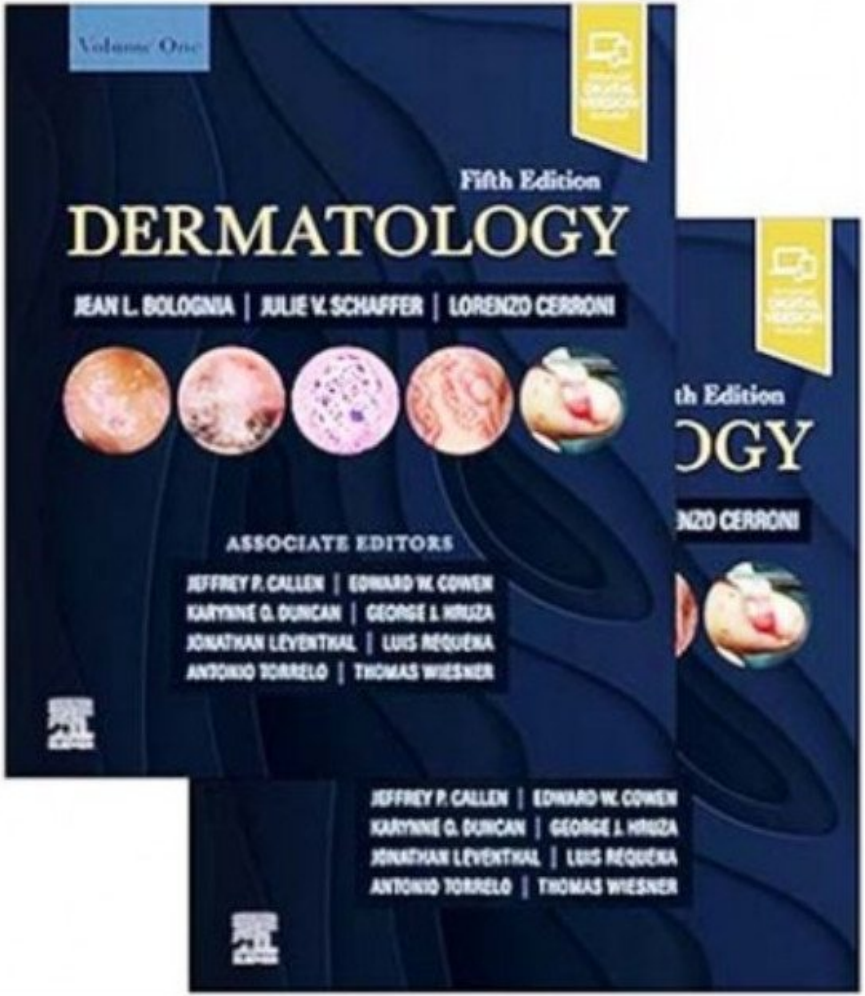
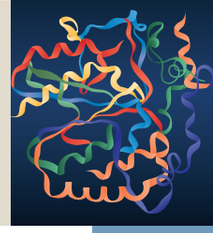

Volume One
Fifth Edition
DERMATOLOGY
JEAN L. BOLOGNIA | JULIE V. SCHAFFER | LORENZO CERRONI
ASSOCIATE EDITORS
JEFFREY P. CALLEN | EDWARD W. COWEN
KARYNNE O. DUNCAN | GEORGE J. HRUZA
JONATHAN LEVENTHAL | LUIS REQUENA
ANTONIO TORRELO | THOMAS WIESNER
JEFFREY P. CALLEN | EDWARD W. COWEN
KARYNNE O. DUNCAN | GEORGE J. HRUZA
JONATHAN LEVENTHAL | LUIS REQUENA
ANTONIO TORRELO | THOMAS WIESNER


الجولان

Biology of the Extracellular Matrix

95



Alexander Nyström and Leena Bruckner-Tuderman

Key features

- Extracellular matrices (ECMs) represent specifically organized networks of collagens, elastin, glycoproteins, and proteoglycans that have distinct structural roles and specific functional properties
- ECMs are biologically active, interact with cells, and regulate their functions during development, regeneration, and normal tissue turnover
- Mutations in ECM genes cause a broad spectrum of human diseases, from Ehlers–Danlos syndrome to epidermolysis bullosa. ECM components are also targeted in autoimmune diseases, e.g., bullous pemphigoid, bullous systemic lupus erythematosus, lichen sclerosus
- The collagen family contains 28 different subtypes. All collagens consist of three polypeptide α-chains folded into a triple helix. In each chain, every third amino acid is glycine (Gly), and thus the sequence can be expressed as $(Gly\text{-}X\text{-}Y)_n$. A hallmark of collagens is the presence of hydroxyproline (Hyp) in the Y position of this repeat sequence. Collagens are expressed in all tissues of the human body, and distinct sets of collagens co-polymerize into highly organized suprastructures, e.g., fibrils and filaments, in a tissue-specific manner
- Elastin provides tissues with elasticity. Elastin monomers contain repetitive hydrophobic sequences and are highly cross-linked. The cross-links between several individual molecules provide both elasticity and insolubility to elastic fibers, which can be stretched by 100% or more and still return to their original form. The elastic fibers in the dermis contain a microfibrillar component that connects the fibers to surrounding structures

INTRODUCTION

The different types of extracellular matrix (ECM) represent specifically organized assemblies of the matrix macromolecules listed in Table 95.1. These macromolecules have characteristic patterns of aggregation into insoluble suprastructures with a high degree of order at successive hierarchic levels[1]. Each of these structures is tissue-specific and adapted to the particular needs of a given tissue. The major constituents are often similar in functionally diverse ECMs. However, various types of less abundant proteins associate with the major ECM components, and differences in their relative composition determine tissue-specific organization of ECM suprastructures. The matrix suprastructures can be compared to alloys, with each having metallurgic properties that differ from each other and those of the pure metals.

Individual ECM macromolecules are usually oligomers composed of one or several polypeptides. Intimate contacts between the subunits are formed by coiled-coil structures, such as the collagen triple helix or supercoiled α-helices comprised of three or more polypeptides. In addition, large matrix macromolecules can be regarded as linear sequences of structural modules that are similar in a large variety of proteins[1]. The modules can be recognized by several cellular receptors, but receptor clustering is determined in a tissue-specific manner, and the response may be different in different tissues.

Our knowledge of matrix macromolecules has increased dramatically due to advances in molecular genetics and proteomics. Numerous molecules have been characterized and their expression, regulation, tissue specificity, and functions discerned[2]. The assembled ECM structures are generally adhesive, enabling the attachment of tissue-specific cells, leukocytes, tumor cells, and even microorganisms (Fig. 95.1). Through integrin-mediated interactions with cells, matrix molecules control cell proliferation, differentiation, and migration, especially during development and regenerative processes. Without contact with the ECM, many cells undergo a form of apoptosis known as *anoikis*. Furthermore, the ECM can function as a reservoir of information; certain proteoglycans and proteins bind growth factors (e.g. transforming growth factor [TGF]-β), releasing and activating them as needed to control cellular functions[2]. To date, mutations in >50 different genes encoding ECM molecules have been found to cause heritable disorders in humans and mice.

COMPONENTS OF THE EXTRACELLULAR MATRIX	
Collagens (28 types)	Laminins (15 types)
Elastin	Proteoglycans (Table 95.3)
Fibrillins (3 types)	Glycoproteins (Table 95.4)
LTBPs (4 types)	Integrins
Fibulins* (7 types)	Enzymes that modify ECM assemblies
*Fibulins are believed to function as intra-molecular bridges that stabilize ECM structural networks (e.g. elastic fibers, microfibrils, basement membrane structures).	

Table 95.1 Components of the extracellular matrix (ECM). They belong to several protein superfamilies, and the molecules assemble into mixed fibrils and networks in a tissue-specific manner. Integrins are the main cellular receptors for the ECM. LTBP, latent TGF-β binding protein.

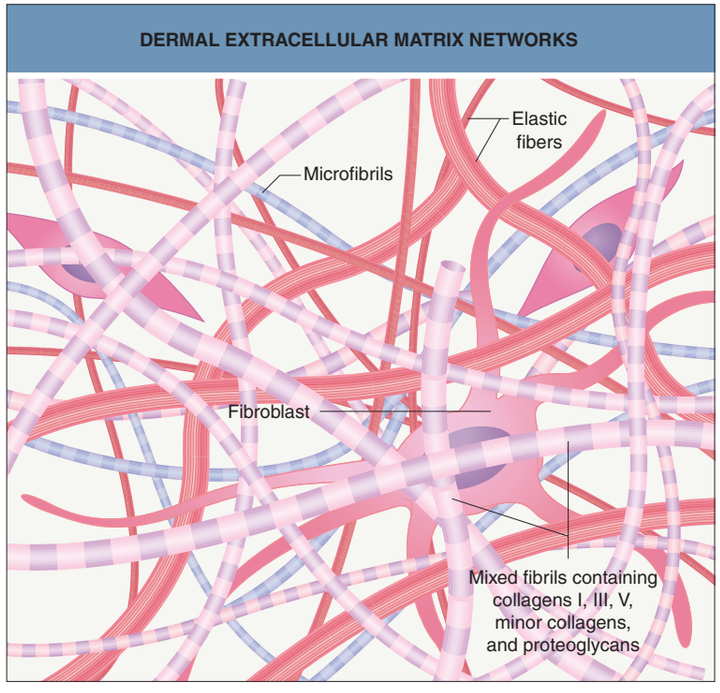


Fig. 95.1 Dermal extracellular matrix networks. Different molecules polymerize into distinct fibril networks and within the mesh of the networks, cells are embedded in the amorphous extrafibrillar matrix. The fibril networks interact with each other, with the extrafibrillar matrix and with the cells. These networks have a dual function: support of the tissue and regulation of cellular functions.

STRUCTURE AND FUNCTION OF THE EXTRACELLULAR MATRIX

Collagens

Collagens play an important role in maintaining the integrity of most tissues. The collagen family includes 28 proteins formally defined as collagens[3] (Table 95.2); they contain 44 distinct polypeptide chains, each encoded by a different gene. At least 15 other proteins have collagen-like domains, e.g. macrophage scavenger receptor 1 and 2, ectodysplasin, pulmonary surfactant proteins.

Collagen triple helix

All collagens consist of three polypeptide chains, known as α-chains, which are folded into a triple helix. In some collagens, the α-chains are identical (homotrimers), while others contain two or three different α-chains (heterotrimers). In the collagenous repeat of each polypeptide chain, every third amino acid is glycine (Gly). The sequence of an α-chain can be expressed as $(Gly\text{-}X\text{-}Y)_n$, where X and Y represent other amino acids and *n* varies according to the length of the repeat. Proline (Pro) and hydroxyproline (Hyp) residues commonly occupy the X and Y positions, respectively, and hydrogen bonds between the hydroxyl groups of Hyp contribute to the stability of the helix. The prototype

THE COLLAGEN FAMILY OF PROTEINS			
Type	**Chains**	**Gene**	**Tissue distribution**
Fibril-forming collagens			
Collagen I	α_1(I), α_2(I)	*COL1A1, COL1A2*	Skin, most ECM
Collagen II	α_1(II)	*COL2A1*	Cartilage, vitreous humor
Collagen III	α_1(III)	*COL3A1*	Skin (including fetal skin), lung, vasculature
Collagen V	α_1(V), α_2(V), α_3(V)	*COL5A1, COL5A2, COL5A3*	Skin, with collagen I heterotypic fibrils
Collagen XI	α_1(XI), α_2(XI)	*COL11A1, COL11A2*	With collagen II heterotypic fibrils
Collagen XXIV	α_1(XXIV)	*COL24A1*	Developing bone and cornea
Collagen XXVII	α_1(XXVII)	*COL27A1*	Cartilage, eye, ear, lung
FACITs			
Collagen IX	α_1(IX), α_2(IX), α_3(IX)	*COL9A1, COL9A2, COL9A3*	With collagen II heterotypic fibrils
Collagen XII	α_1(XII)	*COL12A1*	Skin, tissues containing collagen I
Collagen XIV	α_1(XIV)	*COL14A1*	Skin, tissues containing collagen I
Collagen XVI	α_1(XVI)	*COL16A1*	Skin, many tissues
Collagen XIX	α_1(XIX)	*COL19A1*	Basement membranes, fetal muscle
Collagen XX	α_1(XX)	*COL20A1*	Skin, cornea, cartilage, tendon
Collagen XXI	α_1(XXI)	*COL21A1*	Many tissues, including skin
Collagen XXII	α_1(XXII)	*COL22A1*	Tissue junctions (including between the anagen hair follicle and dermis)
Basement membrane collagen			
Collagen IV	α_1(IV), α_2(IV), α_3(IV), α_4(IV), α_5(IV), α_6(IV)	*COL4A1, COL4A2, COL4A3, COL4A4, COL4A5, COL4A6*	All basement membranes, isoforms vary Skin: α_1(IV), α_2(IV), α_5(IV), and α_6(IV)
Microfibrillar collagen			
Collagen VI	α_1(VI), α_2(VI), α_3(VI)	*COL6A1, COL6A2, COL6A3, COL6A5,COL6A6*	Skin, other microfibril-containing tissues
Network-forming collagens			
Collagen VIII	α_1(VIII), α_2(VIII)	*COL8A1, COL8A2*	Skin, subendothelial matrices
Collagen X	α_1(X)	*COL10A1*	Hypertrophic cartilage
Anchoring fibril collagen			
Collagen VII	α_1(VII)	*COL7A1*	Skin, mucous membranes, cornea
Transmembrane collagens			
Collagen XIII	α_1(XIII)	*COL13A1*	Skin, many tissues
Collagen XVII	α_1(XVII)	*COL17A1*	Skin, mucous membranes, cornea
Collagen XXIII	α_1(XXIII)	*COL23A1*	Lung, cornea, brain, skin, tendon, kidney
Collagen XXV	α_1(XXV)	*COL25A1*	Brain, neurons
Multiplexins			
Collagen XV	α_1(XV)	*COL15A1*	Many tissues; parent molecule of restin*
Collagen XVIII	α_1(XVIII)	*COL18A1*	Many tissues, including skin, subendothelial matrices; parent molecule of endostatin*
Other collagens			
Collagen XXVI	α_1(XXVI)	*COL26A1*	Testis, ovary
Collagen XXVIII	α_1(XXVIII)	*COL28A1*	Schwann cells; fetal skin and calvaria

*Inhibitors of angiogenesis.

Table 95.2 The collagen family of proteins. The names of types found in the skin are in ***bold italics***. Multiplexins are collagens with multiple triple helix domains and interruptions. ECM, extracellular matrix; FACITs, fibril-associated collagens with interrupted triple helices.

collagen (type I) has an uninterrupted Gly-X-Y repeat sequence of almost 1000 amino acid residues; this forms a rigid, rodlike structure with a diameter of 1.5 nm and length of 300 nm. In some collagens, the $(Gly\text{-}X\text{-}Y)_n$ repeats are interrupted by one or more amino acids. The interruptions may be numerous and longer than the $(Gly\text{-}X\text{-}Y)_n$ repeats and they provide the molecule with flexibility, which is important for its specific functions[3].

Biosynthesis of collagens

Collagen biosynthesis involves a number of post-translational modifications (Fig. 95.2). Some collagens are first synthesized as procollagens that have propeptide extensions at their N-terminus, C-terminus, or both. The main intracellular steps in collagen biosynthesis include the following:

- cleavage of signal peptides
- hydroxylation of certain Pro and lysine (Lys) residues to 4-Hyp, 3-Hyp, and hydroxylysine (Hyl)
- glycosylation of some of the Hyl residues to galactosyl-Hyl and glucosylgalactosyl-Hyl
- glycosylation of certain asparagine residues
- association of the α-chains in a specific manner
- formation of intra- and interchain disulfide bonds
- folding of the triple helix

After the chains have become associated and sufficient Hyp residues have been formed in each chain, a nucleus of the triple helix forms (usually in the C-terminal region), and the triple helix propagates towards the other end of the molecule in a zipper-like fashion[4]. The procollagen molecules are then transported from the endoplasmic reticulum across the Golgi apparatus without leaving the lumen of the Golgi cisternae. During this transport, the triple helices begin to aggregate laterally and form early fibrils ready for secretion[5]. The folding and transport of these large, rigid collagens require special machinery[6,7]. Deficiencies in the proteins that interact with collagens during these intracellular events can lead to phenotypes similar to collagen deficiency disorders[8]. The *extracellular* steps in biosynthesis include cleavage of the N- and/or C-terminal propeptides, assembly into suprastructures with other collagens and non-collagenous components, and formation of covalent cross-links.

The specific enzymes involved in the biosynthesis of collagens include prolyl-4-hydroxylase and prolyl-3-hydroxylase, which hydroxylate Pro residues to Hyp, and three lysyl hydroxylases, which hydroxylate Lys residues to Hyl. These enzymes require O_2, Fe^{2+}, α-ketoglutarate, and ascorbate as cofactors. In the rough endoplasmic reticulum, glycosyltransferases add glucosylgalactosyl disaccharides onto the α-chains. The same intracellular enzymes modify all collagen chains[4], whereas extracellular processing enzymes have a higher substrate specificity. Procollagen I N-proteinase cleaves the N-propeptide of procollagens I and II. This enzyme is a member of the disintegrin and metalloproteinase (ADAM) proteinase family and is also referred to as ADAM with *t*hrombospondin type 1 motif (ADAMTS)-2. Procollagen C-proteinases that cleave the C-propeptide of collagens I, II, III, V, and VII belong to the astacin family and include bone morphogenetic protein-1 (BMP-1) and tolloid-like proteins; meprins in this family can cleave both N- and C-termini of collagens[9].

Cross-linking between collagen molecules involves the ε-amino groups of Lys and Hyl and is catalyzed by lysyl oxidase, a copper-requiring enzyme[4]; this process can be regulated by proteoglycans[10]. Another enzyme that catalyzes cross-linking of some collagens is tissue transglutaminase[3].

The collagen family

The length and continuity of the triple helical domains vary among the collagen types. For practical purposes, the collagens have been divided into groups according to their ability to form supramolecular aggregates (Fig. 95.3). The types and tissue distributions of the collagens in each group are listed in Table 95.2, and more detailed information is available in reviews[1,3,4].

Collagens of the skin

Collagens account for 75% of the dry weight and 20%–30% of the volume of the dermis. Different collagens polymerize into distinct suprastructures and have specific functions in the dermis as well as in epidermal and vascular basement membranes. Collagen fibrils are always mixtures of several collagens and other molecules, e.g.,

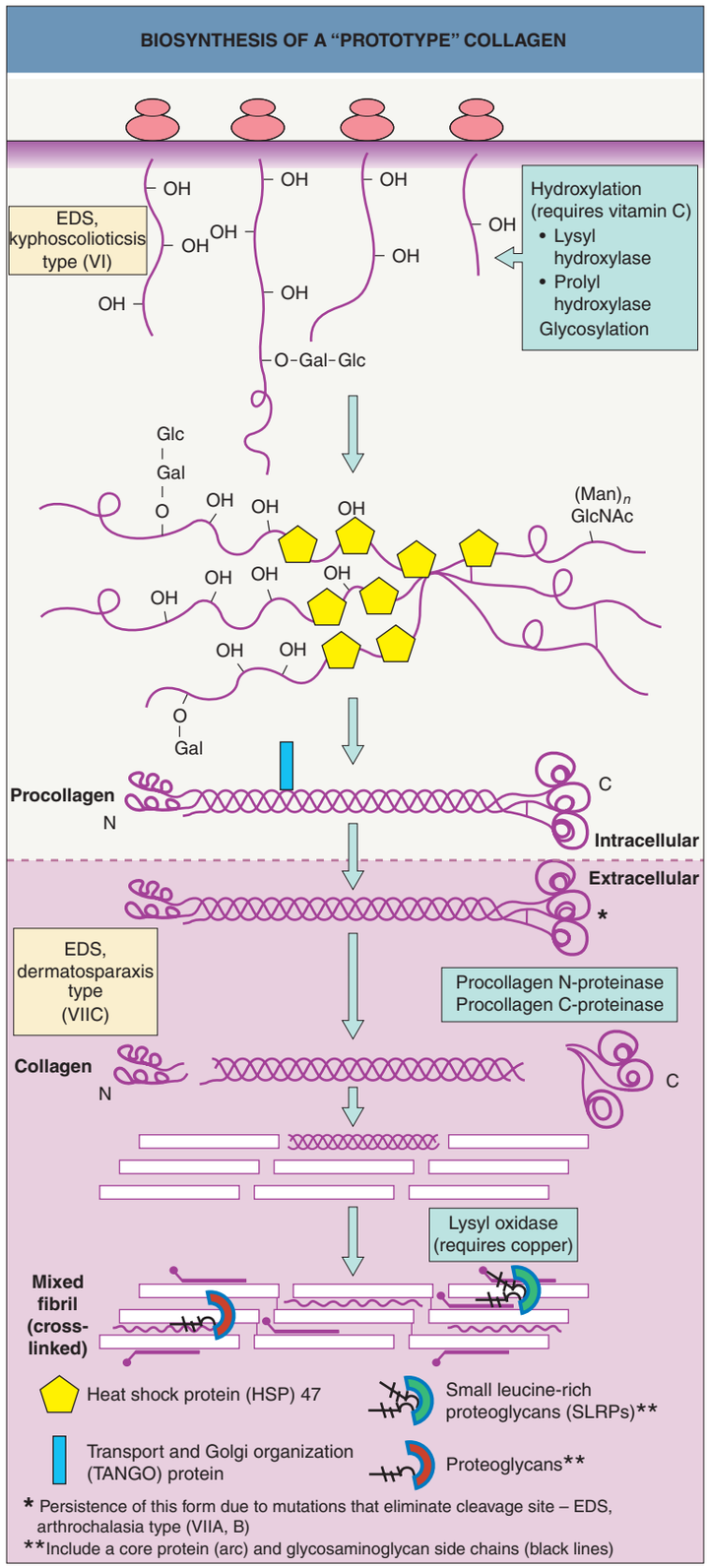


Fig. 95.2 Biosynthesis of a "prototype" collagen. The procollagen α-chains are synthesized by ribosomes in the rough endoplasmic reticulum (ER). Already during the synthesis of the nascent polypeptide, certain prolyl and lysyl residues are hydroxylated and modified by glycosylation. Three α-chains associate to form a trimer and fold into a triple helix. This process is facilitated by heat shock protein (HSP) 47, a collagen-specific molecular chaperone in the ER. The transport and Golgi organization (TANGO) protein 1 mediates secretion of the newly formed triple helical procollagen into the extracellular space, where the N- and C-terminal propeptides are cleaved by specific proteases. The mature collagen molecules assemble to form mixed fibrils with other collagens and non-collagenous molecules. The suprastructures are stabilized by covalent cross-links. Small leucine-rich proteoglycans (SLRPs) and other proteoglycans have roles in the regulation of collagen fibrillogenesis and cross-linking. EDS, Ehlers–Danlos syndrome. *Adapted from Myllyharju J, Kivirikko KI. Collagens, modifying enzymes and their mutations in humans, flies and worms. Trends Genet 2004;20:33–43.*

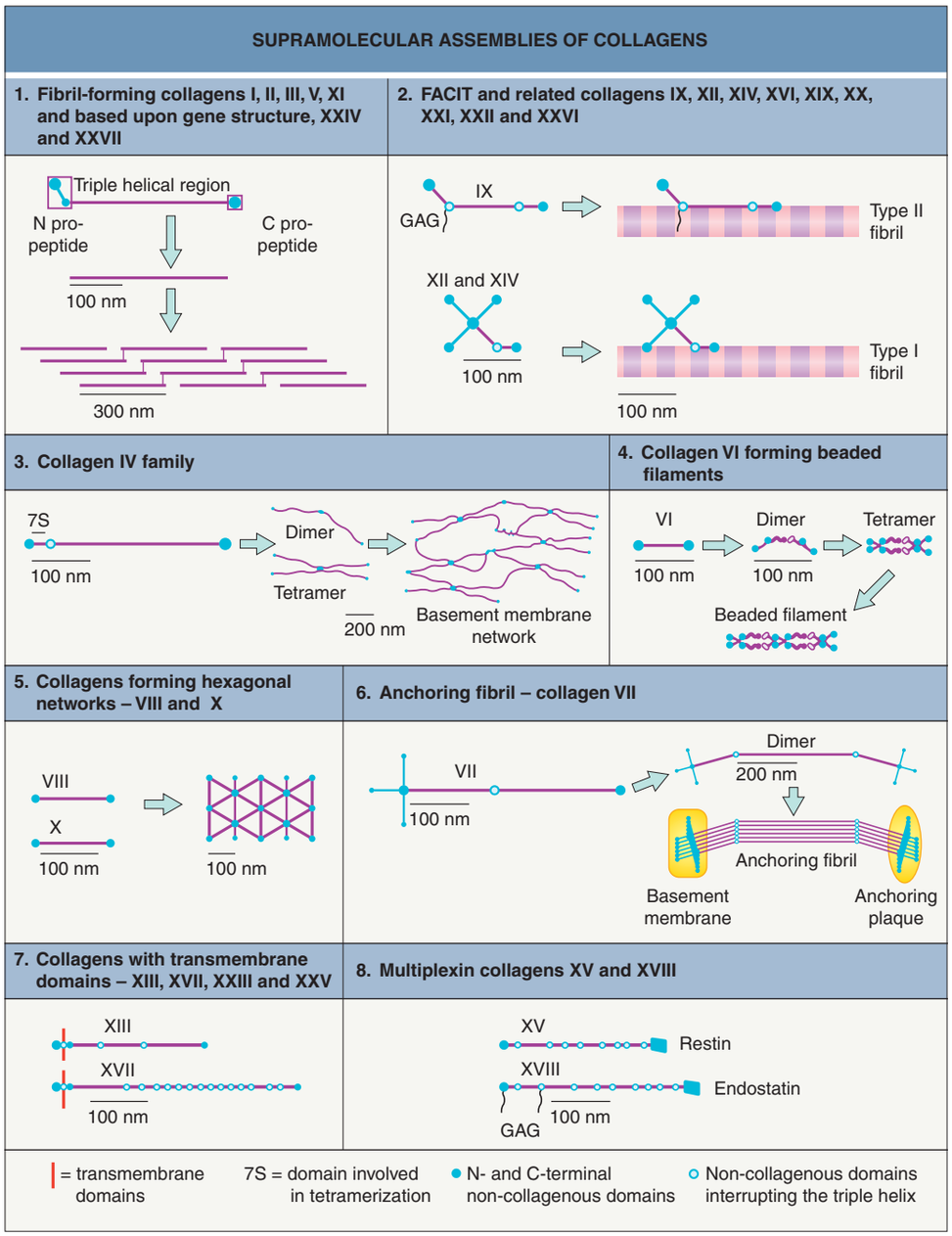


Fig. 95.3 Supramolecular assemblies of collagens. The suprastructures formed by different collagens are shown. Non-collagenous components also interact with the fibrils and networks. The suprastructural organization of the transmembrane collagens XIII and XVII and the multiplexin collagens XV and XVIII is not known yet (panels 7 and 8). These collagens are in close vicinity to basement membranes and are likely to participate and/or interact with the different basement membrane networks. FACIT, fibril-associated collagens with interrupted triple helices; GAG, glycosaminoglycans. *Adapted from Myllyharju J, Kivirikko KI. Collagens, modifying enzymes and their mutations in humans, flies and worms. Trends Genet 2004;20:33–43.*

proteoglycans[1]. Classic, ultrastructurally recognizable, cross-banded fibrils in the dermis contain collagens I, III, V, XII, and XIV. The characteristic cross-banding with a periodicity of 64 nm results from precise lateral packing of the different collagens within the fibrils (Fig. 95.4; see Fig. 95.3). Collagen I is the major component of the fibrils, and the amount of other collagens varies. For example, during embryonic development and wound repair, the relative content of collagen III increases.

Collagen VI, a highly glycosylated and disulfide-bonded collagen, is a component of almost all tissues, including the skin. *In vitro*, it polymerizes to form beaded filaments (see Fig. 95.3), but *in vivo* in the dermis, the ultrastructure of the collagen VI fibrils is reminiscent of microfibrils.

The collagen IV molecules in different basement membranes contain six genetically distinct but structurally homologous α-chains, which form three major networks – α_1/α_2, $\alpha_3/\alpha_4/\alpha_5$, and $\alpha_1/\alpha_2/\alpha_5/\alpha_6$[3]. In the skin, the α_1/α_2 network dominates within the dermal–epidermal junction (see Ch. 28), but the $\alpha_1/\alpha_2/\alpha_5/\alpha_6$ network is also present[11].

Two collagens are essential for the cohesion of the epidermis and dermis (see Ch. 28). Collagen VII is the major, if not sole, component of the anchoring *fibrils* that connect the basement membrane to the dermal ECM. Collagen XVII (also known as bullous pemphigoid antigen 2) is a component of the anchoring *filaments* that bind the basal keratinocytes to the lamina densa of the basement membrane. It is a transmembrane collagen in type II orientation with a long extracellular C-terminal region containing a multiply-interrupted triple helix referred to as collagenous domains 1–15 (see Fig. 31.9). The ectodomains of collagen XVII can be cleaved by transmembrane proteases and then shed, a process important for regulating cell adhesion and migration. Basal keratinocytes also express other transmembrane collagens, such as collagens XIII, a component of focal contacts, and XXIII[12].

The vascular basement membranes in the skin contain collagens VIII and XVIII. Collagen VIII forms hexagonal networks (see Fig. 95.3) below the endothelial basement membranes, thereby strengthening the vascular wall. Collagen XVIII is present in both epidermal basement membranes and the dermal side of vascular basement membranes. Its C-terminal fragment, endostatin, is proteolytically released from the collagen molecule and has independent antiangiogenic and anti-scarring activities[3].

Most collagens in the skin are synthesized by dermal fibroblasts. Exceptions include: (1) collagen XVII, a surface component of epidermal keratinocytes; (2) collagen VII, which is synthesized by both keratinocytes and fibroblasts; and (3) collagens VIII and XVIII, which can also be produced by endothelial cells. Several genetic and acquired diseases are associated with abnormalities of skin collagens or the enzymes that process them (see Table 95.5 & 95.6 and below).

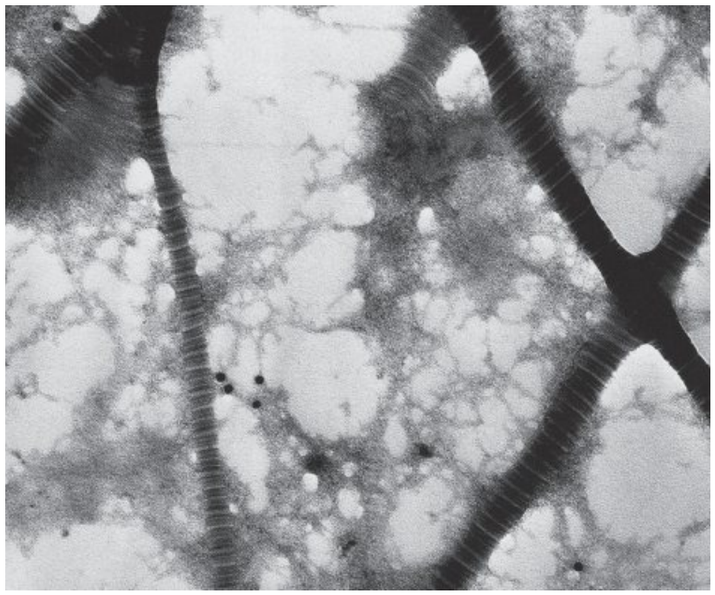


Fig. 95.4 Fibrillar and filamentous networks extracted from human skin. The large cross-banded fibrils represent dermal mixed fibrils containing collagens I, III, V, other minor collagens, and decorin (a proteoglycan). The cross-banding has a characteristic periodicity of 64 nm. The filamentous network in the background contains microfibrillar and basement membrane components. In this immuno-electron photomicrograph, the black dots are colloidal gold particles coupled to anti-collagen IV antibodies, indicating that basement membrane networks are strongly associated with the dermal fibrillar networks. *Courtesy Dr Uwe Hansen.*

Elastic Fibers

The elasticity of many tissues, including the skin, depends upon the structure of elastic fibers, which have variable compositions. A characteristic property of these fibers is that they can be stretched by 100% or more and still return to their original form. Their main components are elastin and microfibrils.

Elastin

Elastin is a highly cross-linked protein[13]. Its monomer, tropoelastin, exists in several tissue-specific splice variants. Ala- and Lys-rich repeats form critical cross-linking domains within a background of hydrophobic amino acid repeats. Lysyl oxidase, the same enzyme that catalyzes collagen cross-linking, catalyzes the formation of desmosine cross-links between elastin molecules, which account for the elasticity and insolubility of the elastic fibers. Elastin makes up ~90% of mature elastic fibers. During fiber assembly, tropoelastin self-assembles and interacts with fibulins 4 and 5, fibrillin 1, and microfibril-associated glycoprotein-1 (MAGP-1). A model for this spatially and temporally regulated process is shown in Fig. 95.5[13].

Microfibrils

Microfibrils (10 to 12 nm in diameter) insert into the basement membrane in a perpendicular orientation (classically referred to as "oxytalan fibers") and extend into the papillary dermis, where they gradually merge with the elastic fibers that form a plexus parallel to the dermal–epidermal junction (classically referred to as "elaunin fibers"). These fibers appear to be continuous with the elastic fibers in the reticular dermis, which contain more abundant elastin. Microfibrils consist mainly of fibrillins[13] but also contain and associate with other

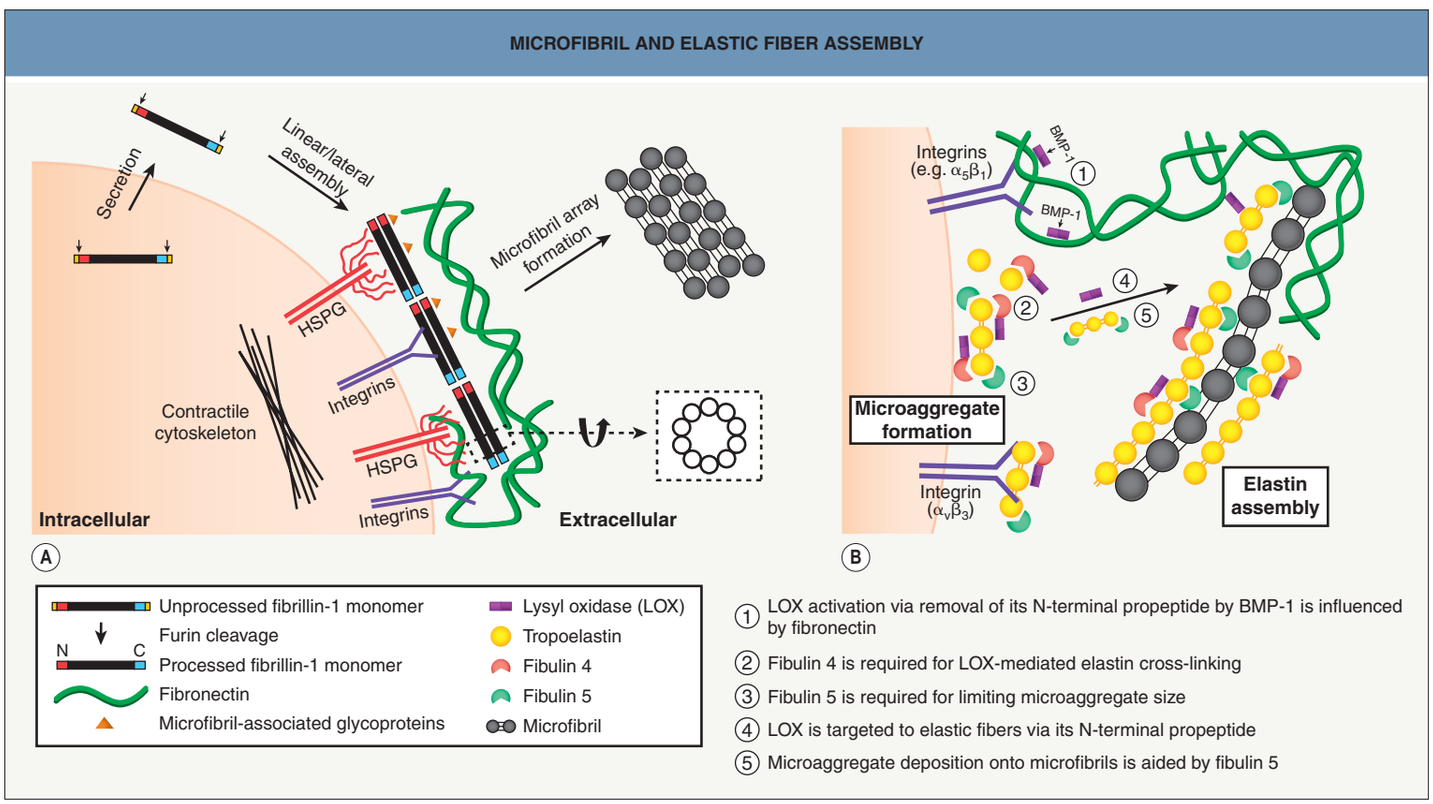


Fig. 95.5 Microfibril and elastic fiber assembly. A Following secretion of fibrillin 1, its N- and C-termini are processed by furin and then interact homotypically; this leads to axial and lateral fibrillin 1 assembly to form microfibrils. Beads may arise from folding of terminal regions, and transglutaminase cross-links provide stabilization. Fibronectin is thought to act as a microfibril assembly template and/or to facilitate assembly at fibrillar adhesions by stimulating cytoskeletal tension through $\alpha_5\beta_1$ integrin. Fibrillin 1 interacts with $\alpha_5\beta_1$, $\alpha_v\beta_3$, and $\alpha_v\beta_6$ integrins during microfibril assembly. Heparan sulfate proteoglycans (HSPGs) are thought to facilitate cell surface–fibrillin 1 interactions, and heparin inhibits microfibril assembly. Fibrillin 1 also binds microfibril-associated glycoproteins, tropoelastin, fibulins, and latent transforming growth factor (TGF)-β binding protein. **B** Elastic fiber formation includes pericellular elastin "microassembly" and subsequent "macroassembly" on a microfibrillar scaffold. Secreted tropoelastin forms globules at the cell surface, which become cross-linked by lysyl oxidase (LOX); this process may involve $\alpha_v\beta_3$ integrin interactions with tropoelastin, as well as interactions of HSPGs with integrins and tropoelastin. Fibulin 4 and fibulin 5 contribute to elastin cross-linking by lysyl oxidase and are also thought to direct the deposition of elastin globules onto preformed fibrillin-containing microfibrils, thereby forming elastic fibers. Microfibrils and elastic fibers are important matrix storage sites for bone morphogenic proteins (BMPs) and latent TGF-β1. *Adapted from Baldwin AK, Simpson A, Steer R, et al. Elastic fibres in health and disease. Expert Rev Mol Med 2013;15:e8.*

proteins, such as MAGPs, latent TGF-β binding proteins (LTBPs), fibulins, elastin microfibril interface (EMILIN)-1, and (in the papillary dermis) collagen XVI[3,13]. Fibrillins 1–3 are large glycoproteins that contain both epidermal growth factor (EGF) and cysteine (Cys) repeats. The EGF repeats bind calcium, which is required for protein stabilization. Fibrillin 1 interacts with perlecan in the epidermal basement membrane to attach microfibrils to the dermal–epidermal junction. Fibrillin interactions with heparan sulfate proteoglycans and integrin receptors also contribute to microfibril assembly (see Fig. 95.5)[13,14].

In addition to guiding elastic fiber assembly and providing structural support, fibrillins function together with LTBPs to regulate cell signaling[13]. The four members of the LTBP family are high-molecular-weight glycoproteins characterized by EGF-like and 8-Cys repeats, and they all associate with the small latent complex of TGF-β (see below; Fig. 95.6). The LTBP-1/latent TGF-β complex (referred to as the large latent complex) binds to fibrillin-containing microfibrils. Together, they control the bioavailability of TGF-β in the skin and other tissues. LTBPs contain multiple proteinase-sensitive sites, providing the means to solubilize the large latent complex from ECM structures. Another group of signaling molecules that can bind to fibrillins are bone morphogenetic proteins (BMPs)[13]. BMPs are secreted as cross-linked dimeric complexes that are associated through their prodomains, which interact directly with the N-terminus of fibrillin. Fibrillins and LTBPs, therefore, have important roles in targeting latent, activatable TGF-β and BMPs into different ECMs. Thus, microfibrils serve not only as a force-bearing element and scaffolding for elastin deposition in the dermis, but also as an important repository for signaling molecules in the skin[2,13].

The Extrafibrillar Matrix

The dermal fibril networks and cells are embedded in an amorphous extrafibrillar material that binds water and provides the hydrated consistency of the skin. Previously, this amorphous material was presumed to be biologically unstructured and inert and was called "ground substance". This prediction turned out to be incorrect; the extrafibrillar matrix is molecularly and structurally diverse, highly organized, and biologically active. It contains a number of proteoglycans and glycoproteins, hyaluronic acid, and water. The functions of the extrafibrillar matrix are adapted to the biologic needs of each tissue. For example, during embryonic development, water-binding proteoglycans and glycosaminoglycans (GAGs) provide a hydrated milieu for cell migration and proliferation. During development and tissue remodeling, glycoproteins of the extrafibrillar matrix are essential for the formation of the correct tissue architecture.

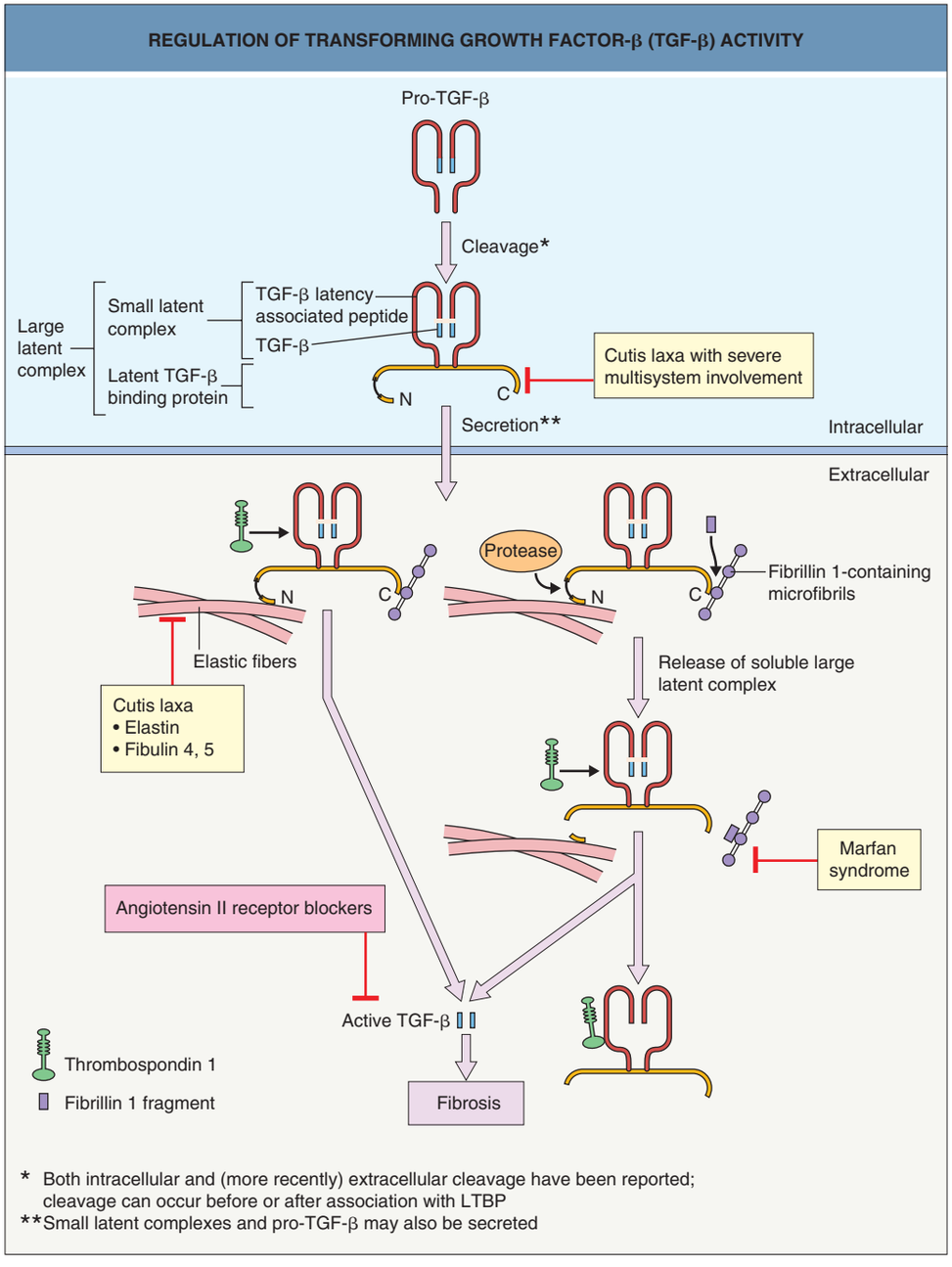


Fig. 95.6 Regulation of transforming growth factor-β (TGF-β) activity. TGF-β is synthesized as an inactive homodimeric propeptide, pro-TGF-β. After cleavage, mature TGF-β is sequestered in an inactive form via its continued association (now noncovalent) with the latency-associated peptide (LAP; forming the small latent complex) and covalent linkage of the LAP to the latent TGF-β binding protein (LTBP; forming the large latent complex). In addition, the large latent complex becomes attached to the extracellular matrix (ECM) via covalent linkage of the LTBP N-terminus with ECM proteins and noncovalent association of the LTBP C-terminus with fibrillin 1 (a member of the LTBP/fibrillin superfamily). Solubilization of the large latent complex from the ECM can occur via proteolytic cleavage of susceptible hinge regions within the LTBP and disruption of the fibrillin 1–LTBP interaction by fibrillin 1 fragments. Binding of ECM glycoproteins such as thrombospondin 1 to the LAP results in the release of active TGF-β that can bind to its receptors and promote fibrosis. *Adapted from August P, Suthanthiran M. Transforming growth factor beta signaling, vascular remodeling, and hypertension. N Engl J Med 2006;354:2721–3.*

Glycosaminoglycans and proteoglycans

GAGs are polysaccharides composed of sulfated and acetylated sugars with negative charges that bind large amounts of ions and water. The most prominent and ubiquitous *protein-free* GAG is hyaluronic acid, a giant polysaccharide composed of thousands of N-acetylglucosamine/glucuronic acid disaccharides. However, other GAGs bind to proteins via a serine hydroxyl group, forming proteoglycans (Fig. 95.7)[15]. There are four classes of proteoglycans based upon their tissue localization: intracellular, cell-surface, pericellular, and extracellular[15]. Proteoglycans differ remarkably in their protein content as well as the number, type, and length of their GAG side chains (Table 95.3).

Four known GAGs can bind proteins to form proteoglycans; they are chondroitin sulfate, dermatan sulfate, keratan sulfate, and heparan sulfate[15]. The correct balance of chondroitin sulfate and dermatan sulfate is necessary for skin function and integrity[16]. Versican, which contains these two GAGs, is an important dermal proteoglycan that can be synthesized by fibroblasts, smooth muscle cells, and epithelial cells. It is associated with the elastic fiber system and forms large complexes with hyaluronic acid, which provide the skin with its tautness (see Fig. 95.7).

Heparan sulfate chains sequester growth factors (e.g. fibroblast growth factors [FGFs], vascular endothelial growth factors [VEGFs]) and present them to their receptors. Perlecan is a major heparan sulfate-containing proteoglycan found in all basement membranes, including the epidermal basement membrane. Collagen XVIII, a collagen/heparan sulfate hybrid, is also present in epidermal and vascular basement membranes as well as the skin[17]. Syndecans are transmembrane heparan sulfate proteoglycans that control cell adhesion to the ECM and cytoskeletal organization. Syndecans 1, 2, and 4 are expressed in the skin and can be found in keratinocytes, dendritic cells, and fibroblasts, where they are thought to mediate "outside-in" cell signaling[15]. Glypicans are membrane-anchored heparan sulfate proteoglycans that interact with growth factors and other extracellular proteins in the skin to regulate developmental and regenerative events[18].

Small leucine-rich proteoglycans (SLRPs) have a protein core of Leu-rich repeats and Cys-bonded loops, with one to five GAG chains. Decorin and biglycan are SLRPs that have multiple functions in the skin via interactions with a variety of proteins, including collagen fibrils (thereby regulating fibrillogenesis), receptor tyrosine kinases, and TGF-β. SLRPs, hyaluronic acid, and versican modulate inflammatory responses through Toll-like receptor signaling[19]. Fibromodulin, keratocan, and lumican are other SLRPs involved in collagen fibril formation, and fibromodulin also regulates intermolecular collagen cross-linking[10,15].

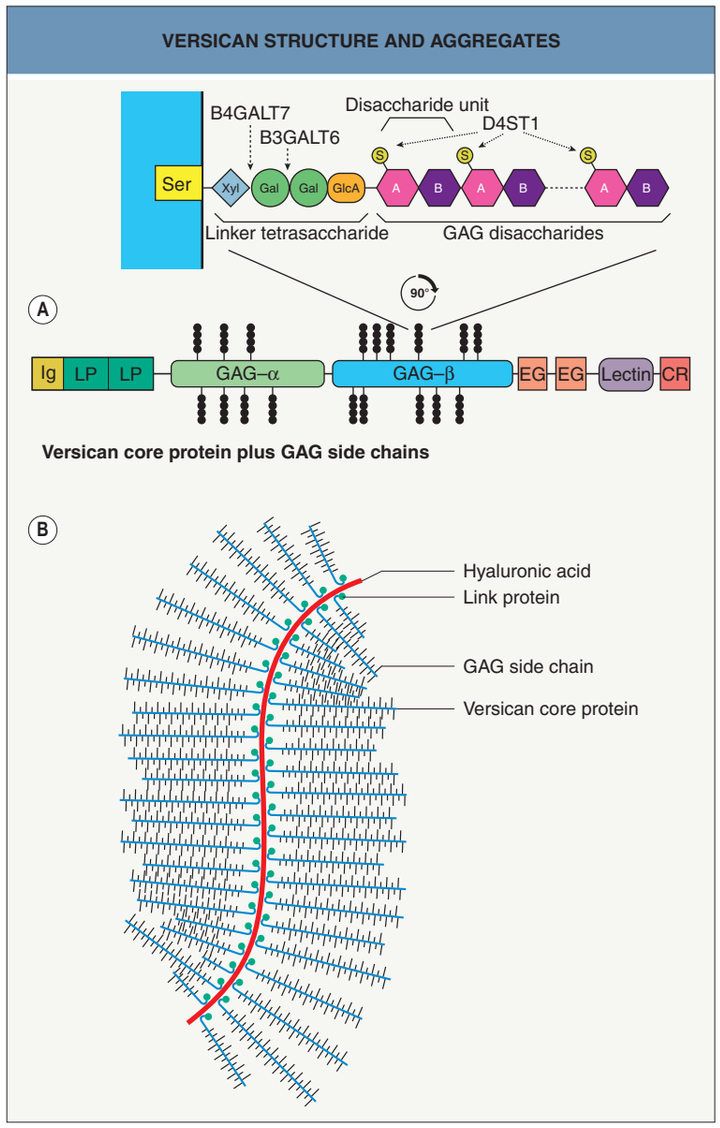


Fig. 95.7 Versican structure and aggregates. A The core protein contains several structural motifs important for glycosaminoglycan (GAG) and ligand binding. The N-terminal immunoglobulin-type repeat (Ig) is followed by two consecutive link-protein type modules (LP), which are involved in mediating the binding of the core protein to hyaluronic acid. The GAG binding domain, which comes in tissue-specific alternative splice variants, GAG-α and/or GAG-β, carries the GAG side chains. It is followed by structural motifs, including two EGF-like repeats (EG), a C-type lectin domain (Lectin), and a complement regulatory protein-like module (CR). The ***inset*** shows an enlarged view of a GAG side chain, which is attached to a serine residue (Ser) of the core protein via a linker tetrasaccharide. In chondroitin sulfate, the disaccharides are composed of N-acetylgalactosamine (GalNAc) [position A] and glucuronic acid [position B]. In dermatan sulfate, the disaccharides are composed of GalNAc [position A] and iduronic acid (IdoA) [position B]. β-1,4-galactosyltransferase 7 (B4GALT7) and β-1,3-galactosyltransferase 6 (B3GALT6) add the first and second galactose (Gal), respectively, to the xylose (Xyl) of the linker tetrasaccharide (dashed arrows). Dermatan-4-sulfotransferase 1 (D4ST1) then adds the active sulfate to the 4-O position of GalNAc (dotted arrows) on dermatan sulfate. Mutations in the genes encoding these enzymes lead to forms of Ehlers–Danlos syndrome (see text and Table 95.5). **B** In the dermis, versican can form huge aggregates with hyaluronic acid (red). The core protein (blue), which carries a number of GAG side chains (black), is bound to hyaluronic acid via its link-protein domain (green; LP module in the scheme in panel **A**). The aggregates can bind large amounts of water, and thus provide for the tautness of the skin. GlcA, glucuronic acid. *Adapted from Iozzo RV. Matrix proteoglycans: from molecular design to cellular function. Ann Rev Biochem 1998;67:609–52; and Miyake N, Kosho T, Matsumoto N. Ehlers-Danlos syndrome associated with glycosaminoglycan abnormalities. Adv Exp Med Biol 2014;802:145–59.*

Laminins and Other Glycoproteins

Laminins, a family of basement membrane molecules with 15 distinct members, are expressed in all tissues. Each laminin isoform is a trimer consisting of an α-, β-, and γ-chain. Combinations of the three chains vary[20,21], with nomenclature based on the chain composition[22]; for example, the laminin composed of α_3, β_3, and γ_2 chains is referred to as laminin 332 (formerly known as laminin 5). In the skin, the epidermal basement membrane contains laminins 332, 311, and 511, and the vascular basement membrane contains laminins 411 and 511. The structure, biologic functions, and genetic defects of laminins expressed in the skin are discussed in more detail in Chapters 28 and 32.

Other glycoproteins with important functions in the skin are listed in Table 95.4[23].

Functions of the Extracellular Matrix

Structural role of the extracellular matrix

In the past, the ECM was simply regarded as a structural scaffold that gave organs their shape and consistency. However, there has been much progress in our understanding of the broad spectrum of ECM suprastructures and their specific functions. Basement membranes are sheets with limited tensile strength but important tissue-specific properties that enable particular cell attachments; they also regulate morphogenesis, differentiation, and barrier functions. At the dermal–epidermal junction, specific basement membrane-associated aggregates ensure strong adhesion of the epidermis to the dermis and thus resistance against external shear forces. In the dermis, different ECM networks are embedded in the water-binding extrafibrillar matrix, maintaining the elasticity, resilience, and tautness of the skin. The specific ECM compositions and post-translational modifications determine the elastic properties and stiffness of a given tissue.

PROTEOGLYCANS OF THE SKIN			
Proteoglycan	**Gene**	**Size of the core protein (kDa)**	**Glycosaminoglycan (GAG) side chains (number)**
Versican	*CSPG2*	265–370, splice variants	Chondroitin/dermatan sulfate (10–30)
Perlecan	*HSPG2*	400–467	Heparan/chondroitin sulfate (3)
Decorin*	*DCN*	40	Chondroitin/dermatan sulfate (1)
Fibromodulin*	*RMOD*	42	Keratan sulfate (2–3)
Lumican*	*LUM*	38	Keratan sulfate (3–4)
Keratocan*	*KERA*	38	Keratan sulfate (3–5)
Biglycan*	*BGN*	40	Chondroitin/dermatan sulfate (2)
Syndecans 1, 2, 4	*SDC1* *SDC2* *SDC4*	35–120	Heparan/chondroitin sulfate (3–5)
Glypican 1	*GPC11*	62	Heparan sulfate (3)
*Small leucine-rich proteoglycan.			

Table 95.3 Proteoglycans of the skin.

GLYCOPROTEINS OF THE SKIN	
Glycoproteins	**Key functions**
Fibronectin	Cell adhesion and migration
Vitronectin	Cell adhesion and migration
Thrombospondins (4 types)	Cell-to-cell and cell-to-matrix communication
Matrilins (4 types)	Matrix assembly, cell adhesion
Tenascins (4 types)	Regulation of cellular function
Cartilage oligomeric matrix protein (COMP)	Matrix assembly, calcium binding, protein folding

Table 95.4 Glycoproteins of the skin.

Regulation of cellular functions

In addition to their structural roles, ECMs are biologically active. *In vitro* studies as well as transgenic and knockout mouse models (see Ch. 3) have demonstrated the importance of ECMs as potent regulators of cellular functions during development, regeneration, wound healing, inflammation, and tumorigenesis. ECM macromolecules can influence a wide range of cellular processes, including adhesion, migration, cytoskeletal organization, division, differentiation, polarization, and apoptosis.

Cells use a variety of receptors, such as integrins and cell surface proteoglycans, to recognize signals from the ECM[2]. The β_1 integrin family represents the most prevalent class of matrix receptors. The α-subunit of the integrin determines the specificity for individual matrix protein ligands, but the affinity and degree of specificity vary. Some integrins recognize only one ligand, while others can bind to several matrix proteins.

"Outside" signals from the ECM can have different effects on the cell[24]. For example, they may induce clustering of integrins on the cell surface and lead to the formation of protein complexes between the cytoplasmic domains of the integrins and the cytoskeleton, thereby influencing cell shape. Alternatively, activation of integrins by the ECM can stimulate signal transduction pathways involving focal adhesion kinase (protein tyrosine kinase 2), paxillin, and tensin. ECM–integrin interactions may also induce mitogen-activated protein kinase-mediated regulation of transcription, cell proliferation, and differentiation. Further regulation of ECM–integrin signaling is mediated by divalent cations, phospholipids, and other agents[25]. Integrins also sense and respond to ECM rigidity through mechanisms involving changes in integrin binding dynamics, stretch-activated ion channels, and unfolding of mechanosensitive proteins (e.g. talin, vinculin) in focal adhesions (see Fig. 28.3B)[24]. These events regulate cell migration and stem cell fate.

Growth factors in the TGF-β family are potent regulators of ECM formation, in addition to their immunomodulatory functions and regulatory role in cell growth[2]. They are secreted from cells as latent complexes containing TGF-β and its propeptide latency-associated peptide (LAP). In most cells, LAP is covalently linked to LTBP, forming the large latent complex (see Fig. 95.6). Secreted large latent complexes associate covalently with ECM proteins. TGF-β can be released from these complexes by a variety of mechanisms including mechanical forces and matrix-degrading proteinases originating from fibroblasts or inflammatory cells. In addition to LTBPs, several other ECM molecules, including proteoglycans and thrombospondin, can bind and modulate the activity of TGF-β.

DISEASES RELATED TO ECM DEFECTS

Molecular studies of the genes and proteins involved in ECM disorders have produced a wealth of information regarding the normal biology of the ECM[13,16,23,26,27]. Putative functions for many matrix macromolecules were found or confirmed when mutations in their genes were defined in diseases. For example, the fundamental roles of collagens VII and XVII in dermal–epidermal adhesion became clear when mutations in the corresponding genes were discovered in patients with hereditary epidermolysis bullosa (EB)[26]. Inherited ECM diseases with cutaneous manifestations are listed in Table 95.5, and the molecular mechanisms and pathophysiology of selected conditions are delineated below. Ehlers–Danlos syndrome (EDS), cutis laxa, and pseudoxanthoma elasticum (PXE) are covered in more depth in Chapter 97, and EB is discussed in Chapter 32.

Ehlers–Danlos syndrome

Collagens and tenascin-X

The quantitatively major components of the collagen fibrils found in the ECMs of many tissues (e.g. skin, tendon, bone, cartilage) are collagens I, II (absent from skin), and III. Smaller amounts of minor collagens (e.g. types V, IX, XI, XII, XIV) are expressed in a tissue-specific manner[3]. Mutations in the genes encoding major and minor collagens can result in distinct abnormalities in different organs[3]. For example, defects in *COL3A1*, which encodes collagen III, are responsible for the vascular type of EDS[16], an autosomal dominant condition that presents with thin translucent skin, excessive bruising, and life-threatening arterial, gastrointestinal, and uterine ruptures. Mutations in *COL3A1* have also been found in patients whose primary clinical manifestation is arterial aneurysms.

Alterations in genes encoding minor fibrillar collagens can also cause severe connective tissue diseases, suggesting pivotal functions for these quantitatively minor components. Collagen V nucleates fibrillogenesis involving collagens I and III; this interaction limits the solubility of macromolecules in fibrils and regulates the geometry of lateral aggregation as well as the overall shapes and sizes of the collagen aggregates. Consistent with this concept, the classical type of EDS occasionally results from mutations in *COL1A1* (encodes the α_1-chain of collagen I), whereas mutations in *COL5A1* and *COL5A2* (encode the α_1- and α_2-chains of collagen V) account for ~50% of patients. Patients with classical EDS exhibit variable degrees of skin hyperelasticity and fragility, atrophic scarring, and joint hypermobility (Fig. 95.8A). Mutations in the gene encoding tenascin-X, a glycoprotein in the extrafibrillar matrix, can cause a recessive form of EDS with similar clinical findings of hyperextensible skin and joint hypermobility[16].

SELECTED GENETIC EXTRACELLULAR MATRIX DISEASES OF THE SKIN				
Protein	**Gene**	**Inheritance**	**Disease**	**Phenotypic features in the skin* and other organs**
Collagen I	*COL1A1*	AD	EDS, arthrochalasia	***Skin hyperextensibility and fragility***, joint hypermobility, congenital hip dislocation†
		AD	EDS, classic (rare cause of this EDS type)	See below
	COL1A2	AD	EDS, arthrochalasia	See above
		AR	EDS, cardiac valvular	Cardiac valve defects, otherwise similar to classic EDS (see below)
Collagen III	*COL3A1*	AD	EDS, vascular	***Translucent, fragile skin with extensive bruising;*** arterial fragility, intestinal and uterine rupture‡
Collagen V	*COL5A1 COL5A2*	AD	EDS, classic	***Skin hyperextensibility and fragility***, joint hypermobility
Collagen VI	*COL6A1, COL6A2, COL6A3*	AD, AR	Ullrich congenital muscular dystrophy Bethlem myopathy	***Puffy skin, atrophic scarring, follicular hyperkeratosis***, distal joint hypermobility, muscular dystrophy
Collagen VII	*COL7A1*	AD, AR	Dystrophic epidermolysis bullosa	***Skin fragility and blistering***
Collagen XII	*COL12A1*	AD, AR	EDS, myopathic Bethlem myopathy	***Soft/doughy skin, atrophic scarring, variable follicular hyperkeratosis***, proximal joint contractures and distal hypermobility, congenital myopathy, hypotonia
Collagen XVII	*COL17A1*	AR	Junctional epidermolysis bullosa	***Skin fragility and blistering***
Fibrillin 1	*FBN1*	AR	Marfan syndrome Marfanoid–progeroid–lipodystrophy syndrome	***Striae***, characteristic body habitus, aortic dilation/dissection‡ ***Skin atrophy***, extreme reduction of subcutaneous fat
Elastin	*ELN*	AD > AR	Cutis laxa, AD > AR	***Lax, redundant skin***
EGF-containing fibulin-like extracellular matrix protein 2 (fibulin 4)	*EFEMP2 (FBLN4)*	AR	Cutis laxa, AR type 1B	***Lax, redundant skin;*** pulmonary emphysema and arterial anomalies
Fibulin 5	*FBLN5*	AR > AD	Cutis laxa, AR type 1A or AD	***Lax, redundant skin;*** pulmonary emphysema and arterial anomalies (AR form)
Latent TGF-β binding protein-4	*LTBP4*	AR	Cutis laxa, AR type 1C	***Lax, redundant skin;*** severe pulmonary, gastrointestinal and urinary abnormalities; dysmorphic facies, joint hyperextensibility, hypotonia
TGF-β receptors 1 & 2, TGF-β2 & -β3, SMAD family member 3	*TGFRB1, TGFRB2, TGFB2, TGFB3, SMAD3*	AD	Loeys–Dietz syndrome‡	***Translucent or velvety skin, easy bruising, atrophic scarring, striae, milia, eczematous dermatitis*** (skin findings vary); aortic aneurysms, arterial tortuosity; craniofacial anomalies (variable), skeletal anomalies, joint hypermobility
Tenascin-X	*TNXB*	AR	EDS, classic-like type 1	***Skin hyperextensibility and fragility***, joint hypermobility, foot deformities, muscle weakness (type 1), osteopenia (type 2)
Aortic carboxypeptidase-like protein	*AEBP1*	AD	EDS, classic-like type 2	
Extracellular matrix protein-1	*ECM1*	AR	Lipoid proteinosis	***Hyalin deposition in the dermis*** and submucosal tissues, ***waxy papules*** on the face (including eyelid margins), ***depressed scars***, hoarse voice, intracranial calcifications
ABCC6 transporter	*ABCC6*	AR	Pseudoxanthoma elasticum (PXE)	***Yellowish papules, lax skin***, retinal angioid streaks, cardiovascular disease
ATPase, Cu^{2+}-transporting, α-polypeptide	*ATP7A*	X-R	Occipital horn syndrome	***Lax skin***, tortuous arteries, joint hypermobility, occipital calcifications
Glucose transporter 10	*GLUT10*	AR	Arterial tortuosity syndrome	***Lax or hyperextensible skin*** (variable), ***telangiectasias on the cheeks***, tortuous arteries, joint hypermobility
Solute carrier family 39, member 13 (zinc transporter ZIP13)	*SLC39A13*	AR	EDS, spondylodysplastic	***Skin hyperextensibility and fragility, wrinkled palms***, joint hypermobility, hypotonia, short stature, developmental delay

*Elastosis perforans serpiginosa can also develop in patients with EDS and pseudoxanthoma elasticum.
†A phenotype with features of both EDS and osteogenesis imperfecta has also been reported.
‡The phenotype of Loeys–Dietz syndrome (LDS) can mimic either Marfan syndrome or vascular EDS; eczematous dermatitis and elevated immunoglobulin E levels suggestive of a hyper-IgE syndrome have also been reported.

Table 95.5 Selected genetic extracellular matrix diseases of the skin.

Continued

SELECTED GENETIC EXTRACELLULAR MATRIX DISEASES OF THE SKIN				
Protein	**Gene**	**Inheritance**	**Disease**	**Phenotypic features in the skin* and other organs**
Lysyl hydroxylase 1	*PLOD1*	AR	EDS, kyphoscoliotic (type VIA[¶])	***Skin hyperextensibility and fragility***, ocular fragility, joint hypermobility, scoliosis
Lysyl hydroxylase 3	*PLOD3*	AR	Generalized connective tissue disorder	***Skin fragility and skin blistering***, bone fragility with contractures, dysmorphic facies, hypoplastic nails, osteopenia, cataracts, delayed growth and development
ADAMTS-2 (procollagen N-proteinase)	*ADAMTS2*	AR	EDS, dermatosparaxis	***Sagging, doughy, fragile skin with easy bruising***; characteristic facies
Dermatan-4-sulfotransferase 1	*CHST14*	AR	EDS, musculocontractural[§]	***Skin hyperextensibility and fragility, wrinkled palms***, ocular fragility, joint contractures and hypermobility, scoliosis, craniofacial abnormalities
Dermatan sulfate epimerase	*DSE*	AR		
Galactosyltransferase-I (β-1,4-galactosyltransferase 7)	*B4GALT7*	AR	EDS, spondylodysplastic (formerly progeroid)	***Skin hyperextensibility***, variable joint hypermobility and contractures, progeroid facies, osteopenia, hypotonia, short stature, developmental delay
Galactosyltransferase-II (β-1,3-galactosyltransferase 6)	*B3GALT6*	AR		
Glucuronosyltransferase I (β-1,3-glucuronyltransferase 3)	*B3GAT3*	AR	Larsen-like syndrome	***Wrinkled acral skin***, joint dislocations, craniofacial dysmorphism, short stature, congenital heart defects
Filamin A (actin-binding protein 280)	*FLNA*	X-D	EDS, periventricular nodular heterotopia variant	***Skin hyperextensibility*** (variable), aortic dilation, periventricular nodular heterotopia, joint hypermobility
Zinc finger protein 469, PR domain-containing protein 5	*ZNF469, PRDM5*	AR	Brittle cornea syndrome	***Soft or hyperextensible skin, wrinkled acral skin, atrophic scarring*** (skin findings vary), thin fragile corneas, blue sclerae, joint hypermobility, scoliosis, hearing loss
FK506-binding protein 14	*FKBP14*	AR	EDS, kyphoscoliotic	***Skin hyperextensibility***, joint hypermobility, progressive kyphoscoliosis, myopathy, hypotonia from birth, impaired hearing
Complement C1r, C1s	*C1R, C1S*	AD	EDS, periodontal	***Excessive bruising, mildly hyperextensible skin***, small joint hypermobility, early-onset periodontitis, marfanoid habitus, increased infections
ATPase, H^+ transporting, lysosomal V0 subunit A2	*ATP6V0A2*	AR	Cutis laxa, AR type 2A Wrinkly skin syndrome	***Lax skin***, facial dysmorphism, large fontanelles, microcephaly, delayed development ± growth, strabismus, joint hypermobility
Pyrroline-5-carboxylate reductase 1	*PYCR1*	AR	Cutis laxa, AR type 2B and 3B (de Barsy syndrome B)	***Lax skin***, facial dysmorphism, large fontanelles, microcephaly, delayed development and growth, joint hypermobility; corneal opacities, cataracts, & athetosis in de Barsy syndrome
Pyrroline-5-carboxylate synthetase	*ALDH18A1*	AD, AR	Cutis laxa, progeroid AD Cutis laxa, AR type 3A (de Barsy syndrome A)	***Lax skin***, facial dysmorphism, delayed development, joint hypermobility, corneal opacities
Ectonucleotide pyrophosphatase/phosphodiesterase 1	*ENPP1*	AR	Generalized arterial calcification of infancy	***Yellowish papules, lax skin***, retinal angioid streaks, severe arterial calcification, hypophosphatemic rickets
γ-glutamyl carboxylase	*GGCX*	AR	PXE-like disorder with multiple coagulation factor deficiency	***Yellowish papules, lax skin***, retinal angioid streaks, cardiovascular disease, bleeding diathesis
Golgin, RAB6-interacting	*GORAB*	AR	Gerodermia osteodysplastica	***Lax skin (primarily on dorsal hands and feet)***, progeroid facies with prognathism, short stature, osteoporosis
Ras and Rab interactor 2	*RIN2*	AR	Macrocephaly, ***alopecia, cutis laxa***, and scoliosis (MACS)	Features in name of disorder, facial dysmorphism, gingival hypertrophy, joint hyperextensibility

[¶]Historical numerical classification of EDS.
[§]Exists on a spectrum with adducted thumb–clubfoot syndrome, which is caused by mutations in the same gene.

Table 95.5 Selected genetic extracellular matrix diseases of the skin. Diseases and phenotypic features are colored based on the primary cutaneous manifestation (when applicable) as follows: *orange*, hyperextensible skin (as in classic EDS); *pink*, extensively bruised skin (as in vascular EDS); *peach-tan*, skin fragility with blistering (as in epidermolysis bullosa); *light blue*, lax skin (as in cutis laxa); *dark blue*, yellowish papules ± lax skin (as in pseudoxanthoma elasticum). ABCC6, ATP-binding cassette subfamily C member 6; AD, autosomal dominant; ADAM, a disintegrin and metalloproteinase; *AEBP1*, adipocyte enhancer binding protein 1; *ALDH18A1*, aldehyde dehydrogenase 18 family, member A1; AR, autosomal recessive; *CHST14*, carbohydrate sulfotransferase 14; EDS, Ehlers–Danlos syndrome; TGF, transforming growth factor; X-D, X-linked dominant; X-R, X-linked recessive.

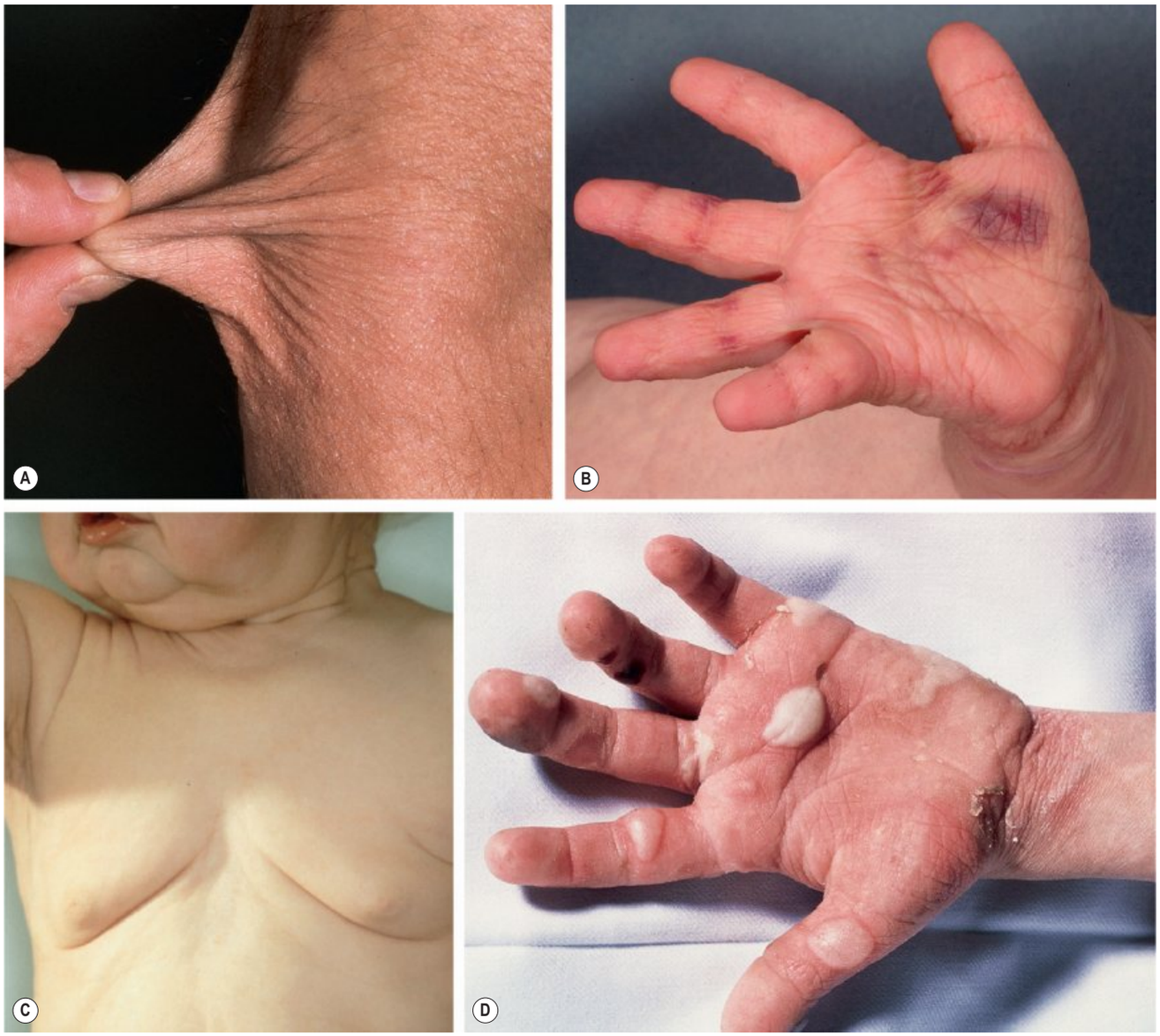


Fig. 95.8 Phenotypic manifestations of genetic extracellular matrix defects. A Ehlers–Danlos syndrome type II with slightly overstretchable skin results from mutations in the collagen V genes. **B** Dermatosparaxis showing fragile skin with purpura and a "doughy" texture due to mutations in the gene for ADAMTS-2. **C** Autosomal dominant cutis laxa is associated with mutations in the elastin gene. **D** Junctional epidermolysis bullosa with skin blisters after minimal friction can be caused by mutations in the collagen XVII gene. *B, Courtesy Julie V. Schaffer MD; C, Courtesy Thomas Schwarz, MD.*

Post-translational modification of collagen

Mutations in genes encoding proteins involved in post-translational modification of collagen (see above and Fig. 95.2) have been found to underlie other forms of EDS. For example, loss-of-function mutations in the lysyl hydroxylase 1 gene lead to abnormal lysyl hydroxylation and glycosylation of collagens in a subset of patients with the kyphoscoliotic type of EDS, a recessive disease characterized by hyperextensible and fragile skin as well as hypermobile joints, scoliosis, and ocular fragility. Failure to cleave the N-propeptide from procollagen I causes the arthrochalasia type of EDS, a dominant disorder that features severe joint hypermobility, including dislocations. The persistence of this propeptide on collagen I drastically alters fibrillogenesis, and the fibrils that form are thin and irregular in diameter. Affected individuals typically have a splice-site mutation in *COL1A1* or *COL1A2* that causes exon skipping and elimination of the cleavage site for ADAMTS-2 (procollagen I N-proteinase) in the proα_1(I) or proα_2(I) chain. Loss-of-function mutations in *ADAMTS2* cause the dermatosparaxis type of EDS (Fig. 95.8B); as in the arthrochalasia type, procollagen I N-propeptides persist and sterically disturb polymerization of the collagen fibrils. Dermatosparaxis has a distinct phenotype that includes characteristic facies and fragile, sagging skin with a doughy consistency. Mutations in the zinc finger protein 469 gene (*ZNF469*) or PR/SET domain 5 (*PRDM5*), which are involved in transcriptional regulation of fibrillar collagens, result in corneal fragility as well as variable skin hyperextensibility and wrinkling[16].

Proteoglycan processing

As discussed above, dermal proteoglycans have important roles in collagen fibril organization. Accordingly, mutations in *B3GALT6* and *B4GALT7*, which encode galactosyltransferases that initiate GAG synthesis, cause a spondylodysplastic type of EDS[16,28,29]. Mutations in *B3GAT3*, which encodes a glucuronosyltransferase that catalyzes the formation GAG-protein linkages, can lead to wrinkled acral skin[30]. The musculocontractural type of EDS is caused by mutations in *CHST14* and *DSE*, which encode dermatan-4-sulfotransferase 1 and dermatan sulfate epimerase, respectively[16,31]. Loss of these enzymes' activity in dermatan sulfate synthesis leads to a reduced dermatan sulfate : chondroitin sulfate ratio, which disrupts decorin function and thereby impairs collagen fibrillogenesis[16].

Cutis laxa

Cutis laxa is an uncommon ECM disease characterized by genetic heterogeneity and clinical variability (see Ch. 97); acquired variants also exist[23]. The primary diagnostic feature is loose, sagging skin with

decreased resilience and elasticity, leading to an appearance of "too large skin" and premature aging (Fig. 95.8C). The skin changes are often accompanied by extracutaneous manifestations, including pulmonary emphysema, bladder diverticula, hernias, and arterial anomalies. Histologically, there is fragmentation or diminution of elastic fibers.

Recessive and dominant forms of cutis laxa can result from mutations in multiple genes, including those that encode the elastic fiber components elastin, fibulin 4, and fibulin 5[32] (see Table 95.5). A severe form of cutis laxa associated with extensive pulmonary, gastrointestinal, and urinary abnormalities is caused by mutations in the latent TGF-β binding protein-4 gene (*LTBP4*), demonstrating the central role of TGF-β signaling in ECM assembly during development[32].

Other inherited disorders are characterized by secondary effects on elastic fiber deposition or degradation[23]. For example, elastic fibers are calcified and fragmented secondary to decreased activity of anti-mineralization proteins in pseudoxanthoma elasticum (see below and Ch. 97). In patients with α_1-antitrypsin deficiency and some forms of acquired atrophoderma, elastic fibers are prematurely degraded due to unregulated elastase activity. Decreased or aberrant deposition of elastic fibers in certain tissues is also characteristic of Marfan syndrome (see below).

Marfan syndrome

Fibrillin 1 is the major component of microfibrils and therefore has an important structural role in elastic fibers. Fibrillin 1 mutations cause Marfan syndrome, an autosomal dominant disorder with variable connective tissue weakness in the skin as well as skeletal, ocular, and cardiovascular systems[13,23]. Cutaneous manifestations include striae and elastosis perforans serpiginosa. In addition to structural disturbances in elastic fibers and microfibrils, fibrillin mutations may decrease the sequestration of latent TGF-β complexes (see Fig. 95.6), thus rendering them more prone to activation. This leads to unproductive tissue remodeling, abnormal cellular behavior, and loss of ECM integrity.

The highly homologous fibrillin 2 exhibits different spatial and temporal expression during development, and the functional relationship between the two molecules is not fully understood. Mutations in the gene encoding fibrillin 2 lead to congenital contractural arachnodactyly, which features skeletal abnormalities in the absence of ocular and cardiovascular features[13].

Loeys–Dietz syndrome

Heterozygous mutations in the genes encoding the TGF-β receptors 1/2 or TGF-β2/3 can cause Loeys–Dietz syndrome, which is characterized by aortic aneurysms, generalized arterial tortuosity, variable craniofacial malformations (e.g. bifid uvula, cleft palate, hypertelorism), skeletal anomalies, and joint laxity. A subset of patients has cutaneous manifestations similar to those of the vascular type of EDS, including translucent skin, easy bruising, and atrophic scarring[13,16]. The phenotypic overlap with Marfan syndrome and vascular EDS is not surprising, considering the association between fibrillin and latent TGF-β and the role of TGF-β in regulating collagen expression.

Other fibrillin-associated syndromes

Genetic mutations that alter the C-terminus of fibrillin 1 cause *marfanoid–progeroid–lipodystrophy syndrome*, which is characterized by an extreme reduction in subcutaneous fat. Mutations affecting the integrin-binding site of fibrillin 1 lead to abnormal microfibril assembly and cause *stiff skin syndrome*, which features diffusely thickened skin since birth, limited joint mobility, nodules over the distal interphalangeal joints, and short stature. In addition, fibrillin 1 deficiency represents a cause of *Weill–Marchesani syndrome*[13], characterized by thick skin, short stature, shortened digits, and ectopia lentis. Mutations in *ADAMTSL2*, which encodes the extracellular ADAMTS-like protein 2 that interacts with TGF-β and fibrillin[33], alter TGF-β bioavailability. This results in *geleophysic dysplasia*, which presents with thick skin, short stature, and joint contractures.

Pseudoxanthoma elasticum

PXE is a heritable disorder characterized by cutaneous, vascular, and ocular involvement that results from the accumulation of fragmented and calcified elastic fibers in the dermis, arterial walls, and Bruch's membrane, respectively (see Ch. 97). The skin findings – laxity and yellowish papules and plaques – are the most common and often the earliest manifestation of PXE.

Although PXE has traditionally been considered as a prototypic heritable ECM disorder, it is caused by mutations in the gene for the ATP-binding cassette (ABC) subfamily C member 6 (ABCC6) transporter, which is primarily expressed in the liver[34]. The absence of functional ABCC6 results in reduced ATP secretion from hepatocytes, which leads to reduced plasma concentrations of inorganic pyrophosphate (PPi), a physiologic inhibitor of mineralization (see Fig. 97.5)[34]. Mutations in the γ-glutamyl carboxylase gene (*GGCX*) can lead to a PXE-like phenotype together with a deficiency in vitamin K-dependent coagulation factors. GGCX catalyzes vitamin K-dependent γ-glutamyl carboxylation, which activates coagulation factors and the matrix gla protein (MGP), an inhibitor of pathologic mineralization.

Epidermolysis bullosa

EB represents a group of hereditary diseases characterized by mechanical fragility of the skin that results in blister formation[26,35] (see Ch. 32). Mutations in the collagen VII gene (*COL7A1*) cause both dominant and recessive forms of *dystrophic EB*[36]. Because collagen VII is a component of the anchoring fibrils, cleavage occurs just below the lamina densa in the uppermost dermis; as a result, blisters tend to heal with scarring. Patients with severe forms of recessive dystrophic EB harbor mutations that lead to premature termination codons[36], and collagen VII and anchoring fibrils are absent. Milder forms of dystrophic EB are associated with missense mutations in one or both copies of *COL7A1* and anchoring fibril dysfunction.

Mutations in *COL17A1*, which encodes the α_1 chain of collagen XVII, a homotrimeric transmembrane collagen localized to the hemidesmosome-anchoring filament complex of basal keratinocytes, can cause *junctional EB*. This recessive EB subtype is characterized by cleavage within the lamina lucida of the basement membrane. Patients with two null alleles of *COL17A1* tend to have widespread blistering (Fig. 95.8D), whereas those with missense mutations and some preservation of collagen XVII function exhibit milder clinical phenotypes[37].

Laminin 332 is a major structural component of the lamina densa, where it secures epidermal adhesion by linking $\alpha_6\beta_4$ integrin on the cell surface to collagen VII of the anchoring fibrils (see Fig. 28.3). Like defects in collagen XVII, mutations in the genes encoding the three polypeptide chains of laminin 332 cause *junctional EB*, with the most severe form resulting from null mutations and a complete lack of laminin 332 in the skin[37].

Other hereditary matrix diseases with skin symptoms

Ullrich congenital muscular dystrophy and *Bethlem myopathy* are caused by mutations in *COL6A1*, *COL6A2*, and *COL6A3* which encode the α_1(VI), α_2(VI), and α_3(VI) chains of collagen VI[3]. This collagen forms microfibrils in several tissues, including muscle and skin. Extramuscular manifestations – a puffy consistency of the skin (primarily in Ullrich), atrophic scarring, and joint hyperlaxity – likely reflect abnormalities of the microfibrillar networks in the dermis and synovia. Deficiency of FK506-binding protein 14, which may act as a chaperone in the endoplasmic reticulum with a role in ECM assembly, leads to a phenotype that includes hyperelastic skin as well as muscular dystrophy.

Via glucosyltransferase and galactosyltransferase activities, lysyl hydroxylase 3 plays a role in the post-translational modification of collagens. Loss-of-function mutations in both copies of *PLOD3*, which encodes lysyl hydroxylase 3, underlie a severe, multi-organ connective tissue disease[38,39]. Affected individuals have fragile skin that is prone to both bruising and blistering, with a reduction in anchoring fibril density and cleavage below the lamina densa similar to that observed in recessive dystrophic EB[39].

Extracellular matrix components as autoantigens

The binding of autoantibodies to ECM components disrupts their supramolecular aggregation or ligand binding, leading to dysfunction and corresponding clinical symptoms. Several ECM components are targeted in autoimmune diseases that affect the kidney, cartilage, and skin (Table 95.6). Autoantigens in these conditions include: the α_3- and α_5-chains of collagen IV in Goodpasture disease[40]; collagen II in relapsing polychondritis; collagen VII in EB acquisita; collagen XVII in bullous pemphigoid; and the γ1-chain of laminin 311 and 511 in

EXTRACELLULAR MATRIX COMPONENTS AS TARGETS IN AUTOIMMUNE DISEASES		
Disease	**Autoantigen**	**Biologic and clinical features**
Goodpasture disease	Collagen IV, α_3 and α_5 chains	Glomerulonephritis, pneumonitis with hemoptysis
Relapsing polychondritis, arthritis	Collagen II; collagen IX	Chondritis of ear, nose, larynx, and trachea; arthritis
Pemphigoid (various subtypes)	Collagen XVII (BP, PG, MMP)*; laminin 332 (MMP), laminin γ1 chain (p200 pemphigoid)	Skin blistering
Epidermolysis bullosa acquisita	Collagen VII	Skin blistering, fragility
Bullous eruption of systemic lupus erythematosus (SLE)	Collagen VII	Skin blistering with underlying SLE
Scleroderma†	Fibrillin 1; PDGF receptor	Skin fibrosis
Lichen sclerosus	Extracellular matrix (ECM) protein-1	Inflammation, epidermal atrophy, hyalinization of the dermis

*Also the autoantigen in linear IgA bullous dermatosis.
†Not confirmed in large patient cohorts.

Table 95.6 Extracellular matrix components as targets in autoimmune diseases. BP, bullous pemphigoid; MMP, mucous membrane (cicatricial) pemphigoid; PDGF, platelet-derived growth factor; PG, pemphigoid gestationis.

anti-p200 (anti-laminin γ1) pemphigoid[37,41]. Antibodies to fibrillin 1 have been described in systemic sclerosis patients, especially those of Choctaw Native American or Japanese descent, and in individuals with linear and generalized subtypes of morphea. The extracellular matrix-1 (ECM-1) protein is the target of autoantibodies in patients with lichen sclerosus and is dysfunctional in individuals with lipoid proteinosis; both conditions feature dermal hyalinization[42]. The immunodominant epitopes in autoimmune diseases are often localized to one or several distinct structural domains, allowing recombinant domains to be employed for diagnostic testing.

Skin aging and other acquired ECM abnormalities

Changes in the dermal ECM contribute to both chronologic and photo-induced skin aging. Morphologic hallmarks of aged skin include reduced microfibrils in the papillary dermis, disorganized elastic fibers, and reduction or weakening of other ECM fibril networks. The structurally perturbed dermal networks cannot bind adequate amounts of hyaluronic acid and, consequently, water, which leads to lax and wrinkled skin. Reduced synthesis of dermal collagens by fibroblasts is a prominent feature of aging that is mediated by decreased TGF-β and connective tissue growth factor (CTGF) signaling. Increased degradation of ECM components also occurs and destabilizes network structures. The deleterious effects of UV irradiation include release of cytokines from the epidermis and generation of reactive oxygen species. These mediators induce inflammatory processes and stimulate expression and activation of matrix metalloproteinases and serine proteinases such as elastase, which can degrade ECM networks[33].

Weakened ECMs lead to disturbed wound healing and a bruising tendency in scurvy, a disease resulting from an insufficient supply of ascorbic acid (vitamin C). This vitamin is an essential cofactor for prolyl- and lysyl-hydroxylases, which modify collagens during their biosynthesis and are required for cross-linking[4].

In fibrotic disorders such as systemic sclerosis (scleroderma) and keloids, thickened skin reflects excessive dermal ECM. Upregulation of ECM synthesis (e.g. collagen, fibrillins, proteoglycans) via TGF-β and CTGF is believed to have a pathogenic role (see Fig. 43.1). The histopathologic abnormalities of keloids due to perturbed ECM assembly and regulation are outlined in Table 98.3.

Animal Models

Mouse models for ECM diseases have provided new insights into pathomechanisms, allowed for further assessment of abnormalities observed in human diseases, and enabled testing of novel therapeutic approaches. For example, fibrillin 1 transgenic mouse models have demonstrated associations of fibrillin 1 with microfibril assembly and TGF-β signaling, showing that a defect in the latter is central to Marfan syndrome pathogenesis and other phenotypes[13,43]. In addition, mice with mutations in the integrin binding sites of fibrillin 1 represent a model of scleroderma[44].

Collagen VII-deficient mice, rats, dogs, and sheep have recapitulated the clinical, genetic, immunohistochemical, and ultrastructural characteristics of recessive dystrophic EB in humans[23]. Collagen VII knockout mice die during the first 2 weeks of life, while mice with hypomorphic mutations have a severe phenotype but live into adulthood[37]. These mice have provided insights into the molecular pathogenesis of recessive dystrophic EB and have been useful for testing cellular and molecular approaches to therapy[45]. Mice with conditional deletion of collagen VII have furthered the understanding of this protein's role in regeneration. Rats with spontaneous *Col7a1* mutations have revealed a gene-dosage effect in dystrophic EB and demonstrated the importance of modifier genes in determining disease phenotype[46,47]. Collagen XVII knockout and mutant mice exhibit a moderately severe form of junctional EB and are also being used to study novel therapeutic approaches.

Mice harboring disrupted proteoglycan genes have demonstrated the importance of these molecules for skin integrity and tautness[15]. The decorin knockout mouse has fragile skin with markedly reduced tensile strength that is associated with irregular, coarse ECM fibers in the skin and tendons; these findings established the fundamental role of decorin in regulating collagen fibrillogenesis *in vivo*.

Abnormalities in collagen-processing enzymes also occur spontaneously in animals. Bovine dermatosparaxis is a recessively inherited connective tissue disorder that, like the human form of the disease, features extremely fragile, doughy skin as well as joint laxity. Both human and bovine dermatosparaxis result from mutations in the gene encoding ADAMTS-2, which excises the N-propeptide of procollagens I and II[23].

Potential for Biologically Valid Molecular Therapies

Genetic, proteomic, and other molecular approaches have led to a better understanding of the mechanisms underlying ECM disorders[48]. This has provided the bases for novel therapies in diseases such as recessive forms of EB caused by a lack of collagen VII, collagen XVII, or laminin 332. Treatment strategies for EB range from employment of gene- and RNA-based technologies to methods utilizing cells or proteins (see Ch. 32). Many of these experimental modalities are currently being evaluated in preclinical models or clinical trials[49].

In a remarkable example of gene therapy, laminin-β3-deficient skin of a child with severe junctional EB was corrected by transplantation of stem cell-enriched epidermal grafts transduced *ex vivo* with a retroviral vector expressing normal *LAMB3* cDNA. Treatment of ~80% of the body surface area resulted in synthesis of functional laminin 332 and an absence of blistering in the corrected epidermis that was sustained for >5 years[50]. *In vivo* topical gene therapy with beremagene geperpavec (B-VEC), a *COL7A1*-containing herpes simplex virus type 1 vector, was recently FDA-approved as a treatment to promote wound healing in patients with dystrophic EB[50a]. Other clinical trials of gene therapy for different types of EB are in progress, and novel vectors and gene editing approaches to correct patient stem cells or induced pluripotent stem (iPS) cells are under development. Intriguingly, patients with junctional and dystrophic EB can develop patches of skin that do not blister due to spontaneous "correction" via revertant mosaicism. This raises the possibility of natural gene therapy by expanding stem cells or generating iPS cells from the corrected patches[51].

Systemic therapy using allogeneic bone marrow-derived stem cell transplantation after total or partial myeloablation has led to homing of donor cells to the skin, increased collagen VII deposition at the dermal–epidermal junction, and variably decreased blistering in children with recessive dystrophic EB[52]. Long-term follow-up studies are needed to evaluate the therapeutic potential of this approach. Alternative strategies under investigation in patients with recessive dystrophic EB include intravenous or intradermal injections of allogeneic mesenchymal stem cells. Protein replacement therapy with intradermal or

intravenous injection of collagen VII has also been explored in animal models of recessive dystrophic EB[53].

For the treatment of dominant disorders, strategies to silence expression of the mutated allele (mitigating dominant-negative effects) or to supplement with the normal protein (correcting haploinsufficiency) hold promise. For dominantly inherited connective tissue disorders, cellular rescue mechanisms such as the unfolded protein response contribute to disease and small molecule therapies such as chemical chaperones may have benefit.

Better understanding of disease mechanisms disclosed an unexpected pharmacologic approach to the treatment of Marfan syndrome[54]. Since excessive TGF-β signaling contributes to the development of aortic aneurysms in affected individuals, it was hypothesized that TGF-β antagonists might prevent or even reverse this disease manifestation. Angiotensin II is known to stimulate TGF-β signaling, and angiotensin II receptor blockers are successfully employed to prevent aortic root dilation in patients with Marfan syndrome[54] (see Fig. 95.6). These agents have also been shown to reduce dermal fibrosis and digital fusion in mice with recessive dystrophic EB[55]. Analogous treatments could potentially be developed for other inherited ECM disorders based on recognition of the pathogenic role of growth factors and other regulatory molecules[56].

Future development of successful therapies for ECM disorders will also depend on the progress in our understanding of functional suprastructure formation by matrix macromolecules. This endeavor will be facilitated not only by the analysis of aggregate formation by matrix macromolecules or their mixtures *in vitro*, but also by the elucidation of further genetic defects and their consequences in animal or human diseases, as well as the generation of transgenic animals as models for human disorders. This information will help us to understand and treat not only inherited ECM diseases but also many common disorders currently considered as acquired.

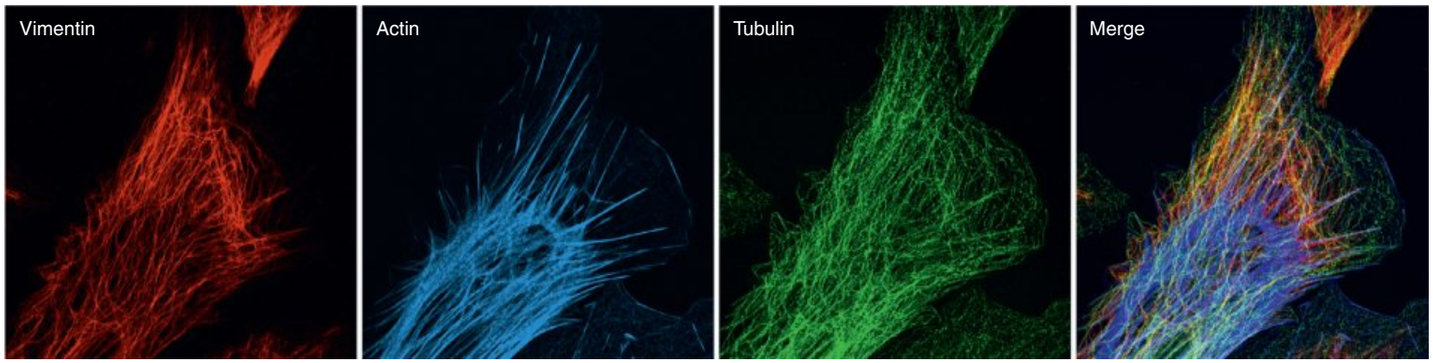
Additional figures available in our eBook (see inside front cover for access code).

REFERENCES

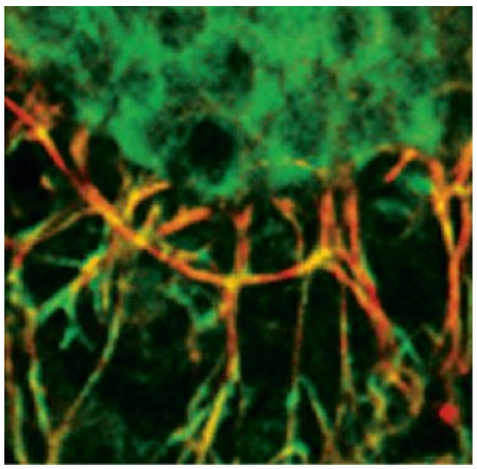
1. Bruckner P. Suprastructures of extracellular matrices: paradigms of functions controlled by aggregates rather than molecules. *Cell Tissue Res*. 2010;339:7–18.
2. Naba A, Clauser KR, Huiming D, et al. The extracellular matrix: tools and insights for the "omics" era. *Matrix Biol*. 2016;49:10–24.
3. Ricard-Blum S. The collagen family. *Cold Spring Harb Perspect Biol*. 2011;3:a004978.
4. Myllyharju J, Kivirikko KI. Collagens, modifying enzymes and their mutations in humans, flies and worms. *Trends Genet*. 2004;20:33–43.
5. Canty EG, Kadler KE. Procollagen trafficking, processing and fibrillogenesis. *J Cell Sci*. 2005;118:1341–1353.
6. Malhotra V, Erlmann P. The pathway of collagen secretion. *Annu Rev Cell Dev Biol*. 2015;31:109–124.
7. Ishikawa Y, Ito S, Nagata K, et al. Intracellular mechanisms of molecular recognition and sorting for transport of large extracellular matrix molecules. *PNAS*. 2016;113:E6036–E6044.
8. Ishikawa Y, Bachinger HP. A molecular ensemble in the rER for procollagen maturation. *Biochim Biophys Acta*. 2013;1833:2479–2491.
9. Prox J, Arnold P, Becker-Pauly C. Meprin α and meprin β: procollagen proteinases in health and disease. *Matrix Biol*. 2015 44–46:7–13.
10. Kalamajski S, Liu C, Tillgren V, et al. Increased C-telopeptide cross-linking of tendon type I collagen in fibromodulin-deficient mice. *J Biol Chem*. 2014;289:18873–18879.
11. Ninomiya Y, Kagawa M, Iyama K, et al. Differential expression of two basement membrane collagen genes, COL4A6 and COL4A5, demonstrated by immunofluorescence staining using peptide-specific monoclonal antibodies. *J Cell Biol*. 1995;130:1219–1229.
12. Nyström A, Kiritsi D. Transmembrane collagens—unexplored mediators of epidermal-dermal communication and tissue homeostasis. *Exp Dermatol*. 2021;30:10–16.
13. Kozel BA, Mecham RP. Elastic fiber ultrastructure and assembly. *Matrix Biol*. 2019;84:31–40.
14. Loeys BL, Gerber EE, Riegert-Johnson D, et al. Mutations in fibrillin-1 cause congenital scleroderma: stiff skin syndrome. *Sci Transl Med*. 2010;2:23ra20.
15. Iozzo RV, Schaefer L. Proteoglycan form and function: a comprehensive nomenclature of proteoglycans. *Matrix Biol*. 2015;42:11–55.
16. Malfait F, De Paepe A. The Ehlers-Danlos syndrome. *Adv Exp Med Biol*. 2014;802:129–143.
17. Heljasvaara R, Aikio M, Ruotsalainen H, Pihlajaniemi T. Collagen XVIII in tissue homeostasis and dysregulation—lessons learned from model organisms and human patients. *Matrix Biol*. 2017:57–58:55–75.
18. Iozzo RV, Sanderson RD. Proteoglycans in cancer biology, tumour microenvironment and angiogenesis. *J Cell Mol Med*. 2011;15:1013–1031.
19. Frey H, Schroeder N, Manon-Jensen T, et al. Biological interplay between proteoglycans and their innate immune receptors in inflammation. *FEBS J*. 2013;280:2165–2179.
20. Miner JH. Laminins and their roles in mammals. *Microsc Res Tech*. 2008;71:349–356.
21. Durbeej M. Laminins. *Cell Tissue Res*. 2010;339:259–268.
22. Aumailley M, Bruckner-Tuderman L, Carter WG, et al. A simplified laminin nomenclature. *Matrix Biol*. 2005;24:326–332.
23. Nyström A, Bruckner-Tuderman L. Matrix molecules and skin biology. *Semin Cell Dev Biol*. 2019;89:136–146.
24. Humphries JD, Chastney MR, Askari JA, Humphries MJ. Signal transduction via integrin adhesion complexes. *Curr Opin Cell Biol*. 2019;56:14–21.
25. Legate KR, Wickstrom SA, Fassler R. Genetic and cell biological analysis of integrin outside-in signaling. *Genes Dev*. 2009;23:397–418.
26. Has C, Bruckner-Tuderman L. The genetics of skin fragility. *Annu Rev Genomics Hum Genet*. 2014;15:245–268.
27. Lindsay ME, Dietz HC. The genetic basis of aortic aneurysm. *Cold Spring Harb Perspect Med*. 2014;4:a015909.
28. Malfait F, Kariminejad A, Van Damme T, et al. Defective initiation of glycosaminoglycan synthesis due to B3GALT6 mutations causes a pleiotropic Ehlers-Danlos-syndrome-like connective tissue disorder. *Am J Hum Genet*. 2013;92:935–945.
29. Nakajima M, Mizumoto S, Miyake N, et al. Mutations in B3GALT6, which encodes a glycosaminoglycan linker region enzyme, cause a spectrum of skeletal and connective tissue disorders. *Am J Hum Genet*. 2013;92:927–934.
30. von Oettingen JE, Tan WH, Dauber A. Skeletal dysplasia, global developmental delay, and multiple congenital anomalies in a 5-year-old boy: report of the second family with B3GAT3 mutation and expansion of the phenotype. *Am J Med Genet A*. 2014;164A:1580–1586.
31. Muller T, et al. Loss of dermatan sulfate epimerase (DSE) function results in musculocontractural Ehlers-Danlos syndrome. *Hum Mol Genet*. 2013;22:3761–3772.
32. Uitto J, Li Q, Urban Z. The complexity of elastic fibre biogenesis in the skin – a perspective to the clinical heterogeneity of cutis laxa. *Exp Dermatol*. 2013;22:88–92.
33. Le Goff C, Cormier-Daire V. From tall to short: the role of TGFbeta signaling in growth and its disorders. *Am J Med Genet C Semin Med Genet*. 2012;160C:145–153.
34. Li Q, Aranyi T, Varadi A, et al. Research progress in pseudoxanthoma elasticum and related ectopic mineralization disorders. *J Invest Dermatol*. 2016;136:550–556.
35. Has C, Bauer JW, Bodemer C, et al. Consensus reclassification of inherited epidermolysis bullosa and other disorders with skin fragility. *Br J Dermatol*. 2020;183:614–627.
36. Bruckner-Tuderman L. Dystrophic epidermolysis bullosa: pathogenesis and clinical features. *Dermatol Clin*. 2010;28:107–114.
37. Bardhan A, Bruckner-Tuderman L, Chapple ILC, et al. Epidermolysis bullosa. *Nat Rev Dis Primers*. 2020;6:78.
38. Salo AM, Cox H, Farndon P, et al. A connective tissue disorder caused by mutations of the lysyl hydroxylase 3 gene. *Am J Hum Genet*. 2008;83:495–503.
39. Vahidnezhad H, Youssefian L, Saeidian AH, et al. Mutations in PLOD3, encoding lysyl hydroxylase 3, cause a complex connective tissue disorder including recessive dystrophic epidermolysis bullosa-like blistering phenotype with abnormal anchoring fibrils and type VII deficiency. *Matrix Biol*. 2019;81:91–106.
40. Pedchenko V, Bondar O, Fogo AB, et al. Molecular architecture of the Goodpasture autoantigen in anti-GBM nephritis. *N Engl J Med*. 2010;363:343–354.
41. Dainichi T, Kurono S, Ohyama B, et al. Anti-laminin gamma-1 pemphigoid. *Proc Natl Acad Sci USA*. 2009;106:2800–2805.
42. Vahidnezhad H, Youssefian L, Uitto J. Lipoid proteinosis. 2016 Jan 21 [Updated 2021 Jul 22] In: Adam MP, Everman DB, Mirzaa GM, et al. (eds). GeneReviews® [Internet]. Seattle: University of Washington, Seattle; 1993–2023. Available from: https://www.ncbi.nlm.nih.gov/books/NBK338540/.
43. Adamo CS, Zuk AV, Sengle G. The fibrillin microfibril/elastic fibre network: a critical extracellular supramolecular scaffold to balance skin homoeostasis. *Exp Dermatol*. 2021;30:25–37.
44. Gerber EE, Gallo EM, Fontana SC, et al. Integrin-modulating therapy prevents fibrosis and autoimmunity in mouse models of scleroderma. *Nature*. 2013;503:126–130.
45. Fritsch A, Loeckermann S, Kern JS, et al. A hypomorphic mouse model of dystrophic epidermolysis bullosa reveals mechanisms of disease and response to fibroblast therapy. *J Clin Invest*. 2008;118:1669–1679.
46. Nystrom A, Velati D, Mittapalli VR, et al. Collagen VII plays a dual role in wound healing. *J Clin Invest*. 2013;123:3498–3509.
47. Nystrom A, Buttgereit J, Bader M, et al. Rat model for dominant dystrophic epidermolysis bullosa: glycine substitution reduces collagen VII stability and shows gene-dosage effect. *PLoS ONE*. 2013;8:e64243.
48. Dengjel J, Bruckner-Tuderman L, Nyström A. Skin proteomics – analysis of the extracellular matrix in health and disease. *Expert Rev Proteomic*. 2020;17:377–391.
49. Bruckner-Tuderman L. Skin fragility: perspectives on evidence-based therapies. *Acta Derm Venereol*. 2020;100:94–101.
50. Kueckelhaus M, Rothoeft T, De Rosa L, et al. Transgenic epidermal cultures for junctional epidermolysis bullosa - 5-year outcomes. *N Engl J Med*. 2021;385 2264–27.

50a. Guide SV, Gonzalez ME, Bağcı IS, et al. Trial of beremagene geperpavec (B-VEC) for dystrophic epidermolysis bullosa. *N Engl J Med*. 2022;387 2211–9.

51. Kiritsi D, Garcia M, Brander R, et al. Mechanisms of natural gene therapy in dystrophic epidermolysis bullosa. *J Invest Dermatol*. 2014;134:2097–2104.
52. Tolar J, Blazar BR, Wagner JE. Concise review: transplantation of human hematopoietic cells for extracellular matrix protein deficiency in epidermolysis bullosa. *Stem Cells*. 2011;29:900–906.
53. Woodley DT, Wang X, Amir M, et al. Intravenously injected recombinant human type VII collagen homes to skin wounds and restores skin integrity of dystrophic epidermolysis bullosa. *J Invest Dermatol*. 2013;133:1910–1913.
54. Ramirez F, Caescu C, Wondimu E, et al. Marfan syndrome: a connective tissue disease at the crossroads of mechanotransduction, TGFβ signaling and cell stemness. *Matrix Biol*. 2018;71–72:82–89.
55. Nyström A, Thriene K, Mittapalli V, et al. Losartan ameliorates dystrophic epidermolysis bullosa and uncovers new disease mechanism. *EMBO Mol Med*. 2015;7:1211–1228.
56. Bowen CJ, Calderón Giadrosic JF, Burger Z. Targetable cellular signaling events mediate vascular pathology in vascular Ehlers-Danlos syndrome. *J Clin Invest*. 2020;130:686–698.



eFig. 95.1 Cytoskeletal organization in a dermal fibroblast. Staining with anti-vimentin (red), anti-actin (blue), and anti-tubulin (green) antibodies. The intracellular cytoskeleton is linked to the extracellular matrix via cell surface receptors such as integrins, and the cytoskeleton is dynamically remodeled in response to ligand occupation and substrate stiffness. *Courtesy Dr Boris Hinz*.



eFig. 95.2 Microfibrils in the papillary dermis. Confocal scanning microscopy of microfibrils which emerge from the epidermis and traverse the papillary dermis perpendicularly. The immunostaining is with antibodies to fibrillin 1 (red) and latent TGF-β complex (green). The orange–yellow color demonstrates co-localization of both proteins on the microfibrils. *Courtesy Dr Michael Raghunath (J Invest Dermatol 1998;111:559–64)*.

Perforating Diseases 96

Ronald P. Rapini

Synonyms: ■ Hyperkeratosis follicularis et parafollicularis in cutem penetrans: Kyrle disease ■ Acquired perforating dermatosis: acquired reactive perforating collagenosis, acquired reactive perforating dermatosis, perforating disorder of uremia

Key features

- Group of disorders with transepidermal elimination of collagen, elastic tissue, or necrotic dermal connective tissue
- Papules or nodules with keratotic plugs
- Elastosis perforans serpiginosa is associated with genetic diseases or penicillamine administration and involves elastic tissue; lesions are typically annular and most commonly occur in flexural sites, in particular the neck
- Reactive perforating collagenosis occurs after minor trauma, involves collagen, and often involves the upper extremities
- Acquired perforating dermatosis is almost always associated with diabetes mellitus and/or the pruritus of chronic kidney disease (stages 4–5); it favors the lower extremities of adults
- Broadband or narrowband UVB phototherapy appears to be the most effective treatment for acquired perforating dermatosis

INTRODUCTION

The perforating diseases are a group of papulonodular skin disorders characterized by keratotic plugs or crusts in which dermal connective tissue "perforates" or is eliminated through the epidermis (Table 96.1). There are two prototypic perforating diseases, both of which can be inherited. *Reactive perforating collagenosis* (RPC) is associated with transepidermal elimination of primarily collagen fibers[1], whereas in *elastosis perforans serpiginosa* (EPS), primarily elastic fibers are extruded through the epidermis. The third major perforating disease is *acquired perforating dermatosis*, which usually develops during adulthood in association with diabetes mellitus and/or the pruritus of chronic kidney disease (stages 4–5)[2]. Many textbooks traditionally list "perforating folliculitis" as the fourth perforating disease[3], but, in the opinion of the author, this seems unjustified. It does not appear to be a specific entity, since perforation or rupture of follicles occurs in a wide variety of diseases classified as folliculitis, regardless of whether the pathogenesis involves bacteria, fungi, *Demodex* mites, drugs, physical trauma, or other mechanisms.

Some authorities have expanded the concept of the preceding so-called "primary" perforating diseases to include a variety of unrelated "secondary" perforating disorders in which transepidermal elimination of a substance occurs as a secondary component of a primary dermatosis (Table 96.2). As in most of the preceding perforating disorders, the epidermis often becomes hyperplastic, eventually surrounds the material to be extruded, and subsequently causes the material's elimination via normal keratinocyte maturation. Some of these disorders are discussed elsewhere in this text and involve perforation of endogenous substances, exogenous foreign material, infectious organisms, granulomas, and even neoplastic cells[4].

HISTORY

In 1916, Kyrle reported a diabetic woman with generalized hyperkeratotic nodules, which he called "hyperkeratosis follicularis et parafollicularis in cutem penetrans". Lutz first described EPS as "keratosis follicularis serpiginosa" in 1953, and, in 1955, Miescher described the histologic findings, naming it "elastoma intrapapillare perforans verruciforme". Mehregan, Schwartz, and Livingood reported the first child with RPC in 1967. A year later, Mehregan and Coskey expanded the concept of perforating disease to include perforating folliculitis in their article.

EPIDEMIOLOGY

The perforating diseases are found worldwide, without any clear racial predilection. The very rare childhood-onset form of RPC is commonly familial, and childhood-onset EPS is occasionally familial. Although the exact inheritance pattern for both is still uncertain, isolated inherited EPS may have an autosomal dominant pattern. EPS affects men more often than women, with a ratio of ~4:1, whereas the sex distribution is nearly equal in RPC and acquired perforating dermatosis. Perforating folliculitis is said to be more common in women. In patients receiving maintenance hemodialysis, acquired perforating dermatosis is observed in an estimated 4.5% to 11% of patients[5]. Acquired perforating dermatosis is more commonly encountered than the inherited perforating disorders.

PATHOGENESIS

The precise pathogenesis underlying the perforating disorders is unknown. As it is unlikely that dermal connective tissue or hair shafts actively perforate into the epithelium, some have argued that "transepidermal elimination" is a more accurate term. The term "perforating" is embedded in the dermatologic lexicon, however, and is easier to say. Epithelium becomes hyperplastic and eventually surrounds the abnormal connective tissue, just as it appears to do with wood splinters or other foreign bodies. In acquired perforating dermatosis, pruritus probably leads to chronic scratching, which results in epithelial hyperplasia, as in prurigo nodularis. Indeed, prurigo nodules are often admixed with classic perforating lesions. The possibility has been raised that enlargement of a hyperkeratotic plug could lead to penetration through the base of the hyperplastic epidermis, i.e. the perforation is caused by the plug above rather than being due to the abnormal connective tissue below.

Primary perforating diseases may be due to either genetic or acquired abnormalities of collagen or elastic fibers. In EPS, as well as some cases of acquired perforating dermatosis in which perforation of elastic fibers is observed, enhanced expression of elastin receptors has been detected in the epidermis surrounding the elastic material[6]. It has been proposed that scratching exposes keratinocytes to *a*dvanced *g*lycation *e*nd product (AGE)-modified extracellular matrix proteins, in particular collagen types I and III. This would then lead to terminal differentiation of keratinocytes via the AGE receptor (CD36), followed by upward movement of keratinocytes along with glycated collagen[7]. Increased levels of AGEs have been detected in the skin of patients with acquired perforating dermatoses[8].

Plasma fibronectin levels are elevated in patients with diabetes mellitus and uremia, and fibronectin is also increased within the skin at sites of transepidermal elimination[9]. This may be significant, since fibronectin plays a role in epithelial cell signaling, locomotion, and differentiation. It binds to type IV collagen (the type found in basement membranes) and to keratinocytes and may incite epithelial proliferation and perforation. In one study of RPC, the investigators demonstrated that the collagen being transepidermally eliminated was type IV collagen[10]. Increased expression of transforming growth factor-β_3 (TGF-β_3), matrix metalloproteinase-1 (MMP-1), and tissue inhibitor of metalloproteinase-1 (TIMP-1) has been observed in lesional skin of acquired RPC[11], but this enhanced expression may be a reflection of concurrent wound healing (see Ch. 141).

MAJOR PERFORATING DISEASES					
Disease	**Incidence**	**Time of onset**	**Most common location**	**Perforating substance**	**Associations**
Familial reactive perforating collagenosis (RPC)	Very rare	Childhood	Arms, hands, sites of trauma	Collagen	None
Elastosis perforans serpiginosa (EPS)	Rare, M > F	Childhood, early adulthood; variable with penicillamine-induced EPS	Neck, face, arms, other flexural areas	Elastic tissue	Genetic diseases (see Fig. 96.13), penicillamine
Perforating folliculitis	Common	Early adulthood	Trunk, extremities	Necrotic material	May simply be ordinary folliculitis with follicular rupture, i.e. not a specific entity
Acquired perforating dermatosis, includes acquired RPC, Kyrle disease*, and rarely, acquired EPS	Common (10% of dialysis patients)	Adulthood	Legs or generalized	Necrotic material, collagen, or uncommonly, elastic tissue	Diabetes, chronic kidney disease (stages 4–5), pruritus, rarely liver disease; may be end stage of perforating folliculitis
Perforating calcific elastosis	Very rare, more common in Black women	Adulthood	Abdomen, periumbilical	Calcified elastic tissue	Multiparity, weight gain, obesity, hypertension

*In the opinion of some authors.

Table 96.1 Major perforating diseases. F, female; M, male.

SECONDARY PERFORATING DISEASES
Endogenous substances
Chondrodermatitis nodularis helicis Hematomas Perforating pseudoxanthoma elasticum Perforating calcinosis Osteoma cutis Gout (urate crystals) Papular mucinosis (mucin)
Granulomas
Perforating granuloma annulare (see Fig. 93.10) Necrobiosis lipoidica Sarcoidosis Rheumatoid nodule
Exogenous foreign material
Silica Wood splinters Tattoo Sutures Injectable soft tissue fillers
Infectious diseases
Chromoblastomycosis Leprosy Schistosomiasis
Tumor cells (more common examples)*
Melanoma Spitz nevus Pilomatricoma
*May be a nonspecific finding in a range of benign and malignant tumors due to "perforation" of the epidermis by complexes of neoplastic cells.

Table 96.2 Secondary perforating diseases. For a more extensive list, see reference 4.

Other proposed pathomechanisms include abnormal vitamin A or D metabolism, enzyme release from neutrophils[12], and microangiopathy related to diabetes. Deposition of uric acid, hydroxyapatite, or silicon[13] has also been implicated in the pathogenesis of perforating disorders.

CLINICAL FEATURES

Reactive Perforating Collagenosis

Familial RPC is a rare disorder that begins during childhood[1,14]. After superficial trauma, patients develop keratotic papules that reach a size of 5–8 mm over the following 3–4 weeks. The Koebner phenomenon may occur, in which injury to the skin results in the formation of new lesions, often in a linear distribution. Koebnerization is more commonly observed with RPC than with the other perforating disorders, but it has been reported with all of them. Arms and hands are the most common sites of involvement in RPC (Fig. 96.1). The papules tend to spontaneously resolve over 6–10 weeks. Verrucous perforating collagenoma (*collagenome perforant verruciformé*) is a very rare non-familial variant of RPC in which severe trauma to the skin results in verrucous papules with transepidermal elimination of collagen[15]. Acquired RPC that begins in adulthood usually occurs in association with diabetes mellitus and/or chronic kidney disease (stages 4–5), and these cases are best classified as acquired perforating dermatosis, even though the histopathology is identical to the inherited form of RPC.



Fig. 96.1 Reactive perforating collagenosis of the arm. Several erythematous papules with a central scale-crust core. *Courtesy Lorenzo Cerroni, MD.*

Elastosis Perforans Serpiginosa

EPS is a rare disorder whose onset is during childhood or early adulthood. About 40% of cases occur in association with other genetic disorders, including Down syndrome, Ehlers–Danlos syndrome, osteogenesis imperfecta, Marfan syndrome (Fig. 96.2), pseudoxanthoma elasticum (PXE), Rothmund–Thomson syndrome, and acrogeria. In a survey of pediatric dermatologists, the majority performed a detailed history and careful physical examination but did not embark upon an extensive search for these genetic disorders in an otherwise healthy child or adolescent with EPS[16].



Fig. 96.2 Elastosis perforans serpiginosa in the setting of Marfan syndrome. Annular papules and plaques developed on the ear.

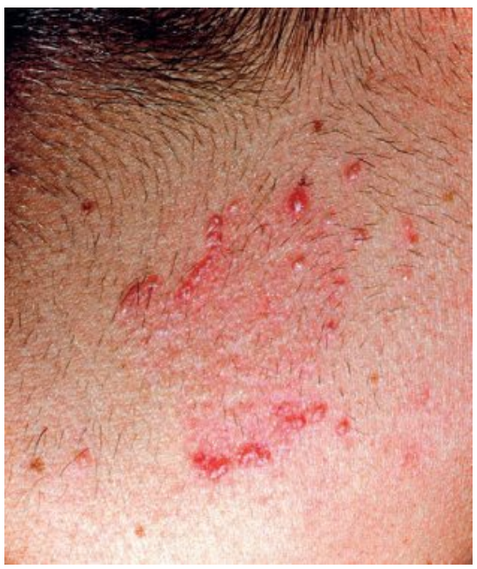


Fig. 96.3 Elastosis perforans serpiginosa. Papules arranged in an annular configuration on the neck.



Fig. 96.4 Penicillamine-induced elastosis perforans serpiginosa. A Multiple annular plaques favoring the antecubital fossae. **B** Closer view with foci of hyperkeratosis at sites of transepidermal elimination.

Very rarely, EPS has been associated with chronic kidney disease (more rarely encountered than the acquired form of RPC) and may overlap with acquired perforating dermatosis. EPS has also been reported following long-term use of penicillamine, usually for 10 or more years. This drug is known to disrupt desmosine cross-links within elastin (see Ch. 97)[17]. Because penicillamine is used to treat Wilson disease, the possibility that abnormal copper metabolism plays a pathogenic role in EPS has been raised. However, EPS has also been observed in patients with cystinuria or rheumatoid arthritis who have received penicillamine.

Lesions of EPS are keratotic, 2- to 5-mm papules that tend to be arranged in a serpiginous or annular pattern, most commonly on the lateral neck (Fig. 96.3), but also on the face, arms (Fig. 96.4), or other flexural areas. The rings of papules may reach several centimeters in diameter. Most patients experience no symptoms or only mild pruritus. Like RPC, the lesions may spontaneously resolve, but in general tend to persist, often for several years.

Acquired Perforating Dermatosis and Kyrle Disease

Acquired perforating dermatosis has been used as a catch-all term for those perforating diseases that arise in adults, usually in association with diabetes mellitus and/or the pruritus of chronic kidney disease (stages 4–5)[2]. The majority of affected patients with established renal failure are receiving dialysis, and most of those with diabetes mellitus have associated nephropathy[18]. In individuals requiring dialysis, predictors for the development of acquired perforating dermatosis include diabetes mellitus, reduced circulating levels of intact parathyroid hormone, hypoalbuminemia, and elevated serum levels of high-sensitivity C-reactive protein[19]. This disorder can also occur in conjunction with other causes of pruritus, from insect bites and scabies to lymphoma and hepatobiliary diseases, including primary biliary cholangitis and hepatocellular carcinoma.

Acquired perforating dermatosis can arise from other forms of trauma (not just scratching), including within sites of healing herpes zoster. In addition, acquired perforating dermatosis and perforating folliculitis may develop following exposure to several classes of drugs including TNF inhibitors, epidermal growth factor receptor inhibitors (e.g. gefitinib, panitumumab) and other kinase inhibitors (e.g. nilotinib), dipeptidyl peptidase-4 inhibitors, antivirals (e.g. telaprevir, indinavir), sirolimus, and several monoclonal antibodies (e.g. natalizumab, bevacizumab). Of note, some of these medications more commonly induce an acneiform eruption with disrupted pilosebaceous units rather than a perforating dermatosis. While an association with hypothyroidism and hyperparathyroidism has been reported, most of these patients also had established risk factors (e.g. diabetes, nephropathy). Lastly, in a series of 22 patients with acquired perforating dermatosis, three were healthy and had no known associated illnesses and two were renal transplant recipients[18].

Acquired perforating dermatosis occurs most commonly on the legs (Fig. 96.5), but generalized or widely scattered papules and nodules can be seen (Figs. 96.6 & 96.7). Extensor surfaces are favored over flexures and the mucous membranes are spared. A clue to the diagnosis is the presence of a central keratotic core, which is sometimes physically removed by the patient. Occasionally, a giant variant is observed,



Fig. 96.5 Acquired perforating dermatosis. **A** Numerous hyperpigmented papules and nodules on the legs in a patient with both chronic kidney disease and diabetes mellitus. **B** The central portion of these lesions can be keratotic or composed of scale-crust. **C** Larger nodules in a patient receiving hemodialysis for end-stage kidney disease. *B, Courtesy Lorenzo Cerroni, MD; C, Courtesy Frank Samarin, MD.*



Fig. 96.6 Acquired perforating dermatosis. Erythematous papules with central keratotic cores in a patient with chronic kidney disease. Sometimes the latter are dislodged by the patient. *Courtesy Lorenzo Cerroni, MD.*



Fig. 96.8 Perforating calcific elastosis. When a biopsy was performed from the elevated edge of this supraumbilical plaque in a multiparous African-American woman, resistance was felt, as well as a grinding sound.



Fig. 96.7 Acquired perforating dermatosis. Note the linear arrangement of the keratotic papules (Koebner phenomenon).

where lesions may reach 2 cm in diameter. Rarely, secondary infections due to bacteria (e.g. *Staphylococcus aureus*), atypical mycobacteria (e.g. *Mycobacterium abscessus*), or fungi (e.g. *Mucor* spp.) have been reported.

Largely on the basis of histologic findings, patients with acquired perforating dermatosis have been variably designated in the literature as having RPC, EPS[2], perforating folliculitis[14], or perforating PXE. However, not only do the pathologic findings vary from lesion to lesion in the same patient, but there are often overlapping features. In addition, since some, but not necessarily all, of these lesions appear to be follicular, and since manipulation of the lesions by patients frequently alters the histologic changes, the term "acquired perforating dermatosis" was proposed to encompass all of these cases. Furthermore, since Kyrle had used the phrase "follicularis et parafollicularis" to emphasize that not all lesions were centered on hair follicles, the eponym Kyrle disease has been used synonymously with acquired perforating dermatosis by some authorities[2]. However, others do not consider Kyrle disease to be an entity or prefer to define it as merely representing the presence of end-stage, excoriated, prurigo nodules of folliculitis[2].

Perforating Calcific Elastosis

This disorder is characterized by plaques that favor the abdomen, especially the periumbilical region of middle-aged, obese, hypertensive, multiparous Black women (Fig. 96.8)[20]. Involvement of the breast in patients with chronic kidney disease has also been observed. The plaques may be verrucous or have keratotic papules at their periphery.

In histologic sections stained with H&E or von Kossa or Verhoeff–van Gieson stains, calcified elastic fibers (identical to those in PXE) are seen undergoing transepidermal elimination. However, affected patients do not manifest other clinical findings of PXE. Similar transepidermal elimination has been observed in patients with dermatitis who applied a commercially available calcium salt water normally used for making bean curd or were exposed to calcium chloride contained in ice-melting salt.

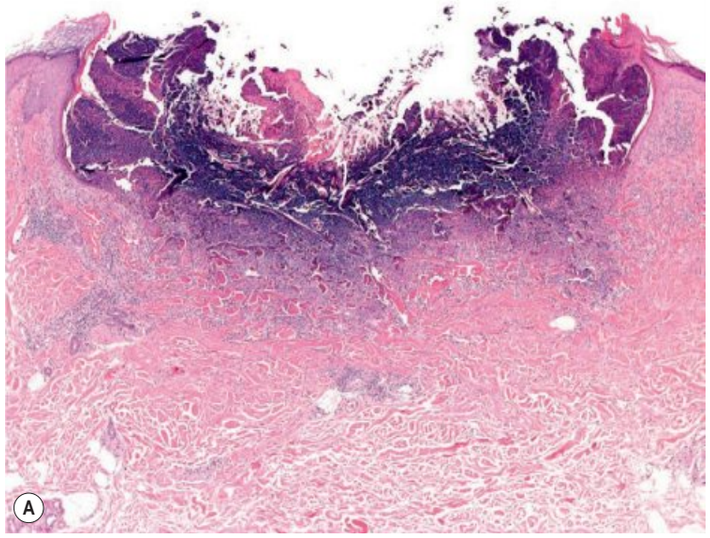
PATHOLOGY

In all the perforating diseases, there is a plug of crusting or hyperkeratosis, with variable parakeratosis, depending upon the stage of the lesion (Fig. 96.9A). As the plug enlarges, epithelial hyperplasia develops, sometimes with dyskeratosis of keratinocytes. At the site of perforation, the epithelial hyperplasia often resembles an elephant snout or crab claw. However, sections from multiple levels through the tissue may need to be examined to find the site of perforation. Some lesions may have aggregates of neutrophils within the dermis, while older lesions, particularly those of EPS, tend to have lymphocytes, macrophages, or multinucleated giant cells in the dermis at the site of perforation.

In RPC, basophilic (degenerative) collagen fibers, some of which are vertically oriented, are seen within the plug or within the epidermis (Figs. 96.9B & 96.10), whereas in EPS, elastic fibers are seen instead (in the same location; Fig. 96.11A). It is important to note, however,



Fig. 96.10 Reactive perforating collagenosis. Transepidermal elimination of red collagen fibers through the spinous layer and into the stratum corneum (Verhoeff–van Gieson stain).



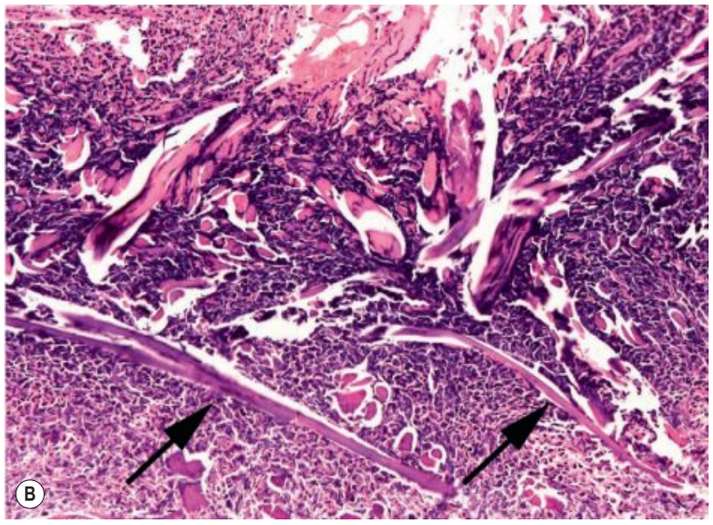
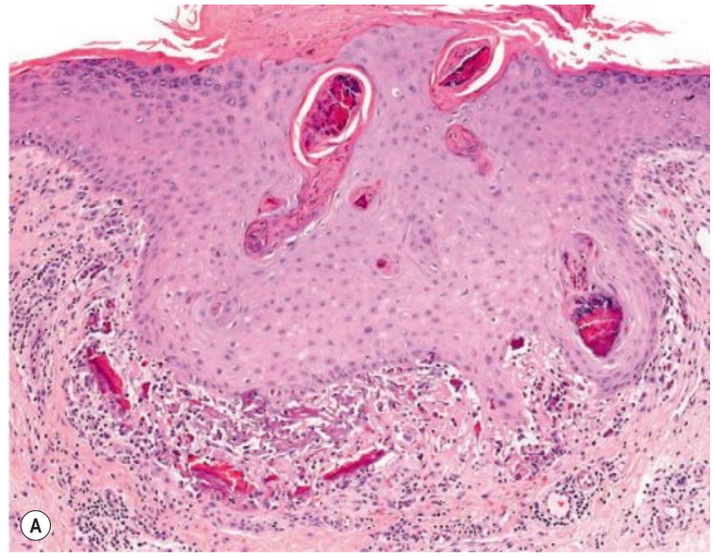


Fig. 96.9 Acquired perforating dermatosis (acquired reactive perforating collagenosis). A Scanning view of a crusted keratotic plug in a patient whose biopsy showed perforating collagen fibers. **B** Higher magnification demonstrating collagen fibers (arrows) extending into the crusted plug. *Courtesy Lorenzo Cerroni, MD.*



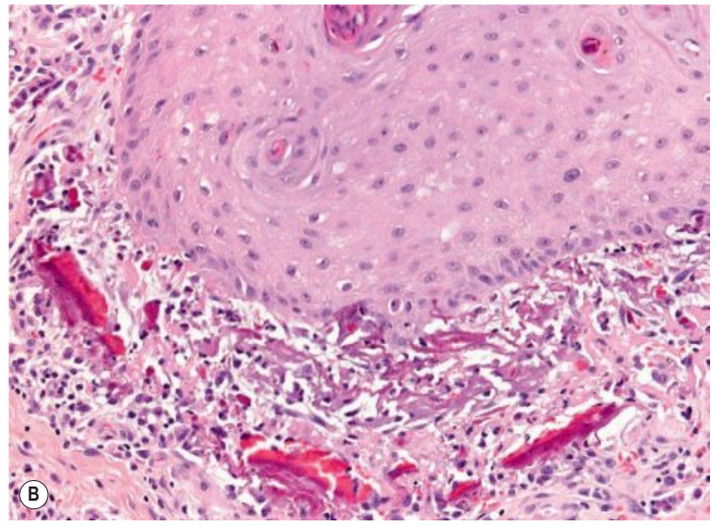


Fig. 96.11 Elastosis perforans serpiginosa. A Hyperplastic epidermis with transepidermal elimination of dermal elastic fibers via channels. Note the surface scale-crust. **B** Characteristic brightly eosinophilic elastic fibers within the superficial dermis. *Courtesy Lorenzo Cerroni, MD.*

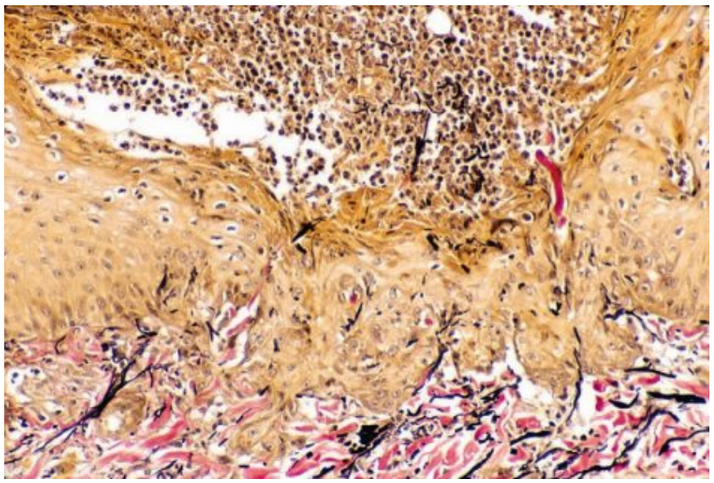


Fig. 96.12 Acquired perforating dermatosis. Transepidermal elimination of both collagen (red) and elastic fibers (black) into a crust with many neutrophils is seen (Verhoeff–van Gieson stain).

DIFFERENTIAL DIAGNOSIS OF PERFORATING DISEASES
Reactive perforating collagenosis and acquired perforating dermatosis
Excoriations from a variety of causes (prurigo simplex)
Prurigo nodularis
Folliculitis
Arthropod bites
Perforation of exogenous foreign material
Perforation of endogenous substances
Multiple keratoacanthomas
Verrucous lupus erythematosus or lichen planus
If Koebner phenomenon: psoriasis, lichen planus, verrucae (autoinoculation)
Elastosis perforans serpiginosa (resembles other annular diseases; see Ch. 19)
Granuloma annulare, Tinea, Sarcoidosis — Common annular diseases
Annular elastolytic giant cell granuloma (actinic granuloma)
Perforating pseudoxanthoma elasticum
Porokeratosis
Discoid lupus erythematosus

Table 96.3 Differential diagnosis of perforating diseases.

that intraepidermal elastic fibers can also be found in other disorders characterized by a hyperplastic epidermis (see below). In RPC, the dermal connective tissue adjacent to the plug appears unremarkable, while in EPS, an increased amount of brightly eosinophilic elastic tissue is often present in the superficial dermis (Fig. 96.11B). The Verhoeff–van Gieson stain is most helpful, because collagen fibers appear red and elastic fibers appear black (Fig. 96.12). However, in EPS, the elastic fibers higher up in the epidermis may lose their ability to stain black. In penicillamine-induced EPS, characteristic "lumpy-bumpy" elastic fibers with lateral buds resembling a "bramble bush" are seen in both lesional and non-lesional skin.

Biopsy findings in acquired perforating dermatosis vary according to the stage of evolution of the lesion. The histology may be identical to childhood RPC or EPS, or to perforating folliculitis. In other cases, it may be less specific, with amorphous degenerated material within the perforations. This material often cannot be clearly identified as collagen or elastic fibers, but sometimes both are present (see Fig. 96.12)[2]. A Japanese consensus group recently proposed classification criteria for perforating disorders based on histologic and clinical findings[21].

DIFFERENTIAL DIAGNOSIS

The differential diagnosis includes other disorders characterized by papules or nodules with central keratotic plugs or crusts, in particular prurigo simplex and prurigo nodularis (Table 96.3). Some authors, including the late A.B. Ackerman, have considered RPC to be a variant of excoriated prurigo. When the Koebner phenomenon occurs, other disorders that can also arise in a linear pattern should be considered, e.g. psoriasis, lichen planus. EPS may be confused with other disorders that are annular or serpiginous (see Ch. 19), but usually the individual keratotic plugs within the ring are distinctive. Histologically, elastic fibers may also be observed within the hyperplastic epidermis of healing wounds, keratoacanthomas, and occasionally hypertrophic lupus erythematosus and lichen simplex chronicus[22].

Since many patients with acquired perforating dermatosis have coexisting folliculitis and prurigo nodularis, there may be several different types of lesions at different stages of development and histologic findings in a single biopsy specimen may not be representative of the entire process.

Fig. 96.13 provides an algorithm for the approach to the patient with a primary perforating disorder.

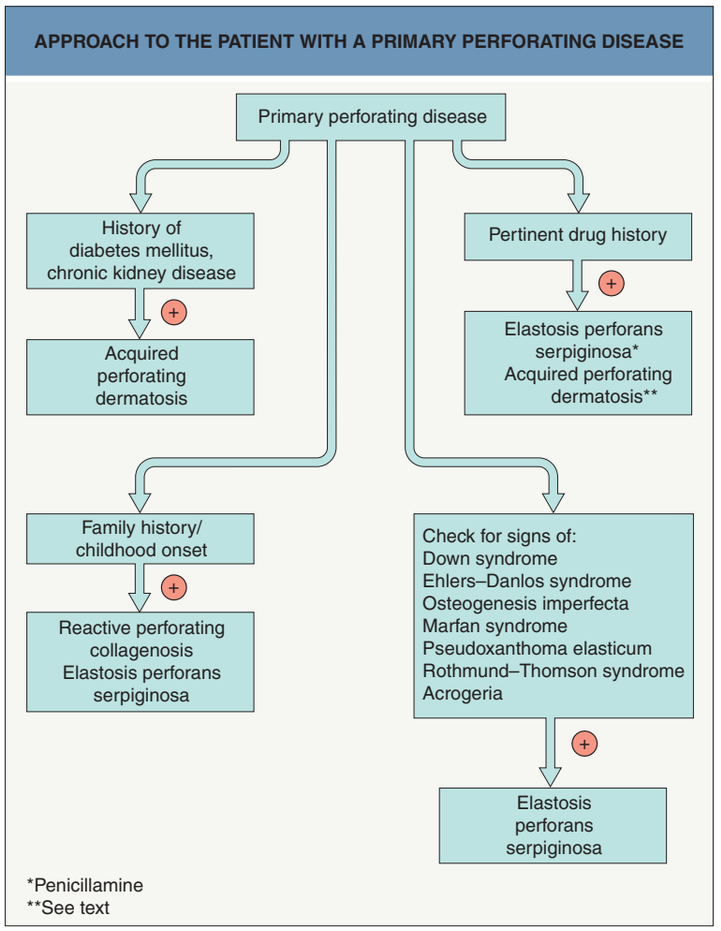


Fig. 96.13 Approach to the patient with a primary perforating disease.

TREATMENT

Table 96.4 summarizes the various treatments that have been reported, most of which are anecdotal or based upon small case series[23–29]. Well-designed, placebo-controlled studies of therapeutic interventions are needed. The inherited forms of RPC and EPS generally remain mild and localized. Sometimes local measures may be successful, but a number of authors have declared treatment to be largely ineffective. The patient with mild RPC may be counseled to simply avoid trauma and wait for lesions to resolve spontaneously.

TREATMENT OF PERFORATING DISEASES Rx
Address contributing factors
If end-stage chronic kidney disease, transplantation may lead to improvement
Discontinue culprit medication, if possible
Topical
Retinoids (e.g. tretinoin, tazarotene)[23] (3)
Corticosteroids (3)
Menthol (3)
Salicylic acid (3)
Sulfur (3)
Benzoyl peroxide (3)
Emollients (3)
Imiquimod (3)
Cantharidin (3)
Systemic
Antihistamines (e.g. doxepin) (3)*
Corticosteroids (intralesional, intramuscular, oral) (2)
Retinoids (vitamin A, acitretin, isotretinoin) (2)
Antibiotics (e.g. doxycycline, clindamycin, erythromycin, rifampin)[24,25] (3)
Dupilumab[26] (3)
Colchicine (3)
Methotrexate (3)
Charcoal (3)
Allopurinol (3)
Other
Avoid trauma and scratching (wearing gloves, trimming fingernails, behavior modification, transcutaneous nerve stimulator) (3)
Cellophane-tape stripping (for EPS) (3)
Phototherapy (broadband or narrowband UVB > UVA1, PUVA)[27,28] (2)
Cryotherapy[29] (3)
Photodynamic therapy (3)
Electrosurgical destruction (3)
Laser ablation (e.g. CO_2, Er:YAG, excimer, pulsed dye) (3)
Excision of larger bothersome lesions (3)
*See Ch. 6 for other anti-pruritic medications.

Table 96.4 Treatment of perforating diseases. Key to evidence-based support: (1) prospective controlled trial; (2) retrospective study or large case series; (3) small case series or individual case reports. EPS, elastosis perforans serpiginosa.

EPS may be treated with local cryotherapy, tangential excision, electrosurgical destruction, laser therapy (e.g. pulsed dye, Er:YAG), or cellophane tape stripping. However, aggressive treatment is more likely to result in scarring. As with RPC, spontaneous resolution of lesions makes it difficult to evaluate therapies.

Treatment of generalized acquired perforating dermatosis or extensive perforating folliculitis is often difficult. Sedating antihistamines and other typical "anti-itch" treatments (see Ch. 6) are often prescribed in an attempt to reduce the associated pruritus. Phototherapy (usually broadband or narrowband UVB) is a particularly good choice for patients with chronic kidney disease, since it often relieves coexisting pruritus. Other therapies that are sometimes helpful include intralesional corticosteroids and oral[15] or topical retinoids. Dupilumab was reported to significantly improve acquired RPC in the setting of adult atopic dermatitis[26]. Anecdotally, some patients have attributed rapid improvement to a change in the type of dialysis tubing or equipment employed, or even an alteration in the methods used during the actual dialysis procedure (personal observation). Occasional dialysis patients with acquired perforating dermatosis have been cured after renal transplantation[13].

Additional figures available in our eBook (see inside front cover for access code).

REFERENCES

1. Flannigan SA, Tucker SB, Rapini RP. Recurrent hyperkeratotic papules from superficial trauma: reactive perforating collagenosis (RPC). *Arch Dermatol*. 1985;121:1554–1555, 1557–1558.
2. Rapini RP, Hebert AA, Drucker CR, et al. Acquired perforating dermatosis. Evidence of combined transepidermal elimination of both collagen and elastic fibers. *Arch Dermatol*. 1989;125:1074–1078.
3. Rubio FA, Herranz P, Robayna G, et al. Perforating folliculitis: report of a case in an HIV-infected man. *J Am Acad Dermatol*. 1999;40:300–302.
4. Karpouzis A, Giatromanolaki A, Sivridis E, Kouskoukis C. Acquired reactive perforating collagenosis: current status. *J Dermatol*. 2010;37:585–592.
5. Cordova KB, Oberg TJ, Malik M, Robinson-Bostom L. Dermatologic conditions seen in end-stage renal disease. *Semin Dial*. 2009;22:45–55.
6. Fujimoto N, Akagi A, Tajima S, et al. Expression of the 67-kDa elastin receptor in perforating skin disorders. *Br J Dermatol*. 2002;146:74–79.
7. Fujimoto E, Kobayashi T, Fujimoto N, et al. AGE-modified collagens I and III induce keratinocyte terminal differentiation through AGE receptor CD36: epidermal-dermal interaction in acquired perforating dermatoses. *J Invest Dermatol*. 2010;130:405–414.
8. Bellinato F, Maurelli M, Gisondi P, Girolomoni G. Acquired perforating dermatoses show increased levels of cutaneous advanced glycation end-products. *Clin Exp Dermatol*. 2022;47:80–85.
9. Bilezikci B, Seckin D, Demirhan B. Acquired perforating dermatosis in patients with chronic renal failure: a possible role for fibronectin. *J Eur Acad Dermatol Venereol*. 2003;17:230–232.
10. Herzinger T, Schirren CG, Sander CA, et al. Reactive perforating collagenosis – transepidermal elimination of type IV collagen. *Clin Exp Dermatol*. 1996;21:279–282.
11. Gambichler T, Birkner L, Stucker M, et al. Up-regulation of transforming growth factor-beta3 and extracellular matrix proteins in acquired reactive perforating collagenosis. *J Am Acad Dermatol*. 2009;60:463–469.
12. Zelger B, Hintner H, Aubock J, et al. Acquired perforating dermatosis. Transepidermal elimination of DNA material and possible role of leukocytes in pathogenesis. *Arch Dermatol*. 1991;127:695–700.
13. Saldanha LF, Gonick HC, Rodriguez HJ, et al. Silicon-related syndrome in dialysis patients. *Nephron*. 1997;77:48–56.
14. Ramesh V, Sood N, Kubba A, et al. Familial reactive perforating collagenosis: a clinical, histopathological study of 10 cases. *J Eur Acad Dermatol Venereol*. 2007;21:766–770.
15. Delacretaz J, Gattlen JM. Transepidermal elimination of traumatically altered collagen. Report of three cases and consideration on the relationship between 'collagenome perforant verruciformé' and reactive perforating collagenosis. *Dermatologica*. 1976;152:65–66.
16. Vearrier D, Buka RL, Roberts B, et al. What is the standard of care in the evaluation of elastosis perforans serpiginosa? A survey of pediatric dermatologists. *Pediatr Dermatol*. 2006;23:219–224.
17. Hellriegel S, Bertsch HP, Emmert S, et al. Elastosis perforans serpiginosa: a case of penicillamine-induced degenerative dermatosis. *JAMA Dermatol*. 2014;150:785–787.
18. Weng CH, Hu CC, Ueng SH, et al. Predictors of acquired perforating dermatosis in uremic patients on hemodialysis: a case-control study. *ScientificWorldJournal*. 2012;2012:158075.
19. Akoglu G, Emre S, Sungu N, et al. Clinicopathological features of 25 patients with acquired perforating dermatosis. *Eur J Dermatol*. 2013;23:864–871.
20. Lopes LC, Lobo L, Bajanca R. Perforating calcific elastosis. *J Eur Acad Dermatol Venereol*. 2003;17:206–207.
21. Kawakami T, Akiyama M, Ishida-Yamamoto A, et al. Clinical practice guide for the treatment of perforating dermatosis. *J Dermatol*. 2020;47:1374–1382.
22. Shah K, Kazlouskaya V, Lal K, et al. Perforating elastic fibers ('elastic fiber trapping') in the differentiation of keratoacanthoma, conventional squamous cell carcinoma and pseudocarcinomatous epithelial hyperplasia. *J Cutan Pathol*. 2014;41:108–112.
23. Outland JD, Brown TS, Callen JP. Tazarotene is an effective therapy for elastosis perforans serpiginosa. *Arch Dermatol*. 2002;138:169–171.
24. Gonul M, Cakmak SK, Gul U, et al. Two cases of acquired perforating dermatosis treated with doxycycline therapy. *Int J Dermatol*. 2006;45:1461–1463.
25. Kasiakou SK, Peppas G, Kapaskelis AM, Falagas ME. Regression of skin lesions of Kyrle's disease with clindamycin: implications for an infectious component in the etiology of the disease. *J Infect*. 2005;50:412–416.
26. Ying Y, Shuang C, Zhen-Ying Z. Dupilumab may be an alternative option in the treatment of acquired reactive perforating collagenosis combined with AD. *Immun Inflamm Dis*. 2022;10:e574.
27. Sehgal VN, Verma P, Battacharya SN, et al. Familial reactive perforating collagenosis in a child: response to narrow-band UVB. *Pediatr Dermatol*. 2013;30:762–764.
28. Mii S, Yotsu R, Hayashi R, et al. Acquired perforating collagenosis successfully treated with narrow-band ultraviolet B. *Acta Derm Venereol*. 2009;89:530–531.
29. Kalkan G, Sahin M, Vahaboglu G, et al. A case of elastosis perforans serpiginosa treatment with cryotherapy. *Int J Dermatol*. 2012;51:1487–1490.



eFig. 96.1 Reactive perforating collagenosis. This keratotic papule on the upper extremity followed minor trauma in a healthy man who had developed similar papules since childhood.



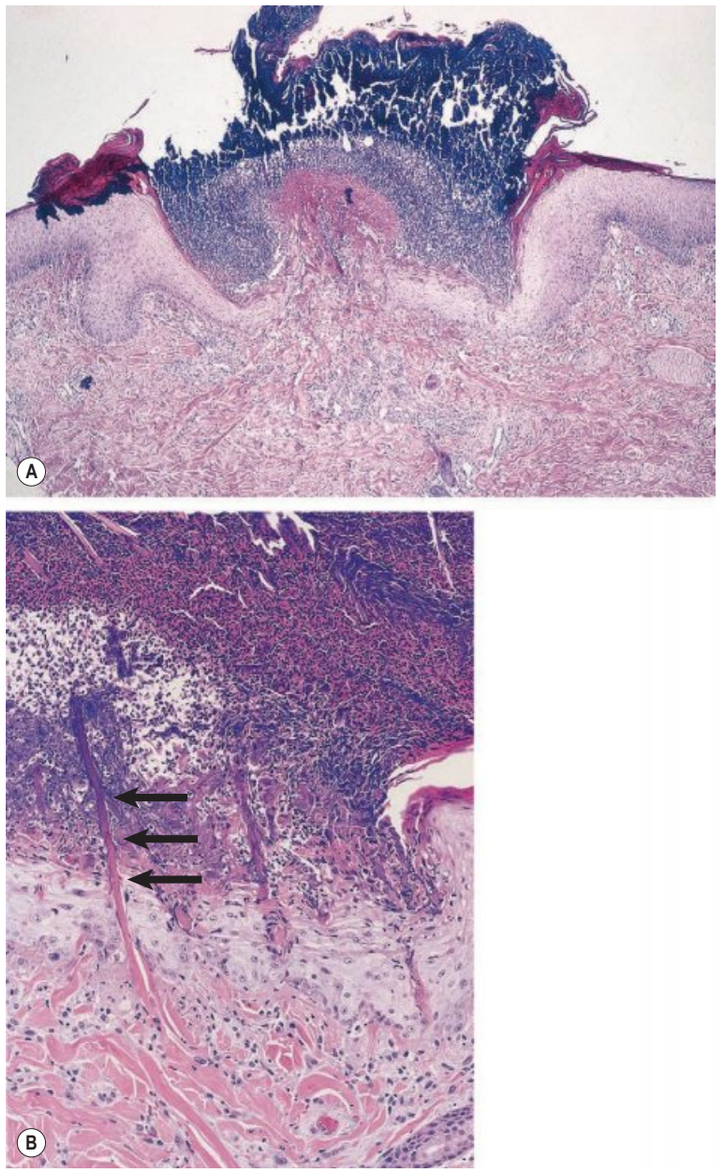
eFig. 96.2 Acquired perforating dermatosis in a patient with diabetes mellitus. *Courtesy Lorenzo Cerroni, MD.*



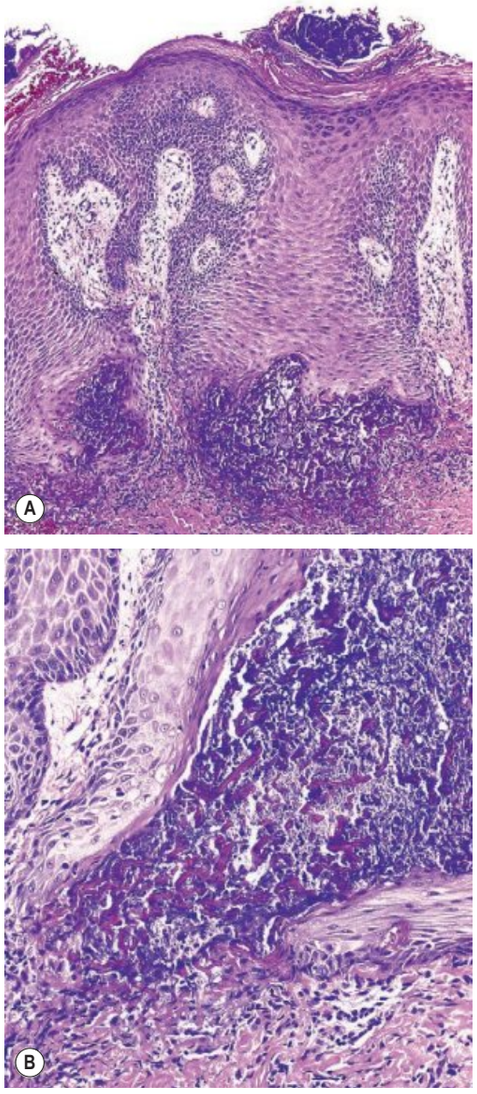
eFig. 96.3 Acquired perforating dermatosis. Erythematous papules with central keratotic cores in a patient with chronic kidney disease. Sometimes the latter are dislodged by the patient. *Courtesy Lorenzo Cerroni, MD.*



eFig. 96.4 Acquired perforating dermatosis. Keratotic papules on the arm of a diabetic woman on hemodialysis. Note the central keratotic core which is sometimes dislodged by the patient.



eFig. 96.5 Acquired perforating dermatosis (acquired reactive perforating collagenosis). A Scanning view of a crusted keratotic plug in a patient whose biopsy showed perforating collagen fibers. **B** Higher magnification demonstrating collagen fibers extending through the epidermis (arrows) into the crusted plug.



eFig. 96.6 Elastosis perforans serpiginosa. **A** Hyperplastic epidermis clutches the increased dermal elastic fibers like a claw. **B** Transepidermal elimination of neutrophils and elastic fibers from the dermis through a channel in the epidermis.

97 Heritable Disorders of Connective Tissue

Nigel P. Burrows, Franziska Ringpfeil and Jouni Uitto†

Chapter Contents

Ehlers–Danlos Syndrome 1714
Pseudoxanthoma Elasticum. 1719
Cutis Laxa 1724

Key features

- Heritable connective tissue disorders with skin involvement comprise a phenotypically diverse group of conditions
- Recognition of characteristic skin findings is often critical to establishing the diagnosis and identifying associated internal involvement, which may include life-threatening cardiovascular disease as in vascular Ehlers–Danlos syndrome and pseudoxanthoma elasticum
- Heritable connective tissue disorders can result from mutations in genes encoding structural extracellular matrix (ECM) proteins (e.g. collagens, components of elastic fibers), enzymes that modify these structural proteins, and other proteins with effects on the ECM (e.g. via transport or regulatory functions)

INTRODUCTION

Heritable connective tissue diseases manifest with a broad range of phenotypic abnormalities, including variable degrees of cutaneous and extracutaneous involvement. At one end of the spectrum, the clinical findings are mild and may be limited to the skin, while in other patients the cutaneous manifestations are part of multi-organ pathology with considerable morbidity and even mortality[1,2]. There have been significant advances in understanding the molecular bases of heritable disorders of connective tissue. This has led to improved classification and prognostication, with better recognition of the phenotypic spectra and relationships among disorders.

Connective tissue is critical for organogenesis during embryonic development and homeostatic maintenance of tissues, with complex protein assembly and cell–matrix interactions. The principal fibrillar components of the extracellular matrix (ECM) of the skin are networks consisting of collagen and elastic fibers (see Ch. 95). The study of heritable disorders of connective tissue has demonstrated the considerable impact of disruption of various individual components of the ECM and related proteins.

Classic, "primary" heritable disorders of connective tissue caused by mutations (pathogenic variants) in the genes encoding collagen and structural components of elastic fibers include several forms of Ehlers–Danlos syndrome (EDS) and cutis laxa, respectively. In addition to defects in the genes that encode these structural proteins and enzymes that modify them, seemingly unrelated pathologic processes can perturb the ECM. Examples of the latter, which can be considered as "secondary" connective tissue disorders, include pseudoxanthoma elasticum (PXE) and homocystinuria.

This chapter provides a detailed review of EDS, PXE, and cutis laxa. In addition, Marfan syndrome, homocystinuria, osteogenesis imperfecta, and Buschke–Ollendorff syndrome are presented in Table 97.1. These and other genetic diseases that affect the ECM of the skin are also summarized in Table 95.5.

EHLERS–DANLOS SYNDROME

Synonym: ■ Cutis hyperelastica

Key features

- Clinically and genetically heterogeneous group of connective tissue disorders due to abnormalities in the synthesis and maintenance of collagens and other ECM components
- Autosomal dominant and autosomal recessive inheritance patterns
- Typical cutaneous features include hyperextensible and fragile skin, easy bruising, and poor wound healing
- Variable extracutaneous features include joint hypermobility, scoliosis, ocular changes, and, particularly in the vascular type, a significant risk of arterial, intestinal, or uterine rupture

History

Patients with features of Ehlers–Danlos syndrome (EDS) were described as early as the mid-1600s. The first comprehensive report of this condition was published in 1892 by Tschernogobow[3]. Drs Ehlers and Danlos, Danish and French dermatologists, respectively, contributed to a comprehensive clinical description in the early 1900s, and this constellation of findings became known as the Ehlers–Danlos syndrome in 1936. The genetic nature of EDS was noted in 1949, and soon thereafter it was suggested that the phenotype resulted from abnormal collagen. The genetic heterogeneity of EDS became evident in the 1960s, and molecular defects in collagen synthesis were first described in 1972[4].

In the past, EDS was divided into 11 subtypes (numbered I–XI) based primarily upon clinical features. In 1997, a consensus conference led to the revised "Villefranche nosology", which included only six subtypes[5]. Following determination of the molecular bases of other forms of EDS[6], an international classification recognizing 13 subtypes due to alterations in 19 genes was proposed in 2017[7], and an additional subtype was identified in 2018 (Table 97.2).

Epidemiology

Features suggestive of EDS (e.g. loose-jointedness) are present in a relatively large number of individuals in the general population. However, more stringent diagnostic criteria that include findings in the skin and joints, at a minimum, estimate the incidence of EDS to be ~1 in 5000.

Pathogenesis

EDS is a genetically as well as clinically heterogeneous group of connective tissue disorders that most often result from disruption of collagen fiber organization and function (Fig. 97.1). The collagen family includes 28 distinct proteins that differ in their tissue distributions and functions[8] (see Ch. 95). Approximately 90% of the collagen within the body is type I, which is expressed in almost all connective tissues and has especially important roles in the skin, tendons, and bones. Each collagen consists of three α-chain polypeptides, many of which are synthesized as precursor pro-α-chains. A trimeric collagen molecule may be either a homotrimer or heterotrimer consisting of the same versus two or three genetically different kinds of α-chains, respectively. There are 45 distinct α-chains, each encoded by a different gene[8].

The pathogenesis of EDS can involve mutations in genes for collagen-processing enzymes as well as those encoding collagen α-chains. The latter result in either dominant-negative effects, e.g. disruption of trimers and fibrils due to incorporation of mutant collagen α-chains, or haploinsufficiency. The precise phenotype depends upon the nature of the mutation(s) and the type of collagen or other protein that is affected.

ADDITIONAL HERITABLE DISORDERS OF CONNECTIVE TISSUE WITH CUTANEOUS FINDINGS				
Disease	**Cutaneous findings**	**Extracutaneous manifestations**	**Inheritance**	**Associated gene/protein product**
Marfan syndrome	Striae, elastosis perforans serpiginosa, decreased subcutaneous fat on extremities	Skeletal abnormalities (e.g. disproportionately long limbs, arachnodactyly, scoliosis), lens subluxations (upward), dilation/dissection of ascending aorta*	AD	*FBN1*/fibrillin 1 defects (the major component of microfibrils)†
Homocystinuria	Malar flush, livedo reticularis, diffuse pigmentary dilution, tissue paper-like scars	Marfanoid habitus, lens subluxations (downward), venous and arterial thrombosis‡, intellectual disability	AR	*CBS*/cystathionine synthase enzyme deficiency (resulting in increased plasma homocysteine¶); rarely, methylenetetrahydrofolate reductase, 5-methyltetrahydrofolate-homocysteine methyltransferase, or 5-methyltetrahydrofolate-homocysteine methyltransferase reductase deficiency (enzymes that convert homocysteine back to methionine)
Osteogenesis imperfecta	Thin skin	Bone fragility, blue sclerae, dentinogenesis imperfecta (in a subset of patients)	AD	*COL1A1*, *COL1A2*/type I collagen defects
Buschke–Ollendorff syndrome	Connective tissue nevi (dermatofibrosis lenticularis disseminata); occasionally cutaneous sclerosis associated with melorheostosis	Osteopoikilosis ("spotted" bones); occasionally melorheostosis (sclerotic bone resembling "dripping candle wax" on radiographs; reflects a postzygotic "second hit" in the *LEMD3* gene); rarely otosclerosis	AD	*LEMD3*/LEM domain-containing 3, an antagonist of bone morphogenic protein (BMP) and TGF-β signaling

*In addition to traditional treatment with β-blockers, angiotensin II receptor blockers (e.g. losartan), which antagonize pathogenic transforming growth factor (TGF)-β signaling, can prevent aortic root dilation in patients with Marfan syndrome; administration of doxycycline, which inhibits metalloproteinases-2 and -9, may also be of benefit.
†Mutations in the genes encoding TGF-β receptors 1 and 2 can lead to a phenotype that mimics Marfan syndrome.
‡Methionine-restricted, cysteine-supplemented diet plus pyridoxine recommended.
¶Elevated plasma homocystine and homocysteine can be detected in patients with homocystinuria, but only homocysteine is elevated in hyperhomocysteinemia.

Table 97.1 Additional heritable disorders of connective tissue with cutaneous findings. Other rare genetic diseases of the extracellular matrix are listed in Table 95.5. AD, autosomal dominant; AR, autosomal recessive.

Several forms of EDS are caused by *dominant-negative* mutations in the genes encoding α-chains of type I (*COL1A1, COL1A2*), type III (*COL3A1*), and type V (*COL5A1, COL5A2*) collagens. Characteristic examples include splice site mutations that can result in an in-frame deletion of a single exon and missense mutations that lead to a glycine substitution in the collagenous domain. The resultant polypeptides are incorporated into the polymeric collagen molecules and disrupt the formation, secretion, and/or thermal stability of triple helices. As a consequence, there may be a reduced amount of collagen as well as structurally and functionally abnormal fibrils.

Haploinsufficiency is caused by a heterozygous loss-of-function mutation, usually associated with a premature termination codon. These types of mutations often result in unstable mRNA that undergoes accelerated decay, leading to an absence of the corresponding polypeptide. Haploinsufficiency can also be caused by a missense mutation encoding a polypeptide that cannot be incorporated into collagen triple helices. Haploinsufficiency occurs when only 50% of the normal amount of collagen is present, which is not enough to form fully functional fibrils and thus results in a disease phenotype.

Vascular EDS can result from either dominant-negative mutations in *COL3A1* or haploinsufficiency of type III collagen, with the latter associated with a delayed onset of arterial complications and prolonged survival[9]. Collagen III is an important component of arterial and intestinal walls and a less abundant component of dermal connective tissue. However, a reduced amount of type III collagen leads to small or variably sized dermal collagen fibrils and thinning of the dermis, emphasizing the role of type III collagen in fibrillogenesis.

Classical EDS can be caused by dominant-negative mutations in *COL5A1* and *COL5A2* or (in 30%–50% of cases) haploinsufficiency of type V collagen (*COL5A1*). The role of type V collagen in collagen fibrillogenesis is to limit fibril diameter, explaining the ~25% increase in fibril diameter that is observed by electron microscopy in affected individuals.

Arthrochalasia EDS results from heterozygous *COL1A1* and *COL1A2* mutations that specifically affect the amino-terminal cleavage site of procollagen I N-peptidase and thereby disrupt processing of type I collagen pro-α-chains. Biallelic loss-of-function mutations in *ADAMTS2*, which encodes this procollagen I N-peptidase, are responsible for *dermatosparaxis* EDS. The latter disorder is characterized by irregular and thin collagen fibrils containing type I collagen with an intact N-propeptide, termed pN-collagen.

Kyphoscoliotic EDS is most often caused by biallelic mutations in *PLOD1*, which encodes another collagen-processing enzyme, lysyl hydroxylase; this leads to reduced hydroxylysine content in collagen polypeptides and altered cross-linking of collagen fibrils. Another form of kyphoscoliotic EDS results from biallelic mutations in *FKBP14*, which encodes an FK506-binding peptidyl-prolyl cis–trans isomerase that catalyzes collagen folding and acts as a chaperone for collagens within the endoplasmic reticulum[10].

Complete tenascin-X deficiency via biallelic null mutations underlies an autosomal recessive *classical-like EDS*[11]. Tenascin-X is an ECM protein that reinforces associations among collagen fibrils and may also regulate the structure and stability of elastic fibers. Another form of classical-like EDS is caused by mutations in *AEBP1*, which encodes an aortic carboxypeptidase-like protein (ACLP) that associates with collagens in the ECM and plays a role in both tissue repair and fibrosis[7].

Spondylodysplastic EDS can result from abnormal glycosaminoglycan processing due to mutations in genes encoding galactosyltransferases (*B4GALT6, B3GALT7*), as well as via disruption of intracellular zinc homeostasis (*SLC39A1*). In addition, defects in glycosaminoglycan biosynthesis due to mutations in dermatan-4-sulfotransferase 1 (*CHST14*) or dermatan sulfate epimerase (*DSE*) cause *musculocontractural EDS*[5]. Lastly, constitutive activation of complement 1 (*C1R, C1S*) in the classical complement pathway underlies *periodontal EDS*[12].

Clinical Features

The general features of EDS include hyperextensible fragile skin and joint hypermobility[4] (Fig. 97.2A,B). The Beighton scale can be utilized to assess the latter[13], and different subtypes of EDS have additional manifestations that facilitate their classification[5,7] (Fig. 97.3). Table 97.2 outlines the currently recognized variants of EDS.

Typical skin findings are present, to a varying degree, in all subtypes of EDS[14]. Skin hyperextensibility is defined as the ability to stretch ≥1.5 cm on the volar surface of the distal forearm or dorsum of the hand; ≥3 cm on the neck, elbow, or knee; and ≥1 cm on the palm[15]. The

2017 INTERNATIONAL CLASSIFICATION OF EHLERS–DANLOS SYNDROME			
EDS subtype	**Clinical features**	**Inheritance**	**Mutated gene/protein**
Classical*	Hyperextensible and soft/doughy skin, joint hypermobility, atrophic scars, easy bruising	AD	*COL5A1, COL5A2*/α_1- and α_2-chains of type V collagen Rarely, *COL1A1*/α_1-chain of type I collagen (associated with vascular fragility)
Classical-like, type 1	Similar to mild classical type but normal scarring; also variable muscle weakness, foot deformities	AR	*TNXB*, tenascin-X
Classical-like, type 2†	Similar to classical EDS; also foot deformities (pes planus, hallux valgus, hammer toes), osteopenia	AR	*AEBP1*/adipocyte enhancer-binding protein 1 (also known as aortic carboxypeptidase-like protein)
Cardiac valvular	Cardiac valve defects, otherwise similar to the classical type	AR	*COL1A2*/α_2-chain of type I collagen
Hypermobile*	Joint hypermobility, pain, and dislocations; less pronounced skin changes, e.g. soft/velvety, mildly hyperextensible; recurrent hernias, variable autonomic dysfunction	AD	Unknown
Vascular*	Thin, translucent skin with excessive bruising; arterial, gastrointestinal, and uterine rupture; small joint hypermobility, varicose veins, characteristic facies	AD	*COL3A1*/α_1-chain of type III collagen
Kyphoscoliotic*	Hyperextensible skin, easy bruising, joint hypermobility, kyphoscoliosis, congenital hypotonia, arterial rupture, blue sclerae, marfanoid habitus *PLOD1*: atrophic scarring, ocular fragility *FKBP14*: follicular hyperkeratosis, myopathy, impaired hearing	AR	*PLOD1*/lysyl hydroxylase‡ *FKBP14*/FK506-binding protein 14
Musculocontractural	Hyperextensible and fragile skin, wrinkled palms, congenital joint contractures, recurrent dislocations, scoliosis, ocular anomalies, craniofacial abnormalities	AR	*CHST14*/dermatan-4-sulfotransferase 1 (allelic with adducted thumb–clubfoot syndrome) *DSE*/dermatan sulfate epimerase
Arthrochalasia*	Hyperextensible and fragile skin, severe joint hypermobility with congenital bilateral hip dislocation, scoliosis	AD	*COL1A1*, *COL1A2*/α_1- and α_2-chains of type I collagen
Dermatosparaxis*	Severe skin fragility, sagging and redundant skin that is soft and doughy, easy bruising, joint hypermobility, short limbs, hernias, distinctive facies	AR	*ADAMTS2*/procollagen I N-peptidase
Periodontal	Mildly hyperextensible skin with prominent vessels, excessive bruising with pretibial plaques, small joint hypermobility, early-onset periodontitis with gingival recession, increased infections, marfanoid habitus	AD	*C1R, C1S*/complement C1r, C1s
Spondylodysplastic (includes former progeroid type)	Soft/doughy, translucent, and/or hyperextensible skin; variable joint hypermobility, hypotonia, limb bowing, short stature, variable tapered fingers, osteopenia, developmental delay *B4GALT6/7*: progeroid facies, joint contractures *SLC39A13*: wrinkled palms, platyspondyly, protuberant eyes	AR	*B4GALT7*/galactosyl transferase-1 *B3GALT6*/ galactosyltransferase-II *SLC39A13*/zinc transporter ZIP13
Brittle cornea syndrome	Soft, translucent skin with variable hyperextensibility and fragility, acral wrinkling, hypermobility of small joints, ocular fragility, keratoglobus/keratoconus, blue sclerae, impaired hearing, scoliosis	AR	*ZNF469*/ zinc finger protein 469 *PRDM5*/ PR domain-containing protein 5
Myopathic	Soft/doughy skin with atrophic scarring, proximal joint contractures and distal hypermobility, congenital myopathy with hypotonia that improves with age	AD or AR	*COL12A1*/α_1-chain of type XII collagen

*Six main types recognized by the 1997 Villefranche consensus classification[4].
†Described after the 2017 international classification.
‡Analysis of the urine for an increased deoxypyridinoline : pyridinoline ratio can be used as a screening test for kyphoscoliotic EDS.

Table 97.2 2017 International classification of Ehlers–Danlos syndrome (EDS)[7]. See reference 7 for full diagnostic criteria. The historical X-linked and fibronectin subtypes have unknown molecular bases and are not included in the current nosology. Other previous EDS subtypes have been reclassified as occipital horn syndrome (see Table 97.7) and familial joint hypermobility syndrome. In addition to recognized forms of EDS, heterozygous mutation in the elastin microfibril interfacer 1 (*EMILIN1*) gene was identified in a patient with increased skin elasticity, aortic aneurysms, sensorimotor peripheral neuropathy, and arthropathy. AD, autosomal dominant; ADAMTS2, *a d*isintegrin-like *a*nd *m*etalloprotease domain with *t*hrombospondin type 1 motif 2; AR, autosomal recessive; COL, collagen; PLOD1, *p*rocollagen-*l*ysine 1, 2-*o*xoglutarate 5-*d*ioxygenase 1.

skin also tends to be fragile, splitting readily due to trauma, particularly on the knees, elbows, shins, and forehead. These wounds present with a gaping, "fish-mouth" appearance; healing may be delayed and dehiscence is common. The resulting scars are typically atrophic and widen over time (Fig. 97.2C), although some affected individuals develop hypertrophic scars. Easy bruising is commonly observed, reflecting the fragility of small blood vessels. Dermatologic disorders that are associated with, but not specific to, EDS include elastosis perforans serpiginosa and piezogenic papules (Fig. 97.2D).

Major subtypes

Classical EDS is inherited in an autosomal dominant fashion and presents with hypermobile joints as well as hyperextensible and fragile skin that is prone to bruising. Scars are typically widened and atrophic, often with a "cigarette paper" appearance. The skin also tends to be soft, with a slightly doughy or velvety texture. Sites of repeated trauma develop a variety of secondary lesions such as molluscoid pseudotumors, which are fleshy nodules composed of redundant skin and fibrous tissue that favor the knees and elbows. Multiple small, hard, mobile

COLLAGEN BIOSYNTHESIS, SECRETION, AND FIBRIL ASSEMBLY – RELATIONSHIP OF PATHOLOGY TO THE MAJOR SUBTYPES OF EHLERS–DANLOS SYNDROME

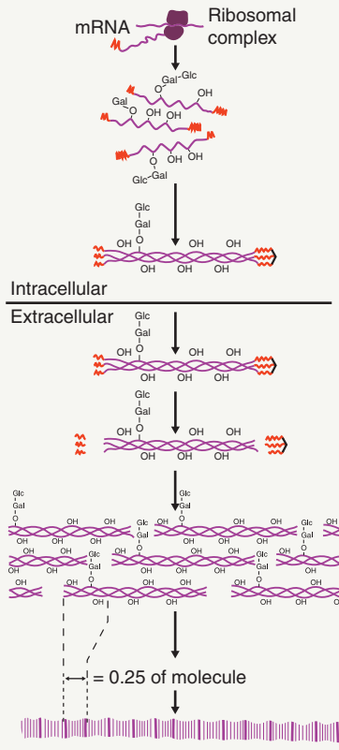
Physiology		Pathology	EDS subtype (mode of inheritance)
	Synthesis, hydroxylation and glycosylation of pro-α polypeptides of type I, III and V collagens	**Lysyl hydroxylase** deficiency results in reduced hydroxylysine content and altered cross-linking profile	Kyphoscoliotic (AR)
	Formation of interchain S-S bonds at the carboxyl ends followed by triple helix formation	Dominant-negative mutations or haploinsufficiency in ***COL3A1*** affect triple helix formation, thermal stability, and secretion of type III collagen molecules	Vascular type (AD)
	Secretion of procollagen	Dominant-negative mutations in the recognition sites for procollagen N-peptidase in ***COL1A1*** and ***COL1A2*** prevent cleavage of amino-terminal propeptides	Arthrochalasia (AD)
	Removal of propeptides by specific proteases	Loss-of-function mutations in **procollagen-N-peptidase** result in the formation of only thin collagen fibrils	Dermatosparaxis (AR)
	Fibril assembly	Dominant-negative mutations in ***COL5A1*** and ***COL5A2*** or haploinsufficiency in ***COL5A1*** result in abnormal or reduced amount of collagen fibrils	Classical type (AD)
		Absence of **tenascin-X** leads to reduced collagen fibril density	Classical type (AR)
	Stabilization of fibrils by intermolecular cross-linking		

Fig. 97.1 Collagen biosynthesis, secretion, and fibril assembly – relationship of pathology to major subtypes of Ehlers–Danlos syndrome. AD, autosomal dominant; AR, autosomal recessive; Glc-Gal, glucosyl-galactosyl residue attached to the hydroxyl group (OH) of lysine residues; S-S bonds, disulfide bonds.

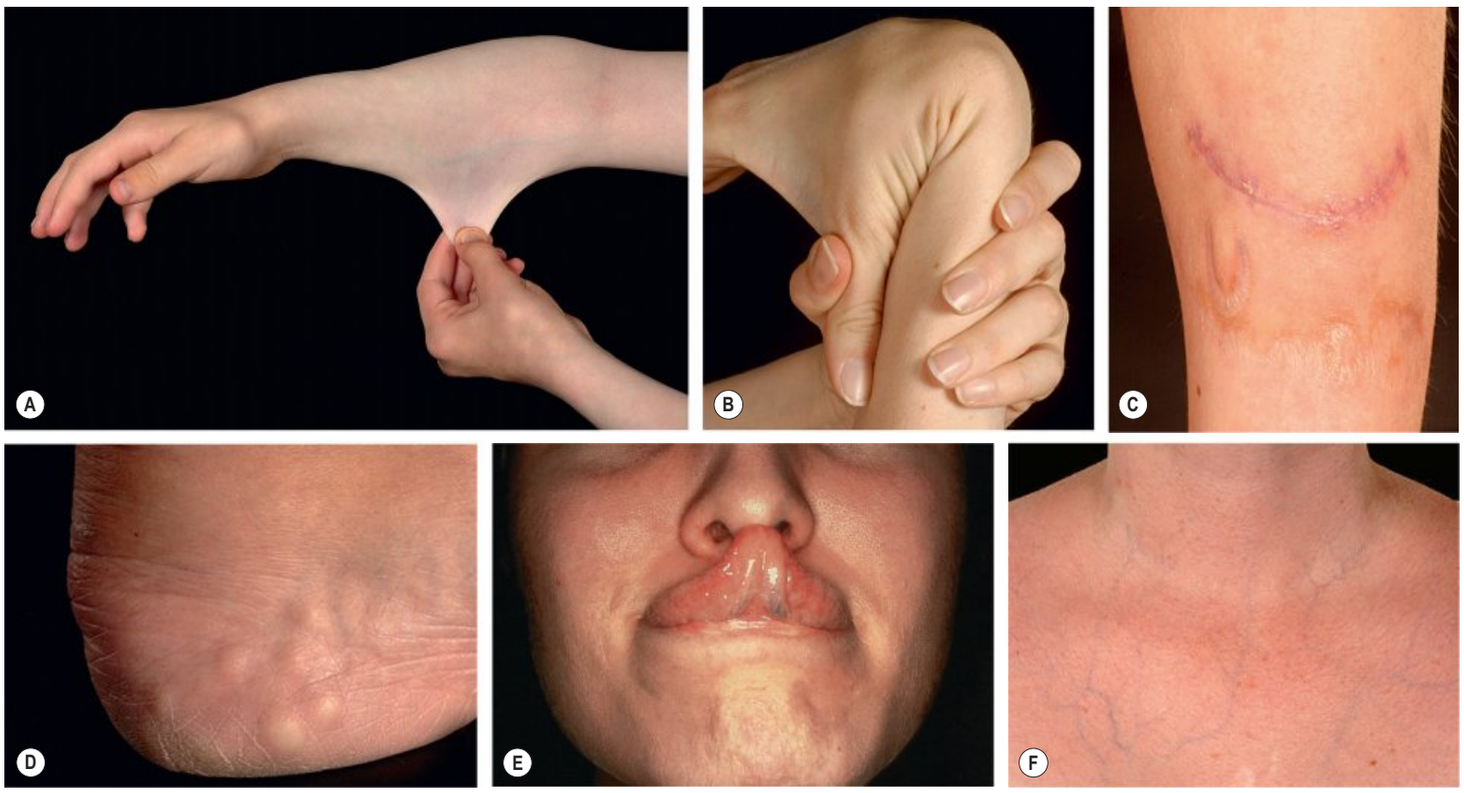


Fig. 97.2 Clinical features of Ehlers–Danlos syndrome (EDS). Patients with classical EDS demonstrating hyperextensible skin (**A**), joint hypermobility at the wrist (**B**), atrophic horseshoe-shaped scars on the shin (**C**), piezogenic papules on the heel (**D**), and the Gorlin sign (**E**). **F** Translucent skin with visible veins on the chest in a patient with vascular EDS. *A–C, F, Courtesy Addenbrooke's Hospital, Cambridge, UK.*

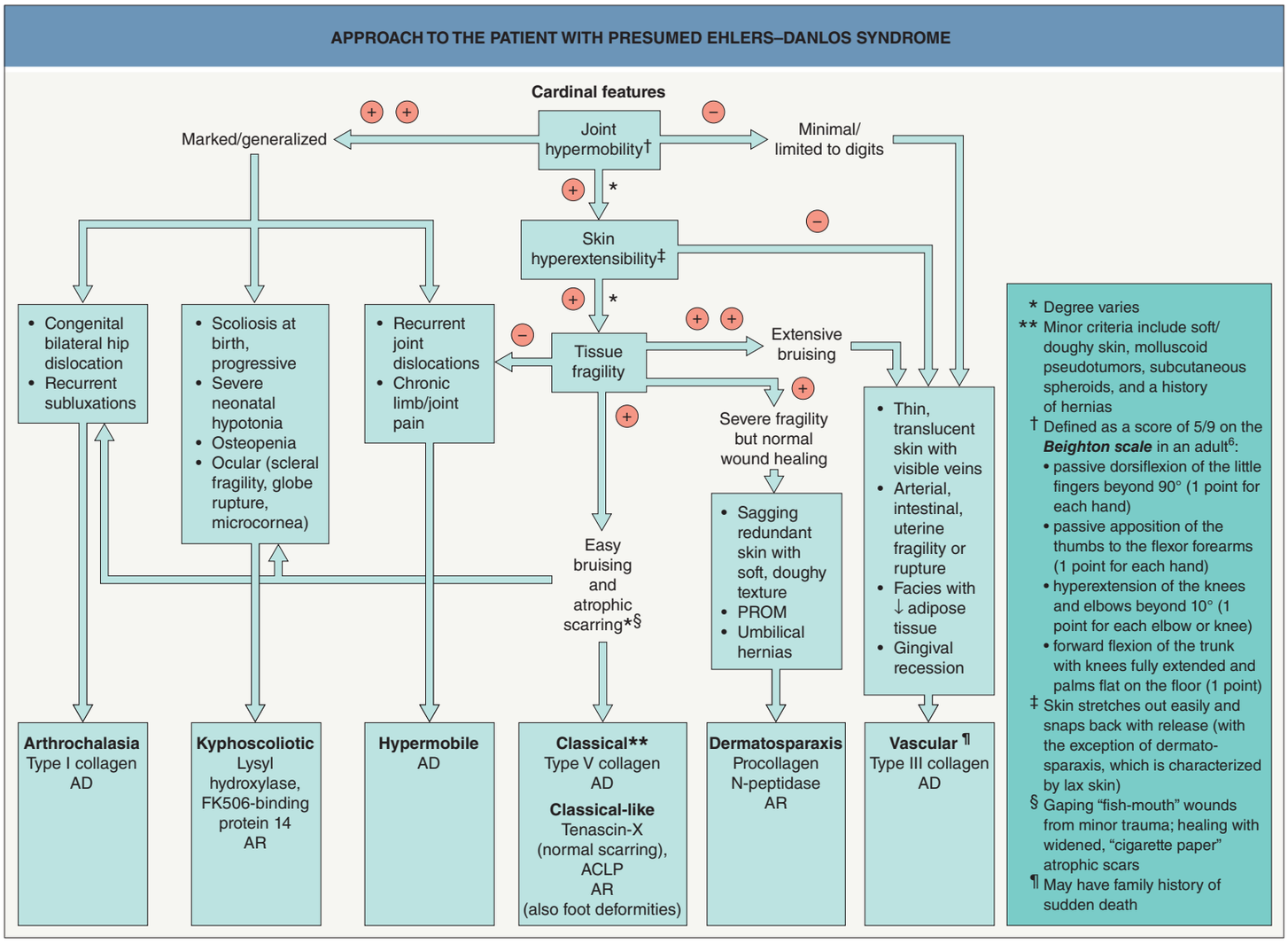


Fig. 97.3 Approach to the patient with presumed Ehlers–Danlos syndrome (EDS). See Table 97.2 for additional rare types of EDS. ACLP, aortic carboxypeptidase-like protein; AD, autosomal dominant; AR, autosomal recessive; PROM, premature rupture of fetal membranes.

papulonodules over bony prominences, such as the ulnar and tibial borders, are also a frequent finding. These subcutaneous spheroids are thought to represent calcified fat. At least half of affected individuals can touch the tip of their nose with their tongue (Gorlin sign), compared to 10% of the general population (Fig. 97.2E). Although classical EDS may be associated with mild aortic root dilation and mitral valve prolapse, each in ~5% of patients, these findings are rarely of clinical significance[16]. Other frequent musculoskeletal manifestations include pes planus, subluxations, and temporomandibular joint dysfunction.

Hypermobile EDS is the most common variant and has autosomal dominant inheritance. The most prominent clinical feature is generalized joint hypermobility, typically leading to recurrent joint dislocations that can cause chronic pain and susceptibility to osteoarthritic changes. Easy bruising is common, and the skin tends to be soft but with only mild hyperextensibility and atrophic scarring. Fatigue is common, and patients may have autonomic dysfunction presenting with orthostatic intolerance and gastrointestinal symptoms[17]; concomitant mast cell activation syndrome has also been described. The 2017 diagnostic criteria distinguish hypermobile EDS from other hypermobility spectrum disorders[18].

Vascular EDS is an autosomal dominant disorder characterized by thin translucent skin (Fig. 97.2F) with extensive bruising and a high risk of arterial, intestinal, and uterine ruptures[19]. Spontaneous arterial rupture has the highest incidence in the third and fourth decades of life but may occur earlier, especially in men, and median survival is ~50 years[9]. Affected individuals often have a characteristic facial appearance, with a "pinched" nose, thin lips, micrognathia, hollow cheeks, and prominent "staring" eyes due to decreased periorbital adipose tissue. Small earlobes and fine scalp hair are additional features.

Less common subtypes

Classical-like EDS, due to either tenascin-X or ACLP deficiency, has autosomal recessive inheritance and an overall phenotype similar to that of classical EDS. Tenascin-X deficiency is characterized by an *absence* of atrophic scarring as well as variable muscle weakness, risk of bowel rupture, and occasional association with congenital adrenal hyperplasia due to deletion of the contiguous gene encoding 21-hydroxylase[20]. Foot deformities are observed in both forms of classical-like EDS, while osteopenia is an additional feature of ACLP deficiency.

Kyphoscoliotic EDS is an autosomal recessive disorder that features skin hyperextensibility, generalized joint hypermobility, severe hypotonia at birth, delayed gross motor development, and progressive congenital scoliosis. Patients with *PLOD1* mutations have scleral fragility that can lead to rupture of the ocular globe, whereas individuals with *FKBP14* mutations present with congenital sensorineural deafness. Additional findings may include atrophic scars, easy bruising, fragility of other tissues (rarely arterial rupture), a marfanoid habitus, and osteopenia.

Arthrochalasia EDS is inherited in an autosomal dominant fashion. The major clinical features include severe generalized joint hypermobility with recurrent subluxations and congenital bilateral hip dislocation. Patients may also present with hyperextensible skin, atrophic scars, easy bruising, hypotonia, scoliosis, and mild osteopenia.

Dermatosparaxis EDS is an autosomal recessive disorder that, unlike other forms of EDS, presents with skin that is sagging and redundant as well as extremely fragile. The skin has a highly characteristic soft, doughy consistency, and it tears and bruises easily (Fig. 97.4). The clinical features of other rare forms of EDS are outlined in Table 97.2.

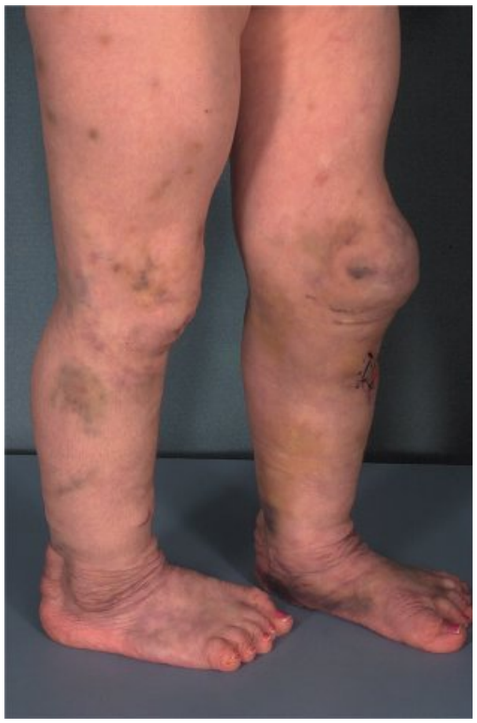


Fig. 97.4 Extensive bruising on the shins in a patient with the dermatosparaxis type of Ehlers–Danlos syndrome (EDS). Similar changes can be seen in vascular EDS. *Courtesy Julie V. Schaffer, MD.*

COMPARISON OF SELECTED CLINICAL FEATURES IN EHLERS–DANLOS SYNDROME AND MARFAN SYNDROME		
	Ehlers–Danlos syndrome	**Marfan syndrome**
Molluscoid pseudotumors	++	–
Skin	Hyperextensibility, "fish-mouth" atrophic scars	Striae
Joint hypermobility	++ (often severe)	+ (mild–moderate)
Easy bruising	++	–
Pectus excavatum	–	++
Scoliosis	+	++
High-arched palate	–	++
Ectopia lentis	+	++
Myopia	+	++
Mitral valve abnormalities	+	++
Stature	Variable	Tall

Table 97.3 Comparison of selected clinical features in Ehlers–Danlos syndrome and Marfan syndrome. ++, common feature; +, occasional feature; –, not a feature.

Pathology and Laboratory Findings

Histopathologic examination of the skin does not usually yield diagnostic findings. Nonspecific increases in elastic fibers have been reported, particularly in areas of repeated trauma or molluscoid pseudotumors. However, in vascular EDS the dermis is often reduced to ~25% of its normal thickness, and immunohistochemical staining may show intracellular accumulation of type III collagen.

Although transmission electron microscopic findings in different EDS subtypes have some overlap, collagen fibrils with variable diameters and occasional large "cauliflower" fibrils with an irregular contour are characteristic of classical EDS[21]. Ultrastructurally, arthrochalasia and dermatosparaxis types of EDS feature angular and "hieroglyphic" appearances of collagen fibrils in cross-section, respectively.

Genetic testing is available for all the major forms of EDS except the hypermobile type[22]. Additional diagnostic methods include: (1) protein electrophoresis of collagens extracted from cultured dermal fibroblasts to assess for specific collagen defects in vascular, arthrochalasia, and dermatosparaxis types of EDS; (2) urine analysis for an increased deoxypyridinoline:pyridinoline ratio in kyphoscoliotic EDS; and (3) ELISA of serum for tenascin-X deficiency[11].

Differential Diagnosis

Several previously described rare forms of EDS, including X-linked and fibronectin subtypes, are no longer included in the EDS nosology due to a lack of clear descriptions of their clinical features and unknown molecular bases. Occipital horn syndrome is now considered to represent a form of cutis laxa (see Table 97.7) rather than EDS. In contrast to cutis laxa, which is characterized by loose and sagging skin with decreased resilience, the skin of patients with EDS (except the dermatosparaxis type) retains its elasticity and recoil. Although some patients with EDS, in particular the kyphoscoliotic type, have a marfanoid body habitus, they do not typically exhibit other findings of Marfan syndrome (Table 97.3), a distinct heritable connective tissue disorder due to mutations in the fibrillin 1 gene (*FBN1*) (see Table 97.1).

The phenotype of Loeys–Dietz syndrome (LDS; formerly known as LDS type II) can mimic that of vascular EDS, with overlapping features including translucent skin, easy bruising, atrophic scarring, joint hypermobility, and arterial rupture (see Table 95.5). However, some patients with LDS have additional features such as a bifid uvula, hypertelorism, and facial milia. Patients with vascular EDS and other types that result in extensive bruising are often suspected to have a bleeding disorder, and they may present to a dermatologist after a hematologic evaluation fails to reveal any abnormalities.

Treatment

Contact sports should be avoided and the use of padding or shin guards may help to decrease trauma to the skin. Delaying suture removal for up to twice as long as usual plus use of two layers of sutures with prolonged tensile strength may improve wound healing and the appearance of surgical scars.

In vascular EDS, affected individuals are at high risk of arterial and bowel ruptures. Use of celiprolol (currently not available in the US), a long-acting β_1-antagonist with partial β_2-agonist properties, may reduce the incidence of arterial dissection; the utility of other β-blockers in vascular EDS remains to be determined[23,24]. Approximately 5% of pregnancies in women with vascular EDS are complicated by fatal uterine or arterial rupture[22]; it is unclear whether elective caesarean section reduces these risks, and patients should be managed in a high-risk obstetric unit with multidisciplinary input. Total abdominal colectomy with end ileostomy or ileorectal anastomosis are considered the safest surgical procedures after colonic perforation, with higher risks of re-perforation and anastomotic leak associated with end colostomy or restoration of colonic continuity[25].

PSEUDOXANTHOMA ELASTICUM

Synonym: ■ Grönblad–Strandberg syndrome

Key features

- An autosomal recessive disorder characterized by clumped, distorted, and calcified elastic fibers
- Cutaneous features include yellowish papules, "cobblestoning," and redundant folds in flexural areas
- Calcification of elastic fibers in the walls of medium-sized arteries can lead to luminal narrowing and clinical sequelae such as intermittent claudication, renovascular hypertension, angina, and less commonly stroke or myocardial infarction
- Angioid streaks reflect breaks in the calcified elastic lamina of Bruch's membrane; choroidal neovascularization and hemorrhage can result in loss of visual acuity
- Gastrointestinal hemorrhage is an occasional complication

History

The French dermatologist Balzer first described the skin manifestations of PXE and associated elastic degeneration in the skin and heart in 1884, which was followed 5 years later by a similar case report by Chauffard. Based on these two cases, Darier coined the name "pseudo-xanthome élastique" in 1896 to differentiate this condition from xanthomas[26]. In the late 1920s, Grönblad[27] and Strandberg[28] recognized the association of the characteristic skin manifestations with angioid streaks, and the cardiovascular manifestations were better defined two decades later. More recently, the molecular defects that underlie PXE were identified, clarifying the mode of inheritance, which had previously been debated[29,30].

Epidemiology

PXE is an autosomal recessive disease, with a prevalence estimated to be from 1 in 25 000 to 1 in 100 000. There is no racial predilection but a slight female preponderance[31]. Skin changes of PXE usually appear during childhood or early adolescence, but the diagnosis is occasionally not made until serious arterial or ocular complications develop in the third or fourth decade of life. Mild cutaneous and ocular findings have also been observed in heterozygous carriers[24].

Pathogenesis

Loss-of-function mutations in both copies of *ABCC6* can be identified in ~90% of patients with PXE. *ABCC6* encodes an ATP-binding cassette (ABC) transporter with a high degree of homology to multidrug resistance-associated proteins. ABCC6 is predominantly expressed in the basolateral plasma membrane of hepatocytes, where it serves as an efflux pump. The absence of functional ABCC6 in PXE patients results in reduced ATP release from hepatocytes[32]. The ectonucleotide pyrophosphatase/phosphodiesterase 1 enzyme (ENPP1) converts extracellular ATP to AMP + inorganic pyrophosphate (PPi), which acts as a physiologic inhibitor of mineralization. Reduced PPi levels in PXE patients result in ectopic calcification of elastic structures in various tissues. PPi is converted to inorganic phosphate (Pi) by tissue nonspecific alkaline phosphatase (TNAP), and inhibition of this enzyme was found to increase PPi levels in a mouse model of PXE[33].

Biallelic mutations in *ENPP1* can cause *generalized arterial calcification of infancy* (GACI), a rare autosomal recessive disorder that is usually lethal during the first six months of life[34]. Occasionally, biallelic *ENPP1* mutations also cause PXE, and *ABCC6* mutations underlie a subset of GACI (GACI-2), thus demonstrating pathogenic and clinical overlap between these two conditions[34–36]. *Arterial calcification due to CD73 deficiency* (ACDC) represents a rare, milder ectopic calcification disorder caused by mutations in *NT5E*, which encodes an ecto-5′-nucleotidase that converts AMP to Pi and adenosine. The latter functions as an inhibitor of TNAP, and lower adenosine levels in ACDC lead to increased TNAP activity that then results in reduced plasma PPi levels. Clinical features of ACDC include calcification of arteries in the lower extremities and calcium hydroxyapatite deposition in juxtaarticular tissues of the hands and vertebrae[37,38].

Biallelic mutations in the γ-glutamyl carboxylase gene (*GGCX*) cause PXE-like skin changes plus deficiency in vitamin K-dependent coagulation factors[39]. A combination of heterozygous mutations in *GGCX* and *ABCC6* has also been identified in patients with cutaneous findings of PXE[40]. The GGCX enzyme catalyzes the vitamin K-dependent γ-glutamyl carboxylation that is necessary for activation of coagulation factors in the liver as well as the matrix gla protein in peripheral connective tissues. When carboxylated (activated), matrix gla protein prevents ectopic mineralization.

In general, the pathogenesis of PXE and related ectopic calcification disorders is related to decreased anti-mineralization activity due to reduced plasma PPi levels. Collectively, this group has been designated as PPi deficiency syndromes[41]. Calcification of elastic fibers in the mid and deep dermis, media and intima of mid-sized arteries, and Bruch's membrane of the eye produces the characteristic clinical and histopathologic changes of PXE (Fig. 97.5).

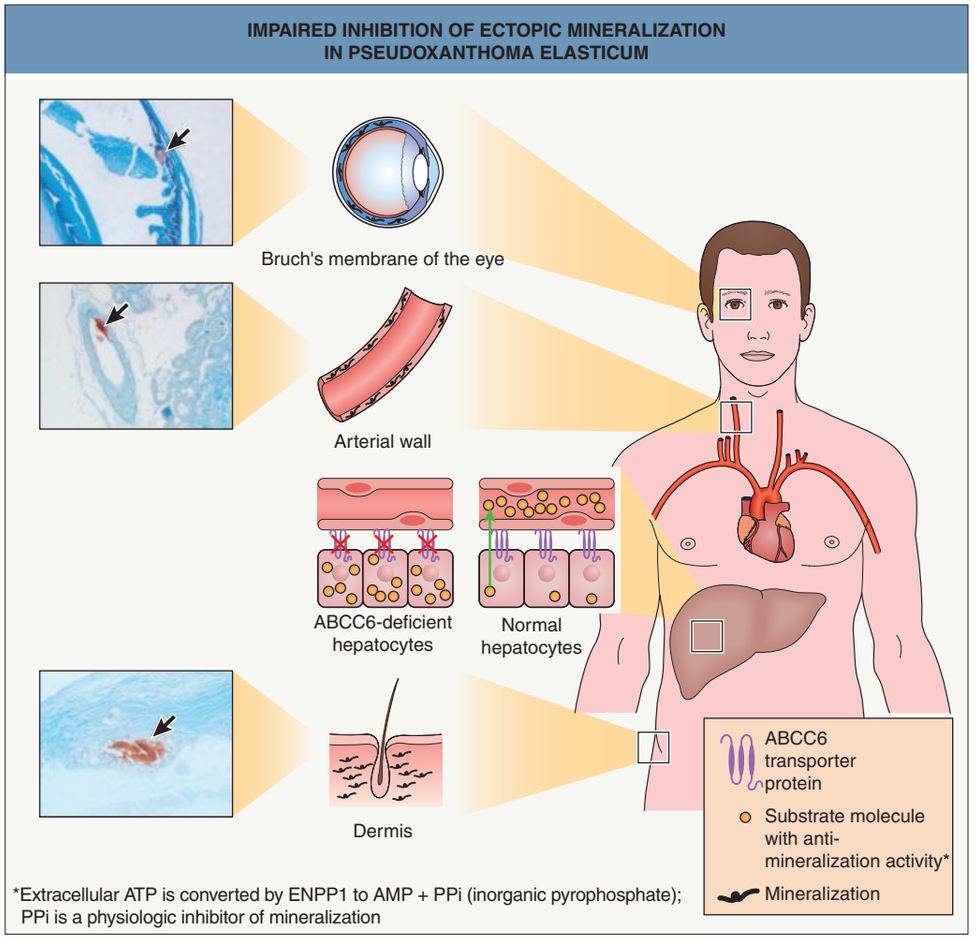


Fig. 97.5 Impaired inhibition of ectopic mineralization in pseudoxanthoma elasticum. The normal liver expresses high levels of the ABC-binding cassette subfamily C member 6 (ABCC6) protein, which serves as an efflux pump on the basolateral surface of hepatocytes, transporting molecules such as ATP from inside these cells to the extracellular space. ATP is rapidly converted to AMP and inorganic pyrophosphate (PPi), with the latter representing a physiologic anti-mineralization factor. In patients with pseudoxanthoma elasticum (PXE), an absence of ABCC6 transporter activity in the liver results in reduced circulating concentrations of PPi, which allows ectopic calcification of connective tissues in the eye, arterial walls (media and intima), and dermis. The presence of calcium is evident on histopathological examination of these tissues (alizarin red staining; see arrows in left panels) in *Abcc6*$^{-/-}$ mice, which recapitulate the features of human PXE. *Adapted from Uitto J, Li Q, Jiang Q. Pseudoxanthoma elasticum: molecular genetics and putative pathomechanisms. J Invest Dermatol 2010;130:661–70.*

Clinical Features

PXE primarily affects the elastic fiber networks of the skin, eyes, and cardiovascular system. There is tremendous variability in severity even among siblings, and sometimes only one or two of these organ systems show signs of the disease.

PXE owes its name to the characteristic cutaneous findings, which bear some resemblance to xanthomas and represent the most frequent manifestation of the condition. Thin, yellowish papules typically begin to appear in flexural areas during the first or second decade of life. Over time, the papules coalesce to form cobblestone-like plaques, giving rise to a "plucked chicken skin" or "cobblestone" appearance (Fig. 97.6). The lateral aspect of the neck is often affected first, with the antecubital and popliteal fossae, wrists, axillae, and groin being additional sites of possible involvement. The periumbilical area may be affected in multiparous women, which should not be confused with *perforating calcific elastosis*, a localized, acquired, purely cutaneous PXE-like condition (Table 97.4; see Ch. 96). Involvement of non-flexural sites can occur in patients with more extensive disease.



Fig. 97.6 Clinical features of pseudoxanthoma elasticum. A–C Yellowish papules and "cobblestoned" plaques on the neck (**A, B**) and in the antecubital fossa (**C**). **D** Pebbling of the skin as well as thickened folds on the neck. **E** Thickened, yellowish, sagging skin in the axilla (**D**). *A, C, Courtesy Addenbrooke's Hospital, Cambridge, UK; D, E, Courtesy Julie V. Schaffer, MD.*

DIFFERENTIAL DIAGNOSIS OF PSEUDOXANTHOMA ELASTICUM

Disorder	Patient characteristics	Clinical features	Histologic features
Actinic elastosis	History of chronic sun exposure; lightly pigmented skin; middle-aged and older adults	Yellow to gray, thickened, lax, finely to coarsely wrinkled skin; photodistribution on the lateral forehead, neck, dorsal aspect of the forearms	Masses of basophilic, amorphous, degenerated elastic fibers in the papillary and upper reticular dermis
Late-onset focal dermal elastosis	7th–9th decades	Multiple 1- to 3-mm yellow papules; may coalesce; neck, axillae, groin, antecubital and popliteal fossae	*Increased* normal-appearing elastic fibers in the mid and deep reticular dermis
PXE-like papillary dermal elastolysis*	6th–9th decades; primarily women	Multiple 2- to 3-mm yellow or skin-colored papules coalescing to form plaques with a cobblestone appearance; neck, flexor forearms, axillae, lower abdomen, inframammary folds	*Decreased* elastic tissue in a band-like distribution in the papillary dermis, with fragmentation and clumping of elastic fibers
White fibrous papulosis of the neck*	5th–9th decades; Japanese men, White women	Multiple 2- to 3-mm whitish papules; lateral and posterior neck > upper trunk	*Decreased* elastic fibers in the papillary and mid reticular dermis; thickened collagen bundles
Elastoderma	3rd–4th decades	Localized areas of lax, pendulous skin; neck, trunk, arm	*Increased* normal- and abnormal-appearing elastic fibers throughout the dermis, extending into the subcutis
Perforating calcific elastosis†	Multiparous Black women; 5th–8th decades‡	Plaque composed of coalescing keratotic papules (most apparent at the periphery); periumbilical area¶	Transepidermal elimination of calcified, distorted elastic fibers

*Within the spectrum of fibroelastolytic diseases of the skin.
†Also referred to as periumbilical perforating PXE.
‡Occasionally associated with an increased calcium–phosphate product in the setting of chronic kidney disease.
¶Similar lesions have been reported on the breasts.

Table 97.4 Differential diagnosis of pseudoxanthoma elasticum (PXE). The differential diagnosis also includes PXE-like skin lesions in patients receiving D-penicillamine, after local exposure to saltpeter, and in chronic kidney disease. In addition, the possibility of underlying β-thalassemia, sickle cell anemia, or primary systemic amyloidosis needs to be considered.



Fig. 97.7 Mucosal lesions in pseudoxanthoma elasticum. Yellow papules on the inner aspect of the lower lip. *Courtesy Addenbrooke's Hospital, Cambridge, UK.*

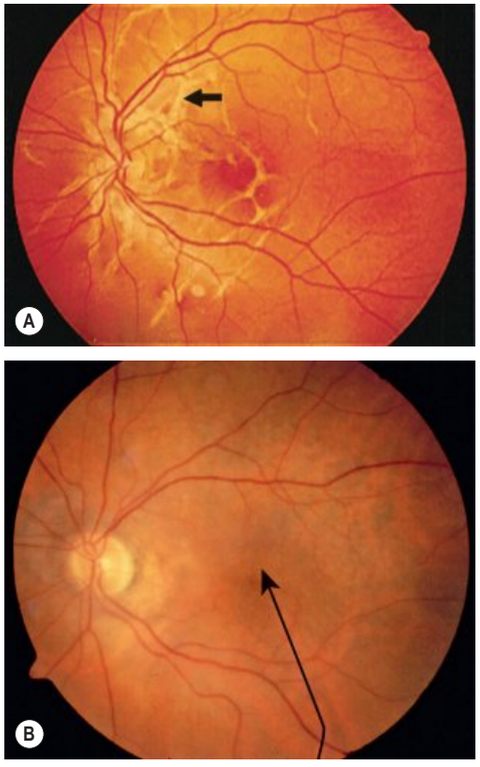


Fig. 97.8 Funduscopic findings in pseudoxanthoma elasticum (PXE). **A** Broad, lightly colored streaks (arrow) represent angioid streaks. **B** Mottling with "peau d'orange" color changes (arrow) over the entire retinal pigment epithelium, which may precede the onset of angioid streaks and represents the most common ophthalmologic finding in PXE.

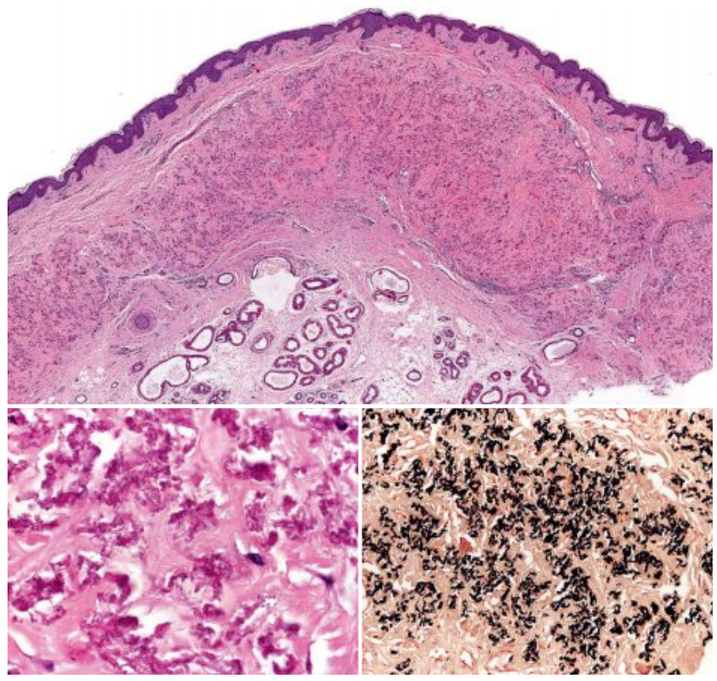


Fig. 97.9 Histopathology of pseudoxanthoma elasticum (PXE). Purple clumps in the mid and deep reticular dermis in H&E-stained sections represent calcium deposits on elastic fibers in advanced PXE (see left inset). An orcein stain highlights the clumped elastic fibers (see right inset). *Courtesy Lorenzo Cerroni, MD.*

With advanced disease, firm papules or plaques may develop due to increased dermal calcium deposition, and extrusion of this yellowish material through the epidermis as "perforating PXE" occasionally occurs. Loss of recoil due to impaired function of the elastic fiber network often leads to sagging of the skin (secondary cutis laxa), which is most notable in the axillae and groin (Fig. 97.6E). Mucosal involvement presents as yellow papules, which are most often apparent on the lower lip (Fig. 97.7). Prominent creases develop on the chin in two-thirds of affected individuals <30 years of age and the vast majority of older patients, contributing to a prematurely aged appearance[42].

The classic ocular finding in PXE is angioid streaks (Fig. 97.8A), which may be evident as early as the first decade of life and can be found in virtually all PXE patients by 30 years of age[31]. Angioid streaks are usually asymptomatic and reflect breaks in the calcified elastic lamina of Bruch's membrane, which is derived from the retina and choroid plexus. These fractures allow choroidal neovascularization, and the newly formed vessels are prone to hemorrhage with subsequent scarring. This process ultimately results in progressive loss of vision, especially within central fields, which usually becomes apparent after 40 years of age and occasionally leads to legal blindness.

Angioid streaks are highly characteristic but not pathognomonic of PXE. They can be encountered, albeit rarely, in a variety of other metabolic and heritable disorders, including Paget disease of the bone, sickle cell anemia, thalassemia, EDS and lead poisoning, as well as in the setting of age-related degeneration of Bruch's membrane. Mottling of the retinal pigment epithelium ("peau d'orange" changes; Fig. 97.8B) due to subconfluent calcification of Bruch's membrane is actually the most prevalent ophthalmologic finding in PXE and may precede the development of angioid streaks. "Coquille d'oeuf" areas reflecting more confluent calcification and "comet" lesions appearing as white bodies in the midperiphery of the fundus represent additional ocular findings that are characteristic of, but not specific to, PXE. Less commonly, macular degeneration, optic drusen, and "owl's eyes" (paired hyperpigmented spots) may be detected.

Cardiovascular manifestations of PXE often cause significant morbidity and occasionally result in premature death. PXE affects primarily mid-sized arteries, especially of the extremities, and progressive calcification of the elastic media and intima leads to the formation of atheromatous plaques. Sequelae may include intermittent claudication, loss of peripheral pulses, renovascular hypertension, angina pectoris, and less often myocardial infarction and stroke; all may occur at a younger age than in the general population. Calcified blood vessels of the gastric and intestinal mucosa have an increased propensity for hemorrhage, and even younger patients may present with gastrointestinal bleeding, particularly from the stomach[31]. Patients with PXE also have an increased prevalence of mitral valve prolapse.

Individuals with *GGCX* mutations have cutaneous, ocular, and cardiovascular findings similar to those of classic PXE. The skin manifestations tend to be more extensive and severe, with involvement of non-flexural areas of the trunk and extremities as well as redundant folds of skin that resemble cutis laxa. Loss of visual acuity secondary to ocular involvement is not typical. Additional hemorrhagic complications may occur secondary to the associated coagulation factor deficiency, including epistaxis, gingival bleeding, menorrhagia, and intracranial hemorrhage.

GACI is typically diagnosed at birth or even prenatally via ultrasound examination. Severe arterial calcification and endothelial proliferation lead to death in the first six months of life due to myocardial ischemia, hypertension, and heart failure. However, surviving children with *ENPP1* mutations may develop skin changes of PXE and angioid streaks as well as hypophosphatemic rickets due to elevated fibroblast growth factor 23 levels[34,43]. Of note, *heterozygous ENPP1* mutations underlie Cole disease, which features punctate palmoplantar keratoderma, guttate hypopigmentation, and variable ectopic calcification (see Ch. 58).

Pathology

Characteristic light microscopic changes in the skin consist of distorted, pleomorphic elastic fibers in the mid and deep reticular dermis. In advanced cases, calcium deposits on these altered elastic fibers are visible in routinely stained sections as purple clumps (Fig. 97.9). Similar changes are observed in the media of mid-sized arteries. In early disease, stains for elastin (orcein and Verhoeff–van Gieson) and calcium (alizarin red and von Kossa) are sometimes necessary to visualize the characteristic alterations in the elastic fibers. In some patients without skin manifestations who are suspected to have PXE because of other findings, such as angioid streaks, biopsy of a preexisting scar can support the diagnosis[44].

Differential Diagnosis

Diagnosis of PXE can be challenging and is often delayed for years after the initial appearance of cutaneous findings. Proposed diagnostic criteria for PXE are presented in Table 97.5[46,47]. Genetic testing of *ABCC6* can be helpful, especially in younger patients and individuals with affected family members. Considering the clinical overlap with other ectopic calcification disorders (see Pathogenesis above), additional genes such as *ENPP1* and *GGCX* should be assessed when pathogenic variants in *ABCC6* are not identified, and use of multigene panels or whole exome sequencing can increase the diagnostic yield[36].

Although characteristic skin lesions are highly suggestive of PXE in younger patients, actinic damage within chronically sun-exposed sites in older individuals may clinically mimic the yellowish plaques of lax skin in PXE. However, the latter findings involve the neck but not the axillae or groin. The differential diagnosis may also include late-onset focal dermal elastosis, PXE-like papillary dermal elastolysis, white fibrous papulosis of the neck, elastoderma, and perforating calcific elastosis (see Table 97.4).

Skin lesions with the same morphology and distribution as PXE and similar histologic features have been observed in patients receiving D-penicillamine (which interferes with desmosine cross-linking in elastin; see below)[48], after local exposure to saltpeter[49], in chronic kidney disease[50], and (historically) in L-tryptophan-induced eosinophilia myalgia syndrome[51]. There is no calcification of the abnormal fibers in D-penicillamine-induced PXE-like skin changes, whereas calcification does occur with saltpeter exposure and chronic kidney disease. Ophthalmologic and cardiovascular findings are absent and the skin lesions may resolve after cessation of the causative exposure or, in patients with renal disease, normalization of the serum calcium–phosphate product.

A PXE-like phenotype is present in up to 20% of the patients with β-thalassemia (Mediterranean populations) or sickle cell anemia[52]. Affected individuals may have characteristic cutaneous involvement as well as angioid streaks and vascular findings, but none of their siblings without a hematologic disorder have signs of PXE, and mutations in *ABCC6* have not been detected. Interestingly, downregulation of ABCC6 expression in the liver has been observed in a mouse model of β-thalassemia, suggesting a possible pathogenic mechanism[53]. PXE-like skin lesions have also been encountered in amyloid elastosis, which typically occurs in the setting of primary systemic amyloidosis; histologic examination reveals amyloid deposits that encase dermal elastic fibers, which may be short and fragmented[54].

Treatment

An approach to the multidisciplinary management of PXE is presented in Table 97.6[55–63]. Several therapies with the goal of preventing progressive mineralization are under investigation[55]. A randomized controlled clinical trial found that etidronate, a PPi analogue, may halt the progression of ectopic arterial calcification in PXE patients[64–66]. Administration of PPi orally, recombinant ENPP1, and TNAP inhibitors represent additional strategies to increase plasma PPi levels[55,67]. Other potential treatments include agents such as inositol that block calcium–phosphate deposition, sodium thiosulfate to chelate calcium,

PROPOSED DIAGNOSTIC CRITERIA FOR PSEUDOXANTHOMA ELASTICUM (PXE; 2014)
Major criteria
Skin findings
• Characteristic pseudoxanthomatous papules and plaques on the neck and/or other flexural sites • Histopathologic evidence of calcified elastic fibers in the mid and lower dermis of affected skin
Eye findings
• Angioid streak(s) >1 disc diameter in length • "Peau d'orange" changes*
Genetic testing
• Biallelic pathogenic variants in *ABCC6*
Minor criteria
• Definite PXE diagnosed in a first-degree relative (especially a sibling) • Pathogenic variant identified in one allele of *ABCC6* • Histopathologic findings of PXE in non-lesional skin
Definite PXE diagnosis* requires either**: Both major skin criteria plus one major eye criterion ***-or- Major genetic criterion ***Probable PXE diagnosis in an individual with an affected first-degree relative* requires either**: Both major skin criteria ***-or-*** One major eye criterion ***Minor criteria can be helpful in suggesting a possible PXE diagnosis***
*In an individual <20 years of age.

Table 97.5 Proposed diagnostic criteria for pseudoxanthoma elasticum (PXE; 2014)[46,47].

A MULTIDISCIPLINARY APPROACH TO MANAGEMENT OF PSEUDOXANTHOMA ELASTICUM
Skin
• No specific treatment is available • Surgical intervention for excessive skin folds[58]
Eyes
Prevention and early detection
• Annual funduscopic examination • Regular use of an Amsler grid to assess for central visual field defects • Use of sunglasses • Diet/vitamins rich in antioxidants • Avoidance of head trauma, heavy straining, and smoking; limited participation in contact and racket sports
Treatment
• Intravitreal injections of VEGF antagonists (e.g. bevacizumab, ranibizumab, aflibercept) to prevent retinal neovascularization (but not mineralization); may stabilize or improve visual acuity[56,57,59,60]
Cardiovascular system
Prevention and early detection
• Baseline electrocardiogram and echocardiogram • Annual cardiovascular examination • Healthy lifestyle with balanced diet, regular exercise, weight control, and avoidance of smoking and excessive alcohol intake • Magnesium supplementation* (e.g. magnesium oxide or citrate)[61–63] • Moderate calcium intake (as appropriate for age) • Low-dose therapy with acetylsalicylic acid if not contraindicated
Treatment
• Correction of hyperlipidemia and hypertension • Low-dose acetylsalicylic acid, pentoxifylline, cilostazol, or clopidogrel for intermittent claudication
*A diet high in magnesium was shown to reduce connective tissue mineralization in a mouse model of PXE[62], and a non-significant trend toward reduced calcification of skin elastic fibers was observed in PXE patients who received magnesium oxide in a small randomized placebo-controlled trial[63].

Table 97.6 A multidisciplinary approach to management of pseudoxanthoma elasticum. VEGF, vascular endothelial growth factor.

and phenylbutyrate to promote maturation of mutant ABCC6[55,68,69]. Overactivation of the DNA damage response/PARP1 pathway has been implicated in aberrant mineralization, and minocycline was recently found to attenuate this signaling and reduce ectopic calcification in PXE fibroblasts as well as *Abcc6*$^{-/-}$ mice and zebrafish[70,71].

Resources for patients and families include PXE International (www.pxe.org), which provides information on ectopic calcification disorders and their management[72].

CUTIS LAXA

Synonyms: ■ Dermatochalasia ■ Dermatomegaly ■ Generalized elastolysis ■ Generalized elastorrhexis

Key features

- Group of conditions characterized by sparse and fragmented elastic fibers
- Both heritable (autosomal dominant, autosomal recessive, and X-linked recessive) and acquired forms
- Features loose, sagging skin with reduced resilience and recoil
- Extracutaneous manifestations include emphysema, arterial and cardiac valvular abnormalities, hernias, diverticula, and craniofacial anomalies

History

The clinical differences between cutis laxa (CL) and EDS were delineated in 1923 by F. Parkes Weber[3], and the generalized nature of the elastolysis and potential for internal involvement were recognized by Goltz and co-workers in 1965[73].

Epidemiology

The heritable forms of CL are rare and no precise estimate of their prevalence is available. There appears to be no racial or ethnic predilection, and inheritance can be autosomal dominant, autosomal recessive, or X-linked recessive. Heritable CL is typically apparent at birth or during early childhood, but the development of lax skin is occasionally delayed until early adulthood in autosomal dominant forms. Acquired CL frequently has a later onset.

Pathogenesis

CL represents a disorder of the elastic fiber network and can involve multiple tissues, including internal organs as well as the skin. Insights into the molecular bases of inherited forms of CL have refined their classification[74,75] (Table 97.7). Mutations in the elastin gene (*ELN*) that lead to qualitative as well as quantitative abnormalities in this protein have been identified as the cause of an autosomal dominant form of CL[76]. Defects in several genes can underlie autosomal recessive CL (ARCL), which tends to be more severe and is divided into groups with different patterns of extracutaneous involvement. ARCL type 1 features potentially fatal involvement of the lungs, vascular abnormalities, and gastrointestinal/genitourinary diverticula, whereas ARCL types 2 and 3 (de Barsy syndrome) are characterized by craniofacial anomalies and delayed growth and development (see Table 97.7).

Fibulins are calcium-dependent glycoproteins that stabilize ECM networks and provide support for elastic fiber assembly. Biallelic mutations in the genes that encode fibulin 5 and fibulin 4 (EGF-containing fibulin-like extracellular matrix protein 2) cause ARCL types 1A and 1B, respectively; a heterozygous duplication within the fibulin 5 gene was also found to underlie CL in one patient[77–79]. Mutations in the latent TGF-β binding protein-4 gene (*LTBP4*) result in ARCL type 1C, which is characterized by severe pulmonary, gastrointestinal, and genitourinary involvement[80]. LTBP4 is an ECM protein that binds to fibrillin and controls the bioavailability of TGF-β, and LTBP4 deficiency leads to aberrant TGF-β activity and defective elastic fiber assembly in many tissues (see Fig. 95.6).

Defects in several intracellular proteins that play a role in metabolic pathways underlie other forms of ARCL. Variable glycosylation abnormalities result from biallelic mutations in *ATP6V0A2*, *ATP6V1E1*, and *ATP6V1A*, which encode subunits of the vacuolar H^+-ATPase, with a phenotypic spectrum that includes ARCL types 2A, 2C, and 2D and features facial dysmorphism, microcephaly, joint hypermobility, and delayed growth and development[75,81]. Mutations in the genes encoding the mitochondrial enzymes pyrroline-5-carboxylate reductase 1 (*PYCR1*) and pyrroline-5-carboxylate synthetase (*P5CS/ALDH18A1*) cause ARCL types 2B/3B and 3A, respectively, with prominent progeroid features and neurodevelopmental manifestations thought to be related to mitochondrial dysfunction[82] (see Table 97.7). *PYCR1* mutations may also lead to features of EDS (e.g. joint hypermobility) and osteogenesis imperfecta[83]. These enzymes are critical for the biosynthesis of proline, which is a major amino acid in collagen and plays a role in an oxidative cycle important to cellular metabolism. In PYCR1 deficiency, there is increased apoptosis of fibroblasts following oxidative stress.

An alternate pathogenic mechanism for CL, in particular acquired variants, is enhanced degradation of elastic fibers. Sagging of the skin, usually with little or no associated internal organ involvement, can develop in the weeks to months following the onset of an inflammatory skin condition such as a drug reaction, chronic urticaria, or Sweet syndrome (Table 97.8). In these cases, release of elastases into the extracellular milieu by inflammatory cells (e.g. neutrophils, monocytes/macrophages) leads to proteolytic degradation of elastic fibers[84]. Generalized or localized CL can develop following a Sweet syndrome-like neutrophilic dermatosis (referred to as Marshall syndrome) and some of these patients may have increased susceptibility to proteolysis due to α_1-antitrypsin deficiency. Immunopathogenic mechanisms may play a role in some cases of acquired CL, as evidenced by the occurrence of acral or generalized CL in association with monoclonal gammopathies and observation of IgG, IgA, or amyloid deposition on elastic fibers in lesional skin[85,86]. In addition, there may be an underlying genetic susceptibility for the development of CL, e.g. polymorphisms or "mild" mutations in the elastin and/or fibulin 5 genes[87].

CL-like cutaneous changes as well as elastosis perforans serpiginosa and PXE-like findings have been observed in patients treated for a prolonged period with high-dose D-penicillamine for conditions such as Wilson disease or cystinuria. D-penicillamine can interfere with elastin cross-linking by two mechanisms. First, D-penicillamine is a copper chelator and can lower serum copper levels, which reduces the activity of lysyl oxidase, an enzyme required for elastin cross-linking (see Ch. 95)[88]. Second, D-penicillamine can chemically block the allysine and lysine residues that come together to form desmosine cross-links. Because of these actions, newly synthesized elastin molecules do not become stably cross-linked. Instead, they are subject to rapid proteolysis, thus precluding the synthesis of functional elastic fibers.

Clinical Features

All forms of CL are characterized by loose, sagging skin with reduced elasticity and resilience. This often gives the affected patient an "aged" facial appearance with down-slanting palpebral fissures and a long philtrum (Fig. 97.10). Cutaneous findings are present at birth in most heritable forms of CL but may develop later in life in autosomal dominant as well as acquired variants. The laxity and wrinkling usually progress over time, although improvement of the skin with age has been noted in ARCL type 2A. Skin involvement is frequently generalized; however, it can be primarily acral, especially in ARCL type 2B or acquired CL.

In some patients with CL, clinical manifestations are limited to the skin, and the phenotype is primarily of cosmetic concern. In other patients, the cutaneous findings are associated with prominent extracutaneous features, which can include emphysema, umbilical and inguinal hernias, gastrointestinal and vesicourinary tract diverticula, arterial and cardiac valvular abnormalities, skeletal or joint involvement, and delayed growth and development. The extracutaneous manifestations, particularly pulmonary complications, can cause considerable morbidity and mortality[89]. Cutaneous and extracutaneous features of specific types of heritable CL are summarized in Table 97.7.

Generalized acquired CL without an identifiable trigger may be clinically indistinguishable from milder heritable forms of CL, e.g.

HERITABLE FORMS OF CUTIS LAXA AND RELATED CONDITIONS					
Disorder	**Inheritance**	**Gene**	**Protein**	**Distribution of cutis laxa**	**Additional features**
Heritable forms of cutis laxa					
ADCL	AD*	*ELN*	Elastin	Generalized	• Cardiac valve abnormalities, aortic dilatation (variable) • Emphysema (uncommon) • Hernias†
		FBLN5 (single patient reported)	Fibulin 5		
ARCL type 1A	AR	*FBLN5*	Fibulin 5	Generalized; large ears with prominent lobes	• Pulmonary emphysema • Stenoses of the supravalvular aorta and pulmonary arteries • Gastrointestinal and vesicourinary diverticula, hernias† • Micrognathia
ARCL type 1B	AR	*FBLN4/EFEMP2*	Fibulin 4	Generalized but less pronounced; may favor skin folds	• Arterial or aortic tortuosity/ aneurysms; aortic isthmus stenosis • Joint hypermobility, arachnodactyly, fractures, high arched palate, micrognathia
ARCL type 1C (Urban–Rifkin–Davis syndrome)	AR	*LTBP4*	Latent TGF-β binding protein-4	Generalized	• Emphysema (severe, often fatal) • Pulmonary arterial stenosis, valvular defects • GI and GU malformations (diverticula, rupture risk) • Micrognathia, large fontanelles • Joint hypermobility, hypotonia • Bitemporal hypotrichosis
ARCL type 2A (Debré type; allelic to wrinkly skin syndrome)	AR	*ATP6V0A2*	Vacuolar H^+-ATPase V0, subunit A2	Generalized; may favor abdomen and dorsal hands; improves over time	• Translucent skin with prominent veins • High myopia (2A); corneal opacities & cataracts (3A/B, PADCL) • Facial dysmorphism‡; triangular face with more progeroid appearance (2B, 3A/B); large fontanelles • Microcephaly, partial pachygyria (2A), absent corpus callosum (2B) • Intellectual disability; seizures, neurologic degeneration (2A); dystonia/ athetosis (3A/B) • Congenital hip dysplasia, joint hypermobility, hypotonia, scoliosis, short stature; osteopenia (2B, 3A/B) • Cranial arterial tortuosity (3A, PADCL) • O- and N-glycosylation defect (2A¶)
ARCL type 2B and 3B (de Barsy syndrome B)	AR	*PYCR1*	Pyrroline-5-carboxylate reductase 1	Generalized; may favor dorsal hands/feet or improve over time; occasionally fat pads (e.g. on buttocks; 3A)	
ARCL type 3A (de Barsy syndrome A) and Progeroid ADCL (PADCL)	AR (3A) AD (PADCL)	*P5CS/ALDH18A1*	Pyrroline-5-carboxylate synthetase		
ARCL types 2C and 2D	AR	*ATP6V1E1* (2C) *ATP6V1A* (2D)	Vacuolar H^+-ATPase V1, subunits E1 and A	Generalized with sparse or subcutaneous fat; large skin folds on extremities, fat pads on buttocks; may improve over time (2D)	• Pneumothorax • Cardiac abnormalities, aortic dilation • "Mask-like" triangular face, hypotonia; variable hip dysplasia, marfanoid habitus • Neurodevelopmental abnormalities (2D)
Gerodermia osteodysplastica (geroderma osteodysplasticum)	AR	*GORAB*	Golgin, RAB6-interacting	Primarily on dorsal hands/ feet	• Malar hypoplasia, prognathism, oblique furrow lateral to eyebrows • Joint hypermobility • Osteoporosis, fractures, dwarfism
Occipital horn syndrome	X-R	*ATP7A*	ATPase, Cu^{2+}-transporting, α-polypeptide	Generalized, most pronounced on face and neck	• Easy bruising, coarse hair (variable) • Arterial tortuosity • Chronic diarrhea; bladder diverticula • Long face, high forehead, hooked nose • Developmental delay • Wedge-shaped occipital calcifications • Joint hypermobility
Macrocephaly, alopecia, CL, and scoliosis (MACS)	AR	*RIN2*	RAS and RAB interactor 2	Generalized, most pronounced on face	• Sparse scalp hair • Gingival hypertrophy, facial dysmorphism • Macrocephaly • Scoliosis, joint hypermobility

Table 97.7 Heritable forms of cutis laxa (CL) and related conditions.

Continued

HERITABLE FORMS OF CUTIS LAXA AND RELATED CONDITIONS					
Disorder	**Inheritance**	**Gene**	**Protein**	**Distribution of cutis laxa**	**Additional features**
Other heritable conditions that feature lax and/or redundant skin					
Arterial tortuosity syndrome	AR	*SLC2A10 (GLUT10)*	Solute carrier family 2, member 10 (a glucose transporter)	Generalized; soft, hyperextensible skin has also been described	• Telangiectasias on cheeks (variable) • Arterial tortuosity • Long face, micrognathia, high-arched palate • Joint hypermobility and contractures
Larsen-like syndrome	AR	*B3GAT3*	Glucuronosyltransferase I	Wrinkled acral skin	• Joint dislocations, craniofacial dysmorphism, short stature • Congenital heart defects
Costello syndrome	AR	*HRAS*	HRAS	Variable, especially on hands and feet	• Deep palmoplantar creases, acanthosis nigricans, periorificial papillomas • Curly or sparse hair, coarse facies • Cardiac malformations • Intellectual disability, short stature • Risk of malignancies, e.g. rhabdomyosarcoma
Donohue syndrome ("leprechaunism"; see Ch. 101)	AR	*INSR*	Insulin receptor	Variable	• Generalized lipodystrophy, hypertrichosis, acanthosis nigricans • Insulin resistance • Distinctive "elfin" facies • Severe growth delay
Finnish-type amyloidosis	AD	*GSN*	Gelsolin	Generalized	• Corneal dystrophy • Polyneuropathy
Cranioectodermal dysplasia (Sensenbrenner syndrome)	AR	*IFT122* *IFT43*	Intraflagellar transport proteins 122 and 43	Generalized; redundant skin folds at neck, ankles, and wrists	• Sparse, fine hair; short, broad nails • Narrow thorax, short proximal limbs, joint hypermobility, brachydactyly, dolichocephaly, dysmorphic facies, dental anomalies • Nephronophthisis, hepatic fibrosis, retinal dystrophy
		WDR35 *WDR19*	WD repeat domain 35 and 19		
Circumferential skin creases, Kunze type	AD, AR	*MAPRE2*	Microtubule-associated protein RP/EB family member 2	Multiple circumferential creases/folds of skin on the extremities (see Fig. 97.13) > neck > trunk (excess rather than lax skin); may resolve over time	• Cleft palate, short stature, dysmorphic facies (e.g. epicanthal folds, small eyes), overfolded helices • Intellectual disability
	AD	*TUBB*	Tubulin-β class I		
Nonsyndromic "Michelin tire baby"	AD	?	?		• Affected skin may have excess fat or smooth muscle, and the latter is often associated with hypertrichosis; elastic fibers are usually normal (fragmentation noted in only one report)

*An AR form of cutis laxa due to a homozygous elastin mutation has been reported in two related families.
†E.g. inguinal, umbilical, diaphragmatic.
‡Features may include a broad forehead and midfacial hypoplasia as well as findings related to the lax skin (e.g. down-slanting palpebral fissures, long philtrum).
¶Can be assessed via analysis of the glycosylation of serum sialotransferrin ± apolipoprotein C-III via isoelectric focusing.

Table 97.7 Heritable forms of cutis laxa (CL) and related conditions. CL can also occur in Williams–Beuren syndrome, which results from deletion of multiple contiguous genes that include *ELN*. In addition to ARCL types 2A and 2C, CL can occur in other congenital disorders of glycosylation, e.g. due to mutations in a component of oligomeric Golgi complex 7 (*COG7*; multiple-system malformations) or steroid 5-α-reductase 3 (*SRD5A3*; also ichthyosis, ocular colobomas, and midline brain malformations). Transaldolase deficiency can present with neonatal CL (generalized or of the forehead) that improves over time as well as hypertrichosis, hepatosplenomegaly, hemolytic anemia, and GU malformations. Features of cutis laxa have also been reported in PURA syndrome. "Neonatal CL with a marfanoid phenotype" was described in an infant who lacked immunohistochemical evidence of laminin-β1 in the skin. AD, autosomal dominant; *ALDH18A1*, aldehyde dehydrogenase 18 family, member A1; AR, autosomal recessive; *EFEMP2*, EGF-containing fibulin-like extracellular matrix protein 2; GI, gastrointestinal; GU, genitourinary; TGF, transforming growth factor; X-R, X-linked recessive.

late-onset autosomal dominant CL. Generalized or localized forms of acquired CL can also occur in association with a plasma cell dyscrasia (see Fig. 97.10B), as a consequence of drug intake (particularly penicillamine), and subsequent to a systemic or cutaneous inflammatory disorder (see Table 97.8). In the latter situation, the inflammatory reaction is followed by progressive sagging of the skin, which can become extensive and lead to a prematurely aged appearance. Acquired CL most commonly develops in adults and when it presents with generalized skin involvement, often beginning on the face and neck, there can be associated internal manifestations such as emphysema and diverticula (e.g. gastrointestinal, vesicourinary). Occasionally, localized CL is found predominantly around the eyes (blepharochalasis) or on the distal extremities, particularly the palms and soles (Fig. 97.11). Marshall syndrome refers to CL in association with a Sweet syndrome-like neutrophilic dermatosis, and it occurs primarily in infants and young children[90].

Pathology

In the skin of patients with CL, the characteristic histopathologic feature is sparse and/or fragmented elastic fibers (Fig. 97.12). This ranges from virtual absence of elastic fibers in a newborn with severe CL (e.g. ARCL type 1) to fragmentation but normal density of fibers in late-onset autosomal dominant CL. Electron microscopy shows irregular

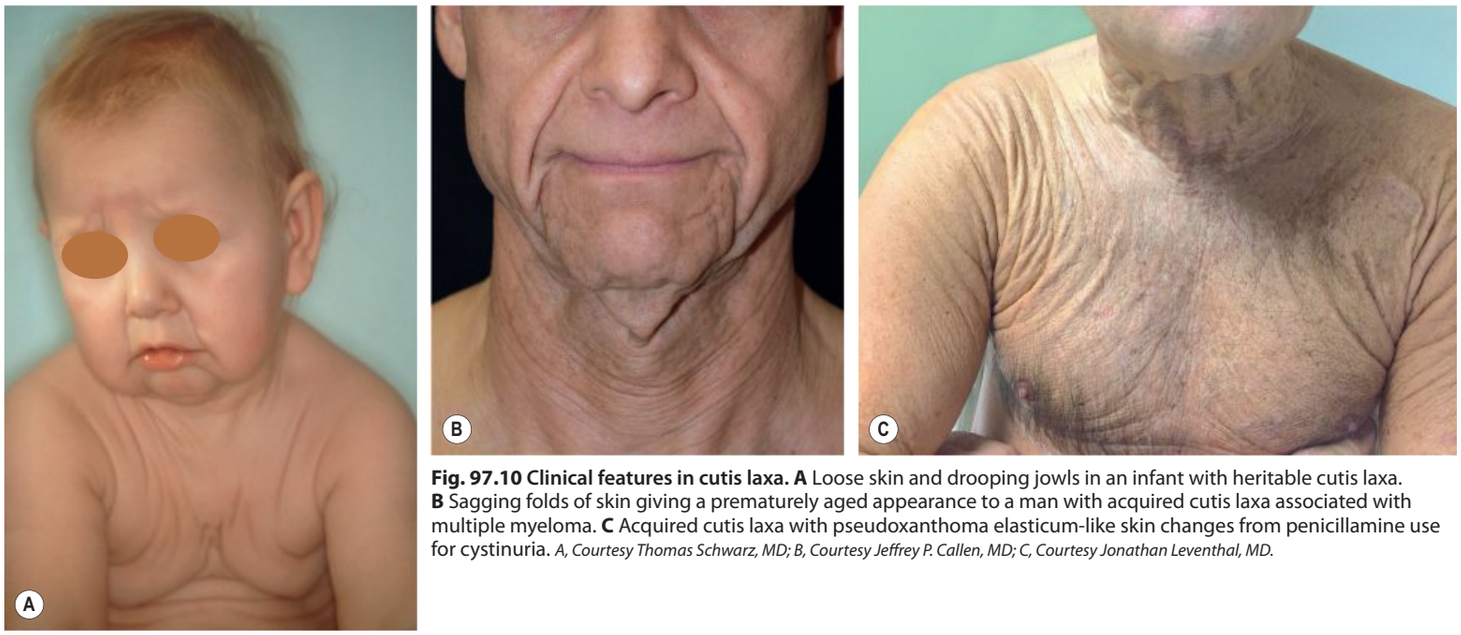


Fig. 97.10 Clinical features in cutis laxa. A Loose skin and drooping jowls in an infant with heritable cutis laxa. **B** Sagging folds of skin giving a prematurely aged appearance to a man with acquired cutis laxa associated with multiple myeloma. **C** Acquired cutis laxa with pseudoxanthoma elasticum-like skin changes from penicillamine use for cystinuria. *A, Courtesy Thomas Schwarz, MD; B, Courtesy Jeffrey P. Callen, MD; C, Courtesy Jonathan Leventhal, MD.*

ACQUIRED CUTIS LAXA: ASSOCIATED CONDITIONS
Skin disorders
• Urticaria and/or angioedema • Drug eruptions (e.g. due to penicillin or an SSRI) • Sweet syndrome-like eruptions (Marshall syndrome*) • Urticarial vasculitis • Arthropod bite reactions • Erythema multiforme • Dermatitis herpetiformis • Lupus panniculitis • Interstitial granulomatous dermatitis • Cutaneous mastocytosis • Cutaneous lymphoma
Extracutaneous inflammatory disorders
• Rheumatoid arthritis • Systemic lupus erythematosus • Nephrotic syndrome • Celiac disease • Sarcoidosis
Hematologic disorders
• Monoclonal gammopathy (especially acral CL; underlying plasma cell dyscrasia)† • Congenital hemolytic anemia
Infectious diseases
• Febrile viral syndrome • *Borrelia burgdorferi* infection • Syphilis • Leprosy
Drug intake (also see drug eruptions above)
• Penicillamine • Isoniazid
*Occurs primarily in infants and young children and is referred to as type II acquired CL, with other forms of acquired CL classified as type I. †Commonly associated with systemic amyloidosis in setting of multiple myeloma.

Table 97.8 Acquired cutis laxa (CL): associated conditions. Generalized or localized CL (including Marshall syndrome) can occur in the setting of α_1-antitrypsin deficiency. SSRI, selective serotonin reuptake inhibitor.



Fig. 97.11 Idiopathic acral localized acquired cutis laxa. The pulp of the digits has loose redundant skin (**A**) and pressure can produce a depression (**B**). The only abnormal finding was an elevated ANA titer. *Courtesy Luis Requena, MD.*

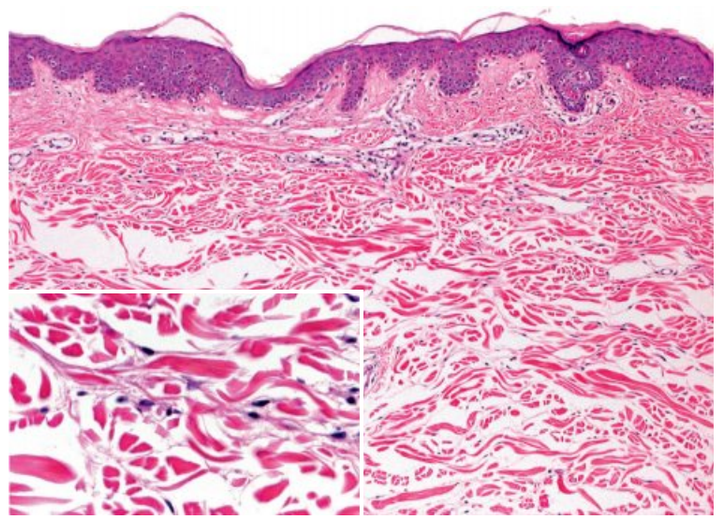


Fig. 97.12 Histologic features of cutis laxa. Dermal elastic fibers are sparse and fragmented. *Courtesy Lorenzo Cerroni, MD.*

fragmentation of the elastic fiber structure. In some patients, elastic fiber abnormalities are accompanied by alterations in collagen fibers, which likely reflect a general perturbation of the ECM and mechanical properties of the skin due to the primary elastic fiber defect.

Differential Diagnosis

Clinical findings similar to CL can develop as a consequence of the normal skin aging. In contrast to CL, the hyperextensible skin of patients with EDS retains elasticity and recoil, with the exception of

the rare dermatosparaxis type. Skin fragility and bruising represent additional features of EDS but not CL. In PXE and the related PXE-like disorder with multiple coagulation factor deficiency, the skin can be loose and sagging without recoil; however, the primary papular lesions at the predilection sites distinguish these conditions from CL.

Mid-dermal elastolysis is an acquired disorder with a predilection for young and middle-aged women that is characterized by circumscribed or diffuse areas of fine wrinkling, most often in sun-exposed sites on the upper trunk, lateral neck, and upper arms (see Ch. 99)[91]. It features the pathognomonic histopathologic finding of a band-like loss of elastic fibers in the mid dermis. Anetoderma presents as focal areas of flaccid skin (typically 1 to 2 cm in diameter) with loss of elastic tissue and may have an antecedent inflammatory process. It is histologically and ultrastructurally identical to CL and may be regarded as a variant of acquired localized CL with smaller, circumscribed lesions.

Additional rare syndromes that can present with lax skin and elastic fiber abnormalities are outlined in Table 97.7[92]. Of note, the "Michelin tire baby" phenotype of congenital circumferential skin creases on the extremities may be reminiscent of CL, but the folds reflect excess tissue rather than cutaneous laxity (Fig. 97.13).

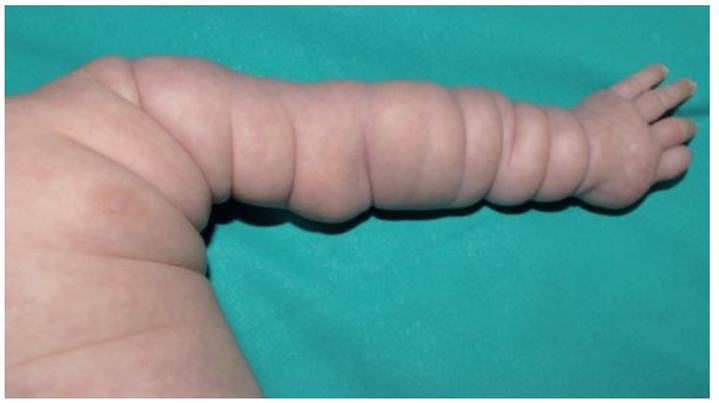


Fig. 97.13 "Michelin tire baby" phenotype. Note the circumferential skin creases on the extremities. *Courtesy Antonio Torrelo, MD.*

Treatment

The redundant and sagging skin may be of major cosmetic concern to patients with CL, and reconstructive surgery can provide improvement with significant psychosocial benefit. Surgical wounds heal with scars that have a normal appearance and tensile strength. However, sagging may reoccur, necessitating additional surgical procedures.

The associated internal organ involvement requires appropriate care through a multidisciplinary approach. All patients should have a baseline echocardiogram and pulmonary assessment, with further investigations such as urinary tract ultrasound (ARCL type 1) and neurologic evaluation (ARCL types 2/3) depending on the subtype and clinical findings[75].

Additional figures and table, Five-point joint hypermobility questionnaire, available in our eBook (see inside front cover for access code).

REFERENCES

1. Sybert VP. *Genetic Skin Disorders*, Vol. 33. Oxford: Oxford University Press; 1997.
2. Pulkkinen L, Ringpfeil F, Uitto J. Progress in heritable skin diseases: molecular bases and clinical implications. *J Am Acad Dermatol*. 2002;47:91–104.
3. McKusick V. *Heritable Disorder of Connective Tissue*. St. Louis: Mosby; 1972:475.
4. Pinnell SR, Krane SM, Kenzora JE, Glimcher MJ. A heritable disorder of connective tissue: hydroxylysine-deficient collagen disease. *N Engl J Med*. 1972;286:1013–1020.
5. Beighton P, De Paepe A, Steinmann B, et al. Ehlers-Danlos syndromes: revised nosology, Villefranche, 1997. Ehlers-Danlos National Foundation (USA) and Ehlers-Danlos Support Group (UK). *Am J Med Genet*. 1998;77:31–37.
6. Malfait F, De Paepe A. The Ehlers-Danlos syndrome. *Adv Exp Med Biol*. 2014;802:129–143.
7. Malfait F, Francomano C, Byers P, et al. The 2017 international classification of the Ehlers-Danlos syndromes. *Am J Med Genet C Semin Med Genet*. 2017;175:8–26.
8. Myllyharju J, Kivirikko KI. Collagens and collagen-related diseases. *Ann Med*. 2001;33:7–21.
9. Pepin MG, Schwarze U, Rice KM, et al. Survival is affected by mutation type and molecular mechanism in vascular Ehlers-Danlos syndrome (EDS type IV). *Genet Med*. 2014;16:881–888.
10. Baumann M, Giunta C, Krabichler B, et al. Mutations in FKBP14 cause a variant of Ehlers-Danlos syndrome with progressive kyphoscoliosis, myopathy, and hearing loss. *Am J Hum Genet*. 2012;90:201–216.
11. Schalkwijk J, Zweers MC, Steijlen PM, et al. A recessive form of the Ehlers-Danlos syndrome caused by tenascin-X deficiency. *N Engl J Med*. 2001;345:1167–1175.
12. Kapferer-Seebacher I, Pepin M, Werner R, et al. Periodontal Ehlers-Danlos syndrome is caused by mutations in C1R and C1S, which encode subcomponents C1r and C1s of complement. *Am J Hum Genet*. 2016;99:1005–1014.
13. Beighton P, Solomon L, Soskolne CL. Articular mobility in an African population. *Ann Rheum Dis*. 1973;32:413–418.
14. Steinmann B, Royce PM. *Connective Tissue and its Heritable Disorders. Molecular Genetic, and Medical Aspects*. New York: Wiley-Liss; 1993.
15. Bowen JM, Sobey GJ, Burrows NP, et al. Ehlers-Danlos syndrome, classical type. *Am J Med Genet C Semin Med Genet*. 2017;175:27–39.
16. Atzinger CL, Meyer RA, Khoury PR, et al. Cross-sectional and longitudinal assessment of aortic root dilation and valvular anomalies in hypermobile and classic Ehlers-Danlos syndrome. *J Pediatr*. 2011;158:826–30. e1.
17. De Wandele I, Rombaut L, Leybaert L, et al. Dysautonomia and its underlying mechanisms in the hypermobility type of Ehlers-Danlos syndrome. *Semin Arthritis Rheum*. 2014;44:93–100.
18. Castori M, Tinkle B, Levy H, et al. A framework for the classification of joint hypermobility and related conditions. *Am J Med Genet C Semin Med Genet*. 2017;175:148–157.
19. Pepin M, Schwarze U, Superti-Furga A, et al. Clinical and genetic features of Ehlers-Danlos syndrome type IV, the vascular type. *N Engl J Med*. 2000;342:673–680.
20. Green C, Ghali N, Akilapa R, et al. Classical-like Ehlers-Danlos syndrome: a clinical description of 20 newly identified individuals with evidence of tissue fragility. *Genet Med*. 2020;22:1576–1582.
21. Angwin C, Ghali N, Baker D, et al. Electron microscopy in the diagnosis of Ehlers-Danlos syndromes: correlation with clinical and genetic investigations. *Br J Dermatol*. 2020;182:698–707.
22. Murray ML, Pepin M, Peterson S, et al. Pregnancy-related deaths and complications in women with vascular Ehlers-Danlos syndrome. *Genet Med*. 2014;16:874–880.
23. Ong KT, Perdu J, De Backer J, et al. Effect of celiprolol on prevention of cardiovascular events in vascular Ehlers-Danlos syndrome: a prospective randomised, open, blinded-endpoints trial. *Lancet*. 2010;376:1476–1484.
24. Gorosabel MC, Dubacher N, Meienberg J, et al. Vascular Ehlers-Danlos syndrome: can the beneficial effect of celiprolol be extrapolated to bisoprolol? *Eur Heart J Cardiovasc Pharmacother*. 2020;6:199–200.
25. Speake D, Dvorkin L, Vaizey CJ, et al. Management of colonic complications of type IV Ehlers-Danlos syndrome: a systematic review and evidence-based management strategy. *Colorectal Dis*. 2020;22:129–135.
26. Darier J. Pseudo-xanthome élastique. *III Congrès Intern de Dermat de Londres*. 1896;5:289–295.
27. Grönblad E. Angioid streaks - pseudoxanthoma elasticum. *Acta Ophthalmol*. 1929;7:329.
28. Strandberg J. Pseudoxanthoma Elasticum. *Z Haut Gechlechtskr*. 1929;31:689–694.
29. Ringpfeil F, Lebwohl MG, Christiano AM, et al. Pseudoxanthoma elasticum: mutations in the MRP6 gene encoding a transmembrane ATP-binding cassette (ABC) transporter. *Proc Natl Acad Sci U S A*. 2000;97:6001–6006.
30. Ringpfeil F, McGuigan K, Fuchsel L, et al. Pseudoxanthoma elasticum is a recessive disease characterized by compound heterozygosity. *J Invest Dermatol*. 2006;126:782–786.
31. Neldner KH. Pseudoxanthoma elasticum. *Clin Dermatol*. 1988;6:1–159.
32. Jansen RS, Kucukosmanoglu A, de Haas M, et al. ABCC6 prevents ectopic mineralization seen in pseudoxanthoma elasticum by inducing cellular nucleotide release. *Proc Nat Acad Sci USA*. 2013;110:20206–20211.
33. Li Q, Huang J, Pinkerton AB, et al. Inhibition of tissue-nonspecific alkaline phosphatase attenuates ectopic mineralization in the Abcc6(-/-) mouse model of PXE but not in the Enpp1 mutant mouse models of GACI. *J Invest Dermatol*. 2019;139:360–368.
34. Nitschke Y, Rutsch F. Generalized arterial calcification of infancy and pseudoxanthoma elasticum: two sides of the same coin. *Front Genet*. 2012;3:302.
35. Li Q, Brodsky JL, Conlin L, et al. Mutations in the ABCC6 gene as a cause of generalized arterial calcification of infancy: genotypic overlap with pseudoxanthoma elasticum. *J Invest Dermatol*. 2014;134:658–665.
36. Saeidian AH, Youssefian L, Huang JH, et al. Genetic heterogeneity of heritable ectopic mineralization disorders in a large international cohort. *Genet Med*. 2022;24:75–86.
37. Markello TC, Pak LK, St Hilaire C, et al. Vascular pathology of medial arterial calcifications in NT5E deficiency: implications for the role of adenosine in pseudoxanthoma elasticum. *Mol Genet Metab*. 2011;103:44–50.
38. Li Q, Price TP, Sundberg JP, et al. Juxta-articular joint-capsule mineralization in CD73 deficient mice: similarities to patients with NT5E mutations. *Cell Cycle*. 2014;13:2609–2615.
39. Vanakker OM, Martin L, Gheduzzi D, et al. Pseudoxanthoma elasticum-like phenotype with cutis laxa and multiple coagulation factor deficiency represents a separate genetic entity. *J Invest Dermatol*. 2007;127:581–587.
40. Li Q, Grange DK, Armstrong NL, et al. Mutations in the GGCX and ABCC6 genes in a family with pseudoxanthoma elasticum-like phenotypes. *J Invest Dermatol*. 2009;129:553–563.
41. Ralph D, van de Wetering K, Uitto J, Li Q. Inorganic pyrophosphate deficiency syndromes and potential treatments for pathologic tissue calcification. *Am J Pathol*. 2022;192:762–770.
42. Lebwohl M, Lebwohl E, Bercovitch L. Prominent mental (chin) crease: a new sign of pseudoxanthoma elasticum. *J Am Acad Dermatol*. 2003;48:620–622.
43. Hoppner J, Kornak U, Sinningen K, et al. Autosomal recessive hypophosphatemic rickets type 2 (ARHR2) due to ENPP1-deficiency. *Bone*. 2021;153:116111.
44. Lebwohl M, Phelps RG, Yannuzzi L, et al. Diagnosis of pseudoxanthoma elasticum by scar biopsy in patients without characteristic skin lesions. *N Engl J Med*. 1987;317:347–350.

45. Li Q, Török L, Kocsis L, et al. Mutation analysis (ABCC6) in a family with pseudoxanthoma elasticum: presymptomatic testing with prognostic implications. *Br J Dermatol*. 2010;163:641–643.
46. Plomp AS, Toonstra J, Bergen AA, et al. Proposal for updating the pseudoxanthoma elasticum classification system and a review of the clinical findings. *Am J Med Genet A*. 2010;152A:1049–1058.
47. Uitto J, Jiang Q, Varadi A, et al. Pseudoxanthoma elasticum: diagnostic features, classification and treatment options. *Expert Opin Orphan Drugs*. 2014;2:567–577.
48. Bolognia JL, Braverman I. Pseudoxanthoma-elasticum-like skin changes induced by penicillamine. *Dermatology*. 1992;184:12–18.
49. Christensen OB. An exogenous variety of pseudoxanthoma elasticum in old farmers. *Acta Derm Venereol*. 1978;58:319–321.
50. Nickoloff BJ, Noodleman FR, Abel EA. Perforating pseudoxanthoma elasticum associated with chronic renal failure and hemodialysis. *Arch Dermatol*. 1985;121:1321–1322.
51. Mainetti C, Masouye I, Saurat JH. Pseudoxanthoma elasticum-like lesions in the L-tryptophan-induced eosinophilia-myalgia syndrome. *J Am Acad Dermatol*. 1991;24:657–658.
52. Aessopos A, Farmakis D, Loukopoulos D. Elastic tissue abnormalities resembling pseudoxanthoma elasticum in beta thalassemia and the sickling syndromes. *Blood*. 2002;99:30–35.
53. Martin L, Douet V, VanWart CM, et al. A mouse model of beta-thalassemia shows a liver-specific down-regulation of Abcc6 expression. *Am J Pathol*. 2011;178:774–783.
54. Sepp N, Pichler E, Breathnach SM, et al. Amyloid elastosis: analysis of the role of amyloid P component. *J Am Acad Dermatol*. 1990;22:27–34.
55. Luo H, Li Q, Cao Y, et al. Therapeutics development for pseudoxanthoma elasticum and related ectopic mineralization disorders: update 2020. *J Clin Med*. 2021;10:14.
56. Bhatnagar P, Freund KB, Spaide RF, et al. Intravitreal bevacizumab for the management of choroidal neovascularization in pseudoxanthoma elasticum. *Retina*. 2007;27:897–902.
57. Verbraak FD. Antivascular endothelial growth factor treatment in pseudoxanthoma elasticum patients. *Dev Ophthalmol*. 2010;46:96–106.
58. Viljoen DL, Bloch C, Beighton P. Plastic surgery in pseudoxanthoma elasticum: experience in nine patients. *Plast Reconstr Surg*. 1990;85:233–238.
59. Sawa M, Gomi F, Tsujikawa M, et al. Long-term results of intravitreal bevacizumab injection for choroidal neovascularization secondary to angioid streaks. *Am J Ophthalmol*. 2009;148:584–590. e2.
60. Gliem M, Birtel J, Herrmann P, et al. Aflibercept for choroidal neovascularizations secondary to pseudoxanthoma elasticum: a prospective study. *Graefes Arch Clin Exp Ophthalmol*. 2020;258:311–318.
61. Li Q, LaRusso J, Grand-Pierre AE, et al. Magnesium carbonate-containing phosphate binder prevents connective tissue mineralization in Abcc6$^{-/-}$ mice: potential for treatment of pseudoxanthoma elasticum. *Clin Transl Sci*. 2009;2:398–404.
62. LaRusso J, Li Q, Jiang Q, et al. Elevated dietary magnesium prevents connective tissue mineralization in a mouse model of pseudoxanthoma elasticum (Abcc6$^{-/-}$). *J Invest Dermatol*. 2009;129:1388–1394.
63. Rose S, On SJ, Fuchs W, et al. Magnesium supplementation in the treatment of pseudoxanthoma elasticum: a randomized trial. *J Am Acad Dermatol*. 2019;81:263–265.
64. Li Q, Kingman J, Sundberg JP, et al. Etidronate prevents, but does not reverse, ectopic mineralization in a mouse model of pseudoxanthoma elasticum (Abcc6(-/-)). *Oncotarget*. 2018;9:30721–30730.
65. Kranenburg G, de Jong PA, Bartstra JW, et al. Etidronate for prevention of ectopic mineralization in patients with pseudoxanthoma elasticum. *J Am Coll Cardiol*. 2018;71:1117–1126.
66. Bartstra JW, de Jong PA, Kranenburg G, et al. Etidronate halts systemic arterial calcification in pseudoxanthoma elasticum. *Atherosclerosis*. 2020;292:37–41.
67. Kozák E, Fülöp K, Tökési N, et al. Oral supplementation of inorganic pyrophosphate in pseudoxanthoma elasticum. *Exp Dermatol*. 2022;31:548–555.
68. Omarjee L, Nitschke Y, Verschuere S, et al. Severe early-onset manifestations of pseudoxanthoma elasticum resulting from the cumulative effects of several deleterious mutations in ENPP1, ABCC6 and HBB: transient improvement in ectopic calcification with sodium thiosulfate. *Br J Dermatol*. 2020;183:367–372.
69. Pomozi V, Brampton C, Szeri F, et al. Functional rescue of ABCC6 deficiency by 4-phenylbutyrate therapy reduces dystrophic calcification in Abcc6(-/-) mice. *J Invest Dermatol*. 2017;137:595–602.
70. Nollet L, Van Gils M, Willaert A, et al. Minocycline attenuates excessive DNA damage response and reduces ectopic calcification in pseudoxanthoma elasticum. *J Invest Dermatol*. 2022;142:1629–1638.
71. Huang J, Ralph D, Boraldi F, et al. Inhibition of the DNA damage response attenuates ectopic calcification in pseudoxanthoma elasticum. *J Invest Dermatol*. 2022;142:2140–2148.e1.
72. Terry SF, Terry PF, Rauen KA, et al. Advocacy groups as research organizations: the PXE International example. *Nat Rev Genet*. 2007;8:157–164.
73. Goltz RW, Hult AM, Goldfarb M, et al. Cutis laxa. A manifestation of generalized elastolysis. *Arch Dermatol*. 1965;92:373–387.
74. Mohamed M, Voet M, Gardeitchik T, et al. Cutis Laxa. *Adv Exp Med Biol*. 2014;802:161–184.
75. Beyens A, Boel A, Symoens S, et al. Cutis laxa: a comprehensive overview of clinical characteristics and pathophysiology. *Clin Genet*. 2021;99:53–66.
76. Tassabehji M, Metcalfe K, Hurst J, et al. An elastin gene mutation producing abnormal tropoelastin and abnormal elastic fibres in a patient with autosomal dominant cutis laxa. *Hum Mol Genet*. 1998;7:1021–1028.
77. Loeys B, Van Maldergem L, Mortier G, et al. Homozygosity for a missense mutation in fibulin-5 (FBLN5) results in a severe form of cutis laxa. *Hum Mol Genet*. 2002;11:2113–2118.
78. Elahi E, Kalhor R, Banihosseini SS, et al. Homozygous missense mutation in fibulin-5 in an Iranian autosomal recessive cutis laxa pedigree and associated haplotype. *J Invest Dermatol*. 2006;126:1506–1509.
79. Hucthagowder V, Sausgruber N, Kim KH, et al. Fibulin-4: a novel gene for an autosomal recessive cutis laxa syndrome. *Am J Hum Genet*. 2006;78:1075–1080.
80. Urban Z, Hucthagowder V, Schurmann N, et al. Mutations in LTBP4 cause a syndrome of impaired pulmonary, gastrointestinal, genitourinary, musculoskeletal, and dermal development. *Am J Hum Genet*. 2009;85:593–605.
81. Kornak U, Reynders E, Dimopoulou A, et al. Impaired glycosylation and cutis laxa caused by mutations in the vesicular H+-ATPase subunit ATP6V0A2. *Nat Genet*. 2008;40:32–34.
82. Guernsey DL, Jiang H, Evans SC, et al. Mutation in pyrroline-5-carboxylate reductase 1 gene in families with cutis laxa type 2. *Am J Hum Genet*. 2009;85:120–129.
83. Vahidnezhad H, Karamzadeh R, Saeidian AH, et al. Molecular dynamics simulation of the consequences of a PYCR1 mutation (p.Ala189Val) in patients with complex connective tissue disorder and severe intellectual disability. *J Invest Dermatol*. 2017;137:525–528.
84. Shapiro SD. Matrix metalloproteinase degradation of extracellular matrix: biological consequences. *Curr Opin Cell Biol*. 1998;10:602–608.
85. Fauconneau A, Sokolowsky N, Camus M, et al. Acquired cutis laxa associated with neutrophilic urticarial dermatosis. *Int J Dermatol*. 2021;60:771–772.
86. Terui H, Yamasaki K, Tamabuchi E, et al. Neutrophil extracellular traps as a possible pathomechanism of generalized acquired cutis laxa associated with IgA-lamda monoclonal gammopathy of undetermined significance. *Acta Derm Venereol*. 2021:101 adv00536.
87. Hu Q, Reymond JL, Pinel N, et al. Inflammatory destruction of elastic fibers in acquired cutis laxa is associated with missense alleles in the elastin and fibulin-5 genes. *J Invest Dermatol*. 2006;126:283–290.
88. Uitto J, Pulkkinen L. Heritable disorders affecting the elastic tissues: cutis laxa, pseudoxanthoma elasticum and related disorders. In: Rimoin DL, Connor JM, Pyeritz RE, eds. *Emery and Rimoin's Principles and Practice of Medical Genetics*. 3rd ed. London: Churchill Livingstone; 2002.
89. Berk DR, Bentley DD, Bayliss SJ, et al. Cutis laxa: a review. *J Am Acad Dermatol*. 2012;66:842. e1–17.
90. Marshall J, Heyl T, Weber HW. Postinflammatory elastolysis and cutis laxa. A report on a new variety of this phenomenon and a discussion of some syndromes characterized by elastolysis. *S Afr Med J*. 1966;40:1016–1022.
91. Rao BK, Endzweig CH, Kagen MH, et al. Wrinkling due to mid-dermal elastolysis: two cases and literature review. *J Cutan Med Surg*. 2000;4:40–44.
92. Morava E, Guillard M, Lefeber DJ, et al. Autosomal recessive cutis laxa syndrome revisited. *Eur J Hum Genet*. 2009;17:1099–1110.



eFig. 97.1 Molluscoid pseudotumors on the knees in a patient with Ehlers–Danlos syndrome.



eFig. 97.2 Atrophic scar in a patient with the classical type of Ehlers–Danlos syndrome.



eFig. 97.3 Typical facial features of the vascular type of Ehlers–Danlos syndrome. *Courtesy Addenbrooke's Hospital, Cambridge, UK.*





eFig. 97.4 Clinical features of pseudoxanthoma elasticum. Yellowish papules and "cobblestoned" plaques in the antecubital fossa (**A**) and neck (**B**). *A, Courtesy Julie V. Schaffer, MD.*



eFig. 97.5 Mucosal lesions in pseudoxanthoma elasticum. Yellow papules on the inner aspect of the lower lip.

FIVE-POINT JOINT HYPERMOBILITY QUESTIONNAIRE
1. Can you now (or could you ever) place your hands flat on the floor without bending your knees?
2. Can you now (or could you ever) bend your thumb to touch your forearm?
3. As a child, did you amuse your friends by contorting your body into strange shapes or could you do the splits?
4. As a child or teenager, did your shoulder or kneecap dislocate on more than one occasion?
5. Do you consider yourself "double-jointed"?
A "yes" answer to ≥2 questions suggests joint hypermobility, with 80%–85% sensitivity and 80%–90% specificity.

eTable 97.1 Five-point joint hypermobility questionnaire[7]. *Adapted from Hakim AJ, Grahame R. Int J Clin Pract 2003;57:163–6.*

98 Dermal Hypertrophies

Salma Machan, Ana María Molina-Ruiz and Luis Requena

Chapter Contents

Hypertrophic Scars and Keloids 1730
Dupuytren Disease 1733
Cutis Verticis Gyrata 1735
Hyaline Fibromatosis Syndrome 1736
Elastic Tissue-Related Disorders 1738

This chapter will discuss disorders in which there are increased amounts of collagen within the skin, followed by those with increased elastin.

HYPERTROPHIC SCARS AND KELOIDS

Key features

- Conventional scars are preceded by injury, form within weeks, remain flat or minimally elevated, and are asymptomatic
- Hypertrophic scars are raised, firm, and confined to the wound margin. Sometimes they improve spontaneously and tend to have a good response to treatment
- Keloids extend beyond the wound margin and are delayed in onset. They seldom resolve spontaneously and response to treatment is often poor

Introduction

All wounds heal with some degree of scar formation, but the mechanisms that govern whether the result will be a fine thin scar, a prominent hypertrophic scar, or a tumor-like keloid remain unclear. The latter represent two forms of abnormal wound healing characterized by local fibroblast proliferation and excessive collagen production in response to cutaneous injury. However, their clinical and histopathologic features differ, as well as proposed pathogeneses.

Epidemiology

Hypertrophic scars develop more often than keloids, and keloids have a higher prevalence in individuals with more darkly pigmented skin including Africans, African-Americans, Hispanics, and Asians[1]. In these populations, an incidence ranging from 4%–16% has been reported[2]. Neither hypertrophic scars nor keloids have a sex predilection, and both entities occur most frequently in those 10 to 30 years of age[3]. Individuals in this age group are more often subjected to trauma and their rate of collagen synthesis is higher. Younger skin also possesses greater tension, as compared to older skin which has less elasticity and is more redundant[2].

Etiology

Proposed etiologic factors include: genetic predisposition; depth, type, and location of the skin injury or wound; degree of tension; local infection or inflammation; and hormonal influences[2,3]. Possible autosomal dominant inheritance with incomplete clinical penetrance and variable expression has been suggested[3]. A range of skin injuries can lead to abnormal scarring, from lacerations, burns, surgical excisions, and skin piercings to injections (vaccines, tattoo inks) and cutaneous inflammation (e.g. acne vulgaris, insect bites)[4]. Moreover, tension is constantly transmitted to the skin from the underlying cartilaginous and bony skeleton, and skin tension can be aggravated by loss of tissue, as occurs with surgical excisions[5]. In addition, hormonal influences have been proposed as an explanation for the appearance of keloids at or after puberty and their resolution following menopause, as well as reports of the onset or enlargement of keloids during pregnancy[2]. Lastly, spontaneous keloids may occur in the absence of any obvious trauma or inflammation, although there is the possibility of unrecognized skin disease (e.g. acne).

Future insights into etiology may come from the genetic disorders in which keloids are an associated feature, including Bethlem myopathy, Rubinstein–Taybi, Warburg–Cinotti and Goeminne syndromes, fronto-metaphyseal dysplasia, and other filamin A-related disorders (see Table 95.5)[6,7]. Patients with polyfibromatosis (see below) can also develop keloids.

Pathogenesis

The ability to heal wounds created by injuries, in particular trauma, offers an evolutionary advantage, with associated scarring being less of an issue. However, cutaneous scarring resulting from surgical procedures is viewed as an unwanted consequence. A regenerative response would be preferred, thereby conceivably providing a superior cosmetic result and avoiding the formation of hypertrophic scars and keloids[8]. Notably, in regenerative healing, there is an absence of inflammation in addition to a lack of scarring. In fetuses, cutaneous wounding during the first and second trimesters of gestation does not lead to scarring, and this is thought to reflect a healing process that is occurring via tissue regenerative pathways in a sterile environment and in the absence of inflammation[9].

Excess scar formation is thought to result from dysregulation during at least one of the three phases of wound healing – inflammatory, proliferative, and remodeling/maturation (see Fig. 141.2)[8–12]. Proinflammatory cytokines such as interleukin-6 (IL-6) and IL-8 have been associated with increased scar formation while the anti-inflammatory cytokine IL-10 can lead to a reduction in scar tissue[8]. Several additional factors have been shown to play a role in enhancing fibroblast-related scar formation, including transforming growth factor (TGF)-β, platelet-derived growth factor (PDGF), the transcription factor homeobox B13, and components of the Wnt signaling pathway[8]. Greater insights into regulation of crucial components of the remodeling phase, e.g. cessation of granulation tissue formation, will hopefully provide targets for preventative or therapeutic interventions for hypertrophic scarring.

Because keloid formation only occurs naturally in humans, the ability to use animal models is limited[9]. In studies utilizing biopsy specimens of keloids, collagen synthesis by fibroblasts is markedly increased as is the production of TGF-β, a key regulatory factor during the proliferative phase of wound healing. However, different TGF-β isoforms may play distinct and even competing roles in wound healing. Expression of TGF-β1 or TGF-β2 may lead to an increase in scarring, whereas expression of TGF-β3 has been associated with a reduction in scarring[13]. This has led to the introduction of therapies that specifically address these different forms of TGF-β (see Table 98.4).

Clinical Features

Distinguishing clinically between a hypertrophic scar and a keloid is usually straightforward, but sometimes it can be difficult if the lesion is small or of recent onset. The characteristic features of hypertrophic scars and keloids are outlined in Table 98.1. Both have a smooth surface, are firm to palpation, and may be pruritic or painful. Occasionally, they can restrict normal movement of adjacent soft tissues. The color can

vary from pink–purple (early lesions) to skin-colored to hypo- or hyperpigmented. While keloids may be more elevated above the skin surface than hypertrophic scars, the key difference is that keloids extend beyond the boundary of the original wound into adjacent normal skin, often with claw-like extensions resembling the pincers of a crab (in Greek, chelè means claw) (Figs. 98.1 & 98.2). In contrast, hypertrophic scars remain confined to the site of the original injury (Fig. 98.3).

Hypertrophic scars usually develop within a few weeks to months after wounding, and they may flatten spontaneously within 1 to 2 years. Most keloids appear within one year of an injury, although the intervening interval may be up to two decades[5]. Of note, keloids do not regress over time. Both hypertrophic scars and keloids favor sites of increased wound tension such as the upper trunk, shoulder, and upper outer arm. However, keloids can also develop in sites such as the earlobe, where there is minimal tension. In addition, keloids can form spontaneously, most often in the midchest region but there is the possibility of unrecognized skin disease (e.g. acne).

CLINICAL FEATURES OF CONVENTIONAL SCARS, HYPERTROPHIC SCARS, AND KELOIDS

	Conventional scar	Hypertrophic scar	Keloid
Preceded by injury	Yes	Yes	Not always
Onset	Within weeks	Few weeks to months	Delayed
Erythema	Temporary	Prominent	Varies
Profile	Flat	Raised	Raised
Symptomatic	No	Yes	Yes
Confined to wound margin	Yes	Yes	No
Spontaneous resolution	N/A	Possible, gradual	Rare
Treatment response	N/A	Good	Poor

Table 98.1 Clinical features of conventional scars, hypertrophic scars, and keloids. N/A, not applicable.

Scar assessment

Scar evaluation ranges from simple scales to technologically advanced devices (e.g. optical coherence tomography) that analyze one or more variables in a reproducible manner[14]. The Vancouver Scar Scale (Table 98.2) and the Patient & Observer Scar Assessment Scale (POSAS) are the most commonly employed assessment tools[14,15]. These scales have significant inter-patient variation because they score subjective features from color to degree of pain and pruritus. More recently, the Japan Scar Workshop (JSW) published the JSW Scar Scale (JSS), a simple and easy tool for objectively diagnosing keloids and hypertrophic scars

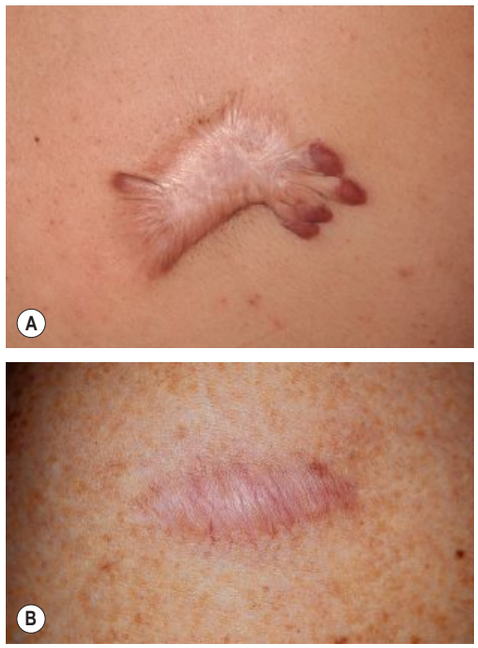


Fig. 98.2 Comparison of a keloid and a hypertrophic scar. A The keloid has claw-like extensions that extend beyond the original wound margin into adjacent normal skin. **B** The hypertrophic scar remains confined to the site of the original surgical wound. *A, Courtesy Edward Cowen, MD; B, Courtesy Jean L. Bolognia, MD.*



Fig. 98.1 Keloids. Common sites include the upper trunk (**A–C**), neck (**D**), and shoulder (**E**). There is a higher prevalence of keloids in patients with darkly pigmented skin, but they can occur in individuals with any skin phototype. Note the extension of the keloids into the normal surrounding skin in a claw-like manner. *C, Courtesy Lorenzo Cerrroni, MD; E, Courtesy Julie V. Schaffer, MD.*

based on risk factors of individual patients and sites of involvement[16]. Non-invasive techniques can also be used to more objectively measure scar color, blood flow, transcutaneous oxygen tension, skin hardness, elasticity, and hydration[17].

Pathology

Distinguishing between a keloid and a hypertrophic scar is important when contemplating treatment, especially more aggressive therapies such as radiation. In some patients, histologic examination is required to make this distinction (Table 98.3). Hypertrophic scars are characterized by an increase in the number of fibroblasts and the density of collagen fibers within the dermis, both of which are oriented parallel to the skin surface. This is accompanied by multiple vertically oriented dermal blood vessels (Fig. 98.4). In keloids, there are whorls and nodules of strikingly thick, glassy, homogeneous collagen bundles that are composed of densely packed fibrils and are oriented haphazardly throughout the dermis (keloidal collagen) (Fig. 98.5). Early on, there are abundant deposits of fibrillary collagen within the reticular dermis of keloids, while mature lesions often have the characteristic thick sclerotic collagen. In longstanding keloids, there may be a return to the earlier fibrillary pattern.

It is noteworthy that keloidal collagen may be absent in up to 45% of keloids[18]. In scars with no detectable keloidal collagen, histologic features that favor a keloid include: no flattening of the epidermis; a lack of fibrosis within the papillary dermis; a tongue-like advancing edge as the scar tissue extends through the reticular dermis; a horizontal cellular fibrous band within the upper reticular dermis with a sharp demarcation from the normal-appearing papillary and reticular dermis; and prominent fascia-like fibrous bands in the deeper portion of the scar[18].

Attempts to differentiate hypertrophic scars from keloids via immunohistochemistry has led to conflicting results[18,19]. In one study, nodules of α-smooth muscle actin (α-SMA)-positive cells (myofibroblasts) were only observed in hypertrophic scars, whereas another investigation found α-SMA expression in both hypertrophic scars (70%) and keloids (45%)[18]. Expression of cyclooxygenase (COX)-1 was observed in 100% of keloids, but it was also expressed in ~50% of hypertrophic scars[19]; thus COX-1 expression favored, but did not specifically identify, keloids. Lastly, *in vitro* differences in fibroblast phenotype, production of extracellular matrix, and CCL5 secretion have been observed[18].



Fig. 98.3 Hypertrophic scar at the site of a knife injury.

Differential Diagnosis

The clinical differential diagnosis of keloids includes the sclerotic form of xanthoma disseminatum, lobomycosis (keloidal blastomycosis; lacaziosis), and the keloidal forms of scleroderma and morphea. Rarely, carcinoma en cuirasse can present as keloidal nodules. Patients with the vascular type of Ehlers–Danlos syndrome may occasionally develop keloidal plaques on their lower extremities, and spontaneous formation of keloids can be a clinical clue to other rare inherited syndromes such as Bethlem myopathy, Rubenstein–Taybi syndrome, and Goeminne syndrome (see above).

Histologically, keloids and hypertrophic scars need to be differentiated from spindle cell tumors, primarily dermatofibroma (DF)[20], dermatofibrosarcoma protuberans (DFSP), dermal fibromatoses, desmoplastic melanoma, and the scar-like variant of squamous cell carcinoma (SCC). Immunostaining for CD34 and factor XIIIa, which is usually positive in DFSP and DF, respectively, is negative in keloids and hypertrophic scars[21]. While there is minimal or no immunostaining for S100 protein in scars, desmoplastic melanomas usually demonstrate strong expression of this marker[22]. Finally, the unusual scar-like variant of SCC may only have focal keratin expression, and a complete panel of keratin stains (to increase sensitivity) may be required for its detection[23].

Treatment

The management of keloids and hypertrophic scars continues to challenge clinicians, and there is no universally accepted treatment algorithm. Potential evidence-based treatments are outlined in Table 98.4[24-33]. Prevention remains the best strategy in predisposed patients, including avoidance of nonessential surgery in high-risk anatomic sites and attention to postsurgical wound care[24]. International guidelines recommend use of silicone gels and sheets in the treatment of both hypertrophic scars and keloids[28]. While potent topical corticosteroids

HISTOPATHOLOGIC FEATURES OF HYPERTROPHIC SCARS AND KELOIDS		
	Hypertrophic scar	**Keloid**
Epidermis	Flattened	Not involved
Papillary dermis	Fibrotic	Not involved
Fibroblasts	Increased	Not increased within keloidal collagen
Collagen bundles	Fine, wavy; orientation is parallel to the epidermis	Large, thick, closely packed; orientation is random relative to the epidermis
Elastic fibers	Diminished or absent	Increased within the deep dermis
Dermal blood vessels	Increased; oriented vertically, perpendicular to the epidermis	Not increased; few, if any, vertically oriented vessels
Inflammatory infiltrate	Sparse, perivascular	Sparse, perivascular
Mast cells	Increased	Increased
Dermal mucin	Increased	Increased
Myofibroblasts	+++	++

Table 98.3 Histopathologic features of hypertrophic scars and keloids. Shading indicates differences.

VANCOUVER SCAR SCALE						
Score for each clinical feature	**0**	**1**	**2**	**3**	**4**	**5**
Pliability	Normal	Supple	Yielding	Firm, solid unit	Banding/"ropes"	Contracture
Height	Flat	<2 mm	2–5 mm	>5 mm	–	–
Vascularity	Normal	Pink	Red	Purple	–	–
Pigmentation	Normal	Hypopigmentation	Hyperpigmentation	–	–	–

Table 98.2 Vancouver Scar Scale. *Adapted from Sullivan T, Smith J, Kermode J, et al. Rating the burn scar. J Burn Care Rehabil 1990;11:256–60.*

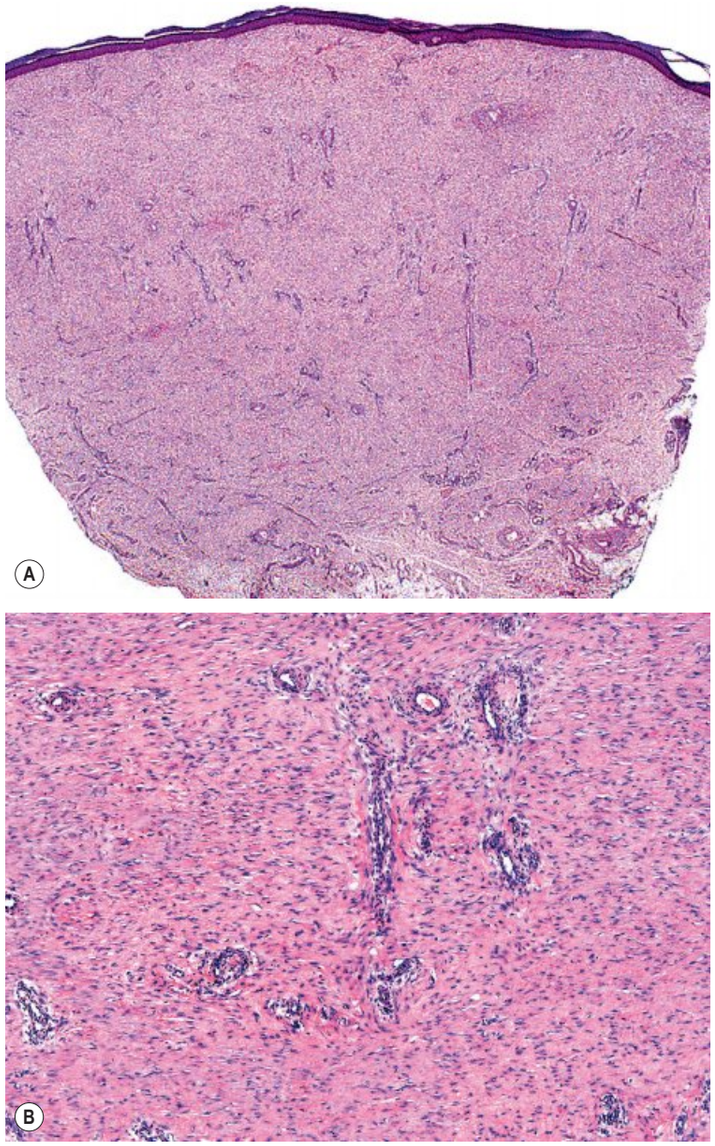


Fig. 98.4 Hypertrophic scar – histopathologic features. A Increased density of collagen fibers within the dermis and vertically oriented blood vessels. **B** Increase in the number of fibroblasts and density of collagen fibers, both of which are oriented horizontally (parallel to the epidermis). The central blood vessel is oriented vertically and there is a sparse perivascular inflammatory infiltrate.

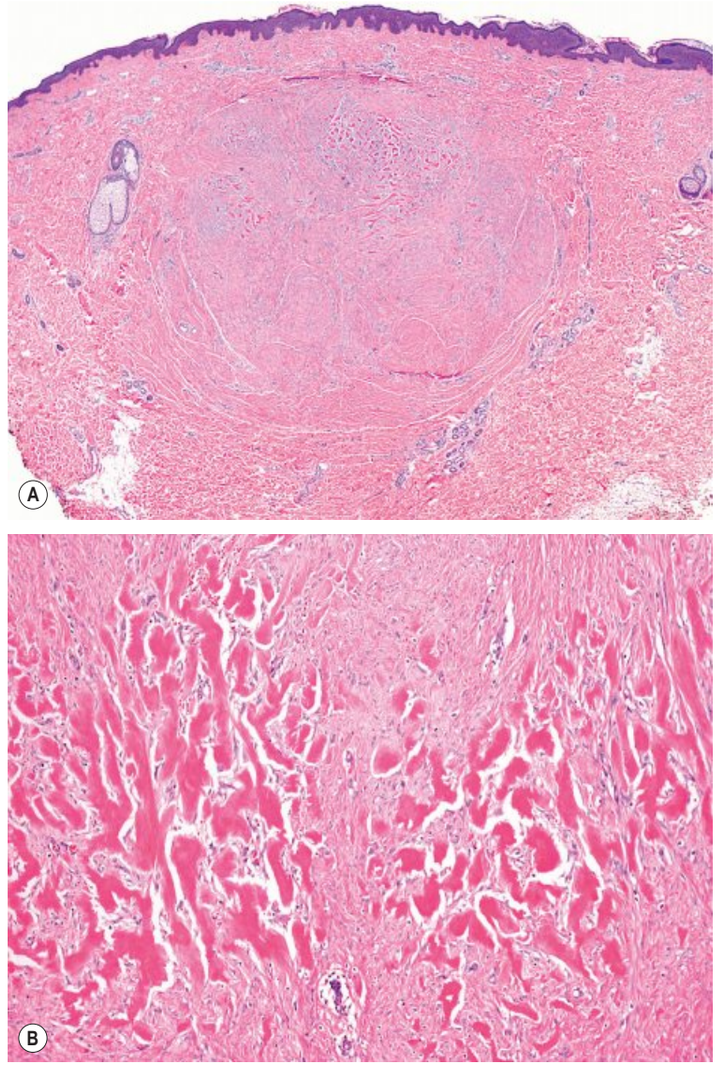


Fig. 98.5 Keloid – histopathologic features. A Nodules of thick collagen bundles are oriented haphazardly within the dermis (keloidal collagen). There is neither flattening of the epidermis nor involvement of the papillary dermis, and a sharp demarcation is seen between the normal-appearing papillary and reticular dermis and the nodules. **B** Strikingly thick, glassy, homogeneous collagen bundles composed of multiple, densely packed fibrils.

are sometimes used to address pruritus, intralesional triamcinolone remains a commonly employed first-line therapy[34]. Incremental increases in triamcinolone concentration may be used to balance flattening effects against the risk of atrophy[29]. An alternative, especially for needle-averse individuals, is clobetasol propionate 0.05% cream under silicone dressing occlusion[30].

Intralesional or topical corticosteroids may be combined with intralesional 5-fluorouracil[31]. For hypertrophic scars and keloids in patients with darker skin color who are at risk for steroid-induced hypopigmentation, intralesional bleomycin and intralesional triamcinolone have been shown to lead to comparable improvement[32]. By reducing muscle tension during wound healing, intralesional botulinum toxin type A can minimize scar formation and reduce associated symptoms[33]; possible explanations include pausing of the fibroblast cell cycle and changes in TGF-β1 expression. Based upon case reports, dupilumab can reduce associated pruritus and may lead to an improvement in appearance[34a].

Surgical revision of hypertrophic scars and keloids can quickly relieve symptoms, but the recurrence rate is quite high. Cryosurgery has been used successfully[24] and is often combined with intralesional triamcinolone. Shave excision followed by contact cryosurgery has also been employed. Pulsed dye laser therapy has become popular as a modality for postsurgical scar reduction and is associated with few side effects. The use of lower cumulative doses has improved the safety of adjuvant postoperative radiation therapy while still maintaining efficacy[25,26] (see Table 98.4 & Ch. 139).

DUPUYTREN DISEASE

Synonyms: ■ Dupuytren's contracture ■ Palmar fibromatosis ■ Dupuytren's diathesis

Key features

- Thickening of palmar and digital fascia
- Progressive flexion contracture of affected digits
- Myofibroblast proliferation followed by excess collagen synthesis
- Treatment includes injections of collagenase, percutaneous needle fasciotomy, and surgical fasciotomy/fasciectomy

History

Henry Cline described thickening of the palmar fascia in 1777 and proposed palmar fasciotomy as a cure. In 1831, Guillaume Dupuytren characterized and popularized this entity.

TREATMENT OPTIONS FOR HYPERTROPHIC SCARS AND KELOIDS		
Treatment	**Mechanism(s) of action**	**Level of evidence**
Silicone sheeting	Reduction in collagen deposition due to an increase in temperature, hydration (reduces water vapor loss), and perhaps oxygen tension	2
Pressure therapy	Pressure-induced hypoxic effects lead to collagen and fibroblast degeneration	2
Onion extract (topical)	Decrease in inflammation and fibroblast proliferation rate	1
Vitamin E (topical)	Antioxidant properties	2
Triamcinolone (intralesional; 10–40 mg/ml)*	Inhibits fibroblast proliferation and collagen synthesis; vasoconstriction; decreases in TGF-β1 and TGF-β2	1
5-Fluorouracil (intralesional; 50 mg/ml not to exceed 100 mg/session; administered weekly)	Inhibits fibroblast proliferation	2
Bleomycin (1.5 IU/ml – multiple puncture technique; maximum 2 ml/cm^2 and 10 IU per session; once monthly)	Direct or indirect, TGF-β-mediated, inhibitory effects on collagen	2
Botulinum toxin (intralesional)	Reduces muscle tension during wound healing, leading to reduction in symptoms, volume and vascularity, presumably due to pausing of the fibroblast cell cycle and changes in TGF-β1 expression	1
Surgical scar revision	Reorientation and construction of multiple tension vectors	2
Cryosurgery (contact and needles more effective than spray; monthly × 3–10 months)*	Direct cellular freezing effects; post-thaw vascular stasis	2
Radiation therapy (postoperative [usually within 72 hours]; 8–10 Gy in a single dose; 6–15 Gy in 3–5 fractions)	Induction of fibroblast apoptosis; restoration of balance between synthesis and degradation of collagen within scar; damage to connective tissue stem cells	2
Laser therapy (pulsed dye laser [PDL] – can begin day of suture removal then every 3–4 weeks; CO_2 fractional laser*; Nd:YAG [1064 nm])	Induces wound contraction and collagen remodeling following thermal necrosis; decreased levels of TGF-β from heat shock response	1 (PDL)
Avotermin (intralesional)†	Recombinant TGF-β3 (form of TGF associated with a reduction in scarring)	1 (phase II trial; no difference in phase III trial)
Human recombinant interleukin-10 (intralesional)†	Anti-inflammatory activity	1‡,¶
Mannose-6-phosphate (intralesional)†	Inhibition of TGF-β1 and TGF-β2 signaling (two forms of TGF associated with an increase in scarring)	1‡
Insulin (intralesional)	Inhibitor of myofibroblasts	1

*Cryotherapy or CO_2 laser sometimes administered prior to intralesional injections of corticosteroids.
†Not commercially available.
‡Based upon phase II trial.
¶In lightly, but not darkly, pigmented individuals.

Table 98.4 Treatment options for hypertrophic scars and keloids. There are also reports of the use of topical retinoic acid, calcineurin inhibitors, imiquimod (deemed ineffective in controlled trials), and tamoxifen; mitomycin C (topical or intralesional); and systemic methotrexate, dupilumab, and calcium channel blockers[75]. Treatments reserved for the treatment of keloids are shaded mid-blue and experimental treatments are shaded dark blue. Key to evidence-based support: (1) prospective controlled trial; (2) retrospective study or large case series; (3) small case series or individual case reports. TGF, transforming growth factor. *Adapted from Tziotzios C, et al. J Am Acad Dermatol 2012;66:13–24.*

Epidemiology

Dupuytren disease is common in White people of northern European ancestry, with a prevalence in Western countries that ranges from 1%–30%; it is rarer in patients with darker skin phototypes. The incidence of Dupuytren disease increases with age and it is most common in middle-aged and older men. Familial associations suggest an autosomal dominant inheritance, but sporadic cases are common. The lesion is associated with other fibromatoses (e.g. plantar fibromatosis, polyfibromatosis; see Ch. 116) as well as diabetes mellitus, liver disease including alcoholic cirrhosis[35], and perhaps epilepsy[35], manual labor[36,37], and cigarette smoking.

Vemurafenib has been linked to new-onset or worsening of Dupuytren disease and plantar fascial fibromatosis. To date, there has been one report of the association of topical timolol with the development of Dupuytren disease and penile fibromatosis[38].

Pathogenesis

Fibrogenic cytokines (e.g. TGF-β1, TGF-β2) are thought to play a role due to their ability to induce collagen production, proliferation of fibroblasts, and the differentiation of fibroblasts into myofibroblasts. Production of tumor necrosis factor (TNF) by M2 macrophages and mast cells in early-stage Dupuytren disease is also thought to activate myofibroblasts, leading to and/or sustaining fibrosis[39]. In genome-wide assays of fibroblasts from Dupuytren disease, the differential expression patterns included genes that encode proteins involved in the extracellular matrix (e.g. collagen), fibrosis (e.g. follistatin), tissue remodeling (e.g. collagenases, matrix metalloproteinases), cellular movement (e.g. kinesins), and signaling pathways (e.g. STAT1, Wnt2), as well as growth factors (e.g. fibroblast growth factor 9)[40]. Activation of the Wnt signaling pathway appears to play a key role as it does in scar formation (see above)[41].

Clinical Features

Patients often present late in the course of their disease with flexion contractures of the affected digits. Lesions usually have an ulnar distribution, and the ring finger is most commonly affected (Fig. 98.6). The disorder begins with a nodule in the fascia of the palm, which grows to produce a cord which then contracts, producing a flexion contracture of the metacarpophalangeal and proximal interphalangeal joints. Complications of Dupuytren disease include nerve injury, loss of joint mobility, and development of complex regional pain syndrome (also referred to as reflex sympathetic dystrophy)[42].



Fig. 98.6 Dupuytren disease. Fibrotic nodule at the base of the fourth finger with an obvious cord extending proximally. In addition to palpation, fibrotic cords can be accentuated by extension of the digit. Eventually, flexion contractures develop.



Fig. 98.7 Cutis verticis gyrata. Cerebriform folding of the skin of the scalp.

Pathology

Histologically, the nodular lesion consists of a proliferation of myofibroblasts, which align along lines of tension. The initial stages are more cellular and there are some mitotic figures; the cells may express α-SMA, indicative of myofibroblastic differentiation. Thicker collagen, fewer myofibroblasts, and scarce to absent mitotic figures characterize later stages[43].

Differential Diagnosis

Although usually the diagnosis is straightforward, one must consider a ganglion cyst, giant cell tumor of the tendon sheath, soft tissue sarcoma (e.g. epithelioid sarcoma), callus, and tenosynovitis. An ultrasonographic hypoechoic mass superficial to a flexor tendon of the third, fourth, or fifth digits at the level of the distal metacarpal, where the length of the lesion is greater than its width, is typical for palmar fibromatosis and helps to exclude other diagnoses[44].

A rare case of lung cancer metastasis simulating Dupuytren disease has been reported[45], and in injection drug users, flexion digital contractures (camptodactyly) due to repeated vascular injury and infection of the digits may mimic Dupuytren disease. Flexion contractures of the hand, along with multiple tender nodules, can develop in the rare paraneoplastic palmar fasciitis and polyarthritis syndrome.

Treatment

Although surgical fasciotomy/fasciectomy to release the joint contracture is the mainstay of treatment, minimally invasive procedures such as percutaneous needle fasciotomy and enzymatic fasciotomy with injectable collagenase (from *Clostridium histolyticum*) are increasingly utilized despite higher recurrence rates[46–51]. Patients receive up to three monthly injections of collagenase per cord, followed by passive finger extension 1–3 days later. Complications include bruising, tendon rupture, ligament or nerve injury, and anaphylaxis. Although some authors have advocated the use of radiotherapy during the early stage of Dupuytren disease, a systematic review found limited evidence to support this approach[52].

A risk score determined by whole genome sequencing may predict postsurgical recurrence[53], while ultrasound findings (e.g. mixed echogenicity, nodular structure) may predict recurrence after minimally invasive treatments[54]. Additional possible treatments include intralesional triamcinolone[55], blue light irradiation (to prevent relapse)[56], correction of vitamin D deficiency[57], and use of inhibitors of TGF-β1[58,59], TGF-β2, TNF[60] and one of its receptors TNFR2, or IL-33[39]. New enzymatic approaches are also in development[61].

CUTIS VERTICIS GYRATA

Key features

- Hypertrophy and folding of the scalp
- Primary (idiopathic) form occurs almost exclusively in males, with an onset at puberty and without facial involvement
- Underlying disorders in the secondary form include endocrinopathies (e.g. acromegaly, myxedema) and genetic disorders (e.g. Turner syndrome)

Clinical Features

Primary cutis verticis gyrata (CVG) consists of overgrowth of the scalp that progresses to produce symmetric gyrate or cerebriform folding of the skin (Fig. 98.7). The folds are usually aligned in an anterior–posterior direction on the crown and vertex and are soft to spongy on palpation. Typically, terminal hair density is reduced on the folds, but not in the furrows. Primary CVG can be subdivided into: (1) isolated CVG; and (2) CVG associated with neurologic and/or ophthalmologic abnormalities. Both subtypes have a male predominance and usually develop around puberty. Secondary CVG is less common and its onset varies from birth to adulthood. In secondary CVG, there is a more equal sex distribution and it may be asymmetric, depending on the underlying etiology (Table 98.5).

Pathology

Biopsy specimens typically show normal skin or diffuse dermal thickening with packed hyalinized collagen and an increased number of fibroblasts. Prominent adnexal structures may be present.

Differential Diagnosis

A cerebriform congenital melanocytic nevus of the scalp may simulate CVG. One must also differentiate the latter from pachydermoperiostosis (primary hypertrophic osteoarthropathy), which is associated with facial involvement, thickening of the skin on the hands and feet, and clubbing of the digits. Patients with pachydermoperiostosis have underlying homozygous or compound heterozygous mutations in *SLCO2A1* or *HPGD*, which encode a prostaglandin transporter and 15-hydroxyprostaglandin dehydrogenase, respectively. Pachydermia is observed in both groups, but exaggerated CVG-like skin changes are associated with mutations in *SLCO2A1* (Fig. 98.8)[62].

Furrowed skin on the scalp, forehead, preauricular areas, neck, trunk, palms, and soles in association with acanthosis nigricans, craniosynostosis, and a prominent umbilical stump characterizes Beare–Stevenson

CUTIS VERTICIS GYRATA – DISEASE ASSOCIATIONS
Primary isolated
• None
Primary with associated anomalies
• Neurologic (e.g. intellectual disability, seizures) • Ophthalmologic (e.g. cataracts, optic atrophy)
Secondary
• Acromegaly, pseudoacromegaly • Myxedema (including cretinism)* • Insulin resistance† and HIV-related lipodystrophy with insulin resistance[76] • Graves disease* • Turner and Noonan syndromes (following resolution of intrauterine lymphedema)* • Fragile X syndrome • Klinefelter syndrome • Hereditary neuralgic amyotrophy • Tuberous sclerosis complex • Hyper-IgE syndrome, autosomal dominant • Rosenthal–Kloepfer syndrome (acromegaloid changes, corneal leukoma) • Vemurafenib (selective BRAF inhibitor) + radiotherapy‡[77] • Paraneoplastic due to metastatic carcinoma
*Increased dermal mucin may also be observed. †May also have acanthosis nigricans. ‡Due to multiple follicular cysts and milia.

Table 98.5 Cutis verticis gyrata – disease associations.

CLINICAL FEATURES OF HYALINE FIBROMATOSIS SYNDROME	
Good prognosis (classic juvenile hyaline fibromatosis)	**Poor prognosis (classic infantile systemic hyalinosis)**
Onset during childhood (<5 years old) and survival into adulthood	Onset during infancy
Firm, pearly papules (favoring the perinasal area and ears)	
Verrucous perianal nodules	
Firm nodules/tumors favoring the scalp, neck, hands, and trunk	Reddish-blue to brown plaques overlying extensor surfaces of joints
	Diffusely thickened skin
Gingival hypertrophy	
Joint contractures	
Osteopenia and osteolytic lesions due to hyaline deposits	
No visceral involvement	Persistent diarrhea
	Recurrent infections
	Visceral involvement
Normal mental development	

Table 98.6 Clinical features of hyaline fibromatosis syndrome.

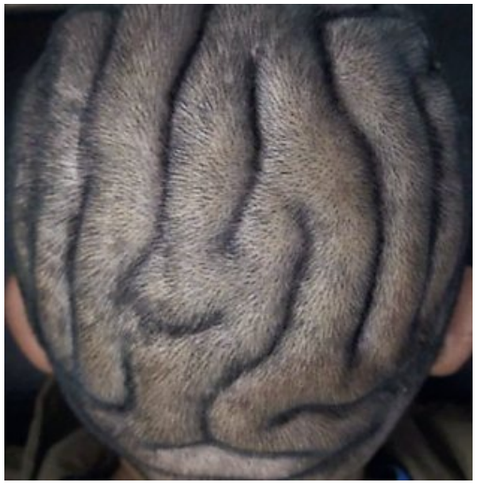


Fig. 98.8 Pachydermoperiostosis (primary hypertrophic osteoarthropathy). There is exaggerated cutis verticis gyrata-like folding of the scalp skin. *Courtesy Dr D. Timaná and Dr J. Valverde, Hospital Docente de Trujillo.*

cutis gyrata syndrome, an autosomal dominant condition caused by mutations in *FGFR2*. Patients with Goeminne syndrome may also have CVG-like folding of the scalp in conjunction with congenital torticollis, multiple keloids, cryptorchidism, and renal dysplasia (TKCR syndrome).

Other potential simulators of CVG include dissecting cellulitis of the scalp, benign hamartomas or tumors (e.g. plexiform neurofibroma, cutaneous neurocristic hamartoma[63], connective tissue nevus, nevus lipomatosus, aggregated cylindromas), primary systemic amyloidosis, leukemia cutis, and malignancies such as folliculotropic mycosis fungoides and angiosarcoma[64]. Based upon patient history, trauma has preceded the development of CVG and there are isolated reports of CVG-like presentations of pemphigus vegetans, Darier disease, scleromyxedema[65], and chronic actinic dermatitis[66] but clinical differentiation is more straightforward.

Treatment

CVG is generally asymptomatic and requires no treatment. Occasionally, surgical excision is performed. Improvement has been reported following injection of hyaluronidase[67].

HYALINE FIBROMATOSIS SYNDROME (JUVENILE HYALINE FIBROMATOSIS AND INFANTILE SYSTEMIC HYALINOSIS)

Synonyms: ■ Murray–Puretic–Drescher syndrome ■ Fibromatosis hyalinica multiplex juvenilis ■ (Juvenile) systemic hyalinosis

Key features

- Rare autosomal recessive disorder with variable phenotypic expression
- Usually presents during infancy or early childhood
- Papulonodules that favor the ears, scalp, neck, hands, and periorificial areas plus gingival hypertrophy and flexion contractures of large joints
- Mutations in the gene that encodes anthrax toxin receptor 2 (*ANTXR2*)
- Treatment consists of excision of nodules and gingivae as needed, but lesions often recur

Introduction

Hyaline fibromatosis syndrome (HFS) is a rare autosomal recessive genodermatosis characterized by hyaline accumulation within the dermis. HFS encompasses both juvenile hyaline fibromatosis (JHF) and infantile systemic hyalinosis (ISH). These two disorders are allelic, i.e. they are due to mutations in the same gene, but differ in severity and visceral involvement[68] (Table 98.6).

History

In 1873, Murray described a condition which he termed "molluscum fibrosum". In 1972, Kitano and colleagues renamed the disorder "juvenile hyaline fibromatosis".

Epidemiology

HFS is a rare disorder that presents during infancy or early childhood.



Fig. 98.9 Juvenile hyaline fibromatosis. Firm pearly papules favor the ears.

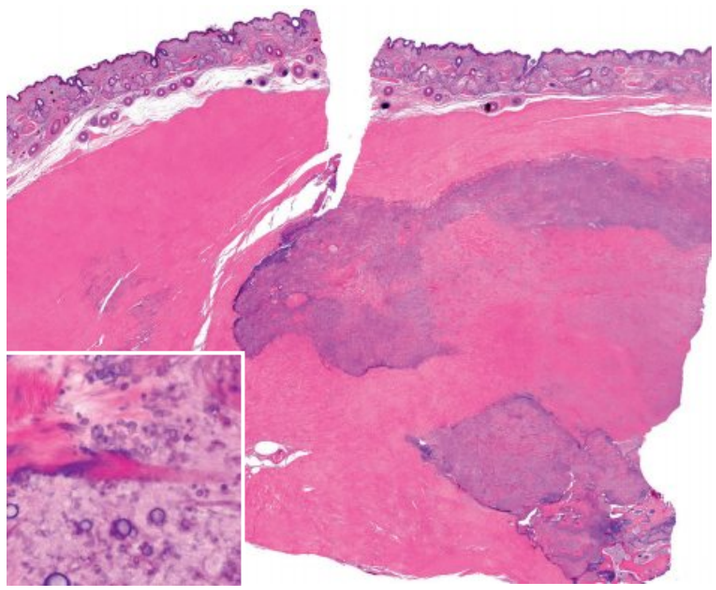


Fig. 98.10 Juvenile hyaline fibromatosis – histopathologic features. Abundant, dense, homogeneous, hyaline (PAS-positive) collagen within the lower dermis and subcutis. Round basophilic calcospherites are also present (inset).

Pathogenesis

Mutations are present in the gene that encodes anthrax toxin receptor 2 (ANTXR2), also referred to as capillary morphogenesis protein-2 (CMG2). ANTXR2 is a transmembrane protein that binds to laminins and types IV and VI collagen (as well as the anthrax toxin). In the skin it is thought to play a role in cell–matrix interactions and basement membrane integrity. Because ANTXR2/CMG2 is thought to target collagen VI for degradation, its dysfunction leads to an accumulation of collagen VI and a subsequent sequestration of inactive matrix metalloproteinases by excess collagen VI, thus leading to fibrosis[69]. As noted previously, mutations in *ANTXR2* can lead to either mild or severe forms of HFS[70]. Missense and other in-frame mutations of the cytoplasmic domain tend to cause a phenotype with a better prognosis (JHF), whereas truncating and missense mutations of the extracellular protein-binding domain lead to a more severe phenotype (ISH). Because ANTXR2 is not expressed in the brain, mental development is not impaired.

Clinical Features

Initially, firm papules and nodules develop on the scalp, ears, neck, and face (particularly perinasal and perioral regions) as well as the perianal area (Fig. 98.9); papulonodules also favor the hands. Patients often suffer severe physical limitations from joint contractures and tumors. Additional clinical features are outlined in Table 98.6. Milder phenotype and later onset has been observed in females[71].

Pathology

Ill-defined nodules composed of dense, homogeneous, hyaline (PAS-positive) collagen are seen within the dermis and, in larger lesions, the subcutaneous tissue (Fig. 98.10). Mononuclear cells and $CD68^+$, osteoclast-like giant cells may be present in a perivascular location in addition to perivascular calcification and eosinophilic globules. Over time, the lesions tend to become more paucicellular, and calcospherites or larger areas of calcification are frequently seen (Fig. 98.10, inset).

Differential Diagnosis

HFS needs to be distinguished from the autosomal recessive disorders MONA (multicentric osteolysis, nodulosis, and arthropathy) and Winchester syndrome which are due to mutations in genes that encode matrix metalloproteinases. Both can have joint contractures, coarse facies, thickened skin and gingival hypertrophy, with painful nodules, especially of the soles, in the former. Histologically, both disorders feature a proliferation of fibroblasts and thickened collagen bundles

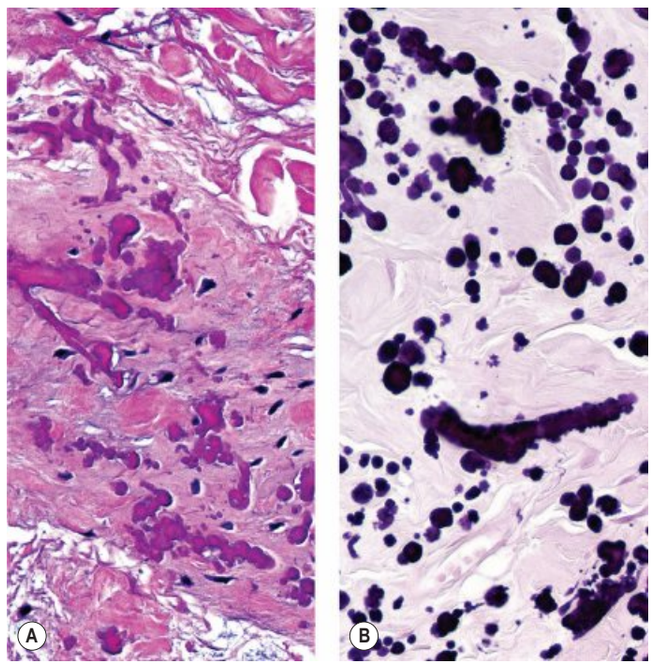


Fig. 98.11 Elastofibroma dorsi – histopathologic features. A Irregular, partially fragmented elastic fibers admixed with swollen collagen bundles. **B** An elastic tissue stain accentuates the fragmented fibers.

extending from the deep dermis to the hypodermis. Other genodermatoses to consider include Farber lipogranulomatosis, lipoid proteinosis, infantile myofibromatosis, terminal osseous dysplasia, and the rarer diffuse variant of stiff skin syndrome that is due to fibrillin-1 mutations and inherited in an autosomal dominant pattern.

Treatment

Treatment options are limited. Surgical excision of nodules and gingival hypertrophy and release of contractures can be performed, but lesions often recur. Diode laser therapy improved skin and mucosal lesions in one patient, but these recurred[72]. Physiotherapy may slow the progression of joint contractures. Injections of corticosteroids into fibromas have met with limited success. Subcutaneous interferon-α-2b therapy improved the skin lesions, gingival hypertrophy, and joint mobility in a patient

DISORDERS CHARACTERIZED BY INCREASED ELASTIC TISSUE FIBERS			
Disorder	**Clinical features**	**Histopathologic features**	**Comments**
Idiopathic or inherited			
Late-onset focal dermal elastosis (focal dermal elastosis)[78]	Multiple 1–3 mm yellow papules that may coalesce Favors the neck and other flexural areas	Increased normal-appearing elastic fibers in the mid and deep reticular dermis	Lacks the systemic features of PXE (see Ch. 97)
Linear focal elastosis (elastotic striae)	Multiple yellow, palpable, striae-like bands Favors the lumbosacral region	Focal increase in number of elongated or fragmented elastic fibers (thickened > thinned) within the mid dermis; the ends of the elastic fibers may be split with a "paintbrush" appearance Early lesions may have inflammation and elastolysis	May represent an excessive regenerative process of elastic fibers, perhaps to repair striae distensae (see Ch. 99)
Elastoderma	Localized areas of lax, pendulous skin with reduced elasticity; neck, trunk, arm	Increased normal- and abnormal-appearing elastic fibers throughout the dermis and subcutis	Lacks the systemic features of PXE (see Ch. 97) Overlaps with cutaneous aging, but earlier onset
Elastofibroma dorsi	Large mass in the deep subcutaneous tissue of the infrascapular area Rarely develops at thoracotomy sites, perhaps related to widened intercostal spaces	Arises within the fascia Increased elastic fibers with a globular and beaded morphology admixed with plump collagen bundles, fibroblasts, and mature fat cells (Fig. 98.11)	Favors older women > men and Japanese Possibly related to chronic mechanical stress Upregulation of TGF-β1 and basic fibroblast growth factor
Elastoma (nevus elasticus)	Firm, skin-colored to yellowish papule(s) which may be clustered Favors the trunk	Accumulation of thick, tortuous, branching elastic fibers within the reticular dermis	Type of connective tissue nevus (see Ch. 116) Associated with Buschke–Ollendorf syndrome (dermatofibrosis lenticularis disseminata)
Elastosis perforans serpiginosa	Annular and polycyclic plaques composed of keratotic papules Favors the neck, face, antecubital fossae, and other flexural areas	Transepidermal or perifollicular channels that contain fragments of elastotic material Increased number of coarse elastic fibers in the superficial dermis No secondary calcium deposition on elastic fibers	Associated with penicillamine (lumpy-bumpy fibers*), Down syndrome and connective tissue disorders (e.g. Ehlers–Danlos syndrome, Marfan syndrome; see Ch. 96)
Pseudoxanthoma elasticum (PXE)	Yellowish skin papules and "cobble-stoned" plaques; redundant folds Favors flexural sites, especially the neck and axillae, and periumbilical region	Distorted and fragmented elastic fibers (elastorrhexis) in mid and deep reticular dermis Calcium deposition on altered elastic fibers	Angioid streaks (Bruch membrane of eye), GI hemorrhage, atherosclerotic cardiovascular disease (see Ch. 97)
Related to cumulative actinic damage (see Fig. 87.24)			
Actinic or solar elastosis (including cutis rhomboidalis nuchae, solar elastotic bands, elastotic nodules of the ear)	Yellow to yellow–white, thickened, coarsely wrinkled skin that favors the lateral forehead, malar region, posterolateral neck, mid extensor arms Bands – forearms Nodules – antihelix > helix	Bluish-grey elastotic material composed of degenerated elastic fibers within the upper and mid dermis In more advanced phases, the elastotic material may aggregate into dense amorphous masses ("actinic elastoma")	Photodamage may be accelerated by medications, e.g. voriconazole (see Ch. 87)
Favré-Racouchot syndrome (nodular elastosis with cysts and comedones)	Bilateral, clustered, open > closed comedones within thickened skin Favors malar prominence and lateral periorbital region	Severe solar elastosis with follicular distention and cystic structures filled with compact keratin	See Ch. 87
Acrokeratoelastoidosis	Bands of waxy or translucent papules and plaques Favors ulnar side of thumb and radial side of forefinger	Shallow depression of the epidermis Usually a decrease in thin and partially fragmented elastic fibers in the mid and deep reticular dermis In some cases, elastic fibers are increased, coarse, and aggregated	May be exacerbated by trauma Also an inherited form that can involve non-sun-exposed sites of the hands and/or feet (see Ch. 58)
Elastoma of Dubreuilh	Yellow to yellow–brown papules or plaques Favor forehead, cheeks, lateral neck	Amorphous masses composed of aggregated elastotic material in the upper dermis	See Ch. 87

*By electron microscopy.

Table 98.7 Disorders characterized by increased elastic tissue fibers. Special stains for elastic fibers include Verhoeff–van Gieson and orcein (acid orcein–Giemsa; see Ch. 0). GI, gastrointestinal.

with JHF. Based on *in vitro* results, proteasome inhibitors may represent a future therapy for HFS patients with ectodomain-related mutations in *ANTXR2*[73].

ELASTIC TISSUE-RELATED DISORDERS

In general, mechanisms which lead to increased dermal elastic tissue are unknown, and the nosology of the elastic tissue-related disorders can be confusing[74]. There are several acquired disorders whose clinical appearance can overlap. Their clinical and histopathologic features are outlined in Table 98.7.

Additional figures and tables on Differences in adult versus fetal wound healing, Treatment options for Dupytren disease, and Differential diagnosis of hyaline fibromatosis syndrome, available in our eBook (see inside front cover for access code).

REFERENCES

1. Sorg H, Tilkorn DJ, Hager S, et al. Skin wound healing: an update on the current knowledge and concepts. *Eur Surg Res*. 2017;58:81–94.
2. English RS, Shenefelt PD. Keloid and hypertrophic scars. *Dermatol Surg*. 1999;25:631–638.
3. Niessen FB, Spauwen PH, Schalkwijk J, Kon M. On the nature of hypertrophic scars and keloids: a review. *Plast Reconstr Surg*. 1999;104:1435–1458.
4. Alster TS, Tanzi EL. Hypertrophic scars and keloids: etiology and management. *Am J Clin Dermatol*. 2003;4:235–243.
5. Nemeth AJ. Keloids and hypertrophic scars. *J Dermatol Surg Oncol*. 1993;19:738–746.
6. Jfri A, Alajmi A. Spontaneous keloids: a literature review. *Dermatology*. 2018;234:127–130.
7. Profyris C, Tziotzios C, Do Vale I. Cutaneous scarring: pathophysiology, molecular mechanisms, and scar reduction therapeutics Part I. The molecular basis of scar formation. *J Am Acad Dermatol*. 2012;66:1–10.
8. Berman B, Maderal A, Raphael B. Keloids and hypertrophic scars: pathophysiology, classification, and treatment. *Dermatol Surg*. 2017;43(Suppl 1):S3–S18.
9. Cole J, Tsou R, Wallace K, et al. Early gene expression profile of human skin to injury using high-density cDNA microarrays. *Wound Repair Regen*. 2001;9:360–370.
10. Schafer M, Werner S. Transcriptional control of wound repair. *Annu Rev Cell Dev Biol*. 2007;23:69–92.
11. Werner S, Grose R. Regulation of wound healing by growth factors and cytokines. *Physiol Rev*. 2003;83:835–870.
12. Shah M, Foreman DM, Ferguson MW. Neutralisation of TGF-beta 1 and TGF-beta 2 or exogenous addition of TGF-beta 3 to cutaneous rat wounds reduces scarring. *J Cell Sci*. 1995;108:985–1002.
13. Brusselaers N, Pirayesh A, Hoeksema H, et al. Burn scar assessment: a systematic review of different scar scales. *J Surg Res*. 2010;164:e115–e123.
14. Van de Kar A, Corion L, Smeulders M, et al. Reliable and feasible evaluation of linear scars by the patient and observer scar assessment scale. *Plast Reconstr Surg*. 2005;116:514–522.
15. Ogawa R, Akita S, Akaishi S, et al. Diagnosis and treatment of keloids and hypertrophic scars: Japan Scar Workshop consensus document 2018. *Burns Trauma*. 2019;7:39.
16. Nguyen DQ, Potokar T, Price P. A review of current objective and subjective scar assessment tools. *J Wound Care*. 2008;17:101–102. 104–6.
17. Lee JY, Yang CC, Chao SC, Wong TW. Histopathological differential diagnosis of keloid and hypertrophic scar. *Am J Dermatopathol*. 2004;26:379–384.
18. Abdou AG, Maraee AH, Saif HF. Immunohistochemical evaluation of COX-1 and COX-2 expression in keloid and hypertrophic scar. *Am J Dermatopathol*. 2014;36:311–317.
19. Limandjaja GC, Niessen FB, Scheper R, et al. Hypertrophic scars and keloids: overview of the evidence and practical guide for differentiating between these abnormal scars. *Exp Dermatol*. 2021;30:146–161.
20. Kuo T, Hu S, Chan H. Keloidal dermatofibroma: report of 10 cases of a new variant. *Am J Surg Pathol*. 1998;22:564–568.
21. Kaneishi NK, Cockerell CL. Histologic differentiation of desmoplastic melanoma from cicatrices. *Am J Dermatopathol*. 1998;20:128–134.
22. Velázquez EF, Werchniack AE, Granter SR. Desmoplastic/spindle cell squamous cell carcinoma of the skin. A diagnostically challenging tumor mimicking a scar: clinicopathologic and immunohistochemical study of 6 cases. *Am J Dermatopathol*. 2010;32:333–339.
23. Tziotzios C, Profyris C, Sterling J. Cutaneous scarring: pathophysiology, molecular mechanisms, and scar reduction therapeutics Part II. Strategies to reduce scar formation after dermatologic procedures. *J Am Acad Dermatol*. 2012;66:13–24.
24. Ogawa R, Tosa M, Dohi T, et al. Surgical excision and postoperative radiotherapy for keloids. *Scars Burn Heal*. 2019;5:2059513119891113.
25. Son Y, Phillips EON, Price KM, et al. Treatment of keloids with a single dose of low-energy superficial X-ray radiation to prevent recurrence after surgical excision: an *in vitro* and *in vivo* study. *J Am Acad Dermatol*. 2020;83:1304–1314.
26. Bao Y, Xu S, Pan Z, et al. Comparative efficacy and safety of common therapies in keloids and hypertrophic scars: a systematic review and meta-analysis. *Aesth Plast Surg*. 2020;44:207–218.
27. de Oliveira GV, Gold MH. Silicone sheets and new gels to treat hypertrophic scars and keloids: a short review. *Dermatol Ther*. 2020;33:e13705.
28. Luther CA, Griffith JL, Kurland E, et al. The infection rate of intralesional triamcinolone and the safety of compounding in dermatology for intradermal and subcutaneous injection: a retrospective medical record review. *J Am Acad Dermatol*. 2020;83:1044–1048.
29. Nor NM, Ismail R, Jamil A, et al. A randomized, single-blind trial of clobetasol propionate 0.05% cream under silicone dressing occlusion versus intra-lesional triamcinolone for treatment of keloid. *Clin Drug Investig*. 2017;37:295–301.
30. Shah VV, Aldahan AS, Mlacker S, et al. 5-Fluorouracil in the treatment of keloids and hypertrophic scars: a comprehensive review of the literature. *Dermatol Ther (Heidelb)*. 2016;6:169–183.
31. Bik L, Sangers T, Greveling K, et al. Efficacy and tolerability of intralesional bleomycin in dermatology: a systematic review. *J Am Acad Dermatol*. 2020;83:888–903.
32. Sohrabi C, Goutos I. The use of botulinum toxin in keloid scar management: a literature review. *Scars Burn Heal*. 2020;6:2059513120926628.
33. Broekstra DC, Groen H, Molenkamp S, et al. A systematic review and meta-analysis on the strength and consistency of the associations between Dupuytren disease and diabetes mellitus, liver disease, and epilepsy. *Plast Reconstr Surg*. 2018;141:367e–379e.
34. Wong TS, Li JZ, Chen S, et al. The efficacy of triamcinolone acetonide in keloid treatment: a systematic review and meta-analysis. *Front Med (Lausanne)*. 2016;3:71.

34a. Peterson DM, Damsky WE, Vesely MD. Treatment of lichen sclerosus and hypertrophic scars with dupilumab. *JAAD Case Rep*. 2022;23:76–78.

35. Mathieu S, Naughton G, Descatha A, et al. Dupuytren's disease and exposure to vibration: systematic review and meta-analysis. *Joint Bone Spine*. 2020;87:203–207.
36. Fadel M, Leclerc A, Evanoff B, et al. Association between occupational exposure and Dupuytren's contracture using a job-exposure matrix and self-reported exposure in the CONSTANCES cohort. *Occup Environ Med*. 2019;76:845–848.
37. Oliphant H, Gouws P. Peyronie's disease and Dupuytren's contracture secondary to topical timolol. *Int Ophthalmol*. 2019;39:683–685.
38. Izadi D, Layton TB, Williams L, et al. Identification of TNFR2 and IL-33 as therapeutic targets in localized fibrosis. *Sci Adv*. 2019;5:eaay0370.
39. Forrester HB, Temple-Smith P, Ham S, et al. Genome-wide analysis using exon arrays demonstrates an important role for expression of extra-cellular matrix, fibrotic control and tissue remodelling genes in Dupuytren's disease. *PLoS ONE*. 2013;8:e59056.
40. Ng M, Thakkar D, Southam L, et al. A genome-wide association study of Dupuytren disease reveals 17 additional variants implicated in fibrosis. *Am J Hum Genet*. 2017;101:417–427.
41. Weinzweig N, Culver JE, Fleegler EJ. Severe contractures of the proximal interphalangeal joint in Dupuytren's disease: combined fasciectomy with capsuloligamentous release versus fasciectomy alone. *Plast Reconstr Surg*. 1996;97:560–566.
42. Requena L, Kutzner H. Fibromatosis. In: Requena L, Kutzner H, eds. *Cutaneous Soft Tissue Tumors*. Philadelphia: Wolters Kluwer Health; 2015:117–126.
43. Morris G, Jacobson JA, Kalume Brigido M, et al. Ultrasound features of palmar fibromatosis or Dupuytren contracture. *J Ultrasound Med*. 2019;38:387–392.
44. Ragois P, Didailler P, Rizzi P. Métastase cutanée d'un cancer pulmonaire simulant une maladie de Dupuytren. *Chir Main*. 2012;31:259–261.
45. Hurst LC, Badalamente MA, Hentz VR, et al. Injectable collagenase *Clostridium histolyticum* for Dupuytren's contracture CORD I Study Group. *N Engl J Med*. 2009;361:968–979.
46. Werlinrud JC, Hansen KL, Larsen S, Lauritsen J. Five-year results after collagenase treatment of Dupuytren disease. *J Hand Surg Eur Vol*. 2018;43:841–847.
47. Soreide E, Murad MH, Denbeigh JM, et al. Treatment of Dupuytren's contracture: a systematic review. *Bone Joint J*. 2018;100:1138–1145.
48. Scherman P, Jenmalm P, Dahlin LB. Three-year recurrence of Dupuytren's contracture after needle fasciotomy and collagenase injection: a two-centre randomized controlled trial. *J Hand Surg Eur Vol*. 2018;43:836–840.
49. Strömberg J, Ibsen Sörensen A, Fridén J. Percutaneous needle fasciotomy versus collagenase treatment for Dupuytren contracture: a randomized controlled trial with a two-year follow-up. *J Bone Joint Surg Am*. 2018;100:1079–1086.
50. Nordenskjöld J, Lauritzson A, Åkesson A, Atroshi I. Collagenase injections for Dupuytren disease: 3-year treatment outcomes and predictors of recurrence in 89 hands. *Acta Orthop*. 2019;90:517–522.
51. Kadhum M, Smock E, Khan A, Fleming A. Radiotherapy in Dupuytren's disease: a systematic review of the evidence. *J Hand Surg Eur Vol*. 2017;42:689–692.
52. Riesmeijer SA, Manley OWG, Ng M, et al. A weighted genetic risk score predicts surgical recurrence independent of high-risk clinical features in Dupuytren's disease. *Plast Reconstr Surg*. 2019;143:512–518.
53. Vanek P, Strömberg J, Fridén J, Aurell Y. Morphological patterns of the pretendinous cord in Dupuytren's disease: a predictor of clinical outcome? *J Plast Surg Hand Surg*. 2018;52:240–244.
54. Krassovka J, Borgschulze A, Sahlender B, et al. Blue light irradiation and its beneficial effect on Dupuytren's fibroblasts. *PLoS One*. 2019;14:e0209833.
55. Seyhan H, Stromps JP, Demir E, et al. Vitamin D deficiency may stimulate fibroblasts in Dupuytren's disease via mitochondrial increased reactive oxygen species through upregulating transforming growth factor-β1. *Med Hypotheses*. 2018;116:40–41.
56. Zhou C, Zeldin Y, Baratz ME, et al. Investigating the effects of pirfenidone on TGF-β1 stimulated non-SMAD signaling pathways in Dupuytren's disease-derived fibroblasts. *BMC Musculoskelet Disord*. 2019;20:135.
57. Chisholm J, Gareau AJ, Byun S, et al. Effect of compound 21, a selective angiotensin II type 2 receptor agonist, in a murine xenograft model of Dupuytren disease. *Plast Reconstr Surg*. 2017;140:686e–696ee.
58. Nanchahal J, Ball C, Davidson D, et al. Anti-tumour necrosis factor therapy for Dupuytren's disease: a randomised dose response proof of concept phase 2a clinical trial. *EBioMedicine*. 2018;33:282–288.
59. Rubin G, Rinott M, Wolovelsky A, et al. A new bromelain-based enzyme for the release of Dupuytren's contracture: Dupuytren's enzymatic bromelain-based release. *Bone Joint Res*. 2016;5:175–177.
60. Sasaki T, Niizeki H, Shimizu A, et al. Identification of mutations in the prostaglandin transporter gene SLCO2A1 and its phenotype-genotype correlation in Japanese patients with pachydermoperiostosis. *J Dermatol Sci*. 2012;68:36–44.
61. Saha D, Kini UA, Kini H. Cutaneous neurocristic hamartoma presenting as cutis verticis gyrata. *Am J Dermatopathol*. 2014;36:e66–e69.
62. Kim JE, Choi KH, Kang SJ, et al. Angiosarcoma mimicking cutis verticis gyrata. *Clin Exp Dermatol*. 2011;36:806–808.
63. Koregol S, Yatagiri RV, Warad SR, Itagi NR. A rare association of scleromyxedema with cutis verticis gyrata. *Indian Dermatol Online J*. 2016;7:186–189.
64. Bourgaux M, Marcaillou M, Matei I, et al. Man of stone: a case of a chronic actinic dermatitis mimicking a cutis verticis gyrata. *J Eur Acad Dermatol Venereol*. 2020;34:e129–e130.
65. Welborn M, Dallo C, Altmeyer M. Cutis verticis gyrata improved with injected hyaluronidase treatments. *Dermatol Arch*. 2018;3:74–76.
66. El-Kamah GY, Fong K, El–Ruby M, et al. Spectrum of mutations in the ANTXR2 (CMG2) gene in infantile systemic hyalinosis and juvenile hyaline fibrosis. *Br J Dermatol*. 2010;163:213–215.
67. Bürgi J, Kunz B, Abrami L, et al. CMG2/ANTXR2 regulates extracellular collagen VI which accumulates in hyaline fibromatosis syndrome. *Nat Commun*. 2017;8:15861.
68. Hanks S, Adams S, Douglas J, et al. Mutations in the gene encoding capillary morphogenesis protein 2 cause juvenile hyaline fibromatosis and infantile systemic hyalinosis. *Am J Hum Genet*. 2003;73:791–800.
69. Cozma C, Hovakimyan M, Iurașcu MI, et al. Genetic, clinical and biochemical characterization of a large cohort of patients with hyaline fibromatosis syndrome. *Orphanet J Rare Dis*. 2019;14:209.
70. Fekrazad R, Fazilat F, Kalhori KA, et al. Juvenile hyaline fibromatosis management with a diode laser: a rare case report. *J Lasers Med Sci*. 2020;11:104–107.
71. Deuquet J, Lausch E, Guex N, et al. Hyaline fibromatosis syndrome inducing mutations in the ectodomain of anthrax toxin receptor 2 can be rescued by proteasome inhibitors. *EMBO Mol Med*. 2011;3:208–221.
72. Andrés-Ramos I, Alegría-Landa V, Gimeno I, et al. Cutaneous elastic tissue anomalies. *Am J Dermatopathol*. 2019;41:85–117.
73. Viera MH, Amini S, Valins W, Berman B. Innovative therapies in the treatment of keloids and hypertrophic scars. *J Clin Aesthet Dermatol*. 2010;3:20–26.

74. Khanijow K, Unemori P, Leslie KS, et al. Cutis verticis gyrata in men affected by HIV-related lipodystrophy. *Dermatol Res Pract*. 2013;2013:941740.
75. Lang N, Sterzing F, Enk AH, Hassel JC. Cutis verticis gyrata-like skin toxicity during treatment of melanoma patients with the BRAF inhibitor vemurafenib after whole-brain radiotherapy is a consequence of the development of multiple follicular cysts and milia. *Strahlenther Onkol*. 2014;190:1080–1081.
76. Knapp M, Carpenter CE, Shea K, et al. Focal dermal elastosis: a proposed update to the nomenclature. *Am J Dermatopathol*. 2020;42:774–775.
77. Yin CY, Yu HM, Wang JP, et al. Long-term follow-up of Dupuytren disease after injection of triamcinolone acetonide in Chinese patients in Taiwan. *J Hand Surg Eur Vol*. 2017;42:678–682.
78. Lah M, Niranjan T, Srikanth S, et al. A distinct X-linked syndrome involving joint contractures, keloids, large optic cup-to-disc ratio, and renal stones results from a filamin A (*FLNA*) mutation. *Am J Med Genet A*. 2016;170:881–890.



eFig. 98.1 Multiple keloids due to acne vulgaris. The neck is a common location for keloids.



eFig. 98.2 Spontaneous generalized keloids. Extensive spontaneous keloids in an African-American man. *Courtesy Claude Burton, MD.*



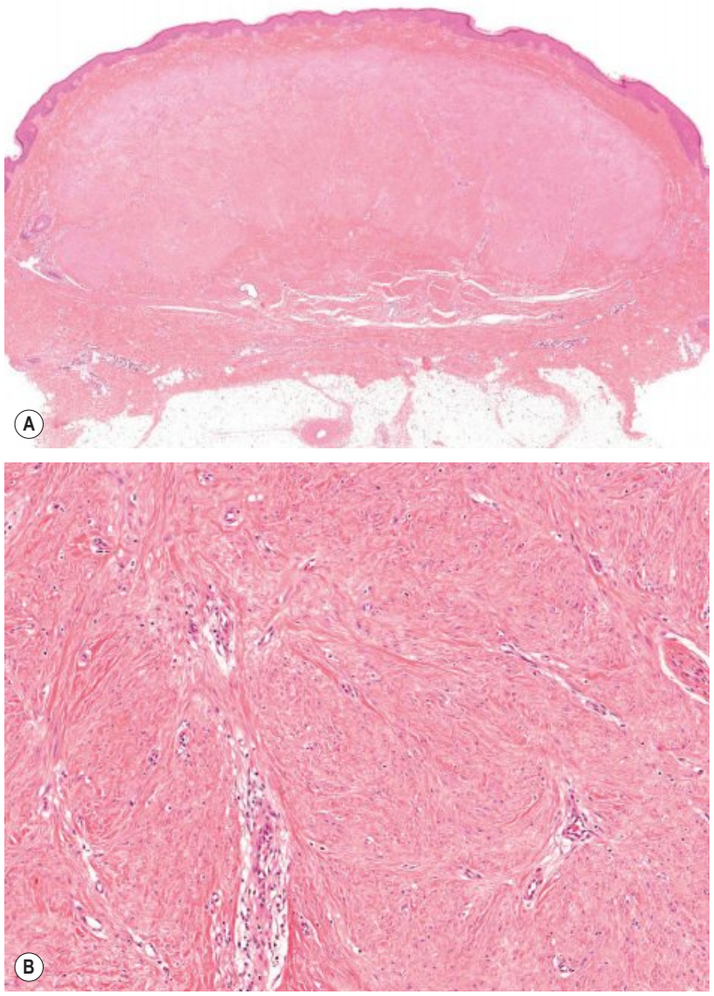
eFig. 98.3 Keloid of the flexor arm in an African-American man. Note the extension of the keloid into the normal surrounding skin in a claw-like manner and the central involution. *Courtesy Claude Burton, MD.*



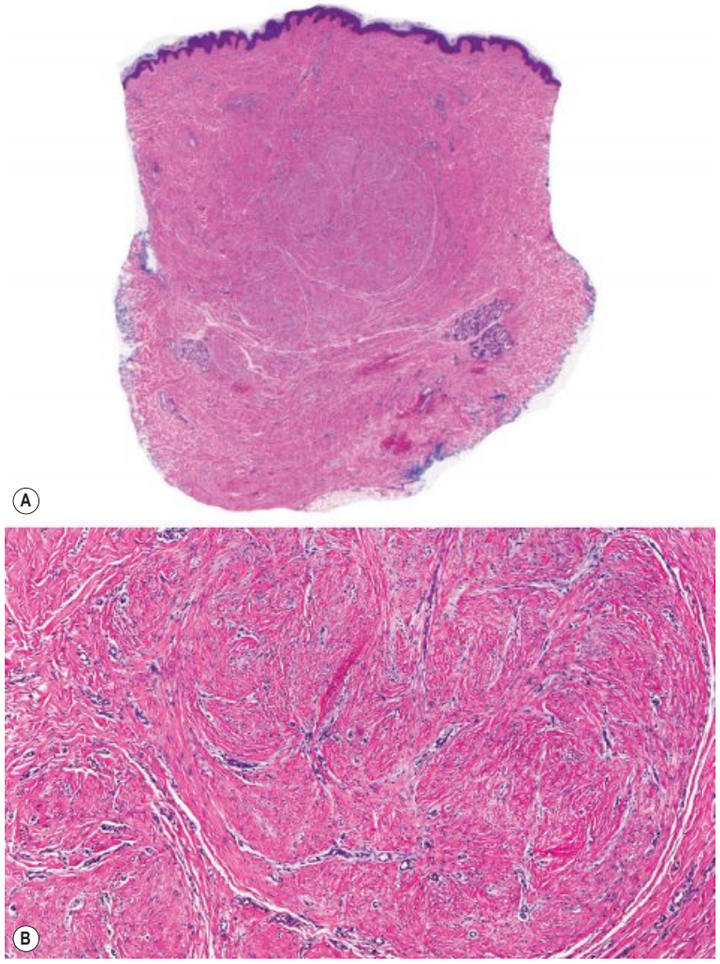
eFig. 98.4 Keloid of the earlobe in an African-American woman. The earlobe, where piercing has been performed for placement of earrings, is a common site for keloid formation. *Courtesy Joyce Rico, MD.*



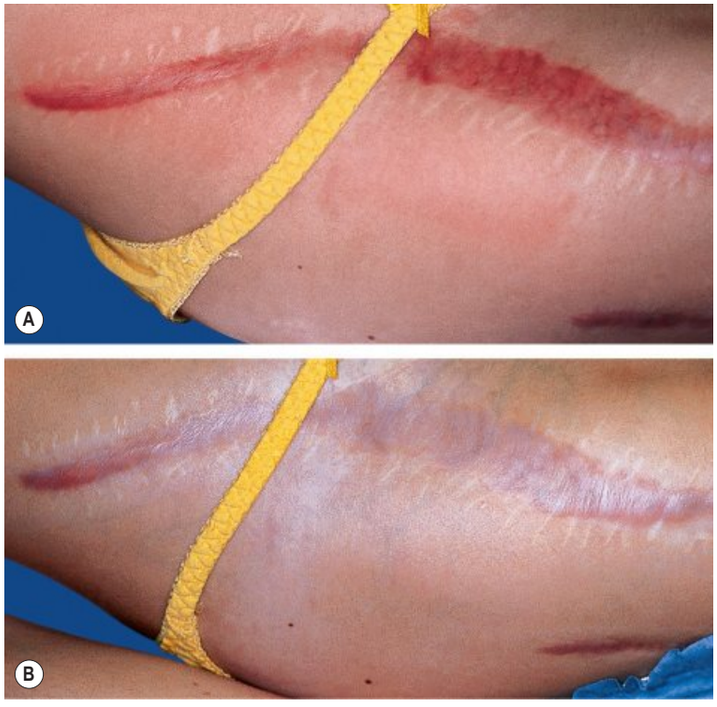
eFig. 98.5 Nodular morphea on the shoulder mimicking keloids. *Courtesy Julie V. Schaffer, MD.*



eFig. 98.6 Hypertrophic scar – histopathologic features. A Replacement of the dermis by hypertrophic bundles of collagen with increased numbers of fibroblasts. **B** Vertically oriented blood vessels, nodules of collagen and fibroblasts. *Courtesy Lorenzo Cerrroni, MD*.



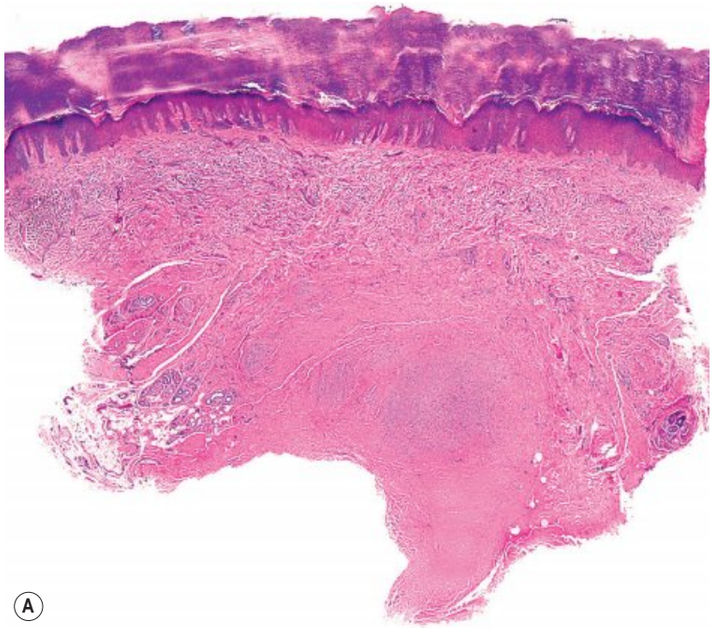
eFig. 98.7 Hypertrophic scar – histopathologic features. A Replacement of the dermis by hypertrophic bundles of collagen with increased numbers of fibroblasts. **B** Nodules of collagen and fibroblasts.

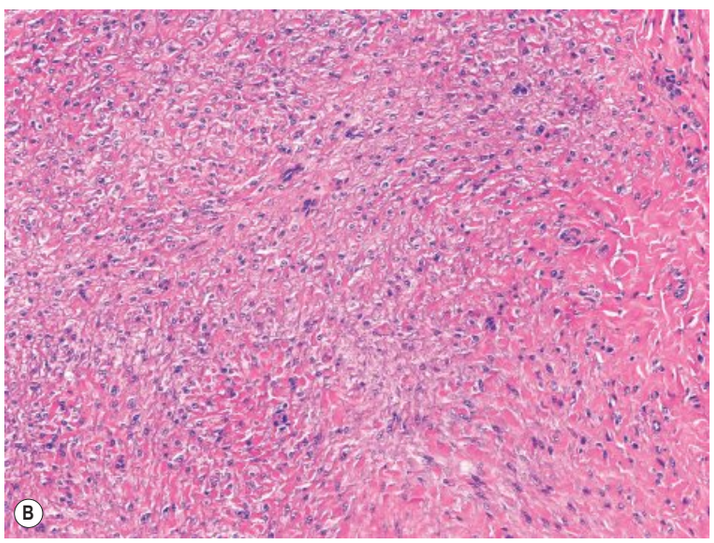


eFig. 98.8 Flashlamp-pumped pulsed dye laser treatment. Hypertrophic scar before (**A**) and after (**B**) treatment with a flashlamp-pumped pulsed dye laser.



eFig. 98.9 Dupuytren disease. There is greater involvement of the fifth finger than the fourth finger. Fibrotic cords can be felt and are accentuated by extension of the digits. Eventually, flexion contractures develop. *Courtesy Jean L. Bolognia, MD*.





eFig. 98.10 Dupuytren disease – histopathologic features. A Acral skin in which there is a dermal nodule of spindle-shaped cells. **B** Fibroblasts with no mitotic figures embedded in a thick collagen matrix.



eFig. 98.11 Juvenile hyaline fibromatosis. Large subcutaneous nodules are most prominent on the hand, wrist, and elbow. The elbow has an obvious joint contracture.

DIFFERENCES IN ADULT VERSUS FETAL WOUND HEALING		
	Adult	**Fetal**
Fluid environment	No	Yes
Sterile environment	No	Yes
Inflammation	Yes	No
Scar formation	Yes	No
pO_2 (mmHg)	>60	20

eTable 98.1 Differences in adult versus fetal wound healing.

TREATMENT OPTIONS FOR DUPUYTREN DISEASE		
Procedure	**Advantages**	**Disadvantages**
Dermofasci*ectomy* (removes diseased fascia including skin)	Addresses severe disease Lower rate of recurrence	Moderate perioperative morbidity Higher rate of complications* Prolonged rehabilitation High cost
Limited fasci*ectomy* (removes diseased fascia)	Addresses moderate to severe disease Low recurrence rate	Moderate perioperative morbidity Increased risk of scarring Prolonged rehabilitation High cost
Open fasci*otomy* (cord incised; diseased tissue is not excised)	Moderately invasive Good visualization Low complication rate*	Recurrence rate higher than with fasciectomy
Needle fasci*otomy* or percutaneous needle aponeurotomy (PNA) with or without lipofilling (cord fragmented by needle then released by manual force; diseased tissue is not excised)	Minimally invasive Outpatient procedure with local anesthesia Rapid recovery Low cost	Steep learning curve Skin tears Less effective for severe disease High rate of recurrences long-term
Enzymatic fasciotomy with collagenase from *Clostridium histolyticum* (Xiaflex® [USA]; Xiaplex® [Europe])	Minimally invasive Rapid Low risk of complications† First-line therapy or second-line therapy after failure of PNA or fasciectomy	Can only perform on a single cord or two thin cords May require multiple procedures High cost
Intralesional corticosteroids	Minimally invasive Softening of nodules after repeated injections Can improve outcome after PNA Low cost	High recurrence rate – at least 50%

*Complications include digital nerve injury or postoperative neurapraxia, flexor tendon injury/rupture, delayed wound healing or skin necrosis, dysvascular digit/arterial injury, hematoma, infection, and complex regional pain syndrome.
†Complications include bruising, tendon rupture, ligament or nerve injury, and anaphylaxis.

eTable 98.2 Treatment options for Dupuytren disease. *Adapted from Mella JR, Guo L, Hung V. Dupuytren's contracture: an evidence based review. Ann Plast Surg 2018;81(6 S Suppl 1):S97–101.*

DIFFERENTIAL DIAGNOSIS OF HYALINE FIBROMATOSIS SYNDROME			
Disease (mode of inheritance)	**Gene**	**Cutaneous manifestations**	**Extracutaneous manifestations**
MONA (multicentric osteolysis, nodulosis, and arthropathy) (AR)	*MMP2*	Painful nodules on the palms and soles, hypertrichosis, gingival hypertrophy	Osteolysis of hand and foot bones, joint contractures, short stature, corneal opacities, coarse facies
Winchester syndrome	*MMP14*	Thickened hyperpigmented skin, hypertrichosis, gingival hypertrophy	
Farber lipogranulomatosis (AR)	*ASAH1*	Subcutaneous nodules, especially periarticular and at sites of trauma	Arthritis, contractures, progressive hoarseness, variable CNS involvement, hepatosplenomegaly
Lipoid proteinosis (AR) (see Ch. 48)	*ECM1*	Vesicles and hemorrhagic crusts followed by pitted scars, yellow papules and nodules favor the face, verrucous lesions on extensor surfaces	Hoarseness, infiltrated tongue with restricted motion, parotitis, loss of teeth, learning difficulties, seizures
Stiff skin syndrome (AD) (see Ch. 43)	*FBN1*	Induration and thickening of the skin – most often of the buttocks and thighs but more widespread than regional/segmental form, hypertrichosis of affected areas	Restricted joint mobility including hip contractures, short stature, internal organs spared
Mucolipidosis II (AR)	*GNPTAB*	Thickened waxy skin especially around the earlobes, gingival hypertrophy, dermal melanocytosis	Short stature, dysostosis multiplex, skeletal abnormalities, cardiac valve disease, developmental delay, coarse facies
Infantile myofibromatosis (see Ch. 116)	*PDGFRB*	Skin-colored to purple nodules – favor the head and neck region and trunk	Lytic metaphyseal lesions, internal organ involvement, e.g. GI tract, kidneys, lung, heart

eTable 98.3 Differential diagnosis of hyaline fibromatosis syndrome. CNS, central nervous system; GI, gastrointestinal.

Atrophies of Connective Tissue 99

Catherine Maari and Julie Powell

Chapter Contents

Mid-dermal Elastolysis 1741
Anetoderma. 1742
Striae 1745
Atrophoderma of Pasini and Pierini 1746
Follicular Atrophoderma 1748
Atrophia Maculosa Varioliformis Cutis 1749
Piezogenic Pedal Papules (Piezogenic Papules) 1749
Other Atrophies of the Connective Tissue 1750

Atrophies of the skin that are due to a diminution or loss of collagen and/or elastic fibers are discussed in this chapter. The areas of involvement can be quite large, as in mid-dermal elastolysis, or punctate, as in follicular atrophoderma. In most disorders, the underlying pathogenesis remains to be discovered.

MID-DERMAL ELASTOLYSIS

Key features

- Uncommon disorder with areas of fine wrinkling
- Usually affects White middle-aged women
- Selective loss of elastic tissue in the mid dermis

Introduction

Mid-dermal elastolysis (MDE) is a rare, acquired disorder of elastic tissue. Clinically, it is usually characterized by diffuse fine wrinkling, most often located on the trunk, shoulders, neck, and arms. Histologically, a clear band of elastolysis with loss of elastic fibers is present in the mid dermis.

History

In 1977, Shelley and Wood reported the first case of "wrinkles due to idiopathic loss of mid-dermal elastic tissue". Their patient, a 42-year-old woman, had circumscribed areas of fine wrinkles that gave her an inappropriately aged appearance[1].

Epidemiology

To date, around 100 cases have been reported in the literature. The vast majority of patients are White women between the ages of 30 and 50 years[2,3].

Pathogenesis

The cause of the acquired elastic tissue degeneration in MDE has yet to be determined. Exposure to UV light, including natural sunlight, UVA (tanning salon), and narrowband UVB phototherapy[4,5], was thought to be a contributing factor in MDE, but this remains unclear[3]. Other hypotheses include defects in the synthesis of elastic fibers, autoimmunity against elastic fibers, and damage to elastic fibers via the release of elastase by inflammatory cells or fibroblasts. Of note, MDE has been observed in the setting of immune reconstitution inflammatory syndrome (IRIS). An imbalance between matrix metalloproteinases (MMPs) and tissue inhibitors of metalloproteinases (TIMPs) may also be playing a role, in addition to $CD34^+$ dendritic fibroblasts[6].

A decrease in lysyl oxidase-like 2 (LOXL2) expression, potentially affecting elastin renewal, has been observed in MDE[7]. There is also a decrease in dermal fibulin-4 and -5, pointing to altered re-assembly of elastic fibers in MDE, and not simply enhanced elastolysis[8]. In sum, the pathogenesis of MDE is likely multifactorial, with genetic predisposition, chronic inflammation, UV irradiation, and/or (auto)immune processes as contributing factors[3].

Clinical Features

Patients can have well-circumscribed to large diffuse areas of fine wrinkling (Fig. 99.1), usually in a symmetric distribution (type I). The wrinkles themselves tend to follow cleavage lines. Discrete perifollicular papules are seen in some patients (type II), with the site of the central hair follicle being indented. Occasionally, erythematous patches, telangiectasias, and reticulated erythema may be present (type III)[3]. Although in the majority of patients there is no history of a prior inflammatory dermatosis, some patients report previous mild to moderate erythema and, rarely, elastolysis is preceded by urticarial lesions or granuloma annulare.

Sites of predilection are the trunk, lateral neck, and upper extremities. Once the patches of wrinkling have appeared, they usually remain stationary. They are asymptomatic and give the skin a prematurely aged appearance. The affected areas usually have normal pigmentation and no associated scaling, induration, or herniation. There is typically no family history of similar lesions and unless linked to an autoimmune disorder, no systemic involvement[2,3]. MDE can lead to significant cosmetic concern.

While diagnosis is usually confirmed via histologic examination of involved skin, non-invasive imaging techniques such as optical coherence microscopy or high-frequency ultrasound may also prove helpful[9].

Pathology

The epidermis is normal in appearance and, occasionally, a mild perivascular infiltrate is noted in the dermis. Elastic tissue stains, such as Verhoeff–van Gieson or Weigert's stain, reveal a selective loss of elastic fibers in the mid dermis (Fig. 99.2). There is preservation of normal elastic tissue in the superficial papillary dermis above, in the reticular dermis below, and along adjacent hair follicles. The preservation of elastic tissue around the hair follicles explains the perifollicular papules observed in some patients.

By electron microscopy, phagocytosis of normal as well as degenerated elastic fiber tissue by macrophages has been described[3]. Elastophagocytosis by macrophages can also be observed by routine histology.

Differential Diagnosis

MDE must be differentiated from other disorders of elastic tissue such as anetoderma, pseudoxanthoma elasticum (PXE), PXE-like papillary dermal elastolysis, elastoderma, and cutis laxa, especially the acquired form (Table 99.1).

Clinically, anetoderma is characterized by soft macules and papules that herniate upon palpation, as opposed to diffuse wrinkling. Histologically, elastolysis can occur in the papillary and/or mid-reticular dermis in anetoderma (see below). Patients with heritable forms of generalized cutis laxa have loose, redundant skin, hanging in folds, and histologic examination shows reduced and fragmented elastic fibers, usually within the entire dermis. Acquired cutis laxa, both generalized and acral, can be a manifestation of an underlying paraproteinemia, with binding of immunoglobulins to elastic fibers (see Table 97.8).

Less often, MDE is confused with solar elastosis or the perifollicular elastolysis that is usually seen on the trunk in association with acne



Fig. 99.1 Mid-dermal elastolysis. A, B Type I – large diffuse patch as well as reticulated areas of fine wrinkling on the upper trunk and proximal arm. The junction of involved and uninvolved skin is marked with an arrow. **C** Types I and II – both circumscribed areas of wrinkling and follicular papules are present. **D** Type II – multiple skin-colored follicular papules. **E** Type III – primarily reticulated erythema. *A, Courtesy Judit Stenn, MD; B, Courtesy Carlo F. Tomasini, MD; C–E, Courtesy Lorenzo Cerroni, MD.*

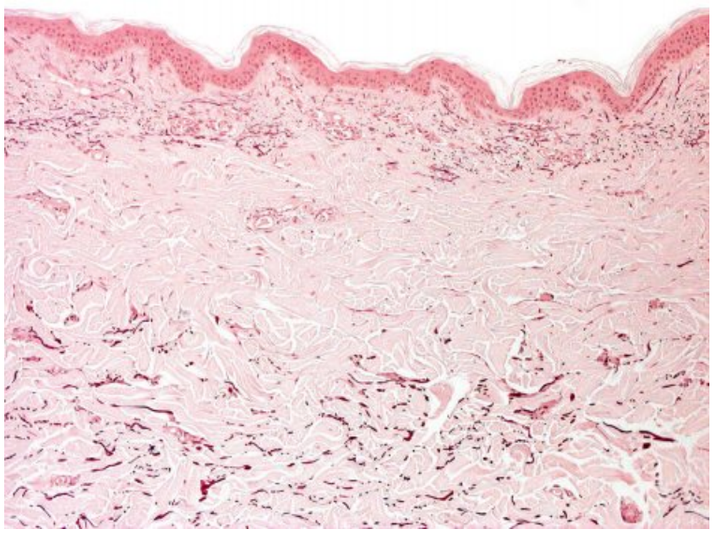


Fig. 99.2 Mid-dermal elastolysis – histopathologic features. A near absence of elastic fibers in a band-like distribution in the mid reticular dermis. Identification of these changes requires an elastic tissue stain (e.g. orcein). *Courtesy Lorenzo Cerroni, MD.*

vulgaris. Solar elastosis differs clinically by its onset in an older age group, restriction to only sun-exposed areas, yellow color, and coarser wrinkling and differs histologically by hyperplasia of abnormal elastic fibers and basophilic degeneration of the collagen in the papillary dermis. Perifollicular elastolysis leads to a selective and almost complete loss of the elastic fibers that surround hair follicles, compared with preservation of elastic fibers around follicles in MDE.

Treatment

Currently, there is no effective treatment for MDE. Sunscreens, colchicine, chloroquine, vitamin E, and topical agents (retinoic acid, corticosteroids) have been tried without success[2]. Topical soybean extract and eicosapentanoic acid are potential future therapies and oral mycophenolate mofetil may be beneficial[2,10].

ANETODERMA

Synonyms: ■ Macular atrophy ■ Anetoderma maculosa ■ Anetoderma maculosa cutis ■ Atrophia maculosa cutis

Key features

- Circumscribed 1–2 cm areas of flaccid skin, which may be elevated, macular, or depressed
- *Primary* anetoderma has classically been divided into inflammatory and non-inflammatory
- *Secondary* anetoderma is associated with infectious and inflammatory cutaneous disorders as well as tumors and autoimmune disorders (e.g. antiphospholipid antibody syndrome)
- Histologically, focal absence of dermal elastic tissue is seen

DISORDERS OF ELASTIC TISSUE			
Condition	**Clinical findings**	**Site of predilection**	**Pathology**
Anetoderma	• Multiple circumscribed areas of flaccid skin • Lesions are often elevated (protruding), but can be macular or depressed	Usually on trunk	Focal or complete loss of elastic tissue in the papillary and/or reticular dermis
Cutis laxa (see Ch. 97)	• Loose, sagging skin folds resulting in prematurely aged appearance • Hereditary or acquired • Internal organ involvement, e.g. pulmonary, in hereditary form and generalized acquired form	Eyelids, cheeks, neck, shoulder girdle and abdomen; distal digits in acquired acral form	Diminished and fragmented elastic fibers usually throughout the dermis
Mid-dermal elastolysis	• Diffuse areas of fine wrinkling (type I), perifollicular papules (type II), and/or reticulated erythema (type III) in middle-aged women	Trunk, arms, and lateral neck	Selective loss of elastic fibers within the mid dermis in a band-like pattern
Pseudoxanthoma elasticum (PXE; see Ch. 97)	• Yellowish coalescing skin papules, "cobblestoning", and redundant folds in flexural sites • Associated ocular and cardiovascular involvement	Lateral neck, axillae, and groin; scars	Clumped and calcified elastic fibers in the mid dermis
PXE-like papillary dermal elastolysis	• Multiple, 2–3 mm, yellow or skin-colored papules that can coalesce into cobblestoned plaques	Neck, flexor forearms, axillae, lower abdomen, inframammary folds	Decreased elastic tissue in the papillary dermis (band-like pattern); clumping and fragmentation of elastic fibers; no calcification of elastic fibers

Table 99.1 Disorders of elastic tissue. For additional entities, see Tables 95.5, 97.4 and 97.7.

Introduction

The term "anetoderma" is derived from *anetos*, the Greek word for slack, and *derma* for skin. Anetoderma is an elastolytic disorder characterized by localized areas of flaccid skin, which may be depressed, macular or papular; the latter can reflect herniation of the subcutaneous tissue. Anetoderma may be idiopathic or associated with an inflammatory disorder of the skin.

History

The first case of primary inflammatory anetoderma was reported by Jadassohn in 1892[11]. A year previously, Schweninger and Buzzi described a 29-year-old woman with multiple, non-inflammatory, sac-like tumors on the trunk and upper extremities[12].

CLASSIFICATION OF ANETODERMA	
Primary anetoderma	• Jadassohn–Pellizzari type: preceding inflammatory lesionsSchweninger–Buzzi type: no preceding inflammatory lesions
Secondary anetoderma	• Associated with a primary dermatosis or cutaneous tumorAssociated with a systemic disease (autoimmune, antiphospholipid syndrome, infectious) or drug
Familial anetoderma	• Both autosomal dominant and autosomal recessive formsUsually develops in first decade of life
Anetoderma of prematurity	• Occurs in extremely premature infants • At sites of monitoring leads or adhesives

Table 99.2 Classification of anetoderma.

Epidemiology

Several hundred cases of anetoderma have been reported in the world literature. Primary anetoderma favors young adults between 15 and 25 years of age and occurs more frequently in women than men. The epidemiology of secondary anetoderma reflects that of the underlying etiologies (see Table 99.3).

Pathogenesis

The pathogenesis of anetoderma is not known. These lesions could be considered unusual scars, since scars also have decreased elastic tissue. The loss of dermal elastin may reflect an impaired turnover of elastin, caused by either increased destruction or decreased synthesis of elastic fibers. There are a number of proposed explanations for the focal elastin destruction, e.g. the release of elastase from inflammatory cells, the release of cytokines such as interleukin-6, an increased production of progelatinases A and B[13], and the phagocytosis of elastic fibers by macrophages. More recently, a decrease in fibulin protein expression was observed, suggesting defective elastic fiber reassembly[6]. Immunologic mechanisms may also play a role, providing an explanation for associated findings such as antiphospholipid antibodies (see below). Based upon a few isolated patients, a link may exist between anetoderma and mutations in genes that encode enzymes in the citric acid cycle[14].

In *primary* anetoderma, there is no underlying associated disorder and lesions arise within clinically normal skin. It has classically been subdivided into two major forms: those with preceding inflammatory lesions (the Jadassohn–Pellizzari type) and those without preceding inflammatory lesions (the Schweninger–Buzzi type) (Table 99.2). This clinical classification is primarily of historical interest, since the two types of lesions can coexist in the same patient and their histopathology is often the same; the presence or absence of clinical inflammation at the onset of the disease is not related to prognosis[15].

Secondary anetoderma can arise in the setting of a primary inflammatory dermatosis, skin infection or cutaneous tumor, as well as in patients with systemic disorders (e.g. autoimmune). Over the past decade, an association with antiphospholipid antibody syndrome has been highlighted. Although the vast majority of cases are sporadic, familial anetoderma has been described and is usually not associated with pre-existing lesions[16].

Clinical Features

The characteristic lesions are flaccid, circumscribed areas of slack skin that are a reflection of a marked reduction or absence of dermal elastic fibers; they can appear as depressions, wrinkling, or sac-like protrusions (Fig. 99.3). These atrophic lesions vary in number from a few to hundreds, and they typically measure 1–2 cm in diameter and are skin-colored to bluish–white in color. The skin surface can be normal in appearance or wrinkled, and a central depression may be seen. Coalescence of smaller lesions can give rise to larger herniations.

The examining finger sinks into a distinct pit with sharp borders as if into a hernia ring. The bulge reappears when the pressure from the finger is released. This clinical finding is referred to as the "buttonhole" sign and is similar to that observed in neurofibromas.

Predilection sites for these asymptomatic lesions are the chest, back, neck, and upper extremities. Primary anetoderma usually develops in young adults, and new lesions often continue to form for many years as the older lesions fail to resolve.

True secondary anetoderma implies that the characteristic atrophic lesion has appeared in the same site as a previous specific skin lesion, e.g. from varicella or leprosy. Some authors also consider lesions associated

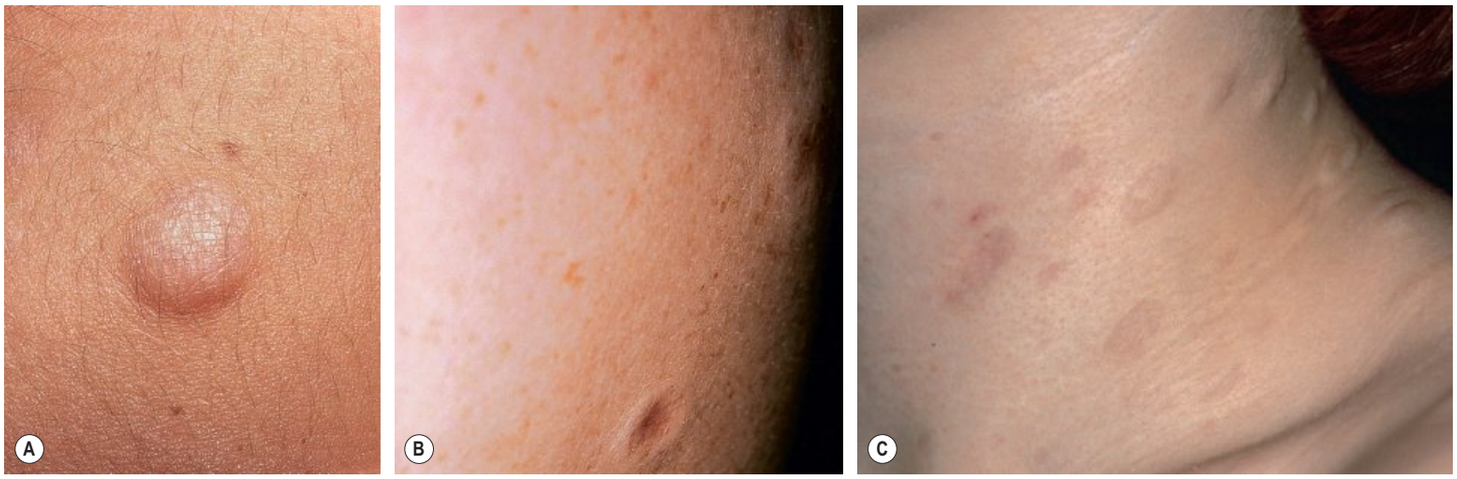


Fig. 99.3 Primary anetoderma. Lesions can range from soft, skin-colored papules that herniate upon palpation (**A**) to flaccid papules that have a central depression (**B**). The upper trunk and neck is a common location for primary anetoderma (**C**). *A, Courtesy Ronald P. Rapini, MD; C, Courtesy Thomas Schwarz, MD.*

with an underlying disease (e.g. HIV infection, antiphospholipid antibody syndrome, autoimmune thyroiditis) as secondary anetoderma; however, in this instance, the atrophic areas do not necessarily develop within areas of known inflammation. Evaluation for the presence of antiphospholipid antibodies should be performed before patients with idiopathic anetoderma are labeled as having primary anetoderma[17]. The range of heterogeneous conditions associated with secondary anetoderma are outlined in Table 99.3. With the exception of distribution (and perhaps size), the clinical features are the same as those of primary anetoderma.

Anetoderma has increasingly been reported in premature infants. In most neonates, it appears to be related to the use of cutaneous monitoring leads or adhesives[18], as well as extreme prematurity[18].

In patients with anetoderma, a variety of systemic abnormalities have been reported, including ocular, endocrinologic, skeletal, cardiac, pulmonary, and gastrointestinal disease. Because there has been no consistency with regard to these associated abnormalities, they are probably coincidental, although the possibility exists that they may reflect a more generalized elastolytic disorder that has yet to be defined.

Pathology

In routinely stained sections, the collagen within the dermis of affected skin appears normal. Perivascular lymphocytes, primarily T helper cells, are often present but do not correlate with clinical findings of inflammation.

The predominant abnormality, revealed by elastic tissue stains, is a focal, more or less complete loss of elastic tissue in the papillary and/or reticular dermis. There are usually some residual abnormal, irregular, and fragmented elastic fibers (Fig. 99.4)[19]. In addition to plasma cells and histiocytes with phagocyted elastic fibers, occasional granuloma formation can be seen.

Direct immunofluorescence sometimes shows linear or granular deposits of immunoglobulins and complement along the dermal–epidermal junction or around the dermal blood vessels in affected skin[20]. However, these findings are not helpful diagnostically.

By electron microscopy, the elastic fibers are fragmented and irregular in shape and occasionally they are engulfed by macrophages.

Differential diagnosis

Anetoderma must be differentiated from other disorders of elastic tissue such as MDE (see Table 99.1) as well as atrophodermas (see below). However, the major differential diagnosis consists of post-traumatic scars and papular elastorrhexis[21]. The latter is an acquired disorder characterized by firm, white, non-follicular papules that measure 2–5 mm in diameter and are evenly scattered on the trunk. The lesions usually appear during adolescence or early adulthood. Histology demonstrates focal degeneration of elastic fibers and normal collagen. There are no associated extracutaneous abnormalities. This disorder is believed by some authors to be a variant of connective tissue nevi or an abortive form of the Buschke–Ollendorff syndrome, while others think that these lesions represent papular acne scars. In contrast to anetoderma, lesions of papular elastorrhexis are firm and non-compressible.

Less often, anetoderma is confused with perifollicular elastolysis (see above), nevus lipomatosus, or focal dermal hypoplasia (Goltz

SECONDARY ANETODERMA – ASSOCIATED CONDITIONS	
Infectious	• Varicella • Folliculitis* • Lepromatous leprosy • Syphilis (cutaneous) • Molluscum contagiosum • Tuberculosis (cutaneous) • HIV infection • Acrodermatitis chronica atrophicans • Post-hepatitis B immunization
Drugs	• Penicillamine • Cabiralizumab (CSF1 receptor antagonist) plus nivolumab**
Inflammatory	• Acne vulgaris • Lichen planus • Neutrophilic dermatoses (Sweet syndrome, pyoderma gangrenosum) • Granuloma annulare • Cutaneous sarcoidosis • Juvenile xanthogranuloma • Cutaneous lymphoid hyperplasia (lymphocytoma cutis) • Insect bites • Prurigo nodularis
Autoimmune	• Cutaneous (e.g. discoid, panniculitis) and systemic lupus erythematosus • Antiphospholipid syndrome • Primary Sjögren syndrome • Addison disease • Graves disease
Tumors and depositions	• Involuted infantile hemangioma • Pilomatricoma • Melanocytic nevus • Schwannoma • Dermatofibroma • Dermatofibrosarcoma protuberans • Primary cutaneous marginal zone B cell lymphoproliferative disorder (formerly primary cutaneous plasmacytoma or immunocytoma) • Mycosis fungoides • Mastocytosis • Nodular amyloidosis • Xanthoma

*May overlap with perifollicular elastolysis.
**Preceding granulomatous inflammation with elastolysis.

Table 99.3 Secondary anetoderma – associated conditions.

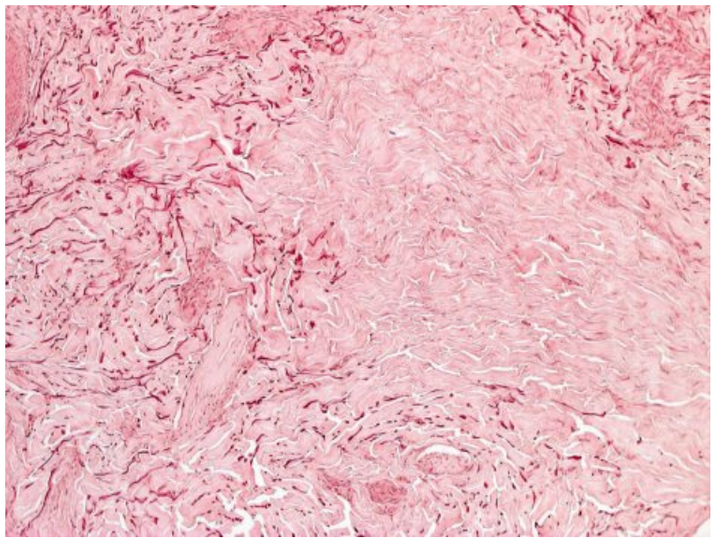


Fig. 99.4 Anetoderma – histopathologic features. A decrease of elastic fibers in both the papillary and reticular dermis (Weigert's stain). *Courtesy Lorenzo Cerroni, MD.*

syndrome). Nevus lipomatosus superficialis of Hoffman and Zurhelle presents as a clustered group of soft, skin-colored to yellow nodules, usually located on the lower trunk and present since birth (see Ch. 117). Histology shows ectopic mature lipocytes located within the dermis. The lesions of Goltz syndrome (including telangiectasias, vermiculate dermal atrophy, hypopigmentation, hyperpigmentation, and fatty herniations/hamartomas) are in a linear array along the lines of Blaschko (see Ch. 62). Histologically, a decrease in dermal content is seen as well as extension or deposition of subcutaneous fat into the dermis.

Treatment

Various therapeutic modalities have been tried, but have not resulted in improvement of existing atrophic lesions; these include intralesional triamcinolone and systemic administration of aspirin, dapsone, phenytoin, penicillin G, vitamin E, and inositol niacinate. Some authors have reported improvement with hydroxychloroquine. Surgical excision of limited lesions may be helpful, with informed consent from the patient regarding the risk of scar formation. The utility of soft tissue fillers is inconclusive. Based upon case reports, fractionated ablative and non-ablative lasers may be beneficial[22,23].

STRIAE

Synonyms: ■ Striae distensae ■ Striae atrophicans ■ "Stretch marks" ■ Striae gravidarum

Introduction

Striae are a very common condition in most age groups. They are linear atrophic depressions of the skin that form in areas of dermal damage produced by stretching of the skin. They are associated with various physiologic states, including puberty, pregnancy, rapid growth, weight gain or loss, obesity[24], and disorders that lead to hypercortisolism. Striae also develop at sites of potent topical corticosteroid application, in particular, occluded intertriginous zones.

History

Striae were first described by Roederer in 1773, and the first histologic descriptions were made by Troisier and Menetrier in 1889.

Epidemiology

Striae are very common and usually develop between the ages of 5 and 50 years. They are seen more commonly in White individuals and occur about twice as frequently in women as in men. They commonly develop during puberty, with a prevalence ranging from 5% to 85%[25], or during pregnancy, with an incidence of up to 90%[26].

Pathogenesis

Factors leading to the development of striae have not been fully elucidated. They are a reflection of "breaks" in the connective tissue that lead to dermal atrophy. A number of factors, including hormones (particularly corticosteroids), mechanical stress and genetic predisposition, appear to play a role. Bevacizumab, an anti-VEGF antibody well known for its negative effect on wound healing, has also been associated with severe ulcerations of corticosteroid-induced striae[27].

Clinical Features

Striae are usually multiple, symmetric, well-defined, linear atrophic lesions that often follow the lines of cleavage. They are usually more of a cosmetic concern, but rarely can ulcerate. Initially, striae appear as red-to-violaceous elevated lines that can be mildly pruritic and are called striae rubrae (Fig. 99.5). Over time, the color gradually fades, and the lesions become atrophic, exhibiting a fine wrinkled appearance. These striae albae are usually permanent, but they may fade somewhat over time[25]. The striae can measure several centimeters in length and a few millimeters to a few centimeters in width.

During puberty, striae appear in areas where there is a rapid increase in size. In girls, the most common sites are the thighs, hips, buttocks and breasts, whereas in boys, they are seen on the shoulders, thighs, buttocks, and lumbosacral region[25] (Fig. 99.6). Other less common sites include the abdomen, upper arms, neck, and axillae.

Striae distensae are a common finding on the abdomen, and less so on the breasts and thighs, of pregnant women, especially during the last trimester. They are more common in younger primigravidas than in older pregnant women, in those who gained more weight during pregnancy, and/or those who had babies with a higher birth weight[26]. The development of striae gravidarum has been associated with an increased risk of laceration during vaginal delivery as well as subsequent pelvic relaxation and clinical prolapse[28,29].

The striae associated with systemic corticosteroid therapy and Cushing syndrome can be larger and more widely distributed (see Ch. 53). Flexural and intertriginous areas are particularly at risk for developing striae from the use of potent topical corticosteroids.

Atrophic striae may become elevated and "worm-like" in the setting of severe edema, including lymphedema. In polymorphic eruption of pregnancy, initial lesions often arise within striae gravidarum.

Pathology

Histologic findings are similar to those of scars and depend upon the stage of evolution of the striae at the time the biopsy is performed. The epidermis can be normal during the early stages, but eventually becomes atrophic with blunted rete ridges. The dermal thickness is decreased, as is the collagen in the upper dermis. The collagen bundles lie parallel to the epidermis. Alterations in elastic fibers are variable, but they can be fragmented, and specific elastin staining can demonstrate a marked reduction compared with adjacent normal dermis[30]. There is an absence of both hair follicles and other adnexal structures.

Differential Diagnosis

The diagnosis of striae distensae is usually straightforward, but the differential diagnosis does include linear focal elastosis (elastotic striae), an entity first described by Burket et al.[31] in 1989. Linear focal elastosis is characterized by rows of yellow, palpable, striae-like bands on the lower back. Unlike striae, the lesions are raised and yellow rather than depressed and white. Elderly men are most commonly affected. Histologically, there is a focal increase in the number of elongated or fragmented elastic fibers as well as a thickened dermis. It is postulated that linear focal elastosis may represent an excessive regenerative process of elastic fibers and could be viewed as a keloidal repair of striae distensae[32].

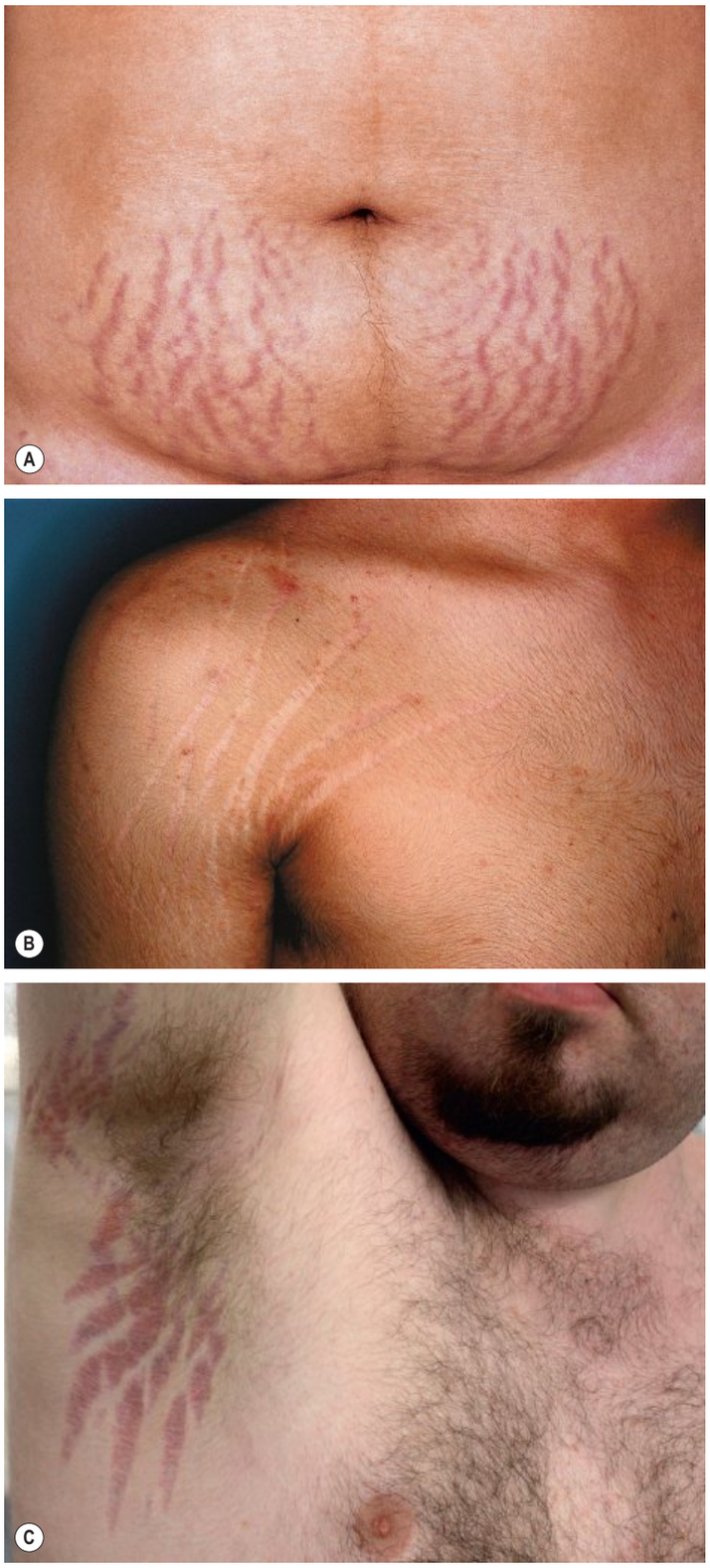


Fig. 99.5 Striae. A Linear erythematous lesions on the abdomen (striae rubrae). **B** Atrophic linear lesions of striae albae in a teenager. **C** Large axillary striae in a patient receiving chronic, high-dose systemic corticosteroids. *B, Courtesy Kalman Watsky, MD.*

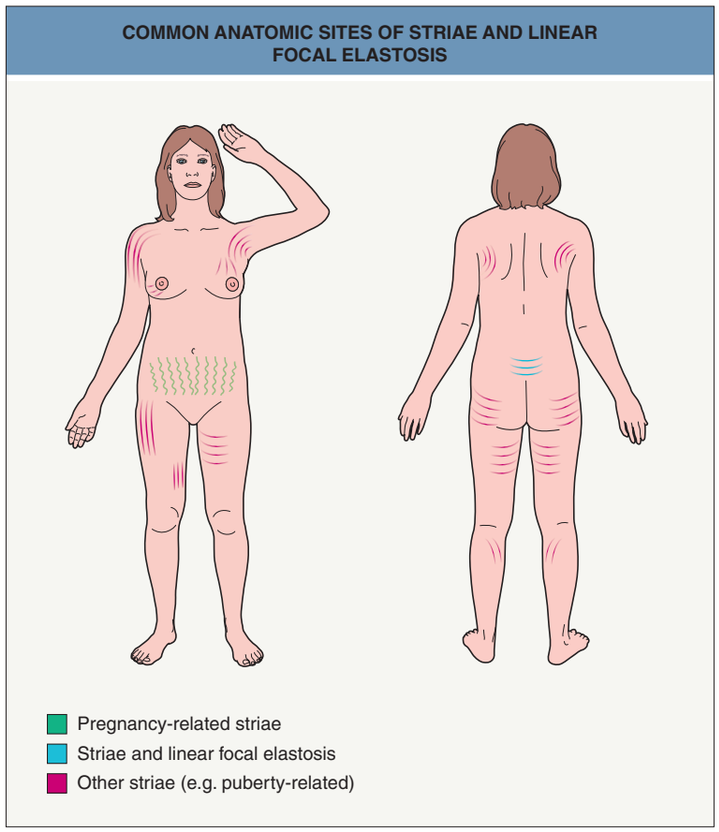


Fig. 99.6 Common anatomic sites of striae and linear focal elastosis. Striae associated with pregnancy are in green and lesions of linear focal elastosis are in blue.

Treatment

Striae distensae have no medical consequences, but they are frequently distressing to those afflicted. As striae tend to improve spontaneously over time, the value of anecdotal therapies without case controls is difficult to assess. Topical treatments that have shown some benefit in early-stage striae include tretinoin 0.1% cream[33] and a combination of 20% glycolic acid with either 0.05% tretinoin or 10% L-ascorbic acid[34]. The evidence for the effect of other topical treatments, either in prevention or treatment of striae, is inconclusive[34].

Several lasers have been used to treat striae: the 585 nm pulsed dye laser may improve the appearance of striae rubrae, but it has no effect on striae albae; secondary pigmentary alterations in darker skin are a potential complication[35]. Improvement of striae albae was noted with fractionated non-ablative lasers, presumably via neocollagenesis[36]. Use of radiofrequency and pulsed magnetic fields may also lead to improvement[37]. However, currently, there is no specific therapy that results in a complete response.

ATROPHODERMA OF PASINI AND PIERINI

Synonyms: ■ Idiopathic atrophoderma of Pasini and Pierini ■ Atrophoderma ■ Sclérodermie atrophique d'emblée ■ Morphea plana atrophica

Key features

- Depressed patches, usually on the posterior trunk and brown in color
- "Cliff-drop" or abrupt transition from normal to diseased skin
- Lesions are asymptomatic and lack induration
- Disorder lasts for many years but has a benign course

Introduction

Atrophoderma of Pasini and Pierini is a form of dermal atrophy that presents as one or more sharply demarcated depressed patches, usually on the back of adolescents or young adults. Whether atrophoderma represents an atypical, primarily atrophic form of morphea or "burnt-out" morphea or a separate distinct entity is still debated.

History

In 1923, Pasini described atrophic cutaneous lesions on the trunk of a 21-year-old woman that he referred to as progressive idiopathic atrophoderma[38]. In 1936, and over the subsequent years, Pierini and associates extensively studied and defined the condition and its possible link to morphea. This prompted Canizares et al.[39] in 1958 to rename this entity "idiopathic atrophoderma of Pasini and Pierini".

Epidemiology

This disorder is more frequently encountered in women than in men, with a ratio of 6:1 in adults[40]. It usually starts insidiously in young individuals during the second or third decade of life. However, a number of cases have been described in children younger than 13 years of age. More recently, rare congenital cases have been reported[41].

Pathogenesis

The etiology of atrophoderma of Pasini and Pierini remains as yet unknown. Some authors have suggested the possible role of *Borrelia burgdorferi* infection, as in acrodermatitis chronica atrophicans, since a positive serology can be found in up to 40%–50% of European patients[42]. However, false-positive results can occur, and results have varied widely. Given some overlap between atrophoderma and morphea, perhaps insights into the pathogenesis of the latter will provide clues to the former.

Clinical features

Lesions usually appear on the trunk, especially the back and lumbosacral region, followed in frequency by the chest, arms, and abdomen[42]. The face, hands, and feet are usually spared. The distribution is often symmetric and bilateral, but a linear pattern along the lines of Blaschko has been described (atrophoderma of Moulin; see Ch. 67).

The lesions are single or multiple and usually round or ovoid, ranging in size from a few centimeters to patches covering large areas of the trunk. They are usually asymptomatic and lack inflammation. When lesions coalesce, they can form large irregular patches. The patches usually have a brown color (Fig. 99.7), but some are blue to violet in color or occasionally hypopigmented[43]. The surface of the skin is normal in appearance, as is the consistency upon palpation. There is a lack of cutaneous induration or sclerosis.

The borders or edges of these lesions are sharply defined, and they are usually described as abrupt "cliff-drop" borders ranging from 1 to 8 mm in depth, although they can have a gradual slant and the depression may be subtle[39]. These depressed patches often give the impression of inverted plateaus, or, if multiple lesions are present, they can have the appearance of Swiss cheese. The lesions are even more apparent when present on the back, because the dermis is thicker in this area. Occasionally, dermal blood vessels are visible within the depressed patches.

The skin surrounding the patches is normal in appearance, and there is no erythema or lilac ring as in morphea. However, typical lesions of morphea, lichen sclerosus, and atrophoderma have been observed to occur simultaneously in the same patient (but in different areas), supporting the view that these conditions are related[44]. In addition, sclerodermatous changes can occasionally appear years later in the center of the depressed lesions, leading to a white, shiny induration[39]. In a series of 139 patients, 17% had a white induration in the central portions of their atrophic lesions, and, in 22%, superficial plaques of morphea coexisted in sites separate from the atrophic foci[40].

The course of this benign disease is progressive, and lesions can continue to appear for decades before reaching a standstill. Transformation to generalized morphea has not been observed.

Pathology

In general, the histologic picture is not diagnostic, so the diagnosis is primarily a clinical one. The epidermis is usually normal or slightly atrophic. Pigmentation of the basal layer may be increased. A perivascular infiltrate consisting of T cells and histiocytes may be seen. Collagen bundles in the reticular dermis show varying degrees of homogenization and clumping. Dermal thickness is reduced when compared with adjacent normal skin[45]. Dermal atrophy is difficult to evaluate on a punch biopsy, but it can be more easily demonstrated if an elliptical biopsy is taken in an area that includes the cliff-drop border and is then sectioned longitudinally to show the transition between normal and lesional skin.



Fig. 99.7 Atrophoderma of Pasini and Pierini. **A, B** Multiple light brown patches on the back; note the subtle depression of the lesions with a "cliff-drop" edge. In A, dermal blood vessels are easily seen within a few patches; the white papule is a healed biopsy site. *A, Courtesy Julie V. Schaffer, MD; B, Courtesy Catherine C. McCuaig, MD.*

In most series, no abnormality has been observed with elastic tissue stains[40,42]; however, a retrospective study described a spectrum of changes, ranging from normal to severe diminution and fragmentation of the elastic fiber network[43]. The adnexal structures are usually preserved. If sclerodermatous changes appear within pre-existing lesions, varying degrees of collagen sclerosis resembling morphea can be seen. Of note, evaluation of collagen and elastic fibers by multiphoton microscopy has suggested that the atrophic appearance of atrophoderma reflects changes in the organization of collagen and elastic fibers, not a variation in their content[46].

Direct immunofluorescence may show nonspecific IgM and C3 staining in the dermal papillary blood vessels in early lesions or at the dermal–epidermal junction[47].

Differential diagnosis

Since the original description, there has been much discussion over whether atrophoderma of Pasini and Pierini is a distinct entity or an atrophic, non-indurated, perhaps "burnt-out" variant of morphea (see Ch. 44). Active lesions of morphea present as indurated, often hyperpigmented plaques with a characteristic peripheral lilac rim.

Although atrophoderma of Pasini and Pierini lacks sclerosis[40,42,44,47], its relationship to morphea is favored by its striking clinical and

histologic similarities to the atrophy seen at sites of regressing plaques of morphea. To some, the different course and outcome of atrophoderma of Pierini and Pasini as compared with morphea justifies preservation of a distinct name.

Anetoderma, also an atrophic dermal process, is easily differentiated by palpation and histology, which consistently shows a loss of elastic fibers in the dermis (as opposed to a loss of collagen).

Treatment

The natural course of the disease is often protracted (10–20 years) but self-healing, making evaluation of therapy difficult. No treatment has been proven effective. In view of the possibility of underlying *Borrelia* infection, penicillin and doxycycline have been used to treat atrophoderma of Pasini and Pierini, but the results have been variable[42,48]. A dramatic response to oral hydroxychloroquine was reported in one patient[49], and Q-switched alexandrite laser may diminish the associated hyperpigmentation[50].

FOLLICULAR ATROPHODERMA

Follicular atrophoderma refers to dimple-like depressions at the follicular orifices. It can occur as an isolated defect of limited extent, in association with a variety of disorders in which hair follicles are plugged with keratin, or with rare genodermatoses.

In 1944, Miescher described follicular atrophoderma in an 8-year-old girl with atypical chondrodystrophy[51]. Six years later, Curth also used the term follicular atrophoderma (although there was no evidence of follicular atrophy but rather follicular agenesis) and further reported in 1978 on the genetics of follicular atrophoderma[52].

Clinical features

Distinctive follicular ice-pick depressions can be seen most commonly on the back of the hands and feet or on the cheeks. These pitted scars are often present at birth or appear during childhood. A family history may be present. Follicular atrophoderma can be associated with Bazex–Dupré–Christol and Conradi–Hünermann–Happle syndromes. When the lesions are found exclusively on the cheeks, the term "atrophoderma vermiculatum" applies. Atrophoderma vermiculatum can in turn be associated with various disorders discussed in the next section.

Atrophoderma Vermiculatum

Atrophoderma vermiculatum, a disorder limited to the face, has been described under a variety of names, including ulerythema acneiforme, acne vermoulante, atrophoderma reticulata symmetrica faciei, folliculitis ulerythema reticulata, folliculitis ulerythemosa, and honeycomb atrophy ("ulerythema" means scar plus redness and "vermiculatum" means worm-eaten).

Atrophoderma vermiculatum may: (1) occur sporadically; (2) be inherited as an autosomal dominant disorder; (3) be part of a group of related diseases that are referred to as "keratosis pilaris atrophicans" (see Table 38.2); or (4) be associated with various syndromes.

Multiple symmetric inflammatory papules on the cheeks, presumably centered around hair follicles, may precede the atrophic lesions. These papules then go on to become pitted, atrophic, depressed scars in a reticulated or honeycomb pattern (Fig. 99.8). The severity of erythema varies, as does the presence of milia and horny follicular plugs. Lesions can extend to the forehead and preauricular regions. Onset is usually in childhood or, less often, around puberty. Both sexes appear to be equally affected[53], and it usually has a slowly progressive course.

Atrophoderma vermiculatum can be associated with a group of closely related disorders referred to as keratosis pilaris atrophicans (see Table 38.2)[54]. This group also includes keratosis follicularis spinulosa decalvans and ulerythema ophryogenes. These conditions are characterized by keratotic follicular papules, variable degrees of inflammation, and secondary atrophic scarring. Ulerythema ophryogenes (or keratosis pilaris atrophicans faciei) differs from atrophoderma vermiculatum by affecting primarily the lateral portion of the eyebrows (ophryogenes) in the form of erythema, follicular papules, and alopecia. The inheritance pattern is autosomal dominant with incomplete penetrance and occasionally autosomal recessive, with progression usually ceasing after puberty. Keratosis follicularis spinulosa decalvans begins during childhood as keratotic follicular papules on the malar area and progresses to involve the eyebrows, scalp, and extremities, with associated scarring alopecia. In most patients, this disorder is inherited in an X-linked recessive fashion.

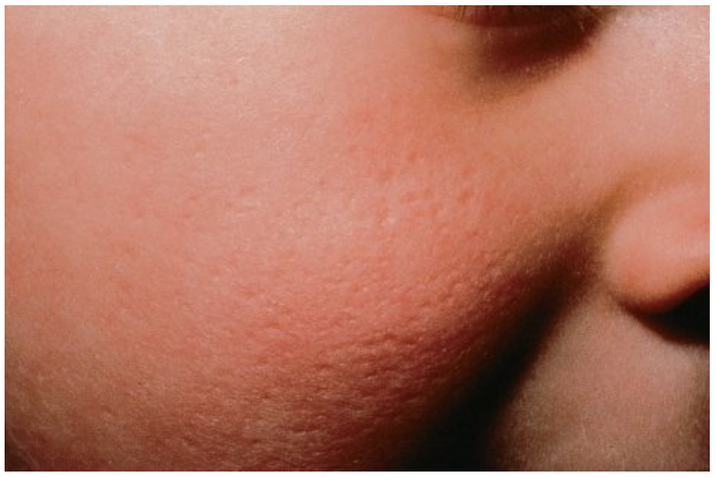


Fig. 99.8 Atrophoderma vermiculatum. Multiple small pitted scars on the cheek of a young girl. Note the honeycomb pattern on the lower inner cheek; the skin is said to appear "worm-eaten". *Courtesy Robert Hartman, MD.*

The underlying pathogenesis in atrophoderma vermiculatum as well as the other disorders in the keratosis pilaris atrophicans group appears to be abnormal follicular hyperkeratinization. The latter occurs in the upper third of the hair follicle, leading to obstruction of the growing hair shaft and production of chronic inflammation. The end result is scarring below the level of obstruction.

Histopathology is usually not very helpful and shows dilated follicles, sometimes associated with plugging, inflammation, and sclerosis of dermal collagen.

Syndromes associated with atrophoderma vermiculatum include Rombo syndrome (milia, telangiectasias, basal cell carcinomas [BCCs], hypotrichosis, acrocyanosis, and, occasionally, trichoepitheliomas) and Loeys–Dietz syndrome (see Ch. 95), in addition to the less well characterized Nicolau–Balus syndrome (syringomas and milia), Tuzun syndrome, and Braun–Falco–Marghescu syndrome (congenital poikiloderma).

The differential diagnosis of atrophoderma vermiculatum includes atrophia maculosa varioliformis cutis, keratosis pilaris rubra of the cheeks, and, in older adults, erythromelanosis faciei.

This disorder is primarily a cosmetic problem. Various topical treatments, including emollients, corticosteroids, tretinoin and keratolytics, have shown no consistent benefit. In some instances, systemic isotretinoin has been shown to stop progression and to induce remission[54]. Dermabrasion, laser therapy (e.g. CO_2, 585 nm pulsed dye), and fillers (e.g. hyaluronic acid, autologous fat) are other options for improving the appearance of the atrophic scars[55].

Bazex–Dupré–Christol Syndrome

Bazex, Dupré and Christol first described this genodermatosis in 1964, not to be confused with Bazex syndrome (acrokeratosis paraneoplastica) in which hyperkeratotic plaques of the ears, nose, cheeks, hands, feet and knees are associated with carcinomas of the upper aerodigestive tract (see Ch. 53). Bazex–Dupré–Christol syndrome is characterized by follicular atrophoderma, milia, multiple BCCs, hypotrichosis, and localized hypohidrosis (above the neck)[56]. It is inherited in an X-linked dominant fashion, and the gene has been linked to Xq24–q27[57]. Additional reported findings include facial hyperpigmentation, hair shaft anomalies, and multiple trichoepitheliomas. Systemic manifestations are absent. Recently, it was suggested that this syndrome might better be classified as an ectodermal dysplasia[58].

The follicular atrophoderma, described as multiple ice-pick marks or patulous follicles, is found most commonly on the dorsal aspect of the hands, but can also be seen on the feet, lower back, elbows, and occasionally the face; it may be present at birth or appear later during childhood. No abnormalities of the elastic fibers have been found (nor any evidence of atrophy of the epidermis, hair or dermis), making the term "follicular atrophoderma" a misnomer. The histopathology usually

shows hair follicles that are abnormally wide, plugged, and surrounded by an inflammatory cell infiltrate and clusters of basaloid cells. Sweat glands can be absent.

BCCs develop in about 40% of patients (primarily on the face) and can resemble melanocytic nevi; the age of onset varies from 9 to 50 years of age. To date, ~20 families with this syndrome have been described.

The differential diagnosis includes other genodermatoses with multiple BCCs: basal cell nevus syndrome (Gorlin syndrome), an autosomal dominant disorder most commonly due to mutations in *PTCH1* (see Ch. 108); Rombo syndrome, an autosomal dominant disorder characterized by BCCs, atrophoderma vermiculatum, milia, hypotrichosis, acrocyanosis, and, occasionally, trichoepitheliomas; and xeroderma pigmentosum (see Ch. 86).

Conradi–Hünermann–Happle Syndrome (X-Linked Dominant Chondrodysplasia Punctata, CDPX2)

Conradi–Hünermann–Happle syndrome is an X-linked dominant disorder that occurs almost exclusively in girls, since it is usually lethal in hemizygous males. This form of chondrodysplasia punctata results from mosaicism for mutations in the gene on the X chromosome that encodes the emopamil-binding protein[59,60]. The clinical manifestations include ichthyosiform streaks (composed of erythema plus feathery, adherent scale) patterned along the lines of Blaschko; they usually resolve during the first year of life and are replaced by bands of follicular atrophoderma[60]. Hyperpigmentation, cataracts, scarring alopecia, saddle-nose deformity, asymmetric limb reduction defects, and stippled calcifications of the epiphyses are additional manifestations (see Ch. 57). Within the ichthyosiform areas in newborns, keratotic follicular plugs containing dystrophic calcification is a distinctive histopathologic feature[59].

ATROPHIA MACULOSA VARIOLIFORMIS CUTIS

Atrophia maculosa varioliformis cutis was first described by Heidingsfeld in 1918[61] and is not as rare as the number of published cases would suggest. It consists of small round "varioliform" and linear facial depressions that are asymptomatic (Fig. 99.9)[62]. It occurs spontaneously on the cheeks and occasionally involves the forehead or chin. There is a gradual increase in the number of lesions, but in the absence of preceding trauma, acne, or inflammatory lesions. A familial variant has been described. Pachydermodactyly and extrahepatic biliary atresia have been associated findings, but this association is probably fortuitous. The pathogenesis is unknown.

The histologic changes include a depression of the epidermis and normal collagen fibers, but a slightly decreased number of elastic fibers. There is usually little or no inflammation. The differential diagnosis includes simple scars, which can be differentiated by history and the presence histologically of dermal fibrosis, and atrophoderma vermiculatum. The latter is harder to differentiate, but it can present with inflammatory papules that are followed by pitted scars, and atrophoderma vermiculatum usually has a honeycombed (rather than sharply linear) pattern and is usually centered on hair follicles. There is no known treatment to prevent the occurrence of these lesions.

PIEZOGENIC PEDAL PAPULES (PIEZOGENIC PAPULES)

Piezogenic pedal papules were first described by Shelley and Rawnsley in 1968[63]. This term is somewhat of a misnomer as piezogenic means "producing pressure", when in fact these lesions are produced by pressure. It is postulated that pressure induces herniation of fat through connective tissue in the dermis of the heels.

These papules are common enough in the general population to be considered normal and have also been described in association with Ehlers–Danlos syndrome, Prader–Willi syndrome, and GATA2 deficiency[64]. An infantile variant characterized by larger nodules on the medial aspect of the heel (present without weight-bearing) has been described[65] and is referred to as pedal papules of infancy and more recently, precalcaneal congenital fibrolipomatous hamartoma (Fig. 99.10). When unilateral, this entity has to be distinguished from juvenile aponeurotic fibroma which can calcify.

Skin-colored papules and nodules are seen on the sides of the heels (Fig. 99.11); they are induced by weight-bearing and disappear when the leg is



Fig. 99.10 Pedal papules of infancy (precalcaneal congenital fibrolipomatous hamartoma). Soft nodules on the medial and plantar surfaces of the foot. *Courtesy Julie V. Schaffer, MD.*



Fig. 99.9 Atrophia maculosa varioliformis cutis. Multiple linear scar-like depressions (between and above arrows) with no history of trauma. *Courtesy Jean L. Bolognia, MD.*



Fig. 99.11 Piezogenic pedal papules. Soft papulonodules on the heel. *Courtesy Benoit Côté, MD.*

raised. The lesions are usually asymptomatic, but pain has been described during weight-bearing, and, in these cases, an orthopedic shoe or surgical excision may help. Similar lesions have been described on the wrists[66].

OTHER ATROPHIES OF THE CONNECTIVE TISSUE

Many systemic conditions (lupus erythematosus, dermatomyositis) and genodermatoses (Rothmund–Thomson syndrome, dyskeratosis congenita, Cockayne syndrome, Hallermann–Streiff syndrome) have cutaneous atrophy (epidermal, dermal, and/or subcutaneous) as an associated finding. Lichen sclerosus is discussed in Chapter 44, progeria in Chapter 63, Ehlers–Danlos syndrome and cutis laxa in Chapter 97, and acrodermatosis chronica atrophicans in Chapter 74. Cutaneous atrophy is also a well-known complication of prolonged use of either systemic or topical corticosteroids (see Ch. 125).

Additional figures available in our eBook (see inside front cover for access code).

REFERENCES

1. Shelley WB, Wood MG. Wrinkles due to idiopathic loss of mid-dermal elastic tissue. *Br J Dermatol*. 1977;97:441–445.
2. Hardin J, Dupuis E, Haber RM. Mid-dermal elastolysis: a female-centric disease; case report and updated review of the literature. *Int J Womens Dermatol*. 2015;1:126–130.
3. Gambichler T, Mamali K, Scheel C. A brief literature update on mid-dermal elastolysis with an emphasis on pathogenetic and therapeutic aspects. *J Clin Aesthet Dermatol*. 2020;13:e53–e58.
4. Snider RL, Lang PG, Maize JC. The clinical spectrum of mid-dermal elastolysis and the role of UV light in its pathogenesis. *J Am Acad Dermatol*. 1993;28:938–942.
5. Vatve M, Morton R, Bilsland D. A case of mid-dermal elastolysis after narrowband ultraviolet B phototherapy. *Clin Exp Dermatol*. 2009;34:263–264.
6. Gambichler T, Breuckmann F, Kreuter A, et al. Immunohistochemical investigation of mid-dermal elastolysis. *Clin Exp Dermatol*. 2004;29:192–195.
7. Gambichler T, Skrygan M. Decreased lysyl oxidase-like 2 expression in mid-dermal elastolysis. *Arch Dermatol Res*. 2013;305:359–363.
8. Gambichler T, Reininghaus L, Skrygan M, et al. Fibulin protein expression in mid-dermal elastolysis and anetoderma: a study of 23 cases. *Acta Derm Venereol*. 2016;96:708–710.
9. Scola N, Goulioumis A, Gambichler T. Non-invasive imaging of mid-dermal elastolysis. *Clin Exp Dermatol*. 2011;36:155–160.
10. Smithson SL, Orchard D, Scardamaglia L. Mycophenolate mofetil to treat mid-dermal elastolysis. *Pediatr Dermatol*. 2018;35:e221–e223.
11. Jadassohn J. Uber eine eigenartige form von 'atrophica maculosa cutis'. *Arch Dermatol Syphilol*. 1892;24:342–358.
12. Schweninger E, Buzzi F. *Multiple benign tumor-like new growths of the skin*. *International Atlas Sellltener Hautkrankheiten, plate 15*. Leipzig: L Voss;; 1891.
13. Venencie PY, Bonnefoy A, Gogly B, et al. Increased expression of gelatinases A and B by skin explants from patients with anetoderma. *Br J Dermatol*. 1997;137:517–525.
14. Brys AK, Rodriguez-Homs LG, Wennerberg S, et al. Anetoderma associated with a succinate dehydrogenase gene mutation: a potental link between anetoderma and citric acid cycle mutations. *JAMA Dermatol*. 2019;155:1317–1318.
15. Venencie PY, Winkelmann RK, Moore BA. Anetoderma: clinical findings, associations, and long-term follow-up evaluations. *Arch Dermatol*. 1984;120:1032–1039.
16. Patrizi A, Neri I, Virdi A, et al. Familial anetoderma: a report of two families. *Eur J Dermatol*. 2011;21:680–685.
17. Hodak E, David M. Primary anetoderma and antiphospholipid antibodies – review of the literature. *Clin Rev Allergy Immunol*. 2007;32:162–166.
18. Gougeon E, Beer F, Gay S, et al. Anetoderma of prematurity: an iatrogenic consequence of neonatal intensive care. *Arch Dermatol*. 2010;146:565–567.
19. Venecie PY, Wilkelmann RK. Histopathologic findings in anetoderma. *Arch Dermatol*. 1984;120:1040–1044.
20. Bergman R, Friedman-Birnbaum R, Hazaz B, et al. An immunofluorescence study of primary anetoderma. *Clin Exp Dermatol*. 1990;15:124–130.
21. Sezer E, Durmaz EO, Sahin S. Papular elastorrhexis: clinical perspectives. *Clin Cosmet Investig Dermatol*. 2018;11:541–544.
22. Cho S, Jung JY, Lee JH. Treatment of anetoderma occurring after resolution of Stevens-Johnson syndrome using an ablative 10,600-nm carbon dioxide fractionated laser. *Dermatol Surg*. 2012;38:677–679.
23. Wang K, Ross NA, Saedi N. Anetoderma treated with combined 595-nm pulsed-dye laser and 1550-nm non ablative fractionated laser. *J Cosmet Laser Ther*. 2016;18:38–40.
24. Hirt PA, Castillo DE, Yosipovitch G, Keri JE. Skin changes in the obese patient. *J Am Acad Dermatol*. 2019;81:1037–1057.
25. Elsedfy H. Striae distensae in adolescents: a mini review. *Acta Biomed*. 2020;91:176–181.
26. Farahnik B, Park K, Kroumpouzos G, Murase J. Striae gravidarum: risk factors, prevention and management. *Int J Womens Dermatol*. 2017;3:77–85.
27. Farber SA, Samimi S, Rosenbach M. Ulcerations within striae distensae associated with bevacizumab therapy. *J Am Acad Dermatol*. 2015;72:e33–e35.
28. Wahman AJ, Finan MA, Emerson SC. Striae gravidarum as a predictor of vaginal lacerations at delivery. *South Med J*. 2000;93:873–876.
29. Salter SA, Batra RS, Rohrer TE, et al. Striae and pelvic relaxation: two disorders of connective tissue with a strong association. *J Invest Dermatol*. 2006;126:1745–1748.
30. Al-Himdani SI, Ud-Din S, Gilmore S, Bayat A. Striae distensae: a comprehensive review and evidence-based evaluation of prophylaxis and treatment. *Br J Dermatol*. 2014;170:527–547.
31. Burket JM, Zelickson AS, Padilla RS. Linear focal elastosis (elastotic striae). *J Am Acad Dermatol*. 1989;20:633–636.
32. Hashimoto K. Linear focal elastosis: keloidal repair of striae distensae. *J Am Acad Dermatol*. 1998;39:309–313.
33. Kang S. Topical tretinoin therapy for management of early striae. *J Am Acad Dermatol*. 1998;39:S90–S92.
34. Ud-Din S, McGeorge D, Bayat A. Topical management of striae distensae (stretch marks): prevention and therapy of straie rubrae and albae. *J Eur Acad Dermatol Venereol*. 2016;30:211–222.
35. Forbat E, Al-Niaimi F. Treatment of striae distensae: an evidence-based approach. *J Cosmet Laser Ther*. 2019;21:49–57.
36. Aldahan AS, Shah VV, Mlacker S, et al. Laser and light treatments for striae distensae: a comprehensive review of the literature. *Am J Clin Dermatol*. 2016;17:239–256.
37. Ramault L, Hoeksema H, Pirayesh A, et al. Microneedling: where do we stand now? A systematic review of the literature. *J Plast Reconstr Aesthet Surg*. 2018;71:1–14.
38. Pasini A. Atrophoderma idiopathica progressiva. *Gior Ital Derm Sif*. 1923;58:785.
39. Canizares O, Sachs PM, Jaimovich L, Torres VM. Idiopathic atrophoderma of Pasini and Pierini. *Arch Dermatol*. 1958;77:42–60.
40. Muntyanu A, Redpath M, Roshdy O, Jfri A. Idiopathic atrophoderma of Pasini and Pierini: case report and literature review. *Clin Case Rep*. 2019;7:258–263.
41. Kang CY. Lam. J. Congenital idiopathic atrophoderma of Pierini and Pasini. *Int J Dermatol*. 2015;54:e44–e46.
42. Buechner SA, Rufli T. Atrophoderma of Pasini and Pierini: clinical and histopathologic findings and antibodies to *Borrelia burgdorferi* in thirty-four patients. *J Am Acad Dermatol*. 1994;30:441–446.
43. Saleh Z, Abbas O, Dahdah MJ, et al. Atrophoderma of Pierini and Pasini: a clinical and histopathological study. *J Cutan Pathol*. 2008;35:1108–1114.
44. Amano H, Nagai Y, Ishikawa O. Multiple morphea coexistent with atrophoderma of Pierini-Pasini (APP): APP could be abortive morphea. *J Eur Acad Dermatol Venereol*. 2007;21:1254–1256.
45. Yokoyama Y, Akimoto S, Ishikawa O. Disaccharide analysis of skin glycosaminoglycans in atrophoderma of Pasini and Pierini. *Clin Exp Dermatol*. 2000;25:436–440.
46. Viera-Damiani G, Lage D, Christofoletti Daldon PE, et al. Idiopathic atrophoderma of Pasini and Pierini: a case study of collagen and elastin texture by multiphoton microscopy. *J Am Acad Dermatol*. 2017;77:930–937.
47. Berman A, Berman GD, Kinnkelmann RK. Atrophoderma (Pasini-Pierini): findings on direct immunofluorescent, monoclonal antibody, and ultrastructural studies. *Int J Dermatol*. 1988;27:487–490.
48. Lee Y, Oh Y, Ahn SY, et al. A case of atrophoderma of Pasini and Pierini associated with *Borrelia burgdorferi* infection successfully treated with oral doxycycline. *Ann Dermatol*. 2011;23:352–356.
49. Carter JD, Valeriano J, Vasey FB. Hydroxychloroquine as a treatment for atrophoderma of Pasini and Pierini. *Int J Dermatol*. 2006;45:1255–1256.
50. Arpey CJ, Patel DS, Stone MS, et al. Treatment of atrophoderma of Pasini and Pierini-associated hyperpigmentation with Q-switched alexandrite laser: a clinical, histologic, and ultrastructural appraisal. *Lasers Surg Med*. 2000;27:206–212.
51. Miescher G. Atypische Chondrodystrophie, Typus morquino kombiniert mit follikularer atrophodermie. *Dermatologica*. 1944;89:38–51.
52. Curth HO. The genetics of follicular atrophoderma. *Arch Dermatol*. 1978;114:1479–1483.
53. Luria RB, Conologue T. Atrophoderma vermiculatum: a case report and review of the literature on keratosis pilaris atrophicans. *Cutis*. 2009;83:83–86.
54. Callaway SR, Lesher JL. Keratosis pilaris atrophicans: case series and review. *Pediatr Dermatol*. 2004;21:14–17.
55. Handrick C, Alster T. Laser treatment of atrophoderma vermiculata. *J Am Acad Dermatol*. 2001;44:693–695.
56. AlSabbagh MM, Baqi MA. Bazex-Dupré-Christol syndrome: review of clinical and molecular aspects. *Int J Dermatol*. 2018;57:1102–1106.
57. Parren LJ, Abuzahra F, Wagenvoort T, et al. Linkage refinement of Bazex-Dupré-Christol syndrome to an 11-4-Mb interval on chromosome Xq25-27.1. *Br J Dermatol*. 2011;165:201–203.
58. Castori M, Castiglia D, Passarelli F, et al. Bazex-Dupré-Christol syndrome: an ectodermal dysplasia with skin appendage neoplasms. *Eur J Med Genet*. 2009;52:250–255.
59. Hoang MP, Carder KR, Pandya AG, Bennettt MJ. Ichthyosis and keratotic follicular plugs containing dystrophic calcification in newborns: distinctive histopathologic features of X-linked dominant chondrodysplasia punctata (Conradi-Hünermann-Happle syndrome). *Am J Dermatopathol*. 2004;26:53–58.
60. Canueto J, Giros M, Ciria S, et al. Clinical, molecular and biochemical characterization of nine Spanish families with Conradi-Hünermann-Happle syndrome: new insights into X-linked dominant chondrodysplasia punctata with a comprehensive review of the literature. *Br J Dermatol*. 2012;166:830–838.
61. Heidingsfeld ML. Atrophia maculosa varioliformis cutis. *J Cutan Dis*. 1918;36:285–288.
62. Kuflik JH, Schwartz RA, Becker KA, Lambert WC. Atrophia maculosa varioliformis cutis. *Int J Dermatol*. 2005;44:864–866.
63. Shelley WB, Rawnsley JM. Painful feet due to herniation of fat. *JAMA*. 1968;205:308–309.
64. Amarnani AA, Poladian KR, Marciano BE, et al. A panoply of rheumatological manifestations in patients with GATA2 deficiency. *Sci Rep*. 2020;10:8305.
65. Greenberg S, Krafchik BR. Infantile pedal papules. *J Am Acad Dermatol*. 2005;53:333–334.
66. Laing VB, Fleischer Jr. AB. Piezogenic wrist papules: a common and symptomatic finding. *J Am Acad Dermatol*. 1991;24:415–417.





eFig. 99.1 Secondary anetoderma. Wrinkling of the skin at sites of sarcoidosis (**A**) and lepromatous leprosy (**B**). *B, Courtesy Louis A. Fragola, Jr, MD.*



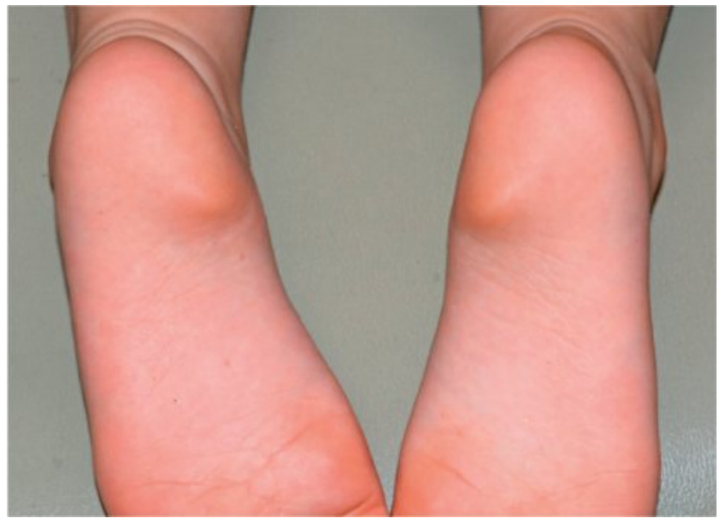
eFig. 99.2 Linear focal elastosis. This is the most common site of involvement. Note that the lesions are elevated and yellowish in color.



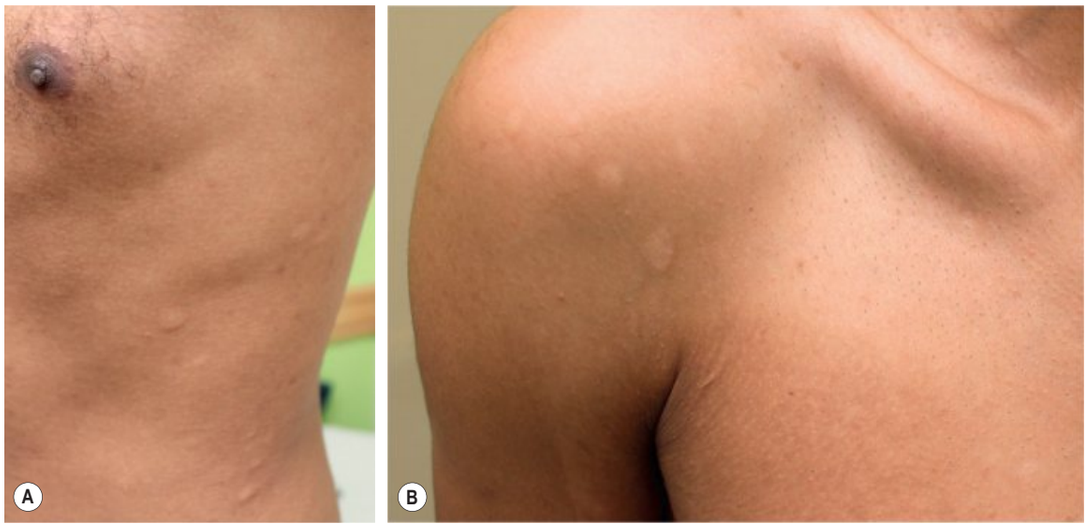
eFig. 99.3 Atrophoderma of Pasini and Pierini. Coalescent hyperpigmented patches on the abdomen.



eFig. 99.4 Piezogenic pedal papules (piezogenic papules). Soft papules, primarily on the medial heel.



eFig. 99.5 Pedal papules of infancy (precalcaneal congenital fibrolipomatous hamartoma). Asymptomatic, symmetric soft nodules on the medial aspect of the heels persist in this 2-year-old child. *Courtesy Julie V. Schaffer, MD.*



eFig. 99.6 Primary anetoderma. Lesions vary, from flat to soft papules that herniate upon palpation, and can appear hypopigmented. *Courtesy Kalman Watsky, MD.*

Panniculitis 100

Luis Requena, Heinz H. Kutzner and James W. Patterson

Chapter Contents

Erythema Nodosum *1751*
Subacute Nodular Migratory Panniculitis *1756*
Morphea/Scleroderma Panniculitis *1756*
Alpha-1 Antitrypsin Deficiency Panniculitis *1757*
Erythema Induratum *1758*
Pancreatic Panniculitis *1760*
Sclerema Neonatorum, Subcutaneous Fat Necrosis of the Newborn, and Post-Steroid Panniculitis *1761*
Lupus Erythematosus Panniculitis (Lupus Panniculitis) *1764*
Panniculitis of Dermatomyositis *1765*
Traumatic Panniculitis *1766*
Lipodermatosclerosis *1767*
Infection-Induced Panniculitis *1769*
Cytophagic Histiocytic Panniculitis *1771*
Malignant Subcutaneous Infiltrates *1771*
Unusual or Newly Described Forms of Panniculitis *1771*

INTRODUCTION

Panniculitis is a diagnostically challenging arena for both dermatologists and pathologists. Terminology is difficult, partly because various names have been applied to the same disorder (e.g. nodular vasculitis and erythema induratum), and partly because new discoveries have resulted in the introduction of new terms and the abandonment of others. From a clinical standpoint, many forms of panniculitis with diverse etiologies closely resemble one another, presenting as tender, erythematous, subcutaneous nodules. Some panniculitides can be a manifestation of different disease processes (erythema nodosum is the classic example), and, even if the type of panniculitis is correctly identified, this is only the first step in a series of investigations required to determine the underlying cause. From a pathologic standpoint, the subcutaneous fat responds to a variety of different insults in a limited number of ways, and, therefore, histopathologic differences among the various forms of panniculitis may be subtle. Management can also be difficult, since there are often at least two therapeutic desiderata:

- specific treatment of the panniculitis
- treatment of the underlying illness.

In this chapter, these issues will be addressed by introducing a schema for the classification of these disorders, recommending an approach to the histopathologic diagnosis, and providing information about the specific forms of panniculitis and their management. The categories are determined partly by clinical characteristics such as anatomic location (Fig. 100.1), partly by histopathology (Fig. 100.2), and partly by etiology. A word should be said about *septal* versus *lobular* panniculitis. These are largely artificial constructs, since there is no purely septal or purely lobular panniculitis.

Table 100.1 provides an approach to the histopathologic diagnosis of an unknown case of panniculitis. When performing a biopsy in a patient with panniculitis, it is absolutely critical that the specimen includes a generous portion of subcutaneous fat. Therefore, excisional biopsies extending through the subcutis or narrow incisional biopsies that incorporate a broad expanse of subcutaneous fat are preferable to punch biopsies.

ERYTHEMA NODOSUM

Synonyms: ■ Erythema contusiformis ■ Erythema nodosum migrans (variant form)

Key features

- Tender, erythematous, subcutaneous nodules
- Usually distributed symmetrically and favor the pretibial areas; occasionally occur elsewhere
- In later stages, lesions acquire a bruise-like appearance
- May be accompanied by fever, arthralgias, and malaise
- Associated with a wide variety of systemic disorders

Introduction

Erythema nodosum is the best known of the various forms of panniculitis, as well as the most common. It typically presents as an acute eruption of tender, erythematous, subcutaneous nodules in the pretibial areas bilaterally. It is widely regarded as a delayed hypersensitivity response to a variety of antigenic challenges[1], although the mechanisms of its development are more complex than this statement would indicate. Histopathologically, it is the prototype of a "septal"

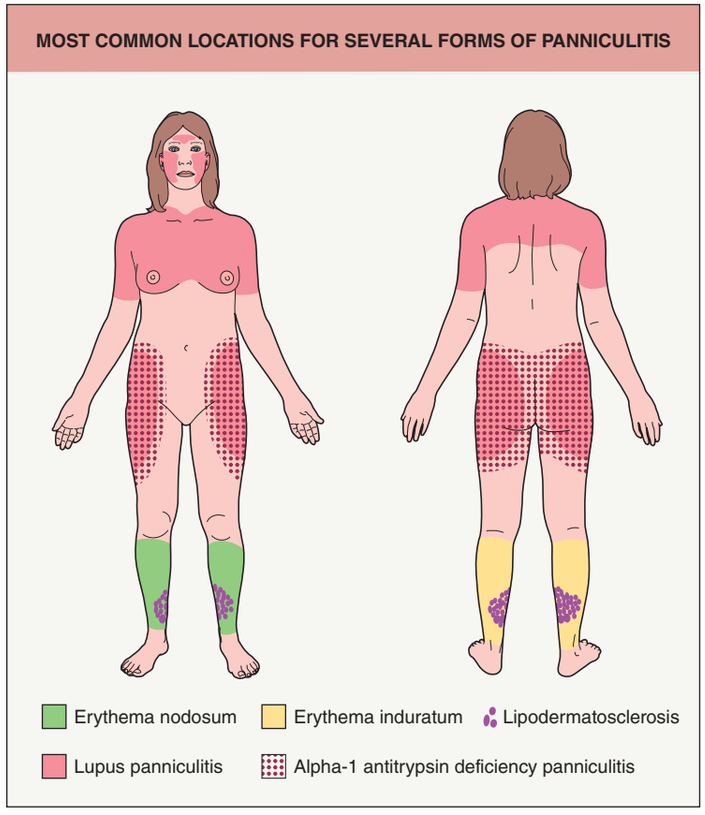
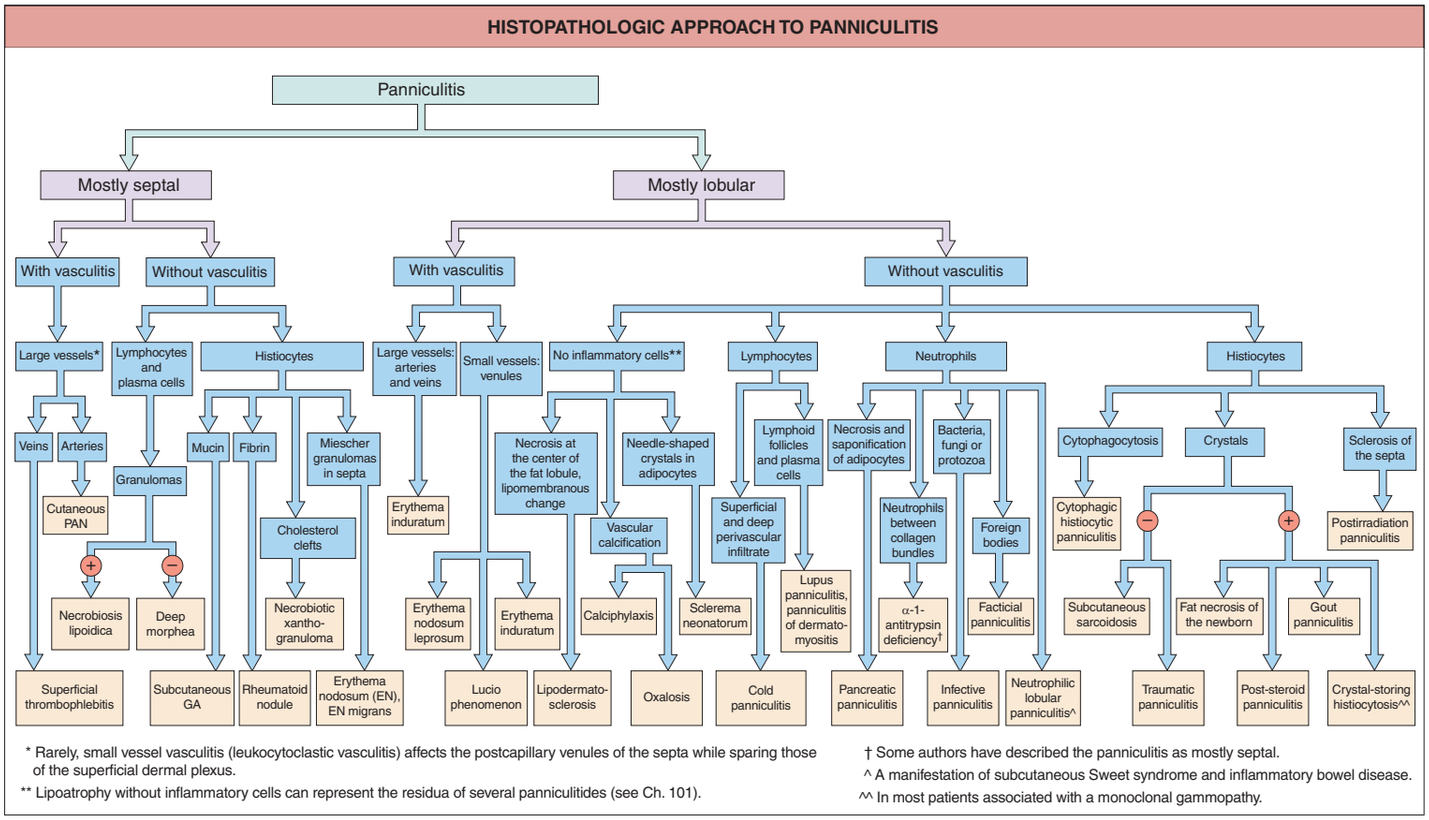


Fig. 100.1 Most common locations for several forms of panniculitis. Classification of panniculitis depends upon multiple factors, including clinical characteristics such as location and ulceration as well as histopathology and etiology.



* Rarely, small vessel vasculitis (leukocytoclastic vasculitis) affects the postcapillary venules of the septa while sparing those of the superficial dermal plexus.

** Lipoatrophy without inflammatory cells can represent the residua of several panniculitides (see Ch. 101).

† Some authors have described the panniculitis as mostly septal.

^ A manifestation of subcutaneous Sweet syndrome and inflammatory bowel disease.

^^ In most patients associated with a monoclonal gammopathy.

Fig. 100.2 Histopathologic approach to panniculitis. Drug-induced panniculitis can be primarily septal or lobular and is reviewed in Table 100.3. Leukemia cutis or lymphoma cutis may mimic panniculitis as in subcutaneous panniculitis-like T cell lymphoma, and the subcutaneous nodules observed in ANCA-associated vasculitides can contain extravascular necrotizing granulomas. GA, granuloma annulare; PAN, polyarteritis nodosa.

AN APPROACH TO THE HISTOPATHOLOGIC DIAGNOSIS OF PANNICULITIS	
Histopathologic aspects to consider	**Conclusions**
Look for the "center of gravity" of the infiltrate	Recommended originally by Pinkus, the purpose is to determine whether or not the inflammatory process is centered in the subcutis (favoring a primary panniculitis), in the dermis, or in the fascia (in which case the panniculitis may be a secondary manifestation of a deeper inflammatory process)
Determine if the panniculitis is predominantly septal, predominantly lobular, or mixed	Generally, a predominantly septal panniculitis narrows the diagnostic considerations. If the panniculitis is lobular or mixed, look for other distinguishing features (see Fig. 100.2)
Determine if there is vasculitis involving a medium-sized vessel, in the face of a lobular or mixed panniculitis	This is characteristic of **erythema induratum (nodular vasculitis)**; caveat: deeper levels are often required in order to demonstrate the involvement of vessels
Look for fat necrosis with saponification and "calcium soap" formation	This is a feature of **pancreatic panniculitis**
Look for needle-shaped clefts within lipocytes	Their presence favors a diagnosis of **sclerema neonatorum, subcutaneous fat necrosis of the newborn**, or **post-steroid panniculitis**
Determine if the panniculitis has a lymphoplasmacytic predominance	This tends to be a feature of **panniculitis due to connective tissue disease**, including lupus erythematosus; beware of lymphocytic predominance in cases of subcutaneous panniculitis-like T cell lymphoma (see Table 100.9)
Check for a "central nidus" of inflammation or evidence of a needlestick injury. Look for vacuolated spaces or foreign material	These are clues to **traumatic panniculitis including factitial panniculitis**. Polarization microscopy can be helpful
Determine if lobular panniculitis has a predominance of neutrophils	**Infection-induced panniculitis, neutrophilic panniculitis** associated with inflammatory bowel disease and rheumatoid arthritis, **subcutaneous Sweet syndrome, traumatic panniculitis, drug-induced panniculitis** (see Table 100.3), **idiopathic neutrophilic lobular panniculitis**; less so in alpha-1 antitrypsin deficiency panniculitis and pancreatic panniculitis
Look for membranocystic changes in the subcutis	This change is characteristic of (though not pathognomonic for) **lipodermatosclerosis**; it can be observed in any panniculitis with prominent degenerative changes
Determine if the panniculitis is associated with substantial cellular necrosis, vascular proliferation, hemorrhage, sweat gland necrosis, or neutrophilic aggregates	These changes are often encountered in **infection-induced panniculitis**. Tissue cultures, special stains, and PCR for organisms may be indicated
Determine if the infiltrating cells are particularly monotonous or atypical in appearance	Consider subcutaneous panniculitis-like T cell lymphoma and other lymphomas with involvement of the subcutaneous fat. Rarely, non-hematologic malignancies mimic panniculitis. Immunohistochemical stains are mandatory for a precise diagnosis
Determine if there are large cells with cytophagic activity	Cytophagic activity (hemophagocytosis) observed primarily in subcutaneous infiltrates of subcutaneous panniculitis-like T cell lymphoma and subcutaneous lesions of primary cutaneous γ/δ T cell lymphoma. This finding was previously termed "cytophagic histiocytic panniculitis"

Table 100.1 An approach to the histopathologic diagnosis of panniculitis.

panniculitis. Identification and treatment of the underlying disorder, if found, is of primary importance, but therapy directed toward the lesions themselves is also an option, especially when idiopathic.

History

At the beginning of the eighteenth century, Robert Willan gave the first clear description of erythema nodosum, and he provided its name in his famous work, *On Cutaneous Disease*[2].

Epidemiology

Erythema nodosum can occur at any age, in both sexes, and in all racial groups. It is more common among women and is more frequently observed during the second through fourth decades of life[3,4]. The relative ranking of underlying causes may vary according to geographic location; for example, in areas where *Coccidioides immitis* is endemic or regions where Behçet disease is more prevalent.

Pathogenesis

Erythema nodosum has been considered a delayed hypersensitivity response to a variety of antigenic stimuli, including bacteria, viruses, and chemical agents[1]. Llorente et al.[5] observed expression of mRNA for Th1 cytokines (interferon-γ, interleukin-2) in the skin lesions and peripheral blood of patients with erythema nodosum, and a Th1 pattern of cytokine synthesis is associated with delayed-type hypersensitivity reactions. However, a complex series of intermediate steps is involved in the development of these lesions. A variety of adhesion molecules and inflammatory mediators appear to be associated with erythema nodosum. For example, in erythema nodosum lesions, vascular cell adhesion molecule-1 (VCAM-1; CD106), platelet endothelial cell adhesion molecule-1 (PECAM-1; CD31), HLA-DR, and E-selectin are expressed on endothelial cells, while very late antigen-4 (VLA-4), L-selectin, and HLA-DR are expressed by inflammatory cells (see Ch. 102)[6].

Neutrophils are often numerous in early lesions, and it has been shown that a higher percentage of circulating neutrophils in patients with erythema nodosum leads to the production of reactive oxygen intermediates; these intermediates, in turn, may provoke inflammation and tissue damage[7]. Support for a pathogenic role for these cells and molecules is provided by studies on the effects of colchicine[8]. This inhibitor of neutrophil chemotaxis has been shown to diminish L-selectin expression on the neutrophil surface, inhibit E-selectin-mediated endothelial adhesiveness for neutrophils, and diminish stimulated expression of ICAM-1 on the endothelium[6].

Additional indirect evidence for the role of inflammatory cells and mediators includes reports of erythema nodosum following treatment with granulocyte colony-stimulating factor[9], and improvement (as well as flares) of erythema nodosum lesions with administration of tumor necrosis factor (TNF) inhibitors[10]. Erythema nodosum, especially in its chronic phase, is characterized by granuloma formation and TNF is known to play a role in granuloma formation. A link between deregulation of TNF production and granuloma formation is further supported by the strong correlation of a polymorphism in the promoter region of the gene that encodes TNF and the development of sarcoidosis-associated erythema nodosum[11].

A wide range of precipitating factors has been linked with erythema nodosum. Infectious causes are common, particularly upper respiratory infections (both streptococcal and non-streptococcal). Other commonly reported causes are listed in Tables 100.2 and 100.3[3,4,12].

Clinical Features

Erythema nodosum presents with bilateral, tender, erythematous nodules. These arise in crops and clearly the most common site is the shins (Fig. 100.3). Other locations are occasionally involved, particularly the thighs and forearms[3]. Nodules may also appear on the trunk, neck, and face[2], but this is sufficiently rare that development of lesions in these locations should prompt consideration of other diagnoses. Unlike other forms of panniculitis, ulceration is not a feature of erythema nodosum. Systemic symptoms may occur that are not necessarily related to a specific coexisting systemic disorder; these include arthritis, arthralgia, fever, and malaise[2].

Because of its close association with a variety of disorders and infections, erythema nodosum is an important skin sign of systemic disease.

CAUSES OF ERYTHEMA NODOSUM

Cause	Comments
Most common	
Idiopathic	Still the largest single category, accounting for a third to a half of cases
Streptococcal infections, especially of the upper respiratory tract	The largest single infectious cause
Other infections: Viral upper respiratory tract infections Bacterial gastroenteritis – *Yersinia* > *Salmonella, Campylobacter*	Overall, infection may account for a third or more of cases
Coccidioidomycosis	Erythema nodosum is associated with a lower incidence of disseminated disease
Drugs	See Table 100.3
Sarcoidosis*	10%–20% of cases in some series
Inflammatory bowel disease	Crohn disease has a stronger association with erythema nodosum than does ulcerative colitis
Uncommon	
Infections: *Brucella melitensis* *Chlamydophila*† *pneumoniae* *Chlamydia trachomatis* *Mycoplasma pneumoniae* *Mycobacterium tuberculosis* *Histoplasma capsulatum* Hepatitis B virus‡	
Neutrophilic dermatoses: Behçet disease Sweet syndrome	"Erythema nodosum" in Behçet disease more closely resembles erythema induratum (nodular vasculitis)
Acne fulminans, including isotretinoin-associated	
Pregnancy	
Rare	
Granulomatous mastitis	
Pernicious anemia	
Diverticulitis	
Infections: *Neisseria gonorrhoeae, N. meningitides* *Escherichia coli, Bartonella henselae, Bordetella pertussis* *Treponema pallidum* Dermatophytes (kerion), *Blastomyces dermatitidis* HIV COVID-19 Giardiasis, amoebiasis (abscesses)	*Erythema nodosum leprosum* is a different disease that is characterized by a cutaneous small vessel vasculitis
MonoMAC syndrome (*GATA2* mutations)	
Malignancy, most often acute myelogenous leukemia, Hodgkin disease	May overlap with Sweet syndrome
Lupus erythematosus	One of several forms of panniculitis reported in LE, in addition to lupus panniculitis

*Löfgren syndrome is an acute, spontaneously resolving form of sarcoidosis characterized by erythema nodosum, hilar lymphadenopathy, fever, polyarthritis and uveitis.
†Previously referred to as *Chlamydia*.
‡Erythema nodosum secondary to the hepatitis B vaccine has also been reported.

Table 100.2 Causes of erythema nodosum. LE, lupus erythematosus; TNF, tumor necrosis factor.

For example, its development may precede or accompany a flare of inflammatory bowel disease. It may also have some value as a prognostic indicator in certain disorders. For example, erythema nodosum is associated with a protective effect against disseminated disease in patients with coccidioidomycosis, and it is closely aligned with a more benign and self-limited form of sarcoidosis[1]. Nevertheless, a significant percentage of cases – more than one-third – have no known disease association, even when followed for a year or more[4]. Clinical or laboratory data that tend to predict that the development of erythema nodosum may be secondary to a systemic disease are listed in Table 100.4.

Erythema nodosum lesions usually last a few days or weeks and then slowly involute, without scar formation. Discoloration suggestive of a bruise may be seen as the erythema subsides. More chronic forms do occur, some of which show a tendency toward migration or centrifugal spread; the latter have been termed *subacute nodular migratory panniculitis* or *erythema nodosum migrans* (see below). Up to one-third of cases of erythema nodosum recur. Annual recurrences are particularly common among idiopathic cases[12].

DRUG-INDUCED PANNICULITIS	
Drug	**Histopathologic patterns**
Estrogens, oral contraceptive pills	EN-like
Antibiotics (e.g. sulfonamides, penicillins)	EN-like
Bromides, iodides	EN-like
TNF inhibitors (e.g. etanercept, infliximab, adalimumab)	EN-like, lupus-like
Immune checkpoint inhibitors (e.g. ipilimumab, nivolumab, pembrolizumab)	EN-like, granulomatous/ sarcoid-like
BRAF inhibitors (e.g. vemurafenib, dabrafenib)	EN-like, neutrophilic lobular
Tyrosine kinase inhibitors (e.g. imatinib, dasatinib, ibrutinib)	EN-like, neutrophilic lobular
Hypomethylating agents (e.g. azacitidine, decitabine, guadecitabine)	Neutrophilic lobular
Bruton's tyrosine kinase (BTK) inhibitors (e.g. ibrutinib, acalabrutinib, zanubrutinib)	Neutrophilic lobular
Gemcitabine	Lipodermatosclerosis-like

Table 100.3 Drug-induced panniculitis. Lesions can develop at multiple sites and is to be distinguished from panniculitis that can develop at sites of injection of medications, e.g. glatiramer acetate, interferon-β, phytonadione (vitamin K), interleukin-2, heparin (eosinophilic panniculitis), pentazocine, vaccines (e.g. tetanus). Additional causes of multiple lesions include G-CSF, nonsteroidal anti-inflammatory drugs (NSAIDs), abatacept, carbamezapine, and leukotriene and proton pump inhibitors. EN, erythema nodosum; TNF, tumor necrosis factor.

Pathology

Erythema nodosum is the prototypic septal panniculitis (Fig. 100.4), but this should not be taken to imply that histopathologic changes are entirely confined to subcutaneous septa[13]. Biopsy specimens of early lesions tend to show edematous septa and mild lymphocytic infiltrates. Of note, neutrophils may predominate in early lesions[6], and a variant with a predominance of eosinophils has been reported[14]. True vasculitis of the type seen in leukocytoclastic vasculitis is not observed, and erythema nodosum is not generally regarded as a vasculitic process. However, "secondary" vasculitis may be observed in lesions when they contain relatively heavy, mixed, or neutrophil-rich inflammatory infiltrates. Erythema nodosum-like lesions in Behçet disease may demonstrate leukocytoclastic or lymphocytic vasculitis involving subcutaneous venules or muscular veins; the latter changes are prone to occur in patients with more severe forms of Behçet disease[15].

In early lesions, one may also find Miescher microgranulomas, a characteristic if not pathognomonic feature of erythema nodosum. These are small collections of cells (macrophages or perhaps "histiocytoid cells" [neutrophil precursors]) that are found within septa or at a septal–lobular interface and tend to surround neutrophils or small cleft-like spaces[16]. Reported variations in the frequency of these granulomas in erythema nodosum[2,16] may result in part from differences in definition, in the acceptance of subtle changes, and in the rigor of the search. In older lesions, Miescher microgranulomas may feature epithelioid and multinucleated giant cells (Fig. 100.4, inset).

As lesions progress, the septa become widened and contain a mixed, partly granulomatous infiltrate. These cells infiltrate the periphery of fat lobules in a lace-like configuration. The extent of lobular involvement may vary, and in some cases can be prominent[6]. Nevertheless, in the case of a lobular panniculitis without the characteristic septal changes, a diagnosis of erythema nodosum should be made with caution.

FINDINGS SUGGESTIVE OF A SYSTEMIC CAUSE FOR ERYTHEMA NODOSUM
• Synovitis • Diarrhea* • Abnormal chest X-ray • Preceding upper respiratory tract infection • Elevated antistreptolysin O and/or anti-DNase B titers • Positive tuberculin skin test or interferon-gamma release assay (e.g. QuantiFERON-TB Gold In-Tube Plus, T-SPOT.TB test)
*Check for fecal blood and white blood cells; stool culture for bacteria and, if indicated, ova and parasites; fecal calprotectin.

Table 100.4 Findings suggestive of a systemic cause for erythema nodosum. Additional evaluation can include viral hepatitis panel and, in women of child-bearing age, serum β-human chorionic gonadotropin.

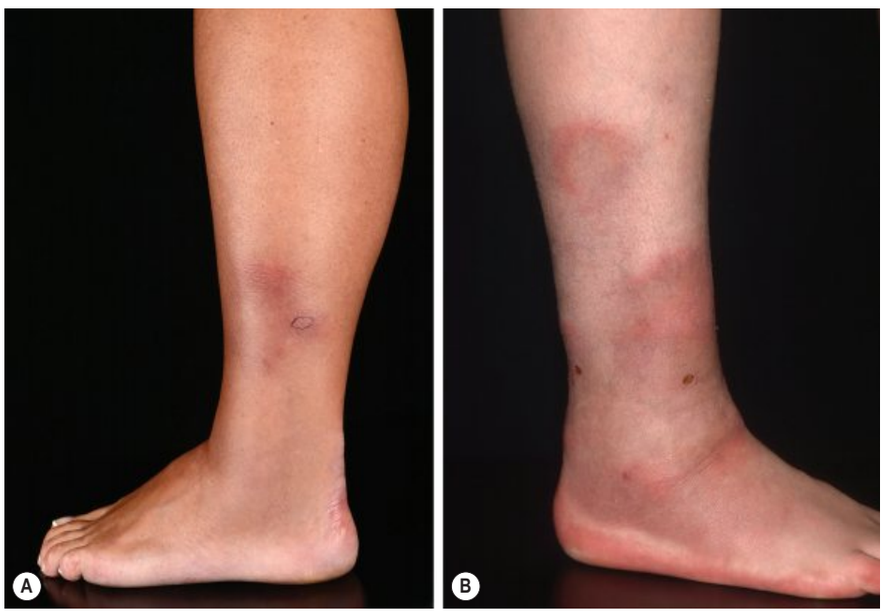


Fig. 100.3 Erythema nodosum – clinical appearance. A Cluster of dull red–brown, tender nodules on the lower leg. **B** The plaques may develop an arciform configuration and bruise-like appearance. *Courtesy Lorenzo Cerrroni, MD.*

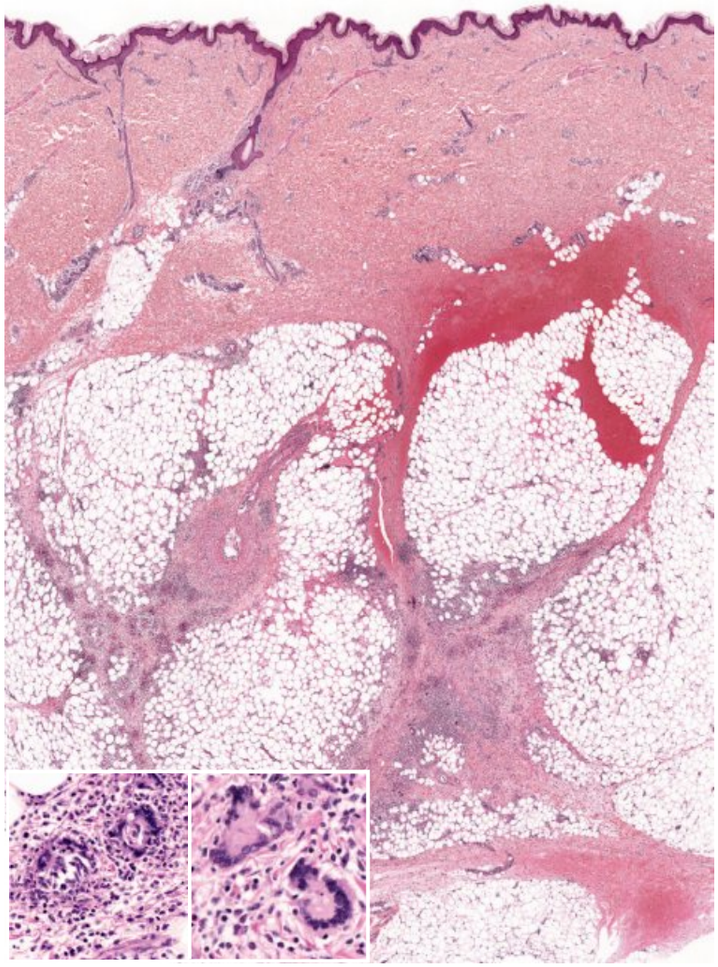


Fig. 100.4 Erythema nodosum – histopathologic features. A predominantly septal panniculitis with Miescher microgranulomas within the septa (left inset). Note the multinucleated giant cells (right inset).

Frequently, there is also a mild to moderate perivascular lymphocytic infiltrate in the overlying dermis. In later stages, the septa become fibrotic, partially replacing the fat lobules. Residual granulomas and lipophages can be observed, and a degree of vascular proliferation may be present[2]. Over the long term, a remodeling process takes place that usually results in minimal residual scarring[2].

Differential Diagnosis

The clinical scenario of an acute eruption of tender subcutaneous nodules over both shins of a young person is highly characteristic of erythema nodosum. However, when lesions are few in number, are located in sites other than the lower legs, or are of longer duration (>6 weeks), erythema nodosum can be difficult to distinguish from other forms of panniculitis. Lesions of erythema induratum (nodular vasculitis) can resemble those of erythema nodosum, but they tend to occur on the posterior aspect of the lower legs and may ulcerate. Ulceration is also a feature of pancreatic panniculitis, which occurs more frequently in other locations (although still favoring the lower legs), is more likely to be accompanied by arthritis and serositis, and is associated with elevated serum amylase and lipase levels.

Histopathologically, the picture of a predominantly septal panniculitis usually limits the differential diagnosis and tends to exclude those conditions that are chiefly lobular or mixed (see Fig. 100.2). Pancreatic panniculitis may show predominantly septal changes in its earliest stages[17], but eventually these lesions exhibit the characteristic fat necrosis, with saponification and "ghost cell" formation. Infection-induced panniculitis can sometimes mimic erythema nodosum, but there are often more extensive neutrophilic infiltrates, cellular necrosis (including sweat gland necrosis), vascular proliferation, and hemorrhage[18].

TREATMENT RECOMMENDATIONS FOR ERYTHEMA NODOSUM	
In all patients	Discontinue possible causative medications Diagnose and treat underlying cause Bed rest and leg elevation Compression
First-line	Nonsteroidal anti-inflammatory medications (3)* Salicylates Potassium iodide (2) (see Table 100.6)
Second-line†	Colchicine (3)‡ Infliximab (3)¶ Hydroxychloroquine (3)§ Adalimumab (3)§ Etanercept (3) Mycophenolate mofetil (3)
Third-line†	Systemic corticosteroids (3) Thalidomide (3)^ Cyclosporine (3) Dapsone (3)

*May trigger a flare of inflammatory bowel disease.
†Immunosuppressives to be used only if underlying infection has been excluded and/or treated.
‡Helpful for erythema nodosum associated with Behçet disease.
¶Helpful for erythema nodosum associated with inflammatory bowel disease.
§Helpful for chronic erythema nodosum.
^May transiently exacerbate erythema nodosum associated with Behçet disease.

Table 100.5 Treatment recommendations for erythema nodosum. Key to evidence-based support: (1) prospective controlled trial; (2) retrospective study or large case series; (3) small case series or individual case reports.

USE OF POTASSIUM IODIDE (KI)
Saturated solution of potassium iodide (SSKI)

• 1000 mg/ml
• Droppers are supplied with calibrations for:
  • 0.3 ml (300 mg)*
  • 0.6 ml (600 mg)
• In adults and older children, common dose = 300 mg TID po with starting dose = 150–300 mg TID
• In infants and young children, common dose = 150 mg TID po
• SSKI should be diluted in water or juice to try to minimize the bitter aftertaste
• Crystallization may occur with cold temperatures, but rewarming and shaking dissolves the crystals; discard if solution turns yellow–brown

Side effects of SSKI
• Acute – nausea, bitter eructation, excessive salivation, urticaria, angioedema, cutaneous small vessel vasculitis • Chronic – enlargement of salivary and lacrimal glands, acneiform eruption, iododerma, hypothyroidism, hyperkalemia, occasionally hyperthyroidism
*0.3 ml = 10 drops from the calibrated dropper supplied with SSKI.

Table 100.6 Use of potassium iodide (KI).

Treatment

Treatments most often recommended for uncomplicated erythema nodosum include bed rest, salicylates, and nonsteroidal anti-inflammatory drugs (NSAIDs; Table 100.5). Potassium iodide has been used with success, with adult dosages ranging from 450 to 1500 mg/day (Table 100.6)[19]. Improvement can be seen within 2 weeks. Potassium iodide may work through inhibition of cell-mediated immunity, as well as via inhibition of neutrophil chemotaxis and suppression of neutrophil-generated oxygen intermediates. In light of this treatment response, reports of erythema nodosum *triggered* by potassium iodide seem contradictory.

Treatment of erythema nodosum is influenced by underlying conditions. Thus, colchicine is useful in management of erythema nodosum that accompanies Behçet disease[6]. Various treatments for inflammatory bowel disease are also effective in managing coexistent erythema nodosum[10,20]. Both etanercept and infliximab have been reported to be effective in treating erythema nodosum[20,21], but paradoxically both have been noted to produce erythema nodosum as a cutaneous side effect[22,23]. In case reports, adalimumab has led to improvement of refractory chronic erythema nodosum[24]. Additional systemic therapies are listed in Table 100.5.

SUBACUTE NODULAR MIGRATORY PANNICULITIS

Synonyms: ■ Erythema nodosum migrans ■ Chronic erythema nodosum

Key features

- Nodules on the lower extremities that migrate or undergo centrifugal spread, with central clearing
- Often unilateral
- Most cases are idiopathic; occasionally associated with streptococcal infection or thyroid disease
- More chronic course than typical erythema nodosum

History and Clinical Features

This condition was first described by Bafverstedt in 1954 and was named *subacute nodular migratory panniculitis* by Vilanova and Piñol Aguade in 1956. Some of its clinical and microscopic characteristics are similar to chronic erythema nodosum, and it is believed by many to represent a variant of the latter[2]. However, others consider it to be a separate disorder[25]. Subacute nodular migratory panniculitis is seen predominantly in women, is often unilateral, and is characterized by nodules that migrate or expand in a centrifugal manner (with central clearing)[2] and may assume a yellowish or morpheaform appearance. Lesions tend to be less tender than those of classic erythema nodosum. There may be few, if any, associated systemic symptoms, though arthralgias have been reported and the ESR may be elevated. Most cases are idiopathic, but some are associated with streptococcal infection (as evidenced by elevated antistreptolysin O and anti-DNase B titers) or thyroid disease[25].

Pathology

Microscopically, the changes are those of a chronic septal panniculitis. However, in contrast to more classic forms of chronic erythema nodosum, subacute nodular migratory panniculitis shows greater septal thickening, more prominent granulomatous inflammation along the borders of widened subcutaneous septa, absence of phlebitis, and rare hemorrhage[25].

Treatment

Untreated, subacute nodular migratory panniculitis can last for months or years. However, treatment with potassium iodide is usually effective, resulting in clearing of lesions within several weeks.

MORPHEA/SCLERODERMA PANNICULITIS

(See also Chs. 43 & 44.)

Clinical Features

Both morphea and systemic sclerosis (scleroderma) can affect the subcutaneous fat (Table 100.7), which is the primary site of involvement in deep morphea (morphea profunda)[26]. Subcutaneous extension also occurs in variants such as disabling pansclerotic morphea of childhood, generalized morphea, and linear morphea. In addition, eosinophilic fasciitis can involve the subcutaneous fat as well as the fascia[27]. These entities may be associated with peripheral eosinophilia, polyclonal gammopathy, and serologic abnormalities[27,28]. It has been proposed that the sclerosing process in systemic sclerosis is initiated by the changes that take place in the subcutis.

Pathology

Table 100.7 outlines the microscopic changes in morphea- and systemic sclerosis-associated septal panniculitis (Fig. 100.5). Lymphocytes and plasma cells predominate[27,29,30], although macrophages and eosinophils may be present. In some cases, the number of plasma cells is striking[29]. In late stages of morphea, the subcutis is largely replaced by hyalinized connective tissue, very often accompanied by changes of lipoatrophy.

Differential Diagnosis

The combination of septal panniculitis with lymphoplasmacytic predominance and dermal and subcutaneous sclerosis is unique, and this helps to separate morphea/systemic sclerosis panniculitis from other septal forms of panniculitis. Differentiation among the several variants outlined above is more difficult, requiring clinical data for accurate classification. Sclerosis with lesser degrees of subcutaneous inflammation characterizes systemic sclerosis, while a predominance of fascial involvement with extension into the subcutis is more typical of eosinophilic fasciitis.

CLINICAL AND MICROSCOPIC FEATURES OF CONNECTIVE TISSUE PANNICULITIS

Disorder	Clinical presentation	Lesion distribution	Relation to systemic disease	Histopathology of panniculitis
Morphea and systemic sclerosis (scleroderma)	Indurated plaques	Extremities, trunk	Occurs in systemic sclerosis, but usually more pronounced in morphea	Septal, with thickening and sometimes mucin deposition; inflammation especially at dermal–subcutaneous interface; lymphocytes and plasma cells; lymphoid follicles in morphea*
Lupus panniculitis	Tender subcutaneous nodules and plaques; may have overlying lesions of discoid LE; lipoatrophy a common sequela	Face (especially cheeks), upper outer arms, shoulders, breasts, hips, buttocks, trunk	Only minority of patients have associated systemic LE	Lobular or mixed lobular/septal; mucin deposition; hyaline necrosis of lobules; lymphocytes, $CD123^+$ plasmacytoid dendritic cells and plasma cells, sometimes with prominent nuclear dust; nodular lymphocytic aggregates or lymphoid follicles
Dermatomyositis	Indurated, painful plaques and nodules; may ulcerate	Buttocks, abdomen, thighs, arms	Can arise in patients with established dermatomyositis or precede other disease manifestations	Lobular or mixed septal/lobular; fat necrosis; lipomembranous changes; sometimes calcification; lymphocytes and plasma cells; sometimes nodular lymphocytic aggregates
Annular atrophic connective tissue panniculitis of the ankles	Subcutaneous atrophy, which may be preceded by induration and tenderness	Circumferential bands around the ankles	Patients often have antinuclear antibodies and/or autoimmune disorders such as thyroiditis or rheumatoid arthritis	Lobular or mixed septal/lobular lymphohistiocytic panniculitis with areas of fat necrosis
Atrophic connective tissue panniculitis	Erythematous, indurated plaques that resolve with subcutaneous atrophy	Favors extremities; may be widespread	As above	As above

*Less often than in lupus panniculitis.

Table 100.7 Clinical and microscopic features of connective tissue panniculitis. LE, lupus erythematosus. *Based on references 27, 29, 81.*

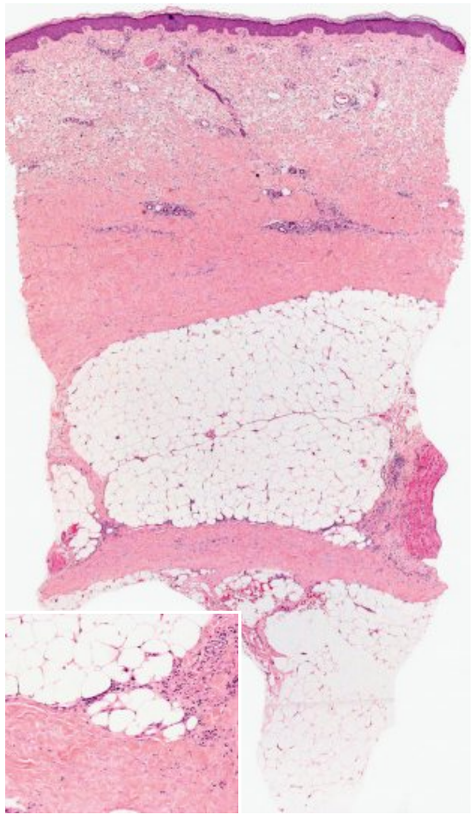


Fig. 100.5 Morphea panniculitis. Septal thickening, mucin deposition and mild lymphocytic infiltrate. Lymphoplasmacytic infiltrates concentrate at the dermal–subcutaneous interface (inset). *Courtesy Lorenzo Cerroni, MD.*

ALPHA-1 ANTITRYPSIN DEFICIENCY PANNICULITIS

Synonym: ■ Alpha-1 protease (proteinase) deficiency panniculitis

Key features

- Erythematous, painful, subcutaneous nodules or plaques that often ulcerate and drain
- Associated with alpha-1 antitrypsin deficiency; patients with the most severe disease are homozygotes for the Z allele of *SERPINA1* (PiZZ)
- A characteristic histopathologic finding is liquefactive necrosis of the dermis and subcutaneous septa, but lobular or mixed septal–lobular changes with neutrophils may occur

Introduction

Alpha-1 antitrypsin deficiency is a well-established, but uncommon, cause of panniculitis. The most severely affected individuals, with markedly decreased levels of the protease inhibitor, are most prone to the development of ulcerating neutrophilic panniculitis. Recognition of the disorder is important not only in the selection of appropriate therapy, but also in addressing other systemic manifestations of the disease and in dealing with its genetic aspects.

History

Alpha-1 antitrypsin deficiency is an inborn error of metabolism that was first delineated by Eriksson and others in the early 1960s. In 1972, Warter and colleagues identified members of a family with alpha-1 antitrypsin deficiency and "Weber–Christian syndrome". Subsequent investigations linked the clinical and microscopic findings to known effects of proteinase inhibitor deficiency.

Epidemiology

In the US, alpha-1 antitrypsin deficiency occurs most commonly in White, followed by Hispanic and Black, individuals. The incidence of panniculitis is approximately equal in men and women[31]. Age of onset ranges from infancy to the eighth decade of life[31].

Pathogenesis

Alpha-1 antitrypsin, a glycoprotein produced in the liver, is the most abundant circulating *ser*ine *p*rotease *in*hibitor (serpin). The more than 120 different alleles of the gene that encodes this protein (SERPINA1; formerly known as PI) are divided into categories based upon the electrophoretic mobility of their protein products (M = medium, S = slow, Z = very slow). The most common protease inhibitor (Pi) phenotype is MM (homozygous for M alleles), which is associated with normal serum levels of alpha-1 antitrypsin (100–200 mg/dl)[32]. Heterozygotes with one copy of the S or Z allele have mild to moderate deficiencies of the inhibitor (PiMS and PiMZ; prevalences of 1%–3% in White populations). Patients who are homozygous for the Z allele (PiZZ; prevalence of 1 : 150–1 : 5000 in White populations) or whose genotype is the rare PiZnull have severe alpha-1 antitrypsin deficiency, with serum levels in the range of 20–45 mg/dl. In these individuals, most of the aberrant alpha-1 antitrypsin protein accumulates within the endoplasmic reticulum of hepatocytes, and the small amounts that enter the circulation have decreased function and a tendency to form inactive polymers that may stimulate neutrophil chemotaxis[33]. Of note, Z-type polymers have been detected in the skin of a patient with alpha-1 antitrypsin deficiency panniculitis, further suggesting a possible proinflammatory role[34].

Alpha-1 antitrypsin acts upon a wide range of proteolytic enzymes that play a direct role in degradation of tissues, including trypsin, collagenase, and elastase[35]. It also has important effects on immune function, e.g. inhibition of membrane-bound serine proteases involved in the activation of lymphocytes and macrophages[36]. It may also inhibit complement activation, both through a direct effect on complement-related proteases[37] and by inhibiting the neutrophil proteases that activate enzymes of the complement system[38].

In addition to panniculitis, the consequences of alpha-1 antitrypsin deficiency include chronic liver disease with cirrhosis (resulting from retention of the aberrant protein within the liver), emphysema, pancreatitis, membranoproliferative glomerulonephritis, rheumatoid arthritis, c-ANCA (cytoplasmic antineutrophil cytoplasmic antibody)-positive vasculitis, other cutaneous vasculitides such as Henoch–Schönlein purpura, and angioedema (resulting from deficiency of the protease inhibitor)[38]. The initiating event in individuals who develop panniculitis is not always clear; trauma appears to play a role in some patients. Postpartum flares of the disease have been reported in genetically susceptible individuals. This is attributed to the estrogen-promoted increase in proteinase inhibitor levels during pregnancy, followed by a precipitous decline to subnormal levels postpartum.

Absence of the alpha-1 antitrypsin protease inhibitor results in activation of lymphocytes and macrophages, lack of restraint upon the complement cascade, release of chemotactic factors, accumulation of neutrophils with release of their proteolytic enzymes, and consequent attack upon fat and nearby connective tissues[33,35]. The subcutis may be particularly vulnerable to this process, since fatty acids make nearby elastin more susceptible to proteolytic degradation[38].

Clinical Features

Large, erythematous to purpuric, tender nodules or plaques appear in a variety of sites (Fig. 100.6), especially the lower trunk and proximal extremities (flanks, buttocks, and thighs)[33,35]. Ulcers develop that may be deep and necrotic, accompanied by an oily discharge[31,33,35]. A history of antecedent trauma can be elicited in approximately one-third of patients[31]. Panniculitis may be accompanied by fever, pleural effusions, and pulmonary emboli[31]. The clinical course of the panniculitis is often prolonged, and lesions are resistant to immunosuppressive therapy. Healing is accompanied by scarring and subcutaneous atrophy[31]. The most severe manifestations arise in those with profound proteinase inhibitor deficiency (PiZZ), although the panniculitis can also occur in heterozygotes.

Pathology

Descriptions of the pathology of alpha-1 antitrypsin deficiency panniculitis have varied. Early, there is a neutrophilic panniculitis, followed rapidly by necrosis and destruction of fat lobules[35]. Splaying of neutrophils



Fig. 100.6 Alpha-1 antitrypsin deficiency panniculitis – clinical appearance. Purpuric nodules on the ankle. *Courtesy Kenneth E. Greer, MD.*

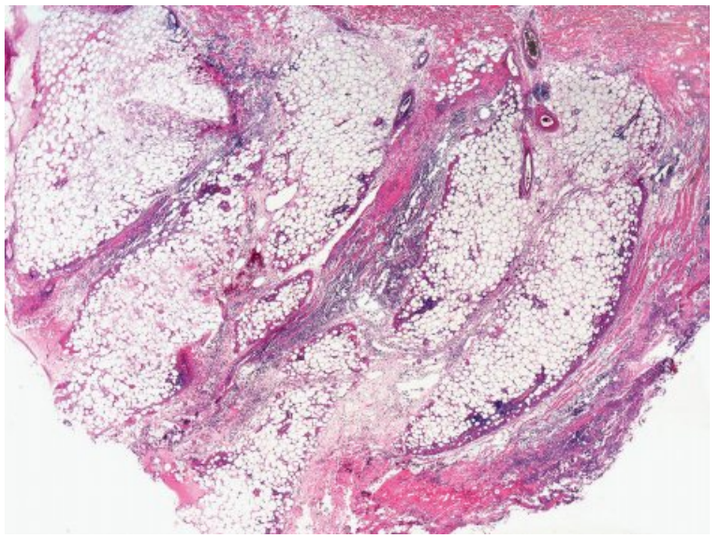


Fig. 100.7 Alpha-1 antitrypsin deficiency panniculitis – histopathologic features. Predominantly septal involvement is seen, with inflammation and collagenolysis of fibrous septa.

between collagen bundles in the reticular dermis has been described as an early clue to the diagnosis[39]. Dissolution of dermal collagen, with resultant liquefactive necrosis and separation of fat lobules from adjacent septa, is a principal change in most cases[40]. Another characteristic feature is the presence of "skip areas" of normal fat adjacent to foci of severe necrotizing panniculitis[35]. Chronic inflammation and hemorrhage may be present at the periphery of areas of involvement[35]. Most authors have not found evidence for *primary* leukocytoclastic vasculitis, although there may be evidence for lymphocytic vasculitis, *secondary* vasculitis in areas of heavy neutrophilic infiltration, or thrombosis[35]. In individuals with intermediate levels of protease inhibitor deficiency, lipophage and giant cell accumulation may be prominent[35]. Lesions heal with scarring and obliteration of fat lobules.

Views differ on whether alpha-1 antitrypsin deficiency panniculitis should be regarded as a primarily septal or lobular panniculitis. Clearly, involvement of fat lobules can be significant, and, as a result, there are authors who have labeled the process a lobular panniculitis. On the other hand, some descriptions have emphasized early septal inflammation, collagenolysis of the fibrous septa (Fig. 100.7)[40], and the prominent septal fibrosis in late-stage lesions[39].

Differential Diagnosis

Clinically, the degrees of inflammation, ulceration, and drainage associated with alpha-1 antitrypsin deficiency panniculitis may actually elicit a differential diagnosis more focused upon ulcerative skin disorders (see Fig. 105.1). Ulcers associated with alpha-1 antitrypsin deficiency generally lack the necrotic, "undermined" borders associated with pyoderma gangrenosum[35]. Tissue culture to exclude infection-induced panniculitis may be required.

Entities in the microscopic differential diagnosis include traumatic (factitial) panniculitis, infection-induced panniculitis, pancreatic panniculitis, and erythema induratum (nodular vasculitis)[35]. Each of these can be associated with infiltrates that include neutrophils and varying degrees of necrosis, yet each has other distinct findings (see below). In the appropriate clinical setting, subcutaneous Sweet syndrome, drug-induced panniculitis, and neutrophilic panniculitis in patients with rheumatoid arthritis or inflammatory bowel disease (IBD) may represent additional diagnostic considerations. Of note, the underlying IBD can be clinically silent. When no underlying disorder is detected, the term idiopathic neutrophilic lobular panniculitis may be applied.

Treatment

Treatments that are usually ineffective include corticosteroids and other immunosuppressants, cytotoxic agents, colchicine, danazol, and hydroxychloroquine[35]. Doxycycline is sometimes effective, particularly in mild cases; one suggested dosage schedule is 200 mg twice daily for 3 months[37,41]. Dapsone may also be beneficial in mild cases, by suppressing neutrophil migration and inhibiting oxidation reactions induced by myeloperoxidase. Reduction of alcohol intake has also been recommended, since ethanol (as a hepatotoxin) may precipitate alpha-1 antitrypsin-associated hepatitis[38].

The most effective therapeutic intervention is replacement of alpha-1 antitrypsin via intravenous infusions. Dosages are generally 60 mg/kg per week, administered over a period of 3 to 7 weeks[31]. Improvement is relatively rapid, in that clearing of the panniculitis can occur after three weekly doses. Recurrences are possible when alpha-1 antitrypsin levels fall below 50 mg/dl, but these typically respond to further replacement therapy. Other successful therapies include plasma exchange and liver transplantation (in appropriate clinical circumstances). There is evidence that autophagy-enhancing drugs, such as carbamazepine, may reduce systemic manifestations, including hepatic fibrosis[42]. Most recently, fazirsiran, an RNA interference therapy, has led to hepatic improvement[42a].

ERYTHEMA INDURATUM

Synonyms: ■ Nodular vasculitis ■ Erythema induratum of Bazin or Bazin disease (tuberculous etiology) ■ Erythema induratum of Whitfield (non-tuberculous etiology)

Key features

- Erythematous nodules or plaques, usually on the posterior lower legs of young to middle-aged women
- Ulceration and drainage may occur
- Microscopic features of lobular or mixed panniculitis with evidence of vasculitis involving arteries or veins
- Classically associated with tuberculosis, but similar lesions can be idiopathic or induced by other infectious agents or drugs

Introduction

Erythema induratum is a condition characterized by nodules on the lower extremities, which may ulcerate and drain. Originally regarded as a tuberculid, detection of mycobacterial DNA within cutaneous lesions in a subset of patients supports its relationship to tuberculosis, at least in a proportion of cases.

History

Erythema induratum was first described by Ernest Bazin in 1861. It was generally regarded as a tuberculid because of a strong association with tuberculosis, although Koch's postulates could not be fulfilled. In

1945, Montgomery and colleagues proposed the term *nodular vasculitis* for cases with similar clinical and pathologic features that were not of tuberculous origin. Since the early 1970s, erythema induratum and nodular vasculitis have generally been considered as synonyms referring to a clinicopathologic entity with several possible causes, one of which is tuberculosis. The detection of mycobacterial DNA in cutaneous lesions has confirmed a tuberculous origin in some patients. There are certain clinicians, however, who prefer to use the term nodular vasculitis when referring to individuals with a non-tuberculous etiology.

Epidemiology

In erythema induratum, an overwhelming female predominance is observed, but men can also develop the disease. There is no apparent racial predilection, and although there is a wide age range among affected patients, the mean is between 30 and 40 years. Erythema induratum of tuberculous etiology occurs more frequently in populations with a high prevalence of tuberculosis.

Pathogenesis

As mentioned previously, some cases have been strongly associated with *Mycobacterium tuberculosis* infection. This can be substantiated by the detection of mycobacterial DNA in skin lesions by PCR[43], with specific primers used to distinguish *M. tuberculosis* complex DNA from that of other mycobacterial pathogens[43]. Non-tuberculous cases have been related to other infectious agents (e.g. *Nocardia*[18], hepatitis C virus[44]) or to drugs (e.g. propylthiouracil[45]). There is a report of erythema induratum being induced by a tuberculin skin test.

Although it has been suggested that erythema induratum results from an immune complex-mediated vasculitis, most investigators believe that the process represents a type IV, cell-mediated response to an antigenic stimulus[46]. Biopsy specimens show a predominance of T lymphocytes, macrophages and dendritic cells, including Langerhans cells[47,48]. One study of peripheral blood mononuclear cells from a patient with erythema induratum and active tuberculosis showed a high proliferative response to purified protein derivative (PPD) and marked production of interferon-γ, suggesting a pathogenic role for these PPD-specific T cells in a delayed hypersensitivity response to mycobacterial antigens[48].

Clinical Features

Erythema induratum is characterized by tender, erythematous to violaceous nodules and plaques that most often develop on the lower legs, especially the calves[47]. Lesions have also been reported on the feet, thighs, buttocks, and arms. An annular arrangement of nodules has been described in *M. tuberculosis*-related cases[49]. Ulceration can occur (Fig. 100.8). Lesions are persistent, tend to heal with scarring, and are prone to recurrence[47,50]. In erythema induratum associated with *M. tuberculosis*, there may be clinical and radiographic evidence for active tuberculosis, positive skin tests to PPD, or a positive interferon-gamma release assay such as the QuantiFERON®-TB Gold Plus test[51]. In addition, other tuberculids, e.g. papulonecrotic, may be present. Clinical differences between tuberculous and non-tuberculous cases are minor.



Fig. 100.8 Erythema induratum – clinical appearance. Inflamed nodular lesions on the lower leg, with evidence of ulceration. *Courtesy Kenneth E. Greer, MD.*

Pathology

Erythema induratum is generally described as a lobular or mixed septal/lobular panniculitis. Inflammation is mixed, and can include neutrophils, lymphocytes, macrophages, and multinucleated giant cells (Fig. 100.9A). Vasculitis is identifiable in the vast majority of cases, and most frequently involves veins or arteries of connective tissue septa and small venules of the fat lobules[52] (Fig. 100.9B). It may be predominantly neutrophilic[47], lymphocytic[50], or granulomatous. Necrosis with a coagulative or caseous appearance may be present, sometimes with palisading granulomas[47]. Necrosis has been described in both tuberculous and non-tuberculous cases, and the incidence and degree of necrosis are greater in those cases that are positive for *M. tuberculosis* DNA by PCR methods[47]. However, this finding is absent in over half of cases.

Differential Diagnosis

Infection-induced panniculitis tends to show a more prominent neutrophilic component, granular basophilic necrosis, sweat gland necrosis and proliferation of small vessels, and organisms may be identified on

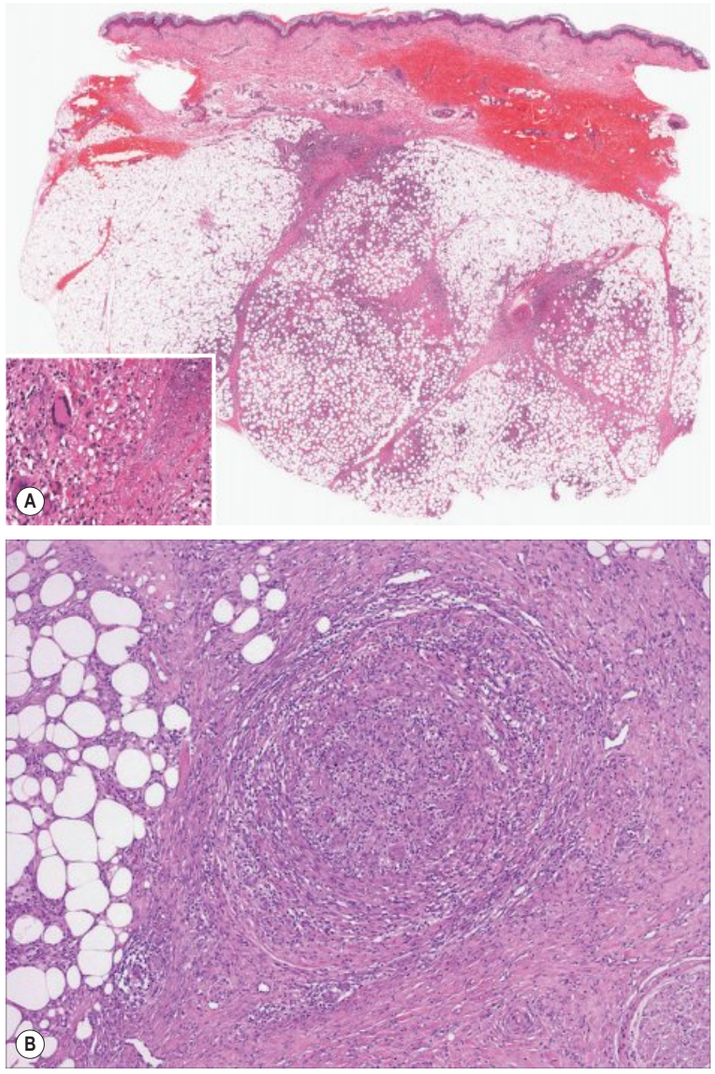


Fig. 100.9 Erythema induratum – histopathologic features. A A predominantly lobular panniculitis is seen with an infiltrate that is lymphocytic and granulomatous; note the multinucleated giant cells (inset). **B** Vasculitis involving a medium-sized vessel in the subcutis.

special staining. Lupus panniculitis tends to be less granulomatous, has a prominent lymphoplasmacellular infiltrate, may show mucin deposits, and frequently has overlying epidermal and dermal changes typical for lupus erythematosus. Both polyarteritis nodosa and thrombophlebitis tend to show inflammation limited to the immediate perivascular zone, in contrast to the extensive lobular panniculitis often encountered in erythema induratum. Histologically, perniosis can be difficult to distinguish from erythema induratum, but there is typically a history of cold exposure[47], and on microscopic examination prominent involvement of dermal vessels is often observed, with "fluffy edema" of their walls.

Treatment

Treatment should be directed at the underlying cause, if found. This includes multi-drug antituberculous therapy[49] (see Ch. 75) and discontinuing possible inciting medications. Therapeutic options for nontuberculous erythema induratum include NSAIDs, corticosteroids, tetracyclines, potassium iodide, and mycophenolate mofetil[53]. Supportive care is similar to that for erythema nodosum (see Table 100.5).

PANCREATIC PANNICULITIS

Synonyms: ■ Pancreatic fat necrosis ■ Enzymatic panniculitis

Key features

- Subcutaneous nodules, sometimes accompanied by fever, arthritis, or abdominal pain
- Associated with pancreatic disorders, including acute and chronic pancreatitis and pancreatic carcinoma
- Mixed septal/lobular panniculitis featuring "ghost cell" formation and the deposition of basophilic material due to saponification of fat by calcium salts
- Treatment primarily directed towards the underlying pancreatic disorder

Introduction

Pancreatic panniculitis is an unusual complication of pancreatic disease. In addition to the symptoms associated with fat necrosis, its chief importance is as a sign of a significant systemic disorder, particularly because the panniculitis may be recognized prior to detection of the underlying pancreatic disease. The association of pancreatitis, panniculitis, and polyarthritis is sometimes referred to as the PPP syndrome.

History

Chiari first described pancreatic panniculitis in 1883. By 1999, fewer than 100 cases had been reported[54,55]. Since then, ~100 additional patients with pancreatic panniculitis have been described, primarily as case reports.

Epidemiology

Panniculitis develops in up to 2% of patients with pancreatic disorders[56]. No geographic, racial or sex predilections have been reported.

Pathogenesis

There is considerable evidence that the enzymes lipase, amylase and trypsin are involved in producing the lesions of pancreatic panniculitis[54]. Elevated enzyme levels have been detected in the blood[55,56], urine[54], and skin lesions[57], even in the absence of detectable pancreatic disease. Lipase has the clearest relationship with the panniculitis, with a number of patients having elevated serum lipase levels but normal amylase levels[55]. Utilizing an anti-pancreatic lipase monoclonal antibody, positive intracellular adipocyte staining was observed in a biopsy of lesional skin[57].

Amylase levels, when elevated, tend to peak 2–3 days after eruption of the skin lesions and return to normal 2–3 days after regression of the lesions. Trypsin and perhaps amylase may act by promoting increased permeability of vessel walls, thereby permitting lipase to hydrolyze neutral fat to form glycerol and free fatty acids, with resulting fat necrosis and inflammation[55,56]. Venous stasis may promote this process, possibly explaining the predilection for the lower extremities. Elevated enzyme levels may not be the complete explanation for the changes of pancreatic panniculitis[58]; immunologic factors probably also play a role.

Clinical Features

Subcutaneous nodules develop in association with acute or chronic pancreatitis, pancreatic carcinoma (acinar cell > other types [e.g. neuroendocrine carcinomas]), pancreatic pseudocysts, pancreas divisum, traumatic pancreatitis, or drug-induced panniculitis (e.g. azathioprine)[55,59]. The possibility of a pancreaticoportal fistula should be considered when panniculitis develops in individuals with chronic pancreatitis, and in some of these patients, an acinar cell carcinoma can also be found. Panniculitis may precede detection of pancreatic disease by 1–7 months[56], and in the case of pancreatic carcinoma, its onset may signal the presence of metastatic disease[55,56].

In pancreatic panniculitis, subcutaneous nodules develop, frequently on the legs (Fig. 100.10) but also on the anterior trunk, arms, and scalp[55,56]. Erythematous, edematous, sometimes painful lesions arise singly or in crops. They can become fluctuant and ulcerate, discharging an oily material[55]. Panniculitis may also involve visceral fat, including the omentum and preperitoneal fat[55]. Associated findings include fever, abdominal pain, inflammatory polyarthritis, ascites, and pleural effusions[55].

The association of subcutaneous nodules, polyarthritis, and eosinophilia is known as Schmid's triad, and it is associated with a poor prognosis. Some patients have radiographic evidence of multiple lytic areas involving the cortical bone near large joints. Cutaneous lesions may involute within a period of weeks, leaving hyperpigmented scars. In acute pancreatitis, the panniculitis resolves as the acute inflammatory phase passes[55]. However, lesions may also persist and expand until the underlying pancreatic abnormality has been treated.



Fig. 100.10 Pancreatic panniculitis – clinical appearance. Multiple painful pink–violet to dark purple nodules and plaques on the shins. There is also evidence of hemorrhage. *Courtesy Sa Rang Kim, MD, and Jean L. Bolognia, MD.*

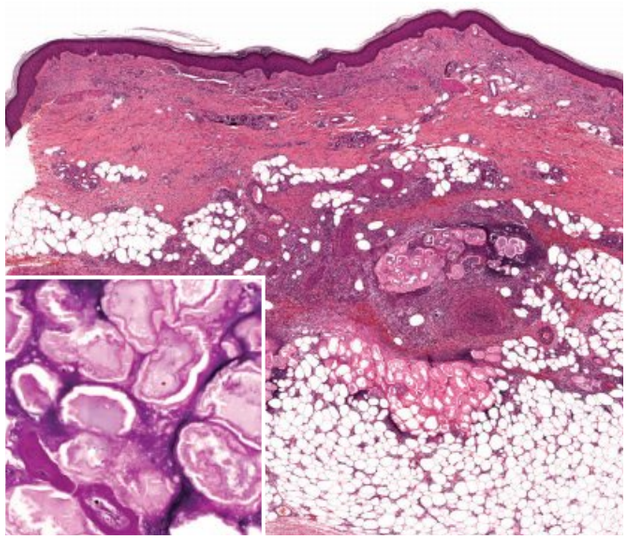


Fig. 100.11 Pancreatic panniculitis – histopathologic features. Lobular and septal panniculitis with neutrophilic inflammation, cellular necrosis, ghost cells (inset), and deposition of homogeneous basophilic material due to saponification of fat by calcium salts (seen here near ghost cells).

Pathology

Pancreatic panniculitis may begin as a septal panniculitis[17], but with progression, the lesion takes on the appearance of a lobular or mixed septal/lobular process. Even in early stages, fat necrosis with liquefaction and microcyst formation is observed[54,58]. Lipocytes lose their nuclei and develop thick, shadowy walls, forming the characteristic "ghost cells". Saponification of fat by calcium salts results in deposition of granular or homogeneous basophilic material (Fig. 100.11). Neutrophils, occasional eosinophils, macrophages, and multinucleated giant cells are sometimes present and may encroach upon the septa. Fibrosis and lipoatrophy are seen in late stages as the process resolves.

Differential Diagnosis

Clinically, the nodules of pancreatic panniculitis can resemble those of a number of other forms of panniculitis. Ulceration and discharge would argue against erythema nodosum, and an association with fever, polyarthritis, and/or abdominal pain should raise suspicion of associated pancreatic disease. Serum amylase and lipase levels, if elevated, may also be helpful. Histologic evidence of "ghost cell" formation and saponification of fat distinguishes pancreatic panniculitis from other panniculitides, with the exception of ghost cell formation in mucormycosis panniculitis. Eosinophilic "hyaline necrosis" is seen in lupus panniculitis, rather than the granular or homogeneous basophilic necrosis typical of pancreatic panniculitis.

Treatment

Although supportive measures such as compression and elevation can be helpful, effective management of pancreatic panniculitis is dependent upon treatment of the underlying pancreatic disease. In chronic pancreatitis, pancreatectomy is curative but is rarely performed because of potential complications. If a fistula or cyst is involved, minimally invasive drainage techniques are initially employed. Somatostatin analogues (e.g. octreotide) can be used to inhibit pancreatic enzyme production[55]. Resection of pancreatic cancer may be followed by regression of the panniculitis.

SCLEREMA NEONATORUM, SUBCUTANEOUS FAT NECROSIS OF THE NEWBORN, AND POST-STEROID PANNICULITIS

Three entities – sclerema neonatorum, subcutaneous fat necrosis of the newborn, and post-steroid panniculitis – are characterized histologically by the formation of needle-shaped clefts within lipocytes. In contrast to adult fat, the subcutaneous fat of infants is thought to be prone to crystal formation because of a higher content of saturated fatty acids, including palmitic and stearic acids, and a relatively lower content of unsaturated fatty acids, such as oleic acid[60]. This increased saturated : unsaturated fatty acid ratio results in a higher melting point for stored fat and promotes crystallization under certain conditions. Microsized crystals (type A) apparently do not produce an inflammatory response; they are actually common (in a widely dispersed form) in healthy infants 6 months of age or less, but are more numerous in sclerema neonatorum. Larger, type B crystals that tend to be arranged in rosettes are capable of eliciting a granulomatous response; these larger crystals are most often seen in subcutaneous fat necrosis of the newborn and post-steroid panniculitis[60]. Crystallization and defects in fat mobilization account for the clinical findings in these disorders.

Sclerema Neonatorum

Key features

- Arises in premature infants
- Skin is diffusely cold, rigid, and board-like
- Microscopically, needle-shaped clefts are present within lipocytes and there is minimal inflammation
- Affected infants are often hypothermic and may have a variety of other medical problems; early death is common

History

Uzembenzius first recognized sclerema neonatorum in 1722, although the classic description is usually attributed to Underwood (1784). Ballantyne provided an early description of the histopathologic changes, and Knopfelmacher noted the presence of needle-shaped crystals in subcutaneous tissue in 1897.

Epidemiology

Sclerema neonatorum presents most often in premature, debilitated infants, usually during the first week of life. There is a slight male predominance, with no substantial sex differences in death rates[61].

Pathogenesis

In infants who develop sclerema, crystallization and hardening of fat occur in the setting of an increased saturated : unsaturated fatty acid ratio and a defective ability to mobilize fatty acids. Precipitating factors are listed in Table 100.8[60].

Clinical features

The clinical features are outlined in Table 100.8[60–62]. Rapid hardening of the subcutaneous tissues leads to firm, rigid skin over most of the body. Low birth weight and hypothermia as well as hemorrhagic phenomena portend a particularly poor prognosis[61].

Pathology

Table 100.8 outlines the microscopic features. Inflammation is usually sparse, and most of the needle-shaped clefts are found within lipocytes rather than within giant cells (Fig. 100.12)[60,62]. At a later stage, thickened connective tissue bands may be the only histologic finding[62].

Differential diagnosis

In contrast to sclerema neonatorum, subcutaneous fat necrosis of the newborn is a localized process with a favorable prognosis; histologically, the latter is distinguished by more prominent inflammation and localization of needle-shaped clefts within giant cells. Scleredema neonatorum is a condition seen in premature infants with congenital heart disease. In this disorder, the skin is distended and wax-like, and on biopsy the dermis appears edematous, with increased amounts of mucin[60]. Other conditions that can present with diffusely indurated skin in the neonatal period include stiff skin syndrome (usually favoring the trunk, buttocks, and thighs), restrictive dermopathy, and Hutchinson–Gilford progeria.

While subcutaneous needle-shaped clefts are generally observed in infants and children, radially arranged needle-shaped clefts

PANNICULITIDES WITH NEEDLE-SHAPED CLEFTS IN THE SUBCUTIS						
Condition	**Patient characteristics**	**Onset**	**Cutaneous findings**	**Associated systemic findings**	**Histopathology**	**Possible precipitating factors**
Sclerema neonatorum	Severely ill premature neonates	First week of life	Widespread, diffuse hardening, sparing only the genitalia, palms and soles; cool, waxy, rigid and board-like skin with purple mottled discoloration	Respiratory difficulties, congestive heart failure, intestinal obstruction, diarrhea; death, usually from septicemia, in three-quarters of patients	Needle-shaped clefts in lipocytes; septal thickening; inflammation sparse to absent (few neutrophils, eosinophils, macrophages or multinucleated giant cells may be seen)	Hypothermia, perinatal asphyxia, defective complement activity, dehydration
Subcutaneous fat necrosis of the newborn	Full-term neonates	First 2–3 weeks of life	Circumscribed, erythematous, indurated subcutaneous nodules favoring the cheeks, shoulders, back, buttocks, thighs; may become fluctuant	Hypercalcemia (onset usually within 2 months), thrombocytopenia, hypertriglyceridemia; severe hypercalcemia may be associated with fever, eosinophilia, and persistent nephrocalcinosis	Lobular panniculitis with neutrophils, lymphocytes, macrophages; needle-shaped clefts in a radial array within lipocytes and giant cells; sometimes foci of calcification, hemorrhage	Hypothermia (including exposure to cooling blankets), hypoglycemia (e.g. due to gestational diabetes), perinatal hypoxemia (e.g. due to meconium aspiration, placenta previa, umbilical cord prolapse, pre-eclampsia)
Post-steroid panniculitis	Children (ages 1–14 years)	1–40 days* after cessation of high-dose systemic corticosteroids	Firm red plaques on the cheeks, arms, trunk; small and discrete or large and confluent lesions; pruritic, tender or asymptomatic	Underlying conditions treated with systemic corticosteroids have included leukemia, cerebral edema, nephrotic syndrome, secretory diarrhea, and acute rheumatic fever as well as chronic obstructive pulmonary disease and Sjögren syndrome in adults	Lobular panniculitis with lymphocytes, macrophages, multinucleated giant cells; needle-shaped clefts in lipocytes and giant cells	Follows rapid withdrawal of systemic corticosteroids

*Usually within 10 days.

Table 100.8 Panniculitides with needle-shaped clefts in the subcutis.

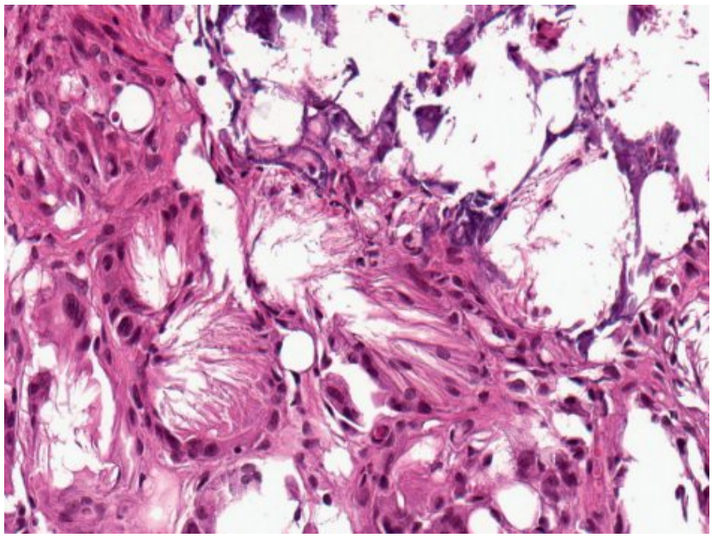


Fig. 100.12 Sclerema neonatorum. Needle-shaped clefts within lipocytes with chronic granulomatous inflammation.

(resembling those of sclerema neonatorum) were reported in an adult with gemcitabine-related thrombotic microangiopathy[63]; however, these crystals were quite small.

Treatment

Attempts to treat this disorder are disappointing[61]. Management includes treatment of sepsis, ventilatory support, correction of fluid and electrolyte imbalances, and maintenance of body temperature[60,64]. Exchange transfusions may be of value in selected instances[60,64]. Systemic corticosteroids are of questionable utility[60,61].

Subcutaneous Fat Necrosis of the Newborn

Key features

- Development of one or more mobile, firm, subcutaneous nodules or plaques during the newborn period
- Sometimes associated with hypercalcemia or thrombocytopenia
- Granulomatous lobular panniculitis with needle-shaped clefts within lipocytes and giant cells
- Prognosis is usually favorable; spontaneous resolution is common

Introduction

In contrast to sclerema neonatorum, subcutaneous fat necrosis is a localized process. Although complications can arise, particularly in relation to hypercalcemia, most cases resolve spontaneously.

History

At the beginning of the twentieth century, Fabyan described "abscesses" that spontaneously resorbed, and he provided the first microscopic description of subcutaneous fat necrosis.

Epidemiology

Subcutaneous fat necrosis of the newborn typically occurs in full-term neonates during the first 2 to 3 weeks of life[65].

Pathogenesis

It is believed that a variety of stresses imposed upon fetal fat, with its high ratio of saturated : unsaturated fatty acids, results in crystallization, adipocyte injury, and granulomatous inflammation. Hypothermia is one potential eliciting factor, as illustrated by cases of subcutaneous fat necrosis that developed following hypothermic cardiac surgery and the use of cooling blankets[66–69]. Other proposed causes are listed in Table 100.8[60,65,67]. The role of birth trauma has been questioned, since many cases have occurred in infants delivered by cesarean section[65].

Clinical features

The clinical features are outlined in Table 100.8. Smooth, circumscribed, mobile, red to violaceous, subcutaneous nodules or plaques develop, sometimes in a symmetrical fashion[60,65] (Fig. 100.13). The areas of fat necrosis can be detected by ultrasonography, CT, and MRI.

Some patients develop hypercalcemia or thrombocytopenia; the former is more common in infants with a higher birth weight and typically appears within two months of skin lesion onset[67,68]. It is believed that the hypercalcemia results from extrarenal production of 1,25-dihydroxyvitamin D_3 (calcitriol) by activated macrophages (expressing 1-α-hydroxylase) within areas of granulomatous panniculitis. This stimulates calcium absorption from the gut and mobilization from the bones[65,70]. The mechanism for thrombocytopenia may be local sequestration in the subcutis, as studies have shown normal bone marrow cellularity and resolution of the thrombocytopenia as the inflammatory process resolves[71]. Spontaneous resolution of lesions is the rule, but some patients develop residual lipoatrophy. Deaths have been reported in those with associated hypercalcemia[71].

Pathology

The microscopic changes are outlined in Table 100.8. They include a predominantly lobular panniculitis with mixed cellularity (Fig. 100.14). Needle-shaped clefts are observed within both lipocytes and giant cells (Fig. 100.14, inset). The crystals are doubly refractile and stain with oil red O[60]. Occasionally, however, needle-shaped clefts are not evident in otherwise typical cases. Eosinophilic granules are sometimes found within multinucleated giant cells; their origin is not entirely certain, but they may be derived from degranulating eosinophils[72].

Differential diagnosis

The extensive cutaneous involvement in sclerema neonatorum is usually distinguishable from the localized, self-limited process of subcutaneous fat necrosis; histologically, inflammation in sclerema is minimal. Post-steroid panniculitis is microscopically indistinguishable from subcutaneous fat necrosis, but it arises in a different clinical setting (see below).

Treatment

Since many lesions resolve spontaneously, the emphasis is on supportive care. Systemic corticosteroids may be indicated to control the inflammation in severe cases[60]. Serial monitoring of calcium levels (for at least 2 months after skin lesion resolution) is recommended[68]. Hypercalcemia is managed by hydration, dietary restriction of both calcium and vitamin D, calcium-wasting diuretics (e.g. furosemide), calcitonin, and bisphosphonates (e.g. etidronate, pamidronate)[65,67,73]. Corticosteroids may be helpful in managing hypercalcemia, by interfering with the metabolism of vitamin D to calcitriol and by inhibiting calcitriol production by macrophages[67].



Fig. 100.13 Subcutaneous fat necrosis of the newborn – clinical appearance. Red–violet indurated plaques, primarily on the back and shoulders. *Courtesy Lorenzo Cerroni, MD.*

Post-Steroid Panniculitis

Key features

- A rare complication of rapid withdrawal of systemic corticosteroids
- Subcutaneous nodules develop on the cheeks, arms, and trunk
- Lesions resolve spontaneously, or when corticosteroids are readministered
- Microscopically, granulomatous lobular panniculitis with needle-shaped clefts within both lipocytes and giant cells

History

In 1956, Smith and Good reported 11 children with acute rheumatic fever who were treated with large doses of corticosteroids that were rapidly tapered. Five children developed pruritic, erythema nodosum-like lesions.

Epidemiology

Post-steroid panniculitis is typically a disorder of children. It occurs in an older age group than either sclerema neonatorum or subcutaneous fat necrosis of the newborn, with reported ages ranging from 20 months to 14 years[74]. Occasionally, the disorder occurs in adults[75].

Pathogenesis

Post-steroid panniculitis occurs after rapid withdrawal of systemic corticosteroids that have been administered either orally or intravenously. For patients who had received prednisone, cumulative dosages ranged from 2000 to 6000 mg[74]. The precise mechanism by which the panniculitis arises is not known.

Clinical features

Patients who have developed this form of panniculitis received corticosteroid therapy for a variety of conditions[74,76], including those listed

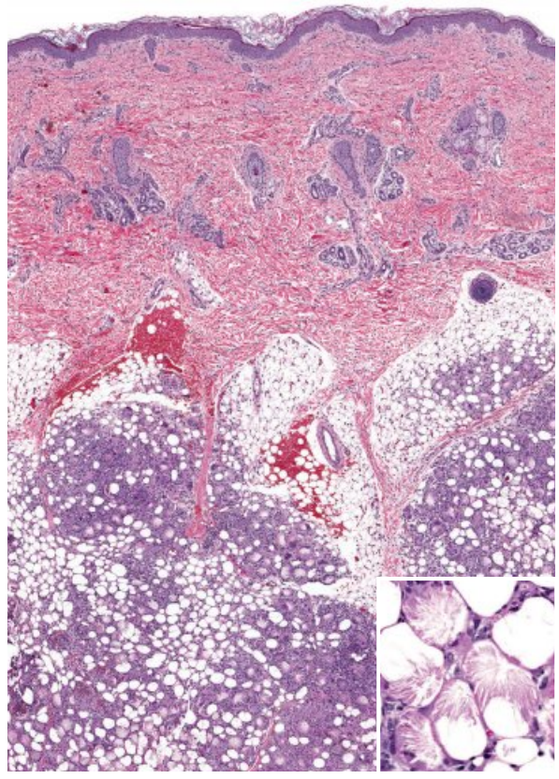


Fig. 100.14 Subcutaneous fat necrosis of the newborn – histopathologic features. A predominantly lobular panniculitis is seen. Needle-shaped clefts in a radial configuration are present within giant cells (inset). Similar findings are seen in post-steroid panniculitis.

in Table 100.8. Lesions appear 1 to 40 days after rapid corticosteroid withdrawal and disappear spontaneously over a period of months to a year[76].

Pathology

Microscopic changes are outlined in Table 100.8[76]. Needle-shaped clefts, some with a "starburst" pattern, can be identified within lipocytes or giant cells.

Differential diagnosis

A less nodular presentation involving the cheeks can mimic non-panniculitic disorders such as erythema infectiosum, atopic dermatitis, lupus erythematosus, or facial cellulitis. The microscopic changes in these conditions would be quite different from those of post-steroid panniculitis. Cold panniculitis has clinical and microscopic similarities, but the history of cold exposure and the lack of needle-shaped clefts histologically permit distinction. The microscopic changes of post-steroid panniculitis are virtually identical to those of subcutaneous fat necrosis of the newborn, although calcification and hemorrhage are more commonly observed in the latter condition. Clinical history allows distinction.

Treatment

Since spontaneous resolution is the rule, treatment is usually unnecessary. Readministration of corticosteroids followed by a more gradual taper may be helpful[76].

LUPUS ERYTHEMATOSUS PANNICULITIS (LUPUS PANNICULITIS)

Synonyms: ■ Lupus profundus ■ Subcutaneous lupus erythematosus

Key features

- Tender subcutaneous nodules and plaques arising on the face, proximal extremities, hips, and trunk
- Associated with discoid lupus erythematosus in at least one-third of patients; less often associated with systemic lupus erythematosus (10%–15% of patients)
- Often precedes onset of other manifestations of lupus erythematosus
- Characteristic microscopic changes include lobular panniculitis with hyaline necrosis and a predominantly lymphoplasmacytic infiltrate; nodular aggregates of lymphocytes are common
- Overlying epidermal or dermal changes of lupus erythematosus are frequently present

History

Kaposi first described the clinical characteristics of lupus panniculitis in 1869. In 1940, it was recognized as a manifestation of lupus erythematosus (LE) by Irgang. Lupus panniculitis was firmly established as a specific subtype of LE in 1956 by Arnold.

Epidemiology

Lupus panniculitis constitutes a small subset of all cases of cutaneous LE, representing 2%–3% of this group[77]. It usually occurs in adults, with a median age of onset of 30–40 years[78]. Children can also develop lupus panniculitis, and an association with neonatal lupus has been described. There is a predominance among women, with a female : male ratio ranging from 2 : 1 to 4 : 1[28,78]. Sometimes there is a family history of either LE or another autoimmune connective tissue disease[77].

Pathogenesis

The autoimmune basis of lupus panniculitis is thought to be similar to that of other types of LE (see Ch. 41). The cells comprising the infiltrates of lupus panniculitis are T lymphocytes and macrophages[79]. Lupus panniculitis, often with a childhood onset and widespread distribution, has been described in patients with partial C4 deficiency[80]. This complement deficiency causes defective opsonization of immune complexes, which may play a role in the pathogenesis of the disease[80]. Immunohistochemical analysis has shown an interferon-driven Th1-biased immune response in active lesions of lupus panniculitis; this may result in recruitment of cytotoxic CXCR3-positive lymphocytes[81].

Clinical Features

Lupus panniculitis is characterized by tender subcutaneous nodules and plaques that may arise in crops (see Table 100.7). A history of trauma can sometimes be elicited. Lesions tend to develop on the face, upper arms, hips, and trunk (Fig. 100.15). Linear scalp lesions are more common among, but not restricted to, East Asian populations. The lack of involvement of the distal extremities is noteworthy[78]. Changes in the overlying skin range from a light pink color to those of discoid LE, i.e. scaling, follicular plugging, dyspigmentation, telangiectasias, atrophy, and scarring. At times, findings of discoid LE are too subtle to be recognized clinically but can be seen on microscopic examination of biopsy specimens. The overlying skin may also be "tethered" to the subcutaneous nodule or plaque, creating a surface depression, and ulceration occasionally occurs. Lupus panniculitis has a chronic, relapsing clinical course. It usually eventuates in subcutaneous atrophy, which can be disfiguring (see Chs. 41 & 101).

Lupus panniculitis often occurs prior to other manifestations of LE and in the absence of other autoimmune connective tissue diseases[78]. For example, lesions of discoid LE have developed up to 10 years after the appearance of the panniculitis. However, manifestations of systemic LE or discoid LE can also occur long before or simultaneously with the panniculitis[28]. There is a closer relationship of lupus panniculitis to other forms of chronic cutaneous LE (e.g. discoid LE) than to systemic LE. Coexistent discoid lesions are observed in at least one-third of patients, whereas only 10%–15% meet the diagnostic criteria for systemic LE[78,82]. Most individuals in the latter group have relatively mild systemic manifestations, usually arthralgias or Raynaud phenomenon[77]. It is common for patients to have low-titer antinuclear antibodies; they can also have other circulating autoantibodies (e.g. anti-dsDNA, anti-RNP), leukopenia, hypocomplementemia, and an elevated ESR[77].

Pathology

Lupus panniculitis is a predominantly lobular process with a variable degree of inflammation (Fig. 100.16A). Nodular aggregates of lymphocytes, usually B cells, are often present (Fig. 100.16B), as are variably



Fig. 100.15 Lupus panniculitis – clinical appearance. Red–brown plaques on the upper outer arm. Note the significant subcutaneous atrophy and overlying lesions of discoid lupus erythematosus. *Courtesy Kenneth E. Greer, MD.*

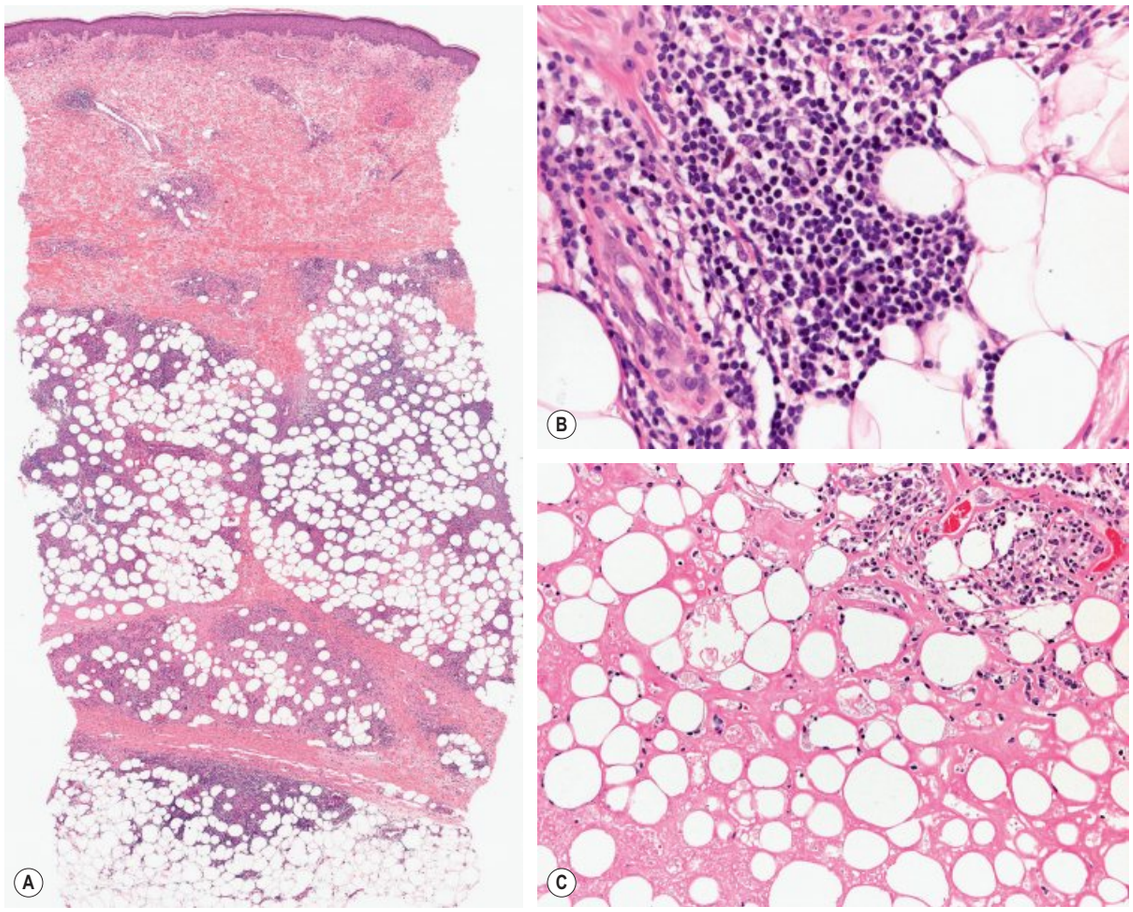


Fig. 100.16 Lupus panniculitis – histopathologic features. **A, B** A primarily lobular panniculitis with nodular aggregates of lymphocytes. **C** Hyaline necrosis of fat lobules is also a characteristic feature. A focus of lipomembranous changes, a nonspecific finding observed in the late stages of several types of panniculitis, is present. *Courtesy Lorenzo Cerroni, MD.*

large clusters of CD123$^+$ plasmacytoid dendritic cells. The characteristic microscopic changes, e.g. hyaline necrosis of the fat lobules (Fig. 100.16C), are outlined in Table 100.7. Granulomas can occur and tend to encroach upon the septa, but they are usually not prominent. Other features include lymphocytic vasculitis and mucin or calcium deposition.

The subcutaneous findings alone are considered sufficiently characteristic to permit a diagnosis of lupus panniculitis. However, overlying epidermal or dermal changes of discoid LE occur in one-half to two-thirds of cases and are also helpful diagnostically[79,82,83]. With direct immunofluorescence, a positive lupus band can be identified in the overlying skin in a high percentage of cases, even in those where the histopathologic changes are nonspecific[83].

Differential Diagnosis

Clinically, lesions of lupus panniculitis can resemble other forms of panniculitis. The rarity of involvement of the distal lower extremities helps to distinguish it from conditions such as erythema nodosum and erythema induratum. It should also be remembered that other forms of subcutaneous inflammation may occur in patients with LE, including erythema nodosum, thrombophlebitis, pancreatic panniculitis, and juxta-articular, rheumatoid nodule-like lesions.

Microscopically, lupus panniculitis can resemble the panniculitis associated with morphea and dermatomyositis (see Table 100.7), traumatic panniculitis (which often has evidence of foreign material), and, in its later stages, localized lipoatrophy due to other etiologies[77]. The most important entity in the differential diagnosis is subcutaneous panniculitis-like T cell lymphoma, as there can be considerable histopathologic overlap between the two disorders. The distinguishing features are outlined in Table 100.9. It should be noted, however, that changes such as vacuolar alteration of the basilar layer and dermal mucin deposition have been reported in panniculitis-like T cell lymphoma[84]. In some cases, overlapping histopathological features of lupus panniculitis and subcutaneous panniculitis-like T cell lymphoma have been reported[85], and these cases probably represent examples of "atypical" lupus panniculitis.

Treatment

Antimalarials are frequently used to treat lupus panniculitis, and they produce improvement in most patients[76]. Addition of a second antimalarial may prove useful in patients who do not respond to a single agent. In view of the chronic, relapsing nature of the disease, treatment may be required for several years[77].

Systemic corticosteroids, when used, are often restricted to initial phases of the disease[77]. Other systemic therapies include dapsone, immunosuppressive agents (e.g. mycophenolate mofetil), thalidomide, IVIg, and rituxumab[78,80,86]. Overlying discoid lesions, if present, can be treated with potent topical or intralesional corticosteroids.

PANNICULITIS OF DERMATOMYOSITIS

Key features

- An uncommon manifestation of dermatomyositis
- More frequently, incidental microscopic changes of panniculitis (in the absence of clinical lesions) are observed
- Can precede or follow other manifestations of dermatomyositis
- Microscopically, it is a lobular or mixed panniculitis with lymphoplasmacytic predominance
- Usually responds to therapy

Introduction

Panniculitis is an uncommon but established clinical manifestation of dermatomyositis. However, there is some evidence that microscopic involvement of subcutaneous fat without overt clinical features of panniculitis is more frequently observed.

LUPUS PANNICULITIS VS SUBCUTANEOUS PANNICULITIS-LIKE T-CELL LYMPHOMA (SPTCL) – DISTINGUISHING FEATURES	
Lupus panniculitis	**SPTCL**
Clinical features	
• Subcutaneous nodules, indurated plaques; sometimes large painful ulcers; lipoatrophy	• Multiple plaques and nodules; usually do not ulcerate
• Proximal extremities, hips, trunk; face and scalp in Asian populations	• Favors the extremities, but can be generalized
• Precedes, accompanies, or follows the development of other manifestations of LE	• Fever, weight loss, and/or hemophagocytic syndrome in a small subset of patients
• Treatment: corticosteroids (intralesional, ultrapotent topical), antimalarials, cyclosporine, dapsone	• Treatment: systemic corticosteroids; cyclosporine; chemotherapy and HSCT reserved for advanced disease
Microscopic and laboratory features	
• Epidermal and dermal changes of LE in half of cases • Lobular lymphocytic panniculitis • Nuclear dust can be observed in later stages	• Epidermal changes occur rarely; changes confined to the subcutis • Lobular lymphocytic involvement • Nuclear dust can be observed in later stages
• Cytologic atypia or adipocyte rimming by lymphocytes: uncommon • Lymphoid follicles: 20%–50% of cases • Clusters of B cells: present	• Cytologic atypia and adipocyte rimming by lymphocytes: seen more frequently • Lymphoid follicles: generally absent • Clusters of B cells: absent
• Staining for MxA: more extensive • Clusters of $CD123^+$ plasmacytoid dendritic cells	• Staining for MxA: less extensive • Clusters of plasmacytoid dendritic cells not observed
• Infiltrate: plasma cells commonly seen, sometimes eosinophils • Fat necrosis: hyaline or lipomembranous • TCR gene rearrangements: polyclonal	• Infiltrate: plasma cells usually absent, granulomas may be seen • Fat necrosis: fibrinoid/coagulative • TCR gene rearrangements: monoclonal

Table 100.9 Lupus panniculitis versus subcutaneous panniculitis-like T cell lymphoma (SPTCL) – distinguishing features. HSCT, hematopoietic stem cell transplant; LE, lupus erythematosus; MxA, human myxovirus resistance protein 1; TCR, T cell receptor.

Clinical Features

The characteristic lesions are persistent, indurated, painful plaques and nodules that may ulcerate and lead to lipoatrophy (see Table 100.7)[87]. They can arise in the setting of established dermatomyositis[87] or represent the initial manifestation of the disease[88]. In affected individuals, the other clinical and laboratory features as well as the incidence of malignancy appear to be similar to those of dermatomyositis patients without panniculitis[87]. Partial or generalized lipoatrophy without preceding clinical lesions of panniculitis (occasionally accompanied by increased abdominal fat) occurs in up to one-quarter of patients with juvenile dermatomyositis, and it is often associated with metabolic abnormalities such as hypertriglyceridemia and insulin resistance (see Ch. 101).

Pathology

The microscopic features are outlined in Table 100.7. Lymphocytic vasculitis has been described, and fat necrosis has been noted in several reports[87]. Membranocystic changes have been observed in some cases (see section on lipodermatosclerosis), and lesions with these changes may be particularly resistant to therapy[87]. Calcification is variable and is an expected finding in cases of dermatomyositis associated with calcinosis of deep soft tissues and skeletal muscle[27,87]. Vacuolar alteration of the basal layer of the overlying epidermis has been described[87], and the dermis may be edematous or mucinous with perivascular lymphocytic inflammation[89]. Direct immunofluorescence is reported to be negative for deposits along the dermal–epidermal junction[87], although immunoreactants have been detected in vessel walls[89].

Differential Diagnosis

Lupus panniculitis is more likely to show hyaline necrosis and lymphoid nodules, but clinical and laboratory findings may be needed to make a distinction. Overlying poikilodermatous changes can occur in both diseases, but lupus is more likely to show appendageal involvement and is associated with positive basement membrane zone fluorescence.

Treatment

Good responses to therapy have generally been reported[89], and treatments include prednisone, methotrexate, azathioprine, JAK inhibitors, cyclosporine, and IVIg[87,89]. Panniculitis lesions have shown variable responses to hydroxychloroquine. Residual facial lipoatrophy has been successfully treated with hyaluronic acid and poly-L-lactic acid dermal fillers.

TRAUMATIC PANNICULITIS

Key features

- Inflammation in the subcutis resulting from external injury
- The injurious event may be accidental, purposeful, or iatrogenic, and it may be a manifestation of an underlying psychiatric disturbance
- A variety of histopathologic changes are observed, depending upon the inciting agent
- Identification of foreign material is of greatest help in diagnosis

Introduction

Extrinsic injury of varying types can produce panniculitis. There are four broad categories: cold panniculitis (Haxthausen disease), sclerosing lipogranuloma, panniculitis due to other injectable substances or therapies (e.g. megavoltage radiation), and panniculitis due to blunt trauma.

History

Lemez described cold panniculitis in 1928, when he noted that newborns and infants up to 6 months of age were particularly susceptible to cold injury, as demonstrated by the production of a subcutaneous nodule following application of an ice cube. In 1941, Haxthausen described a condition occurring in small children a few days after exposure to cold, consisting of firm infiltrated nodules of the cheeks and chin. A similar type of cold injury due to popsicles was reported by Epstein and Oren in 1970.

Injection of foreign lipid material into the skin for cosmetic or other purposes has been performed for centuries. In 1950, Smetana and Bernhard reported 14 cases of what they termed *sclerosing lipogranuloma* of the male genitalia. They believed it was an endogenous process, but subsequent studies demonstrated the presence of mineral oil in similar cases.

Epidemiology

Infants and small children are most at risk for cold panniculitis. A form of the disease also occurs on the thighs of young women who are equestrians[90]. Sclerosing lipogranuloma of the male genitalia is seen mostly in young adults[91]. A sclerosing, pseudosclerodermatous panniculitis has been reported following megavoltage radiation for metastatic carcinoma[92] and as a radiation recall reaction after cyclophosphamide therapy[93].

Pathogenesis

Cold injury to fat favors small children, due in part to the previously discussed characteristics of their fat[94]. Cold injury is also related to

fluctuations in blood flow that occur with declining temperatures (the "hunting phenomenon"), ice crystal formation, and the changes that occur with thawing[94]. Injections of oils (and associated impurities) are known for producing subcutaneous inflammation. Substances include mineral oil (paraffin) as well as camphor, cottonseed, and sesame oils. Even medical grade silicone may contain impurities, and since encapsulation of this material is desirable when used for cosmetic purposes, fibrosis-inducing substances such as olive oil or castor oil are often added. Injected substances responsible for factitial panniculitis have included milk, feces, and a host of other substances.

Panniculitis has also been produced at the sites of injection by numerous therapeutic agents, such as pentazocine, phytonadione (vitamin K)[95], glatiramer acetate, interferon-β, interleukin-2[96], heparin, and vaccines (e.g. tetanus), as well as substances that have been used for tissue augmentation such as bovine collagen[97] or poly-L-lactic acid. More recently, panniculitis due to "mesotherapy" (injection of substances such as phosphatidylcholine and deoxycholate to treat localized fat accumulations; see Ch. 156)[98] and electroacupuncture[99] have been described. In addition to the foreign body response elicited by many of these agents, other immune mechanisms may also be involved. With blunt trauma, granulomas contain material that may be derived from the breakdown of erythrocyte membranes[100].

Clinical Features

In cold panniculitis (including popsicle panniculitis), erythematous, firm nodules develop, particularly on the cheeks and chin[94]. In equestrian cold panniculitis, erythematous to violaceous, tender plaques appear on the thighs following exposure to cold while wearing tight-fitting clothing (Fig. 100.17)[90]. While equestrian cold panniculitis is a commonly used term in the literature, it has been suggested that equestrian perniosis would be a more apt term given that the inflammatory infiltrate is primarily in the dermis.

In lipogranuloma, nodules are sometimes migratory and can be accompanied by varying degrees of swelling, erythema, abscess formation, lymphangitis, and fibrosis. The term *sclerosing lipogranuloma* often refers to lesions arising on the male genitalia due to self-injection of oily materials (see Ch. 94). There has also been a report of a sclerosing lipogranuloma that apparently resulted from topical application of vitamin E cream[101]. In several Japanese patients, Y-shaped induration of the scrotum (in which exogenous lipids could not be detected) was described as eosinophilic sclerosing lipogranuloma[102]. Patients with sclerosing lipogranuloma frequently deny self-injection, making diagnosis difficult. Another variant of lipogranuloma is the *grease gun granuloma*, which results from accidental firing of the grease gun used by mechanics. This results in formation of a verrucous nodule, often on the dorsum of the hand[103].



Fig. 100.17 Cold panniculitis. Violaceous nodules and plaques, some with central crusting, on the thigh of a young woman. Collarettes of scale developed as the lesions healed. While equestrian cold panniculitis is a commonly used term in the literature, it has been suggested that equestrian perniosis would be a more apt term given that the inflammatory infiltrate is primarily in the dermis. *Courtesy Kendra Lesiak, MD.*

Inflamed nodules with varying degrees of pain and fibrosis have been observed in other forms of panniculitis due to injection, with the distribution of lesions sometimes providing a clue to their cause. A dramatic example of this is *Texier disease*, a panniculitis due to phytonadione (vitamin K) injections. In this disorder, sclerotic lesions with lilac-colored borders form on the buttocks and thighs, in a configuration resembling a "cowboy gunbelt and holster"[95]. Lesions due to blunt trauma often have an ecchymotic character and involve locations such as the shin, arm, or hand[100]. Hypertrichosis may also be present, possibly the consequence of local hyperemia or angiogenesis.

Pathology

Table 100.10 outlines the microscopic changes in various forms of traumatic panniculitis[91,93,103–106]. In addition, sclerosing lipogranuloma is discussed in Chapter 94.

Differential Diagnosis

In cold panniculitis, the absence of needle-shaped clefts in lipocytes and location of the most intense inflammation near the dermal–subcutaneous interface help to distinguish this condition from subcutaneous fat necrosis of the newborn. In sclerosing lipogranuloma and related lipogranulomas, distinctive large vacuoles are found in the dermis and subcutis (Fig. 100.18). Mineral oil in non-processed tissue can be identified by infrared spectroscopy[103] or mass spectrometry[107].

Panniculitis due to injectable substances can be diagnosed when foreign material (often identified by polarization microscopy) is present. Cosmetic fillers have distinctive histologic features (see Fig. 94.11), and silicone can be distinguished from other cosmetic fillers by cutaneous ultrasonography[108]. Cases with acute inflammation and necrosis may resemble infection-induced panniculitis, and, in fact, infection may accompany injection panniculitis; special stains and cultures for organisms (including atypical mycobacteria) are useful in this regard. Sclerosing traumatic panniculitis (e.g. due to phytonadione or pentazocine injections) may resemble morphea clinically, but would not present as a septal panniculitis histologically[95].

Treatment

Treatment of these disorders should focus on removal of the inciting stimulus and eradication of any associated infection. Intralesional or systemic corticosteroids can be helpful in controlling the inflammation, and they have been used in the management of sclerosing lipogranuloma and granulomatous panniculitis due to other injected substances[97]. Surgical excision may also be an option for sclerosing lipogranuloma.

LIPODERMATOSCLEROSIS

Synonyms: ■ Sclerosing panniculitis ■ Hypodermitis sclerodermiformis ■ Chronic panniculitis with lipomembranous changes

Key features

- Favors the medial aspect of the lower extremities above the malleolus
- Acute phase with erythema, warmth, and tenderness, which may be misdiagnosed as infectious cellulitis
- Chronic phase with induration and red–brown to violet–brown discoloration
- Usually develops in the setting of chronic venous insufficiency
- Both septal and lobular panniculitis; lipomembranous changes are common, particularly in chronic lesions

Introduction

Erythema, induration, and pigmentary changes have long been known to be associated with venous insufficiency. Because of the variety of clinical appearances and histopathologic findings that can occur at different stages of the disease, a number of diagnostic terms have been

MICROSCOPIC FEATURES OF TRAUMATIC PANNICULITIS		
Condition	**Microscopic features**	**Special considerations**
Cold panniculitis	Septal/lobular inflammation, especially at the dermal–subcutaneous border and periadnexally; lymphocytes, neutrophils, foamy macrophages, poorly developed granulomas; mucin, adipocyte necrosis, microcysts	Needle-shaped clefts are not observed
Lipogranuloma	*Sclerosing lipogranuloma* – granulomatous lobular panniculitis with marked fibrosis and numerous round or oval vacuoles of various sizes in the dermis and subcutis, producing a "Swiss cheese" appearance (Fig. 100.18); nodular aggregates of lymphocytes, plasma cells, eosinophils, macrophages or giant cells often present *Grease gun granuloma* – also pseudoepitheliomatous hyperplasia	Exogenous oils within the vacuoles can be identified in frozen sections stained with oil red O, silver bromide and osmium tetroxide; infrared spectroscopy; mass spectrometry
Injection-induced panniculitis	Central nidus of subcutaneous inflammation; sometimes fibrosis* or polarizing foreign material	*Povidone panniculitis* – gray–blue material within macrophages on routine staining that also stains with Congo red and chlorazol-fast pink *Cancer vaccines*, *heparin* – eosinophils may be numerous
Panniculitis due to aluminum in vaccines	Nonspecific lobular panniculitis with fibrosis; formation of numerous lymphoid follicles; may resemble lupus panniculitis, pseudolymphoma (see Table 121.1)	Macrophages display grayish to violaceous, granular cytoplasm due to lysosomes that contain aluminum salts; can be identified using X-ray microanalysis or possibly aluminum staining
Panniculitis due to injectable aesthetic microimplants	Diffuse granulomatous infiltrate that may involve the dermis and subcutis; focal areas of collagen degeneration	Different "fillers" can have specific histopathologic features (see Fig. 94.11 & Table 94.5)
Blunt trauma	Organizing hematoma, focal granuloma	Deposits of glycosaminoglycans (mucopolysaccharides) and iron can be seen
Postirradiation or radiation recall panniculitis	Deep fibrosis, mixed inflammation	Inflammation includes lymphocytes, plasma cells, macrophages, eosinophils

*Especially with phytonadione (vitamin K) and pentazocine injections; lipid-containing vacuoles, fat necrosis, foam cells, thrombosis and endarteritis are also observed in the latter.

Table 100.10 Microscopic features of traumatic panniculitis.

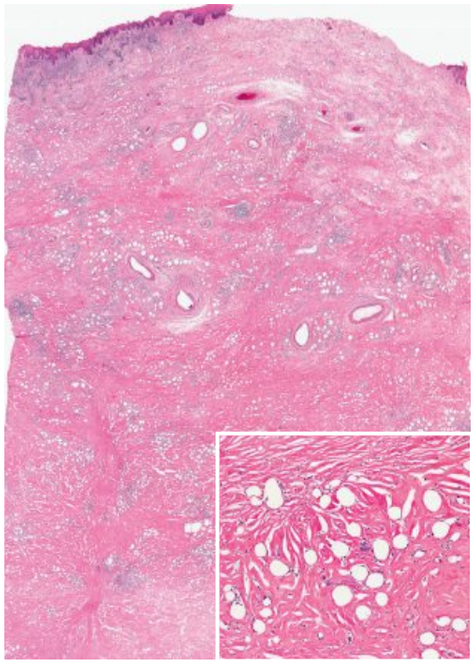


Fig. 100.18 Mineral oil granuloma (paraffinoma). There is sclerosis throughout the dermis and subcutis as well as numerous vacuolated spaces (inset). Scattered histiocytes and lymphocytes are also seen. *Courtesy Lorenzo Cerroni, MD.*

employed to explain the changes. Recently, the various manifestations of this panniculitis have been consolidated under the heading of *lipodermatosclerosis* or *sclerosing panniculitis*.

History

In 1955, Huriez drew attention to a related indurated lesion, which he termed *hypodermitis sclerodermiformis*.

Epidemiology

Most patients are women over the age of 40 years, but appearance after the age of 75 years has also been reported[109,110].

Pathogenesis

There is considerable evidence for venous insufficiency in patients with lipodermatosclerosis[111], and fibrinolytic abnormalities are also present in these individuals. Venous hypertension leads to a compromised ability to reduce foot vein pressure during exercise. This results in increased capillary permeability, which causes leakage of fibrinogen, its polymerization to form fibrin cuffs around vessels, impedance of oxygen exchange, and tissue anoxia (see Ch. 105)[110]. Pericapillary fibrin deposits can be seen in uninvolved, clinically normal extremities of patients with healed venous ulcers of the opposite extremity, suggesting that this abnormality precedes the clinical changes of lipodermatosclerosis[112].

There may also be an abnormal regulation of angiogenesis within lesions of lipodermatosclerosis. In particular, increased expression of vascular endothelial growth factor receptor 1 (VEGFR-1), which can act as a negative regulator of VEGF-mediated angiogenesis, has been observed, along with increased expression of angiopoietin-2 (Ang-2)[113]. Additional factors contributing to the pathogenesis of lipodermatosclerosis may include protein C and S deficiencies[114], local stimulation of collagen synthesis[110], including an increased number of cells expressing procollagen type 1 mRNA[115], and obesity.

Clinical Features

The acute phase of lipodermatosclerosis presents with pain, warmth, erythema, and some induration (Fig. 100.19), most often initially on the medial lower leg above the malleolus. Other dependent sites such as the lower aspect of the abdominal pannus can also develop lipodermatosclerosis. At this point, the changes are relatively diffuse[110]. In the chronic phase, there is marked sclerosis of the dermis and subcutis, resulting in induration that is more sharply demarcated from adjacent normal skin. Brown discoloration due to hemosiderin deposition may also be present[109]. These features give the affected leg the appearance of an inverted wine bottle[116].

Pathology

Early lesions show mid-lobular ischemic necrosis, a lymphocytic infiltrate in the septa that rims the fat lobules, variable degrees of capillary congestion and thrombosis, and hemorrhage with

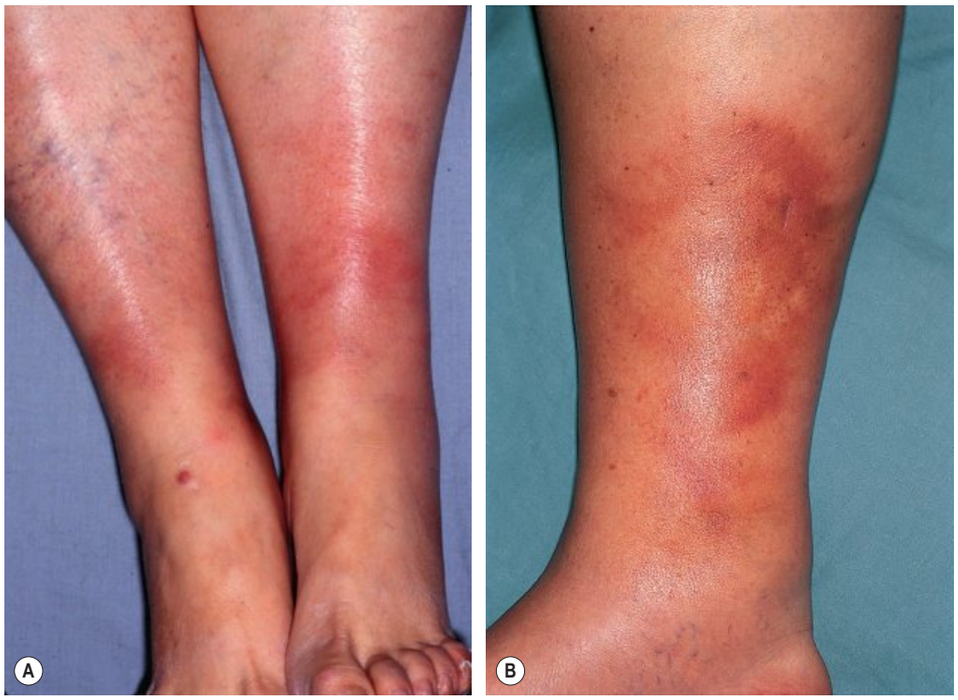


Fig. 100.19 Lipodermatosclerosis – clinical appearance. A Acute phase with tender erythematous plaques on both lower extremities. **B** Chronic phase with sclerotic red–brown plaque on the lower medial leg. *B, Courtesy Kenneth E. Greer, MD.*

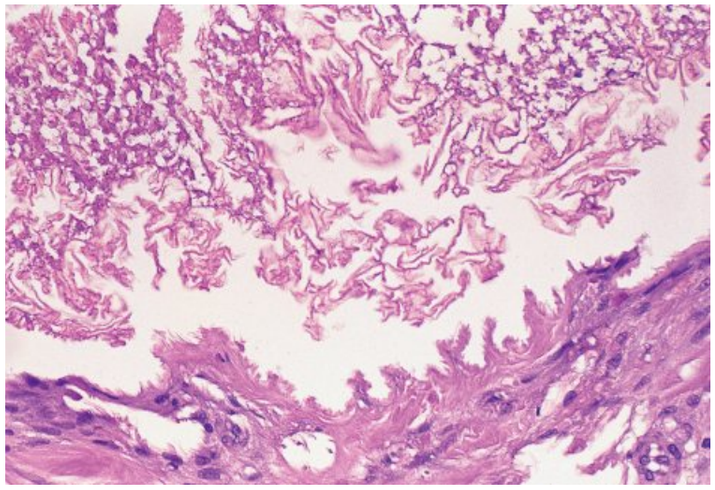


Fig. 100.20 Lipodermatosclerosis – histopathologic features. Lipomembranous change, consisting of cystic formation with elaborate papillary configurations.

hemosiderin deposition. With progression, septal thickening, hyaline sclerosis involving lipocytes, lipophage formation, and mixed inflammatory cell infiltrates appear[109]. Advanced lesions show marked septal sclerosis and membranocystic change in the face of a marked reduction in inflammation.

Membranocystic change is a key feature in lipodermatosclerosis[117]. This consists of thickened, undulating membranes that form cysts and papillary configurations (Fig. 100.20). The membranes are believed to result from degenerated cell membranes of lipocytes and/or macrophages. The material comprising the membranes is ceroid, an oxidation product of unsaturated fatty acids[118].

Short, frayed elastic fibers can be present within the subcutaneous septa, and these may be calcified, features that resemble pseudoxanthoma elasticum[119]. Myospherulosis, a foreign-body type of granulomatous reaction to lipid-containing material and blood, has been described in lesions of lipodermatosclerosis[120]. By phosphotungstic acid–hematoxylin stain or by immunofluorescent methods, pericapillary fibrin can also be demonstrated in lesions of lipodermatosclerosis[117]. Dermal changes include fibrosis, tortuous thick-walled veins, and superficial and deep perivascular inflammation[109]. Biopsy should be avoided if the diagnosis is obvious, since poor wound healing and ulceration frequently result. When necessary, a thin elliptical excision should be obtained from the margin of a lesion.

Differential Diagnosis

Difficulties in clinical diagnosis arise most often in early lesions, when the process is more diffuse and erythematous. At this stage, consideration is often given to infectious cellulitis, erythema nodosum, or erythema induratum[109,110,116]. Persistence of a lesion, association with stasis changes, and lack of response to antimicrobials suggest the correct diagnosis, perhaps aided by studies of venous function[111].

As induration develops and progresses, differentiation from morphea and scleromyxedema may be necessary. In morphea, subcutaneous involvement is predominantly septal, and lipophagic and lipodystrophic changes are not as prominent as they are in lipodermatosclerosis[109]. Membranocystic changes, when present, can be of great diagnostic help; however, these findings can occur in a variety of other conditions, including lupus and dermatomyositis panniculitis, liposarcoma, erythema nodosum, and diabetic dermopathy[118].

Treatment

Leg elevation and consistent compression therapy are the mainstays of treatment for lipodermatosclerosis[110]. Traditional anti-inflammatory therapies are usually ineffective in this condition[109], although intralesional corticosteroids (e.g. triamcinolone 5–10 mg/cc) may be of benefit when used in conjunction with compression therapy. Good results were reported with the anabolic steroid stanozolol[110] especially in the earlier phases of the disease, but this medication is no longer commercially available. As a result, danazol has been used (successfully) as a substitute[121]. Anabolic steroids enhance fibrinolysis, and they can reduce pain, extent of involvement, and induration of the skin. However, side effects of sodium retention, lipid profile abnormalities, hepatotoxicity, and virilization in women do limit their use. Oxandrolone, an anabolic steroid with less hepatotoxicity and fewer androgenic effects, represents another therapeutic option[113]. Other reported treatments include ultrasound, pentoxifylline, fasciotomy, and phlebectomy[110,122].

INFECTION-INDUCED PANNICULITIS

Synonym: ■ Infective panniculitis

Key features

- A wide variety of infectious agents has been reported to produce panniculitis
- Some degree of immunosuppression is common, but not invariable
- Histopathologic findings vary, but often include mixed septal/lobular panniculitis, neutrophilic infiltration, hemorrhage, and necrosis
- Special staining and culture of drainage and tissue can provide a definitive diagnosis

Introduction

Panniculitis can result from a distant focus of infection (a classic example being erythema nodosum) or panniculitis can be *directly* induced by an infectious agent. The latter can produce a variety of clinical and microscopic appearances, although there are some features that infection-induced lesions have in common, regardless of the etiologic agent.

History

While multiple reports of panniculitis directly caused by infectious agents have been published, most early studies of deep skin infections did not focus upon the changes in the subcutaneous fat. In 1989, Patterson et al.[18] studied 15 cases of infection-induced panniculitis, with an emphasis upon the histopathologic features in the subcutis. Since that time, additional reports of panniculitis due to infection have continued to appear.

Epidemiology

There appears to be no age, sex, or racial predilection among cases of infection-induced panniculitis. Many of these patients are immunosuppressed[18] or have predisposing medical conditions such as diabetes mellitus.

Pathogenesis

In this group of disorders, infectious agents are considered to be directly responsible for the panniculitis. Examples of reported microorganisms to date are listed in Table 100.11[18,123–126].

Involvement of the subcutis can result from direct inoculation or septicemia. Other potential modes of spread include transfascial from an enteric source, in the case of abdominal panniculitis or via "persorption", a proposed mechanism by which *Candida* migrates across intact endothelium from the gut to a subcutaneous site[124]. Immunosuppression is common, but not invariable, among individuals with infection-induced panniculitis.

Clinical Features

Patients develop local swelling and erythema. There may be one or more fluctuant nodules that ulcerate and drain. Lesions on the legs and feet are common, but other sites of involvement include the gluteal region, abdomen, axillae, arm, or hand. In addition to sepsis, underlying conditions include diabetes mellitus, leukemias or solid tumors, autoimmune connective tissue disease, AIDS, and organ transplantation.

Pathology

Individual cases can mimic other primary forms of panniculitis. Common changes (regardless of the infectious agent) include a mixed septal/lobular panniculitis, neutrophilic infiltration, vascular proliferation, hemorrhage, and necrosis that involves lipocytes, inflammatory cells, and eccrine sweat coils[18] (Fig. 100.21). In Q fever due to *Coxiella burnetii*, there may be a "doughnut-like" granulomatous lobular panniculitis, in which fibrin and inflammatory cells form a ring around a central clear space; similar changes have been found in the liver and bone marrow of patients with Q fever[123]. In lobular panniculitis due to *Stenotrophomonas maltophilia* (previously *Pseudomonas maltophilia*), phagocytosis of bacteria leads to foamy histiocytes whose cytoplasm is filled with bluish, granular material.

INFECTION-INDUCED PANNICULITIS – REPORTED CAUSATIVE AGENTS
Bacteria
Staphylococcus aureus Group A *Streptococcus* *Pseudomonas aeruginosa* *Stenotrophomonas maltophilia* *Brucella melitensis* *Nocardia asteroides* *Tropheryma whipplei* (causative agent of Whipple disease)
Mycobacteria
M. tuberculosis *M. marinum, M. avium-intracellulare, M. chelonae, M. fortuitum, M. ulcerans*
Coxiella
C. burnetii
Borrelia
B. burgdorferi
Fungi
Blastomyces dermatitidis, Histoplasma capsulatum *Microsporum* spp. (including *M. canis*) *Candida* spp. (including *C. albicans*) *Cryptococcus neoformans* *Aspergillus* spp. (including *A. flavus*), *Mucor* or related zygomycetes, *Fusarium* spp., *Aureobasidium pullulans*
Helminths & protozoa
Nematodes (*Gnathostoma* spp.) Trematodes (*Fasciola hepatica*, *Schistosoma* spp.)

Table 100.11 Infection-induced panniculitis – reported causative agents.

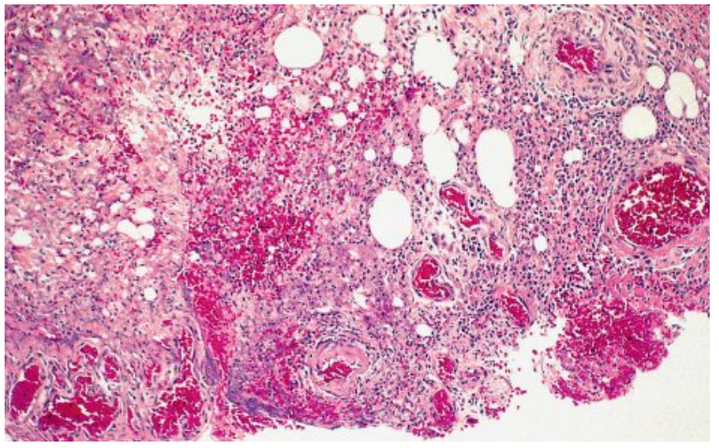


Fig. 100.21 Infection-induced panniculitis. Bacterial panniculitis, showing heavy neutrophilic infiltration, basophilic necrosis, vascular proliferation, and hemorrhage.

Differential Diagnosis

Fluctuant, ulcerating nodules also occur in pancreatic panniculitis, traumatic panniculitis, and alpha-1 antitrypsin deficiency panniculitis. Clinical and laboratory data can usually permit distinction. As noted previously, traumatic panniculitis may be accompanied by infection. Examples of infection-induced panniculitis with predominantly septal involvement or vasculitis could be confused with acute erythema nodosum or erythema induratum, respectively. Panniculitis due to mucormycosis may feature "ghost cells" and granular calcium deposits and thus resemble pancreatic panniculitis; it can also mimic gouty panniculitis due to the presence of intracellular crystalline deposits[126]. Special stains for organisms and cultures of drainage and tissue are keys to the diagnosis. In one study, special stains were positive for organisms in 14 of 15 cases[18].



Fig. 100.22 Cytophagic histiocytic panniculitis – clinical appearance. Subcutaneous nodules with purpura. *Courtesy Kenneth E. Greer, MD.*

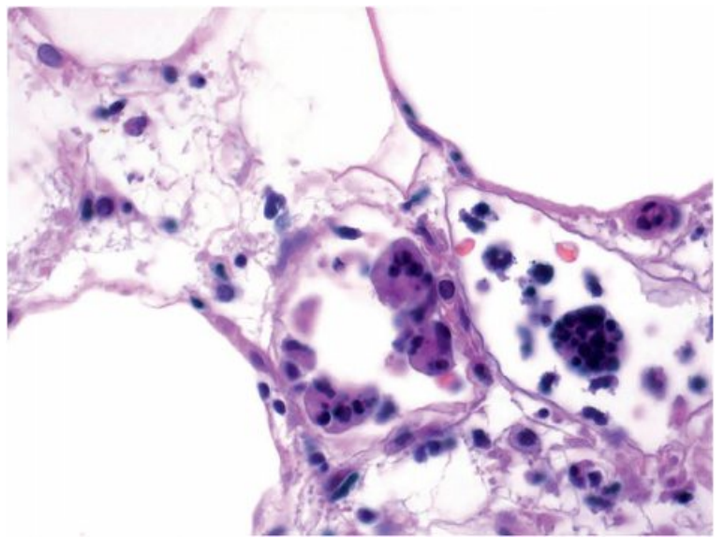


Fig. 100.23 Cytophagic histiocytic panniculitis – histopathologic features. Macrophages engaged in cytophagic activity. Some of them have the appearance of "bean bag" cells.

Treatment

Treatment consists of appropriate antimicrobial therapy. Surgery may be indicated for isolated lesions caused by grain-forming fungi or bacteria, such as mycetoma or botryomycosis. A more radical surgical approach has been used successfully in treating abdominal panniculitis due to enteric bacteria.

CYTOPHAGIC HISTIOCYTIC PANNICULITIS

The term "cytophagic histiocytic panniculitis" (CHP) has been used to describe subcutaneous nodules or plaques that on histologic examination show infiltrates of macrophages containing erythrocytes, lymphocytes, and/or karyorrhectic debris, i.e. exhibiting hemophagocytosis (Figs. 100.22 & 100.23)[127]. These macrophages with cytophagic activity have been referred to as "bean bag" cells. With the advent of immunophenotyping and genetic techniques, it has become apparent that the vast majority of patients have lymphoma, with atypical lymphoid cells also present within the panniculus[128]. In general, the lymphomas represent subcutaneous involvement of primary cutaneous γ/δ T cell lymphoma or EBV-associated extranodal NK/T cell lymphoma, nasal type (see Ch. 120)[129]. Occasionally, patients have subcutaneous panniculitis-like T cell lymphoma, and, rarely, no lymphoma[130]. Individuals in the latter group may still have a fatal course due to a hemophagocytic syndrome that involves the liver, spleen, and bone marrow (leading to pancytopenia). Mutations in a number of genes can predispose individuals to the development of hemophagocytic syndrome, including that which encodes perforin (see Table 91.1). Of note, a child with microscopic findings of CHP but no evidence of lymphoma was found to have a heterozygous nonsense mutation in the gene that encodes perforin[131].

MALIGNANT SUBCUTANEOUS INFILTRATES

Malignant infiltrates may involve the subcutis, mimicking the clinical and microscopic appearance of panniculitis. The best known of these is subcutaneous panniculitis-like T cell lymphoma (see Ch. 120). While cytophagia can be seen in the latter disorder, it is particularly characteristic of subcutaneous involvement of primary cutaneous γ/δ T cell lymphoma and EBV-associated extranodal NK/T cell lymphoma, nasal type (see above). Other lymphomas (e.g. B cell), leukemias, and metastatic solid tumors may infiltrate the subcutis. Obviously, clinical information is crucial in such cases.

Histopathologic clues include the recognition of significant pleomorphism or monotony among infiltrating cells in the subcutis, infiltration between collagen bundles of the dermis or around adnexal structures, and supporting immunohistochemical studies. Of note, the diagnosis of subcutaneous panniculitis-like T cell lymphoma can sometimes be elusive as the initial impression may be lupus panniculitis (see Table 100.9) or even a nonspecific panniculitis with lipomembranous changes[132].

UNUSUAL OR NEWLY DESCRIBED FORMS OF PANNICULITIS

Table 100.12 lists several more recently described or unusual forms of panniculitis. In addition, there is an ever-expanding list of drugs that can induce panniculitis, especially with the introduction of immuno- and targeted therapies (see Table 100.3). When a patient presents with panniculitis that is not readily classifiable, it may be worthwhile to consider these alternative diagnoses. Several of them probably do not actually represent distinct entities but rather overarching terms that include established forms of panniculitis. For example, plasma cell panniculitis could include not only morphea and postirradiation pseudosclerodermatous panniculitis but also other autoimmune connective tissue diseases or infectious diseases. The fasciitis–panniculitis syndrome is a term that has appeared from time to time, primarily in the non-dermatology literature. While sometimes discussed as if it were a single entity, fasciitis–panniculitis syndrome has been used to include eosinophilic fasciitis, morphea profunda, lupus panniculitis, lipodermatosclerosis, and a variety of other conditions. Sweet syndrome and Lyme disease are established entities that can occasionally have panniculitis as a significant finding. Two other more recently described conditions, atypical lymphocytic lobular panniculitis and panniculitic bacterid, may require further study and experience before being widely accepted as distinct entities. No doubt this list will change as disease mechanisms are better understood and disorders are reclassified or absorbed into other classification schemes.

Additional figures and table on Classification of the panniculitides, available in our eBook (see inside front cover for access code).

UNUSUAL OR RECENTLY DESCRIBED FORMS OF PANNICULITIS			
Type of panniculitis	**Clinical features**	**Microscopic findings**	**Comments**

Crystal deposition panniculitis	Red nodules, sometimes with necrosis; may have drainage; legs and elsewhere	Necrotizing and/or granulomatous panniculitis; calcium oxalate crystals in subcutaneous vessels; subcutaneous deposits of sodium urate crystals
		Crystals of Igs in the cytoplasm of histiocytes
			• Metabolic
			  • Oxalosis: primary (inherited) or secondary (chronic renal failure)
			  • Urate deposition: may be an isolated cutaneous finding in gout
			• Paraneoplastic
			  • Crystal-storing histiocytosis: associated with hematologic malignancies

Idiopathic palmoplantar hidradenitis (see Ch. 39)	Sudden onset of painful erythematous nodules; soles > palms Self-limited	Neutrophilic eccrine hidradenitis	More common in children Precipitated by trauma (mechanical, thermal) Mimicked by erythema nodosum, pseudomonas hot-foot syndrome, cold panniculitis
Sweet panniculitis (subcutaneous Sweet syndrome)*	Erythematous nodules that may be painful; extremities; associated with leukemias (e.g. AML, hairy cell leukemia), treatment of acute promyelocytic leukemia with all-*trans*-retinoic acid, and, rarely, solid tumors	Predominantly neutrophilic lobular panniculitis, without vasculitis; immature myeloid forms have been described	Must exclude other neutrophil-rich forms of panniculitis, such as infection-induced, traumatic, alpha-1 antitrypsin deficiency and pancreatic panniculitides
Panniculitic bacterid	Sudden onset of tender subcutaneous nodules; lower extremities; polyclonal hypergammaglobulinemia, cold agglutinins, cryofibrinogens	Lobular panniculitis, predominantly neutrophils with microabscesses; angiopathy; extravascular granulomas	Triggered by non-tuberculous infections; underlying disorders include atopy, antiphospholipid antibody syndrome
Plasma cell panniculitis	Hyperpigmentation and induration; trunk and extremities	Sclerosis of subcutaneous septa; plasma cells prominent component of infiltrate	Not a single entity; manifestation of morphea profunda, other autoimmune connective tissue disorders, and postirradiation pseudosclerodermatous panniculitis
Panniculitis of Lyme disease	Tender nodules or diffuse fasciitis; fever, chills, photophobia, polyarthritis	Acute septal panniculitis; may contain eosinophils, plasma cells; lymphocytic vasculopathy	Detection of *Borrelia* spp. in tissues; positive serologies confirm the diagnosis
Fasciitis–panniculitis syndrome	Subcutaneous induration, sometimes with regional pain	Chronic inflammation, accompanied by replacement of fat lobules by fibrous tissue; thickening of fascia	Term used primarily in the rheumatologic literature; encompasses several autoimmune connective tissue diseases; also described as a paraneoplastic syndrome with hematologic, pancreatic, and gastrointestinal malignancies
Atypical lymphocytic lobular panniculitis	Recurrent, infiltrative plaques; lower extremities, abdomen	Interstitial subcutaneous infiltrate with well-differentiated lymphocytes; no significant fat necrosis	Molecular studies show clonal or oligoclonal profile; no progression to lymphoma; considered T cell dyscrasia
Infantile-onset panniculitis with uveitis and systemic granulomatosis	High fever, anemia, hepatosplenomegaly, uveitis, arthritis	Histiocytic lobular panniculitis, with lymphocytes and neutrophils initially; granulomas in later stage	Resemblance to Blau syndrome, but lacks *NOD2/CARD15* mutations; may respond to TNF inhibitors
*Neutrophilic panniculitis also may precede the lipodystrophy of proteasome-associated autoinflammatory syndrome/CANDLE (chronic atypical neutrophilic dermatosis with lipodystrophy and elevated temperature) syndrome (see Table 45.7).			

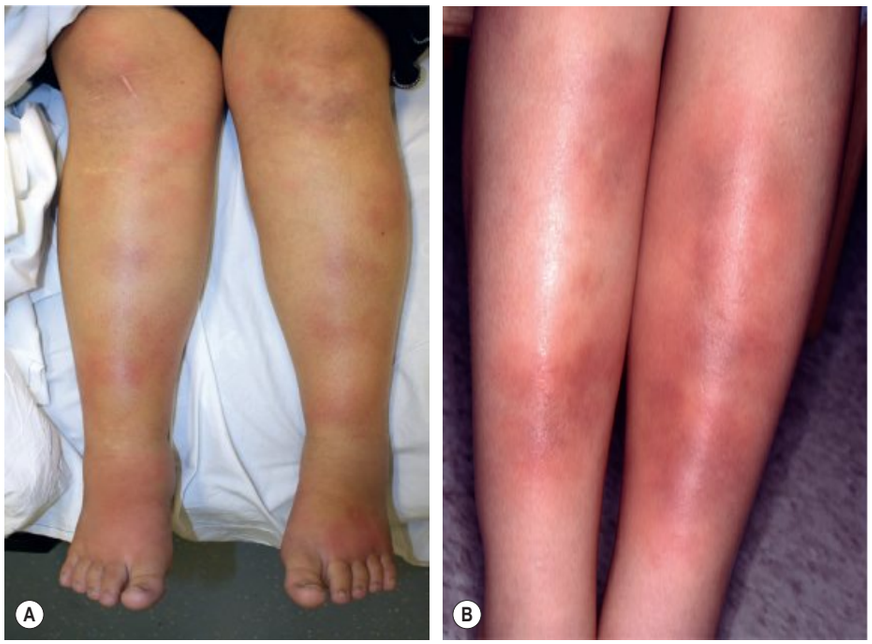
Table 100.12 Unusual or recently described forms of panniculitis. AML, acute myelogenous leukemia; TNF, tumor necrosis factor.

REFERENCES

1. Braverman IM. Protective effects of erythema nodosum in coccidioidomycosis. *Lancet*. 1999;353:168.
2. White WL, Hitchcock MG. Diagnosis: erythema nodosum or not? *Semin Cutan Med Surg*. 1999;18:47–55.
3. Cribier B, Caille A, Heid E, et al. Erythema nodosum and associated diseases. A study of 129 cases. *Int J Dermatol*. 1998;37:667–672.
4. Garcia-Porrua C, Gonzalez-Gay MA, Vazquez-Caruncho M, et al. Erythema nodosum: etiologic and predictive factors in a defined population. *Arthritis Rheum*. 2000;43:584–592.
5. Llorente L, Richaud-Patin Y, Alvarado C, et al. Elevated Th1 cytokine mRNA in skin biopsies and peripheral circulation in patients with erythema nodosum. *Eur Cytokine Netw*. 1997;8:67–71.
6. Senturk T, Aydintug O, Kuzu I, et al. Adhesion molecule expression in erythema nodosum-like lesions in Behçet's disease. A histopathological and immunohistochemical study. *Rheumatol Int*. 1998;18:51–57.
7. Kunz M, Beutel S, Brocker E. Leucocyte activation in erythema nodosum. *Clin Exp Dermatol*. 1999;24:396–401.
8. Wallace SL. Erythema nodosum treatment with colchicine. *JAMA*. 1967;202:1056.
9. Nomiyama J, Shinohara K, Inoue H. Erythema nodosum caused by the administration of granulocyte colony-stimulating factor in a patient with refractory anemia. *Am J Hematol*. 1994;47:333.
10. Winter HS. Treatment of pyoderma gangrenosum, erythema nodosum, and aphthous ulcerations. *Inflamm Bowel Dis*. 1998;4:71.
11. Labunski S, Posern G, Ludwig S, et al. Tumor necrosis factor-alpha promoter polymorphism in erythema nodosum. *Acta Derm Venereol*. 2001;81:18–21.
12. Mert A, Ozaras R, Tabak F, et al. Erythema nodosum: an experience of 10 years. *Scand J Infect Dis*. 2004;36:424–427.
13. Thurber S, Kohler S. Histopathologic spectrum of erythema nodosum. *J Cutan Pathol*. 2006;33:18–26.
14. Egawa T, Okuyama R, Tagami H, et al. Erythema nodosum with eosinophilic panniculitis. *Int J Dermatol*. 2010;49:965–967.
15. Misago N, Tada Y, Koarada S, et al. Erythema nodosum-like lesions in Behçet's disease: a clinicopathological study of 26 cases. *Acta Derm Venereol*. 2012;92:681–686.
16. Sanchez Yus E, Sanz Vico MD, de Diego V. Miescher's radial granuloma. A characteristic marker of erythema nodosum. *Am J Dermatopathol*. 1989;11:434–442.
17. Ball NJ, Adams SP, Marx LH, et al. Possible origin of pancreatic fat necrosis as a septal panniculitis. *J Am Acad Dermatol*. 1996;34:362–364.
18. Patterson JW, Brown PC, Broecker AH. Infection-induced panniculitis. *J Cutan Pathol*. 1989;16:183–193.
19. Horio T, Imamura S, Danno K, et al. Potassium iodide in the treatment of erythema nodosum and nodular vasculitis. *Arch Dermatol*. 1981;117:29–31.
20. Banks PA, Present DH. Treatment of erythema nodosum, aphthous stomatitis, and pyoderma gangrenosum in patients with IBD. *Inflamm Bowel Dis*. 1998;4:73.
21. Boyd AS. Etanercept treatment of erythema nodosum. *Skinmed*. 2007;6:197–199.
22. Rosen T, Martinelli P. Erythema nodosum associated with infliximab therapy. *Dermatol Online J*. 2008;14:3.
23. Rajakulendran S, Deighton C. Adverse dermatological reactions in rheumatoid arthritis patients treated with etanercept, an anti-TNFalpha drug. *Curr Drug Saf*. 2006;1:259–264.
24. Benitez-Gutierrez L, Tutor-de Ureta P, Mellor-Pita S, et al. Refractory chronic erythema nodosum treated with adalimumab. *Rev Clin Esp*. 2013;213:466–467.
25. de Almeida Prestes C, Winkelmann RK, Su WP. Septal granulomatous panniculitis: comparison of the pathology of erythema nodosum migrans (migratory panniculitis) and chronic erythema nodosum. *J Am Acad Dermatol*. 1990;22:477–483.
26. Su WP, Person JR. Morphea profunda. A new concept and a histopathologic study of 23 cases. *Am J Dermatopathol*. 1981;3:251–260.
27. Winkelmann RK. Panniculitis in connective tissue disease. *Arch Dermatol*. 1983;119:336–344.
28. Peters MS, Su WP. Eosinophils in lupus panniculitis and morphea profunda. *J Cutan Pathol*. 1991;18:189–192.

29. Vincent F, Prokopetz R, Miller RA. Plasma cell panniculitis: a unique clinical and pathologic presentation of linear scleroderma. *J Am Acad Dermatol*. 1989;21:357–360.
30. Fleischmajer R, Nedwich A. Generalized morphea. I. Histology of the dermis and subcutaneous tissue. *Arch Dermatol*. 1972;106:509–514.
31. Pittelkow MR, Smith KC, Su WP. Alpha-1-antitrypsin deficiency and panniculitis. Perspectives on disease relationship and replacement therapy. *Am J Med*. 1988;84:80–86.
32. American Thoracic Society, European Respiratory Society. American Thoracic Society/European Respiratory Society statement: standards for the diagnosis and management of individuals with alpha-1 antitrypsin deficiency. *Am J Respir Crit Care Med*. 2003;168:818–900.
33. Irvine C, Neild V, Stephens C, et al. Alpha-1-antitrypsin deficiency panniculitis. *J R Soc Med*. 1990;83:743–744.
34. Gross B, Grebe M, Wencker M, et al. New findings in PiZZ alpha1-antitrypsin deficiency-related panniculitis. Demonstration of skin polymers and high dosing requirements of intravenous augmentation therapy. *Dermatology*. 2009;218:370–375.
35. Su WP, Smith KC, Pittelkow MR, et al. Alpha 1-antitrypsin deficiency panniculitis: a histopathologic and immunopathologic study of four cases. *Am J Dermatopathol*. 1987;9:483–490.
36. Arora PK, Miller HC, Aronson LD. Alpha 1-antitrypsin is an effector of immunological stasis. *Nature*. 1978;274:589–590.
37. Breit SN, Penny R. The role of alpha 1 protease inhibitor (alpha 1 antitrypsin) in the regulation of immunologic and inflammatory reactions. *Aust N Z J Med*. 1980;10:449–453.
38. Smith KC, Pittelkow MR, Su WP. Panniculitis associated with severe alpha 1-antitrypsin deficiency. Treatment and review of the literature. *Arch Dermatol*. 1987;123:1655–1661.
39. Geller JD, Su WP. A subtle clue to the histopathologic diagnosis of early alpha 1-antitrypsin deficiency panniculitis. *J Am Acad Dermatol*. 1994;31:241–245.
40. Hendrick SJ, Silverman AK, Solomon AR, et al. Alpha 1-antitrypsin deficiency associated with panniculitis. *J Am Acad Dermatol*. 1988;18:684–692.
41. Humbert P, Faivre B, Gibey R, et al. Use of anti-collagenase properties of doxycycline in treatment of alpha 1-antitrypsin deficiency panniculitis. *Acta Derm Venereol*. 1991;71:189–194.
42. Hidvegi T, Ewing M, Hale P, et al. An autophagy-enhancing drug promotes degradation of mutant 1-antitrypsin Z and reduces hepatic fibrosis. *Science*. 2010;329:229–232.
42a. Strnad P, Mandorfer M, Choudhury G, et al. Fazirsiran for liver disease associated with alpha1-antitrypsin deficiency. *N Engl J Med*. 2022;387:514–24.
43. Baselga E, Margall N, Barnadas MA, et al. Detection of *Mycobacterium tuberculosis* DNA in lobular granulomatous panniculitis (erythema induratum–nodular vasculitis). *Arch Dermatol*. 1997;133:457–462.
44. Gimenez-Garcia R, Sanchez-Ramon S, Sanchez-Antolin G, Velasco Fernandez C. Red fingers syndrome and recurrent panniculitis in a patient with chronic hepatitis C. *J Eur Acad Dermatol Venereol*. 2003;17:692–694.
45. Wolf D, Ben-Yehuda A, Okon E, et al. Nodular vasculitis associated with propylthiouracil therapy. *Cutis*. 1992;49:253–255.
46. Ollert MW, Thomas P, Korting HC, et al. Erythema induratum of Bazin. Evidence of T-lymphocyte hyperresponsiveness to purified protein derivative of tuberculin: report of two cases and treatment. *Arch Dermatol*. 1993;129:469–473.
47. Schneider JW, Jordaan HF. The histopathologic spectrum of erythema induratum of Bazin [see comments]. *Am J Dermatopathol*. 1997;19:323–333.
48. Koga T, Kubota Y, Kiryu H, et al. Erythema induratum in a patient with active tuberculosis of the axillary lymph node: IFN-gamma release of specific T cells. *Eur J Dermatol*. 2001;11:48–49.
49. Jacinto SS, Nograles KB. Erythema induratum of Bazin: role of polymerase chain reaction in diagnosis. *Int J Dermatol*. 2003;42:380–381.
50. Shaffer N, Kerdel FA. Nodular vasculitis (erythema induratum): treatment with auranofin. *J Am Acad Dermatol*. 1991;25:426–429.
51. Na SY, Park SY, Cho HH, et al. Application of IFN-gamma releasing assay for the diagnosis of erythema induratum of Bazin. *J Eur Acad Dermatol Venereol*. 2014;28:41–45.
52. Segura S, Pujol RM, Trindade F, Requena L. Vasculitis in erythema induratum of Bazin: a histopathologic study of 101 biopsy specimens from 86 patients. *J Am Acad Dermatol*. 2008;59:839–851.
53. Taverna JA, Radfar A, Pentland A, et al. Case reports: nodular vasculitis responsive to mycophenolate mofetil. *J Drugs Dermatol*. 2006;5:992–993.
54. Forstrom T, Winkelmann RK. Acute, generalized panniculitis with amylase and lipase in skin. *Arch Dermatol*. 1975;111:497–502.
55. Heykarts B, Anseeuw M, Degreef H. Panniculitis caused by acinous pancreatic carcinoma. *Dermatology*. 1999;198:182–183.
56. Francombe J, Kingsnorth AN, Tunn E. Panniculitis, arthritis and pancreatitis. *Br J Rheumatol*. 1995;34:680–683.
57. Dhawan SS, Jimenez-Acosta F, Poppiti Jr RJ, Barkin JS. Subcutaneous fat necrosis associated with pancreatitis: histochemical and electron microscopic findings. *Am J Gastroenterol*. 1990;85:1025–1028.
58. Berman B, Conteas C, Smith B, et al. Fatal pancreatitis presenting with subcutaneous fat necrosis. Evidence that lipase and amylase alone do not induce lipocyte necrosis. *J Am Acad Dermatol*. 1987;17:359–364.
59. García-Romero D, Vanaclocha F. Pancreatic panniculitis. *Dermatol Clin*. 2008;26:465–470.
60. Fretzin DF, Arias AM. Sclerema neonatorum and subcutaneous fat necrosis of the newborn. *Pediatr Dermatol*. 1987;4:112–122.
61. Milunsky A, Levin SE. Sclerema neonatorum: a clinical study of 79 cases. *S Afr Med J*. 1966;40:638–641.
62. Pasyk K. Sclerema neonatorum. Light and electron microscopic studies. *Virchows Arch A Pathol Anat Histol*. 1980;388:87–103.
63. Mir-Bonafe JM, Roman-Curto C, Santos-Briz A, et al. Gemcitabine-associated livedoid thrombotic microangiopathy with associated sclerema neonatorum-like microscopic changes. *J Cutan Pathol*. 2012;39:707–711.
64. Ferguson CK. Care of the infant with sclerema neonatorum. *JOGN Nurs*. 1983;12:391–394.
65. Burden AD, Krafchik BR. Subcutaneous fat necrosis of the newborn: a review of 11 cases. *Pediatr Dermatol*. 1999;16:384–387.
66. Chuang SD, Chiu HC, Chang CC. Subcutaneous fat necrosis of the newborn complicating hypothermic cardiac surgery. *Br J Dermatol*. 1995;132:805–810.
67. Hicks MJ, Levy ML, Alexander J, et al. Subcutaneous fat necrosis of the newborn and hypercalcemia: case report and review of the literature. *Pediatr Dermatol*. 1993;10:271–276.
68. Stefanko NS, Drolet BA. Subcutaneous fat necrosis of the newborn and associated hypercalcemia: a systematic review of the literature. *Pediatr Dermatol*. 2019;36:24–30.
69. Silverman AK, Michels EH, Rasmussen JE, et al. Subcutaneous fat necrosis in an infant, occurring after hypothermic cardiac surgery. *J Am Acad Dermatol*. 1986;15:331–336.
70. Bachrach LK, Lum CK. Etidronate in subcutaneous fat necrosis of the newborn. *J Pediatr*. 1999;135:530–531.
71. Wolach B, Raas-Rothschild A, Vogel R, et al. Subcutaneous fat necrosis with thrombocytopenia in a newborn infant. *Dermatologica*. 1990;181:54–55.
72. Tajirian A, Ross R, Zeikus P, Robinson-Bostom L. Subcutaneous fat necrosis of the newborn with eosinophilic granules. *J Cutan Pathol*. 2007;34:588–590.
73. Khan N, Licata A, Rogers D. Intravenous bisphosphonates for hypercalcemia accompanying subcutaneous fat necrosis: a novel treatment approach. *Clin Pediatr (Phila)*. 2001;40:217–219.
74. Roenigk Jr HH, Haserick JR, Arundell FD. Poststeroid panniculitis. *Arch Dermatol*. 1964;90:387–391.
75. Kim ST, Kim TK, Lee JW, et al. Post-steroid panniculitis in an adult. *J Dermatol*. 2008;35:786–788.
76. Silverman RA, Newman AJ, LeVine MJ, et al. Poststeroid panniculitis: a case report. *Pediatr Dermatol*. 1988;5:92–93.
77. Peters MS, Su WP. Lupus erythematosus panniculitis. *Med Clin North Am*. 1989;73:1113–1126.
78. Martens PB, Moder KG, Ahmed I. Lupus panniculitis: clinical perspectives from a case series. *J Rheumatol*. 1999;26:68–72.
79. Riccieri V, Sili Scavalli A, Spadaro A, et al. Lupus erythematosus panniculitis: an immunohistochemical study. *Clin Rheumatol*. 1994;13:641–644.
80. Burrows NP, Walport MJ, Hammond AH, et al. Lupus erythematosus profundus with partial C4 deficiency responding to thalidomide. *Br J Dermatol*. 1991;125:62–67.
81. Wenzel J, Proelss J, Wiechert A, et al. CXCR3-mediated recruitment of cytotoxic lymphocytes in lupus erythematosus profundus. *J Am Acad Dermatol*. 2007;56:648–650.
82. Ng PP, Tan SH, Tan T. Lupus erythematosus panniculitis: a clinicopathologic study. *Int J Dermatol*. 2002;41:488–490.
83. Sanchez NP, Peters MS, Winkelmann RK. The histopathology of lupus erythematosus panniculitis. *J Am Acad Dermatol*. 1981;5:673–680.
84. Pincus LB, LeBoit PE, McCalmont TH, et al. Subcutaneous panniculitis-like T-cell lymphoma with overlapping clinicopathologic features of lupus erythematosus: coexistence of 2 entities? *Am J Dermatopathol*. 2009;31:520–526.
85. Bosisio F, Boi S, Caputo V, et al. Lobular panniculitic infiltrates with overlapping histopathologic features of lupus panniculitis (lupus profundus) and subcutaneous T-cell lymphoma: a conceptual and practical dilemma. *Am J Surg Pathol*. 2015;39:206–211.
86. Espirito Santo J, Gomes MF, Gomes MJ, et al. Intravenous immunoglobulin in lupus panniculitis. *Clin Rev Allergy Immunol*. 2010;38:307–318.
87. Santos-Briz A, Calle A, Linos K, et al. Dermatomyositis panniculitis: a clinicopathological and immunohistochemical study of 18 cases. *J Eur Acad Dermatol Venereol*. 2018;32:1352–1359.
88. Solans R, Cortes J, Selva A, et al. Panniculitis: a cutaneous manifestation of dermatomyositis. *J Am Acad Dermatol*. 2002;46:S148–S150.
89. Molnar K, Kemeny L, Korom I, et al. Panniculitis in dermatomyositis: report of two cases. *Br J Dermatol*. 1998;139:161–163.
90. Beacham BE, Cooper PH, Buchanan CS, et al. Equestrian cold panniculitis in women. *Arch Dermatol*. 1980;116:1025–1027.
91. Oertel YC, Johnson FB. Sclerosing lipogranuloma of male genitalia. Review of 23 cases. *Arch Pathol Lab Med*. 1977;101:321–326.
92. Pielasinski U, Machan S, Camacho D, et al. Postirradiation pseudosclerodermatous panniculitis: three new cases with additional histopathologic features supporting the radiotherapy etiology. *Am J Dermatopathol*. 2013;35:129–134.
93. Borroni G, Vassallo C, Brazzelli V, et al. Radiation recall dermatitis, panniculitis, and myositis following cyclophosphamide therapy: histopathologic findings of a patient affected by multiple myeloma. *Am J Dermatopathol*. 2004;26:213–216.
94. Rajkumar SV, Laude TA, Russo RM, et al. Popsicle panniculitis of the cheeks. A diagnostic entity caused by sucking on cold objects. *Clin Pediatr (Phila)*. 1976;15:619–621.
95. Pang BK, Munro V, Kossard S. Pseudoscleroderma secondary to phytomenadione (vitamin K1) injections: Texier's disease. *Australas J Dermatol*. 1996;37:44–47.
96. Baars JW, Coenen JL, Wagstaff J, et al. Lobular panniculitis after subcutaneous administration of interleukin-2 (IL-2), and its exacerbation during intravenous therapy with IL-2. *Br J Cancer*. 1992;66:698–699.
97. Garcia-Domingo MI, Alijotas-Reig J, Cistero-Bahima A, et al. Disseminated and recurrent sarcoid-like granulomatous panniculitis due to bovine collagen injection. *J Investig Allergol Clin Immunol*. 2000;10:107–109.
98. Tan J, Rao B. Mesotherapy-induced panniculitis treated with dapsone: case report and review of reported adverse effects of mesotherapy. *J Cutan Med Surg*. 2006;10:92–95.
99. Jeong KH, Lee MH. Two cases of factitial panniculitis induced by electroacupuncture. *Clin Exp Dermatol*. 2009;34:e170–e173.
100. Winkelmann RK, Barker SM. Factitial traumatic panniculitis. *J Am Acad Dermatol*. 1985;13:988–994.
101. Foucar E, Downing DT, Gerber WL. Sclerosing lipogranuloma of the male genitalia containing vitamin E: a comparison with classical 'paraffinoma'. *J Am Acad Dermatol*. 1983;9:103–110.
102. Takihara H, Takahashi M, Ueno T, et al. Sclerosing lipogranuloma of the male genitalia: analysis of the lipid constituents and histological study. *Br J Urol*. 1993;71:58–62.
103. Henrichs WD, Helwig EB. Grease gun granulomas. *Mil Med*. 1986;151:78–82.
104. Kaufman HL, Harandi A, Watson MC, et al. Panniculitis after vaccination against CEA and MUC1 in a patient with pancreatic cancer. *Lancet Oncol*. 2005;6:62–63.
105. Chong H, Brady K, Metze D, Calonje E. Persistent nodules at injection sites (aluminum granuloma) – clinicopathological study of 14 cases with a diverse range of histological reaction patterns. *Histopathology*. 2006;48:182–188.
106. Requena L, Requena C, Christensen L, et al. Adverse reactions to injectable soft tissue fillers. *J Am Acad Dermatol*. 2011;64:1–34.
107. Dytkiewitz E, Morlock GE. Analytical strategy for rapid identification and quantification of lubricant additives in mineral oil by high-performance thin-layer

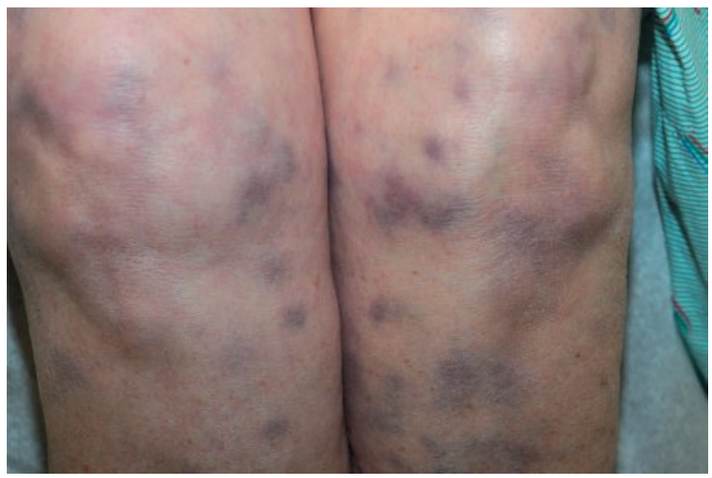
chromatography with UV absorption and fluorescence detection combined with mass spectrometry and infrared spectroscopy. *J AOAC Int*. 2008;91:1237–1243.
108. Wortsman X, Wortsman J, Orlandi C, et al. Ultrasound detection and identification of cosmetic fillers in the skin. *J Eur Acad Dermatol Venereol*. 2012;26:292–301.
109. Jorizzo JL, White WL, Zanolli MD, et al. Sclerosing panniculitis. A clinicopathologic assessment. *Arch Dermatol*. 1991;127:554–558.
110. Kirsner RS, Pardes JB, Eaglstein WH, et al. The clinical spectrum of lipodermatosclerosis. *J Am Acad Dermatol*. 1993;28:623–627.
111. Greenberg AS, Hasan A, Montalvo BM, et al. Acute lipodermatosclerosis is associated with venous insufficiency. *J Am Acad Dermatol*. 1996;35:566–568.
112. Stacey MC, Burnand KG, Bhogal BS, et al. Pericapillary fibrin deposits and skin hypoxia precede the changes of lipodermatosclerosis in limbs at increased risk of developing a venous ulcer. *Cardiovasc Surg*. 2000;8:372–380.
113. Herouy Y, Kreis S, Mueller T, et al. Inhibition of angiogenesis in lipodermatosclerosis: implication for venous ulcer formation. *Int J Mol Med*. 2009;24:645–651.
114. Falanga V, Bontempo FA, Eaglstein WH. Protein C and protein S plasma levels in patients with lipodermatosclerosis and venous ulceration. *Arch Dermatol*. 1990;126:1195–1197.
115. de Giorgio-Miller AM, Treharne LJ, McAnulty RJ, et al. Procollagen type I gene expression and cell proliferation are increased in lipodermatosclerosis. *Br J Dermatol*. 2005;152:242–249.
116. Segal S, Cooper J, Bolognia J. Treatment of lipodermatosclerosis with oxandrolone in a patient with stanozolol-induced hepatotoxicity. *J Am Acad Dermatol*. 2000;43:558–559.
117. Alegre VA, Winkelmann RK, Aliaga A. Lipomembranous changes in chronic panniculitis. *J Am Acad Dermatol*. 1988;19:39–46.
118. Ishikawa O, Tamura A, Ryuzaki K, et al. Membranocystic changes in the panniculitis of dermatomyositis. *Br J Dermatol*. 1996;134:773–776.
119. Walsh SN, Santa Cruz DJ. Lipodermatosclerosis: a clinicopathologic study of 25 cases. *J Am Acad Dermatol*. 2010;62:1005–1012.
120. Flagothier C, Piérard GE, Quatresooz P. Cutaneous myospherulosis and membranous lipodystrophy: extensive presentation in a patient with severe steroid-induced dermal atrophy. *J Eur Acad Dermatol Venereol*. 2006;20:457–460.
121. Hafner C, Wimmershoff M, Landthaler M, Vogt T. Lipodermatosclerosis: successful treatment with danazol. *Acta Derm Venereol*. 2005;85:365–366.
122. Goldman MP. The use of pentoxifylline in the treatment of systemic sclerosis and lipodermatosclerosis: a unifying hypothesis? *J Am Acad Dermatol*. 1994;31:135–136.
123. Galache C, Santos-Juanes J, Blanco S, et al. Q fever: a new cause of 'doughnut' granulomatous lobular panniculitis. *Br J Dermatol*. 2004;151:685–687.
124. Ginter G, Rieger E, Soyer HP, et al. Granulomatous panniculitis caused by *Candida albicans*: a case presenting with multiple leg ulcers. *J Am Acad Dermatol*. 1993;28:315–317.
125. Canal L, Fuente Dde L, Roriguez-Moreno J, et al. Specific cutaneous involvement in Whipple disease. *Am J Dermatopathol*. 2014;36:344–346.
126. Requena L, Sitthinamsuwan P, Santonja C, et al. Cutaneous and mucosal mucormycosis mimicking pancreatic panniculitis and gouty panniculitis. *J Am Acad Dermatol*. 2012;66:975–984.
127. Winkelmann RK, Bowie EJ. Hemorrhagic diathesis associated with benign histiocytic, cytophagic panniculitis and systemic histiocytosis. *Arch Intern Med*. 1980;140:1460–1463.
128. Wick MR, Patterson JW. Cytophagic histiocytic panniculitis – a critical reappraisal. *Arch Dermatol*. 2000;136:922–924.
129. Willemze R, Cerroni L, Kempf W, et al. The 2018 update of the WHO-EORTC classification for primary cutaneous lymphomas. *Blood*. 2019;133:1703–1714.
130. Craig AJ, Cualing H, Thomas G, et al. Cytophagic histiocytic panniculitis – a syndrome associated with benign and malignant panniculitis: case comparison and review of the literature. *J Am Acad Dermatol*. 1998;39:721–736.
131. Chen RL, Hsu YH, Ueda I, et al. Cytophagic histiocytic panniculitis with fatal haemophagocytic lymphohistiocytosis in a paediatric patient with perforin gene mutation. *J Clin Pathol*. 2007;60:1168–1169.
132. Weenig RH, Ng CS, Perniciaro C. Subcutaneous panniculitis-like T-cell lymphoma: an elusive case presenting as lipomembranous panniculitis and a review of 72 cases in the literature. *Am J Dermatopathol*. 2001;23:206–215.



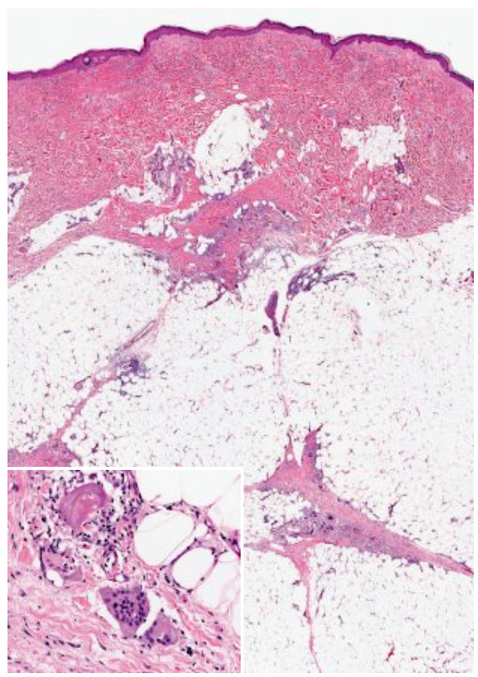
eFig. 100.1 Erythema nodosum – clinical appearance. **A** Erythematous, tender nodules bilaterally on the shins and dorsal feet; the patient is pregnant. **B** The nodules and plaques may develop a bruise-like appearance. *A, Courtesy Ian Odell, MD, PhD; B, Courtesy Kalman Watsky, MD.*



eFig. 100.2 Erythema nodosum in a patient with sarcoidosis. Tender pink to pink–violet nodules and plaques primarily on the shins. *Courtesy David Khalil, MD.*



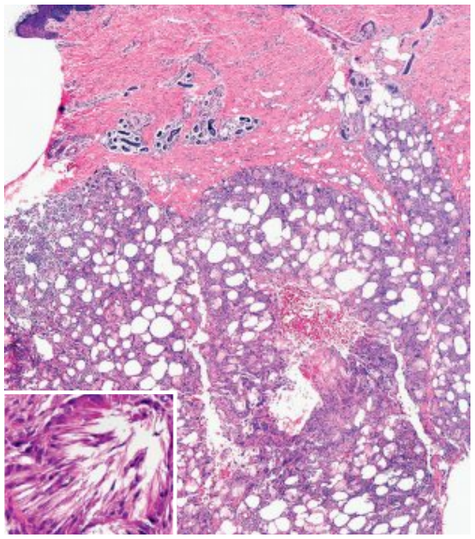
eFig. 100.3 Erythema nodosum with bruise-like appearance. *Courtesy Kalman Watsky, MD.*



eFig. 100.4 Erythema nodosum – histopathologic features. A predominantly septal panniculitis with Miescher microgranulomas within the septa. Note the multinucleated giant cells (inset). *Courtesy Lorenzo Cerroni, MD.*



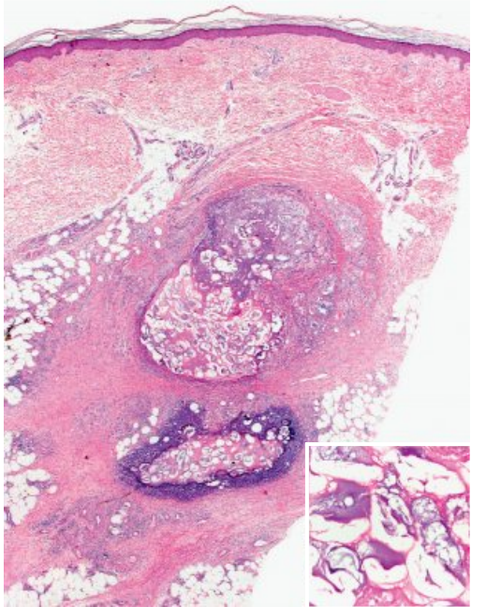
eFig. 100.5 Superficial thrombophlebitis in the setting of saphenous varicosities. A Dull pink-brown areas of inflammation overlying sites of thrombophlebitis. **B** Overlying acute inflammation can mimic panniculitis (see arrow in **A**). *Courtesy Kalman Watsky, MD.*



eFig. 100.6 Subcutaneous fat necrosis of the newborn – histopathologic features. A predominantly lobular panniculitis is seen. Needle-shaped clefts in a radial configuration are present within giant cells (inset). Similar findings are seen in post-steroid panniculitis.



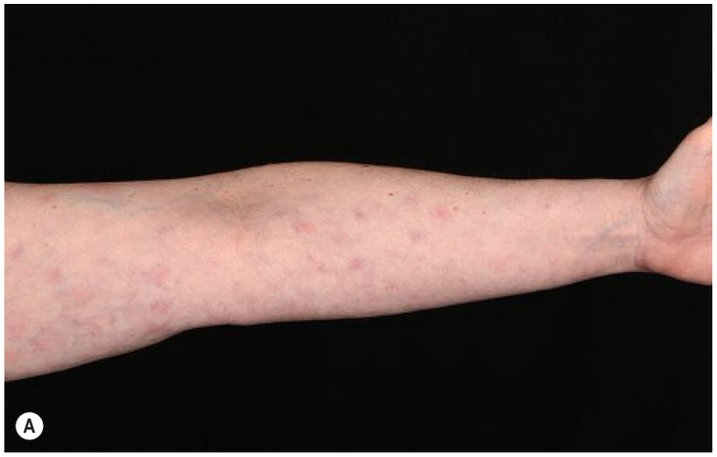
eFig. 100.7 Subcutaneous fat necrosis of the newborn – clinical features. Indurated plaques on the trunk.



eFig. 100.8 Pancreatic panniculitis – histopathologic features. Lobular and septal panniculitis with neutrophilic inflammation, cellular necrosis, ghost cells (inset), and deposition of homogeneous basophilic material due to saponification of fat by calcium salts. *Courtesy Lorenzo Cerroni, MD.*



eFig. 100.9 Lupus panniculitis. Erythematous plaque involving the orbital area.





eFig. 100.10 Drug-induced panniculitis – clinical and histopathologic findings. **A** Erythematous papulonodules on the arm of a 44-year-old woman with metastatic melanoma treated with dabrafenib and trametinib. **B** A lobular panniculitis with a predominance of neutrophils within the inflammatory infiltrate (inset). *Courtesy Lorenzo Cerroni, MD.*



eFig. 100.11 Pancreatic panniculitis – clinical appearance. Multiple red to violet–brown nodules on the arm. There is also postinflammatory desquamation.

CLASSIFICATION OF THE PANNICULITIDES
Predominantly septal panniculitis
• Erythema nodosum   • Erythema nodosum migrans (subacute nodular migratory panniculitis) • Panniculitis of morphea/systemic sclerosis • Alpha-1 antitrypsin deficiency panniculitis*
Lobular and mixed septal–lobular panniculitis

• With vasculitis involving septal veins or arteries, lobular venules or small veins
  • Erythema induratum (nodular vasculitis)
• With necrosis as an early finding
  • Pancreatic panniculitis
• With needle-shaped clefts within lipocytes
  • Sclerema neonatorum
  • Subcutaneous fat necrosis of the newborn
  • Post-steroid panniculitis
• Associated with autoimmune connective tissue disease
  • Lupus erythematosus panniculitis (lupus profundus)
  • Panniculitis of dermatomyositis
• Lipodystrophic panniculitis (see Ch. 101)
  • Lipoatrophy
  • Lipohypertrophy
• Traumatic panniculitis, including factitial panniculitis
  • Cold panniculitis (popsicle panniculitis, Haxthausen disease)
  • Sclerosing lipogranuloma (including grease gun granuloma)
  • Panniculitis due to other injectable substances
  • Panniculitis due to blunt trauma
• Lipodermatosclerosis
• Infection-induced panniculitis
• Malignancy-related panniculitis-like infiltrates
  • Subcutaneous panniculitis-like T cell lymphoma (see Ch. 120)
  • Other lymphomas with involvement of subcutaneous tissues

*Descriptions vary; some authors regard this as a lobular or mixed septal–lobular panniculitis.

eTable 100.1 Classification of the panniculitides. The categories for classification of panniculitis are determined partly by clinical characteristics such as location and associated diseases and partly by histopathology. This classification scheme does not include Weber–Christian disease as cases initially assigned this designation have subsequently been reclassified as other forms of panniculitis, including alpha-1 antitrypsin deficiency, lipodermatosclerosis, lupus panniculitis, and traumatic panniculitis.

101 Lipodystrophies

Suat Hoon Tan, Hong Liang Tey and Joel Hua Liang Lim

Subtypes: ■ Lipodystrophy: lipoatrophy, lipohypertrophy

Key features

- Lipodystrophies are inherited or acquired disorders characterized by a paucity or complete absence of fat that may be generalized, partial, or localized; lipohypertrophy may accompany the lipoatrophy
- Though the terms lipodystrophy and lipoatrophy are often used interchangeably, lipoatrophy should be used specifically for selective loss of fat, with lipodystrophy implying a redistribution of fat, in part due to a hypertrophic compensation of the non-atrophic fat
- Lipodystrophy syndromes represent a heterogeneous group of disorders that are characterized by lipoatrophy ± fat accumulation in characteristic body distribution patterns
- Fat is a metabolically active organ, thus fat loss can be associated with metabolic derangements, which parallel the extent and duration of lipoatrophy
- Lipodystrophy is often accompanied by the metabolic syndrome, which includes insulin resistance, diabetes mellitus, hyperinsulinemia, dyslipidemia, cardiovascular disease, and hepatic steatosis
- In addition to the metabolic syndrome, systemic manifestations of generalized and partial lipodystrophy syndromes include hormonal abnormalities, organ dysfunction, anabolic features, glomerulonephritis, and autoimmune disorders
- A distinct syndrome of peripheral lipoatrophy, central obesity, breast hypertrophy, dorsocervical fat pad enlargement, hyperlipidemia and insulin resistance occurs in patients with HIV infection undergoing treatment with antiretroviral therapy (ART)
- Isolated or localized lipoatrophy can occur at the site of medication injection, trauma or pressure, in association with autoimmune connective tissue disease, or following certain panniculitic inflammatory or neoplastic processes
- Microscopically, there may be a complete absence of subcutaneous fat or a decrease in adipocyte size and number. An inflammatory panniculitis may be seen in early disease

INTRODUCTION

Lipodystrophy describes a heterogeneous group of diseases characterized by a selective fat loss in a characteristic body distribution pattern, often accompanied by secondary fat accumulation. Adipose tissue has crucial metabolic and endocrine functions, in addition to its role in mechanical protection. The loss of subcutaneous fat and a compensatory accumulation of visceral fat is closely associated with insulin resistance, diabetes mellitus, dyslipidemia, hypertension, and coronary artery disease. These metabolic abnormalities and their sequelae constitute the metabolic syndrome and underscore the important functions of fat, in its role as a diverse and crucial body organ.

More than a century after the first description of lipodystrophy[1] and then delineation of generalized lipodystrophy into congenital and acquired forms[2], the genetic bases of several of the inherited lipodystrophies have now been elucidated. Mutations have been found in genes ranging from those encoding proteins essential for adipocyte differentiation to those encoding nuclear lamins (see below).

Clinically, lipodystrophy can be broadly classified into inherited or acquired forms and then further subclassified based on the extent of fat loss, in conjunction with genetic mutations, age of onset, and systemic manifestations (Fig. 101.1 & Table 101.1). Based upon the distribution pattern, lipodystrophy may be subdivided into three major groups: (1) generalized; (2) partial (extensive, but not generalized); and (3) localized (involving an isolated area).

Localized lipodystrophy, which may be due to injections of medications or vaccines, pressure, previous surgery, trauma or panniculitis, is the most commonly encountered form. It typically presents as lipoatrophy but occasionally lipohypertrophy develops, e.g. at sites of insulin injection (see Table 21.22). Less often, lipodystrophy associated with antiretroviral therapy (ART) for human immunodeficiency virus (HIV) infection[3] and with administration of immune checkpoint inhibitors are seen. Dermatologists may also play a key role in diagnosing acquired generalized lipodystrophy and its preceding panniculitis. Finally, there are several rare genetic syndromes that will be discussed (see Table 101.1).

PATHOGENESIS

Adipose tissue functions as an endocrine organ via its secretion of hormones and adipocytokines, such as leptin, TNF, interleukin (IL)-6, and adiponectin. Altered expression and activity of these factors play a role in the development of insulin resistance and other metabolic sequelae seen in lipodystrophic syndromes, which are similar to those observed in the metabolic syndrome and obese individuals[4,5].

There appears to be a final common pathway of defective adipocyte triglyceride storage in conditions characterized by fat loss as well as fat excess. This defect can result from impaired triglyceride synthesis due to an enzyme deficiency (e.g. 1-acylglycerol-3-phosphate *O*-acyltransferase 2), defective adipocyte development caused by mutations in genes critical to adipocyte differentiation (e.g. *BSCL2/seipin, PPARG, LMNA*), adipocyte apoptosis, or autoimmune- or drug-mediated adipocyte destruction. These various processes impair normal adipocyte differentiation, development, lifespan, and/or function[6].

The destruction or impaired differentiation of adipocytes leads to a cascade of hormonal and metabolic consequences. Adiponectin, the protein product of *ADIPOQ*, is expressed in and secreted exclusively by differentiated adipocytes. It plays a positive role in regulating insulin sensitivity and glucose and lipid homeostasis. Plasma adiponectin levels are inversely correlated with fasting insulin levels and insulin resistance[7]. Serum adiponectin and leptin levels are reduced both in murine models of lipoatrophy with insulin resistance and in humans with congenital and acquired lipodystrophies,[8] including HIV/ART-related lipodystrophy[9,10]. Leptin replacement has been shown to reverse insulin resistance in mouse models with a deficiency of mRNAs that encode leptin.[11] This replacement also results in significant and sustained improvements in hyperglycemia, dyslipidemia, and hepatic steatosis in patients with different forms of lipodystrophy[12,13].

Congenital Generalized Lipodystrophy (Berardinelli–Seip Congenital Lipodystrophy, Berardinelli–Seip Syndrome)

Congenital generalized lipodystrophy (CGL) is an autosomal recessive disorder with four known genetic subtypes. The two major forms, types 1 and 2, are due to mutations in *AGPAT2*, which encodes 1-acylglycerol-3-phosphate *O*-acyltransferase 2, and *BSCL2/seipin*, respectively (see Table 101.1). It has been postulated that these genetic mutations cause lipodystrophy primarily by affecting adipocyte differentiation or lipid droplet formation in adipose tissue. In type 1, aberrant AGPAT2

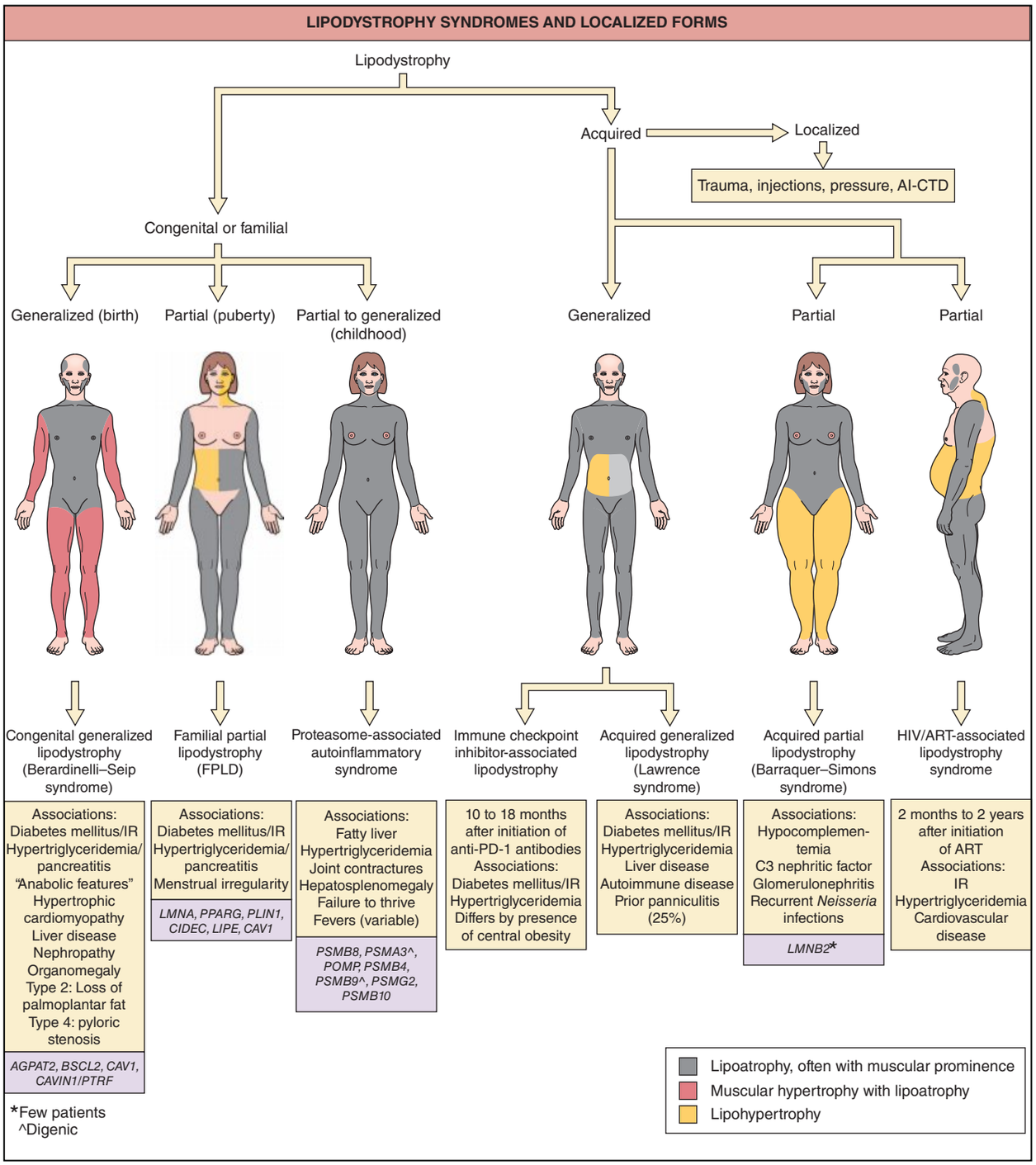


Fig. 101.1 Lipodystrophy syndromes and localized forms. Schematic representation of the predominant sites of lipoatrophy and lipohypertrophy. Additional syndromes, including familial partial lipodystrophy with mandibuloacral dysplasia, are outlined in Table 101.1. Tables 63.9 and 63.10 review progeroid syndromes in which lipoatrophy can be seen. AI-CTD, autoimmune connective tissue disease; ART, antiretroviral therapy; IR, insulin resistance; PD, programmed cell death. *AGPAT2*, encodes 1-acylglycerol-3-phosphate *O*-acyltransferase 2 (triglyceride and phospholipid synthesis); *BSCL2*, encodes seipin (lipid droplet formation); *CAV1*, encodes caveolin 1 (binds fatty acids and translocates them to lipid droplets); *CAVIN1/PTRF*, encodes caveolae associated protein 1 (biogenesis of caveolae and expression of caveolins 1 and 3); *CIDEC*, encodes cell death-inducing DNA fragmentation factor-like effector C (adipocyte apoptosis); *LIPE*, encodes lipase E, hormone sensitive type (hydrolysis of triglycerides to free fatty acids); *LMNA*, encodes lamins A/C (structural integrity of the nuclear lamina); *LMNB2*, encodes lamin B2 (structural integrity of the nuclear lamina); *PLIN1*, encodes perilipin 1 (formation, maturation, and function of lipid droplets within adipocytes); *POMP*, encodes proteasome maturation protein; *PPARG*, encodes peroxisome proliferator-activated receptor-gamma (essential role in lipogenesis); *PSMA3*, encodes proteasome subunit alpha 3; *PSMB4, -B8, -B9, -B10*, encode proteasome subunit beta 4, 8, 9, 10; *PSMG2*, encodes proteasome subunit gamma 2.

enzyme activity causes a marked reduction in triglyceride and phospholipid synthesis, resulting in abnormal adipocyte function[14]. In type 2, *BSCL2* mutations affect the endoplasmic reticulum membrane protein seipin which is critical for lipid droplet morphology.

In types 3 and 4 CGL, genetic mutations alter the function of caveolae, which are invaginations of the plasma membrane involved in signal transduction and endocytosis, including internalization of the insulin receptor. Patients with type 3 CGL have mutations in *CAV1* which encodes caveolin 1[15]; caveolins are essential components of caveolae and caveolin 1 binds fatty acids and translocates them to lipid droplets. Type 4 CGL is due to mutations in *CAVIN1/PTRF*, whose protein product is involved in the biogenesis of caveolae and the expression of caveolins 1 and 3[16].

Differences in the molecular basis of CGL may account for the phenotypic heterogeneity[17]. *AGPAT2* has been found to be highly expressed in human omental adipose tissue, which may explain the preferential loss

LIPODYSTROPHY SYNDROMES							
Syndrome	**Age of onset**	**Sex**	**Genetics**	**Distribution of fat changes**	**Metabolic derangements**	**Systemic associations**	**Additional cutaneous and systemic features**
Inherited							
Congenital generalized lipodystrophy (CGL; Berardinelli–Seip syndrome)	Birth	F = M	AR Type 1: *AGPAT2* Type 2: *BSCL2/seipin* Type 3: *CAV1* Type 4: *CAVIN1/PTRF*	Fat: face, trunk, extremities, viscera Types 1, 3, 4: loss of metabolically active adipose tissue in the skin and viscera, but preservation of mechanical adipose tissue (palmoplantar, retro-orbital) Type 2: both metabolically active and mechanical adipose tissue are lost Types 1, 2: lack of bone marrow fat Types 3, 4: preserved bone marrow fat	+++: IR, DM, ↑ TG; anabolic features; ↑ metabolic rate	Type 3: associated with vitamin D resistance	Hypertrophic cardiomyopathy, liver failure/cirrhosis, acute pancreatitis, organomegaly,osteosclerosis, proteinuric nephropathy (see Table 101.3) More severe disease in type 2, with higher incidence of intellectual disability and cardiomyopathy Type 4: prominent skin veins, cardiac conduction defects, pyloric and esophageal stenosis, muscle weakness
Familial partial lipodystrophy (FPLD; previously referred to as Köbberling–Dunnigan syndrome)	Puberty	F > M	AD FPLD1 (Köbberling type): not known FPLD2 (Dunnigan type): *LMNA* [lamin A/C] FPLD3: *PPARG* FPLD4: *PLIN1* FPLD7: *CAVI* AR* FPLD5: *CIDEC* FPLD6: *LIPE*	FPLD1: ↓ fat on extremities ± ↑ fat on face/neck, trunk FPLD2: ↓ fat on extremities ± trunk, ↑ fat on face/neck (double chin), muscular hypertrophy FPLD3: ↓ fat on extremities/buttocks (less severe than FPLD2); trunk/viscera spared FPLD4: ↓ fat on lower extremities with small adipocytes and increased fibrosis of adipose tissues FPLD5: ↓ fat on lower extremities/buttocks; small, multilocular lipid droplets histologically FPLD6: ↓ fat on lower extremities, ↑ fat of abdomen and axillae	IR, DM, ↑ TG, ↓ HDL (more severe in FPLD3 than FPLD2)	None preceding	Chylomicronemia syndrome with acute pancreatitis, eruptive xanthomas Clinical findings and metabolic complications more severe in women
Familial partial lipodystrophy with mandibuloacral dysplasia (MAD)	Childhood or puberty	M > F	AR Type A: *LMNA* Type B: *ZMPSTE24*	fat on extremities Type B – may have generalized lipodystrophy	IR, DM, ↑ TG, ↓ HDL in some patients	None preceding	Premature aging, hypoplasia of mandible, clavicles and terminal digits, short stature, scleroderma-like skin lesions with mottled skin pigmentation
Proteasome-associated autoinflammatory disorders (PRAAS; PRAAS1 has also been referred to as CANDLE syndrome and Nakajo–Nishimura syndrome)	Childhood	M = F	AR PRAAS1: *PSMB8, PSMA3* (digenic) PRAAS2: *POMP* PRAAS3: *PSMB4*, *PSMB9* (digenic) PRAAS4: *PSMG2* PRAAS5: *PSMB10*	Common features: ↓ facial fat, partial lipoatrophy involving upper half of body Occasionally, generalized lipoatrophy	↑ TG, ↓ HDL cholesterol	None preceding	Panniculitis, pernio-like lesions, eyelid edema and erythema Hepatosplenomegaly, basal ganglia calcifications (for additional features see text)

Table 101.1 Lipodystrophy syndromes.

Continued

LIPODYSTROPHY SYNDROMES							
Syndrome	**Age of onset**	**Sex**	**Genetics**	**Distribution of fat changes**	**Metabolic derangements**	**Systemic associations**	**Additional cutaneous and systemic features**
Acquired							
Acquired generalized lipodystrophy (Lawrence syndrome)	Childhood or adolescence	F > M 3 : 1	None known	↓ Fat: face, trunk, extremitiesPreservation of fat within the bone marrow	++: IR, DM, ↑ TG (correlates with the degree of lipodystrophy)	1/3 have a preceding autoimmune disease (e.g. juvenile dermatomyositis, Sjögren syndrome) or infection; 25% have a preceding panniculitis; rarely associated with CVID	Liver failure/cirrhosis, proteinuric nephropathy
Acquired partial lipodystrophy (Barraquer–Simons syndrome)	Childhood or adolescence Rarely adults	F > M 3 : 1	Sporadic or AD: *LMNB2* (Lamin B2)	Fat: face, upper extremities, trunk, with spread in a cephalocaudal direction Spares lower extremities Fat: hips and legs Hemilipodystrophic variants	Rare IR, DM, ↑ TG	Often preceded by a febrile illness; 1/5 have mesangiocapillary glomerulonephritis Almost all have low levels of C3 and presence of circulating C3 nephritic factor Autoimmune disease associations include SLE, dermatomyositis	Sequelae of renal abnormalities
HIV/ART-associated lipodystrophy syndrome	2 months to 2 years after initiation of combination antiretroviral therapy (ART) Adults > children	M = F overall, F > M central adiposity	None known	Fat: face, extremities Fat: central (trunk/viscera), dorsocervical ("buffalo hump"), breasts Lipomas (e.g. pubic)	++: IR, ↑ TG, ↑ LDL, ↓ HDL; ± DM	HIV infection	Cardiovascular disease
Immune checkpoint inhibitor-associated lipodystrophy	Reflects underlying neoplasm	Reflects underlying neoplasm	–	↓ Fat: face, limbs, ↑ fat of abdomen	IR, DM, ↑ TG	Underlying neoplasm	Hepatic steatosis

*Provisional for FPLD5 and FPLD6.

Table 101.1 Lipodystrophy syndromes. Facial lipoatrophy can be seen in patients with POEMS (polyneuropathy, organomegaly, endocrinopathy, monoclonal gammopathy, skin changes) syndrome and generalized lipoatrophy in children who have undergone an allogeneic hematopoietic stem cell transplant. AR, autosomal recessive; AD, autosomal dominant; *AGPAT2*, 1-acylglycerol-3-phosphate O-acyltransferase 2; *BSCL2*, Berardinelli–Seip congenital lipodystrophy 2 (Seipin) gene; CANDLE, chronic atypical neutrophilic dermatosis with lipodystrophy and elevated temperature; *CAV1*, caveolin 1 gene; *CAVIN1*, caveolae associated protein 1; *CIDEC*, cell death-inducing DFFA-like effector C; CVID, combined variable immunodeficiency; DM, diabetes mellitus; HDL, high-density lipoproteins; HIV, human immunodeficiency virus; LDL, low-density lipoproteins; IR, insulin resistance; *LIPE*, lipase, hormone-sensitive; PI, protease inhibitor; *PLIN*, perilipin 1; *PPARG*, peroxisome proliferator-activated receptor-γ; PTRF, polymerase I and transcript release factor; POMP, proteasome maturation protein; *PSMA*, proteasome subunit alpha; *PSMB*, proteasome subunit beta; *PSMG*, proteasome subunit gamma; SLE, systemic lupus erythematosus; TG, triglycerides; *ZMPSTE24*, gene that encodes a zinc metalloproteinase.

of metabolically active intra-abdominal adipose tissue but preservation of mechanical palmoplantar adipose tissue in patients with type 1 CGL. *BSCL2* has been found to also be highly expressed in the brain[18], which may account for the higher prevalence of intellectual disability in type 2 patients.

Familial Partial Lipodystrophy

Familial partial lipodystrophy (FPLD) is a heterogeneous group of autosomal dominantly, and rarely autosomal recessively, inherited disorders (see Table 101.1). The most prevalent subtype is FPLD2, which is due to mutations in *LMNA*[19]. *LMNA* encodes lamins A/C, with lamins belonging to the intermediate filament family of structural proteins that compose the nuclear lamina. *LMNA* mutations lead to a disruption in nuclear function, resulting in apoptosis and premature cell death of adipocytes, and they lead to alterations in the extracellular matrix of adipose tissue. There is also aberrant TGF-β signaling and this is associated with abnormal responses to metabolic requirements. Decreased plasma leptin and increased fasting plasma insulin and C-peptide levels are additional findings[20], as is premature senescence of vascular cells; the latter contributes to the observed cardiovascular complications[21]. Of note, *LMNA* mutations are responsible for a group of disorders known as laminopathies that includes premature aging syndromes (e.g. progeria), muscular dystrophies, cardiomyopathies, and one form of Charcot–Marie–Tooth neuropathy (see Tables 63.9 & 63.10). The clinical phenotype/syndrome is determined by the site and type of *LMNA* mutation(s)[22].

While the genetic basis of FPLD1 is unknown, FPLD3 results from heterozygous missense mutations of the gene that encodes peroxisome proliferator-activated receptor-γ (PPAR-γ)[23]. PPAR-γ plays an essential role in adipogenesis (see Fig. 101.14), but the entire pathogenesis remains unclear. Although this subtype has a milder phenotype than FPLD2, with a later age of onset and involvement confined to the distal

extremities, metabolic abnormalities are more severe, suggesting that *PPARG* mutations may have additional effects on metabolism.

In patients with FPLD4, heterozygous loss-of-function mutations have been described in the gene that encodes perilipin-1 (*PLIN1*)[24,25]. Perilipin is responsible for the formation, maturation, and function of lipid droplets within adipocytes. Lipoatrophy of the lower extremities is accompanied by marked hypertriglyceridemia and severe insulin resistance with type 2 diabetes.

To date, FPLD5 and FPLD6 are based on a single patient and three sets of siblings, respectively, and because of homozygous mutations (missense, nonsense) or deletions (FPLD5, FPLD6) and consanguinity (FPLD6), an autosomal recessive pattern is favored. The associated genes encode a member of the cell death-inducing DNA fragmentation factor-like effector family (*CIDEC*) that is thought to play a role in adipocyte apoptosis[26] and lipase E, hormone sensitive type (*LIPE*). While homozygous mutations in *CAV1* lead to congenital generalized lipodystrophy (see above), patients with FPLD7 are heterozygotic for *CAV1* mutations.

Partial lipodystrophy may also be seen in association with mandibuloacral dysplasia (MAD), an autosomal recessive syndrome associated with mutations in *LMNA* (type A), or with mutations in *ZMPSTE24*, which encodes a zinc metalloproteinase involved in post-translational proteolytic processing of prelamin A (type B)[27]. The latter has been associated with severe mandibuloacral dysplasia, premature aging, and generalized lipodystrophy.

Mesangiocapillary glomerulonephritis type 2 (MCGN II) has been reported in a case of partial lipodystrophy due to a mutation in *LMNA*, suggesting that partial lipodystrophy of both the sporadic and familial subtypes may predispose to this condition and the observed renal abnormalities and hypocomplementemia may be secondary to other factors associated with lipodystrophy[28].

Acquired Generalized Lipodystrophy (Lawrence Syndrome)

There is no known genetic defect. A third of patients have an antecedent autoimmune disease or viral or bacterial infection, but a causal relationship with the latter has not been established. The preceding panniculitis observed in 25% of patients (see Table 101.1)[29] and the frequent association of autoimmune disease imply immunologically mediated lipolysis. Autoantibodies against the adipocyte membrane have been reported in one patient with this condition[30], and anti-perilipin 1 antibodies in a second.[31] This autoimmune diathesis could also explain the high incidence of type 1 diabetes mellitus and reports of co-existing common variable immunodeficiency (CVID)[32].

Acquired Partial Lipodystrophy Syndrome (Barraquer–Simons Syndrome)

Acquired partial lipodystrophy syndrome occurs sporadically or may be autosomal dominant, with mutations in *LMNB2* detected in some patients[33]. Subcutaneous fat is often lost acutely after a viral illness. The exact pathogenesis is not known, but it may be related to adipsin, a protein produced by adipocytes which is identical to factor D (a component of the alternative complement pathway; see Ch. 60), as well as C3 nephritic factor (C3NeF), an IgG autoantibody against an alternative pathway enzyme. There is dysregulated activation of the alternative pathway, associated with C3NeF binding to the rate-limiting C3 convertase enzyme (C3bBb). This results in unopposed activation of the alternative complement pathway, excessive consumption of C3, and complement-dependent lysis of adipocytes.

Regional differences in factor D expression parallel the regional distribution of adipocyte loss in partial lipodystrophy, which may explain the cephalocaudal distribution of fat. Renal cells also express complement components, and a similar mechanism of complement-mediated injury may be responsible for the MCGN II seen in these patients[28].

Localized Lipoatrophy

The pathogenesis of localized lipoatrophy is heterogeneous. Circumscribed areas of lipoatrophy may follow inflammation from pyogenic abscesses, lobular panniculitides due to autoimmune connective tissue diseases (e.g. lupus erythematosus, dermatomyositis), or subcutaneous panniculitis-like T cell lymphoma.

Iatrogenic causes include traumatic and inflammatory responses to injected medications (Table 101.2). Anti-sense oligonucleotides (AONs), which modulate protein expression via hybridization with cellular RNA, represent the most recent addition to this list. One example of AONs is the experimental drug drisapersen[34].

In the case of insulin lipoatrophy, it may be induced by impurities and is significantly associated with the presence of anti-insulin antibodies[35]; mononuclear infiltrates near insulin injections suggest a localized immune response. Because repeated use of the same injection site increases the risk of lipoatrophy, the latter can be largely prevented by regular rotation of injection sites. Of note, lipoatrophy is fairly rare with the use of human insulin and insulin pump therapy. Lipoatrophy may also occur at injection sites of growth hormone and glatiramer acetate due to a direct lipolytic effect and panniculitis, respectively.

Lipoatrophia semicircularis may represent repetitive trauma or pressure-induced changes (Fig. 101.2), due to constant or intermittent pressure from leaning against the edges of furniture, basins and counters, or from tight-fitting clothing and elastic undergarments. Both resolution of the lesions when trauma is avoided and the occurrence of similar lesions in multiple employees in the same workplace provide support for microtrauma as the etiology[36]. Local hyperproduction of

INJECTED MEDICATIONS THAT CAN CAUSE LOCALIZED LIPOATROPHY
Most common
• Insulin*
• Non-human ≫ human, insulin analogues
• Rarely, can occur at distant sites
• Corticosteroids
Less common
• Antibiotics
• Benzathine penicillin†
• Amikacin
• Immunomodulatory drugs
• Glatiramer acetate (multiple sclerosis)
• Methotrexate†
• Vaccines
• Diphtheria–pertussis–tetanus vaccine
• Quadrivalent human papillomavirus vaccine
• Growth hormone
• Heparin
• Iron dextran
• Anti-sense oligonucleotides
• Anti-programmed cell death protein 1 (PD-1) antibodies
• Exogenous material
*Lipohypertrophy can also occur.
†Including semicircular lipoatrophy.

Table 101.2 Injected medications that can cause localized lipoatrophy. Lipoatrophy can also be seen at sites of acupuncture.



Fig. 101.2 Lipoatrophia semicircularis (semicircular lipoatrophy). Bilateral slightly curved depressions on the anterolateral thighs. *Courtesy Diane Thaler, MD.*



Fig. 101.3 Localized lipoatrophy of the upper lateral calf due to pressure. A fairly common finding in women who cross their legs while seated. *Courtesy Jean L. Bolognia, MD.*



Fig. 101.4 Congenital generalized lipodystrophy syndrome (Berardinelli–Seip syndrome). A Lipoatrophy of the trunk leading to muscle definition. **B** Extensive acanthosis nigricans. *Courtesy Edward Cowen, MD.*

TNF by macrophages has been implicated[37]. Localized lipoatrophy of the upper and lateral calf due to pressure is commonly observed in women who cross their legs when seated (Fig. 101.3).

Up to 60% of *involutional lipoatrophy* (see below) may be associated with prior local injections, suggesting a trauma-related phenomenon[38]. Although lipophagocytizing macrophages seen by electron microscopy suggest an initial stimulation by injectable material, an active foreign body reaction is typically absent.

Lipodystrophia centrifugalis abdominalis infantilis is usually idiopathic, but has been reported to be associated with mechanical trauma or focal infection. Predominance of this condition in East Asia is notable and reports in twins and siblings point to the possibility of an HLA predisposition. In one patient with lipodystrophia centrifugalis abdominalis infantilis, positive immunohistochemical staining for Fas, Bcl-2 and p53, as well as terminal transferase-mediated dUTP nick end-labeling (TUNEL) in degenerating fatty tissue, suggested apoptosis as a possible factor[39].

CLINICAL FEATURES

Congenital Generalized Lipodystrophy (CGL)

CGL is rare, with an estimated prevalence of <1 case in 10 million[40]. As an autosomal recessive disorder, there is often consanguinity. All subtypes are characterized by generalized loss or absence of metabolically active subcutaneous fat from birth, resulting in a cadaveric facies and distinctive muscular-appearing body habitus (Fig. 101.4A). Anabolic features are evident in early childhood (Table 101.3). There is also a deficiency of bone marrow fat (types 1, 2) and visceral fat (types 1, 3, 4). Type 2 CGL also lacks mechanical fat, in addition to metabolically active fat.

The inability to store sufficient fat in the adipocytes results in the metabolic syndrome (see Table 53.5), which becomes more profound during puberty[40]. Diabetes mellitus is evident by adolescence, but hyperinsulinemia can be detected as early as infancy. Clitoromegaly is seen in women and may be associated with polycystic ovarian syndrome and infertility. Hepatosplenomegaly is typical and may be associated with umbilical herniation. Cutaneous findings (see Table 101.3) include acanthosis nigricans, which is noted by adolescence and may be extensive (Fig. 101.4B). Serious medical complications and metabolic derangements include cirrhosis from fatty liver, premature atherosclerosis, sequelae of diabetes, pancreatitis from hypertriglyceridemia, osteosclerosis[41], and a high mortality rate from hypertrophic cardiomyopathy[40]. Type 2 appears to be a more severe disorder that is associated with intellectual disability, hypertrophic cardiomyopathy, and a higher incidence of premature death while type 4 patients have arrhythmias from myocardial fibrofatty infiltration, esophageal dysmotility, and pyloric stenosis[16]. In one series of CGL, there was an ~35-year reduction in lifespan, with liver disease and infection as the most common causes of death[42].

Familial Partial Lipodystrophy

Familial partial lipodystrophy (FPLD) was first described by Dunnigan and Köbberling[42], who outlined the clinical characteristics of large Scottish and German pedigrees with familial syndromes of partial lipodystrophy. FPLD is classified based upon genetic mutations and clinical phenotype (see Table 101.1). This group of disorders differs from other forms of inherited lipodystrophy by a later onset (after puberty) and fat loss predominantly affecting the extremities, with sparing of the face[40]. FPLD is a rare disorder, with a prevalence of <1 in 15 million[40].

In FPLD2, a normal childhood is followed by a progressive, symmetric loss of subcutaneous fat; the latter uniformly involves the extremities and variably extends to the trunk (anterior > posterior). Compensatory accumulation of excess fat occurs and results in a fat head and neck, with a round face, as well as increased supraclavicular fat (see Fig. 101.1). Acromegalic facies with submental fullness ("double chin") is characteristic. As a result of the loss of fat in the limbs, there is an accentuation of subcutaneous veins and muscular prominence (Fig. 101.5). Although FPLD3 has milder clinical features and an onset after the second decade of life, the metabolic disturbances may be more severe[40].

Metabolic disturbances in FPLD are similar to those in the generalized lipodystrophy syndromes. Glucose intolerance, ranging from mild to severe, develops during young adulthood. Acute pancreatitis and hepatic steatosis and cirrhosis may occur, with complications from diabetes mellitus, atherosclerotic cardiovascular disease, or hypertrophic cardiomyopathy leading to premature death[40]. When compared to men, affected women have been reported to have more severe triglyceride elevations (chylomicronemia syndrome)[43]. Dermatologic manifestations include tuberous xanthomas, acanthosis nigricans and hirsutism, while gynecologic findings include menstrual irregularities, polycystic ovaries, and fat hypertrophy within the labia majora.

Familial partial lipodystrophy with mandibuloacral dysplasia is a rare variant of partial lipodystrophy characterized by mandibular and clavicular hypoplasia, short stature, a high-pitched voice, and ectodermal abnormalities of the skin, teeth, nails, and hair[27,40]. There are multiple craniofacial defects, including dental overcrowding and bird-like facies. Skeletal abnormalities include osteolysis of the clavicles, acro-osteolysis, delayed closure of cranial sutures, and joint contractures. Mottled hyperpigmentation, alopecia, atrophy of extremity skin, and nail dysplasia are the characteristic cutaneous findings. Less common clinical features include sensorineural hearing loss, delayed puberty, a high-arched palate, and cutaneous calcinosis. Features of the metabolic syndrome may be present (see Table 53.5).

FEATURES OF CONGENITAL GENERALIZED LIPODYSTROPHY
Lipodystrophic features
• Lack of fat in the buccal region, resulting in a cadaveric facies • MRI studies show near total absence of subcutaneous fat and other metabolically active adipose tissues • Preservation of fat deposits in "mechanical" sites (types 1, 3, 4): orbit, palms, soles, tongue, breasts, vulva, and in periarticular and epidural regions • Muscular body habitus due to the extreme paucity of subcutaneous fat
Anabolic features
• Muscular hypertrophy with prominent superficial veins • Acromegalic facial and acral features • Voracious appetite • Increased basal metabolic rate • Heat intolerance • Accelerated growth with a normal to slightly increased adult height • Advanced bone and dental age • Osteosclerotic and lytic skeletal changes • Masculine features in females (clitoromegaly rare) • Enlarged genitalia (usually limited to infancy and childhood)
Metabolic disturbances
• Insulin resistance and severe fasting or postprandial hyperinsulinemia from early infancy • Insulin levels may decrease after several years, due to exhaustion of pancreatic β cells • Very insulin-resistant diabetes mellitus: noted at puberty with growth cessation • Impaired glucose tolerance is noted around age 8–10 years • Hypertriglyceridemia and sequelae (chylomicronemia, pancreatitis) • Hyperlipidemia accelerates at puberty (with growth cessation) • Low HDL-cholesterol levels (accurate assessment may be hindered by the increased TGs) • Low plasma leptin levels, corresponding to decreased body fat • Osteosclerosis (increased density)
Dermatologic manifestations
• Acanthosis nigricans, often early onset and widespread • Hypertrichosis, including increased (often curly) scalp hair at birth • Hyperhidrosis • Coarse skin on the upper body • Hyperkeratotic epidermal papillomatosis (may represent an exaggerated form of acanthosis nigricans) • Xanthomas
Gynecologic disturbances
• Oligomenorrhea • Polycystic ovaries • Infertility (females)
Organomegaly and organ dysfunction
• Hypertrophic cardiomyopathy (often fatal) • Fatty liver, hepatomegaly, cirrhosis, liver failure • Organomegaly: tonsils and adenoids, lymph nodes, spleen, kidneys, adrenals, pancreas, ovaries • Central nervous system abnormalities: hypothalamic–pituitary dysfunction, ventricular dilation, below average intelligence, ± mild mental retardation • Proteinuric nephropathy

Table 101.3 Features of congenital generalized lipodystrophy.[2,33] HDL, high-density lipoprotein; MRI, magnetic resonance imaging; TG, triglyceride.

Proteasome-Associated Autoinflammatory Syndromes

To date, five types of proteasome-associated autoinflammatory syndrome (PRAAS) have been identified and are due to mutations in seven genes that encode proteasome-associated proteins (see Table 45.7). PRAAS1 has also been referred to as CANDLE (chronic atypical neutrophilic dermatosis with lipodystrophy and elevated temperature) syndrome[44] and Nakajo–Nishimura syndrome[45]. In addition to recurrent fevers, annular violaceous plaques, eyelid erythema, and pernio-like lesions that begin during infancy or early childhood[46], patients can develop panniculitis-induced lipodystrophy. Partial (e.g. PRAAS1) or generalized (e.g. PRAAS4) lipoatrophy has been described. In biopsy specimens of nodules, a dense dermal infiltrate of atypical myeloid cells that resembles leukemia cutis or "histiocytoid" Sweet syndrome is seen, along with mature neutrophils. Treatment options include JAK inhibitors, corticosteroids, and methotrexate.



Fig. 101.5 Lipoatrophy of the lower extremities, leading to muscular prominence. *Courtesy William D. James, MD.*

Recurrent lipoatrophic panniculitis of children

In this syndrome, painful subcutaneous nodules are accompanied by fever, malaise, abdominal pain, and arthralgias[47]. Localized lipoatrophy then develops at the sites of nodules. Histopathologically, there is a lobular panniculitis with a mixed infiltrate composed of neutrophils, lymphocytes, macrophages, and mononuclear myeloid cells. Methotrexate and/or corticosteroids led to clinical improvement. The authors proposed that this constellation may represent an autoinflammatory disease. Of note, whole genome sequencing did not detect a form of PRAAS (see previous section)[47].

Acquired Generalized Lipodystrophy (Lawrence Syndrome)

To date, ~80 cases of acquired generalized lipodystrophy (AGL) have been reported in the English literature. New diagnostic criteria for AGL have been proposed, as well as a sub-classification into three subtypes (Table 101.4).

In approximately one-third to one-half of patients, there is a preceding systemic illness, in particular, a viral or bacterial infection or an autoimmune disorder (e.g. a connective tissue disease, thyroiditis)[40]. The rare patients who also have CVID can have recurrent infections (see Ch. 60). Drug-induced lipodystrophy, e.g. due to immune checkpoint inhibitors, needs to be excluded (see below).

Clinical features of AGL are similar to those of the congenital variant, but are of later onset and milder. The lipoatrophy typically does not become apparent until childhood or adolescence and rarely develops during adulthood. This disorder is three times as common in women. Large areas of the face, trunk, and extremities have fat loss (Fig. 101.6), and the palms and soles may even be involved. Loss of acral subcutaneous fat as well as perinephric and intra-abdominal fat can be documented by MRI scans. However, bone marrow fat is preserved, and this feature can be helpful in differentiating AGL from CGL types 1 and 2.

Tender subcutaneous nodules of panniculitis may precede the lipoatrophy in the type 1 variant and there may be an overlap in the

panniculitic and autoimmune subtypes. Progression can occur rapidly or over an extended period. When the lipodystrophy becomes generalized, metabolic abnormalities begin to manifest. Although the latter are less severe in AGL than in CGL, the period between the appearance of lipoatrophy and development of frank diabetes (~4 years) is shorter in AGL[40]. The extent of fat loss mirrors the severity of insulin resistance and hypertriglyceridemia.

Compared to the autoimmune and idiopathic types of AGL, the panniculitic variant may have less severe fat loss and a lower prevalence of diabetes and hypertriglyceridemia (see Table 101.4)[30]. In addition, the associated anabolic features are variable and less prominent and its severity is less striking when the condition starts in later childhood or adulthood.

In AGL, hepatic steatosis is commonly present in affected children, leading to a higher incidence of hepatomegaly, cirrhosis, and liver-related mortality than in CGL. Gynecologic abnormalities include true or pseudo-clitoromegaly (the latter due to fat loss), polycystic ovarian syndrome, and menstrual irregularities. Premature coronary artery disease and carotid or peripheral arterial disease may occasionally be seen. Renal and central nervous system abnormalities are usually absent.

ACQUIRED GENERALIZED LIPODYSTROPHY: PROPOSED DIAGNOSTIC CRITERIA AND SUBTYPES
Essential criterion
Selective loss of fat involving large regions of the body beginning during childhood or adolescence
Supportive criteria

• Clinical
  • Loss of subcutaneous fat from the palms and soles
  • Acanthosis nigricans
  • Hepatosplenomegaly
  • Panniculitis prior to onset (by clinical history and/or histologic confirmation; see below)
  • Associated autoimmune diseases (see below)
• Laboratory
  • Diabetes mellitus or impaired glucose tolerance
  • Severe hyperinsulinemia (fasting and/or postprandial)
  • Increased serum triglyceride and/or decreased HDL-cholesterol levels
  • Reduced serum leptin and/or adiponectin levels
  • Anthropometric or MRI evidence of large regions of fat loss
  • MRI evidence of preserved bone marrow fat

Subtypes

• Panniculitic variant (type 1)
  • Panniculitis precedes the onset of lipoatrophy, which may be noted in the center of expanding annular lesions or at distant sites
  • Mean age of onset is 7 years; slight female predominance (~1.5-fold)
  • Associated symptoms include low-grade fever, malaise, arthralgias, and abdominal pain
  • May be associated with autoimmune diseases (see below)
  • Relatively mild metabolic derangements and leptin abnormalities
  • Histopathologic evaluation reveals a mostly lobular lymphohistiocytic subcutaneous infiltrate ± granulomatous foci
• Autoimmune variant (type 2)
  • Concurrent or prior autoimmune disease without preceding panniculitis; associated with juvenile dermatomyositis, Sjögren syndrome, juvenile idiopathic arthritis, vitiligo, chronic urticaria/angioedema, and autoimmune thyroiditis, hepatitis or hemolytic anemia
  • Mean age of onset is 15 years; female predominance (~3-fold)
  • Hepatomegaly is invariably present; hypertriglyceridemia and diabetes mellitus occur in most patients
  • Laboratory abnormalities may be observed without clinical evidence of autoimmune disease, including antinuclear, anti-smooth muscle, antiglomerular basement membrane, anti-salivary duct, antimitochondrial, and anti-adrenal/ovary/placenta/testis antibodies
• Idiopathic (type 3)
  • No evidence of panniculitis or autoimmune disease
  • Mean age of onset is 20 years (range, <2–60 years); female predominance (~3-fold)

Table 101.4 Acquired generalized lipodystrophy: proposed diagnostic criteria and subtypes. *Adapted from reference 29.*

Dermatologic features of AGL, in addition to panniculitis and lipoatrophic areas, include acanthosis nigricans, localized or generalized hyperpigmentation, eruptive xanthomas, telangiectasias, mild palmar/plantar keratoderma, and hair abnormalities, including mild hirsutism, curly hair, and occasional alopecia. The acanthosis nigricans begins in childhood and involves the neck, axillae, groin, umbilicus, and nipples. Associated autoimmune diseases include juvenile dermatomyositis, Sjögren syndrome, and vitiligo. In addition, patients may have chronic urticaria and angioedema (see Table 101.4).

Acquired Partial Lipodystrophy (Barraquer–Simons Syndrome)

Acquired partial lipodystrophy, also known as progressive lipodystrophy or cephalothoracic lipodystrophy, is the second most common type of non-localized lipodystrophy, after HIV/ART-related lipodystrophy. It has been reported worldwide, with more than 250 patients described in the literature[40,48].

Three phenotypic subtypes have been noted: (1) fat loss in the upper half of the body; (2) fat loss in the upper half of the body, with hypertrophy of adipose tissue in the lower half; and (3) hemi-lipodystrophy, where one half of the face or body is affected.

Lipodystrophy begins during childhood or pre-puberty (median age at diagnosis is 8–10 years) and sometimes follows a viral illness. It is characterized by an insidious onset, with symmetric and progressive loss of subcutaneous fat in a cephalocaudal direction (Fig. 101.7). Extension of the lipoatrophy usually takes place over a 1- to 2-year period, but can occur over many years. Physical findings may be apparent by adolescence, although the onset may be delayed until 40 years of age. Women are affected three times more often than men.

The face is usually affected first, with sunken eyes due to loss of retro-orbital and periorbital fat. This is accentuated by concurrent loss of buccal and temporal fat, resulting in a progeria-like or cadaveric appearance (Fig. 101.8). The hips and legs tend to be spared, and often demonstrate fat hypertrophy, especially in women. Growth delay or stunted growth is not characteristic of this disorder.

MCGN II with nephritic syndrome, seen in approximately one-fifth of patients, may occur many years, usually about eight, after the onset of lipodystrophy. Almost all patients with acquired partial lipodystrophy have low levels of C3 in addition to circulating C3 nephritic factor (C3NeF), composed of polyclonal IgG[28]. This leads to unopposed activation of the alternative complement pathway (see above) and C3NeF-induced lysis of adipocytes. The low C3 level also predisposes



Fig. 101.6 Acquired generalized lipodystrophy. There is loss of subcutaneous fat, resulting in a muscular appearance of the legs and accentuation of the tendons. *Courtesy Jacqueline Junkins-Hopkins, MD.*



Fig. 101.7 Acquired partial lipodystrophy syndrome in a patient with nephritic factor and renal disease. Lipoatrophic features are most prominent on the face. There is obvious loss of buccal fat. The patient also had axillary acanthosis nigricans. *Courtesy Kenneth E. Greer, MD.*



Fig. 101.8 Acquired partial lipodystrophy syndrome in a patient with Sjögren syndrome. Lipoatrophy of the face with sunken eyes and loss of temporal and buccal fat pads. The facial pigmentation is related to lichen planus. *Courtesy Priya Sen, MD.*

these patients to recurrent *Neisseria meningitidis* infections and repeat vaccinations may be required.

Other autoimmune associations include systemic lupus erythematosus, juvenile dermatomyositis, systemic sclerosis, Sjögren syndrome, pernicious anemia, hypothyroidism, celiac disease, dermatitis herpetiformis, temporal arteritis, and small vessel vasculitis.

Metabolic syndrome is less common in APL than in other lipodystrophies, but acanthosis nigricans, menstrual abnormalities, hirsutism, insulin resistance, type 2 diabetes mellitus, and hyperlipidemia may be seen.

Localized Lipoatrophy

Localized lipoatrophy presents as one or multiple depressed areas, usually on the proximal extremities, ranging from under a few centimeters to greater than 20 cm in diameter. *Drug-induced lipoatrophy* is most commonly due to injections of corticosteroids and non-human insulin (see Table 101.2); it may be accompanied by local lipohypertrophy. Of note, multifocal lipoatrophy due to intravenous corticosteroid use has been described and insulin injection-related lipoatrophy can appear at distant sites.





Fig. 101.9 Localized lipoatrophy secondary to lupus panniculitis. **A** An area of depression on the cheek due to burnt-out lupus panniculitis; note the dyspigmentation and scarring from an overlapping lesion of discoid lupus erythematosus. **B** Circular depressions on the upper arm, a common location for lupus panniculitis. *A, Courtesy National Skin Centre, Singapore.*

Involutional lipoatrophy is an idiopathic lipoatrophy characterized clinically by non-inflammatory focal loss of fat. Based on reported cases, there is a strong female predominance. Focal oval areas of lipoatrophy, 2 to 8 cm in diameter, occur predominantly on the buttocks and proximal extremities, especially the upper arm, corresponding to locations frequently used as injection sites. Although it is estimated that up to 60% of cases of involutional lipoatrophy may be associated with prior local injections (see above), this type of lipoatrophy may occur without prior injections.

Atrophic connective tissue panniculitis is rare, and it often occurs on the upper or lower extremities. In "pure" cases of this condition, there is no prior clinical inflammation although there is evidence histologically of lymphocytic panniculitis. In other patients, the lipoatrophy may be the direct result of clinical panniculitis. The latter is common on the head and neck or proximal extremities if associated with lupus panniculitis (also referred to as lupus profundus; Fig. 101.9). Other associated autoimmune diseases include dermatomyositis, thyroiditis, juvenile idiopathic arthritis, vitiligo, and insulin-dependent diabetes mellitus.

Lipoatrophia semicircularis (semicircular lipoatrophy) has been reported primarily in women in their 20s to 30s and rarely in children. It presents as symmetric, asymptomatic, 4–8 cm curvilinear horizontal depressions on the anterolateral thighs (see Fig. 101.2). Infrequent presentations include two or three parallel depressions, a unilateral distribution, or symptoms of cramps, pain after sports, heavy legs, or a burning sensation. The lesions usually appear over a few weeks and spontaneously resolve between 9 months to 4 years. The lipoatrophy may recur. MRI can assist in differentiating this from an inflammatory panniculitis.

Annular lipoatrophy presents with a deep, persistent, pseudosclerotic band approximately 9–11 cm in length that encircles the arm or ankle[49]. More extensive lesions have been reported that were 14–16 cm in length. It may be preceded by tenderness and swelling of the limb, or be associated with discomfort and arthritis. This entity may represent a variant or end-stage presentation of atrophic connective tissue disease panniculitis. Thus, there may be patients with associated autoimmune diatheses.



Fig. 101.10 Lipodystrophia centrifugalis abdominalis infantilis (centrifugal lipodystrophy). A 5-year-old Malay boy with a two-year history of progressive lipoatrophy involving the groin bilaterally and the lower abdomen. The veins in the involved area are readily visible. *Courtesy National Skin Centre, Singapore.*

Lipodystrophia centrifugalis abdominalis infantilis (centrifugal lipodystrophy) has largely been reported from East Asia, with most patients of Japanese, Korean, or Chinese origin[50]. Onset is usually before 3 years of age, with >90% of patients presenting by age 5 years. In Koreans, there is a four-fold female predominance[51]. Although lipodystrophia centrifugalis abdominalis infantilis affects primarily Asian children, it may occasionally occur in Caucasians and in adults.

Clinically, a well-demarcated area of lipoatrophy with a periphery of erythema and scale is seen on the abdomen or elsewhere on the trunk, often with associated regional lymphadenopathy. The lipoatrophy begins on the lower abdomen or in the groin region (and may include the genitalia) in about 80% of patients, and in the axillary region in about 20% of patients; it spreads onto the abdomen or chest, respectively, in a centrifugal fashion (Fig. 101.10). The underlying blood vessels become visible and ulceration may occur within the depressed areas. Contrary to its original name, this condition can affect non-abdominal sites such as the face, neck, and lumbosacral region (Fig. 101.11A), and it is not limited to infants. The lesions may progress slowly over several years, then often cease enlarging by 13 years of age[49]. Although there is no specific therapy, >60% of patients spontaneously improve (Fig. 101.11B).

Progressive hemifacial atrophy (Parry–Romberg syndrome) is considered to be a form of severe linear morphea (see Ch. 44). In addition to lipoatrophy, there may be atrophy of the underlying muscle and bone as well as the potential for ophthalmologic, dental, and neurologic involvement. An association with *Borrelia burgdorferi* infection has been reported in Europe.

Non-progressive late-onset linear hemifacial lipoatrophy occurs on the malar cheek, primarily in elderly individuals.

Inflammatory reactions due to material injected for cosmetic purposes or from self-inflicted injections of foreign material can lead to lipoatrophy which may be associated with scarring and dyschromia.

Lipohypertrophy

Lipohypertrophy remains a frequent complication of insulin therapy, irrespective of the insulin source and mode of administration[52]. As with insulin lipoatrophy, anti-insulin antibodies are associated with lipohypertrophy in children and adolescents with type 1 diabetes. The clinical consequence is that injection of insulin into a site of lipohypertrophy, while painless, may lead to erratic absorption of the insulin with poor glycemic control and rebound phenomenon[52]. Of note, insulin-induced nodular amyloidosis may have a clinical appearance similar to lipohypertrophy.

Injection of pegvisomant, a growth hormone receptor antagonist used to treat acromegaly, is another cause of lipohypertrophy (Table 101.5).



Fig. 101.11 Lipodystrophia centrifugalis infantilis (centrifugal lipodystrophy) of the face. A A 2-year-old girl with a serpentine violaceous band involving the cheek in association with lipoatrophy. **B** The same child two years later, with spontaneous resolution. The most common location for lipodystrophia centrifugalis infantilis is the abdomen (see Fig. 101.10). *Courtesy National Skin Centre, Singapore.*

CAUSES OF LIPOHYPERTROPHY
• **Insulin therapy –** risk factors include duration of therapy, frequent injections, failure to rotate sites of injections, and poor injection technique
• **Pegvisomant (growth hormone receptor antagonist) injections***
• **Growth hormone injections**
• **Excess corticosteroids** – includes Cushing disease (excessive ACTH production by the pituitary gland) and Cushing syndrome (iatrogenic, adrenal tumors, nodular adrenal hyperplasia, ectopic ACTH production)
• **HIV/ART-associated** – risk factors include extended exposure to nucleoside reverse transcriptase inhibitors, exposure to protease inhibitors, age ≥40 years, longer duration of therapy, higher body mass index before onset of therapy, and presence of metabolic derangements (elevated serum triglyceride and insulin levels; depressed serum testosterone levels)
• **Lipodystrophy syndromes** – familial partial lipodystrophy (neck and face), acquired partial lipodystrophy (hips and lower extremities)
*Used to treat acromegaly.

Table 101.5 Causes of lipohypertrophy.

PATHOLOGY

Generally speaking, the histologic picture of the various lipodystrophy syndromes (see Table 101.1) is non-inflammatory. In *generalized lipodystrophy*, there is complete or near-complete loss of subcutaneous fat, with the dermis and fascia in direct apposition. Less often,

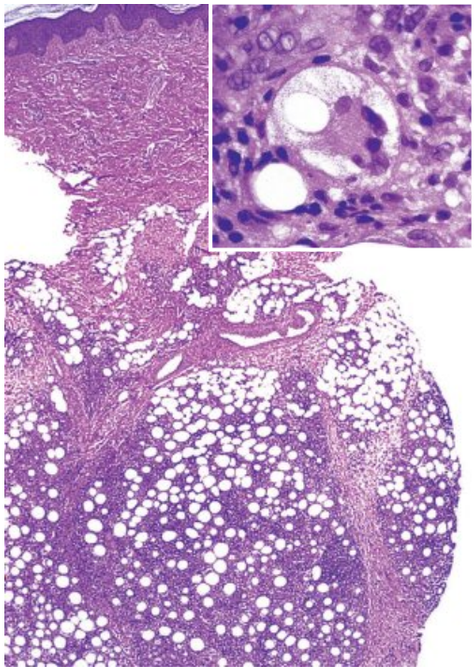


Fig. 101.12 Histopathologic features of the preceding panniculitis in type 1 acquired generalized lipodystrophy. Lobular panniculitis with infiltrate of lymphocytes, histiocytes, multinucleated giant cells, and lipophages. There is also cytoplasmic vacuolization of the fat cells (inset). See Table 101.4 for three types. *Courtesy Jacqueline Junkins-Hopkins, MD.*

biopsy specimens appear to have no overt abnormalities, except for an increased amount of collagen, which has replaced the subcutaneous fat. In contrast, biopsies of *acquired generalized lipodystrophy*, in particular type 1, may show a lobular panniculitis (Fig. 101.12; see Table 101.4).

In *acquired generalized lipodystrophy* and areas of lipoatrophy in some forms of *partial lipodystrophy*, two histologic patterns have been recognized: (1) non-inflammatory with involutional changes of the fat; and (2) inflammatory in the form of a lobular panniculitis with lymphocytes, lipophages, and plasma cells[53]. Whether these two patterns are stage-related remains to be clarified, as even in patients without panniculitis clinically, biopsies of early lesions may show inflammation, but it is usually mild.

Involutional changes of the subcutaneous fat are characterized by small fat lobules with a reduction in the size and number of adipocytes (Fig. 101.13). *Involutional lipoatrophy* can be further divided into two histologic subtypes[38]. In the first type, the lobules may be composed of faintly acidophilic, small fat cells that retract from one another as well as the surrounding connective tissue, leading to an appearance similar to embryonic fat; the lobules often have an eosinophilic appearance. These histologic findings are more prominent at the periphery of the clinically depressed area, with tiny acidophilic fat cells present more centrally. Inflammation is absent to sparsely mononuclear. The second type, with indistinguishable clinical features, shows small atrophic adipocytes with a normal fat cell membrane surrounded by prominent vasculature. At scanning magnification, the lobules are collapsed (with an orientation parallel to the skin surface) and surrounded by numerous capillaries. Acid mucopolysaccharide deposition within the fat lobules and fibrosis of the septae may be seen, as well as occasionally lipomembranous changes.

Although birefringent, non-crystalline material may occasionally be observed, foreign body giant cells and lipophages are typically absent in both subtypes of involutional lipoatrophy. $CD68^+$ macrophages can be demonstrated with immunohistochemical staining. Ultrastructural studies have shown that these are lysosomally active macrophages adjacent to lipocytes and likely containing degenerated lipid remnants[38]. In *localized lipodystrophy*, a loss of fatty tissue is seen, along with a variable degree of fibrosis. There is usually no inflammatory infiltrate, although panniculitis has been reported in a few cases. Deposits of immunoreactants can be seen within blood vessel walls or the basement membrane, particularly in the inflammatory type.

Histologically, well-developed areas of *lipodystrophia centrifugalis abdominalis infantilis* show a diminution of subcutaneous fat with scant or absent inflammation. The erythematous rim tends to correspond to a moderate or marked lymphohistiocytic infiltrate in the subcutaneous fat; a deep dermal and peri-eccrine lymphocytic infiltrate

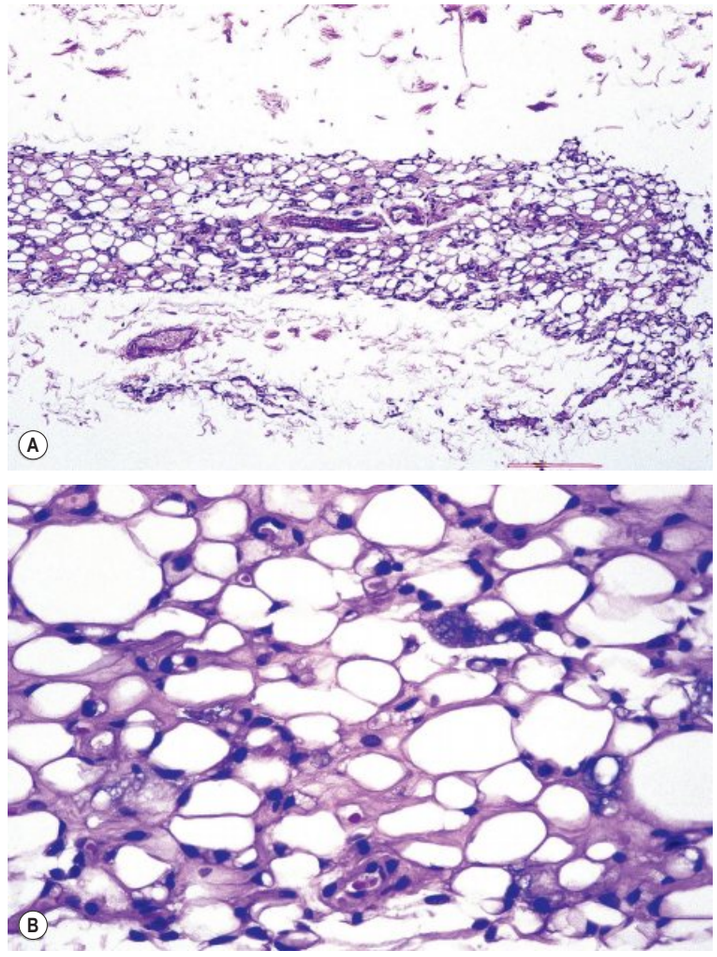


Fig. 101.13 Histopathologic features of involutional lipoatrophy secondary to corticosteroid injection. A There is marked diminution and collapse of the fat lobules, without inflammation. **B** Higher power demonstrates decreased size of fat cells with eosinophilic thickened cell walls with a hyalinized and mucinous stroma. *Courtesy Jacqueline Junkins-Hopkins, MD.*

is an uncommon finding. There may be fibrosis and thickening of the septae within the subcutis. The few adipocytes that are present may have myxoid changes.

Other localized variants such as *lipoatrophia semicircularis* (semicircular lipoatrophy) and *drug-induced lipoatrophy* usually show a loss of fatty tissue and replacement by collagen, with no features of panniculitis. There are often scattered lipophages. However, at sites of glatiramer acetate injections, panniculitis that resembles lupus profundus histologically can be seen. Lastly, HIV/ART-associated lipodystrophy resembles the non-inflammatory pattern of lipodystrophy.

DIFFERENTIAL DIAGNOSIS

There are a variety of other complex syndromes that present with lipoatrophy along with a number of other physical and systemic features (see below). A detailed discussion of these syndromes is beyond the scope of this chapter.

The excessive fat accumulation seen in patients with FPLD2 and HIV/ART-associated lipodystrophy could be confused with Cushing syndrome and obesity. Acromegaly can have overlapping features with generalized lipodystrophy.

In an infant with generalized lipodystrophy, the following conditions should also be considered:

- *Leprechaunism* (Donohue syndrome) is included in some lipodystrophy classifications, as the patients present with generalized lipodystrophy, severe insulin resistance, acanthosis nigricans, and hirsutism. In contrast to CGL, these patients have a distinct elfin facies, severe intrauterine growth retardation, prominent nipples, cutis laxa, mutations in the insulin receptor gene, and death during infancy.

- *SHORT syndrome* (*s*hort stature, *h*yperextensible joints or *h*ernia, *o*cular depression, *R*ieger anomaly [iridocorneal mesodermal dysgenesis], and *t*eething delay) is also included in some lipodystrophy classifications, as there is congenital lipoatrophy of the face and upper body. This condition is distinguished by the above-outlined abnormalities, intrauterine growth retardation, delayed bone age, mutations in *PIK3R1*, and a dysmorphic facies, which includes a triangular shape, micrognathia, deep-set eyes, and anteverted ears. Metabolic abnormalities are rare to absent.
- *Progeria-type syndromes* are characterized by limb lipoatrophy, cardiovascular disease and diabetes, but they are accompanied by muscle wasting, sclerodermatous changes, cataracts, and other signs of premature aging. Some of the progeric syndromes have *LMNA* mutations similar to those associated with FPLD, and may be considered as part of a broader group of disorders termed laminopathies (see Table 63.10).
- In *Cockayne syndrome*, lipoatrophic changes are accompanied by growth delay, retinal abnormalities, photosensitivity, and defects in DNA repair (see Chs. 63 & 87).
- *AREDYLD syndrome*: congenital generalized lipoatrophic diabetes is associated with an acrorenal field defect and ectodermal dysplasia.

In the case of partial lipodystrophy, there was a report of diffuse, symmetrical lipoatrophy of the lower extremities following extensive inflammation due to lobular panniculitis[54]. Neither underlying autoimmune diseases nor exogenous causes were identified.

Localized lipodystrophies should be differentiated from initial phases of progressive lipodystrophy, morphea, lupus panniculitis, and atrophoderma of Pasini and Pierini. Although there is overlap amongst the various types of localized lipodystrophy, the distribution and morphology combined with a history of injections, the presence clinically or histologically of panniculitis, and associated autoimmune disorders may aid in the diagnosis.

Poland syndrome is a rare congenital disorder consisting of unilateral partial or total absence of a breast and/or pectoralis major muscle plus ipsilateral symbrachydactyly, which may simulate lipoatrophy. Lipohypoplasia, as is seen in disorders such as Proteus syndrome, can also mimic lipoatrophy.

Lastly, whole-body MRI has been shown to assist in differentiating the various subtypes of lipodystrophies, based upon the amount and extent of residual adipose tissue and the absence or preservation of marrow fat[55]. This information, in combination with the clinical phenotype and especially genetic testing, improves diagnostic accuracy and prognostication.

TREATMENT

Therapeutic interventions for lipodystrophy syndromes focus on three aspects: (1) cosmetic concerns; (2) metabolic derangements; and (3) systemic associations[56]. For volume loss due to lipoatrophy, soft tissue fillers and autologous fat transplantation can be helpful, albeit temporarily[57,58]. Solid synthetic volumetric midfacial implants, constructed using computer-aided design and manufacturing technology, may offer a more durable correction of the defects[59]. A conservative approach can be undertaken when spontaneous improvement may occur as in pressure-induced or traumatic lipoatrophy. For lipohypertrophy, liposuction and lipectomy represent moderately effective treatments[60]. Switching to purified human insulin may improve lipoatrophy at sites of insulin injections, but it may require 1 to 3 years[52].

The treatment of metabolic abnormalities requires input from dieticians and endocrinologists[56]. Several medications are used to address insulin resistance and glucose control including thiazolidinediones, metformin, sulfonylureas, dipeptidyl peptidase 4 inhibitors ("gliptins"), glucagon-like peptide 1 agonists, sodium-glucose cotransporter-2 inhibitors (gliflozins), and insulin[56]. Treatment of hypertriglyceridemia includes diet, fibrates, omega-3 fatty acids, niacin, and statins[56,61]. For refractory metabolic disease, bariatric surgery can be considered[62].

Of note, recombinant methionyl human leptin (metreleptin) is FDA-approved for the treatment of congenital or acquired *generalized* lipodystrophy. Metreleptin binds to hypothalamic leptin receptors, leading to decreased appetite and increased insulin sensitivity. Marked improvements in glycemic control, hyperlipidemia, hepatic steatosis, and diabetic complications such as proteinuria have been reported[63]. Metreleptin is generally well tolerated, with sustained effects as long as neutralizing anti-metreleptin antibodies do not develop. There is also a black box warning regarding risk of lymphoma. It has also been shown to be an effective steroid-sparing therapy for the acquired generalized lipodystrophy that can follow allogeneic hematopoietic stem cell transplantation[64].

In acquired partial lipodystrophy, longitudinal evaluation will allow identification of associated autoimmune connective tissue diseases (e.g. lupus, dermatomyositis), thyroid disease, or renal disease that requires treatment. Such treatment may halt the progression of the lipodystrophy. If proteinuria, a low serum C3, and C3 nephritic factor (C3NeF) are detected, a renal biopsy to exclude MCGN II may be required. Encouraging results following the use of IVIg have been reported, presumably due to the IVIg containing neutralizing antibodies against C3NeF[65]. When no secondary cause is found, treatment is limited.

Additional potential therapies include volanesorsen, an antisense oligonucleotide that binds to apoC-III mRNA and is EMA-approved for familial chylomicronemia syndrome but not FDA-approved because of the risk of thrombocytopenia. Both evinacumab, a human angiopoietin-like 3 (ANGPTL3) blocking antibody that is currently FDA-approved for homozygous familial hypercholesterolemia, and gemcabene calcium, a dialkyl ether dicarboxylic acid which has orphan drug designation for the same indication, have also shown efficacy in patients with severe hypertriglyceridemia[56]. Setmelanotide, a melanocortin-4 receptor agonist, is FDA-approved for obesity due to deficiencies of proopiomelanocortin (POMC), proprotein convertase subtilisin/kexin type 1 (PCSK1), or leptin receptor (LEPR) and may reduce triglyceride levels.

ACQUIRED LIPODYSTROPHY DUE TO OTHER CAUSES

Medications

HIV/ART-associated lipodystrophy

Worldwide, HIV/ART-associated lipodystrophy is still the most common form of non-localized lipodystrophy. Fortunately, its incidence has fallen significantly with the advent of new ARTs and increased awareness of its association with protease inhibitors (PI) and nucleoside analogue reverse transcriptase inhibitors (NRTIs) such as stavudine and didanosine. There are several proposed mechanisms to explain this particular type of lipodystrophy (Fig. 101.14; Table 101.6) and they include:

- impaired pre-adipocyte differentiation and increased adipocyte apoptosis[66,67]
- impaired insulin-stimulated lipogenesis and increased lipolysis[66], leading to decreased adipocyte size
- mitochondrial toxicity[68].

HIV/ART-associated lipodystrophy reflects an interplay of several factors including the type of ART administered, direct effects of HIV proteins, and other host factors such as age and severity of HIV infection. The key contributor is extended use of higher-risk ARTs, in particular the older-generation NRTIs (e.g. stavudine, didanosine), early PIs (e.g. indinavir, full-dose ritonavir), and raltegravir (an integrase strand transfer inhibitor [INSTI])[69]. Host risk factors include an age >40 years and more severe HIV infection (e.g. $CD4^+$ count <200/mcl, higher nadir viral load) at the onset of therapy[70,71]. Baseline subcutaneous body fat composition prior to ART also plays a role, with a higher risk of lipoatrophy in individuals with lower body fat and a higher risk of lipohypertrophy in those with higher body fat[70,71].

The clinical findings in HIV/ART-associated lipodystrophy include: (1) irreversible lipoatrophy of peripheral sites, primarily the face, extremities, heel pads, and buttocks (Fig. 101.15 & 101.16); (2) central lipohypertrophy or adipose tissue accumulation, especially dorsocervical, supraclavicular and mammary, as well as intra-abdominal and visceral (e.g. liver); and (3) development of metabolic abnormalities. In cross-sectional studies utilizing DEXA scans and computed tomography, a 15%–65% prevalence of central lipohypertrophy was noted within 1 to 2 years of initiation of ART[70]. Patient self-report, in concert with physician examination, represent the earliest and best indicators of body contour changes. The latter are a major cause of both social stigmatization and reduced drug adherence.

Distinct clinical syndromes of fat redistribution can result, depending upon the particular drug or combination of drugs. In patients who developed lipohypertrophy, INSTIs were associated with increased weight

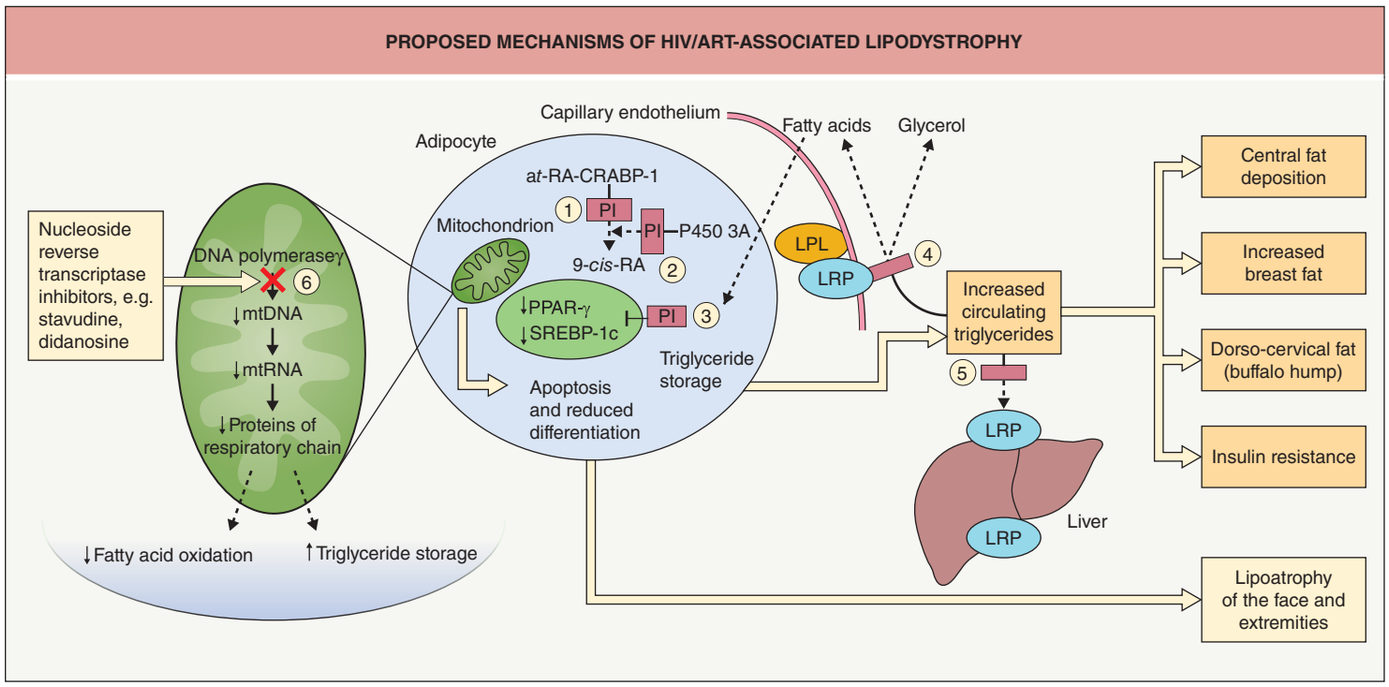


Fig. 101.14 Proposed mechanisms of HIV/ART-associated lipodystrophy. The combination of decreased PPAR-γ expression and decreased fatty acid oxidation capacity resulting from drug exposure could explain how these drugs cause adipocyte toxicity and lipoatrophy. See Table 101.6 for additional details. The numbers represent sites of drug effects. ART, antiretroviral therapy; *at*-RA, all-*trans*-retinoic acid; CRABP-1, cytoplasmic retinoic acid binding protein type 1; LPL, lipoprotein lipase; LRP, low-density lipoprotein receptor-related protein; mtRNA, mitochondrial RNA; mtDNA, mitochondrial DNA; PIs, protease inhibitors; PPAR-γ, peroxisome proliferator-activated receptor-γ; RXR, retinoid X receptor; SREBP-1c, sterol regulatory element-binding protein-1c. *Adapted from Carr A. HIV protease inhibitor-related lipodystrophy syndrome. Clin Infect Dis 2000;30:S135–42.*

MECHANISMS OF ANTIRETROVIRAL THERAPY (ART)-ASSOCIATED LIPOATROPHY			
	HIV drugs implicated	**Drug-induced effect**	**Cellular response**
↓ Adipocyte differentiation*	PIs, NRTIs	Defect in lamin A/C processing and/or RXR-PPAR-γ heterodimer activation decreases function of SREBP-1c & other downstream transcription factors	↓ Production of new mature fat cells → ↓ fat cell number
↑ Adipocyte apoptosis+	PIs, NRTIs	↑ TNF-α signaling (as well as mechanism described above for ↓ differentiation)	↑ Fat cell death → ↓ fat cell number
↑ Lipolysis*	PIs, NRTIs	↓ Expression of perilipin	↑ Release of stored TGs as FFAs and glycerol into circulation →↓ fat cell size
↓ Lipogenesis	PIs, NRTIs	↓ Expression and function of lipogenic SREBP-1c	↓ FFA uptake by adipocytes → ↓ fat cell size
Mitochondrial toxicity	NRTIs	Inhibition of mitochondrial DNA polymerase-γ	↑ Catabolic pathways (lipolysis), altered production of hormones and cytokines (↓ adiponectin, ↑ TNF-α), ↓ adipocyte differentiation, ↑ adipocyte apoptosis

*Also represent sequelae of mitochondrial toxicity.

Table 101.6 Mechanisms of antiretroviral therapy (ART)-associated lipoatrophy. FFA, free fatty acids; HIV, human immunodeficiency virus; NRTI, nucleoside reverse transcriptase inhibitor; PI, protease inhibitor; PPAR-γ, peroxisome proliferator-activated receptor-γ; RXR, retinoid X receptor; SREBP-1c, sterol regulatory element-binding protein-1c; TG, triglycerides; TNF, tumor necrosis factor. *From refs. 60–62,64,65.*

gain compared to PIs and NNRTIs[72]. Amongst the NRTIs, tenofovir alafenamide led to more weight gain than did tenofovir disoproxil fumarate, abacavir, or zidovudine[72]. With regard to lipoatrophy, NRTIs, especially stavudine, were more likely to result in peripheral fat wasting. Of note, older NRTIs are associated with multiple complications related to mitochondrial toxicity, including myopathy, polyneuropathy, liver steatosis, pancreatitis, hyperlactatemia, bone marrow toxicity and a Fanconi-like syndrome.

Similar to inherited lipodystrophy syndromes, fat redistribution in HIV/ART-associated lipodystrophy may precede the development of metabolic complications. These include insulin resistance, diabetes, dyslipidemia, and bone disorders such as osteopenia, osteoporosis, and avascular necrosis. The insulin resistance may arise via either the direct effects of PIs on insulin-mediated whole-body glucose uptake or the indirect effects of dyslipidemia, mitochondrial toxicity, and changes in body fat composition. Adipocytokines, in particular leptin and adiponectin, affect insulin sensitivity, and low levels of both factors have been observed in HIV/ART-associated lipodystrophy[5,9,73]. Genetic variation in resistin production by adipose tissue is also implicated in HIV/ART-associated obesity and insulin resistance[74]. In HIV-infected patients receiving ART, the prevalence of metabolic syndrome has been reported to be 15%–25%, resulting in an increased risk for cardiovascular disease[40]. For example, the Data Collection on Adverse Events of Anti-HIV Drugs (DAD) study found an ~25% increase in the rate of myocardial infarctions per year during the first 4–6 years of ART exposure[75].

Immune Checkpoint Inhibitor-Associated Lipodystrophy

Two anti-PD-1 antibodies, nivolumab and pembrolizumab, have been associated with the development of lipodystrophy[76]. Following at least 10 months of administration, generalized lipoatrophy developed in

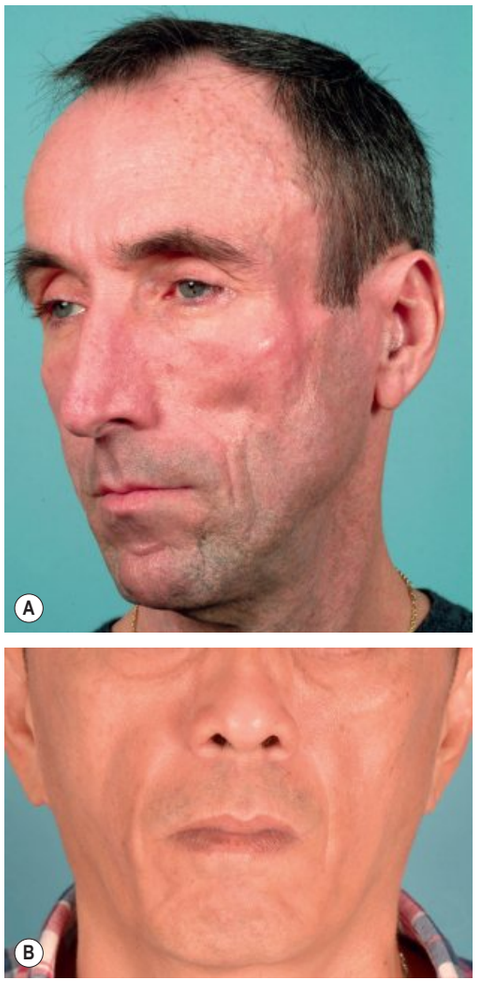


Fig. 101.15 HIV/ART-associated lipoatrophy. A The side view highlights the loss of temporal fat. **B** There is symmetric loss of buccal and parotid fat, resulting in prominent zygomata and a cachectic appearance, in a second patient. *A, Courtesy Ken Katz, MD; B, Courtesy National Skin Centre, Singapore.*

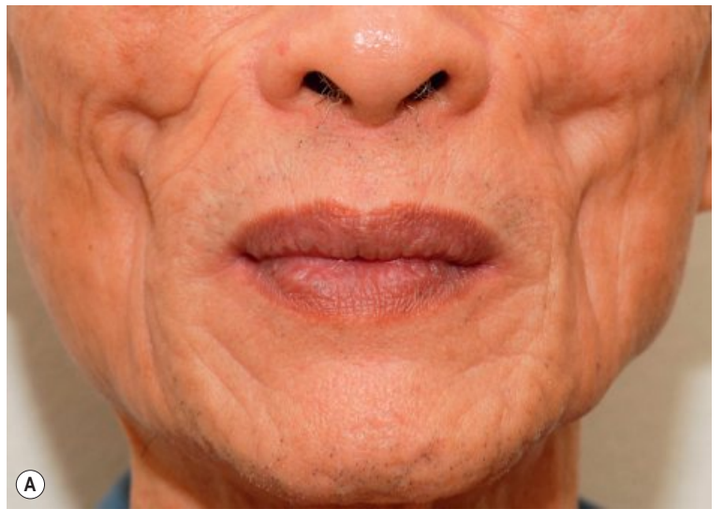




Fig. 101.16 HIV/ART-associated lipoatrophy. A Marked indentation of the medial cheeks in an older patient, with redundant melolabial folds. **B** Lower extremities with prominent veins and defined musculature. *A, Courtesy Priya Sen, MD.*

association with diabetes mellitus, insulin resistance, hypertriglyceridemia, and central obesity. These clinical manifestations persisted despite discontinuation of the medication.

POEMS Syndrome

Acquired partial lipodystrophy that preferentially affects the face is one of the more recently recognized cutaneous manifestations of POEMS syndrome (polyneuropathy, organomegaly, endocrinopathy, monoclonal gammopathy, and skin changes). Symmetric lipoatrophy of the face has been noted in up to half of patients[77]. Treatment of the underlying paraproteinemia usually arrests its progression but does not lead to reversal.

Allogeneic Hematopoietic Stem Cell Transplantation-Associated Lipodystrophy

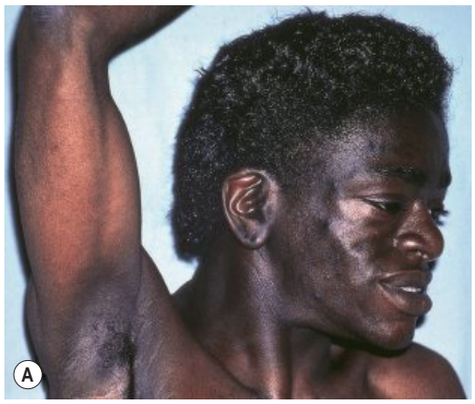
Acquired partial lipodystrophy and associated metabolic abnormalities have been observed following allogeneic hematopoietic stem cell transplantation, primarily in children[78]. The cutaneous findings resemble those of FPLD with lipoatrophy of the gluteal region and extremities and retention of fat in the face and abdomen. It may reflect a graft-versus-host (GVHD) reaction at the adipocyte level.

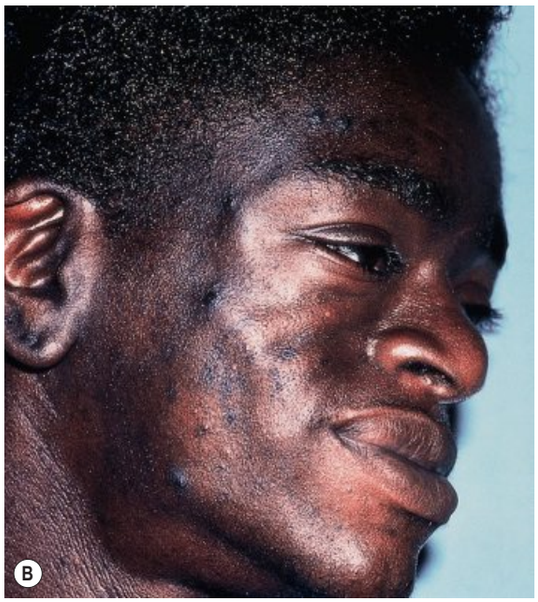
Additional figures available in our eBook (see inside front cover for access code).

REFERENCES

1. Mitchell SW. Singular case of absence of adipose matter in the upper half of the body. *Am J Med Sci*. 1885;90:105–106.
2. Seip M, Trygstad O. Generalized lipodystrophy, congenital and acquired (lipoatrophy). *Acta Paediatr Suppl*. 1996;413:2–28.
3. Carr A, Samaras K, Burton S, et al. A syndrome of peripheral lipodystrophy, hyperlipidemia and insulin resistance in patients receiving HIV protease inhibitors. *AIDS*. 1998;12:F51–F58.
4. Wauters M, Considine RB, van Gaal LF. Human leptin: from an adipocyte hormone to an endocrine mediator. *Eur J Endocrinol*. 2000;143:293–311.
5. Vigouroux C, Maachi M, Nguyen TH, et al. Serum adipocytokines are related to lipodystrophy and metabolic disorders in HIV-infected men under antiretroviral therapy. *AIDS*. 2003;17:1503–1511.
6. Simha V, Garg A. Lipodystrophy: lessons in lipid and energy metabolism. *Curr Opin Lipidol*. 2006;17:162–169.
7. Weyer C, Funahashi T, Tanaka S, et al. Hypoadiponectinemia in obesity and type 2 diabetes: close association with insulin resistance and hyperinsulinemia. *J Clin Endocrinol Metab*. 2001;86:1930–1935.
8. Haque WA, Shimomura I, Matsuzawa Y, Garg A. Serum adiponectin and leptin levels in patients with lipodystrophies. *J Clin Endocrinol Metab*. 2002;87:2395–2398.
9. Addy CL, Gavrila A, Tsiodras S, et al. Hypoadiponectinemia is associated with insulin resistance, hypertriglyceridemia, and fat redistribution in human immunodeficiency virus-infected patients treated with highly active antiretroviral therapy. *J Clin Endocrinol Metab*. 2003;88:627–636.
10. Nagy S, Tsiodras S, Martin L, et al. Leptin is independently associated with lipodystrophy in HIV-1 infected patients treated with HAART. *Clin Infect Dis*. 2003;36:795–802.
11. Shimomura I, Hammer RE, Ikemoto S, et al. Leptin reverses insulin resistance and diabetes mellitus in mice with congenital lipodystrophy. *Nature*. 1999;401:73–76.

12. Chong AY, Lupsa BC, Cochran EK, Gorden P. Efficacy of leptin therapy in the different forms of human lipodystrophy. *Diabetologia*. 2010;53:27–35.
13. Javor ED, Cochran EK, Musso C, et al. Long-term efficacy of leptin replacement in patients with generalized lipodystrophy. *Diabetes*. 2005;54:1994–2002.
14. Agarwal AK, Garg A. Genetic basis of lipodystrophies and management of metabolic complications. *Annu Rev Med*. 2006;57:297–311.
15. Kim CA, Delepine M, Boutet E, et al. Association of a homozygous nonsense caveolin-1 mutation with Berardinelli-Seip congenital lipodystrophy. *J Clin Endocrinol Metab*. 2008;93:1129–1134.
16. Patni N, Vuitch F, Garg A. Postmortem findings in a young man with congenital generalized lipodystrophy type 4 due to CAVIN1 mutations. *J Clin Endocrinol Metab*. 2019;104:957–960.
17. Agarwal AK, Simha V, Oral SA, et al. Phenotypic and genetic heterogeneity in congenital generalized lipodystrophy. *J Clin Endocrinol Metab*. 2003;88:4840–4847.
18. van de Warrenburg BP, Scheffer H, van Eijk JJ, et al. *BSCL2* mutations in two Dutch families with overlapping Silver syndrome-distal hereditary motor neuropathy. *Neuromuscul Disord*. 2006;16:122–125.
19. Peters JM, Barnes R, Bennett L, et al. Localization of the gene for familial partial lipodystrophy (Dunnigan variety) to chromosome 1q21–22. *Nat Genet*. 1998;18:292–295.
20. Hegele RA, Cao H, Huff MW, Anderson CM. LMNA R482Q mutation in partial lipodystrophy associated with reduced plasma leptin concentration. *J Clin Endocrinol Metab*. 2000;855:3089–3093.
21. Vigouroux C, Guénantin AC, Vatier C, et al. Lipodystrophic syndromes due to LMNA mutations: recent developments on biomolecular aspects, pathophysiological hypotheses and therapeutic perspectives. *Nucleus*. 2018;9:235–248.
22. Garg A, Vinaitheerthan M, Weatherall PT, Bowcock AM. Phenotypic heterogeneity in patients with familial partial lipodystrophy (Dunnigan variety) related to the site of missense mutations in lamin A/C gene. *J Clin Endocrinol Metab*. 2001;86:59–65.
23. Agarwal AK, Garg A. A novel heterozygous mutation in peroxisome proliferator-activated receptor-gamma gene in a patient with familial partial lipodystrophy. *J Clin Endocrinol Metab*. 2002;87:408–411.
24. Gandotra S, Le Dour C, Bottomley W, et al. Perilipin deficiency and autosomal dominant partial lipodystrophy. *N Engl J Med*. 2011;364:740–748.
25. Kozusko K, Tsang V, Bottomley W, et al. Clinical and molecular characterization of a novel PLIN1 frameshift mutation identified in patients with familial partial lipodystrophy. *Diabetes*. 2015;69:299–310.
26. Rubio-Cabezas O, Puri V, Murano I, et al. Partial lipodystrophy and insulin resistant diabetes in a patient with a homozygous nonsense mutation in CIDEC. *EMBO Mol Med*. 2009;1:280–287.
27. Agarwal AK, Fryns JP, Auchus RJ, Garg A. Zinc metalloproteinase, ZMPSTE24, is mutated in mandibuloacral dysplasia. *Hum Mol Genet*. 2003;12:1995–2001.
28. Corvillo F, Akinci B. An overview of lipodystrophy and the role of the complement system. *Mol Immunol*. 2019;112:223–232.
29. Misra A, Garg A. Clinical features and metabolic derangements in acquired generalized lipodystrophy: case reports and review of the literature. *Medicine (Baltimore)*. 2003;82:129–146.
30. Hubler A, Abendroth K, Keiner T, et al. Dysregulation of insulin like growth factors in a class of generalized acquired lipoatrophic diabetes mellitus (Lawrence syndrome) connected with autoantibodies against adipocyte membranes. *Exp Clin Endocrinol Diabetes*. 1998;106:79–84.
31. Corvillo F, Aparicio V, López-Lera A, et al. Autoantibodies against perilipin 1 as a cause of acquired generalized lipodystrophy. *Front Immunol*. 2018;199:2142.
32. Halpern B, Nery M, Pereira MAA. Case report of acquired generalized lipodystrophy associated with common variable immunodeficiency. *J Clin Endocrinol Metab*. 2018;103:2807–2810.
33. Gao J, Li Y, Fu X, Luo X. A Chinese patient with acquired partial lipodystrophy caused by a novel mutation with LMNB2 gene. *J Pediatr Endocrinol Metab*. 2012;25:375–377.
34. Nguyen AL, Morren M, van Doorn R. Severe lipodystrophy following prolonged subcutaneous administration of antisense oligonucleotides. *JAMA Dermatol*. 2019;155:1084–1086.
35. Raile K, Noelle V, Landgraf R, Schwarz HP. Insulin antibodies are associated with lipoatrophy but also with lipohypertrophy in children and adolescents with type 1 diabetes. *Exp Clin Endocrinol Diabetes*. 2001;109:393–396.
36. Gómez-Espejo C, Pérez-Bernal A, Camacho-Martínez F. A new case of semicircular lipoatrophy associated with repeated external microtraumas and review of the literature. *J Eur Acad Dermatol Venereol*. 2005;19:459–461.
37. Becker C, Barbulescu K, Hildner K, et al. Activation and methotrexate-mediated suppression of the TNF alpha promoter in T cells and macrophages. *Ann N Y Acad Sci*. 1998;859:311–314.
38. Dahl PR, Zalla MJ, Winkelmann RK. Localized involutional lipoatrophy: a clinicopathologic study of 16 patients. *J Am Acad Dermatol*. 1996;35:523–528.
39. Okita H, Ohtsuka T, Yamakage A, Yamazaki S. Lipodystrophia centrifugalis abdominalis infantilis – immunohistochemical demonstration of an apoptotic process in the degenerating fatty tissue. *Dermatology*. 2000;201:370–372.
40. Hussain I, Patni N, Garg A. Lipodystrophies, dyslipidaemias and atherosclerotic cardiovascular disease. *Pathology*. 2019;51:202–212.
41. Zou W, Rohatgi N, Brestoff JR, et al. Congenital lipodystrophy induces severe osteosclerosis. *PLoS Genet*. 2019;15e1008244.
42. Lima JG, Nobrega LHC, Lima NN, et al. Causes of death in patients with Berardinelli-Seip congenital generalized lipodystrophy. *PLoS One*. 2018;8:13. e0199052.
43. Chait A, Eckel RH. The chylomicronemia syndrome is most often multifactorial: a narrative review of causes and treatment. *Ann Intern Med*. 2019;170:626–34..
44. Cardis MA, Montealegre Sanchez GA, Goldbach-Mansky R, et al. Recurrent fevers, progressive lipodystrophy, and annular plaques in a child. *J Am Acad Dermatol*. 2019;80:291–295.
45. Kanazawa N, Honda-Ozaki F, Saito MK. Induced pluripotent stems cells representing Nakajo-Nishimura syndrome. *Inflamm Regen*. 2019;39:1835–1850.
46. Brehm A, Krüger E. Dysfunction in protein clearance by the proteasome: impact on autoinflammatory diseases. *Semin Immunopathol*. 2015;37:323–333.
47. Torrelo A, Noguera-Morel L, Hernández-Martín A, et al. Recurrent lipoatrophic panniculitis of children. *J Eur Acad Dermatol Venereol*. 2017;31:536–543.
48. Misra A, Peethambaram A, Garg A. Clinical features and metabolic and autoimmune derangements in acquired partial lipodystrophy. Report of 35 cases and review of the literature. *Medicine (Baltimore)*. 2004;83:18–34.
49. Lamam Bennani Z, Boussofara L, Denguezli M, et al. Annular lipoatrophy of the ankles. *Ann Dermatol Venereol*. 2011;138:512–515.
50. Imamura S. Lipodystrophia centrifugalis abdominalis infantilis: statistical analysis of 168 cases. *Pediatr Dermatol*. 2012;29:437–441.
51. Chang SE, Bae GY, Jeong YI, et al. Lipodystrophia centrifugalis abdominalis in Korea. *Pediatr Dermatol*. 2004;21:538–541.
52. Gupta SS, Gupta KS, Gathe SS, et al. Clinical implications of lipohypertrophy among people with type 1 diabetes in India. *Diabetes Technol Ther*. 2018;20:483–491.
53. Peters MS, Winklemann RK. The histopathology of localized lipoatrophy. *Br J Dermatol*. 1986;114:27–36.
54. Camacho D, Pielasinski U, Revelles JM, et al. Diffuse lower limb lipoatrophy. *J Cutan Pathol*. 2011;38:270–274.
55. Altay C, Seçil M, Demir T, et al. Determining residual adipose tissue characteristics with MRI in patients with various subtypes of lipodystrophy. *Diagn Interv Radiol*. 2017;23:428–434.
56. Akinci B, Meral R, Oral EA. Update on therapeutic options in lipodystrophy. *Curr Diab Rep*. 2018;18:139.
57. Brown RJ, Araujo-Vilar D, Cheung PT, et al. The diagnosis and management of lipodystrophy syndromes: a multi-society practice guideline. *J Clin Endocrinol Metab*. 2016;101:4500–4511.
58. Wolfort FG, Cetrulo CL, Nevarre DR. Suction-assisted lipectomy for lipodystrophy syndromes attributed to HIV-protease inhibitor use. *Plast Reconstr Surg*. 1999;104:1814–1820.
59. Binder WJ, Bloom DC. The use of custom-designed midfacial and submalar implants in the treatment of facial wasting syndrome. *Arch Facial Plast Surg*. 2004;6:394–397.
60. Akinci B, Sahinoz M, Oral E, et al. *Lipodystrophy syndromes: presentation and treatment. Endotext [Internet]*. South Dartmouth: MDText.com, Inc; 2000.
61. Macallan DC, Baldwin C, Mandalia S, et al. Treatment of altered body composition in HIV-associated lipodystrophy: comparison of rosiglitazone, pravastatin, and recombinant human growth hormone. *HIV Clin Trials*. 2008;9:254–268.
62. Melvin A, Adams C, Flanagan C, et al. Roux-en-Y gastric bypass surgery in the management of familial partial lipodystrophy type 1. *J Clin Endocrinol Metab*. 2017;102:3616–3620.
63. Brown RJ, Oral EA, Cochran E, et al. Long-term effectiveness and safety of metreleptin in the treatment of patients with generalized lipodystrophy. *Endocrine*. 2018;60:479–489.
64. Shibata Y, Nakatsuka A, Eguchi J, et al. Acquired partial lipoatrophy as graft-versus-host disease and treatment with metreleptin: two case reports. *J Med Case Rep*. 2018;1412:368.
65. Bacchi VF, Maillet F, Berlan L, et al. Neutralising antibodies against C3NeF in intravenous immunoglobulin. *Lancet*. 1992;340:63–64.
66. Grigem S, Fischer-Posovszky P, Debatin KM, et al. The effect of the HIV protease inhibitor ritonavir on proliferation, differentiation, lipogenesis, gene expression and apoptosis of human preadipocytes and adipocytes. *Horm Metab Res*. 2005;37:602–609.
67. Caron M, Auclair M, Lagathu C, et al. The HIV-1 NRTI stavudine and zidovudine alter adipocyte functions *in vitro*. *AIDS*. 2004;18:2127–2136.
68. Brinkman K, Smeitink I, Romijn J, Reiss P. Mitochondrial toxicity induced by NRTI is a key factor in the pathogenesis of ART-related lipodystrophy. *Lancet*. 1999;354:1112–1115.
69. Alikhani A, Morin H, Matte S, et al. Association between lipodystrophy and length of exposure to ARTs in adult HIV-1 infected patients. *BMC Infect Dis*. 2019;1819:820.
70. Miller J, Carr A, Emery S, et al. HIV lipodystrophy: prevalence, severity and correlates of risk in Australia. *HIV Med*. 2003;4:293–301.
71. Lichtenstein KA. Refining lipodystrophy syndrome. *J Acquir Immune Defic Syndr*. 2005;39:395–400.
72. Sax PE, Erlandson KM, Lake JE, et al. Weight gain following initiation of antiretroviral therapy: risk factors in randomized comparative clinical trials. *Clin Infect Dis*. 2020;71:1379–1389.
73. Sweeney LL, Brennan AM, Mantzoros CS. The role of adipokines in relation to HIV lipodystrophy. *AIDS*. 2007;21:895–904.
74. Ranade K, Geese WJ, Noor M, et al. Genetic analysis implicates resistin in HIV lipodystrophy. *AIDS*. 2008;22:1561–1568.
75. Friis-Møller N, Weber R, Reiss P, et al. DAD study group. Cardiovascular disease risk factors in HIV patients – association with antiretroviral therapy. Results from the DAD study. *AIDS*. 2003;17:1179–1193.
76. Haddad N, Vidal-Trecan T, Baroudjian B, et al. Acquired generalized lipodystrophy under immune checkpoint inhibition. *Br J Dermatol*. 2020;182:477–480.
77. Barete S, Mouawad R, Choquet S, et al. Skin manifestations and vascular endothelial growth factor levels in POEMS syndrome: impact of autologous hematopoietic stem cell transplantation. *Arch Dermatol*. 2010;146:615–623.
78. Hosokawa M, Shibata H, Hosokawa T, et al. Acquired partial lipodystrophy with metabolic disease in children following hematopoietic stem cell transplantation: a report of two cases and a review of the literature. *J Pediatr Endocrinol Metab*. 2019;32:537–541.





eFig. 101.1 Congenital generalized lipodystrophy syndrome. **A** Extensive acanthosis nigricans, facial and extremity lipodystrophy, and muscular habitus. **B** Close-up view demonstrating loss of buccal and temporal fat. *Courtesy Kenneth E. Greer, MD.*



eFig. 101.3 Congenital generalized lipodystrophy syndrome (Berardinelli–Seip syndrome). Extensive acanthosis nigricans. *Courtesy Edward Cowen, MD.*



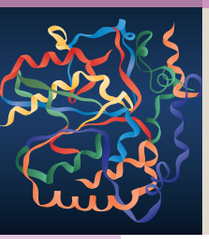
eFig. 101.2 Congenital generalized lipodystrophy (Berardinelli–Seip syndrome). This woman has extensive acanthosis nigricans, well-defined muscles, prominent superficial veins and clitoromegaly. *Courtesy Regional Dermatology Training Centre, Moshi, Tanzania.*



eFig. 101.4 HIV/ART-associated lipodystrophy. The side view highlights the loss of temporal fat. *Courtesy National Skin Centre, Singapore.*



eFig. 101.5 Facial lipoatrophy due to lupus panniculitis. *Courtesy Jeffrey P. Callen, MD.*



102 Vascular Biology

Benedikt Weber, Satoshi Hirakawa and Michael Detmar

Chapter Contents

Structure and Function of Cutaneous Blood Vessels *1790*
Vascular Development *1791*
Structure and Function of the Cutaneous Lymphatic Vascular System *1796*
Angiogenesis- and Lymphangiogenesis-Related Diseases *1798*
Antiangiogenic Therapies *1798*

Key features

- Cutaneous blood vessels and lymphatic vessels play essential roles in skin inflammation, wound healing, and tumor progression
- Vascular endothelial growth factor-A (VEGF-A) and placental growth factor (PlGF) are major skin angiogenesis factors
- The expression of VEGF and PlGF by keratinocytes is upregulated in psoriasis, healing wounds, and cutaneous squamous cell carcinomas
- VEGF-C and VEGF-D induce skin lymphangiogenesis via interaction with VEGF receptor-3 on lymphatic endothelium
- Mutations in several genes including *FLT4*, which encodes VEGF receptor-3, have been identified in congenital lymphedema
- Therapeutic modulation of angiogenesis is of increasing interest for anti-cancer, anti-inflammatory, and chronic wound therapies

STRUCTURE AND FUNCTION OF CUTANEOUS BLOOD VESSELS

Blood vessels are essential for supplying sufficient oxygen and nutrients, maintaining normal tissue homeostasis and function, and meeting the increased nutritional needs in various pathologic conditions. Blood flows from arteries and arterioles through capillary loops to postcapillary venules and veins. For practical and didactic purposes, the vascular system of the skin has been divided into a superficial and a deep vascular plexus (Fig. 102.1), with additional vascular networks surrounding sweat glands and hair follicles.

The architecture of the cutaneous vascular system varies in different areas of the body. In the presence of pronounced epidermal rete ridges, such as in the skin overlying the extensor aspects of the joints or on the palms and soles, straight capillary loops extend into the elongated dermal papillae. In contrast, rete ridge formation and papillary loop formation are less pronounced in sites such as abdominal skin. The shape of the papillary microvessels reflects the three-dimensional architecture of the epidermal rete ridges, typically with one or two loops within each dermal papilla[1]. The inner diameter of papillary blood vessels averages between 5 and 10 microns. In contrast to the idealized architectural model of the cutaneous vascular system, vascular perfusion studies (Fig. 102.2) and light-sheet fluorescence microscopy studies (Fig. 102.3) revealed a rather continuous, sometimes irregular meshwork of interconnecting cutaneous blood vessels. Consistently, blood vessels are found immediately below the non-vascularized epidermis.

Anagen hair follicles are highly vascularized. The often single blood vessel within the mesenchymal hair papilla is derived from the lower vascular plexus, whereas the dense vascular network surrounding the hair follicle is predominantly derived from the upper vascular plexus (Fig. 102.4). The relatively small blood vessels found in the telogen resting phase elongate and enlarge during the anagen growth phase and then extend towards the subcutis together with the growing hair follicle[2]. In the catagen phase, hair follicle involution is associated with regression of perifollicular blood vessels and with increased rates of endothelial cell apoptosis. The extent of perifollicular vascularization may directly influence the size of the hair follicles[2].

The cutaneous vasculature also plays a systemic role in regulating body temperature and blood pressure. Arterioles have precapillary muscular sphincters that, upon contraction, shunt the blood via arteriovenous anastomoses directly to venules, thereby bypassing the capillary networks. Arteriovenous anastomoses are frequently found in the fingertips, where they form the glomi or glomus bodies[1]. Glomi have autonomous innervation and control peripheral blood flow via modulation of their muscular contraction levels.

In the extremities, venous blood vessels have valves that consist of thin, half-moon-shaped folds composed primarily of collagen and covered on both sides by endothelium. These valves are required for the efficient return of blood proximally and ensure unidirectional flow. Initially, it was thought that venous valves were limited to larger veins. However, a series of investigations revealed that (micro)valves are also present in small postcapillary venous networks in the skin, down to a vessel diameter of just less than 100 microns. These valves prevent venous reflux from postcapillary venules into the capillary bed and arteriovenous anastomoses[3].

All blood vessels contain a continuous inner monolayer of flat endothelial cells that are surrounded, on the external side, by a continuous basement membrane. Smaller vessels have a second, sometimes discontinuous, layer of perivascular cells called pericytes, which are surrounded

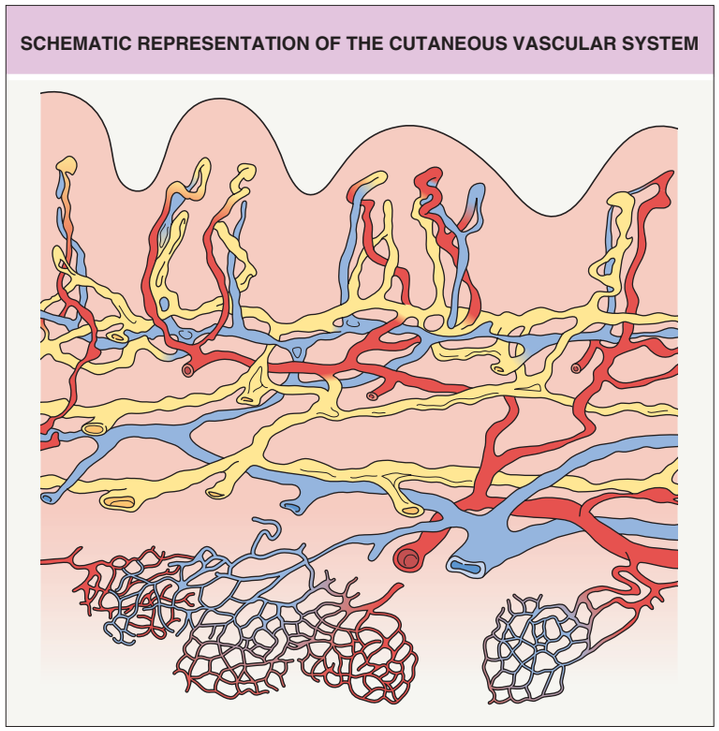


Fig. 102.1 Schematic representation of the cutaneous vascular system. The superficial vascular plexus feeds vessels in the dermal papillae; arteries (red) and veins (blue) are closely associated with lymphatic vessels (yellow). The capillary networks of the subcutaneous adipose tissue are depicted at the base of the schematic.

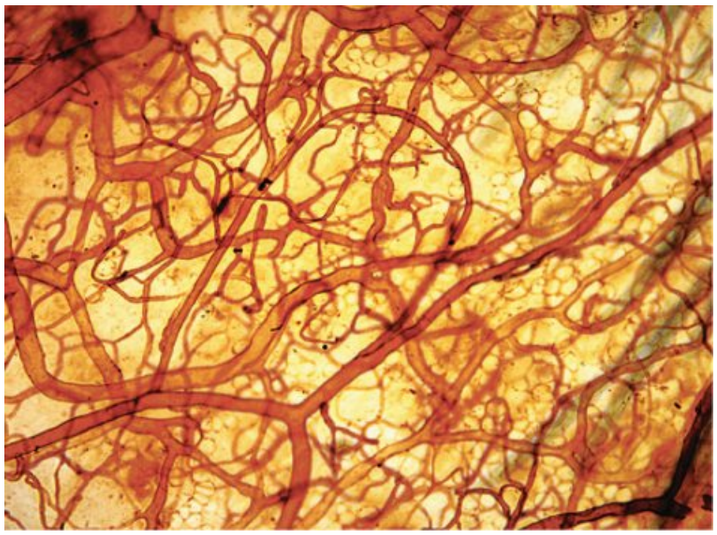


Fig. 102.2 Intravascular perfusion of murine skin with the lectin *Lycopersicon esculentum*. The perfusion highlights dense irregular vascular networks.

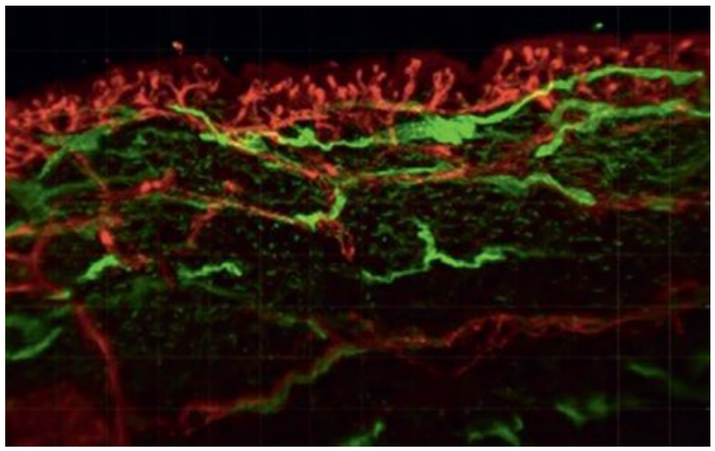


Fig. 102.3 Light-sheet fluorescent microscopy depicting distinct staining of cutaneous blood vessels and lymphatic vessels in human skin. The blood vessels stain positively for von Willebrand factor (red) while the lymphatic vessels stain positively for LYVE-1 (green). Multiple capillary loops are seen in the dermal papillae (top).

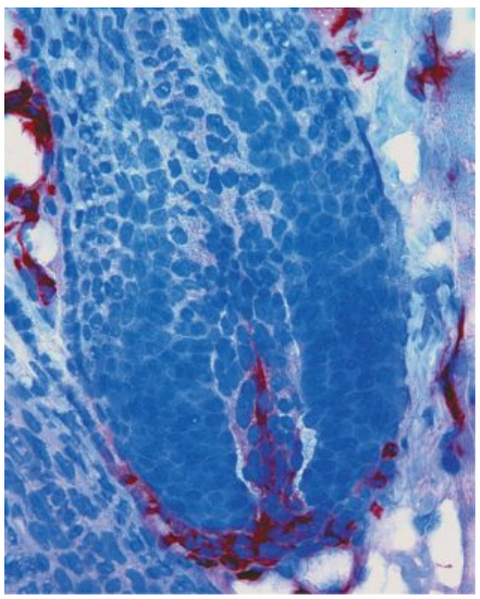


Fig. 102.4 Blood supply of the hair follicle. A single vascular loop extends into the dermal papilla of the hair follicle, while a mesh of blood vessels surrounds the anagen hair follicle (CD31 immunohistochemical stain).

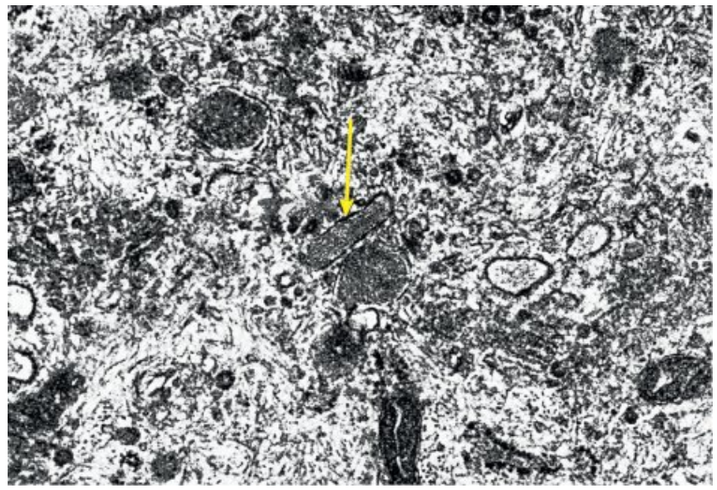


Fig. 102.5 Ultrastructural visualization of a rod-shaped Weibel–Palade body (WPB; arrow) within the cytoplasm of a human endothelial cell.

by a basement membrane that is continuous with the endothelial basement membrane. Pericytes play an important role in maintaining mature blood vessels, and detachment of pericytes from endothelial cells is an early event during sprouting angiogenesis (outgrowth of new capillaries from pre-existing blood vessels). Pericytes also surround arterioles and venules, and they can be visualized by staining for platelet-derived growth factor receptor-β (PDGFR-β), NG2 (chondroitin sulfate proteoglycan 4), α-smooth muscle actin, and desmin. The walls of most arterioles, larger venules, and veins contain contractile smooth muscle cells surrounded by a basement membrane. Vascular basement membranes contain collagen types IV, XV and XVIII, laminin, fibronectin, and other extracellular matrix proteins (see Ch. 95).

At the ultrastructural level, endothelial cells are characterized by tight junctions between adjacent cells and by specialized organelles, the rod-shaped Weibel–Palade bodies (Fig. 102.5). These Weibel–Palade bodies are storage organelles for the coagulation factor von Willebrand factor (also known as factor VIII-related antigen); they also contain P-selectin, angiopoietin-2, and endothelin-1. Activation of endothelial cells by proinflammatory cytokines or pro-angiogenic factors leads to translocation of Weibel–Palade bodies to the cell membrane, with consecutive enhanced membrane expression of P-selectin and release of von Willebrand factor. Other characteristic ultrastructural features include caveolae (minute invaginations of the membrane surface), pinocytotic vesicles, and the formation of vesiculo-vacuolar organelles (VVOs)[4]. Circulating macromolecules cross the endothelium through interendothelial cell gaps and transendothelial cell pores, some of which arise from VVOs. Endothelial cell fenestrations, areas with direct apposition of the endothelial cell membranes without intervening cytoplasm, are rarely seen in normal skin except in angiogenic perifollicular blood vessels during the growth phase of the hair follicle. However, fenestrated endothelial cells are frequently seen in skin diseases with pronounced angiogenesis and vascular hyperpermeability, including psoriasis.

Several markers are utilized for immunohistochemical staining of blood vascular endothelial cells (Table 102.1). In normal human skin, the most specific markers for cutaneous *blood vessels* appear to be von Willebrand factor (see Fig. 102.3), CD34, and PV-1 (plasmalemma vesicle-associated protein-1); the latter is recognized by the PAL-E (Pathologische Anatomie Leiden-Endothelium) antibody. Double immunofluorescence stains for the pan-endothelial cell marker CD31 (PECAM-1) plus the lymphatic vessel endothelial hyaluronan receptor-1 (LYVE-1) or the glycoprotein podoplanin (recognized by the widely used D2-40 antibody) also allow for the selective visualization of LYVE-1-negative (or podoplanin-negative), CD31-positive blood vessels in the skin. As a result, blood vessels can be distinguished from lymphatic vessels (see Fig. 102.15).

VASCULAR DEVELOPMENT

During embryogenesis, the first blood vessels are formed through *vasculogenesis*, defined as the differentiation of undifferentiated angioblasts into endothelial cells that form a primitive vascular network.

IMMUNOHISTOCHEMICAL MARKERS FOR LYMPHATICS AND FOR BLOOD VESSELS		
Marker	**Lymphatics**	**Blood vessels**
CD31 (PECAM-1)	+	++
CD34	–	++
von Willebrand factor	–	+
PV-1 (PAL-E antibody)	–	+
VEGFR-3	+	–
Podoplanin (D2-40 antibody)	++	–
LYVE-1	++	–
Prox1	++	–

Table 102.1 Immunohistochemical markers for lymphatics and for blood vessels. The medium shading and the dark shading highlight markers that distinguish blood vessels and lymphatics, respectively. LYVE-1, lymphatic vessel endothelial hyaluronan receptor-1; PAL-E, Pathologische Anatomie Leiden-Endothelium; PECAM-1, platelet-endothelial cell adhesion molecule-1; Prox1, prospero-related homeobox 1; PV-1, plasmalemma vesicle-associated protein-1; VEGFR, vascular endothelial growth factor receptor.

Angioblasts originate from blood islands in the extraembryonic mesoderm of the yolk sac. Blood islands are clusters of epithelioid cells; the outer cells differentiate into angioblasts, whereas the inner cells differentiate into primitive hematopoietic cells, suggesting that both cell types originate from a common embryonic precursor cell, the hemangioblast[5] (Fig. 102.6). Hemangioblasts are derived from earlier precursor cells under the influence of fibroblast growth factors (FGFs), and they already express the high-affinity receptor for vascular endothelial growth factor-A (VEGF-A) – vascular endothelial growth factor receptor-2 (VEGFR-2; KDR [human]; Flk-1 [murine]).

Angioblasts develop under the influence of stimulation by VEGF-A and express several vascular endothelial cell markers, including the Tie-1 and Tie-2 receptors, vascular endothelial (VE)-cadherin, and the high-affinity VEGF receptors 1 (Flt-1), 2 (KDR), and 3 (Flt-4). Within the embryo, angioblasts that appear along the anterior intestinal portal and the lateral edges of the somites coalesce to form the dorsal aorta and the large vessel primordia of the body. Angioblasts are highly migratory "prevascular" endothelial cells and are found throughout the embryo with the exception of tissues such as cartilage and epithelia.

When angioblasts form a lumen, they become endothelial cells with a polarized phenotype and production of a basal lamina. Interaction of integrin receptors on the endothelial surface with the basement membrane is critical for the formation of the primordial vascular plexus, while vascular endothelial (VE)-cadherin is required for the formation of interendothelial adherence junctions. The early vascular system consists of sinusoidal capillaries arranged in a polygonal honeycomb pattern (see Fig. 102.6). This primordial vascular plexus then becomes surrounded by mesenchymal cells that give rise to pericytes and vascular smooth muscle cells. In a next step, profound remodeling of the primordial vascular plexus takes place under the influence of VEGF-A, angiopoietins, and ephrins (see below). Remodeling involves both the formation and regression of blood vessels as well as apoptosis of vascular endothelial cells.

Angiogenesis, the sprouting of new blood vessels from existing primordial vessels, represents the major mechanism for new blood vessel formation[6]. During this process, specialized endothelial cells, so-called tip cells, extend filopodia and sense the environment for guidance cues such as VEGF-A (Fig. 102.7). Tip cells are followed by stalk cells which extend the sprout by proliferation and form a lumen[6,7]. Tip cells can connect with neighboring tip cells to form new vascular branches[8]. The specification of tip and stalk cells is regulated by Notch signaling. Activation of VEGFR-2 on tip cells by VEGF-A results in increased expression of the Notch ligand Delta-like 4 (Dll4), which binds to Notch expressed on neighboring stalk cells. Notch signaling in stalk cells leads to reduced VEGFR-2 expression, rendering these cells less responsive to VEGF-A (see Fig. 102.7). This is a highly dynamic process in which endothelial cells compete for the tip cell position[6,7]. In addition, glycolysis plays a vital role in the regulation of vascular sprouting, in parallel with genetic cues[9].

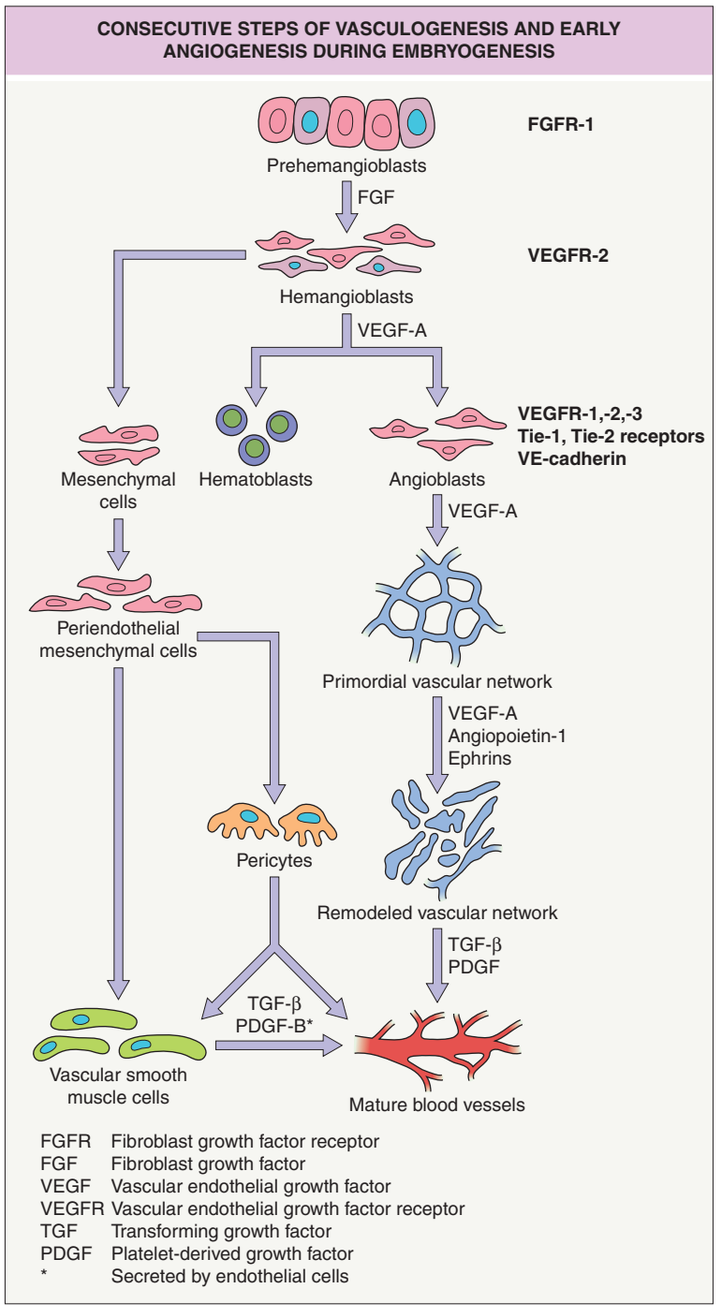


Fig. 102.6 Consecutive steps of vasculogenesis and early angiogenesis during embryogenesis: formation and remodeling of primordial vascular networks.

The Tie-2 receptor tyrosine kinase present on endothelial cells also plays a crucial role in vascular sprouting and remodeling during early embryonic angiogenesis. Pericyte-derived angiopoietin-1 (Ang-1) activates the Tie-2 receptor, whereas Ang-2 can act as an inhibitor of Ang-1 under angiogenic conditions (Fig. 102.8). In addition, Eph–ephrin receptor interactions, via bidirectional signaling, play an important role in vascular remodeling and in the determination of vascular identity. Ephrin B2 is specifically expressed by arterial endothelium, whereas its receptor, Eph-B4, is expressed by venous endothelium. Both molecules are involved in the definition of boundaries between arterial and venous endothelial cells.

Additional molecules are involved in the control of embryonic angiogenesis and vascular remodeling, including semaphorins, transforming growth factor-β (TGF-β), endoglin (the low-affinity receptor for TGF-β), and activin receptor-like kinase-1. Dysfunction of the latter two proteins is seen in hereditary hemorrhagic telangiectasia (see below). Platelet-derived growth factor subunit B (PDGF-B), secreted by endothelial cells, plays a critical role in the recruitment and differentiation of pericytes and periendothelial smooth muscle cells that contribute to the stability of mature blood vessels[6].

Regulation of Skin Angiogenesis

Angiogenesis is a common feature of developing skin during embryogenesis. In contrast, the blood vessels in healthy adult skin are predominantly quiescent, except for the expansion and involution of perifollicular blood vessels during the hair cycle[2]. However, adult skin retains the capacity for brisk initiation of angiogenesis in the setting of wound healing, inflammation, and neoplastic growth. Angiogenesis occurs as: (1) the sprouting outgrowth of new capillaries from pre-existing postcapillary venules; or (2) non-sprouting remodeling of pre-existing blood vessels either through circumferential growth/vascular enlargement or through the formation of intravascular endothelial cell pillars (intussusception). Angiogenesis is a multistep process that often involves as a first step the induction of microvascular hyperpermeability, i.e. increased vascular leakage, leading to extravasation of plasma proteins such as fibrinogen and prothrombin (Table 102.2). Fibrinogen is then further processed to fibrin and serves as a provisional matrix for migrating endothelial cells, whereas the generation of thrombin acts as an initiator of the extrinsic coagulation cascade, leading to cleavage and activation of several matrix proteins[10]. Together, these processes lead to the generation of a highly angiogenic stroma.

A major function of pericytes appears to be the maintenance of mature and quiescent blood vessels (a function which is interrupted during angiogenesis). In normal adult skin, pericytes secrete Ang-1, which leads to phosphorylation of the Tie-2 receptor (a receptor exclusively expressed on endothelial cells) and maintenance of the mature vascular architecture with low vascular permeability (see Fig. 102.8). In turn, endothelial cells secrete growth factors that mediate the recruitment of pericytes, including PDGFB that binds to the PDGFR-β on pericytes. During angiogenesis, endothelial cells express high amounts of Ang-2, a functional antagonist of Ang-1 in activated endothelium, thereby blocking the maturation-inducing effect of Ang-1 and leading to detachment of pericytes from vascular endothelial cells[11]. In the presence of VEGF-A, endothelial cells then undergo the consecutive steps of angiogenesis, whereas in the absence of VEGF-A, vascular endothelial cells undergo apoptosis (see Fig. 102.8). Both VEGF-A and Ang-2 expression are upregulated in angiogenic skin diseases, including psoriasis, and keratinocyte-derived VEGF-A and placental growth factor (PlGF; see below) both potently induce the expression of Ang-2 in dermal microvascular endothelial cells. Bone marrow-derived progenitor cells also contribute to the angiogenic response, with most of these cells differentiating into perivascular macrophages that secrete angiogenic factors, including VEGF-A.

The vascular basement membrane serves as a natural barrier that prevents sprouting of endothelial cells from quiescent vessels, with pericytes assisting in the maintenance of the quiescent state. An early step in the angiogenic response involves the degradation of vascular basement membrane components such as collagen type IV by the concerted action of activated proteases, including matrix metalloproteinase (MMP)-2 and MMP-9[7]. Integrin receptors on the surface of activated endothelial cells, in particular the $\alpha_1\beta_1$, $\alpha_2\beta_1$, and $\alpha_v\beta_3$ integrins, then interact with either native or degraded matrix molecules (e.g. collagen type I, fibronectin) to facilitate endothelial cell migration[12]. The migration of endothelial cells is directed towards a gradient of angiogenesis factors that are usually produced by the epidermis, but may also be secreted by macrophages and other stromal cells. Endothelial cells then undergo a series of cell divisions, promoted by potent angiogenesis factors such as VEGF-A and basic fibroblast growth factor (bFGF). Finally, the endothelial cells form vascular lumina and mature new blood vessels with basement membranes and pericytes.

In normal skin, vascular quiescence is maintained by the dominant influence of potent endogenous angiogenesis inhibitors over angiogenic stimuli. Angiogenesis is induced by increased secretion of angiogenic

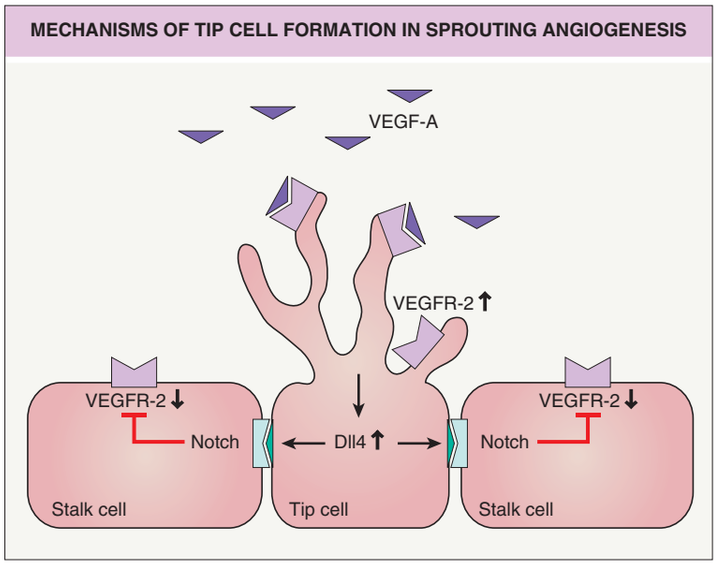


Fig. 102.7 Mechanisms of tip cell formation in sprouting angiogenesis. Activation of VEGFR-2 by VEGF-A in vascular tip cells promotes filopodia formation and increased expression of the Notch ligand Delta-like 4 (Dll4). Dll4 activates Notch signaling in neighboring stalk cells, leading to reduced VEGFR-2 expression and diminished sensitivity to VEGF-A.

THE STEPWISE INDUCTION OF ANGIOGENESIS
1. Induction of microvascular hyperpermeability
2. Enzymatic degradation of vascular basement membrane and interstitial matrix
3. Endothelial cell migration
4. Endothelial cell proliferation
5. Formation of mature blood vessels

Table 102.2 The stepwise induction of angiogenesis.

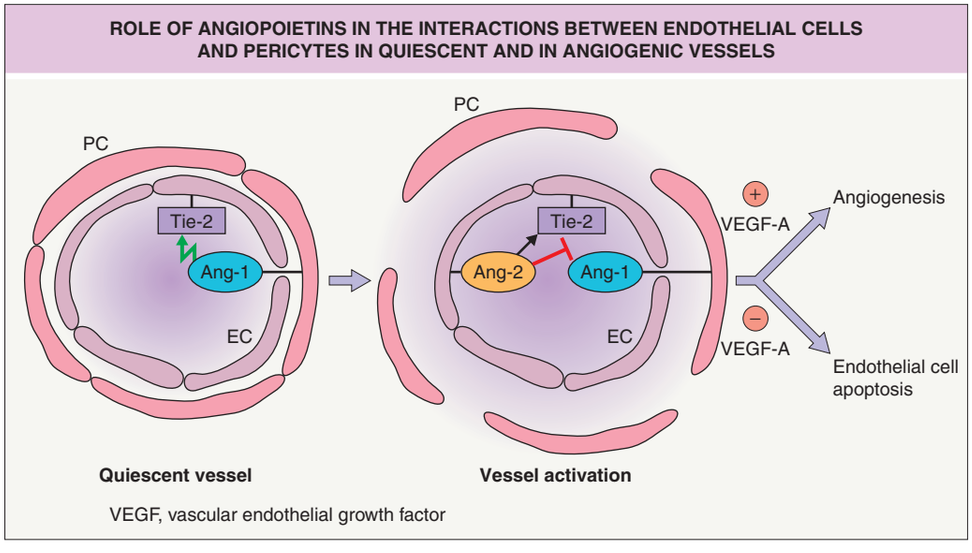


Fig. 102.8 Role of angiopoietins in the interactions between endothelial cells and pericytes in quiescent and in angiogenic vessels. Activation of the endothelial Tie-2 receptor by pericyte (PC)-derived angiopoietin-1 (Ang-1) maintains vessel maturation. Upregulation of angiopoietin-2 (Ang-2) in angiogenic endothelial cells (EC) blocks the vessel-stabilizing effect of pericyte-derived Ang-1 via the endothelial Tie-2 receptor. Both VEGF-A and Ang-2 expression are upregulated in angiogenic skin diseases, including psoriasis.

factors and/or by downregulation of angiogenesis inhibitors. The major skin angiogenesis factor, VEGF-A, was originally discovered as vascular permeability factor (VPF) due to the activity of tumor cell-conditioned media to induce accumulation of ascites fluid[13]. VEGF-A is a homodimeric, heparin-binding glycoprotein with at least four isoforms of 121, 165, 189, and 201 amino acids (due to alternative splicing) found in human skin. VEGF-A binds to two type III tyrosine kinase receptors that are expressed predominantly on vascular endothelial cells: Flt-1/VEGF receptor-1 (VEGFR-1) and KDR/Flk-1/VEGFR-2 (Fig. 102.9). In addition, VEGF-A165 also binds to the neuropilin-1 receptor on endothelial and other cells.

In vitro, VEGF-A acts as a specific mitogen for human dermal microvascular endothelial cells and induces endothelial cell migration. *In vivo*, VEGF-A enhances microvascular permeability and angiogenesis. VEGF-A is expressed at low levels in normal epidermis, whereas in healing wounds and in skin diseases associated with angiogenesis and vascular hyperpermeability, particularly psoriasis, VEGF-A expression by epidermal keratinocytes is markedly increased[14]. The expression and biologic activity of VEGF-A are controlled by several distinct molecular mechanisms. Hypoxia results in transcriptional activation (via hypoxia-inducible factors) and stabilization of VEGF-A mRNA. In the skin, hypoxia leads to upregulation of VEGF-A expression by epidermal keratinocytes, dermal fibroblasts, and dermal endothelial cells. This mechanism is likely important for the induction of epidermal VEGF-A expression during wound healing and in hypoxic areas of skin cancers.

Keratinocyte VEGF-A expression is also induced by growth factors that mediate epidermal hyperplasia. In psoriasis, healing wounds, and squamous cell carcinomas (SCCs), TGF-α and other ligands of the epidermal growth factor receptor (EGFR) are released by suprabasal keratinocytes. In an autocrine loop, these growth factors induce hyperplasia of the epidermis. Simultaneously, they induce VEGF-A gene expression and protein secretion by epidermal keratinocytes, which leads to paracrine induction of angiogenesis via interaction with VEGF receptors on cutaneous microvessels (see Fig. 102.9). This mechanism links epidermal hyperplasia with increased vascularization, thereby providing enhanced vascular support to meet the enhanced nutritional needs of proliferating keratinocytes[14]. Several other growth factors that stimulate keratinocyte proliferation, including keratinocyte growth factor (KGF), bFGF, and hepatocyte growth factor (HGF), can also promote VEGF-A production by epidermal keratinocytes.

The biologic importance of epidermis-derived VEGF-A for cutaneous angiogenesis *in vivo* has been confirmed in genetic mouse models designed to have overexpression of VEGF-A in epidermal keratinocytes. VEGF-A transgenic mice are characterized by elongated and tortuous dermal blood vessels that are hyperpermeable to circulating plasma proteins. These mice are unable to downregulate experimentally induced cutaneous inflammation and develop chronic inflammatory skin lesions that closely resemble those of human psoriasis[15]. Many human cancers are characterized by increased expression of VEGF-A by tumor cells and by increased expression of VEGF receptors by tumor-associated blood vessels. VEGF-A also promotes skin carcinogenesis, in that selective transgenic overexpression of VEGF-A in epidermal keratinocytes resulted in enhanced tumor development and metastasis[16].

Placental growth factor (PlGF) is a member of the VEGF family and two isoforms, PlGF-1 (149 amino acids) and PlGF-2 (170 amino acids), are expressed in human skin. Similar to VEGF-A, PlGF expression is upregulated in cutaneous SCCs, epidermal keratinocytes at the advancing wound edge, and hyperplastic psoriatic epidermis. In contrast to VEGF, PlGF does not activate VEGFR-2 (KDR) but selectively binds to VEGFR-1 (see Fig. 102.9). In addition, the heparin-binding isoform PlGF-2 binds to the neuropilin-1 receptor. Evidence from genetic mouse models indicates that PlGF and VEGF-A act in synergy to induce both angiogenesis and vascular leakage and that PlGF exerts proinflammatory effects[17]. A number of additional pro-angiogenic molecules are upregulated in angiogenic skin conditions, including interleukin-8, PDGF, bFGF, and several angiogenic chemokines[18].

Thrombospondin (TSP)-1 and TSP-2 are major inhibitors of cutaneous angiogenesis that are expressed in normal human skin. These matricellular proteins mediate interactions between extracellular matrix molecules and cellular integrin receptors. TSP-1 inhibits endothelial cell proliferation *in vitro* and angiogenesis *in vivo*. In normal human skin, TSP-1 is expressed by dermal cells and by epidermal keratinocytes. It is deposited within the dermal–epidermal basement membrane zone, contributing to the barrier that prevents ingrowth of blood vessels into the epidermis. TSP-1 expression is downregulated in cutaneous SCCs, and reintroduction of *TSP-1* into SCCs inhibits tumor growth in mice, in association with inhibition of tumor angiogenesis and enhanced tumor cell death[19]. Overexpression of TSP-1 in the skin of transgenic mice results in impaired granulation tissue formation and wound vascularization, delayed and reduced skin carcinogenesis, and diminished photodamage from chronic UVB irradiation. Interestingly, UVB irradiation of human skin results in an angiogenic switch with upregulation of VEGF-A and downregulation of TSP-1[20]. The mechanisms by which TSP-1 inhibits skin angiogenesis include the induction of endothelial cell apoptosis through specific interactions with the endothelial CD36 receptor, the activation of latent TGF-β, and the inhibition of matrix metalloproteinase activity.

TSP-2 also acts as an endogenous inhibitor of angiogenesis. Mice deficient in TSP-2 show increased skin vascularization, enhanced and prolonged inflammatory reactions, and increased skin carcinogenesis, confirming the important role of endogenous TSP-2 in controlling skin angiogenesis. Accordingly, targeted overexpression of TSP-2 within murine epidermis protects from skin cancer development and inhibits the growth of established skin cancers[21]. Antiangiogenic activity has also been reported for several cleavage products of molecules that are expressed in the vascular basement membrane, including fragments of collagens type IV (tumstatin), XV, and XVIII (endostatin).

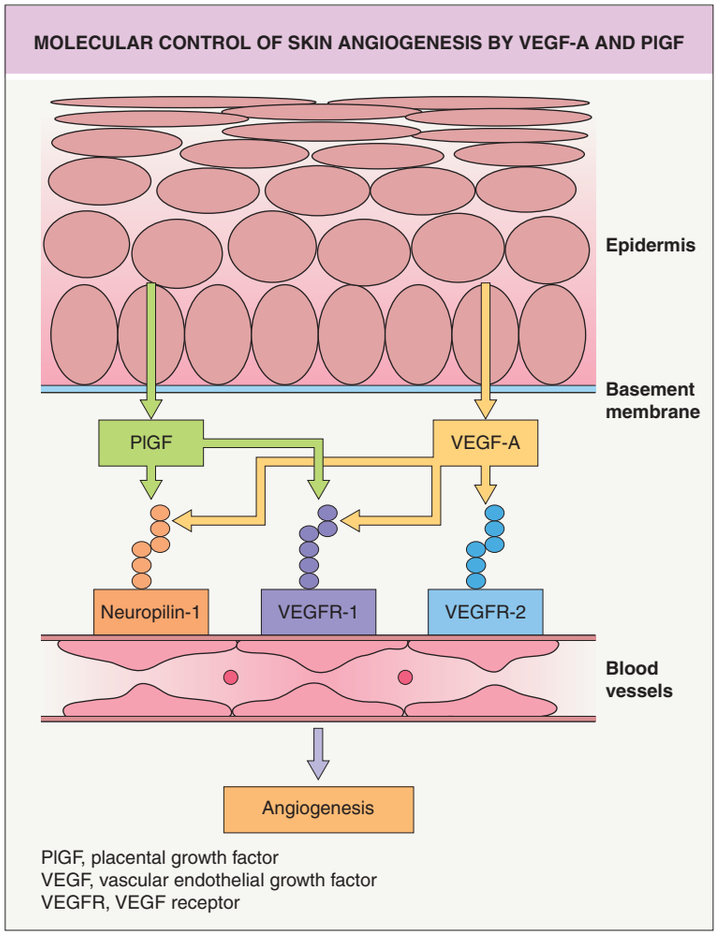


Fig. 102.9 Molecular control of skin angiogenesis by vascular endothelial growth factor-A (VEGF-A) and placental growth factor (PlGF).

Angiogenesis and Wound Healing

Capillary growth from pre-existing vasculature is an essential component of the proliferative phase of cutaneous wound healing (see Fig. 141.3). After exposure to thrombin, endothelial cells release matrix metalloproteinase-2 (gelatinase-A), which causes local dissolution of the basement membrane and extracellular matrix (ECM), allowing endothelial cells

to migrate through the basement membrane. Capillary sprouts then invade the ECM and the fibrin clot in the wound bed, and within a few days, a new stroma forms. This so-called granulation tissue is characterized by the proliferation of blood vessels, fibroblast migration, and collagen synthesis. In this neostroma, the angiogenic sprouts organize into a dense microvascular network, thereby supporting cells with nutrition and oxygen.

The process of vascular sprouting within the premature wound matrix is controlled by several factors including hypoxia (due to microvascular damage) as well as various growth factors and cytokines released from platelets or produced by neutrophils, macrophages, fibroblasts, and keratinocytes during the inflammatory stage of wound healing (Fig. 102.10)[22]. The low oxygen gradient between injured and healthy tissues induces the transcriptional activator hypoxia-inducible factor-1 (HIF-1) which promotes angiogenesis via multiple mechanisms. The latter include: (1) upregulation of a large number of proangiogenic target genes; and (2) production of pro-angiogenic growth factors such as VEGF-A and stromal cell derived factor-1 (SDF-1 or CXCL12; see Fig. 102.10). In addition to hypoxia, cellular disruption also initiates angiogenesis via release of fibroblast growth factors (FGF-1/2). Endothelial progenitor cells are also recruited to the wound site, where they differentiate into mature endothelial cells.

During these initial phases of wound healing, the pro-angiogenic environment creates an immature microvascular network characterized by high vessel tortuosity, often resulting in dead-end flow pathways. The newly formed microvascular network has a density of blood vessels that exceeds that of normal skin. However, after this maximum density of blood vessels during the initial phases, microvascular regression is observed due to the release of several antiangiogenic factors including pigment epithelium-derived factor (PEDF), IFN-γ-inducible protein-10 (CXCL10), or Sprouty-2[23].

At the same time, vascular interstitial cells, including smooth muscle cells and pericytes, stabilize the newly formed microvascular capillaries. The major growth factor that supports the stabilization of this new vascular network is PDGF-B which stimulates pericyte differentiation and has been used therapeutically in the treatment of diabetic wounds. Furthermore, the angiopoietins Ang-1 and Ang-2, together with their receptor Tie-2, regulate the angiogenic response throughout cutaneous wound healing. Additional soluble factors that have been reported to be involved in the orchestration of the angiogenic phase of cutaneous wound repair are depicted in Fig. 102.10. Defects in cutaneous angiogenesis impair the formation of granulation tissue and delay healing, leading to the development of a non-healing environment in several types of chronic cutaneous wounds[24].

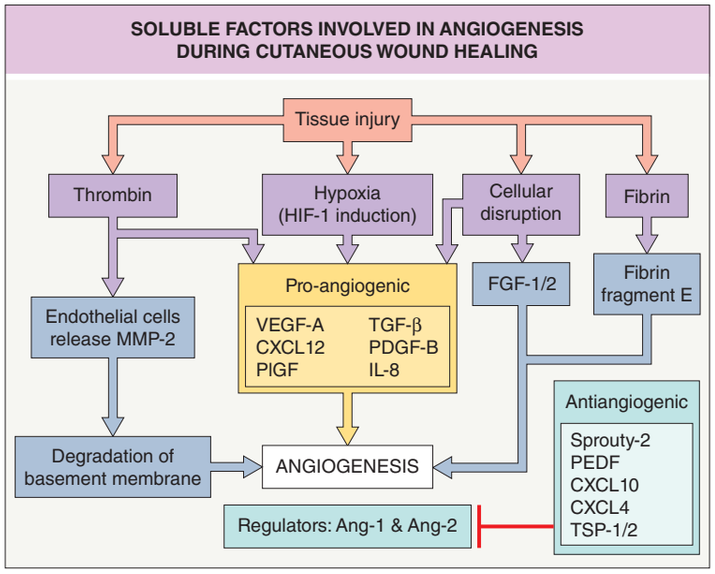


Fig. 102.10 Soluble factors involved in angiogenesis during cutaneous wound healing. Following tissue injury, multiple pro-angiogenic as well as antiangiogenic factors modulate cutaneous wound healing. Ang-1/2, angiopoietin-1/2; CXCL4/10/12, C-X-C motif chemokine ligand 4/10/12; FGF-1/2, fibroblast growth factor-1/2; HIF-1, hypoxia-inducible factor-1; IL-8, interleukin-8; MMP-2, matrix metalloproteinase-2; PEDF, pigment epithelium-derived factor; PlGF, placental growth factor; PDGF-B, platelet-derived growth factor-B; TSP-1/2, thrombospondin-1/2; TGF-β, transforming growth factor-β; VEGF-A, vascular endothelial growth factor A. Stromal cell derived factor-1 (SDF-1) is also known as CXCL12.

Regulation of Leukocyte–Endothelial Cell Interactions

Accumulation of leukocytes is a prominent feature of acute and chronic inflammatory skin diseases and represents a rate-limiting step in the inflammatory response. Leukocyte recruitment is a multistep process controlled by the sequential activation of a number of adhesion molecules on both leukocytes and vascular endothelial cells, as well as by several inflammatory cytokines and chemokines. Leukocyte extravasation occurs primarily in the postcapillary venules of the skin as they are particularly sensitive to the induction of adhesion molecules. The specific cell-type expression, ligands, and function of the major adhesion molecules involved in leukocyte–endothelial cell interactions are summarized in Table 102.3.

MAJOR ADHESION MOLECULES INVOLVED IN LEUKOCYTE–ENDOTHELIAL CELL INTERACTIONS: CELL-TYPE SPECIFIC EXPRESSION, LIGANDS, AND FUNCTION

Adhesion molecule	Cell type	Ligands	Function
Integrin family			
LFA-1 (CD11a/CD18)	Leukocytes	ICAM-1, ICAM-2, JAM-A	Adhesion, crawling, transmigration
Mac-1 (CD11b/CD18)	Granulocytes, monocytes	ICAM-1, ICAM-2, JAM-C	Adhesion, crawling, transmigration
VLA-4 (CD49d/CD29)	Lymphocytes, monocytes, eosinophils, basophils	VCAM-1, JAM-B	Adhesion, crawling, transmigration
Selectin family			
E-selectin (CD62E)	Endothelial cells	ESL-1, PSGL-1, CD44	Capture, rolling
P-selectin (CD62P)	Endothelial cells	PSGL-1	Capture, rolling
L-selectin (CD62L)	Leukocytes	CD34, GlyCAM-1, MAdCAM, PSGL-1	Capture, rolling
Ig supergene family			
ICAM-1 (CD54)	Endothelial cells, monocytes	LFA-1, Mac-1, CD43	Adhesion, crawling
ICAM-2 (CD102)	Endothelial cells	LFA-1, Mac-1	Adhesion, crawling, transmigration
VCAM-1 (CD106)	Endothelial cells	VLA-4	Adhesion, crawling
PECAM-1 (CD31)	Endothelial cells	PECAM-1	Adhesion, transmigration
Junctional adhesion molecules			
JAM-A	Endothelial cells	LFA-1	Adhesion, crawling
JAM-B	Endothelial cells	VLA-4	Adhesion, crawling, transmigration
JAM-C	Endothelial cells	Mac-1	Adhesion, crawling

Table 102.3 Major adhesion molecules involved in leukocyte–endothelial cell interactions: cell-type specific expression, ligands, and function. CLA, cutaneous lymphocyte-associated antigen; ESL, E-selectin ligand; GlyCAM, glycosylation-dependent cell adhesion molecule; ICAM, intercellular adhesion molecule; JAM, junctional adhesion molecule; LFA, lymphocyte function-associated antigen; Mac-1, macrophage-1 antigen; MAdCAM, mucosal addressin cell adhesion molecule; PECAM, platelet–endothelial cell adhesion molecule; PSGL, P-selectin glycoprotein ligand; VCAM, vascular cell adhesion molecule; VLA, very late activation antigen.

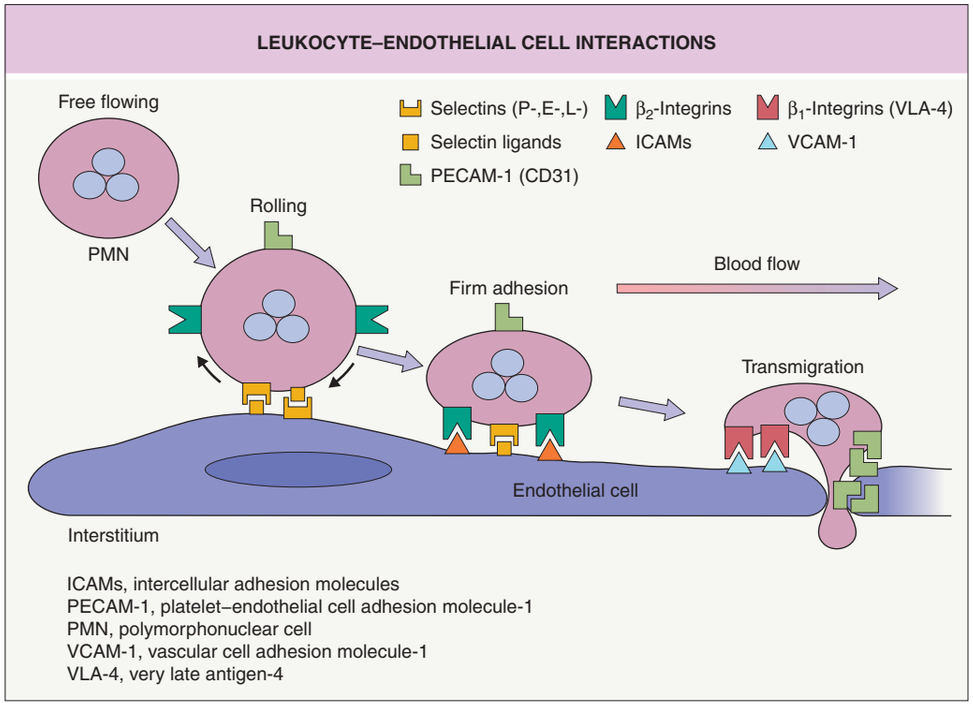


Fig. 102.11 The multistep process of leukocyte–endothelial cell interactions that leads to leukocyte recruitment into inflamed skin. Leukocyte extravasation involves tethering and rolling, largely mediated by selectins and their ligands. This is followed by firm adhesion and transmigration, largely mediated by adhesion molecules and their integrin ligands. Selectin ligands on leukocytes include E-selectin ligand-1 (ESL-1) and P-selectin glycoprotein ligand (PSGL-1).

As the first step in leukocyte extravasation, relatively weak adhesive interactions between leukocytes and endothelial cells, involving distinct selectins and their ligands, lead to tethering and rolling of leukocytes on the vessel wall (Fig. 102.11). In a second step, leukocytes become firmly attached to the vessel wall, which is mainly mediated by the interaction of adhesion molecules of the immunoglobulin superfamily and their ligands. The switch from the rolling phase to firm luminal adhesion and crawling requires activation of integrins, in which they switch from a low-affinity to a high-affinity conformation. This activation is mediated by signaling via chemokines that are either expressed by endothelial cells themselves and presented on their surface or expressed by perivascular cells and transcytosed by the endothelium.

Finally, leukocytes migrate into the dermis through spaces between adjacent endothelial cells. Junctions between endothelial cells are usually very tight due to interactions of vascular endothelial (VE)-cadherin, junctional adhesion molecules (JAMs), and others, and they need to be opened transiently for leukocytes to be able to transmigrate. During this process, vascular endothelial-protein-tyrosine phosphatase (VE-PTP) plays a major role. VE-PTP is normally associated with VE-cadherin but becomes transiently separated from it during leukocyte transmigration[25].

STRUCTURE AND FUNCTION OF THE CUTANEOUS LYMPHATIC VASCULAR SYSTEM

The cutaneous lymphatic system develops in parallel with the blood vascular system through a process termed lymphangiogenesis, and lymphatic vessels are not present in avascular structures such as epidermis, hair, and nails[26]. The lymphatic system is composed of a vascular network of thin-walled capillaries that drain protein-rich lymph from the extracellular space and play a crucial role in maintaining normal tissue pressure. Lymphatic vessels also play an essential role in mediating the transport of immune cells from the skin to the regional lymph nodes. The lymphatic system also plays a role in the metastatic spread of cutaneous malignancies, with anti-lymphangiogenic therapy representing a potential strategy for some cancer types[27].

Lymphatic capillaries are lined by a continuous single-cell layer of overlapping endothelial cells and lack a continuous basement membrane. In the initial lymphatic vessels, overlapping flaps at the borders of oak leaf-shaped endothelial cells lack junctions at their tips but are anchored on the sides by discontinuous button-like junctions; the latter differ from the conventional, continuous, zipper-like junctions found in larger collecting lymphatics and blood vessels[28]. Lymph returns to the venous circulation via larger lymphatic collecting vessels that contain a muscular and adventitial layer as well as numerous valves. The thoracic duct and right lymphatic duct are connected via lymphovenous valves to the subclavian veins.

The lymphatic vessels of the skin form two horizontal plexuses. The superficial plexus collects lymph from lymphatic capillaries and is located in close vicinity to the superficial cutaneous arterial plexus. Vertical lymphatic vessels connect the superficial plexus with the larger collecting vessels in the lower dermis and upper subcutis, whereas few lymphatics are found within the subcutis (see Fig. 102.1). The deep lymphatic vessels are located below the deep arterial system and contain valves to ensure unidirectional fluid transport.

The structure of the cutaneous lymphatics is dependent on the structure of the skin at a particular site and can vary significantly. Lymphatic vessels have a regular, uniform shape where the skin is firm and thick, whereas the shapes are more variable in regions where the skin is thin and loose. Certain areas, such as the fingers, genitalia, and palms and soles, appear to have a more abundant lymphatic network.

Lymphatic capillaries respond to increased tissue fluid content by widening their lumina (Fig. 102.12), an action mediated by anchoring filaments that connect the lymphatic endothelial cells with the surrounding interstitium. In normal skin, the majority of lymphatic vessels are collapsed. Whereas elevation of the interstitial pressure up to +2 mmHg results in both distention of lymphatic vessels and increased lymph flow, higher interstitial fluid pressure results in edema formation. The detection of enlarged lymphatics in the skin, however, does not allow predictions about their function because overextended lymphatics can be dysfunctional, as in some types of lymphedema[29]. Increased fluid load in the tissue is thought to activate lymphatic drainage via mechanosensors in lymphatic endothelium[30].

The peripheral lymphatic system is thought to originate from primary lymph sacs which arise from endothelial cells that bud from veins during early development. They then spread by endothelial sprouting into the surrounding tissues and organs. Non-venous progenitor cells may also contribute to the formation of cutaneous lymphatic vessels[31]. The homeobox gene *Prox1* is a specific marker for lymphatic endothelial cells. *Prox1* is first expressed during embryonic development in a polarized manner by a subset of venous endothelial cells. The latter bud off from the cardinal veins, migrate through the tissues, and finally form lymphatic vessels (Fig. 102.13). In adults, specific expression of Prox1 is maintained by cutaneous lymphatic endothelial cells and – together with podoplanin – appears to be the most specific marker for lymphatic vascular differentiation in the skin (see Table 102.1)[32]. Of note, Prox1 deficiency results in complete absence of a lymphatic

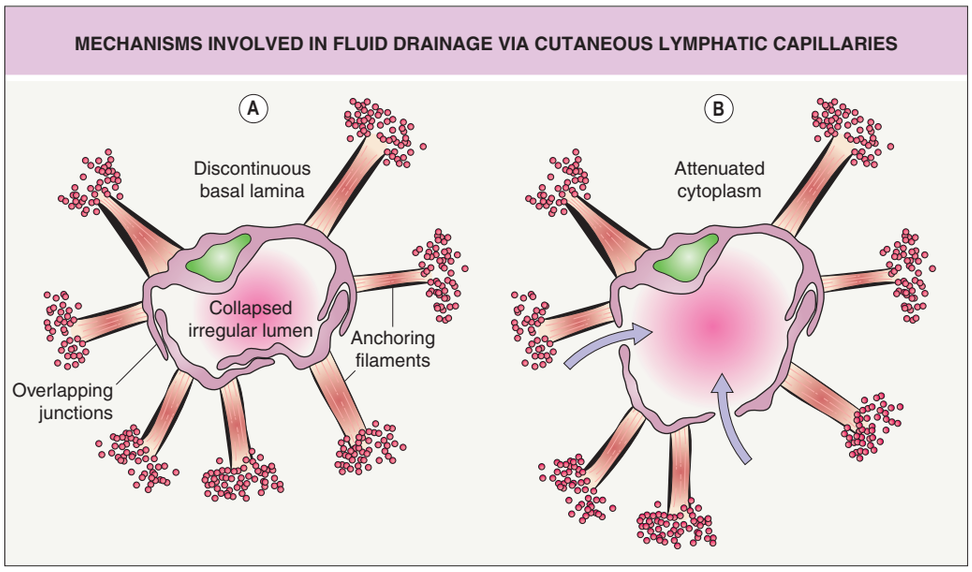


Fig. 102.12 Mechanisms involved in fluid drainage via cutaneous lymphatic capillaries. A Normal skin. **B** Skin with increased interstitial fluid content.

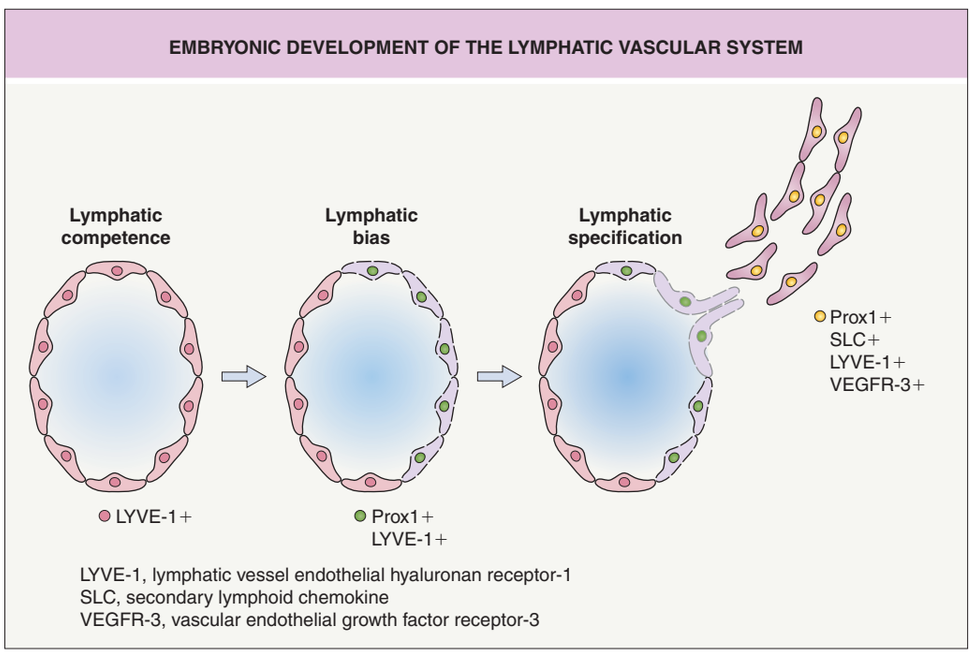


Fig. 102.13 Embryonic development of the lymphatic vascular system.

system in mice, among other defects, and Prox1 activity is needed to maintain the lymphatic vessel phenotype after birth[33].

Other markers, in addition to Prox1, have been identified that are predominantly or exclusively expressed by lymphatic endothelial cells in the skin (see Table 102.1). *VEGFR-3* (vascular endothelial growth factor receptor-3, Flt-4) is expressed on lymphatic vessels in normal skin and serves as a receptor for the lymphangiogenesis factors VEGF-C and VEGF-D[34] (Fig. 102.14). *Podoplanin*, a transmembrane glycoprotein, is a specific marker for the cutaneous lymphatic vasculature. The antibody D2-40 recognizes podoplanin and specifically stains lymphatic vessels (but not blood vessels) in normal and diseased human skin[35]. Of note, podoplanin plays an important role in the separation of the lymphatic and blood vascular systems by inducing platelet aggregation via its receptor CLEC2 on platelets; this prevents the influx of blood into the lymphatic vascular system. Indeed, either specific podoplanin deficiency in the lymphatic vessels of mice or the absence of CLEC2 in platelets results in blood filling of the lymphatic vascular system[36,37].

The *lymphatic vessel endothelial hyaluronan receptor-1* (LYVE-1), a CD44 homolog, has been identified as a specific cell surface protein of lymphatic endothelial cells. Although some specialized blood vascular endothelial cells that are involved in hyaluronic acid metabolism (e.g. sinusoidal endothelial cells in the liver, vascular endothelium in the lung) also express LYVE-1, its expression is specific for lymphatics in most organs, including the skin (Fig. 102.15; see Fig. 102.3). The expression of LYVE-1 is stronger in lymphatic capillaries than in larger lymphatic collecting vessels. Some of the markers discussed here, including VEGFR-3 and LYVE-1, can also be expressed by distinct subsets of leukocytes such as macrophages, particularly under inflammatory conditions. Thus, double staining with markers such as LYVE-1 plus the endothelial marker PECAM-1 (platelet–endothelial cell adhesion molecule-1, CD31), which is expressed by both blood vessel and lymphatic endothelial cells, is recommended for the unequivocal identification of lymphatic vessels (see Table 102.1).

Several molecules have been discovered that regulate the growth and function of lymphatic vessels. Both VEGF-C and VEGF-D activate the receptor tyrosine kinase VEGFR-3 (Flt-4) on lymphatic endothelial cells and, after proteolytic cleavage, the receptor tyrosine kinase VEGFR-2 (KDR) on blood vessels and lymphatic endothelium[34] (see Fig. 102.14). Transgenic mice with targeted overexpression of either VEGF-C or VEGF-D within the skin exhibited hyperplastic cutaneous lymphatic vessels, whereas no major abnormalities of blood vessels were found. Conversely, blockade of both VEGF-C and VEGF-D by transgenic overexpression of a soluble VEGFR-3 in the skin results in the absence of a cutaneous lymphatic system and development of lymphedema[38].

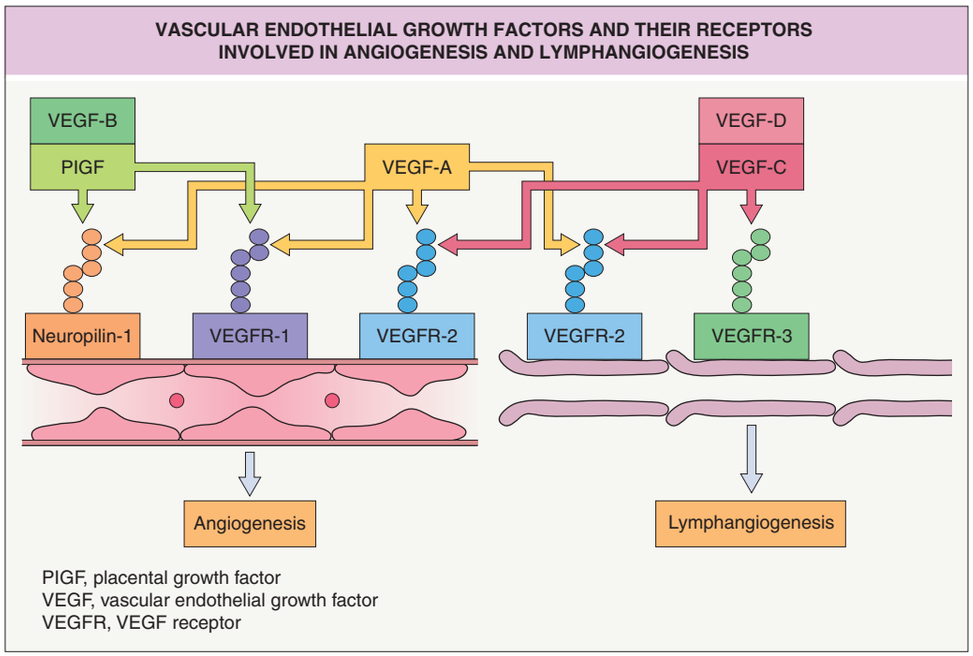


Fig. 102.14 Vascular endothelial growth factors and their receptors involved in angiogenesis and lymphangiogenesis. Heterozygous inactivating missense mutations of the gene encoding VEGFR-3, the receptor for the lymphangiogenesis factors VEGF-C and VEGF-D, have been found in families affected by primary lymphedema/lymphatic malformation 1, which is characterized by chronic swelling of the extremities.

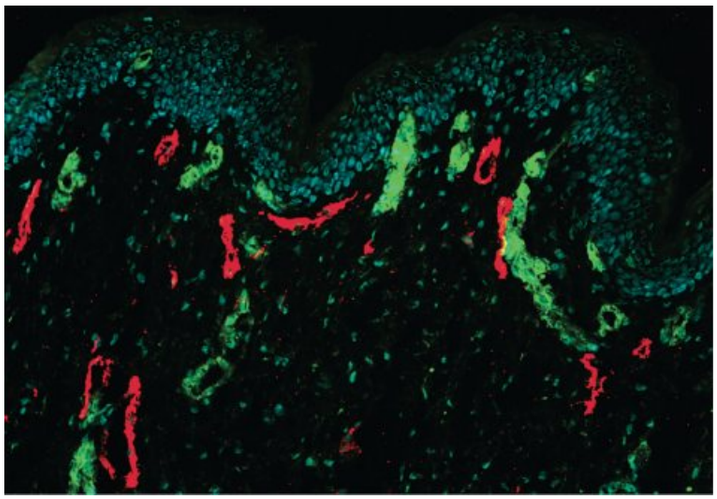


Fig. 102.15 Specific immunofluorescence staining of CD31-positive blood vessels (green) that are LYVE-1-negative and of CD31-positive/LYVE-1-positive lymphatic vessels (red) in human foreskin. Nuclei are stained blue.

Additional lymphangiogenesis factors have been identified, including VEGF-A, angiopoietin-1, bFGF, HGF, and sphingosine-1-phosphate[32].

ANGIOGENESIS- AND LYMPHANGIOGENESIS-RELATED DISEASES

Angiogenesis is a characteristic feature of tissue repair as well as numerous diseases, including inflammatory skin disorders (e.g. psoriasis, contact dermatitis), cutaneous neoplasias (e.g. SCC, melanoma, Kaposi sarcoma, infantile hemangiomas), and chronic wounds. Moreover, several other diseases are characterized by prominent visible blood vessels, including rosacea and basal cell carcinomas (BCCs). Genetic mutations that lead to dysfunction of the vascular Tie-2 receptor have been associated with vascular malformations[39] (see Ch. 104), and mutations in the genes that encode the low-affinity TGF-β receptor endoglin and activin receptor-like kinase (ALK)-1 lead to the formation of vascular malformations in patients with hereditary hemorrhagic telangiectasia types I and II, respectively[40].

Impairment of lymphatic function leads to the development of several diseases, most prominently to lymphedema with its associated impaired immune function, impaired wound healing, and fibrotic changes[41]. Heterozygous inactivating missense mutations of the gene encoding VEGFR-3 have been found in families affected by primary lymphedema/lymphatic malformation 1 characterized by chronic swelling of the extremities (see Table 105.7)[42]. In lymphedema–distichiasis, lymphatic vessel function fails due to mutations in the gene that encodes the forkhead transcription factor FOXC2[43]. Recessive and dominant forms of hypotrichosis–lymphedema–telangiectasia are also caused by dysfunction of a transcription factor, SOX18[44]. Additional gene mutations involved in lymphatic anomalies include *CCBE1*, *FAT4*, or *ADAMTS3* (Hennekam lymphangiectasia–lymphedema syndrome), *GJC2* (hereditary lymphatic malformation 3), *PTPN11* (Noonan syndrome), and *GATA2* (primary lymphedema with myelodysplasia [Emberger syndrome])[45].

Insufficient angiogenesis has also been shown to play a fundamental role in chronic wounds, particularly in patients with diabetes mellitus. In diabetic wounds, VEGF-A levels and the Ang-1 : Ang-2 ratio are decreased, while systemic PEDF levels are increased[46]. This results in a significant impairment of angiogenesis and wound healing.

Tumor-induced lymphangiogenesis promotes sentinel lymph node metastasis and reduces overall survival in patients with melanomas and various types of carcinomas[27,47]. Finally, impaired function of lymphatic vessels has been identified in chronic inflammation, and activation of lymphatic vessel function has shown promising results in the treatment of chronic inflammatory diseases including experimental skin inflammation and arthritis[32,48].

ANTIANGIOGENIC THERAPIES

Because induction of angiogenesis is essential for tumor progression, inhibition of tumor angiogenesis has become a target for cancer therapy[49]. Despite the identification of several distinct tumor angiogenesis factors, including interleukin-8 and bFGF, the majority of approved anti-tumor angiogenesis therapies rely on targeting VEGF-A. The latter is generally considered to represent the major angiogenic factor in the majority of solid tumors.

The anti-VEGF-A humanized monoclonal antibody *bevacizumab* was the first FDA-approved angiogenesis inhibitor (Fig. 102.16). Beneficial effects were observed in patients with metastatic colon cancer when bevacizumab was combined with chemotherapy[7]. Subsequently, bevacizumab has been approved for the treatment of other solid tumors including metastatic breast cancer, non-small-cell lung cancer (NSCLC), ovarian cancer, and cervical cancer as well as glioblastoma and renal cell carcinoma[50]. *Ramucirumab*, a monoclonal antibody that targets human VEGFR-2, has been approved for advanced gastric cancer, hepatocellular carcinoma, and metastatic forms of NSCLC and colorectal cancer. *Afilbercept*, a soluble VEGF receptor fusion protein ("VEGF trap"), is approved for both colorectal cancer and wet macular degeneration. In

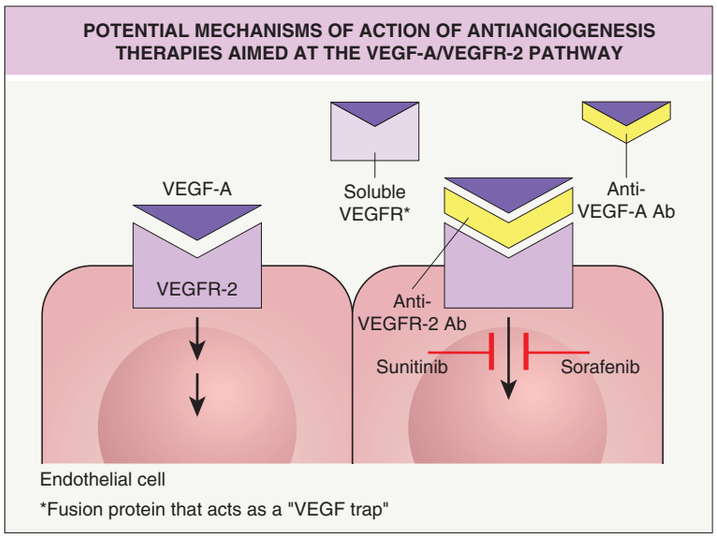


Fig. 102.16 Mechanisms of action of antiangiogenesis therapies aimed at the VEGF-A/VEGFR-2 pathway. Examples of anti-VEGF-A antibodies are bevacizumab and ranibizumab and an example of an anti-VEGFR-2 antibody is ramucirumab. Aflibercept acts as a soluble VEGF receptor fusion protein ("VEGF trap"). Tyrosine kinase inhibitors that block the VEGFR signaling pathway include cabozantinib, lenvatinib, pazopanib, and regorafenib as well as sorafenib and sunitinib.

addition, several tyrosine kinase inhibitors (e.g. cabozantinib, lenvatinib, pazopanib, regorafenib, sorafenib, sunitinib) have been approved, primarily for renal cell carcinoma, but also for thyroid, hepatocellular, and colorectal carcinomas (see Fig. 102.16). However, these inhibitors are not specific for VEGFR tyrosine kinases but also inhibit other tyrosine kinases (see Table 21.16). In addition, the mTOR inhibitor everolimus, a moderate angiogenesis inhibitor, is approved for several solid organ carcinomas.

Although anti-VEGF-A therapies have been beneficial in a range of carcinomas, as a monotherapy they have been ineffective due to the development of resistance. However, combined inhibition of VEGF-A plus other pro-angiogenic signaling pathways has resulted in improved response rates. For example, *vanucizumab*, a humanized anti-VEGF/Ang-2 bi-specific monoclonal antibody, has been shown in initial studies to suppress revascularization and tumor progression in solid tumors. Combined inhibition of both FGF and VEGF pathways has also led to greater efficacy. In addition to their antiangiogenic effects, VEGF-A inhibitors may also increase response rates to immunotherapy – an approach that is currently under investigation for various cancer types, including melanoma[51].

Although it has been proposed that inhibition of tumor angiogenesis leads to normalization of blood vessels and increased tumor delivery of chemotherapeutic drugs, antiangiogenic cancer therapy has not been as successful as originally envisioned. Mechanisms mediating primary or secondary tumor resistance to antiangiogenic approaches include[52]: (1) upregulation of additional angiogenesis factors (e.g. FGFs, HGF) and activation of alternative angiogenic signaling pathways; (2) recruitment of bone marrow-derived progenitor cells and other cell types with proinflammatory/pro-angiogenic phenotypes; (3) hypoxia-driven cancer cell invasion and metastasis; (4) co-opting of existing vessels by tumor cells; and (5) the formation of perfused vessels by tumor cells themselves, called "vascular mimicry".

Non-malignant skin diseases have also emerged as potential targets for treatments aimed at vascular endothelium. The mechanisms by which propranolol, a non-selective β-adrenergic receptor blocker, induces regression of hemangiomas are not fully understood, but it may induce endothelial cell apoptosis and interfere with the VEGF-A/VEGFR signaling pathway as well as reduce plasma renin levels (see Ch. 103). Sirolimus (rapamycin), an mTOR inhibitor, has been successfully used to treat patients with tufted angiomas/kaposiform hemangioendotheliomas who develop Kasabach–Merritt phenomenon as well as lymphatic malformations and kaposiform lymphangiomatosis.

In addition to these potential dermatologic applications, antiangiogenesis has become a promising new therapeutic approach in ophthalmology. Diabetes mellitus is frequently associated with intraocular neovascularization, and new blood vessel growth is the principal cause of visual loss in the wet form of age-related macular degeneration, the most common cause of blindness in Western countries. Nowadays, intravitreal injection of VEGF-A inhibitors (e.g. ranibizumab, aflibercept) are used to prevent progression of this disease and can even improve vision.

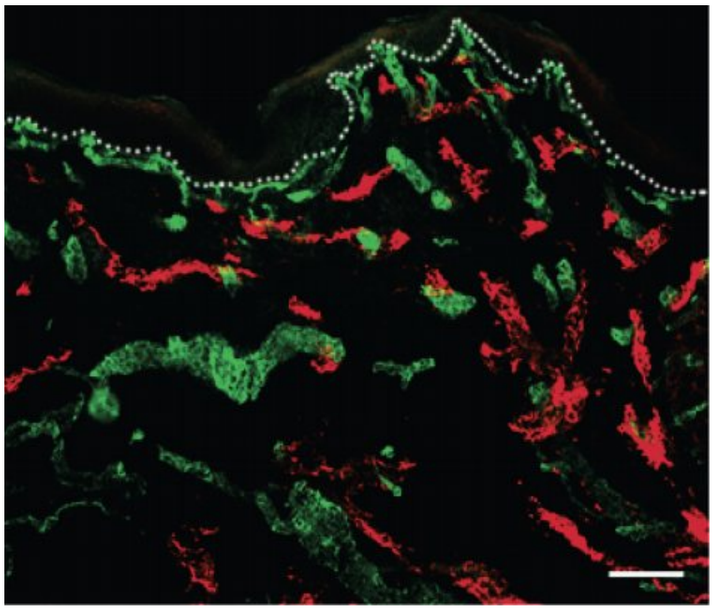
Additional figures available in our eBook (see inside front cover for access code).

REFERENCES

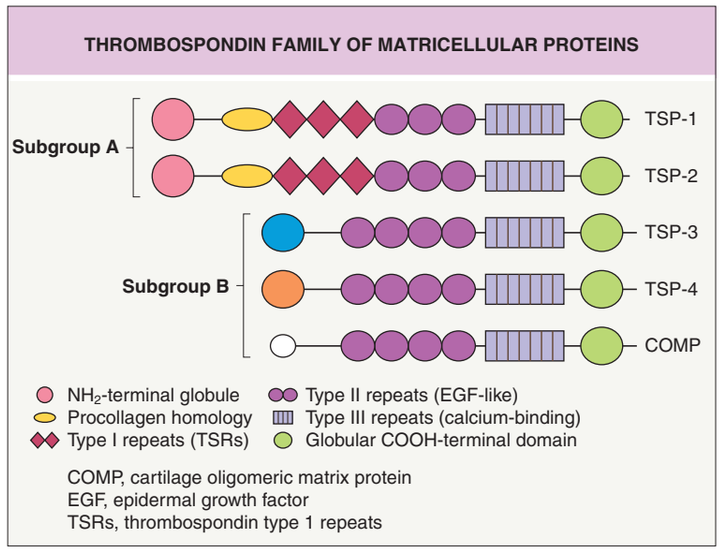
1. Ryan TJ. Cutaneous circulation. In: Goldsmith LA, ed. *Biochemistry and Physiology of the Skin*. New York: Oxford University Press; 1983. p. 817–877.
2. Yano K, Brown LF, Detmar M. Control of hair growth and follicle size by VEGF-mediated angiogenesis. *J Clin Invest*. 2001;107:409–417.
3. Vincent JR, Jones GT, Hill GB, van Rij AM. Failure of microvenous valves in small superficial veins is a key to the skin changes of venous insufficiency. *J Vasc Surg*. 2011;54(6 Suppl):62S–69S.
4. Dvorak HF, Brown LF, Detmar M, Dvorak AM. Vascular permeability factor/vascular endothelial growth factor, microvascular hyperpermeability, and angiogenesis. *Am J Pathol*. 1995;146:1029–1039.
5. Flamme I. Molecular biology of vasculogenesis and early angiogenesis. In: Rubanyi GM, ed. *Angiogenesis in Health and Disease: Basic Mechanisms and Clinical Applications*. New York: Marcel Dekker; 2000. p. 1–30.
6. Potente M, Gerhardt H, Carmeliet P. Basic and therapeutic aspects of angiogenesis. *Cell*. 2011;146: 873–887.
7. Welti J, Loges S, Dimmeler S, Carmeliet P. Recent molecular discoveries in angiogenesis and antiangiogenic therapies in cancer. *J Clin Invest*. 2013;123:3190–3200.
8. Betz C, Lenard A, Belting HG, Affolter M. Cell behaviors and dynamics during angiogenesis. *Development*. 2016;143:2249–2260.
9. De Bock K, Georgiadou M, Carmeliet P. Role of endothelial cell metabolism in vessel sprouting. *Cell Metab*. 2013;18:634–647.
10. Dvorak HF. Tumors: wounds that do not heal. Similarities between tumor stroma generation and wound healing. *N Engl J Med*. 1986;315:1650–1659.
11. Holash J, Maisonpierre PC, Compton D, et al. Vessel cooption, regression, and growth in tumors mediated by angiopoietins and VEGF. *Science*. 1999;284:1994–1998.
12. Senger DR, Perruzzi CA, Streit M, et al. The alpha(1) beta(1) and alpha(2)beta(1) integrins provide critical support for vascular endothelial growth factor signaling, endothelial cell migration, and tumor angiogenesis. *Am J Pathol*. 2002;160:195–204.
13. Senger DR, Galli SJ, Dvorak AM, et al. Tumor cells secrete a vascular permeability factor that promotes accumulation of ascites fluid. *Science*. 1983;219:983–985.
14. Detmar M, Brown LF, Claffey KP, et al. Overexpression of vascular permeability factor/vascular endothelial growth factor and its receptors in psoriasis. *J Exp Med*. 1994;180:1141–1146.
15. Kunstfeld R, Hirakawa S, Hong YK, et al. Induction of cutaneous delayed-type hypersensitivity reactions in VEGF-A transgenic mice results in chronic skin inflammation associated with persistent lymphatic hyperplasia. *Blood*. 2004;104:1048–1057.
16. Hirakawa S, Kodama S, Kunstfeld R, et al. VEGF-A induces tumor and sentinel lymph node lymphangiogenesis and promotes lymphatic metastasis. *J Exp Med*. 2005;201:1089–1099.
17. Carmeliet P, Moons L, Luttun A, et al. Synergism between vascular endothelial growth factor and placental growth factor contributes to angiogenesis and plasma extravasation in pathological conditions. *Nat Med*. 2001;7:575–583.
18. Huggenberger R, Detmar M. The cutaneous vascular system in chronic skin inflammation. *J Investig Dermatol Symp Proc*. 2011;15:24–32.
19. Lawler J, Detmar M. Tumor progression: the effects of thrombospondin-1 and -2. *Int J Biochem Cell Biol*. 2004;36:1038–1045.
20. Yano K, Kadoya K, Kajiya K, et al. Ultraviolet B irradiation of human skin induces an angiogenic switch that is mediated by upregulation of vascular endothelial growth factor and by downregulation of thrombospondin-1. *Br J Dermatol*. 2005;152: 115–121.
21. Kunstfeld R, Hawighorst T, Streit M, et al. Thrombospondin-2 overexpression in the skin of transgenic mice reduces the susceptibility to chemically induced multistep skin carcinogenesis. *J Dermatol Sci*. 2014;74:106–115.
22. Eming SA, Brachvogel B, Odorisio T, Koch M. Regulation of angiogenesis: wound healing as a model. *Prog Histochem Cytochem*. 2007;42:115–170.
23. DiPietro LA. Angiogenesis and wound repair: when enough is enough. *J Leukoc Biol*. 2016;100:979–984.
24. Veith AP, Henderson K, Spencer A, et al. Therapeutic strategies for enhancing angiogenesis in wound healing. *Adv Drug Deliv Rev*. 2019;146:97–125.
25. Broermann A, Winderlich M, Block H, et al. Dissociation of VE-PTP from VE-cadherin is required for leukocyte extravasation and for VEGF-induced vascular permeability in vivo. *J Exp Med*. 2011;208:2393–2401.
26. Cueni LN, Detmar M. The lymphatic system in health and disease. *Lymphat Res Biol*. 2008;6:109–122.
27. Karaman S, Detmar M. Mechanisms of lymphatic metastasis. *J Clin Invest*. 2014;124:922–928.
28. Baluk P, Fuxe J, Hashizume H, et al. Functionally specialized junctions between endothelial cells of lymphatic vessels. *J Exp Med*. 2007;204:2349–2362.
29. Gousopoulos E, Proulx ST, Scholl J, et al. Prominent lymphatic vessel hyperplasia with progressive dysfunction and distinct immune cell infiltration in lymphedema. *Am J Pathol*. 2016;186:2193–2203.



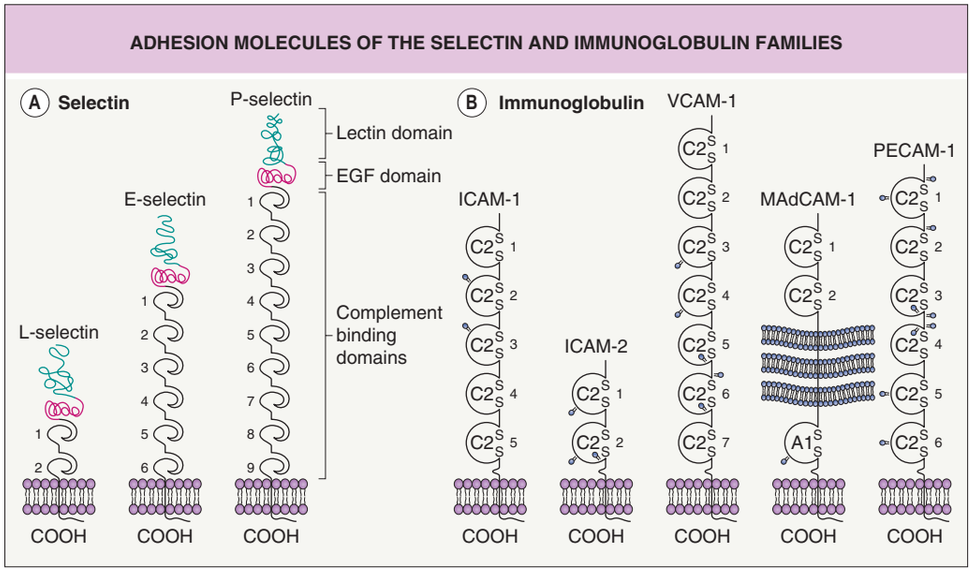
30. Planas-Paz L, Strilic B, Goedecke A, et al. Mechanoinduction of lymph vessel expansion. *EMBO J*. 2012;31:788–804.
31. Martinez-Corral I, Ulvmar MH, Stanczuk L, et al. Nonvenous origin of dermal lymphatic vasculature. *Circ Res*. 2015;116:1649–1654.
32. Dieterich LC, Seidel CD, Detmar M. Lymphatic vessels: new targets for the treatment of inflammatory diseases. *Angiogenesis*. 2014;17:359–371.
33. Yang Y, Oliver G. Development of the mammalian lymphatic vasculature. *J Clin Invest*. 2014;124:888–897.
34. Zheng W, Aspelund A, Alitalo K. Lymphangiogenic factors, mechanisms, and applications. *J Clin Invest*. 2014;124:878–887.
35. Schacht V, Dadras SS, Johnson LA, et al. Up-regulation of the lymphatic marker podoplanin, a mucin-type transmembrane glycoprotein, in human squamous cell carcinomas and germ cell tumors. *Am J Pathol*. 2005;166:913–921.
36. Bianchi R, Russo E, Bachmann SB, et al. Postnatal deletion of podoplanin in lymphatic endothelium results in blood filling of the lymphatic system and impairs dendritic cell migration to lymph nodes. *Arterioscler Thromb Vasc Biol*. 2017;37:108–117.
37. Hess PR, Rawnsley DR, Jakus Z, et al. Platelets mediate lymphovenous hemostasis to maintain blood-lymphatic separation throughout life. *J Clin Invest*. 2014;124:273–284.
38. Makinen T, Jussila L, Veikkola T, et al. Inhibition of lymphangiogenesis with resulting lymphedema in transgenic mice expressing soluble VEGF receptor-3. *Nat Med*. 2001;7:199–205.
39. Limaye N, Wouters V, Uebelhoer M, et al. Somatic mutations in angiopoietin receptor gene TEK cause solitary and multiple sporadic venous malformations. *Nat Genet*. 2009;41:118–124.
40. Mallet C, Lamribet K, Giraud S, et al. Functional analysis of endoglin mutations from hereditary hemorrhagic telangiectasia type 1 patients reveals different mechanisms for endoglin loss of function. *Hum Mol Genet*. 2015;24:1142–1154.
41. Mortimer PS, Rockson SG. New developments in clinical aspects of lymphatic disease. *J Clin Invest*. 2014;124:915–921.
42. Karkkainen MJ, Ferrell RE, Lawrence EC, et al. Missense mutations interfere with VEGFR-3 signalling in primary lymphoedema. *Nat Genet*. 2000;25:153–159.
43. Petrova TV, Karpanen T, Norrmen C, et al. Defective valves and abnormal mural cell recruitment underlie lymphatic vascular failure in lymphedema distichiasis. *Nat Med*. 2004;10:974–981.
44. Irrthum A, Devriendt K, Chitayat D, et al. Mutations in the transcription factor gene SOX18 underlie recessive and dominant forms of hypotrichosis-lymphedema-telangiectasia. *Am J Hum Genet*. 2003;72:1470–1478.
45. Brouillard P, Boon L, Vikkula M. Genetics of lymphatic anomalies. *J Clin Invest*. 2014;124:898–904.
46. Okonkwo UA, DiPietro LA. Diabetes and wound angiogenesis. *Int J Mol Sci*. 2017;18:1419.
47. Dadras SS, Paul T, Bertoncini J, et al. Tumor lymphangiogenesis: a novel prognostic indicator for cutaneous melanoma metastasis and survival. *Am J Pathol*. 2003;162:1951–1960.
48. Huggenberger R, Ullmann S, Proulx ST, et al. Stimulation of lymphangiogenesis via VEGFR-3 inhibits chronic skin inflammation. *J Exp Med*. 2010;207:2255–2269.
49. Chung AS, Lee J, Ferrara N. Targeting the tumour vasculature: insights from physiological angiogenesis. *Nat Rev Cancer*. 2010;10:505–514.
50. Garcia J, Hurwitz HI, Sandler AB, et al. Bevacizumab (Avastin®) in cancer treatment: a review of 15 years of clinical experience and future outlook. *Cancer Treat Rev*. 2020;86:102017.
51. Lopes-Coelho F, Martins F, Pereira SA, Serpa J. Anti-angiogenic therapy: current challenges and future perspectives. *Int J Mol Sci*. 2021;22:3765.
52. Jain RK. Antiangiogenesis strategies revisited: from starving tumors to alleviating hypoxia. *Cancer Cell*. 2014;26:605–622.



eFig. 102.1 Distinct staining of cutaneous blood vessels (PAL-E; green) and lymphatic vessels (LYVE-1; red) in human neonatal foreskin. The dotted line indicates the approximate location of the basement membrane. The white bar represents 50 microns.



eFig. 102.2 The thrombospondin (TSP) family of matricellular proteins. TSP-1 and TSP-2 are potent endogenous inhibitors of skin angiogenesis.



eFig. 102.3 Adhesion molecules of the selectin (A) and immunoglobulin (B) families. EGF, epidermal growth factor; MAdCAM, mucosal addressin cell adhesion molecule; ICAM, intercellular adhesion molecule; PECAM, platelet–endothelial cell adhesion molecule; VCAM, vascular cell adhesion molecule.

Infantile Hemangiomas 103

Anita N. Haggstrom, Sheilagh M. Maguiness and Maria C. Garzon

Synonyms: ■ Hemangioma of infancy ■ Hemangioma

Key features

- The most common benign soft tissue tumor of infancy
- Characteristic growth pattern with early proliferation followed by gradual, spontaneous involution and variable residual skin changes
- Distinct histopathologic and immunohistochemical features that differentiate them from other vascular anomalies in children
- May be associated with extracutaneous findings when occurring at certain anatomic sites (e.g. the face, neck, lumbosacral area), especially when lesions have a segmental pattern
- Management is tailored to each patient as suggested in published guidelines
- Systemic β-blockers are first-line therapy for most children with complicated hemangiomas

INTRODUCTION

Infantile hemangiomas (IHs) are benign proliferations of endothelial cells and their supporting tissues and they represent the most common tumors arising in the neonatal period. IHs are characterized by significant growth during the first several months of life, followed by slow spontaneous involution over the ensuing years. This natural history differentiates them from vascular malformations (Table 103.1). Studies highlighting the potential roles of specific IH stem cells and hypoxia have provided new insights into their pathophysiology.

HISTORY

The terms "infantile hemangioma" and "hemangioma of infancy" describe a specific group of vascular tumors that arise during infancy and demonstrate characteristic clinical and histologic features. IHs have been recognized in the medical literature for centuries, and they have been given various names such as *strawberry nevus* and *capillary hemangioma*. Despite early attempts to make distinctions among different types of vascular lesions, the term "hemangioma" was applied to a wide variety of congenital and acquired vascular anomalies including vascular malformations, without consideration of differences in their biologic behavior.

One of the important developments in the study of vascular "birthmarks", including lesions that become apparent during early infancy, was the acceptance of a biologic classification scheme. In 1982, Mulliken and Glowacki[1] first proposed that vascular birthmarks should be categorized according to their biologic and clinical behavior. The International Society for the Study of Vascular Anomalies has modified and periodically updated this classification to reflect new insights, including the genetic bases of multiple types of vascular anomalies (Table 103.2)[2].

Under this organization scheme, vascular birthmarks are divided into three categories: *vascular tumors*, *vascular malformations*, and a smaller group of "*provisionally unclassified*" lesions. Vascular tumors are characterized by cellular proliferation and include IH, pyogenic granuloma, and less common neoplasms such as tufted angioma and kaposiform hemangioendothelioma (see Table 103.2 and Ch. 114). Vascular malformations, on the other hand, are believed to represent errors in vascular morphogenesis. They are frequently noted during the neonatal period, but, unlike IHs, they do not rapidly proliferate in the first year of life nor do they resolve spontaneously (see Table 103.1; see Fig. 104.1). Vascular malformations are characterized by the type of anomalous vessels they contain and by their flow properties (see Ch. 104).

The biologic classification includes histopathologic, immunohistochemical, and genetic features that aid in distinguishing IHs from other vascular anomalies as well as predicting the clinical behavior and prognosis of these vascular lesions. The current classification serves as a framework for understanding vascular birthmarks but is evolving as new insights emerge.

EPIDEMIOLOGY

IHs arise during the first year of life and are the most common tumor of infancy. They develop in 4%–5% of infants, with lesions usually noted within the first several weeks of life[3]. IHs may occur more commonly in White infants than in other racial groups. A female : male ratio of 2–5 : 1 has been noted in multiple retrospective studies as well as prospective studies conducted in dermatology practices; however, a hospital-based prospective birth-cohort study found no female predominance among infants who developed an IH[3]. A higher female : male ratio of 7–9 : 1 has been reported for patients with severe, complicated IHs.

IHs also develop more frequently in premature infants. Low birth weight represents an independent IH risk factor, and IHs affect 25%–30% of infants with a birth weight <1000 g and 15% of those with a birth weight between 1000 and 1500 g[4]. Factors associated with placental insufficiency (e.g. preeclampsia, placenta previa) are also associated with IH development, while prematurity and multiple gestation pregnancies are linked with the development of multifocal IHs[3,5–7]. One study found a threefold increased incidence in infants born following chorionic villus sampling compared to those born following amniocentesis or without a history of prenatal instrumentation[8]. A higher maternal age has also been associated with hemangioma development[6,7].

IHs typically arise sporadically, although a family history has been reported in up to a third of patients[9]. The frequent occurrence of hemangiomas in the general population makes it difficult to assess the true familial incidence, and no specific genes have been consistently implicated.

PATHOGENESIS

IHs represent localized or regional areas of abnormal vascular development and proliferation. Their development involves *de novo* formation of vessels from multipotent hemangioma-derived stem cells (HemSCs) and endothelial progenitor cells (vasculogenesis) as well as formation of new vessels from existing ones (angiogenesis)[10,11]. Other cell types in the hemangioma's environment, including monocytes, fibroblasts, pericytes, mesenchymal cells, adipocytes and mast cells, can influence endothelial cell proliferation and may have a role in hemangioma formation and/or involution.

The overlapping immunohistochemical phenotype of hemangioma cells and human placental endothelium has led to the suggestion that hemangioma cells may be of placental origin or undergo differentiation toward a placental microvascular phenotype. North and co-workers[12,13] reported that glucose transporter protein-1 (GLUT1) is expressed by IHs during all phases of their development (proliferating, involuting, involuted) as well as by the placenta, but not by other vascular tumors or malformations. Additional placenta-associated vascular antigens, including merosin, FcγRII, and Lewis Y antigen, are present in hemangioma specimens and placental chorionic villi but absent in microvessels of the normal skin and subcutis[13]. However, hemangiomas do not express placental *trophoblastic* markers (e.g. human placental lactogen)[14] and are not thought to represent placental emboli.

DIFFERENCES BETWEEN INFANTILE HEMANGIOMAS AND VASCULAR MALFORMATIONS		
	Infantile hemangioma	**Vascular malformation**
Clinical	• Usually absent at birth or subtle precursor lesion present; only occasionally well formed • Rapid proliferation in first 2–5 months of life • Spontaneous involution over years	• Usually evident at birth • Slower expansion, with increase in area proportionate to the child's growth • Persists into adulthood
Epidemiology	More common in: • Girls (2–5 : 1) • Premature and/or low-birth-weight infants • Infants whose mothers were older, underwent chorionic villus sampling, or had preeclampsia	No sex or gestation predilection
Pathology	**Proliferating**: endothelial cell hyperplasia, lobule formation, mast cells, prominent basement membrane **Involuting**: fibrofatty tissue replacement, decreased mast cells when fully involuted	Dependent upon type, often irregular vascular channels
Immunohistochemistry	Positive for GLUT1, Lewis Y antigen, merosin, and FcγRII, Wilms tumor protein 1 (WT1)	Negative for GLUT1, Lewis Y antigen, merosin, and FcγRII, WT1

Table 103.1 Differences between infantile hemangiomas and vascular malformations.

BIOLOGIC CLASSIFICATION OF VASCULAR BIRTHMARKS
Vascular tumors
Benign • Infantile hemangioma • Congenital hemangioma (rapidly involuting, non-involuting, partially involuting) • Tufted angioma • Pyogenic granuloma • Spindle cell hemangioma • Others Locally aggressive or borderline • Kaposiform hemangioendothelioma • Others, e.g. retiform or composite hemangioendothelioma
Vascular malformations

Simple
• Capillary malformations (CMs)
• Venous malformations (VMs)
  • Common, glomuvenous, others
• Lymphatic malformations (LMs)
  • Common: macrocystic, microcystic, mixed; others
• Arteriovenous malformations, arteriovenous fistula (AVMs, AVFs; high flow)
Combined
• CVM, CLM, LVM, CAVM, CLAVM, others
Of major named vessels
Associated with other anomalies
• Sturge–Weber syndrome, Klippel–Trenaunay syndrome, others

Provisionally unclassified
• Angiokeratomas • Multifocal lymphangioendotheliomatosis with thrombocytopenia • Others

Table 103.2 Biologic classification of vascular birthmarks. Updated based on the International Society for the Study of Vascular Anomalies (ISSVA) Classification of Vascular Anomalies[2]. Vascular malformations are discussed in Chapter 104 and other vascular tumors in Chapter 114. CAVM, capillary–arteriovenous malformation; CLAVM, capillary–lymphatic–arteriovenous malformation; CLM, capillary–lymphatic malformation; CVM, capillary–venous malformation; LVM, lymphatic–venous malformation

Role of Hypoxia

The role of hypoxia in the pathogenesis of IHs is supported by their association with hypoxic placental changes, prematurity/low birth weight (often caused by placental insufficiency), retinopathy of prematurity (GLUT1-positive, hypoxia-induced neovascularization), and regional arterial insufficiency in PHACE(S) and LUMBAR syndromes (see below)[15,16]. Hypoxia upregulates expression of GLUT1 and vascular endothelial growth factor (VEGF), leading to mobilization of endothelial progenitor cells. Moreover, the combination of hypoxia and estrogen has a synergistic effect on hemangioma endothelial cell proliferation *in vitro*[15], potentially explaining the predilection of IHs for female infants. Investigators have also found that hypoxia inducible factor (HIF)-1α and its downstream effectors are upregulated in IHs during their proliferative phase[17].

Signaling Pathways

Several signaling pathways play a role in IH development. Studies have confirmed the importance of VEGF (also known as VEGF-A) signaling, with a shift from expression of VEGF receptor 1 (VEGFR-1), which binds VEGF with high affinity but transmits a very weak signal, to VEGFR-2, which strongly stimulates endothelial cell proliferation upon VEGF binding[18]. VEGFR-2 signaling activates the phosphatidylinositol 3-kinase (PI3K)-mechanistic target of rapamycin (mTOR) pathway, leading to upregulation of HIF-1α and increased levels of VEGF. Accordingly, treatment of hemangioma endothelial cells *in vitro* with the mTOR inhibitor sirolimus (rapamycin) results in reduced proliferation[19].

Hemangiomas also have increased expression of the endothelial cell-specific Tie-2 tyrosine kinase receptor and dysregulated production of angiopoietin-2, which may promote angiogenesis and inhibit vessel maturation (see Ch. 102)[20]. The Notch pathway is thought to mediate differentiation of HemSCs into pericytes/vascular smooth muscle cells[21], and the latter appear to have pro-angiogenic properties and support IH development[22]. The renin–angiotensin system (RAS) has also been implicated in IH proliferation via activation of angiotensin II receptor 2[23], and treatment of IH with β-blockers reduces plasma renin levels[24].

Genetic Factors

A variety of genetic factors may be involved in the development of IH. There have been reports of *somatic* mutations in genes that encode proteins involved in VEGF signaling (e.g. VEGFRs) and other pathways that affect vascular development within hemangioma tissue[25]. Heterozygous *germline* mutations in *VEGFR2* and *ANTXR1* (anthrax toxin receptor 1), which encodes an integrin-like endothelial cell receptor, have been identified in a small subset of IH patients and may represent hemangioma predisposition factors[18].

Factors Influencing Natural History

Hemangiomas have been studied during different phases of their clinical course to gain insights into the mechanisms that govern their growth and involution. In the proliferative phase, hemangiomas express markers of proliferation such as proliferating cell nuclear antigen (PCNA) and increased levels of pro-angiogenic molecules such as VEGF and basic fibroblast growth factor (bFGF)[26–28]. In addition, other angiogenesis mediators, proteins found within the perivascular extracellular matrix, and enzymes involved in matrix remodeling are produced at higher levels during proliferation (Table 103.3)[26,29–32].

The factors that govern the transition of hemangiomas from proliferation to involution and the mechanisms of the associated decrease in

MARKERS OF PROLIFERATING AND INVOLUTING HEMANGIOMAS
Proliferative phase
• General markers of proliferation, e.g. proliferating cell nuclear antigen (PCNA)
• Vascular endothelial growth factor (VEGF), basic fibroblast growth factor (bFGF)*,†
• Monocyte chemoattractant protein-1†
• Adhesion molecules on endothelial cells – E-selectin, ICAM-3†
• Matrix metalloproteinase-2 and -9 (extracellular matrix remodeling)‡
• Vitronectin (found in the perivascular extracellular matrix)
• Indoleamine 2,3-dioxygenase (inhibits T cell activation)
• Apoptosis inhibitors
Involution
• Interferon-regulated gene products (interferons are known to inhibit angiogenesis)
• bFGF (early in involution)
• Increased mast cells (early in involution)
• Tissue inhibitor of matrix metalloproteinases-1 (inhibits angiogenesis)
• Apoptosis promoters
*VEGF and bFGF, but not the angiogenesis inhibitor interferon-β, are also expressed by the hyperplastic epidermis overlying proliferating hemangiomas. †Angiogenesis mediators. ‡Increased levels also found in blood and urine.

Table 103.3 Markers of proliferating and involuting hemangiomas. Lymphatic vessel endothelial hyaluronan receptor (LYVE)-1 has been identified in perivascular dendritic cells in hemangiomas of various stages. ICAM, intercellular adhesion molecule.

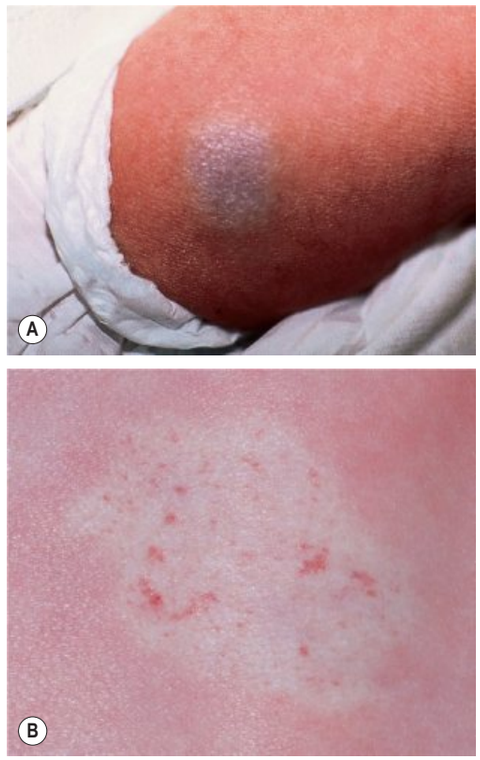


Fig. 103.1 Infantile hemangioma precursors. These premonitory lesions can have a "bruised" (**A**) or blanched (**B**) appearance. *B, Courtesy Julie V. Schaffer, MD.*

pro-angiogenic factors are not fully understood[26,30]. Increased expression of angiogenesis inhibitors and apoptosis promoters has been observed in involuting hemangiomas (see Table 103.3)[26,33]. Depending on the extracellular environment, mesenchymal stem cells may contribute to endothelial cell proliferation during the hemangioma growth phase or differentiate into adipocytes contributing to fibrofatty residua in involuting hemangiomas[34].

CLINICAL FEATURES

Presentation

Most IHs have a typical presentation and growth pattern. Lesions usually become apparent during the first few weeks of life, although the proportion of hemangiomas that are "congenital" in published series has ranged from 15% to 60%[35]. IHs evident at birth most often appear as precursor lesions, which are apparent in up to 65% of IHs[35], but occasionally they present as relatively well-formed typical IHs that subsequently demonstrate variable proliferation then slow involution. Precursor IH lesions include telangiectasias surrounded by a vasoconstricted halo, areas of pallor, pink macules, and blue bruise-like patches (Fig. 103.1). Pink macules and patches may mimic a capillary malformation, and repeat examination over the ensuing weeks is essential to determine the diagnosis (Fig. 103.2). Rapidly involuting, partially involuting, and non-involuting *congenital hemangiomas* (RICH/PICH/NICH) represent distinct entities that are discussed below.

Occasionally, an area of ulceration in the diaper area, in other skin folds, or on the lip may herald the onset of an IH[36], and in a newborn infant these lesions may be confused with bacterial or viral infections. Continued observation usually clarifies the diagnosis. With dermoscopy, the characteristic findings of red lacunae separated by white septae in superficial IHs and violaceous to blue lacunae in deeper IHs may be helpful when the diagnosis is not clear[37].

Hemangiomas may occur anywhere on the skin and mucosal surfaces. Although overall they most commonly develop on the trunk[3], ~50% of the IHs that present to a pediatric dermatologist are located on the head and neck[7]. The clinical appearance of an IH is influenced by its location within the skin and subcutaneous tissues. *Superficial* hemangiomas are situated in the upper dermis and are bright red in color during their proliferating phase. The surface is finely lobulated, and the term "strawberry hemangioma" has been used to describe them[1] (Fig. 103.3).

Deep hemangiomas are located in the deep dermis and/or subcutis. They usually are not apparent in the immediate newborn period, often



Fig. 103.2 Segmental superficial infantile hemangioma mimicking a port-wine birthmark. This 3-week-old girl is at risk of PHACE(S) syndrome. *Courtesy Julie V. Schaffer, MD.*

becoming evident a few weeks or even months after birth. They present as warm, ill-defined, light blue–purple masses with minimal or no overlying skin changes, making them more difficult to diagnose than superficial or mixed hemangiomas (Fig. 103.4). The presence of dilated veins or telangiectasias overlying a deep hemangioma provides a clue that the lesion is of vascular origin. Larger deep hemangiomas often have significant arterial blood supply during the proliferative phase, and detection of high flow by Doppler ultrasonography can help to confirm the diagnosis. Mixed hemangiomas have both superficial and deep components, often presenting during the proliferative phase as a well-delineated red vascular plaque overlying a larger, poorly circumscribed violaceous or light blue nodule.

Superficial hemangiomas are the most common type, accounting for ~50%–60% of IHs. An additional 25%–35% of hemangiomas are mixed and 15% are deep[38]. Approximately 25% of patients have multiple

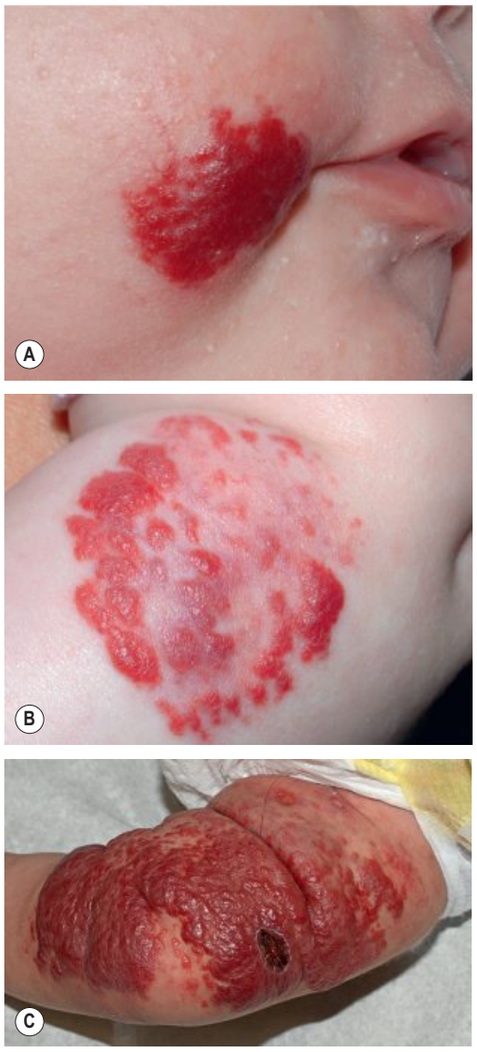


Fig. 103.3 Superficial infantile hemangiomas. Lesions can be focal (**A**,**B**) or have a broader segmental distribution (**C**). Note the bright red color and finely lobulated surface, irrespective of size. Involvement may be diffuse or discontiguous. *Courtesy Julie V. Schaffer, MD.*

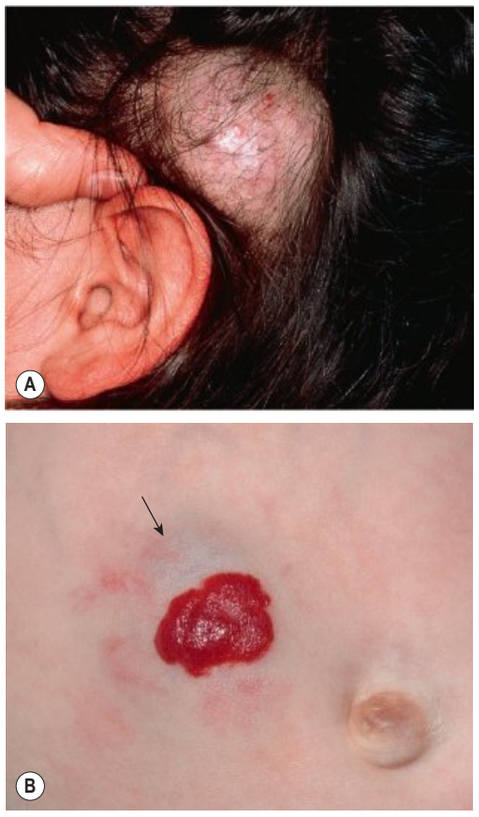


Fig. 103.4 Deep and mixed infantile hemangiomas. A Skin-colored deep hemangioma with overlying telangiectasias and alopecia on the scalp. **B** Mixed hemangioma composed of a well-demarcated, bright red superficial plaque plus a broader, ill-defined underlying deep nodule with a subtle light blue–purple hue (arrow) and scattered telangiectasias. *B, Courtesy Julie V. Schaffer, MD.*

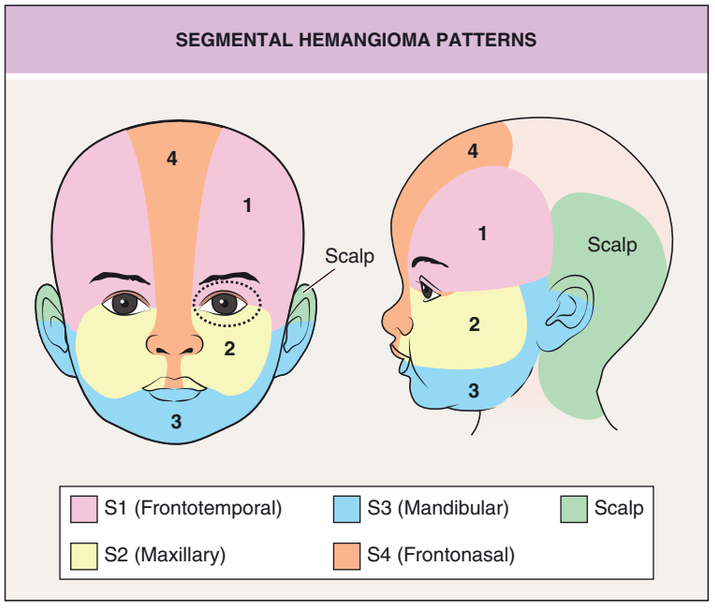


Fig. 103.5 Segmental hemangioma patterns. Based upon a prospective study (n = 165) of image analyses of hemangiomas. *Adapted with permission from Endicott AA, Chamlin SL, Drolet BA, et al. Mapping of segmental and partial segmental infantile hemangiomas of the face and scalp. JAMA Dermatol 2021;157:1328–34.*

lesions, which are occasionally associated with hemangiomas in the liver or other internal organs (see below).

IHs can also be categorized based upon the pattern of involvement, which may help to predict prognosis[39–41]. The two main pattern subtypes are: (1) *focal* – arising from a single localized nidus (see Fig. 103.3A,B); and (2) *segmental* – covering a broad area or developmental unit in a "plaque-like" manner (see Fig. 103.3C). Lesions that are difficult to classify are designated as *indeterminate* and may represent *partial segmental* lesions that respect anatomic boundaries similar to their larger segmental counterparts[42]. The majority of IHs are focal lesions, and those on the face may show predilection for embryonic fusion lines[39]. The distribution patterns of segmental hemangiomas on the face resemble classic embryonic facial prominences, differing the most on the upper face. Investigators have identified four primary segments for facial hemangiomas, S1 to S4 (Fig. 103.5)[43]. Involvement of these segments may be incomplete, and some hemangiomas encompass more than one segment. A C-shaped pattern extending from the posterior auricular area to the posterolateral scalp has also been observed[42].

Segmental hemangiomas often begin as broad patches of confluent or reticulated erythema and/or telangiectasias. Within a few weeks, bright red papules and plaques arise within this "field". Segmental hemangiomas are more likely to be associated with regional extracutaneous anomalies, including PHACE(S) and LUMBAR syndromes (see below)[40]. On the extremities, smaller segmental hemangiomas typically spare the distal digits in a "biker glove" pattern (Fig. 103.6), while larger lesions that encompass the distal digits are associated with a higher risk of extracutaneous anomalies[44]. Rhabdomyomatous mesenchymal hamartomas presenting as a papule or atrophic plaque in the midline anterior neck/trunk or sacrum in association with segmental hemangiomas have also been described[45].

Natural History

Studies have documented the typical growth pattern of IHs. The phases include *early proliferation* with a rapid increase in size, *late proliferation* with continued growth at a slower rate, *plateau* (existence as a distinct phase debated), and *involution*[41]. Hemangiomas tend to "mark out their territory" early on, subsequently undergoing primarily volumetric rather than centrifugal growth[35,41]. During the proliferative phase, hemangiomas frequently become warmer and firmer in texture, and the surface of superficial hemangiomas may appear tense. Mixed and deep hemangiomas in the proliferative phase often feel firmer and look larger when the infant is crying or active. Deep hemangiomas tend to



Fig. 103.6 "Biker glove" pattern of an acral infantile hemangioma with minimal or arrested growth. Note the characteristic sparing of the distal fingers.

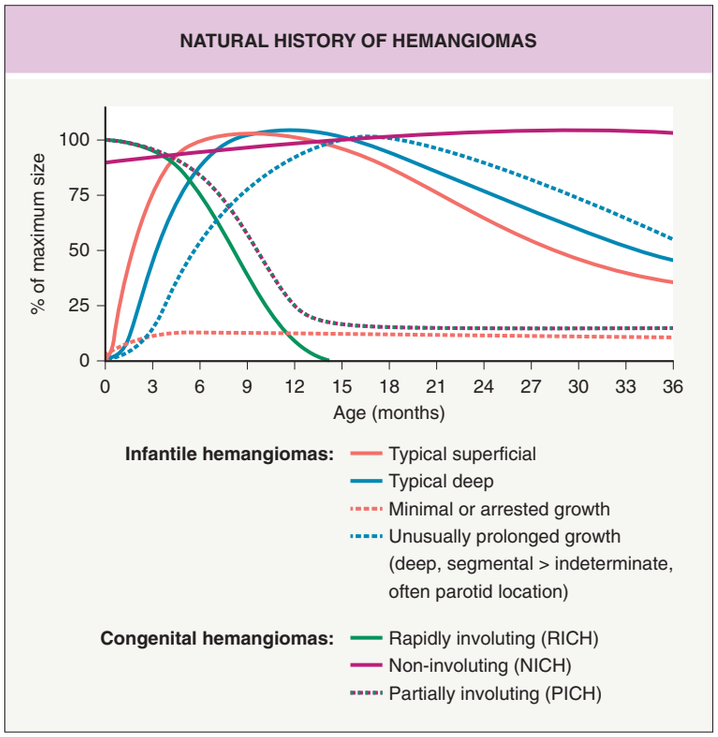


Fig. 103.7 Natural history of infantile and congenital hemangiomas.

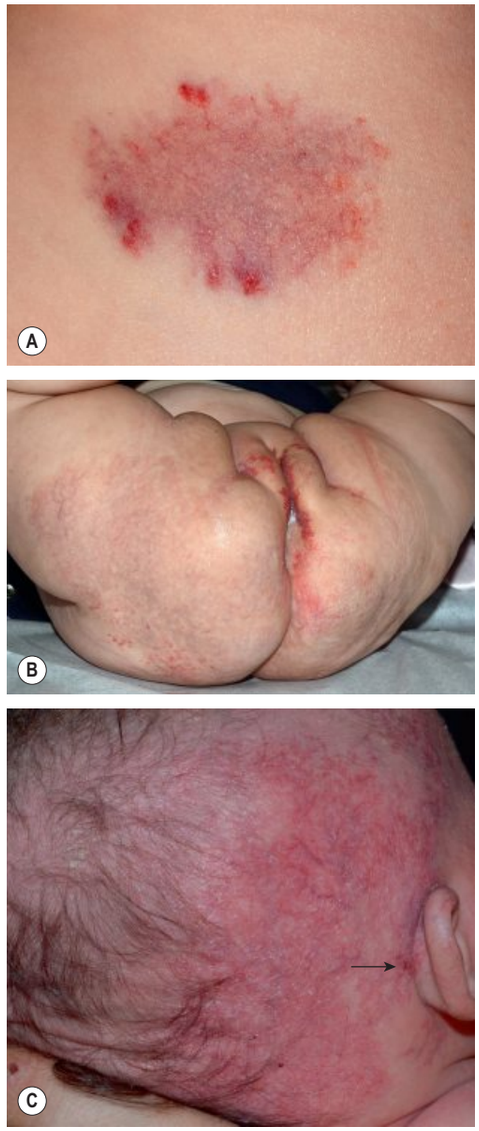


Fig. 103.8 Infantile hemangiomas with minimal or arrested growth (IH-MAG). Telangiectasias and larger ectatic vessels are evident. Focal small bright red papules cover <25% of the surface area and are evident at the periphery (**A**); on the vulva and upper buttock (**B**); and behind the ear (**C**, arrow). Presence of these papules (which may be subtle or absent), reticulated erythema, and characteristic fine to coarse telangiectasias help to distinguish these lesions from capillary–venous malformations. *Courtesy Julie V. Schaffer, MD.*

proliferate for a longer period of time than do superficial hemangiomas, and the deep component of mixed lesions often continues to grow even after the superficial component has plateaued (Fig. 103.7).

The majority of hemangiomas reach 80% of their final size by the end of the early proliferative phase, which occurs at a mean age of 3 months, and growth is usually most rapid from 5 to 8 weeks of age[35,41]. The small minority of hemangiomas that grow after 9 months of age (rarely as late as ≥3 years of age) tend to have a deep component and/or segmental morphology, and IHs in the parotid gland area are particularly prone to this behavior[41,46,47].

A subset of hemangiomas referred to as *IH with minimal or arrested growth (IH-MAG)* (previously described as "*abortive*" or "*reticular*") display little or no growth beyond patches of reticulated erythema with coarse and/or fine telangiectasias, often superimposed on a background of pallor (Fig. 103.8)[48,49]. If present, the proliferative component involves <25% of the surface area, often presenting as small red papules at the periphery[48]. Development of eczematous dermatitis localized to a IH-MAG has been described[50]. These hemangiomas favor the lower body and may develop recalcitrant ulceration or (if larger and segmental) be associated with LUMBAR or PHACE(S) syndrome (see below)[51]. They are GLUT1-positive and involute at a pace similar to classic IHs, although larger ectatic vessels may persist.

Involution of IHs may begin as early as the first year of life and continues for several years. A color change from bright red to gray–purple (Fig. 103.9) and flattening of the surface are often the earliest signs of involution in superficial lesions. As the tumor involutes, deeper lesions become less firm[52].

Classic studies on the natural history of untreated hemangiomas demonstrated that 30% of lesions involute fully by 3 years of age, 50% by 5 years, 70% by 7 years, and >90% by 9 years[52]. However, more recent studies have concluded that the median age of completed involution is 36 months, with >90% of children showing no further improvement after 4 years of age[53]. Some hemangiomas involute completely, while others leave residual telangiectasias, atrophy/anetoderma, fibrofatty tissue, redundant skin, or (if previously ulcerated) scarring (Fig. 103.10). Predicting whether the residual lesion will be significant is a challenging aspect of hemangioma management. Risk factors for more prominent sequelae include an abrupt "step" border, "cobblestoned" surface, and mixed IH subtype[54].

Complications

The majority of hemangiomas are small lesions that require little or no intervention. However, some hemangiomas are problematic due to their size, location, or association with other anomalies. The age of the patient and the growth pattern of the hemangioma are additional factors that help to determine the risk of complications and need for systemic therapy[55] (see Table 103.7).

Ulceration

Ulceration occurs in up to 10% of all IHs and represents the most common complication[56]. Although hemangiomas in any location can be affected, those on the lip and in the anogenital region or other skin folds (e.g. the neck) have the greatest tendency to ulcerate (Fig. 103.11). Ulceration develops more commonly within large, mixed (superficial and deep), or segmental hemangiomas[56]. For example, ulceration occurs in up to 30% of segmental extremity lesions (see Fig. 103.3C)[44]. In addition, IHs-MAG are prone to ulceration, which may be recalcitrant.

Ulceration of IHs occurs most commonly during the proliferative phase, with most ulcers developing within the first 6 months of life[57]. Whitish discoloration of hemangiomas in infants younger than 3 months of age may be a sign of impending ulceration[58]. In addition to causing pain, ulcers increase the risk of infection and result in scarring. Bleeding rarely occurs and can usually be controlled with firm pressure. The management of ulcerated hemangiomas may be challenging (see below)[57,59]. Large hemangioma size, segmental morphology, and ulceration extending over a greater surface area are associated with longer healing times[57].



Fig. 103.9 Infantile hemangioma during involution. Note the patchy lightening in surface color and softening.

Disfigurement and interference with function related to IH size and/or location

Large hemangiomas can distort tissues, interfere with function, and lead to significant long-term sequelae. In addition, regional extracutaneous abnormalities may occur, primarily in association with segmental hemangiomas (see below). High-output congestive heart failure represents a rare complication that occurs primarily in patients with extensive hepatic hemangiomas.

Even small IHs may cause complications if they arise in vulnerable locations. *Periocular* hemangiomas can result in ophthalmologic complications (Fig. 103.12). Most commonly, periocular hemangiomas cause astigmatism by compressing the globe and deforming the cornea, which results in asymmetric refractive errors. They may also cause visual abnormalities by obstructing the visual axis or by invading the orbital musculature, which can lead to light-deprivation amblyopia and strabismus, respectively. Proptosis is a rare presentation of an orbital hemangioma, potentially leading to corneal exposure; the diagnosis of hemangioma may be difficult clinically when a cutaneous lesion is not present. Infants with periocular hemangiomas should be evaluated by an ophthalmologist at baseline with appropriate follow-up during the proliferative stage.

Hemangiomas on the *nasal tip* are particularly challenging (Fig. 103.13A). Deep and mixed hemangiomas can distort the underlying cartilage and leave significant fibrofatty residua upon involution. The resultant "Cyrano-nose" deformity may require reconstructive surgery. In rare cases, superficial hemangiomas located along the *columella* may ulcerate and lead to destruction of underlying cartilage, which may be heralded by the appearance of a horizontal crease in the inferior columella.



Fig. 103.10 Residua of infantile hemangiomas. Hemangioma with ulcer (**A**), which involuted leaving minimal hypopigmentation (arrows) and a circular scar at site of ulceration in the same patient 20 years later (**B**); **C, D** telangiectasias; and **E** atrophy and fibrofatty changes. *A, B, Courtesy Ronald P. Rapini, MD; D, Courtesy Jean L. Bolognia, MD.*

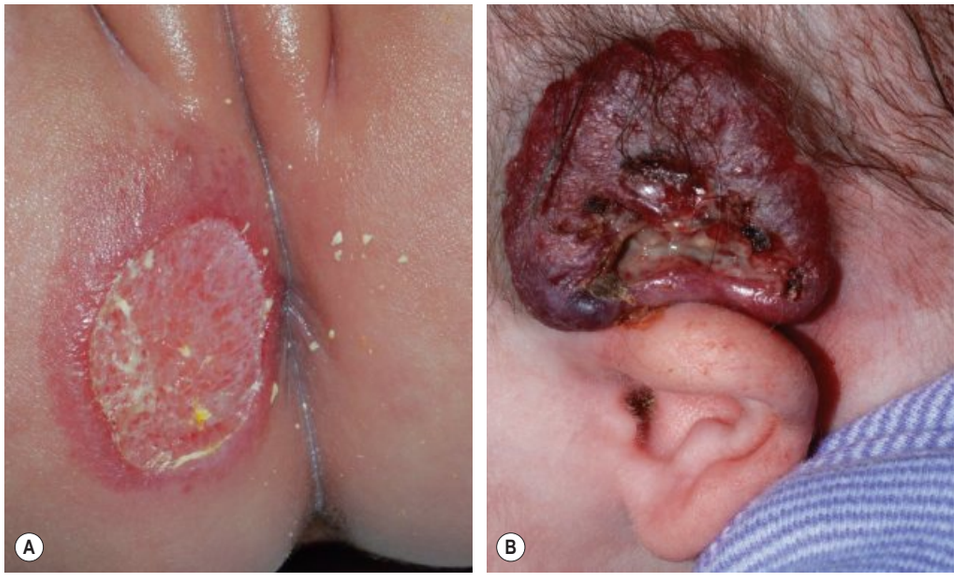


Fig. 103.11 Ulcerated hemangiomas. A Ulcerated early superficial hemangioma on the buttock. Because the hemangioma component may not be obvious, this diagnosis should be considered when an infant presents with an ulcer in the diaper area. **B** Ulcerated thick superficial hemangioma above the ear. Note the distortion of the pinna. *Courtesy Julie V. Schaffer, MD.*



Fig. 103.12 Infantile hemangiomas affecting the eyelids. These superficial segmental **(A)** and deep **(B)** infantile hemangiomas are obstructing the visual axis. *Courtesy Julie V. Schaffer, MD.*



Fig. 103.13 Infantile hemangiomas in facial sites with increased risk of disfigurement. A Nasal deformity can result from mixed or deep hemangiomas on the nasal tip. **B** The lip is a sensitive site, especially when lesions cross the vermilion border or involve the philtrum, and hemangiomas in this location are prone to ulceration. *Courtesy Julie V. Schaffer, MD.*

Lip hemangiomas are often superficial or mixed lesions; painful ulceration is common as they proliferate, which leads to feeding difficulties. Local factors, including friction and moisture, may contribute to ulceration. Distortion of the vermilion border or lengthening of the lip can result in significant cosmetic residua, eventually requiring surgical correction (Fig. 103.13B)[60].

Hemangiomas located on the *pinna* may ulcerate and become infected, increasing the risk of scarring and distortion of normal structures. Conductive hearing loss can result from obstruction of the external auditory canal by a hemangioma.

Hemangiomas located on the *breast* pose a particular challenge in girls. These lesions may affect the underlying breast bud, and residual masses may lead to the appearance of breast asymmetry. Early surgical intervention is not advised, as it may ultimately affect normal breast development.

Anogenital hemangiomas are often complicated by painful ulceration, and wound care may be difficult in this region. Large hemangiomas of the *limbs* may also ulcerate, and residual excess tissue and rarely limb-length discrepancy can remain upon involution.

Extracutaneous involvement

Large hemangiomas on the head and neck, most commonly segmental lesions >5 cm in diameter, can pose challenges beyond the complications noted above. In particular, they are often associated with extracutaneous anomalies[61]. These hemangiomas may present as segmental telangiectatic patches (e.g. IH-MAG), plaques, or deep masses. A relationship between facial hemangiomas and structural or vascular CNS anomalies was recognized >45 years ago[62]. Since then, other associated congenital anomalies have been identified. In 1996[63], the acronym *PHACE(S) syndrome* was coined for this spectrum of findings: *P, p*osterior fossa and other structural brain malformations; *H, h*emangioma; *A, a*rterial anomalies of cervical and cerebral vessels; *C, c*ardiac defects (especially *c*oarctation of the aorta); *E, e*ye anomalies; and *S, s*ternal defects and *s*upraumbilical raphe (Fig. 103.14). Impaired hearing, dysphagia, speech/language delay, dental anomalies, and endocrine abnormalities such as hypopituitarism and hypothyroidism are additional less commonly observed features[64,65]. Diagnostic criteria for PHACE(S) syndrome were established by a multidisciplinary group of specialists in 2009 and updated in 2016[66] (Table 103.4).

In a prospective study of 108 infants (age <1 year) with large facial hemangiomas (≥22 cm^2), 31% had PHACE(S) syndrome. The vast majority (91%) of affected individuals had more than one extracutaneous manifestation (major ± minor criteria), and the most common findings were cerebrovascular (91%), cardiovascular (67%), and structural brain (52%) anomalies[61]. The cerebrovascular anomalies typically occur ipsilateral to the hemangioma and most commonly involve the internal carotid artery, highlighting the need for both head and neck imaging[67]. Of note, in other studies, the prevalence of PHACE(S) in infants with segmental IHs of the head and neck was as high as 58%[68].

An approach to the evaluation of infants at risk for PHACE(S) syndrome is presented in Fig. 103.15, and there are consensus-derived recommendations for evaluation and ongoing care[66]. Cerebrovascular and cardiovascular changes may be progressive, with potential complications including ischemic stroke and neurovascular sequelae in adulthood (e.g. atypical migraines, hearing loss)[69,70]. Affected individuals should be followed by specialists as clinically appropriate.

Lower facial or "beard" hemangiomas often serve as markers of airway hemangiomas, which typically involve the subglottis. The risk of airway hemangiomas can be estimated by the extent of cutaneous involvement in this region (Fig. 103.16)[71], but occasionally they are associated with segmental hemangiomas that primarily involve the upper face or small hemangiomas in the "beard" area[72]. The onset of respiratory symptoms such as noisy breathing or biphasic stridor ranges from weeks to months of age[71]. Infants with lower facial hemangiomas of concern should be referred for otolaryngologic evaluation.

Hemangiomas located in the *midline lumbosacral area* (Fig. 103.17) are a marker for occult spinal dysraphism. The risk of spinal dysraphism in an infant or child with an isolated midline lumbosacral hemangioma or residuum of an involuted hemangioma >2.5 cm in diameter is ~35%[73]. Factors that further increase the risk include a larger or ulcerated hemangioma and the presence of additional cutaneous markers such as a deviated gluteal cleft, lipoma, or skin appendage (see Ch. 64)[73].

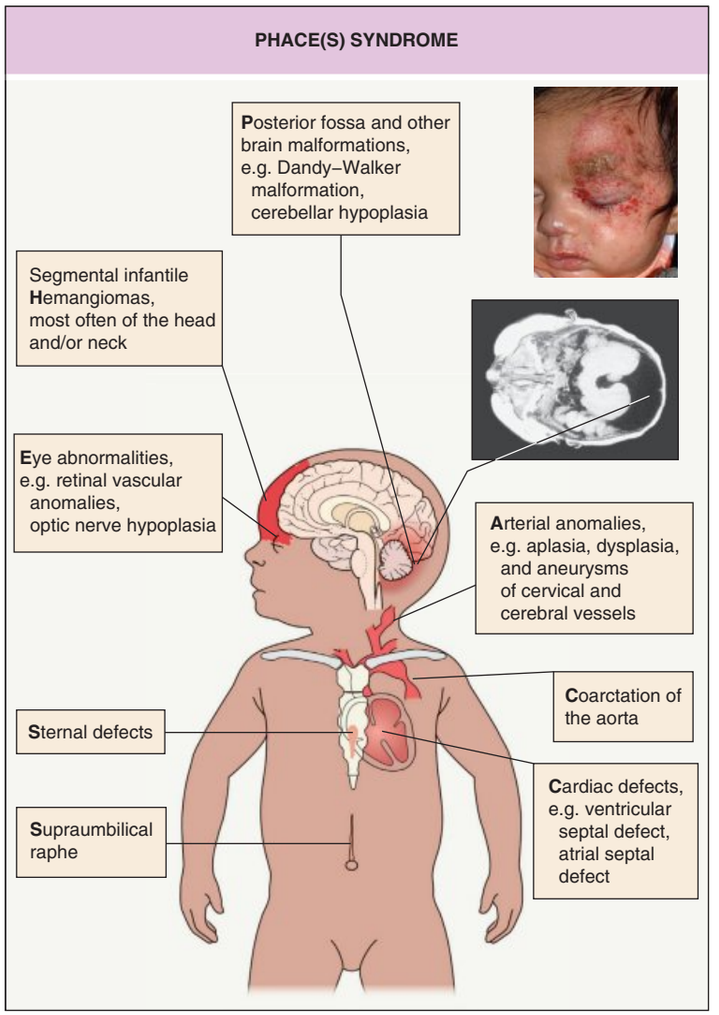


Fig. 103.14 PHACE(S) syndrome. Major clinical features are illustrated. Additional possible associated features include hearing impairment, dysphagia, speech/language delay, dental anomalies, and endocrine abnormalities such as hypopituitarism and hypothyroidism. *Inset, courtesy Julie V. Schaffer, MD.*

Large hemangiomas on the lower body, especially extensive segmental IHs, are associated with a broad spectrum of regional extracutaneous abnormalities, analogous to those of the upper body in PHACE(S) syndrome. Several acronyms have been proposed for this group of findings, and the most inclusive is *LUMBAR syndrome*: *L, l*ower body/*l*umbosacral hemangioma and *l*ipomas or other cutaneous anomalies (e.g. "skin tags"); *U, u*rogenital anomalies and *u*lceration of the hemangioma; *M, m*yelopathy (spinal dysraphism); *B, b*ony deformities; *A, a*norectal and *a*rterial anomalies; and *R, r*enal anomalies[74] (Fig. 103.18). Recommendations for evaluation of infants with hemangiomas in a midline lumbosacral location and/or a segmental distribution on the lower body are summarized in Fig. 103.15.

Multifocal lesions are found in 10%–25% of infants with hemangiomas and may be associated with visceral involvement[75]. Most infants with both internal and skin involvement have many small, superficial cutaneous hemangiomas that range from a few millimeters to a few centimeters in diameter (Fig. 103.19). Historically, the terms *"diffuse"* and *"benign" neonatal hemangiomatosis* were used for infants who had multiple cutaneous hemangiomas with or without visceral lesions, respectively. However, some cases reported as diffuse neonatal hemangiomatosis actually represented other vascular anomalies (e.g. multifocal lymphangiomatosis with thrombocytopenia; see Ch. 114)[76]. To avoid confusion, *multifocal infantile hemangiomas with or without extracutaneous hemangiomas* is now the preferred term.

The liver is by far the most common site of internal hemangiomas in patients with multifocal IHs (Fig. 103.20). Because a larger number of cutaneous IHs increases the risk of hepatic involvement, evaluation

DIAGNOSTIC CRITERIA FOR PHACE(S) SYNDROME		
Definite PHACE(S):		
• Hemangioma >5 cm in diameter of the head including scalp PLUS 1 major criterion or 2 minor criteria • Hemangioma of the neck, upper trunk, or trunk and proximal upper extremity PLUS 2 major criteria		
Possible PHACE(S):		
• Hemangioma >5 cm in diameter of the head including scalp PLUS 1 minor criterion • Hemangioma of the neck, upper trunk, or trunk and proximal upper extremity PLUS 1 major criterion or 2 minor criteria • No hemangioma PLUS 2 major criteria		
Organ system	**Major criteria**	**Minor criteria**
Arterial	• Anomalies of major cerebral or cervical arteries* – dysplasia†, hypoplasia, stenosis/occlusion, aberrant origin/course • Persistent carotid–vertebrobasilar anastomosis (e.g. proatlantal segmental, hypoglossal, otic, trigeminal arteries)	• Aneurysm of cerebral arteries
Structural brain	• Posterior fossa anomalies – Dandy–Walker complex, other hypoplasia/dysplasia of the mid or hind brain	• Midline anomalies • Malformation of cortical development
Cardiovascular	• Aortic arch anomalies • Aberrant origin of subclavian artery ± vascular ring	• Ventricular septal defect • Right/double aortic arch • Systemic venous anomalies
Ocular	• Posterior segment anomalies – persistent hyperplastic primary vitreous/persistent fetal vasculature, retinal vascular anomalies, optic nerve hypoplasia, morning glory disc anomaly	• Anterior segment anomalies, e.g. sclerocornea, cataract, coloboma, microphthalmia
Ventral or midline	• Sternal defect/pit/cleft • Supraumbilical raphe	• Hypopituitarism • Ectopic thyroid • Midline sternal papule/hamartoma
*Includes internal carotid artery; middle, anterior, or posterior cerebral artery; and vertebrobasilar system. †Includes kinking, looping, tortuosity, and/or dolichoectasia.		

Table 103.4 Diagnostic criteria for PHACE(S) syndrome[66].

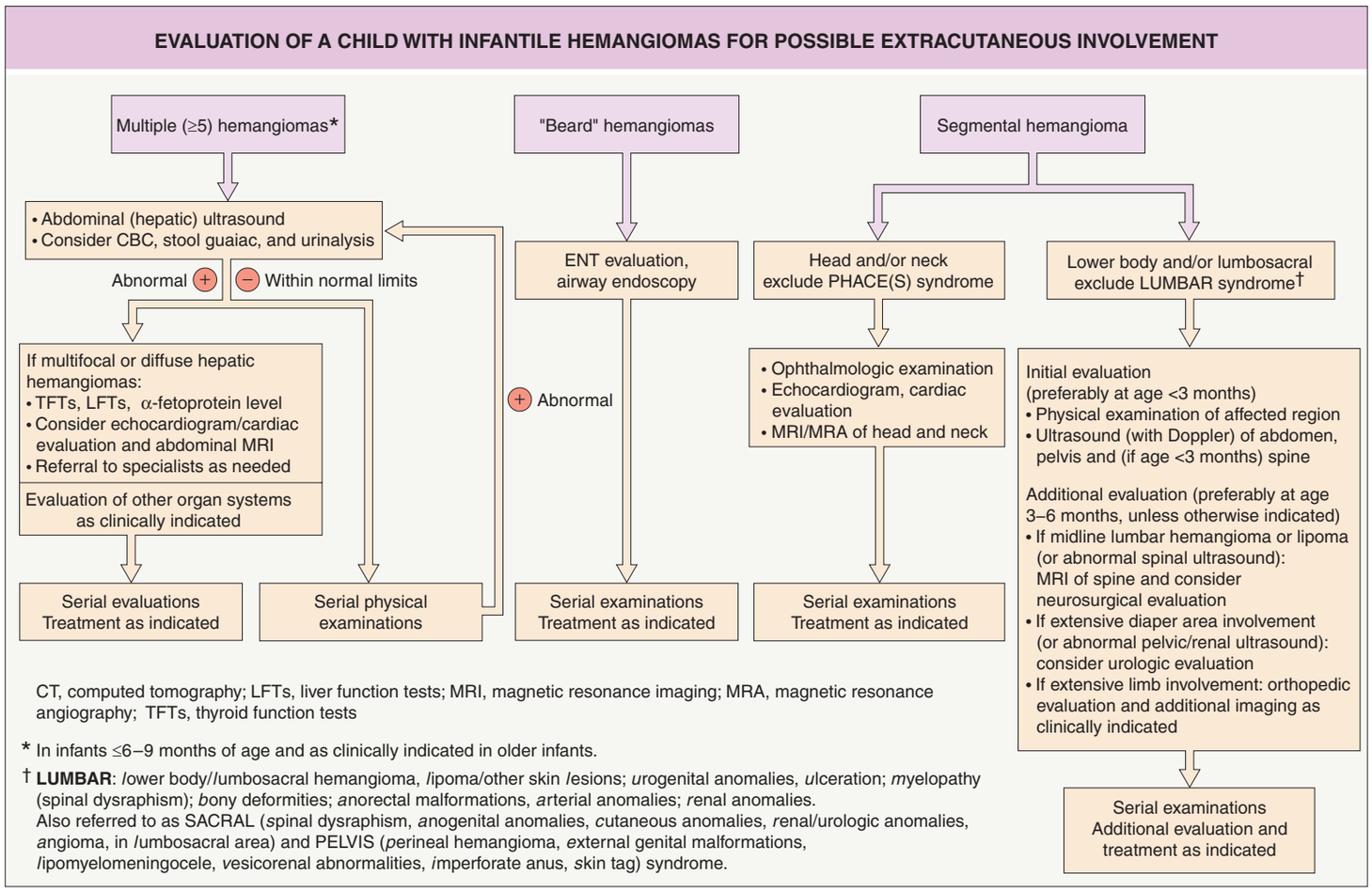


Fig. 103.15 Evaluation of a child with infantile hemangiomas for possible extracutaneous involvement.

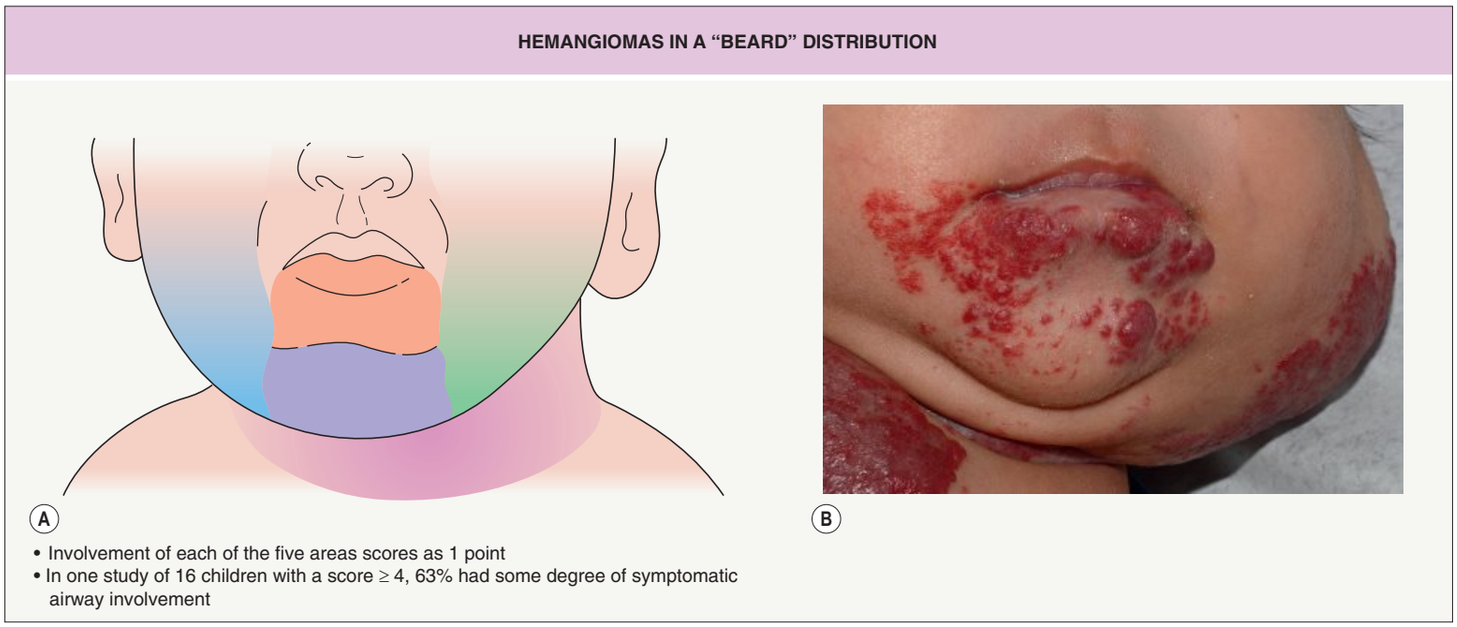


Fig. 103.16 Hemangiomas in a "beard" distribution. A Anatomic sites associated with risk of an airway hemangioma. **B** Infant with a laryngeal hemangioma in addition to cutaneous lesions in a "beard" distribution. *A, Adapted, with permission, from ref. 71; B, Courtesy Julie V. Schaffer, MD.*



Fig. 103.17 Segmental lumbosacral hemangioma. This child is at risk for LUMBAR syndrome. *Courtesy Julie V. Schaffer, MD.*

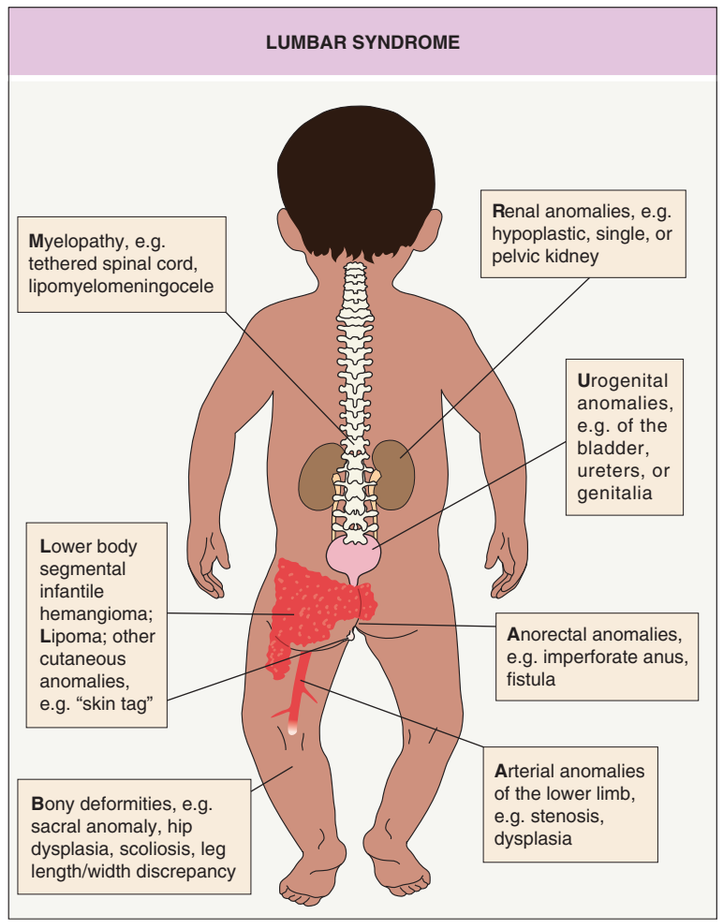


Fig. 103.18 LUMBAR syndrome. Major clinical features are illustrated. The segmental hemangioma is often ulcerated.

with abdominal ultrasonography is recommended when ≥5 skin lesions are present (see Fig. 103.15)[77,78]. Rarely, infants with a large IH or fewer than 5 small IHs have liver involvement.

Liver hemangiomas are classified as focal, multifocal, or diffuse. Focal hepatic hemangiomas are likely distinct from IHs, undergoing early involution similar to rapidly involuting congenital hemangiomas (RICH; see below)[79]. Multifocal and especially diffuse hepatic hemangiomas are associated with a risk of high-output cardiac failure due to arteriovenous or arterioportal shunts, as well as hypothyroidism (see below) and abdominal compartment syndrome due to massive hepatomegaly[79]. Management of patients with hepatic hemangiomas requires interdisciplinary care, which typically includes serial ultrasounds, clinical assessments and laboratory evaluation, with treatment as indicated[79].

Extracutaneous hemangiomas occasionally occur in infants with a single large cutaneous hemangioma, usually a segmental facial lesion, with or without associated PHACE(S). For example, segmental cutaneous hemangiomas may be associated with segmental hemangiomas in the gastrointestinal tract, most often in the distribution of the superior mesenteric artery and potentially complicated by bleeding[80]. IHs within the CNS are very rare and typically represent intracranial or intraspinal extension of an overlying IH, which may be a segmental lesion. Associated hydrocephalus has been reported, but invasion into the CNS parenchyma does not typically occur[81]. Additional sites of internal involvement rarely observed in association with segmental hemangiomas of the skin include the mediastinum and lungs.



Fig. 103.19 Multifocal infantile hemangiomas with extracutaneous hemangiomas. In this child, many small, superficial skin lesions were present in a miliary pattern and hemangiomas were present in the liver. Historically, this was referred to as "diffuse neonatal hemangiomatosis". *Courtesy Julie V. Schaffer, MD.*

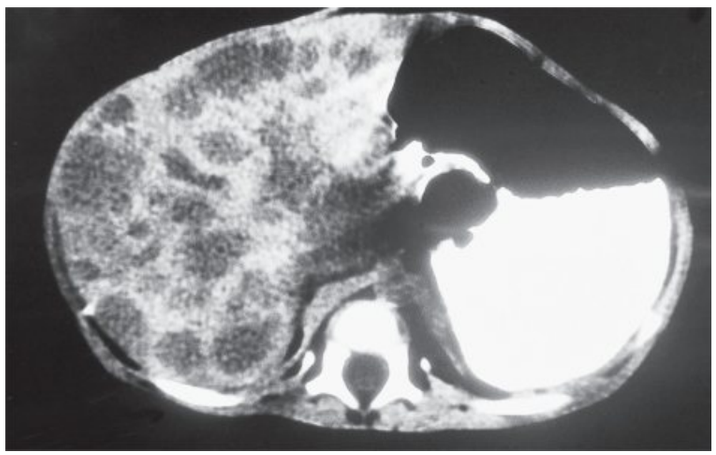


Fig. 103.20 Multifocal hepatic hemangiomas. CT scan demonstrating multiple hepatic hemangiomas in a child with multifocal cutaneous infantile hemangiomas ("diffuse neonatal hemangiomatosis"). *Courtesy Amy Paller, MD.*

Hemangiomas may also develop in a variety of other locations, including mucosal surfaces and the eyes. Extracutaneous hemangiomas may also occur in the absence of skin lesions. Typically, IHs in extracutaneous sites follow the same course of proliferation and involution as cutaneous lesions.

Increased levels of type 3 iodothyronine deiodinase, an enzyme that deactivates thyroid hormone, have been identified in tissue from proliferating hemangiomas. This can lead to hypothyroidism in infants with large-volume proliferative-phase lesions[82]. The consumptive nature of the hypothyroidism often makes it difficult to correct, but it resolves as the tumor regresses. Screening for hypothyroidism in the immediate neonatal period is inadequate, as hemangiomas are typically only beginning to develop at that time. Although consumptive hypothyroidism is usually associated with hepatic hemangiomas, it has been described in patients with large hemangiomas in the parotid area, and type 3 iodothyronine deiodinase activity has been noted in cutaneous hemangiomas[83]. Consequently, it has been recommended that evaluation for hypothyroidism be considered in infants with large cutaneous hemangiomas or hepatic hemangiomas[82].

RADIOLOGIC FEATURES

Most superficial and mixed IHs are diagnosed based upon their clinical features. Ultrasonography or MRI may be helpful in confirming the diagnosis and extent of deep IHs that lack superficial changes. It is important to consider the phase of growth when assessing hemangiomas radiographically, because proliferating hemangiomas demonstrate different characteristics than their involuting and involuted counterparts.

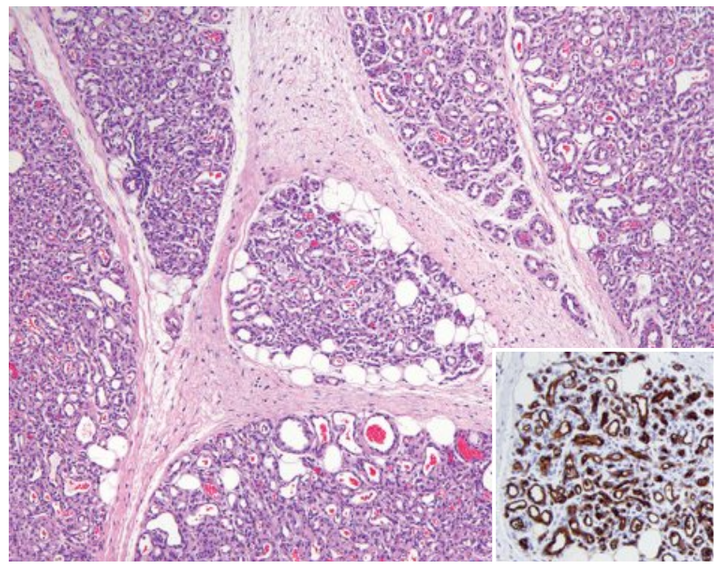


Fig. 103.21 Histologic features of a proliferating infantile hemangioma. Collections of endothelial cells forming vascular lumens, separated by fibrotic septae. The inset shows positive GLUT1 staining of endothelial cells. *Courtesy Matthew Kuhar, MD.*

MRI with contrast is the most useful imaging technique for helping to define the extent and tissue characteristics of vascular anomalies, and the use of contrast can help to differentiate a hemangioma from other tumors. If MRI does not confirm the diagnosis of hemangioma or there are concerns regarding a possible malignancy, histologic examination of the tumor is recommended. MRI and/or MR angiography (MRA) can also be used to determine the presence of hemangiomas within internal organs and to detect other structural abnormalities, including CNS malformations and arterial anomalies.

PATHOLOGY

The histopathologic features of IH correlate with the stage of hemangioma development (see Table 103.1). IHs may extend from the superficial dermis to the deep subcutaneous tissue; in some locations, there may be involvement of surrounding tissues such as salivary glands and muscle. Biopsy specimens of proliferating hemangiomas demonstrate well-defined non-encapsulated masses composed of proliferating plump endothelial cells and pericytes. Small vascular lumens may be noted focally throughout the tumor, but lumen formation may be more difficult to appreciate in early proliferating lesions.

Later in the proliferating stage, lobules of endothelial masses separated by fibrous septae become more prominent (Fig. 103.21). Larger feeding and draining vessels are noted within the septae, and mitotic figures and apoptotic bodies may be present within the tumor mass. Although abnormal mitotic figures are not typical of proliferating hemangiomas, some authors have noted that mitotic activity and mild nuclear pleomorphism may be present in IHs and should not be a cause for concern if other typical histopathologic features are also present. An increased number of mast cells is often present within proliferating hemangiomas, and some studies have found even higher numbers of mast cells during early involution[31].

The involution phase is marked by flattening of the endothelium and reduced numbers of mitotic figures. Eventually, the vessels decrease in number and lose their tightly packed appearance, with fibrous and fatty tissue separating the vessels within and between lobules. The feeding and draining vessels within the septae may persist. Fully involuted lesions display fibrofatty tissue and a few persistent vessels at sites where tumor lobules and septae previously existed.

Immunohistochemical analysis is useful for confirming the diagnosis of IH. A high level of GLUT1 immunoreactivity is present in the endothelia within IHs of all phases (see Fig. 103.21). GLUT1 staining is

absent in most other types of vascular tumors and vascular malformations. Wilms tumor 1 (WT1) expression is also observed in IH but not vascular malformations, with the exception of arteriovenous malformations. In addition, other placenta-associated vascular proteins, including FcγRII, merosin and Lewis Y antigen, are present in IHs but absent in vascular malformations and pyogenic granulomas. These placental markers are also absent in normal vessels of the skin and subcutis[12,31].

DIFFERENTIAL DIAGNOSIS

Superficial and mixed hemangiomas are usually diagnosed based upon their characteristic clinical features. Hemangioma precursors and early proliferating lesions may sometimes be misdiagnosed as capillary malformations or telangiectasias. Pyogenic granulomas (PGs) occur commonly in children and may mimic a superficial hemangioma; however, PGs usually arise after the first few months of life, are typically pedunculated, and tend to bleed. Other vascular lesions of infancy that may be in the differential diagnosis of superficial hemangioma include tufted angioma, multifocal lymphangioendotheliomatosis with thrombocytopenia, infantile hemangiopericytoma, spindle cell hemangioma, verrucous venulocapillary malformation ("verrucous hemangioma"), and eccrine angiomatous hamartoma.

Deep hemangiomas provide a greater diagnostic challenge, and radiographic evaluation may be helpful. Other vascular anomalies that may be considered in the differential diagnosis of a deep hemangioma include a venous, lymphatic, or combined venous–lymphatic malformation (see Ch. 104) as well as a congenital hemangioma (see below; Table 103.5) or kaposiform hemangioendothelioma (see Ch. 114). Kasabach–Merritt phenomenon (KMP), a potentially life-threatening thrombocytopenic coagulopathy, typically presents during the first months to year of life with a rapidly enlarging, ecchymotic mass (see Ch. 114); KMP is now known to be primarily associated with kaposiform hemangioendotheliomas and less often tufted angiomas, but not IHs as historically assumed.

Congenital fibrosarcoma is often firm and blue–purple in color and can have ectatic superficial veins, which may lead to misdiagnosis as a hemangioma. In addition, some patients with this malignancy present with disseminated intravascular coagulation, which further confuses the clinical picture. Rhabdomyosarcoma, neuroblastoma, primitive neuroectodermal tumor, lymphoblastic lymphoma, and dermatofibrosarcoma protuberans are other neoplasms that may have a vascular appearance due to overlying telangiectasias or a blue–red color. Additional entities that may be mistaken for a hemangioma include: infantile myofibromatosis – solitary or multiple red to pink plaques or nodules; lipoblastoma – an enlarging skin-colored or (less often) erythematous mass; and nasal glial heterotopia – classically a congenital blue–red mass on the bridge of the nose. Radiographic studies, especially MRI, may be useful in differentiating these tumors from a hemangioma. However, if the diagnosis is not clarified by clinical and radiographic examinations, or if the lesions are atypical, then histologic examination is indicated.

KEY FEATURES OF INFANTILE AND CONGENITAL HEMANGIOMAS

Infantile hemangioma	Rapidly involuting congenital hemangioma (RICH)	Non-involuting congenital hemangioma (NICH)
Usually absent or precursor lesion at birth	Fully developed at birth	Fully developed at birth
Rapid postnatal proliferation	Intrauterine proliferation	Intrauterine proliferation then proportionate postnatal growth
Slow spontaneous involution	Rapid involution during the first year*	Do not involute spontaneously Tardive growth during childhood in ~10%
More common in girls	Equal prevalence in boys and girls	Equal prevalence or slightly more common in girls
Lobular endothelial proliferation during proliferative phase; fibrous and fatty tissue during involution	Capillary lobules within fibrotic stroma containing thin-walled vessels, hemosiderin	Lobules of small, thin-walled vessels with large central vessel; dilated, dysplastic veins between lobules; "hobnailed" endothelial cells lining intralobular vessels
Positive GLUT1 and Lewis Y antigen	Negative GLUT1 and Lewis Y antigen	Negative GLUT1 and Lewis Y antigen

*Occasionally associated with thrombocytopenia during the neonatal period.

Table 103.5 Key features of infantile and congenital hemangiomas. Partially involuting congenital hemangiomas (PICHs) represent an intermediate form that undergoes incomplete involution.

TREATMENT

IHs manifest with a wide spectrum of clinical severity, and their management needs to be individualized. The Hemangioma Activity Scale and Hemangioma Severity Scale were developed to help objectively assess IHs and their response to therapy[84,85]. Active intervention is recommended for IHs with a greater risk of developing local or systemic complications (Table 103.6)[86]. The major goals of management include: (1) preventing or reversing life- or function-threatening complications; (2) treating ulcerations; (3) preventing permanent disfigurement; (4) minimizing psychosocial distress to patients and their families; and (5) avoiding overly aggressive, potentially scarring procedures for lesions that have a strong probability of involuting without significant residua[87].

Active Non-Intervention

Small, uncomplicated hemangiomas carry an excellent prognosis and are often managed with active non-intervention, especially in extrafacial sites[88]. However, physicians should recognize that even small, seemingly trivial lesions may be troubling to parents and cause significant distress. Active non-intervention includes addressing parental concerns as well as discussing the expected natural history of IHs, indications for treatment, types of therapy, and why such interventions are or are not appropriate for their child. The hemangioma can be followed with periodic clinical assessment and photography. Reviewing photographic examples of the evolution of hemangiomas may be helpful for families. Many parents are fearful of bleeding; therefore, reviewing the care for superficial bleeding, along with reassurance that it is rarely problematic, is worthwhile.

Management of Ulceration

Ulceration is the most frequent complication of IHs (see Fig. 103.11). Management should be directed at healing the ulceration, preventing infection, and reducing pain. Multiple modalities are often used concurrently, with no single therapy proven to be most effective[59]. Components of management include wound care, treatment of infection (relatively uncommon), specific therapies (e.g. topical or systemic β-blockers), and pain control.

Wound care

Many small, superficial ulcerations can be managed with local wound care. Saline solution compresses may be used to gently debride thick

REASONS TO CONSIDER SYSTEMIC THERAPY FOR INFANTILE HEMANGIOMAS

Threatened vital functions
- Vision
- Airway

Increased potential for disfigurement
- Nasal tip/columella
- Lip, especially if the lesion crosses the vermilion border
- Large (≥2 cm)/rapidly growing lesion, especially if on the face (>1 cm if age ≤3 months) or with an abrupt "step" border
- Breast, especially if a larger lesion involves the nipple in a girl

Recalcitrant/severe ulceration

High-output cardiac failure

Table 103.6 Reasons to consider systemic therapy for infantile hemangiomas.

crusts. Although infection is uncommon, topical antibacterial ointments (e.g. mupirocin) can be applied for occlusive as well as antimicrobial effects. If clinical signs of infection develop, a bacterial culture should be obtained. Occlusive dressings (e.g. hydrocolloid, foam, silicone-based) aid in healing and pain control. They can be applied after the topical antibiotic or petrolatum at sites that are amenable (see Ch. 145). Thin hydrocolloid dressings are often favored because of the ease of application over curved surfaces and the ability to leave them in place for a few days. Inexpensive petrolatum-impregnated gauze is another option and it is especially helpful for perineal ulcers, but needs to be changed frequently.

Specific therapy

Modalities that are utilized to treat hemangiomas for other indications (see below) may be helpful in treating ulcerated lesions. Application of topical timolol can aid in healing of small ulcerated IHs, but caution must be taken regarding systemic absorption[89–91] (see below).

Oral propranolol therapy is often useful for ulcers that are extensive or have failed local therapies. In one study of ulcers present for a mean of 7 weeks, the median time to healing after initiating propranolol was 4 weeks and most patients achieved pain relief within 15 days[92]. Although early propranolol therapy may help to prevent ulceration of IHs in high-risk locations, precipitation or worsening of ulceration in such lesions has also been described with propranolol administration[93]. Initiation of propranolol at a low dose with slow escalation is recommended for IHs with ulceration or at high risk of ulceration – a recent retrospective study found that ulcer healing time was shorter with a propranolol dose of ≤1 mg/kg/day compared to higher doses[57,93].

Pulsed dye laser has been used for the treatment of ulcerated hemangiomas, especially in combination with other modalities. Some uncontrolled studies demonstrated healing of ulcerations and resolution of pain after two to three treatments[94]. However, others observed mixed results, with 50% showing improvement and 5% experiencing worsening of the ulceration[59]. Excisional surgery may be considered for small or pedunculated ulcerated lesions.

Pain control

An important consideration in the treatment of ulcerated hemangiomas is pain control. Local wound care, and especially occlusive dressings, can provide some pain relief. Oral acetaminophen and topical lidocaine 2%–5% ointment may also help to alleviate the discomfort. Lidocaine ointment should be used sparingly (e.g. maximum of a pea-sized amount) to prevent systemic lidocaine toxicity. Eutectic mixture of local anesthetics is not recommended for the treatment of ulcerated hemangiomas because it should not be applied to eroded or ulcerated skin[59]. In severe cases, consultation with a pain management specialist may be required.

Local Therapies

Topical β-blockers

Topical application of timolol maleate, a non-selective β-blocker, can be of benefit in the treatment of IHs, especially small superficial lesions that are <1 mm in thickness[91,95] (Fig. 103.22). Timolol is available in several ophthalmic formulations, including 0.5% solution and 0.5% gel-forming solution (GFS; extended-release), with one drop (0.25 mg) twice daily of the latter most commonly utilized to treat IHs. A randomized control study found this dosing of timolol 0.5% GFS to be an effective and safe therapy for small (<2.5 cm), thin, non-ulcerated cutaneous IHs in infants 5–24 weeks of age, with benefit seen after 8–16 weeks of treatment[96].

A pharmacokinetic study found that as hemangiomas with a prominent superficial component increased in thickness, higher plasma concentrations of topically applied timolol were observed[97]. Although topical timolol treatment guidelines have not been established, it is recommended that the dose be limited to a maximum of 2 drops of timolol 0.5% GFS daily or <0.25 mg/kg/day[98,99]. Despite systemic absorption, topical timolol treatment is generally well tolerated and serious adverse events are rare.

Intralesional corticosteroids

Historically, intralesional corticosteroids were commonly used to treat localized IHs; however, this modality is now utilized infrequently considering the efficacy of β-blocker therapy. Intralesional corticosteroids (e.g. triamcinolone <3 mg/kg per treatment session) may be employed for selected small, focal hemangiomas. However, serious complications, including retinal and ophthalmic artery occlusion leading to permanent vision loss, as well as local atrophy and necrosis, have limited the use of this modality in the periorbital area[100].

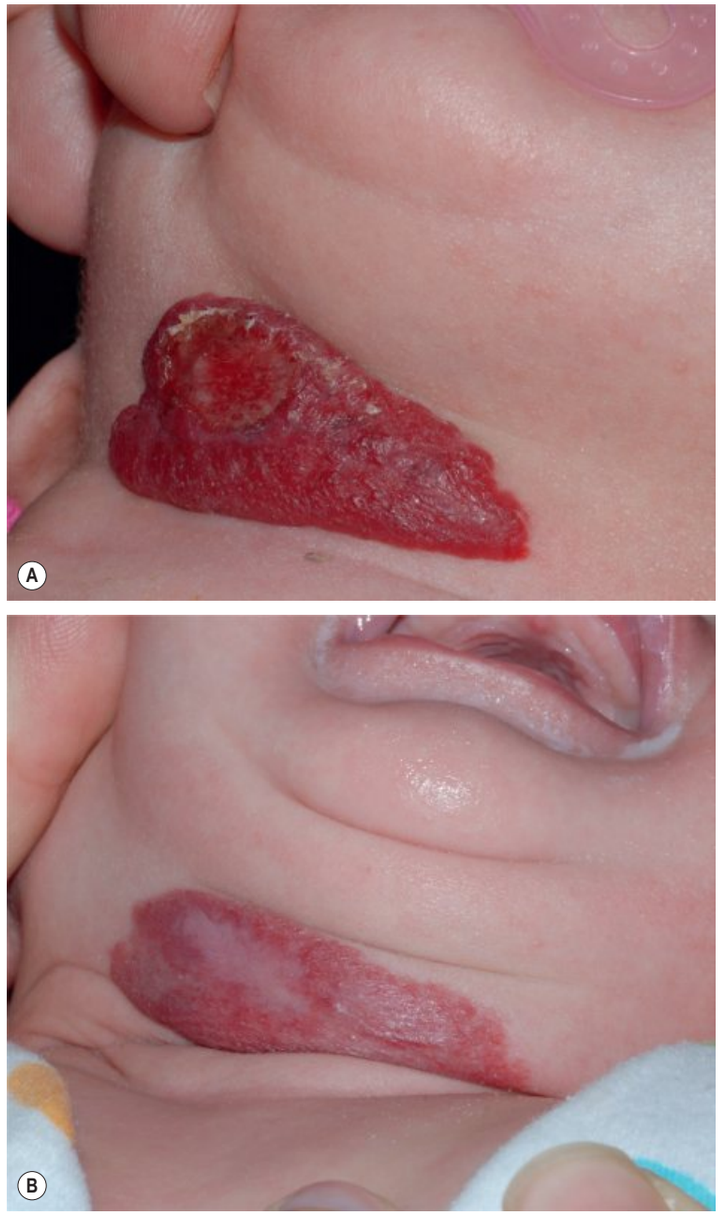


Fig. 103.22 Ulcerated superficial hemangioma treated with topical timolol. **A** An ulcerated superficial infantile hemangioma on the neck of a 10-week-old girl. **B** Four weeks after institution of topical timolol 0.5% gel, with one small drop applied twice daily. Note the healing of the ulcer, which occurred within two weeks, as well as the lighter color and decreased thickness of the hemangioma. *Courtesy Julie V. Schaffer, MD.*

Systemic Therapies

Systemic β-blockers

The serendipitous discovery of the non-selective β-blocker propranolol as a treatment for IH in 2008 has revolutionized the management of this common tumor, and it currently represents the first-line systemic therapy for IHs[101]. In 2014, propranolol (Hemangeol™) became the first FDA-approved treatment for IHs. Oral β-blockers are effective in halting growth and expediting regression of cutaneous, ocular, airway, and hepatic IHs as well as for complications such as ulceration.

The mechanisms of action of propranolol are thought to be multifaceted. The color change from red to purple and softening that are observed within the first few days of treatment are likely related to immediate vasoconstrictive effects via β_2-adrenergic receptors on hemangioma pericyte cells. Subsequent progressive reduction in volume and redness may be due to decreases in serum concentration of VEGF, bFGF, and renin as well as induction of endothelial cell apoptosis[102–105].

Compared to systemic corticosteroids, propranolol has superior efficacy and a more favorable side-effect profile[106]. Potentially serious adverse effects such as hypotension, bradycardia, hypoglycemia, and bronchospasm are uncommon. β-blockers may mask early signs of hypoglycemia, so infants should be fed in conjunction with medication administration[107]. More common side effects include sleep disturbances (e.g. restless sleep, nightmares), cold extremities, diarrhea, and somnolence (especially in the first few days of therapy). There are rare reports of hyperkalemia associated with propranolol treatment of large ulcerated hemangiomas[108,109]. Long-term studies have found no evidence of cognitive, developmental, or growth impairment in 4- to 7-year-old children who received propranolol treatment for hemangiomas during infancy[110,111].

Table 103.7 outlines recommendations for propranolol administration, although clinical practices regarding evaluation, dosing, and monitoring vary[112,113]. Patients at risk of PHACE(S) syndrome should undergo evaluation for cardiovascular and cerebrovascular anomalies that may merit caution given the theoretical risk for hypotension. Most infants with PHACE(S) syndrome can be successfully treated with propranolol[114]. However, depending on their extracutaneous manifestations, these patients may need to be managed together with cardiologists and/or neurologists, proceeding cautiously with dose escalation in individuals at increased risk for complications such as stroke[115]. A history of airway reactivity or asthma may not be an absolute contraindication to propranolol therapy, but such patients require closer monitoring and consultation with a pulmonologist.

Propranolol dosing is weight-based, usually with a target dose of 2–3 mg/kg/day (see Table 103.7). In infants with ulcerated hemangiomas, doses of ≤1 mg/kg/day may reduce healing time[57]. Treatment

ADMINISTRATION OF PROPRANOLOL FOR INFANTILE HEMANGIOMAS (IHs): COUNSELING, RISK ASSESSMENT, DOSING, AND MONITORING

Counseling for parents

- Discuss potential risks of propranolol, including bradycardia, hypotension, hypoglycemia, sleep disturbances, and bronchospasm
- Review signs of hypoglycemia – *early* (may be masked by β-blockade): sweating, rapid heart rate, shakiness, fussiness; *late*: lethargy, poor feeding, hypothermia, seizures
- Emphasize the need to administer propranolol during or immediately after a feeding; twice daily doses should be ≥9 hours apart
- Dose should be lowered or therapy suspended during intercurrent illnesses with decreased oral intake or vomiting
- Provide written anticipatory guidance: https://pedsderm.net/site/assets/files/1028/12_spd_propranolol_color_web-final.pdf

Assessment of risk for complications of β-blocker therapy

Standard risk

- Age ≥5 weeks (using corrected age for premature infants)
- Normal birthweight and weight gain
- IH pattern and distribution does not confer risk of PHACE
- Normal cardiovascular and respiratory examination/history†
- Caregiver is able to understand and adhere to outpatient protocols

Higher risk

- Age <5 weeks (using corrected age for premature infants)
- IH pattern and distribution at risk for PHACE*
- History of recent or persistent hypoglycemia
- Cardiovascular disease, reactive airway disease/bronchospasm†, or brain malformation
- Extensive hepatic hemangiomas
- First degree relative with congenital heart disease, sudden death, or arrhythmia
- Maternal history of connective tissue disorder

Dosing and course

- Initial: usually ~1 mg/kg/day divided into 2 (or 3) doses‡
- Target: 2–3 mg/kg/day divided into 2 (or 3) doses‡; the target dose may be lower (~1 mg/kg/day) for ulcerated lesions, and the FDA-approved maximum is 3.4 mg/kg/day
- For a proliferating IH, treatment is typically continued for 6–12 months, depending on the clinical setting and course¶
  - The dose should be adjusted to account for weight gain to maintain the goal dose/kg
- Taper over 2–4+ weeks before discontinuing, primarily to assess for rebound growth

Monitoring

- Outpatient initiation of therapy
  - FDA recommendations include monitoring heart rate and blood pressure for 2 hours after the initial dose or a significant dose increase§
  - Measure heart rate and blood pressure every 4–8 weeks while on a stable dose
  - Normal ranges for pediatric vital signs are available at: www.emedicinehealth.com/pediatric_vital_signs/article_em.htm
- Consider a brief inpatient stay (e.g. 1–2 days) with telemetry for initiation of treatment if <5 weeks corrected age and/or complications such as cardiovascular or cerebrovascular anomalies

*Hemangioma ≥5 cm in diameter on the head or upper body (see Table 103.4). For at-risk patients, perform MRI/MRA of head/neck and echocardiogram to exclude arterial and cardiovascular anomalies (see Fig. 103.15); if abnormal, consult with a neuroradiologist, neurologist, and/or cardiologist as indicated.

†Contraindications include bradycardia (<80 beats/minute), blood pressure <50/30 mmHg, >1st degree heart block, and decompensated heart failure. Reactive airway disease/bronchospasm is a relative contraindication to propranolol therapy that may require consultation with a pulmonologist.

‡The dose is typically increased in increments of 1 mg/kg/day weekly in an outpatient setting or after 1–3 doses in an inpatient setting, until reaching the target dose; a lower starting/target dose and slower escalation may be required for patients at higher risk of complications. For at-home initiation (e.g. via telemedicine), a starting dose of 0.5 mg/kg/day increased by 0.5 mg/kg/day every 3–4 days until the target dose is reached has been recommended[112].

¶A longer duration of treatment may be required for IHs with prolonged growth or rebound growth after reduction/discontinuation of propranolol.

§A multicenter retrospective study found that in-office monitoring of vital signs upon propranolol initiation and dose escalation rarely changed management and did not predict adverse events[139].

Table 103.7 Administration of propranolol for infantile hemangiomas: recommendations for counseling, risk assessment, dosing, and monitoring. Practices for evaluation, dosing, and monitoring vary widely. The patient's age, hemangioma-related issues, and medical comorbidities affect management. A dosing chart is provided for FDA-approved Hemangeol™ 4.28 mg/ml solution (https://hemangeol.com/physician/dosing-administration/); generic propranolol 20 mg/5 ml (4 mg/ml) solution is also available.

is typically continued for 6–12 months, followed by gradual tapering. Approximately 25% of IHs undergo rebound growth after cessation of propranolol, with a higher risk if the lesion is deep or therapy is discontinued before 9 months of age[116–118].

β-blockers that do not cross the blood–brain barrier because they are hydrophilic (rather than lipophilic like propranolol) may potentially produce less CNS effects such as sleep disturbance. These agents include atenolol (β_1-selective) and nadolol (non-selective), neither of which is currently FDA-approved for IH treatment. Randomized controlled studies of atenolol and nadolol treatment of IH have demonstrated efficacy and safety similar to that of propranolol, with a faster response to nadolol[119–121]. Because nadolol is excreted primarily in the feces, bowel movement frequency should be monitored and the medication held if substantial constipation[122]. A recent study found that the R(+) enantiomers of propranolol and atenolol, which do not have β-blocker activity, inhibited formation of IH-like blood vessels from hemangioma stem cells in a murine xenograft model, suggesting the possibility of these agents' utility for IH treatment[123].

Systemic corticosteroids

Systemic corticosteroids, usually prednisolone or prednisone, were traditionally employed for the treatment of life- or function-threatening hemangiomas (see Table 103.6). Corticosteroids suppress VEGF production by hemangioma-derived stem cells and inhibit vasculogenesis in a murine model[124]. Although no longer a first-line therapy, systemic corticosteroids are still occasionally utilized when β-blocker therapy is contraindicated or in combination with β-blockers, e.g. for airway or diffuse hepatic hemangiomas[106]. Initial doses equivalent to 2–3 mg/kg/day of prednisone are typically administered, with variable duration of therapy, tapering schedules, and monitoring. Adverse effects of systemic corticosteroids include cushingoid facies, irritability, disruption of sleep, gastrointestinal symptoms, hypertension, hypothalamic–pituitary–adrenal (HPA) axis suppression, and increased susceptibility to opportunistic infections (see Ch. 125).

Other systemic therapies

Sirolimus (rapamycin) inhibits the mTOR signaling pathway, which plays an important role in cell growth and proliferation (see Fig. 61.12). Oral sirolimus is emerging as a second-line systemic treatment for recalcitrant life- or function-threatening IHs. There have been reports of its successful use for large facial IHs that failed to respond to β-blocker therapy[125,126]. Potential adverse effects include mucositis, hyperlipidemia, headaches, hepatotoxicity, and neutropenia. Laboratory monitoring is necessary including complete blood counts, serum creatinine, liver function tests and lipid panels, as well as sirolimus serum levels.

Vincristine and recombinant interferon-α (2a and 2b) represent historical therapies for severe, recalcitrant IHs that are no longer used because of potential complications such as peripheral neuropathy and spastic diplegia, respectively[127].

Surgical Therapy

Pulsed dye laser (PDL) therapy (585–600 nm wavelength, usually 0.45–1.5 ms pulse duration) is effective for the treatment of capillary malformations. Although PDL therapy may have some benefit for superficial IHs, there is risk for ulceration when it is used early in the growth phase. Multiple treatment sessions, usually every few weeks, are required during the proliferative phase to produce improvement. Considering the superior efficacy of β-blockers, PDL is currently not a first-line therapy for proliferating IHs. However, PDL therapy is often helpful for residual telangiectasias following propranolol therapy and/or involution of the IH. Potential adverse effects from PDL therapy include pigmentary alteration and atrophic scarring as well as ulceration. The Nd:YAG laser has also been used to treat IHs, either alone or in combination with the PDL; however, the higher risk of scarring limits its utility.

The fractional CO_2 laser has been used to improve the texture of residual atrophy and scarring following IH involution. Multiple treatments are typically required and may not be well tolerated without sedation.

Surgical excision may be employed for involuted or partially involuted lesions to remove fibrofatty tissue and redundant skin. The optimal timing of surgery depends upon multiple factors, including the location, size, and morphology (e.g. pedunculated vs sessile) of the lesion. In a retrospective study of 112 IHs resected by a single surgeon, 87% of the lesions were located on the head or neck, 38% of patients had received other treatments during the proliferative phase, and most excisions were performed at 2–3 years of age[128].

Surgical excision during the proliferative phase is controversial and usually reserved for situations in which: (1) a function-threatening hemangioma, e.g. a periocular lesion blocking the visual axis or lip lesion interfering with feeding or speech, failed to respond to pharmacologic therapy; or (2) pharmacologic therapy is believed to pose a greater risk to the patient than surgical excision. Other settings where early surgery may be appropriate include pedunculated lesions for which resection will be inevitable and small, persistently ulcerated lesions that have failed conservative therapy. The ultimate management goal is to achieve as normal an appearance as possible, considering the expected surgical scar as well as the predicted time course and outcome of involution. Therefore, just as with other treatment modalities, the surgical management of IHs needs to be individualized.

RAPIDLY INVOLUTING AND NON-INVOLUTING CONGENITAL HEMANGIOMAS

Infants are occasionally born with a fully developed hemangioma. These congenital hemangiomas (CHs) have features that are clinically, histologically, immunohistochemically, and genetically distinct from IHs (see Table 103.5). Most notably, CHs are GLUT1-negative and have different natural histories, most commonly rapidly involuting (RICH) or non-involuting (NICH) subtypes[129,130] (see Fig. 103.7). Lesions often have somatic gain-of-function mutations in *GNAQ* or *GNA11*, which encode G protein α-subunits that increase signaling via the MAPK pathway[131].

Rapidly involuting congenital hemangiomas (RICHs) are characterized by intrauterine development, with little, if any, postnatal growth and rapid involution within the first year of life. They are equally common in boys and girls. Intrauterine growth may be noted by prenatal ultrasonography as early as 12 weeks' gestation, and prenatal Doppler ultrasonography may reveal high vascularity and fast flow[129]. This tumor can appear at birth as a raised violaceous mass with prominent radiating veins, a hemispheric nodule with coarse telangiectasias surrounded by a pale rim, or a firm, pink to violaceous plaque that is often located on the lower extremity (Fig. 103.23). Small, firm, violaceous papules may be present on the surface, and superimposed milia or hypertrichosis are occasionally noted. Possible complications include necrosis, ulceration, transient thrombocytopenia, and potentially life-threatening hemorrhage that may be heralded by focal crusting[129,132].

Non-involuting congenital hemangiomas (NICHs) typically grow proportionately with the child and, unlike IHs, do not involute spontaneously[130]. These lesions may have a slight female predominance and most often develop on the trunk and extremities[133]. They typically present at birth as a well-circumscribed, pink to blue–violet plaque or nodule with overlying coarse telangiectasias, surrounded by a pale or bluish rim and often draining veins; a "patch" subtype has a flat surface and minimal induration[133] (Fig. 103.24). NICHs are warm to palpation and may be painful. The diagnosis is often established retrospectively when involution fails to occur. Up to 10% of NICHs undergo tardive (delayed) growth, most often between 2 and 10 years of age; lesions may also develop red papules, overlying pyogenic granulomas, and superficial bleeding[134]. In addition, some CHs that initially show regression soon after birth fail to fully involute and have been termed *partially involuting congenital hemangioma* (PICH)[135].

Although CHs may be recognized by prenatal ultrasonography during the second and third trimesters, misdiagnosis as other vascular anomalies such as lymphatic or arteriovenous malformations is common[136]. Postnatal ultrasonographic evaluation of a RICH or NICH typically reveals dense vascularity with a fast-flow component[137]. Compared to IH, CHs tend to have a more heterogeneous appearance with visible vessels and sometimes (especially in RICH) calcifications[138]. MRI reveals features similar to IHs[130], although CHs may be less well-defined and occasionally demonstrate fat stranding[138].

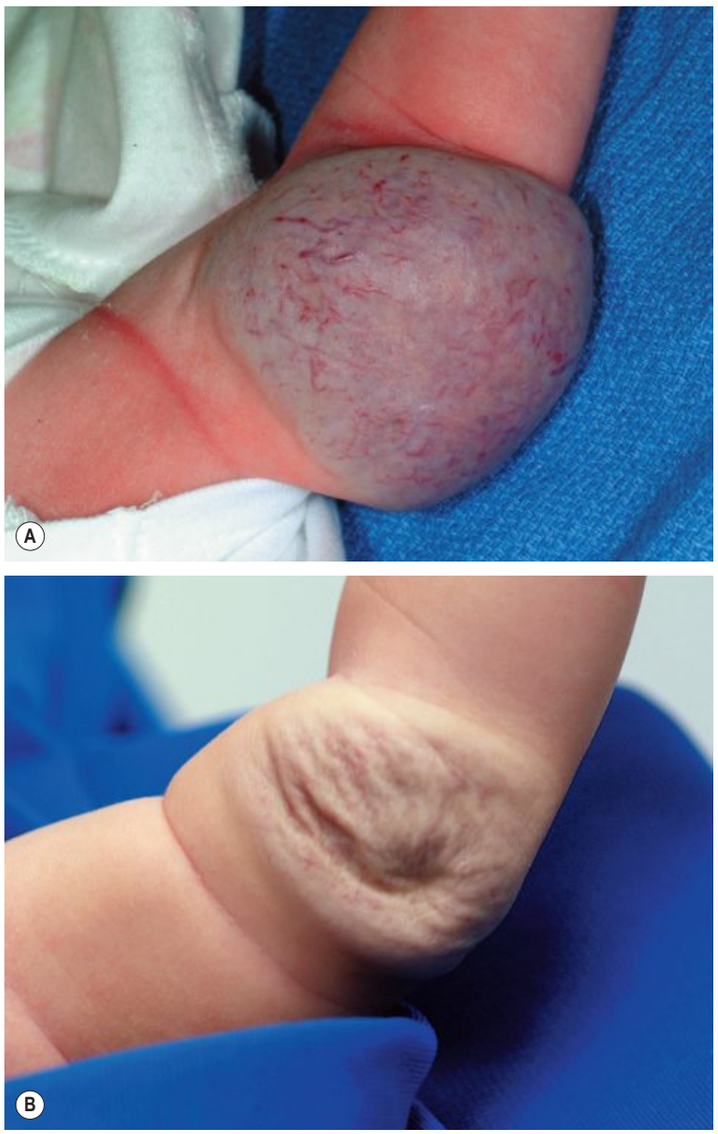


Fig. 103.23 Rapidly involuting congenital hemangioma (RICH). A Violaceous tumor on the upper extremity with surface telangiectasias in a neonate. **B** Spontaneous involution at 5 months of age, with fibrofatty residua. *Courtesy Annette Wagner, MD.*

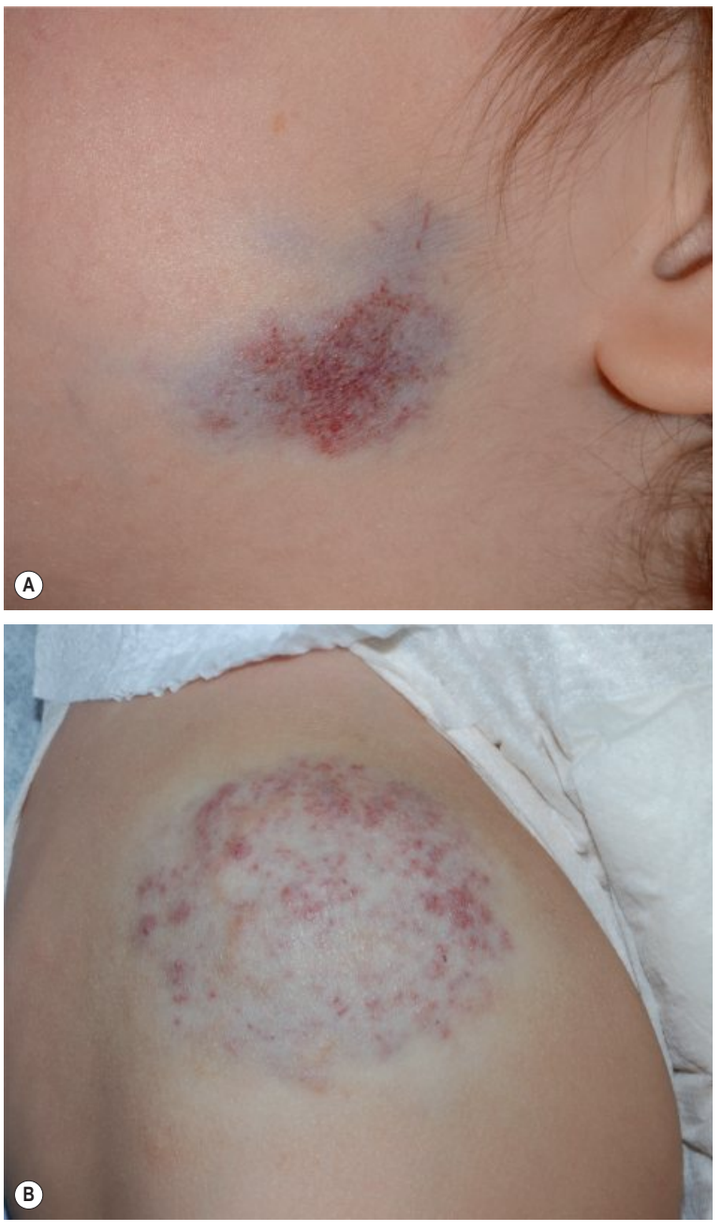


Fig. 103.24 Non-involuting congenital hemangiomas. Light blue–violet vascular plaques with overlying coarse telangiectasias and a pale rim, located on the cheek (**A**) and thigh (**B**). *Courtesy Julie V. Schaffer, MD.*

Histologically and immunophenotypically, CHs have several features that are distinct from IHs (see Table 103.5). These include striking lobularity with densely fibrotic stroma, stromal hemosiderin deposits, focal thrombosis and sclerosis of capillary lobules, fewer mast cells, and the coexistence of proliferating vasculature with multiple thin-walled vessels. Moreover, CHs lack immunoreactivity to GLUT1 and Lewis Y antigen. Some tumors do, however, demonstrate zones of involution.

Most CHs do not require treatment, and medical therapies such as propranolol are generally not effective. Surgical excision may be an option for a well-defined NICH, although residual tumor and persistent pain are possible.

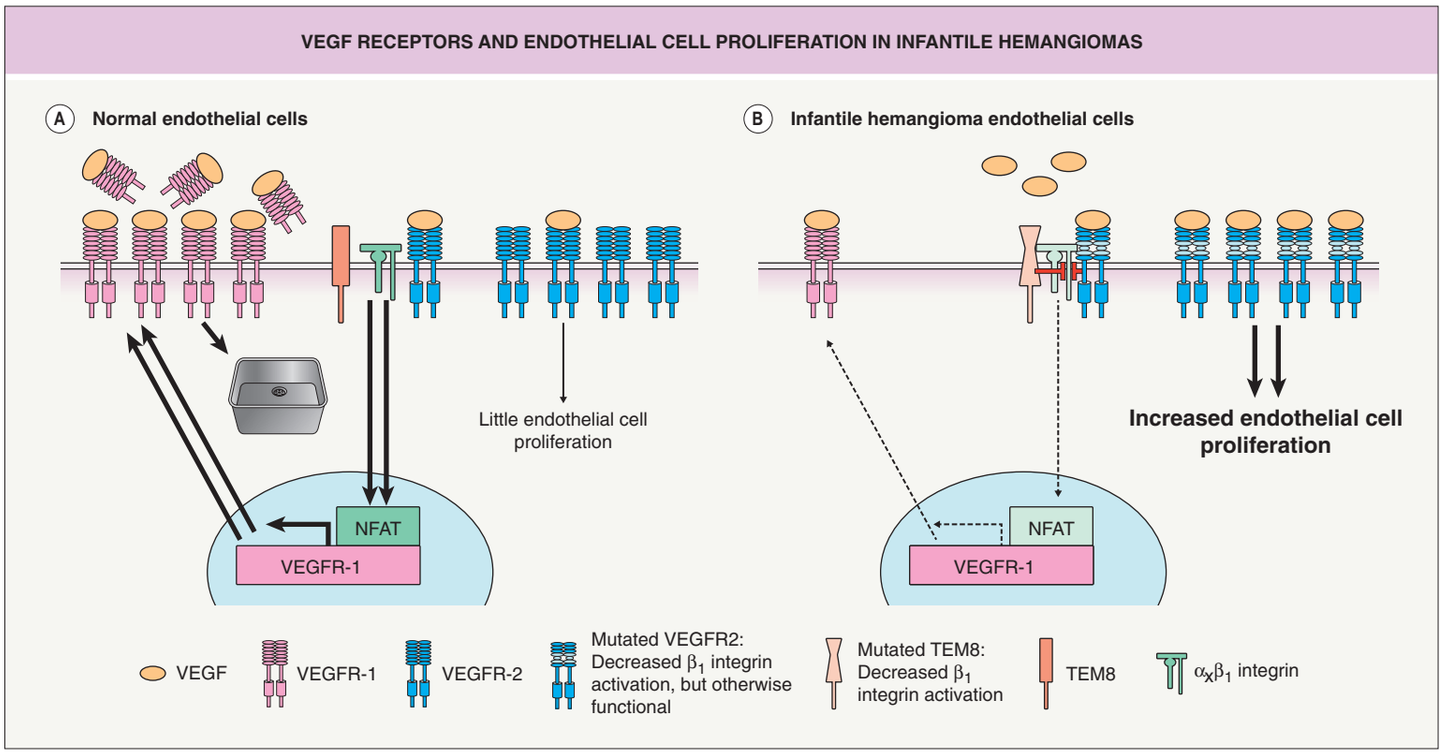
Additional figures and a table on Imaging of infantile hemangiomas, available in our eBook (see inside front cover for access code).

REFERENCES

1. Mulliken JB, Glowacki J. Hemangiomas and vascular malformations in infants and children: a classification based on endothelial characteristics. *Plast Reconstr Surg*. 1982;69:412–420.
2. ISSVA Classification of Vascular Anomalies, 2018. International Society for the Study of Vascular Anomalies. <https://issva.org/classification>.
3. Munden A, Butschek R, Tom WL, et al. Prospective study of infantile haemangiomas: incidence, clinical characteristics and association with placental anomalies. *Br J Dermatol*. 2014;170:907–913.
4. Drolet BA, Swanson EA, Frieden IJ. Infantile hemangiomas: an emerging health issue linked to an increased rate of low birth weight infants. *J Pediatr*. 2008;153:712–715.
5. Garzon MC, Drolet BA, Baselga E, et al. Comparison of infantile hemangiomas in preterm and term infants: a prospective study. *Arch Dermatol*. 2008;144:1231–1232.
6. Hunjan MK, Schoch JJ, Anderson KR, et al. Prenatal risk factors for infantile hemangioma development. *J Invest Dermatol*. 2017;137:954–957.
7. Hemangioma Investigator Group, Haggstrom AN, Drolet BA, et al. Prospective study of infantile hemangiomas: demographic, prenatal and perinatal characteristics. *J Pediatr*. 2007;150:291–294.
8. Burton BK, Schulz CJ, Angle B, Burd LI. An increased incidence of hemangiomas in infants born following chronic villus sampling (CVS). *Prenat Diagn*. 1995;15:209–214.
9. Castrén E, Salminen P, Vikkula M, et al. Inheritance patterns of infantile hemangioma. *Pediatrics*. 2016;138:e20161623.

10. Yu Y, Flint AF, Mulliken JB, et al. Endothelial progenitor cells in infantile hemangioma. *Blood*. 2004;103:1373–1375.
11. Khan ZA, Boscolo E, Pcard A, et al. Multipotential stem cells recapitulate human infantile hemangioma in immunodeficient mice. *J Clin Invest*. 2008;118:2592–2599.
12. North PE, Waner M, Mizeracki A, Mihm MC. GLUT1: a newly discovered immunohistochemical marker for juvenile hemangiomas. *Hum Pathol*. 2000;31:11–22.
13. North PE, Waner M, Mizeracki A, et al. A unique microvascular phenotype shared by juvenile hemangiomas and human placenta. *Arch Dermatol*. 2001;137:559–570.
14. Bree AF, Siegfried E, Sotelo-Avila C, Nahass G. Infantile hemangiomas: speculation on placental trophoblastic origin. *Arch Dermatol*. 2001;137:573–577.
15. Drolet BA, Frieden IJ. Characteristics of infantile hemangiomas as clues to pathogenesis: does hypoxia connect the dots? *Arch Dermatol*. 2010;146:1295–1299.
16. Colonna V, Resta L, Napoli A, Bonifazi E. Placental hypoxia and neonatal haemangioma: clinical and histological observations. *Br J Dermatol*. 2010;162:208–209.
17. Kleinman ME, Greives MR, Churgin SS, et al. Hypoxia-induced mediators of stem/progenitor cell trafficking are increased in children with hemangioma. *Arterioscler Thromb Vasc Biol*. 2007;27:2664–2670.
18. Jinnin M, Medici D, Park L, et al. Suppressed NFAT-dependent VEGFR1 expression and constitutive VEGFR2 signaling in infantile hemangioma. *Nat Med*. 2008;14:1236–1246.
19. Medici D, Olsen BR. Rapamycin inhibits proliferation of hemangioma endothelial cells by reducing HIF-1-dependent expression of VEGF. *PLoS ONE*. 2012;7:e42913.
20. Calicchio ML, Collins T, Kozakewich HP. Identification of signaling systems in proliferating and involuting phase infantile hemangiomas by genome-wide transcriptional profiling. *Am J Pathol*. 2009;174:1638–1649.
21. Boscolo E, Stewart CL, Greenberger S, et al. JAGGED1 signaling regulates hemangioma stem cell-to-pericyte/vascular smooth muscle cell differentiation. *Arterioscler Thromb Vasc Biol*. 2011;31:2181–2192.
22. Boscolo E, Mulliken JB, Bischoff J. Pericytes from infantile hemangioma display proangiogenic properties and dysregulated angiopoietin-1. *Arterioscler Thromb Vasc Biol*. 2013;33:501–509.
23. Itinteang T, Brasch HD, Tan ST, Day DJ. Expression of components of the renin-angiotensin system in proliferating infantile haemangioma may account for the propranolol-induced accelerated involution. *J Plast Reconstr Aesthet Surg*. 2011;64:759–765.
24. Sulzberger L, Baillie R, Itinteang T, et al. Serum levels of renin, angiotensin-converting enzyme and angiotensin II in patients treated by surgical excision, propranolol and captopril for problematic proliferating infantile haemangioma. *J Plast Reconstr Aesthet Surg*. 2016;69:381–386.
25. Walter JW, North PE, Waner M, et al. Somatic mutation of vascular endothelial growth factor receptors in juvenile hemangioma. *Genes Chromosomes Cancer*. 2002;33:295–303.
26. Takahashi K, Mulliken JB, Kozakewich HPW, et al. Cellular markers that distinguish the phases of hemangiomas during infancy and childhood. *J Clin Invest*. 1994;93:2357–2364.
27. Chang J, Most D, Bresnick S, et al. Proliferative hemangiomas: analysis of cytokine gene expression and angiogenesis. *Plast Reconstr Surg*. 1999;103:1–9.
28. Zhang L, Lin X, Wang W, et al. Circulating level of vascular endothelial growth factor in differentiating hemangioma from vascular malformation patients. *Plast Reconstr Surg*. 2005;116:200–204.
29. Salcedo R, Ponce ML, Young HA, et al. Human endothelial cells express CCR2 and respond to MCP-1: direct role of MCP-1 in angiogenesis and tumor progression. *Blood*. 2000;96:34–40.
30. Verkarre V, Patey-Mariaud de Serre N, Vazeux R, et al. ICAM-3 and E-selectin endothelial cell expression differentiate two phases of angiogenesis in infantile hemangiomas. *J Cutan Pathol*. 1999;26:17–24.
31. Tan ST, Velickovic M, Ruger BM, Davis BF. Cellular and extracellular markers of hemangioma. *Plast Reconstr Surg*. 2000;106:529–538.
32. Marler JJ, Fishman SJ, Kilroy SM, et al. Increased levels of urinary matrix metalloproteinases parallels the extent and activity of vascular anomalies. *Pediatrics*. 2005;116:38–45.
33. Razon MJ, Kraling BM, Mulliken JB, Bischoff J. Increased apoptosis coincides with onset of involution in infantile hemangiomas. *Microcirculation*. 1998;5:189–195.
34. Yu Y, Fuhr J, Boye E, et al. Mesenchymal stem cells and adipogenesis in hemangioma involution. *Stem Cells*. 2006;24:1605–1612.
35. Tollefson MM, Frieden IJ. Early growth of infantile hemangiomas: what parents' photographs tell us. *Pediatrics*. 2012;130:e314–e320.
36. Liang MG, Frieden IJ. Perineal and lip ulcerations as the presenting manifestation of hemangioma of infancy. *Pediatrics*. 1997;99:256–259.
37. Natsis NE, Gordon SC, Kaushik A, Seiverling EV. A practical review of dermoscopy for pediatric dermatology part II: vascular tumors, infections, and inflammatory dermatoses. *Pediatr Dermatol*. 2020;37:798–803.
38. Esterly NB. Cutaneous hemangiomas, vascular stains and malformations, and associated syndromes. *Curr Probl Dermatol*. 1995;7:69–107.
39. Waner M, North PE, Scherer KA, et al. The nonrandom distribution of facial hemangiomas. *Arch Dermatol*. 2003;139:869–875.
40. Chiller KG, Passaro D, Frieden IJ. Hemangiomas of infancy: clinical characteristics, morphologic subtypes and their relationship to race, ethnicity and sex. *Arch Dermatol*. 2002;138:1567–1576.
41. Chang LC, Haggstrom AN, Drolet BA, et al. Growth characteristics of infantile hemangiomas: implications for management. *Pediatrics*. 2008;122:360–367.
42. Endicott AA, Chamlin SL, Drolet BA, et al. Mapping of segmental and partial segmental infantile hemangiomas of the face and scalp. *JAMA Dermatol*. 2021;157:1328–1334.
43. Haggstrom AN, Lammer EJ, Schneider RA, et al. Patterns of infantile hemangiomas: new clues to hemangioma pathogenesis and embryonic facial development. *Pediatrics*. 2006;117:698–703.
44. Weitz NA, Bayer ML, Baselga E, et al. The "biker-glove" pattern of segmental infantile hemangiomas on the hands and feet. *J Am Acad Dermatol*. 2014;71:542–547.
45. Stefanko NS, Davies OMT, Beato MJ, et al. Hamartomas and midline anomalies in association with infantile hemangiomas, PHACE, and LUMBAR syndromes. *Pediatr Dermatol*. 2020;37:78–85.
46. Brandling-Bennett HA, Metry DW, Baselga E, et al. Infantile hemangiomas with unusually prolonged growth phase: a case series. *Arch Dermatol*. 2008;144:1632–1637.
47. O'Brien KF, Shah SD, Pope E, et al. Late growth of infantile hemangiomas in children >3 years of age: a retrospective study. *J Am Acad Dermatol*. 2019;80:493–499.
48. Suh KY, Frieden IJ. Infantile hemangiomas with minimal or arrested growth: a retrospective case series. *Arch Dermatol*. 2010;146:971–976.
49. Corella F, Garcia-Navarro X, Ribe A, et al. Abortive or minimal-growth hemangiomas: immunohistochemical evidence that they represent true infantile hemangiomas. *J Am Acad Dermatol*. 2008;58:685–690.
50. Roncone K, Kindley KJ, Zlotoff B. Eczematous dermatitis in an infantile hemangioma with minimal or arrested growth. *Pediatr Dermatol*. 2018;35:261–262.
51. Mulliken JB, Marler JJ, Burrows PE, et al. Reticular infantile hemangioma of the limb can be associated with ventral-caudal anomalies, refractory ulceration, and cardiac overload. *Pediatr Dermatol*. 2007;24:356–362.
52. Bowers RE, Graham EA, Tomlinson KM. The natural history of the strawberry nevus. *Arch Dermatol*. 1960;82:667–680.
53. Couto RA, Maclellan RA, Zurakowski D, Greene AK. Infantile hemangioma: clinical assessment of the involuting phase and implications for management. *Plast Reconstr Surg*. 2012;130:619–624.
54. Baselga E, Roe E, Coulie J, et al. Risk factors for degree and type of sequelae after involution of untreated hemangiomas of infancy. *JAMA Dermatol*. 2016;152:1239–1243.
55. Krowchuk DP, Frieden IJ, Mancini AJ, et al. Subcommittee on the Management of Infantile Hemangiomas. Clinical Practice Guideline for the management of infantile hemangiomas. *Pediatrics*. 2019;143:e20183475.
56. Chamlin SL, Haggstrom AN, Drolet BA, et al. Multicenter prospective study of ulcerated hemangiomas. *J Pediatr*. 2007;151:684–689.
57. Fernández Faith E, Shah S, Witman PM, et al. Clinical features, prognostic factors, and treatment interventions for ulceration in patients with infantile hemangioma. *JAMA Dermatol*. 2021;157:566–572.
58. Maguiness SM, Hoffman WY, McCalmont TH, Frieden IJ. Early white discoloration of infantile hemangioma: a sign of impending ulceration. *Arch Dermatol*. 2010;146:1235–1239.
59. Kim HJ, Colombo M, Frieden IJ. Ulcerated hemangiomas: clinical characteristics and response to therapy. *J Am Acad Dermatol*. 2001;44:962–972.
60. O TM, Scheuermann-Poley C, Tan M, Waner M. Distribution, clinical characteristics, and surgical treatment of lip infantile hemangiomas. *JAMA Facial Plast Surg*. 2013;15:292–304.
61. Haggstrom AN, Garzon MC, Baselga E, et al. Risk for PHACE syndrome in infants with large facial hemangiomas. *Pediatrics*. 2010;126:e418–e426.
62. Pascual-Castroviejo I. Vascular and nonvascular intracranial malformations associated with external capillary hemangiomas. *Neuroradiology*. 1978;16:82–84.
63. Frieden IJ, Reese V, Cohen D. PHACE syndrome: the association of posterior fossa brain malformations, hemangiomas, arterial anomalies, coarctation of the aorta and cardiac defects, and eye abnormalities. *Arch Dermatol*. 1996;132:307–311.
64. Goddard DS, Liang MG, Chamlin SL, et al. Hypopituitarism in PHACES association. *Pediatr Dermatol*. 2006;23:476–480.
65. Duffy KJ, Runge-Samuelson C, Bayer ML, et al. Association of hearing loss with PHACE syndrome. *Arch Dermatol*. 2010;146:1391–1396.
66. Garzon MC, Epstein LG, Heyer GL, et al. PHACE syndrome: consensus-derived diagnosis and care recommendations. *J Pediatr*. 2016;178:24–33, e2.
67. Hess CP, Fullerton HJ, Metry DW, et al. Cervical and intracranial arterial anomalies in 70 patients with PHACE syndrome. *AJNR Am J Neuroradiol*. 2010;31:1980–1986.
68. Forde KM, Glover MT, Chong WK, Kinsler VA. Segmental hemangioma of the head and neck: high prevalence of PHACE syndrome. *J Am Acad Dermatol*. 2017;76:356–358.
69. Siegel DH, Tefft KA, Kelly T, et al. Stroke in children with posterior fossa brain malformations, hemangiomas, arterial anomalies, coarctation of the aorta and cardiac defects, and eye abnormalities (PHACE) syndrome: a systematic review of the literature. *Stroke*. 2012;43:1672–1674.
70. Stefanko NS, Cossio ML, Powell J, et al. Natural history of PHACE syndrome: a survey of adults with PHACE. *Pediatr Dermatol*. 2019;36:618–622.
71. Orlow SJ, Isakoff MS, Blei F. Increased risk of symptomatic hemangiomas of the airway in association with cutaneous hemangiomas in a "beard" distribution. *J Pediatr*. 1997;131:643–646.
72. Darrow DH. Management of infantile hemangiomas of the airway. *Otolaryngol Clin North Am*. 2018;51:133–136.
73. Drolet BA, Chamlin SA, Garzon MC, et al. Prospective study of spinal anomalies in children with infantile hemangiomas of the lumbosacral skin. *J Pediatr*. 2010;157:789–794.
74. Iacobas I, Burrows PE, Frieden IJ, et al. LUMBAR: association between cutaneous infantile hemangiomas of the lower body and regional cutaneous anomalies. *J Pediatr*. 2010;157:795–801.
75. Achauer BM, Chang C, Vander Kam VM. Management of hemangiomas of infancy: review of 245 patients. *Plast Reconstr Surg*. 1997;99:1301–1308.
76. Glick ZR, Frieden IJ, Garzon MC, et al. Diffuse neonatal hemangiomatosis: an evidence-based review of case reports in the literature. *J Am Acad Dermatol*. 2012;67:898–903.
77. Horii KA, Drolet BA, Frieden IJ, et al. Prospective study of the frequency of hepatic hemangiomas in infants with multiple cutaneous hemangiomas. *Pediatr Dermatol*. 2011;28:245–253.
78. Ji Y, Chen S, Yang K, et al. Screening for infantile hepatic hemangioma in patients with cutaneous infantile hemangioma: a multicenter prospective study. *J Am Acad Dermatol*. 2020:S0190–9622(20)33116–9.
79. Iacobas I, Phung TL, Adams DM, et al. Guidance document for hepatic hemangioma (infantile and congenital) evaluation and monitoring. *J Pediatr*. 2018;203:294–300.e2.
80. Drolet BA, Pope E, Juern AM, et al. Gastrointestinal bleeding in infantile hemangioma: a complication of segmental, rather than multifocal, infantile hemangiomas. *J Pediatr*. 2012;1601021–6, e3.
81. Viswanathan V, Smith ER, Mulliken JB, et al. Infantile hemangiomas involving the neuraxis: clinical and imaging findings. *AJNR Am J Neuroradiol*. 2009;30:1005–1013.
82. Huang SA, Tu HM, Harney JW, et al. Severe hypothyroidism caused by type 3 iodothyronine deiodinase in infantile hemangiomas. *N Engl J Med*. 2000;343:185–189.
83. De Corti F, Crivellaro C, Zanon GF, Luzzatto C. Consumptive hypothyroidism associated with parotid infantile hemangioma. *J Pediatr Endocrinol Metab*. 2015;28:467–469.
84. Semkova K, Kazandjieva J, Kadurina M, Tsankov N. Hemangioma Activity and Severity Index (HASI), an instrument for evaluating infantile hemangioma:

development and preliminary validation. *Int J Dermatol*. 2015;54:494–498.
85. Haggstrom AN, Beaumont JL, Lai JS, et al. Measuring the severity of infantile hemangiomas: instrument development and reliability. *Arch Dermatol*. 2012; 148:197–202.
86. Frieden IJ, Eichenfield LF, Esterly NB, et al. Guidelines of care for hemangiomas of infancy. *J Am Acad Dermatol*. 1997;37:631–637.
87. Luu M, Frieden IJ. Haemangioma: clinical course, complications and management. *Br J Dermatol*. 2013;169:20–30.
88. Tanner JL, Dechert MP, Freiden IJ. Growing up with a facial hemangioma: parent and child coping and adaptation. *Pediatrics*. 1998;101:446–451.
89. Boos MD, Castelo-Soccio L. Experience with topical timolol maleate for the treatment of ulcerated infantile hemangiomas (IH). *J Am Acad Dermatol*. 2016;74:567–570.
90. Weibel L, Barysch MJ, Scheer HS, et al. Topical timolol for infantile hemangiomas: evidence for efficacy and degree of systemic absorption. *Pediatr Dermatol*. 2016;33:184–190.
91. Püttgen K, Lucky A, Adams D, et al. Topical timolol maleate treatment of infantile hemangiomas. *Pediatrics*. 2016;138:e20160355.
92. Saint-Jean M, Leaute-Labreze C, Mazereeuw-Hautier J, et al. Propranolol for treatment of ulcerated infantile hemangiomas. *J Am Acad Dermatol*. 2011;64:827–832.
93. Meyer-Mueller C, Nicholson C, Polcari I, et al. Worsening ulceration of infantile hemangioma after initiation or escalation of propranolol. *Pediatr Dermatol*. 2022;39:255–259.
94. David LR, Malek MM, Argenta LC. Efficacy of pulse dye laser therapy for the treatment of ulcerated hemangiomas: a review of 78 patients. *Br J Plast Surg*. 2003;56:317–327.
95. Chakkittakandiyil A, Phillips R, Frieden IJ, et al. Timolol maleate 0.5% or 0.1% gel-forming solution for infantile hemangiomas: a retrospective, multicenter, cohort study. *Pediatr Dermatol*. 2012;29:28–31.
96. Chan H, McKay C, Adams S, Wargon O. RCT of timolol maleate gel for superficial infantile hemangiomas in 5- to 24-week-olds. *Pediatrics*. 2013;131:e1739–e1747.
97. Drolet BA, Boakye-Agyeman F, Harper B, et al. Systemic timolol exposure following topical application to infantile hemangiomas. *J Am Acad Dermatol*. 2020;82:733–736.
98. Borok J, Gangar P, Admani S, et al. Safety and efficacy of topical timolol treatment of infantile haemangioma: a prospective trial. *Br J Dermatol*. 2018;178:e51–e52.
99. Frommelt P, Juern A, Siegel D, et al. Adverse events in young and preterm infants receiving topical timolol for infantile hemangioma. *Pediatr Dermatol*. 2016;33:405–414.
100. Egbert JE, Schwartz GS, Walsh AW. Diagnosis and treatment of ophthalmic artery occlusion during an intralesional injection of corticosteroid into an eyelid capillary hemangioma. *Am J Ophthamol*. 1996;121:638–642.
101. Léauté-Labrèze C, Dumas de la Roque E, Hubiche T, et al. Propranolol for severe hemangiomas of infancy. *N Engl J Med*. 2008;358:2649–2651.
102. Babiak-Choroszczak L, Giżewska-Kacprzak K, Gawrych E, et al. Serum concentrations of VEGF and bFGF in the course of propranolol therapy of infantile hemangioma in children: are we closer to understand the mechanism of action of propranolol on hemangiomas? *Adv Clin Exp Med*. 2018;27:703–710.
103. Chim H, Armijo BS, Miller E, et al. Propranolol induces regression of hemangioma cells through HIF-1α-mediated inhibition of VEGF-A. *Ann Surg*. 2012;256:146–156.
104. Sharifpanah F, Saliu F, Bekhite MM, et al. β-adrenergic receptor antagonists inhibit vasculogenesis of embryonic stem cells by downregulation of nitric oxide generation and interference with VEGF signalling. *Cell Tissue Res*. 2014;358:443–452.
105. England RW, Hardy KL, Kitajewski AM, et al. Propranolol promotes accelerated and dysregulated adipogenesis in hemangioma stem cells. *Ann Plast Surg*. 2014;73:S119–S124.
106. Bauman NM, McCarter RJ, Guzzetta PC, et al. Propranolol vs prednisolone for symptomatic proliferating infantile hemangiomas: a randomized clinical trial. *JAMA Otolaryngol Head Neck Surg*. 2014;140:323–330.
107. Holland KE, Frieden IJ, Frommelt PC, et al. Hypoglycemia in children taking propranolol for the treatment of infantile hemangioma. *Arch Dermatol*. 2010;146:775–778.
108. Girón-Vallejo O, López-Gutiérrez JC, Fernández-Pineda I, et al. Dental caries as a side effect of infantile hemangioma treatment with propranolol solution. *Pediatr Dermatol*. 2010;27:672–673.
109. Cavalli R, Buffon RB, de Souza M, et al. Tumor lysis syndrome after propranolol therapy in ulcerative infantile hemangioma: rare complication or incidental finding? *Dermatology*. 2012;224:106–109.
110. Moyakine AV, Kerstjens JM, Spillekom-van Koulil S, van der Vleuten CJ. Propranolol treatment of infantile hemangioma (IH) is not associated with developmental risk or growth impairment at age 4 years. *J Am Acad Dermatol*. 2016;75:59–63.
111. González-Llorente N, Del Olmo-Benito I, Muñoz-Ollero N, et al. Study of cognitive function in children treated with propranolol for infantile hemangioma. *Pediatr Dermatol*. 2017;34:554–558.
112. Drolet BA, Frommelt PC, Chamlin SL, et al. Initiation and use of propranolol for infantile hemangioma: report of a consensus conference. *Pediatrics*. 2013;131:128–140.
113. Frieden IJ, Püttgen KB, Drolet BA, et al. Management of infantile hemangiomas during the COVID pandemic. *Pediatr Dermatol*. 2020;37:412–418.
114. Olsen GM, Hansen LM, Stefanko NS, et al. Evaluating the safety of oral propranolol therapy in patients with PHACE syndrome. *JAMA Dermatol*. 2020;156:186–190.
115. Metry D, Frieden IJ, Hess C, et al. Propranolol use in PHACE syndrome with cervical and intracranial arterial anomalies: collective experience in 32 infants. *Pediatr Dermatol*. 2013;30:71–89.
116. Giachetti A, Garcia-Monaco R, Sojo M, et al. Long-term treatment with oral propranolol reduces relapses of infantile hemangiomas. *Pediatr Dermatol*. 2014;31:14–20.
117. Shah SD, Baselga E, McCuaig C, et al. Rebound growth of infantile hemangioma after propranolol therapy. *Pediatrics*. 2016;137:e20151754.
118. Shehata N, Powell J, Dubois J, et al. Late rebound of infantile hemangioma after cessation of oral propranolol. *Pediatr Dermatol*. 2013;30:587–591.
119. Ábarzúa-Araya A, Navarrete-Dechent CP, Heusser F, et al. Atenolol versus propranolol for the treatment of infantile hemangiomas: a randomized controlled study. *J Am Acad Dermatol*. 2014;70:1045–1049.
120. Pope E, Lara-Corrales I, Sibbald C, et al. Noninferiority and safety of nadolol vs propranolol in infants with infantile hemangioma: a randomized clinical trial. *JAMA Pediatr*. 2022;176:34–41.
121. Ji Y, Chen S, Yang K, et al. Efficacy and safety of propranolol vs atenolol in infants with problematic infantile hemangiomas: a randomized clinical trial. *JAMA Otolaryngol Head Neck Surg*. 2021;147:599–607.
122. McGillis E, Baumann T, LeRoy J. Death associated with nadolol for infantile hemangioma: a case for improving safety. *Pediatrics*. 2020;145:e20191035.
123. Seebauer CT, Graus MS, Huang L, et al. Non-beta blocker enantiomers of propranolol and atenolol inhibit vasculogenesis in infantile hemangioma. *Clin Invest*. 2022;132:e151109.
124. Greenberger S, Boscolo E, Adini I, et al. Corticosteroid suppression of VEGF-A in infantile hemangioma-derived stem cells. *N Engl J Med*. 2010;362:1005–1013.
125. Kaylani S, Theos AJ, Pressey JG. Treatment of infantile hemangiomas with sirolimus in a patient with PHACE syndrome. *Pediatr Dermatol*. 2013;30:e194–e197.
126. Dávila-Osorio VL, Iznardo H, Roé E, et al. Propranolol-resistant infantile hemangioma successfully treated with sirolimus. *Pediatr Dermatol*. 2020;37:684–686.
127. Payarols P, Masferrer P, Bellvert G. Treatment of life-threatening hemangiomas with vincristine. *N Engl J Med*. 1995;333:69.
128. Lee AH, Hardy KL, Goltsman D, et al. A retrospective study to classify surgical indications for infantile hemangiomas. *J Plast Reconstr Aesthet Surg*. 2014;67:1215–1221.
129. Boon LM, Enjolras O, Mulliken JB. Congenital hemangioma: evidence of accelerated involution. *J Pediatr*. 1996;128:329–335.
130. Enjolras O, Mulliken JB, Boon LM, et al. Noninvoluting congenital hemangioma: a rare cutaneous vascular anomaly. *Plast Reconstr Surg*. 2001;107:1647–1654.
131. Ayturk UM, Couto JA, Hann S, et al. Somatic activating mutations in GNAQ and GNA11 are associated with congenital hemangioma. *Am J Hum Genet*. 2016;98:789–795.
132. Baselga E, Cordisco MR, Garzon M, et al. Rapidly involuting congenital haemangioma associated with transient thrombocytopenia and coagulopathy: a case series. *Br J Dermatol*. 2008;158:1363–1370.
133. Lee PW, Frieden IJ, Streicher JL, et al. Characteristics of noninvoluting congenital hemangioma: a retrospective review. *J Am Acad Dermatol*. 2014;70:899–903.
134. Cossio ML, Dubois J, McCuaig CC, et al. Non-involuting congenital hemangiomas (NICH) with postnatal atypical growth: a case series. *Pediatr Dermatol*. 2019;36:466–470.
135. Nasseri E, Piram M, McCuaig CC, et al. Partially involuting congenital hemangiomas: a report of 8 cases and review of the literature. *J Am Acad Dermatol*. 2014;70:75–79.
136. Marler JJ, Fishman SJ, Upton J, et al. Prenatal diagnosis of vascular anomalies. *J Pediatr Surg*. 2002;37:318–326.
137. Rogers M, Lam A, Fischer G. Sonographic findings in a series of rapidly involuting congenital hemangiomas (RICH). *Pediatr Dermatol*. 2002;19:5–11.
138. Gorincour G, Kokta V, Rypens F, et al. Imaging characteristics of two subtypes of congenital hemangiomas: rapidly involuting congenital hemangiomas and non-involuting congenital hemangiomas. *Pediatr Radiol*. 2005;35:1178–1185.
139. Püttgen KB, Hansen LM, Lauren C, et al. Limited utility of repeated vital sign monitoring during initiation of oral propranolol for complicated infantile hemangioma. *J Am Acad Dermatol*. 2021;85:345–352.



eFig. 103.1 VEGF receptors and endothelial cell proliferation in infantile hemangiomas. A In normal endothelial cells, β_1 integrin (which forms a complex with the integrin-like receptor TEM8 and VEGFR-2) increases transcription of VEGFR-1 via activation of NFAT. Binding of VEGF to VEGFR-2 stimulates endothelial cell proliferation, but VEGF binding to VEGFR-1 (which exists in soluble and transmembrane forms) is of higher affinity and does not transmit a signal. VEGFR-1 thereby acts as a VEGF "sink" or decoy receptor that decreases the amount of VEGF available to activate VEGFR-2. **B** Hemangioma endothelial cells have decreased β_1 integrin activity and, consequently, markedly reduced expression of VEGFR-1. This leads to increased VEGF-dependent activation of VEGFR-2 and enhanced endothelial cell proliferation. In a subset of hemangioma patients, the low β_1 integrin activity can be explained by a germline mutation in the *VEGFR2* or *TEM8* gene; such mutations result in increased interactions among β_1 integrin, TEM8, and VEGFR-2 as well as inhibition of β_1 integrin function. NFAT, nuclear factor of activated T cells; VEGF, vascular endothelial growth factor; VEGFR, VEGF receptor; TEM8, tumor endothelial marker 8.

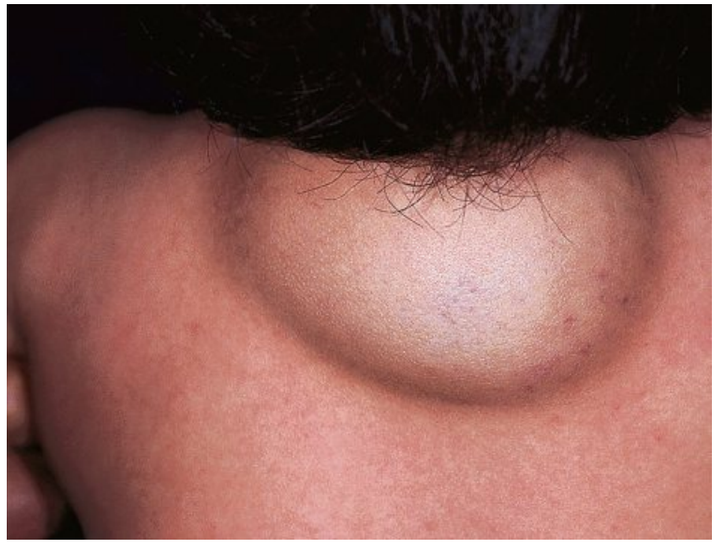




eFig. 103.2 Segmental superficial infantile hemangiomas. *B, Courtesy Julie V. Schaffer, MD.*



eFig. 103.3 Superficial infantile hemangioma mimicking a capillary malformation. This lesion's segmental configuration would warrant consideration of PHACE(S) syndrome.



eFig. 103.4 Deep infantile hemangioma. *Courtesy Anthony Mancini, MD.*







eFig. 103.5 Infantile hemangiomas with minimal or arrested growth (IH-MAG). Telangiectasias and larger ectatic vessels are evident. Note the focal crusting (**A**) and small bright red papules that cover <25% of the surface area (**B,C**). *C, Courtesy Julie V. Schaffer, MD.*



eFig 103.6 Infantile hemangioma with minimal or arrested growth (IH-MAG). There is reticulated erythema with scattered telangiectasias as well as a background of pallor. *Courtesy Julie V. Schaffer, MD.*



eFig. 103.7 Exophytic, pedunculated infantile hemangioma in involution phase. Lesions with a mushroom-like shape are more likely to leave redundant skin and fibrofatty tissue. *Courtesy Julie V. Schaffer, MD.*



eFig. 103.8 Residual telangiectasias following involution of a segmental infantile hemangioma. *Courtesy Julie V. Schaffer, MD.*



eFig. 103.9 Residua of an infantile hemangioma. Note the atrophy and fibrofatty changes. *Courtesy Ronald P. Rapini, MD.*





eFig. 103.10 Ulcerated mixed hemangiomas.



eFig. 103.11 Ulcerated infantile hemangioma on the arm. *Courtesy Kalman Watsky, MD.*



eFig. 103.12 Ulcerated early superficial hemangioma on the buttock. The vascular component of such lesions may be subtle. *Courtesy Julie V. Schaffer, MD.*



eFig. 103.13 Lip hemangioma crossing the vermilion border.



eFig. 103.14 Infantile hemangioma on the lip. This is a cosmetically sensitive site and hemangiomas in this location are prone to ulceration. *Courtesy Julie V. Schaffer, MD.*



eFig 103.15 Infantile hemangioma in a beard distribution. Involvement of this site is associated with the risk of an airway hemangioma. *Courtesy Julie V. Schaffer, MD.*



eFig 103.16 Lumbosacral hemangioma associated with tethered cord. *Photograph courtesy Ilona Frieden, MD.*



eFig. 103.17 Multifocal infantile hemangiomas with extracutaneous hemangiomas. In this child, multiple small, superficial skin lesions were present in a miliary pattern and hemangiomas were present in the liver. Historically, this was referred to as "diffuse neonatal hemangiomatosis". *Courtesy Ronald P. Rapini, MD.*





eFig. 103.18 Rapidly involuting congenital hemangioma (RICH). A Violaceous nodule with coarse telangiectasias and peripheral blanching in a neonate. **B** Significant involution at 5 months of age, with a residual depression. *Courtesy Julie V. Schaffer, MD.*



eFig. 103.19 Non-involuting congenital hemangioma (NICH) on the forehead of a school-aged child. There is a subtle pale rim. *Courtesy Julie V. Schaffer, MD.*



eFig. 103.20 Non-involuting congenital hemangioma (NICH) in a school-aged child. This lesion was fully formed at birth and remained warm and firm to palpation. Note the coarse telangiectasias and pallor. *Courtesy Julie V. Schaffer, MD.*



eFig. 103.21 Kaposiform hemangioendothelioma associated with Kasabach–Merritt phenomenon in a 5-week-old boy. Progressive induration and ecchymosis developed rapidly over a 24-hour period. An eczematous eruption is also evident. *Courtesy Julie V. Schaffer, MD.*

IMAGING FINDINGS IN INFANTILE HEMANGIOMAS						
Lesion	**Magnetic resonance imaging**				**Doppler sonography**	**Computed tomography**
	T1-weighted	**Contrast enhancement**	**T2-weighted**	**Gradient**		
Proliferating	STM, iso- or hypointense to muscle Flow voids	Uniform intense enhancement	Lobulated STM Increased signal Flow voids	HFV within and around STM	Discrete STM containing HFV Decreased arterial resistance	Uniformly enhancing STM Dilated feeding and draining vessels
Involuting	Variable fat content	As above	Variable fat content	As above	As above	Variable fat content
Involuted	High signal (fat)	No enhancement	Decreased signal (fat)	No HFV	Echogenic avascular STM	Fat density No enhancement

eTable 103.1 Imaging findings in infantile hemangiomas. HFV, high-flow vessels; STM, soft tissue mass. *Adapted with permission from Burrows PE, Laor T, Paltiel H, et al. Diagnostic imaging in the evaluation of vascular birthmarks. Dermatol Clin 1998;16:455–88.*

104 Vascular Malformations

Eulalia Baselga

Synonyms: ■ Vascular birthmarks; mature angiomas [misnomer]; angiodysplasias ■ Capillary malformation (CM): port-wine birthmark [preferred], port-wine stain, nevus flammeus ■ Venous malformation (VM): cavernous angioma [misnomer], cavernous hemangioma [misnomer], phlebectasia ■ Lymphatic malformation (LM): lymphangioma, lymphangioma circumscriptum, lymphangioma simplex, cystic hygroma, cavernous lymphangioma [historical terms/misnomers] ■ Arteriovenous malformation (AVM): cirsoid aneurysm, cirsoid hemangioma [misnomer]

Key features

- Although both were once called "angiomas", vascular malformations differ from the vascular tumors seen in infants and children
- In slow-flow malformations, capillaries, veins, and/or lymphatic channels are anomalous; most lesions are either apparent at birth or become evident within the first few months or years of life
- In fast-flow malformations, there is arteriovenous shunting; some lesions are apparent at birth, but the majority become evident later in childhood or adulthood
- Vascular malformations are lifelong and may worsen over time, creating cosmetic consequences and functional impairment
- Vascular malformations are occasionally found together with other abnormalities as a part of a complex syndrome

INTRODUCTION

According to the classification system adopted by the International Society for the Study of Vascular Anomalies (ISSVA), there are two types of vascular anomalies: vascular tumors (most commonly the infantile hemangioma) and vascular malformations[1] (Table 104.1; see Table 103.2). Vascular malformations are localized defects of vascular morphogenesis, likely caused by dysfunction in pathways regulating the formation of vascular channels during embryonic development, including effects on endothelial cell growth and survival. True angiogenesis may occur in some of these lesions, potentially explaining their propensity to thicken and even expand over time. However, in general, vascular malformations do not exhibit the markers of endothelial cell proliferation seen in infantile hemangiomas during their proliferative phase (Fig. 104.1). The suffix "oma" (meaning "tumor") has therefore been deemed inaccurate for vascular malformations, and terms such as "angioma", "lymphangioma", and "hemangioma" should not be used for these lesions.

In the current ISSVA classification system[2,3], which was updated in 2018, vascular malformations are categorized depending on the predominant type(s) of anomalous vessels:

- **capillary** (CM), classically a port-wine birthmark (PWB), but also including telangiectasias, cutis marmorata telangiectatica congenita (CMTC), and nevus simplex
- **venous** (VM): a misnomer for this entity is "cavernous hemangioma", a term with a long history of use to describe deep infantile hemangiomas
- **lymphatic** (LM): this category includes microcystic and macrocystic lesions, which were previously termed lymphangioma and cystic hygroma (respectively), along with more extensive forms with visceral or bone involvement. Central conducting lymphatic anomalies and primary lymphedema are also included in this category.
- **arteriovenous** (AVM): fast-flow lesions characterized by malformed arteries, veins, and capillaries with direct communications that produce arteriovenous shunting.

Vascular malformations are further divided into four groups: (1) *simple* – containing only one type of vessel or an AVM; (2) *combined* – composed of ≥2 types of vessels, e.g. capillary–venous (CVM), capillary–lymphatic (CLM), capillary–lymphatic–venous (CLVM), lymphatic–venous (LVM), capillary–arteriovenous (C-AVM), or capillary–lymphatic–arteriovenous (CL-AVM); (3) *major named vessels* involved; and (4) *associated with other anomalies* as a part of a complex syndrome, which have classically been referred to with eponyms such as Sturge–Weber and Klippel–Trenaunay syndromes (see Table 103.2). In a few scenarios, vascular tumors and malformations occur together, such as spindle cell hemangiomas and VMs in patients with Maffucci syndrome or pyogenic granulomas superimposed on a CM or AVM. Co-segregation of infantile hemangiomas and vascular malformations within families has also been observed.

Vascular malformations may occur in any body part or organ system. They are most easily identified in the skin and mucous membranes, with some of these lesions invading deep into underlying muscles, bones, or joints. Others are found in visceral locations. Vascular malformations can appear as localized lesions of varying sizes, occur within a segmental distribution, or be dispersed as multifocal or disseminated lesions.

Vascular malformations are persistent and some worsen over time if not treated. Categorizing a lesion as a CM, LM, VM, AVM, or combined lesion is important, since diagnostic modalities as well as treatment differ depending on the type(s) of vessels involved[1]. The genetic bases of multiple types of vascular malformations and associated syndromes have been elucidated (Table 104.2, Fig. 104.2). This has been incorporated in the ISSVA classification and provides the foundation for targeted approaches to therapy[4]. In many patients, a multidisciplinary team is required to provide optimal management. Cure is rarely achievable. A realistic aim is improvement and minimization of cosmetic or functional consequences. Many patients require longitudinal care from infancy through adulthood[1].

HISTORY

In the medical literature addressing vascular malformations, lesions and syndromes were originally delineated based on clinical features. Many authors played a major role in their description, including Virchow, Trélat, Monod, Klippel, Trenaunay, Weber, Sturge, Bockenheimer, Maffucci, Bell, and Malan. Unfortunately, pathologists and clinicians did not work together. Consequently, multiple nomenclatures became an obstacle to communication among physicians treating these patients. In 1976, John B. Mulliken (a plastic surgeon in the US), Anthony E. Young (a vascular surgeon in the UK), and Jean-Jaques Merland (a neurointerventional radiologist in France) joined forces to convene the first of many Workshops on Vascular Anomalies. The ISSVA, created in 1992, is dedicated to analyzing the clinical, radiologic, biologic, and pathologic characteristics of vascular lesions and improving diagnosis and treatment via multidisciplinary and international collaboration.

EPIDEMIOLOGY

Little is known regarding the exact prevalence of vascular malformations in the general population. The most common types are CMs, then VMs. The least common are AVMs. Vascular malformations have no sex predilection.

PATHOGENESIS

An initial embryologic process, vasculogenesis, creates the primitive vascular plexus. Then angiogenesis, the secondary sprouting of

DIFFERENCES BETWEEN VASCULAR MALFORMATIONS AND INFANTILE HEMANGIOMAS		
Characteristics	**Vascular malformations**	**Infantile hemangiomas**
Clinical features	CM: red, macular during infancy VM: blue, compressible, fills with dependency LM: vesicles or large cysts AVM: four stages: stage 1 – dormant: red, warm; macular (mimics CM) or slightly infiltrated (mimics involuting infantile hemangioma) stage 2 – expansion: warm mass with thrill/throbbing, dilated draining veins stage 3 – destruction: pain, ulceration; occasional bone lysis and fracture stage 4 – cardiac decompensation; high-output cardiac failure; also signs of stage(s) 2 ± 3	Premonitory markers at birth in 50%: red telangiectatic, bluish bruise-like, or white/anemic macules Superficial hemangioma: bright red, "strawberry"-like papules and plaques (during proliferative phase) Deep hemangioma: warm, rubbery mass under normal-colored or bluish skin
Sex prevalence	Female : male ratio 1 : 1	Female : male ratio 2 : 1 to 5 : 1
Natural history	Usually evident at birth Lifelong persistence, with commensurate growth during childhood and often slow worsening over time AVM: may worsen with puberty, trauma, and pregnancy	Precursor lesion or no evidence at birth Postnatal proliferation over 5–9 months, then slow involution over years Reach stable involuted stage
Radiology	VM or LM (slow flow): hypersignal on MRI T2-weighted sequence VM: thrombi and phleboliths (MRI, CT); gadolinium enhancement on MRI AVM (fast flow): flow voids on MRI T1- and T2-weighted sequences; arteriovenous shunts on Doppler ultrasound	Well-defined mass Some flow voids on MRI T1-weighted sequences (high-flow vessels)
Pathology (see Fig. 104.25)	CM: ectatic capillaries VM or LM: distorted, interconnected malformed channels AVM: AV fistulae and increased capillaries Typically no increase in cellular turnover	Dense lobular proliferation of endothelial cells forming capillaries with tiny lumens Increased cellular turnover in proliferating lesions can be demonstrated by elevated levels of markers of proliferation (PCNA, Ki-67), ECM remodeling (collagenase, urokinase), and vascular growth (bFGF, VEGF)
Immunophenotype	GLUT1-negative	GLUT1-positive
Hematology	VM or LVM: chronic LIC, occasional DIC Treatment of flares with low-molecular-weight heparin Possible benefit of low-dose aspirin as prophylaxis	(Kasabach–Merritt phenomenon is not linked to infantile hemangiomas, but to other vascular tumors such as kaposiform hemangioendotheliomas and tufted angiomas, both of which are GLUT1-negative; see Ch. 114)
Molecular biology	CMs (including SWS): somatic *GNAQ* > *GNA11* mutation Sporadic VMs: somatic *TEK* (~50%) or *PIK3CA* (~25%) mutation LMs: somatic *PIK3CA* mutation AVMs: somatic *MAP2K1, NRAS, KRAS, BRAF* Familial vascular malformations and overgrowth syndromes: see Tables 104.2 and 104.5	Rare families with autosomal dominant inheritance linked to 5q, and *somatic* loss of heterozygosity of 5q in some hemangiomas *Germline* mutation in *VEGFR2* or *TEM8* in some patients *Somatic* mutation in *VEGFR2* or *FLT4*/*VEGFR3* (5q34) in some hemangiomas Clonality in some hemangiomas

Table 104.1 Differences between vascular malformations and infantile hemangiomas. AVM, arteriovenous malformation; bFGF, basic fibroblast growth factor; CM, capillary malformation; CT, computed tomography; DIC, disseminated intravascular coagulation; ECM, extracellular matrix; *FLT4*, fms-related tyrosine kinase 4; *GNAQ/11*, G protein subunit α q or 11; LIC, localized intravascular coagulation; LM, lymphatic malformation; *MAP2K1*, mitogen-activated protein kinase kinase 1; MRI, magnetic resonance imaging; PCNA, proliferating cell nuclear antigen; *PIK3CA*, phosphatidylinositol-4,5-biphosphate 3-kinase catalytic subunit α; SWS, Sturge–Weber syndrome; *TEM8*, tumor endothelial marker 8; VEGF, vascular endothelial growth factor; VM, venous malformation.

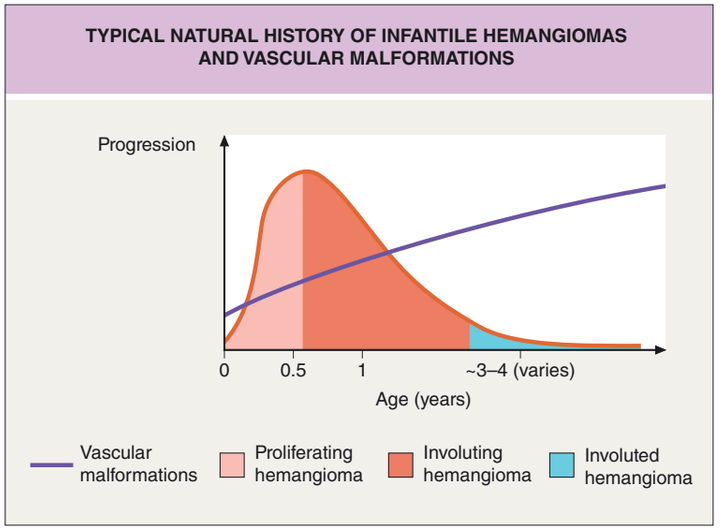


Fig. 104.1 Typical natural history of infantile hemangiomas and vascular malformations.

mesoderm-derived endothelial cells, forms new vessels from existing ones, thereby generating most blood and lymphatic vessels. Endothelial cells differentiate and recruit smooth muscle cell precursors to ensheathe them and build vessel walls. Changes in channel size, morphology, and rheology then create capillaries, veins, and arteries.

Vascular malformations constitute a heterogeneous group of disorders that result from alterations in the formation of blood or lymphatic channels. Dysfunction in signaling processes that regulate migration, differentiation, maturation, adhesion, and survival of the cells of vascular walls is thought to have a pathogenic role. Markers of cellular proliferation are not elevated in vascular malformations. In the cephalic region of the embryo, mural cells associated with endothelial cells come from the neural crest; therefore, a vascular malformation complex involving the head, such as Sturge–Weber syndrome (SWS), is caused by a somatic mutation in the embryo's anterior neural crest or adjacent cephalic mesenchyma. Identification of the genetic defects underlying various types of vascular malformations and the functions of the encoded proteins has provided insights into regulatory pathways critical to vascular morphogenesis (see Table 104.2)[5].

Sporadic vascular malformations may be caused by somatic mutations in the same or different genes than those implicated in the less common familial forms of the same type of malformation. For example, *somatic*

VASCULAR ANOMALIES FOR WHICH THE MOLECULAR BASIS IS KNOWN				
Vascular malformation	**Mode of inheritance**	**Mutated gene(s)**	**Type of mutation**	**Protein and function**
Capillary and/or arteriovenous malformations				
Port-wine birthmark/Sturge–Weber syndrome	Mosaic	*GNAQ* *GNA11*	Gain-of-function	Q-class G protein α-subunits
Port-wine birthmark/phakomatosis pigmentovascularis type II or overgrowth (e.g. of an extremity)		*GNAQ* *GNA11*		
AKT3-associated capillary malformation	Mosaic	*AKT3*	Gain-of-function	Activates AKT/mTOR pathway
Capillary malformation–arteriovenous malformation, including Parkes Weber syndrome	AD	*RASA1* *EPHB4**	Loss-of-function	p120-Ras-GAP protein and EPH receptor B4 in endothelial cells – interact and modulate MAPK signaling
Cerebral cavernous malformation (CCM)†	AD	CCM1: *KRIT1* CCM2: *CCM2* CCM3: *PDCD10*	Loss-of-function	KRIT-1 interacts with KREV-1, RAP-1A and malcavernin (the *CCM2* gene product) – roles in MAPK and integrin signaling
Hereditary hemorrhagic telangiectasia (HHT; Osler–Weber–Rendu)	AD	HHT1: *ENG* HHT2: *ACVRL1/ALK1* HHT5: *GDF2*	Loss-of-function	Endoglin and activin A receptor-like type 1 are two TGF-β receptors with roles in vessel wall integrity, which are activated by GDF2
Juvenile polyposis with HHT	AD	*SMAD4*	Loss-of-function	SMAD4 tumor suppressor protein – role in TGF-β signaling
Microcephaly–capillary malformation syndrome‡	AR	*STAMBP*	Loss-of-function	STAM-binding protein, a deubiquitinating enzyme
Arteriovenous malformations	Mosaic	*MAP2K1* *BRAF* *KRAS* *HRAS*	Gain-of-function	Activate MAPK pathway
Venous malformations				
Cutaneous and mucosal venous malformations (VMCM)	AD	*TEK*	Gain-of-function	TIE-2, an endothelial cell-specific tyrosine kinase receptor that binds angiopoietins
Blue rubber bleb nevus syndrome	Mosaic with double (cis) somatic mutations			
Venous malformations¶	Mosaic, sometimes with double (cis) somatic mutations	*TEK* *PIK3CA*	Gain-of-function	See above for TIE-2; PIK3CA activates AKT/mTOR pathway
Glomuvenous malformations	AD	*GLMN*	Loss-of-function	Glomulin is a component of a multiprotein complex – role in vascular morphogenesis
Verrucous venous malformation	Mosaic	*MAP3K3*	Gain-of-function	Activates MAPK pathway
Lymphatic anomalies				
Lymphatic malformations (microcystic, macrocystic, generalized lymphatic anomalies)	Mosaic	*PIK3CA*	Gain-of-function	Activates AKT/mTOR pathway
Kaposiform lymphangiomatosis	Mosaic	*NRAS*	Gain-of-function	Activates MAPK pathway
Congenital lymphedema (Milroy disease)	AD > AR	*FLT4*	Loss-of-function	VEGFR-3 – a tyrosine kinase receptor in lymphatic vessels
Milroy-like disease	AD	*VEGFC*	Loss-of-function	VEGF-C – a ligand for VEGFR-3
Lymphedema–distichiasis	AD	*FOXC2*	Loss-of-function	Forkhead family transcription factor C2
Hereditary lower extremity lymphedema	AD (female predominance)	*CELSR1*	Loss-of-function	Cadherin involved in lymphatic valve formation
Hypotrichosis–lymphedema–telangiectasia syndrome	AR, AD	*SOX18*	Loss-of-function or dominant-negative	SRY-box 18 transcription factor
Hennekam lymphangiectasia–lymphedema syndrome§	AR	*CCBE1* *FAT4* *ADAMTS3*	Loss-of-function	Collagen & calcium-binding EGF domain-containing protein 1; FAT atypical cadherin 4; protease that cleaves pro-VEGF-C
Generalized lymphatic dysplasia	AR	*PIEZO1*	Loss-of-function	Ion channel involved in lymphatic development

*Mutations in *EPHB4* can also result in nonimmune hydrops fetalis and postnatal lymphatic dysfunction.
†Cutaneous vascular malformations, including hyperkeratotic capillary–venous malformations (associated primarily with *KRIT1* mutations) and venous malformations (less common), occur in ~10% of patients.
‡Features multiple small capillary malformations, hypoplastic distal phalanges, severe intellectual disability, and intractable seizures.
¶Somatic mutations in *GJA4* (gap junction protein alpha 4) encoding connexin 37 have also been reported in cutaneous and hepatic venous malformations.
§Presents with generalized lymphedema, lymphangiectasias (intestinal and pulmonary), facial anomalies (flat face, depressed nasal bridge, hypertelorism), and intellectual disability.

Table 104.2 Vascular malformations for which the molecular basis is known.

Continued

VASCULAR ANOMALIES FOR WHICH THE MOLECULAR BASIS IS KNOWN				
Vascular malformation	**Mode of inheritance**	**Mutated gene(s)**	**Type of mutation**	**Protein and function**
Hereditary lymphedema	AD	*GJC2*	Loss-of-function	Connexin 47 in gap junctions of lymphatic vessels
Oculo-dento-digital dysplasia	AD	*GJA1*	Missense	Connexin 43 in gap junctions
Lymphedema–choanal atresia	AR	*PTPN14*	Loss-of-function	Protein tyrosine phosphatase that may interact with VEGFR-3
Microcephaly, lymphedema, chorio-retinal dysplasia syndrome	AD	*KIF11*	Loss-of -function	Kinesin family member 11
Arteriopathy				
CADASIL	AD	*NOTCH3* *HTRA1*	Loss-of-function	Accumulation of NOTCH-3 protein in vascular smooth muscle cells; serine peptidase dysfunction

Table 104.2 Vascular malformations for which the molecular basis is known. Vascular malformations also occur in patients with the overgrowth syndromes presented in Table 104.5. Lymphedema is a feature of other disorders such as Noonan syndrome/other RASopathies (see Table 61.3), GATA2 deficiency (see Table 60.13), and a subset of hypohidrotic ectodermal dysplasia with immunodeficiency (see Ch. 63). *Aagenaes syndrome* is an autosomal recessive disorder linked to 15q that manifests with infantile cholestasis and childhood-onset lymphedema. Unless otherwise noted, the mosaic conditions above are characterized by a heterozygous somatic mutation in lesional tissue. Some AD conditions (e.g. cutaneous and mucosal venous malformations, glomuvenous malformations) feature a "second hit" mutation in lesional tissue. AD, autosomal dominant; *ADAMTS3*, ADAM metallopeptidase with thrombospondin type 1 motif 3; AR, autosomal recessive; CADASIL, cerebral autosomal dominant arteriopathy with subcortical infarcts and leukoencephalopathy; *CELSR1*, cadherin EGF LAG seven-pass G-type receptor 1; *FLT4*, fms-related tyrosine kinase 4; *GDF2*, growth differentiation factor 2; *PIK3CA*, phosphatidylinositol-4,5-biphosphate 3-kinase catalytic subunit α; MAPK, mitogen-activated protein kinase; *MAP2K1*, MAPK kinase 1; *MAP3K3*, MAPK kinase kinase kinase 3; mTOR, mechanistic target of rapamycin; *PDCD10*, programmed cell death 10; *PIEZO1*, piezo-type mechanosensitive ion channel component 1; TGF-β, transforming growth factor-β; VEGF(R), vascular endothelial growth factor (receptor); VM, venous malformation.

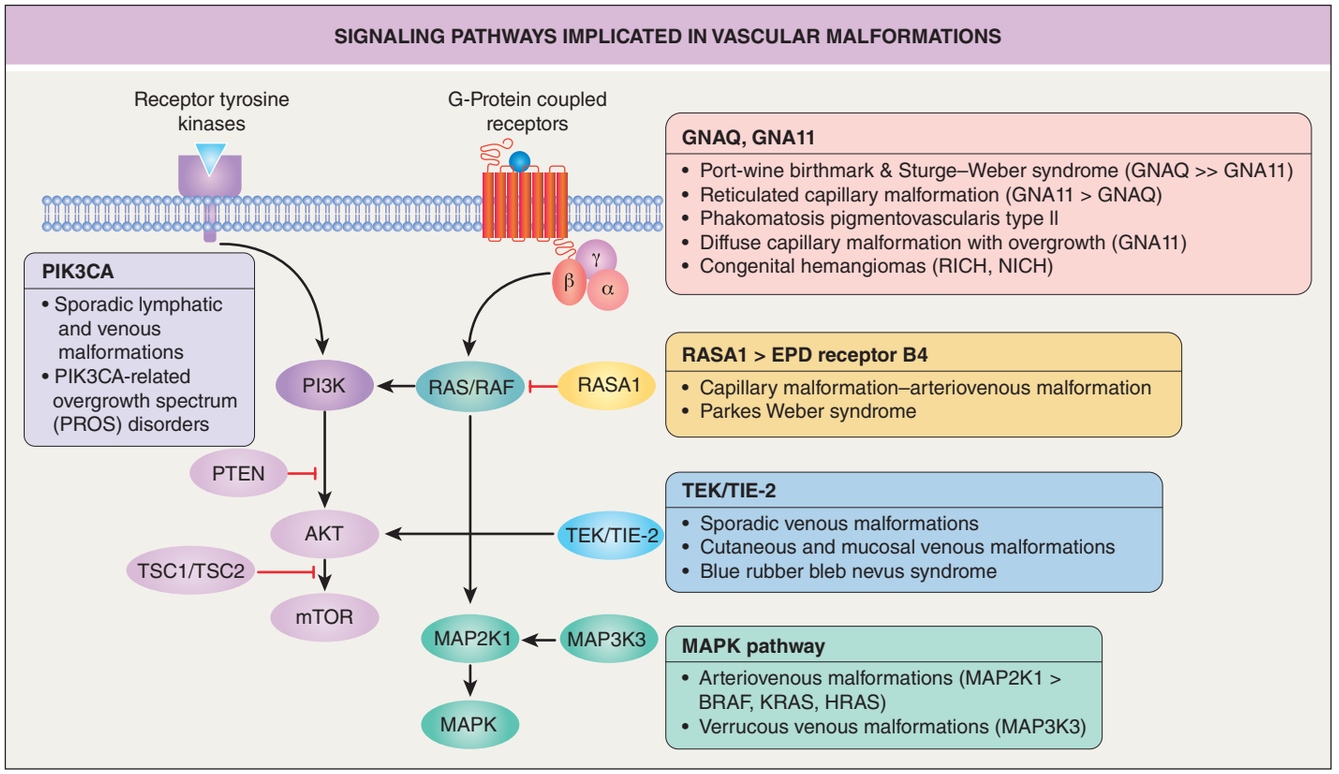


Fig. 104.2 Signaling pathways implicated in vascular malformations. MAPK, mitogen-activated protein kinase; *MAP2K1*, MAPK kinase 1; *MAP3K3*, MAPK kinase kinase kinase 3; mTOR, mechanistic target of rapamycin; *PIK3CA*, phosphatidylinositol-4,5-biphosphate 3-kinase catalytic subunit α.

TEK mutations that cause constitutive activation of the endothelial cell tyrosine kinase receptor TIE-2 are found in lesional tissue (but not the peripheral blood) in approximately half of patients with sporadic VM. Individuals with blue rubber bleb nevus syndrome and a subset of those with sporadic VMs (multifocal > unifocal lesions) have *two somatic* gain-of-function *TEK* mutations within the *same* allele (double [*cis*])[6,7]. While familial cutaneous and mucosal VMs (VMCM) result from a *germline* gain-of-function *TEK* mutation, a second-hit mutation in the same or other *TEK* allele has been documented in a few individuals[6,7]. Advances in our understanding of the pathogenesis of vascular malformations has provided the basis for targeted treatment strategies[4,6–9].

CLINICAL FEATURES

Most vascular malformations can be correctly categorized based on their clinical features. This helps in selection of the most appropriate investigative tools (Table 104.3), avoiding redundant and unnecessary diagnostic imaging procedures. In addition, genetic analysis may be of utility in patients with vascular malformations associated with clinical manifestations that may potentially benefit from targeted systemic therapy as well as those with familial transmission. A sample of affected tissue is typically required for genetic testing in conditions caused by a somatic mutation, and massively parallel/next-generation sequencing

INVESTIGATIVE TOOLS FOR VASCULAR MALFORMATIONS				
Tool	**Vascular lesion**			
	Capillary malformation	**Lymphatic malformation**	**Venous malformation**	**Arteriovenous malformation**
Ultrasonography	+/–	++++	+++	++++
CT with contrast	–	++	++	++
MRI with gadolinium	–*	+++ (no gadolinium enhancement)	++++ (gadolinium enhancement)	+++
3D-angio CT or 3D-angio MRI	–	–	++	++++
Dynamic magnetic resonance lymphangiography (MRL)	–	++++	–	–
Arteriography	–	–	–	++++
Phlebography	–	–	+/–	–
Lymphography (isotopic)	–	+/–	–	–
Biopsy	+/–	+/–	–	–

*See text for recommended imaging to evaluate for possible Sturge–Weber syndrome (SWS).

Table 104.3 Investigative tools for vascular malformations. Multidetector CT and 3-dimensional MR venography may help to determine the extent of involvement in patients with Klippel–Trenaunay syndrome. A larger number of +'s indicates increased utility. CT, computed tomography; MRI, magnetic resonance imaging.

(NGS) panels are available for overgrowth syndromes and lymphedema (see Appendix).

Capillary Malformations

The ISSVA CM category includes nevus simplex, PWBs, reticulate CMs, CMTC, CM of CM-AVM, and telangiectasias[3]; additional clinical variants such as "geographic" and "diffuse" CMs have also been described[10]. Occasionally, CMs represent the most obvious sign of a complex syndrome. An approach to the evaluation of a patient with a presumed CM of the head and neck region is shown in Fig. 104.3.

Nevus simplex

Nevus simplex (salmon patch) is a very common congenital vascular birthmark evident in 30%–80% of neonates[11]. Although classified as a CM by the ISSVA, nevus simplex is thought to represent remnants of the fetal circulation rather than a mosaic condition due to a somatic mutation. These pink-to-red macules and patches with somewhat indistinct borders have characteristic locations on the forehead/glabella in a V-shape ("angel kiss"), eyelids, philtrum, occiput, nape ("stork bite"), and lumbosacral area (Fig. 104.4A,B). They often become more prominent with crying or vigorous activity. The term *nevus simplex complex* has been proposed for extensive lesions[12].

Facial nevus simplex tends to fade spontaneously between 1 and 3 years of age, but extrafacial and some glabellar lesions are more persistent. During infancy, eczematous dermatitis may preferentially or solely develop within a nevus simplex. The vast majority of children with a nevus simplex do not have associated abnormalities; however, a prominent or persistent midfacial nevus simplex is a feature of several syndromes, including Beckwith–Wiedemann and megalencephaly–CM. Although there has been controversy regarding whether a lumbosacral nevus simplex represents a possible sign of occult spinal dysraphism, most authors do not recommend spinal imaging in the absence of additional cutaneous findings (see Ch. 64)[13,14].

Port-wine birthmark (PWB) and variants

A somatic activating mutation in *GNAQ* (Q-class G protein subunit α) or, occasionally, *GNA11* (G protein subunit α 11) in affected skin (especially the blood vessels) ± regional extracutaneous tissues (e.g. brain, eyes) underlies isolated PWBs and Sturge–Weber syndrome (SWS)[15]. These mutations (most often of R183 residues) lead to increased mitogen-activated protein kinase (MAPK) signaling (see Fig. 104.2), which results in increased cell proliferation and decreased apoptosis[16].

PWBs typically present at birth as well-demarcated, bright or deep red macules and patches, with their color resembling that of port wine. Fainter red or pink birthmarks have been termed "*nevus roseus*" because their color resembles that of rosé wine[17]. Some light red–pink birthmarks are not solid but finely reticulated, often with a blotchy appearance and indistinct borders; these *reticulated CMs* are distinct from CMTC, which has a more well-defined, purplish net- or tram track-like pattern and is often associated with cutaneous atrophy. Reticulated CMs can be due to somatic gain-of-function mutations in *GNA11* and, less commonly, *GNAQ* or *PIK3CA*[15,18].

The growth of PWBs is commensurate with the child's growth. They can be localized, have a segmental pattern, or be multifocal and widespread. The distribution patterns of facial PWBs are thought to reflect the prominences that form during embryonic craniofacial development and their associated vasculature. Because these regions resemble the dermatomes of the trigeminal nerve, the following areas were classically recognized: V1 – forehead and upper eyelid; V2 – maxillary region (Fig. 104.4C); and V3 – mandibular region.

Over time, PWBs, especially those in the maxillary and mandibular areas, often develop a deeper red hue, changing from pinkish-red at birth to purplish-red by adulthood. Affected skin may thicken and become nodular (Fig. 104.5), and superimposed pyogenic granulomas occasionally appear. In a study of 173 patients with PWBs, thickening was observed in 11% (median age 32 years), nodularity in 24% (median age 44 years), and both in 6% (median age 45 years)[19]. These changes are rarely observed in the lighter "nevus roseus" or in PWBs located on the trunk and limbs. Overgrowth of the soft tissues and facial bones underlying a PWB can also occur, creating problems such as an open-bite deformity. Affected gums and lips may enlarge, potentially resulting in epulides, gingival bleeding, macrocheilia, and lip incompetence. As with nevus simplex, eczematous dermatitis may have a predilection for areas of skin affected by the PWB.

PWBs are congenital in the vast majority of patients. However, *acquired port wine-like lesions* have been described in adolescents and adults, and onset of such lesions may be precipitated by trauma[20]. Of note, early morphea, especially the linear variant, occasionally presents with a red vascular patch that mimics an acquired *port wine-like lesion*[21].

A CM can be admixed with a network of blanched macules representing a nevus anemicus (*nevus vascularis mixtus*; Fig. 104.6). The association of a CM with dermal melanocytosis (Fig. 104.7) or a nevus spilus (speckled lentiginous nevus) is referred to as *phakomatosis pigmentovascularis (PPV)* (Table 104.4)[22,23]. Patients with PPV type II (*cesioflammea*) have the same activating mutation, either in *GNAQ* or *GNA11*, in both the PWB and dermal melanocytosis. Likewise, mosaic mutations in *PTPN11* (protein tyrosine phosphatase nonreceptor type 11) have been found to underlie both the nevus roseus and nevus spilus in patients with PPV type III[23a]. Hypertension due to renal artery stenosis has been described in patients with extensive PWBs[15].

Sturge–Weber syndrome

SWS is a sporadic neurologic disorder in which a facial PWB is associated with ipsilateral leptomeningeal/brain and ocular vascular anomalies. Although all three components constitute a diagnosis of "complete" SWS, patients with a PWB plus CNS involvement alone are also typically diagnosed as having SWS, whereas those with a facial PWB

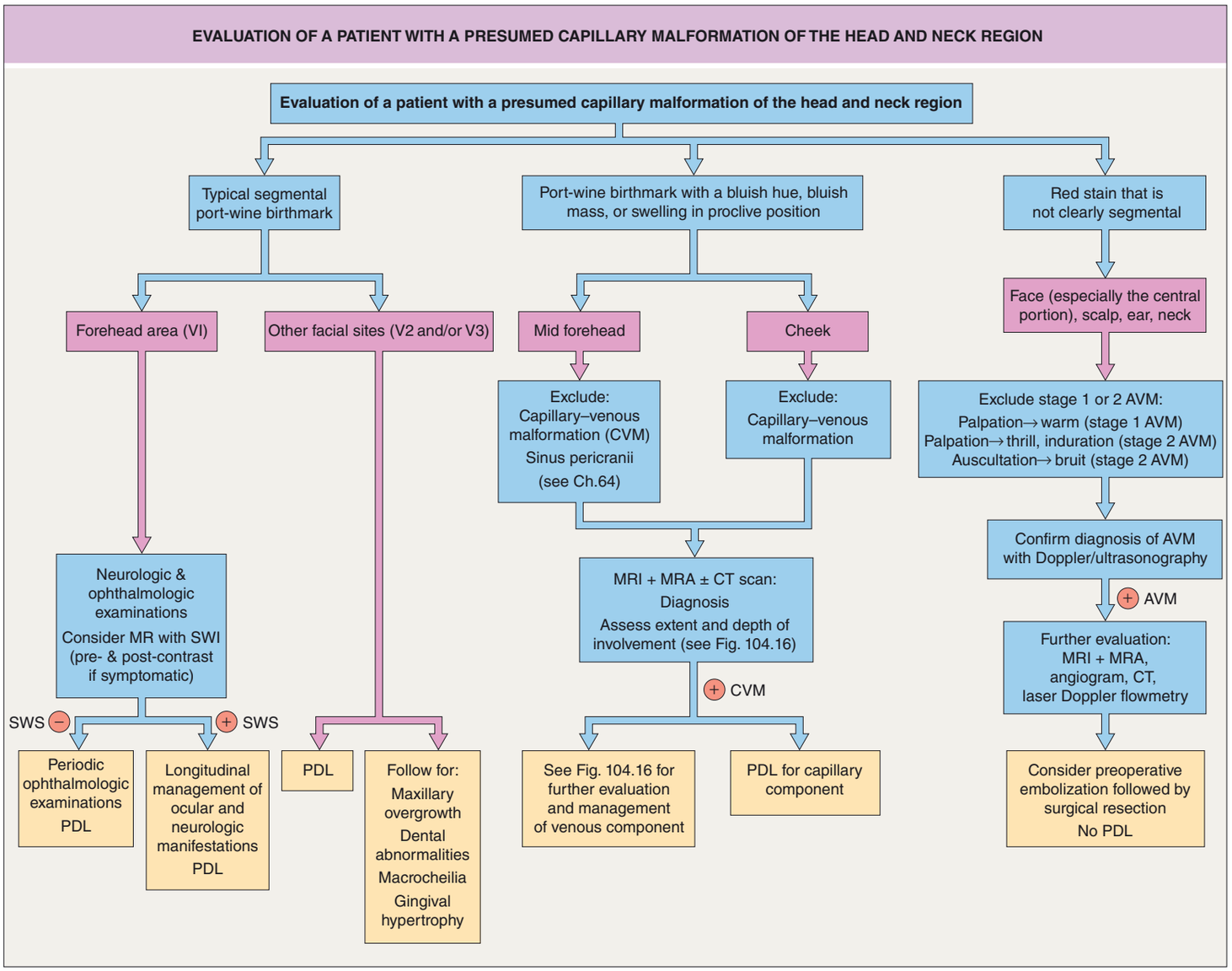


Fig. 104.3 Evaluation of a patient with a presumed capillary malformation of the head and neck region. AVM, arteriovenous malformation; CT, computed tomography; PDL, flashlamp-pumped pulsed dye laser; MRA, magnetic resonance arteriography; MRI, magnetic resonance imaging; SWI, susceptibility-weighted imaging; SWS, Sturge–Weber syndrome.



Fig. 104.4 Nevus simplex versus port-wine birthmark (PWB). A Involvement of the central face in a symmetric pattern is typical of a nevus simplex (salmon patch); such lesions usually fade over the first few years of life but are sometimes misdiagnosed as a PWB. **B** Nevus simplex in the nape area ("stork bites") tend to be more persistent. **C** In this young infant with a PWB in the maxillary region, the affected skin is smooth. This lesion will be persistent. *B, Courtesy Julie V. Schaffer, MD.*



Fig. 104.5 Facial port-wine birthmark in the maxillary region in an adult. Hyperplasia and nodularity are prominent. *Courtesy Pablo Boixeda, MD.*

plus ocular involvement alone are often classified separately. The brain and/or ocular manifestations of SWS rarely occur without an associated PWB. Mosaicism due to a somatic activating mutation in *GNAQ* (or rarely *GNA11*) represents the cause of both SWS and non-syndromic facial PWBs (see above), with the former resulting from a mutation that arises earlier in development and affects the vasculature of the eye and CNS as well as the skin[16].

Facial PWBs associated with SWS were classically considered to involve the V1 region, which includes the forehead and upper eyelid[1], often with extension unilaterally or bilaterally over more of the face (Fig. 104.8). More recent studies have shown that involvement of the "forehead area", which includes the upper eyelid and is delineated inferiorly by a line drawn from the outer canthus to the top of the ear, represents the best clinical predictor for SWS (Fig. 104.9)[24]. This risk area encompasses portions of V2/V3 as well as V1 and is thought to correspond with the embryonic *frontonasal prominence*[25]. The latter includes neural crest-derived vasculature and develops in conjunction with the forebrain, which gives rise to the cerebral cortex and optic vesicles. A somatic *GNAQ* mutation occurring in the frontonasal area prior to migration of embryonic neural crest derivatives, which also include the leptomeninges and choroid, may therefore explain the forehead location of CMs associated with cerebral and ocular vascular malformations. Some SWS patients also have PWBs on the extremities and trunk. In addition, SWS occasionally occurs in the setting of PPV type II (see Table 104.4).



Fig. 104.6 Port-wine birthmark intermingled with a nevus anemicus on the shoulder. This man had phakomatosis pigmentovascularis type IIb, with additional features including an upper facial port-wine birthmark, Sturge–Weber syndrome, and extensive dermal melanocytosis.



Fig. 104.7 Phakomatosis pigmentovascularis type IIa (cesioflammea). A large port-wine birthmark and extensive dermal melanocytosis are seen.

PHAKOMATOSIS PIGMENTOVASCULARIS (PPV)				
Type	**Descriptive name**	**Proportion of reported cases**	**Major cutaneous components**	**Other reported cutaneous components**
Ia/b	*	<5%*	Epidermal nevus + **PWB**	
IIa/b	Phakomatosis cesioflammea	75%	Dermal melanocytosis (aberrant Mongolian spots) + **PWB**	Nevus anemicus, hypotrichosis, lipohypoplasia, hypoplastic nails
IIIa/b	Phakomatosis spilorosea or melanorosea	10%	Nevus spilus (macular type) + **light red–pink CM ("nevus roseus")**	Nevus anemicus, lymphedema, hypotrichosis
IVa/b	Phakomatosis melanovascularis or unclassifiable	10%	Café-au-lait macule + **CM** Variable, sometimes with features of II + III or II + V	Nevus anemicus, nevoid hyper- or hypopigmentation, nevus sebaceus
Va/b	Phakomatosis cesiomarmorata	<5%	Dermal melanocytosis + **cutis marmorata telangiectatica congenita**	

*Existence as a type of PPV has been challenged considering that epidermal nevi are not melanocytic lesions; epidermal nevi can occur together with vascular malformations in Proteus, PTEN hamartoma tumor, and CLOVES syndromes (see Table 104.5), which are not generally considered as PPV.

Table 104.4 Phakomatosis pigmentovascularis (PPV). a = cutaneous abnormalities only; b = cutaneous and extracutaneous abnormalities (e.g. of Sturge–Weber syndrome, Klippel–Trenaunay syndrome, or ocular, as well as nevus of Ota). Vascular lesions are in bold. CM, capillary malformation; PWB, port-wine birthmark.



Fig. 104.8 Infant at risk for Sturge–Weber syndrome (SWS). The port-wine birthmark covers most of the left side of the face.

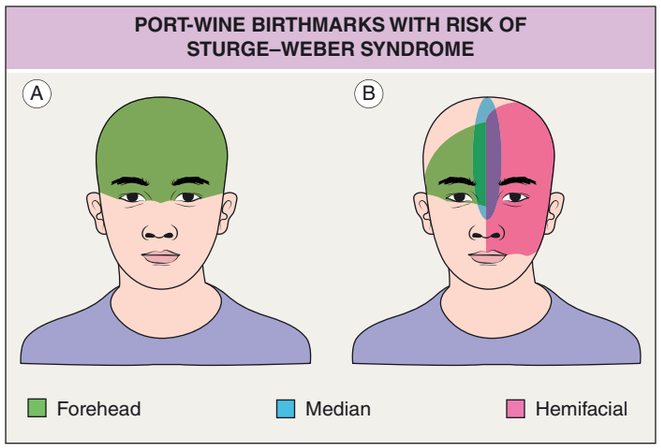


Fig. 104.9 Port-wine birthmarks (PWBs) with risk of Sturge–Weber syndrome (SWS). Involvement of the "forehead area" (**A**), which includes the upper eyelids and is delineated inferiorly by a line drawn from the outer canthus to the top of the ear, is associated with risk of SWS. Hemifacial and median forehead (**B**) as well as bilateral forehead lesions are associated with highest risk.

Ocular involvement in SWS can result in enlarged venous vessels affecting the conjunctiva, episclera, retina, and/or choroid. The most common ocular manifestation is glaucoma, which affects 30%–60% of patients with a PWB on the forehead and/or eyelids; choroidal hemorrhage and retinal detachment are rare complications. Ocular involvement is more frequent when the PWB affects both the V1 and V2 regions. Glaucoma may be detected at birth because of buphthalmos (enlargement of the globe), and acute glaucoma with a cloudy cornea can be an infantile emergency. Usually, however, increased eye pressure develops slowly. As a result, glaucoma may become evident during late childhood, adolescence, or even adulthood. Thus, periodic lifelong assessment of visual function and pressure of both eyes, as contralateral glaucoma occasionally occurs, is mandatory.

Neurologic symptoms can result from hypoperfusion of the ipsilateral brain due to CVMs within the pia mater, absence of superficial cortical veins, and dilated deep draining veins. Over time, chronic hypoxia may lead to cerebral hemiatrophy and calcifications, with the occipital region being the most frequent location. The most common neurologic manifestation is seizures, which are most often focal motor, either affecting the side of the body opposite to the vascular anomaly or generalized. The seizures typically develop in the first two years of life and affect ≥75% of children with SWS[26]; they may be difficult to control with anticonvulsants, especially early on. Additional findings can include stroke-like episodes with contralateral hemiparesis or hemiplegia; developmental delay affecting motor and cognitive skills; emotional and behavioral problems; attention deficit disorder; and migraine headaches. Endocrine dysfunction such as central hypothyroidism and growth hormone deficiency may also occur, even in patients with normal neuroimaging[27].

The risk of ocular and/or neurologic manifestations of SWS is ~25%–50% when a unilateral PWB affects most of the forehead area; it is lower when the PWB involves a smaller portion of this area and higher (>50%) for a hemifacial lesion or a bilateral PWB covering the forehead and both upper eyelids[25,28,29] (see Fig. 104.9). One prospective study also found an increased risk of SWS in patients with PWBs on the median forehead (a distribution reminiscent of nevus simplex), whereas linear PWBs on the forehead were not associated with SWS[25].

A recent consensus statement on the management of SWS recommended referral of any infant or child with a high-risk facial PWB (see above) to a pediatric neurologist and ophthalmologist for baseline evaluation and periodic follow-up (see Fig. 104.3)[30]. In newborns and infants with a high-risk PWB but no history of seizures or neurologic symptoms, neuroimaging should be considered in selected individuals (e.g. with an extensive bilateral facial PWB or if presymptomatic treatment is contemplated) rather than on a routine basis[29]. In such patients, a non-sedated, non-contrast screening MRI including T1 and T2 (± fluid attenuation inversion recovery [FLAIR]) and susceptibility-weighted imaging (SWI) ± diffusion-weighted imaging (DWI) is recommended. These modalities can demonstrate early leptomeningeal changes with enlargement of transmedullary and periventricular veins; although sensitivity in asymptomatic patients is limited in the first few months of life, leptomeningeal involvement can be excluded by ≥1 year of age. In patients with neurologic symptoms, pre- and post-contrast MRI that includes high-resolution volumetric sequences in addition to SWI and post-contrast FLAIR imaging is recommended[29]. Gyriform calcifications and atrophy develop during childhood in SWS patients and are visible by CT scans and other neuroimaging modalities.

Early diagnosis of SWS is important, as prophylactic aspirin administration may reduce the frequency of stroke-like episodes and seizures[31,32]. Some infants and children with SWS have cognitive deficits that are more severe than anticipated based upon their limited cortical involvement on conventional MRI studies. Functional cerebral imaging, e.g. SPECT (single photon emission computed tomography) that evaluates regional cerebral blood flow or PET (positron emission tomography) that demonstrates metabolism of glucose, can provide additional prognostic information. Quantitative electroencephalography (EEG) may also aid in screening for brain involvement in asymptomatic infants at risk of SWS[33].

Capillary malformations associated with overgrowth, including the PIK3CA-related overgrowth spectrum (PROS)

PWBs and reticulated CMs on the trunk and extremities may be associated with regional overgrowth and other syndromic features (Table 104.5)[34]. Mosaicism for mutations that result in activation of the phosphatidylinositol 3-kinase (PI3K)/AKT pathway have been found to underlie several of these conditions (see Figs. 104.2 and 113.1), including those in the *PIK3CA*-related overgrowth spectrum (PROS). The various terms and eponyms used for overgrowth syndromes are likely to be refined as the molecular etiologies are further clarified.

Diffuse capillary malformation with overgrowth

Diffuse CM with overgrowth (DCMO) is a term proposed for a widespread reticulated CM associated with proportional soft tissue and/or bony hypertrophy (Fig. 104.10A)[35]. Unlike Klippel–Trenaunay syndrome (KTS), the overgrowth is not progressive and does not correlate with the location of the CM; in addition, although some DCMO patients have clinically prominent subcutaneous veins, they do not have a true VM or LM. In contrast to megalencephaly–CM, DCMO patients are normocephalic and do not have associated neurologic abnormalities. The pale red–pink, reticulated CM in DCMO involves multiple contiguous anatomic regions, often with a sharp midline demarcation on the anterior trunk, and may lighten over the first few months of life; approximately half of patients have additional areas with a confluent CM, usually in acral sites. Somatic activating mutations in *GNA11* and *PIK3CA* (phosphatidylinositol-4,5-biphosphate 3-kinase catalytic subunit α) have been reported to cause diffuse CM associated with mild and more significant overgrowth, respectively[15,36,37].

OVERGROWTH SYNDROMES WITH VASCULAR MALFORMATIONS								
	DCMO	***PIK3CA*-Related Overgrowth Spectrum (PROS)**				***PIK3R1*-Related Overgrowth**	**Proteus**	**PHTS**
		M-CM	**KTS**	**CLOVES**	**CLAPO**			
Gene	*GNA11* or *GNAQ*	*PIK3CA*, mosaic	*PIK3CA*, mosaic	*PIK3CA*, mosaic	*PIK3CA*, mosaic	*PIK3R1*, mosaic	*AKT1*, mosaic	*PTEN* germline with somatic second mutation
Asymmetric/segmental overgrowth								
At birth	+	+	+	+	+	+	–/minimal	+
Progressive	–	–	+	+	+	+	+++	+
Correlates with site(s) of vascular malformation	–	–	+	+	+	variable	–	variable
Digital abnormalities	30%: syndactyly, sandal gap, macrodactyly	Syndactyly > polydactyly, macrodactyly; sandal gap	Occasional macrodactyly, syndactyly (associated with deep venous anomalies)	Broad hands/feet, macrodactyly (especially 3rd toe), sandal gap	–	Macrodactyly of 2nd toe, syndactyly, sandal gap	Macrodactyly with distorted/deformed digits	–
Macrocephaly	–	+; (hemi)megalencephaly, dolichocephaly	–	30% with (hemi) megalencephaly	–	–	Dolichocephaly	+
Capillary malformations	Reticulated ± confluent areas; widespread, block-like	Reticulated; widespread, block-like; persistent nevus simplex	Geographic, well-demarcated, dark (associated with LM) or blotchy light; on extremity ± extension	Geographic, well-demarcated, dark; on trunk overlying lipomatous mass	Well-demarcated, outlining lower lip with "sawtooth" border	Well-demarcated or reticulated; often on lower extremity	Well-demarcated; often on trunk	Variable
Venous anomalies	Variable prominent veins	Variable prominent veins	VM*; often persistent lateral marginal vein, abnormal deep venous system	VM* of superficial, deep thoracic, and often major central veins	VM* of neck	VM in most patients	Variable VM*	Variable VM; dilated draining veins associated with high-flow lesions
Lymphatic anomalies	–	–	Often LM with overlying vesicles, lymphedema	Truncal LM within lipomatous mass; overlying vesicles	LM of tongue, face, and/or neck	Variable LM	Variable LM	Variable LM, lymphedema
Arteriovenous malformations	–	–	–	Variable spinal/paraspinal AVM	–	–	–	Fast-flow "PTEN hamartoma of soft tissue" with intramuscular involvement and ectopic fat
Other cutaneous features	–	Hyperelastic, soft/doughy skin	–	Lipomatous truncal masses, epidermal nevi, furrowed soles	–	Lipomatosis	Cerebriform connective tissue nevi of palms/soles, epidermal nevi, lipomatous overgrowth, regional lipohypoplasia	Lipomatosis, epidermal nevi, pigmented macules of genitalia; later tricholemmomas, acral keratoses, oral papillomas, neuromas, sclerotic fibromas

*Associated with a high risk of venous thrombosis and pulmonary embolism; may have chronic intravascular coagulopathy.

Table 104.5 Overgrowth syndromes with vascular malformations.

Continued

OVERGROWTH SYNDROMES WITH VASCULAR MALFORMATIONS								
	DCMO	*PIK3CA*-Related Overgrowth Spectrum (PROS)				*PIK3R1*-Related Overgrowth	Proteus	PHTS
		M-CM	KTS	CLOVES	CLAPO			
Other extracutaneous features	–	Polymicrogyria, ventriculomegaly, cerebellar tonsillar ectopia/Chiari malformation, hydrocephalus, hypotonia, seizures, developmental delay; frontal bossing, joint hypermobility	–	Variable polymicrogyria, seizures, and other features of M-CM	–	Variable developmental delay	Lung bullae; hyperostoses, megaspondylodysplasia with scoliosis; long face with ptosis, depressed nasal bridge, anteverted nares, and open mouth at rest	See Table 63.3
Tumors	–	Rare Wilms tumor†	–	Rare Wilms tumor†	–	–	Parotid monomorphic adenoma, ovarian cystadenoma, testicular tumors, meningioma	Increased risk of thyroid, breast, endometrial, renal, and GI carcinomas

†Surveillance with abdominal ultrasound every 3–4 months until 8 years of age is recommended.

Table 104.5 Overgrowth syndromes with vascular malformations. PTEN hamartoma tumor syndrome (PHTS) includes Cowden and Bannayan–Riley–Ruvalcaba syndromes as well as SOLAMEN syndrome – *s*egmental *o*vergrowth, *l*ipomatosis, *a*rteriovenous *m*alformation, and *e*pidermal *n*evus (see Ch. 63). Additional entities in the *PIK3CA*-related overgrowth spectrum that have dermatologic manifestations include hemihyperplasia multiple lipomatosis, fibroadipose hyperplasia, and isolated tissue overgrowth related to a LM, VM, or lipomatosis. CLOVES, *c*ongenital *l*ipomatous *o*vergrowth, *v*ascular anomalies, *e*pidermal nevi, *s*coliosis/*s*keletal abnormalities; DCMO, *d*iffuse *c*apillary *m*alformation with *o*vergrowth; GI, gastrointestinal; KTS, Klippel–Trenaunay syndrome; LM, lymphatic malformation; M-CM, megalencephaly–capillary malformation; *PIK3CA*, phosphatidylinositol-4,5-biphosphate 3-kinase catalytic subunit α; *PTEN*, phosphatase and tensin homolog; VM, venous malformation.

Klippel–Trenaunay syndrome

Klippel–Trenaunay syndrome (KTS) is currently defined by the triad of a PWB, anomalous veins (representing a VM), and progressive overgrowth of the affected extremity. However, this eponym has also been erroneously used for any capillary malformation associated with limb hypertrophy. The vascular malformation in KTS is a combined CVM or CLVM, which may be localized or more extensive. Somatic mutations in *PIK3CA* have been identified in CLVMs associated with KTS[38]. In addition, somatic mutations in *PIK3R1* (phosphoinositide-3-kinase regulatory subunit 1) have been identified in patients with C(L)VMs and overgrowth of the affected extremity[39] (see Table 104.5).

A well-demarcated, dark red-to-purple birthmark with irregular borders, referred to as a *geographic CM*, favors the lateral aspect of the thigh and is usually associated with a lymphatic component. Superimposed purple papules or hemorrhagic vesicles frequently develop and, especially if a persistent lateral marginal vein is evident on the outer aspect of the knee, a geographic CM predicts more severe, progressive overgrowth and a higher likelihood of complications such as cellulitis[40,41] (Fig. 104.11A). Other children have pink-to-red, blotchy capillary birthmarks, which are associated with a better prognosis (Fig. 104.11B); in the absence of a VM, these patients may be more appropriately classified as having DCMO (see above) or simply a PWB with associated overgrowth. Foot and hand malformations in KTS are usually associated with deep venous system anomalies[42].

With lower extremity KTS, leg length discrepancy is progressive and requires ongoing orthopedic care. Lymphedema can lead to massive limb overgrowth and cellulitis. Some severely affected individuals have capillary–venous or lymphatic anomalies affecting the anogenital area, bladder, pelvis, retroperitoneum, and gastrointestinal tract that may bleed and result in anemia. A protein-losing enteropathy has also been described.

Like simple VMs (see below), the anomalous venous network in KTS may be associated with a chronic intravascular coagulopathy with high D-dimer and variably low fibrinogen levels. Patients with specific anomalies such as the presence of the lateral marginal vein, insufficient perforator veins, or intramuscular involvement are at higher risk of deep vein thrombosis, chronic thromboembolic pulmonary hypertension, and even life-threatening pulmonary embolism[40,43,44]. Prophylactic anticoagulation should be considered in KTS patients, especially those with evidence of hypercoagulability, when they have additional risk factors for venous thromboembolism such as surgery, trauma, or pregnancy[45]. Periodic echocardiography to assess for pulmonary hypertension has also been recommended by some authors[46].

Duplex ultrasonography is useful in investigating the vascular anomalies underlying KTS (see Table 104.3). Multidetector computed tomography (MDCT) and three-dimensional magnetic resonance venography (MRV) can help to determine the extent of musculoskeletal, thoracic, and abdominopelvic involvement as well as to characterize bone density changes, limb asymmetry, and the presence/patency of the deep venous system. Lymphoscintigraphy is rarely indicated. In patients with GI bleeding, colonoscopy or capsule endoscopy may reveal capillary patches, extensive dilated venous channels, and microcystic LM in the intestines.

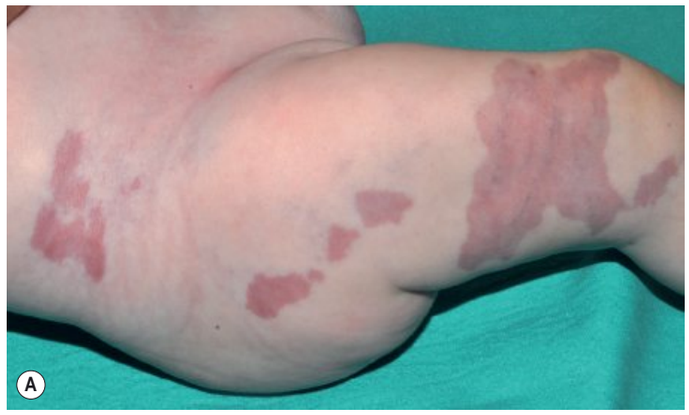
CLOVES syndrome

This "Proteus-like" syndrome is characterized by asymmetric, progressive, infiltrative *c*ongenital *l*ipomatous *o*vergrowth that is typically truncal; *v*ascular anomalies; *e*pidermal nevi; *s*coliosis/*s*keletal abnormalities that include broad hands and feet; *s*pinal/paraspinal arteriovenous lesions; and *s*eizures[47,48]. CLOVES syndrome is caused by somatic activating mutations in *PIK3CA*[49], and the clinical findings overlap considerably with those of other forms of PROS, such as KTS and megalencephaly–CM (see Table 104.5)[50]. LMs are often present within the lipomatous truncal mass of CLOVES, with variable extension into the retroperitoneum and mediastinum. Well-demarcated, dark red, geographic CMs/CLMs usually overlie the mass, which is also typically associated with both aberrant superficial veins and phlebectasia of the thoracic or major central veins; the latter result in increased risk of pulmonary embolism, especially when undergoing surgery[51].





Fig. 104.10 Reticulated capillary malformations. A Diffuse capillary malformation with overgrowth. This normocephalic infant has an extensive reticulated capillary malformation involving the trunk, one arm, and both legs. **B** Megalencephaly–capillary malformation syndrome. This boy has hemihypertrophy of the side of the body opposite to the capillary malformation. *Courtesy Julie V. Schaffer, MD.*



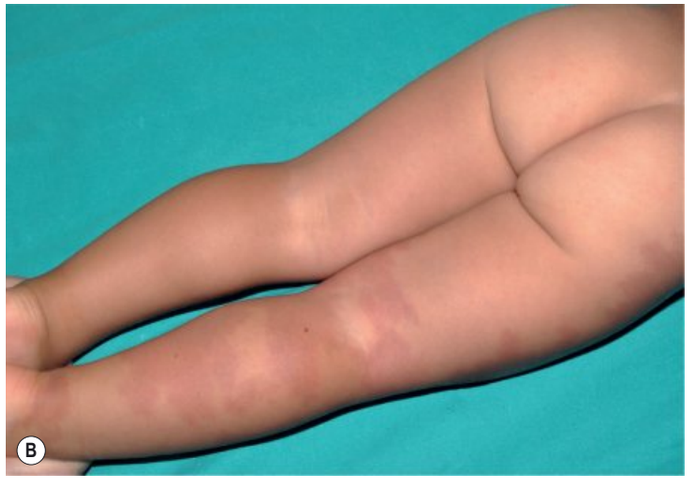


Fig. 104.11 Klippel–Trenaunay syndrome. A Darker red–purple, well-demarcated geographic capillary birthmark on the thigh associated with dilated veins and an enlarged lower limb. **B** Light red, blotchy capillary birthmark associated with enlargement of the lower extremity. Compared to blotchy CMs, geographic CMs are more likely to be associated with lymphatic malformations as well as tissue overgrowth.

Megalencephaly–capillary malformation

Megalencephaly–CM, which was previously known as macrocephaly–CM and macrocephaly–CMTC, features asymmetric overgrowth, progressive (hemi)megalencephaly, and a widespread reticulated CM, often with a characteristic midline demarcation on the abdomen (Fig. 104.10B). Additional features include a persistent midfacial nevus simplex, frontal bossing, neonatal hypotonia, developmental delay, syndactyly (especially 2nd–3rd toes), polydactyly, joint laxity, and hyperelastic skin[52]. Neuroimaging characteristically shows ventriculomegaly, acquired cerebellar tonsillar ectopia ± herniation, polymicrogyria, and cerebral asymmetry. Megalencephaly–CM is caused by postzygotic mutations in *PIK3CA*[53,54].

CLAPO syndrome

CLAPO syndrome features a *C*M of the lower lip and *L*M of the tongue and neck, together with *a*symmetry and *p*artial *o*vergrowth of the face and extremities[55]. The CM of the lower lip is always midline and symmetrical; it may affect the entire lip and usually extends to the adjacent skin (Fig. 104.12). The LM may not be apparent in affected neonates, becoming evident later in life. Somatic mutations in *PIK3CA* are responsible for CLAPO syndrome[56].

Proteus syndrome

Proteus syndrome is characterized by progressive overgrowth over time and a mosaic distribution of anomalies (see Ch. 62)[57]. It is caused by somatic activating mutations in *AKT1*, which encodes a protein that positively regulates cellular growth and proliferation[58]. Manifestations are minimal at birth, typically becoming apparent at 6–18 months of age. Asymmetric, disproportionate bone overgrowth leads to consequences such as megaspondylodysplasia with scoliosis, knee deformities, asymmetric macrodactyly, and cranial hyperostosis. In addition to vascular malformations with variable capillary, venous, and lymphatic components, cutaneous features include highly characteristic cerebriform connective tissue nevi of the palms and soles (Fig. 104.13), epidermal nevi, lipomatous overgrowth, and regional absence of fat. Bullous pulmonary degeneration, specific neoplasms (e.g. ovarian cystadenoma, parotid monomorphic adenoma), and a facial phenotype with ptosis and anteverted nares represent other findings. Deep vein thrombosis results in premature death in up to 20% of patients[59]. The differential diagnosis of Proteus syndrome includes PROS as well as PTEN hamartoma tumor syndrome (see Table 104.5).

Cutis marmorata telangiectatica congenita

CMTC is characterized by a dark purple to red–purple, broad reticulated vascular pattern intermingled with telangiectasias and occasionally prominent veins (Fig. 104.14). It commonly affects one or more limbs and the corresponding quadrant(s) of the trunk. Unlike physiologic cutis marmorata, CMTC persists upon warming an affected infant. Atrophic depressions may be evident within the net-like pattern (see Fig. 104.14C), especially over joints, and can result in ulceration and scarring. CMTC often lightens after the first year of life, but some residual violaceous network is common[1,60]. Up to 50% of patients have hypoplasia (girth > length) of the affected limb(s) or additional vascular

malformations. Other skeletal (e.g. syndactyly), ocular (e.g. glaucoma), and neurologic defects have been reported, especially in patients with generalized CMTC; however, these associations may reflect misdiagnosis of CM-associated syndromes as CMTC. *Adams–Oliver syndrome* features CMTC or a reticulated CM together with distal transverse limb defects, variable cardiac malformations, and scalp/skull defects (aplasia cutis congenita; see Ch. 64).

A somatic *AKT3* mutation has been identified in patients with CMs reminiscent of CMTC but more sharply delineated, linear, and located on the lateral side of the trunk or an extremity[61]. Associated soft tissue atrophy and variable megalencephaly were also observed. Lastly, relatively short-lived skin findings resembling CMTC have been observed in patients with neonatal lupus.





Fig. 104.12 CLAPO syndrome. A Capillary malformation on the lower lip and chin, with swelling of the neck due to a lymphatic malformation. **B** Microcystic lymphatic malformation on the tongue. *A, Courtesy Julie V. Schaffer, MD.*

Telangiectasias

Telangiectasias are dilated capillary-type blood vessels (see Ch. 106). These punctate, stellate, or linear red lesions may have a localized, segmental, or widespread distribution. In some disorders, they tend to affect particular anatomic sites. For example, *angioma serpiginosum* features clusters of tiny punctate telangiectasias in serpiginous patterns with a predilection for the extremities, whereas *unilateral nevoid telangiectasia* usually refers to a segmental configuration favoring the face, neck, chest, and arms. The lesions of *hereditary benign telangiectasia* (HBT) may mimic those of hereditary hemorrhagic telangiectasia



Fig. 104.13 Plantar cerebriform connective tissue nevus in a man with Proteus syndrome.







Fig. 104.14 Cutis marmorata telangiectatica congenita (CMTC). Note the hypoplasia of the affected limb (**A**,**B**) and associated cutaneous atrophy leading to a depression (**C**). The color of the broad vascular network can be red–purple (**A**,**C**) or, as seen in this infant of Caribbean descent, brownish-purple (**B**). *C, Courtesy Richard Antaya, MD.*

(HHT; see below), but the former is not associated with epistaxis or visceral hemorrhage. In addition, some kindreds initially reported as having HBT actually had capillary malformation–arteriovenous malformation (CM-AVM; see below)[62].

Hereditary hemorrhagic telangiectasia

Hereditary hemorrhagic telangiectasia (HHT; Osler–Weber–Rendu disease) is an autosomal dominant disorder characterized by visceral AVMs and mucocutaneous telangiectasias, which actually represent small AVMs; these AVMs have a propensity to bleed. Phenotypes vary considerably, even within a given family[63–65]. The first manifestation of HHT is usually epistaxis during childhood or adolescence, beginning at a mean age of 12 years[65]. Multiple telangiectasias of the skin and oral mucosa usually appear after puberty and may not be evident until adulthood, with ~50% of affected children <10 years of age having at least one evident telangiectasia[66]. The telangiectasias most commonly affect the face, lips, tongue, palms and fingers, including periungual areas and the nail bed. These dark red lesions are either round, slightly elevated papules or ill-defined, stellate macules.

It is important to screen individuals suspected to have HHT for visceral AVMs (Table 104.6). In particular, AVMs in the lungs and brain are often asymptomatic prior to the sudden development of life-threatening complications[63–65]. Pulmonary AVMs can result in hypoxemia, hemorrhage, and cerebral abscesses or strokes due to paradoxical emboli. Transcatheter embolotherapy of pulmonary AVMs is recommended[65]. Lethal intracranial hemorrhage from cerebral AVMs can occur as early as infancy[64], and acute paraplegia due to spinal AVMs has also been described in children with HHT. Treatment strategies for AVMs of the CNS include embolization, microsurgery, and stereotactic radiation. Gastrointestinal or (less often) genitourinary tract bleeding typically occurs in mid adulthood and often presents as iron deficiency anemia. Lastly, hepatic AVMs may lead to high-output heart failure, portal hypertension, and biliary disease.

Classic HHT is due to heterozygous mutations in *ENG* (endoglin; HHT1) or *ACVRL1* (activin A receptor-like type 1, also known as *ALK1*; HHT2). Both genes encode glycoprotein components of endothelial transforming growth factor-β (TGF-β) receptors. A genotype–phenotype correlation has been established, with a higher risk of pulmonary (especially in women) and cerebral AVMs in HHT1 and a higher risk of liver AVMs in HHT2. A few reported patients with HHT-like manifestations but somewhat larger and more widespread cutaneous telangiectasias/AVMs had underlying mutations in *GDF2* (growth differentiation factor 2), which encodes a protein that binds to endoglin and ACVRL1. In addition, mutations in *SMAD4*, which encodes a protein that transmits signals from the TGF-β receptor, underlie a disorder that features juvenile gastrointestinal polyposis and HHT. Genetic testing can establish the diagnosis of HHT in children and young adults who do not yet meet clinical criteria (see Table 104.6). Information on medical centers and laboratories that specialize in HHT is available at curehht.org.

Ataxia–telangiectasia

Ataxia–telangiectasia is an autosomal recessive disorder that occurs in approximately 1 in 40000 births and is due to mutations in *ATM* (see Ch. 60). Ataxia is the initial symptom and usually presents in toddlers. Telangiectasias typically begin to appear at 4–6 years of age, primarily on the conjunctivae, face, and ears. Immunoglobulin deficiencies (e.g. IgA, IgG) and defective cell-mediated immunity explain the frequent sinopulmonary infections. Patients are at high risk for the development of lymphoma and leukemia. Elevated levels of circulating α-fetoprotein are found in affected individuals. Heterozygote carriers of a mutated *ATM* gene also have an increased risk of breast cancer and hematologic malignancies.

STUDIES RECOMMENDED TO SCREEN FOR SYSTEMIC INVOLVEMENT AND ASSIST IN THE DIAGNOSIS OF HEREDITARY HEMORRHAGIC TELANGIECTASIA (HHT)

Study	Indication(s)	Purpose of study	Intervention(s) if positive study
Transthoracic contrast echocardiography (bubble study)*	Definite or suspected HHT†	Detect **pulmonary** AVMs, which lead to right-to-left shunting (15%–50% of HHT patients)	• Transcatheter embolotherapy in all adults and in children with AVMs that are large or associated with hypoxemia • Antibiotic prophylaxis for procedures with risk of bacteremia, precautions to avoid air bubbles during intravenous access, and avoidance of SCUBA diving
Brain MRI with and without contrast‡	Definite or suspected HHT†	Detect **cerebral** AVMs and other vascular malformations (~25% of HHT patients)	• Referral to a center with neurovascular expertise for consideration of invasive testing and treatment
Annual hemoglobin and hematocrit testing	Adult HHT patients and children with recurrent bleeding and/or symptoms of anemia	Detect substantial bleeding related to **gastrointestinal** (GI) AVMs (~25% of HHT patients; less common before age 40 years)	• Esophagogastroduodenoscopy if anemia disproportionate to epistaxis • Iron supplementation • Treatment considerations for GI bleeding include endoscopic argon plasma coagulation, antifibrinolytics, and bevacizumab
Doppler ultrasonography, multiphase contrast CT, or contrast MRI of liver	(1) Adults with definite or suspected HHT† (2) HHT patients with signs/symptoms of heart failure or hepatobiliary disease	Detect **hepatic** AVMs (present in 30%–80% but symptomatic in <10% of HHT patients)	• Additional testing and treatment directed by findings and symptoms; liver biopsy should be avoided
Genetic analysis of *ENG* and *ACVRL1* ± *SMAD4* and/or *GDF2*	(1) "Index case" in HHT family (2) Patients at risk because of an affected first-degree relative¶ (e.g. who do not meet HHT criteria† or desire prenatal testing) (3) Patients clinically suspected to have HHT who do not meet criteria†	Detect underlying mutation in *ENG* or *ACVRL1* (~75% of HHT patients) > *SMAD4* (1%–3% of HHT patients) or *GDF2*	• Identification of a specific mutation facilitates genetic analysis in family members, including prenatal testing • Further screening for systemic involvement if diagnosis established

*If negative, repeat screening should be considered after puberty, within the 5 years preceding a planned pregnancy, after pregnancy, and otherwise every 5–10 years.
†Clinical diagnostic criteria are: spontaneous recurrent epistaxis, characteristic mucocutaneous telangiectasias, visceral telangiectasias/AVMs, and HHT in a first-degree relative; definite HHT if ≥3 criteria (met by ≥90% of HHT patients by age 40 years) and possible/suspected HHT if 1–2 criteria (especially for children and young adults).
‡Some authors have recommended omission of contrast in the initial MRI screening of children (especially those <2 years of age), and repeat screening with contrast at ~age 18 can be considered for children with negative studies; MRI screening for spinal AVFs can also be considered in children.
¶The causative mutation should first be identified in an "index case" from the family.

Table 104.6 Studies recommended to screen for systemic involvement and assist in the diagnosis of hereditary hemorrhagic telangiectasia (HHT). AVF, arteriovenous fistula; AVM, arteriovenous malformation; CT, computed tomography; GDF2, growth differentiation factor 2; MRI, magnetic resonance imaging. Based on the 2020 Second International HHT Guidelines[65].

Angiokeratomas

Angiokeratomas are currently categorized by ISSVA as a provisionally unclassified vascular anomaly. They consist of ectasias of dermal vessels plus an acanthotic and hyperkeratotic overlying epidermis (see Ch. 114). Immunohistochemical studies have shown that most angiokeratomas stain positively with lymphatic markers. These dark red-to-purple, papular vascular anomalies vary considerably in size, depth, and location[1]. The two most common types are *solitary papular angiokeratoma* and *angiokeratomas of the scrotum and vulva*. The former is often found on the lower extremity, and clinically it may be mistaken for a melanoma.

In *angiokeratoma circumscriptum*, clusters of ectasias form a plaque or linear array, usually on an extremity and often present at birth. A congenital hyperkeratotic vascular anomaly resembling angiokeratoma circumscriptum, but with a deeper dermal component consisting of thick-walled blood vessels larger than capillaries, may represent a *verrucous venulocapillary malformation* (*"verrucous hemangioma"*; see below and Ch. 114), which can be caused by somatic *MAP3K3* (mitogen-activated protein kinase kinase 3 gene) mutations. Grouped tiny lesions are also seen in *angiokeratoma of Mibelli*, which favors the toes, fingers, knees, and elbows.

Angiokeratoma corporis diffusum is characterized by more widespread lesions, often in a bathing trunk distribution; it can be associated with several hereditary lysosomal storage disorders such as *Fabry disease*, an X-linked recessive condition due to deficiency of α-galactosidase A, and *α-fucosidase deficiency* (see Table 63.7). Angiokeratoma-like lesions as well as microcystic lymphatic lesions may develop on the surface of geographic CMs in KTS (see above).

Venous Malformations

There are two major types of VMs: (1) common and familial VMs, together accounting for ~95% of VMs; and (2) glomuvenous malformations (GVMs). VMs may be confused with deep infantile hemangiomas or, when they involve a large portion of an extremity, KTS. Common and familial VMs are recognized clinically by their blue hue, softness, compressibility, and tendency to fill with dependency (Fig. 104.15). They are most often focal or segmental but may have a widespread distribution in forms with autosomal dominant inheritance. Somatic activating mutations in the *TEK* and *PIK3CA* genes account for ~50% and ~25% of sporadic common VMs, respectively; VMs due to mutations in the former gene are more likely to affect the surface of the skin[67]. VMs are best imaged using T2-weighted MRI (see Table 104.3)[1]. Fig. 104.16 provides an approach to the evaluation and management of patients with VMs.

Cephalic venous malformation

These lesions frequently lead to cosmetic and functional problems that worsen over time[1]. In addition to the skin, they may affect the lips, oral mucosa, and deeper structures such as muscles, the infratemporal fossa, and the orbit (see Fig. 104.16). Cephalic VMs expand when the head is in dependent position. With time, distortion of facial features often becomes conspicuous. Patients with parapharyngeal and laryngeal VMs should be monitored for sleep apnea, which can put them at risk of sudden death during sleep. Approximately 20% of patients with extensive cephalic VMs have defects of the underlying skull[1], which must be identified before performing sclerotherapy to avoid embolization through the defect.

Approximately 25% of patients with extensive cephalic VMs have developmental venous anomalies, previously referred to by the misnomer "venous angiomas", compared to <1% of the general population[1]. These are uncommon functional trajectories of venous drainage from the brain, usually with enlarged deep venous channels. Developmental venous anomalies may cause headaches, but they do not confer risk of cerebral hemorrhage and treatment is not needed. Of note, patients with cephalic VMs are not at increased risk of CCM-type cerebral vascular malformations (see below).

Trunk and limb venous malformation

VMs of the trunk and limbs often have cosmetic and functional consequences (see Fig. 104.17). VMs form spongy masses of saggy ectatic venous channels, which are easily emptied by elevating and massaging the affected region (see Fig. 104.16). However, permeation deep into muscles, joints, and bones is common[1]. Muscle involvement is associated with episodes of pain after motion and in the morning. The pain is linked to thromboses inside the low-flow channels, leading to phlebolith formation (round calcifications). Half of patients with large VMs have a chronic localized intravascular coagulopathy with elevated D-dimer levels[68,69]. Joint involvement usually becomes symptomatic before 10 years of age, with complications such as effusions and hemarthrosis. Limb VMs are commonly misdiagnosed as KTS, but undergrowth of a limb affected by a simple VM is more common than overgrowth.

Sinusoidal hemangioma

Sinusoidal "hemangioma" is thought to represent a distinctive type of venous malformation that typically presents in adults, especially



Fig. 104.15 Venous malformations (VMs). A Distortion of the tongue and lower lip has led to an open bite. **B** The skin and muscles of the entire arm are affected, with soft bluish nodules and obvious swelling in the dependent position. **C** This VM has a segmental distribution on the right trunk and involvement of the ipsilateral arm.

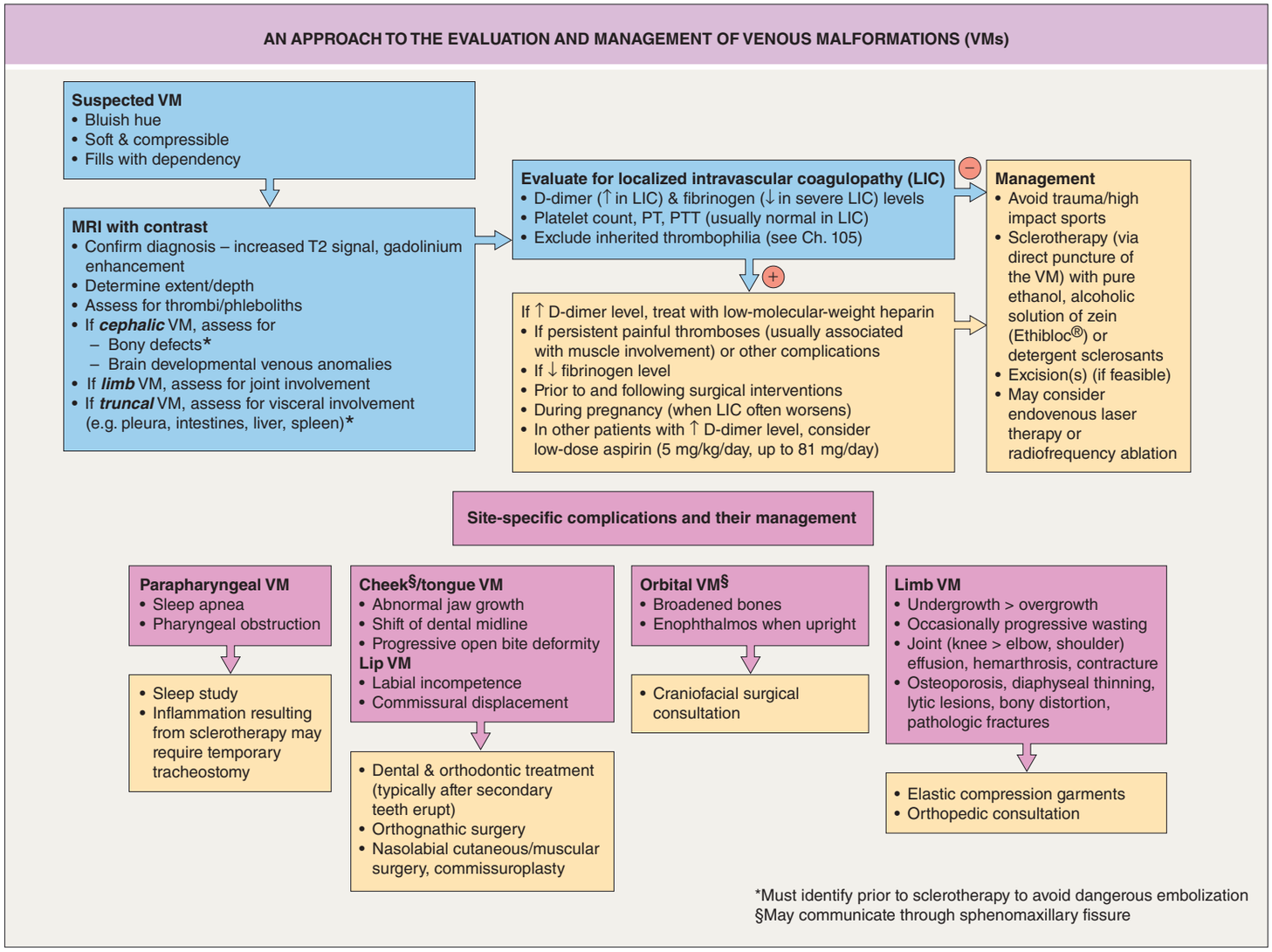


Fig. 104.16 An approach to the evaluation and management of venous malformations (VMs).

middle-aged women, with deep bluish nodules that favor the breast and extremities (see Ch. 114). Diagnosis is based on histologic features: well-circumscribed lobules composed of densely packed, large, thin-walled, blood-filled venous channels. Sinusoidal patterns have also been observed in congenital VMs.

Fibro-adipose vascular anomaly (FAVA)

FAVA presents between birth and early adulthood with a painful intramuscular mass, most often on the calf and in association with a contracture[70]. Histopathologically, there is a combination of fat, abnormal venous channels with perivascular fibrosis, and lymphoplasmacytic aggregates within atrophied skeletal muscle. Treatment options include excision or image-guided percutaneous cryoablation. Underlying somatic mutations in *PIK3CA* have been reported[38].

Verrucous venulocapillary malformation (verrucous VM, verrucous "hemangioma")

Verrucous VM (see Ch. 114) is included in the ISSVA classification as a subtype of VM, and an underlying somatic mutation in *MAP3K3* has been identified in a subset of these lesions (see Fig. 104.2)[71]. This malformation presents as a purple red birthmark, often with a segmental distribution on an extremity, and hyperkeratosis develops over time. The clinical appearance overlaps with that of angiokeratoma circumscriptum and the hyperkeratotic cutaneous capillary–venous malformation associated with familial cerebral cavernous malformation. Red vascular dots are seen with dermoscopy, which helps to distinguish verrucous VM from a CM or LM[72].

Syndromes associated with venous malformations

Familial cutaneous and mucosal venous malformation (VMCM)

Familial VMCM is an autosomal dominant condition in which multiple VMs affect the skin, oral mucosa, and muscles. Visceral VMs (e.g. of intestines, lungs, CNS) and cardiac malformations have been observed in a few families[73]. The disorder is caused by heterozygous germline mutations in *TEK* that result in hyperphosphorylation and constitutive activation of TIE-2, a vascular endothelium-specific tyrosine kinase receptor (see Fig. 104.2); the downstream signaling of this receptor is also altered[8,73]. Interestingly, approximately half of *sporadic* VMs have *somatic* activating *TEK* mutations within lesional tissue[8].

Blue rubber bleb nevus syndrome (BRBNS; Bean syndrome)

BRBNS is a sporadic disease characterized by the progressive appearance of dark blue papules and nodules and skin-colored compressible protuberances ("rubber blebs") in a widespread distribution, in addition to larger VMs affecting subcutaneous tissues and muscle (Fig. 104.17). Some patients have a large congenital VM with a characteristic darker purple–blue fern-shaped pattern on the surface[74]. Gastrointestinal lesions bleed and result in iron deficiency anemia. Other sites of visceral involvement (CNS, lungs, heart) are uncommon. BRBNS was recently found to be caused by double (cis) somatic activating *TEK* mutations, i.e. two mutations within the same allele of the gene[7].

Maffucci syndrome

Maffucci syndrome is a sporadic condition that features VMs, which present as blue to skin-colored nodules, and enchondromas similar to those of Ollier disease, which can lead to orthopedic consequences



Fig. 104.17 Blue rubber bleb nevus syndrome. Multiple scattered small blue venous nodules, several of which are superimposed on a larger subcutaneous venous malformation. *Courtesy Juan Carlos López, MD.*



Fig. 104.18 Maffucci syndrome. A Both nodular venous malformations and enchondromas distort the hand. **B** A radiograph demonstrates an enchondroma and multiple phleboliths.

(Fig. 104.18). It most commonly affects the extremities; however, cephalic lesions with severe neuro-ophthalmologic complications may also occur. Histologically, the cutaneous nodules demonstrate features of both a VM and a vascular tumor, the spindle cell hemangioma (see Ch. 114).



Fig. 104.19 Plaque-type glomuvenous malformation on the distal lower extremity.

Heterozygous somatic mutations in *IDH1* (NADP(+)-dependent isocitrate dehydrogenase 1) have been identified in affected tissues, with the same mutation in the spindle cell hemangiomas and enchondromas[75]; the latter lesions also rarely have underlying *IDH2* mutations.

Glomuvenous malformation (GVM)

GVMs (previously known as glomangiomas) represent a variant of VM with rows of glomus cells around distorted venous channels (see Ch. 114). They occur as small solitary lesions, widely scattered blue–purple nodules, or (less commonly) large segmental plaques (Fig. 104.19). GVMs may be evident at birth, especially larger plaques, or appear from childhood to adolescence; they often enlarge over time[76,77]. In contrast to classic VMs, GVMs tend to be painful when palpated, partially (rather than fully) compressible, and hyperkeratotic with a cobblestone-like appearance (especially on the extremities). GVMs do not typically affect viscera or joints, and they are not associated with a coagulopathy. Mucosal involvement with deep intraoral lesions and superficial invasion of muscles occasionally occurs. Approximately two-thirds of patients with GVMs, but only 1% of those with classic VMs, have a family history of similar lesions. GVMs result from a heterozygous germline mutation in the glomulin gene (*GLMN*), which is passed from generation to generation in an autosomal dominant manner, *plus* a somatic "second hit" (loss of heterozygosity) in this gene within lesional skin (see Table 104.2)[78].

Cerebral cavernous malformation and hyperkeratotic cutaneous capillary–venous malformation

A distinctive hyperkeratotic cutaneous capillary–venous malformation (HCCVM) occurs in a subgroup of patients with familial cerebral cavernous malformation (CCM)[79,80]. Neurologic manifestations, which develop at a mean age of 30 years (range, 2–72 years), may include headaches, seizures, and cerebral hemorrhage[79]. This autosomal dominant disorder can be caused by mutations in three different genes (see Table 104.2): *KRIT1* (*CCM1*), *CCM2* (malcavernin), and *PDCD10* (*CCM3*). Among the ~10% of familial CCM patients who have *cutaneous* capillary and/or venous malformations, ~90% have a *KRIT1* mutation[80].

HCCVMs occur almost exclusively in patients with *KRIT1* mutations, with one report to date in an individual with a *PDCD10* mutation. These irregularly shaped, dark crimson or reddish-purple plaques with surrounding bluish discoloration are typically congenital and located on the extremities; GLUT1-positivity has been described[81]. Smaller reddish-brown macules with peripheral telangiectatic puncta have also been observed[80]. Less frequently, children and adults with mutations in any of the three genes develop dark blue cutaneous papules and nodules reminiscent of the blue rubber bleb nevus syndrome, which represent VMs[80]. The differential diagnosis includes a verrucous VM.

Lymphatic Malformations

The spectrum of LMs includes primary lymphedema, common LMs, generalized lymphatic anomaly (GLA), and central conducting lymphatic anomalies (CCLAs; channel-type LMs)[82]. The targetoid

hemosiderotic lymphatic malformation (hobnail "hemangioma") is discussed in Chapter 114. Lymphedema results from inadequate drainage of lymph due to hypoplasia, aplasia, or disruption of lymphatic channels. Lymphedema is divided into *primary* forms due to abnormal lymphatic development and *secondary* forms due to acquired disruption of lymphatic drainage (see Ch. 105). In contrast, LMs are due to hyperplasia of the lymphatic network. This hyperplasia most commonly results in cysts, including smaller microcystic and/or larger macrocystic lesions; these cysts can develop within the skin, mucous membranes, muscles, bone, or occasionally viscera[1]. Somatic activating mutations in *PIK3CA* underlie most common LMs[38]. CCLAs affecting structures such as the cisterna chyli and thoracic duct result in lymphatic leakage that leads to pleural or pericardial effusions and ascites.

Primary lymphedema

Patients with primary lymphedema usually accumulate lymph fluid in the extremities (lower > upper); cephalic and genital involvement occasionally occurs. Affected individuals are at risk for bacterial infections and septicemia. Generalized lymphedema may be associated with intestinal or pulmonary lymphangiectasias, exudative enteropathy, and pleural effusions.

Primary lymphedema may be classified according to its age of onset into congenital, peripubertal (praecox), and late-onset (tarda; >35 years of age) forms[83], but since the time of onset can vary even within the same family, genetic bases are now more commonly used for classification (see Table 105.7). Table 104.2 outlines the multiple genes that have been implicated in isolated and syndromic forms of lymphedema. Many of the proteins encoded by these genes act in the vascular endothelial growth factor receptor-3 (VEGFR3) signaling pathway[82,83] (see Ch. 102).

The most common congenital form, classically referred to as *Milroy disease*, presents with lymphedema below the knees, prominent veins, and upslanting toenails. *Lymphedema–distichiasis syndrome* due to *FOXC2* mutations features lymphedema of peripubertal onset, congenital distichiasis (aberrant eyelashes arising from the meibomian glands lead to a double row of eyelashes), venous varicosities, and occasionally yellow nails. Lymphedema, chylothorax, and chylous ascites are also variably seen in Turner syndrome (see Ch. 55) and RASopathies including Noonan, cardio-facio-cutaneous, Costello, and rarely CM-AVM syndromes (see below and Table 61.3).

Macrocystic lymphatic malformation ("cystic hygroma")

Macrocystic LMs represent collections of large, interconnected lymphatic cysts lined by a thin endothelium. The most common locations are the neck, axilla, and lateral chest wall (Fig. 104.20A). Prenatal detection by ultrasound is possible as early as the first trimester of pregnancy. Some patients who are diagnosed prenatally have malformation syndromes caused by chromosomal abnormalities or other genetic disorders (e.g. Turner syndrome, Noonan syndrome). A macrocystic LM appears as a large, soft, translucent mass under normal skin. The diagnosis can be confirmed by ultrasound, CT, or MRI (see Table 104.3) as well as by direct puncture and cytologic analysis of the fluid. Hemorrhage inside a cyst can create sudden swelling, with the mass becoming tender, tense, firm, and purple to yellowish in color.

Microcystic lymphatic malformation ("lymphangioma circumscriptum")

These ill-defined aggregates of relatively small, abnormal lymphatic channels are the most common type of LM. They favor the proximal limbs and chest but can occur in any cutaneous site or in the mouth,

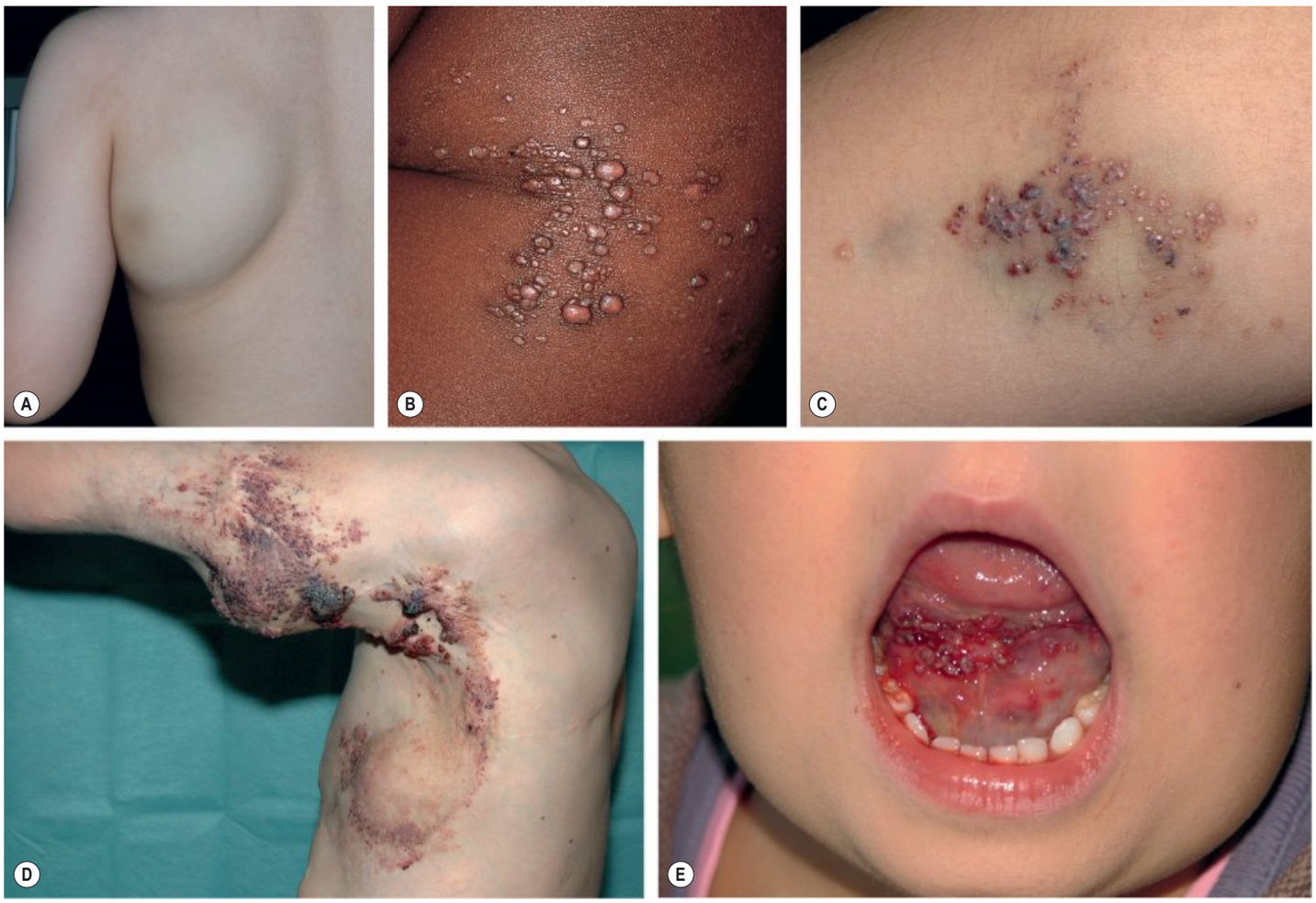


Fig. 104.20 Lymphatic malformations (LMs). A Macrocystic LM on the lateral trunk. The mass was soft except for a focal firm area of hemorrhage associated with bruise-like discoloration of the overlying skin. **B–E** Microcystic LMs presenting as clusters of clear or hemorrhagic vesicles, with active bleeding from lesions in the mouth (**E**). The crops of vesicles in (**D**) recurred years after surgical resection (utilizing grafting and linear closure) of a large microcystic LM affecting the skin and deeper structures of the arm and thorax. *A, C, Courtesy Julie V. Schaffer, MD.*

including the tongue, buccal mucosa, lips, and oral floor. Plaques with crops of clear or hemorrhagic vesicles scattered on their surface vary over time, both in size and in the number and color of superimposed vesicles (Fig. 104.20B–E). Additional clinical findings are intermittent swelling, hemorrhage, and leakage of lymph from superficial vesicles. Lesions are often much more extensive than clinically expected from the number of vesicles. Complications include erysipelas-like reactions following minor injuries, other inflammatory flares, and infections.

Combined microcystic and macrocystic lymphatic malformation

Extensive cervicofacial combined LMs commonly have bony involvement. This can lead to mandibular overgrowth and prognathism, resulting in a long or asymmetric face, bite deformities, and abnormal occlusal planes[84]. Intraoral combined LMs are frequently complicated by inflammatory flares or spontaneous bleeding in the setting of upper respiratory or dental infections. This can result in sudden expansion of the lesions, particularly those in the tongue. Local infections can lead to cellulitis or even septicemia. In some patients with massive oropharyngeal combined LMs, airway compromise (extrinsic or intrinsic) requires tracheostomy. Hypersalivation and dental caries are common, with the potential for loss of teeth. Speech, mastication, and swallowing may be impaired. In addition to swelling, pain, and infections, specific complications of combined LMs in the orbital region include chemosis, strabismus, amblyopia, proptosis, and visual loss[85].

On the trunk and limbs, combined LMs tend to worsen as the child grows. When a minor wound on the affected extremity becomes infected, the inflammatory reaction results in expansion of the LM, as also occurs in patients with limb lymphedema. Perineal and gluteal cleft LMs, which are particularly prone to fluid leakage and infection, severely impair quality of life. Extensive combined LMs, in particular those with a venous component, may be associated with a chronic localized intravascular coagulopathy with elevated D-dimer levels (see above).

Generalized lymphatic anomaly (GLA)

GLA, previously referred to as "lymphangiomatosis", represents an extensive, multifocal abdominal and thoracic LM that extends into viscera such as the spleen, liver, intestines, and pleura/lung; the bones are often involved, but the cortex is typically spared. GLA may have a lethal outcome due to expansion, chylous effusions, visceral complications, and vertebral compression.

Kaposiform lymphangiomatosis (KLA)

KLA is currently considered to represent an aggressive subtype of GLA that is characterized by progressive involvement of the mediastinum, lungs, pleura, retroperitoneum, spleen, bones, soft tissue, and skin[86]. Histologically, it features clusters or sheets of hemosiderotic, spindled lymphatic endothelial cells oriented in a parallel fashion amid abnormal dilated lymphatic channels. Circulating angiopoietin-2 levels are elevated in KLA and may serve as a biomarker.

Patients present at a median age of 6 years (range, birth to fifth decade) with respiratory symptoms, thrombocytopenia, hypofibrinogenemia, and life-threatening hemorrhagic pericardial and pleural effusions[87]. An enlarging subcutaneous mass may be evident, sometimes with an overlying red–purple birthmark and lymphatic vesicles. An underlying somatic *NRAS* mutation is present in most affected individuals[87,88]. The reported 5-year survival is ~20%–50%[86,87], and successful treatment with sirolimus (rapamycin) and MEK inhibitors has been described (see Fig. 113.1).

Gorham–Stout disease

In *Gorham–Stout (disappearing bone)* disease, a LM creates progressive radiolucent bone lesions with cortical involvement and eventually massive osteolysis. This results in pathological fractures and deformities. Involvement of the thoracic skeleton may be associated with pulmonary lymphangiectasia. A somatic activating *KRAS* mutation has been identified in affected tissue from a patient with Gorham-Stout disease.

Central conducting lymphatic anomalies (CCLAs; channel-type LMs)

CCLAs are characterized by dilation, dysfunction, or obstruction of major thoracic or abdominal lymphatic channels. The manifestations depend on the site of the anomaly and can include chylothorax, chylous ascites, protein-losing enteropathy, peripheral lymphedema, lymphorrhea, and cutaneous vesicles. Underlying mutations have been identified in genes encoding various components of the RAS–*m*itogen-*a*ctivated *p*rotein *k*inase (MAPK) pathway (germline or mosaic; see Fig. 55.4) as well as other proteins with roles in lymphatic development (e.g. MyoD family inhibitor domain containing protein, piezo-type mechanosensitive ion channel component 1)[89,90].

Arteriovenous Malformations

AVMs are fast-flow vascular malformations with direct communications (AV shunting) between arteries and veins, creating an AV nidus. They are rare and constitute the most dangerous group of vascular anomalies. Schobinger staging was adopted by the ISSVA in order to classify AVMs according to their clinical severity[1,2,91]. The stages are: (1) *quiescent/dormant* – macular or slightly infiltrated, red, warm lesions mimicking a CM (Fig. 104.21A,B); (2) *expansion* – warm masses with throbbing and thrills over dilated draining veins (Fig. 104.21C); (3) *destruction* – necrosis, hemorrhage, ulceration and (occasionally) lytic bone lesions (plus findings of stage 2) (Fig. 104.21D); (4) *cardiac decompensation* (plus findings of stage 2 ± 3). Initial evaluation with ultrasonography and MRI studies can confirm the diagnosis and delineate the extent of the lesion (see Table 104.3). Somatic activating mutations in *MAP2K1* and less commonly *KRAS*, *NRAS*, or *BRAF* have been found to underlie AVMs[92,93] (see Fig. 104.2).

In 40% of patients, AVMs are visible at birth; the remainder appear later in life. Features that can help to distinguish an early-stage AVM from a CM include heterogeneous color saturation, peripheral pallor, sharply demarcated "archipelago-like" borders (see Fig. 104.21A), and warmth to touch as well as associated soft tissue swelling/overgrowth (see Fig. 104.21B) and prominent veins[94]. The most frequent location is cephalic (~70% of patients; Fig. 104.22)[91]. Puberty (75% of patients), pregnancy (25% of women), and trauma may result in worsening of AVMs[91]. In an analysis of 65 patients with cephalic AVMs (Odile Enjolras, personal data), 39 were centrofacial and 7 were hemifacial; 10 affected the forehead, 10 the ear, and 4 the scalp.

Stage 3 cephalic AVMs are disfiguring and function- or even life-threatening lesions, and those on an ear or extremity may lead to amputation[95]. Multifocal AVMs affecting an extremity can lead to cardiac overload and distal ischemia. Attempted treatment with arterial or venous ligatures, partial excision, or proximal (rather than selective distal) embolization often precipitates complications. *Stewart–Bluefarb syndrome* represents *acroangiodermatitis* (pseudo-Kaposi sarcoma; see Ch. 105) occurring in association with an AVM of the lower extremity.

Syndromes associated with arteriovenous malformations

Cobb syndrome

This rare sporadic condition features cutaneous, intraspinal (intramedullary ± meningeal), and vertebral AVMs in the same segment. These findings can occur as a manifestation of CM-AVM syndrome due to *RASA1* mutations (see below). Congenital red or red–brown vascular birthmarks mimicking a CM, but actually representing stage 1 AVMs (Fig. 104.23), or throbbing masses with dilated veins (stage 2 AVMs) are present in 20% of patients with spinal AVMs. Neurologic deficits typically develop during young adulthood due to a mass effect of the expanding AVM on the spinal cord or subarachnoid hemorrhage. Neurologic signs range from back pain and radiculalgia to rectal and bladder dysfunction to paraparesis and paraplegia. MRI and angiography establish the presence of the spinal AVM. Endovascular embolization of the spinal AVM may improve the prognosis.

Bonnet–Dechaume–Blanc syndrome (BDBS; Wyburn–Mason syndrome)

This rare segmental AVM extends from the craniofacial region to the orbit and brain. Incomplete forms of the disease also exist. The brain AVM may remain asymptomatic or manifest as seizures or hemiparesis/hemiplegia. In 12 BDBS patients between 5 and 51 years of age, the facial AVMs (stage 1, 2, or 3) were midfacial in 3, hemifacial in 3, and both midfacial and hemifacial in 6 (Odile Enjolras, personal observations). The presence of an orbital AVM was an inconsistent finding (4 patients), but brain AVMs of the chiasm, choroid plexus, or thalamus

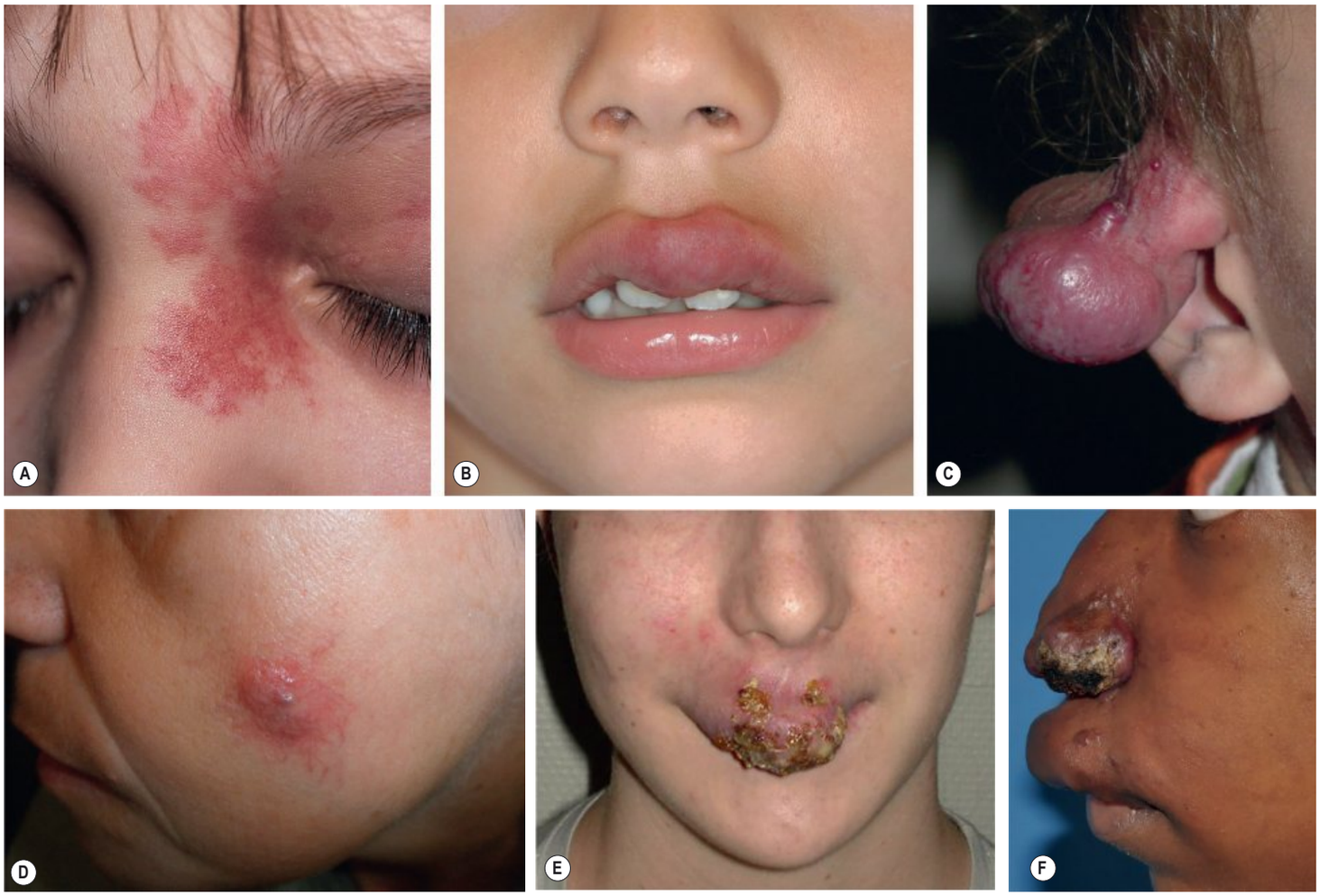


Fig. 104.21 Arteriovenous malformations (AVMs). A,**B** Dormant (stage 1) AVMs mimicking a port-wine birthmark (**A**) and infantile hemangioma (**B**). **C**, **D** Expanding (stage 2) AVMs on the external ear and cheek. **E, F** Destructive (stage 3) AVMs that have led to cutaneous necrosis. *D, Courtesy, Fernando Alfageme, MD; E, Courtesy Juan Carlos López, MD.*

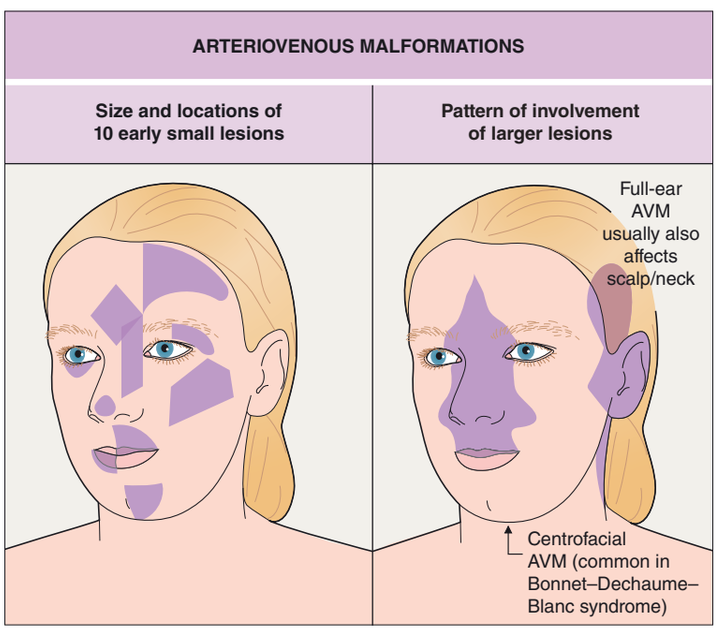


Fig. 104.22 Arteriovenous malformations – size, locations, and patterns.



Fig. 104.23 Cobb syndrome. This birthmark on the nape has an appearance reminiscent of a salmon patch, but it was warm and superimposed darker red macules progressively appeared. Doppler ultrasonography, MRI, and arteriography confirmed the presence of a arteriovenous malformation of the skin and spine.

were present in all 12 individuals and led to cerebral hemorrhage in 4 patients. In a second series of 15 patients with BDBS[96], orbital AVMs were present in 14 and frequently affected the optic nerve (13 patients) and retina (11 patients); symptoms in this group included reduced visual acuity or fields, blindness, recurrent epistaxis, nasal obstruction, and gingival hemorrhage.

Parkes Weber syndrome

In this rare *fast-flow* vascular malformation syndrome, limb overgrowth (in length and girth) occurs secondary to arteriovenous fistulae (AVF); this must be differentiated from the purely *slow-flow* malformations of KTS. A red CM, excess fat, and lymphatic anomalies may also be observed in Parkes Weber syndrome. Lytic bone lesions and cardiac failure often develop, and prognosis is poor after puberty. Over 50% of patients with Parkes Weber syndrome have a germline *RASA1* or *EPHB4* mutation plus an early somatic "second hit" mutation in the same gene underlying their larger AVM/AVF (see Ch. 62); these individuals also display the characteristic features of the CM-AVM syndrome (see below)[9,52].

Capillary malformation–arteriovenous malformation (CM-AVM) syndrome

This autosomal dominant disorder is caused by mutations in *RASA1* (~50% of patients; CM-AVM1) and less often in *EPHB4* (CM-AVM2) (see Table 104.2 and Fig. 104.2)[97,98]. Multiple, scattered small cutaneous CMs are evident at birth and continue to appear during childhood and adolescence. These CMs present as pink to red–brown macules, often with a narrow blanched border or in CM-AVM2 a blanched central region, as well as hypotrichosis of the affected skin (Fig. 104.24). Some macules are warmer than adjacent uninvolved skin, and pulsed Doppler may show decreased peripheral vascular resistance, suggesting a pre-AVM lesion. Histologically, the macules have numerous thick-walled arterioles in the superficial dermis, suggestive of an incipient AVM rather than a CM[99].

Patients sometimes have numerous punctate red macules, each surrounded by a white halo, located primarily on the extremities[97]. Patients with CM-AVM2 may also have telangiectasias favoring the lips, perioral area, and upper trunk. Approximately 35% and 15%–20% of individuals with CM-AVM1 and 2, respectively, also have high-flow lesion(s)[9,52]. Among 138 patients from 68 families with CM-AVM1, >90% had multifocal small CMs, 6% had a solitary "atypical" CM, 18% had an AVM/AVF of the skin/subcutaneous tissue (extremities > face/neck), 5% had Parkes Weber syndrome, and 15% had an intracranial or intraspinal AVM[62,97]. The CNS AVMs may lead to neurologic symptoms, which typically develop in the first decade of life and can include headaches, seizures, and sensorimotor deficits. MRI of the brain/spine is recommended for asymptomatic infants and young children with CM-AVM as well as patients of any age with neurologic manifestations[100].

PTEN hamartoma tumor syndrome (PHTS)

PHTS due to *PTEN* mutations encompasses the autosomal dominant Bannayan–Riley–Ruvalcaba and Cowden syndromes as well as the type 2 mosaic *s*egmental *o*vergrowth, *l*ipomatosis, *AVM*s, and *e*pidermal *n*evus (SOLAMEN) syndrome (see Ch 63)[101,102]. Affected individuals are often macrocephalic, and they are predisposed to the development of malignancies, especially of the breast, thyroid, and endometrium. Cutaneous manifestations with onset at birth or in childhood include genital pigmented macules, segmental excess of hypervascularized fat, and vascular malformations. The latter are typically multifocal, intramuscular, fast-flow lesions associated with ectopic fat and focal segmental dilatation of draining veins[103]. By both imaging and histopathologic features, these vascular malformations differ from sporadic AVMs and they have been renamed *PTEN hamartomas of soft tissue*. Oral sirolimus has been used to treat these lesions[104]. Cerebral developmental venous anomalies are also common in PHTS patients, and additional mucocutaneous lesions in affected adolescents and adults include tricholemmomas, acral keratoses, sclerotic fibromas, neuromas, and oral papillomas.

PATHOLOGY

The histologic characteristics of the four major types of vascular malformations are illustrated in Fig. 104.25[1].

Capillary Malformations

A CM is composed of ectatic capillaries within the papillary and reticular dermis, lined by a flat continuous endothelium. Thickening of affected skin can occur over time due to a progressive increase in the diameter of the capillaries, involvement of the dermis and subcutis, fibrosis of the dermis, and, occasionally, venous channels in the subcutis.

Venous Malformations

Large convoluted and interconnected anomalous venous channels dissect the normal connective tissues and muscles. Organized thrombi, phleboliths (round calcifications), and intravascular papillary endothelial hyperplasia are frequently observed. Anomalous vessels of a VM have a continuous flat endothelium and a thin basement membrane. Their walls have discontinuous media due to foci with a relative lack or absence of smooth muscle cells.

Lymphatic Malformations

LMs of the *microcystic* type exhibit enlarged, distorted, irregular lymphatic channels with varying numbers of smooth muscle cells in their walls and a very thin endothelium, sometimes barely visible. Larger polyhedral lymphatic vessels may exhibit valves, and they are usually separated by fibrous septa. Lymphatic clefts dissect the host connective tissues. Hyperkeratotic epidermis may overlie some clusters of dermal lymphatic vesicles. LMs of the *macrocystic* type are composed of large lymphatic cisterns, often interconnected with thinner channels. Vesicles and large cysts in LMs usually contain watery fluid, lymphocytes, and macrophages; hemorrhage can also be seen. Lymphatic endothelium can be identified by immunohistochemical staining for podoplanin, LYVE-1, and Prox1 (see Ch. 102).



Fig. 104.24 Capillary malformation–arteriovenous malformation (CM-AVM) due to a *RASA1* mutation. Multiple pink–red (**A,B**) to brownish (**C**) macules. A subtle blanched halo is often evident at the periphery of the lesions. *B, Courtesy Margarita Larralde, MD.*

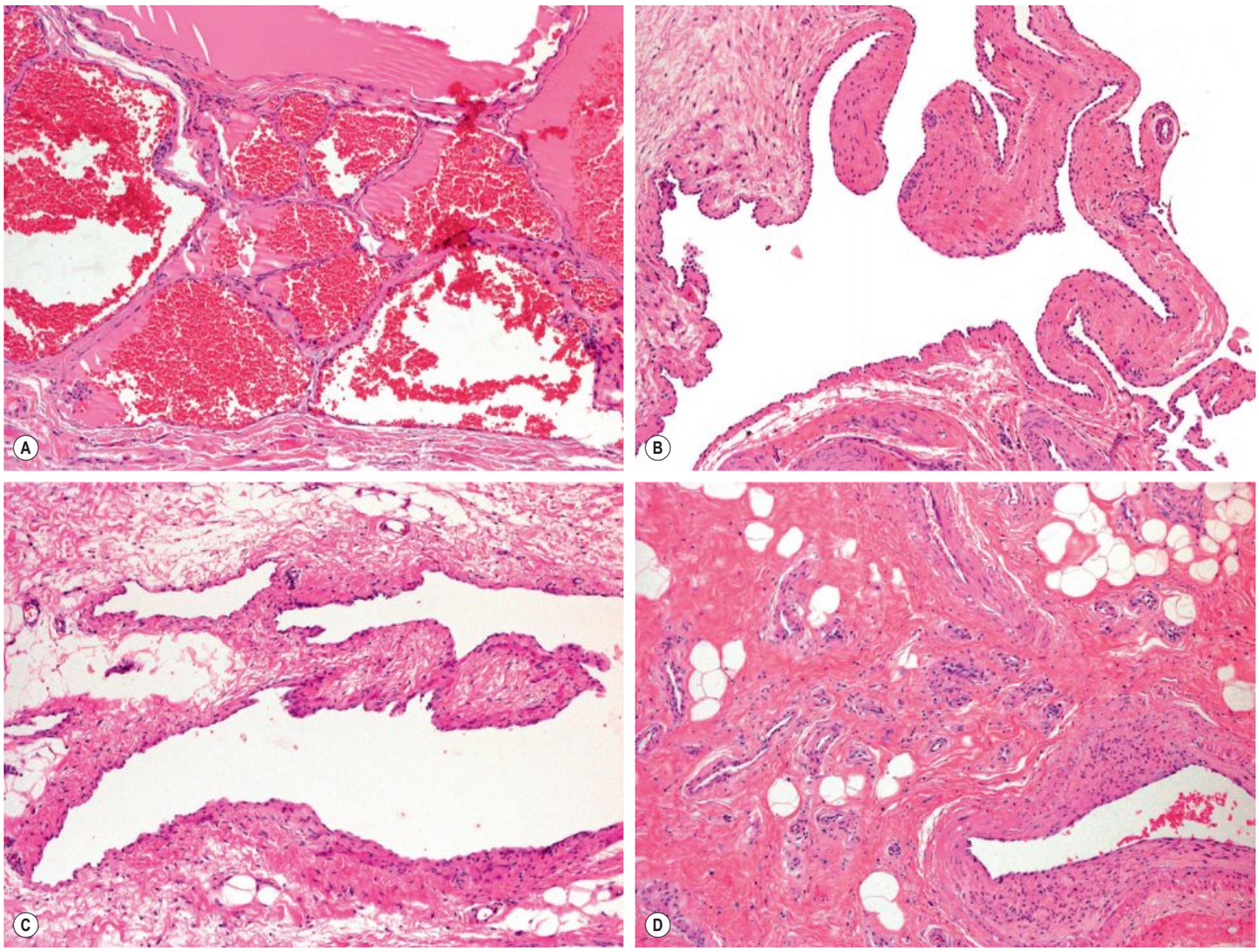


Fig. 104.25 Histologic features of vascular malformations. A Capillary malformation in an adult that was thickened and nodular. An increased number of dilated capillaries are present in the dermis. **B** Venous malformation composed of large, irregularly shaped, thin-walled channels. **C** Lymphatic malformation with large, irregularly shaped channels. **D** Arteriovenous malformation demonstrating an area of intense capillarogenesis near the AV nidus. This finding is sometimes misinterpreted as a "capillarovenous" malformation. *A–D, Courtesy Lorenzo Cerroni, MD.*

Arteriovenous Malformations

AVMs have irregularly thickened walls and are usually randomly distributed in the dermis and other involved tissues. Direct communications between vessels with different elastic components, typically arteries and veins, may be evident. A capillary component is often obvious in the overlying papillary dermis, and it may have a lobular architecture.

DIFFERENTIAL DIAGNOSIS

Vascular malformations must be distinguished from vascular neoplasms. Superficial infantile hemangiomas at the beginning of their proliferative phase or with minimal/arrested growth may resemble CMs, whereas deep infantile hemangiomas and other vascular tumors such as kaposiform hemangioendothelioma, infantile hemangiopericytoma, and benign lymphangioendothelioma (acquired progressive lymphangioma) can mimic VMs, LMs, and LVMs (see Chs. 103 & 114). Multifocal lymphangioendotheliomatosis with thrombocytopenia should be considered in patients with multiple vascular malformations, especially when associated with gastrointestinal bleeding (see Ch. 114).

Occasionally, other neoplasms and inflammatory disorders are misdiagnosed as vascular anomalies. A red or blue color and/or a mass underneath normal skin can represent potentially misleading clinical signs. For example, erythematous lesions of lupus erythematosus, plaque-type angiofibromas, telangiectasia macularis eruptiva perstans, and other telangiectatic conditions can mimic CMs (see Ch. 106). Dermal melanocytosis has a deep blue color that may lead to misdiagnosis as a VM. Masses beneath normal skin that may be erroneously diagnosed as a macrocystic LM in infants and children include a lipoblastoma, teratoma, bronchogenic cyst, branchial cleft cyst, thyroglossal duct cyst, myofibroma, rhabdomyosarcoma, and fibrosarcoma.

Acquired cutaneous lymphangiectasia imitating a LM can develop in several settings (Table 104.7).

TREATMENT

No single treatment exists for this heterogeneous group of lesions.

Capillary Malformations

PWBs and telangiectasias are best treated with a pulsed dye laser (PDL; see Ch. 137)[105–107]. This treatment of PWBs, which is typically initiated early in life for facial lesions to decrease potential psychosocial impact and avoid lesional thickening, is often very effective. However, not all lesions respond well; PWBs on the central face and distal limbs tend to be more resistant to therapy than those in other sites. PDL treatment is safe, producing temporary purpura but a low risk of hypo- or hyperpigmentation and scarring[106]. Although the latter side effects

CAUSES OF ACQUIRED CUTANEOUS LYMPHANGIECTASIA
Inflammatory causes
Crohn disease (favors perineal area) Orofacial granulomatosis Morphea profunda Systemic sclerosis
Infectious causes
Tuberculosis (e.g. scrofuloderma) Recurrent erysipelas/cellulitis
Neoplastic causes
Intralymphatic metastases (e.g. breast carcinoma, melanoma)
Iatrogenic causes
Surgical resection, lymphadenectomy, and/or radiotherapy for cancer (e.g. of the breast, prostate, bladder, cervix) Amputations Corticosteroid-induced atrophy ± photoaging Penicillamine-induced dermopathy
Other causes
Pregnancy (vulvar) Cirrhotic ascites (abdominal) Porphyrias (e.g. porphyria cutanea tarda, variegate porphyria; centrofacial) Spontaneous development in elderly patients (genital)

Table 104.7 Causes of acquired cutaneous lymphangiectasia. In the literature, this is sometimes referred to as acquired lymphangioma circumscriptum.

are more common in individuals with darkly pigmented skin (e.g. skin phototype V), these patients may have a good response and should not be excluded from PDL treatment.

Intervention during infancy with modified PDL therapy using a longer wavelength, increased pulse duration, higher fluence (11–12 J/cm^2), and dynamic cooling spray can maximize lightening or clearing of PWBs[107]. Use of a topical anesthetic (see Ch. 143), together with the anesthetic effect of the cryogen spray, helps to reduce the need for general anesthesia in children. In a longitudinal study of 51 patients whose facial CM was treated with classic PDL, redarkening was evident in one-third of the lesions after a median follow-up period of 10 years[108]. Relapses may be less common in patients treated at a younger age. If treatment is delayed, facial and gingival PWBs may develop hyperplastic changes that require additional dermatologic (e.g. dermabrasion prior to PDL treatment) as well as orthodontic and surgical interventions (e.g. to correct open-bite deformities and macrocheilia). For PWBs resistant to PDL, other lasers such as the alexandrite or Nd:YAG may be of utility. Topical application of sirolimus in conjunction with PDL may also provide additional benefit[109] (see Ch. 129).

Multidisciplinary care is necessary for patients with SWS[30]. Anticonvulsants are the mainstay of treatment for seizures, although selected patients with severe, uncontrolled seizures may benefit from surgical management. Low-dose aspirin (3–5 mg/kg) can also be considered in symptomatic and presymptomatic patients with brain involvement[110]. Oral sirolimus also has potential benefit for uncontrolled seizures, cognitive impairment, and perhaps as a preventive treatment in SWS patients with extensive leptomeningeal involvement[111,112]. Glaucoma usually responds to medical or surgical treatment. As discussed above, PDL therapy for PWBs can begin during infancy[113]. Psychological counseling may be helpful for patients and families affected by SWS, and support is also available through the Sturge–Weber Foundation (www.sturge-weber.org).

Venous Malformations

Satisfactory treatment of a cephalic VM typically requires multiple sclerotherapy procedures over a period of years, often spanning from childhood to adulthood, combined with surgical excisions (see Fig. 104.16)[1]. The aims are to maintain facial symmetry, preserve muscular functions, and restore the dynamics of the smile. Limb VMs may also benefit from sclerotherapy and resection; however, many are too extensive and invasive for such interventions to be advisable. Use of elastic compression garments helps to reduce swelling and pain in the affected extremity. Treatment with low-molecular-weight heparin can control chronic coagulopathy associated with VMs, especially before surgery and during painful thrombotic events[68,69]. Low-dose aspirin (3–5 mg/kg/day, up to 81 mg/day) may be of some benefit in patients with a mild coagulopathy[114].Treatment of VMs with oral sirolimus or the PI3K inhibitor alpelisib has also been reported to improve the associated coagulopathy as well as reduce lesion size and pain[115], although sirolimus appears to have greater benefit for combined lesions with a lymphatic component[116].

Lymphatic Malformations

The choice and outcome of treatment depend on the type and extent of the LM[84,85]. Macrocystic LMs are best treated with percutaneous sclerotherapy utilizing agents such as killed bacteria (picibanil/OK-432), alcoholic solution of zein (Ethibloc®), sodium tetradecyl sulfate, pure ethanol, doxycycline, or bleomycin. This creates an inflammatory reaction with subsequent fibrosis and shrinkage of the treated cyst; repeated procedures are usually necessary. Surgical excision can be employed if sclerotherapy fails or gives incomplete results.

Surgical excision is the treatment of choice for microcystic LMs, either with direct closure or (for large lesions) use of skin grafts or tissue expanders. However, incomplete excisions occur in virtually all cases, whether because of concern regarding functional consequences of extensive surgeries or underestimation of the extent of the LM (see Fig. 104.21D). Other techniques that are often used in combination include laser therapy (e.g. CO_2, surface application or intralesional bare fiber Nd:YAG, diode), radiofrequency ablation, cryoablation, and sclerotherapy[117–119]. Topical application of sirolimus may have benefit for the superficial component of microcystic LMs, with case series noting reductions in vesicle volume, lymphatic leakage, and bleeding[120]. Microcystic LMs of the tongue and floor of the mouth are particularly difficult to treat, and careful dental hygiene is important. Transient inflammatory swelling of LMs usually responds to therapy with NSAIDs, corticosteroids, and/or antibiotics.

Patients with complex lymphatic anomalies may need replacement of albumin and immunoglobulins. A low-fat diet and substitution of long-chain fatty acids with medium-chain fatty acids may benefit those with intestinal lymphangiectasia. Oral sirolimus has been used with success in patients with LMs, GLA, and Gorham–Stout disease[116,121,122], and PI3K inhibition with alpelisib represents another promising therapeutic strategy[123]. Sildenafil treatment has led to variable decreases in volume and softening of large LMs in some patients[124], but no responses were seen in other series[125]. Zoledronate may be of benefit for osteolysis secondary to LMs in Gorham–Stout disease.

Arteriovenous Malformations

In general, stage 2 and 3 AVMs of the head and neck should be excised completely after careful preoperative embolization using arterial ± direct puncture approaches to prevent excessive intraoperative bleeding. Reconstruction often requires techniques such as skin grafting, preoperative tissue expansion, and free tissue transfer[1,91]. Subtotal excision frequently results in subsequent progression of the AVM, with recruitment of adjacent vessels and apparent angiogenesis. Stage 1 and early stage 2 AVMs are often managed conservatively if postsurgical cosmetic results might be worse than the lesion itself. However, resection of early-stage AVMs can prevent further progression.

Embolization alone usually cannot cure a superficial AVM. The most effective embolic agent, pure ethanol, poses substantial risks (especially at higher doses) that include renal or pulmonary toxicity and cardiac arrest. For AVMs that begin to hemorrhage, embolization may be life-saving. Distal hand or foot AVMs are rarely controlled long-term by embolotherapy, and ischemic complications resulting in extreme pain, necrosis, and bleeding may require amputation. In one report, treatment of a diffuse AVM in the arm of a young girl using a metalloproteinase inhibitor (Marimastat®) with antiangiogenic effects produced sustained improvement over a 12-year period, including reconstruction of affected bones and without adverse effects[126]. Treatment with trametinib, a

MEK inhibitor, was beneficial in a child with a large, progressive truncal *MAP2K1*-related AVM and a young woman with cardiac compromise due to CM-AVM syndrome[127].

Combined Malformations and the PIK3CA-Related Overgrowth Spectrum (PROS)

A combined vascular malformation of a limb requires an individualized management plan. Longitudinal orthopedic evaluation is essential for lower extremity lesions in growing children. Carefully timed epiphysiodesis before the end of the growth period can potentially correct a leg-length discrepancy in KTS, but it may worsen vascular disease in Parkes Weber syndrome. Treatment of a component of the vascular malformation (e.g. surgery for varicose veins in KTS or embolization of the AV nidus in Parkes Weber syndrome) often has suboptimal results. Elastic support garments and a compensatory shoe-lift are indispensable conservative interventions.

The PI3K inhibitor alpelisib is FDA-approved for patients ≥2 years of age with severe manifestations of PROS[128]. In a retrospective study in 32 patients with PROS, alpelisib therapy for 24 weeks led to improvement in vascular malformations and overgrowth in 79% and 74% of patients, respectively, with 38% achieving a ≥20% reduction in the volume of PROS lesions. Treatment of Proteus syndrome patients with miransertib, an oral AKT inhibitor, has led to stabilization of overgrowth and pain improvement[129]. Additional clinical trials and long-term follow-up studies are needed to provide further data on the benefits of targeted therapies in these overgrowth syndromes.

Acknowledgment

The author wishes to acknowledge the late Odile Enjolras, MD for her valuable contribution to this chapter in the previous editions.

APPENDIX

EXAMPLE OF A GENETIC PANEL: ADDITIONAL CODES	
VANSeq Panel*	**Genes**
Capillary malformations – 7 genes	*AKT1, EPHB4, GNA11, GNAQ, PIK3CA, PIK3R1, RASA1*
Lymphatic malformations, venous malformations, arteriovenous malformations (LM/VM/AVM) – 17 genes	*ACVRL1, ARAF, BRAF, ELMO2, ENG, EPHB4, GDF2, GLMN, HRAS, KRAS, MAP2K1, MAP3K3, NRAS, PIK3CA, PTEN, RASA1, TEK (TIE2)*
Lymphedema – 23 genes	*ARAF, BRAF, CCBE1, CELSR1, DCHS1, EPHB4, FAT4, FLT4, FOXC2, GATA2, GJC2, HGF, HRAS, KIF11, KRAS, MAP2K1, MET, NRAS, PIEZO1, PTPN14, RASA1, SOX18, VEGFC*
Vascular tumor – 10 genes	*BRAF, CTNNB1, GNA11, GNA14, GNAQ, HRAS, IDH1, IDH2, KRAS, NRAS*
VANseq expanded – 47 genes	*ACVRL1, AKT1, ARAF, BRAF, CCBE1, CCM2, CELSR1, CTNNB1, DCHS1, ELMO2, ENG, EPHB4, FAT4, FGFR1, FLT4, FOXC2, GATA2, GDF2, GJA4, GJC2, GLMN, GNA11, GNA14, GNAQ, HGF, HRAS, IDH1, IDH2, KIF11, KRAS, KRIT1, MAP2K1, MAP3K3, MET, NRAS, PDCD10, PDGFRB, PIEZO1, PIK3CA, PTEN, PTPN11, PTPN14, RASA1, SMAD4, SOX18, TEK, VEGFC*
*Modifed from the Seattle Children's Hospital vascular anomalies sequencing panel.	

Example of a genetic panel: additional codes. Panels vary depending on the laboratory.

Additional figures available in our eBook (see inside front cover for access code).

REFERENCES

1. Enjolras O, Wassef M, Chapot R. *A Color Atlas of Vascular Tumors and Vascular Malformations*. New York: Cambridge University Press; 2007.
2. Wassef M, Blei F, Adams D, et al. Vascular anomalies classification: recommendations from the International Society for the Study of Vascular Anomalies. *Pediatrics*. 2015;136:e203–e214.
3. ISSVA Classification of Vascular Anomalies, 2018. International Society for the Study of Vascular Anomalies. Available at <https://issva.org/classification>.
4. Dekeuleneer V, Seront E, Van Damme A, et al. Theranostic advances in vascular malformations. *J Invest Dermatol*. 2020;140:756–763.
5. Uebelhoer M, Boon LM, Vikkula M. Vascular anomalies: from genetics toward models for therapeutic trials. *Cold Spring Harb Perspect Med*. 2012;2:pii: a009688.
6. Limaye N, Wouters V, Uebelhoer M, et al. Somatic mutations in angiopoietin receptor gene *TEK* cause solitary and multiple sporadic venous malformations. *Nat Genet*. 2009;41:118–124.
7. Soblet J, Kangas J, Nätynki M, et al. Blue rubber bleb nevus (BRBN) syndrome is caused by somatic TEK (TIE2) mutations. *J Invest Dermatol*. 2017;137:207–216.
8. Irrthum A, Brouillard P, Enjolras O, et al. Linkage disequilibrium narrows locus for venous malformation with glomus cells (VMGLOM) to a single 1.48 Mbp YAC. *Eur J Hum Genet*. 2001;9:34–38.
9. Eerola L, Boon LM, Mulliken JB, et al. Capillary malformation-arteriovenous malformation: a new clinical and genetic disorder caused by *RASA1* mutations. *Am J Hum Genet*. 2003;73:1240–1249.
10. Rozas-Muñoz E, Frieden IJ, Roé E, et al. Vascular stains: proposal for a clinical classification to improve diagnosis and management. *Pediatr Dermatol*. 2016;33:570–584.
11. Kanada KN, Merin MR, Munden A, et al. A prospective study of cutaneous findings in newborns in the United States: correlation with race, ethnicity, and gestational status using updated classification and nomenclature. *J Pediatr*. 2012;161:240–245.
12. Juern AM, Glick ZR, Drolet BA, Frieden IJ. Nevus simplex: a reconsideration of nomenclature, sites of involvement, and disease associations. *J Am Acad Dermatol*. 2010;63:805–814.
13. Guggisberg D, Hadj-Rabia S, Viney C, et al. Skin markers of occult spinal dysraphism in children: a review of 54 cases. *Arch Dermatol*. 2004;140:1109–1115.
14. Chern JJ, Kirkman JL, Shannon CN, et al. Use of lumbar ultrasonography to detect occult spinal dysraphism. *J Neurosurg Pediatr*. 2012;9:274–279.
15. Jordan M, Carmignac V, Sorlin A, et al. Reverse phenotyping in patients with skin capillary malformations and mosaic *GNAQ* or *GNA11* mutations defines a clinical spectrum with genotype-phenotype correlation. *J Invest Dermatol*. 2020;140:1106–1110.
16. Shirley MD, Tang H, Gallione CJ, et al. Sturge-Weber syndrome and port-wine stains caused by somatic mutation in GNAQ. *N Engl J Med*. 2013;368:1971–1979.
17. Happle R. Capillary malformations: a classification using specific names for specific skin disorders. *J Eur Acad Dermatol Venereol*. 2015;29:2295–2305.
18. Siegel DH, Cottrell CE, Streicher JL, et al. Analyzing the genetic spectrum of vascular anomalies with overgrowth via cancer genomics. *J Invest Dermatol*. 2018;138:957–967.
19. Klapman MH, Yao JF. Thickening and nodules in port-wine stains. *J Am Acad Dermatol*. 2001;44:300–302.
20. Millán-Cayetano JF, Del Boz J, García-Montero P, de Troya-Martín M. Acquired port-wine stain (Fegeler syndrome): a report of 3 cases. *Actas Dermosifiliogr*. 2017;108:954–955.
21. Nijhawan RI, Bard S, Blyumin M, et al. Early localized morphea mimicking an acquired port-wine stain. *J Am Acad Dermatol*. 2011;64:779–782.
22. Fernández-Guarino M, Boixeda P, de Las Heras E, et al. Phakomatosis pigmentovascularis: clinical findings in 15 patients and review of the literature. *J Am Acad Dermatol*. 2008;58:88–93.
23. Happle R. Phacomatosis pigmentovascularis revisited and reclassified. *Arch Dermatol*. 2005;141:385–388.
23a. Polubothu S, Bender N, Muthiah S, et al. PTPN11 mosaicism causes a spectrum of pigmentary and vascular neurocutaneous disorders and predisposes to melanoma. *J Invest Dermatol*. 2023;143:1043–1051.
24. Waelchli R, Aylett SE, Robinson K, et al. New vascular classification of port wine stains: improving prediction of Sturge-Weber risk. *Br J Dermatol*. 2014;171:861–867.
25. Dutkiewicz AS, Ezzedine K, Mazereeuw-Hautier J, et al. A prospective study of risk for Sturge-Weber syndrome in children with upper facial port-wine stain. *J Am Acad Dermatol*. 2015;72:473–480.
26. Sudarsanam A, Ardern-Holmes SL. Sturge-Weber syndrome: from the past to the present. *Eur J Paediatr Neurol*. 2014;18:257–266.
27. Miller RS, Ball KL, Comi AM, Germain-Lee EL. Growth hormone deficiency in Sturge-Weber syndrome. *Arch Dis Child*. 2006;91:340–341.
28. Mazereeuw-Hautier J, Syed S, Harper J. Bilateral facial capillary malformation associated with eye and brain abnormalities. *Arch Dermatol*. 2006;142:994–998.
29. Boos MD, Bozarth XL, Sidbury R, et al. Forehead location and large segmental pattern of facial port-wine stains predict risk of Sturge-Weber syndrome. *J Am Acad Dermatol*. 2020;83:1110–1117.
30. Sabeti S, Ball KL, Bhattacharya SK, et al. Consensus statement for the management and treatment of Sturge-Weber syndrome: neurology, neuroimaging, and ophthalmology recommendations. *Pediatr Neurol*. 2021;121:59–66.
31. Bay MJ, Kossoff EH, Lehmann CU, et al. Survey of aspirin use in Sturge-Weber syndrome. *J Child Neurol*. 2011;26:692–702.
32. Lance EI, Sreenivasan AK, Zabel TA, et al. Aspirin use in Sturge-Weber syndrome: side effects and clinical outcomes. *J Child Neurol*. 2013;28:213–218.
33. Ewen JB, Kossoff EH, Crone NE, et al. Use of quantitative EEG in infants with port-wine birthmark to assess for Sturge-Weber brain involvement. *Clin Neurophysiol*. 2009;120:1433–1440.
34. Enjolras O, Chapot R, Merland JJ. Vascular anomalies and the growth of limbs: a review. *J Pediatr Orthop B*. 2004;13:349–357.
35. Lee MS, Liang MG, Mulliken JB. Diffuse capillary malformation with overgrowth: a clinical subtype of vascular anomalies with hypertrophy. *J Am Acad Dermatol*. 2013;69:589–594.
36. Couto JA, Ayturk UM, Konczyk DJ, et al. A somatic GNA11 mutation is associated with extremity capillary malformation and overgrowth. *Angiogenesis*. 2017;20:303–306.
37. Goss JA, Konczyk DJ, Smits P, et al. Diffuse capillary malformation with overgrowth contains somatic PIK3CA variants. *Clin Genet*. 2020;97:736–740.

38. Luks VL, Kamitaki N, Vivero MP, et al. Lymphatic and other vascular malformative/overgrowth disorders are caused by somatic mutations in PIK3CA. *J Pediatr*. 2015;166:1048–1054. e1–5.
39. Corsmeier DJ, Avenarius M, Dudley JN, et al. Somatic *PIK3R1* variation as a cause of vascular malformations and overgrowth. *Genet Med*. 2021;23:1882–1888.
40. Redondo P, Aguado L, Martinez-Cuesta A. Diagnosis and management of extensive vascular malformations of the lower limb: part II. Systemic repercussions [corrected], diagnosis, and treatment. *J Am Acad Dermatol*. 2011;65:909–923.
41. Maari C, Frieden IJ. Klippel-Trenaunay syndrome: the importance of "geographic stains" in identifying lymphatic disease and risk of complications. *J Am Acad Dermatol*. 2004;51:391–398.
42. Redondo P, Bastarrika G, Aguado L, et al. Foot or hand malformations related to deep venous system anomalies of the lower limb in Klippel-Trénaunay syndrome. *J Am Acad Dermatol*. 2009;61:621–628.
43. Huiras EE, Barnes CJ, Eichenfield LF, et al. Pulmonary thromboembolism associated with Klippel-Trenaunay syndrome. *Pediatrics*. 2005;116:e596–e600.
44. Zwerink LGJM, Te Loo DMWM, Praster R, et al. Aberrant venous anatomy as a risk factor for thromboembolic events in patients with Klippel-Trénaunay syndrome: case-control study within a cohort study. *J Am Acad Dermatol*. 2021;84:1470–1472.
45. Redondo P, Aguado L, Marquina M, et al. Angiogenic and prothrombotic markers in extensive slow-flow vascular malformations: implications for antiangiogenic/antithrombotic strategies. *Br J Dermatol*. 2010;162:350–356.
46. Rodriguez-Manero M, Aguado L, Redondo P. Pulmonary arterial hypertension in patients with slow-flow vascular malformations. *Arch Dermatol*. 2010;146:1347–1352.
47. Sapp JC, Turner JT, van de Kamp JM, et al. Newly delineated syndrome of congenital lipomatous overgrowth, vascular malformations, and epidermal nevi (CLOVE syndrome) in seven patients. *Am J Med Genet*. 2007;143A:2944–2958.
48. Alomari AT. Characterization of a distinct syndrome that associates complex truncal overgrowth, vascular, and acral anomalies: a descriptive study of 18 cases of CLOVES syndrome. *Clin Dysmorphol*. 2009;18:1–7.
49. Kurek KC, Luks VL, Ayturk UM, et al. Somatic mosaic activating mutations in PIK3CA cause CLOVES syndrome. *Am J Hum Genet*. 2012;90:1108–1115.
50. Keppler-Noreuil KM, Sapp JC, Lindhurst MJ, et al. Clinical delineation and natural history of the PIK3CA-related overgrowth spectrum. *Am J Med Genet A*. 2014;164:1713–1733.
51. Alomari AI, Burrows PE, Lee EY, et al. CLOVES syndrome with thoracic and central phlebectasia: increased risk of pulmonary embolism. *J Thorac Cardiovasc Surg*. 2010;140:459–463.
52. Wright DR, Frieden IJ, Orlow SJ, et al. The misnomer "macrocephaly-cutis marmorata telangiectatica congenita syndrome": report of 12 new cases and support for revising the name to macrocephaly-capillary malformations. *Arch Dermatol*. 2009;145:287–293.
53. Mirzaa GM, Riviere JB, Dobyns WB. Megalencephaly syndromes and activating mutations in the PI3K-AKT pathway: MPPH and MCAP. *Am J Med Genet C Semin Med Genet*. 2013;163C:122–130.
54. Riviere JB, Mirzaa GM, O'Roak BJ, et al. De novo germline and postzygotic mutations in AKT3, PIK3R2 and PIK3CA cause a spectrum of related megalencephaly syndromes. *Nat Genet*. 2012;44:934–940.
55. López-Gutiérrez JC, Lapunzina P. Capillary malformation of the lower lip, lymphatic malformation of the face and neck, asymmetry and partial/generalized overgrowth (CLAPO): report of six cases of a new syndrome/association. *Am J Med Genet*. 2008;146A:2583–2588.
56. Rodriguez-Laguna L, Ibañez K, Gordo G, et al. CLAPO syndrome: identification of somatic activating PIK3CA mutations and delineation of the natural history and phenotype. *Genet Med*. 2018;20:882–889.
57. Turner JT, Cohen MM, Biesecker LG. Reassessment of the Proteus syndrome literature: application of diagnostic criteria to published cases. *Am J Med Genet*. 2004;130A:111–122.
58. Lindhurst MJ, Sapp JC, Teer JK, et al. A mosaic activating mutation in AKT1 associated with the Proteus syndrome. *N Engl J Med*. 2011;365:611–619.
59. Cohen MM Jr. Proteus syndrome: an update. *Am J Med Genet C Semin Med Genet*. 2005;137C:38–52.
60. Ben Amitai D, Fichman S, Merlob P. Cutis marmorata telangiectatica congenita: clinical findings in 85 patients. *Pediatr Dermatol*. 2000;17:100–104.
61. Davies OMT, Garzon MC, Frieden IJ, et al. Cutaneous vascular anomalies associated with a mosaic variant of *AKT3*: genetic analysis continues to refine the diagnosis, nomenclature, and classification of vascular anomalies. *J Am Acad Dermatol*. 2022;87:162–164.
62. Revencu N, Boon LM, Mulliken JB, et al. Parkes Weber syndrome, vein of Galen aneurysmal malformation and other fast-flow vascular anomalies are caused by *RASA1* mutations. *Hum Mutat*. 2008;29:959–965.
63. Sabbà C, Pasculli G, Lenato GM, et al. Hereditary hemorrhagic telangiectasia: clinical features in *ENG* and *ALK1* mutation carriers. *J Thromb Haemost*. 2007;5:1149–1157.
64. Morgan T, McDonald J, Anderson C, et al. Intracranial hemorrhage in infants and children with hereditary hemorrhagic telangiectasia (Osler-Weber-Rendu syndrome). *Pediatrics*. 2002;109:e12.
65. Faughnan ME, Mager JJ, Hetts SW, et al. Second International Guidelines for the diagnosis and management of hereditary hemorrhagic telangiectasia. *Ann Intern Med*. 2020;173:989–1001.
66. Gonzalez CD, Cipriano SD, Topham CA, et al. Localization and age distribution of telangiectases in children and adolescents with hereditary hemorrhagic telangiectasia: a retrospective cohort study. *J Am Acad Dermatol*. 2019;81:950–955.
67. Limaye N, Kangas J, Mendola A, et al. Somatic activating PIK3CA mutations cause venous malformation. *Am J Hum Genet*. 2015;97:914–921.
68. Mazoyer E, Enjolras O, Bisdorff A, et al. Coagulation disorders in patients with venous malformation of limbs and trunk (a study in 118 patients). *Arch Dermatol*. 2008;144:861–867.
69. Dompmartin A, Acher A, Thibon P, et al. Association of localized intravascular coagulopathy with venous malformations. *Arch Dermatol*. 2008;144:873–877.
70. Alomari AI, Spencer SA, Arnold RW, et al. Fibro-adipose vascular anomaly: clinical-radiologic-pathologic features of a newly delineated disorder of the extremity. *J Pediatr Orthop*. 2014;34:109–117.
71. Couto JA, Vivero MP, Kozakewich HP, et al. A somatic MAP3K3 mutation is associated with verrucous venous malformation. *Am J Hum Genet*. 2015;96:480–486.
72. Boccara O, Ariche-Maman S, Hadj-Rabia S, et al. Verrucous hemangioma (also known as verrucous venous malformation): a vascular anomaly frequently misdiagnosed as a lymphatic malformation. *Pediatr Dermatol*. 2018;35:e378–e381.
73. Wouters V, Limaye N, Uebelhoer M, et al. Hereditary cutaneomucosal venous malformations are caused by *TIE2* mutations with widely variable hyper-phosphorylating effects. *Eur J Hum Genet*. 2010;18:414–420.
74. Ivars M, Martin-Santiago A, Baselga E, et al. Fern-shaped patch as a hallmark of blue rubber bleb nevus syndrome in neonatal venous malformations. *Eur J Pediatr*. 2018;177:1395–1398.
75. Pansuriya TC, van Eijk R, d'Adamo P, et al. Somatic mosaic IDH1 and IDH2 mutations are associated with enchondroma and spindle cell hemangioma in Ollier disease and Maffucci syndrome. *Nat Genet*. 2011;43:1256–1261.
76. Boon LM, Mulliken JB, Enjolras O, Vikkula M. Glomuvenous malformation (glomangioma) and venous malformation: distinct clinicopathologic and genetic entities. *Arch Dermatol*. 2004;140:971–976.
77. Mallory SB, Enjolras O, Boon LM, et al. Congenital plaque-type glomuvenous malformations presenting in childhood. *Arch Dermatol*. 2006;142:892–896.
78. Brouillard P, Ghassibé M, Penington A, et al. Four common glomulin mutations cause two thirds of glomuvenous malformations ("familial glomangiomas"): evidence for a founder effect. *J Med Genet*. 2005; 42:e13.
79. Revencu N, Vikkula M. Cerebral cavernous malformation: new molecular and clinical insights. *J Med Genet*. 2006;43:716–721.
80. Sirvente J, Enjolras O, Wassef M, et al. Frequency and phenotypes of cutaneous vascular malformations in a consecutive series of 417 patients with familial cerebral cavernous malformations. *J Eur Acad Dermatol Venereol*. 2009;23:1066–1072.
81. Matarneh B, Cottrell CE, Choi S, et al. KRIT1-positive hyperkeratotic cutaneous capillary venous malformation. *Pediatr Dermatol*. 2022;39:250–254.
82. Makinen T, Boon LM, Vikkula M, Alitalo K. Lymphatic malformations: genetics, mechanisms and therapeutic strategies. *Circ Res*. 2021;129:136–154.
83. Gordon K, Varney R, Keeley V, et al. Update and audit of the St George's classification algorithm of primary lymphatic anomalies: a clinical and molecular approach to diagnosis. *J Med Genet*. 2020;57:653–659.
84. Edwards PD, Rahbar R, Ferraro NF, et al. Lymphatic malformation of the lingual base and oral floor. *Plast Reconstr Surg*. 2006;115:1906–1915.
85. Greene AK, Burrows PE, Smith L, Mulliken JB. Periorbital lymphatic malformation: clinical course and management in 42 patients. *Plast Reconstr Surg*. 2005;115:22–30.
86. Croteau SE, Kozakewich HP, Perez-Atayde AR, et al. Kaposiform lymphangiomatosis: a distinct aggressive lymphatic anomaly. *J Pediatr*. 2014;164:383–388.
87. Perez-Atayde AR, Debelenko L, Al-Ibraheemi A, et al. Kaposiform lymphangiomatosis: pathologic aspects in 43 patients. *Am J Surg Pathol*. 2022;46:963–976.
88. Barclay SF, Inman KW, Luks VL, et al. A somatic activating NRAS variant associated with kaposiform lymphangiomatosis. *Genet Med*. 2019;21:1517–1524.
89. Liu M, Smith CL, Biko DM, et al. Genetics etiologies and genotype phenotype correlations in a cohort of individuals with central conducting lymphatic anomaly. [published correction appears in *Eur J Hum Genet 2022;30:1094]. Eur J Hum Genet*. 2022;30:1022–1028.
90. Byrne AB, Brouillard P, Sutton DL, et al. Pathogenic variants in MDFIC cause recessive central conducting lymphatic anomaly with lymphedema. *Sci Transl Med*. 2022;14:eabm4869.
91. Enjolras O, Logeart I, Gelbert F, et al. Malformations artérioveineuses: étude de 200 cas. *Ann Dermatol Venereol*. 2000;127:17–22.
92. Al-Olabi L, Polubothu S, Dowsett K, et al. Mosaic RAS/MAPK variants cause sporadic vascular malformations which respond to targeted therapy. *J Clin Invest*. 2018;128:5185.
93. Couto JA, Huang AY, Konczyk DJ, et al. Somatic MAP2K1 mutations are associated with extracranial arteriovenous malformation. *Am J Hum Genet*. 2017;100:546–554.
94. Galligan ER, Baselga E, Frieden IJ, et al. Characterization of vascular stains associated with high flow. *J Am Acad Dermatol*. 2021;84:654–660.
95. Wu JK, Bisdorff A, Gelbert F, et al. Auricular arteriovenous malformation: evaluation, management, and outcome. *Plast Reconstr Surg*. 2005;115:985–995.
96. Bhattacharya JJ, Luo CB, Suh DC, et al. Wyburn-Mason or Bonnet-Dechaume-Blanc as cerebrofacial arteriovenous metameric syndromes (CAMS). *Interv Neuroradiol*. 2001;7:5–17.
97. Revencu N, Boon LM, Mendola A, et al. RASA1 mutations and associated phenotypes in 68 families with capillary malformation-arteriovenous malformation. *Hum Mutat*. 2013;34:1632–1641.
98. Amyere M, Revencu N, Helaers R, et al. Germline loss-of-function mutations in EPHB4 cause a second form of capillary malformation-arteriovenous malformation (CM-AVM2) deregulating RAS-MAPK signaling. *Circulation*. 2017;136:1037–1048.
99. Valdivielso-Ramos M, Torrelo A, Martin-Santiago A, et al. Histopathological hallmarks of cutaneous lesions of capillary malformation-arteriovenous malformation syndrome. *J Eur Acad Dermatol Venereol*. 2020;34:2428–2435.
100. Orme CM, Boyden LM, Choate KA, et al. Capillary malformation–arteriovenous malformation syndrome: review of the literature, proposed diagnostic criteria, and recommendations for management. *Pediatr Dermatol*. 2013;30:409–415.
101. Wanner M, Celebi JT, Peacocke M. Identification of a PTEN mutation in a family with Cowden syndrome and Bannayan-Zonana syndrome. *J Am Acad Dermatol*. 2001;44:183–187.
102. Pezzolesi MG, Li Y, Zhou XP, et al. Mutation-positive and mutation-negative patients with Cowden and Bannayan-Riley-Ruvalcaba syndromes associated with distinct 10q haplotypes. *Am J Hum Genet*. 2006;79:923–934.
103. Tan WH, Baris HN, Burrows PE, et al. The spectrum of vascular anomalies in patients with PTEN mutations: implications for diagnosis and management. *J Med Genet*. 2007;44:594–602.
104. Iacobas I, Burrows PE, Adams DM, et al. Oral rapamycin in the treatment of patients with hamartoma syndromes and PTEN mutation. *Pediatr Blood Cancer*. 2011;57:321–323.
105. Nguyen CM, Yohn JJ, Huff C, et al. Facial port wine stains in childhood: prediction of the rate of improvement as a function of the age of the patient, size and location of the port wine stain and the number of treatments with the pulsed dye (585 nm) laser. *Br J Dermatol*. 1998;138:821–825.
106. Seukeran DC, Collins P, Sheehan-Dare RA. Adverse reactions following pulsed tunable dye laser treatment of port wine stains in 701 patients. *Br J Dermatol*. 1997;136:725–729.

107. Chapas AM, Eickhorst K, Geronemus RG. Efficacy of early treatment of facial port wine stains in newborns: a review of 49 cases. *Lasers Surg Med*. 2007;39:563–568.
108. Huikeshoven M, Koster PH, de Borgie CA, et al. Redarkening of port-wine stains 10 years after pulsed-dye-laser treatment. *N Engl J Med*. 2007;356:1235–1240.
109. Marqués L, Núñez-Córdoba JM, Aguado L, et al. Topical rapamycin combined with pulsed dye laser in the treatment of capillary vascular malformations in Sturge-Weber syndrome: phase II, randomized, double-blind, intraindividual placebo-controlled clinical trial. *J Am Acad Dermatol*. 2015;72:151–158.
110. Bachur CD, Comi AM. Sturge-Weber syndrome. *Curr Treat Options Neurol*. 2013;15:607–617.
111. Triana Junco PE, Sánchez-Carpintero I, López-Gutiérrez JC. Preventive treatment with oral sirolimus and aspirin in a newborn with severe Sturge-Weber syndrome. *Pediatr Dermatol*. 2019;36:524–527.
112. Sun B, Han T, Wang Y, et al. Sirolimus as a potential treatment for Sturge-Weber syndrome. *J Craniofac Surg*. 2021;32:257–260.
113. Sabeti S, Ball KL, Burkhart C, et al. Consensus statement for the management and treatment of port-wine birthmarks in Sturge-Weber syndrome. *JAMA Dermatol*. 2021;157:98–104.
114. Nguyen JT, Koerper MA, Hess CP, et al. Aspirin therapy in venous malformation: a retrospective cohort study of benefits, side effects, and patient experiences. *Pediatr Dermatol*. 2014;31:556–560.
115. Boscolo E, Limaye N, Huang L, et al. Rapamycin improves TIE2-mutated venous malformation in murine model and human subjects. *J Clin Invest*. 2015;125:3491–3504.
116. Maruani A, Tavernier E, Boccara O, et al. Sirolimus (rapamycin) for slow-flow malformations in children: the observational-phase randomized clinical PERFORMUS trial. *JAMA Dermatol*. 2021;157:1289–1298.
117. Peters DA, Courtemanche DJ, Heran MKS, et al. Treatment of cystic lymphatic vascular malformations with OK-432 sclerotherapy. *Plast Reconstr Surg*. 2006;118:1441–1446.
118. Leboulanger N, Roger G, Caze A, et al. Utility of radiofrequency ablation for haemorrhagic lingual lymphangioma. *Int J Pediatr Otorhinolaryngol*. 2008;72:953–958.
119. Shiels WE 2nd, Kenney BD, Caniano DA, Besner GE. Definitive percutaneous treatment of lymphatic malformations of the trunk and extremities. *J Pediatr Surg*. 2008;43:136–139.
120. García-Montero P, Del Boz J, Baselga-Torres E. Use of topical rapamycin in the treatment of superficial lymphatic malformations. *J Am Acad Dermatol*. 2019;80:50815.
121. Triana P, Dore M, Cerezo VN, et al. Sirolimus in the treatment of vascular anomalies. *Eur J Pediatr Surg*. 2017;27:86–90.
122. Ricci KW, Hammill AM, Mobberley-Schuman P, et al. Efficacy of systemic sirolimus in the treatment of generalized lymphatic anomaly and Gorham-Stout disease. *Pediatr Blood Cancer*. 2019;66:e27614.
123. Delestre F, Venot Q, Bayard C, et al. Alpelisib administration reduced lymphatic malformations in a mouse model and in patients. *Sci Transl Med*. 2021;13:eabg0809.
124. Swetman GL, Berk DR, Vasanawala SS, et al. Sildenafil for severe lymphatic malformations. *N Engl J Med*. 2012;366:384–386.
125. Koshy JC, Eisemann BS, Agrawal N, et al. Sildenafil for microcystic lymphatic malformations of the head and neck: a prospective study. *Int J Pediatr Otorhinolaryngol*. 2015;79:980–982.
126. Burrows PE, Mulliken JB, Fishman SJ, et al. Pharmacological treatment of a diffuse arteriovenous malformation of the upper extremity in a child. *J Craniofac Surg*. 2009;20:1597–2002.
127. Lekwuttikarn R, Lim YH, Admani S, et al. Genotype-guided medical treatment of an arteriovenous malformation in a child. *JAMA Dermatol*. 2019;155:256–257.
128. Venot Q, Blanc T, Rabia SH, et al. Targeted therapy in patients with PIK3CA-related overgrowth syndrome. *Nature*. 2018;558:540–546.
129. Keppler-Noreuil KM, Sapp JC, Lindhurst MJ, et al. Pharmacodynamic study of miransertib in individuals with Proteus syndrome. *Am J Hum Genet*. 2019;104:484–491.



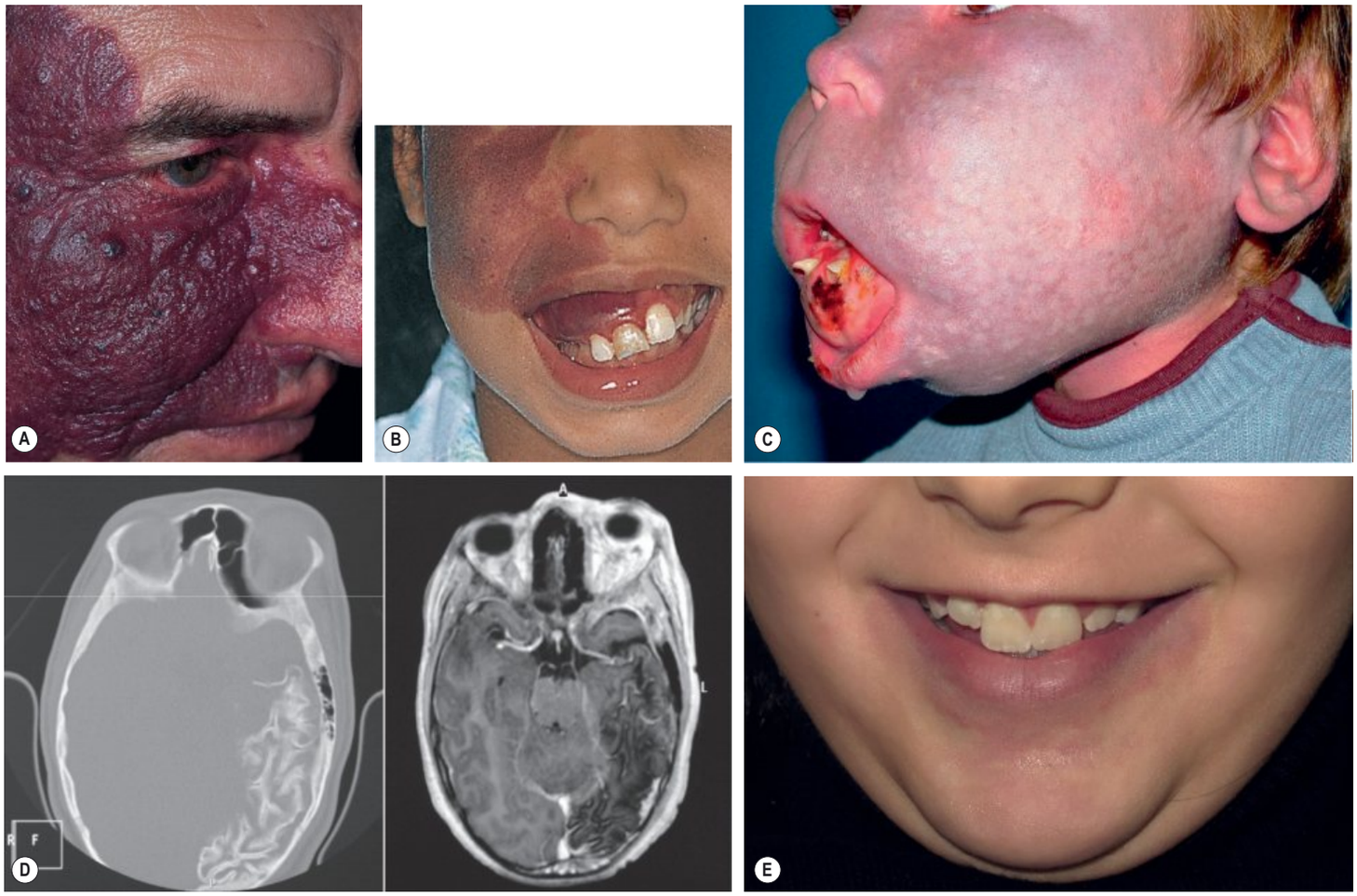
eFig. 104.1 Nevus simplex (stork bite) with overlying eczema. *Courtesy Julie V. Schaffer, MD.*



eFig. 104.2 Port-wine birthmark involving the majority of the left side of the face. Involvement of the "forehead area" is associated with risk for Sturge–Weber syndrome. *Courtesy Julie V. Schaffer, MD.*



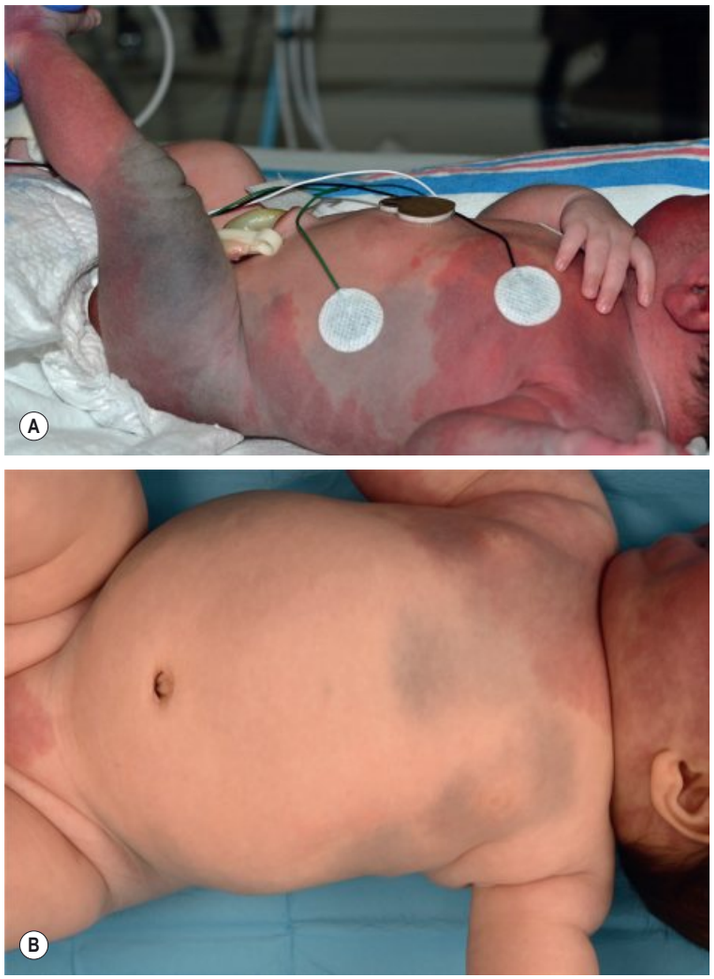
eFig. 104.3 Port-wine birthmark of the maxillary region in an infant. *Courtesy Julie V. Schaffer, MD.*



eFig. 104.4 Facial port-wine birthmarks (PWBs) with associated hypertrophy and other manifestations. A Hyperplasia and nodularity are prominent in this adult. **B** Note the enlarged gingiva on the right and overgrowth of the right maxilla. **C** Severe hypertrophy of the gingiva, soft tissues, and bone in a child with a diffuse facial PWB. This has resulted in an open bite and dental abnormalities. **D** Brain imaging in Sturge–Weber syndrome. A head CT scan (left) shows gyriform calcifications in the involved hemisphere. MRI in the same patient (right) demonstrates the corresponding cerebral hemiatrophy and vascular anomaly. **E** *C*apillary malformation of the lower lip as a manifestation of the *L*ymphatic malformation of the tongue/neck *A*symmetry *P*artial *O*vergrowth (CLAPO) syndrome. This girl presented with a capillary malformation on the lower lip and chin together with a lymphatic malformation on the tongue.



eFig. 104.5 Phakomatosis pigmentovascularis IIa (cesioflammea) with widespread PWBs and dermal melanocytosis.



eFig. 104.6 Phakomatosis pigmentovascularis type II. A,B A combination of a port-wine birthmark and extensive dermal melanocytosis are seen. *A, Courtesy Julie V. Schaffer, MD.*





eFig. 104.7 Klippel–Trenaunay syndrome. A–C These dark red–purple geographic birthmarks are associated with lymphatic as well as venous malformations, with variable degrees of overgrowth. Note the hemorrhagic lymphatic vesicles (**C**). *A, Courtesy Julie V. Schaffer, MD.*



eFig. 104.8 Reticulated capillary malformation in a patient with megalencephaly–capillary malformation syndrome. Note the sharp midline demarcation on abdomen. This girl has hemihypertrophy of the same side of the body, syndactyly of the 2nd–3rd toes, and a sandal gap.



eFig. 104.9 Cutis marmorata telangiectatica congenita (CMTC) in a neonate. Note the broad purple reticulated network. *Courtesy Rosa Maria Cordisco, MD.*



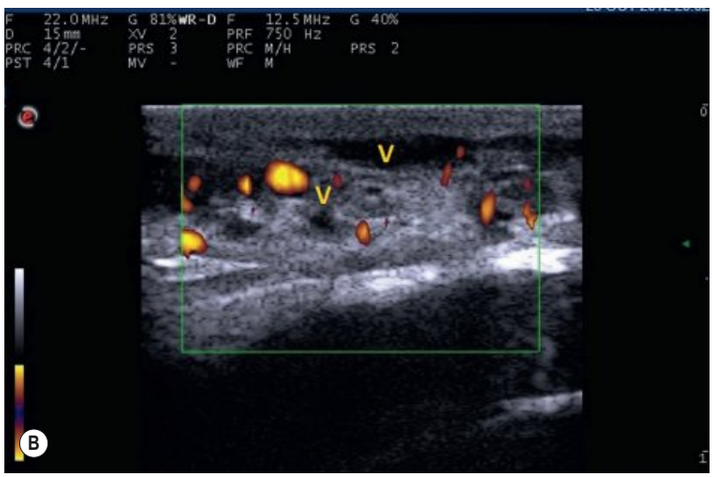
eFig. 104.10 Cutis marmorata telangiectatica congenita (CMTC). Reticulated red–purple vascular pattern on the arm. The lesions near the elbow are depressed due to associated cutaneous atrophy. *Courtesy Noah Hornick, MD, PhD.*

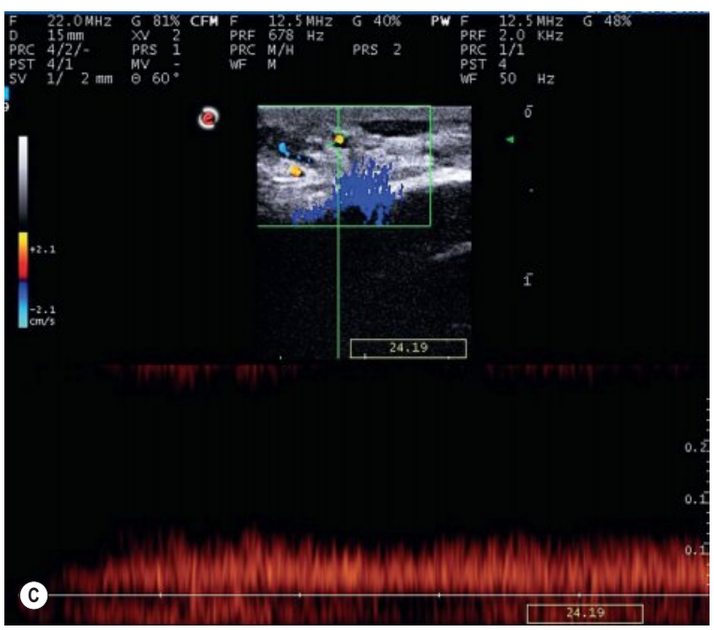




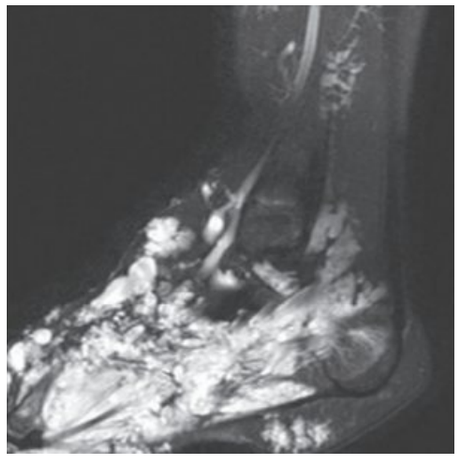
eFig. 104.11 Venous malformations. Bluish compressible lesions on the genitalia (**A**) and arm (**B**).



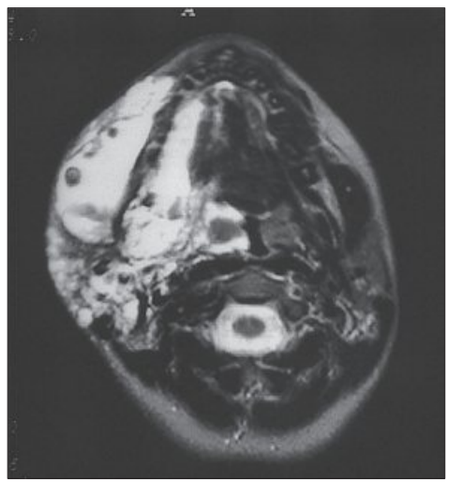




eFig. 104.12 Demonstration of venous malformation as a low-flow vascular lesion. A Cluster of compressible blue–violet papulonodules present since birth (a central scar is also present). **B** Subcutaneous channel-like structures (V) with increased flow observed by Mode B and Power Doppler ultrasound, respectively. **C** Spectral Doppler demonstrating a phasic sinusoidal venous flow pattern. *Courtesy Dr. Fernando Alfageme.*



eFig. 104.13 MRI, T2 – SE sequence of a venous malformation on the foot. Diffuse cutaneous and intramuscular involvement is evident.



eFig. 104.14 T2-weighted MRI sequence clearly shows venous malformation (VM) in the neck (white hypersignals). The black dots in the white areas of VMs are phleboliths.





eFig. 104.15 Blue rubber bleb nevus syndrome. A Small blue venous nodules are superimposed on a large subcutaneous venous malformation in this girl. **B** This neonate has a venous malformation (VM) involving the entire arm, gastrointestinal VMs, scattered smaller blue papules on the knee and foot, and coagulopathy. *B, Courtesy Aicha Salhi, MD.*



eFig. 104.16 Glomuvenous malformations. Blue–purple papules and plaques with a cobblestone-like appearance on the feet (**A**,**B**) and in a segmental pattern on the trunk and arm (**C**).



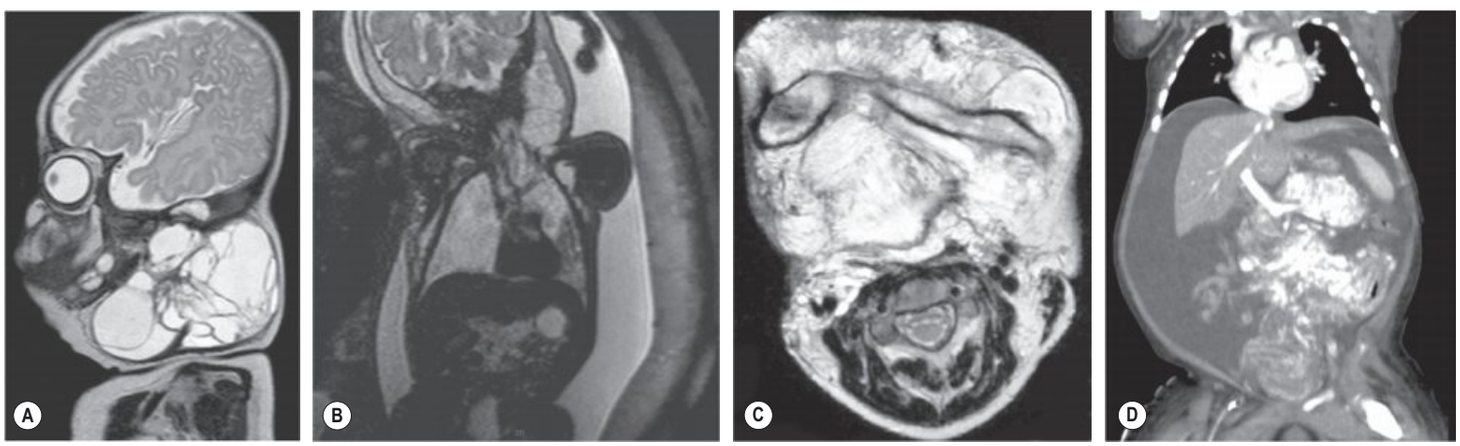




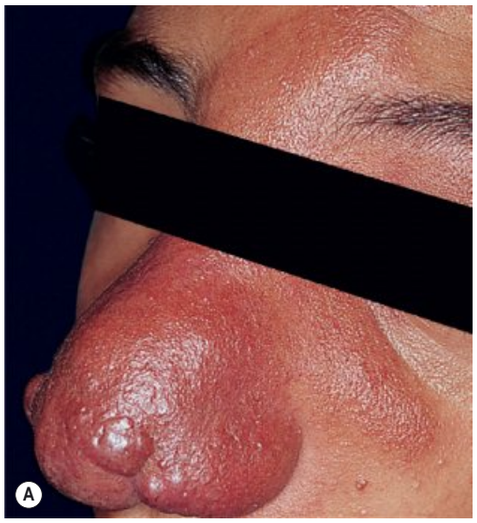
eFig. 104.17 Lymphatic malformations (LMs). A Clusters of small skin-colored lymphatic vesicles in a microcystic LM. **B** Massive congenital macrocystic LM involving the soft tissue and some bones of the left neck, thorax, and arm. The patient died from uncontrolled LM-associated coagulopathy. **C** LM vesicles in the mouth, which bleed frequently.



eFig. 104.18 Gorham–Stout disease. Purplish papules and plaques representing combined capillary–lymphatic malformations.



eFig. 104.19 MRI of lymphatic malformations (LMs). A Neonate with well-delineated, hyper-T2 LM macrocysts. **B** Prenatal 2nd trimester MRI-T2 showing a diffuse LM of the head, neck, lungs, and abdomen; the fetus later died *in utero*. **C** MRI-T2 showing a massive microcystic LM blurring soft tissues and distorting bones of the mouth and pharynx. **D** MRI-T1 with contrast demonstrates a diffuse LM of the abdomen with ascites, a condition with poor prognosis that is often mislabeled as lymphangiomatosis.





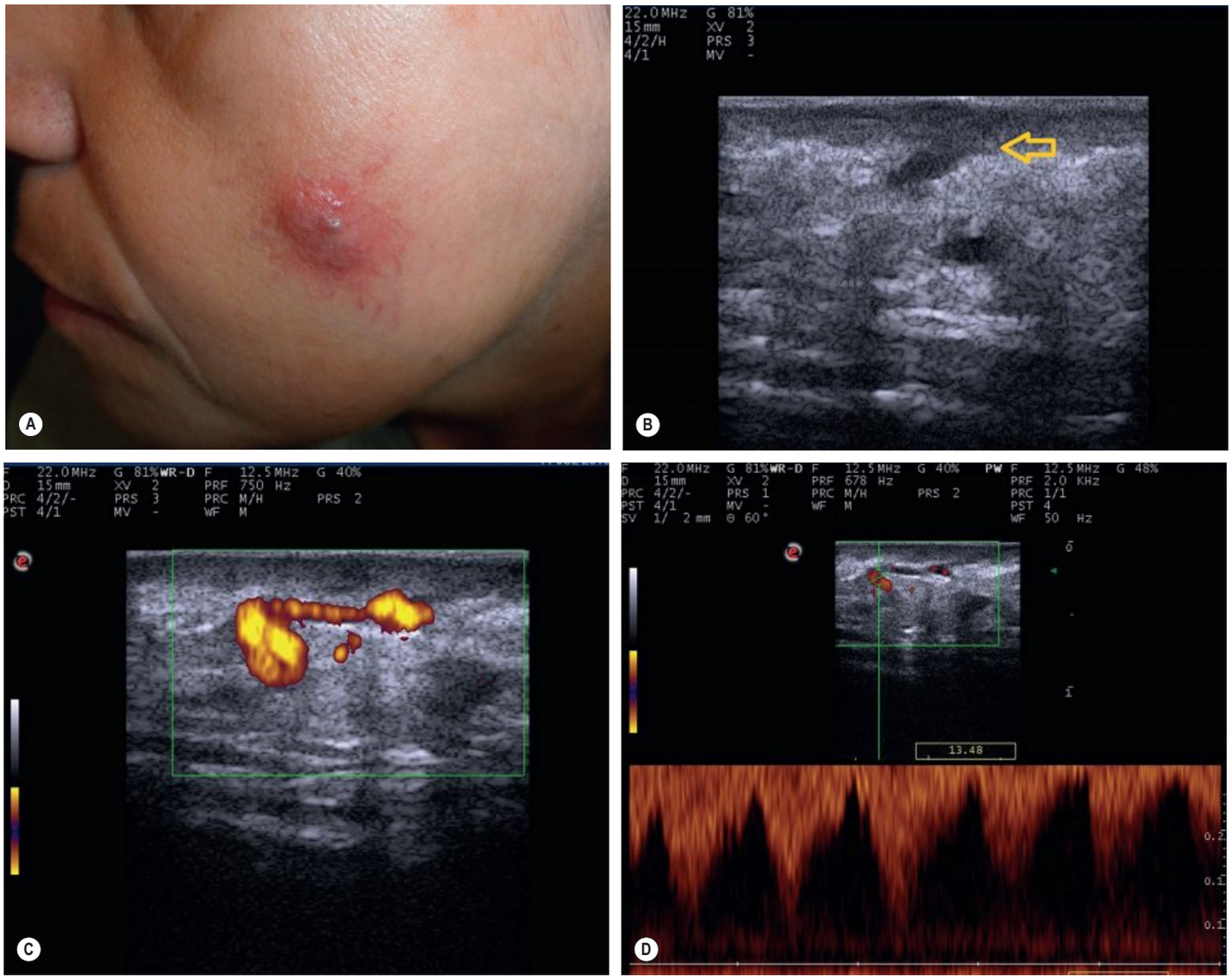
eFig. 104.20 Arteriovenous malformations (AVMs). A Stage 2 centrofacial AVM associated with AVMs of the retina and brain in a boy with Bonnet–Dechaume–Blanc syndrome. **B** Stage 3–4 facial AVM before and after treatment. *B, Courtesy Juan Carlos López, MD.*







eFig. 104.21 Capillary malformation–arteriovenous malformation (CM-AVM) due to a *RASA1* mutations. Large (**A**) and small (**B**) pink patches on the thigh with peripheral white halos. **C** Red warm patch on the forearm representing a quiescent AVM. *A, Courtesy Margarita Larralde, MD.*



eFig. 104.22 Demonstration of an arteriovenous malformation as a high-flow vascular lesion. A Slowly growing erythematous nodule with telangiectasias present since birth. **B** Hypoechoic (arrow) dermal and subcutaneous lesion by Mode B ultrasound. **C** Increased blood flow by Power Doppler ultrasound. **D** Spectral Doppler demonstrating an arterial biphasic curve flow pattern. *Courtesy Dr. Fernando Alfageme.*

105 Ulcers

Ariela Hafner and Eli Sprecher

Chapter Contents

Venous Ulcers 1844
Lymphedema 1852
Arterial Ulcers 1854
Diabetic (and Neuropathic) Ulcers 1855
Ulcers Due to Physical Factors 1857
Other Causes of Skin Ulceration 1859

Synonyms: ■ Ulcer – wound, sore ■ Venous ulcer – ulcer due to venous insufficiency/venous hypertension ■ Arterial ulcer – ulcer due to atherosclerosis ■ Neuropathic ulcer – mal perforans ■ Livedoid vasculopathy – atrophie blanche, livedoid vasculitis ■ Pressure ulcer – decubitus ulcer, pressure sore, bed sore

Key features

- The history should include onset, course, symptoms, exacerbating and alleviating factors, past medical history, family history, social history, travel, and medications
- Important aspects of the physical examination include location, size, shape and depth of the ulcer, characteristics of the ulcer edge and base, and associated physical findings
- Helpful laboratory evaluation includes vascular studies, blood tests (e.g. for thrombophilia), microbial cultures, and biopsy
- A biopsy of non-healing chronic ulcers is indicated to exclude carcinoma or other underlying diseases
- In addition to local care, therapy of ulcers should aim to correct or treat the underlying cause:
  - Venous insufficiency: compression
  - Arterial insufficiency: revascularization
  - Neuropathic or pressure ulcer: relief of pressure or other local factor that might be causing or exacerbating the ulceration
  - Infection: antibiotics
  - Neoplasm: surgery, chemotherapy, radiotherapy
  - Vasculopathy: treat the underlying cause of the occlusive disorder
  - Vasculitis or other inflammatory process (e.g. pyoderma gangrenosum): corticosteroids, immunosuppressive agents
- A key factor in therapy is the promotion of wound healing:
  - Debridement: mechanical, enzymatic, autolytic
  - Dressings: maintain a moist wound environment
  - Infection control: antibiotics
  - Skin grafting or skin substitutes
  - Growth factors

INTRODUCTION

A chronic wound is defined as one that fails to progress through a normal orderly and timely sequence of repair or a wound that passes through the repair process without restoring a functional result[1]. A cutaneous ulcer is a wound that is associated with loss of both epidermal and dermal tissues. Chronic ulcers, which are due to a variety of systemic and/or local factors, can represent both a diagnostic and therapeutic challenge to the dermatologist. The majority of ulcers occur on the lower extremities, and most are related to venous insufficiency/venous hypertension, peripheral artery disease, or peripheral neuropathy (Table 105.1). Less common causes are outlined in Figure 105.1 and sites other than the legs may be involved (e.g. pressure-induced ulcers).

Wound therapy has advanced considerably over the past few decades with the advent of innovative dressings and technologies, but the key factor in the management of chronic ulcers remains proper patient evaluation and correction of the underlying cause, when identified.

VENOUS ULCERS

Chronic venous disease is a common problem in adults, with its prevalence increasing with age. Due in large part to a lack of standardized diagnostic criteria, the prevalence varies considerably, from <1% to 17% in men and from <1% to 40% in women[2].

Risk factors for chronic venous disease include family history, age, female sex, obesity, pregnancy, prolonged standing, and height[3]. Venous hypertension and venous insufficiency represent the most common cause of chronic leg ulcerations. Venous ulcers tend to recur, are sometimes painful, and clearly have an impact on quality of life[4]. Because of their prevalence and chronicity, there are significant healthcare costs, estimated to be ~$3 billion per year in the US[3].

Pathogenesis

The venous system of the lower extremities consists of an interconnected network of superficial veins, deep veins, and perforator or communicating veins which connect the superficial and deep systems[5] (see Ch. 155). Throughout the superficial, communicating and deep veins, one-way bicuspid valves ensure unidirectional flow toward the deep system, thus allowing blood to flow in a cephalad direction and preventing reflux (Fig. 105.2A). It is primarily the contraction of calf muscles that drives blood from the leg toward the heart[4].

During standing, as leg muscles relax, venous pressure in the legs may reach up to 80 to 90 mmHg[3]. Calf muscle contractions, e.g. when walking, transiently increase pressure within the deep leg veins, propelling blood towards the heart. When pressure rises within the deep system, the valves close, preventing retrograde flow and transmission of high pressure to the superficial system[4]. When the deep system empties, the deep vein pressure abruptly falls to <30 mmHg and the valves open, enabling flow from the superficial into the deep system[3,4].

In the absence of competent valves, however, the decrease in venous pressure with leg movements is attenuated, and high pressures generated in the deep veins by calf muscle contraction are transmitted to the superficial venous system and to the microcirculation within the skin[3]. A sustained elevation in venous pressure is responsible for the typical clinical picture seen in chronic venous disease and is termed *venous hypertension* or *venous insufficiency*.

In most patients, venous hypertension is caused by reflux through incompetent valves (Fig. 105.2B), whether primary (congenital) or secondary to deep vein thromboses or recurrent trauma. Additional causes of venous hypertension include venous outflow obstruction and failure of the calf muscle pump due to obesity or leg immobility[3].

Although venous hypertension appears to be central to the skin changes seen in chronic venous disease, the exact pathogenic cascade from valvular incompetence to frank ulceration remains obscure. A few pathomechanisms have been suggested, but it is still unclear whether they represent causative factors or epiphenomena[6]. One proposal was that cuffs of fibrin around dermal capillaries (due to leakage of fibrinogen) could impede the diffusion of oxygen and nutrients to

COMPARISON OF CLINICAL FINDINGS IN THE THREE MAJOR TYPES OF LEG ULCERS			
	Venous	**Arterial**	**Neuropathic/mal perforans***
Location	Medial malleolar region	Pressure sites Distal points (toes)	Pressure sites
Morphology	Usually shallow Irregular borders Yellow fibrinous base	Dry, necrotic base Well-demarcated ("punched out")	"Punched out"
Surrounding skin	Yellow–brown to brown discoloration due to hemosiderin deposits Pinpoint petechiae ("stasis purpura") Lipodermatosclerosis	Shiny atrophic skin with hair loss	Thick callus
Other physical examination findings	Varicosities Leg/ankle edema Acroangiodermatitis ± Stasis dermatitis ± Lymphedema	Weak/absent peripheral pulses Cool feet Prolonged capillary refill time (>3–4 seconds) Pallor on leg elevation (45° for 1 min) Dependent rubor	Peripheral neuropathy with decreased sensation ± Foot deformities

*Most commonly due to diabetes mellitus.

Table 105.1 Comparison of clinical findings in the three major types of leg ulcers. *Adapted from Phillips TJ, Dover JS. Leg ulcers. J Am Acad Dermatol 1991;25:965–87.*

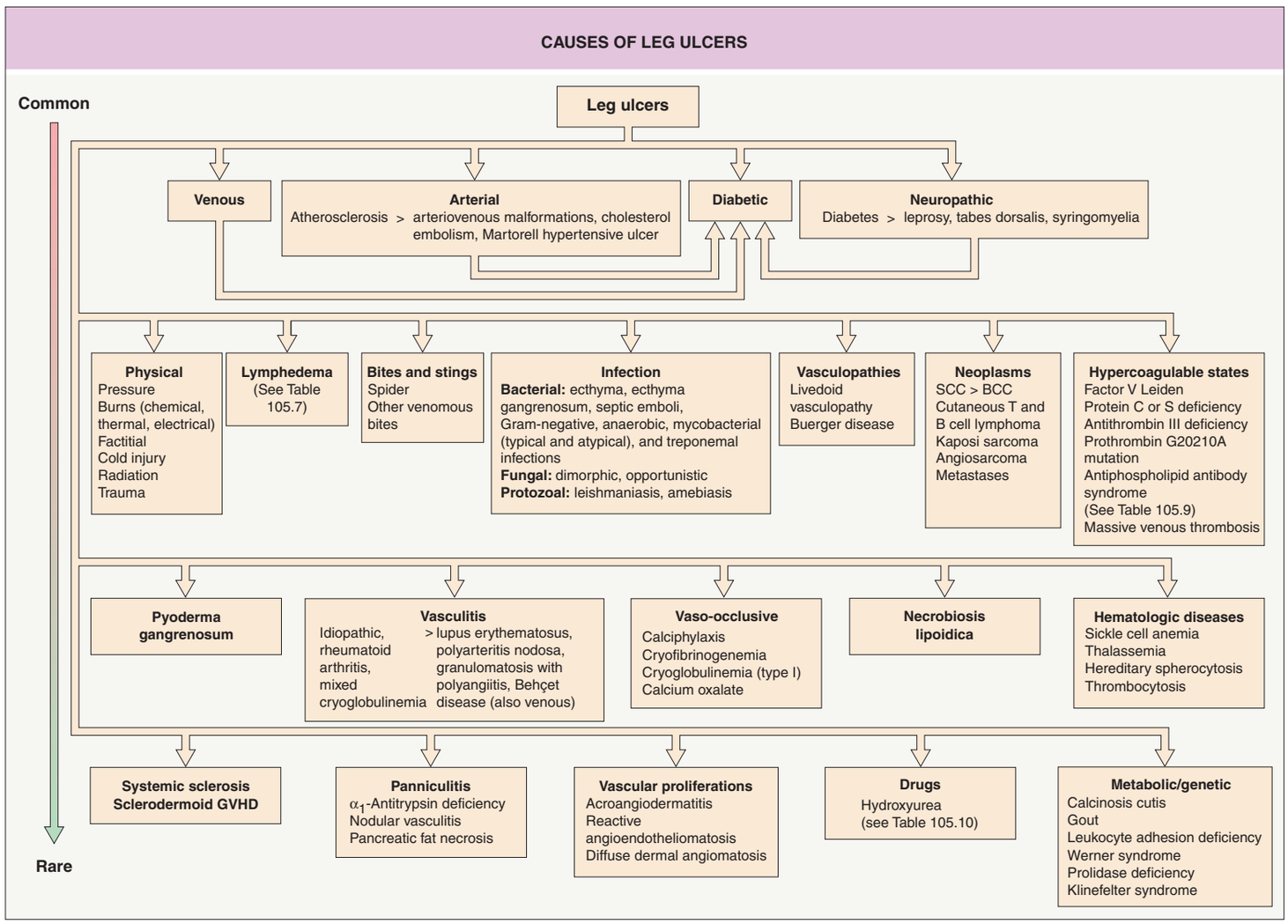


Fig. 105.1 Causes of leg ulcers. Patients with Behçet disease develop lower extremity ulcers due to vasculitis and/or venous insufficiency related to deep vein thromboses, and, occasionally, erosive pustular dermatosis is a cause of leg ulcers. Hydroxyurea-induced leg ulcers are often on the malleolus or tibial crest, exceedingly painful, and surrounded by atrophic skin. Additional genetic syndromes associated with ulceration are listed in Table 105.10. GVHD, graft-versus-host disease.

surrounding tissues and lead to degenerative skin changes[7]. Other investigators suggested that venous pooling induced inter-endothelial space widening and deposition of fibrin and other macromolecules that then "trapped" growth factors, rendering them unavailable for wound repair[8].

Nowadays, however, the predominant theory is that chronic inflammation plays a key role in chronic venous ulcers (Fig. 105.3)[3]. With elevated venous pressure, shear stress on the endothelial wall is altered, leading to glycocalyx disruption and endothelial cell activation. As a result, there is release of vasoactive mediators, proinflammatory

molecules (e.g. chemokines), and prothrombotic precursor proteins. Increased expression of adhesion molecules such as ICAM-1, VCAM-1, and platelet-endothelial leukocyte adhesion molecule-1 (PECAM-1) on endothelial cells leads to leukocyte recruitment followed by diapedesis into the dermis (see Fig. 102.11). This inflammatory response then leads to further venous wall damage[9].

Increased expression and activity of matrix metalloproteinases (MMPs) also contribute to the breakdown of the extracellular matrix, which promotes the formation of ulcers and impairs healing. Elevated levels of cytokines such as transforming growth factor-beta (TGF-β) and vascular endothelial growth factor (VEGF) translate into increased dermal fibrosis and proliferation of dermal capillaries, respectively (see Fig. 141.3). Capillary hyperpermeability and extravasation of red blood cells lead to deposition of ferric iron within affected skin, resulting in brown discoloration.

While the persistent inflammatory response gives rise to ulcer formation (see above), continued production of MMPs and cytokines (e.g. interleukin-1, tumor necrosis factor [TNF]) leads to impaired fibroblast function and increased degradation of growth factors necessary for wound healing. In addition, oxidative stress-induced premature aging and dysfunction of wound fibroblasts contribute to the chronicity of venous ulcers[10,11].

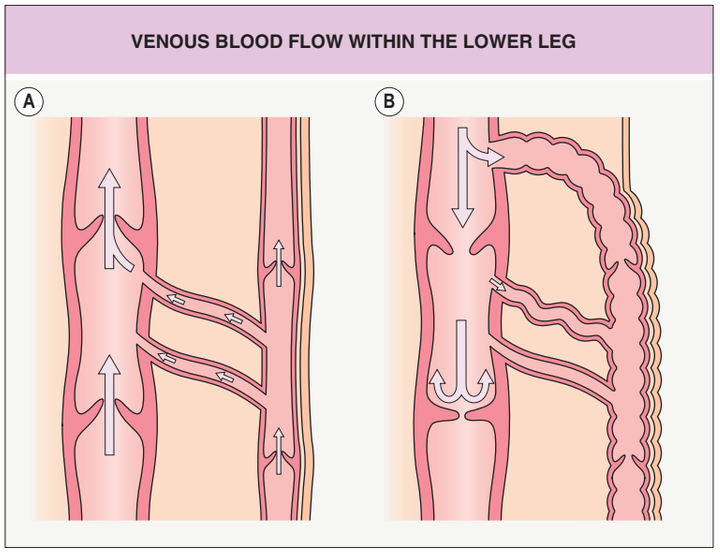


Fig. 105.2 Venous blood flow within the lower leg. A Under normal circumstances, blood is pumped against gravity towards the heart by the calf muscles. Blood flows from the superficial veins to the deep venous system via the perforating veins. Bicuspid valves ensure the unidirectionality of the blood flow. **B** When the valves are incompetent and/or hydrostatic pressure is elevated, blood flows back into the superficial venous system, leading to the formation of varicose veins.

Clinical Features

Chronic venous disease is associated with a wide spectrum of clinical findings, ranging from uncomplicated telangiectasias and varicose veins to lipodermatosclerosis and large chronic ulcerations[5]. Patients with venous ulcers often complain of swelling and aching of the legs, typically worsened by dependency and prolonged standing but improved by leg elevation, use of gradient support stockings or walking, all of which decrease venous pressure. Additional symptoms sometimes ascribed to chronic venous disease include muscle cramps, pruritus, and restless legs[4,5].

Most commonly, venous ulcers are located above the medial malleolus (Fig. 105.4). The ulcer is usually shallow with a border that is typically irregular; the wound bed is often covered by a yellow, fibrinous exudate. If the latter is appropriately debrided, a base of healthy, non-ischemic granulation tissue is usually seen. When untreated, venous ulcers tend

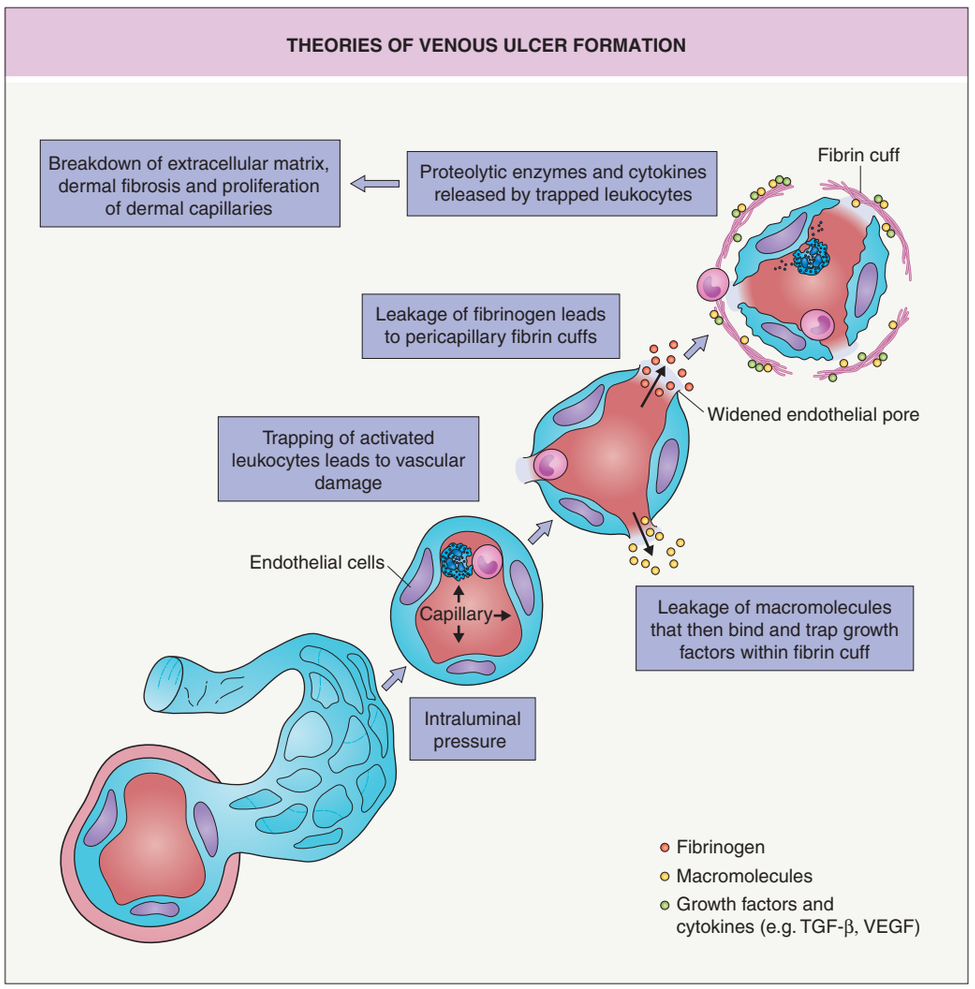


Fig. 105.3 Theories of venous ulcer formation. The theories include the presence of pericapillary cuffs due to leakage of fibrinogen, binding of growth factors by leaked molecules, and the trapping of leukocytes, with subsequent chronic inflammation, dermal changes, and ulcer formation. TGF, transforming growth factor; VEGF, vascular endothelial growth factor.



Fig. 105.4 Venous ulcer and stasis dermatitis. Note the erythema, crusting, and scaling of the skin surrounding the ulcer of the medial malleolus. There is a yellowish fibrinous exudate and granulation tissue is seen in 15%–20% of the ulcer bed. In a chronic ulcer, the thickened rolled border is referred to as epibole.

to become larger than most other chronic wounds and can even become circumferential on the lower extremity[4]. Pedal pulses are usually palpable. If they are not palpable because of induration or edema, an ankle–brachial index (see below) should be obtained to exclude concomitant peripheral artery disease[5].

Characteristic associated features include (Fig. 105.5): (1) varicose veins of varying severity (see Ch. 155); (2) pinpoint petechiae superimposed on a yellow–brown discoloration due to extravasation of red blood cells and deposition of hemosiderin within macrophages (see Fig. 22.7), which is sometimes accompanied by hyperpigmentation; (3) edema; and (4) stasis dermatitis with pruritus, erythema, scaling, and weeping (see Ch. 13). Of note, stasis dermatitis is sometimes aggravated by allergic contact dermatitis to topically applied medications, e.g. neomycin. The smooth, ivory-white, sclerotic plaques of atrophie blanche that are often surrounded by punctate telangiectasias and/or brown discoloration are observed in up to 40% of patients with chronic venous insufficiency[12].

Patients with longstanding venous hypertension and insufficiency may develop chronic lipodermatosclerosis (also known as sclerosing panniculitis) with induration and fibrosis that begins on the lower medial aspect of the leg above the malleolus (see Fig. 105.5C, D). Eventually, the entire lower third of the leg may become involved, leading to an appearance that has been likened to an "inverted champagne bottle". Some authors believe the degree of lipodermatosclerosis correlates with delayed wound healing. Chronic lipodermatosclerosis may be preceded or accompanied by an acute inflammatory stage characterized by warm, erythematous, firm plaques that are tender and painful and are often misdiagnosed as cellulitis or another type of panniculitis, especially erythema nodosum[4].

Lipodermatosclerosis, along with ulcerations, is not limited to the lower extremities, as these changes can be seen in other sites such as the most dependent portion of the pannus (Fig. 105.6).

Laboratory Evaluation

Standardized evaluation of patients with chronic venous disease is based on the CEAP classification system which generates scores derived from objective clinical signs (C), etiology (E), anatomic (A) location of the affected veins, and pathophysiology (P) (reflux, obstruction, or both)[13]. Table 155.1 outlines the details of the CEAP classification system.

Color duplex ultrasonography, preferably performed with the patient in a standing position, is useful for assessing both reflux and obstruction within the deep, superficial, and perforating veins, from the inferior vena cava to the calf veins[14]. It provides information that is necessary when determining the CEAP score. For most indications, color duplex ultrasonography has replaced venography. The latter is an invasive test that can provide a detailed view of the venous system in preparation for reconstructive surgery and stenting procedures.

Pathology

In the skin surrounding the ulceration, nonspecific features are seen including reactive epithelial hyperplasia, dermal fibrosis, and an inflammatory infiltrate, along with a proliferation of capillaries, extravasation of red blood cells, and deposits of hemosiderin within macrophages. Biopsies are occasionally performed to exclude a neoplastic, vasculitic, vasculopathic, or infectious process.

Differential Diagnosis

A significant number of patients may have a combination of venous and arterial insufficiency, so before treatments such as compression stockings are prescribed, the latter should be excluded (see below). In patients with livedoid vasculopathy (Fig. 105.7) or recurrent deep vein thromboses, the possibility of thrombophilia (hypercoagulability) as a contributing factor needs to be considered (see Table 105.9 & Ch. 23). Additional clues from the history, e.g. rate of expansion, and physical examination aid in narrowing the differential diagnosis (Table 105.2). Histologic examination of a longstanding or recalcitrant ulcer is recommended to exclude other diagnoses, such as squamous cell carcinoma[12] or atypical mycobacterial infection (see Fig. 105.1), and the biopsy specimen should include surrounding non-ulcerated skin.

Treatment

Most of the therapeutic principles described in the following sections can be applied to the care of other types of cutaneous ulcers, unless otherwise specified. In general, normal wound healing requires adequate perfusion, good nutritional and immune status, and avoidance of deleterious mechanical forces[15]. The initial step in the approach to an ulcer should be to address all systemic and local factors that may impair healing.

Moisture and occlusion

In the past, the mainstay of wound management was to dry the wound bed with absorptive gauzes. A major breakthrough in the management of chronic wounds was the realization that a moist environment is critical for wound healing and occlusive dressings do not increase the risk of infection[16]. Moist retentive wound dressings stimulate collagen synthesis, promote angiogenesis by creating a hypoxic environment, encourage re-epithelialization, and decrease pain. By serving as a barrier against external contamination and by lowering wound pH, occlusive dressings actually decrease wound infection rates[15].

Dressings should be changed based on their potential for absorbency and the amount of exudate, with attention to the delicate balance between overhydration and excessive dryness. For example, occlusive dressings applied to highly exudative wounds may cause maceration and erosion of the surrounding skin, possibly leading to further deterioration of the wound. In addition, chronic wound fluid can perpetuate cytokine and MMP production (see above), thereby affecting the function of fibroblasts and growth factors and contributing to chronicity. It is therefore important to protect the skin surrounding the wound bed with an ointment in order to preserve barrier integrity[15].

Debridement

Debridement consists of the removal of necrotic, non-viable, or infected tissue from the wound bed in order to promote healing. In a sense, debridement is an attempt to shift the wound from a chronic state (with a milieu characterized by an abnormal extracellular matrix, an excess of proteolytic enzymes, and senescent cells) into an acute state. Debridement can be surgical (sharp debridement), mechanical (wet-to-dry), autolytic, chemical (enzymatic), and biologic (maggot therapy)[17].

Sharp debridement with surgical instruments represents the most rapid method for debriding a wound and is most appropriate for large necrotic and/or infected wounds. It also enables the clinician to estimate the extent and severity of a wound. Although damage to viable tissue is possible, sharp debridement performed by a skilled physician is usually highly selective[17]. Caution is advised in the case of arterial



Fig. 105.5 Associated findings in patients with venous hypertension and venous insufficiency. **A** Venulectasias of the instep referred to as corona phlebectasia. **B** Brown discoloration of the foot and ankle due to hemosiderin deposits within dermal macrophages in addition to hyperpigmentation. Note the cut-off at Wallace's line. **C** Lipodermatosclerosis with violet–brown discoloration, tenderness, and induration that typically begins above the medial malleolus. **D** Stasis dermatitis and chronic lipodermatosclerosis with serous crusts and the "inverted champagne bottle" or "bowling pin" configuration. **E** Acroangiodermatitis (pseudo-Kaposi sarcoma). Violaceous plaque in a patient with venous hypertension. Histologically, these lesions can resemble Kaposi sarcoma. *A, B, Courtesy Jean L. Bolognia, MD; C, Courtesy Kalman Watsky, MD.*

ulcers because of the potential risk for tissue desiccation and ulcer enlargement[15]. Sharp debridement may be associated with bleeding and pain and may necessitate analgesia.

Wet-to-dry (mechanical) debridement consists of placing gauze moistened with saline over the wound, allowing the gauze to dry, and then removing the dry gauze along with adherent non-viable tissue. It is relatively fast and easy to perform but is painful and does not discriminate between viable and non-viable tissue. It is indicated for wounds with large amounts of necrotic tissue.

Autolytic debridement is the process by which the body uses its own proteolytic enzymes and phagocytic cells to clear necrotic debris. The process is enhanced by moist retentive wound dressings and may require weeks to accomplish. Autolytic debridement is selective, painless, and suited primarily for wounds with minimal debris. It is contraindicated if the wound is infected[17].

Enzymatic (chemical) debridement utilizes topically applied proteolytic enzyme preparations such as papain–urea or collagenase to digest necrotic tissue, collagen, fibrin, and wound exudate. Chemical debridement is a gradual process. The papain–urea preparation contains papain, which is derived from the plant *Carica papaya* and is a non-selective cysteine protease. It is active over a broad pH range and is associated with an intense inflammatory response and digestion of viable tissue; local pain or a burning sensation is often described. Therefore, the product should be applied only to the wound bed and not to the surrounding intact skin. Collagenase preparations are derived from *Clostridium histolyticum*; they specifically target native collagen and are active within a narrow pH range of 6 to 8. These preparations are highly selective and do not harm viable cells[16]. Prior to application, it is advisable to cross-hatch the eschar, if present, in order to increase penetration[15].



Fig. 105.6 Lipodermatosclerosis, chronic ulceration and lymphedema of the dependent portion of the pannus. The changes are similar to those seen on the distal lower extremities. *Courtesy Jean L. Bolognia, MD.*

POINTS TO INCLUDE IN THE HISTORY AND PHYSICAL EXAMINATION OF PATIENTS WITH A LEG ULCER	
History	**Physical examination**

• Onset and clinical course of ulcer
• Symptoms, including those of vascular disease or neuropathy
• Alleviating factors
• Exacerbating factors
• Past medical history, e.g. diabetes mellitus, ASCVD, autoimmune CTD
• Family history
• Medications, topical and systemic
• Personal habits (e.g. smoking, alcohol intake)
• Nutritional status
	General, emphasizing the following:
	• Ulcer characteristics
	  • Location and size
	  • Morphology, including depth, shape, border, and base
	  • Type and amount of exudate
	  • Surrounding skin, e.g. edema, dermatitis, fibrosis, cellulitis, necrosis
	• Peripheral pulses
	• Capillary refill time
	• Evidence of peripheral neuropathy
	• Deep tendon reflexes

Table 105.2 Points to include in the history and physical examination of patients with a leg ulcer. ASCVD, atherosclerotic cardiovascular disease; CTD, connective tissue disease. *Courtesy Tania Phillips, MD.*





Fig. 105.7 Livedoid vasculopathy. A Multiple hemorrhagic crusts and small, very painful ulcers associated with brown discoloration due to hemosiderin deposits. **B** Stellate, porcelain-white atrophic scars with peripheral telangiectatic papules, referred to as atrophie blanche. *B, Courtesy Julie V. Schaffer, MD.*

For therapy-resistant, chronic ulcers with marked necrosis and slough, *maggot debridement* therapy can be considered. Essentially, it exploits the ability of maggots to decompose necrotic tissue (benign myasis), but the debridement is done in a controlled manner so as to avoid undesirable effects on healthy tissues[18]. Degradation via proteinases that are in larval excretory/secretory products is thought to contribute to wound debridement[19]. It is important to select larval strains that feed preferentially on necrotic tissue and to avoid applying too many larvae to a wound. The flies most often employed are facultative calliphorids, in particular the green bottle blowfly, *Lucilia sericata*[18].

Maggots are used to treat various types of chronic ulcers, including pressure ulcers, venous ulcers, and neurovascular diabetic ulcers, as well as traumatic and postsurgical wounds. In a multicenter, randomized, open study that compared the clinical effectiveness of larval therapy to a standard debridement technique (hydrogel) for "sloughy" or necrotic leg ulcers, larval therapy did not improve the rate of healing or reduce bacterial load, but it did significantly reduce the time to debridement and increase ulcer pain[20].

Novel approaches to wound debridement are currently under investigation, including both hydrosurgery and ultrasound- and radiofrequency-based techniques[21].

Wound dressings

The ideal wound dressing should: (1) provide a moist retentive environment; (2) absorb excess exudate without causing maceration of surrounding skin; (3) protect against bacteria; (4) leave no residual debris but cause no trauma when removed; (5) decrease odor; and (6) relieve pain. In addition, the ideal wound dressing should be cost-effective, easy to handle, and be neither irritating nor allergenic. While there is no single dressing that can fulfill all these criteria throughout the entire healing process, a vast array of dressings exists, and the choice of a dressing depends upon the wound type and its characteristics at a given time (Table 105.3)[15,16].

Management of wound infection

The presence of a microbial infection is always detrimental to wound healing. However, all chronic open wounds are colonized with bacteria and it is important, although often difficult, to distinguish true infection from bacterial colonization. Of note, colonization is defined by the presence of replicating bacteria and adherent microorganisms, but without evidence of tissue damage.

Critical colonization is a relatively new concept in which the bacterial burden within a chronic wound does not elicit the typical symptoms or signs of an infection but does delay healing. The presence of $>10^6$ colony-forming units of bacteria/gram of tissue predicts delayed wound healing and a high risk for developing an infection[16]. More recent studies have demonstrated that in many chronic wounds, bacteria persist in the form of biofilms. The latter represent communities of bacteria, protected by an adhesive polymeric matrix cover, that communicate with each other

TYPES OF WOUND DRESSINGS			
Dressing type	**Properties**	**Disadvantages**	**Indications**

Gauzes	• Good absorption
	• Can be impregnated with:
	  • NaCl to become highly absorbent, discourage bacterial overgrowth, and prevent formation of excess granulation tissue
	  • petrolatum so less drying and adherent, but then less absorbent
	  • iodine or silver as an antiseptic
		• Adhere to wound bed and promote desiccation
		• Can cause pain and trauma, including removal of epithelium, upon removal
			• Wet wounds with heavy exudate
			• May serve as a secondary dressing

Films	• Semi-occlusive, thin polyurethane membranes • Maintain moisture • Permeable only to vapors, not to liquids • Transparency enables wound visualization	• Non-absorbent • Can cause maceration if applied to wounds with heavy exudate	• Wounds with minimal exudate • As a secondary dressing
Hydrogels	• Maintain a moist environment • Promote autolytic debridement • Non-adhesive • Relieve pain	• Can lead to maceration of skin surrounding wound if used in exudative wounds	• Dry wound • Wound with minimal exudate
Hydrocolloids	• Adhesive, occlusive dressings that absorb exudates with the formation of hydrophilic gel • Provide a moist environment	• Not suitable for wounds with heavy exudate or infected wounds • May produce a brown, malodorous exudate • May be traumatic on removal • Excess granulation tissue with prolonged use	• Wounds with a mild to moderate exudate
Alginates	• Fibrous dressings derived from brown seaweed • Highly absorbent and require moisture to function • Ion exchange between calcium in the alginate and sodium in the wound fluid leads to the formation of a moist retentive gel • Hemostatic	• May adhere to dry wounds • May leave fibrous debris in the wound • Can lead to maceration around the wound unless cut to the size of the wound bed	• Wounds with a moderate to heavy exudate • Undermined or tunneling wounds
Foams (polyurethane)	• Good absorbance capacity • Non-traumatic upon removal • Provide thermal and shear protection	• May produce malodorous drainage • Maceration around wound possible	• Wounds with a moderate to heavy exudate
Collagens	• Collagen matrix that physically entraps MMPs and facilitates growth factor activity	• Nonspecific inhibition of MMPs	• Clean, non-infected, recalcitrant chronic wounds

Table 105.3 Types of wound dressings. For additional details, see Chapter 145. MMPs, matrix metalloproteinases.

via water channels. Through these communication channels, bacteria are able to regulate the transcription of genes and protein products in a manner that is beneficial to them, but which can delay healing (quorum sensing)[16]. Biofilms are particularly resistant to antimicrobial therapy.

Wounds become clinically infected when host defenses are overwhelmed. Signs and symptoms of infection include an increased exudate, purulent discharge, pain, and surrounding erythema and swelling. However, sometimes an increase in ulcer size and malodorous or friable granulation tissue are the only clues to the presence of an active infection within a chronic wound. Systemic signs of infection such as fever, chills, tachycardia, and leukocytosis may suggest that the infection has progressed to a bacteremia or septicemia, although the former may be subtle in elderly patients, necessitating a high index of suspicion.

Most chronic wounds have a polymicrobial flora. Bacterial cultures usually grow aerobic Gram-positive cocci, which are often mixed with Gram-negative bacilli and sometimes anaerobes[22]. Clinically infected wounds should be cultured and treated initially with broad-spectrum systemic antibiotics. The antibiotic regimen is then adjusted based on the results of sensitivity testing.

In properly treated, non-healing wounds that demonstrate critical colonization, topical antimicrobials should be considered. Topical antimicrobial agents are divided into two major categories: antiseptics and antibiotics. Antiseptics have a broad antimicrobial spectrum as well as multiple microbial targets, but they are often toxic to host tissues. Topical antibiotics have specific cellular targets and a narrower spectrum of activity; they are not toxic to human cells but are more likely to induce bacterial resistance. Commonly used *topical antibiotics* include bacitracin, neomycin, mupirocin, retapamulin, ozenoxacin, gentamicin, and fusidic acid. However, topical antibiotics can cause allergic contact dermatitis, in particular neomycin and bacitracin. It is also preferable to avoid topical antimicrobials that have a systemic counterpart[22].

Commonly used *antiseptics* include hydrogen peroxide, chlorhexidine, iodine-based preparations (e.g. povidone-iodine, cadexomer iodine), and silver-releasing agents. Hydrogen peroxide and povidone-iodine have a broad antimicrobial spectrum with minimal resistance but may be cytotoxic. Cadexomer iodine is a complex of 0.9% elemental iodine plus cadexomer microbeads which are composed of a modified starch-based polymer. Upon absorption of exudate, the cadexomer beads swell and slowly release iodine into the wound bed, thus maintaining non-toxic iodine concentrations[23].

Silver is an effective antiseptic agent with broad-spectrum activity, including against methicillin-resistant *Staphylococcus aureus* (MRSA), vancomycin-resistant enterococci (VRE), and extended-spectrum β-lactamase producers. Resistance has rarely been reported, primarily with Gram-negative species[22]. Only the ionized form of silver (Ag^+) has antimicrobial properties, so exposure to wound fluid or exudate is required if the source is metallic silver[24]. Silver ions kill bacteria by damaging bacterial cell walls and intracellular and nuclear membranes as well as denaturing bacterial DNA, RNA, and key enzymes (e.g. respiratory enzymes)[15,24]. Silver may also promote cellular proliferation and re-epithelialization by inducing the production of metallothionein by epidermal cells. Metallothionein increases zinc- and copper-dependent enzymes required for cellular proliferation and matrix remodeling[24]. Silver has been incorporated into various dressing products (e.g. gauzes, hydrocolloids, alginates, foams) in addition to creams, gels, and barrier protectants which differ in their solubility and the rate at which silver ions are released into the wound bed[15]. Disadvantages of silver products include potential irritation, permanent blue–gray discoloration (localized argyria), and cost. Topical silver sulfadiazine has induced neutropenia in children which was reversible once the cream was discontinued[16].

Lastly, as chronic wounds may serve as a portal of entry for *Clostridium tetani*, it is recommended that the tetanus immune status of patients with chronic leg ulcers be assessed[25].

Adjuncts to wound care

Compression

Compression therapy is a mainstay in the treatment of venous insufficiency. Compression stockings improve venous return, reduce edema, stimulate healthier granulation tissue within venous ulcers[15], and improve quality of life[15]. A Cochrane meta-analysis of 39 randomized controlled trials concluded that compression therapy increased ulcer healing rates when compared to no compression[26].

Elastic stockings, preferably with graduated compression, are available in a wide range of compressive pressures (15 to 60 mmHg), lengths, and materials (Table 105.4). Lower levels of compression (20 to 30 mmHg) are sufficient for preventing mild edema, whereas higher levels of compression (30 to 40 mmHg) are required to control stasis dermatitis or lead to the healing of ulcers. Compression stockings also prevent the recurrence of venous ulcers once healed. Therefore, lifelong use of compression is recommended for patients with a history of venous ulcers[5]. In addition to stockings, there are other forms of compression such as bandages and wraps, as outlined in Tables 105.5 and 105.6. Of note, early endovascular ablation of superficial venous reflux as an adjunct to compression therapy led to faster healing of venous ulcers than compression therapy alone[27].

It is important to remember that compression therapy in patients with undiagnosed arterial insufficiency can lead to ulcer worsening, gangrene, or even limb amputation. As many patients with venous disease have concomitant arterial insufficiency, clinically significant arterial disease must be excluded before prescribing compression therapy. The latter is also relatively contraindicated in patients with uncompensated congestive heart failure[15].

Manual lymph drainage

Edema is a significant cause of delayed healing of venous ulcers. Identifying the cause of the edema is instrumental in choosing the appropriate therapy, which in turn is critical for ulcer resolution. However, even with identification and treatment of contributing factors (e.g. afterload reduction, diuretics), edema may be persistent.

Manual lymph drainage is a massage technique in which lymph conduits are contracted more frequently and lymphatic fluid is moved away from affected lymphedematous regions toward more centrally located, functioning lymph basins, thereby reducing edema volume. This manual drainage is employed during the early, intensive phase of lymphedema therapy and is combined with short-stretch compression bandaging applied immediately after treatment. The regimen also includes a series of exercises to increase lymphatic flow through functioning collateral pathways, skin care, and sometimes the use of intermittent pneumatic compression. This intensive, short-term

CLASSES OF COMPRESSION STOCKINGS		
Class	**Pressure at the ankle**	**Indication**
I	20–30 mmHg	Simple varicose veins
		Mild edema
		Leg fatigue
II	30–40 mmHg	Moderate edema
		Severe varicosities
		Moderate venous insufficiency
III	40–50 mmHg	Severe edema
		Severe venous insufficiency
		Post-thrombotic lymphedema
IV	50–60 mmHg	Elephantiasis

Table 105.4 Classes of compression stockings. *Adapted from Phillips TJ. Current approaches to venous ulcers and compression. Dermatol Surg 2001;27:611–21.*

TYPES OF COMPRESSION THERAPY		
Bandage	**Advantages**	**Disadvantages**
Elastic wraps (e.g. ACE™ bandage)	Inexpensive Can be reused	Often applied incorrectly by the patient Tend to unravel Do not maintain sustained compression Lose elasticity after washing
Self-adherent wraps (e.g. Coban™)	Self-adherent Maintain compression	Expensive Cannot be reused
Unna boot	Comfortable Protects against trauma Full maintenance of ambulatory outpatient status Minimal interference with regular activities Substitutes for a failing pump	Pressure changes over time Needs to be applied by well-trained physicians and nurses Does not accommodate highly exudative wounds
Four-layer bandage	Comfortable Can be left in place for 7 days Protects against trauma Maintains a constant pressure for 7 days because of the overlap and elasticity of the bandages Useful for highly exudative wounds	Needs to be applied by well-trained physicians and nurses Expensive
Graduated compression stockings	Reduce the ambulatory venous pressure Increase venous refilling time Improve calf pump function Different types of stockings accommodate different types of leg disorders Dressings underneath can be changed frequently	Often cannot monitor patient compliance Difficult to put on, unless have zipper or Velcro® straps
Orthotic device	Adjustable compression Sustained pressure Easily put on and removed Comfortable	Expensive Bulky appearance
Compression pump	Augments venous return Improves hemodynamics and microvascular functions Enhances fibrinolytic activity Prevents postoperative thromboembolic complications in high-risk patients	Expensive Requires immobility for a few hours per day

Table 105.5 Types of compression therapy. *Adapted from Choucair M, Phillips TJ. Compression therapy. Dermatol Surg 1998;24:141–8.*

CLASSES OF COMPRESSION BANDAGES	
Class	**Properties**
Class I	Lightweight and conforming
	Stretch and simple dressing retention properties
Class II	Also known as short stretch bandages
	Act like rigid, non-elastic bandages
	Used for light support
Class III	
• Class IIIA	Light compression bandages
• Class IIIB	Moderate compression bandages
• Class IIIC	Extra-high performance
	Achieve 40 mmHg at the ankle
	Useful for severe varicosities, severe edema, post-phlebitic syndrome

Table 105.6 Classes of compression bandages.

therapy is referred to as "complete decongestive physiotherapy" and is followed by a maintenance phase that consists of skin care, elastic compression, and exercise[28,29].

Topical negative pressure wound therapy

In topical negative pressure therapy, ideally performed using a vacuum-assisted closure (VAC) system, negative pressure is applied to hasten wound healing. It is used primarily for ulcers that are due to venous disease or diabetes. The system includes an open pore foam conduit (cut to the wound size) sealed with a semi-occlusive drape which is then attached to a vacuum source via a tube (see Fig. 145.13). When subatmospheric pressure (100–125 mmHg) is applied to the foam–wound interface (continuously or intermittently), accumulated fluid is transferred to a canister. Topical negative pressure therapy promotes wound healing by creating mechanical forces that stimulate a biological response while maintaining a moist environment. It also removes exudate, reduces edema, increases local perfusion, decreases the bacterial count, and enhances granulation tissue formation[15,30].

Before application, the wound must be debrided of necrotic tissue in order to prevent infection. Topical negative pressure therapy is contraindicated for ischemic wounds and ulcerated malignancies because it may cause necrosis of the wound edges and tumor growth, respectively. The foam should be changed every 48 to 72 hours. Sometimes, new granulation tissue grows into the foam, which can result in pain during foam changing. If this occurs, then the foam should be changed more frequently or a denser foam employed. In up to 25% of patients, there are complications such as pain, odor, periwound irritation or maceration, infection, bleeding, and necrosis; most of these problems can be avoided with careful patient selection and skilled management[30,31].

Skin substitutes

Patients with recalcitrant chronic ulcers can sometimes benefit from autologous skin grafting, especially when the ulcers are due to venous disease (see Ch. 148). However, there has been an increase in the use of biologic dressings and synthetic skin substitutes in such patients. Living skin substitutes are tissue-engineered products that contain a cellular component of autologous or allogeneic origin plus a biodegradable scaffold, and they serve as a replacement for the epidermis, dermis or both. These skin mimetics provide temporary wound coverage, serving primarily as a source for growth factors and extracellular matrix. Although effective in wound repair, their clinical use is still limited due to their high cost and complex technology (see Ch. 145)[32]. In general, these living skin substitutes are indicated for venous and diabetic ulcers.

There are also biologic dressings that consist of just an extracellular matrix (i.e. they have no cellular component). Structural extracellular matrix components, such as collagen, fibronectin, and proteoglycans, provide a temporary scaffold that supports cellular proliferation and migration. In addition, they contain cytokines, e.g. TGF-β, bFGF, which promote wound healing. These dressings are also used for diabetic and venous ulcers.

Another approach is a bio-inspired artificial hydrogel matrix that utilizes natural enzymatic reactions to become bioactive. It is able to incorporate and then deliver biomolecules (e.g. MMPs, growth factors) and at the same time be degraded and remodeled by them, ultimately being replaced by newly formed tissue. Emerging therapies include application of bone marrow-derived mesenchymal cells, mesenchymal stem cell-derived extracellular vesicles, and spraying of autologous fibroblasts and keratinocytes onto the wound[33,34].

Topical and oral medications

Daily, short-contact application of topical tretinoin solution (0.05%; currently requires compounding) was reported to stimulate granulation tissue formation and healing of chronic leg ulcers[35]. Application of small amounts of 0.025% tretinoin cream was also observed to induce neovascularization in ischemic wound beds[15]. Daily application of 0.5% timolol maleate solution (one drop per 2 cm of wound perimeter) can also improve healing of chronic diabetic and venous leg ulcers via promotion of keratinocyte migration[36]. Topical growth factors, in particular PDGF, have been utilized to enhance wound healing (see below).

Pentoxifylline, a drug that targets inflammatory cytokine release, leukocyte activation and platelet aggregation at the microcirculatory level, is occasionally a component of the treatment regimen for chronic venous insufficiency. Although evidence of a beneficial effect when the drug is used as monotherapy is largely lacking, pentoxifylline has been shown (at a dose of 1200 mg/day), in conjunction with compression therapy, to modestly improve ulcer healing as compared to compression plus placebo[37]. This effect has been attributed to the drug's fibrinolytic properties, antithrombotic effects, and/or ability to inhibit the production of proinflammatory cytokines.

The use of veno-active drugs, especially flavonoids such as micronized purified flavonoid fraction (MPFF), either alone or in combination with compression, may lead to improved healing of venous ulcers and a reduction in edema[38]. The proposed mechanism is inhibition of leukocyte trapping and as a consequence, a decrease in the release of proinflammatory molecules that damage the endothelium and increase capillary permeability.

Ulcers secondary to livedoid vasculopathy may benefit from antiplatelet and anticoagulant agents including aspirin, direct oral anticoagulants (DOACs), and low-molecular-weight heparin, as well as fibrinolytics, vasodilators, and immunosuppressants or immunomodulators (e.g. IVIg) (see Ch. 23).

Figure 105.8 outlines an approach to the patient with a presumed venous ulcer.

LYMPHEDEMA

Lymphedema is the accumulation of lymph fluid within the interstitium that is due to a reduction in lymph drainage in the presence of *normal* capillary filtration. Lymphedema should be differentiated from edema which results from an imbalance between capillary filtration and lymph drainage.

Lymphedema can be primary or secondary (Table 105.7). **Primary** lymphedema can be further subdivided based on age at time of clinical presentation, but because the time of onset may vary, even within the same family, genetic bases when known are currently used for classification[39]. *Congenital lymphedema* usually appears before 1 year of age and is sporadic or familial (e.g. lymphatic malformation 1 [Milroy disease]; Fig. 105.9). Meige disease (lymphatic malformation 5), classically a type of *lymphedema praecox*, is the most common form of primary lymphedema and it usually presents around puberty and more often affects girls. *Lymphedema tarda* usually presents after 35 years of age and is probably the result of an environmental trigger such as trauma or infection superimposed on inherently weakened lymphatics.

Common causes for **secondary** or acquired lymphedema are malignancy, radiation, and surgical lymph node dissection, as well as recurrent cellulitis, trauma, filariasis, morbid obesity, and chronic venous insufficiency (Fig. 105.10). Filariasis, due to infection of the lymphatics by the nematode *Wuchereria bancrofti*, is the most common cause of lymphedema in low-income tropical and subtropical countries. Podoconiosis, due to pedal exposure to volcanic soils, occurs most commonly in eastern Africa (Fig. 105.11A).

Clinically, lymphedema begins as painless pitting edema of the dorsal aspect of the foot which then progresses proximally. Over time, the skin becomes indurated due to fibrosis, and the affected areas are prone to ulceration and secondary infection. Recurrent infections lead to worsening of the lymphedema and a vicious cycle is established[28].

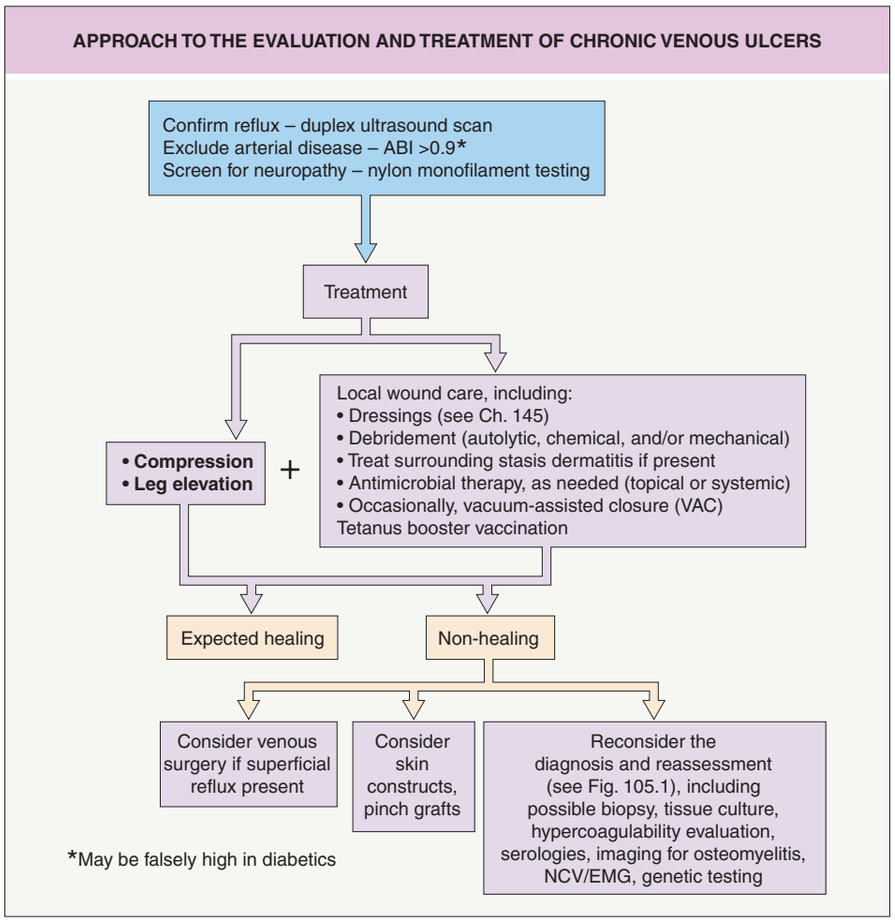


Fig. 105.8 Approach to the evaluation and treatment of chronic venous ulcers. See Table 105.8 for determination and interpretation of the ankle–brachial index (ABI). EMG, electromyography; NCV, nerve conduction velocity test.

CAUSES OF LYMPHEDEMA	
Primary lymphedema	**Secondary lymphedema**
Congenital lymphedema (presents at birth or within first 1–2 years of life)*	• Recurrent lymphangitis and cellulitis • Parasitic infections, e.g. filariasis • Lymph node dissection, e.g. for melanoma or breast cancer • Malignant obstruction, e.g. lymphoma, Kaposi sarcoma, retroperitoneal sarcoma • Radiation injury • Obesity • Surgical excisions, e.g. mastectomy, prostatectomy • Podoconiosis (exposure to mineral microparticles in volcanic soils) • Acne vulgaris and acne rosacea (midface) • Granulomatous disease (e.g. Crohn disease, granuloma inguinale, sarcoidosis)
• Congenital aplasia of the thoracic duct • Hypoplasia of peripheral lymphatics • Congenital abnormalities of the abdominal or thoracic lymphatics *Genetic disorders:* • Lymphatic malformation 1† (AD; *FLT4*), 2 (AD), 3 (AD; *GJC2*), 4 (AD; *VEGFC*), 5‡, 6 (AR; *PIEZO1*), 7 (AD; *EPHB4*), 8 (AR; *CALCRL*), 9 (AD; *CELSR1*), 10 (AD; *ANGPT2*), 11 (AD; *TIE*), 12 (AR; *MDFIC*) • Turner syndrome (see Ch. 55) • Noonan syndrome and other RASopathies (see Ch. 55) • Ectodermal dysplasia and immunodeficiency 1 (XLR; *IKBKG*)	
Lymphedema praecox (presents around puberty)*	
• Yellow nail syndrome • Lymphedema–distichiasis syndrome/lymphedema–distichiasis syndrome with renal disease and DM: AD (*FOXC2*) • Hypotrichosis–lymphedema–telangiectasia syndrome: AR or AD (with renal defect) (*SOX18*)	
Lymphedema tarda (presents after age 35 years)	

*Original classification was based upon age of onset, with an early onset termed Milroy disease and an onset around puberty termed Meige disease, but time of onset varied even within the same family so genetic bases now used for classification.
†Also referred to as Milroy disease.
‡Also referred to as Meige disease.

Table 105.7 Causes of lymphedema. In distichiasis, there is abnormal growth of eyelashes from the orifices of meibomian glands, leading to a double row of eyelashes. Table 104.2 lists additional forms of hereditary lymphedema, e.g. Hennekam lymphangiectasia–lymphedema syndrome 1, 2, 3 (*CCBE1*, *FAT4*, *ADAMTS3*), microcephaly with or without chorioretinopathy, lymphedema, or mental retardation (*KIF11*), and lymphedema, primary, with myelodysplasia (*GATA2*). WILD syndrome is discussed in Chapter 79, with the L representing lymphedema. AD, autosomal dominant; AR, autosomal recessive; DM, diabetes mellitus; XLR, X-linked recessive.

Elephantiasis nostras verrucosa is a complication of chronic lymphedema and most commonly affects the feet and distal lower extremities. In addition to profound non-pitting edema and progressive fibrosis of the dermis and subcutaneous tissue, there are verrucous changes with papillomatosis and hyperkeratosis (Fig. 105.11B). The skin acquires a mossy or cobblestone appearance and discrete firm fibrous papules or nodules may develop. Colonization with bacteria and fungi often results in ulcers becoming crusted and malodorous[40].

Elephantiasis nostras verrucosa is difficult to treat. Compression stockings, pneumatic pumps, and manual lymph drainage (see above)

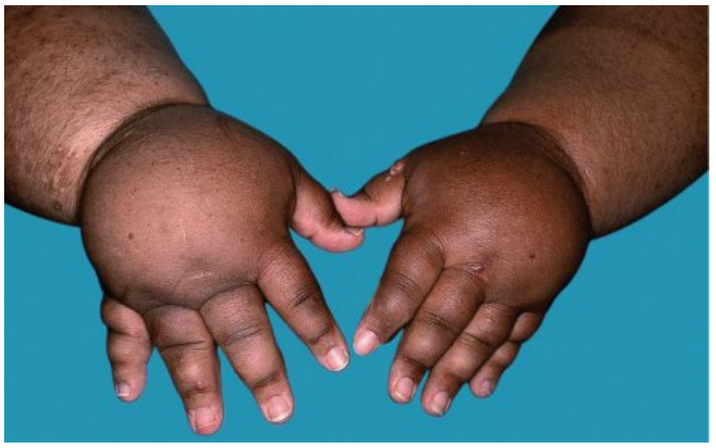


Fig. 105.9 Bilateral primary lymphedema due to lymphatic malformation 1 (also referred to as Milroy disease).



Fig. 105.10 Lymphedema secondary to morbid obesity associated with myxedema.



Fig. 105.11 Elephantiasis nostras verrucosa. A Podoconiosis (endemic, nonfilarial elephantiasis) due to pedal exposure to volcanic soils. **B** The patient had both lymphedema and venous insufficiency. Note the involvement of the foot. *A, Courtesy Claire Fuller, MD.*

are used to decrease lymph accumulation. Topical keratolytics or humectants, such as salicylic acid and urea, may improve the hyperkeratosis[40]. Oral retinoids have been reported to be of benefit for both the verrucous changes and the lymphedema[41]. Surgical management of lymphedema includes physiologic procedures such as lymphaticovenous anastomosis for relatively early (stage I) lymphedema. Debulking and reduction surgery with preservation of perforators are reserved for patients with advanced (stage III) disease[42].



Fig. 105.12 Lipedema. This middle-aged woman has bilateral "stovepipe" enlargement of the legs and minimal involvement of the feet. Note the sharp demarcation between normal and abnormal tissue at the ankle, referred to as the "cuff sign". *Courtesy Jean L. Bolognia, MD.*

The differential diagnosis includes lipedema[43], in which there is an abnormal deposition of subcutaneous fat and lymphatic vessel dysfunction with sparing of the feet (Fig. 105.12), thyroid dermopathy (pretibial myexedema), and obesity-associated lymphedematous mucinosis, where there can be dermal mucin deposition in the absence of thyroid disease.

ARTERIAL ULCERS

Peripheral arterial disease (PAD) is a common manifestation of atherosclerosis. Cigarette smoking and diabetes mellitus are the strongest risk factors, with hypertension, dyslipidemia, and hyperhomocysteinemia representing additional risk factors[44]. Up to 25% of patients with leg ulcers have PAD, and a significant number of patients have a combination of arterial and venous insufficiencies[15].

Pathogenesis

A lack of blood perfusion decreases tissue resilience and leads to tissue necrosis; it also impedes wound healing by reducing the supply of oxygen, nutrients, and soluble mediators involved in the repair process. Although PAD alone infrequently precipitates ulceration, arterial insufficiency plays a major role in delayed wound healing and complications including gangrene. Ischemic foot ulcers are often precipitated by trauma in a patient with relatively mild symptoms of arterial insufficiency. In such an individual, the degree of skin perfusion is sufficient to maintain cutaneous integrity but is not adequate enough to support proper wound healing. In such a setting, the ulcer will inevitably progress into a chronic wound or gangrene unless perfusion is restored[45].

Clinical Manifestations

Most patients with significant PAD are symptom-free. Intermittent claudication, defined as leg pain induced by ambulation and relieved by resting, represents the earliest and the most common presenting symptom of PAD of the lower extremities. With disease progression, patients begin to complain of pain at rest, especially when the legs are elevated in bed at night, which is ameliorated by dependency. While symptoms of claudication are usually localized to the calf or the thigh, pain at rest is often felt in the feet. In advanced stages of PAD, the reduction in cutaneous blood supply may lead to ischemic ulceration and gangrene, and this may necessitate amputation[46].

Arterial ulcers are usually round with a sharply demarcated border and are characterized by an absence of bleeding (Fig. 105.13). These wounds typically occur on the distal lower extremities, often over bony prominences. The surrounding skin may be hairless, shiny, and atrophic. Wound pain is often significant and is exacerbated by limb elevation.



Fig. 105.13 Arterial ulcer. The punched-out appearance and surrounding smooth shiny skin are common features.



Fig. 105.14 Cholesterol emboli. Ischemia of the toes and necrosis with early ulcer formation.

DETERMINATION AND INTERPRETATION OF THE ANKLE–BRACHIAL INDEX

- With the patient in a supine position, the systolic blood pressure is measured in the:
  - brachial arteries (right and left)
  - dorsalis pedis and posterior tibial arteries (right and left)
- The ABI is determined by:

$$\frac{\text{the highest of the systolic pressures from the dorsalis pedis or posterior tibial arteries}}{\text{the higher of the brachial artery systolic pressures}}$$

- Interpretation of the ABI:
  - 0.91–1.40 = normal range
  - >1.40 = suggests incompressible tibial arteries due to medial calcification (diabetes mellitus, chronic renal insufficiency, older age; in these patients the toe–brachial index is measured)
  - <0.9 = indicative of peripheral artery disease (PAD)
  - 0.71–0.90 = mild PAD
  - 0.41–0.70 = moderate PAD
  - 0.00–0.40 = severe PAD

Table 105.8 Determination and interpretation of the ankle–brachial index (ABI).

Additional manifestations of impaired arterial perfusion to the foot include diminished or absent pedal pulses, cool feet, pallor of the foot with elevation of the leg and then subsequent redness with lowering (dependent rubor), sluggish refilling of toe capillaries, thickened nails, and absence of toe hair (see Table 105.1)[15,45].

Laboratory Evaluation

The ankle–brachial pressure index, more commonly referred to as the ankle–brachial index (ABI), is a simple, non-invasive test that is widely used for diagnosis of PAD and to assess its severity. The ABI is calculated by dividing the systolic blood pressure in the ankle by the systolic blood pressure in the arm while the patient is in a resting supine position (Table 105.8). A decrease in arterial blood pressure at the ankle (relative to the central blood pressure) implicates arterial stenosis at any point between the aorta and the ankle[47]. The normal range for the ABI is 0.91 to 1.40, with a reading <0.9 being indicative of PAD[48].

Depending on the patient's presentation and symptoms, further non-invasive imaging techniques may be employed, including duplex ultrasound, computed tomography angiography (CTA), and magnetic resonance angiography (MRA). Both CTA and MRA produce images of vascular structures in cross-sectional slices that can be reconfigured into three-dimensional angiographic images. CTA is less expensive than MRA, with higher spatial resolution. However, CTA involves ionizing radiation and the use of iodinated contrast material. The gold standard for diagnosis and evaluation of PAD is invasive digital subtraction angiography[44], but amongst radiologists, it is being replaced by CTA and MRA.

Measurement of transcutaneous oxygen pressure (TcPO2) quantifies skin oxygenation and indirectly assesses blood flow. The reduction in TcPO2 correlates with the severity of lower extremity ischemia[49], and when the TcPO2 is <40 mmHg, wound healing is impaired.

Differential Diagnosis

Patients with PAD can also develop cutaneous ulcers due to *cholesterol emboli* (Fig. 105.14) and risk factors include arterial or coronary catheterization and anticoagulation (see Ch. 23). In *Buerger disease*, ulcers occur distally on both the upper and lower extremities, with smoking as a risk factor. *Martorell hypertensive ischemic ulcers* result from arteriolosclerosis and in contrast to arterial ulcers, they are typically located on the posterolateral leg. These ulcers are characterized by excruciating pain and patients have treatment-resistant hypertension. Histologically, subcutaneous stenotic arteriolosclerosis and medial calcinosis are prominent. Treatment includes surgical debridement, skin grafting, and pain and blood pressure control.

Additional disorders to consider are shown in Figure 105.1, including diffuse dermal angiomatosis (see below).

Treatment

Arterial ulcers can benefit from restoration of peripheral arterial blood flow, either by endovascular interventions (e.g. percutaneous angioplasty, stent placement, cryoplasty) or by more invasive surgical reconstruction (e.g. femoral popliteal bypass)[15]. In principle, local treatment of arterial ulcers is similar to that of other types of skin ulcers, with two major exceptions: (1) sharp debridement should be performed very cautiously or avoided in order to prevent further necrosis and ulcer enlargement; and (2) VAC therapy should be avoided as it can lead to worsening of the ulcer. Additional interventions include smoking cessation, exercise training, antiplatelet drugs (e.g. aspirin, clopidogrel), cilostazol, and treatment of diabetes, hyperlipidemia, and hypertension.

DIABETIC (AND NEUROPATHIC) ULCERS

Patients with diabetes mellitus have a 10%–25% lifetime risk of developing a foot ulcer. These foot ulcers constitute a major medical and economical burden, with a substantial morbidity and impaired quality of life. Approximately 15% of diabetic patients with foot ulcers will eventually undergo a lower extremity amputation. The rising incidence of both type 1 and type 2 diabetes has made diabetic foot ulcers the most important risk factor for lower extremity amputation in high-income countries[50,51].

Pathogenesis

The etiology of diabetic ulcer formation is multifactorial. Although ischemia, trauma, and infection have traditionally been incriminated as underlying pathogenic factors, nowadays diabetic neuropathy is considered to be the major cause of foot ulcers in diabetic patients[52].

Diabetic neuropathy typically involves the sensory, motor and autonomic nerves, with *sensory* neuropathy substantially impairing the patient's perception of touch, deep pressure, temperature, and joint position. With the loss of protective sensation, foot trauma is unrecognized and this can lead to ulceration. Peripheral *motor* neuropathy results in weakness and atrophy of the intrinsic muscles of the feet, producing altered biomechanics and structural deformities that, in the presence of sensory neuropathy, increase the risk for skin injury and ulceration from repetitive mechanical stress. Continuous pressure to the skin overlying bony prominences typically results in the formation of a thick, keratotic plaque (callus), which eventually breaks down and ulcerates[15,52]. *Autonomic* neuropathy also plays a role because it can lead to a loss of sweating, with the resultant dry skin being susceptible to cracks and fissures that serve as a portal of entry for bacteria[52]. In addition, a potential consequence of autonomic neuropathy is arteriovenous shunting within the skin microcirculation which results in decreased cutaneous perfusion and oxygen saturation, thus contributing to ulceration and an impaired response to infection[50]. Moreover, this abnormal vascular autoregulation, coupled with sensory neuropathy, contributes to the development of Charcot joints (degenerative arthropathy), further adding to the risk of ulceration from an abnormal distribution of pressure forces and foot deformities[53].

Diabetes is also associated with an increased risk of developing PAD, which characteristically affects vessels between the knee and the ankle[51]. Although microcirculatory dysfunction occurs early on in the course of diabetes, it is primarily atherosclerotic macrovascular disease that accounts for ischemic complications in these patients[50]. In general, diabetic foot ulcers are not purely related to vascular occlusion; rather, mechanical damage that typically occurs to the insensate foot, in the presence of a decreased blood supply, rapidly results in neuroischemic ulcers. PAD also contributes to an altered response to foot infections and poor wound healing. The combination of a depressed immune response plus a decrease in cutaneous blood supply plays a key role in the development of cellulitis, abscesses, and osteomyelitis, all of which increase the risk of limb amputation[53].

Occasionally, patients with diabetes develop ulcerations within lesions of necrobiosis lipoidica as well as ulcers due to streptococcal infections.

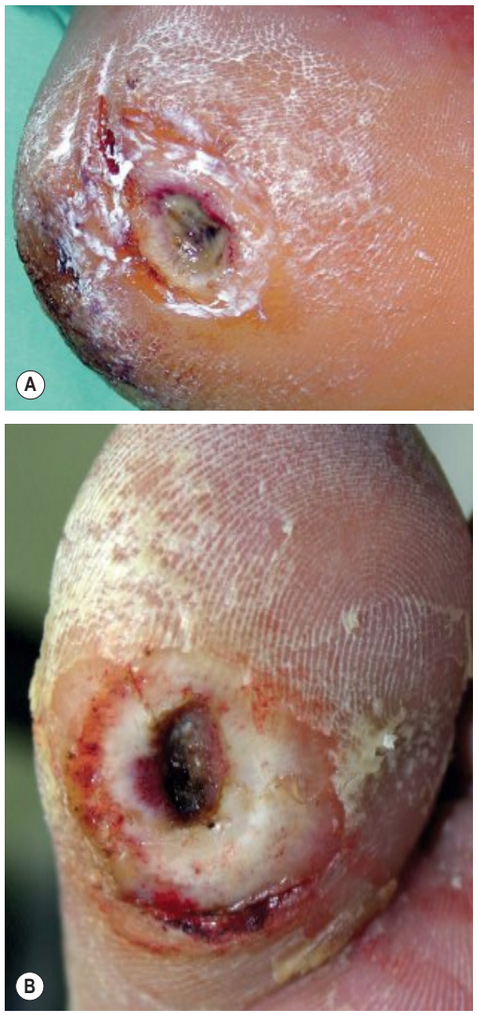


Fig. 105.15 Neuropathic ulcers (mal perforans) in patients with diabetes mellitus and peripheral neuropathy. Common locations are the plantar surface of the heel (**A**) and the great toe (**B**). Note the thick rim of callus.

Clinical Features

Diabetic ulcers are usually located on pressure points and bony prominences such as the metatarsal heads, great toes, and heels (Fig. 105.15). They often arise within exuberant, moist, malodorous calluses (mal perforans). In the absence of peripheral atherosclerotic disease, the diabetic foot is warm, with good color and palpable pulses, but with decreased sensation. Foot deformities are frequently present, e.g. hammer toes, claw toes, collapse of the longitudinal arch (Charcot foot).

Laboratory Evaluation

Because diabetic ulcers are heterogeneous in nature, a thorough evaluation of the patient is crucial in determining the underlying causes. More specifically, peripheral neuropathy can be detected via a neurologic examination of the lower extremities that includes the use of a 10 g monofilament to test for sensation[54]. More invasive testing, i.e. nerve conduction studies/electromyography, is sometimes required. The degree to which vascular perfusion is compromised can be assessed via determination of the ABI (see above).

A complete blood count, ESR, C-reactive protein level, and blood glucose level are obtained when assessing for a possible associated infection. Of note, sometimes an elevated blood glucose level is the only sign of infection[55]. Microbial cultures (bacterial, mycobacterial, and fungal) should be obtained from the wound bed. Although swabs are often used, deep tissue specimens, obtained aseptically, are preferable[54].

Diagnostic imaging, including plain radiographs of both feet, bone scintigraphy, MRI, CT and sometimes ultrasound, is used to better define the presence or absence of a bone or deep soft tissue infection. Of these, MRI is the most accurate test for diagnosing osteomyelitis. If osteomyelitis is suspected, a bone biopsy processed for culture and histology is the gold standard[51,52].

Treatment

Conservative treatment of diabetic foot ulcers consists of providing a proper wound healing environment, eradication of infection, and avoidance of repetitive trauma by alleviating the mechanical load on ulcers (off-loading). Methods of off-loading include bed rest and the use of a wheelchair, crutches, total contact casting, cast walkers, felted foam, half-shoes, or therapeutic shoes. Total contact casting is considered to be the best approach as it enables pressure redistribution and continuous off-loading of the ulcer area. The inability of the patient to remove the cast ensures compliance and reduces the level of activity[54,56]. However, total contact casting is somewhat impractical because it is expensive and requires skill and experience. In addition, as the edema subsides, cast changing and size adjustments are often required (usually twice a week or more often). Total contact casting is contraindicated if the wound is infected or has a significant exudate and it can lead to new ulcerations over bony prominences[52].

Another approach to off-loading is the use of specialized shoes that reduce pressure about the forefoot and heel and multilayered insoles that enhance shock absorption[52]. Half-shoes assist in off-loading forefoot plantar ulcers as they support only the rear and mid foot, while the forefoot is left suspended in the air[54].

Initial wound management consists of cleansing the wound and proper debridement of any necrotic material, including the callus; the latter can contribute to increased pressure on the insensate foot. In addition, debridement promotes wound healing at the cellular level by removing excess extracellular matrix, thus liberating trapped growth factors and facilitating cell migration[53]. Moist wound healing is recommended as with other types of chronic ulcers but avoidance of maceration of surrounding skin is of particular importance.

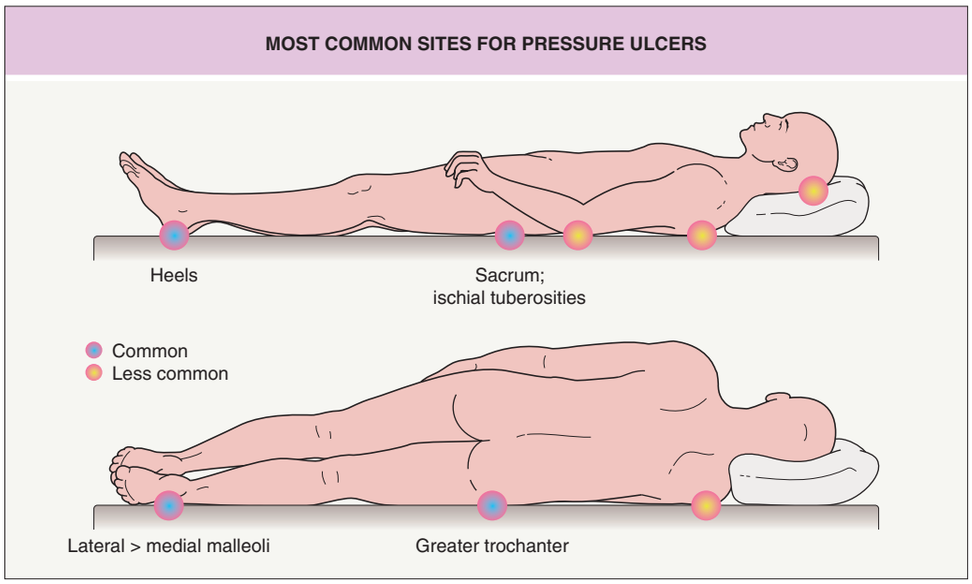


Fig. 105.16 Most common sites for pressure ulcers.

Apart from standard therapies (see above), hyperbaric oxygen has been shown to be of specific benefit to patients with diabetic foot ulcers. While it is unclear to what extent it benefits other types of ulcers[57], hyperbaric oxygen therapy has been shown to be effective in the treatment of diabetic foot ulcers, with a decrease in healing time and amputation rate. Oxygen (100%) at supra-atmospheric pressures is intermittently inhaled, either in a full-body (monoplace) chamber or in a multiplace chamber via a gas mask. In theory, tissue hypoxia impairs wound healing and hyperbaric oxygen therapy leads to an increase in the blood oxygen level within the wound. In addition, there is reallocation of blood flow to hypoxic areas due to hyperoxic vasoconstriction of surrounding normal tissue[58]. Side effects include oxygen toxicity to the brain (e.g. seizures) and lungs, and barotrauma to the lungs, ears, sinuses, and eyes (transient myopia)[15].

As endogenous growth factors are often degraded or trapped within chronic wounds, genetically engineered exogenous growth factors have been used to try to enhance wound healing[59]. Becaplermin gel (Regranex®) is recombinant platelet-derived growth factor whose biologic activity is similar to its endogenous counterpart, with stimulation of granulation tissue production and release of other growth factors important to wound repair. It is the only growth factor currently approved for use in chronic neuropathic diabetic ulcers[15]. In the setting of best wound care, becaplermin gel has been shown to increase healing rates and shorten healing time of diabetic ulcers[60]. However, in routine clinical practice, becaplermin has not been as successful and it has an FDA black box warning of an increased risk of cancer mortality (when exposed to three or more tubes). More recently, strategies have focused on improving growth factor activity and protecting these factors from degradation[32].

Living skin equivalents (e.g. Apligraf®, Dermagraft®) are bioengineered products that act as delivery systems for growth factors and extracellular matrix (see Ch. 145)[61–63]. Both are indicated for recalcitrant diabetic foot ulcers that have no exposed muscle, bone or tendon, are not infected, and have had aggressive debridement.

Prevention

Preventing wound recurrence is of critical importance. The risk of ulceration and/or amputation is increased in patients who have had diabetes for >10 years, are male, have poor glucose control, or have target organ complications. Foot-related conditions that are associated with an increased risk of amputation are peripheral neuropathy, altered biomechanics, evidence of increased pressure, foot deformity, PAD, history of an ulcer or previous amputation, and severe nail pathology[64]. Tight control of glucose levels is required in order to prevent diabetic complications that are due to microvascular changes, as the latter predispose the patient to neuropathy, ischemia, and infection. Lower HbA1c values are associated with a decrease in healing times for leg and foot ulcers[65]. Smoking cessation and control of low-density lipoprotein (LDL) and total cholesterol levels are also important in the prevention of atherosclerotic vascular disease.

All diabetic patients should receive an annual foot examination to assess neurologic and vascular status, biomechanics, skin integrity, and the presence and types of foot deformities. Patients with significant risk factors for ulcer formation should be evaluated more frequently. Education regarding daily foot care that includes inspection for any scratch, blister or erythema, daily washing in warm water, appropriate footwear selection (e.g. avoiding pointed shoes), skin moisturizing, and treatment of nail and foot fungal infection should be provided.

ULCERS DUE TO PHYSICAL FACTORS

Any form of mechanical trauma to the skin can result in the formation of an ulcer if factors that compromise the skin's ability to recover from physical insults are present. The most common form of physical injury which leads to ulceration is prolonged pressure due to immobilization. The resultant ulcer is commonly referred to as a *pressure ulcer* or *decubitus ulcer* (decubitus means lying down in Latin). These ulcers are caused by unrelieved pressure to soft tissues compressed between a bony prominence and an external surface. The most common bony prominences involved are the sacrum, ischial tuberosities, greater trochanters, heels, and lateral malleoli[66] (Fig. 105.16). A special type of pressure ulcer, often presenting as a pear- or butterfly-shaped ulcer in the sacral area, is termed a Kennedy terminal ulcer because it often precedes death.

Approximately 1.5–3 million people in the US have pressure ulcers, with an annual cost of treatment of up to $5 billion[66]. It has also been estimated that 10% of hospitalized patients and 25% of nursing home residents have pressure ulcers, with most developing during the first few weeks of hospitalization. An estimated 70% of pressure ulcers occur in patients over 70 years of age; 95% are located on the lower portion of the body: 65% in the pelvic girdle area (Fig. 105.17) and 30% on the lower limbs (Fig. 105.18). Risk factors that predispose to the development of pressure ulcers include prolonged immobility, sensory deficit, circulatory disturbance, and poor nutrition[66].

Pathogenesis

Four major etiologic factors have been identified as playing an important role in the development of pressure ulcers: external pressure, shearing forces, friction, and moisture.

Interstitial pressures >32 mmHg (normal capillary pressure range = 12–32 mmHg) usually compromise oxygenation and microcirculation. There is an inverse time–pressure curve, with slow ulcer



Fig. 105.17 Pressure ulcer (stage III) over the sacral area.



Fig. 105.18 Black eschar of the heel at site of pressure necrosis.

formation at low pressures and rapid ulcer formation at high pressures (>70 mmHg). The length of continuous exposure of the skin to pressure is also of critical importance, thus explaining why intermittent relief of the pressure can prevent ulcer formation. Because subcutaneous tissues are most susceptible to the damaging effects of prolonged exposure to pressure, deep tissue trauma can occur with relatively little superficial damage that would alert caregivers to the extent of tissue injury[66].

Shearing forces result from the sliding and relative displacement of two apposing surfaces. Although externally applied pressure is more effective than shearing forces alone in reducing skin arteriolar blood flow, these two factors can combine to enhance vascular occlusion. When the head of a supine patient is raised more than 30°, shearing forces occur in the sacral and coccygeal areas. Sliding of the torso transmits pressure to the sacrum and deep fascia, as the outer sacral skin is fixed because of friction with the bed. Vessels within the deeper portion of the superficial fascia angulate and thrombose, which manifests clinically as undermining of the ulcer[66].

Friction is often associated with shearing and it reflects the degree of resistance generated when two surfaces move across each other. When a bedridden patient is dragged across the bed sheets, friction is produced. Damage to the protective stratum corneum enhances ulcer formation by compromising the skin barrier.

Moisture results from perspiration due to fevers and from urine and feces. It has been shown to increase the risk of pressure ulcer formation fivefold[66].

Clinical Features

Pressure ulcers are usually classified according to a four-stage system designed by the National Pressure Ulcer Advisory Panel (NPUAP) (Fig. 105.19). Of note, the ulcers do not necessarily progress sequentially from stage I to stage IV, nor do they necessarily heal from stage IV to stage I[67].

- *Stage I*: non-blanchable erythema of intact skin which heralds skin ulceration. For individuals with more darkly pigmented skin, warmth, edema, discoloration of the skin, and induration may serve as indicators of impending ulceration[66,67].
- *Stage II*: partial-thickness skin loss involving the epidermis, dermis, or both. This superficial lesion presents as an erosion, blister, or shallow ulcer[66,67].
- *Stage III*: full-thickness skin loss with damage to the subcutaneous tissue, extending down to (but not including) the underlying fascia. This deep lesion presents as a crater-like ulcer and sometimes involves adjacent tissue[66,67].
- *Stage IV*: full-thickness skin loss and extensive tissue necrosis with destruction extending to muscle, bone, or supporting structures such as tendons or joint capsules. Undermining or sinus tracts can be present[66,67].

As mentioned previously, a major limitation in the clinical classification of pressure ulcers stems from the fact that extensive deep tissue damage may be accompanied initially by minimal superficial manifestations. Adequate evaluation may also be hampered by the presence of an eschar, which should be debrided for full assessment[66].

Pathology

When the diagnosis is in doubt or when a secondary malignancy is suspected in the setting of a longstanding lesion, histologic examination is indicated. In all four stages, the histopathologic findings are rather nonspecific. When there is *blanchable* erythema clinically, the superficial dermal capillaries and venules are dilated. Mild to moderate edema within the papillary dermis is seen in association with a mild perivascular lymphocytic infiltrate. The epidermis, pilosebaceous structures, and reticular dermis remain normal. At the stage of *non-blanchable* erythema, engorgement of capillaries and venules with red blood cells, platelet thrombi, and hemorrhage are observed in the papillary dermis. Although the epidermis still appears normal, sweat gland and subcutaneous fat degeneration is often present[66]. Subepidermal separation can occur with formation of a subepidermal bulla. In early ulcers, the epidermis is lost and acute inflammation of the papillary and reticular dermis is seen. Chronic ulcers have a diffusely fibrotic dermis with a loss of adnexa. The surface may have a hemorrhagic crust containing acute inflammatory cells or a thin zone of coagulation necrosis. In the black eschar stage, full-thickness destruction of the skin occurs. General dermal architecture is preserved, but there is obliteration of cellular details.

Treatment

Pressure ulcers are preventable, primarily by relief of pressure on the skin. This can be accomplished by frequent position changes in addition to use of a variety of support surfaces to relieve pressure; the latter include air- or liquid-filled flotation devices, foam products, and pillows or foam wedges as positioning devices. Adequate nutrition, education, pain management, and psychosocial support are also important interventions. Causes of immobility and systemic conditions that interfere with wound healing or decrease tissue perfusion must be addressed, including congestive heart failure, diabetes, and/or spastic paresis.

The general principles of ulcer and chronic wound care discussed previously also apply to pressure ulcer management. Briefly, debridement may be accomplished via mechanical, enzymatic, and/or autolytic means (see above). Wounds should be cleansed as non-traumatically as possible, and normal saline for irrigation is preferred rather than cytotoxic agents such as hydrogen peroxide or povidone-iodine.

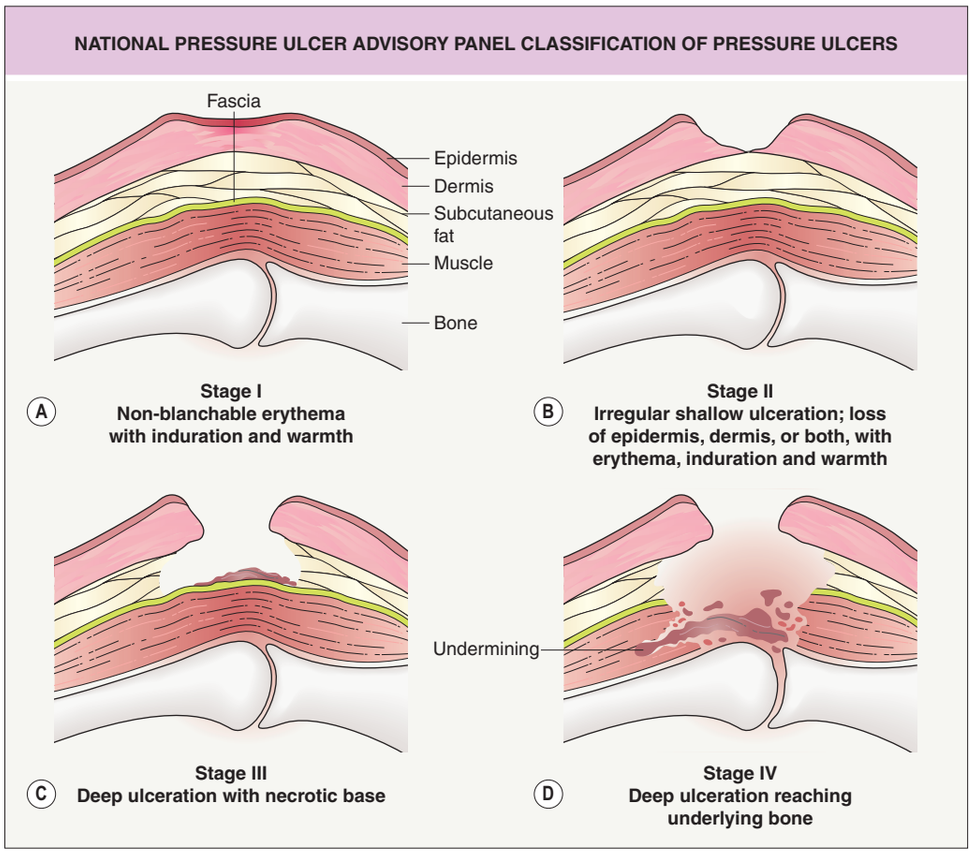


Fig. 105.19 National Pressure Ulcer Advisory Panel classification of pressure ulcers. A Stage I: non-blanchable erythema of intact skin. This lesion is the heralding sign of impending skin ulceration. For darker-skinned individuals, other signs may be indicators and include warmth, edema, discoloration of the skin, and induration. **B** Stage II: partial-thickness skin loss involving the epidermis, dermis or both. This superficial lesion presents as an abrasion, blister, or shallow crater. **C** Stage III: full-thickness skin loss, in which subcutaneous tissue is damaged or necrotic and may extend down into, but not including, the underlying fascia. This deep lesion presents as a crater and sometimes involves adjacent tissue. **D** Stage IV: full-thickness skin loss and extensive tissue necrosis, destruction to muscle, bone, or supporting structures such as a tendon or joint capsule. Undermining or sinus tracts can be present.

As always, bacterial colonization and infection must be controlled. Dressings should provide a moist, but not macerated, environment and occlusive dressings are often utilized.

In general, stage I, II, and III pressure ulcers are more likely to heal with local therapy, whereas stage IV ulcers, particularly those over the ischial tuberosities, often require surgical intervention. Adjuvant therapies such as laser, ultrasound, hyperbaric oxygen, and UV irradiation are investigational and to date cannot be considered as standard of care. The application of growth factors, cultured keratinocyte grafts, and skin substitutes is promising, but these are also still in the investigational stage.

OTHER CAUSES OF SKIN ULCERATION

Ulcers that are apparently recalcitrant to prescribed treatments should be reevaluated regarding compliance with the program of care, and when non-compliance is excluded, then rare or unusual causes should be considered (Fig. 105.20; see Fig. 105.1).

Diffuse Dermal Angiomatosis

Diffuse dermal angiomatosis is an unusual manifestation of vascular atherosclerosis. There is rather rapid development of one or several violaceous plaques in a reticulated pattern, often with central ulceration. The lesions are typically painful and are usually located on the lower extremities, but they may appear elsewhere (e.g. breast, forearm) (see Fig. 105.20A). Histologically, a diffuse interstitial proliferation of CD31-positive endothelial cells is present within the papillary and reticular dermis, with focal formation of small vascular channels. Cytologic atypia and atypical mitoses are absent.

Interventions to correct the underlying PAD, such as femoral artery angioplasty or femoral popliteal bypass surgery, lead to rapid resolution. Less often, lesions resolve without therapy[68].

Hematologic Disorders

Anemia is a major and often underrecognized cause for delayed wound healing. It prevents proper tissue oxygenation. In addition, some forms of anemia are associated with a marked tendency for ulcer formation, such as the hemoglobinopathies (see Fig. 105.20C)[69]. Hematologic malignancies are also associated with ulcerative processes including pyoderma gangrenosum, vasculitis, and cryoglobulinemia (particularly type I). Clotting abnormalities can play a direct role in the formation of ulcers (e.g. antiphospholipid antibody syndrome)[70,71], as well as serving as a predisposing factor for more common types of cutaneous ulcerations such as venous ulcers[72,73]. Acute massive venous thrombosis, also known as phlegmasia cerulea dolens, can lead to massive edema in the legs, with subsequent ischemia and ulceration due to venous limb gangrene[74]. Table 105.9 summarizes the recommended evaluation when thrombophilia is suspected.

Tropical Ulcers

These ulcers are found in children and adults residing in the tropics who typically live in rural areas and are malnourished or otherwise debilitated. They may also occur in travelers returning from those areas. Although many tropical diseases manifest with chronic ulceration, the term "tropical ulcer" is often used to describe a phagedenic ulcer, usually located on the leg, which often occurs secondarily to minor trauma[75]. The ulcer is invariably associated with a polymicrobial infection including *Fusobacterium* spp., other anaerobic bacteria, and spirochetes.

Tropical ulcers are always painful and progress rapidly to often involve deep tissues. The edges are undermined and violaceous, and malignant degeneration can occur. Assessment includes a smear and cultures plus soft tissue and bone imaging when deep involvement is suspected. These ulcers are best managed with systemic antibiotics

EVALUATION FOR THROMBOPHILIA/HYPERCOAGULABILITY			
Disorder	**%***	**Screening tests**	**Potential confounding conditions**
Inherited			
Factor V Leiden	5	Activated protein C (APC) resistance†	Warfarin, heparin, DOACs, OCP, pregnancy, ↑ factor VIII level, lupus anticoagulant†
	5	Factor V Leiden mutation (AD) [reflex text if APC detected]	–
Prothrombin G20210A	2	Prothrombin G20210A mutation (AD)	–
Hyperhomocysteinemia	>5	↑ Homocysteine level (may have homozygous *MTHFR* C677T mutation or be compound heterozygote > heterozygous *CBS* mutation)	Deficient folate, B_{12} or B_6; older age, smoking
Protein C deficiency	0.3	↓ Protein C activity (AD)	Warfarin, DOACs, OCP, pregnancy, liver disease, ↑ factor VIII level, lupus anticoagulant
Protein S deficiency	0.05	↓ Free protein S antigen level and/or activity (AD)	Warfarin, DOACs, OCP, pregnancy, liver disease, ↑ factor VIII level, lupus anticoagulant, acute thrombosis
Antithrombin III deficiency	0.1	↓ Antithrombin III activity (AD)	Heparin, DOACs, liver disease, acute thrombosis
Excess factor VIII	10	↑ Factor VIII level	Acute phase response, OCP, pregnancy, old age
Excess fibrinogen	ND	↑ Fibrinogen level	Acute phase response, pregnancy, smoking, older age
Dysfibrinogenemia	ND	↓ Functional fibrinogen; ↑ thrombin time	Recent birth, liver disease
Excess factor IX or XI	ND	↑ Factor IX or XI level	Warfarin (factor IX)
Plasminogen deficiency	ND	↓ Plasminogen	–
Excess plasminogen activator inhibitor-1 (PAI-1)	ND 10	↑ PAI-1 *PAI* 4 G/4 G, 4 G/5 G, or 5 G/5 G promoter region polymorphism	Wide range of normal values and diurnal variation
Excess lipoprotein (a)	10	↑ Lipoprotein (a) level	–
Tissue factor pathway inhibitor (TFPI)	10	↓ TFPI	–
Thrombin-activatable fibrinolysis inhibitor	ND	↑ Thrombin-activatable fibrinolysis inhibitor	–
Thrombomodulin deficiency	ND	↓ Thrombomodulin	–
Acquired			
Lupus anticoagulant‡	ND	↑ RVVT (dilute), sensitive PTT, or kaolin clotting time¶	Warfarin, heparin, DOACs
Anticardiolipin antibodies‡	ND	IgG or IgM anticardiolipin antibodies at moderate–high levels, on ≥2 occasions ≥12 weeks apart	Various infectious diseases
Anti-β_2-glycoprotein I antibodies‡	ND	Anti-β_2-glycoprotein I antibodies present, on ≥2 occasions ≥12 weeks apart	–
Cryoglobulinemia, type I	ND	Type I cryoglobulins present	–
Heparin-induced thrombocytopenia§	ND§	• *Screening*: anti-heparin/platelet factor 4 (PF4) antibodies • *Confirmatory*: serotonin release assay	–
Cryofibrinogenemia	ND	Cryofibrinogens present	Acute phase response

*Approximate percentage of general population with the defect.
†Factor V Leiden accounts for ~95% of patients with APC resistance when the latter is assessed by "second generation" assays, which are not limited by most potential confounding conditions.
‡Antiphospholipid antibodies.
¶Confirmed by: (1) failure to correct the prolonged coagulation time in mixing studies; and (2) correction with the addition of excess phospholipids.
§Exposure to heparin or low-molecular-weight heparin.

Table 105.9 Evaluation for thrombophilia/hypercoagulability. Shaded areas represent first-tier screening tests. The initial laboratory evaluation should also include a complete blood count with differential and platelet count, examination of a peripheral blood smear, ESR, activated partial thromboplastin time (PTT), and hepatic and renal function panels. Testing for anti-neutrophil cytoplasmic antibodies (ANCA) can be considered for patients with retiform purpura, as ANCA-positive vasculitides occasionally present with minimally inflammatory lesions; patients with levamisole-induced vasculopathy may have anti-phospholipid antibodies (as well as ANCA). Infections can also lead to coagulopathy (e.g. COVID-19-associated) in which abnormalities such as elevated fibrinogen or antiphospholipid antibodies are detected. Additional inherited causes of hypercoagulability include polymorphisms in the genes encoding the endothelial protein C receptor, the protein Z-dependent protease inhibitor, and E-selectin. AD, autosomal dominant; CBS, cystathionine β-synthase; DOACs, direct-acting oral anticoagulants; MTHFR, methylenetetrahydrofolate reductase; ND, not determined; OCP, oral contraceptive pills; RVVT, Russell viper-venom time.



Fig. 105.20 Additional causes of ulcers. A Diffuse dermal angiomatosis develops most often in pendulous breasts (note the scars from previous breast reduction surgery) and the lower extremities in association with atherosclerosis. **B** Systemic sclerosis with an ulcer of the fingertip. **C** Multiple ulcers in a patient with sickle cell anemia. **D** Necrobiosis lipoidica. Controversy exists about the exact risk of diabetes mellitus in such patients, but it is more strongly associated with diabetes than is granuloma annulare. **E** Prolidase deficiency with spontaneous ulcers and scarring from previous ulcerations. **F** Ulceration of the lateral malleolus in a patient receiving hydroxyurea. **G** Henoch–Schönlein purpura in an adolescent. *A, Courtesy Margo Peters, MD; D, Courtesy Jeffrey P. Callen, MD; E, Courtesy Duygu Gülseren, MD; F, Courtesy Karynne O. Duncan, MD; G, Courtesy Julie V. Schaffer, MD.*

(e.g. tetracycline, metronidazole) and non-adherent dressings; they occasionally require surgical debridement.

The differential diagnosis of tropical ulcers[76] includes other common causes of ulceration in tropical areas such as bacterial (including anthrax), mycobacterial, deep fungal, and parasitic (leishmaniasis) infections as well as non-infectious causes such as sickle cell anemia, venous insufficiency, neuropathy, and trauma.

Additional Causes

A variety of physical, inflammatory, infectious, metabolic, and inherited disorders are also associated with cutaneous ulceration (see Fig. 105.20B, D–G) and they are outlined in Fig. 105.1 and Table 105.10.

Additional figures available in our eBook (see inside front cover for access code).

ADDITIONAL CAUSES OF CUTANEOUS ULCERATION		
Cause	**Favored anatomic site**	**Location of review**
Physical		
Burns – thermal, electrical, chemical	Site of exposure	Chapters 15, 16, 88
Cold injury (e.g. frostbite)	Acral	Chapter 88
Radiation (e.g. orthovoltage)	Site of exposure	Chapter 139
Inflammatory		
Vasculitis (small and medium-sized vessels, primary and secondary)	Lower extremities	Chapter 24; Fig. 105.20G
Pyoderma gangrenosum	Lower extremities, sites of trauma	Chapter 25
Necrobiosis lipoidica	Lower extremities	Chapter 93; Fig. 105.20D
Behçet disease	Lower extremities	Chapter 25
Panniculitis, (e.g. nodular vasculitis, equestrian cold panniculitis/perniosis)	For the two examples, calves and outer thighs	Chapter 100
Vascular		
Raynaud phenomenon and systemic sclerosis	Digital, extensor surface of joints	Chapter 43; Fig. 105.20B
Hemoglobinopathies (e.g. sickle cell anemia)	Lower extremities	Fig. 105.20C
Diffuse dermal angiomatosis	Lower extremities, pendulous breasts	Fig. 105.20A
Infectious		
Bacterial (e.g. *Streptococcus* spp., *Treponema* spp.), mycobacterial, viral (e.g. chronic HSV), fungal, parasitic	Exposed sites Pressure sites in the case of leprosy and tertiary syphilis*	Chapters 74–83; Fig. 105.1
Bites and stings		Chapter 85
Neoplastic		
BCC, SCC > metastases, other primary cutaneous malignancies (epithelial and non-epithelial), cutaneous T and B cell lymphomas	For BCC and SCC, sites of chronic sun exposure For SCC, chronic ulcers, scars, sites of chronic inflammation or oncogenic HPV infection	Chapters 108, 119–122
Metabolic		
Examples: calcinosis cutis, calciphylaxis, gout	Varies from juxta-articular (calcinosis cutis, gout) to "fatty" areas (calciphylaxis)	Chapters 48, 50
Genodermatoses		
Examples: Adams–Oliver syndrome, prolidase deficiency, laryngo-onycho-cutaneous syndrome, familial tumoral calcinosis, Werner syndrome, familial chilblain lupus (*TREX1* mutations), Klinefelter syndrome, leukocyte adhesion deficiency, SAVI	Varies from scalp due to aplasia cutis congenita to lower extremity	Chapters 41, 45, 50, 60, 63, 64; Fig. 105.20E
Drugs		
Hydroxyurea	Lower extremities	Chapters 21, 23; Fig. 105.20F
Methotrexate	Psoriatic plaques	
Warfarin	"Fatty" areas, e.g. breasts	
Heparin	Sites of injection and distant sites	
All-*trans* retinoic acid (systemic), anti-angiogenic multi-kinase inhibitors (e.g. cabozantinib, sunitinib)	Scrotum > vulva	
Interferon, glatiramer acetate, bortezomib, anti-sense oligonucleotides	Sites of sc injection†	
NSAIDs (e.g. diclofenac), penicillin, hydroxyzine, vitamin K, bismuth salts	Sites of IM injection†	
Photodamage		
Erosive pustular dermatosis	Usually hairless scalp, but occasionally lower extremity	Chapter 25

*Due to neuropathy.
†Associated with ischemia in a livedo pattern in Nicolau syndrome.

Table 105.10 Additional causes of cutaneous ulceration. In addition to lower extremity ulcers, patients with prolidase deficiency develop diffuse telangiectasias, dermatitis, lymphedema and manifestations of systemic lupus erythematosus. BCC, basal cell carcinoma; HPV, human papillomavirus; HSV, herpes simplex virus; IM, intramuscular; SAVI, STING (*st*imulator of *in*terferon *g*enes)-associated vasculopathy with onset in infancy; sc, subcutaneous; SCC, squamous cell carcinoma.

REFERENCES

1. Lazarus GS, Cooper DM, Knighton DR, et al. Definitions and guidelines for assessment of wounds and evaluation of healing. *Arch Dermatol*. 1994;130:489–493.
2. Beebe-Dimmer JL, Pfeifer JR, Engle JS, Schottenfeld D. The epidemiology of chronic venous insufficiency and varicose veins. *Ann Epidemiol*. 2005;15:175–184.
3. Bergan JJ, Schmid-Schonbein GW, Smith PD, et al. Chronic venous disease. *N Engl J Med*. 2006;355:488–498.
4. Valencia IC, Falabella A, Kirsner RS, Eaglstein WH. Chronic venous insufficiency and venous leg ulceration. *J Am Acad Dermatol*. 2001;44:401–421. quiz 422–4.
5. Raju S, Neglen P. Clinical practice. Chronic venous insufficiency and varicose veins. *N Engl J Med*. 2009;360:2319–2327.
6. Mekkes JR, Loots MA, Van Der Wal AC, Bos JD. Causes, investigation and treatment of leg ulceration. *Br J Dermatol*. 2003;148:388–401.
7. Browse NL, Burnand KG. The cause of venous ulceration. *Lancet*. 1982;2:243–245.
8. Falanga V, Eaglstein WH. The "trap" hypothesis of venous ulceration. *Lancet*. 1993;341:1006–1008.
9. Raffetto JD. Pathophysiology of chronic venous disease and venous ulcers. *Surg Clin North Am*. 2018;98:337–347.
10. Clark RA. Oxidative stress and "senescent" fibroblasts in non-healing wounds as potential therapeutic targets. *J Invest Dermatol*. 2008;128:2361–2364.
11. Wall IB, Moseley R, Baird DM, et al. Fibroblast dysfunction is a key factor in the non-healing of chronic venous leg ulcers. *J Invest Dermatol*. 2008;128:2526–2540.
12. Barron GS, Jacob SE, Kirsner RS. Dermatologic complications of chronic venous disease: medical management and beyond. *Ann Vasc Surg*. 2007;21:652–662.
13. Meissner MH, Gloviczki P, Bergan J, et al. Primary chronic venous disorders. *J Vasc Surg*. 2007;46:54S–67S. Suppl S.
14. Alavi A, Sibbald RG, Phillips TJ, et al. What's new: management of venous leg ulcers: approach to venous leg ulcers. *J Am Acad Dermatol*. 2016;74:627–640. quiz 641–2.
15. Fonder MA, Lazarus GS, Cowan DA, et al. Treating the chronic wound: a practical approach to the care of nonhealing wounds and wound care dressings. *J Am Acad Dermatol*. 2008;58:185–206.
16. Panuncialman J, Falanga V. The science of wound bed preparation. *Surg Clin North Am*. 2009;89:611–626.
17. Falabella AF. Debridement and wound bed preparation. *Dermatol Ther*. 2006;19:317–325.
18. Sherman RA, Hall MJ, Thomas S. Medicinal maggots: an ancient remedy for some contemporary afflictions. *Annu Rev Entomol*. 2000;45:55–81.
19. Chambers L, Woodrow S, Brown AP, et al. Degradation of extracellular matrix components by defined proteinases from the greenbottle larva Lucilia sericata used for the clinical debridement of non-healing wounds. *Br J Dermatol*. 2003;148:14–23.
20. Dumville JC, Worthy G, Bland JM, et al. Larval therapy for leg ulcers (VenUS II): randomised controlled trial. *BMJ*. 2009;338:b773.
21. Madhok BM, Vowden K, Vowden P. New techniques for wound debridement. *Int Wound J*. 2013;10:247–251.
22. Lipsky BA, Hoey C. Topical antimicrobial therapy for treating chronic wounds. *Clin Infect Dis*. 2009;49:1541–1549.
23. Zhou LH, Nahm WK, Badiavas E, et al. Slow release iodine preparation and wound healing: in vitro effects consistent with lack of in vivo toxicity in human chronic wounds. *Br J Dermatol*. 2002;146:365–374.
24. Lansdown AB. A review of the use of silver in wound care: facts and fallacies. *Br J Nurs*. 2004;13:S6–S19.
25. Korber A, Graue N, Rietkotter J, et al. Insufficient tetanus vaccination status in patients with chronic leg ulcers. Results of a prospective investigation in 100 patients. *Dermatology*. 2008;217:69–73.
26. O'Meara S, Tierney J, Cullum N, et al. Four layer bandage compared with short stretch bandage for venous leg ulcers: systematic review and meta-analysis of randomised controlled trials with data from individual patients. *BMJ*. 2009;338:b1344.
27. Gohel MS, Heatley F, Liu X, et al. A randomized trial of early endovenous ablation in venous ulceration. *N Engl J Med*. 2018;378:2105–2114.
28. Kerchner K, Fleischer A, Yosipovitch G. Lower extremity lymphedema update: pathophysiology, diagnosis, and treatment guidelines. *J Am Acad Dermatol*. 2008;59:324–331.
29. Mayrovitz HN. The standard of care for lymphedema: current concepts and physiological considerations. *Lymphat Res Biol*. 2009;7:101–108.
30. Hunter JE, Teot L, Horch R, Banwell PE. Evidence-based medicine: vacuum-assisted closure in wound care management. *Int Wound J*. 2007;4:256–269.
31. Venturi ML, Attinger CE, Mesbahi AN, et al. Mechanisms and clinical applications of the vacuum-assisted closure (VAC) device: a review. *Am J Clin Dermatol*. 2005;6:185–194.
32. Rizzi SC, Upton Z, Bott K, Dargaville TR. Recent advances in dermal wound healing: biomedical device approaches. *Expert Rev Med Devices*. 2010;7:143–54.
33. Sharma P, Kumar A, Dey AD. Cellular therapeutics for chronic wound healing: future for regenerative medicine. *Curr Drug Targets*. 2022;23(16):1489–1504. https://doi.org/10.2174/1389450123092062314462O. PMID: 35748548.
34. Kirsner RS, Marston WA, Snyder RJ, et al. Spray-applied cell therapy with human allogeneic fibroblasts and keratinocytes for the treatment of chronic venous leg ulcers: a phase 2, multicentre, double-blind, randomised, placebo-controlled trial. *Lancet*. 2012;380:977–985.
35. Paquette D, Badiavas E, Falanga V. Short-contact topical tretinoin therapy to stimulate granulation tissue in chronic wounds. *J Am Acad Dermatol*. 2001;45:382–386.
36. Thomas B, Kurien JS, Jose T, et al. Topical timolol promotes healing of chronic leg ulcer. *J Vasc Surg Venous Lymphat Disord*. 2017;5:844–850.
37. Jull A, Waters J, Arroll B. Pentoxifylline for treatment of venous leg ulcers: a systematic review. *Lancet*. 2002;359:1550–1554.
38. Bush R, Comerota A, Meissner M, et al. Recommendations for the medical management of chronic venous disease: the role of micronized purified flavanoid fraction (MPFF). *Phlebology*. 2017;32:3–19.
39. Brice G, Child AH, Evans A, et al. Milroy disease and the VEGFR-3 mutation phenotype. *J Med Genet*. 2005;42:98–102.
40. Sisto K, Khachemoune A. Elephantiasis nostras verrucosa: a review. *Am J Clin Dermatol*. 2008;9:141–146.
41. Zouboulis CC, Biczo S, Gollnick H, et al. Elephantiasis nostras verrucosa: beneficial effect of oral etretinate therapy. *Br J Dermatol*. 1992;127:411–416.
42. Schaverien MV, Coroneos CJ. Surgical treatment of lymphedema. *Plast Reconstr Surg*. 2019;144:738–758.
43. Langendoen SI, Habbema L, Nijsten TE, Neumann HA. Lipoedema: from clinical presentation to therapy. A review of the literature. *Br J Dermatol*. 2009;161:980–986.
44. White C. Clinical practice. Intermittent claudication. *N Engl J Med*. 2007;356:1241–1250.
45. Sumpio BE. Foot ulcers. *N Engl J Med*. 2000;343:787–793.
46. Ouriel K. Peripheral arterial disease. *Lancet*. 2001;358:1257–1264.
47. Al-Qaisi M, Nott DM, King DH, Kaddoura S. Ankle brachial pressure index (ABPI): an update for practitioners. *Vasc Health Risk Manag*. 2009;5:833–841.
48. Grenon SM, Gagnon J, Hsiang Y. Video in clinical medicine. Ankle-brachial index for assessment of peripheral arterial disease. *N Engl J Med*. 2009;361:e40.
49. Nishio H, Minakata K, Kawaguchi A, et al. Transcutaneous oxygen pressure as a surrogate index of lower limb amputation. *Int Angiol*. 2016;35:565–572.
50. Alavi A, Sibbald RG, Mayer D, et al. Diabetic foot ulcers: part II. Management. *J Am Acad Dermatol*. 2014;70(21):e1–e4; quiz 45–6.
51. Cavanagh PR, Lipsky BA, Bradbury AW, Botek G. Treatment for diabetic foot ulcers. *Lancet*. 2005;366:1725–1735.
52. Andersen CA, Roukis TS. The diabetic foot. *Surg Clin North Am*. 2007;87:1149–1177, x.
53. Falanga V. Wound healing and its impairment in the diabetic foot. *Lancet*. 2005;366:1736–1743.
54. Boulton AJ. Pressure and the diabetic foot: clinical science and offloading techniques. *Am J Surg*. 2004;187:17S–24S.
55. Richard JL, Sotto A, Lavigne JP. New insights in diabetic foot infection. *World J Diabetes*. 2011;2:24–32.
56. Boulton AJ, Kirsner RS, Vileikyte L. Clinical practice. Neuropathic diabetic foot ulcers. *N Engl J Med*. 2004;351:48–55.
57. Kranke P, Bennett M, Roeckl-Wiedmann I, Debus S. Hyperbaric oxygen therapy for chronic wounds. *Cochrane Database Syst Rev*. 2004:CD004123.
58. Thackham JA, McElwain DL, Long RJ. The use of hyperbaric oxygen therapy to treat chronic wounds: a review. *Wound Repair Regen*. 2008;16:321–330.
59. Tecilazich F, Dinh TL, Veves A. Emerging drugs for the treatment of diabetic ulcers. *Expert Opin Emerg Drugs*. 2013;18:207–217.
60. Steed DL. Clinical evaluation of recombinant human platelet-derived growth factor for the treatment of lower extremity ulcers. *Plast Reconstr Surg*. 2006;117:143S–149SS. discussion 150S–51S.
61. Dinh TL, Veves A. The efficacy of Apligraf in the treatment of diabetic foot ulcers. *Plast Reconstr Surg*. 2006;117:152S–157SS; discussion 158S–9S.
62. Marston WA. Dermagraft, a bioengineered human dermal equivalent for the treatment of chronic nonhealing diabetic foot ulcer. *Expert Rev Med Devices*. 2004;1:21–31.
63. White R, McIntosh C. A review of the literature on topical therapies for diabetic foot ulcers. Part 2: advanced treatments. *J Wound Care*. 2009;18:335–341.
64. Mayfield JA, Reiber GE, Sanders LJ, et al. Preventive foot care in diabetes. *Diabetes Care*. 2004;27(Suppl 1):S63–S64.
65. Markuson M, Hanson D, Anderson J, et al. The relationship between hemoglobin A(1c) values and healing time for lower extremity ulcers in individuals with diabetes. *Adv Skin Wound Care*. 2009;22:365–372.
66. Olesen CG, de Zee M, Rasmussen J. Missing links in pressure ulcer research--an interdisciplinary overview. *J Appl Physiol*. 1985;2010(108):1458–1464.
67. Morton LM, Phillips TJ. Wound healing and treating wounds: differential diagnosis and evaluation of chronic wounds. *J Am Acad Dermatol*. 2016;74:589–605; quiz 606.
68. Draper BK, Boyd AS. Diffuse dermal angiomatosis. *J Cutan Pathol*. 2006;33:646–648.
69. Trent JT, Kirsner RS. Leg ulcers in sickle cell disease. *Adv Skin Wound Care*. 2004;17:410–416.
70. Nakano J, Nakamura M, Ito T, et al. A case of antiphospholipid syndrome with cutaneous ulcer and intrauterine fetal growth retardation. *J Dermatol*. 2003;30:533–537.
71. Schwartzfarb EM, Romanelli P. Hyperhomocysteinemia and lower extremity wounds. *Int J Low Extrem Wounds*. 2008;7:126–136.
72. Darvall KA, Sam RC, Adam DJ, et al. Higher prevalence of thrombophilia in patients with varicose veins and venous ulcers than controls. *J Vasc Surg*. 2009;49:1235–1241.
73. Hafner J, Kuhne A, Schar B, et al. Factor V Leiden mutation in postthrombotic and non-postthrombotic venous ulcers. *Arch Dermatol*. 2001;137:599–603.
74. Musani MH, Musani MA, Verardi MA. Venous gangrene a rare but dreadful complication of deep venous thrombosis. *Clin Appl Thromb Hemost*. 2011;17:E1–E3.
75. Lupi O, Madkan V, Tyring SK. Tropical dermatology: bacterial tropical diseases. *J Am Acad Dermatol*. 2006;54:559–578; quiz 578–80.
76. Zeegelaar JE, Faber WR. Imported tropical infectious ulcers in travelers. *Am J Clin Dermatol*. 2008;9:219–232.



eFig. 105.1 Brown discoloration of the shins due to hemosiderin deposition. This occurs in the setting of venous hypertension and previous solar and traumatic purpura. Note the demarcation at the upper edges of her socks. *Courtesy Karynne O. Duncan, MD.*



eFig. 105.2 Acroangiodermatitis (pseudo-Kaposi sarcoma). Violaceous plaques in a patient with venous hypertension. *Courtesy David Khalil, MD.*



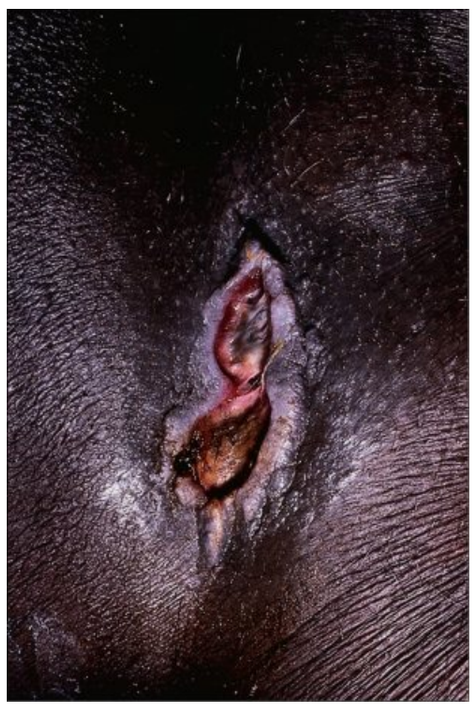
eFig. 105.3 Venous ulcer of the medial malleolus. This is a common site for this type of ulcer. Induration due to lipodermatosclerosis, hemosiderin deposition, and atrophie blanche scars were present in the surrounding skin. *Courtesy Jean L. Bolognia, MD.*



eFig. 105.4 Elephantiasis nostras verrucosa. Multiple fibrotic papules and nodules. *Courtesy Jean L. Bolognia, MD.*



eFig. 105.5 Mal perforans. Neuropathic ulcerations at pressure points on the plantar surface of the great toes in a patient with diabetic neuropathy. Note the thick rim of callus.



eFig. 105.6 Sacral decubitus ulcer. *Courtesy Ronald P. Rapini, MD.*



eFig. 105.7 Pressure ulcer on the back in a wheelchair-bound patient. *Courtesy Julie V. Schaffer, MD.*



eFig. 105.8 Diffuse dermal angiomatosis. Ulcerations can develop within the reticulated violaceous plaques. Note that the breasts are pendulous. *Courtesy Luis Requena, MD.*



eFig. 105.9 Phlegmasia cerulean dolens. Reticulated violaceous discoloration of the distal foot due to deep venous thrombosis. Ulceration can develop within the areas of ischemia.



eFig. 105.10 Prolidase deficiency with spontaneous ulcers and scarring from previous ulcerations. *Courtesy Edward Cowen, MD.*

106 Other Vascular Disorders

Robert Kelly and Christopher Baker

Chapter Contents

Livedo Reticularis and Livedo Racemosa 1864
Flushing 1867
Erythromelalgia 1868
Telangiectasias 1870
Venous Lakes 1873
Nevus Anemicus 1873
Angiospastic Macules (Bier Spots) 1874

INTRODUCTION

This chapter will cover several disorders of the skin vasculature, including livedo reticularis, flushing, and erythromelalgia, as well as vascular ectasias such as telangiectasias and venous lakes. Some of the diseases described here are important skin signs of systemic disease, while others are incidental findings. Additional disorders of blood vessels are covered elsewhere, e.g. infantile hemangiomas (Ch. 103), vascular malformations (Ch. 104), and vascular neoplasms and proliferations (Ch. 114).

LIVEDO RETICULARIS AND LIVEDO RACEMOSA

Key features

- Livedo reticularis – may be physiologic or pathologic, presenting as an even and complete reticulated vascular network; due to slow flow and subsequent accumulation of blood within the cutaneous vasculature, with histologic findings that are generally unremarkable
- Livedo racemosa – due to pathologic changes within cutaneous vessels that are identifiable histologically, leading to disruption of cutaneous blood flow; presents as an uneven and fragmented reticular vascular pattern
- Appropriate investigations depend on the clinical context and associated findings

Introduction

The term "livedo" refers solely to a color change, but it is commonly combined with a modifier to describe two different net-like patterns of blanchable, red–purple discoloration. These two types are livedo reticularis (LRe) and livedo racemosa (LRa). LRe is an extremely common finding and usually results from a physiologic vasospastic response to cold exposure. It presents as an even and complete red–purple net-like pattern. Among normal healthy individuals, the predisposition to LRe will vary. However, it can also be a reflection of a number of underlying systemic diseases.

LRa is less common and is associated with underlying pathology. A broken reticular vascular pattern with a disrupted branching appearance is observed. The distribution is often patchy, and depending on the underlying cause and severity, LRa may be accompanied by retiform purpura.

Both LRe and LRa can vary with changes in external temperature, i.e. disappearing with warming and reappearing with cooling. The reticular vascular pattern can become more prominent with rest or it may become less pronounced with exercise or leg elevation due to reduced stasis of blood within cutaneous vessels.

History

The term "livedo reticularis" was first used by Hebra over a century ago to describe a violaceous skin discoloration caused by an abnormality of the cutaneous circulation. Renault (1883) and later Unna (1896) and Spalteholz (1927) suggested that a cone arrangement of the cutaneous microvasculature served as an explanation for the occurrence and pattern of LR[1].

Pathogenesis

Both LRe and LRa result from alterations in blood flow through the cutaneous microvasculature (Fig. 106.1). The latter consists of arterioles that are oriented perpendicularly to the skin surface. The vessels ultimately divide into capillary beds that in turn drain into a subpapillary plexus. It has been proposed that this arrangement of vessels gives rise to a series of 1- to 3-cm cones with the ascending arteriole at the apex of each cone. At the edge of the cone, the venous plexus is more prominent, and the arterial bed is diminished. Any process that either reduces blood flow to and through the skin or reduces drainage of blood out of the skin will result in the accumulation of deoxygenated blood in the venous plexus, leading to the clinical appearance of LRe or LRa[1–3].

There are a number of causes of LRe and LRa (Table 106.1), and the clinical pattern can vary with the nature of the underlying cause.

A complete fine network, as seen in LRe, is indicative of alterations in blood flow caused by vasospasm or by factors within the blood that alter the viscosity and flow through the vessels. On the other hand, vessel wall pathology and intraluminal obstruction can give rise to the irregular, disrupted, patchy pattern of LRa (Figs. 106.2 & 106.3). When LRa is widespread, disorders such as lymphocytic thrombophilic arteritis[4,5], Sneddon syndrome, and antiphospholipid antibody syndrome (APS)[6,7] should be strongly considered.

Clinical Features

Livedo reticularis

Congenital livedo reticularis

Cutis marmorata telangiectatica congenita

Cutis marmorata telangiectatica congenita (CMTC) is characterized by a persistent reticulated vascular pattern that is often limited to one extremity (see Ch. 104), but can be more widespread. Lesions are usually noted at birth, and, when the trunk is involved, there may be a sharp cut-off at the midline. Associated anomalies include other vascular malformations, limb asymmetry, and occasionally neurologic or ocular abnormalities[8,9]. Cutaneous vascular changes can improve during the first few years of life, with 20% of patients showing complete resolution.

Acquired livedo reticularis

Cutis marmorata/physiologic livedo reticularis

These terms are synonymous and refer to a normal pattern of LRe that is due to vasospasm in response to cold (Fig. 106.4A). It is often more marked in neonates, infants, and young children[2,3], with the term *cutis marmorata* often used to describe LRe in children. The LRe is often widespread, particularly on the lower extremities. There is significant fluctuation with changes in temperature, and the vascular pattern generally disappears with warming. Although frequently physiologic in nature, secondary causes such as vasospasm in the setting of lupus erythematosus and Raynaud phenomenon need to be considered (see Table 106.1)[2,3]. In adults, it may be associated with a tendency towards acrocyanosis and chilblains.

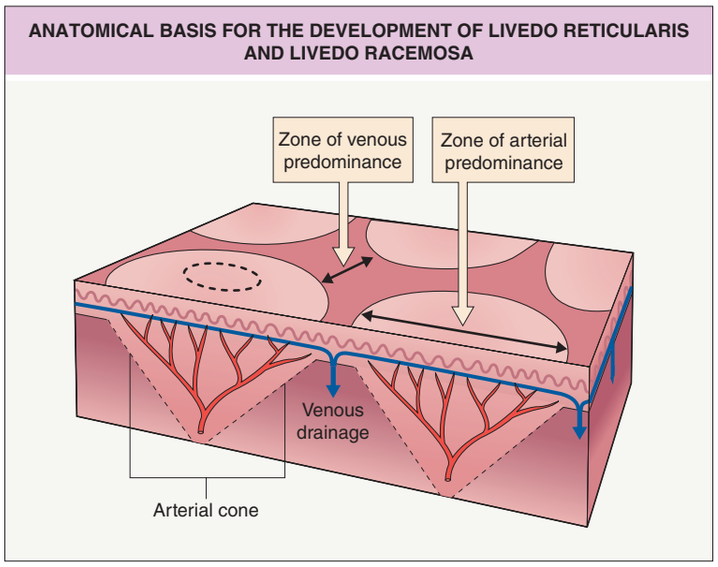


Fig. 106.1 Anatomical basis for the development of livedo reticularis and livedo racemosa. An elliptical biopsy from the paler central "hole" in the net pattern is necessary in order to sample the affected arterioles (dashed oval); serial sectioning may be required.

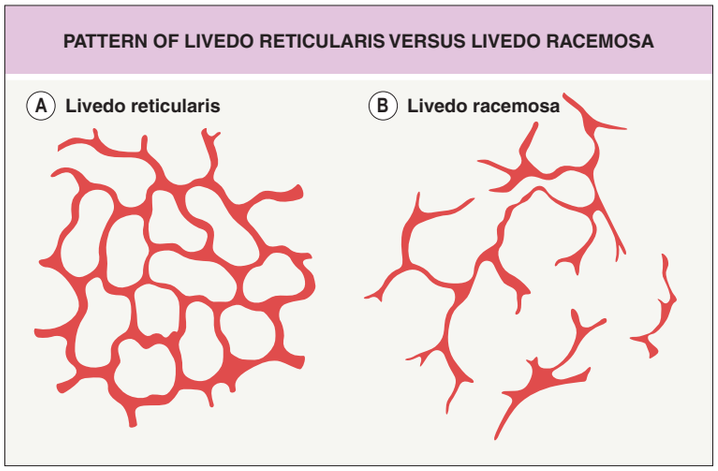


Fig. 106.2 Pattern of livedo reticularis (A) versus livedo racemosa (B).



Fig. 106.3 Livedo racemosa in a patient with lymphocytic thrombophilic arteritis. A more irregular, broken, and branching pattern is seen, as compared to livedo reticularis.

CAUSES OF LIVEDO RETICULARIS AND LIVEDO RACEMOSA

Livedo reticularis

Congenital

- Cutis marmorata telangiectatica congenita

Acquired

Vasospasm

- Cutis marmorata/physiologic livedo reticularis
- Autoimmune connective tissue diseases (e.g. SLE)
- Raynaud phenomenon/disease

Intraluminal pathology

- Increased normal blood components
  - Thrombocythemia
  - Polycythemia vera
- Abnormal proteins
  - Cryoglobulins
  - Cryofibrinogens
  - Cold agglutinins
  - Other paraproteins (e.g. IgM)

Livedo racemosa

Vessel wall pathology

- Vasculitis
  - Cutaneous polyarteritis nodosa (cutaneous arteritis)
  - Systemic polyarteritis nodosa
  - Cryoglobulinemic vasculitis
  - Autoimmune connective tissue disease-associated vasculitis (e.g. rheumatoid arthritis, SLE, Sjögren syndrome)
- Lymphocytic thrombophilic arteritis (macular arteritis, macular lymphocytic arteritis)
- Calciphylaxis
- Sneddon syndrome
- Deficiency of adenosine deaminase 2
- VEXAS syndrome
- Livedoid vasculopathy (also intraluminal obstruction)

Intraluminal pathology

- Thrombophilia/hypercoagulability (see Table 105.9)
  - Antiphospholipid antibody syndrome
  - Protein S and C deficiencies
  - Antithrombin III deficiency
  - Factor V Leiden mutation
  - Homocystinuria, hyperhomocysteinemia
  - Disseminated intravascular coagulation
  - SARS-CoV-2
- Thrombotic thrombocytopenic purpura
- Embolic
  - Cholesterol emboli
  - Septic emboli
  - Atrial myxoma
  - Nitrogen (decompression sickness)
  - Carbon dioxide arteriography
- Hyperoxaluria/oxalosis
- Intralymphatic histiocytosis

Additional causes of livedo reticularis and livedo racemosa

- Medications (e.g. amantadine, norepinephrine, gemcitabine, interferon)
- Infections (e.g. hepatitis C [vasculitis], *Mycoplasma* spp. [cold agglutinins], syphilis)
- Neoplasms (e.g. pheochromocytoma)
- Neurologic disorders (e.g. complex regional pain syndrome [reflex sympathetic dystrophy], paralysis)
- Moyamoya disease

Table 106.1 Causes of livedo reticularis and livedo racemosa. SLE, systemic lupus erythematosus; VEXAS, vacuoles, E1 enzyme, X-linked, autoinflammatory, somatic.

Livedo reticularis due to intraluminal pathology

LRe can result from circulating proteins or cells that slow intravascular blood flow. Abnormal circulating proteins (e.g. cryoglobulins[10], cryofibrinogens, cold agglutinins, IgM paraproteins) can lead to increased blood viscosity. Additionally, an increase in normal blood components in disorders such as polycythemia vera[11] and thrombocythemia

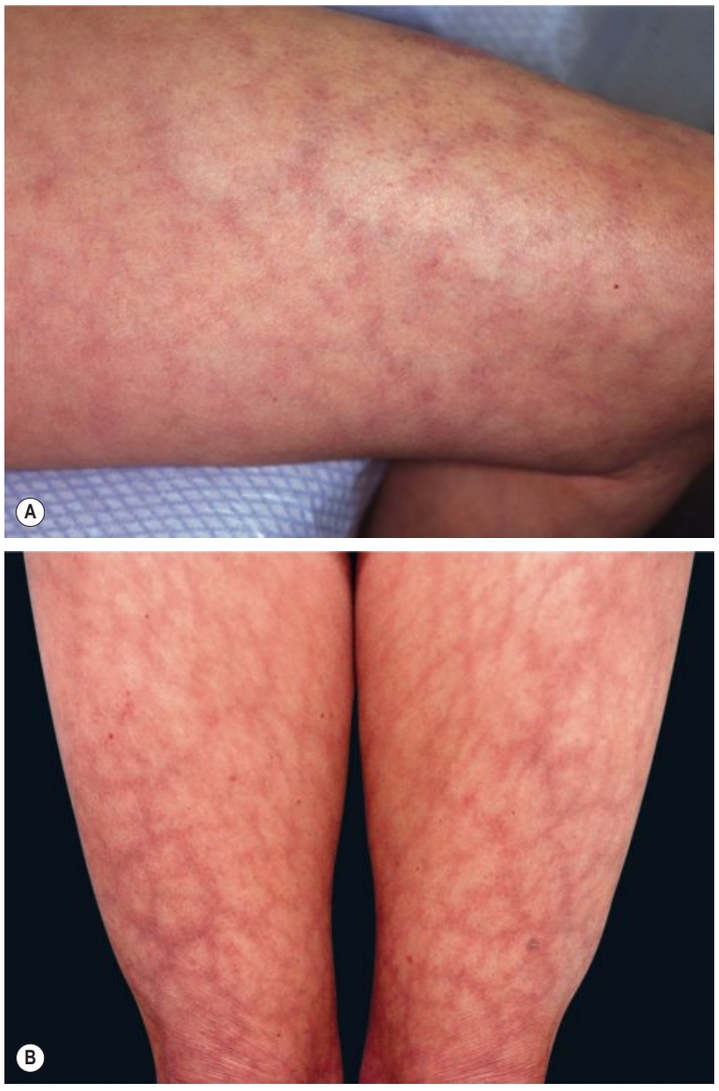


Fig. 106.4 Livedo reticularis. A An even, net-like pattern is seen on the thigh in physiologic livedo reticularis. **B** Livedo reticularis in a patient with systemic lupus erythematosus. *B, Courtesy Jeffrey P. Callen, MD.*

(essential thrombocytosis) may result in altered blood flow. LRe of the lower extremities is often seen in patients with neurologic conditions that lead to immobility of the lower limbs and intravascular stasis.

Livedo racemosa

Livedo racemosa due to vessel wall pathology

LRa results from more significant disruption of blood flow, either from narrowing or complete obstruction of vessel lumina. The most common cause is *vasculitis* involving the medium-sized arterioles at the dermal–subcutaneous junction or in the deep dermis. It is a characteristic finding in cutaneous polyarteritis nodosa (cPAN; more recently renamed cutaneous arteritis)[12], in which there is predominantly involvement of medium-sized arterioles, but can also be seen in systemic PAN and ANCA-associated vasculitides (see Ch. 24). In cPAN, the LRa often has a "starburst" pattern with scattered separate reticulated red–purple patches.

Lymphocytic thrombophilic arteritis, also known as macular arteritis or macular lymphocytic arteritis, often presents with widespread blanchable LRa (see Fig. 106.3)[4,5,13]. Additional clinical findings include patches of macular pigmentation and focal areas of cutaneous ulceration[4]. The vascular inflammation is lymphocytic rather than neutrophilic, and this allows distinction from cPAN. *Livedoid vasculopathy* may also be associated with LRa, but the vascular pattern is usually limited to the lower extremities (see Ch. 23)[14].

Sneddon syndrome is rare and is characterized by widespread LRa as well as multiple transient cerebral ischemic attacks and infarctions. The latter can lead to progressive neurologic impairment[6,7] (see Ch. 23). The LRa is often located on the trunk, buttocks, and proximal



Fig. 106.5 Calciphylaxis in a patient with end-stage chronic renal disease. There is retiform purpura and a large black eschar overlying cutaneous necrosis. Note the violaceous reticulated pattern on the inner thighs. Because the patient was also receiving warfarin, the differential diagnosis included warfarin necrosis. *Courtesy Alicia Little, MD.*

extremities, with a typically large branching pattern. Histologically, there is vessel wall thickening due to intimal smooth muscle proliferation and luminal narrowing. Because this thickening can be preceded by partial or complete vessel occlusion by fibrin thrombi, there is overlap with intraluminal pathology (see below).

ADA2 deficiency is due to homozygous or compound heterozygous mutations in *CECR1* which encodes adenosine deaminase 2 (see Ch. 45). This disorder is also known as vasculitis, autoinflammation, immunodeficiency, and hematologic defects syndrome (VAIHS). It usually presents during childhood and the vascular inflammation favors the skin and central nervous system; a PAN-like presentation with LRa and nodules is accompanied by early-onset cerebrovascular accidents (CVAs; see Fig. 45.11). In addition to hepatosplenomegaly, patients may have fevers, hypogammaglobulinemia, and cytopenias[15,16].

Calciphylaxis consists of calcium deposition within the walls of blood vessels (see Ch. 50). It is most commonly seen in the setting of end-stage chronic kidney disease complicated by secondary hyperparathyroidism. Calciphylaxis may initially commence with LRa that then becomes purpuric and subsequently necrotic (Fig. 106.5)[17].

Livedo racemosa due to intraluminal pathology

Complete obstruction of the vessel lumen can result from either emboli (e.g. cholesterol emboli derived from atheromata[18]) or thromboses within vessels due to thrombophilia (hypercoagulability). As outlined in Table 105.9, causes of thrombophilia include APS[19] and deficiencies of protein C[20], protein S, or antithrombin III[21]. Exposure to either heparin or warfarin can also lead to thrombosis-induced cutaneous necrosis. In patients with severe SARS-CoV-2 infection, a thrombotic vasculopathy can develop, with both LRe and LRa having been observed[22].

Intracellular crystal deposition is seen in hyperoxaluria and this also gives rise to luminal obstruction and LRa[23]. A patchy, discontinuous pattern is seen and it may subsequently become purpuric with areas of infarction and necrosis.

Other causes of livedo reticularis and livedo racemosa

There are numerous causes of LRe and LRa cited in the literature, and for most, one of the above mechanisms can generally be implicated. The other causes include drugs such as amantadine[24] and norepinephrine (noradrenaline), as well as infections. The latter can lead to: the production of cryoglobulins, cold agglutinins, or antiphospholipid antibodies; the induction of immune vasculitis; or septic vasculitis or septic emboli. Neoplasms may also be an underlying trigger via hypercoagulability or paraproteinemia as well as vasospasm (e.g. pheochromocytoma). Lastly, these vascular patterns may be seen in several neurologic conditions (e.g. complex regional pain syndrome) as a result of vasospasm or vasodilation (this is in addition to stasis arising from immobility).

Differential Diagnosis

Erythema ab igne is a heat-induced skin disease that begins as a reversible LRe, then with continued heat exposure, it evolves into a fixed reticulated hyperpigmentation. The sites of involvement reflect the source of exposure, e.g. heating pad, laptop computer, space heater. Various cutaneous eruptions may have a reticulated pattern and might be considered in the differential diagnosis, including reticulated erythematous mucinosis (favors mid central trunk) and some viral exanthems (e.g. erythema infectiosum). Poikilodermatous conditions may also have a reticulated pattern (e.g. dermatomyositis, mycosis fungoides); however, the presence of epidermal changes and telangiectasias help to distinguish these conditions.

Pathology

The histology of LRe and LRa varies depending on the underlying cause. In general, no specific abnormality is evident in LRe, but there may be ectasia of superficial blood vessels. With LRa, a number of abnormalities may be seen, including vasculitis, calcium deposition within vessel walls (calciphylaxis; see Fig. 50.6), intravascular eosinophilic plugging (monoclonal cryoglobulinemia; see Fig. 23.4), intraluminal thromboses (hypercoagulable states), cholesterol clefting (cholesterol emboli; see Fig. 23.5), and crystal deposition (oxalosis). In Sneddon syndrome, an occlusive vasculopathy is followed by subendothelial smooth muscle hyperplasia with partial or complete occlusion of affected arterioles. However, in order to find these histopathologic changes, it is necessary to sample the affected arterioles. An elliptical incisional biopsy from the paler central "hole" in the net pattern is necessary and serial sectioning may be required (see Fig. 106.1).

Treatment

Identification of the underlying cause or associated disorder determines the appropriate treatment options.

FLUSHING

Key features

- Flushing is a physiologic response, but in an exaggerated form causes clinical symptoms
- Common triggers (e.g. heat, emotion, exercise, some foods) will exacerbate flushing of any cause
- Causes of excessive flushing include exogenous medications, menopause, neurologic disorders, and systemic diseases (e.g. carcinoid syndrome)

Introduction

Flushing is the term used to describe transient and episodic reddening of the skin, most commonly of the face, and less often the neck, ears, and upper chest. It is the visible sign of a generalized increase in cutaneous blood flow. The greater visibility and capacitance of the superficial cutaneous vasculature of the face and adjacent areas accounts for the limited distribution[25]. In the evaluation of an affected patient, there are a number of causes to consider, including underlying systemic disorders (Table 106.2).

Pathogenesis

An increase in cutaneous blood flow occurs with relaxation of vascular smooth muscle. This may occur via the autonomic nervous system[26] (usually leading to active vasodilation), endogenous vasoactive agents (such as histamine and serotonin), or exogenous agents (Table 106.3). Alcohol-induced flushing may result from the direct effect of alcohol as well as cutaneous vasodilation from elevated blood levels of acetaldehyde; the latter occurs in those with alcohol dehydrogenase deficiency (prevalent in East Asians) and in the "disulfiram reaction" induced by some medications. Flushing from fermented alcoholic drinks may be caused by vasoactive substances such as tyramine. Vasodilation mediated by the autonomic nervous system is often accompanied by eccrine sweating due to a direct effect on both sweat glands and blood vessels (wet flush)[27]. Direct vasodilation by vasoactive agents is usually not associated with increased sweating (dry flush).

CAUSES OF FLUSHING

• Physiologic
• Exogenous agents (see Table 106.3)
• Menopause
• Neurologic disorders
  • Anxiety
  • Autonomic dysfunction, including CNS-driven*
  • Tumors (e.g. hypogonadal pituitary tumors)
  • Migraine
  • Frey syndrome (auriculotemporal syndrome)
• Dumping syndrome due to rapid gastric emptying
• Systemic diseases
  • Carcinoid syndrome
  • Mastocytosis
  • Pheochromocytoma
  • Medullary carcinoma of the thyroid
  • Thyrotoxicosis
  • POEMS syndrome
  • Pancreatic tumors (e.g. VIPomas)
  • Prostaglandin-secreting renal cell carcinoma

*May be rapidly fluctuating in the setting of increased intracranial pressure, head trauma, or benzodiazepine withdrawal-induced catatonia.

Table 106.2 Causes of flushing. Rosacea may be associated with pronounced flushing, but usually fixed erythema, papulopustules, edema, and/or telangiectasia are present to some degree. Patients with rubeosis facei diabeticorum may note facial warmth. CNS, central nervous system; POEMS, *p*olyneuropathy, *o*rganomegaly, *e*ndocrinopathy, *M*-protein (monoclonal gammopathy), *s*kin changes; VIP, vasoactive intestinal polypeptide.

EXOGENOUS AGENTS THAT CAN CAUSE FLUSHING

• Alcohol
• Drugs
  • Angiotensin-converting enzyme (ACE) inhibitors
  • Calcium channel blockers
  • Calcitonin
  • Chlorpropamide*
  • Cholinergic agonists (e.g. pilocarpine)
  • Cyclosporine
  • Dupilumab*
  • Disulfiram*
  • Fumaric acid esters
  • Gold ("nitritoid reactions")
  • Hormone therapy (e.g. anastrozole, tamoxifen)
  • Hydralazine
  • Metronidazole*
  • Nicotinic acid
  • Nitrates (e.g. glyceryl trinitrate)
  • Opiates
  • Prostaglandins
  • Sildenafil, tadalafil, vardenafil
  • Tamoxifen
  • Topical calcineurin inhibitors*
  • Serotonin syndrome (usually combination of two drugs such as MAO inhibitor plus SSRI)
• Foods
  • Spoiled scombroid fish
• Food additives
  • Monosodium glutamate (MSG), sodium nitrite, sulfites

*With alcohol intake.

Table 106.3 Exogenous agents that can cause flushing. MAO, monoamine oxidase; SSRI, selective serotonin reuptake inhibitor.

Clinical Features

Blushing is a common emotionally triggered form of flushing associated with embarrassment and anxiety and is considered an exaggerated physiologic response. *Physiologic flushing* also occurs as part of normal

thermoregulation in response to heat or exercise. *"Hot flashes"* refer to flushing associated with menopause, which lasts for a few minutes and is usually associated with sweating[28].

Flushing of any cause may be exacerbated or triggered by a number of common factors such as heat, hot drinks, exercise, anxiety, food additives (e.g. sulfites), and alcohol. Affected patients often report a feeling of heat and burning of the skin during episodes and find the color change a social hindrance. Some patients become anxious that they will flush at inopportune times and this further exacerbates the problem. Repeated flushing may result in permanent "fixed" erythema and telangiectasias.

Carcinoid tumors that secrete vasoactive agents (e.g. serotonin) are associated with the carcinoid syndrome (Table 106.4). This syndrome includes flushing, which is often severe[29], and it may be precipitated by common triggers of flushing. The classic "carcinoid flush" occurs with ~10% of *midgut* tumors (small intestine, appendix, proximal colon), but only when there are associated liver metastases; it lasts minutes and consists of erythema and pallor as well as a cyanotic hue. Type III *gastric* carcinoid tumors are associated with a pruritic, patchy, bright red flush admixed with white patches and probably mediated by histamine. *Bronchial* tumors are associated with a prolonged (hours to days), intensely red to purple flush. Hindgut tumors (distal colon, rectum) are rarely, if ever, associated with the carcinoid syndrome and flushing, even with liver metastases.

An approach to the clinical assessment of flushing and relevant investigations are listed in Table 106.5.

SIGNS AND SYMPTOMS OF THE CARCINOID SYNDROME

• Cutaneous
  • Flushing
  • Vascular rosacea-like changes
  • Pellagra
  • Edema and induration of the face > extremities
• Bronchospasm
• Diarrhea
• Cardiac dysfunction (right-sided)
• Hypotension
• Peptic ulcers

Table 106.4 Signs and symptoms of the carcinoid syndrome.

CLINICAL APPROACH TO THE EVALUATION OF FLUSHING

1. Identify provocative factors
  • Direct questioning
  • Patient diary (food, medications, activities)
2. Check for associated symptoms
  • Sweating
  • Fever
  • Urticaria
  • Diarrhea
  • Bronchospasm
3. Investigation (not required in all cases)
  Indicated if flushing:
  • Of sudden or recent onset
  • Severe
  • Associated with systemic symptoms
  Investigations to consider:
  • Complete blood count with differential and platelets
  • Thyroid function tests
  • Serum estrogen, FSH, LH
  • Serum tryptase [M]; serum chromogranin A levels [C]; plasma free metanephrines [P]
  • 24-hour urine collection for:
  • Serotonin metabolites such as 5-hydroxyindole acetic acid (5-HIAA) [C]
  • Fractionated metanephrines (more specific but less sensitive than plasma) [P]
  • Histamine metabolites such as methylimidazole acetic acid (MeImAA) [M]
  • CT/MRI scans; octreotide/somatostatin receptor scintigraphy (using radiolabeled octreotide)
4. Elimination
  • Exclude suspected drugs and food additives

Table 106.5 Clinical approach to the evaluation of flushing. C, carcinoid; FSH, follicle stimulating hormone; LH, luteinizing hormone; M, mastocytosis; P, pheochromocytoma.

Differential Diagnosis

Fixed erythema, and sometimes telangiectasias, of the face and neck are seen in fair-skinned individuals with photodamage as well as patients with seborrheic dermatitis and photosensitive autoimmune connective tissue diseases (e.g. dermatomyositis). Affected individuals may complain of the persistent redness and burning of the skin rather than actual flushing. Rosacea may be associated with pronounced flushing, but usually fixed erythema, papulopustules, edema, and/or telangiectasias are present to some degree.

Treatment

The clinician should consider and eliminate any suspected exogenous cause (see Table 106.3). Underlying systemic causes, although rare, should be considered (see Table 106.2). Triggers of flushing are likely to be clinically relevant in most patients and should be avoided where possible. Non-selective β-blockers (e.g. nadolol, propranolol) or clonidine may be effective in idiopathic flushing. Anxiolytics may be helpful, particularly if emotional symptoms or anxiety are triggers. Menopausal flushing may respond to hormone replacement therapy, clonidine, or selective serotonin reuptake inhibitors (SSRIs). In troublesome cases unresponsive to these measures, transthoracic endoscopic sympathectomy may be considered.

ERYTHROMELALGIA

Synonyms: ■ Erythermalgia ■ Erythralgia

Key features

- Characterized by painful burning and erythema of the distal extremities (lower > upper)
- Precipitated by heat and relieved by cooling
- May be idiopathic, familial, or arise secondarily due to an underlying condition (e.g. thrombocythemia)

Introduction

Erythromelalgia is an episodic condition characterized by a burning sensation, erythema, and increased skin temperature. It affects acral sites, particularly the lower extremities. Classically, there are three major forms, including:

- type 1 – associated with thrombocythemia
- type 2 – primary or idiopathic form
- type 3 – associated with underlying causes other than thrombocythemia.

History

The term "erythromelalgia" was first coined by Mitchell in 1878. It was used to describe redness (erythros), involvement of extremities (melos), and pain (algos). The diagnostic criteria were established by Thompson[30] in 1979: (1) burning pain in the extremities; (2) pain aggravated by warming; (3) pain relieved by cooling; (4) erythema of affected skin; and (5) increased temperature of affected skin.

Epidemiology

In Norway, the estimated incidence of erythromelalgia is 0.25/100 000 with a prevalence of 2/100 000[31]. While types 1 and 3 usually appear during adulthood, type 2 may appear in childhood and may be familial. The female : male incidence varies from 2 : 1 to almost 3 : 1. In one study, the mean age of onset was 56 years (range, 5–91 years) with 4% having their symptoms begin during childhood.

Pathogenesis

While the discovery of *SCN9A* mutations in patients with primary familial erythromelalgia has provided insights into this disorder, in general, the pathogenesis of erythromelalgia is not entirely understood. Firstly, it may

vary depending on the underlying cause and between different patient subgroups. For example, in patients with thrombocythemia, the pathophysiology is likely to be related to both increased numbers of platelets as well as abnormalities in platelet function. Of note, one explanation for why type 1 erythromelalgia does not respond to heparin or warfarin is that the microthrombi that form do not require thrombin activation[32].

In other types of erythromelalgia, changes in vascular dynamics may be a factor. It has been proposed that hyperemia results from increased blood flow through arteriovenous shunts with a resultant reduction in blood flow within nutritional vessels, thus leading to cutaneous hypoxia[31,33]. Another proposed mechanism is vasoconstriction (as occurs in Raynaud phenomenon), but in erythromelalgia this is followed by a prolonged phase of hyperemia[34]. A temperature-triggered release of vasoactive substances and chemical pain mediators may also play a role.

In 2004, gain-of-function missense mutations in *SCN9A*, which encodes the voltage-gated sodium channel alpha subunit Nav1.7, were first described in patients with primary familial erythromelalgia[35]. Nav1.7 produces threshold currents and is expressed primarily within dorsal root ganglia of sensory neurons (especially nociceptors) and sympathetic ganglion neurons. Mutations lead to lowered thresholds and "over-excitability" of pain-signaling sensory neurons[36] while at the same time producing "under-excitability" of sympathetic neurons. Certain mutations that produce a lesser effect on sodium channel activation and subsequent neuron excitability are associated with a later onset of clinical signs and symptoms[37].

Another dominantly inherited pain syndrome, paroxysmal extreme pain disorder, has also been found to be due to gain-of-function mutations in *SCN9A*, whereas loss-of-function mutations in both copies of this gene lead to a recessively inherited insensitivity to pain[38]. Lastly, there exist additional families that are not linked to chromosome 2q31–32 (*SCN9A* locus), suggesting genetic heterogeneity[39].

Associations in secondary erythromelalgia include myelodysplastic syndromes, diabetes mellitus, peripheral arterial disease, vasculitis, systemic lupus erythematosus, and other autoimmune connective tissue diseases.

Clinical Features

Erythromelalgia is characterized by burning, erythema, and warmth of acral sites (Fig. 106.6). Attacks most commonly occur late in the day, last through the night, and frequently impair sleep. The symptoms are usually episodic, although occasionally they may be continuous. The feet are involved in 90% of patients, whereas the hands are affected in 25%. Less commonly, there is also involvement of the head and neck. Type 1 erythromelalgia may be unilateral and is more frequently associated with progression to ischemic necrosis. In contrast, the idiopathic form is more likely to be bilateral. The pain is precipitated by minor elevations in temperature (between 32°C and 36°C). Other exacerbating factors include exercise, standing, walking, fever, and limb dependency. Cooling and limb elevation generally reduce the symptoms.

The affected areas will often appear red and swollen. Other findings include acrocyanosis, livedo reticularis, facial flushing, cutaneous necrosis, and ulceration. In up to 40% of patients, the limb may appear normal between attacks. Prolonged immersion in water can lead to extensive maceration and contribute to ulcer formation.

Prognosis is variable. In one long-term study, ~30% of patients fell into each of three categories: worsening, no change, and improvement. A further 10% had complete resolution of their symptoms[40].

Pathology

In type 1 erythromelalgia, vessels may show intimal proliferation and occlusive thrombosis followed by complete fibrosis of the affected arterioles. In general, however, biopsies are not required and histology is nonspecific.

Differential Diagnosis

Complex regional pain syndrome (CRPS; reflex sympathetic dystrophy) may sometimes have features similar to erythromelalgia (see Ch. 6). Abnormal warmth, erythema, and burning pain may be seen in both, but CRPS does not have the characteristic close relationship to temperature and tends to be constant rather than episodic. Peripheral neuropathy may also cause tingling and burning and may require differentiation by nerve conduction studies. Calcium channel blockers, autonomic dysfunction, acrodynia, and mushroom poisoning, as well as occlusive vascular diseases such as thromboangiitis obliterans, may be associated with erythromelalgia-like symptoms. It is important to consider underlying causes of erythromelalgia – in particular, chronic myeloproliferative disorders – as erythromelalgia may be the first sign of the latter.

Treatment

Although numerous treatments have been reported as possible therapies for erythromelalgia, no single therapy is consistently effective and many cases can prove difficult to control. The assistance of a specialist pain clinic can be valuable. Various methods of cooling the limbs during attacks, such as fans, wet dressings, and ice packs wrapped in towels, should be explored and have often already been tried by the time of presentation. Frequent periods of leg elevation can be helpful in reducing both discomfort and leg edema, whereas prolonged periods of leg dependency should be avoided. Simple oral analgesia is also important.

Aspirin can be effective for type 1 erythromelalgia and treatment for the thrombocythemia with medications such as hydroxyurea and (based upon mutational analysis) JAK inhibitors should also be considered. Topical therapies include capsaicin cream, 1%–2% amitriptyline/0.5% ketamine gel, and lidocaine patches, while possible oral medications include SSRIs (e.g. venlafaxine), tricyclic antidepressants (e.g. amitriptyline), anticonvulsants (e.g. gabapentin, carbamazepine), calcium channel blockers (e.g. diltiazem), the prostaglandin analogue misoprostol, and especially



Fig. 106.6 Erythromelalgia. Red hot painful hand (**A**) and feet (**B**) in two patients with erythromelalgia. *A, Courtesy Agustin Aloma, MD.*

in primary inherited erythromelalgia, sodium channel blocking agents (e.g. mexiletine, flecainide)[41,42]. With the report of functional expression studies (based upon a specific mutation) correlating with clinical responsiveness to carbamazepine or mexiletine, the possibility exists of utilizing such assays in the future to guide therapy. Rizatriptan, a selective agonist of serotonin 5-HT_{1B} and 5-HT_{1D} receptors, can be used for acute pain attacks in patients with primary erythromelalgia. In addition, there are ongoing trials of Nav1.7 channel blockers, both oral and topical.

Several intravenous therapies have been used for more severe cases, including nitroprusside, prostaglandin E1, and lidocaine (combined with oral mexiletine). More invasive approaches include epidural infusions of bupivacaine and opiates, lumbar sympathetic blocks, and bilateral lumbar sympathectomies[43]. Oral medications should be tried initially, but more invasive procedures may be necessary for more severe cases.

TELANGIECTASIAS

Key features

- Telangiectasia is due to persistently dilated dermal vessels and not angiogenesis
- Can occur as a primary process, a result of cutaneous damage, or secondary to systemic disease

Introduction

Telangiectasia refers to abnormal, small, persistently dilated blood vessels visible in the skin (Fig. 106.7). Individual vessels can be discerned and range in color from light red to deep purple and will usually empty with pressure. They occur as a result of vascular dilation rather than new vessel growth and are thought to arise from capillaries, venules, or small arteriovenous malformations. Telangiectasias are seen in a range of clinical settings (Table 106.6).

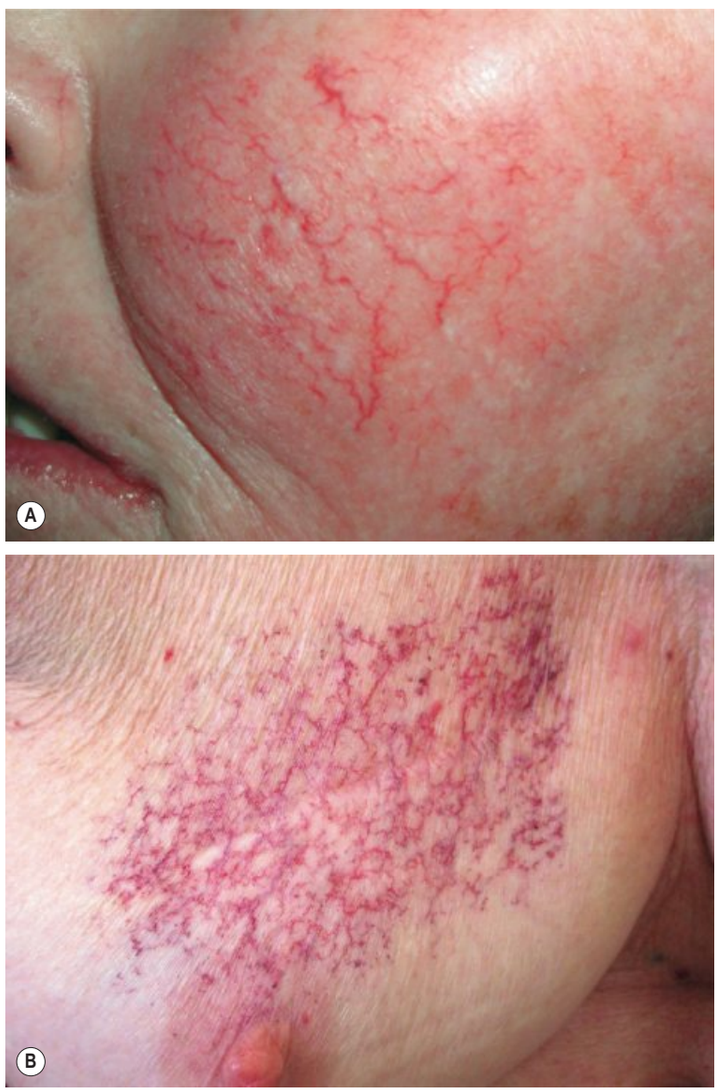


Fig. 106.7 Telangiectasias. A Sun-induced telangiectasias on the cheek. **B** Prominent telangiectasias on the breast following radiation therapy.

CAUSES OF TELANGIECTASIAS
Primary
• Spider telangiectasias (also associated with estrogen excess) • Hereditary benign telangiectasia (Fig. 106.8)* • Costal fringe • Angioma serpiginosum • Unilateral nevoid telangiectasia • Generalized essential telangiectasia • Cutaneous collagenous vasculopathy
Secondary to physical changes or damage
• Photodamage • Post radiation therapy • Traumatic • Venous hypertension
Skin disease
• Telangiectatic rosacea • Incipient or involuted infantile hemangiomas • Basal cell carcinoma
Hormonal/metabolic

• Estrogen-related
  • Liver disease
  • Pregnancy
  • Exogenous estrogens
• Corticosteroids (topical, systemic, Cushing syndrome)

Anti-neoplastic agents
• Tesirine† (e.g. loncastuximab tesirine-lpyl) • Ado-trastuzumab emtansine†
Systemic conditions

• Carcinoid syndrome
• Mastocytosis (telangiectasia macularis eruptiva perstans)
• Autoimmune connective tissue diseases
  • Lupus erythematosus
  • Dermatomyositis
  • CREST syndrome/systemic sclerosis
• Mycosis fungoides, including poikilodermatous
• B cell lymphomas
• TEMPI syndrome
• Angiolupoid sarcoidosis
• GVHD (in the context of poikiloderma)
• HIV infection (anterior chest)

Congenital malformations and genodermatoses
• Cutis marmorata telangiectatica congenita • Klippel–Trenaunay syndrome • Hereditary hemorrhagic telangiectasia • Ataxia–telangiectasia • Hypotrichosis–lymphedema–telangiectasia syndrome • Rombo syndrome • Bloom syndrome • Rothmund–Thomson syndrome • Poikiloderma with neutropenia • Dyskeratosis congenita • Xeroderma pigmentosum • Goltz syndrome (in lines of Blaschko) • GM1-gangliosidosis (also associated with angiokeratoma corporis diffusum) • Prolidase deficiency
*Childhood onset of multiple punctate, linear, or arborizing telangiectasias favoring sun-exposed areas of the face and upper extremities; the vermilion lips and palate are occasionally affected, but there is no visceral involvement. †Cytotoxic payload in monoclonal antibody drug conjugates.

Table 106.6 Causes of telangiectasias. GVHD, graft-versus-host disease; TEMPI, telangiectasias, elevated erythropoietin and erythrocytosis, monoclonal gammopathy, perinephric fluid collections, and intrapulmonary shunting.



Fig. 106.8 Hereditary benign telangiectasia. Fine linear and branching telangiectasias are seen on the cheeks bilaterally in this five-year-old boy. There is no associated visceral involvement. *Courtesy Julie V. Schaffer, MD.*

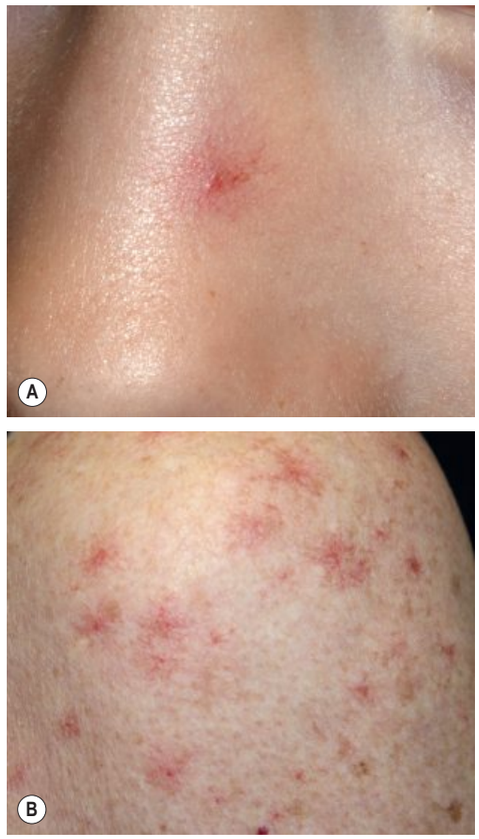


Fig. 106.9 Spider telangiectasia. They are characterized by a central arteriole with radiating telangiectatic "legs". **A** Single lesion on the nose of a young child. **B** Multiple lesions on the shoulder of an adult with liver disease. *A, Courtesy Julie V. Schaffer, MD; B, Courtesy Jeffrey P. Callen, MD.*

Treatment is often not required; however, options include cosmetic camouflage, light or fine wire diathermy, injection sclerotherapy, and laser or intense pulsed light therapies.

Spider Telangiectasia

Synonyms: ▪ Nevus araneus ▪ Spider nevus ▪ Spider angioma

This localized lesion has a slightly raised central red papule (which often becomes more prominent with time) and multiple small, radiating, dilated vessels ("legs")[44] (Fig. 106.9). The lesion can vary from several millimeters to more than a centimeter in diameter. They are commonly located on the face, neck, upper trunk, and hands.

Spider telangiectasias represent a form of telangiectasia with a central feeding arterial vessel. They are usually seen in otherwise healthy individuals, especially women and children. Lesions, often multiple, commonly occur with pregnancy, liver disease, and oral contraceptive pills (OCPs). Spontaneous resolution may occur, especially after pregnancy. Treatment options include electrosurgery or vascular lasers.

Generalized Essential Telangiectasia

This is a primary disorder that typically affects adult women but may commence during childhood. Initially, the limbs are affected, especially the distal lower extremities, with sheets of asymptomatic blanchable telangiectasias (Fig. 106.10)[45,46]. The involvement is usually symmetric. Over time, there is often a progression proximally such that the telangiectasias become more widespread. Although the telangiectasias are persistent, patients do not have associated systemic illnesses.

The differential diagnosis includes cutaneous collagenous vasculopathy; typically it is not confused with telangiectasia macularis eruptiva perstans. While improvement with vascular lasers is possible, the progressive nature must be considered and the cost of treating extensive involvement may prove prohibitive.



Fig. 106.10 Generalized essential telangiectasia. Bilateral sheets of asymptomatic blanchable telangiectasias. The initial site of involvement is usually the distal lower extremity. *Courtesy Jean L. Bolognia, MD.*

Cutaneous Collagenous Vasculopathy

Cutaneous collagenous vasculopathy (CCV) was first described in 2000[47]. Clinically, it can resemble generalized essential telangiectasia (GET). However, based upon the limited number of reported cases, there is not a female predominance, the telangiectasias may involve just the trunk and/or proximal extremities, and history of an "upward march" of lesions is lacking (Fig. 106.11A)[48]. The etiology is unknown and there is no clear association with any underlying systemic illness or medication.

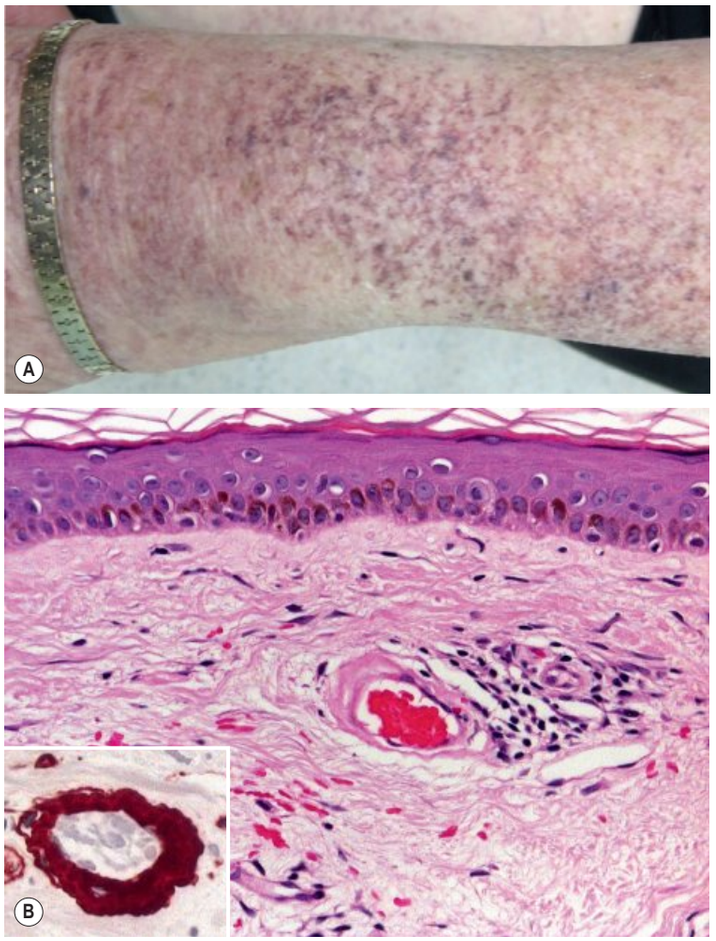


Fig. 106.11 Cutaneous collagenous vasculopathy – clinical and histologic features. A Multiple violaceous branching telangiectasias on the forearm; the patient also had involvement of the thighs, abdomen, and back. **B** In the upper dermis, there are some extravasated red blood cells and clumped RBCs within an ectatic blood vessel. Note the concentric hyaline deposits at the periphery of the affected blood vessel. Immunohistochemical staining with antibodies to collagen type IV highlight the deposits (inset). *B, Courtesy Lorenzo Cerrroni, MD.*



Fig. 106.12 Unilateral nevoid telangiectasia. Note the segmental, unilateral distribution pattern of discrete telangiectasias. *Courtesy Robert Hartman, MD.*



Fig. 106.13 Angioma serpiginosum. Grouped dark red puncta on the arm in a serpiginous pattern.

CCV does have unique histopathologic findings consisting of ectatic superficial blood vessels with hyalinized and laminated, concentric concretions surrounding the basement membrane of affected vessels. With special staining, this material is PAS-positive and diastase-resistant, and by immunohistochemistry, it reacts with antibodies against collagen type IV (Fig. 106.11B). Ultrastructurally, the deposits have been shown to consist of collagen with abnormal banding patterns (Luse bodies)[48].

This condition, like generalized essential telangiectasia, is benign in nature. There are scattered case reports of improvement following pulsed dye laser therapy.

Unilateral Nevoid Telangiectasia

Telangiectasias in this condition are usually confined to the trigeminal or upper cervical dermatomes (Fig. 106.12) and may follow the lines of Blaschko[49,50]. Congenital and acquired forms are recognized. It has been proposed that an increase in estrogen receptors on blood vessels in affected areas and/or an increase in estrogen levels is causative. Situations of relative estrogen excess such as pregnancy, puberty, and liver disease are associated with the acquired form.

Angioma Serpiginosum

Angioma serpiginosum is a rare vascular disorder with a characteristic appearance[51,52]. It is usually sporadic, but familial cases have been reported. Typically, the condition affects female patients and commences during the first two decades of life. Multiple, small, asymptomatic, non-palpable, deep-red to purple puncta occur in small clusters and sheets (Fig. 106.13). The arrangement and extension of the lesions may produce a serpiginous pattern. The extremities are most commonly affected, initially with a unilateral distribution; over months to years, the involvement may become more widespread. The palms, soles, and mucous membranes are not involved.

The puncta represent dilated, non-inflamed capillaries within the dermal papillae. These can be seen with dermoscopy. Incomplete blanching occurs with pressure, but lesions are not purpuric. The differential diagnosis includes pigmented purpuric eruptions, particularly the Majocchi variant (purpura annularis telangiectoides), which is more likely to be bilateral and on biopsy has perivascular lymphocytes and extravasated erythrocytes. Treatment is not necessary, but lesions can be improved with the pulsed dye laser.

Hereditary Hemorrhagic Telangiectasia

Synonyms: ■ Osler–Weber–Rendu disease ■ Osler–Rendu–Weber disease

Hereditary hemorrhagic telangiectasia (HHT) is an autosomal dominant condition in which there are multiple mucocutaneous and gastrointestinal telangiectasias (which are actually arteriovenous malformations)

as well as variable visceral involvement (lung, liver, and CNS). The diagnosis may first be suspected in children who have repeated episodes of epistaxis; however, the initial presentation can occur during the second or third decades of life. The characteristic mat-like and papular telangiectasias on the mucous membranes are first seen during adolescence[53]. Cutaneous lesions usually appear after puberty or even later in life.

Lesions, which increase in size and number as the patient ages, are most commonly seen on the face, tongue, lips, nasal mucosa, hands, and fingertips (Fig. 106.14). They frequently occur throughout the gastrointestinal tract and may result in obvious hemorrhage or iron deficiency anemia. Hemorrhage from vascular lesions in the lung, liver, CNS, spleen, and urinary tract may occur, as well as paradoxical emboli due to pulmonary arteriovenous malformations.

HHT can result from mutations in several genes, most commonly *HHT1* and *HHT2* which encode endoglin and ALK-1, respectively (see Table 104.2). Both of these glycoproteins are TGF-β receptors expressed by vascular endothelium, and they are thought to play a role in angiogenesis and vessel wall integrity.

Treatment of the mucocutaneous vascular lesions may not be required. Destructive treatments such as diathermy, cautery, or laser may be used to treat individual lesions. Surgical management or embolization may be required for uncontrolled hemorrhage from mucosal lesions or complications arising from visceral lesions. Initial and longitudinal evaluation of patients with HHT is outlined in Table 104.6.

Ataxia–Telangiectasia

Synonym: ■ Louis-Bar syndrome

Ataxia–telangiectasia was first described by Louis-Bar in 1941. It is an autosomal recessive disorder characterized by cerebellar ataxia, chromosomal instability (frequent translocations between chromosomes 7 and 14), growth retardation, oculocutaneous telangiectasias, pulmonary infections (including bronchiectasis), immunodeficiency, and the development of lymphomas[54].

It is covered in more detail in Chapter 60. Linear telangiectasias first appear on the bulbar conjunctivae between 4 and 6 years of age. Cutaneous telangiectasias favor the head and neck region, and they are most common on the malar prominences, ears, and eyelids in addition to the popliteal and antecubital fossae. Patients may have poikiloderma (hypopigmentation, hyperpigmentation, atrophy, telangiectasia), premature hair graying, and decreased subcutaneous fat.



Fig. 106.14 Hereditary hemorrhagic telangiectasia. The tongue and lips are a common location for the mat-like and papular telangiectasias that actually represent small arteriovenous malformations.

VENOUS LAKES

Venous lakes are small, dark-blue, slightly elevated, soft lesions that are predominantly localized on the lips (Fig. 106.15), ears, or face of older adults. They can usually be emptied of most of their blood content by persistent pressure[55,56]. Pathologically, venous lakes represent telangiectasias in the dermis. Either one great, dilated venule or several communicating dilated spaces that contain erythrocytes are seen. Thrombosis is sometimes present. Optional treatment with electrosurgery or a hemoglobin-targeting laser is usually effective.

NEVUS ANEMICUS

Nevus anemicus is a congenital pale area of skin, most commonly found on the upper to mid trunk. These patches have an irregular border and an average diameter of 5–10 cm (Fig. 106.16). Within the body of the lesion, local blood vessels are very sensitive to endogenous catecholamines and are permanently vasoconstricted[57]. The border and extent of the lesion become imperceptible with pressure (or diascopy) sufficient to cause blanching of surrounding skin. Conversely, application of heat or an ice cube will often accentuate the lesion; the border becomes hyperemic during warming, while the lesion stays pale. The pale appearance of the lesion (rather than an absence of pigmentation) and the results of the above clinical maneuvers allow nevus anemicus to be differentiated from vitiligo and nevus depigmentosus, respectively. Interestingly, islands of sparing may be present within the lesion, and skin transplanted within the nevus anemicus retains the characteristics



Fig. 106.15 Venous lake on the lip. The lesion is soft and, with compression, can be emptied of most of its blood content. *Courtesy Ronald P. Rapini, MD.*



Fig. 106.16 Nevus anemicus. Pale area of vasoconstriction with irregular borders on the back.



Fig. 106.17 Angiospastic macules (Bier spots). Multiple pale spots with an erythematous background on the forearm.

of the donor site (donor dominance). No histologic abnormalities have been reported. No treatment is required or effective. Of note, nevus anemicus can co-exist with vascular malformations and is seen in up to half of patients with neurofibromatosis type 1.

ANGIOSPASTIC MACULES (BIER SPOTS)

These were first described by Bier in 1898 and represent a pattern of vascular mottling consisting of white macular areas surrounded by a red to occasionally blue cyanotic background. Bier spots most commonly occur on the arms and legs of young adults (Fig. 106.17), but may also occur on the trunk. They are more noticeable in patients with lightly pigmented skin. Angiospastic macules may be induced by venous congestion and can be elicited by placing a limb in a dependent position or by placing a tourniquet around a limb. The spots disappear with limb elevation or release of the tourniquet. As with nevus anemicus, the border of the lesion becomes imperceptible with pressure (diascopy). The vascular pattern is thought to result from a benign physiological response consisting of vasoconstriction. Bier spots have also been associated with pregnancy, lymphedema, cryoglobulinemia, capillary malformation-arteriovenous malformation syndrome (especially type 2 due to *EPHB4* mutations), tuberous sclerosis complex, and aortic hypoplasia. *BASCULE* syndrome features *B*ier *a*nemic *s*pots, *c*yanosis (acral), and an *u*rticaria-*l*ike *e*ruption in association with orthostatic intolerance.

Additional figures available in our eBook (see inside front cover for access code).

REFERENCES

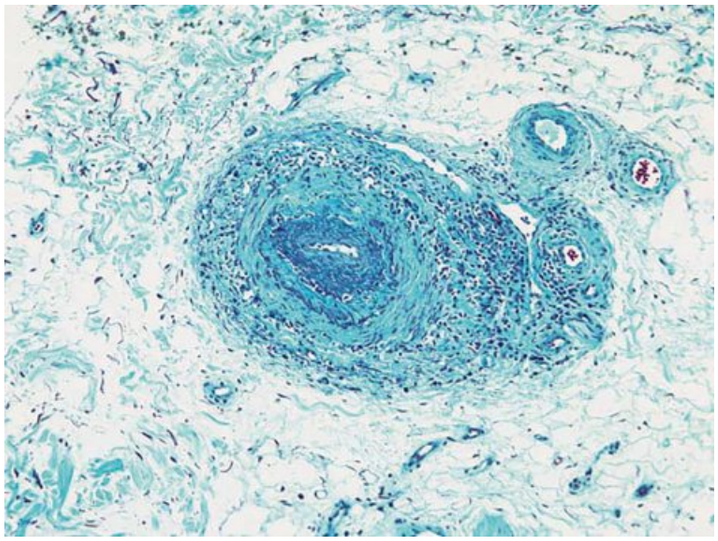
1. Fleischer Jr AB, Resnick SD. Livedo reticularis. *Dermatol Clin*. 1990;8:347–354.
2. Gibbs MB, English JC, Zirwas MJ. Livedo reticularis: an update. *J Am Acad Dermatol*. 2005;52:1009–1019.
3. Bashir S, Chew A. Cutaneous reactions to cold and heat. In: Griffiths C, Barker J, Bleiker T, et al., editors. *Textbook of Dermatology*. 8th ed. Blackwell Science; 2017. p. 125.6.
4. Kelly RI, Wee E, Balta S, Williams RA. Lymphocytic thrombophilic arteritis and cutaneous polyarteritis nodosa: clinicopathologic comparison with blinded histologic assessment. *J Am Acad Dermatol*. 2020;83:501–508.
5. Lee JS, Kossard S, McGrath MA. Lymphocytic thrombophilic arteritis: a newly described medium-sized vessel arteritis of the skin. *Arch Dermatol*. 2008;144:1175–1182.
6. Francés C, Piette JC. The mystery of Sneddon syndrome: relationship with antiphospholipid syndrome and systemic lupus erythematosus. *J Autoimmun*. 2000;15:139–143.
7. Francés C, Papo T, Wechsler B, et al. Sneddon syndrome with or without antiphospholipid antibodies: a comparative study in 46 patients. *Medicine (Baltimore)*. 1999;78:209–219.
8. Devillers AC, de Waard-van der Spek FB, Oranje AP. Cutis marmorata telangiectatica congenita: clinical features in 35 cases. *Arch Dermatol*. 1999;135:34–38.
9. Gerritsen MJP, Steijlen PM, Brunner HG, Rieu P. Cutis marmorata telangiectatica congenita: report of 18 cases. *Br J Dermatol*. 2000;142:366–369.
10. Speight EL, Lawrence CM. Reticulate purpura, cryoglobulinaemia and livedo reticularis. *Br J Dermatol*. 1993;129:319–323.
11. Filo V, Brezová D, Hlavcák P, Filová A. Livedo reticularis as a presenting symptom of polycythemia vera. *Clin Exp Dermatol*. 1999;24:428.
12. Bauzá A, España A, Idoate M. Cutaneous polyarteritis nodosa. *Br J Dermatol*. 2002;146:694–699.
13. Vakili S, Zampella JG, Kwatra SG, et al. Lymphocytic thrombophilic arteritis: a review. *J Clin Rheumatol*. 2019;25:147–152.
14. Anavekar NS, Kelly R. Heterozygous prothrombin gene mutation associated with livedoid vasculopathy. *Australas J Dermatol*. 2007;48:120–123.
15. Zhou Q, Yang D, Ombrello AK, et al. Early-onset stroke and vasculopathy associated with mutations in ADA2. *N Engl J Med*. 2014;370:911–920.
16. Navon Elkan P, Pierce SB, Segel R, et al. Mutant adenosine deaminase 2 in a polyarteritis nodosa vasculopathy. *N Engl J Med*. 2014;370:921–931.
17. Nigwekar SU, Kroshinsky D, Nazarian RM, et al. Calciphylaxis: risk factors, diagnosis, and treatment. *Am J Kidney Dis*. 2015;66:133–146.
18. Rosman HS, Davis TP, Reddy D, Goldstein S. Cholesterol embolization: clinical findings and implications. *J Am Coll Cardiol*. 1990;15:1296–1299.
19. Gibson GE, Su WPD, Pittelkow MR. Antiphospholipid syndrome and the skin. *J Am Acad Dermatol*. 1997;36:970–982.
20. Weir NU, Snowden JA, Greaves M, Davies-Jones GAB. Livedo reticularis associated with hereditary protein C deficiency and recurrent thromboembolism. *Br J Dermatol*. 1995;132:283–285.
21. Donnet A, Khalil R, Terrier G, et al. Cerebral infarction, livedo reticularis, and familial deficiency in antithrombin-III. *Stroke*. 1992;23:611–612.
22. Freeman EF, Devon E, Lipoff JB, et al. The spectrum of COVID-19 associated dermatologic manifestations: an international registry of 716 patients from 31 countries. *J Am Acad Dermatol*. 2020;83:1118–1129.
23. Spiers EM, Sanders DY, Omura EF. Clinical and histologic features of primary oxalosis. *J Am Acad Dermatol*. 1990;22:952–956.
24. Sladden MJ, Nicolaou N, Johnston GA, Hutchinson PE. Livedo reticularis induced by amantadine. *Br J Dermatol*. 2003;149:655–680.
25. Wilkin JK. Why is flushing limited to a mostly facial cutaneous distribution? *J Am Acad Dermatol*. 1988;19:309–313.
26. Freeman R, Waldorf HA, Dover JS. Autonomic neurodermatology (Part II): disorders of sweating and flushing. *Semin Neurol*. 1992;12:394–407.
27. Wilkin JK. The red face: flushing disorders. *Clin Dermatol*. 1993;11:211–223.
28. Wilkin JK. Flushing reactions. *Recent Adv Dermatol*. 1983;6:157–187.
29. Clement D, Ramage J, Srirajaskanthan R. Update on pathophysiology, treatment, and complications of carcinoid syndrome. *J Oncol*. 2020;2020;8341426.
30. Thompson GH, Hahn G, Rang M. Erythromelalgia. *Clin Orthop Relat Res*. 1979;144:249–254.
31. Kvernebo K. Erythromelalgia: a condition caused by microvascular arteriovenous shunting. *Vasa*. 1998(Suppl. 51):1–40.
32. van Genderen PJ, Lucas IS, van Strik R, et al. Erythromelalgia in essential thrombocythemia is characterized by platelet activation and endothelial cell damage but not by thrombin generation. *Thromb Haemost*. 1996;76:333–338.
33. Mork C, Asker CL, Salerud EG, Kvernebo K. Microvascular arteriovenous shunting is a probable pathogenetic mechanism in erythromelalgia. *J Invest Dermatol*. 2000;114:643–646.
34. Berlin AL, Pehr K. Coexistence of erythromelalgia and Raynaud's phenomenon. *J Am Acad Dermatol*. 2004;50:456–460.
35. Yang Y, Wang Y, Li S, et al. Mutations in *SCN9A*, encoding a sodium channel alpha subunit, in patients with primary erythermalgia. *J Med Genet*. 2004;41:171–174.
36. Choi JS, Dib-Hajj SD, Waxman SG. Inherited erythermalgia: limb pain from an S4 charge-neutral Na channelopathy. *Neurology*. 2006;67:1563–1567.
37. Han C, Dib-Hajj SD, Lin Z, et al. Early- and late-onset inherited erythromelalgia: genotype-phenotype correlation. *Brain*. 2009;132:1711–1722.
38. Fischer TZ, Waxman SG. Familial pain syndromes from mutations of the NaV1.7 sodium channel. *Ann N Y Acad Sci*. 2010;1184:196–207.
39. Burns TM, Te Morsche RH, Jansen JB, Drenth JP. Genetic heterogeneity and exclusion of a modifying locus at 2q in a family with autosomal dominant primary erythermalgia. *Br J Dermatol*. 2005;153:174–177.
40. Davis MDP, O'Fallon WM, Rogers III RS, Rooke TW. Natural history of erythromelalgia. *Arch Dermatol*. 2000;136:330–336.
41. Iqbal J, Bhat MI, Charoo BA, et al. Experience with oral mexiletine in primary erythromelalgia in children. *Ann Saudi Med*. 2009;29:316–318.
42. Natkunarajah J, Atherton D, Elmslie F, et al. Treatment with carbamazepine and gabapentin of a patient with primary erythermalgia (erythromelalgia) identified to have a mutation in the *SCN9A* gene, encoding a voltage-gated sodium channel. *Clin Exp Dermatol*. 2009;34:e640–e642.
43. Cohen JS. Erythromelalgia: new theories and new therapies. *J Am Acad Dermatol*. 2000;43:841–847.
44. Bean WB. *Vascular Spiders and Related Lesions of the Skin*. Oxford: Blackwell Scientific; 1958.
45. Rothe MJ, Grant-Kels JM. Nomenclature of the primary telangiectasias. *Int J Dermatol*. 1992;31:320.
46. McGrae Jr JD, Winkelmann RK. Generalized essential telangiectasia: report of a clinical and histochemical study of 13 patients with acquired cutaneous lesions. *J Am Med Assoc*. 1963;185:909–913.
47. Salama S, Rosenthal DJ. Cutaneous collagenous vasculopathy with generalized telangiectasia: an immunohistochemical and ultrastructural study. *J Cutan Pathol*. 2000;27:40–48.
48. Davis TL, Mandal RV, Bevona C, et al. Collagenous vasculopathy: a report of three cases. *J Cutan Pathol*. 2008;35:967–970.
49. Wilken JK. Unilateral dermatomal superficial telangiectasia. *Arch Dermatol*. 1984;120:579–580.
50. Uhlin SR, McCarty Jr KS. Unilateral nevoid telangiectatic syndrome: the role of estrogen and progesterone receptors. *Arch Dermatol*. 1983;119:226–228.
51. Hunt SJ, Santa Cruz DJ. Acquired benign and 'borderline' vascular lesions. *Dermatol Clin*. 1992;10:97–115.
52. Marriott PJ, Munro DD, Ryan T. Angioma serpiginosum: familial incidence. *Br J Dermatol*. 1975;93:701–706.
53. Abrahamian LM, Rothe MJ, Grant-Kels JM. Primary telangiectasia of childhood. *Int J Dermatol*. 1992;31:307–313.
54. Smith LL, Conerly SL. Ataxia-telangiectasia or Louis-Bar syndrome. *J Am Acad Dermatol*. 1985;12:681–696.
55. Bean WB, Walsh JR. Venous lakes. *Arch Dermatol*. 1956;74:459–463.
56. Alcalay J, Sandbank M. The ultrastructure of cutaneous venous lakes. *Int J Dermatol*. 1987;26:645–646.
57. Mountcastle EA, Diestelmeier MR, Lupton GP. Nevus anemicus. *J Am Acad Dermatol*. 1986;14:628–632.



eFig. 106.1 Sneddon syndrome. The characteristic irregular, broken, branching pattern of livedo racemosa is seen on the back and arms. *Courtesy Norbert Sepp, MD*.



eFig. 106.3 Livedo racemosa in a patient with lymphocytic thrombophilic arteritis.



eFig. 106.2 Sneddon syndrome. A connective tissue stain highlights a subcutaneous artery with subendothelial proliferation of smooth muscle, leading to almost complete luminal occlusion.



eFig. 106.4 Reticulate purpura and cutaneous necrosis due to calciphylaxis. These patients also often have patchy areas of livedo reticularis. *Courtesy Norbert Sepp, MD*.



eFig. 106.5 Hereditary benign telangiectasia. Fine linear and punctate telangiectasias are seen on the cheeks and vermilion lips bilaterally in this child. There is no associated visceral involvement. *Courtesy Antonio Torrelo, MD.*



eFig. 106.7 Generalized essential telangiectasia. Bilateral sheets of asymptomatic blanchable telangiectasias. The initial site of involvement is usually the distal lower extremity. *Courtesy Kalman Watsky, MD.*





eFig. 106.6 Spider telangiectasia. A Central arteriole with radiating telangiectatic "legs" on the cheek of a young child. **B** Multiple lesions in a jaundiced patient with liver disease. *A, Courtesy Phillip Bekhor, MD; B, Courtesy Ronald P. Rapini, MD.*



eFig. 106.8 Generalized essential telangiectasia. The site of initial involvement is usually the distal lower extremities. Sheets of asymptomatic blanchable telangiectasias appear bilaterally and over time can become widespread. *Courtesy Jean L. Bolognia, MD.*







eFig. 106.9 Hereditary hemorrhagic telangiectasia (HHT). A–C Multiple telangiectasias of the hand. The telangiectasias actually represent small arteriovenous malformations. *Courtesy Irwin Braverman, MD.*

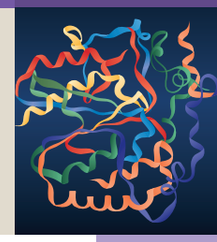




eFig. 106.10 Nevus anemicus. A Pale area of vasoconstriction with irregular borders on the back. **B** Obliteration of the border via application of pressure. *Courtesy Kalman Watsky, MD.*

Principles of Cutaneous Tumor Biology

107



Thomas Tüting and Andreas Dominik Braun

Chapter Contents

The Genome Perspective *1875*
The Cell Perspective *1878*
The Tissue Perspective *1881*
Pathogenesis of Keratinocyte Carcinomas *1884*
Current Developments and Future Perspectives *1885*

Key features

- Over time, cancer genomes gradually accumulate somatic mutations, and oncogenic driver mutations that increase cell fitness are selected in a process termed Darwinian cancer evolution
- Cancer evolution is also driven by complex chromosomal rearrangements (chromothripsis, chromoplexy) and mutational storms (kataegis) that occur in a single catastrophic cell division, a process called punctuated genome evolution
- Oncogenic driver mutations usually activate proliferative signaling, initiate cell division, and reprogram cellular metabolism to support cell growth and proliferation
- Mutations in tumor suppressor genes often deregulate cell cycle checkpoints, help cells evade physiologic mechanisms of cellular senescence and programmed cell death, and increase genome instability
- By deregulating developmental signaling pathways and cell–cell communication networks, cancer cells create novel tumor ecosystems
- Immune cells can sense DNA damage, specifically recognize mutated cancer cells, and enforce the adaptation and selection of cancer cell subpopulations with immune evasive phenotypes
- Chromosomal instability of cancer cells and a protumorigenic inflammatory microenvironment increase cancer cell plasticity, foster epithelial–mesenchymal transitions, and enable cancer cell invasion and metastasis
- Basal cell carcinomas (BCCs) arise as a result of oncogenic mutations in the Hedgehog signaling pathway, and they often have additional mutations in *TP53* and the Notch pathway
- Cutaneous squamous cell carcinomas (cSSCs) often carry loss-of-function mutations in the Notch pathway, *TP53*, and *CDKN2A*

INTRODUCTION

Worldwide, skin cancer is the most common type of cancer in fair-skinned individuals. This chapter will introduce our current understanding of the fundamental principles underlying cancer development. Notably, skin cancer research has provided significant contributions to the unraveling of the cellular and molecular mechanisms by which environmental carcinogens can cause cancer[1]. The following sections review the remarkable advances in cancer genetics, cancer biology, and cancer immunology made during the 21st century that have initiated a revolution in cancer therapy.

To facilitate our understanding of these novel insights, an increasing number of "hallmarks of cancer" have been defined[2,3]. As a conceptual framework, these hallmarks are presented along three dimensions of biologic organization: (1) the evolution of cancer genomes; (2) the biology of cancer cells; and (3) the development of cancer ecosystems (Fig. 107.1). This is followed by a review of recent insights into the molecular pathogenesis of keratinocyte carcinomas. The chapter concludes with a brief survey of ongoing technological advances that will shape the future of patient care, enabling improved prevention, earlier detection, and patient-specific therapeutic interventions.

THE GENOME PERSPECTIVE

The DNA Sequencing Revolution

Publication of the human genome sequence in 2001 and assembly of a reference sequence of the human genome in April 2003 provided a new foundation for biological research and launched a new era in biomedicine. The subsequent development of massively parallel DNA sequencing technologies (next-generation sequencing; see Ch. 3) has revolutionized genomic research. While completion of the human genome project took 13 years, today it is possible to sequence several whole human genomes in as little as a day.

A recent milestone in human genome research was a series of publications in 2020 by the Genome Aggregation Database (gnomAD) Consortium which delineated the sequences of 125 748 exomes (the protein-coding regions of the human genome) and 15 708 whole genomes[4]. This collection provided unprecedented insights into human genome variation at both the population and individual level. In the same year, the international ICGC/TCGA Pan-Cancer Analysis of Whole Genomes (PCAWG) Consortium published a landmark paper describing the generation and integrative analyses of 2658 cancer whole genomes (and matched normal tissues) across 38 tumor types[5]. Together with several companion papers, this resulted in new insights into the mechanisms of cancer development, extension of the list of oncogenes, and confirmation of the importance of oncogenic mutations in known cancer driver genes.

The ability to sequence and compare whole cancer genomes also revealed the significance of *structural* genomic alterations that affect the topology of the genome and alter "non-coding" sequences; the latter do not contain information for the production of proteins yet comprise 97% of the human genome. These aberrations include simple structural alterations such as deletions, tandem duplications, and unbalanced translocations, in addition to complex structural alterations that are rearranged in local clusters and inserted distantly in the genome. Structural aberrations are thought to play a previously underestimated role in driving cancer development via amplifications of oncogenes, deletions of tumor suppressor genes, creation of fusion genes, or aberrant insertion of oncogenes at transcriptionally active sites[6].

The number of DNA sequences generated from whole genomes of malignant and normal tissues of cancer patients, as well as from different tissues of otherwise healthy individuals, is increasing rapidly. At the same time, new tools for computational analyses are enabling increasingly sophisticated interrogations of large genomic data sets, thereby revealing an enormous complexity and heterogeneity of genomic alterations in cancer cells. These analyses have revealed large differences between different tumor types, between different patients with the same tumor type, and even between spatially or temporally distinct tumor regions in a single patient. In addition, an increasing number of variations in the human genome were associated with inherited cancer predisposition. However, this is just the beginning in our understanding of the functional implications of genomic alterations that underlie cancer development and the complex mechanisms that shape their evolution.

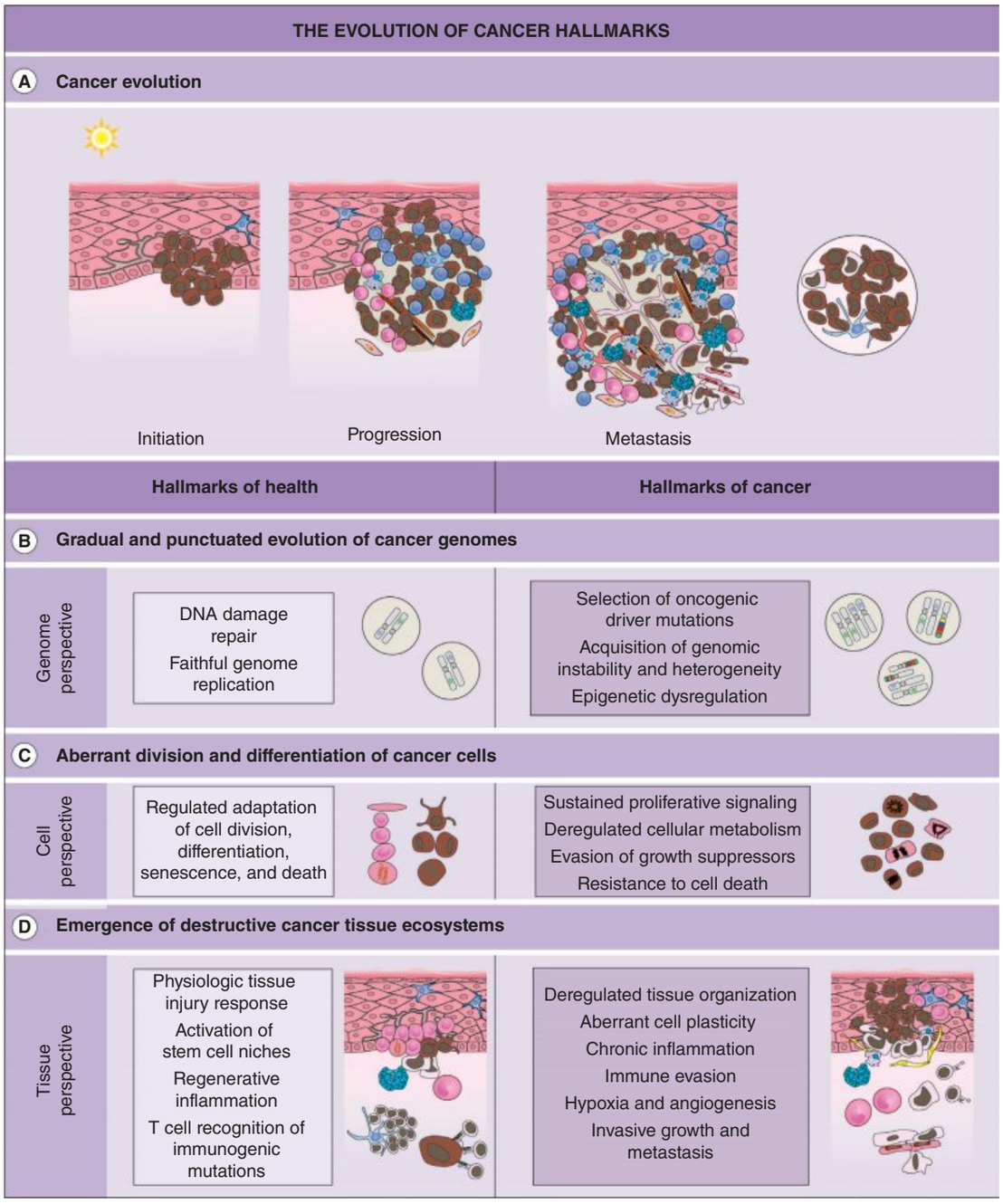


Fig. 107.1 The evolution of cancer hallmarks. A Schematic representation of the cancer initiation, local progression, and metastatic dissemination of skin cancer using melanoma as an example. **B–D** A simplified view integrating the concepts of cancer evolution and cancer hallmarks. Cancer development disrupts three principal levels of biological organization: genomes, cells, and tissues.

Types of Somatic Mutations

Cancer genomes accumulate a heterogeneous and complex array of somatic mutations

Cancer cells originate from normal precursor cells within tissues. In the process of malignant transformation, cancer cells acquire an increasing number of alterations in their genome, which are collectively called *somatic mutations*. Somatic mutations are distinguished from *germline pathogenic variants (mutations)*, which are already present in the fertilized egg and carry inherited information from both parents. Somatic mutations in cancer genomes are identified by direct comparison with the corresponding genomes of normal cells (usually obtained from blood). Mutations in cancer cells can be grouped into different categories according to their size[7]:

- *Single base substitutions* or point mutations are the most frequent alterations and correspond to single nucleotide variants (SNVs) in the germline. Cancer cells derived from tissues that are exposed to carcinogens (e.g. skin exposed to UV radiation) contain a high number of somatic single base substitutions.
- Small insertions or deletions of DNA (*indels*) are the second most frequent alteration and have a size of up to 50 base pairs (bps).
- *Structural variations* include alterations of larger DNA segments such as large insertions and deletions (>50 bps), somatic copy number alterations (SCNAs), and complex rearrangements.

Chromosomal alterations that are microscopically visible by cytogenetic techniques are a characteristic feature of cancer cells derived from patients with advanced disease. These include numerical and structural alterations of chromosomes (aneuploidy), gains and losses of chromosomal regions, and translocations (Fig. 107.2A). Such karyotype aberrations are uncommon in normal cells. Next-generation sequencing technologies have revealed numerous structural variations that are not detected by microscopic cytogenetic analyses, yet are important in cancer development and contribute to the heritable variation present in human genomes.

The Darwinian Model of Gradual Cancer Evolution

Rare oncogenic driver mutations are selected during cancer evolution

The generation of genome-wide catalogs of somatic mutations in various cancer types has provided new opportunities for studying the mechanisms by which somatic mutations arise in cancer genomes. Sequencing of single cell genomes revealed that a few mutations arise

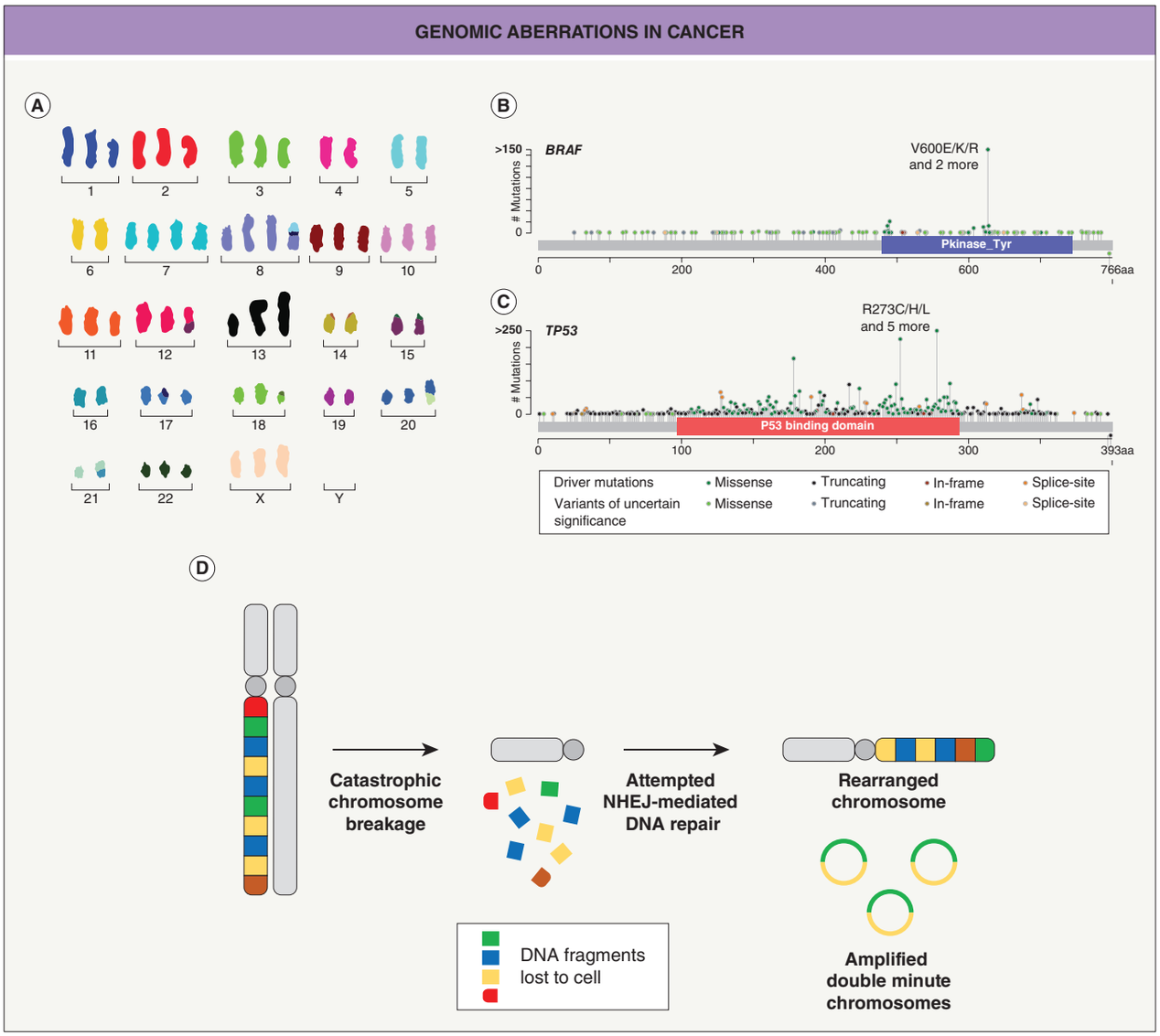


Fig. 107.2 Genomic aberrations in cancer. A Cancers often have highly abnormal karyotypes with extra copies of several chromosomes as well as various structural aberrations, which result from translocation events. **B** Mutations in *BRAF*, illustrating the typical mutation pattern in an oncogene. The vast majority of mutations affect valine at amino acid position 600 in the tyrosine kinase domain, resulting in a constitutively active protein. Mutations with low frequency are often of uncertain significance and without functional relevance. **C** Mutations in *TP53*, illustrating the typical mutation pattern in a tumor suppressor gene. Compared to an oncogene, the mutations are more widely distributed within the gene with hotspots affecting the p53 DNA-binding domain. Note that low frequency mutations are often truncating mutations resulting in a non-functional protein. **D** During chromothripsis, one or multiple chromosomes are fragmented into multiple pieces during a single cataclysmic event. Subsequently, these fragments are stitched together in a near-random orientation using non-homologous end joining or microhomologous repair mechanisms. This results in the generation of grossly altered chromosomes, double minute chromosomes, and loss of some DNA fragments. NHEJ, non-homologous DNA end-joining. *A, Adapted and redrawn from Lodish H, et al. Molecular Biology of the Cell, 9th edn. Austin: W. H. Freeman & Company, 2021 and from Abdel-Rahman WM, et al. Spectral karyotyping suggests additional subsets of colorectal cancers characterized by pattern of chromosome rearrangement. Proc Natl Acad Sci 2001;98:2538–43; B, C, Adapted from cBioPortal of Cancer Genomics; D, Adapted from Rausch T, et al. Genome sequencing of pediatric medulloblastoma links catastrophic DNA rearrangements with TP53 mutations. Cell 2012;148:59–71.*

spontaneously during each cell division due to errors by the molecular machinery of DNA replication. When cells are exposed to endogenous and exogenous mutagens, these errors are significantly accelerated because the resulting DNA damage is occasionally improperly repaired. Importantly, the efficiency of DNA repair can be compromised by inherited germline variants or by acquired somatic alterations in "*caretaker*" *genes* that coordinate DNA damage responses and DNA replication. As a result, each individual cancer genome carries a unique set of somatic mutations that have accumulated during aging and malignant transformation, reflecting the history of different DNA damage and repair processes.

Computational algorithms are able to discriminate at least 30 different mutational signatures and can reveal a history of exposure to exogenous mutagens and mechanisms of DNA repair defects[7]. A prominent example are skin cancer genomes, which bear large numbers of C-to-T and CC-to-TT transitions that are typically caused by UVB irradiation (see Fig. 86.15). Interestingly, the local density of mutations varies up to fivefold amongst different genomic regions, indicating an uneven distribution across the genome. Initial analyses found that this variance in mutational burden correlates with chromatin accessibility and modification, as well as replication timing.

In cancer genomes, the process of malignant transformation is reflected in non-random patterns of somatic alterations. For example, single base substitutions are recurrently detected at unique mutational hotspots within oncogenes (e.g. *BRAF*) and a significantly increased mutation density is seen in several exons of well-known tumor suppressor genes (e.g. *TP53*; Fig. 107.2B,C). In addition, copy number alterations accumulate with tumor type-specific patterns, most notably *amplifications* of genomic regions encoding oncogenes (e.g. *BRAF*, *MYC*, cyclins) as well as *deletions* of genomic regions encoding tumor suppressor genes such as *TP53* or *CDKN2A*[5].

The emergence of these mutational patterns can be explained by the concept of Darwinian evolution at the level of the cancer cell. According to this concept, somatic mutations arise accidentally as a result of

genome replication errors and the effects of exogenous or endogenous DNA mutagens. If a somatic mutation confers a competitive advantage for growth or survival within the population of tissue cells, it will be positively selected over time. In the context of cancer biology, positively selected mutations are called "*oncogenic drivers*", whereas somatic mutations that have no biological effects and are not selected are called "*passenger mutations*". To date, bioinformatic analyses have focused on mutational patterns that indicate a selection of oncogenic driver genes. These patterns include the clustering of base pair substitutions at hotspots or in small genomic regions that alter the structure of encoded proteins or deregulate their expression. Deciphering the functional impact of these somatic mutations on cellular functions has greatly contributed to our understanding of cancer biology.

Single Catastrophic Events in Genome Evolution

Complex chromosomal rearrangements can arise after a single catastrophic cell division error

Evidence is accumulating that during cancer evolution cells can acquire complex genomic rearrangements within very short periods of time, i.e. one cell division. One such process is termed *chromothripsis* and occurs in a single catastrophic cell division. Chromothripsis describes the shattering (thripsis in Greek) of chromosomes and the subsequent reassembly in a random order to produce derivative chromosomes with complex rearrangements (Fig. 107.2D)[8]. It can result from chromosome mis-segregation during cell division, and this can lead to the generation of small micronuclei with unstable nuclear envelopes that are prone to irreversible disruption. Chromosomes within micronuclei accumulate extensive DNA damage and are susceptible to shattering during the next mitosis. This generates multiple chromosomal fragments that are subsequently reassembled by DNA double-strand break repair to form derivative chromosomes (see Fig. 107.2D). Chromothripsis is observed with a frequency of 20% across various cancer types and in more than half of advanced melanomas[9]. A related process is termed *chromoplexy*, in which co-occurring double-stranded DNA breaks in different chromosomes are randomly reassembled, resulting in shuffled chains of rearrangements[5].

Another process, termed *kataegis* (Greek for thunderstorm), is a process of local hypermutations that results in clustered, strand-biased nucleotide substitutions[10]. The mutation clusters are typically several hundred bps long and alternate between a wide range of CT or GA substitutional patterns, suggesting that kataegis occurs in only one of the two template strands during DNA replication. Kataegis is observed with a frequency of 60% in various cancer types with a high prevalence in acral melanomas.

Gradual Cancer Evolution Versus Punctuated Evolution and Catastrophic Events

The discovery that complex genomic rearrangements with multiple somatic mutations can occur in cancer genomes during one or a few catastrophic cell divisions questioned the prevailing Darwinian theory of cancer evolution[11], as the latter assumes the sequential acquisition of mutations in a gradual fashion over time. Such evolutionary jumps have been postulated by evolutionary biologists as a means of initiating speciation in the heavily debated theory of punctuated equilibrium. In punctuated equilibrium, a few rapid changes result in the generation of novel species.

Nowadays, whole genome sequencing enables a partial reconstruction of the evolutionary history of cancer based upon the patterns of how somatic mutations accumulate, with the mutations serving as molecular clocks. These analyses revealed that long phases of gradual mutational "microevolution" (the Darwinian model of cancer evolution) can alternate with short periods of intense mutational "macroevolution" (single catastrophic events such as chromothripsis, chromoplexy, or kataegis), whereby cancer genomes can acquire multiple strong oncogenic driver mutations (Fig. 107.3)[11]. Using this approach, it was shown that phenotypically healthy skin already contains clonally expanded keratinocytes and melanocytes with a high burden of UVB-induced somatic mutations and positively selected oncogenic drivers, indicating that cancer genome evolution begins earlier than previously thought[12].

The relative importance of gradual versus punctuated cancer genome evolution differs between cancer entities. For example, a predominantly gradual genome evolution occurs in melanomas such as lentigo maligna that arise in photodamaged skin of older adults and carry a high mutational load. As noted previously, the observation that healthy skin already contains clonal populations of melanocytes harboring weakly oncogenic mutations indicates that the latter are acquired gradually over a lifetime, consistent with the Darwinian model. In contrast, a more punctuated genome evolution is found in acral and uveal melanomas as they harbor numerous structural variants and a significantly lower mutational load[13,14]. In the majority of melanomas, both gradual and punctuated genome evolution are thought to occur in a sequential manner, with oncogenic hotspot mutations generally occurring before copy number gains. The acquisition of complex genomic alterations and genomic instability that is frequently associated with a shift in mutational signatures promotes metastatic tumor progression.

THE CELL PERSPECTIVE

Functional Capabilities Acquired by Cancer Cells

Oncogenic driver mutations alter the physiologic behavior of cells

The comprehensive analysis of large numbers of cancer genomes has increased the number of oncogenic driver mutations within protein coding sequences to several hundreds. Mechanistic studies in cell culture systems and in model organisms have helped to understand how these alterations contribute to the malignant phenotype of cancer cells. Such endeavors have provided fundamental insights into the biology of cell behavior analogous to how the study of pathogens has elucidated the mechanisms of immune defense.

Many oncogenic driver mutations were found to alter the function of proteins that regulate cell division, faithful genome replication, and cell survival, confirming the concept that oncogenic driver mutations confer a selective growth advantage during cancer evolution. A limited number of oncogenic signaling pathways have emerged that control these essential cellular processes and serve as a map to functionally classify oncogenic driver genes. Prominent examples include the RTK–RAS–MAPK (receptor tyrosine kinase–RAS–mitogen-activated protein kinase) and the PI3K–AKT–mTOR growth factor signaling pathways (see Figs. 55.3, 55.4 & 113.1), in addition to p53–Rb cell cycle control (Fig. 107.4) and DNA damage response pathways[15].

To better illustrate the complex molecular mechanisms that contribute to malignant transformation, a set of hallmark capabilities has been defined that reflect the biologic consequences of oncogenic driver mutations, particularly aberrant proliferation and survival of cancer cells. Predominantly intrinsic cellular capabilities are sustained proliferative signaling, deregulated metabolism, evasion of growth suppressors, and resistance to cell death, as well as acquisition of replicative immortality and genome instability (see Fig. 107.1)[3]. This section reviews the fundamental principles of how oncogenic driver mutations compromise the physiologic regulation of cell division and genome replication, with a focus on the development of skin cancer.

Sustaining Proliferative Signaling

Oncogenic mutations constitutively activate growth factor signaling and drive cell division

Oncogenic driver genes that activate growth factor signaling were initially discovered as cellular homologs of genes identified in RNA tumor viruses[16,17]. The discovery that point mutations in *ras* also occur in human cancers led to an intensive effort to understand the underlying mechanisms by which these mutations promote uncontrolled cell growth. Functional analyses characterized Ras proteins as simple, binary, on-off switches that connect the activity of growth factors bound to their cell surface receptors to growth responses. For example, activation of *receptor tyrosine kinases* (RTKs) turns on Ras proteins, which then activate a cascade of *mitogen-activated protein kinases* (MAPKs) and subsequently a set of transcription factors in the nucleus (see Fig. 113.1).

Oncogenic mutations in *Ras* genes impair the GTPase activity of Ras proteins, which is tightly controlled in normal cells. Mutated

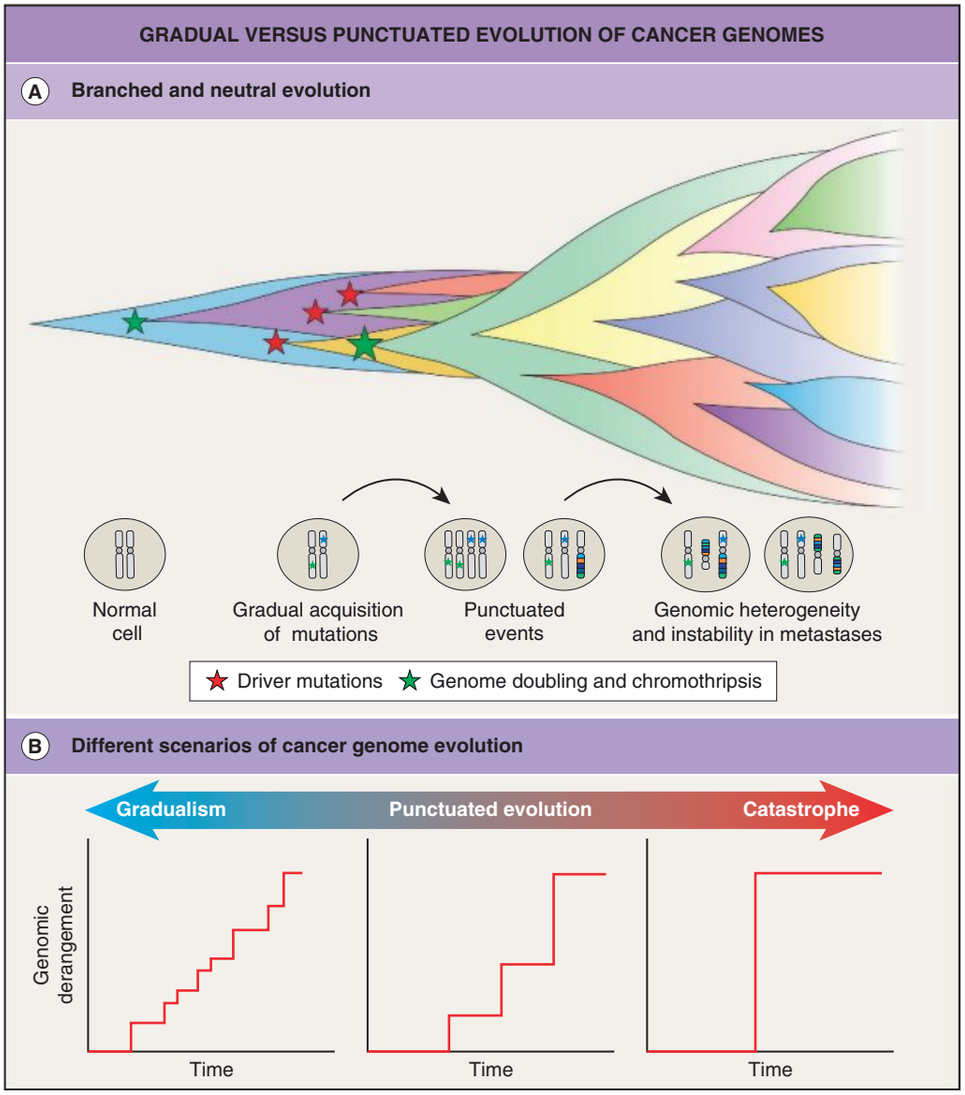


Fig. 107.3 Gradual versus punctuated evolution of cancer genomes. A Muller diagram of a hypothetical evolutionary trajectory of cancer genomes. The evolutionary progression of skin cells towards cancer often begins by acquisition of UV-induced mutations acquired during a lifetime in a gradual evolution. Once regulatory cell cycle checkpoints and DNA damage responses are impaired, gross alterations of the genome (e.g. genome doubling) or catastrophic single events (e.g. chromothripsis, kataegis) may occur. This leads to increased genomic heterogeneity, a key feature of advanced and metastatic cancer. **B** Illustration of different scenarios of cancer genome evolution. Left: oncogenic driver mutations accumulate gradually (Darwinian model of gradual cancer evolution). Middle: progression via punctuated events that induce more drastic chromosomal alterations such as chromoplexis. Right: cancer arising after a single catastrophic event such as chromothripsis. *A, Adapted from Niida A, et al. A unified simulation model for understanding the diversity of cancer evolution. PeerJ 2020;8:e8842; B, Adapted from Baca SC, et al. Punctuated evolution of prostate cancer genomes. Cell 2013;153:666–77.*

Ras proteins are locked in a constitutively active, GTP-bound state that signals independently of upstream activation of growth factor receptors. Genomic analyses revealed large numbers of diverse oncogenic driver mutations that deregulate different components of the RTK–RAS–MAPK pathway in many cancer types[5]. Proliferative signals generated by oncogenic mutations in the RTK–RAS–MAPK pathway ultimately activate several transcription factors that orchestrate cell cycle entry and progression. The development and clinical implementation of small molecule inhibitors of mutated BRAF to treat melanoma has unequivocally demonstrated the importance of oncogenic growth factor signaling in cancer cell proliferation (see Fig. 113.1).

Deregulating Cellular Metabolism

Oncogenic signaling reprograms metabolic pathways to support cellular proliferation

Oncogenic signaling has also been found to activate the molecular machinery required to synthesize the large amounts of RNA, DNA, proteins, and membrane lipids necessary to produce a new cell. This requires increased uptake of glucose, lipids, and essential amino acids[18]. The glycolytic conversion of glucose to lactate under oxygen-rich conditions (*aerobic glycolysis*) was first described by Otto Warburg nearly 100 years ago. Importantly, glycolytic metabolites not only provide a source for the generation of energy in mitochondria, but also serve as building blocks for the synthesis of many macromolecules.

The important role of an activated MAPK pathway in the metabolic activity of cancer cells is impressively demonstrated by the ability of BRAF inhibitors to abrogate the uptake of radiolabeled glucose as visualized in a PET-CT scan. Oncogenic driver mutations in the PI3K–AKT signaling pathway also support glycolysis via post-translational modifications and increased transcription of glucose transporters and glycolytic enzymes[19]. Understanding the metabolic adaptations and the alterations in protein translation during cancer progression is an emerging field of study that holds the potential for future novel therapeutic approaches[20].

Mutations in p53 and Rb Tumor Suppressor Pathways Deregulate Cell Cycle Control

Oncogenic mutations in growth factor signaling pathways initiate the cell cycle machinery that orchestrates the replication of genomic DNA and the subsequent segregation of chromosomes into two daughter cells[17,21,22]. In normal cells, cyclins, cyclin-dependent kinases (CDKs), and cyclin-dependent kinase inhibitors (CKIs) tightly control the following: the decision to enter the cell cycle at the G1/S checkpoint; the process of DNA synthesis during the S phase; the decision to initiate mitosis at the G2/M DNA damage checkpoint; and the process of chromosome segregation during the M-phase. A network of tumor suppressor genes tightly regulates the G1/S and the G2/M cell cycle checkpoints to ensure the generation and distribution of identical genomes (see Fig. 107.4), and it is frequently inactivated in cancer cells[21,22].

Central players in this network include p53, Rb, and p16 (one of the protein products of *CDKN2A*). p53 was initially thought to enhance growth of tumor cells but was later found to be primarily a tumor suppressor[23]. Loss-of-function mutations in *TP53* represent the most frequent oncogenic alteration across multiple tumor types[5]. Today, p53

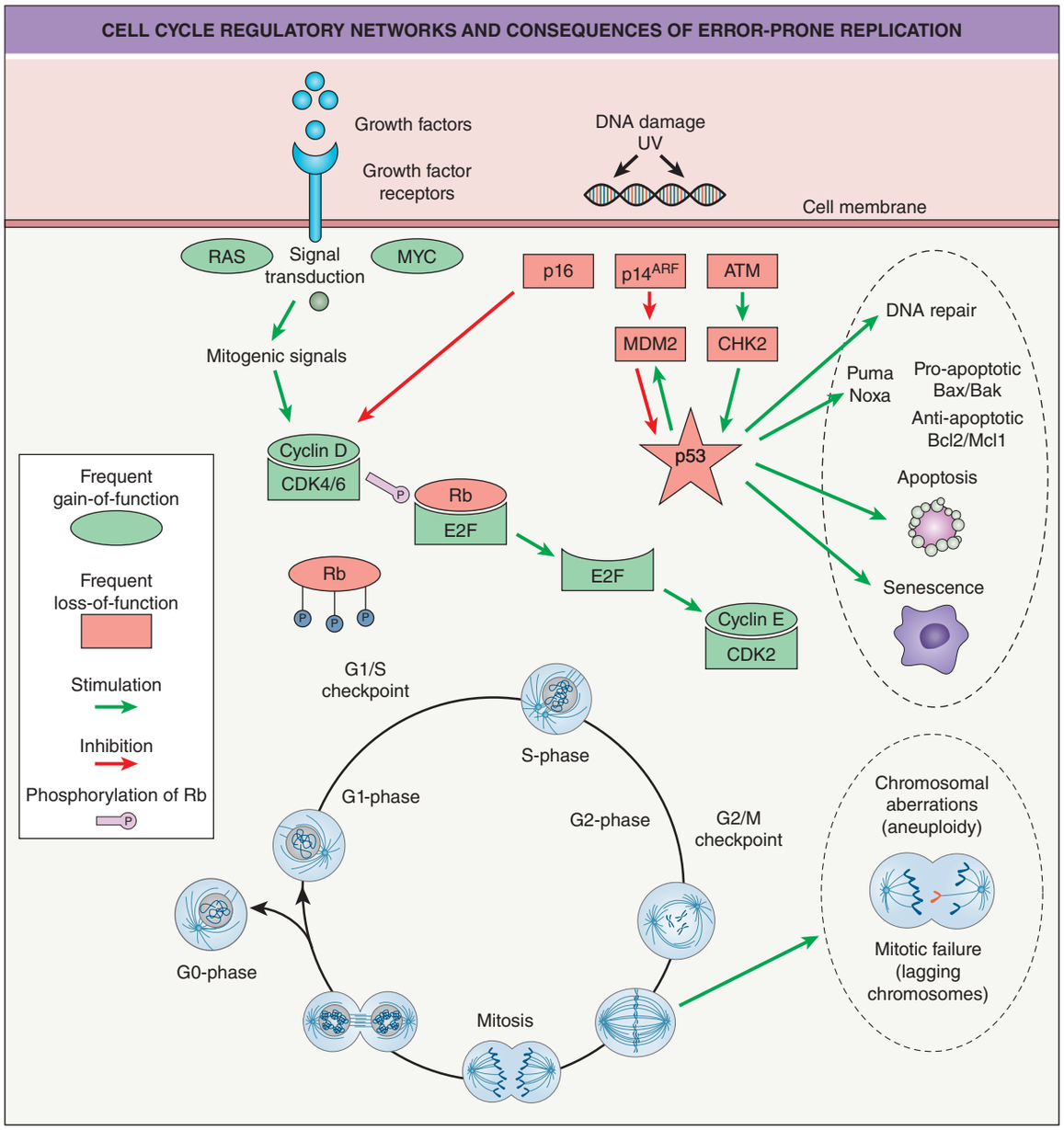


Fig. 107.4 Cell cycle regulatory networks and consequences of error-prone replication. Growth signals promote the activity of CDK4/6 and Cyclin D and drive cell cycle progression. DNA damage responses activate the p53–Rb network of tumor suppressors and arrest cells at the G1/S checkpoint of the cell cycle. If DNA damage is irreversible, cells enter a senescent state and ultimately activate the mitochondrial apoptotic signaling cascade leading to apoptotic cell death. Oncogenic driver mutations frequently deactivate the p53–Rb tumor suppressor network, thereby overriding cell cycle checkpoints. This predisposes cells to mitotic errors that can lead to chromosomal aberrations with numerical or structural aneuploidy.

is considered to be the *guardian of the genome* due to its important role in pathways that sense irreparable DNA damage and initiate programmed cell senescence or cell death (see Fig. 107.4). The *CDKN2A* and *RB* tumor suppressor genes, whose protein products control the G1/S cell cycle checkpoint, are also inactivated in the majority of cancer cells[22,24]. As a result, cancer cells do not exit from the cell cycle and continue to divide despite damage in their genomic DNA.

Resisting Cell Death

The proliferative capacity of healthy cells is tightly regulated by physiologic mechanisms of cell senescence and death. Cell senescence is a form of irreversible exit from the cell cycle in response to external or internal cellular stress and DNA damage. Senescence can be induced by carcinogens, reactive oxygen species, oncogene-induced replicative stress, or telomere attrition. At the molecular level, senescence is regulated by activation of the $p14^{ARF}$/MDM2/p53 and p16/pRb tumor suppressor pathways (see Fig. 107.4)[25,26]. Increased expression of p53 and p16 proteins are hallmarks of preneoplastic cells and represent a barrier for cancer development. Inactivation of these pathways allows cells to progress towards malignancy. Loss of p53 function also dysregulates the molecular machinery of programmed apoptotic cell death, which is critical for organismal development and the maintenance of tissue homeostasis.

In normal tissues, the balance between cell death and survival is maintained by tight regulation of members of the BH3-only and BCL-2-like families. In the absence of p53, the activity of the pro-apoptotic protein Bax is inhibited, thereby impairing apoptosis and promoting cell survival. Apoptosis is an important orderly process, which begins with the activation of orchestrating initiator caspases such as caspase 8 and 9. The latter in turn activate effector caspases, nucleases, and other lytic enzymes, resulting in the ordered degradation of genomic DNA and proteins including cytoskeleton components such as actin and lamins. Recently, multiple novel types of programmed cell death pathways such as ferroptosis, necroptosis, and pyroptosis have been described, with each exerting different effects on surrounding tissues[27].

Genome Instability and Mutation

Oncogenic alterations that disrupt the p53 and Rb tumor suppressor pathways impair DNA damage and repair responses, thus rendering cancer cells particularly susceptible to errors in DNA replication and chromosome segregation during mitotic division. For example, impairment of the mitotic spindle assembly checkpoint leads to chromosome mis-segregation and subsequently daughter cells with numerically and structurally altered chromosomes, a condition termed *aneuploidy*. A frequent early event during cancer evolution is whole genome doubling, which predisposes cancer cells with defective cell cycle

control to acquire additional chromosomal alterations and ultimately to develop chromosomal instability (see Fig. 107.4)[28–31].

The functional impact of aneuploidy on cancer progression is context-dependent[29]. Initially, leakage of DNA fragments from ruptured micronuclei into the cytosol, a frequent event in aneuploid cells, activates innate immune responses. This activation occurs via the cytosolic DNA-sensing cGAS–STING pathway and the production of interferons. Later during cancer evolution, the cGAS–STING pathway predominantly activates proinflammatory transcriptional responses that support immune evasion and metastatic dissemination[30,31].

THE TISSUE PERSPECTIVE

Architectures in Cancer Ecosystems

Oncogenic signaling alters the physiologic organization of cells in tissues and organs

A characteristic pathologic feature of advanced cancer is the disruption of normal tissue and organ architecture. Cancer cells often have increased morphologic heterogeneity, impaired cellular differentiation, and the phenotypic plasticity of their lineage progenitors[2]. The surrounding tumor microenvironment is frequently characterized by numerous inflammatory immune cells, newly formed vessels, and altered structure of the extracellular matrix. As similar features are observed in wound healing, cancer is thought to behave like a chronic wound that does not heal[32]. The identification of oncogenic driver mutations which dysregulate intercellular communication networks of ligands, receptors, and signaling mediators that have several functions – determining cell-fate decisions and morphologic patterning during embryogenesis, orchestrating tissue regeneration following injury or stress, and maintaining homeostasis in adult tissues – provides an explanation for this observation[33].

The evolution of cancer cells with increased transcriptional and epigenetic plasticity is critically shaped by reciprocal interactions with each other and with immune cells, endothelial cells, and fibroblasts within different niches of the tumor microenvironment[34]. The various cell phenotypes and their niches create a dynamic cancer tissue ecosystem that is coordinated by an altered intercellular communication network. Within this ecosystem, malignant and non-malignant cells dynamically adapt their phenotypes in response to the changing microenvironmental conditions during cancer progression and in response to therapeutic intervention. This includes the sensing of DNA damage in cancer cells by innate immune cells, as well as the subsequent genetic selection and phenotypic adaptation of cancer cells exposed to cytotoxic T cells that specifically recognize cancer mutations[30,35]. In addition, hypoxia promotes the release of angiogenic factors and initiates neovascularization. Inflammation and hypoxia promote cancer cell plasticity and epithelial-to-mesenchymal transitions that activate cellular migration programs and support invasive growth and metastatic spread[34].

Phenotypic Plasticity and Epigenetic Reprogramming

Increased cell state heterogeneity and plasticity is a hallmark of progressive tumor growth

The skin epithelium continuously self-renews through the activity of a long-lived population of adult stem cells that reside in microenvironmental niches. Adult stem cells undergo asymmetric cell divisions to give rise to transiently proliferating progeny and eventually to terminally differentiated cells that perform skin-specific functions. Keratinocytes, for example, continuously regenerate and eventually undergo programmed cell death to form the stratum corneum. Melanocytes and intraepithelial leukocytes have a longer lifespan and predominantly expand following tissue injury.

Physical damage, chemical toxins, and pathogens induce cellular stress and activate stem cell niches in the skin to increase their proliferative output, replace damaged cells, and restore tissue homeostasis. A typical example is the response to sunburning UV irradiation (Fig. 107.5). Importantly, tissue damage repair responses involve a transiently increased plasticity of stem cell states that allows precursor cells to adapt their differentiation pathways[36]. The underlying molecular mechanisms of tissue organization also govern the development of cancer and represent an additional bottleneck for the evolution of cancer genomes.

The accumulation of UV radiation-induced oncogenic driver mutations can only occur in cells that are capable of long-term self renewal and the generation of an entire cancer ecosystem. Lineage tracing experiments in genetically engineered mouse tumor models as well as in cancer-patient derived xenografts are beginning to reveal how somatic mutations that deregulate developmental signaling pathways in cancer cells increase the plasticity of stem cells and alter the differentiation trajectories of their cellular progeny. Reciprocal communication of keratinocyte carcinoma cells with fibroblasts as well as immune and endothelial cells through Hedgehog and Notch signaling are prominent examples in skin cancer (Figs. 107.6 & 107.7). These signals also orchestrate epithelial-to-mesenchymal transitions (EMT) during development and in response to tissue injury[37,38]. Both genetic and epigenetic dysregulation of these developmental signaling pathways promote tumor progression, from initiation and maintenance to metastatic spread and growth at distant sites.

Avoiding Immune Destruction

The cellular immune system can specifically recognize and eliminate mutated cancer cells

Based on experimental observations in the 1970s that immune cells can specifically recognize and eliminate virally induced cancer cells in mice, it was hypothesized that the immune system also controls the development of human cancer. In the first two decades of the 21st century this theory of cancer immunosurveillance advanced from wishful thinking pursued by very few scientists to a general principle in oncology.

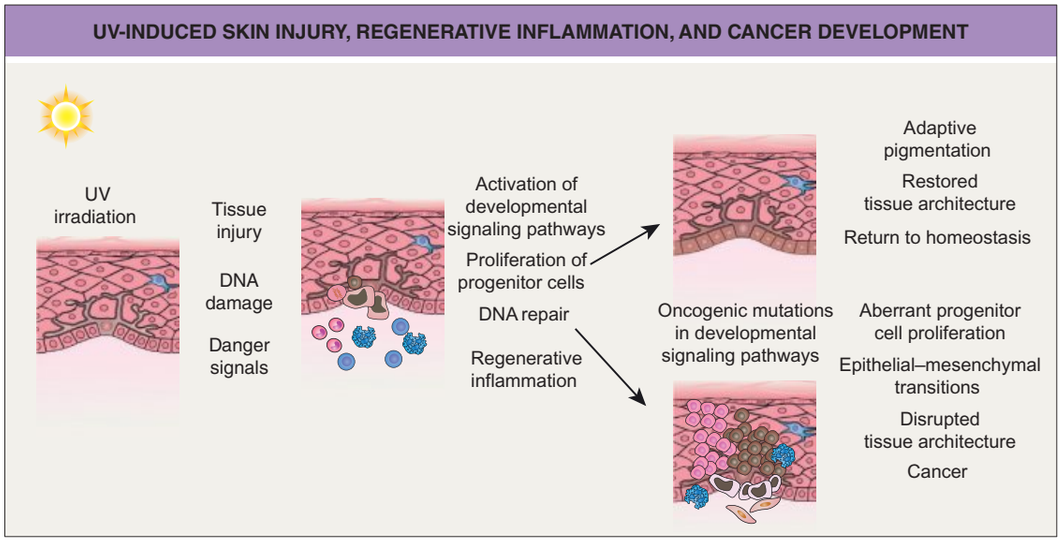


Fig. 107.5 UV-induced skin injury, regenerative inflammation, and cancer development. UV irradiation causes tissue injury and DNA damage. This results in the proliferation of progenitor cells and the activation of developmental signaling pathways that orchestrate tissue repair and restore tissue architecture. Oncogenic mutations in these signaling pathways promote aberrant proliferation of precursor cells within stem and progenitor cell niches, disrupt normal tissue architecture, and foster epithelial–mesenchymal transitions, thus leading to carcinoma.

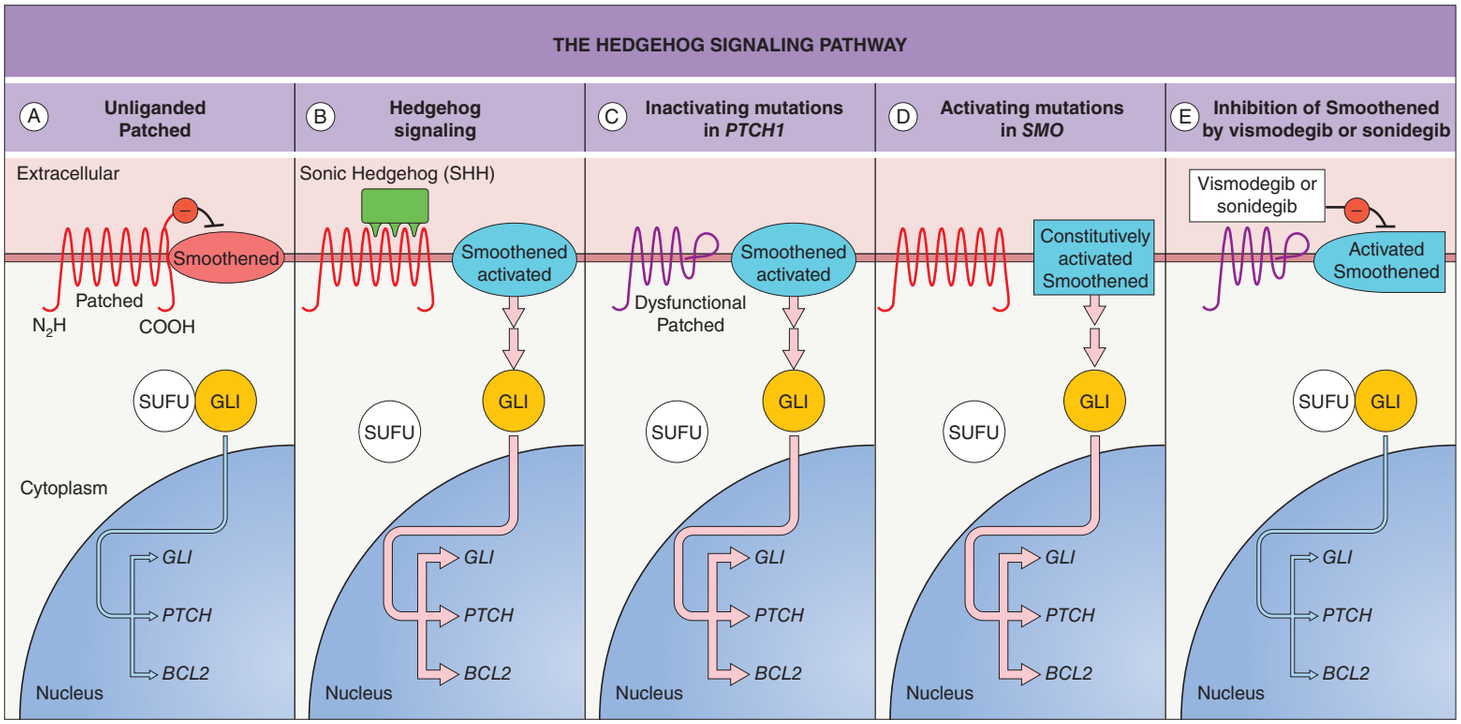


Fig. 107.6 The Hedgehog signaling pathway. A Unbound Patched silences Smoothened (SMO) signaling. **B** As Hedgehog binds to its receptor Patched, the repression of SMO is removed and signals are transduced via GLI to the nucleus. **C** Inactivating mutations in *PTCH1* (or rarely *PTCH2*) lead to dysfunctional Patched and this mimics Hedgehog binding and results in constitutive activation of GLI and downstream target genes. **D** An activating mutation in *SMO* results in constitutive signaling via GLI to activate downstream target genes. Such mutations are detected in sporadic BCCs in which *PTCH1* is intact. **E** Vismodegib and sonidegib are inhibitors of SMO that have been used to treat patients with BCNS as well as metastatic or locally advanced BCCs. At least 50% of advanced BCCs develop resistance to vismodegib, commonly via acquiring mutations in *SMO*.

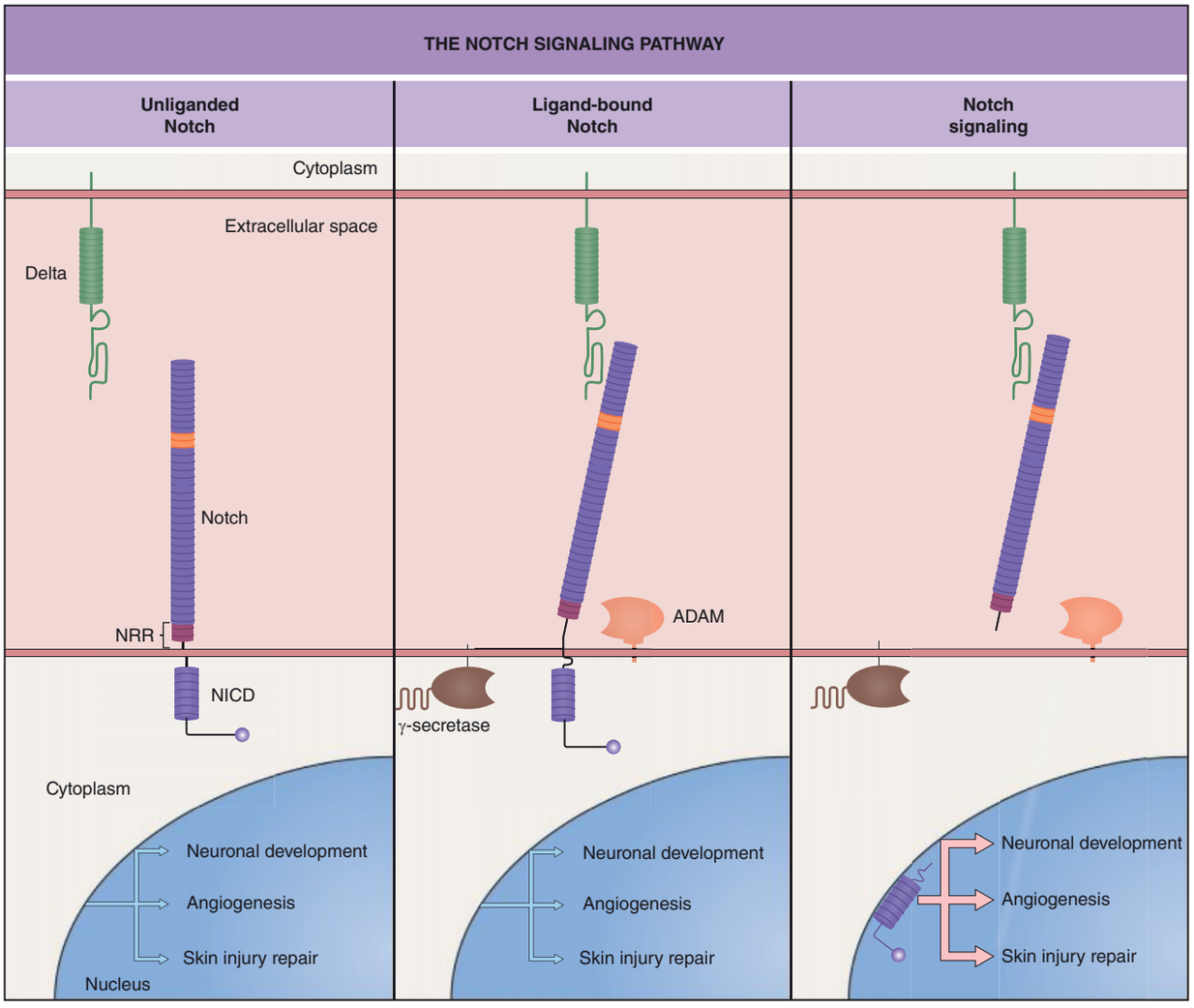


Fig. 107.7 The Notch signaling pathway. Notch signaling is inactivated in the majority of keratinocytes. The membrane-bound (juxtacrine) ligands of the Delta-like and Jagged family interact with the Notch receptor on the target cell and promote the cleavage of Notch both on the extracellular surface via ADAM (a disintegrin and metalloprotease) and on the intracellular surface via γ-secretase. The Notch intracellular domain (NICD) translocates into the nucleus and activates the transcription factor CSL. The extracellular, ligand-bound domain of Notch is repurposed by phagocytosis.

Initial proof-of-principle for the ability of T cells to specifically eradicate human cancer was obtained in studies where lymphocytes were isolated from melanoma metastasis tissues, expanded *ex vivo* and reinfused into patients. The clinical efficacy of monoclonal antibodies targeting the immunoregulatory receptors CTLA-4 and PD-1 (immune checkpoint blockade) on T cells represented a breakthrough for T cell immunotherapies and is currently changing the treatment of many cancer patients[39–41].

DNA damage in cancer cells triggers the cGAS–Sting pathway and alerts the innate immune system[30,31]. This also activates dendritic cells that take up cancer cell fragments and induces their migration to the regional lymph nodes (Fig. 107.8A). Here, dendritic cells present tumor antigens to naive T cells and stimulate their expansion and differentiation into effector T cells. These cells of the adaptive immune system home into tumor tissues where they can eradicate the malignant cell population[35,39]. The ability of tumor-specific T cells to broadly recognize mutated peptides, which stochastically arise as a consequence of genomic alterations in cancer cells, represents a cornerstone of modern tumor immunology. These mutated peptides (termed *neoantigens*) are presented to T cells in the binding groove of MHC molecules in a similar manner as viral antigens (see Ch. 4). This explains why the efficacy of T cell immunotherapies directly correlates with the mutational burden of cancer cells.

Tumor-specific T cells also recognize self-antigens derived from normal gene products that are expressed only in specific cell types. Melanosomal enzymes such as tyrosinase that are recognized by melanoma-specific T cells are typical examples of lineage differentiation antigens. Proteins of the *MAGE* gene family, which are physiologically expressed in embryonic tissues and are restricted to reproductive organs in adults (termed *cancer testis antigens*), represent another class of tumor antigens recognized by T cells and are frequently re-expressed in cancer cells due to epigenetic alterations[35,39].

Detailed immunohistopathologic investigations revealed that cancer tissues vary widely with respect to the infiltration of T cells and other immune cells. Recently, clinical and experimental evidence has accumulated that oncogenic driver mutations orchestrate the tumor immune landscape. For example, mutations that activate the Wnt signaling pathway or *MYC* promote evasion of cellular immunity by preventing T cells from entering tumor tissues, a phenomenon called *T cell exclusion*[42]. However, the interaction between tumor and immune cells is not unidirectional, and immune cells may also secrete cytokines that are conducive to cancer cell survival and proliferation.

Today, it is well documented that the anti-tumoral T cell response imposes a critical cell-extrinsic barrier to malignant transformation[43]. Current immunotherapies partially resurrect this barrier by reactivating

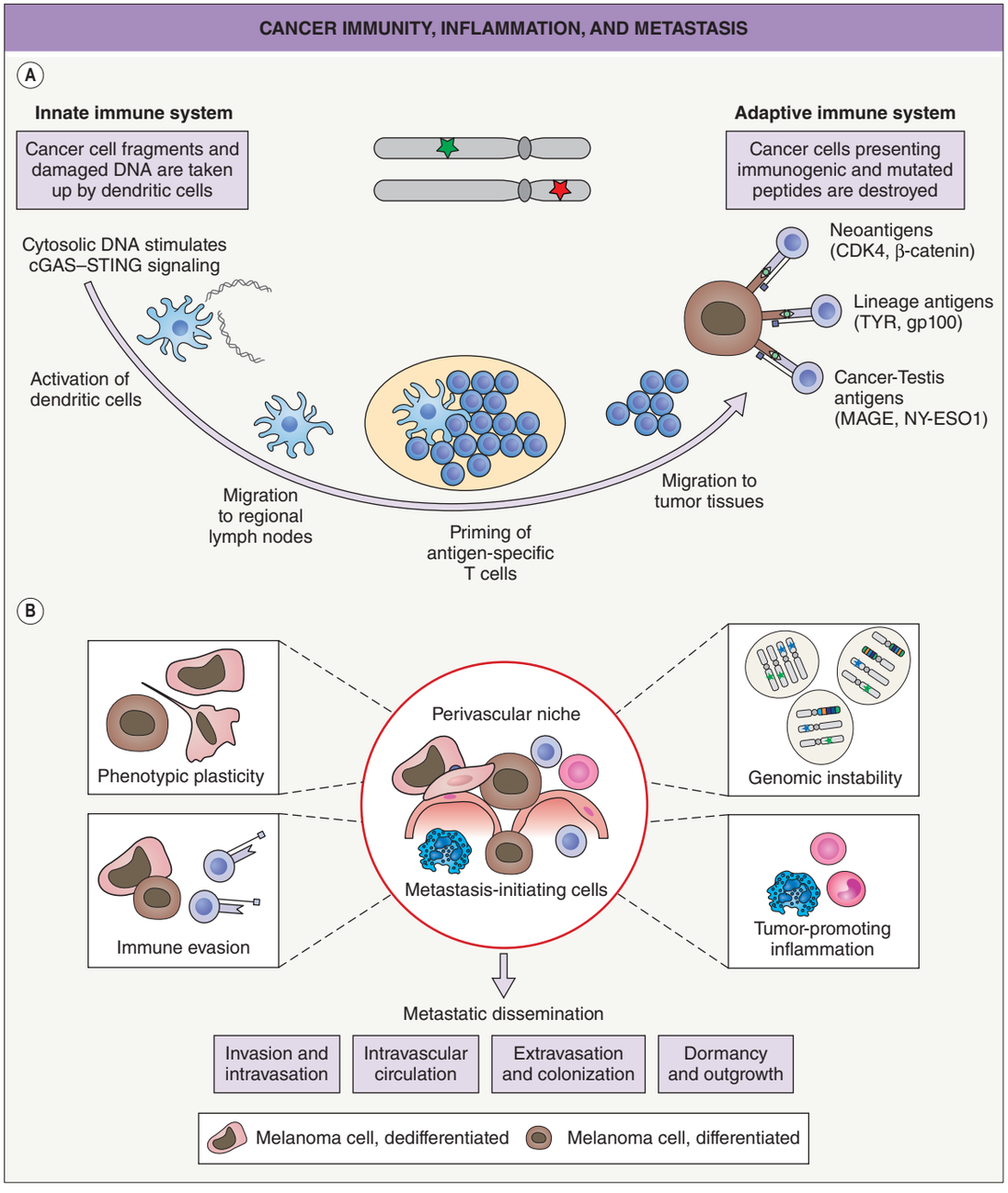


Fig. 107.8 Cancer immunity, inflammation, and metastasis. A Dynamics of innate and adaptive immune recognition of cancer cells by the cellular immune system. **B** In the process of metastasis, cancer cells depend on several cell-intrinsic and cell-extrinsic factors that support extravasation, survival in the circulation, dormancy at sites of organ colonization, and outgrowth to clinically apparent distant metastases. Shown here is the perivascular niche, which plays a key role in promoting cancer cell survival.

the effector functions of tumor-infiltrating T cells. However, cancer cells in turn evade T cell immunity through a variety of mechanisms, including transcriptional downregulation of genes involved in antigen presentation and the acquisition of dedifferentiated, stem cell-like phenotypes[44–46]. In this process, T cells drive phenotypic adaptations of cancer cells and shape their genomic evolution through Darwinian selection of subpopulations with genetically hardwired immune evasive properties, e.g. loss-of-function mutations in MHC molecules[43].

Cancer-Promoting Inflammation

A growth-promoting inflammatory microenvironment can drive cancer progression

Progressively growing cancer cells engage in dynamic reciprocal interactions with surrounding immune cells, creating a microenvironment that fosters their survival and proliferation[47]. This is driven in part by cancer cell-intrinsic oncogenic signaling and the secretion of growth-promoting, proinflammatory cytokines and chemokines. In addition, cancer-promoting inflammatory microenvironments can result from repetitive tissue injury due to the action of physical and chemical carcinogens. The potential role of inflammatory cells within cancer tissues in promoting malignant progression was already recognized by Rudolph Virchow in 1863 in his "irritation theory of cancer". This was experimentally verified using chemical carcinogens and UV irradiation as initiators and inflammatory promotors.

Chronic inflammation, both intrinsic and extrinsic to cancer cells, increases the recruitment of myeloid immune cell populations with T cell suppressive phenotypes that normally orchestrate tissue regeneration. DNA damage responses and genomic instability of cancer cells contribute to a protumorigenic inflammatory response, for example due to leakage of extrachromosomal double-stranded DNA into the cytosol, which activates innate antiviral immune responses via the cGAS–STING pathway. Activation of this signaling pathway in cancer-associated dendritic cells can stimulate antigen-specific T cells, while activation in cancer cells with chromosomal instability supports cancer cell survival and evasion of T cell immunity[30].

Inducing or Accessing Vasculature

Hypoxic environments activate proangiogenic signaling pathways

Increased blood supply of oxygen and nutrients is required for continuous tumor growth. The identification of vascular endothelial growth factor (VEGF) as one of the principle molecular regulators of tumor angiogenesis represents a milestone in cancer research[48]. Cancer cells produce VEGF in response to hypoxic conditions that stabilize and activate this hypoxia-inducible factor. Binding of VEGF to its receptor VEGFR2 on endothelial cells initiates the formation of new blood vessels through neoangiogenesis. Mechanistically, this is orchestrated by motile endothelial cells, called tip cells, that break down the surrounding extracellular matrix (ECM) and initiate the growth of new vascular sprouts. This process is tightly regulated by Notch signaling via the secretion of the delta ligand-like 4 (DLL4) by endothelial tip cells (see Fig. 102.7).

However, newly formed blood vessels in tumors are mostly abnormal, both structurally and functionally. Their architecture is chaotic, tortuous, and leaky due to a lack of normal pericyte coverage, resulting in irregular blood flow, decreased perfusion, and chronic hypoxia. The cross-talk between hypoxic cancer cells and endothelial cells is also critically shaped by proangiogenic and proinflammatory mediators secreted by cells of the immune system in the tumor microenvironment. For example, macrophages and neutrophils can secrete VEGF-A and other proangiogenic factors such as angiopoietin-1 (ANGPT1) and hepatocyte growth factor (HGF). Therapeutic inhibition of proangiogenic signaling has been shown to normalize the tumor vasculature and improve the efficacy of chemo- and immunotherapies. Conversely, effective immunotherapies can contribute to vessel normalization[49].

Activating Invasion and Metastasis

Phenotypic plasticity enables cancer cell invasion, migration, and metastasis

If cancers are detected early, patients can be cured by surgical excision. This is frequently achieved for cancers in the skin that are immediately visible. However, in some cases cancer cells are able to invade adjacent tissue, enter lymph and blood vessels, spread throughout the body, and colonize distant organs before they are locally resected. Histologically distinct cancer entities differ in their propensity and their patterns of metastatic dissemination. This was already noted in the late 19th century by the English surgeon Stephen Paget who proposed that the organ preference of cancer metastasis might result from favorable interactions between metastatic cancer cells and the unique tissue microenvironments in different organs. This "seed and soil" theory was complemented later to include the impact of mechanical factors such as the anatomy of vascular and lymphatic drainage from the site of a primary tumor. Research over the past several decades has provided insights into cellular and molecular mechanisms that drive cancer metastasis[50–52]. The characterization of cancer cell subpopulations that initiate and sustain the development of metastases represented a key conceptual advance. These rare metastasis-initiating cells display the stem cell-like phenotype and plasticity of their lineage progenitors that helps them to survive the adverse physical and metabolic conditions in the circulation and evade immune cell recognition and destruction[51].

Metastasis-initiating cancer cells undergo reversible epithelial-to-mesenchymal transitions and enter slow-cycling and dormant cell states during the metastatic cascade. The switch of adhesion molecules from epithelial to mesenchymal cell states, most notably from E-cadherin to N-cadherin, is regarded as a critical step in initiating migration and invasion of carcinoma cells. Inflammatory cells in the microenvironment contribute to the disassembly of the extracellular matrix (ECM) and its constituents via enzymes such as matrix metalloproteinases (MMPs), thereby facilitating invasive growth. Supportive interactions with endothelial cells promote cancer cell migration and proliferation along blood vessel surfaces, increasing the likelihood of intravasation and dissemination through the circulation. Dynamic adaptation of cell adhesion networks protects cancer cells from anoikis, a type of apoptosis-like destruction of cells that have lost their cell-matrix contact. Only very few circulating metastasis-initiating cells are finally able to colonize distant organs. Here, they survive and remain dormant for longer periods of time within perivascular niches, before they grow out as clinically apparent metastases (Fig. 107.8B)[51].

Despite impressive advances in our understanding of the biology underlying cancer metastasis, patients with metastatic disease frequently develop resistance to currently available treatments. Progressive growth of disseminated cancer cells remains responsible for the majority of cancer-associated deaths. Current large scale sequencing studies of cancer metastases reveal an increasingly heterogeneous and complex picture of genomic alterations at this late stage of cancer evolution. These studies found that the majority of oncogenic driver mutations occur before metastatic dissemination. However, chromosomal instability and copy-number variations such as whole genome doubling were more frequently observed in metastatic cancer cells from many tumor types[53]. Evidence is accumulating that the unique microenvironments in different organs, most notably the metabolic conditions and the immune cell composition that determine therapy responses, also shape the evolution of cancer genomes during metastatic progression. Integrated analyses of the whole cancer ecosystems are required to fully understand metastatic disease as a prerequisite for the development of patient-specific therapeutic strategies.

PATHOGENESIS OF KERATINOCYTE CARCINOMAS

Keratinocyte carcinomas derive from epidermal keratinocytes and worldwide represent the most common cancer type in fair-skinned populations. The majority of keratinocyte carcinomas are basal cell carcinomas (BCCs), which are locally destructive and only rarely develop metastases. Cutaneous squamous cell carcinomas (cSCCs) are less common, but more likely to metastasize and are responsible for the majority of deaths from keratinocyte carcinomas (see Ch. 108).

Genomic sequencing of keratinocyte carcinomas has revealed the highest mutational burden of any cancer type, with molecular signatures of UV-induced DNA damage. This is consistent with lifelong sun exposure as the most important environmental risk factor[54,55]. It is now known that epidermal keratinocytes in clinically normal-appearing, UV-exposed skin can tolerate a surprisingly high number of mutations in known cancer genes[12], indicating powerful mechanisms

that prevent malignant transformation at the tissue level. Recent experiments in genetically engineered mouse models suggest that oncogenic signaling induces keratinocyte differentiation and physiologic death as a mechanism of tumor suppression[56].

Molecular Pathogenesis of Basal Cell Carcinoma (BCC)

Genetic linkage studies in families with basal cell nevus syndrome (BCNS or Gorlin syndrome; see Ch. 108), a rare inherited disorder in which multiple BCCs develop comparatively early in life, provided an initial insight into the specific molecular pathogenesis of BCC – this was beyond the known mutations in *TP53* that are present in all keratinocyte carcinomas. These studies identified *PTCH1* as a tumor suppressor gene that is inactivated in BCNS patients and whose protein product is an inhibitor of the Hedgehog signaling pathway (see Fig. 107.6). Subsequent studies identified loss-of-function mutations in *PTCH1* as a frequent event in sporadic BCCs[57].

The Hedgehog signaling pathway was discovered in *Drosophila*, is highly conserved during evolution, and plays an important role in tissue patterning and cell fate during embryonal development. In the skin, Hedgehog signaling is responsible for the developmental regulation of hair follicles and sebaceous glands. In adult tissues, it is involved in epithelial and neural stem cell maintenance as well as in tissue repair responses. Oncogenic activation of Hedgehog signaling is observed in various types of cancer, including BCC, medulloblastoma, and pancreatic, breast, colon, ovarian, and small cell lung carcinomas. Experimental activation of Hedgehog signaling in epidermal keratinocytes from genetically engineered mice leads to skin tumors with a BCC phenotype, demonstrating the functional importance of this pathway *in vivo*[58].

Whole exome sequencing studies confirmed BCCs as the tumor entity with the highest number of mutations and provided a comprehensive picture of the landscape of oncogenic driver mutations in BCC metastases (Fig. 107.9A). In addition to driver mutations that activate the Hedgehog pathway in 85% of BCCs, these studies identified mutations in target genes of N-Myc as well as the Notch and Hippo-YAP pathways[54]. These findings are thought to provide an explanation for the phenotypic variation of BCCs. Recently, it was shown that in genetically engineered mice, combined experimental activation of the Hedgehog and Notch signaling pathways, together with overexpression of N-Myc, was able to drive progressive and unrestrained growth of BCCs[59]. These observations support a model in which the aggressive growth of BCCs is the result of multiple complementary genetic alterations, consistent with the concept of cancer evolution (Fig. 107.9B).

Molecular Pathogenesis of Cutaneous Squamous Cell Carcinoma (cSCC)

The pathogenesis of cSSC has been studied experimentally for decades in mice using mutagenic chemicals such as dimethylbenzanthrene (DMBA) and UV irradiation in two-stage carcinogenesis models. The identification of oncogenic *Hras* mutations in cSCCs arising in DMBA-exposed mice represents a milestone in skin cancer biology[1]. Subsequent murine studies demonstrated an important role for loss-of-function mutations in *p53* in Ras-driven cSCCs, enabling chromosomal alterations and genomic instability. Initial studies in a limited number of human cSCCs confirmed recurrent oncogenic driver mutations in *HRAS* and *TP53*. Deeper insights into the molecular pathogenesis of cSCCs and the identification of additional oncogenic drivers had to await the comprehensive characterization of a larger number of cSCCs using next-generation sequencing of whole exomes. Initial reports identified frequent mutations in genes of the Notch pathway[60].

The Notch signaling pathway was first described in *Drosophila* (see Fig. 107.7). More than a century ago, Thomas Hunt Morgan identified mutant fruit flies with a characteristic notching of their wings, giving the gene its name. In the 1980s, Notch genes were identified and found to orchestrate an ancient cell signaling pathway that is highly conserved within the animal kingdom. Notch signaling plays an important role in cell–cell communication during embryogenesis and is critically required for the development of many tissues and organs including the brain, the heart and vasculature, the hematopoietic system, and the skin. It promotes the self-renewal of stem and progenitor cells, orchestrates cell fate decisions, and regulates cell differentiation in a cell context-dependent manner. Notch signaling is maintained at a low level in adult organisms and is rapidly upregulated during repair responses following tissue injury.

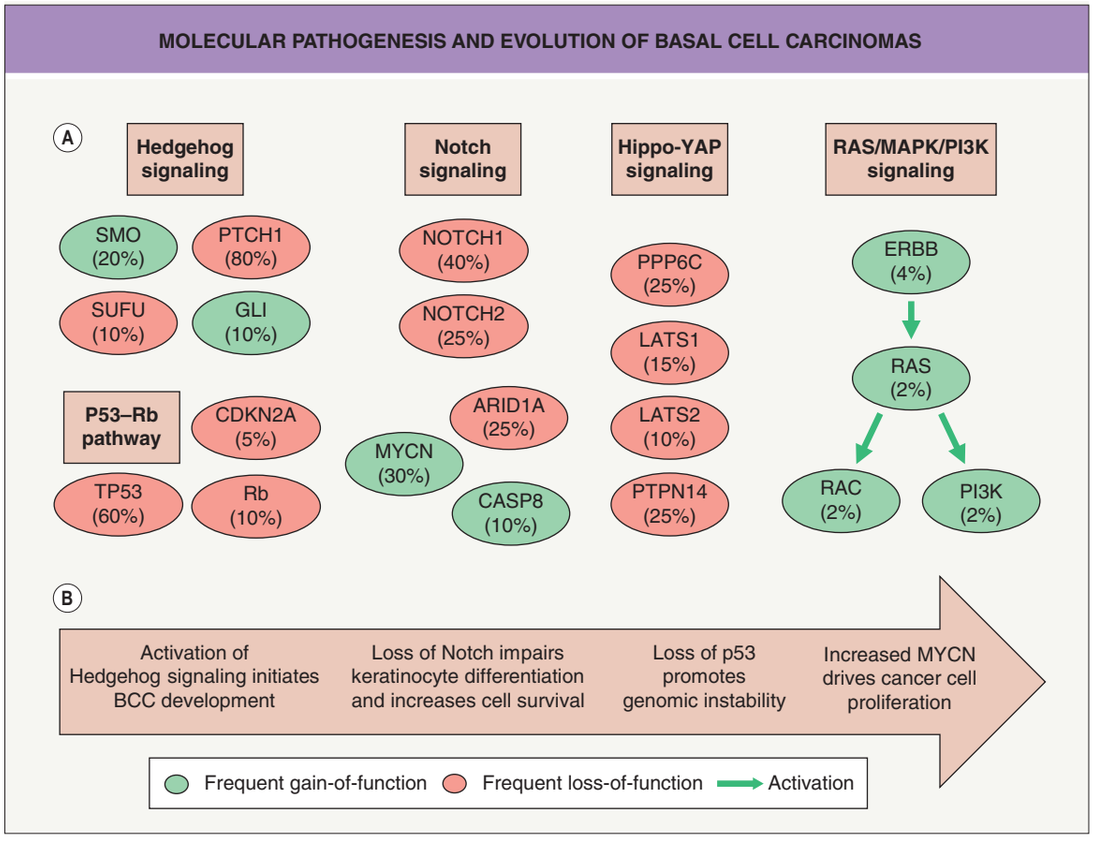


Fig. 107.9 Molecular pathogenesis and evolution of basal cell carcinomas (BCCs). A Genomic alterations in signaling pathways involved in BCC pathogenesis. **B** Hypothetical model of the evolutionary trajectory of BCC. *A, Adapted from Bonilla X, et al. Genomic analysis identifies new drivers and progression pathways in skin basal cell carcinoma. Nat Genet 2016;48:398–406.*

Importantly, mutations in Notch pathway genes are observed in a wide range of malignancies, most notably in multiple non-cutaneous carcinomas, leukemias, and brain tumors. The oncogenic activity of Notch signaling depends on the cellular context. Initial studies showed that increased Notch signaling is oncogenic in leukemias. In contrast, Notch signaling has tumor suppressor activity in the skin, most likely because it supports keratinocyte differentiation.

A recent comprehensive bioinformatics analysis of available genome sequencing data for cSCCs provided a comprehensive overview of the landscape of oncogenic driver mutations, confirming the important role of mutations in Notch pathway genes as the second most frequent group of oncogenic drivers after *TP53* and *Rb* (Fig. 107.10A)[55]. Today, sequential acquisition of oncogenic driver mutations in genes that encode proteins in the p53–Rb and Notch pathways, followed by mutations in epigenetic regulators and the acquisition of structural and numerical chromosome alterations, are thought to represent the evolutionary trajectory of cSCC development (Fig. 107.10B,C). Progressively growing carcinomas acquire chromosomal alterations, aberrantly activate the phenotypic plasticity of their stem and progenitor cells, recruit suppressive T cells that subvert anti-tumoral immunity, and engage with endothelial cells to support metastatic dissemination.

CURRENT DEVELOPMENTS AND FUTURE PERSPECTIVES

Mapping the Evolution of Cancer Ecosystems in Space and Time

Recent advances in single-cell and spatially resolved technologies have enabled analysis of tumor specimens at an unprecedented resolution. The next frontier in cancer research is to use these techniques to further understand the spatial and chronologic complexity of cancer. Current projects such as the NIH Human Biomolecular Atlas Program (HuBMAP) aim to generate references of human tissues by combining (epi-)genomic, transcriptomic, proteomic, and metabolomics analyses with single-cell and spatial resolution[61]. In analogy to the first human reference genome created more than 20 years ago, these frameworks may serve as invaluable tools for understanding the dynamics of tissue development.

Similar approaches focusing on cancer rather than healthy tissues are attempting to reconstruct the heterogeneity and complex interactions between cancer cells and their host organisms[62]. This wealth of information is already catalyzing the development of novel bioinformatical analysis tools and promoting the convergence of diverse scientific disciplines with the potential to once again revolutionize our understanding of cancer. The aforementioned projects may have the capability of answering some of the key riddles of cancer in the coming decade: the mechanisms of metastatic spread, the tissue specificity of oncogenic events, the cell(s) of origin of cancer, and the influence of the cancer microenvironment.

The Microbiome and Cancer

Although the discovery of microbiota influencing tumor development dates back more than 100 years, only recent discoveries have suggested a far deeper relationship between cancer cells and surrounding microbes. Due to the low biomass compared to the tumor cells themselves, and the diverse strains of microbiota colonizing different areas of the bodies and tumor types, the study of cancer-associated microbiota has proven to be challenging. However, recent technological advances have enabled their study, highlighting that microbiota have the capacity to modulate multiple aspects of cancer development, progression, and therapeutic response[63].

As an example, correlations have been observed between specific bacterial strains in the gut and responses to immunotherapy, suggesting that the microbiome profoundly influences host immune responses and thereby therapeutic efficacy. Additionally, metastatic dissemination has been shown to be influenced by intracellular bacteria. As lifestyle

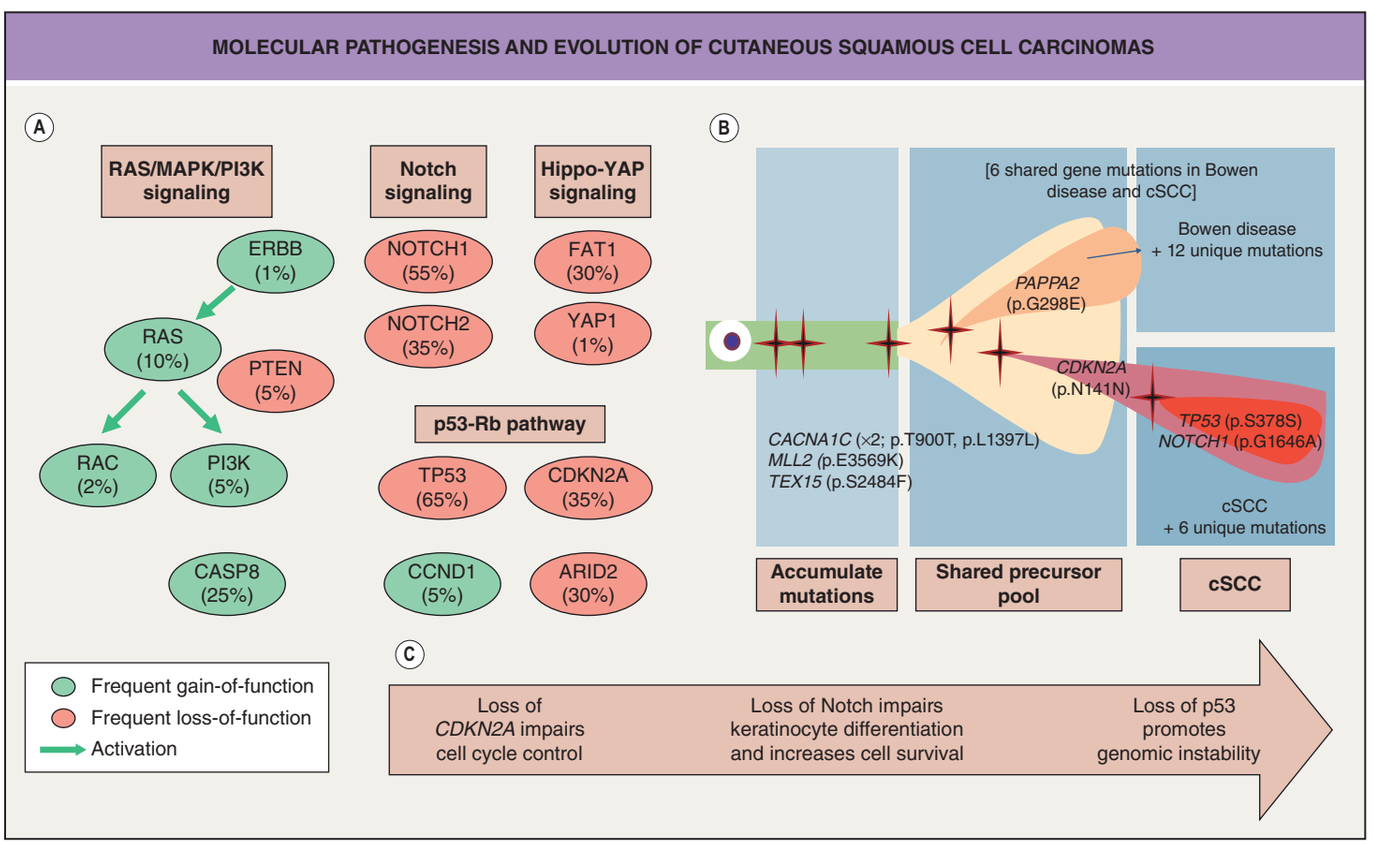


Fig. 107.10 Molecular pathogenesis and evolution of cutaneous squamous cell carcinomas (cSCCs). A Genomic alterations in signaling pathways involved in cSCC pathogenesis. **B** Evolutionary trajectory of a cSCC. **C** Hypothetical model of the evolutionary trajectory of cSCC. *A, Adapted from Chang D, et al. The landscape of driver mutations in cutaneous squamous cell carcinoma. NPJ Genom Med 2021;16:61; B, Adapted from Albibas AA, et al. Subclonal evolution of cancer-related gene mutations in p53 immunopositive patches in human skin. J Invest Dermatol 2018;138:189–98.*

factors such as diet or smoking modulate the microbiome, these findings open new avenues of patient-centric therapeutic approaches. In the near future, synthetic biology approaches using engineered bacteria as cancer therapeutics may complement the current arsenal of targeted and immune therapies.

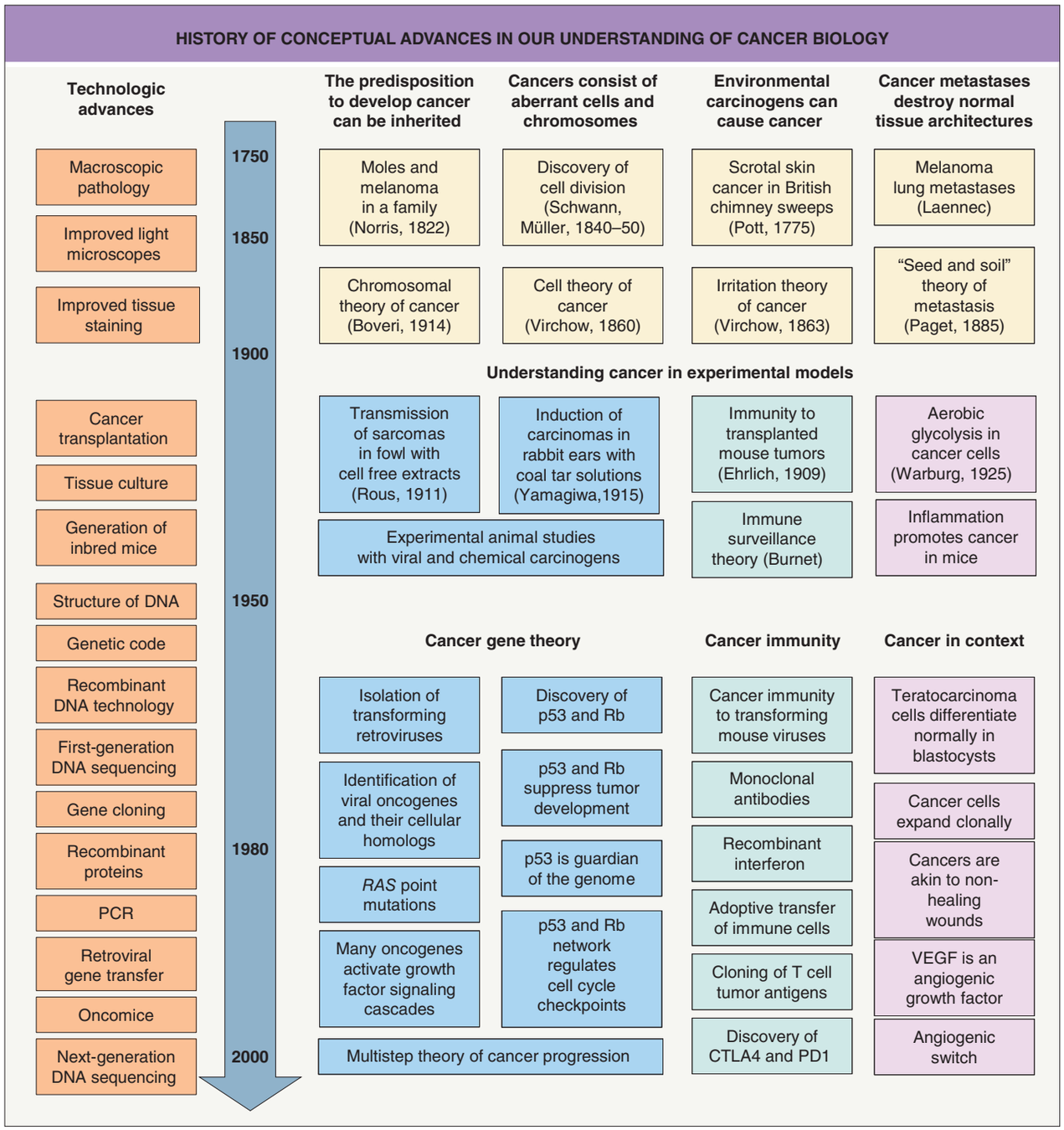
Future Perspectives for Clinical Translation

Despite the astounding technologic progress that has allowed the analysis of molecular profiles of tumors at an unprecedented depth, the clinical application of these methods is currently lagging behind. To bridge this gap, new projects are addressing the applicability and usefulness of molecular information in patient care. Studies such as the Tumor Profiler Trial are attempting to combine bulk and single-cell DNA and RNA sequencing, immunofluorescence, mass cytometry imaging, and pharmacologic analyses into a molecular research report that can be used to guide therapeutic decisions[64].

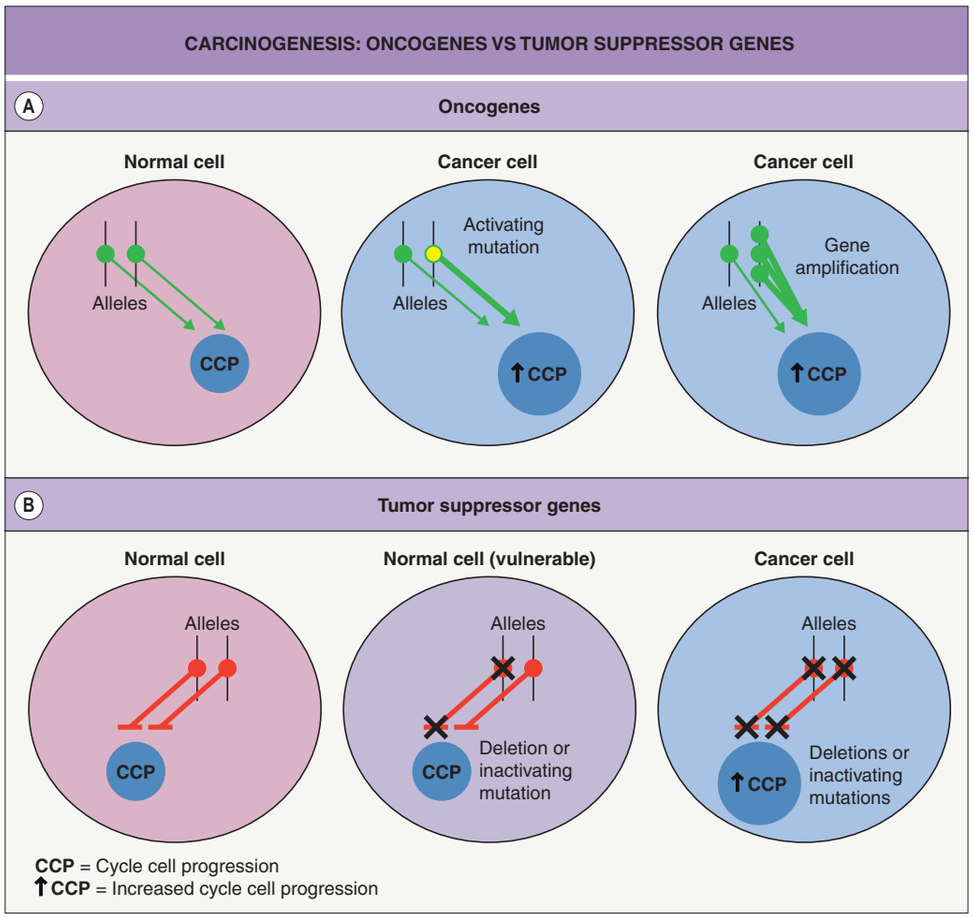
Additional figures available in our eBook (see inside front cover for access code).

REFERENCES

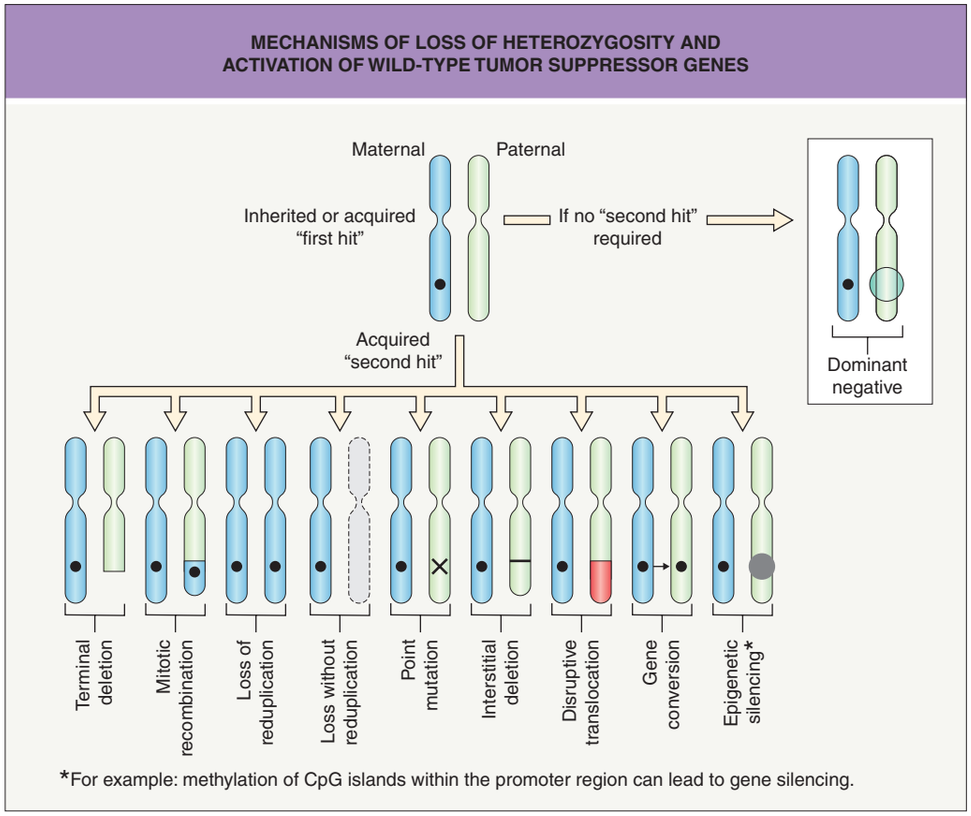
1. Balmain A, Yuspa SH. Milestones in skin carcinogenesis: the biology of multistage carcinogenesis. *J Invest Dermatol*. 2014;134:E2–E7.
2. Hanahan D. Hallmarks of cancer: new dimensions. *Cancer Discovery*. 2022;12:31–46.
3. Hanahan D, Weinberg RA. Hallmarks of cancer: the next generation. *Cell*. 2011;144:646–674.
4. Karczewski KJ, Francioli LC, Tiao G, et al. The mutational constraint spectrum quantified from variation in 141,456 humans. *Nature*. 2020;581:434–443.
5. Campbell PJ, Getz G, Korbel JO, et al. Pan-cancer analysis of whole genomes. *Nature*. 2020;578:82–93.
6. Li Y, Roberts ND, Wala JA, et al. Patterns of somatic structural variation in human cancer genomes. *Nature*. 2020;578:112–121.
7. Alexandrov LB, Kim J, Haradhvala NJ, et al. The repertoire of mutational signatures in human cancer. *Nature*. 2020;578:94–101.
8. Umbreit NT, Zhang CZ, Lynch LD, et al. Mechanisms generating cancer genome complexity from a single cell division error. *Science*. 2020;368eaba0712.
9. Cortés-Ciriano I, Lee JJK, Xi R, et al. Comprehensive analysis of chromothripsis in 2,658 human cancers using whole-genome sequencing. *Nature Genet*. 2020;52:331–341.
10. Roberts SA, Gordenin DA. Hypermutation in human cancer genomes: footprints and mechanisms. *Nat Rev Cancer*. 2014;14:786–800.
11. Vendramin R, Litchfield K, Swanton C. Cancer evolution: Darwin and beyond. *EMBO J*. 2021;40:e108389.
12. Martincorena I, Roshan A, Gerstung M, et al. Tumor evolution. High burden and pervasive positive selection of somatic mutations in normal human skin. *Science*. 2015;348:880–886.
13. Newell F, Wilmott JS, Johansson PA, et al. Whole-genome sequencing of acral melanoma reveals genomic complexity and diversity. *Nat Commun*. 2020;11:5259.
14. Field MG, Durante MA, Anbunathan H, et al. Punctuated evolution of canonical genomic aberrations in uveal melanoma. *Nat Commun*. 2018;9:116.
15. Vogelstein B, Papadopoulos N, Velculescu VE, et al. Cancer genome landscapes. *Science*. 2013;339:1546–1558.
16. Fernández-Medarde A, De Las Rivas J, Santos E. 40 Years of RAS—a historic overview. *Genes*. 2021;12:681.
17. Pylayeva-Gupta Y, Grabocka E, Bar-Sagi D. RAS oncogenes: weaving a tumorigenic web. *Nat Rev Cancer*. 2011;11:761–774.
18. Pavlova NN, Thompson CB. The emerging hallmarks of cancer metabolism. *Cell Metab*. 2016;23:27–47.
19. Hoxhaj G, Manning BD. The PI3K–AKT network at the interface of oncogenic signalling and cancer metabolism. *Nat Rev Cancer*. 2020;20:74–88.
20. Faubert B, Solmonson A, DeBerardinis RJ. Metabolic reprogramming and cancer progression. *Science*. 2020;368eaaw5473.
21. Malumbres M, Barbacid M. RAS oncogenes: the first 30 years. *Nat Rev Cancer*. 2003;3:459–465.
22. Matthews HK, Bertoli C, de Bruin RAM. Cell cycle control in cancer. *Nat Rev Mol Cell Biol*. 2022;23:74–88.
23. Levine AJ, Oren M. The first 30 years of p53: growing ever more complex. *Nat Rev Cancer*. 2009;9:749–758.
24. Sherr CJ, McCormick F. The RB and p53 pathways in cancer. *Cancer Cell*. 2002;2:103–112.
25. He S, Sharpless NE. Senescence in health and disease. *Cell*. 2017;169:1000–1011.
26. Mooi WJ, Peeper DS. Oncogene-induced cell senescence – halting on the road to cancer. *N Engl J Med*. 2006;355:1037–1046.
27. Strasser A, Vaux DL. Cell death in the origin and treatment of cancer. *Mol Cell*. 2020;78:1045–1054.
28. Holland AJ, Cleveland DW. Boveri revisited: chromosomal instability, aneuploidy and tumorigenesis. *Nat Rev Mol Cell Biol*. 2009;10:478–487.
29. Ben-David U, Amon A. Context is everything: aneuploidy in cancer. *Nat Rev Genet*. 2020;21:44–62.
30. Bakhoum SF, Cantley LC. The multifaceted role of chromosomal instability in cancer and its microenvironment. *Cell*. 2018;174:1347–1360.
31. Tijhuis AE, Johnson SC, McClelland SE. The emerging links between chromosomal instability (CIN), metastasis, inflammation and tumour immunity. *Mol Cytogenet*. 2019;12:17.
32. Schäfer M, Werner S. Cancer as an overhealing wound: an old hypothesis revisited. *Nature Reviews Molecular Cell Biology*. 2008;9:628–638.
33. Malta TM, Sokolov A, Gentles AJ, et al. Machine learning identifies stemness features associated with oncogenic dedifferentiation. *Cell*. 2018;173:338–354. e15.
34. Prager BC, Xie Q, Bao S, Rich JN. Cancer stem cells: the architects of the tumor ecosystem. *Cell Stem Cell*. 2019;24:41–53.
35. Coulie PG, Van den Eynde BJ, van der Bruggen P, Boon T. Tumour antigens recognized by T lymphocytes: at the core of cancer immunotherapy. *Nat Rev Cancer*. 2014;14:135–146.
36. Ge Y, Gomez NC, Adam RC, et al. Stem cell lineage infidelity drives wound repair and cancer. *Cell*. 2017;169:636–650. e14.
37. Aiello NM, Stanger BZ. Echoes of the embryo: using the developmental biology toolkit to study cancer. *Dis Model Mech*. 2016;9:105–114.
38. Dongre A, Weinberg RA. New insights into the mechanisms of epithelial–mesenchymal transition and implications for cancer. *Nat Rev Mol Cell Biol*. 2019;20:69–84.
39. Chen DS, Mellman I. Elements of cancer immunity and the cancer–immune set point. *Nature*. 2017;541:321–330.
40. Galon J, Bruni D. Tumor immunology and tumor evolution: intertwined histories. *Immunity*. 2020;52:55–81.
41. Waldman AD, Fritz JM, Lenardo MJ. A guide to cancer immunotherapy: from T cell basic science to clinical practice. *Nat Rev Immunol*. 2020;20:651–668.
42. Spranger S, Gajewski TF. Impact of oncogenic pathways on evasion of antitumour immune responses. *Nat Rev Cancer*. 2018;18:139–147.
43. Birkbak NJ, McGranahan N. Cancer genome evolutionary trajectories in metastasis. *Cancer Cell*. 2020;37:8–19.
44. Landsberg J, Kohlmeyer J, Renn M, et al. Melanomas resist T-cell therapy through inflammation-induced reversible dedifferentiation. *Nature*. 2012;490:412–416.
45. Li J, Stanger BZ. How tumor cell dedifferentiation drives immune evasion and resistance to immunotherapy. *Cancer Research*. 2020;80:4037–4041.
46. Miao Y, Yang H, Levorse J, et al. Adaptive immune resistance emerges from tumor-initiating stem cells. *Cell*. 2019;177:1172–1186. e14.
47. Greten FR, Grivennikov SI. Inflammation and cancer: triggers, mechanisms, and consequences. *Immunity*. 2019;51:27–41.
48. De Palma M, Biziato D, Petrova TV. Microenvironmental regulation of tumour angiogenesis. *Nat Rev Cancer*. 2017;17:457–474.
49. Magnussen AL, Mills IG. Vascular normalisation as the stepping stone into tumour microenvironment transformation. *Br J Cancer*. 2021;125:324–336.
50. Lambert AW, Pattabiraman DR, Weinberg RA. Emerging biological principles of metastasis. *Cell*. 2017;168:670–691.
51. Massagué J, Ganesh K. Metastasis-initiating cells and ecosystems. *Cancer Discov*. 2021;11:971–994.
52. Massagué J, Obenauf AC. Metastatic colonization by circulating tumour cells. *Nature*. 2016;529:298–306.
53. Nguyen B, Fong C, Luthra A, et al. Genomic characterization of metastatic patterns from prospective clinical sequencing of 25,000 patients. *Cell*. 2022;185:563–575. e11.
54. Bonilla X, Parmentier L, King B, et al. Genomic analysis identifies new drivers and progression pathways in skin basal cell carcinoma. *Nat Genet*. 2016;48:398–406.
55. Chang D, Shain AH. The landscape of driver mutations in cutaneous squamous cell carcinoma. *NPJ Genom Med*. 2021;6:1–10.
56. Ying Z, Sandoval M, Beronja S. Oncogenic activation of PI3K induces progenitor cell differentiation to suppress epidermal growth. *Nat Cell Biol*. 2018;20:1256–1266.
57. Epstein EH. Basal cell carcinomas: attack of the hedgehog. *Nat Rev Cancer*. 2008;8:743–754.
58. Sánchez-Danés A, Hannezo E, Larsimont JC, et al. Defining the clonal dynamics leading to mouse skin tumour initiation. *Nature*. 2016;536:298–303.
59. Trieu KG, Tsai SY, Eberl M, et al. Basal cell carcinomas acquire secondary mutations to overcome dormancy and progress from microscopic to macroscopic disease. *Cell Reports*. 2022;39:110779.
60. South AP, Purdie KJ, Watt SA, et al. NOTCH1 mutations occur early during cutaneous squamous cell carcinogenesis. *J Invest Dermatol*. 2014;134:2630–2638.
61. HuBMAP Consortium. The human body at cellular resolution: the NIH Human Biomolecular Atlas Program. *Nature*. 2019;574:187–192.
62. Rozenblatt-Rosen O, Regev A, Oberdoerffer P, et al. The human tumor atlas network: charting tumor transitions across space and time at single-cell resolution. *Cell*. 2020;181:236–249.
63. Sepich-Poore GD, Zitvogel L, Straussman R, et al. The microbiome and human cancer. *Science*. 2021;371eabc4552.
64. Irmisch A, Bonilla X, Chevrier S, et al. The Tumor Profiler Study: integrated, multi-omic, functional tumor profiling for clinical decision support. *Cancer Cell*. 2021;39:288–293.



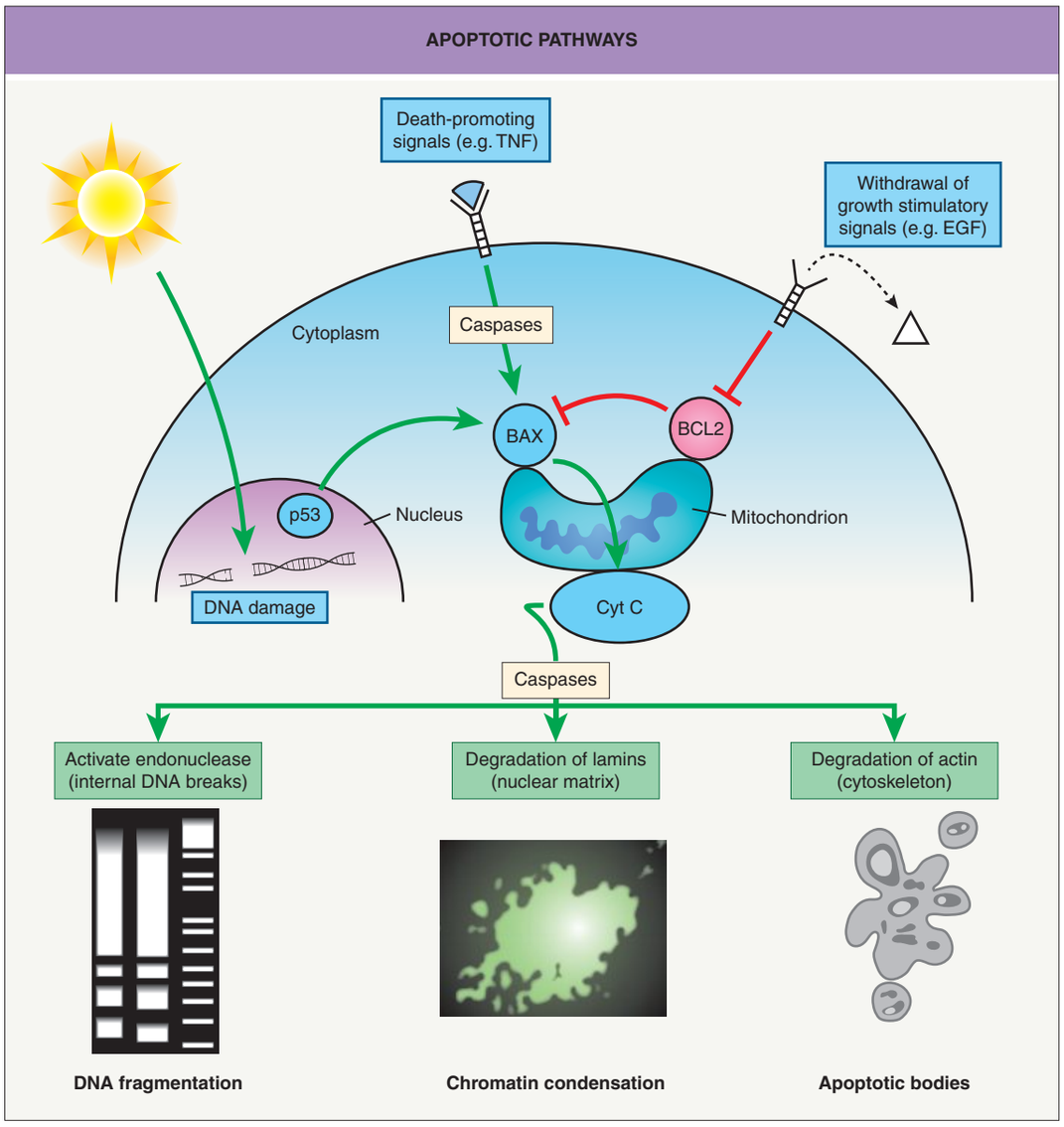
eFig. 107.1 History of conceptual advances in the understanding of cancer biology. Key technologic advances (left) are accompanied by a selection of groundbreaking observations in the fields of cancer biology, cancer genetics, and cancer immunology (right).



eFig. 107.2 Carcinogenesis: oncogenes versus tumor suppressor genes. A Under physiologic conditions, proto-oncogenes control the rate of cell cycle progression (left). Oncogenes are proto-oncogenes that have acquired activating mutations, represented by the yellow dot within the second allele (center) or gene amplifications (right). Oncogenes function in a dominant fashion, meaning that activating alterations in only one allele are sufficient for the gene to gain oncogenic potential. **B** A tumor suppressor gene acts as a brake on the cell cycle, decreasing cell proliferation. Tumor suppressor genes are inactivated by mutations in both alleles. Tumor suppressor genes function in a recessive manner, meaning that a mutation in only one allele is not sufficient for loss of gene function. eFig. 107.3 demonstrates the various mechanisms by which the "second hit" occurs in tumor suppressor genes.



eFig. 107.3 Mechanisms of loss of heterozygosity and inactivation of wild-type tumor suppressor genes. Mechanisms depicted by which both copies of a gene can be inactivated (bottom). With loss of heterozygosity (LOH), the resultant changes are best explained by the absence of wild-type protein. While translocations usually activate oncogenes or generate new fusion proteins, they can also be associated with microdeletions. An alternative mechanism exists (right) in which the wild-type allele is rendered non-functional. That is, some mutations can lead to expressed truncated proteins, and the latter may have dominant-negative effects or may be partially functional. An example would be the p53 protein. *Adapted and redrawn from Foulkes WD. Inherited susceptibility to common cancers. N Engl J Med 2008;359:2143–53.*



eFig. 107.4 Apoptotic pathways. Various triggering events are depicted within blue-colored boxes. Consequences of induced apoptosis are shown at the bottom of the figure within green-colored boxes. Fragmentation of genomic DNA by endonucleases results in a discrete ladder of DNA fragments of decreasing lengths as seen in the left two lanes compared to the DNA standard ladder in the right-most lane. Cyt, cytochrome; EGF, epidermal growth factor; TNF, tumor necrosis factor.

108 Actinic Keratosis, Basal Cell Carcinoma, and Squamous Cell Carcinoma

Ingrid H. Wolf, H. Peter Soyer, Erin K. McMeniman and Peter Wolf

Chapter Contents

Actinic Keratosis and Squamous Cell Carcinoma *1892*
Basal Cell Carcinoma *1900*

Synonyms: ■ Solar keratosis and senile keratosis are non-preferred synonyms for actinic keratosis (solar keratosis is abbreviated to SK, causing confusion with seborrheic keratosis) ■ Bowen disease: squamous cell carcinoma *in situ*, intraepidermal carcinoma ■ Basal cell epithelioma and rodent ulcer are antiquated synonyms for basal cell carcinoma ■ Basal cell nevus syndrome: nevoid basal cell carcinoma syndrome, Gorlin syndrome, Gorlin–Goltz syndrome

Key features

- Keratinocyte carcinoma, also referred to as non-melanoma skin cancer (NMSC), includes basal cell carcinoma (BCC), cutaneous squamous cell carcinoma (cSCC), and variants such as verrucous carcinoma; it represents the most common malignancy among White individuals
- The major risk factor for BCCs and cSCCs is exposure to ultraviolet radiation (UVR); other factors include exposure to ionizing radiation, arsenic or organic chemicals, human papilloma virus infection, immunosuppression, and genetic predisposition
- Prevention efforts are aimed at lowering incidence and morbidity via educational programs and sun protection campaigns
- If neglected or inappropriately managed, keratinocyte carcinomas can cause significant morbidity and even death
- Surgery remains a mainstay of treatment, but additional modalities include topical chemotherapy and immunomodulators, photodynamic therapy, radiation therapy, and systemic medications (e.g. targeted drugs, immune checkpoint inhibitors)

INTRODUCTION

Keratinocyte carcinomas, specifically basal cell carcinoma (BCC) and cutaneous squamous cell carcinoma (cSCC), represent the most frequently observed malignancy among White individuals. In individuals with fair skin, ~75%–80% of these malignancies are BCCs and up to 25% are SCCs[1]. The incidence of both continues to rise, leading to an increasing burden of disease. In this chapter, cSCC includes SCCs that arise on the lower vermilion lip.

HISTORY

In 1775, Sir Percivall Pott noted an etiologic relationship between SCC and chimney soot exposure in his short treatise *Chirurgical Observations Relative to the Cancer of the Scrotum*. During the Industrial Revolution, links to arsenic, coal tar, shale oil, and creosote were also identified. In the late 1800s, Paul Unna noted a connection to UVR, when he described skin cancer development in chronically sun-exposed sites in sailors.

Evidence of the basal cell nevus syndrome (BCNS), consisting of jaw cysts, syndactyly and bifid ribs, has been identified in Egyptian mummies almost 4000 years old. In the 1850s, Lebert first used the term "rodent ulcer" to describe untreated BCCs of long duration. Several years later, Sir Jonathan Hutchinson published a review of 42 cases of BCCs, identifying the tumor as a single entity with many different clinical and histopathologic forms. Krompecher first suggested that a BCC arose from the cells of the basal layer of the epidermis, but there were additional theories regarding the site of origin of this tumor, including from the hair follicle and other adnexal structures.

EPIDEMIOLOGY

Keratinocyte carcinomas occur worldwide in all races and ethnicities. They represent the most common malignancy in the US and are associated with substantial morbidity and a relatively small but significant mortality rate. An estimated 5.5 million NMSCs occurred in ~3.3 million individuals in the US in 2012[2], with one in five Americans developing skin cancer during their lifetime[3] (>95% will be NMSC). In a more recent analysis, the incidence of NMSC was noted to be significantly higher in Americans >65 years of age, with a rate of 45 individuals with NMSC/1000 persons and a case rate of 75 cases of NMSC/1000 persons[4].

The most important factor related to development of these neoplasms appears to be skin phenotype (Table 108.1)[5–12], but other factors also play a significant role. As an example, the incidence is about ten times higher in White versus Hispanic men and five times higher in White versus Hispanic women[13]. However, deriving precise data is hampered by the fact that these neoplasms are not routinely included in most state cancer registries and patients with NMSC are often treated in private offices rather than hospitals.

The average amount of annual UVR correlates with the incidence of skin cancer. There is also a direct relationship between incidence and latitude, in that the closer individuals are to the equator, the greater their exposure to UVR. In Australia, in 2002, the cumulative risk by age 70 years of having at least one BCC or cSCC was 70% for men and 58% for women. Incidence also increases with age, with a sharp increase in BCCs in men after the age of 60 years. In those under 40 years of age, the majority of NMSC is found in women, but, by age 80, the incidence in men exceeds that in women by a 2–3 : 1 ratio[13].

Actinic keratoses (AKs) are most often found in fair-skinned individuals, but can be seen in all races. AKs are so common that it has been estimated that up to 12% of individuals in the US have them[14]. AKs are also very common in other countries with large fair-skinned populations. For example, in Austria when 4449 outpatients >30 years of age were screened, an overall AK prevalence of 39% in men and 24% in women was observed, with prevalence increasing with age in both sexes[15].

Over 80% of AKs occur in sites with the most cumulative sun exposure, e.g. the bald scalp, superior helices of the ears, face, dorsal hands, extensor forearms. Risk factors include skin phototypes I and II, significant cumulative sun exposure, a prior history of AKs, increasing age, immunosuppression, and male sex[16]. AKs are also markers for an increased risk of developing invasive cSCC[17], but the rates of transformation are low and difficult to assess (see below)[18].

The demographics of *cSCC* are similar to those of AKs, with the majority of SCC occurring on the head, neck, upper extremities[19], or shins. In light-skinned populations, the degree of UV exposure is related to SCC development, while chronic irritation or injury can play a role in all populations. cSCC is found more frequently in men (M : F = 3 : 1), especially in younger age groups, and the incidence increases significantly after age 60 years[13]. The incidence of cSCC has been rising worldwide in all age groups over the last several decades at an estimated 3%–10% per year, with >400 000 cases of invasive SCC diagnosed annually in the US[20]. Similar incidence trends have been noted worldwide.

Weinstock[21] reported an age-adjusted mortality rate for confirmed cases of cSCC in Rhode Island of 0.26/100 000. SCC-associated mortality is

INFLUENCE OF SKIN PIGMENTATION ON EPIDEMIOLOGY OF NMSC AND CUTANEOUS MELANOMA		
Characteristic	**Lightly pigmented individuals**	**Darkly pigmented individuals**
NMSC – annual incidence per 100 000	230	3.4
BCC : SCC ratio	4 : 1	1.1 : 1 to 2 : 1
BCC male : female ratio	1.5 : 1	1.3 : 1
SCC male : female ratio	2 : 1 to 5 : 1	1.3 : 1
% of SCCs developing in scars and chronic non-healing ulcers	<2	30–40
NMSC incidence rates	Increasing	?
NMSC mortality rates	Decreasing until 2000; possibly increasing since 2010	Decreasing until 2000; possibly increasing since 2010
Melanoma – annual incidence per 100 000	29	1
Deaths due to melanoma – annual incidence per 100 000	4.3	0.2

Table 108.1 Influence of skin pigmentation on epidemiology of non-melanoma skin cancer (NMSC) and cutaneous melanoma. BCC, basal cell carcinoma; SCC, squamous cell carcinoma. From references 3,5–12.

higher in White individuals and older persons, and men have a 3 : 1 greater SCC mortality rate as compared with women[21]. In some studies, SCCs located on the ear, lip, and genitalia appear to have a higher risk of death. While melanoma among White individuals is responsible for 90% of skin cancer deaths before 50 years of age, in adults over 85 years of age, the majority of skin cancer deaths are attributable to cSCC[6]. A population-based analysis of CDC data revealed that mortality rates due to NMSC had been decreasing through 2000, were relatively stable until 2010, and then significantly increased by 44% through 2017[22]. Possible explanations included a true increase due to factors such as an aging population and an increase in immunosuppressed patients in addition to changes in cause of death documentation. For the period studied, the NMSC mortality rate was 1.24/100 000 persons/year (0.62, 0.38, and 0.23 for sun-exposed, genital, and perianal sites, respectively). At all three sites, mortality rates due to NMSC increased in White, but not in Black, individuals.

BCC is the most common skin cancer in humans, and men generally have higher rates of BCC than do women (1.5–2 : 1)[23]. Over the last 30–40 years, it is estimated that incidence rates have risen between 20% and 80%. In the US, a disproportionate increase has been observed in young women. Similar increases in incidence rates have been noted worldwide, with the incidence doubling in Finland and Switzerland and increasing in Wales by 50% over this time period.

Incidence rates for BCC also increase with age, and the median age at diagnosis is 68 years. In 2002, an incidence rate for BCC of 884 per 100 000 per year was observed in Australia. In this geographic location, cSCC typically occurs at half the rate of BCC among men and at about one-third the rate among women.

Mortality from BCC is quite rare and occurs primarily in immunocompromised patients and individuals with BCNS. Cases of metastatic BCC are more likely from tumors with aggressive histopathologic patterns (morpheaform, infiltrating, metatypical, basosquamous). Perineural growth, also referred to as perineural invasion, may be an indicator of aggressive disease[24]. Metastases often involve regional lymph nodes, lungs, bone, and skin. The mean age at the time of death is higher than with cSCC, and the age-adjusted mortality rate for BCC has been estimated at 0.12 per 100 000. Mortality risk is related to increasing age, lighter skin phototypes, and male sex (>2 compared with women).

PATHOGENESIS

See Chapter 107.

RISK FACTORS FOR THE DEVELOPMENT OF BASAL CELL CARCINOMAS (BCCs) AND CUTANEOUS SQUAMOUS CELL CARCINOMAS (cSCCs)		
	cSCC	**BCC**
Environmental exposures		
Exposure to UVR	+	+
Other exposures to UV light (PUVA, tanning beds)	+	+
Ionizing radiation	+	+
Chemicals, including arsenic, mineral oil, coal tar, soot, mechlorethamine (nitrogen mustard), polychlorinated biphenyls, 4,4′ bipyridyl, psoralen (plus UVA)[39]	+	+
Medications (e.g. voriconazole, azathioprine, BRAF inhibitors, hydrochlorothiazide*, hydroxyurea, other immunosuppressants)	+	(+)
Human papillomavirus (HPV)	+	(+)
Cigarette smoking	+	
Pigmentary phenotype		
Fair skin, always burns, never tans	+	+
Freckling	+	+
Red hair	+	+
Genetic syndromes		
Xeroderma pigmentosum	+	+
Oculocutaneous albinism	+	+
Epidermodysplasia verruciformis	+	(+)
Ferguson–Smith syndrome	+	
Muir–Torre syndrome	+**	+**
Basal cell nevus syndrome		+
Bazex–Dupré–Christol and Rombo syndromes		+
Dyskeratosis congenita	+	
Kindler syndrome	+	
Bloom syndrome	+	
Keratitis–ichthyosis–deafness syndrome	+	
Rothmund–Thomson syndrome	+	+
Predisposing clinical settings		
Chronic non-healing wounds	+	
Longstanding discoid lupus erythematosus, lichen planus (particularly mucosal), or lichen sclerosus	+	
Dystrophic epidermolysis bullosa (primarily recessive)	+	
Porokeratosis (most commonly Mibelli and linear)	+	
Nevus sebaceus	+ (rare)	+†
Immunosuppression		
Organ transplantation	+	+
Other (e.g. chronic lymphocytic leukemia treated with fludarabine, AIDS patients with HPV infection)	+	(+)

*Photosensitizing medication, but conflicting data.
**Both cSCCs (keratoacanthoma type) and BCCs typically have sebaceous differentiation.
†More often trichoblastomas.

Table 108.2 Risk factors for the development of basal cell carcinomas (BCCs) and cutaneous squamous cell carcinomas (cSCCs). UVR, ultraviolet radiation.

RISK FACTORS (TABLE 108.2)

Environmental Exposures

Ultraviolet radiation (UVR)

Exposure to UVR is the predominant cause of BCC and cSCC as evidenced by migrant studies, the correlation of incidence to latitude, and animal studies. There is, however, a difference in the type of UV

exposure. For BCCs, intermittent intense episodes of UV exposure and sunburns at any age appear to increase risk, whereas cumulative long-term UV exposure and childhood sunburns increase the risk for developing cSCCs and AKs[25,26].

Sun exposure early in life appears to have a greater influence on subsequent skin cancer risk than at a later age. For example, individuals born in countries with high ambient UV radiation such as Australia have significantly higher incidence rates of BCC and cSCC as compared to those with a similar genetic background (e.g. British, northern Europeans) who migrated to these areas later in life from countries with lower ambient UV radiation[25,27,28].

Indoor tanning usage

Multiple studies have demonstrated an increased risk for the development of BCCs and cSCCs in those who are exposed to artificial sources of UVR. Intentional tanning has been shown to increase the risk of SCC development[29] and Karagas et al.[30] demonstrated that any use of tanning devices was associated with odds ratios of 2.5 for SCC and 1.5 for BCC, even after adjustment for history of sunburns, sunbathing, and sun exposure. A systematic review and meta-analysis of 12 studies (n = 9328 cases of NMSC) fundamentally confirmed these findings[31]. In response, many countries have passed legislation aimed at regulating indoor tanning facilities. Notably, Australia has actually completely banned this commercial industry while some states in the US prohibit minors from indoor tanning[32].

Therapeutic UVR exposure

Individuals with psoriasis have been shown to be at increased risk for the development of keratinocyte carcinomas. Whereas long-term follow-up of psoriasis patients who were treated with UVR plus tar (Goeckerman) or narrowband UVB found no increased risk[33], long-term PUVA therapy was associated with a significant, dose-related risk of cSCC development (adjusted relative risk = 8.6 for an accumulated exposure of between 100 and 337 treatments)[34]. With prolonged PUVA therapy, a slightly increased risk for BCC development was noted as well. In addition to the direct effects of PUVA, PUVA-induced immunosuppression may also play a role.

Ionizing radiation

Exposure to ionizing radiation leads to a threefold increased risk for BCC and cSCC[35]. The risk is in proportion to the radiation dose. Larger fractionated doses (>12–15 Gy) are thought to be necessary to induce tumor formation, so the risk with a given total dose may be less if a larger number of smaller fractionated doses are given. Most SCCs and BCCs that arise after exposure to ionizing radiation do so after a long latency period of up to several decades, with most tumors appearing ~20 years after the initial exposure.

Treatment of tinea capitis with radiation (prior to the discovery of effective systemic antifungal medications) has been linked to the development of multiple BCCs. In a study of 2224 children given X-ray therapy for tinea capitis (compared with a control group of 1380 tinea capitis patients given only topical medications), the relative risk for developing BCC of the head and neck among irradiated White individuals was 3.6[36].

Patients with BCNS are exquisitely sensitive to ionizing radiation and it should be avoided if possible (see below).

Occupational risk factors

Persons with outdoor occupations have a higher risk of developing skin cancer[37]. Based upon decades-old evidence, airline pilots, who are also exposed to ionizing radiation at flight altitudes, have about twice the risk of developing keratinocyte carcinomas than the general population[38]. Other occupations associated with an increased risk for NMSC include agricultural workers, gardeners, sailors, and locomotive engineers.

Chemical exposures

Multiple organic chemicals have been associated with an increased risk for the development of keratinocyte carcinomas[39] (see Table 108.2). Occupational chemical exposures which can lead to skin cancer most commonly involve pesticides, asphalt, tar, and polycyclic aromatic hydrocarbons, and they typically result in SCC. The skin cancers induced by chemical exposures are usually localized as well as multiple, most often appearing on the arms[40].

Arsenic is a well-defined cause of SCC (see Ch. 88). A clue to arsenic exposure is the presence of palmoplantar arsenical keratoses. BCC has also been reported following extensive arsenic exposure. The typical latency period from exposure to tumor development is 20–40 years[41].

Human Papillomavirus Infection

Human papillomaviruses (HPV) represent a large group of DNA tumor viruses that infect the epithelia of both skin and mucosae, inducing hyperproliferative lesions, most commonly warts. HPV is associated with anogenital SCCs, particularly in HIV-infected patients. Individuals with the genetic condition epidermodysplasia verruciformis (EV) are known to have a significantly increased risk of developing SCCs, especially in sun-exposed sites. Infection with the HPV types referred to as EV- or beta-types (see Table 79.1) is also observed in the general population, in particular in immunosuppressed solid organ transplant recipients[42]. Because these specific HPV subtypes are thought to act as facilitators for the accumulation of UVR-induced mutations during the development of SCC[43], a goal is to design therapeutic HPV vaccines[44].

Immunosuppression

Organ transplantation

Solid organ transplant recipients have a markedly increased incidence of skin cancer, primarily cSCC. The incidence of BCC in organ transplant recipients is up to 5–10 times greater than in the general population, while the incidence of SCC is 30–250 times greater. Risk factors include skin phototypes I/II, cumulative sun exposure, previous history of skin cancer, age at transplantation, and the degree and the length of immunosuppression.

cSCC is a significant cause of morbidity and mortality in transplant recipients[45,46]. The pathogenesis of skin cancer in transplant recipients is multifactorial, involving decreased immunity, direct carcinogenic effects of immunosuppressive medications, and HPV infection in addition to UVR exposure. Transplant recipients are prone to developing numerous lesions and are more likely to suffer local and regional recurrences and metastases[45]. AKs and SCCs begin to appear with increasing frequency several years after transplantation. Lesions are often multiple and usually develop in sun-exposed areas. cSCCs from transplant recipients frequently contain HPV DNA, but it can be from a range of HPV strains including those that occur in common benign cutaneous warts (HPV types 1 and 2), EV (HPV-5 and others; see above), high-risk oncogenic warts (HPV types 16 and 18), and low-risk oncogenic genital warts (HPV types 6 and 11). Sometimes, several HPV types are detected within a single tumor. More recently, a role for polyomaviruses in the development of cSCCs has been proposed.

In one series of renal transplant patients from the US, 5% of the patients died of skin cancer. In another series of heart transplant patients from Australia, 27% died of skin cancer. Two-thirds of these deaths were due to cSCC. Several studies have shown that in renal transplant patients sirolimus, an mTOR inhibitor, reduced the development of cSCCs when compared to calcineurin inhibitors (e.g. cyclosporine, tacrolimus)[47]. However, the impact may be related to the number of previous SCCs[48]. More recently, belatacept, a fusion protein that prevents CD28 activation, was also observed to reduce skin cancer risk in renal transplant recipients[49]. Based upon currently available data, sirolimus and belatacept appear to be preferable in patients with a history of SCCs or strong risk factors. Additional interventions include reduction in immunosuppression, aggressive screening, discontinuing hydrochlorothiazide (HCTZ), and instituting acitretin. Of note, in Ireland a progressive decline in the incidence of keratinocyte carcinomas in organ transplant recipients from 1994 to 2014 was observed[50].

Patients who receive hematopoietic transplants do not experience this marked increase in skin cancer incidence (unless they have received long-term voriconazole), presumably because of a shorter duration of immunosuppression.

Immunosuppressive drugs

Use of immunosuppressive drugs, including systemic immunomodulators (e.g. TNF inhibitors, alemtuzumab, JAK inhibitors), increases the risk for the development of skin cancer. Risk of cSCC development is directly related to the length and degree of immunosuppressive drug usage. Given

the long-lasting mutations and increased risk of NMSC associated with thiopurines (e.g. azathioprine, 6-mercaptopurine)[51], their use in patients with significant photodamage should be avoided when possible.

HIV infection

Patients with HIV infection are at increased risk for the development of several cancers, including HPV-related SCC of the anus. These tumors can be aggressive and monitoring that incorporates anal cytology is recommended[52].

Other Risk Factors, Including BRAF Inhibitors

Up to 25% of patients receiving selective *BRAFV600 inhibitors* (e.g. vemurafenib, dabrafenib) can develop either cSCCs or keratoacanthomas (KAs). They develop primarily in individuals with cutaneous photodamage and can appear within weeks of beginning the kinase inhibitor. Fortunately, the combination of a selective BRAF inhibitor with a MEK inhibitor, as is routinely done nowadays, significantly reduces the incidence of side effects of both drugs, including the formation of SCCs and KAs. *Voriconazole* is also associated with the development of UVR-induced skin cancers, possibly a result of the phototoxic moieties of its metabolites. Due to the small, but statistically significant, increase in the risk of NMSC (hazard rate of 1.04 for SCC and 1.09 for BCC) associated with the use of *HCTZ*[53], the FDA revised its labeling in 2020.

Other possible risk factors include residence at high altitudes, thermal burns, chronic ulcers, and tobacco use[54]. While evidence from animal models suggested a relationship between fat intake and skin cancer incidence, results from subsequent epidemiologic studies were inconsistent and failed to show any strong evidence for either this association or for other dietary factors (e.g. vitamins, minerals)[55–57].

Genetic Risk Factors

Genetic predisposition

Phenotypic characteristics such as red hair, light skin, poor ability to tan, and freckling have been identified as risk factors for melanoma as well as NMSC[25]. Pigmentation is a polygenic trait, with polymorphisms in several genes leading to the variation observed in the human race (see Ch. 65). A key gene encodes the human melanocortin-1 receptor (MC1R) which is expressed on the cell surface of melanocytes. Population-based studies in diverse ethnic groups have shown that the coding region of the human *MC1R* is remarkably polymorphic. In White individuals, there is a strong association between nine common *MC1R* variant alleles and the red hair/fair skin phenotype, thus placing these individuals at higher risk of photocarcinogenesis[58]. Based upon genome-wide association studies and candidate gene studies (see Ch. 54), ~30 and at least 11 susceptibility loci for BCC and cSCC, respectively, have been identified, and they include multiple pigmentation loci.

Genetic syndromes associated with an increased risk of BCCs and/or cSCCs

Xeroderma pigmentosum

Xeroderma pigmentosum (XP) consists of a group of autosomal recessive disorders characterized by defects in unscheduled DNA repair (see Ch. 86). A markedly increased incidence of keratinocyte carcinoma and melanoma is observed in these individuals, if they are exposed to sunlight. cSCCs and BCCs appear at an early age (median age, 8 years), and in affected individuals who are <20 years of age the risk is 4800 times that of the general population. Strict UV avoidance can significantly decrease skin cancer formation.

Oculocutaneous albinism

Oculocutaneous albinism encompasses a group of autosomal recessive disorders in which there is a variable degree of pigmentary dilution of the skin, eyes, and hair (see Ch. 66). At a relatively early age, NMSC, especially SCC, and cutaneous melanoma develop with increased frequency. As in XP, strict sun avoidance for life can greatly minimize tumor development. However, for these patients metastatic cSCC is still a significant problem in areas of the world such as equatorial Africa.

Epidermodysplasia verruciformis

Epidermodysplasia verruciformis (EV) is a rare, usually recessively inherited disorder due to mutations in *TMC6* or *TMC8*, which encode transmembrane channels. There is widespread colonization of the skin by HPVs of multiple subtypes, most often 5 and 8 (see Ch. 79). Evidence for an association between cutaneous HPV infection and cSCC was first reported in these patients. One-third to one-half of patients will develop SCCs as adults, usually in sun-exposed regions, and several decades earlier than is typical for SCC development in the general population. Aggressive biologic behavior, including perineural spread, metastases, and death, have been reported.

Dystrophic epidermolysis bullosa

Dystrophic epidermolysis bullosa with significant scarring can result from both dominant and recessive mutations in the type VII collagen gene. cSCCs more commonly appear in the recessive forms, where they are the most common cause of death. Tumors usually develop during the third to fifth decades of life, are frequently multiple, and demonstrate aggressive behavior in terms of recurrences and metastases.

Basal cell nevus syndrome (BCNS)

BCNS is an autosomal dominant disorder due to an inactivating mutation in *PTCH1*[59] or rarely *PTCH2* while *SUFU* mutations can also lead to multiple hereditary infundibulocystic BCC syndrome (see Fig 107.6). Manifestations of BCNS include multiple or early-onset BCCs, odontogenic keratocysts of the jaw, palmoplantar pits, calcification of the falx cerebri, and skeletal anomalies (Table 108.3; Fig. 108.1). Affected individuals may also develop specific neoplasms such as medulloblastomas, bilateral ovarian fibromas, and cardiac fibromas. Recognition of the early clinical signs of BCNS such as macrocephaly and palmar pits allows for additional screening of at-risk individuals[59].

BCCs usually appear after puberty, but they may develop during childhood. The number of BCCs in a single patient varies from a few

DIAGNOSTIC CRITERIA FOR BASAL CELL NEVUS SYNDROME (BCNS)
Major criteria
1. One basal cell carcinoma (BCC) before the age of 20 years or excessive number of BCCs*
2. Odontogenic keratocysts of the jaw (proven by histology; detected by orthopantogram)
3. Two or more palmar or plantar pits (may be enhanced by soaking of the hands)
4. Lamellar calcification of the falx cerebri before the age of 20 years (on anterior–posterior skull X-rays)
5. Childhood medulloblastoma
6. First-degree relative with BCNS
Minor criteria
1. Macrocephaly (determined after adjustment for height; OFC >97th percentile)
2. Skeletal malformations (e.g. preaxial or postaxial polydactyly)
3. Vertebral/rib anomalies observed on chest X-ray and/or spinal X-ray: bifid/splayed/extra ribs; bifid vertebrae
4. Ocular anomalies (e.g. cataract, developmental defects, pigmentary changes of the retinal epithelium)
5. Cleft lip or palate
6. Ovarian or cardiac fibromas
7. Lympho-mesenteric or pleural cysts
*Need to take into account decreased risk in darkly pigmented individuals and increased risk in those with significant photodamage.

Table 108.3 Diagnostic criteria for basal cell nevus syndrome (BCNS). The diagnosis of BCNS requires *two major plus one minor or one major plus three minor criteria*. With the presence of one major criterion, identification of a heterozygous germline pathogenic variant in *PTCH1* or *SUFU* establishes the diagnosis. The occasional variants in *PTCH2* may not be conclusive and pathogenic variants in *SUFU* may not always cause typical BCNS (see text). Other skeletal abnormalities include frontal bossing, moderate or severe hypertelorism, Sprengel deformity (unilateral elevation of smaller-sized scapula), marked syndactyly of the digits, and marked pectus deformity. *Adapted from Varon R, Demuth I, Chrzanowska KH. Nijmegen Breakage Syndrome. 1999 May 17 [Updated 2017 Feb 2]. In: Adam MP, Mirzaa GM, Pagon RA, et al., editors. GeneReviews® [Internet]. Seattle (WA): University of Washington, Seattle; 1993-2022. www.ncbi.nlm.nih.gov/books/NBK1151 and ref. 59.*

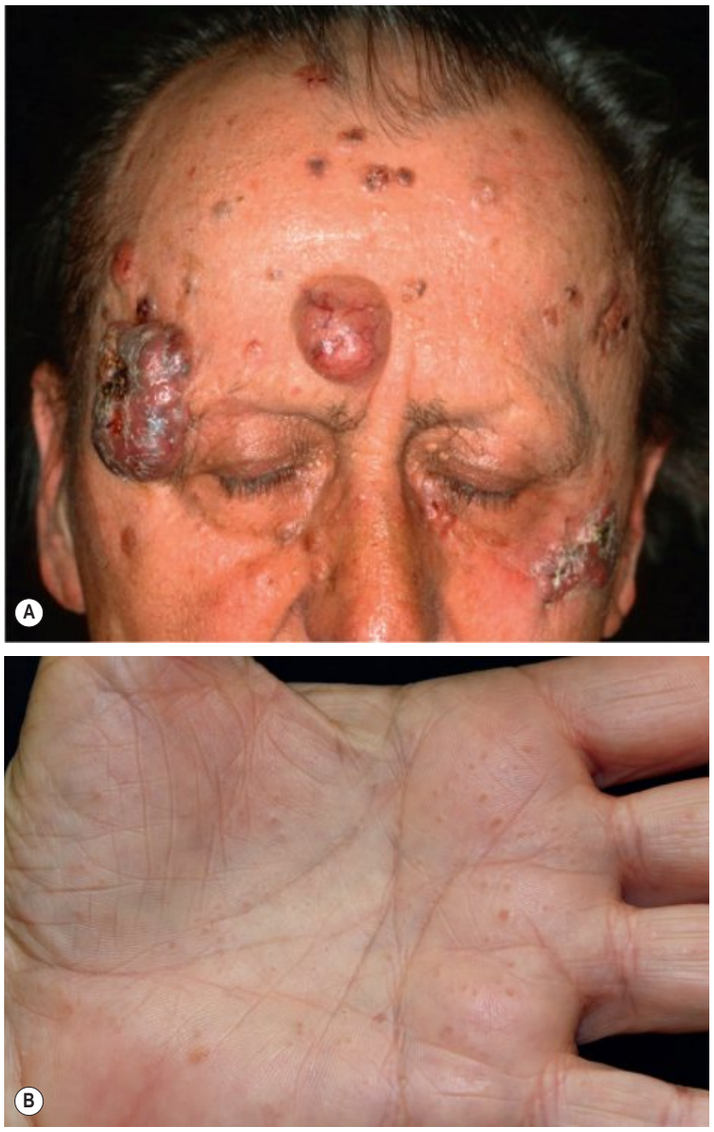


Fig. 108.1 Basal cell nevus syndrome. A Numerous small and several large nodular BCCs on the face. **B** Multiple palmar pits. *B, Courtesy Jeffrey P. Callen, MD.*

to more than a thousand and the size from pinpoint to >5 cm (see Fig. 108.1A). The BCCs favor the sun-exposed areas of the face, neck, and upper trunk, but may occur in sun-protected sites. As in the general population, nodular BCCs usually occur on the face, while superficial BCCs are found primarily on the torso. Individual lesions may be papulonodular, pedunculated, pigmented, eroded, ulcerated, or have a combination of these features. The pigmented BCCs are sometimes misdiagnosed clinically as melanocytic nevi (see Fig. 108.20). The clinical course of the cutaneous tumors is usually indolent prior to puberty, after which they enlarge and eventually ulcerate, as in the general population. Individuals with BCNS are exquisitely sensitive to ionizing radiation, and hundreds of tumors can develop in children within sites of radiation following radiotherapy for medulloblastoma. Additional cutaneous findings include epidermoid (infundibular) cysts and facial milia.

Bazex–Dupré–Christol syndrome and Rombo syndrome

Bazex–Dupré–Christol syndrome is a rare condition, consisting of follicular atrophoderma (usually occurring as circumscribed areas on the dorsal aspect of the hands and feet), hypotrichosis, localized hypohidrosis, milia, epidermoid cysts, and multiple, primarily facial, BCCs. The BCCs develop during the second decade of life and frequently have a trichoepithelioma-like histopathologic appearance. In most families, the inheritance pattern is X-linked dominant and mutations in *ACTRT1* have been detected, resulting in aberrant activation of the hedgehog signaling within primary cilia[60]. Sometimes a source of semantic confusion is the completely different Bazex syndrome (acrokeratosis paraneoplastica), in which psoriasiform plaques of the fingers, toes, ears, and nose are often associated with SCC of the upper aerodigestive tract.

The so-called *Rombo syndrome* has many of the features of Bazex–Dupré–Christol syndrome. Patients have an atrophoderma vermiculatum-like appearance on the cheeks, with evidence of sweat duct proliferation histologically. In addition, they often have hypotrichosis, blepharitis, peripheral (facial/acral) telangiectatic erythema, milia, trichoepitheliomas, and BCCs.

Bloom syndrome

Bloom syndrome (congenital telangiectatic erythema) is a rare autosomal recessive disorder due to mutations in *BML* which encodes the DNA helicase RecQL3 (see Ch. 87). In addition to malar erythema and telangiectasias, short stature and photosensitivity, patients can develop cSCCs as well as leukemia and malignancies of the gastrointestinal tract[61].

Rothmund–Thomson syndrome (RTS)

During the first few months of life, patients develop photodistributed erythema, edema, and vesicles of the cheeks and face (see Ch. 87)[61]. Additional cutaneous findings include gradual appearance of poikiloderma, thinning of scalp hair, and hypoplastic nails. While osteosarcoma develops in type II RTS (due to dysfunction of the DNA helicase RecQL4), NMSC can develop in both types. Mutations in *ANAPC1*, whose protein product mediates ubiquitination and controls progression through mitosis and G1 of the cell cycle, are responsible for type I RTS.

Keratitis–ichthyosis–deafness (KID) syndrome

In addition to congenital sensorineural hearing loss, patients present with a transient erythroderma at birth or during infancy followed by discrete plaques of erythrokeratoderma as well as palmoplantar keratoderma (see Ch. 57)[61]. Mutations in genes that encode connexins lead to KID syndrome (see Ch. 58); these gap junction proteins are expressed in ectoderm-derived epithelia of the inner ear, cornea, and epidermis. Patients have an increased susceptibility to viral, bacterial, and fungal infections and can develop the follicular occlusion triad, proliferating pilar tumors, and early-onset mucocutaneous SCCs (see Table 57.5).

Risk of Additional Cancers

Individuals who have had a BCC or cSCC are at increased risk for the development of additional BCCs and SCCs[62], compared to the general population. They are also at increased risk for developing cutaneous melanoma[63]. Based upon epidemiologic studies, persons with a history of BCCs or SCCs may be at increased risk for developing and dying from other (non-skin) cancers[64–66].

Field cancerization

In field cancerization, areas of the skin with significant photodamage (e.g. the bald scalp) have multiple clusters of p53-mutated keratinocytes[67] and they may or may not be clinically apparent. The presence of multiple actinic keratoses points to the diagnosis. Treatment regimens should focus not just on specific tumors but on the entire affected anatomical site (see below).

ACTINIC KERATOSIS AND SQUAMOUS CELL CARCINOMA

Clinical Features

Actinic keratosis

Actinic keratoses (AKs) were initially described as solar keratoses (due to their suspected cause) and senile keratoses (due to the age of onset). The term "actinic keratosis" is preferred over solar keratosis, partly because the abbreviation SK also stands for seborrheic keratosis.

AKs have historically been characterized as being "precancerous" or "premalignant" because the atypical keratinocytes within these lesions are confined to the epidermis. There is no risk of metastasis until these lesions evolve into invasive carcinoma, but AKs are viewed as potential precursors of cSCC. The likelihood of a solitary AK progressing into an invasive cSCC is difficult to predict, with estimates varying widely from 0.1% to 20%.

AKs present on sun-damaged skin of the head, neck, upper trunk, and extremities (Fig. 108.2A–D). Individuals at higher risk of developing

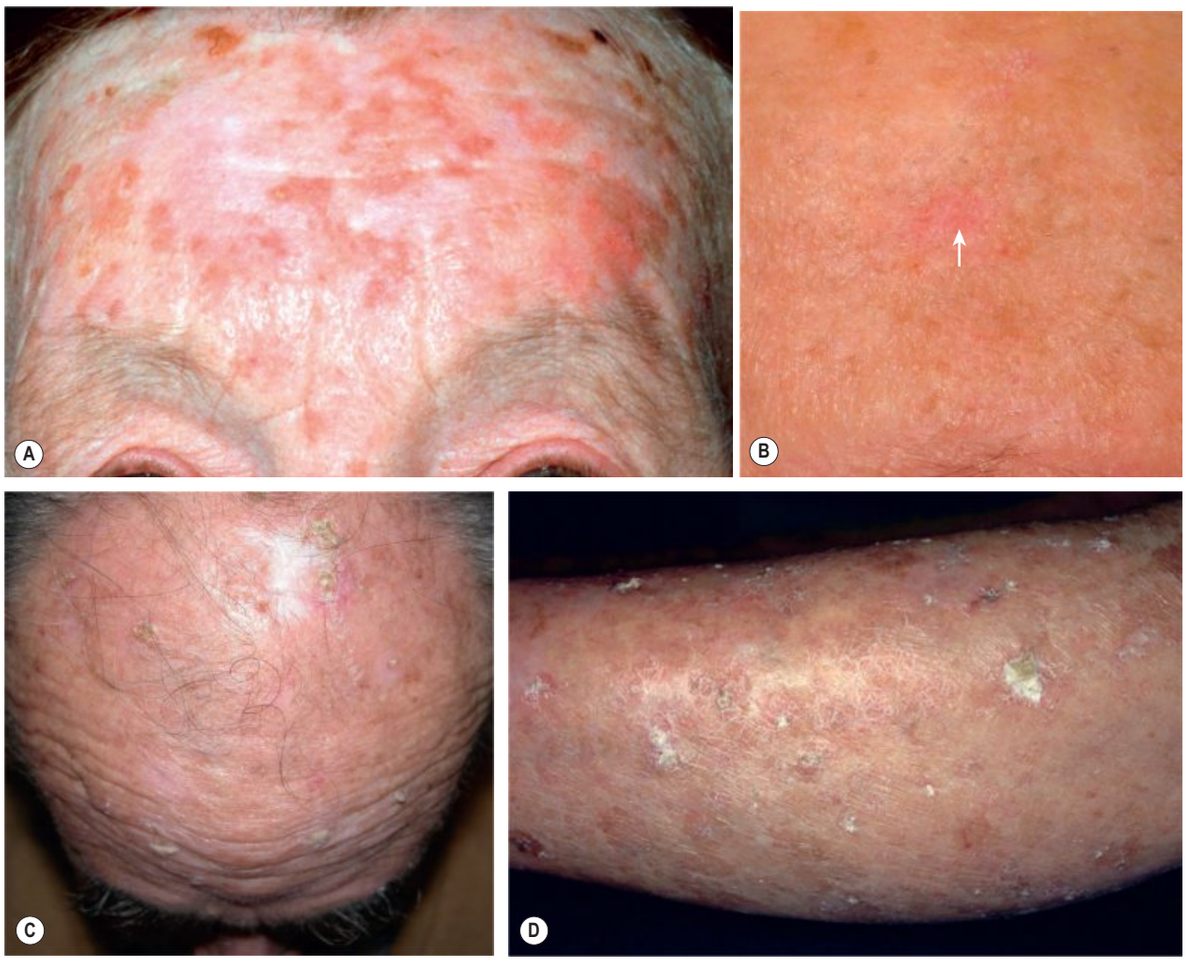


Fig. 108.2 Actinic keratoses (AKs). A Multiple AKs on the forehead of an elderly woman with fair complexion, blue eyes, and severe photodamage; the AKs vary in size from a few millimeters to over a centimeter. On the left forehead, the eroded pink plaque with scale represents a superficial SCC. **B** Pink-colored atrophic AK with minimal scale on the forehead. **C** Multiple AKs on the bald scalp, some of which are hyperkeratotic; the area of hypopigmentation represents a site of previous treatment and due to the field defect, recurrence at the edge is commonly observed. **D** Multiple, large hypertrophic AKs on the shin of an elderly woman; note the thick scale. *A, Courtesy, Medical University of Graz; B, Courtesy Iris Zalaudek, MD; D, Courtesy Jean L. Bolognia, MD.*

AKs include the elderly, those with lighter skin phototypes, and those with a history of chronic sun exposure. The typical lesion is a rough erythematous macule or papule with white to yellow scale. Patients may report tenderness, but this occurs more commonly with hypertrophic lesions (see Fig. 108.2D). AKs can range in size from a few millimeters to large confluent patches several centimeters in diameter, especially in patients with severe photodamage (see Fig. 108.2A). Dermoscopic features, such as the strawberry pattern seen on the face, can assist in diagnosis (see below).

One of the earliest signs is slight erythema with almost imperceptible scale (see Fig. 108.2B), although some lesions are devoid of visible erythema and present only as slight scale with indistinct borders. Advanced lesions are typically thicker and well-defined with more visible hyperkeratosis and erythema. Lesions are frequently clustered in areas of highest cumulative sun exposure, such as the superior helices of the ears, upper forehead, supraorbital ridge, nasal bridge, malar eminences, dorsal hands, extensor forearms, shins, and the bald scalp (see Fig. 108.2C). Of note, clinically, AKs may spontaneously regress, but then can reappear at the same site.

Visual inspection is best performed with simultaneous palpation to detect lesions that may not be readily apparent. This is especially true in individuals with significant background erythema from chronic sun exposure or rosacea. Clinical subtypes of AKs include the classic variant already described, hypertrophic (often hyperkeratotic), pigmented, lichenoid, atrophic, and actinic cheilitis.

Hypertrophic (hyperkeratotic) AKs are easily identified on visual inspection as papules and plaques with scale or scale-crust and an erythematous base (see Fig. 108.2D). The erythematous base often extends beyond the overlying hyperkeratosis. The hyperkeratotic scale can become white or yellow–brown over time. Due to their thickness, patients often find these lesions to be bothersome. Occasionally, a hyperkeratotic AK may develop a cutaneous horn that manifests as a column of thick cornified material that protrudes above the skin. The major entity in the differential diagnosis of a hyperkeratotic AK is a cSCC.

Pigmented AKs represent a subtype that often lacks associated erythema and has a hyperpigmented or reticulated appearance (Fig. 108.3). These lesions can at times be difficult to distinguish from reticulated seborrheic keratoses, lentigines, or even the lentigo maligna subtype of cutaneous melanoma. Dermoscopy may be a useful adjunct in these situations (see Ch. 0). Clinical clues are the location on sun-exposed skin, background solar changes, and hyperkeratosis that is sometimes appreciable by palpation. In cases in which the diagnosis is questionable, a biopsy is required to exclude the possibility of melanoma.

Lichenoid AKs have a clinical appearance similar to that of the classic form of AKs but with more erythema at the base of the lesion. Patients may relate pruritus or tenderness. Histology shows a lichenoid infiltrate in a pre-existing AK. The differential diagnosis includes a lichen planus-like keratosis, which also arises within areas of sun-damaged skin and can be pruritic, multiple, and even eruptive (see Ch. 109).

Atrophic AKs usually have minimal surface change and appear as pink to red, slightly scaly macules (see Fig. 108.2B). Histology shows an atrophic epidermis.

Actinic cheilitis is the term used to describe the characteristic changes that occur on the lower vermilion lip of individuals with moderate to severe photodamage. Actinic cheilitis may present as well-demarcated, erythematous patches or thin plaques with scale. In other patients, the erythema and especially the scale is more diffuse and can involve the entire lower vermilion lip; areas of leukoplakia may also be present (Fig. 108.4). The potential for evolving into invasive SCC is relatively higher than for AKs elsewhere (see Fig. 108.8).

Cutaneous squamous cell carcinoma in situ

cSCC *in situ* is commonly called Bowen disease (Fig. 108.5). The characteristic presentation of SCC *in situ* is an erythematous scaly patch or slightly elevated plaque that often arises within photodamaged sun-exposed skin. However, it can also develop in sun-protected sites (Fig. 108.6). The head and neck region and extremities are the most common sites, followed by the trunk. Lesions can become crusted and

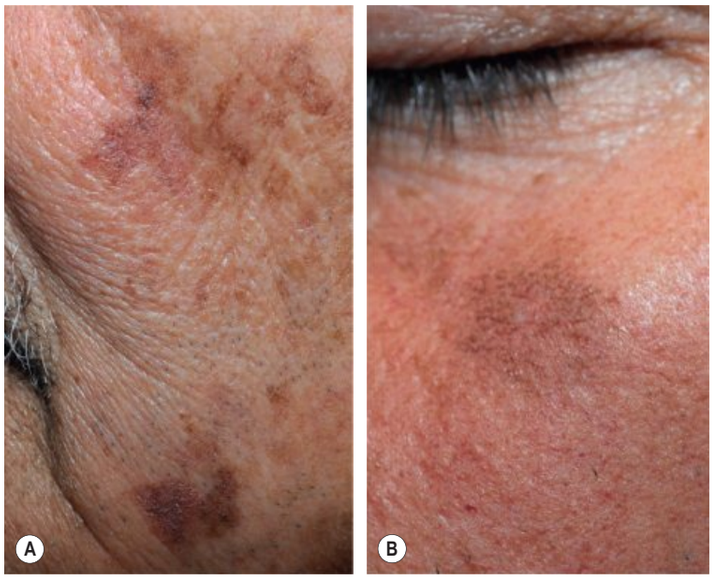


Fig. 108.3 Pigmented actinic keratoses. A, B The hyperpigmentation can have a reticulated appearance and there may be associated scale but an absence of erythema. *Courtesy Kalman Watsky, MD.*



Fig. 108.4 Actinic cheilitis. Erythema and scale of the entire lower vermilion lip with erosions and areas of leukoplakia. *Courtesy Kalman Watsky, MD.*



Fig. 108.5 Squamous cell carcinomas *in situ*, Bowen disease type. A Scaly red plaque on the chest with skip areas and background photodamage. **B** Erythematous plaque with thick yellow scale-crust on the distal lower extremity that may be misdiagnosed as psoriasis or dermatitis. **C** Larger broken-up pink plaque with scale-crust in the pubic region, a sun-protected site. This type of lesion is often misdiagnosed as dermatitis or psoriasis and treated with topical corticosteroids. **D** Bright red, well-demarcated plaque on the proximal nail fold with associated horizontal nail ridging; the possibility of HPV infection needs to be considered. **E** Dermoscopic findings of tiny dotted vessels in the upper half of the lesion combined with superficial scales. **F** Extensive involvement of the finger which was misdiagnosed clinically as an inflammatory dermatosis and treated for years with corticosteroid creams. *B, Courtesy Kalman Watsky, MD; E, Courtesy Iris Zalaudek, MD.*

erosions may be prominent within mucosal lesions in the anogenital region (see Ch. 73).

Clinical distinction of cSCC *in situ* from superficial BCC, psoriasis, or chronic eczema may at times be difficult (see Fig. 108.5B,F). Generally, superficial BCCs often have a more translucent quality with slight elevation of the leading edge as well as characteristic dermoscopic features (see Ch. 0). Patients with psoriasis and diffuse actinic damage can pose a diagnostic dilemma, as concomitant psoriatic papules and plaques may clinically resemble AKs and Bowen disease.

Arsenic-induced SCC in situ resembles the classic variant clinically but has a marked tendency to be multifocal and to arise in sun-protected areas of the trunk. Associated findings include palmoplantar keratoses and guttate hypopigmentation superimposed on hyperpigmentation (see Ch. 88).

Bowenoid papulosis is a squamous intraepithelial neoplasm linked to human papillomaviruses, most commonly HPV type 16 (see Table 79.1). The clinical appearance can vary from small brown papules of the penis to perianal pink papules to corrugated pink to brown plaques of the inguinal creases (see Fig. 73.13). It favors young adults and spontaneous regression can occur. However, the histopathologic findings are those of a high-grade squamous intraepithelial lesion or SCC *in situ*.

Other variants of SCC *in situ* include a pigmented variant often seen in individuals with darker skin types and a verrucous form. Pigmented SCC *in situ* may be mistaken for a superficial melanoma, and verrucous SCC *in situ* may simulate a seborrheic keratosis or a wart.

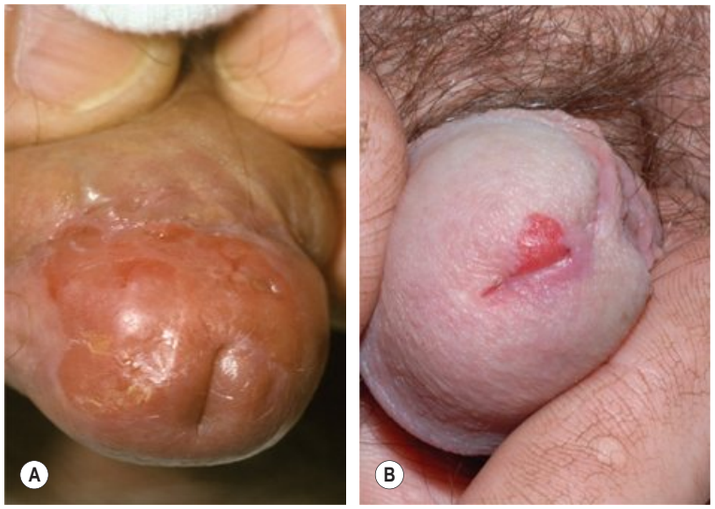


Fig. 108.6 Penile squamous cell carcinoma *in situ* (also referred to as erythroplasia of Queyrat). A Glistening, dull red, thin plaque of the glans penis. **B** Small, well demarcated paraurethral red plaque.

Invasive cutaneous squamous cell carcinoma

Invasive cSCC usually arises within a background of sun-damaged skin, most commonly on the bald scalp, face, neck, extensor forearms, dorsal hands, and shins (Fig. 108.7A,B). The color usually varies from erythematous to skin-colored; rarely there are pigmented variants. SCCs are often papulonodular, but can be plaque-like, papillomatous, or even vegetating (Figs. 108.7C,G and 108.8). The degree of scale varies, with some lesions becoming quite hyperkeratotic (Fig. 108.7E,F); secondary changes include crusting, erosions, and ulcerations (Fig. 108.7D,H). Dermoscopic features are outlined in Chapter 0.

The natural history of cSCCs also varies, from slowly enlarging to rapidly growing with significant tenderness and even pain. Of note, paresthesias, anesthesia, and pain may be signs of perineural invasion. The clinical differential diagnosis, in addition to hypertrophic AK, includes inflamed seborrheic keratosis or verruca vulgaris, atypical fibroxanthoma, prurigo nodularis, Merkel cell carcinoma, and hypertrophic lichen planus or cutaneous lupus. Staging is most often based upon the American Joint Committee on Cancer (AJCC) TNM system which focuses on cSCC of the head and neck (Table 108.4). Because the majority of cSCCs assessed by dermatologists do not have lymph node metastases, the major focus consists of determining if the primary tumor is T1, T2, or T3. In the Brigham and Women's Hospital staging system, high-risk factors are employed to further subdivide T2 into T2a

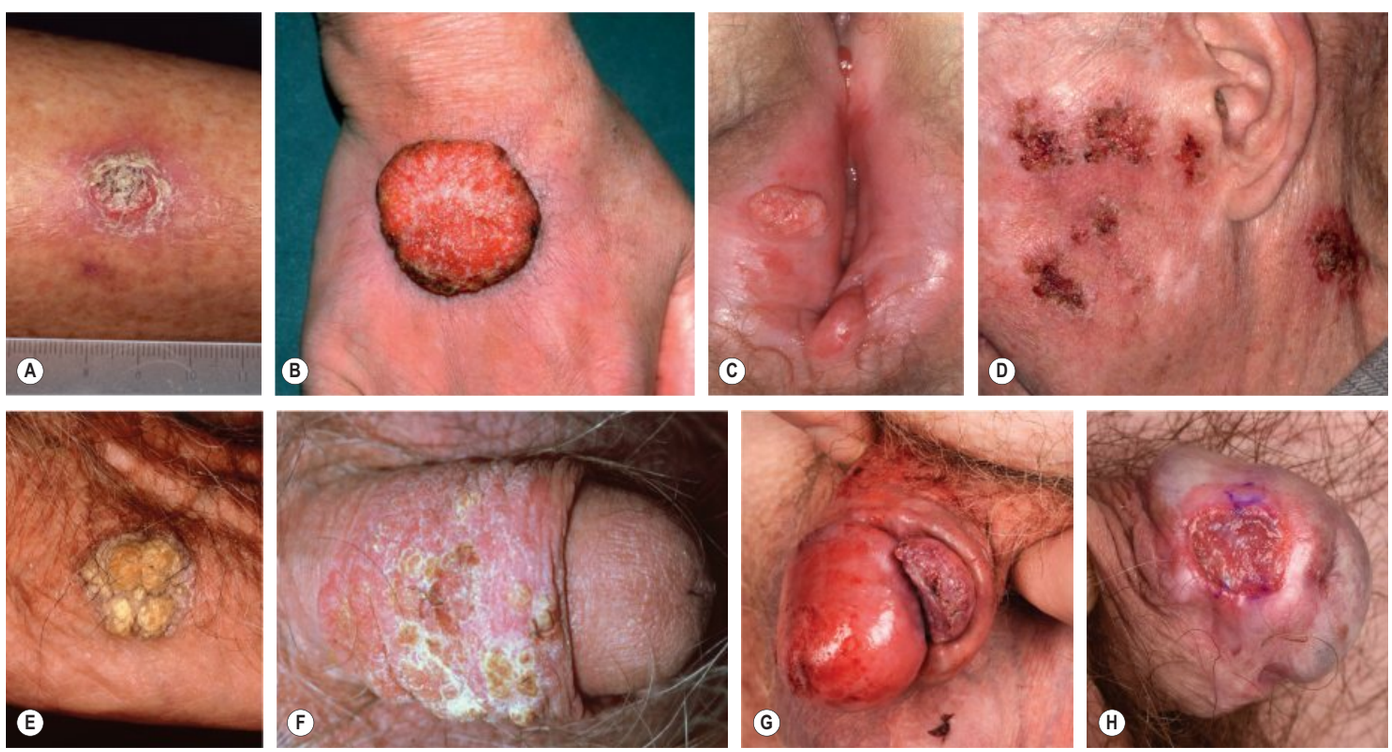


Fig. 108.7 Clinical spectrum of cutaneous squamous cell carcinoma (SCC). A Eroded and keratotic nodule that developed rapidly at the site of trauma on the shin. The differential diagnosis includes atypical squamous proliferation. **B** Large, fungating nodule on the dorsum of the hand. **C** Eroded, slightly vegetating, thick plaque arising within lichen sclerosis of the vulva. **D** Multiple eroded superficial SCCs in association with actinic damage and sites of previous treatment on the cheek and neck of an elderly man. **E** Keratotic verrucous nodule on the dorsal hand. **F–H** As in photodamaged skin, SCC of the genitalia can vary from a pink scaly plaque to an eroded nodule to an ulcer. *A, Courtesy Jean L. Bolognia, MD.*



Fig. 108.8 Squamous cell carcinoma (SCC) of the lower lip. A Extensive hyperkeratosis and leukoplakia of the lower vermilion lip; histopathologically, the SCC was superficially invasive and well-differentiated. **B** Verrucous and eroded nodule on the lower vermilion lip in a heavy smoker.

and T2b (Table 108.5)[68]. Nonetheless, clinical examination of patients with invasive cSCC includes palpation of regional lymph nodes for enlargement and firmness, followed by assessment of size if enlarged.

Keratoacanthoma

Keratoacanthomas (KAs) are considered by some to be a variant of cSCC and by others to represent benign tumors (i.e. a pseudomalignancy). The exact nosology is still uncertain, although there are some data that support its differentiation from "conventional" SCC. Typically, a rapidly enlarging papule evolves into a sharply circumscribed, crateriform nodule with a keratotic core over a period of a few weeks (Fig. 108.9A–D), and then it may resolve slowly over months to leave an atrophic scar. Most lesions occur on the head and neck or in sun-exposed areas of the extremities, with or without symptoms of pain or tenderness.

There are several distinct clinical presentations of KA, including solitary, multiple, grouped, keratoacanthoma centrifugum marginatum (Fig. 108.9E), giant (Fig. 108.9F), multiple spontaneously regressing (Ferguson–Smith), multiple non-regressing, and generalized eruptive (Grzybowski). Occasionally, KAs develop in a subungual, palmoplantar, or intraoral location. KAs are also seen in patients with Muir–Torre syndrome and they may have sebaceous differentiation (see Ch. 63). In addition, multiple KAs have been associated with chemical exposures, immunosuppression, BRAF inhibitors, and HPV infection.

By far the most common presentation is the solitary KA. While most of these tumors are small (5 to 15 mm), some KAs (e.g. keratoacanthoma centrifugum marginatum [see Fig. 108.9E]) may reach several centimeters in diameter, persist for months before resolution, and heal with prominent scarring. Grouped KAs may resolve more slowly than solitary KAs, while subungual KAs have been associated with underlying bony destruction.

STAGING OF CUTANEOUS SQUAMOUS CELL CARCINOMA (cSCC) OF THE HEAD AND NECK			
T, N, M			
Primary tumor (T)			
TX	Primary tumor cannot be identified		
Tis	Carcinoma *in situ*		
T1	Tumor <2 cm in greatest dimension		
T2	Tumor 2 cm or larger, but smaller than 4 cm in greatest dimension		
T3	Tumor 4 cm or larger in maximum dimension or minor bone erosion or perineural invasion or deep invasion*		
T4	Tumor with gross cortical bone/marrow invasion (4a); skull base invasion and/or skull base foramen involvement (4b)		
Regional lymph nodes (clinical) (cN)			
NX	Regional lymph nodes cannot be assessed		
N0	No regional lymph node metastasis		
N1	Metastasis in a single ipsilateral lymph node, ≤3 cm in greatest dimension and ENE(–)		
N2	Metastasis in a single ipsilateral lymph node, >3 cm but <6 cm in greatest dimension and ENE(–) (2a); or in multiple ipsilateral lymph nodes, none >6 cm in greatest dimension and ENE(–) (2b); or in bilateral or contralateral lymph nodes, none >6 cm in greatest dimension and ENE(–) (2c)		
N3	Metastasis in a lymph node, >6 cm in greatest dimension and ENE(–) (3a); or metastasis in any node(s) and ENE(+) (3b)		
Distant metastasis (M)			
M0	No distant metastasis		
M1	Distant metastasis		
Stage			
	T	***N***	***M***
0	Tis	N0	M0
I	T1	N0	M0
II	T2	N0	M0
III	T3	N0	M0
	T1	N1	M0
	T2	N1	M0
	T3	N1	M0
IV	T1	N2	M0
	T2	N2	M0
	T3	N2	M0
	T Any	N3	M0
	T4	N Any	M0
	T Any	N Any	M1

*Deep invasion is defined as invasion beyond the subcutaneous fat or >6 mm (as measured from the granular layer of adjacent normal epidermis to the base of the tumor); perineural invasion for T3 classification is defined as tumor cells within the nerve sheath of a nerve lying deeper than the dermis or measuring 0.1 mm or larger in caliber, or presenting with clinical or radiographic involvement of named nerves without skull base invasion or transgression.

Table 108.4 Staging of cutaneous squamous cell carcinoma of the head and neck. ENE, extranodal extension. *Adapted from American Joint Committee on Cancer (AJCC), 8th edition (2017).*

The Ferguson–Smith syndrome is an autosomal dominant condition due to mutations in *TGFBR1* which encodes TGF-β receptor type 1. Multiple KAs develop within sun-exposed areas, usually beginning during the third decade of life. Lesions typically regress over weeks to months, but rare examples of metastases have been reported. Multiple KAs of the Grzybowski type present as hundreds of papules resembling milia or early eruptive xanthomas. They develop rapidly and may slowly

resolve over a period of months. Patients often have scarring, ectropion, and a mask-like facies.

Verrucous carcinoma

Verrucous carcinoma is a rare, well-differentiated variant of SCC which tends to occur in middle-aged and older adults. It is considered a low-grade malignancy with three major subtypes: (1) epithelioma cuniculatum (plantar surface of the foot); (2) giant condyloma acuminatum of the genitalia (also known as Buschke–Löwenstein tumor; see Ch. 79); and (3) oral florid papillomatosis (oral mucosa). Of note, the "cuniculatum" refers to the rabbit burrow-like appearance with crevices.

Clinically, verrucous carcinomas present as large (sometimes huge), exophytic tumors with a papillomatous or verrucous surface (Fig. 108.10A,B). They are commonly associated with HPV infection, and distinguishing between a verrucous carcinoma and a large wart or condyloma acuminatum can be challenging. Gradual penetration of verrucous carcinomas into underlying tissues can result in destruction of subcutis, fascia, and bone. These tumors can arise within scars and amputation stumps (Fig. 108.10C) as well as in association with fistulae of osteomyelitis and chronic venous insufficiency. Verrucous carcinomas often recur after attempted removal, but they usually do not metastasize, except for recurrent or irradiated tumors with anaplastic transformation. Some authors consider subungual KAs, proliferating tricholemmal cysts (proliferating pilar tumors), and papillomatosis cutis carcinoides (which favors the shins and dorsal feet) to be subtypes of verrucous carcinoma.

HIGH RISK FACTORS FOR CUTANEOUS SQUAMOUS CELL CARCINOMA
• Vertical tumor thickness >6 mm
• Tumor diameter ≥2 cm*
• Location: ear, lips, oral or genital mucosa
• Histopathologic features: poorly differentiated*, presence of desmoplasia, invasion beyond subcutaneous fat*
• Perineural invasion of nerves with a diameter of ≥0.1 mm*
• Bone invasion
• Immunosuppression
*One of four high-risk factors (HRFs) in the Brigham and Women's Hospital grading system; T1 = 0 HRFs; T2a = 1 HRF; T2b = 2–3 HRFs; T3 = ≥4 HRFs or bone invasion.

Table 108.5 High-risk factors for cutaneous squamous cell carcinoma. *Adapted from Stratigos AJ et al.*[84]

Lymphoepithelioma-like carcinoma of the skin

Lymphoepithelioma-like carcinoma of the skin (LELCS) is an uncommon neoplasm that shows histopathologic similarities to lymphoepithelioma-like carcinoma (LELC), an undifferentiated nasopharyngeal carcinoma associated with EBV infection. LELCS has the potential for both sweat glandular and follicular differentiation. Clinically, it presents as a dermal papule or nodule arising in the head and neck region. In contrast to LELC, EBV genome integration is not found in LELCS, and metastases are rare. Evidence of HPV infection is also usually absent. LELCS is considered by some to be a variant of cSCC, while others view it as a type of cutaneous adnexal carcinoma.

Histologically, LELCSs are localized within the dermis or subcutis, with involvement of the overlying epidermis having been observed in only a few cases. The tumor consists of clusters of epithelial cells (with large vesicular nuclei and prominent nucleoli) intermingled with a prominent inflammatory infiltrate that sometimes forms germinal centers. However, classic signs of squamous differentiation such as

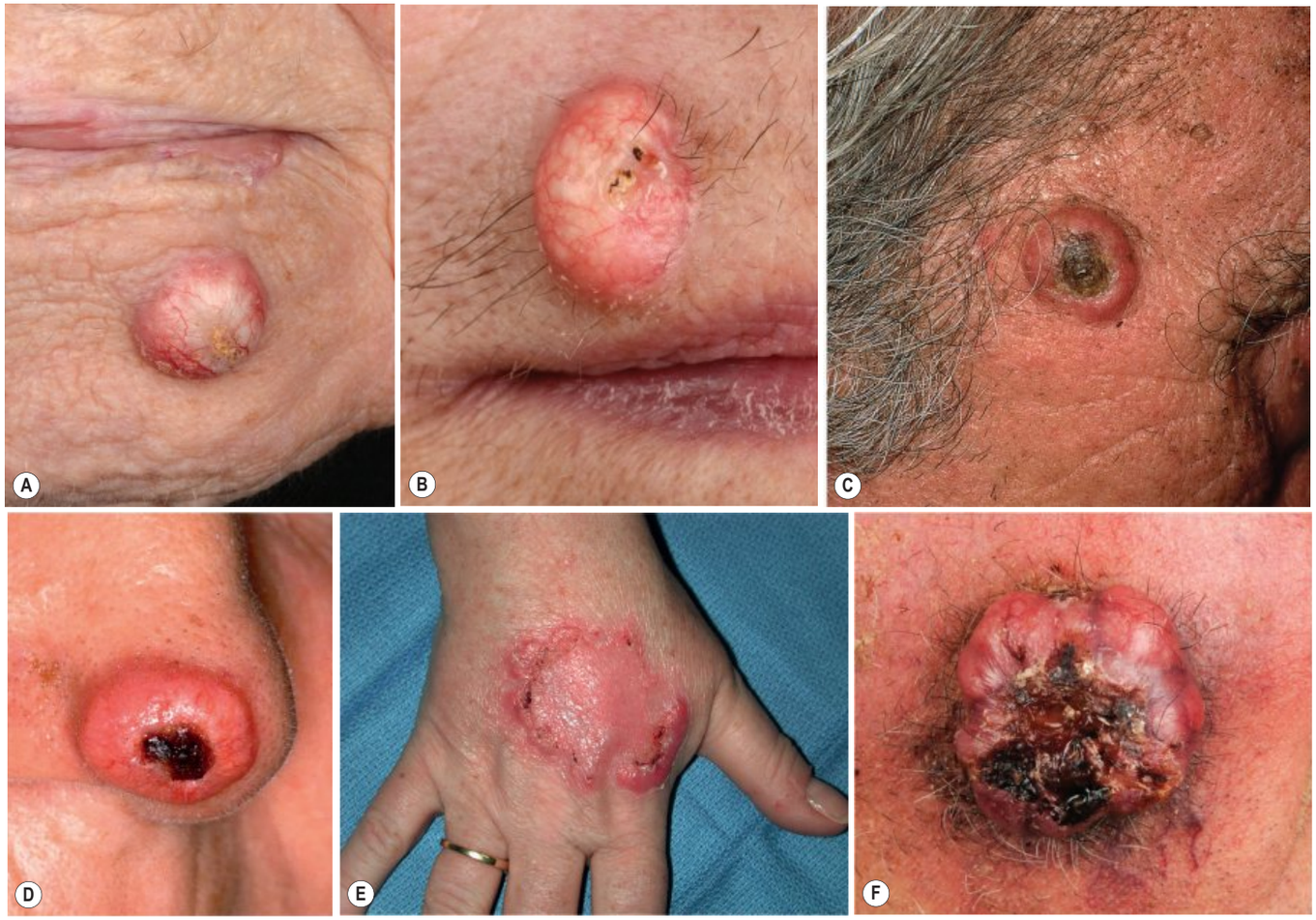


Fig. 108.9 Clinical spectrum of keratoacanthomas. A, B Erythematous nodules that are yellow–white centrally with a keratotic core; telangiectasias are also seen. **C, D** Rapidly growing, erythematous crateriform nodules with a rolled border and larger central keratotic core. The lesions may be tender. **E** Progressive peripheral expansion and central involution with residual atrophy characterize keratoacanthoma centrifugum marginatum. **F** Giant keratoacanthoma with a yellow–red color, multilobed rolled border, central ulceration, and a history of rapid growth.



Fig. 108.10 Verrucous carcinoma. A Longstanding large nodule on the plantar surface with a rabbit burrow-like appearance; such a tumor is also referred to as an epithelioma cuniculatum. **B** Keratotic and ulcerated plaque on the ventromedial aspect of the great toe. **C** A classic location in an amputation stump. In general, these well-differentiated SCCs enlarge slowly.

keratin "pearls", dyskeratotic cells, or intercellular bridges are absent. Neoplastic cells express cytokeratin and epithelial membrane antigen while stromal lymphocytes express leukocyte common antigen (CD45). The histopathologic differential diagnosis includes lymphocytoma cutis, follicle center lymphoma, and carcinoma with thymus-like differentiation.

In vivo Imaging Methods

Dermoscopy

Dermoscopy of invasive cSCC reveals linear-irregular vessels, elongated vessels resembling hairpins, dotted vessels, or a combination of these findings (polymorphous or atypical vascular pattern). Typically, vessels are surrounded by a whitish halo; the latter is the dermoscopic hallmark of all keratinizing tumors and is also found in KAs and in seborrheic keratoses (see Ch. 0). Ulceration and hemorrhagic crusts appear as red-, brown-, or black-colored surface blotches. Rare pigmented cSCCs may have a scaly surface, diffuse or homogenous blue pigmentation, and/or irregularly distributed blue–gray granular structures. AKs on the face can demonstrate a so-called "strawberry pattern" (an erythematous pseudonetwork surrounding hair follicle orifices filled with yellowish keratotic plugs; see Fig. 0.39H) as well as a "red starburst pattern" (central mass of keratin and hairpin vessels). In other body sites, AKs often display surface scales and dotted vessels. Bowen disease typically has a scaly surface and glomerular vessels (see Fig. 0.39D).

Reflectance confocal microscopy

Reflectance confocal microscopy (RCM) is an imaging technique which allows non-invasive horizontal imaging of the epidermis and superficial dermis at almost the same resolution as routine histology. However, RCM (and dermoscopic) features of keratinizing tumors are often difficult to visualize due to the surface scaling which obscures underlying structures. In AKs and cSCCs, key findings consist of areas with an irregular honeycomb pattern and atypia of keratinocytes; blood vessels display the "button hole" sign[69].

Pathology

Actinic keratosis

There is partial thickness involvement of the epidermis by atypical keratinocytes with nuclear pleomorphism, especially in the basal layer, as well as disordered maturation. Hyperkeratosis and parakeratosis are constant findings. Acrosyringia and acrotrichia are often *uninvolved*, resulting in orthokeratosis above the ostia of these structures (Fig. 108.11A). In the dermis, actinic elastosis is seen. A minority of dermatopathologists employ a grading system – early AK (grade I), AK involving the lower two-thirds of the epidermis (grade II), full-thickness atypia of the epidermis (grade III; SCC *in situ*) – but this classification has not gained widespread acceptance.

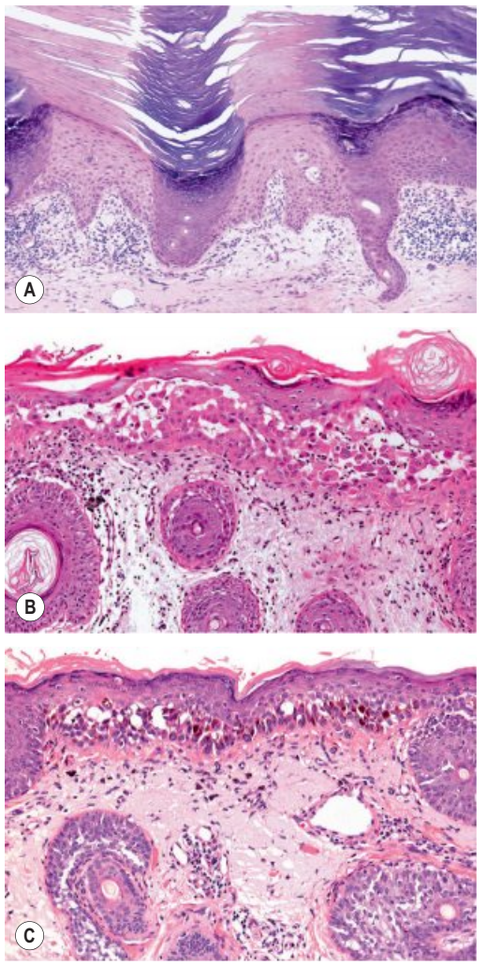


Fig. 108.11 Histopathology of actinic keratoses (AKs). A Hyperkeratotic AK with alternating pink and blue colors in the cornified layer; the pink-colored parakeratotic columns within the stratum corneum are located above the atypical keratinocytes in the spinous layer, while the blue-colored columns of orthohyperkeratosis are above the acrosyringia. Atypical epidermal keratinocytes also display a pinkish color that contrasts with the color of the basophilic, normal keratinocytes of the acrosyringia. **B** Acantholytic variant with clefts within the stratum spinosum. **C** Pigmented actinic keratosis with increased melanin pigmentation within the basal layer. Note the solar elastosis in the dermis. *B, C, Courtesy Lorenzo Cerroni, MD.*

In addition to atrophic and bowenoid AKs, several other histopathologic variants have been described, including acantholytic (Fig. 108.11B), hypertrophic (hyperkeratotic), pigmented, and lichenoid. In *hypertrophic* AKs, marked hyperkeratosis with associated parakeratosis is evident. If pronounced, this can lead to cutaneous horn formation. *Pigmented* AKs additionally show basilar pigmentation in a pattern similar to a solar lentigo (Fig. 108.11C). *Lichenoid* AKs demonstrate a band-like infiltrate of lymphocytes in the papillary dermis directly beneath the dermal–epidermal junction. *Actinic cheilitis* arises on the vermilion lips, primarily the lower one, and intraepithelial atypical keratinocytes, usually associated with inflammation, are observed.

Squamous cell carcinoma in situ

SCC *in situ* (Bowen disease), by definition, demonstrates full-thickness atypia of the epidermis over a broad zone (Fig. 108.12). Dyskeratosis, nuclear pleomorphism, and apoptosis are often more florid than in AKs, and mitoses are frequent. The epidermis commonly exhibits acanthosis. Atypical keratinocytes extend down the adnexa, and diffuse confluent parakeratosis is also observed. Lastly, in contrast to AKs, the basal layer of the epidermis is usually spared and, at least focally, is composed of small compressed basaloid keratinocytes arranged in a palisade.

Invasive cutaneous squamous cell carcinoma

In well-differentiated cSCC, there is a downward proliferation of lobules with aggregations of glassy, brightly eosinophilic keratinocytes containing nuclei with some degree of pleomorphism and mitoses (Fig. 108.13A). Keratin pearls and apoptotic cells are observed. The degrees of nuclear atypia and cellular differentiation vary within and among tumors (Fig. 108.13B). The pink quality of the cytoplasm arises from abundant high-molecular-weight keratin. The inflammatory infiltrate differs considerably in intensity and consists primarily of lymphocytes and plasma cells. At their margins, many well-differentiated

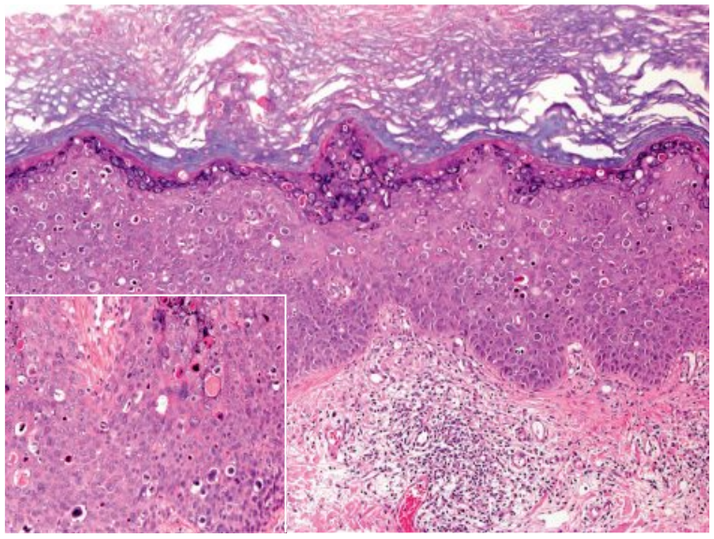


Fig. 108.12 Histopathology of Bowen disease (squamous cell carcinoma *in situ*). Irregular epidermal hyperplasia with atypical pleomorphic keratinocytes throughout the entire epidermal thickness. Note several necrotic keratinocytes (inset). *Courtesy Lorenzo Cerroni, MD.*

cSCCs exhibit contiguity with an AK. When invasive cSCC arises from Bowen disease, the intradermal tumor cells often have a more basophilic appearance.

Poorly differentiated cSCCs display progressive and overlapping features, ending in highly infiltrative tumors that lack overt keratinization and sometimes have a spindle cell morphology. Perineural infiltration (Fig. 108.13C) and desmoplastic or sclerotic stromal change become more common in these forms. Neurotropic SCCs behave in a more aggressive manner, with local recurrence rates approaching 50%. Poorly differentiated tumors (cytokeratin$^+$) generally require immunohistochemistry to distinguish them from spindle-cell melanoma (Melan-A$^+$, SOX-10$^+$, S100$^+$), atypical fibroxanthoma (cytokeratin$^-$, Melan-A$^-$, SOX-10$^-$, S100$^-$; CD10$^+$), leiomyosarcoma (smooth muscle actin$^+$, desmin$^+$), and other malignant tumors (exclusionary immunohistology).

There are several variants of SCC. The acantholytic type (Fig. 108.13D) and the related adenoid (pseudoglandular) SCC may have a worse prognosis, but this has been questioned[70]. Other variants of SCC include lesions with overlying cutaneous horn formation as well as bowenoid, clear cell, pseudovascular, desmoplastic, mucinous, adenosquamous, pigmented, and spindle cell types. The latter probably has a worse prognosis. Marjolin's ulcer is an SCC that occurs in a chronic wound or scar, including from a thermal burn.

A large, prospective study focusing on risk factors that predict metastasis and local recurrence in cSCC reported overall rates of 4% for metastasis and 3% for local recurrence[71]. Only tumors >2 mm in vertical

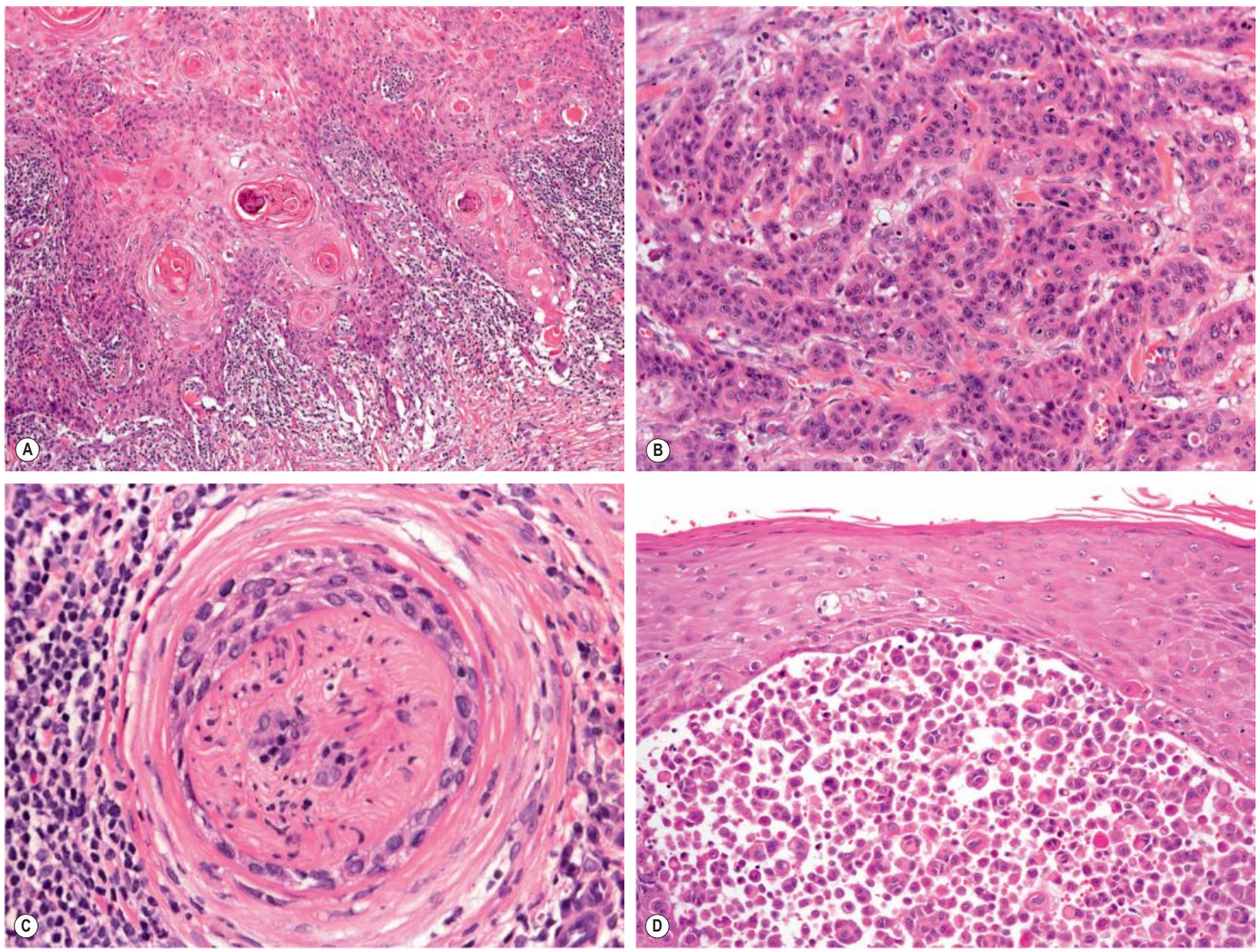


Fig. 108.13 Squamous cell carcinoma (SCC): range of histopathologic findings. A Well-differentiated SCC with numerous horn pearls (eosinophilic parakeratotic keratinization). **B** Poorly differentiated SCC with strands and cords of epithelial cells with prominent nuclear atypia and no signs of keratinization. **C** Perineural growth and neurotropism of a poorly differentiated SCC. **D** Acantholytic SCC characterized by epithelial aggregations composed of atypical keratinocytes with acantholysis. *Courtesy Lorenzo Cerroni, MD.*

thickness had a significant risk of developing metastases. For SCCs whose thickness was between 2.1 and 6 mm, the metastatic rate was 4%, and it was 16% for lesions thicker than 6 mm. Other risk factors for metastasis included location on the ear or mucosa, increased horizontal size, and immunosuppression (see Table 108.5). Tumor thickness and the presence of a desmoplastic stroma were found to be risk factors for local recurrence. For example, of 51 patients with desmoplastic SCC, 24% developed local recurrences, compared to 1% of 564 patients with non-desmoplastic SCCs.

Keratoacanthoma

A keratoacanthoma (KA) typically has a "volcano-like" architecture. The tumor is comprised of well-differentiated keratinocytes with a brightly eosinophilic glassy cytoplasm, surrounding a core filled with cornified material (Fig. 108.14). An inflammatory infiltrate of lymphocytes, and often eosinophils, is usually present. Small intratumoral abscesses of neutrophils are common, and neurotropism may be observed. As the lesion regresses, the dome-shaped architecture flattens and fibrosis develops at the base of the lesion. Cytologic atypia is usually not pronounced in a KA. If hyperchromatic nuclei or abnormal mitoses are prominent, then the diagnosis of an invasive KA-like SCC should be rendered.

Verrucous carcinoma

Verrucous carcinoma is defined as a well-differentiated and distinct clinicopathologic variant of SCC (Fig. 108.15). However, this term should not be applied to every SCC that has a warty appearance. Cytologic atypia is minimal, and the tumor has a pushing border as opposed to an infiltrating invasive edge. Verrucous carcinoma can be associated with HPV infection, and histopathologic distinction from a large wart or condyloma is often difficult and may be impossible if the entire tumor is not available for microscopic examination. The major distinguishing features of a verrucous carcinoma are the massiveness and depth of the lesion, as well as the pronounced irregular architecture.

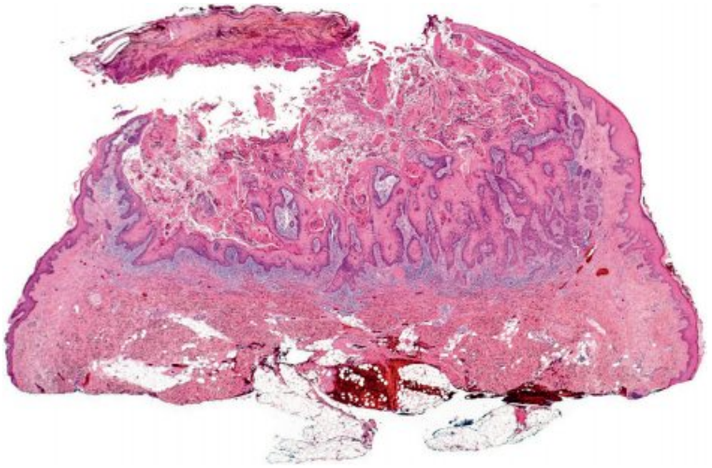


Fig. 108.14 Histopathology of keratoacanthoma. Scanning magnification of a stereotypical keratoacanthoma with a keratin-filled crater encompassed by epithelial lips. *Courtesy Lorenzo Cerroni, MD.*

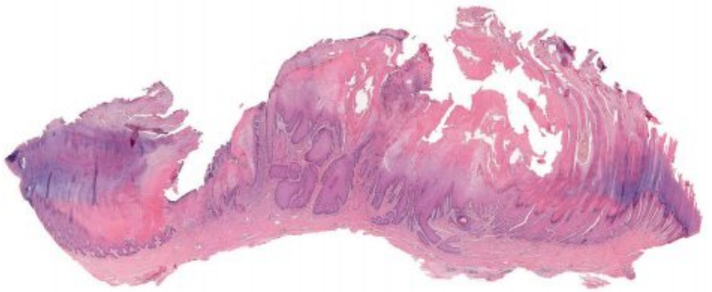


Fig. 108.15 Histopathology of verrucous carcinoma. A markedly irregular epithelial hyperplasia with prominent hyperkeratosis is seen. For the histopathologic diagnosis of verrucous carcinoma, the size of the lesion and architectural features are more important than cytomorphology, which usually does not show prominent atypia, thus emphasizing the need for large excisional biopsies in order to make a proper diagnosis. *Courtesy Lorenzo Cerroni, MD.*

Histopathologic simulators of SCC

There are a number of histopathologic simulators of SCC, including seborrheic keratosis, verruca vulgaris, inverted follicular keratosis, prurigo nodularis, hypertrophic lichen planus, hypertrophic lupus erythematosus, and the pseudocarcinomatous hyperplasia that can occur in a range of disorders (e.g. dimorphic fungal infections, healing wounds, tattoos, some non-keratinocyte tumors). Architectural pattern and recognition of cellular and nuclear features of malignancy are critical in establishing a diagnosis. In some cases, only clinical correlation allows a distinction between SCC and some of these conditions. Of note, SCC may occur in the setting of a pre-existing benign tumor (e.g. seborrheic keratosis) as well as within chronic pseudoepitheliomatous hyperplasia related to hypertrophic lichen planus or hypertrophic lupus erythematosus.

Atypical squamous proliferation

Atypical squamous proliferation (ASP) is a term used to describe the histologic findings found in papulonodules and thick plaques that develop within markedly sun-damaged skin, usually on the shins and following trauma. This term is preferred over keratoacanthoma-like squamous proliferations as they often lack a central keratotic core. Although ASPs are associated with less cytologic atypia than cSCCs[72], distinction can prove challenging. Immunohistochemical staining for p53 may be helpful with positivity in basal and immediately suprabasal layers in ASP, in contrast to full-thickness positivity in cSCC. Presumably growth factors released during wound healing, including following surgical excision, trigger proliferation of keratinocytes with UV-induced mutations.

BASAL CELL CARCINOMA

Clinical Features

Basal cell carcinoma (BCC) is a tumor that usually arises within sun-damaged skin. However, it may also develop in sites with minimal sun exposure, e.g. inner canthus, retroauricular; rarely BCCs occur on the palms, soles, and mucous membranes. Currently, despite the description of multiple subtypes of BCC, a universally accepted classification scheme is lacking, but a standardization of terminology has recently been proposed[73]. Nonetheless, four major distinctive clinicopathologic types are commonly recognized, namely, nodular, superficial, morpheaform, and fibroepithelial (also referred to as fibroepithelioma of Pinkus)[74]. Combinations of the latter three types with nodular BCC can occur. While all types of BCC may ulcerate, ulceration is observed more often in the nodular type. Also, variable amounts of melanin may be present within these tumors, even though the majority of BCCs are amelanotic; pigmented BCCs are observed more commonly in those with darker skin phototypes. When one attempts to classify BCCs, a significant confounding factor is the number of different histopathologic patterns that become entwined with clinical subtypes. Examples are cystic, mucinous, micronodular, and basosquamous BCCs. Although these patterns may be seen in all four major clinicopathologic types of BCC, they are observed more frequently in the nodular type.

Nodular basal cell carcinoma

Nodular BCC is the most common subtype, accounting for ~50% of all BCCs. Lesions typically present as a shiny, pearly papule or nodule with a smooth surface and the presence of arborizing telangiectasias (Fig. 108.16). With time, the tumor can enlarge and ulcerate (rodent ulcer, phagedenic ulcer), but an elevated rolled border usually remains and is a clinical clue to the diagnosis. A variable degree of pigmentation may be seen within the tumor (Fig. 108.17A–C). Sites of predilection are the face, especially the cheeks, nose, nasolabial folds, forehead and eyelids, but nodular BCCs may arise in any hair-bearing area of the skin. They rarely occur in non-hair-bearing sites, e.g. oral or genital mucosa, palms and soles.

The clinical differential diagnosis of non-ulcerated lesions includes adnexal neoplasms (see Ch. 111), fibrous papules, intradermal melanocytic nevi, lichen keratoses, and amelanotic melanomas; for ulcerated lesions, see Table 45.3 and Fig. 105.1.



Fig. 108.16 Clinical spectrum of nodular basal cell carcinoma. A Translucent papulonodule with prominent telangiectasias on the infraorbital cheek. **B** Classic presentation with a pearly rolled border and central hemorrhagic crust. **C** Larger plaque with rolled borders and multiple telangiectasias. **D** Nodulo-ulcerative tumor of the preauricular region with translucent rolled borders, most obvious at "12 o'clock"**. E** Depressed scar on the nose. **F** Dermoscopy of a nodular basal cell carcinoma of the forehead. The arborizing telangiectasias are in sharp focus (inset). *A, Courtesy Stanley J. Miller, MD; E, Courtesy Kalman Watsky, MD.*

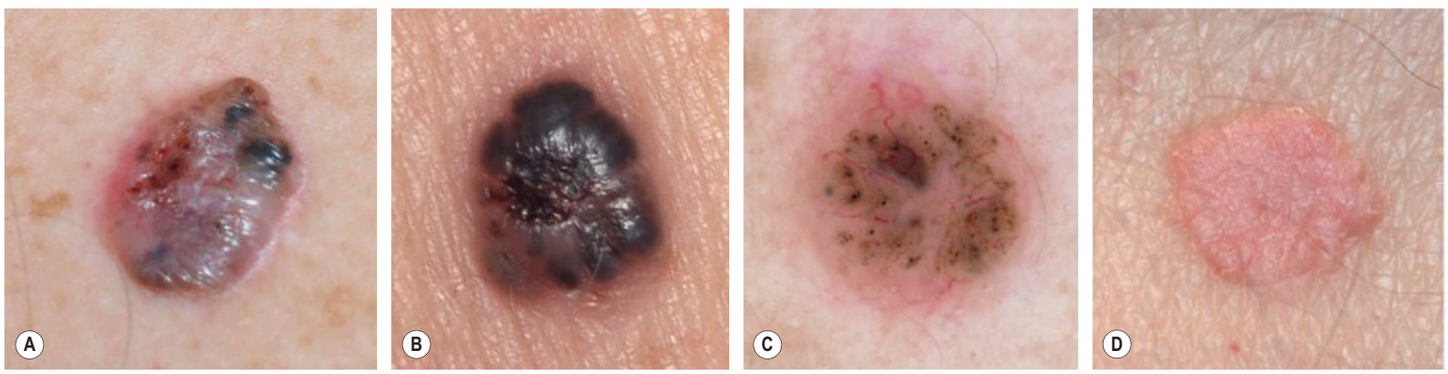


Fig. 108.17 Additional variants of basal cell carcinoma (BCC) – pigmented and fibroepithelial (fibroepithelioma of Pinkus). A, B Pigmented nodular BCCs with varying degrees of melanin pigmentation that may clinically resemble cutaneous melanoma. However, the glassy translucency, in concert with characteristic dermoscopic features such as arborizing telangiectasias and multiple blue–gray ovoid globules (**C**), point to the diagnosis of pigmented BCC. **D** A soft, skin-colored to light pink, broad, sessile plaque on the lower back is a classic presentation for a fibroepithelial BCC. *A, Courtesy Kalman Watsky, MD; C, Courtesy Giuseppe Argenziano, MD; D, Courtesy Oscar Colegio, MD.*

Superficial basal cell carcinoma

Superficial BCCs typically present as a well-circumscribed, erythematous, macule/patch or thin papule/plaque, with the diameter varying from a few millimeters to several centimeters (Fig. 108.18). Additional findings include focal crusts and/or scale, a thin rolled border, and variable amounts of melanin; in larger lesions, areas of spontaneous regression may be present, characterized by atrophy and hypopigmentation. The mean age at diagnosis is in the mid 50 s, a younger age than for other types of BCC, and in younger age groups, superficial BCC is the most common subtype. This BCC variant favors the trunk and extremities; less often, it occurs in the head and neck region. Multiple lesions may be present.

The growth pattern of superficial BCCs is primarily horizontal, but tumors may occasionally become deeply invasive, with induration, ulceration, and nodule formation. Subclinical lateral spread accounts for the significant recurrence rate of these tumors after routine surgical treatment. The clinical differential diagnosis includes solitary lichenoid keratosis and Bowen disease (more scale) as well as inflammatory diseases such as psoriasis, dermatitis, and cutaneous lupus erythematosus.

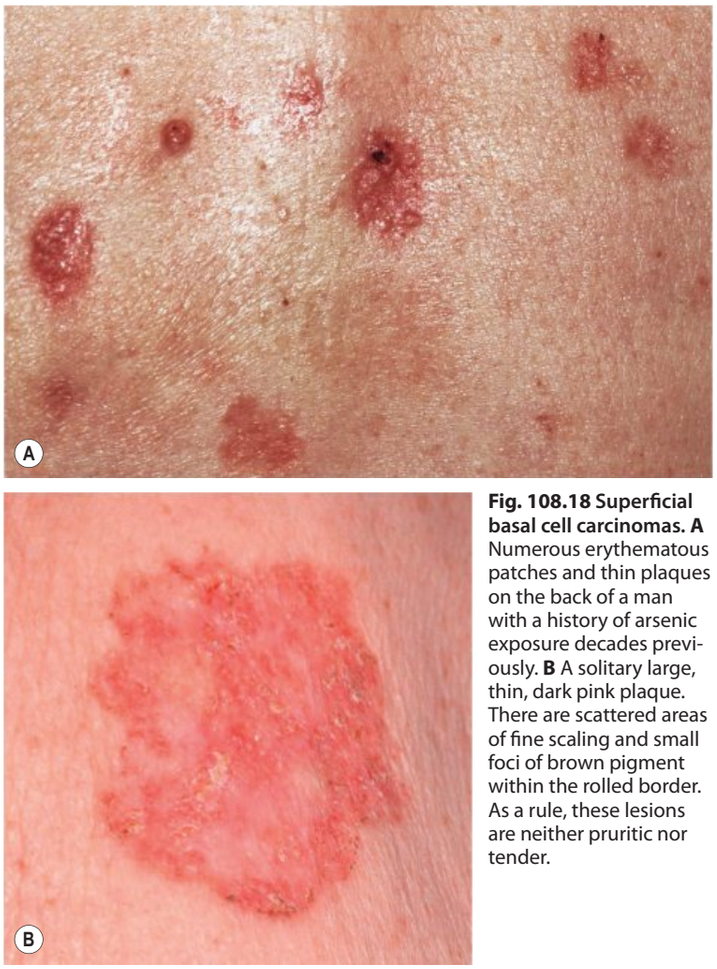


Fig. 108.18 Superficial basal cell carcinomas. A Numerous erythematous patches and thin plaques on the back of a man with a history of arsenic exposure decades previously. **B** A solitary large, thin, dark pink plaque. There are scattered areas of fine scaling and small foci of brown pigment within the rolled border. As a rule, these lesions are neither pruritic nor tender.



Fig. 108.19 Morpheaform basal cell carcinomas. A Recurrent tumor two years after microscopically controlled surgery; note the scar-like appearance with superimposed glassy pink and brown papules. **B** Oval hypopigmented firm plaque that resembles a scar (e.g. post electrodesiccation and curettage). While there is a light pink color between 9 and 12 o'clock, no translucency or rolled border is present. **C** A classic example with indistinct borders and scar-like appearance.



Fig. 108.20 Dermoscopy of pigmented "nevoid" basal cell carcinomas of the abdomen in a patient with basal cell nevus syndrome. There are pigment globules, maple leaf structures, and one arborizing telangiectasia as well as a pink background color (inset).

Morpheaform basal cell carcinoma

This less common subtype of BCC frequently presents as a slightly elevated to even depressed area of induration that is usually light pink to white in color and has ill-defined borders; it may resemble a scar or plaque of morphea (Fig. 108.19). The surface of the lesion is typically smooth, although crusts with underlying erosions or ulcerations as well as superimposed papules may be observed. While an elevated pearly border is typically absent, telangiectasias may be present. The biologic behavior is usually more aggressive, with extensive local destruction.

Fibroepithelial basal cell carcinoma (fibroepithelioma of Pinkus)

This rare variant of BCC usually presents as a skin-colored or pink, sessile plaque or pedunculated papulonodule with a smooth surface (Fig. 108.17D). It favors the trunk, especially the lower back. Fibroepithelial BCCs often occur in individuals with multiple superficial BCCs. The clinical differential diagnosis includes an intradermal melanocytic nevus or large fibroepithelial polyp (skin tag). Of note, some experts believe that fibroepithelioma of Pinkus is a variant of trichoblastoma (not BCC).

In vivo Imaging Methods

Dermoscopy

Dermoscopy provides a demonstrated benefit in the diagnosis of non-pigmented and pigmented BCCs[75]. The dermoscopic hallmark of BCC is the presence of well-focused arborizing vessels in conjunction with foci of microulceration (see Fig. 108.16F). Additional findings with a high specificity for BCC include large blue–gray ovoid nests, multiple blue–gray globules, leaf-like structures, and spoke-wheel areas (Fig. 108.20; see Ch. 0); a pigment network is absent. Short, fine superficial telangiectasias as well as concentric structures and multiple, "in-focus" blue–gray dots have also been described.

Reflectance confocal microscopy (RCM)

The following reflectance confocal microscopy (RCM) features have been described for all BCCs, regardless of subtype (Fig. 108.21)[69]: (1) variable architectural disarray of the epidermis; (2) a streaming pattern of elongated monomorphic nuclei that are polarized along the same axis; (3) tightly packed cells in the papillary dermis with a nodular/cord-like growth pattern; (4) palisading of tumor cell nuclei; (5) peritumoral dark cleft-like spaces (representing peritumoral mucinous edema); and (6) the presence of bright dendritic cells and melanophages (in pigmented BCC). RCM can also be used to determine surgical margins prior to excision.

Pathology

All types of BCC have, as a least common denominator, the presence of aggregations of basaloid keratinocytes within a variably fibromyxoid

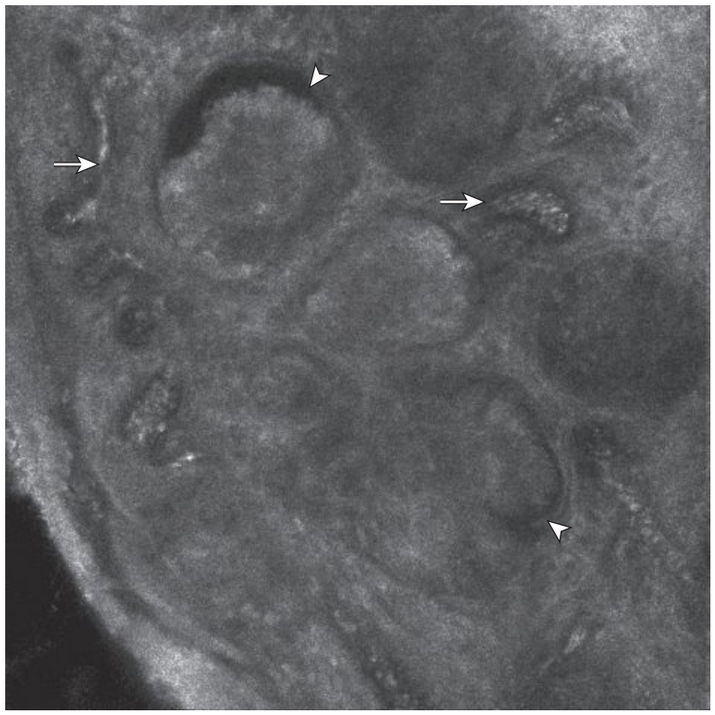


Fig. 108.21 Reflectance confocal microscopy of a basal cell carcinoma. A 0.5 × 0.5 mm image at a depth of 85 microns. Aggregations of basaloid cells with hyporeflective cleft-like peritumoral spaces (arrowheads) and dilated tortuous blood vessels can be seen (arrows). *Courtesy Claudia Curchin, MBBS.*

stroma. A connection to the epidermis is usually observed, at least focally (Fig. 108.22A). The tumor cells have large, relatively uniform nuclei and scant cytoplasm; cellular borders are indistinct and desmosomes are inapparent. Apoptotic cells are common. The fibromyxoid stroma is intimately associated with the tumor islands, often showing increased cellularity. A characteristic feature of BCC is retraction of the stroma around the tumor islands, creating microscopically visible clefts (Fig. 108.22B). Although this latter feature may not be seen in all instances, when present it is useful in differentiating BCCs from histopathologic simulators.

In *nodular BCC*, large, round or oval aggregations of basaloid keratinocytes extend from the epidermis into the dermis (Fig. 108.22C). Overlying ulceration with an associated inflammatory response may be present. Peripheral palisading is usually prominent and peritumoral clefts are often conspicuous in nodular BCC (Fig. 108.22D). Centrally, the nuclei lack organization and are more randomly distributed. In larger tumor islands, central areas of necrosis may develop, leading to the formation of cystic spaces. *True cystic or nodulocystic BCCs* contain mucin pools within the tumor islands (Fig. 108.22E). Micronodular BCCs are composed of tumor islands much smaller than those of nodular BCC (Fig. 108.22F). The cellular features are similar.

Superficial BCCs are characterized by small, superficially located buds of basaloid cells extending no more deeply than the papillary dermis, with or without clefting (see Fig. 108.22A,B). In a given two-dimensional plane of section, there are skip areas along the epidermis, hence the synonym "superficial multifocal BCC". There is evidence that many of these multifocal buds connect in a net-like pattern, such that most tumors are not truly multifocal.

Pigmented BCCs usually have the overall architecture of a nodular BCC. They contain aggregates of melanin, often irregularly distributed, and sometimes an increased number of intratumoral melanocytes (Fig. 108.22G). Melanophages are frequently dispersed within the dermis.

Morpheaform, sclerosing and infiltrative BCCs share similar histopathologic features. A common finding is a pattern of strands and cords of basaloid keratinocytes extending between collagen bundles (Fig. 108.22H). These tumor islands may be composed of very few cells and may surround nerves. A peripheral palisaded pattern of tumor cells is absent and stromal retraction (cleft formation) is also frequently not evident.

Fibroepithelial BCC (fibroepithelioma of Pinkus) is a variant of BCC characterized by thin anastomosing strands and cords of tumor cells that project downward from the epidermis in a fenestrated pattern and are embedded in a fibrovascular stroma (Fig. 108.22I). Both peripheral palisading and peritumoral retraction are less prominent. The differential diagnosis includes eccrine syringofibroadenoma and reticulated seborrheic keratosis.

Infundibulocystic BCCs have cords of follicular germs with small infundibular cysts that display differentiation towards hair follicle structures. Although they can be difficult to differentiate from trichoepitheliomas or other follicular adnexal neoplasms, immunostaining for PHLDA1, a marker of epithelial follicular stem cells, is stronger and more diffuse in trichoepitheliomas[76]. Multiple hereditary infundibulocystic BCC syndrome has been associated with a germline mutation in *SUFU*.

Additional histopathologic subtypes of BCC

Basosquamous carcinoma

Basosquamous carcinoma (metatypical BCC, keratotic BCC) is a tumor that has histopathologic features of both BCC and cSCC (Fig. 108.22J). These tumors may behave biologically more like an SCC than a BCC, i.e. they have more aggressive behavior with a greater likelihood of both recurring after treatment and metastasizing. It has been estimated that this variant constitutes 1% of all keratinocyte carcinomas. When metastases occur, they may have the same microscopic appearance as the original tumor or may resemble a poorly differentiated SCC.

Micronodular basal cell carcinoma

This histopathologic term applies to BCCs in which smaller aggregations of basaloid cells infiltrate the dermis (see Fig.108.22F). Micronodular BCCs possess a destructive behavior, with subclinical spread and high rates of recurrence. Clinically, they may present as infiltrated macules, papules/nodules, or plaques and are basically indistinguishable from nodular BCCs. A recent consensus project suggested that infiltrating, sclerosing, and micronodular subtypes should be grouped together under the umbrella term "infiltrating BCCs"[73].

Histopathologic simulators of BCC

Other basaloid tumors that may simulate BCC include adnexal neoplasms, in particular trichoblastoma (Table 108.6). In contrast to BCC, clefts in trichoblastoma are located within the stroma and not in direct proximity to the basaloid tumor islands. In addition, follicular germs and papillae, simulating rudimentary hair follicles, are commonly found in trichoblastomas. Basaloid induction within dermatofibromas and reactive folliculocentric basaloid proliferation may also simulate BCC histopathologically.

TREATMENT

Several national and international organizations have established guidelines of care for BCCs and cSCCs. When available, these guidelines are based upon evidence but are oftentimes developed via expert consensus[77–79].

Evaluation and Risk Assessment

Evaluation of a suspected NMSC requires a history, physical examination, and biopsy of the suspicious lesion. The history should assess duration, rate of growth, and any prior therapy, as well as any personal or family history of prior skin cancers. Localized neurologic symptoms, although rare, may suggest the possibility of perineural involvement. Any history of prior radiation therapy to the area should be elicited. Current medical problems (e.g. chronic lymphocytic leukemia), medications (e.g. voriconazole, hydroxyurea), and allergies should be reviewed. Evidence of immunosuppression (e.g. organ transplantation, immunosuppressive medications, HIV infection) should be determined, and any of the risk factors listed in Table 108.2 identified.

Physical examination should include observation and palpation of the tumor to determine exact location and size, and whether it appears to have any connection to underlying structures such as muscle, cartilage, or bone. An assessment should be done of how well or poorly defined the tumor borders are, whether there is physical evidence of prior surgery or other therapeutic interventions (indicating the possibility of

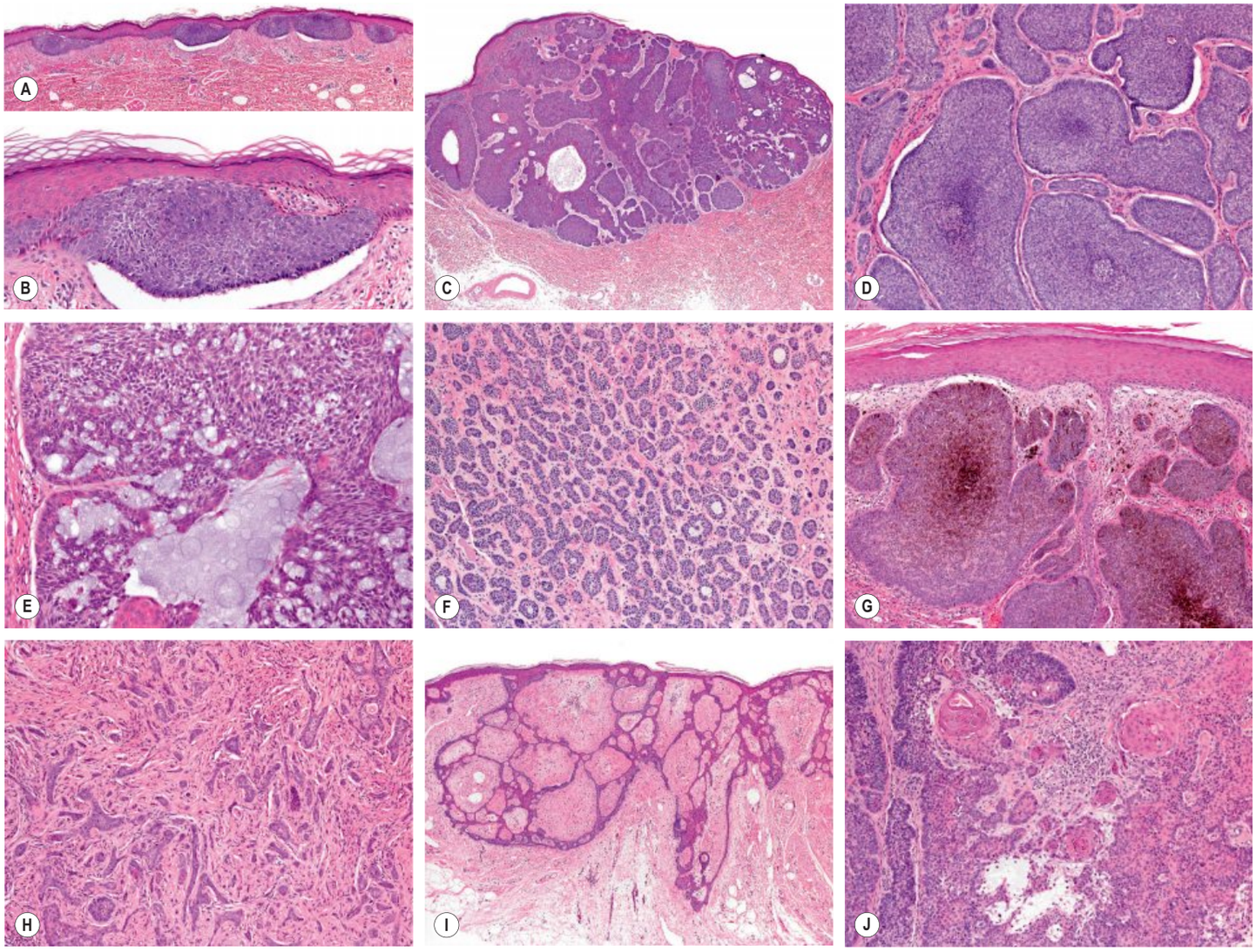


Fig. 108.22 Basal cell carcinoma (BCC): range of histopathologic findings. A *Superficial* type with a few basaloid buds and stromal retraction spaces. **B** A single basaloid aggregation with all the morphologic findings (e.g. peripheral palisading of nuclei, retraction between the tumor and surrounding stroma) characteristic of a *superficial* BCC. **C** *Nodular* BCC with large, partly confluent aggregations of basaloid cells as well as a few cystic spaces. **D** Nodular aggregations of basaloid cells with peripheral palisading and retraction spaces commonly seen in conventional *nodular* BCCs. **E** Nodular aggregations of basaloid cells with mucin deposition within the epithelial component, referred to as *mucinous* BCC. **F** *Micronodular* BCC characterized by numerous, densely packed, small nodular aggregations of basaloid cells. **G** *Pigmented* BCC with nodular aggregations of basaloid cells that contain brown melanin pigment. **H** *Morpheaform* BCC with numerous basaloid strands and cords with an irregular jagged outline embedded within a fibrous stroma. **I** *Fibroepithelial* BCC (fibroepithelioma of Pinkus) with a fenestrated pattern of anastomosing epithelial cords. **J** *Basosquamous* BCC in which both basaloid cells with peripheral palisading and eosinophilic cells with slightly pleomorphic nuclei and foci of keratinization ("horn pearls") are present. *Courtesy Lorenzo Cerroni, MD.*

recurrence), and if the tumor has developed within a site of chronic inflammation or scar. Careful inspection of the surrounding skin to exclude the presence of satellite lesions is necessary, as is examination of the draining lymph nodes, especially for high-risk tumors, since in-transit and distant metastases are more common in these patients. In all patients, a full skin examination is required, to exclude other cutaneous malignancies.

Skin cancers are often identifiable visually by an experienced clinician. Nevertheless, a properly performed biopsy is essential to the diagnosis and management of any lesion. Numerous biopsy techniques, including excisional, incisional, shave, saucerization, and punch, may be employed (see Ch. 146). For obvious skin cancers, especially in elderly patients, a tissue specimen is sometimes obtained at the same time as definitive therapy. If a superficial process (such as a superficial BCC or SCC *in situ*) is suspected, or if shallow therapy (such as curettage and electrodesiccation) is being contemplated, a shave biopsy is usually adequate for establishing a diagnosis. In most other instances, a punch biopsy or deep saucerization that extends to subcutaneous fat is preferred. AKs, on the other hand, are often treated without prior biopsy unless invasive NMSC is suspected; clinical judgment determines which AKs require treatment and which can be left untreated.

For both BCC and cSCC, the pathology report should include an assessment of the histopathologic subtype and status of the surgical margins. If present, ulceration and perineural or vascular involvement should be noted. In cSCC, the degree of differentiation and tumor depth should be assessed; the latter may consist of an anatomic estimate of depth or an actual measurement of tumor thickness in millimeters and can be prognostically useful. Even though clinical responses to immune checkpoint inhibitors have been observed irrespective of programmed cell death-ligand 1 (PD-L1) expression by the tumor cells of cSCC, immunohistochemical staining for PD-L1 is still oftentimes performed as several studies have observed a higher response rate in PD-L1$^+$ tumors[79a,79b].

Based upon clinical and pathologic parameters, a specific tumor may be stratified into a low-risk or high-risk category (Table 108.7). High-risk tumors, particularly SCCs (see Table 108.5), need to be treated aggressively. For larger and deeper tumors, preoperative radiographic imaging studies should be considered. Sentinel lymph node biopsy may provide additional prognostic information, but longer-term studies are needed to determine sensitivity, specificity, and any survival benefit. Because of the risk of post-therapeutic tumor recurrence and the elevated risk for subsequent skin cancers, patients are typically followed regularly for life.

HISTOLOGIC SIMULANTS OF BASAL CELL CARCINOMA (BCC)	
	Major distinguishing features
Adenoid cystic carcinoma	Cribriform pattern; EMA-positive
Ameloblastoma	Location in mouth
Basaloid follicular hamartoma	Multiple small papules; positive family history; loose to fibrotic stroma
Budding of atypical keratinocytes in actinic keratoses (may simulate superficial BCC)	No clefts around tumor complexes
Cloacogenic carcinoma	Anal location
Basaloid induction in epidermis overlaying a dermatofibroma*	Typical features of dermatofibroma in the dermis
Eccrine carcinoma	Small sweat ducts
Folliculocentric basaloid proliferation	Focal follicular budding
Merkel cell carcinoma and other neuroendocrine carcinomas	Punctate keratin (CK20-positive) in cytoplasm; positivity for Merkel cell polyomavirus (subset of cutaneous cases)
Metastatic breast carcinoma	History; single filing; expression of CK7, mammoglobulin, gross cystic disease fluid protein-15
Microcystic adnexal carcinoma	Small keratin cysts, absent stromal retraction, ductal differentiation
Mucinous carcinoma	Pools of mucin with floating basaloid islands
Nevus sebaceus	Basaloid induction; trichoblastomas and BCCs may arise within a nevus sebaceus
Sebaceous carcinoma	Adipophilin-positive sebocytes
Trichoblastoma	Clefts within the stroma; hair germs and papillae; PHLDA1-positive
Trichoepithelioma and desmoplastic trichoepithelioma	Horn cysts, absent stromal retraction, papillary mesenchymal bodies; PHLDA1 positivity; peritumoral CD34 positivity; positive family history when multiple
*Genuine BCC may rarely develop within a dermatofibroma.	

Table 108.6 Histologic simulants of basal cell carcinoma (BCC). CK, cytokeratin; EMA, epithelial membrane antigen.

RISK FACTORS FOR RECURRENCE OF NMSC		
	Low risk	**High risk**
Clinical risk factors		
Location (see Fig. 150.2) and size	Area L <20 mm	Area L ≥20 mm
	Area M <10 mm	Area M ≥10 mm
	Area H <6 mm	Area H ≥6 mm
Borders	Well defined	Poorly defined
Primary vs recurrent	Primary	Recurrent
Tumor at site of prior radiation therapy	Negative	Positive
Tumor at site of chronic inflammatory process (SCC only)	Negative	Positive
Rapidly growing tumor (SCC only)	Negative	Positive
Neurologic symptoms: pain, paresthesia, paralysis (SCC only)	Negative	Positive
Immunosuppression	Negative	Positive
Pathologic risk factors		
Perineural involvement	Negative	Positive
Subtype (BCC only)	Nodular, superficial	Micronodular, infiltrating, sclerosing
Degree of differentiation (SCC only)	Well differentiated	Moderately or poorly differentiated
Desmoplasia (SCC only)	Negative	Positive
Adenoid, adenosquamous, or desmoplastic (SCC only)	Negative	Positive
Tumor thickness (SCC only)	<2 mm	≥2 mm (see text)
Area L: low risk for recurrence: trunk, extremities. **Area M:** middle risk for recurrence: cheeks, forehead, neck, scalp. **Area H:** high risk for recurrence: "mask areas" of face (central face, eyelids, eyebrows, periorbital, nose, lips, chin, mandible, preauricular and postauricular skin/sulci, ear, temple), genitalia, hands, and feet.		

Table 108.7 Risk factors for recurrence of non-melanoma skin cancer (NMSC). BCC, basal cell carcinoma; SCC, squamous cell carcinoma. *Adapted from Miller SJ. The National Comprehensive Cancer Network guidelines of care for nonmelanoma skin cancers. Dermatol Surg 2000;26:289–92 and Brantsch KD, Meisner C, Schonfisch B, et al. Analysis of risk factors determining prognosis of cutaneous squamous-cell carcinoma: a prospective study. Lancet Oncol 2008;9:713–20.*

Surgical and Destructive Procedures

Standard excision

Cutaneous squamous cell carcinoma

Low-risk cSCC should be excised with a surgical margin of 4–6 mm. Standard excision without micrographic assessment of the complete margin (see Fig. 150.1) may be considered for select high-risk tumors, but strong caution is advised. US guidelines of care consider available data insufficient for evaluation of standard excision for high-risk tumors[78].

Basal cell carcinoma

Surgical excision is the standard treatment for most primary BCCs. In 98% of cases of non-morpheaform BCCs <2 cm in diameter, 4-mm margins are adequate for removal[79]. However, for facial lesions, simple excision with narrow margins is often not adequate for effective removal. For high-risk BCCs, US guidelines of care recommend Mohs micrographic surgery[77] while European guidelines recommend a surgical margin of 5–15 mm (depending on tumor characteristics) when micrographic surgery is not available[79].

Curettage alone

Barlow et al.[80] reported a 5-year cure rate of 96% when 302 biopsy-proven BCCs were treated by a single investigator with curettage alone. Minimal hypopigmentation and scarring was observed. If the deep margin of the shave biopsy specimen had >50% involvement with tumor, there was an increased risk of recurrence. Some clinicians combine curettage with application of topical agents such as imiquimod postoperatively.

Curettage with electrodesiccation

Curettage with electrodesiccation is frequently used by dermatologists to treat BCCs. Cure rates as high as 97%–98% have been reported[81], but careful selection of appropriate lesions (e.g. those without extension into the deep dermis) is necessary. In terminal hair-bearing sites, extension of neoplastic cells down follicular structures could also lead to incomplete removal. Curettage and electrodesiccation can be used for smaller SCCs *in situ* and well-differentiated primary SCCs <1 cm in diameter.

Mohs micrographic surgery

Mohs micrographic surgery results in superior histopathologic verification of complete removal of the tumor and allows for maximum conservation of tissue (see Ch. 150). Although Mohs micrographic surgery remains cost-effective when compared to either excisions done in a surgical center or hospital operating room or radiation therapy, it is more expensive than in-office standard excision. In one series of BCCs treated with Mohs micrographic surgery, a recurrence rate of only 1% over 5 years was observed. This was superior to all other modalities, including excision (10%), curettage and desiccation (8%), radiation therapy (9%), and cryotherapy (7.5%). However, percentages do vary

among studies, depending in part on the physicians involved and the types of lesions selected for inclusion.

Although direct comparison of different studies is difficult, Mohs micrographic surgery clearly has the highest cure rate when all tumor types as well as recurrent tumors are taken into consideration[82]. In one series of recurrent BCCs, Mohs micrographic surgery had a long-term recurrence rate of 5.6%, superior to all other modalities, including excision (17%), radiation therapy (10%), and curettage with electrodesiccation (40%). Mohs micrographic surgery is the preferred treatment for morpheaform, poorly demarcated, incompletely removed, or recurrent BCCs, as well as for those sites in which tissue conservation is paramount and there is a need for reliable clear margins. Mohs micrographic surgery is similarly indicated in cases of high-risk primary or recurrent SCC.

Radiation therapy

Radiation therapy is a therapeutic option for patients with a BCC or cSCC who are not well suited for surgery (see Ch. 139)[83,84]. Before choosing this therapy, both function and cosmetic outcome are considered. Advantages include avoidance of an invasive procedure in a patient who may not be able to tolerate surgery or is unwilling to undergo surgery. Disadvantages include lack of margin control, poor cosmesis in some patients, a prolonged course of therapy, and increased risk for future skin cancers. Scars from radiation therapy tend to worsen with time, in contrast to surgical scars, which improve over time.

Radiation is often used as an adjuvant modality following treatment of aggressive or high-risk cSCC with surgery, especially when perineural involvement is identified, to reduce local or locoregional recurrence[84a]. Verrucous carcinomas, which are well differentiated and rarely metastasize, are usually not treated with radiotherapy, since there is concern that cellular transformation may result in a worse prognosis. Radiotherapy is not well suited for morpheaform BCCs, as they are relatively radioresistant, or for patients with BCNS since X-rays can lead to mutations in the second *PTCH* allele, with subsequent tumorigenesis.

Cryosurgery

Cryosurgery is a mainstay of treatment for AKs, but has also been used to treat BCCs and cSCCs (see Ch. 138). It has the advantage of being a relatively easy to perform and quick procedure (particularly in the case of AKs) and is advantageous for those patients wishing to avoid invasive surgery. Complications may include hypertrophic scarring and postinflammatory pigmentary changes. A serious potential adverse outcome is recurrent carcinoma that can become extensive because of concealment by the fibrous scar tissue.

Photodynamic therapy

Photodynamic therapy (PDT) is FDA-approved for the treatment of multiple AKs (see Ch. 135). In the European Union and elsewhere, it is also approved for cSCC *in situ* and BCC. PDT is used primarily for superficial BCCs and occasionally as second-line therapy for nodular BCCs when surgery is not clinically recommended. Guidelines of care address clinical indications, photosensitizer administration, and light exposure specifications[85]. Daylight PDT, which is less painful than classic PDT, can be particularly useful in patients with numerous AKs and field cancerization. In organ transplant recipients, a systematic review found that PDT was the most effective treatment for AKs, when compared to topical imiquimod, ingenol mebutate, diclofenac sodium, and 5-fluoruracil[86]. However, in a randomized trial in immunocompetent patients, topical 5-fluorouracil was more effective than PDT, topical imiquimod, or topical ingenol mebutate for the treatment of AKs[87].

Laser

Laser surgery is an uncommon treatment for BCCs and cSCCs, with limited data in the literature and restriction to low-risk tumors.

Non-Surgical Treatments

Topical therapies

Table 108.8 outlines treatment options for AKs, including the dosing and side effects of FDA-approved topical agents.

5-fluorouracil (5-FU) is used primarily for the treatment of AKs and occasionally for superficial BCCs and selected cSCCs *in situ*. In a randomized trial in immunocompetent patients, 5-FU was more effective for the treatment of AKs than other standard therapies (see above)[87]. Side effects are usually limited to significant local skin reactions (see Ch. 129).

Diclofenac sodium, a nonsteroidal anti-inflammatory drug (NSAID), is also an effective option for the treatment of AKs. However, longer treatment cycles are required.

Imiquimod is a Toll-like receptor 7 agonist whose major side effect is a local skin reaction that can include erosions and crusting (see Ch. 129). The 5% formulation is FDA-approved for the treatment of superficial BCCs while 2.5%, 3.75%, and 5% formulations are approved for non-hypertrophic AKs on the face and scalp. Over a three-year period, imiquimod was superior to diclofenac sodium in clearing AKs and preventing histologic progression and recurrences. However, in a controlled trial evaluating AK treatments, it was less effective than topical 5-FU (see above)[87]. When compared to surgery in a randomly controlled trial of 501 patients with BCCs, tumor clearance was 82.5% in the imiquimod group versus 98% in the surgery group[88]. For SCC *in situ*, clearance rates of 73%–88% at 3–6 months have been reported[89].

Tirbanibulin, a drug that inhibits Src kinase signaling and tubulin polymerization, has been recently approved as a 1% ointment for the treatment of AKs. In two phase III trials, complete clearance of lesions after 5 days of application was observed in 44% to 54% of study participants[90].

Topical agents currently under investigation include the hedgehog pathway inhibitor ***patidegib*** for the treatment of BCCs[91]. Application of 2% or 4% patidegib gel has shown promising results, especially in patients with BCNS. Additional compounds under development for the treatment of AKs are ***sinecatechin***, which is derived from green tea leaves, and ***tuvatexib***, a hexokinase inhibitor.

Combination therapy

Combining more than one therapeutic modality has the potential advantage of enhancing the cure rate while minimizing adverse effects and maximizing cosmetic results. Both topical 5-FU cream and 5% imiquimod cream have been used to pretreat BCC sites prior to Mohs micrographic surgery, leading to a decrease in tumor size before surgical removal. Imiquimod cream has also been used, in conjunction with topical 5-FU cream, for the treatment of cSCC *in situ* in transplant recipients. Excellent cosmetic results have been reported when BCCs were treated with just curettage followed by 6 weeks of topical 5% imiquimod cream. In patients with AKs, combination therapy with calcipotriene (calcipotriol) 0.005% ointment plus 5% 5-FU cream twice daily for four consecutive days led to a response rate of 88%[92]. When PDT was combined with other topical agents (e.g. imiquimod), higher AK clearance rates were observed in comparison to monotherapy[85]; this approach has also been employed for actinic cheilitis.

Chemowraps

To treat multiple AKs, especially on the extremities and in the setting of field cancerization, wraps composed of zinc oxide-impregnated gauze can be used to occlude 5-FU cream[93]. In one series of 25 patients with widespread AKs, a response rate of 60% was achieved following weekly 5-FU chemowraps. Monitoring of patients for severe local reactions and systemic toxicity is recommended[94].

Intralesional treatment

There are reports describing the effectiveness of directly injecting NMSCs with cytostatic drugs such as methotrexate, bleomycin, and 5-FU, or injecting immunomodulators such as interferon alpha 2b, with response rates of about 80%[95]. Because of a limited level of evidence, the use of intratumoral agents should be considered in selected patients (Table 108.9).

Systemic Therapy

Treatment of advanced cutaneous SCC

Systemic therapy is utilized when tumors are neither surgically resectable nor curable by radiotherapy or when metastases have

COMMON TREATMENT OPTIONS FOR ACTINIC KERATOSES

Localized/lesion-targeted treatments*

Lesion-targeted treatment	*Comments*
Liquid nitrogen cryosurgery	• No cutting or anesthesia necessary • 10- to 14-day healing period • Risk of hypopigmentation
Curettage (> curettage + electrodesiccation)	• Requires local anesthesia • Risk of hypopigmentation and scarring (less so if curettage alone)
Shave excision	• Requires local anesthesia • Risk of hypopigmentation and scarring

Topical field treatments†,‡

Although these are the recommended FDA dosing schedules, if the patient develops significant burning with application or significant erosive erythema, the treatment should be held or discontinued

Topical agent	*Dosing*	*Comments*
5-Fluorouracil	• 0.5% cream – apply in the evening × 4 weeks • 1% or 5% cream – apply twice a day for 2–4 weeks • 2% and 5% solutions – apply twice a day for 2–4 weeks • When treating extensor extremities, pretreatment with a topical retinoid for 1–2 weeks may be required or occluded "chemowraps" may be used	• Warn of photosensitivity, which can be severe • Optimal results occur if treatment continues until there is significant inflammation or superficial erosions • Healing usually occurs within 2 weeks of stopping treatment • Solution is best for hair-bearing areas, such as the scalp
Imiquimod	• 2.5% or 3.75% cream – apply at bedtime for 2 weeks; take a 2-week break, and then repeat 2-week application cycle • 5% cream – apply 2 times per week for 16 consecutive weeks • Recommended treatment area is 25 cm^2	• May cause systemic flu-like symptoms • Not recommended if patient has an underlying autoimmune condition • May cause hypopigmentation at the treated site
Diclofenac sodium	• 3% gel – apply twice a day for 90 days • A maximum amount of 8 g daily should not be exceeded	• Do not use if patient is allergic to nonsteroidal anti-inflammatory drugs (NSAIDs) • Although it may have a less severe cutaneous reaction, compliance is an issue given a longer application period
Tirbanibulin	• 1% ointment – apply once daily for 5 consecutive days (face and scalp)	• May have less severe local cutaneous reaction

Procedural field treatments†,‡

Procedure	*Comments*
Photodynamic therapy (PDT; 5-ALA + blue light or red light or day light; MAL + red light or day light)	• Can be painful • Requires 24 hours of no outdoor exposure post-treatment • Relatively quick recovery over 1–2 weeks
Chemical peels (e.g. trichloroacetic acid)	• May require local anesthesia • May cause significant irritation and temporary discoloration • Healing typically over 7 days
Ablative laser techniques (e.g. ablative fractional lasers, erbium:YAG laser)	• Requires local anesthesia • Depending on the technique, recovery period varies • Hypopigmentation a potential complication

*Most appropriate for an isolated or limited number of actinic keratoses.
†Most appropriate for numerous or larger AK lesions.
‡In practice, combination or sequential therapy is sometimes used (e.g. liquid nitrogen to several thicker lesions followed by imiquimod or 5-fluorouracil applied to the entire forehead).

Table 108.8 Common treatment options for actinic keratoses. Addition of calcipotriene (calcipotriol) 0.005% to 5-fluorouracil may increase efficacy and shortens duration of treatment. Other compounds under development are sinecatechin, which is derived from green tea leaves, and tuvatexib, a hexokinase inhibitor. Ingenol mebutate has been removed from the market. ALA, 5-aminolevulinic acid. Daylight-activated PDT is discussed in Ch. 135.

developed. Currently, there are no consensus-based recommendations regarding the best treatment for advanced cSCC.

Immunotherapy with immune checkpoint inhibitors

Response rates of >40% in advanced cSCCs have been reported with anti-PD-1 antibodies including cemiplimab, pembrolizumab, and nivolumab[96]. For example, cemiplimab led to overall response rates (ORRs) of 44% and 45% for locally advanced cSCC and metastatic cSCC, respectively. As a result, cemiplimab is FDA approved for both indications. In patients who received pembrolizumab, ORRs of 42% and 32% were observed in patients with unresectable cSCC and recurrent or metastatic cSCC, respectively; it is now FDA-approved for the latter group of patients. Of note, in more than one study, patients with PD-L1$^+$ tumors had significantly higher response rates than those with negative tumors[79b], leading to the suggestion that immunohistochemical evaluation of PD-L1 be performed when considering immunotherapy. Use of cemiplimab as *neoadjuvant* therapy for stage II to IV cSCC led to a pathologic complete response rate of 51%[96a]. Side effects associated with immune checkpoint inhibitors are reviewed in Chapters 113 and 128.

In patients with advanced cSCC, anti-PD-1 antibodies have resulted in significantly better outcomes when compared to chemotherapeutic agents (e.g. carboplatin, paclitaxel, capecitabine) or tyrosine kinase inhibitors. The epidermal growth factor receptor inhibitor cetuximab, in combination with chemotherapy or radiation therapy, represents a potential second-line regimen for advanced cSCC.

Treatment of advanced BCC

Hedgehog signaling pathway inhibition

As with SCC, advanced BCC is defined as locally advanced or metastatic. When locally advanced, tumors are neither surgically

INTRALESIONAL ADMINISTRATION OF 5-FLUOROURACIL AND METHOTREXATE	
5-Fluorouracil (5-FU; 50 mg/ml)	• Maximum injection: 50–100 mg per lesion per session • Injection every week for 3–8 treatments
Methotrexate (MTX; 25 mg/ml)	• Check renal function prior to administration • Maximum injection: 1 ml per lesion per session • Injections every 2–4 weeks for 1–4 treatments
Both 5-FU and MTX	• Inject into base of lesion and lesion should blanch • Multiple injections into a single lesion may be required (e.g. each quadrant) • To avoid intravascular injection, pull back on syringe

Table 108.9 Intralesional administration of 5-fluorouracil and methotrexate.

resectable (e.g. due to involvement of vital structures) nor curable by radiotherapy. Inactivating mutations in *PTCH1*, *PTCH2*, or *SUFU* or activating mutations in *SMO* lead to activation of the hedgehog signaling pathway and have been associated with the development of BCCs (see Fig. 107.6); mutations in the first three genes can lead to BCNS. The hedgehog pathway inhibitors vismodegib (Fig. 108.23) and sonidegib are quite effective systemic treatments for advanced BCC.

Vismodegib was first reported to have antitumor activity in locally advanced or metastatic BCC in 2009[97]. Of the 33 patients treated with vismodegib in the phase I trial, two had a complete response (6%) while 16 had a partial response (48%). There was a reduction in the number of new BCCs as well as the size of existing BCCs. In further studies, individuals with metastatic BCC and locally advanced BCC had ORRs of ~30% and ~40%–45%, respectively. Nearly all patients in these trials reported adverse reactions (Table 108.10), leading to treatment discontinuation in about 30% of study participants. More recently two intermittent vismodegib regimens have been evaluated in patients with multiple BCCs and BCNS; these individual drug modifications (with non-dosing periods) led to equal efficacy but a lower rate of adverse events[98]. ***Sonidegib***, another hedgehog signaling inhibitor (via smoothened antagonism), also demonstrated efficacy in locally advanced and metastatic BCC.

Immunotherapy with immune checkpoint inhibitors

BCCs contain a high mutational tumor burden due to chronic UV-induced damage to DNA. This leads to an abundance of tumor neoantigens, providing a rationale for the use of immune checkpoint inhibitors, in particular anti-PD-1 antibodies[99]. Pembrolizumab, nivolumab, and cemiplimab have been investigated, and cemiplimab is currently FDA-approved for locally advanced or metastatic BCC in patients previously treated with a hedgehog pathway inhibitor or for whom a hedgehog pathway inhibitor is inappropriate. When cemiplimab was used as second-line therapy for locally advanced BCC (e.g. following development of resistance to hedgehog inhibitors), an ORR of 31% was observed[100]. Neoadjuvant immunotherapy may also be an option with the goal of reducing the size of the BCC thereby enabling subsequent surgical excision[99].

Prophylaxis

In high-risk patients, the most commonly used agents are low-dose acitretin to reduce the number of cSCCs[101] and nicotinamide to reduce the number of AKs and NMSCs[102]. However, in a study of immunosuppressed organ-transplant recipients, oral niacinamide did not lead to a reduction in the number of AKs and NMSCs[102a]. Other options include celecoxib and low-dose capecitabine, an oral prodrug of 5-FU[77–79]. However, the degree of efficacy of these agents remains controversial.

Reduction of immunosuppression

Reduction or cessation of immunosuppressive drugs has been associated with a decrease in the number of skin cancers and improved outcome in patients with pre-existing skin cancers[103]. When immunosuppression is essential, e.g. in organ transplant recipients, use of sirolimus or belatacept can lead to a reduction in NMSCs (see above).

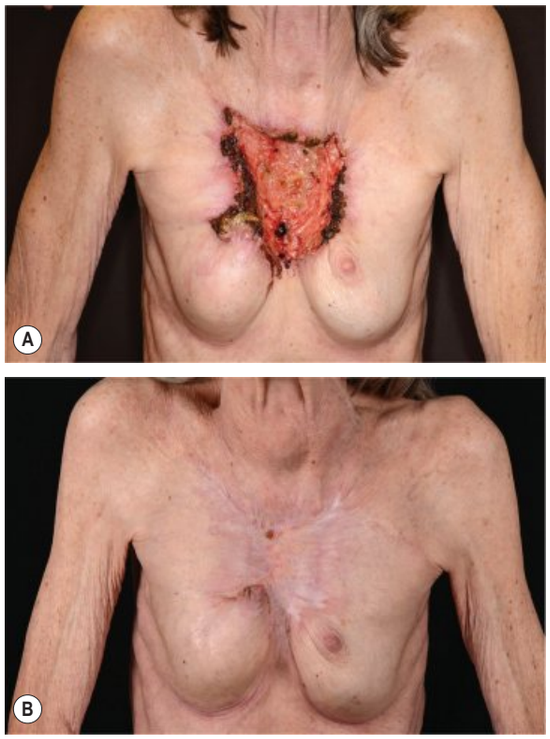


Fig. 108.23 Locally advanced basal cell carcinoma treated with vismodegib. **A** Large ulcerated tumor of the central chest. **B** Nearly complete regression following administration of vismodegib (150 mg daily) for 10 weeks.

SIDE EFFECTS OF VISMODEGIB AND SONIDEGIB	
Common	
• Dysguesia* (>40% of patients)	• Nausea, reduced appetite, and weight loss
• Muscle spasms	• Diarrhea
• Alopecia	• Fatigue
Less common	
• cSCCs, including phenotypic switch of BCC to cSCC	• Keratoacanthomas
• Cough	• Amenorrhea
• Congestive heart failure	• Hyponatremia
• Pneumonia	• Arthralgia
• Thromboembolism	• Pruritus
*Due to altered cell turnover of adult tongue epithelium.	

Table 108.10 Side effects of vismodegib and sonidegib. Both medications can lead to birth defects or fetal death. BCC, basal cell carcinoma; cSCC, cutaneous squamous cell carcinoma.

Prevention

Primary prevention programs focused on lowering UV exposure appear to be having a beneficial effect in reducing the incidence of skin cancer. Consistent use of sunscreens has been shown to decrease the incidence of SCC, but to have no effect or only a weak effect on the incidence of BCC in both immunocompetent individuals and immunocompromised organ transplant recipients[104]. Lastly, educational programs for medical professionals and the public are also important interventions.

Acknowledgment

The editors wish to thank Dr. Darrell S. Rigel for his valuable contributions to this chapter in the previous editions.

Additional figures and tables on Uncommon cutaneous neoplasms that can mimic differentiated or undifferentiated invasive squamous cell carcinoma (SCC), and Histopathologic patterns observed in nodular basal cell carcinomas, available in our eBook (see inside front cover for access code).

REFERENCES

1. Staples MP, Elwood M, Burton RC, et al. Non-melanoma skin cancer in Australia: the 2002 national survey and trends since 1985. *Med J Aust*. 2006;184:6–10.
2. Rogers HW, Weinstock MA, Feldman SR, Coldiron BM. Incidence estimate of nonmelanoma skin cancer (keratinocyte carcinomas) in the US population, 2012. *JAMA Dermatol*. 2015;151:1081–1086.
3. Rigel DS, Friedman RJ, Kopf AW. Lifetime risk for development of skin cancer in the U.S. population: current estimate is now 1 in 5. *J Am Acad Dermatol*. 1996;35:1012–1013.
4. Rogers H, Beveridge M, Puente J, et al. Incidence of nonmelanoma skin cancer in the United States population aged 65 years and older, 2014. *J Am Acad Dermatol*. 2021;85:741–743.
5. Hannuksela-Svahn A, Pukkala E, Karvonen J. Basal cell skin carcinoma and other nonmelanoma skin cancers in Finland from 1956 through 1995. *Arch Dermatol*. 1999;135:781–786.
6. Weinstock MA. Death from skin cancer among the elderly: epidemiological patterns. *Arch Dermatol*. 1997;133:1207–1209.
7. Stern RS. The mysteries of geographic variability in nonmelanoma skin cancer incidence. *Arch Dermatol*. 1999;135:843–844.
8. Halder RM, Bridgeman-Shah S. Skin cancer in African Americans. *Cancer*. 1995;75:667–673.
9. Alam M, Ratner D. Cutaneous squamous-cell carcinoma. *N Engl J Med*. 2001;344:975–983.
10. Bang KM, Halder RM, White JE, et al. Skin cancer in black Americans: a review of 126 cases. *J Natl Med Assoc*. 1987;79:51–58.
11. Kwa RE, Campana K, Moy RL. Biology of cutaneous squamous cell carcinoma. *J Am Acad Dermatol*. 1992;26:1–26.
12. Lukowiak TM, Aizman L, Perz A, et al. Association of age, sex, race, and geographic region with variation of the ratio of basal cell to cutaneous squamous cell carcinomas in the United States. *JAMA Dermatol*. 2020;156:1–7.
13. Harris RB, Griffith K, Moon TE. Trends in the incidence of nonmelanoma skin cancers in southeastern Arizona, 1985–1996. *J Am Acad Dermatol*. 2001;45:528–536.
14. Bickers DR, Lim HW, Margolis D, et al. The burden of skin diseases: 2004 a joint project of the American Academy of Dermatology Association and the Society for Investigative Dermatology. *J Am Acad Dermatol*. 2006;55:490–500.
15. Eder J, Prillinger K, Korn A, et al. Prevalence of actinic keratosis among dermatology outpatients in Austria. *Br J Dermatol*. 2014;171:1415–1421.
16. Green A. Epidemiology of actinic keratosis. *Curr Probl Dermatol*. 2015;46:1–7.
17. Chen GJ, Feldman SR, Williford PM, et al. Clinical diagnosis of actinic keratosis identifies an elderly population at high risk of developing skin cancer. *Dermatol Surg*. 2005;31:43–47.
18. Werner RN, Sammain A, Erdmann R, et al. The natural history of actinic keratosis. *Br J Dermatol*. 2013;169:502–518.
19. Lebwohl M. Actinic keratosis: epidemiology and progression to squamous cell carcinoma. *Br J Dermatol*. 2003;149(Suppl. 66):31–33.
20. Karia PS, Han J, Schmults CD. Cutaneous squamous cell carcinoma: estimated incidence of disease, nodal metastasis, and deaths from disease in the United States, 2012. *J Am Acad Dermatol*. 2013;68:957–966.
21. Weinstock MA. Controversies in the public health approach to keratinocyte carcinomas. *Br J Dermatol*. 2006;154(Suppl. 1):3–4.
22. Misitzis A, Beatson M, Weinstock MA. Keratinocyte carcinoma mortality in the United States as reported in death certificates, 2011–2017. *Dermatol Surg*. 2020;46:1135–1140.
23. Scrivener Y, Grosshans E, Cribier B. Variations of basal cell carcinomas according to gender, age, location and histopathological subtype. *Br J Dermatol*. 2002;147:41–47.
24. Buchanan L, De'Ambrosis B, DeAmbrosis K, et al. Defining incidental perineural invasion: the need for a national registry. *Australas J Dermatol*. 2014;55:107–110.
25. Almahroos M, Kurban AK. Ultraviolet carcinogenesis in nonmelanoma skin cancer. Part I: incidence rates in relation to geographic locations and in migrant populations. *Skinmed*. 2004;3:29–35.
26. Zanetti R, Rosso S, Martinez C, et al. Comparison of risk patterns in carcinoma and melanoma of the skin in men: a multi-centre case-case-control study. *Br J Cancer*. 2006;94:743–751.
27. Kricker A, Armstrong BK, English DR, Heenan PJ. Pigmentary and cutaneous risk factors for non-melanocytic skin cancer – a case-control study. *Int J Cancer*. 1991;48:650–662.
28. Dallas R, English DR, Armstrong BK, et al. Demographic characteristics, pigmentary and cutaneous risk factors for squamous cell carcinoma of the skin: a case-control study. *Int J Cancer*. 1998;76:628–634.
29. Hemminki K, Zhang H, Czene K. Time trends and familial risks in squamous cell carcinoma of the skin. *Arch Dermatol*. 2003;139:885–889.
30. Karagas MR, Stannard VA, Mott LA, et al. Use of tanning devices and risk of basal cell and squamous cell skin cancers. *J Natl Cancer Inst*. 2002;94:224–226.
31. Wehner MR, Shive ML, Chren MM, et al. Indoor tanning and non-melanoma skin cancer: systematic review and meta-analysis. *BMJ*. 2012;345:e5909.
32. American Academy of Dermatology. Indoor tanning. <www.aad.org/media/stats-indoor-tanning>.
33. Hearn RMR, Kerr AC, Rahim KF, et al. Incidence of skin cancers in 3867 patients treated with narrow-band ultraviolet B phototherapy. *Br J Dermatol*. 2008;159:931–935.
34. Stern RS, Liebman EJ, Vakeva L. Oral psoralen and ultraviolet-A light (PUVA) treatment of psoriasis and persistent risk of nonmelanoma skin cancer. PUVA follow-up study. *J Natl Cancer Inst*. 1998;90:1278–1284.
35. Lichter MD, Karagas MR, Mott LA, et al. Therapeutic ionizing radiation and the incidence of basal cell carcinoma and squamous cell carcinoma. The New Hampshire Skin Cancer Study Group. *Arch Dermatol*. 2000;136:1007–1011.
36. Shore RE, Moseson M, Xue X, et al. Skin cancer after X-ray treatment for scalp ringworm. *Radiat Res*. 2002;157:410–418.
37. Loney T, Paulo MS, Modenese A, et al. Global evidence on occupational sun exposure and keratinocyte cancers: a systematic review. *Br J Dermatol*. 2021;184:208–218.
38. Miura K, Olsen CM, Rea S, et al. Do airline pilots and cabin crew have raised risks of melanoma and other skin cancers? Systematic review and meta-analysis. *Br J Dermatol*. 2019;181:55–64.
39. Yuspa SH. Cutaneous chemical carcinogenesis. *J Am Acad Dermatol*. 1986;15:1031–1044.
40. Lei U, Masmas TN, Frentz G. Occupational non-melanoma skin cancer. *Acta Derm Venereol*. 2001;81:415–417.
41. Wong SS, Tan KC, Goh CL. Cutaneous manifestations of chronic arsenicism: review of seventeen cases. *J Am Acad Dermatol*. 1998;38:179–185.
42. Ramezani M, Baharzadeh F, Almasi A, Sadeghi M. A systematic review and meta-analysis: evaluation of the β-human papillomavirus in immunosuppressed individuals with cutaneous squamous cell carcinoma. *BioMedicine*. 2020;10:1–10.
43. Rollison DE, Viarisio D, Amorrortu RP, et al. An emerging issue in oncogenic virology: the role of beta human papillomavirus types in the development of cutaneous squamous cell carcinoma. *J Virology*. 2019;93:e01003–18..
44. Boilesen DR, Nielsen KN, Holst PJ. Novel antigenic targets of HPV therapeutic vaccines. *Vaccines*. 2021;9:1262.
45. Berg D, Otley CC. Skin cancer in organ transplant recipients: epidemiology, pathogenesis, and management. *J Am Acad Dermatol*. 2002;47:1–17.
46. Comeau S, Jensen L, Cockfield SM, et al. Non-melanoma skin cancer incidence and risk factors after kidney transplantation: a Canadian experience. *Transplantation*. 2008;86:535–541.
47. Dantal J, Morelon E, Rostaing L, et al. Sirolimus for secondary prevention of skin cancer in kidney transplant recipients: 5-year results. *J Clin Oncol*. 2018;36:2612–2620.
48. Hoogendijk-van den Akker JM, Harden PN, Hoitsma AJ, et al. Two-year randomized controlled prospective trial converting treatment of stable renal transplant recipients with cutaneous invasive squamous cell carcinomas to sirolimus. *J Clin Oncol*. 2013;31:1317–1323.
49. Wang M, Mittal A, Colegio OR. Belatacept reduces skin cancer risk in kidney transplant recipients. *J Am Acad Dermatol*. 2020;82:996–998.
50. Menzies S, O'Leary E, Callaghan G, et al. Declining incidence of keratinocyte carcinoma in organ transplant recipients. *Br J Dermatol*. 2019;181:983–991.
51. Peyrin-Biroulet L, Khosrotehrani K, Carrat F, et al. Increased risk for nonmelanoma skin cancers in patients who receive thiopurines for inflammatory bowel disease. *Gastroenterology*. 2011;141:1621–1628.
52. Goncalves JCN, Macedo AC, Madeira K, et al. Accuracy of anal cytology for diagnosis of precursor lesions of anal cancer: systematic review and meta-analysis. *Dis Colon Rectum*. 2019;62:112–120.
53. Eworuke E, Haug N, Bradley M, et al. Risk of nonmelanoma skin cancer in association with use of hydrochlorothiazide-containing products in the United States. *JNCI Cancer Spectr*. 2021;5:pkab009.
54. Freiman A, Bird G, Metelitsa AI, et al. Cutaneous effects of smoking. *J Cutan Med Surg*. 2004;8:415–423.
55. Granger RH, Blizzard L, Fryer JL, Dwyer T. Association between dietary fat and skin cancer in an Australian population using case-control and cohort study designs. *BMC Cancer*. 2006;6:141.
56. McNaughton SA, Marks GC, Green AC. Role of dietary factors in the development of basal cell cancer and squamous cell cancer of the skin. *Cancer Epidemiol Biomarkers Prev*. 2005;14:1596–1607.
57. Ibiebele TI, van der Pols JC, Hughes MC, et al. Dietary fat intake and risk of skin cancer: a prospective study in Australian adults. *Int J Cancer*. 2009;125:1678–1684.
58. Sturm RA. Skin colour and skin cancer – MC1R, the genetic link. *Melanoma Res*. 2002;12:405–416.
59. Gold NB, Campbell IM, Sheppard SE, Tan W-H. Proposed criteria for nevoid basal cell carcinoma syndrome in children assessed using statistical optimization. *Sci Rep*. 2021;11:19791.
60. Park H-S, Papanastasi E, Blanchard G, et al. ARP-T1-associated Bazex-Dupré-Christol syndrome is an inherited basal cell cancer with ciliary defects characteristic of ciliopathies. *Commun Biol*. 2021;4:544.
61. Schierbeck J, Vestergaard T, Bygum A. Skin cancer associated genodermatoses: a literature review. *Acta Derm Venereol*. 2019;99:360–369.
62. Marcil I, Stern RS. Risk of developing a subsequent nonmelanoma skin cancer in patients with a history of nonmelanoma skin cancer: a critical review of the literature and meta-analysis. *Arch Dermatol*. 2000;136:1524–1530.
63. Marghoob AA, Slade J, Salopek TG, et al. Basal cell and squamous cell carcinomas are important risk factors for cutaneous malignant melanoma. Screening implications. *Cancer*. 1995;75:707–714.
64. Nugent Z, Demers AA, Wiseman MC, et al. Risk of second primary cancer and death following a diagnosis of nonmelanoma skin cancer. *Cancer Epidemiol Biomarkers Prev*. 2005;14:2584–2590.
65. Chen J, Ruczinski I, Jorgensen TJ, et al. Nonmelanoma skin cancer and risk for subsequent malignancy. *J Natl Cancer Inst*. 2008;100:1215–1222.
66. Barton V, Armeson K, Hampras S, et al. Nonmelanoma skin cancer and risk of all-cause and cancer-related mortality: a systematic review. *Arch Dermatol Res*. 2017;309:243–251.
67. Willenbrink TJ, Ruiz ES, Cornejo CM, et al. Field cancerization: definition, epidemiology, risk factors, and outcomes. *J Am Acad Dermatol*. 2020;83:709–717.
68. Ruiz ES, Karia PS, Besaw R, Schmults CD. Performance of the American Joint Committee on Cancer Staging Manual, 8th Edition vs the Brigham and Women's Hospital tumor classification system for cutaneous squamous cell carcinoma. *JAMA Dermatol*. 2019;155:819–825.
69. Shahriari N, Grant-Kels JM, Rabinovitz H, et al. Reflectance confocal microscopy: diagnostic criteria of common benign and malignant neoplasms, dermoscopic and histopathologic correlates of key confocal criteria, and diagnostic algorithms. *J Am Acad Dermatol*. 2021;84:17–31.
70. Ogawa T, Kiuru M, Konia TH, Fung MA. Acantholytic squamous cell carcinoma is usually associated with hair follicles, not acantholytic actinic keratosis, and is not "high risk": diagnosis, management, and clinical outcomes in a series of 115 cases. *J Am Acad Dermatol*. 2017;76:327–333.
71. Brantsch KD, Meisner C, Schonfisch B, et al. Analysis of risk factors determining prognosis of cutaneous squamous-cell carcinoma: a prospective study. *Lancet Oncol*. 2008;9:713–720.
72. Ko C, Glusac EJ, McNiff JM, et al. Squamous proliferations on the legs of women: qualitative examination of histopathology, TP53 sequencing, and implications for diagnosis in a series of 30 cases. *J Am Acad Dermatol*. 2017;77:1126–1132.
73. Fernández-Figueras MT, Malvehi J, Tschandl P, et al. Position paper on a simplified histopathological classification of basal cell carcinoma: results of the European Consensus Project. *J Eur Acad Dermatol Venereol*. 2022;36:351–359.

74. Ackerman AB, Reddy VB, Soyer HP. *Neoplasms with Follicular Differentiation*. New York: Ardor Scribendi; 2001.
75. Reiter O, Mimouni I, Dusza S, et al. Dermoscopic features of basal cell carcinoma and its subtypes: a systematic review. *J Am Acad Dermatol*. 2021;85:653–664.
76. Yeh I, McCalmont TH, LeBoit PE. Differential expression of PHLDA1 (TDAG51) in basal cell carcinoma and trichoepithelioma. *Br J Dermatol*. 2012;165:1106–1110.
77. Bichakjian C, Armstrong A, Baum C, et al. Guidelines of care for the management of basal cell carcinoma. *J Am Acad Dermatol*. 2018;78:540–559.
78. Alam M, Armstrong A, Baum C, et al. Guidelines of care for the management of cutaneous squamous cell carcinoma. *J Am Acad Dermatol*. 2018;78:560–578.
79. Peris K, Fargnoli MC, Garbe C, et al. Diagnosis and treatment of basal cell carcinoma: European consensus-based interdisciplinary guidelines. *Eur J Cancer*. 2019;118:10–34.

79a. Migden MR, Khushalani NI, Chang ALS, et al. Cemiplimab in locally advanced cutaneous squamous cell carcinoma: results from an open-label, phase 2, single-arm trial. *Lancet Oncol*. 2020;21:294–305.

79b. Maubec E, Boubava M, Petrow P, et al. Phase II study of pembrolizumab as first-line, single-drug therapy for patients with unresectable cutaneous squamous cell carcinomas. *J Clin Oncol*. 2020;38:3051–3061.

80. Barlow JO, Zalla MJ, Kyle A, et al. Treatment of basal cell carcinoma with curettage alone. *J Am Acad Dermatol*. 2006;54:1039–1045.
81. Spiller WF, Spiller RF. Treatment of basal cell epithelioma by curettage and electrodesiccation. *J Am Acad Dermatol*. 1984;11:808–814.
82. Xiong DD, Beal BT, Varra V, et al. Outcomes in intermediate-risk squamous cell carcinomas treated with Mohs micrographic surgery compared with wide local excision. *J Am Acad Dermatol*. 2020;82:1195–1204.
83. Cho M, Gordon L, Rembielak A, Woo TC. Utility of radiotherapy for treatment of basal cell carcinoma: a review. *Br J Dermatol*. 2014;171:968–973.
84. Stratigos AJ, Garbe C, Dessinioti C, et al. European interdisciplinary guideline on invasive squamous cell carcinoma of the skin: Part 2. Treatment. *Eur J Cancer*. 2020;128:83–102.

84a. Stevenson ML, Criscito MC, Wilken R, et al. Use of adjuvant radiotherapy in the treatment of high-risk cutaneous squamous cell carcinoma with perineural invasion. *JAMA Dermatol*. 2020; 156:918–921.

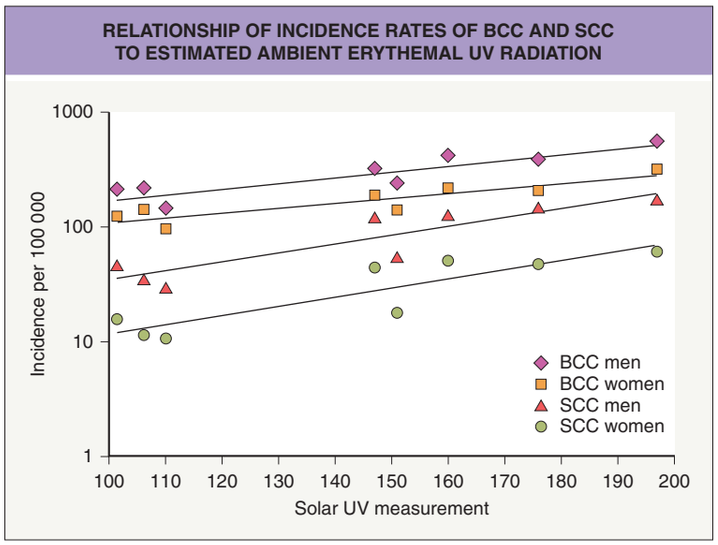
85. Morton CA, Szeimies RM, Basset-Seguin N, et al. European Dermatology Forum guidelines on topical photodynamic therapy 2019 Part 1: treatment delivery and established indications – actinic keratoses, Bowen's disease and basal cell carcinomas. *J Eur Acad Dermatol Venereol*. 2019;33:2225–2238.
86. Heppt MV, Steeb T, Niesert AC, et al. Local interventions for actinic keratosis in organ transplant recipients: a systematic review. *Br J Dermatol*. 2019;180:43–50.
87. Jansen MHE, Kessels JPHM, Nelemans PJ, et al. Randomized trial of four treatment approaches for actinic keratosis. *N Engl J Med*. 2019;380:935–946.
88. Williams HC, Bath-Hextall F, Ozolins M, et al. Surgery versus 5% imiquimod for nodular and superficial basal cell carcinoma: 5-year results of the SINS randomized controlled trial. *J Invest Dermatol*. 2017;137:614–619.
89. Love WE, Bernhard JD, Bordeaux JS. Topical imiquimod or fluorouracil therapy for basal and squamous cell carcinoma: a systematic review. *Arch Dermatol*. 2009;145:1431–1438.
90. Blauvelt A, Kempers S, Lain E, et al. Phase 3 trials of tirbanibulin ointment for actinic keratosis. *N Engl J Med*. 2021;384:512–520.
91. Cosio T, Di Prete M, Di Raimondo C, et al. Patidegib in dermatology: a current review. *Int J Mol Sci*. 2021;22:10725.
92. Cunningham TJ, Tabacchi M, Eliane J-P, et al. Randomized trial of calcipotriol combined with 5-fluorouracil for skin cancer precursor immunotherapy. *J Clin Invest*. 2017;127:106–116.
93. Goon PKC, Clegg R, Yong ASW, et al. 5-Fluorouracil "chemowraps" in the treatment of multiple actinic keratoses: a Norwich experience. *Dermatol Ther (Heidelb)*. 2015;5:201–205.
94. Peuvrel L, Saint-Jean M, Quereux G, et al. 5-Fluorouracil chemowraps for the treatment of multiple actinic keratoses. *Eur J Dermatol*. 2017;27:635–640.
95. Metterle L, Nelson C, Patel N. Intralesional 5-fluorouracil (5-FU) as a treatment for nonmelanoma skin cancer (NMSC): a review. *J Am Acad Dermatol*. 2016;74:552–557.
96. Sadowsky LM, Kosche C, West DP, Choi JN. Current evidence for safety and efficacy of anti-programmed cell-death 1 agents in the treatment of cutaneous squamous cell carcinoma: a systematic review. *J Am Acad Dermatol*. 2020;82:522–524.

96a. Gross ND, Miller DM, Khushalani NI, et al. Neoadjuvant cemiplimab for stage II to IV cutaneous squamous-cell carcinoma. *N Engl J Med*. 2022;387:1557–1568.

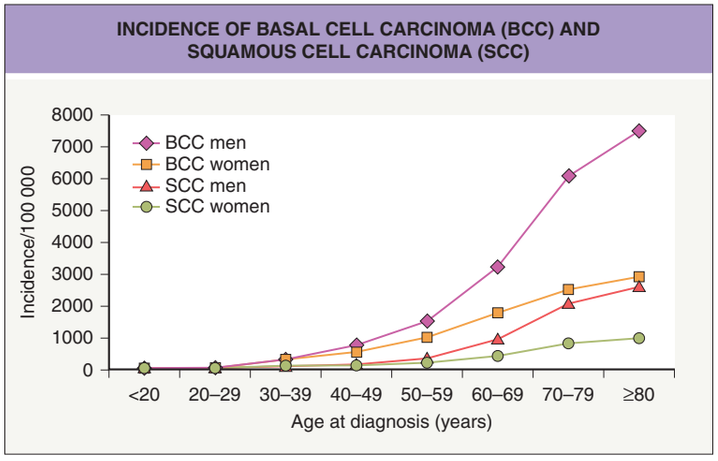
97. Von Hoff DD, LoRusso PM, Rudin CM, et al. Inhibition of the hedgehog pathway in advanced basal-cell carcinoma. *N Engl J Med*. 2009;361:1164–1172.
98. Dréno B, Kunstfeld R, Hauschild A, et al. Two intermittent vismodegib dosing regimens in patients with multiple basal-cell carcinomas (MIKIE): a randomised, regimen-controlled, double-blind, phase 2 trial. *Lancet Oncol*. 2017;18:401–412.
99. Ligtenberg KG, Hu JK, Damsky W, et al. Neoadjuvant anti-programmed cell death 1 therapy for locally advanced basal cell carcinoma in treatment-naïve patients: a case series. *JAAD Case Rep*. 2020;6:628–633.
100. Stratigos AJ, Sekulic A, Peris K, et al. Cemiplimab in locally advanced basal cell carcinoma after hedgehog inhibitor therapy: an open-label, multi-centre, single-arm phase II trial. *Lancet Oncol*. 2021;22:848–857.
101. Harwood CA, Leedham-Green M, Leigh IM. Low-dose retinoids in the prevention of cutaneous squamous cell carcinomas in organ transplant recipients. A 16-year retrospective study. *Arch Dermatol*. 2005;141:456–464.
102. Chen AC, Martin AJ, Choy B, et al. A phase 3 randomized trial of nicotinamide for skin-cancer chemoprevention. *N Engl J Med*. 2015;373:1618–1626.

102a. Allen NC, Martin AJ, Snaidr VA, et al. Nicotinamide for skin-cancer chemoprevention in transplant recipients. *N Engl J Med*. 2023;388:804–812.

103. Otley CC, Maragh SL. Reduction of immunosuppression for transplant-associated skin cancer: rationale and evidence of efficacy. *Dermatol Surg*. 2005;31:163–168.
104. Collins A, Savas J, Doerfler L. Nonsurgical treatments for nonmelanoma skin cancer. *Dermatol Clin*. 2019;37:435–441.



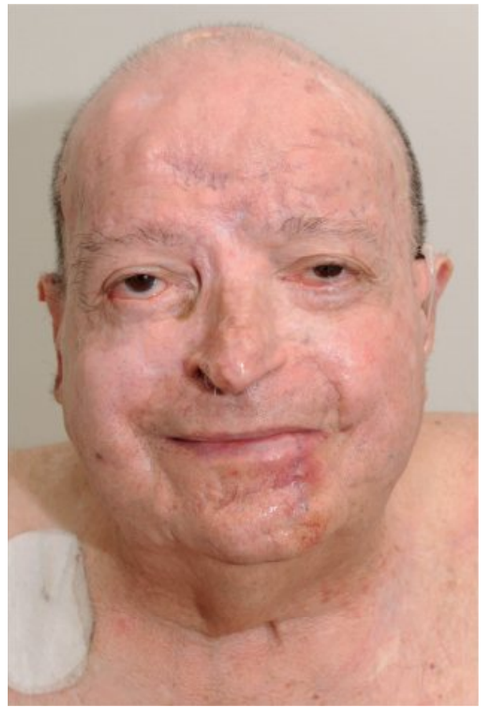
eFig. 108.1 Relationship of incidence rates of basal cell carcinoma (BCC) and squamous cell carcinoma (SCC) to estimated ambient erythemal UV radiation as measured in ten cities in the US. *From Armstrong BK, Kricker A. J Photochem Photobiol B 2001;63:8–18.*



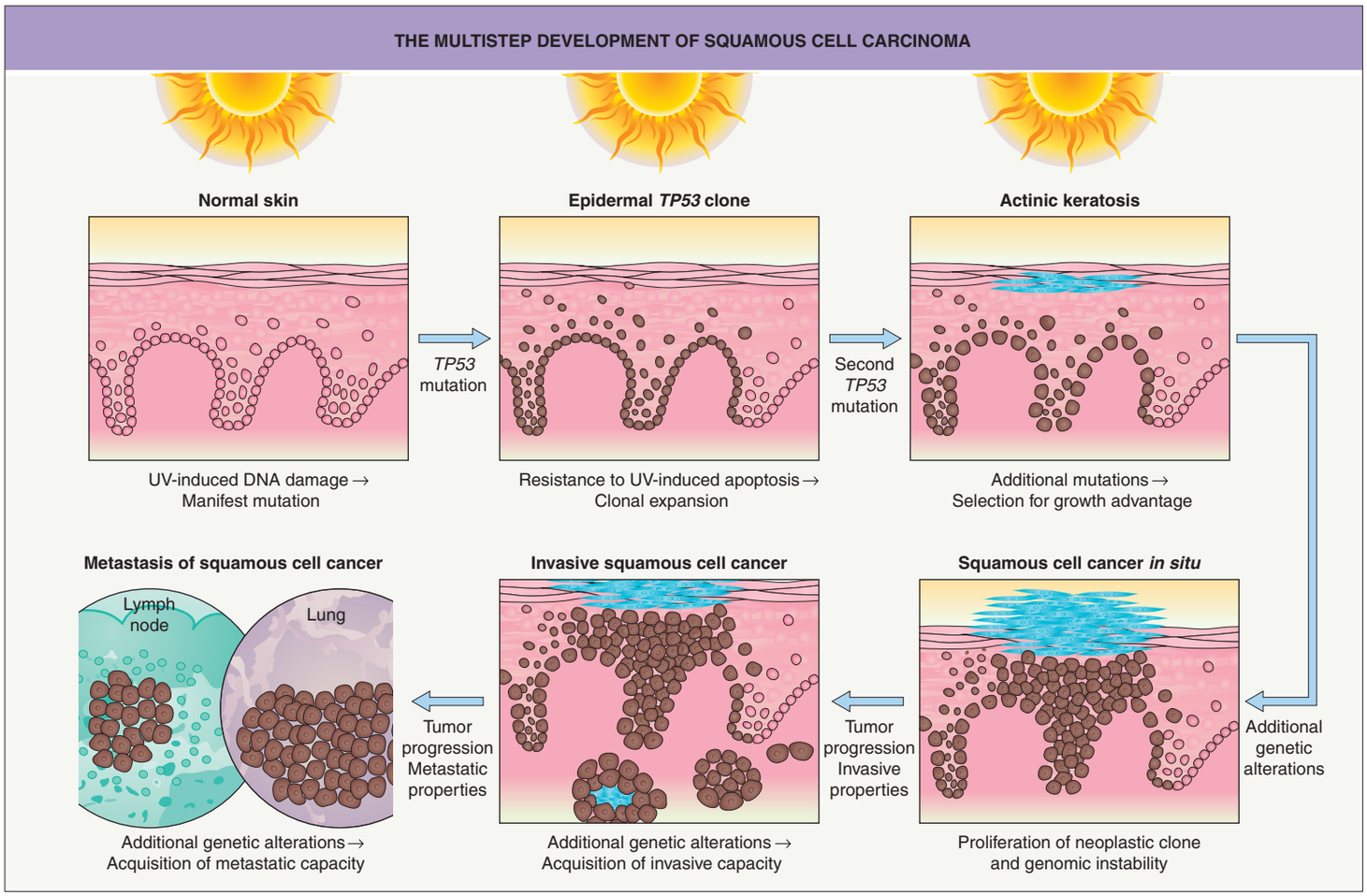
eFig. 108.2 Incidence of basal cell carcinoma (BCC) and squamous cell carcinoma (SCC) by age and sex.



eFig. 108.3 Basal cell nevus syndrome (BCNS). Three superficial BCCs and one large nodular BCC on the chest of a younger man.



eFig. 108.4 Basal cell nevus syndrome. Frontal bossing and hypertelorism, with multiple scars from previous excisions of BCCs.



eFig. 108.5 The multistep development of squamous cell carcinoma. UV irradiation of normal skin induces mutations in keratinocytes and facilitates clonal expansion of keratinocytes with a mutated *TP53* gene. Additional mutations (including a second *TP53* mutation) that affect genes controlling proliferation, cell migration and cell death provide for selective growth advantage and cause genomic instability. The final result is metastatic tumor cells, capable of growing in regional lymph nodes and internal organs.



eFig. 108.6 Actinic keratoses (AKs). Numerous hypertrophic AKs on the bald scalp with hypopigmentation at sites of previous treatment.



eFig. 108.7 Actinic cheilitis. Erosions, scaling and leukoplakia of the lower vermilion lip. *Courtesy Carl M. Allen, MD.*



eFig. 108.8 Squamous cell carcinoma *in situ* (Bowen disease). Pink plaque with white scale and a hemorrhagic crust arising within photodamaged skin. *Courtesy Kalman Watsky, MD.*



eFig. 108.9 Cutaneous horn arising within a squamous cell carcinoma *in situ* on the helix. *Courtesy Kalman Watsky, MD.*



eFig. 108.10 Squamous cell carcinoma *in situ* of the nail unit. Hyperkeratosis and hemorrhagic crusting of the lateral nail bed and nail fold. *Courtesy Kalman Watsky, MD.*



eFig. 108.11 Pigmented squamous cell carcinoma *in situ* (Bowen disease). This lesion may be diagnosed as a cutaneous melanoma clinically. The pink depressed area is a biopsy site. *Courtesy Kalman Watsky, MD.*





eFig. 108.12 Clinical spectrum of cutaneous squamous cell carcinoma (SCC). A A large keratotic nodule of the supraorbital region in an elderly woman; note the coarse wrinkling and solar elastosis of the face. **B** Firm, eroded, red plaque on the scrotum; histopathologically, the SCC was moderately differentiated.







eFig. 108.13 Clinical spectrum of cutaneous squamous cell carcinoma (SCC). A Smooth-surfaced erythematous nodule in the preauricular area. **B** Large scaly plaque developing in a background of photodamage and actinic keratoses on the dorsal hand. **C** Pink verrucous plaque arising within a burn scar.



eFig. 108.14 Squamous cell carcinoma (SCC) of the lower lip. The patient subsequently died from metastatic SCC. Note the severe solar elastosis.



eFig. 108.15 Recurrent squamous cell carcinoma in a patient who had received a solid organ transplant. *Courtesy John Carucci, MD.*







eFig. 108.16 Keratoacanthomas. A,B Rapidly growing, erythematous crateriform nodules with a rolled border and central keratotic core**. C** Central ulceration rather than keratotic core. Lesions may be tender and note the yellow color in **B**.



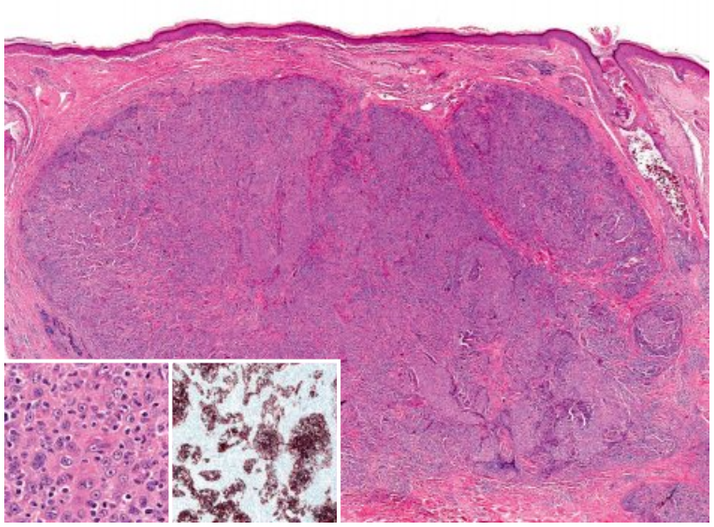
eFig. 108.17 Keratoacanthoma. Giant keratoacanthoma with a yellow–red color and a history of rapid growth.



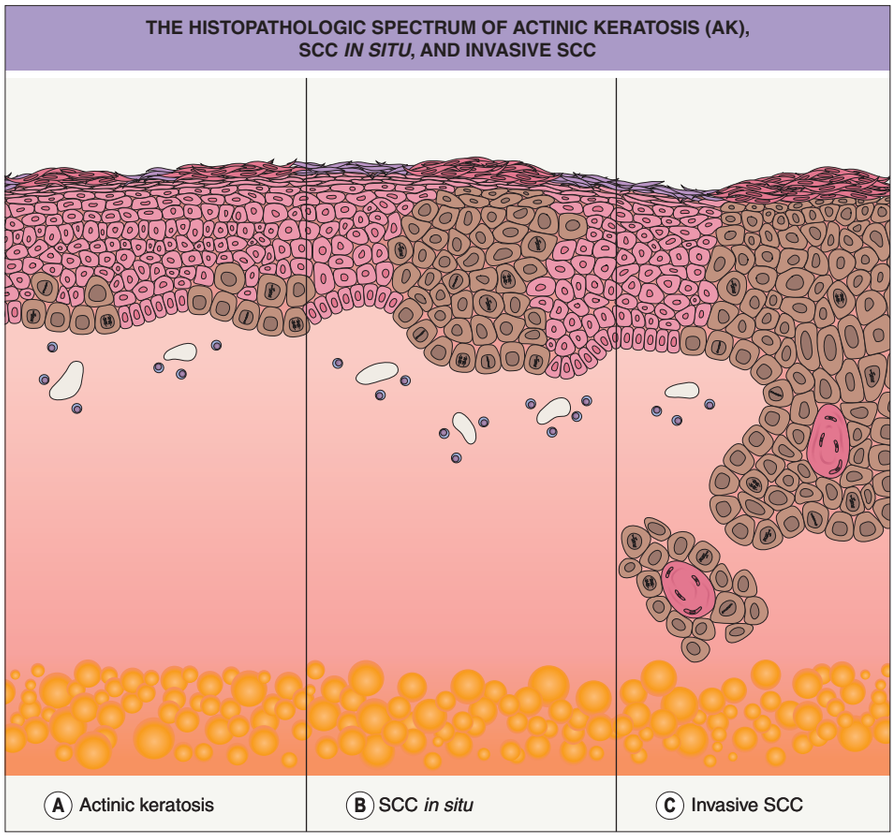
eFig. 108.18 Generalized eruptive keratoacanthomas (Grzybowski). *Courtesy Maria Paula Migliorini, MD, and Renata Scarabucci Janones, MD.*



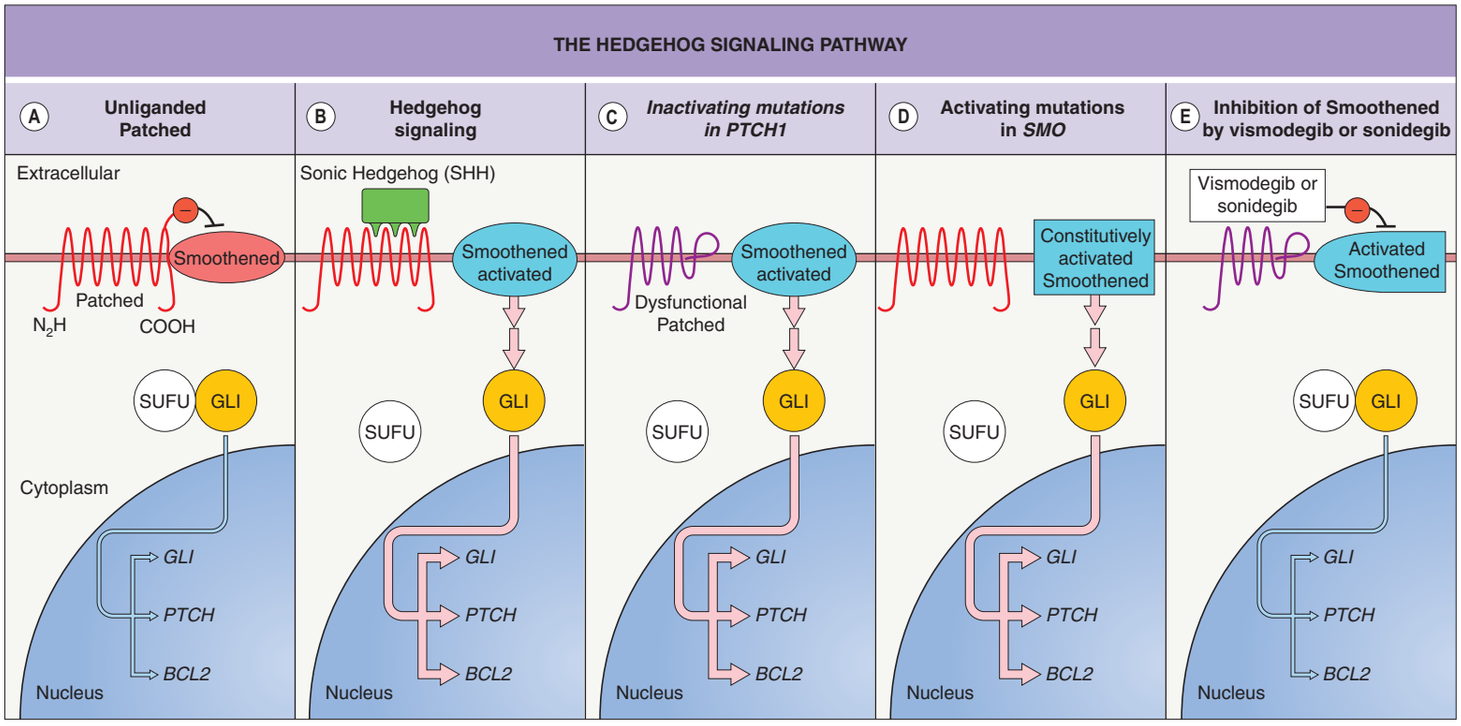
eFig. 108.19 Verrucous carcinoma, Buschke–Löwenstein variant. Large, cauliflower-like tumor in the genital region. *Courtesy Helmut Kerl, MD.*



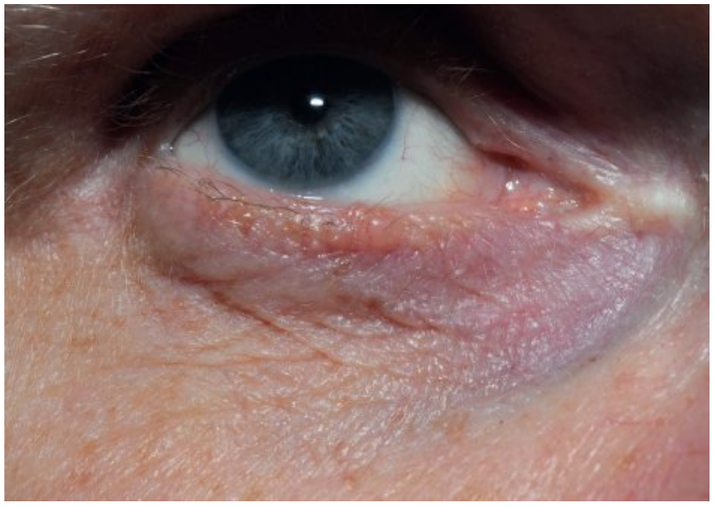
eFig. 108.20 Lymphoepithelioma – histopathologic features. A dermal tumor without a connection to the epidermis, comprised of mononuclear cells with vesicular nuclei and prominent nucleoli (inset left) that are admixed with large numbers of small lymphocytes, focally masking the tumor complexes. A staining for pan-cytokeratin (inset right) highlights the neoplastic epithelial cells. *Courtesy Lorenzo Cerrroni, MD*.



eFig. 108.21 The histopathologic spectrum of actinic keratosis (AK), SCC *in situ*, and invasive SCC. A An AK consists of a lower epidermal proliferation of cytologically abnormal keratinocytes; the adnexal epithelium is notably spared. **B** In SCC *in situ*, the atypical keratinocytes occupy the entire epidermis and intraepidermal portion of adnexal structures, without invasion into the dermis. **C** Invasive SCC is distinguished by the extension of the malignant keratinocytes into the dermis. If an invasive SCC is clinically suspected, the biopsy specimen should be deep enough to determine the extent of dermal invasion.



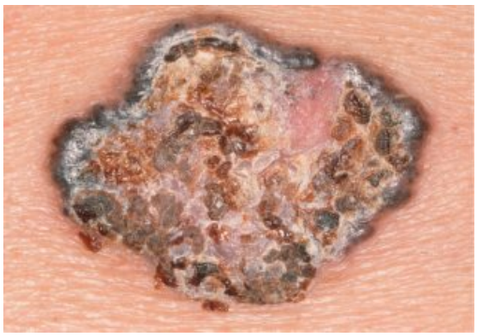
eFig. 108.22 The Hedgehog signaling pathway. A Unbound Patched silences Smoothened (SMO) signaling. **B** As Hedgehog binds to its receptor Patched, the repression of SMO is removed and signals are transduced via GLI to the nucleus. **C** Inactivating mutations in *PTCH* lead to dysfunctional Patched and this simulates Hedgehog binding and results in constitutive activation of GLI and downstream target genes. **D** An activating mutation in *SMO* results in constitutive signaling to GLI and downstream target genes. Such mutations are detected in sporadic BCCs in which *PTCH1* is intact. **E** Vismodegib and sonidegib are inhibitors of SMO that have been used to treat patients with BCNS as well as metastatic or locally advanced BCCs (see Fig. 108.23). At least 50% of advanced BCCs develop resistance to vismodegib, commonly via acquiring mutations in *SMO*.



eFig. 108.23 Subtle papules of basal cell carcinoma of the eyelid margin.
Courtesy Kalman Watsky, MD.



eFig. 108.24 Superficial basal cell carcinoma. An erythematous plaque that may resemble dermatitis. The trunk is a common location for this type of basal cell carcinoma. *Courtesy Rhonda Pomerantz, MD.*



eFig. 108.25 Pigmented basal cell carcinoma. In addition to the admixture of scale and hemorrhagic crusts centrally, there is a translucent and black rolled border superiorly.



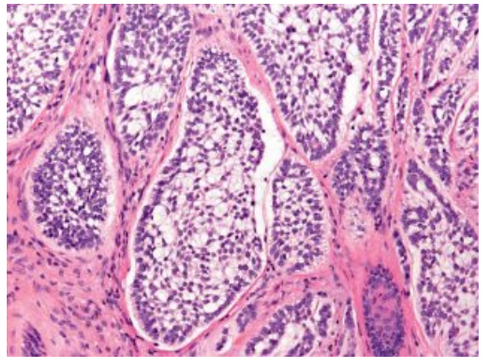
eFig. 108.26 Fibroepithelioma of Pinkus. This soft, skin-colored to light pink, broad, sessile nodule on the lower back representing a fibroepithelial BCC is adjacent to a classic nodular BCC.



eFig. 108.27 Fibroepithelioma of Pinkus. Soft, skin-colored, sessile plaque on the lower back.



eFig. 108.28 Dermoscopy of a nodular basal cell carcinoma. Pearly pink papule above the eyebrow. Dermoscopy shows telangiectatic vessels, erythema, and cystic spaces (inset).



eFig. 108.29 Histopathologic features of a clear cell basal cell carcinoma. Basaloid aggregations with pronounced clear cell differentiation. *Courtesy Lorenzo Cerroni, MD.*

UNCOMMON CUTANEOUS NEOPLASMS THAT CAN MIMIC DIFFERENTIATED OR UNDIFFERENTIATED INVASIVE SQUAMOUS CELL CARCINOMA (SCC)	
Neoplasm	**Clues to the diagnosis/comments**
Adnexal carcinomas	
• Microcystic adnexal carcinoma	Evidence of ductal differentiation Perineural infiltration in deeper areas Luminal CEA positivity in the ducts
• Syringomatous carcinoma	Evidence of ductal differentiation Perineural infiltration in deeper areas Luminal CEA positivity in the ducts
Atypical fibroxanthoma	Often a diagnosis of exclusion Some authors consider it to be an undifferentiated variant of SCC CD10 (+), CK (–), Melan-A (–), SOX10 (–), S100 (–) Sometimes SMA (+)
Carcinosarcoma	May be an undifferentiated SCC Stromal cells are pan-CKs (+), e.g. AE1/AE3, MNF116
Desmoplastic melanoma	Melanoma *in situ* may be present at dermal–epidermal junction Patchy lymphoid aggregates S100 (+), SOX-10 (+), p75 (+)
Epithelioid angiosarcoma	Hemorrhage and focal vascular lumina ERG (+), CD31 (+) podoplanin (+); may be CK (+)
Leimyosarcoma, undifferentiated	Evidence of smooth muscle differentiation in more differentiated areas SMA (+), desmin (+)
Lymphoepithelial-like carcinoma	May be an undifferentiated SCC CK (+) in the cellular aggregates within the lymphoid nodules

eTable 108.1 Uncommon cutaneous neoplasms that can mimic differentiated or undifferentiated invasive squamous cell carcinoma (SCC). See Table 122.4 for evaluation of cutaneous metastases. CEA, carcinoembryonic antigen; CK, cytokeratin; SMA, smooth muscle actin.

HISTOPATHOLOGIC PATTERNS OBSERVED IN NODULAR BASAL CELL CARCINOMAS			
I. Epithelial patterns		**II. Cytologic characteristics**	
Adamantinoid	Labyrinthine	***Nuclear features***	***Cytoplasmic features***
Adenoid	Macronodular	Bowenoid	Basosquamous
Adenoid–cystic (adeno-cystic)	Micronodular	Cuboid	Clear
Anastomosing	Multimicrocystic	Oval	Granular
Arboriform	Nodular	Round	Signet-ring
Cribriform (sieve-like)	Petaloid	Spindle	Scant
Columnar	Racemiform	**III. Non-epithelial (stromal) findings**	
Cord-like	Retiform (reticulated)	Amyloid	Keloidal tissue
Comedo-like	Strand-like	Calcification	Mucin deposition
Cystic	Trabecular	Cartilaginous metaplasia	Osseous metaplasia
Frond-like	Tubular	Fibrosis (fibroplasia)	Sclerosis
Fenestrated		Granulation tissue-like	

eTable 108.2 Histopathologic patterns observed in nodular basal cell carcinomas. Adapted from ref. 74.

Benign Epidermal Tumors and Proliferations 109

Luis Requena, Celia Requena and Clay J. Cockerell

Chapter Contents

Solar Lentigo 1911
Seborrheic Keratosis 1913
Lichenoid Keratosis 1916
Dermatosis Papulosa Nigra 1917
Stucco Keratosis 1917
Porokeratosis 1918
Flegel Disease 1922
Acrokeratosis Verruciformis 1923
Cutaneous Horn 1923
Clear Cell Acanthoma 1923
Inverted Follicular Keratosis 1925
Warty Dyskeratoma 1925
Acantholytic (Dyskeratotic) Acanthoma 1926
Epidermolytic Acanthoma 1926
Large Cell Acanthoma 1927
Epidermal Nevus 1928
Inflammatory Linear Verrucous Epidermal Nevus 1929
Nevus Comedonicus 1930
Acanthosis Nigricans 1931
Nevoid Hyperkeratosis of the Nipple and Areola 1931
Confluent and Reticulated Papillomatosis 1931
Terra Firma-Forme Dermatosis 1932
Clear Cell Papulosis 1932

The majority of entities in this chapter can be further classified according to the algorithm in Fig. 109.1.

SOLAR LENTIGO

Synonyms: ■ Lentigo senilis ■ Liver spot ■ Senile freckle

Key features

- Tan to brown to black macules in sites of exposure to UVR
- Histologically, the rete ridges often have club-shaped or bud-like extensions, in addition to increased basal layer pigmentation
- Solar lentigines and macular seborrheic keratoses exist along a continuum

Epidemiology

Solar lentigines are present in 90% of White individuals over the age of 60 years, and their incidence increases with advancing age. They also occur, but less often, in younger individuals and in Asians as a consequence of acute or chronic sun exposure. Inherited patterned lentiginosis favors African-Americans with lighter skin phototypes, including those with mixed Native American heritage.

Pathogenesis

Solar lentigines result from epidermal hyperplasia, with variable proliferation of melanocytes and accumulation of melanin within keratinocytes, in response to chronic exposure to UVR. Similar to seborrheic keratoses, activating somatic mutations in *FGFR3* and *PIK3CA* have been detected in solar lentigines (Table 109.1)[1]. As with ephelides, variants in the melanocortin-1 receptor gene are also linked to the development of solar lentigines.

Clinical Features

Solar lentigines are well-circumscribed, round, oval or irregularly shaped macules that vary in color from tan to dark brown or black. More lightly pigmented lesions are usually homogeneous, whereas darker ones tend to have a mottled appearance. Solar lentigines almost always present as multiple lesions. They usually vary in diameter from 3 mm to 2 cm and can become confluent. Solar lentigines occur in sun-exposed sites, predominantly the dorsal aspects of the hands and forearms, face, upper trunk, and shins (Fig. 109.2A).

By tangential lighting, a reticulated pigment pattern may be appreciated, and Wood's lamp illumination enhances both visible and inapparent lesions. The dermoscopic features of a solar lentigo may include the following: a diffuse light brown structureless area, sharply demarcated and/or moth-eaten borders, fingerprinting, and a reticular pattern with thin lines that are occasionally short and interrupted[2]. A particular variant that has been termed hypermelanotic or "ink spot" solar lentigo is characterized by a striking jet-black color and a stellate outline. By dermoscopy, a black branching pattern is seen.

While solar lentigines may fade slightly after cessation of exposure to UVR, they usually persist indefinitely. Solar lentigines have been shown to be an independent risk factor for the development of cutaneous melanoma. Histologic overlap suggests that both lichenoid keratoses and reticulated seborrheic keratoses can evolve from solar lentigines.

Associated Diseases and Special Forms

A PUVA (psoralen + UVA) lentigo is a well-defined hyperpigmented macule that commonly develops in individuals undergoing long-term PUVA photochemotherapy (see Ch. 134). These lentigines can arise in any site exposed to UVA light and often persist for years after discontinuation of PUVA therapy. In contrast to solar lentigines, PUVA lentigines usually exhibit a darker brown color and more of a stellate appearance, clinical features that may suggest cutaneous melanoma. Histologically, PUVA lentigines display lentiginous hyperplasia of large melanocytes that often exhibit mild cytologic atypia and often contain *BRAF* mutations[3]. Numerous solar lentigines are also seen in patients with xeroderma pigmentosum, and they are often an initial cutaneous finding (see Ch. 87).

Pathology

The rete ridges often have club-shaped or bud-like extensions (Fig. 109.2B), as well as branching or fusing of rete ridges, forming a reticulated pattern. The epidermis between the rete ridges may appear thinned. There is increased basal layer pigmentation, especially in the basaloid cells of the rete ridges, and the lesional keratinocytes are larger than those of adjacent, non-involved epidermis. In some (but not all) cases, the melanocytes are slightly increased in number. Melanocytes in DOPA-stained sections of solar lentigines exhibit increased melanogenesis, and these cells have more numerous as well as longer and thicker dendritic processes than the melanocytes

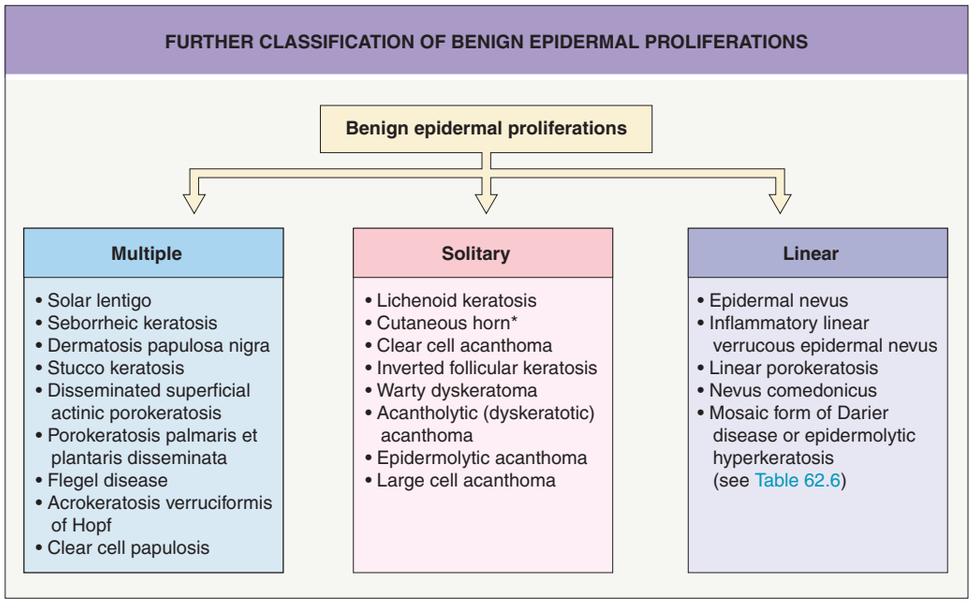


Fig. 109.1 Further classification of benign epidermal proliferations. Although the term solitary lichenoid keratosis is sometimes used, patients may develop multiple lesions, especially those with skin phototypes I or II and significant actinic damage. *When arising from a verruca or seborrheic keratosis.

SOMATIC ACTIVATING MUTATIONS IN BENIGN EPIDERMAL TUMORS

Tumor	Gene(s)
Solar lentigines	*FGFR3**, *PIK3CA*†
PUVA lentigines	*BRAF*
Seborrheic keratoses	*FGFR3*, *PIK3CA* > *KRAS*, *HRAS*, *EGFR*, *AKT1*
Lichenoid keratosis‡	*FGFR3*, *PIK3CA*, *HRAS* > *KRAS*
Dermatosis papulosa nigra	*FGFR3*
Stucco keratoses	*PIK3CA*
Epidermolytic acanthoma	*KRT10*
Acantholytic (dyskeratotic) acanthoma	*ATP2A2*, *ATP2C1*
Epidermal nevi with hyperkeratosis, acanthosis and papillomatosis (but no epidermolytic hyperkeratosis) histologically; also referred to as non-epidermolyic verrucous epidermal nevi (NEVEN) or keratinocytic epidermal nevi (see Table 62.6)	*FGFR3*, *FGFR2*, *PIK3CA*, *HRAS* > *KRAS* > *NRAS*; primarily in syndromic forms: *AKT1*, *PTEN* > *BRAF*
Acneiform nevus (Munro acne nevus)	*FGFR2*
Nevus comedonicus	*NEK9*
See Table 62.6 for genes underlying nevus sebaceus and epidermal nevi with epidermolytic hyperkeratosis, acantholytic dyskeratosis, or associated overgrowth syndromes	

*Germline mutations in this gene lead to skeletal dysplasia syndromes associated with acanthosis nigricans.
†Germline mutations in this gene are often lethal, but occasionally can lead to a Cowden syndrome-like phenotype.
‡Related to benign lentigo, SK, or actinic keratosis; the latter can have *RAS* mutations.

Table 109.1 Somatic activating mutations in benign epidermal tumors. Phosphatidylinositol-4,5-bisphosphate 3-kinase functions downstream of FGFR3. FGFR3, fibroblast growth factor receptor 3; NEK9, NIMA-related kinase 9; PIK3CA, phosphatidylinositol-4,5-bisphosphate 3-kinase, catalytic subunit alpha.



Fig. 109.2 Solar lentigines. A Multiple, round to irregularly shaped, brown macules on the dorsal aspect of the hands in an older woman. **B** The rete ridges have club-shaped extensions and the epidermis between the rete ridges appears thinned. There is increased basal layer pigmentation, but the number of melanocytes is normal or only slightly increased. *B, Courtesy Lorenzo Cerroni, MD.*

of normal skin. The superficial dermis often contains melanophages and occasionally a mild perivascular infiltrate of lymphocytes. Solar elastosis is also prominent. Electron microscopic studies reveal abundant melanosome complexes in keratinocytes which appear to be larger than in normal surrounding skin.

Differential Diagnosis

The clinical differential diagnosis of a solar lentigo includes an ephelid, macular seborrheic keratosis, pigmented actinic keratosis, lentigo maligna, simple lentigo, junctional melanocytic nevus, and large cell acanthoma. Table 112.1 outlines the similarities and differences between solar lentigines and ephelides. There is essentially a continuum extending from solar lentigo to macular seborrheic keratosis. The presence of a keratotic surface and horn cysts points to a seborrheic keratosis. Pigmented actinic keratoses are more likely to have a scaly rough surface. Lentigo maligna often exhibits greater variation in pigmentation and irregularity of borders compared with solar lentigo, and by dermoscopy, rhomboidal structures and irregular pigmented

dots around hair follicles can be seen, in particular on the face. Simple lentigines are often smaller and more heavily pigmented than solar lentigines, and they arise during childhood with less relationship to UVR exposure (see Ch. 112).

Treatment

Although a solar lentigo is a benign lesion of cosmetic concern only, it is an indication of cumulative UVR exposure which dictates monitoring of the patient for cutaneous carcinomas. Bleaching agents (e.g. hydroquinone) are not effective. Both cryotherapy and laser surgery (e.g. frequency doubled Q-switched Nd:YAG) can lead to significant improvement[4], but caution must be used to prevent post-treatment dyspigmentation. Preventive measures include sunscreens, physical barriers, and limitation of sun exposure.

SEBORRHEIC KERATOSIS

Key features

- Common benign lesions that typically begin to appear during the fourth decade of life
- Develop anywhere except mucous membranes, palms, and soles
- Tan to black, macular, papular or verrucous lesions; often have a waxy "stuck-on" appearance
- May become irritated or inflamed
- Large variation in clinical appearance and can simulate melanocytic neoplasms

Introduction

Seborrheic keratoses (SKs) are common benign skin lesions that are almost ubiquitous among older individuals. They develop in hair-bearing skin, invariably sparing the mucosal surfaces and the palms and the soles. Thus, SKs can appear on the head and neck, extremities, and trunk, especially the upper back and submammary region (in women).

Many clinical and histologic variants of SK have been described, and although they are usually easily recognized clinically, some lesions may prove difficult to diagnose by inspection alone, so biopsy for histopathologic examination may be required. This is especially true when there is a history of recent change or if there is inflammation. Larger dark lesions are sometimes biopsied when there is concern about the possibility of melanoma, but with the advent of dermoscopy, nowadays this occurs less frequently.

History

The date of the initial description of SKs is uncertain. In 1927, Freudenthal delineated their clinical and histologic features.

Epidemiology

Autosomal dominant inheritance with incomplete penetrance has been postulated to explain an apparent familial predisposition. Despite their frequent occurrence, there are few large-scale statistical analyses regarding prevalence or sex and racial predilection. In part, this is because epidemiologic studies often view SKs as coincidental findings. They have been reported to be more common in White populations and to affect men and women equally[5]. Their appearance prior to the fourth decade is uncommon, with lesions continuing to develop throughout one's lifetime.

Pathogenesis

SKs are considered a sign of aging and overexpression of amyloid precursor protein within SKs has been reported. While SKs can occur in sun-protected sites (e.g. inframammary fold), sun exposure has also been implicated in their development. Supporting evidence comes from the more frequent occurrence and earlier age of onset of SKs in individuals residing in tropical climates. An Australian study found a higher prevalence of SKs within sun-exposed areas in contrast to non-sun-exposed areas in the same subjects. A higher frequency and an earlier age of onset were also observed in their Australian study group population compared to a UK study group[6].

Alterations in the distribution of epidermal growth factor receptors have been observed in SKs, and based upon androgen receptor polymorphisms, a clonal origin was detected in over half of lesions evaluated, suggesting a neoplasm rather than hyperplasia[7]. Importantly, similar to solar lentigines, somatic activating mutations in two genes – *FGFR3*, which encodes fibroblast growth factor receptor 3[8], and *PIK3CA*, whose protein product is the alpha subunit of phosphoinositide-3-kinase[9] – have been detected within SKs (see Table 109.1). The enhanced activity of these two proteins leads to increased AKT activity[10]. Less frequently, mutations in *KRAS*, *HRAS*, *EGFR*, and *AKT1* oncogenes as well as within the promoters for *TERT* and *DPH3* have been identified.

In irritated SKs, apoptosis within areas of squamous differentiation has been implicated as a cause of the irritation[11]. Although SKs are often clinically verrucous, human papillomavirus (HPV) has been detected infrequently, except in lesions in the genital region. It is likely that these latter lesions actually represent condyloma acuminatum, as the two entities may appear similar both clinically and histopathologically[12].

Clinical Features

Although occasionally solitary, SKs more commonly present as multiple, pigmented, sharply marginated lesions. On the back, raindrop-like and streaming patterns can be seen (Fig. 109.3). SKs may be macules, papules, or plaques, depending on their stage of development. Even within the same lesion there may be a marked variation in color. They are usually light brown in color but may appear white to waxy yellow



Fig. 109.3 Seborrheic keratoses. A Multiple seborrheic keratoses of the posterior trunk that vary in size and color. **B** Sharply demarcated, pigmented papule and plaques with a papillomatous surface and pseudohorn cysts. Note the "stuck-on" appearance.

to brown–black. SKs typically evolve from a macule and may progress to become papular or verrucous. Keratotic plugging, a "stuck-on" appearance, and/or overlying scale are helpful features in distinguishing SKs from melanocytic neoplasms, noting that occasionally keratotic plugging can be seen in compound and intradermal melanocytic nevi. Dermoscopic features are reviewed in Ch. 0.

Individual lesions may be of any size but usually measure about 1 cm in diameter. They can become quite large, i.e. >5 cm in diameter. SKs may become inflamed or irritated due to friction or trauma, but rarely from secondary bacterial infection. Although usually asymptomatic, irritated or inflamed lesions can become tender, pruritic, erythematous, crusted, and rarely, pustular. Sometimes inflammation reflects an underlying diathesis, e.g. psoriasis.

Spontaneous regression, although observed, is not a common feature of SKs, even following inflammation. With trauma, the lesion may crumble, explaining reports of SKs "falling off". Conditions associated with an abrupt appearance or increase in number of lesions, followed by regression when the condition resolves, include pregnancy, coexisting inflammatory dermatoses (in particular erythroderma)[13], and malignancy (next section)[14].

Seborrheic Keratosis and Malignancy

Instances of malignant neoplasms arising within and adjacent to SKs were reported as early as 1932[15]. Invasive and *in situ* squamous cell carcinoma (SCC), cutaneous melanoma, basal cell carcinoma (BCC), and keratoacanthoma have all been observed in association with SKs. This most likely represents a coincidental neoplasm developing within adjacent skin, i.e. a collision lesion, although it is possible that the various cell types present in an SK could develop into their respective neoplasms. In theory, the basaloid cells could give rise to BCC, the spinous cells to SCC, and melanocytes to melanoma[15]. While several histopathologic studies have found BCC to be the most frequently associated neoplasm[15], the neoplasms most commonly misdiagnosed clinically as SKs were SCC *in situ* (e.g. 60 [1.4%] of 4310 specimens[16]) and invasive SCC. In one investigation, 4.6% of SCCs were clinically diagnosed as SKs, and in some of these, features of SK were seen in association with the SCC. The "collision" theory, when two distinct neoplasms develop separately at the same site, has been proposed as a possible explanation for this occurrence, especially given the prevalence of keratinocyte carcinomas and SKs in the population at large[17]. Others believe that BCCs and SKs are both derived from the infundibular portion of the hair follicle, cells of which could evolve into either neoplasm, and in some cases, both concurrently.

The sign of Leser–Trélat is a rare cutaneous marker of internal malignancy, most commonly adenocarcinomas of the gastrointestinal tract and less often other solid organ malignancies and lymphoma. It is considered to be a paraneoplastic cutaneous syndrome characterized by an abrupt and striking increase in the number and/or size of SKs occurring before, during, or after an internal malignancy has been detected[18,19]. Associated pruritus has been documented in over 40% of cases and the majority of the lesions are located on the back, followed by the extremities, face, and abdomen[20,21]. Malignant acanthosis nigricans, another paraneoplastic syndrome, may appear at the same time or shortly after the sign of Leser–Trélat in ~20% of patients[20].

Since its initial description in 1900, the validity of the sign of Leser–Trélat as a reliable marker of internal malignancy has been challenged, given the frequency of both neoplasia and SKs in the elderly population, in whom the condition is usually observed[21]. Its description is also loosely defined, which is problematic as there are no standards for quantifying the number of lesions required for the diagnosis. In addition, determining the magnitude of a patient-reported increase in number can be difficult. The few studies investigating SKs and their link with internal malignancy have largely been inconclusive. One retrospective review examined 1752 consecutive patients with the diagnosis of SK, and of these, 62 individuals were diagnosed with an internal malignancy within 1 year before or after the diagnosis of SK. Of those 62 patients, six patients presented with findings consistent with the sign of Leser–Trélat. However, an age- and sex-matched control group demonstrated similar findings[22].

The pathogenesis of the sign of Leser–Trélat is uncertain, but it is thought to be related to secretion of a growth factor by the neoplasm which leads to epithelial hyperplasia[20], as in malignant acanthosis nigricans. To qualify as a paraneoplastic process, the cutaneous findings need to coincide with the presence of the malignancy, resolve when the primary tumor is excised or successfully treated, and reappear with its recurrence or metastasis, i.e. fulfill Curth's postulates (see Ch. 53).

Pathology

There are at least six histologic types of SK: acanthotic, hyperkeratotic, reticulated, irritated, clonal, and melanoacanthoma. Different histopathologic features are often present in the same lesion, resulting in diverse appearances. There are varying degrees of hyperkeratosis, acanthosis, and papillomatosis. Pseudohorn cysts, the product of cross-sectioned epidermal invaginations, are highly characteristic, though not invariably present. Generally, the base of an SK lies on a flat horizontal plane flanked by normal epidermis. The characteristic acanthosis is the result of an accumulation of benign squamous and basaloid keratinocytes, typically projecting outward and upward in an irregular fashion. The sharp demarcation at the base of most lesions has been called the "string" sign. The marked papillomatosis and hyperkeratosis are often likened to "church spires" with shadows of retained cornified material at their peaks.

The squamous cells of many SKs are representative of those found in the normal-appearing epidermis, but some SKs may contain basaloid cells that have a smaller size, uniform appearance, and large oval-shaped nuclei. When slight intercellular edema is present, intercellular bridges are easily visualized. Cytologic atypia is usually not a feature of most SKs. Mild keratinocyte atypia and mitotic figures, when present, are usually associated with irritation and inflammation. The papillary dermis in most instances is unremarkable.

The *acanthotic* SK is the most common histologic type. It usually presents as a smooth-surfaced, dome-shaped papule. Slight hyperkeratosis and papillomatosis are often present, while the greatly thickened epidermis typically contains a preponderance of basaloid cells (Fig. 109.4A). Papillae may be narrow in some lesions, while others may be composed of interwoven aggregates of epithelial cells surrounding islands of connective tissue in a retiform pattern. Invaginated pseudohorn cysts are most prevalent in this variant. Melanin is often increased in the acanthotic type of SK; it is primarily concentrated within keratinocytes, having been transferred from neighboring melanocytes. Deeply pigmented lesions contain abundant melanin in basaloid cells.

The *hyperkeratotic* type of SK, also known as a digitated, serrated or papillomatous type, is almost the morphologic reverse of the acanthotic type. Acanthosis is present but there is more prominent hyperkeratosis and papillomatosis (Fig. 109.4B). A preponderance of squamous cells relative to basaloid cells is seen. Abundant pigmentation is unusual, and keratinizing pseudocysts are observed less frequently than in acanthotic SKs. The hyperkeratotic type is the variant often described as having epidermal projections resembling "church spires", a finding also seen in acrokeratosis verruciformis.

The *reticulated* or *adenoid* type of SK is characterized histologically by delicate strands of epithelium that extend from the epidermis in an interlacing pattern (Fig. 109.4C). They are composed of a double row or more of basaloid cells that may be hyperpigmented. Pseudohorn cysts, although less common than in the acanthotic variant, may be observed. Often, a solar lentigo is seen at the lateral margins of the lesion, supporting the notion that reticulated SK evolves from a solar lentigo.

A lymphoid infiltrate is often present in the dermis of *inflamed* or *irritated* SKs (Fig. 109.4D). It may be perivascular, diffuse, or lichenoid. Spongiosis is often present and there may be necrosis of keratinocytes. Squamous eddies are common findings as well and these consist of whorls of eosinophilic keratinocytes. Irritated SKs often lack the sharply demarcated horizontal base seen with most SKs.

Clonal SKs are considered by some to represent a variant of irritated SK. The clonal, or nested, type of SK is characterized by having well-defined nests of loosely packed cells within the epithelium (Fig. 109.4E). The nests are composed predominantly of variably sized keratinocytes that are often paler than adjacent cells and have a uniform appearance. Nests may also contain melanocytes.

There is a rare variant of SK with numerous basal clear cells that histologically can mimic melanoma *in situ*[23,24]. However, these clear cells demonstrate negative immunostaining for Melan-A/MART-1, MITF, SOX10, and S100 protein.

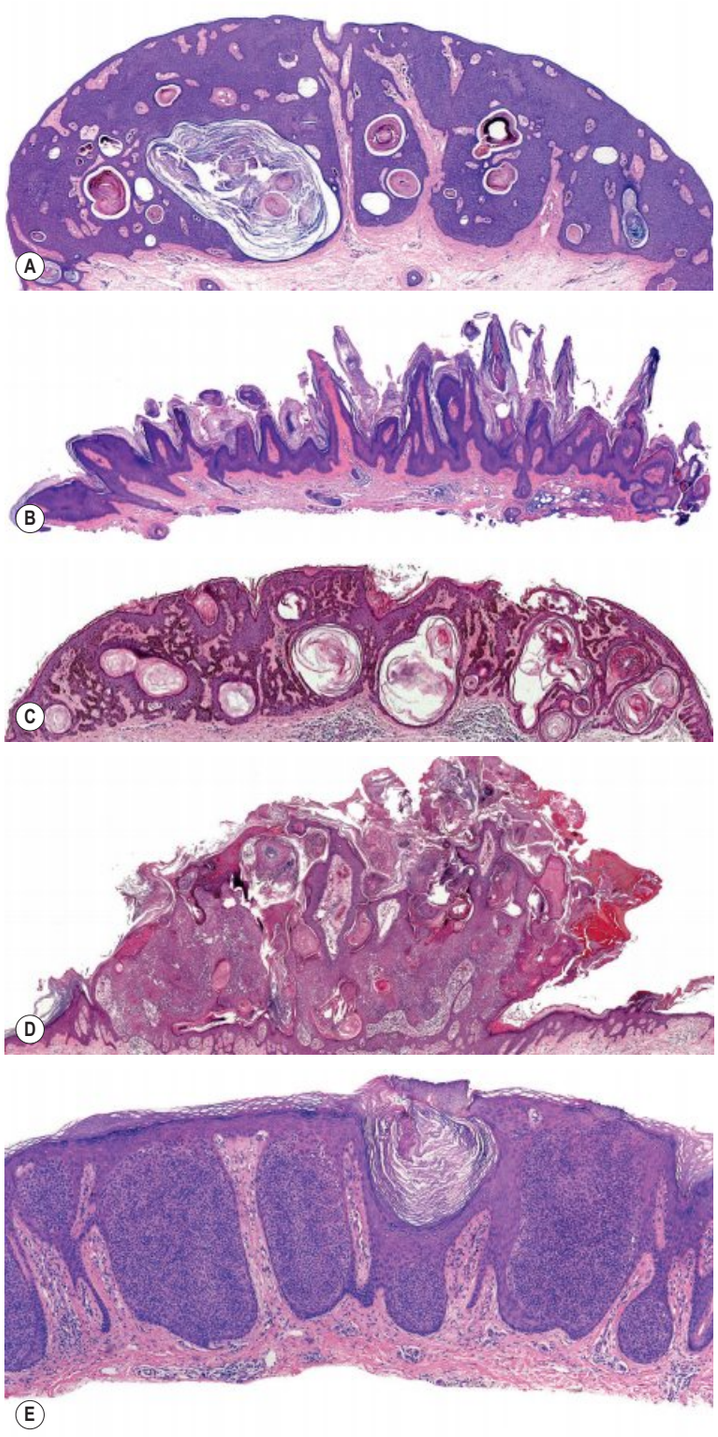


Fig. 109.4 Seborrheic keratoses (SKs) – spectrum of histologic subtypes. **A** Acanthotic type with lobular hyperplasia with prominent horn cysts. **B** Papillomatous or hyperkeratotic type with church spires of papillomatosis and hyperkeratosis. **C** Reticulated or adenoid type with delicate, lace-like strands of interconnecting epithelium and interspersed pseudohorn cysts. **D** Irritated seborrheic keratosis. Exophytic lesion with papillomatosis, hyperkeratosis, hemorrhagic crust, and dermal inflammation. Mild keratinocyte atypia and mitotic figures, when present in SKs, are usually associated with irritation and inflammation. **E** Clonal type with Borst–Jadassohn phenomenon characterized by well-demarcated nests of keratinocytes within the epidermis. *C, D, Courtesy Lorenzo Cerroni, MD.*

Differential Diagnosis

Most SKs are easily identified clinically, although there are entities that may have a similar appearance. Conditions thought to be variants of SKs include dermatosis papulosa nigra, stucco keratoses, and inverted follicular keratoses. They are discussed in this chapter under their respective headings. The clinical differential diagnosis of SK includes solar lentigo, verruca vulgaris, condyloma acuminatum, Bowen disease, SCC, melanocytic nevus, melanoma, acrochordon, and tumor of the follicular infundibulum.

Clinical differentiation between macular SKs, solar lentigines, and melanocytic neoplasms such as melanoma may at times be impossible. Solar lentigines are neither keratotic nor elevated, but some are considered to represent an incipient reticulated type of SK. Over time, solar lentigines can develop into SKs as the buds of pigmented basaloid cells become thicker and there is greater acanthosis. Dermoscopy can prove useful in distinguishing these entities (see Ch. 0).

A review of 20 cases of verrucous melanoma demonstrated how difficult it may be to distinguish between benign and malignant tumors. Of interest, 50% of these verrucous melanomas were thought to represent SKs clinically and a histopathologic diagnosis of a benign nevus was assigned to 10%. A broad spectrum of histopathologic findings, including hyperkeratosis, pseudoepitheliomatous hyperplasia, asymmetry, and an exophytic papillomatous growth pattern, were present in these cases[25].

Acanthotic and irritated types of SK should be distinguished from eccrine poroma. On occasion, SKs may demonstrate "poroid" differentiation. Histologically, poromas are comprised of homogeneous, small basophilic cells with a delicate fibrovascular stroma and narrow ductal lumina with eosinophilic, PAS-positive, diastase-resistant cuticles (see Ch. 111).

Differentiation between an irritated SK, an SCC *in situ* (Bowen disease), and SCC may require histopathologic examination. An irritated SK may be misdiagnosed as an SCC if atypia is present. Although squamous eddies may be abundant in both tumors, there should be no evidence of involvement of the dermis in irritated SKs. Bowen disease demonstrates a preponderance of atypical keratinocytes with vacuolated cytoplasm, close crowding of nuclei, abundant mitoses, and parakeratosis. The adnexal epithelium is also involved.

The Borst–Jadassohn pattern of clonal SK is also seen in some examples of Bowen disease. In general, Bowen disease with a clonal or nested pattern has greater atypia of the individual keratinocytes.

Melanoacanthoma was originally described by Bloch and named "non-nevoid melano-epithelioma, type 1". It is now regarded as a heavily pigmented SK by most authorities. In this variant, melanocytes are distributed throughout the lesion. While the keratinocytes contain melanin, the bulk of the pigment is present within melanocytes, many of which also have long dendrites[26]. Although the melanocytes are prominent, there is no significant increase in their number. The heavy pigmentation of melanoacanthoma has been explained by a possible blockage in the transfer of melanin to keratinocytes.

Intraoral melanoacanthoma or melanoacanthosis was first described in 1979. These lesions bear a striking clinical resemblance to the melanoacanthoma type of SK. Histologically, they are distinct from the cutaneous variant by having only minimal epithelial hyperplasia. Their histologic features are most like those of a heavily pigmented lentigo simplex, with a proliferation of dendritic melanocytes within the basal layer of the epithelium[27].

Verrucae and condylomata acuminata are hyperplasias caused by HPV. Both can clinically mimic SKs but differ in that they most frequently occur in younger individuals. Verrucae often present as rough papules with pinpoint red or black dots that represent tiny intracorneal hemorrhages. Verrucae favor acral locations, while condylomata acuminata occur primarily in the anogenital region. As noted previously, HPV has been reported in anogenital lesions with histologic features of SK[28]. Koilocytic changes of perinuclear vacuolization with nuclear pyknosis in the superficial epidermis may not be present in some verrucae, but are helpful if present. An SK generally tends to be oriented in a more horizontal than vertical fashion, often has pseudohorn cysts, and lacks koilocytes.

Tumor of the follicular infundibulum is distinguished from an SK by a superficial distinct plate-like epithelial proliferation. The latter consists of multiple slender epidermal connections composed of basaloid or pale cells, without as much hyperkeratosis as an SK. The reticulated type of SK has a similar pattern but lacks the distinct plate-like growth. Skin-colored SKs, especially in flexural sites, can easily be mistaken for an acrochordon, which has a pedunculated shape and is usually smoother and smaller in size.

Other conditions with papillated epidermal hyperplasia histologically are readily distinguished on a clinical basis. Some of these include

acanthosis nigricans, epidermal nevus, and confluent and reticulated papillomatosis. Epidermal nevi tend to follow the lines of Blaschko, appearing in a linear arrangement on the extremities and a whorled pattern on the trunk. Although histologic sections of epidermal nevi typically exhibit acanthosis and hyperkeratosis, they usually lack the pseudocysts seen in many SKs. Epidermal nevi are also usually apparent at birth or shortly thereafter, unlike SKs, which are seen in adults.

Acrokeratosis verruciformis of Hopf has a "church spire" configuration similar to that described for hyperkeratotic SK[29], but it is an autosomal dominant disorder and lesions are usually limited to the distal extremities (see Ch. 59). Acanthoma fissuratum may clinically resemble a large SK, but histopathologic analysis reveals irregular epidermal hyperplasia due to friction.

Treatment

Treatment of asymptomatic SKs is largely performed for cosmetic reasons. Symptomatic lesions are usually removed by destruction, curettage, or shave excision. The most common method of destruction is cryotherapy. Other methods include electrodesiccation and laser vaporization (e.g. erbium:YAG). More recently, a topical solution of 40% hydrogen peroxide was FDA-approved for SK removal[30]. Inhibitors of AKT activity have been shown to induce apoptosis in cultured intact seborrheic keratoses and may possibly represent a future topical therapy[10].

LICHENOID KERATOSIS

Synonyms: ■ Lichen planus-like keratoses (LPLK) ■ Solitary lichenoid keratosis (SLK) ■ Benign lichenoid keratosis (BLK)

Key features

- A pink to red–brown scaly papule that arises in sun-exposed sites, most commonly the forearms and upper chest
- Histologically, it appears almost identical to lichen planus, but is distinguished by clinical correlation
- Represents an inflammatory stage of a solar lentigo, SK, or actinic keratosis

History

In 1966, two independent groups reported solitary asymptomatic lesions with the histologic features of lichen planus. These two groups referred to these lesions as solitary lichen planus and solitary lichen planus-like keratosis.

Epidemiology

In one series, 85% of lichenoid keratoses (LKs) developed between the ages of 35 and 65 years[31]. Women are diagnosed with the condition twice as frequently as men, and the vast majority of lesions are seen in White individuals. Occasionally, patients with a fair complexion and significant photodamage develop multiple LKs.

Pathogenesis

LKs have been thought to represent inflammation of a solar lentigo, SK, or actinic keratosis. *FGFR3*, *PIK3CA*, and *RAS* mutations have been detected in ~50% of LKs, providing support for this relationship (see Table 109.1)[32]. Because some of the lesions are related to "precancerous" actinic keratoses, the term lichenoid keratosis is preferred over the term benign lichenoid keratosis. Lesions are best referred to as a lichenoid actinic keratosis when there is significant keratinocyte cytologic atypia or other classic features of an actinic keratosis, and as an irritated SK when a lichenoid infiltrate is associated with other features of an SK.

Increased numbers of Langerhans cells have been observed in the epidermis of LKs. This has led to the suggestion that the lichenoid infiltrate of lymphocytes is secondary to a stimulus from an unidentified epidermal antigen. This mechanism is similar to that proposed for lichen planus.

Clinical Features

LKs occur primarily as solitary pink to red–brown, often scaly, papules ranging from 0.3 to 1.5 cm in diameter (Fig. 109.5A). An astute clinician can oftentimes suspect the diagnosis before the biopsy is performed. LK most closely resembles Bowen disease or BCC, and for this reason, these lesions are frequently biopsied. They are usually asymptomatic, although occasionally patients complain of slight pruritus or stinging[33]. The most common sites are the forearms and upper chest, with less frequent occurrence on the shins (in women) and other chronically sun-exposed sites. Dermoscopic findings include light brown pseudonetworks due to residual solar lentigo and overlapping pinkish areas related to lichenoid inflammation. Annular granular structures and gray pseudonetworks are present in the early regressing stage, while blue–gray fine dots can be seen in the late regressing stage. Blue–gray dots or globules, representing melanophages, are also considered typical of an LK.

Pathology

LK has a lichenoid infiltrate composed primarily of lymphocytes with scattered histiocytes (Fig. 109.5C). Eosinophils and plasma cells are sometimes present. All other elements of an interface dermatitis are observed, including basal vacuolar alteration, melanin incontinence, and colloid bodies. When melanin incontinence is prominent, the term pigmented lichenoid keratosis is sometimes used. Parakeratosis may be seen, unlike in typical lichen planus. Sometimes there is frank separation of the epidermis from the infiltrate in the dermis, giving rise to a subepidermal cleft or blister cavity. Basal cell proliferation is absent, and keratinocyte atypia is either mild or absent. Changes of a solar lentigo or macular SK are often present at the periphery of the specimen.

Occasionally, the histopathologic findings in an LK may mimic mycosis fungoides due to the presence of Pautrier-like microabscesses, alignment of lymphocytes along the basal layer, and epidermotropism of the infiltrate. When the entire lesion is excised, in contrast to mycosis fungoides the infiltrate in lichenoid keratosis ends abruptly at the lateral edges of the lesion (Fig. 109.5C) (this feature cannot be observed in incisional biopsies). There is also an atrophic variant, and sometimes the lesion may mimic lupus erythematosus (LE) histopathologically[34].

LKs may undergo regression, and thus, histologically, they may be confused with other regressing tumors, especially melanoma. The regressed LK usually displays a loosely fibrotic papillary dermis with scattered lymphocytes and melanophages. Regressed melanoma typically has a dense band of melanophages with lymphocytes and dilated blood vessels; usually there is also a thin epidermis overlying

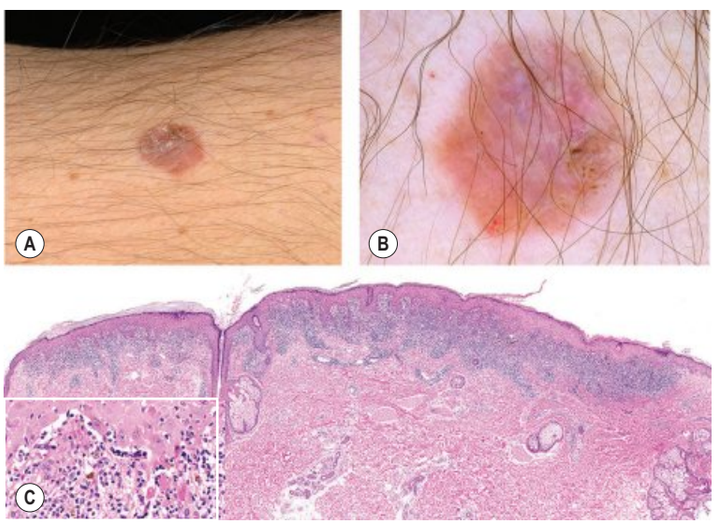


Fig. 109.5 Lichenoid keratosis. A Pink and light brown flat papule with focal scale-crust. **B** Dermoscopy demonstrates irregular granular pigmentation and whitish areas corresponding to focal hypergranulosis and hyperkeratosis. **C** Well-circumscribed lichenoid infiltrate; several necrotic keratinocytes and a few melanophages are present (inset). *Courtesy Lorenzo Cerroni, MD.*

effaced rete ridges. In states of partial regression, histopathologic clues to the proper diagnosis remain, but the end stages of both tumors may not be distinguishable. Careful search for elements of superficial BCC is also advisable.

Differential Diagnosis

Frequently cited clinical impressions include Bowen disease, actinic keratosis, BCC, irritated SK, melanoma (including amelanotic), and melanocytic nevus. Development of inflammation or color change within a pigmented lesion may lead the clinician to suspect an atypical melanocytic nevus or melanoma[31]. Even when a melanocytic neoplasm is not in the clinical differential diagnosis, the pathologist must take care to ensure that the lichenoid infiltrate is not obscuring melanoma *in situ* or even melanoma involving the superficial dermis, as the latter may become heavily inflamed. Multiple LKs may be misdiagnosed as a lichenoid drug eruption and can be a cause of pruritus in elderly patients[35].

Histologically, LK resembles other conditions with a band-like inflammatory (lichenoid) reaction pattern, including lichen planus, "lichenoid" LE, lichenoid fixed drug reactions, and mycosis fungoides. Clinical correlation is very useful in excluding these conditions, e.g. LK occurs as a single lesion in the majority of patients. While lichen planus may be virtually identical to LK histologically, there is usually more wedge-shaped hypergranulosis and less parakeratosis in lichen planus.

Treatment

Once the diagnosis of LK is made, no further therapy is necessary. Any remaining lesion may be destroyed by any method.

DERMATOSIS PAPULOSA NIGRA

Key features

- Most common in individuals of African descent with darkly pigmented skin
- Multiple hyperpigmented papules on the face
- Considered to be a variant of SK
- Cryotherapy can result in hypopigmentation; optimal treatment is scissor snip, curettage, or light electrodesiccation, when desired

Introduction

Dermatosis papulosa nigra (DPN) presents as multiple, hyperpigmented, filiform to sessile, smooth-surfaced papules measuring from 1 to 5 mm. The lesions typically develop on the face of darkly pigmented individuals.

History

DPN was first described by Castellani in 1925 based on his observations during visits to Central America and Jamaica.

Epidemiology

DPN has a strong familial predisposition and, in selected populations, reported incidences have ranged from 10% to 75%. This variability in incidence may be a reflection of sampling, as African-Americans with lighter skin phototypes are affected less commonly. In addition to those with African heritage, the condition has also been reported in Filipinos, Vietnamese, Europeans, and Mexicans. Women are twice as likely to be affected as men and it rarely occurs in children. DPN is not related to any systemic disease or syndrome.

Pathogenesis

The cause of DPN is unknown. It tends to have an earlier age of onset than that of SKs, but otherwise is similar and probably represents a variant of SK. Some authors have viewed it as a variant of multiple acrochordons. However, an *FGFR3* mutation was detected in two samples of DPN, supporting its relationship to SKs (see Table 109.1)[36].



Fig. 109.6 Dermatosis papulosa nigra. Multiple hyperpigmented papules with typical location on the cheeks.

Clinical Features

Pigmented papules are distributed symmetrically on the malar eminences and forehead (Fig. 109.6). Less often, lesions are on the neck, chest and back. The papules usually appear during adolescence and gradually increase in size and number over time, peaking in the sixth decade.

Pathology

DPN is characterized by acanthosis, papillomatosis, and hyperkeratosis in a pattern quite similar to the acanthotic type of SK. Pseudohorn cysts, however, are not a common feature.

Differential Diagnosis

The differential diagnosis of DPN includes primarily multiple SKs and acrochordons. Occasionally, verrucae, melanocytic nevi, adnexal tumors (e.g. trichoepitheliomas, fibrofolliculomas, tricholemmomas, basaloid follicular hamartomas, syringomas), and angiofibromas might be considered clinically (see Fig. 111.5).

Treatment

Treatment of DPN is generally performed for cosmetic purposes, although individual lesions may be troublesome. Care should be exercised to avoid treatments that may result in dyspigmentation, so initially it may be best to treat just a small number of lesions. Snip excision with scissors, curettage, and light electrodesiccation are the most common treatment modalities. Hypopigmentation after cryotherapy can be particularly problematic, since melanocytes are more sensitive to freeze damage than are keratinocytes.

STUCCO KERATOSIS

Synonym: ■ Keratosis alba

Key features

- Gray–white papules
- Typically on the lower extremities of older adults, especially the ankles
- Lesions are "stuck on", and when scraped off, there is minimal bleeding
- Probably a variant of SK

Introduction

Stucco keratoses are discrete, gray–white papules that are hard and opaque, with the latter reflecting focal accumulations of cornified material. They are usually distributed symmetrically below the knee, especially on the ankle and dorsal aspect of the foot.

History

In 1958, Kocsard was the first to describe stucco keratoses and eight years later he coined the term *stucco keratosis* to reflect its "stuck-on" appearance. Although early accounts of stucco keratoses described elastotic changes in the upper dermis, this has been shown to represent solar elastosis.

Epidemiology

There is no familial predilection for stucco keratoses. They can become more apparent during cold winter months, most likely due to lower humidity and more xerotic skin. They occur primarily in middle-aged to elderly individuals and are usually first observed after 40 years of age. Men are four times more likely to be affected than women. Although precise epidemiologic data are lacking, most descriptions have been in White individuals. There are no known associated diseases or syndromes.

Pathogenesis

Histochemical studies suggest an acquired focal abnormality of keratinization, and a *PIK3CA* mutation was detected in three of five samples of stucco keratoses[37]. There was a single case report of several HPV types within multiple keratoses detected by PCR, but the significance of this finding is unclear as HPV DNA is purported to be detectable in at least 20% of normal skin specimens[38]. Ultrastructural examination has revealed no viral particles[39].

Sun exposure has been proposed to be a factor in the formation of stucco keratoses, as most affected individuals have evidence of solar damage. However, this may be a reflection of the age and phototype of the patients. Heat and petroleum products such as tar have also been implicated, but none of these theories explain the distribution pattern.

Clinical Features

Usually tens, but sometimes hundreds, of gray–white papules are present on the lower extremities of older adults (Fig. 109.7). They favor the ankles and dorsal feet but may extend to the thighs. Occasionally, stucco keratoses appear on the forearms. The lesions are usually small, measuring from 1 to 4 mm; rarely larger plaques are seen. The lesions may be scraped or flicked off the skin surface with a fingernail and there is usually minimal, if any, bleeding. A collarette of dry scale may remain. On occasion, brown, pink, and deep yellow shades have been described.



Fig. 109.7 Stucco keratoses. Multiple gray–white keratotic papules, primarily on the ankle and dorsal foot.

Pathology

Stucco keratoses display prominent orthokeratotic hyperkeratosis and papillomatosis, often imparting a peaked "church spire" pattern. Acanthosis is usually present, but to a lesser degree than in some SKs. The granular layer may be thickened. Horn cysts are usually absent and cytologic atypia is not a feature.

Differential Diagnosis

Stucco keratoses may resemble SKs, acrokeratosis verruciformis of Hopf, verruca plana, or epidermodysplasia verruciformis. SKs tend to be larger and pigmented with a surface that appears "waxy", in contrast to stucco keratoses, which are smaller and have a dry, rough surface. The differential diagnosis also includes the disorder multiple minute digitate hyperkeratosis. In addition to flattened or dome-shaped keratotic papules, patients have numerous nonfollicular, hyperkeratotic, filiform projections measuring 1–2 mm in diameter. Histologically, stucco keratoses resemble hyperkeratotic SKs and acrokeratosis verruciformis; all three may demonstrate papillomatosis and digitation, giving an appearance similar to "church spires". As discussed below, the lesions of acrokeratosis verruciformis favor the dorsal aspects of the hands (as well as the feet).

Treatment

As with SKs, treatment is generally for cosmetic reasons, although symptomatic lesions may require removal. Curettage, or local destruction with cryosurgery or electrodesiccation, are the usual forms of treatment. In older patients, initial treatment of a few lesions allows assessment of healing time. Topical application of urea, lactic acid, or retinoids may reduce the hard scale, but the actual lesions persist.

POROKERATOSIS

Key features

- At least eight clinical variants of porokeratosis are recognized
- The prototype, *porokeratosis of Mibelli*, is a plaque that appears during infancy or childhood, usually on an extremity
- *Disseminated superficial actinic porokeratosis* (DSAP) is the most common type, with multiple thin papules appearing in chronically sun-exposed skin of the extremities
- *Disseminated superficial porokeratosis* has a widespread distribution pattern but lesions do not exclusively involve chronically sun-exposed sites
- *Solar facial porokeratosis* is a variant with thin papules on the face of young women, especially Asians
- *Linear porokeratosis* develops during infancy or childhood and follows the lines of Blaschko
- *Punctate porokeratosis* appears during or after adolescence as 1–2 mm papules of the palms and soles
- *Porokeratosis palmaris et plantaris disseminata* (PPPD) is a variation of punctate porokeratosis, with lesions also present on other areas of the body
- *Porokeratosis ptychotropica* is a rare variant that favors the intergluteal cleft and buttocks
- Some forms are inherited in an autosomal dominant fashion (e.g. DSAP)
- A thread-like raised hyperkeratotic border is characteristic and its histologic correlate is the cornoid lamella, a thin column of parakeratosis
- Development of SCC is possible but in most variants rare

Introduction

Porokeratosis consists of a disease spectrum in which lesions can vary significantly in size and distribution but characteristically share a thin keratotic rim. The latter is a clinical reflection of the cornoid lamella, the

diagnostic column of parakeratosis seen histologically. An explanation for the gradual centrifugal expansion of lesions is the migration of a clone of "mutated" keratinocytes. The disorder was erroneously named porokeratosis because the cornoid lamella was initially described as being present over a sweat pore, which of course is a fixed structure that cannot expand peripherally. Clinically, at least eight types of porokeratosis have been recognized (Table 109.2). Previous reports of more than one type of porokeratosis developing in the same patient[40] and in multiple members of an affected family[41] can be explained by more recent genetic studies.

History

In 1893, Mibelli first described what is now considered classic porokeratosis: one to several discrete plaques that may occur anywhere on the skin or mucous membranes, usually appearing during infancy or childhood. That same year, Respighi reported a superficial and disseminated form of the disease while Chernosky defined disseminated superficial actinic porokeratosis (DSAP) nearly 70 years later. In the 1970s, porokeratosis palmaris et plantaris disseminata (PPPD) and punctate porokeratosis were described. Porokeratosis ptychotropica is a more recently recognized form.

CLINICAL VARIANTS OF POROKERATOSIS

Variant	Clinical features
Porokeratosis of Mibelli	Plaque that arises during infancy or childhood, usually on a distal extremity; often several cm in diameter; a distinct keratotic rim may not be apparent (Fig. 109.9A)
Disseminated superficial actinic porokeratosis (DSAP)	Pink to brown papules and plaques with peripheral scale; arise in sun-exposed sites, especially the extensor forearms and shins; usually measure from a few mm to 1 cm in diameter; familial form has autosomal dominant inheritance pattern (Fig. 109.9B–D)
Solar facial porokeratosis	Thin papules on the face of young women, especially Asians, and may be pigmented (Fig. 109.9E,F)
Disseminated superficial porokeratosis (DSP)	Widespread distribution similar to DSAP but lesions do not exclusively involve sun-exposed sites
Linear porokeratosis	Streaks along the lines of Blaschko; arise during infancy or childhood; risk of development of squamous cell carcinoma (Fig. 109.9G)
Punctate porokeratosis	Palmoplantar papules that measure 1–2 mm in diameter; arise during adolescence or adulthood (Fig. 109.9H)
Porokeratosis palmaris et plantaris et disseminata (PPPD)	Palmoplantar papules in addition to involvement of the trunk, extremities, and even mucous membranes; onset during childhood or adolescence
Porokeratosis ptychotropica	Red to brown papules or plaques in the intergluteal cleft and on the buttocks; there may be coalescence of lesions centrally with scattered papules peripherally; a distinct keratotic rim may not be apparent (Fig. 109.9I)
Localized genital porokeratosis	Most commonly found on the scrotum followed by the penis; genital involvement may also be seen in other variants
Eruptive disseminated porokeratosis	Abrupt onset of numerous, widespread, inflamed keratoses; may be pruritic and can spontaneously regress; possibly a sign of an associated malignancy in up to ~30% of patients
Porokeratoma	Favors extremities but can occur on buttocks or in the intergluteal cleft

Table 109.2 Clinical variants of porokeratosis. Lesions that resemble porokeratosis are also seen in CDAGS syndrome: *c*raniosynostosis and clavicular hypoplasia, *d*elayed closure of the fontanelle, *a*nal anomalies, *g*enitourinary malformations, and *s*kin eruption[55]. Additional variants include follicular (cornoid lamellae within follicular ostia) and reticulated. Color can vary from pink to brown and several variants may develop a verrucous appearance.

Epidemiology

Porokeratosis can be inherited as an autosomal dominant disorder, including DSAP and PPPD, but many cases appear to be sporadic. Porokeratosis of Mibelli affects boys more than girls, but DSAP is more commonly diagnosed in women. Although PPPD is inherited in an autosomal dominant manner, it is twice as common in males than in females, perhaps reflecting an environmental factor. Given its relationship to sun exposure, DSAP is more frequently observed in patients with skin phototypes I and II and is rare in individuals with phototypes V and VI.

Pathogenesis

Heterozygous germline mutations in genes that encode enzymes in the mevalonate pathway – mevalonate kinase (MVK), phosphomevalonate kinase (PMVK), mevalonate diphosphate decarboxylase (MVD), and farnesyl diphosphate synthase (FDPS) – have been detected in different forms of porokeratosis, both familial and sporadic (Fig. 109.8)[42,43]. Cholesterol, an isoprenoid, is the end product of this metabolic pathway, and isoprenoids play an essential role in cellular proliferation and differentiation as well as cytoskeleton organization. Whether it is a deficiency of end products such as cholesterol, an accumulation of toxic intermediate metabolites, or both that leads to lesions of porokeratosis is not known. To date, germline mutations in one additional gene that encodes a vesicular nucleotide transporter, *SLC17A9*, have been reported in familial DSAP[44].

As anticipated given its distribution along the lines of Blaschko, a postzygotic somatic mutation in *MVD* or *PMVK*, i.e. a "second hit", was identified within lesions of linear porokeratosis in individuals who possessed respective germline heterozygous mutations (see Fig. 62.2)[45]. An explanation for the early appearance of linear porokeratosis is the occurrence of a single second hit during embryogenesis. In contrast, differing acquired second hits in patients with DSAP, who possess germline heterozygous mutations in *MVK* or *MVD*, represent UV-signature point mutations or somatic homologous recombinations[46]. The latter leads to biallelic deficiency.

Within lesions of DSAP, the concentration of epidermal cells with a second hit was found to be higher within their central portions than in the annular rings[46]. How these findings relate to the formation of the peripheral cornoid lamella remains speculative.

Clinical Features

Classic *porokeratosis of Mibelli* is a rare condition, appearing during infancy or childhood as an asymptomatic, small, brown to skin-colored keratotic papule that gradually enlarges over a period of years to form a plaque that may measure several centimeters in diameter. There is a raised, sharply demarcated, keratotic, thready border with a longitudinal furrow (Fig. 109.9A). The center of the lesion may be hyperpigmented, hypopigmented, atrophic, and/or anhidrotic. Lesions may occur anywhere on the body, including mucous membranes, but the extremities are most frequently involved. Multiple lesions may be present, but they are almost always regionally localized and unilateral.

Disseminated superficial actinic porokeratosis (DSAP) is much more common than the Mibelli type. Small asymptomatic or mildly pruritic keratotic papules, usually ranging from 3 to 10 mm in diameter, appear during the third to fourth decades of life. They are typically skin-colored to tan–brown to pink–red in color. As the lesions progress, they expand radially, and the older, central area becomes atrophic while the well-demarcated border develops a thin, elevated, furrowed keratotic rim (Fig. 109.9B–D). The lesions occur exclusively in sun-exposed areas, most commonly the shins and extensor forearms. In more extensive disease, there is involvement of the upper outer arms, upper trunk, and thighs. Facial sparing is characteristic, with the exception of the solar facial variant (Fig. 109.9E,F; see Table 109.2).

Some patients report that lesions of DSAP become more prominent and erythematous during the summer[47], and there are reports of patients with psoriasis receiving UVB or PUVA treatments developing DSAP. In individuals with skin phototypes I and II, DSAP may resemble and coexist with actinic keratoses, but, unlike actinic keratoses, DSAP almost always involves the legs and rarely the face, whereas patients

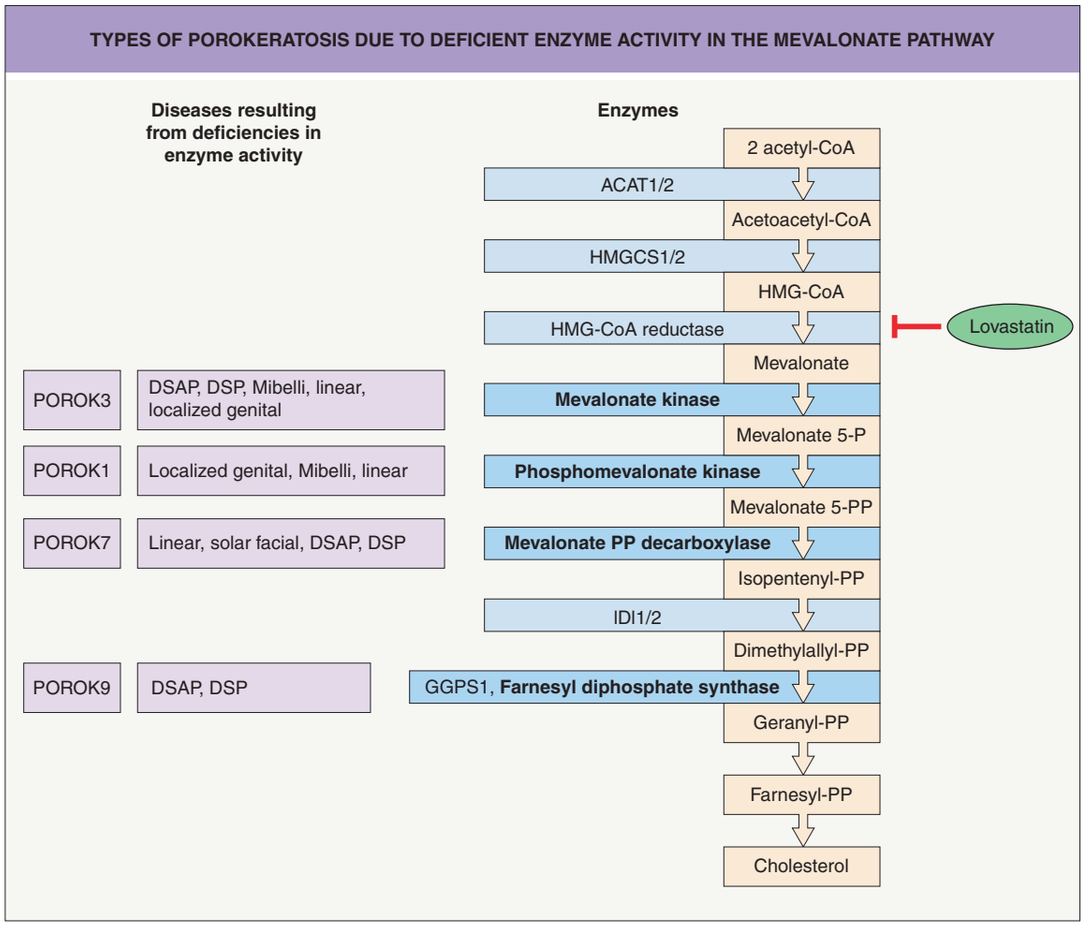


Fig. 109.8 Types of porokeratosis due to deficient enzyme activity in the mevalonate pathway. To date, enzymes in **bold** are dysfunctional in four forms of porokeratosis. POROK corresponds to the OMIM classification of porokeratoses; to date underlying genetic mutations for the following forms have not been detected: POROK2: porokeratosis palmaris et plantaris disseminata (PPPD); POROK4, POROK5: disseminated superficial actinic porokeratosis (DSAP); POROK6: linear, PPPD. Mutations in *SLC17A9* are associated with POROK8. ACAT, acetyl-coenzyme A acetyltransferase; DSP, disseminated superficial porokeratosis; GGPS, geranyl diphosphate synthase; HMGCS, HMG-CoA synthase; IDI, isopentyl-diphosphate isomerase; PP, diphosphate.

with actinic keratoses on the legs almost always have them on the face as well[48]. Rarely, DSAP has been reported in association with hepatitis C viral infection or systemic lupus erythematosus.

Disseminated superficial porokeratosis (DSP), like DSAP, has a more widespread pattern than the other types of porokeratosis. DSP usually involves the extremities bilaterally and symmetrically, sparing the palms, soles, and mucous membranes.

Linear porokeratosis arises during infancy or childhood, and it consists of one or more plaques that are similar in appearance to classic porokeratosis; however, the plaques follow the lines of Blaschko, most commonly on the extremities (Fig. 109.9G). The distribution pattern is a reflection of genetic mosaicism (see above). When an individual has both DSAP and linear porokeratosis, the latter represents type 2 mosaicism (see Fig. 62.2). Thicker plaques of linear porokeratosis have been associated with *PMVK* mutations and thinner plaques with *MVD* mutations[45].

PPPD is uncommon and individual lesions resemble those of porokeratosis of Mibelli except they are smaller and have a less pronounced keratotic border. They may be asymptomatic or pruritic, and generally arise during childhood or adolescence. As the name suggests, the palms and soles are initially affected, but any surface, including mucous membranes, may be involved.

Punctate porokeratosis is the most difficult type to diagnose clinically because of the small size of the lesions. It appears during adolescence or adulthood as small "seed-like" keratotic papules with a peripheral raised rim on the palms and/or soles[49] (Fig. 109.9H). Clinically, it may resemble punctate keratoderma, Darier disease, Cowden syndrome, or arsenical keratoses, but the presence of a cornoid lamella histologically narrows the differential diagnosis. There are two other palmoplantar disorders that also have parakeratotic columns – spiny keratoderma, where lesions resemble the spines of an old-fashioned music box, and porokeratotic eccrine ostial and dermal duct nevus (PEODDN; also referred to as porokeratotic adnexal ostial nevus) – but clinically these entities are easily discernible.

Porokeratosis ptychotropica is an unusual variant in which pruritic, red to brown papules and plaques develop in the intergluteal cleft and on the buttocks (Fig. 109.9I)[50]. There may be coalescence of lesions centrally. Histologically, multiple cornoid lamellae are seen rather than a single peripheral cornoid lamella.

Development of SCC within lesions of porokeratosis has been reported in all variants except punctate and ptychotropica. Lesions in older patients, those of longstanding duration, and linear variants all have higher rates of malignant degeneration. DSAP has the lowest risk of malignant change[51]. SCC generally appears as a papule or plaque arising in contiguity with the individual lesion of porokeratosis, leading to asymmetry.

In the setting of immunosuppression, multiple lesions of porokeratosis can appear and they may attain a large size (see Fig. 109.9B,C)[52]. Uncommon clinical variants of porokeratosis include a reticular form[53] and a follicular variant[54]. In CDAGS (*c*raniosynostosis and clavicular hypoplasia, *d*elayed closure of the fontanelle, *a*nal anomalies, *g*enitourinary malformations, and *s*kin eruption) syndrome, a very rare autosomal recessive disorder, patients develop erythematous plaques on the face and extremities that histologically resemble porokeratosis (see Table 109.2)[55].

Pathology

Identification of the cornoid lamella is the *sine qua non* for the histologic diagnosis of porokeratosis, although it may be seen in other conditions such as verruca vulgaris and actinic keratosis. It is characterized by a thin column of tightly packed parakeratotic cells extending from an invagination of the epidermis through the stratum corneum, often protruding above the surface of the adjacent skin (Fig. 109.10). Under the cornoid lamella, the granular layer is either absent or markedly attenuated, but it is of normal thickness in other areas of the lesion. Dyskeratosis and pyknotic keratinocytes with perinuclear edema are present in the spinous layer beneath the cornoid lamella. The superficial portion of the cornoid lamella trails toward the center of the lesion in



Fig. 109.9 Porokeratosis – clinical variants. A Porokeratosis of Mibelli on the hand of a child. **B** Large-sized actinic porokeratosis in a renal transplant recipient with significant solar damage; the narrow elevated rim is obvious. **C** Large-sized actinic porokeratosis with a prominent rim in a second immunocompromised patient. **D** Multiple lesions of disseminated superficial actinic porokeratosis (DSAP) with obvious peripheral keratotic rims; lesions can range in color from light brown to pink. **E** Multiple thin pigmented lesions in an Asian patient with the solar facial variant. **F** Dermoscopy of the solar facial variant with visualization of the narrow keratotic border. **G** Several streaks of linear porokeratosis on the lower extremity. **H** Multiple keratotic papules of the plantar surface due to punctate porokeratosis. **I** Porokeratosis ptychotropica with pink to brown papules localized to the intergluteal cleft and buttocks. *B, Courtesy Jean L. Bolognia, MD; E and H, Courtesy Kalman Watsky MD; F, Courtesy Nan Ring, MD; I, Courtesy César Cosme Álvarez Cuesta, MD.*

a pattern that has been likened to smoke coming out of a moving train as the "clone" of epidermal cells advances centrifugally. The cornoid lamella corresponds to the clinically observed raised keratotic border. The clinician should include this portion of the lesion in the biopsy to establish the diagnosis. Sometimes, cornoid lamellae are found in multiple locations throughout the lesion in addition to the periphery.

Compared to classic porokeratosis of Mibelli, the invagination from which the cornoid lamella extends is less pronounced in variants. Corresponding to the less prominent border seen in DSAP, the cornoid lamella in DSAP often does not protrude above the surface of the adjacent stratum corneum. The epidermis in the central portion of a porokeratotic lesion may be normal, hyperplastic, or atrophic, with effacement of rete ridges. The dermis contains lymphocytes that may be perivascular, localized beneath the cornoid lamella, or lichenoid in the central portion of the lesion.

Differential Diagnosis

Porokeratosis can resemble other annular lesions (see Table 19.1) as well as actinic keratoses, but dermoscopy can assist in detection of the furrowed keratotic rim as can application of ink to the skin surface. Linear porokeratosis may be confused with other linear lesions such as inflammatory linear epidermal nevus, incontinentia pigmenti (stage II), and linear lichen planus (see Ch. 62), but none of these have a cornoid lamella. Although cornoid lamellae can be found in actinic keratoses, in the latter, partial epidermal cytologic atypia is invariably present. Verruca vulgaris often has mounds of parakeratosis that are sometimes identical to cornoid lamellae, but koilocytosis is usually present along with other histologic features of warts. Porokeratotic eccrine ostial and dermal duct nevus (PEODDN) is a separate entity (see Ch. 111).

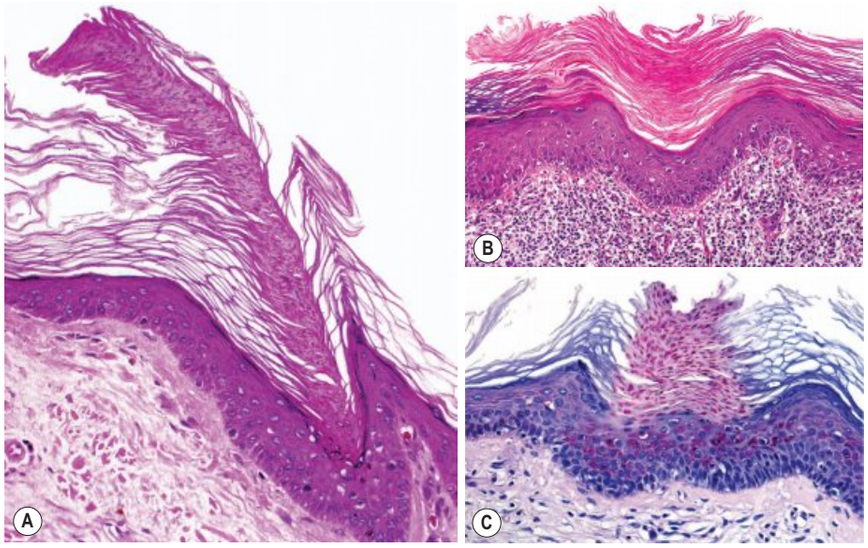


Fig. 109.10 Porokeratosis – histopathologic features. The cornoid lamella, a narrow column of parakeratotic cells, is the typical histologic feature of porokeratosis. It can vary in length and discernibility. **A** An obvious cornoid lamella. **B** More subtle cornoid lamella that becomes more obvious with a PAS stain (**C**).

Treatment

Cryotherapy[47], topical 5-fluorouracil (5-FU)[48], topical retinoids or calcipotriene (calcipotriol) in combination with 5-FU, topical imiquimod, topical tacrolimus[56], photodynamic or laser therapy, shave excision, curettage, and depending upon circumstances, linear excision[57] and dermabrasion[58] have all been used with variable degrees of success. Unless the abnormal clone of keratinocytes is destroyed, lesions tend to recur, and they are more difficult to eradicate than are actinic keratoses. Topical cholesterol 2%/lovastatin 2% cream or ointment is a newly described pathogenesis-directed therapy[59]. In widespread or refractory lesions, administration of oral acitretin may be beneficial, although the disease will recur following its discontinuation[60]. Photoprotection should be recommended, especially for patients with DSAP and linear porokeratosis.

FLEGEL DISEASE

Synonym: ■ Hyperkeratosis lenticularis perstans

Key features

- Very rare disorder; possible autosomal dominant inheritance pattern
- Multiple keratotic papules with a disc-like appearance in a symmetric distribution
- Predilection for the dorsal aspect of the feet and the distal extremities of adults

Introduction

In 1958, Flegel described this rare disorder in which asymptomatic, disc-shaped, keratotic papules appear most commonly on the distal extremities of adults. The name hyperkeratosis lenticularis perstans refers to the disc or lens shape (lenticularis) of the papules and their persistent nature (perstans).

Epidemiology

Flegel disease is possibly inherited in an autosomal dominant pattern, although it also develops sporadically. Lesions are usually not evident until mid to late adulthood, but they have been described in individuals as young as 13 years of age[61,62]. No racial predilection has been reported.

Pathogenesis

By electron microscopy, lamellar granules (Odland bodies) have been shown to be either absent or altered[63]. The lipid byproducts within lamellar granules influence stratum corneum desquamation, and, if they are absent or abnormal, hyperkeratosis may develop.

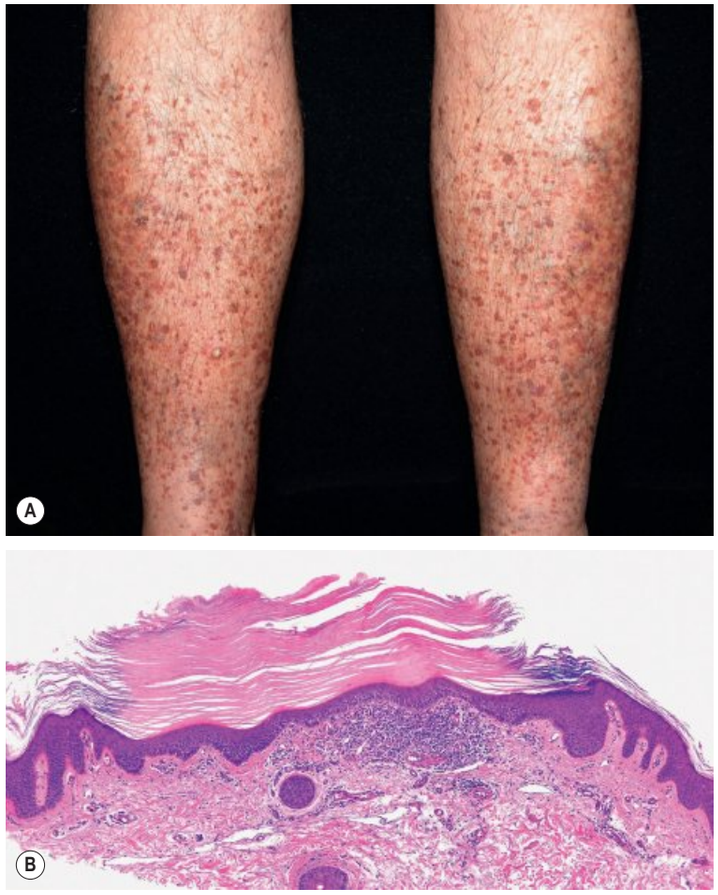


Fig. 109.11 Flegel disease. A Multiple symmetric hyperpigmented keratotic papules are present on the shins. **B** Thinned and flattened epidermis with overlying marked hyperkeratosis and an underlying patchy lichenoid infiltrate within the papillary dermis.

Clinical Features

In Flegel disease, numerous red–brown keratotic papules appear in a symmetric pattern (Fig. 109.11A); rarely, a unilateral distribution has been observed. Lesions most commonly develop on the dorsal aspect of the feet and distal legs and arms, including the palms and soles.

Involvement of the pinna and oral mucosa has also been described. Individual papules are small, typically measuring from 1 to 5 mm in diameter while lesions on the palms or soles often appear as fine pits. The papules have attached scale which may be more prominent at the peripheral margin. Removal of this scale can result in bleeding. Although lesions are usually asymptomatic, occasionally patients complain of pruritus. Flegel disease has reportedly been associated with endocrine disorders such as diabetes mellitus and hyperthyroidism[64].

Pathology

The papules consist of a discrete zone of ortho-hyperkeratosis, contrasting with the normal basket-weave cornified layer of the surrounding normal epidermis in most locations (Fig. 109.11B). There is often focal parakeratosis and hypogranulosis. The thin atrophic stratum spinosum is usually sharply indented or depressed at its lateral margins. A lichenoid infiltrate of lymphocytes is often present in the papillary dermis, along with dilated blood vessels. A slight degree of hyperchromatism or nuclear infoldings, resembling Sézary cells, has been described in some cases of Flegel disease[65].

Differential Diagnosis

Stucco keratoses present as whitish-gray papules on the dorsal feet and legs, but histologically there is papillomatosis not atrophy of the epidermis. Also, there is no inflammation unless lesions have become irritated. Perforating disorders have more prominent central keratotic plugs instead of disc-shaped hyperkeratosis, and there is a transepidermal elimination of connective tissue (see Ch. 96). With the exception of perforating granuloma annulare, perforating diseases rarely, if ever, occur on the palms or soles. DSAP typically occurs on the legs, but there is a keratotic rim due to the cornoid lamella. Although the dermal changes in Flegel disease may overlap with other lichenoid diseases (see Ch. 11), the clinical presentation allows differentiation. Without clinical correlation, cases with lymphocyte atypia could be misdiagnosed as cutaneous T cell lymphoma.

Treatment

Treatment of Flegel disease is problematic as lesions tend to resist all but destructive therapy. Application of topical 5-fluorouracil cream is moderately effective, although it may not be well tolerated because of irritation. Oral retinoids or PUVA in combination with oral retinoids or calcipotriene yielded unsuccessful or inconsistent results.

ACROKERATOSIS VERRUCIFORMIS

Key features

- Multiple small, skin-colored, warty papules primarily on the dorsal aspect of the hands and feet
- Rare autosomal dominant disorder of keratinization that is due to a mutation in *ATP2A2* and is allelic with Darier disease
- "Church spire" hyperkeratosis, papillomatosis, and acanthosis

Clinical Features and Pathogenesis

Acrokeratosis verruciformis of Hopf is a rare autosomal dominant disorder that has its onset during early childhood. Multiple small, skin-colored, warty papules appear on the dorsal aspect of the hands and feet and less commonly on the extensor surfaces of the forearms and legs (see Fig. 59.14). It can be seen in patients with Darier disease, and patients with acrokeratosis verruciformis may also have small, keratin-filled depressions on the palms and soles, as well as nail involvement. These observations are not surprising given that the two disorders are allelic, with both due to mutations in *ATP2A2* (see Fig. 59.1). However, to date, the same missense mutation – leading to a Pro602Leu substitution in ATP2A2 – has been detected in families with acrokeratosis verruciformis, but not in those with Darier disease[66].

Pathology

There is hyperkeratosis, papillomatosis, and acanthosis, often with hyperpigmentation. The hyperkeratosis may be quite prominent, and a "church spire" configuration, similar to that described for hyperkeratotic SK and stucco keratosis, is a frequent finding.

Differential Diagnosis

Histologic features similar to those of SK include hyperkeratosis, papillomatosis, and acanthosis as well as some degree of hyperpigmentation. Clinicopathologic correlation is necessary to distinguish between these disorders.

Treatment

Treatment is similar to that described for SKs and stucco keratoses.

CUTANEOUS HORN

Synonym: ■ Cornu cutaneum

Key features

- Clinical term for a white to yellow, hard, keratotic conical lesion; the base may be a papule, plaque, or nodule
- Most commonly in sun-exposed areas and arising from a hyperkeratotic actinic keratosis
- *In situ* or invasive SCC is present in up to 20% of lesions
- Other common causes include verruca and SK

Clinical Features

Cutaneous horn is a clinical term for a white to yellow, hard, keratotic conical lesion (Fig. 109.12A) whose base is a papule, plaque, or nodule that ranges from a few millimeters to several centimeters in diameter. The histologic correlate is an abnormal accumulation of keratin in an elongated, vertically oriented column overlying an abnormality of the underlying spinous layer. Cutaneous horns may arise anywhere on the body, but favor chronically sun-exposed sites. Men are affected more frequently than women. Individuals with a fair complexion and the elderly are particularly predisposed[67].

Pathology

A cutaneous horn consists of hyperkeratosis and parakeratosis associated with variable acanthosis (Fig. 109.12B), usually in association with the atypical keratinocytes of an actinic keratosis. Up to 20% of cutaneous horns arise in an *in situ* or invasive SCC[67]. Other lesions that may give rise to cutaneous horns include verrucae, SKs, and less commonly, other epithelial neoplasms, including those derived from follicular epithelium, especially tricholemmomas.

Treatment

Shave excision with local destruction is the most common treatment. The former must be done deeply enough to allow the pathologist to evaluate the dermis beneath the horn in order to determine if there is an invasive SCC. An elliptical excision can be performed, especially if the base is nodular or indurated. Treatment of AKs and SCCs is outlined in Chapter 108. Cryotherapy alone may fail because the base may not be adequately treated unless the horn is pared first.

CLEAR CELL ACANTHOMA

Synonym: ■ Degos acanthoma





Fig. 109.12 Cutaneous horn. A This cutaneous horn arose from an actinic keratosis. **B** Striking column of hyperkeratosis with hyperplasia of the underlying epidermis.



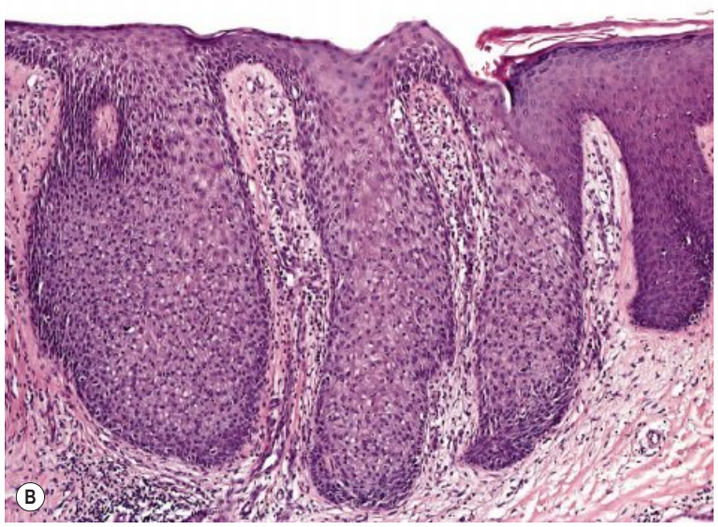


Fig. 109.13 Clear cell acanthoma. A Well-demarcated, dark red, shiny papule with a wafer-like collarette of scale. **B** Epidermal hyperplasia consisting of large pale keratinocytes. Note the sharp transition to normal skin. *B, Courtesy Lorenzo Cerroni, MD.*

Key features

- Uncommon, usually solitary, papule or plaque on the leg
- Lesions are blanchable, erythematous, and discrete; they may have attached "wafer-like" scale at their periphery
- Psoriasiform histology with well-demarcated zone containing clear to pale keratinocytes that stain positively with PAS

Introduction

First described by Degos in 1962, clear cell acanthoma is an uncommon red papule or plaque, usually on the leg. It may be suspected by astute clinicians, but usually a biopsy is required to establish the diagnosis.

Epidemiology

Clear cell acanthoma has no sex predilection and generally develops during middle-age, peaking in incidence by 50 to 60 years of age. It has not been described in children and neither an ethnic nor racial preference has been identified. Familial predisposition is rare, although there is one report of a French kinship with multiple affected family members having disseminated lesions[68].

Pathogenesis

The etiology of clear cell acanthoma is unknown. Although it was once thought to be induced by crude coal tar and UV light, there is no proof of a link with environmental trauma, drugs, toxic substances, or viruses. Given its abundant clear cytoplasm, it was originally thought to exhibit eccrine differentiation, but immunohistochemical and ultrastructural findings are more consistent with tricholemmal differentiation or features of the interfollicular epidermis[69,70]. It may be regarded as a variant of SK in which there are abundant glycogen-containing keratinocytes[71].

Others have proposed that clear cell acanthoma may actually be a localized, nonspecific, reactive inflammatory dermatosis. Several benign hyperproliferative dermatoses, including psoriasis, share a cytokeratin staining pattern similar to that seen in clear cell acanthoma. Furthermore, similarities in the histopathologic features between psoriasis and clear cell acanthoma suggest a common abnormality in the maturation of keratinocytes[72]. However, clear cell acanthomas do not develop following trauma and do not exhibit koebnerization, suggesting they are not simply a variant of localized psoriasis.

Clinical Features

Clear cell acanthoma presents as an asymptomatic, erythematous, rounded papule or plaque that appears "stuck on", similar to an SK (Fig. 109.13A)[73]. A "wafer-like" scale is often appreciated, especially at the periphery[74]. The majority of clear cell acanthomas are solitary and on the leg, but they may be found on the face, forearm, and trunk as well as in the inguinal region. Occasionally they are slightly eroded and a serous exudate may be present on the surface. There is often prominent vascularity as in a pyogenic granuloma, but the erythema can be blanched with application of pressure. By dermoscopy, the looped blood vessels within the dermal papillae create red dots in lines, referred to as a "string-of-pearls" (see Fig. 0.40C). Polarizing-specific white lines can also be seen.

Clear cell acanthomas usually develop slowly, often over a period of 2–10 years. They range in size from 0.3 to 2 cm in diameter, although rarely larger lesions have been reported, one of which had a diameter of 6 cm. Multiple lesions are also rare, with only about two dozen cases reported in the English literature, and these acanthomas may be either few in number or numerous and widespread[75]. Disseminated forms have been categorized as either discrete (<12 lesions) or eruptive (>30 lesions)[76]. One patient developed ~400 lesions[75] and another with eruptive acanthomas experienced spontaneous regression[77].

Clear cell acanthomas with cystic, pigmented, or polypoid features have been described, but these are uncommon. They have also been noted to develop in areas of pre-existing dermatoses, within epidermal nevi, after trauma, and following insect bites. SCC *in situ* has been rarely documented in association with clear cell acanthoma.

Pathology

Clear cell acanthoma displays a zone of sharply demarcated, thickened epidermis with regular psoriasiform hyperplasia composed of enlarged pale keratinocytes (Fig. 109.13B). The epidermis is eroded and neutrophils extend from the papillary dermis into the stratum spinosum, aggregating in the overlying thin crust. The granular layer is diminished and the rete ridges are elongated. PAS stains the pale cytoplasm of the keratinocytes red. The material that stains with PAS is diastase-sensitive, confirming it is glycogen. Electron microscopy also demonstrates abundant glycogen within the cytoplasm. The dermis contains dilated blood vessels and sparse perivascular lymphocytes.

Differential Diagnosis

Clear cell acanthoma may be clinically confused with a traumatized hemangioma, inflamed SK or verruca, BCC, SCC, pyogenic granuloma, poroma, amelanotic melanoma, or psoriasis; dermoscopy can assist in establishing the diagnosis. Histologically, other clear cell neoplasms may occasionally cause confusion, although the overall psoriasiform pattern of a clear cell acanthoma usually allows for distinction. Tricholemmomas usually appear on the face and consist of an inwardly growing lobule of pale keratinocytes lacking other features of psoriasis. The sebocytes of sebaceous neoplasms have a multiloculated cytoplasm containing lipid instead of glycogen, and they stain positively for epithelial membrane antigen or adipophilin.

Clear cell acanthoma-like lesions of the nipple/areola share histopathologic features with classic clear cell acanthomas but eosinophils are present and clinically the lesions resemble eczema of one or both nipples and areolae[78]. Resolution following application of corticosteroid cream has been reported.

Treatment

Shave excision or curettage combined with electrofulguration is a common and adequate form of treatment. Most lesions do not recur.

INVERTED FOLLICULAR KERATOSIS

Key features

- Asymptomatic, firm, white–tan to pink papule
- Typically solitary; most commonly on the face and neck of middle-aged and older adults
- Benign endophytic variant of irritated SK
- Histologically, squamous eddies and inflammation are common findings

History

Helwig was the first to delineate the features of inverted follicular keratosis (IFK) in 1955.

Epidemiology

IFK is seen most commonly in middle-aged to older White individuals. Men are affected twice as frequently as women.

Pathogenesis

In 1963, Duperrat and Mascaro proposed that the tumor was derived from the infundibulum of the hair follicle, although the cause is unclear.

Clinical Features

IFK is typically an asymptomatic, firm, white–tan to pink papule. It is found on the face in ~85% of cases, in particular on the cheek and upper lip. This is followed in frequency by other sites in the head and neck region. IFKs are usually <1 cm in diameter, but rarely they may reach up to 8 cm. They are typically stable and persistent lesions, but may regress.

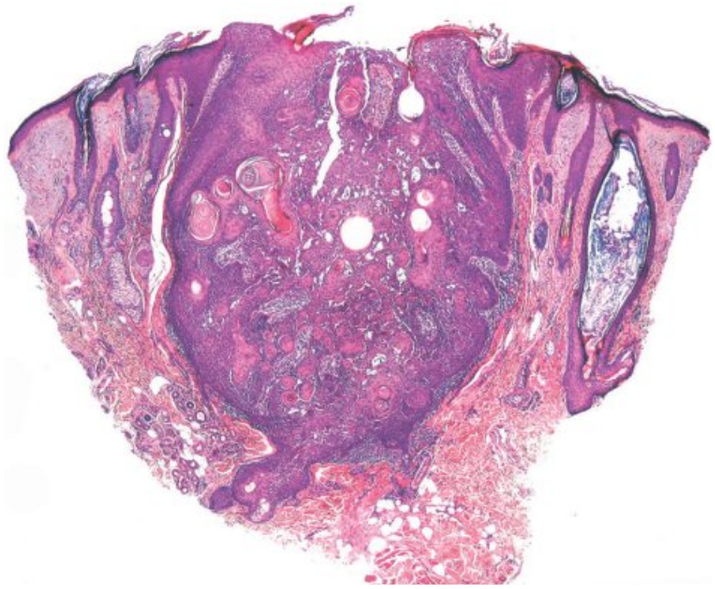


Fig. 109.14 Inverted follicular keratosis. An endophytic proliferation of keratinocytes with prominent squamous eddies is seen.

Pathology

IFK exhibits an endophytic, somewhat bulbous proliferation of eosinophilic keratinocytes with basaloid or squamous differentiation (Fig. 109.14). The keratinocyte proliferation seems to surround one or several follicular canals that open to the surface. There may be inflammation and squamous eddies are commonly seen.

Differential Diagnosis

The clinical differential diagnosis of IFK includes verruca, SK, tricholemmoma and other follicular adnexal tumors, BCC, and SCC. Tricholemmoma has a predominance of clear cells, often with a palisade of basal cells and a thickened basement membrane. Rare mitotic figures may be appreciated in an IFK, but overt cellular atypia as in SCC is absent.

WARTY DYSKERATOMA

Key features

- Uncommon, usually solitary papule or nodule with a central keratotic plug
- Favor the head and neck region
- Acantholytic dyskeratosis at the base and sides of a cup-like epidermal invagination

Introduction

Usually found on the head or neck, warty dyskeratoma is an uncommon solitary papule or nodule with a comedo-like plug and acantholysis with dyskeratosis histologically.

History

Helwig coined the term "isolated Darier's disease" in 1954. Three years later, the lesion was given the name warty dyskeratoma to indicate its solitary verrucous nature.

Epidemiology

Warty dyskeratomas are uncommon and demonstrate no genetic predisposition. They are more prevalent in men, usually appearing between the fifth and seventh decades of life. They occur more commonly in White individuals.

Pathogenesis

The pathogenesis of the acantholytic dyskeratosis in warty dyskeratomas has not been elucidated, although abnormal adhesion of keratinocytes has been demonstrated. Now that the gene responsible for Darier disease has been cloned, abnormalities in the function of its protein product could potentially be investigated in related entities like warty dyskeratoma.

Clinical Features

Warty dyskeratoma presents as a solitary (rarely multiple), verrucous, often crusted, skin-colored to red–brown papule or nodule with a central pore containing a keratotic plug. They grow slowly and are located most commonly on the scalp, face, or postauricular area[79]. Lesions have been found beneath the nail plate and in the mouth, especially on the hard palate and alveolar ridge. Warty dyskeratomas typically range in size from several millimeters to 2 cm in diameter. The scalp is the most common site for multiple lesions.

Most warty dyskeratomas are asymptomatic, but patients may occasionally complain of pruritus or burning. Bleeding and discharge of foul-smelling cornified material may occur. They have been reported to coexist with other skin lesions, including verruciform xanthoma, actinic keratosis, SCC, BCC, and adnexal carcinomas. To date, malignant degeneration in a warty dyskeratoma has not been reported.

Pathology

It is well circumscribed and usually involves at least one dilated folliculosebaceous unit. There is a central cup-like invagination lined with epithelium displaying acantholysis as well as individual cell necrosis, corps ronds and grains, most closely resembling Darier disease (Fig. 109.15). The central crater is filled with cornified debris. Villous-like papillae, sometimes composed of only a single layer of basal cells, often project upward from the invaginated hyperplastic base.

Differential Diagnosis

Warty dyskeratomas may resemble other epithelial neoplasms and proliferations such as a verruca, epidermal inclusion cyst, SK, hypertrophic actinic keratosis, or SCC. Histologically, other conditions with suprabasilar acantholytic dyskeratosis must be excluded, such as Darier disease, Grover disease, Hailey–Hailey disease, familial dyskeratotic comedones, acantholytic acanthoma, acantholytic actinic keratosis, and acantholytic SCC. Most of these entities are quite different clinically.

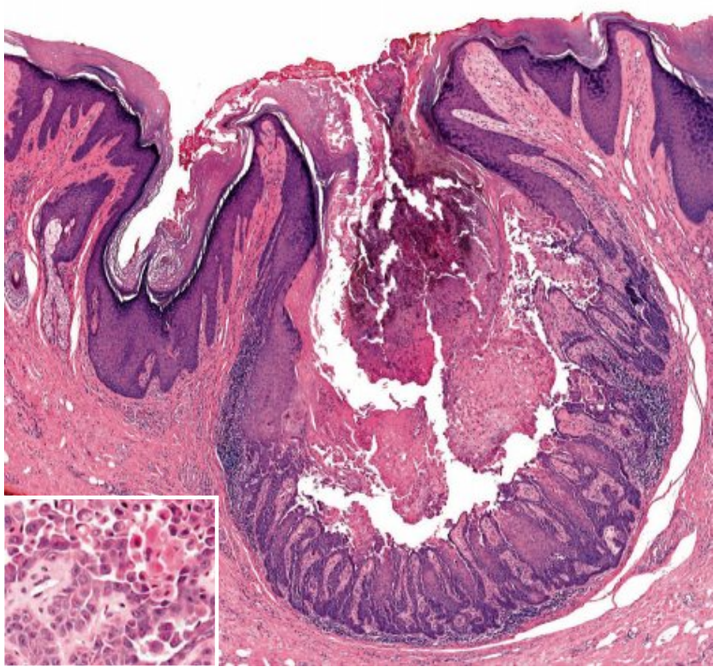


Fig. 109.15 Warty dyskeratoma. A cup-shaped invagination with a central keratotic plug. The lower portion of the wall has multiple villi. The epithelium demonstrates acantholysis and dyskeratosis (inset). *Courtesy Lorenzo Cerroni, MD.*

Treatment

Given its benign nature, treatment depends upon the clinical situation. Lesions are often biopsied to exclude the possibility of a malignancy.

ACANTHOLYTIC (DYSKERATOTIC) ACANTHOMA

Key features

- Often a solitary papule on the trunk of adults; may present as multiple lesions in the genital area
- Variant of a solitary keratosis with histopathologic findings of acantholysis, with or without dyskeratosis, in a hyperplastic epidermis with an overall flat architecture

An acantholytic (dyskeratotic) acanthoma is usually a solitary papule on the trunk of adults, and biopsy is often performed to exclude a BCC. Occasionally, there are multiple lesions in the genital area that can be confused with condylomata acuminata. Postzygotic mutations in *ATP2A2* or *ATP2C1* have been detected in these acanthomas; when germline, mutations in these genes lead to Darier disease and Hailey-Hailey disease, respectively. Histologically, there is acantholysis with or without dyskeratosis. Unlike warty dyskeratoma, there is neither a cup-shaped architecture nor an association with a hair follicle. In contrast to acantholytic actinic keratosis, there is no keratinocyte atypia.

EPIDERMOLYTIC ACANTHOMA

Key features

- Discrete keratotic papules in adults, with epidermolytic hyperkeratosis seen histologically
- Two varieties: an isolated form and a disseminated form

Epidemiology

Epidermolytic acanthomas may appear any time during adulthood. No particular race or sex is favored. To date, there are no reports of familial cases.

Pathogenesis

Because its clinical and histopathologic features may resemble those of verrucae, a viral origin was originally suspected, but HPV DNA has not been detected in the lesions[80]. Exogenous factors such as UVR, other viruses[81], and trauma[82] have all been suggested as causes of acquired epidermolytic hyperkeratosis. Recently, hotspot mutations in the Arg156 position of *KRT10*, known to cause epidermolytic ichthyosis, were detected in several epidermolytic acanthomas[83].

Clinical Features

The isolated form was initially described in 1970, while the disseminated form was described in 1973. Both forms present as pigmented keratotic papules that may resemble verrucae or SKs (Fig. 109.16A). Individual lesions are generally 1 cm or less in diameter. When isolated, they may appear on any body site. Discrete lesions, when in a cluster, are still categorized as the isolated variant. The disseminated form has a predilection for the trunk, especially the back; it has also been reported in the genital region where it can mimic condylomata acuminata[84]. Lesions are usually asymptomatic, but they may be pruritic.

Pathology

The histologic pattern of epidermolytic hyperkeratosis (Fig. 109.16B) consists of four components:

- clear spaces of varying size surrounding nuclei in the stratum spinosum and stratum granulosum

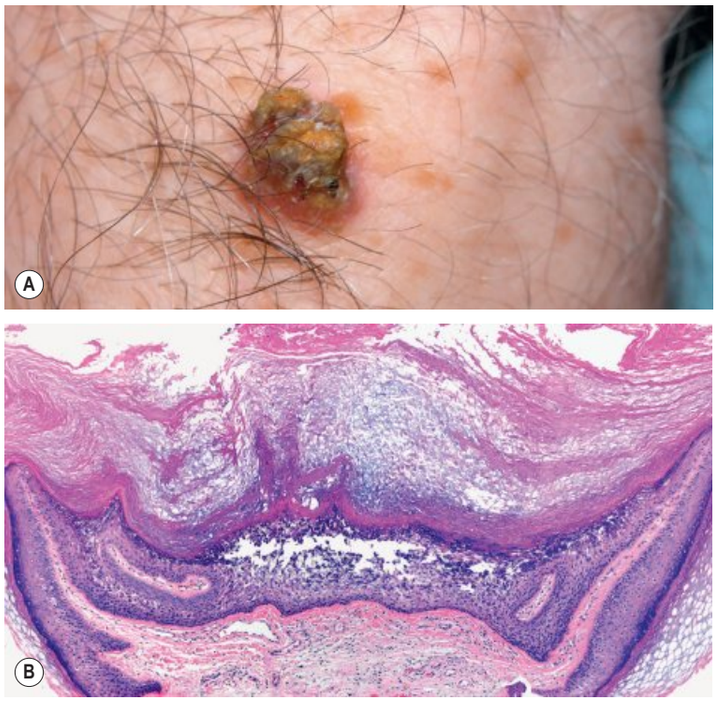


Fig. 109.16 Solitary epidermolytic acanthoma. A Keratotic papulonodule on the chest. **B** Marked hyperkeratosis and epidermolytic hyperkeratosis within the underlying epidermis.

- indistinct cellular boundaries consisting of reticulated, lightly staining material
- a markedly thickened granular zone containing an increased number of small and large, irregularly shaped, basophilic keratohyaline-like bodies
- compact hyperkeratosis.

The basal layer is normal. Epidermolytic acanthomas generally demonstrate more papillomatosis than is typically seen in other conditions with the histologic pattern of epidermolytic hyperkeratosis. There is often a slight superficial perivascular lymphocytic infiltrate in the dermis.

Differential Diagnosis

Clinically epidermolytic acanthomas resemble verrucae and SKs. Because they do not have a characteristic clinical appearance, the diagnosis is not usually made until after a biopsy is performed. Epidermolytic hyperkeratosis is a histologic finding common to several conditions, including epidermolytic ichthyosis (bullous congenital ichthyosiform erythroderma) as well as particular forms of epidermal nevi and palmoplantar keratoderma. It is seen incidentally in normal skin and in lesions such as follicular cysts, SKs, atypical nevi, actinic keratoses, and cutaneous horns.

Treatment

Treatment is not required as the lesions are benign. Destruction, shave excision, or linear excision is successful, although recurrence may follow superficial removal.

LARGE CELL ACANTHOMA

Key features

- Skin-colored, hyperpigmented, or hypopigmented papule or plaque
- Located on sun-exposed skin of older individuals
- Likely a variant of solar lentigo or SK

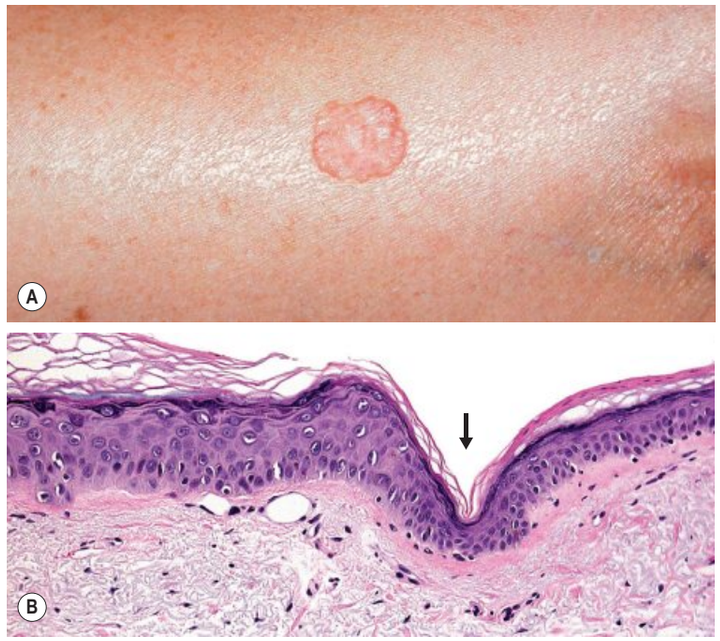


Fig. 109.17 Large cell acanthoma. A Well-demarcated, thin, pink–brown plaque. **B** Slight epidermal hyperplasia with uniformly enlarged keratinocytes; the latter have abundant cytoplasm and enlarged nuclei (left side). Arrow points to the border of the acanthoma. *Courtesy Lorenzo Cerroni, MD.*

Introduction

Large cell acanthoma is a benign keratinocytic lesion that is asymptomatic and often ignored[85]. Some dermatopathologists make the diagnosis frequently, while others do not believe that this is a specific entity.

History

Pinkus first described the lesion in 1967 during a lecture on benign epidermal neoplasms in which he coined the term[86].

Epidemiology

Large cell acanthomas most commonly arise in sun-damaged skin of middle-aged to elderly individuals, with ages at diagnosis ranging from 30 to 90 years and a mean age in the mid-60s. Women have a slightly higher incidence and most affected patients have skin phototypes I or II.

Pathogenesis

The pathogenesis of large cell acanthoma is unknown. Genetic studies have demonstrated low-grade aneuploidy, a finding typically associated with malignancy. Nevertheless, large cell acanthoma has generally been considered to be clinically benign. Some investigators have proposed that it is a variant of Bowen disease[87]. Still others classify it as a variant of solar lentigo in a stage evolving into a reticulated SK or lichen planus-like keratosis[88].

Clinical Features

It typically presents as a solitary, sharply demarcated, skin-colored, hyperpigmented, or hypopigmented papule or plaque (Fig. 109.17A). These acanthomas are most commonly located on the face or neck, including the eyelid, but can be extrafacial[87]. Rarely, multiple lesions are scattered on the extremities.

As it is asymptomatic and often ignored, the time to diagnosis is quite variable, ranging from 3 months to 15 years[85].

Pathology

Histologically, large cell acanthomas are well demarcated, with uniformly large keratinocytes with abundant cytoplasm and enlarged nuclei (Fig. 109.17B). Mild cytologic atypia may be present. There is

variable hyperkeratosis, papillomatosis, epidermal rete ridge elongation, and basal layer hyperpigmentation. Some lesions have minimal hyperkeratosis with flattened rete ridges and only small dermal papillae[87].

Differential Diagnosis

The differential diagnosis includes solar lentigo (histologically), SK, actinic keratosis, Bowen disease, and melanoma.

Treatment

Shave or simple excision as well as destruction are options.

EPIDERMAL NEVUS (SEE CH. 62)

Synonyms: ■ Keratinocytic nevus – nevus verrucosus, verrucous nevus, nevus unius lateris (multiple, unilateral), ichthyosis hystrix (extensive, bilateral)

Key features

- Onset typically within the first year of life
- Most commonly, hyperpigmented papillomatous papules and plaques appear in a linear array along the lines of Blaschko

Introduction

Within dermatology, the term nevus (plural, nevi) has three definitions: (1) a congenital lesion (birthmark) or lesion arising early in life; (2) a benign tumor of melanocytes; or (3) a hamartoma. The latter is a benign malformation with an excess or deficiency of structural elements normally found in the affected area, e.g. epidermis, connective tissue, adnexa. In most hamartomas, one element is predominant.

Epidemiology

The incidence of epidermal nevus is estimated to be 1 in 1000 infants. The vast majority of epidermal nevi develop sporadically, although familial cases have been reported. However, a familial pattern is more characteristic of the papular epidermal nevus with a "skyline" basal cell layer that presents with scattered rather than linear lesions[89,90]. There is no sex predilection.

Pathogenesis – see Ch. 62 and Table 62.6

Clinical Features

In a review of 131 patients with epidermal nevi, the age of onset ranged from birth to 14 years, with 80% evident within the first year of life[91], although the lesions may occasionally become apparent during adulthood[92]. Epidermal nevi most commonly present as a single linear lesion, but sometimes multiple unilateral or bilateral linear plaques are seen (see Ch. 62). Most lesions consist of well-circumscribed, hyperpigmented, papillomatous, keratotic, or velvety papules and plaques that are usually asymptomatic (Fig. 109.18A,B). The earliest lesions may be macular and confused with linear and whorled nevoid hypermelanosis. Rarely, epidermal nevi are hypopigmented. Once developed, the nevi may thicken and become more verrucous, especially over joints and in flexural areas such as the neck. Epidermal nevi follow the lines of Blaschko and may have an abrupt midline demarcation (Fig. 109.18C).

Epidermal nevus syndrome, a concept proposed by Solomon and Esterly in 1968, is diagnosed when epidermal nevi occur in combination with other developmental anomalies (see Ch. 62). These abnormalities most commonly involve the central nervous or musculoskeletal systems. Excluding cutaneous manifestations, a study of 119 patients with epidermal nevi found that 33% had abnormalities in one organ system, 6% in two, 5% in three, and 5% in five or more. Several overgrowth syndromes can present with epidermal nevi, including Proteus, CLOVES, and PTEN hamartoma-tumor syndromes (see Chs. 62 & 104).



Fig. 109.18 Epidermal nevi. A Obvious papillomatosis in a single thin linear plaque; this is the most common clinical presentation. **B** Larger sized verrucous hyperpigmented plaque. **C** Multiple verrucous hyperpigmented plaques that clearly follow the lines of Blaschko. Note the midline demarcation. **D** The most common histologic pattern is epidermal hyperplasia with papillomatosis and hyperkeratosis.
A, Courtesy Julie V. Schaffer, MD; B, Courtesy Kalman Watsky, MD; C, Courtesy Kathryn Schwarzenberger, MD.

Pathology

At least ten histologic patterns have been observed in epidermal nevi, and more than one may be present in the same lesion[93,94]. Virtually all are characterized by epidermal hyperplasia, hyperkeratosis, acanthosis, papillomatosis, and variable parakeratosis (Fig. 109.18D). Other findings such as epidermolytic hyperkeratosis and focal acantholytic dyskeratosis may be prominent features when there is mosaicism for mutations in *KRT1* or *KRT10* and *ATP2A2*, respectively. Inflammatory linear verrucous epidermal nevus (ILVEN) may have clinical and histologic features very similar to psoriasis (see the following section).

Neoplasms such as BCC, SCC, and keratoacanthoma may rarely develop in association with epidermal nevi. This malignant change occurs less commonly in epidermal nevi than in the closely related nevus sebaceus. Malignancy, when it does occur, typically develops after puberty[95]. Examples of BCC arising in epidermal and sebaceous nevi may actually be trichoblastomas, representing a manifestation of the hamartomatous nature of the neoplasm[96,97].

Differential Diagnosis

Nevus sebaceus, usually found on the head instead of the trunk or extremities, can be considered a subtype of epidermal nevus but with additional hamartomatous components of sebaceous and apocrine glands accompanying the papillomatous epidermis (see Ch. 111). Organoid nevi combine features of both epidermal nevus and nevus sebaceus, with variation often depending upon anatomic site (e.g. head and neck versus trunk). RAVEN (rounded and velvety epidermal nevus), also referred to as nevoid acanthosis nigricans, is a rare entity due to postzygotic mosaicism for FGFR3 or FGFR2 mutations in which lesions have a distinctive rounded outline. Lichen striatus is an acquired lesion, has less papillomatosis and acanthosis as well as more dyskeratosis and spongiosis, and does not persist indefinitely. There are other nevoid conditions that are distributed along the lines of Blaschko and therefore may simulate epidermal nevi, depending on the type and degree of epidermal proliferation. Examples include PEODDN, linear lichen planus, and X-linked dominant chondrodysplasia punctata. Small lesions must be distinguished from SKs, psoriasis, condylomata acuminata, and verrucae vulgares, especially if there is Koebner phenomena. The histologic differential diagnosis also includes hyperkeratosis of the nipple.

Treatment

Infants and children with epidermal nevi, particularly multiple or extensive lesions, require a thorough evaluation for systemic abnormalities in conjunction with a pediatrician (see Ch. 62). Full-thickness surgical excision is curative, but recurrence is common when only the epidermis is removed (e.g. by shave excision or curettage) because the hamartomatous process also involves at least the papillary dermis. However, surgical excision can be complicated by hypertrophic scars or keloid formation. Topical therapies such as corticosteroids, retinoic acid, tars, anthralin, 5-fluorouracil, and podophyllin have all been used, but they are of limited benefit. Chronic therapy with oral retinoids has been reported to be effective at decreasing the thickness of systematized epidermal nevi, although it does not result in resolution. Laser ablation may also be undertaken, but to be effective, it must induce scarring and fibrosis of at least the papillary dermis. Therefore, this treatment is often not cosmetically acceptable to patients and test sites are recommended. Most recently, topical sirolimus was reported to lead to improvement but results are modest.

INFLAMMATORY LINEAR VERRUCOUS EPIDERMAL NEVUS

Key features

- Linear, psoriasiform papules or plaques, usually on one extremity
- 75% of these nevi appear before the age of 5 years
- Usually persists for years despite attempts at treatment
- Histologically, psoriasiform hyperplasia with alternating parakeratosis and orthokeratosis

Introduction

Inflammatory linear verrucous epidermal nevus (ILVEN) is a relatively rare, linear, psoriasiform plaque that usually presents during childhood.

History

Altman and Mehregan are credited with the first description of ILVEN in 1971.

Pathogenesis

At least one patient with ILVEN was shown to have a postzygotic mutation in *GJA1*, which encodes connexin 43[98]. Germline mutations in this gene lead to erythrokeratodermia variabilis. In 2 of 15 patients with ILVEN, mosaicism for mutations in CARD14 was detected[99]. Germline mutations in this gene lead to CAPE (CARD14-associated papulosquamous eruption) which has features of both psoriasis and pityriasis rubra pilaris. Two additional patients, who subsequently developed psoriasis, were found to have a germline heterozygous CARD14 mutation plus a postzygotic hotspot mutation in KRT10 while the second had a postzygotic hotspot mutation in HRAS[99a].

Clinical Features

ILVEN has a psoriasiform appearance and may be associated with significant pruritus. Scaly, erythematous papules coalesce to form a linear plaque, usually on a limb (Fig. 109.19A), although occasionally the trunk may be involved. Lesions are almost always unilateral. In ~75% of patients, onset is before the age of 5 years and is often within the first six months of life[100]. Isolated instances of adult onset have been reported[101] and, rarely, there may be a familial predisposition[102]. In earlier studies, ILVEN was observed more commonly in females[102]. Most lesions tend to be persistent. A possible association of ILVEN with arthritis has been described[103].

Pathology

The psoriasiform histology of ILVEN correlates with its psoriasiform clinical appearance. Epidermal rete ridges are elongated, and broad zones of parakeratosis without an underlying granular layer alternate abruptly with depressed regions of orthokeratosis and hypergranulosis (Fig. 109.19B). There is often exocytosis of lymphocytes and neutrophils into the spongiotic papillomatous epidermis and occasionally Munro microabscesses are seen.

Differential Diagnosis

At least three other variants of epidermal nevi with inflammation have been described, including lichenoid epidermal nevus, psoriasis superimposed on an epidermal nevus, and epidermal nevi in X-linked dominant *c*ongenital *h*emidysplasia with *i*chthyosiform nevus and *l*imb *d*efects (CHILD) syndrome. Lichenoid epidermal nevus is typically a verrucous plaque with a lichenoid lymphocytic dermal infiltrate. It is debatable whether lichenoid epidermal nevus truly represents linear lichen planus. The age of onset, distribution, resistance to therapy, and lack of family history are all features of ILVEN. Patients with linear (nevoid) psoriasis or *CARD14* mutations can have or develop classic plaques of psoriasis elsewhere.

It has been suggested that ILVEN may be a forme fruste of CHILD syndrome because rarely, ipsilateral skeletal anomalies are seen in patients with ILVEN. Also, although large areas of ichthyosiform erythema characteristically involve one-half of the body with an affinity for skin folds (ptychotropism), patients with CHILD syndrome can have linear keratotic plaques along the lines of Blaschko that have an appearance similar to ILVEN. CHILD syndrome differs histologically from ILVEN in that it has features of verruciform xanthoma, especially when biopsy specimens are from body folds[104], as well as vacuoles within the cells of the lower stratum corneum ultrastructurally. However, electron microscopy is rarely performed nowadays, and in a series of 5 patients initially diagnosed as having ILVEN, 2 were found to have germline *NSDHL* mutations, i.e. CHILD syndrome[99a]. This might explain the previous reports of female predominance.



Fig. 109.19 Inflammatory linear verrucous epidermal nevus (ILVEN). A Linear erythematous scaly plaque with a psoriasiform appearance on the leg. **B** Epidermal hyperplasia and broad zones of parakeratosis alternating with ortho-hyperkeratosis.

Treatment

As with other epidermal nevi, ILVEN is difficult to treat. Treatments that are successful in psoriasis are only partially effective for ILVEN[103]. Surgical excision is effective but results in scarring. The pulsed dye laser has been used successfully in some cases. Its mechanism of action is thought to involve destruction of small blood vessels in the papillary dermis that supply the overlying epidermis[105]. Combination therapy with topical tretinoin and 5-fluorouracil creams has also been employed with beneficial results, but long-term success can only be achieved with maintenance therapy[106]. Topical synthetic derivatives of vitamin D_3, such as calcipotriene, may also be partially effective[107,108]. There are anecdotal reports of improvement with crisaborole ointment, TNF inhibitors, and other lasers (e.g. excimer, fractionated CO_2, ablative CO_2). In a patient with mosaicism for a *CARD14* mutation, ustekinumab led to significant improvement[99].

Arthritis in association with ILVEN, although rare, can lead to significant morbidity. Early recognition is critical. Treatment is the same as for psoriatic arthritis[103].

NEVUS COMEDONICUS

Synonyms: ■ Comedo nevus ■ Comedonal nevus

Key features

- Benign hamartoma, usually arising before the age of 10 years
- Multiple grouped comedones in a linear array, most commonly on the face, trunk, or neck
- Histologically, epidermal invaginations containing keratin plugs and underdeveloped hair shafts

Introduction

Nevus comedonicus is a rare hamartoma of the folliculosebaceous unit resulting in numerous dilated, keratin-filled comedones.

History

Kofmann, in 1895, was the first to delineate the features of nevus comedonicus. In 1914, White attempted to change the name to "nevus follicularis keratosis" as he thought the comedo-like lesions did not represent true comedones, as sebaceous glands were either rudimentary or absent in most cases.

Epidemiology

Approximately half of the cases of nevus comedonicus are evident at birth, with others appearing during childhood, usually before the age of 10 years. Onset in adulthood, albeit rare, is often associated with irritation or trauma. There is no racial or sex predilection. Although most cases arise sporadically, familial clustering has been reported[109].

Pathogenesis

Nevus comedonicus is thought to represent growth dysregulation affecting the mesodermal portion of the pilosebaceous unit. The epithelial-lined invaginations, incapable of forming mature terminal hairs and sebaceous glands, accumulate a soft cornified ostial product resulting in a comedo-like plug.

In 2016, mosaic activating mutations in the NIMA-related kinase 9 gene (*NEK9*) were identified in the affected skin of patients with classic nevus comedonicus (see Table 62.6)[110]. Two decades earlier, *FGFR2* mutations had been detected in lesional but not adjacent normal skin of an acneiform nevus referred to as the Munro acne nevus, also providing evidence for genetic mosaicism[111]. In contrast to a classic nevus comedonicus, the Munro acne nevus tends to have pre-existing linear hypopigmentation, peripubertal onset of the acne lesions, and histopathologic findings of an atrophic comedonal wall with prominent associated sebaceous lobules. Of note, patients with Apert syndrome, sporadic or inherited in an autosomal dominant manner and due to mutations in *FGFR2*, may have comedones and severe cystic acne (see Table 62.6).

Clinical Features

There is usually a single circumscribed area (Fig. 109.20A) or linear streak composed of clusters of dilated follicular ostia that contain firm, darkly pigmented, cornified material. Occasionally, multiple linear plaques may be seen with midline demarcation. The overall size is variable and can range from a few centimeters in diameter to extensive lesions affecting half of the body. The site most commonly affected is the face, followed by the trunk, neck, and upper extremity. These nevi may also arise in areas that are devoid of hair follicles such as the palms, soles, and glans penis. When present on the elbows and knees, lesions can be verrucous in appearance. Inflammatory papules and cysts are often admixed with the comedones. Hormonal influences of puberty often worsen the condition. Development of SCC or keratoacanthoma within the nevus is exceedingly rare.

Pathology

Nevus comedonicus consists of grouped undeveloped hair follicles, presenting as dilated invaginations filled with cornified debris devoid of

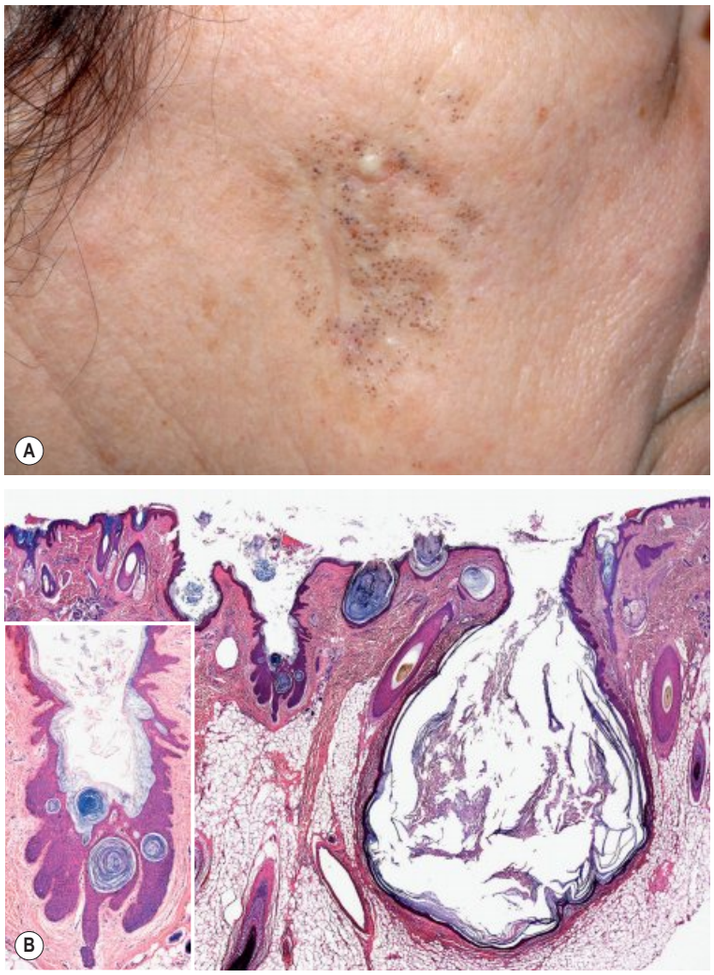


Fig. 109.20 Nevus comedonicus. A Numerous comedones as well as two cysts within a circumscribed area on the right cheek. **B** Dilated infundibula filled with orthokeratotic keratin. Occasionally, the wall of the comedo will display epithelial hyperplasia (inset). *A, Courtesy Lorenzo Cerroni, MD.*

hair shafts (Fig. 109.20B). Epidermolytic hyperkeratosis may sometimes be present in the follicular epithelium.

Differential Diagnosis

Many skin conditions present with comedones, and these must be differentiated from nevus comedonicus. Distinctive features of *acneiform nevus* are discussed under Pathogenesis. *Infantile acne* typically presents on the face between the ages of 3 and 24 months. The comedones, pustules, and papules in this disorder are not linear, and they are self-limited. Chloracne is associated with exposure to toxins that lead to the formation of comedones, generally located on both sides of the face and commonly behind the ears.

Familial dyskeratotic comedones is a rare autosomal dominant disorder in which comedones arise during childhood or adolescence and are widely scattered on the trunk and extremities without a linear configuration. Histologically, acantholytic dyskeratosis in the comedo wall is seen.

The *dilated pore nevus* resembles nevus comedonicus clinically but differs histologically by containing dilated follicular cysts. *Porokeratotic eccrine ostial and dermal duct nevi* also may be confused with nevus comedonicus, especially when the latter involves the palms or soles. These lesions are comprised of dilated eccrine ducts containing parakeratotic debris. The keratinocyte cytoplasm is typically vacuolated and the granular layer is absent.

Treatment

As with other epidermal nevi, treatment of nevus comedonicus is problematic. Localized lesions can be surgically excised, although it is often difficult to excise larger lesions. Manual comedo extraction, dermabrasion, and the use of keratolytic agents (e.g. salicylic acid, tretinoin, ammonium lactate[112]) may be helpful, but they are not curative. Isotretinoin is not usually recommended owing to the long-term treatment required, but it may be beneficial in preventing cyst formation. Antibiotics may be necessary to treat secondary infections.



Fig. 109.21 Nevoid hyperkeratosis of the nipple and areola. Diffuse seborrheic keratosis-like thickening and hyperpigmentation of the areola. *Courtesy Lorenzo Cerroni, MD.*

ACANTHOSIS NIGRICANS

Acanthosis nigricans is discussed in detail in Chapter 53. Histologically, it may be misinterpreted as an SK, epidermal nevus, or confluent and reticulated papillomatosis, unless appropriate clinical correlation is provided.

NEVOID HYPERKERATOSIS OF THE NIPPLE AND AREOLA

This unusual condition of unknown etiology affects women more frequently than men. It is usually bilateral, but can be unilateral (Fig. 109.21). Progressive diffuse thickening of the skin of both areolas, which appears hyperpigmented, often begins after puberty. Histologically, there is irregular basaloid acanthosis with elongation and anastomosis of rete ridges, orthokeratotic hyperkeratosis, and hyperpigmentation of the basal layer, mimicking a seborrheic keratosis. Nevoid hyperkeratosis may become more evident during pregnancy and it may also occur in men receiving hormonal therapy. Although no uniformly effective treatment exists, there are case reports of improvement with topical retinoids, cryotherapy, or radiofrequency ablation.

CONFLUENT AND RETICULATED PAPILLOMATOSIS

Synonym: ■ Confluent and reticulated papillomatosis of Gougerot and Carteaud

Key features

- Onset typically during puberty
- Multiple brown, verrucous, thin papules or plaques in a confluent and/or reticulated pattern, most commonly on the central chest and upper abdomen
- Oral minocycline is effective in ~50% of patients

History

Confluent and reticulated papillomatosis of Gougerot and Carteaud (CARP) was first described in 1927.

Epidemiology

The typical onset of CARP is during puberty[113]. Depending upon the series, young women are affected more frequently than young men and vice versa; racial predisposition also varies. Occurrence of CARP is mostly sporadic, although familial cases have been reported.

Pathogenesis

Some think CARP may be caused by an endocrine imbalance, especially insulin resistance, because of its association with conditions such as obesity, menstrual irregularities, and diabetes mellitus as well as pituitary and thyroid disorders. In addition, there is a clinical resemblance to acanthosis nigricans. However, many patients are otherwise healthy. Another hypothesis is that CARP is a disorder of keratinization. This theory arose because a number of patients have been successfully treated with topical and systemic retinoids[114]. An abnormal host response to *Malassezia furfur* has also been suggested, as this organism is sometimes prevalent within areas of involvement in its yeast (and less often hyphal) forms and because treatment with topical selenium sulfide has sometimes been successful[115]. The majority of cases, however, demonstrate no evidence of *M. furfur* proliferation.

Clinical Features

The initial lesions of CARP are 1–2 mm papules, first appearing in the intermammary area or less frequently the interscapular or epigastric regions. Lesions rapidly enlarge to 4–5 mm and become brown, keratotic, verrucous papules, patches, or thin plaques. The papules coalesce and become confluent centrally and reticulated peripherally (Fig. 109.22). There can be involvement of the neck, upper trunk, and other flexural areas. Oral lesions have not been reported. The eruption is asymptomatic or, rarely, mildly pruritic.



Fig. 109.22 Confluent and reticulated papillomatosis (CARP). Multiple thin hyperpigmented papules of the upper back that are confluent centrally and have a reticulated pattern peripherally. *Courtesy Ronald Savin, MD.*

Pathology

There is hyperkeratosis, acanthosis, and papillomatosis. Sparse superficial perivascular infiltrates of lymphocytes are also seen. A characteristic feature is the club-shaped, bulbous epidermal rete ridges that protrude slightly into the papillary dermis with pigment at their bases ("dirty feet").

Differential Diagnosis

CARP can clinically resemble acanthosis nigricans, tinea versicolor, and Darier disease. Acanthosis nigricans has thicker, more velvety plaques involving intertriginous areas; it also lacks the reticulated pattern of CARP. Acanthosis nigricans is most commonly associated with insulin resistance and improves with weight loss; some authors refer to this form of the disease as pseudoacanthosis nigricans. Tinea versicolor may be related to CARP because of its brownish scale and association with *M. furfur*, but it is neither reticulated nor papillomatous. Occasionally, retention hyperkeratosis, also referred to as terra firma-forme, may be confused with CARP, but the former can be easily removed with an alcohol swab.

Histologically, CARP may be misinterpreted as an SK, epidermal nevus, acanthosis nigricans, or other papillomatous epithelial proliferation, unless appropriate clinical information is provided.

Treatment

Treatment of CARP is often frustrating because it may not respond to therapeutic interventions or recurs after cessation of therapy. No single agent has been uniformly successful at providing long-term resolution. Temporary improvement has been reported with the use of various oral antibiotics (e.g. tetracyclines) and oral retinoids (e.g. isotretinoin, acitretin)[114,116] as well as topical salicylic acid, hydroquinone, tacrolimus[117], sirolimus, antifungals (e.g. selenium sulfide)[115], vitamin D_3 analogues, and 5-fluorouracil. Oral minocycline has been reported to be effective in ~50% of patients, with some reporting no recurrences, while others experienced disease-free intervals for up to 18 months[118]. Oral retinoids are no more successful than oral antibiotics at maintaining a disease-free state, and given their potential for causing hypertriglyceridemia and teratogenicity, they are generally considered to be second- or third-line agents.

TERRA FIRMA-FORME DERMATOSIS

Terra firma-forme dermatosis is a benign skin disease characterized by brown papules and plaques, often in a corrugated pattern. Histopathologic examination is not necessary as lesions can be removed via rubbing with 70% isopropyl alcohol pads.

CLEAR CELL PAPULOSIS

Key features

- Extremely rare condition, mainly described in Asian children
- Hypopigmented macules and papules arranged along the milk lines
- Histologically, large clear cells are scattered along the basal layer of the epidermis and within the malpighian layer

Epidemiology

Clear cell papulosis (CCP) is an extremely rare condition that preferentially affects Chinese and other Asian children[119].

Pathogenesis

The pathogenesis of CCP is unknown. The arrangement of lesions along the so-called milk lines and the appearance of clear cells in lesional skin suggest a histogenetic relationship with Toker cells. Some authors have considered this process as the benign counterpart of extramammary Paget disease[120].

Clinical Features

CCP is characterized by multiple, asymptomatic, white macules or papules that are 2–10 mm in diameter and favor the anterior chest, abdomen, and lumbar region (see Fig. 66.31). The lesions are often arranged along the milk lines. In rare cases, the face may be also involved.

Pathology

Lesions of CCP are mildly acanthotic and have a slightly disorganized arrangement of epidermal keratinocytes. Numerous clear cells are scattered primarily along the basal layer of the epidermis, but also within its upper layers. These clear cells are larger than adjacent keratinocytes and have cytoplasmic vacuolization due to abundant mucin within their cytoplasm; the latter may be highlighted by PAS, mucicarmine, Alcian blue, or colloidal iron stains. Immunohistochemically, clear cells of CCP express carcinoembryonic antigen, cytokeratins ($CK7^+$, $AE1/AE3^+$, $CAM5.2^+$), epithelial membrane antigen (EMA), and gross cystic disease fluid protein-15 (GCDFP-15), but are negative for expression of CD1a, S100 protein, and HMB45[119].

Differential Diagnosis

Clinically, CCP should be differentiated from hypopigmented lesions of tinea versicolor, pityriasis lichenoides chronica, guttate lichen sclerosus, achromic verrucae plana, and confetti lesions of tuberous sclerosis (see Table 66.5). Histologically, CCP needs to be distinguished from extramammary Paget disease and pagetoid dyskeratosis. Neoplastic cells of extramammary Paget disease are more atypical and pleomorphic than those of CCP. Pagetoid dyskeratosis is a disorder of keratinization characterized by clear and pale eosinophilic keratinocytes scattered within the epidermis; it is an incidental histopathologic finding without any clinical significance.

Treatment

CCP is a benign process and no treatment is necessary. Most patients experience at least a partial regression[121].

Acknowledgment

The authors would like to acknowledge Raymond Barnhill, MD, for his contribution to the solar lentigo section of this chapter.

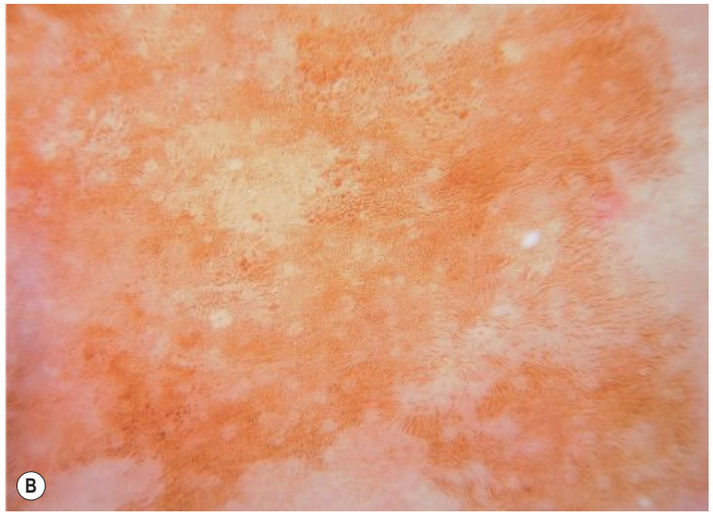
Additional figures available in our eBook (see inside front cover for access code).

REFERENCES

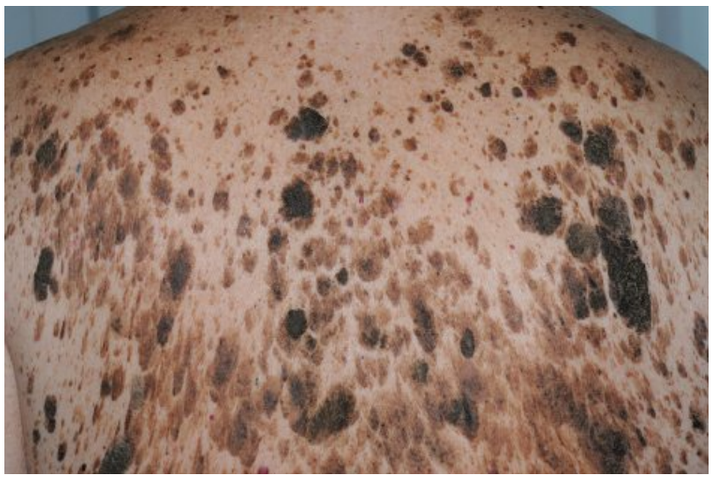
1. Hafner C, Stoehr R, van Oers JM, et al. FGFR3 and PIK3CA mutations are involved in the molecular pathogenesis of solar lentigo. *Br J Dermatol*. 2009;160:546–551.
2. Wang SQ, Rabinovitz H, Oliviero MC, Marghoob AA. Solar lentigines, seborrheic keratoses, and lichen planus-like keratosis. In: Marghoob AA, Malvehy J, Braun B, eds. *Atlas of Dermoscopy*. 2nd ed. London: Informa Healthcare; 2012.
3. Lassacher A, Worda M, Kaddu S, et al. T1799A BRAF mutation is common in PUVA lentigines. *J Invest Dermatol*. 2006;126:1915–1917.
4. Todd MM, Rallis TM, Gerwels JW, et al. A comparison of three lasers and liquid nitrogen in the treatment of solar lentigines. *Arch Dermatol*. 2000;136:841–846.
5. Verhagen ARHB, Koten JW, Chaddah VK, Patel RI. Skin diseases in Kenya: a clinical and histopathological study of 3,168 patients. *Arch Dermatol*. 1968;98:577–586.
6. Yeatman J, Kilkenny M, Marks R. The prevalence of seborrhoeic keratoses in an Australian population: does exposure to sunlight play a part in their frequency? *Br J Dermatol*. 1997;137:411–414.
7. Nakamura H, Hirota S, Adachi S, et al. Clonal nature of seborrheic keratosis demonstrated by using the polymorphism of the human androgen receptor locus as a marker. *J Invest Dermatol*. 2001;116:506–510.
8. Hafner C, Hartmann A, van Oers JMM, et al. *FGFR3* mutations in seborrheic keratoses are already present in flat lesions and associated with age and localization. *Mod Pathol*. 2007;20:895–903.
9. Heidenreich B, Denisova E, Rachakonda S, et al. Genetic alterations in seborrheic keratoses. *Oncotarget*. 2017;8:36639–36649.
10. Neel VA, Todorova K, Wang J, et al. Sustained Akt activity is required to maintain cell viability in seborrheic keratosis, a benign epithelial tumor. *J Invest Dermatol*. 2016;136:696–705.
11. Pesce C, Scalora S. Apoptosis in the areas of squamous differentiation of irritated seborrheic keratosis. *J Cutan Pathol*. 2000;27:121–123.
12. Leonardi C, Zhu W, Kinsey W, Penneys N. Seborrheic keratoses from the genital region may contain human papillomavirus DNA. *Arch Dermatol*. 1991;127:1203–1206.
13. Schwengle L, Rampen F. Eruptive seborrheic keratoses associated with erythrodermic pityriasis rubra pilaris: possible role of retinoid therapy. *Acta Derm Venereol*. 1988;68:443–445.
14. Winkelmann R. Superficial spreading (and disappearing) seborrheic keratosis. *Cutis*. 1999;63:235–237.
15. Díaz-Cascajo C, Reichel M, Sanchez J. Malignant neoplasms associated with seborrheic keratoses. An analysis of 54 cases. *Am J Dermatopathol*. 1996;18:278–282.
16. Sloan J, Jaworsky C. Clinical misdiagnosis of squamous cell carcinoma in situ as seborrheic keratosis. A prospective study. *J Dermatol Surg Oncol*. 1993;19:413–416.
17. Rao B, Freeman R, Poulos E, et al. The relationship between basal cell epithelioma and seborrheic keratosis. A study of 60 cases. *J Dermatol Surg Oncol*. 1994;20:761–764.
18. Vielhauer V, Herzinger T, Korting HC. The sign of Leser-Trélat: a paraneoplastic cutaneous syndrome that facilitates early diagnosis of occult cancer. *Eur J Med Res*. 2000;5:512–516.
19. Grob JJ, Rava MC, Gouvernet J, et al. The relation between seborrheic keratoses and malignant solid tumours. A case-control study. *Acta Derm Venereol*. 1991;71:166–169.
20. Yeh J, Munn S, Plunkett T, et al. Coexistence of acanthosis nigricans and the sign of Leser-Trélat in a patient with gastric adenocarcinoma: a case report and literature review. *J Am Acad Dermatol*. 2000;42:357–362.
21. Schwartz R. Sign of Leser-Trélat. *J Am Acad Dermatol*. 1996;35:88–95.
22. Lindelof B, Sigurgeirsson B, Melander S. Seborrheic keratoses and cancer. *J Am Acad Dermatol*. 1992;26:947–950.
23. Neuhaus IM, LeBoit PE, McCalmont TM. Seborrheic keratosis with basal clear cells: a distinctive microscopic mimic of melanoma in situ. *J Am Acad Dermatol*. 2006;54:132–135.
24. Haspeslagh M, De Schepper S, De Wispelaere I, Degryse N. Seborrheic keratosis with basal clear cells: a peculiar microscopic mimic of melanoma in situ. *J Cutan Pathol*. 2013;40:768–769.
25. Blessing K, Evans AT, al-Nafussi A. Verrucous naevoid and keratotic malignant melanoma: a clinico-pathological study of 20 cases. *Histopathology*. 1993;23:453–458.
26. Simón P, Requena L, Sánchez Yus E. How rare is melanoacanthoma? *Arch Dermatol*. 1991;127:583–584.
27. Tomich C, Zunt S. Melanoacanthosis (melanoacanthoma) of the oral mucosa. *J Dermatol Surg Oncol*. 1990;16:231–236.
28. Li J, Ackerman AB. "Seborrheic keratoses" that contain human papillomavirus are condylomata acuminata. *Am J Dermatopathol*. 1994;16:398–405.
29. Schueller W. Acrokeratosis verruciformis of Hopf. *Arch Dermatol*. 1972;106:81–83.
30. Baumann LS, Blauvelt A, Draelos ZD, et al. Safety and efficacy of hydrogen peroxide topical solution, 40% (w/w), in patients with seborrheic keratoses: results from 2 identical, randomized, double-blind, placebo-controlled, phase 3 studies (A-101-SEBK-301/302). *J Am Acad Dermatol*. 2018;79:869–877.
31. Berger TG, Graham JH, Goette DK. Lichenoid benign keratosis. *J Am Acad Dermatol*. 1984;11:635–638.
32. Groesser L, Herschberger E, Landthaler M, Hafner C. FGFR3, PIK3CA and RAS mutations in benign lichenoid keratosis. *Br J Dermatol*. 2012;166:784–788.
33. Prieto VG, Casal M, McNutt NS. Lichen planus-like keratosis: a clinical and histologic reexamination. *Am J Surg Pathol*. 1993;17:259–263.
34. Morgan MB, Stevens GL, Switlyk S. Benign lichenoid keratosis. A clinical and pathologic reappraisal of 1040 cases. *Am J Dermatopathol*. 2005;27:387–392.
35. Pitney L, Weedon D, Pitney M. Multiple lichen planus-like keratoses: lichenoid drug eruption simulant and under-recognised cause of pruritic eruptions in the elderly. *Australas J Dermatol*. 2016;57:54–56.
36. Metin SA, Lee BW, Lambert WC, Parish LC. Dermatosis papulosa nigra: a clinically and histopathologically distinct entity. *Clin Dermatol*. 2017;35:491–496.
37. Hafner C, Landthaler M, Mentzel T, Vogt T. FGFR3 and PIK3CA mutations in stucco keratosis and dermatosis papulosa nigra. *Br J Dermatol*. 2010;162:508–512.
38. Astori G, Lavergne D, Benton C, et al. Human papillomaviruses are commonly found in normal skin of immunocompetent hosts. *J Invest Dermatol*. 1998;110:752–755.
39. Shall L, Marks R. Stucco keratoses. A clinico-pathological study. *Acta Derm Venereol*. 1991;71:258–261.
40. Dover JS, Phillips TJ, Burns DA. Disseminated superficial actinic porokeratosis: coexistence with other porokeratotic variants. *Arch Dermatol*. 1986;122:887–889.
41. Lucker GP, Steiflen PM. The coexistence of linear and giant porokeratosis associated with Bowen's disease. *Dermatology*. 1994;189:78–80.
42. Zhang Z, Li C. Genomic variations of the mevalonate pathway in porokeratosis. *eLife*. 2015;4:e06322.
43. Zhang SQ, Jiang T, Li M, et al. Exome sequencing identifies MVK mutations in disseminated superficial actinic porokeratosis. *Nat Genet*. 2012;44:1156–1160.
44. Cui H, Li L, Wang W, et al. Exome sequencing identifies SCL17A9 pathogenic gene in two Chinese pedigrees with disseminated superficial actinic porokeratosis. *J Med Genet*. 2014;51:699–704.
45. Atzmony L, Khan HM, Lim YH, et al. Second-hit, postzygotic *PMVK* and *MVD* mutations in linear porokeratosis. *JAMA Dermatol*. 2019;155:548–555.
46. Kubo A, Sasaki T, Suzuki H, et al. Clonal expansion of second-hit cells with somatic recombinations or C>T transitions form porokeratosis in MVD or MVK mutant heterozygotes. *J Invest Dermatol*. 2019;139:2458–2466.
47. Shumack SP, Commens CA. Disseminated superficial actinic porokeratosis: a clinical study. *J Am Acad Dermatol*. 1989;20:1015–1022.

48. McDonald SG, Peterka ES. Porokeratosis (Mibelli): treatment with topical 5-fluorouracil. *J Am Acad Dermatol*. 1983;8:107–110.
49. Rahbari H, Cordero A, Mehregan A. Punctate porokeratosis. A clinical variant of porokeratosis of Mibelli. *J Cutan Pathol*. 1977;4:338–341.
50. Yeo J, Winhoven S, Tallon B. Porokeratosis ptychotropica: a rare and evolving variant of porokeratosis. *J Cutan Pathol*. 2013;40:1042–1047.
51. Sasson M, Krain A. Porokeratosis and cutaneous malignancy: a review. *Dermatol Surg*. 1996;22:339–342.
52. Han YW, Kim YJ, Kim HO, Park YM. Clinical study of porokeratosis associated with immunosuppressive therapy in renal transplant recipients. *Ann Dermatol*. 2008;20:167–171.
53. Helfman RJ, Poulos EG. Reticulated porokeratosis: a unique variant of porokeratosis. *Arch Dermatol*. 1985;121:1542–1543.
54. de Almeida Jr HL, Guarenti MIM, de Castro LAS, Rocha NM. Follicular involvement in porokeratosis. *J Eur Acad Dermatol Venereol*. 2007;21:109–111.
55. Mendoza-Londono R, Lammer E, Watson R, et al. Characterization of a new syndrome that associates craniosynostosis, delayed fontanel closure, parietal foramina, imperforate anus, and skin eruption: CDAGS. *Am J Hum Genet*. 2005;77:161–168.
56. Parks AC, Conner KJ, Armstrong CA. Long-term clearance of linear porokeratosis with tacrolimus 0.1% ointment. *JAMA Dermatol*. 2014;150:194–196.
57. Rabbin PE, Baldwin HE. Treatment of porokeratosis of Mibelli with CO_2 laser vaporization versus surgical excision with split-thickness skin graft: a comparison. *J Dermatol Surg Oncol*. 1993;19:199–202.
58. Spencer JM, Katz BE. Successful treatment of porokeratosis of Mibelli with diamond fraise abrasion. *Arch Dermatol*. 1992;128:1187–1188.
59. Atzmony L, Lim YH, Hamilton C, et al. Topical cholesterol/lovastatin for the treatment of porokeratosis: a pathogenesis-directed therapy. *J Am Acad Dermatol*. 2020;82:123–131.
60. Goldman GD, Milstone LM. Generalized linear porokeratosis treated with etretinate. *Arch Dermatol*. 1995;131:496–497.
61. Bean S. Hyperkeratosis lenticularis perstans: a clinical, histopathologic, and genetic study. *Arch Dermatol*. 1969;99:705–709.
62. Miranda-Romero A, Sanchez Sambucety P, Bajo del Pozo C, et al. Unilateral hyperkeratosis lenticularis perstans (Flegel's disease). *J Am Acad Dermatol*. 1998;39:655–657.
63. Jang K, Choi J, Sung K, et al. Hyperkeratosis lenticularis perstans (Flegel's disease): histologic, immunohistochemical, and ultrastructural features in a case. *Am J Dermatopathol*. 1999;21:395–398.
64. Bortoluzzi P, Cusini M, Veraldi S, Nazzaro G. Hyperkeratosis lenticularis perstans (Flegel's disease): our experience and review of the literature. *Int J Dermatol*. 2021;60:33–38.
65. Langer K, Zonzits E, Konrad K. Hyperkeratosis lenticularis perstans (Flegel's disease). *J Am Acad Dermatol*. 1992;27:812–816.
66. Ronan A, Ingrey A, Murray N, Chee P. Recurrent ATP2A2 p.(Pro602Leu) mutation differentiates acrokeratosis verruciformis of Hopf from the allelic condition Darier disease. *Am J Med Genet A*. 2017;173:1975–1978.
67. Sathyanarayana SA, Deutsch GB, Edelman M, Cohen-Kashi KJ. Cutaneous horn: a malignant lesion? A brief review of the literature. *Dermatol Surg*. 2012;38:285–287.
68. Balus L, Cainelli T, Cristiani R, et al. Multiple familial clear cell acanthoma. *Ann Dermatol Venereol*. 1984;111:665–666.
69. Hashimoto T, Inamoto N, Nakamura K, et al. Involucrin expression in skin appendage tumours. *Br J Dermatol*. 1987;117:325–332.
70. Akiyama M, Hayakawa K, Watanabe Y, et al. Lectin-binding sites in clear cell acanthoma. *J Cutan Pathol*. 1990;17:197–201.
71. Kwittken J. Clear cell acanthoma: a metabolic variant of seborrheic keratosis. *Mt Sinai J Med*. 1980;47:49–51.
72. Finch TM, Tan CY. Clear cell acanthoma developing on a psoriatic plaque: further evidence of an inflammatory aetiology? *Br J Dermatol*. 2000;142:842–844.
73. Degos R, Civatte J. Clear-cell acanthoma. Experience of 8 years. *Br J Dermatol*. 1970;83:248–254.
74. Fine R, Chernosky M. Clinical recognition of clear-cell acanthoma (Degos'). *Arch Dermatol*. 1969;100:559–563.
75. Innocenzi D, Barduagni F, Cerio R, et al. Disseminated eruptive clear cell acanthoma – a case report with review of the literature. *Clin Exp Dermatol*. 1994;19:249–253.
76. Naeyaert J, de Bersaques J, Geerts M, et al. Multiple clear cell acanthomas. A clinical, histological, and ultrastructural report. *Arch Dermatol*. 1987;123:1670–1673.
77. García-Gavín J, González-Vilas D, Montero I, et al. Disseminated eruptive clear cell acanthoma with spontaneous regression: further evidence of an inflammatory origin? *Am J Dermatopathol*. 2011;33:599–602.
78. Kuo KL, Lo CS, Lee LY, Yang CH, Kuo TT. Clear cell acanthoma (CCA)-like lesions of the nipple/areola: a clinicopathological study of 12 cases supporting a nonneoplastic eczematous disease. *J Am Acad Dermatol*. 2019;80:749–755.
79. Kaddu S, Dong H, Mayer G, Kerl H, Cerroni L. Warty dyskeratoma—"follicular dyskeratoma": analysis of clinicopathologic features of a distintive follicular adnexal neoplasm. *J Am Acad Dermatol*. 2002;47:423–428.
80. Lee TJ, Wu YH. Multiple epidermolytic acanthomas mimicking condyloma: a retrospective study of 8 cases. *Int J Dermatol*. 2018;57:28–33.
81. Metzler G, Sonnichsen K. Disseminated epidermolytic acanthoma. *Hautarzt*. 1997;48:740–742.
82. Banky JP, Turner RJ, Hollowood K. Multiple scrotal epidermolytic acanthomas; secondary to trauma? *Clin Exp Dermatol*. 2004;29:489–491.
83. Cheraghiou S, Atzmony L, Roy SF, et al. Mutations in KRT10 in epidermolytic acanthoma. *J Cutan Pathol* 202;47:524–9.
84. Bogale SR, Chan CS, McIntire H, Hsu S. Epidermolytic acanthoma of the scrotum: a rare mimicker of condyloma acuminatum. *Dermatol Online J*. 2011;17:6.
85. Sanchez Yus E, de Diego V, Urrutia S. Large cell acanthoma. A cytologic variant of Bowen's disease? *Am J Dermatopathol*. 1988;10:197–208.
86. Pinkus H. Epidermal mosaic in benign and precancerous neoplasia (with special reference to large-cell acanthoma). *Acta Dermatol (Kyoto)*. 1970;65:75–81.
87. Sanchez Yus E, del Rio E, Requena L. Large-cell acanthoma is a distinctive condition. *Am J Dermatopathol*. 1992;14:140–148.
88. Fraga GR, Amin SM. Large cell acanthoma: a variant of solar lentigo with cellular hypertrophy. *J Cutan Pathol*. 2014;41:733–739.
89. Meschia JF, Junkins E, Hofman KJ. Familial systematized epidermal nevus syndrome. *Am J Med Genet*. 1992;44:664–667.
90. Santos Silva LF, Miroux-Catarino A, Pimentel B, et al. Familial cases of PENS: a review of the literature. *Am J Dermatopathol*. 2020;42:593–596.
91. Rogers M, McCrossin I, Commens C. Epidermal nevi and the epidermal nevus syndrome. A review of 131 cases. *J Am Acad Dermatol*. 1989;20:476–488.
92. Adams B, Mutasim D. Adult onset verrucous epidermal nevus. *J Am Acad Dermatol*. 1999;41:824–826.
93. Su W. Histopathologic varieties of epidermal nevus. A study of 160 cases. *Am J Dermatopathol*. 1982;4:161–170.
94. Submoke S, Piamphongsant T. Clinico-histopathological study of epidermal naevi. *Australas J Dermatol*. 1983;24:130–136.
95. Solomon L, Esterly N. Epidermal and other congenital organoid nevi. *Curr Probl Pediatr*. 1975;6:1–56.
96. Levin A, Amazon K, Rywlin A. A squamous cell carcinoma that developed in an epidermal nevus. Report of a case and a review of the literature. *Am J Dermatopathol*. 1984;6:51–55.
97. Braunstein B, Mackel S, Cooper P. Keratoacanthoma arising in a linear epidermal nevus. *Arch Dermatol*. 1982;118:362–363.
98. Umegaki-Arao N, Sasaki T, Fujita H, et al. Inflammatory linear verrucous epidermal nevus with a postzygotic *GJA1* mutation is a mosaic erythrokeratodermia variabilis et progressiva. *J Invest Dermatol*. 2017;137:967–970.
99. Riachi M, Polubothu S, Stadnik P, et al. Molecular genetic dissection of inflammatory linear verrucous epidermal naevus leads to successful targeted therapy. *J Invest Dermatol*. 2021;141:2979–2983.
99a. Atzmony L, Ugwu N, Hamilton C, et al. Inflammatory linear verrucous epidermal nevus (ILVEN) encompasses a spectrum of inflammatory mosaic disorders. *Pediatr Dermatol*. 2022;39:903–907.
100. Lee SH, Rogers M. Inflammatory linear verrucous epidermal naevi: a review of 23 cases. *Australas J Dermatol*. 2001;42:252–256.
101. Kawaguchi H, Takeuchi M, Ono H, et al. Adult onset of inflammatory linear verrucous epidermal nevus. *J Dermatol*. 1999;26:599–602.
102. Goldman K, Don P. Adult onset of inflammatory linear verrucous epidermal nevus in a mother and her daughter. *Dermatology*. 1994;189:170–172.
103. Al-Enezi S, Huber A, Krafchik B, et al. Inflammatory linear verrucous epidermal nevus and arthritis: a new association. *J Pediatr*. 2001;138:602–604.
104. Happle R. The group of epidermal nevus syndromes Part I. Well defined phenotypes. *J Am Acad Dermatol*. 2010;63:1–22.
105. Altster T. Inflammatory linear verrucous epidermal nevus: successful treatment with the 585 nm flashlamp-pumped pulsed dye laser. *J Am Acad Dermatol*. 1994;31:513–514.
106. Kim J, Chang M, Shwayder T. Topical tretinoin and 5-fluorouracil in the treatment of linear verrucous epidermal nevus. *J Am Acad Dermatol*. 2000;43:129–132.
107. Gatti S, Carrozzo AM, Orlandi A, et al. Treatment of inflammatory linear verrucous epidermal naevus with calcipotriol. *Br J Dermatol*. 1995;132:837–839.
108. Mitsuhashi Y, Katagiri Y, Kondo S. Treatment of inflammatory linear verrucous epidermal naevus with topical vitamin D3. *Br J Dermatol*. 1997;136:134–135.
109. Ferrari B, Taliercio V, Restrepo P, et al. Nevus comedonicus: a case series. *Pediatr Dematol*. 2015;32:216–219.
110. Levinsohn JL, Sugarman JL, Yale Center for Mendelian Genomics, et al. Somatic mutations in *NEK9* cause nevus comedonicus. *Am J Hum Genet*. 2016;98:1030–1037.
111. Munro CS, Wilkie AO. Epidermal mosaicism producing localised acne: somatic mutation in *FGFR2*. *Lancet*. 1998;352:704–705.
112. Inoue Y, Miyamoto Y, Ono T. Two cases of nevus comedonicus: successful treatment of keratin plugs with a pore strip. *J Am Acad Dermatol*. 2000;43:927–929.
113. Scheinfeld N. Confluent and reticulated papillomatosis. A review of the literature. *Am J Clin Dermatol*. 2006;7:305–313.
114. Buynzeel-Koomen CAFM, de Wit RFE. Confluent and reticulated papillomatosis successfully treated with aromatic etretinate. *Arch Dermatol*. 1984;120:1236–1237.
115. Nordby AC, Mitchell AJ. Confluent and reticulated papillomatosis responsive to selenium sulfide. *Int J Dermatol*. 1986;25:194–199.
116. Lee MP, Stiller MJ, McClain SA, et al. Confluent and reticulated papillomatosis: response to high-dose oral isotretinoin therapy and reassessment of epidemiologic data. *J Am Acad Dermatol*. 1994;31:327–331.
117. Tirado-Sánchez A, Ponce-Olivera RM. Tacrolimus in confluent and reticulated papillomatosis of Gougerot Carteaud. *Int J Dermatol*. 2013;52:513–514.
118. Chang SN, Kim SC, Lee SH, Lee WS. Minocycline treatment for confluent and reticulated papillomatosis. *Cutis*. 1996;57:454–457.
119. Wang D, Ho MS, Koh MJ, Giam YC. A case report of clear cell papulosis and a review of the literature. *Ann Acad Med Singap*. 2017;46:160–166.
120. Yu Y, Sukhatme S, Loo DS. Clear cell papulosis: a connection of clear cells to Toker cells or Paget disease. *Arch Dermatol*. 2009;145:1066–1068.
121. Tseng FW, Kuo TT, Lu PH, et al. Long-term follow-up study of clear cell papulosis. *J Am Acad Dermatol*. 2010;63:266–273.





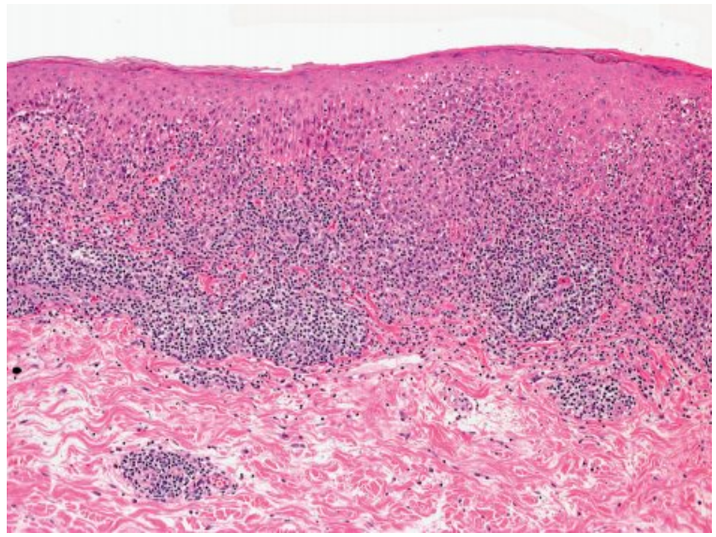
eFig. 109.1 Solar lentigines. A Sharply demarcated, uniform, tan macules on sun-exposed skin. **B** Dermoscopically, moth-eaten borders, fingerprinting, and a reticular pattern with thin lines, short and interrupted.



eFig. 109.2 Seborrheic keratoses. Multiple seborrheic keratoses on the back in a pattern that has been likened to raindrops.



eFig. 109.3 Seborrheic keratoses. Multiple seborrheic keratoses of the anterior trunk that vary in size and color.



eFig. 109.4 Lichenoid keratosis – histopathologic features. A lichenoid infiltrate beneath the epidermis with formation of a few Civatte bodies. Focal compact hyperkeratosis is also present, as well as many intraepidermal lymphocytes. Because the basal layer is often obscured, a careful search for a melanocytic lesion, including lentigo maligna, is warranted. *Courtesy Lorenzo Cerroni, MD.*



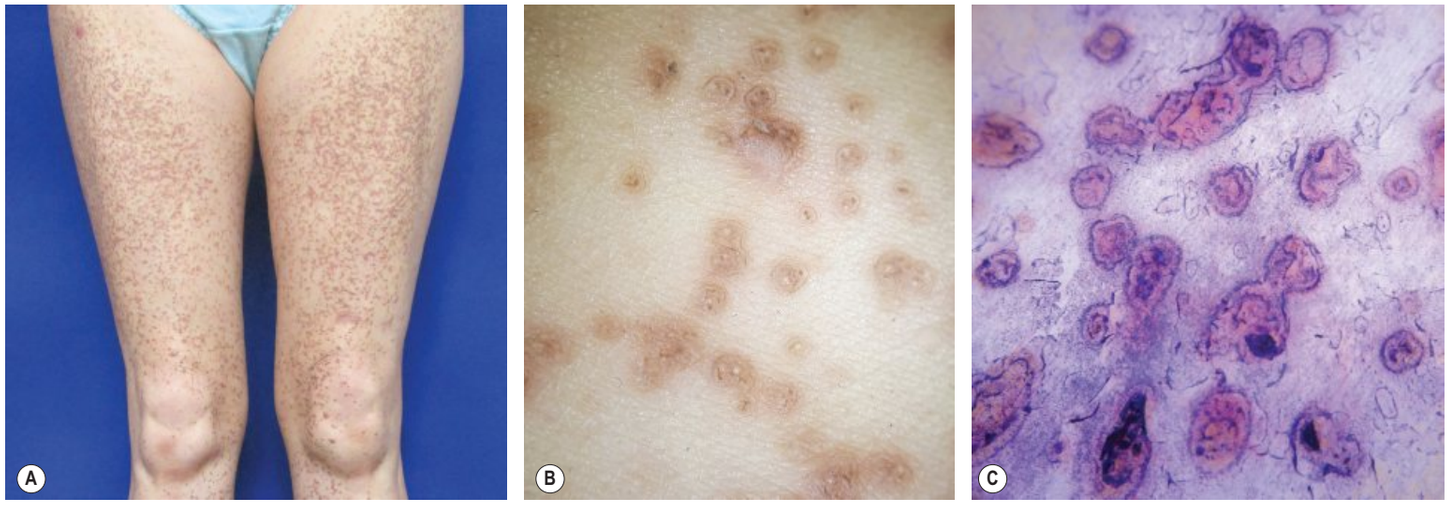
eFig. 109.5 Dermatosis papulosis nigra. Multiple hyperpigmented papules with typical location on the cheeks.



eFig. 109.6 Stucco keratoses. Multiple gray–white keratotic papules on the ankle and dorsal foot. *Courtesy Jean L. Bolognia, MD.*



eFig. 109.8 Disseminated superficial actinic porokeratosis. The shins are a common location and lesions can vary in color from pink to brown.



eFig. 109.7 Eruptive disseminated porokeratosis. A Numerous small pink papules in a symmetric pattern. **B** By dermoscopy, the characteristic border is visualized. **C** Addition of ink accentuates dermoscopic findings. *Courtesy Tessy Melissa Bernaola Prudencio, MD and Betty Sandoval Angelino, MD.*



eFig. 109.9 Dermoscopy of disseminated superficial actinic porokeratosis. The narrow keratotic border is easily visualized. *Courtesy Nan Ring, MD.*



eFig. 109.10 Linear porokeratosis in a patient who also has disseminated superficial actinic porokeratosis. This is an example of type 2 mosaicism (see Ch. 62). *Courtesy Kalman Watsky, MD.*



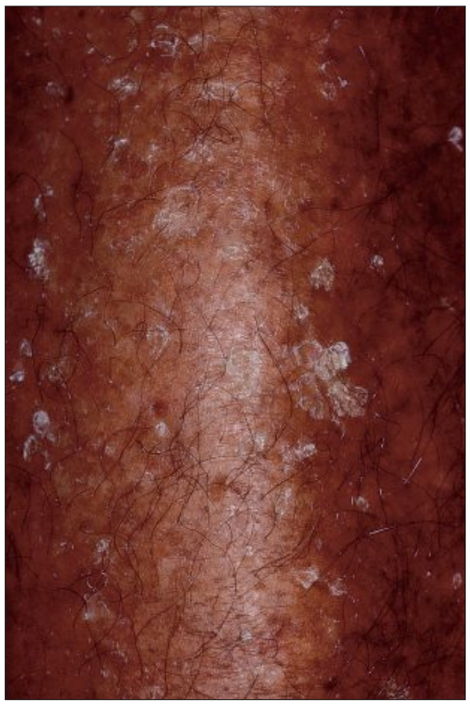
eFig. 109.11 Linear porokeratosis. Multiple brown streaks in a reticular (and linear) pattern on the lower extremity. *Courtesy Emily Berger, MD.*



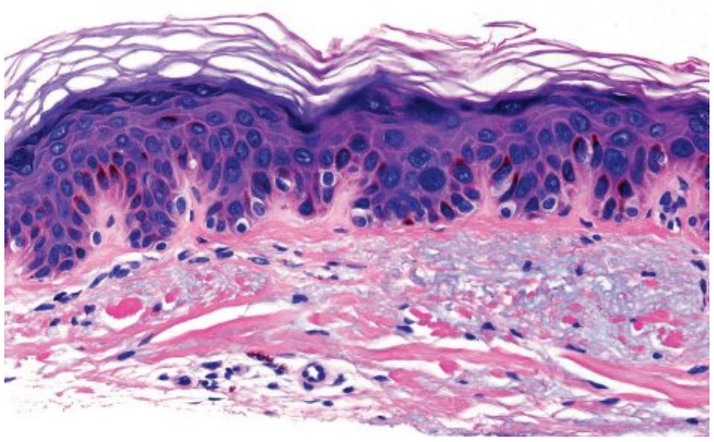
eFig. 109.12 Actinic porokeratosis in a renal transplant patient with significant solar damage. Note the narrow, elevated rim. *Courtesy Jean L. Bolognia, MD.*



eFig. 109.13 Porokeratosis – histopathologic features. The cornoid lamella, a narrow column of parakeratotic cells, is the typical histopathologic feature of porokeratosis. Note the absence of the granular layer beneath the cornoid lamella. *Courtesy Lorenzo Cerroni, MD.*



eFig. 109.14 Flegel disease (hyperkeratosis lenticularis perstans). Multiple symmetric keratotic papules are seen on the shins.



eFig. 109.15 Large cell acanthoma. Slight epidermal hyperplasia with enlarged cells, centrally and to the left.



eFig. 109.16 Epidermal nevus. Linear array of waxy papillomas on the left upper eyelid along the lines of Blaschko. Development of the central elevated verrucous papule prompted evaluation. *Courtesy Karynne O. Duncan, MD.*



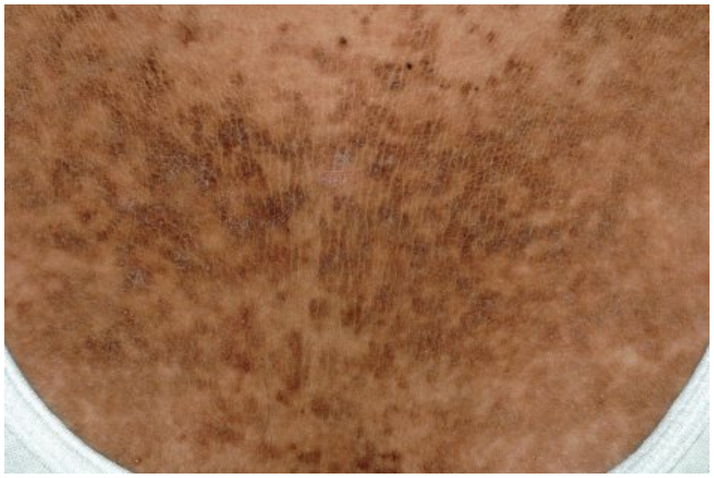
eFig. 109.17 Inflammatory linear verrucous epidermal nevus (ILVEN). Linear erythematous scaly plaques on the medial aspect of the right thigh. Some of the lesions have a psoriasiform appearance.



eFig. 109.18 Inflammatory linear verrucous epidermal nevus (ILVEN). Linear discontinuous dull pink plaque with scale along the lines of Blaschko. *Courtesy Department of Dermatology, Medical University of Graz.*



eFig. 109.19 Confluent and reticulated papillomatosis (CARP). Multiple hyperpigmented verrucous papules form a reticulated pattern.



eFig. 109.20 Confluent and reticulated papillomatosis (CARP). Multiple hyperpigmented papules on the chest that have a ridged pattern centrally and a reticulated pattern peripherally. *Courtesy Julie V. Schaffer, MD.*



eFig. 109.21 Confluent and reticulated papillomatosis (CARP). Multiple thin hyperpigmented papules of the chest and neck that have become confluent centrally and assume a reticulated pattern peripherally. *Courtesy Lorenzo Cerroni, MD*

110 Cysts

Mary Seabury Stone

Chapter Contents

Cysts with a Lining of Stratified Squamous Epithelium *1935*
Cysts Lined with Non-Stratified Squamous Epithelium *1942*
Cysts without an Epithelial Lining *1945*

Key features

- Cutaneous cysts present as circumscribed dermal or subcutaneous papules or nodules
- Cysts may be lined by either stratified squamous epithelium or non-stratified squamous epithelium; cystic structures without an epithelial lining are better classified as pseudocysts
- Histologic features of the cyst lining and the anatomic location determine the type of cyst
- Treatment of cysts, when indicated, is primarily surgical

INTRODUCTION

Cysts are common cutaneous lesions. Patients with cysts may present to clinicians because of medical or cosmetic concerns, or due to discomfort from mechanical irritation or inflammation of the cyst. The definitive diagnosis of a cyst requires histologic examination, as many other dermal and subcutaneous tumors can form cyst-like nodules. Cysts can be classified by anatomic location (as they may occur in virtually any organ of the body), by embryologic derivation, or by histologic features. As the histologic features determine the definitive diagnosis, that scheme will be used in this chapter, which is limited to cutaneous cysts.

True cysts have an epithelial lining that may be composed of stratified squamous epithelium or other forms of epithelia while "pseudocysts" have no epithelial lining at all. Cutaneous cysts can be divided into three main categories based on the presence or absence and composition of the cyst wall (Table 110.1; Fig. 110.1). Many non-dermatologists refer to epidermoid and pilar cysts as "sebaceous cysts", possibly believing erroneously that the hydrated white keratinized contents of many epithelial-lined cysts is of sebaceous origin. The only true sebaceous cyst is the steatocystoma. The term "sebaceous cyst" is best avoided.

CYSTS WITH A LINING OF STRATIFIED SQUAMOUS EPITHELIUM

Epidermoid Cyst

Synonyms: ■ Epidermal inclusion cyst ■ Infundibular cyst ■ Epidermal cyst

Epidermoid cysts are the most common cutaneous cysts. They can occur anywhere on the skin, but are most common on the face and upper trunk. These lesions are well-demarcated, skin-colored to yellowish dermal nodules, and they may have a clinically visible punctum representing the follicle from which the cyst is derived (Fig. 110.2). Epidermoid cysts range from a few millimeters to several centimeters in diameter. Tiny superficial epidermoid cysts are known as milia (see below). These cysts derive from the follicular infundibulum, hence

THE THREE MAIN CATEGORIES OF CUTANEOUS CYST

Category	Type	Most common location
Stratified squamous epithelium	Epidermoid (infundibular) cyst	Face; upper trunk
	Milium	Face
	Tricholemmal cyst	Scalp
	Proliferating tricholemmal cyst	Scalp (favors elderly women)
	Proliferating epidermoid (infundibular) cyst	Pelvic (anogenital)
	Vellus hair cyst	Trunk (chest)
	Steatocystoma	Trunk; axillae; groin
	Cutaneous keratocyst	No characteristic location
	Pigmented follicular cyst	Face (men)
	Dermoid cyst	Face along embryonic fusion planes, e.g. lateral eyebrow (infants)
	Verrucous cyst	Face; upper trunk; plantar surface (HPV-infected epidermoid cysts)
	Ear pit cyst Pilonidal cyst	Preauricular Upper gluteal cleft; sacrococcygeal area
Non-stratified squamous epithelium	Hidrocystoma	
	• Eccrine	Face (lower eyelid, cheek)
	• Apocrine	Face (eyelid margin)
	Bronchogenic cyst	Suprasternal notch (infants)
	Thyroglossal duct cyst	Midline anterior neck
	Branchial cleft cyst	Lateral neck; preauricular; mandibular (teenagers, young adults)
	Cutaneous ciliated cyst	Lower extremities (young women)
	Ciliated cyst of the vulva	Labia majora
	Median raphe cyst	Ventral glans and penile shaft
	Omphalomesenteric duct cyst	Umbilical; periumbilical
Absence of epithelium (pseudocysts)	Mucocele	Oral mucosa (lower labial)
	Digital mucous cyst (pseudocyst)	Dorsal aspect of distal phalanx of finger (occasionally toe)
	Ganglion	Wrist
	Pseudocyst of the auricle	Scaphoid fossa of the ear (adult men)
	Cutaneous metaplastic synovial cyst (pseudocyst)	Sites of surgical trauma

Table 110.1 The three main categories of cutaneous cyst.

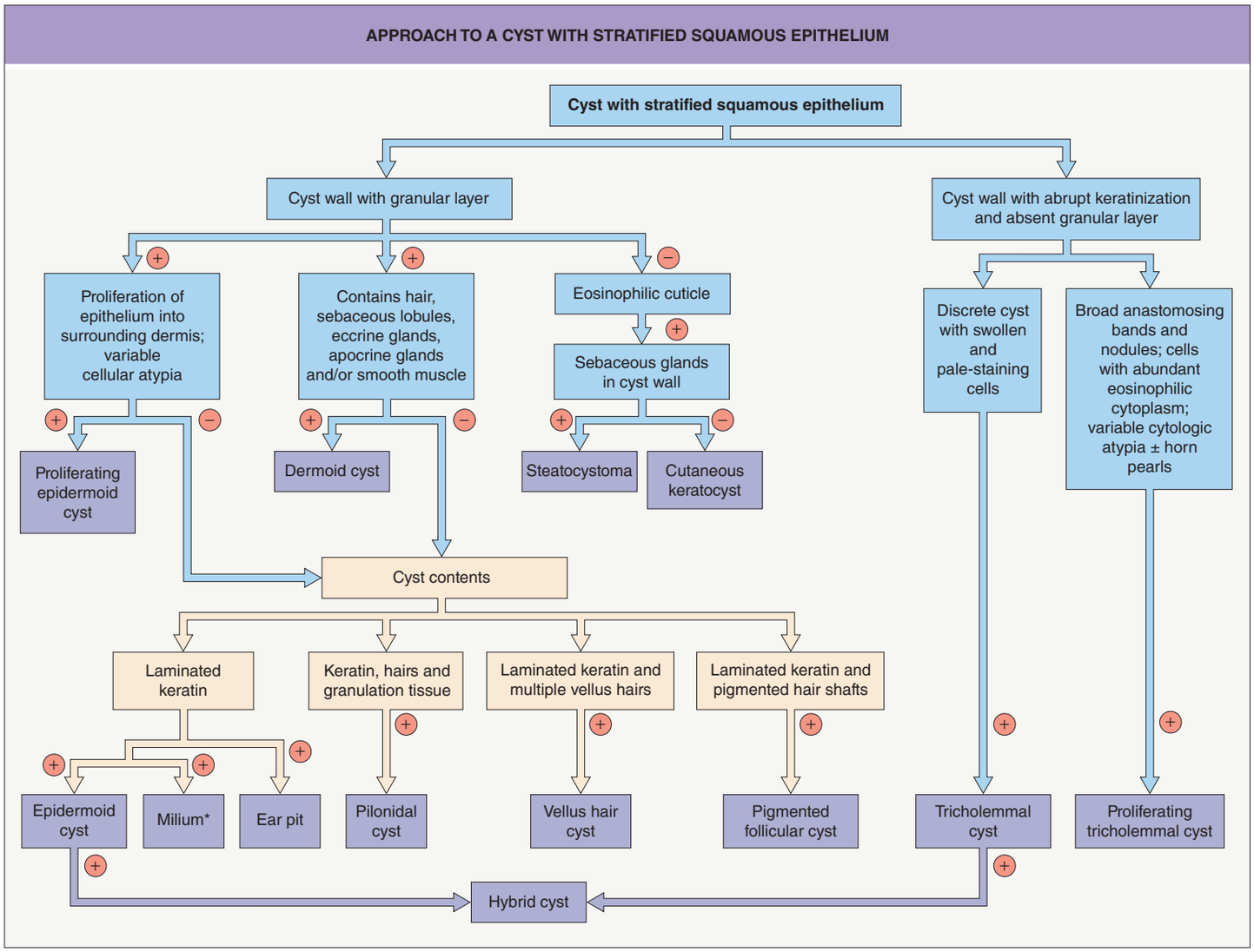


Fig. 110.1 Approach to a cyst with stratified squamous epithelium. *Diameter 1–2 mm.



Fig. 110.2 Epidermoid cyst. Typical clinical appearance of an epidermoid cyst with a yellowish hue. Two pores are present in this example.

the synonym infundibular cysts (Fig. 110.3). They may be primary, or they may arise from disrupted follicular structures or traumatically implanted epithelium (hence the synonym epidermal "inclusion" cyst).

As follicular disruption is important in the pathogenesis of many epidermoid cysts, multiple epidermoid cysts may occur in individuals with a history of significant acne vulgaris. Multiple cysts may also occur in the setting of Gardner syndrome (familial adenomatous polyposis) and in basal cell nevus syndrome[1,2]. Patients receiving cyclosporine to prevent solid organ transplant rejection or BRAF inhibitors, both non-selective (e.g. sorafenib) and selective (e.g. vemurafenib), can develop multiple epidermoid cysts or milia, often on the face[3]. Multiple scrotal cysts (Fig. 110.4) may lead to scrotal calcinosis via dystrophic calcification[4].

Non-inflamed epidermoid cysts are usually asymptomatic, but with pressure, cyst contents may be expressed that may have an objectionable odor. Rupture of the cyst wall can result in an intensely painful inflammatory reaction, and this is a common reason for presentation to a physician (Fig. 110.5). Development of a basal cell carcinoma (BCC) or squamous cell carcinoma (SCC) within an epidermoid cyst is a very rare event.

Pathology

Histologic examination shows a cystic cavity filled with laminated keratin lined by a stratified squamous epithelium that includes a granular layer (Fig. 110.6). A surrounding inflammatory response with both acute suppurative and chronic granulomatous inflammation as well as variable fibrosis may be seen as evidence of prior rupture. In individuals with Gardner syndrome, some cysts have, as a characteristic feature, columns of pilomatricoma-like shadow cells projecting into the cyst cavity[1].

Treatment

If treatment is desired, excision is curative. Removal may be accomplished by simple excision, or incision and expression of the cyst contents and wall through the surgical defect. If the entire cyst wall is not removed, the cyst may recur. Excision is best performed when the cyst is non-inflamed ("cold"). Inflamed epidermoid cysts may require incision and drainage, and occasionally, antibiotic therapy. Intralesional injections of triamcinolone may speed resolution of the inflammation.

Dilated Pore of Winer

Dilated pore of Winer presents as a single dilated comedo, primarily occurring on the face of adults.

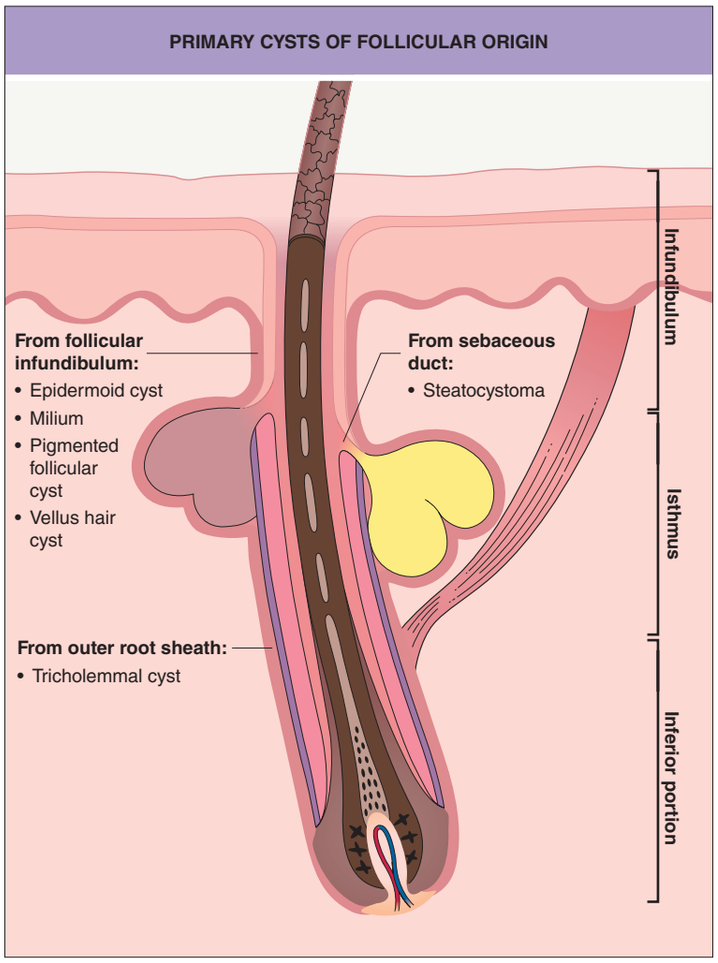


Fig. 110.3 Primary cysts of follicular origin. Anatomic origin of cysts derived from the pilosebaceous unit. *Adapted from Requena L, Sanchez Yus E. Follicular hybrid cysts. An expanded spectrum. Am J Dermatopathol 1991;13:228–33.*



Fig. 110.4 Multiple epidermoid cysts of the scrotum. *Courtesy Lorenzo Cerroni, MD.*

Pathology

A dilated follicular opening, filled with keratinous debris and lined by squamous epithelium with a granular layer, is seen. The lining is acanthotic with finger-like projections pushing into the surrounding dermis.



Fig. 110.5 Inflamed epidermoid cyst. Such painful inflammatory reactions to cyst rupture are a frequent cause for presentation to a physician.

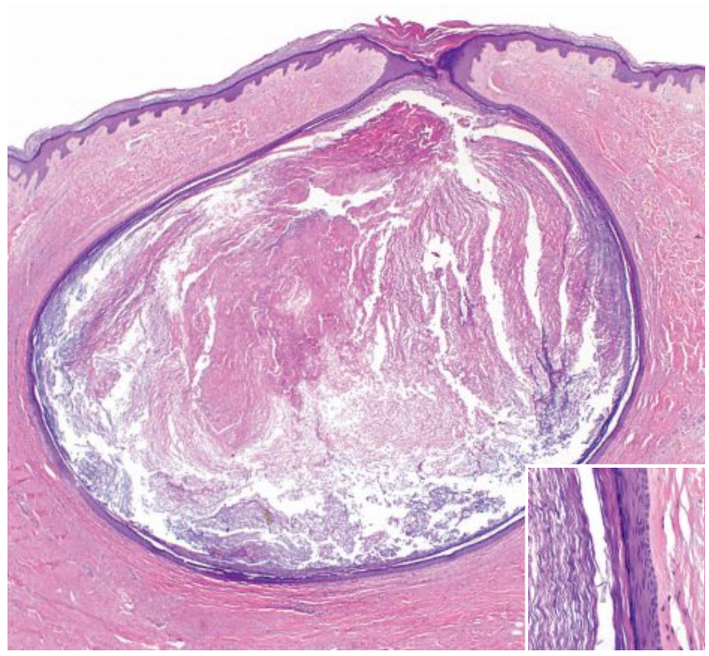


Fig. 110.6 Histopathology of an epidermoid cyst. Laminated keratin within an epithelial-lined cyst in the dermis. The cyst wall shows infundibular keratinization including a granular layer (inset).

Differential diagnosis

Although there is usually a more papular component, an obvious pore can be seen in a pilar sheath acanthoma, trichoepithelioma, and large-pore BCC.

Treatment

If treatment is desired, excision is curative.

Milium

Milia are small superficial cysts and are quite common, occurring in individuals of all ages. They may originate from the infundibulum of hair follicles or from eccrine ducts, and in the mouth from minor salivary gland ducts or from epithelium entrapped within embryologic fusion planes. Milia present as 1–2 mm, firm, white to yellow, subepidermal papules (Fig. 110.7).

Between 40% and 50% of infants will have milia, most commonly on the face. Most milia in newborns will resolve spontaneously during the first 4 weeks of life. Milia in newborns may also occur on the hard palate (Epstein pearls) or on the alveolar ridges (Bohn nodules). These also resolve spontaneously. Milia may occur as a primary phenomenon, especially on the face, or as secondary phenomena following blistering processes (e.g. porphyria cutanea tarda, epidermolysis bullosa acquisita) or superficial ulceration from trauma or cosmetic procedures. Milia



Fig. 110.7 Milia. Tiny (1–2 mm), white, dome-shaped papules on the face.

may also occur in areas of topical corticosteroid-induced atrophy[5], in follicular mycosis fungoides, and as a side effect of BRAF inhibitors (see above).

Milia en plaque is characterized by multiple milia within an erythematous edematous plaque, and the most common location is the postauricular area. Numerous milia in an infant may be a sign of oral–facial–digital syndrome type 1, an X-linked disorder that is lethal in males, in which milia are associated with facial and skull malformations, cleft lip and palate, a lobulated tongue, developmental delay, and polycystic kidneys; the associated alopecia follows the lines of Blaschko on the scalp. Milia are also seen in the setting of a number of other syndromes, including the BCC-associated syndromes basal cell nevus syndrome, Rombo syndrome, and Bazex–Dupré–Christol syndrome, as well as atrichia with papular lesions, Loeys–Dietz syndrome, basaloid follicular hamartoma syndrome, Basan syndrome, hypohidrotic ectodermal dysplasia, and a subset of Brooke–Spiegler syndrome (Rasmussen syndrome).

Pathology

Histologic features are those of a small epidermoid cyst with a stratified squamous epithelial lining that includes a granular layer. The cyst contents consist of laminated keratin.

Treatment

Milia may be removed by incising the epidermis over the milium with a needle, scalpel, or lancet and expressing the milium. The latter can be aided by the use of a comedo extractor. Laser ablation and electrodesiccation are also reported options. For multiple facial milia, topical retinoid therapy may be helpful in reducing the number of new milia and aiding in the ease of removal.

Tricholemmal Cyst

Synonyms: ■ Trichilemmal cyst ■ Pilar cyst ■ Wen ■ Isthmus–catagen cyst

Tricholemmal cysts are clinically indistinguishable from epidermoid cysts, but they are fourfold to fivefold less common. Ninety percent of tricholemmal cysts are located on the scalp (Fig. 110.8A). They may be solitary, but frequently are multiple, and they may be inherited as an autosomal dominant trait due to a germline variant of *PLCD1*, which encodes phospholipase C delta 1a. Interestingly, the somatic mutations in the cysts were found to be on the same chromosome as the germline variant[5a].

Pathology

The walls of tricholemmal cysts show keratinization analogous to that of the outer root sheath of the hair follicle at the isthmus *and* the sac surrounding catagen and telogen hairs (hence the synonym isthmus–catagen cyst). Tricholemmal cysts are lined by stratified squamous epithelial cells that become swollen and pale close to the cystic cavity and show abrupt keratinization without an intervening granular layer (Fig. 110.9). The cyst contents consist of homogeneous, eosinophilic, compact material that often contains foci of calcification. A suppurative and/or granulomatous response may surround the cyst if prior wall rupture has occurred. Occasionally, if the outermost epithelial portion of the cyst wall separates from the remainder of the cyst, the histologic features can resemble a hidrocystoma.



Fig. 110.8 Tricholemmal cyst versus proliferating tricholemmal cyst. A A tricholemmal cyst is a well circumscribed, mobile, mid dermal nodule with a smooth surface. **B** A proliferating tricholemmal cyst presenting as a large skin-colored to light-pink nodule on the scalp. Both types of cyst favor the scalp. *B, Courtesy Luis Requena, MD.*

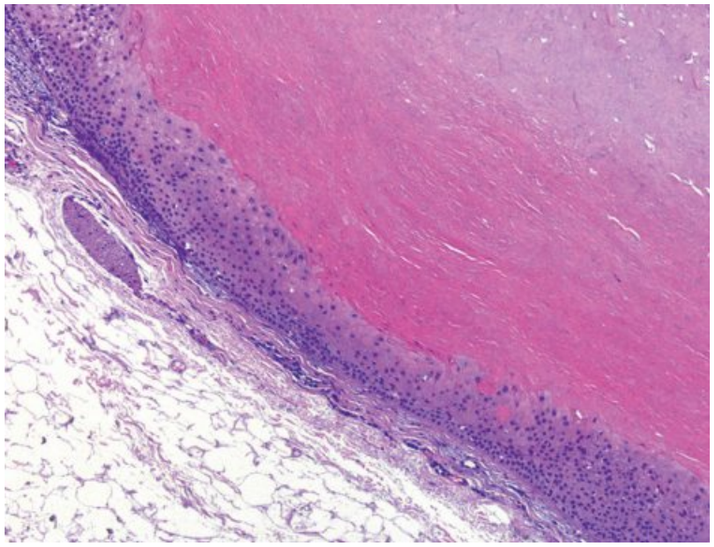


Fig. 110.9 Histopathology of a tricholemmal cyst. The cyst wall shows swollen keratinocytes with abrupt keratinization without formation of a granular layer. Compact, eosinophilic keratin fills the cyst. *Courtesy Luis Requena, MD.*

Differential diagnosis

In addition to epidermoid cysts, ruptured pilar cysts of the scalp can overlap with alopecic and aseptic nodules of the scalp.

Treatment

Treatment is by excision. Tricholemmal cysts typically "deliver" themselves through an incision without rupture more easily than do epidermoid cysts, and, therefore, the distinction between a tricholemmal cyst and an epidermoid cyst can often be correctly made at the time of excision.

Verrucous Cyst

HPV infection of the lining of an epidermoid, or rarely a tricholemmal, cyst can lead to a verrucous cyst. Verrucous cysts occur most commonly

on the face, upper trunk, and plantar surface and may harbor a number of different HPV types, including those associated with epidermodysplasia verruciformis. In verrucous plantar cysts, HPV 60 has been the most commonly reported HPV type. Verrucous cysts have also been observed in association with proliferating epidermoid cysts and have been hypothesized to be a possible precursor[6].

Pathology

In addition to features of an epidermoid or tricholemmal cyst, these cysts have a lining with verrucous features including acanthosis, papillomatosis, focal hypergranulosis with coarse keratohyalin granules, and occasionally koilocytes.

Treatment

Excision is curative.

Proliferating Tricholemmal Cyst

Synonyms: ■ Proliferating trichilemmal cyst ■ Proliferating tricholemmal tumor ■ Proliferating pilar tumor ■ Proliferating follicular cystic neoplasm

A proliferating tricholemmal cyst classically occurs as a slow-growing nodule on the scalp (see Fig. 110.8B). Ninety percent occur on the scalp and ~85% occur in women, with a median age of 63 years[7]. Proliferating tricholemmal cysts vary in size from a few millimeters to up to 25 cm in diameter. These tumors generally behave in a benign fashion, although on occasion, aggressive local growth with recurrences and metastases has been observed[7,8]. Extremely rarely, spindle cell carcinomas may develop within a proliferating tricholemmal cyst[9]. Distant metastases are rare.

Pathology

The histologic features of a proliferating tricholemmal cyst consist of broad anastomosing bands and nodules of squamous epithelium (Fig. 110.10). The epithelium consists of a proliferation of cells with abundant eosinophilic cytoplasm; the cells undergo abrupt keratinization and form dense homogeneous keratin that fills cystic spaces. There may be areas of epidermoid keratinization with formation of horn pearls as well as areas of foreign body giant cell reaction. One-quarter of cases show an epidermal connection[5]. Cytologic atypia can vary markedly. Most tumors show well-circumscribed, pushing borders surrounded by compressed collagen. The lack of infiltrative growth into the surrounding stroma and abrupt tricholemmal keratinization helps to differentiate these cysts from SCC. Areas of marked atypia and infiltrative borders are features associated with a potential for aggressive behavior[10].

Treatment

Treatment is by complete surgical excision.

Proliferating Epidermoid Cyst

Synonyms: ■ Proliferating epithelial cyst ■ Proliferating infundibular cyst

Proliferating epidermoid cysts were first described in detail in 1995[7]. Unlike proliferating tricholemmal cysts, proliferating epidermoid cysts are observed more commonly in men and only 20% occur on the scalp. The most common location is the anogenital region. They range in size from 0.5 to 15 cm. In a series of 30 patients for whom follow-up was available, 20% of the cysts recurred, some multiple times, and one patient died of intractable local disease[7]. None of the patients developed metastatic disease.

Pathology

Histologically, almost half of cases show an epidermal connection, usually with a narrow opening or connection to a dilated follicle. Most tumors show areas of typical epidermoid cyst wall. In addition, areas of squamous proliferation with squamous eddy formation are seen, with formation of a granular layer and production of loose laminated keratin. The epithelium tends to proliferate peripherally into the surrounding dermis, rather than centrally as seen in proliferating tricholemmal cysts. Degrees of cellularity and atypia are variable, and frank carcinomatous change with an infiltrative growth pattern may be seen.



Fig. 110.10 Histopathology of a proliferating tricholemmal cyst. Well-circumscribed nodules of squamous epithelium in the dermis. Within their central portions, abrupt keratinization is seen. *Courtesy Lorenzo Cerroni, MD.*

Treatment

Treatment is by complete surgical excision.

Vellus Hair Cysts

Vellus hair cysts, described by Esterly, Fretzin, and Pinkus in 1977[11], most commonly present as numerous, small, dome-shaped papules, ranging from skin-colored to darkly pigmented (Fig. 110.11). These cysts are most commonly located on the trunk, and they may be inherited in an autosomal dominant pattern. Multiple lesions are known as "eruptive" vellus hair cysts; occasionally, solitary cysts are seen. Although some lesions may resolve via transepidermal elimination of cyst products, most lesions persist indefinitely. Vellus hair cysts may become inflamed, but in general, they are asymptomatic except for cosmetic concerns.

Eruptive vellus hair cysts may be seen in conjunction with steatocystoma multiplex, and both types of cysts have been reported in the setting of pachyonychia congenita, most commonly PC-17 (see Ch. 58).

Pathology

Histologically, one sees a small cystic structure lined by stratified squamous epithelium with epidermoid (infundibular) keratinization. The cysts contain loose laminated keratin and numerous vellus hair shafts (Fig. 110.12). A follicle may be found entering the lower portion of the cyst.

Visualization of the vellus hair shafts via microscopic examination of expressed cyst contents allows for a bedside diagnosis.

Treatment

Vellus hair cysts may be treated by a number of modalities, including incision and drainage, needle evacuation, puncture followed by forceps-assisted extraction, topical retinoic or lactic acid, and laser ablation.



Fig. 110.11 Eruptive vellus hair cysts. Admixture of pigmented, skin-colored, and yellow–white papules of varying sizes on the trunk.



Fig. 110.12 Histopathology of a vellus hair cyst. A cyst shows epidermoid keratinization of its wall as well as laminated keratin and several vellus hair shafts within its cavity (inset).

Steatocystoma

Steatocystomas occur as single (steatocystoma simplex) or multiple (steatocystoma multiplex) lesions. They tend to be a few millimeters to a centimeter in diameter and appear as cysts within the dermis that drain oily fluid if punctured (Fig. 110.13A–C). Steatocystomas are most numerous on the chest and in the axillae and groin. There are unusual facial and acral variants as well as a rare congenital linear form. Steatocystomas persist indefinitely, and they are usually asymptomatic except for cosmetic concerns.

Steatocystoma multiplex can be inherited as an autosomal dominant condition, and is due to mutations in *KRT17*. It may occur in association with eruptive vellus hair cysts and pachyonychia congenita, most frequently PC-17 (see Fig. 58.11)[12,13].

Pathology

Biopsy specimens show a dermal cyst lined by a thin stratified squamous epithelium without a granular layer. The epithelium is surmounted by a thin, irregular, corrugated eosinophilic cuticle (Fig. 110.13D). Small sebaceous lobules are found in or immediately adjacent to the cyst wall. Cysts with the typical corrugated eosinophilic lining of steatocystoma, but with no adjacent sebaceous glands, have been termed cutaneous keratocyst or sebaceous duct cyst. The latter can be seen in patients with the basal cell nevus syndrome.

Treatment

Lesions can be excised or incised with removal of the cyst wall.

Follicular Hybrid Cyst

Synonym: ■ Hybrid cyst

Follicular hybrid cysts are not distinctive clinically, but rather represent a histologic variant of cysts with a stratified squamous lining in which there is transition in the cyst wall between epidermoid keratinization and tricholemmal or matrical keratinization[14,15]. They were originally described by Brownstein[15]. Hybrid cysts with features of both an epidermoid cyst and a keratocyst have been associated with the basal cell nevus syndrome[16].

Pigmented Follicular Cyst

Pigmented follicular cysts, described by Mehregan and Medenica[17], are usually solitary and occur primarily on the face of men. They are often deeply pigmented and may be confused clinically with a melanocytic nevus.

Histologically, these cysts have a pore-like connection to the epidermis, are lined by stratified squamous epithelium that includes a granular layer, and contain pigmented hair shafts. The clinical presentation, epidermal connection, and pigmented terminal hair shafts rather than vellus hair shafts distinguish the pigmented follicular cyst from vellus hair cysts.

Dermoid Cyst

Cutaneous dermoid cysts typically present in an infant along an embryonic fusion plane as a discrete, subcutaneous nodule (see Ch. 64). Dermoid cysts are usually 1–4 cm in diameter. The most common location is around the eyes.

Pathology

Histologically, dermoid cysts are lined by stratified squamous epithelium that includes a granular layer. They contain other normal cutaneous structures such as hair, sebaceous lobules, eccrine glands, apocrine glands, and/or smooth muscle.

Treatment

Treatment is by excision. However, as the differential diagnosis includes neural heterotopias, imaging studies may be appropriate prior to excision in order to exclude a connection to the CNS (see Ch. 64).

Ear Pit

Synonyms: ■ Preauricular cyst ■ Congenital auricular fistula ■ Preauricular fistula

Ear pits are congenital defects, and they may present as a true cystic nodule or an invagination in the preauricular area (Fig. 110.14). During development, the ear is formed by the fusion of six tubercles: three each from the first two branchial arches. Preauricular cysts reflect defective embryologic fusion with epithelial entrapment. These defects are relatively common, occurring in ~0.5%–1% of the normal population, and they may be transmitted in an autosomal dominant fashion[18]. Ear pits are usually unilateral and right-sided. Infection with tenderness and purulent drainage may prompt presentation to a physician.

Although ear pits are usually not associated with other significant abnormalities, they can occur in conjunction with deafness or with deafness plus renal anomalies in the branchio-otic syndrome and branchio-oto-renal syndrome, respectively. Ear pits are also seen in a number of other congenital syndromes, including Treacher Collins, Goldenhar, and cat-eye syndromes.

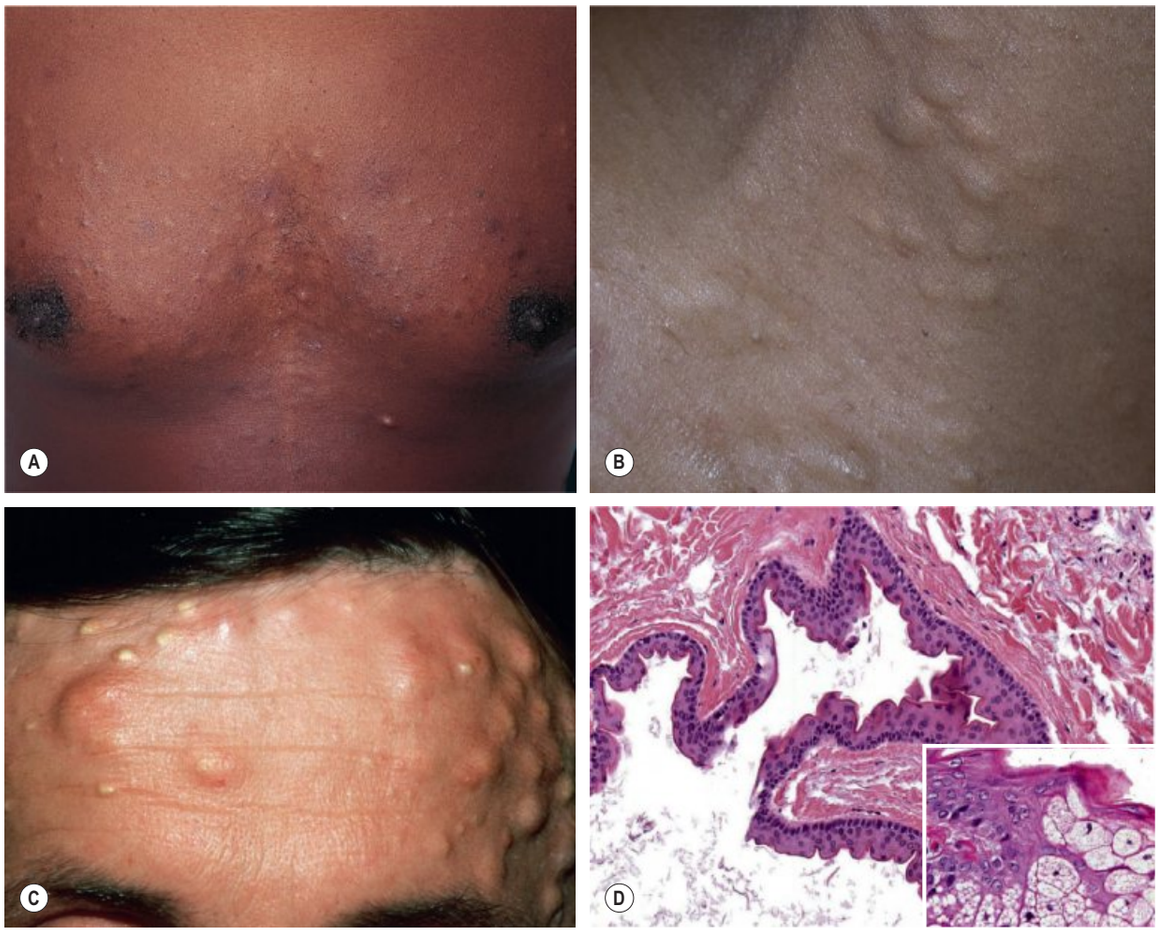


Fig. 110.13 Steatocystoma multiplex. A, B Numerous cystic papules on the trunk and multiple cystic nodules on the neck. **C** Larger cystic nodules on the forehead. **D** Histopathology of steatocystoma. The cyst wall is characterized by an undulated, thin stratified epithelium lacking a stratum granulosum and lined by an eosinophilic cuticle. A search may be required to identify small sebaceous lobules in or immediately adjacent to the cyst wall (inset). *C, Courtesy Luis Requena, MD; D, Courtesy Lorenzo Cerroni, MD.*



Fig. 110.14 Ear pit. *Courtesy Julie V. Schaffer, MD.*

Pathology

Histologically, preauricular pits or cysts are lined by stratified squamous epithelium with a granular layer.

Treatment

If removal is desired, simple excision is curative. Although most ear pits are incidental findings, in a newborn, a physical examination to exclude one of the associated syndromes and an evaluation for hearing loss is indicated. Infected lesions may require antibiotic therapy.

Pilonidal Cyst

Synonyms: ■ Pilonidal sinus ■ Pilonidal disease ■ Barber's interdigital pilonidal sinus (when located in the interdigital spaces)

Pilonidal cysts typically present as an inflamed, painful, cystic swelling in the upper gluteal cleft or sacrococcygeal area, but they have been described in other locations. They most commonly occur in White individuals and in males who are hirsute[19]. Pilonidal cysts usually present clinically during the second decade of life.

The etiology of pilonidal cysts and sinuses has been a controversial issue. Some authors have argued that they are congenital, essentially representing a dermoid cyst, whereas most authors now believe that the vast majority of lesions are acquired, representing a foreign body response to entrapped hair. A pilonidal cyst can be seen as part of the "follicular inclusion tetrad" which consists of acne conglobata, hidradenitis suppurativa, dissecting cellulitis (perifolliculitis capitis abscedens et suffodiens), and pilonidal cyst (see Ch. 38). Persistent exogenous hairs in the interdigital space of barbers or dog groomers may incite an encompassing epidermal proliferation, giving rise to a pilonidal cyst.

Pathology

Histologic features are those of an epidermal-lined cyst or sinus tract. Cyst cavities contain hair and keratin debris and are surrounded by fibrosis, granulation tissue, and mixed inflammation.

Treatment

Treatment is surgical.

CYSTS LINED WITH NON-STRATIFIED SQUAMOUS EPITHELIUM

Hidrocystoma

Synonyms: ■ Cystadenoma ■ Sudoriferous cyst ■ Moll gland cyst

Hidrocystomas typically present as translucent, skin-colored to bluish cysts on the face, although they may occur in other sites. Hidrocystomas are traditionally divided into apocrine and eccrine hidrocystomas based upon histologic features, and as solitary (Smith type) or multiple (Robinson type). Hidrocystomas may be associated with specific syndromes of ectodermal dysplasia, including Schöpf–Schulz–Passarge syndrome.

Apocrine hidrocystomas are usually solitary (Fig. 110.15), whereas eccrine hidrocystomas may be solitary or multiple and are occasionally quite numerous (Fig. 110.16). Eccrine hidrocystomas can enlarge with heat exposure or during the summer and regress with cooler temperatures. In general, eccrine hidrocystomas are thought to develop from cystic dilation of eccrine ducts due to retention of eccrine secretions, while apocrine hidrocystomas are thought to represent adenomas of apocrine gland coils[20]. Apocrine hidrocystomas are sometimes referred to as cystadenomas, although it has been recommended that this term be reserved for lesions with true papillomatous projections histologically[21]. Lesions along the lower eyelid margin are also known as Moll gland cysts.

Pathology

Histologically, *apocrine* hidrocystomas are unilocular to multilocular dermal cysts lined by two layers of epithelial cells that show luminal bulbous protrusions ("snouting") and decapitation secretion (Fig. 110.17). Similarly lined papillary projections may extend into the cyst lumen. Histologic features of *eccrine* hidrocystomas are those of a uniloculate cyst containing clear fluid, lined by two layers of cuboidal to flattened epithelium (Fig. 110.18). Hidrocystomas that appear by light microscopy to be eccrine include a subset of lesions that stain positively for milk fat globulin 1, as in lesions of apocrine origin[20].

Treatment

Hidrocystomas may be removed by simple excision, including via Gradle scissors, or by electrodesiccation. Multiple eccrine hidrocystomas may also be treated with daily application of topical 1% atropine in aqueous solution, although lesions reappear within days of discontinuing therapy[22]. Flattening after botulinum toxin A injections has been reported[23].

Bronchogenic Cyst

Cutaneous bronchogenic cysts are most commonly found in the suprasternal notch, and rarely they appear on the anterior neck or chin (see

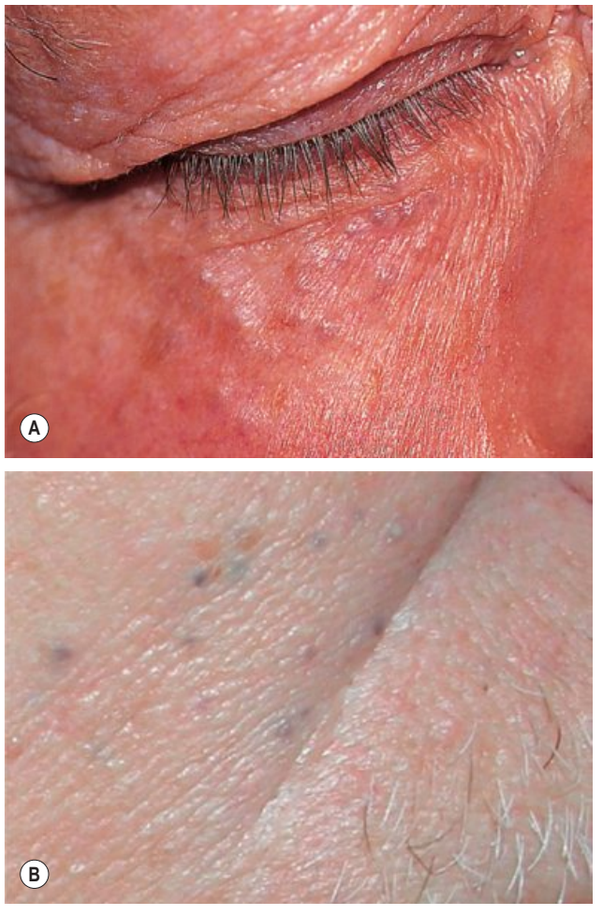


Fig. 110.16 Eccrine hidrocystomas. Numerous, tiny, translucent or bluish papules on the lower eyelid (**A**) or the cheek (**B**).

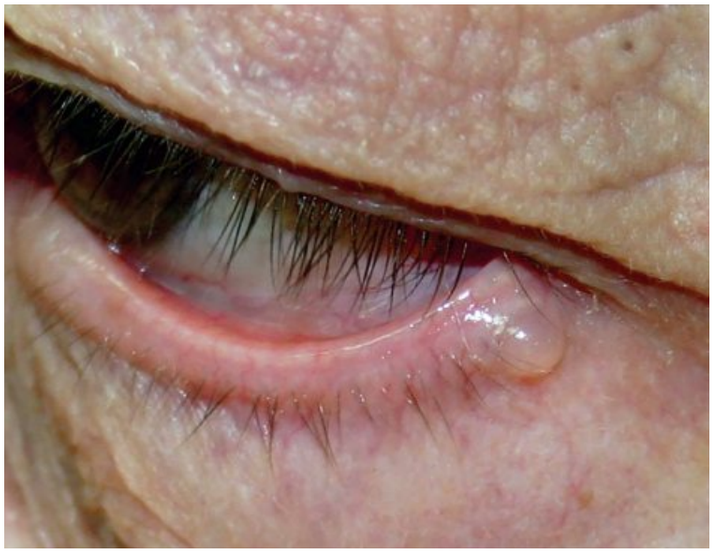


Fig. 110.15 Apocrine hidrocystoma. A single, clear fluid-filled cyst on the lateral lower eyelid margin.

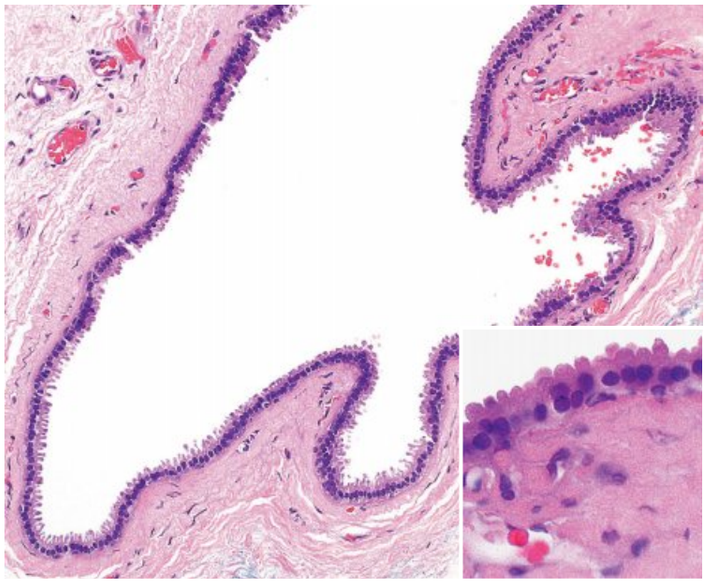


Fig. 110.17 Histopathology of an apocrine hidrocystoma. A unilocular cyst whose wall shows typical apocrine decapitation secretion (inset).

Fig. 64.2). A fistulous tract may connect to the epidermis. Rarely, they present as a pedunculated growth[24]. Bronchogenic cysts are solitary, and they are typically noted at birth. Malignant transformation is very rare. They represent respiratory epithelium sequestered during embryologic development of the tracheobronchial tree.

Pathology

Bronchogenic cysts are lined by pseudostratified, ciliated, columnar epithelium with interspersed goblet cells. The cyst wall often contains smooth muscle and mucous glands and rarely cartilage.

Treatment

Treatment is by excision.

Thyroglossal Duct Cyst

Thyroglossal duct cysts present as deep midline cystic nodules on the anterior neck in children or young adults (see Fig. 64.2). During development, the thyroid gland descends from the floor of the pharynx to the anterior neck. The tract it forms is known as the thyroglossal duct. Thyroglossal duct cysts arise from remnants of the thyroglossal duct. A tract connecting these cysts to the hyoid bone is frequently present, resulting in characteristic movement of the cyst with swallowing. Rarely, thyroid carcinoma may originate in a thyroglossal duct cyst[25].

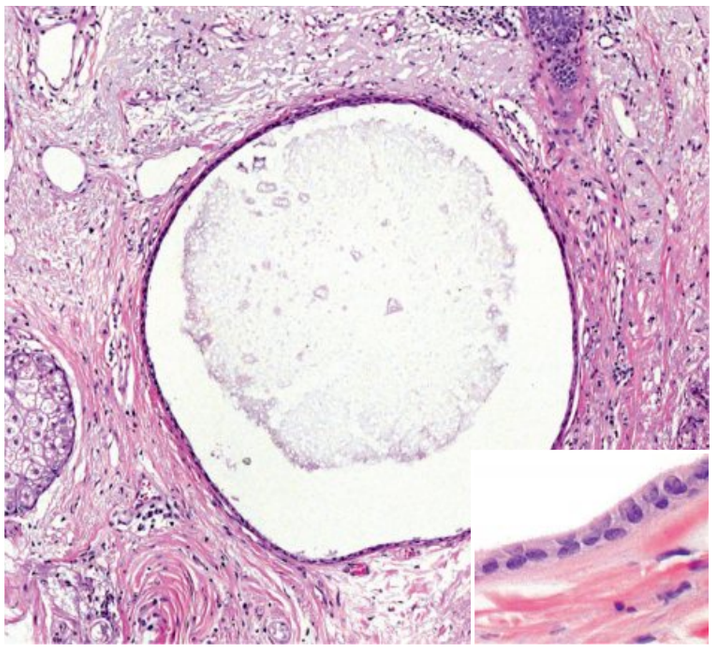


Fig. 110.18 Histopathology of an eccrine hidrocystoma. Two layers of flattened epithelium form the cell wall (inset).

Pathology

Histologically, thyroglossal duct cysts may be lined with cuboidal, columnar, or stratified squamous epithelium, and it may contain some ciliated columnar cells. The characteristic histologic feature is the presence of thyroid follicles, characterized by low cuboidal cells surrounding homogeneous pink material, in the cyst wall (Fig. 110.19).

Treatment

Treatment is surgical, with excision of the cyst and any residual tract.

Branchial Cleft Cyst

Synonyms: ■ Lymphoepithelial cyst ■ Lateral cervical cyst

Branchial cleft cysts occur in the preauricular area, mandibular region, or along the anterior border of the sternocleidomastoid muscle (see Fig. 64.2). The origin of these cysts is controversial. There are two major theories regarding their origin:

- they arise from branchial cleft remnants
- they represent cystic alteration of embryologic epithelium or tonsillar epithelium within cervical lymph nodes[26].

Branchial cleft cysts most commonly manifest during the second or third decade of life. Infection of these cysts is a frequent cause of presentation to a physician.

Pathology

Histologically, these cysts are lined by stratified squamous epithelium or by pseudostratified ciliated columnar epithelium, and they are surrounded by lymphoid tissue.

Treatment

Treatment is by excision of the cyst and its associated tract after delineation of the extent of the lesion by CT or MRI[27].

Cutaneous Ciliated Cyst and Ciliated Cyst of the Vulva

Synonyms: ■ Cutaneous müllerian cyst ■ Cutaneous ciliated cystadenoma ■ Paramesonephric mucinous cyst of the vulva

Cutaneous ciliated cysts are uncommon cysts that typically occur on the lower extremities of young women, although a few cases have been reported in men. They are usually a few centimeters in diameter and,

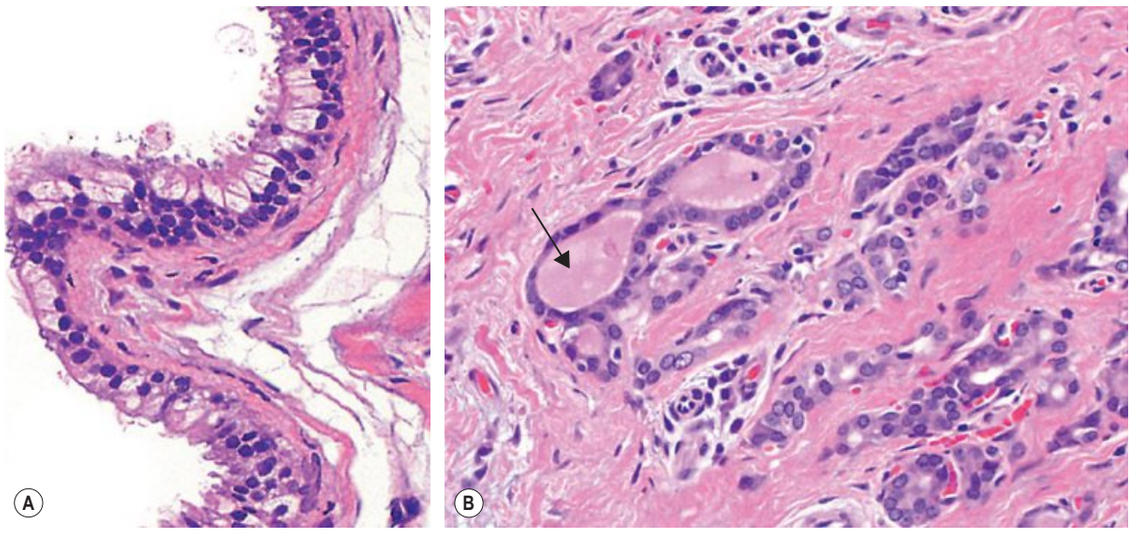


Fig. 110.19 Histopathology of a thyroglossal duct cyst. A The cyst is lined by ciliated columnar epithelium; some of the cells contain clear cytoplasm. **B** Thyroid follicles are present in the tissue surrounding the cyst; note the homogeneous colloid within the lumina (arrow).

on rupture, drain clear to amber fluid. The histogenesis of these cysts is controversial. Most authors have suggested a müllerian duct origin, hence the term cutaneous müllerian cyst. However, the few occurrences in men and the rare reports of ciliated cysts on the scalp have led to the alternative hypothesis that some cases represent ciliated metaplasia of eccrine glands[28].

Ciliated cysts of the vulva are müllerian heterotopias, and they are located most commonly on the labia majora. They usually measure between 1 and 3 cm in diameter.

Pathology

Cutaneous ciliated cysts may be unilocular or multiloculated. The cyst wall is composed of simple cuboidal to columnar ciliated epithelium that may have papillary projections into the cyst lumen (Fig. 110.20).

Differential diagnosis

Bartholin gland cysts and abscesses occur on either side of the vaginal opening and are more common than ciliated cysts of the vulva.

Treatment

Excision is curative.

Median Raphe Cyst

Median raphe cysts are solitary and usually only a few millimeters in diameter, although they may extend over several centimeters linearly. They occur in young men on the ventral aspect of the penis, most commonly on or near the glans. These cysts are thought to develop from aberrant urethral epithelium, but do not connect to the urethra[29].

Pathology

Histologically, median raphe cysts are lined by stratified columnar epithelium (one to four cell layers thick) without a connection to the overlying epithelium. Occasionally, mucin-containing cells are seen in the lining. Very rarely, a ciliated lining has been observed[30]. Positive immunohistochemical staining of the cyst wall epithelium for cytokeratin 7 and GATA3 supports the urothelial origin of these cysts[30a].

Treatment

Excision is curative.

Omphalomesenteric Duct Cyst

Synonyms: ■ Vitelline cyst ■ Omphalomesenteric duct remnant

Omphalomesenteric duct cysts represent a developmental defect in the closure of the omphalomesenteric duct. The omphalomesenteric duct is the fetal connection between the midgut and the yolk sac. It is usually obliterated and loses its intestinal attachment by 6 weeks of gestation[31]. Remnants of this duct may occur anywhere along its course between the intestines and the umbilicus. The spectrum of defects resulting from this faulty closure includes Meckel diverticulum, umbilical–enteric fistulae, umbilical sinuses, and omphalomesenteric duct cysts (internal or external); the latter can present as an umbilical polyp (Fig. 110.21A).

Pathology

These lesions are characterized histologically by ectopic gastrointestinal mucosa (Fig. 110.21B) and must be distinguished from umbilical metastases of gastrointestinal adenocarcinomas.

Differential diagnosis

In postmenarcheal female patients, the possibility of cutaneous endometriosis should be considered.

Treatment

Management of omphalomesenteric duct cysts includes appropriate radiologic studies to exclude communication to the gastrointestinal tract prior to surgical excision.

Urachal Cyst

The urachus is a tube connecting the fetal bladder to the umbilicus and it normally closes during development, resulting in a fibrous tract. A persistent urachus presents during infancy with urine leakage from the umbilicus. A urachal cyst results from an incomplete urachal duct remnant. Urachal cysts are rare, and they usually present as a painful umbilical mass due to secondary infection. The diagnosis can be established by ultrasound in the majority of patients[32].

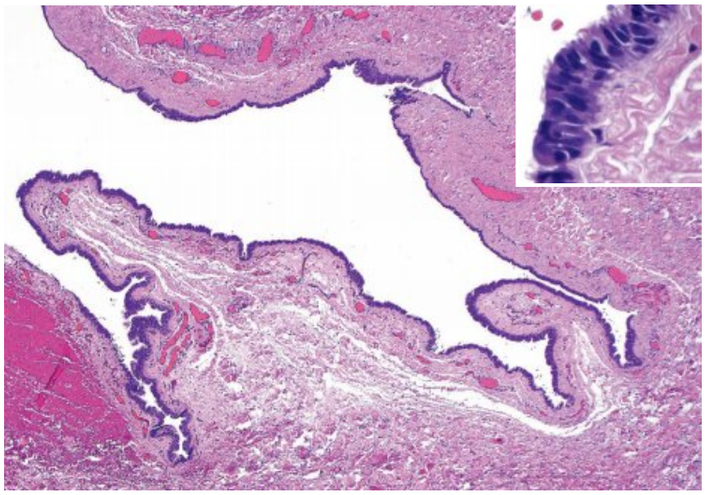


Fig. 110.20 Histopathology of a ciliated cyst of the vulva. The cyst wall is composed of columnar ciliated epithelium (inset).



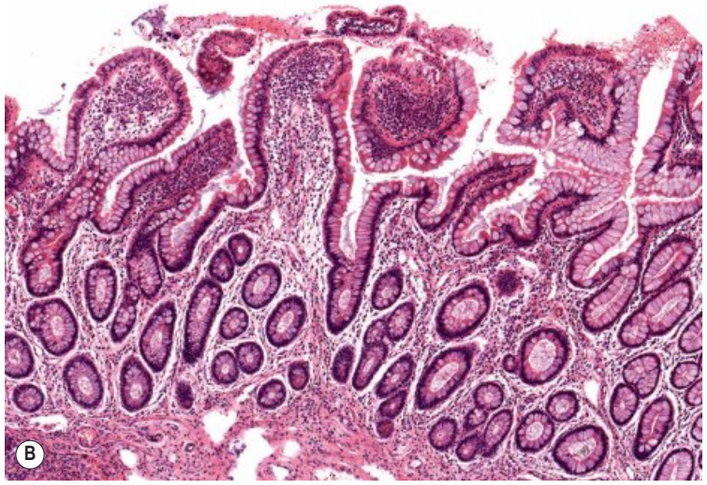


Fig. 110.21 Omphalomesenteric duct cyst. A An umbilical pink papule in an infant. The clinical differential diagnosis includes an umbilical (pyogenic) granuloma and urachal cyst/remnant. **B** Histologically, ectopic gastrointestinal epithelium is seen; note the villi and goblet cells. *B, Courtesy Luis Requena, MD.*

Pathology

These cysts are characterized by a urothelial lining of cuboidal or columnar cells.

Treatment

Excision is recommended to prevent secondary infections as well as late development of adenocarcinoma[32].

CYSTS WITHOUT AN EPITHELIAL LINING

Mucocele

Synonyms: ■ Mucous cyst of oral mucosa ■ Ranula (when located on the floor of the mouth)

Mucoceles most frequently develop on the lower labial mucosa, but they also occur on the floor of the mouth, buccal mucosa, and tongue. They appear as dome-shaped, mucosa-colored to bluish, translucent papules or nodules that range in size from a few millimeters to over a centimeter (Fig. 110.22; see Fig. 72.22). Mucoceles arise as a result of disruption of the ducts of minor salivary glands. This disruption leads to an accumulation of mucinous material, a reactive inflammatory response, and the development of surrounding granulation and fibrous tissue. Multiple mucoceles can develop in patients with GVHD.

A variant of mucocele, superficial mucocele, presents as a clear tense vesicle that is a few millimeters in diameter. Superficial mucoceles are most commonly found on the retromolar pad, posterior buccal mucosa, and soft palate. These lesions are short-lived, asymptomatic, and recurrent. They may be confused clinically with an immunobullous or viral process.

Pathology

Biopsy specimens of mucoceles show one or several spaces within the connective tissue filled with mucinous material, but without an epithelial lining. The spaces are surrounded by chronic inflammation and mucin-containing macrophages, as well as granulation and fibrous tissue. A salivary duct may be seen at the periphery of these findings. Adjacent minor salivary glands may show chronic inflammation and fibrosis. The mucinous material is sialomucin, and the latter contains both neutral and acid mucopolysaccharides, which stain with PAS (diastase-resistant) and with Alcian blue or colloidal iron, respectively.

Histologically, a superficial mucocele shows a subepithelial vesicle filled with mucin and a surrounding sparse to moderate mixed inflammatory infiltrate. Salivary gland ducts are seen opening into the vesicle or immediately adjacent to the vesicle.

Treatment

Mucoceles may resolve spontaneously. If they do not, treatment options include excision, marsupialization, electrodesiccation, intralesional corticosteroid injection, or cryosurgery.



Fig. 110.22 Mucocele. A bluish to mucosa-colored translucent papule on the lower mucosal lip.

Digital Mucous Cyst (Pseudocyst)

Synonyms: ■ Digital myxoid cyst ■ Cutaneous myxoid cyst

Digital mucous cysts (pseudocysts) most commonly occur on the dorsal surface of the distal phalanx of the finger (Fig. 110.23). Toe lesions are less commonly observed. A characteristic longitudinal depression in the nail plate may be seen distal to the cyst. These cysts are skin-colored to bluish and drain clear gelatinous material when punctured. The etiology of digital mucous cysts is controversial, with some authors stating that they are degenerative in origin while others believe they extend from the distal interphalangeal joint space. A pedicle connecting the cyst to the adjacent joint space can usually be demonstrated[33].

Pathology

Histologically, a digital mucous cyst resembles focal mucinosis, often with clefts in the dermis; an epithelial lining is absent (Fig. 110.24). The clefts and the surrounding loose connective tissue contain abundant acid mucopolysaccharides, which can be highlighted by Alcian blue or colloidal iron stains.



Fig. 110.23 Digital mucous cyst. Translucent cystic papule overlying the distal interphalangeal joint. *Courtesy Lorenzo Cerroni, MD.*

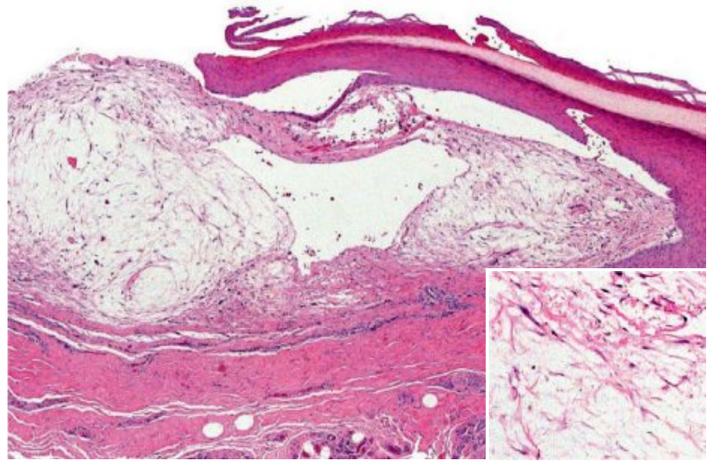


Fig. 110.24 Histopathology of a digital mucous cyst. A subepidermal cystic cavity is surrounded by mucin-rich dermis (inset). Note the prominent stratum lucidum of acral skin. *Courtesy Lorenzo Cerroni, MD.*



Fig. 110.25 Ganglion (cyst) – clinical presentation and histologic features. **A** A skin-colored, compressible, subcutaneous nodule is present on the wrist (arrow), the most common location. **B** A cystic space of acral skin is surrounded by fibrous tissue. *A, Courtesy Jean L. Bolognia, MD; B, Courtesy Lorenzo Cerroni, MD.*

Treatment

Resolution may be seen after intralesional injection of corticosteroids, injection of sclerosing agents, or repeated puncture and drainage[34]. Surgical excision may lead to even higher success rates.

Ganglion

Synonyms: ■ Ganglion cyst ■ Synovial cyst

Ganglia are soft cystic masses up to 4 cm in diameter that most commonly occur on the dorsal aspect of the wrist; they may also be found on the volar wrist or fingers, the dorsal aspect of the feet, or the knees (Fig. 110.25A). Ganglia rarely develop on the lateral elbow or anterior shoulder. They occur more commonly in women and may cause discomfort with activity, impairment of mobility, or cosmetic concerns. In the rare disorder cystic ganglionosis, multiple lesions appear during childhood or adolescence.

Ganglia are frequently attached to a tendon sheath or the joint capsule, but usually do not communicate with the joint space[35,36]. The mucin present within a ganglion is thought to be produced by local fibroblasts.

Pathology

Myxoid change is seen within the connective tissue that ultimately forms cystic spaces. These spaces coalesce into a dominant cystic space lined by variably thick fibrous tissue (Fig. 110.25B), sometimes with a synovial lining.

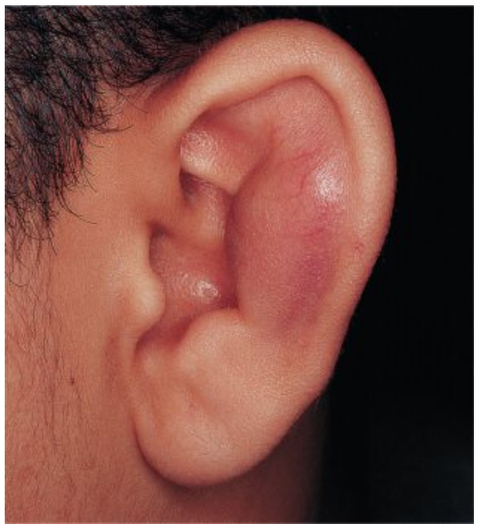


Fig. 110.26 Pseudocyst of the auricle. Erythematous firm nodule on the ear.

Treatment

Early lesions may respond to several weeks of compression therapy[35]. Other options include aspiration plus intralesional corticosteroid injection or excision. Recurrences are common, even with excisional therapy.

Pseudocyst of the Auricle

Synonyms: ■ Endochondral pseudocyst ■ Cystic chondromalacia ■ Intracartilaginous cyst

Pseudocyst of the auricle usually arises in the scaphoid fossa of the ear in middle-aged men. Lesions are usually unilateral. They present as a painless swelling (Fig. 110.26), and they tend to arise over the course of a few weeks. The etiology of pseudocyst of the auricle is unknown, but chronic trauma as well as a developmental defect have been suggested.

Pathology

Biopsy specimens show a cavity within the auricular cartilage (without an epithelial lining) that contains clear fluid. Fibrous tissue and granulation tissue may be found in the cavity as well. The cartilage lining the cavity may show degenerative changes. No inflammation is seen within the cartilage, a feature that distinguishes a pseudocyst from relapsing polychondritis, which may be in the clinical differential diagnosis.

Treatment

Treatment options include aspiration, with or without intralesional injection of corticosteroids, as well as incision and drainage with destruction of the cavity. Each of these modalities should be followed by pressure dressings[36].

Cutaneous Metaplastic Synovial Cyst (Pseudocyst)

Cutaneous metaplastic synovial cysts (pseudocysts) typically present as a solitary tender subcutaneous nodule, although multiple lesions have been reported[37,38]. They occur primarily in areas of prior trauma, particularly prior surgical trauma. Frequently, the preoperative diagnosis is that of a suture granuloma.

Pathology

A cystic cavity is seen within the dermis that is not lined by epithelium. The cavity may communicate with the overlying epidermis via fistulas. Variably cellular villous structures mimicking hyperplastic synovium protrude into the cavity. These villi are covered with a fibrinous exudate. The base of the villi tends to merge with surrounding scar tissue.

Treatment

Excision is curative.

Additional figures available in our eBook (see inside front cover for access code).

REFERENCES

1. Cooper PH, Fechner RE. Pilomatricoma-like changes in the epidermal cysts of Gardner's syndrome. *J Am Acad Dermatol*. 1983;8:639–644.
2. Gorlin RJ. Nevoid basal cell carcinoma syndrome. *Dermatol Clin*. 1995;13:113–125.
3. Boussemart L, Routier E, Mateus C, et al. Prospective study of cutaneous side-effects associated with the BRAF inhibitor vemurafenib: a study of 42 patients. *Ann Oncol*. 2013;24:1691–1697.
4. Shah V, Shet T. Scrotal calcinosis results from calcification of cysts derived from hair follicles: a series of 20 cases evaluating the spectrum of changes resulting in scrotal calcinosis. *Am J Dermatopathol*. 2007;29:172–175.
5. Langley RG, Walsh NM, Ross JB. Multiple eruptive milia: report of a case, review of the literature, and a classification. *J Am Acad Dermatol*. 1997;37:353–356.

5a. Kolodney MS, Coman GC, Smolkin MB, et al. Hereditary trichilemmal cysts are caused by two hits to the same copy of the phospholipase C delta 1 gene *(PLCD1)*. *Sci Rep*. 2020;10:6035.

6. Richey PM, Ferguson NN, Stone MS. Verrucous cysts: possible precursor of proliferating epidermoid cyst. *J Cutan Pathol*. 2019;46:457–459.
7. Sau P, Graham JH, Helwig EB. Proliferating epithelial cysts. Clinicopathological analysis of 96 cases. *J Cutan Pathol*. 1995;22:394–406.
8. Satyaprakash AK, Sheehan DJ, Sangueza OP. Proliferating trichilemmal tumor: a review of the literature. *Dermatol Surg*. 2007;33:1102–1108.
9. Mori O, Hachisuka H, Sasai Y. Proliferating trichilemmal cyst with spindle cell carcinoma. *Am J Dermatopathol*. 1990;12:479–484.
10. Ye J, Nappi O, Swanson PE, et al. Proliferating pilar tumors: a clinicopathologic study of 76 cases with a proposal for definition of benign and malignant variants. *Am J Clin Pathol*. 2004;122:566–574.
11. Esterly NB, Fretzin DF, Pinkus H. Eruptive vellus hair cysts. *Arch Dermatol*. 1977;113:500–503.
12. Sharma VM, Stein SL. A novel mutation in K6b in pachyonychia congenita type 2. *J Invest Dermatol*. 2007;127:2060–2062.
13. McLean WH, Rugg EL, Lunny DP, et al. Keratin 16 and keratin 17 mutations cause pachyonychia congenita. *Nat Genet*. 1995;9:273–278.
14. Requena L, Sanchez Yus E. Follicular hybrid cysts. An expanded spectrum. *Am J Dermatopathol*. 1991;13:228–233.
15. Brownstein MH. Hybrid cyst: a combined epidermoid and trichilemmal cyst. *J Am Acad Dermatol*. 1983;9:872–875.
16. Tirado M, Stander S, Metze D. Histologic and immunohistochemical characteristics of cutaneous cysts in Goltz-Gorlin syndrome: clues for differentiation of nonsyndromic cysts. *Am J Dermatopathol*. 2014;36:892–898.
17. Mehregan AH, Medenica M. Pigmented follicular cysts. *J Cutan Pathol*. 1982;9:423–427.
18. Scheinfeld NS, Silverberg NB, Weinberg JM, Nozad V. The preauricular sinus: a review of its clinical presentation, treatment, and associations. *Pediatr Dermatol*. 2004;21:191–196.
19. da Silva JH. Pilonidal cyst: cause and treatment. *Dis Colon Rectum*. 2000;43:1146–1156.
20. de Viragh PA, Szeimies RM, Eckert F. Apocrine cystadenoma, apocrine hidrocystoma, and eccrine hidrocystoma: three distinct tumors defined by expression of keratins and human milk fat globulin 1. *J Cutan Pathol*. 1997;24:249–255.
21. Sugiyama A, Sugiura M, Piris A, et al. Apocrine cystadenoma and apocrine hidrocystoma: examination of 21 cases with emphasis on nomenclature according to proliferative features. *J Cutan Pathol*. 2007;34:912–917.
22. Sanz-Sanchez T, Dauden E, Perez-Casas A, et al. Efficacy and safety of topical atropine in treatment of multiple eccrine hidrocystomas. *Arch Dermatol*. 2001;137:670–671.
23. Woolery-Lloyd H, Rajpara V, Nijhawan RI. Treatment for multiple periorbital eccrine hidrocystomas: botulinum toxin A. *J Drugs Dermatol*. 2009;8:71–73.
24. Miller III OF, Tyler W. Cutaneous bronchogenic cyst with papilloma and sinus presentation. *J Am Acad Dermatol*. 1984;11:367–371.
25. Dedivitis RA, Guimaraes AV. Papillary thyroid carcinoma in thyroglossal duct cyst. *Int Surg*. 2000;85:198–201.
26. Golledge J, Ellis H. The aetiology of lateral cervical (branchial) cysts: past and present theories. *J Laryngol Otol*. 1994;108:653–659.
27. Thaller SR, Bauer BS. Cysts and cyst-like lesions of the skin and subcutaneous tissue. *Clin Plast Surg*. 1987;14:327–340.
28. Reserva JL, Carrigg AB, Schnebelen AM, et al. Cutaneous ciliated cyst of the scalp: a case report of a cutaneous ciliated eccrine cyst and a brief review of the literature. *Am J Dermatopathol*. 2014;3:679–682.
29. Asarch RG, Golitz E, Sausker WF, Kreye GM. Median raphe cysts of the penis. *Arch Dermatol*. 1979;115:1084–1086.
30. Fernández-Aceñero MJ, Garcia-Gonzales J. Median raphe cyst with ciliated cells: report of a case. *Am J Dermatopathol*. 2003;25:175–176.

30a. Carrasco L, Torre-Castro J, Ortiz S, et al. Median raphe cysts: a clinico-pathologic and immunohistochemical study of 52 cases. *J Cutan Pathol*. 2023;50:536–543.

31. Larralde de Luna M, Cicioni V, Herrera A, et al. Umbilical polyps. *Pediatr Dermatol*. 1987;4:341–343.
32. Ekwueme KC, Parr NJ. Infected urachal cyst in an adult: a case report and review of the literature. *Cases J*. 2009;2:6422.
33. de Berker D, Lawrence C. Ganglion of the distal interphalangeal joint (myxoid cyst): therapy by identification and repair of the leak of joint fluid. *Arch Dermatol*. 2001;137:607–610.
34. Park SE, Park EJ, Kim SS, et al. Treatment of digital mucous cysts with intralesional sodium tetradecyl sulfate injection. *Dermatol Surg*. 2014;40:1249–1254.
35. Soren A. Clinical and pathologic characteristics and treatment of ganglia. *Contemp Orthop*. 1995;31:34–38.
36. Secor CP, Farrell HA, Haydon III RC. Auricular endochondral pseudocysts: diagnosis and management. *Plast Reconstr Surg*. 1999;103:1451–1457.
37. Singh SR, Ma AS, Dixon A. Multiple cutaneous metaplastic synovial cysts. *J Am Acad Dermatol*. 1999;41:330–332.
38. Fukuyama M, Sato Y, Hayakawa J, Ohyama M. Cutaneous metaplastic synovial cyst: case report and literature review from the dermatological point of view. *Keio J Med*. 2017;66:9–13.



eFig. 110.1 Epidermoid cyst of the face with two small pores. Note the central yellow color. *Courtesy Lorenzo Cerroni, MD.*



eFig. 110.2 Multiple epidermoid cysts of the scrotum. They may be associated with dystrophic calcification. *Courtesy Joyce Rico, MD.*



eFig. 110.3 Milium of the nipple. Note the white color. *Courtesy Julie V. Schaffer, MD.*



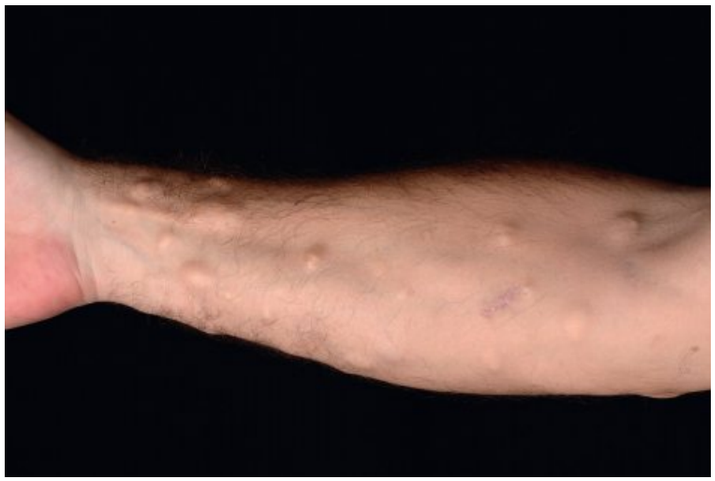
eFig. 110.4 Multiple milia in a patient with epidermolysis bullosa. *Courtesy Luis Requena, MD.*



eFig. 110.5 Proliferating tricholemmal cyst of the forehead. Skin-colored to yellow nodule with telangiectasias. *Courtesy Luis Requena, MD.*



eFig. 110.6 Proliferating tricholemmal cyst of the scalp. A large skin-colored nodule on the scalp. *Courtesy Luis Requena, MD.*



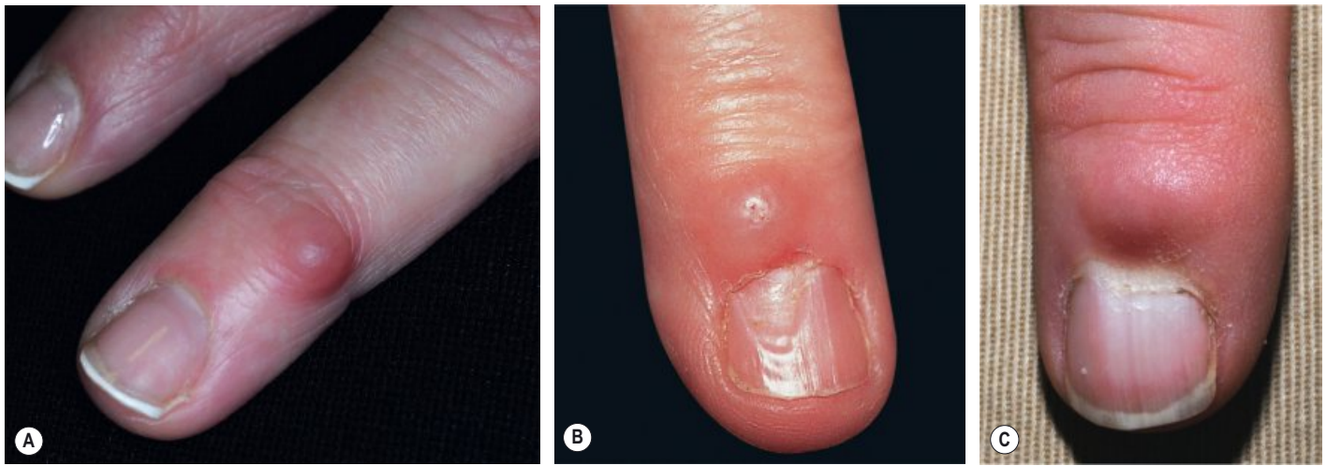
eFig. 110.8 Steatocystoma multiplex. Multiple cystic nodules on the arm. *Courtesy Lorenzo Cerroni, MD.*



eFig. 110.7 Eruptive vellus hair cysts. Pigmented small papules on the thigh of a young woman, a few of which are inflamed.



eFig. 110.9 Apocrine hidrocystoma. A single, slightly bluish, translucent papule on the lower eyelid near the lateral canthus.

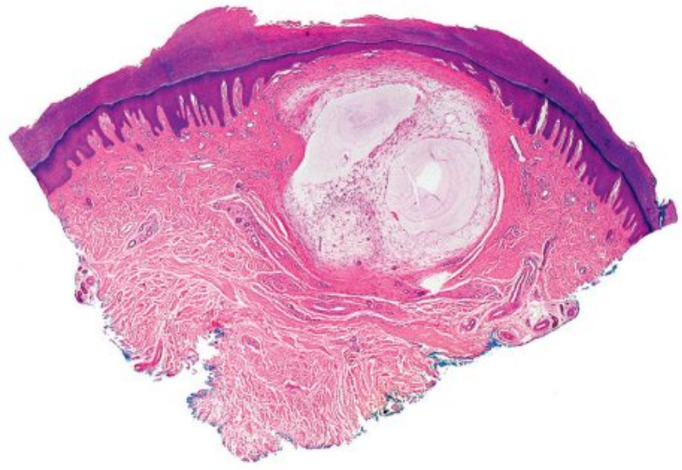


eFig. 110.10 Digital mucous cysts. A A compressible pink papule overlying the distal interphalangeal joint. **B** A translucent papule on the dorsal distal phalanx of the finger causing a depression in the nail plate. **C** Skin-colored papule adjacent to the proximal nail fold. There is associated nail plate depression. *A, Courtesy Jean L. Bolognia, MD ; C, Courtesy Kalman Watsky, MD.*

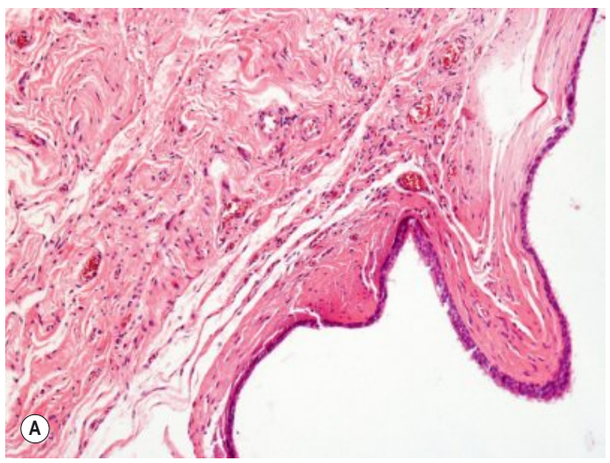


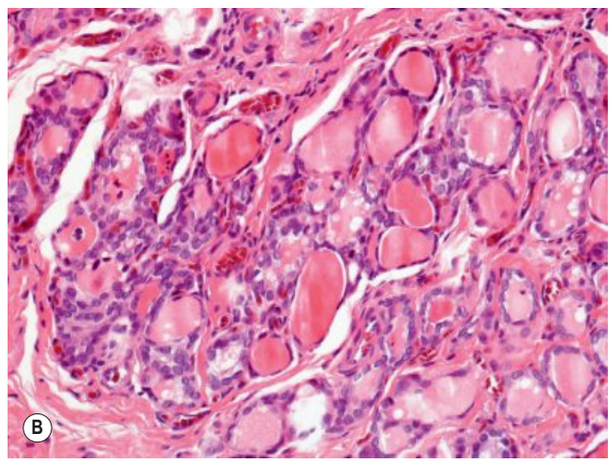


eFig. 110.11 Digital mucous cysts of the toes. A Compressible, pink, translucent papule abutting the proximal nail fold. **B** When located on the toes, mucous cysts are more likely to have superimposed changes due to trauma. *A, Courtesy Luis Requena, MD; B, Courtesy Lorenzo Cerroni, MD.*



eFig. 110.12 Histopathology of a digital mucous cyst. A subepidermal cystic cavity that contains mucin. The prominent stratum corneum is indicative of acral skin. *Courtesy Luis Requena, MD.*





eFig. 110.13 Histopathology of a thyroglossal duct cyst. A The cyst is lined by ciliated columnar epithelium; some of the cells contain clear cytoplasm. **B** Thyroid follicles are present in the tissue surrounding the cyst; note the homogeneous colloid within the lumina. *Courtesy Luis Requena, MD.*

111 Adnexal Neoplasms

Timothy H. McCalmont and Laura B. Pincus

Chapter Contents

Neoplasms and Proliferations with Follicular Differentiation . . . *1948*
Neoplasms and Proliferations with Sebaceous Differentiation . . *1960*
Neoplasms and Proliferations with Apocrine (or Eccrine) Differentiation *1962*
Neoplasms and Proliferations with Eccrine Differentiation *1969*

Key features

- Terminology and classification of adnexal tumors has varied considerably according to different authorities
- Adnexal neoplasms can differentiate toward the folliculosebaceous-apocrine unit or the eccrine apparatus
- As a reflection of joint ontogeny, tumors often exhibit combinations of follicular, sebaceous, and apocrine differentiation
- Many adnexal tumors historically classified as eccrine are probably apocrine

The nosology of adnexal neoplasms has been confused for decades, and a key problem has been the lack of a logical classification scheme. Postulated classifications and inferences regarding lineage have often been contradictory, a reflection of the fact that broad conclusions regarding lineage and classification were formerly based on enzyme histochemical attributes of dubious specificity[1,2].

The crucial principle to keep in mind when considering adnexal neoplasms is that the development of the eccrine apparatus is distinct from the folliculosebaceous-apocrine unit. Eccrine glands develop directly from embryonic epidermal anlage during early months of fetal development[3]. Follicles arise directly from the epidermis concurrently, but their development differs in that mesenchymal cells, precursors of the follicular papilla, descend jointly into the dermis with the developing follicle (see Ch. 2 and Fig. 2.4). Subsequently, sebaceous and apocrine glands and their ducts elaborate as secondary structures from bulges on the side of the developing follicle.

These ontogenetic relationships reflect relationships observed repeatedly in clinical disease[1]. As one would expect from ontogeny, follicular, sebaceous, and apocrine differentiation occur conjointly, and combinations of eccrine and folliculosebaceous differentiation probably do not exist.

Both the differentiation of the tumor (Fig. 111.1) and the topography of adnexal structures offer insights into logical classification. There is striking variation in anatomic distribution among adnexal neoplasms, and some of these differences hold implications regarding lineage. Based on topography, it is nonsensical to pigeonhole spiradenoma, a tumor that commonly occurs within apocrine skin and rarely, if ever, develops within acral skin, as an eccrine tumor. In contrast, an acral predilection suggests that poroma is commonly of eccrine lineage[4].

Lastly, microscopy and morphology play a role in the assessment of lineage. For some lines of differentiation, the meaning ascribed to specific attributes is indisputable. Cells with coarsely vacuolated cytoplasm and scalloped nuclei signify sebaceous differentiation. Follicular differentiation is established by the presence of bulbar basaloid cells accompanied by mesenchymal cells resembling the follicular papilla. Follicular lineage is also connoted by attributes such as matrical or outer sheath differentiation. In contrast, there are no specific attributes that permit recognition of eccrine or apocrine differentiation, although decapitation configuration at the luminal border can be considered suggestive of apocrine differentiation.

More recently, molecular pathology has been employed given the various alterations, including gene fusions, that have been observed in benign and malignant adnexal tumors[5].

NEOPLASMS AND PROLIFERATIONS WITH FOLLICULAR DIFFERENTIATION

Follicular and Folliculosebaceous-Apocrine Hamartomas

Hamartomas are benign proliferations composed of cellular elements, native to a site, in aberrant proportion. A congenital hamartoma, such as nevus sebaceus, is properly referred to as a *nevus*. Hamartomas can be acquired and present in a tumor-like fashion, although such lesions do not represent authentic neoplasms.

Proliferations of the folliculosebaceous-apocrine unit are commonly hamartoma-like. The folliculosebaceous-apocrine unit incorporates follicular epithelial, follicular mesenchymal, and sebaceous and apocrine elements; thus its microscopically diverse progeny is not surprising. Many follicular proliferations that we consider neoplastic, such as trichoblastoma, have integral stroma, and thus the distinction between follicular hamartoma and follicular neoplasm is sometimes blurred.

Hair follicle nevus

Introduction

Hair follicle nevi are authentic hamartomas, usually congenital, in which hairs and the follicles that ensheath them have abnormal morphology or size or are present in increased numbers. Recently, postzygotic gain-of-function variants in *FGFR2* were described in two patients with hair follicle nevi[5a].

Clinical features

Hair follicle nevus, also known as *vellus hamartoma*, presents as a small papule(s) from which fine hairs protrude evenly from the surface. Lesions typically involve the face and commonly reside near the ear[6]. *Accessory tragus* overlaps with hair follicle nevus, and it has been suggested that the two entities are the same[7]. *Nevus pilosus* designates hamartomas characterized by closely set, non-vellus hairs.

Pathology

Microscopically, hair follicle nevi display a domed surface with an increase in normally formed vellus follicles. The configuration may resemble normal skin. Accessory tragi exhibit an identical pattern but are uniquely identifiable if deep subjacent hyaline cartilage is present and can be found. Nevus pilosus is characterized by closely set terminal follicles.

Treatment

No therapy is required. Excision can be considered for cosmesis. In the evaluation of a hair follicle nevus or accessory tragus in a small child, parents can be counseled that the *relative* size of the lesion will diminish with time. That is, the child will grow disproportionately faster than the lesion.

Trichofolliculoma

Introduction

Trichofolliculoma does not represent an authentic neoplasm. Rather, the term designates a group of follicular hamartomas in which follicular structures emanate from a central dilated infundibular space.

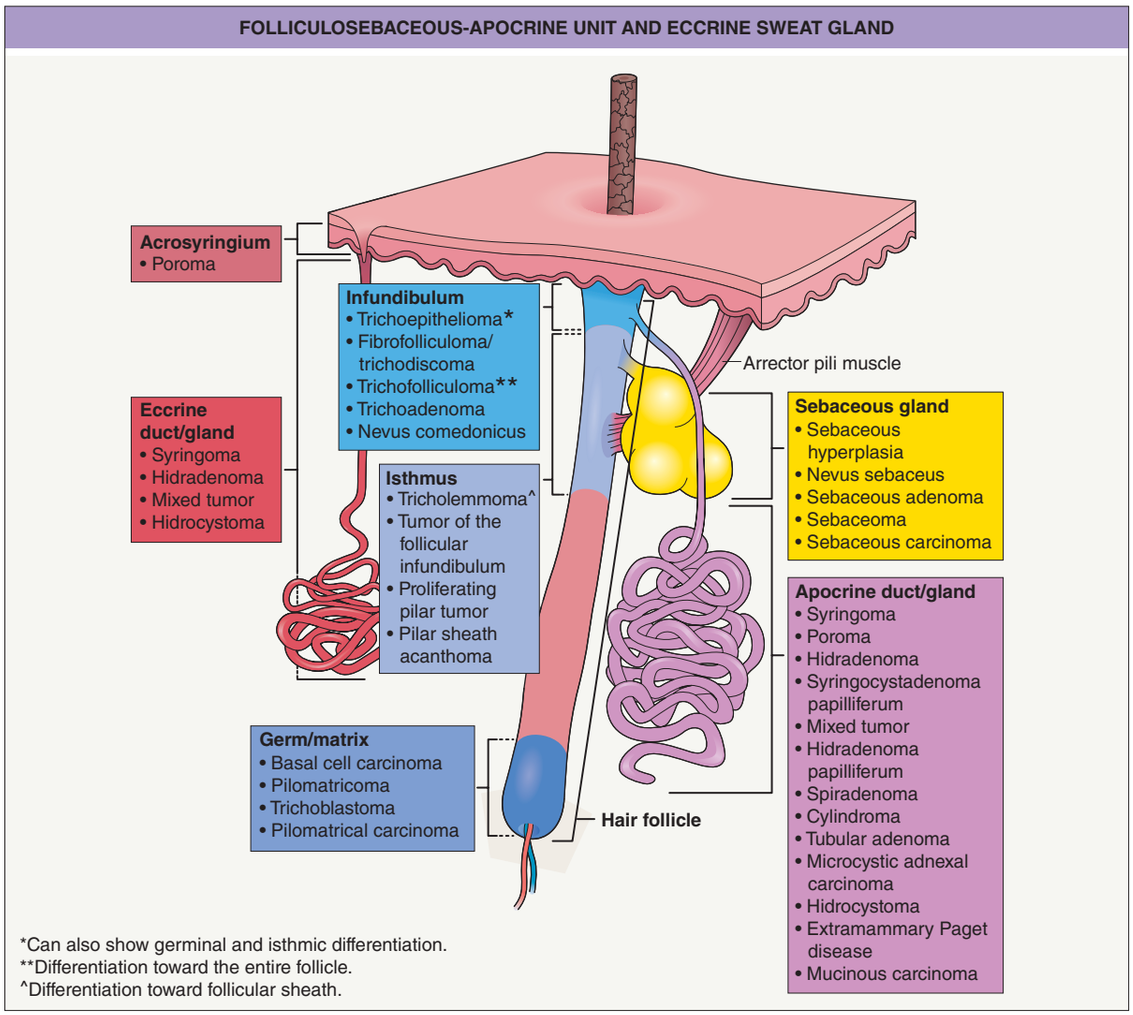


Fig. 111.1 The folliculosebaceous-apocrine unit and eccrine sweat gland with examples of adnexal tumors that differentiate toward the hair follicle, sebaceous gland, apocrine gland, and eccrine gland. *Courtesy Christine Ko, MD.*

Clinical features

Trichofolliculoma presents as a papule or nodule involving the face, scalp, or upper trunk. Many examples are not clinically distinctive. Sometimes, a central follicular ostium or punctum may be identifiable and it may harbor a small tuft of more lightly pigmented hairs (Fig. 111.2). Rarely, the clinical presentation will be as a large nodule or cyst or as multiple lesions in uncommon sites. By dermoscopy, white vellus hairs protrude from a well-defined pinkish papule and this has been likened to a "moldy peach"[8].



Fig. 111.2 Trichofolliculoma. Wispy vellus hairs emerge from a skin-colored papule with a dilated central pore.

Pathology

Prototypically, a trichofolliculoma consists of a central cystic space with infundibular cornification and central orthokeratin. Sometimes, cross-sections of hair shafts are identifiable within the cyst. Relatively well-developed and occasionally oddly formed vellus follicles protrude in radial fashion from the central structure (Fig. 111.3). The follicles usually display a bulb and papilla and exhibit inner and outer sheath and isthmic differentiation. The entire structure, including the central cyst and its associated radiating follicles, is enveloped by a vascularized fibrous (angiofibroma-like) stroma.

The radiating follicles are frequently cut on tangent, thus creating considerable microscopic variation, and deeper sections through the tissue block sometimes are required for diagnosis. If the radiating follicles are accompanied by sebaceous glands, the hamartoma can be termed a *sebaceous trichofolliculoma*[9]. This diagnostic embellishment is not of any clinical import.

The term *folliculosebaceous cystic hamartoma* has been applied to a group of nodular and cystic lesions described independently from trichofolliculoma[10–12]. Folliculosebaceous cystic hamartoma shows a central infundibular cyst from which follicular and sebaceous elements emanate, and the encompassing stroma may be fibrous or myxoid and often contains adipocytes. Rather than a unique entity, it seems likely that folliculosebaceous cystic hamartoma represents a large cystic sebaceous trichofolliculoma[10].

Pilar sheath acanthoma is characterized by a cystically dilated follicular configuration that opens to the surface epithelium, much like trichofolliculoma. However, in pilar sheath acanthoma, the lobules of cells that radiate from the cystic dilation recapitulate only the follicular isthmus and outer sheath rather than forming full follicular structures. In addition, a pilar sheath acanthoma does not have the investing fibrous stroma of a trichofolliculoma.

Treatment

Trichofolliculoma is wholly benign and no treatment is needed. If a trichofolliculoma is discovered by biopsy, no further intervention is required.

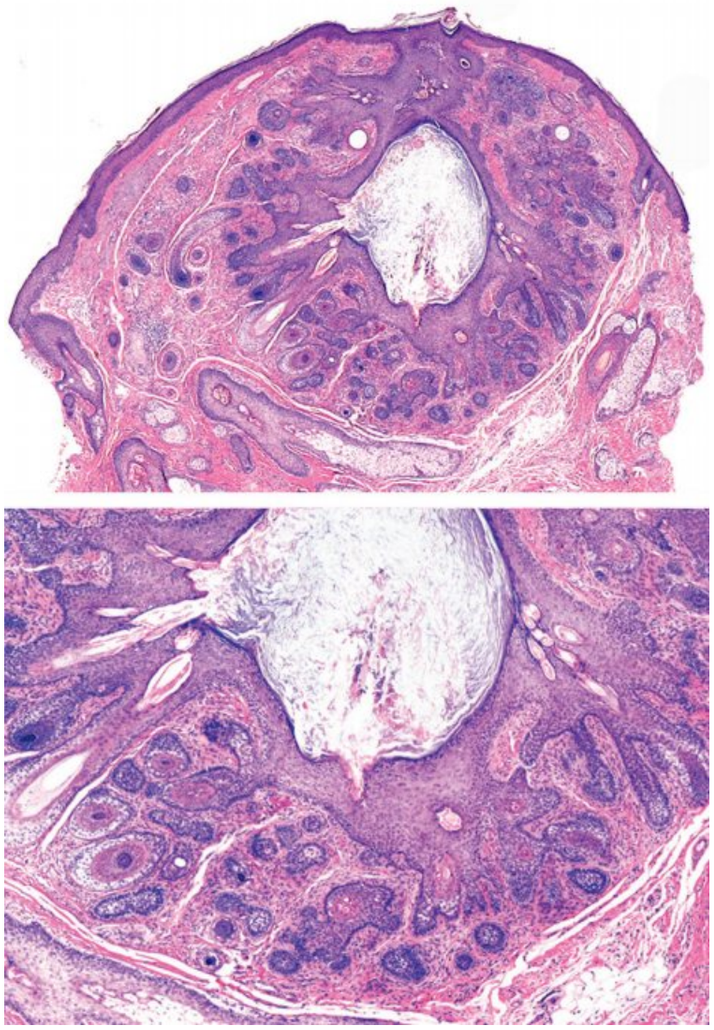


Fig. 111.3 Trichofolliculoma. There is a central patulous follicular infundibulum, from which fully formed or nearly fully formed follicles radiate. *Courtesy Luis Requena, MD.*

Fibrofolliculoma, perifollicular fibroma, and trichodiscoma

Introduction

Fibrofolliculoma represents an adnexal hamartoma that includes both follicular epithelial and mesenchymal elements. Perifollicular fibroma and trichodiscoma were described independently but probably represent purely mesenchymal proliferations on the same spectrum as fibrofolliculoma. Some authorities consider perifollicular fibroma to be related to angiofibroma.

Clinical features

Fibrofolliculomas, perifollicular fibromas, and trichodiscomas are not clinically distinctive. All present as small, skin-colored to hypopigmented papules that involve the head and neck or upper trunk. The papules commonly present in multiplicity (Fig. 111.4A–D). In this context, strong consideration should be given to the possibility of the Birt–Hogg–Dubé syndrome (Fig. 111.5), an autosomal dominant disorder typified by multiple fibrofolliculomas, trichodiscomas, and acrochordon-like lesions. The major systemic manifestations are renal tumors, the majority of which are oncocytomas or renal cell carcinomas of the chromophobe or hybrid chromophobe–oncocytoma type, pulmonary cysts, and spontaneous pneumothoraces (Table 111.1). Colonic polyps and connective tissue nevi have also been reported in affected patients as have multiple primary cutaneous melanomas[13]. However, it has not yet been determined if there is a significant increased risk for melanoma compared to the general population. Heterozygous mutations in the tumor suppressor gene *FLCN*, which encodes folliculin, a protein involved in cell–cell adhesion, underlie this syndrome (see Table 111.1).

Multiple papules of the face and pinnae can also be seen in patients with *familial multiple discoid fibromas*, but there are no systemic manifestations or mutations in *FLCN*. Mutations have been detected in *FNIP1*, which encodes a folliculin interacting protein.

Pathology

At low magnification, *fibrofolliculoma* displays slender strands of follicular mantle cells that emanate from a folliculosebaceous unit at the level of the isthmus (Fig. 111.4E). Usually, the strands are composed of cells with a slightly basaloid appearance, and sometimes, tiny integrated collections of mature sebocytes are identifiable. The epithelial component may assume a mitt-like morphology in some instances, encasing the vascularized fibrous stroma.

Perifollicular fibroma consists almost exclusively of stroma that is identical to the stromal elements of fibrofolliculoma and angiofibroma. Lesions consist of spindled and stellate cells arrayed concentrically around follicles and distributed amongst thickened collagen bundles with a proportionate number of intervening small thin-walled vessels. Sometimes, a concurrent component of follicular epithelial hyperplasia is identifiable, although the epithelium tends to be inconspicuous in comparison to fibrofolliculoma. Trichodiscoma was thought by Pinkus to represent a unique proliferation with differentiation toward the *haarscheibe* (hair disk), which is probably a mythical structure. More recently, *trichodiscomas* have been interpreted as fibrofolliculomas or perifollicular fibromas with myxoid rather than fibrous stroma. Lastly, the so-called neurofollicular hamartoma is now considered to be a type of trichodiscoma with a predominance of spindle cells.

Treatment

Fibrofolliculomas, perifollicular fibromas, and trichodiscomas are all benign and require no surgical treatment. Superficial electrodesiccation, laser ablation, or dermabrasion can be utilized to ameliorate multiple lesions. Unlike the angiofibromas of tuberous sclerosis, topical rapamycin did not result in cosmetic improvement in the fibrofolliculomas of Birt–Hogg–Dubé syndrome[14].

Nevus sebaceus

Introduction

Originally known as *organoid nevus*, nevus sebaceus is commonly thought of as a sebaceous lesion and historically has been the first entity discussed in chapters describing sebaceous tumors. In truth, nevus sebaceus is a non-neoplastic malformation that includes follicular, sebaceous, and apocrine elements[15] as well as epidermal hyperplasia.

Clinical features

Nevus sebaceus represents a classic *nevus* or congenital malformation. At birth, lesions are only slightly raised and subtly discernible. Nevus sebaceus involves the scalp or face commonly, the neck occasionally, and the trunk rarely. Lesions that are linear are distributed along the lines of Blaschko, although this may be difficult to appreciate if small in size. On the scalp, a nevus will remain hairless, or mostly so, as the infant's hair grows normally around it. During childhood, the nevus thickens slightly and assumes a yellow or orange hue (Fig. 111.6). At adolescence, progressive thickening occurs and the surface becomes pebbly or verrucous. Especially when there is more extensive involvement with nevus sebaceus, the possibility of Schimmelpenning syndrome or phakomatosis pigmentokeratotica needs to be considered (see Ch. 62).

In a study of 65 sebaceous nevi, postzygotic somatic mutations were detected in *HRAS* (95% of nevi) and *KRAS* (5%)[16]. Mosaicism for *HRAS* and *KRAS* mutations was also detected in individuals with Schimmelpenning syndrome. The more common mutations were shown to lead to activation of the MAPK and PI3K-AKT pathways (see Fig. 113.1). A syringocystadenoma papilliferum or trichoblastoma that arises within a nevus sebaceus carries the same *HRAS* mutation as the underlying nevus[17].

Nevus sebaceus represents a fertile field for the development of secondary adnexal neoplasms, commonly benign but occasionally malignant[18–20]. Past generations of dermatologists were taught that secondary carcinoma develops in 10% or more of these lesions over time, although this figure was poorly substantiated. The vast majority of secondary proliferations represent benign follicular germinative (trichoblastoma-like) foci; the actual incidence of secondary basal



Fig. 111.4 Fibrofolliculomas in association with Birt–Hogg–Dubé syndrome – clinical and histopathologic findings. A, B Multiple, small, skin-colored to white papules on the ear and neck. **C** Multiple smooth papules of the cheek and nose that are skin-colored to relatively hypopigmented; they lack the telangiectasias of the background skin. **D** Dozens of white–gray papules of the midface, some of which have become confluent. **E** Strands of basaloid cells emanate from a folliculosebaceous unit and form a mitt-like configuration encasing delicate fibrous stroma. *B, Courtesy Kalman Watsky, MD; C, Courtesy Barry Goldberg, MD; D, Courtesy Edward Cowen, MD.*

cell carcinoma (BCC) is <1%[18,19]. Historically, syringocystadenoma papilliferum (papillary syringoadenoma) was believed to represent the most common secondary proliferation (Fig. 111.7), but recent analyses indicate that trichoblastoma occurs more frequently[18,19]. Other common secondary neoplasms include tricholemmoma, desmoplastic tricholemmoma, sebaceous adenoma, apocrine adenoma, and poroma. Only rarely does secondary sebaceous carcinoma or apocrine carcinoma arise in a nevus sebaceus. Malignancy probably develops only in longstanding or neglected lesions but exceptionally can be a source of mortality.

When a nodule develops within a nevus sebaceus and large blue–gray ovoid nests are noted by dermoscopy, then the pattern of the nests should be assessed. If the entire lesion is a blue–gray nest (symmetric pattern) trichoblastoma is favored whereas an asymmetric pattern of nests favors BCC.

Pathology

In nevus sebaceus, the principal malformation is of individual follicular units. An infantile nevus sebaceus can be microscopically subtle, particularly if the biopsy specimen includes only lesional skin, as the malformed follicular units are small and deviate little from normal. In an excisional specimen from the scalp during later childhood, tiny misshapen lesional follicles provide a stark contrast to normal terminal follicles at the periphery of the biopsy. Small apocrine glands may be identifiable in a specimen of sufficient depth. The epidermis also thickens and becomes progressively more papillated, gradually assuming a configuration akin to an epidermal nevus.

By late adolescence, nevus sebaceus displays an epidermal pattern identical to that of an epidermal nevus, typified by acanthosis and fibroplasia of the papillary dermis. There may be enlarged sebaceous glands in contiguity with the dermal–epidermal junction (Fig. 111.8). Buds of follicular germinative cells may jut from the junction as well. The underlying follicular units remain smallish and appear distorted but their sebaceous lobules increase in prominence. Dilated apocrine glandular structures with inspissated secretions are not uncommonly identifiable in the reticular dermis. This histopathology remains stable into adulthood.

Over time, some patients develop exaggerated verrucous epidermal hyperplasia much like a verruca vulgaris. It has been suggested that this is a consequence of human papillomavirus infection[21]. Secondary neoplasms are common, and trichoblastoma, tricholemmoma, and syringocystadenoma are frequently observed[18,19]. The strong association between syringocystadenoma and nevus sebaceus warrants careful scrutiny any time the diagnosis of syringocystadenoma is rendered, to ascertain whether a nevus sebaceus can be found in the same specimen.

Treatment

As carcinoma was formerly reputed to commonly develop within nevus sebaceus, the risk of transformation was used as justification for complete excision. In truth, the risk of development of secondary carcinoma is low[18]. However, the risk for the development of a secondary benign neoplasm, such as syringocystadenoma or trichoblastoma, is relatively high. In addition, it is clear that nevus sebaceus becomes increasingly verrucous and conspicuous over time. In light of this, conservative complete excision during late childhood represents a commonly utilized, but not required, approach. Lesions within the scalp may be difficult for the patient to follow clinically. For facial lesions, consideration can be given to excision during childhood, before the development of secondary verrucous alteration. The excisional margins can be narrow. Removal by shave or laser ablation is usually not successful.

Mixed tumor (chondroid syringoma)

Introduction

Cutaneous mixed tumor, also known as *chondroid syringoma*, represents an acquired hamartoma with folliculosebaceous-apocrine differentiation that has been interpreted as an adnexal adenoma since its

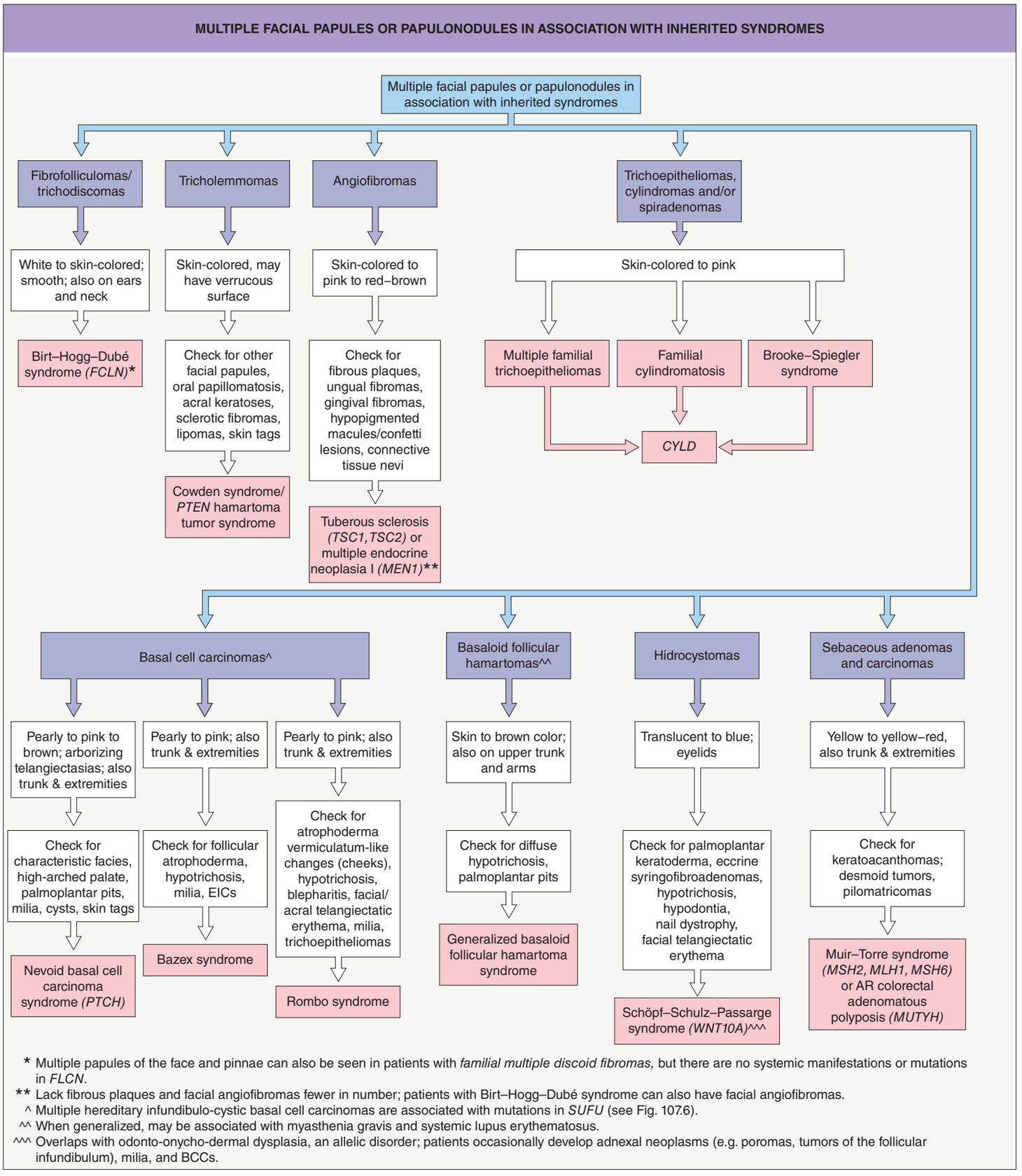


Fig. 111.5 Multiple facial papules or papulonodules in association with inherited syndromes. Patients with Gardner syndrome can develop multiple epidermoid inclusion cysts (sometimes with foci of pilomatrical differentiation) and osteomas in the head and neck region. Multiple syringomas occur with an increased frequency in patients with Down syndrome. AR, autosomal recessive; EICs, epidermoid inclusion cysts.

description. Despite this legacy, in the opinion of the authors, mixed tumor is best pigeonholed as a hamartoma. However, the presence of *PLAG1* fusion genes, including *NDRG1-PLAG1* and *TRPS1-PLAG1*, supports their classification as true neoplasms. The fusion genes lead to overexpression of PLAG1 (pleomorphic adenoma gene 1), a zinc finger transcription factor.

The stroma of a mixed tumor is always abundant and generally comprises half of the surface area of a given lesion in conventional

GUIDELINES FOR THE DIAGNOSIS AND EVALUATION OF BIRT–HOGG–DUBÉ SYNDROME (BHDS)
Diagnostic criteria
Major
• Five or more fibrofolliculomas/trichodiscomas, with at least one confirmed microscopically • Identification of a heterozygous pathogenic variant in *FLCN*
Minor
• Multiple lung cysts – bilateral basally located lung cysts with no apparent cause, with or without spontaneous primary pneumothorax • Early-onset renal cancer (age <50 years) • Multifocal or bilateral renal cancer • Renal cancer with mixed chromophobe and oncocytic histomorphology • First-degree relative with BHDS
Evaluation
Imaging studies for pulmonary and renal involvement
• Pulmonary: high-resolution CT scan of the chest to detect cysts • Renal: renal MRI scan (preferred) or abdominal/pelvic CT scan to detect tumors
Suggested surveillance and recommendations

• Cutaneous: full body skin examination
• Pulmonary: smoking cessation and judicious use of general anesthesia to reduce risk of pneumothorax
• Renal: annual renal MRI scan (preferred) or abdominal/pelvic CT scan, but if no family history of renal tumors plus 2–3 negative annual scans, screening can be done every 2 years
  • Tumors <3 cm in diameter monitored by periodic imaging
  • Tumors >3 cm in diameter treated with surgical excision

Table 111.1 Guidelines for the diagnosis and evaluation of Birt–Hogg–Dubé syndrome (BHDS). According to the European Birt–Hogg–Dubé Consortium, one major or two minor criteria are required for diagnosis whereas other diagnostic criteria require identification of a pathogenic variant in *FLCN*. CT, computed tomography; MRI, magnetic resonance imaging. *Adapted from Sattler EC, Steinlein OK. Birt-Hogg-Dubé syndrome – GeneReviews® – NCBI Bookshelf; 2020 (www.ncbi.nlm.nih.gov/books/NBK1522).*



Fig. 111.6 Nevus sebaceus. Orange, waxy, hairless plaque in a linear configuration on the scalp of a child. *Courtesy Julie V. Schaffer, MD.*



Fig. 111.7 Syringocystadenoma papilliferum arising within a nevus sebaceus. Yellow–brown verrucous plaque in which an eroded, pink, lobulated papulonodule developed. *Courtesy Kalman Watsky, MD.*

sections, and the epithelial component is commonly heterogeneous[22]. An analogy has been drawn between cutaneous mixed tumor and mixed tumor (pleomorphic adenoma) of the salivary gland. Because they have fusion genes in common, the comparison has some validity. However, it is important to note that pleomorphic adenoma of the salivary gland functions as a neoplasm in a biological sense, as it holds a tendency for local recurrence if incompletely extirpated as well as the potential for evolution to malignancy. In contrast, chondroid syringoma represents an indolent process virtually devoid of proliferative capacity, and it rarely recurs after enucleation.

Some authors consider chondroid syringoma and cutaneous myoepithelioma to represent two ends of a spectrum, and this concept is supported by the fact that some chondroid syringomata are particularly rich in myoepithelial cells[23]. In addition, some authors consider cutaneous and salivary mixed tumors to be related myoepithelial neoplasms because they can have similar gene rearrangements involving *PLAG1*[24].

Clinical features

The clinical presentation of a mixed tumor is indistinctive. The lesions present as cutaneous papulonodules that can be misconstrued as cysts (Fig. 111.9). Involvement of the head and neck is common and lesions may also develop on the trunk or within axillary or genital skin.

Pathology

Mixed tumor presents pathologically as a well-circumscribed nodule that resides within the deep reticular dermis or subcutis. Its biphasic morphology includes epithelial structures encompassed by ample varied stroma[22]. There is always a prominent collagenous component to the stroma, but myxoid and adipocytic zones can also be found. Despite its name, stromal hyaline cartilage is found in less than half of all chondroid syringomata.

The epithelial component of a mixed tumor displays two primary patterns. Most mixed tumors demonstrate large inter-anastomosing and branching tubules lined by two cell layers – columnar cells with decapitation secretion at the luminal border and cuboidal cells peripherally; this configuration has been dubbed apocrine mixed tumor[25] (Fig. 111.10). Less commonly, mixed tumors show an epithelial component that includes many small, rounded, cuticulated ducts (Fig. 111.11). Such lesions have been interpreted by some as eccrine. Rather, it seems likely that all mixed tumors are hamartomas of folliculosebaceous-apocrine lineage and that the configuration of the epithelial component can vary.

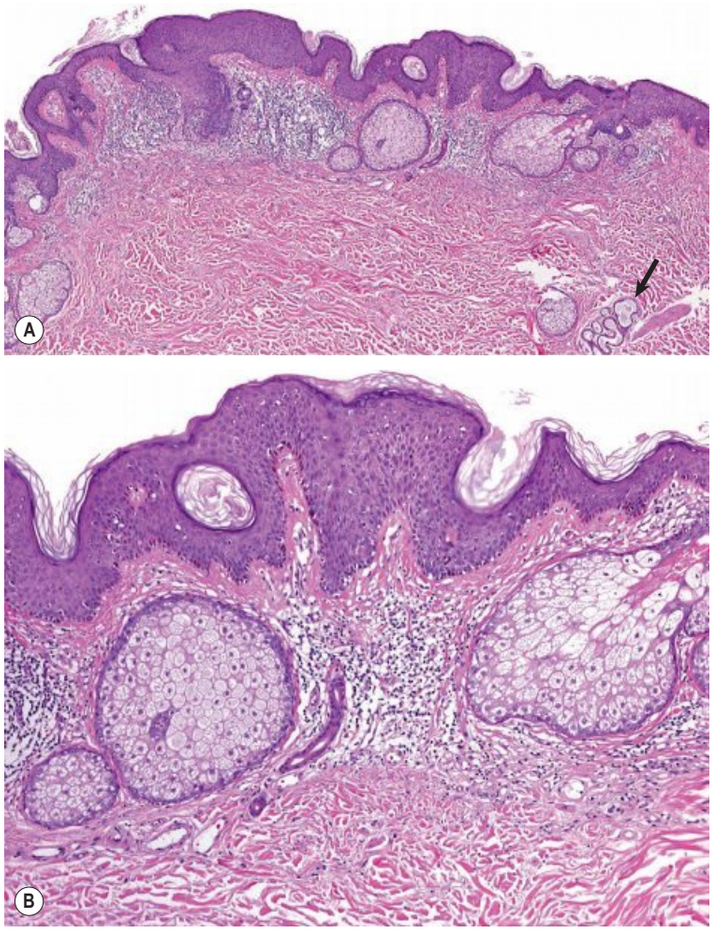


Fig. 111.8 Nevus sebaceus. A Hyperplasia of the epidermis in a papillated fashion, much like the pattern of an epidermal nevus. This is accompanied by adnexal malformation, with enlarged sebaceous lobules. Note the apocrine glands (arrow). **B** The coarsely vacuolated cytoplasm is diagnostic of sebocytes.



Fig. 111.9 Chondroid syringoma (mixed tumor). Exophytic lobulated nodule on the upper cutaneous lip. Note the several whitish areas within the lesion and telangiectatic blood vessels. *Courtesy Lorenzo Cerroni, MD.*

The epithelial component of an apocrine mixed tumor also commonly includes follicular and sebaceous elements[22,26]. Follicular differentiation can consist of small clusters of follicular germinative cells, lobules of outer sheath cells, cystic foci with isthmic or infundibular keratinization, and clusters of matrical cells. Small collections of sebocytes may also be found.

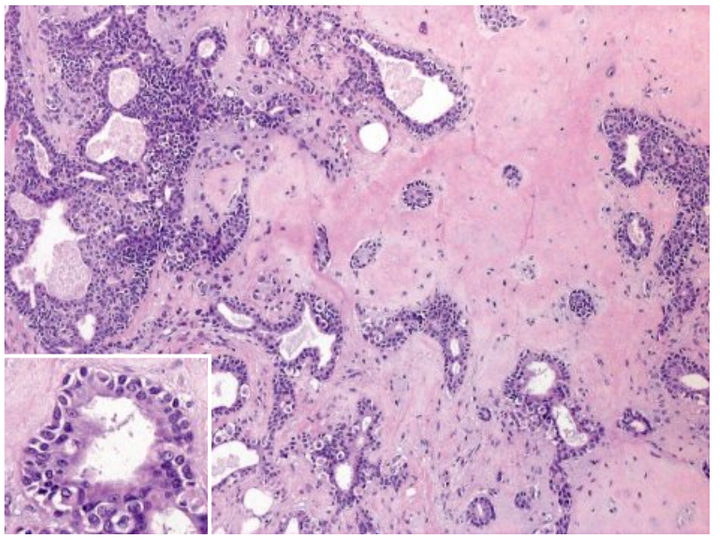


Fig. 111.10 Mixed tumor (chondroid syringoma) with overt apocrine differentiation. Clusters of dilated, branching tubules within a hyalinized stroma. The tubules are lined by columnar cells and contain secretory material within their lumina. Conspicuous apocrine differentiation with a "decapitation" pattern is evident (inset).

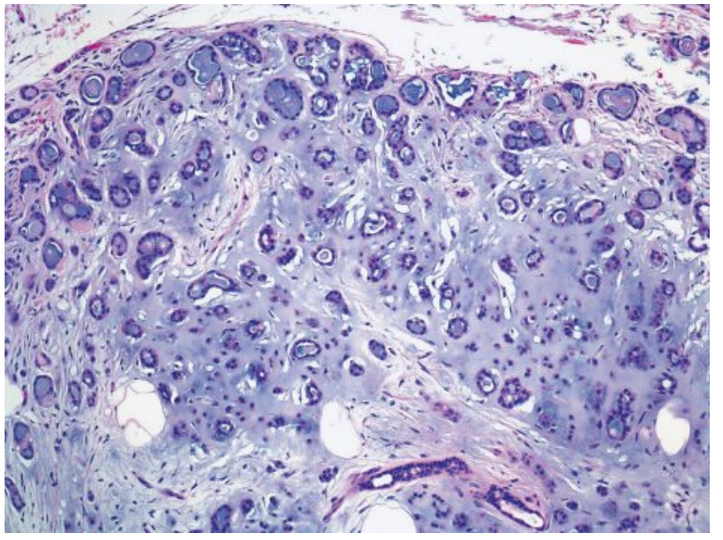


Fig. 111.11 Mixed tumor (chondroid syringoma) with ductal differentiation. This pattern, commonly referred to as the "eccrine" type of mixed tumor, shows small syringoma-like ducts within ample stroma reminiscent of hyaline cartilage.

The number of myoepithelial cells in chondroid syringomas varies. Rare tumors composed exclusively of myoepithelial cells are classified as cutaneous myoepithelioma (see below).

Treatment

Mixed tumor is benign and indolent. Most lesions are treated by simple enucleation, and the risk for persistence/recurrence is minimal. In contrast to mixed tumors of salivary origin, there is no need for excision with margins.

Neoplasms and Proliferations with Follicular Germinative Differentiation

Trichoepithelioma/trichoblastoma

Introduction

Trichoepithelioma and trichoblastoma are terms that refer to benign neoplasms with mostly follicular germinative differentiation[27]. Historically, the term *trichoepithelioma* is older and represents the name ascribed to a solitary lesion of the multiple familial form of

trichoepithelioma (epithelioma adenoides cysticum), and thus the term trichoepithelioma is clinically useful in this context. The designation *trichoblastoma* was coined more recently and was originally applied to neoplasms that showed follicular bulbar differentiation almost exclusively. Although trichoepithelioma is still used, *trichoblastoma* has evolved to be an overarching label for benign proliferations with follicular germinative differentiation[27]. For many, in the current dermatopathologic lexicon, trichoepithelioma represents a variant of trichoblastoma.

Various authors have described subtle variations within the spectrum of follicular germinative neoplasms, thereby birthing terms such as trichogerminoma, trichoblastic fibroma, and lymphadenoma (adamantinoid trichoblastoma)[27]. For purposes of this discussion, these variants will be considered as falling within the larger spectrum of trichoblastoma.

Clinical features

A classic trichoepithelioma usually presents as a skin-colored papule or nodule on the face or upper trunk. Lesions have a predilection for the nose (Fig. 111.12). When in multiplicity, constituting epithelioma adenoides cysticum or Brooke-Spiegler syndrome, lesional density is always greatest in the central face, with sparing of perioral skin. The cylindromatosis gene (*CYLD*), whose protein product functions as a tumor suppressor, underlies epithelioma adenoides cysticum. *CYLD* encodes a deubiquitinating enzyme that impedes the nuclear factor (NF)-κB and c-Jun N-terminal kinase (JNK) pathways[28]. Specifically, missense mutations lead to amino acid substitutions within the ubiquitin (Ub)-specific protease (USP) domain of the CYLD protein in patients with multiple familial trichoepitheliomas. Epithelioma adenoides cysticum can be cosmetically troublesome and is associated with a risk of secondary BCCs and parotid gland neoplasms[29]. Patients can also develop cylindromas and spiradenomas (see Fig. 111.5). The molecular features of *sporadic* trichoepitheliomas are largely unknown, with occasional tumors displaying somatic mutations in *PTCH1* (inactivating) or *CTNNB1* (activating), which have been described primarily in BCCs and pilomatricomas, respectively.

Lesions described historically as *trichoblastomas* were often larger and deeper than simple trichoepitheliomas.

Pathology

All trichoepitheliomas and trichoblastomas have in common the architectural attributes of a benign neoplasm, namely: relative symmetry, circumscription, and a lack of substantial cytologic atypicality. In addition, all are linked by a prominence of follicular germinative cells with enveloping fibrocytic stroma that varies in degree[27,30]. In classic trichoepithelioma, the fibrocytic stroma is conspicuous and constitutes as much as half of the cellularity of the lesion in a given cross-section. In other lesions that simulate BCC, follicular germinative cells may be arrayed as either small or large nodules with only scant intervening sclerotic stroma. The coarse fibrous stroma typically maintains tightly adherent contact to the lesional follicular germinative cells[30]. This is in distinct contrast to the pattern of BCC, in which clefts between basaloid cells and stromal elements often serve as a diagnostic clue.

In classic trichoepithelioma, follicular germinative cells are often disposed as small clusters or as reticulate and cribriform cords (Fig. 111.13). There are usually foci of pronounced bulbar differentiation, emulating the follicular bulb and papilla; these structures have been termed *papillary mesenchymal bodies*[30,31]. Classic trichoepithelioma does not typically show follicular germinative differentiation exclusively. Rather, small cornifying cystic spaces with surrounding pinkish keratinocytes, reflecting concurrent infundibular or isthmic differentiation, are also apparent.

In small or large nodular trichoblastoma, follicular germinative cells comprise the majority of the surface area, papillary mesenchymal bodies may be inconspicuous, and superficial follicular differentiation may be absent. *Trichoblastic fibroma* is a designation used to characterize small nodular trichoblastomas with exaggerated fibrous stroma that often constitutes over half of the cross-sectional area of the lesion[32]. Papillary mesenchymal bodies may be conspicuous in trichoblastic fibroma. With close scrutiny, other modes of differentiation can occasionally be found in a trichoblastoma. There may be tiny collections of mature sebocytes, reflecting concurrent sebaceous differentiation, and (apocrine) ductal differentiation may also be noted.

The differential diagnosis often includes BCC and differentiation is best accomplished by light microscopy. Nonetheless, the role of immunohistochemical staining with markers such as CK20 and PHLDA1 (*p*leckstrin *h*omology-*l*ike *d*omain, family *A*, member *1*) protein, a follicular stem cell marker, has been investigated. Positive

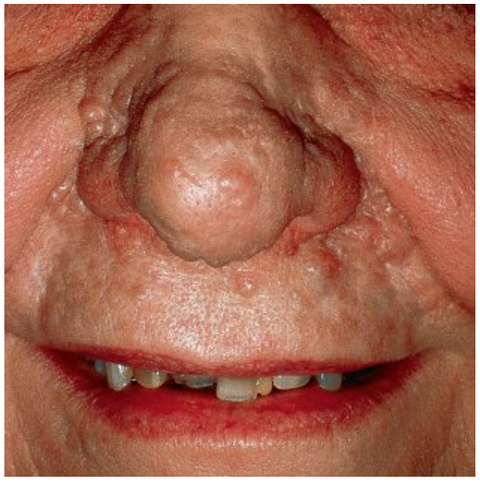


Fig. 111.12 Multiple familial trichoepitheliomas. Numerous skin-colored papules and nodules on the midface. Patients have inactivating mutations in the tumor suppressor gene *CYLD*.

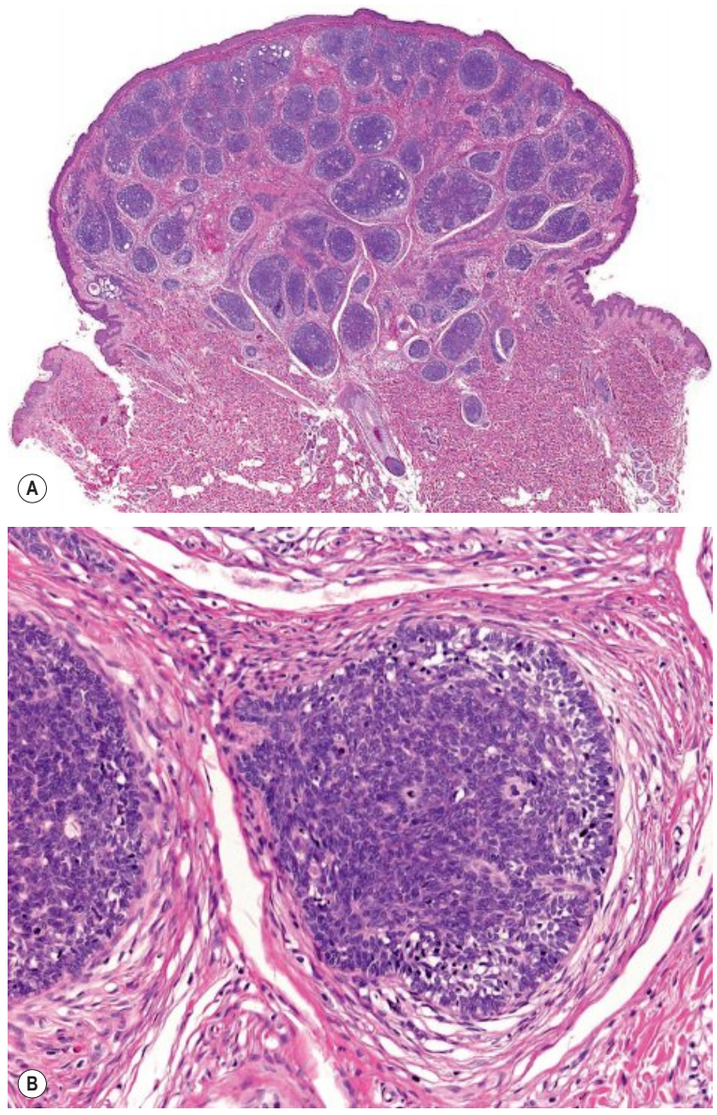


Fig. 111.13 Trichoepithelioma (trichoblastoma). A Dome-shaped papule composed primarily of clusters of follicular germinative cells. **B** A cluster of follicular germinative cells. Note that the clefts are between stromal elements, in contrast to the clefts between tumor and stroma that are characteristic of basal cell carcinoma.

CK20 labeling of Merkel cells colonizing basaloid aggregates has been shown to favor trichoepithelioma/trichoblastoma over BCC[33], and positive staining for PHLDA1 protein was observed in desmoplastic trichoepitheliomas but not in morpheaform BCCs[34]. However, a subsequent study found that while morpheaform BCCs did not express PHLDA1, a sizable minority of micronodular BCCs did[35], thus this marker appears to be most helpful if the pattern in consideration is a morpheaform BCC. The differential diagnosis of some types of trichoblastoma may also include microcystic adnexal carcinoma, syringoma, and spiradenoma.

Treatment

Trichoblastoma is benign and provokes no imperative for surgical treatment. Multiple facial trichoepitheliomas can be cosmetically disabling and many affected patients desire some type of intervention. Longitudinal evaluation for the possibility of secondary BCC is warranted[29]. Because of the number of lesions, conventional excision is not indicated. Other ablative approaches, including laser or electrosurgical destruction, have been employed with some success[36]. Partial responses with topical sirolimus (1% cream; 0.2% gel), topical imiquimod (5% cream), or oral vismodegib, either alone or in combination with CO_2 laser, have been described in case reports or small series[37].

Desmoplastic trichoepithelioma (desmoplastic trichoblastoma)

Introduction

Originally termed *sclerosing epithelial hamartoma*, desmoplastic trichoepithelioma represents a variant of trichoblastoma with exaggerated stromal sclerosis (desmoplasia)[38]. It can easily be misinterpreted as morpheaform BCC by the uninitiated.

Clinical features

Desmoplastic trichoepithelioma commonly presents as a firm skin-colored to erythematous annular plaque with a central dell. The cheek of a woman represents a stereotypical context[38]. Most examples do not exceed 1 cm in diameter. Nearly all desmoplastic trichoepitheliomas are solitary. Multiplicity is a rarity.

Pathology

Desmoplastic trichoepitheliomas are composed of cords of basaloid cells, often two cells wide, arrayed interstitially amongst coarsened collagen bundles (Fig. 111.14)[27,38]. The lesions are relatively circumscribed and are often confined to the upper two-thirds of the reticular dermis, although this is difficult to appreciate in biopsies *en parte*. Small cystic foci of isthmic or infundibular keratinization may be present, and if these cystic spaces are predominant, the designation *trichoadenoma* is apt (see below). The cornifying cysts can rupture and elicit a granulomatous reaction, and small secondary foci of calcification may also be identified[27,38]. In ~20% of cases, dermal nests of a melanocytic nevus are intermingled with complexes of the desmoplastic trichoepithelioma.

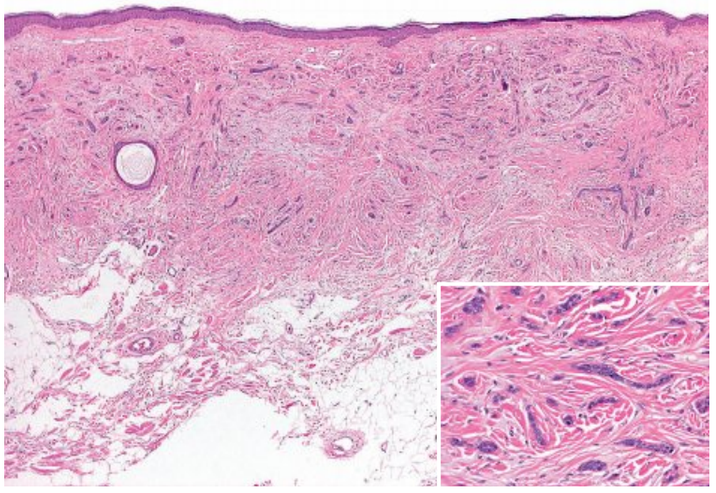


Fig. 111.14 Desmoplastic trichoepithelioma. In the upper and mid reticular dermis, thin strands of basaloid (follicular germinative) cells are arrayed within sclerotic stroma. Much like conventional trichoepithelioma, there are foci of superficial follicular keratinization, with keratinizing cystic spaces. Higher magnification of the thin strands and sclerotic stroma (inset). *Courtesy Lorenzo Cerroni, MD.*

Treatment

Desmoplastic trichoepithelioma is benign. Small or partial biopsies may yield diagnostic uncertainty with respect to morpheaform BCC or microcystic adnexal carcinoma as a consideration in the differential diagnosis, and re-excision or resampling may be necessary when the interpretation is ambiguous. Negative staining for PHLDA1 (see previous section) supports the diagnosis of morpheaform BCC. Temporary improvement has been observed with topical imiquimod.

Neoplasms and Proliferations with Matrical Differentiation

Pilomatricoma (pilomatrixoma, trichomatrioma, calcifying epithelioma)

Introduction

Pilomatricoma is a benign neoplasm or cyst typified by follicular matrical cornification. It has been demonstrated that activating mutations in *CTNNB1*, the gene that encodes β-catenin, are generally present in matrical neoplasms, including pilomatricomas[39]. β-catenin is a component of a key signaling pathway that influences cell differentiation and proliferation (see Ch. 55). Pilomatricomas also commonly demonstrate trisomy 18[40]. Some patients with multiple familial pilomatricomas have germline missense gain-of-function mutations in *PLCD1*.

Clinical features

Pilomatricoma usually presents as a solitary skin-colored, yellow, or bluish papule or nodule (Fig. 111.15). Rarely, multiple lesions are evident, sometimes in association with myotonic dystrophy, Turner syndrome, Rubinstein–Taybi syndrome, or familial adenomatosis polyposis-related syndromes including Gardner syndrome (when cystic)[41]. Firmness is typical and reflects secondary calcification as well as accompanying fibrosis and granulomatous inflammation. Some lesions are "rock-hard" and plate-like on palpation. An angulated shape can be appreciated by stretching the overlying skin ("tent sign"). Although pilomatricomas may develop on any hair-bearing surface, the majority occur on the head or upper trunk[42]. Most tumors appear during childhood and adolescence, but pilomatricomas may develop at any age and can simulate BCC, clinically or microscopically, especially in later adulthood. In rats and humans, pilomatricomas have been observed in association with vismodegib administration. Occasionally, the dermis overlying a pilomatricoma will develop anetoderma.

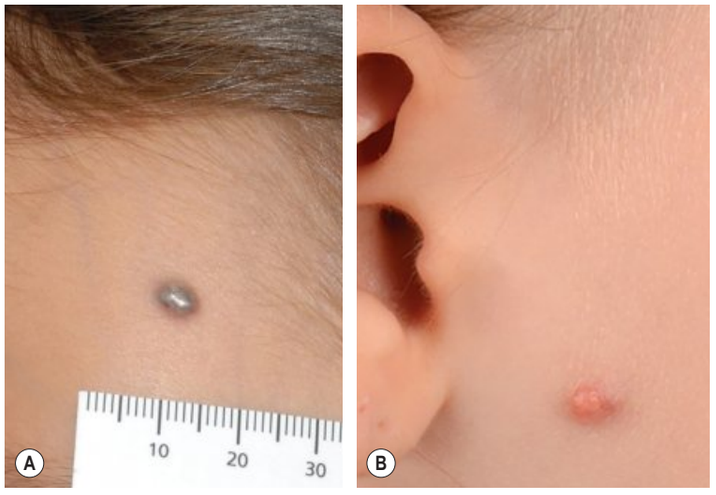


Fig. 111.15 Pilomatricomas in two children. A Firm blue–black papule on the forehead. **B** Firm yellow–pink papule in a preauricular location in a child. *Courtesy Lorenzo Cerroni, MD.*

Pathology

Histopathologically, an early pilomatricoma frequently presents as a cyst with central matrical cornification. The cyst wall consists of basaloid matrical cells that show an abrupt transition to central eosinophilic, cornified matrical cells in which barely discernible nuclear outlines remain (Fig. 111.16). Sometimes, pink trichohyalin granules, illustrative of matrical cornification, are identifiable at the transition point. The central anucleate cornified cells are commonly referred to as *ghost* or *shadow* cells.

In fully developed pilomatricomas, a cystic configuration is commonly lost. Solid collections of basaloid matrical cells and matrical corneocytes are present in varying degrees. The cornified matrical cells elicit considerable fibrosis and a secondary granulomatous infiltrate, which can become predominant in longstanding lesions. Matrical cells have a proliferative capacity as high as any human tissue and can display numerous cells in mitosis. The designation *proliferating pilomatricoma* refers to a pilomatricoma with a high mitotic index. At times, such lesions can be misinterpreted as carcinoma[43], but in contrast to pilomatrical carcinomas, they lack an infiltrative growth pattern and marked tumor necrosis. In late lesions, basaloid matrical cells may be lacking. An involutional pilomatricoma at times can present with only a few shadow cells buried in a larger fibrosing granulomatous reaction. Calcification, ossification, and occasionally transepidermal elimination also ensue in late lesions.

By immunohistochemistry, specific nuclear expression of β-catenin is found in the basaloid cells, when they are present.

Treatment

Pilomatricoma is a benign lesion that is usually treated by simple enucleation. A pilomatricoma may recur after limited excision. If multiple recurrences are observed, complete excision (with negative margins) should be performed to exclude pilomatrical carcinoma.

Pilomatrical carcinoma

Introduction

Pilomatrical (matrical) carcinoma is an uncommon malignancy that exhibits matrical cornification, much like pilomatricoma[44]. Mutations in *CTNNB1* (encodes β-catenin) are common in matrical carcinomas[39]. This suggests a partial common pathogenesis for pilomatricoma and matrical carcinoma. Although on a practical basis no clear association exists, there is a theoretical risk for the possibility of matrical carcinoma developing from conventional pilomatricoma.

Clinical features

Matrical carcinoma is typically a disease of adulthood. Lesions develop on the head and neck, often in the retroauricular area. Although a pathogenic link with ultraviolet irradiation has not been established, many matrical carcinomas develop within severely sun-damaged skin. If a diagnosis of matrical carcinoma is offered in a child or young adult at an age when the diagnosis is improbable, the case should be reassessed for the possibility of pilomatricoma.

Pathology

Much like pilomatricoma, matrical carcinomas include both basaloid matrical cells and anucleate matrical corneocytes. In contrast to pilomatricoma, the matrical carcinoma cells usually display nuclear pleomorphism. An infiltrative configuration or poor circumscription is usually apparent, especially in an excisional biopsy. Tumor necrosis is commonly present. There may be considerable squamous cornification as well, and parts of a given lesion may resemble conventional squamous cell carcinoma (SCC).

Matrical carcinoma should be distinguished microscopically from BCC with matrical differentiation[45]. The latter entity represents an otherwise conventional BCC in which small foci of matrical cornification are identifiable. The clinical behavior of this variant is thought to be identical to that of conventional BCC. As in pilomatricomas, nuclear expression of β-catenin is seen in the basaloid cells of matrical carcinomas, as well as in a relevant proportion of BCCs. Thus, negative staining of basaloid cells points to a BCC.

Treatment

Matrical carcinoma is a low-grade form of adnexal carcinoma that poses some risk for metastasis, although the risk is believed to be low[44]. Complete extirpation with negative margins represents standard care.

Neoplasms and Proliferations with Follicular Sheath (Tricholemmal) Differentiation

Tricholemmoma (trichilemmoma)

Introduction

Tricholemmoma constitutes a form of benign adnexal neoplasm with differentiation toward the follicular outer sheath[46]. Some have averred that tricholemmoma is merely a viral wart based upon conventional

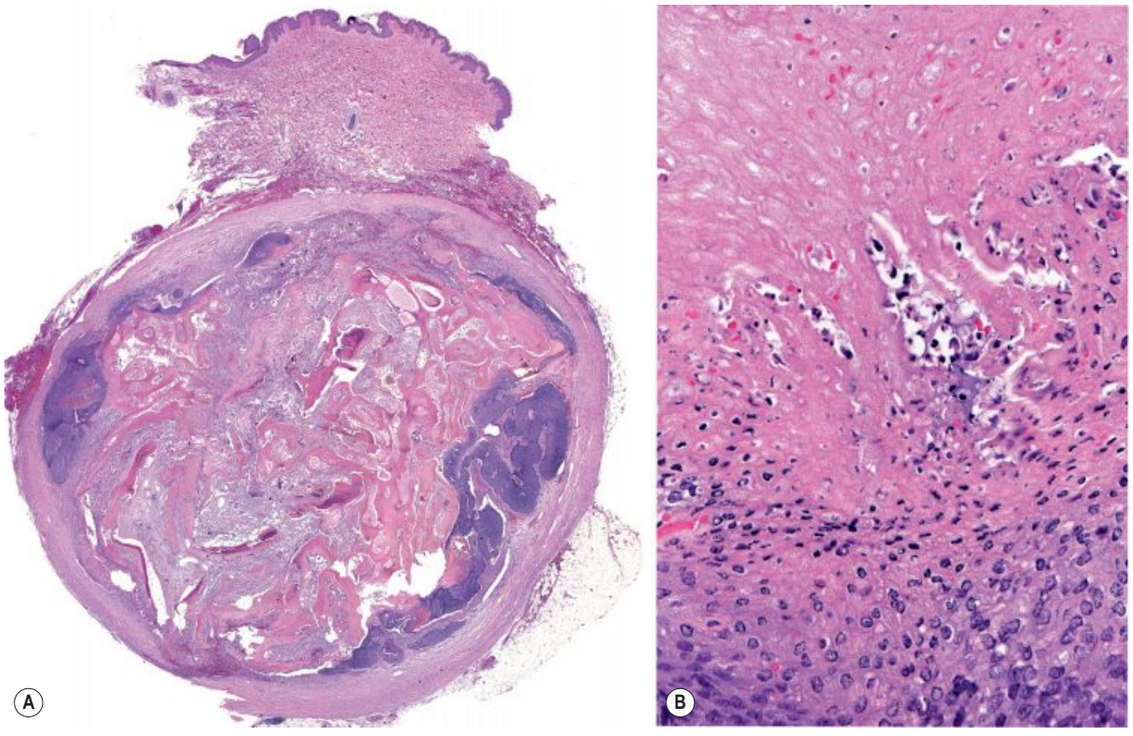


Fig. 111.16 Pilomatricoma. A At low magnification, a well-circumscribed, epithelial-lined cystic nodule is seen. A portion is lined by basaloid matrical cells. Centrally, there are anucleate keratinized matrical cells ("shadow" cells). **B** Transition between matrical cells (lower) and central anucleate "shadow" cells (upper). *Courtesy Lorenzo Cerroni, MD.*

histopathology[27]. Although one study found human papillomavirus (HPV) DNA within lesions by PCR, in general molecular analysis has failed to demonstrate intralesional HPV DNA and thus viral causation seems unlikely[47].

Clinical features

Tricholemmomas may arise as single or as multiple papules that usually have similar coloration to surrounding normal skin (see Fig. 63.3)[46,48]. Individual lesions may display hyperkeratosis or a verrucous surface. Most are distributed on the central face, including the nose or upper lip, but any non-glabrous site may be affected. Tricholemmomas can also present on genital skin and simulate condylomata acuminata if multiple. This tumor may occur as a secondary neoplasm within nevus sebaceus. The variant *desmoplastic tricholemmoma* is especially common in this context[49]. Both sporadic and nevus sebaceus-associated tricholemmomas often contain *HRAS* mutations.

Multiple tricholemmomas typically present on facial or genital skin. Multiple tricholemmomas are a common manifestation of Cowden syndrome/PTEN hamartoma tumor syndrome (see Ch. 63 & Fig. 111.5)[46,50]. In addition to tricholemmomas, manifestations of Cowden syndrome include sclerotic fibromas, acral keratoses, and adenocarcinoma of the breast, thyroid gland, or gastrointestinal tract[51]. Loss of PTEN expression within a tricholemmoma, as assessed by immunohistochemistry, is suggestive that the patient has Cowden syndrome[52].

Pathology

Microscopically, tricholemmomas present as small circumscribed lobular proliferations composed of pallid, glycogen-containing outer root sheath cells. There is often a broad connection to the surface epidermis (Fig. 111.17)[46,48,50]. A papillated surface is common, and there may be verrucous hyperplasia with hypergranulosis, thereby simulating the pattern of a verruca in a superficial biopsy. Squamous eddies are not uncommon. There is a palisade of small, compact basal keratinocytes at the periphery of a lesional lobule, and a flanking thickened basement membrane that is PAS-D (periodic acid Schiff with diastase)-positive is commonly present. Outer root sheath differentiation can also be recognized through use of CD34 immunostaining.

In desmoplastic tricholemmoma, small central angular clusters of outer root sheath cells are arrayed in an infiltrative pattern with enveloping sclerotic stroma. This creates a configuration that at times simulates carcinoma[49,53]. Most commonly, a desmoplastic focus is accompanied or surrounded by areas of conventional tricholemmoma that serve as the basis for accurate interpretation, but the diagnosis can be deceptive in partial or superficial biopsies.

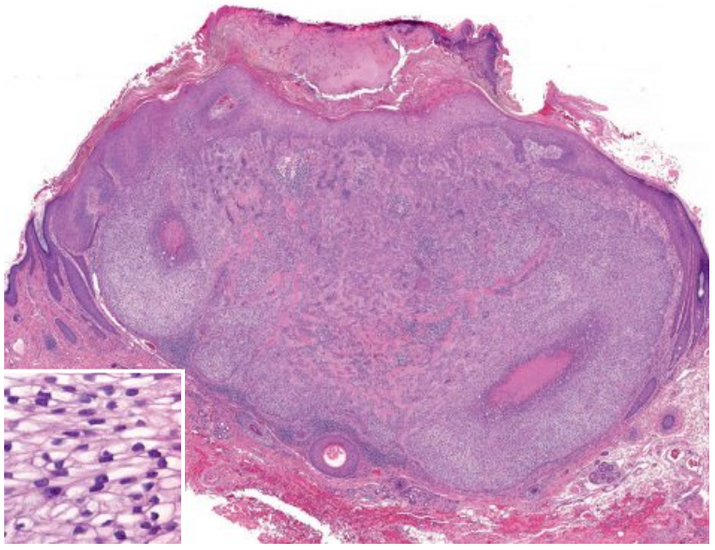


Fig. 111.17 Tricholemmoma. Circumscribed nodular proliferation of pale-staining cells with a broad connection to the overlying epidermis. There is also surface crust and focal areas of necrosis within the tumor. Sometimes these lesions are misdiagnosed as superficial carcinomas. The cells contain glycogen and display outer root sheath differentiation (inset). *Courtesy Lorenzo Cerroni, MD.*

Treatment

Tricholemmoma is a benign adnexal neoplasm with limited proliferative capacity. After recognition by biopsy, no further treatment is needed unless there is uncertainty regarding the diagnosis. If there is a desire for ablation, cryotherapy, electrosurgical destruction, shave, curettage, or excision may be employed.

Tricholemmal (trichilemmal) carcinoma

This malignant analogue of tricholemmoma represents an invasive lesion composed in part of glycogen-containing clear cells, similar to cells of the follicular outer sheath. If a thickened, PAS-positive, prominent basement membrane can be identified peripheral to areas of clear cell change, it is probably of considerable diagnostic significance. CD34 immunopositivity may also be of potential diagnostic value. Many of these carcinomas show accompanying keratinization and thus there is considerable overlap with lesions that have been pigeonholed as clear cell SCC.

Treatment

Tricholemmal carcinoma represents a carcinoma with limited metastatic potential. These lesions are probably best considered equivalent to SCC and treated as such.

Neoplasms and Proliferations with Superficial Follicular (Infundibular and Isthmic) Differentiation

Tumor of follicular infundibulum (infundibuloma; isthmicoma)

Introduction

This benign lesion is commonly known as *tumor of follicular infundibulum* (TFI) or *infundibuloma*, but the designation *isthmicoma* is more apt, as the proliferation primarily shows follicular isthmic differentiation.

Clinical features

TFI prototypically presents clinically as a subtle macule, thin papule, or plaque[54,55]. Lesions are skin-colored or sometimes slightly hypopigmented and may appear slightly atrophic[54]. Many examples are diagnosed incidentally within skin cancer excision specimens where no known clinical lesion was even identifiable. TFI may occur in multiplicity (Fig. 111.18A) and assume a reticulated pattern; patients with this presentation may defy diagnosis for a time because of the subtlety of both the clinical and the microscopic findings[54–56]. Patients with multiple atrophic-appearing TFI may display a clinical pattern reminiscent of disseminated superficial porokeratosis or multiple actinic keratoses. TFI is rarely present in Cowden syndrome.

Pathology

TFI consists of a plate-like proliferation of eosinophilic isthmic keratinocytes arrayed in reticulate fashion in the superficial dermis, in broad, but intermittent, continuity with both the surface epidermis and extant follicular structures[54]. Most of the constituent keratinocytes have cytoplasm similar to keratinocytes of the follicular isthmus, follicles in catagen phase, or the cells of an isthmic (pilar) cyst (Fig. 111.18B). The keratinocytes are paler than those of the surface epidermis, and often a few scattered dyskeratotic keratinocytes are present. Some lesions will display tricholemmal foci in which pallid keratinocytes or a thickened basement membrane can be found, and occasionally a hybrid of TFI and tricholemmoma may be encountered. Additionally, small buds of follicular germinative cells may jut from the undersurface of a TFI.

Rarely, small clusters of sebocytes may be found within TFI[57]. Sebaceous or apocrine ducts have also been documented[56].

Treatment

TFI is a benign adnexal proliferation with negligible proliferative capacity. If desired, lesions may be removed by cryotherapy, shave, or electrosurgical destruction. For multiple lesions, superficial laser ablation can be considered[54].

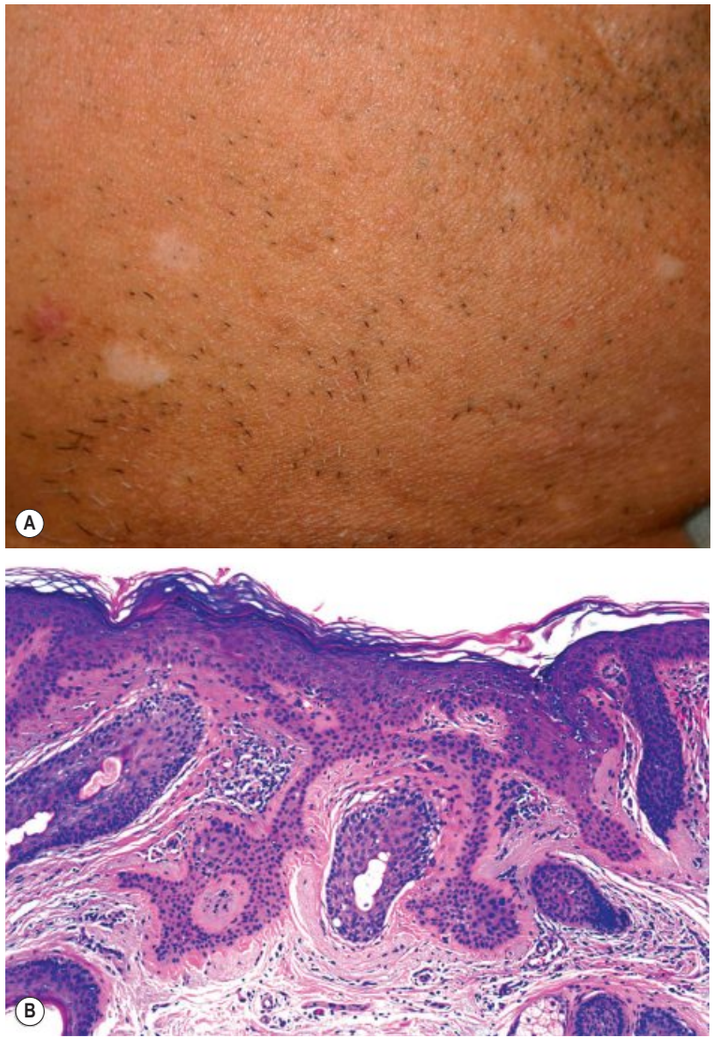


Fig. 111.18 Tumor of follicular infundibulum. A Multiple hypopigmented thin papules on the cheek. **B** The microscopic pattern is subtle, resembling a reticulated seborrheic keratosis. Strands of pale eosinophilic keratinocytes display multifocal attachment to the epidermal surface and also commonly interconnect with existent follicular structures.

Trichoadenoma (trichoadenoma of Nikolowski)

Introduction

The term *trichoadenoma* is a misnomer, as there are no adenomas of follicular lineage since the hair follicle is not a structure that exhibits glandular differentiation. Trichoadenoma represents a benign follicular neoplasm with sclerotic stroma that consists largely of small cystic spaces that exhibit infundibular and isthmic differentiation[58].

Clinical features

The clinical presentation of trichoadenoma is not distinctive. The neoplasm presents as a skin-colored papule or small plaque.

Pathology

Trichoadenoma is usually positioned in the superficial dermis. Cornifying cysts with infundibular or isthmic keratinization comprise the bulk of the proliferation (Fig. 111.19)[58]. The sclerotic stroma is often accompanied by thin strands of basaloid cells, similar to the cords observed in desmoplastic trichoepithelioma. Trichoadenoma and desmoplastic trichoepithelioma have many overlapping histopathologic features, and, in their "pure" forms, likely represent opposite poles of the spectrum of the same entity.

Treatment

Trichoadenoma is a benign adnexal neoplasm with negligible proliferative capacity. No further treatment is necessary unless the patient desires removal.

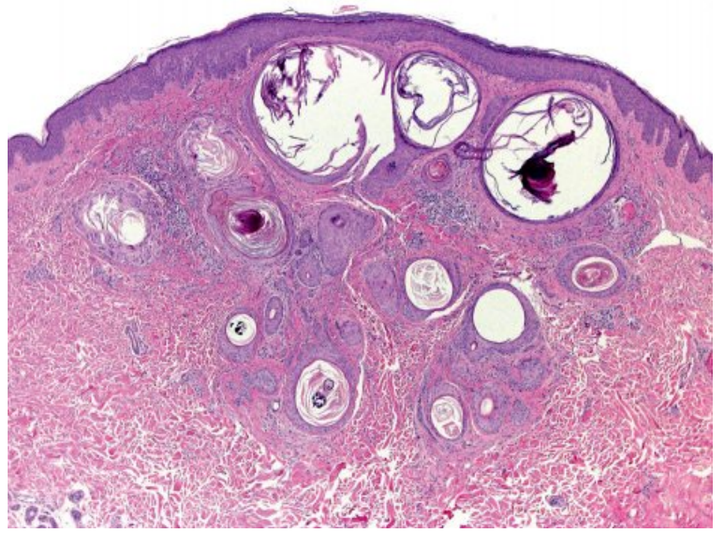


Fig. 111.19 Trichoadenoma. This lesion consists primarily of small keratinizing cystic spaces. There are also lobules and a few cords of basaloid cells. Both are surrounded by sclerotic stroma, similar to the pattern observed in desmoplastic trichoepithelioma. *Courtesy Lorenzo Cerroni, MD.*

Proliferating pilar tumor (proliferating follicular-cystic neoplasm)

Introduction

Known for decades as *proliferating pilar tumor (PPT)*, *proliferating tricholemmal cyst* or *proliferating pilar cyst*, the designation *proliferating follicular-cystic neoplasm (PFCN)* was proposed by Ackerman as a more apt designation[27]. This term describes a group of nodular/cystic neoplasms characterized microscopically by abrupt keratinization akin to that of the follicular isthmus or in a follicle in catagen phase[59]. In the past, it was known that PPT could simulate SCC microscopically, but the entity was generally regarded as a benign process, although it was recognized that, occasionally, locally destructive behavior could occur[59].

Recently, this concept has been called into question, and a proposal has been issued that PFCN represents a mix of benign and malignant neoplasms grouped together under one rubric[27]. The proposal further iterates that a benign PFCN should be designated as *proliferating follicular-cystic acanthoma* (PFCA), while a malignant PFCN should be designated as *proliferating follicular-cystic carcinoma* (PFCC). As some examples of PFCN share features with carcinoma, including clinical characteristics such as locally destructive behavior, microscopic characteristics such as nuclear atypicality, and molecular characteristics such as aberrations in ploidy, this proposal seems diagnostically practical[60,61]. Of note, an activating *PIK3CA* mutation was detected in a metastatic PFCC[61a].

Clinical features

PPT presents as a nodule, usually no more than a few centimeters in size, although there have been reports of lesions exceeding 20 cm in diameter. The lesions can develop in men but a female predominance is seen in most series. Roughly 90% of cases arise in the scalp, probably as a reflection of the density of follicles at that locale. The prototypical presentation is as a nodule on the scalp of an elderly woman. The tumors are usually well circumscribed but may be multinodular. Their circumscription is reflected in smooth borders and the fact that lesions generally shell out from adjacent tissues during surgical excision.

Pathology

PPT consists of a large and/or deep nodule that resides in the dermis or subcutis[59]. Because of its large size, the laboratory commonly receives fragmented specimens. Both solid and cystic patterns are usually evident at low magnification, with cystic areas exhibiting the pattern of an isthmic (pilar) cyst (Fig. 111.20). The constituent keratinocytes are mostly isthmic keratinocytes with dense eosinophilic cytoplasm, and centrally there is an abrupt transition to compact keratin with little intervening granular layer. Rarely, shadow cells, implying matrical keratinization, can be found. There may be focal necrosis and calcification.

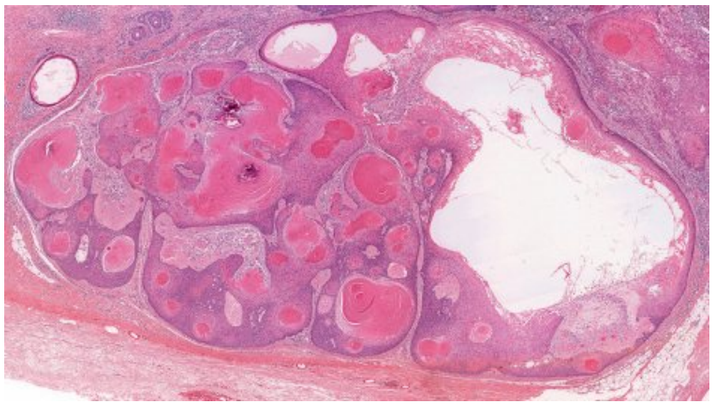


Fig. 111.20 Proliferating follicular-cystic neoplasm. This complex multicystic neoplasm shows abrupt keratinization, similar to the pattern exhibited at the follicular isthmus (proliferating pilar tumor, proliferating tricholemmal cyst). Although it can be difficult to determine whether these lesions are benign or malignant, this example was well circumscribed and showed no cytological atypia (proliferating folliculo-cystic acanthoma). *Courtesy Lorenzo Cerroni, MD.*

The degree of cytologic atypicality varies among lesions and amongst different areas of a given lesion. Commonly, the neoplastic cells contain enlarged vesicular nuclei with prominent nucleoli and some degree of nuclear hyperchromasia; mitotic figures are usually identified, but overt anaplasia is usually not present. Since some examples of PPT represent low-grade forms of carcinoma, tumors with marked cytologic atypicality, extensive necrosis, a lack of circumscription, or extraordinary numbers of mitotic figures warrant designation as PFCC[60].

Treatment

As noted, some examples of PPT may represent carcinoma. If a lesion has been enucleated in its entirety or near entirety, is circumscribed, and lacks substantial cytologic atypia, it can be interpreted as PFCA and additional surgical therapy is not necessary. If a given lesion lacks circumscription, shows substantial cytologic atypia or necrosis, or has been sampled *en parte*, then complete excision is warranted, as PFCC remains a concern.

NEOPLASMS AND PROLIFERATIONS WITH SEBACEOUS DIFFERENTIATION

Sebaceous gland hyperplasia

Introduction

Sebaceous gland hyperplasia (SGH) does not represent a true neoplasm. It represents benign enlargement of sebaceous glands. Numerous lesions can develop following systemic administration of immunosuppressive medications, in particular calcineurin inhibitors.

Clinical features

SGH is relatively common and presents with one or multiple yellowish, occasionally telangiectatic papules, usually on the central or upper face and sometimes on the upper trunk (Fig. 111.21). Commonly, the clinical lesions display a central dell that corresponds to a central follicular infundibular ostium. *Beaded lines* represent a unique expression of SGH in which a linear array of hyperplastic sebaceous glands is present in the vicinity of the clavicle or on the neck[62]. Biopsy is occasionally indicated to exclude BCC, but the dermoscopic findings of a crown of blood vessels, rather than arborizing vessels, assist in the diagnosis (see Ch. 0).

Pathology

The sebaceous gland in SGH shows normal morphology, with a thin rim of seboblasts surrounding the remainder of the gland, composed of mature sebocytes. The enlarged sebaceous lobules usually circumferentially surround a central infundibulum.

Treatment

If treatment is desired, lesions can be removed or diminished by shave, light electrosurgical destruction, cryotherapy, or laser ablation[63]. Long-term topical retinoid application may be beneficial. A short course of oral isotretinoin has been utilized for patients with extensive or disfiguring lesions.



Fig. 111.21 Sebaceous hyperplasia. A Skin-colored to yellowish papules with a central dell. **B** Numerous lesions of sebaceous hyperplasia in a solid organ transplant recipient receiving long-term cyclosporine. *B, Courtesy Oscar Colegio, MD, PhD.*

Sebaceous adenoma, sebaceoma, and sebaceous epithelioma

Introduction

The term *adenoma* designates a benign neoplasm with glandular differentiation, and any benign proliferation with predominance of sebaceous differentiation can be grouped under this rubric. Commonly, the term sebaceous adenoma has been applied to superficial benign sebaceous neoplasms with a predominance of mature sebocytes, while sebaceous epithelioma and sebaceoma have been applied to sebaceous neoplasms with a predominance of seboblasts. Troy and Ackerman[64] coined *sebaceoma* as an alternative to describe a group of benign sebaceous proliferations that were generally more deeply situated than superficial sebaceous adenomas and in which a vertically oriented microscopic pattern was identifiable.

The dated term sebaceous epithelioma is inherently confusing, as the diagnosis has been utilized differently by various authorities. To some, a sebaceous epithelioma represents a low-grade form of sebaceous carcinoma or BCC with sebaceous differentiation. Others have utilized the term to characterize sebaceoma or sebaceous proliferations of uncertain potential. We believe that the designation sebaceous epithelioma should be abandoned.

In this chapter, the term *sebaceous adenoma* is used in broad fashion to encompass both conventional sebaceous adenoma and sebaceoma.

Clinical features

Sebaceous adenomas present clinically as papules or nodules, usually less than a centimeter in diameter, distributed on the head or neck and sometimes on the upper trunk. The lesions are not clinically distinctive except when there is a yellowish color, which is often not apparent. Superficial sebaceous adenomas are usually relatively small and papular, while sebaceomas may present as a deep nodule[64,65]. Multiple sebaceous neoplasms, especially cystic ones, may be a presenting sign of the Muir–Torre syndrome (MTS; see Table 63.5), in which patients can also develop multiple keratoacanthomas and visceral carcinomas, especially colonic adenocarcinoma[66,67]. Sebaceous neoplasms with a keratoacanthoma-like pattern point to the diagnosis of MTS (see below).

Pathology

Conventional *sebaceous adenoma* is usually captured in continuity with the surface epidermis and is relatively small and circumscribed. The relative proportions of basaloid seboblastic cells and mature sebocytic cells varies, but sebocytes usually predominate. Seboblasts comprise a thin multilayer of cells at the periphery of each lobule. Mitotic figures can be found in seboblasts but are not conspicuous. Necrosis is not typically evident in an adenoma unless the lesion has been traumatized. Significant necrosis, whether of single cells or *en masse*, raises concern for the possibility of carcinoma.

Sebaceoma is usually more deeply situated, often involving the deep reticular dermis and sometimes the superficial subcutis[64]. The lesions are sharply circumscribed in an excisional specimen, but this may be difficult to fully appreciate in a biopsy *en parte*. Seboblasts predominate in sebaceoma and sebocytic differentiation may be only focal, yielding a microscopic pattern not unlike a large nodular trichoblastoma (Fig. 111.22). If sebaceous differentiation is only focal, then epithelial membrane antigen (EMA) or adipophilin immunoperoxidase staining can be considered as a diagnostic supplement. EMA labels mature sebocytes in the normal sebaceous gland, while adipophilin labels multivacuolated lipid-containing cells.

Use of immunohistochemistry to assess for loss of expression of mismatch repair proteins encoded by MTS-associated genes, e.g. MSH2, MSH6, MLH1, and PMS2, has been reported to be an effective screening technique[68]. However, it should be noted that loss of expression, as detected by immunohistochemistry, does not necessarily reflect underlying germline mutations. Occasionally, mutations can occur in sporadic neoplasms[69]. Additionally, protein expression can sometimes be detected within tumors in patients who actually harbor a germline mutation in the gene encoding that particular protein; this is usually due to the presence of a protein that, despite being dysfunctional, can react with the antibody utilized for the test[68]. For these reasons, assessment for loss of expression of a mismatch repair protein is most helpful as a screening technique for MTS, but, if found, is not fully diagnostic, and confirmatory genetic testing should be considered after assessing risk for MTS (see Table 63.5). In the same context, assessment of microsatellite instability may also serve as a screening technique.

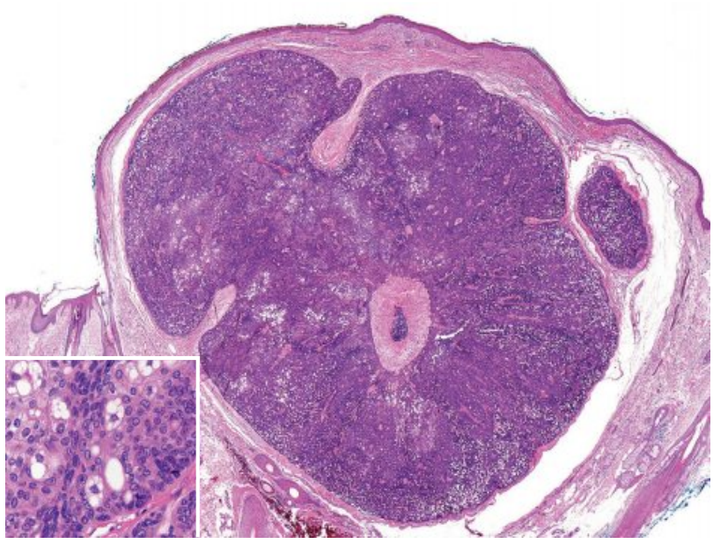


Fig. 111.22 Sebaceous adenoma (sebaceoma). Well-circumscribed proliferation of both basaloid seboblastic cells and scattered mature sebocytes with coarsely vacuolated cytoplasm (inset).

Treatment

Once a definite microscopic diagnosis has been achieved, no further treatment is obligatory. It is often difficult to establish the circumscription of lesions captured in superficial or partial biopsies. Complete excision of such lesions is appropriate to exclude the possibility of BCC with sebaceous differentiation or sebaceous carcinoma. Deeply situated lesions of MTS may be prone to rapid growth.

Sebaceous carcinoma

Introduction

The term sebaceous carcinoma designates an adenocarcinoma with sebaceous differentiation. By historical convention, these carcinomas have been separated into ocular and extraocular types. Originally, periorbital sebaceous carcinomas were thought to hold a graver prognosis, but more recent data suggest that tumors in this location have a similar overall survival rate as sebaceous carcinomas arising elsewhere[70].

Clinical features

The clinical presentation of sebaceous carcinoma is not distinctive. Typical clinical lesions include erythematous nodules or plaques that may be ulcerated or crusted and only occasionally display yellowish coloration. More commonly, the lesions display an erythematous or pearly morphology that is indistinguishable from common forms of keratinocyte carcinoma. Early in presentation, ocular lesions are very commonly misdiagnosed as blepharitis or ocular rosacea.

Sebaceous carcinomas commonly develop in the periorbital area but also occur elsewhere on the head and neck and less commonly on the trunk. Carcinomas from the trunk often display a nodular pattern, and superficial biopsies from such lesions may be deceptive and can be misinterpreted[70]. Sebaceous carcinoma can occur in patients with Muir–Torre syndrome (MTS), but the identification of a sebaceous carcinoma alone is not sufficient to diagnose the syndrome[66]. However, any unusual sebaceous neoplasm is probably sufficient provocation for consideration of the disease (see Table 63.5).

Pathology

Like many malignancies, sebaceous carcinoma often exhibits asymmetry, a lack of circumscription, and areas with an infiltrative pattern. In nodular sebaceous carcinoma, cells are arrayed as large nests and lobules. In infiltrative sebaceous carcinomas, jagged nests and thin strands are found. Sebaceous carcinoma can involve the surface epidermis or conjunctiva in a pagetoid pattern, especially in ocular lesions[71,72]. This can be confused with Bowen disease or melanoma.

The degree of sebaceous differentiation in sebaceous carcinoma varies greatly, as does the degree of nuclear atypicality (Fig. 111.23). Some carcinomas display obvious sebocytic differentiation, while other examples may be largely seboblastic or undifferentiated in appearance. Differentiation from sebaceous adenoma may be difficult, but loss of expression of bcl-2 and p21 as well as higher p53 and Ki-67 expression represent useful immunohistochemical markers that point to sebaceous carcinoma. Recently, it has been shown that TERT promoter mutations are present in a minority of sebaceous carcinomas and absent in sebaceous adenomas[73].

Stains for lipid, such as oil red O or Sudan black, have been utilized in the past as a tool to confirm sebaceous differentiation through labeling of cytoplasmic fat. However, such stains have little routine practical applicability as they require the use of frozen tissue substrate. EMA and adipophilin immunohistochemical staining represent the best supplemental tests for confirmation of sebaceous differentiation. When authentic sebaceous differentiation is present, coarsely vacuolated cytoplasmic positivity can be seen with either stain.

Crateriform or cystic sebaceous neoplasms that display a clinical appearance and microscopic architecture reminiscent of keratoacanthoma are uncommon lesions that probably represent low-grade carcinomas[66]. Sebaceous neoplasms with a keratoacanthoma-like pattern probably only occur in the context of MTS.

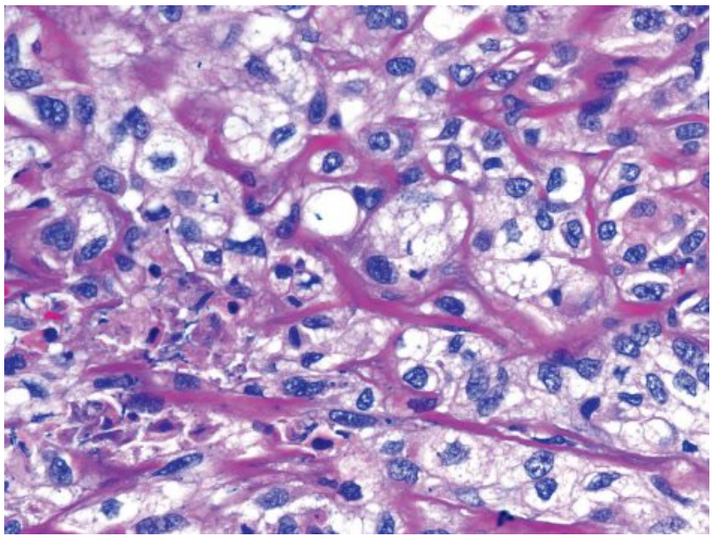


Fig. 111.23 Sebaceous carcinoma. At high magnification, there are cells with atypical nuclei and ample coarsely vacuolated cytoplasm. There are also many necrotic cells with pyknotic nuclei.

Treatment

Sebaceous carcinoma is an adnexal carcinoma with significant, albeit variable, metastatic potential. The primary treatment remains surgical extirpation, including removal via Mohs micrographic surgery. Although the risk of metastatic disease was formerly believed to be high, particularly for ocular carcinomas, the data contained within many older reports may be skewed by inclusion of carcinomas diagnosed late in their evolution. Extensive disease of the eye has been treated with ocular enucleation, especially when ocular conjunctival involvement was present. The metastatic potential of both superficial sebaceous carcinoma and sebaceous carcinoma with an infiltrative pattern may be limited, although additional study will be necessary to fully establish this as well as the possibility that missense mutations in *PCDH15* are associated with metastatic ocular sebaceous carcinoma.

NEOPLASMS AND PROLIFERATIONS WITH APOCRINE (OR ECCRINE) DIFFERENTIATION

In most textbooks, adnexal neoplasms with glandular and ductular differentiation have been rigorously separated into eccrine and apocrine neoplasms. Commonly, the distinction was based upon enzyme histochemistry, an imprecisely applied technique that is no longer available. Discrimination has also been based upon conventional microscopic assessment, a useful but imprecise tool, at least for the distinction of eccrine and apocrine attributes.

A few authorities have responded to this difficulty by grouping apocrine and eccrine neoplasms together, in recognition of the fact that it is impossible to determine whether a given lesion, such as a given syringoma, is of apocrine or eccrine lineage. In the sections that follow, the traditional categorization as apocrine or eccrine will be maintained, but areas of overlap will be expressly noted. For entities such as syringoma, poroma, and hidradenoma, which can be of either apocrine or eccrine lineage, the presentation will be included in the discussion of apocrine lesions.

Benign Neoplasms and Proliferations with Apocrine (or Eccrine) Ductal and Tubular Differentiation

Syringoma

Introduction

Syringoma represents a benign adnexal neoplasm with mostly ductal (syringeal) differentiation. Historically, syringomas have been interpreted as neoplasms of eccrine lineage[74,75]. The term syringoma can be used to describe neoplasms of either apocrine or eccrine lineage, and it is currently impossible to judge the lineage of any given lesion other than by its context[1,2].



Fig. 111.24 Syringomas. **A** Aggregated skin-colored papules with a periorbital distribution. **B** Multiple skin-colored to pink, smooth papules on the neck and upper chest. The lesions favor the ventral surface of the trunk, a distribution pattern referred to as *"en demi-cuirasse"*. *B, Courtesy Jean L. Bolognia, MD.*

Clinical features

A syringoma manifests clinically as a small, firm, skin-colored papule. Syringomas commonly present in multiplicity (Fig. 111.24) and may be eruptive[76]. The lesions are removed from women more commonly than men, although it is not clear that this represents treatment bias. There is an increased incidence in Asian populations as well as an association with Down syndrome. Clear cell syringomas are associated with diabetes mellitus. Patients with Nicolau–Balus and Costello syndromes can also develop syringomas (see Chs. 99 and 55), and rarely they are seen in patients with Brooke–Spiegler syndrome (see below).

Syringomas may occur at any site on the body but are prone to occur in the periorbital area, especially the eyelids[77]. Sometimes, lesions involve the upper trunk (favoring the ventral surface) or genital skin[76,78]. Eruptive syringomas most commonly involve the trunk but may involve the extremities, including the palms and soles. Some cases of eruptive syringomas may be familial with autosomal dominant inheritance. Acral syringomas, which are rare, are those that are most clearly of eccrine lineage, as the acini of glabrous (non-hair-bearing) skin are exclusively eccrine[79].

Syringoma-like foci can be found in biopsy specimens of cicatricial alopecias. Although initially thought to represent authentic syringomas and to play a role in pathogenesis[80], later studies aptly demonstrated that, in fact, these foci represented reactive changes in response to the inflammation and scarring from the cicatricial alopecia. That is, these foci were simply bystanders[81]. Occasionally, syringoma-like changes can also be seen in non-scarring alopecia.

Pathology

From scanning magnification, a syringoma is small and circumscribed and is usually confined to the superficial dermis. The encompassing stroma is sclerotic. The epithelial component of the proliferation is composed of cells with pale or pinkish cytoplasm forming nests and

tubules of relatively uniform size. Depending upon the exact plane of section, the nests of a syringoma vary in shape, and some nests may assume a morphology that resembles a comma or a tadpole (Fig. 111.25). Tubular areas exhibit ductular differentiation with central lumina lined by a compact eosinophilic cuticle. Typically, half or more of the nests in a given plane of section will show central ductal differentiation.

Usually, a syringoma lacks keratinization, although at times superficial cornification can be seen. Syringomas also typically lack evidence of follicular differentiation. If either follicular differentiation or keratinization is identified, other differential diagnostic possibilities should be strongly considered. The combination of superficial cornification, poor circumscription, and extension into the deep reticular dermis (or subcutis) favors microcystic adnexal carcinoma over syringoma. A lesion with strands of basaloid cells, focal superficial cornification, and focal calcification probably represents desmoplastic trichoepithelioma rather than syringoma. If there are only cornifying cysts present and authentic ductal differentiation is lacking, then the most likely diagnosis is trichoadenoma.

Treatment

Syringoma is a benign adnexal neoplasm with negligible proliferative capacity. After definitive diagnosis, no further surgical intervention is needed unless adnexal carcinoma remains a clinicopathologic consideration. Syringomas may be treated with careful application of trichloroacetic acid, cryotherapy, punch excision or electrosurgical destruction, with variable results. This can be difficult in the common situation in which multiple lesions are present on eyelids. Disseminated lesions can be cosmetically disabling and therapeutically challenging, and laser ablation might be the best choice[82].

Poroma

Introduction

Poroma designates a group of benign adnexal neoplasms with poroid (terminal ductal) differentiation. Like syringomas, poromas were widely interpreted historically as neoplasms of eccrine lineage because of dubious enzyme histochemistry[74,75]. The words *eccrine* and *poroma* became seemingly inextricably linked in the dermatologic lexicon, and thus poromas are often referred to as eccrine in reflexive fashion[2]. Poroma can be a proliferation of either apocrine or eccrine lineage[83–85]. Eccrine and apocrine poromas probably occur in nearly equal numbers.

The term *acrospiroma* is used by some authorities as a synonym for poroma and is used by other authorities as a broad designation that encompasses both poroma and hidradenoma.

Clinical features

Poromas usually present as solitary papules, plaques, or nodules (Fig. 111.26)[4]. When sessile vascular plaques surrounded by thin indented moats appear on the palms and soles, an astute dermatologist can strongly suspect the diagnosis. They can appear on any cutaneous surface, where they are less readily identified with specificity. The scalp is another common site, with or without an associated nevus sebaceus[18]. Presumably, poromas arising secondarily within nevus sebaceus represent apocrine poromas. Occasionally, a poroma will be pigmented. Poromas commonly display highly vascularized stroma, and a clinical pattern suggestive of pyogenic granuloma is common, especially in poromas that involve acral skin. Rarely, multiple poromas will develop, either in an acral or in a widespread distribution, a clinical pattern referred to as poromatosis. Poromatosis can occur following chemotherapy and/or radiation therapy.

Up to 90% of sporadic poromas contain *YAP1-MAML2* and *YAP1-NUTM1* fusion genes that can lead to tumorigenesis presumably via transactivation of the transcription factor TEAD[86]. Less often, *WWTR1-NUTM1* fusions and additional fusions involving *NUTM1* are detected. NUT immunohistochemical staining may be used to differentiate poroid neoplasms with *NUTM1* fusions from other types of adnexal tumors[86a].

Pathology

The principal finding in all forms of poroma consists of a circumscribed proliferation of compact cuboidal keratinocytes with small monomorphous nuclei and scant eosinophilic cytoplasm. Poromas can be wholly intraepidermal, a pattern known historically as hidroacanthoma simplex; can occur in broad continuity with the epidermis (juxta-epidermal poroma; Fig. 111.27); or can develop wholly (or nearly so)

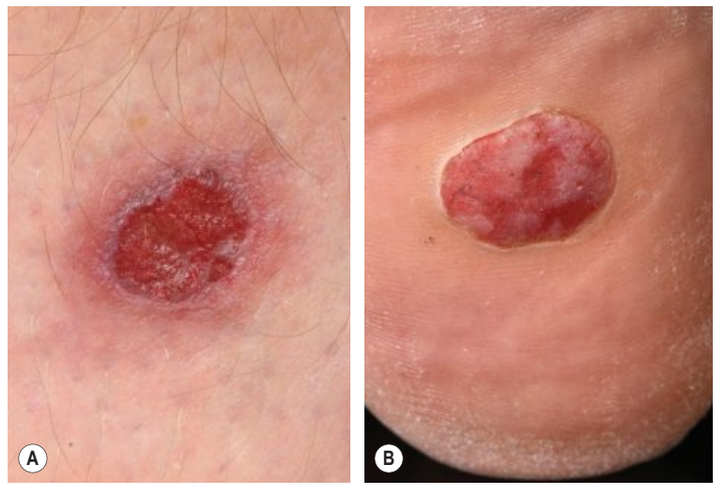


Fig. 111.26 Poromas. Solitary eroded red plaques on the distal lower extremity (**A**) and the plantar surface (**B**). There is resemblance to granulation tissue and a distinct rim is seen. The differential diagnosis often includes amelanotic melanoma and pyogenic granuloma. *A, Courtesy Department of Dermatology, Medical University of Graz; B, Courtesy Lorenzo Cerroni, MD.*

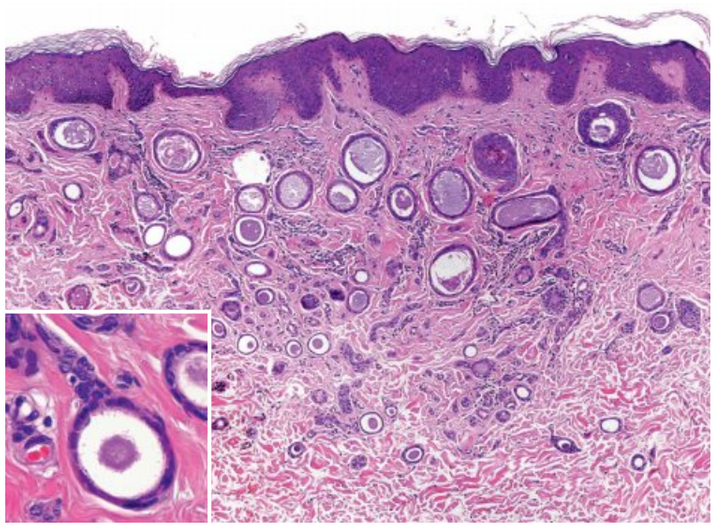


Fig. 111.25 Syringoma. This superficial adnexal neoplasm consists of multiple nests of cells with pale cytoplasm positioned within sclerotic stroma. Many nests show central ductal differentiation with a compact eosinophilic cuticle. A tadpole shape may be seen (inset).

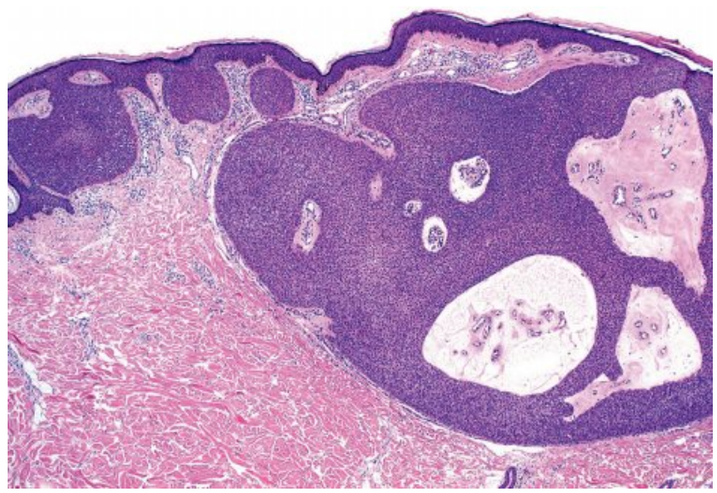


Fig. 111.27 Poroma, juxta-epidermal pattern. This poroma displays a pattern common to both eccrine and apocrine poroma. There are inter-anastomosing cords composed of small compact "poroid" cells, and the intervening stroma is well vascularized.

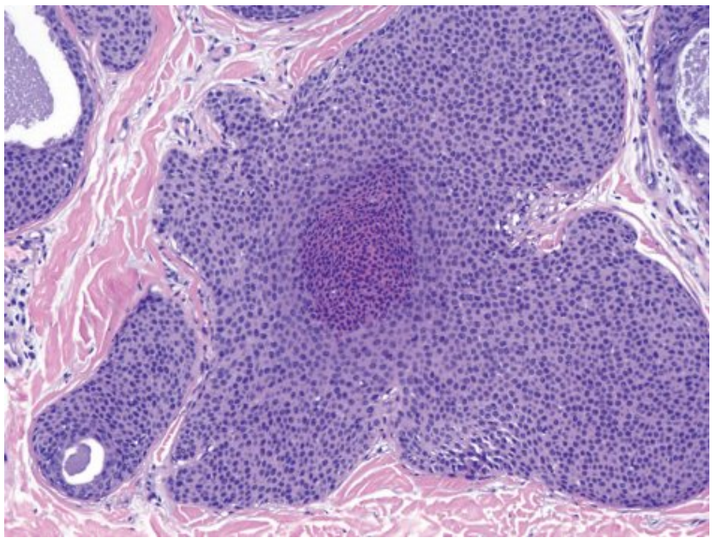


Fig. 111.28 Poroma, intradermal pattern. At low magnification, this lesion was a well-circumscribed dermal nodule. This higher magnification shows conspicuous foci of ductal differentiation at the edges and also a central focus of necrosis *en masse*, a finding common to poroma that is uncommon in other benign neoplasms.

within the dermis (intradermal poroma; Fig. 111.28), a pattern known historically as dermal duct tumor[3]. Accompanying stroma may be scant in association with intraepidermal poroma.

The degree of ductal differentiation varies greatly in individual neoplasms. Some poromas display innumerable foci in which poroid cells form small cuticulated ductal spaces. In other lesions, ducts may be difficult to identify, and a resemblance to seborrheic keratosis may ensue. Expression of GATA3 has been proposed as a useful feature for distinguishing clonal seborrheic keratosis (negative) from hidroacanthoma simplex (positive)[87]. Carcinoembryonic antigen (CEA) immunostaining, which labels the luminal surface of both apocrine and eccrine ducts, can be employed as a tool to confirm the presence of ductal differentiation. Poromas may occasionally display tubular (rather than ductal) foci in which a central cuticle is lacking. If such tubular foci are lined by columnar cells with holocrine secretion at the luminal border, a presumptive diagnosis of apocrine poroma can be offered.

At times, a poroma may display striking clear cell change. The constituent nuclei in such lesions are small but are surrounded by ample pale cytoplasm. Poromas are an exception to the rule that necrosis *en masse* is a clue to a malignancy. Curiously, poromas commonly display small collections of cells in coagulation necrosis. In malignant tumors, necrosis is usually a consequence of rapid growth (growth beyond the capacity of perfusion), but this is an unlikely explanation for necrosis in poroma, in which cellular proliferation is low. Poromas may occasionally display small foci of sebaceous differentiation, which usually consists of clusters of mature sebocytes near the lesion base[83,88].

Treatment

Poroma is a benign adnexal neoplasm and thus treatment is optional. Superficial lesions may be treated by shave or electrosurgical destruction. Superficial or deeper lesions may also be treated with simple excision.

Hidradenoma

Introduction

Hidradenoma is a form of benign adnexal neoplasm that is a close relative of poroma but is usually characterized by cells with ample cytoplasm, is never wholly intraepidermal, and does not commonly have a broad-based connection to the epidermis. As has been mentioned, some authorities use the broad designation *acrospiroma* to refer to both hidradenoma and poroma jointly. Although commonly classified as an eccrine neoplasm, hidradenomas are thought to be of either apocrine or eccrine lineage[74,75]. The majority of hidradenomas show histopathologic features suggestive of apocrine lineage[1,89]. In approximately half of hidradenomas, a t(11;19) translocation, resulting in a *CRTC1-MAML2* fusion gene, is present[90,91]. Fusions of *CRTC3-MAML2* or *EWSR1-POU5F1* have also been described.

Clinical features

Hidradenoma lacks any distinctive clinical attributes. The lesion presents as a solitary dermal or subcutaneous nodule; sometimes, a cystic quality or serous drainage can be detected.

Pathology

Hidradenomas are mostly dermal neoplasms with a nodular, sharply circumscribed pattern when viewed at low magnification. Some hidradenomas may display a juxta-epidermal pattern superficially with multifocal attachment to the epidermis, much like poroma. Although the stroma of hidradenoma is commonly sclerotic and may contain ectatic vessels, usually the granulation tissue-like quality that typifies the stroma of a poroma is not present. If desmoplastic stroma is conspicuous and exaggerated, the designation *desmoplastic hidradenoma* is recommended. The cells of hidradenoma are large with ample cytoplasm but uniform nuclei, which are generally somewhat larger than the nuclei of poroma. Overt clear cell change (clear cell hidradenoma) is common, as is cystic degeneration (solid-cystic hidradenoma)[92] (Fig. 111.29). Ductal differentiation can be found with scrutiny, although the degree observed may be minimal. Some lesions contain tubules lined by columnar cells with a decapitation pattern along their luminal border; such lesions can be designated as apocrine hidradenoma without question. Not surprisingly, tumors with features of both hidradenoma and poroma can be encountered, and the term *poroid hidradenoma* has been applied in this setting to denote a variant of poroma with some features of hidradenoma[93].

Treatment

Hidradenoma is a benign adnexal neoplasm. Complete conservative excision is curative. There are rare reports of hidradenomas with extension isolated to regional lymph nodes[94]; the possibility of a primary nodal hidradenoma has also been raised.

Benign Neoplasms with Apocrine Differentiation

Apocrine adenoma

Introduction

Any benign neoplasm with apocrine differentiation, including poroma and hidradenoma, could be grouped under the broad roof of this rubric. On a practical basis, only adenomas with conspicuous glandular differentiation are included in this category. Usually, these proliferations exhibit abundant apocrine epithelium and conspicuous decapitation secretion, in which part of the cytoplasm pinches off into a lumen. Apocrine adenomas may present with a tubular or papillary microscopic pattern or a combination of the two. Entities within this conglomeration include *tubular adenoma, papillary adenoma, syringocystadenoma papilliferum*, and *hidradenoma papilliferum*. The latter entity, also known as *papillary hidradenoma*, is a source of potential semantic confusion with conventional hidradenoma. Papillary hidradenoma (hidradenoma papilliferum) is an apocrine adenoma that usually exhibits a pronounced frond-like pattern with apocrine epithelium lining the constituent papillae. In contrast, conventional hidradenoma (acrospiroma) exhibits a mostly solid configuration.

Tubular, papillary, or tubulopapillary adenomas with conspicuous apocrine differentiation may develop within the parenchyma or secretory apparatus of the breast. Apocrine adenomas in continuity with the nipple commonly exhibit a tubulopapillary pattern and have been referred to as *erosive adenomatosis*[95,96]. In addition to a tubulopapillary pattern, apocrine adenomas of the nipple may display small foci with solid and cribriform patterns, but usually necrosis is not identifiable. Since such lesions are usually solitary, as erosion is commonly not present, and as the designation erosive adenomatosis is somewhat provocative, it is probably best to employ the simple term *nipple adenoma* in this context. The distinction between nipple adenoma and ductal adenocarcinoma can sometimes be challenging, and consultation with an experienced breast pathologist should be sought in difficult cases.

Clinical features

The presentation of *tubular or papillary adenoma* is not distinctive. These tumors present as smooth papules or nodules, and biopsy is required for diagnosis.



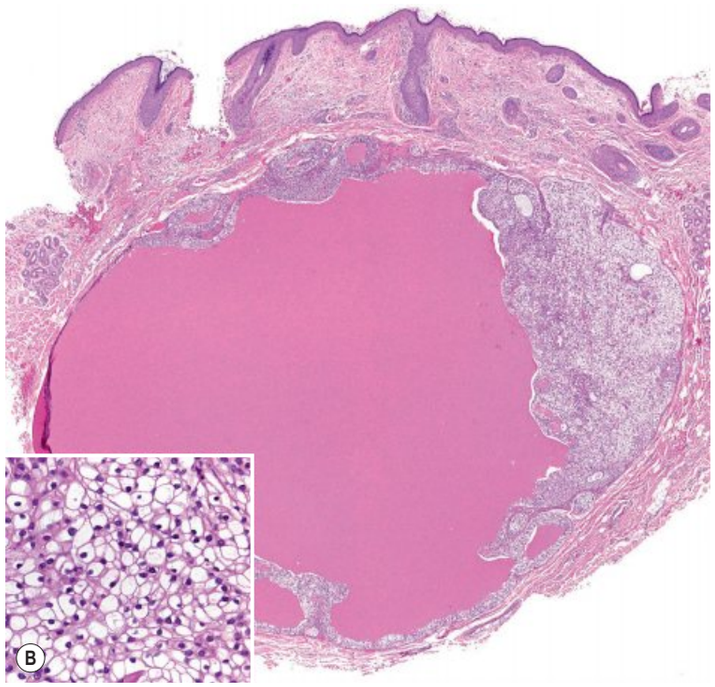


Fig. 111.29 Hidradenoma. A Solitary violaceous nodule on the abdomen with serous drainage. **B** Well-circumscribed nodule with prominent cystic architecture in this solid-cystic variant of hidradenoma. The cells have small uniform nuclei and ample cytoplasm that often is pale or shows overt clear cell change (inset). *B, Courtesy Lorenzo Cerroni, MD.*



Fig. 111.30 Syringocystadenoma papilliferum. Grouped papules and nodules with scale-crust. The possibility of an associated nevus sebaceus needs to be considered.

Syringocystadenoma papilliferum presents as a papule or plaque almost exclusively on the head or neck. Syringocystadenomas usually exhibit a crusted surface that may ooze serosanguinous fluid (Fig. 111.30); this is a reflection of the fact that the papillae of a syringocystadenoma are in continuity with the epidermal surface, permitting extrusion of secretory products. Most papillary syringocystadenomas present on the scalp in association with nevus sebaceus (see Fig. 111.7)[18,97]. Sporadic forms of syringocystadenoma papilliferum can harbor either *BRAF* V600E mutations or activating mutations in *HRAS* (or less often *KRAS*), while those that arise within a nevus sebaceus carry the same *HRAS* mutation as the underlying nevus[17].

Hidradenoma papilliferum usually presents as a smooth dermal or subcutaneous nodule, usually no more than a centimeter in diameter. Most papillary hidradenomas arise on the vulva, but development within skin of the breast, axilla, and inguinal or perianal areas has also been documented[98].

Pathology

At low magnification, *tubular and papillary adenomas* are usually well-circumscribed neoplasms positioned within the dermis, the superficial subcutis, or a combination of the two. Adenomas with a tubular pattern are composed mostly of rounded glandular spaces that vary in size and are lined by one or several layers of cuboidal cells with pale cytoplasm and small nuclei. Most spaces have small lumina and some display columnar apocrine cells apically. Papillary adenomas contain conspicuous tufts, with luminal cells that display an apocrine pattern. A combination of tubular and papillary patterns is not uncommon.

Papillary syringocystadenoma (*syringocystadenoma papilliferum*) is distinctive for its wide papillary fronds that are in continuity with the surface squamous epithelium (Fig. 111.31A,B). Syringocystadenomas are only rarely cystic. The fronds are lined by a bilayer, with basal cuboidal cells and apical columnar apocrine cells, and the cores of fronds virtually always contain a dense infiltrate of lymphocytes and plasma cells (Fig. 111.31C). A plasmacytic infiltrate commonly accompanies neoplasms of apocrine lineage, and thus the mere presence of plasma cells in a given lesion is not sufficient to confirm a diagnosis of syringocystadenoma.

At low magnification, *papillary hidradenoma* (*hidradenoma papilliferum*) consists of a well-circumscribed nodule within the dermis and usually lacks both a connection to the surface epithelium and the prominent plasmacytic infiltrate of syringocystadenoma papilliferum. Both tubules and papillary fronds are usually present, and broad elongated fronds with delicate fibrous cores are usually identifiable (Fig. 111.32). Both tubules and fronds are usually lined by a bilayer, with basal cuboidal myoepithelial cells and apical apocrine cells, and the apical cells usually display a conspicuous holocrine secretion. At least some of the basal layer cells represent authentic myoepithelial cells with contractile function, and labeling of the myoepithelial layer through immunohistochemical staining for actin filaments can sometimes be of diagnostic value in the distinction from adenocarcinoma, which often lacks a complete myoepithelial layer.

Treatment

Apocrine adenomas are completely benign lesions. Complete conservative excision is curative.

Undifferentiated Neoplasms of Apocrine Lineage

Most adnexal neoplasms contain foci of differentiation that may be rudimentary but that are readily interpretable as representing normal structures. For example, while trichoblastoma is largely undifferentiated, it contains foci such as papillary mesenchymal bodies that clearly indicate follicular germinative lineage. In contrast, two closely related entities, spiradenoma and cylindroma, display either a general lack of differentiation or display differentiation not readily identifiable as indicative of a normal structure. Both spiradenoma and cylindroma

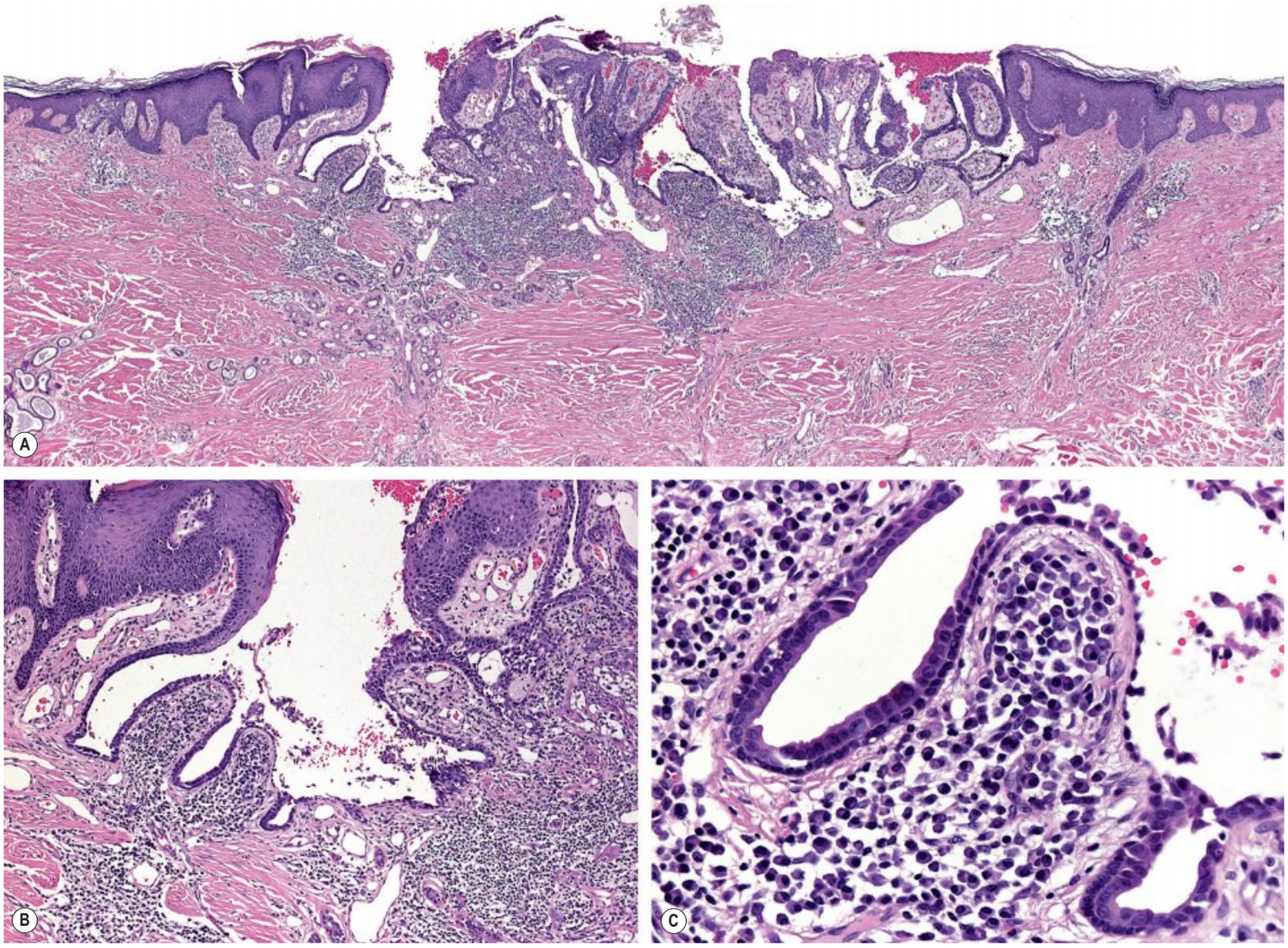


Fig. 111.31 Syringocystadenoma papilliferum. A This neoplasm has an eroded surface and consists of multiple papillary projections composed of dilated ducts surrounded by dense inflammatory infiltrates. **B, C** The papillae are lined by columnar cells that usually display overt apocrine differentiation. The dermal cores of papillae are usually stuffed with lymphocytes and typically many plasma cells. *Courtesy Lorenzo Cerroni, MD.*

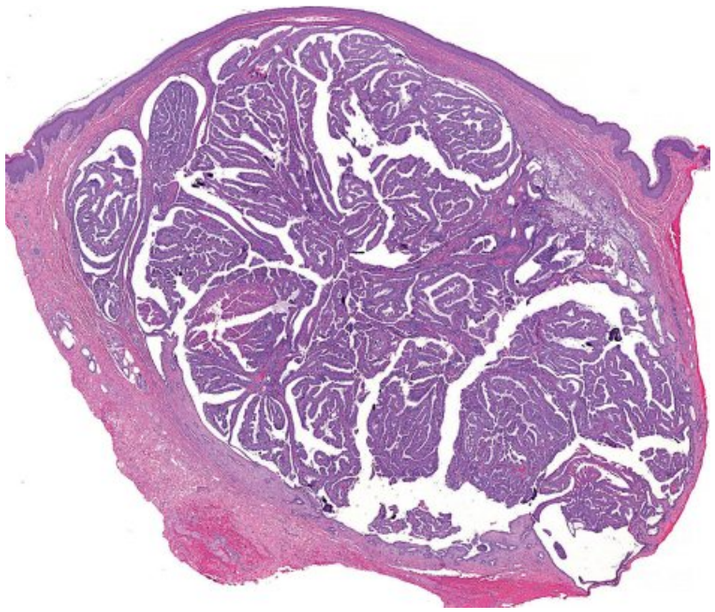


Fig. 111.32 Hidradenoma papilliferum. This well-circumscribed dermal nodule is composed of anastomosing and arborizing glandular and papillary structures. *Courtesy Lorenzo Cerroni, MD.*

occasionally display tubular foci with a decapitation luminal pattern, suggesting apocrine lineage, but mostly these neoplasms display uninterpretable/unrecognizable differentiation.

Spiradenoma

Definition

The term *spiradenoma* connotes a benign adnexal neoplasm that has been historically designated as being of eccrine lineage, although reassessment indicates an apocrine process[1,74,75]. Spiradenoma not uncommonly occurs jointly with cylindroma and both occur jointly with trichoepithelioma/trichoblastoma (see Fig. 111.5); the most parsimonious explanation for this complex juxtaposition is that both spiradenoma and cylindroma are of folliculosebaceous-apocrine lineage[99]. Both spiradenomas and cylindromas occur jointly with trichoepitheliomas in the Brooke–Spiegler syndrome that is due to mutations in *CYLD*, again implying kinship rather than disparate lineage. To date, spiradenoma has never been observed on glabrous (non-hair-bearing) skin. If spiradenoma were truly eccrine, occurrence on the palm or sole would be the rule and not the exception.

Clinical features

Spiradenoma typically presents as a dermal or subcutaneous papule or nodule in nearly any location; extraordinary lesions may achieve a diameter of several centimeters. Sometimes, spiradenomas are painful. The clinical lesions are not distinctive and biopsy is required for diagnosis, although an astute dermatologist can suspect the diagnosis in the setting of a painful nodule with a bluish hue. Spiradenomas may occur in multiplicity and

in concert with cylindromas and trichoepitheliomas/trichoblastomas, and multiple lesions should prompt consideration of a diagnosis of Brooke–Spiegler syndrome. In sporadic spiradenomas, *CYLD* mutations have also been described as has a recurrent, mutually exclusive, missense mutation in the kinase domain of *ALPK1* (α-kinase 1).

Pathology

At low magnification, spiradenoma assumes a multinodular pattern with relatively large nodules positioned within the dermis and subcutis. Although the nodules may be asymmetrically distributed, each is sharply circumscribed. The nodules are composed of basaloid cells without obvious differentiation, although tubular apocrine foci can be observed on occasion. Upon close scrutiny, individual nodules exhibit a trabecular internal morphology, with compact basophilic cells lining the borders of trabeculae and larger cells with scant pale cytoplasm within their centers (Fig. 111.33). Usually, small lymphocytes are scattered throughout trabecular areas. Some large (giant) spiradenomas develop cystic areas of degeneration or striking vascular ectasia as secondary events. Compact eosinophilic basement membrane material, arrayed either as tiny PAS-positive droplets or as circumferential bands, can occasionally be found within a spiradenoma, although such deposits are more commonplace in cylindroma.

Treatment

Spiradenoma is a benign adnexal neoplasm. Despite its basaloid appearance, spiradenoma holds negligible proliferative capacity and recurrence is uncommon after simple enucleation or conservative excision.

Cylindroma

Introduction

The term *cylindroma* describes a form of benign adnexal neoplasm that is closely related to spiradenoma.

Clinical features

Cylindromas can present singly or in multiplicity and are not clinically distinctive; thus a biopsy is required for diagnosis. Solitary lesions commonly appear on the head and neck, especially the scalp (Fig. 111.34), but they can also develop within skin of the trunk or genitalia. Multiple cylindromas may coalesce and form giant mosaic plaques on the scalp, which has been pejoratively referred to as a turban tumor[100,101]. The recognition of multiple cylindromas should prompt consideration of the Brooke–Spiegler syndrome or multiple cylindromatosis (both autosomal dominant conditions), most examples of which are associated with *CYLD* mutations. An *MYB–NFIB* gene fusion, similar to that identified in adenoid cystic carcinoma of the breast or the head and neck, has been described in sporadic cylindromas by some, but not all, investigators.

Pathology

At low magnification, cylindromas consist of sharply circumscribed nodules arrayed within the dermis and/or subcutis. The nodules are composed of nests of basaloid cells in close apposition, arrayed in a complex pattern that has been likened to a jigsaw puzzle. A rim of densely eosinophilic, PAS-positive basement membrane material commonly envelops the individual nests, and droplets of similar composition are often scattered in the centers of small nests (Fig. 111.35). Foci of ductular and apocrine tubular differentiation can sometimes be found but are inconspicuous.

Treatment

Cylindroma is a benign adnexal proliferation. Despite its basaloid appearance, cylindroma holds negligible proliferative capacity and recurrence is uncommon after complete excision.

Carcinomas of apocrine lineage

Introduction

Adnexal carcinomas with tubular and ductular differentiation (adnexal adenocarcinomas) are relatively uncommon, and their rarity has contributed to confusion with respect to diagnosis, classification, and therapy. Adnexal carcinomas can develop *de novo* or they can arise in association with extant benign adnexal neoplasms. The semantics of carcinomas that arise in association with benign neoplasms has been

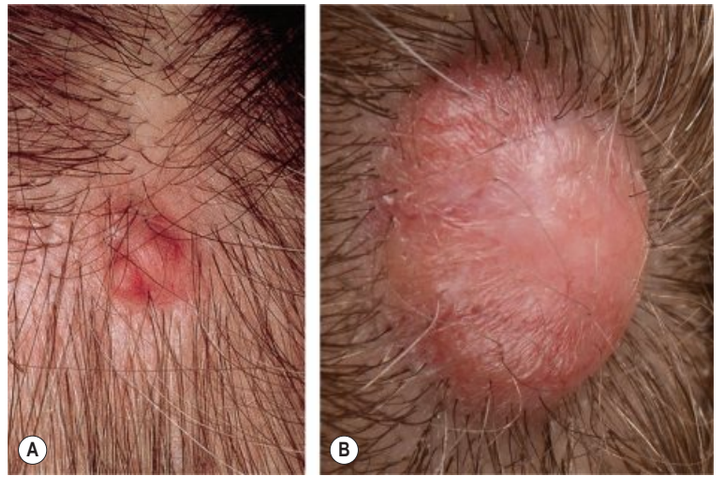


Fig. 111.34 Cylindromas. A, B While numerous tumors aggregated on the scalp are called turban tumors, solitary lesions usually present as smooth erythematous nodules which can vary in size. *B, Courtesy Lorenzo Cerroni, MD.*

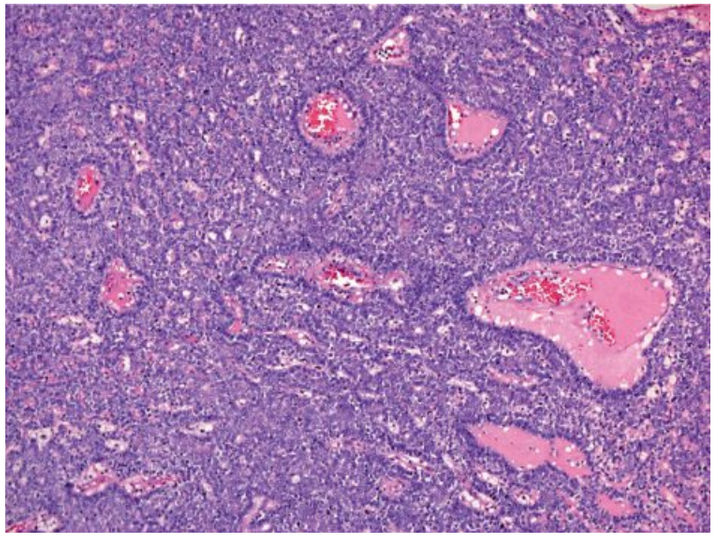


Fig. 111.33 Spiradenoma. Basaloid cells arranged partly in trabecular and mostly in cohesive aggregates with ductal differentiation. Note in larger lumina eosinophilic secretory material. *Courtesy Lorenzo Cerroni, MD.*

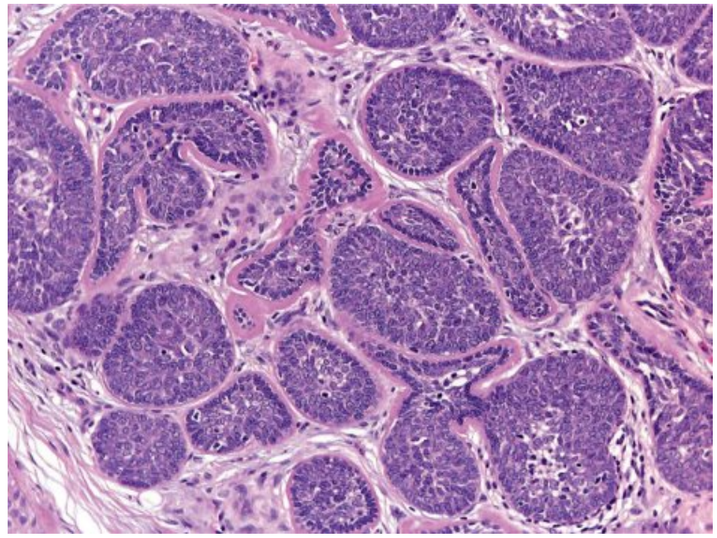


Fig. 111.35 Cylindroma. Nests of basaloid cells in a jigsaw puzzle-like pattern. Many nests are circumferentially enveloped by a dense eosinophilic cylinder of basement membrane material.

problematic, as there has been a historical tendency to create an oxymoronic nomenclature by modifying the name of the benign analogue with the simple addition of the adjective *malignant*. Going forward, correct designations such as porocarcinoma and spiradenocarcinoma should be employed while the oxymoronic designations malignant poroma and malignant spiradenoma should be eschewed[2].

For certain types of adnexal carcinoma, such as spiradenocarcinoma or cylindrocarcinoma, the adenocarcinomas that develop from the benign neoplasm often lack a decisive pattern of differentiation and may only be specifically diagnosable through recognition of a remnant of the residual benign lesion. A spiradenocarcinoma in the absence of detectable spiradenoma will likely only be recognizable as poorly differentiated adenocarcinoma. Some forms of adnexal adenocarcinoma, such as porocarcinoma, display distinctive differentiation that is recognizable in a *de novo* lesion or in a carcinoma that developed within an existent tumor.

Clinical features

In general, the presentation of adnexal adenocarcinomas is not distinctive. Patients who develop adnexal carcinoma within an existent benign neoplasm often relate a history of recent rapid (or explosive) enlargement of a previously stable, longstanding plaque or nodule (Fig. 111.36). Ulceration and bleeding are common associated findings. Adnexal adenocarcinoma presents as a plaque or nodule, and biopsy and microscopy are required for diagnosis.

Perhaps the most is known about the presentation of *microcystic adnexal carcinoma* (MAC), a low-grade form of adnexal carcinoma (also known as *sclerosing sweat duct carcinoma*) that has been carefully evaluated in several large series[102]. MAC typically presents in young or middle-aged adults, most commonly in women and occasionally in children, and lesions slowly enlarge over years and are often misdiagnosed prior to the time of definitive recognition (Fig. 111.37)[102]. The most common location is the lip. Curiously, a left-sided predominance was noted in the largest series from the US, suggesting that UV light exposure (from driving) might be contributory to carcinogenesis, much like common forms of keratinocyte carcinoma.

Pathology

All forms of adnexal adenocarcinoma share architectural attributes of malignancy, such as asymmetry, lack of circumscription, and an infiltrative configuration. There is considerable variability in the degree of cytologic atypia, and no standard currently exists for the grading of these neoplasms. Some forms of adnexal carcinoma may display overtly anaplastic cytomorphology while other carcinomas, such as MAC or syringomatous carcinoma, display very subtle nuclear atypia.

Syringomatous carcinoma refers to a rare form of carcinoma with distal ductal differentiation[103,104]. It may be of either apocrine or eccrine lineage, and generally lineage cannot be discerned microscopically. Syringomatous carcinoma is characterized by poor circumscription and an infiltrative pattern at low magnification and is composed of small nests and tubules of pale cells with central cuticulated ducts. The degree of nuclear atypia is usually modest, and thus a superficial biopsy, which hides the lack of circumscription, can lead to misinterpretation as syringoma. To date, syringomatous carcinoma has only been observed as a *de novo* malignancy.

MAC is a close relative of syringomatous carcinoma that is distinctive for its biphasic or multiphasic differentiation. MAC displays a ductal component identical to that of syringomatous carcinoma coupled with follicular and (sometimes) sebaceous differentiation (Fig. 111.38)[102,105,106]. The follicular component of MAC consists most notably of small cystic (microcystic) foci with follicular infundibular and isthmic keratinization, similar to the superficial follicular keratinization observed in desmoplastic trichoepithelioma or trichoadenoma. Areas resembling the follicular outer sheath may also be present. Extensive infiltration of the reticular dermis and perineural extension of tumor cells are common findings. Although desmoplastic trichoepithelioma and MAC exhibit overlapping features and both are characterized by foci of superficial follicular keratinization, follicular germinative (basaloid) cells are a hallmark of trichoepithelioma but are rarely, if ever, present in MAC. In a minority of cases of MAC, mutually exclusive molecular alterations – inactivation of *TP53* or insertions within *JAK1* – are observed.



Fig. 111.36 Porocarcinoma. Rapid growth and erosion or ulceration accompany this malignant adnexal tumor.



Fig. 111.37 Microcystic adnexal carcinoma. This tumor presents as a slowly expanding, firm plaque that can be subtle clinically.

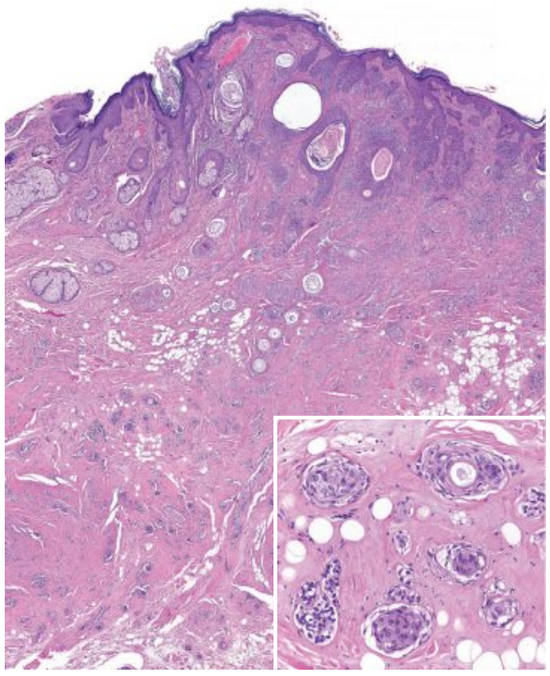


Fig. 111.38 Microcystic adnexal carcinoma. This deeply infiltrative carcinoma shows a biphasic microscopic pattern, with both ductular differentiation and superficial follicular keratinization. The high-magnification inset shows conspicuous ductal differentiation without cytologic atypism, which sometimes leads to misdiagnosis as a benign lesion. *Courtesy Lorenzo Cerroni, MD.*

Porocarcinoma may develop *de novo* or in association with an existent poroma[107]. Like poroma, porocarcinoma may be of apocrine or eccrine lineage, and it is generally impossible to determine the exact lineage of any given tumor. The degree of cytologic atypia is variable[104,108], and some examples of porocarcinoma display little cytologic atypia. Thus, close attention must be paid to other attributes of malignancy and small or partial biopsies may defy exact diagnosis. Porocarcinoma is composed of nests of eosinophilic or pallid cuboidal cells that infiltrate the dermis and perhaps subjacent deeper tissues, and ductal differentiation is usually conspicuous (Fig. 111.39). Porocarcinoma may display intraepidermal growth, with a pagetoid or nested pattern within the epidermis in some cases[104,108]. The same molecular alterations observed in poromas have been described in porocarcinoma (see above), together with mutations in *TP53, RB1, CDKN2A,* and *HRAS* (see Ch. 107).

Hidradenocarcinoma may develop *de novo* or in association with an existent hidradenoma. Hidradenocarcinoma may be of apocrine or eccrine lineage. Cases reported in the older literature were notable for the presence of marked clear cell change, much like clear cell hidradenoma. *CRTC1–MAML2* fusion genes (also seen in up to half of hidradenomas) and amplification of *ERBB2* have been described. The differential diagnosis includes cutaneous metastases of mucoepidermoid carcinoma of the salivary glands.

Spiradenocarcinoma and *cylindrocarcinoma* are usually poorly differentiated carcinomas that develop *de novo* or more commonly in association with an existent spiradenoma or cylindroma[109,110]. Both are extremely rare and may come to medical attention late in their course, as their evolution within longstanding stable lesions may contribute to a delay in pursuit of care by the patient. In addition to the molecular alterations found in their benign counterparts (with the possible exception of *MYB–NFIB* gene fusions), loss-of-function *TP53* mutations and *ALPK1* hotspot mutations have been described in spiradenocarcinoma.

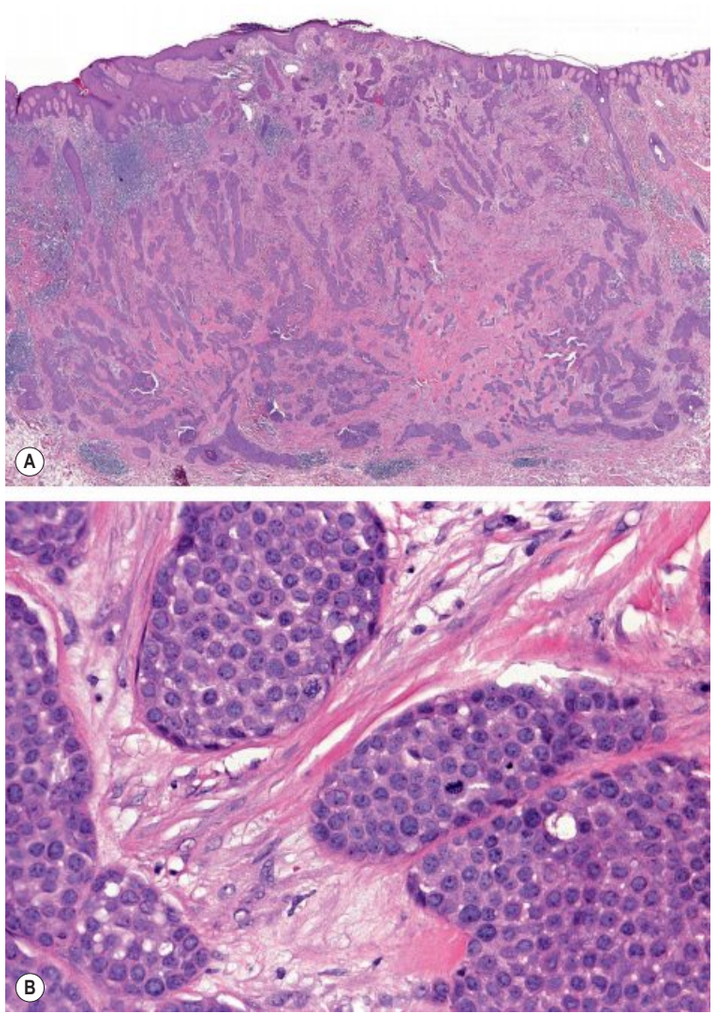


Fig. 111.39 Porocarcinoma. A There are irregularly shaped nests and strands of neoplastic cells that infiltrate deeply. **B** The largest nest shows foci of ductular differentiation. *Courtesy Lorenzo Cerroni, MD.*

Adenoid cystic carcinoma is a type of relatively undifferentiated adnexal carcinoma that resembles micronodular BCC but is generally distinctive for the presence of cribriform (net-like) glandular differentiation and a paucity of accompanying myxoid stroma. Primary cutaneous adenoid cystic carcinomas have been misinterpreted as metastatic lesions. Although initially postulated to represent a type of eccrine carcinoma, most authorities believe the entity represents a neoplasm of apocrine lineage. Adenoid cystic carcinoma tends to display considerable local invasiveness and most examples remain confined to the skin over years or even decades, but metastasis to lymph nodes and parenchymal organs can also rarely occur[111]. CD117 immunopositivity has been reported in association with adenoid cystic carcinoma and may be of value in providing additional diagnostic support. Fusion genes involving *NF1B*, most commonly mutually exclusive *MYB–NFIB* or *MYBL1–NFIB* fusions, have been reported.

Primary cutaneous cribriform carcinoma is a partially circumscribed tumor composed of interconnected solid aggregations of basophilic epithelial cells perforated by empty round spaces resulting in a sieve-like or cribriform pattern. Intraluminal bridges are typically present. This tumor has some resemblance to adenoid cystic carcinoma and is often in the differential diagnosis of the latter. The most reliable microscopic findings that favor adenoid cystic carcinoma over cribriform carcinoma include a poorly circumscribed pattern of growth, the presence of basophilic mucinous material within lacunae, and a lack of intraluminal bridges.

Mucinous carcinoma, another form of adnexal adenocarcinoma, is characterized by small collections of epithelial cells floating in large pools of mucin. The epithelial cells can sometimes assume a cribriform configuration. An associated *in situ* component is present in some cases. In our view, the relatively recently described entity *endocrine mucin-producing sweat gland carcinoma* is a variant of mucinous carcinoma rather than a unique entity. Lastly, *extramammary Paget disease* may represent extension of an underlying apocrine carcinoma and this entity is discussed in detail in Chapter 73.

Secretory carcinoma of the skin is another form of adnexal adenocarcinoma[111a]. It is characterized by a well-circumscribed proliferation of relatively cytologically bland cells configured as nodules. The nodules contain tubular and microcystic spaces with abundant eosinophilic secretions. Foci of more solid growth are also seen. Most cases of secretory carcinoma of the skin are associated with an *ETV6-NTRK3* fusion gene[111b].

Treatment

As a generality, the majority of adnexal adenocarcinomas are low-grade forms of carcinoma that are locally invasive but pose a low risk for metastasis. Many adnexal carcinomas that yield metastatic spread are large or were diagnosed late in their evolution. Surgical extirpation, including removal via Mohs micrographic surgery, remains the primary therapeutic modality. Careful microscopic classification is crucial to developing experience with larger groups of histopathologically homogeneous lesions in order to assess natural history as well as proper medical and surgical care.

NEOPLASMS AND PROLIFERATIONS WITH ECCRINE DIFFERENTIATION

Eccrine nevus (hamartoma)

Nevi or malformations with an eccrine glandular component are extremely uncommon. The clinical morphology of such lesions is not distinctive. Some lesions are alleged to maintain function of the eccrine apparatus. This can manifest clinically as mucinous discharge or localized hyperhidrosis.

Microscopically, the judgment as to whether eccrine glands are normal in number or increased can be difficult, especially in a partial biopsy. The absolute number of eccrine units is increased and the constituent units are of increased size in eccrine nevi. The surrounding stroma may be exclusively fibrotic or may include adipocytes. When the stroma also harbors an increase in small vascular channels, the designation *eccrine angiomatous hamartoma* can also be applied (see Fig. 39.5). For skin tag-like lesions on the coccygeal area, the term *coccygeal polypoid eccrine nevus* has been applied.



Fig. 111.40 Porokeratotic eccrine ostial and dermal duct nevus. Markedly hyperkeratotic spines arise from dilated eccrine ostia, corresponding to the histologic findings of cornoid lamellae. Note the linearity of several of the lesions. *Courtesy Julie V. Schaffer, MD.*

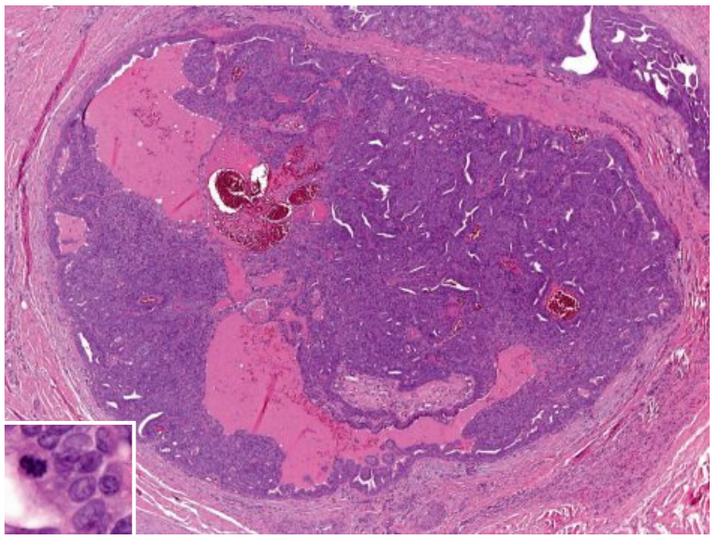


Fig. 111.41 Papillary adenocarcinoma of the digit. Partly cystic, irregular tumor with tubular and papillary foci. Mitotic figures are easily identified (inset). *Courtesy Lorenzo Cerroni, MD.*

So-called porokeratotic eccrine ostial and dermal duct nevi are probably not eccrine nevi at all. These lesions are typically congenital and present as papules or plaques on the hands or feet, with digitate hyperkeratosis (Fig. 111.40). The focal hyperkeratosis corresponds to cornoid lamellae that are often situated within acanthotic acrosyringia. Eccrine acini are qualitatively and quantitatively normal in porokeratotic nevi, suggesting that these lesions should not be classified as a form of adnexal nevus. From the standpoint of nosology, these lesions probably fit best on the spectrum of epidermal nevi. Somatic mosaicism for mutations in *GJB2*, which encodes connexin 26 (see Ch. 58), has been reported in patients with porokeratotic eccrine ostial and dermal duct nevi.

Treatment

Eccrine nevi are benign and require no treatment. Excision can be completed as an optional step.

Syringoma, poroma, hidradenoma, adnexal adenocarcinoma

(See above.)

Syringofibroadenoma

Syringofibroadenomas are rare tumors, usually located on the limbs. They may be associated with Clouston syndrome or Schöpf–Schulz–Passarge syndrome. They are characterized by an irregular network of thin cords and strands of epithelial cells extending down from the epidermis. Ductal structures are usually present. A similar pattern may be observed in some cases of chronic stasis dermatitis or in a site of trauma or chronic ulceration. This has prompted some authorities to view syringofibroadenoma as a reactive process rather than an authentic neoplasm.

Papillary adenoma and adenocarcinoma

Introduction

The concept of *papillary adenoma* was originally put forth under the designation *aggressive digital papillary adenoma*[112–114]. These neoplasms are uncommon and often occur on acral skin of the fingers, toes, palms and soles, a topographic restriction that suggests that many or most are of eccrine lineage. Papillary adenoma was deemed aggressive because the neoplasms were prone to local recurrence if not completely excised, and some lesions were found to erode bone or infiltrate adjacent soft tissue[113]. Some neoplasms first classified as aggressive papillary adenoma have metastasized[114], and thus it appears this spectrum includes both adenomas and adenocarcinomas. It has also been suggested that all acral papillary lesions represent adenocarcinomas, but this seems biologically unlikely. Of note, human papillomavirus 42 has recently been described as a tumor driver in aggressive digital papillary adenocarcinoma[115].

Clinical features

Papillary adenoma/adenocarcinoma presents as a solitary nodular lesion in an adult of any age. Lesions up to several centimeters in diameter have been observed. There is a male predilection. The lesions may be deeply situated and can impinge upon or erode underlying bone. The favored metastatic route appears to be hematogenous, and metastases involving the lung can occur.

Pathology

Papillary adenocarcinomas are extraordinarily cellular and display a combination of solid and papillary areas; they are occasionally cystic (Fig. 111.41)[113]. A cribriform pattern can sometimes be found. For carcinomas with a largely cribriform or tubular configuration, the designation tubulopapillary carcinoma can be employed. Irrespective of the architecture of the lesion, its constituent cells have hyperchromatic nuclei and relatively little cytoplasm, and mitotic figures are usually readily identifiable. There may be necrosis of individual cells or necrosis *en masse*. The enveloping stroma is commonly sclerotic. In overtly malignant lesions, vascular invasion or infiltration of bone may be observed. However, superficial biopsies that contain the cystic portions of the tumor may fail to show atypical features and can lead to the misdiagnosis of hidrocystoma or cystadenoma.

Treatment

It is difficult to predict the clinical course based upon the microscopic pattern. Complete surgical extirpation of papillary adenocarcinoma remains the standard of care, sometimes requiring partial amputation of the affected finger or toe. Because of diagnostic ambiguity, papillary adenomas should also be fully excised.

Additional figures available in our eBook (see inside front cover for access code).

REFERENCES

1. McCalmont TH. A call for logic in the classification of adnexal neoplasms. *Am J Dermatopathol*. 1996;18:103–109.
2. McCalmont TH. Batman and adnexal tumors. *J Cutan Pathol*. 2010;37:401–402.
3. Montagna W. Embryology and anatomy of the cutaneous adnexa. *J Cutan Pathol*. 1984;11:350–351.
4. Hyman AB, Brownstein MH. Eccrine poroma. An analysis of forty-five new cases. *Dermatologica*. 1969;138:29–38.
5. Plotzke JM, Adams DJ, Harms PW. Molecular pathology of skin adnexal tumours. *Histopathology*. 2022;80:166–183.

5a. Cheng Q, Yang F, Xue R, et al. Postzygotic gain-of-function variants in FGFR2 in two patients with hair

follicle nevus. *Br J Dermatol*. 2023:ljad267. doi:10.1093/bjd/ljad267.
6. Labandeira J, Peteiro C, Toribio J. Hair follicle nevus: case report and review. *Am J Dermatopathol*. 1996;18:90–93.
7. Ban M, Kamiya H, Yamada T, Kitajima Y. Hair follicle nevi and accessory tragi: variable quantity of adipose tissue in connective tissue framework. *Pediatr Dermatol*. 1997;14:433–436.
8. Ye H, Song Z, Chen S, Huang C. 'Mouldy peach' dermoscopic pattern in trichofolliculoma. *J Eur Acad Dermatol Venereol*. 2022;36:e726–e727.
9. Plewig G. Sebaceous trichofolliculoma. *J Cutan Pathol*. 1980;7:394–403.
10. Schulz T, Hartschuh W. Folliculo-sebaceous cystic hamartoma is a trichofolliculoma at its very late stage. *J Cutan Pathol*. 1998;25:354–364.
11. Kimura T, Miyazawa H, Aoyagi T, Ackerman AB. Folliculosebaceous cystic hamartoma. A distinctive malformation of the skin. *Am J Dermatopathol*. 1991;13:213–220.
12. Bolognia JL, Longley BJ. Genital variant of folliculosebaceous cystic hamartoma. *Dermatology*. 1998;197:258–260.
13. Cocciolone RA, Crotty KA, Andrews L, et al. Multiple desmoplastic melanomas in Birt-Hogg-Dubé syndrome and a proposed signaling link between folliculin, the mTOR pathway, and melanoma susceptibility. *Arch Dermatol*. 2010;146:1316–1318.
14. Gijezen LM, Vernooij M, Martens H, et al. Topical rapamycin as a treatment for fibrofolliculomas in Birt-Hogg-Dubé syndrome: a double-blind placebo-controlled randomized split-face trial. *PLoS ONE*. 2014;9:e99071.
15. Prioleau PG, Santa Cruz DJ. Sebaceous gland neoplasia. *J Cutan Pathol*. 1984;11:396–414.
16. Groesser L, Herschberger E, Ruetten A, et al. Postzygotic HRAS and KRAS mutations cause nevus sebaceous and Schimmelpenning syndrome. *Nat Genet*. 2012;44:783–787.
17. Shen AS, Peterhof E, Kind P, et al. Activating mutations in the RAS/mitogen-activated protein kinase signaling pathway in sporadic trichoblastoma and syringocystadenoma papilliferum. *Hum Pathol*. 2015;46:272–276.
18. Jaqueti G, Requena L, Sanchez Yus E. Trichoblastoma is the most common neoplasm developed in nevus sebaceus of Jadassohn: a clinicopathologic study of a series of 155 cases. *Am J Dermatopathol*. 2000;22:108–118.
19. Cribier B, Scrivener Y, Grosshans E. Tumors arising in nevus sebaceus: a study of 596 cases. *J Am Acad Dermatol*. 2000;42:263–268.
20. Alessi E, Wong SN, Advani HH, Ackerman AB. Nevus sebaceus is associated with unusual neoplasms. An atlas. *Am J Dermatopathol*. 1988;10:116–127.
21. Carlson JA, Cribier B, Nuovo G, Rohwedder A. Epidermodysplasia verruciformis-associated and genital-mucosal high-risk human papillomavirus DNA are prevalent in nevus sebaceus of Jadassohn. *J Am Acad Dermatol*. 2008;59:279–294.
22. Akasaka T, Onodera H, Matsuta M. Cutaneous mixed tumor containing ossification, hair matrix, and sebaceous ductal differentiation. *J Dermatol*. 1997;24:125–131.
23. Naujokas A, Charli-Joseph Y, Ruben BS, et al. SOX-10 expression in cutaneous myoepitheliomas and mixed tumors. *J Cutan Pathol*. 2014;41:353–363.
24. Antonescu CR, Zhang L, Shao SY, et al. Frequent PLAG1 gene rearrangements in skin and soft tissue myoepithelioma with ductal differentiation. *Genes Chromosomes Cancer*. 2013;52:675–682.
25. Hassab-el-Naby HM, Tarn S, White WL, Ackerman AB. Mixed tumors of the skin. A histological and immunohistochemical study. *Am J Dermatopathol*. 1989;11:413–428.
26. Gianotti R, Coggi A, Alessi E. Cutaneous apocrine mixed tumor: derived from the apocrine duct of the folliculo-sebaceous-apocrine unit? *Am J Dermatopathol*. 1998;20:53–55.
27. Ackerman AB, Reddy VB, Soyer HP. *Neoplasms with Follicular Differentiation*. 2nd ed. New York: Ardor Scribendi; 2001:1109.
28. Blake PW, Toro JR. Update of cylindromatosis gene (*CYLD*) mutations in Brooke-Spiegler syndrome: novel insights into the role of deubiquitination in cell signaling. *Hum Mutat*. 2009;30:1025–1036.
29. Pincus LB, McCalmont TH, Neuhaus IM, et al. Basal cell carcinomas arising within multiple trichoepitheliomas. *J Cutan Pathol*. 2008;35:59–64.
30. Bettencourt MS, Prieto VG, Shea CR. Trichoepithelioma: a 19-year clinicopathologic re-evaluation. *J Cutan Pathol*. 1999;26:398–404.
31. Brooke JD, Fitzpatrick JE, Golitz LE. Papillary mesenchymal bodies: a histologic finding useful in differentiating trichoepitheliomas from basal cell carcinomas. *J Am Acad Dermatol*. 1989;21:523–528.
32. Requena L, Renedo G, Sarasa J, et al. Trichoblastic fibroma. *J Cutan Pathol*. 1990;17:381–384.
33. Collina G, Eusebi V, Capella C, Rosai J. Merkel cell differentiation in trichoblastoma. *Virchows Arch*. 1998;433:291–296.
34. Sellheyer K, Krahl D. PHLDA1 (TDAG51) is a follicular stem cell marker and differentiates between morpheaform basal cell carcinoma and desmoplastic trichoepithelioma. *Br J Dermatol*. 2011;164:141–147.
35. Yeh I, McCalmont TH, LeBoit PE. Differential expression of PHLDA1 (TDAG51) in basal cell carcinoma and trichoepithelioma. *Br J Dermatol*. 2012;167:1106–1110.
36. Sajben FP, Ross EV. The use of the 1.0 mm handpiece in high energy, pulsed CO_2 laser destruction of facial adnexal tumors. *Dermatol Surg*. 1999;25:41–44.
37. Lobo Y, Blake T, Wheller L. Management of multiple trichoepithelioma: a review of pharmacological therapies. *Aust J Dermatol*. 2021;62:e192–e200.
38. Brownstein MH, Shapiro L. Desmoplastic trichoepithelioma. *Cancer*. 1977;40:2979–2986.
39. Lazar AJ, Calonje E, Grayson W, et al. Pilomatrix carcinomas contain mutations in *CTNNB1*, the gene encoding beta-catenin. *J Cutan Pathol*. 2005;32:148–157.
40. Agoston AT, Liang CW, Richkind KE, et al. Trisomy 18 is a consistent cytogenetic feature in pilomatricoma. *Mod Pathol*. 2010;23:1147–1150.
41. Ciriacks K, Knabel K, Waite MB, et al. Syndromes associated with multiple pilomatricomas: when should clinicians be concerned? *Pediatr Dermatol*. 2020;37:9–17.
42. Danielson-Cohen A, Lin SJ, Hughes CA, et al. Head and neck pilomatrixoma in children. *Arch Otolaryngol Head Neck Surg*. 2001;127:1481–1483.
43. Kaddu S, Soyer HP, Wolf IH, Kerl H. Proliferating pilomatricoma. A histopathologic simulator of matrical carcinoma. *J Cutan Pathol*. 1997;24:228–234.
44. Hardisson D, Linaves MD, Cuevas-Santos J, Contreas F. Pilomatrix carcinoma: a clinicopathologic study of six cases and review of the literature. *Am J Dermatopathol*. 2001;23:394–401.
45. Aloi FG, Molinero A, Pippione M. Basal cell carcinoma with matrical differentiation. Matrical carcinoma. *Am J Dermatopathol*. 1988;10:509–513.
46. Brownstein MH. Trichilemmoma. Benign follicular tumor or viral wart? *Am J Dermatopathol*. 1980;2:229–231.
47. Leonardi CL, Zhu WY, Kinsey WH, Penneys NS. Trichilemmomas are not associated with human papillomavirus DNA. *J Cutan Pathol*. 1991;18:193–197.
48. Brownstein MH, Shapiro L. Trichilemmoma. Analysis of 40 new cases. *Arch Dermatol*. 1973;107:866–869.
49. Roson E, Gomez Centeno P, Sanchez Aguilar D, et al. Desmoplastic trichilemmoma arising within a nevus sebaceus. *Am J Dermatopathol*. 1998;20:495–497.
50. Brownstein MH, Mehregan AH, Bikowski JB, et al. The dermatopathology of Cowden's syndrome. *Br J Dermatol*. 1979;100:667–673.
51. Requena L, Gutierrez J, Sanchez Yus E. Multiple sclerotic fibromas of the skin. A cutaneous marker of Cowden's disease. *J Cutan Pathol*. 1992;19:346–351.
52. Al-Zaid T, Ditelberg JS, Prieto VG, et al. Trichilemmomas show loss of PTEN in Cowden syndrome but only rarely in sporadic tumors. *J Cutan Pathol*. 2012;39:493–499.
53. Hunt SJ, Kilzer B, Santa Cruz DJ. Desmoplastic trichilemmoma: histologic variant resembling invasive carcinoma. *J Cutan Pathol*. 1990;17:45–52.
54. Vin-Christian K, Grekin R, McCalmont T. Hypopigmented papules of the cheeks, neck, and shoulders. *Arch Dermatol*. 1999;135:463–464. 466–7.
55. Kolenik 3rd SA, Bolognia JL, Castiglione Jr FM, Longley BJ. Multiple tumors of the follicular infundibulum. *Int J Dermatol*. 1996;35:282–284.
56. Horn TD, Vennos EM, Bernstein BD, Cooper PH. Multiple tumors of follicular infundibulum with sweat duct differentiation. *J Cutan Pathol*. 1995;22:281–287.
57. Mahalingam M, Bhawan J, Finn R, Stefanato CM. Tumor of the follicular infundibulum with sebaceous differentiation. *J Cutan Pathol*. 2001;28:314–317.
58. Rahbari H, Mehregan A, Pinkus A. Trichoadenoma of Nikolowski. *J Cutan Pathol*. 1977;4:90–98.
59. Brownstein MH, Arluk DJ. Proliferating trichilemmal cyst: a simulant of squamous cell carcinoma. *Cancer*. 1981;48:1207–1214.
60. Sethi S, Singh UR. Proliferating trichilemmal cyst: report of two cases, one benign and the other malignant. *J Dermatol*. 2002;29:214–220.
61. Sleater J, Beers B, Stefan M, et al. Proliferating trichilemmal cyst. Report of four cases, two with nondiploid DNA content and increased proliferation index. Am J Dermatopathol. 1993;15:423–428.
61a. Gallant JN, Sewell A, Almodovar K, et al. Genomic landscape of a metastatic malignant proliferating tricholemmal tumor and its response to PI3K inhibition. *NPJ Precis Oncol*. 2019;3:5.
62. Finan MC, Apgar JT. Juxta-clavicular beaded lines: a subepidermal proliferation of sebaceous gland elements. *J Cutan Pathol*. 1991;18:464–468.
63. Bader RS, Scarborough DA. Surgical pearl: intralesional electrodesiccation of sebaceous hyperplasia. *J Am Acad Dermatol*. 2000;42:127–128.
64. Troy JL, Ackerman AB. Sebaceoma. A distinctive benign neoplasm of adnexal epithelium differentiating toward sebaceous cells. *Am J Dermatopathol*. 1984;6:7–13.
65. Misago N, Narisawa Y. Rippled-pattern sebaceoma. *Am J Dermatopathol*. 2001;23:437–443.
66. Rutten A, Burgdorf W, Hugel H, et al. Cystic sebaceous tumors as marker lesions for the Muir-Torre syndrome: a histopathologic and molecular genetic study. *Am J Dermatopathol*. 1999;21:405–413.
67. Misago N, Narisawa Y. Sebaceous neoplasms in Muir-Torre syndrome. *Am J Dermatopathol*. 2000;22:155–161.
68. Mathiak M, Rütten A, Mangold E, et al. Loss of DNA mismatch repair proteins in skin tumors from patients with Muir-Torre syndrome and MSH2 or MLH1 germline mutations: establishment of immunohistochemical analysis as a screening test. *Am J Surg Pathol*. 2002;26:338–343.
69. Morales-Burgos A, Sánchez JL, Figueroa LD, et al. MSH-2 and MLH-1 protein expression in Muir Torre syndrome-related and sporadic sebaceous neoplasms. *P R Health Sci J*. 2008;27:322–327.
70. Dasgupta T, Wilson LD, Yu JB. A retrospective review of 1349 cases of sebaceous carcinoma. *Cancer*. 2009;115:158–165.
71. Kohler S, Rouse RV, Smoller BR. The differential diagnosis of pagetoid cells in the epidermis. *Mod Pathol*. 1998;11:79–92.
72. Nguyen GK, Mielke BW. Extraocular sebaceous carcinoma with intraepidermal (pagetoid) spread. *Am J Dermatopathol*. 1987;9:364–365.
73. Muñoz-Jiménez MT, Blanco L, Ruano Y, et al. TERT promoter mutation in sebaceous neoplasms. *Virchows Arch*. 2021;479:551–558.
74. Hashimoto K, Lever WF. Histogenesis of skin appendage tumors. *Arch Dermatol*. 1969;100:356–369.
75. Hashimoto K, Lever WF. Skin appendage tumors. *Arch Dermatol*. 1970;101:252–253.
76. Soler-Carrillo J, Estrach T, Mascaro JM. Eruptive syringoma: 27 new cases and review of the literature. *J Eur Acad Dermatol Venereol*. 2001;15:242–246.
77. Ciarloni L, Frouin E, Bodin F, Cribier B. Syringoma: a clinicopathological study of 244 cases. *Ann Dermatol Venereol*. 2016;143:521–528.
78. Di Lernia V, Bisighini G. Localized vulvar syringomas. *Pediatr Dermatol*. 1996;13:80–81.
79. Garcia C, Krunic AL, Grichnik J, et al. Multiple acral syringomata with uniform involvement of the hands and feet. *Cutis*. 1997;59:213–214. 216.
80. Shelley WB, Wood MG. Occult syringomas of scalp associated with progressive hair loss. *Arch Dermatol*. 1980;116:843–844.
81. Mehregan AH, Mehregan DA. Syringoma-like sweat duct proliferation in scalp alopecias. *J Cutan Pathol*. 1990;17:355–357.
82. Goyal S, Martins CR. Multiple syringomas on the abdomen, thighs, and groin. *Cutis*. 2000;66:259–262.
83. Harvell JD, Kerschmann RL, LeBoit PE. Eccrine or apocrine poroma? Six poromas with divergent adnexal differentiation. *Am J Dermatopathol*. 1996;18:1–9.
84. Azma A, Tawfik O, Casparian JM. Apocrine poroma of the breast. *Breast J*. 2001;7:195–198.
85. Kamiya H, Oyama Z, Kitajima Y. Apocrine poroma: review of the literature and case report. *J Cutan Pathol*. 2001;28:101–104.
86. Sekine S, Kiyono T, Ryo E, et al. Recurrent YAP1-MAML2 and YAP1-NUTM1 fusions in poroma and porocarcinoma. *J Clin Invest*. 2019;129:3827–3832.
86a. Macagno N, Kervarrec T, Sohier P, et al. NUT is a specific immunohistochemical marker for the diagnosis of YAP1-NUTM1- rearranged cutaneous poroid neoplasms. *Am J Surg Pathol*. 2021;45:1221–1227.
87. Lin C-Y, Kuo TT, Chang Y-C. Comparative immunohistochemical study of hidroacanthoma simplex and clonal seborrheic keratosis with GATA3 and p63. *Am J Dermatopathol*. 2022;44:17–20.

88. Lee NH, Lee SH, Ahn SK. Apocrine poroma with sebaceous differentiation. Am J Dermatopathol. 2000;22:261–263.
89. Gianotti R, Alessi E. Clear cell hidradenoma associated with the folliculo-sebaceous-apocrine unit. Histologic study of five cases. Am J Dermatopathol. 1997;19:351–357.
90. Winnes M, Mölne L, Suurküla M, et al. Frequent fusion of the CRTC1 and MAML2 genes in clear cell variants of cutaneous hidradenomas. Genes Chromosomes Cancer. 2007;46:559–563.
91. Kyrpychova L, Kacerovska D, Vanecek T, et al. Cutaneous hidradenoma: a study of 21 neoplasms revealing neither correlation between the cellular composition and CRTC1-MAML2 fusions nor presence of CRTC3-MAML2 fusions. Ann Diagn Pathol. 2016;23:8–13.
92. Wolff K, Winkelmann RK, Decker RH. Solid-cystic hidradenoma: an enzyme histochemical, biochemical, and electron microscopic study. *Acta Dermatol Kyoto Engl Ed*. 1968;63:309–322.
93. Requena L, Sanchez M. Poroid hidradenoma: a light microscopic and immunohistochemical study. Cutis. 1992;50:43–46.
94. Stefanato CM, Ferrara G, Chaudhry IH, et al. Clear cell nodular hidradenoma involving the lymphatic system: a tumor of uncertain malignant potential or a novel example of "metastasizing" benign tumor? *Am J Surg Pathol*. 2012;36:1835–1840.
95. Brownstein MH, Phelps RG, Magnin PH. Papillary adenoma of the nipple: analysis of fifteen new cases. *J Am Acad Dermatol*. 1985;12:707–715.
96. Diaz NM, Palmer JO, Wick MR. Erosive adenomatosis of the nipple: histology, immunohistology, and differential diagnosis. *Mod Pathol*. 1992;5:179–184.
97. Koga T, Kubota Y, Nakayama J. Syringocystadenoma papilliferum without an antecedent naevus sebaceous. *Acta Derm Venereol*. 1999;79:237.
98. Vang R, Cohen PR. Ectopic hidradenoma papilliferum: a case report and review of the literature. *J Am Acad Dermatol*. 1999;41:115–118.
99. Goette DK, McConnell MA, Fowler VR. Cylindroma and eccrine spiradenoma coexistent in the same lesion. *Arch Dermatol*. 1982;118:273–274.
100. Nerad JA, Folberg R. Multiple cylindromas. The 'turban tumor. *Arch Ophthalmol*. 1987;105:1137.
101. Reingold IM, Keasbey LE, Graham JH. Multicentric dermal-type cylindromas of the parotid glands in a patient with florid turban tumor. *Cancer*. 1977;40:1702–1710.
102. Chiller K, Passaro D, Scheuller M, et al. Microcystic adnexal carcinoma: forty-eight cases, their treatment, and their outcome. *Arch Dermatol*. 2000;136:1355–1359.
103. Hoppenreijs VP, Reuser TT, Mooy CM, et al. Syringomatous carcinoma of the eyelid and orbit: a clinical and histopathological challenge. *Br J Ophthalmol*. 1997;81:668–672.
104. Urso C, Bondi R, Paglierani M, et al. Carcinomas of sweat glands: report of 60 cases. *Arch Pathol Lab Med*. 2001;125:498–505.
105. Nickoloff BJ, Fleischmann HE, Carmel J, et al. Microcystic adnexal carcinoma. Immunohistologic observations suggesting dual (pilar and eccrine) differentiation. *Arch Dermatol*. 1986;122:290–294.
106. van der Horst MPJ, Brenn T. Update on malignant sweat gland tumors. *Surg Pathol Clin*. 2017;10:383–397.
107. Spencer DM, Bigler LR, Hearne DW, et al. Pedal papule. Eccrine porocarcinoma (EPC) in association with poroma. *Arch Dermatol*. 1995;131:214.
108. Robson A, Greene J, Ansari N, et al. Eccrine porocarcinoma (malignant eccrine poroma): a clinicopathologic study of 69 cases. *Am J Surg Pathol*. 2001;25:710–720.
109. Granter SR, Seeger K, Calonje E, et al. Malignant eccrine spiradenoma (spiradenocarcinoma): a clinicopathologic study of 12 cases. *Am J Dermatopathol*. 2000;22:97–103.
110. Durani BK, Kurzen H, Jaeckel A, et al. Malignant transformation of multiple dermal cylindromas. Br J Dermatol. 2001;145:653–656.
111. Kato N, Yasukawa K, Onozuka T. Primary cutaneous adenoid cystic carcinoma with lymph node metastasis. *Am J Dermatopathol*. 1998;20:571–577.
111a. Brandt SM et al. Secretory carcinoma in the axilla: probable origin from axillary skin appendage glands in a young girl. *Am J Surg Pathol*. 2009; 33:950–953.
111b. Kastnerova L, Luzar B, Goto K, et al. Secretory carcinoma of the skin: report of 6 cases, including a case with a novel NFIX-PKN1 translocation. *Am J Surg Pathol*. 2019;43:1092–1098.
112. Smith KJ, Skelton HG, Holland TT. Recent advances and controversies concerning adnexal neoplasms. Dermatol Clin. 1992;10:117–160.
113. Kao GF, Helwig EB, Graham JH. Aggressive digital papillary adenoma and adenocarcinoma. A clinicopathological study of 57 patients, with histochemical, immunopathological, and ultrastructural observations. J Cutan Pathol. 1987;14:129–146.
114. Duke WH, Sherrod TT, Lupton GP. Aggressive digital papillary adenocarcinoma (aggressive digital papillary adenoma and adenocarcinoma revisited). Am J Surg Pathol. 2000;24:775–784.
115. Leiendecker L, Neumann T, Jung PS, et al. Human papillomavirus 42 drives digital papillary adenocarcinoma and elicits a germ-cell like program conserved in HPV-positive cancers. Cancer Discov. 2023;13:70–84.



eFig. 111.1 Fibrofolliculomas in association with Birt–Hogg–Dubé syndrome. Multiple smooth papules of the lateral cheek that are relatively hypopigmented and lack the telangiectasias of the background skin.



eFig. 111.3 Fibrofolliculomas in association with Birt–Hogg–Dubé syndrome. *Courtesy Kalman Watsky, MD.*



eFig. 111.2 Fibrofolliculomas in association with Birt–Hogg–Dubé syndrome. Numerous skin-colored to white papules in the head and neck region. The patient also had a history of spontaneous pneumothoraces and benign renal cysts. *Courtesy Jonathan S. Leventhal, MD.*



eFig. 111.4 Nevus sebaceus. An oval yellow–pink verrucous plaque on the scalp. Note the alopecia.



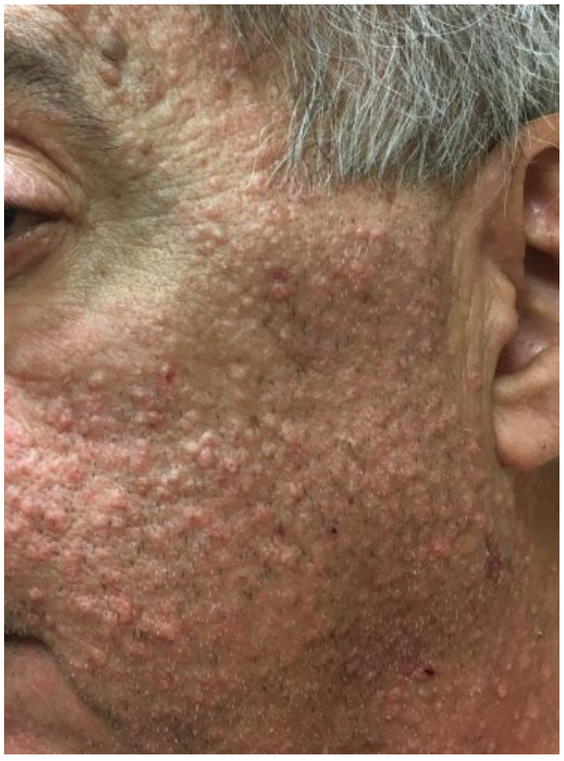
eFig. 111.5 Pilomatricoma. A firm papule on the cheek of a child.



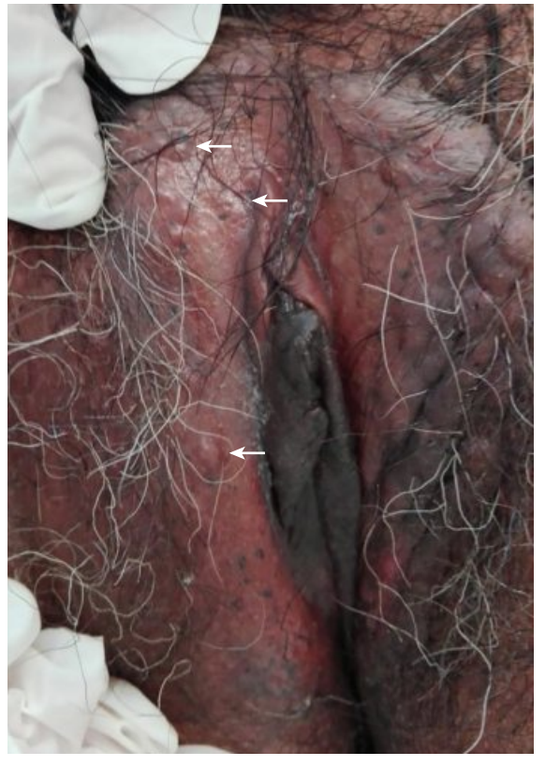
eFig. 111.6 Tumors of the follicular infundibulum. The hypopigmented papules can resemble fibrofolliculomas clinically. *Courtesy Lorenzo Cerroni, MD.*



eFig. 111.8 Sebaceous adenoma of the nose in a patient with Muir–Torre syndrome. Note the slightly lobulated surface. *Courtesy Jonathan S. Leventhal, MD.*



eFig. 111.7 Sebaceous hyperplasia. Numerous lesions in a patient receiving long-term cyclosporine. *Courtesy Dennis Cooper, MD.*



eFig. 111.9 Vulvar syringomas. Multiple skin-colored papules on the labia majora (arrows) in addition to lentiginous melanosis. *Courtesy Diana Carolina Palacios Narváez, MD and María Elisa Vega Memije, MD.*



eFig. 111.10 Poroma. A biopsy specimen is necessary to establish a definitive diagnosis.

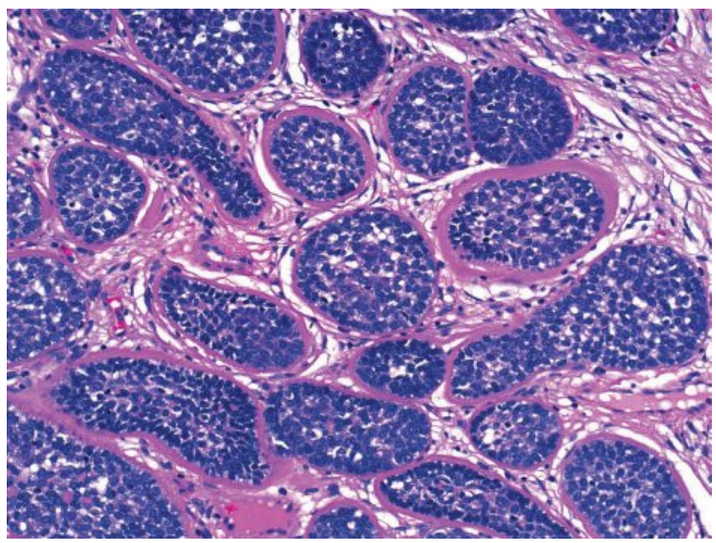


eFig. 111.11 Poroma. A solitary eroded red plaque on the plantar surface.





eFig. 111.12 Porokeratotic eccrine ostial and dermal duct nevus. A Linear keratotic plaques on the palm. **B** Markedly keratotic spines arise from dilated eccrine ostia, corresponding to the histologic findings of cornoid lamellae.



eFig. 111.13 Cylindroma. Nests of basaloid cells in a jigsaw puzzle-like pattern. Many nests are circumferentially enveloped by a dense eosinophilic cylinder of basement membrane material.

Benign Melanocytic Neoplasms and Melanotic Lesions

112

Thomas Wiesner and Raymond L. Barnhill

Chapter Contents

Circumscribed Melanotic Lesions *1973*
- Ephelides *1973*
- Café-Au-Lait Macules *1974*
- Becker Melanosis (Nevus) *1975*
- Solar Lentigines *1976*
- Lentigo Simplex and Mucosal Melanotic Macules *1976*
- Dermal Melanocytosis *1979*
- Nevus of Ota, Nevus of Ito, and Related Conditions *1980*

Melanocytic Nevi *1982*
- Blue Nevus and Its Variants *1982*
- Pigmented Epithelioid Melanocytoma *1984*
- Common Acquired Melanocytic Nevi *1984*
- Genital Nevus and Nevi of Special Sites *1987*
- Acral Nevus *1987*
- Spitz Nevus and Atypical Spitz Tumor *1988*
- Pigmented Spindle Cell Nevus *1990*
- WNT-Activated Deep Penetrating/Plexiform Nevus *1991*
- BAP1-Inactivated Melanocytic Nevus *1992*
- Atypical (Dysplastic) Melanocytic Nevus *1993*
- Congenital Melanocytic Nevus *1996*
- Nevus Spilus *2000*
- Halo Nevus *2001*
- Combined Nevus *2002*
- Recurrent Melanocytic Nevus *2003*

INTRODUCTION

Melanocytic nevi are benign melanocytic neoplasms that most commonly develop within the epidermis or dermis. Histologically, there is a proliferation of melanocytes, both in nests and as solitary cells, with the nests defined as aggregates of three or more melanocytes in direct contact. Melanocytic nevi are usually caused by genomic aberrations (oncogenic mutations or translocations) that activate oncogenes and result in a clonal proliferation of affected melanocytes.

The non-nevus melanotic lesions discussed in this chapter can also be tan to dark brown or black in color, but in contrast to melanocytic nevi, they have minimal, if any, increase in melanocyte density. In addition, there is no nesting of melanocytes. Their hyperpigmentation is due to an increase in melanin synthesis and its subsequent transfer to keratinocytes. Other benign and malignant tumors (e.g. seborrheic keratoses, keratinocyte carcinomas) that can also be hyperpigmented are discussed in Chapters 108–111 and 115.

CIRCUMSCRIBED MELANOTIC LESIONS

EPHELIDES

Synonym: ■ Freckles

Key features

- Small, uniformly pigmented macules in sun-exposed sites
- More common in fair-skinned individuals and more noticeable in summer than in winter
- Hyperpigmentation of the basal layer of the epidermis without an increase in melanocyte density

Epidemiology and Pathogenesis

Ephelides are common in fair-skinned individuals, especially those with red hair, and occur more frequently in women. They first appear in early childhood and usually stabilize in number during adulthood, followed by gradual fading. Ephelides result from an increase in sun-induced melanin synthesis and transport of melanosomes from melanocytes to keratinocytes. Frequent sunburns and variants of the melanocortin-1 receptor gene (*MC1R*) play an important role in the development of ephelides (see Fig. 65.13)[1].

Clinical Features

Ephelides are limited to sun-exposed sites – primarily the face, upper trunk, and dorsal aspects of the arms. Ephelides are well demarcated, uniformly pigmented, oval to irregular-shaped macules that are usually 1 to 3 mm in size. Depending upon the intensity of sun exposure, ephelides vary in color from light to medium brown. In the summer, they are more conspicuous and then fade during the winter. Ephelides are benign with no potential for malignant transformation. However, higher numbers of ephelides correlate with an increased risk of acquired melanocytic nevi and melanoma[2].

Pathology

There is hyperpigmentation of the basal layer of the epidermis without an increase in the number of melanocytes. Compared to adjacent uninvolved epidermis, melanocytes in ephelides are larger and have more branching of dendrites and stronger DOPA positivity, indicating increased activity[3].

Differential Diagnosis

Ephelides must be distinguished from simple lentigines, solar lentigines, small café-au-lait macules, and junctional nevi. In addition to being confined to sun-exposed skin, the clinical appearance of ephelides varies depending upon the amount of exposure to UVR (Table 112.1). Café-au-lait macules are usually solitary and larger than ephelides.

Treatment

If ephelides are a cosmetic concern, sun exposure should be minimized and use of sunscreens, hats, and protective clothing recommended. Topical retinoids and hydroquinone may lighten lesions, but it is difficult to achieve an homogeneous clinical effect and potential side effects (e.g. irritation, dyspigmentation) need to be considered. Pigment-specific lasers represent an additional treatment option, but recurrences are common[4].

COMPARATIVE CLINICAL FEATURES OF EPHELIDES AND SOLAR LENTIGINES		
	Ephelides (freckles)	**Solar lentigines (see Ch. 109)**
Epidemiology		
Age of appearance	Early childhood	By 20–30 years (I, II)
Skin color	Light pigmentation	Light to dark pigmentation
Hair color	Often red or blond hair	Any type
Skin phototype	More common in I, II	More common in I and II, but also in III and IV
History		
Precipitating factors	Bursts of high-intensity sun exposure activate latent predetermined melanocytes, leading to permanent freckles	Repeated sun exposure over time alters melanocytes within a circumscribed area to overproduce melanin
Duration of lesions	Fade without sun exposure	Persist for life
Relation to season	Much darker in summer, fade in winter and over time with aging	May darken in summer but do not fade in winter
Heredity	Probably AD; also AR when related to *MC1R* variants	No data
Physical examination		
Type of lesion	Macule	Macule
Size	1–5 mm	5–15 mm or larger
Color	Light or medium brown	Medium or dark brown
Shape	Oval to irregular	Oval to irregular
Border	Smooth to jagged	Smooth to jagged
Distribution	Favor the face, extensor forearms, and back; rare on the dorsal aspect of the hands	Sites of chronic sun exposure, especially the face, arms (including dorsal aspect of the hands), and upper trunk
Dermoscopic features		
	Uniform pigmentation and a moth-eaten edge	Diffuse light brown structureless areas, sharply demarcated and/or moth-eaten borders, fingerprinting, and a reticular pattern with thin lines that are occasionally short and interrupted

Table 112.1 Comparative clinical features of ephelides and solar lentigines. I, II, III, IV = skin phototypes (see Ch. 134); AD, autosomal dominant; AR, autosomal recessive; MC1R, melanocortin-1 receptor.

CAFÉ-AU-LAIT MACULES

Key features

- Well-circumscribed, uniformly light to dark brown macules or patches
- Usually 2 to 5 cm in diameter (in adults), but can vary from a few mm to >20 cm in size
- Hyperpigmentation of the basal layer of the epidermis without an increase in melanocyte density
- Found in 10%–20% of the normal population, but multiple lesions raise the possibility of an underlying genetic disorder

Epidemiology

Café-au-lait macules (CALMs) may be present at birth, but usually become clinically apparent during the first year of life. The number of CALMs in an individual can vary from one to more than a dozen. Single CALMs are found in 10% to 20% of the normal population, and up to 1% of healthy children have up to three CALMs, especially African-American children[5].

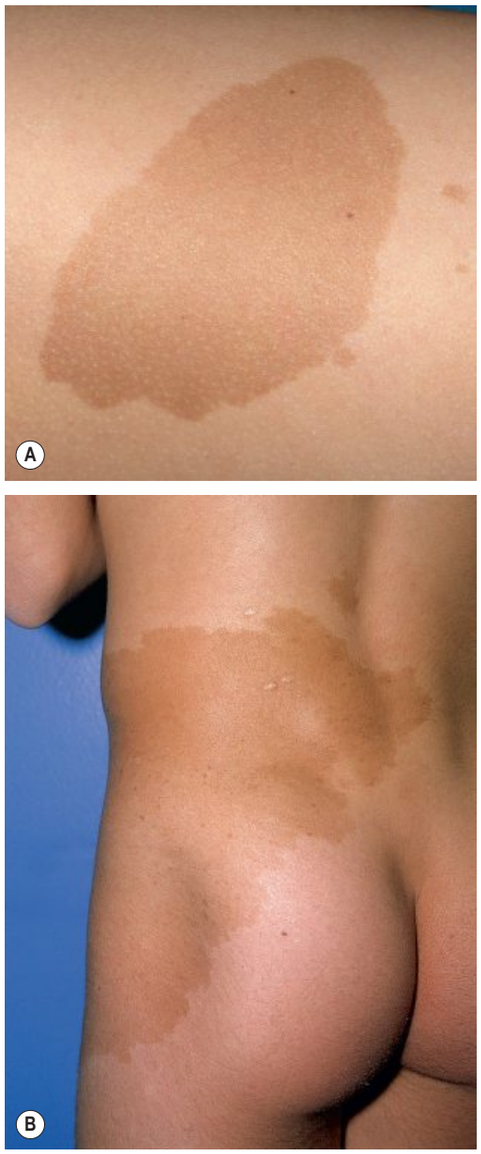


Fig. 112.1 Café-au-lait macules (CALMs). **A** Typical CALM with well-defined and regular margins in a patient with neurofibromatosis 1. **B** Large tan patch in a geographic pattern on the lateral trunk. The patient did not have McCune–Albright syndrome. *A, Courtesy Julie V. Schaffer, MD.*

Pathogenesis

The hyperpigmentation observed in CALMs is due to an increase in the melanin content within keratinocytes. While the underlying pathogenesis is not fully understood, UVR-independent mediators that stimulate melanin synthesis and transfer are likely involved (see Ch. 65). In patients with neurofibromatosis 1, biallelic *NF1* inactivation has been identified in melanocytes from CALMs (see Fig. 61.8), and in patients with McCune–Albright syndrome, affected skin contains activating mutations in the gene that encodes $G_s\alpha$ (see Fig. 65.14).

Clinical Features

The term café-au-lait refers to the characteristic homogeneous color of CALMs, reminiscent of coffee with milk. Their color varies from light to dark brown and correlates with the individual's background constitutive pigmentation. CALMs are macular and most have an oval shape with a distinct regular border and uniform color ("typical" CALMs; Fig. 112.1A). CALMs are usually 2–5 cm in diameter in adults but can vary from freckle-like lesions (≤2 mm) to patches that are >20 cm in diameter (Fig. 112.1B). CALMs enlarge proportionately with overall body growth and then remain stable in size during adulthood.

CALMs are benign lesions that may be located anywhere on the body, with the exception of the mucous membranes. By dermoscopy, a homogeneous brown patch is seen with perifollicular hypopigmentation; a faint reticular pattern may also be present. When multiple CALMs are present, the possibility of an underlying genetic disorder needs to be considered (Table 61.3). Compared with neurofibromatosis type 1 (NF1), the CALMs of McCune–Albright syndrome are typically fewer in number, larger, have a midline demarcation, and tend to be unilateral. If present, superimposed lentigines (due to widespread "freckling" extending beyond the axillae) can point to NF1-associated CALMs.

Pathology

Light microscopy shows a normally configured epidermis with a slight increase in melanin within basilar keratinocytes, but no or a minimal increase in melanocyte number. The adnexal epithelium is spared of hyperpigmentation. Melanin macroglobules (large pigment particles resulting from fusion of autophagosomes containing varying numbers of melanosomes) are often seen in NF-associated CALMs[6], but are also found in normal skin, isolated CALMs, and other pigmented lesions.

Differential Diagnosis

Hyperpigmented macules or patches that might be confused with CALMs include pigmentary mosaicism (segmental pigmentation disorder, Blaschko-linear hyperpigmentation), early nevus spilus (before the "speckles" have appeared), Becker melanosis (without obvious hypertrichosis), mastocytoma, mosaic (segmental) neurofibromatosis, and postinflammatory hyperpigmentation. Smaller lesions may resemble lentigines or acquired melanocytic nevi, while larger lesions may be confused with relatively flat congenital melanocytic nevi. Café-noir spots are hyperpigmented patches that have an even darker hue (relative to background skin) than CALMs and are seen in LEOPARD syndrome (Noonan syndrome with multiple lentigines) and Carney complex.

Treatment

Topical agents (e.g. hydroquinone) and sun protection have no effect on CALMs. The clinical response to pigment-specific laser therapy is difficult to predict (see Ch. 137), and recurrence rates are frequent[4]. In addition to recurrence, risks of laser surgery include transient hyperpigmentation or hypopigmentation, slight scarring, permanent hyperpigmentation, and incomplete clearance.

BECKER MELANOSIS (NEVUS)

Synonyms: ■ Becker's nevus ■ Becker's pigmentary hamartoma ■ Nevoid melanosis

Key features

- Unilateral, hyperpigmented, often hypertrichotic patch or slightly elevated plaque
- Most commonly on the anterior or posterior chest of male patients
- Onset usually during adolescence

Epidemiology

Becker melanosis occurs in ~1 in 200 individuals, with no racial predilection. This cutaneous hamartoma is usually unilateral and can initially appear as a light brown patch during late childhood to adolescence, followed by an increase in thickness, pigmentation, and hair growth. The latter changes are thought to reflect its androgen dependence. While Becker melanosis is often reported to be six times more common in males than in females, a more equal sex distribution has been suggested with androgen-dependent changes leading to a higher incidence of its diagnosis in men[7].

Pathogenesis

Postzygotic mutations in *ACTB*, which encodes beta-actin, have been detected in the majority of Becker nevi and in Becker nevus syndrome. There is some evidence that the *ACTB* mutations may lead to activation of the Hedgehog signaling pathway in these organoid hamartomas[8]. Other investigators observed an increase in androgen receptors in dermal fibroblasts, and an increased sensitivity to androgens has been postulated[9]. This would provide an explanation for the onset of Becker melanosis during or after puberty, as well as its clinical and histologic manifestations, which include hypertrichosis, dermal thickening, acne, and hypertrophic sebaceous glands.

Clinical Features

The onset of Becker melanosis is usually noted during the second decade of life. Lesions are usually unilateral and involve an upper quadrant of the anterior or posterior chest (Fig. 112.2A,B). However, they have also

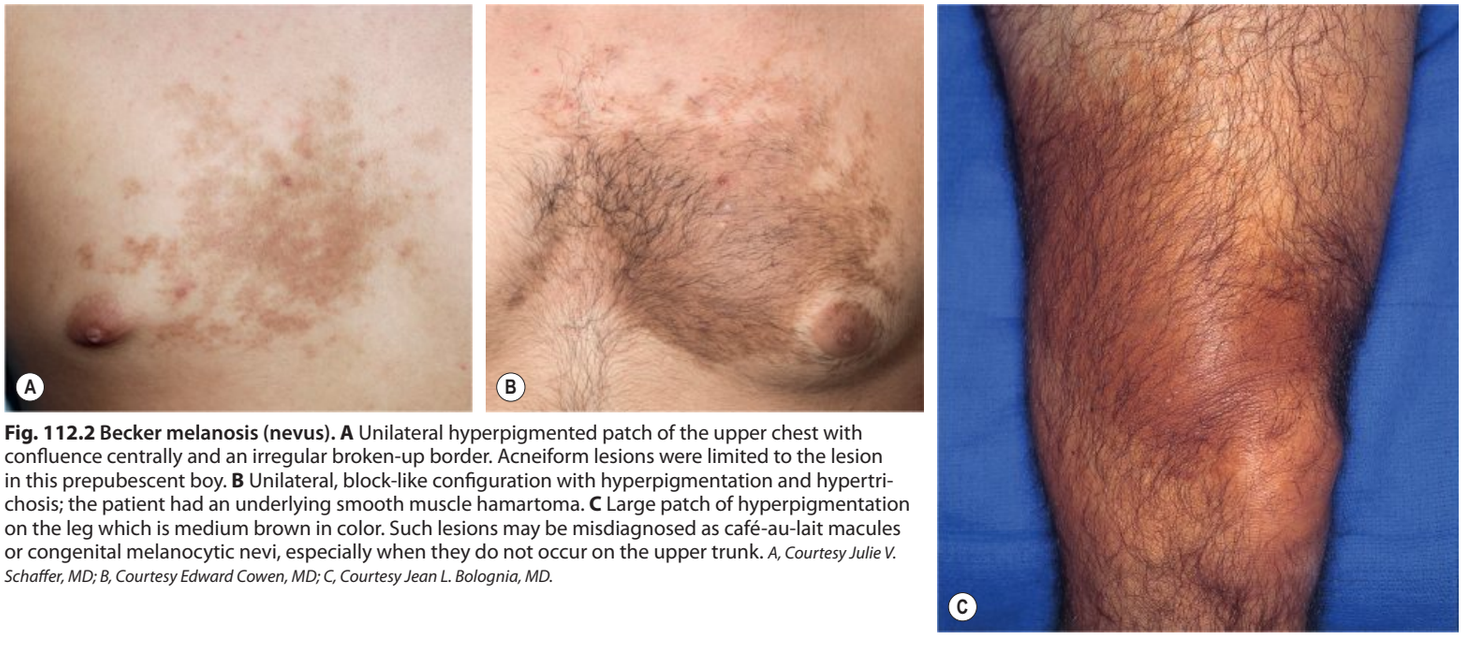


Fig. 112.2 Becker melanosis (nevus). A Unilateral hyperpigmented patch of the upper chest with confluence centrally and an irregular broken-up border. Acneiform lesions were limited to the lesion in this prepubescent boy. **B** Unilateral, block-like configuration with hyperpigmentation and hypertrichosis; the patient had an underlying smooth muscle hamartoma. **C** Large patch of hyperpigmentation on the leg which is medium brown in color. Such lesions may be misdiagnosed as café-au-lait macules or congenital melanocytic nevi, especially when they do not occur on the upper trunk. *A, Courtesy Julie V. Schaffer, MD; B, Courtesy Edward Cowen, MD; C, Courtesy Jean L. Bolognia, MD.*

been described on the face, neck, lower trunk, extremities, and buttocks (Fig. 112.2C). Normally, Becker melanosis appears as a single lesion, but multiple lesions have occasionally been observed. The diameter ranges from a few centimeters to >15 cm, and the most common configuration is block-like, although linear patterns have been reported.

The hyperpigmentation varies from uniformly tan to dark brown, and while the lesions are well demarcated, the margins are usually irregular. The center of the lesion may show slight thickening and corrugation of the skin. Hypertrichosis usually develops after the hyperpigmentation, and the hairs become coarser and darker with time (see Fig. 112.2B). Sometimes, the hypertrichosis is subtle and can only be appreciated by comparison with the contralateral side. The hypertrichosis and pigmentation may not overlap completely. After its initial appearance, Becker melanosis may enlarge slowly for a year or two but then remains stable in size. The color can fade with time, but hypertrichosis usually persists.

Normally, Becker melanosis is asymptomatic, but some patients report pruritus. Firmness to palpation may point to an associated smooth muscle hamartoma. In some patients, perifollicular papules may be a sign of coexistent proliferation of the arrector pili muscle. Acneiform lesions strictly limited to the area of hyperpigmentation have also been reported.

Becker melanosis is a benign lesion, and malignant transformation has not been reported. In contrast to the hyperplasia of the ectodermal and mesodermal tissues in Becker melanosis, developmental anomalies that are generally hypoplastic in nature have occasionally been associated with Becker melanosis (often referred to as Becker nevus syndrome). These abnormalities include hypoplasia of the ipsilateral breast, areola, nipple and arm, ipsilateral arm shortening, lumbar spina bifida, thoracic scoliosis, and pectus carinatum, as well as enlargement of the ipsilateral foot. Accessory scrotum and supernumerary nipples have also been reported. In cases of Becker melanosis with associated abnormalities, the male : female ratio is reversed at 2 : 5 (in comparison to the reported 6 : 1 in those without abnormalities)[10].

Pathology

There is a variable degree of acanthosis, hyperkeratosis, and sometimes mild papillomatosis. Regular elongation of the rete ridges and hyperplasia of the pilosebaceous unit may be observed. The melanin content of the keratinocytes is increased, whereas the number of melanocytes is normal or only slightly increased, without nesting. Melanophages may be found in the papillary dermis. A concomitant smooth muscle hamartoma is often, but not invariably, present in the dermis.

Differential Diagnosis

The differential diagnosis primarily includes CALM, congenital melanocytic nevus, plexiform neurofibroma, and congenital smooth muscle hamartoma. The latter hamartoma tends to be smaller in size, but some authors consider Becker melanosis and congenital smooth muscle hamartoma to be two ends of a clinical spectrum (see Ch. 117). Surface corrugation, noted with side-lighting, is not seen in CALMs. A congenital melanocytic nevus, plexiform neurofibroma, and congenital smooth muscle hamartoma can all have cutaneous hyperpigmentation plus hypertrichosis. By dermoscopy, Becker melanosis, as compared to congenital nevi, is less likely to have focal thickening of network lines, globules, or homogeneous diffuse pigmentation. In an occasional patient, histologic evaluation is required to confirm the diagnosis, especially if the lesion is in an unusual location and there is an associated smooth muscle hamartoma.

Treatment

Patients with Becker melanosis should be examined for possible soft tissue and bone abnormalities (see above). When there are cosmetic concerns, electrolysis, waxing, camouflage makeup, and laser treatments represent therapeutic options. The hypertrichosis is often easier to address than the hyperpigmentation via laser therapy (see Ch. 137). As with CALMs, incomplete clearance and recurrences are commonly observed[4].

SOLAR LENTIGINES

Synonyms: ■ Lentigo senilis ■ Liver spot ■ Old age spot ■ Senile freckle

Key features

- Tan to dark brown or black macules, primarily in sun-exposed sites in middle-aged and older adults
- Hyperpigmentation of the basal layer of the epidermis, usually in association with elongation of the rete ridges
- No or only a slight increase in the number of melanocytes

Solar lentigines are common benign lesions resulting from chronic UVR exposure that results in epidermal hyperplasia. These lesions are found in >90% of the White population older than 60 years of age (Fig. 112.3 & Fig. P1), but are also seen in Asians, especially on the face (see Ch. 87). The clinical differential diagnosis includes macular seborrheic keratosis (oftentimes considered on a spectrum with solar lentigo), pigmented actinic keratosis, pigmented Bowen disease, and lentigo maligna as well as benign pigmented lesions such as lentigo simplex, ephelis, small CALM, and junctional melanocytic nevus. Solar lentigines are discussed in detail in Chapter 109.

LENTIGO SIMPLEX AND MUCOSAL MELANOTIC MACULES

Synonyms:

- Lentigo simplex: • simple lentigo • lentiginosis (if multiple)
- Mucosal melanotic macules: • mucosal melanotic lesions • lentiginosis • melanosis
- Anatomic subtypes: • oral melanotic macules • labial melanotic macules • genital lentiginosis • anogenital lentiginosis

Key features

- Persistent brown macule that appears at an early age (when compared to a solar lentigo)
- Little or no relationship to sun exposure
- Hyperpigmentation of basilar keratinocytes with a slightly increased number of singly arranged melanocytes

Epidemiology

Lentigines are more common in those with lightly pigmented skin, but can occur in all skin phototypes. There is no sex predilection. Lentigines often appear during childhood and then increase in number



Fig. 112.3 Solar lentigines. Numerous light brown macules, some of which have an irregular border, on chronically sun-exposed skin.

from puberty into early adulthood. Of note, isolated lesions may be present at birth. Sometimes there is an eruptive form called lentiginosis, with or without obvious precipitating factors. After melanocyte activation, lentigo simplex represents the most common histology in matrix biopsies of longitudinal melanonychia (see Ch. 71). In darkly pigmented individuals, lentigo simplex is the most common histologic pattern for cutaneous pigmented lesions in acral sites.

Oral melanotic macules are found primarily in adults over 40 years of age. The most common sites are the vermilion border, followed by the gingiva, the buccal mucosa, and the palate. From 30% to 60% of melanomas within the oral cavity are preceded by melanosis for several months or years. The *labial (lip) melanotic macule* usually appears between the second and fourth decades of life and has a strong predilection for White women.

The incidence of *lentiginosis or melanosis* of the female *genital area* is probably higher than reported. For example, 15% of 106 females between the ages of 16 and 42 years had genital "nevi", and in a study of 100 random autopsies, three cases showed melanosis of the genitalia. Most lesions are found on the labia minora, but they can also occur on the labia majora, the vaginal introitus, the cervix, the periurethral area, and the perineum as well as perianally. In general, lentiginosis and melanosis of the female genitalia are benign conditions; atypia is uncommon and progression to melanoma has rarely been observed[11].

In a study of 10 000 men between 17 and 25 years, 14% were noted to have "pigmented nevi" of the genitalia[12]. It is uncertain what proportion represented penile lentiginosis or melanosis since no clinical descriptions or histologic studies were reported. In the literature, the ages of patients with penile lentiginosis or melanosis range from 15 to 75 years. The glans penis, penile shaft, and perianal region are the most common sites of involvement of anogenital lentiginosis in men.

The incidence of primary acquired melanosis (PAM) of the *conjunctiva* is unknown. It is nearly always unilateral and is subdivided into two groups: PAM with no atypia and PAM with atypia. The latter can progress to melanoma. PAM must be distinguished from conjunctival nevi (thicker and more circumscribed) and complexion-associated melanosis (bilateral and around the limbus) as well as melanoma.

Pathogenesis

Hyperpigmentation of the basilar keratinocytes likely arises from an increased production of melanin and the slightly increased number of singly arranged melanocytes. To date, insights into lentigo formation have not been forthcoming despite the discovery of the genetic bases of several syndromes associated with lentiginosis. In contrast to solar lentigines (see Ch. 109), somatic activating mutations in *FGFR3* or *PIK3CA* are absent in lentigo simplex[13]. Some penile lesions have been reported to follow injury, irritation, or PUVA therapy; in women, hormonal factors are thought to play a role. Acral lentigines may be influenced by genetic factors since they are frequently found in darkly pigmented individuals.

Clinical Features

Lentigines simplex are light brown to black, homogeneously pigmented macules. They are well circumscribed and round or oval, have regular borders, and are usually <5 mm (often <3 mm) in diameter. These lentigines can occur anywhere on the body, including palmoplantar skin, without any predilection for sun-exposed sites. Mucosal melanotic macules frequently have irregular, ill-defined borders as well as mottled non-homogeneous pigmentation with areas devoid of pigment (Fig. 112.4); in contrast to cutaneous lesions, they can slowly increase in size over months to years, with or without changes in the degree of pigmentation. By dermoscopy, mucosal lentigines have a fingerprint pattern with narrow parallel lines and broader track-like pigmentation interrupted by dots and globules.

Lentigines simplex occur as solitary or multiple lesions. Multiple or generalized lentigines may be an isolated phenomenon, either present at birth or appearing during childhood or adulthood, or it may be a sign of a genetic disorder (Table 112.2).



Fig. 112.4 Genital lentiginosis. Biopsy of the clinically most atypical lesion (at 7 o'clock) showed no cellular atypia. Over a period of 10 years, several of the macules faded. *Courtesy Jean L. Bolognia, MD.*

DISORDERS ASSOCIATED WITH MULTIPLE LENTIGINES	
Disorders	**Comments**
Generalized	
LEOPARD syndrome (now referred to as Noonan syndrome with multiple lentigines)	• Autosomal dominant inheritance (high penetrance, variable expressivity); mutations in *PTPN11* > *RAF1* > *BRAF* • *L*entigines present in infancy/early childhood • Café-noir macules • *E*CG changes (conduction defects, hypertrophic cardiomyopathy), *o*cular hypertelorism, *p*ulmonary stenosis, *a*bnormal genitalia, growth *r*etardation and *d*eafness
Generalized lentigines	• Autosomal dominant inheritance; mapped to 4q21.1–q22.3 • Café-au-lait macules
Deafness plus lentiginosis*	• ? Forme fruste of LEOPARD syndrome
Carney complex (NAME/LAMB syndrome)	• Autosomal dominant inheritance; mutations in *PRKAR1A* (second locus on 2p16) • Lentigines, mucocutaneous myxomas, blue nevi (including epithelioid) • Psammomatous melanotic schwannomas • Atrial myxoma • Myxoid mammary fibroadenomas • Pigmented nodular adrenocortical disease; testicular (calcifying Sertoli cell), thyroid, and pituitary tumors
Arterial dissection plus lentiginosis	• ? Inheritance pattern • Cutaneous lentigines with onset in childhood • Dissection of aortic, internal carotid, and vertebral arteries

Table 112.2 Disorders associated with multiple lentigines.

Continued

DISORDERS ASSOCIATED WITH MULTIPLE LENTIGINES	
Disorders	**Comments**
Generalized	
Gastrocutaneous syndrome*	• Autosomal dominant inheritance; see Table 61.3 for details
Tay syndrome*	• ? Autosomal recessive inheritance • Growth retardation, intellectual disability; triangular face; cirrhosis; trident hands • Café-au-lait macules; premature canities; vitiligo
Pipkin syndrome*	• Autosomal dominant inheritance • Nystagmus; strabismus
Localized	
Head and neck (including oral mucosa) ± acral	
Peutz–Jeghers syndrome	• Autosomal dominant inheritance; mutations in *STK11* • Lentigines favor perioral region†, oral mucosa‡ and hands; longitudinal melanonychia • Multiple hamartomatous GI polyps • Pancreatic carcinoma; ovarian (adenoma malignum)/testicular tumors
Bandler syndrome*	• Autosomal dominant inheritance • Distribution of lentigines similar to Peutz–Jeghers • GI bleeding with small intestine "hemangiomas" rather than polyps
Laugier–Hunziker syndrome	• Similar distribution of lentigines as in Peutz–Jeghers, including lips, oral mucosa, and digits • Longitudinal melanonychia and genital melanosis
Hyperkeratosis-hyperpigmentation (Cantú) syndrome	• Autosomal dominant inheritance • Punctate palmoplantar keratoderma • Multiple small (1 mm) macules on the face, forearms, hands/feet
Cowden disease	• Autosomal dominant inheritance; mutations in *PTEN* • Periorificial and acral pigmented macules (see Table 63.3)
Centrofacial lentiginosis (neurodysraphic)	• Autosomal dominant inheritance • Lentigines in a butterfly distribution on the nose, cheeks > forehead, eyelids, upper lip • Onset in infancy; increase in number in childhood • Possibly associated with neuropsychiatric illness and osseous anomalies
Inherited patterned lentiginosis	• Autosomal dominant inheritance • African-Americans with light brown skin • Pigmented macules appear in early childhood • Present on central face and lips > buttocks, elbows, hands/feet • Rare oral mucosal involvement
Cronkhite–Canada syndrome	• Typically affects older men • Lentigines of buccal mucosa, face, hands/feet • Alopecia (diffuse, non-scarring), nail dystrophy, intestinal polyposis, diarrhea, malabsorption
Genital	
Bannayan–Riley–Ruvalcaba syndrome	• Autosomal dominant inheritance; mutations in *PTEN* • Penile > vulvar pigmented macules (see Table 63.3)
"Photodistribution"	
Xeroderma pigmentosum	• Autosomal recessive inheritance; mutations in genes encoding proteins that repair UV-induced DNA damage • Lentigines favor, but are not limited to, chronically sun-exposed sites • Multiple skin cancers
Segmental	
Partial unilateral lentiginosis (PUL)	• Multiple lentigines in a segmental distribution • Café-au-lait macules in same distribution • Both PUL and "zosteriform" speckled lentiginous nevus can be seen in patients with mosaic NF1 (segmental NF)

*To date, observed in 1–2 families.
†May fade.
‡Persists.

Table 112.2 Disorders associated with multiple lentigines. ECG, electrocardiogram; GI, gastrointestinal; LEOPARD, *l*entigines/*E*CG abnormalities/*o*cular hypertelorism/*p*ulmonary stenosis/*a*bnormalities of genitalia/*r*etardation of growth/*d*eafness syndrome; NAME, *n*evi/*a*trial myxoma/*m*yxoid neurofibroma/*e*phelides syndrome; LAMB, *l*entigines/*a*trial myxoma/*m*ucocutaneous myxoma/*b*lue nevi syndrome. *Adapted from Bolognia JL. Disorders of hypopigmentation and hyperpigmentation. In: Harper J, Oranje A, Prose N (eds). Textbook of Pediatric Dermatology, 2nd edn. Oxford: Blackwell Science, 2006:997–1040.*

Associated syndromes

In *LEOPARD syndrome* (now referred to as Noonan syndrome with multiple lentigines), the acronym refers to: *l*entigines, *e*lectrocardiographic conduction defects, *o*cular hypertelorism, *p*ulmonary stenosis, *a*bnormalities of genitalia, *r*etardation of growth, and *d*eafness (see Table 112.2). Multiple lentigines are present at birth or appear during early infancy and may increase in number during childhood. The lesions are generalized, occurring in both sun-exposed and sun-protected sites, including genitalia, palms, and soles.

The *Carney complex* is an autosomal dominant syndrome characterized by multiple lentigines and multiple neoplasias, including: myxomas of the skin, heart (atrial), and breast; psammomatous melanotic schwannomas; epithelioid blue nevi of skin and mucosae; growth hormone-producing pituitary adenomas; and testicular Sertoli cell tumors (Fig. 112.5A). Components of the Carney complex have been described previously as the *NAME* (*n*evi, *a*trial myxoma, *m*yxoid neurofibroma, *e*phelides) and *LAMB* (*l*entigines, *a*trial myxoma, *m*ucocutaneous myxoma, *b*lue nevi) syndromes.



Fig. 112.5 Genetic disorders associated with multiple lentigines. A Numerous, variably shaped, tan to dark brown lentigines, with the greatest number on the midface in a patient with Carney complex (NAME/LAMB syndrome). **B** Lentiginosis of the vermilion and mucosal lips in a patient with Peutz–Jeghers syndrome. *Courtesy Edward Cowen, MD.*

Peutz–Jeghers syndrome is also an autosomal dominant disorder characterized by mucocutaneous lentigines which are present at birth or appear during childhood in combination with intestinal polyposis (Fig. 112.5B). The skin lesions have an acrofacial distribution pattern and favor the perioral region (see Fig. 53.31). Mucosal lesions may affect the palate, tongue, buccal mucosa, and conjunctivae. The major differential diagnosis is *Laugier–Hunziker syndrome* in which there are acromucosal lentigines and longitudinal melanonychia, but no consistent internal manifestations (Fig. 112.6).

In *partial unilateral lentiginosis*, also referred to as segmental lentiginosis, there is unilateral clustering of lentigines, suggesting a developmental abnormality of melanocytes. The onset is often during childhood. There is no background hyperpigmentation (as in nevus spilus) and the lesion can expand in a wavefront-like manner. Patients with facial lesions may have ocular involvement and CALMs may also be present. Partial unilateral lentiginosis may be associated with mosaic (segmental) NF1 (see Table 61.2).

Pathology

Lentigo simplex is characterized by increased melanin in the basal layer and sometimes even in the upper layers of the epidermis and the stratum corneum. The number of melanocytes in the basal layer is slightly increased, but there are no melanocytic nests. Melanophages and a mild inflammatory infiltrate are often present in the superficial dermis.

Lesions on mucous membranes, including the lips, show acanthosis with or without elongation of the rete ridges (Fig. 112.7). Slight melanocytic hyperplasia is usually observed, but may be absent. Hyperkeratosis, telangiectasia, activated fibroblasts, and large dendritic melanocytes have been described in labial melanotic macules. Ultrastructurally, melanin macroglobules have been observed within the melanocytes, as well as in keratinocytes and melanophages. These are not specific for lentigo simplex since they have been described in other pigmented lesions (see above).

Differential Diagnosis

The differential diagnosis of a solitary lentigo simplex consists primarily of a junctional melanocytic nevus, a flat form of compound melanocytic nevus, solar lentigo, and ephelis. In some instances, cutaneous melanoma, pigmented spindle cell nevus, and cutaneous intracorneal hemorrhage might enter into the differential diagnosis. Although there is a continuum from simple lentigo to junctional melanocytic nevus, the former is often smaller than the latter and it may not show distorted skin markings when viewed with side-lighting. Lentigo simplex is usually distinguished from a solar lentigo by its smaller size, symmetry, uniform pigmentation, and lack of relationship to sun-exposed sites. However, this clinical distinction may not be possible in some instances.



Fig. 112.6 Labial and acral lentigines in two patients with Laugier–Hunziker syndrome. A Multiple hyperpigmented macules on the lower lip and a few on the tongue; Peutz–Jeghers syndrome can have a similar clinical appearance. **B** Numerous lentigines on the palms. *B, Courtesy Drs. Tello Flores and Sánchez Félix.*

Treatment

In general, there is no need to treat a benign-appearing lentigo simplex. Lesions on acral or mucous membranes should be evaluated carefully and, if clinically atypical, should be considered for biopsy to assess for melanocytic atypia. Patients with both generalized and localized lentiginosis should undergo investigation to exclude systemic disease (see Table 112.2).

DERMAL MELANOCYTOSIS

Synonyms: ■ Congenital dermal melanocytosis: • Mongolian spot

Key features

- Blue to blue–gray patch present at birth that is most commonly located in the lumbosacral region
- Usually resolves during childhood
- More common in Asians
- Sparse dendritic melanocytes in the deeper dermis

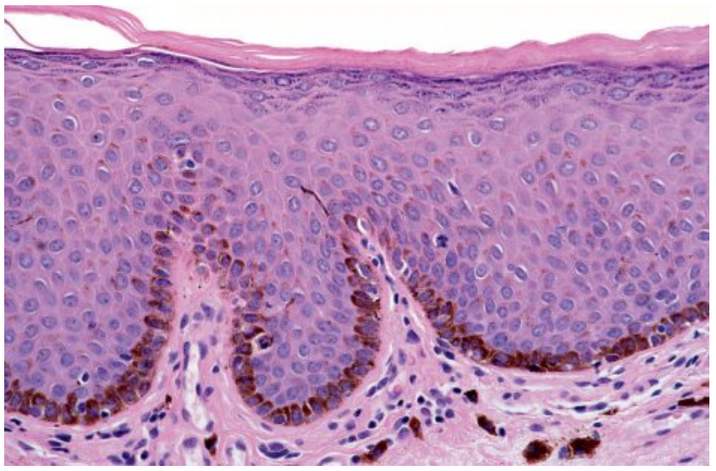


Fig. 112.7 Labial melanotic macule (lentigo) – histopathologic features. Hyperpigmented rete ridges are broader than in the typical lentigo. In addition to basilar hyperpigmentation and melanophages, a few dendritic processes of melanocytes are seen. *Courtesy Lorenzo Cerroni, MD.*

Epidemiology

Dermal melanocytosis is usually present at birth or appears within the first weeks of life; rarely, lesions appear after early childhood. Dermal melanocytosis usually regresses during early childhood, but it can persist and was seen in 4% of Japanese males between 18 and 22 years of age. While there is no sex predilection, the frequency varies widely depending upon ethnicity, e.g. 100% in Malaysians, 90%–100% in Mongolians, Japanese, Chinese and Koreans, 87% in Bolivian Indians, 65% of Black individuals in Brazil, 17% of White individuals in Bolivia, but only 1.5% of White persons in Brazil. These differences suggest that genetic factors influence survival of dermal melanocytes. Microscopically, histologic findings consistent with dermal melanocytosis can be found in the presacral area of 100% of newborns, irrespective of race[14].

Pathogenesis

The blue color in dermal melanocytosis is secondary to melanin-producing melanocytes in the middle to lower dermis. Melanocytes appear in the dermis during the 10th week of gestation and then either migrate into the epidermis or undergo cell death, except for melanocytes in the dermis of the scalp, extensor aspects of the distal extremities, and the sacral area. The latter is the most common site for dermal melanocytosis. The bluish coloration results from the Tyndall phenomenon: dermal pigmentation appears blue because of decreased reflectance of light in the longer-wavelength region compared with the surrounding skin. Longer wavelengths, such as red, orange and yellow, are not reflected, compared with the shorter wavelengths of blue and violet, which are reflected.

Clinical Features

The classic location is the sacrococcygeal and lumbar regions and the buttocks, followed by the back. Dermal melanocytosis may consist of a single or multiple patches and usually involves <5% of the body surface area. The lesions are macular and have a round, oval, or angulated shape. The size varies from a few to more than 20 cm with the color varying from light blue to dark blue to blue–gray. Extrasacral variants tend to be more persistent, and there is overlap between persistent lesions and the entities adult-onset dermal melanocytoses, nevus of Ito, and patch blue nevus. Extensive dermal melanocytosis should raise the possibility of phakomatosis cesioflammea (type II phakomatosis pigmentovascularis [PPV]) and phakomatosis cesiomarmorata (type V PPV; see Table 104.4). When CALMs and satellite congenital melanocytic nevi reside within areas of dermal melanocytosis, a rim that lacks dermal melanocytes may be seen around each lesion (Fig. 112.8).

Pathology

Bipolar, pigmented dendritic melanocytes are dispersed singly in the lower half of the dermis. These melanocytes are DOPA-positive and lie parallel to the epidermis between the collagen bundles without disturbing the normal architecture of the skin. Occasionally, persistent dermal melanocytosis has the histology of a blue nevus with involvement of the subcutis, muscle, and fascia by melanocytes, but lacks thick collagen bundles. On electron microscopy, dermal melanocytosis shows fully developed melanocytes with mature, electron-dense melanosomes and few premelanosomes.



Fig. 112.8 Dermal melanocytosis (Mongolian spots) in a child with neurofibromatosis 1. Surrounding each café-au-lait macule there is an absence of the characteristic blue discoloration.

Differential Diagnosis

The differential diagnosis of dermal melanocytosis includes nevus of Ota, nevus of Ito, and patch blue nevus. The latter has many names in the literature, including dermal melanocyte hamartoma, acquired dermal melanocytosis, and acquired linear dermal melanocytosis; clearly there is overlap with the rare adult-onset dermal melanocytosis. The clinical differential diagnosis may also include venous malformations or deep infantile hemangiomas and a contusion. Although the distinctive clinical presentation of dermal melanocytosis generally allows easy distinction from these entities, there have been reports of the misdiagnosis of child abuse.

Treatment

Persistent lesions may be treated with cover-up cosmetics or lasers (see nevus of Ota).

NEVUS OF OTA, NEVUS OF ITO, AND RELATED CONDITIONS

Synonyms:

- Nevus of Ota: • nevus fuscoceruleus ophthalmomaxillaris • oculodermal melanocytosis • congenital melanosis bulbi • oculomucodermal melanocytosis
- Nevus of Ito: • nevus fuscoceruleus acromiodeltoideus
- Nevus of Ota-like macules: • Hori nevus

Key features

- Blue to blue–gray to blue–brown unilateral patch on the face (nevus of Ota) or the shoulder region (nevus of Ito)
- More common in Asians
- More dermal dendritic melanocytes than in dermal melanocytosis, but less than in blue nevus

Nevus of Ota

Epidemiology

Nevus of Ota occurs predominantly in individuals with darker skin phototypes, especially in Asians, but has also been described in White individuals[15]. Approximately 80% of all reported cases have been in women; however, this figure may be somewhat skewed as a result of greater cosmetic concerns in women. In Japan, nevus of Ota is seen in ~0.4%–0.8% of all dermatologic patients. The lesion has two peaks of onset: the first (~50%–60% of all cases) is during infancy (before the age of 1 year), with the majority present at birth, and the second (40%–50%) is around puberty. Although rare familial forms of nevus of Ota have been reported, the condition is generally not considered hereditary.

Pathogenesis

The blue to blue–gray color in nevus of Ota is due to melanin-producing melanocytes in the dermis. The larger concentration of melanocytes in nevus of Ota in comparison to dermal melanocytosis is thought to indicate a hamartoma. Somatic activating mutations in *GNA11* or *GNAQ* were detected in up to 15% of cases of nevus of Ota, as compared to 65%–75% of blue nevi (primarily *GNAQ*) and 80%–85% of primary uveal melanomas[16]. In mice, germline mutations in *Gnaq* lead to an increase in dermal pigmentation. The possibility of a hormonal influence in women has been raised.

Clinical features

Nevus of Ota is usually characterized by a confluence of individual macules varying from pinhead-sized to several millimeters in diameter (Fig. 112.9A). The shape of the individual macules may be round, oval, or serrated, whereas the overall appearance is that of an irregularly demarcated and often mottled patch. The overall size varies from a few centimeters to extensive unilateral and occasionally bilateral involvement. The color varies from shades of brown to gray, blue, black, and purple.

Nevus of Ota is usually unilateral and favors the distribution of the first two branches of the trigeminal nerve. The most common sites of involvement are the periorbital area, temple, forehead, malar area, earlobe, pre- and retroauricular regions, nose, and conjunctivae. In approximately two-thirds of patients, the ipsilateral sclera is involved. Rarely, nevus of Ota affects the cornea, iris, fundus oculi, retrobulbar fat, periosteum, retina, and optic nerve. Iris mammillations and glaucoma (~10% of patients)[17] have been reported, but vision is usually not impaired. Other frequent sites of involvement include the tympanum (55%), nasal mucosa (30%), pharynx (25%), and palate (20%). Occasionally, the external auditory canal, mandibular area, lips, neck, and thorax are involved. In 5% to 15% of patients, the lesion is bilateral.

Nevus of Ota may extend over time and persists for life. Variations in color intensity have been described, especially in association with periods of hormonal flux such as menstruation, puberty, or menopause.

Melanomas arising within nevi of Ota are unusual, with uveal melanomas estimated at 1 in 400 in White individuals and even less often in Asians. Cutaneous melanomas are rare, but typically have presented as new subcutaneous nodules, although other tumors such as atypical cellular blue nevi have also been described[18]. In addition to the uveal tract, primary melanomas of the orbit, chiasma, and meninges have been observed in association with nevus of Ota, as it is one of the entities that can have associated neuromelanosis and meningeal melanocytomas. Of note, *BAP1* mutations have been detected in cases that progressed to melanoma, pointing to a role in malignant transformation.

Pathology

The non-infiltrated areas in nevus of Ota show pigmented, elongated, and dendritic melanocytes scattered between the collagen bundles (Fig. 112.9B). In comparison to dermal melanocytosis, the cells are more numerous and located within the upper third of the reticular dermis. Occasionally, cells are found also in the papillary dermis and deep in the subcutaneous fat.

Hyperpigmentation of the basal epidermis and an increase in basilar melanocytes may occur. The DOPA reactivity of the melanocytes in nevus of Ota varies: slightly pigmented cells are often strongly reactive, whereas heavily pigmented melanocytes often are not reactive, indicating minimal residual enzymatic activity. Melanocytes can be found clustering around blood vessels as well as sweat and sebaceous glands. Raised or infiltrated areas show a larger number of dendritic melanocytes forming cellular aggregates or clumps resembling blue nevi histologically.



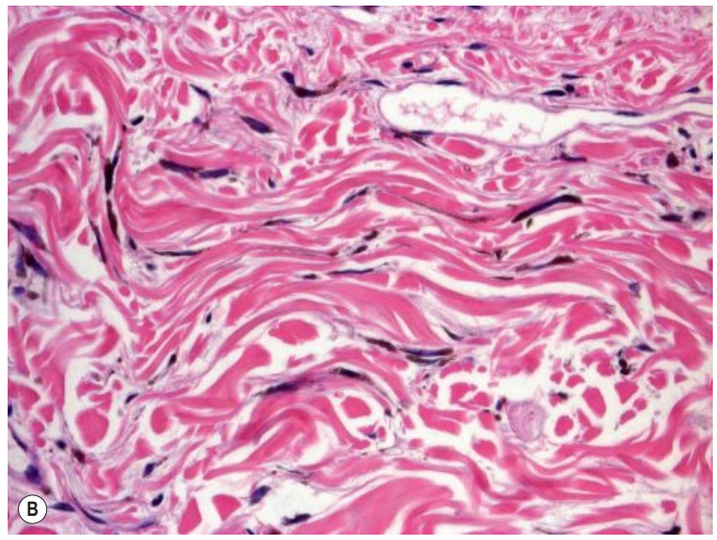


Fig. 112.9 Nevus of Ota (oculodermal melanocytosis) – clinical and histopathologic features. A Unilateral blue–gray discoloration of the face, which is either mottled or confluent. There is also involvement of the sclera. **B** Scattered pigmented elongated and dendritic melanocytes within the reticular dermis. *B, Courtesy Lorenzo Cerroni, MD.*

Differential diagnosis

The differential diagnosis of nevus of Ota includes dermal melanocytosis (Mongolian spot), adult-onset dermal melanocytosis, blue nevus (patch or plaque), melasma, partial unilateral lentiginosis (when it involves the face), a nevus spilus that develops blue nevi, venous malformations, and ecchymoses. Dermal melanocytosis differs from nevus of Ota and other dermal melanocytoses due to its location in the lumbosacral region and its spontaneous regression during childhood.

Treatment

Nevus of Ota and nevus of Ota-like macules have been treated successfully by Q-switched ruby, alexandrite, and Nd:YAG lasers[4,19]. Although malignant changes are rare in patients with nevus of Ota, patients with eye involvement should be followed more carefully by an ophthalmologist, since the majority of associated melanomas are ocular in origin and some patients develop glaucoma. Suspicious lesions, especially a new subcutaneous nodule, should be biopsied. Any complaint of neurologic symptoms requires further investigation.

Nevus of Ito and Related Conditions

Nevus of Ito involves the shoulder with extension onto the lateral upper trunk, corresponding to the distribution of the lateral cutaneous and

posterior supraclavicular brachial nerves. While its location differs from that of nevus of Ota, the clinical appearance and histologic features are the same. Occasionally, there is an associated ipsilateral or bilateral nevus of Ota.

Acquired nevus of Ota-like macules (Hori nevus) are characterized by bilateral, grouped, blue–gray to gray–brown macules of the zygomatic area. Less often, similar lesions are on the forehead, upper outer eyelids, and nose. This entity has been reported primarily in Chinese or Japanese women ranging from 20 to 70 years of age. In contrast to nevus of Ota, the eye and oronasal mucosa are not involved. It is often misdiagnosed as melasma, but the distinction is important as nevus of Ota-like macules can be successfully treated with laser surgery, similar to nevus of Ota.

Patch blue nevus overlaps with the rare disorder adult-onset dermal melanocytosis and presents as a diffusely gray–blue area that may have superimposed darker macules. The age of onset and sites of involvement vary, with some lesions having a linear distribution.

MELANOCYTIC NEVI

The term "nevus" is used to describe a hamartoma (e.g. epidermal nevus, sebaceous nevus) or a proliferation of melanocytes. Melanocytic nevi are defined histologically by nests of melanocytes, with a nest representing an aggregate of three or more melanocytes in direct contact. Melanocytic nevi are usually caused by genomic aberrations (mutations, translocations) that activate oncogenes, resulting in a clonal proliferation of melanocytes (Table 112.3). Genetic syndromes in which patients develop numerous melanocytic nevi are summarized in Table 112.4.

BLUE NEVUS AND ITS VARIANTS

Synonyms: ■ Blue nevus of Jadassohn–Tièche ■ Dermal melanocytoma ■ Nevus bleu ■ Blue neuronevus

Key features

- Blue to blue–black, firm papule, nodule or plaque, often with an onset during childhood or adolescence
- Aggregates of heavily pigmented, dendritic, spindled, or epithelioid melanocytes within the dermis

Epidemiology

In White populations, the estimated prevalence of blue nevi is 0.5%–1% while in Japanese adults, it is up to 4%. The ratio of common blue nevi to cellular blue nevi is at least 5 : 1. In general, congenital blue nevi are unusual, with most blue nevi arising during childhood or adolescence and up to a quarter first appearing in middle-aged adults. However, ~25% of cellular blue nevi are congenital, and they are more common in women (female : male ratio = 2 : 1).

Pathogenesis

Blue nevi are benign tumors of dermal melanocytes[20]. During the second half of gestation, dermal melanocytes disappear, but some residual melanin-producing cells remain in the dermis of the scalp, sacral region, and dorsal aspect of the distal extremities. These are the sites where blue nevi most commonly occur. The blue coloration is the result of the Tyndall phenomenon (see above).

Blue nevi frequently contain somatic activating mutations in *GNAQ* (50–60%) or *GNA11* (7–15%); less commonly there are mutations in *CYSLTR2* (~3%), *NRAS* (~3%), or *BRAF* (~1%) and *GRM1* fusions (see Table 112.3)[21,21a].

Clinical Features

Common *blue nevi* are well-circumscribed, dome-shaped papules that are blue, blue–gray, or blue–black in color (Fig. 112.10A–D)[15]. They are usually 0.5 to 1.0 cm in diameter, rarely larger. These nevi may occur anywhere, but about 50% are found on the dorsal aspect of the hands and feet, with other common sites the face and scalp. Blue nevi have also been observed in the oral and genital mucosae, cervix, prostate, spermatic cord, and lymph nodes. Over time, hypopigmentation may develop within the center of blue nevi, and an "achromic" variant has been described.

Usually, blue nevi are solitary, but they may be multiple, agminated, or arise within a nevus spilus or plaque blue nevus. Concentric, target-like lesions (target blue nevi) have also been described. Dermoscopically, a blue nevus is characterized by homogeneous blue–gray to blue–black pigmentation (see Ch. 0).

Cellular blue nevi are blue to blue–gray or black nodules or plaques, generally 1 to 2 cm in diameter but sometimes larger (Fig. 112.11A,B)[20]. Their surface is often smooth but sometimes irregular. The most common sites are the buttocks, sacrococcygeal area, and scalp, followed by the face and feet. Rarely, a cellular blue nevus can have satellitosis.

Occasionally, lymph nodes draining the anatomic site of a cellular blue nevus contain blue nevus cells. The foci, found either in the marginal sinuses or in the capsule, are usually small and discrete. They may result from passive transport or represent arrested migration from the neural crest. This type of nodal involvement ("benign metastasis") has been described in a minority of the reported cases of cellular blue nevi.

GENES AND GENE FUSIONS IMPLICATED IN THE DEVELOPMENT OF MELANOCYTIC NEVI	
Genes or gene fusions	**Type of melanocytic nevus**
Genes	
BRAF	Common acquired melanocytic nevi (65%–80%); small minority of blue nevi
NRAS	Congenital melanocytic nevi (~80%), small minority of common acquired melanocytic nevi and blue nevi, congenital melanocytic nevus with hypophosphatemia (single case)
HRAS	Spitz nevi*,† (~15%), deep penetrating nevi (6%), nevus spilus/speckled lentiginous nevi (100% in one series); also phakomatosis pigmentokeratotica
GNAQ	Blue nevi (50%–60%, depending upon the study); also nevus of Ota and related conditions, phakomatosis pigmentovascularis
GNA11	Blue nevi (7%–15%); also nevus of Ota and related conditions, phakomatosis pigmentovascularis
CYSLTR2	Small minority of blue nevi
PRKAR1A	Pigmented epithelioid melanocytomas, epithelioid blue nevi (mutation in the second allele in Carney complex); sometimes a second mutation in a combined melanocytic nevus
BAP1	BAP1-inactivated melanocytic nevi
CTNNB1	WNT-activated deep penetrating/plexiform nevi
PTEN	Nevi in patients with xeroderma pigmentosum (~60%)
Gene fusions	
• Spitz nevi/tumors: translocations (fusions) of receptor tyrosine kinases (*ROS1*, *NTRK1/2/3*, *ALK*, *RET*, *MET*, *MERTK*) or kinases in the MAPK pathway (*BRAF*, *RAF1*, *MAP3K8*) • Pigmented spindle cell nevi: fusions of *NTRK3*, less commonly involving *MERTK*, *RET*, or *ROS1* • Minority of blue nevi: fusions of *GRM1*[21a] • Group of dermal melanocytic tumors that histologically resemble clear cell sarcoma or metastatic melanoma, but have an indolent behavior: CRTC1::TRIM11 fusion[86]	
*Also copy number increases of chromosome 11p where *HRAS* resides. †Also Spitz nevi arising within a nevus spilus (sometimes mistakenly termed "agminated Spitz nevi").	

Table 112.3 Genes and gene fusions implicated in the development of melanocytic nevi. NTRK3, neurotrophic receptor tyrosine kinase 3.

GENETIC SYNDROMES ASSOCIATED WITH NUMEROUS ACQUIRED MELANOCYTIC NEVI
Familial atypical mole and melanoma syndrome*
BAP1 cancer syndrome – atypical epithelioid nevi/tumors, uveal melanomas, mesothelioma
Carney complex (NAME/LAMB syndromes) – see Table 112.2
Turner syndrome – webbed neck, congenital lymphedema (partial or complete loss of X chromosome in females)
Noonan syndrome (mutations in multiple genes including *PTPN11*, *RAF1*, *KRAS*, *SOS1*) > other RASopathies (e.g. LEOPARD [Noonan with multiple lentigines] syndrome, cardiofaciocutaneous syndrome, Costello syndrome; see Ch. 55)
Ectrodactyly, ectodermal dysplasia, and cleft lip/palate syndrome (EEC syndrome; *TP63* mutations)
Goeminne syndrome – torticollis, keloids, cryptorchidism, and renal dysplasia
Kuskokwim syndrome – congenital joint contractures, skeletal deformities (*FKBP10* mutations)
Mulvihill Smith syndrome – progeroid short stature with pigmented nevi
Trichorhinophalangeal syndrome type II (Langer–Giedion syndrome)
Tricho-odonto-onychial dysplasia
*OMIM designation is "Susceptibility to cutaneous melanoma".

Table 112.4 Genetic syndromes associated with numerous acquired melanocytic nevi. *Adapted from reference 87.*

Pathology

Common blue nevi are composed of elongated, often slightly wavy melanocytes with long, branching dendrites (Fig. 112.10E,F). The melanocytes, with their long axes parallel to the epidermis, lie grouped or in bundles in the upper and mid dermis. Occasionally, they extend into the subcutaneous tissue or approach the epidermis but do not alter it. Most melanocytes are filled with fine melanin granules that obscure their nuclei and extend into their dendrites. Variable numbers of melanin-laden macrophages are also present. The amount of collagen is usually increased, giving the lesion a fibrotic or sclerotic appearance. In the hypopigmented variant, melanin content is minimal centrally[20].

Cellular blue nevi are well-circumscribed, nodular dermal tumors that are larger in diameter and have a higher cellular density than common blue nevi. Most often, well-defined nests of fusiform to ovoid melanocytes are surrounded by collagen and numerous melanophages (see Fig. 112.11C). Most of the melanocytes are usually lightly pigmented, with the majority of pigment residing in melanophages.

Aggregates of spindle cells may be arranged in intersecting bundles extending in various directions, a disposition resembling the storiform pattern of a neurofibroma. In cellular blue nevi, penetration of rounded, well-defined cellular islands into the subcutaneous tissue is frequently noted. Some of the cells may appear atypical, with nuclear pleomorphism accompanied by multinucleated giant cells, rare mitoses, and inflammatory infiltrates. Lastly, while there are classic histopathologic differences between common and cellular blue nevi, overlapping features are seen in some lesions[20].

Atypical cellular blue nevi demonstrate one or more of the following features compared to conventional cellular blue nevi: larger size (>1–2 cm), asymmetry, ulceration, infiltrating features, cytologic atypia, mitoses, and necrosis[22]. Such lesions have been associated with lymph node metastases and evolution to frank melanoma.

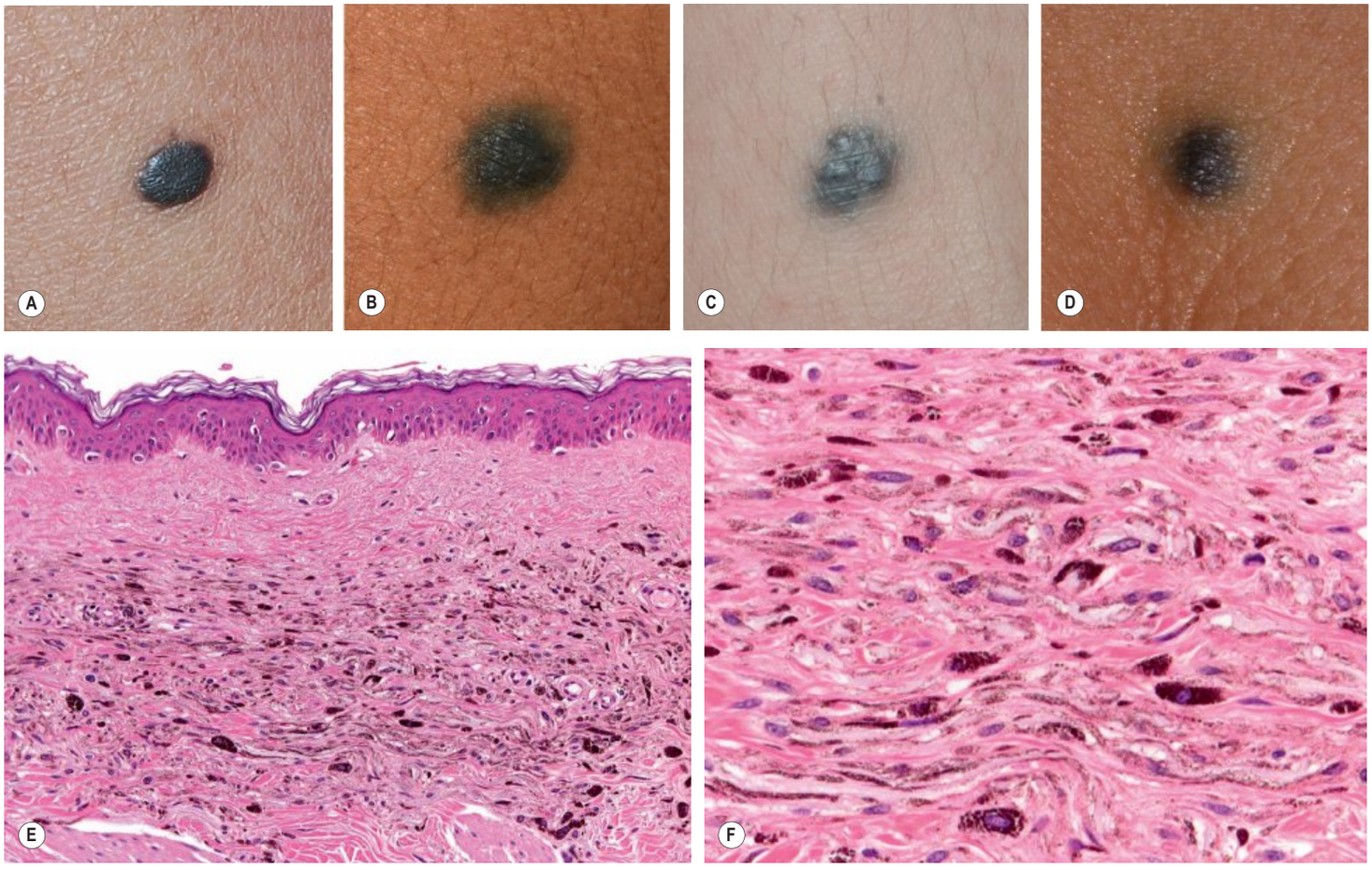


Fig. 112.10 Common blue nevi – clinical and histopathologic features. A Well-circumscribed, dark blue flat papule. **B** Dark blue–black papule in a patient with more darkly pigmented skin. **C** Blue papule with an irregular, micropapular surface. **D** Congenital blue–black papule superior to the gluteal cleft. **E, F** Heavily pigmented, spindle-shaped melanocytes as well as melanophages within the dermis; the melanocytes are denser than in dermal melanocytosis or nevus of Ota. *A–D, Courtesy Julie V. Schaffer, MD; E, F, Courtesy Lorenzo Cerroni, MD.*

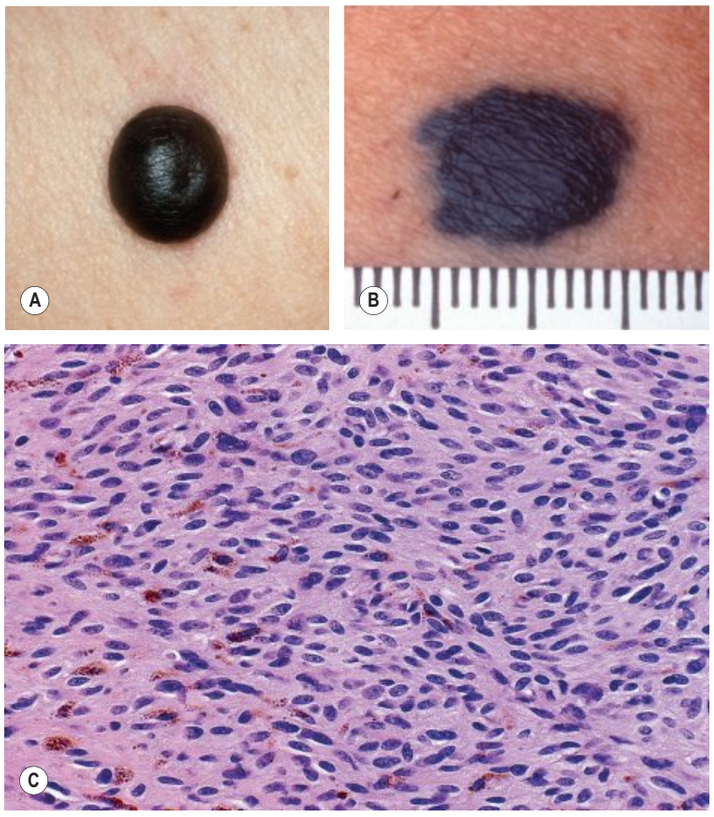


Fig. 112.11 Cellular blue nevi – clinical and histopathologic features. A A black nodule. **B** A firm blue plaque is a common presentation. **C** Plump spindled melanocytes devoid of melanin pigment and arranged within bundles are present within the dermis. Scattered melanin-containing melanophages are also present. *A, C, Courtesy Lorenzo Cerroni, MD; B, Courtesy Jean L. Bolognia, MD.*

Melanoma arising from blue nevus (MBN) refers to a melanoma arising within a pre-existing blue nevus, nearly always the cellular type. Classically, a rapidly growing, large (>2 cm) nodule arises on the scalp (followed by the face and trunk) in an adult who is usually >45 years of age. MBNs are often aggressive, with frequent metastasis to regional lymph nodes and the liver. In addition to the *GNAQ* or *GNA11* mutations in blue nevi, MBN often show additional genomic aberrations in *BAP1* or *SF3B1*[23].

Differential Diagnosis

The clinical differential diagnosis of a common blue nevus includes traumatic tattoo, vascular lesions including venous lake and angiokeratoma, combined nevus, sclerosing hemangioma, primary or metastatic melanoma, pigmented spindle cell nevus, atypical nevus, pigmented dermatofibroma, papular pigmented basal cell carcinoma, and glomus tumor. Cellular blue nevi also need to be distinguished from nevus of Ota, when on the face, as well as cutaneous neurocristic hamartoma, a complex proliferation of nevus cells, Schwann cells, and pigmented dendritic and spindled cells. Histologically, an atypical cellular blue nevus needs to be distinguished from MBN. Occasionally, a cutaneous melanoma metastasis may resemble a blue nevus.

Treatment

Blue nevi that are <1 cm in diameter, clinically stable, located in a typical anatomic site, and have no atypical features do not require removal. Histologic evaluation should be considered for lesions that appear *de novo*, are multinodular or plaque-like, or have undergone change. Atypical cellular blue nevi should be resected completely in order to prevent recurrence and because of the risk for malignant transformation or metastases. The approach to typical cellular blue nevi varies, but if observation is difficult (e.g. lesions on the scalp), excision can be considered.

PIGMENTED EPITHELIOID MELANOCYTOMA

Synonyms: ■ Epithelioid blue nevus ■ PRKAR1A-inactivated melanocytoma ■ Animal-type melanoma

Key features

- Rare tumor that usually presents as a slowly growing pigmented papulonodule
- Characterized by inactivation of *PRKAR1A*

Epidemiology and Pathogenesis

The term pigmented epithelioid melanocytoma (PEM) encompasses tumors previously referred to as epithelioid blue nevus and "animal-type", "melanophagic", or "pigment synthesizing" melanoma. PEMs are rare tumors that occur in both sexes with diverse ethnic backgrounds. The majority of PEMs have a loss of PRKAR1A immunoreactivity or inactivating mutations in *PRKAR1A*. The latter lead to activation of protein kinase A catalytic subunits (PRKACA, PRKABA) and induce melanocyte proliferation, differentiation, and pigmentation. Inactivation of PRKAR1A is usually combined with kinase fusions or mutations in genes (e.g. *BRAF*, *NRAS*, *NF1*, *CYSLTR2*, *GNAQ*, *GNA11*) involved in other melanocytic tumors (see Table 112.3)[24].

Clinical Features and Pathology

PEM presents as a slowly growing pigmented papule or nodule. It usually arises in the second or third decade, with the extremities being the most common site. Although PEMs were first described as a feature of Carney complex (see Table 112.2), they also may occur sporadically[25,26]. Histologically, a PEM is composed of pigmented epithelioid melanocytes with large vesicular nuclei. These cells are often admixed with heavily pigmented spindled and dendritic melanocytes as well as melanophages. Cytologic atypia and dermal mitoses may be present. PEMs frequently metastasize to regional lymph nodes but rarely spread extranodally and are almost never fatal.

The clinical appearance of a PEM is similar to a cellular blue nevus. Histologically, it needs to be differentiated from primary or metastatic melanoma as well as tumoral melanosis due to complete or almost complete regression of melanoma.

COMMON ACQUIRED MELANOCYTIC NEVI

Synonyms: ■ Nevocellular nevus ■ "Mole"

Key features

- A junctional nevus is a brown to black macule with melanocytic complexes at the dermoepidermal junction
- An intradermal nevus is a skin-colored to light pink or brown papule with complexes of melanocytes in the dermis
- A compound nevus is a brown papule with combined histologic features of junctional and intradermal nevi

Epidemiology

The prevalence of melanocytic nevi depends on age, ethnicity, genetic, and environmental factors. In early childhood, only a few nevi are present, but their number then increases and reaches a peak in the third decade of life; thereafter, nevi disappear with age[27]. There is a period of particularly rapid development of nevi at puberty. A study in Scotland noted that, in the first decade of life, girls had an average of three nevi and boys two nevi. For the peak age interval of 20 to 29 years, women and men had mean nevus counts of 33 and 22, respectively. In the seventh decade of life, women had a mean of 6 nevi and men 4 nevi, reflecting a progressive decline.

White individuals generally have greater numbers of nevi than populations with more darkly pigmented skin, e.g. African-Americans and Asians. In White individuals, the number of nevi is highest in those with skin phototype II. Additionally, melanocytic nevi (includes lentigines) on the palms and soles, nail beds, and conjunctivae are more prevalent in Africans and Asians. The mean acral "nevus" count for Africans in Uganda was 11, versus 2 to 8 for African-Americans.

Genetic factors also play a role in the prevalence of nevi: increased numbers of nevi have been shown to cluster in families, especially those with familial melanoma. Although an autosomal dominant mode of inheritance has been postulated for clinically atypical nevi in hereditary melanoma families, the pattern of inheritance may be more complex. Environmental factors such as sun exposure influence the development of melanocytic nevi as exemplified by the nevus counts of the outer versus inner arm or the back versus buttocks. However, genetic factors seem to directly determine an individual's potential for developing melanocytic nevi, and the final expression of this potential is influenced by solar exposure. In addition, individuals appear to inherit different propensities for nevogenesis[27], e.g. there is a higher correlation of nevus counts in monozygotic twins (r = 0.94) as compared to dizygotic twins (r = 0.60)[28].

Pathogenesis

The majority of melanocytic nevi arise from an activation of oncogenes that allows a clonal proliferation of affected melanocytes. In common acquired nevi, the initiating oncogenic event is usually an activating mutation in *BRAF* (80%) or *NRAS* (5%). Factors leading to the onset of melanocytic nevi are poorly understood but include the genetic influences alluded to earlier and environmental agents, principally UV exposure (Table 112.5). In genome-wide association studies (GWAS), a correlation was found between the number of melanocytic nevi and certain single nucleotide polymorphisms (SNPs) located near the *MTAP*, *PLA2G6*, *IRF4*, and *KITLG* genes.

Clinical Features

Melanocytic nevi are well-circumscribed, round to ovoid lesions, generally measuring from 2 to 6 mm in diameter. In general, they are symmetric and have a homogeneous appearance. While some common nevi may display slight asymmetry, the borders are usually regular and well-defined. *Junctional* nevi are macular lesions with a uniform, medium-to-dark brown color and slight accentuation of skin markings visible with side-lighting (Fig. 112.12A). The dermoscopic features of a junctional nevus include a uniform pigment network thinning out towards the periphery (see Table 0.15) (Fig. P2). *Compound* nevi show variable degrees of elevation and in general somewhat lighter shades of brown than do junctional nevi (Fig. 112.12C). Dermoscopically, compound nevi are characterized by a globular architecture with multiple round to ovoid globules sometimes forming a cobblestone pattern (see Table 0.15). *Intradermal* nevi are usually more elevated and show lighter shades of brown or even skin-colored tones compared to compound nevi (Fig. 112.12E). These nevi can also be pink in color. The dermoscopic features of an intradermal nevus predominantly consist of focal globules or globular-like structures. In addition, pale to whitish structureless areas and fine linear or comma vessels may be present (Fig. P3). In addition to clinical and dermoscopic overlap amongst all three types of nevi, intradermal nevi (and to a lesser degree compound nevi) may be papillomatous with pseudo-horn cysts.

Nevi, especially acquired "congenital-appearing" nevi, contain hairs that are coarse and dark compared to those in the surrounding skin. Nevi of the palms and soles are often macular or only slightly raised, have regular and well-defined borders, and show uniform or linear brown coloration (see below). Melanocytic nevi of the nail matrix usually present as uniformly pigmented, brown longitudinal bands (melanonychia striata, longitudinal melanonychia) with regular and distinct margins (Fig. 112.13; see Ch. 71).

Melanocytic nevi associated with epidermolysis bullosa

Distinctive melanocytic nevi termed "epidermolysis bullosa (EB) nevi" or "EB nevi" may develop at the sites of antecedent bullae or erosions primarily in patients with forms of EB that are recessively inherited (see Ch. 32)[29]. These nevi can have a strikingly large size (up to 3 cm) as well as asymmetry, border irregularity, dark color, and satellitosis. Their development may be related to repetitive disruption of the basement membrane zone with the promotion of proliferation or dispersion of melanocytes into the blister cavity with their subsequent proliferation in its floor. Although there are no reports of cutaneous melanoma developing at the sites of EB nevi, melanoma can occasionally arise within the setting of EB; thus longitudinal observation is warranted.

TRIGGERS FOR THE DEVELOPMENT AND/OR GROWTH OF MELANOCYTIC NEVI
Exposure to ultraviolet light
• Sun exposure leading to multiple or severe sunburns*
• Intermittent intense sun exposure (e.g. on sunny holidays)
• Chronic moderate sun exposure (e.g. residence at lower latitudes)
• Neonatal phototherapy
Blistering processes (other than severe sunburns)
• Toxic epidermal necrolysis/Stevens–Johnson syndrome*
• Epidermolysis bullosa – junctional (particularly generalized atrophic benign) > recessive dystrophic > recessive simplex*
• Bullae secondary to sulfur mustard (mustard gas) exposure*
Scarring/fibrosing processes
• Genital lichen sclerosus†
Systemic immunosuppression
• Chemotherapy, particularly for childhood hematologic malignancies and capecitabine*,†,‡
• Allogeneic bone marrow transplantation‡
• Solid organ transplantation, particularly renal and with the use of azathioprine*,‡
• HIV infection/AIDS*
• Chronic myelogenous leukemia*
• TNF inhibitor therapy*,‡
• Cyclosporine, azathioprine*
Increased hormone levels
• Pregnancy*,¶
• Growth hormone (increased size, not number, of nevi)
• Addison disease*
• Thyroid hormone*
• α-Melanocyte stimulating hormone analogue (afamelanotide)*
Other
• Sorafenib, vemurafenib, sunitinib, encorafenib, radotinib, regorafenib, nilotinib*
• Rituximab
• Atopic dermatitis in children (conflicting results in different studies)
• Postoperative fever*
• Seizures or electroencephalographic abnormalities*
*Eruptive nevi have been reported.
†An increased number of atypical nevi may also be seen.
‡Nevi have a predilection for the palms and soles.
¶Relative immunosuppression may also play a role; an increase in the size or number of nevi has not been clearly demonstrated for pregnant women in general, with the exception of areas that enlarge such as the abdomen. Melanoma may grow at an accelerated pace during pregnancy.

Table 112.5 Triggers for the development and/or growth of melanocytic nevi. TNF, tumor necrosis factor. *Adapted from Schaffer JV, Bolognia JL. The biology of melanocytic nevi. In: Nordlund JJ, Boissy RE, Hearing VJ, et al. (eds). The Pigmentary System: Physiology and Pathophysiology, 2nd edn. Oxford: Blackwell Publishing, 2006:1092–125.*

Melanocytic nevi associated with lichen sclerosus

Occasionally, melanocytic nevi develop within areas of genital lichen sclerosus[30]. The lesions are often dark brown to black in color, irregular in outline, and can measure ≥6 mm. As a result, the possibility of melanoma is frequently considered clinically, and histologic distinction is not always easy.

Pathology

Melanocytic nevi contain intraepidermal and/or dermal nests of melanocytes (Fig. 112.12B,D,F). The cells within the junctional nests have round, ovoid, or fusiform shapes and are arranged in cohesive nests. These melanocytes often contain melanin or occasionally may be

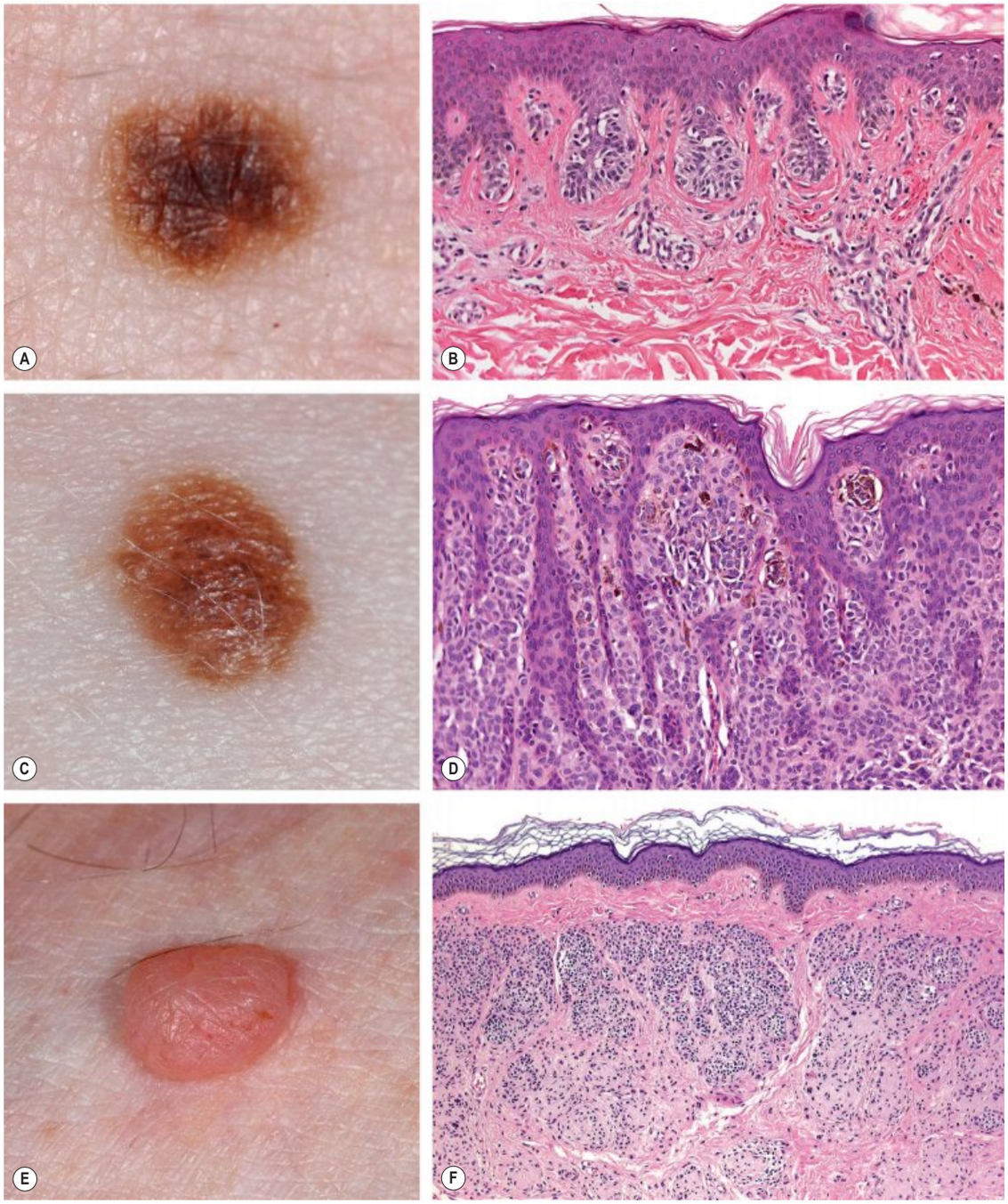


Fig. 112.12 Common acquired melanocytic nevi – clinical and histopathologic features. **A, B** Junctional nevus – dark brown macule with lighter brown rim and regular nests of small, uniform melanocytes at the dermal–epidermal junction. **C, D** Compound nevus – light to medium brown papule and both junctional and dermal nests of melanocytes. **E, F** Intradermal nevus – soft light pink papule and nests of melanocytes within the dermis. *B, D, F, Courtesy Lorenzo Cerroni, MD.*

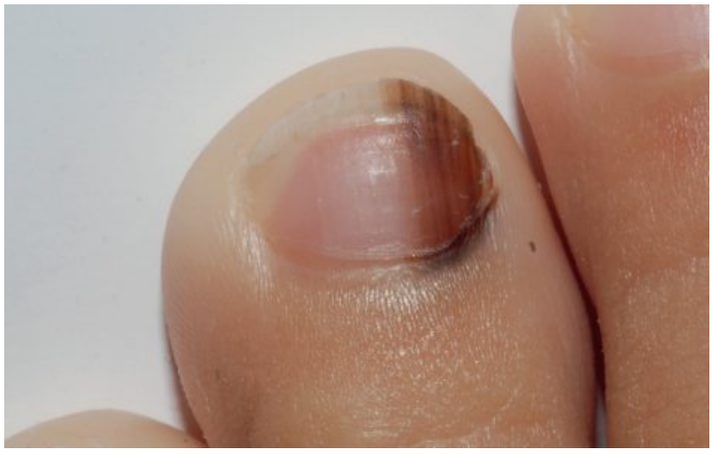


Fig. 112.13 Longitudinal melanonychia due to a benign melanocytic nevus of the nail matrix. Note the pseudo-Hutchinson sign. *Courtesy Julie V. Schaffer, MD.*

non-pigmented. In the superficial dermis, the melanocytes usually have epithelioid cell characteristics and contain amphophilic cytoplasm and, frequently, granular melanin. The nuclei have uniform chromatin with a slightly clumped texture. Deeper in the dermis, the melanocytes have less cytoplasm and appear smaller. There may be a further transition to cells separated by fine connective tissue and assuming a spindled configuration, similar to fibroblasts or Schwann cells.

EB nevi are best considered as exaggerated variants of recurrent/persistent melanocytic nevi (see below). They usually exhibit asymmetry and considerable variation in the overall architecture, including the junctional nests. Pagetoid melanocytosis and cytologic atypia may be present, as well as fibroplasia, a lymphocytic infiltrate, and melanophages.

In *melanocytic nevi associated with lichen sclerosus* (LS), the features of a genital nevus are superimposed on the changes of LS, which can vary from subtle to obvious. Irregular and confluent junctional nests are often accompanied by cytologic atypia. The changes of LS may suggest regression, and if the inflammatory component is significant, it may hinder assessment of the nevus cells. Findings that favor a genital nevus (rather than melanoma) include: a diameter <5 mm; relative symmetry;

sharp circumscription; nests located predominantly at the dermal–epidermal junction which predominate over melanocytes arranged as solitary units; low-grade cytologic atypia of melanocytes; a conventional dermal nevus component; absence of significant dermal mitoses; and limitation of the nevus to the area of LS.

Differential Diagnosis

The differential diagnosis of melanocytic nevi includes the full spectrum of pigmented and skin-colored lesions (see Ch. 0). Raised nevi, potentially confused with seborrheic keratoses, are less likely to have a verrucoid surface and pseudo-horn cysts and do not have a cerebriform surface when examined by dermoscopy. Dermatofibromas are usually differentiated from nevi by their very firm consistency, "dimpling" with lateral compression, preference for the lower extremities, and central white patch by dermoscopy. Both neurofibromas and fibroepithelial polyps may be indistinguishable from skin-colored or slightly pigmented, pedunculated intradermal nevi. In general, typical melanocytic nevi are distinguishable from atypical nevi and melanoma by smaller size, overall symmetry and orderly appearance, homogeneous coloration, and regular, well-defined borders. Furthermore, red, blue, gray, and black colors are not usually seen in common acquired nevi and should alert one to a potentially atypical lesion.

Treatment

Indications for removing melanocytic nevi include a changing lesion (e.g. enlarging, new color) and an atypical clinical appearance suspicious for melanoma. Nevi are also removed when they are bothersome (e.g. site of repeated trauma) or for cosmetic concerns. Even though the total number of melanocytic nevi correlates with the risk of melanoma (see Fig. 113.5), there is no reason to remove nevi on a routine basis.

GENITAL NEVUS AND NEVI OF SPECIAL SITES

Key features

- Benign melanocytic nevi that occur in "special" anatomic sites; the latter include the genitalia as well as the scalp, ear, nipple, umbilicus, and acral and flexural sites (e.g. axilla)
- Atypical clinical and histologic features make a reliable distinction from melanoma difficult and may lead to higher excision rates

Clinical Features

Melanocytic nevi occurring in genital sites, especially the vulva, often have distinctive clinical and histopathologic features compared to nevi from non-genital sites. Similar nevi may also occur in other locations such as the scrotum and perineum as well as the scalp, ear, nipple, umbilicus, and acral and flexural sites (e.g. axilla). These special-site nevi appear to be uncommon, perhaps accounting for <10% of nevi removed, but data could be biased by selection factors. Compared to common acquired nevi, nevi of special sites are often larger in size, may have irregular borders, and often have a complex mahogany color, i.e. an admixture of tan, brown, and red[31]. However, it is important to remember that melanoma can also arise in these sites, especially in middle-aged to older adults.

Pathology

In general, nevi of special sites have architectural features that differ from those of common acquired nevi and overlap with those of dysplastic nevi and melanoma. These atypical features include asymmetry, irregular arrangement of junctional melanocytic nests (including along the lateral aspects of the rete ridges), bridging of nests, discohesive melanocytes within nests, lentiginous proliferation, follicular involvement, pagetoid spread, dermal lamellar fibroplasia, and cytologic atypia[32].

Differential Diagnosis

The differential diagnosis includes primarily melanoma, Spitz nevus, and nevi associated with genital LS (see above). Vulvar melanoma tends to occur in older women (average age ~65 years) and is quite rare in young patients.

ACRAL NEVUS

Synonyms: ■ Melanocytic nevus of acral skin ■ Melanocytic acral nevus with intraepidermal ascent of cells (MANIAC)

Key features

- Benign melanocytic neoplasm of the non-hair-bearing skin of the hands and feet
- Histologically, about one-third of acral nevi demonstrate intraepidermal upward migration of melanocytes and other architectural changes that can resemble melanoma

Epidemiology and Pathogenesis

Acral nevi are common, occurring in up to one-third of the population. Their incidence peaks in the third and fourth decades of life. They are more common in individuals with darker skin phototypes. As in common acquired nevi, acral nevi have mutations in *BRAF* or *NRAS* in a mutually exclusive pattern.

Clinical Features

Acral nevi are usually macular or only slightly elevated. They may display a uniform brown or dark brown color, but often have linear striations. The characteristic dermoscopic features of acral nevi are due to the unique anatomy of acral skin. Both the palms and soles have parallel ridges (mountains) and furrows (valleys), with the intraepidermal eccrine ducts passing through the ridges (Fig. 112.14). In acral nevi, the nests of nevus cells are situated around the furrows. The three major dermoscopic patterns seen in acral nevi are the parallel furrow (Fig. 112.15), the lattice-like (Fig. P4), and the fibrillar pattern (Table 112.6)[33].

Pathology

Acral nevi are usually relatively small (<5–6 mm), well-circumscribed, symmetric compound nevi. Occasionally, the junctional nests are somewhat enlarged, but they usually have a fairly uniform round or oval shape and are similar in size and spacing. Lentiginous melanocytic

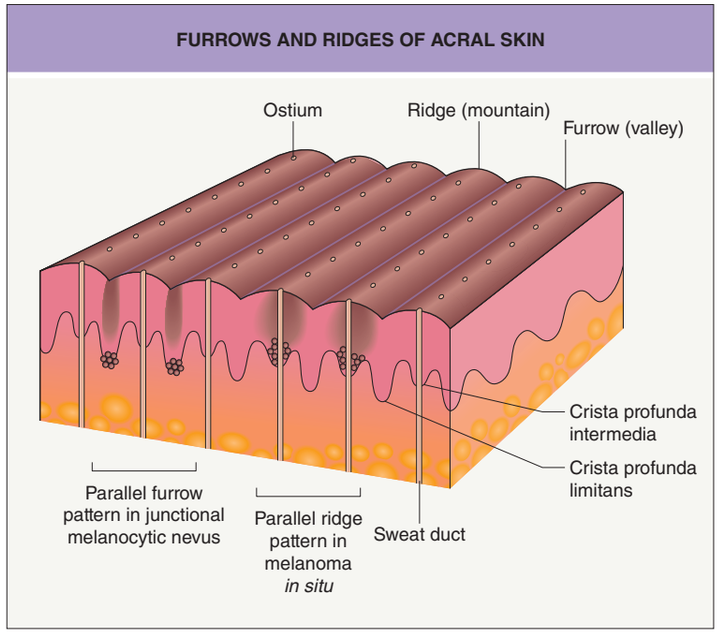


Fig. 112.14 Furrows and ridges of acral skin.

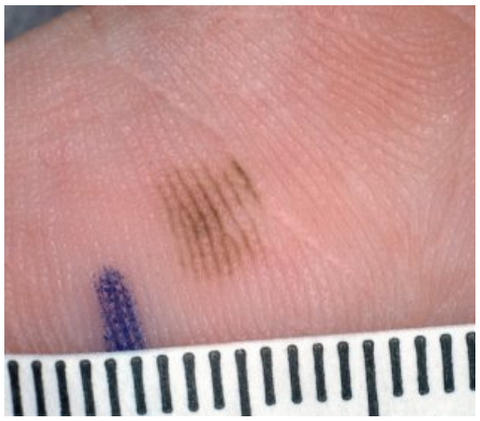


Fig. 112.15 Acral melanocytic nevus. The parallel furrow pattern is evident with a small focus of the lattice pattern. The ostia of the eccrine ducts within the epidermal ridges can also be seen, especially at the site of blue ink. *Courtesy Jean L. Bolognia, MD.*

ACRAL NEVI – COMMON DERMOSCOPIC PATTERNS	
Pattern	**Dermoscopy features**
Parallel furrow (most common)	Parallel rows of linear pigmentation along furrows/valleys (sulci of the surface skin markings; see Fig. 112.14 & 112.15)
Lattice-like	Parallel furrows plus lines of pigmentation crossing the parallel lines (see Fig. P4)
Fibrillar	Densely packed, fine parallel lines of pigmentation, often set in a direction that crosses the skin markings

Table 112.6 Acral nevi – common dermoscopic patterns.

proliferation and some degree of upward migration of melanocytes are features commonly observed in acral nevi. One should be cautious in over-interpreting the latter changes unless prominent architectural disorder and cytologic atypia are also present. The dermal component of acral nevi is often characterized by round nests of melanocytes[33].

SPITZ NEVUS AND ATYPICAL SPITZ TUMOR

Synonyms for Spitz nevus: ■ Epithelioid cell nevus ■ Spindle cell nevus ■ Spindle and epithelioid cell nevus ■ Spitz's juvenile melanoma ■ Benign juvenile melanoma

Key features

- Pink, red, or pigmented papule or nodule, usually in children or young adults
- Composed of epithelioid and/or spindled melanocytes with a regular architecture
- Often harbor tyrosine kinase fusions (e.g. involving *ALK*, *ROS1*, *NTRK1/2/3*, *BRAF*) or activating *HRAS* mutations

Epidemiology

The prevalence of Spitz nevus in the general population has not been accurately documented[34]. However, of the melanocytic lesions that have been surgically excised, ~1% exhibit the histologic characteristics of Spitz nevus. In data from Australia, it has been estimated that Spitz nevus accounts for 1.4 cases per 100 000 population, as compared with an annual incidence of 25.4 melanomas per 100 000 population. The vast majority of Spitz nevi are acquired, with congenital Spitz nevi being exceedingly rare. Spitz nevi occur in all age groups, but are uncommon beyond 40 to 50 years of age. In one series, 36% of the individuals with Spitz nevi were under the age of 10 years, 33% were between the ages of 10 and 20 years, and 31% were older than 20 years of age[34]. There is no sex predilection and Spitz nevi occur in all skin phototypes.

Pathogenesis

Spitz nevi are clonal proliferations of melanocytes, and most Spitz nevi are caused by structural genomic rearrangements that lead to gene fusions, activating either receptor tyrosine kinases (*ROS1*, *ALK*, *NTRK1/2/3*, *MET*, *MERTK*, *RET*) or kinases in the MAPK pathway (*BRAF*, *RAF1*, *MAP3K8*) (see Table 112.3). These kinase fusions can then activate various oncogenic pathways, including the MAPK signaling pathway. In addition, a subset of Spitz nevi harbors activating mutations in *HRAS* that are often accompanied by copy number gains of the mutant *HRAS* allele[35].

Widespread eruptive Spitz nevi have been associated with HIV infection, Addison disease, chemotherapy, pregnancy, puberty, and trauma, many of the same triggers as for common acquired nevi (see Table 112.5). The eruption of Spitz nevi during pregnancy and puberty suggests a possible role for hormonal activation.

Clinical Features

Spitz nevi vary in size from 2 mm to >10 mm, with an average diameter of ~8 mm[34]. Typically, they are well-circumscribed, dome-shaped papules or nodules that vary in color from pink to tan to dark brown or black (Fig. 112.16). Generally, the color is homogeneous and the margins are well defined. The surface topography may be smooth or, in some instances, verrucous. Relatively flat, polypoid, and pedunculated morphologies have also been described. Occasional lesions may have erosions and scale-crust while others may be firm due to sclerosis and resemble dermatofibromas (i.e. desmoplastic)[36]. Telangiectasia is a frequent finding. While Spitz nevi may develop anywhere on the body, they are frequently observed on the lower extremities as well as in the head and neck region, particularly in children. In most instances, there is a history of recent onset, but a small percentage of Spitz nevi have been present for many years.

Multiple Spitz nevi may occur in an agminated (grouped) or disseminated pattern[37]. *Disseminated Spitz nevi* can number in the hundreds, erupt suddenly, and involve the entire integument except for the palms, soles, and mucous membranes. The papules tend to be polymorphous, affect adults, and spontaneously regress over several years. To date, no case reports of malignant degeneration of grouped or disseminated Spitz nevi have been published, although disseminated Spitz nevi have been associated with seizures.

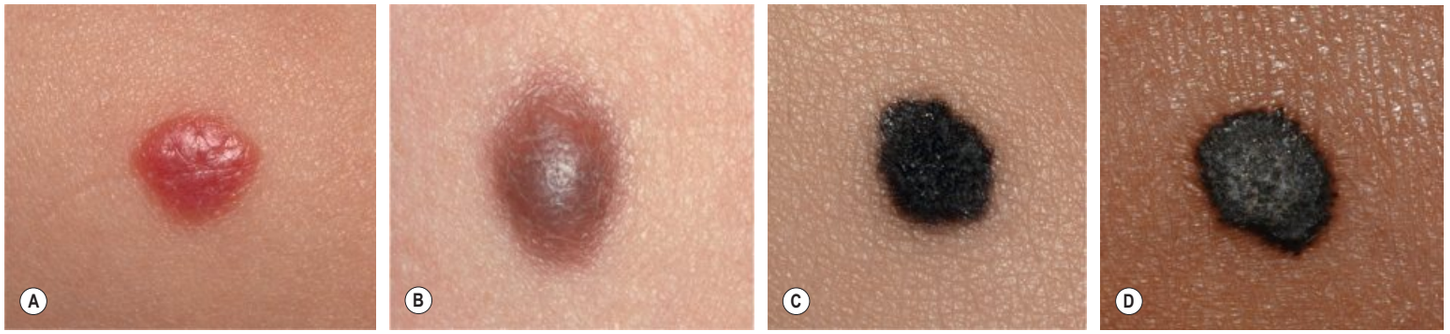


Fig. 112.16 Spitz nevi. A Red, symmetric, dome-shaped papule on the thigh of a child. **B** Medium-brown, symmetric, dome-shaped papule with a thinner rim in an adolescent. **C** Darkly pigmented Spitz nevus in a child with a flatter surface. **D** Sometimes there is a verrucous surface. *A, C, D, Courtesy Julie V. Schaffer, MD; B, Courtesy Lorenzo Cerroni, MD.*



Fig. 112.17 Agminated Spitz nevi. The grouped papules have arisen on normally pigmented skin.

Agminated (grouped) Spitz nevi are characterized by varying numbers of individual, raised nevi occurring in a localized or segmental distribution and arising in otherwise clinically normal skin (Fig. 112.17). Some confusion has arisen in the literature as lesions arising within a CALM-like tan background have been referred to as agminated Spitz nevi; however, these lesions would be better termed Spitz nevi within a nevus spilus (speckled lentiginous nevus). Spindle and epithelioid cell proliferations can also develop within large/giant congenital nevi.

Atypical Spitz tumor (Spitz melanocytoma) refers to a melanocytic neoplasm that morphologically and genetically lies between Spitz nevus and Spitz melanoma. Atypical Spitz tumors have one or more atypical features that deviate from conventional Spitz nevi[38]; these include: large size (>5–10 mm in diameter); asymmetry; deep involvement of the dermis or subcutis; ulceration; easily found dermal mitoses (>2–3 mitoses/mm^2), especially deep; significant pagetoid spread; prominent confluence and high cellular density of melanocytes in the dermis; and lack of maturation. Genetically, atypical Spitz tumors harbor the same genetic alterations as Spitz nevi (i.e. kinase fusions) and additional genomic aberrations such as inactivation of the tumor suppressor gene *CDKN2A*.

Spitz melanoma are rare lesions and the diagnosis is best established by integrating clinical, histologic, and molecular criteria (see Ch. 113)[39]. Compared to atypical Spitz tumors, Spitz melanomas exhibit even greater asymmetry, poor circumscription, and higher degrees of nuclear atypia with numerous mitoses.

Pathology

Spitz nevi are usually symmetric, sharply circumscribed, and composed of large epithelioid and/or spindled melanocytes. The melanocytes usually extend from the epidermis into the reticular dermis in an inverted-wedge configuration. The closely apposed nests of cells within a uniformly hyperplastic epidermis often contribute to a so-called "raining-down" appearance (Fig. 112.18). Both mononuclear and multinucleated giant epithelioid cells are frequently observed. These cells extend into the dermis as nests, fascicles, or single cells. In general, there is orderly infiltration of the dermal collagen by melanocytic complexes with so-called maturation, i.e. gradual diminution of nuclear and cellular sizes as well as the size of nests.

The individual cells usually have abundant cytoplasm that stains slightly bluish or pink and nuclei with open chromatin patterns. Rather uniform nucleoli are usually also noted. Intraepidermal eosinophilic globules (Kamino bodies) are commonly found in Spitz nevi, but may occasionally be encountered in other melanocytic tumors including cutaneous melanoma. Kamino bodies represent altered components of the basement membrane, including collagen types IV and VII.

In Spitz nevi, some histopathologic patterns are associated with particular genetic features. For example, a plexiform pattern typically corresponds to the molecular presence of *ALK* fusions and to positivity for ALK by immunohistochemistry[40].

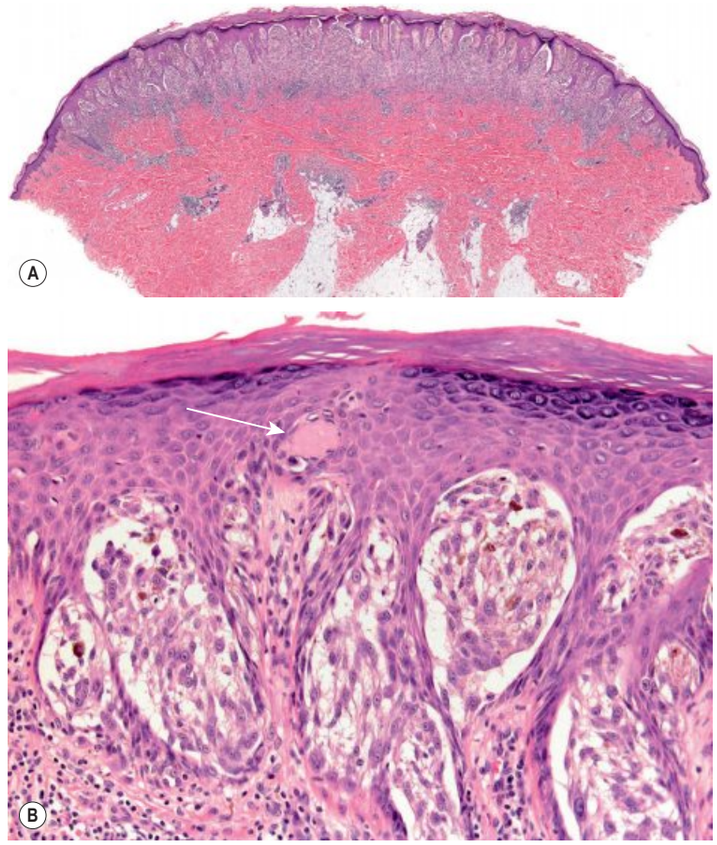


Fig. 112.18 Spitz nevus – histopathologic features. A Dome-shaped with sharply demarcated and symmetric proliferation of spindled and epithelioid melanocytes at the dermal–epidermal junction and within the papillary dermis; there is also regular epidermal hyperplasia. **B** Nests of cohesive spindled and epithelioid melanocytes with clefts between the nests and the hyperplastic epidermis. Note a "Kamino body" (arrow). *Courtesy Lorenzo Cerroni, MD.*

Differential Diagnosis

The clinical differential diagnosis of Spitz nevi is wide and includes other melanocytic nevi, particularly intradermal nevi, hemangiomas, pyogenic granulomas, verrucae, mollusca contagiosa, juvenile and adult xanthogranulomas, dermatofibromas, mastocytomas, and adnexal tumors. The fundamental diagnostic problem is the histologic differentiation of Spitz nevus from cutaneous melanoma, which is one of the most difficult problems in pathology. A number of clinical and histopathologic parameters are summarized in Table 112.7. Spitz nevi are differentiated from BAP1-inactivated melanocytic tumors by immunohistochemical positivity for BAP1 (see below).

Treatment

Because of the frequent diagnostic difficulty in classifying these lesions, histologic evaluation of the entire lesion is recommended. Recurrence rates from 5% to 15% have been observed when lesions are incompletely excised. Some authors recommend complete excision with tumor-free margins for all Spitz nevi, whereas others reserve this recommendation for lesions with atypical features (clinically or histologically) or for Spitz nevi in adults. For highly atypical or histologically ambiguous variants, a margin of ~1 cm is recommended. It is also advisable that patients with atypical lesions have periodic evaluations every 6 to 12 months. Sentinel lymph node biopsy, although controversial, may be considered on a case-by-case basis for clearly atypical lesions with a Breslow depth ≥1 mm. However, there is mounting evidence that sentinel lymph node involvement by Spitz tumors is not necessarily analogous to conventional metastatic melanoma[38], as almost all of the cases studied to date have not shown progression of disease beyond the sentinel lymph nodes.

Whole-genome sequencing followed by targeted therapy has also been employed. In a patient with unresectable "agminated" Spitz nevi and GOPC-ROS1 fusion, the oral tyrosine kinase inhibitor crizotinib led to improvement.

COMPARISON OF SPITZ NEVUS AND MELANOMA		
Parameter	**Spitz nevus**	**Melanoma**
Clinical features		
Age	Young age, especially prepubertal, favors a benign process	Exceedingly rare in pre-pubertal children; outnumber Spitz nevi in patients >30 years of age
Anatomic site	May occur anywhere, but favors the lower extremities and particularly in children the head and neck region	Most often on the trunk (back) in men and distal lower extremities in women; favors intermittently sun-exposed skin, but may occur anywhere
Size	Often <5–6 mm, usually <10 mm	Often >6 mm, but early lesions may be smaller; large size favors melanoma
Symmetry	Usually symmetric	Increasing asymmetry favors melanoma
Histopathologic features		
Architecture	Dome-shaped, plaque-like, wedge-shaped in dermis, plexiform	Heterogeneous and complex (with exceptions)
Circumscription	Usually well demarcated with peripheral junctional nests	Often poorly demarcated ending in single-cell patterns
Epidermal features	Regular hyperplasia; intraepidermal eosinophilic globules common, numerous, and large-sized	Irregular epidermal pattern; intraepidermal eosinophilic globules uncommon, few in number, and small-sized
Maturation	Overall reduction in cellular density with depth; orderly dispersion and regular spacing of nests and cells among collagen bundles with depth; nests become progressively smaller, finally resulting in single melanocytes at the base of lesion; cells and nuclei also diminish in size with depth; maturation may be absent in a subset of Spitz nevi	Little or no maturation; confluence of melanocytes is not lost with depth; irregular spacing and disorderly arrangements of cells
Pagetoid spread	Less frequent than in melanoma; orderly; often confined to the epidermis over the central part of the lesion; nested patterns may be more frequent than single cells	Common; disorderly; the melanoma cells often reach the granular layer; higher cellular density
Zonation	Uniformity of cytologic features across horizontal strata of lesion	Heterogeneity of features
Mitotic figures in dermal component	Limited in number, superficial, usually not atypical	Greater in number, deeply located, atypical
Cytologic features	Abundant ground-glass or opaque cytoplasm; polyangular, rhomboidal; occasional dendrites	Variable amount of cytoplasm; often granular or "dusty" and abundant in epithelioid cells; scant cytoplasm in spindled cells
Nuclear features	Enlarged nuclei; uniform dispersed chromatin pattern; nucleoli may be prominent but usually uniform; reniform, multilobulated, multinucleate and giant bizarre forms occur	Pleomorphism; often high nuclear to cytoplasmic ratios; hyperchromatism; prominent variable nucleoli commonly multiple; thickened nuclear membranes
Genetic features		
	Translocations (fusions) of receptor tyrosine kinases (*ROS1*, *ALK*, *NTRK1/2/3*, *MET*, *MERTK*, *RET*) or kinases of the MAPK pathway (*BRAF*, *RAF1*, *MAP3K8*) *HRAS* activating mutations (often seen in desmoplastic Spitz tumors)	Oncogenic mutations in *BRAF* (~ 35%–50%), *NRAS* (~10%–25%), *NF1* (~10%) *TERT* promoter mutations Inactivation of *CDKN2A*, *PTEN*, *TP53*

Table 112.7 Comparison of Spitz nevus and melanoma.

PIGMENTED SPINDLE CELL NEVUS

Synonyms: ■ Pigmented spindle cell tumor of Reed ■ Pigmented variant of Spitz nevus

Key features

- Dark brown to black thin papule, usually <6 mm in diameter
- A spindle cell variant of Spitz nevus with heavily pigmented spindle-shaped melanocytes in the epidermis ± the superficial dermis

Epidemiology and Pathogenesis

Pigmented spindle cell nevi are classified by some authors as a subtype of Spitz nevi and in this case account for <20% of Spitz nevi[41]. A few have been noted at birth; however, the mean age at diagnosis is 25 years (the age range in one series was 3 to 66 years). Women are affected more often than men. Pigmented spindle cell nevi are most commonly located on the extremities (70% of cases in one study), with the thigh being the most frequent site. About 20% of pigmented spindle cell nevi are found on the trunk, and ~10% occur in the head and neck region.

Pigmented spindle cell nevi are initiated by activating kinase fusions, most commonly involving *NTRK3* which encodes neurotrophic receptor tyrosine kinase 3. In one study, genomic fusions involving *NTRK3* were found in 80% of cases; other less common fusions involved *MERTK*, *ROS1*, and *RET*[42].

Clinical Features

The pigmented spindle cell nevus is usually a relatively flat or slightly raised, well-circumscribed lesion with an average diameter of 3 mm (range 1.5 to 10 mm). The color is usually dark brown or black and homogeneous. The most common dermoscopic patterns include the following: a dark structureless area almost to the periphery of the lesion, a central dark structureless area with symmetric pseudopods or radial streaming (starburst pattern), and/or a peripheral globular pattern (see Fig. 0.37). Irregularity of pigmentation is rare but may be found in atypical variants of pigmented spindle cell nevi. There is often a history of recent development or change. In one study, lesions had been present on average for about 6 months, although some were of longstanding duration.

Congenital forms of pigmented spindle cell nevi, although unusual, have been recognized. The occurrence of atypical varieties of pigmented spindle cell nevi and the presence of remnants of pigmented spindle cell nevi in association with cutaneous melanoma are circumstantial evidence that pigmented spindle cell nevi can undergo rare

transformation to cutaneous melanoma. In a long-term (mean 8.8 years) follow-up of 15 patients with excised pigmented spindle cell nevi, there was no evidence of recurrence. In our experience, these lesions have almost never recurred. Thus, unless a lesion has been incompletely excised, recurrence strongly suggests an atypical process, possibly cutaneous melanoma.

Pathology

Pigmented spindle cell nevi display a well-circumscribed and orderly appearance (Fig. 112.19). Lesions are usually only slightly raised with nevus cells confined to the epidermis, although they may involve the papillary dermis. The lesion is well circumscribed and is typified by fascicles of uniform, slender spindle cells that are closely aggregated (Fig. 112.19, inset). The cells usually contain fine, granular melanin and their nuclei have delicate chromatin and small inconspicuous nucleoli. There may be clefting around the intraepidermal fascicles. Numerous melanophages are usually present in the papillary dermis. Upward migration of nevus cells throughout the epidermis is sometimes noted, but usually these cells are confined to the lower half of the epidermis. Atypical variants exhibit prominent single-cell hyperplasia extending peripherally along the basal layer of the epidermis and in a pagetoid pattern throughout the epidermis. Cytologic atypia may also be present to a varying degree in these atypical variants.

Differential Diagnosis

The clinical differential diagnosis of pigmented spindle cell nevi includes early melanoma, atypical nevus, blue nevus, angiokeratoma, and pigmented basal cell carcinoma. In general, the borders of pigmented spindle cell nevi are regular and well-defined. The color is also homogeneous in most instances. However, atypical forms of pigmented spindle cell nevi may have irregular borders and variation in color. Although spindle cell nevi have a characteristic dermoscopic pattern, histopathologic examination is required for diagnosis. It must be emphasized, however, that the clinicopathologic presentation of typical pigmented spindle cell nevi is distinctive. Its history is that of a recently developed or changing, small, well-circumscribed, black lesion on the thigh of a young woman (usually in her 20 s). These lesions are often conspicuous because of the dearth of pigmented lesions elsewhere on the body.

Treatment

The proper treatment of pigmented spindle cell nevi is complete excision with clear margins. The reason for this recommendation is to prevent recurrence, since the pathology of recurring lesions may be alarming and difficult to distinguish from melanoma. For pigmented spindle cell nevi with atypical features, wider surgical margins are advised. For example, we advocate resection margins of 5 to 10 mm for markedly atypical forms of pigmented spindle cell nevus because histopathologic distinction from melanoma may be exceedingly difficult. Periodic follow-up, i.e. every 6 to 12 months, is also strongly advised for patients with atypical variants of pigmented spindle cell nevus.

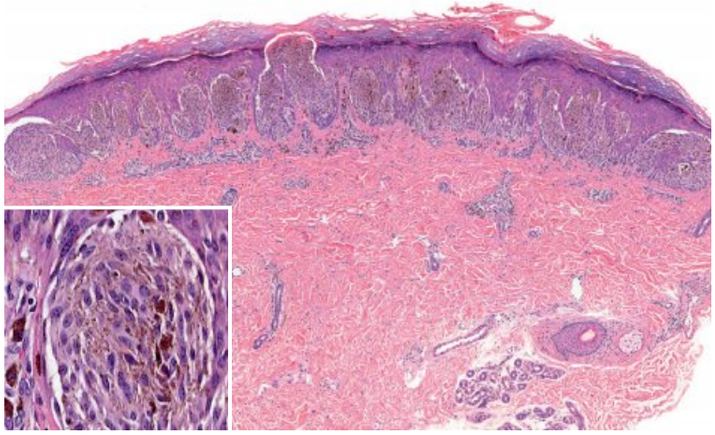


Fig. 112.19 Pigmented spindle cell nevus – histopathologic features. A predominantly junctional melanocytic proliferation that is characterized by well-defined margins, symmetry, and an overall plate-like configuration. Several nests have a vertical configuration and some may show "perforation" of the epidermis. Inset: the melanocytes are spindle-shaped and heavily pigmented. *Courtesy Lorenzo Cerroni, MD.*

WNT-ACTIVATED DEEP PENETRATING/ PLEXIFORM NEVUS

Synonyms: ■ Deep penetrating nevus/melanocytoma ■ Plexiform spindle cell nevus/melanocytoma

Key features

- Well-circumscribed, symmetric, darkly pigmented papule measuring 5–10 mm in diameter
- Due to concomitant activation of the WNT signaling pathway (typically due to a *CTNNB1* mutation) and the MAPK pathway (typically due to a *BRAF* mutation)
- Histologically characterized by spindled and/or epithelioid melanocytes extending into the deep reticular dermis and arranged in a wedge-shaped or plexiform pattern

Epidemiology and Pathogenesis

WNT-activated deep penetrating/plexiform nevi are rare tumors that occur in all age groups, with a mean age of 30 years and a slight predominance in women[43]. Most lesions arise from common acquired nevi due to an additional mutation that activates the WNT signaling pathway. In more than 90% of cases, these mutations affect a critical domain of *CTNNB1*, which encodes β-catenin. In rare cases, this pathway is activated by loss-of-function mutations in *APC*. The additional MAPK pathway activation is due to mutations in *BRAF* or rarely mutations in *MAP2K1* or *HRAS*, or *BRAF* fusions. WNT pathway activation leads to an increase in pigmentation, cell volume, and nuclear cyclin D1 levels, thereby altering the phenotype of a *BRAF*-mutated common acquired nevus into a WNT-activated deep penetrating/plexiform nevus[44].

Clinical Features

These nevi occur most commonly in the head and neck region, followed by the extremities and trunk. They are typically symmetric, well-circumscribed, darkly pigmented papules with a diameter that is <10 mm[45].

Pathology

WNT-activated deep penetrating/plexiform nevi are predominantly dermal melanocytic neoplasms. In most lesions, a junctional component and variably large areas of a conventional nevus are present, i.e. the histopathologic features of a "combined" nevus. Nests of enlarged epithelioid to spindle-shaped pigmented melanocytes are admixed with melanophages. The *deep penetrating subtype* is often wedge-shaped with bulbous extension into the deep reticular dermis or subcutis, with melanocytes extending along adnexal and neurovascular structures. In the *plexiform spindle cell subtype*, the melanocytes are located more superficially and are arranged in a fascicular-plexiform pattern. By immunohistochemistry, nuclear positivity for β-catenin or LEF1, which is also involved in WNT signaling, may help establish the diagnosis (cytoplasmic positivity is not specific)[45].

Differential Diagnosis

The clinical differential diagnosis includes melanoma and other types of melanocytic nevi, especially blue nevi, combined nevi, pigmented Spitz nevi, and pigmented epithelioid melanocytomas. However, the fundamental diagnostic issue is histologic differentiation from melanoma. Compared to melanomas, these nevi usually occur in younger patients, are smaller, have a regular, symmetric, and plexiform architecture,

and display monomorphous cells with low-grade atypia and a mitotic rate of ≤2 mitoses/mm[2,45]. True bona fide melanomas derived from a WNT-activated deep penetrating/plexiform melanocytoma appear to be extremely rare.

Treatment

These nevi usually exhibit a benign clinical behavior. However, atypical lesions may spread to regional lymph nodes and eventually have an unfavorable clinical outcome[43]. Consequently, some authors recommend complete excision, whereas others reserve this recommendation for lesions with clinically or histologically atypical features. In the case of partial biopsies, patient age, size of the lesion, and clinical and histopathologic features can be considered, but it is important to note that histopathologic differentiation from melanoma may be very difficult or even impossible when the entire lesion is not examined.

BAP1-INACTIVATED MELANOCYTIC NEVUS

Synonyms: ■ BAP1-inactivated melanocytic tumor ■ BAP1-inactivated melanocytoma ■ BAPoma ■ Melanocytic BAP1-mutated atypical intradermal tumor (MBAIT) ■ Wiesner nevus

Key features

- Skin-colored to reddish-brown, dome-shaped, 5–10 mm papule
- Caused by a bi-allelic inactivation of the *BAP1* tumor suppressor gene, usually in combination with a *BRAF* mutation
- Histologically characterized by an epithelioid cell morphology

Epidemiology and Pathogenesis

BAP1-inactivated melanocytic nevi are rare tumors, but their exact prevalence is unknown. They can occur sporadically or in association with the *BAP1* tumor predisposition syndrome (BAP1-TPDS), which is a rare autosomal dominant tumor syndrome due to germline *BAP1* mutations[46].

These nevi usually arise from a bi-allelic inactivation of *BAP1* in a conventional nevus, which usually has a *BRAF* mutation, or less commonly a *NRAS* mutation or *RAF1* fusion. The *BAP1* inactivation results in an epithelioid cell morphology of the clonally expanding melanocytes[47]. In sporadic tumors, bi-allelic *BAP1* inactivation often occurs through a loss-of-function mutation in one *BAP1* allele and a chromosomal deletion in the remaining wild-type *BAP1* allele. In patients with BAP1-TPDS, bi-allelic BAP1 loss is due to inactivation of the remaining wild-type *BAP1* allele.

Clinical Features

BAP1-inactivated melanocytic nevi can occur anywhere on the skin, but are more commonly observed in chronically sun-exposed sites. They usually present as inconspicuous, skin-colored to reddish-brown, dome-shaped papules measuring 5–10 mm in diameter (Fig. 112.20). Some lesions have small brown areas at their periphery, representing remnants of a conventional nevus. By dermoscopy, they usually appear as: (1) structureless pink-to-tan lesions, sometimes with irregular eccentric dots/globules or peripheral vessels; (2) a network with raised structureless pink-to-tan areas; or (3) a globular pattern[48].

Solitary BAP1-inactivated melanocytic nevi occur sporadically and are usually not associated with an increased cancer risk. In contrast, multiple BAP1-inactivated melanocytic nevi are associated with the BAP1-TPDS. Genetic testing for *BAP1* germline mutations should be considered in patients with multiple such nevi or with a family history of BAP1-TPDS-associated cancers, most commonly uveal or cutaneous melanoma, mesothelioma, and renal cell carcinoma[46].

Pathology

BAP1-inactivated melanocytic nevi are predominantly intradermal melanocytic proliferations with occasional junctional involvement. The majority have remnants of an adjacent conventional nevus (e.g. small nevoid cells) plus larger epithelioid cells (Fig. 112.21A–C), i.e. features of a "combined" nevus. The minority have no remnants of a conventional nevus.



Fig. 112.20 BAP1-inactivated melanocytic nevus. Reddish-brown, elevated, slightly asymmetric papule on the upper arm.

The characteristic cells are large, epithelioid melanocytes with well-defined cytoplasmic borders, large amounts of eosinophilic cytoplasm, and vesicular nuclei with prominent nucleoli. The BAP1-inactivated melanocytes reside within the dermis and are typically not pigmented. They can show varying degrees of nuclear size, including nuclear pleomorphism with dispersed chromatin patterns and prominent nucleoli. The mitotic activity is low, and tumor-infiltrating lymphocytes are frequently present.

In the epithelioid cells, bi-allelic *BAP1* inactivation typically leads to complete loss of nuclear BAP1 expression by immunohistochemistry, and this is a good surrogate for demonstration of *BAP1* inactivation at a molecular level. In combined cases, BAP1 immunoreactivity is retained within the nevoid compartment (Fig. 112.21D)[49].

Differential Diagnosis

The differential diagnosis includes intradermal nevi, neurofibromas, and fibroepithelial polyps. However, the notable diagnostic issue is the histologic differentiation from spitzoid lesions and melanoma. In some cases with spitzoid cytomorphology, BAP1-inactivated melanocytic nevi may resemble a Spitz nevus; however, Kamino bodies are absent and typically there is a lack of the wedge-shaped silhouette of Spitz nevi as well as lack of expression of BAP1. Combined BAP1-inactivated melanocytic nevi may be confused with melanoma arising in a nevus. Helpful clues are recognition of the typical epithelioid melanocytes and loss of BAP1 expression by immunohistochemistry in the absence of malignant features. However, because BAP1-inactivated melanoma, sometimes in association with a pre-existing melanocytic nevus, may occasionally be observed, BAP1 inactivation *per se* is not a criterion for benignity.

Treatment

BAP1-inactivated melanocytic nevi typically have an indolent clinical course[50]. However, the increased incidence of BAP1-inactivated cutaneous melanomas in patients with multiple BAP1-inactivated melanocytic nevi indicates an increased risk of progression to melanoma. In the setting of a partial biopsy, histopathologic features, patient age, and size of the residual lesion should be considered when making recommendations regarding re-excision.

Cancer screening criteria for uveal and cutaneous melanoma, mesothelioma, renal cell carcinoma, and cholangiocarcinoma have been proposed for carriers of *BAP1* germline pathogenic variants. Of note, BAP1-inactivated melanocytic nevi often precede the onset of other tumors[46].

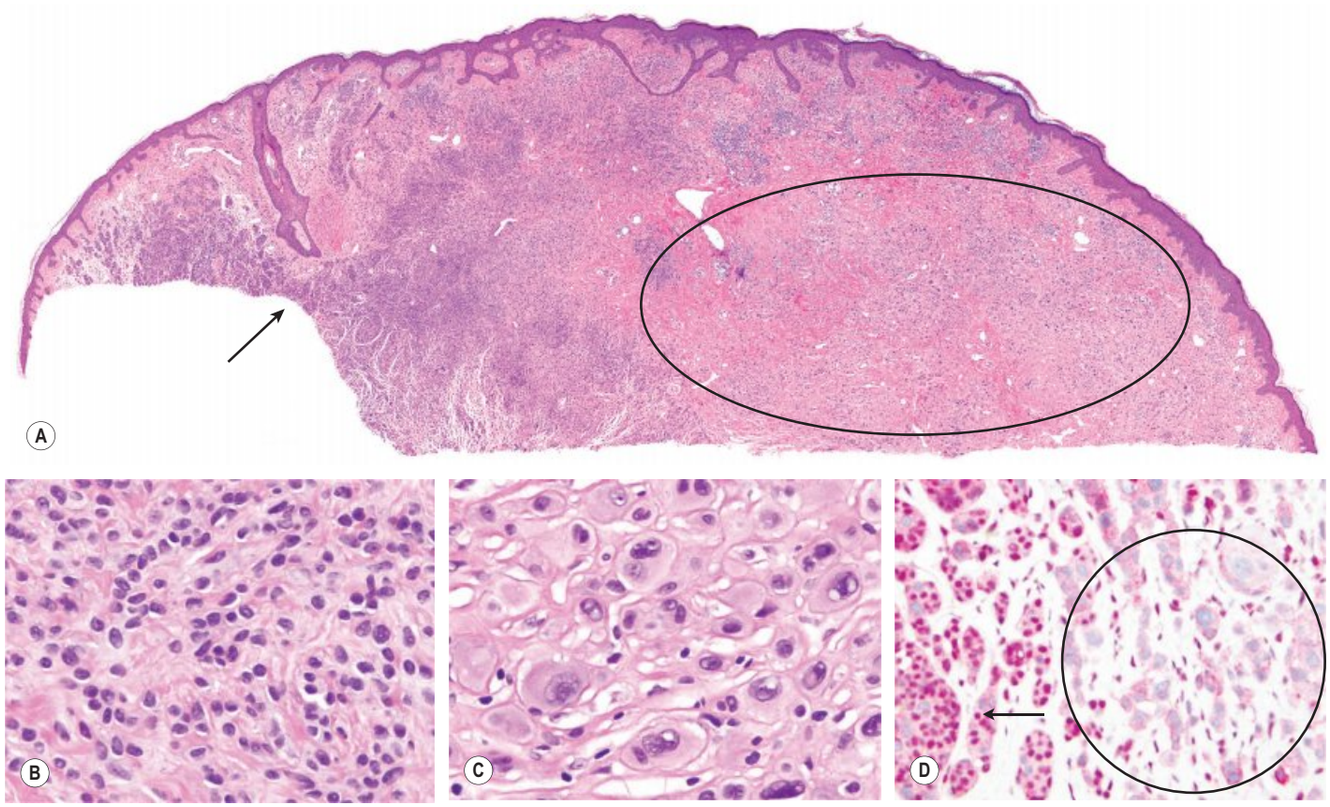


Fig. 112.21 Combined BAP1-inactivated melanocytic nevus. A The conventional nevus (left; arrow) consists of small oval melanocytes, whereas the BAP1-inactivated nevus (right; oval) consists of large, nonpigmented epithelioid melanocytes. **B** Higher magnification of the small oval melanocytes of the conventional nevus. **C** Higher magnification of the large, non-pigmented epithelioid melanocytes with large pleomorphic nuclei, vesicular chromatin, abundant cytoplasm, distinct cell borders, and a sparse infiltrate of lymphocytes. **D** BAP1 immunohistochemistry shows nuclear immunoreactivity in the conventional nevus component (left; arrow) and loss of nuclear immunoreactivity in the BAP1-inactivated component (right; circle).

ATYPICAL (DYSPLASTIC) MELANOCYTIC NEVUS

Synonyms: ■ Nevus with architectural disorder and cytologic atypia ■ Atypical nevus ■ Clark's nevus ■ Atypical mole ■ "Dysplastic" melanocytic nevus ■ B-K mole ■ The mole of FAMM (familial atypical mole and melanoma) syndrome

Key features

- A controversial clinical term for nevi that have atypical morphologic features such as asymmetry, irregular borders, and color variation
- Also a controversial pathologic term used for nevi with atypical architectural features and cytologic atypia
- The diagnostic threshold for melanoma versus atypical nevus remains a gray area due to a lack of consensus concerning precise differentiating criteria

History

Since the description of atypical or "dysplastic" melanocytic nevi in melanoma-prone families more than 40 years ago, and subsequently in individuals outside such kindreds, these lesions have remained a controversial topic[51–53]. The controversy arose primarily because no consensus could be reached regarding the nature of these lesions and it was not possible to formulate precise, commonly accepted diagnostic criteria. This relates both to criteria for individual lesions (what are the essential morphologic criteria required for diagnosis?) and for the so-called "dysplastic nevus syndrome" (how many clinically atypical melanocytic nevi are needed?). A particular problem, dating back to the original studies of atypical ("dysplastic") melanocytic nevi in hereditary kindreds, has been the tendency to consider the histopathologic diagnosis of atypical melanocytic nevi as the gold standard. However, it has been shown that the histopathologic criteria ascribed to atypical melanocytic nevi lack specificity and the correlation between *clinically* atypical melanocytic nevi and *histopathologically* atypical melanocytic nevi is poor. Thus, the term atypical melanocytic nevus does not describe a distinct clinicopathologic entity, but rather encompasses a heterogeneous group of nevi including:

- nevi with atypical *clinical* features, which have been termed simply "atypical nevi"; in general, these atypical nevi can clinically simulate melanoma; this group of nevi includes not only atypical ("dysplastic") nevi, but also some congenital and combined melanocytic nevi, Spitz nevi, and pigmented spindle cell nevi
- nevi with abnormal *histopathologic* features
- nevi with *both* abnormal clinical and histopathologic features

Many studies have found that, irrespective of histology, melanoma risk correlates with both: (1) the number of ordinary nevi (e.g. >50 or >100; see Fig. 113.6); and (2) the presence and number of clinically atypical nevi, as defined by several features including size (e.g. >5, 6, or 10 mm), irregular or ill-defined borders, and variation in color (Tables 112.8 & 112.9; see Fig. 113.7)[54–58]. Despite the seemingly logical conclusion that *histopathologically* atypical nevi should be associated with an increased risk of melanoma, thus far relatively limited data have shown such a relationship[59]. Currently, the assessment of a patient's melanoma risk is based almost exclusively

MELANOCYTIC NEVUS PHENOTYPES		
	Common pattern	**Atypical pattern**
Number	None to few (<25) nevi	Many (>50) nevi
Size	<5 mm	Variable: small to large, often several >5 mm
Color	Uniform, homogeneous color	Some to many melanocytic nevi with irregular or haphazard color, erythema within the nevus
Borders	Well circumscribed	Irregular or ill-defined borders

Table 112.8 Melanocytic nevus phenotypes.

MELANOMA RISK ASSOCIATED WITH CLINICALLY ATYPICAL MELANOCYTIC NEVI: COMPARISON OF OCCURRENCE IN MELANOMA PATIENTS VERSUS CONTROLS					
Study	**Country**	**Definition**	**Melanoma patients (%)**	**Controls (%)**	**Relative risk**
Roush et al. & Nordlund et al.	Australia	>5 mm, irregular border, and haphazard pigmentation	34	7	7.7
MacKie et al.	Scotland	>5 mm and either irregular pigmentation or inflammation	38	20	2.1–4.5*
Holly et al.	US	At least 3 of 6 criteria: ill-defined border, irregular border, irregular pigmentation, >5 mm, erythema, accentuated skin margins	55	17	3.8–6.3†
Halpern et al.	US	>4 mm, macular component, variegation of color, and irregular or indistinct border	39	7	8.8
Garbe et al.	Germany	At least 3 of 5 criteria: >5 mm, irregular margins, ill-defined border, color variation, macular and papular components	45	5	7

*Relative risk for one or two atypical nevi, 2.1; for three or more atypical nevi, 4.5.
†Relative risk for one to five atypical nevi, 3.8; for six or more atypical nevi, 6.3.

Table 112.9 Melanoma risk associated with clinically atypical melanocytic nevi: comparison of occurrence in melanoma patients versus controls[54–58]. A more recent study found statistically significant adjusted odds ratios of 2.57, 2.59, and 3.08 for multicomponent dermoscopic features, size >8mm, and anterior truncal location, respectively[58a].

on a total body skin examination that assesses the total number of nevi and number of atypical melanocytic nevi, plus risk factors, in particular a personal and/or family history of melanoma and degree of photodamage (see Ch. 113).

Epidemiology

Estimates of the incidence of atypical melanocytic nevi cover a wide range, as would be expected given the lack of consensus regarding definitions. Most estimates are in the 10% range for the general population but up to 40% in patients with melanoma. Atypical melanocytic nevi may be single or multiple. In the general population, atypical nevi may arise in a "sporadic" fashion, i.e. without a history of familial melanoma, versus in the context of a family history of atypical moles and/or melanoma. In both clinical settings, there is agreement that these nevi indicate some increase in melanoma risk.

Sporadic atypical melanocytic nevi may occur at any time, while persons with a family history of atypical melanocytic nevi and/or melanoma usually manifest their atypical lesions by the end of the second decade. In contrast to common acquired nevi that tend to appear in increasing numbers around puberty, atypical melanocytic nevi may appear, even in an eruptive fashion, as late as the sixth decade. Histologic contiguity of atypical melanocytic nevi to melanomas was frequently observed in several studies[60], but the development of melanoma in association with an individual atypical melanocytic nevus in the sporadic setting seems to be an uncommon event and not more frequent than the development of melanoma in other types of melanocytic nevi. One study estimated that the annual transformation rate of any single melanocytic nevus into melanoma ranged from ≤1 in 200 000 (≤0.0005%) to ≤1 in 33 000 (≤0.003%)[60a].

Pathogenesis

The pathogenesis of atypical nevi is not well understood. As in common acquired nevi, the driver mutation is frequently a *BRAF* V600E mutation, and less frequently an oncogenic *BRAF* non-V600E or *NRAS* mutation. In addition, mutations in the *TERT* promoter or loss of the tumor suppressor *CDKN2A* may be present. Atypical nevi appear to have a higher mutation rate than common acquired nevi or congenital melanocytic nevi, but a lower mutation rate than melanoma[53].

Clinical Features

Atypical nevi occupy an intermediate position on a continuum with common nevi at one end and cutaneous melanoma at the other end, and, as a result, they overlap with both. No single feature is diagnostic of atypical melanocytic nevi; rather, a constellation of clinical and dermoscopic findings is required for their recognition (Figs. 112.22 & see Fig. P9). Some authors recommend the following criteria: a macular component plus at least three of the following features: size >5 mm, color variegation, ill-defined border, uneven peripheral contour, and erythema[61]. By

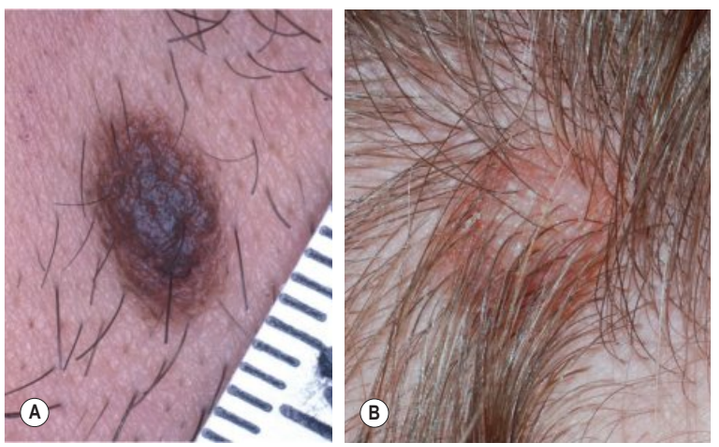


Fig. 112.22 Atypical melanocytic nevi. A Although this "fried egg" nevus is at least 7 mm in size, it is symmetric and does not need to be excised. **B** "Eclipse" nevi, characterized by a tan center and brown rim, are commonly found on the scalp of children who go on to develop numerous melanocytic nevi. The associated dermoscopic patterns are those seen in benign melanocytic nevi. *A, Courtesy Jean L. Bolognia, MD; B, Courtesy Julie V. Schaffer, MD.*

definition, these lesions have a flat component representing junctional proliferation, and there is often a central raised portion that represents a dermal component resulting in the resemblance to a "fried egg" or a "head with shoulders". The more clinical abnormalities present, the greater the likelihood that the lesion will prove to be histologically atypical.

The following gross morphologic features are commonly seen in atypical melanocytic nevi:

- *Asymmetry*: atypical melanocytic nevi often lack mirror-image symmetry.
- *Size*: atypical melanocytic nevi can be of any size, but generally range from 5 to 15 mm in diameter.
- *Borders*: atypical melanocytic nevi often have irregular and ill-defined borders, but not typically the notched or scalloped borders of melanoma.
- *Coloration*: atypical melanocytic nevi commonly have irregular pigmentation with two or three shades of brown, e.g. tan, brown, and dark brown (Fig. 112.23A). They may also have pink, gray, brown–black, or skin-colored areas. However, some atypical melanocytic nevi present with fairly uniform coloration and an erythematous appearance.

Atypical melanocytic nevi appear most commonly on the trunk, especially the back, but are also found on the scalp. Their numbers may range from one or two to hundreds (Fig. 112.23B). When multiple large lesions are present, their prominence is noteworthy, and while there may be variability, patients often have a "signature" nevus, clinically and histologically. Localized patterns such as linear tracts, clusters, or figurate arrays may also be seen in patients with numerous nevi.





Fig. 112.23 Atypical melanocytic nevi. **A** There is asymmetry as well as several shades of brown, simulating the clinical features seen in cutaneous melanoma. **B** In addition to multiple atypical nevi, patients can have numerous banal nevi.

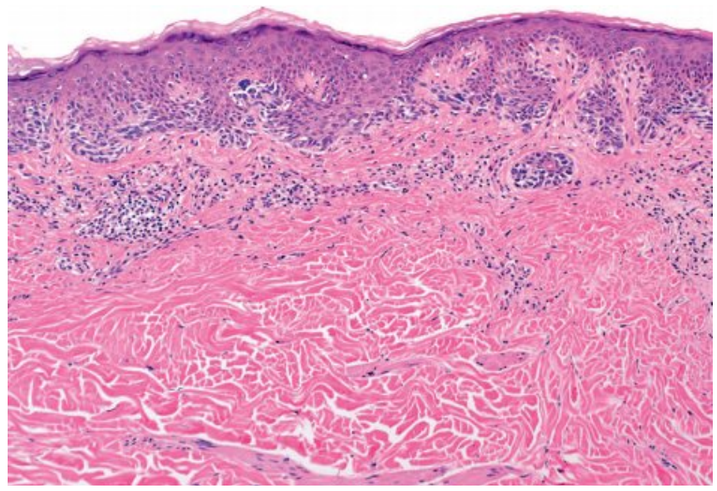


Fig. 112.24 Atypical melanocytic nevus – histopathologic features. Note confluent nests of melanocytes at the dermal–epidermal junction with so-called "bridging" of rete ridges (confluence of melanocytic nests parallel to the epidermis bringing together two or more rete ridges) as well as scattered solitary melanocytes in the lower portion of the epidermis. *Courtesy Lorenzo Cerroni, MD.*

The overwhelming majority of atypical melanocytic nevi are clinically stable. However, there is evidence that some lesions eventuate in cutaneous melanoma. Progressive abnormalities in DNA content, cytogenetic alterations, and increased expression of melanocyte-associated antigens by immunohistochemistry have been correlated with progressive degrees of histologic atypia[60]. Although findings suggest a progression of atypical melanocytic nevi toward melanoma, atypical melanocytic nevi are not inevitable precursors to melanoma, and their presence can be viewed as a phenotypic marker of "an entire skin at risk".

Pathology

Prototypic atypical melanocytic nevi are characterized by several architectural features. Compared to ordinary nevi, these nevi are often larger (commonly >5 mm in diameter), poorly circumscribed, slightly asymmetric, relatively flat (especially at the periphery of the lesion), and often show heterogeneity. In atypical melanocytic nevi, the junctional component frequently extends beyond the dermal component (the "shoulder" phenomenon).

Of particular importance is architectural disorder of the intraepidermal component, which occurs in two patterns that are often present simultaneously to a varying degree (Fig. 112.24). The *first* is lentiginous melanocytic proliferation that is almost always associated with elongated epidermal rete ridges. In general, the basilar melanocytes are concentrated in the lowermost portions of the rete ridges, and the frequency of basilar melanocytes varies greatly, e.g. from one melanocyte per one to two keratinocytes to the melanocytes replacing the basilar keratinocytes and resulting in a confluent, clustered, or multilayered cellular appearance.

The *second* pattern consists of melanocytic nests that are irregularly disposed along and between the rete ridges, as compared to ordinary nevi. These nests vary in size and shape, are often elongated, commonly have their long axes oriented along the dermal–epidermal junction, and contain variable numbers of cells. Colliding nests of melanocytes frequently fuse or "bridge". Discohesion of cells within these nests is also common; this feature contrasts with the cohesive appearance of junctional nests of melanocytes in ordinary nevi. Atypical nevi often have a higher density of melanocytes in the intraepidermal component than do ordinary nevi.

Atypical melanocytic nevi often exhibit cytologic atypia. The latter is discontinuous and variable, from only a small percentage of melanocytes demonstrating nuclear atypia to most cells being atypical. Cytologic atypia often correlates with the degree of architectural abnormality. Pleomorphism of the nuclei (i.e. variation in size, shape, and staining properties) is the most characteristic attribute of the nuclear changes in atypical melanocytic nevi. However, nuclear enlargement and hyperchromatism also occur. The cells are frequently typified by a perinuclear clear space resulting from cytoplasmic shrinkage, which is an artifact of tissue processing. Criteria for grading the degree of cytologic atypia and even architectural abnormality have been proposed, but there is neither consensus regarding using a grading system nor how to define different grades of atypia.

The dermal component of atypical melanocytic nevi may be composed of typical nevus cells, as in any acquired nevus, or of cells that may exhibit atypia. In addition to the abnormal architectural disorder and cytologic atypia, atypical melanocytic nevi usually exhibit changes related to host response. Two forms of collagenous change occur in the papillary dermis and a mixture of the two patterns is not uncommon. The most common pattern, termed *concentric fibrosis*, is a condensation of collagen around the epidermal rete. A less common pattern, termed *lamellar fibroplasia*, consists of finely layered or laminated collagen beneath the rete tips with fibroblasts arranged in a linear array along the laminated collagen fibers. Both patterns can also be observed in melanoma. Lymphocytic infiltrates, usually distributed in a perivascular fashion and less commonly in a band-like pattern, are also frequently observed. Finally, atypical melanocytic nevi usually have prominent vascularity throughout the papillary dermis, which is due to dilation and hypertrophy of existing vascular channels, rather than angiogenesis.

Differential Diagnosis

The differential diagnosis of pigmented lesions with a similar size includes both melanocytic and keratinocytic lesions. Lichen planus-like keratoses, pigmented seborrheic keratoses, solar lentigines, pigmented actinic keratoses, pigmented Bowen disease, and basal cell carcinomas may exhibit pink, tan, brown, or dark brown colors. Among melanocytic proliferations, the principal diagnostic considerations are common acquired nevi, small congenital nevi, and cutaneous melanoma. The atypical melanocytic nevus is characterized by haphazard, irregular coloration, including hues of pink, tan, brown and even black, and irregularity in shape (features it shares with melanoma). The other non-melanoma lesions either show symmetry and/or uniformity of coloration or, when irregularly colored, show orderly gradations or patterns of pigmentation.

Dermoscopy plays an important role in the evaluation of atypical melanocytic nevi (Fig. P5). Although atypical melanocytic nevi can clinically resemble melanoma, many of these lesions fall into one of the benign dermoscopic melanocytic patterns (see Fig. P9). Features employed to evaluate a melanocytic nevus include colors, symmetry, and organization. Benign melanocytic lesions tend to have few colors and are symmetric with regard to the distribution of colors and structures. When these structures are symmetrically distributed and there are fewer than three colors (light brown, dark brown, and black) noted, they create a pattern seen in many benign lesions. The most common benign patterns are reticular, globular, and homogeneous (see Fig. 0.37). In addition, there are the subset patterns of reticular–homogeneous, reticular–globular, and globular–homogeneous (see Fig. P9)[62]. Finally, another subset of atypical melanocytic nevi is characterized by uncertain melanocytic dermoscopic patterns. Just as the clinical and histologic features of atypical melanocytic nevi are a continuum, so too are the features with dermoscopy. These lesions should either be excised or serially monitored.

The histopathological differential diagnosis of atypical (dysplastic) melanocytic nevi from melanoma may be very difficult and may be influenced by the threshold of a given dermatopathologist for the diagnosis of early melanoma. For example, some cases classified as "dysplastic nevus with severe architectural and morphologic atypia" in one center may be diagnosed as "melanoma *in situ*" by another. Immunohistochemical stains may be helpful, and strong positivity for PRAME (*pr*eferential expressed *a*ntigen of *me*lanoma) in the majority of neoplastic cells is a strong criterion for the histopathologic diagnosis of melanoma. In addition, atypical nevi located on chronic sun-damaged skin and/or the face should be judged with caution, as the likelihood of melanoma is significant in these settings.

Treatment

As within any area of medicine, the physician is first obliged to do no harm. Such an approach is particularly important in patients with atypical melanocytic nevi with avoidance of overly aggressive procedures, surgery, and follow-up. Common sense should prevail at all times and consideration should be given to whether the intervention has an impact on potentially reducing melanoma mortality. Treatment depends upon several factors including: (1) whether the patient presents with one or a few nevi versus numerous nevi; (2) whether the patient has a personal history of melanoma; and (3) whether there exists a familial setting of atypical melanocytic nevi and/or melanoma. The risk of melanoma is probably continuous and increases with the number of nevi, clinical atypia of nevi, and personal and familial occurrence of atypical nevi and melanoma.

Regardless of the risk group, any pigmented lesion suspicious for melanoma and any significantly changing lesion should, in the authors' opinion, be excised completely with free margins. Some authors have advocated "deep" shave excision (saucerization) for superficial lesions, which is acceptable as long as the lesion is removed entirely, including its base. As opposed to partial punch biopsy, which should be discouraged, the latter allows for assessment of the overall architecture of the lesion and leads to less sampling error.

A helpful rule of thumb in following patients with many atypical melanocytic nevi is to search for lesions that clearly stand out as different from the patient's other (baseline) nevi ("ugly duckling"); such lesions should be examined carefully. It should be kept in mind that new nevi will continue to develop and nevi may enlarge and change with time, especially in young individuals. One must use common sense in assessing this normal evolution of nevi and not be overly aggressive in removing such nevi. An acceptable practice is to follow such patients on a regular schedule with a total body skin examination plus dermoscopy, baseline photography, and/or digital dermoscopy, as preferred by the clinician. Computerized assessment and comparison of clinical photographs is increasingly being employed. The frequency of follow-up examinations is individualized and is based on the previously mentioned risk factors, i.e. numbers and clinical atypia of nevi, lesion stability, and personal and family history of melanoma.

For any melanocytic lesion, it is important to know if the lesion has been adequately sampled and if the lesion was considered to be clinically atypical. If lesions are "severely" atypical, re-excision is recommended because of frequent overlap with, and difficult distinction from, melanoma *in situ*. For atypical melanocytic nevi with lesser degrees of atypia, the answer regarding whether to re-excise is controversial. In general, if lesions are "mildly" atypical, no re-excision is recommended, as long as no significant residuum of the nevus is clinically apparent. If lesions are "moderately" atypical, the decision to re-excise is particularly difficult. Studies show that dermatologists tend to re-excise moderately atypical lesions if a biopsy margin is positive[63]. Despite this propensity for re-excision, available data do not necessarily support re-excision of moderately atypical nevi. Independent retrospective studies examining the utility of re-excision of moderately atypical nevi conclude that re-excision of these nevi rarely results in a change in diagnosis[64]. In a study of 1809 mildly and moderately atypical nevi, 765 were found to have positive margins and of these 495 underwent re-excision. Of the 495 re-excisions, only a single case resulted in a clinically significant change[65]. Therefore, the current data may not support a blanket recommendation to re-excise all moderately atypical nevi even if there are positive margins.

Unfortunately, the discussion of whether or not to re-excise dysplastic nevi is greatly confounded by the lack of a uniform grading system amongst pathologists. Often this leaves dermatologists erring on the side of caution when it comes to this clinical decision. Therefore, even when no residual lesion is clinically obvious, re-excision might be considered, depending upon a number of factors: the initial degree of concern clinically, the size of the nevus (versus the size of the biopsy), the color (more inclined with amelanotic lesions as assessing residuum is more difficult), the site (easy or difficult to visualize by the patient), the patient's ability and interest in following the site, and the patient's prior personal and family history of melanoma.

In general, follow-up of patients with multiple atypical nevi, especially in the context of a personal or family history of melanoma, should be every 3 to 12 months, depending on the clinical situation. One should consider documentation of nevi by body charts and clinical photography as judged appropriate, with periodic updating. Individual photographs of the most atypical or difficult-to-follow nevi are particularly helpful. Additional tools such as dermoscopy and/or digital imaging devices may be useful diagnostic aids. Finally, individuals presenting with atypical melanocytic nevi should have a family history taken for the presence of atypical melanocytic nevi and/or melanoma. First-degree blood relatives should be examined both for documentation and to assess and potentially diminish their own risks of developing melanoma.

CONGENITAL MELANOCYTIC NEVUS

Synonyms:

- Congenital nevomelanocytic nevus
- Large or giant congenital melanocytic nevus: • Bathing trunk nevus • Garment nevus

Key features

- Small congenital nevi are <1.5 cm in diameter (in adults)
- Medium-sized congenital nevi are between 1.5 and 20 cm in diameter (in adults)
- Large (>20 to 40 cm in adults) and giant congenital nevi (>40 cm in adults) have a higher risk for developing melanoma than do ordinary nevi
- Neurocutaneous melanosis may occur in patients with multiple medium-sized congenital nevi and those with large/giant congenital nevi, especially when in a posterior axial location and accompanied by satellite lesions

Introduction

Congenital melanocytic nevi are benign proliferations of melanocytes that are present at birth and may be intraepidermal, dermal, or both[66,67]. Lesions indistinguishable from congenital nevi may appear up to 2 years after birth and are therefore referred to as *tardive congenital nevus*. Finally, histopathologic features of congenital nevi may be observed in melanocytic tumors acquired during childhood or adolescence, with dermatopathologists often referring to them as melanocytic nevi with a congenital pattern.

Some congenital melanocytic nevi may be just a few millimeters in size and appear clinically indistinguishable from common acquired nevi. In general, congenital melanocytic nevi are classified as small (<1.5 cm), intermediate- or medium-sized (1.5 to 20 cm), large (>20 to 40 cm), and giant (>40 cm), based upon their size in adults[68]. Given the eventual size, a congenital nevus ≥9 cm on the scalp or ≥6 cm on the trunk in a newborn is assigned to the large/giant category; with extensive involvement (e.g. the entire trunk), assignment to the giant category is self-evident. Some authors base the distinction between small, intermediate, and large/giant congenital nevi on their ease of removal. In this scheme, small congenital nevi generally may be removed by simple excision, medium-sized nevi often require staged excisions for closure, and large/giant nevi often cannot be removed or require multiple staged excisions and/or tissue expanders for removal.

Patients with ≥3 small or medium-sized congenital melanocytic nevi or a giant congenital melanocytic nevus may have associated neurocutaneous melanosis (see below).

Epidemiology

The prevalence of congenital melanocytic nevi varies widely depending on the study, ranging from 0.5% to 30%[67], but in our experience occur in ~1% of newborns. Most lesions are 3 to 4 cm in diameter. Large/giant congenital nevi are rare, with an estimated incidence of 0.005% (1 in 20 000). Patients with large/giant nevi often have multiple smaller (satellite) nevi, with greater numbers correlating with an increased risk of neurocutaneous melanosis (see below). Familial aggregation of congenital nevi has occasionally been reported.

Pathogenesis

The majority of congenital melanocytic nevi have oncogenic *NRAS* mutations. *BRAF* mutations are detected in up to 7% of cases while *KRAS* mutations and kinase fusions are rare[69]. Individual melanocytes begin to appear in fetal skin before 40 days' gestation. Given the observation of congenital divided nevi of the eyelid and the fact that the eyelids open during the sixth month of gestation, it appears that congenital melanocytic nevi can develop prior to the sixth month of gestation. Patients with a large/giant congenital nevus and/or multiple satellite lesions should be thought of as having a systemic disease (Fig. 112.25), as nevus cells can be found in sites beyond the skin and central nervous system (CNS), such as the retroperitoneum.



Fig. 112.25 Congenital melanocytic nevi associated with neurocutaneous melanosis. A Multiple medium-sized nevi. The patient had 25–30 such lesions. This presentation is most commonly associated with neurocutaneous melanosis. **B** Giant congenital nevus in an axial location with numerous satellite nevi, some of which have hypertrichosis. This patient died of intractable ascites due to the migration of melanocytes from the brain to the peritoneal cavity via his VP shunt. In the perianal region, the nevus was softer and somewhat "spongy" due to neurotization. *Courtesy Jean L. Bolognia, MD.*

Clinical Features

Small and medium-sized congenital nevi are usually round or oval, fairly symmetric, slightly raised, and tan in color (Fig. P6). They may or may not have associated hypertrichosis (Fig. 112.26), and perifollicular hypo- or hyperpigmentation may be seen. Some congenital melanocytic nevi have rugose or pebbly surfaces (see Fig. 112.26A,B). Lesions that are initially minimally elevated often become thicker and darker in color and may develop a verrucous appearance.

After an initial darkening during the first year of life, some congenital melanocytic nevi may become lighter in color with aging, including satellite lesions. In addition, congenital nevi can develop the halo phenomenon (see below), and occasionally, congenital nevi completely regress, even without forming a halo. As hamartomas, congenital nevi can exhibit asymmetry and color variation, develop papules and nodules (e.g. proliferative nodules), and change over time (see Fig. 112.26); however, histologic examination of any concerning areas is recommended (Table 112.10). Areas within congenital nevi can also undergo neurotization and develop compressible, boggy plaques or nodules (Fig. 112.27).

The dermoscopic structures seen in congenital nevi include the following: globules, diffuse background pigmentation (structureless), milia-like cysts, hypertrichosis, hyphae-like structures, and perifollicular pigment changes. The most common dermoscopic patterns are reticular, globular, reticular–globular (see Fig. P6), diffuse brown pigmentation, and multicomponent. The multicomponent pattern is often difficult to distinguish from melanoma and requires either monitoring or biopsy.

Varying numbers of satellite lesions often accompany large/giant congenital melanocytic nevi (see Fig. 112.25B). Such lesions typically resemble small or medium-sized congenital melanocytic nevi. Of note, some patients present with multiple medium-sized congenital nevi in the absence of a large congenital nevus (see Fig. 112.25A), and these individuals are at greatest risk for neurocutaneous melanosis (up to 70% in one study).

Neurocutaneous melanosis (melanocytosis)

In neurocutaneous melanosis, there can be diffuse involvement of the leptomeninges that cover the brain and/or the spinal cord. In addition, intraparenchymal melanosis or solid tumors within the brain parenchyma may be observed. The melanocytes can be benign or malignant and can result in obstruction (with hydrocephalus) or a mass effect. In addition, a variety of intracranial and intraspinal anomalies (e.g. Dandy–Walker malformation, extensive arachnoid cysts) can be seen in association with neurocutaneous melanosis[66,67].

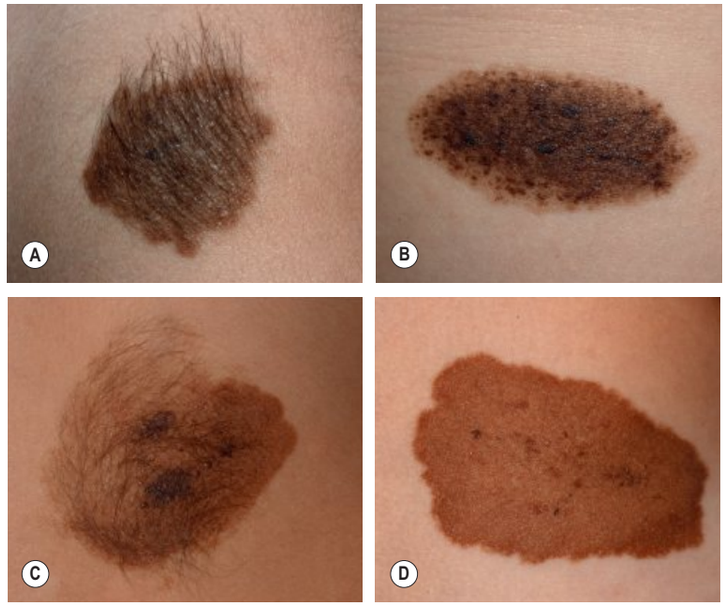


Fig. 112.26 Medium-sized congenital melanocytic nevi. A Hypertrichosis and slight heterogeneity in pigmentation. **B, C** More marked heterogeneity in pigmentation, topography, and hypertrichosis, reflecting the hamartomatous nature of congenital nevi. **D** Hyperpigmented papules of varying sizes and color. *Courtesy Julie V. Schaffer, MD.*

MANAGEMENT OF CHILDREN WITH GIANT CONGENITAL MELANOCYTIC NEVI
Surgical excision versus long-term clinical examination
• Consider surgical excision of the nevus (staged and/or with tissue expanders), typically in children at least 6 months of age in order to avoid the period of highest general anesthesia risk • If not excised or partial excision, lifelong examination of the nevus (including palpation) every 6 to 12 months plus baseline photography • Histologic examination of enlarging firm papulonodules and new areas of induration or ulceration*
MRI of head and spine for the detection of neurocutaneous melanosis† (NCM) and other CNS abnormalities‡

• Risk factors for NCM
  • multiple satellite lesions (≥20)¶
  • giant/"garment" nevus (>40 cm projected adult size)
  • posterior axial location (in some but not all studies)
• If no risk factors and no neurologic symptoms, MRI not necessary
• If at least one risk factor but asymptomatic, MRI should be considered prior to 4–6 months of age for highest sensitivity
• In asymptomatic patients with intermediate risk (e.g. <10–20 satellites, 20–40 cm nevus as an adult), MRI can be considered on a case-by-case basis
• Patients with symptomatic NCM should have MRI performed
• See Fig. 112.28 for recommendations regarding further evaluation

*Ulceration at birth or during the first week of life in areas prone to trauma may be due to immaturity of the skin but should heal over a few weeks. †Also referred to as neurocutaneous melanocytosis. ‡Need to check renal function given association with genitourinary malformations. ¶Highest risk of NCM in those with multiple satellite nevi but no giant congenital nevus. Some authors consider MRI if ≥3 congenital nevi whereas others do so if ≥2 congenital nevi (see Fig. 112.28)

Table 112.10 Management of children with giant congenital melanocytic nevi (GCMN). CNS, central nervous system; MRI, magnetic resonance imaging.

Based upon MRI screening of at-risk infants (Fig. 112.28), preferably done during the first 6 months of life, ~80% of infants have no abnormalities, ~15%–20% have intraparenchymal melanosis, and <10% have other abnormalities (e.g. diffuse leptomeningeal involvement, masses)[70]. This latter group has a poor prognosis with associated seizures and neurodevelopmental delay as well as the highest risk for developing CNS melanoma. However, MRI cannot always predict or exclude the possibility of future symptoms[66,67].



Fig. 112.27 Several areas of "neurotization" within a giant congenital nevus. The edges of the boggy plaques or nodules are demarcated by arrowheads. This phenomenon should not be confused with how cells of acquired nevi can display a neuroid differentiation within conventional intradermal nevi, sometimes characterized by Schwann cell-like features.

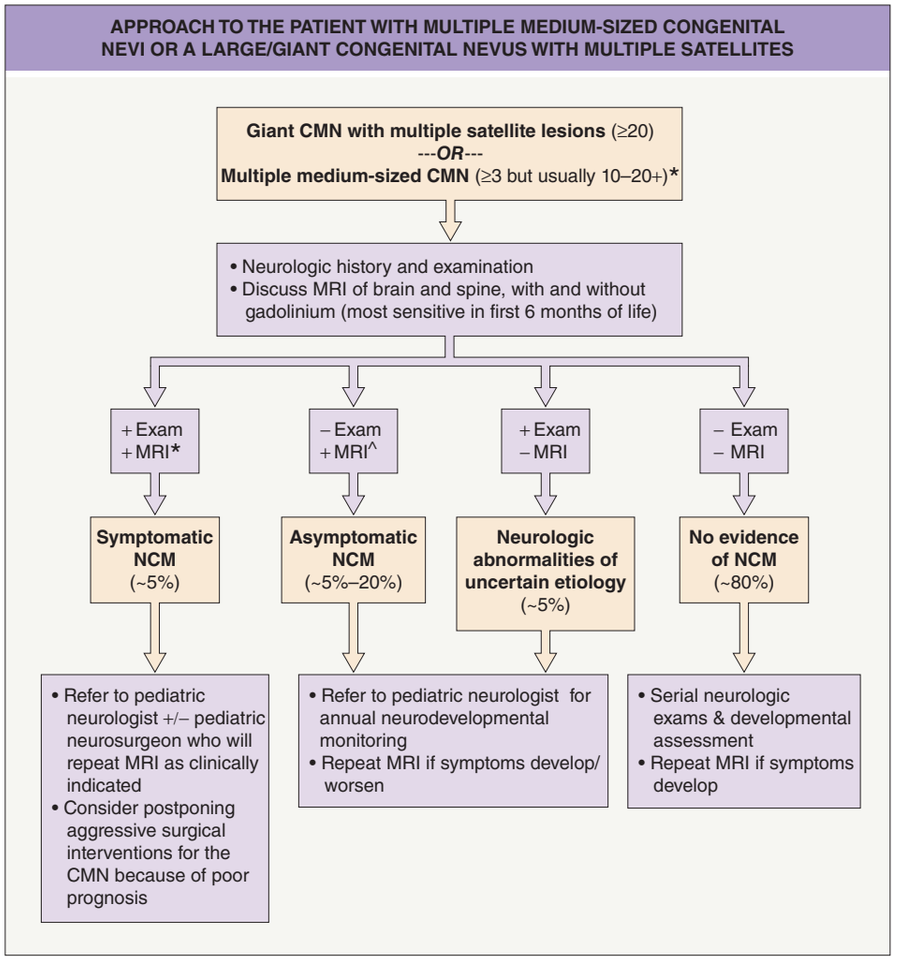


Fig. 112.28 Approach to the patient with multiple medium-sized congenital nevi or a large/giant congenital nevus with multiple satellites. *A relatively high percentage of these patients have NCM; some authors use the criterion of ≥2 CMN. **Diffuse leptomeningeal involvement and masses. ^Usually intraparenchymal melanosis. CMN, congenital melanocytic nevus; NCM, neurocutaneous melanosis.

As noted previously, neurocutaneous melanosis occurs primarily in patients with ≥3 small or medium-sized congenital melanocytic nevi or a giant congenital melanocytic nevus with satellitosis. In one series of 33 patients with neurocutaneous melanosis associated with giant congenital melanocytic nevi, all nevi had a posterior axial location (involving the head, neck, back, and/or buttocks); 31 of 33 patients had satellite nevi. In another study, 80% had posterior axis involvement and 55% had more than 20 satellite nevi. Of note, neurocutaneous melanosis can also be seen in patients with nevus of Ota and phakomatosis pigmentovascularis.

Melanoma arising in congenital nevi

Although all sizes of congenital melanocytic nevi may be associated with melanoma, historical estimates of melanoma risk have been exaggerated because of referral and selection bias and misdiagnosis. The risk of melanoma increases with the size of the nevus, with most studies reporting an incidence rate of melanoma in small/medium congenital melanocytic nevi of <1%. For example, a prospective study of 230 medium-sized congenital melanocytic nevi in 227 patients, followed on average for 6.7 years, failed to document the development of a single case of melanoma. Similarly, in a longitudinal cohort study of 265 patients with medium-sized congenital melanocytic nevi, none developed melanoma.

On the other hand, several studies have noted substantial melanoma risk linked to large or giant congenital melanocytic nevi. In a prospective study of 92 patients with large/giant congenital melanocytic nevi, three patients developed melanoma in extracutaneous sites (brain, CNS, retroperitoneum) during follow-up averaging 5.4 years. The authors calculated the cumulative 5-year life-table risk for melanoma to be 4.5% and the standardized morbidity ratio to be 239, leading to the recommendation for continuous surveillance[71]. A comprehensive review of 14 studies that examined the development of melanoma in patients with congenital melanocytic nevi reported an overall risk of melanoma of 0.7% (in those with congenital melanocytic nevi of all types), with a risk of 2.5% and 3.1% in large and giant nevi, respectively[72].

When a cutaneous melanoma develops in a relatively small congenital melanocytic nevus, it appears most commonly at the dermal–epidermal junction in a pattern similar to that of other conventional melanomas. However, cutaneous melanomas arising in larger congenital melanocytic nevi can develop within the dermis, subcutaneous fat, or even deeper, as a distinct nodule[73]. Rarely, other malignant tumors may arise in these lesions, including rhabdomyosarcomas, malignant peripheral nerve sheath tumors, fibrosarcomas, leiomyosarcomas, osteogenic sarcomas, and liposarcomas.

Leptomeningeal melanomas can arise in patients with neurocutaneous melanosis and most commonly involve the frontal and temporal lobes. As expected, these melanomas have a poor prognosis.

Abnormalities associated with congenital nevi

Patients with large/giant congenital nevi can also have urinary tract anomalies, obstruction of orifices by the nevus (e.g. perianal), and infiltration of lymph nodes and the mother's placenta by nevus cells.

Pathology

In contrast to common acquired nevi, which are confined to the papillary and upper reticular dermis, congenital nevi may have infiltration of the lower reticular dermis, subcutaneous fat, fascia, and even deeper (Fig. 112.29). It is characteristic to observe melanocytes in a single-cell array throughout the middle or lower reticular dermis and even extending into the septa of the subcutis. Melanocytes often surround (cuffing) and/or infiltrate blood vessels, adnexal structures such as hair follicles, sebaceous glands and sweat glands, and cutaneous muscles and nerves. There is often maturation and diminished cellularity with increasing depth within the dermis. Uncommonly, congenital melanocytic nevi may show striking neural differentiation suggesting a peripheral nerve sheath tumor such as a neurofibroma or schwannoma. Structures resembling Meissner corpuscles, Verocay bodies, or neuroid tubules may be observed.

In some patients, nodular proliferations can arise within congenital nevi ("proliferating nodules"), particularly those that are medium-sized, large, or giant. These nodules can be very difficult to distinguish from melanoma arising in a congenital nevus, both clinically and histopathologically. Proliferating nodules usually arise during the first few years of life or are present at birth. They tend to blend well with the remaining nevus and have only slight atypia and occasional mitoses. When analyzed by array comparative genomic hybridization (aCGH), proliferating nodules contain gains and losses of entire chromosomes, in contrast to melanomas that contain several gains and losses, but only of portions of chromosomes.

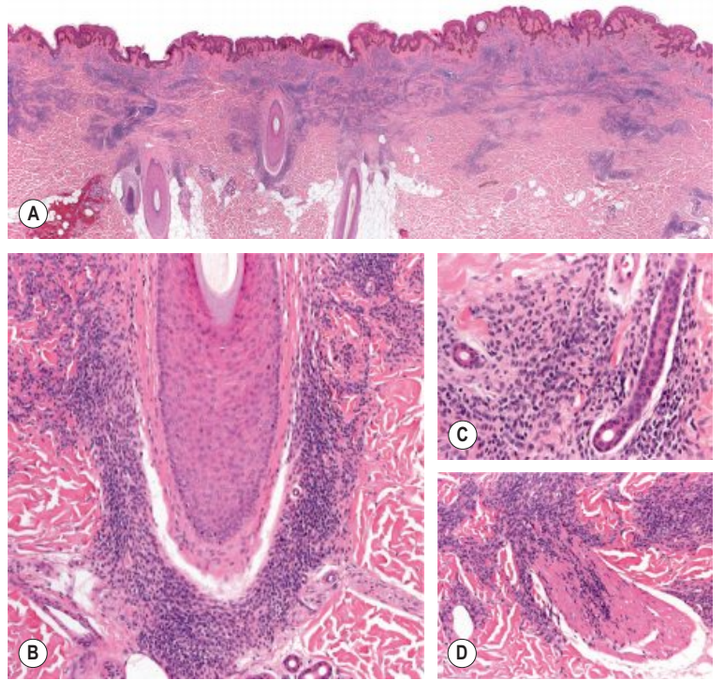


Fig. 112.29 Congenital melanocytic nevus – histopathologic features. **A** Scanning view with complexes of nevus cells extending into the deep reticular dermis and down adnexal structures. Melanocytes surround a hair follicle (**B**), extend along eccrine sweat ducts (**C**), and surround and infiltrate an arrector pili muscle (**D**). *Courtesy Lorenzo Cerroni, MD.*

Differential Diagnosis

The differential diagnosis of small congenital nevi includes congenital smooth muscle hamartoma, neurofibroma, atypical nevus, and melanoma. For medium-sized congenital nevi, an additional entity to consider is Becker melanosis, including those with an associated smooth muscle hamartoma. Large/giant congenital melanocytic nevi are occasionally misdiagnosed as plexiform neurofibromas, as the latter can have both hyperpigmentation and hypertrichosis. Of course, the possibility of melanoma exists for any clinically atypical area (e.g. darkening, nodularity) within a congenital nevus. The differences between melanoma and a proliferating nodule are outlined in the Pathology section.

Treatment

The treatment of congenital melanocytic nevi is primarily related to two factors: their cosmetically disfiguring appearance and their increased risk for progression to melanoma. The decision to remove a congenital nevus is individualized and based on melanoma risk, age, anatomic location (especially proximity to vital structures), presence or absence of neurocutaneous melanosis, anticipated cosmetic outcome, and complexity of removal. In the absence of a cosmetic concern, the routine excision of uniform-appearing small and medium-sized congenital nevi no longer seems justified due to the low melanoma risk. An acceptable alternative to surgical excision is baseline photography, education, and yearly examination.

The treatment of large/giant congenital nevi is more problematic, since melanoma risk is present from birth. If such large/giant nevi are to be excised, most authorities recommend delaying the procedure for

at least 6 months so as to decrease the risk from general anesthesia (see Table 112.10). Since the prognosis of patients with *symptomatic* neurocutaneous melanosis is poor, excisions of large/giant congenital melanocytic nevi should be delayed. In neonates with either large/giant congenital melanocytic nevi with multiple satellite nevi (especially if ≥20) or multiple medium-sized congenital nevi, MRI is routinely performed to detect neurocutaneous melanosis. For patients with asymptomatic neurocutaneous melanosis, individualized care is indicated (see Fig. 112.28).

In the past, dermabrasion was sometimes performed, resulting in a more lightly pigmented and less elevated congenital nevus. Repeat curettage performed in the first few weeks of life (when there is a cleavage plane in the upper dermis) has led to similar results. Scarring and prolonged healing in the case of large lesions are the drawbacks. Lasers (e.g. Q-switched ruby, Q-switched alexandrite) have also been used to treat congenital nevi, but recurrence of pigmentation is an issue as is persistence of nevus cells[74].

Suspected proliferating nodules should be evaluated histologically. As mentioned previously, when melanoma supervenes in a large congenital nevus, it may involve the dermal or subcutaneous component and be difficult to detect early. Cutaneous melanoma arising in the smaller types of congenital melanocytic nevi usually begins in the epidermis and can be detected more readily.

As with Spitz nevi, whole-genome sequencing followed by targeted therapy has been tried for large/giant congenital nevi. There is at least one report of a MEK inhibitor leading to a decrease in size and thickness.

NEVUS SPILUS

Synonyms: ■ Speckled lentiginous nevus ■ Zosteriform lentiginous nevus (based upon distribution pattern)

Key features

- Tan patch containing a variable number of more darkly pigmented macules and papules, which range from lentigines to junctional and compound nevi to Spitz and blue nevi
- Occasionally, atypical nevi and small and medium-sized congenital nevi are seen within a larger nevus spilus

Epidemiology

The prevalence of nevus spilus varies from 0.2% to 3%, and it has no sex or ethnic predilection. Lesions are usually present at birth or appear within the first few years of life. Therefore, nevus spilus is classified as a type of congenital melanocytic nevus[75].

Pathogenesis

A nevus spilus often has an oval shape, but it may have a block-like configuration or follow the lines of Blaschko (see Ch. 62). Nevi in the latter patterns are sometimes referred to as zosteriform speckled lentiginous nevi and their configuration suggests a molecular event affecting melanoblasts during embryogenesis. Melanocytes in both the background café-au-lait patch and the smaller nevi contain a mosaic of activating *HRAS* mutations[76]. In theory, these secondary genomic alterations contribute to the development of the nevi. As an example, in a nevus spilus in which Spitz nevi developed, amplification of *HRAS* was identified in the Spitz nevi.

Clinical Features

Nevus spilus usually occurs on the trunk and extremities. The tan macular area typically ranges from 1 to 4 cm in diameter (Fig. 112.30A,B), but can be >20 cm and involve an entire extremity or half the trunk

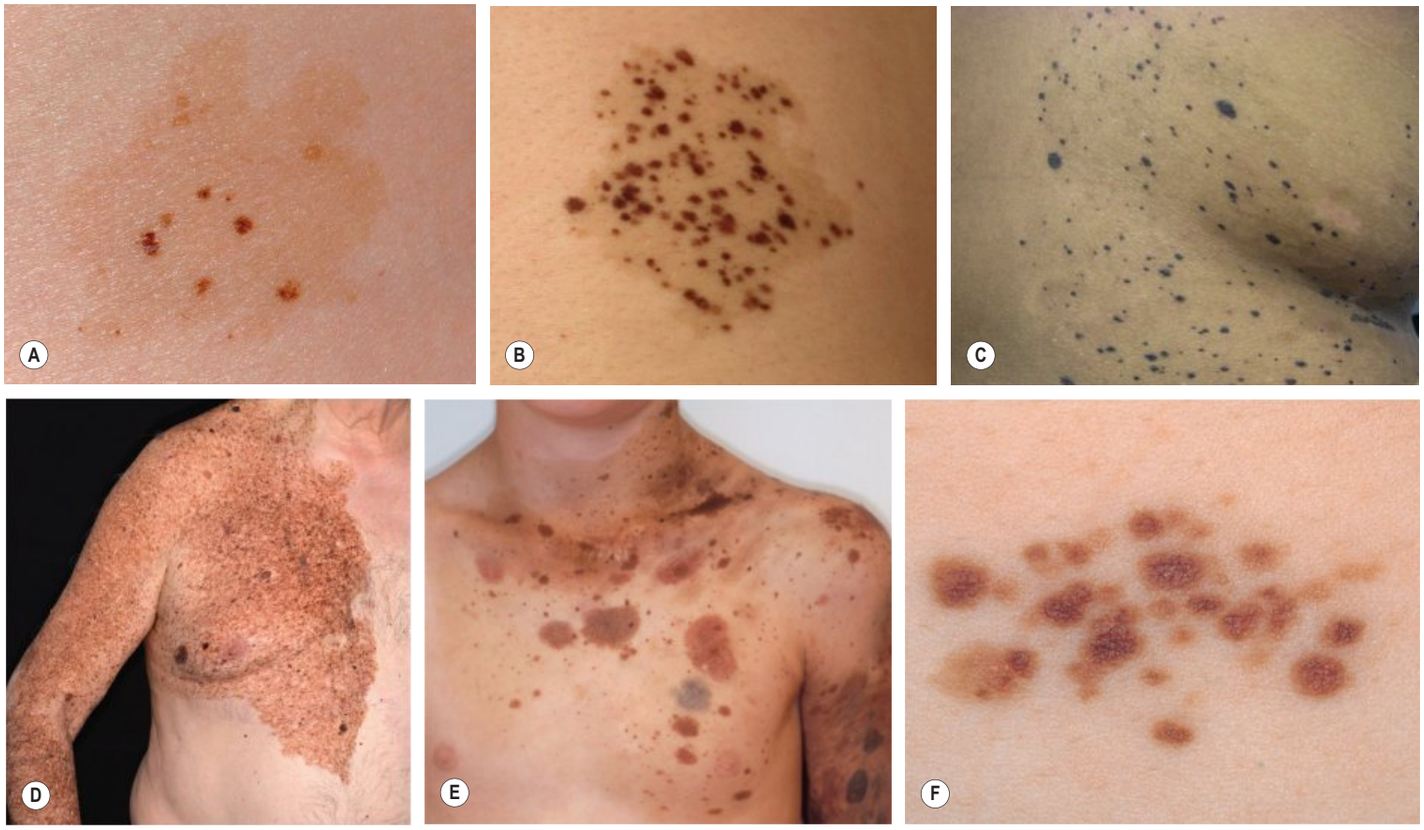


Fig. 112.30 Nevus spilus (speckled lentiginous nevus) – range of presentations and comparison to agminated nevi. A, B A few versus numerous medium to dark brown macules and papules superimposed upon a tan patch. **C** Larger lesion of the lateral trunk with dark brown to black nevi of varying sizes; sometimes the tan background is subtle and not initially recognized. **D** Zosteriform variant with more extensive involvement of the chest and arm. **E** The "speckles" can be larger and resemble small and medium-sized congenital nevi. The larger lesions were present at birth while the smaller nevi have appeared over time. **F** Agminated melanocytic nevi – grouped brown macules and papules in the absence of background hyperpigmentation (see also Fig. 112.17). *B, C, E, F, Courtesy Jean L. Bolognia, MD; D, Courtesy Luis Requena, MD.*

(Fig. 112.30C,D)[75]. Although the darker speckles are usually macules or papules that are 1–6 mm in diameter, larger lesions that resemble small and medium-sized congenital nevi are occasionally seen (Fig. 112.30E).

At birth, only a subtle lightly pigmented CALM-like patch may be seen. Over time, there is usually an increase in "speckling". Cutaneous melanoma may arise within a nevus spilus, and on occasion melanocytic dysplasia has been noted in the nevus spilus adjacent to the site of melanoma development. As with conventional congenital melanocytic nevi, the risk of melanoma may be related to size, but it may also be related to the type of "speckles".

Nevus spilus maculosus, characterized by macular speckles, is seen in patients with phacomatosis spilorosea (phakomatosis spilorosea: phakomatosis pigmentovascularis type III; see Ch. 104) whereas the papular variant favors those with phakomatosis pigmentokeratotica. The latter patients also have organoid nevi, which combine features of epidermal nevi and sebaceous nevi. Patients with speckled lentiginous nevi may have ipsilateral dysesthesia, muscular weakness, or hyperhidrosis, a combination referred to as the "speckled lentiginous nevus syndrome".

Pathology

The tan patch of nevus spilus is characterized by elongated epidermal rete ridges plus lentiginous melanocytic hyperplasia. In the hyperpigmented macular foci, either lentiginous melanocytic hyperplasia or a junctional nevus is present, whereas the papular foci represent compound, dermal, blue, Spitz, and/or atypical nevi. Histopathologic features characteristic of congenital melanocytic nevi can also be seen.

Differential Diagnosis

The major entities in the differential diagnosis are agminated melanocytic nevi and partial unilateral lentiginosis (Fig. 112.30F). However, neither has an associated tan patch as a background, and agminated nevi have less variation in the types of nevi present. Sometimes Wood's lamp examination is required to make the distinction.

Treatment

Nevus spilus is a benign melanocytic neoplasm. Patients with larger lesions or nevi with atypical features should undergo longitudinal evaluation, as there are reports of cutaneous melanoma developing within a nevus spilus. Individual pigmented lesions with atypical features or a suspicious change should be evaluated histologically.

HALO NEVUS

Synonym: ■ Sutton nevus

Key features

- Circumferential depigmentation (white halo) around a nevus
- Most common on the trunk in teenagers with an increased number of nevi
- Inflammatory infiltrate within the nevus

Epidemiology

The prevalence of halo nevi in the general population is ~1%. Halo nevi generally develop in individuals under the age of 20 years, with a mean age at presentation of ~15 years. There is no sex predilection, but patients who develop halo nevi have a higher number of melanocytic nevi. Approximately 20% of individuals with halo nevi have vitiligo and their nevi are less often associated with atypical features[77].

Pathogenesis

Development of a halo of depigmentation is thought to be an immunologic reaction against nevus cells. The inflammatory infiltrate usually consists predominantly of T cells, especially cytotoxic $CD8^+$ T cells[78]. Although the basis for nevus cell destruction in halo nevi is poorly understood, both humoral and cellular immunologic factors have been implicated. Individuals with regressing halo nevi have antibodies directed against melanoma cells and lymphocytes isolated from patients with halo nevi are cytotoxic to melanoma cells *in vitro*. Transcriptome analysis of halo nevi did reveal immune mechanisms similar to vitiligo[79].

Clinical Features

Halo nevi are most commonly observed in teenagers and young adults, and they are often initially noted in the summer. This is likely because tanning leads to greater contrast with the halo. The trunk is the most common location and 25%–50% of affected individuals have two or more halo nevi. Numerous eruptive halo nevi is a rare phenomenon. In older adults, a distinction is made between persistent halo nevi versus new-onset halo nevi (see below).

Halo nevi are characterized by a central melanocytic nevus component that may be relatively flat or raised and dark brown to pink in color. The nevus may exhibit surface scale or crusting. Surrounding the central nevus is a well-circumscribed annulus of hypo- or depigmented skin (Fig. 112.31A,B). Erythema occasionally precedes the development of the depigmented halo, which is thought to appear over a period of weeks to months. In typical halo nevi, the central nevus often measures 3–6 mm in diameter, has smooth and well-defined borders, and has a homogeneous color (stage I). By dermoscopy, globular and/or homogeneous patterns that typify benign nevi in children and young adults are usually observed[80]. The white halo is often symmetric with a uniform width that may vary from a few millimeters up to several centimeters (uncommon), but it can be asymmetric (Fig. 112.31C). A Wood's lamp can enhance or discern the halo and allow for assessment of the number of halo nevi. Dermoscopically, the halo is white and structureless (Fig. P7). The development of circumscribed poliosis involving scalp hairs, eyebrows, or eyelashes can be a clue to the presence of a halo nevus in these locations.

After the development of a halo nevus, its subsequent course is variable. Usually the nevus regresses over months to years, leaving a

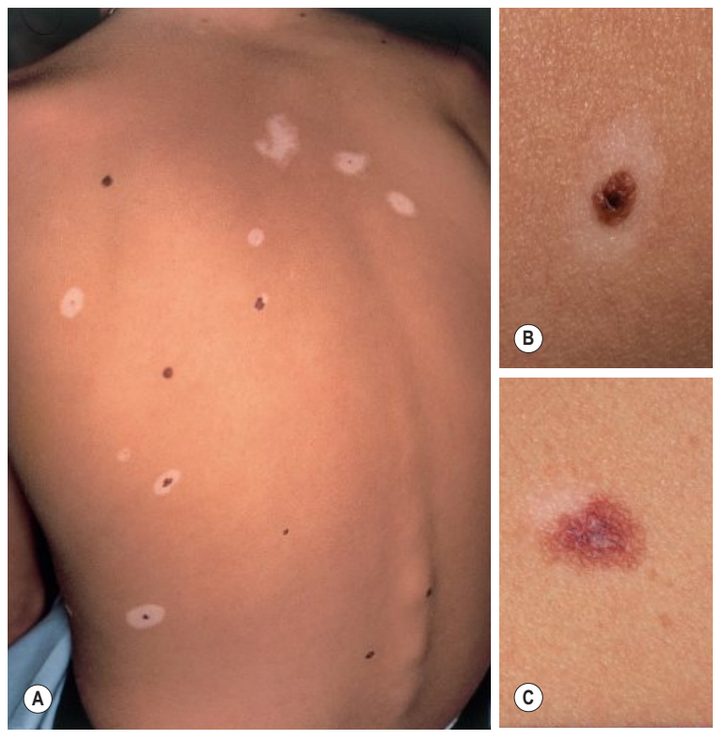


Fig. 112.31 Halo melanocytic nevi. A Stage I (central brown nevus), II (central pink nevus), III (depigmented macule), and early IV (partially repigmented skin) halo nevi are present. Multiple halo nevi are seen most commonly in children and young adults with numerous nevi. **B** Two-tone compound nevus surrounded by an oval ring of hypopigmentation. **C** A benign compound nevus with an asymmetric halo. *B, Courtesy Edward Cowen, MD; C, Courtesy Jean L. Bolognia, MD.*

white macule (stage III). The central nevus may first become irregular or pink in color (stage II). Complete repigmentation of the skin is seen in the majority of patients, but the process may take years to decades (stage IV). Rarely, the central nevus persists and the halo repigments.

In most patients, halo nevi occur as an isolated phenomenon in the setting of multiple melanocytic nevi. However, a relationship to vitiligo, melanoma, and atypical nevi has been well documented. Multiple halo nevi may be a sign of an ocular or cutaneous melanoma elsewhere, especially in older adults whose lesions are of recent onset. Occasionally, halo nevi appear following immunotherapy for melanoma or administration of other medications, e.g. imatinib, tocilizumab.

Pathology

The halo nevus may be junctional, compound, or dermal. In the fully evolved stages, the central nevus is associated with a well-circumscribed, dense infiltrate of lymphocytes and histiocytes, which occupies the papillary dermis and penetrates the nests of nevus cells. The lymphohistiocytic infiltrate can be so prominent that the nevus cells are difficult to distinguish from surrounding cells without special stains. Degenerating nevus cells can sometimes be identified in this zone.

Differential Diagnosis

Common acquired melanocytic nevi with halo phenomenon must be distinguished from: (1) other melanocytic proliferations with halos, such as congenital melanocytic nevi, atypical nevi, blue nevi, Spitz nevi, primary melanomas, or melanoma metastases; and (2) non-melanocytic lesions with halos, such as dermatofibromas, seborrheic keratoses, flat warts, mollusca contagiosa, basal cell carcinomas, lichen planus, psoriasis, or sarcoidosis. When a solitary halo lesion develops, especially in an older adult, the possibility of melanoma needs to be considered and a biopsy performed if there are atypical features. However, in adolescents, halo nevi are exceedingly more common than halo primary melanomas.

Treatment

Halo nevi are benign melanocytic lesions and the approach to patients with halo nevi is individualized and depends upon the clinical setting. All persons with halo nevi should be questioned regarding a personal or family history of cutaneous melanoma, atypical nevi, and vitiligo. Each halo nevus should be inspected carefully for features of an atypical melanocytic nevus or melanoma. The patient also should undergo a comprehensive skin examination for evidence of other halo nevi, atypical nevi, melanoma, or vitiligo. If no atypical features are observed, the patient should be followed with periodic skin examinations. Clinically atypical halo nevi should be examined histologically. Individuals beyond 40 years of age with new-onset halo nevi should be examined carefully for melanoma (ocular, mucosal, and cutaneous). A possible association with other malignancies has been noted for post-adolescent patients with eruptive halo nevi[81].

COMBINED NEVUS

Synonyms: ■ Biphasic melanocytic nevus ■ Biphenotypic nevus ■ Melanocytic nevus with phenotypic heterogeneity ■ Clonal nevus ■ Inverted type A nevus

Key features

- A benign melanocytic neoplasm with two or more phenotypically distinct tumor cell populations
- Usually <6 mm in diameter with variegated pigmentation

Introduction and Epidemiology

Combined melanocytic nevus refers to the simultaneous presence of at least two distinct nevus components in a single melanocytic neoplasm[82]. While any combination of conventional nevus, blue nevus, or Spitz nevus may potentially be observed, a common combination is a conventional compound nevus plus a blue nevus. Of note, some lesions diagnosed as combined nevi in the past are nowadays classified differently, e.g. as BAP1-inactivated tumors, WNT-activated deep penetrating/plexiform nevi, pigmented epithelioid melanocytomas.

The exact incidence of combined nevi is unknown, but has been estimated to be <1% of all melanocytic nevi sampled for histopathologic examination. Combined nevi can develop at any age, but typically present in young adults, with a mean age of ~30 years. There is no sex predilection[83].

Clinical Features

Combined nevi may arise at any site, but they have a predilection for the head and neck region, especially those with a blue nevus component. The clinical features reflect the types of nevi that are present. A smooth, blue–gray to blue–brown to blue–black papule or nodule is a common presentation, as is a discrete dark brown to black focus within an otherwise uniformly tan or brown common acquired nevus (Fig. 112.32). A papule or nodule may also arise within any type of melanocytic nevus including atypical and congenital nevi.

Pathology

The histologic features also vary depending on the types of nevi present. Most often, a banal compound or intradermal nevus is either admixed with a dermal population of pigmented epithelioid or spindled melanocytes or it overlies a more discrete pigmented spindle and epithelioid component (Fig. 112.33). Cytologic atypia and mitotic activity are rare[83].

Differential Diagnosis and Treatment

Both clinically and histologically, the presence of two or more components in a melanocytic lesion raises the possibility of melanoma, including melanoma arising within a nevus. If the lesion is sufficiently suspicious, a biopsy that includes the entire tumor should be performed. The clinical differential diagnosis also includes blue nevus, pigmented Spitz nevus, pigmented spindle cell nevus, pigmented basal cell carcinoma, benign vascular tumor, the hemosiderotic variant of dermatofibroma, and melanoma metastasis. Immunohistochemistry can assist in excluding other types of combined melanocytic neoplasms, e.g. BAP1 for BAP1-inactivated tumors, β-catenin and LEF1 for WNT-activated deep penetrating/plexiform nevi, PRKAR1A for pigmented epithelioid melanocytomas.



Fig. 112.32 One variant of combined melanocytic nevus. Dark brown to black papule within an otherwise uniformly pigmented light brown nevus. The differential diagnosis includes the possibility of a melanoma developing in a nevus. Some clinicians refer to nevi with this clinical appearance and the histologic features seen in Fig. 112.33 as clonal nevi. *Courtesy Lorenzo Cerroni, MD.*

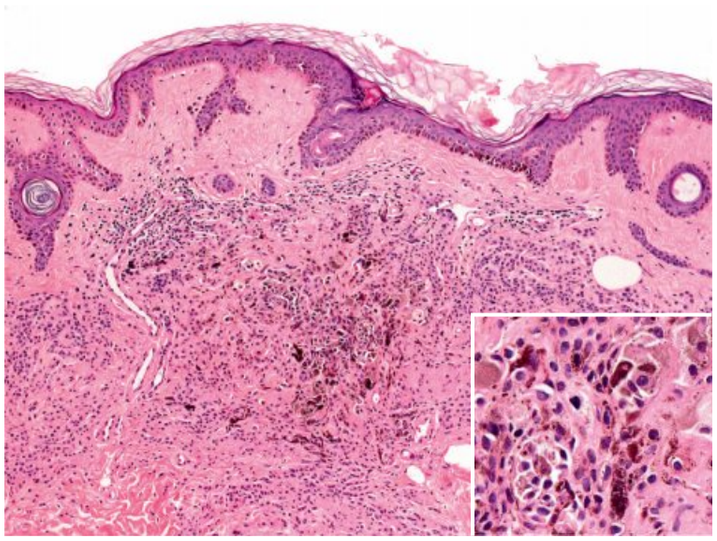


Fig. 112.33 Combined nevus – histopathologic features. Within this intradermal nevus is a focal collection of pigmented epithelioid dermal melanocytes and melanophages. The cells are benign in appearance (inset). Close examination of the focal collection of pigmented cells is recommended to exclude the possibility of melanoma. *Courtesy Lorenzo Cerroni, MD.*

RECURRENT MELANOCYTIC NEVUS

Synonyms: ■ Persistent melanocytic nevus ■ Pseudomelanoma

Key features

- A benign melanocytic nevus that recurs after incomplete removal, including following excisional or laser surgery
- Overlying scar tissue, heavily pigmented melanocytes proliferate within the epidermis, often with upward migration, and may resemble melanoma histologically

Epidemiology

Recurrent nevi are most often observed in women aged 20–30 years, reflecting the greater number of nevi removed from women and a higher prevalence in younger patients. Recurrent nevi are most commonly observed on the trunk, followed by the head and neck region. Most recurrences occur after shave excisions and are evident within 6 months of the surgical procedure[84]. When the recurrence develops >12 months after the original procedure and/or extends beyond the scar, the original biopsy should be re-evaluated and if unavailable, repeat histologic examination performed.

Pathogenesis

The recurrence of melanocytic nevi reflects migration of residual nevus cells into the epidermis, followed by proliferation. These residual cells originate from the underlying dermal component or periphery of the original incompletely excised nevus. Hence, the alternative term persistent nevus. Trophic factors stimulating melanocyte migration, melanocyte proliferation, or both, may be related to mechanisms of wound healing or scar formation.

Clinical Features

Recurrent nevi are characterized by circumscribed hyperpigmentation within a scar. The scar is usually secondary to a surgical procedure, but can follow attempted laser removal, application of chemical irritants, or significant trauma (Fig. 112.34A). Most recurrent nevi are macular and measure 2 to 5 mm in diameter. They can be circular, especially when perifollicular, or irregular in outline (Fig. P8) and most have a

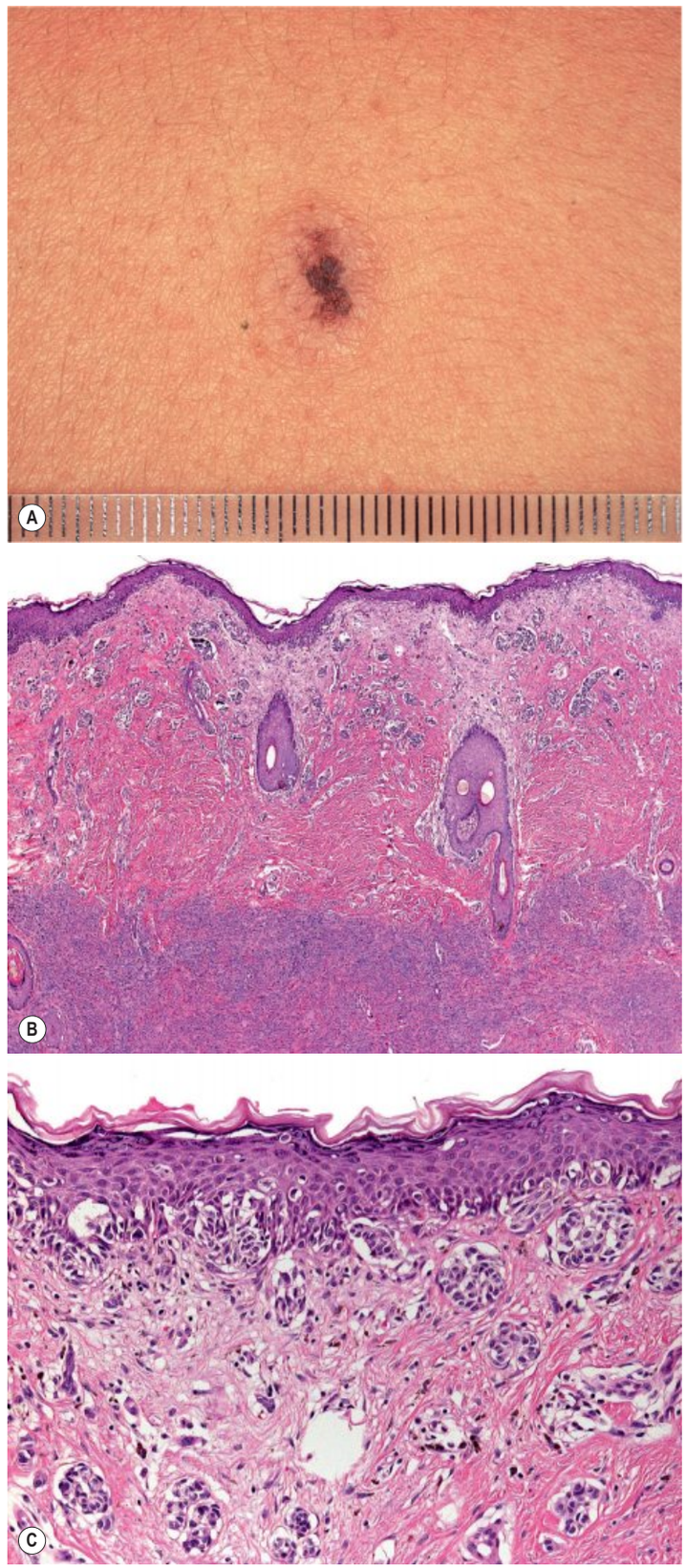


Fig. 112.34 Recurrent melanocytic nevus – clinical and histopathologic features. A Irregular dark brown pigmentation within the center of a circular scar; the pigmentation reflects the proliferation of melanocytes within the epidermis. Note that there is no extension of the recurrence beyond the scar itself, one of the signs that favors observation rather than repeat biopsy. **B** Histologically, an irregular junctional and superficial dermal melanocytic proliferation overlies a dermal scar and more deeply located residual dermal nevus. **C** At higher magnification, both junctional nests of melanocytes and single melanocytes are noted along the flattened dermal–epidermal junction as well as focally in suprabasal layers. The melanocytes are enlarged polygonal cells and show some low-grade nuclear pleomorphism. *A, Courtesy Jean L. Bolognia, MD; B, C, Courtesy Lorenzo Cerroni, MD.*

single shade of brown. However, recurrences following shave excision of darker brown compound melanocytic nevi can be black in color. When the recurrent nevus has varied pigmentation or extends beyond the associated scar, the possibility of an atypical nevus or melanoma should be considered. The dermoscopic features of recurrent/persistent nevi are sometimes difficult to distinguish from melanoma.

Most recurrent nevi are stable for years after development and then may fade. No increased melanoma risk has been associated with recurrent nevi. Clinical features that point to the need for a repeat biopsy include progressive enlargement, extension beyond the confines of the surgical scar, and a longer time interval before recurrence (>12 months)[85].

Pathology

Corresponding to the clinical features, one frequently observes intraepidermal melanocytic proliferation confined to the area above a dermal scar (Fig. 112.34B,C). The epidermis exhibits effacement of the rete pattern and variable lentiginous or nested proliferation of melanocytes. The presence of intraepidermal melanocytes extending beyond the dermal scar is suspicious for melanoma. Often, the cells contain abundant melanin and have relatively uniform, small nuclei. Occasionally, low-to-moderate grade cytologic atypia may be noted, but mitotic activity is rare. Upward migration of epidermal melanocytes may occur.

Frequently, there are residual dermal nevus cells beneath the superficial dermal scar and cytologically they resemble the junctional component (see Fig. 112.34B). Staining for PRAME is negative. In general, re-evaluation of the original biopsy, if one had been performed, is considered part of the histopathologic assessment of recurrent melanocytic tumors.

Differential Diagnosis

The differential diagnosis of recurrent nevi includes the lentiginous melanocytic proliferations and pigmented streaks due to basilar hyperpigmentation that can both develop in surgical excision scars (including those for melanoma). Additional entities to consider are traumatized nevi, recurrent atypical melanocytic nevi, and recurrent melanoma. In general, a recurrent melanocytic nevus is confined to the area of the surgical scar, appears within 6 months of surgery, and exhibits a bland histologic picture. Recurrent atypical nevi may have more disordered intraepidermal melanocytic proliferation (even a pagetoid pattern) and greater cytologic atypia than conventional recurrent nevi. Clinical features suggesting melanoma include irregular pigmentation, progressive enlargement, extension beyond the confines of the surgical scar, and a longer time interval before recurrence (>12 months). Strong PRAME-positivity of most melanocytes is considered very suspicious for melanoma.

Treatment

Establishing the etiology of the scar (see above) is integral to the diagnosis. Review of the previous biopsy specimen is mandatory if any atypicality is noted histologically or if the lesion arises >12 months after the attempt at removal. It is also a preferred practice for all recurrent nevi. Clinical features that point to the need for a repeat biopsy are outlined above and histopathologic findings guide the need for further re-excision.

Additional figures and table on Assessment of atypical Spitz tumors in children and adolescents for risk for metastasis, available in our eBook (see inside front cover for access code).

REFERENCES

1. Bastiaens M, ter Huurne J, Gruis N, et al. The melanocortin-1-receptor gene is the major freckle gene. *Hum Mol Genet*. 2001;10:1701–1708.
2. Praetorius C, Sturm RA, Steingrimsson E. Sun-induced freckling: ephelides and solar lentigines. *Pigment Cell Melanoma Res*. 2014;27:339–350.
3. Breathnach AS, Wyllie LM. Electron microscopy of melanocytes and melanosomes in freckled human epidermis. *J Invest Dermatol*. 1964;42:389–394.
4. Passeron T, Genedy R, Salah L, et al. Laser treatment of hyperpigmented lesions: position statement of the European Society of Laser in Dermatology. *J Eur Acad Dermatol Venereol*. 2019;33:987–1005.
5. Lalor L, Davies OMT, Basel D, Siegel DH. Café au lait spots: when and how to pursue their genetic origins. *Clin Dermatol*. 2020;38:421–431.
6. Jimbow K, Szabo G, Fitzpatrick TB. Ultrastructure of giant pigment granules (macromelanosomes) in the cutaneous pigmented macules of neurofibromatosis. *J Invest Dermatol*. 1973;61:300–309.
7. Happle R. Becker's nevus and lethal beta-actin mutations. *J Invest Dermatol*. 2017;137:1619–1621.
8. Cai ED, Sun BK, Chiang A, et al. Postzygotic mutations in beta-actin are associated with Becker's nevus and Becker's nevus syndrome. *J Invest Dermatol*. 2017;137:1795–1798.
9. Sarpa HG, Harris R, C Hansen D, et al. Androgen receptor expression patterns in Becker's nevi: an immunohistochemical study. *J Am Acad Dermatol*. 2008;59:834–838.
10. Torchia D. Becker nevus syndrome: a 2020 update. *J Am Acad Dermatol*. 2021;85:e101–e103.
11. Haugh AM, Merkel EA, Zhang B, et al. A clinical, histologic, and follow-up study of genital melanosis in men and women. *J Am Acad Dermatol*. 2017;76:836–840.
12. Barnhill RL, Albert LS, Shama SK, et al. Genital lentiginosis: a clinical and histopathologic study. *J Am Acad Dermatol*. 1990;22:453–456.
13. Hafner C, Stoehr R, van Oers JMM, et al. The absence of BRAF, FGFR3, and PIK3CA mutations differentiates lentigo simplex from melanocytic nevus and solar lentigo. *J Invest Dermatol*. 2009;129:2730–2735.
14. Cordova A. The Mongolian spot. *Clin Pediatr*. 1981;20:714–719.
15. Baykal C, Yılmaz Z, Sun GP, Büyükbabani N. The spectrum of benign dermal dendritic melanocytic proliferations. *J Eur Acad Dermatol Venereol*. 2019;33:1029–1041.
16. Van Raamsdonk CD, Griewank KG, Crosby MB, et al. Mutations in *GNA11* in uveal melanoma. *N Engl J Med*. 2010;363:2191–2199.
17. Teekhasaenee C, Ritch R, Rutnin U, Leelawongs N. Ocular findings in oculodermal melanocytosis. *Arch Ophthalmol*. 1990;108:1114–1120.
18. Gerami P, Pouryazdanparast P, Venmula S, Bastian BC. Molecular analysis of a case of nevus of Ota showing progressive evolution to a melanoma with intermediate stages resembling cellular blue nevus. *Am J Dermatopathol*. 2010;32:301–305.
19. Chan HH, Leung RS, Ying SY, et al. A retrospective analysis of complications in the treatment of nevus of Ota with the Q-switched alexandrite and Q-switched Nd: YAG lasers. *Dermatol Surg*. 2000;26:1000–1006.
20. Murali R, McCarthy SW, Richard A, Scolyer RA. Blue nevi and related lesions: a review highlighting atypical and newly described variants, distinguishing features and diagnostic pitfalls. *Adv Anat Pathol*. 2009;16:365–382.
21. Möller I, Murali R, Müller H, et al. Activating cysteinyl leukotriene receptor 2 (CYSLTR2) mutations in blue nevi. *Mod Pathol*. 2017;30:350–356.

21a. Kervarrec T, Lo Bello G, Pissaloux D, et al. GRM1 gene fusions as an alternative molecular driver in blue nevi and related melanomas. *Mod Pathol*. 2023;36:100264.

22. Barnhill RL, Argenyi Z, Berwick M, et al. Atypical cellular blue nevi (cellular blue nevi with atypical features): lack of consensus for diagnosis and distinction from cellular blue nevi and malignant melanoma ("malignant blue nevus"). *Am J Surg Pathol*. 2008;32:36–44.
23. Griewank KG, Müller H, Jackett LA, et al. SF3B1 and BAP1 mutations in blue nevus-like melanoma. *Mod Pathol*. 2017;30:928–939.
24. de la Fouchardiere A, Tirode F, Castillo C, et al. Attempting to solve the pigmented epithelioid melanocytoma (PEM) conundrum: PRKAR1A inactivation can occur in different genetic backgrounds (common, blue, and Spitz subgroups) with variation in their clinicopathologic characteristics. *Am J Surg Pathol*. 2022;46:1106–1115.
25. Carney JA, Ferreiro JA. The epithelioid blue nevus: a multicentric familial tumor with important associations, including cardiac myxoma and psammomatous melanotic schwannoma. *Am J Surg Pathol*. 1996;20:259–272.
26. Zembowicz A, Carney JA, Mihm MC. Pigmented epithelioid melanocytoma: a low-grade melanocytic tumor with metastatic potential indistinguishable from animal-type melanoma and epithelioid blue nevus. *Am J Surg Pathol*. 2004;28:31–40.
27. Whiteman DC, Pavan WJ, Bastian BC. The melanomas: a synthesis of epidemiological, clinical, histopathological, genetic, and biological aspects, supporting distinct subtypes, causal pathways, and cells of origin. *Pigment Cell Melanoma Res*. 2011;24:879–897.
28. Zhu G, Duffy DL, Eldridge A, et al. A major quantitative-trait locus for mole density is linked to the familial melanoma gene CDKN2A: a maximum-likelihood combined linkage and association analysis in twins and their sibs. *Am J Hum Genet*. 1999;65:483–492.
29. Lanschuetzer CM, Laimer M, Nischler E, Hintner H. Epidermolysis bullosa nevi. *Dermatol Clin*. 2010;28:179–183.
30. Carlson JA, Mu XC, Slominski A, et al. Melanocytic proliferations associated with lichen sclerosus. *Arch Dermatol*. 2002;138:77–87.
31. Merkel EA, Martini MC, Amin SM, Lee CY, Gerami P. Evaluation of dermoscopic features for distinguishing melanoma from special site nevi of the breast. *J Am Acad Dermatol*. 2016;75:364–370.
32. Ahn CS, Guerra A, Sangüeza OP. Melanocytic nevi of special sites. *Am J Dermatopathol*. 2016;38:867–881.
33. Kim NH, Choi YD, Seon HJ, Lee JB, Yun SJ. Anatomic mapping and clinicopathologic analysis of benign acral melanocytic neoplasms: a comparison between adults and children. *J Am Acad Dermatol*. 2017;77:735–745.
34. Weedon D, Little J. Spindle and epithelioid cell nevi in children and adults. A review of 211 cases of the Spitz nevus. *Cancer*. 1977;40:217–225.
35. Goto K, Pissaloux D, Tirode F, de la Fouchardière A. Spitz nevus with a novel TFG-NTRK2 fusion: the first case report of NTRK2-rearranged Spitz/Reed nevus. *J Cutan Pathol*. 2021;48:1193–1196.
36. Barr R, Morales R, Graham J. Desmoplastic nevus. A distinct histologic variant of mixed spindle and epithelioid cell nevus. *Cancer*. 1980;46:557–564.
37. Dawe RS, Wainwright NJ, Evans AT, Lowe JG. Multiple widespread eruptive Spitz naevi. *Br J Dermatol*. 1998;138:872–874.
38. Ludgate MW, Fullen DR, Lee J, et al. The atypical Spitz tumor of uncertain biologic potential: a series of 67 patients from a single institution. *Cancer*. 2009;115:631–641.
39. Benton S, Zhao J, Zhang B, et al. Impact of next-generation sequencing on interobserver agreement and diagnosis of spitzoid neoplasms. *Am J Surg Pathol*. 2021;45:1597–1605.
40. Busam KJ, Kutzner H, Cerroni L, Wiesner T. Clinical and pathologic findings of Spitz nevi and atypical Spitz tumors with ALK fusions. *Am J Surg Pathol*. 2014;38:925–933.

41. Ferrara G, Argenziano G, Soyer HP, et al. The spectrum of Spitz nevi: a clinicopathologic study of 83 cases. *Arch Dermatol*. 2005;141:1381–1387.
42. VandenBoom T, Quan VL, Zhang B, et al. Genomic fusions in pigmented spindle cell nevus of Reed. *Am J Surg Pathol*. 2018;42:1042–1051.
43. Cosgarea I, Griewank KG, Ungureanu L, et al. Deep penetrating nevus and borderline-deep penetrating nevus: a literature review. *Front Oncol*. 2020;10:837.
44. Yeh I, Lang UE, Durieux E, et al. Combined activation of MAP kinase pathway and β-catenin signaling cause deep penetrating nevi. *Nat Commun*. 2017;8:644.
45. Ebbelaar CF, Schrader AMR, van Dijk M, et al. Towards diagnostic criteria for malignant deep penetrating melanocytic tumors using single nucleotide polymorphism array and next-generation sequencing. *Mod Pathol*. 2022;35:1110–1120.
46. Walpole S, Pritchard AL, Cebulla CM, et al. Comprehensive study of the clinical phenotype of germline BAP1 variant-carrying families worldwide. *J Natl Cancer Inst*. 2018;110:1328–1341.
47. Wiesner T, Obernauf AC, Murali R, et al. Germline mutations in BAP1 predispose to melanocytic tumors. *Nature Genet*. 2011;43:1018–1021.
48. Yélamos O, Navarrete-Dechent C, Marchetti MA, et al. Clinical and dermoscopic features of cutaneous BAP1-inactivated melanocytic tumors: results of a multicenter case-control study by the International Dermoscopy Society. *J Am Acad Dermatol*. 2019; 80:1585–1593.
49. Wiesner T, Murali R, Fried I, et al. A distinct subset of atypical Spitz tumors is characterized by BRAF mutation and loss of BAP1 expression. *Am J Surg Pathol*. 2012;36:818–830.
50. Murali R, Wiesner T, Scolyer RA. Tumours associated with BAP1 mutations. *Pathology*. 2013;45:116–126.
51. Elder DE. Dysplastic naevi: an update. *Histopathology*. 2010;56:112–120.
52. Drozdowski R, Spaccarelli N, Peters MS, Grant-Kels JM. Dysplastic nevus part I: historical perspective, classification, and epidemiology. *J Am Acad Dermatol*. 2023;88:1–10.
53. Spaccarelli N, Drozdowski R, Peters MS, Grant-Kels JM. Dysplastic nevus part II: dysplastic nevi: molecular/genetic profiles and management. *J Am Acad Dermatol*. 2023;88:13–20.
54. Roush GC, Nordlund JJ, Forget B, et al. Independence of dysplastic nevi from total nevi in determining risk for nonfamilial melanoma. *Prev Med*. 1988;17:273–279.
55. MacKie RM, Freudenberger T, Aitchison TC. Personal risk-factor chart for cutaneous melanoma. *Lancet*. 1989;2:487–490.
56. Holly EA, Kelly JW, Shpall SN, Chiu SH. Number of melanocytic nevi as a major risk factor for malignant melanoma. *J Am Acad Dermatol*. 1987;17:459–468.
57. Halpern AC, Guerry 4th D, Elder DE, et al. Dysplastic nevi as risk markers of sporadic (nonfamilial) melanoma. A case-control study. *Arch Dermatol*. 1991;127:995–999.
58. Garbe C, Buttner P, Weiss J, et al. Risk factors for developing cutaneous melanoma and criteria for identifying persons at risk: multicenter case-control study of the central malignant melanoma registry of the German Dermatological Society. *J Invest Dermatol*. 1994;102:695–699.
58a. Rishpon A, Navarrete-Dechent C, Marghoob AA, et al. Melanoma risk stratification of individuals with a high-risk naevus phenotype - a pilot study. *Australas J Dermatol*. 2019; 60:e292–e297.
59. Shors AR, Kim S, White E, et al. Dysplastic naevi with moderate to severe histological dysplasia: a risk factor for melanoma. *Br J Dermatol*. 2006;155:988–993.
60. Shain AH, Yeh I, Kovalyshyn I, Sriharan A. The genetic evolution of melanoma from precursor lesions. *N Engl J Med*. 2015;373:1926–1936.
60a. Tsao H, Bevona C, Goggins W, Quinn T. The transformation rate of moles (melanocytic nevi) into cutaneous melanoma: a population-based estimate. *Arch Dermatol*. 2003;139:282–288.
61. Gandini S, Sera F, Cattaruzza MS, et al. Meta-analysis of risk factors for cutaneous melanoma: I. Common and atypical naevi. *Eur J Cancer*. 2005;41:28–44.
62. Hoffman-Wellenhof R, Blum A, Wolf IH, et al. Dermoscopic classification of atypical melanocytic nevi. *Arch Dermatol*. 1992;137:1575–1580.
63. Duffy KL, Mann DJ, Petronic-Rosic V, Shea CR. Clinical decision making based on histopathologic grading and margin status of dysplastic nevi. *Arch Dermatol*. 2012;148:259–260.
64. Reddy KK, Farber MJ, Bhawan J, et al. Atyptical (dysplastic) nevi outcomes of surgical excision and association with melanoma. *JAMA Dermatol*. 2013;149:928–934.
65. Strazzula L, Vedak P, Hoang MP, et al. The utility of re-excising mildly and moderately dysplastic nevi: a retrospective analysis. *J Am Acad Dermatol*. 2014;71:1071–1076.
66. Alikhan A, Ibrahimi OA, Eisen DB. Congenital melanocytic nevi: where are we now? Part I. Clinical presentation, epidemiology, pathogenesis, histology, malignant transformation, and neurocutaneous melanosis. *J Am Acad Dermatol*. 2012;67:495. e1–17.
67. Ibrahimi OA, Alikhan A, Eisen DB. Congenital melanocytic nevi: where are we now? Part II. Treatment options and approach to treatment. *J Am Acad Dermatol*. 2012;67:515. e1–13.
68. Krengel S, Scope A, Dusza SW, et al. New recommendations for the categorization of cutaneous features of congenital melanocytic nevi. *J Am Acad Dermatol*. 2013;68:441–451.
69. Martins da Silva V, Martinez-Barrios E, Tell-Martí G, et al. Genetic abnormalities in large to giant congenital nevi: beyond NRAS mutations. *J Invest Dermatol*. 2019;139:900–908.
70. Kinsler VA, O'Hare P, Bulstrode N, et al. Melanoma in congenital melanocytic nevi. *Br J Dermatol*. 2017;176:1131–1143.
71. Marghoob AA, Schoenbach SP, Kopf AW, et al. Large congenital melanocytic nevi and the risk for the development of malignant melanoma. A prospective study. *Arch Dermatol*. 1996;132:170–175.
72. Krengel S, Hauschild A, Schäfer T. Melanoma risk in congenital melanocytic naevi: a systematic review. *Br J Dermatol*. 2006;155:1–8.
73. Egan CL, Oliveria S, Elenitsas R, et al. Cutaneous melanoma risk and phenotypic changes in large congenital nevi: a follow-up study of 46 patients. *J Am Acad Dermatol*. 1998;39:923–932.
74. Kishi K, Okabe K, Ninomiya R, et al. Early serial Q-switched ruby laser therapy for medium-sized to giant congenital melanocytic naevi. *Br J Dermatol*. 2009;161:345–352.
75. Schaffer JV, Orlow SJ, Lazova R, Bolognia JL. Speckled lentiginous nevus: within the spectrum of congenital melanocytic nevi. *Arch Dermatol*. 2001;137:172–178.
76. Sarin KY, McNIff JM, Kwok S, et al. Activating *HRAS* mutation in nevus spilus. *J Invest Dermatol*. 2014;134:1766–1768.
77. Herd RM, Hunter JA. Familial halo naevi. *Clin Exp Dermatol*. 1998;23:68–69.
78. Zeff RA, Freitag A, Grin CM, Grant-Kels JM. The immune response in halo nevi. *J Am Acad Dermatol*. 1997;37:620–624.
79. Pan C, Shang J, Jiang H, et al. Transcriptome analysis reveals the molecular immunological characteristics of lesions in patients with halo nevi when compared to stable vitiligo, normal nevocytic nevi and cutaneous melanoma. *J Inflamm Res*. 2021;14:4111–4124.
80. Kolm I, Di Stefani A, Hofmann-Wellenhof R, et al. Dermoscopy patterns of halo nevi. *Arch Dermatol*. 2006;142:1627–1632.
81. Lorentzen HF. Eruptive halo naevi: a possible indicator of malignant disease in a case series of post-adolescent patients. *Acta Derm Venereol*. 2020:100 adv00228.
82. Baran JL, Duncan LM. Combined melanocytic nevi: histologic variants and melanoma mimics. *Am J Surg Pathol*. 2011;35:1540–1548.
83. Scolyer RA, Zhuang L, Palmer AA, et al. Combined naevus: a benign lesion frequently misdiagnosed both clinically and pathologically as melanoma. *Pathology*. 2004;36:419–427.
84. Park HK, Leonard DD, Arrington 3rd JH, Lund HZ. Recurrent melanocytic nevi: clinical and histologic review of 175 cases. *J Am Acad Dermatol*. 1987;17:285–292.
85. Blum A, Hofmann-Wellenhof R, Marghoob AA, et al. Recurrent melanocytic nevi and melanomas in dermoscopy: results of a multicenter study of the International Dermoscopy Society. *JAMA Dermatol*. 2014;150:138–145.
86. Hanna J, Ko JS, Billings SD, et al. Cutaneous melanocytic tumor with CRTC1::TRIM11 translocation: an emerging entity analyzed in a series of 41 cases. *Am J Surg Pathol*. 2022;46:1457–1466.
87. Marghoob AA, Orlow SJ, Kopf AW. Syndromes associated with melanocytic nevi. *J Am Acad Dermatol*. 1993;29:373–388.



Fig. P1 Solar lentigines. Sharply demarcated, uniform, tan macules on sun-exposed skin. Dermoscopically, moth-eaten borders, fingerprinting, and a reticular pattern with thin lines, short and interrupted.

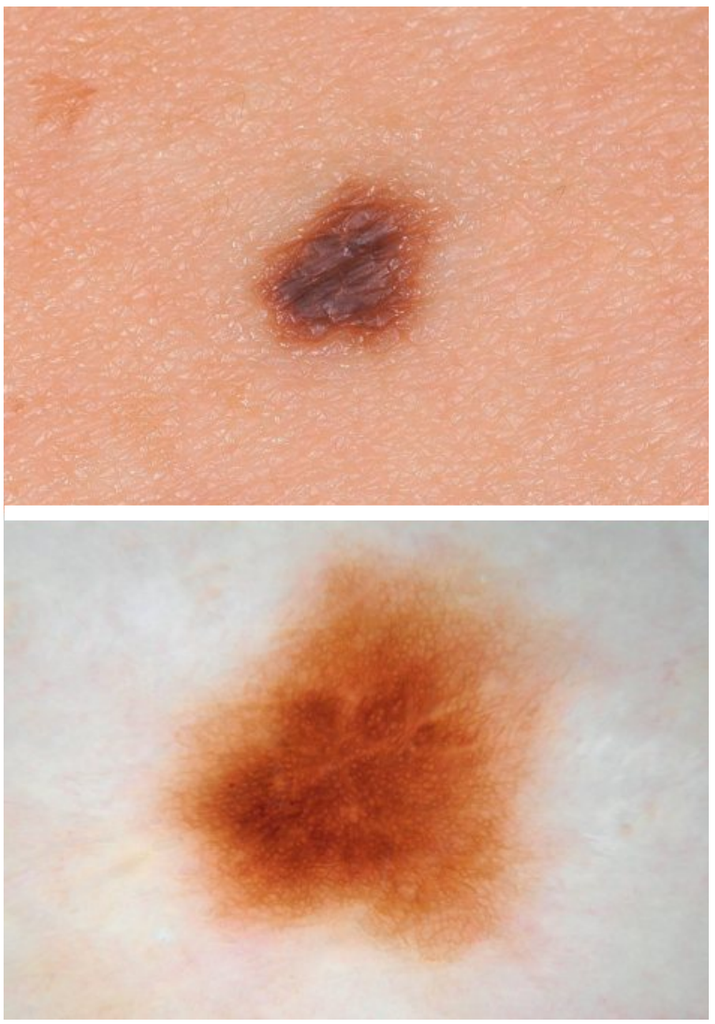


Fig. P2 Junctional nevus. Clinically, a brown macule with central hyperpigmentation. Dermoscopically, a uniform pigment network.



Fig. P3 Intradermal nevus. A light tan, soft, raised papule. Dermoscopically, focal globular-like structures, whitish structureless areas, and fine comma vessels.



Fig. P4 Melanocytic nevus of acral skin. A brown macule on the sole of the foot. Dermoscopically, a lattice-like pattern.

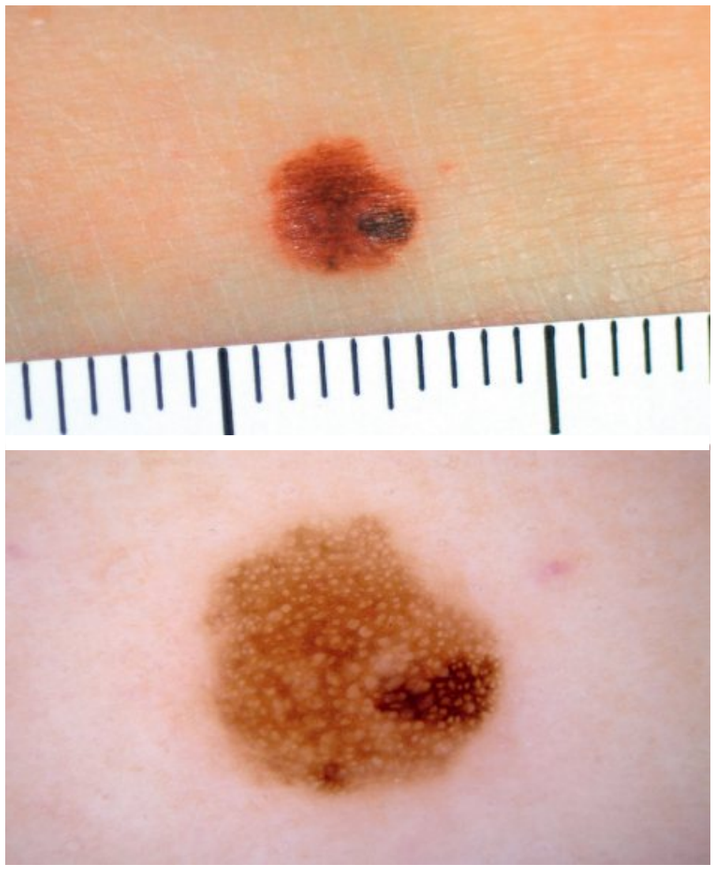


Fig. P5 Clinically atypical melanocytic nevus. The dermoscopy pattern is reticular–disorganized and can be seen with uncertain lesions.



Fig. P6 Medium-sized congenital nevus. Dermoscopically, a globular pattern with hyphae-like structures.

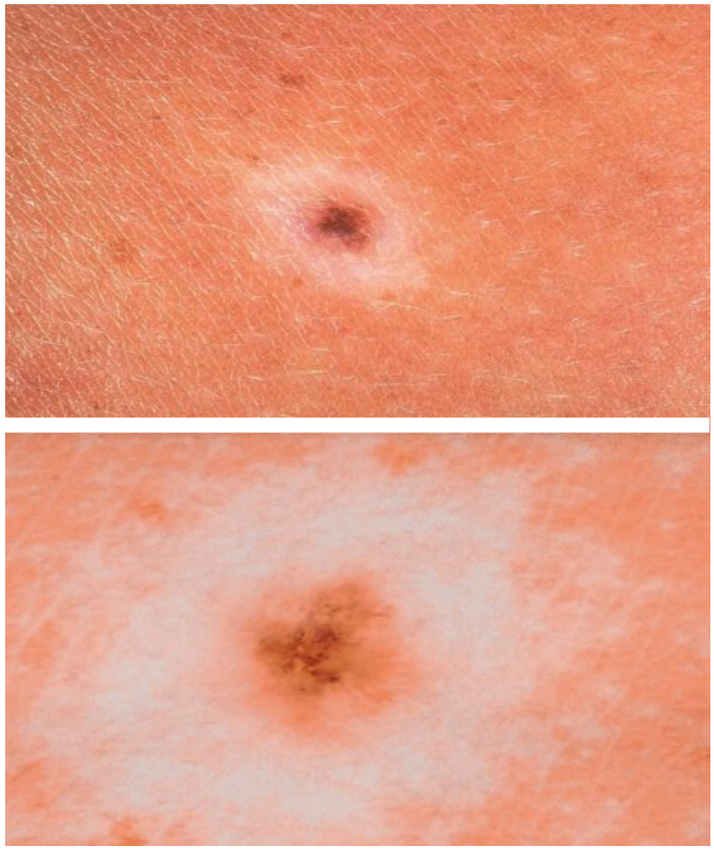


Fig. P7 Halo nevus. A depigmented macular halo surrounding a central dark brown papule. Dermoscopically, a symmetric white structureless area surrounding the remaining network of the nevus.



Fig. P8 Recurrent melanocytic nevus. A brown papule with areas of scarring. Dermoscopically, asymmetric pigmentation within the confines of the scar.

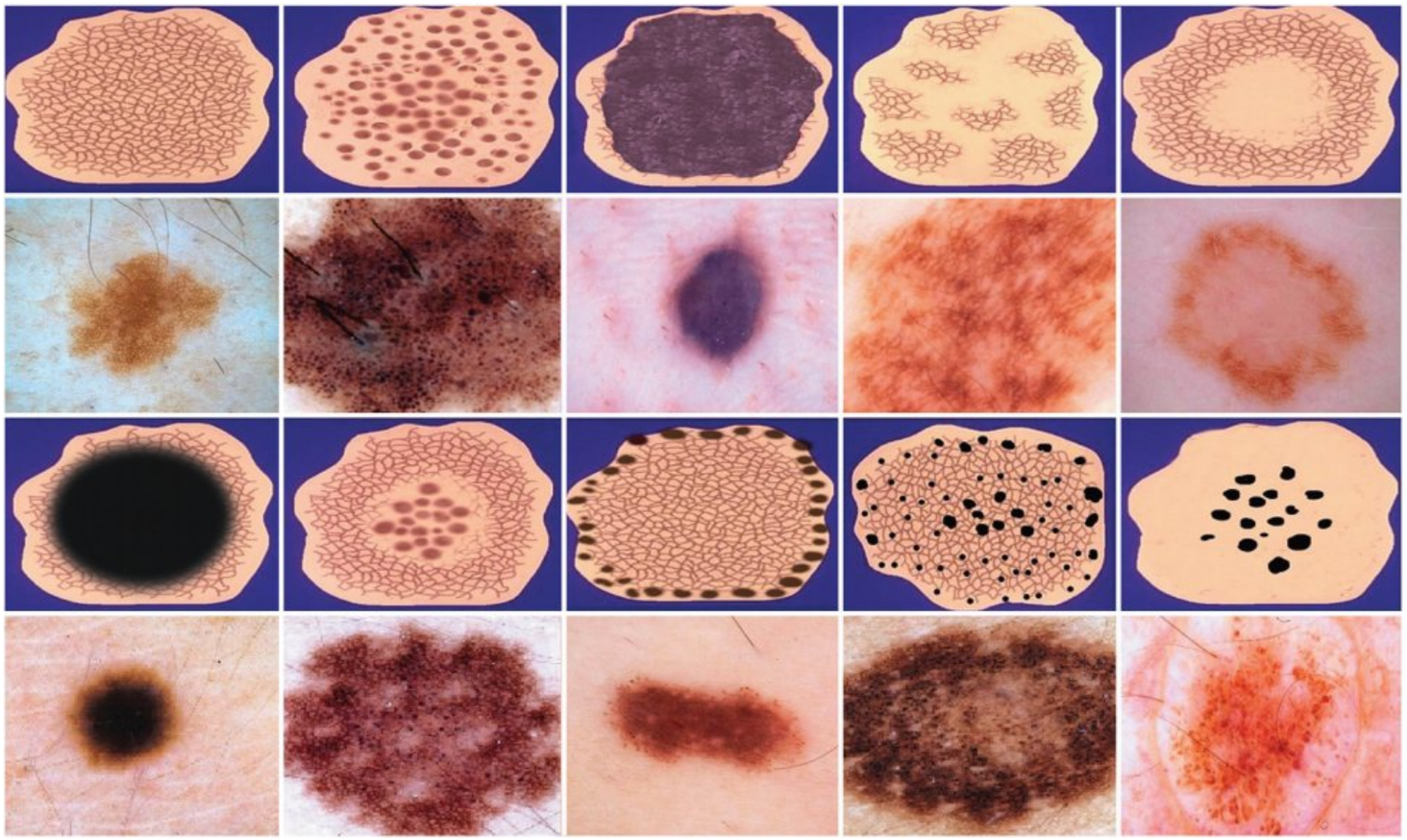
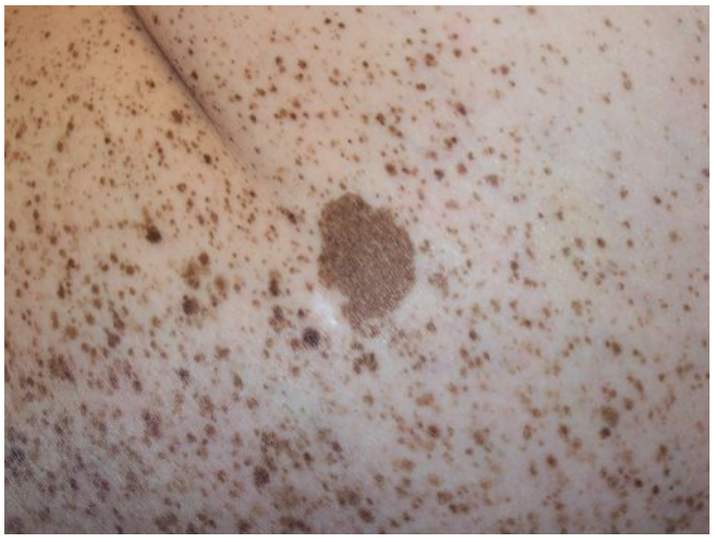


Fig. P9 Atypical melanocytic nevi with dermoscopic patterns commonly seen in benign melanocytic nevi. *Courtesy the AAD Dermoscopy Group.*



eFig. 112.1 Segmental café-au-lait macules. Although this may represent a mosaic form of neurofibromatosis type 1 (NF1), a minority of patients have limited extracutaneous manifestations of NF1. *Courtesy Julie V. Schaffer, MD.*



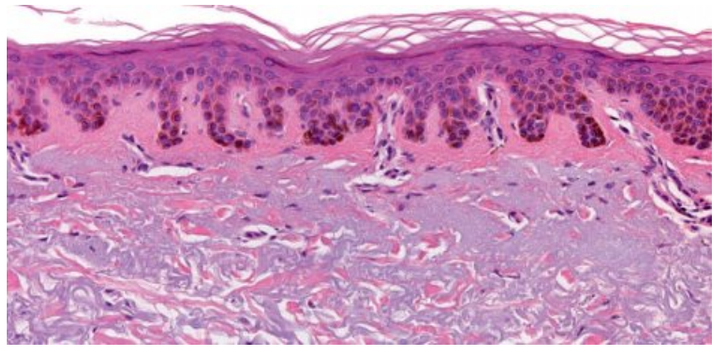
eFig. 112.2 Café-noir lesion in a patient with Carney complex. When compared to uninvolved skin, café-noir lesions are a darker shade than CALMs. *Courtesy Jean L Bolognia, MD.*



eFig. 112.3 Becker melanosis (nevus). Hyperpigmented patch with hypertrichosis and an irregular, broken-up border. *Courtesy Julie V. Schaffer, MD.*



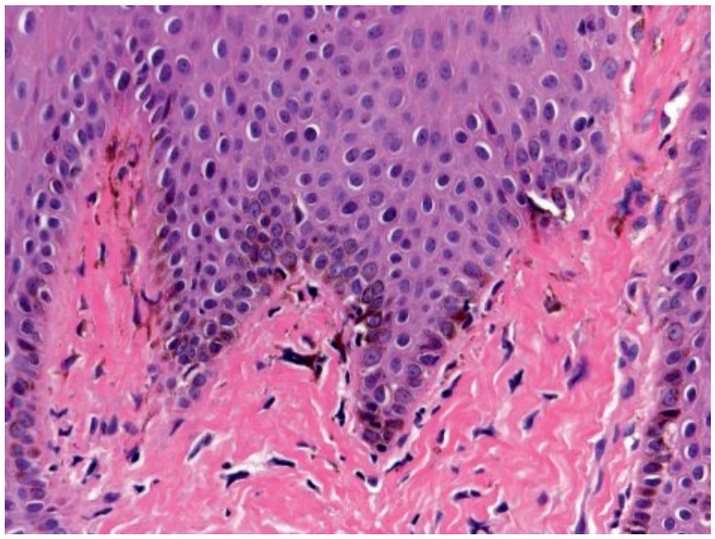
eFig. 112.4 Solar lentigines. Numerous light brown macules, some of which have an irregular border, on chronically sun-exposed skin. *Courtesy of Jean L. Bolognia MD.*



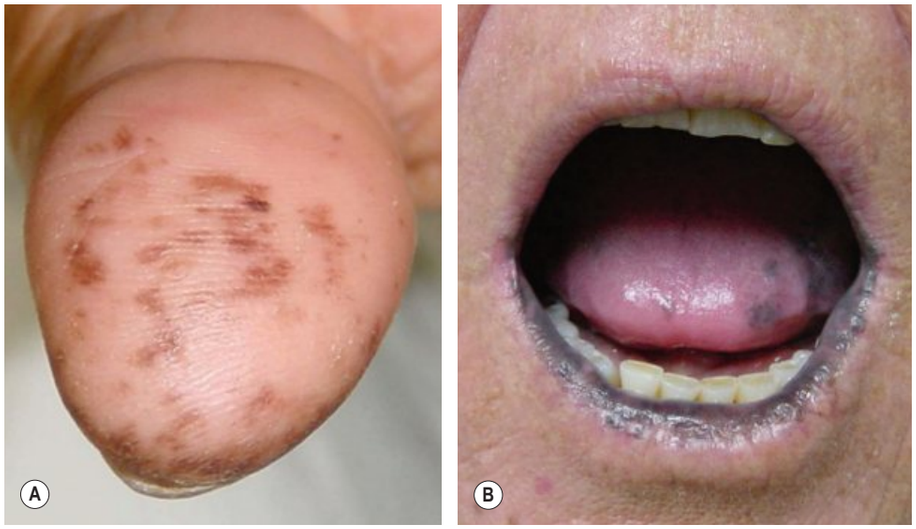
eFig. 112.5 Solar lentigo – histopathologic features. Hyperpigmented elongated rete ridges as well as solar elastosis. *Courtesy Lorenzo Cerroni, MD.*



eFig. 112.6 Penile lentiginosis (melanosis). *Courtesy Sonya K. Burton, MD.*



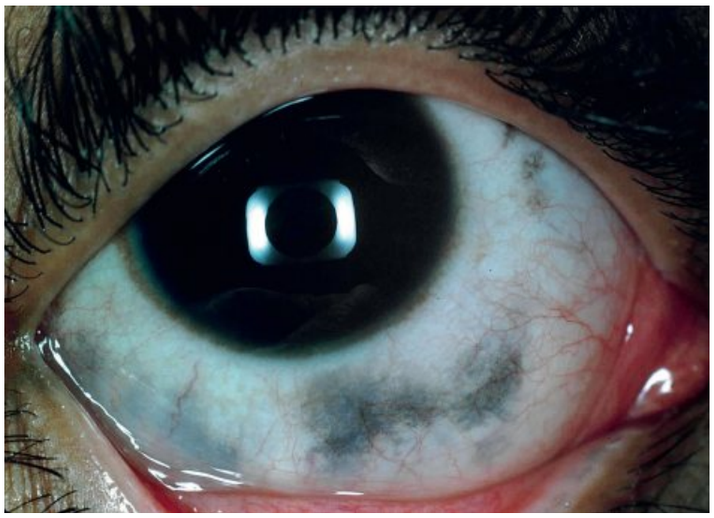
eFig. 112.8 Labial melanotic macule (lentigo) – histopathologic features. Hyperpigmented rete ridges are broader than in a typical lentigo. Basilar hyperpigmentation and melanophages are seen. *Courtesy Lorenzo Cerroni, MD.*



eFig. 112.7 Laugier–Hunziker syndrome. A, B Oral and acral lentigines. The lentigines on the vermilion lower lip are nearly confluent.



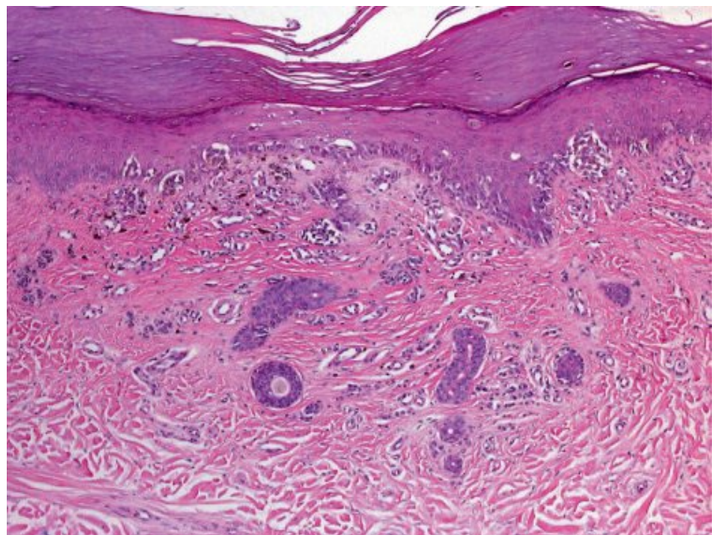
eFig. 112.9 Nevus of Ota. Unilateral blue–gray discoloration of the upper face accompanied by blue and blue–gray discoloration of the sclera. *Courtesy Kalman Watsky, MD.*



eFig. 112.10 Nevus of Ota – ocular involvement. Blue discoloration of the sclera. *Courtesy Jean L. Bolognia, MD.*



eFig. 112.11 Nevus of Ito. Similar color and histology as nevus of Ota but located on the shoulder with extension onto the arm and upper lateral trunk. *Courtesy Luis Requena, MD.*



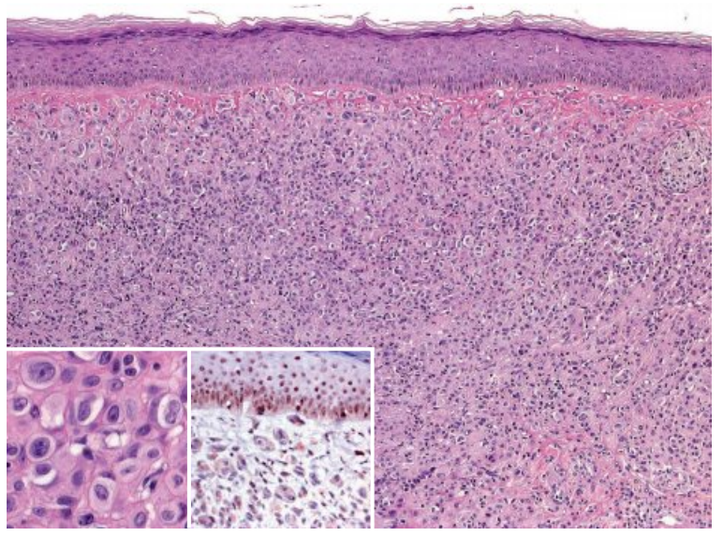
eFig. 112.12 Acral melanocytic nevus – histopathologic features. Proliferation of nevoid and epithelioid melanocytes within the epidermis and superficial dermis. Note the single melanocytes and small complexes of melanocytes within the upper layers of the epidermis. *Courtesy Lorenzo Cerroni, MD.*



eFig. 112.13 Spitz nevus. Red dome-shaped papule on the ear of a child. *Courtesy Ronald P. Rapini, MD.*



eFig. 112.14 Spitz nevus. Pink symmetric papule in a child. *Courtesy Julie V. Schaffer, MD.*



eFig. 112.16 Epithelioid cell nevus/tumor associated with BAP1 loss – histopathologic features. There is a dermal proliferation of epithelioid melanocytes. The two insets show details of cellular morphology and of loss of BAP1 expression (note normal nuclear staining of keratinocytes within the epidermis). *Courtesy Lorenzo Cerroni, MD.*



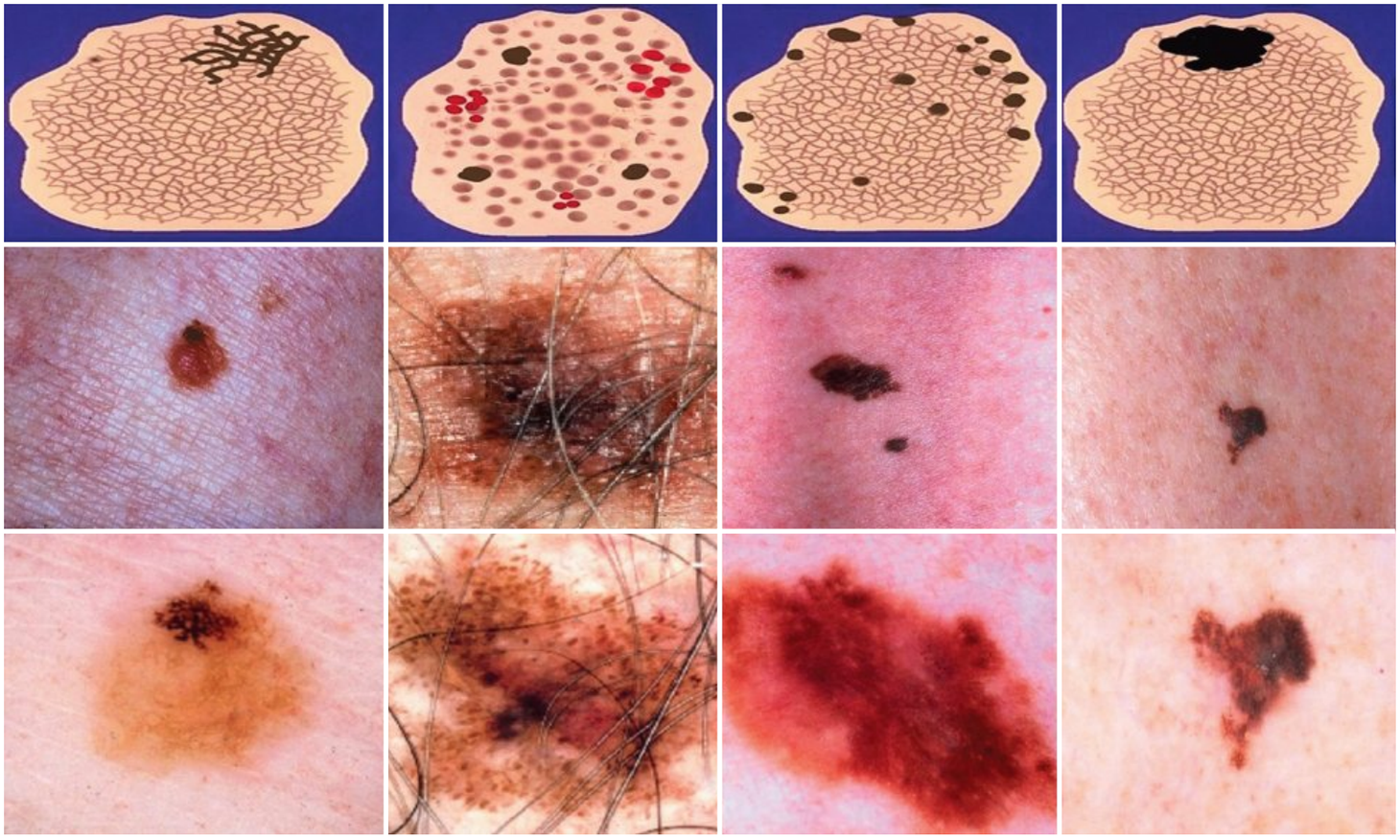
eFig. 112.15 BAP1-inactivated melanocytic nevus (BAPoma). The patient had a mesothelioma in the setting of the *BAP1* tumor predisposition syndrome. *Courtesy Edward Cowen, MD.*



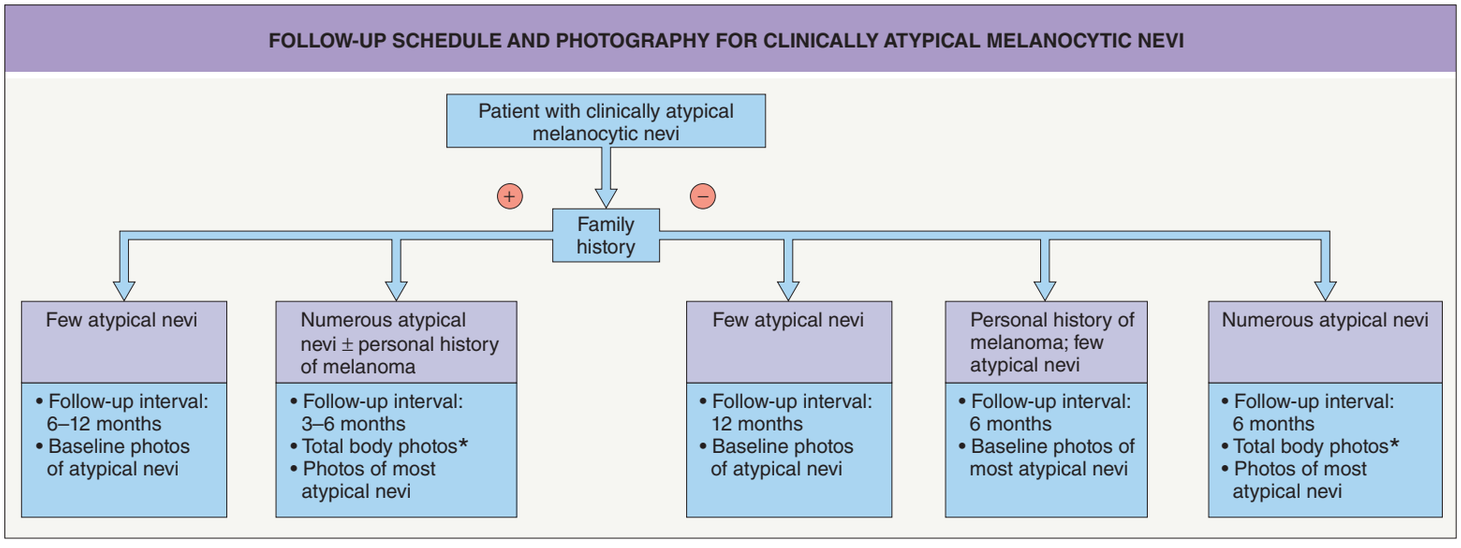
eFig. 112.17 Erythematous variant of atypical melanocytic nevus.



eFig. 112.18 Eclipse nevus on the scalp. Note the discontinuous rim. *Courtesy Julie V. Schaffer, MD.*



eFig. 112.19 Atypical melanocytic nevi with dermoscopic patterns often associated with melanoma. From top to bottom, schematic, normal illumination, and dermoscopy. *Courtesy the AAD Dermoscopy Group*.



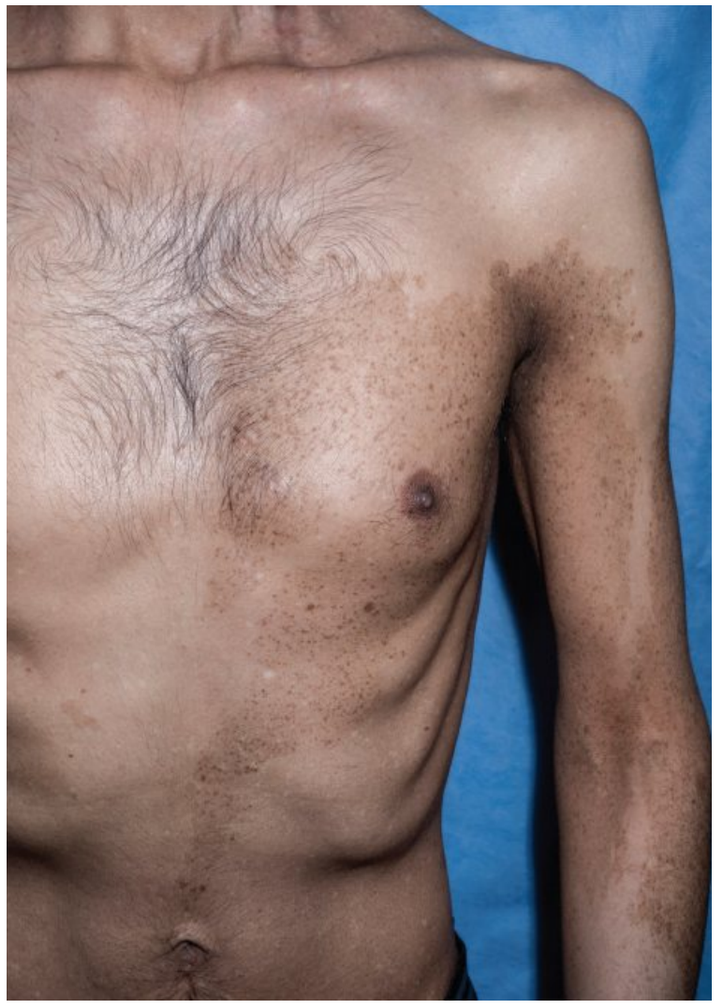
eFig. 112.20 Follow-up schedule and photography for clinically atypical melanocytic nevi. *Advocated by some authors, but not standard of care.



eFig. 112.21 Small congenital melanocytic nevus. Note the hypertrichosis and slight heterogeneity in pigmentation, reflecting its hamartomatous nature. *Courtesy Lorenzo Cerroni, MD.*



eFig. 112.22 Small congenital melanocytic nevus. Note the hypertrichosis and somewhat irregular pigmentation, reflecting its hamartomatous nature. *Courtesy Jean L. Bolognia MD.*



eFig. 112.24 Nevus spilus (speckled lentiginous nevus). Large tan patch on the left torso and arm with numerous more darkly pigmented macules. This type of lesion is sometimes referred to as zosteriform but can follow the lines of Blaschko. *Courtesy Edward Cowen, MD.*



eFig. 112.23 Giant congenital melanocytic nevus with multiple satellite nevi. The infant also had neurocutaneous melanosis. *Courtesy Jeffrey P. Callen, MD.*

ASSESSMENT OF ATYPICAL SPITZ TUMORS IN CHILDREN AND ADOLESCENTS FOR RISK FOR METASTASIS	
Parameter	**Score**
Age (years)	
Pre-pubertal	0
Post-pubertal	1
Diameter (mm)	
0–10	0
>10	1
Involvement of subcutaneous fat	
Absent	0
Present	2
Ulceration	
Absent	0
Present	2
Mitotic activity (per mm^2)	
0–5	0
6–8	2
≥9	5

eTable 112.1 Assessment of atypical Spitz tumors in children and adolescents for risk for metastasis. Total score and risk for metastasis: 0–2, low risk; 3–4, intermediate risk; 5–11, high risk.

113 Melanoma

Lisa C. Zaba, Jennifer Y. Wang and Susan M. Swetter

Chapter Contents

Molecular Pathogenesis *2009*
Host Immune Response to Melanoma *2010*
Epidemiology *2010*
Risk Factors for Cutaneous Melanoma *2012*
Types of Primary Melanomas *2016*
Other Melanoma Variants *2019*
Melanoma and Pregnancy *2022*
Melanoma in the Pediatric and Adolescent Population *2022*
Diagnosis *2022*
Pathology *2025*
Staging *2030*
Prognosis *2031*
Evaluation of a Patient with Suspected Melanoma *2031*
Management *2034*
Melanoma Surveillance *2040*

Abbreviations:

CGH, comparative genomic hybridization
FISH, fluorescence *in situ* hybridization
GEP, gene expression profiling
NGS, next generation sequencing

Key features

- Melanoma represents a malignant tumor that arises from melanocytes and is responsible for the majority of skin cancer deaths
- The incidence rates of melanoma have increased over the past four decades by five- to seven-fold, whereas mortality rates began to stabilize in the early 1990s and more recently have declined due to effective therapies for advanced disease
- Dermoscopy has led to an improvement in diagnostic accuracy as have bedside imaging technologies and molecular tests, performed both before and after skin biopsy
- Early-stage melanomas are usually curable by surgical excision
- A greater understanding of molecular pathophysiology has translated into improved melanoma risk assessment, diagnosis, prognostication, and targeted therapies
- For metastatic melanoma, the advent of oral therapies that target mutant signaling pathways (e.g. BRAF and MEK inhibitors) and immunotherapies that act as checkpoint inhibitors (e.g. anti-CTLA-4, -PD-1, and -PD-L1 antibodies) has resulted in improved overall survival

INTRODUCTION

Melanoma is a malignant tumor that arises from melanocytes and is most commonly cutaneous in origin. It can also arise on mucosal surfaces (e.g. oral, conjunctival, vaginal) and within the uveal tract of the eye as well as the leptomeninges.

Rising incidence rates of cutaneous melanoma have been observed worldwide over the past four decades in White populations. While mortality rates increased slightly in the US and Europe during the 1970s and 1980s, a stabilization of mortality rates has been observed in a number of countries since the 1990s. The latter is due primarily to increased early detection of thinner cutaneous melanomas that have a lower likelihood of metastasis. Melanoma is also one of the most common forms of cancer in young adults. It therefore represents a significant public health concern in this age group, especially with respect to potential years of life lost. After decades of minimal progress, the recent introduction of effective targeted and immune therapies has led to a significant decline in mortality rates in patients with advanced disease.

MOLECULAR PATHOGENESIS

Cancer usually develops through a stepwise evolutionary process, with tumor progression involving both genetic instability and selective growth of cells with advantageous mutations. Additional contributing factors include genetic predisposition, mutagenic environmental events, and antitumor host response. As discussed in Chapter 107, the hallmarks of cancer can be acquired by the activation of oncogenes or the inactivation of tumor suppressor genes via point mutations, genomic rearrangements (e.g. deletions, inversions, duplications, fusions, and translocations), and epigenetic mechanisms such as microRNA expression and promoter methylation. Genome-wide analysis of genetic aberrations has revolutionized our understanding of the complex interplay of signaling pathways[1].

In melanoma, initiating oncogenic events frequently affect genes involved in the mitogen-activated protein kinase (MAPK) and phosphoinositide 3-kinase (PI3K) signaling pathways (Fig. 113.1). While these alterations may initially result in senescence, secondary genetic alterations can then result in progression into a malignant tumor[2]. The constitutive activation of MAPK or PI3K signaling that commonly occurs can be due to mutations in several kinase genes or fusions that disrupt the regulatory domain of a kinase gene, as well as copy number alterations. Other mechanisms include: upregulation of telomerase genes which results in unlimited replicative potential; changes in chromatin remodeling that lead to increased gene expression; and disruption of cell cycle regulation via mutations in genes that encode cyclin D1, p16/p14^{ARF}, or p53[3]. Table 113.1 lists some of the key primary and secondary driver mutations identified in melanomas[2].

Melanomas from different anatomic sites with varying degrees of UV radiation (UVR) damage differ in their characteristic driver mutations (see Table 113.1). Recognition of several distinct mechanisms of melanoma pathogenesis has inspired the current taxonomy of melanocytic neoplasia reflected in the 2018 WHO Classification of Skin Tumours, which integrates site of origin (epithelium- versus non-epithelium-associated) and role of cumulative sun damage (CSD; high-, low-, or non-CSD-related), along with mole phenotype (high vs low nevus count) and frequency of BRAF, NRAS, and other relevant mutations[2,4–6].

Advances in our understanding of the molecular basis of melanoma have paved the way for the era of targeted therapy. For example, discovery of the *BRAF* V600E mutation, which substitutes a glutamic acid (E) for valine (V) at codon 600, leading to activation of the MAPK pathway, has led to the use of BRAF inhibitors for *BRAF*-mutant melanomas. These agents are combined with MEK inhibitors, which act downstream of BRAF in the MAPK pathway, for improved efficacy and tolerability. For melanomas lacking the typical point mutations in *BRAF*, *NRAS*, or *NF1* (so-called "pan-negative" melanomas), identification of MAPK-activating kinase gene fusions in a subset of these melanomas

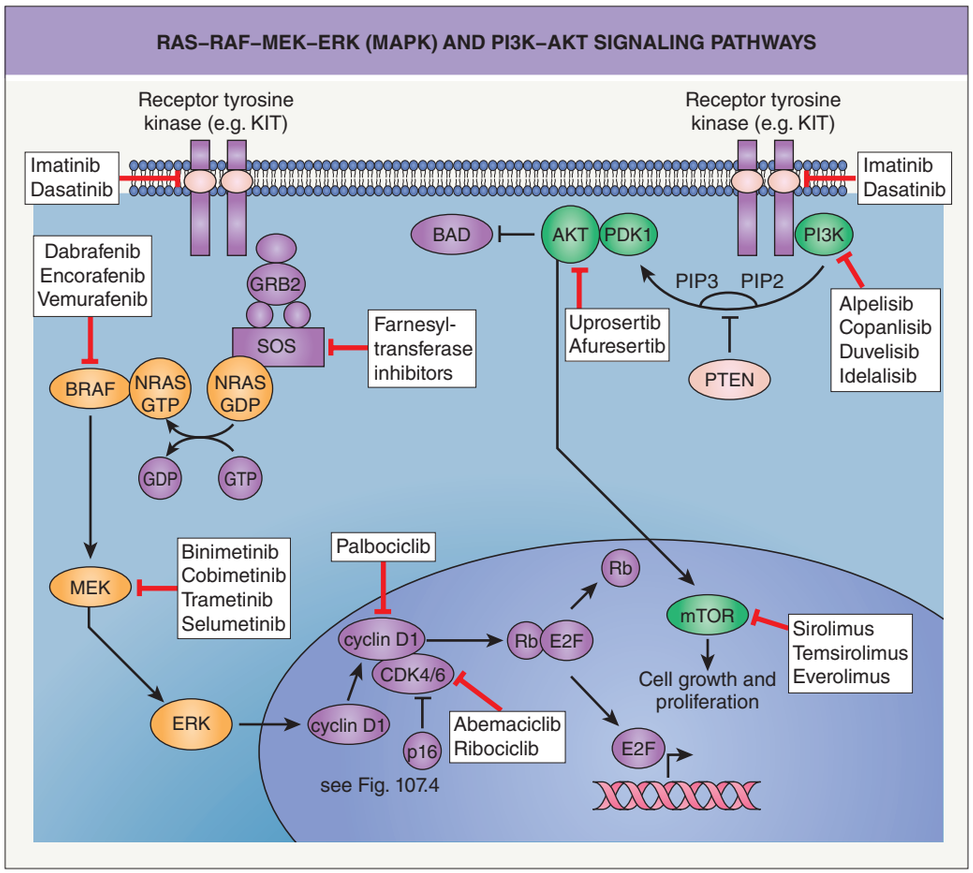


Fig. 113.1 RAS–RAF–MEK–ERK (MAPK) and PI3K–AKT signaling pathways. The *m*itogen-*a*ctivated *p*rotein *k*inase (MAPK) pathway (orange color), also referred to as the MAP kinase pathway, is physiologically activated by growth factor binding to receptor tyrosine kinases. The stimulus is relayed to the nucleus via the GTPase activity of NRAS and the kinase activity of BRAF, MEK, and ERK. Within the nucleus, this results in increased transcription of genes involved in cell growth, proliferation, and migration. The central role of this pathway in melanocytic neoplasia is highlighted by the fact that either *NRAS* or *BRAF* is mutated in up to 80% of all cutaneous melanomas and melanocytic nevi. The PI3K–AKT pathway is another important regulator of cell survival, growth, and apoptosis (green color). A key inhibitor of this pathway is PTEN and inactivation of the gene that encodes PTEN via mutations, deletions, or promoter methylation also occurs in cutaneous melanomas. As a result, there is increased activity of the PI3K–AKT signaling pathway. Examples of farnesyltransferase inhibitors are tipifarnib and lonafarnib. BAD, BCL-2 associated agonist of cell death; CDK, cyclin-dependent kinase; E2F, transcription factor that controls transcription of cyclins; ERK, extracellular signal-regulated kinase; GDP, guanosine-5-diphosphate; GRB2, growth factor receptor-bound protein 2, an adaptor protein that contains one Src homology 2 (SH2) domain and two SH3 domains; GTP, guanosine-5-triphosphate; MEK, MAPK kinase; mTOR, mammalian target of rapamycin (aka sirolimus); p16, protein product of *CDKN2A*; PDK1, phosphoinositide-dependent kinase-1; PI3K, phosphatidylinositol 3-kinase; PIP2, phosphatidylinositol 4,5-bisphosphate; PIP3, phosphatidylinositol 3,4,5-triphosphate; PTEN, phosphatase and tensin homolog; Rb, retinoblastoma protein; SOS, son of sevenless.

may permit their treatment with other kinase inhibitors. For example, melanomas harboring *NTRK* fusions can be treated with larotrectinib, a selective TRK inhibitor approved for TRK fusion-positive tumors[7].

HOST IMMUNE RESPONSE TO MELANOMA

Melanoma is a highly immunogenic tumor, making it ideal for immune-based therapeutic approaches (Fig. 113.2). Multiple melanoma antigens, recognized by autologous T cells or antibodies, have been described including: (1) mutant tumor antigens (e.g. mutant p16 [CDKN2A]); (2) shared tumor-specific antigens of the cancer/testis family (e.g. MAGE-1, MAGE-3, NY-ESO-1); and (3) cell type-specific differentiation antigens (e.g. tyrosinase, PMEL17/gp100, MART-1/Melan-A). These proteins are processed and presented on the melanoma cell surface as MHC/peptide complexes. $CD8^+$ cytotoxic T cells recognize these antigens via their T cell receptors (TCRs) and, if appropriately activated by costimulatory signals, are able to kill tumor cells. $CD4^+$ T helper cells and antibodies also play a critical role.

Activation of melanoma-specific $CD8^+$ T cells is dependent on the migration of tumor antigen-loaded dendritic cells to a draining lymph node. Here, melanoma antigens are presented to $CD8^+$ T cells in the presence of a costimulatory signal; the latter consists of the binding of B7 on the antigen-presenting cell to CD28 on the T cell (see Ch. 4). Cytotoxic T lymphocyte-associated antigen-4 (CTLA-4) is an inhibitory homolog of CD28 that is upregulated following T cell activation and acts as natural inhibitor of T cell activation by removing the costimulatory signal. Programmed cell death protein 1 (PD-1) is another inhibitory receptor in the CD28 family (see Fig. 128.9). The interaction of PD-1 with its ligands PD-L1 and PD-L2 promotes apoptosis of tumor antigen-specific T cells and reduces apoptosis in regulatory T cells.

Immunotherapy based upon CTLA-4, PD-1, and PD-L1 blockade was first introduced for the treatment of melanoma (see below), beginning with ipilimumab, an anti-CTLA-4 antibody. This was followed by the approval of anti-PD-1 antibodies (nivolumab, pembrolizumab) as first-line monotherapy for metastatic and locally advanced melanoma. Combining anti-CTLA-4 and anti-PD-1 antibodies leads to greater efficacy, but a significant increase in immune-related adverse events (irAEs). Of note, vitiligo is a melanocyte-targeted irAE that occurs in 2%–25% of patients and its development correlates with improved progression-free survival[8].

Insights into mechanisms of melanoma-specific host immune responses and immune escape have clearly led to improved immunotherapy in the form of checkpoint inhibitors and hopefully will result in other more effective therapies, including vaccines. However, overcoming the range of immune escape mechanisms still remains a challenge (Table 113.2).

EPIDEMIOLOGY

Cutaneous melanoma develops primarily in individuals with lightly pigmented skin. While melanoma is relatively uncommon amongst more darkly pigmented individuals of African, Asian, or Hispanic origin, its incidence has been slowly rising in some of these populations[9].

In 2015, over 350 000 new cases of melanoma were diagnosed worldwide, corresponding to an age-standardized incidence rate of 5 per 100 000 individuals, and nearly 60 000 deaths were attributable to melanoma. Globally, Australia, New Zealand, North America, and Europe bear the greatest burden of disease, with the highest incidence rates in Australia/New Zealand (~54/100 000) and Northern Europe (~25–26/100 000)[10]. Based upon the Surveillance Epidemiology and End Results (SEER) database, an estimated 99 780 men and women in the US are expected to be diagnosed with invasive cutaneous melanoma in 2022, with a projected 7650 melanoma-associated deaths[11].

Over the past several decades, the incidence rates of cutaneous melanoma have increased significantly (Fig. 113.3A)[12]. Whereas the annual increase in melanoma incidence varies depending upon the population, in general it has been estimated to be between 3% and 7%. These estimates predict a doubling of rates every 10–20 years, making cutaneous melanoma the most rapidly increasing cancer in White populations. However, an increase in skin screening, biopsy rates, and histopathologic diagnosis likely also contribute to this rise[13]. The trend of increasing incidence rates is predicted to continue for at least the next decade, although several countries have begun to observe stabilizing or declining rates in recent years[14].

Since 2006, the overall incidence of melanoma in the US has risen at a slower rate of ~1% per year. Although melanoma incidence rates have

GENETIC MUTATIONS IN MELANOMAS			
Gene	**Genomic alteration(s)**	**Molecular effect**	**Clinical significance**
BRAF	Point mutation, kinase fusion	Constitutive kinase activity, leading to activation of MAPK pathway	• 50%–60% of cutaneous melanomas, including 70% of non-CSD melanomas (*BRAF* V600E most common) • V600K and non-V600E mutations seen in high-CSD melanomas • Also in acquired melanocytic nevi and atypical (dysplastic) nevi
NRAS	Point mutation	Constitutive kinase activity, leading to activation of MAPK and PI3K pathways	• 15%–20% of melanomas, including high-CSD (most common mutation), low-CSD, acral lentiginous, and mucosal melanomas • Also in majority of large/giant congenital melanocytic nevi and melanoma arising in congenital nevi
KIT	Point mutation, amplification	Constitutive activation or increased expression of RTK, leading to MAPK pathway activation	• 15%–40% of acral lentiginous, mucosal, and high-CSD melanomas
GNAQ, GNA11	Point mutation	Constitutive G protein activity, leading to activation of downstream protein kinase C and MAPK pathways	• 80%–90% of uveal melanomas • Also in blue nevi and melanomas arising within blue nevi
NF1	Deletion	Loss of NF1 tumor suppressor function, leading to activation of MAPK and PI3K pathways	• 25% of desmoplastic melanomas • 30% of high-CSD melanomas
HRAS	Point mutation	Constitutive kinase activity, leading to activation of MAPK pathway	• Spitz melanomas
NTRK1/3	Kinase fusion	Constitutive activation of RTK, leading to increased activation of MAPK and PI3K pathways	• Spitz melanomas • Subset of BRAF/NRAS/NF1-negative melanomas
CDKN2A	Deletion	Loss of p16 tumor suppressor function, leading to increased Rb phosphorylation, E2F transcription factor activation, and expression of cell cycle progression genes	• *Most common germline mutation* in familial melanoma • Accounts for ~2% of cutaneous melanomas • Also in atypical (dysplastic) nevi, atypical Spitz tumors
CCND1	Amplification	Increased phosphorylation of Rb, leading to activation of transcription factor E2F and expression of cell cycle progression genes	• *Melanoma susceptibility gene* • Copy number gains common in high-CSD and acral lentiginous melanomas
CDK4	Amplification	Same as *CCND1*	• *Melanoma susceptibility gene*
BAP1	Deletion	Loss of BAP1 deubiquitinase function, leading to altered histone modifications and deregulated gene expression	• *Melanoma susceptibility gene* (BAP1 tumor syndrome) • Nearly 50% of uveal melanomas
TERT	Promoter mutation, amplification	Increased telomerase enzyme activity, leading to telomere elongation and impaired cell senescence	• *Melanoma susceptibility gene* • Amplifications commonly present in acral lentiginous melanomas
MITF	Point mutation, amplification	Alteration of transcription factor function, leading to dysregulation of melanin biosynthesis and upregulation of *CDK4*, *CDKN2A*, and *BCL2* transcription	• *E318K germline mutation* associated with lightly pigmented skin, elevated melanocytic nevus count, and increased melanoma risk, including amelanotic melanoma
POT1	Point mutation	Increased telomerase enzyme activity, activation of DNA damage	• *Germline mutations* associated with an increased risk of cutaneous melanoma
PTEN	Point mutation, deletion	Loss of PTEN tumor suppressor function, leading to increased activation of PI3K pathway	• *Germline mutations* (e.g. Cowden syndrome) associated with increased risk of cutaneous melanoma

Table 113.1 Genetic mutations in melanomas. Germline mutations in BRAC2 may be associated with a slightly increased risk of melanoma. The genes in the darker shade can be inherited as melanoma susceptibility genes. See Figs. 65.4, 67.22, and Fig. 113.1 for sites of activity of protein products. CSD, cumulative sun damage; MAPK, mitogen-activated protein kinase; PI3K, phosphatidylinositol-3 kinase; Rb, retinoblastoma; RTK, receptor tyrosine kinase. From references 2, 4, 26, and 30.

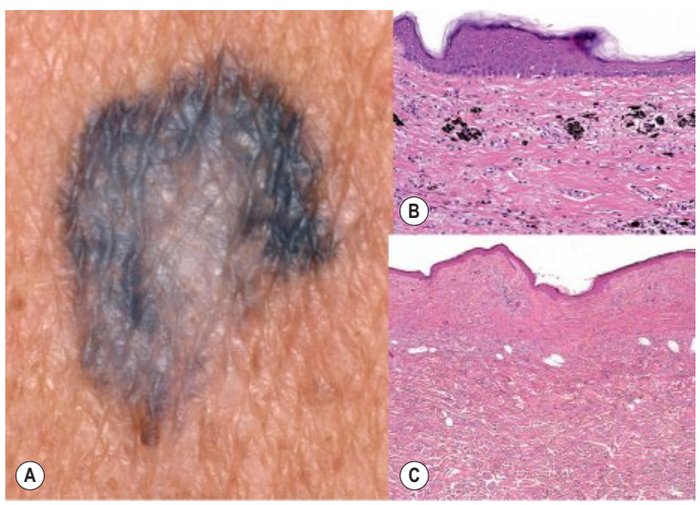


Fig. 113.2 Completely regressed cutaneous melanoma. A, B The gray-black arciform area had only melanophages in the upper dermis; although there were no remaining cells of melanoma, the patient already had nodal metastases. **C** The central hypopigmented area had fibrosis with sparse inflammation. Complexes of a pre-existing melanocytic nevus were present focally below the zone of regression. *Courtesy, Department of Dermatology, Medical University of Graz.*

ESCAPE MECHANISMS OF MALIGNANT TUMORS, INCLUDING MELANOMA
Loss of tumor-specific antigens
Loss of MHC class I molecules
Secretion of immuno-inhibitory cytokines (e.g. IL-10, TGF-β)
Upregulation of inhibitory costimulatory molecules and ligands on tumor or immune cells (e.g. CTLA-4, PD-L1, PD-1)

Table 113.2 Escape mechanisms of malignant tumors, including melanoma. IL, interleukin; MHC, major histocompatibility complex; TGF, transforming growth factor.

decreased in younger populations, they have significantly increased among older individuals, specifically non-Hispanic White men >55 years of age and White women >45 years of age[15]. Invasive melanomas, particularly thick melanomas, have also increased significantly over the past two decades among Hispanics in regions of high UVR exposure (e.g. California, Florida)[16].

Despite the continued increase in melanoma incidence worldwide, melanoma mortality has generally stabilized and in some countries declined in recent years. After increasing during the 1980s in most European countries as well as in North America (Fig. 113.3B),

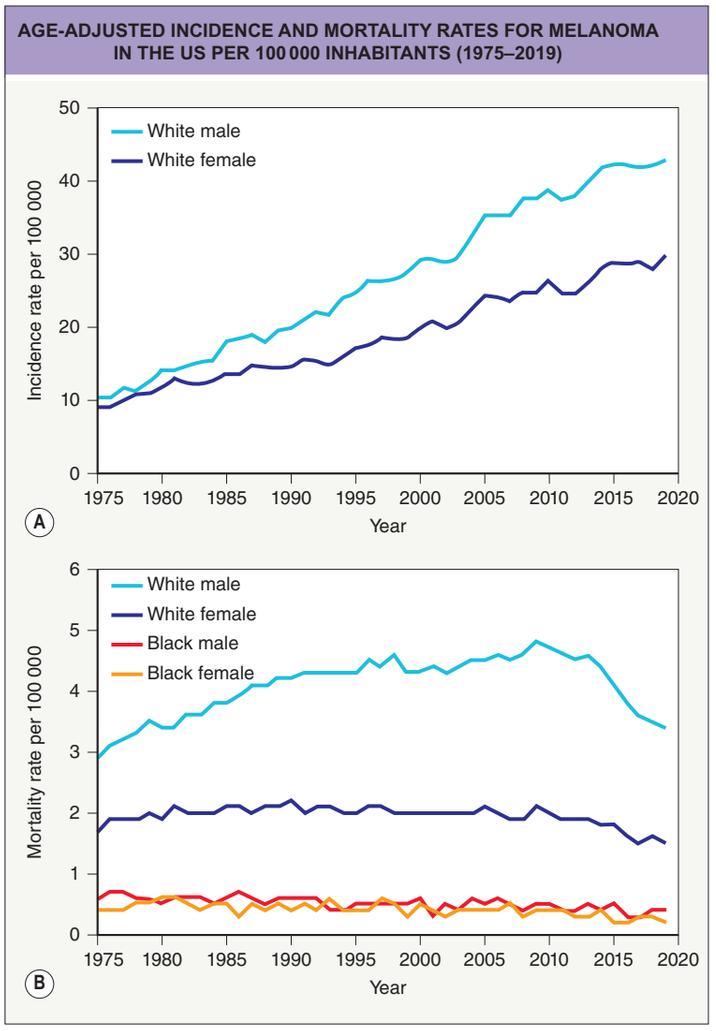


Fig. 113.3 Age-adjusted incidence rates and mortality rates for melanoma in the US per 100 000 inhabitants (1975–2019). A, B While the incidence of melanoma has increased significantly in White men and women over the past four decades, there has been a modest increase in mortality, primarily in middle-aged to older White men and individuals of lower socioeconomic status, across all racial and ethnic groups[12]. *Data from https://seer.cancer.gov/statistics-network/explorer.*

RISK FACTORS FOR THE DEVELOPMENT OF CUTANEOUS MELANOMA
Epidemiologic factors
• Male sex • >60 years of age
Genetic factors
• Family history of cutaneous melanoma, pancreatic cancer, astrocytoma, uveal melanoma, and/or mesothelioma • Lightly pigmented skin (Fitzpatrick I–II phototypes) • Tendency to burn, inability to tan • Red hair color and blue eyes (pheomelanin-predominant) • Personal history of melanoma • DNA repair defects (e.g. xeroderma pigmentosum) • Predisposing germline mutations or polymorphisms (e.g. *CDKN2A, CDK4, BAP1, TERT, MITF*)
Environmental factors
• Intense intermittent sun exposure • Multiple and/or blistering sunburns, including during childhood • Chronic sun exposure • Residence in equatorial latitudes • Tanning bed use, especially under the age of 35 years • Iatrogenic or acquired immunosuppression (e.g. solid organ transplant recipients, HIV infection)
Phenotypic expressions of gene/environment interactions

• Melanocytic nevi and solar lentigines:
  • Increased total number of acquired melanocytic nevi (MN)
  • >100 MN, relative risk ~8- to 10-fold increased
  • Atypical melanocytic nevi (AMN)
  • 5 AMN, relative risk ~4- to 6-fold increased
  • Actinic keratosis or keratinocyte carcinoma
  • Multiple solar lentigines (SL)
  • Multiple SL, relative risk ~3- to 4-fold increased

Table 113.3 Risk factors for the development of cutaneous melanoma.

Australia, and New Zealand, mortality rates from melanoma peaked in the early 1990s. Subsequently, trends have been less uniform, with mortality rates still rising in several European countries but stabilizing or decreasing in others as well as in Australia and the US. Worldwide, there has been a widening sex disparity over the past three decades, with male death rates continuing to rise in contrast to stable or decreasing female death rates. Several countries have also observed increasing mortality rates among older adults, but stable or decreasing rates among younger adults[17]. Similar trends have been noted in the US, where mortality rates for non-Hispanic White individuals have decreased in women and younger age groups but continue to increase in men over age 65 years[18]. However, with the advent of effective therapies, notable reductions in mortality have been observed since 2013 in non-Hispanic White individuals, including older men[19]. Melanoma survival among non-White populations continues to significantly lag behind White populations[20], and in several countries lower socioeconomic status has also been associated with higher mortality rates.

Vertical tumor thickness (Breslow depth) is the most important prognostic factor in primary cutaneous melanoma. Tumor thickness at initial diagnosis is somewhat age-dependent[21], with the percentage of thick melanomas increasing significantly with age, reaching 20% by age 80 years in both sexes. In the US, populations with the greatest mortality rates – older men, non-White individuals, and those in lower socioeconomic groups – have experienced a disproportionate increase in the incidence of thicker, more advanced melanomas at diagnosis[22,23].

Over the past several decades, a progressive reduction in mean tumor thickness has occurred as a result of more effective detection of melanoma at an earlier stage[24]. In Germany, for example, there has been a trend towards diagnosing thinner melanomas since the 1980s, with the median tumor thickness decreasing from 1.81 mm (1980s) to 0.53 mm (2000). The percentages of *in situ* and thin (T1; ≤1 mm) melanomas also increased[24]. Diagnosing thinner tumors should translate into stable or decreasing mortality rates, despite the rise in incidence rates. However, US data indicate that incidence rates among all tumor thickness categories have significantly increased over the past few decades (although most prominently for thin melanomas), suggesting that enhanced detection of thin melanomas cannot entirely account for the continued rise in overall melanoma incidence[22,23].

RISK FACTORS FOR CUTANEOUS MELANOMA

Recognition of risk factors for the development of melanoma is important from a public health and a clinical care perspective (Table 113.3)[25]. Identification of high-risk cohorts improves the efficiency and efficacy of public health efforts. Individual risk assessment influences clinical decision-making, including the threshold for performing a biopsy, prevention counseling, and surveillance. Risk factors may be divided into three categories: (1) genetic factors; (2) phenotypic manifestations of gene–environment interactions; and (3) environmental factors.

Genetic Risk Factors

Germline genetic mutations and polymorphisms can predispose individuals to melanoma, but detection of inherited genetic susceptibility is relatively uncommon. Approximately 5%–10% of melanomas develop in individuals with a family history of melanoma, though it is not necessarily due to transmission of a single genetic mutation[26,27]. The genes involved range from the rare high-penetrance genes responsible for some familial clustering of melanoma (e.g. *CDKN2A*) to the more common pigmentation genes responsible for the relative propensity of light-skinned individuals to develop melanoma (e.g. *MC1R*).

The major high-penetrance susceptibility gene locus associated with familial melanoma is *CDKN2A*. Approximately 2% of cutaneous melanomas can be specifically attributed to pathogenic germline mutations in *CDKN2A*[28]. This locus encodes two distinct protein products, p16 and $p14^{ARF}$, with the latter via an alternative reading frame, hence the designation ARF. p16 and $p14^{ARF}$ exert regulatory effects on cell cycle progression through the retinoblastoma protein (Rb) and p53 pathways, respectively (see Fig. 107.4). Germline *CDKN2A* mutations have been observed in 20%–40% of familial melanoma kindreds, ranging from 5% to 70% depending on the population studied[27,29] (Fig. 113.4). The penetrance of *CDKN2A* mutations is modified by germline variants of other genes, including *MC1R*. In some families, carriers of germline *CDKN2A* mutations are also at increased risk of developing pancreatic cancer[29].

Less common high-risk melanoma susceptibility genes have been identified, including the cell cycle regulator *CDK4*, the BRCA1-associated protein 1 gene (*BAP1*; see below), and telomere maintenance genes such as *TERT* and *POT1* (see Fig. 113.4). There is increasing recognition that germline mutations in these loci may not only confer an increased risk of cutaneous melanoma but also an increased risk of other internal malignancies, with melanoma possibly considered a "sentinel" cancer[30]. Although the full spectrum of potential malignancies remains to be fully characterized for some of these mutations, greater understanding of these melanoma-cancer complexes will impact future management and cancer surveillance of affected individuals.

Various pigmentation genes confer a low to moderate level of melanoma susceptibility. Specific germline variants of the melanocortin 1 receptor gene (*MC1R*) have been found to correlate with melanoma risk above and beyond clinically apparent skin phenotype (see Ch. 65). A strong association between *MC1R* as a susceptibility gene and the risk of developing *BRAF*-mutant melanomas has also been observed. While the risk of developing any cutaneous melanoma lies between 1.5- and 3-fold for individuals with *MC1R* variants, the risk of developing *BRAF*-mutant melanomas was as high as 17-fold for those with two *MC1R* germline variants[31]. In addition to *MC1R*, single nucleotide polymorphisms in the tyrosinase gene (*TYR*), tyrosinase-related protein 1 gene (*TYRP1*), and *SLC45A2* are significantly associated with melanoma risk (see Ch. 65). A rare functional variant in the gene that encodes microphthalmia-associated transcription factor (*MITF*), p.E318K, has also been associated with a light-skin phenotype and predisposes to cutaneous melanoma as well as renal cell carcinoma[32].

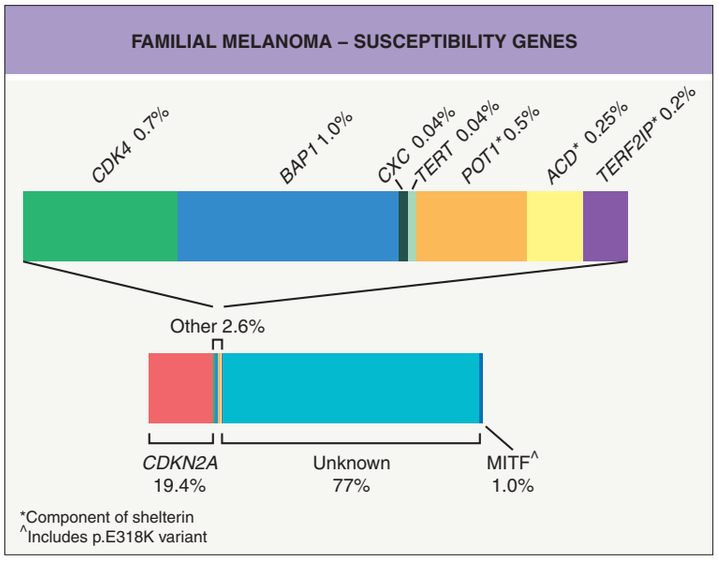


Fig. 113.4 Familial melanoma – susceptibility genes. Germline *CDKN2A* mutations are observed in 20%–40% of familial melanoma kindreds. Note the significant percentage of families for whom the genetic basis is unknown, a point that should be discussed with patients contemplating genetic screening. Patients with mutations in *CDKN2A* (p16), *CDKN2A* ($p14^{ARF}$), and *MITF* can also develop pancreatic carcinoma, neural tumors, and renal cell carcinoma, respectively, while those with *BAP1* mutations can develop uveal melanoma, mesothelioma, renal cell carcinoma, cholangiocarcinoma, meningioma, and basal cell carcinoma (at an early age). *POT1* mutations are associated with chronic lymphocytic leukemia, gliomas, and cardiac angiosarcomas. Screening recommendations are based upon the detected genetic mutation. ACD, adrenocortical dysplasia protein homolog; BAP1, BRCA1 associated protein 1; CDK4, cyclin-dependent kinase 4; CXC, CXC motif chemokine; MITF, microphthalmia-associated transcription factor; POT1, protection of telomeres 1; TERF2IP, telomeric repeat binding factor 2 interacting protein; TERT, telomerase reverse transcriptase (mutations in promoter). *Adapted from Potrony M, Badenas C, Agulilaera P, et al. Update in genetic susceptibility in melanoma. Ann Transl Med 2015;3:210.*

BAP1 tumor syndrome

Among the better-characterized melanoma-cancer complexes is the BAP1 tumor syndrome. BAP1, a deubiquitylase involved in cell cycle regulation and DNA damage response pathways, was originally implicated in the pathogenesis of aggressive uveal melanomas. Germline mutations in *BAP1* have subsequently been associated with an increased risk of cutaneous melanoma, uveal melanoma, mesothelioma, and renal cell carcinoma. Affected individuals are also at slightly increased risk of basal cell carcinoma, meningioma, and cholangiocarcinoma[33].

A characteristic finding in this syndrome is the progressive appearance of small, red–orange to skin-colored papules, which histologically demonstrate distinctive epithelioid melanocytes with loss of BAP1 nuclear staining by immunohistochemistry. These benign skin lesions, termed melanocytic *BAP1*-mutated atypical intradermal tumors (MBAITs; also "BAPomas" or *BAP1*-inactivated melanocytomas), may occur sporadically or as part of the BAP1 tumor syndrome. Up to two-thirds of patients with the BAP1 tumor syndrome may present with multiple MBAITs during the first decades of life[30].

Genetic screening in familial melanoma

The decision to perform genetic testing in cases of familial melanoma is multifaceted and must take into account the pretest probability of an underlying genetic basis, patient wishes, and the perceived risks, benefits, and limitations of current testing strategies. Consultation with a qualified cancer genetic counselor or specialist is recommended to fully explore these issues and provide important patient education and counseling, regardless of whether testing is actually performed.

Currently, there is limited evidence as to whether genetic screening is harmful or helpful[34]. Identification of germline mutations, particularly those associated with other malignancies, may be helpful in guiding additional specialist evaluation and cancer surveillance. However, in addition to the high proportion of familial melanomas with an unknown genetic basis, testing may not identify pathogenic mutations in known susceptibility genes and variants of unknown significance may lead to greater uncertainty for both clinicians and patients. Although some have argued that knowledge of mutation status may not necessarily change dermatologic management, such as the frequency of skin examinations or sun protection education, studies of *CDKN2A* germline testing have found improved adherence to dermatologic screening and precautionary behaviors among both mutation-positive and mutation-negative patients[35].

While numerous assays for *CDKN2A* mutations are commercially available, they do not capture potentially relevant germline mutations in other melanoma susceptibility genes. Multi-gene panels are thus preferred for genetic risk assessment of familial melanoma and associated internal malignancies, with the caveat that formal guidelines for subsequent cancer surveillance may currently be lacking in some scenarios.

Regional variances in the background incidence of melanoma and penetrance of melanoma susceptibility genes make it difficult to create a single guideline for genetic testing that is applicable worldwide[28]. The 2019 American Academy of Dermatology (AAD) Melanoma Clinical Practice Guidelines included recommended selection criteria for genetic counseling (Table 113.4)[34]. For regions with moderate to high melanoma incidence rates, such as the US, the "rule of 3" identifies those with a high likelihood of a *CDKN2A* germline mutation who may benefit from testing. This includes individuals with three or more primary invasive melanomas as well as families with at least one invasive melanoma and two or more other diagnoses of invasive melanoma and/or pancreatic cancer among first- or second-degree relatives (on the same side of the family)[28]. A "3 by 40" modification of this rule has been suggested to focus testing on individuals under age 40 years, since multiple melanomas in older individuals are more likely to be related to cumulative UVR exposure[26,] and a "rule of 2" variation may be considered in regions with low melanoma incidence rates[28].

RECOMMENDATIONS FOR GENETIC SCREENING FOR FAMILIAL MELANOMA
Consider genetic testing for patients with cutaneous melanoma who have: • 2 or more relatives, particularly first-degree relatives, with a history of invasive cutaneous melanoma and/or pancreatic cancer (i.e. ≥3 affected family members on same side of the family) • Personal history of ≥3 primary invasive cutaneous melanomas, including 1 tumor before age 45 • ≥1 MBAIT/"BAPoma" and family history of mesothelioma, meningioma, and/or uveal melanoma • ≥2 MBAITs/"BAPomas"
Genetic counseling should be performed by a qualified genetic risk counselor
Use of multi-gene panels is preferred over single-gene testing (e.g. *CDKN2A*)

Table 113.4 Recommendations for genetic screening for familial melanoma. MBAIT, melanocytic BAP1-mutated atypical intradermal tumor. From reference 34.

Genetic counseling may also be considered for individuals in whom the BAP1 tumor syndrome is suspected – specifically, individuals with two or more histologically proven MBAITs or at least one MBAIT and a personal or family history of mesothelioma, meningioma, or uveal melanoma.

For patients with detected germline mutations, specialist referrals for risk-appropriate malignancy screening may be warranted, and a multidisciplinary approach with input from genetic counselors can be helpful in guiding specific management. Carriers of *CDKN2A* mutations, particularly those with a family history of pancreatic cancer, may benefit from evaluation by gastroenterology specialists and earlier screening for pancreatic cancer. For *BAP1* mutation carriers, referral to ophthalmology for ocular melanoma surveillance should be offered, in addition to other specialist evaluations for possible internal malignancy screening[34].

Phenotypic Risk Factors Reflecting Gene/Environment Interactions

The strongest independent risk factors for the development of cutaneous melanoma are those that reflect a combination of genetic and phenotypic susceptibility plus environmental exposure, i.e. melanocytic nevi, atypical/dysplastic melanocytic nevi, ephelides, and solar lentigines. Both an increased number of common/typical melanocytic nevi and the presence of clinically atypical/histologically dysplastic melanocytic nevi are independent risk factors for melanoma, as is the presence of solar lentigines. Acquired melanocytic nevi play a dual role as a risk factor: (1) they are indicators of UV exposure and DNA damage; and (2) they can be formal precursors of melanoma. However, remnants of benign melanocytic nevi are found in only a minority of melanomas. Based on epidemiologic data, the risk of malignant transformation in an individual melanocytic nevus has been estimated to be one melanoma in hundreds of atypical nevi and one in thousands of common nevi[36,37]. Consequently, prophylactic removal of clinically and dermoscopically banal melanocytic nevi is not justified given the low percentage of melanomas that arise in association with nevi.

Common melanocytic nevi

Although performed on populations from different regions and with varying skin phototypes, studies have consistently reported a continuous and almost linear increase in melanoma risk with greater numbers of common melanocytic nevi, particularly larger nevi (diameter >5 mm)[38,39] (Fig. 113.5). Light-skinned populations have higher melanocytic nevus counts than do darker-skinned populations. For those with >50 common melanocytic nevi, the relative melanoma risk has ranged from ~7 in southern Spain[40] to ~54 in Scotland[41]. Nonetheless, the dose-dependent relationship between number of common melanocytic nevi and risk of cutaneous melanoma holds true for all White populations.

The association of increased nevus counts and melanoma risk is strongest for superficial spreading and nodular subtypes, more recently classified as melanomas of low cumulative sun damage (CSD)[4]. This is in contrast to lentigo maligna melanoma (high-CSD melanoma) which is highly correlated with skin phototype and hair color[41]. These

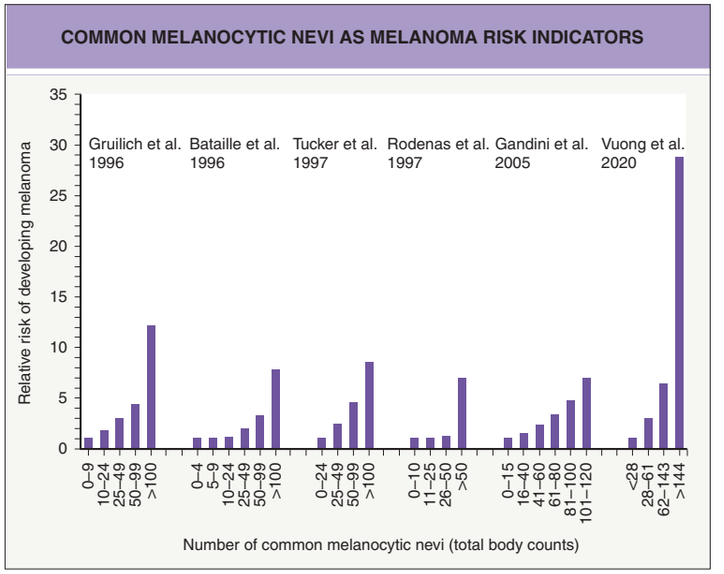


Fig. 113.5 Common melanocytic nevi as melanoma risk indicators. Relative risk of developing melanoma for a given number of common/typical melanocytic nevi (total body counts) as determined by five epidemiologic studies and one meta-analysis (Gandini et al.[47]). Nevus count studies have mostly been conducted in lighter skinned White populations; however, one study was conducted in southern Spain (Rodenas et al.[40]) Melanoma risk increases almost linearly with the number of common melanocytic nevi, rendering common nevi valuable as risk indicators.

findings suggest that there are additional genetic susceptibility factors and molecular mechanisms involved in the formation of melanoma in chronically versus intermittently sun-exposed skin. Melanoma at a particular anatomic site is more strongly related to the number of melanocytic nevi within that respective site than to the number of nevi in other body sites[40,41], highlighting the key role of local mutagenic effects of UVR in addition to genetic susceptibility (see below).

Atypical melanocytic nevi

Since the original description of BK-mole syndrome in 1978[42], several definitions of atypical melanocytic nevi as well as the atypical mole syndrome have been published. Although clinically atypical nevi often exhibit features of dysplasia histologically, the vast majority of histologically dysplastic nevi are benign and do not progress to melanoma. There is also significant variability in the histopathologic interpretation of dysplastic nevi, leading to much confusion regarding their role as melanoma precursor lesions. One study of 187 pathologists experienced in melanocytic lesion interpretation found *inter*observer concordance rates below 50% in the diagnosis of moderately dysplastic nevi, severely dysplastic nevi, melanoma *in situ*, and superficially invasive melanoma. *Intra*observer reproducibility rates for these diagnostic classes were also poor, ranging from 35% to 63%[43]. As a result of this diagnostic uncertainty, it becomes difficult to draw definitive conclusions regarding the relationship between histologically dysplastic nevi and melanoma risk[39].

In general, a diagnosis of clinically atypical melanocytic nevi is based upon the presence of at least three of the following criteria: (1) diameter ≥5 mm; (2) ill-defined borders; (3) an irregular margin; (4) varying shades within the lesion; and (5) the simultaneous presence of papular and macular components[44]. Distinguishing atypical nevi from melanoma can be aided by dermoscopy, with specific dermoscopic patterns having been identified within benign atypical nevi (e.g. reticular patchy, reticular with central hypo- or hyperpigmentation, homogeneous, peripheral reticular with central globules, peripheral globular, globular, two- or multi-component pattern; see Fig. 112.P9). A relative risk of up to 500-fold for developing cutaneous melanoma has been described for specific subgroups of the atypical mole syndrome[45]. However, sporadic atypical melanocytic nevi are commonly observed in individuals outside of the setting of the atypical mole syndrome. One possible explanation for the range of estimates of risk is the use of different definitions of clinically "atypical" melanocytic nevi by various investigators.

Several studies have found clinically atypical and/or histologically dysplastic nevi to be associated with increased melanoma risk outside of the context of familial melanoma (Fig. 113.6). The maximum reported relative risk for developing melanoma was as high as 32-fold when there were 10 or more atypical melanocytic nevi[46]. The consistency of these findings among multiple studies and across geographic locations supports the significance of clinically atypical/histologically dysplastic melanocytic nevi as an independent risk factor for sporadic melanoma.

In contrast to the continuous increase in melanoma risk with greater numbers of common melanocytic nevi, for atypical melanocytic nevi, a threshold level of five or more such lesions was associated with a clearly higher relative risk in several studies; however, there was no significant increase in risk beyond this number[44]. This finding suggests that at least five clinically atypical melanocytic nevi are needed to establish the diagnosis of atypical mole syndrome[47]; they are typically observed in conjunction with an increased mole count of at least 50, and often >100, common nevi. In patients with familial melanoma, atypical melanocytic nevi are an indicator of a markedly elevated melanoma risk.

Environmental Risk Factors

Ultraviolet radiation

The total risk for developing melanoma is determined by a complex interplay between genetic factors and exposure to UVR. It is well established that chronic suberythemal doses of UVR cause DNA mutations in skin cells. In mouse skin, repeated UVB irradiation at 10%–20% of the minimal erythema dose induced DNA damage. This damage persisted in the dermis and epidermis for several weeks following discontinuation of UVB exposure[48]. Therefore, low-dose UVB exposure in a repeated fashion could cause skin cancer. Initial indications of an etiologic role for UVR in melanoma development came from the observation that melanoma incidence was increased in White populations living closest to the equator. For example, melanoma incidence and mortality rates in Australia are 5–10 times higher than in Europe.

At the same time, numerous observations suggested factors other than chronic sun exposure played a role in melanomagenesis. Case–control studies demonstrated that melanoma risk was closely associated with the number of melanocytic nevi and with the occurrence of sunburns in childhood[49,50]. Interestingly, sunburns during childhood and adolescence significantly elevated the risk for melanoma development, but additional sunburns during adulthood did not contribute to any further risk elevation, suggesting that melanoma risk may incur primarily during childhood. Other studies found only a modest increase in melanoma risk in association with occupational or total sun exposure, but a significantly increased risk associated with intermittent sun exposure[51]. These findings were further supported by a large population-based study in New Zealand, which observed two divergent populations with high melanoma burden: young to middle-aged adults, who tended to develop melanoma in intermittently sun-exposed areas, and older adults with melanoma predominantly in areas of chronic sun exposure[52].

A bimodal age and site distribution of melanomas suggested two distinct mechanisms of UV-induced pathogenesis and this has been supported by genetic studies[53]. Early-onset melanomas, typically occurring in middle-aged adults at sites of low CSD, frequently demonstrate somatic *BRAF* or *NRAS* mutations and are often associated with an increased nevus count. In contrast, late-onset melanomas, typically lentigo maligna type, tend to occur on sites with high CSD such as the head and neck. The genomic changes seen in high-CSD melanomas are distinct from those seen in low-CSD melanomas and more clearly illustrate the role of cumulative UV damage in their pathogenesis, as evidenced by their higher mutational burden and more frequent UV signature mutations[2,54]. In comparison, the development of low-CSD melanomas appears largely related to intermittent UVR exposure during childhood.

Epidemiologic studies in young children have demonstrated a relationship between the frequency and duration of sun exposure and high numbers of melanocytic nevi early in life[55,56]. They also pointed to even moderate sun exposure as sufficient for the induction of nevi in children. The sites of subsequent melanomas often reflect the distribution pattern of melanocytic nevi[57], with both low-CSD melanomas and acquired nevi commonly harboring *BRAF* activating mutations[6]. Within acquired nevi, the high frequency of the specific *BRAF* V600E driver mutation, itself a low-probability event, suggests a high mutational burden is present in melanocytes at a young age[2]. Accumulation of additional UV-induced mutations affecting *TERT*, *CDKN2A*, and other key regulatory genes may contribute to eventual melanoma development during middle age[2,4]. It is interesting to note that the *BRAF* V600E mutation is not itself a UV signature mutation, suggesting a role for indirect UV-related mechanisms or other complex factors in the development of low-CSD melanoma.

The unique melanocyte response to UV damage, although not fully characterized, may provide additional explanations for melanoma development at both low- and high-CSD sites. In contrast to keratinocytes, which undergo apoptosis following severe UV damage, melanocytes do not undergo apoptosis as readily. Their function is to provide protective melanin to the surviving cells and so they are retained within the epidermis, even with damage that may have been sustained through either frequent, low-intensity UV exposures or infrequent, high-intensity exposures. Subsequently, melanoma can arise in anatomic sites with intermittent sun exposure.

Both UVB and UVA radiation are associated with the development of cutaneous melanoma, with UVB believed to be the stronger contributor. Data supporting *UVB* as a causative factor come from: (1) animal studies in which UVB was shown to induce melanoma in susceptible mice and in xenografted human skin engineered to express melanocytic growth factors[58,59]; and (2) the fact that there is a higher incidence of cutaneous melanoma in equatorial regions where UVB is most intense. Data implicating *UVA* in the development of cutaneous melanoma derive from: (1) studies in which UVA was shown to initiate melanoma (fish) and melanocytic hyperplasia (pigmented opossums)[60,61]; and (2) epidemiological studies showing an increased incidence of melanoma developing in users of indoor tanning beds and perhaps recipients of PUVA.

The risk of melanoma from artificial UVR exposure from tanning bed use is well documented. An estimated 10 000 melanoma cases each year in the US, Europe, and Australia are attributable to indoor tanning[62]. Indoor tanning is common among adolescents and young adults, with 55% of university students and 19% of adolescents in 2013 reporting any prior tanning bed use, and exposure to tanning beds before the age of 35 years has a statistically significant association with melanoma development. Large-scale meta-analyses have demonstrated an odds ratio of 1.16 for melanoma associated with any prior tanning bed use, with a significantly increased risk associated with >10 tanning sessions[63]. In 2009, the World Health Organization (WHO) International Agency for Research on Cancer (IARC) categorized tanning

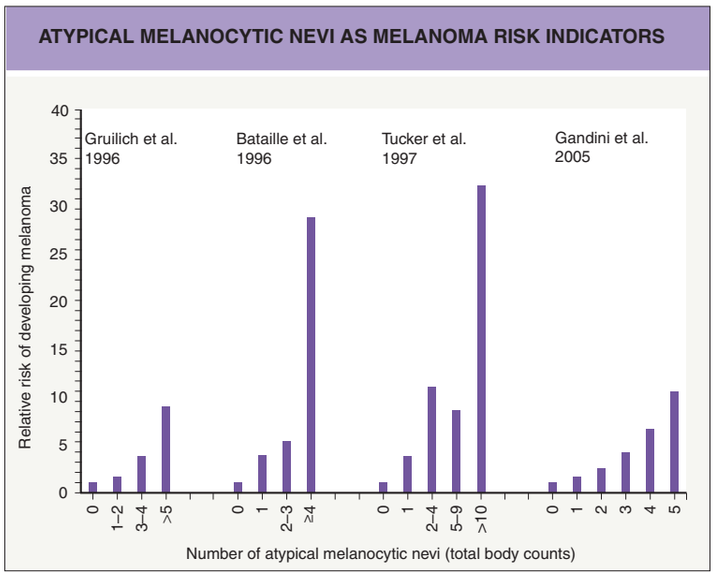


Fig. 113.6 Atypical melanocytic nevi as melanoma risk indicators. Relative risk of developing melanoma for a given number of atypical melanocytic nevi (total body counts) as determined by three epidemiologic studies and one meta-analysis (Gandini et al.[47]) An elevated risk is associated with relatively small numbers of atypical nevi. The relative risk as indicated by the number of atypical nevi is independent from the total number of melanocytic nevi, and it is related in a multiplicative fashion to the risk based on the total number of nevi. In other words, the individual risk for developing melanoma is calculated by multiplying the risk related to the total number of nevi times that due to the number of atypical nevi (see Table 113.3).

beds as a human carcinogen. Following this announcement and legislative changes limiting tanning bed access, tanning bed use worldwide has decreased by ~70% in adolescents and 35% in adults[64]. In the US, legislation banning indoor tanning among minors is state-dependent, with 24 states and the District of Columbia banning tanning bed use in individuals under 18 years (as of 2023)[65]. Additional efforts to improve legislative impact and public education will be important in addressing this ongoing public health concern.

Sun protection

Regular use of sunscreen and other sun protective measures has been shown to decrease the development of actinic keratoses and cutaneous SCCs, but evidence regarding sunscreen's ability to prevent cutaneous melanoma was not demonstrated until the results of the Nambour Skin Cancer Prevention trial were published in 2010 (see Ch. 132). This prospective randomized controlled trial (RCT) conducted in Queensland, Australia found that the daily application of SPF 16 sunscreen to the head and arms in half of 1621 adults (versus discretionary use in the other half) over a 4.5-year period reduced the incidence of new primary cutaneous melanoma by 50%–73%, 10 years after completion of the trial. This single RCT provides evidence for sunscreen efficacy in preventing melanoma development[66]. Given the low-SPF sunscreens and inferior UV filters available during the intervention period (1992–1996), as well as the age of the study population (25–75 years), it is likely that long-term use of improved broad-spectrum sunscreens in children and adolescents could have even greater benefits.

Sunscreen use is not without controversy. Some studies have raised potential safety concerns regarding chronic sunscreen use, including absorption through the skin[67] and possible endocrine-disrupting properties of some UV filters, although evidence for the latter is currently limited to studies of high-dose ingestion in rats[68]. Other studies have revealed the potential negative environmental impact of certain chemical UV filters, including potential damage to coral reefs through direct contact. Therefore, additional sun protective measures should be encouraged, including physical means of blocking the sun (e.g. non-transparent clothing, hats, eyewear) and reducing UV radiation exposure when possible (e.g. shade coverings, limiting outdoor activities between the hours of 10:00 a.m. and 4:00 p.m.).

TYPES OF PRIMARY MELANOMAS

Four major subtypes of primary cutaneous melanoma were originally described based upon their predominant growth patterns[69] (Table 113.5). The 2023 WHO Classification of Skin Tumours now recognizes nine major subtypes of melanoma based on their proposed etiopathogenesis: (1) low-CSD melanoma; (2) lentigo maligna melanoma (high-CSD melanoma); (3) desmoplastic melanoma; (4) Spitz melanoma; (5) acral melanoma; (6) mucosal melanoma; (7) melanoma arising in a giant congenital nevus; (8) melanoma arising in a blue nevus; and (9) ocular (uveal, conjunctival) melanoma[2,4–6]. Additional forms include primary CNS, nodular, nevoid, and dermal melanomas. Nonetheless, previous growth pattern-based classifications remain helpful, including for earlier clinical recognition.

FREQUENCY OF FOUR DIFFERENT SUBTYPES OF PRIMARY CUTANEOUS MELANOMA IN FOUR RACIAL GROUPS

Affected individuals	Superficial spreading	Nodular	Lentigo maligna	Acral lentiginous
Median age (years)	54	61	69	64
Average percentage	68%	16%	14%	2%
NHW (n, % by race/ethnicity)	84790 (69%)	19260 (16%)	17226 (14%)	1822 (1.5%)
HW (n, % by race/ethnicity)	1993 (62%)	689 (21%)	250 (8%)	300 (9%)
Black (n, % by race/ethnicity)	218 (37%)	106 (18%)	46 (8%)	215 (37%)
Asian/PI (n, % by race/ethnicity)	364 (48%)	160 (21%)	69 (9%)	168 (22%)

Table 113.5 Frequency of four different subtypes of primary cutaneous melanoma in four racial groups. See text for the seven major subtypes of cutaneous melanoma in the 2023 WHO Classification of Skin Tumours. Based upon Surveillance, Epidemiology, and End Results (SEER) data (n = 127 676)[263]. NHW, Non-Hispanic White; HW, Hispanic White; Asian/PI, Asian and Pacific Islanders.

Superficial Spreading Melanoma

Superficial spreading melanoma (SSM) – which in general corresponds to low-CSD melanoma – is the most common type of cutaneous melanoma in light-skinned individuals (Fig. 113.7) and is diagnosed most frequently between the ages of 40 and 60 years. It accounts for ~60%–70% of all melanomas and occurs at any site, but is most frequently observed on the trunk (mainly back) of men and the legs and trunk of women. It begins as an asymptomatic brown to black macule with color variations and irregular, notched borders (Fig. 113.8). SSM can arise *de novo* or in a pre-existing nevus (Fig. 113.9). When *in situ*, the melanoma is usually macular with an irregular outline and variable pigmentation (Fig. 113.10). SSMs may have a diameter ≤5 mm (Fig. 113.11). After a typically slow horizontal (radial) growth phase limited to the epidermis or focally within the papillary dermis, a more rapid vertical growth phase, which presents clinically with the development of a papule or nodule, can then occur. In up to two-thirds of tumors, regression (visible as gray, hypo- or depigmentation) of part of the lesion is observed, reflecting the interaction of the host immune system with the progressing tumor (see Fig. 113.2). SSM/low-CSD melanomas are the most likely subtype to arise in association with a pre-existing nevus, with one study demonstrating this relationship in about half of SSMs[70]. However, the likelihood of an individual nevus progressing to melanoma is exceedingly low (see above).

Nodular Melanoma

Nodular melanoma (NM) is the second most common subtype in individuals with lightly pigmented skin, although the lentigo maligna melanoma subtype accounts for a higher percentage in older individuals. NM is diagnosed most frequently during the sixth decade of life and more often in men than in women. It accounts for ~15%–25% of all melanomas (see Table 113.5) and occurs at any body site, but is most frequently seen on the trunk, head, and neck. While nodular melanoma does not appear to correlate with UV exposure specifically, histologically a nodular pattern may be evident in most of the subtypes in the 2023 WHO classification (see above)[4]. NM typically presents as a blue, brown, or black papule or nodule that may ulcerate and bleed (Fig. 113.12), but can also be clinically amelanotic, i.e. pink to red. Lesions typically develop rapidly over weeks to months. Although NM is rare in prepubertal children, it is often clinically amelanotic in this age group, particularly in non-White children[71].

Nodular melanoma is believed to arise as a *de novo* vertical growth phase tumor, without the pre-existing horizontal growth phase that characterizes the other histologic types. These melanomas tend to elude early detection and are often diagnosed at thicker, more advanced stages with an associated worse prognosis. Although overall NM only accounts



Fig. 113.7 Longstanding superficial spreading melanoma. Note asymmetry, irregular borders, variation in colors, scar-like regression zones, and an inferior pink papule, indicating vertical growth phase.

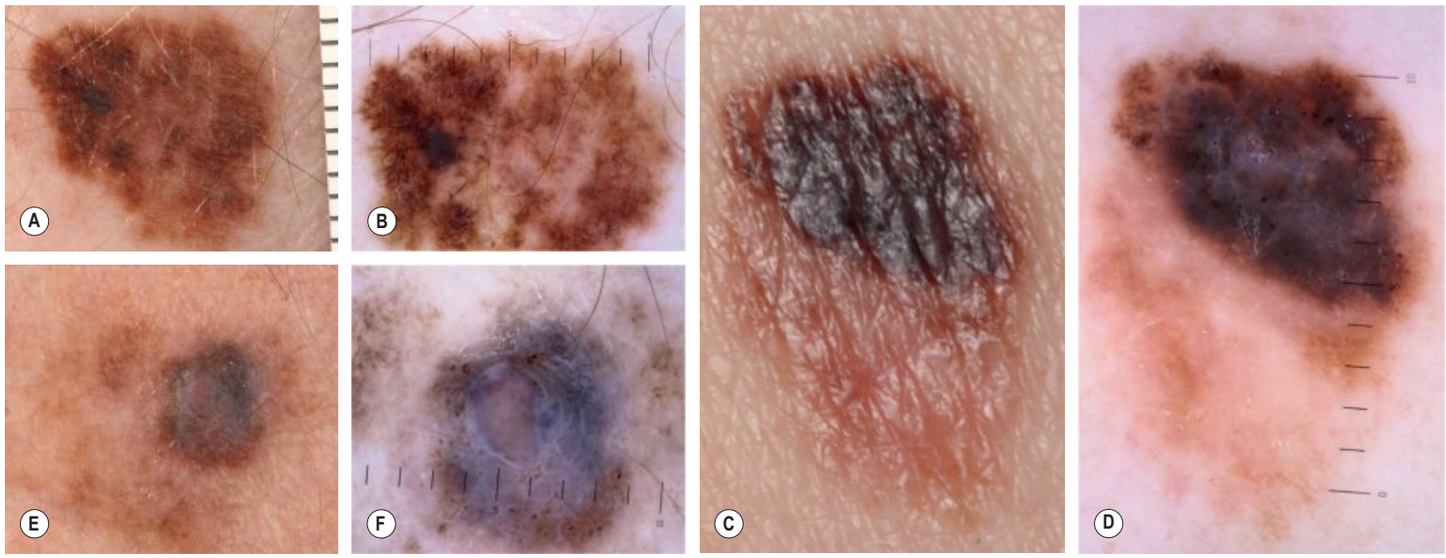


Fig. 113.8 Superficial spreading melanomas. Clinically, all of these lesions demonstrate asymmetry due to variation in color and irregularity in outline. Breslow depths for **A**, **C**, **E** were <0.5 mm, 0.58 mm, and 1.60 mm, respectively. **B**, **D**, **F** By dermoscopy, there is asymmetry, atypical pigment networks, irregular blotches, and multiple colors; in **D** and **F** a blue–white veil is present. *Courtesy Claus Garbe, MD and Jürgen Bauer, MD.*

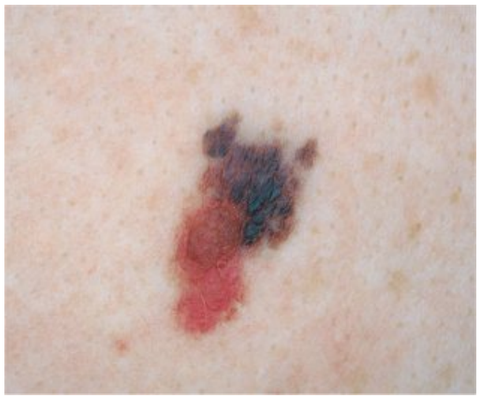


Fig. 113.9 Superficial spreading melanoma arising in a pre-existing melanocytic nevus. Note the irregular outline and variable pigmentation. The central brown papule represents the pre-existing melanocytic nevus; both the superior irregular brown-black plaque and the inferior erythematous plaque represent the melanoma.

for 10%–15% of histopathologically subtyped melanomas, it represents almost 50% of melanomas >2 mm in depth at diagnosis and nearly 40% of ultimately fatal cases[72,73]. Despite the seemingly "aggressive" behavior of NM, biological differences among melanoma subtypes have not been clearly linked to melanoma-specific survival (MSS), but rather to differences in clinical presentation that affect early detection.

Lentigo Maligna Melanoma

Although currently estimated to account for 10%–15% of cutaneous melanomas, with an aging population the incidence of lentigo maligna melanoma (LMM; corresponding to high-CSD melanoma) is on the rise (see Table 113.5). Although LMM is diagnosed most frequently during the seventh decade of life, it often occurs in younger patients who have had significant cumulative sun exposure. LMM develops within chronically sun-damaged skin, most commonly on the face, particularly the nose and cheek, as well as the scalp in older men with androgenetic alopecia. LMM usually appears as a slowly growing, asymmetric, tan to brown to black macule with color variation and an irregular, indented border. Invasive LMM typically presents as a papule or nodule in association with the macular precursor lesion (Fig. 113.13). The latter is termed lentigo maligna or melanoma *in situ*, lentigo maligna [MIS, LM] type (Fig. 113.14A,C,E). It has been estimated that 5% of LM lesions progress to invasive melanoma, but true rates of progression from the *in situ* precursor are unknown[74]. Because MIS, LM typically arises within a background of photodamaged skin, it can be difficult to distinguish from atypical/actinic melanocytic hyperplasia histologically. This phenomenon frequently confounds surgical margin assessment (see Fig. 150.4).

Lentigo maligna displays characteristic features on dermoscopic examination, although differentiation from pigmented actinic keratosis



Fig. 113.10 Melanoma *in situ* on the dorsal foot of an 84-year-old man. A, B The lesion is asymmetric and not well circumscribed. **C** The dermoscopic findings include asymmetry, variation in color, atypical pigment network, and irregular brown blotches. *Courtesy, Department of Dermatology, Medical University of Graz.*

is not always possible (Fig. 113.14B,D,F). In facial skin, hyperpigmented follicular openings (circle in a circle) are slowly overgrown by irregular pigmented dots around the follicles (annular granular pattern)[75]. Rhomboidal structures can also be seen (see Table 0.15).

Acral Lentiginous Melanoma

Acral lentiginous melanoma (ALM) is a relatively uncommon type of cutaneous melanoma and is diagnosed most frequently in the seventh decade of life. It typically occurs on the palms and soles or in and around the nail apparatus (e.g. subungual melanoma). ALM accounts for ~2%–5% of all melanomas, and the incidence of ALM is similar across all racial and ethnic groups. However, since individuals with darker skin phototypes develop fewer UV-related melanomas, ALM represents a disproportionate *percentage* of melanomas diagnosed in Black (up to 36%), Asian (up to 22%), and Hispanic (up to 9%) patients compared to only 2% of melanomas in non-Hispanic White patients (see Table 113.5)[76].

ALM typically presents as an asymmetric, brown to black macule with color variation and irregular borders (Fig. 113.15A). A higher percentage of ALMs are diagnosed at an advanced stage, likely related to: (1) lack of awareness of melanoma risk on acral sites, particularly in those with more darkly pigmented skin and an overall low risk of melanoma; (2) difficulty in clinically distinguishing this subtype from benign lesions and traumatic skin changes (Fig. 113.15B); and (3) an elevated threshold for biopsy due to the morbidity associated with surgery in acral sites. Primary misdiagnosis of ALM occurs in about one-third of all patients and leads to substantial delay in establishing the correct diagnosis. For example, when there are verrucous features, this can result in ALMs being treated as warts.

Melanoma of the nail matrix (subungual melanoma) can present as longitudinal melanonychia (Fig. 113.16) or as hyperpigmentation extending onto the hyponychium or beyond the lateral or proximal nail fold (Hutchinson sign) (see Ch. 71). The possibility of melanoma should be considered when pigmented nail bands have atypical features, in



Fig. 113.11 Melanoma *in situ*. This melanoma *in situ* measured <3 mm in diameter. Small melanomas can be easily overlooked, especially if they are less heavily pigmented. This lesion was the "ugly duckling" (outlier) among this patient's nevi. Dermoscopy assists in making an earlier diagnosis. *Courtesy Claus Garbe, MD and Jürgen Bauer, MD.*



Fig. 113.13 Lentigo maligna melanoma. A Asymmetric pigmented lesion on the earlobe, with irregular borders and significant variation in pigmentation; the Breslow depth was 0.45 mm. **B** Larger triangular brown patch in which there are multiple dark brown, black, and blue–gray papules and plaques. Breslow depth was 1.1 mm. *A, Courtesy Claus Garbe, MD and Jürgen Bauer, MD; B, Courtesy Kalman Watsky, MD.*

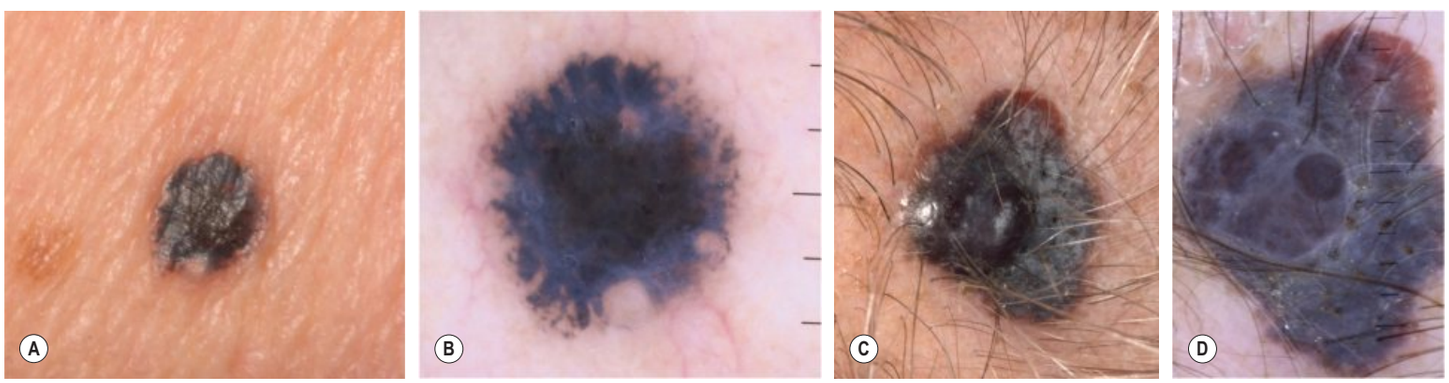


Fig. 113.12 Nodular melanomas. A Darkly pigmented papule measuring ~3 mm in diameter with a Breslow depth of 0.95 mm. **B** By dermoscopy, blue color, atypical pigment network, and streaks are seen. **C** Darkly pigmented plaque on the scalp with an eccentric nodule; Breslow depth was 2.75 mm. **D** By dermoscopy, multiple colors including blue–gray are seen. *Courtesy Claus Garbe, MD and Jürgen Bauer, MD.*

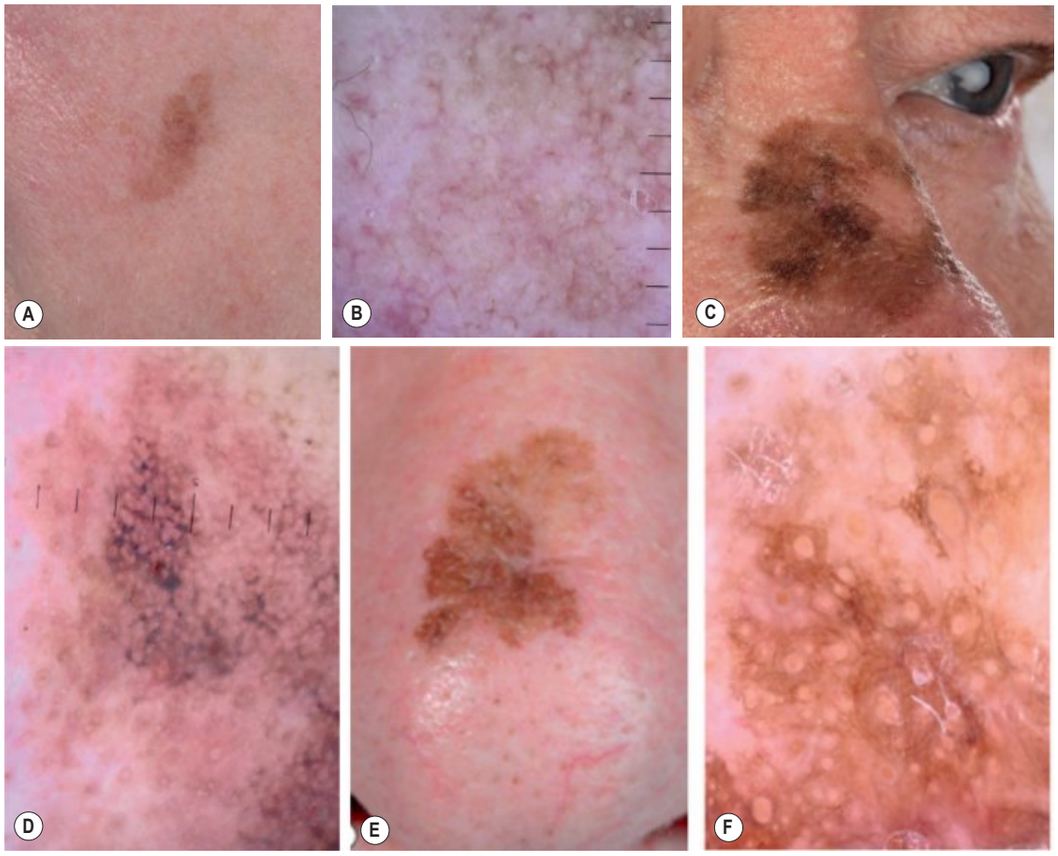


Fig. 113.14 Lentigo maligna (melanoma *in situ*, lentigo maligna type). A, **C** An early lentigo maligna presenting as a light brown patch with subtle, asymmetric pigmentation is compared to a more obvious lesion with readily apparent variation in pigmentation. **B**, **D** By dermoscopy, follicular openings surrounded by annular pigmentation are seen, referred to as a "circle in a circle". Findings are more subtle in **B** and a few rhomboidal structures are seen in **D**. **E** A pigmented lesion on the dorsal nose, with irregular borders, light to dark brown color, and marked asymmetry. **F** Dermoscopy demonstrating annular structures corresponding to follicular openings surrounded by melanoma cells ("circle in a circle"). *Courtesy Claus Garbe, MD and Jürgen Bauer, MD.*

particular if they are solitary, darkly pigmented, have irregular pigmentation, and/or have a width ≥3 mm.

ALM is a genetically distinct subtype of melanoma and clearly differs from the other types of cutaneous melanoma. It harbors more and different genetic changes than the other types and can display activating *KIT* mutations in exons 11, 13, and 17, which was hoped to lead to the successful use of KIT-inhibiting drugs (e.g. imatinib, sunitinib; see Fig. 113.1). Unfortunately, they have demonstrated limited efficacy in the treatment of metastatic disease[77].

OTHER MELANOMA VARIANTS

There are cutaneous melanomas that may present with unusual manifestations. Some of these are defined by clinical features, others by histologic findings.

Amelanotic Melanomas

Fortunately, the majority of melanomas are clinically pigmented, which aids in visual recognition and diagnosis. Melanomas lacking clinically evident pigment are termed "amelanotic" (Fig. 113.17). All four major histologic subtypes of melanoma discussed above can have amelanotic variants that may confound clinical diagnosis; recognition of dermoscopic features in amelanotic melanoma can be useful (see Figs. 0.38 and 0.39). Amelanotic SSMs, NMs, and LMMs are often biopsied due to clinical suspicion of basal or squamous cell carcinomas. Amelanotic ALMs, including subungual type, are especially challenging and may be mistaken for warts or SCC (see Fig. 113.15B). Amelanotic melanomas do not differ from pigmented melanomas in terms of prognosis or therapy.

Melanoma with Features of a Spitz Nevus (Spitzoid Melanoma and Spitz Melanoma)

Spitzoid melanomas comprise a heterogeneous category of melanomas demonstrating histomorphologic features suggestive of a Spitz nevus, e.g. well-circumscribed margins and epithelioid melanocytes that do not mature with progressively deeper dermal extension. However, unlike benign Spitz nevi, spitzoid melanomas may have features such as a large clinical diameter, deep infiltration into the dermis or subcutis, marked cytologic atypia of dermal melanocytes, or mitotic figures at the base of the lesion (see Table 112.7).

Within the category of "spitzoid melanoma" is Spitz melanoma, defined by the 2023 WHO classification as the malignant counterpart of the Spitz nevus based upon genetic characteristics[4]. Genomic analyses have revealed that many cases of *spitzoid melanomas* (e.g. with morphologic features of Spitz nevi) demonstrate genetic features of low-CSD melanoma, including *BRAF* and *NRAS* mutations not typically present in Spitz nevi. In contrast, *Spitz melanomas* demonstrate a distinct spectrum of MAPK-activating alterations more closely associated with Spitz lineage, such as mutations or fusions involving *HRAS*, *ALK*, *BAP1*, *ROS1* and *NTRK1/3*, among others[78].

A subset of spitzoid lesions demonstrate histopathologic features intermediate between benign Spitz nevi and melanoma and may present a significant diagnostic challenge, particularly since they present more often in pediatric, adolescent, and young adult populations. In the 2023 WHO classification, these lesions are termed *Spitz melanocytomas* whereas in the past, they were referred to by several terms including *a*typical *S*pitz *t*umors (ASTs), "*mel*anocytic *t*umors of *u*ncertain *m*alignant *p*otential" (MelTUMPs), or "*s*pitzoid *t*umors of *u*ncertain *m*alignant *p*otential" (STUMPs). These ambiguous lesions are considered to have biologically indeterminate behavior and are frequently treated with complete excision. Some ASTs may metastasize to regional lymph nodes, further confounding their distinction from melanoma. However, ASTs generally follow a more benign course than melanoma, even with nodal metastases, and the diagnostic and prognostic value of sentinel lymph node biopsy (SLNB) for this class of lesions has been questioned in recent years[79]. In the absence of widely accepted histomorphologic diagnostic criteria, several molecular approaches have been taken in attempts to distinguish these entities from melanoma, e.g. immunohistochemistry, fluorescence *in situ* hybridization (FISH), comparative genomic hybridization (CGH), gene expression profiling (GEP), next generation sequencing (NGS) analysis (see below).

Desmoplastic Melanoma

Desmoplastic melanoma (DM) is defined histologically by the presence of spindled melanocytes and prominent stromal fibrosis. The typical clinical lesion is a skin-colored, pink, or red plaque or nodule located on sun-exposed

skin. The lack of classic clinical findings for melanoma may result in a delay in diagnosis. DM may develop: (1) *de novo*; (2) in conjunction with an overlying LM, ALM, or other radial growth phase melanoma; or (3) rarely in mucosal sites. Deep tissue samples are necessary to establish the diagnosis (Fig. 113.18), as superficial portions of the tumor show subtle or non-diagnostic findings which may be mistaken for the fibrosis of a scar or other spindle cell neoplasms. Based upon the degree of desmoplasia and spindled melanocytes within the tumor, "pure" (>90% of tumor consists of a proliferation of spindle cells in a desmoplastic stroma) and "mixed" (<90% of the tumor has a desmoplastic stroma and focally there are nodules of melanoma cells) forms of DM have been described, with differing clinical behavior in the two forms (see below).

Compared to SSM and LMM subtypes, DM is more infiltrative and typically thicker at the time of diagnosis. Incomplete excision and local recurrences commonly occur. A subset of DMs may demonstrate neurotropism (i.e. perineural invasion), with associated higher rates of local recurrence following surgical resection; adjuvant radiation therapy may be considered to improve local control[80]. While deep DMs have significant potential for distant metastasis, conventional T-staging tends to overestimate the likelihood for metastasis. When matched for thickness, several studies have demonstrated improved melanoma-specific survival (MSS) for pure DMs as compared to other melanoma subtypes[81]. Prognosis appears to be worse for the mixed subtype compared to the pure subtype, although data are somewhat conflicting[82]. Regional lymph node metastases are generally uncommon in DM, but mixed DM is significantly more likely than pure DM to have nodal involvement, with positive SLNB rates comparable to conventional melanomas in some studies[82]. Lymphovascular invasion is also more commonly observed in the mixed form[83].



Fig. 113.15 Acral lentiginous melanoma. A Irregularly pigmented lesion on the plantar surface of the foot. Dermoscopic findings include irregular diffuse pigmentation and a parallel ridge pattern (see Fig. 112.14). **B** Crusted pink nodule on the heel that had been treated for several months as a wart prior to diagnosis. *A, Courtesy Claus Garbe, MD and Jürgen Bauer, MD; B, Courtesy Department of Dermatology, Medical University of Graz.*

Clear Cell Sarcoma ("Melanoma of Soft Parts")

Clear cell sarcoma is an uncommon soft tissue malignancy that demonstrates substantial histopathologic overlap with melanoma, including

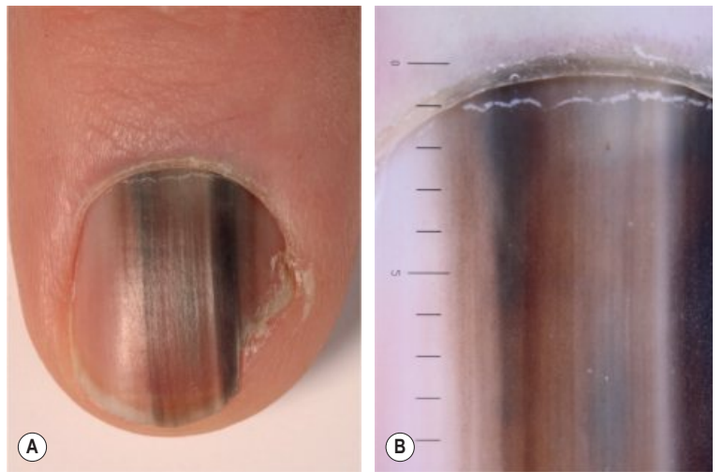


Fig. 113.16 Melanoma of the nail matrix. A, **B** The longitudinal pigmentation of the nail plate is non-homogeneous, both clinically and dermoscopically. Histologically, the Breslow depth was 0.7 mm. *Courtesy Claus Garbe, MD and Jürgen Bauer, MD.*

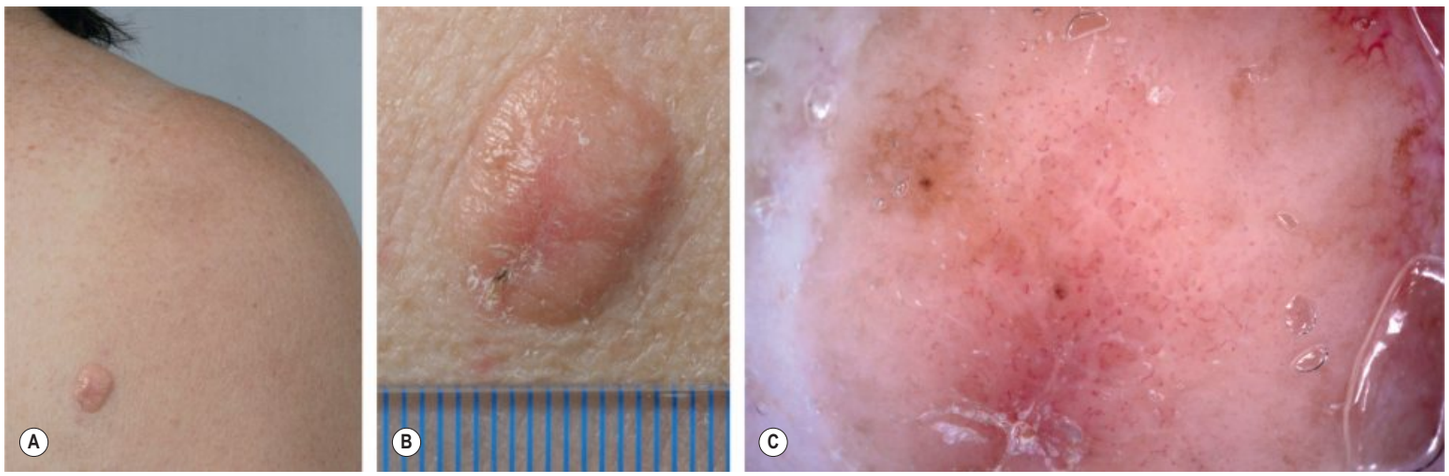


Fig. 113.17 Amelanotic melanoma. A, B Skin-colored to light pink nodule on the right scapula of a female patient; tumor thickness was 4 mm. **C** By dermoscopy, some pigmented globules allow one to identify the tumor as a melanocytic lesion. Dotted, point, and linear-irregular vessels are suggestive of melanoma. *Courtesy Claus Garbe, MD and Jürgen Bauer, MD.*

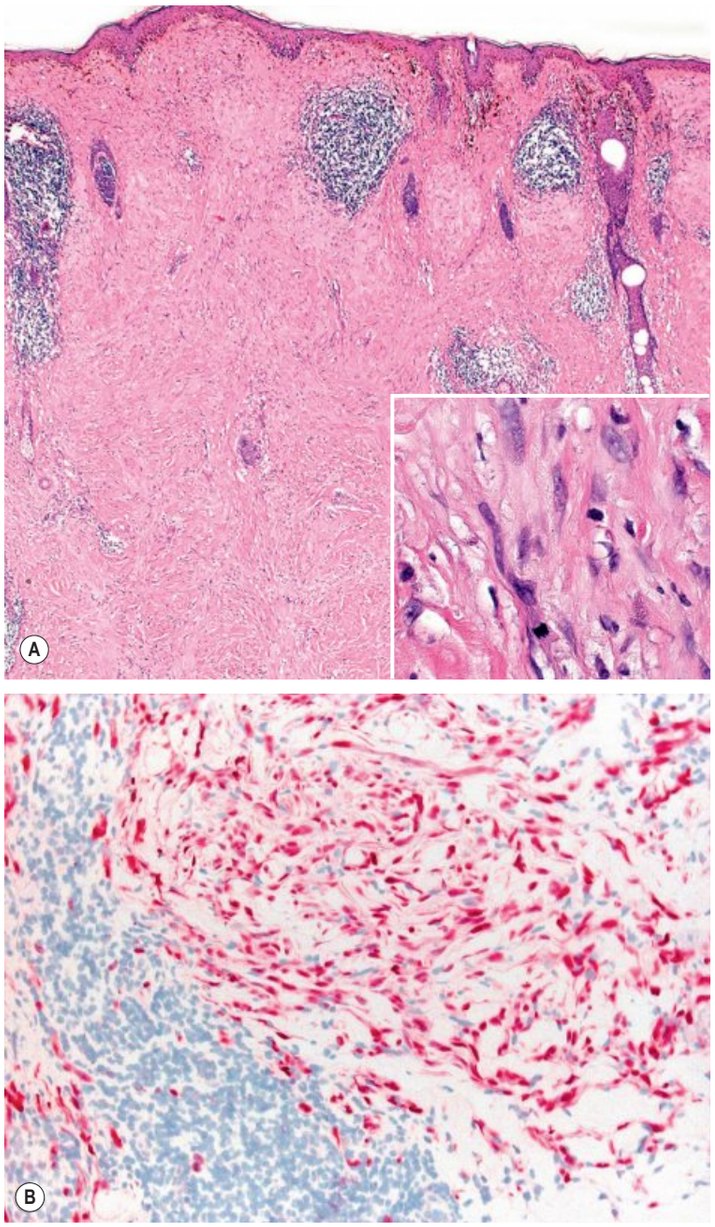


Fig. 113.18 Histopathologic features of a desmoplastic melanoma. A Loosely textured spindle cells (inset) within fibroblastic stroma. In the epidermis and follicular epithelium, there are changes of melanoma *in situ* with proliferation of atypical melanocytes. Note the lymphoid infiltrates. **B** S100-positive spindle cells within the dermis. *Courtesy Lorenzo Cerroni, MD.*

the presence of melanosomes by electron microscopy and immunohistochemical expression of S100, HMB-45, Melan-A, and other melanocytic markers[84,85]. Despite its close histopathologic resemblance to melanoma, leading to the designation "melanoma of soft parts", the exact cell of origin remains unknown, and its clinical presentation is distinctive from conventional melanoma.

Clear cell sarcoma most often presents on the distal extremities of adolescents and young adults, typically arising within the deep soft tissue in association with tendons and aponeuroses. Tumors are composed of nests and fascicles of oval to spindled cells with vesicular nuclei, basophilic nucleoli, and eosinophilic to clear cytoplasm. Multinucleated giant cells and melanin can frequently be seen. Rare cases of superficial clear cell sarcoma may be histologically challenging to distinguish from primary dermal melanomas or melanoma metastases. However, unlike melanoma, clear cell sarcoma demonstrates characteristic rearrangements of *EWSR1*; most frequently a reciprocal translocation t(12; 22)(q13; q12) results in a *EWS–ATF1* fusion gene[84]. These tumors tend to be aggressive, with a high likelihood of regional and distant metastases.



Fig. 113.19 Melanoma arising in a cellular blue nevus (blue nevus-like melanoma). Satellite (lymphatic) metastases are also present. *Courtesy Helmut Kerl, MD.*

Melanoma Arising in a Blue Nevus (Blue Nevus-Like Melanoma)

Blue nevus-like melanoma, also known as melanoma arising in blue nevus and formerly as malignant blue nevus, is a rare dermal tumor of melanocytes. It is most commonly located on the head and particularly the scalp (Fig. 113.19). The tumor presents as a blue–black, deeply situated nodule, generally >1 cm in diameter. Histologically, elements of a benign cellular blue nevus are associated with nodular areas of atypical spindle-shaped and bipolar dendritic melanocytes, mitotic figures, necrosis, and melanophages. The clinical course is characterized by a high rate of recurrence and metastasis. The associated cellular blue nevus may have mutations in *GNAQ* or less often *GNA11* (see Table 112.3), with mutations in *BAP1*, *SF3B1*, and *EIFA1X* detectable within the malignant portion.

Primary Dermal Melanoma

Although rare, dermal-based melanomas may mimic cutaneous or lymphatic metastases histologically and appear clinically similar to a cyst or other dermal tumor. These so-called "primary dermal melanomas" are characterized by a lack of overlying epidermal involvement and no regressive features, and they may be misclassified as stage III or IV melanoma at the outset. Although primary dermal melanomas present with an average Breslow depth of 3–9 mm, depending on the study[86,87], current evidence suggests a more favorable prognosis when compared to equivalently staged conventional primary melanomas – notably an estimated 5-year survival of 80%–100%. Histologic distinction between primary dermal melanoma and cutaneous metastasis may be challenging, if not impossible, and clinical exclusion of metastatic disease (often via imaging) is essential. Findings of an associated intradermal nevus and focal or weak immunohistochemical staining for proliferation-related markers (cyclin D1, Ki-67, and p53) have been described as potential distinguishing features of primary dermal melanoma[86,87].

Ocular Melanoma

Primary ocular melanomas, which are relatively rare (5% of all melanomas), can be divided into conjunctival melanomas and uveal melanomas (iris, choroidal, and ciliary body melanomas). Uveal melanomas frequently (up to 85%) harbor somatic activating mutations in *GNA11* or *GNAQ*. These genes encode members of the q class of G protein α-subunits. Heterotrimeric G proteins are involved in mediating signals between G-protein-coupled receptors (GPCRs) and downstream effectors (see Fig. 65.14)[88]. As noted previously, *GNAQ* (more frequently than *GNA11*) mutations have been detected in blue nevi but not in cutaneous melanomas.

Although biopsy of the primary tumor is not generally needed for diagnosis, it may be considered for prognostication purposes, with molecular testing via chromosomal analysis or GEP preferred over cytology alone[89]. Chromosomal changes of prognostic significance in ocular melanoma include monosomy 3 and alterations of 8q and 6p. Monosomy 3 reduces the 5-year survival from ~100% to <50%, and a particularly poor outcome has been associated with combined abnormalities in chromosomes 3 and 8[90]. However, chromosomal studies of fine needle biopsies can be limited due to sampling error resulting from tumor heterogeneity and technical failures.

Uveal melanomas can be divided into Class 1 (low metastatic risk) and Class 2 (high metastatic risk) based upon a GEP of 15 genes[91]. The GEP of Class 1 uveal melanomas resembles normal uveal melanocytes with >95% of patients free of metastasis at 4 years. In contrast, the GEP of Class 2 uveal melanomas resembles primitive neural/ectodermal stem cells with <20% of these patients free of metastasis at 4 years[92]. *BAP1* mutations are associated with Class 2 uveal melanomas[93].

The management of uveal melanoma has shifted to eye-sparing approaches, without significantly impacting patient survival. Radiotherapy with proton beams has replaced eye enucleation as the standard treatment. Unfortunately, immune checkpoint inhibitors have not led to responses similar to those seen in cutaneous melanoma. Tebentafusp, a bispecific engager that brings together $CD3^+$ T cells and melanoma cells with the gp100/HLA-A*02:01 complex, is approved for unresectable or metastatic uveal melanoma in HLA-A*02:01-positive adults. Surveillance imaging with contrast-enhanced magnetic resonance imaging or ultrasound is primarily directed at the liver, the most frequent site of uveal melanoma metastasis.

Mucosal Melanoma

Mucosal melanomas are rare lesions that may occur in the mouth, nasopharynx, larynx, and anogenital mucosae. They tend to occur near the mucocutaneous junctions of squamous and columnar epithelia and account for ~1% of melanomas. As many as 35% of mucosal melanomas are reportedly amelanotic, further complicating clinical diagnosis[94]. Not surprisingly, these tumors tend to be diagnosed at a locally advanced stage with associated poor prognosis. Similar to ALM, mucosal melanomas are a genetically distinct subtype of melanoma. They harbor more and different DNA copy number changes than do cutaneous melanomas and they can harbor activating *KIT* mutations, which could make the tumor sensitive to KIT-inhibiting drugs (e.g. imatinib; see Fig. 113.1)[77]. However, as with ALM, response rates to KIT inhibitors have so far been limited.

MELANOMA AND PREGNANCY

Melanoma accounts for 25%–30% of all cancers diagnosed during pregnancy, and the incidence has been increasing[95,96]. Although 10% of women experience darkening of their melanocytic nevi during the first 3 months of pregnancy[97], proportionate enlargement of nevi occurs within skin that has expanded due to the pregnancy (e.g. abdomen, breasts)[98]. Both biopsy and wide local excision (WLE) with small amounts of lidocaine and epinephrine (adrenaline) are considered safe to perform during pregnancy and should not be delayed. If SLNB is indicated, US National Comprehensive Cancer Network (NCCN) and AAD (2019) guidelines suggest waiting until at least the second trimester to avoid potential fetal complications of general anesthesia[34]. Both isosulfan blue and methylene blue are contraindicated in pregnancy due to risk of fetal harm, but use of radiotracer is supported by limited data, although fetal radiation dose is not known. Alternatively, in lieu of immediate SLNB, regional surveillance ultrasound can be safely utilized to monitor the draining nodal basin(s) until SLNB can be safely performed. For surveillance and imaging, non-ionizing radiation modalities such as MRI and ultrasound are preferred, as exposure to radiation from CT, X-ray, and PET scans may lead to an increased risk of fetal carcinogenesis.

An association between hormonal changes during pregnancy and development of melanoma or worsening of the prognosis of an existing melanoma has not been demonstrated in stage 0–III disease[99]. Moreover, there are no studies demonstrating that exogenous hormones (e.g. oral contraceptives, hormone-containing contraceptive devices/implants, postmenopausal hormone replacement therapy, hormones associated with assisted reproductive technology) increase the risk of developing cutaneous melanoma. There is also no evidence to suggest that subsequent pregnancies after a cutaneous melanoma diagnosis result in an increased risk of recurrence or development of additional primary melanomas. In fact, higher parity is associated with decreased risk of developing melanoma[100]. That said, in women diagnosed with stage II/III melanomas, consideration of a 2- to 3-year waiting period may be practical given that most recurrences occur during that time period. Lastly, with systemic treatments such as immune checkpoint inhibitors and targeted agents there may be increased risk of fetal toxicity[101,102].

MELANOMA IN THE PEDIATRIC AND ADOLESCENT POPULATION

Childhood melanoma is very rare. Approximately 2% of melanomas occur in patients younger than 20 years of age, and 0.3% in those younger than 14 years[103]. Risk factors for melanoma in children parallel those in adults. The exceedingly rare conditions of xeroderma pigmentosum and giant congenital melanocytic nevi contribute minimally to the prepubertal incidence of melanoma.

Pediatric melanomas, especially in prepubertal children, were found in a series of 70 patients to frequently lack conventional criteria. As a result, alternative ABCD criteria were proposed: **A** – amelanotic; **B** – bleeding, bump; **C** – color uniformity; and **D** – *de novo* appearance, any diameter[104]. In one prospective series, non-White children and adolescents were more likely to present with melanomas that were clinically amelanotic, on the extremities, and nodular subtype, compared to White children and adolescents, who presented more frequently with superficial spreading melanomas[71].

Histologically, melanomas in children may resemble those of adults, but melanomas with features resembling Spitz nevus or deep penetrating nevus are reported to be more common in this age group. As noted above, the differentiation of melanoma from atypical Spitz tumor (Spitz melanocytoma), pigmented epithelial melanocytoma, or other indeterminate melanocytic neoplasms remains a diagnostic challenge. Additional molecular tests (e.g. CGH, FISH, GEP, NGS [see below]) are often required to avoid overdiagnosis of childhood melanoma[105]. Prognosis and survival of pediatric melanoma is stage-dependent, similar to that in adults[106]. As such, treatment should follow the same rationale, regardless of age.

DIAGNOSIS

Early detection is a key factor for improving survival in patients with melanoma. The clinical diagnosis of cutaneous melanoma continues to be based on visual inspection and dermoscopy. A history of change in the color, shape, or size of a pigmented skin lesion over the course of months or years is the most sensitive clinical sign for melanoma, and it may be detected by the patient or by serial screening examinations plus dermoscopy. In high-risk patients, the latter may be supplemented with comparison of stored digital and dermoscopic images and/or total body photography.

Public awareness campaigns have highlighted the ABCDEs of melanoma: **A**symmetry, **B**order irregularity, **C**olor variegation, **D**iameter >5 mm, and **E**volution. It has been shown that patients more commonly recognize a melanoma by the development of a new pigmented lesion or by an increase in size or change in color of a pre-existing lesion, highlighting the importance of "E"[107]. Additionally, the ABCD features broadly overlap with clinically atypical melanocytic nevi, including those that are banal and have low-grade histologic dysplasia, making ABCD less specific as warning signs for melanoma in certain patients.

Dermatologists often unconsciously rely on cognitive (overall pattern) and comparative (ugly duckling sign) processes rather than an algorithm of morphologic criteria (ABCD). A diagnostic clue is the so-called *"ugly duckling" sign*, which focuses on the morphologic differences between a single striking lesion and the surrounding benign "signature" nevi[108]. There is a good interobserver reproducibility of this sign, supporting the significance of recognizing the "outlier" nevus[109].

Two other helpful clinical clues are the *"Little Red Riding Hood" sign* and the *"EFG" rule*. The former represents the finding of erythema or inflammation that at times will surround a cutaneous melanoma[110]. "EFG" stands for an **E**levated, **F**irm, or **G**rowing lesion and is helpful to keep in mind for accurately diagnosing a clinically amelanotic nodular melanoma.

MELANOCYTIC LESIONS THAT SIMULATE MELANOMAS		
Melanocytic lesion	**Clinical simulators**	**Histopathologic simulators**
• Acral nevi	√	√
• Ancient nevi		√
• Atypical (dysplastic, Clark's) nevi	√	√
• Atypical Spitz tumors	√	√
• Black (hypermelanotic) nevi	√	
• Blue nevi and variants	√	*
• Combined nevi	√	√
• Congenital nevi	√	√ (when biopsied shortly after birth)
• Deep penetrating nevi	√	√
• Halo nevi	√	√
• Hyperplasia of melanocytes in sun-damaged skin		√
• Longitudinal melanonychia	√	
• Melanocytic proliferation overlying a benign neoplasm		√
• Melanosis of mucosal regions	√	
• Nevi exposed to UV radiation		√
• Nevi and lentigines in anogenital regions	√	√
• Nevi in other "special sites", e.g. milk line, flexures, on or around the ear		√
• Nevi in patients with epidermolysis bullosa or lichen sclerosus	√	√
• Pigmented streaks in melanoma scars	√	
• Proliferating nodules within congenital nevi	√	√
• Recurrent nevi	√	√
• Reticulated (ink-spot) lentigo	√	
• Spitz nevi	√	√

*Some melanoma metastases are histologically indistinguishable from common blue nevi.

Table 113.6 Melanocytic lesions that simulate melanomas.

NON-MELANOCYTIC CLINICAL SIMULATORS OF MELANOMA
Simulating superficial spreading melanoma
• Solar lentigo • Seborrheic keratosis • Thrombosed hemangioma, angiokeratoma • Pigmented superficial basal cell carcinoma • Pigmented actinic keratosis • Extramammary Paget disease • Bowen disease including pigmented variant
Simulating nodular melanoma
• Seborrheic keratosis • Pyogenic granuloma • Dermatofibroma • Thrombosed hemangioma, angiokeratoma • Pigmented basal cell carcinoma • Pigmented poroma and pigmented porocarcinoma • Pigmented pilomatricoma and melanocytic matricoma • Pigmented dermatofibrosarcoma protuberans (Bednar tumor)
Simulating lentigo maligna/lentigo maligna melanoma
• Solar lentigo/macular seborrheic keratosis • Actinic keratosis, including the pigmented variant • Lichenoid keratosis • Pigmented superficial basal cell carcinoma
Simulating acral lentiginous melanoma of the palms and soles
• Black heel (hemorrhage in stratum corneum caused by trauma) • Plantar warts • Trophic ulcers • Plantar callosity • Tinea nigra
Simulating subungual acral lentiginous melanoma
• Subungual hematoma • Bowen disease • Verruca • Paronychia • Drug-induced nail pigmentation
Simulating desmoplastic melanoma
• Basal cell carcinoma • Squamous cell carcinoma • Dermatofibrosarcoma protuberans • Pseudolymphoma • Ruptured hair follicle/cyst • Adnexal tumor • Arthropod bite reaction (persistent)

Table 113.7 Non-melanocytic clinical simulators of melanoma. In addition to the keratinocytic carcinomas and other tumors listed above, the differential diagnosis of amelanotic melanomas includes warts, ruptured cysts, and persistent arthropod reactions.

It is important to keep in mind that not all cutaneous melanomas present with typical clinical clues. Based on visual inspection alone, accuracy for the clinical diagnosis of melanoma does not exceed 75% and may be increased to up to 90% with the use of dermoscopy by experts. However, 10%–25% of melanomas may still be missed despite these diagnostic efforts. The term "featureless melanoma" has been coined for early and difficult-to-diagnose melanomas and may partially explain this statistic[111]. Sometimes, patients are the first to recognize these featureless cutaneous melanomas, and there should be a low threshold for biopsying any persistent lesion that arouses patient concern for "being different" from the rest.

Differential Diagnosis

A variety of conditions may simulate melanoma, either clinically or histopathologically, or both. Awareness of these simulators is of great practical importance in order to avoid misdiagnosis or overdiagnosis of melanoma. Tables 113.6 and 113.7 list several melanocytic and non-melanocytic lesions that can mimic melanomas.

Dermoscopy

Dermoscopy, also known as skin surface microscopy or epiluminescence microscopy (ELM), is an essential, non-invasive tool for diagnosing pigmented skin lesions and for recognizing cutaneous melanoma (see Figs. 113.8, 113.10, 113.12, 113.14). Clinical diagnostic sensitivity is significantly enhanced by the use of dermoscopy, and the correct diagnosis of melanoma is improved by nearly 50% in the hands of experienced/trained practitioners who utilize this diagnostic technique. It therefore can prevent unnecessary biopsies[112].

In one form of dermoscopy, a magnifying lens system is combined with a fluid interface in order to eliminate skin surface reflection. Hand-held lenses or cameras equipped with lenses and coupled with digital imaging systems are used. A glass plate makes direct contact with the skin, and ultrasound contact gel or a disinfectant spray can be used for the fluid interface. Morphologic structures within the epidermis, the dermal–epidermal junction, and the superficial dermis can be visualized with this technique. An alternative and more commonly employed form of dermoscopy uses polarized light to eliminate the surface reflection so that neither a liquid interface nor direct skin contact is required. The magnifications of these instruments range from 6- to 100-fold, but the most widely used dermoscope provides a 10-fold magnification, which is sufficient for routine assessment of most pigmented skin lesions.

The dermoscopic evaluation of cutaneous pigmented lesions involves a two-step algorithm. First, the observer determines whether the lesion under investigation is of melanocytic origin or not. For a lesion to be

considered melanocytic, it needs to have at least one of the following dermoscopic structures/features: pigment network, streaks, aggregated globules, homogeneous blue pigment, or parallel pattern (acral lesions). If the lesion does not possess one of the aforementioned melanocytic features, then it needs to be evaluated further to determine if it has any dermoscopic characteristics consistent with other entities such as a seborrheic keratosis, dermatofibroma, or pigmented basal cell carcinoma (see Tables 0.14 & 0.15). However, if the lesion does not have any features of a melanocytic lesion *and* it does not have any features of a non-melanocytic tumor, then, by default, the lesion is considered to be of melanocytic origin.

Once a lesion is deemed to be melanocytic in origin, the second step of the algorithm is to differentiate between a benign melanocytic nevus and melanoma. To this end, multiple algorithms have been created, including pattern analysis, the ABCD rule, Menzies method, and the 7-point checklist, among others, which assist the clinician in deciding which lesions require a biopsy (see Tables 0.17–0.20)[75]. Several typical dermoscopic patterns have been described for benign nevi, including those with low-grade clinical atypia/histologic dysplasia, recognition of which can prevent unnecessary biopsy (see above).

The major dermoscopic criteria for melanoma can be broken down into global features, patterns, and local features. Global features of melanoma include dermoscopic asymmetry and the presence of multiple colors. Patterns seen by dermoscopy include reticular, globular, reticular–globular, homogeneous, reticular–homogeneous, and starburst. In melanoma, the most common patterns are the multicomponent pattern (three or more dermoscopic structures distributed asymmetrically), asymmetric starburst pattern, and nonspecific pattern (does not fit one of the known benign patterns). Lastly, the presence of any of the following local features should raise concern for melanoma: atypical network, negative pigment network, streaks, atypical dots or globules, irregular blood vessels, regression structures, crystalline structures, and blue–white veil (Table 113.8).

Over the past several years, dermoscopic criteria have been further refined in order to recognize difficult-to-diagnose melanomas such as ALMs and subungual melanomas[113]. Additionally, diagnostic clues for early nodular melanomas and for amelanotic melanomas have been described, as these melanomas do not display the classic features (see above)[114]. As with clinical examination, not all melanomas can be clearly recognized by dermoscopy and "featureless" melanomas exist[111].

Photography

In high-risk patients, especially those with complex mole patterns, total body digital photography can be a helpful adjunct in the identification of new and changing lesions[115]. The availability of baseline images for comparison, including dermoscopic images, permits the detection of melanomas that are growing or changing without manifesting obvious clinical characteristics, while simultaneously avoiding the removal of stable clinically atypical nevi[115]. Future adoption of new and developing technologies, including automated two- and three-dimensional total body photography, sequential digital dermoscopic imaging, and computer-assisted diagnostic algorithms that incorporate artificial intelligence, may further enhance longitudinal evaluation of melanocytic lesions[116].

DERMOSCOPIC CRITERIA AND THEIR CORRESPONDING HISTOPATHOLOGIC FEATURES			
Criterion	**Morphologic definition**	**Associated histopathologic changes**	**Diagnosis**
Pigment network	Network of brownish lines over a diffuse tan background	Pigmented rete ridges	Melanocytic lesion
Typical network	Brown-colored, regularly meshed and narrowly spaced network	Regular and elongated rete ridges	Benign melanocytic lesion
Atypical network	Black, brown, or gray network with irregular meshes and thick lines	Irregular and broadened rete ridges	Melanoma
Dots/globules	Black, brown, and/or gray, round to oval, variably sized structures regularly or irregularly distributed within the lesion	Pigment aggregates within the stratum corneum, epidermis, dermal–epidermal junction or papillary dermis	If regular: benign melanocytic lesion; if irregular: melanoma
Streaks	Irregular, linear structures not clearly combined with pigment network lines at the margins	Confluent junctional nests of melanocytes	Melanoma
Blue–white veil	Irregular, confluent, gray–blue to whitish-blue diffuse pigmentation	Acanthotic epidermis with focal hypergranulosis above sheets of heavily pigmented melanocytes in the dermis	Melanoma
Blotches	Black-, brown-, and/or gray-colored areas with regular or irregular shape/distribution	Hyperpigmentation throughout the epidermis and/or upper dermis	If regular: benign melanocytic lesion; if irregular: melanoma
Regression structures	White (scar-like) areas, blue (pepper-like) areas or combinations of both	Thickened papillary dermis with fibrosis and/or variable amounts of melanophages	Melanoma
Milia-like cysts	White–yellowish, roundish dots	Intraepidermal horn globules, also called horn pseudocysts	Seborrheic keratosis (occasionally observed in papillomatous melanocytic nevi)
Comedo-like openings	Brown–yellowish, round to oval or even irregularly shaped, sharply circumscribed structures	Keratin plugs situated within dilated follicular openings	Seborrheic keratosis
Leaf-like areas	Brown–gray to gray–black patches revealing a leaf-like configuration	Pigmented, solid aggregations of basaloid cells in the papillary dermis	Basal cell carcinoma
Red–blue lacunas	Sharply demarcated, roundish to oval areas with a reddish, red–bluish, or red–black color	Dilated vascular spaces situated in the upper dermis	Vascular lesion
Vascular structures	Comma-like vessels		Benign melanocytic lesion
	Arborizing vessels		Basal cell carcinoma
	Hairpin vessels		Seborrheic keratosis
	Dotted or irregular vessels		Melanoma

Table 113.8 Dermoscopic criteria and their corresponding histopathologic features. *With permission from Argenziano & Soyer, Lancet Oncol 2001;2:443–9. © 2001 Elsevier.*

Non-Invasive Diagnostic Imaging

Non-invasive diagnostic imaging modalities are increasingly being utilized for melanoma detection. These technologies have the potential to augment clinical diagnosis and triage, decreasing unnecessary biopsies and excisions. However, their performance in "real-world" clinical settings remains to be seen, and they do not replace the gold standard of histopathologic diagnosis; widespread availability of novel imaging techniques is another limitation. While many are still in development, two modalities have been FDA-approved for clinical use: reflectance confocal microscopy and electrical impedance spectroscopy.

Reflectance confocal microscopy (RCM) uses a near-infrared, low-intensity diode laser designed for non-invasive *in vivo* imaging of the skin. Structures within the epidermis and papillary dermis are visualized with high resolution, producing images akin to traditional histology (see Ch. 0). This technique has been used to analyze various cutaneous tumors, including melanoma (Fig. 113.20), with a pooled sensitivity of 92% and pooled specificity of 70% for melanoma detection in a recent meta-analysis[117]. RCM improves diagnostic accuracy for cutaneous melanoma compared to clinical and dermoscopic examination, preventing over half of benign lesions from unnecessary removal[116]. RCM may also enable more accurate intraoperative assessment of subclinical extension of LMM, with excellent agreement (>80%) between RCM mapping and histopathologic margin assessment during staged excision[118]. Additional applications of RCM include evaluation of dermoscopically equivocal lesions in difficult-to-biopsy situations (e.g. cosmetically sensitive areas, acral sites, young children) as well as short-term clinical monitoring of suspected lentigo maligna or amelanotic lesions whose initial RCM imaging appears negative for melanoma[119].

Electrical impedance spectroscopy (EIS) relies on the different electrical properties of normal and abnormal tissue to distinguish between benign nevi and melanoma. A hand-held probe with "microinvasive" electrode pins that penetrate the stratum corneum delivers an imperceptible low-level electrical current through the skin to measure the bioimpedance of the area of interest. EIS demonstrates high sensitivity: >96% melanoma detection for lesions deemed suspicious for melanoma on clinical and dermoscopic examination. However, specificity is much lower (~35% in one prospective trial[120]). Notably, seborrheic keratoses may display a high false-positive rate with EIS, underscoring the importance of clinical judgment when adopting these imaging technologies.

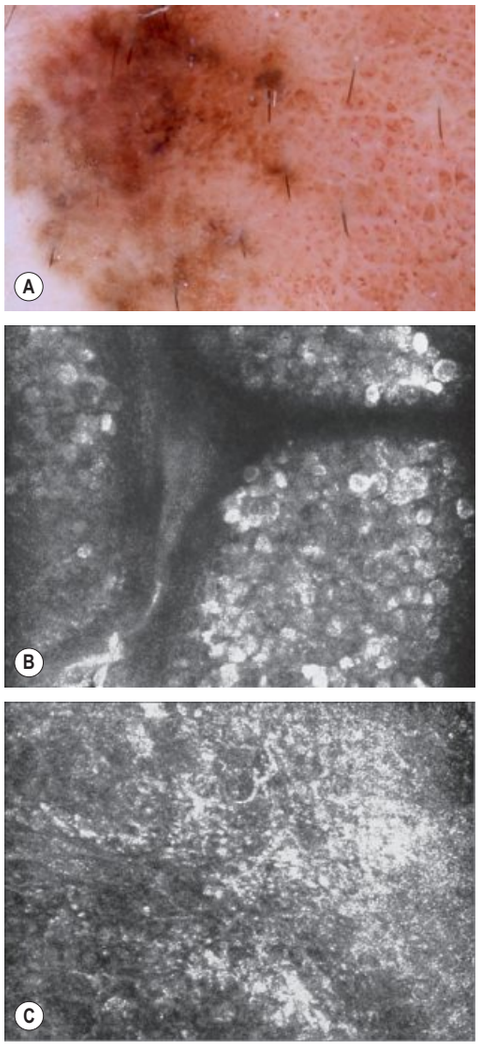


Fig. 113.20 Cutaneous melanoma arising within a compound melanocytic nevus – dermoscopy and reflectance confocal microscopy (RCM). A By dermoscopy, the nevus has a regular cobblestone pattern (right) whereas the melanoma component has a disorganized pattern with an atypical pigment network as well as atypical dots and globules (left). **B** RCM of the nevus portion demonstrates regularly organized collections of reflective melanocyte cells within nests. **C** In the melanoma portion, there is architectural disorder of the epidermis with large round solitary atypical refractive (pagetoid) cells as well as bright atypical dendritic cells. *Courtesy Anthony Rossi, MD and Ashfaq Marghoob, MD.*

PATHOLOGY

Histopathology remains the gold standard for melanoma diagnosis, although studies have demonstrated significant interobserver variability in the application of diagnostic criteria for melanocytic neoplasms ranging from moderately dysplastic nevi to *in situ* and thin (T1) melanomas[43]. While most melanomas are readily distinguished from melanocytic nevi based on standard criteria (Table 113.9), some melanocytic lesions remain diagnostically challenging despite incorporation of immunohistochemistry and various molecular techniques.

It has been proposed that melanomas progress through two phases. The first is the radial (horizontal) growth phase (RGP), characterized by centrifugal spread of neoplastic melanocytes within the epidermis and infiltration of the papillary dermis by single cells or small nests. The second, vertical growth phase (VGP) is characterized by the presence of dermal nests/nodules of atypical melanocytes that are larger than and/or cytologically distinct from their intraepidermal counterparts. It has been further postulated that the RGP lacks metastatic potential even in the presence of dermal invasion, whereas the VGP correlates with the capacity for metastasis. The major histologic types of melanoma described above differ with regard to the presence and morphology of the RGP. However, because the value of RGP versus VGP in assessing prognosis has not been confirmed by larger studies, the "growth phase" is not part of current classification schemes.

CRITERIA FOR THE HISTOPATHOLOGIC DIAGNOSIS OF MELANOMA
Architectural pattern
• Asymmetry • Poor circumscription of intraepidermal melanocytic component • Silhouette of tumor base is uneven (except in nevoid melanoma) • No maturation of melanocytes with progressive descent into the dermis (maturation may be present in some nevoid melanomas) • Nests of melanocytes within the epidermis are not equidistant from one another • Nests of melanocytes vary in size and shape • Some nests of melanocytes become confluent • Scatter of melanocytes above the dermal–epidermal junction • Melanocytes arranged as solitary units predominate over nests within the epidermis • Melanocytes in some nests are not cohesive • Melanocytes extend down adnexal epithelium • Sheets of melanocytes within the dermis • Nests at the base of lesion are occasionally large
Cytomorphology
• Atypical melanocytes (with pleomorphic nuclei) • Mitotic figures • Necrotic melanocytes
Other features
• Signs of regression (especially if extensive [>75%] or extending beneath measured Breslow thickness) • Actinic (solar) elastosis (i.e. CSD vs non-CSD melanoma), particularly if pushed down by newly formed collagen containing complexes of melanocytes (sign of a recent growth) • "Dusty" melanin within tumor cells • Melanin is not distributed in a uniform fashion • Plasma cells at the base of the lesion

Table 113.9 Criteria for the histopathologic diagnosis of melanoma. CSD, cumulative sun damage. *Adapted from Ackerman A, Cerroni L, Kerl H. Pitfalls in Histopathologic Diagnosis of Malignant Melanoma. Philadelphia: Lea & Febiger, 1994.*

Typically, cutaneous melanoma is asymmetric, poorly circumscribed, and characterized by nests of melanocytes within the epidermis that are not equidistant from one another, vary in size and shape, and focally become confluent (Fig. 113.21)[69]. Within the epidermis, solitary melanocytes often predominate over nests. Some solitary melanocytes and nests of melanocytes are found well above the dermal–epidermal junction, at times extending into the upper epidermis, even the cornified layer; this is referred to as "pagetoid" scatter. These findings define melanoma *in situ* (Fig. 113.22). The presence of such features along with atypical melanocytes within the dermis constitute invasive melanoma. One element of histologic asymmetry in melanoma is the extension of the intraepidermal tumor cells far from the invasive intradermal component. Similar findings are present in the adnexal epithelium of folliculosebaceous units and eccrine ducts. Within the dermis, the melanocyte nuclei do not become smaller within the deeper portions of the tumor (absence of maturation). In parallel, the nests of melanocytes also do not become smaller with progressive descent.

In SSM, the radial growth phase predominates histologically with broad, horizontal extension of atypical melanocytic nests and single cells within the epidermis and superficial dermis. As these tumors frequently represent low-CSD melanomas, solar elastosis within the dermis is usually minimal. In nodular melanoma, the tumor extends vertically in the dermis with a comparatively limited involvement of the overlying epidermis (Fig. 113.23). Overall, the tumor may exhibit a nodular, polypoid, or pedunculated architecture.

LMM (high-CSD melanoma) differs from the prototypic melanoma by the presence of marked solar elastosis (a sign of chronic sun damage) as well as the tendency to have little pagetoid spread within the epidermis. Tumor cells show lentiginous spread, i.e. solitary tumor cells in the epidermal basal layer predominate over tumor cell nests within the epidermis. The atypical melanocytes are commonly present within the epithelium of adnexal structures, especially along the outer root sheath of hair follicles (Fig. 113.24). The invasive component is more often composed of spindle cells, although any morphology is possible. Reflecting the role of high CSD in the pathogenesis of this subtype, epidermal atrophy, in addition to solar elastosis in the upper dermis, is commonly observed.

ALM often has a proliferation of atypical melanocytes within the basal layer of a hyperplastic epidermis, i.e. a lentiginous spread of single melanoma cells (Fig. 113.25). These findings may be subtle in early lesions or at the tumor's periphery. In volar and subungual sites, this lentiginous component may contain strikingly dendritic melanocytes with hyperchromatic, vertically elongated nuclei and irregular dendritic processes that may reach the mid spinous layers. Throughout the lesion, atypical melanocytes are arranged singly and in irregularly shaped nests at all levels of the epidermis ("pagetoid scatter"), with a predominance of single cells. In the cornified layer, numerous melanocytes and melanin granules are diffusely scattered. These findings are in contrast to the mild cytomorphologic atypia that may characterize benign acral nevi and nevi in other "special sites" (e.g. genitalia, milk line), a finding commonly referred to as "special site atypia". For example, while some pagetoid scatter may be present in acral nevi, this is typically confined to the skin furrows ("columnar scatter"), whereas in melanoma it is present throughout the lesion, involving both ridges and furrows ("diffuse scatter").

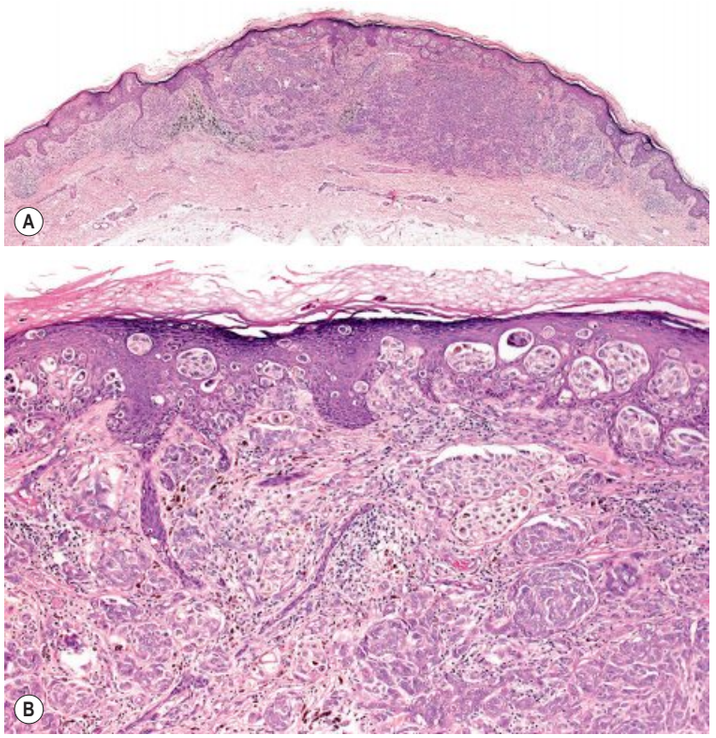


Fig. 113.21 Histopathologic features of a typical superficial spreading (low-CSD) cutaneous melanoma. A Asymmetric melanocytic tumor with asymmetry in both distribution of melanocytic complexes and pigment. **B** Pagetoid melanocytes organized as solitary units and nests varying in size and shape are present throughout the entire epidermis. Neoplastic melanocytes extend into the dermis. There is absence of maturation at deeper levels of the dermis. *Courtesy Lorenzo Cerroni, MD.*

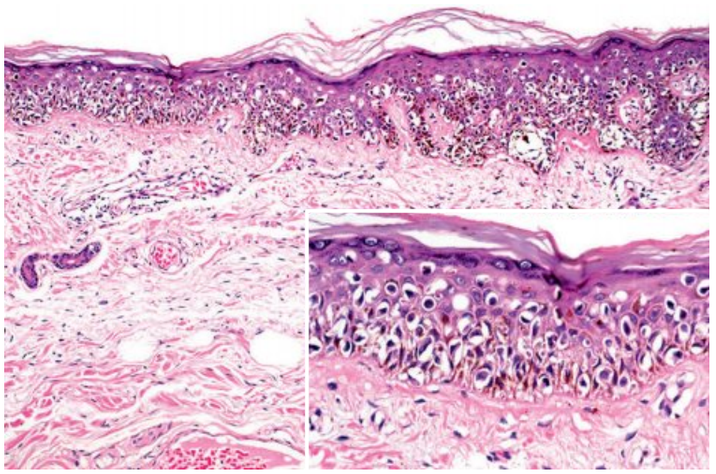


Fig. 113.22 Histopathologic features of a melanoma *in situ*. Increased number of melanocytes with atypical nuclei not only in the basal layer, but also at all levels of the epidermis. Note the predominance of single cells over nests. *Courtesy Lorenzo Cerroni, MD.*

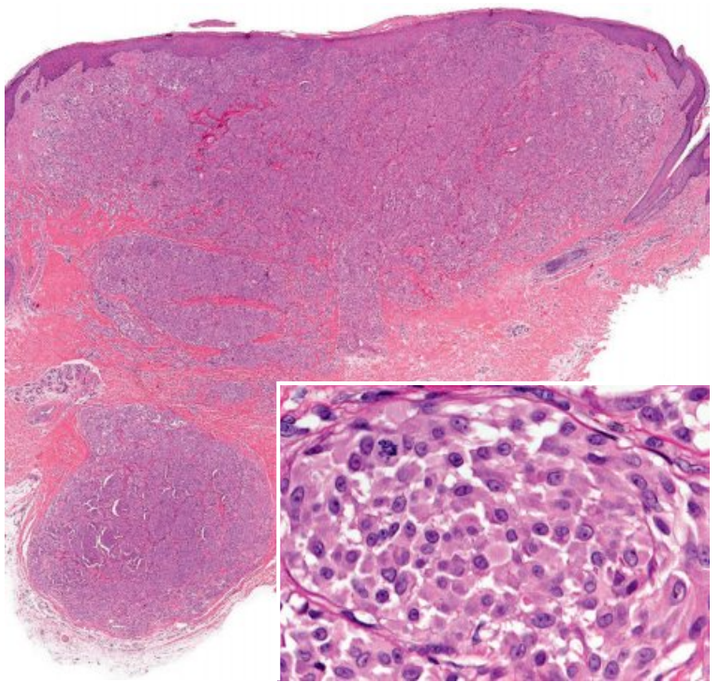


Fig. 113.23 Histopathologic features of a nodular melanoma. Relatively well-circumscribed tumor primarily within the dermis. Confluent complexes of atypical melanocytes extend throughout the entire dermis and into the superficial portion of the subcutaneous fat. Note the atypical epithelioid melanocytes and one mitotic figure (inset). *Courtesy Lorenzo Cerroni, MD.*

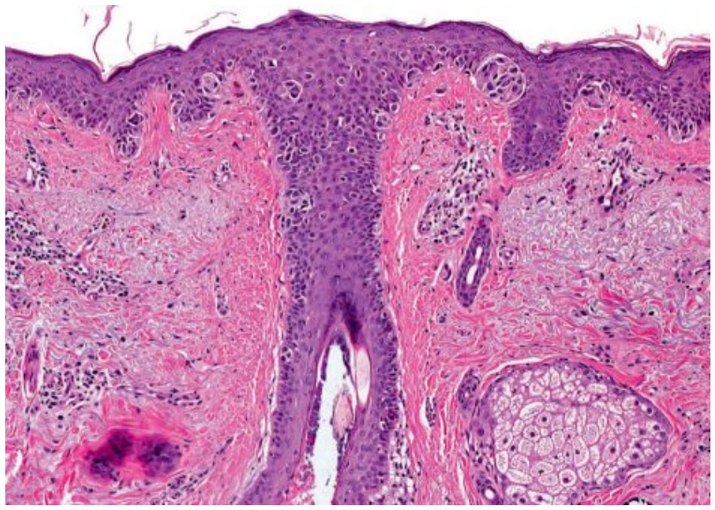


Fig. 113.24 Histopathologic features of a lentigo maligna (melanoma *in situ* of sun-damaged skin). Proliferation of atypical melanocytes within the epidermis, with single cells predominating over nests. Note the extension of the atypical melanocytes into the hair follicle epithelium and the solar elastosis in the dermis. *Courtesy Lorenzo Cerroni, MD.*

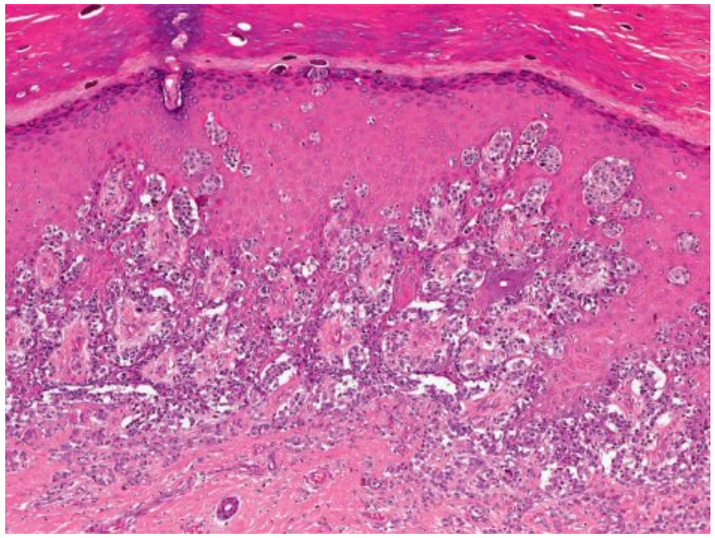


Fig. 113.25 Histopathologic features of an acral lentiginous melanoma. Irregular, sometimes confluent, nests of atypical melanocytes within a hyperplastic epidermis. Some of the melanocytes are hyperchromatic and are also present within the cornified layer. Note the thick stratum corneum typical of acral skin. *Courtesy Lorenzo Cerroni, MD.*

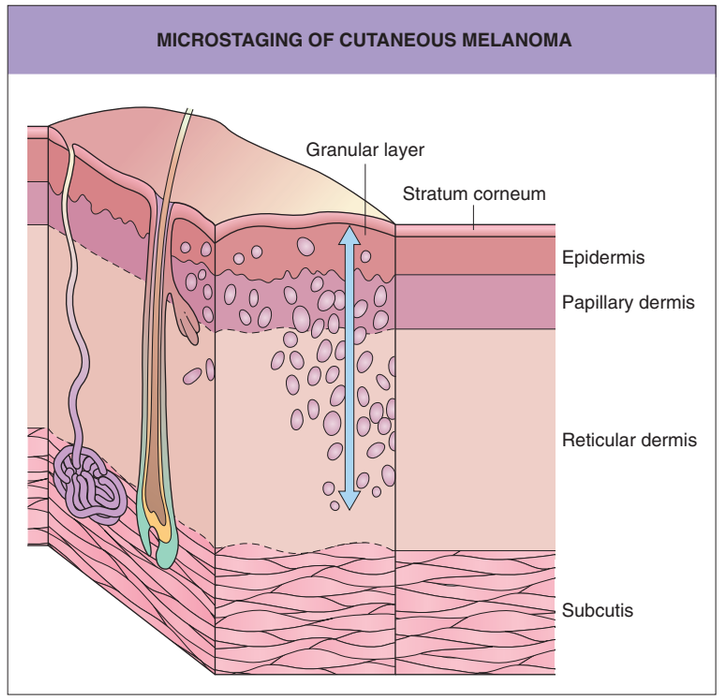


Fig. 113.26 Microstaging of cutaneous melanoma: Breslow tumor thickness. Breslow method: measure from the granular layer of the epidermis to the deepest part of the tumor.

Microstaging

Of the histologic features in a primary cutaneous melanoma, Breslow depth (i.e. tumor thickness) is the strongest predictor of survival. Melanoma thickness is measured in millimeters from the top of the granular cell layer of the epidermis (or the base of an ulcer) to the deepest point of tumor penetration, using an ocular micrometer (Fig. 113.26). In addition to tumor thickness, a number of other histologic features should be noted such as ulceration and involvement of margins[121–123]. Tumor thickness and ulceration are major determinants of T-stage in the current AJCC-8/UICC staging system, with ulceration defined histologically as the absence of an intact epidermis overlying a major portion of the primary tumor plus an associated host response (e.g. fibrinous exudate, acute inflammatory infiltrate).

Although dermal mitotic count (measured according to the "hot spot" method and reported as number/mm^2) does not currently upstage primary melanoma, it was viewed as a prognostic factor in the previous AJCC staging system. Guidelines for the histopathologic examination and reporting of melanoma features have been published by the International Collaboration on Cancer Reporting and the College of American Pathologists[121–123]. However, a number of experienced dermatopathologists only report criteria essential for the current staging classification – tumor thickness, ulceration (if present), satellites (if present), and assessment of margins.

Immunohistopathology

Immunohistochemical studies can be helpful in the assessment of diagnostically difficult cases of primary melanoma as well as in the assessment of metastatic tumors of unknown origin (see Tables 0.13 & 122.4). However, the diagnosis of cutaneous melanoma is based upon routine H&E staining, as immunostaining patterns alone cannot clearly differentiate between benign and malignant lesions. A wide range of melanoma-associated antigens have been identified for which immunohistochemical stains are available. Melanocyte differentiation antigens, e.g. PMEL17/gp100 (HMB45), tyrosinase, MART-1/Melan-A, MITF, are useful for: (1) distinguishing cells of melanocytic lineage from other tumor types; (2) visualizing the full extent of tumor cells of a primary melanoma; and (3) identifying minute foci of melanoma in sentinel lymph node biopsies. HMB45, which recognizes the melanosome-specific glycoprotein PMEL17/gp100, has high specificity for melanocytes and nevus cells, but its utility is limited by its heterogeneous staining pattern and limited sensitivity. Transfer of melanosomes to keratinocytes can also lead to positive staining for tyrosinase and PMEL17/gp100 (HMB45) in keratinocytes. Because MITF is a transcription factor in melanocytes, it does not stain melanosome-containing keratinocytes. Of note, HMB45, tyrosinase, MART-1/Melan-A, and MITF may all be negative in desmoplastic melanoma, representing an important potential pitfall.

Staining for S100, a calcium-binding protein, has high sensitivity for melanocytes and melanoma, including desmoplastic or spindled cell melanoma. However, this protein is also expressed by Langerhans cells, other dendritic cells, eccrine glands, Schwann cells, chondrocytes, and adipose tissue. SOX10, a transcription factor, has emerged as a popular alternative to S100 and other melanocytic markers due to easier interpretation of its nuclear staining pattern. Although SOX10 is not entirely melanocyte-specific (expressed in myoepithelial cells and other cells of Schwannian lineage), it will identify the spindled component of most desmoplastic melanomas. There is also less background staining of dermal fibrohistiocytic cells by SOX10 compared to S100, making SOX10 useful in distinguishing residual desmoplastic melanoma from

scar. In sum, the use of panels of these antibodies improves sensitivity and specificity, but remains diagnostically imperfect.

More recently, immunohistochemical staining for PRAME (PReferentially expressed Antigen in MElanoma) was introduced. Initially identified in tumor-reactive T cells from patients with cutaneous melanoma, *PRAME* was one of the few GEP genes that discriminated between melanoma and benign melanocytic neoplasms. Immunohistochemical staining for PRAME is generally negative in benign nevi, solar lentigines, melanocytic hyperplasia in sun-damaged skin, and other melanocytic lesions with intermediate histopathologic features[124]. In contrast, the majority of primary cutaneous melanomas and their metastases demonstrate diffuse nuclear PRAME immunostaining, which appears to be strongly concordant with abnormal cytogenetic test results[125]. PRAME may be a useful marker in the assessment of melanoma surgical margins (including LM), in distinguishing melanoma micrometastases from nodal nevi in sentinel lymph nodes, and in the evaluation of ambiguous melanocytic lesions[126]. Potential exceptions include desmoplastic melanomas, of which only a third may be PRAME-positive, and spitzoid neoplasms, in which PRAME positivity may correlate less strongly with histopathologic features[124]. Although it currently appears to be a promising immunohistochemical marker for melanoma, because a minority of melanocytic nevi are PRAME-positive, correlation with conventional histopathologic features is paramount for proper classification of both PRAME-positive and PRAME-negative lesions.

Molecular Analysis

Some cutaneous melanomas prove challenging to diagnose, and differentiation between atypical Spitz tumor (AST)/Spitz melanocytoma and spitzoid melanoma or between deep penetrating nevus or atypical blue nevus and melanoma can be difficult based upon histopathology. In such cases, CGH or FISH in addition to newer molecular techniques (NGS, GEP) may be helpful (Table 113.10).

CGH is a method for the genome-wide assessment of DNA copy number changes in tumor cells. Fluorescence-labeled tumor DNA and reference DNA from a healthy donor are hybridized onto metaphase chromosomes or on arrays of oligonucleotides (array CGH). From the relative fluorescence copy number, gains or losses within the tumor can be calculated. The oligonucleotide spots on the array can be mapped to the respective position within the human genome. CGH analysis of benign melanocytic nevi typically shows *no* clonally expanded chromosomal aberrations, while in the vast majority of melanomas, *gains and losses* of particular segments of chromosomes or entire chromosomes are found, including copy number gains of 1q, 6p, 7p, 7q, 8q, 17q, and 20q and losses of chromosomes 6q, 8p, 9p, and 10q[127]. As an exception, ~20% of Spitz nevi show an increase in copy number of chromosome 11p (corresponding to *HRAS* activation) or an isolated loss of chromosome 3 (corresponding to loss of *BAP1*), aberrations not typically found in cutaneous melanoma[127–129].

FISH can also assist in differentiating between benign and malignant melanocytic tumors (see Fig. 3.8). These assays often focus on chromosomal loci that are frequently affected by copy number changes in melanoma. Studies have shown that FISH assays that target various combinations of 6p25 (*RREB1*), 6q23 (*MYB*), 8q24 (*cMYC*), 11q13 (*CCND1*), CEP6 (centromere of chromosome 6), and 9p21/CEP9 (*CDKN2A*) discriminate between benign nevi and melanoma with high sensitivity and specificity[130–132]. The disadvantage of FISH is that only gains and losses involving a limited number of chromosomes are detected. However, compared to CGH, FISH is typically faster, less expensive, and requires less tumor tissue to perform.

NGS has also been used to further characterize the genomic landscape of multiple tumors, including melanoma and various spitzoid tumors[133,134]. This method allows for the analysis of hundreds of genes in a single study (see Fig. 3.5), and it can potentially point to new prognostic markers or therapeutic targets. NGS has facilitated the discovery of various fusion kinases that underly the pathogenesis of some melanocytic neoplasms, including spitzoid neoplasms. Due to the immense data infrastructure and bioinformatics expertise required for NGS, its availability is currently limited to a few commercial laboratories and academic research centers.

A frequent application of the above molecular techniques is in the evaluation of AST versus spitzoid melanoma. One or multiple methods can be utilized given that complementary information is provided by each assay[135]. For FISH, inclusion of the 9p21/CEP9 probe significantly increases sensitivity for spitzoid melanoma, as homozygous loss of this locus has been associated with advanced locoregional disease or death. Gains of 8q24 and 11q13 also correlate with an aggressive clinical course, but the risk is lower than with homozygous 9p21 deletions[136]. In cases with ambiguous or negative FISH results, CGH may provide additional information regarding other copy number alterations supportive of melanoma. Identification of *TERT* promoter mutations via NGS is also suggestive of more aggressive clinical behavior, with one study demonstrating a significant association with extranodal metastasis and death[137]. In the assessment of ASTs, identification of an underlying *BRAF* or *NRAS* mutation by NGS may favor a conventional melanoma with spitzoid features over AST[138]. Regardless of which techniques are used, definitive classification of ASTs remains a significant challenge.

DIFFERENTIAL DIAGNOSIS OF MELANOMA – MOLECULAR DIAGNOSTICS THAT CAN BE UTILIZED

Test	Detects	Advantages	Disadvantages
Comparative genomic hybridization (CGH) – FFPE tissue	Chromosomal gains and losses (DNA copy number changes)	Genome-wide screening for chromosomal gains and losses without prior knowledge of the genomic aberrations	• No detection of mutations (single nucleotide changes), small gains or deletions, balanced translocations, and polyploidy • A low percentage of neoplastic cells in the specimen leads to false negative results
Fluorescent *in situ* hybridization (FISH; see Fig. 3.8) – FFPE tissue	Deletions, amplifications, translocations	Each cell nucleus is evaluated individually so that even tumors with a low percentage of neoplastic cells can be analyzed without the risk of false-negative results	• Prior knowledge of the genomic aberrations necessary to build the probe • Poor interobserver reproducibility • No detection of mutations or small copy number aberrations • Analyzes only a limited number of chromosomal loci (usually 4–6)
Next generation sequencing (NGS; see Fig. 3.5) – FFPE	Sequence of nucleotides in RNA or DNA, eiither n specific regions or entire genome	Most comprehensive method for genomic analysis and gene expression prolifiling	• Currently quite expensive and labor intensive • Performed primarily in academic centers (e.g. for identification of therapeutic targets)
Gene expression profiling (GEP) *Post biopsy* – FFPE tissue *Pre biopsy* – tape stripping	Gene expression levels of selected genes	• May provide information regarding risk of metastasis for uveal and cutaneous melanomas* • May distinguish benign melanocytic nevi from cutaneous melanomas	• Evaluates gene expression levels, but gives no information regarding the underlying genomic aberrations • In selected, unequivocal benign or malignant lesions, the sensitivity and specificity appears to be ~80%–90%, but the diagnostic value for ambiguous lesions remains undetermined

*Currently used to predict metastatic risk in uveal melanomas.

Table 113.10 Differential diagnosis of melanoma – molecular diagnostics that can be utilized. These tests have been used to assist in the diagnosis of ambiguous and/or controversial melanocytic tumors as well as for prognostication; the latter is primarily GEP for melanomas. Next generation sequencing is covered in the text. FFPE, formalin-fixed, paraffin-embedded.

Gene Expression Profiling (GEP)

GEP has gained attention as a potentially useful molecular technique in the field of melanoma, and GEP assays for diagnosis as well as prognostication have been developed. Whereas diagnostic GEP aims to classify an undiagnosed melanocytic lesion as benign, intermediate, or malignant, prognostic GEP aims to provide further clinical risk stratification for melanomas beyond AJCC stage and other clinicopathologic factors. GEP assays typically use quantitative reverse transcriptase PCR (qRT-PCR) to measure the mRNA expression levels of a limited panel of genes; the latter have been correlated with pre-specified outcomes, such as benignity, tendency to metastasize, or SLNB risk prediction, and the goal is to accurately predict this outcome in the queried lesion. Ideally, during development of prognostic GEP assays, fully annotated cohorts of archival melanoma tissue samples would be analyzed, with subsequent prospective validation among separate melanoma cohorts as well as comparison against all known clinicopathologic factors and AJCC stage to determine prognostic accuracy and clinical utility.

Gene expression profiling for diagnosis

Development of diagnostic GEP assays was based on several DNA microarray studies that demonstrated disparate gene expression patterns when benign melanocytic lesions were compared to melanoma[139–142]. There are currently two commercially available diagnostic GEP tests, a 3-gene assay (DermTech Smart Stickers™) that was initially a 2-gene assay, and a 23-gene expression signature (23-GES) assay (myPath® Melanoma). Both the initial 2-gene assay and the current 3-gene assay use adhesive tape stripping pre-biopsy to determine the likelihood of malignancy (and need for biopsy) of a melanocytic neoplasm based on melanoma-associated genes – *LINC*, *PRAME*, and more recently, *TERT*. The original 2-gene assay demonstrated a sensitivity of 91% and specificity of 69% in the classification of suspicious melanocytic lesions[143], with subsequent real-world studies demonstrating even higher specificity (91%) and high negative predictive value (99%) without decreased sensitivity for melanoma[144]. The addition of *TERT* to the 3-gene assay was reported to increase diagnostic sensitivity to 97% in a study of 103 pigmented skin lesions clinically suspicious for melanoma[145].

The 23-GES assay uses formalin-fixed paraffin-embedded tissue samples from diagnostic biopsies, when histopathologic analysis is indeterminate for melanoma[146]. Some studies of the 23-GES assay have demonstrated high sensitivity (93%) and specificity (96%) in distinguishing melanoma from benign nevi, with clinically proven outcomes[147]. However, other studies have noted its limitations in more ambiguous melanocytic lesions, including spitzoid tumors[148]. Given the novelty of diagnostic GEP assays and limited experience in clinical settings, current appropriate use criteria published by US dermatology and dermatopathology societies maintain an uncertain role for qRT-PCR-based assays in melanoma diagnosis[149,150].

Gene expression profiling for prognosis

Current AJCC-8 melanoma staging and international guidelines use primary tumor histologic factors, e.g. Breslow thickness, ulceration, and pathologic status of the regional lymph nodes (via SLNB) to estimate patient prognosis. Prognostic GEP aims to improve on AJCC melanoma staging by classifying metastatic risk and predicting disease recurrence, potentially identifying patients who would benefit from surveillance imaging and/or adjuvant therapy.

Currently, there are three commercially available prognostic GEP tests including the 31-gene DecisionDx®-Melanoma (US) and 11-gene MelaGenix (Europe). These two assays use a dichotomous class assignment of risk for metastasis (class 1 vs class 2 or low risk vs high risk) rather than calculating an estimated MSS as is done with AJCC staging and other risk-based predictive nomograms. The third Merlin Test combines an 8-gene GEP test with Breslow thickness and patient age to predict SLNB positivity or negativity, with the potential goal of reducing unnecessary SLNBs in patients at low risk of a positive result; prospective validation studies are ongoing[151]. The 11-GEP MelaGenix assay was studied in Europe and reported as an independent prognostic factor for MSS, along with tumor thickness and age, in 291 stage I–III melanoma tumors, suggesting a potential role for this assay in clinical decisions regarding adjuvant therapy[152].

Currently, in the US, the majority of prognostic GEP testing is performed with the 31-gene panel. Most clinicians who order this test report an increased frequency of clinical or imaging surveillance in patients designated as having class 2 disease, regardless of AJCC stage[153]. However, the clinical utility of prognostic GEP testing and its impact on patient outcomes remains uncertain, and routine prognostic GEP testing is not recommended in current US national guidelines (NCCN and AAD)[25,34].

A major criticism of current GEP tests is their relatively low positive predictive value in stage I melanoma, particularly thin (T1) tumors[154]. A meta-analysis of melanomas tested with 31-GEP demonstrated a true positive rate of 1% (6/623) and false positive rate of 10% (61/623) for stage I melanomas[155]; this means that 100 stage I melanomas would need to be tested to identify one that will metastasize while 10 individuals would be falsely identified as having high-risk melanoma. Stage II melanomas had a better prognostic performance with a true positive rate of 28% (59/212) and false positive rate of 37% (78/212), suggesting that GEP testing may ultimately prove more useful in guiding adjuvant therapy use and/or surveillance imaging in this subset of patients. However, stage II melanoma patients are typically followed more intensely than those with stage I due to their increased chance of disease recurrence.

In thin melanomas, the lower positive predictive values of available GEP tests may be related to low numbers of metastases in the cohorts of stage I melanomas used to train and validate the models (e.g. 9% and 3%, respectively)[156]. Alternatively, predicting metastatic potential based upon mRNA expression may represent a biological obstacle for earlier stage melanomas, i.e. a small percentage of cells conferring metastatic potential is not detectable with existing technology platforms[157]. An additional criticism is that designation of a dichotomous value (e.g. class 1 vs class 2) to a continuous variable (e.g. disease-free survival) leads to assignment of equal risk to heterogeneous populations[158]. The major argument for testing thin melanomas with 31-GEP is the high negative predictive value (87%), which could provide additional reassurance to patients. However, the contribution of GEP testing beyond AJCC-8 staging and other known clinicopathologic factors (e.g. primary tumor mitotic rate, lymphovascular invasion, patient age, biologic sex) is unclear. In addition, the implications of a false-positive result should be discussed with the patient, preferably in a multidisciplinary care setting.

There is great interest in risk prediction for SLN-positivity in order to reduce the number of unnecessary SLNBs performed. Two commercially available GEP tests have been studied in this regard: (1) the 8-gene Merlin Test (combined with Breslow thickness and patient age)[159]; and (2) a modified i-31-GEP DecisionDx® that uses artificial intelligence to integrate a continuous GEP score with clinicopathologic factors (age, biologic sex, anatomic location, Breslow thickness, mitotic rate, ulceration, subtype, tumor infiltrating lymphocytes, deep margin transection). Three US and European validation cohort studies with 208, 210, and 421 patients[159–161] have been performed, with the largest study reporting a 35% SLNB reduction rate (via a low risk score) in patients with T1–T2 melanomas (95% CI, 29.4–41.8), with a negative predictive value of 96.5% (95% CI: 90.0–99.3). In a validation cohort of 1674 T1–T4 melanomas from 25 surgical and 5 dermatology centers, the i-31-GEP model identified an additional 19% of tumors (compared with T-stage alone) with <5% SLNB risk, for which the procedure would not be recommended[162]. A recent decision-analytic study suggested that the i-31-GEP model could help to risk stratify patients with T1b melanoma, identifying 23% who could safely forego SLNB (using a 5% risk threshold), though its role in patients with T1a and T2 melanoma requires further study[155]. Various SLNB risk calculators have been developed worldwide that incorporate relevant clinicopathologic factors (e.g. Breslow thickness, ulceration, age, melanoma subtype, lymphovascular invasion) and may provide additional means to more easily predict SLN-positivity[163,164].

While current data are insufficient to support the use of available prognostic/predictive GEP tests to determine the need for SLNB, surveillance imaging, and/or adjuvant treatment, the field is rapidly evolving. There is consensus that further investigation of existing and novel GEP tests should meet certain criteria before being routinely incorporated into clinical practice[165,166]. The latest NCCN guidelines note the need for ongoing study of large data sets of unselected patients to determine whether a combination of GEP testing and clinicopathologic variables provides clinically actionable information, given the previously cited limitations in stage I melanoma[25,165,167]. As GEP testing is further

refined and newer technologies (e.g. circulating tumor DNA) evolve, there is great promise that clinical decision-making will be guided by molecular tumor classifications.

STAGING

Accurate staging of melanoma is essential for clinical prognostication and management. The current tumor–node–metastases (TNM) staging system was introduced by the American Joint Committee on Cancer (AJCC) in 2001 and most recently revised in 2017 (AJCC-8; Table 113.11)[168,169].

The two main factors that determine the **T** classification are: (1) Breslow depth; and (2) histopathologic evidence of ulceration. The **N** classification reflects the extent of tumor within the regional lymph node basin. The most important prognostic factors in the **N** classification are: (1) the number of metastatic lymph nodes; (2) whether the lymph node involvement is clinically occult (microscopic) versus clinically detectable (macroscopic); and (3) the presence or absence of satellite, in-transit, and microsatellite metastases. The **M** classification refers to metastatic disease and is based on three important features: (1) the anatomic site of the distant metastases; (2) the serum lactate dehydrogenase (LDH) level; and (3) the presence or absence of central nervous system (CNS) metastasis. The **T**, **N**, **M** classifications are combined to determine the AJCC stage (Table 113.12), and this allows one to predict survival and assists in selecting the most appropriate treatment. Fig. 113.27 includes 10-year MSS curves for stage I–III melanomas based on the international melanoma database and AJCC-8[169]. Stage IV survival estimates were not included in this model given the recent introduction of novel immune and targeted therapies that lead to markedly improved survival.

AJCC MELANOMA TNM CLASSIFICATION (2017)

Definition of primary tumor (T)

T category	*Thickness*	*Ulceration status*
TX (primary tumor thickness cannot be assessed*)	NA	NA
T0 (no evidence of primary tumor†)	NA	NA
Tis (melanoma *in situ*)	NA	NA
T1	≤1.0 mm	Unknown or unspecified
T1a	<0.8 mm	Without ulceration
T1b	<0.8 mm 0.8–1.0 mm	With ulceration With or without ulceration
T2	>1.0–2.0 mm	Unknown or unspecified
T2a	>1.0–2.0 mm	Without ulceration
T2b	>1.0–2.0 mm	With ulceration
T3	>2.0–4.0 mm	Unknown or unspecified
T3a	>2.0–4.0 mm	Without ulceration
T3b	>2.0–4.0 mm	With ulceration
T4	>4.0 mm	Unknown or unspecified
T4a	>4.0 mm	Without ulceration
T4b	>4.0 mm	With ulceration

Definition of regional lymph node (N)

N category	*Extent of regional lymph node and/or lymphatic metastasis*	
	Number of tumor-involved regional lymph nodes	*Presence of in-transit, satellite, and/or microsatellite metastases*¶
NX	Regional nodes not assessed‡	No
N0	No regional metastases detected	No
N1	One tumor-involved node – *or* – in-transit, satellite, and/or microsatellite metastases with no tumor-involved nodes	
N1a	One clinically occult (i.e. detected by SLN biopsy)	No
N1b	One clinically detected	No
N1c	No regional lymph node disease	Yes
N2	Two or three tumor-involved nodes – *or* – in-transit, satellite, and/or microsatellite metastases with one tumor-involved node	
N2a	Two or three clinically occult (i.e. detected by SLN biopsy)	No
N2b	Two or three, at least one of which was clinically detected	No
N2c	One clinically occult or clinically detected	Yes
N3	Four or more tumor-involved nodes – *or* – in-transit, satellite, and/or microsatellite metastases with two or more tumor-involved nodes – *or* – any number of matted nodes without or with in-transit, satellite, and/or microsatellite metastases	
N3a	Four or more clinically occult (i.e. detected by SLN biopsy)	No
N3b	Four or more, at least one of which was clinically detected, or presence of any number of matted nodes	No
N3c	Two or more clinically occult or clinically detected and/or presence of any number of matted nodes	Yes

Table 113.11 AJCC melanoma TNM classification (2017).

AJCC MELANOMA TNM CLASSIFICATION (2017)		
Definition of distant metastasis (M)		
M category	***M criteria***	
	Anatomic site	***LDH level[§]***
M0	No evidence of distant metastasis	NA
M1	Evidence of distant metastases	
M1a	Distant metastasis to skin, soft tissue including muscle, and/or non-regional lymph node	Not recorded or unspecified
M1a(0)		Not elevated
M1a(1)		Elevated
M1b	Distant metastasis to lung with or without M1a sites of disease	Not recorded or unspecified
M1b(0)		Not elevated
M1b(1)		Elevated
M1c	Distant metastasis to non-CNS visceral sites with or without M1a or M1b sites of disease	Not recorded or unspecified
M1c(0)		Not elevated
M1c(1)		Elevated
M1d	Distant metastasis to CNS with or without M1a, M1b or M1c sites of disease	Not recorded or unspecified
M1d(0)		Not elevated
M1d(1)		Elevated

*For example, diagnosis by curettage.
†For example, unknown primary or completely regressed melanoma.
‡For example, SLN biopsy not performed or regional nodes previously removed for another reason; exception: pathological N category is not required for most T1 melanomas, use cN when SLNB is not performed.
¶In-transit metastases are >2 cm from the primary tumor but not beyond the regional lymph nodes, while satellite lesions are within 2 cm of the primary, although both represent lymphatic metastasis with similar prognosis. Satellite lesions can be detected clinically or microscopically; the latter are referred to as microsatellite metastases.
§Suffixes for M category: (0) LDH not elevated, (1) LDH elevated. No suffix is used if LDH is not recorded or is unspecified.

Table 113.11 AJCC melanoma TNM classification (2017). Histologic evaluation of lymph nodes must include at least one immunohistochemical marker (e.g. HMB45, MART-1/Melan-A). CNS, central nervous system; LDH, lactic dehydrogenase; NA, not applicable; SLN, sentinel lymph node. *Adapted from AJCC Cancer Staging Manual. American Joint Committee on Cancer, 8th edn. Springer, 2017:563–85.*

Stage 0 represents melanoma *in situ* and stages I and II represent localized cutaneous disease. Distinction is made between stage IA patients (T1a: Breslow depth <0.8 mm without ulceration), who are *not* generally considered for sentinel node biopsy, and stage IB (T1b: <0.8 mm with ulceration, 0.8–1 mm with or without ulceration; T2a: >1.0–2.0 mm without ulceration) or stage II patients for whom SLNB is typically discussed and offered (Table 113.13). Stage III represents regional nodal and/or lymphatic (microsatellite/satellite/in-transit) metastases. Stage IV represents distant metastases, including distant skin, nodal, visceral, and/or brain metastasis.

PROGNOSIS

The prognosis of a patient with melanoma depends upon the stage at diagnosis. Prognosis for patients with surgically resected localized primary cutaneous melanoma and no nodal or distant metastases (stage I or II) is generally excellent (see Table 113.12). Patients with stage IA melanoma have a 5-year survival expectancy of 99% per the AJCC-8 international database, compared to patients with thick (>4 mm), ulcerated melanoma (T4b N0) who have a 5-year survival rate of 82%[170]. Although dermal mitotic rate is not incorporated into AJCC-8 staging, it is an independent prognostic factor for survival; for example, a mitotic rate of ≥1/mm^2 decreases 5-year survival in node-negative T1–T4 melanoma to 84%[170]. In addition to the microstaging variables discussed above, clinical variables with prognostic significance in stage I/II disease include sex, age, and anatomic site (Table 113.14). For example, women with stage I/II disease tend to have a better MSS than men. Location of the primary melanoma on the trunk, head (particularly scalp), or neck portends a poorer prognosis than melanoma on the extremities.

Stage III melanoma patients are a heterogeneous group with respect to risk for distant metastases and MSS. Per AJCC-8 data, the 5-year survival rates range from 93% for patients with pathologic stage IIIA melanoma (non-ulcerated primary tumor ≤2 mm in depth and up to 3 nodal micrometastases [T1a/b–T2a N1a–N2a M0]) to a low of ~32% for patients with pathologic stage IIID melanoma (ulcerated T4 primary tumor plus four or more clinically occult or detected lymph nodes ± lymphatic metastasis [T4b N3a/b/c M0])[170]. However, with the advent of newer targeted agents and immune checkpoint inhibitors, survival rates for both stage III and IV melanoma have increased over the past decade. Major prognostic factors in stage III melanoma are primary tumor characteristics (thickness and ulceration), the number of lymph nodes with metastases, and tumor burden. The latter is based on whether nodal metastases are clinically occult (micrometastases, as detected by SLNB) or clinically palpable (macrometastases), in addition to the presence or absence of lymphatic (microsatellite/satellite/in-transit) metastasis.

In stage IV patients, the major prognostic factor is the site of distant metastases, with a poorer prognosis for visceral than for non-visceral (e.g. skin, subcutaneous, distant lymph node) metastases. Prior to the use of more effective systemic agents over the past decade, the median survival for stage IV patients was 9 months, and the estimated 5-year survival rate was <10% when the serum LDH level was abnormally elevated. Variables that influence survival are initial site of metastasis, disease-free interval before distant metastases, stage of disease preceding distant metastases, and tumor burden at the time of diagnosis. Lower tumor burden in patients with unresectable stage III/IV melanoma (defined as normal serum LDH level and <3 organ sites with metastasis) is associated with improved response to targeted therapy, suggesting that earlier detection and treatment of metastatic disease may improve long-term survival[171].

EVALUATION OF A PATIENT WITH SUSPECTED MELANOMA

Medical History

A thorough medical history should be taken, focusing especially on risk factors for the development of melanoma such as a personal or family history of melanoma, skin phototype I/II, tanning bed use, childhood history of sunburns, and iatrogenic or acquired immunosuppression (see Table 113.3). A thorough review of symptoms should

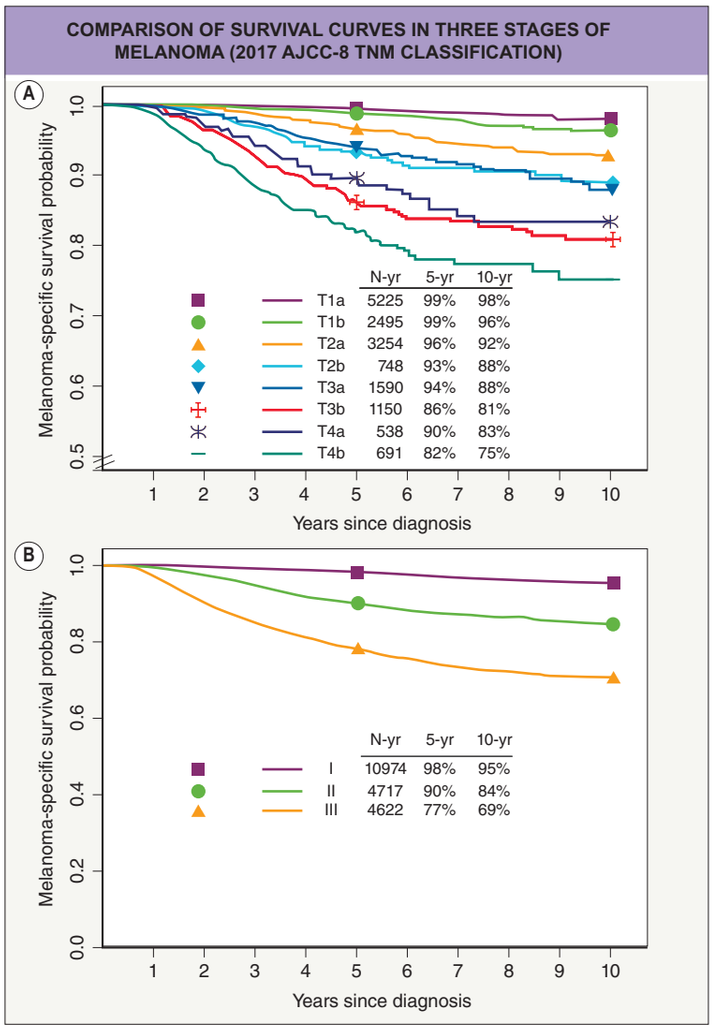


Fig. 113.27 Comparison of survival curves in three stages of melanoma based upon 2017 AJCC-8 melanoma TNM classification and prior to FDA approval of targeted therapy or immunotherapy for stage III disease. These curves represent melanoma-specific survival probabilities prior to FDA approval of targeted therapy or immunotherapy for stage III disease. **A** Melanoma-specific survival curves according to T subcategory for patients with stage I and II cutaneous melanoma from AJCC-8 international melanoma database. Data for T2–T4 patients filtered to include only those with negative SLNB; T1 patients included regardless of whether SLNB performed. **B** Melanoma-specific survival curves according to stage in patients with stage I to III melanoma from AJCC-8 international melanoma database. *With permission from Gershenwald JE, Scolyer RA, Hess KR, et al. Melanoma staging: Evidence-based changes in the American Joint Committee on Cancer Eighth Edition Cancer Staging Manual. CA Cancer J Clin 2017;67:472–92.*

AJCC-8 STAGE GROUPINGS FOR CUTANEOUS MELANOMA (2017)

	Survival (%)*	Clinical staging†			Pathologic staging‡		
		T	N	M	T	N	M
0		Tis	N0	M0	Tis	N0	M0
IA	99	T1a	N0	M0	Tla	N0	M0
					T1b		
IB	99	T1b	N0	M0	T2a	N0	M0
	96	T2a					
IIA	93	T2b	N0	M0	T2b	N0	M0
	94	T3a			T3a		
IIB	86	T3b	N0	M0	T3b	N0	M0
	90	T4a			T4a		
IIC	82	T4b	N0	M0	T4b	N0	M0
III¶		Any T, Tis	≥N1	M0			
IIIB					T0	N1b, N1c	M0
IIIC					T0	N2b, N2c, N3b or N3c	M0
IIIA	93				T1a/b–T2a	N1a or N2a	M0
IIIB	83				T1a/b–T2a	N1b/c or N2b	M0
					T2b/T3a	N1a–N2b	
IIIC	69				T1a–T3a	N2c or N3a/b/c	M0
					T3b/T4a	Any N ≥ N1	
					T4b	N1a–N2c	
IIID	32				T4b	N3a/b/c	M0
IV	§	Any T	Any N	M1	Any T, Tis	Any N	M1

*Estimated 5-year melanoma-specific survival is based on the AJCC-8 international melanoma database and TMN classification; of note, they predate the use of newer systemic therapies for stage III disease.
†Clinical staging includes microstaging of the primary melanoma and clinical/radiologic evaluation for metastases. By convention, it should be used after complete excision of the primary melanoma with clinical assessment for regional and distant metastases. Stage 0 and T1a melanomas (with exceptions) are clinically staged; T1b melanoma may be considered for pathologic staging with sentinel lymph node biopsy.
‡Pathologic staging includes microstaging of the primary melanoma and pathologic information about the regional lymph nodes following sentinel lymph node biopsy (for T2a–T4b melanoma in the AJCC-8 database) or following complete or therapeutic lymphadenectomy. Pathologic stage 0 or stage IA patients are the exception.
¶There are no stage III subgroups for clinical staging.
§Survival estimates for stage IV disease were not included in AJCC-8 data given incorporation of targeted and immune therapies associated with markedly improved melanoma-specific survival.

Table 113.12 AJCC-8 staging groups for cutaneous melanoma (2017). *Adapted from Gershenwald JE, Scolyer RA, Hess KR, et al. Melanoma staging: Evidence-based changes in the American Joint Committee on Cancer Eighth Edition Cancer Staging Manual. CA Cancer J Clin 2017;67:472–92*

SENTINEL LYMPH NODE BIOPSY (SLNB) CONSIDERATIONS

Clinical stage*		Breslow depth (mm)	Ulceration (present/absent)	Probability of positive SLNB	SLNB recommendation
0	Tis	NA	NA	0	No
IA	T1a	<0.8	–	<5%	Not typically†
IB	T1b	<0.8	+	5%–10%	Discuss and consider
		0.8–1.0	–		
	T2a	1.1–2.0	–	>10%	Discuss and offer
IIA	T2b	1.1–2.0	+		
	T3a	2.1–4.0	–		
IIB	T3b	2.1–4.0	+		
	T4a	>4.0	–		
IIC	T4b	>4.0	+		

*Based upon AJCC-8.
†Consider offering if one or more high-risk features: mitotic index ≥2/mm^2 (particularly in a young patient), lymphovascular invasion, and incomplete microstaging (deep margin diffusely involved and/or large clinical residual lesion following partial biopsy).

Table 113.13 Sentinel lymph node biopsy (SLNB) considerations. NA, not applicable.

diffusely

MELANOMA – MAJOR INDEPENDENT PROGNOSTIC FACTORS FOR SURVIVAL IN MULTIVARIATE ANALYSES	
Prognostic factor	**Commentary**
Tumor thickness	≤1 mm, low risk; >1 mm, higher risk
Ulceration	Worse prognosis with ulceration
Mitotic rate	Worse prognosis with high mitotic rate (e.g. 5-year survival of 84% with ≥11 mitoses/mm^2)
Age	Worse prognosis with older age
Sex	Men have poorer prognosis (only for localized disease)
Anatomic site	Trunk, head (particularly scalp), and neck associated with poorer prognosis than extremities
Number of involved lymph nodes	Cut-off points: 1, 2–3, 4 or more lymph nodes (see Table 113.11)
Regional lymph node tumor burden	Clinically detectable (palpable) nodal metastases with poorer prognosis than clinically occult (microscopic) nodal metastases
Site of distant metastases	Visceral metastases associated with poorer prognosis than non-visceral metastases (skin, subcutaneous, distant lymph nodes)

Table 113.14 Cutaneous melanoma – major independent prognostic factors for survival in multivariate analyses.

address unintentional weight loss, fatigue, headache, and other constitutional symptoms, although cutaneous melanoma rarely presents with synchronous distant metastasis. Other family members should be screened if either melanoma or atypical melanocytic nevi are present, with a detailed history of malignancies, especially pancreatic cancer, that may warrant *CDKN2A* and/or multi-gene testing for hereditary cancer syndromes. All individuals at risk should be educated about the clinical features of melanoma, skin self-examination practices, and routine sun protection measures.

Skin Investigation and Clinical Diagnosis

A total body skin examination (TBSE) should be performed to estimate the total number of melanocytic nevi and the number of clinically atypical nevi, as well as the presence of congenital nevi. Atypical pigmented lesions should be examined by dermoscopy. Any lesion suspected of being melanoma or severely dysplastic should undergo excisional/complete biopsy, when possible.

Excisional biopsy is intended to completely remove the tumor with narrow (1–3 mm) peripheral margins and adequate depth to avoid histologic transection. Complete biopsy is recommended for suspected melanomas to prevent sampling error (e.g. missing a focus of melanoma arising in a precursor benign lesion) and to enable the pathologist to assess the overall architecture of the lesion and accurately microstage the tumor. Excisional/complete biopsy may be performed via full-thickness elliptical, disc, or punch technique or with deep shave/saucerization to the level of the deep reticular dermis; the latter is the biopsy technique most commonly used by US dermatologists.

Superficial shave biopsies should generally be avoided for palpable lesions in order to avoid histologic transection and underestimation of tumor thickness. However, a broad shave biopsy may optimize histopathologic assessment of suspected MIS, LM type, to exclude potential microinvasion. One must keep in mind that malignant melanocytes grow along adnexal structures in MIS, LM type, and therefore they commonly reach the basal resection margin of a shave biopsy.

The specimen should be sent to a pathologist experienced in the diagnosis of melanocytic tumors, preferably a board-certified dermatopathologist. A second opinion is sometimes necessary for difficult cases. Since cutaneous melanoma most commonly metastasizes to regional lymph nodes, palpation of lymph node basins should also be routinely performed, both initially and longitudinally.

Laboratory Investigations and Imaging

Worldwide evidence-based clinical practice guidelines[25,172] are uniform in recommending against *baseline* imaging or laboratory tests in asymptomatic patients with cutaneous melanoma of any thickness. Evaluation should be pursued for any signs or symptoms concerning for regional nodal and/or distant metastasis, but this is seldom encountered in most newly diagnosed patients. There is some variation among international guidelines regarding *surveillance* imaging and laboratory tests, although the consensus opinion is that appropriate studies should be done as clinically warranted for signs/symptoms concerning for disease recurrence.

The NCCN and AAD (2019) guidelines consider surveillance imaging (generally CT with contrast of the chest/abdomen/pelvis or whole-body FDG PET-CT) in asymptomatic patients with stage IIB melanoma and higher, recognizing its potential merits of surveillance in patients at higher risk for disease recurrence[25,34]. However, it remains to be proven that pre-symptomatic detection of metastatic recurrences is associated with improved patient outcomes, although as noted previously, there is some evidence that systemic targeted therapy is more efficacious in the setting of lower tumor burden[171]. Of note, in a single-center study of 353 stage IIB–IIIC patients treated with immune checkpoint inhibitors, improved MSS was observed in those who underwent intensive imaging surveillance for detection of asymptomatic recurrences, as compared to those with symptomatic recurrences[173].

An effective and noninvasive examination technique which was first introduced in Europe is lymph node ultrasound[174]. The scar of the primary cutaneous melanoma, the lymphatic drainage areas, and the regional lymph node basin are examined by ultrasound with a 7.5–10 MHz probe. In one-third of patients, metastases can be detected before they become palpable with this technique. In some European countries, lymph node ultrasound is recommended for staging and follow-up of patients with melanomas >1 mm in thickness[175]. NCCN guidelines recognize the merits of nodal ultrasound when clinical lymph node examination is equivocal for concerning adenopathy (at baseline or in follow-up) or completion lymph node dissection (CLND) is not pursued following a positive SLNB (see below). There may be additional value in obtaining regional nodal ultrasound in stage II (T2b/T3/T4) patients who do not undergo SLNB or when the procedure is not successful. However, regional nodal ultrasound assessment should only be performed if radiologic expertise is available[25].

Several serum markers for metastatic melanoma have been investigated. The most frequently employed biomarkers are LDH (US and Australia/New Zealand) and protein S100B and melanoma inhibitory activity (MIA; Europe). Since 2002, testing for LDH has been a standard component of the AJCC subclassification of stage IV melanoma, as LDH is an important predictor of survival and response to therapy in this subgroup[169,171]. However, LDH determination is not recommended in lower stage patients due to low sensitivity and specificity for detection of metastasis[34]. Primarily in Europe, protein S100B is employed as a serum biomarker for the detection of metastasis in patients at higher risk for recurrence[175].

In the future, circulating tumor DNA (ctDNA) may be utilized to monitor tumor burden/disease progression and thereby predict residual melanoma following surgical resection and risk for disease recurrence[176]. After sequencing the patient's primary tumor for tumor-specific mutations, RT-PCR is performed on peripheral blood to look for the presence of these mutations. Because ctDNA has a very short half-life (hours to days), it assesses active disease.

Investigation of stage III/IV melanoma patients may include radiologic investigations such as whole-body FDG PET-CT, ultrasound of the nodal basin, CT scan with contrast of the chest, abdomen and pelvis, and CT or MRI of the brain (Table 113.15). Chest radiography lacks sensitivity for metastatic detection but may be considered for pulmonary screening in certain patients. While the current average costs of PET-CT and CT scans in the US are ~$5750 and $3200, respectively (newchoicehealth.com), median specificity for identification of metastatic disease for CT scans was ~20% less than for PET-CT, and sensitivity was ~5% less for both primary staging and surveillance. For routine staging, a meta-analysis of 74 studies (n = 10 528 patients) determined that PET-CT had the highest sensitivity for detection of distant metastasis (80%, 95% CI 53%–93%) and specificity (87%, 95% CI 54%–97%), and nodal basin ultrasound had the highest sensitivity for detecting nodal involvement (60%, CI 33%–83%, specificity 97%, CI 98%–99%)[177]. Therefore, when possible, PET-CT is the preferred imaging modality for staging and surveillance of higher stage melanomas, although CT scans are less costly and frequently performed. MRI with contrast is preferred

SYMPTOMS AND DIAGNOSTIC TESTS FOR METASTATIC MELANOMA		
Metastatic site (TNM)	**Symptoms**	**Diagnostic tests***
Skin, soft tissue metastasis (TxNxM1a), in-transit metastasis (TxN1–3cM0)	Papules or nodules that vary in color from skin-toned to pink–red to blue, brown, or black; secondary ulceration or bleeding	Biopsy or fine needle aspiration for histopathologic confirmation; radiologic imaging as indicated for metastatic evaluation (CT C/A/P with contrast or PET-CT)
Brain metastasis (TxNxM1d)	Headache, nausea, seizures, focal weakness, visual disturbance, paresthesias	MRI with contrast (preferred), CT with contrast; neurosurgical consultation for tissue confirmation
Lung metastasis (TxNxM1b)	Mostly asymptomatic; rarely, chest pain, dyspnea, cough, hemoptysis	CT with contrast or PET-CT; chest X-ray not preferred but may be used for pulmonary screening in lower risk patients; bronchoscopy or interventional radiology for tissue confirmation
Gastrointestinal or liver metastasis (TxNxM1c)	• GI: abdominal pain, signs of anemia (e.g. fatigue, chest pain), vomiting, constipation, melena	• CBC, CT with contrast or PET-CT; colonoscopy for tissue confirmation
	• Liver: abdominal pain, jaundice	• Liver function tests, LDH; CT with contrast, PET-CT, or MRI; liver biopsy for tissue confirmation
Bone metastasis (TxNxM1c)	Pain, spontaneous fractures	Bone scan or PET-CT; biopsy for tissue confirmation

*Always include a thorough medical history and physical examination as well as complete blood count (CBC) and blood chemistry including lactate dehydrogenase (LDH). A multidisciplinary approach involving cutaneous, surgical, medical, and radiation oncologists is recommended to determine the most appropriate metastatic evaluation.

Table 113.15 Symptoms and diagnostic tests for metastatic melanoma. C/A/P, chest/abdomen/pelvis; CT, computed tomography; MRI, magnetic resonance imaging; PET, positron emission tomography.

for evaluation of brain metastases or special clinical situations such as deciding on the operability of soft tissue metastases[178].

MANAGEMENT

The management of cutaneous melanoma has rapidly changed over the past decade with the advent of molecular tests that aid in diagnosis, in addition to the paradigm-changing use of targeted therapy for *BRAF*-mutant melanoma and immune checkpoint blockade.

Management of the Primary Melanoma (Stage I and II)

Following histologic diagnosis, the primary cutaneous melanoma site should be re-excised with an appropriate surgical margin determined by the tumor thickness (Table 113.16). The rationale for excisional margins is based on the capacity of melanoma cells to migrate away from the tumor origin, i.e. melanoma may extend wider or deeper than is visibly apparent. The major goal is to prevent local recurrence, including persistent disease-type and satellite (lymphatic) metastasis.

Beginning in 1980, several prospective RCTs led to an evolution of surgical margins, although these studies, with one exception, excluded MIS and invasive melanoma in acral and head/neck sites. In the prior era, invasive melanoma was often excised with a wide margin of 5 cm, independent of tumor thickness. Then a WHO randomized trial demonstrated that 1 cm surgical margins (compared with 3 cm margins) were safe and effective for melanomas <1 mm in thickness and for melanomas up to 2 mm in depth[179,180]. A subsequent RCT focusing on intermediate-thickness melanoma (1 to 4 mm) found that 2 cm margins

SURGICAL TREATMENT OF PRIMARY CUTANEOUS MELANOMA		
Tumor thickness	**Excision margins (cm)**	**Comments**
In situ	0.5–1.0	• Melanoma *in situ*, lentigo maligna type, may require wider surgical margins (≥1 cm) for histologic clearance • Surgical techniques allowing for comprehensive peripheral and deep margin assessment (Mohs micrographic surgery, staged excision with permanent sections) may enhance local control • Topical treatment with imiquimod and radiation therapy are considered second-line modalities and may be used when surgery is not possible or postoperatively (in the case of imiquimod)
≤1 mm	1.0	• Thin, minimally invasive (T1a) lentigo maligna melanoma: Mohs micrographic surgery may be considered for tumors on the face or other anatomically constrained sites • Other cutaneous melanomas: Mohs micrographic surgery has not yet been prospectively studied in comparison to staged excision with permanent sections or conventional wide excision
>1–2 mm	1.0–2.0	
>2 mm	2.0	

Table 113.16 Surgical treatment of primary cutaneous melanoma. Evidence from available randomized trials is insufficient to address the optimal margins for the excision of primary cutaneous melanoma, but multiple expert international committees have produced fairly consistent guidelines, as summarized here. Of note, further investigative efforts will likely alter the standards of care over time. *Adapted from National Comprehensive Cancer Network. Melanoma: Cutaneous. NCCN Clinical Practice Guidelines in Oncology (NCCN Guidelines) Version 2.2023: https://www.nccn.org/professionals/physician_gls/pdf/cutaneous_melanoma.pdf.*

were as effective as 4 cm margins in preventing local metastatic recurrence[181]. Another RCT demonstrated the long-term safety of a 2 cm excision margin for thick melanomas (>2 mm thickness) at a median follow-up of 19.6 years, essentially confirming a maximum of 2 cm surgical margins for T3/T4 melanomas[182]. While current randomized trial evidence is non-existent for MIS (typically excised with 0.5 to 1 cm margins) and insufficient with regard to optimal surgical margins for T1 melanoma, expert international committees have produced fairly consistent guidelines, as summarized in Table 113.16[172,175].

Surgical margins in anatomically constrained sites such as the face, ears, digits, and mucous membranes may be narrower to preserve function and/or cosmesis[183]. For MIS of the face, which is typically LM/CSD type, Mohs micrographic surgery (MMS) or staged excision techniques with permanent sections may be employed to provide complete circumferential peripheral and deep histologic margin assessment (CCPDMA), while providing the narrowest possible margins. At the same time, subclinical extension of MIS, LM type, may require margins of 1 cm or greater for complete histologic clearance[184]. Similarly, lentiginous acral and mucosal melanomas are often poorly defined clinically and multifocal in nature. As a result, local recurrences are more frequent in these melanoma subtypes.

Mohs micrographic surgery (MMS)

In the US, the use of MMS for melanoma has nearly tripled over the past two decades[185]. As noted previously, MMS and staged excision using paraffin-embedded permanent section analysis may be considered for the treatment of MIS, LM type, especially in the head and neck region, as well as MIS in acral sites. Utilization of CCPDMA in these surgically challenging sites with significant photodamage has been associated with lower rates of persistent-disease type local recurrence[184]. The use of frozen section immunohistochemistry for MART-1 or other melanocytic markers has further improved intraoperative assessment of tumor clearance, although melanocyte hyperplasia in the setting of chronic actinic damage may complicate histopathologic interpretation of margins[186]. For MIS in non-anatomically constrained sites (e.g. trunk, extremities) and/or with distinct clinical margins (e.g. superficial spreading type), 5 mm surgical margins are typically performed, and MMS/CCPDMA is not generally needed for histologic clearance[34].

The role of MMS for invasive melanoma remains controversial. Proponents have argued that CCPDMA often results in surgical margins greater than those recommended for conventional excisions, ensuring full tumor resection[187]. Retrospective analyses of the National Cancer Database (NCD) have demonstrated improved overall survival (measured by all-cause mortality) for thin (T1a) invasive melanomas of the head and neck treated with MMS as compared to excision with >1 cm margins[188,189], but importantly, MSS is not assessed in the NCD. Other retrospective studies using SEER and NCD data have found similar MSS rates between MMS and standard excision, suggesting at least non-inferiority of MMS in melanoma treatment[190,191]. Of note, these studies do not provide information about the specific MMS technique employed, the precise surgical margins or other treatment details, local recurrence types (persistent disease vs satellitosis), and MSS rates.

A more recent systematic review and meta-analysis assessed local recurrence following MMS, staged excision, or conventional WLE for nearly 14 000 head and neck melanomas (100 published studies); 51.0% (7138) were treated by WLE, 34.5% (4826) by MMS, and 14.5% (2034) by staged excision[192]. Local recurrence rates were the lowest for MMS (0.61%; 95% CI, 0.1%–1.4%), followed by staged excision (1.8%; 95% CI, 1.0%–2.9%) and WLE (7.8%; 95% CI, 6.4%–9.3%), although definitions of local recurrence and proportions of invasive melanomas varied, with marked heterogeneity among the studies. A subsequent critical review of quality and data reporting in the MMS/staged excision literature noted serious or critical bias in 98% of publications eligible for analysis when modified "risk of bias in non-randomized studies of interventions" (ROBINS-I) criteria were employed[193]. The authors cited the need for longer follow-up periods, clear tumor classifications, and prospective, randomized study designs to improve the quality of future research.

Large, prospective, head-to-head comparisons of MMS and other margin control techniques versus conventional excision are now being proposed. Presently, there is insufficient evidence for national guidelines to recommend the use of MMS to treat invasive melanoma. Current NCCN guidelines do recognize the value of comprehensive histologic margin assessment for MIS, LM/CSD and acral types, along with minimally invasive (T1a) LMM in anatomically constrained sites[25]. It anticipated that greater consensus will emerge from further investigations.

Topical imiquimod

Another area of debate is the treatment of LM with topical imiquimod, a Toll-like receptor (TLR)-7 agonist, rather than with surgical excision. An important distinction is its use in the primary setting (in lieu of surgical resection) versus in the adjuvant setting (after optimal surgery has been performed). *Primary* therapy is most often utilized in elderly patients with limited function or life expectancy and/or comorbidities that prevent surgical excision, in addition to facial lesions where surgical removal would lead to disfigurement. *Adjuvant* use of imiquimod may be initiated when the surgical margin is histologically narrow (≤1 mm) or transected, but clinically no residual tumor is evident. Imiquimod may also be used as a neoadjuvant therapy so as to shrink the tumor preoperatively.

Because most published studies consist of case series, there is significant variation in: (1) frequency and duration of applications; (2) pre-treatment and post-treatment disease assessments; (3) use of combination therapies (e.g. cryotherapy, topical 5-fluorouracil); and (4) duration of surveillance. In two studies that described imiquimod as a neoadjuvant therapy prior to staged excision with a 2 mm margin, an 82%–83% histologic clearance rate and 4% recurrence rate were reported; however, an initial excisional biopsy was performed so the application of imiquimod was actually more adjuvant in nature[194,195].

In recent analyses, when imiquimod was used as a *primary* therapy with similar mean follow-up times, clinical clearance rates of 72%–84% were reported[196–199]. In a single-arm, phase II trial of primary imiquimod for LM diagnosed by partial punch biopsy, histologic clearance rates were somewhat lower at 37% after application 5 days per week for 12 weeks. However, distinguishing residual LM from actinic melanocytic hyperplasia in excisional specimens was a noted challenge in this study, which did not assess long-term response rates[200]. In an open-label, nonrandomized prospective study of 89 patients with MIS, LM type, treated until significant inflammation developed and followed for a median of 4.8 years, 16 (18%) relapsed; a greater number of lesional melanocytes (counted in biopsy specimens) was associated with an increased risk of local recurrence[201]. Two recent systematic reviews suggest the importance of cumulative dose and treatment intensity, with at least 60 applications of imiquimod at >5 times per week associated with the highest likelihood of complete clinical and histologic clearance[202,203].

In the *adjuvant* setting, i.e. following surgery, the clinical clearance rate in one retrospective study was 94% with a mean follow-up of 43 months[204]. Use of imiquimod versus radiation therapy as second-line therapy for LM is currently under investigation in an RCT in Australia, when staged surgical excision with 5 mm margins is not possible, declined by the patient, or fails to clear the tumor histologically (RADICAL Trial, www.clinicaltrials.gov/ct2/show/NCT02394132).

Adjuvant Therapy Considerations for Stage II Melanoma

Based upon results of a phase 3, randomized, double-blind trial, adjuvant pembrolizumab was recently approved for resected stage IIB (T3b/T4aN0) and IIC (T4bN0) melanoma. The trial involved 976 patients ≥12 years of age who underwent pathologic staging with SLNB to confirm node-negative status. They were treated with adjuvant pembrolizumab (200 mg IV every 3 weeks) for one-year (17 cycles) versus placebo. At a median follow-up of 20.9 months, adjuvant pembrolizumab significantly reduced the risk of recurrence or death (hazard ratio 0.61, 95% CI, 0.45–0.82); the 18-month recurrence-free survival rate was 85.8% for pembrolizumab and 77.0% for placebo[205]. Similar quality-of-life measures were observed in the two study arms, along with manageable immunotoxicities – 16% of patients developed grade 3–4 immune-related adverse events (irEAs), similar to adjuvant immunotherapy trials in stage III melanoma. However, careful discussion of risk/benefit ratio and referral to medical oncology is recommended to determine the most appropriate stage II melanoma patients for adjuvant therapy.

Local Recurrences

It is critical to understand the biologic differences between local recurrence from inadequate excision of the primary tumor (termed *persistent disease-type* or "true" local recurrence) from that due to lymphatic metastasis in or around the scar (termed *satellitosis*). Persistent disease-type local recurrence abuts the surgical excision scar, is histologically defined by *in situ* and/or radial growth phase, and should be surgically managed according to Breslow thickness of the recurrence (Fig. 113.28A). Local satellite recurrence is an intralymphatic recurrence within or adjacent (≤2 cm) to the excision scar, although AJCC-8 recognizes this distance as arbitrary, since satellite and in-transit (lymphatic) metastases have similar survival outcomes (Fig. 113.29)[169]. Importantly, local satellite recurrence reclassifies the melanoma as stage III, prompting staging via imaging, referral for WLE and possible SLNB, and discussion of adjuvant therapy.

Melanomas with a higher frequency of subclinical extension, e.g. acral lentiginous, LM, are at higher risk of persistent disease-type local recurrence (Figs. 113.28A-C & 113.30), whereas melanomas that are thicker, ulcerated, have a higher mitotic rate, and/or lymphovascular invasion are at increased risk of metastatic local recurrence (satellites) despite prior adequate surgical margins. Thick desmoplastic melanomas with "pure" desmoplastic histology, extensive perineural invasion/neurotropism, and/or head and neck location may exhibit either type of local recurrence (Fig. 113.28D) and thus are sometimes considered for adjuvant radiation therapy following initial resection.

Satellitosis presents as one or more indurated papulonodules within or immediately surrounding the melanoma scar (generally within 2 cm) and is strongly associated with the development of in-transit, regional, and distant metastases. As noted previously, satellite recurrence reclassifies the melanoma as stage III, with consideration of subsequent systemic therapy. There is no evidence that patient survival is adversely affected if local recurrence results from incomplete excision of the primary melanoma (i.e. persistent disease), provided that the recurrent *in situ* and/or radial growth phase tumor is promptly re-excised and there is no evidence of nodal or distant disease.

Local recurrences of melanoma, particularly the persistent disease-type, can occur several years (rarely decades) after excision of the primary lesion. When a lesion previously diagnosed histologically as a melanocytic nevus recurs locally more than two years after removal, re-evaluation for possible melanoma should be considered.

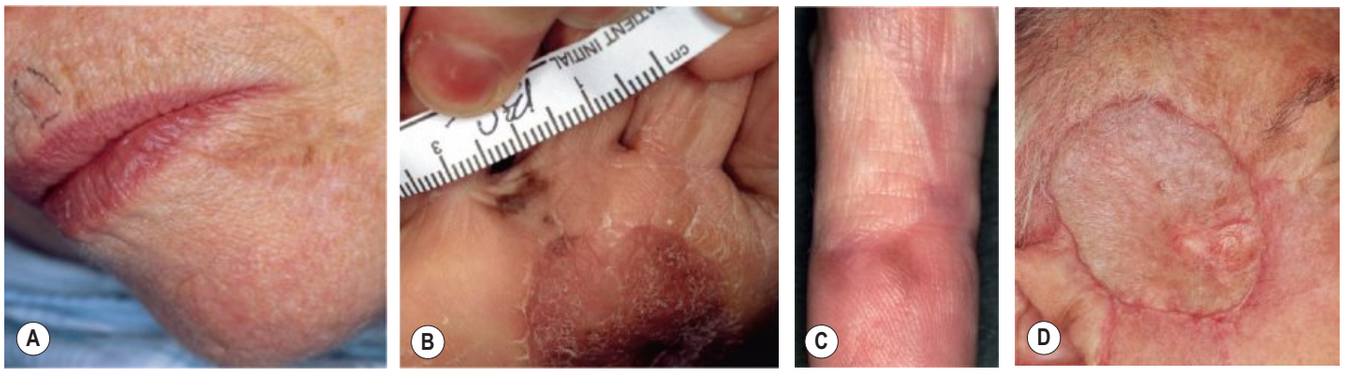


Fig. 113.28 Local recurrences of cutaneous melanoma. A Persistent disease-type local recurrence of lentigo maligna (melanoma *in situ*) along the upper lateral margin of the excision of the chin; inked lesion on the central upper lip is an actinic keratosis. **B** Recurrent *in situ* acral lentiginous melanoma at the 10 o'clock position on the split-thickness skin graft. **C** Recurrent acral lentiginous melanoma on the second finger. The lentiginous types of melanoma have a propensity to recur locally due to persistence of subclinical melanoma (mainly *in situ*) as well as the presence of "field melanocytes" that harbor the same genetic alterations as the primary tumor but are morphologically indistinguishable from normal melanocytes, thus leading to "false negative" histologic margins. Staining with PRAME may highlight positive nevoid melanocytes at the site of the tumor, possibly reducing the risk of recurrence, but data are still very limited. **D** Amelanotic nodule representing local recurrence of a desmoplastic melanoma under the skin graft. *A,B,D, Courtesy Jean L. Bolognia, MD; C, Courtesy Department of Dermatology, Medical University of Graz.*

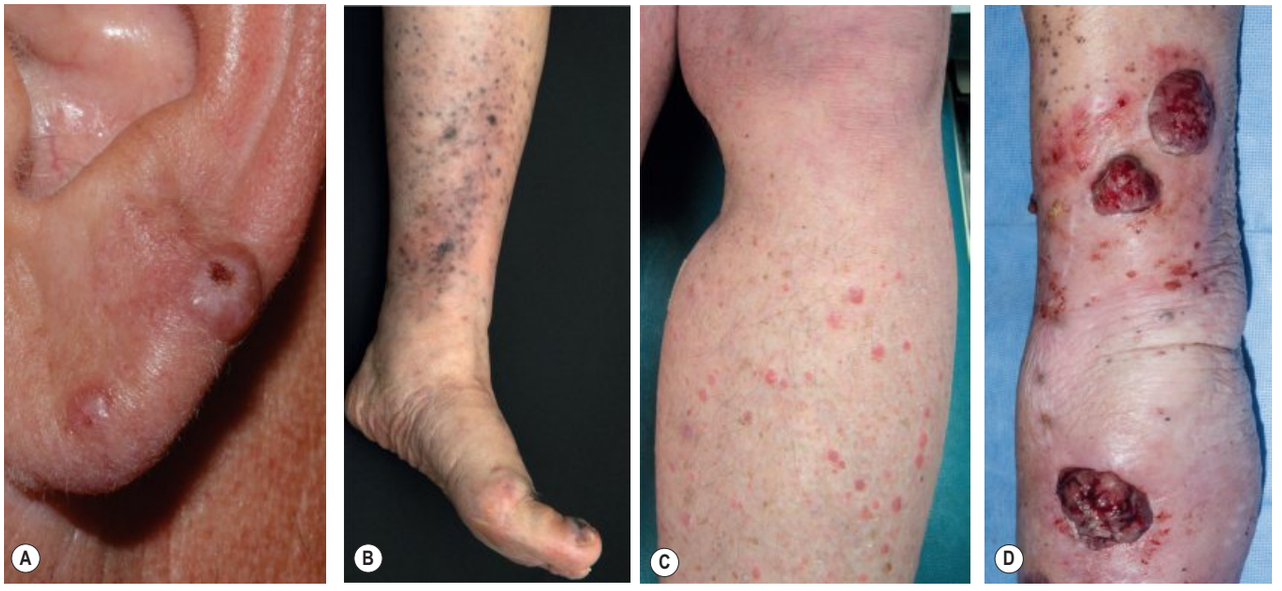


Fig. 113.29 Satellite and in-transit (lymphatic) metastases of cutaneous melanoma. A Amelanotic melanoma of the external ear with satellitosis. **B** Ulcerated melanoma of the hallux with multiple in-transit metastases on the shin and calf, consisting of numerous brown to gray-black patches, papules, and small plaques. **C** In-transit metastases consisting of multiple firm pink papules on the leg. **D** In-transit metastases consisting of multiple friable tumors on the arm as well as smaller blue–gray papules. *A, Courtesy Sonya K. Burton, MD; C, Courtesy, Department of Dermatology, Medical University of Graz; D, Courtesy Edward Cowen, MD.*

Management of Regional Metastatic Melanoma (Stage III)

In ~70% of patients, metastatic spread of melanoma is locoregional, i.e. confined to the site of the primary melanoma, its draining lymph nodes, and the lymphatics between the primary tumor and regional lymph nodes. Locoregional metastasis may manifest as clinically occult lymph node micrometastasis, clinically evident (i.e. palpable) lymph node macrometastasis, or as satellite/in-transit metastasis (discussed above). The vast majority of stage III patients are identified with microscopic nodal disease following SLNB.

Sentinel lymph node biopsy (SLNB) and completion lymph node dissection

SLNB was introduced in the 1990s as a method for determining whether the melanoma had microscopically spread to regional nodes and was based upon the presumed migration of melanoma cells from the primary tumor to an initial draining regional lymph node(s). SLNB thereafter replaced elective lymph node dissection (ELND), which was previously considered standard of care for intermediate thickness melanoma until four multicenter, randomized, prospective trials failed to show a survival benefit for patients treated with ELND plus wide excision compared to wide excision alone[206–209].

Approximately 15%–20% of patients with clinically node-negative cutaneous melanoma >1 mm in depth will exhibit microscopic lymph node involvement on SLNB[210]. Increased rates of SLNB-positivity occur with greater tumor thickness and other adverse histologic features in the primary melanoma, e.g. ulceration, high mitotic index, lymphovascular invasion. SLNB is optimally performed in the same operative setting as the surgical excision. Preoperative lymphatic mapping is performed to identify the first draining lymph node(s) within the lymph node basin(s) using technetium sulfur colloid and/or blue dye injected into the skin surrounding the melanoma biopsy site. Lymphoscintigraphy demonstrates the lymphatic drainage pattern from a given melanoma site and can be combined with 3D CT imaging. The tumor typically drains to one lymph node basin and 1–2 nodes within that basin, although there can be multiple draining nodal basins in areas of lymphatic overlap such as the mid trunk or head and neck.

The sentinel lymph nodes are intraoperatively defined as: (1) any pathologically enlarged nodes based on palpation; (2) nodes dyed blue (following injection of dye); (3) the node with the highest emission of radiotracer; and (4) any nodes that emit ≥10% of radiotracer compared to the hottest node. Intraoperatively, a small incision is made overlying the

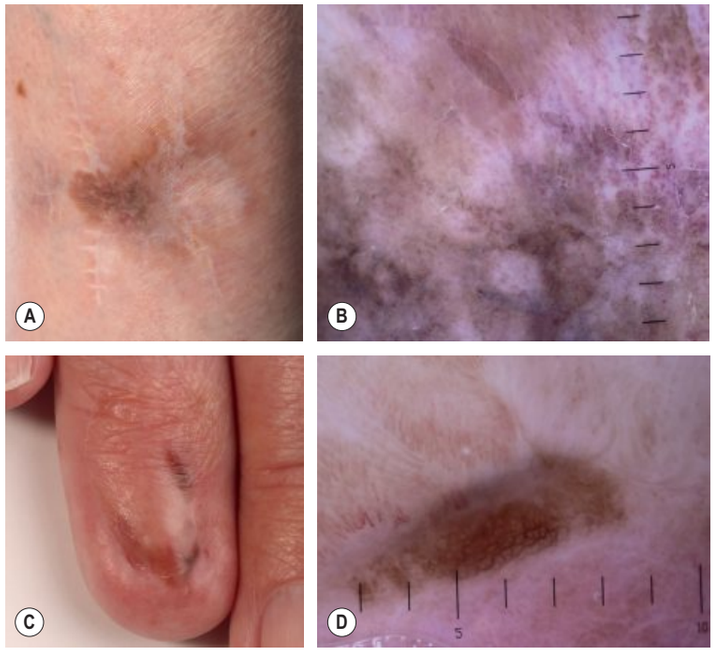


Fig. 113.30 Local recurrences of cutaneous melanoma. A Recurrent lentigo maligna on the lower leg; note the depressed scar due to repeated excisions. **B** By dermoscopy, an asymmetric pattern with multiple colors, ranging from light brown to dark blue–gray. **C** Recurrent acral lentiginous melanoma of the nail unit. The lentiginous types of melanoma have a propensity to recur locally due to persistence of subclinical melanoma (mainly *in situ* and/or in radial growth phase). **D** By dermoscopy, an asymmetric pattern with an atypical network inferiorly and multiple colors including blue–gray and gray–white. *Courtesy Claus Garbe, MD and Jürgen Bauer, MD.*

nodal basin and visual inspection, palpation, and a hand-held gamma counter are used to identify and then remove the sentinel nodes in their entirety, followed by histopathology to identify microscopic deposits of tumor via cytomorphologic and immunohistochemical analyses[121,123].

Pathologic staging of the sentinel lymph nodes is considered standard for staging and prognostication of primary cutaneous melanomas ≥1 mm in thickness. Numerous publications have identified the status of the sentinel lymph node(s) as the strongest prognostic factor for survival and recurrence[211,212]. For melanomas ≥1 mm thickness, pathologic nodal staging is recommended in practice guidelines worldwide and by the AJCC and UICC, taking into account patient factors such as age, functional status, and life expectancy (see Table 113.11 & 113.12)[169]. For example, if a patient has a medical condition such as dementia or comorbid factors that preclude general anesthesia or raise operative risk, it would be reasonable to forgo SLNB.

The role of SLNB for thinner (T1) melanomas is less clear. It may be considered in AJCC-8 T1b melanoma (<0.8 mm with ulceration or 0.8–1.0 mm with or without ulceration), although rates of SLNB-positivity in this group are still relatively low. T1a melanomas (<0.8 mm without ulceration) rarely exhibit a high mitotic index (>2/mm^2) or lymphovascular invasion. However, if these histologic factors are evident, SLNB may also be considered, particularly in younger patients who may be more likely to pursue adjuvant therapy and/or surveillance imaging[25].

Apart from select subgroups of patients with regional nodal disease in the MSLT-1 trial, SLNB has not been demonstrated to improve overall survival and is considered a prognostic, rather than therapeutic, procedure[213,214]. However, identification of occult stage III disease via SLNB now allows for adjuvant therapies that improve relapse-free survival and may ultimately result in increased MSS. Risks of SLNB include those associated with general anesthesia, surgical site seroma, infection, and rarely, lymphedema in an extremity.

Pursuit of completion lymph node dissection (CLND) following a positive SLNB has declined worldwide following two RCTs (DeCOG and MSLT-2) that failed to show an overall survival benefit in SLNB-positive patients who underwent CLND versus those who were observed but followed with regional nodal ultrasound examination[215,216]. Where radiologic expertise is available, surveillance nodal ultrasound (or cross-sectional imaging) is generally recommended in lieu of CLND for SLNB-positive patients per current NCCN guidelines, but imaging does not provide pathologic information regarding non-sentinel lymph node status.

Skin satellite and in-transit metastases

As noted previously, satellite and in-transit metastases occur within the lymphatic vessels located between the primary melanoma and the draining lymph node basin. They represent stage III disease and are associated with increased risk for the development of regional nodal and distant metastasis.

In the past, the treatment of choice for satellite/in-transit metastasis was surgical, but intralesional therapy with immune-activating injectables such as talimogene laherparepvec (TVEC) and the TLR9 agonist tilsotolimod and/or systemic therapies can now be used in a neoadjuvant fashion if numerous or extensive lesions are not initially surgically resectable. TVEC is a genetically engineered herpes virus that replicates in cancer cells, causing them to burst and produce GM-CSF, thus stimulating an immune response against the cancer. For locally unresectable disease in a patient who wishes to avoid the side effects of systemic neoadjuvant therapy, TVEC may be an appropriate choice. TVEC was FDA-approved based upon a phase III study that demonstrated a 32% response rate with a complete remission in 17%[217]; other studies have shown a response rate of up to 88%[218]. TVEC has also been investigated in combination with immune checkpoint inhibitors.

For multiple in-transit metastases on an extremity, isolated limb perfusion with melphalan, with or without tumor necrosis factor (TNF), has palliative value[219]. The procedure may be curative, as indicated by reported 5- and 10-year survival rates of 40% and 30%, respectively. Nowadays, however, intralesional and systemic immunotherapies and targeted agents are more commonly employed.

Clinically detectable regional lymph node metastases

If regional lymph node metastases are diagnosed clinically (i.e. palpable) or via imaging, confirmatory core biopsy or fine needle aspiration is recommended. Therapeutic lymph node dissection (TLND) has been considered standard therapy for bulky regional adenopathy and consists of an anatomically complete dissection of the involved nodal basin[164,167]. The extent of the TLND may be modified according to the anatomic area of lymph node involvement. While TLND has been the standard of care for local basin control of bulky lymphadenopathy, the approach to clinically apparent/macroscopic nodal disease (as well as resectable distant metastases) now includes *neoadjuvant* immunotherapy and targeted therapy prior to surgical excision[25,220,221].

Adjuvant therapy

The goal of adjuvant therapy is the elimination of clinically inapparent micrometastases, primarily in resected high-risk stage II or III melanoma and occasionally resected stage IV melanoma. Prior to the advent of more effective systemic therapies (see below), there was limited success with chemotherapy and immunostimulants such as bacille Calmette–Guérin (BCG) or *Corynebacterium parvum*. The latter were tried because of the finding that melanoma cells express tumor antigens recognizable by the immune system. In 1995, the FDA approved the use of high-dose interferon alpha (IFN-α) for adjuvant treatment of stage IIB and III melanoma (per AJCC staging at the time), and in 1998, high-dose interleukin 2 (IL-2) was approved for unresectable melanoma. Flu-like symptoms, including profound malaise, and depression often led to dose reductions of IFN-α while IL-2 was associated with hypotension and capillary leak syndrome. Prior to the 2010s, adjuvant IFN-α (low- and intermediate-dose in Europe and high-dose in the US) was standard treatment for resected stage III melanoma[222–224].

Based upon the discovery of genetic mutations in melanomas, including *BRAF* V600E, there was a paradigm shift in treatment strategies. While the combination of BRAF and MEK inhibitors was initially approved for unresectable stage III and IV melanoma, in 2018, dabrafenib plus trametinib was approved for adjuvant treatment of resected stage III BRAF V600-mutant disease[225]. The second key discovery was the ability of immune checkpoint blockade to selectively stimulate activated T cells (see below). This eventually led to the approval of anti-CTLA-4 (ipilimumab) and anti-PD-1 antibodies (nivolumab, pembrolizumab) as adjuvant therapies for resected stage III melanoma[226–228]. Based on demonstration of durable relapse-free survival in the seminal prospective randomized trials[229–232], adjuvant therapy is considered a standard treatment option for appropriate patients with high-risk resected stage III and stage IV melanoma, although to date overall survival benefit has not been reported.

Management of Distant Metastases (Stage IV)

Over the past decade, effective targeted and immune therapies have revolutionized the treatment of advanced melanoma, leading to marked improvement in relapse-free and overall survival[226–228]. There is a rapid and high response rate to oral kinase inhibitors (initially targeting BRAF), but development of resistance is an issue. On the other hand, immune checkpoint inhibitors have a slower response rate (apart from dual anti-CTLA-4/PD-1 blockade), but the response is often long-lasting. Prior to the introduction of these therapies, the prognosis of stage IV melanoma was poor, with a 5-year survival rate of <10% and median survival of about 9 months[233]. Within the AJCC substages, differential survival is observed, with soft tissue metastases only (M1a) having a better prognosis than visceral and CNS metastases (M1b, M1c, M1d). For each of these disease sites, i.e. across M categories, an abnormal LDH level is associated with a poorer prognosis, as are a greater number of metastases, multi-organ involvement, and older age at diagnosis (see Table 113.11)[233]. In a small proportion of patients with few metastases involving only one or two organs, surgical or other ablative treatment strategies with curative intent may be considered.

Surgery

Despite melanoma's tendency to disseminate to multiple organs, resection of limited metastases (metastasectomy) may provide palliation and potential long-term survival benefit[234]. Numerous studies have demonstrated clear and durable survival advantages for patients undergoing complete resection of metastatic melanoma, particularly isolated pulmonary, nodal or skin metastases, although modern systemic therapeutic approaches are also an option. Factors that positively influence prognosis are isolated non-visceral metastasis and complete resection with free surgical margins. For certain indications, such as isolated lung metastases, median 5-year survival can approach 30% after surgical treatment, with adjuvant systemic therapy further improving relapse-free survival. For brain metastases, surgical resection alone may extend median survival to about 10 months, with a significant improvement in quality of life[235], but nowadays stereotactic radiosurgery is commonly employed as are systemic therapies (see below). While targeted and immune therapy have become standard of care for resectable and unresectable stage IV melanoma, there are ongoing investigations of combinatorial approaches including neoadjuvant systemic therapy prior to surgery.

Radiation therapy

Although radiation therapy (RT) is rarely indicated for localized cutaneous melanoma, it may be used for primary treatment of unresectable MIS, LM type, and in the adjuvant setting for desmoplastic melanoma at high-risk of recurrence[25]. In the past, adjuvant RT was routinely administered following surgical resection of bulky nodal disease, but then it was found to have no relapse-free or overall survival benefit in a large international RCT[236]. Long-term follow-up did confirm the benefit of RT for improved local control of the lymph node basin, but at the expense of both short- and long-term adverse side effects[236,237]. For stage III disease, the use of RT has been largely replaced by improved adjuvant systemic therapies.

In stage IV melanoma, RT is used primarily for palliation of symptoms related to distant metastases in patients with incurable disease. Specific indications include pain control as well as spinal cord compression, stabilization of bones affected by metastasis, and brain metastases. The latter are typically treated via stereotactic radiosurgery and fractionated stereotactic radiotherapy; these methods are preferred as both primary and adjuvant treatments due to their superior efficacy and improved side effect profile compared to whole brain radiotherapy. Whole brain radiotherapy is reserved for palliation when stereotactic radiosurgery is not possible or when systemic therapy has failed[25].

Systemic therapy

Systemic therapy is the mainstay of treatment in patients with distant metastases, with surgery and RT playing a more limited role (see above). Both small-molecule kinase inhibitors that target BRAF and MEK and immune checkpoint inhibitors (ICIs) have revolutionized treatment strategies (Table 113.17). These therapies are far superior and generally less toxic than chemotherapy and systemic IL-2, and they are considered first-line treatments for unresectable stage III and IV melanoma. Clinical trials have or are currently evaluating regimens in which ICIs and BRAF/MEK inhibitors are administered in combination or sequentially as well as possible advantages of pulse-dosing targeted agents to improve efficacy, combat resistance, and reduce side effects. Of note, severe drug hypersensitivity reactions have been observed when BRAF inhibitors were administered soon after ICIs, with ~20% of patients fulfilling the criteria for DRESS (drug reaction with eosinophilia and systemic symptoms), compared to 5% of patients who received BRAF inhibitors without ICI priming[238].

TARGETED THERAPIES AND IMMUNE CHECKPOINT INHIBITORS		
Targeting the MAPK pathway (see Fig. 113.1)		**FDA approved for advanced melanoma as of August 2023**
BRAF inhibitors (selective*) – combined with a MEK inhibitor	Dab*raf*enib	√
	Enco*raf*enib	√
	Vemu*raf*enib	√
MEK inhibitors – combined with a BRAF inhibitor	Bini*met*inib	√
	Cobi*met*inib	√
	Tra*met*inib	√
Immune checkpoint inhibitors (see Fig. 128.9)		
Anti-CTLA-4 antibodies	Ipilimumab	√
	Tremelimumab	
Anti-PD-1 antibodies	Nivolumab	√
	Pembrolizumab	√
	Dostarlimab	
	Retifanlimab	Approved for metastatic Merkel cell carcinoma
Anti-PD-L1 antibodies	Atezolizumab	√ (in combination with BRAF inhibitor + MEK inhibitor)
	Avelumab	Approved for metastatic Merkel cell carcinoma
	Cemiplimab	Approved for locally advanced or metastatic BCC and cutaneous SCC
	Durvalumab	
Anti-LAG3 antibody	Relatlimab	√ (in combination with nivolumab)

*Target melanomas that have specific amino acid substitutions at position 600 in BRAF, most commonly V600E and less often V600D or V600K.

Table 113.17 Major systemic treatments for metastatic melanoma – targeted therapies and immune checkpoint inhibitors. Pembrolizumab is also approved for metastatic Merkel cell carcinoma. BCC, basal cell carcinoma; MAPK, mitogen-activated protein kinase; SCC, squamous cell carcinoma.

Molecularly targeted therapy

Tumor genotyping indicates that ~45% of cutaneous melanomas harbor activating mutations in *BRAF* and ~15% have activating mutations in *NRAS*, leading to constitutive activation of the RAS–RAF–MEK–ERK (MAPK) signaling pathway that regulates cell proliferation (see Fig. 113.1). A specific point mutation in *BRAF*, which leads to the substitution of glutamic acid (E) for valine (V) at codon 600, hence V600E, accounts for 90% of *BRAF* mutations. Three small molecule inhibitors that selectively target the mutant BRAF kinase have been EMA- and FDA-approved, beginning in 2011. Approval was based upon the results of phase III clinical trials that initially compared dabrafenib and vemurafenib to dacarbazine (DTIC)[239,240].

The three BRAF inhibitors – vemurafenib, dabrafenib, and encorafenib – exhibit similar rapid therapeutic responses and side effect profiles (see Table 21.16), although photosensitivity to UVA and pyrexia are more common with vemurafenib and dabrafenib, respectively. Unfortunately patients treated with BRAF inhibitor monotherapy develop tumor resistance after an average of six months of treatment. Furthermore, due to paradoxical activation of the MAPK pathway in keratinocytes with wild-type BRAF and oftentimes *RAS* mutations, cutaneous SCCs and keratoacanthomas develop in up to 25% of patients treated with BRAF inhibitor monotherapy.

Mechanisms of resistance to selective BRAF inhibitors include increased MEK activity, either via mutational activation or overexpression of COT, as well as expression of truncated forms of BRAF (which dimerize and activate the MAPK pathway) and overexpression of platelet-derived growth factor. MEK inhibitors are therefore combined with BRAF inhibitors in an effort to postpone development of resistance (see Table 113.17). Because this combination of kinase inhibitors prolongs the average time to development of treatment resistance to 10 months[241,242] and improves efficacy, it is considered standard of care for locally advanced or metastatic *BRAF*-mutated melanoma. Importantly, the cutaneous side effects of the selective BRAF inhibitors, including squamous papillomas, plantar keratoses, and cutaneous SCCs, are significantly reduced with the dual regimen. For patients whose melanomas have activating *BRAF* (V600) mutations, initial combination targeted therapy may be used when a rapid clinical response is needed in life-threatening situations, but ICIs are normally preferred as first-line therapy, independent of mutational status[242a].

In patients with *NRAS* mutations, BRAF inhibitors are ineffective, but administration of MEK inhibitor monotherapy can result in objective tumor responses in ~25% of patients. A subgroup of melanoma patients, especially those with acral lentiginous or mucosal melanoma, have amplifications and/or mutations in *KIT* which lead to enhanced activity of the KIT receptor and potential targeted therapy (see above and Fig. 113.1)[129].

Immunotherapy

Immunotherapy is based on the concept that the immune system is able to fight cancer, and melanoma is one of the prototypic and most highly immunogenic malignancies. Therefore, a therapeutic effect might be achieved by infusing effectors of the immune system such as antibodies, cytokines, or killer cells. Not only has the advent of ICIs transformed the treatment of melanoma, it has positively impacted numerous other cancers. Additional anti-melanoma immunotherapies include injection of oncolytic agents (see above), cancer vaccination, and adoptive cell therapy. In the latter, non-myeloablative lymphodepleting chemotherapy is followed by infusion of expanded autologous tumor-infiltrating lymphocytes.

Immune checkpoint blockade

Currently, ICIs are considered first-line therapy in patients with unresectable stage III or IV disease, either with or without an activating *BRAF* mutation[25]. While the anti-CTLA-4 antibody ipilimumab was the first to be FDA- and EMA-approved for advanced melanoma (see Table 113.17), it has largely been supplanted by anti-PD-1 antibodies (nivolumab, pembrolizumab). As single agents, the latter have superior efficacy and less toxicity when compared to ipilimumab alone. Combined anti-CLTA-4/-PD-1 blockade is also considered first-line and is associated with a significantly greater response rate but higher incidence of side effects.

These antibodies *antagonize inhibitory* receptors on T cells, thus leading to stimulation of existing immune responses against melanoma antigens via activation of cytotoxic $CD8^+$ T cells (see Fig. 128.9). This strategy is in contrast to simply enhancing existing immunostimulatory mechanisms as was done for decades in melanoma vaccine trials.

Cytotoxic T lymphocyte-associated antigen-4 (CTLA-4) blockade. Full T cell activation requires stimulation through the T cell receptor as well as a costimulatory signal provided by the binding of B7 on an antigen-presenting cell to CD28 on the T cell. CTLA-4 is a homolog of CD28 and is an inhibitory T cell receptor that is upregulated following T cell activation. The normal function of CTLA-4 is to compete with CD28 to bind B7 in order to downregulate T cell activation, acting as a natural "brake" by removing the costimulatory signal. The CTLA-4–B7 interaction can be blocked with an anti-CTLA-4 monoclonal antibody, which has a higher affinity for CTLA-4 than B7 (see Fig. 128.9). Thus, the *inhibitory signal is prevented* and the "brake" on T cell activation released.

Two fully human anti-CTLA-4 monoclonal antibodies (mAbs) have been investigated, tremelimumab and ipilimumab, with the latter receiving FDA and EMA approval for the treatment of metastatic melanoma[243,244]. As a single agent, objective response rates of 11% were achieved and a significant portion of these responses were durable. At three years, the survival rate for ipilimumab plus dacarbazine was 21% versus 12% for dacarbazine alone. Although responses to anti-CTLA-4 mAbs may persist, they may take as long as 12 weeks or even longer to develop[245].

Side effects from CTLA-4 blockade are autoimmune-related and include colitis, hepatitis, thyroiditis, hypophysitis, myocarditis, and a wide range of skin reactions from dermatitis to leukoderma. Of note, development of vitiligo-like leukoderma is correlated with an improved clinical response[246]. Additional cutaneous and systemic side effects are outlined in Table 21.18. Systemic corticosteroids or steroid-sparing agents are often employed to treat these autoimmune-related phenomena. Although the combination of ipilimumab plus the anti-PD-1 antibody nivolumab can lead to an enhanced objective response (61%) when compared to ipilimumab alone (11%), it results in a significant increase in grade 3 and grade 4 side effects[247]. Newer regimens have employed alternative dosing of combination ipilimumab and nivolumab to try to reduce toxicity while maintaining efficacy[248].

Blockade of programmed cell death 1 (PD-1) and its ligand (PD-L1). PD-1 is an inhibitory immune receptor of the CD28 family that plays an important role in the immune escape of tumors. The interaction of PD-1 (CD279) with its ligand PD-L1 (B7-H1; CD274) inhibits T cell proliferation and effector functions and induces apoptosis of tumor-specific T cells. Blockade of either PD-1 or PD-L1 can restore the immune functions of dysfunctional T cells, including enhancement of cytokine production and cytolysis. Since PD-L1 is widely expressed on tumor cells, this blockage focuses on T cell–cancer cell interactions, i.e. the T cell's effector phase (see Fig. 128.9).

Two anti-PD-1 antibodies, nivolumab and pembrolizumab, have been approved as first-line monotherapy for metastatic melanoma (see Table 113.17), with markedly less toxicity compared to ipilimumab. As with ipilimumab, anti-PD-1 therapy works equally well in *BRAF*-wild type and *BRAF*-mutated melanomas. Compared to an overall one-year survival rate of 42% in dacarbazine-treated patients, the one-year survival rate for patients who received nivolumab was 73%[249], and the objective response rate was 40% (compared to 14% for dacarbazine). As monotherapies, nivolumab and pembrolizumab are more effective than ipilimumab, e.g. nivolumab led to a median progression-free survival (PFS) of 6.9 months versus 2.9 months for ipilimumab[224] while pembrolizumab resulted in an objective response of 33% versus 12% for ipilimumab[250]. A more provocative finding was the enhanced clinical response and reduced incidence of colitis seen in patients receiving anti-PD-1 checkpoint inhibitors who had a diverse microbiome, and the use of oral antibiotics within one month of starting ICIs could impair therapeutic effectiveness[251]. This is presumably because intestinal bacteria play a role in the development of a T cell immune response.

The irAEs seen with anti-PD-1 antibodies overlap with those of anti-CTLA-4 antibodies and include dermatitis, pneumonitis, and nephritis (see Table. 21.18). However, a higher proportion of patients receiving CTLA-4 inhibitors experience grade 3 or higher irAEs compared to those treated with PD-1 inhibitors. As with ipilimumab, patients who had an objective response were more likely to develop vitiligo-like leukoderma. Utilizing antibodies that target PD-L1 rather than PD-1 represents another strategy and these antibodies have been approved for the treatment of other carcinomas that express PD-L1 (see Table 113.17). Of note, in patients with PD-L1-negative tumors, the combination of nivolumab plus ipilimumab prolonged median PFS to a greater extent than did nivolumab alone (11.2 months vs 5.3 months) whereas the two treatment regimens led to a similar PFS in patients with PD-L1-positive tumors[224]. However, further data did not support PD-L1 expression as a biomarker for response to ICIs, and melanoma guidelines do not recommend utilizing PD-L1 expression in clinical decision-making[252]. Lastly, given the durable survival benefit with single agent immunotherapy in pivotal anti-CTLA-4 and -PD-1 antibody trials, ICIs are recommended as frontline therapy over targeted agents in patients with metastatic or unresectable disease[242a,253,254].

Blockade of other immune checkpoints. There are multiple ligand-receptor interactions between T cells and dendritic cells that represent potential therapeutic targets. Recently, the combination of relatlimab, an inhibitor of LAG3 on T cells, plus nivolumab was approved for the treatment of unresectable or metastatic melanoma. Fewer grade 3–4 irAEs were observed compared to dual checkpoint blockade with nivolumab plus ipilimumab. Progression-free survival with the combination was 10.1 months compared to 4.6 months for nivolumab alone[255]. Additional potential treatments include sotigalimab, which interrupts interactions between CD40L on T cells and CD40 on dendritic cells. Given the rapidly evolving immunotherapeutic options in melanoma, attention to guidelines-based care is critical.

Cancer vaccines

Cancer vaccines have long been pursued in the hope of enhancing immune recognition and effector antitumor immune responses via improved antigen presentation and elicitation of effector memory T cell responses that are durable. Increased knowledge of the relevant antigenic epitopes capable of eliciting antitumor immunity has prompted a variety of vaccine approaches. Although vaccines are well tolerated, they rarely have been monitored with methods that are now recognized to be critical for detecting whether or not the vaccine induced an immune response. Not surprisingly, the large phase III trials of older crude autologous tumor cell vaccines did not demonstrate clinical evidence of antitumor activity, either in advanced disease or in the adjuvant setting.

Peptide vaccines have been studied in large, multicenter ECOG trials in the US[256] and led to the induction of immune responses in more than a third of vaccinated patients. However, none showed an improvement in overall survival, with the exception of a combination of gp100 peptide vaccine plus IL-2, which improved progression-free survival compared with IL-2 alone[257]. More recently, mRNA vaccines are being investigated for induction of antitumor immunity in a variety of cancers and hold promise for melanoma[258].

Chemotherapy

Over the past four decades, cytotoxic chemotherapy has demonstrated a low but reproducible level of activity against metastatic melanoma. Drugs most commonly employed include dacarbazine (DTIC)/temozolomide, carboplatin/cisplatin, vindesine/vinblastine, BCNU/fotemustine, and paclitaxel/docetaxel. Unfortunately, despite the identification of multiple chemotherapeutic agents with activity against melanoma both *in vitro* and in phase I/II clinical trials[259,260], to date no significant impact on survival exists for any chemotherapeutic regimen. In those countries where targeted therapy and ICIs are readily available, chemotherapy is now administered as salvage therapy. However, in lower-income countries, chemotherapy may be a first-line treatment due to the high cost of newer agents.

The most widely used single chemotherapeutic agent remains dacarbazine (DTIC). It has shown the greatest effectiveness as a single agent in most trials – an ~10%–15% response rate can be achieved with a median response duration of 5 to 6 months. The oral alkylating agent temozolomide (a prodrug of MTIC, the active metabolite of DTIC) has some efficacy in treating CNS metastases and is equal in efficacy to DTIC[261,262]. Fotemustine is a member of the nitrosourea family and has some activity against melanoma, including brain metastases.

MELANOMA SURVEILLANCE

Protocols for the longitudinal care of melanoma patients vary worldwide and generally depend on the risk of disease recurrence and development of new primary melanomas. Lifelong follow-up of these patients is important because of: (1) the risk of second primary cutaneous melanomas (3.5%–4.5%, depending on nevus phenotype and/or genetic factors); (2) the risk of local and/or metastatic recurrence (greatest in the first 2–5 years after initial diagnosis and stage-dependent); (3) the risk of late recurrence (>10–15 years) which is uncommon but does occur; and (4) the increased risk of other cutaneous malignancies (e.g. cutaneous SCC, BCC).

Most stage I/II cutaneous melanomas will present with locoregional recurrence, while stage III/IV patients most often present with systemic metastases. The latter group is typically followed by an oncologist, although ongoing dermatologic assessment is important for detection of disease recurrence and new primary melanomas, as well as recognition and treatment of cutaneous side effects from targeted and immune therapies. Recommendations for the frequency of dermatologic visits varies internationally and amongst practitioners. As 90% of recurrences occur during the first 5 years following primary diagnosis (with the greatest risk in the first 2 years), most experts recommend dermatologic visits one to four times per year for 2 years after diagnosis (depending on risk of disease recurrence and alternating with oncologic visits in those with higher stage disease), then every 6 to 12 months through year 5 following diagnosis, then at least annually thereafter. Clinical surveillance frequency is also influenced by the number of melanocytic nevi (common and atypical), number of primary cutaneous melanomas, and genetic susceptibility, which increases the risk of additional primary melanomas.

Dermatologic visits should include: (1) updates on the medical history; (2) review of systems (e.g. any new or changing lesions, new "lumps or bumps" in or around the melanoma excision site or in nodal basins, unanticipated weight loss, fatigue, headache or other CNS symptoms, shortness of breath); (3) total body skin examination; (4) examination and palpation of the melanoma scar/excision site and surrounding area for local recurrences or in-transit metastases; (5) examination of regional and distant lymph nodes; and (6) laboratory and radiologic tests as indicated by concerning signs and/or symptoms. Patients should be counseled to adhere to sun-protective measures; perform skin self-examinations at home; and to take an oral vitamin D_3 supplement, particularly if they are practicing regular sun protection. Family members should also be encouraged to undergo routine skin examinations.

While early detection of asymptomatic melanoma metastasis has not been clearly associated with improved survival, most data pertain to the era of minimally effective systemic therapies. The future of melanoma diagnosis and treatment will likely involve molecular techniques that accurately demonstrate residual disease (e.g. ctDNA) or have proven validity for prognosis and staging to determine which patients require SLNB, surveillance imaging, and/or adjuvant therapy following resection of the primary tumor.

The merits of early detection of primary melanoma cannot be understated. Diagnosis of melanoma when thin and most curable will reduce patient morbidity and associated costs of care. Primary prevention aimed at avoiding natural and artificial sources of UVR, and early detection strategies for this visible and largely recognizable cutaneous tumor should be at the forefront of public health measures.

Additional figures and table on Invasive cutaneous melanoma - components of the histopathologic report, available in our eBook (see inside front cover for access code).

REFERENCES

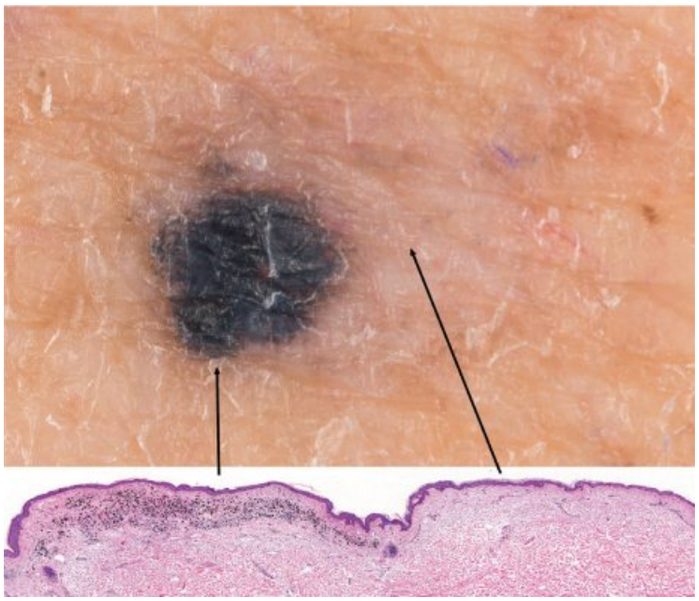
1. Hodis E, Watson IR, Kryukov GV, et al. A landscape of driver mutations in melanoma. *Cell*. 2012;150:251–263.
2. Bastian BC. The molecular pathology of melanoma: an integrated taxonomy of melanocytic neoplasia. *Ann Rev Pathol*. 2014;9:239–271.
3. Shain AH, Joseph NM, Yu R, et al. Genomic and transcriptomic analysis reveals incremental disruption of key signaling pathways during melanoma evolution. *Cancer Cell*. 2018;34:45–55.e44.
4. Elder DE, Bastian BC, Cree IA, et al. The 2018 World Health Organization classification of cutaneous, mucosal, and uveal melanoma: detailed analysis of 9 distinct subtypes defined by their evolutionary pathway. *Arch Pathol Lab Med*. 2020;144:500–522.
5. Whiteman DC, Watt P, Purdie DM, et al. Melanocytic nevi, solar keratoses, and divergent pathways to cutaneous melanoma. *J Natl Cancer Inst*. 2003;95:806–812.
6. Maldonado JL, Fridlyand J, Patel H, et al. Determinants of BRAF mutations in primary melanomas. *J Natl Cancer Inst*. 2003;95:1878–1890.
7. Drilon A, Laetsch TW, Kummar S, et al. Efficacy of larotrectinib in TRK fusion-positive cancers in adults and children. *N Engl J Med*. 2018;378:731–739.
8. Chan L, Hwang SJE, Byth K, et al. Survival and prognosis of individuals receiving programmed cell death 1 inhibitor with and without immunologic cutaneous adverse events. *J Am Acad Dermatol*. 2020;82:311–316.
9. Wu X-C, Eide MJ, King J, et al. Racial and ethnic variations in incidence and survival of cutaneous melanoma in the United States, 1999-2006. *J Am Acad Dermatol*. 2011;65:S26–S37.
10. Karimkhani C, Green AC, Nijsten T, et al. The global burden of melanoma: results from the Global Burden of Disease Study 2015. *Br J Dermatol*. 2017;177:134–140.
11. Siegel RL, Miller KD, Fuchs HE, Jemal A. Cancer statistics, 2021. *CA Cancer J Clin*. 2021;71:7–33.
12. Sitenga JL, Aird G, Ahmed A, et al. Socioeconomic status and survival for patients with melanoma in the United States: an NCDB analysis. *Int J Dermatol*. 2018;57:1149–1156.
13. Leiter U, Eigentler T, Garbe C. Epidemiology of skin cancer. *Adv Exp Med Biol*. 2014;810:120–140.
14. Whiteman DC, Green AC, Olsen CM. The growing burden of invasive melanoma: projections of incidence rates and numbers of new cases in six susceptible populations through 2031. *J Invest Dermatol*. 2016;136:1161–1171.
15. Holman DM, Freeman MB, Shoemaker ML. Trends in melanoma incidence among non-Hispanic whites in the United States, 2005 to 2014. *JAMA Dermatol*. 2018;154:361–362.
16. Hu S, Parmet Y, Allen G, et al. Disparity in melanoma: a trend analysis of melanoma incidence and stage at diagnosis among whites, Hispanics, and blacks in Florida. *Arch Dermatol*. 2009;145:1369–1374.
17. Yang DD, Salciccioli JD, Marshall DC, et al. Trends in malignant melanoma mortality in 31 countries from 1985 to 2015. *Br J Dermatol*. 2020;183:1056–1064.
18. Jemal A, Saraiya M, Patel P, et al. Recent trends in cutaneous melanoma incidence and death rates in

the United States, 1992-2006. *J Am Acad Dermatol*. 2011;65:S17–25.e11–13.
19. Berk-Krauss J, Stein JA, Weber J, et al. New systemic therapies and trends in cutaneous melanoma deaths among US whites, 1986–2016. *Am J Public Health*. 2020;110:731–733.
20. Dawes SM, Tsai S, Gittleman H, et al. Racial disparities in melanoma survival. *J Am Acad Dermatol*. 2016;75:983–991.
21. Wellbrock C. Melanoma and the microenvironment: age matters. *N Engl J Med*. 2016;375:696–698.
22. Shaikh WR, Dusza SW, Weinstock MA, et al. Melanoma thickness and survival trends in the United States, 1989 to 2009. *J Natl Cancer Inst*. 2015;108:djv294.
23. Linos E, Swetter SM, Cockburn MG, et al. Increasing burden of melanoma in the United States. *J Invest Dermatol*. 2009;129:1666–1674.
24. Buettner PG, Leiter U, Eigentler TK, Garbe C. Development of prognostic factors and survival in cutaneous melanoma over 25 years: an analysis of the Central Malignant Melanoma Registry of the German Dermatological Society. *Cancer*. 2005;103:616–624.
25. National Comprehensive Cancer Network. Melanoma: Cutaneous. NCCN Clinical Practice Guidelines in Oncology (NCCN Guidelines) Version 2.2023. Available at: https://www.nccn.org/professionals/physician_gls/pdf/cutaneous_melanoma.pdf.
26. Soura E, Eliades PJ, Shannon K, et al. Hereditary melanoma: update on syndromes and management. Genetics of familial atypical multiple mole melanoma syndrome. *J Am Acad Dermatol*. 2016;74:395–407. quiz 408–10.
27. Rossi M, Pellegrini C, Cardelli L, et al. Familial melanoma: diagnostic and management implications. *Dermatol Pract Concept*. 2019;9:10–16.
28. Leachman SA, Carucci J, Kohlmann W, et al. Selection criteria for genetic assessment of patients with familial melanoma. *J Am Acad Dermatol*. 2009;61:677. e1–14.
29. Goldstein AM, Chan M, Harland M, et al. Features associated with germline CDKN2A mutations: a GenoMEL study of melanoma-prone families from three continents. *J Med Genet*. 2007;44:99–106.
30. Soura E, Eliades PJ, Shannon K, et al. Hereditary melanoma: update on syndromes and management. Emerging melanoma cancer complexes and genetic counseling. *J Am Acad Dermatol*. 2016;74:411–420. quiz 421–2.
31. Fargnoli MC, Fargnoli MC, Pike K, et al. MC1R variants increase risk of melanomas harboring BRAF mutations. *J Invest Dermatol*. 2008;128:2485–2490.
32. Yokoyama S, Woods SL, Boyle GM, et al. A novel recurrent mutation in MITF predisposes to familial and sporadic melanoma. *Nature*. 2011;480:99–103.
33. Walpole S, Pritchard AL, Cebulla CM, et al. Comprehensive study of the clinical phenotype of germline BAP1 variant-carrying families worldwide. *J Natl Cancer Inst*. 2018;110:1328–1341.
34. Swetter SM, Tsao H, Bichakjian CK, et al. Guidelines of care for the management of primary cutaneous melanoma. *J Am Acad Dermatol*. 2019;80:208–250.
35. Aspinwall LG, Leaf SL, Dola ER, et al. CDKN2A/p16 genetic test reporting improves early detection intentions and practices in high-risk melanoma families. *Cancer Epidemiol Biomarkers Prev*. 2008;17:1510–1519.
36. Bauer J, Garbe C. Risk estimation for malignant transformation of melanocytic nevi. *Arch Dermatol*. 2004;140:127 author reply 127.
37. Tsao H, Bevona C, Goggins W, Quinn T. The transformation rate of moles (melanocytic nevi) into cutaneous melanoma: a population-based estimate. *Arch Dermatol*. 2003;139:282–288.
38. Grob JJ, Gouvernet J, Aymar D, et al. Count of benign melanocytic nevi as a major indicator of risk for nonfamilial nodular and superficial spreading melanoma. *Cancer*. 1990;66:387–395.
39. Rosendahl CO, Grant-Kels JM, Que SKT. Dysplastic nevus: fact and fiction. *J Am Acad Dermatol*. 2015;73:507–512.
40. Ródenas JM, Delgado-Rodríguez M, Farinas-Alvarez C, et al. Melanocytic nevi and risk of cutaneous malignant melanoma in southern Spain. *Am J Epidemiol*. 1997;145:1020–1029.
41. Swerdlow AJ, English J, MacKie RM, et al. Benign melanocytic naevi as a risk factor for malignant melanoma. *Br Med J (Clin Res Ed)*. 1986;292:1555–1559.
42. Clark WH, Reimer RR, Greene M, Ainsworth AM, Mastrangelo MJ. Origin of familial malignant melanomas from heritable melanocytic lesions. 'The B-K mole syndrome'. *Arch Dermatol*. 1978;114:732–738.
43. Elmore JG, Barnhill RL, Elder DE, et al. Pathologists' diagnosis of invasive melanoma and melanocytic proliferations: observer accuracy and reproducibility study. *Br Med J (Clin Res Ed)*. 2017;357:j2813.
44. Garbe C, Büttner P, Weiss J, et al. Risk factors for developing cutaneous melanoma and criteria for identifying persons at risk: multicenter case-control study of the Central Malignant Melanoma Registry of the German Dermatological Society. *J Invest Dermatol*. 1994;102:695–699.
45. Kraemer KH, Tucker M, Tarone R, Elder DE, Clark WH. Risk of cutaneous melanoma in dysplastic nevus syndrome types A and B. *N Engl J Med*. 1986;315:1615–1616.
46. Tucker MA, Halpern A, Holly EA, et al. Clinically recognized dysplastic nevi. A central risk factor for cutaneous melanoma. *JAMA*. 1997;277:1439–1444.
47. Gandini S, Sera F, Cattaruzza MS, et al. Meta-analysis of risk factors for cutaneous melanoma: I. Common and atypical naevi. *Eur J Cancer*. 2005;41:28–44.
48. Mitchell DL, Greinert R, de Gruijl FR, et al. Effects of chronic low-dose ultraviolet B radiation on DNA damage and repair in mouse skin. *Cancer Res*. 1999;59:2875–2884.
49. Osterlind A, Tucker MA, Stone BJ, Jensen OM. The Danish case-control study of cutaneous malignant melanoma. II. Importance of UV-light exposure. *Int J Cancer*. 1988;42:319–324.
50. Green A, MacLennan R, Siskind V. Common acquired naevi and the risk of malignant melanoma. *Int J Cancer*. 1985;35:297–300.
51. Elwood JM, Jopson J. Melanoma and sun exposure: an overview of published studies. *Int J Cancer*. 1997;73:198–203.
52. Bulliard JL. Site-specific risk of cutaneous malignant melanoma and pattern of sun exposure in New Zealand. *Int J Cancer*. 2000;85:627–632.
53. Anderson WF, Pfeiffer RM, Tucker MA, Rosenberg PS. Divergent cancer pathways for early-onset and late-onset cutaneous malignant melanoma. *Cancer*. 2009;115:4176–4185.
54. Valejo Coelho MM, Matos TR, Apetato M. The dark side of the light: mechanisms of photocarcinogenesis. *Clin Dermatol*. 2016;34:563–570.
55. Harrison SL, MacLennan R, Buettner PG. Sun exposure and the incidence of melanocytic nevi in young Australian children. *Cancer Epidemiol Biomarkers Prev*. 2008;17:2318–2324.
56. Bauer J, Büttner P, Wiecker TS, et al. Risk factors of incident melanocytic nevi: a longitudinal study in a cohort of 1,232 young German children. *Int J Cancer*. 2005;115:121–126.
57. Whiteman DC, Stickley M, Watt P, et al. Anatomic site, sun exposure, and risk of cutaneous melanoma. *J Clin Oncol*. 2006;24:3172–3177.
58. De Fabo EC, Noonan FP, Fears T, Merlino G. Ultraviolet B but not ultraviolet A radiation initiates melanoma. *Cancer Res*. 2004;64:6372–6376.
59. De Fabo EC. Initial studies on an in vivo action spectrum for melanoma induction. *Prog Biophys Mol Biol*. 2006;92:97–104.
60. Ley RD. Dose response for ultraviolet radiation A-induced focal melanocytic hyperplasia and nonmelanoma skin tumors in Monodelphis domestica. *Photochem Photobiol*. 2001;73:20–23.
61. Mitchell D, Paniker L, Sanchez G, et al. The etiology of sunlight-induced melanoma in Xiphophorus hybrid fish. *Mol Carcinogen*. 2007;46:679–684.
62. Wehner MR, Chren M-M, Nameth D, et al. International prevalence of indoor tanning: a systematic review and meta-analysis. *JAMA Dermatol*. 2014;150:390–400.
63. Colantonio S, Bracken MB, Beecker J. The association of indoor tanning and melanoma in adults: systematic review and meta-analysis. *J Am Acad Dermatol*. 2014;70:847–857.e1–18.
64. Rodriguez-Acevedo AJ, Green AC, Sinclair C, et al. Indoor tanning prevalence after the International Agency for Research on Cancer statement on carcinogenicity of artificial tanning devices: systematic review and meta-analysis. *Br J Dermatol*. 2020;182:849–859.
65. Aim at Melanoma Foundation. Indoor Tanning Legislation 2023. Available at: https://www.aimatmelanoma.org/legislation-policy-advocacy/indoor-tanning.
66. Green AC, Williams GM, Logan V, Strutton GM. Reduced melanoma after regular sunscreen use: randomized trial follow-up. *J Clin Oncol*. 2011;29:257–263.
67. Matta MK, Zusterzeel R, Pilli NR, et al. Effect of sunscreen application under maximal use conditions on plasma concentration of sunscreen active ingredients: a randomized clinical trial. *JAMA*. 2019;321:2082–2091.
68. Lim HW, Arellano-Mendoza M-I, Stengel F. Current challenges in photoprotection. *J Am Acad Dermatol*. 2017;76:S91–S99.
69. Clark WH, From L, Bernardino EA, Mihm MC. The histogenesis and biologic behavior of primary human malignant melanomas of the skin. *Cancer Res*. 1969;29:705–727.
70. Skender-Kalnenas TM, English DR, Heenan PJ. Benign melanocytic lesions: risk markers or precursors of cutaneous melanoma? *J Am Acad Dermatol*. 1995;33:1000–1007.
71. Afanasiev OK, Tu JH, Chu DH, Swetter SM. Characteristics of melanoma in white and nonwhite children, adolescents, and young adults: analysis of a pediatric melanoma institutional registry, 1995-2018. *Pediatric Dermatol*. 2019;36:448–454.
72. Demierre M-F, Chung C, Miller DR, Geller AC. Early detection of thick melanomas in the United States: beware of the nodular subtype. *Arch Dermatol*. 2005;141:745–750.
73. Shaikh WR, Xiong M, Weinstock MA. The contribution of nodular subtype to melanoma mortality in the United States, 1978 to 2007. *Arch Dermatol*. 2012;148:30–36.
74. Weinstock MA, Sober AJ. The risk of progression of lentigo maligna to lentigo maligna melanoma. *Br J Dermatol*. 1987;116:303–310.
75. Argenziano G, Soyer HP, Chimenti S, et al. Dermoscopy of pigmented skin lesions: results of a consensus meeting via the internet. *J Am Acad Dermatol*. 2003;48:679–693.
76. Bradford PT, Goldstein AM, McMaster ML, Tucker MA. Acral lentiginous melanoma: incidence and survival patterns in the United States, 1986–2005. *Arch Dermatol*. 2009;145:427–434.
77. Curtin JA, Fridlyand J, Kageshita T, et al. Distinct sets of genetic alterations in melanoma. *N Engl J Med*. 2005;353:2135–2147.
78. Raghavan SS, Peternel S, Mully TW, et al. Spitz melanoma is a distinct subset of spitzoid melanoma. *Mod Pathol*. 2020;33:1122–1134.
79. Lallas A, Kyrgidis A, Ferrara G, et al. Atypical Spitz tumours and sentinel lymph node biopsy: a systematic review. *Lancet Oncol*. 2014;15:e178–e183.
80. Spillane A, Hong A, Fogarty G. Re-examining the role of adjuvant radiation therapy. *J Surg Oncol*. 2019;119:242–248.
81. Howard MD, Wee E, Wolfe R, et al. Differences between pure desmoplastic melanoma and superficial spreading melanoma in terms of survival, distribution and other clinicopathologic features. *J Eur Acad Dermatol Venereol*. 2019;33:1899–1906.
82. Nicolson NG, Han D. Desmoplastic melanoma. *J Surg Oncol*. 2019;119:208–215.
83. Conic RZ, Ko J, Allam SH, et al. Mixed versus pure variants of desmoplastic melanoma: the Cleveland Clinic experience. *Ann Plast Surg*. 2018;80:277–281.
84. Hantschke M, Mentzel T, Rütten A, et al. Cutaneous clear cell sarcoma: a clinicopathologic, immunohistochemical, and molecular analysis of 12 cases emphasizing its distinction from dermal melanoma. *Am J Surg Pathol*. 2010;34:216–222.
85. Hisaoka M, Ishida T, Kuo T-T, et al. Clear cell sarcoma of soft tissue: a clinicopathologic, immunohistochemical, and molecular analysis of 33 cases. *Am J Surg Pathol*. 2008;32:452–460.
86. Sidiropoulos M, Obregon R, Cooper C, et al. Primary dermal melanoma: a unique subtype of melanoma to be distinguished from cutaneous metastatic melanoma: a clinical, histologic, and gene expression-profiling study. *J Am Acad Dermatol*. 2014;71:1083–1092.
87. Cassarino DS, Cabral ES, Kartha RV, Swetter SM. Primary dermal melanoma: distinct immunohistochemical findings and clinical outcome compared with nodular and metastatic melanoma. *Arch Dermatol*. 2008;144:49–56.
88. Van Raamsdonk CD, Bezrookove V, Green G, et al. Frequent somatic mutations of GNAQ in uveal melanoma and blue naevi. *Nature*. 2009;457:599–602.
89. National Comprehensive Cancer Network. Uveal Melanoma. NCCN Clinical Practice Guidelines in Oncology (NCCN Guidelines) Version 1; 2023. Available at. https://www.nccn.org/professionals/physician_gls/pdf/uveal.pdf.
90. Schoenfield L, Pettay J, Tubbs RR, Singh AD. Variation of monosomy 3 status within uveal melanoma. *Arch Pathol Lab Med*. 2009;133:1219–1222.
91. Harbour JW, Chen R. The DecisionDx-UM Gene Expression profile test provides risk stratification and individualized patient care in uveal melanoma. *PLoS Curr*. 2013:5.
92. Onken MD, Worley LA, Char DH, et al. Collaborative Ocular Oncology Group report number 1: prospective validation of a multi-gene prognostic assay in uveal melanoma. *Ophthalmology*. 2012;119:1596–1603.
93. Decatur CL, Ong E, Garg N, et al. Driver mutations in uveal melanoma: associations with gene expression profile and patient outcomes. *JAMA Ophthalmol*. 2016;134:728–733.

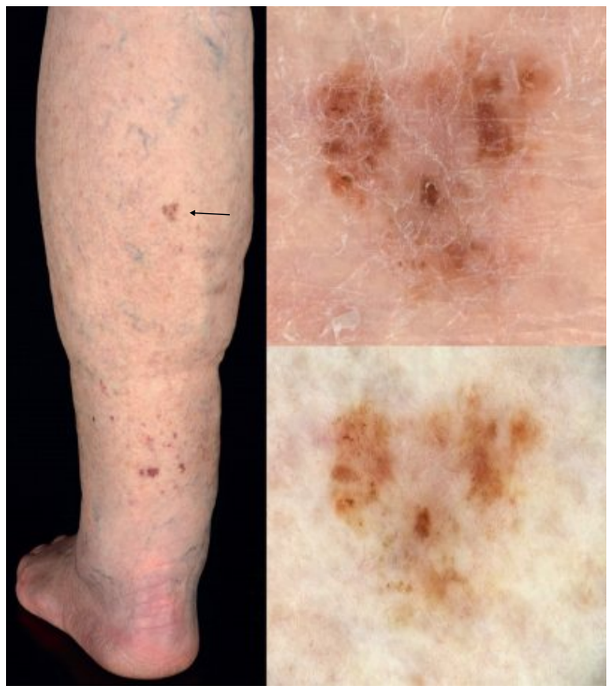
94. Tomicic J, Wanebo HJ. Mucosal melanomas. *Surg Clin North Am*. 2003;83:237–252.
95. Stensheim H, Møller B, van Dijk T, Fosså SD. Cause-specific survival for women diagnosed with cancer during pregnancy or lactation: a registry-based cohort study. *J Clin Oncol*. 2009;27:45–51.
96. Andersson TM-L, Johansson ALV, Fredriksson I, Lambe M. Cancer during pregnancy and the postpartum period: a population-based study. *Cancer*. 2015;121:2072–2077.
97. Sanchez JL, Figueroa LD, Rodriguez E. Behavior of melanocytic nevi during pregnancy. *Am J Dermatopathol*. 1984;6:89–91.
98. Pennoyer JW, Grin CM, Driscoll MS, et al. Changes in size of melanocytic nevi during pregnancy. *J Am Acad Dermatol*. 1997;36:378–382.
99. Jones MS, Lee J, Stern SL, Faries MB. Is pregnancy-associated melanoma associated with adverse outcomes? *J Am Coll Surg*. 2017;225:149–158.
100. Gandini S, Iodice S, Koomen E, et al. Hormonal and reproductive factors in relation to melanoma in women: current review and meta-analysis. *Eur J Cancer*. 2011;47:2607–2617.
101. Grunewald S, Jank A. New systemic agents in dermatology with respect to fertility, pregnancy, and lactation. *J Dtsch Dermatol Ges*. 2015;13:277–289. quiz 290.
102. Poulet FM, Wolf JJ, Herzyk DJ, DeGeorge JJ. An evaluation of the impact of PD-1 pathway blockade on reproductive safety of therapeutic PD-1 inhibitors. *Birth Defects Res B Dev Reprod Toxicol*. 2016;107:108–119.
103. Pappo AS. Melanoma in children and adolescents. *Eur J Cancer*. 2003;39:2651–2661.
104. Cordoro KM, Gupta D, Frieden IJ, et al. Pediatric melanoma: results of a large cohort study and proposal for modified ABCD detection criteria for children. *J Am Acad Dermatol*. 2013;68:913–925.
105. Paradela S, Fonseca E, Pita S, et al. Spitzoid melanoma in children: clinicopathological study and application of immunohistochemistry as an adjunct diagnostic tool. *J Cutan Pathol*. 2009;36:740–752.
106. Averbook BJ, Lee SJ, Delman KA, et al. Pediatric melanoma: analysis of an international registry. *Cancer*. 2013;119:4012–4019.
107. Liu W, Hill D, Gibbs AF, et al. What features do patients notice that help to distinguish between benign pigmented lesions and melanomas?: the ABCD(E) rule versus the seven-point checklist. *Melanoma Res*. 2005;15:549–554.
108. Grob JJ, Bonerandi JJ. The 'ugly duckling' sign: identification of the common characteristics of nevi in an individual as a basis for melanoma screening. *Arch Dermatol*. 1998;134:103–104.
109. Scope A, Dusza SW, Halpern AC, et al. The "ugly duckling" sign: agreement between observers. *Arch Dermatol*. 2008;144:58–64.
110. Giuffrida R, Uranitsch M, Schmid K, et al. Hypomelanotic melanoma detected by the "little red riding hood sign" in a patient with neurofibromatosis type 1. *Dermatol Pract Concept*. 2017;7:71–73.
111. Kittler H, Guitera P, Riedl E, et al. Identification of clinically featureless incipient melanoma using sequential dermoscopy imaging. *Arch Dermatol*. 2006;142:1113–1119.
112. Kittler H, Pehamberger H, Wolff K, Binder M. Diagnostic accuracy of dermoscopy. *Lancet Oncol*. 2002;3:159–165.
113. Phan A, Dalle S, Touzet S, et al. Dermoscopic features of acral lentiginous melanoma in a large series of 110 cases in a white population. *Br J Dermatol*. 2010;162:765–771.
114. Menzies SW, Kreusch J, Byth K, et al. Dermoscopic evaluation of amelanotic and hypomelanotic melanoma. *Arch Dermatol*. 2008;144:1120–1127.
115. Truong A, Strazzulla L, March J, et al. Reduction in nevus biopsies in patients monitored by total body photography. *J Am Acad Dermatol*. 2016;75:135–143.e135.
116. Fried L, Tan A, Bajaj S, et al. Technological advances for the detection of melanoma: advances in diagnostic techniques. *J Am Acad Dermatol*. 2020;83:983–992.
117. Pezzini C, Kaleci S, Chester J, et al. Reflectance confocal microscopy diagnostic accuracy for malignant melanoma in different clinical settings: systematic review and meta-analysis. *J Eur Acad Dermatol Venereol*. 2020;34:2268–2279.
118. Navarrete-Dechent C, Cordova M, Aleissa S, et al. Lentigo maligna melanoma mapping using reflectance confocal microscopy correlates with staged excision: a prospective study. *J Am Acad Dermatol*. 2023;88:371–379.
119. Waldman RA, Grant-Kels JM, Curiel CN, et al. Consensus recommendations for the use of non-invasive melanoma detection techniques based on results of an international DELPHI process. *J Am Acad Dermatol*. 2021;85:745–749.
120. Malvehy J, Hauschild A, Curiel-Lewandrowski C, et al. Clinical performance of the Nevisense system in cutaneous melanoma detection: an international, multicentre, prospective and blinded clinical trial on efficacy and safety. *Br J Dermatol*. 2014;171:1099–1107.
121. Scolyer R, Balamurgan T, Busam K, et al. *Invasive Melanoma, Histopathology Reporting Guide*. 2nd Edition. Sydney, Australia: International Collaboration on Cancer Reporting; 2019. Available at: http://www.iccr-cancer.org/datasets/published-datasets/skin/invasive-melanoma.
122. Shon W, Frishberg D, Gershenwald J, et al. *Protocol for the Examination of Biopsy Specimens from Patients with Melanoma of the Skin, version 4.2.0.0*. College of American Pathologists (CAP); 2020. Available at: https://documents.cap.org/protocols/cp-skin-melanoma-biopsy-20-4200.pdf.
123. Shon W, Frishberg D, Gershenwald J, et al. *Protocol for the Examination of Excision Specimens from Patients with Melanoma of the Skin, version 4.3.0.2*. College of American Pathologists (CAP); 2021. Available at: https://documents.cap.org/protocols/Skin.Melanoma_4.3.0.2.REL_CAPCP.pdf.
124. Raghavan SS, Wang JY, Kwok S, et al. PRAME expression in melanocytic proliferations with intermediate histopathologic or spitzoid features. *J Cutan Pathol*. 2020;47:1123–1131.
125. Gradecki SE, Slingluff CL, Gru AA. PRAME expression in 155 cases of metastatic melanoma. *J Cutan Pathol*. 2021;48:479–485.
126. Lezcano C, Pulitzer M, Moy AP, et al. Immunohistochemistry for PRAME in the distinction of nodal nevi from metastatic melanoma. *Am J Surg Pathol*. 2020;44:503–508.
127. Bastian BC, Olshen AB, LeBoit PE, Pinkel D. Classifying melanocytic tumors based on DNA copy number changes. *Am J Pathol*. 2003;163:1765–1770.
128. Bastian BC, Wesselmann U, Pinkel D, Leboit PE. Molecular cytogenetic analysis of Spitz nevi shows clear differences to melanoma. *J Invest Dermatol*. 1999;113:1065–1069.
129. Wiesner T, Murali R, Fried I, et al. A distinct subset of atypical Spitz tumors is characterized by BRAF mutation and loss of BAP1 expression. *Am J Surg Pathol*. 2012;36:818–830.
130. Gerami P, Scolyer RA, Xu X, et al. Risk assessment for atypical spitzoid melanocytic neoplasms using FISH to identify chromosomal copy number aberrations. *Am J Surg Pathol*. 2013;37:676–684.
131. Gerami P, Mafee M, Lurtsbarapa T, et al. Sensitivity of fluorescence in situ hybridization for melanoma diagnosis using RREB1, MYB, Cep6, and 11q13 probes in melanoma subtypes. *Arch Dermatol*. 2010;146:273–278.
132. Minca EC, Al-Rohil RN, Wang M, et al. Comparison between melanoma gene expression score and fluorescence in situ hybridization for the classification of melanocytic lesions. *Mod Pathol*. 2016;29:832–843.
133. Wiesner T, Kutzner H, Cerroni L, et al. Genomic aberrations in spitzoid melanocytic tumours and their implications for diagnosis, prognosis and therapy. *Pathology*. 2016;48:113–131.
134. Siroy AE, Boland GM, Milton DR, et al. Beyond BRAF(V600): clinical mutation panel testing by next-generation sequencing in advanced melanoma. *J Invest Dermatol*. 2015;135:508–515.
135. Cho-Vega JH. A diagnostic algorithm for atypical spitzoid tumors: guidelines for immunohisto-chemical and molecular assessment. *Mod Pathol*. 2016;29:656–670.
136. Gerami P, Li G, Pouryazdanparast P, et al. A highly specific and discriminatory FISH assay for distinguishing between benign and malignant melanocytic neoplasms. *Am J Surg Pathol*. 2012;36:808–817.
137. Lee S, Barnhill RL, Dummer R, et al. TERT promoter mutations are predictive of aggressive clinical behavior in patients with spitzoid melanocytic neoplasms. *Sci Rep*. 2015;5:11200.
138. Quan VL, Zhang B, Zhang Y, et al. Integrating next-generation sequencing with morphology improves prognostic and biologic classification of spitz neoplasms. *J Invest Dermatol*. 2020;140:1599–1608.
139. Koh SS, Opel ML, Wei JP, et al. Molecular classification of melanomas and nevi using gene expression microarray signatures and formalin-fixed and paraffin-embedded tissue. *Mod Pathol*. 2009;22:538–546.
140. Bittner M, Meltzer P, Chen Y, et al. Molecular classification of cutaneous malignant melanoma by gene expression profiling. *Nature*. 2000;406:536–540.
141. Talantov D, Mazumder A, Yu JX, et al. Novel genes associated with malignant melanoma but not benign melanocytic lesions. *Clin Cancer Res*. 2005;11:7234–7242.
142. Wachsman W, Morhenn V, Palmer T, et al. Noninvasive genomic detection of melanoma. *Br J Dermatol*. 2011;164:797–806.
143. Gerami P, Yao Z, Polsky D, et al. Development and validation of a noninvasive 2-gene molecular assay for cutaneous melanoma. *J Am Acad Dermatol*. 2017;76:114–120.e112.
144. Ferris LK, Gerami P, Skelsey MK, et al. Real-world performance and utility of a noninvasive gene expression assay to evaluate melanoma risk in pigmented lesions. *Melanoma Res*. 2018;28:478–482.
145. Cullison SRJ, Jansen B, Yao Z, Ferris LK. Risk stratification of severely dysplastic nevi by non-invasively obtained gene expression and mutation analyses. *SKIN*. 2020;4:105–110.
146. Clarke LE, Warf MB, Flake DD 2nd, et al. Clinical validation of a gene expression signature that differentiates benign nevi from malignant melanoma. *J Cutan Pathol*. 2015;42:244–252.
147. Ko JS, Matharoo-Ball B, Billings SD, et al. Diagnostic distinction of malignant melanoma and benign nevi by a gene expression signature and correlation to clinical outcomes. *Cancer Epidemiol Biomarkers Prev*. 2017;26:1107–1113.
148. Castillo SA, Pham AK, Dagrosa AT, et al. Concordance analysis of the 23-gene expression signature (myPath Melanoma) with fluorescence in situ hybridization assay and single nucleotide polymorphism array in the analysis of challenging melanocytic lesions: results from an academic medical center. *Am J Dermatopathol*. 2020;42:939–947.
149. Vidal CI, Armbrect EA, Andea AA, et al. Appropriate use criteria in dermatopathology: initial recommendations from the American Society of Dermatopathology. *J Cutan Pathol*. 2018;45:563–580.
150. Fung MA, Vidal CI, Armbrecht EA, et al. Appropriate use criteria for ancillary diagnostic testing in dermatopathology: New recommendations for 11 tests and 220 clinical scenarios from the American Society of Dermatopathology Appropriate Use Criteria Committee. *J Cutan Pathol*. 2022;49:231–245.
151. Bellomo D, Arias-Mejias SM, Ramana C, et al. Model combining tumor molecular and clinicopathologic risk factors predicts sentinel lymph node metastasis in primary cutaneous melanoma. *JCO Precision Oncol*. 2020;4:319–334.
152. Gambichler T, Tsagoudis K, Kiecker F, et al. Prognostic significance of an 11-gene RNA assay in archival tissue of cutaneous melanoma stage I-III patients. *Eur J Cancer*. 2020;143:11–18.
153. Berger AC, Davidson RS, Poitras JK, et al. Clinical impact of a 31-gene expression profile test for cutaneous melanoma in 156 prospectively and consecutively tested patients. *Curr Med Res Opin*. 2016;32:1599–1604.
154. Kovarik CL, Chu EY, Adamson AS. Gene expression profile testing for thin melanoma: evidence to support clinical use remains thin. *JAMA Dermatol*. 2020;156:837–838.
155. Marchetti MA, Coit DG, Dusza SW, et al. Performance of gene expression profile tests for prognosis in patients with localized cutaneous melanoma: a systematic review and meta-analysis. *JAMA Dermatol*. 2020;156:953–962.
156. Gerami P, Cook RW, Wilkinson J, et al. Development of a prognostic genetic signature to predict the metastatic risk associated with cutaneous melanoma. *Clin Cancer Res*. 2015;21:175–183.
157. Schatton T, Murphy GF, Frank NY, et al. Identification of cells initiating human melanomas. *Nature*. 2008;451:345–349.
158. Chan WH, Tsao H. Consensus, controversy, and conversations about gene expression profiling in melanoma. *JAMA Dermatol*. 2020;156:949–951.
159. Mulder EEAP, Dwarkasing JT, Tempel D, et al. Validation of a clinicopathological and gene expression profile model for sentinel lymph node metastasis in primary cutaneous melanoma. *Br J Dermatol*. 2021;184:944–951.

160. Yousaf A, Tjien-Fooh FJ, Rentroia-Pacheco B, et al. Validation of CP-GEP (Merlin Assay) for predicting sentinel lymph node metastasis in primary cutaneous melanoma patients: a U.S. cohort study. *Int J Dermatol*. 2021;60:851–856.
161. Johansson I, Tempel D, Dwarkasing JT, et al. Validation of a clinicopathological and gene expression profile model to identify patients with cutaneous melanoma where sentinel lymph node biopsy is unnecessary. *Eur J Surg Oncol*. 2022;48:320–325.
162. Whitman ED, Koshenkov VP, Gastman BR, et al. Integrating 31-gene expression profiling with clinicopathologic features to optimize cutaneous melanoma sentinel lymph node metastasis prediction. *JCO Precision Oncol*. 2021;5:1466–1479.
163. Lo SN, Ma J, Scolyer RA, et al. Improved risk prediction calculator for sentinel node positivity in patients with melanoma: The Melanoma Institute Australia nomogram. *J Clin Oncol*. 2020;38:2719–2727.
164. El Sharouni MA, Varey AHR, Witkamp AJ, et al. Predicting sentinel node positivity in patients with melanoma: external validation of a risk-prediction calculator (the Melanoma Institute Australia nomogram) using a large European population-based patient cohort. *Br J Dermatol*. 2021;185:412–418.
165. Grossman D, Okwundu N, Bartlett EK, et al. Prognostic gene expression profiling in cutaneous melanoma: identifying the knowledge gaps and assessing the clinical benefit. *JAMA Dermatol*. 2020;156:1004–1011.
166. Grossman D, Kim CC, Hartman RI, et al. Prognostic gene expression profiling in melanoma: necessary steps to incorporate into clinical practice. *Melanoma Manag*. 2019:6 MMT32.
167. Ferris LK, Farberg AS, Middlebrook B, et al. Identification of high-risk cutaneous melanoma tumors is improved when combining the online American Joint Committee on Cancer Individualized Melanoma Patient Outcome Prediction Tool with a 31-gene expression profile-based classification. *J Am Acad Dermatol*. 2017;76:818–825.e813.
168. Balch CM, Gershenwald JE, Soong S-J, et al. Final version of 2009 AJCC melanoma staging and classification. *J Clin Oncol*. 2009;27:6199–6206.
169. Gershenwald JE, Scolyer RA, Hess KR, et al. Melanoma of the skin. In: Amin MB, Edge SB, Greene FL, eds. *AJCC Cancer Staging Manual*. 8th ed. New York, NY: Springer International Publishing; 2017.
170. Gershenwald JE, Scolyer RA, Hess KR, et al. Melanoma staging: evidence-based changes in the American Joint Committee on Cancer eighth edition cancer staging manual. *CA Cancer J Clin*. 2017;67:472–492.
171. Long GV, Flaherty KT, Stroyakovskiy D, et al. Dabrafenib plus trametinib versus dabrafenib monotherapy in patients with metastatic BRAF V600E/K-mutant melanoma: long-term survival and safety analysis of a phase 3 study. *Ann Oncol*. 2017;28:1631–1639.
172. Cancer Council Australia. Melanoma Guidelines Working Party. Clinical practice guidelines for the diagnosis and management of melanoma. Sydney: Melanoma Institute Australia. Available at: https://wiki.cancer.org.au/australia/Guidelines:Melanoma.
173. Ibrahim AM, Le May M, Bosse D, et al. Imaging intensity and survival outcomes in high-risk resected melanoma treated by systemic therapy at recurrence. *Ann Surg Oncol*. 2020;27:3683–3691.
174. Blum A, Schlagenhauff B, Stroebel W, et al. Ultrasound examination of regional lymph nodes significantly improves early detection of locoregional metastases during the follow-up of patients with cutaneous melanoma: results of a prospective study of 1288 patients. *Cancer*. 2000;88:2534–2539.
175. Garbe C, Peris K, Hauschild A, et al. Diagnosis and treatment of melanoma: European consensus-based interdisciplinary guideline. *Eur J Cancer*. 2010;46:270–283.
176. Marczynski GT, Laus AC, Dos Reis MB, et al. Circulating tumor DNA (ctDNA) detection is associated with shorter progression-free survival in advanced melanoma patients. *Sci Rep*. 2020;10:18682.
177. Xing Y, Bronstein Y, Ross MI, et al. Contemporary diagnostic imaging modalities for the staging and surveillance of melanoma patients: a meta-analysis. *J Natl Cancer Inst*. 2011;103:129–142.
178. Müller-Horvat C, Radny P, Eigentler TK, et al. Prospective comparison of the impact on treatment decisions of whole-body magnetic resonance imaging and computed tomography in patients with metastatic malignant melanoma. *Eur J Cancer*. 2006;42:342–350.
179. Veronesi U, Cascinelli N, Adamus J, et al. Thin stage I primary cutaneous malignant melanoma. Comparison of excision with margins of 1 or 3 cm. *N Engl J Med*. 1988;318:1159–1162.
180. Veronesi U, Cascinelli N. Narrow excision (1-cm margin). A safe procedure for thin cutaneous melanoma. *Arch Surg*. 1991;126:438–441.
181. Balch CM, Soong SJ, Smith T, et al. Long-term results of a prospective surgical trial comparing 2 cm vs. 4 cm excision margins for 740 patients with 1-4 mm melanomas. *Ann Surg Oncol*. 2001;8:101–108.
182. Utjés D, Malmstedt J, Teras J, et al. 2-cm versus 4-cm surgical excision margins for primary cutaneous melanoma thicker than 2 mm: long-term follow-up of a multicentre, randomised trial. *Lancet*. 2019;394:471–477.
183. Ross MI. Excision of primary melanoma. In: Balch CM, Houghton AN, Sober AJ, Soong SJ, eds. *Cutaneous Melanoma*. 5th ed. St. Louis: CRC Press; 2009:251–274.
184. Kunishige JH, Doan L, Brodland DG, Zitelli JA. Comparison of surgical margins for lentigo maligna versus melanoma in situ. *J Am Acad Dermatol*. 2019;81:204–212.
185. Lee MP, Sobanko JF, Shin TM, et al. Evolution of excisional surgery practices for melanoma in the United States. *JAMA Dermatol*. 2019;155:1244–1251.
186. Zalla MJ, Lim KK, Dicaudo DJ, Gagnot MM. Mohs micrographic excision of melanoma using immunostains. *Dermatol Surg*. 2000;26:771–784.
187. Maher IA. Improving survival for patients with early-stage melanoma. *JAMA Dermatol*. 2019;155:1229–1230.
188. Hanson J, Demer A, Liszewski W, et al. Improved overall survival of melanoma of the head and neck treated with Mohs micrographic surgery versus wide local excision. *J Am Acad Dermatol*. 2020;82:149–155.
189. Cheraghlou S, Christensen SR, Agogo GO, Girardi M. Comparison of survival after Mohs micrographic surgery vs wide margin excision for early-stage invasive melanoma. *JAMA Dermatol*. 2019;155:1252–1259.
190. Trofymenko O, Bordeaux JS, Zeitouni NC. Melanoma of the face and Mohs micrographic surgery: nationwide mortality data analysis. *Dermatol Surg*. 2018;44:481–492.
191. Demer AM, Hanson JL, Maher IA, Liszewski W. Association of Mohs micrographic surgery vs wide local excision with overall survival outcomes for patients with melanoma of the trunk and extremities. *JAMA Dermatol*. 2021;157:84–89.
192. Bittar PG, Bittar JM, Etzkorn JR, et al. Systematic review and meta-analysis of local recurrence rates of head and neck cutaneous melanomas after wide local excision, Mohs micrographic surgery, or staged excision. *J Am Acad Dermatol*. 2021;85:681–692.
193. Adalsteinsson JA, Stoj VJ, Algzan H, et al. Limitations in the literature regarding Mohs surgery and staged excision for melanoma: a critical review of quality and data reporting. *J Am Acad Dermatol*. 2023;88:404–413.
194. Flores S, Luby NJ, Bowen GM. Comparison of melanocyte density counts in topical imiquimod-treated skin surrounding lentigo maligna vs control biopsy specimens. *JAMA Dermatol*. 2018;154:482–484.
195. Donigan JM, Hyde MA, Goldgar DE, et al. Rate of recurrence of lentigo maligna treated with off-label neoadjuvant topical imiquimod, 5%, cream prior to conservatively staged excision. *JAMA Dermatol*. 2018;154:885–889.
196. Papanikolaou M, Lawrence CM. Long-term outcomes of imiquimod-treated lentigo maligna. *Clin Exp Dermatol*. 2019;44:631–636.
197. Tio D, van Montfrans C, Ruijter CGH, et al. Effectiveness of 5% topical imiquimod for lentigo maligna treatment. *Acta Derm Venereol*. 2019;99:884–888.
198. Rajpar SF, Marsden JR. Imiquimod in the treatment of lentigo maligna. *Br J Dermatol*. 2006;155:653–656.
199. Read T, Noonan C, David M, et al. A systematic review of non-surgical treatments for lentigo maligna. *J Eur Acad Dermatol Venereol*. 2016;30:748–753.
200. Marsden JR, Fox R, Boota NM, et al. Effect of topical imiquimod as primary treatment for lentigo maligna: the LIMIT-1 study. *Br J Dermatol*. 2017;176:1148–1154.
201. Gautschi M, Oberholzer PA, Baumgartner M, et al. Prognostic markers in lentigo maligna patients treated with imiquimod cream: a long-term follow-up study. *J Am Acad Dermatol*. 2016;74:81–87.e81.
202. Tio D, van der Woude J, Prinsen CAC, et al. A systematic review on the role of imiquimod in lentigo maligna and lentigo maligna melanoma: need for standardization of treatment schedule and outcome measures. *J Eur Acad Dermatol Venereol*. 2017;31:616–624.
203. Mora AN, Karia PS, Nguyen BM. A quantitative systematic review of the efficacy of imiquimod monotherapy for lentigo maligna and an analysis of factors that affect tumor clearance. *J Am Acad Dermatol*. 2015;73:205–212.
204. Swetter SM, Chen FW, Kim DD, Egbert BM. Imiquimod 5% cream as primary or adjuvant therapy for melanoma in situ, lentigo maligna type. *J Am Acad Dermatol*. 2015;72:1047–1053.
205. Luke JJ, Rutkowski P, Queirolo P, et al. Pembrolizumab versus placebo as adjuvant therapy in completely resected stage IIB or IIC melanoma (KEYNOTE-716): a randomised, double-blind, phase 3 trial. *Lancet*. 2022;399:1718–1729.
206. Veronesi U, Adamus J, Bandiera DC, et al. Delayed regional lymph node dissection in stage I melanoma of the skin of the lower extremities. *Cancer*. 1982;49:2420–2430.
207. Veronesi U, Adamus J, Bandiera DC, et al. Inefficacy of immediate node dissection in stage 1 melanoma of the limbs. *N Engl J Med*. 1977;297:627–630.
208. Sim FH, Taylor WF, Pritchard DJ, Soule EH. Lymphadenectomy in the management of stage I malignant melanoma: a prospective randomized study. *Mayo Clin Proc*. 1986;61:697–705.
209. Balch CM, Soong SJ, Bartolucci AA, et al. Efficacy of an elective regional lymph node dissection of 1 to 4 mm thick melanomas for patients 60 years of age and younger. *Ann Surg*. 1996;224:255–263. discussion 263–6.
210. Mraz-Gernhard S, Sagebiel RW, Kashani-Sabet M, et al. Prediction of sentinel lymph node micrometastasis by histological features in primary cutaneous malignant melanoma. *Arch Dermatol*. 1998;134:983–987.
211. Leiter U, Buettner PG, Bohnenberger K, et al. Sentinel lymph node dissection in primary melanoma reduces subsequent regional lymph node metastasis as well as distant metastasis after nodal involvement. *Ann Surg Oncol*. 2010;17:129–137.
212. Kettlewell S, Moyes C, Bray C, et al. Value of sentinel node status as a prognostic factor in melanoma: prospective observational study. *BMJ*. 2006;332:1423.
213. Morton DL, Thompson JF, Cochran AJ, et al. Sentinel-node biopsy or nodal observation in melanoma. *N Engl J Med*. 2006;355:1307–1317.
214. Morton DL, Thompson JF, Cochran AJ, et al. Final trial report of sentinel-node biopsy versus nodal observation in melanoma. *N Engl J Med*. 2014;370:599–609.
215. Leiter U, Stadler R, Mauch C, et al. Complete lymph node dissection versus no dissection in patients with sentinel lymph node biopsy positive melanoma (DeCOG-SLT): a multicentre, randomised, phase 3 trial. *Lancet Oncol*. 2016;17:757–767.
216. Faries MB, Thompson JF, Cochran AJ, et al. Completion dissection or observation for sentinel-node metastasis in melanoma. *N Engl J Med*. 2017;376:2211–2222.
217. Andtbacka RHI, Collichio F, Harrington KJ, et al. Final analyses of OPTiM: a randomized phase III trial of talimogene laherparepvec versus granulocyte-macrophage colony-stimulating factor in unresectable stage III-IV melanoma. *J Immunother Cancer*. 2019;7:145.
218. Franke V, Berger DMS, Klop WMC, et al. High response rates for T-VEC in early metastatic melanoma (stage IIIB/C-IVM1a). *Int J Cancer*. 2019;145:974–978.
219. Alexander HR, Fraker DL, Bartlett DL, et al. Analysis of factors influencing outcome in patients with in-transit malignant melanoma undergoing isolated limb perfusion using modern treatment parameters. *J Clin Oncol*. 2010;28:114–118.
220. Patel SP, Othus M, Chen Y, et al. Neoadjuvant-adjuvant or adjuvant-only pembrolizumab in advanced melanoma. *N Engl J Med*. 2023;388:813–823.
221. Menzies AM, Amaria RN, Rozeman EA, et al. Pathological response and survival with neoadjuvant therapy in melanoma: a pooled analysis from the International Neoadjuvant Melanoma Consortium (INMC). *Nat Med*. 2021;27:301–309.
222. McMasters KM, Egger ME, Edwards MJ, et al. Final results of the Sunbelt Melanoma Trial: a multi-institutional prospective randomized phase III study evaluating the role of adjuvant high-dose interferon alfa-2b and completion lymph node dissection for patients staged by sentinel lymph node biopsy. *J Clin Oncol*. 2016;34:1079–1086.
223. Wheatley K, Ives N, Eggermont A, et al. Interferon-α as adjuvant therapy for melanoma: an individual patient data meta-analysis of randomised trials. *J Clin Oncol*. 2007;25:8526.
224. Larkin J, Chiarion-Sileni V, Gonzalez R, et al. Combined nivolumab and ipilimumab or monotherapy in untreated melanoma. *N Engl J Med*. 2015;373:23–34.
225. Long GV, Hauschild A, Santinami M, et al. Adjuvant dabrafenib plus trametinib in stage III BRAF-mutated melanoma. *N Engl J Med*. 2017;377:1813–1823.

226. Eggermont AM, Chiarion-Sileni V, Grob JJ, et al. Prolonged survival in stage iii melanoma with ipilimumab adjuvant therapy. *N Engl J Med*. 2016;375:1845–1855.
227. Weber J, Mandala M, Del Vecchio M, et al. Adjuvant nivolumab versus ipilimumab in resected stage III or IV melanoma. *N Engl J Med*. 2017;377:1824–1835.
228. Eggermont AMM, Blank CU, Mandala M, et al. Adjuvant pembrolizumab versus placebo in resected stage III melanoma. *N Engl J Med*. 2018;378:1789–1801.
229. Ascierto PA, Del Vecchio M, Mandalá M, et al. Adjuvant nivolumab versus ipilimumab in resected stage IIIB-C and stage IV melanoma (CheckMate 238): 4-year results from a multicentre, double-blind, randomised, controlled, phase 3 trial. *Lancet Oncol*. 2020;21:1465–1477.
230. Zimmer L, Livingstone E, Hassel JC, et al. Dermatologic Cooperative Oncology Group. Adjuvant nivolumab plus ipilimumab or nivolumab monotherapy versus placebo in patients with resected stage IV melanoma with no evidence of disease (IMMUNED): a randomised, double-blind, placebo-controlled, phase 2 trial. *Lancet*. 2020;395:1558–1568.
231. Dummer R, Hauschild A, Santinami M, et al. Five-year analysis of adjuvant dabrafenib plus trametinib in stage III melanoma. *N Engl J Med*. 2020;383:1139–1148.
232. Eggermont AMM, Blank CU, Mandalà M, et al. EORTC Melanoma Group. Adjuvant pembrolizumab versus placebo in resected stage III melanoma (EORTC 1325-MG/KEYNOTE-054): distant metastasis-free survival results from a double-blind, randomised, controlled, phase 3 trial. *Lancet Oncol*. 2021;22:643–654.
233. Neuman HB, Patel A, Ishill N, et al. A single-institution validation of the AJCC staging system for stage IV melanoma. *Ann Surg Oncol*. 2008;15:2034–2041.
234. Young SE, Martinez SR, Essner R. The role of surgery in treatment of stage IV melanoma. *J Surg Oncol*. 2006;94:344–351.
235. Staudt M, Lasithiotakis K, Leiter U, et al. Determinants of survival in patients with brain metastases from cutaneous melanoma. *Br J Cancer*. 2010;102:1213–1218.
236. Burmeister BH, Henderson MA, Ainslie J, et al. Adjuvant radiotherapy versus observation alone for patients at risk of lymph-node field relapse after therapeutic lymphadenectomy for melanoma: a randomised trial. *Lancet Oncol*. 2012;13:589–597.
237. Henderson MA, Burmeister BH, Ainslie J, et al. Adjuvant lymph-node field radiotherapy versus observation only in patients with melanoma at high risk of further lymph-node field relapse after lymphadenectomy (ANZMTG 01.02/TROG 02.01): 6-year follow-up of a phase 3, randomised controlled trial. *Lancet Oncol*. 2015;16:1049–1060.
238. Lamiaux M, Scalbert C, Lepesant P, et al. Severe skin toxicity with organ damage under the combination of targeted therapy following immunotherapy in metastatic melanoma. *Melanoma Res*. 2018;28:451–457.
239. Chapman PB, Hauschild A, Robert C, et al. Improved survival with vemurafenib in melanoma with BRAF V600E mutation. *N Engl J Med*. 2011;364:2507–2516.
240. Hauschild A, Grob J-J, Demidov LV, et al. Dabrafenib in BRAF-mutated metastatic melanoma: a multicentre, open-label, phase 3 randomised controlled trial. *Lancet*. 2012;380:358–365.
241. Larkin J, Ascierto PA, Dréno B, et al. Combined vemurafenib and cobimetinib in BRAF-mutated melanoma. *N Engl J Med*. 2014;371:1867–1876.
242. Long GV, Stroyakovskiy D, Gogas H, et al. Combined BRAF and MEK inhibition versus BRAF inhibition alone in melanoma. *N Engl J Med*. 2014;371:1877–1888.
242a. Atkins MB, Lee SJ, Chmielowski B, et al. Combination dabrafenib and trametinib versus combination nivolumab and ipilimumab for patients with advanced BRAF-mutant melanoma: The DREAMseq Trial-ECOG-ACRIN EA6134. *J Clin Oncol*. 2023;41:186–197.
243. Hodi FS, O'Day SJ, McDermott DF, et al. Improved survival with ipilimumab in patients with metastatic melanoma. *N Engl J Med*. 2010;363:711–723.
244. Robert C, Thomas L, Bondarenko I, et al. Ipilimumab plus dacarbazine for previously untreated metastatic melanoma. *N Engl J Med*. 2011;364:2517–2526.
245. Sarnaik AA, Weber JS. Recent advances using anti-CTLA-4 for the treatment of melanoma. *Cancer J*. 2009;15:169–173.
246. Teulings HE, Limpens J, Jansen SN, et al. Vitiligo-like depigmentation in patients with stage III-IV melanoma receiving immunotherapy and its association with survival: a systematic review and meta-analysis. *J Clin Oncol*. 2015;33:773–781.
247. Postow MA, Chesney J, Pavlick AC, et al. Nivolumab and ipilimumab versus ipilimumab in untreated melanoma. *N Engl J Med*. 2015;372:2006–2017.
248. Lebbe C, Meyer N, Mortier L, et al. Evaluation of two dosing regimens for nivolumab in combination with ipilimumab in patients with advanced melanoma: results from the phase IIIb/IV CheckMate 511 trial. *J Clin Oncol*. 2019;37:867–875.
249. Robert C, Long GV, Brady B, et al. Nivolumab in previously untreated melanoma without BRAF mutation. *N Engl J Med*. 2015;372:320–330.
250. Robert C, Schachter J, Long GV, et al. Pembrolizumab versus ipilimumab in advanced melanoma. *N Engl J Med*. 2015;372:2521–2532.
251. Elkrief A, El Raichani L, Richard C, et al. Antibiotics are associated with decreased progression-free survival of advanced melanoma patients treated with immune checkpoint inhibitors. *Oncoimmunol*. 2019;8:e1568812.
252. Larkin J, Chiarion-Sileni V, Gonzalez R, et al. Five-year survival with combined nivolumab and ipilimumab in advanced melanoma. *N Engl J Med*. 2019;381:1535–1546.
253. Wolchok JD, Chiarion-Sileni V, Gonzalez R, et al. Long-term outcomes with nivolumab plus ipilimumab or nivolumab alone versus ipilimumab in patients with advanced melanoma. *J Clin Oncol*. 2022;40:127–137.
254. Atkins MB, Lee SJ, Chmielowski B, et al. DREAMseq (Doublet, Randomized Evaluation in Advanced Melanoma Sequencing): a phase III trial—ECOG-ACRIN EA6134. *J Clin Oncol*. 2021;39:36 (suppl):356154.
255. Tawbi HA, Schadendorf D, Lipson EJ, et al. Relatlimab and nivolumab versus nivolumab in untreated advanced melanoma. *N Engl J Med*. 2022;386:24–34.
256. Kirkwood JM, Lee S, Moschos SJ, et al. Immunogenicity and antitumor effects of vaccination with peptide vaccine+/-granulocyte-monocyte colony-stimulating factor and/or IFN-alpha2b in advanced metastatic melanoma: Eastern Cooperative Oncology Group Phase II Trial E1696. *Clin Cancer Res*. 2009;15:1443–1451.
257. Schwartzentruber DJ, Lawson DH, Richards JM, et al. gp100 peptide vaccine and interleukin-2 in patients with advanced melanoma. *N Engl J Med*. 2011;364:2119–2127.
258. Bafaloukos D, Gazouli I, Koutserimpas C, et al. Evolution and progress of mRNA Vaccines in the treatment of melanoma: Future prospects. *Vaccines (Basel)*. 2023;11:636.
259. Jilaveanu LB, Aziz SA, Kluger HM. Chemotherapy and biologic therapies for melanoma: do they work? *Clin Dermatol*. 2009;27:614–625.
260. Yang AS, Chapman PB. The history and future of chemotherapy for melanoma. *Hematol Oncol Clin North Am*. 2009;23:583–597. x.
261. Middleton MR, Grob JJ, Aaronson N, et al. Randomized phase III study of temozolomide versus dacarbazine in the treatment of patients with advanced metastatic malignant melanoma. *J Clin Oncol*. 2000;18:158–166.
262. Quirt I, Verma S, Petrella T, Bak K, Charette M. Temozolomide for the treatment of metastatic melanoma: a systematic review. *Oncologist*. 2007;12:1114–1123.
263. Wang Y, Zhao Y, Ma S. Racial differences in six major subtypes of melanoma: descriptive epidemiology. *BMC Cancer*. 2016;16:691.



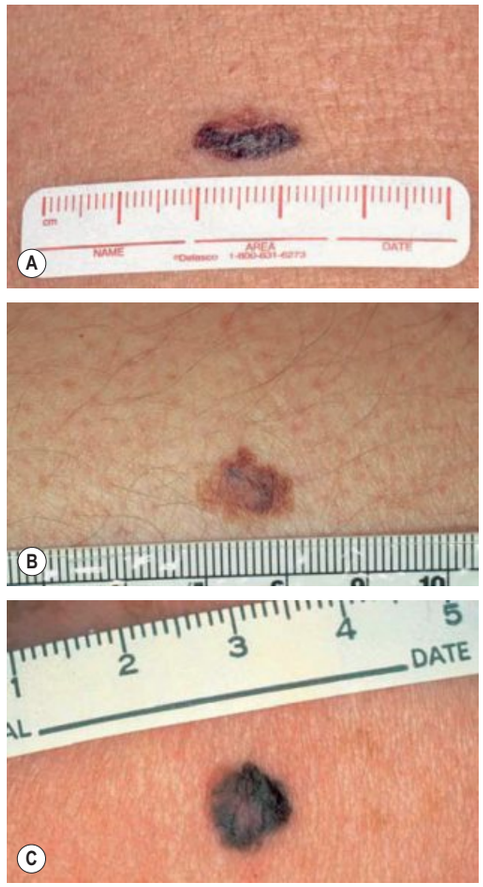
eFig. 113.1 Completely regressed cutaneous melanoma on the back of an 84-year-old man. The gray-black circular area on the left corresponds histologically to a band-like infiltrate of melanophages whereas the hypopigmentation on the right has fibrosis with sparse inflammation. There were no remaining cells of melanoma, but the patient already had nodal and visceral metastases. *Courtesy, Department of Dermatology, Medical University of Graz.*



eFig. 113.3 Melanoma *in situ* on the lower leg of an 82-year-old woman. The pigmented lesion is asymmetric and poorly circumscribed. The dermoscopic findings include asymmetry, multiple colors, irregular blotches, and areas of regression. *Courtesy, Department of Dermatology, Medical University of Graz.*



eFig. 113.2 Cutaneous melanoma with regression. An asymmetric, irregularly pigmented melanocytic lesion. The central depigmented zone is due to tumor regression and histopathologically, fibrosis can be seen. *Courtesy Claus Garbe, MD and Jürgen Bauer, MD.*



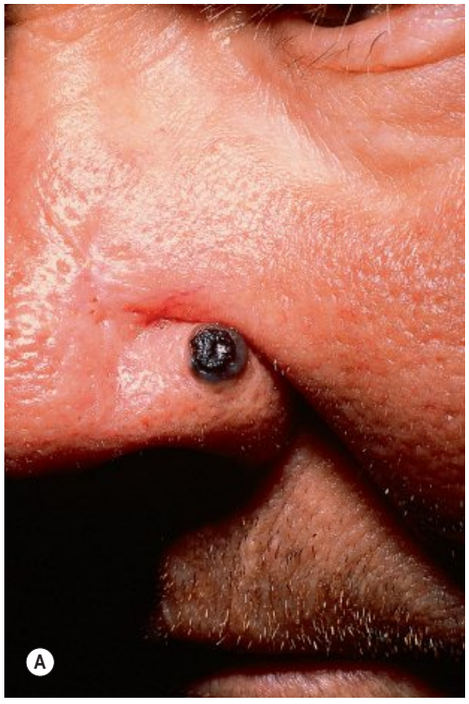
eFig. 113.4 Early superficial spreading melanomas. All of these lesions demonstrate asymmetry due to variation in color and irregularity in outline. In addition, there is pink discoloration in **C**. **A** and **B** were less than 0.5 mm in thickness and **C** was 0.8 mm. *A, Courtesy Kalman Watsky MD; B, C, Courtesy Jean L. Bolognia, MD.*



eFig. 113.5 Minimally invasive melanoma (Breslow depth 0.3 mm) with a diameter <5 mm. *Courtesy Frank O. Nestle, MD and Allan C. Halpern, MD.*



eFig. 113.6 Nodular melanoma (T4). The majority of the lesion is gray–black in color. *Courtesy Kalman Watsky, MD.*





eFig. 113.7 Nodular melanomas. A Ulcerated black nodule on the nose. **B** Blue–black nodule with hemorrhagic crust. *A, Courtesy Ronald P. Rapini, MD.*



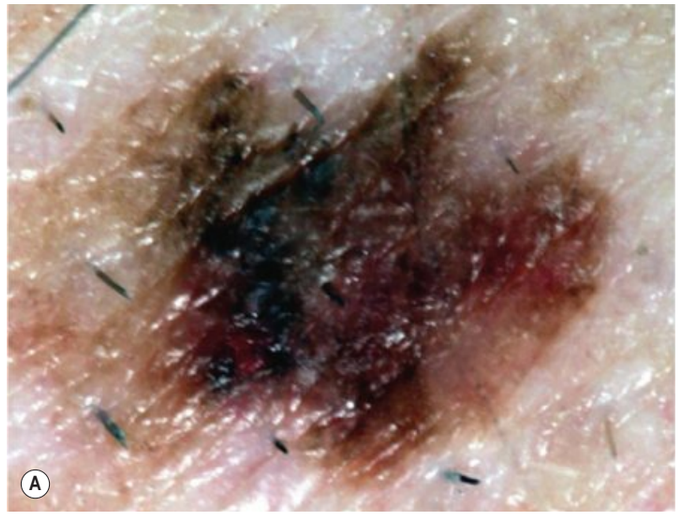
eFig. 113.8 Blue–black ulcerated nodular melanoma. Inferiorly, there is a thinner plaque with varying shades of brown. *Courtesy Sonya K. Burton, MD.*

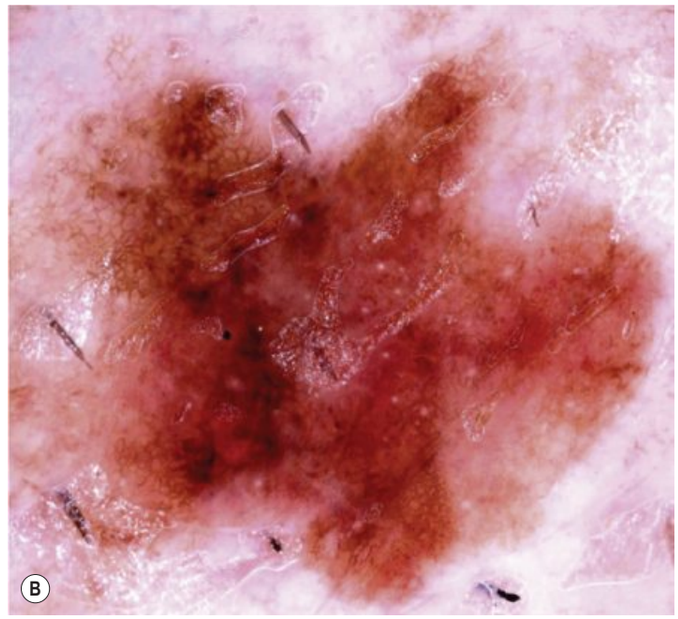


eFig. 113.9 Amelanotic nodular melanoma. Pink, slightly scaly, thick plaque on the dorsal aspect on the third toe. Melanoma may not be the initial clinical diagnosis for such lesions.



eFig. 113.10 Amelanotic melanoma on the ear. *In situ* or minimally invasive squamous cell carcinoma might be the initial clinical diagnosis. *Courtesy Karynne O. Duncan, MD.*





eFig. 113.11 Melanoma *in situ*. A Note the asymmetry, border irregularity, color variation, and erythema ("Little Red Riding Hood" sign). **B** The dermoscopic findings include a broadened network, dots, and some globules inside this asymmetric lesion. *Courtesy Claus Garbe, MD and Jürgen Bauer, MD.*

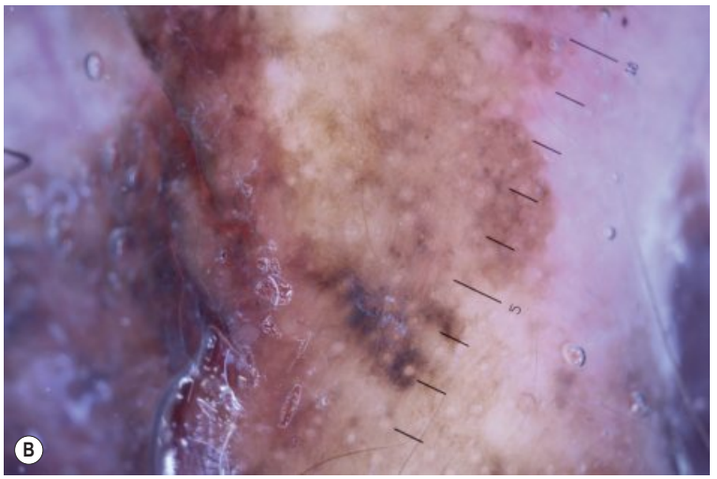


eFig. 113.12 Melanoma *in situ*, lentigo maligna type. Large brown patch on the forehead with asymmetry and variation in color. *Courtesy, Department of Dermatology, Medical University of Graz.*



eFig. 113.13 Lentigo maligna (melanoma in situ, lentigo maligna type). Large-sized brown patch with areas of dark brown and blue–gray color.





eFig. 113.14 Lentigo maligna melanoma (LMM). A A more advanced LMM on the ear (Breslow depth = 0.86 mm). **B** Corresponding dermoscopy with annular structures corresponding to follicular openings surrounded by melanoma cells ("circle in a circle"). *Courtesy Claus Garbe, MD and Jürgen Bauer, MD.*



eFig. 113.15 Nodular melanoma arising within a lentigo maligna. *Courtesy Kalman Watsky, MD.*



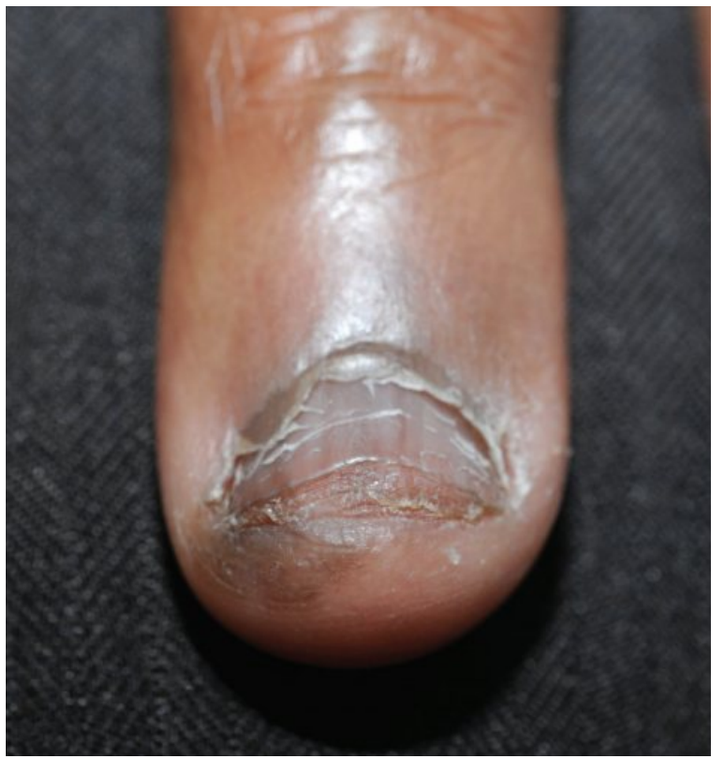
eFig. 113.16 Acral lentiginous melanoma on the plantar surface of the foot. *Courtesy Kalman Watsky, MD.*



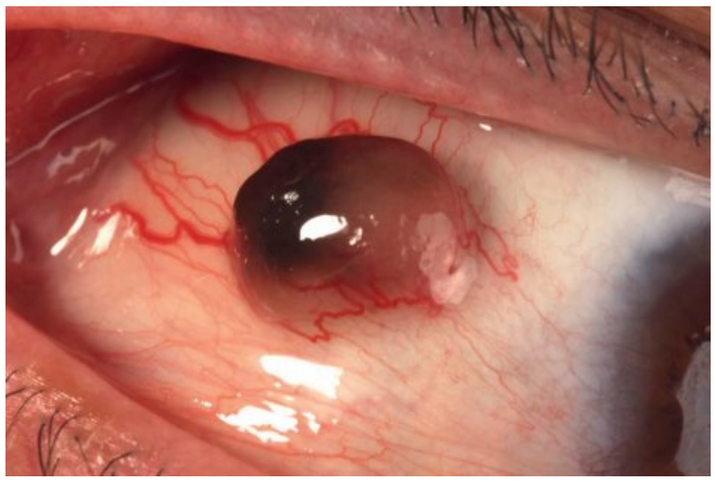
eFig. 113.17 Acral lentiginous melanoma. Ulceration of the plantar surface of the foot; there is brown pigmentation both within and extending beyond the ulceration. *Courtesy Kalman Watsky, MD.*



eFig. 113.18 Large-sized acral lentiginous melanoma on the plantar surface of the foot. In addition to multiple shades of brown and black, there is ulceration and central regression. *Courtesy Sonya K. Burton, MD.*



eFig. 113.19 Melanoma of the nail unit presenting as longitudinal melanonychia. Extension of pigment onto the fingertip is a helpful diagnostic sign. *Courtesy Kalman Watsky, MD.*



eFig. 113.20 Conjunctival melanoma.



eFig. 113.21 Persistent disease-type local recurrence of melanoma at the edge of a graft and a flap. *Courtesy Jean L. Bolognia, MD.*



eFig. 113.22 In-transit metastases of cutaneous melanoma. Multiple large blue–black nodules along the lymphatics. *Courtesy Jean L. Bolognia MD.*

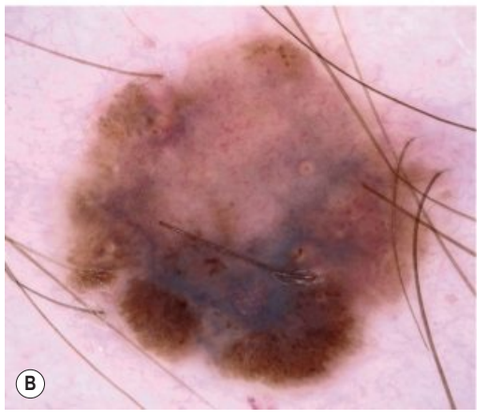


eFig. 113.23 Primary melanoma of the scalp (unresected) with multiple lymphatic metastases. The patient had a complete response to ipilimumab plus nivolumab and on biopsy, only dermal melanin remained at the sites of metastases. *Courtesy Kalman Watsky, MD.*

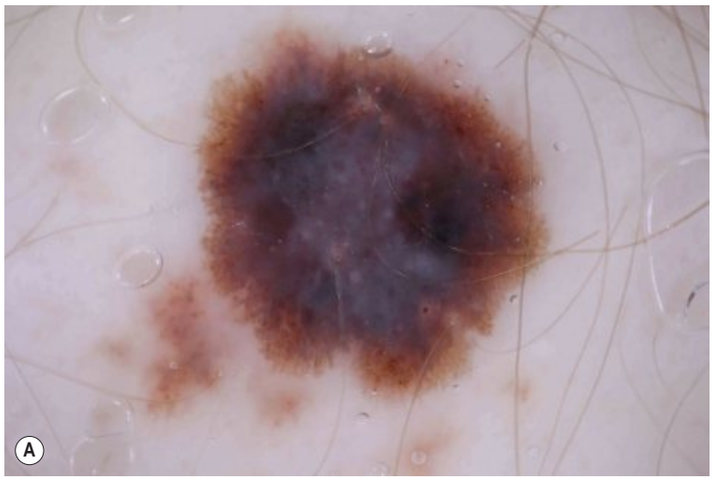


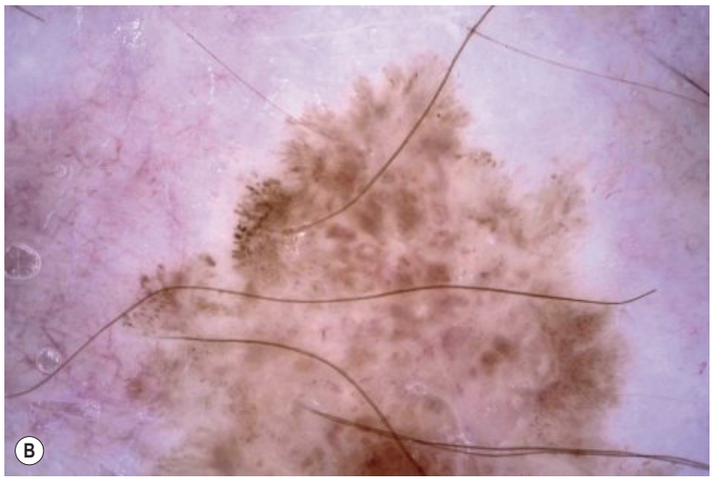
eFig. 113.24 Melanuria in a patient with stage IV metastatic melanoma.

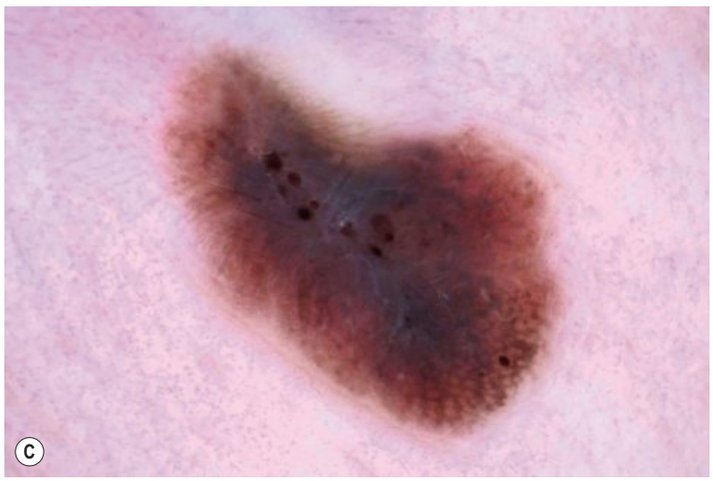




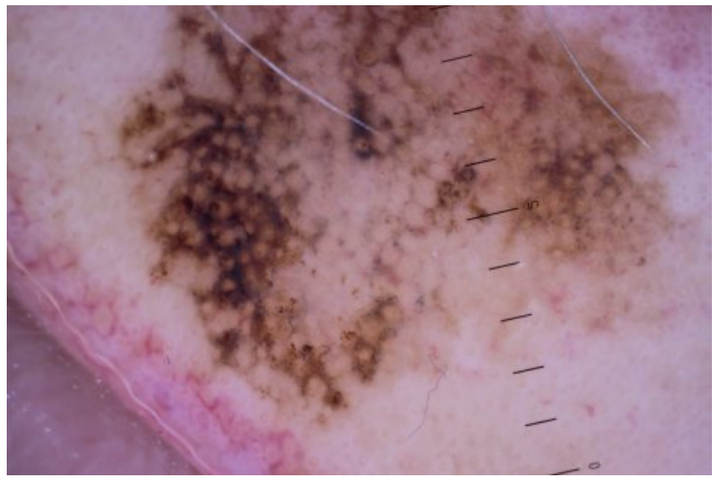
eFig. 113.25 Illustration of dermoscopy. This pair of images illustrates the clinical appearance (**A**), and the same lesion viewed with dermoscopy (**B**). Greater detail can be appreciated at 10- to 20-fold magnification. This lesion is an early invasive melanoma with sharp demarcation, asymmetry, and a central blue–whitish veil. *Courtesy Claus Garbe, MD and Jürgen Bauer, MD.*



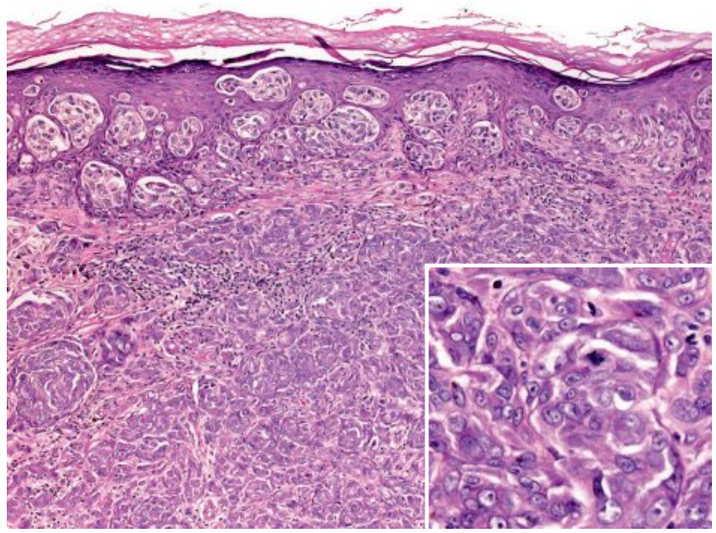




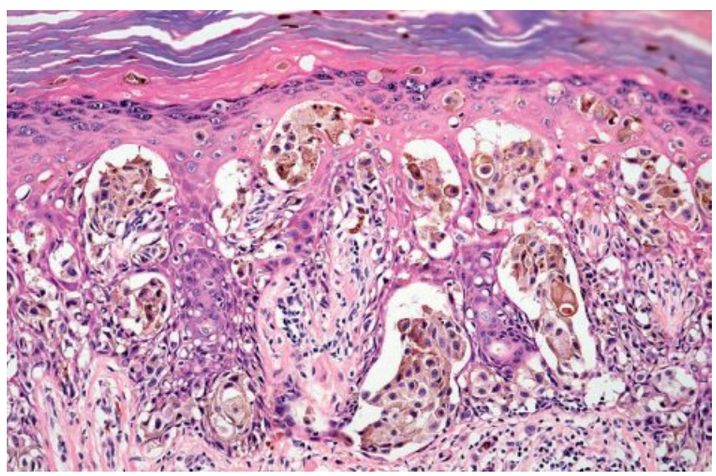
eFig. 113.26 Dermoscopic appearance of superficial spreading cutaneous melanomas. A Striking asymmetry and streaks at the periphery. The latter have also been called radial streaming and pseudopods. **B** Streaks and blue–whitish veil. **C** Streaks, blue–whitish veil, and irregular blotches. *Courtesy Claus Garbe, MD and Jürgen Bauer, MD.*



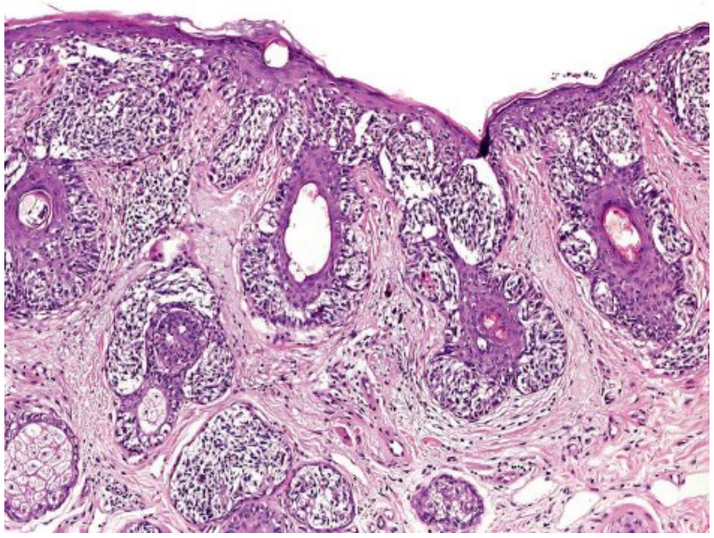
eFig. 113.27 Dermoscopy of lentigo maligna melanoma (Breslow depth = 0.45 mm). There is asymmetric pigmentation of the follicular openings and annular granular structures. Corresponds to Fig. 113.13A. *Courtesy Claus Garbe, MD and Jürgen Bauer, MD.*



eFig. 113.28 Superficial spreading ("conventional") melanoma – histopathologic features. Irregular intraepidermal nests and confluent dermal complexes of atypical melanocytes. Some of the atypical melanocytes have prominent nucleoli and one mitosis can be seen (inset). *Courtesy Lorenzo Cerroni, MD.*



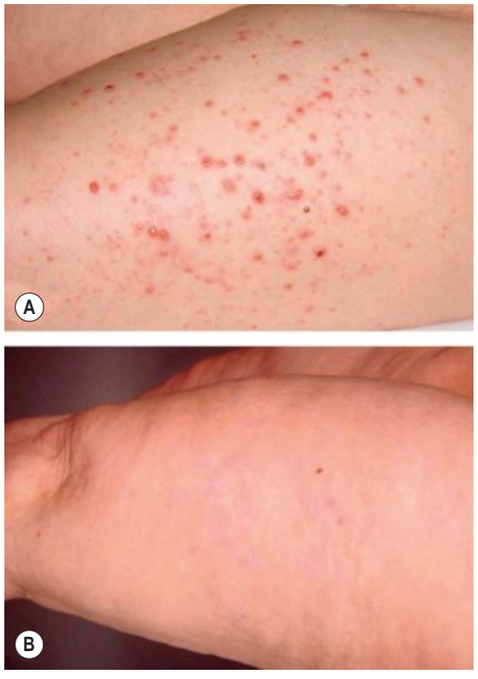
eFig. 113.29 Acral lentiginous melanoma – histopathologic features. Atypical pigmented melanocytes arranged in irregular nests and as solitary units involve all layers of the epidermis and are also visible within the horny layer. *Courtesy Lorenzo Cerroni, MD.*



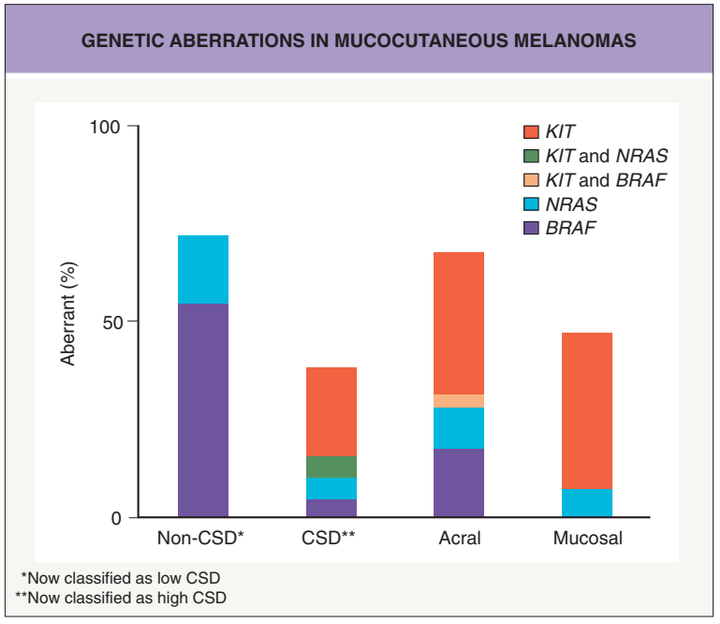
eFig. 113.30 Melanoma in situ with extensive adnexal involvement of hair follicles. Large, confluent complexes of melanocytes are within the epidermis and the epithelium of several hair follicles. Seemingly intradermal complexes are likely still connected to the hair follicles, but the connection may not be visible in some sections. *Courtesy Lorenzo Cerroni, MD.*



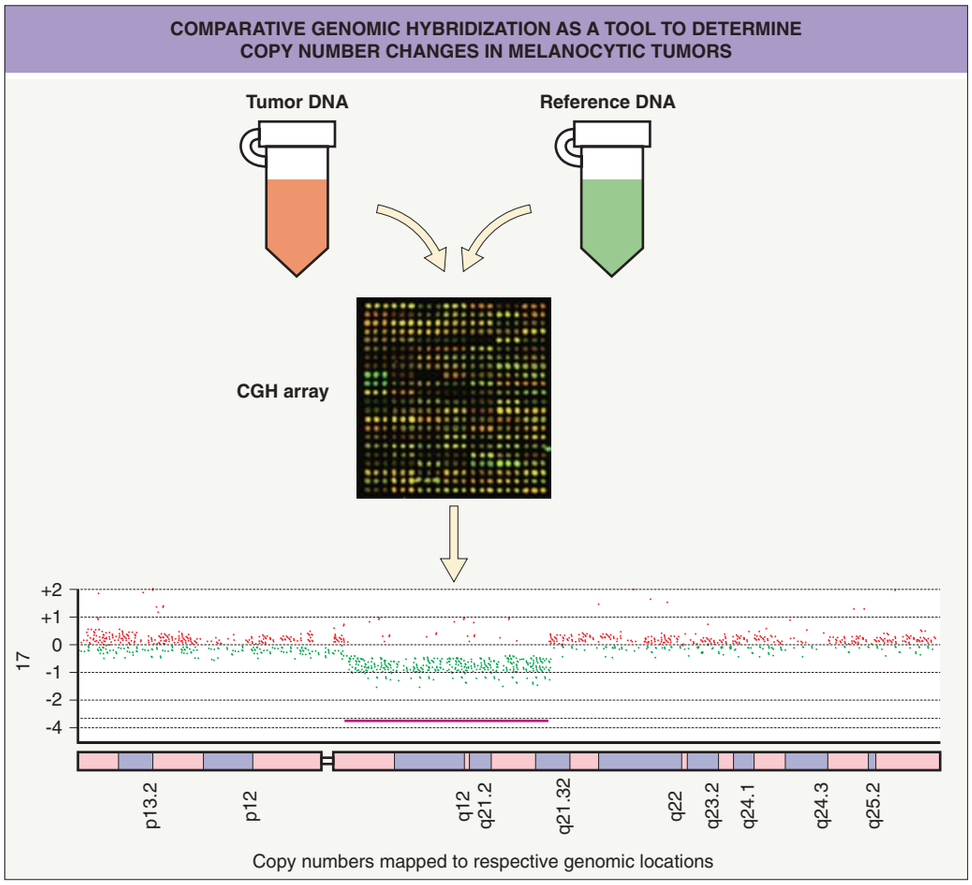
eFig. 113.32 Black heel. Traumatically induced hemorrhage within the stratum corneum can simulate an acral melanoma.



eFig. 113.31 Intralesional interleukin-2 treatment. **A** Multiple in-transit metastases were treated with intralesional low-dose IL-2 for 6 weeks. **B** Complete remission after 1 year, which persisted during the follow-up period of 7 years. *Courtesy Claus Garbe, MD and Jürgen Bauer, MD.*



eFig. 113.33 Genetic aberrations in mucocutaneous melanomas – original findings. Of melanomas with somatic mutations in *BRAF*, at least 80% lead to substitution of glutamic acid (E) for valine (V) at codon 600, i.e. V600E. CSD, cumulative sun damage, such as marked solar elastosis; non-CSD, skin without cumulative sun damage. *From Curtin JA, Busam K, Pinkel D, Bastian BC. J Clin Oncol 2006;24:4340–6.*



eFig. 113.34 Comparative genomic hybridization (CGH) as a tool to determine copy number changes in melanocytic tumors. Total genomic DNA is isolated from the tumor and from healthy reference samples, and labeled with fluorescent dyes. The mixture of test and reference DNA is hybridized onto a genome-wide microarray of oligonucleotides. Tumor and reference DNA bind to the complementary oligonucleotides and the ratio of their fluorescence intensities is approximately proportional to the ratio of the copy numbers of the corresponding DNA sequences in the tumor and reference genomes. The copy number ratio can be mapped to the genomic location of the array element.

INVASIVE CUTANEOUS MELANOMA – COMPONENTS OF THE HISTOPATHOLOGIC REPORT
Essential
Tumor thickness (Breslow depth), to the nearest 0.1 mm*
Ulceration (present or absent)*
Presence of macroscopic (gross specimen) or microscopic satellites*
Peripheral and deep margin status (involved/uninvolved with *in situ* and/or invasive melanoma, broad vs focal transection of invasive melanoma at deep margin)
Additional features that are encouraged
Mitotic rate (“hot spot” method), #/mm^2
Lymphovascular/angiolymphatic invasion
Histopathologic subtype of melanoma (if desmoplastic, “pure” or “mixed”)
Regression, if extensive (>75%)
Neurotropism/perineural invasion
Tumor-infiltrating lymphocytes (none, brisk, non-brisk)
Associated nevus
*These elements determine T- or N-stage and are required. Other elements are useful for prognostication and management.

eTable 113.1 Invasive cutaneous melanoma – components of the histopathologic report. From references 25,121–123.

Vascular Neoplasms and Neoplastic-Like Proliferations

114

Paula E. North

Chapter Contents

Benign Vascular Neoplasms and Reactive Hyperplasias *2045*
Borderline and Low-Grade Malignant Vascular Neoplasms *2060*
Malignant Vascular Neoplasms *2067*
Perivascular Neoplasms and Neoplastic-Like Proliferations *2070*

INTRODUCTION

In this chapter we use the term *neoplasm* synonymously with *tumor* in a general, albeit imperfect[1], sense, consistent with its common usage: *an abnormal proliferation ("new growth") of cells that appears to be relatively autonomous (i.e. not reactive)*. Of note, common infantile hemangiomas are discussed separately (see Ch. 103) as are telangiectatic lesions (see Ch. 106) and vascular malformations (see Ch. 104); however, in some patients, vascular malformations may be associated with a number of the cellular vascular proliferations discussed herein. The chapter also includes a review of vascular lesions that were previously designated as vascular tumors (angiomas) but have since been reclassified as distinctive vascular malformations, e.g. glomuvenous malformation (previously "glomangioma"), verrucous venulocapillary malformation (previously verrucous "hemangioma"). In addition, several entities with established or suspected features of reactive processes that mimic neoplasms are discussed as is Kaposi sarcoma, a virus-associated process of as-yet-uncertain position on the hyperplasia–neoplasia spectrum, but with an associated mortality rate. Two benign vascular proliferations of more seemingly straightforward infectious etiology (bacillary angiomatosis and verruga peruana) are covered elsewhere (see Ch. 74). With these caveats in mind, a broad working classification of vascular neoplasms and neoplastic-like conditions is presented in Table 114.1. Selected vascular neoplasms and neoplastic-like proliferations with their associated syndromes and characteristic laboratory findings are outlined in Fig. 114.1.

BENIGN VASCULAR NEOPLASMS AND REACTIVE HYPERPLASIAS

Intravascular Papillary Endothelial Hyperplasia (PEH)

Synonyms: ■ Masson's pseudoangiosarcoma ■ Masson's tumor

Key features

- Not a specific disease entity, but rather a distinct histopathological pattern that can be confused with angiosarcoma
- The primary or "pure" form is not associated with a pre-existing vascular anomaly and appears as a solitary, slowly growing, often painful nodule located within a dilated dermal, subcutaneous, or submucosal vein
- Secondary forms are associated with venous malformations and other vascular anomalies prone to thrombosis
- Rare forms are extravascular, probably arising within hematomas
- Thought to represent an unusual, exuberant response of endothelial cells to organizing thrombus

Introduction

Masson first described this process in 1923 in hemorrhoidal veins, terming it *hemangio-endotheliome vegetant intravasculaire*, and interpreted it as a neoplastic process mimicking angiosarcoma. In 1932, Henschen re-interpreted the process as reactive, and in 1971 Kauffman and Stout noted its occurrence not only in thrombosed vessels but also in a hematoma, further demonstrating the potential for confusion with soft tissue angiosarcoma. A lymphatic vessel counterpart of Masson's lesion was reported in 1979 in a cystic lymphatic malformation[2].

Epidemiology

Papillary endothelial hyperplasia (PEH) shows a slight female predominance, most pronounced for the rare extravascular examples[3]. Although lesions can occur at any age, most are in adults, with an average age of 35 years. A history of trauma is elicited in a small minority of patients[3].

Pathogenesis

Areas of papillary endothelial hyperplasia can, in most cases, be seen to merge with definitive thrombus material, in support of the notion that they represent an unusual form of thrombus organization.

Clinical features

Primary lesions of superficial tissues appear as solitary, firm masses, often with red or blue discoloration of the overlying skin or mucosa. The history is typically one of slow growth over a period of several months or years. These occur most commonly within veins of the head and neck and, interestingly, the fingers, but they may also arise elsewhere[3]. In a study of 314 cases, 56% were of the primary form, 40% were associated with other vascular lesions, and 4% appeared extravascularly[3]. Clinical features of the secondary forms are those of the underlying vascular anomaly.

Pathology

Intravascular examples may be limited to the confines of a single thin-walled vein or may arise, often multifocally, within pre-existing vascular lesions such as venous malformations, glomuvenous malformations, spindle cell hemangiomas, and pyogenic granulomas (Fig. 114.2). Foci of intravascular PEH are extremely common in venous malformations and serve to distinguish these low-flow lesions from high-flow arteriovenous malformations. Rarely, the involved vessel wall is ruptured, allowing the proliferative vascular process to spill out into the adjacent stroma. Extravascular examples that on serial sectioning show no evidence of a surrounding blood vessel wall may have arisen within an organizing hematoma[3].

Early lesions show growth of endothelial sprouts into fibrinous thrombus material, dividing it into papillary fronds lined by a single layer of plump endothelial cells with minimal mitotic activity and no significant cytologic atypia. The early fibrin cores of the papillae become collagenized and hyalinized with time, and the endothelial lining becomes thin and attenuated. Lesional papillae may fuse to form an anastomosing meshwork of vessels separated by connective tissue stroma that mimics angiosarcoma (Fig. 114.2, inset). However, the relatively high mitotic rate, striking pleomorphism, and necrosis that characterize angiosarcoma are lacking[4].

Differential diagnosis

The clinical appearance of these lesions is nonspecific, and diagnosis relies on microscopic examination. The most important consideration for the pathologist is well-differentiated angiosarcoma.

A WORKING CLASSIFICATION OF CUTANEOUS VASCULAR ANOMALIES
Reactive conditions
• ***Intravascular papillary endothelial hyperplasia***
• ***Reactive angioendotheliomatosis***
• ***Intravascular reactive angioendotheliomatosis***
• ***Diffuse dermal angiomatosis***
• Eruptive pseudoangiomatosis (self-limited exanthem of bright-red angioma-like lesions, originally described in children, can follow viral infections or vaccines)
• Pseudo-Kaposi sarcoma (acroangiodermatitis of Mali, Stewart–Bluefarb syndrome)
Telangiectasias (see Ch. 106)
• ***Angiokeratoma*** (exception is angiokeratoma circumscriptum, which represents a capillary/lymphatic or capillary malformation)
• Generalized essential telangiectasia
• Cutaneous collagenous vasculopathy
• Unilateral nevoid telangiectasia
• Hereditary hemorrhagic telangiectasia
• Hereditary benign telangiectasia
• Cutis marmorata telangiectatica congenita
• Angioma serpiginosum
• Spider nevus
• Venous lake
Vascular malformations (see Tables 104.2 & 104.5 for associated mutated genes)
• Capillary malformation (CM), includes subtypes nevus simplex, port-wine birthmark, reticulated CM, and geographic CM (see Ch. 104)
• Venous malformation
• Lymphatic malformation (microcystic and macrocystic)
• Mixed capillary/venous/lymphatic malformation
• Arteriovenous malformation
• Capillary malformation–arteriovenous malformation (CM-AVM)
• ***Targetoid hemosiderotic lymphatic malformation*** (previously classified as hobnail "hemangioma" or targetoid hemosiderotic "hemangioma")
• ***Verrucous venulocapillary malformation*** (previously classified as verrucous "hemangioma")
Benign vascular neoplasms and neoplastic-like proliferations
• Infantile hemangioma (see Ch. 103 for details)
• Congenital hemangioma (includes non-involuting congenital hemangioma [NICH], rapidly involuting congenital hemangioma [RICH], and partially involuting congenital hemangioma; see Ch. 103 for details and mutated genes)
• ***Pyogenic granuloma (lobular capillary hemangioma)****[*]
• ***Cherry angioma***
• ***Tufted angioma (likely a superficial form of kaposiform hemangioendothelioma)***
• ***Glomeruloid hemangioma****[*]
• ***Microvenular hemangioma****[*]
• ***Epithelioid hemangioma (angiolymphoid hyperplasia with eosinophilia [ALHE])****[*]
• ***Multifocal lymphangioendotheliomatosis with thrombocytopenia***[†]
• ***Sinusoidal hemangioma***[‡]
• ***Spindle cell hemangioma***[¶]
• Epithelioid angiomatous nodule (debate as to whether it is a variant of epithelioid hemangioma)
• Papillary hemangioma
• Acquired elastotic hemangioma (capillary-like appearance in association with solar elastosis)
• Poikilodermatous plaque-like hemangioma (pelvic girdle or lower extremities, favors the elderly)
• Cutaneous pseudoangiomatous stromal hyperplasia (primarily encountered in the breast)
• ***Post-radiation atypical vascular lesions of the skin*** (see Table 114.4)
Borderline and low-grade malignant vascular neoplasms
• ***Kaposiform hemangioendothelioma (KHE)***
• ***Papillary intralymphatic angioendothelioma (PILA)*** (Dabska-type hemangioendothelioma, Dabska tumor)
• ***Retiform hemangioendothelioma (RHE)***
• ***Composite hemangioendothelioma (CHE)***
• ***Pseudomyogenic hemangioendothelioma***
• ***Kaposi sarcoma***
Malignant vascular neoplasms
• ***Epithelioid hemangioendothelioma (EHE)***[§]
• ***Angiosarcoma***
Perivascular neoplasms and neoplastic-like proliferations
• ***Glomus tumor (proper)***
• ***Glomuvenous malformation ("glomangioma")***
• ***Glomangiosarcoma***
• ***Infantile-type hemangiopericytoma/myofibromatosis***
• Adult-type hemangiopericytoma
• Glomangiopericytoma
• Myopericytoma
• PEComa (perivascular epithelioid cell tumor)[‖]
*Also viewed as a reactive condition.
†Not clear if a multifocal vascular neoplasm or malformation.
‡Likely a sinusoidal pattern of intravascular endothelial hyperplasia within a pre-existing low-flow vascular malformation.
¶Also viewed as a vascular malformation.
§Reclassified by the WHO as a malignant, rather than intermediate or borderline, vascular tumor.
‖A spectrum of mesenchymal tumors that includes clear cell "sugar" tumor of the lung, angiomyolipoma, lymphangiomyomatosis, clear cell myomelanocytic tumor, and the rare cutaneous tumors with a similar morphology and phenotype; nab-sirolimus approved for treatment of advanced malignant PEComas.

Table 114.1 A working classification of cutaneous vascular anomalies. Entities covered in this chapter are in ***bold italics***.

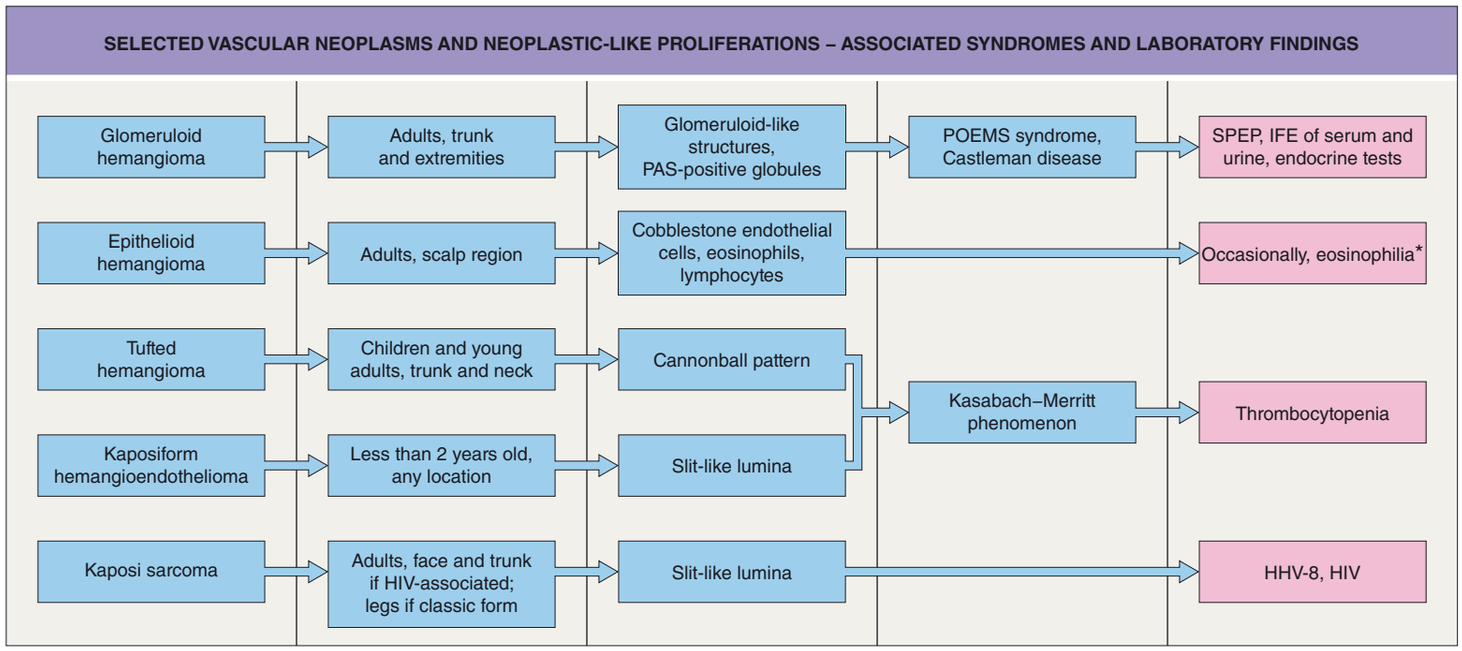


Fig. 114.1 Selected vascular neoplasms and neoplastic-like proliferations – associated syndromes and laboratory findings. *If eosinophilia present, need to consider Kimura disease. IFE, immunofixation electrophoresis; SPEP, serum protein electrophoresis; HHV-8, human herpesvirus 8; HIV, human immunodeficiency virus; PAS, periodic acid Schiff stain.

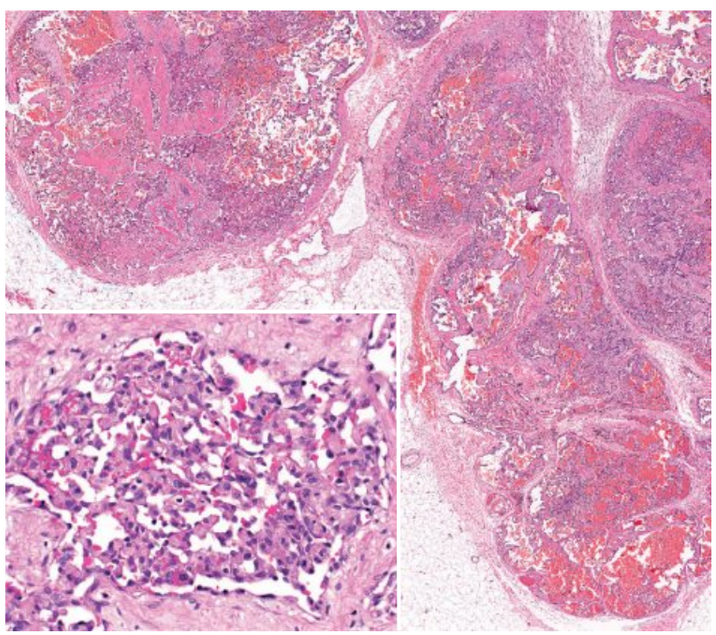


Fig. 114.2 Papillary endothelial hyperplasia (PEH) in a large venous malformation – histopathologic features. Large vascular spaces with remnants of old fibrin thrombi and prominent, irregular recanalization. Networks of recanalizing endothelial cells may mimic angiosarcoma (inset).

Treatment

Surgical excision is usually curative. Local recurrences may occur when the lesion is superimposed on a vascular malformation that may generate new foci of endothelial hyperplasia.

Reactive Angioendotheliomatosis

Key features

- Uncommon, self-limited process occurring exclusively in the skin and characterized histologically by a dense proliferation of small capillaries
- The most common form is predominantly intravascular, resulting in luminal obliteration of pre-existing dermal vessels; many of these patients have vaso-occlusive disorders or systemic infections
- Should be distinguished from *intravascular large cell lymphoma (B or NK/T)*, an angiotropic lymphoma erroneously termed *malignant angioendotheliomatosis* prior to the advent of discriminating immunohistochemistry
- The diffuse dermal angiomatosis variant occurs most commonly on the leg or the breast and is associated with atherosclerosis, cigarette smoking, and large pendulous breasts

Introduction

Angioendotheliomatosis has historically been considered to be a single disease entity, divided into benign and malignant variants. As such, the large pleomorphic cells found within blood vessels in malignant angioendotheliomatosis were thought to be transformed endothelial cells. However, immunohistochemical studies have convincingly demonstrated that these cells are neoplastic lymphocytes. Accordingly, *malignant angioendotheliomatosis* has been renamed *intravascular large cell lymphoma (B or NK/T)* (see Ch. 119). The benign form is a true angioendotheliomatosis and is considered reactive.

Epidemiology

Reactive angioendotheliomatosis is rare and although it can occur at any age, the age of onset often reflects that of any associated systemic disorder. While many cases are idiopathic, this vascular proliferation may be associated with systemic disorders such as bacterial endocarditis, monoclonal gammopathies (including type I cryoglobulinemia), antiphospholipid syndrome, and calciphylaxis as well as renal transplantation, hepatic disease, and rheumatoid arthritis. The diffuse dermal angiomatosis variant occurs most commonly on the leg or the breast[5,6] and is associated with atherosclerosis, cigarette smoking, and large pendulous breasts.

Pathogenesis

Reactive angioendotheliomatosis is a benign, self-limited process. Its frequent association with various systemic conditions has led some investigators to propose that the capillary proliferation may be caused by a circulating angiogenic factor[7]. However, the fact that many of the disorders associated with this process cause vascular occlusion or tissue ischemia suggests that a local, hypoxia-induced increase in vascular endothelial growth factor (VEGF) may be playing a role[8]. In addition, immunological factors may contribute to the proliferative process.

Clinical features

Although erythematous nodules or plaques, often with superimposed petechiae or ecchymoses, are the characteristic primary lesions, the spectrum ranges from erythematous macules to tumor-like masses. Sites of involvement can vary, but the most common is the lower extremities. Focal ulceration may be evident, especially in the diffuse dermal angiomatosis variant (see Fig. 105.20). In this latter variant, reticulated thin violaceous plaques with telangiectasias are often seen (Fig. 114.3A).

Pathology

In this predominantly dermal, but also occasionally subcutaneous, process, there is a poorly marginated proliferation of closely packed capillaries lined by plump endothelial cells rimmed by small numbers of pericytes. The pattern of proliferation is highly variable both within and between lesions and is typically described as diffuse and/or lobular[9]. Focally, more dilated capillaries may be present and foci of hemosiderin deposition, fibrin microthrombi, and/or mild chronic inflammation are relatively common. Immunohistochemical positivity for endothelial markers such as CD31 and von Willebrand factor, and focally for pericyte/smooth muscle-associated actins, confirms the cellular composition. Expression of markers of lymphatic endothelial differentiation (e.g. Prox1, podoplanin) is consistently negative[10]. Cytologic atypia is absent and mitotic figures are rare to absent.

The capillary lumina are small and may be occluded by fibrin thrombi and bulging endothelial cells (Fig. 114.3B). In many cases, the proliferating capillaries appear to be contained within a larger, pre-existing vessel, obliterating its lumen, but sometimes the proliferation extends directly between collagen bundles (Fig. 114.3C). Cases associated with cryoglobulinemia typically show intraluminal and intracellular eosinophilic globules, but this finding can also be seen in the absence of cryoglobulinemia.

Differential diagnosis

The clinical differential diagnosis includes vascular tumors (e.g. Kaposi sarcoma, angiosarcoma) as well as other causes of ulceration (see Fig. 105.1). Histologically, one must consider other forms of intravascular endothelial proliferation, including intravascular pyogenic granuloma, papillary intralymphatic angioendothelioma, and intravascular PEH. Intralymphatic histiocytosis can be distinguished by the presence of CD68-positive histiocytes within dilated Prox1- and podoplanin-positive lymphatic vessels[10]. Malignant intravascular proliferations (e.g. intravascular large cell lymphoma [B or NK/T], intralymphatic metastases, intravascular complexes of Merkel cell carcinoma) can be easily distinguished via morphology and immunohistochemistry[11].

Treatment

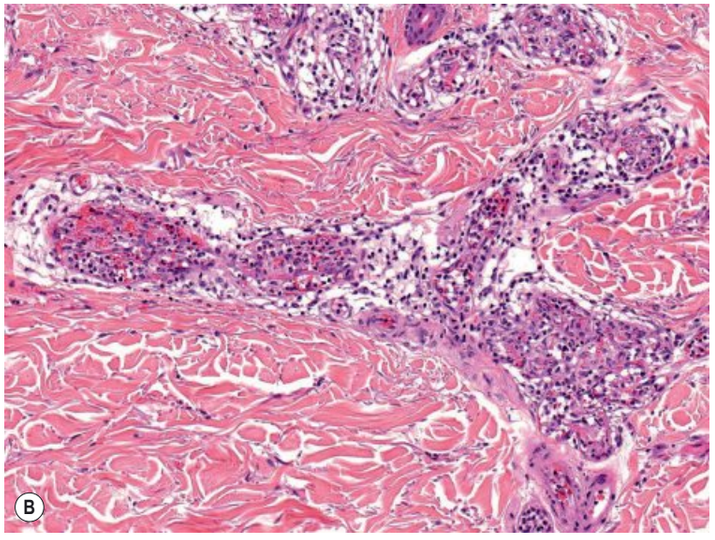
Evaluation for known associated systemic disorders is important because lesions may regress upon resolution of the underlying condition, e.g. revascularization of an ischemic limb. In case reports, oral isotretinoin has led to improvement, possibly due to its antiangiogenic properties, with consideration of potential side effects[12,13].

Angiokeratomas

Key features

- Small, dark, vascular, and variably keratotic lesions that result from dilation of superficial vessels
- Angiokeratoma circumscriptum is a capillary–lymphatic or capillary malformation
- Angiokeratoma corporis diffusum results from several lysosomal storage disorders and is associated with systemic manifestations





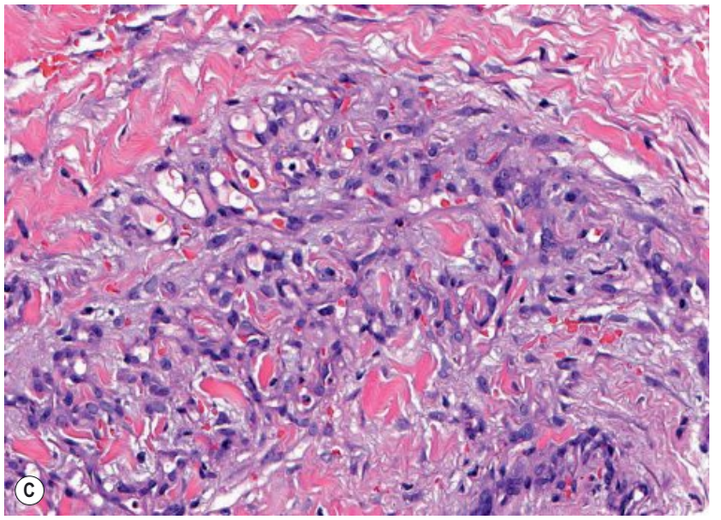


Fig. 114.3 Reactive angioendotheliomatosis – clinical and histopathologic features. A Reticulated violaceous plaques with punctate telangiectasias in a patient with diffuse dermal angiomatosis of the pendulous breast. **B** Intravascular variant with proliferation of grouped capillaries along the course of a dermal blood vessel. The endothelial cells lack atypia and within several capillaries there is an intraluminal proliferation of endothelial cells admixed with erythrocytes occluding the lumina. **C** Diffuse dermal angiomatosis variant with proliferation of hyperplastic endothelial cells without atypical features infiltrating the dermis and forming small vascular lumina. *A, Courtesy Department of Dermatology, Medical University of Graz; B, Courtesy Heinz Kutzner, MD; C, Courtesy Lorenzo Cerroni, MD.*

Introduction

Angiokeratomas are well-circumscribed vascular lesions consisting of superficial vascular ectasia and hyperkeratosis. Five variants have been recognized. With the exception of angiokeratoma circumscriptum (which represents a capillary–lymphatic or capillary malformation), angiokeratomas result from ectatic dilation of pre-existing vessels in the papillary dermis.

Clinical features

Solitary or multiple angiokeratomas

Most commonly, they present as a small, warty, black papule on the lower extremities, but may occur anywhere on the body (Fig. 114.4). The lesions are thought to result from injury to or chronic irritation of the wall of a venule in the papillary dermis. Solitary lesions may be confused with melanoma due to their dark color. Dermoscopy will readily distinguish between these two entities (see Ch. 0).

Genital Angiokeratomas

Synonym: ■ Angiokeratoma of Fordyce

These angiokeratomas may arise in the second or third decade but are most commonly seen in older age groups. In women, angiokeratomas occur most commonly on the labia majora and rarely the clitoris while in men, they develop primarily on the scrotum and rarely the penis[14,15]. The lesions are red–purple to black in color, may be single or multiple, and arise along superficial vessels (Fig. 114.5). In some patients, they may be associated with thrombophlebitis, varicoceles, and inguinal hernias. Vulvar lesions may be associated with vulvar varicosities, hemorrhoids, or increased venous pressure during pregnancy.

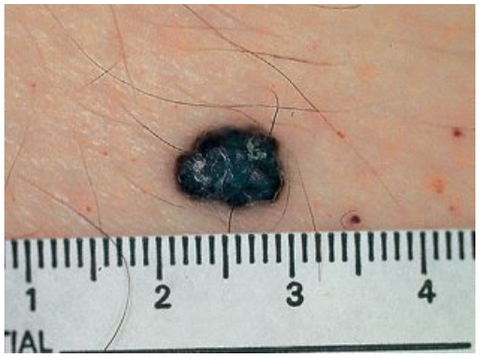


Fig. 114.4 Solitary angiokeratoma. Because of their dark color, these lesions may resemble cutaneous melanoma. Dermoscopy will readily distinguish between these two entities. *Courtesy Jean L. Bolognia, MD.*



Fig. 114.5 Scrotal angiokeratomas. These lesions typically arise along superficial vessels.

Angiokeratoma corporis diffusum

This disorder is characterized by the development of multiple, often clustered angiokeratomas, usually in a bathing trunk distribution. Lesions vary in number (from only a few to numerous) and usually begin to appear during late childhood or adolescence. X-linked recessive Fabry disease is the best-known entity with this clinical presentation and results from a deficiency of the lysosomal enzyme α-galactosidase A (see Ch. 63). This leads to the accumulation of the neutral glycolipid ceramide trihexidose within lysosomes of multiple cell types. Other enzyme deficiencies associated with angiokeratoma corporis diffusum are outlined in Table 63.7.

Angiokeratoma of Mibelli

Lesions usually develop between the ages of 10 and 15 years and are most commonly situated on the dorsal and lateral aspects of the fingers and toes. They may also occur on the dorsa of the hands and feet and rarely on the elbows and knees. Angiokeratoma of Mibelli may be associated with chilblains and acrocyanosis. In rare instances, ulceration of the fingertips can occur. There is a familial predisposition and the disorder may be transmitted in an autosomal dominant fashion with variable penetrance.

Angiokeratoma circumscriptum

This entity usually develops during infancy or childhood as either a plaque of multiple discrete papules (Fig. 114.6) or hyperkeratotic papules and nodules that often become confluent. They occur on the trunk, arms, or legs and are unilateral in most patients. There is a female predominance.

Pathology

Marked dilatation of the papillary dermal vessels is seen in association with an acanthotic, variably hyperkeratotic epidermis. Elongated rete ridges may partially or completely enclose vascular channels, and a collarette may be present at the margin of the lesions. In Fabry disease, vacuoles can be detected within endothelial cells and pericytes. The amount of glycolipid is small and may be difficult to detect in routinely prepared sections. However, the deposits stain positively with PAS and anti-GB3 antibody. They can also be demonstrated by electron microscopy.

Differential diagnosis

Clinically, angiokeratomas should be distinguished from other vascular lesions as well as acral pseudolymphomatous angiokeratomas (see Ch. 121). Darkly colored or thrombosed angiokeratomas may resemble cutaneous melanoma.

Treatment

Patients may request removal for cosmetic reasons. This may be achieved by shave excision, diathermy or laser therapy, the choice of which would largely depend on the size of the lesion.



Fig. 114.6 Angiokeratoma circumscriptum. These grouped red–violet papules had been present since childhood. *Courtesy Jean L. Bolognia, MD.*

Targetoid Hemosiderotic Lymphatic Malformation (Hobnail "Hemangioma")

Synonyms: ■ Targetoid hemosiderotic hemangioma ■ Superficial hemosiderotic lymphovascular malformation ■ Hobnail lymphatic malformation

Key features

- Uncommon acquired vascular lesion that usually presents as a red–blue or brown papule, most commonly on the extremities and often with a history of local trauma
- The papule is sometimes surrounded by a pale ring and then an ecchymotic halo
- Biphasic pattern of dilated, thin-walled vessels with hobnail endothelial cells in the superficial dermis, transitioning to smaller, slit-like vessels in the deeper dermis and lateral portions of the lesion
- Lesional endothelial cells strongly express the lymphoendothelial marker podoplanin and have minimal expression of CD34, consistent with lymphatic differentiation



Fig. 114.7 Targetoid hemosiderotic lymphatic malformation (hobnail "hemangioma"). There is a target-like appearance with a central violet papule surrounded by a pale rim whose color reflects hemosiderin deposition and then a purpuric halo. *Courtesy Department of Dermatology, Medical University of Graz.*

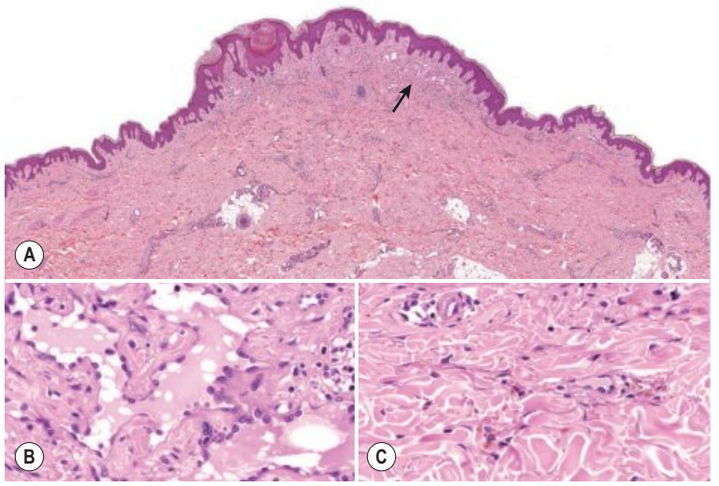


Fig. 114.8 Targetoid hemosiderotic lymphatic malformation (hobnail "hemangioma") – histopathologic features. A Biphasic appearance with dilated superficial dermal vessels lined by hobnailed endothelial cells in the center of the lesion (arrow; **B**), merging with smaller slit-like vessels that dissect between collagen bundles in deeper and lateral portions of the dermis (**C**). *Courtesy Lorenzo Cerroni, MD.*

Introduction and history

The original description in 1988 coined the term *targetoid hemosiderotic hemangioma* to emphasize the targetoid clinical appearance and hemosiderin deposition. Since then it has become apparent that only a minority of these lesions have an ecchymotic halo and hemosiderin deposition is variable. The term *hobnail hemangioma* was proposed to encompass lesions with the characteristic biphasic growth pattern and marked hobnail endothelial morphology, with or without a targetoid clinical appearance and/or marked hemosiderin deposition[16,17]. A benign clinical course has been observed in the over 100 cases that have been reported to date[17,18]. Recently, this "hemangioma" was reclassified as a *targetoid hemosiderotic lymphatic malformation* (THLM)[19].

Epidemiology

There is no sex predilection[17]. In a series of 62 patients, their ages ranged from 6 to 72 years (median, 32 years)[18].

Pathogenesis

This vascular anomaly was thought to represent the benign end of a spectrum of vascular tumors that have hobnail endothelial cells and which includes papillary intralymphatic angioendothelioma (PILA) and retiform hemangioendothelioma (see Table 114.1)[16]. However, the endothelial cells of THLM and PILA, but not retiform hemangioendothelioma, stain positively for several markers of lymphatic differentiation[18,20]. In addition, the endothelial cells of THLM are generally negative for Wilms tumor-1 (WT-1) and have a low Ki-67 proliferation index. The latter explains its reclassification as a vascular malformation based upon International Society for the Study of Vascular Anomalies (ISSVA)-sanctioned restriction of the suffix "angioma" to intrinsically proliferative vascular tumors[19].

Trauma may stimulate the appearance of a THLM, with microshunts between small lesional blood vessels and adjacent lesional lymphatic vessels explaining the presence of erythrocytes within lymphatic vessels and hemosiderin deposits[20].

Clinical features

Most lesions are asymptomatic, solitary, well-circumscribed, red–blue to violet–brown papules that are initially 2 to 3 mm in diameter and then slowly increase in size. In some cases, the papule is surrounded by a thin pale ring and then an ecchymotic halo (Fig. 114.7). The ecchymotic ring may fade and eventually disappear over time, and some lesions undergo cycles of spontaneous regression and recurrence. Favored sites, in decreasing order of frequency, are the lower extremities, upper extremities, back, buttock/hip, and chest wall. Lesions have also been reported on the tongue and gingiva[17].

Pathology

There is a biphasic histologic pattern (Fig. 114.8A), consisting of: (1) dilated, thin-walled vessels containing small numbers of red blood cells and lined by prominent hobnail endothelial cells within the superficial dermis (Fig. 114.8B); and (2) smaller, more slit-like vessels that dissect between collagen bundles in deeper and lateral portions of the dermis (Fig. 114.8C). Extravasated red blood cells and hemosiderin deposits are common but may be absent. Although the superficial vessels occasionally have delicate intraluminal papillary fronds, the more complex, multilayered endothelial tufts of PILA are lacking. The endothelial cells of both the dilated and the slit-like vessels stain positively for the lymphoendothelial marker podoplanin (see Ch. 102), but show little, if any, reactivity for the blood vascular marker CD34[18,20].

Differential diagnosis

The clinical differential diagnosis includes melanocytic nevus, sclerosing hemangioma, and benign vascular neoplasms and proliferations in Table 114.1[17]. Histopathologically, it must be distinguished from patch-stage and lymphangioma-like variants of Kaposi sarcoma, well-differentiated angiosarcoma, retiform hemangioendothelioma, PILA, and microcystic lymphatic malformation.

Treatment

Treatment consists of simple excision. Longitudinal evaluation of 35 patients, ranging from 1 to 4 years, revealed no local recurrence or systemic metastasis[18].

Verrucous Venulocapillary Malformation (Verrucous "Hemangioma")

Synonym: ■ Verrucous venous malformation

Key features

- Rare congenital vascular anomaly that has been reclassified as a vascular malformation
- Somatic missense mutations in *MAP3K3* (mitogen-activated protein kinase kinase kinase 3) detected in some lesions
- Isolated, grouped, or confluent red-to-purple papules with reactive hyperkeratosis; often darkens with age
- Most commonly occurs on the distal extremity and can be complicated by ulceration and bleeding but not local tissue hypertrophy
- Histologically, dilated capillaries and venules are present within the papillary and investing dermis as well as the deep reticular dermis and subcutis; the overlying epidermis is acanthotic

Introduction and history

This rare, but increasingly well-recognized, vascular anomaly was originally thought to be a "hemangioma", but has since been reclassified as a vascular malformation. The debate arose in part because these lesions may show evidence of cellular proliferation during their evolution. Mulliken and colleagues recommended use of the term *verrucous venous malformation*[21] while others prefer the designation *verrucous venulocapillary malformation*, congruent with the predominant component vessels.

Epidemiology

There are no sex, racial, or ethnic predilections.

Pathogenesis

Somatic missense mutations in *MAP3K3* (mitogen-activated protein kinase kinase kinase 3) were detected in 6 of 10 verrucous venulocapillary malformations[21]. The mutant allele frequencies ranged from 6% to 19% in affected tissue and these mutations were not found in unaffected tissue or other types of vascular anomalies. Of note, studies in *MAP3K3* knockout mice had previously implicated MAP3K3 in vascular development.

Clinical features

Verrucous venulocapillary malformations are congenital and present as isolated, grouped, or confluent red-to-purple papules that can sometimes be extensive. The vast majority occur on the distal extremities, particularly the leg (Fig. 114.9A); the trunk is a rare location[22]. They progressively darken and become hyperkeratotic during childhood, often increasingly complicated by ulceration, bleeding, and scarring. They do not regress and are not associated with local tissue hypertrophy or other developmental anomalies.

Pathology

Features can vary with age, in particular the appearance of secondary orthohyperkeratosis and verrucous epidermal hyperplasia, but consistently there are dilated capillaries and venules (without a smooth muscle layer) within the papillary dermis and occasionally the investing dermis around adnexae. There is sparing of most of the reticular dermis, with the dilated blood vessels reappearing in the deep dermis and subcutis, where they are usually smaller in caliber, often grouped, and sometimes have intraluminal thrombi (Fig. 114.9B). The superficial dermal vessels are usually the most obviously dilated with expansion of the dermal papillae (Fig. 114.9C). A purely subcutaneous variant has been described[23].

Endothelial cells consistently express markers of blood vascular differentiation, including CD31 and CD34. Focal positivity for lymphatic endothelial markers, e.g. Prox1, podoplanin, has been observed in some, but not all, studies[24,25]. Mitotic activity is very low. Many verrucous venulocapillary malformations have light, focal immunoreactivity for GLUT1, in contrast to the intense endothelial GLUT1 positivity seen in infantile hemangiomas[26,27]; staining for CD15 and indolamine 2,3 deoxygenase is negative (personal observation).

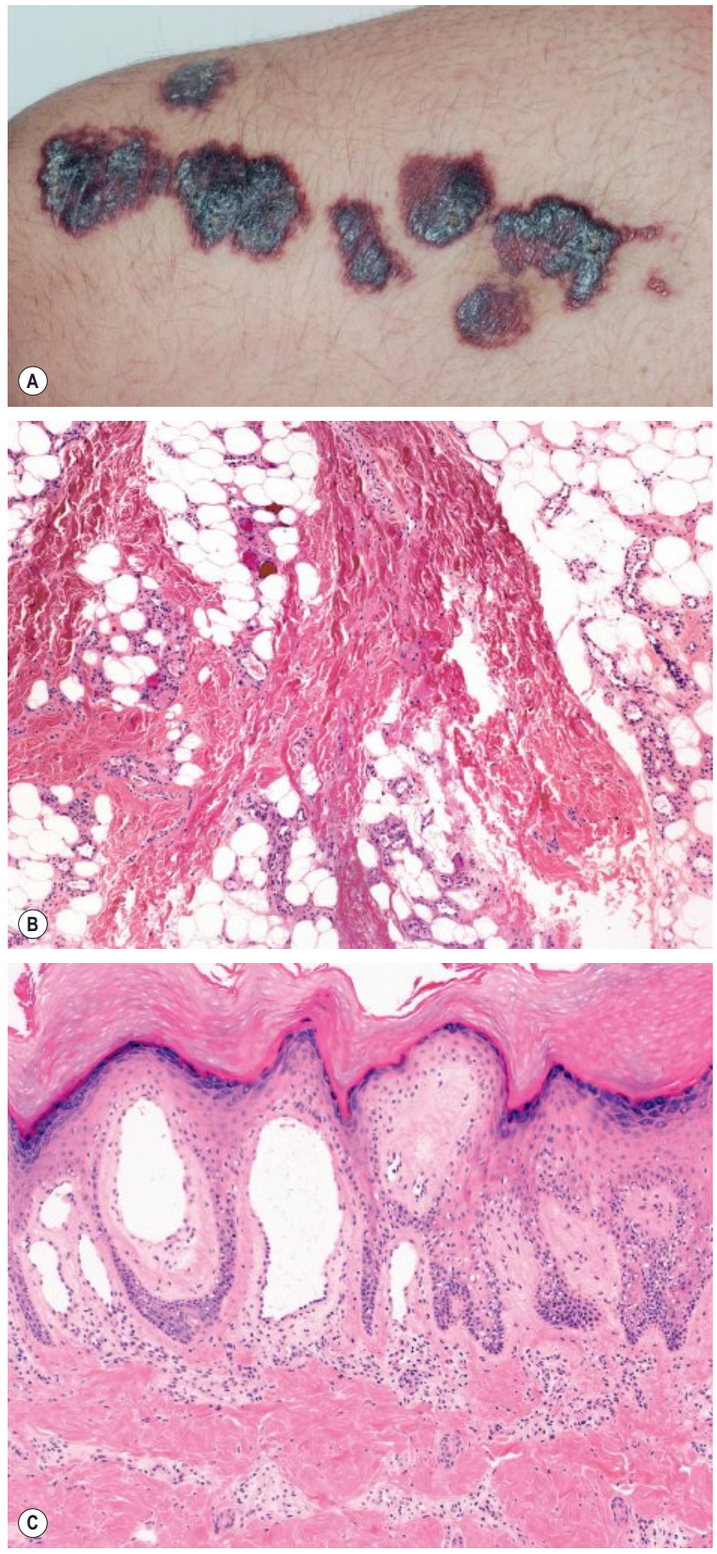


Fig. 114.9 Verrucous venulocapillary malformation (verrucous "hemangioma") – clinical and histopathologic features. A Linear array of purple plaques on the thigh; the thicker portions of the plaques are darker in color with overlying scale. **B** Ectatic venules and capillaries infiltrate the subcutis. **C** Ectatic capillaries and venules expand the papillary dermis; note the hyperkeratosis. *A, Courtesy Julie V. Schaffer, MD.*

Differential diagnosis and treatment

The differential diagnosis includes other venous and venulocapillary malformations, lymphatic and mixed venous–lymphatic malformations (see Ch. 104), non-involuting congenital hemangioma, infantile hemangioma (see Ch. 103), and verrucous epidermal nevus (see Ch. 109). Current first-line therapeutic options include surgical excision

and treatment of the superficial component with pulsed dye, long-pulsed Nd:YAG, and/or carbon dioxide lasers. However, treatment is challenging for extensive lesions. More recently, topical and oral sirolimus have been utilized with variable results[28–30].

Pyogenic Granuloma

Synonyms: ■ Lobular capillary hemangioma ■ Granuloma pyogenicum

Key features

- Rapidly growing, friable, red papule or polyp of skin or mucosa that frequently ulcerates; most common in children and young adults
- Those arising on the gingiva of pregnant women (*granuloma gravidarum*) are considered a separate clinical subgroup, but are histologically indistinguishable
- The characteristic single lesion may spontaneously regress as well as recur whereas multiple lesions can arise, even repeatedly, within pre-existing vascular malformations or congenital hemangiomas
- Neither infectious in etiology nor granulomatous histologically but occasionally associated with trauma or hormonal factors; historically considered a reactive vascular hyperplasia
- Somatic *BRAF* and *RAS* mutations have been detected in sporadic lesions and more often in secondary pyogenic granulomas arising within capillary malformations, pointing to at least a partially neoplastic etiology rather than purely reactive hyperplasia
- Consists of lobules of small benign capillaries set in a fibromyxoid matrix, often distinctly exophytic and bounded by a collarette of hyperplastic epithelium
- Occasionally found in subcutaneous or intravascular locations

Introduction and history

Poncet and Dor are credited with the initial description in 1897, and they believed the cause was a *Botryomyces* infection. The term *granuloma pyogenicum* was coined in 1904 by Hartzell to describe four similar cases that he thought represented a nonspecific granulation tissue-type response to any type of pyogenic agent[31]. Although the etiology of these common lesions remains controversial and potentially heterogeneous, the term *pyogenic granuloma* is clearly a misnomer. There is no evidence to implicate any infectious agent, and the histologic appearance is not granulomatous.

Epidemiology

Pyogenic granulomas (PGs) can develop at any age but are more common in children and young adults. There may be a slight male predominance, but no racial or familial predisposition. Gingival lesions may arise during pregnancy (see Fig. 27.11C). Rarely, neonates develop extensive multifocal PGs.

Pathogenesis

PGs exhibit several clinical features suggestive of reactive neovascularization, including a common association with pre-existing injury or irritation, limited capacity for growth, and a propensity for multiple eruptive lesions that may be localized or disseminated. The occasional appearance of PGs within other vascular anomalies, especially capillary[32] and arteriovenous malformations or congenital hemangiomas, suggests that abnormalities in blood flow or background somatic mutations within the underlying lesion may play a role.

In one study, 8 of 10 PGs arising within a capillary malformation (CM) had a *BRAF* c.1799T>A mutation and 1 of 10 an *NRAS* c.182A>G mutation[33]. All of these secondary PGs also had the underlying CM-specific *GNAQ* c.548G>A mutation, pointing to their derivation from the cells of the CM as well as the independent occurrence of a *BRAF* mutation within the PG[33]. The same *BRAF* c.1799T>A mutation was also found in 3 of 25 sporadic PGs suggesting its possible role as a driver mutation in primary and secondary PGs. *BRAF* c.1799T>A mutation leads to BRAF V600E and immunohistochemical staining for this protein can be used to confirm the presence of BRAF V600E within the endothelial cells of a PG and its absence in adjacent perilesional normal epidermis. Activation of the MAPK signaling pathway (see Fig. 113.1) points to a neoplastic rather than purely reactive process[33], at least for some PGs, taking into account the background level of MAPK signaling due to external factors (e.g., trauma, irritation).

Clinical features

The lesion presents as a solitary red papule or polyp that grows rapidly over the course of several weeks or months, stabilizes, and then may decrease in size (Fig. 114.10). Its final size is rarely >1 cm, and it may persist indefinitely if not removed. Approximately one-third develop following minor trauma. In one series of 289 cases, the most common sites, in decreasing order of frequency, were the gingiva, fingers, lips, face, and tongue[34]. They are extremely friable, frequently ulcerate, and may bleed profusely with minor trauma. Multiple satellite lesions occasionally develop near a primary PG, usually after destruction of that lesion[35]. Rarely, PGs arise within the subcutis, develop intravascularly, or erupt in a disseminated fashion[36]. PGs have been reported in association with vascular malformations (see above) as well as multiple drugs including systemic retinoids[37], indinavir, and BRAF, EGFR, HER2, MEK and mTOR inhibitors. Medication-induced lesions are often in a periungual location and are sometimes referred to as pseudo-PGs.

Pathology

The quintessential cutaneous or mucosal lesion is a well-circumscribed, exophytic, sometimes pedunculated proliferation of small capillaries, often arranged in a lobular pattern (Fig. 114.11). Lesional capillaries are lined by flattened to slightly plump endothelial cells, rimmed by pericytes, and surrounded by a variably edematous fibromyxoid interstitial stroma containing fibroblasts. Endothelial and stromal cell mitotic activity is highly variable and depends on the stage of growth; a variably dense infiltrate of lymphocytes, plasma cells, neutrophils, and mast cells is usually present. Capillary lumina within the lobules vary from small and angular to branching and ectatic, and foci of thrombosis and intravascular PEH may be present. A few larger vessels with smooth muscle walls, usually venous (but often including a small ascending arterial feeder), are frequently present at the base of the lesion. Thick, intervening bands of dense fibrous tissue sharply define the lobularity and help distinguish pyogenic granuloma from other lobular forms of capillary proliferation such as infantile hemangioma. The lateral margins are often defined by epithelial "collarettes".

Differential diagnosis

The diagnosis of PG can be made clinically if the red, bleeding papule is coupled with the characteristic location and history. Otherwise, they can be easily confused with amelanotic melanoma and, in the immunosuppressed patient, bacillary angiomatosis or Kaposi sarcoma. Glomus



Fig. 114.10 Pyogenic granuloma – clinical features. A Eroded pink–red papulonodule with a narrow base on the scalp. **B** Pedunculated papule on the finger, a common site. **C** Bright red nodule with hemorrhagic crusting and narrow base. By dermoscopy, red homogeneous areas are intersected by white lines (see Ch. 0). *A, Courtesy Julie V. Schaffer, MD; C, Courtesy Department of Dermatology, Medical University of Graz.*

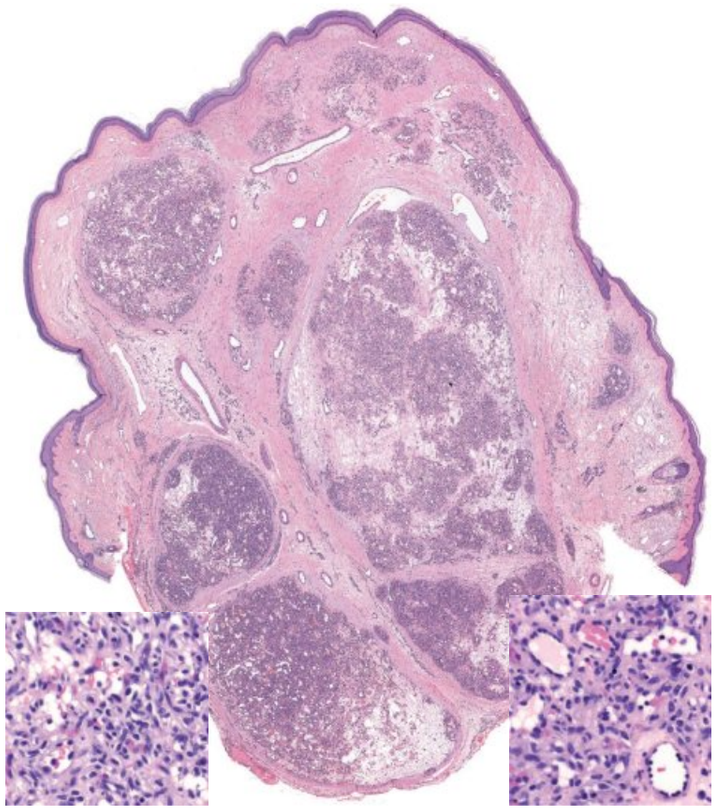


Fig. 114.11 Pyogenic granuloma – histopathologic features. Proliferating capillaries (insets) are often grouped into lobules by dense fibrous bands, hence the synonym lobular capillary hemangioma. *Courtesy Lorenzo Cerroni, MD.*

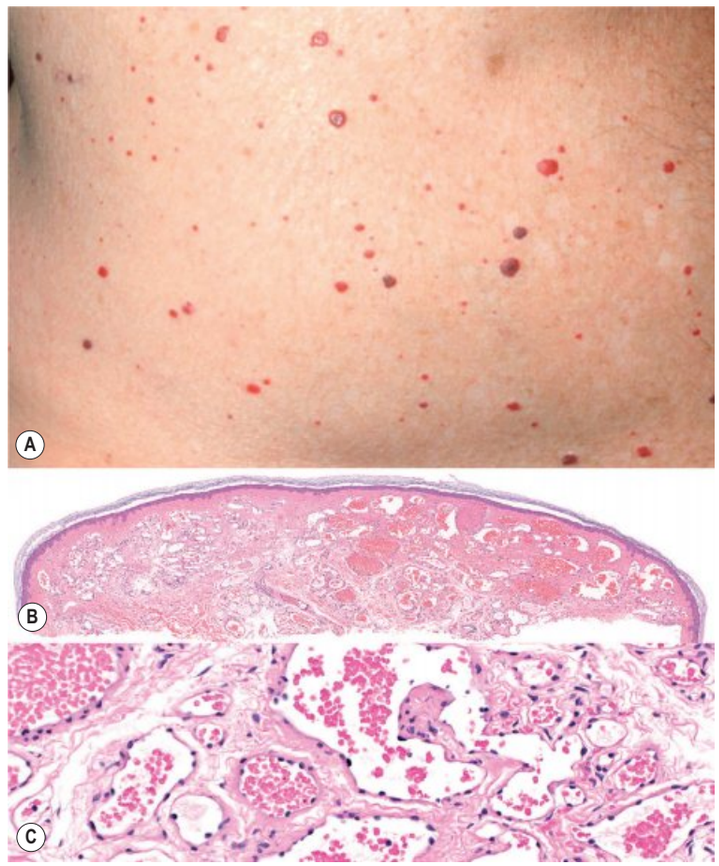


Fig. 114.12 Cherry angiomas. A Multiple compressible red papules of varying sizes on the abdomen. **B,C** Histologically, congested capillaries and postcapillary venules expand the papillary dermis. *Courtesy Lorenzo Cerrroni, MD.*

tumors, infantile hemangiomas, and irritated melanocytic nevi and warts can all mimic PGs. Histologic confirmation is always helpful in cases where the diagnosis is in question.

Treatment

Shave excision followed by electrosurgery of the base under local anesthesia is sufficient for most lesions. Patients and parents should be alerted to the possibility of recurrence after removal. Excision with suturing may result in less postoperative bleeding and a lower recurrence rate.

Pulsed dye laser has also been shown to be a safe and effective treatment for small PGs and may be particularly useful in children[38]. Topical β-blockers (e.g. timolol) or silver nitrate cauterization may be helpful for targeted cancer therapy-induced pseudo-PGs or small PGs in children. Successful sclerotherapy in nine patients using monoethanolamine oleate was reported, with inconspicuous scar formation and no recurrence[39].

Cherry Angioma

Synonyms: ■ Cherry hemangioma ■ Senile angioma ■ Campbell–De Morgan spot

Key features

- Bright red, dome-shaped to polypoid papules up to several millimeters in diameter that begin appearing during adult life, most commonly on the trunk and upper extremities
- A common, benign lesion found in most individuals by the age of 60 years, sometimes in large numbers
- Consist of dilated, congested capillaries and postcapillary venules within the papillary dermis

Introduction and history

Cherry angiomas are the most common of the acquired cutaneous vascular proliferations. They can be unattractive and when eruptive may rarely herald an underlying systemic abnormality.

Epidemiology

Both sexes are affected equally. Although they may occasionally develop during adolescence, cherry angiomas usually first appear during the third decade of life or later, and then increase in number over time. Most people over 60 years of age have one or more such lesions.

Pathogenesis

An increased number of cherry angiomas often appear during pregnancy and may involute in the postpartum period, suggesting that hormonal factors may be important in their pathogenesis. Two women with hundreds of eruptive cherry hemangiomas, both of whom had increased serum levels of prolactin, have also been reported[40]. Most angiomas that appear in the setting of POEMS syndrome are cherry angiomas, often in association with glomeruloid hemangiomas. Mutually exclusive somatic mutations in three *GNA* genes – *GNA11*, *GNA14*, and *GNAQ* – have been identified in the majority of cherry angiomas[41,42]. Of note, these genes have been associated with a variety of other benign (but not malignant) vascular anomalies, e.g. *GNAQ* and CMs[43]. In ~20% of cherry angiomas, somatic *HRAS* and *KRAS* mutations have been detected[33]. As with PGs, these findings suggest that cherry angiomas are more appropriately considered neoplastic rather than purely reactive in nature, although incidence and phenotypic variability could be influenced by the cell type harboring the mutation and external factors (e.g. trauma, hormones, gammopathy)[33].

Clinical features

Cherry angiomas are round to oval, bright red to purple, dome-shaped papules ranging in size from barely visible to several millimeters in diameter (Fig. 114.12A). Well-developed lesions may be polypoid. They most commonly develop on the trunk and proximal extremities and are rare on the hands, feet, and face. It is not unusual for elderly adults to have 50–100 cherry angiomas on their trunk. Rarely, a segmental distribution pattern, possibly reflecting mosaicism, is seen.

Patients are usually aware of the benign nature of these extremely common lesions and bring them to a physician's attention only when concerned about their appearance. They are generally asymptomatic but may occasionally bleed when traumatized.

Pathology

Histologically, congested, ectatic capillaries and postcapillary venules are seen within the papillary dermis and superficial reticular dermis (Fig. 114.12B,C). Early lesions are characterized by small lumina and plump endothelial cells. With maturation, the vessels dilate and the endothelial cell cytoplasm flattens, often producing slightly hobnailed nuclei. Vessel diameter decreases with descent into the reticular dermis. There is loss of epidermal ridges centrally and peripherally adnexal epithelial collarettes are seen.

Differential diagnosis

The distinctive clinical and dermoscopic findings (see Ch. 0) limit other diagnostic considerations. Glomeruloid hemangiomas, although similar in clinical appearance, can be distinguished histologically. Tiny cherry angiomas may resemble petechiae.

Treatment

Patients may request removal of cosmetically undesirable or chronically traumatized cherry angiomas. This can be accomplished by shave excision, electrodesiccation, or laser ablation, and recurrences are unusual.

Tufted Angioma

Synonyms: ■ Acquired tufted angioma ■ Angioblastoma of Nakagawa ■ Tufted hemangioma

Key features

- Usually presents as an acquired lesion in children and young adults, but may be congenital
- Non-homogeneous pink to red patches and plaques with superimposed papules that spread slowly, often to involve large areas, then stabilize; rarely completely regress
- Most commonly located on neck or trunk
- When congenital can be associated with Kasabach–Merritt phenomenon (syndrome)
- Thought to represent a mild superficial form of kaposiform hemangioendothelioma
- Characterized histologically by tightly packed tufts of tiny capillaries distributed within the dermis and subcutis in a "cannonball" pattern; foci of spindled endothelial cells may be present

Introduction

Tufted angioma has often been lumped erroneously with infantile hemangioma under the generic term "capillary hemangioma". However, a distinction is important given its association with Kasabach–Merritt phenomenon (KMP) in some infants. In older children and adults, it may clinically mimic Kaposi sarcoma. Current opinion is that tufted angioma falls within a spectrum shared by kaposiform hemangioendothelioma (KHE), with the latter usually having deeper involvement of soft tissues. From a practical standpoint, many pathologists favor a unified histopathologic diagnosis for these two variants.

History

Tufted angioma was first described in 1989 by Wilson-Jones and Orkin[44]. Apparently identical lesions had been described many years previously as angioblastoma and progressive capillary hemangioma. The association of tufted angioma with KMP, shared by KHE, is now widely recognized[45].

Epidemiology

Most lesions occur in young adults and children, many during the first year of life. Over 50% present before 5 years of age[44], and ~15% are congenital[44]. Rarely, lesions appear late in life[46]. Although one family with several affected family members has been reported[47], the vast majority of cases are sporadic.

Pathogenesis

Tufted angioma and KHE have a significant degree of overlap in histologic features, with resection specimens of KHE often demonstrating dermal changes that would have been interpreted in small biopsy specimens as tufted angioma. The virtually exclusive association of these two entities with KMP, plus their histologic and molecular overlap, provides convincing evidence that tufted angioma likely represents a more superficial, milder form of KHE (see KHE section for discussion of molecular studies)[45,48–51].

Clinical features

Tufted angiomas appear as mottled red patches or plaques with superimposed angiomatous papules, typically on the neck, trunk or shoulders, that grow slowly by lateral extension over a period of 5 months to 10 years[44] (Fig. 114.13). Occasionally, lesions have an associated growth of lanugo hair or CM-like areas[52]. Platelet trapping (KMP) may develop in congenital cases, although less commonly than in KHE. Lesions eventually stabilize in size, then may persist unchanged, shrink, or leave a fibrotic residuum. Rarely, complete spontaneous regression has been observed[52]. Occasionally lesions are painful, and exacerbations of pain may occur during periods of uncontrolled platelet trapping[53].

Pathology

Tufted angiomas, as originally described in the dermatology literature, are characterized by multiple discrete lobules of capillaries set within the dermis and often the subcutis in a so-called "cannonball" pattern (Fig. 114.14). Borders of the area of tissue involvement are poorly defined. The dermal collagen and subcutis separating capillary lobules may be histologically normal but are often fibrotic. The lobules are composed of tiny capillaries with pinpoint lumina, occasionally containing fibrin microthrombi, that are tightly packed together without intervening stroma (Fig. 114.14, inset), and they frequently bulge into peripherally placed thin-walled vessels. Mitotic figures are rare.

Endothelial cells may be focally spindled, but less prominently than in KHE. The sweeping spindled cell fascicles and epithelioid nodules of KHE are typically absent in tufted angioma[50,54]. Although the number of spindled endothelial cells differs when tufted angioma is compared to KHE, they share an identical phenotype: Prox1$^{\pm}$ (nuclear), podoplanin and LYVE-1^{+} (cytoplasmic), CD31^{+}, CD34^{+}, and smooth muscle actin (SMA)$^{-}$. In both tumors, it has been suggested that the proportion of spindled endothelial cells and degree of podoplanin/Prox1 positivity correlates with aggressiveness and active KMP, but this has not been definitely demonstrated[45,50,54].

Of note, endothelial cells of tufted angioma do not immunoreact for infantile hemangioma-associated antigens such as GLUT1 and Lewis Y antigen[27]. Ultrastructural studies have demonstrated classical Weibel–Palade bodies. In cases associated with KMP, platelet trapping has been confirmed with CD61 immunoreaction[55].

Differential diagnosis

Congenital/early infantile tufted angiomas must be differentiated from infantile hemangiomas, the most common tumors of infancy (see Ch. 103).

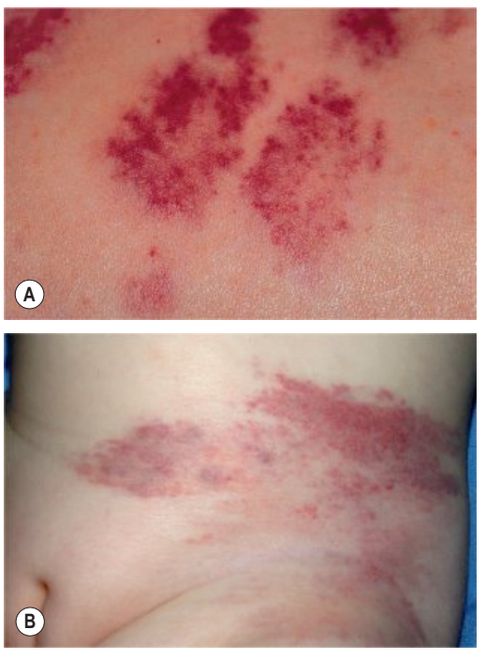


Fig. 114.13 Tufted angioma – clinical features. A Mottled red patches and superimposed papules are typical clinical features. **B** Pink–red to violet plaque in an infant that is broken up into smaller papules. *B, Courtesy Julie V. Schaffer, MD.*

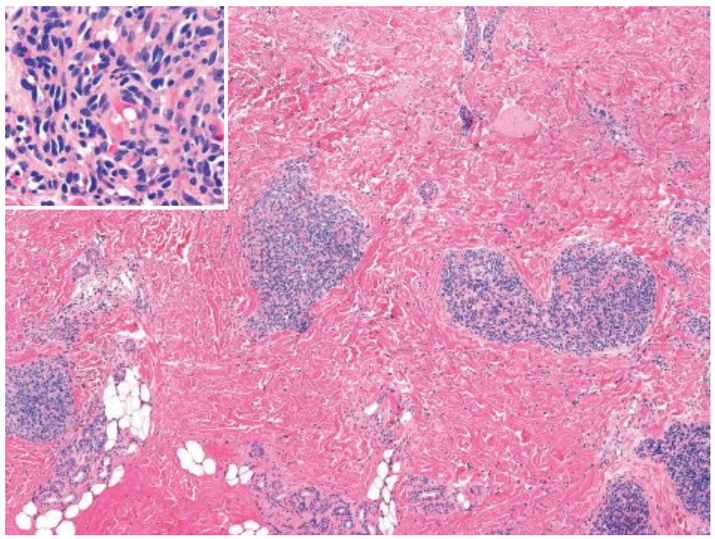


Fig. 114.14 Tufted angioma – histopathologic features. Within the dermis, there is typically a cannonball distribution of dense capillary lobules (inset). *Courtesy Luis Requena, MD.*

The latter are positive for placental capillary-associated endothelial markers (e.g. GLUT1) and show more rapid growth (without lateral extension) during the first year of life, followed by spontaneous, slow involution[27]. Infantile hemangiomas are transiently positive for the lymphatic-associated marker LYVE-1 early in their course, presumably as an expression of their embryonic, cardinal vein-type endothelial phenotype[56], but lack other lymphatic markers such as podoplanin and Prox1[56,57].

Other entities that may mimic the clinical appearance of tufted angioma include pyogenic granuloma arising within a vascular malformation and Kaposi sarcoma. Pyogenic granuloma can be distinguished histologically by its characteristic edematous stroma, granulation tissue-type changes, common presence of inflammation, lack of association with lymphatic markers, and generally larger, more loosely packed lesional vessels. Kaposi sarcoma differs in its lack of tufting, presence of a plasma cell infiltrate, and prominence of fascicles of spindle cells forming slit-like spaces. KHE, although overlapping in histology and likely synonymous in pathogenesis, is traditionally described as a more bulky, deeply seated lesion that tends to infiltrate across multiple tissue planes and has more prominent spindled endothelial cells[50].

Treatment

Complete surgical excision is the treatment of choice for small tufted angiomas, but recurrence is common. Topical sirolimus (rapamycin), an mTOR inhibitor, can be tried (see Ch. 129). Use of the pulsed dye laser has been ineffective[53,58], although the argon tunable dye laser with its higher risk of scarring has been used successfully. Both aggravation and improvement have been reported with the Nd:YAG laser. Historically, high-dose systemic corticosteroids were sometimes employed[59], even though generally ineffective. Interferon-α may produce partial regression, but its use is no longer recommended given the risk of inducing permanent spastic diplegia in infants (see Ch. 103)[58]. For patients with tufted angioma/KHE who develop KMP, first-line therapy consists of oral sirolimus plus prednisolone[60,61]; vincristine plus prednisone is another option[60–62]. Aspirin may also help to control the platelet interaction, pain, and growth of tufted angiomas[53].

Glomeruloid Hemangioma

Key features

- A histologically distinct type of hemangioma that occurs primarily in patients with POEMS syndrome
- In POEMS syndrome, multiple, firm, angiomatous papules or plaques are scattered most often on the trunk and proximal extremities
- Characterized histologically by nests of capillaries within dilated dermal vessels, resembling renal glomeruli
- Likely induced by increased circulating levels of VEGF

POEMS SYNDROME – CLINICAL CRITERIA, CUTANEOUS FINDINGS, AND ASSOCIATED VASCULAR LESIONS
Diagnostic criteria
***M*onoclonal plasmaproliferative disorder** – *and* – **Sensorimotor *p*olyneuropathy** plus at least one other major criterion and one minor criterion
Major criteria
• Sclerotic bone lesions • Castleman disease • Increased circulating levels of VEGF
Minor criteria
• Extravascular volume overload (peripheral edema, pleural effusions, ascites) • Thrombocytosis or polycythemia • Papilledema • *O*rganomegaly (hepatosplenomegaly) or lymphadenopathy • *E*ndocrinopathy (e.g. adrenal, pituitary, gonadal, parathyroid) • Skin changes (characteristic)
Cutaneous findings
• Vascular lesions • More common: diffuse hyperpigmentation, induration, hypertrichosis, hyperhidrosis • Less common: clubbing, livedo reticularis, acrocyanosis, flushing, acquired facial lipoatrophy, leukonychia
Types of cutaneous vascular lesions
• Cherry hemangiomas • Glomeruloid hemangiomas • Other: reactive angioendotheliomatosis, intravascular papillary endothelial hyperplasia, lobular capillary hemangiomas, microvenular hemangiomas

Table 114.2 POEMS syndrome – clinical criteria, cutaneous findings, and associated vascular lesions. Patients with AESOP (*a*denopathy and *e*xtensive *s*kin patch *o*verlying a *p*lasmacytoma) syndrome may fulfill the criteria for POEMS syndrome. Patients with TEMPI syndrome also have a monoclonal gammopathy (M) but they develop telangiectasias (T) as well as elevated erythropoietin and erythrocytosis (E), perinephric fluid collections (P), and intrapulmonary shunting (I). VEGF, vascular endothelial growth factor.

Introduction and history

The term *glomeruloid hemangioma* was coined by Chan et al.[63] in 1990 to describe a distinctive vascular proliferation that occurs primarily in patients with POEMS syndrome (*p*olyneuropathy, *o*rganomegaly, *e*ndocrinopathy, *m*onoclonal gammopathy, and *s*kin lesions). Although the majority of patients with POEMS syndrome have an underlying plasma cell dyscrasia, this lesion occurs more commonly in those with multicentric Castleman disease. There is some overlap with reactive angioendotheliomatosis, but glomeruloid hemangioma is discussed separately because of its highly distinctive histologic features and well-recognized clinical association.

Clinical features

The reported incidences of angiomas in patients with POEMS syndrome range from 25% to 45%. These appear as multiple, firm, dome-shaped, red to purple papules or plaques ranging in diameter from a few millimeters to a few centimeters; they are scattered predominantly over the trunk and proximal extremities (see Ch. 53). Additional cutaneous manifestations of POEMS syndrome are outlined in Table 114.2, as are the types of vascular lesions that occur in these patients. True glomeruloid hemangiomas appear to be fairly specific for POEMS syndrome, and rarely they may appear years prior to recognition of the syndrome[64]. In addition, there are reports of a solitary variant that is not associated with POEMS syndrome.

Pathogenesis

Glomeruloid hemangiomas are thought to be reactive, rather than neoplastic. Patients with POEMS syndrome often have increased circulating levels of VEGF[65] such that this elevation represents a major diagnostic criterion (see Table 114.2). Most cases of POEMS syndrome associated with multicentric Castleman disease (~90%) have evidence

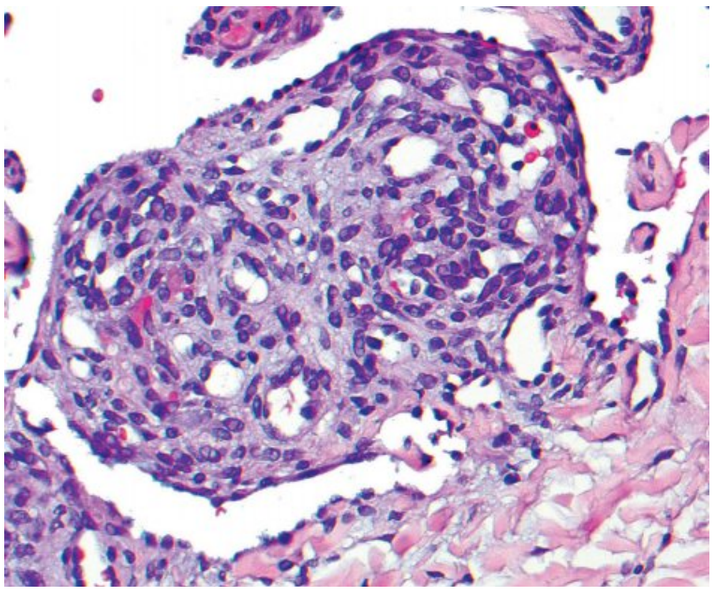


Fig. 114.15 Histology of a glomeruloid hemangioma in a patient with POEMS syndrome. Dilated dermal vessels are filled with congeries of small capillaries reminiscent of renal glomeruli.

of human herpesvirus-8 (HHV-8) infection by PCR. It is suspected that viral interleukin (IL)-6 produced by HHV-8 may indirectly promote angiogenesis by inducing VEGF expression[66]. There was also a case report of a patient with Erdheim–Chester disease and elevated circulating levels of VEGF who developed a glomeruloid hemangioma, further implicating the pathogenic role of VEGF[67].

Pathology

Most of the angiomas seen in patients with POEMS syndrome are found upon histologic examination to be consistent with common cherry angiomas, with numerous dilated dermal capillaries lined by flattened endothelial cells (see above). Only a few demonstrate the distinctive features of glomeruloid hemangioma. These consist of dilated dermal vessels filled by small, well-formed capillary loops that lead to structures reminiscent of renal glomeruli (Fig. 114.15).

The capillaries comprising these glomeruloid formations are lined by flat endothelial cells surrounded by an outer layer of pericytes and are separated by a scant stroma containing large cells with lightly eosinophilic cytoplasm and multiple eosinophilic globules. The latter are PAS-positive, diastase-resistant, and by immunohistochemistry positive for polytypic immunoglobulin, presumably derived from the associated paraprotein[63]. Of note, these interstitial, immunoglobulin-containing cells are of endothelial derivation. Lastly, since many POEMS syndrome patients have both cherry angiomas and glomeruloid hemangiomas, and the cherry angiomas may display focal glomeruloid formation, it is likely that these two histologic subsets reflect variants or different stages of the same process[63].

Differential diagnosis

The clinical differential diagnosis includes other vascular proliferations and tumors (see Table 114.1), while the histologic differential diagnosis of glomeruloid hemangioma is essentially that described above for reactive angioendotheliomatosis. A more recently described entity, *papillary hemangioma*, also enters the histologic differential diagnosis[68]. The latter is characterized by intravascular papillary growths of capillaries, pericytes, and stromal cells within ectatic dermal vessels, accompanied by hyaline globules (features reminiscent of glomeruloid hemangioma), but it differs by being solitary, being confined to the head and neck region, and having neither a true glomeruloid architecture nor an association with POEMS syndrome.

Treatment

Treatment is not required, although shave excision, cryosurgery, electrodesiccation, or pulsed dye laser surgery will remove the vascular tumors.

Microvenular Hemangioma

Synonym: ■ Microcapillary hemangioma

Key features

- An uncommon, acquired, slowly growing, benign vascular tumor of young to middle-aged adults
- Presents as a small, usually solitary, sharply circumscribed red papulonodule or plaque on the trunk or extremities, with a predilection for the forearms
- Consists of small branching capillaries and venules with collapsed lumina and conspicuous pericytes infiltrating the full thickness of the reticular dermis
- May be subject to hormonal influences in some women

Introduction and history

Microvenular hemangioma was first described by that name in 1991 by Hunt, Santa Cruz, and Barr[69], although cases reported as microcapillary hemangiomas are probably identical.

Epidemiology

Reported cases have been in young and middle-aged adults of both sexes. Some cases in women have been temporally related to pregnancy or oral contraceptive use, although this has not been widely corroborated.

Pathogenesis

Microvenular hemangiomas have been noted in patients with POEMS syndrome[40], suggesting that these lesions, like glomeruloid hemangiomas, may be of reactive etiology. Observations that some microvenular hemangiomas affecting women present in association with pregnancy or oral contraceptive use arguably suggest a hormonal influence.

Clinical features

Microvenular hemangioma typically presents as a solitary, purple to red, slowly enlarging papule, plaque, or small nodule on the trunk or extremities (rarely the face). Multiple lesions have occasionally been observed. There appears to be a particular predilection for the forearms, and most lesions are <2 cm in diameter[40]. Although the majority are asymptomatic, mild erythema and tenderness have been reported.

Pathology

Histologically, lesions are poorly circumscribed proliferations of small, relatively monomorphous, branching capillaries and venules involving the full thickness of the reticular dermis. Unlike port-wine birthmarks, in which vascular ectasia is prominent, the vascular lumina of this tumor are inconspicuous and often collapsed. Cells lining the vessels show no atypia, are strongly positive for endothelial markers and WT-1, and are associated with SMA-positive pericytes. The vessels are not as delicate or angulated as the lymphatic-like vessels of Kaposi sarcoma or the vessels of microcystic lymphatic malformations, and they often contain red blood cells. The pericytic component is obvious even in routine H&E-stained sections.

Differential diagnosis

The major histologic differential diagnostic consideration for these acquired lesions is patch-stage Kaposi sarcoma. Kaposi sarcoma differs by the presence of delicate lymphatic-like vessels, plasma cells, eosinophilic globules, interstitial fascicles of spindle cells, and positivity for HHV-8.

Treatment

Surgical excision has been effective in reported cases.

Epithelioid Hemangioma

Recommended Synonym: ■ Angiolymphoid hyperplasia with eosinophilia (ALHE) subtype of epithelioid hemangioma

Historical Synonyms: ■ Angiolymphoid hyperplasia with eosinophilia ■ Pseudopyogenic granuloma ■ Inflammatory angiomatous nodule ■ Papular angioplasia ■ Inflammatory arteriovenous hemangioma ■ Intravenous atypical vascular proliferation ■ Nodular angioblastic hyperplasia with eosinophilia and lymphofolliculosis ■ Histiocytoid hemangioma

Key features

- Benign angiomatous nodules or plaques, often multiple and grouped; usually located in the head and neck region, especially around the ears
- May be painful, pruritic, or pulsatile, and often recur after excision
- Characterized histologically by proliferations of capillary-sized vessels with epithelioid endothelial cells surrounding larger, thick-walled vessels, accompanied by eosinophils and lymphocytes
- Associated with arteriovenous shunts and sometimes trauma
- Kimura disease now considered to be a separate clinicopathological entity

Introduction and history

Epithelioid hemangioma was initially described as *angiolymphoid hyperplasia with eosinophilia (ALHE)* in 1969 by Wells and Whimster and subsequently referred to as *histiocytoid hemangioma*. Although originally thought to be a late stage of Kimura disease, it is now generally accepted that these represent two separate entities.

Epidemiology

Epithelioid hemangioma occurs in young to middle-aged adults without sex or ethnic predilection. Previous reports of a female predominance are not supported by more recent series. A history of trauma can be elicited in some patients[70].

Pathogenesis

Both the WHO and the ISSVA classify epithelioid hemangiomas as benign vascular tumors[71,72]. Genetic heterogeneity correlates with morphologic subtypes and locations, supporting the concept that distinct entities exist within the "epithelioid hemangioma" group. Lesions arising within deep soft tissue and bone often demonstrate *FOS* or *FOSB* rearrangements[73,74] while these rearrangements are not observed in cutaneous lesions[74]. The latter display several features that suggest a significant reactive, as opposed to neoplastic, component; for example, there is frequently mural damage to or rupture of large intralesional vessels, suggesting that trauma and/or arteriovenous shunting may play a pathogenic role[70]. In addition, cutaneous epithelioid hemangiomas have been observed in association with pre-existing arteriovenous fistulas and malformations. It is possible that cutaneous epithelioid hemangiomas represent a heterogeneous group of histologically overlapping disorders, some neoplastic and others reactive due to arteriovenous (AV) shunting. There are rare reports of *TEK* (*TIE2*) mutations in epithelioid hemangiomas, but additional studies have not corroborated this finding[75].

Clinical features

Epithelioid hemangiomas typically present as papules or nodules that are tan, brown, pink, or dull red in color and are located predominantly in the head and neck region, especially around the ears and on the forehead and scalp (Fig. 114.16). Less commonly, lesions have been observed in the mouth and on the trunk, distal extremities, vulva, and penis. Most papulonodules are dermal or subcutaneous in location; occasionally, epithelioid hemangiomas involve deeper soft tissues or bone or arise from vessels[4]. Approximately half of the patients with dermal or subcutaneous papulonodules have multiple lesions, generally in a clustered pattern[4]. The skin lesions can be either asymptomatic or painful, pruritic or pulsatile[70]. Some patients have regional lymph node enlargement and peripheral eosinophilia.



Fig. 114.16 Epithelioid hemangioma (angiolymphoid hyperplasia with eosinophilia) – clinical features. Multiple pink papulonodules are often seen on the scalp.

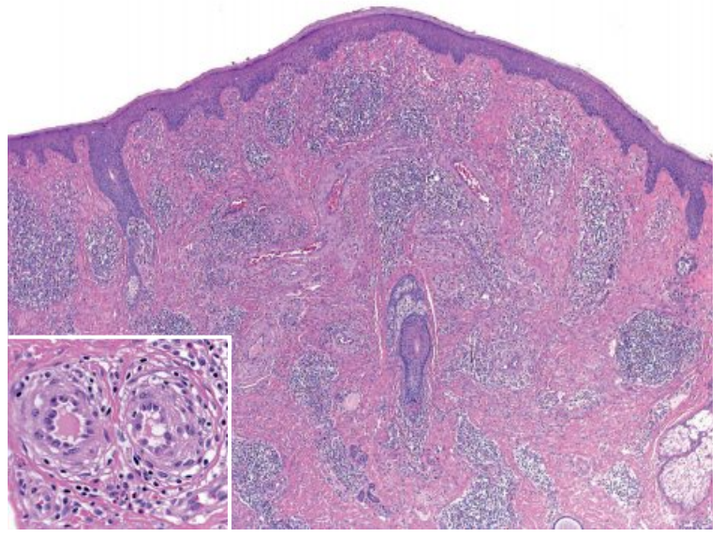


Fig. 114.17 Histology of epithelioid hemangioma (angiolymphoid hyperplasia with eosinophilia) – histopathologic features. Dermal proliferation of vessels accompanied by dense inflammatory infiltrates. Enlarged endothelial cells with cytoplasmic vacuolization protrude into the lumen of the central blood vessels, producing a scalloped or "cobblestone" appearance (inset); note also the infiltrate of lymphocytes and eosinophils surrounding the vessels. *Courtesy Lorenzo Cerroni, MD.*

Pathology

Typical lesions involving the dermis and subcutaneous tissue are of the ALHE subtype and present as well-circumscribed, vaguely lobular proliferations of capillary-sized vessels surrounding larger central blood vessels. There is a variably dense perivascular inflammatory infiltrate rich in lymphocytes and eosinophils (Fig. 114.17). Scattered ectatic lymphatic vessels are variably present. Mast cells and plasma cells are usually also present, and nodular lymphoid aggregates, with or without germinal centers, may be prominent, particularly in subcutaneous lesions. The stroma is fibrous, and the larger vessels have thick walls with prominent myxoid degeneration.

Many of the vessels, particularly the larger ones, are lined by enlarged endothelial cells with cytoplasmic vacuolization that protrude into the lumen, producing a scalloped or "cobblestone" appearance (Fig. 114.17, inset). These epithelioid endothelial cells are responsible for use of the descriptors epithelioid and, previously, histiocytoid. Inflammatory infiltration of medium- to large-sized arteries, with variable luminal occlusion, damage to elastic laminae, and even mural rupture, is common. In older lesions, fibrosis is more prominent, with a reduction in the inflammatory and vascular elements. Over 50% of cases of cutaneous epithelioid hemangioma have strong diffuse immunopositivity for FOSB although they lack molecular rearrangements[76].

Differential diagnosis

Epithelioid hemangioma may resemble cutaneous lymphoid hyperplasia, lymphoma cutis, sarcoidosis, epithelioid hemangioendothelioma, epithelioid angiosarcoma, Kimura disease, and richly vascularized metastatic tumors. Kimura disease is now considered to be a separate entity that is usually located on the posterior neck and histologically has much larger lymphoid follicles.

Treatment

Although rare instances of spontaneous regression have been reported, surgical excision is generally required. About one-third of lesions recur after excision[4], sometimes due to incomplete excision of an underlying nidus of AV shunting, e.g. an AV malformation or AV fistula. Intraoperative bleeding can be problematic. Various lasers (e.g. CO_2, pulsed dye, copper vapor) have been used with variable success. In a small case series, treatment with polidocanol sclerotherapy (for the deep vascular component) plus radiofrequency ablation was reportedly successful[77]. Other reported therapies include intralesional corticosteroids, oral propranolol, and radiation therapy.

Multifocal Lymphangioendotheliomatosis with Thrombocytopenia

Synonym: ■ Congenital cutaneovisceral angiomatosis with thrombocytopenia

Key features

- Cutaneous vascular lesions are typically present at birth, along with visceral involvement and chronic mild to moderate thrombocytopenia
- Numerous, widely distributed, red–brown to burgundy, flat or indurated papules and plaques, often with central pallor
- Gastrointestinal bleeding is common and may be life-threatening
- Distinctive histopathological features that resemble benign lymphangioendothelioma, with variable expression of lymphatic-associated markers

Introduction and history

Initially described in 2004 by North et al.[78], the term *multifocal lymphangioendotheliomatosis with thrombocytopenia* (MLT) reflected its highly characteristic histology, multifocal tissue involvement, consistent expression of the lymphatic-associated marker LYVE-1, and associated thrombocytopenia. Based upon a similar series of cases, the term *congenital cutaneovisceral angiomatosis with thrombocytopenia* (CCAT) was proposed[79]. In the current ISSVA classification, MLT is listed as a "provisionally unclassified vascular anomaly"[72].

Epidemiology

MLT is a sporadic disorder with no known racial or sex predilections. Although lesions are usually apparent at birth, they often slowly enlarge and increase in number over time.

Pathogenesis

It is not yet clear if MLT is best classified as a tumor or malformation. Lesional endothelial cells coexpress CD34 and LYVE-1 and may focally express podoplanin, making blood–vascular versus lymphatic–vascular differentiation ambiguous[80]. As with KHE/tufted angioma, this mixed endothelial phenotype may be linked to the associated selective thrombocytopenia (see below)[45,48,78].

Clinical features

Cutaneous lesions, often numbering in the hundreds at birth, are flat or indurated, red–brown to burgundy papules or plaques (Fig. 114.18A), often with pallor and occasionally scar-like areas centrally. Both a slow progression of pre-existing lesions and the appearance of new lesions is typical, without evidence of regression. Similar lesions in the gastrointestinal tract lead to severe gastrointestinal bleeding and anemia, beginning during infancy. Some patients have extensive pulmonary involvement complicated by hemoptysis; less often, other sites are affected, e.g. muscle, synovium, liver, spleen, kidney, bone[48,79,81]. The thrombocytopenia is chronic but fluctuates and is mild-to-moderate, especially in infants. Serum fibrinogen levels and PT/PTT are essentially normal.

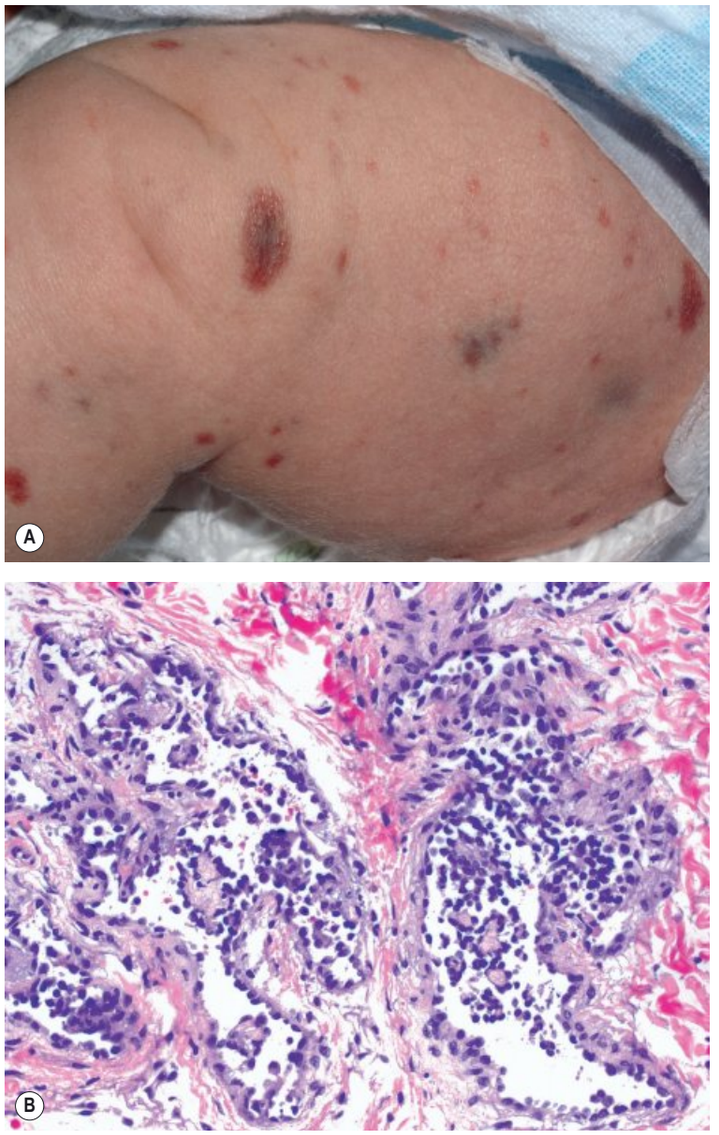


Fig. 114.18 Multifocal lymphangioendotheliomatosis with thrombocytopenia. A Multiple red–brown to red–purple papules and plaques in a widespread distribution. **B** Thin-walled vessels focally form intraluminal papillary projections. When the projections are complex, the endothelium that lines them can appear to float within the vascular lumen. *A, Courtesy Julie V. Schaffer, MD.*

Pathology

Thin-walled vessels are scattered throughout the dermis and subcutis and are lined by a monolayer of slightly hobnailed endothelial cells that focally form papillary projections (Fig. 114.18B). Some of the papillary formations are complex and appear to float within the lumina. However, lumina, especially the smaller ones, are largely devoid of red blood cells. Endothelial cells show strong immunopositivity for CD31, CD34, and LYVE-1, light to absent positivity for podoplanin, and negativity for GLUT1[78]. Mitotic figures are rare or absent, although Ki-67 expression may be increased.

Differential diagnosis

This entity must be differentiated from a "blueberry muffin baby" (see Table 121.4) as well as other disorders with multifocal vascular lesions that present during infancy or childhood, including multifocal infantile hemangiomas, blue rubber bleb nevus syndrome, glomuvenous malformations, and Maffucci syndrome. However, the skin lesions of MLT

are unique in their clinical and histologic appearance and are far more numerous than would be typical for any of these vascular disorders except for multifocal infantile hemangiomas.

Treatment

Gastrointestinal bleeding may spontaneously stabilize or require segmental resection to control. Corticosteroids, sirolimus, everolimus, vincristine, thalidomide, and bevacizumab have been reported to be of possible value in some, but not all, cases[78,79,82–84].

Sinusoidal Hemangioma

Synonyms: ■ Variant sinusoidal hemangioma ■ Sinusoidal venous malformation

Key features

- Relatively rare, small, well-demarcated acquired lesion most commonly seen in the subcutis of middle-aged women and traditionally described as a variant of "cavernous hemangioma" (venous malformation)
- Probably malformative with a delayed presentation, rather than neoplastic or reactive in etiology
- Histologically distinguished by dilated, interconnecting venous channels exhibiting a prominent sieve-like or sinusoidal pattern
- Similar sinusoidal patterns are seen focally in many venous malformations
- May be confused with well-differentiated angiosarcoma, but distinguished from the latter by lack of significant cytologic atypia, infiltrative growth, and endothelial multilayering

Introduction and history

In 1991, sinusoidal hemangioma was described as a distinctive subset of so-called "cavernous hemangioma" (historic term as now recognized to be a venous malformation). In contrast to typical venous malformations of childhood, sinusoidal hemangiomas presented during adulthood and had an unusually prominent sinusoidal or sieve-like histologic pattern. Some authors believe that sinusoidal hemangioma may represent PEH within a pre-existing vascular malformation.

Epidemiology

These adult-onset lesions have most commonly been observed in middle-aged women and are relatively rare. The not uncommon occurrence in breast subcutaneous tissue has emphasized the need to differentiate these lesions from angiosarcoma.

Pathogenesis

Because of the typical presentation during adulthood, a neoplastic or reactive etiology has been suggested. However, the strong histologic parallels with venous malformations of childhood suggest that these mitotically quiescent vascular lesions are probably congenital developmental disorders that become evident later in life due to remodeling, thrombosis, recanalization, and progressive vascular dilation. Focal sinusoidal patterns have also been described in congenital venous malformations.

Clinical features

Sinusoidal hemangiomas, as traditionally defined, are relatively well-demarcated, solitary, deep dermal or subcutaneous papulonodules that are freely mobile. The color varies from red (superficial lesions) to bluish or skin-colored (subcutaneous lesions). They most commonly develop in adult women and favor the arms and torso (including the breast). Longitudinal studies have revealed no evidence of metastasis or of local recurrence following resection.

Pathology

Generally well-defined lobules of dilated, thin-walled veins with scant mural smooth muscle form characteristic interconnected, "emphysematous", sieve-like spaces. Lining endothelial cells are flattened, single-layered, and mitotically inactive. Organizing thrombi are common, with occasional superimposed changes of PEH. There is no significant cytologic atypia. Central infarction and necrosis have been reported.

Differential diagnosis

Given the typical presentation during adulthood and anastomosing vascular pattern, the most clinically significant simulant is well-differentiated angiosarcoma. The latter is distinguished by a more infiltrative pattern, endothelial multilayering, mitotic activity, and cytologic atypia.

Treatment

Complete surgical resection, which is facilitated by its typical obvious demarcation, is curative.

Spindle Cell Hemangioma

Synonym: ■ Spindle cell hemangioendothelioma (not recommended)

Key features

- Blue–red nodules typically develop within the dermal and subcutaneous tissue of the distal extremities of young adults and children and tend to multiply locally
- Occurs in Klippel–Trenaunay syndrome and especially Maffucci syndrome; in the latter setting, the spindle cell hemangiomas often have somatic *IDH1/2* mutations
- Composed of thin-walled cavernous veins containing organizing thrombi, interspersed with fascicles of spindle cells and occasional aggregates of vacuolated epithelioid cells
- Originally interpreted as a low-grade angiosarcoma (*spindle cell hemangioendothelioma*), but now viewed as a benign lesion without metastatic potential (*spindle cell hemangioma*)
- Currently regarded by many as a vascular malformation complicated by thrombosis and irregular vascular collapse

Introduction and history

This entity was first described by Weiss and Enzinger in 1986 as *spindle cell hemangioendothelioma* given its spindle cell morphology and the fact that one case from their series of 26 had metastasized to a regional lymph node. Results of larger studies with extended follow-up have led to the current view that this tumor has no inherent malignant potential[4,85]. In 1996, Perkins and Weiss suggested that it be renamed *spindle cell hemangioma*[85].

Epidemiology

Spindle cell hemangiomas usually occur in children and young adults, although in a series of 78 patients[85], the ages ranged from 8 to 78 years, with a median age of 32 years. However, those presenting during late adulthood appear to represent previously occult, longstanding lesions. There is no sex predilection. These hemangiomas occur in association with varicose veins and various vascular malformations, including in patients with Klippel–Trenaunay syndrome (capillary–venous or capillary–venous–lymphatic malformation)[86] and Maffucci syndrome (venous malformation)[87].

Pathogenesis

In the 2014 ISSVA classification scheme, spindle cell hemangioma is categorized as a benign vascular tumor[72]. Nonetheless, it has long been thought to represent a vascular malformation altered by thrombosis and irregular vascular collapse[4,85]. Its association with vascular malformation syndromes (see above) further supports this hypothesis. Typical development of multiple nodules over time within a given anatomic region suggests intravascular propagation[85].

In patients with Maffucci syndrome, somatic alterations in 2p22.3, 2q24.3, and 14q11.2 have been described[87], and in tumoral tissue, including spindle cell hemangiomas and endochondromas, heterozygous

somatic mutations in *IDH1* (rarely *IDH2*) were detected in 10 of 13 patients[88]. The latter encode NADP(+)-dependent isocitrate dehydrogenases and mutations can lead to epigenetic modifications (see Ch. 54)[87,89]. *IDH1/2* mutations have also been reported in sporadic spindle cell hemangiomas (in the absence of Maffucci syndrome), suggesting that these mutations are specifically linked to the vascular lesion rather than Maffucci syndrome[90].

Clinical features

Most spindle cell hemangiomas begin as a solitary, firm, red–blue nodule in the subcutaneous tissue and dermis of the distal upper or lower extremity, then slowly develop multifocally within a localized area (Fig. 114.19). Rarely there is involvement of skeletal muscle and occasionally tumors develop on the trunk, head and neck, or proximal limbs. They may be asymptomatic or painful, and ~60% recur following resection[85].

Pathology

Hemorrhagic, often multiple, nodules are seen within the dermis and subcutaneous tissue and are composed of two basic histologic elements (in variable combinations): (1) thin-walled, cavernous spaces containing organizing thrombi; and (2) more cellular areas containing spindle cells and occasional aggregates of vacuolated epithelioid cells (Fig. 114.20). The spindled areas stain focally for actin, form slit-like vascular spaces, and appear to consist of fibroblastic cells, pericytes, and collapsed vessels[4]. The epithelioid interstitial cells, as well as the flattened cells lining the cavernous spaces, stain positively for endothelial markers[86]. Cavernous vessels may show foci of intravascular PEH and phleboliths consistent with the presence of organizing thrombus material. Frequently, remnants of residual vascular walls rim the lesion, suggesting intravascular development.



Fig. 114.19 Spindle cell hemangioma – clinical features. Clustered blue–red multifocal nodules are typical.

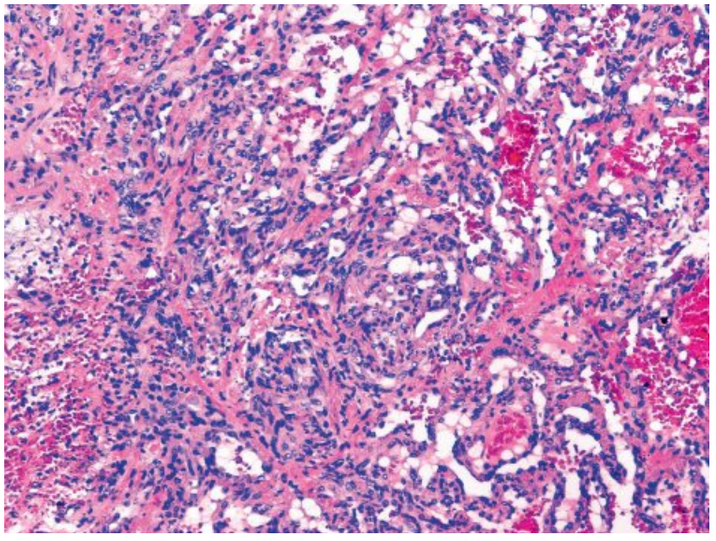


Fig. 114.20 Spindle cell hemangioma – histopathologic features. Partly dilated, partly collapsed vessels lined by spindled and epithelioid cells.

Differential diagnosis

These tumors may resemble nodular lesions of Kaposi sarcoma, but the latter lack cavernous vascular spaces and vacuolated epithelioid endothelial cells and are positive for HHV-8. The frequent presence of foci of secondary intravascular PEH within a spindle cell hemangioma may lead to misdiagnosis. A primary lesion of intravascular PEH is solitary and lacks epithelioid endothelial cells (see above).

Treatment

Based upon the large series of Perkins and Weiss[85], simple surgical excision is successful in some patients (~40%). The frequent local recurrences may reflect the inherent multifocality, with growth within vessels leading to discontinuous locoregional sites[85]. There is one report of the successful use of intralesional and intra-arterial IL-2, with no signs of recurrence at 24 months[91].

BORDERLINE AND LOW-GRADE MALIGNANT VASCULAR NEOPLASMS

Kaposiform Hemangioendothelioma

Synonyms: ■ Infantile kaposiform hemangioendothelioma ■ Kaposi-like infantile hemangioendothelioma

Key features

- Rare infiltrative tumor of infancy and childhood that crosses tissue planes and can involve the skin, subcutis, and deeper soft tissues
- Depending upon level of involvement, presents as an ill-defined, often indurated, violaceous stain, plaque, or bulging mass; may wax and wane but does not spontaneously involute
- Locally aggressive and occasionally multifocal along lymphatic pathways, but thought not to truly metastasize
- Overlapping histologic features (e.g. expression of mixed blood vascular and lymphatic endothelial markers) and likely synonymous in pathogenesis with tufted angioma, with the latter designation traditionally ascribed to more superficial lesions
- Complete surgical excision is recommended where feasible
- In some patients is associated with Kasabach–Merritt phenomenon (syndrome), requiring treatment with sirolimus or vincristine plus prednisone

Introduction and history

Kaposiform hemangioendothelioma (KHE) was described as such by Zukerberg et al.[49] in 1993, although equivalent lesions had been previously reported as "hemangioma with Kaposi's sarcoma-like features"[92] and "Kaposi-like infantile hemangioendothelioma". Many lesions of this type were previously misdiagnosed as infantile hemangioma.

Epidemiology

Most tumors present in children <2 years of age, and some are congenital. In one literature review of patients with skin involvement[93], the average age at presentation was 43 months. Tumors that are bulky and congenital are most likely to be associated with Kasabach–Merritt phenomenon (KMP), with KMP said to only develop in those patients with congenital/early infantile lesions. Patients with more deeply seated tumors, particularly in the retroperitoneum, are also at increased risk for KMP[93]. Occasionally KHE has been described in adults, all to date without evidence of KMP[94]. There is no sex predilection.

Pathogenesis

KMP was originally defined as life-threatening thrombocytopenic purpura occurring in the setting of an enlarging "hemangioma".

Decades later, with improved categorization of vascular tumors and malformations, it became clear that KMP develops in association with tufted angioma and KHE[45,49] – not the common infantile hemangioma. Rarely, KMP occurs in patients with a congenital fibrosarcoma or congenital hemangiopericytoma.

In KMP, there is profound sustained thrombocytopenia, sometimes accompanied by microangiopathic hemolytic anemia and secondary consumption of fibrinogen and coagulation factors (see Ch. 22). It differs from the localized chronic consumptive coagulopathy that may complicate large venous or venous–lymphatic malformations in which platelet counts are normal or only slightly decreased, but D-dimers are elevated and in more severe cases, fibrinogen levels are low.

As noted previously, KHE and tufted angioma, given their striking overlap histologically and mutual association with KMP, are widely thought to be, at a minimum, closely related and are likely biologically synonymous[45,49,50,92,95,96]. Molecular studies provide a degree of support for this concept, although further investigation is clearly warranted. For example, when 5 KHEs and 2 tufted angiomas were compared to a variety of vascular malformations (n=14) via next generation sequencing and genome-wide methylation analysis, a similar methylation cluster pattern was present in KHEs and tufted angiomas, indicating that they are epigenetically related and distinct from the vascular malformation cluster; an *NRAS* mutation was also found in one tufted angioma and a *RAD50* mutation in one KHE[51]. Of note, no *GNA14* mutations, which are present in benign vascular lesions such as cherry hemangiomas, were detected[51]. This is in contrast to a second study in which *GNA14* mutations were observed in 3 cases of KHE/tufted angioma[97]. Thus, to date there is no consistent mutational pattern in these tumors as *PIK3CA* mutations have also been described in single case reports.

Platelet trapping within the vascular beds of these lesions is thought to play a role in the selective thrombocytopenia of KMP. The strong endothelial expression of Prox1, LYVE-1, and focally podoplanin (all lymphatic-associated antigens) as well as for the blood vascular marker CD34 supports the concept that these tumors have a mixed, partially lymphatic endothelial phenotype. This mixed endothelial phenotype may explain the propensity for platelet trapping as podoplanin is the natural ligand of CLEC-2, a platelet-bound receptor[98].

The paradoxical worsening of KMP observed in some patients following platelet transfusions suggests that platelet activation within the tumor may stimulate vascular proliferation[45], presumably by release of platelet-associated angiogenic agonists. In theory, a self-sustaining cycle of platelet trapping and tumor growth may exist.

Clinical features

KHE usually involves the skin, subcutis, and deeper soft tissues (Fig. 114.21). Cutaneous and subcutaneous forms present as locally infiltrative vascular stains or plaques that can develop nodules. Deeper soft tissue lesions can appear as bulging, indurated masses or may be undetectable on physical examination. KHE occasionally presents as a bulky body cavity or retroperitoneal mass and rarely with bony or splenic involvement. Patients with KMP often have purpura and ecchymoses.

Due to rare reports of spread along (or perhaps multifocal involvement of) local lymphatic chains, KHE is categorized as an "intermediate (locally aggressive)" soft tissue tumor by the WHO[71]. To date, no true distant metastases have been reported, although to date one patient did have spread to regional lymph nodes[99].

The two most common causes of death from KHE are complications of thrombocytopenia and direct tumor infiltration[93]. Clinical evaluation of suspected cases, for instance new-onset vascular tumors in children >3 months of age[93], should include magnetic resonance imaging (MRI), a complete blood cell count, coagulation studies to detect coexistent KMP, and, if not prohibited by severe thrombocytopenia, biopsy for histopathologic diagnosis. By MRI, KHE is usually diffusely enhancing and T2 hyperintense, with ill-defined margins that cross tissue planes.

Following treatment of KMP, residual KHE has been subclassified into: type I – resembles a port-wine birthmark and may overlie fibrotic infiltration; type II – minor soft tissue swelling and telangiectasias; and type III – sclerotic or infiltrative, depending upon depth.

Pathology

KHE is characterized by ill-defined, frequently coalescing nodules composed of fascicles of moderately plump spindled endothelial cells with eosinophilic to clear cytoplasm and bland nuclei that form elongated, slit-like lumina containing erythrocytes, reminiscent of Kaposi sarcoma (Fig. 114.22A). The spindle cells often encompass nests of more epithelioid endothelial cells and pericytes that are surrounding platelet-rich microthrombi (which can be highlighted by CD61 immunostaining). At the margin of the lesion, the spindle cells may infiltrate into the surrounding adipose tissue and between collagen bundles, or they may be encased by desmoplastic stroma. The spindle cells are strongly immunoreactive for the pan-endothelial marker CD31, the blood vascular marker CD34, and the lymphatic endothelial markers podoplanin (Fig. 114.22B), LYVE-1, VEGFR-3, and Prox1[50].

Mitotic activity is variable, but generally low. Focally, lobules of small, rounded capillaries lined by flat endothelia merge with the spindled areas. Extravasated erythrocytes and hemosiderin granules are typically present, and tumor cells may contain intracytoplasmic erythrocyte fragments and hyaline globules. Often there is a prominent component of dilated vessels with a lymphatic morphology that intermingles with the tumor lobules, but these vessels are often most obvious within the marginal soft tissues. Residual KHE, i.e. remaining after successful medical treatment, represents a dormant, often sclerotic, version of the original disease process.



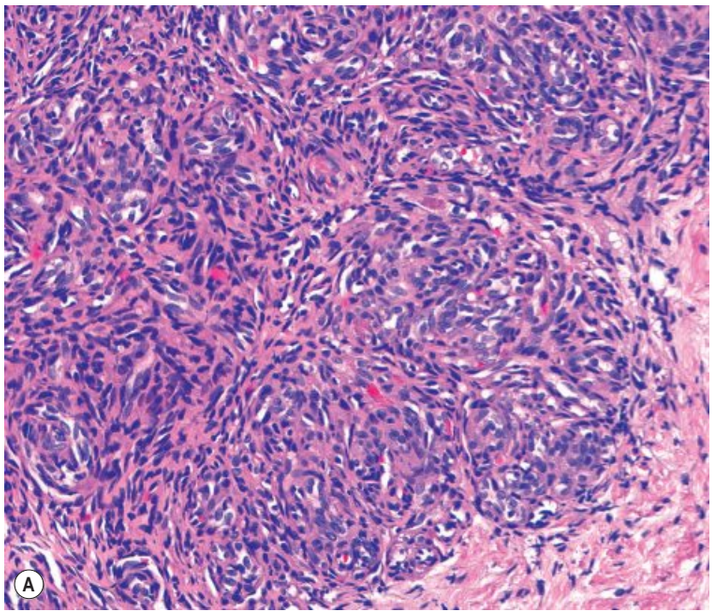
Fig. 114.21 Kaposiform hemangioendothelioma complicated by Kasabach–Merritt phenomenon in a 5-week-old boy. Progressive induration and ecchymosis developed rapidly over a 24-hour period. An eczematous eruption is also evident. *Courtesy Julie V. Schaffer, MD.*

Differential diagnosis

In addition to tufted angioma, the differential diagnosis includes infantile hemangioma, congenital hemangiomas (e.g. rapidly involuting [RICH], non-involuting [NICH]), and Kaposi sarcoma. Infantile hemangiomas, unlike KHE, express an unusual and complex endothelial phenotype shared only by placental capillaries, most commonly manifested by immunohistochemical staining for GLUT1[26,27]. Infantile hemangiomas also lack both fascicles of spindle cells and foci with a mixed lymphatic–blood vascular phenotype. Tufted angioma is thought to be a milder, more superficial form of KHE that is distinguished by a relative scarcity of endothelial spindling and an absence of pericyte-rich epithelioid nodules. Kaposi sarcoma, which is rare in children (outside of Africa), lacks the lobularity of KHE, characteristically contains plasma cell infiltrates, and is positive for HHV-8.

Treatment

Tufted angiomas and KHEs that are localized and superficial can be cured by wide local excision. However, tumors in deeper soft tissues, the mediastinum, or retroperitoneum are often large and unresectable. As with tufted angioma, first-line therapy for associated KMP consists of sirolimus[60,61] or vincristine[62] plus prednisone. Treatment of small lesions without KMP is controversial.



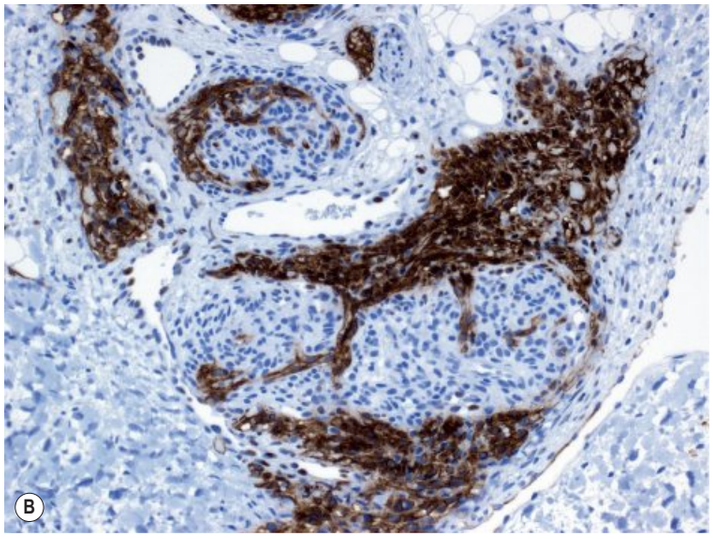


Fig. 114.22 Histology of kaposiform hemangioendothelioma. A Fascicles of spindled endothelial cells forming slit-like lumina surround nests of more epithelioid areas rich in pericytes. **B** The endothelial cells show evidence of lymphatic differentiation, here evidenced by positivity for podoplanin.

Papillary Intralymphatic Angioendothelioma (PILA)

Synonyms: ■ Dabska-type hemangioendothelioma ■ Dabska tumor ■ Endovascular papillary angioendothelioma ■ Malignant endovascular papillary angioendothelioma ■ Hobnail hemangioendothelioma

Key features

- Rare neoplasm with at least partial lymphatic differentiation and very low metastatic potential that occurs primarily in children
- Enlarging dermal or subcutaneous mass or plaque, often on distal extremities
- Histologically defined by prominent papillary intralymphatic growth and peculiar rosette-like clusters of hobnail, columnar endothelial cells

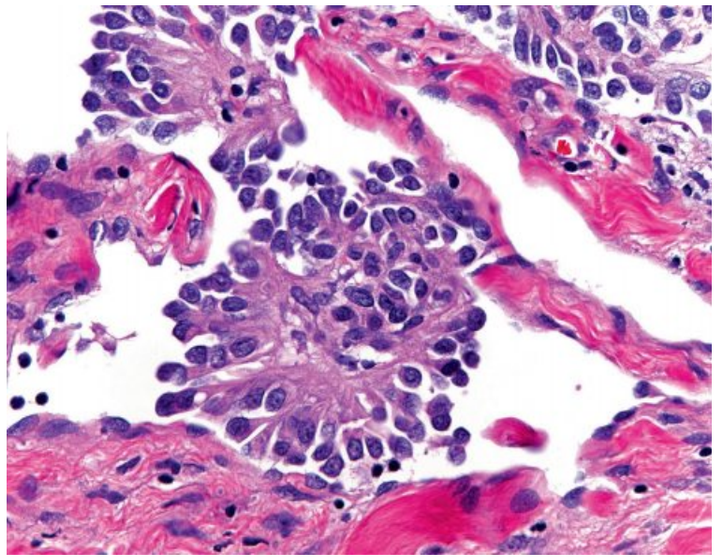


Fig. 114.23 Histology of papillary intralymphatic lymphangioendothelioma (PILA). Rosette-like intravascular clusters of hobnailed, columnar endothelial cells.

Introduction and history

Maria Dabska first described tumors of this type as *malignant endovascular papillary angioendothelioma* in 1969 based on a series of six cases, all in children. Two patients in this original series had lymph node metastases, and one of them later developed distant metastases and died. Subsequently reported cases have behaved in a benign fashion, although follow-up for some has been limited[100]. Based on the prominent presence of lymphatic vessels, the tentative potential for malignant or borderline clinical behavior, and the defining presence of papillary intravascular proliferation, the currently favored designation for this tumor is *papillary intralymphatic angioendothelioma* (PILA)[100]; this term has also been adopted by the WHO[71]. Because of their shared hobnail endothelial morphology and similar biologic behavior, Weiss and Goldblum[4] have suggested that the term *hobnail hemangioendothelioma* be used to embrace both PILA and retiform hemangioendothelioma. However, the lack of convincing evidence of lymphatic differentiation in the latter has seriously undermined any potential relatedness of these two entities[101].

Epidemiology

Compilations of reported cases have shown no clear sex predilection, with ~75% of patients being children and the remainder primarily young adults. Tumors may be present at birth. A more recent series of 12 patients in which the mean age was 30 years suggests a wider age range[100].

Clinical features

These tumors most commonly originate within the soft tissues of an extremity and rarely other sites such as bone or spleen. Lesions can present as either enlarging, diffuse, firm swellings of skin and subcutaneous tissue or as soft intradermal plaques; sometimes there is also a pink or blue discoloration of the skin. The size range is wide (up to 40 cm)[100]. A number of cases appear to have arisen within pre-existing lymphatic malformations.

The WHO currently classifies PILA as an intermediate (rarely metastasizing) vascular tumor[71], and in the 2014 ISSVA classification scheme[72] it is considered a locally aggressive or borderline tumor.

Pathology

The unifying microscopic feature is presence within the dermis and/or subcutis of intercommunicating, thin-walled vessels lined by hobnail endothelial cells, with the latter forming characteristic intraluminal papillary projections that focally assume a rosetting or matchstick-like pattern (Fig. 114.23). Lesional vessels are variable in size. Hyaline papillary stromal cores stain positively for collagen type IV, and, in some cases, focal actin-positive pericytes may be present within the papillary projections[100]. Lymphocytes may cluster along the endothelial lining of

the vessels and infiltrate into the surrounding stroma; large lymphoid aggregates are common. There is strong endothelial immunopositivity for VEGFR-3 and podoplanin in the hobnail endothelial proliferations of these tumors[102], indicative of lymphatic differentiation. CD34 expression is low.

Differential diagnosis

PILA must be differentiated histologically from other entities with hobnail endothelial architecture, including targetoid hemosiderotic lymphatic malformation, hemangioma with dabskoid features, retiform hemangioendothelioma, and well-differentiated angiosarcoma. Targetoid hemosiderotic lymphatic malformation is a smaller, more superficial dermal process, without exuberant papillary tufts. Retiform hemangioendothelioma usually occurs in adults and intravascular papillary tufts are infrequent and poorly developed. Of note, regional lymph node disease has been documented in both PILA and retiform hemangioendothelioma. Angiosarcoma, even when well differentiated, may display intravascular papillary growths that suggest PILA, but classic hobnail endothelial cells are absent. In children, angiosarcomas are extremely uncommon and are usually visceral (especially cardiac or pericardial).

Treatment

Optimal therapy is relatively conservative surgical excision with clear margins, supplemented by close follow-up. Local recurrences following excision are common (~40%).

Retiform Hemangioendothelioma (RHE) and Composite Hemangioendothelioma (CHE)

Synonym: ■ Hobnail hemangioendothelioma for RHE (no longer recommended)

Key features

- Rare neoplasms with very low metastatic potential and a wide age range that favor young adults
- Present as a slowly growing exophytic tumor or multinodular plaque that is often on the distal extremity
- A morphologic spectrum characterized in RHE by a diffuse infiltration of the dermis and/or subcutis by elongated vessels with hobnail endothelial cells arborizing in a pattern resembling normal rete testis that in CHE is admixed with other vascular patterns
- Rearrangements of *YAP1* are common, in particular *YAP1–MAML2* fusions
- Local recurrence following excision occurs in ~60% of cases but regional lymph node spread is rare; a neuroendocrine variant of CHE is more aggressive

Introduction and history

RHE was first described as an entity in 1994 by Calonje et al.[16] based on a series of 15 cases and was interpreted as a low-grade angiosarcoma. RHE is currently classified by the WHO and ISSVA as a vascular tumor of intermediate (rarely metastasizing) type[71] and a locally aggressive or borderline vascular tumor[72], respectively. Very rarely, there is a complex admixture of the features of RHE with a variety of other distinct vascular patterns, especially epithelioid changes reminiscent of epithelioid hemangioendothelioma, resulting in CHE[103,104].

Epidemiology

RHE and CHE occur most commonly in young adults, although the age range is wide. There is no clear sex predilection.

Pathogenesis

As noted in the previous section, use of the term *hobnail hemangioendothelioma* (not to be confused with hobnail "hemangioma") to encompass both PILA and RHE has been proposed[4]. However, increasingly convincing evidence that RHE endothelial cells, unlike those of PILA, usually do not express lymphatic markers has weakened this proposal. In an RHE from an apparently immunocompetent patient, HHV-8 sequences were detected[105].

More recently, 5/13 (38%) of RHEs and 3/11 (27%) of CHEs arising within soft tissue were found to have rearrangements of *YAP1*, with five (including all three CHEs) having a *YAP1–MAML2* fusion. Such findings support the inclusion of RHE and CHE within a morphologic spectrum[106]. Additional reported gene fusions in neuroendocrine CHEs are *PTBP1–MAML2* and *EPC1–PCH2*[106,107].

Clinical features

The clinical appearance of both RHE and CHE is not specific and the vascular nature may not be suspected clinically. RHE typically presents as a solitary, slow-growing, reddish blue plaque, exophytic mass or dermal/subcutaneous nodule, most commonly on the extremities. Most CHEs also appear on the distal extremities, typically appearing as a nodular mass or ill-defined swelling. Rarely, these tumors occur in viscera.

In the original series of RHEs, nearly 60% recurred locally, and 1 of 14 patients followed longitudinally developed lymph node involvement[16]. To date, there have been no RHE-related deaths. Following surgical excisions, there may be multiple recurrences of CHEs, with the potential for lymph node metastasis. Those CHEs that contain angiosarcoma-like areas are much less aggressive than conventional angiosarcomas[104] while a "neuroendocrine" variant of CHE that coexpresses synaptophysin and endothelial markers is more clinically aggressive with distant metastases in 50% of cases[107].

Pathology

RHE is one of a small group of vascular anomalies characterized by endothelial cells with a so-called hobnail appearance; this group also includes targetoid hemosiderotic lymphatic malformation and PILA. Overall, there is a diffuse infiltration of the reticular dermis and/or subcutis by an arborizing network of elongated, thin-walled vessels forming a pattern reminiscent of normal rete testis. The margins are ill-defined. Higher magnification of the lesional vessels reveals a lining of bland endothelial cells with prominent apical nuclei that protrude into the lumina in a hobnail or "matchstick" fashion. Mitotic figures are rare, and cytologic atypia is minimal, or rarely, mild. Solid foci of spindle cells expressing endothelial markers are often present, as are occasional intravascular papillae. Unless the tumor arises within the background of a vascular malformation, cavernous lymphatic-like vessels are absent as are the prominent intravascular proliferations characteristic of PILA. The endothelial cells of RHE consistently express pan-endothelial markers such as CD31 and ERG, but usually do not express lymphatic markers such as podoplanin, VEGFR3, and Prox1[101].

CHEs are infiltrative tumors that by definition must be composed of at least two morphologically distinct vascular tumor patterns, most commonly resembling RHE and epithelioid hemangioendothelioma, but occasionally resembling spindle cell hemangioma, angiosarcoma, or vascular/lymphatic malformations[103]. CHEs consistently express CD31 and ERG and variably express podoplanin[103]. The more aggressive "neuroendocrine" variant contains, in addition to RHE-like areas, a strikingly nested pattern of epithelioid-to-slightly spindled endothelial cells plus solid sheets of epithelioid endothelial cells unaccompanied by the myxochondroid to hyalinized matrix characteristic of epithelioid hemangioendothelioma and epithelioid hemangioma[107].

Differential diagnosis

Important entities to exclude are epithelioid hemangioendothelioma and low-grade angiosarcoma. The former is distinguished by epithelioid endothelial cells with glassy cytoplasm embedded in a myxochondroid matrix. Well-differentiated angiosarcomas are distinguished by subtle cytologic atypia, multilayered endothelial cells, mildly increased mitotic activity, and lack of hobnail endothelial cells.

Treatment

Wide excisional biopsy with follow-up is appropriate. However, local recurrence is common.

Pseudomyogenic Hemangioendothelioma

Key features

- Rare neoplasm with intermediate biologic potential and male predominance that favors young adults and the lower extremities
- Solitary, or more commonly multiple, nodules that cross tissue planes – usually the skin, often skeletal muscle, and less often bone
- Infiltrative sheets and fascicles of loosely arranged spindled to polygonal cells with abundant eosinophilic cytoplasm resembling a myoid tumor or epithelioid sarcoma
- Immunohistochemical staining: ERG$^+$; AE1/AE3$^+$; CD31$^+$ (less consistently); FOSB$^+$ (diffuse nuclear); CD34$^-$; podoplanin$^-$, LYVE-1$^-$, Prox1$^-$; desmin$^-$; S100$^-$; EMA$^-$
- Associated with *SERPINEE1–FOSB* fusions or, more commonly in solitary lesions, with *ACTB–FOSB* fusions; both lead to upregulation of FOSB expression

Introduction and epidemiology

Pseudomyogenic hemangioendothelioma (PMHE) was first included as an entity in the 2013 WHO Classification of Soft Tissue and Bone and was classified as a tumor of intermediate biologic potential. The age range is wide, but most commonly diagnosed in the second to fifth decades. There is a male predominance.

Pathogenesis

Two gene fusions – *SERPINEE1–FOSB* and *ACTB–FOSB* – have been identified in PMHEs. Both result in upregulation of FOSB expression[108,109]. The FOS family of proteins (e.g. FOS, FOSB) dimerize with JUN proteins to form the AP-1 transcriptional factor complex that has been implicated in the genesis of multiple tumor types.

Clinical features

Most patients present with subcutaneous nodules, often multiple, that involve the skin and skeletal muscle. The lesions tend to cross tissue planes and favor the distal lower extremities. They may resemble dermatofibromas, nodular fasciitis, or a vascular neoplasm[110]. While solitary lesions are more likely to have *ACTB–FOSB* fusions rather than *SERPINE1–FOSB* fusions, genetic variants appear similar clinically[108,111]. Local recurrence following resection occurs in ~60% of patients but lymph node and distant metastases are uncommon[111].

Pathology

The architecture of dermal PMHE ranges from loosely fascicular to focally plexiform or storiform, with infiltrative borders. There are sheets, nests, and short intersecting fascicles of plump spindled cells with ample eosinophilic cytoplasm and vesicular nuclei with prominent nucleoli within the mid and deep reticular dermis, often with extension along connective tissue septa into the subcutis[110]. Focally, clusters of more epithelioid, rounded cells with slightly atypical vesicular nuclei and rhabdomyoblast-like appearance may be present. The epidermis can be normal or hyperplastic. There is consistent coexpression of endothelial markers and cytokeratins, including expression by most tumor cells of CD31, ERG, FLI-1, and cytokeratin AE1/AE3[110]. In nearly all cases, there is diffuse nuclear FOSB expression.

Differential diagnosis

The histologic differential diagnosis of PMHE includes epithelioid sarcoma, epithelioid hemangioendothelioma, and epithelioid angiosarcoma[110]. Unlike PMHE, epithelioid sarcoma shows moderate cytologic atypia and is EMA$^+$, CD34$^+$, INI-1$^-$, and CD31$^-$. Epithelioid hemangioendothelioma has epithelioid cells with prominent cytoplasmic vacuolization, myxohyaline stroma, CD34 positivity, and characteristic *WWTR1–CAMTA1* fusions. Epithelioid angiosarcoma has marked cytologic atypia, frequent mitotic figures, and positivity for CD34. Diffuse nuclear FOSB immunostaining points to the diagnosis of PMHE[111].

Treatment

Treatment options include simple surgical excision, amputation (multifocal disease), chemotherapy[112], and radiotherapy. Partial responses to everolimus[113] and sirolimus[114] have been reported.

Kaposi Sarcoma

Key features

- It is controversial whether Kaposi sarcoma (KS) represents neoplasia or hyperplasia; all clinical variants are viewed as a virally induced disease, with HHV-8 the causative agent
- A multifocal systemic disease with four principal clinical variants: (1) chronic or classic KS; (2) African endemic KS, including a fulminant lymphadenopathic type; (3) KS due to iatrogenic immunosuppression; and (4) AIDS-related epidemic KS
- Cutaneous lesions can vary from pink patches to dark violet plaques, nodules, or polyps, depending on clinical variant and stage
- The histologic features of KS do not vary significantly between clinical subtypes, but do vary with stage of the lesion
- Most cases in children, with or without HIV infection, are of the lymphadenopathic type and are rapidly fatal due to visceral dissemination
- Because of multifocality, treatment with chemotherapy and/or radiation is favored over surgery

Introduction and history

In 1872 Moritz Kaposi described five men with an unusual multifocal sarcoma of the skin which he termed "idiopathic multiple pigmented sarcoma of the skin". This disease entity became known as *Kaposi sarcoma* and historically has been considered a chronic, protracted disease primarily affecting elderly men, generally Jewish (Ashkenazi) or of Mediterranean/Eastern European descent. Despite occasional reports regarding its occurrence in organ transplant recipients and its endemic form in Africa, KS received little attention until it became epidemic among men who have sex with men and was recognized as a sign of acquired immunodeficiency syndrome (AIDS). A new human herpesvirus (HHV-8), also referred to as KS-associated herpesvirus, was recognized as the probable inductive agent of all clinical variants of KS. The mechanisms that control the clinical variability of KS are likely to involve a number of interrelated factors modulated by the patient's immune status and have yet to be fully defined.

Epidemiology

The epidemiologic aspects of the four major types of Kaposi sarcoma are outlined in Table 114.3.

Pathogenesis

Immunohistochemical and ultrastructural studies have firmly established the endothelial nature of KS, but it remains controversial whether this endothelial phenotype is vascular, lymphatic, or perhaps a composite of both. Moreover, many, if not most cells forming the substance of a plaque or nodule of KS are spindled cells distinctly unlike normal endothelial cells in morphology, although expressing pan-endothelial markers like CD31. These spindled cells also coexpress markers of blood vascular differentiation (CD34) and lymphatic differentiation (VEGFR-3[102,115], podoplanin[116], LYVE-1[117]). A seminal discovery was that, *in vitro*, Kaposi sarcoma herpesvirus (taxonomical name HHV-8) can infect both lymphatic and blood vascular endothelial cells and induce transcriptional reprogramming, leading to expression of lymphangiogenic molecules in infected blood vascular endothelial cells[118] and a more blood vascular profile in infected lymphatic endothelial cells[119]. This potentially explains the mixed lymphatic/blood vascular phenotype of KS, but also emphasizes the difficulty in precisely assigning endothelial cell derivation based solely on marker studies[120].

HHV-8 can also induce aberrant expression of mesenchymal markers in endothelial cells (endothelial-to-mesenchymal transition) via Notch-dependent signaling[121]. This may provide an explanation for why poorly differentiated KS endothelial cells express mesenchymal and macrophage as well as endothelial markers[122]. Of note, there is also evidence that HHV-8 may cause a mesenchymal-to-endothelial transition, transforming mesenchymal stem cells into KS endothelial cells[123]. The relative contributions of these transitions in cellular differentiation to the pathogenesis of KS remain unclear.

EPIDEMIOLOGIC ASPECTS OF THE FOUR MAJOR TYPES OF KAPOSI SARCOMA
Classic
• Predominantly in individuals of Jewish (Ashkenazi) descent and/or of Mediterranean/Eastern European descent • Male : female (M : F) ratio varies from 15 : 1 (older literature) to 3 : 1 or 1 : 1 (more recent observations) • Two-thirds of patients develop disease after the age of 50 years
African endemic
• Incidence amongst Black Africans ranges from 1% to 10%, with a clear male predominance • Accounts for up to 9% of all reported cancers in equatorial Africa • The lymphadenopathic variant affects primarily children, with a M : F ratio of approx. 1 : 1
Due to iatrogenic immunosuppression
• Individuals are immunosuppressed secondary to systemic medications, e.g. calcineurin inhibitors, prednisone, cytotoxic agents, JAK inhibitors • Cyclosporine is associated with a higher incidence and more rapid onset of disease • Lesions can regress following cessation of immunosuppressive therapy • Estimated incidences of post-transplantation KS in Western countries and the Near East are <1% and 4%, respectively • Men are slightly more often affected than women
AIDS-related epidemic
• Occurs primarily in men who have sex with men • To a lesser degree, seen in female partners of affected men and in women from certain regions of Africa and the Caribbean who became HIV-infected via heterosexual contact • Up to 40% of men who have sex with men with AIDS can develop KS, compared with <5% in other risk groups and 4% in children • Can flare in the setting of immune reconstitution inflammatory syndrome • Occasionally develops in HIV-infected patients receiving chronic antiretroviral therapy, perhaps due to immunosenescence

Table 114.3 Epidemiologic aspects of the four major types of Kaposi sarcoma (KS). A fifth type has been proposed – nonepidemic KS in HIV-seronegative men who have sex with men. *Adapted from Dispenzieri A. Blood Rev 2007;21:285–99.*



Fig. 114.24 Classic Kaposi sarcoma. Red macules and patches on the plantar surface of the foot, with violaceous plaques on the ankle.



Fig. 114.25 Kaposi sarcoma in a patient with AIDS. Multiple violet to violet–brown plaques that are usually more widely distributed than in classic KS. On the uppermost trunk, there are several oval lesions whose long axes are parallel to skin tension lines. *Courtesy Luis Requena, MD.*

It also remains unclear whether KS is essentially hyperplastic or neoplastic in nature, or both. While some studies employing X-chromosome inactivation (methylation) patterns have supported singular, presumably disseminated, clones[124], others utilizing the same methodology in examining sets of multiple lesions from single patients have found either oligoclonal composition within a given lesion or dissimilar, presumably independently developing, clones[125]. Despite these lingering uncertainties about both endothelial phenotype transitions and clonality, it is noteworthy how much compelling molecular, clinical, and epidemiological evidence has accumulated to confirm that infection with HHV-8 causes, or at least strongly influences, the development of KS[126]. This virus is known to be present in most patients with all clinical types of KS, and seroreactivity to HHV-8 is not present to a significant degree in the normal population. The HHV-8 genome, when detected in the blood of HIV-positive men, strongly predicts their subsequent development of KS.

HHV-8 contains homologs of cellular genes that can stimulate cell proliferation, inflammation, and angiogenesis and perhaps inhibit apoptosis[127]. *In vitro*, HHV-8 enhances the proliferation of primary endothelial cells or extends their life span, while not producing complete oncogenic transformation[128]. The host immune response and cytokines (particularly fibroblast growth factor) released by the virally infected cells may further support tumor growth in an autocrine and paracrine manner[129–131]. The role of inflammation in KS is supported by the observation that in patients with AIDS, pre-existing KS can get worse, at least transiently, in the setting of the immune reconstitution inflammatory syndrome (IRIS; see Ch. 78)[132].

Clinical features

Classic KS typically presents as slowly growing, pink to red–violet macules on the distal lower extremities that may coalesce to form large plaques (Fig. 114.24), or develop into nodules or polypoid tumors. Initially unilateral lesions progress to a more widely disseminated multifocal pattern. Early lesions may regress, while others evolve, leading to lesions in different stages at the same time. Patients with longstanding KS may have lesions in the mouth and gastrointestinal tract that are usually asymptomatic as well as lymphedema.

African endemic KS can be classified into four subgroups: nodular, florid, infiltrative, and lymphadenopathic. The nodular variant resembles classic KS in course and appearance, whereas the florid and infiltrative types are more biologically aggressive. The lymphadenopathic type is notably different in several regards: it predominantly affects children, the primary tumors involve the lymph nodes (although skin and mucosal lesions may also be present), and its course is fulminant and fatal.

KS due to iatrogenic immunosuppression (transplantation-associated KS) is generally clinically similar to classic KS. It may resolve completely upon removal of immunosuppressive therapy. KS associated with prolonged high-dose immunosuppression may behave in a more aggressive fashion, causing death in patients who develop internal involvement.

AIDS-related epidemic KS most commonly affects HIV-infected patients with advanced immune impairment and $CD4^+$ T cell counts of <500 cells/cubic millimeter[133]. Clinical features of KS in the HIV-infected patient are protean. While some patients experience only a single lesion, others have disseminated cutaneous disease. Individual lesions range from faint erythematous macules, papules, and plaques to purple–black tumors and nodules. Macules and plaques are frequently oval to lanceolate and may array along lines of cleavage of the skin (Fig. 114.25). Coalescing papules and plaques occasionally form extensive armor-like constricting plaques that may impair the function of extremities and cause lymphedema.

While any skin surface may be involved, the trunk and midface (particularly the nose) are common sites, causing significant cosmetic disfigurement (see Ch. 78). Bluish to violaceous macules, plaques, and tumors can arise intraorally. Plaques and tumors at any site may

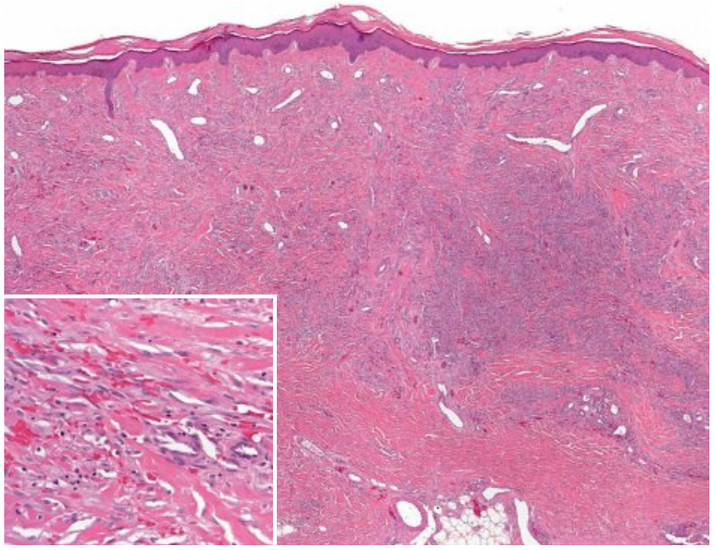


Fig. 114.26 Histology of Kaposi sarcoma – plaque stage. In the reticular dermis, there is a spindle cell vascular proliferation characterized by slit-like vascular spaces with extravasated erythrocytes (inset). *Courtesy Lorenzo Cerroni, MD.*

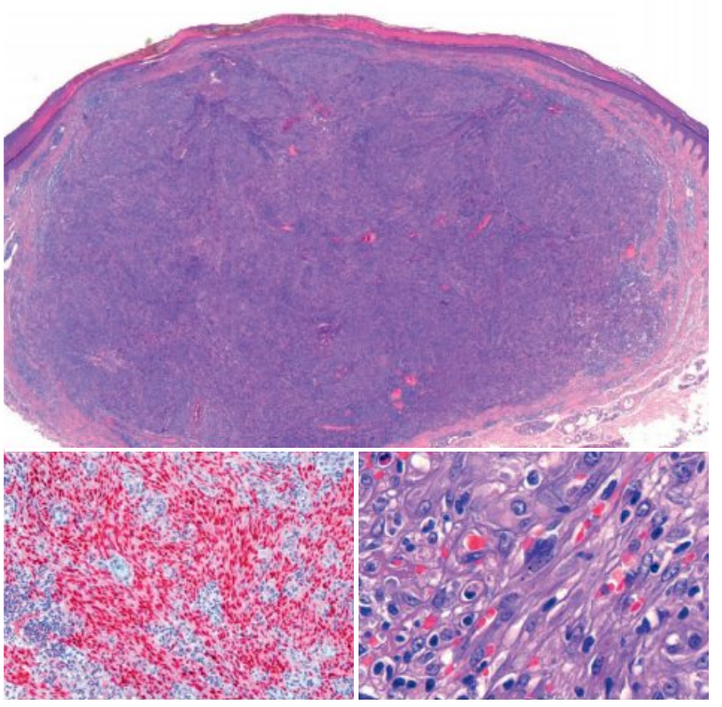


Fig. 114.27 Histology of Kaposi sarcoma – nodular stage. Nodular dermal proliferation of spindled and epithelioid cells admixed with extravasated erythrocytes (right inset). Note the positivity for the latency-associated nuclear antigen (LANA-1) of HHV-8 (left inset). *Courtesy Luis Requena, MD.*

ulcerate and become secondarily infected. KS frequently involves the viscera, including the gastrointestinal tract, lymph nodes, and lungs. The prognosis of pulmonary disease is grave.

Pathology

The histologic appearance of KS does not vary significantly between the different clinical subtypes, but does vary with stage of the lesion. The *patch* stage is characterized by a superficial dermal proliferation of small, angulated vessels lined by inconspicuous endothelial cells, suggestive of lymphatics. These delicate but "jagged" vessels tend to separate collagen bundles and are accompanied by a sparse infiltrate of lymphocytes and plasma cells as well as small numbers of spindle cells expressing endothelial markers. In the more advanced *plaque* stage, the vascular proliferation extends to include the deeper dermis and may involve the subcutis (Fig. 114.26). The spindled endothelial cell population also expands among the ramifying small vessels.

In the *nodular* phase, there is replacement of dermal collagen by these spindled endothelial cells. Pleomorphism and significant numbers of mitotic figures are absent. The spindle cells form intersecting fascicles and are separated by characteristic slit-like spaces containing erythrocytes (Fig. 114.27). The resulting sieve-like pattern of vascular spaces is highly characteristic of KS. Intracellular and extracellular hyaline globules are thought to represent degenerated erythrocytes[4]. The tumor nodules are often rimmed by ectatic or crescentic vessels, hemosiderin deposits, lymphocytes and plasma cells, and may be compartmentalized by fibrous bands. Some tumors contain prominent ectatic meshworks of vessels and have been referred to as "lymphangioma-like" KS. Tumors with a frankly sarcomatous appearance, nuclear pleomorphism, and brisk mitotic activity may occur either as a late stage within previously indolent lesions or as an initial presentation, with the latter most commonly observed in African endemic cases.

Demonstration of expression of the latency-associated nuclear antigen (LANA-1) of HHV-8 has proved to be a highly sensitive and specific marker of KS and other HHV-8-associated disorders such as multicentric Castleman disease and primary effusion lymphoma in both HIV-positive and HIV-negative patients (see Fig. 114.27, left inset)[134,135]. Immunohistochemical detection of this antigen in vascular tumors is more diagnostically useful than detection of the HHV-8 genome by PCR since a few non-KS vascular tumors in both immunocompromised and immunocompetent patients have been found to be positive for HHV-8 by PCR, but not for LANA-1 by immunohistochemical staining, presumably due to detection of HHV-8 within blood cells circulating through the tumors[134].

Differential diagnosis

For patch stage KS, the clinical differential diagnosis includes capillary malformations, an early stage of several of the vascular tumors in Table 114.1, and when on the lower extremities, changes secondary to venous hypertension. Histologically, patch stage KS must be distinguished from stasis changes, well-differentiated angiosarcoma, and benign vascular proliferations and tumors; positivity for LANA-1 points to the diagnosis of KS.

Histologically, the most important differential diagnostic considerations in nodular stage KS are KHE, spindle cell hemangioma, and moderately differentiated angiosarcoma, all of which are negative for LANA-1 of HHV-8. Although KS and spindle cell hemangioma are both characterized by proliferations of spindle cells, KS lacks the cavernous spaces of the latter. KHE is almost exclusively a disease of infancy and childhood and is distinguished from KS by a strongly lobular architecture and lack of plasma cell infiltrates. Angiosarcoma is characterized by endothelial atypia and mitotic activity, both absent in KS.

Late-stage KS may both clinically and histologically resemble pseudo-Kaposi sarcoma, i.e. acroangiodermatitis of Mali that is related to chronic venous insufficiency and Stewart–Bluefarb syndrome that can be associated with an arteriovenous malformation. These reactive, hyperplastic entities differ from KS in that the hyperplasia can be seen to derive from pre-existing vasculature and staining for HHV-8 is negative. Late-stage KS lesions can also be confused histologically with a number of non-vascular spindle cell sarcomas such as fibrosarcoma and leiomyosarcoma. In these cases, demonstration of CD31 immunoreactivity helps confirm the vascular differentiation of KS.

Other entities that can mimic KS clinically but which can be easily distinguished on the basis of histologic features include cutaneous metastases, leukemia or lymphoma cutis, venous and lymphatic malformations, and the cutaneous manifestations of polyarteritis nodosa and erythema elevatum diutinum.

Treatment

In many patients with KS, obtaining a complete cure may be an unrealistic expectation, since recurrence rates are high. Treatment of visible lesions, even in HIV-positive patients with widely disseminated disease, improves appearance, heightens self-esteem, and provides patients with a sense of control in an otherwise difficult situation. In older immunocompetent patients with static disease, observation and close follow-up is an option. Surgery is only useful for tissue diagnosis and removal of solitary lesions. Cryotherapy, laser surgery, photodynamic therapy, intralesional vinblastine or vincristine, and topical alitretinoin, timolol and

imiquimod as well as low-dose oral propranolol have been used to treat superficial patches and plaques[136,137,137a]. Cryotherapy must usually be sufficiently vigorous to cause epidermal ulceration, and the resulting scar seems to replace the vascular proliferation of KS. Extensive, multifocal disease often requires systemic treatment (see below).

Radiation therapy is an option for multifocal, but relatively localized, cutaneous KS. Reported regimens include single-dose radiation (8 to 12 Gy) delivered to an extended field and total skin electron beam therapy (4 Gy fractions weekly) for 6 to 8 weeks (see Ch. 139). Radiation therapy also plays a role in the treatment of localized oral KS, but may have a briefer effect in AIDS-related KS than in classic KS[138].

Rapidly progressive KS (defined by development of 10 or more new cutaneous lesions per month), pulmonary KS, symptomatic visceral involvement, and significant lymphedema are indications for systemic chemotherapy. Liposomal anthracyclines, paclitaxel, and vinblastine are used singly or in combination; less often vincristine, gemcitabine, vinorelbine, etoposide, and/or bleomycin are administered[139,140]. High-dose interferon-α is sometimes employed, but its use is frequently limited by side effects[141]. Immunomodulatory drugs (IMiDs) that inhibit growth of blood vessels such as pomalidomide have also been used successfully for cutaneous and oral KS. Additional potential therapies include sirolimus (see below) and tyrosine kinase inhibitors (e.g. pazopanib). Antiretroviral therapy has clearly helped to alleviate AIDS-related KS, probably indirectly by decreasing viral load and by increasing the CD4 count, but the exact mechanism is unclear. As noted previously, flares of KS can occur as a manifestation of IRIS (see Ch. 78), but this does not necessarily translate into a poor prognosis.

Organ transplant patients with KS pose a particular therapeutic challenge, that of balancing the risk of graft rejection with the benefit of improvement in KS. In addition to reduction of immunosuppression[142], substitution of sirolimus for cyclosporine can also lead to clinical improvement of KS. In 15 renal transplant recipients, this substitution led to resolution of all of the KS lesions in all of the patients, both clinically (by 3 months) and histologically (by 6 months). The authors observed neither episodes of rejection nor changes in kidney graft function[143]. This observation has been independently corroborated by additional studies, albeit not always with equally impressive response rates[144]. It is not yet clear if the beneficial effect of sirolimus reflects lessened immunosuppression or possibly a more direct antitumor effect related to inhibition of HHV-8-induced effects (e.g. PI3K and AKT phosphorylation)[120]. Organ transplant patients with KS also respond to conventional local and systemic therapies used in other forms of KS.

MALIGNANT VASCULAR NEOPLASMS

Epithelioid Hemangioendothelioma

Key features

- Malignant, but relatively indolent, vascular tumor that typically arises in adults
- Skin involvement uncommon and usually associated with more deeply seated disease
- Histologically, cords and nests of epithelioid endothelial cells within a myxoid or hyalinized stroma
- Although ~30% of patients develop metastases within regional lymph nodes, lung, liver, or bone, <50% of patients with metastases die of their disease

Introduction and history

Traditionally, the term *hemangioendothelioma* denoted a vascular tumor of intermediate malignant potential. The original description of *epithelioid hemangioendothelioma* (EHE) incorporated this definition as these tumors can give rise to metastases but their biologic behavior may be relatively indolent[145]. The WHO and ISSVA have recently reclassified EHE as a malignant, rather than intermediate or borderline, vascular tumor. Only angiosarcoma shares that designation (see Table 114.1)[71,72], although EHE is clearly associated with a better prognosis than classic angiosarcoma.

Epidemiology

EHE typically arises in adults, but in a younger age group than angiosarcoma[146]. Occurrence in preadolescent children is exceedingly rare. Unlike angiosarcoma, women appear to be affected slightly more frequently than men.

Pathogenesis

EHE is a clonal neoplastic proliferation of endothelial cells. Most classical cases have a t(1;3)(p36.3;q25) translocation which generates a WWTR1–CAMTA1 fusion protein that is likely an early causative event in oncogenesis[147–149]. *WWTR1* (3q25) encodes a transcriptional coactivator[150] while *CAMTA1* (1p36) encodes a calmodulin-binding transcription activator[151,152]. There is a *WWTR1–CAMTA1* fusion-negative subset of EHE that arises primarily in young adults; compared to classic EHE, more well-developed vascular structures and voluminous eosinophilic cytoplasm are present[153]. This subset contains an alternative gene fusion, *YAP1-TFE3*[153].

To date, the *WWTR1–CAMTA1* and *YAP1–TFE3* fusions have not yet been detected in other neoplasms, in particular the morphologic mimics of EHE such as epithelioid angiosarcoma, epithelioid sarcoma-like hemangioendothelioma, and epithelioid hemangioma. However, it is not yet certain that these fusions are unique to EHE[147,148]. Notably, both the *WWTR1–CAMTA1* and *YAP1–TFE3* gene fusions are reliably detected by FISH and/or RT-PCR[154].

Clinical features

Most tumors present as a slightly painful mass within deep soft tissues, but lesions can develop in the skin, viscera, or bone and are multifocal in up to 50% of patients[155]. Skin involvement is usually associated with an underlying soft tissue or bone tumor, but purely cutaneous examples do occur[145], primarily on the extremities. Skin tumors can be multinodular, and they need to be distinguished from cutaneous metastasis from a visceral primary tumor[156]. Some cases are closely associated with or arise from a vessel, usually a vein. Occlusion of that vessel may lead to secondary symptoms (e.g. edema, thrombophlebitis).

Overall, ~30% of patients develop metastases within the regional lymph nodes, lung, liver, or bone, and <50% of patients with metastases have died of their disease. One study of 30 patients suggested that dermal tumors may have a better prognosis than more deeply seated lesions[145].

Pathology

Similar to its more common counterparts involving soft tissue and bone, cutaneous EHE has an infiltrative growth pattern of epithelioid tumor cells with eosinophilic cytoplasm that form poorly canalized nests and cords within a distinctive myxohyaline stroma (Fig. 114.28). An important clue to their endothelial origin is the presence of small

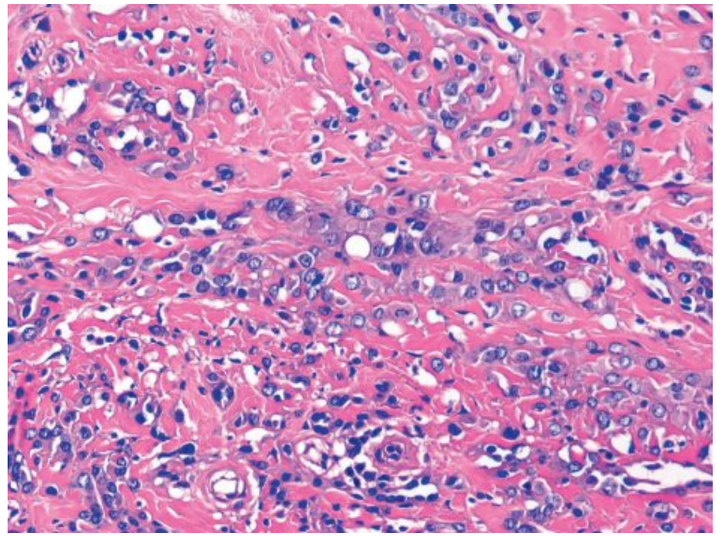


Fig. 114.28 Histology of epithelioid hemangioendothelioma. Poorly canalized cords and nests of endothelial cells forming small intracytoplasmic vacuoles as a sign of primitive vascular differentiation. *Courtesy Luis Requena, MD.*

intracytoplasmic vacuoles containing red blood cells. The nuclei are vesicular with little or no atypia and contain small, inconspicuous nucleoli. An angiocentric growth pattern may be present, but is less commonly observed in cutaneous tumors. Unlike epithelioid hemangioma, inflammation is sparse. Mitotic rate is variable and only weakly correlates with clinical outcome[145].

The tumor cells of EHE are positive for endothelial markers such as ERG, CD31, and CD34 and may also be positive for podoplanin, LYVE-1, and Prox1 (at least focally), suggesting lymphatic or mixed lymphatic–blood vascular differentiation[157,158]. Electron microscopy shows that EHE cells, unlike normal endothelial cells, contain abundant cytoplasmic intermediate filaments[159]. These filaments can cause immunopositivity for cytokeratins and/or smooth muscle antigen, leading to misdiagnosis[146].

Differential diagnosis

The differential diagnosis is broad and includes epithelioid sarcoma, metastatic signet ring adenocarcinoma, melanoma, and epithelioid angiosarcoma. An essential criterion for diagnosis of EHE is immunohistochemical evidence of endothelial differentiation[145]. Differentiation from epithelioid angiosarcomas may be problematic and relies upon recognition of the typical architectural pattern of EHE throughout the lesion plus an absence of the more atypical cells of angiosarcoma that frequently show apoptosis and abnormal mitotic figures in addition to the lack of *WWTR1-CAMTA1* or *YAP1-TFE3* gene fusions.

Treatment

Appropriate therapy involves wide local excision without adjuvant chemotherapy or radiotherapy, given the typically low-grade nature of these tumors. Regional lymph nodes should also be evaluated since these represent a common site for metastases. Anecdotally, stabilization of disease has been observed with interferon, celecoxib, and thalidomide[150]. Updated clinical practice guidelines were published in 2021[160].

Angiosarcoma

Synonyms: ■ Malignant hemangioendothelioma ■ Hemangiosarcoma ■ Lymphangiosarcoma

Key features

- Uncommon malignant neoplasm of endothelium, accounting for <1% of all sarcomas
- Unlike most sarcomas, has a predilection for skin and superficial soft tissue
- Most commonly affects the scalp and face of the elderly and areas of chronic lymphedema or radiodermatitis; rare in children
- Cutaneous forms are usually well to moderately differentiated lesions composed of anastomosing vessels that dissect between bundles of collagen
- Approximately 50% of cases express markers of lymphatic differentiation
- Prognosis is extremely poor, with <15% of patients surviving 5 years
- Most long-term survivors received early radical ablative surgery

Introduction and history

The term *angiosarcoma* has traditionally been used to denote all biologically high-grade malignant neoplasms of endothelial derivation, regardless of the evidence of lymphatic or blood vascular differentiation. However, even though EHE has recently been reclassified as a malignant, rather than intermediate or borderline, vascular tumor[71,72], it has a much better prognosis than angiosarcoma as well as distinct molecular underpinnings. Therefore, EHE is not considered an angiosarcoma variant.

Angiosarcomas were first described systematically by Caro and Stubenrauch in 1945. Only 3 years later, Stewart and Treves described the association between angiosarcoma and post-mastectomy lymphedema. The cutaneous form of angiosarcoma that primarily affects the face and scalp of the elderly was characterized by Wilson-Jones in 1964.

Epidemiology

Angiosarcomas are unusual neoplasms that occur more often in White men and develop primarily in middle-aged or older adults, with the highest incidence in individuals >70 years of age[161]. Those rare examples that occur during childhood or adolescence are more likely to arise in or around viscera (especially the heart or pericardium)[162] or in association with other disease states[163], including chronic or congenital lymphedema, chronic radiodermatitis, and immunosuppression.

Pathogenesis

Angiosarcomas are clonal proliferations of malignantly transformed cells expressing endothelial differentiation. When compared with other sarcomas, distinct upregulation of vascular-specific receptor tyrosine kinase genes, including *TIE1*, *KDR*, *FLT1* and *TEK*, has been observed in angiosarcomas[164]. Furthermore, high-level *MYC* amplification (chromosome 8q24) is consistently seen in radiation-induced and lymphedema-associated angiosarcomas[165,166]. *MYC* amplification leads to upregulation of the miR-17-92 cluster, which downregulates thrombospondin-1, a potent inhibitor of angiogenesis[167]. The *WWTR1–CAMTA1* gene fusion typically seen in EHE has not been detected in angiosarcomas, including epithelioid angiosarcomas[148]. Mechanisms underlying the association between chronic lymphedema and angiosarcoma remain uncertain. Theories include induction of neoplastic change by unknown carcinogens in accumulated lymphatic fluid and the idea that areas with chronic lymphedema are "immunologically privileged sites" due to loss of afferent lymphatic connections.

Radiotherapy has been shown to be an independent risk factor for angiosarcoma development, best exemplified in breast cancer patients (see below). Environmental chemical exposures linked to angiosarcoma, particularly of the liver, include vinyl chloride, thorium dioxide, arsenic, radium, and anabolic steroids[168]. Lastly, neither HHV-8 infection nor cumulative sun exposure appears to be associated with angiosarcoma.

Clinical features

The most common form of angiosarcoma is cutaneous angiosarcoma (without lymphedema) in the elderly. Approximately 70% of these tumors occur in patients over 40 years of age, with the highest incidence in those >70 years of age. About 50% involve the head and neck (Fig. 114.29). Lesions typically present as a deceptively benign-appearing bruise-like patch on the central face, forehead, or scalp. Facial swelling and edema may be present. More advanced lesions are violaceous nodules that bleed easily and may ulcerate. The area of involvement spreads centrifugally, eventually covering large portions of the head and neck. The prognosis is invariably poor, with a less than 15% survival over a 5-year period[161]. In contrast, pediatric cutaneous angiosarcomas tend to be small, unifocal, and favor girls and the lower extremity[163].



Fig. 114.29 Angiosarcoma. Erythematous and purple hemorrhagic plaques as well as grouped vesicles with clear or hemorrhagic fluid (reminiscent of microcystic lymphatic malformation) are present. There is also induration and a pink hue to the left side of the face in addition to evidence of previous excisions and radiotherapy. *Courtesy Lorenzo Cerroni, MD.*

Angiosarcomas that arise in the setting of chronic lymphedema present as firm, coalescing violaceous nodules or an indurated plaque on a background of brawny, non-pitting edema. More than 90% of all angiosarcomas associated with lymphedema arise after mastectomy and lymph node dissection (Stewart–Treves syndrome). In these cases, the inner aspect of the upper arm is the most common site of involvement. Other forms of chronic lymphedema are associated with angiosarcoma, including congenital, filarial, traumatic, and idiopathic. The duration of lymphedema prior to appearance of angiosarcoma ranges from 5 to 25 years.

Even though the incidence is very low (<0.05% in a recent survey of breast cancer patients)[169], the greater use of breast-sparing surgery paired with irradiation has translated into an increase in post-irradiation sarcomas. The latter arise within breast parenchyma and overlying skin, with an average post-treatment interval of 6 years. Post-irradiation angiosarcomas appear as infiltrative plaques or nodules in or near the area of irradiated tissue and share the poor prognosis of all forms of angiosarcoma (Fig. 114.30). These are aggressive, infiltrative, multicentric tumors that enlarge incessantly. Local recurrence and metastasis to regional lymph nodes and lung are common.

Angiosarcomas of skin and soft tissue have also been reported in association with benign and malignant nerve sheath tumors[170], defunctionalized arteriovenous shunts in renal transplant patients[171], long-term exposure to various foreign materials[172], xeroderma pigmentosum[173], and bilateral retinoblastoma[174].

MRI, which shows a nonspecific decreased or variable signal intensity in T1 images, an increased signal in T2 images, and enhancement with gadolinium, is more useful than CT in accurately delineating the extent of local disease, including involvement of neurovascular structures and joints. It is also the imaging modality of choice for evaluating tumor response to preoperative radiation or chemotherapy.

Pathology

Angiosarcomas involving the skin, although highly variable in degree of endothelial differentiation both between and within individual tumors, do not vary in histology as a class; the latter includes those of the "usual type" not associated with lymphedema, those associated with chronic lymphedema, and those associated with chronic radiodermatitis. Well-differentiated areas display an anastomosing network of sinusoidal vessels, often bloodless, lined by a single layer of endothelial cells of slight to moderate nuclear atypia. These exhibit a highly infiltrative pattern, splitting apart collagen bundles and groups of adipose cells. In less well-differentiated areas, the endothelial cells with more pronounced nuclear pleomorphism and mitotic activity pile up and form papillary projections (Fig. 114.31). In poorly differentiated areas, luminal formation may be non-apparent and mitotic activity may be high, mimicking other high-grade sarcomas, carcinoma, or melanoma. Hemorrhage and blood-filled cavities may be present.

Most angiosarcomas stain positively for CD31, CD34, ERG, c-MYC, and Fli-1[175–177], with CD31 and ERG generally considered the most useful markers. Immunohistochemical detection of factor VIII-related antigen, although highly specific for endothelial cells, lacks sensitivity for vascular neoplasms and is negative or very weak even in well-differentiated angiosarcomas.

In tumors associated with chronic lymphedema, networks of small lymphatics lined by endothelial cells with hyperchromatic nuclei may ramify through adjacent soft tissues and have been interpreted as premalignant change. Angiosarcomas developing in this setting may retain lymphatic characteristics (Fig. 114.32). While angiosarcomas arising within a background of chronic lymphedema are often presumed to originate from lymphatics, many angiosarcomas outside of this setting are thought to have mixed lineage due to expression of lymphatic markers, e.g. podoplanin, Prox1 (usually to a minor degree), in addition to pan-endothelial markers and markers more typical of blood vascular endothelium (e.g. CD34)[178]. Until this issue is further clarified, use of the more generic term *angiosarcoma*, rather than *lymphangiosarcoma* or *hemangiosarcoma*, seems prudent.

More recently, a category of purely "lymphatic-type angiosarcoma" was proposed based on a distinctive subset of 21 tumors arising within

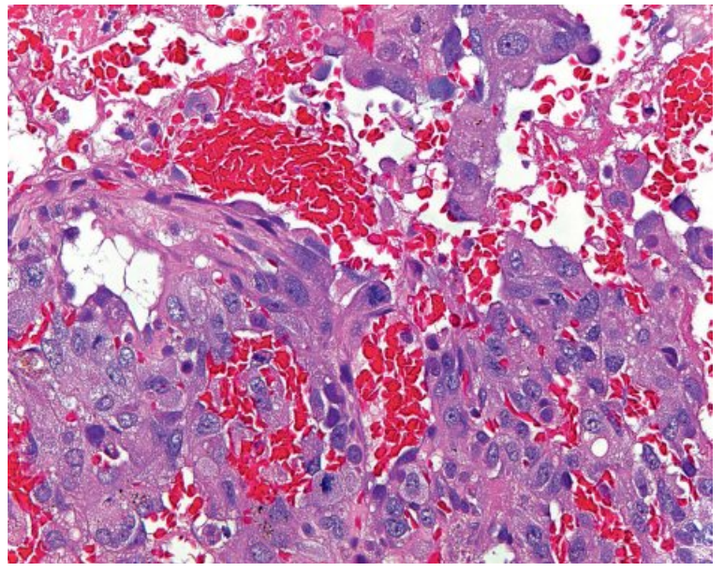


Fig. 114.31 Histology of angiosarcoma. Ill-defined vascular spaces filled with erythrocytes and lined by atypical, piled-up endothelial cells.



Fig. 114.30 Post-radiation angiosarcoma. Red–violet patches and plaques on the breast. The clinicopathologic differential diagnosis is primarily post-radiation atypical vascular proliferation of the skin, an entity that may represent a precursor of post-radiation angiosarcoma (Table 114.4). *Courtesy Celia Requena, MD.*

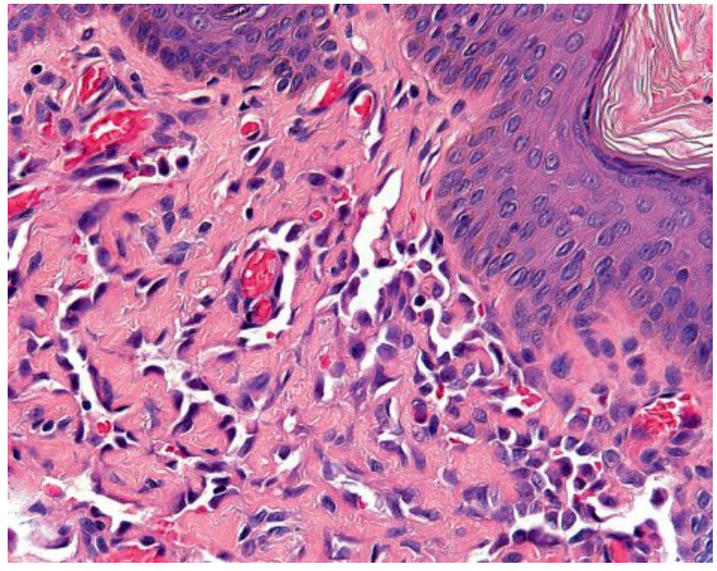


Fig. 114.32 Histology of angiosarcoma with lymphatic characteristics ("lymphangiosarcoma"). Some of the vascular channels are angular and lack erythrocytes. Also note the hyperchromatic atypical endothelial cells.

FEATURES OF RADIATION-INDUCED ANGIOSARCOMA OF THE BREAST (COMPARED TO POST-RADIATION ATYPICAL VASCULAR LESIONS OF THE SKIN)
Clinical features: • thicker and more indurated plaques
Histopathologic features: • cellular atypia • multilayering of vessels • positivity for c-MYC • high Ki-67 proliferation index

Table 114.4 Features of radiation-induced angiosarcoma of the breast (compared to post-radiation atypical vascular lesions of the skin).

the skin and subcutis of the head and neck region in adults. The tumors were defined by the growth characteristics of angiosarcoma (low-to-high grade), cytologic features of lymphatic differentiation (e.g. hobnail-type endothelium), dense intratumoral and peritumoral T cell infiltrates, and diffuse endothelial expression of at least one lymphatic marker – most commonly podoplanin (89%) and/or Prox1 (100%). Although somewhat reminiscent of RHE histologically, this angiosarcoma subgroup displayed more cytologic atypia and a more aggressive course (albeit less aggressive than conventional angiosarcoma).

Highly aggressive angiosarcomas with an epithelioid appearance occasionally occur in the skin[179], although this variant is more common in deep soft tissues. These so-called "epithelioid angiosarcomas" consist of large, rounded cells with prominent eosinophilic nucleoli in which the only morphologic evidence of vascular differentiation may be the presence of occasional intracytoplasmic vacuoles. Cytokeratin positivity is present in about one-third of epithelioid angiosarcomas[180,181], making distinction from carcinoma problematic. Fortunately, this distinction can be accomplished by demonstration of coexistent CD31 and/or ERG expression. The proportion of purely epithelioid cutaneous angiosarcomas appears to be higher among pediatric cases (90%) compared to adult cases (30%)[182].

Differential diagnosis

Early recognition and histologic diagnosis are crucial in the treatment of angiosarcoma. In sites of previous radiation, it can be difficult to distinguish angiosarcomas from atypical vascular lesions. Well-differentiated angiosarcomas, which display only slight cytologic atypia despite their high-grade biologic behavior, may also closely resemble microcystic lymphatic malformation. Other vascular neoplasms that must be distinguished from angiosarcoma histologically include PILA, RHE, epithelioid hemangioendothelioma, and KHE/tufted angioma. Intravascular proliferation of atypical endothelial cells is not a feature of KS and HHV-8 is negative in angiosarcoma. Nuclear staining for c-MYC can be useful for distinguishing angiosarcoma (positive in the majority of cases) from its mimickers (negative). Distinguishing post-radiation atypical vascular lesions of the skin from radiation-induced angiosarcoma of the breast can sometimes be challenging (Table 114.4).

Treatment

Surgical excision with wide margins is indicated. Even with negative margins by histologic examination, the recurrence rate and chance of metastatic disease are high. This may in part reflect the tendency for multifocality. Systemic therapies are limited and include taxanes (+/– radiotherapy) and anthracyclines[183,184]. There are also isolated reports of the successful use of IMiDs, targeted therapies (e.g. pazopanib), and immune checkpoint inhibitors. Radiotherapy alone may be palliative, but does not improve survival. Complete and partial responses to propranolol plus vinblastine-based metronomic chemotherapy were observed in seven patients with advanced angiosarcoma[185].

PERIVASCULAR NEOPLASMS AND NEOPLASTIC-LIKE PROLIFERATIONS

Glomus Tumors and Glomuvenous Malformations

Synonyms: ■ Glomus tumor: solitary glomus tumor, solid glomus tumor ■ Glomuvenous malformation: glomangioma, infiltrating glomus tumor, multiple glomus tumors

Key features

- A heterogeneous group of benign tumors and malformations characterized by the presence of glomus cells
- Two major subgroups are *glomus tumor* and *glomuvenous malformation (*previously termed "glomangioma")
- The glomus tumor typically presents in young adults, is a *solitary*, *painful* papule or nodule on the extremities with a predilection for subungual sites, and consists of a relatively *solid proliferation of glomus cells* associated with *small vessels*
- The less common glomuvenous malformation typically presents in infancy or childhood, is often *multiple* and *asymptomatic* and histologically resembles a venous malformation in which *dilated vessels* are rimmed by a *few glomus cells*
- Histologic variants in which glomus cells merge with well-differentiated smooth muscle cells are referred to as glomangiomyomas
- Extremely rare atypical and malignant forms have been described

Introduction

Tumors distinguished by the presence of benign glomus cells have been subclassified in the past into a number of descriptive types, such as solid, solitary, multiple, adult, pediatric, and diffuse. Current evidence supports division of these tumors into two major disparate categories: (1) the glomus tumor proper, a cellular lesion that tends to be well circumscribed, solitary, and subungual; and (2) the glomuvenous malformation (GVM), a frequently multifocal lesion, traditionally termed a "glomangioma", that most commonly presents in infants or children and histologically resembles a venous malformation in which lesional vessels are rimmed by glomus cells.

Epidemiology

Solitary glomus tumors can occur at any age, but are most common in young adults. Although these tumors in general show no sex predilection, subungual lesions are more common in women. GVMs are less common (accounting for 10%–20% of all glomus cell lesions) and typically present in children without sex predilection; many are evident at birth.

Pathogenesis

The fact that the most common site of occurrence of glomus tumors (the subungual region of the finger) corresponds to one of the densest areas of distribution of the normal glomus body suggests that many glomus tumors represent neoplastic proliferations originating from pre-existing normal glomus cell populations. However, the occasional occurrence of glomus tumors at sites where normal glomus bodies may not be found, including bone, gastrointestinal tract, trachea, and nerve, suggests that some glomus tumors may arise from pluripotent mesenchymal cells or even ordinary smooth muscle cells.

Despite the shared presence of benign glomus cells, glomus tumors and GVMs differ widely in clinical and histopathologic features and are likely unrelated in pathogenesis. The resemblance to venous malformations plus the early presentation of GVMs strongly supports their now widely accepted malformative etiology as well as abandonment of the traditional term *glomangioma*.

Familial GVM is inherited in an autosomal dominant fashion, with patients tending to have multiple lesions that continue to appear later in life, sometimes in response to trauma[186]. At least 40 different germline mutations in *GLMN*, which resides on chromosome 1p22.1 and encodes glomulin, have been detected; glomulin may function as an immunophilin ligand[187–190]. In one study, the most common *GLMN* mutation was present in ~45% of families[191]. The frequent multifocality, incomplete but high (~90%) penetrance, and delayed development in familial GVM suggest a paradominant inheritance pattern in which somatic mutations likely serve as "second hits". Interestingly, in a recent study of 28 cases of familial GVM, second hits were identified in 16 lesions. Although these included a few intragenic mutations and deletions as well as one interstitial deletion containing *GLMN*, the majority of identified mutations represented acquired uniparental isodisomy, with a breakpoint region near the centromere at 1p13.1–1p12. The latter led to duplication of the germline *GLMN* mutation

at 1p22.1 without causing quantitative loss of other genes[192]. It is assumed that somatic mutations within or affecting *GLMN* are the likely cause of sporadic GVMs.

Knock-out mouse studies have shown that glomulin is essential for the viability and appropriate development of the embryonic vasculature during vascular remodeling[193]. In embryonic and adult mice, glomulin is expressed primarily in vascular smooth muscle cells[194].

Clinical features

The ***glomus tumor*** is a benign lesion that usually presents in young adults (20–40 years of age) as a small (<2 cm), blue–red papule or nodule in the deep dermis or subcutis of the distal upper or lower extremities. They are tender to touch, and may be associated with severe paroxysmal pain in response to temperature changes and pressure. The hand, especially the nail beds and palm, is most commonly affected (Fig. 114.33), but cutaneous lesions can also occur at other sites. Unusual extracutaneous glomus tumors have been reported in the gastrointestinal tract, bone, mediastinum, trachea, mesentery, cervix, and vagina. Extremely rare instances of malignant transformation within glomus tumors, with documented metastasis, have been described[195].

Radiographs are of limited usefulness in diagnosis, but subungual tumors often show bony erosion and may show increased distance between the nail and the dorsum of the phalanx. MRI is frequently the primary diagnostic imaging modality of choice (Fig. 114.34), followed by contrast-enhanced CT. Glomus tumors are strongly enhancing masses by both CT and MRI.

GVMs may be present at birth or become evident during childhood or adolescence and tend to be multiple. They are generally asymptomatic lesions that vary widely in appearance, from multiple, soft, red to blue nodules that may be widely distributed or confluent to multifocal, pink to deep blue plaque-like lesions (Figs. 114.35 & 114.36); occasionally, single punctate lesions are seen. Although they clinically resemble venous malformations, GVMs differ in appearance from the latter in a number of aspects[196]: they tend to be more nodular or cobblestone-like in appearance, more blue and less compressible, and they do not swell with exercise or dependency. Lesions typically thicken and become more blue in color with time. Although less painful than the glomus tumor, GVMs may be tender to palpation, and bouts of pain may occur in association with menstruation and pregnancy. All reported cases have behaved in a benign fashion.

Pathology

The common ***glomus tumor*** is a generally well-circumscribed proliferation of solid sheets and clusters of uniform glomus cells focally clustering around a variable number of capillary-sized, endothelium-lined vessels (Fig. 114.37). The stroma can be myxoid or hyalinized and may contain numerous small nerve twigs. A dense fibrous pseudocapsule may be present. The glomus cells are distinctive in their uniformly rounded or polygonal shape, centrally placed and rounded nuclei, and pale eosinophilic cytoplasm. PAS staining reveals basement membrane material around individual tumor cells. Mitotic figures may be present, but are normally configured. In that glomus cells represent modified smooth muscle cells with myofilaments, there is consistent expression of vimentin and muscle actin isoforms, and variably reported expression of desmin. Examples demonstrating gradual transition from rounded glomus cells to elongated, well-differentiated smooth muscle cells have been termed glomangiomyomas[197].

Although the great majority of glomus tumors display no significant cytologic atypia, some have atypical or frankly malignant features. Based on an analysis of 52 atypical and malignant glomus tumors[198], a histopathologic classification of glomus tumors with unusual features has been proposed, with *malignant glomus tumors* defined as those of large size (>2 cm) and deep location, or those with marked atypia and a high mitotic rate (≥5/50 HPF), or those with atypical mitotic figures. Malignant examples show a compressed rim of benign glomus



Fig. 114.33 Glomus tumor. The lesion presented with pain and ill-defined subungual erythema. *Courtesy Ronald P. Rapini, MD.*



Fig. 114.35 Glomuvenous malformation ("glomangioma"). Note the cluster of slightly compressible blue papules.

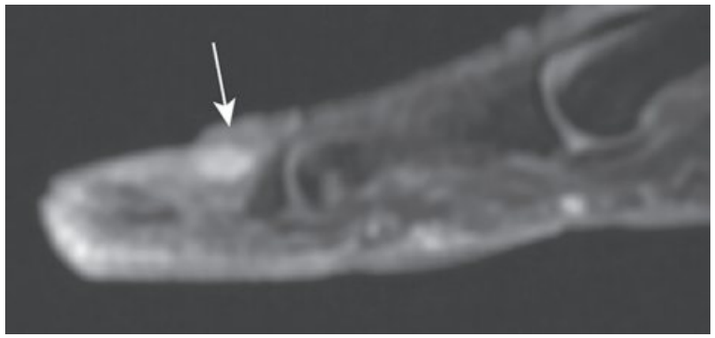


Fig. 114.34 MRI of a glomus tumor located in the proximal portion of the nail bed and matrix. While there was a low signal lesion noted in T1-weighted images of the left index finger, the lesion was very bright in T2-weighted images with diffuse homogeneous enhancement with gadolinium (arrow). *Courtesy Kalman Watsky, MD.*



Fig. 114.36 Glomuvenous malformation ("glomangioma"). Large cluster of blue papulonodules becoming confluent centrally.

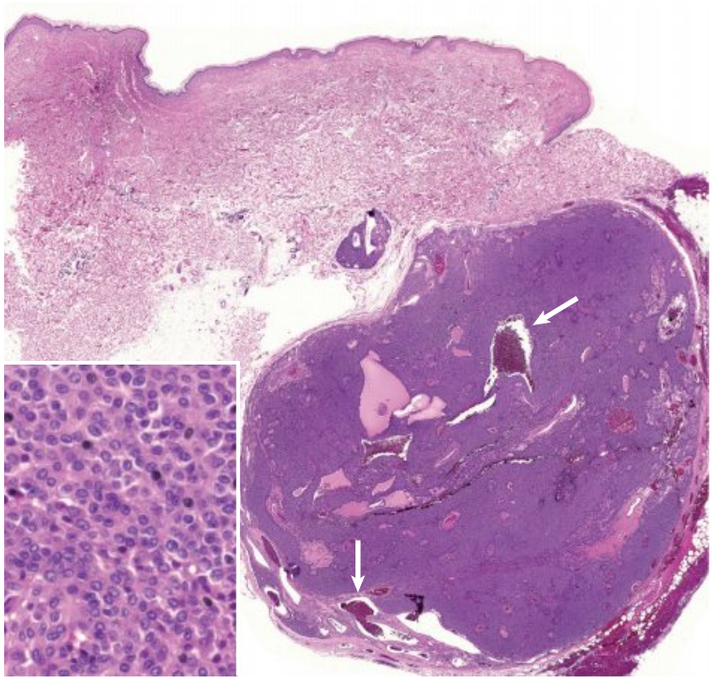


Fig. 114.37 Histology of a glomus tumor. Well-defined subcutaneous nodule composed of dense cellular aggregates encompassing several vascular lumina (arrows). There is a predominance of monomorphous glomus cells with round nuclei and scarce cytoplasm (inset). *Courtesy Lorenzo Cerroni, MD.*

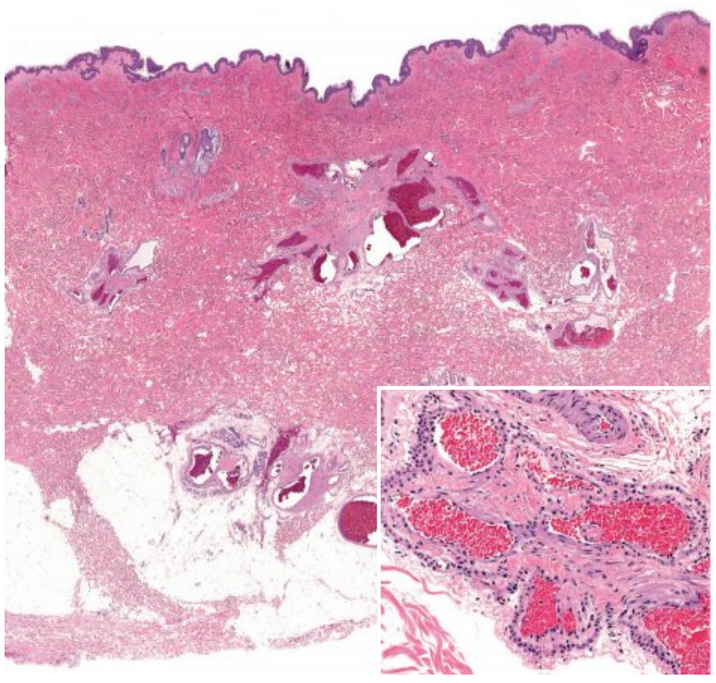


Fig. 114.38 Histology of a glomuvenous malformation ("glomangioma"). Several aggregates of vascular structures in the dermis and superficial subcutaneous fat, most of which are filled with erythrocytes. The vascular walls are composed of one or more layers of round, monomorphous glomus cells (inset). *Courtesy Lorenzo Cerroni, MD.*

tumor around the malignant areas in about one-half of cases, consistent with malignant transformation from a pre-existing benign tumor. In some cases, the presence of nuclear pleomorphism without mitoses is thought to represent a degenerative phenomenon ("ancient" changes), and tumors with these characteristics have been termed "symplastic" glomus tumors.

GVMs consist of large, dilated, thin-walled veins in the dermis and subcutaneous tissue, histologically equivalent to those comprising venous malformations, but surrounded by one or more layers of uniform, cuboidal glomus cells (Fig. 114.38). Some microscopic fields may lack the glomus cells and be indistinguishable from common venous malformations. They are less circumscribed than solitary glomus tumors and may be distributed as separate nodules in the same anatomic area. Like venous malformations without glomus cells, many GVMs contain organizing thrombi or phleboliths.

Differential diagnosis

Solitary glomus tumors may clinically be confused with other painful nodules such as eccrine spiradenomas and leiomyomas which can readily be distinguished from glomus tumors histologically and immunohistochemically. From a histologic point of view, solid forms of hidradenoma may closely resemble glomus tumors, especially when sweat ducts contain erythrocytes, but can be distinguished by their keratin expression. Cellular glomus tumors are occasionally mistaken for pseudoangiomatous intradermal nevi, but the latter are positive for melanocytic markers.

GVMs must be distinguished from ordinary venous malformations that lack glomus cells by histologic examination, although several clinical features of these lesions also help make this distinction (see section above). It is likely that many cases of the so-called blue rubber bleb nevus syndrome, a familial disorder characterized by multiple venous malformations, actually represent examples of multiple GVMs.

Treatment

Solitary glomus tumors can be treated successfully by local surgical excision. Other options include electrodesiccation and sclerotherapy.

GVMs are less amenable to surgery than are common glomus tumors, due to their more extensive and multifocal nature. In a series of large facial "glomangiomas"[196], MRI was the best modality for definition of the extent of the lesions and their relationship to other anatomic structures. In this same series, surgical resection reduced the area of discoloration and improved facial contour, while sclerotherapy was less effective than for venous malformations[196]. Laser surgery employing CO_2, KTP, Nd:YAG, and pulsed dye lasers may also be helpful. In a retrospective study of 17 patients with GVMs who were treated with dual wavelength pulsed dye–Nd:YAG laser therapy, a reduction of at least 60% was observed[196]. Residual lesions following subtotal resections may slowly re-expand[196].

Infantile Hemangiopericytoma

Synonym: ■ Congenital hemangiopericytoma

Key features

- Benign neoplasm of perivascular myoid differentiation that usually presents at birth or in the first years of life
- Closely related to infantile myofibromatosis
- Clinical appearance is that of single or multiple dermal and subcutaneous nodules that may be alarmingly large at birth or grow rapidly
- Differs in both histology and clinical behavior from adult-type hemangiopericytoma, which rarely involves the skin
- Histologically, multilobulated tumor with cellular areas of spindle cells and antler-like branching blood vessels, merging with less cellular areas containing plump myofibroblasts
- Behaves in a benign fashion, despite frequent focal necrosis and increased mitotic activity

Introduction and history

The concept of hemangiopericytoma as an entity has been controversial since these tumors were described in 1942 by Stout and Murray, who considered them to be composed mainly of pericytes. Congenital or infantile hemangiopericytoma was recognized as a separate entity from adult-type hemangiopericytoma in 1976 by Enzinger and Smith

due to its distinguishing clinical and histologic features. Classic adult-type hemangiopericytomas will not be discussed here because of their extreme rarity in superficial tissues.

Epidemiology

Infantile hemangiopericytomas are uncommon tumors that typically appear in the first year of life and are usually congenital. There is a male predominance by ~2:1. Examples in older children have occasionally been reported.

Pathogenesis

The frequent zonal pattern of myofibroblastic differentiation in infantile hemangiopericytomas has led to the proposal that infantile hemangiopericytoma and infantile myofibromatosis may lie upon a continuous spectrum of myofibroblastic lesions[199]. In addition, a family of adult tumors with perivascular myoid differentiation has been described that overlaps histologically with infantile myofibromatosis and includes two newer entities, termed *glomangiopericytoma* and *myopericytoma*. Granter et al.[200], in support of similar observations by Requena and colleagues[201], have proposed that this widening spectrum of tumors and their distinctive cellular components might be better explained by derivation from a pluripotent periendothelial cell capable of differentiating along smooth muscle, pericytic, and glomus cell lines, rather than from myofibroblasts.

Clinical features

Infantile hemangiopericytomas are nodules that primarily occur in the subcutaneous and dermal tissues of the head and neck. Congenital examples may be alarming in size at birth or grow rapidly thereafter. Multicentric cases have been reported and have in some instances been misinterpreted as examples of distant metastasis. Although benign behavior appears to be the rule, large tumors may be problematic if they hemorrhage or threaten vital structures. Lesions in the tongue and in deeply seated sites, such as the mediastinum and abdomen, have been reported. Rare multisystemic forms in neonates may be lethal. Local recurrence after excision is common, although spontaneous tumor regression has also been documented.

Pathology

Infantile-type hemangiopericytomas, unlike the adult type, are usually dermal or subcutaneous in location and are often multilobulated. They typically show a biphasic growth pattern in which primitive hemangiopericytomatous areas resembling the adult tumors (short spindle cells arranged around thin-walled, branching vessels) blend with less cellular areas containing plump myofibroblast-like cells set within a collagenous matrix. Focal necrosis and significant mitotic activity may be present, but are not indicative of poor prognosis.

Differential diagnosis

Infantile hemangiopericytomas demonstrate nonspecific clinical and radiologic features and require histologic examination for definitive diagnosis. They may be confused clinically with an infantile hemangioma due to rapid postnatal growth, and large congenital lesions may suggest a rapidly involuting congenital hemangioma or infantile fibrosarcoma. Further diagnostic considerations include infantile myofibromatosis and subcutaneous pyogenic granuloma.

Treatment

Conservative treatment following establishment of the diagnosis via histologic examination is generally recommended given the potential for spontaneous regression. Complete surgical resection is a reasonable option in some cases, although there appears to be a conflicting tendency of these tumors to both locally recur and spontaneously regress.

Additional figures available in our eBook (see inside front cover for access code).

REFERENCES

1. Ackerman AB. *Resolving Quandaries in Dermatology, Pathology, and Dermatopathology*. New York: Ardor Scribendi; 2001.
2. Kuo T, Gomez LG. Papillary endothelial proliferation in cystic lymphangiomas. A lymphatic vessel counterpart of Masson's vegetant intravascular hemangioendothelioma. *Arch Pathol Lab Med*. 1979;103:306–308.
3. Pins MR, Rosenthal DI, Springfield DS, Rosenberg AE. Florid extravascular papillary endothelial hyperplasia (Masson's pseudoangiosarcoma) presenting as a soft-tissue sarcoma. *Arch Pathol Lab Med*. 1993;117:259–263.
4. Weiss SW, Goldblum JR. *Enzinger and Weiss's Soft Tissue Tumors*. 4th ed. St Louis: Mosby; 2001.
5. Yang H, Ahmed I, Verghese M, Schroeter AL. Diffuse dermal angiomatosis of the breast. *Arch Dermatol*. 2006;142:343–347.
6. Ferreli C, Atzori L, Caputo V, Rongioletti F. Diffuse dermal angiomatosis of the breast: an emerging entity in the setting of cutaneous angiomatoses. *Clin Dermatol*. 2021;39:271–277.
7. Pasyk K, Depowski M. Proliferating systematized angioendotheliomatosis of a 5-month-old infant. *Arch Dermatol*. 1978;114:1512–1515.
8. Bali R, Wali GN, Ieremia E. The spectrum of cutaneous reactive angiomatoses in end stage renal failure. *Am J Dermatopathol*. 2021;43:576–578.
9. McMenamin ME, Fletcher CDM. Reactive angioendotheliomatosis: a study of 15 cases demonstrating a wide clinicopathologic spectrum. *Am J Surg Pathol*. 2002;26:685–697.
10. Requena L, El-Shabrawi-Caelen Walsh SN, et al. Intralymphatic histocytosis. A clinicopathologic study of 16 cases. *Am J Dermatopathol*. 2009;31:140–151.
11. Vilas Boas P, Cerroni L, Requena L. Intravascular cutaneous disorders. A clinicopathologic review. *Am J Dermatopathol*. 2021;43:119–136.
12. McLaughlin ER, Morris R, Weiss SW, Arbiser JL. Diffuse dermal angiomatosis of the breast: response to isotretinoin. *J Am Acad Dermatol*. 2001;45:462–465.
13. Karadag AS, Parish LC, Lambert WC. Isotretinoin in retrospect. *Clin Dermatol*. 2017;35:335–339.
14. Sadowsky LM, Socik A, Burnes A, et al. Genital angiokeratomas in adult men and women: prevalence and predisposing factors. *J Cutan Med Surg*. 2019;23:513–518.
15. Cohen PR, Celano NJ. Penile angiokeratomas (PEAKERS) revisited: a comprehensive review. *Dermatol Ther (Heidelb)*. 2020;10:551–567.
16. Calonje E, Fletcher CD, Wilson-Jones E, Rosai J. Retiform hemangioendothelioma. A distinctive form of low-grade angiosarcoma delineated in a series of 15 cases. *Am J Surg Pathol*. 1994;18:115–125.
17. Guillou L, Calonje E, Speight P, et al. Hobnail hemangioma: a pseudomalignant vascular lesion with a reappraisal of targetoid hemosiderotic hemangioma. *Am J Surg Pathol*. 1999;23:97–105.
18. Mentzel T, Partanen TA, Kutzner H. Hobnail hemangioma ('targetoid hemosiderotic hemangioma'): clinicopathologic and immunohistochemical analysis of 62 cases. *J Cutan Pathol*. 1999;26:279–286.
19. Al Dhaybi R, Lam C, Hatami A, et al. Targetoid hemosiderotic hemangiomas (hobnail hemangiomas) are vascular lymphatic malformations: a study of 12 pediatric cases. *J Am Acad Dermatol*. 2012;66:116–120.
20. Franke FE, Steger K, Marks A, et al. Hobnail hemangiomas (targetoid hemosiderotic hemangiomas) are true lymphangiomas. *J Cutan Pathol*. 2004;31:362–367.
21. Couto JA, Vivero MP, Kozakewich HP, et al. A somatic MAP3K3 mutation is associated with verrucous venous malformation. *Am J Hum Genet*. 2015;96:480–486.
22. Tennant LB, Mulliken JB, Perez-Atayde AR, Kozakewich HP. Verrucous hemangioma revisited. *Pediatr Dermatol*. 2006;23:208–215.
23. Schmidt B, El Zein S, Cuoto J, et al. Verrucous venous malformation – subcutaneous variant. *Am J Dermatopathol*. 2021;43:e181–e184.
24. Wang L, Gao T, Wang G. Verrucous hemangioma: a clinicopathological and immunohistochemical analysis of 74 cases. *J Cutan Pathol*. 2014;41:823–830.
25. Laing EL, Brasch HD, Steel R, et al. Verrucous hemangioma expresses primitive markers. *J Cutan Pathol*. 2013;40:391–396.
26. North PE, Waner M, Mizeracki A, Mihm Jr. MC. GLUT1: a newly discovered immunohistochemical marker for juvenile hemangiomas. *Hum Pathol*. 2000;31:11–22.
27. North PE, Waner M, Mizeracki A, et al. A unique microvascular phenotype shared by juvenile hemangiomas and human placenta. *Arch Dermatol*. 2001;137:559–570.
28. Le Sage S, David M, Dubois J, et al. Efficacy and absorption of topical sirolimus for the treatment of vascular anomalies in children: a case series. *Ped Dermatol*. 2018;35:472–477.
29. Geeurickx M, Labarque V. A narrative review of the role of sirolimus in the treatment of congenital vascular malformations. *J Vasc Surg Venous Lymphat Disord*. 2021;9:1321–1333.
30. Al-Furaih I, Al-Marzoug A, Al-Qadri N. Sirolimus for the management of verrucous venous malformation. *Case Rep Dermatol*. 2021;13:298–303.
31. Hartzell MB. Granuloma pyogenicum (botryomycosis of French authors). *J Cutan Dis*. 1904;22:520–523.
32. Katta R, Bickle K, Hwang L. Pyogenic granuloma arising in port-wine stain during pregnancy. *Br J Dermatol*. 2001;144:644–645.
33. Groesser L, Peterhof E, Evert M, et al. BRAF and RAS mutations in sporadic and secondary pyogenic granuloma. *J Invest Dermatol*. 2016;136:481–486.
34. Kerr DA. Granuloma pyogenicum. *Oral Surg Oral Med Oral Pathol*. 1951;4:158.
35. Warner J, Jones EW. Pyogenic granuloma recurring with multiple satellites. A report of 11 cases. *Br J Dermatol*. 1968;80:218–227.
36. Wilson BB, Greer KE, Cooper PH. Eruptive disseminated lobular capillary hemangioma (pyogenic granuloma). *J Am Acad Dermatol*. 1989;21:391–394.
37. Campbell JP, Grekin RC, Ellis CN, et al. Retinoid therapy is associated with excess granulation tissue responses. *J Am Acad Dermatol*. 1983;9:708–713.
38. Tay YK, Weston WL, Morelli JG. Treatment of pyogenic granuloma in children with the flashlamp-pumped pulsed dye laser. *Pediatrics*. 1997;99:368–370.
39. Matsumoto K, Nakanishi H, Seike T, et al. Treatment of pyogenic granuloma with a sclerosing agent. *Dermatol Surg*. 2001;27:521–523.
40. Requena L, Sangueza OP. Cutaneous vascular proliferation. Part II. Hyperplasias and benign neoplasms. *J Am Acad Dermatol*. 1997;37:887–919.
41. Klebanov N, Lin WM, Artomov M, et al. Use of targeted next-generation sequencing to identify activating hot spot mutations in cherry angiomas. *JAMA Dermatol*. 2019;155:211–215.

42. Liau J-Y, Lee J-C, Tsai J-H, et al. High frequency of *GNA14*, *GNAQ*, and *GNA11* mutations in cherry hemangioma: a histopathological and molecular study of 85 cases indicating *GNA14* as the most commonly mutated gene in vascular neoplasms. *Mod Pathol*. 2019;32:1657–1665.
43. Jansen P, Müller H, Lodde GC, et al. *GNA14*, *GNA11*, and *GNAQ* mutations are frequent in benign but not malignant cutaneous vascular tumors. *Front Genet*. 2021;12:1–8.
44. Wilson-Jones E, Orkin M. Tufted angioma (angioblastoma). A benign progressive angioma, not to be confused with Kaposi's sarcoma or low-grade angiosarcoma. *J Am Acad Dermatol*. 1989;20:214–225.
45. Enjolras O, Wassef M, Mazoyer E, et al. Infants with Kasabach-Merritt syndrome do not have 'true' hemangiomas. *J Pediatr*. 1997;130:631–640.
46. Hebeda CL, Scheffer E, Starink TM. Tufted angioma of late onset. *Histopathology*. 1993;23:191–193.
47. Heagerty AH, Rubin A, Robinson TW. Familial tufted angioma. *Clin Exp Dermatol*. 1992;17:344–345.
48. Sarkar M, Mulliken JB, Kozakewich HP, et al. Thrombocytopenic coagulopathy (Kasabach-Merritt phenomenon) is associated with Kaposiform hemangioendothelioma and not with common infantile hemangioma. *Plast Reconstr Surg*. 1997;100:1377–1386.
49. Zukerberg LR, Nickoloff BJ, Weiss SW. Kaposiform hemangioendothelioma of infancy and childhood. An aggressive neoplasm associated with Kasabach-Merritt syndrome and lymphangiomatosis. *Am J Surg Pathol*. 1993;17:321–328.
50. Le Huu AR, Jokinen CH, Ruben BP, et al. Expression of Prox1, lymphatic endothelial nuclear transcription factor, in kaposiform hemangioendothelioma and tufted angioma. *Am J Surg Pathol*. 2010;34:1563–1573.
51. Broek RWT, Koelsche C, Eijkelenboom A, et al. Kaposiform hemangioendothelioma and tufted angioma – (epi)genetic analysis including genome-wide methylation profiling. *Ann Diagn Pathol*. 2020;44:151434.
52. Browning J, Frieden I, Baselga E, et al. Congenital self-regressing tufted angioma. *Arch Dermatol*. 2006;142:749–751.
53. Leaute-Labreze C, Bioulac-Sage P, Labbe L, et al. Tufted angioma associated with platelet trapping syndrome: response to aspirin. *Arch Dermatol*. 1997;133:1077–1079.
54. Feito-Rodriguez M, Sanchez-Orta A, De Lucus R, et al. Congenital tufted angioma: a multicenter retrospective study of 30 cases. *Ped Dermatol*. 2018;35:808–816.
55. Seo SK, Suh JC, Na GY, et al. Kasabach-Merritt syndrome: identification of platelet trapping in a tufted angioma by immunohistochemistry technique using monoclonal antibody to CD61. *Pediatr Dermatol*. 1999;16:392–394.
56. Dadras SS, North PE, Bertoncini J, et al. Infantile hemangiomas are arrested in an early developmental vascular differentiation state. *Mod Pathol*. 2004;17:1068–1079.
57. North PE. Vascular tumors and malformations of infancy and childhood. *Pathol Case Rev*. 2008;13:213–235.
58. Suarez SM, Pensler JM, Paller AS. Response of deep tufted angioma to interferon alfa. *J Am Acad Dermatol*. 1995;33:124–126.
59. Munn SE, Jackson JE, Jones RR. Tufted haemangioma responding to high-dose systemic steroids: a case report and review of the literature. *Clin Exp Dermatol*. 1994;19:511–514.
60. Adams DM, Trenor CC, Hammill AM, et al. Efficacy and safety of sirolimus in the treatment of complicated vascular anomalies. *Pediatrics*. 2016;137:e20153257.
61. Ji Y, Chen S, Xiang B, et al. Sirolimus for the treatment of progressive kaposiform hemangioendothelioma: a multicenter retrospective study. *Int J Cancer*. 2017;141:848–855.
62. Fahrtash F, McCahon E, Arbuckle S. Successful treatment of kaposiform hemangioendothelioma and tufted angioma with vincristine. *J Pediatr Hematol Oncol*. 2010;32:506–510.
63. Chan JK, Fletcher CD, Hicklin GA, Rosai J. Glomeruloid hemangioma. A distinctive cutaneous lesion of multicentric Castleman's disease associated with POEMS syndrome. *Am J Surg Pathol*. 1990;14:1036–1046.
64. Chung W-K, Lee D-W, Yang J-H, et al. Glomeruloid hemangioma as a very early presenting sign of POEMS syndrome. *J Cutan Pathol*. 2009;36:1126–1128.
65. Watanabe O, Maruyama I, Arimura K, et al. Overproduction of vascular endothelial growth factor/vascular permeability factor is causative in Crow-Fukase (POEMS) syndrome. *Muscle Nerve*. 1998;21:1390–1397.
66. Belec L, Mohamied AS, Authier F-J, et al. Human herpesvirus 8 infection in patients with POEMS syndrome-associated multicentric Castleman's disease. *Blood*. 1999;93:3643–3653.
67. Legendre P, Norkowski E, Le Pelletier F, et al. Glomeruloid haemangioma: a possible consequence of elevated VEGF in POEMS and Erdheim-Chester disease. *Eur J Dermatol*. 2018;28:784–789.
68. Suurmeijer AJH, Fletcher CDM. Papillary hemangioma: a distinctive cutaneous hemangioma of the head and neck area containing hyaline globules. *Histopathology*. 2007;51:638–648.
69. Hunt SJ, Santa Cruz DJ, Barr RJ. Microvenular hemangioma. *J Cutan Pathol*. 1991;18:235–240.
70. Olsen TG, Helwig EB. Angiolymphoid hyperplasia with eosinophilia. A clinicopathologic study of 116 patients. *J Am Acad Dermatol*. 1985;12:781–796.
71. Antonescu CR, Bridge JA, Cunha IW, et al. *Soft Tissue Tumours*. *WHO Classification of Tumours of Soft Tissue and Bone*. 5th ed. Lyon: IARC Press; 2020:2–3.
72. Wassef M, Blei F, Adams D, et al. Vascular Anomalies Classification: recommendations from the International Society for the Study of Vascular Anomalies. *Pediatrics*. 2015;136:e203–e214.
73. van IJzendoorn DGP, de Jong D, Romagosa C, et al. Fusion events lead to truncation of FOS in epithelioid hemangioma of bone. *Genes Chromosomes Cancer*. 2015;54:565–574.
74. Huang SC, Zhang L, Sung YS, et al. Frequent FOS gene rearrangements in epithelioid hemangioma: a molecular study of 58 cases with morphologic reappraisal. *Am J Surg Pathol*. 2015;39:1313–1321.
75. Antonescu C. Malignant vascular tumors – an update. *Mod Pathol*. 2014;27:S30–S38.
76. Hung YP, Fletcher CD, Hornick JL. FOSB is a useful diagnostic mjarker for pseudomyogenic hemangioendothelioma. *Am J Surg Pathol*. 2017;41:596–606.
77. Khunger N, Pahwa M, Jain RK. Angiolymphoid hyperplasia with eosinophilia treated with a novel combination technique of radiofrequency ablation and sclerotherapy. *Dermatol Surg*. 2010;36:422–425.
78. North PE, Kahn T, Cordisco MR, et al. Multifocal lymphangioendotheliomatosis with thrombocytopenia: a newly recognized clinicopathological entity. *Arch Dermatol*. 2004;140:599–606.
79. Prasad V, Fishman SJ, Mulliken JB, et al. Cutaneovisceral angiomatosis with thrombocytopenia. *Pediatr Dev Pathol*. 2005;8:407–419.
80. North PE. Vascular tumors and malformations. *Surg Pathol Clin*. 2010;3:455–494.
81. Maronn M, Catrine K, North P, et al. Expanding the phenotype of multifocal lymphangioendotheliomatosis with thrombocytopenia. *Pediatr Blood Cancer*. 2009;52:531–534.
82. Droitcourt C, Boccara O, Fraitag S, et al. Multifocal lymphangioendotheliomatosis with thrombocytopenia: clinical features and response to sirolimus. *Pediatrics*. 2015;136:e517–e522.
83. Kline RM, Buck LM. Bevacizumab treatment in multifocal lymphangioendotheliomatosis with thrombocytopenia. *Pediatr Blood Cancer*. 2009;52:534–536.
84. Nava FB, Barrial M, Munoz AJ, et al. Multifocal lymphangioendotheliomatosis with thrombocytopenia: phenotypic variability and response to rapamycin. *Cir Pediatr*. 2021;34:105–110.
85. Perkins P, Weiss SW. Spindle cell hemangioendothelioma. An analysis of 78 cases with reassessment of its pathogenesis and biologic behavior. *Am J Surg Pathol*. 1996;20:1196–1204.
86. Fletcher CD, Beham A, Schmid C. Spindle cell haemangioendothelioma: a clinicopathological and immunohistochemical study indicative of a non-neoplastic lesion. *Histopathology*. 1991;18:291–301.
87. Amyere M, Dompmartin A, Wouters V, et al. Common somatic alterations identified in Maffucci syndrome by molecular karyotyping. *Mol Syndromol*. 2014;5:259–267.
88. Pansuriya TC, van Eijk R, d'Adamo P, et al. Somatic mosaic IDH1 and IDH2 mutations are associated with enchondroma and spindle cell hemangioma in Ollier disease and Maffucci syndrome. *Nat Genet*. 2011;43:1256–1261.
89. Schaap FG, Frech PJ, Bovée JV. Mutations in the isocitrate dehydrogenase genes IDH1 and IDH2 in tumors. *Adv Anat Pathol*. 2013;20:32–38.
90. Kurek KC, Pansuriya TC, van Ruler MAJH, et al. R132C IDH1 mutations are found in spindle cell hemangiomas and not in other vascular tumors or malformations. *Am J Pathol*. 2013;182:1494–1500.
91. Setoyama M, Shimada H, Miyazono N, et al. Spindle cell hemangioendothelioma: successful treatment with recombinant interleukin-2. *Br J Dermatol*. 2000;142:1238–1239.
92. Niedt GW, Greco MA, Wieczorek R, et al. Hemangioma with Kaposi's sarcoma-like features: report of two cases. *Pediatr Pathol*. 1989;9:567–575.
93. Vin-Christian K, McCalmont TH, Frieden IJ. Kaposiform hemangioendothelioma. An aggressive, locally invasive vascular tumor that can mimic hemangioma of infancy. *Arch Dermatol*. 1997;133:1573–1578.
94. Mentzel T, Mazzoleni G, Dei Tos AP, Fletcher CD. Kaposiform hemangioendothelioma in adults. Clinicopathologic and immunohistochemical analysis of three cases. *Am J Clin Pathol*. 1997;108:450–455.
95. Lyons LL, North PE, Mac-Moune Lai F, et al. Kaposiform hemangioendothelioma: a study of 33 cases emphasizing its pathologic, immunophenotypic, and biologic uniqueness from juvenile hemangioma. *Am J Surg Pathol*. 2004;28:559–568.
96. Enjolras O, Mulliken JB, Wassef M, et al. Residual lesions after Kasabach-Merritt phenomenon in 41 patients. *J Am Acad Dermatol*. 2000;42:225–235.
97. Lim YH, Baccchiocchi A, Qiu J, Straub R, et al. GNA somatic mutation causes congenital sporadic vascular umors by MAPK activation. *Am J Hum Genet*. 2016;99:443–450.
98. Pollitt AY, Poulter NS, Gitz E, et al. Syk and Src family kinases regulate C-type lectin receptor 2 (CLEC-2)-mediated clustering of podoplanin and platelet adhesion to lymphatic endothelial cells. *J Biol Chem*. 2014;289:35695–35710.
99. Lai FM, Allen PW, Yuen PM, Leung PC. Locally metastasizing vascular tumor. Spindle cell, epithelioid, or unclassified hemangioendothelioma? *Am J Clin Pathol*. 1991;96:660–663.
100. Fanburg-Smith JC, Michal M, Partanen TA, et al. Papillary intralymphatic angioendothelioma (PILA): a report of twelve cases of a distinctive vascular tumor with phenotypic features of lymphatic vessels. *Am J Surg Pathol*. 1999;23:1004–1010.
101. Parsons A, Sheehan DJ, Sangueza OP. Retiform hemangioendotheliomas usually do not express D2–40 and VEGFR-3. *Am J Dermatopathol*. 2008;30:31–33.
102. Folpe AL, Veikkola T, Valtola R, Weiss SW. Vascular endothelial growth factor receptor-3 (VEGFR-3): a marker of vascular tumors with presumed lymphatic differentiation, including Kaposi's sarcoma, kaposiform and Dabska-type hemangioendotheliomas, and a subset of angiosarcomas. *Mod Pathol*. 2000;13:180–185.
103. Rubin BP, Folpe AL. Composite hemangioendothelioma. In: WHO Classification of Tumours Editorial Board. *World Health Organization Classification of Tumors 5th Edition: Soft Tissue and Bone Tumors*. Lyon, France: IARC Press; 2020:163–165.
104. Nayler SJ, Rubin BP, Calonje E, et al. Composite hemangioendothelioma: a complex, low-grade vascular lesion mimicking angiosarcoma. *Am J Surg Pathol*. 2000;24:352–361.
105. Schommer M, Herbst RA, Brodersen JP, et al. Retiform hemangioendothelioma: another tumor associated with human herpesvirus 8? *J Am Acad Dermatol*. 2000;42:290–292.
106. Antonescu CR, Dickson BC, Sung Y-S, et al. Recurrent YAP1 and MAML2 gene rearrangements in retiform and composite hemangioendothelioma. *Am J Surg Pathol*. 2020;44:1677–1684.
107. Perry KD, Al-Ibraheemi A, Rubun BP, et al. Composite hemangioendothelioma with neuroendocrine marker expression: an aggressive variant. *Mod Pathol*. 2017;30:1589–1602.
108. Agaram NP, Zhang L, Cotzia P, et al. Expanding the spectrum of genetic alterations in pseudomyogenic hemangioendothelioma with recurrent novel ACTB-FOSB gene fusions. *Am J Surg Pathol*. 2018;42:1653–1661.
109. Zhu G, Benayed R, Ho C, et al. Diagnosis of known sarcoma fusions and novel fusion partners by targeted RNA sequencing with identification of a recurrent ACTB-FOSB fusion in pseudomyogenic hemangioendothelioma. *Mod Pathol*. 2019;32:609–620.
110. Requena L, Santonja C, Martinez-Amo JL, et al. Cutaneous epithelioid sarcoma-like (pseudomyogenic) hemangioendothelioma: a little known low-grade cutaneous vascular neoplasm. *JAMA Dermatol*. 2013;149:459–465.
111. Kallen ME, Hornick JL. The 2020 WHO Classification: what's new in soft tissue tumor pathology? *Am J Surg Pathol*. 2020;45:e1–e23.
112. Joseph J, Wang WL, Patnana M, et al. Cytotoxic and targeted therapy for treatment of pseudomyogenic hemangioendothelioma. *Clin Sarcoma Res*. 2015;5:22.

113. Ozeki M, Nozawa A, Kanda K, et al. Everolimus for treatment of pseudomyogenic hemangioendothelioma. *J Pediatr Hematol Oncol*. 2017;39:328–331.
114. Gabor KM, Sapi Z, Tiszlavicz LG, et al. Sirolimus therapy in the treatment of pseudomyogenic hemangioendothelioma. *Pediatr Blood Cancer*. 2018:65.
115. Jussila L, Valtola R, Partanen TA, et al. Lymphatic endothelium and Kaposi's sarcoma spindle cells detected by antibodies against the vascular endothelial growth factor receptor-3. *Cancer Res*. 1998;58:1599–1604.
116. Weninger W, Partanen TA, Breiteneder-Geleff S, et al. Expression of vascular endothelial growth factor receptor-3 and podoplanin suggests a lymphatic endothelial cell origin of Kaposi's sarcoma tumor cells. *Lab Invest*. 1999;79:243–251.
117. Xu H, Edwards JR, Espinosa O, et al. Expression of a lymphatic endothelial cell marker in benign and malignant vascular tumors. *Hum Pathol*. 2004;35:857–861.
118. Carroll PA, Brazeau E, Lagunoff M. Kaposi's sarcoma-associated herpesvirus infection of blood endothelial cells induces lymphatic differentiation. *Virology*. 2004;328:7–18.
119. Wang H-W, Trotter MWB, Lagos D, et al. Kaposi sarcoma herpesvirus-induced cellular reprogramming contributes to the lymphatic gene expression in Kaposi sarcoma. *Nat Genet*. 2004;36:687–693.
120. Ganem D. KSHV and the pathogenesis of Kaposi sarcoma: listening to human biology and medicine. *J Clin Invest*. 2010;120:939–949.
121. Gasperini P, Espigol-Frigole G, McCormick PJ, et al. Kaposi sarcoma herpesvirus promotes endothelial-to-mesenchymal transition through Notch-dependent signaling. *Cancer Res*. 2012;72:1157–1169.
122. Cancian L, Hansen A, Boshoff C. Cellular origin of Kaposi's sarcoma and Kaposi's sarcoma-associated herpesvirus-induced cell reprogramming. *Trends Cell Biol*. 2013;23:421–432.
123. Li Y, Zhong C, Liu D, et al. Evidence for Kaposi sarcoma originating from mesenchymal stem cells through KSHV-induced mesenchymal-to-endothelial transition. *Can Res*. 2018;78:230–245.
124. Rabkin CS, Janz S, Lash A, et al. Monoclonal origin of multicentric Kaposi's sarcoma lesions. *N Engl J Med*. 1997;336:988–993.
125. Duprez R, Lacoste V, Brière J, et al. Evidence for a multiclonal origin of multicentric advanced lesions of Kaposi sarcoma. *J Natl Cancer Inst*. 2007;99:1086–1094.
126. Weiss RA, Whitby D, Talbot S, et al. Human herpesvirus type 8 and Kaposi's sarcoma. *J Natl Cancer Inst Monogr*. 1998;23:51–54.
127. Moore PS, Chang Y. Kaposi's sarcoma-associated herpesvirus-encoded oncogenes and oncogenesis. *J Natl Cancer Inst Monogr*. 1998;23:65–71.
128. Wang L, Damania B. Kaposi sarcoma-associated herpesvirus confers a survival advantage to endothelial cells. *Cancer Res*. 2008;68:4640–4648.
129. Sciacca FL, Sturzl M, Bussolino F, et al. Expression of adhesion molecules, platelet-activating factor, and chemokines by Kaposi's sarcoma cells. *J Immunol*. 1994;153:4816–4825.
130. Masood R, Cai J, Tulpule A, et al. Interleukin 8 is an autocrine growth factor and a surrogate marker for Kaposi's sarcoma. *Clin Cancer Res*. 2001;7:2693–2702.
131. Schulz TF, Cesarman E. Kaposi sarcoma-associated herpesvirus: mechanisms of oncogenesis. *Curr Opin Virol*. 2015;14:116–128.
132. Bower M, Nelson M, Young AM, et al. Immune reconstitution inflammatory syndrome associated with Kaposi's sarcoma. *J Clin Oncol*. 2005;23:5224–5228.
133. Tappero JW, Conant MA, Wolfe SF, Berger TG. Kaposi's sarcoma. Epidemiology, pathogenesis, histology, clinical spectrum, staging criteria and therapy. *J Am Acad Dermatol*. 1993;28:371–395.
134. Hammock L, Reisenauer A, Wang W, et al. Latency-associated nuclear antigen expression and human herpesvirus-8 polymerase chain reaction in the evaluation of Kaposi sarcoma and other vascular tumors in HIV-positive patients. *Mod Pathol*. 2005;18:463–468.
135. Dupin N, Fisher C, Kellam P, et al. Distribution of human herpesvirus-8 latently infected cells in Kaposi's sarcoma, multicentric Castleman's disease, and primary effusion lymphoma. *Proc Natl Acad Sci USA*. 1999;96:4546–4551.
136. Régnier-Rosencher E, Guillot B, Dupin N. Treatments for classic Kaposi sarcoma: a systematic review of the literature. *J Am Acad Dermatol*. 2013;68:313–331.
137. Brambilla L, Bellinvia A, Tourlaki A, et al. Intralesional vincristine as first-line therapy for nodular lesions in classic Kaposi sarcoma: a prospective study in 151 patients. *Br J Dermatol*. 2009;162:854–859.
137a. Salido-Vallejo R, González-Menchen A, Alcántara-Reifs C, et al. Treatment with oral propranolol for refractory classic cutaneous Kaposi sarcoma. *JAMA Dermatol*. 2022;158:832–834.
138. Antman K, Chang Y. Kaposi's sarcoma. *N Engl J Med*. 2000;342:1027–1038.
139. Krown SE. Acquired immunodeficiency syndrome-associated Kaposi's sarcoma. Biology and management. *Med Clin North Am*. 1997;81:471–494.
140. Vanni T, Sprinz E, Machado MW, et al. Systemic treatment of AIDS-related Kaposi sarcoma: current status and perspectives. *Cancer Treat Rev*. 2006;32:445–455.
141. Gascon P, Schwartz RA. Kaposi's sarcoma. New treatment modalities. *Dermatol Clin*. 2000;18:169–175.
142. Qunibi WY, Barri Y, Alfurayh O, et al. Kaposi's sarcoma in renal transplant recipients: a report on 26 cases from a single institution. *Transplant Proc*. 1993;25:1402–1405.
143. Stallone G, Schena A, Infante B, et al. Sirolimus for Kaposi sarcoma in renal-transplant patients. *N Engl J Med*. 2005;352:1317–1323.
144. Lebbe C, Euvrard S, Barrou B, et al. Sirolimus conversion for patients with post-transplant Kaposi's sarcoma. *Am J Transplant*. 2006;6:2164–2168.
145. Mentzel T, Beham A, Calonje E, et al. Epithelioid hemangioendothelioma of skin and soft tissues: clinicopathologic and immunohistochemical study of 30 cases. *Am J Surg Pathol*. 1997;21:363–374.
146. Quante M, Patel NK, Hill S, et al. Epithelioid hemangioendothelioma presenting in the skin: a clinicopathologic study of eight cases. *Am J Dermatopathol*. 1998;20:541–546.
147. Tanas MR, Sboner A, Oliveira AM, et al. Identification of a disease-defining gene fusion in epithelioid hemangioendothelioma. *Sci Transl Med*. 2011;3:98.
148. Errani C, Zhang L, Sung YS, et al. A novel WWTR1-CAMTA1 gene fusion is a consistent abnormality in epithelioid hemangioendothelioma of different anatomic sites. *Genes Chromosomes Cancer*. 2011;50:644–653.
149. Mitelman F, Johansson B, Mertens F. The impact of translocations and gene fusions on cancer causation. *Nat Rev Cancer*. 2007;7:233–245.
150. Chan SW, Lim CJ, Chen L, et al. The Hippo pathway in biological control and cancer development. *J Cell Physiol*. 2011;226:928–939.
151. Attiyeh EF, London WB, Mosse YP, et al. Chromosome 1p and 11q deletions and outcome in neuroblastoma. *N Engl J Med*. 2005;353:2243–2253.
152. Barbashina V, Salazar P, Holland EC, et al. Allelic losses at 1p36 and 19q13 in gliomas: correlation with histologic classification, definition of a 150-kb minimal deleted region on 1p36, and evaluation of CAMTA1 as a candidate tumor suppressor gene. *Clin Cancer Res*. 2005;11:1119–1128.
153. Antonescu CR, Le Loarer F, Mosquera JM, et al. Novel YAP1-TFE3 fusion defines a distinct subset of epithelioid hemangioendothelioma. *Genes Chromosomes Cancer*. 2013;52:775–784.
154. Flucke U, Vogels RJ, de Saint Aubain Somerhausen N, et al. Epithelioid hemangioendothelioma: clinicopathologic, immunhistochemical, and molecular genetic analysis of 39 cases. *Diagn Pathol*. 2014;9:131.
155. Lau K, Massad M, Pollak C, et al. Clinical patterns and outcome in epithelioid hemangioendothelioma with or without pulmonary involvement: insights from an internet registry in the study of a rare cancer. *Chest*. 2011;140:1312–1318.
156. Vignon-Pennamen MD, Varroud-Vial C, Janssen F, et al. Cutaneous metastases of hepatic epithelioid hemangioendothelioma. *Ann Dermatol Venereol*. 1989;116:864–866.
157. Miettinen M, Wang ZF. Prox1 transcription factor as a marker for vascular tumors - evaluation of 314 vascular endothelial and 1086 nonvascular tumors. *Am J Surg Pathol*. 2012;36:351–359.
158. Naqvi J, Ordonez NG, Luna MA, et al. Epithelioid hemangioendothelioma of the head and neck: role of podoplanin in the differential diagnosis. *Head Neck Pathol*. 2008;2:25–30.
159. Vasquez M, Ordóñez NG, English GW, Mackay B. Epithelioid hemangioendothelioma of soft tissue: report of a case with ultrastructural observations. *Ultrastruct Pathol*. 1998;22:73–78.
160. Stacchiotti S, Miah AB, Frezza AM, et al. Epithelioid hemangioendothelioma, an ultra-care cancer: a concensus paper from the community of experts. *ESMO Open*. 2021;6:1–14.
161. Holden CA, Spittle MF, Jones EW. Angiosarcoma of the face and scalp, prognosis and treatment. *Cancer*. 1987;59:1046–1057.
162. Deyrup AT, Miettinen M, North PE, et al. Angiosarcomas arising in the viscera and soft tissue of children and young adults. *Am J Surg Pathol*. 2009;33:264–269.
163. Deyrup AT, Miettinen M, North PE, et al. Pediatric cutaneous angiosarcomas: a clinicopathological study of 10 cases. *Am J Surg Pathol*. 2011;35:70–75.
164. Antonescu CR, Yoshida A, Guo T, et al. KDR activating mutations in human angiosarcomas are sensitive to specific kinase inhibitors. *Cancer Res*. 2009;69:7175–7179.
165. Manner J, Radlwimmer B, Hohenberger P, et al. *MYC* high level gene amplification is a distinctive feature of angiosarcomas after irradiation or chronic lymphedema. *Am J Surg Pathol*. 2010;176:34–39.
166. Guo T, Zhang L, Chang N-E, et al. Consistent *MYC* and *FLT4* gene amplification in radiation-induced angiosarcoma but not in other radiation-associated atypical vascular lesions. *Genes Chromosomes Cancer*. 2011;50:25–33.
167. Italiano A, Thomas R, Breen M, et al. The miR-17–92 cluster and its target THBS1 are differentially expressed in angiosarcomas dependent on MYC amplification. *Genes Chromosomes Cancer*. 2012;51:569–578.
168. Young RJ, Brown NJ, Reed MW, et al. Angiosarcoma. *Lancet Oncol*. 2010;11:983–991.
169. Marchal C, Weber B, de Lafontan B, et al. Nine breast angiosarcomas after conservative treatment for breast carcinoma: a survey from French Comprehensive Cancer Centers. *Int J Radiat Oncol Biol Phys*. 1999; 44:113–119.
170. Brown RW, Tornos C, Evans HL. Angiosarcoma arising from malignant schwannoma in a patient with neurofibromatosis. *Cancer*. 1992;70:1141–1144.
171. Bessis D, Sotto A, Roubert P, et al. Endothelin-secreting angiosarcoma occurring at the site of an arteriovenous fistula for haemodialysis in a renal transplant recipient. *Br J Dermatol*. 1998;138:361–363.
172. Jennings TA, Peterson L, Axiotis CA, et al. Angiosarcoma associated with foreign body material. A report of three cases. *Cancer*. 1988;62:2436–2444.
173. Leake J, Sheehan MP, Rampling D, et al. Angiosarcoma complicating xeroderma pigmentosum. *Histopathology*. 1992;21:179–181.
174. Dunkel IJ, Gerald WL, Rosenfield NS, et al. Outcome of patients with a history of bilateral retinoblastoma treated for a second malignancy: the Memorial Sloan-Kettering experience. *Med Pediatr Oncol*. 1998;30:59–62.
175. Folpe AL, Chand EM, Goldblum JR, Weiss SW. Expression of Fli-1, a nuclear transcription factor, distinguishes vascular neoplasms from potential mimics. *Am J Surg Pathol*. 2001;25:1061–1066.
176. DeYoung BR, Swanson PE, Argenyi ZB, et al. CD31 immunoreactivity in mesenchymal neoplasms of the skin and subcutis: report of 145 cases and review of putative immunohistologic markers of endothelial differentiation. *J Cutan Pathol*. 1995;22:215–222.
177. Miettinen M, Lindenmayer AE, Chaubal A. Endothelial cell markers CD31, CD34, and BNH9 antibody to H- and Y-antigens–evaluation of their specificity and sensitivity in the diagnosis of vascular tumors and comparison with von Willebrand factor. *Mod Pathol*. 1994;7:82–90.
178. Breiteneder-Geleff S, Soleiman A, Kowalski H, et al. Angiosarcomas express mixed endothelial phenotypes of blood and lymphatic capillaries: podoplanin as a specific marker for lymphatic endothelium. *Am J Pathol*. 1999;154:385–394.
179. Suchak R, Thway K, Zelger B, et al. Primary cutaneous epithelioid angiosarcoma: a clinicopathological study of 13 cases of rare neoplasm occurring outside the setting of conventional angiosarcomas and with predilection for the limbs. *Am J Surg Pathol*. 2011;35:60–69.
180. Gray MH, Rosenberg AE, Dickersin GR, Bhan AK. Cytokeratin expression in epithelioid vascular neoplasms. *Hum Pathol*. 1990;21:212–217.
181. Meis-Kindblom JM, Kindblom LG. Angiosarcoma of soft tissue: a study of 80 cases. *Am J Surg Pathol*. 1998;22:683–697.
182. Deyrup AT, McKenney JK, Tighiouart M, et al. Sporadic cutaneous angiosarcomas: a proposal for risk stratification based on 69 cases. *Am J Surg Pathol*. 2008;32:72–77.
183. Saroha S, Litwin S, von Mehren M. Retrospective review of treatment for angiosarcoma at Fox Chase Cancer Center over the past 15 years. *J Clin Oncol*. 2007;25:10034.
184. Seo T, Kitamura S, Yanagi T, Ujiie H. Efficacy of a combination of paclitaxel and radiation therapy

against cutaneous angiosarcoma: a single-institution retrospective study of 21 cases. *J Dermatol*. 2022;49:383–386.
185. Lee ATJ, Huang PH, Pollack SM, Jones RL. Effective management of advanced angiosarcoma by the synergistic combination of propranolol and vinblastine-based metronomic chemotherapy: a bench to bedside study. *EBioMedicine*. 2016;6:4–5.
186. Boon LM, Mulliken JB, Enjolras O, et al. Glomulovenous malformation (glomangioma) and venous malformation: distinct clinicopathologic and genetic entities. *Arch Dermatol*. 2004;140:971–976.
187. Irrthum A, Brouillard P, Enjolras O, et al. Linkage disequilibrium narrows locus for venous malformation with glomus cells (VMGLOM) to a single 1.48 Mbp YAC. *Eur J Hum Genet*. 2001;9:34–38.
188. Brouillard P, Olsen BR, Vikkula M. High-resolution physical and transcript map of the locus for venous malformations with glomus cells (VMGLOM) on chromosome 1p21-p22. *Genomics*. 2000;67:96–101.
189. Brouillard P, Boon LM, Vikkula M. Mutations in a novel factor, glomulin, are responsible for glomuvenous malformations ("glomangiomas"). *Am J Hum Genet*. 2002;70:866–874.
190. Nguyen H-L, Boon LM, Vikkula M. Genetics of vascular malformations. *Semin Pediatr Surg*. 2014;23:221–226.
191. Brouillard P, Boon LM, Revencu N, GVM Study Group. Genotypes and phenotypes of 162 families with a glomulin mutation. *Mol Syndromol*. 2013;4:157–164.
192. Amyere M, Aerts V, Brouillard P, et al. Somatic uniparental isodisomy explains multifocality of glomuvenous malformations. *Am J Hum Genet*. 2013;92:188–196.
193. Tron AE, Arai T, Duda DM, et al. The glomuvenous malformation protein glomulin binds Rbx1 and regulates cullin RING ligase-mediated turnover of Fbw7. *Mol Cell*. 2012;46:67–78.
194. McIntyre BA, Brouillard P, Aerts V, et al. Glomulin is predominantly expressed in vascular smooth muscle cells in the embryonic and adult mouse. *Gene Expr Patterns*. 2004;4:351–358.
195. Brathwaite CD, Poppiti Jr. RJ. Malignant glomus tumor. A case report of widespread metastases in a patient with multiple glomus body hamartomas. *Am J Surg Pathol*. 1996;20:233–238.
196. Mounayer C, Wassef M, Enjolras O, et al. Facial 'glomangiomas': large facial venous malformations with glomus cells. *J Am Acad Dermatol*. 2001;45:239–245.
197. Yang JS, Ko JW, Suh KS, Kim ST. Congenital multiple plaque-like glomangiomyoma. *Am J Dermatopathol*. 1999;21:454–457.
198. Folpe AL, Fanburg-Smith JC, Miettinen M, Weiss SW. Atypical and malignant glomus tumors: analysis of 52 cases, with a proposal for the reclassification of glomus tumors. *Am J Surg Pathol*. 2001;25:1–12.
199. Mentzel T, Calonje E, Nascimento AG, Fletcher CD. Infantile hemangiopericytoma versus infantile myofibromatosis. Study of a series suggesting a continuous spectrum of infantile myofibroblastic lesions. *Am J Surg Pathol*. 1994;18:922–930.
200. Granter SR, Badizadegan K, Fletcher CD. Myofibromatosis in adults, glomangiopericytoma, and myopericytoma: a spectrum of tumors showing perivascular myoid differentiation. *Am J Surg Pathol*. 1998;22:513–525.
201. Requena L, Kutzner H, Hugel H, et al. Cutaneous adult myofibroma: a vascular neoplasm. *J Cutan Pathol*. 1996;23:445–457.



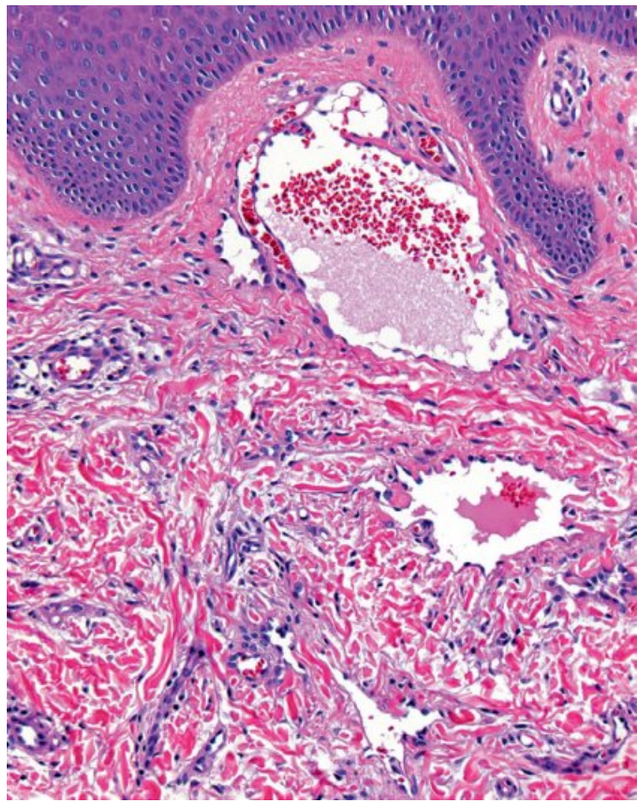
eFig. 114.1 Diffuse dermal angiomatosis. Reticulated violaceous plaques of the breasts with punctate telangiectasias. *Courtesy Department of Dermatology, Medical University of Graz.*



eFig. 114.2 Diffuse dermal angiomatosis. Violaceous plaques with a central blue–black plaque bulla. Ulcerations can develop within areas of involvement. *Courtesy Luis Requena, MD.*



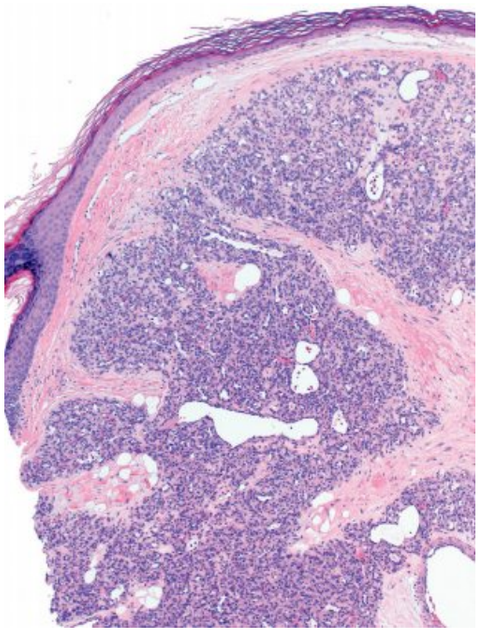
eFig. 114.3 Targetoid hemosiderotic lymphatic malformation (hobnail "hemangioma"). Note the target-like appearance. *Courtesy Ronald P. Rapini, MD.*



eFig. 114.4 Targetoid hemosiderotic lymphatic malformation (hobnail "hemangioma") – histopathologic features. Dilated superficial dermal vessels lined by hobnailed endothelial cells, merging with smaller slit-like vessels in the lower dermis.



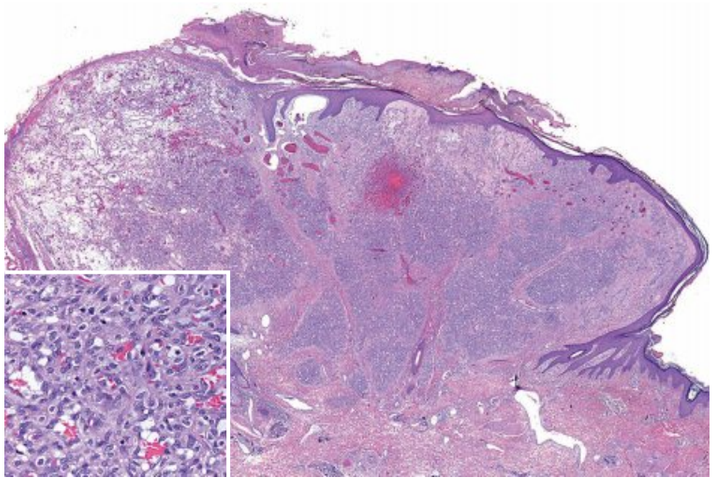
eFig. 114.5 Pyogenic granuloma arising within the nasal vestibule. *Courtesy Sonya K. Burton, MD.*



eFig. 114.6 Histology of pyogenic granuloma (lobulary capillary hemangioma). Proliferating capillaries are often grouped into lobules by dense fibrous bands, hence the synonym lobular capillary hemangioma. The lesion is often clutched by an epithelial collarette.



eFig. 114.9 Tufted angioma. Dull pink–red to violet plaque on the distal thigh and knee of an infant.



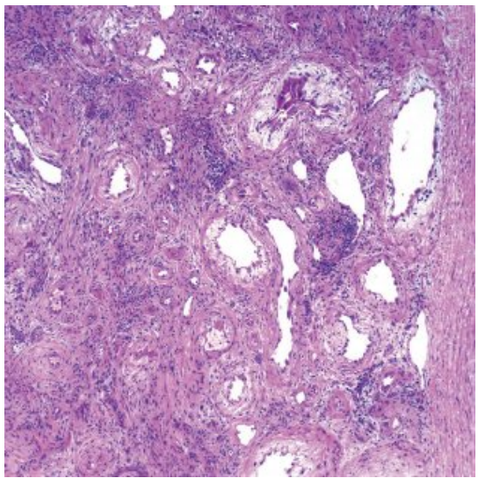
eFig. 114.7 Histology of pyogenic granuloma (lobulary capillary hemangioma). Exophytic nodule characterized by lobules of capillaries delineated by fibrous bands (hence the synonym lobular capillary hemangioma). The lesions are often clutched by an epithelial collarette and are commonly ulcerated. The inset shows the proliferation of small capillaries. *Courtesy Lorenzo Cerroni, MD.*



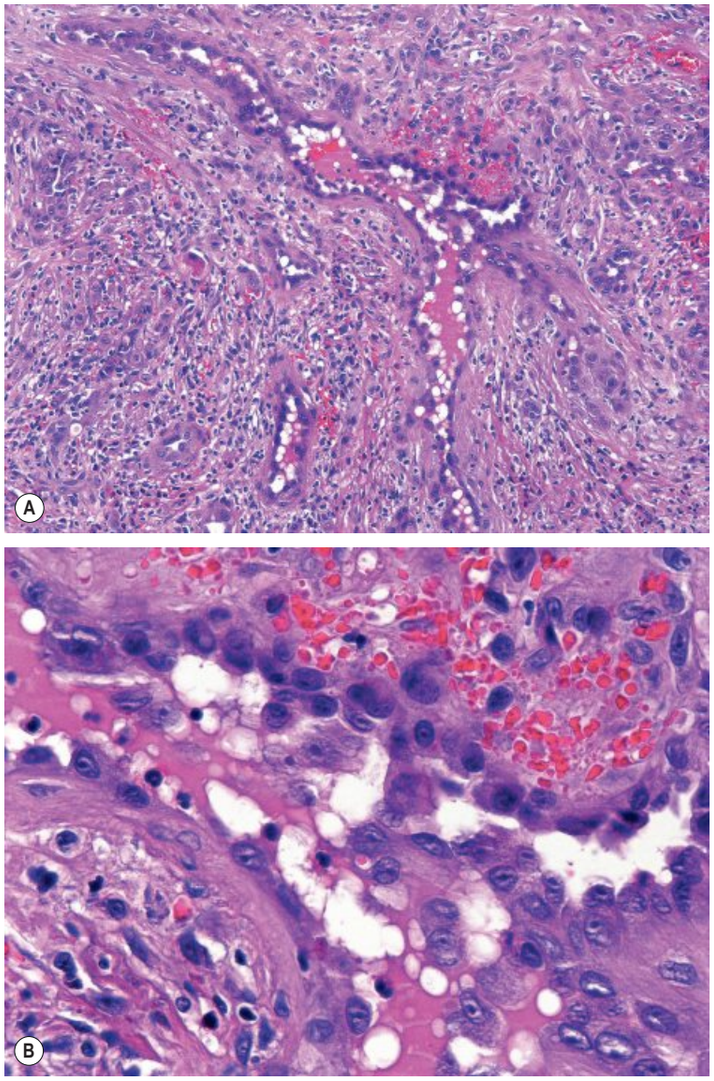
eFig. 114.10 Epithelioid hemangioma (angiolymphoid hyperplasia with eosinophilia). Multiple skin-colored and pink papulonodules and tumors on the scalp. *Courtesy Karynne O. Duncan, MD.*



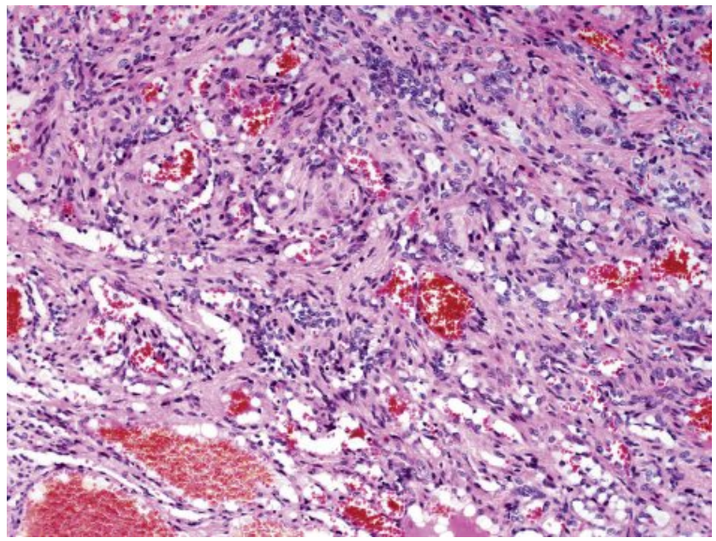
eFig. 114.8 Tufted angioma. Dull red–violet plaque on the flank in a neonate.



eFig. 114.11 Histology of epithelioid hemangioma (angiolymphoid hyperplasia with eosinophilia). Proliferation of vessels characterized by enlarged endothelial cells and surrounded by inflammatory infiltrates.



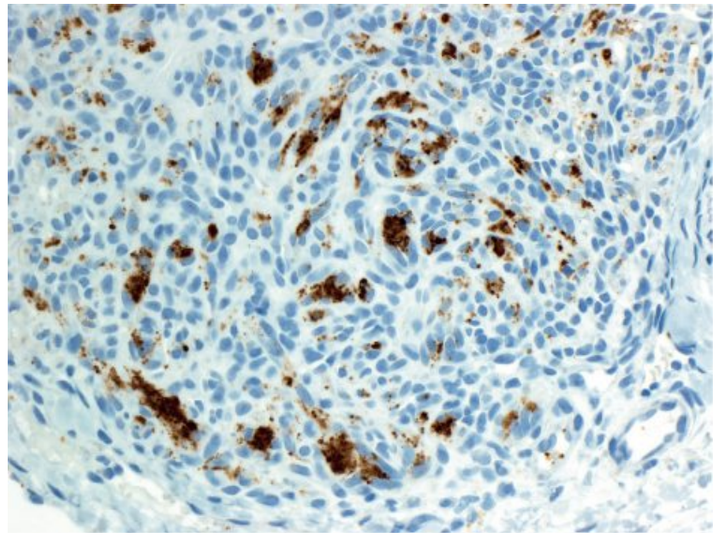
eFig. 114.12 Histology of epithelioid hemangioma (angiolymphoid hyperplasia with eosinophilia). A Proliferation of vessels surrounded by inflammatory infiltrates. **B** The vessels are characterized by enlarged endothelial cells protruding into the lumen. *Courtesy Luis Requena, MD.*



eFig. 114.13 Histology of spindle cell hemangioma. Collapsed veins containing organizing thrombi alternate with more cellular spindled areas and occasional vacuolated epithelioid cells.



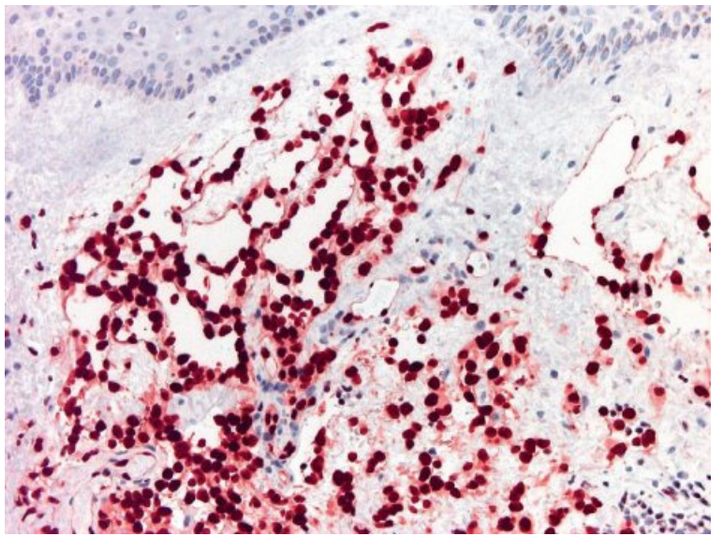
eFig. 114.14 Kaposiform hemangioendothelioma complicated by Kasabach–Merritt phenomenon. A large red–purple mass on the upper flank of an infant.



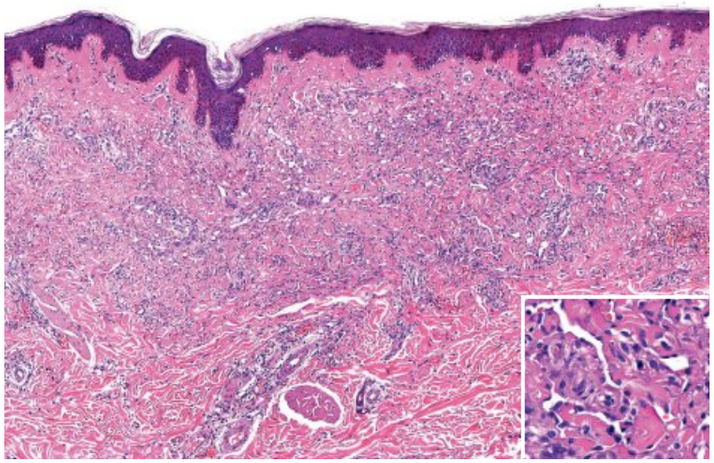
eFig. 114.15 Kaposiform hemangioendothelioma. CD61 immunostain highlights the platelets trapped in lesional vessels, representing the histologic correlate of Kasabach–Merritt phenomenon.



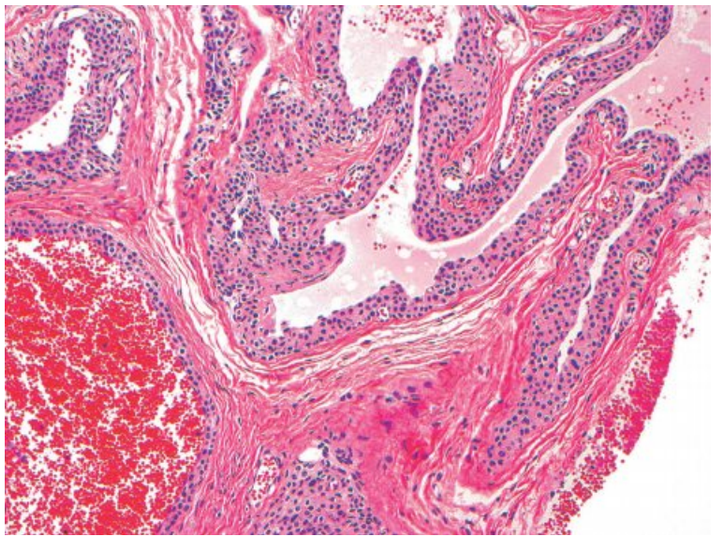
eFig. 114.16 Kaposi sarcoma – classic type. Violaceous plaque with superimposed papules. *Courtesy Jean L. Bolognia, MD.*



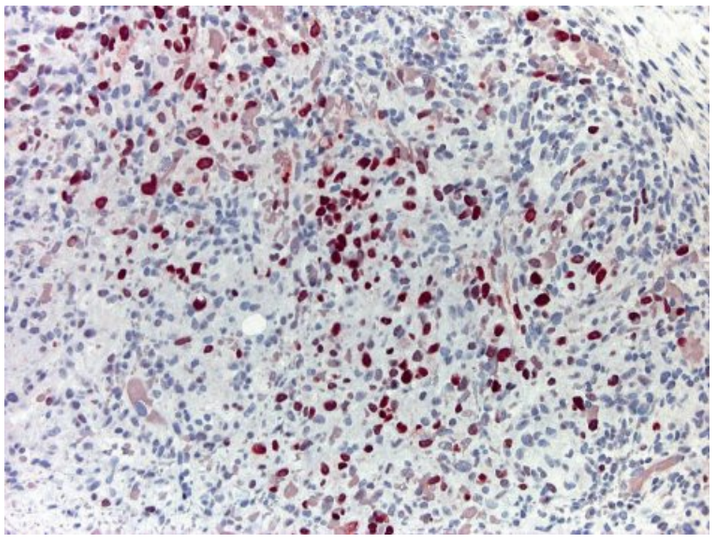
eFig. 114.19 Cutaneous angiosarcoma. Strong nuclear immunostaining of neoplastic cells for ERG. *Courtesy Lorenzo Cerroni, MD.*



eFig. 114.17 Histology of Kaposi sarcoma – patch stage. In the upper reticular dermis, there is a vascular proliferation characterized by slit-like vascular spaces (inset) with hemorrhage. *Courtesy Luis Requena, MD.*



eFig. 114.20 Histology of a glomuvenous malformation ("glomangioma"). One or more, often incomplete, layers of glomus cells rim abnormal venous channels that are otherwise histologically consistent with a venous malformation.



eFig. 114.18 Cutaneous angiosarcoma. Immunostaining for c-MYC shows nuclear positivity of many neoplastic cells. *Courtesy Lorenzo Cerroni, MD.*



eFig. 114.21 Pyogenic granuloma. Grouped red papules on the lip.



eFig. 114.22 Genital angiokeratomas. In men, the scrotum is the most common location. *Courtesy Kalman Watsky, MD.*



eFig. 114.23 Angiosarcoma. Large ulcerated plaque with hemorrhage. *Courtesy Catherine Baker, MD, and Noel Turner, MD.*

Neural and Neuroendocrine Neoplasms (Other than Neurofibromatosis) 115

Andrea Saggini, Tomoko Akaike, Paul Nghiem and Zsolt B. Argenyi

Chapter Contents

Classification, Terminology, and Histogenesis 2077
Neuromas 2077
Schwannoma 2081
Neurofibroma 2083
Nerve Sheath Myxoma and Cellular Neurothekeoma 2084
Granular Cell Tumor 2085
Perineurioma 2086
Malignant Peripheral Nerve Sheath Tumor 2087
Merkel Cell Carcinoma 2087
Heterotopic Neural Tissue of the Skin 2090
Primitive Neuroectodermal Tumors 2092

In the past, neural tumors were often misdiagnosed histopathologically because of confusing classifications. As a result, their clinical relevance was poorly understood. Clinically, cutaneous neural tumors often look alike and most of them are benign. However, their correct diagnosis can be helpful in recognizing important clinical syndromes and this can contribute to better patient management[1].

CLASSIFICATION, TERMINOLOGY, AND HISTOGENESIS

Cutaneous neural tumors can be classified into two major groups: those derived from peripheral nerves and those derived from ectopic or heterotopic neural tissue (Table 115.1). The former group were classically subdivided into true nerve sheath neoplasms and hamartomatous tumors, although this classification may be specious due to evidence that most hamartomas are driven by clonal expansion of a neoplastic cell population[2,3].

Cutaneous neural tumors tend to differentiate toward one or more elements of the nervous system; as a result, they recapitulate to varying degrees the morphogenesis of normal peripheral nerves. Therefore, knowledge of the organization of the normal peripheral nerve (Fig. 115.1) is crucial to understanding the histogenesis of cutaneous neural tumors[2].

The basic element of a peripheral nerve is the nerve fiber, which is composed of an axon and its surrounding Schwann cell layer. A peripheral nerve can be compared to a conventional telephone cable, in which each axon and its surrounding Schwann cell layer correspond to a telephone wire and its insulation, respectively. Nerve fibers are bundled within nerve fascicles by the perineurium, a sheath composed of specialized perineurial cells (see Fig. 115.1). Inside the nerve fascicle, the space between individual nerve fibers is referred to as the endoneurium. The bundles of nerve fascicles are further encased in a supportive fibrous sheath called the epineurium. To a variable extent, this architectural arrangement is recognizable in many cutaneous neural neoplasms.

The most important constituent cells are the Schwann cell, the perineurial cell, and the various nonspecific mesenchymal cells, such as fibroblasts and mast cells. These cells are capable of proliferation and malignant transformation. Other elements of the peripheral nerve, which are cell parts or products (i.e. axons and myelin, respectively), cannot duplicate. Schwann cells are derived from the neural crest and perineurial cells appear to be modified fibroblasts of mesodermal origin. This difference in histogenesis is also reflected in the distinct antigenic expression of these cells. Schwann cells express S100 protein and SOX10 but not perineurial markers (e.g. epithelial membrane antigen, GLUT1, claudin-1), whereas perineurial cells stain positively for perineurial markers but not S100 protein and SOX10. Axons contain a specific type of intermediate filament called neurofilament, and myelinated axons contain myelin basic protein, both of which can be detected by immunohistochemistry. These and other immunohistochemical markers often can help to establish the correct diagnosis.

In the following sections, each clinically relevant neural neoplasm is discussed (Tables 115.2–115.4).

NEUROMAS

Key features

Traumatic neuroma

- Develops at the site of previous trauma
- Skin-colored papule or nodule that is often painful or sensitive
- Circumscribed histologically, but not encapsulated
- Regenerative proliferation of axons and Schwann cells within fibrous scar tissue

Solitary circumscribed neuroma

- Formerly known as "palisaded encapsulated neuroma"
- Solitary papule or nodule, usually on the face of adults
- Circumscribed histologically; partially or completely encapsulated
- Compactly arranged fascicles of spindle cells with only vague palisading of nuclei

Introduction

Neuromas are proliferations of neural tissue in which the ratio of axons to Schwann cells is only slightly less than the normal 1 : 1 ratio. There are two major subtypes: *traumatic (or amputation) neuroma* and *solitary circumscribed neuroma* (SCN). Traumatic neuromas are complex regenerative proliferations of nerve fibers that follow injury. SCN, formerly known as palisaded encapsulated neuroma, is a benign peripheral nerve sheath tumor whose development is not preceded by apparent tissue injury.

History

The current view of traumatic neuroma was introduced by Huber and Lewis based on the concept of Wallerian degeneration. SCN was described by Reed and co-workers in 1972[4].

Epidemiology

Traumatic neuromas are relatively uncommon but can occur at any age and in either sex. They are more prevalent in professions with a high probability of physical injuries. SCN develops spontaneously and gradually without obvious preceding trauma. These tumors appear during adulthood (mean age, 45 years), and there is no sex predisposition or association with known tumor predisposition syndromes[2–4].

Pathogenesis

The term "neuroma" refers to a benign nerve sheath tumor characterized by a relatively balanced proliferation of Schwann cells and axons, resulting in an axon to Schwann cell ratio close to the normal 1 : 1 ratio[5].

CLASSIFICATION OF CUTANEOUS NEURAL AND NEUROENDOCRINE TUMORS	
Tumors of the peripheral nerve sheath and related structures	**Neural heterotopias**
Neuromas	Meningeal
• Traumatic (amputation) • Solitary circumscribed (palisaded encapsulated) • Multiple mucocutaneous (non-encapsulated) • Epithelial sheath	• Meningocele • Rudimentary meningocele (type 1 meningioma)
	Neuroglial
	• Nasal glial heterotopia ("nasal glioma")
Schwannomas	**Neuroblastic/ganglionic tumors**
• Common • Ancient • Cellular • Plexiform • Epithelioid • Microcystic/reticular • Psammomatous melanotic (malignant melanotic schwannian tumor)	• Primary primitive neuroectodermal tumor • Neuroblastoma • Ganglioneuroma
	Miscellaneous neural and neuroendocrine tumors
Neurofibromas	• Meningioma (type II and type III) • Primary low-grade neuroendocrine carcinoma of the skin (primary cutaneous carcinoid tumor) • Neuroendocrine carcinoma of the skin (Merkel cell carcinoma) • Pigmented neuroectodermal tumor of infancy
• Common (localized cutaneous) • Diffuse • Intraneural (localized) • Plexiform • Ancient (with cytological atypia) • Atypical neurofibromatous neoplasm of uncertain biologic potential (ANNUBP)	
Nerve sheath myxoma* Granular cell tumor Perineurioma • Soft tissue • Sclerosing • Other variants Hybrid peripheral nerve sheath tumor Malignant peripheral nerve sheath tumor	

*Cellular neurothekeoma is now regarded as a distinct entity with no evidence of neural differentiation.

Table 115.1 Classification of cutaneous neural and neuroendocrine tumors.

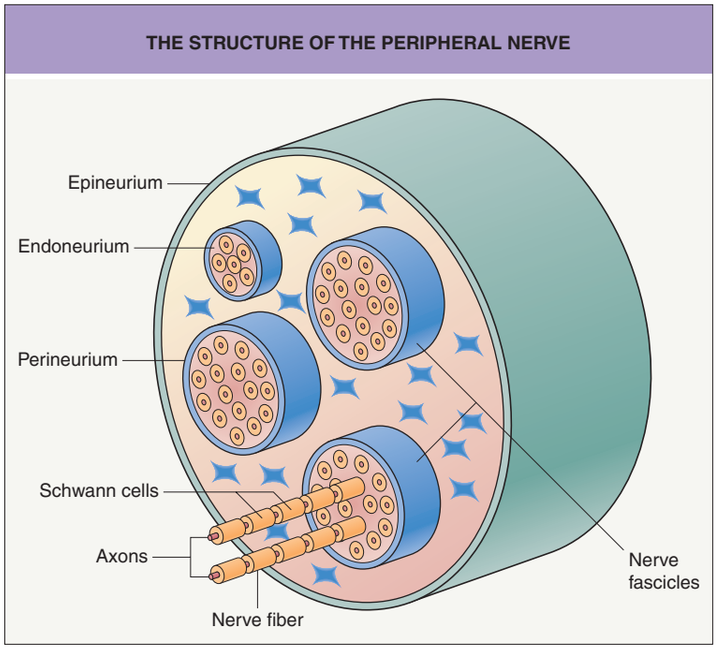


Fig. 115.1 The structure and components of the peripheral nerve.



Fig. 115.2 Traumatic neuroma. A painful, firm papule that appeared after a deep puncture injury.

Traumatic neuromas represent exuberant proliferations of nerve fibers that develop in response to an extrinsic nerve injury. Ideally, a severed nerve is reestablished via an orderly growth of axons and proliferating Schwann cells from the proximal to the distal end of the nerve[6]. If the two nerve ends are not maintained in close apposition, the reparative process fails, resulting in a tangle of irregularly proliferating proximal nerve fascicles embedded within scar tissue.

In SCN there is a coupled proliferation of Schwann cells and axons within the confinement of the perineurium. Its exact pathomechanism remains to be determined. Although a reactive process following minor tissue injury (e.g. facial acne) has been postulated, no definite traumatic origin has been demonstrated[2].

Clinical Features

Traumatic neuromas are usually solitary, skin-colored or reddish purple, firm papules or nodules at sites of wounds, surgical scars, and amputations[7,8] (Fig. 115.2). On the lower extremities, they may be multiple[7]. Early lesions are asymptomatic, but after a few months they gradually become painful, frequently with a lancinating character. Variable tingling and itching can be associated with the pain.

In neonates and young infants, similar lesions may be located on the lateral surface of a normal digit, most commonly the ulnar side of the fifth digit. Such tumors, also referred to as "rudimentary supernumerary digits", have traditionally been regarded as traumatic neuromas secondary to amputation of supernumerary digits *in utero*[9] (see Fig. 64.24). However, on histologic examination, there is no evidence of a pre-existing supernumerary digit, leading some authors to propose that these lesions may represent true congenital malformations.

SCNs present as asymptomatic, rubbery to firm, skin-colored to pink papules or nodules ranging in diameter from 2 to 6 mm[4]. Approximately 90% are located on the face, primarily around the nose, but they also occur on the cheek, chin, lips, and oral mucosa[10]. The remaining 10% occur elsewhere, including the trunk and extremities.

In MEN2B, also referred to as multiple mucosal neuroma syndrome or MEN type 3, numerous soft, skin- or mucosa-colored papules and nodules appear on the eyelid margins, mucosal lips, tongue, and conjunctivae, as well as the nasal and laryngeal mucosae (see Fig. 63.2). Additional findings include pheochromocytomas, medullary carcinoma of the thyroid, gastrointestinal ganglioneuromatosis, rare perinasal cutaneous neuromas, and palpable foci of dermal hyperneury (see Table 63.2). Multiple mucocutaneous neuromas with a predilection for the face and distal extremities may also be a manifestation of the PTEN hamartoma tumor syndrome (see Tables 63.3 & 63.4).

Pathology

Traumatic neuromas are usually well-circumscribed nodules located at any level of the dermis or the subcutis. They are encased by a fibrous sheath, although the distal end can be poorly defined. The proliferation is composed of a chaotic, poorly organized tangle of fascicles of various

CLINICAL FEATURES OF BENIGN NEURAL NEOPLASMS							
	Traumatic (amputation) neuroma	**Solitary circumscribed neuroma (SCN)**	**Schwannoma**	**Neurofibroma**	**Nerve sheath myxoma**	**Cellular neurothekeoma***	**Granular cell tumor**
Incidence	Uncommon	Rare	Uncommon	Very common	Rare	Rare	Rare
Age	Any	Adults (30–60 years)	Adults (30–50 years)	Adults (20–60 years)	Any	Early adulthood (mean age, 24 years)	Adults (30–50 years)
Sex	M:F = 1:1	M:F = 1:1	M:F = 1:1	M:F = 1:1	M:F = 1:1	F:M = 2:1	F>M
Number	Usually solitary	Usually solitary	Usually solitary (>90%)	Usually solitary	Usually solitary	Usually solitary	Usually solitary (10% multiple)
Location	At sites of trauma, surgical scars, amputations	90% face, 10% elsewhere	Flexor aspect of an extremity, head	Trunk, head (solitary type)	Distal extremities	Predominantly on head and upper extremities	25% tongue, 75% elsewhere, mainly head and neck
Size	0.5–2.0 cm	0.2–0.6 cm	0.5–3.0 cm	0.2–2.0 cm	0.5–1.0 cm	0.5–3.0 cm	0.5–3.0 cm
Clinical appearance	Skin-colored to reddish purple, firm papule or nodule	Skin-colored or pink, rubbery to firm papule or nodule	Soft, skin-colored to pink or yellow, smooth-surfaced nodule or tumor	Skin-colored, soft or rubbery papule or nodule, sometimes pedunculated	Soft, skin-colored papule or nodule	Pink, red, or brown, firm papule or nodule	Skin-colored to brownish red, firm papulo-nodule; may have ulcerated or verrucous surface
Symptoms	Variable; tingling, pruritus, lanci-nating pain	Asymptomatic	Asymptomatic; occasionally painful or tender; rarely paresthesias; occasionally freely movable	Asymptomatic; "buttonhole" sign may be present	Asymptomatic	Usually asymp-tomatic, rarely painful or pruritic	Asymptomatic or occasionally tender or pruritic
Association	NA	Multiple (non-encapsu-lated) neuromas in MEN2B (mucosal) and PTEN hamartoma tumor syndrome (mucocuta-neous)	Neurofibromatosis type 2, schwan-nomatosis	If multiple, may be sign of one of the various forms of neurofibro-matosis (see Ch. 61)	NA	NA	Multiple tumors more frequently occur in African-Americans and RASopathies (NF1, Noonan syndrome, Noonan syndrome with multiple lentigines)
Clinical differential diagnosis	Hypertrophic scar, derma-tofibroma, foreign body granuloma, granular cell tumor, neurothekeoma, phantom limb pain (amputation)	Basal cell carcinoma, adnexal tumor, IDN, neurofibroma, schwannoma, nerve sheath myxoma; when multiple, adnexal tumors (see Fig. 111.5)	Neurofibroma, lipoma, angio-lipoma, cyst (epidermoid, pilar, dermoid, ganglion), IDN, adnexal tumors (including sebaceous), SCN, leiomyoma	IDN, soft fibroma, schwannoma, fibrolipoma, SCN, nerve sheath myxoma, anetoderma, lipoma, cyst (epidermoid, pilar)	IDN, neuro-fibroma, schwannoma, lipoma, cyst (myxoid, ganglion, epidermoid, pilar)	Dermatofibroma (including sclerosing heman-gioma variant), adnexal tumor, hypertrophic scar, keloid, granular cell tumor, SCN, fibrosed dermal or compound melanocytic nevus	Tongue: irritation (traumatic) fibroma, verruca, SCC Elsewhere: dermatofibroma, regressing verruca, adnexal tumor, prurigo nodularis, fibrosed melano-cytic nevus, SCC
Other	"Rudimentary supernu-merary digit" is considered a variant (Ch. 64)		Melanotic schwannoma is a distinct entity and may be associated with Carney complex	Plexiform variant is pathogno-monic for NF1		Gene expression profile suggests fibrohistiocytic differentiation	Visceral forms occur; true malignant trans-formation rare

*Cellular neurothekeoma is no longer considered to be a neural neoplasm.

Table 115.2 Clinical features of benign neural neoplasms. NA, not applicable; IDN, intradermal melanocytic nevus; MEN2B, multiple endocrine neoplasia, type 2B; NF1, neurofibromatosis type 1; SCC, squamous cell carcinoma.

sizes and shapes (Fig. 115.3). Between the fibers are variable amounts of fibrous tissue with or without inflammatory cells and mucin[5]. The constituent cells are Schwann cells and accompanying perineurial cells with spindle-shaped nuclei and cytoplasm. Special stains show several axons in an irregular, haphazard pattern[1,2].

SCNs present as well-circumscribed, ovoid or round nodules within the mid dermis, although some lesions may extend into the subcutis; occasionally, there is a multinodular, plexiform growth pattern. The tumor appears at least partially encapsulated by a thin connective tissue sheath composed of perineurial cells[10] (Fig. 115.4). The parenchyma consists of interwoven fascicles of spindled cells. Fascicles are compactly and relatively uniformly arranged, occasionally separated by clefts. The stroma is relatively monomorphous, and in contrast to traumatic neuromas, there is no evidence of inflammation, granulation tissue, or scarring[5].

HISTOLOGIC DIFFERENTIAL DIAGNOSTIC FEATURES OF COMMON CUTANEOUS NEURAL NEOPLASMS				
	Traumatic neuroma	**Solitary circumscribed neuroma**	**Schwannoma**	**Neurofibroma (localized cutaneous variant)**
Location in the skin	Any level of dermis or subcutis	Mid dermis, occasionally extending into subcutis	Deep dermis or subcutis	Any location in the dermis
Growth pattern	Usually well circumscribed but may be poorly defined at the distal end	Well circumscribed, nodular, rarely plexiform	Well circumscribed, nodular or ovoid	Poorly to well circumscribed
Encapsulation	Usually encased by a fibrous sheath	Yes, by perineurium	Yes, by perineurium	Not encapsulated in the dermis
Architecture	Chaotic, poorly organized tangle of fascicles of various sizes and shapes	Compactly arranged fascicles; frequent clefts between fascicles	Hypercellular areas (Antoni A), fascicles in various patterns, hypocellular areas (Antoni B), edematous, myxoid	Fine fibrillary lattice of haphazardly arranged spindle cells in variably dense matrix
Constituent cell types	Schwann cells, perineurial cells, fibroblasts, mast cells, macrophages	Schwann cells (99%), perineurial cells (in capsule only)	Schwann cells (99%), perineurial cells (in capsule only)	Schwann cells, perineurial cells, fibroblasts, mast cells
Cytologic features	Spindle cells with indistinct cytoplasmic contours and tapered slender nuclei	Spindle cells with indistinct cytoplasmic contours and tapered slender nuclei	Spindle cells with indistinct cytoplasmic contours and slender nuclei	Spindle cells with slender nuclei, plump fibroblasts
Nuclear palisading	None	Usually present, but indistinct	Yes (Antoni A areas)	Rarely
Verocay bodies	None	None	Often	None
Nerve fibers (axons)	Yes; abundant, irregular pattern	Yes; abundant, often in a parallel arrangement	Yes; very rare, more frequent at the site of the connecting nerve	Yes; rare, scattered
Other important features	Nerve of origin frequently present, extensive fibrosis	Nerve of origin frequently present, no fibrosis	Mast cells; may have extensive degenerative changes (e.g. hyalinization, hemorrhage) in Antoni B areas ("ancient changes")	Variable fibrosis and myxoid changes, mast cells, occasional blood vessels
Histopathologic differential diagnosis	Hypertrophic scar, neurofibroma, schwannoma, palisaded encapsulated neuroma	Traumatic neuroma, schwannoma, angioleiomyoma, myofibroma	Palisaded encapsulated neuroma, angiomyoma, fibrous histiocytoma, traumatic neuroma	Melanocytic nevus with neuroid differentiation, dermatofibroma, hypertrophic scar, dermatofibrosarcoma protuberans, traumatic neuroma

Table 115.3 Histologic differential diagnostic features of common cutaneous neural neoplasms.

IMMUNOHISTOCHEMICAL STAINING OF CUTANEOUS NEURAL NEOPLASMS AND THE MAJOR TUMORS IN THE DIFFERENTIAL DIAGNOSIS							
Neoplasm	**Immunohistochemical stain**						
	NF (for axons)	**S100**	**SOX10**	**EMA***	**CD34**	**Melan-A**	**SMA**
Traumatic neuroma	+	+	+	±	–	–	–
Solitary circumscribed neuroma	+	+	+	+ (peripheral capsule)	–	–	–
Schwannoma and variants	–†	+	+	+ (peripheral capsule)	–	–^	–
Neurofibroma and variants‡	±	+	+	±	±	–	–
Nerve sheath mixoma	–†	+	+	± (peripheral capsule)	±	–	–
Cellular neurothekeoma	–	–	–	–	–	–	±
Perineurioma	–	–	–	+ (neoplastic cells)	±	–	–
Granular cell tumor	–	+	+	–	–	–	–
Malignant peripheral nerve sheath tumor¶	±	±	±	–	–	–	–
Melanocytic nevus with neural differentiation	–	+	+	–	–	+	–
Dermatofibrosarcoma protuberans	–	–^^	–	–	+	–	–
Leiomyoma	–	–	–	–	–	–	+

*Similar pattern of immunoreactivity may be observed with GLUT1 and claudin-1
†Very sparse axons may be demonstrated in serial immunostained sections
‡In some variants, staining pattern may be variable
¶The rare perineurial variant is S100(–) / SOX10(–) / EMA(+)
^Positive in psammomatous melanotic schwannomas.
^^In the pigmented variant (Bednar tumor), scattered S100-/SOX10-/Melan-A-positive dendritic melanocytes are seen but the neoplastic cells are negative.

Table 115.4 Immunohistochemical staining of cutaneous neural neoplasms and the major tumors in the differential diagnosis. EMA, epithelial membrane antigen; Melan-A, melanocyte-related antigen; NF, neurofilament; S100, S100 protein; SMA, smooth muscle actin. +, positive; –, negative.

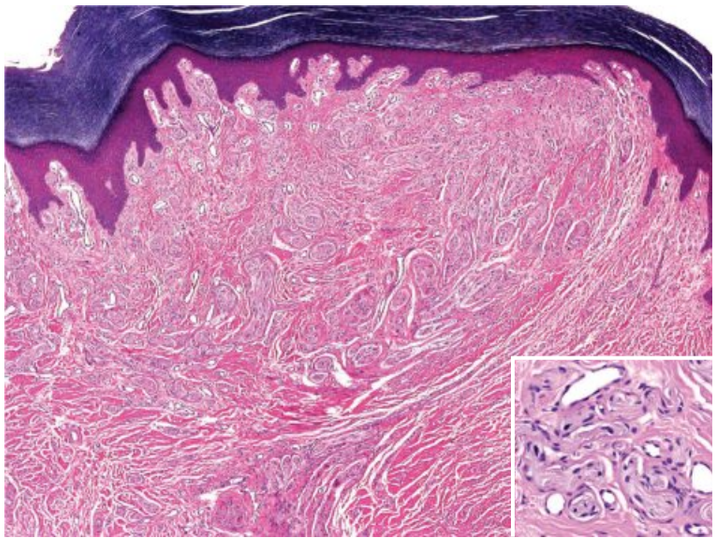


Fig. 115.3 Traumatic neuroma. Acral lesion with a chaotic proliferation of nerve fascicles is embedded in a fibrous stroma. Note nerve fascicles within a fibrotic stroma (inset). *Courtesy Lorenzo Cerroni, MD.*

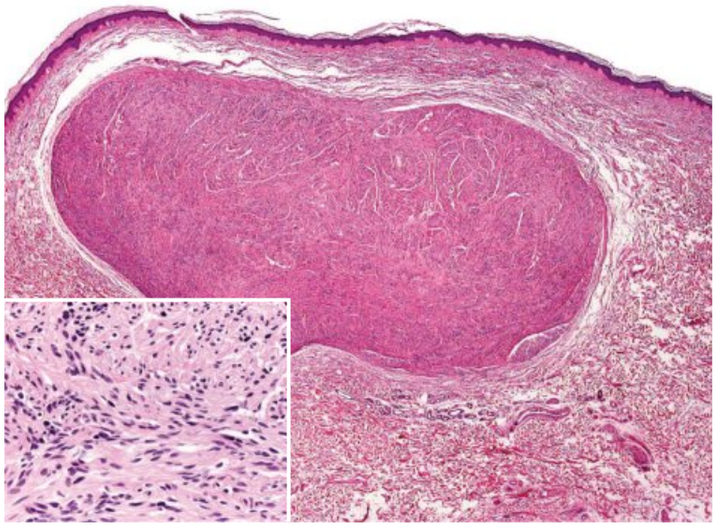


Fig. 115.4 Solitary circumscribed neuroma. The well-circumscribed dermal nodule appears encapsulated. Note nerve fascicles (inset). *Courtesy Lorenzo Cerroni, MD.*

The nuclei of the spindle-shaped tumor cells are elongated and wavy with tapered ends and an evenly basophilic chromatin pattern. Occasionally, a parallel arrangement of the nuclei is present, but distinct palisading or Verocay body formation is unusual[11–13]. No appreciable nuclear pleomorphism or mitotic activity is observed. In contrast to schwannomas, abundant axons throughout the tumor nodules may be highlighted via special stains[11] (Fig. 115.5).

Mucosal neuromas in MEN2B consist of non-encapsulated, tortuous proliferations of nerve bundles with a prominent perineurium, while dermal hyperneury is characterized by an increased number of enlarged and haphazardly arranged dermal nerves. Epithelial sheath neuroma represents a more recently described entity in which there is hyperplasia of mature nerve fascicles within the dermis (akin to dermal hyperneury), but each fascicle is surrounded by an aberrant sheath of squamous epithelium instead of normal perineurium; these features must be distinguished from perineural invasion by malignant tumors[14].

Differential Diagnosis

The diagnosis of traumatic neuroma is usually suspected by the history of a painful or symptomatic papulonodule at a site of injury and is confirmed by pathologic examination. Clinically, SCNs may resemble a BCC, adnexal tumor, intradermal melanocytic nevus, or neurofibroma (see Table 115.2). The diagnosis usually depends upon histologic examination (see Table 115.3).

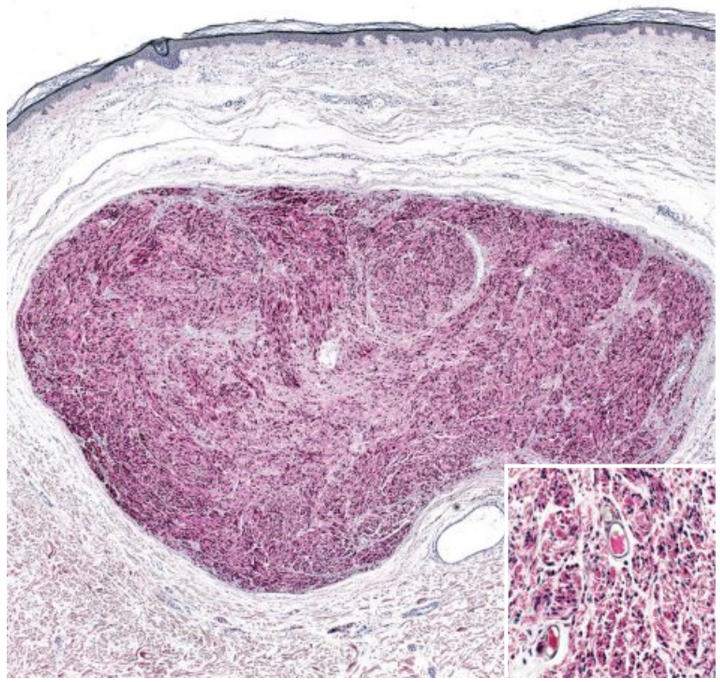


Fig. 115.5 Solitary circumscribed neuroma. Diffuse positivity for S100 within the dermal nodule. Note expression of S100 by the nerve fascicles (inset). *Courtesy Lorenzo Cerroni, MD.*

Treatment

Surgical excision of traumatic neuromas is recommended, with an attempt to reposition the proximal nerve stump into a scar-free area[7]. SCNs are easily excised, and some can even be enucleated from the surrounding dermis or subcutaneous tissue[4].

SCHWANNOMA

Synonyms: ■ Neurilemmoma ■ Neurolemmoma ■ Schwann cell tumor ■ Acoustic neuroma

Key features

- Solitary papulonodule that usually appears on the flexural aspect of an extremity, along a peripheral nerve
- Occasionally painful or tender
- Deep dermal or subcutaneous location
- Histologically, there is an encapsulated spindle cell proliferation with biphasic Antoni A and B areas, palisading of nuclei, and Verocay bodies; rare axons are present

Introduction

Schwannomas are benign encapsulated nerve sheath neoplasms nearly entirely composed of differentiated Schwann cells.

History

Stout coined the term "neurilemoma", referring to the closely applied sheath and covering of the tumor[15]. Because nearly the entire tumor is composed of Schwann cells, the designation "schwannoma" is preferred.

Epidemiology

Schwannomas may occur at any age, with a peak incidence during the fourth to sixth decades of life. There is no sex or racial predilection. Approximately 90% of schwannomas are solitary and occur sporadically[2]. Multiple schwannomas can be a manifestation of neurofibromatosis type 2 (NF2) or schwannomatosis, with both disorders having a mosaic (segmental) form. Patients with NF2, an autosomal dominant disorder, can develop meningiomas and bilateral vestibular schwannomas ("acoustic neuromas") (see Table 61.5)[2,16–19]. The latter tumors are unusual in schwannomatosis which is sporadic in the majority of patients (see below).

Psammomatous melanotic schwannoma (also more recently referred to as "malignant melanotic schwannian tumor") is a variant that typically arises from spinal and autonomic nerves[20]. This tumor may occur sporadically as well as in the setting of Carney complex (see Ch. 112). *Primary cutaneous* psammomatous melanotic schwannomas are exceedingly rare and appear to have a more indolent behavior than extracutaneous counterparts.

Pathogenesis

Because a schwannoma is a neoplastic proliferation of periaxonal or endoneurial Schwann cells, it develops as an encapsulated mass within the confines of the perineurium. Normal nerve fascicles are passively displaced to the periphery, with the bulk of the tumor appearing devoid of other normal peripheral nerve components[2]. Only after careful dissection can the attached nerve trunk be demonstrated.

Loss of expression of merlin, the oncosuppressor protein encoded by *NF2*[21,22], leads to the development of schwannomas. *Somatic* inactivating mutations in *NF2* occur in 50%–75% of sporadic schwannomas, while *germline* inactivating mutations lead to NF2. Both inherited and sporadic (~40% of patients) schwannomatosis are associated with germline mutations in either *SMARCB1* or *LZTR1*, coupled with somatic biallelic inactivation of *NF2* in each tumor[17–19]. The development of psammomatous melanotic schwannomas, either sporadically or in association with Carney complex, is related to inactivation of *PRKAR1A*.

Clinical Features

Schwannomas present as solitary, soft, skin-colored to pink or yellow, smooth-surfaced, dermal or subcutaneous papulonodules (Fig. 115.6). In general, their diameter ranges between 0.5 and 3 cm[23]. They are most commonly found on the flexor aspect of extremities along a larger nerve trunk, followed by the head and neck region[24]. Tumors are usually asymptomatic, but occasionally pain and tenderness occur, in particular if forceful movements place the attached nerve under tension. Motor disturbances and paresthesias are extremely rare[25].

Pathology

Schwannomas are well-circumscribed, nodular or ovoid tumors composed of differentiated Schwann cells. They are located in the deep dermis or subcutis and are almost always encapsulated. The tumors are composed of hypercellular (also called Antoni A-type tissue) and hypocellular (Antoni B-type tissue) areas[2]. Within areas of Antoni A-type tissue, there is proliferation of spindle cells with indistinct cytoplasmic contours and uniform nuclei[26]. Nuclear palisading is a typical finding and palisaded nuclei arranged in double rows can result in characteristic "Verocay bodies"[2,3] (Fig. 115.7). Mitotic figures are absent or rare.

Antoni B-type tissue areas have characteristic large, irregularly spaced vessels with thickened fibrotic walls, as well as variable degrees of edematous, mucinous, cystic, xanthomatous, and fibrotic changes within the hypocellular stroma. Such degenerative changes, which are often associated with some degree of cytologic atypia, are the predominant feature in so-called *ancient schwannomas*. These latter tumors should not be confused with *cellular schwannomas*, a histologic subtype composed largely of Antoni A-type tissue but lacking Verocay bodies, that rarely occur in the skin[27]. Axons are sparse in schwannomas and may be best detected at the tumor's periphery in proximity to nerve attachments[28].

Additional less common subtypes of schwannomas include plexiform, epithelioid (frequently associated with loss of SMARCB1 expression), and microcystic/reticular schwannomas[29–31]. In psammomatous melanotic schwannoma, a mixture of spindled and epithelioid cells that resembles syncytial tissue is seen. The cells have variable pleomorphism and nuclear atypia, and focal areas may demonstrate typical neural organization, i.e. nuclear palisading and whorl formation. Melanin deposition is often heavy, obscuring cytologic details. Psammomatous structures, consisting of eosinophilic laminated and whorled structures with variable calcification, are a frequent and characteristic finding. The cells stain positively for S100 protein and SOX10 and in psammomatous melanotic schwannomas also stain positively for Melan-A, HMB-45, and tyrosinase[32].

Differential Diagnosis

The clinical differential diagnosis includes neurofibroma, lipoma, angiolipoma, adnexal tumor, cyst (epidermoid, pilar, dermoid, ganglion), and intradermal melanocytic nevus. The diagnosis is made by histopathologic examination. Clinically, a psammomatous melanocytic schwannoma may resemble a blue, combined, or atypical melanocytic nevus.



Fig. 115.6 Solitary cutaneous schwannoma. Skin-colored nodule on the plantar surface of the great toe. *Courtesy Julie V. Schaffer, MD.*

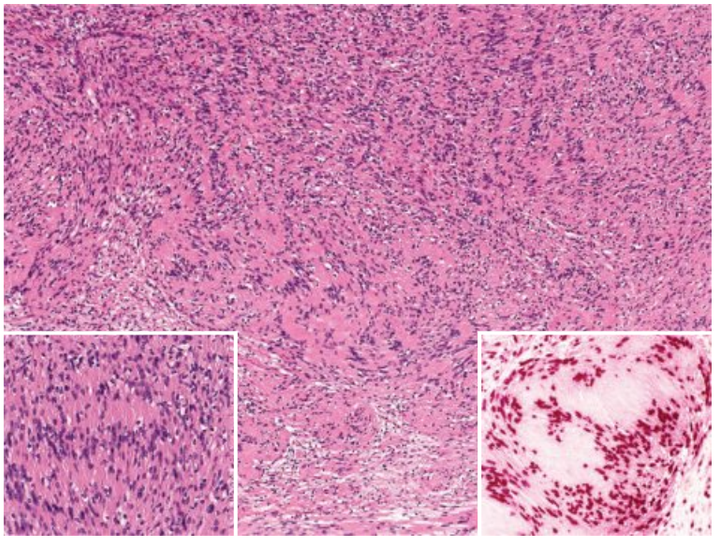


Fig. 115.7 Solitary cutaneous schwannoma. Hypercellular areas often show nuclear palisading and Verocay bodies. Detail of Verocay bodies and the nuclear expression of SOX10 (insets). *Courtesy Lorenzo Cerroni, MD.*

Treatment

Schwannomas are benign and a simple excision is curative. If the clinical diagnosis is suspected, the tumor should be removed by enucleation, preserving normal nerve function.

NEUROFIBROMA

Variants/synonyms: ■ Solitary neurofibroma – sporadic neurofibroma, solitary nerve sheath tumor ■ Plexiform neurofibroma

Key features

Solitary type

- Skin-colored to tan–violet papule or nodule
- May be pedunculated or have the "buttonhole" sign
- Predilection for the trunk and head
- Spindle cell proliferation with variable mixture of the components of the peripheral nerve, including residual axons
- Fibrosis and mucinous changes are common

Plexiform type

- Pathognomonic of NF1
- Large, occasionally pigmented, bag-like mass
- Favors the trunk and proximal extremities
- The plexiform variant has similar cytologic constituents as the solitary or sporadic type, but carries a risk of malignant transformation

Introduction

Neurofibromas are benign nerve sheath tumors composed of a complex proliferation of neuromesenchymal cells (Schwann cells, perineurial cells, fibroblasts, and mast cells), along with residual interspersed axons[2]. Cutaneous neurofibromas are common, especially as solitary lesions. The presence of multiple neurofibromas raises the possibility of one of the several types of neurofibromatosis, including the mosaic form (see Ch. 61). Plexiform neurofibromas are pathognomonic of NF1.

History

Neurofibromas were originally described as fibrous tumors by von Recklinghausen. A neuroectodermal origin was suggested by Verocay and eventually confirmed by immunohistochemical and ultrastructural studies.

Epidemiology

Localized cutaneous neurofibromas are the most common peripheral nerve sheath tumors, and have neither age nor sex preference. Diffuse and plexiform neurofibromas are considered to be of congenital origin.

Pathogenesis

Neurofibromas differ from schwannomas in that several cell types are involved in their histogenesis. Regardless of the histologic subtype of neurofibromas (e.g. localized cutaneous, diffuse, plexiform), the basic process is proliferation of the entire "neuromesenchyme", which includes Schwann cells, perineurial cells, endoneurial fibroblasts, and mast cells[2]. Axons are easily found in neurofibromas, although the axon to Schwann cell ratio is significantly lower than the normal 1 : 1 ratio. Within a neurofibroma, only a subpopulation of Schwann cells is neoplastic, carrying a clonal biallelic inactivation of *NF1*. Nullizygosity ($NF1^{-/-}$) of Schwann cells is a prerequisite, but is not sufficient, for neurofibroma formation; the latter may require the promoting effect of a $NF1^{+/-}$ microenvironment, in particular *NF1*-haploinsufficient mast cells[33] (see Fig. 61.2). The pathogenesis of sporadic cutaneous neurofibromas remains unclear, as most of them show retained expression of neurofibromin[34].

Clinical Features

Clinically, *localized cutaneous* neurofibromas present as asymptomatic, skin-colored, soft or rubbery papulonodules. They range in size from 0.2 to 2 cm and may become pedunculated[2]. These tumors grow slowly and the "buttonhole" sign is often present[2], i.e. the tumor is easily invaginated. Approximately 10% of patients develop multiple localized cutaneous neurofibromas, with some of these patients having one of the several types of neurofibromatosis (see Ch. 61). Additional clinicopathologic subtypes of neurofibroma include diffuse, intraneural, and plexiform variants. The diffuse subtype may present as indurated or soft nodules and plaques, while the intraneural variant presents as solitary fusiform masses. Except for plexiform neurofibromas, these subtypes rarely undergo malignant change.

Plexiform neurofibromas are especially important because they are considered pathognomonic of NF1 and carry a significant risk of transformation into malignant peripheral nerve sheath tumors (MPNSTs)[2]. These neurofibromas affect large segments of a nerve, distorting it into a "bag of worms", and present as baggy or pedunculated subcutaneous masses that can feel rope-like on palpation and are frequently hyperpigmented (Fig. 115.8). Involvement of an entire extremity leads to elephantiasis neuromatosa. Recognition and correct patient management is crucial in these cases, especially in subtle forms of NF1, where the other cutaneous stigmata may not be obvious. The exact incidence of malignant transformation is not known but it is estimated to occur in 2%–30% of NF1 patients, depending on disease severity in the population studied[2].

Pathology

Neurofibromas are poor- to well-circumscribed, nodular or oblong tumors that can be located anywhere within the dermis and subcutis[2,3]. Even when localized grossly, they lack a capsule and tend to infiltrate surrounding soft tissues. The common *localized cutaneous* variant usually has its center in the superficial dermis, creating a dome-shaped or polypoid elevation of its surface (Fig. 115.9). The tumor is composed of a fine fibrillary lattice of haphazardly arranged slender spindle cells[35], and the stroma can be variably vascular, fibrotic, edematous or myxomatous. In addition to Schwann cells and perineurial cells, plump fibroblasts and mast cells are present. Vague palisading of nuclei may occur, occasionally with true Verocay body formation, and can be regarded as hybrid neurofibroma/schwannoma tumors[2,35]. Mitotic figures are absent or rare. By utilizing special stains, rare scattered axons may be demonstrated, as in all other variants.

The *diffuse* variant lacks a well-defined growth pattern as it infiltrates the dermis and subcutis; characteristically, Meissner body-like structures may be observed in the deeper parts of these tumors. Intraneural neurofibromas are well-circumscribed masses along a peripheral nerve, being encapsulated by perineurium or epineurium[2]. *Plexiform* neurofibromas consist of a tortuous mass of neurofibromatous tissue with



Fig. 115.8 Plexiform neurofibroma in a patient with neurofibromatosis type 1. Soft, pendulous mass with "bag of worms" appearance. *Courtesy Lorenzo Cerroni, MD.*

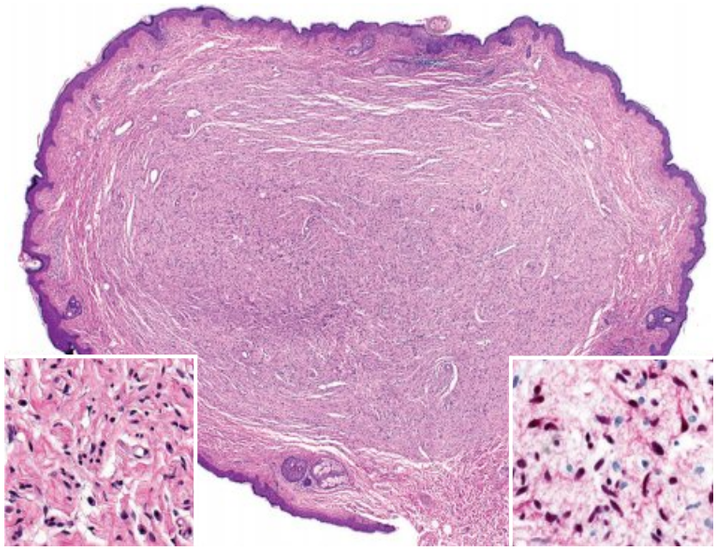


Fig. 115.9 Neurofibroma. Unencapsulated dermal proliferation of spindle cells separated from the overlying epidermis by a grenz zone. The tumor contains a diffuse proliferation of spindle cells with slender, ovoid nuclei in a mast cell-rich fibrillary matrix (inset lower left). Note expression of S100 by spindle cells (inset lower right). *Courtesy Lorenzo Cerroni, MD.*

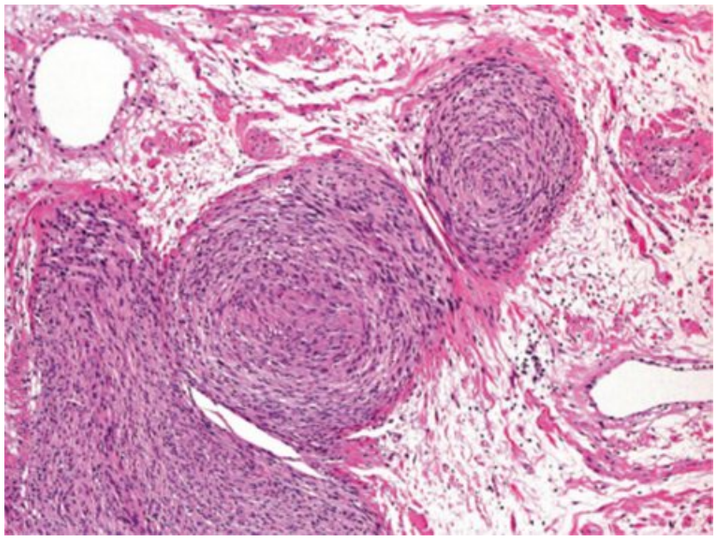


Fig. 115.10 Plexiform neurofibroma. Irregularly expanded, twisted fascicles of neoplastic cells arranged in lobular structures. *Courtesy Lorenzo Cerroni, MD.*

an intraneural origin (Fig. 115.10). The neoplastic tissue progressively expands within the nerve branch then extends into the surrounding soft tissue, resulting in the frequent combination of intraneural and diffuse extraneural growth patterns.

MPNSTs may develop from pre-existing plexiform neurofibromas via deletions of the *CDKN2A/CDKN2B* locus. While cytological atypia alone in neurofibromas is not worrisome ("ancient neurofibromas"), malignant transformation is heralded by an intermediate histopathologic step (so-called "atypical neurofibromatous neoplasm of uncertain biologic potential" [ANNUBP]), which is defined by a variable combination of nuclear atypia, increased cellularity, and increased mitotic activity[36].

Differential Diagnosis

The clinical differential diagnosis of a solitary neurofibroma includes an intradermal melanocytic nevus, schwannoma, soft fibroma, and fibrolipoma (see Table 115.2). The majority of solitary or sporadic neurofibromas have similar clinical and histologic features to the multiple papular neurofibromas seen in patients with NF1. Plexiform neurofibromas with overlying hyperpigmentation and hypertrichosis can resemble congenital melanocytic nevi. As the latter can undergo neurotization and may be accompanied by satellite lesions, examination of the patient for Lisch nodules, axillary freckling, and café-au-lait macules is essential. Histologically, a plexiform neurofibroma must be differentiated from other plexiform tumors, including plexiform schwannoma, plexiform SCN, and desmoplastic melanoma.

Treatment

Neurofibromas are usually treated by simple excision. The evaluation and management of plexiform neurofibromas and neurofibromatosis is discussed in Chapter 61.

NERVE SHEATH MYXOMA AND CELLULAR NEUROTHEKEOMA

Synonyms: ■ Myxoma of the nerve sheath ■ Neurothekeoma

Key features

- Two distinct entities previously classified as morphologic variants within the same spectrum
- Nerve sheath myxoma is a true benign nerve sheath tumor with schwannian differentiation
- Cellular neurothekeoma is a non-neural neoplasm of presumptive fibrohistiocytic differentiation
- Both tumors present as nonspecific skin-colored to red–brown papulonodules
- Histologically, both tumors have a lobular or fascicular pattern with variable deposition of extracellular mucin
- Benign behavior, but local recurrences may occur

Introduction

Classic (myxoid) nerve sheath myxoma and cellular neurothekeoma were initially regarded as subtypes of the same neuromesenchymal entity ("nerve sheath myxoma"), characterized by the proliferation of nerve sheath cells in a variably myxomatous stroma[37]. There is now sufficient evidence to state that cellular neurothekeoma is not related to nerve sheath myxoma or to the neural crest, but rather represents a non-neural mesenchymal neoplasm, perhaps of fibrohistiocytic differentiation[38]. As such, the term "neurothekeoma" is a misnomer.

History

Nerve sheath myxoma was first described as a specific entity by Harkin and Reed in 1969. The term "cellular neurothekeoma" was coined by Rosati and colleagues in 1986[2].

Epidemiology

True nerve sheath myxomas are rare, affecting all ages and both sexes equally[39]. Cellular neurothekeoma has a predilection for adolescents and young adults (<40 years of age) and is nearly twice as common in women as men[40].

Pathogenesis

True *nerve sheath myxomas* are superficial peripheral nerve sheath tumors characterized by a benign proliferation of schwannian cells in a plexiform/multinodular growth pattern plus abundant myxoid degeneration. A thin, incomplete layer of perineurial cells may surround the nodules, as in SCN[39,41]. The extreme mucin production may explain the difficulty in detecting axons in these tumors.

Cellular neurothekeoma has a controversial histogenesis. Despite its morphologic similarities to nerve sheath myxoma, there is no expression of schwannian differentiation markers (e.g. S100 protein, SOX10)[40,42]. Based upon gene expression profile analyses, cellular neurothekeoma is more closely related to fibrohistiocytic neoplasms[38].



Fig. 115.11 Cellular neurothekeoma of the scalp, presenting as a small, firm, erythematous nodule.

Clinical Features

Nerve sheath myxoma is a soft, skin-colored papule or nodule, generally 5 to 10 mm in diameter and typically located on the distal extremities[39].

Cellular neurothekeomas favor the head and neck region as well as the upper extremities, although cases from a variety of anatomic sites have been reported. These tumors are described as firm papulonodules that are pink, red, or brown in color and range in size from 0.5 to 3 cm (Fig. 115.11). Symptoms are nonspecific and seem to relate to the size and firmness of the tumor[40].

Pathology

Nerve sheath myxoma is a well-defined, lobular or plexiform neoplasm that is usually located in the reticular dermis (Fig. 115.12). It often appears encapsulated by a compression of the surrounding fibrous tissue[39]. There is a hypocellular myxoid stroma with rare scattered spindled, stellate, or dendritic cells. The cells usually have scant pale cytoplasm with indistinct cytoplasmic contours and hyperchromatic, ovoid, or angulated nuclei[39,41]. Nucleoli are small and mitotic figures are rare or absent. On occasion, multinucleated giant cells with eosinophilic cytoplasm can be identified. Histochemically, the myxoid stroma stains strongly positive for acidic mucopolysaccharides (see Ch. 46)[39]. In a minority of cases, scattered neurofilament-positive axons may be detected[41]. The tumor cells are positive for S100 protein, SOX10, and collagen type IV and the capsule has a weak and discontinuous expression of epithelial membrane antigen (EMA) and other perineurial markers[2,41].

Cellular neurothekeomas are composed of ill-defined multilobular masses or fascicles in the reticular dermis[40] (Fig. 115.13). In some cases, the growth pattern can be frankly infiltrative or dissecting without any hint of a residual capsule, and there may be involvement of the superficial subcutis[42,43]. Cytologically, the predominant cell types are epithelioid or polygonal cells with ample eosinophilic cytoplasm and round nuclei with an open chromatin pattern[40,43]. Many cells have prominent nucleoli. Less often, the constituent cells are spindle-shaped with hyperchromatic nuclei, resembling those observed in nerve sheath myxomas. Mitotic figures are often present but are usually normal morphologically. Rare cases with increased mitotic figures and cytologic atypia have been reported[43]. The stroma can be markedly fibrotic or even hyalinized. There is no detectable connection with peripheral nerves.

The tumor does not have a consistent immunohistochemical profile, with the nonspecific marker NKI/C3 expressed in essentially all cases. Expression of PGP9.5 (neuron-specific peptide), microphthalmia transcription factor (MITF; see Ch. 65), and smooth muscle actin may be observed in individual cases. Importantly, expression of S100 protein, SOX10, and perineurial markers is consistently absent[40,44,45].

Differential Diagnosis

A nerve sheath myxoma is usually asymptomatic and clinically is often mistaken for an intradermal melanocytic nevus, neurofibroma, lipoma, or cyst (e.g. myxoid, ganglion) (see Table 115.2). Clinically, a cellular neurothekeoma usually resembles a dermatofibroma (including the sclerosing hemangioma variant), hypertrophic scar, keloid, or granular cell tumor.

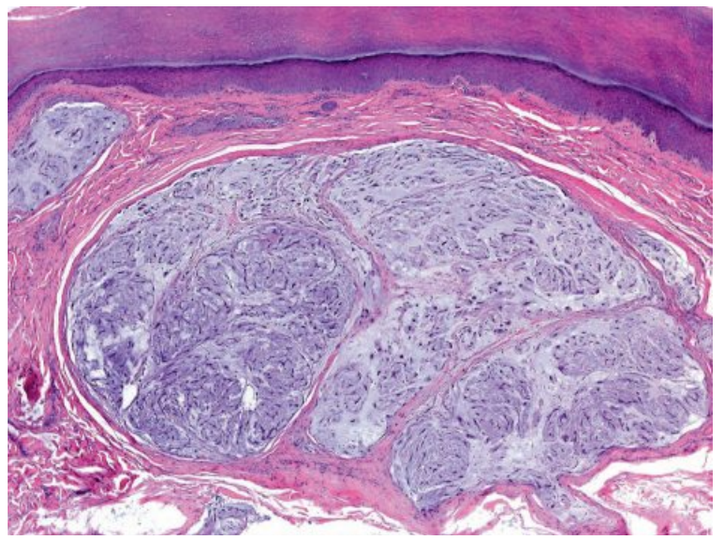


Fig. 115.12 Nerve sheath myxoma. Well-defined fascicles with myxoid stroma. *Courtesy Lorenzo Cerroni, MD.*

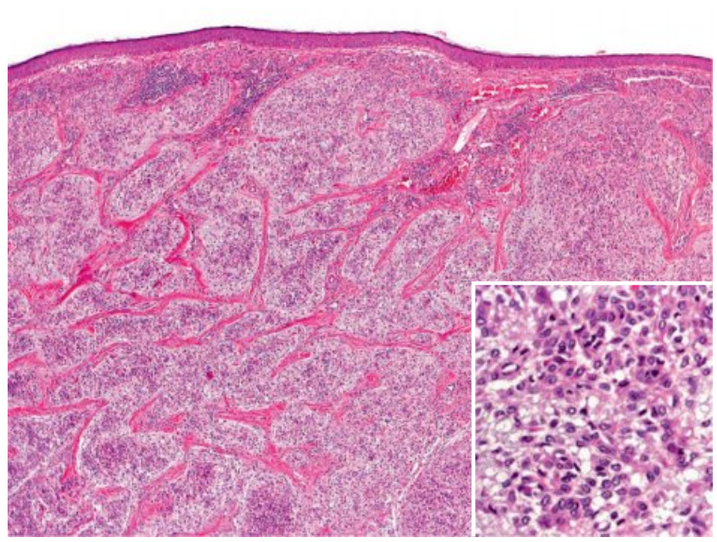


Fig. 115.13 Cellular neurothekeoma. Epithelioid nests are dispersed in a hyalinized stroma. Whorl-like arrangement of epithelioid cells with nuclear pleomorphism (inset). *Courtesy Lorenzo Cerroni, MD.*

Treatment

These lesions are usually treated by simple excision; however, if incompletely removed, a nerve sheath myxoma may recur. There have been a few case reports of atypical variants of cellular neurothekeoma with postulated uncertain behavior, in which case complete excision is recommended.

GRANULAR CELL TUMOR

Synonym: ■ Abrikossoff's tumor

Key features

- Seen more commonly in adults, women, and African-Americans
- Predilection for the head and neck, tongue, and breast, but may occur anywhere, including the viscera
- Malignant transformation is rare and usually occurs with deep-seated lesions
- Histologically, an ill-defined, infiltrative tumor, often with associated pseudoepitheliomatous (pseudocarcinomatous) hyperplasia
- Large polygonal cells with finely granular eosinophilic cytoplasm; the granules are PAS-positive, diastase-resistant

Introduction

Granular cell tumor is a neoplasm with neuroectodermal differentiation consisting of epithelioid to polygonal cells with granular change due to cytoplasmic accumulation of lysosomal granules. The exceedingly rare "cutaneous non-neural granular cell tumor" is a morphologically indistinguishable neoplasm that lacks expression of S100 protein or SOX10 and has frequent *ALK* (anaplastic lymphoma kinase gene) rearrangements[46]. Occasionally, granular cell change may occur in a variety of unrelated neoplasms as a secondary phenomenon (see below)[47].

History

This tumor was originally thought by Abrikossoff, who used the term "granular cell myoblastoma", to be derived from muscle[48]. Feyrter first suggested a neural origin.

Epidemiology

Granular cell tumor is a relatively rare tumor that occurs primarily in adults (age 30–50 years) and favors men and African-Americans. Up to 10% of patients have multiple lesions, and ~70% of tumors are located in the head and neck region, including 25% on the tongue[2]. Other common locations are the breast (5%–15%) and proximal extremities. Visceral lesions may develop in the gastrointestinal and upper respiratory tracts.

Pathogenesis

The neural origin of granular cell tumor has been a subject of debate, but immunohistochemical and ultrastructural studies have clearly proven its schwannian differentiation. Granular cells express S100 protein, SOX10, and CD57 (a neuronally expressed adhesion molecule), like Schwann cells[49–51]. Loss-of-function mutations in the V-ATPase accessory genes *ATP6AP1* (60%) and *ATP6AP2* (10%) have been detected in the majority of cutaneous and extracutaneous neural granular cell tumors, irrespective of anatomic site and biological behavior[52,53]. How inactivation of these membrane proton pumps leads to accumulation of lysosomes and tumorigenesis requires further investigation. Multiple cutaneous granular cell tumors can be seen in patients with RASopathies such as NF1, Noonan syndrome, and Noonan syndrome with multiple lentigines (LEOPARD syndrome), thus implying a role of the RAS/MAPK pathway in their pathogenesis[54] (see Fig. 55.4).

Clinical Features

A granular cell tumor presents as an asymptomatic or occasionally tender or pruritic, skin-colored to brownish-red, firm dermal or subcutaneous papulonodule, ranging in diameter from 0.5 to 3 cm. Occasionally, the surface will be ulcerated or verrucous. Granular cell tumors are slowly growing and in general have a benign behavior. Rarely, malignant behavior is observed (local infiltration or metastasis), more often when the tumor arises from a visceral or deep location. Malignant granular tumors may develop *de novo* or via malignant transformation of a pre-existing benign lesion[55].

Pathology

The dermis contains a poorly circumscribed nodule composed of polygonal, pale-staining cells that may infiltrate into the adjacent subcutis. The cells have abundant, granular, faintly eosinophilic cytoplasm with round, dark nuclei (Fig. 115.14)[56]. Characteristic larger cytoplasmic granules are called pustulo-ovoid bodies. With the PAS reaction, the granules are positive, but they are diastase-resistant. Occasionally, a perineurial growth pattern is present; however, the tumor is devoid of axons. Increased numbers of mast cells are present in some lesions, and the overlying epidermis is frequently hyperplastic. Rarely, a plexiform growth pattern has been described[56]. Histopathologic criteria predictive of aggressive behavior are not well established, but may include necrosis, increased mitotic rate, spindling of the cells, high nuclear:cytoplasmic ratio, vesicular nuclei, and nuclear pleomorphism[2,55,57].

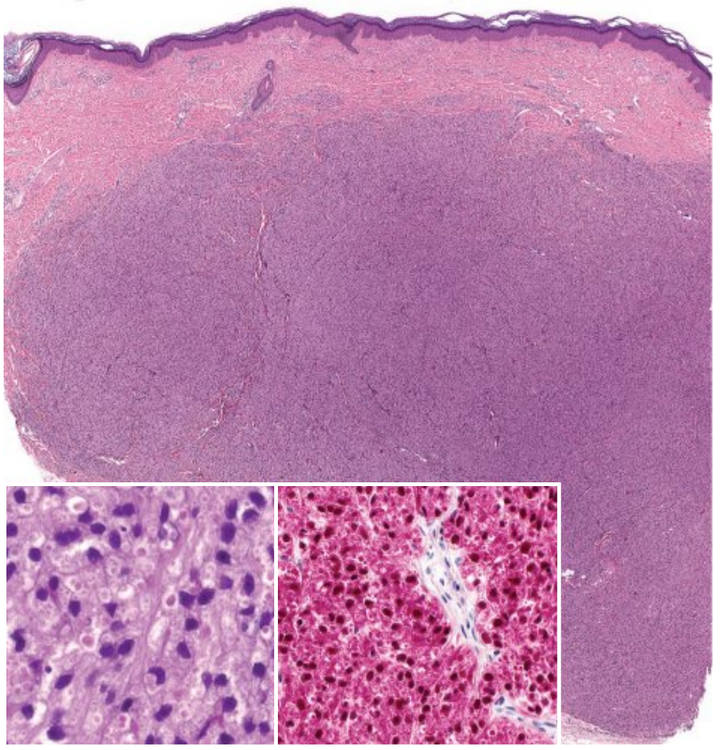


Fig. 115.14 Granular cell tumor. The tumor may show a nodular or infiltrative growth pattern. The large polygonal cells have finely granular cytoplasm, pustulo-ovoid bodies, and round nuclei (left inset) that stain positively for S100 (right inset). *Courtesy Lorenzo Cerroni, MD.*

True (neural) granular cell tumors express S100 protein, SOX10, PGP9.5 (neuron-specific peptide), and nerve growth factor receptor. The cells may stain positively for CD68 and NKI/C3, but are negative for the lineage-restricted histiocytic marker CD163 as well as melanocytic differentiation markers Melan-A and HMB-45. There may be diffuse nuclear reactivity for MITF and TFE3, posing a diagnostic challenge with *TFE3*-rearranged tumors and PEComas[58,59].

Differential Diagnosis

The clinical differential diagnosis of lingual lesions includes an irritation fibroma, verruca, and squamous cell carcinoma (SCC). Elsewhere, this tumor may resemble a dermatofibroma, regressing verruca, or adnexal neoplasm (see Table 115.2). Granular cell tumors can induce considerable pseudoepitheliomatous (pseudocarcinomatous) hyperplasia of the overlying epithelium, and superficial biopsy samples have been mistaken for SCC, especially on the tongue[60]. A variety of epithelial and mesenchymal neoplasms can show granular cell change, including BCCs, leiomyomas, dermatofibromas, and leiomyosarcomas[47].

Treatment

The treatment is complete excision. If incompletely excised, this tumor has a high local recurrence rate, due to the plexiform or perineurial growth pattern.

PERINEURIOMA

Synonyms: ■ Storiform perineurial fibroma ■ Fibrolamellar nerve sheath tumor ■ Localized hypertrophic neuropathy

Introduction

Perineuriomas represent a proliferation of perineurial cells, with both intraneural and extraneural growth patterns. These tumors are rare and Table 115.5 outlines their features.

KEY FEATURES OF SOFT TISSUE (EXTRANEURAL) PERINEURIOMAS OF INTEREST TO DERMATOLOGISTS
Clinical features
• Solitary, nondescript, skin-colored, soft tissue mass • Occurs primarily on the trunk and extremities of adults, with the sclerosing variant favoring the hands of young men
Histopathologic features
• Predominant cell type is the perineurial cell, which is a modified fibroblastic cell • In classic soft tissue perineurioma, there is a well-circumscribed (but non-encapsulated) proliferation of slender, elongated spindle cells within the dermis and/or subcutis; the latter form tightly woven fascicles, sometimes with a lamellar or storiform pattern (Fig. 115.15), and the intertwining stroma can be hyalinized or myxoid • In the sclerosing variant, there may be epithelioid cells alternating with spindle cells, intermixed with thick collagen bundles • Reticular perineurioma, another variant, is characterized by a lace-like arrangement of cells that leads to the formation of microscopic cysts • Hybrid benign peripheral nerve sheath tumors may show a perineurial neoplastic population closely intermingled with a schwannomatous (or more rarely neurofibromatous) population • Only very infrequent atypical cases have significant atypia and/or increased mitotic activity
Immunohistochemistry
• Cells stain positively for EMA, GLUT1, and claudin-1 • CD34 may be positive (60% of cases); S100 protein and SOX10 are invariably negative (with the exception of hybrid benign peripheral nerve sheath tumors)
Clinical differential diagnosis
• Benign soft tissue tumors (e.g. lipoma) and soft tissue sarcomas
Histologic differential diagnosis
• Neurofibromas with extensive fibrosis (S100-, SOX10-, and NF-positive), DFSP (EMA-, GLUT1-, and claudin-1-negative; CD34-positive), sclerosing fibroma (EMA-, GLUT1-, and claudin-1-negative)
Treatment
• Complete excision – biologic behavior usually benign, rarely malignant

Table 115.5 Perineuriomas – key features of extraneural variants of interest to dermatologists. DFSP, dermatofibrosarcoma protuberans; EMA, epithelial membrane antigen; NF, neurofilament. Claudin-1 is a tight junction-associated protein. Based upon references 122, 123, & 124.

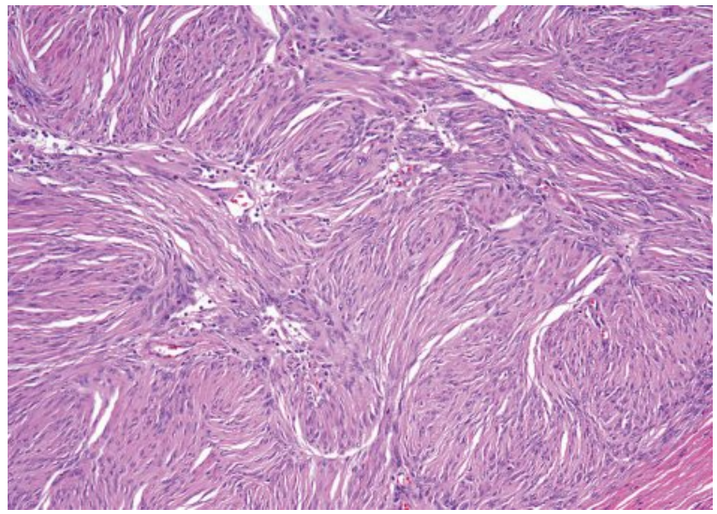


Fig. 115.15 Soft tissue perineurioma. Compact proliferation of spindle cells with lobular and storiform pattern.

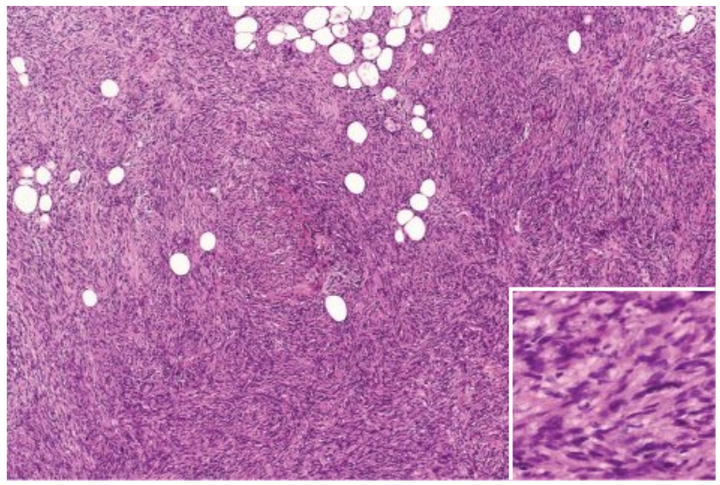


Fig. 115.16 Malignant peripheral nerve sheath tumor. Overall, the intersecting fascicles create a "herringbone" pattern. There is marked cellular pleomorphism with cytologic atypia and mitotic activity (inset). *Courtesy Lorenzo Cerroni, MD.*

MALIGNANT PERIPHERAL NERVE SHEATH TUMOR

Synonyms: ■ Neurosarcoma ■ Malignant schwannoma

The term "malignant peripheral nerve sheath tumor" (MPNST) is preferable to the widely used but confusing synonyms above. This is because any cellular component of the peripheral nerve can give rise to these tumors, including perineurial or endoneurial fibroblasts (rather than Schwann cells)[61,62]. MPNST is primarily a tumor of deep soft tissues and rarely involves the skin. Despite its rarity, MPNST has clinical relevance for dermatologists because this malignancy develops within 2%–30% of plexiform neurofibromas, which are associated with NF1[63] (see Ch. 61).

A definitive diagnosis requires histologic examination, usually in conjunction with immunohistochemistry and molecular biologic analysis. Histologically, in the most common form, there is a proliferation of atypical spindle cells, often arranged in a "herringbone" pattern. There is variable cytologic atypia, numerous abnormal mitotic figures, and areas of necrosis and hemorrhage (Fig. 115.16)[61,62]. Staining for S100 protein and SOX10, if positive, is only patchy or focal[51]. Regardless of the clinical setting (sporadic, NF1-associated, or radiotherapy-associated), MPNSTs show frequent and concurrent loss-of-function mutations in *NF1*, *CDKN2A/CDKN2B*, and the polycomb repressive complex 2 (PRC2)-related genes *EED* or *SUZ12*[63]. Complete loss of PRC2 activity and an associated lack of immunohistochemical expression of the epigenetic marker H3K27me3 (trimethylation of lysine 27 on histone H3 which represses transcription) are observed in >80% of high-grade MPNSTs and may represent a useful tool for its differentiation from other soft tissue sarcomas[64].

MERKEL CELL CARCINOMA

Synonyms: ■ Primary neuroendocrine carcinoma of the skin ■ Trabecular carcinoma of the skin ■ Primary small cell carcinoma of the skin ■ Cutaneous apudoma

Key features

- Predilection for the head and neck region of older adults
- Solitary, rapidly growing nodule
- Histologically, tumor is composed of small, round blue cells, often with a nested or trabecular growth pattern
- High mitotic rate, frequent single-cell or zonal necrosis, often perinuclear dot-like CK20-positivity (pathognomonic)
- Approximately 40% of patients develop local, nodal, or distant metastasis

Introduction

Merkel cell carcinoma (MCC) is an aggressive cutaneous carcinoma that shares ultrastructural and immunohistochemical features with other neuroendocrine tumors. Although rare, the incidence of MCC is rapidly increasing along with the aging population. These tumors display nonspecific clinical features and highly aggressive behavior. Early recognition and adequate therapy are therefore critical.

History

This tumor was originally described by Toker and given the name "trabecular carcinoma" based on its lattice-like and infiltrative growth pattern[65]. Subsequently, the neuroendocrine nature of this tumor was recognized. Similarities to the normal Merkel cell of the skin led to its name[66].

Epidemiology

The male:female ratio is 1.5:1 and its incidence increases strikingly with age, e.g. MCC is 10 000 times more likely to arise in an 80-year-old individual than in a 20-year-old[67]. Other risk factors include lightly pigmented skin, extensive sun exposure, and chronic immunosuppression (e.g. organ transplantation recipients, hematologic malignancies)[68].

Pathogenesis

The cells of MCC and the normal Merkel cell, a touch-sensing cell located in the basal layer of the epidermis, share several features. However, the MCC's cell of origin is unclear and it appears unlikely that normal Merkel cells give rise to this carcinoma[66]. This tumor is also referred to as "primary neuroendocrine carcinoma of the skin", a term that is often used in pathology reports.

In 2008, a landmark discovery revealed the association of MCC with a novel polyomavirus, now referred to as Merkel cell polyomavirus (MCPyV)[69]. In humans, this polyomavirus is ubiquitous as it can be readily detected within the normal skin of most healthy people where it exists in an episomal form. Very rarely, a clonal integration event leads to critical portions of the virus being spliced into a human chromosome, ultimately resulting in MCC. Of note, the integration event must be accompanied by mutation(s) that lead to truncation of the large T antigen and inactivation of its helicase domain. If not inactivated, the helicase domain would initiate DNA replication at the integration site which would then lead to cell death. Inhibition of viral oncoproteins in polyomavirus-infected tumor cells results in a cessation of proliferation, suggesting that ongoing viral protein expression is required for MCCs[70].

In the US, ~80% of MCCs are driven by this polyomavirus[71], while the remaining 20% are virus-negative. The latter tumors arise in chronically sun-damaged skin and contain very high numbers of UV-signature mutations[72]. Interestingly, only about 40% of MCCs in Australia are virus-induced, with the majority related to ultraviolet exposure. In contrast, in Asian countries, where people have more pigmented skin, 90% of MCCs are virus-driven.

Clinical Features

This cutaneous carcinoma can develop at any site, but favors the head and neck region, followed by the extremities and the buttocks. It usually presents as a pink–red to violaceous, firm, dome-shaped, solitary nodule that has grown rapidly (Fig. 115.17)[67]. Ulceration can occur. Overall, the behavior is that of an aggressive tumor, with significant risk of local, regional, and/or distant recurrence and metastasis.

In an analysis of 9387 cases of MCC, 65% of patients presented with local disease whereas 26% and 8% presented with nodal or distant metastases, respectively[73]. Prior to the advent of immunotherapy,



Fig. 115.17 Merkel cell carcinoma (primary neuroendocrine carcinoma of the skin). A Exophytic violet tumor on the posterior thigh; the clinical differential diagnosis included lymphoma. **B** Minimally elevated violaceous plaque with peripheral blue color arising within the sun-protected skin of the buttocks; the clinical differential diagnosis included a vascular tumor. **C** Hemorrhagic purple nodule within sun-damaged skin on the scalp. **D–F** Large pink to red nodules arising in older adults within obvious photodamaged skin. The lesions can have a lobulated surface, central ulceration, or telangiectasias. *A–E, Courtesy Department of Dermatology, University Graz.*

five-year overall survival for these three groups was 50% (local disease), 35% (nodal disease), and 15% (distant disease). Tumor diameter at the time of diagnosis influences prognosis, with lesions >2 cm (but without invasion of fascia) having a 40% overall survival at five years (compared to 55% for tumors ≤2 cm; Table 115.6)[73].

Occasionally, paraneoplastic syndromes, similar to those seen with other neuroendocrine carcinomas, occur in patients with MCC. These include malignancy-associated hyponatremia and Lambert–Eaton myasthenic syndrome.

Pathology

The tumor appears as a poorly defined dermal mass, often infiltrating the subcutaneous fat, fascia, and even muscle. While it may show various growth patterns, a sheet-like growth pattern is seen most commonly, followed by nested and trabecular patterns (Fig. 115.18A)[74]. Characteristically, the edge of the tumor shows a trabecular infiltrating pattern[65]. The tumor is composed of monotonously uniform, small, round to oval cells that are about two to three times larger than mature lymphocytes[65,66]. Their cytoplasm is scant and faintly amphophilic. The nuclei of these cells are ovoid with a finely dispersed chromatin pattern and distinct nuclear membranes (Fig. 115.18B). Nucleoli are usually not prominent, but mitotic figures are abundant. Extensive areas of necrosis, individual cell necrosis, and characteristic crush or drying artifacts are common[74]. Intralymphatic involvement by tumor cells is not uncommon, sometimes distant from the main tumor mass. In some cases, single neoplastic cells or tiny aggregates are present at the edge of the biopsy specimen, rendering evaluation of the surgical margin difficult without the aid of immunohistochemistry (see below).

Various types of differentiation have been described in MCC, including rosette-like structures resembling Homer Wright rosettes of neuroblastoma, epidermotropic involvement with pagetoid spread, and eccrine and squamoid differentiation[75,76]. Immunohistochemically, there is a characteristic perinuclear globule upon staining for low-molecular-weight cytokeratins (CK) such as CK20, CK5/6, and CK7 (Fig. 115.18C). This corresponds to the ultrastructural distribution of paranuclear whorls of intermediate filaments[74,75]. In addition, there is positive staining for various neuroendocrine markers, including chromogranin, synaptophysin, somatostatin, calcitonin, and vasoactive intestinal peptide[75]. These peptides are associated with ultrastructurally demonstrable, membrane-bound, dense-core secretory granules.

The tumor also expresses neuron-specific enolase and occasionally neural filaments, CD56, and CD99; however, immunostaining for S100 protein is characteristically negative[75]. Likewise, a negative reaction for thyroid transcription factor 1 (TTF-1) helps to differentiate MCC from cutaneous metastases of other small cell carcinomas (pulmonary and extrapulmonary); the latter are characteristically positive for this marker[75]. Recognition of MCPyV, which can be detected by immunohistochemical (e.g. T antigen) and molecular biologic methods[77], provides an additional tool for diagnosis; however, false-positive PCR results are possible given the ubiquitous nature of the virus. For prognostication, increased p63 expression may portend clinically aggressive behavior, but to date has not altered prognosis based upon stage (Table 115.6)[78]. Negativity for MCPyV may associated with a somewhat poorer prognosis, whereas ALK-positive MCC (which is usually accompanied by MCPyV positivity) appears to have a less aggressive behavior[72,79]. A dataset for the reporting of MCCs has recently been proposed[79a].

Differential Diagnosis

The differential diagnosis of early-stage MCCs includes keratinocyte carcinomas, epidermoid cysts, adnexal tumors, and amelanotic melanoma. When tumors are violaceous or hemorrhagic, the differential

MERKEL CELL CARCINOMA – 8TH AJCC STAGING SYSTEM				
Stage		**Primary tumor**	**Lymph node**	**Distant metastasis**
0		*In situ* (only within the epidermis)	No regional lymph node metastasis	No
I	Clinical*	≤2 cm maximum tumor dimension	Nodes negative by clinical examination (no pathologic examination performed)	No
I	Pathologic†	≤2 cm maximum tumor dimension	Nodes negative by pathologic examination	No
IIA	Clinical	>2 cm tumor dimension	Nodes negative by clinical examination (no pathologic examination performed)	No
IIA	Pathologic	>2 cm tumor dimension	Nodes negative by pathologic examination	No
IIB	Clinical	Primary tumor invades bone, muscle, fascia, or cartilage	Nodes negative by clinical examination (no pathologic examination performed)	No
IIB	Pathologic	Primary tumor invades bone, muscle, fascia, or cartilage	Nodes negative by pathologic examination	No
III	Clinical	Any size/depth tumor	Nodes positive by clinical examination (no pathologic examination performed)	No
IIIA	Pathologic	Any size/depth tumor	Nodes positive by pathologic examination only (nodal disease not apparent by clinical examination)	No
		Not detected ("unknown primary")	Nodes positive by clinical examination; confirmed by pathologic examination	No
IIIB	Pathologic	Any size/depth tumor	Nodes positive by clinical examination and confirmed by pathologic examination – *or* – In-transit metastasis‡	No
IV	Clinical	Any	Regional nodal involvement +/–	Distant metastasis detected clinically
IV	Pathologic	Any	Regional nodal involvement +/–	Distant metastasis confirmed by pathologic examination

*Clinical detection of nodal or metastatic disease may be via inspection, palpation, and/or imaging.
†Pathologic detection/confirmation of nodal disease may be via sentinel lymph node biopsy and pathologic confirmation of metastatic disease may be via biopsy of the suspected metastasis.
‡In-transit metastasis: a tumor distinct from the primary lesion and located either: (1) between the primary lesion and the draining regional lymph nodes; or (2) distal to the primary lesion.

Table 115.6 Merkel cell carcinoma – 8th American Joint Committee on Cancer (AJCC) staging system. While more extensive lymph node involvement portends a poorer prognosis, the number of positive lymph nodes is not factored into the staging of MCC. *Adapted from www.merkelcell.org/staging and Harms KL, Healy MA, Nghiem P, et al. Analysis of prognostic factors from 9387 Merkel cell carcinoma cases forms the basis for the new 8th edition AJCC staging system. Ann Surg Oncol 2016;23:3564–71.*

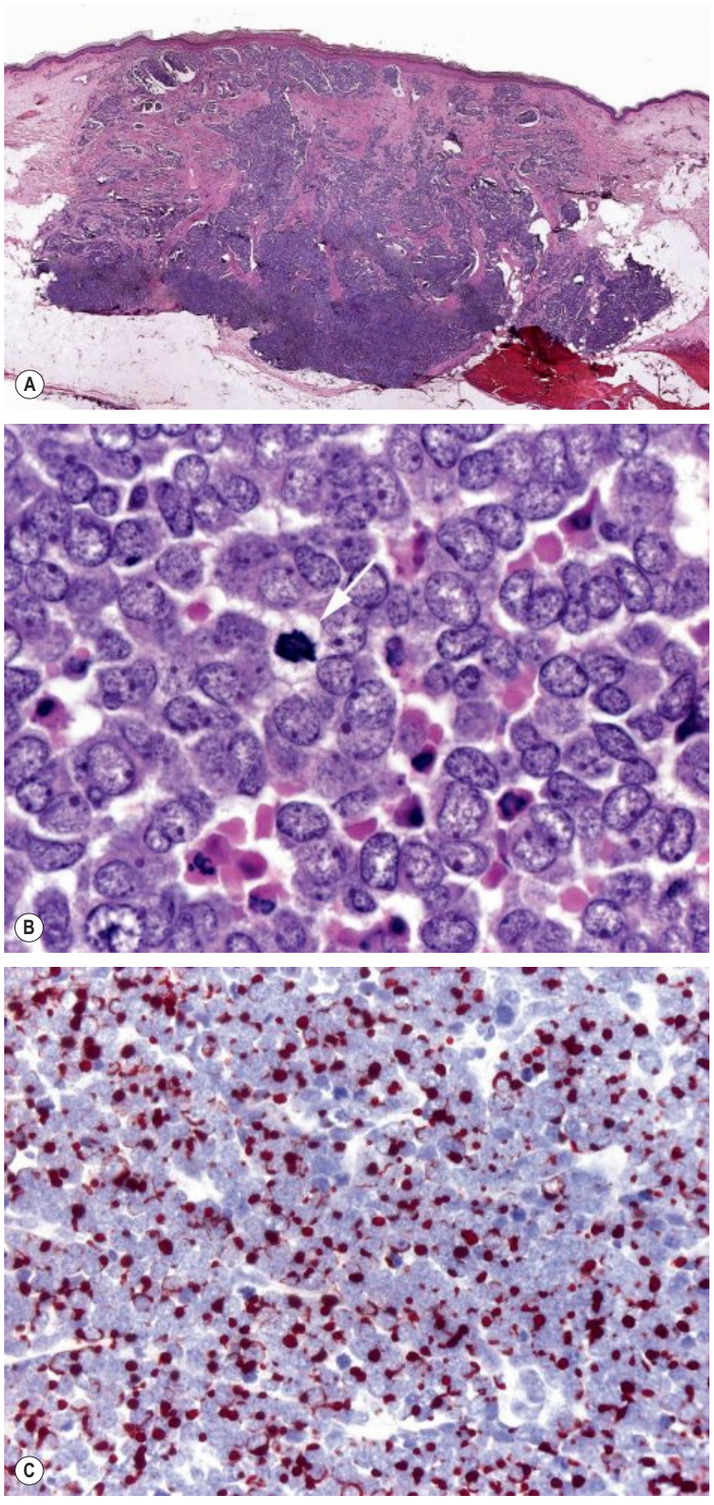


Fig. 115.18 Merkel cell carcinoma (primary neuroendocrine carcinoma of the skin). A Nodular infiltrate of basaloid cell aggregates and strands throughout the dermis, extending into the superficial subcutis. **B** Small, round to ovoid basaloid cells with vesicular nuclei and small nucleoli; note several necrotic (apoptotic) cells and a mitotic figure (white arrow). **C** Immunohistochemical stain for cytokeratin 20 demonstrates a characteristic perinuclear dot pattern. *Courtesy Lorenzo Cerroni, MD.*

diagnosis also includes pyogenic granuloma, hemangioma, angiosarcoma, and lymphoma (see Fig. 115.17A–C). Histologically, there is a broad spectrum of small, round, blue cell tumors of diverse histogenesis that can be confused with MCC[75]. These include metastatic neuroendocrine carcinoma of the lung (small cell or oat cell carcinoma), poorly differentiated eccrine carcinoma, lymphoma, metastatic neuroblastoma, primary peripheral primitive neuroectodermal tumor, Ewing sarcoma, melanoma, and poorly differentiated SCC[74,75].

Treatment

For newly diagnosed locoregional MCC, surgery remains the principal initial therapy. Excision of the primary tumor plus sentinel lymph node biopsy (SLNB) are recommended for most patients (Fig. 115.19), with these procedures also providing prognostic information[80–82]. SLNB positivity at the time of the initial MCC diagnosis is estimated to be 35%[83]. Age >65 years, immunosuppression, primary tumor on the trunk, and larger tumor size are associated with higher rates of SLN positivity[83,84]. However, even tumors ≤5 mm are associated with a positive SLNB in ~15% of patients[83]. Surgery is often followed by radiation therapy to the primary site and in some patients, the draining lymph node basin (see Fig. 115.19).

The management of MCC often requires a multidisciplinary approach with involvement of surgeons, medical and radiation oncologists, and dermatologists. Updated guidelines are readily available[85] and Fig. 115.19 provides a current algorithm for evaluation and treatment[86–93].

Prior to the advent of immunotherapy, cytotoxic chemotherapy was the primary option for advanced stage disease, but responses were not durable[94]. Several clinical trials, in which anti-PD-1 and anti-PD-L1 antibodies demonstrated significantly improved progression-free survival and overall survival compared to historical data for conventional chemotherapy[90–93,93a], led to FDA approval of avelumab, pembrolizumab, and retifanlimab. These antibodies are now considered first-line therapies for advanced MCC[85]. However, primary or acquired resistance to immunotherapy remains a major challenge, ultimately affecting >50% of treated patients[90–93,93b].

Careful surveillance is important because MCC recurs in up to 40% of patients[95] and effective treatments are now available. A baseline determination (within a few months of initial therapy) of the presence or absence of circulating antibodies against the Merkel virus oncoprotein is recommended[96]. In seropositive patients, antibody titers correlate with tumor burden and represent a sensitive and specific assay that can be followed longitudinally[96,97]. However, ~50% of patients do not produce these antibodies[96,97] and surveillance via imaging is required in these seronegative patients. The latter group may have an ~40% higher risk of recurrence compared to seropositive patients of the same stage.

Over 80% of recurrences of MCC arise within the first 3 years after diagnosis[95]. There is a web-based recurrence risk calculator (merkelcell.org/recur) that factors in stage as well as the disease-free interval since treatment, immune status, sex, age, and location of the primary site. This calculator provides an accurate assessment of a patient's ongoing risk of recurrence and assists in planning frequency of surveillance testing.

HETEROTOPIC NEURAL TISSUE OF THE SKIN

These rare lesions develop from embryologically misplaced neural tissue within the skin.

Nasal Glial Heterotopia

Synonyms: ■ Nasal glioma ■ Nasal neuroglial heterotopia ■ Nasal heterotopic brain tissue

Key features

- Rare, benign, congenital lesion
- Most common near the root of the nose, but can be intranasal
- Solitary, firm, smooth, skin-colored to red–purple papulonodule
- Microscopically, lobulated neuroglial tissue

History

The term "nasal glioma" was introduced by Schmidt in 1900.

Epidemiology

These extracranial rests of brain tissue are rare and usually manifest at the time of birth.

Pathogenesis

Nasal glial heterotopia (NGH) is the result of embryologic displacement of brain tissue, usually along the cranial closure lines and without apparent communication with underlying structures (see Figs. 64.1 & 64.8)[98]. It has

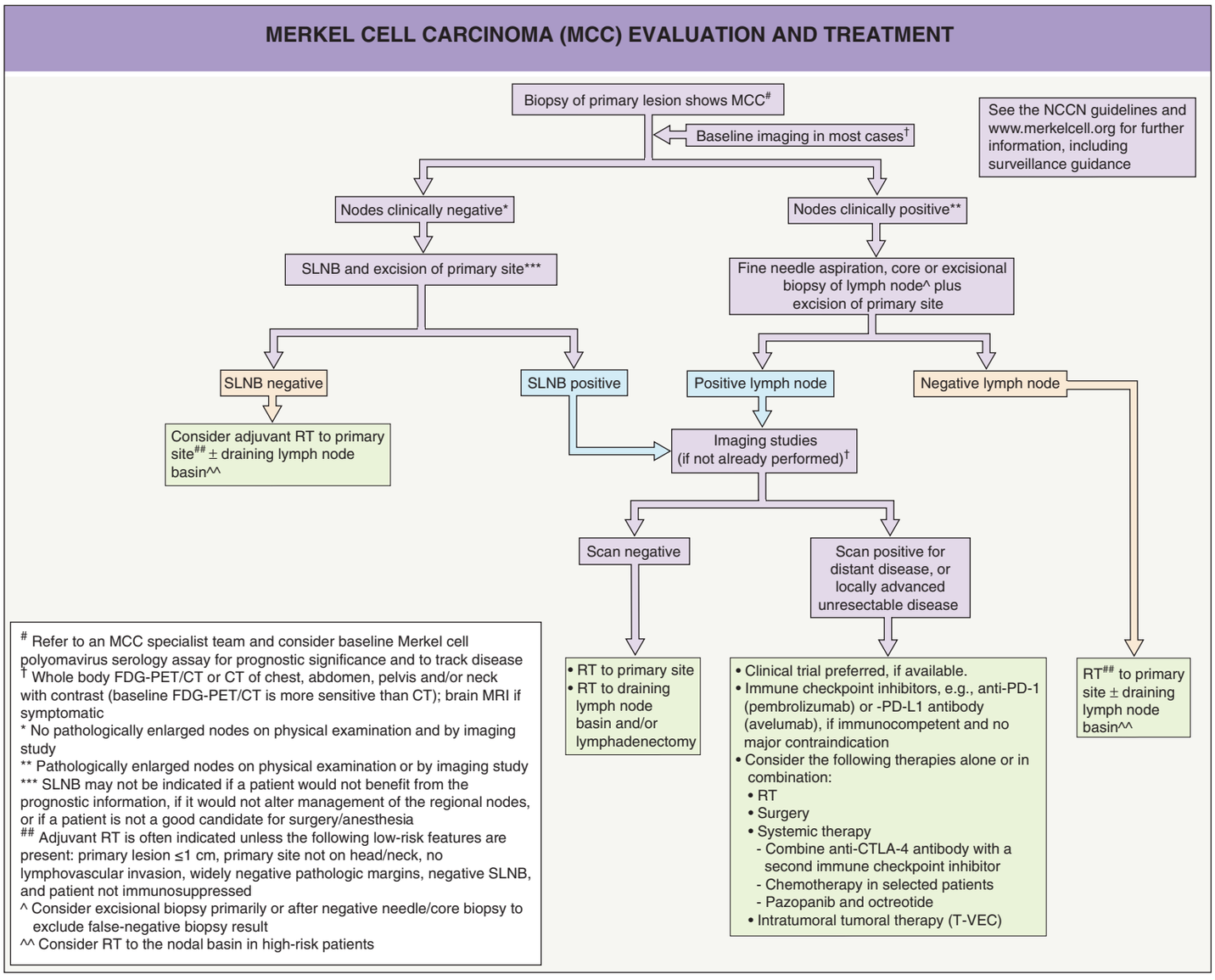


Fig. 115.19 Merkel cell carcinoma (MCC) evaluation and treatment algorithm. CT, computerized tomography; FDG-PET, fluorodeoxyglucose-positron emission tomography; NCCN, National Comprehensive Cancer Network; RT, radiotherapy; SLNB, sentinel lymph node biopsy.

a predilection for the perinasal area; therefore, it is commonly referred to as a nasal "glioma". As this is not a true neoplasm, the term is misleading[99].

Clinical features

NGHs are firm, smooth-surfaced, skin-colored to red–violet papulonodules that may have obvious telangiectasias and range in size from 1 to 3 cm. Approximately 60% are located on the bridge of the nose (Fig. 115.20), with the remainder usually located intranasally or in both locations[99,100].

Pathology

In a NGH, an ill-defined, non-encapsulated neuropil-like mass is seen within the dermis and subcutis. The neuropil-like tissue is composed of nests and strands of pale-staining, finely vacuolated or fibrillary matrix in which various types of astrocytes can be found[98]. Gemistocytic astrocytes, with polygonal, eosinophilic cytoplasm and eccentric nuclei, as well as multinucleated giant cells, are relatively common. Mature neurons are present in variable numbers[99]. Occasionally, residual meningoendothelial cells, ependymal cells, choroid plexus-like structures, and pigmented cells can be identified[100]. No mitotic activity or aggressive growth pattern has been described.

Differential diagnosis

Clinically, the lesion must be differentiated from other facial midline lesions (see Ch. 64)[99,101] as well as an infantile hemangioma, dermoid cyst, and nasal polyp (see Table 64.1).



Fig. 115.20 Nasal glial heterotopia ("nasal glioma") in a newborn. Pink to violet soft nodule.

Treatment

Most cutaneous neural malformations can be effectively treated by excision. Cranial imaging is recommended before these lesions are biopsied or removed[102], because NGHs can communicate with the

intracranial space, and therefore cerebrospinal fluid leakage and subsequent meningoencephalitis and other neurologic damage may occur after biopsy[99].

Heterotopic Meningeal Tissue

Synonym: ■ Rudimentary meningocele

Key features

- Rare disorder that usually presents in neonates and infants and favors the scalp, forehead, and dorsal midline
- Soft to firm, skin-colored nodule, often with partial alopecia and/or the "hair collar" sign when on the scalp
- Can be associated with other developmental anomalies
- Histologically, solid nests and strands, whorls of epithelioid or spindle cells, and psammoma bodies

History

The concept of rudimentary meningocele was introduced by Lopez et al.[103].

Epidemiology

Meningeal heterotopias are rare lesions, usually apparent at or shortly after birth[103].

Pathogenesis

Rudimentary meningoceles are thought to result from herniation of the meningeal lining into the skin and subcutaneous tissues during embryologic development, usually with no residual communication with the CNS (see Fig. 64.8)[104]. Although these lesions are sometimes classified as type I cutaneous meningiomas[103], considering their non-neoplastic nature, they are better classified as rudimentary meningoceles[104].

Clinical features

Rudimentary meningoceles most commonly present on the scalp of neonates and infants at the sites of cranial closure (see Fig. 64.1). Less often they occur on the forehead (midline) or overlie the spine. Skin-colored papules or nodules on the scalp are often associated with alopecia and/or the "hair collar" sign[105].

Pathology

A rudimentary meningocele is an ill-defined mass of cavernous, pseudovascular spaces embedded in a markedly collagenous stroma[104,106]. The spaces may be lined by elongated meningoendothelial cells characterized by eosinophilic cytoplasm, round or ovoid nuclei, and a fine chromatin pattern. Similar cells dissect or wrap around collagen fibers, producing "collagen bodies". No significant cytologic atypia or mitotic activity is present. Focal calcification and psammoma bodies (eosinophilic laminated and whorled structures with variable calcification) may occur. Meningothelial cells consistently express vimentin and EMA, whereas immunoexpression of S100 protein is variable.

Differential diagnosis

In neonates and infants, rudimentary meningoceles must be distinguished from "atretic" meningoceles (an intermediate form with an intracranial connection), membranous aplasia cutis congenita, heterotopic brain tissue, dermoid cysts, and infantile hemangiomas. Type II and type III meningiomas are in the histologic differential diagnosis. They usually develop on the scalp of adults, either along the course of a cranial nerve (type II) or as a cutaneous "metastasis" or direct extension of a primary meningioma of the arachnoid lining (type III)[103,105,107]. Within the deep dermis or subcutis, there is a multinodular mass, often with an infiltrative growth pattern[108–110]. The cells may show a variable degree of differentiation, and in the most common form, the spindle cells have a concentric, whorl-like arrangement[108]; psammoma bodies are often present[108–110]. Mitotic figures are rare in type II and variably increased in type III. Clinically, these nodular tumors may have associated alopecia and can resemble an epidermoid or pilar cyst, adnexal tumor, or cutaneous metastasis. They may occur in the setting of neurofibromatosis (types I and II)[111]. Lastly, the deeper portions of rudimentary meningoceles may have an infiltrative growth pattern with pseudovascular spaces, with a resemblance to angiosarcoma.

Treatment

As with nasal glial heterotopia, imaging studies are required prior to biopsy or excision. The latter is performed primarily by neurosurgeons.

PRIMITIVE NEUROECTODERMAL TUMORS

Synonyms: ■ Neuroblastoma (primary or metastatic) ■ Neuroepithelioma ■ Ganglioneuroma

Key features

- The third most common malignant neoplasm in children
- Cutaneous metastases (children) are seen more frequently than primary cutaneous tumors (adults)
- Cutaneous metastases present as multiple, blue to purple dermal nodules in association with elevated serum and urine catecholamines
- Histologically, small, round, blue cells in a nested or infiltrative growth pattern, with formation of Homer Wright rosettes
- Prognosis depends on the patient's age, clinical stage, and specific genetic abnormalities (e.g. *MYCN* oncogene amplification)

Introduction

Neuroblastic–ganglionic tumors are derived from the germinal neuroepithelium and/or from the neural crest. They display a wide spectrum of clinicopathologic features based on their relative degree of differentiation, ranging from very primitive neuroectodermal tumors to more mature forms such as neuroblastomas.

History

The concept of neuroectodermal tumors was introduced by Stout in 1918. Since then, different terms have been used for tumors with cytologically similar features, reflecting the controversy regarding this entity. Dehner performed a comprehensive review of the nosology of this diverse group of lesions, suggesting the term "primitive neuroectodermal tumors" (PNET)[112]. This concept was then further expanded following the recognition that PNET and extraosseous Ewing sarcoma can have similar immunohistochemical and chromosomal abnormalities (e.g. translocations involving *EWSR1*), and therefore nowadays they are considered within the same neoplastic spectrum[113].

Epidemiology

Neuroblastoma is the third most commonly observed childhood malignancy, and cutaneous metastases are frequent[3]. Most neuroblastomas develop as sporadic tumors, although familial cases have been reported. Primary cutaneous PNETs are tumors of adulthood (mean age, 40 years) and are exceedingly rare[3]. Cutaneous ganglioneuroma has a predilection for the trunk.

Pathogenesis

PNETs of the skin either represent metastases from a PNET of the adrenals and/or ganglionic chain (traditionally designated as neuroblastomas) or develop *de novo* from heterotopic neural crest cells[2]. In the latter case, they are referred to as peripheral PNETs or as peripheral neuroblastomas. *ALK* is implicated in the tumorigenesis of many familial and some sporadic cases of neuroblastoma. In addition, DNA ploidy and specific genetic abnormalities, such as *MYCN* oncogene amplification or aberrations of chromosomes 11q or 1p, influence prognosis[114]. Cutaneous ganglioneuroma is best regarded as resulting from abnormal migration and differentiation of neural crest cells.

Clinical Features

In children, the cutaneous metastases of neuroblastoma often manifest as multiple, blue to purple, dermal papules or nodules that resemble the "blueberry muffin" lesions seen with congenital infections or hematologic disorders[4] (see Ch. 121). These nodules may blanch upon stroking and develop an erythematous halo[115,116]. Serum and urine catecholamine levels are typically elevated. In children, complete spontaneous regression has been described in stage IV-S neuroblastoma, including cutaneous metastases[117].

In adults, PNETs are rapidly growing dermal or subcutaneous nodules that favor the trunk or head. Ulceration is common. These highly aggressive neoplasms have an almost invariably fatal outcome.

Pathology

In metastatic neuroblastoma, an ill-defined or infiltrative mass is present in the dermis and/or the subcutis. However, when smaller and more superficial, deposits are more defined. The tumor mass is composed of atypical, small, dark cells with scant cytoplasm[2,112]. The cells have larger nuclei than mature lymphocytes (with a coarse chromatin pattern) and they form irregular nests, cords, or poorly cohesive sheets. Rosette formation, by concentrically arranged tumor cells in double or multiple circles, is common. The center of the rosettes contains converging fine fibrillary material characteristic of Homer Wright-type rosettes[2] (Fig. 115.21). Mitotic activity is high, and abnormal mitoses are abundant. Extensive areas of necrosis and hemorrhage are common.

As the tumor differentiates, the relative proportion of neuroblastoma components decreases, and the ganglioneuromatous elements increase. Eventually, the tumor may show features indistinguishable from a ganglioneuroma[117]. Cutaneous ganglioneuromas are characterized by mature ganglion cells immersed in a Schwann cell-rich stroma. Lesions consisting of only ganglion cells may also occur and are referred to as "ganglion cell choristomas". Ganglion cells are round-to-polygonal with vesicular nuclei and abundant pale cytoplasm; the latter contains Nissl granules which may be highlighted by a toluidine blue stain. Immunohistochemically, the cells of neuroblastomas and ganglioneuromas react variably with neural and neuroendocrine markers, depending on their state of differentiation. These markers include neuron-specific enolase, S100 protein, neurofilaments, synaptophysin, chromogranin, and CD99 (see Ch. 0)[114].

Primary cutaneous PNETs have similar histopathologic features to those of the classic neuroblastoma, but ganglionic or neuromatous differentiation is not characteristic. These two tumors also share major immunohistochemical features. However, MIC-2(013) is commonly expressed by PNETs, but not by neuroblastomas, facilitating their distinction[114,117–120].

Differential Diagnosis

In children, the clinical differential diagnosis includes other types of cutaneous metastasis, extramedullary hematopoiesis, and mastocytosis, whereas in adults it includes adnexal tumors, lymphoma, and soft tissue sarcomas. Histologically, both metastatic neuroblastoma and primary cutaneous PNET must be differentiated from other small, round, blue cell tumors that form rosettes and may involve the skin[120,121] (see discussion in MCC section). Cutaneous ganglioneuroma must be distinguished from cutaneous metastases of neuroblastoma, with age of onset and other clinical history required for distinction.

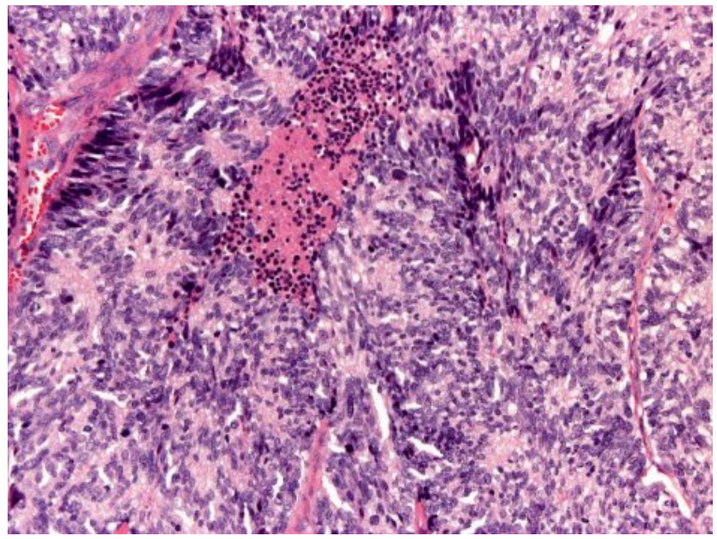


Fig. 115.21 Cutaneous neuroblastoma. The tumor is composed of small cells with small, round to ovoid nuclei that can be arranged in rosettes. The fibrillary material in the center of Homer Wright-type rosettes is characteristic. In the upper mid-portion of the figure there is a large area of necrosis. *Courtesy Lorenzo Cerroni, MD.*

Treatment

The effective treatment of neuroblastoma requires an interdisciplinary team that includes oncologists, surgeons, and radiation therapists. The overall prognosis of localized tumor involvement has improved with combined surgical excision, multiagent chemotherapy, differentiating agents (e.g. 13-cis-retinoic acid), immunotherapy (e.g. dinutuximab), hematopoietic stem cell transplantation, and radiopharmaceuticals[114]. Important prognostic factors include the age, stage, histologic differentiation, specific genetic abnormalities (e.g. *MYCN* oncogene amplification, 11q aberration), and response to initial chemotherapy[2].

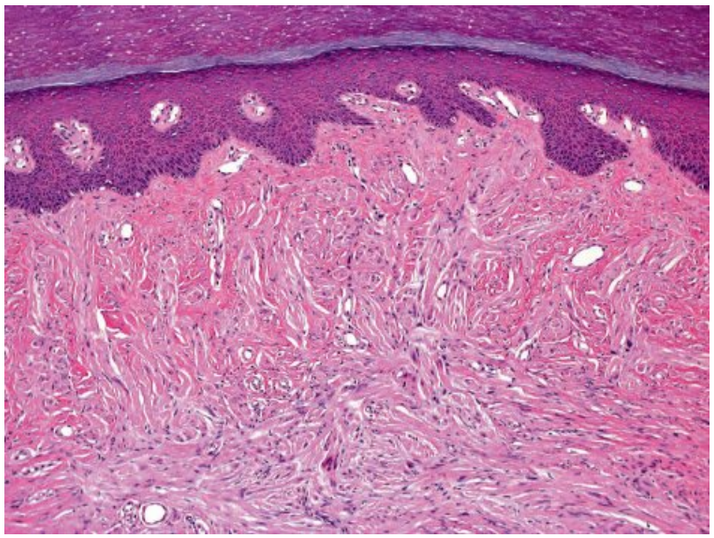
Additional figures and table on Tumors and tumor-like conditions of ectopic and heterotopic neural tissue involving the skin, available in our eBook (see inside front cover for access code).

REFERENCES

1. Cates JM, Coffin CM. Neurogenic tumors of soft tissue. *Pediatr Dev Pathol*. 2012;15:62–107.
2. Goldblum JR, Folpe AL, Weiss SW. *Benign Tumors of Peripheral Nerves. Enzinger & Weiss's Soft Tissue Tumors*. 7th ed. Philadelphia: Elsevier; 2020:885–958.
3. Rodriguez FJ, Folpe AL, Giannini C, et al. Pathology of peripheral nerve sheath tumors: diagnostic overview and update on selected diagnostic problems. *Acta Neuropathol*. 2012;123:295–319.
4. Reed RJ, Fine RM, Meltzer HD. Palisaded, encapsulated neuromas of the skin. *Arch Dermatol*. 1972;106:865–870.
5. Argenyi ZB, Santa Cruz D, Bromley C. Comparative light-microscopic and immunohistochemical study of traumatic and palisaded, encapsulated neuromas of the skin. *Am J Dermatopathol*. 1992;14:504–510.
6. Höke A. Mechanisms of disease: what factors limit the success of peripheral nerve regeneration in humans? *Nat Clin Pract Neurol*. 2006;2:448–454.
7. Matthews GJ, Osterholm JL. Painful traumatic neuromas. *Surg Clin North Am*. 1972;51:1313–1324.
8. Burtner DD, Goodman M. Traumatic neuroma of the nose. *Arch Otolaryngol*. 1972;103:108–109.
9. Shapiro L, Juklin EA, Brownstein HM. Rudimentary polydactyly. *Arch Dermatol*. 1973;108:223–225.
10. Leblebici C, Savli TC, Yeni B, et al. Palisaded encapsulated (solitary circumscribed) neuroma: a review of 30 cases. *Int J Surg Pathol*. 2019;27:506–514.
11. Argenyi ZB. Immunohistochemical characterization of palisaded encapsulated neuroma. *J Cutan Pathol*. 1990;17:329–335.
12. Argenyi ZB, Cooper PH, Santa Cuz D. Plexiform and other unusual variants of palisaded encapsulated neuroma. *J Cutan Pathol*. 1993;20:34–39.
13. Argenyi ZB. Newly recognized neural neoplasms relevant to the dermatopathologist. *Dermatol Clin*. 1992;10:219–234.
14. Requena L, Grosshans E, Kutzner H, et al. Epithelial sheath neuroma; a new entity. *Am J Surg Pathol*. 2000;24:190–196.
15. Stout AP. The peripheral manifestations of specific nerve sheath tumor (neurilemoma). *Am J Cancer*. 1935;24:751–796.
16. Halliday D, Parry A, Evans DG. Neurofibromatosis type 2 and related disorders. *Curr Opin Oncol*. 2019;31:562–567.
17. Plotkin SR, Wick A. Neurofibromatosis and schwannomatosis. *Semin Neurol*. 2018;38:73–85.
18. Hulsebos TJM, Plomp AS, Wolterman RA, et al. Germline mutations of *INI1/SMARCB1* in familial schwannomatosis. *Am J Hum Genet*. 2007;80:805–810.
19. Piotrowski A, Xie J, Liu YF, et al. Germline loss-of-function mutations in LZTR1 predispose to an inherited disorder of multiple schwannomas. *Nat Genet*. 2014;46:182–187.
20. Torres-Mora J, Dry S, Li X, et al. Malignant melanotic schwannian tumor: a clinicopathologic, immunohistochemical, and gene expression profiling study of 40 cases, with a proposal for the reclassification of "melanotic schwannoma". *Am J Surg Pathol*. 2014;38:94–105.
21. Sainz J, Huynh PD, Figueroa K, et al. Mutations of the neurofibromatosis type 2 gene and lack of the gene product in vestibular schwannomas. *Hum Mol Genet*. 1994;3:885–891.
22. Agnihotri S, Jalali S, Wilson MR, et al. The genomic landscape of schwannoma. *Nat Genet*. 2016;48:1339–1348.
23. Das Gupta TK, Brasfield RD, Strong EW, et al. Benign solitary schwannomas (neurilemomas). *Cancer*. 1969;24:355–366.

24. Whitaker WG, Droulias C. Benign encapsulated neurilemoma: a report of 76 cases. *Am Surg*. 1976;42:675–678.
25. Jacobs RL, Barmada R. Neurilemoma: a review of the literature with six case reports. *Arch Surg*. 1971;102:181–186.
26. Vilanova JR, Burgos-Bretones JJ, Alvarez JA, et al. Benign schwannomas: a histopathological and morphometric study. *Pathology*. 1982;137:281–286.
27. Argenyi ZB, Balogh K, Abraham AA. Degenerative ("ancient") changes in benign cutaneous schwannoma: a light microscopic, histochemical and immunohistochemical study. *J Cutan Pathol*. 1993;20:148–153.
28. Nascimento AF, Fletcher CD. The controversial nosology of benign nerve sheath tumors: neurofilament protein staining demonstrates intratumoral axons in many sporadic schwannomas. *Am J Surg Pathol*. 2007;31:1363–1370.
29. Berg JC, Schethauer BW, Spinner RJ, et al. Plexiform schwannoma: a clinicopathologic overview with emphasis on the head and neck region. *Hum Pathol*. 2008;39:633–640.
30. Jo VY, Fletcher CDM. SMARCB1/INI1 loss in epithelioid schwannoma: a clinicopathologic and immunohistochemical study of 65 cases. *Am J Surg Pathol*. 2017;41:1013–1022.
31. Luzar B, Tanaka M, Schneider J, Calonje E. Cutaneous microcystic/reticular schwannoma: a poorly recognized entity. *J Cutan Pathol*. 2016;43:93–100.
32. Cohen JN, Yeh I, LeBoit PE. Melanotic schwannoma of the vulva: a case report and review of the literature. *Am J Dermatopathol*. 2020;42:46–51.
33. Fletcher JS, Pundavela J, Ratner N. After *Nf1* loss in Schwann cells, inflammation drives neurofibroma formation. *Neuro-oncol Adv*. 2020;2(Suppl 1):i23–i32.
34. Anastasaki C, Dahiya S, Gutmann DH. KIR2DL5 mutation and loss underlies sporadic dermal neurofibroma pathogenesis and growth. *Oncotarget*. 2017;8:47574–47585.
35. Megahed M. Histopathological variants of neurofibroma. A study of 114 lesions. *Am J Dermatopathol*. 1994;16:486–495.
36. Miettinen MM, Antonescu CR, Fletcher CDM, et al. Histopathologic evaluation of atypical neurofibromatous tumors and their transformation into malignant peripheral nerve sheath tumor in patients with neurofibromatosis 1: a consensus overview. *Hum Pathol*. 2017;67:1–10.
37. Barnhill RL, Mihm Jr. MC. Cellular neurothekeoma. A distinctive variant of neurothekeoma mimicking nevomelanocytic tumors. *Am J Surg Pathol*. 1990;14:113–120.
38. Sheth S, Li X, Binder S, Dry SM. Differential gene expression profiles of neurothekeomas and nerve sheath myxomas by microarray analysis. *Mod Pathol*. 2011;24:343–354.
39. Fetsch JF, Laskin WB, Miettinen M. Nerve sheath myxoma: a clinicopathologic and immunohistochemical analysis of 57 morphologically distinctive, S-100 protein- and GFAP-positive, myxoid peripheral nerve sheath tumors with a predilection for the extremities and a high local recurrence rate. *Am J Surg Pathol*. 2005;29:1615–1624.
40. Fetsch JF, Laskin WB, Hallman JR, et al. Neurothekeoma: an analysis of 178 tumors with detailed immunohistochemical data and long-term patient follow-up information. *Am J Surg Pathol*. 2007;31:1103–1114.
41. Laskin WB, Fetsch JF, Miettinen M. The "neurothekeoma": immunohistochemical analysis distinguishes the true nerve sheath myxoma from its mimics. *Hum Pathol*. 2000;31:1230–1241.
42. Stratton J, Billings SD. Cellular neurothekeoma: analysis of 37 cases emphasizing atypical histologic features. *Mod Pathol*. 2014;27:701–710.
43. Hornick JL, Fletcher CD. Cellular neurothekeoma: detailed characterization in a series of 133 cases. *Am J Surg Pathol*. 2007;31:329–340.
44. Fried I, Sitthinamsuwan P, Muangsomboon S, et al. SOX-10 and MiTF expression in cellular and 'mixed' neurothekeoma. *J Cutan Pathol*. 2014;41:640–645.
45. Fox MD, Billings SD, Gleason BC, et al. Expression of MiTF may be helpful in differentiating cellular neurothekeoma from plexiform fibrohistiocytic tumor (histiocytoid predominant) in a partial biopsy specimen. *Am J Dermatopathol*. 2012;34:157–160.
46. Cohen JN, Yeh I, Jordan RC, et al. Cutaneous non-neural granular cell tumors harbor recurrent ALK gene fusions. *Am J Surg Pathol*. 2018;42:1133–1142.
47. Cardis MA, Ni J, Bhawan J. Granular cell differentiation: a review of the published work. *J Dermatol*. 2017;44:251–258.
48. Abrikossoff A. Myomas originating from transversely striated voluntary musculature. *Virchows Arch Pathol Anat*. 1926;260:215–233.
49. Fisher ER, Wechsler H. Granular cell myoblastoma – a misnomer. Electron-microscopic and histochemical evidence concerning its Schwann cell derivation and nature (granular cell schwannoma). *Cancer*. 1962;15:936–954.
50. Heerema MG, Suurmeijer AJ. Sox10 immunohistochemistry allows the pathologist to differentiate between prototypical granular cell tumors and other granular cell lesions. *Histopathology*. 2012;61:997–999.
51. Karamchandani JR, Nielsen TO, van de Rijn M, West RB. Sox10 and S100 in the diagnosis of soft-tissue neoplasms. *Appl Immunohistochem Mol Morphol*. 2012;20:445–450.
52. Pareja F, Brandes AH, Basili T, et al. Loss-of-function mutations in ATP6AP1 and ATP6AP2 in granular cell tumors. *Nat Commun*. 2018;9:3533.
53. Sekimizu M, Yoshida A, Mitani S, et al. Frequent mutations of genes encoding vacuolar H^+-ATPase components in granular cell tumors. *Genes Chromosomes Cancer*. 2019;58:373–380.
54. Gunson TH, Hashim N, Sharpe GR. Generalized lentiginosis, short stature, and multiple cutaneous nodules–quiz case. LEOPARD syndrome (LS) associated with multiple granular cell tumors (GCTs). *Arch Dermatol*. 2010;146:337–342.
55. Machado I, Cruz J, Lavernia J, et al. Solitary, multiple, benign, atypical, or malignant: the "Granular Cell Tumor" puzzle. *Virchows Arch*. 2016;468:527–538.
56. Mentzel T, Wadden C, Fletcher CD. Granular cell change in smooth muscle tumors of skin and soft tissue. *Histopathology*. 1994;24:223–231.
57. Fanburg-Smith JC, Meis-Kindblom JM, Fante R, Kindblom LG. Malignant granular cell tumor of soft tissue. Diagnostic criteria and clinicopathologic correlation. *Am J Surg Pathol*. 1998;22:779–794.
58. Gleason BC, Nascimento AF. HMB-45 and Melan-A are useful in the differential diagnosis between granular cell tumor and malignant melanoma. *Am J Dermatopathol*. 2007;29:22–27.
59. Schoolmeester JK, Lastra RR. Granular cell tumors overexpress TFE3 without corollary gene rearrangement. *Hum Pathol*. 2015;46:1242–1243.
60. Van der Wal N, Baak JP, Schipper NW, et al. Morphometric study of pseudoepitheliomatous hyperplasia in granular cell tumors of the tongue. *J Oral Pathol Med*. 1989;18:8–10.
61. Erlandson RA, Woodruff JM. Peripheral nerve sheath tumors: an electron microscopic study of 43 cases. *Cancer*. 1982;49:273–287.
62. Wanebo JE, Malik JM, Vandenberg SE, et al. Malignant peripheral nerve sheath tumors: a clinicopathologic study of 28 cases. *Cancer*. 1993;71:1247–1253.
63. Lee W, Teckie S, Wiesner T, et al. PRC2 is recurrently inactivated through EED or SUZ12 loss in malignant peripheral nerve sheath tumors. *Nat Genet*. 2014;46:1227–1232.
64. Lyskjaer I, Lindsay D, Tirabosco R, et al. H3K27me3 expression and methylation status in histological variants of malignant peripheral nerve sheath tumours. *J Pathol*. 2020;252:151–164.
65. Toker C. Trabecular carcinoma of the skin. *Arch Dermatol*. 1972;105:107–110.
66. Becker JC, Stang A, DeCaprio JA, et al. Merkel cell carcinoma. *Nat Rev Dis Primers*. 2017;3:17077.
67. Paulson K, Park S, Vandeven N, et al. Merkel cell carcinoma: current US incidence and projected increases based on changing demographics. *J Am Acad Dermatol*. 2018;78:457–463.
68. Schadendorf D, Lebbe C, Hausen A, et al. Merkel cell carcinoma: epidemiology, prognosis, therapy and unmet medical needs. *Eur J Cancer*. 2017;71:53–69.
69. Feng H, Shuda M, Chang Y, Moore PS. Clonal integration of a polyomavirus in human Merkel cell carcinoma. *Science*. 2008;319:1096–1100.
70. Harms P, Harms K, Moore P, et al. The biology and treatment of Merkel cell carcinoma: current understanding and research priorities. *Nat Rev Clin Oncol*. 2018;15:763–776.
71. Kassem A, Schöpflin A, Diaz C, et al. Frequent detection of Merkel cell polyomavirus in human Merkel cell carcinomas and identification of a unique deletion in the *VP1* gene. *Cancer Res*. 2008;68:5009–5013.
72. Harms PW, Collie AM, Hovelson DH, et al. Next generation sequencing of cytokeratin 20-negative Merkel cell carcinoma reveals ultraviolet-signature mutations and recurrent TP53 and RB1 inactivation. *Mod Pathol*. 2016;29:240–248.
73. Harms KL, Healy MA, Nghiem P, et al. Analysis of prognostic factors from 9387 Merkel cell carcinoma cases forms the basis for the new 8th edition AJCC staging system. *Ann Surg Oncol*. 2016;23:3564–3571.
74. Wick MR, Scheithauer BW. Primary neuroendocrine carcinoma of the skin. In: Wick MR, ed. *Pathology of Unusual Malignant Cutaneous Tumors*. New York: Marcel Dekker; 1985:107–172.
75. Cheuk W, Kwan MY, Suster S, Chan JK. Immunostaining for thyroid transcription factor 1 and cytokeratin 20 aids the distinction of small cell carcinoma from Merkel cell carcinoma, but not pulmonary from extrapulmonary small cell carcinomas. *Arch Pathol Lab Med*. 2001;125:228–231.
76. LeBoit PE, Crutcher WA, Shapiro PE. Pagetoid intraepidermal spread in Merkel cell (primary neuroendocrine) carcinoma of the skin. *Am J Surg Pathol*. 1992;16:584–592.
77. Duncavage EJ, Le BM, Wang D, Pfeifer JD. Merkel cell polyomavirus: a specific marker for Merkel cell carcinoma in histologically similar tumors. *Am J Surg Pathol*. 2009;33:1771–1777.
78. Stetsenko G, Malekirad J, Paulson G, et al. p63 expression in Merkel cell carcinoma predicts poorer survival yet may have limited clinical utility. *Am J Clin Pathol*. 2013;140:838–844.
79. Moshiri A, Doumani R, Blom A, et al. Polyomavirus-negative Merkel cell carcinoma: a more aggressive subtype based on analysis of 282 cases using multimodal tumor virus detection. *J Invest Dermatol*. 2017;137:819–827.
79a. Busam KJ, Judge MJ, Bichakjian CK, et al. Dataset for the reporting of Merkel cell carcinoma: recommendations from the International Collaboration on Cancer Reporting (ICCR). *Am J Surg Pathol*. 2022;46:1583–1591.
80. Duker I, Starz H, Bachter D, Balda BR. Prognostic and therapeutic implications of sentinel lymphonodectomy and S-staging in Merkel cell carcinoma. *Dermatology*. 2001;202:225–229.
81. Gupta SG, Wang LC, Penas LC, et al. Sentinel lymph node biopsy for evaluation and treatment of patients with Merkel cell carcinoma: the Dana-Farber experience and meta-analysis of the literature. *Arch Dermatol*. 2006;142:771–774.
82. Gunaratne DA, Howle JR, Veness MJ. Sentinel lymph node biopsy in Merkel cell carcinoma: a 15-year institutional experience and statistical analysis of 721 reported cases. *Br J Dermatol*. 2016;174:272–281.
83. Iyer J, Storer BE, Paulson KG, et al. Relationships between primary tumor size, number of involved nodes and survival among 8,044 cases of Merkel cell carcinoma. *J Am Acad Dermatol*. 2014;70:637–643.
84. Conic R, Ko J, Saridakis S, et al. Sentinel lymph node biopsy in Merkel cell carcinoma: predictors of sentinel lymph node positivity and association with overall survival. *J Am Acad Dermatol*. 2019;81:364–372.
85. National Comprehensive Cancer Network. Merkel Cell Carcinoma (Version 1.2023), April 2023. <www.nccn.org/login?ReturnURL=https://www.nccn.org/professionals/physician_gls/pdf/mcc.pdf>.
86. Singh N, Alexander NA, Lachance K, et al. Clinical benefit of baseline imaging in Merkel cell carcinoma: analysis of 584 patients. *J Am Acad Dermatol*. 2021;84:330–339.
87. Tarabadkar ES, Thomas H, Blom A, et al. Clinical benefit from tyrosine kinase inhibitors in metastatic Merkel cell carcinoma: a case series of 5 patients. *Am J Case Rep*. 2018;19:505–511.
88. Akaike T, Qazi J, Anderson A, et al. High somatostatin receptor expression and efficacy of somatostatin analogues in patients with metastatic Merkel cell carcinoma. *Br J Dermatol*. 2021;184:319–327.
89. LoPiccolo J, Schollenberger M, Dakhil S, et al. Rescue therapy for patients with anti-PD-1-refractory Merkel cell carcinoma: a multicenter, retrospective case series. *J Immunother Cancer*. 2019;7:170.
90. Nghiem PT, Bhatia S, Lipson EJ, et al. PD-1 blockade with pembrolizumab in advanced Merkel-cell carcinoma. *N Engl J Med*. 2016;374:2542–2552.
91. Nghiem P, Bhatia S, Lipson EJ, et al. Durable tumor regression and overall survival in patients with advanced Merkel cell carcinoma receiving pembrolizumab as first-line therapy. *J Clin Oncol*. 2019;37:693–702.
92. Kaufman H, Russell J, Hamid O, et al. Avelumab in patients with chemotherapy-refractory metastatic Merkel cell carcinoma: a multicentre, single-group, open-label, phase 2 trial. *Lancet Oncol*. 2016;17:1374–1385.
93. D'Angelo SP, Russell J, Lebbe C, et al. Efficacy and safety of first-line avelumab treatment in patients with stage IV metastatic Merkel cell carcinoma: a preplanned interim analysis of a clinical trial. *JAMA Oncol*. 2018;4:e180077.

93a. Kang C. Retifanlimab: First approval. *Drugs*. 2023;83: 731–737.
93b. Nghiem P, Bhatia S, Lipson EJ, et al. Three-year survival, correlates and salvage therapies in patients receiving first-line pembrolizumab for advanced Merkel cell carcinoma. *J Immunother Cancer*. 2021;9:e002478.
94. Iyer JG, Blom A, Doumani R, et al. Response rates and durability of chemotherapy among 62 patients with metastatic Merkel cell carcinoma. *Cancer Med*. 2016;5:2294–2301.
95. Bichakjian CK, Lowe L, Lao CD, et al. Merkel cell carcinoma: critical review with guidelines for multidisciplinary management. *Cancer*. 2007;110:1–12.
96. Paulson KG, Lewis CW, Redman MW, et al. Viral oncoprotein antibodies as a marker for recurrence of Merkel cell carcinoma: a prospective validation study. *Cancer*. 2017;123:1464–1474.
97. Samimi M, Molet L, Fleury M, et al. Prognostic value of antibodies to Merkel cell polyomavirus T antigens and VP1 protein in patients with Merkel cell carcinoma. *Br J Dermatol*. 2016;174:813–822.
98. Patterson K, Kapur S, Chandra RS. "Nasal gliomas" and related brain heterotopias: a pathologist's perspective. *Pediatr Pathol*. 1986;5:353–362.
99. Yeoh GPS, Bale PM, de Silva M. Nasal cerebral heterotopia: the so-called nasal glioma or sequestered encephalocele and its variants. *Pediatr Pathol*. 1989;9:531–549.
100. Orkin M, Fisher I. Heterotopic brain tissue (heterotopic neural rest): case report with review of related anomalies. *Arch Dermatol*. 1966;94:699–708.
101. Fletcher CDM, Carpenter G, McKee PH. Nasal glioma: a rarity. *Am J Dermatopathol*. 1986;8:341–346.
102. Kennard CD, Rasmussen JE. Congenital midline nasal masses: diagnosis and management. *J Dermatol Surg Oncol*. 1990;16:1025–1036.
103. Lopez DA, Silvers DN, Helwig EB. Cutaneous meningiomas: a clinicopathologic study. *Cancer*. 1974;34:728–744.
104. Sibley DA, Cooper PH. Rudimentary meningocele: a variant of "primary cutaneous meningioma". *J Cutan Pathol*. 1989;16:72–80.
105. Berry III AD, Patterson W. Meningoceles, meningomyeloceles, and encephaloceles: a neuro-dermatopathologic study of 132 cases. *J Cutan Pathol*. 1991;18:164–177.
106. Marrogi AJ, Swanson PE, Kyriakos M, et al. Rudimentary meningocele of the skin: clinicopathologic features and differential diagnosis. *J Cutan Pathol*. 1991;18:178–188.
107. Argenyi ZB. Cutaneous neural heterotopias and related tumors relevant for the dermatopathologist. *Semin Diagn Pathol*. 1996;13:60–71.
108. Nochomovitz LE, Jannotta F, Orenstein JM. Meningioma of the scalp: light and electron microscopic observations. *Arch Pathol Lab Med*. 1985;109:92–95.
109. Theaker JM, Fleming KA. Meningioma of the scalp: a case report with immunohistological features. *J Cutan Pathol*. 1987;14:49–53.
110. Gelli MC, Pasquinelli G, Martinelli G, et al. Cutaneous meningioma: histochemical, immunohistochemical and ultrastructural investigation. *Histopathology*. 1993;23:576–578.
111. Argenyi ZB, Thielberg MD, Hayes CM, Whitaker DC. Primary cutaneous meningioma associated with von Recklinghausen disease. *J Cutan Pathol*. 1994;21:549–556.
112. Dehner LP. Peripheral and central primitive neuroectodermal tumors: a nosologic concept seeking a consensus. *Arch Pathol Lab Med*. 1986;110:997–1005.
113. Dehner LP. Primitive neuroectodermal turmor and Ewing's sarcoma. *Am J Surg Pathol*. 1993;17:1–13.
114. Mueller S, Matthay KK. Neuroblastoma: biology and staging. *Curr Oncol Rep*. 2009;11:431–438.
115. Shown TE, Durfee MF. Blueberry muffin baby: neonatal neuroblastoma with subcutaneous metastases. *J Urol*. 1970;104:193–195.
116. Hawthorne HC, Nelson JS, Witzelben CL, et al. Blanching subcutaneous nodules in neonatal neuroblastoma. *J Pediatr*. 1970;77:297–300.
117. Ahmed AA, Zhang L, Reddivalla N, Hetherington M. Neuroblastoma in children: update on clinicopathologic and genetic prognostic factors. *Pediatr Hematol Oncol*. 2017;29:1–21.
118. Esiashvili N, Goodman M, Ward K, et al. Neuroblastoma in adults: Incidence and survival analysis based on SEER data. *Pediatr Blood Cancer*. 2007;49:41–46.
119. Argenyi ZB, Bergfeld WF, McMahon JT, et al. Primitive neuroectodermal tumor in the skin with features of neuroblastoma in an adult patient. *J Cutan Pathol*. 1986;13:420–430.
120. Nguyen AV, Argenyi ZB. Cutaneous neuroblastoma: peripheral neuroblastoma. *Am J Dermatopathol*. 1993;15:7–14.
121. Banerjee SS, Agbamu DA, Eyden BP, Harris M. Clinicopathological characteristics of peripheral primitive neuroectodermal tumour of skin and subcutaneous tissue. *Histopathology*. 1997;31:355–366.
122. Macarenco RS, Ellinger F, Oliveira AM. Perineuroma. A distinctive and underrecognized peripheral nerve sheath neoplasm. *Arch Pathol Lab Med*. 2007;131:625–636.
123. Hornick JL, Fletcher CD. Soft tissue perineurioma: clinicopathologic analysis of 81 cases including those with atypical histologic features. *Am J Surg Pathol*. 2005;29:845–858.
124. Hornick JL, Bundock EA, Fletcher CD. Hybrid schwannoma/perineurioma: clinicopathologic analysis of 42 distinctive benign nerve sheath tumors. *Am J Surg Pathol*. 2009;33:1554–1561.



eFig. 115.1 Amputation neuroma (digit). Note the proliferation of nerve fascicles within a fibrotic stroma and the lack of bony structures. *Courtesy Lorenzo Cerroni, MD.*



eFig. 115.2 Mosaic form of neurofibromatosis type 1. Multiple pink–brown papules in a linear arrangement. *Courtesy Kalman Watsky, MD.*



eFig. 115.3 Plexiform neurofibromas. The pink–brown plaques are soft, and large lesions often have a sagging bag-like appearance. *Courtesy Julie V. Schaffer, MD.*



eFig. 115.4 Plexiform neurofibroma in a child with neurofibromatosis type 1. Pendulous, bag-like mass with overlying patches of hyperpigmentation.





eFig. 115.5 Merkel cell carcinomas (primary neuroendocrine carcinomas). A A rapidly growing, violaceous nodule on the toe. **B** Large, eroded, erythematous nodule arising within sun-damaged skin of the cheek. *B, Courtesy Lorenzo Cerroni, MD*.



eFig. 115.6 Merkel cell carcinoma (primary neuroendocrine carcinoma). A red–violet nodule arising within sun-damaged skin of the left fifth finger in a 70-year-old man.

TUMORS AND TUMOR-LIKE CONDITIONS OF ECTOPIC AND HETEROTOPIC NEURAL TISSUE INVOLVING THE SKIN				
	Nasal glial heterotopia ("nasal glioma")*	**Rudimentary meningocele**	**Cutaneous meningioma (types II and III)**	**Peripheral neuroblastoma**
Incidence	Rare	Rare	Extremely rare	Extremely rare
Age	Neonates	Neonates or infants	Usually adults	Late adulthood
Location	Most commonly near the root of the nose but can be intranasal	Scalp, forehead, paravertebral area	Scalp	Head and trunk
Size	1.0–3.0 cm	0.5–3.0 cm	0.5–4.0 cm	0.5–5.0 cm
Clinical appearance	Firm, smooth, skin-colored to red–purple nodule	Soft to firm nodule, often with alopecia or the "hair collar" sign; occasionally cystic; blue–red hue common	Soft to firm nodule, often with alopecia	Soft, skin-colored to red, often ulcerated nodule
Clinical differential diagnosis	Infantile hemangioma, nasal polyp, juvenile xanthogranuloma, dermoid cyst	Membranous aplasia cutis, heterotopic brain tissue, dermoid cyst, infantile hemangioma	Epidermoid or pilar cyst, adnexal tumors, cutaneous metastasis	Adnexal tumors, lymphoma, soft tissue sarcoma, cutaneous metastasis
Associations	Intracranial connection in ~20% ("atretic" encephalocele)	An intracranial connection may be present ("atretic" meningocele)	May be associated with neurofibromatosis (types I and II)	NA
Other	NA	NA	Metastasis of CNS meningioma must be excluded	Metastasis of ganglionic or adrenal neuroblastoma and extension of olfactory neuroblastoma must be excluded, especially in children
Histopathologic features	Lobulated neural tissue (glial cells, astrocytes, rarely true neurons)	Cystic or cavernous spaces, scattered meningothelial cells, pseudovascular pattern, psammoma bodies	Solid nests and strands, whorls of epithelioid or spindle cells, psammoma bodies	Rosette-like (Homer Wright-type) structures of small, round, blue cells, extensive infiltration and necrosis
Biologic course	Benign	Benign	Locally aggressive and destructive	Extremely malignant with widespread metastases

*Heterotopic brain tissue can also be located in the midline scalp, orbit, lip, and oropharynx.

eTable 115.1 Tumors and tumor-like conditions of ectopic and heterotopic neural tissue involving the skin.

116 Fibroblastic, Myofibroblastic, and "Fibrohistiocytic" Proliferations and Neoplasms of the Skin

Bernadette Liegl-Atzwanger and Heinz H. Kutzner

Chapter Contents

Skin Tags 2096
Cutaneous Angiofibroma 2096
Dermatofibroma 2097
Acral Fibrokeratoma 2099
Acral Fibromyxoma 2099
Sclerotic Fibroma of the Skin 2099
Pleomorphic Fibroma of the Skin 2101
Multinucleate Cell Angiohistiocytoma 2102
Dermatomyofibroma 2103
Tenosynovial Giant Cell Tumor (Localized Type) 2103
Fibroma of Tendon Sheath 2104
Nodular Fasciitis 2104
Connective Tissue Nevus 2105
Inclusion Body Fibromatosis 2106
Infantile Myofibromatosis 2106
Myopericytoma 2107
Calcifying Aponeurotic Fibroma 2107
Fibrous Hamartoma of Infancy 2108
Fibromatoses 2108
Plexiform Fibrohistiocytic Tumor 2109
Atypical Fibroxanthoma 2110
Dermatofibrosarcoma Protuberans 2111
Giant Cell Fibroblastoma 2112
Fibrosarcoma 2113
Epithelioid Sarcoma 2113

Key features

- Proliferations and tumors categorized as fibroblastic, myofibroblastic, and "fibrohistiocytic" commonly develop in the skin
- These tumors are composed of fibroblasts, myofibroblasts, histiocytes, dermal dendritic cells, collagen fibers, elastic fibers, and connective tissue mucin, with each component present in variable proportions depending upon the particular neoplasm
- Benign proliferations of these cells, as in nodular fasciitis, can mimic malignant neoplasms
- Immunohistochemical staining for CD34, α-smooth muscle actin, factor XIIIa, and CD68 assists in confirming fibroblastic/myofibroblastic differentiation, with staining for keratins, S100, and SOX10 performed to exclude epithelial or melanocytic differentiation
- When differentiating the various tumors within this group, immunohistochemistry provides limited discrimination
- For some tumors (e.g. dermatofibrosarcoma protuberans, nodular fasciitis), RT-PCR, fluorescent *in situ* hybridization (FISH), and next generation sequencing (NGS) can detect translocations and fusion genes, allowing for more precise diagnoses
- While focusing primarily on proliferations and neoplasms commonly encountered by dermatologists, tumors of soft tissue are also reviewed

SKIN TAGS

Synonyms: ■ Acrochordons ■ Fibroepithelial polyps

Clinical Features

Skin tags are very common, presenting as soft, skin-colored to slightly hyperpigmented, pedunculated papules that favor the neck, axilla, and groin (Fig. 116.1). Skin tags are usually asymptomatic but can become painful secondary to irritation or infarction.

Epidemiology

Men and women are equally affected, and close to 50% of all individuals have at least one skin tag[1]. Although skin tags were once thought to be associated with colonic polyps, more recent studies have not confirmed this relationship[2]. Skin tags have also been reported as a cutaneous marker for diabetes mellitus[3].

Pathology

Histologically, skin tags are polypoid with loose to dense collagenous stroma and thin-walled blood vessels.

In Birt–Hogg–Dubé syndrome and Cowden syndrome, patients can have typical skin tags, but sometimes the "skin tags" represent fibrofolliculomas, trichodiscomas or perifollicular fibromas versus sclerotic fibromas, respectively[4].

Treatment

Unless irritated or infarcted, skin tags are more of a cosmetic issue than a clinical concern and can be removed by scissor excision.

CUTANEOUS ANGIOFIBROMA

Synonyms: ■ Fibrous papule ■ Pearly penile papule ■ Ungual fibroma (Koenen tumor) ■ Fibrous papule of the nose

Cutaneous angiofibroma is a descriptive term for a group of lesions with different clinical presentations and implications, but similar histologic findings.

Clinical Features

Fibrous papules are solitary, dome-shaped and shiny, skin-colored to reddish papules located on the face of adults, most commonly on the nose (Fig. 116.2)[5]. Clinically, they can mimic small intradermal melanocytic nevi, basal cell carcinomas (BCCs), or adnexal tumors. By dermoscopy, a white color is often seen.

Pearly penile papules are pearly, white, dome-shaped, closely aggregated small papules located on the glans penis, commonly in a multilayered and circumferential manner on the corona (Fig. 116.3). They are found in up to 30% of young postpubertal adults and are more common in uncircumcised men[6]. They can be mistaken for condylomata acuminata or hypertrophied sebaceous glands.

Multiple facial angiofibromas are seen in tuberous sclerosis (TS), multiple endocrine neoplasia type 1, Birt–Hogg–Dubé syndrome[7], and



Fig. 116.1 Multiple skin tags in the axilla. The lesions are skin-colored, soft and pedunculated.



Fig. 116.2 Fibrous papule of the nose. A smooth, dome-shaped, skin-colored papule.



Fig. 116.3 Pearly penile papules. Multiple small white papules along the corona of the glans penis. Note the multilayered distribution. *Courtesy Kalman Watsky, MD.*

rarely, neurofibromatosis type 2 or as an isolated finding. They are usually distributed bilaterally on the cheeks, nasolabial folds, nose and chin. In TS, facial angiofibromas usually appear during early to mid childhood and characteristically spare perioral skin. Patients with TS can also have multiple *ungual angiofibromas*. Both facial (≥3) and ungual (≥2) angiofibromas represent major diagnostic criteria for TS (see Table 61.7).

Pathology

All angiofibromas are dome-shaped lesions composed of a dermal proliferation of plump or stellate fibroblasts in a collagenous stroma with an increase in the number of thin-walled, dilated blood vessels (Fig. 116.4). The collagen fibers can be arranged in a concentric fashion around hair follicles and blood vessels (a variant known as perifollicular fibroma). Elastic fibers are decreased in number. Some fibroblasts can be multinucleated. Granular and clear-cell variants have been described.

DERMATOFIBROMA

Synonyms: ■ Benign fibrous histiocytoma (preferred terminology in soft tissue pathology) ■ Fibroma simplex ■ Sclerosing hemangioma ■ Nodular subepidermal fibrosis ■ Histiocytoma ■ Dermal dendrocytoma

Clinical Features

Dermatofibromas occur primarily in adults and often develop on the lower extremities. They are firm, minimally elevated to dome-shaped papules that are usually <1 cm in diameter, but occasionally are >2 cm. The lesions are commonly hyperpigmented (Fig. 116.5). On palpation, they may seem attached to the subcutaneous tissue; pinching the lesion gently usually results in apparent downward movement of the tumor, also known as the "dimple sign". By dermoscopy, a central white scar-like patch or white network surrounded by a delicate pigment network is most commonly observed (see Ch. 0).

Although some dermatofibromas are thought to arise at sites of trauma or arthropod bites, their precise etiology is unknown. Multiple eruptive dermatofibromas have been observed in patients with autoimmune disorders (e.g. lupus erythematosus) and atopic dermatitis and in the setting of immunosuppression (e.g. HIV infection)[8]. Clinically, dermatofibromas can be confused with cysts or melanocytic nevi, especially those with fibrosis. In the case of larger lesions, the possibility of dermatofibrosarcoma protuberans (DFSP), which is less well defined and multilobed, may be considered.

Pathology

Dermatofibromas are characterized by a nodular dermal proliferation, predominantly composed of spindle-shaped fibroblasts and myofibroblasts arranged as short intersecting fascicles (Fig. 116.6).

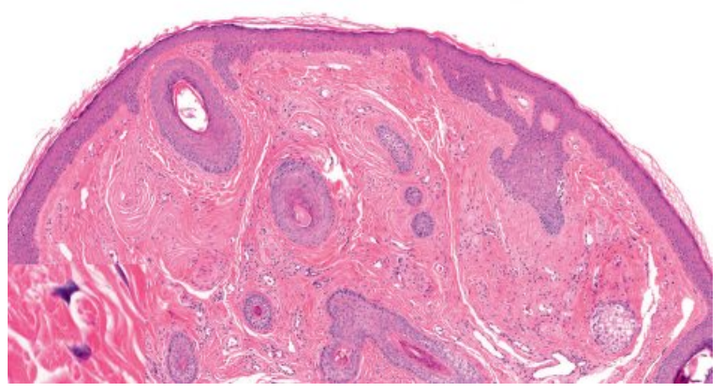


Fig. 116.4 Angiofibroma. A dome-shaped silhouette with a densely packed collagenous stroma and a diffuse array of fusiform and stellate fibroblasts is seen. These features plus dilated postcapillary venules are characteristic of an angiofibroma. *Courtesy Lorenzo Cerroni, MD.*



Fig. 116.5 Dermatofibroma. Firm papule on the lower extremity with peripheral hyperpigmentation. Accentuation of pigmentation at the periphery of the lesion is typical of dermatofibroma. *Courtesy Lorenzo Cerroni, MD.*

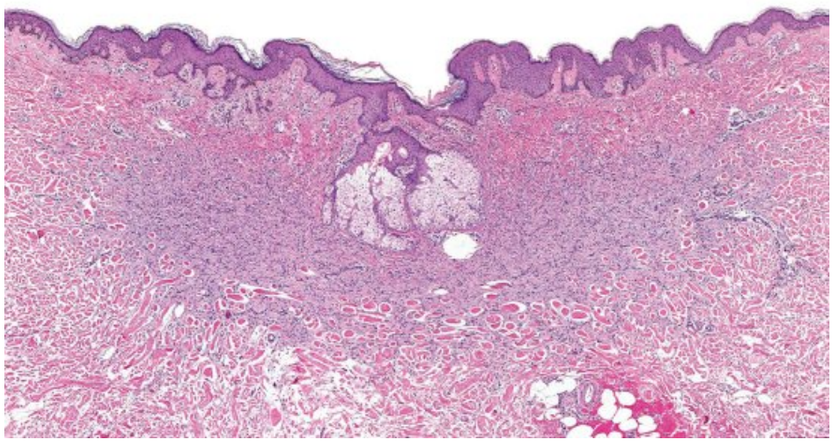


Fig. 116.6 Dermatofibroma. Symmetric, dermal proliferation of spindled fibroblasts in the dermis, with hyperplasia and hyperpigmentation of the overlying epidermis. Note a sebaceous gland "induced" by the fibroblastic proliferation. *Courtesy Lorenzo Cerroni, MD.*

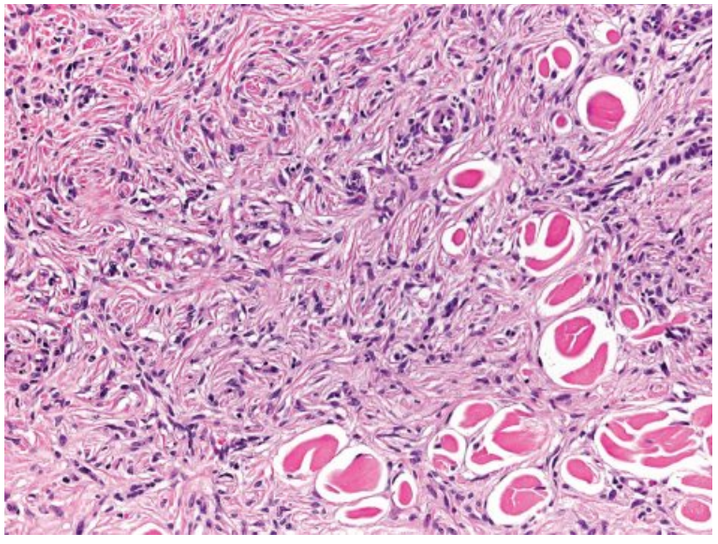


Fig. 116.7 Dermatofibroma. Thick "entrapped" collagen bundles at the outer margin of a cellular proliferation of small fusiform cells is typical of a dermatofibroma. *Courtesy Lorenzo Cerroni, MD.*

The fibroblasts and myofibroblasts have plump oval nuclei with small nucleoli and mitoses may be present. An admixture of these cells with mono- or multinucleated histiocytes with vacuolated (xanthomatous) cytoplasm can be seen, hence the synonym benign fibrous histiocytoma. "Keloidal" collagen bundles, which are refractile with polarized light, are seen at the periphery (Fig. 116.7); the presence of peripheral "entrapped" collagen bundles is considered a classic hallmark of dermatofibroma. Hemorrhage into a dermatofibroma explains the common finding of hemosiderin.

The overlying epidermis is usually hyperplastic. Sometimes there are aggregates of basaloid cells with follicular differentiation emanating from the epidermis (follicular and basaloid "induction"). This finding may be confused with a superficial BCC. There are, however, a few reported cases of true BCCs evolving within longstanding dermatofibromas[9]. Histologic variants of dermatofibroma are listed in Table 116.1.

Positive immunohistochemical reactions for vimentin, factor XIIIa[10–12], muscle-specific actin and CD68, as well as a negative reaction for CD34 (in the center of the lesion), support the diagnosis of dermatofibroma. Evolving cellular dermatofibromas may stain strongly for α-smooth muscle actin (SMA). The histologic differential diagnosis includes keloid, scar, connective tissue nevus, dermatomyofibroma, DFSP (CD34-positive), and nodular Kaposi sarcoma (HHV8-positive, ERG-positive). Of note, dermatofibromas may show CD34 positivity at the periphery while the center is usually CD34-negative, in contrast to DFSP which is homogeneously CD34-positive.

Whether dermatofibromas are reactive or neoplastic has been an area of controversy for a long time. The detection of clonality in a subset of fibrous histiocytomas in addition to a large size, mitotic activity, and/or high recurrence rate in some dermatofibromas and the very rare metastatic potential suggest that fibrous histiocytoma is a tumor rather than a reactive inflammatory process[13–17]. In addition, epithelioid fibrous histiocytomas, formerly classified as a variant of fibrous histiocytoma, have been shown to demonstrate recurrent *ALK* fusions[18]. Mutations in *F13A1*, which encodes coagulation factor XIII subunit A, have also been detected in families with autosomal

CLINICAL AND HISTOPATHOLOGIC VARIANTS OF DERMATOFIBROMA/FIBROUS HISTIOCYTOMA
Clinical variants
• Annular hemosiderotic dermatofibroma • *Deep dermatofibroma* • Delled ("atrophic") dermatofibroma • Dermatofibroma with satellitosis • Disseminated multiple dermatofibromas • Erosive and ulcerated dermatofibroma • Giant dermatofibroma • Hyperkeratotic dermatofibroma • Hyperpigmented nodular dermatofibroma • *Lipidized fibrous histiocytoma ("ankle-type" histiocytoma)* • Multinodular hemosiderotic dermatofibroma • Multiple grouped dermatofibromas • Nonpigmented dermatofibroma • Pedunculated or polypoid dermatofibroma • Unusual locations for dermatofibromas: *face*, finger, subungual, palmoplantar, scalp
Histopathologic variants
• Adenodermatofibroma • *Aneurysmal fibrous histiocytoma (hemorrhagic or hemosiderotic dermatofibroma)* • Balloon cell dermatofibroma • Cellular dermatofibroma (fibrous histiocytoma) • Cholesterotic dermatofibroma • Clear cell dermatofibroma • Combined dermatofibroma • *Deep dermatofibroma* • Delled ("atrophic") dermatofibroma • Dermatofibroma mimicking hemangiopericytoma • *Dermatofibroma with atypical cells (with "monster" cells or pseudosarcomatous dermatofibroma)* • Dermatofibroma with calcification or metaplastic ossification • Dermatofibroma with elastophagocytosis • Dermatofibroma with eosinophilic infiltrate • Dermatofibroma with follicular and/or sebaceous induction • Dermatofibroma with lymphoid follicles • Dermatofibroma with myofibroblastic differentiation • Dermatofibroma with osteoclast-like giant cells • Dermatofibroma with proliferation of nerve fibers • Dermatofibroma with prominent vascular component (sclerosing "hemangioma") • *Epithelioid fibrous histiocytoma* • Granular cell dermatofibroma • Lichenoid, erosive, and ulcerated dermatofibroma • *Metastasizing fibrous histiocytoma* • Myxoid dermatofibroma • Palisading dermatofibroma • Poorly cellular dermatofibroma (fibrous, hyalinizing, and keloidal dermatofibromas) • Signet-ring cell dermatofibroma • Xanthomatous dermatofibroma

Table 116.1 Clinical and histopathologic variants of dermatofibroma/fibrous histiocytoma. Entities in *italics* are reviewed in Table 116.2. *Adapted from Requena L, Kutzner H. Cutaneous soft tissue tumors. Philadelphia: Wolters Kluwer, 2014.*

dominantly inherited multiple dermatofibromas[19]. It has been hypothesized that a resultant conformational change in the subunit may lead to enhanced α4-integrin binding.

Treatment

Dermatofibromas may be biopsied or excised to exclude a melanocytic proliferation, a fibrosed cyst, or other mesenchymal neoplasm. Undisturbed, dermatofibromas usually persist, but with time may undergo partial regression, especially centrally.

Variants of Dermatofibroma

The many clinical and histologic variants of dermatofibroma are listed in Table 116.1 and key features of selected variants are outlined in Table 116.2.

ACRAL FIBROKERATOMA

Synonym: ■ Acquired digital fibrokeratoma

Clinical Features

This uncommon lesion presents as a solitary, skin-colored to pink, slightly keratotic, exophytic papulonodule with a collarette of elevated skin (Fig. 116.10). Acquired fibrokeratomas usually occur in middle-aged adults and the most common site is the finger[20]. Clinically, they can resemble a supernumerary digit (see Ch. 64), ungual fibroma, or verruca.

Pathology

Acral fibrokeratomas are composed of thick collagen bundles surrounded by blood vessels, oriented perpendicularly to the epidermis (Fig. 116.10, inset)[21]. The histopathologic differential diagnosis includes ungual fibroma and supernumerary digit[22].

ACRAL FIBROMYXOMA

Synonyms: ■ Superficial acral fibromyxoma ■ Digital fibromyxoma

Clinical Features

Acral fibromyxoma is a rare tumor of acral sites first described in 2001[23]. There is a 2:1 male:female ratio, with a broad range for age of onset[24–27]. The tumor presents as a slowly enlarging, often painful mass, with an average size of 1–2 cm. It usually develops on the toes or fingers, with two-thirds of tumors occurring close to or involving the nail bed[24–26]; 3% of tumors invade adjacent bone[24,27]. Less common sites include the palm or heel[28]. The clinical differential diagnosis includes primarily ungual fibroma and verruca.

Pathology

Acral fibromyxomas are located within the dermis with extension into the subcutis. There are non-encapsulated, poorly circumscribed masses composed of spindled to stellate cells arranged in a vague storiform or loosely fascicular growth pattern (Fig. 116.11). The stroma is myxoid to fibromyxoid with prominent blood vessels and frequent mast cells. Most tumors have alternating areas of fibrous and myxoid stroma[24]. Minimal cellular atypia is common, and occasionally scattered larger cells with so-called "degenerative change" are present[24]. Mitotic figures are rare. Significant pleomorphism, neural/perineural infiltration, and necrosis are not seen. In cases involving the nail bed, there is often papillary hyperplasia of the nail bed epithelium[28].

The majority of these tumors stain strongly for CD34 with occasional expression of epithelial membrane antigen (EMA) and SMA; expression of CD99, CD10[25], nestin, and desmin has also been reported (see Ch. 0)[24,28]. By immunohistochemistry, the majority of cases demonstrate loss of retinoblastoma 1 (RB1) expression due to deletion of *RB1*[29] (Table 116.3). The histologic differential diagnosis includes cellular digital fibroma, myxoid neurofibroma, superficial angiomyxoma, and DFSP.

Treatment

These tumors follow a benign course, with ~25% recurring after complete excision[24]. Neither malignant transformation nor metastasis has been reported[24].

SCLEROTIC FIBROMA OF THE SKIN

Synonym: ■ Storiform collagenoma

HISTOLOGIC VARIANTS OF DERMATOFIBROMA/FIBROUS HISTIOCYTOMA			
Variant	**Clinical features**	**Histopathologic features**	**DDx/Comments**
Aneurysmal fibrous histiocytoma (hemorrhagic or hemosiderotic dermatofibroma)[e1]	Large size and nodular or dome-shaped with a history of recent rapid growth	• Large blood-filled spaces rimmed by densely aggregated siderophages but without the typical endothelial lining of vascular structures (pseudovascular spaces; hemorrhagic pseudocysts; Fig. 116.8) • Extravasation of erythrocytes • Sheets of large histiocytes & brown, Prussian blue-positive siderophages interspersed with small capillaries without endothelial atypia • Siderophages may be multi-nucleated • Also conventional features of histiocyte-rich fibrous histiocytoma	• Clinically and histologically may be confused with malignant vascular tumors or angiomatoid fibrous histiocytoma • IHC staining with the endothelial marker CD31 may lead to confusion as also stains phagocytic histiocytes and siderophages
Deep dermatofibroma (extending into subcutaneous tissue)[88]	• Usually on the trunk and proximal extremities • 1–2 cm in diameter	• Similar features to common DF, but extension of dermal components into subcutis • Extension via two patterns: 1. ~70% of cases – vertical or horizontal fashion, predominantly along septa which become wedge-shaped 2. ~30% of cases – well-circumscribed base with smooth deep margin	• Clinically, may resemble lipoma or DFSP • Histologically, absence of the multilayered & "honeycomb" patterns characteristic of DFSP
Dermatofibroma with atypical cells (with "monster" cells or pseudosarcomatous dermatofibroma)[e2–e7,17]	• Middle-aged adults • Slightly >1 cm in diameter	• Architectural pattern & components of a common DF plus atypical mono- and multinucleated cells with large pleomorphic and hyperchromatic nuclei, some of which have prominent nucleoli (Fig. 116.9) • Cells have abundant vacuolated cytoplasm, often with hemosiderin deposits • Rare mitotic figures and no atypical mitoses	• Current recommendation is to treat with clinical caution • If in addition to features of a DF with atypical cells, there are numerous mitoses and many of the mitoses are atypical, then the tumor should be labeled as atypical fibrohistiocytic tumor with a genuine, but exceeding low, metastatic potential
Epithelioid fibrous histiocytoma (epithelioid cell histiocytoma)[e8,e9,19]	• Firm, sessile or polypoid papules or nodules • 0.5–1.5 cm in diameter	• Dome-shaped or polypoid dermal nodules with peripheral adnexal collarettes • Monomorphous population of large, stellate and triangular, epithelioid cells with eosinophilic cytoplasm & oval nuclei with small nucleoli; some cells have 2 or more nuclei; no nesting of cells • Rare mitotic figures • Cells separated by delicate collagen fibers & variable amounts of mucin • Proliferation of small blood vessels can be seen	• When vascular in appearance, pyogenic granuloma or sclerosing hemangioma • Spitz nevus/tumor • *ALK* rearrangement and overexpression • The major entity in the differential diagnosis is intradermal Spitz nevus
Fibrous histiocytoma of the face[e10]	Dermal/subcutaneous plaque	• Predominance of distinct cellular fascicles & bundles of spindle-shaped tumor cells plus classic features of a fibrous histiocytoma • Often extend into the subcutaneous fat and deeper soft tissues, including striated muscle	Compared to classic fibrous histiocytomas located elsewhere, excised with wider margins because of diffuse infiltration, involvement of deeper tissues, and increased rate of local recurrences
Lipidized fibrous histiocytoma ("ankle-type" fibrous histiocytoma, "ankle-type" dermatofibroma)[e11]	Striking predilection for the lower extremity, in particular the ankle	• Large foam cells and interspersed siderophages predominate • Focally, features of an ordinary fibrous histiocytoma (e.g. peripheral "entrapped" dermal collagen) can be seen	Prognosis excellent
Metastasizing fibrous histiocytoma[e2–e7,17,18]	Metastases are well-documented but exceedingly rare	• To date, no specific histologic feature predicts metastatic behavior • Warning signs – large primary tumor, extension into subcutis with infiltrative peripheral borders, high proliferation rate (Ki67) & mitotic activity, & multiple recurrences • Includes aneurysmal, cellular, and atypical fibrous histiocytomas	• Cytogenetic aberrations detected via aCGH may reflect a biologic continuum with 0 in common fibrous histiocytomas to some in atypical fibrous histiocytomas to many in malignant fibrous histocytomas/sarcomas • In metastasizing fibrous histiocytomas, genetic aberrations were seen in 2 to 3 chromosomes

Table 116.2 Histologic variants of dermatofibroma/fibrous histiocytoma. aCGH, array comparative genomic hybridization; ALK, anaplastic lymphoma kinase; DDx, differential diagnosis; DF, dermatofibroma; DFSP, dermatofibrosarcoma protuberans; IHC, immunohistochemical.

Clinical Features

This distinct, very collagenous variant of fibroma was originally reported as a component of Cowden syndrome (PTEN hamartoma tumor syndrome). However, a sporadic solitary form has also been described[30].

In Cowden syndrome, the sclerotic fibromas can be solitary or multiple. They appear on the skin and/or mucous membranes as pearly papules or nodules that measure from a few to up to 10 mm in diameter.

Pathology

Sclerotic fibromas are well-circumscribed, dome-shaped, dermal hypocellular nodules composed predominantly of sclerotic thick collagen bundles. The bundles are arranged as short intersecting stacks in a parallel arrangement and are separated by spaces containing connective tissue mucin (plywood-like or whorl-like pattern; Fig. 116.12). Between the collagen bundles, there are thin spindled cells.

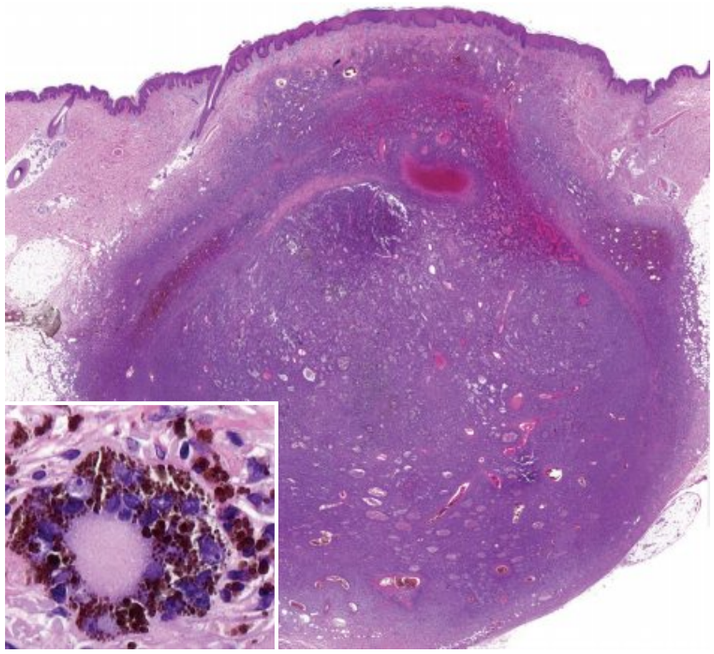


Fig. 116.8 "Aneurysmal" dermatofibroma. There are multiple blood-filled spaces and lacunae without an endothelial lining amidst a cellular proliferation replete with siderophages and foamy macrophages (inset).

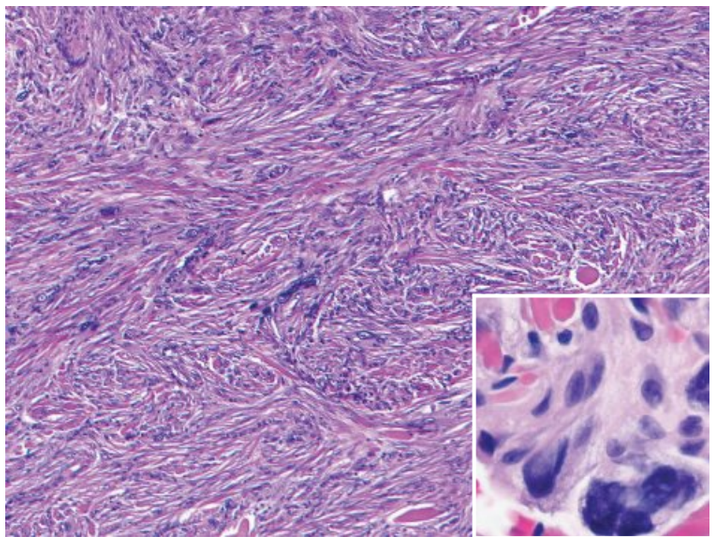


Fig. 116.9 Dermatofibroma with atypical cells ("monster" cells). There are histiocyte-like cells with large hyperchromatic (inset) and pleomorphic nuclei as well as scattered fibroblasts. Mitoses are not present.

The spindle cells react positively for vimentin, muscle-specific actin, and CD34[31]. Positivity for CD34 may result in the misdiagnosis of early DFSP.

PLEOMORPHIC FIBROMA OF THE SKIN

Clinical Features

This unusual variant of a fibroma was described by Kamino et al.[32] in 1989. Pleomorphic fibromas of the skin usually present in adults, with a slight preponderance in women. They favor the extremities and appear as asymptomatic, solitary, skin-colored, dome-shaped or polypoid papules which measure from a few millimeters to nearly 2 cm in diameter. Clinically, they resemble skin tags, neurofibromas,

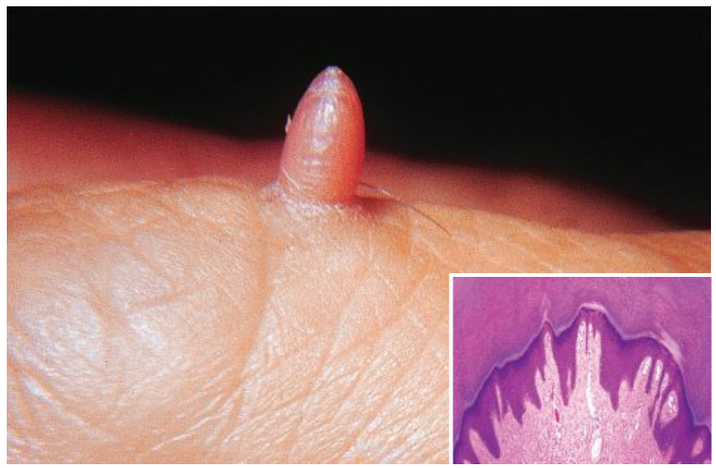


Fig. 116.10 Acral fibrokeratoma. A light pink exophytic papule arising from the dorsal surface of the finger. Histologically, there is a digitated fibrovascular core with vertically arranged collagen bundles lined by epidermal hyperplasia; note the thick stratum corneum (inset). *Courtesy Hideko Kamino, MD.*

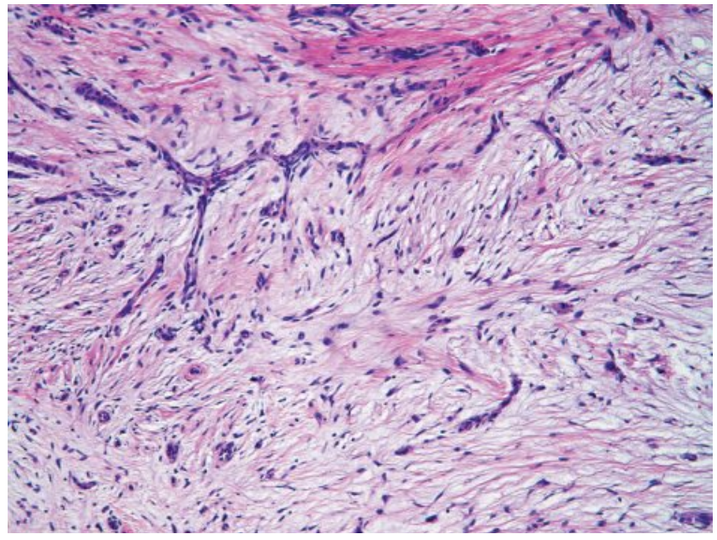


Fig. 116.11 Acral fibromyxoma. The lesion is composed of spindled and stellate cells arranged in a loose storiform pattern with a myxoid collagenous matrix. *Courtesy Shane Meehan, MD.*

or intradermal melanocytic nevi but are firmer to palpation. Treatment is simple excision, and to date there have been no reports of recurrence.

Pathology

Pleomorphic fibromas are polypoid or dome-shaped, well-circumscribed dermal lesions characterized by low cellularity with a predominance of thick collagen bundles in a haphazard array. There are scattered spindled cells and irregularly shaped multinucleated cells with scanty cytoplasm, indistinct cellular borders, and large pleomorphic and hyperchromatic nuclei (Fig. 116.13). Some of the multinucleated cells have multilobed nuclei. Mitotic figures are rare.

The spindle-shaped cells and the irregularly shaped, multinucleated cells are positive for vimentin and CD34[33], and the spindle-shaped cells react positively for muscle-specific actin. The differential diagnosis includes dermatofibroma with atypical cells, atypical fibroxanthoma, and neurofibroma with atypical cells. Superficial variants of pleomorphic lipoma or cutaneous atypical lipomatous tumor (ALT) have similar histologic features as pleomorphic fibroma albeit with larger numbers of entrapped adipocytes as well as occasional lipoblasts in ALT. In ALT, nuclear expression of MDM2 and CDK4 is seen.

FIBROBLASTIC, MYOFIBROBLASTIC AND "FIBROHISTIOCYTIC" PROLIFERATIONS AND NEOPLASMS – MUTATED GENES AND GENE FUSION PARTNERS			
Neoplasm/Proliferation	**Gene**	**Protein product**	**Protein function/dysfunction**
Epithelioid fibrous histiocytoma	*ALK*	Anaplastic lymphoma receptor tyrosine kinase	Rearrangements lead to overexpression of ALK
Acral fibromyxoma	*RB1*	Retinoblastoma 1	Loss of tumor suppressor function
Tenosynovial giant cell tumor (localized type)	*CSF1*	Colony-stimulating factor 1	Attracts macrophages
	COL6A3	Collagen type VI α-3 chain	Subunit of collagen
Nodular fasciitis	*MYH9*	Myosin heavy chain 9	Subunit of myosin
	USP6	Ubiquitin specific peptidase 6	Induces production of MMPs
Inherited infantile myofibromatosis	*PDGFRB*	Platelet-derived growth factor receptor-β	Ligand-independent receptor kinase activity
	NOTCH3	Notch receptor 3	Increased PDGFRB expression
Cellular/atypical myofibromas	*SRF*	Serum response factor	Vascular smooth muscle cell differentiation
	RELA	RELA proto-oncogene, NF-κB subunit	Pathologic activation of NF-κB pathway
Calcifying aponeurotic fibroma	*FN1*	Fibronectin 1	Allegedly drives inappropriate expression of EGF
	EGF	Epidermal growth factor (EGF)	Activation of signaling pathways via EGF receptor
Desmoid type fibromatosis (extra-abdominal fibromatosis)	*CTNNB1*	β-catenin	Nuclear accumulation stimulates target genes in WNT/β-catenin signaling pathway
DFSP, giant cell fibroblastoma	*COL1A1*	Collagen type I α-1 chain	Subunit of collagen
	PDGFB	Platelet derived growth factor subunit B	Continued expression leads to activation of PDGF receptor B
Fibrosarcomas	See Table 116.4		
Epithelioid sarcoma	*SMARCB1/ INI1*	SWI/SNF-related, matrix-associated, actin-dependent regulator of chromatin, subfamily B, member 1/integrase interactor 1	Regulates transcription as part of a complex that relieves repression of chromatin structures

Table 116.3 Fibroblastic, myofibroblastic and "fibrohistiocytic" proliferations and neoplasms – mutated genes and gene fusion partners. Tumors with gene fusion partners are shaded in peach; the protein that is overexpressed is shaded in blue. DFSP, dermatofibrosarcoma protuberans; MMPs, matrix metalloproteinases; SWI/SNF, SWItch Sucrose Non-Fermentable chromatic remodeling complex.

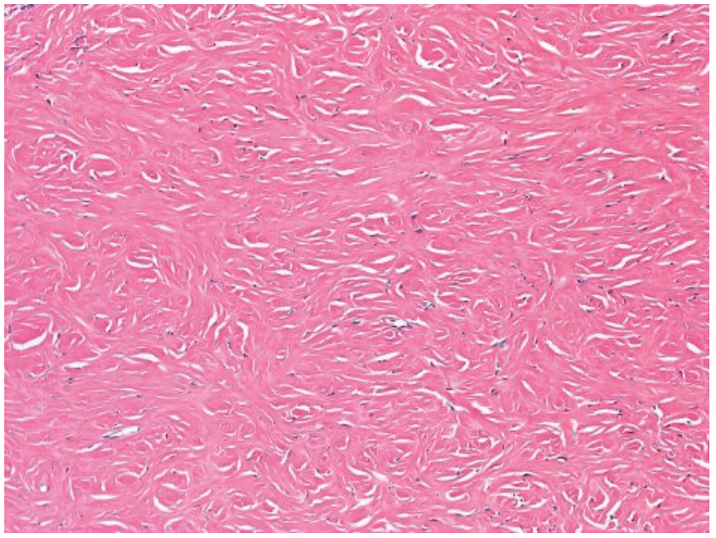


Fig. 116.12 Sclerotic fibroma. The collagen bundles in this hypocellular tumor are arranged in short parallel bundles, leading to a laminated or "plywood" appearance. *Courtesy Lorenzo Cerroni, MD.*

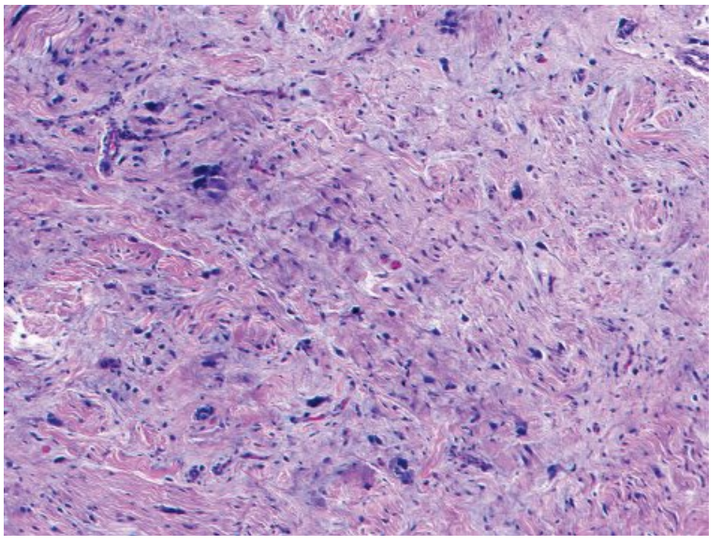


Fig. 116.13 Pleomorphic fibroma. There are delicate interwoven collagen bundles with a few interspersed large mononucleated and multinucleated atypical fibroblasts. The stroma is dominated by mesenchymal mucin.

MULTINUCLEATE CELL ANGIOHISTIOCYTOMA

Clinical Features

The typical clinical presentation of multinucleate cell angiohistiocytomas is that of slowly growing, multiple, discrete but grouped, red to violaceous papules, usually on the lower extremities or the dorsal aspect of the hands (Fig. 116.14). The lesions may be unilateral or bilateral, and typically affect women over 40 years of age[34]. A generalized form has also been described[35]. Clinically, lesions may resemble piloleiomyomas, Kaposi sarcoma, granuloma annulare, or sarcoidosis.

Pathology

These lesions are composed of a proliferation of dilated capillaries and small venules in the superficial to mid dermis within thickened collagen bundles (Fig. 116.15). The characteristic cell is a multinucleated giant cell, sometimes with peripheral palisading of the nuclei within eosinophilic cytoplasm (Fig. 116.15, inset). The histopathologic differential diagnosis includes dermatofibroma, angiofibroma, hemangioma, and interstitial granuloma annulare.



Fig. 116.14 Multinucleate cell angiohistiocytoma. Red–brown macules and papules on the dorsum of the hand.

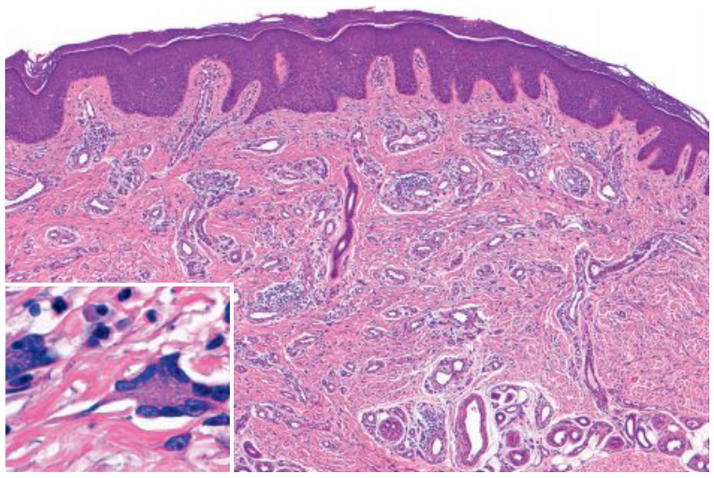


Fig. 116.15 Multinucleate cell angiohistiocytoma. There is a proliferation of dilated blood vessels with a sparse inflammatory infiltrate, an increase in fibroblasts, and the presence of stellate and angulated giant cells (inset). Resemblance to an incipient, richly vascularized dermatofibroma is striking.

Treatment

These lesions are benign. If left untreated, most cases progress slowly without evidence of spontaneous resolution.

DERMATOMYOFIBROMA

This tumor was described as plaque-like dermal fibromatosis in 1991 by Hügel[36] and as dermatomyofibroma by Kamino et al.[37]. It is a benign fibroblastic/myofibroblastic dermal neoplasm[38].

Clinical Features

Dermatomyofibromas most commonly occur in young women and favor the shoulder area, axilla, upper arm, and neck. Occasionally, these tumors arise during childhood. They are asymptomatic, well-circumscribed, oval or annular, skin-colored to red–brown plaques that have a smooth surface and measure 1–2 cm in diameter.

Pathology

Dermatomyofibromas are well-circumscribed plaques involving the reticular dermis and the upper portion of the subcutaneous septae; they are composed of well-defined, long fascicles of spindle-shaped cells parallel to the skin surface (Fig. 116.16). The cells have a very uniform appearance, with elongated nuclei having rounded or pointed ends and one or two small nucleoli. There is no evidence of nuclear atypia, and mitoses are rare. The cells are separated by thin collagen fibers and elastic fibers are preserved.

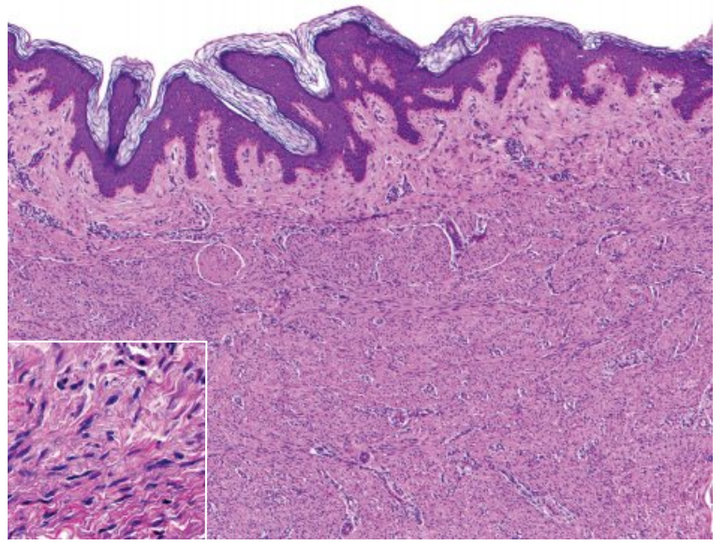


Fig. 116.16 Dermatomyofibroma. The myofibroblasts are arranged in long intersecting fascicles that are parallel to the skin surface. The cells have a uniform appearance, with elongated nuclei having rounded or pointed ends (inset). *Courtesy Luis Requena, MD.*

The fascicles, spindle-shaped cells, collagen fibers, and elastic fibers may have a wavy appearance. The adnexal structures are spared.

With Verhoeff–van Gieson stain, the elastic fibers appear slightly increased in number. The spindle-shaped cells react positively for vimentin and are variably positive for muscle-specific actin; staining for desmin, factor XIIIa, and CD34 is negative. These results support a fibroblastic/myofibroblastic differentiation rather than smooth muscle differentiation[36–38]. The histologic differential diagnosis includes dermatofibroma, DFSP, myofibroma, smooth muscle tumors, fibrous hamartoma of infancy, fibromatoses, and fibroblastic connective tissue nevus.

Treatment

The treatment is simple excision. Recurrence is uncommon even when marginally or incompletely excised[38].

TENOSYNOVIAL GIANT CELL TUMOR (LOCALIZED TYPE)

Synonyms: ■ Giant cell tumor of tendon sheath ■ Localized nodular tenosynovitis

Clinical Features

This tumor usually presents as a firm nodule on the hand or finger (Fig. 116.17), but can also occur on the toes and other periarticular sites. It is typically slowly growing and fixed to subcutaneous structures without attachment to the overlying skin, except on the distal fingers and toes. Although usually asymptomatic, there can be pain, numbness, or stiffness of the affected digit.

Localized tenosynovial giant cell tumor is the most common tumor of the hand and can present at any age, but usually appears in adults 30 to 50 years of age and is more common in women than in men[39].

Pathology

The localized type of tenosynovial giant cell tumor is lobulated and well circumscribed (Fig. 116.18). It is composed of mononuclear cells, multinucleated osteoclast-like giant cells, foamy histiocytes, and inflammatory cells set in a variably collagenized stroma. The characteristic multinucleated giant cells are typically scattered throughout the tumor

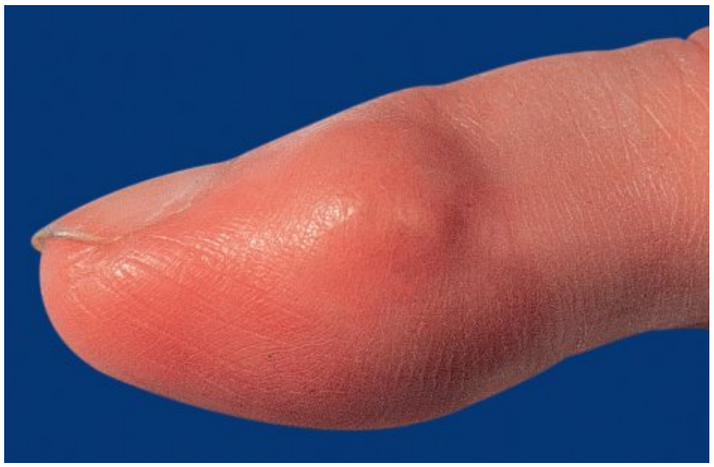


Fig. 116.17 Tenosynovial giant cell tumor (localized type). A skin-colored nodule on the lateral aspect of the index finger. This tumor was previously referred to as giant cell tumor of tendon sheath.

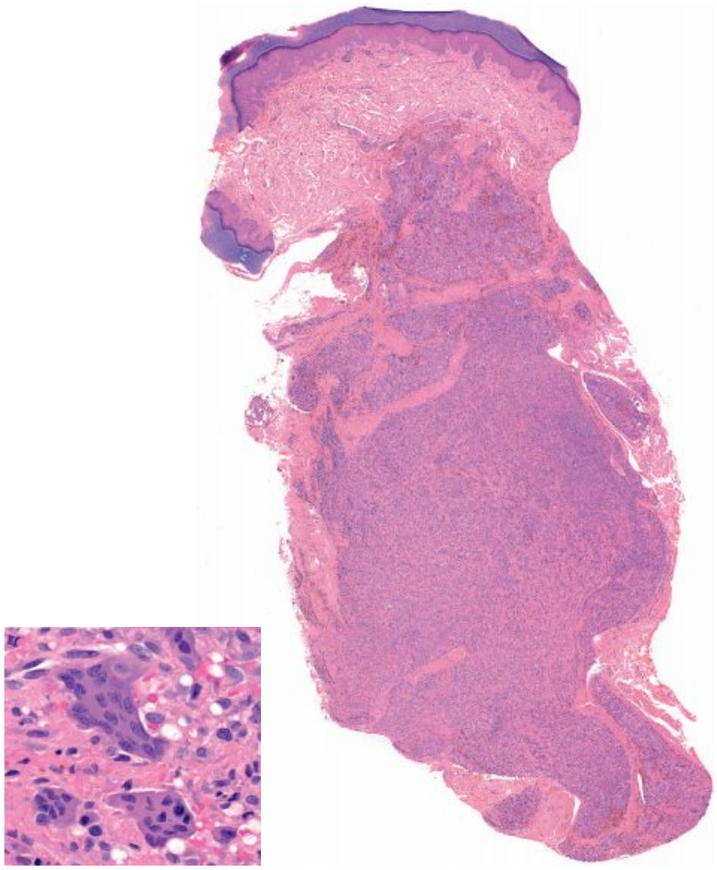


Fig. 116.18 Tenosynovial giant cell tumor (localized type). The tumor is composed of sheets of epithelioid histiocytes with a variable number of the characteristic multinucleated osteoclast-like giant cells (inset). Some of the histiocytes may have pale foamy cytoplasm. This tumor was previously referred to as giant cell tumor of tendon sheath. *Courtesy Lorenzo Cerroni, MD.*

in variable densities. These cells have eosinophilic cytoplasm and from a few to 50 nuclei (Fig. 116.18, inset). There are also both large and small mononucleated histiocytes with abundant vacuolated cytoplasm containing variable amounts of hemosiderin deposits. Stromal clefts, mitotic figures, and, rarely, vascular involvement may be observed.

By immunohistochemistry, the larger mononuclear cells express clusterin, which highlights their dendritic processes, and rarely stain positively for desmin. The smaller cells are positive for CD68, CD163, and CD45 (see Ch. 0). Remarkably, there is always a focal leukocyte common antigen (LCA)-positive lymphocytic infiltrate. Cytogenetically, this tumor has characteristic translocations, in particular t(1;2)(p13;q37) which fuses two genes – *CSF1* at 1p13 encoding colony-stimulating factor-1 and *COL6A3* at 2q37 encoding collagen type VI α-3[40–42]. This fusion leads to an overexpression of CSF1, which attracts large numbers of macrophages to the tumor site (see Table 116.3). The histologic differential diagnosis includes epithelioid sarcoma, synovial sarcoma, deep dermatofibroma, and tumors with myogenic differentiation.

Treatment

This tumor is benign, with a local recurrence rate of 30%. It can be treated by simple excision[39].

FIBROMA OF TENDON SHEATH

Synonym: ■ Tenosynovial fibroma

Clinical Features

This benign tumor presents as a small subcutaneous nodule. It is most frequently found on the hands and feet, with the most common site of involvement being the thumb. While usually asymptomatic, there can be limitation in the range of motion of involved joints[43].

This fibroma usually presents in those 20 to 50 years of age. Men develop these tumors three times more often than women. The clinical differential diagnosis includes localized type of tenosynovial giant cell tumor, neuroma, ganglion cyst, rheumatoid nodule, and subcutaneous granuloma annulare.

Pathology

The tumor has a well-circumscribed lobular appearance and is attached to a tendon sheath. It is composed of dense hyalinized collagen with scattered spindle-shaped fibroblasts/myofibroblasts and stromal clefts. There are characteristic elongated slit-like vessels as well as occasional giant cells and foci of myxoid change. Tumor cells stain focally for α-smooth muscle actin. In some cellular variants, *USP6* rearrangements similar to those in nodular fasciitis have been reported, raising the question if such variants represent tenosynovial nodular fasciitis[44].

Treatment

This tumor is benign, with a recurrence rate of ~25%. Some authors believe that this tumor may represent a sclerotic end-stage of the localized type of tenosynovial giant cell tumor[45].

NODULAR FASCIITIS

Synonyms: ■ Benign nodular (pseudosarcomatous) fasciitis
■ Subcutaneous pseudosarcomatous fibromatosis
■ Pseudosarcomatous fasciitis

Clinical Features

Nodular fasciitis is a benign transient tumor ("transient neoplasia")[46] that occurs in young to middle-aged adults. It presents as a rapidly growing (but self-limited) subcutaneous nodule measuring from 1 to 5 cm in diameter, and the upper extremity is the most common site. In children, the head and neck region is a frequent location[47]. Clinicopathologic variants include intradermal nodular fasciitis, intravascular fasciitis, and cranial fasciitis[48–50]. The latter variant develops predominantly in infants <2 years of age. It typically involves the outer table of the skull and contiguous soft tissue of the scalp but may extend through the inner table into the meninges.

Pathology

There is an unencapsulated, well-circumscribed or infiltrative, subcutaneous, fascial, or intramuscular nodule with a stellate appearance. A proliferation of plump spindle and stellate fibroblasts and myofibroblasts with oval nuclei is seen. In early lesions, the cells are loosely arranged in an edematous, myxomatous stroma imparting a "feathered" appearance (Fig. 116.19A,B), with a proliferation of small blood vessels, scattered lymphocytes, and extravasated erythrocytes ("tissue culture pattern"). Mitoses are frequent, but atypical mitoses are not seen. Intradermal fasciitis, intravascular fasciitis, and cranial fasciitis are similar histologically to nodular fasciitis.

The fibroblasts and myofibroblasts react positively for vimentin and muscle-specific actin and, to a lesser degree, for α-smooth muscle actin; rarely, desmin expression is seen. The interstitial monocytic round cells are positive for CD68[51]. An immunophenotypic pattern consisting of a loosely arranged α-smooth muscle actin-positive myofibroblastic proliferation sprinkled with $CD68^+$ macrophages and histiocytes is highly characteristic of nodular fasciitis (Fig. 116.19C,D). Cytogenetically, *USP6* rearrangements with formation of the fusion gene *MYH9-USP6* occur in most examples of nodular fasciitis (see Table 116.3)[42,46]. Mapping of *USP6* via FISH or next generation sequencing is a useful adjunct in the diagnosis of nodular fasciitis[42,52].

Treatment

Nodular fasciitis is treated with a conservative excision. The recurrence rate is ~1%[53].

CONNECTIVE TISSUE NEVUS

Variants/synonyms: ■ Collagen nevus: collagenoma, shagreen patch ■ Elastic tissue nevus: elastoma, dermatofibrosis lenticularis disseminata (Buschke–Ollendorf syndrome) ■ Mucin nevus: mucinous connective tissue nevus ■ Fibroblastic nevus: fibroblastic connective tissue nevus

Clinical Features

Connective tissue nevi are firm, solitary or multiple, skin-colored papules, nodules, or plaques that usually present at birth or arise during childhood (Fig. 116.20). A linear arrangement occasionally occurs. These nevi may represent hamartomas rather than neoplasms. Clinically and histologically, they may be subtle and even resemble normal skin. Several variants have been described, based upon the dominant tissue component present, and they are listed above, along with their synonyms.

The shagreen patch of tuberous sclerosis most commonly presents as a pebbly plaque with a "pigskin" appearance on the lower back (see Ch. 61). In the Buschke–Ollendorf syndrome, multiple skin-colored or slightly yellowish papules are seen and are referred to as dermatofibrosis lenticularis disseminata. This syndrome is due to loss-of-function mutations in *LEMD3* which then lead to loss of antagonism of the TGF-β and bone morphogenic protein signaling pathways[54]. The disorder is inherited in an autosomal dominant pattern and the papules begin at an early age. In radiograms, a characteristic stippled appearance to the bone is seen, called osteopoikilosis (Fig. 116.21). This abnormality is asymptomatic.

Connective tissue nevus is the sole category A criterion for Proteus syndrome. The nevi occur most commonly on the plantar surface and acquire a cerebriform appearance, but can be seen elsewhere (e.g. hands, abdomen; see Fig. 104.10).



Fig. 116.20 Connective tissue nevus. Coalescence of multiple tan papules and plaques on the lower back. The lesion was firm to palpation and histologically had increased collagen.

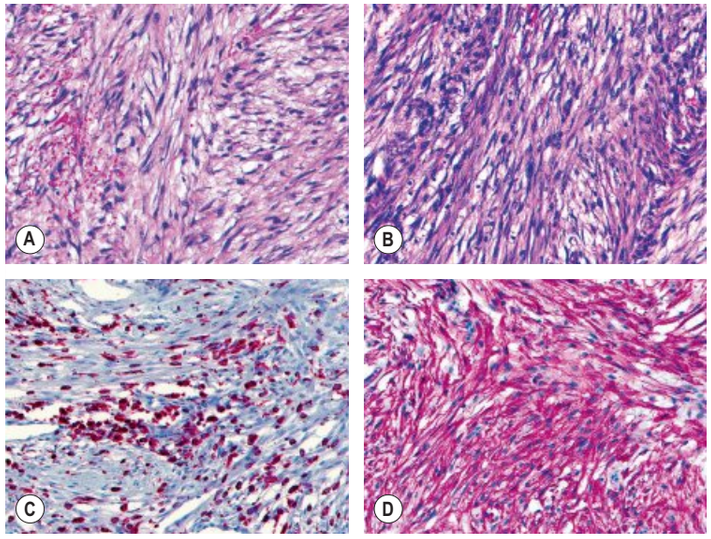


Fig. 116.19 Nodular fasciitis. A,B Proliferation of spindle-shaped and plump fibroblasts arranged in a haphazard array with focally myxoid stroma. The plump and spindle-shaped fibroblasts within the myxoid stroma have a vague "tissue culture-like" appearance. **C** Typical clusters of $CD68^+$ macrophages that are amidst a dense proliferation of α-smooth muscle actin-positive myofibroblasts (**D**).



Fig. 116.21 Osteopoikilosis. In this radiograph, multiple asymptomatic round to oval areas ("islands") of increased bone density are seen in the tibia. *Courtesy Jean L. Bolognia, MD.*

Pathology

There is usually a poorly demarcated area of increased dermal collagen bundles without an apparent increase in fibroblasts. Those lesions with a prominent collagen component are designated as *collagenomas*. A variant with increased elastic fibers has been called *elastoma*. Many of the cutaneous lesions in Buschke–Ollendorf syndrome tend to have increased elastic fibers, but some appear to be primarily collagenous. *Mucinous connective tissue nevi* are characterized by increased mucin deposition within the dermis. *Fibroblastic connective tissue nevus* is a recently delineated variant that presents as a solitary, slowly growing, asymptomatic, firm plaque or nodule. It has a smooth surface and is tan–white to light brown in color. These nevi most commonly occur on the trunk and in the head and neck region of children, with involvement of the deep dermis and superficial subcutis[55]. There is an intradermal proliferation of bland $CD34^+$ fibroblastic/myofibroblastic cells arranged in short-intersecting fascicles. It must be distinguished from $CD34^+$ plaque-like dermal fibroma (medallion-like dermal dendrocyte hamartoma; see eTable 116.1), DFSP, and dermatomyofibroma.

Differential Diagnosis

Although the differential diagnosis includes fibromatoses, fibrous hamartoma of infancy, infantile myofibromatosis, and dermatofibromas, clinicopathologic correlation usually establishes the diagnosis fairly easily.

INCLUSION BODY FIBROMATOSIS

Synonyms: ■ Infantile digital fibroma ■ Recurring digital fibrous tumor of childhood

Clinical Features

Inclusion body fibromatosis commonly presents as multiple, firm, smooth, skin-colored, dome-shaped nodules on the dorsolateral aspects of the fingers and toes (Fig. 116.22). They can be up to several centimeters in diameter and tend to spare the thumb and great toe.

Almost all cases occur in infants under 1 year of age. Rare adult cases of a histologically similar tumor have been reported at extradigital sites[56]. Multiple lesions may be seen in patients with terminal osseous dysplasia with pigmentary defects.



Fig. 116.22 Inclusion body fibromatosis. Firm skin-colored nodule on the dorsolateral aspect of the second toe in a young child. This entity was previously referred to as infantile digital fibroma.

Pathology

These fibromas are poorly circumscribed proliferations of spindle-shaped myofibroblasts, arranged as interwoven fascicles with a collagenous stroma within the dermis or subcutaneous tissue. The cells have uniform, spindle-shaped, wavy nuclei without nuclear atypia or mitoses. The pathognomic feature is the presence of eosinophilic intracytoplasmic inclusions (Fig. 116.23), which are often perinuclear and are red-purple in color with Masson's trichrome stain.

Treatment

In general, the clinical course is benign, although functional impairment is possible. Spontaneous regression within 2–3 years is the usual natural history[57]. Contractures can be problematic. Recommended treatment options include conservative excision or observation (after histologic confirmation), with additional surgery as necessary for recurrences[58].

INFANTILE MYOFIBROMATOSIS

Synonyms: ■ Infantile fibromatosis ■ Congenital multicentric fibromatosis ■ Congenital generalized fibromatosis ■ Infantile myofibroma/myofibromatosis

Clinical Features

Clinically, *infantile myofibromatosis* presents as one or more, firm to rubbery, skin-colored to purple, dermal or subcutaneous nodules, commonly located in the head and neck region or on the trunk (Fig. 116.24). Some patients have a multicentric form *without visceral involvement* where multiple lesions develop in the skin, subcutaneous tissue, bone, and/or muscles. The multicentric (generalized) form *with visceral involvement* represents the most severe expression of the disease and is characterized by multiple lesions in the skin, subcutaneous tissue, muscles, and/or bones as well as involvement of one or more internal organs, in particular the lungs, heart, and gastrointestinal tract. Skeletal involvement, which occurs in approximately half of patients with multicentric disease, typically presents as lytic metaphyseal lesions.

Approximately 50% of patients have lesions present at birth, with more appearing during the first two years of life. Familial cases have been

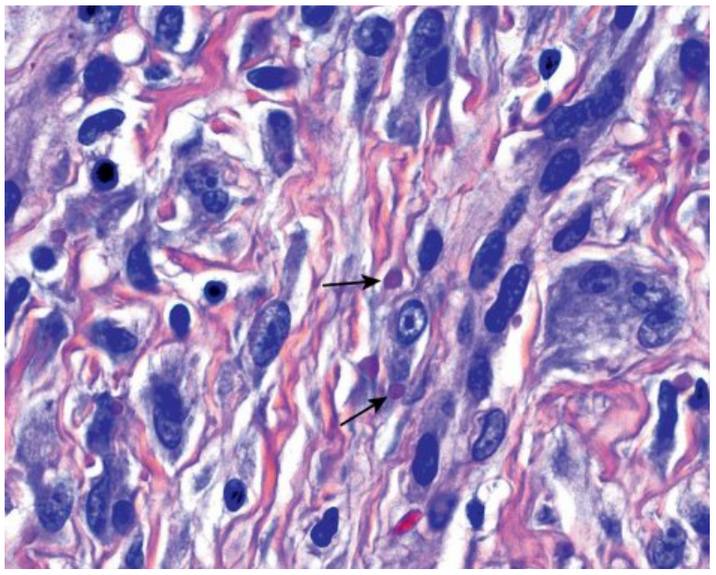


Fig. 116.23 Inclusion body fibromatosis. Myofibroblasts have pathognomonic cytoplasmic eosinophilic hyalin globules (arrows). This entity was previously referred to as infantile digital fibroma. *Courtesy Hideko Kamino, MD.*

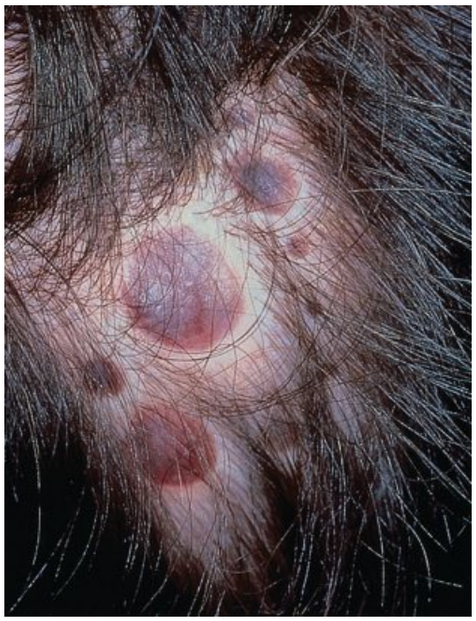


Fig. 116.24 Infantile myofibromatosis. Multiple firm violaceous papulonodules on the scalp.

reported, with an autosomal dominant inheritance pattern (see below), and female infants have a greater tendency for visceral involvement[59]. Evaluation for internal involvement includes skeletal radiographs, electrocardiogram, and CT scan of the chest and abdomen or whole-body MRI. The multicentric form without visceral involvement (and the solitary form) typically undergo spontaneous regression but can recur, whereas the visceral form is associated with a mortality rate of up to 75%.

Solitary myofibromas represent the third and the most common form of infantile myofibromatosis (~75% of cases). They exist on a spectrum with *myopericytomas*, may also develop in older children or adults, and have a good prognosis (see below)[60].

Pathology

In the 5th edition of the WHO classification of soft tissue and bone tumors, myofibromas are categorized within the group of pericytic/perivascular tumors. These tumors are composed of circumscribed nodules with a biphasic appearance. Areas of plump spindle-shaped myofibroblasts with abundant cytoplasm, arranged in fascicles within a collagenous stroma, blend with more cellular areas composed of smaller, rounder cells having less cytoplasm and an associated stag-horn pattern of dilated branching blood vessels. Mitotic figures, necrosis, intravascular growth, and stromal hyalinization can be present.

Immunohistochemically, the spindle and rounded cells are positive for vimentin and SMA, with negative staining for desmin, as is seen in myofibroblasts. The histologic differential diagnosis includes infantile hemangiopericytoma, which some authors suggest exists on a continuum with myofibromatosis (see Ch. 114).

PDGFRB plays a role in tumor pathogenesis, with germline mutations in this gene detected in the autosomal dominant form of infantile myofibromatosis[61]. A *NOTCH3* mutation that leads to increased PDGFRB expression has also been reported in familial infantile myofibromatosis[62], and *SRF-RELA* gene fusions have been noted in cellular/atypical myofibromas (see Table 116.3)[63]. Lastly, gain-of-function mutations in *PDGFRB* have been detected in solitary pediatric myofibromas[64].

Treatment

Patients with only soft tissue and bony involvement have a good prognosis, as the tumors regress spontaneously within months via massive apoptosis[65]. Those with visceral involvement have a high mortality rate within the first 4 months owing to the compromise of vital organ function (e.g. cardiopulmonary failure). However, if patients survive beyond this period to when the tumors begin to regress, the prognosis is much improved. Because the tumors tend to regress, debulking surgery is recommended only for symptomatic lesions. Targeted tyrosine kinase inhibitors (e.g. imatinib) and combination chemotherapy have been used in severe cases[59].

MYOPERICYTOMA

Synonyms: ■ Cutaneous adult myofibroma ■ Perivascular myoma ■ Glomangiopericytoma

Clinical Features

This tumor is the adult counterpart of infantile myofibromatosis, but as noted previously can be seen in older children[60,66–69]. It presents as a solitary, firm, deep dermal nodule and is often diagnosed clinically as a dermatofibroma, cyst, or angioleiomyoma. Multicentric variants are rare.

Pathology

These perivascular tumors possess a broad morphologic spectrum: at one end is a myoid nodular proliferation resembling an angioleiomyoma and at the other end is a hemangiopericytoma-like, richly vascularized, biphasic tumor with both myoid basophilic spindle cell nodules and richly vascularized myopericytic sheets. A highly characteristic finding is the "spinning off" of the outer vessel wall of small myopericytic cells. Myopericytomas may have degenerative changes including symplastic nuclear atypia, hyalinization, and cystic changes.

The term myopericytomatosis has been introduced for an apparently benign variant of myopericytoma characterized by innumerable, discrete microscopic myopericytomatous nodules that typically diffusely involve superficial soft tissue in adults. *PDGFRB* alterations are present in a subset of myopericytomas/myopericytomatosis and infantile myofibromatosis/myofibromas. Therefore these entities appear to lie within a histogenetic continuum. When *PDGFRB* alterations are present, tyrosine kinase inhibitors represent a potential therapeutic strategy, if needed[61,70].

Treatment

Myopericytoma can be interpreted as infantile myofibromatosis "en miniature". Lesions are benign, with malignant variants being exceedingly rare. Treatment consists primarily of local excision.

CALCIFYING APONEUROTIC FIBROMA

Synonyms: ■ Juvenile aponeurotic fibroma ■ Calcifying fibroma ■ Cartilage analogue of fibromatosis

Clinical Features

This is a very rare entity that presents as a solitary, slowly growing, asymptomatic, firm subcutaneous nodule that is usually fixed to underlying structures. It occurs primarily on the hands, and sometimes on the feet. A characteristic radiologic finding is the presence of stippled calcifications. Most cases occur in young children and adolescents, and boys are affected more frequently than girls[71].

Pathology

The tumor is poorly circumscribed with an infiltrating border. It is composed of sheets of spindled and epithelioid fibroblasts with parallel nuclei in a collagenous stroma. The biphasic pattern of plump epithelioid cells in conjunction with slender spindle cells can be striking. Most cases have a myofibroblastic immunophenotype with expression of α-smooth muscle actin.

In addition, there are characteristic islands of calcifications surrounded by palisaded epithelioid fibroblasts (Fig. 116.25). In older lesions, these areas of calcification can undergo chondroid and osseous metaplasia. *FN1-EGF* gene fusions have been reported in these tumors and can facilitate diagnosis in unusual cases[72].

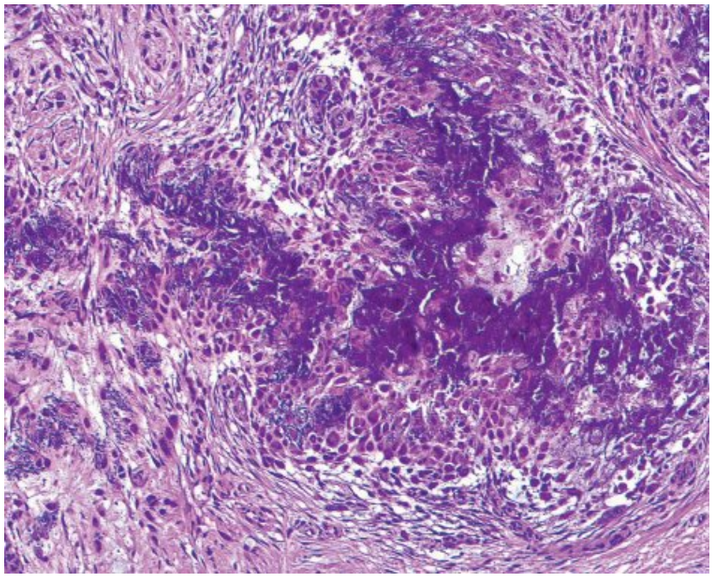


Fig. 116.25 Calcifying aponeurotic fibroma. Islands of calcification are surrounded by palisaded and osteoclast-like fibroblasts. In between these areas are sheets of spindled and epithelioid fibroblasts in a collagenous stroma.

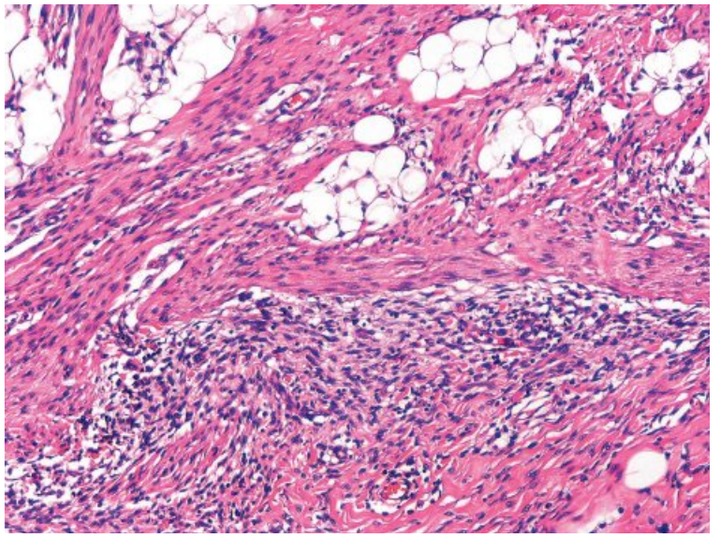


Fig. 116.26 Fibrous hamartoma of infancy. It is composed of a mixture of elongated bundles of spindle-shaped myofibroblasts, clusters of smaller immature mesenchymal cells in a myxoid stroma, and mature adipocytes.

Treatment

These tumors are benign, with a local recurrence rate of ~50%[71]. Treatment consists of local excision, with re-excision for recurrences.

FIBROUS HAMARTOMA OF INFANCY

Synonym: ■ Subdermal fibromatous tumor of infancy

Clinical Features

This tumor typically presents as a solitary, painless, skin-colored subcutaneous nodule. It favors the axilla, shoulder, and upper arm, although it can appear in other sites such as the groin[73,74]. There is a variable rate of growth, and a fibrous hamartoma can become quite large. Fixation to underlying structures may be observed. Occasionally, hyperhidrosis and hypertrichosis are present[75].

Most of these tumors appear within the first year of life, but some are congenital. Boys are affected three times as often as girls[73,76]. Fibrous hamartomas may mimic other subcutaneous malignancies of infancy such as rhabdomyosarcoma and cutaneous metastases (e.g. neuroblastoma, leukemia) as well as other fibromatoses and subcutaneous fat necrosis.

Pathology

This tumor is not well circumscribed, and it is composed of three distinctive elements in variable proportions: (1) a proliferation of spindle-shaped, α-smooth muscle actin-positive myofibroblasts arranged as broad fascicles within a collagenous stroma; (2) nests and aggregates of smaller, round to plump, spindle-shaped, immature mesenchymal cells within a myxoid matrix (primitive-appearing cells can express CD34); and (3) mature adipocytes (Fig. 116.26). Hyalinized zones with cracking artifact, mimicking giant cell fibroblastoma, are frequently observed[77].

Treatment

Fibrous hamartoma of infancy is benign and the usual treatment is local excision, with recurrence being fairly uncommon[76]. If left untreated, the tumor continues to grow and stabilizes in size by mid-childhood. In rare cases, the presence of "sarcomatous" areas provides evidence that these are complex neoplasms rather than hamartomas[77].



Fig. 116.27 Knuckle pads. Note the localization to the skin overlying the knuckles. *Courtesy Ronald P. Rapini, MD.*

FIBROMATOSES

Synonyms/subtypes:

- Superficial fascial fibromatosis:
  - palmar fibromatosis (Dupuytren disease)
  - plantar fibromatosis (Ledderhose disease)
  - penile fibromatosis (Peyronie disease)
  - knuckle pads (holoderma)
  - pachydermodactyly
- Deep musculoaponeurotic fibromatosis:
  - desmoid type fibromatosis (extra-abdominal fibromatosis) [synonym: aggressive fibromatosis]

Clinical Features

Fibromatoses are slowly growing tumors. The superficial variants may reach up to several centimeters in greatest diameter[78]. They appear as firm nodules, plaques, or cord-like tumors along the flexor tendons.

Palmar and plantar fibromatoses usually appear during adulthood and the incidence increases with age. Flexion contractures, especially



Fig. 116.28 Pachydermodactyly. A form of digital fibromatosis characterized by soft tissue swelling of the lateral aspects of the fingers, usually in the area of the proximal interphalangeal joints of the second to fourth fingers. *Courtesy Julie V. Schaffer, MD.*

of the fourth and fifth fingers, can result (see Ch. 98). Although nuclear β-catenin expression is observed in a subset of tumors, neither *CTNNB1* nor *ABC* mutations have been detected.

Penile fibromatosis is more common in middle-aged to elderly men; pain and erectile dysfunction are common.

Knuckle pads affect the extensor surfaces of the interphalangeal and metacarpophalangeal joints (Fig. 116.27) and may be associated with palmar and plantar fibromatosis. While often idiopathic, they may also be a reflection of trauma. In Bart–Pumphrey syndrome, knuckle pads are seen in association with palmoplantar keratoderma, hearing loss, and leukonychia (see Ch. 58).

Pachydermodactyly is an uncommon form of digital fibromatosis. It typically presents in adolescent boys as soft tissue swelling of the lateral aspects of the proximal interphalangeal joints of the second to fourth fingers (Fig. 116.28). This disorder may be related to mechanical trauma[79].

Deep musculoaponeurotic fibromatoses or *desmoid tumors* are usually rather large – up to 25 cm in diameter. There are abdominal and extra-abdominal variants. They may present in postsurgical scars, within the abdominal wall following trauma or pregnancy, and as mesenteric fibromatosis in Gardner syndrome (due to *APC* mutations; see Ch. 63). Up to 95% of sporadic desmoid tumors harbor mutations in *CTNNB1* which encodes β-catenin[80].

Pathology

Fibromatoses consist of large, poorly circumscribed, dermal and subcutaneous plaques and nodules composed of long sweeping fascicles of monotonous fibroblasts and myofibroblasts, along with compressed and elongated vessels (Fig. 116.29). The neoplastic cells usually infiltrate the adjacent aponeurosis, fascia, and skeletal muscle.

In general, tumor cells in all types of fibromatoses stain variably for muscle-specific actin and α-smooth muscle actin, depending upon the extent of myofibroblastic differentiation. In palmar and plantar fibromatoses, at least 50% of tumor cells may show nuclear immunopositivity for β-catenin[81], but in the absence of a mutation; in desmoid tumors (desmoid-type fibromatosis), ~70%–75% of cell nuclei stain positively for β-catenin[81]. As noted previously, the vast majority of sporadic desmoid tumors have mutations in *CTNNB1*[80].

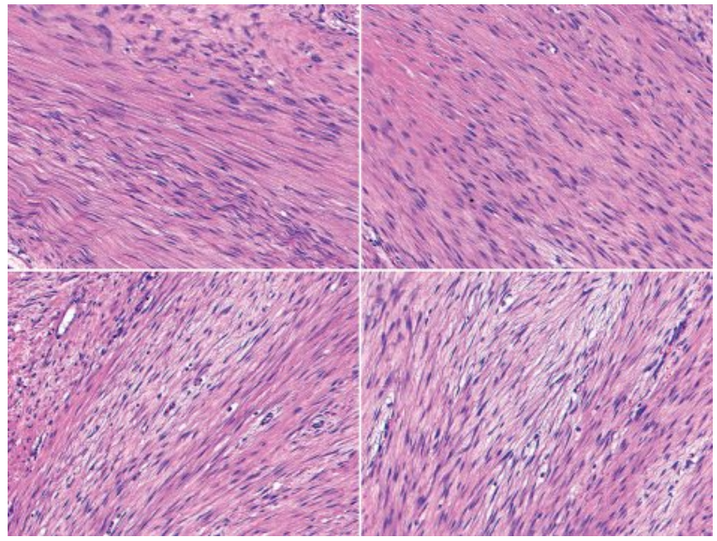


Fig. 116.29 Extra-abdominal desmoid tumor (fibromatosis). There is a distinct cellular proliferation of bland spindled cells arranged in ill-defined long fascicles. These cells have bland nuclear features.

Cytogenetic abnormalities have been identified less frequently in superficial fibromatoses as compared to their deep counterparts, and in the former, usually exhibit simple numerical changes, especially gains of chromosome 8[82].

Treatment

Surgical excision with fasciectomy is standard therapy for palmar and plantar fibromatosis, with the goal of reducing functional impairment rather than complete disease removal. Injection of collagenase (from *Clostridium histolyticum*) represents a nonsurgical option for Dupuytren contractures, with response rates of 45%–65%[83]. Penile fibromatoses may resolve spontaneously in approximately a third of patients[84]. Therefore, a waiting period is recommended before injections of collagenase, surgical excision, or laser therapy. The deep musculoaponeurotic fibromatoses have a higher recurrence rate and appropriate treatment of these is beyond the scope of this book[85].

PLEXIFORM FIBROHISTIOCYTIC TUMOR

Clinical Features

A plexiform fibrohistiocytic tumor typically presents as a slowly growing, firm, painless mass in a child or young adult[86]. It is usually <3 cm in diameter and usually occurs on an extremity. This tumor is regarded as having intermediate biologic behavior with a tendency to recur locally but only rarely metastasizing.

Pathology

The tumor develops at the dermal/subcutaneous junction and appears as an infiltrative mass that may invade muscle. It is composed of small nodules of histiocytes and multinucleated giant cells surrounded by fascicles of spindled cells in variable proportions. These spindle cells express SMA. Mitotic figures and mild nuclear pleomorphism may be seen as well as lymphovascular invasion. Based on shared morphologic and phenotypic features, there is growing evidence to suggest that cellular neurothekeoma and plexiform fibrohistiocytic tumor exist on a continuum[87].

Treatment

These tumors are locally aggressive with high rates of recurrence, requiring excision with wider margins and long-term evaluation[88].

ATYPICAL FIBROXANTHOMA

Clinical Features

This tumor usually presents as a rapidly growing, exophytic, dome-shaped nodule that measures from 1 to 2 cm in diameter (Fig. 116.30). Secondary changes include serosanguineous crusts and ulceration[89]. In the 5th edition of the WHO classification of soft tissue and bone tumors, atypical fibroxanthoma (AFX) is defined as a dermal-based mesenchymal neoplasm of uncertain differentiation that develops within photodamaged skin. It is viewed as existing on a disease spectrum with pleomorphic dermal sarcoma. However, when strict diagnostic criteria are applied, AFX generally behaves in a benign fashion[90–92].

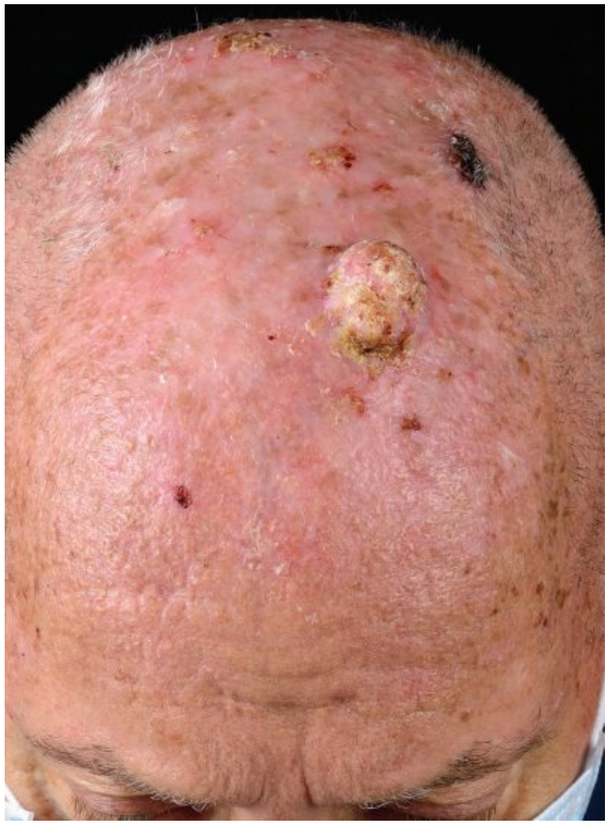


Fig. 116.30 Atypical fibroxanthoma. A crusted nodule on the scalp arising within a background of chronic photodamage with multiple actinic keratoses and diffuse scarring. *Courtesy Lorenzo Cerroni, MD.*

Pathology

This dermal-based tumor is well circumscribed and commonly ulcerated, and it usually has a collarette of hyperplastic epithelium. The neoplasm is confined to the dermis, with minimal to no infiltration of the subcutaneous fat; extensive infiltration of fatty tissue actually excludes the diagnosis of AFX. The tumor can push both adnexal structures and abnormal elastic fibers (solar elastosis) to the bottom of the lesion.

AFX is composed of atypical spindle-shaped cells with moderate amounts of cytoplasm and large atypical cells with abundant pale-staining vacuolated cytoplasm. The cells have large pleomorphic and hyperchromatic nuclei and some of them are multinucleated (Fig. 116.31A). Several morphologic variants of AFX exist – spindle-cell non-pleomorphic, clear cell, pigmented, myxoid, osteoclast-like giant cell-rich, keloidal, and granular cell (Fig. 116.31B–D)[93–98].

Tumor cells can express muscle-specific actin, CD68, and CD10[99]. However, these markers are considered to be nonspecific in the context of an AFX. As a rule, the diagnosis of AFX must be established by exclusion, in particular of squamous cell carcinoma and its variants, cutaneous melanoma, angiosarcoma, myxofibrosarcoma, variants of fibrous histiocytoma, pleomorphic fibroma, non-neural granular cell tumor, and superficial leiomyosarcoma[91]. An AFX is characteristically negative for all types of cytokeratins, melanocytic markers, the endothelial marker ERG, and desmin.

Tumors whose pathologic features are similar to AFX but demonstrate subcutaneous invasion, necrosis, and/or lymphovascular or perineural invasion are thought to be associated with an adverse outcome and are better regarded as *pleomorphic dermal sarcoma* or *undifferentiated pleomorphic sarcoma of skin*[92].

Treatment

The behavior of AFX is benign in the vast majority of patients, provided that strict diagnostic criteria are applied[91]. Because the incidence of local recurrences is very low and metastases are rare[99], AFX is usually cured by complete excision, including via Mohs micrographic surgery. In contrast, pleomorphic dermal sarcoma/undifferentiated pleomorphic sarcoma should be excised with wide tumor-free margins, and patients should be followed closely as these sarcomas have a local recurrence

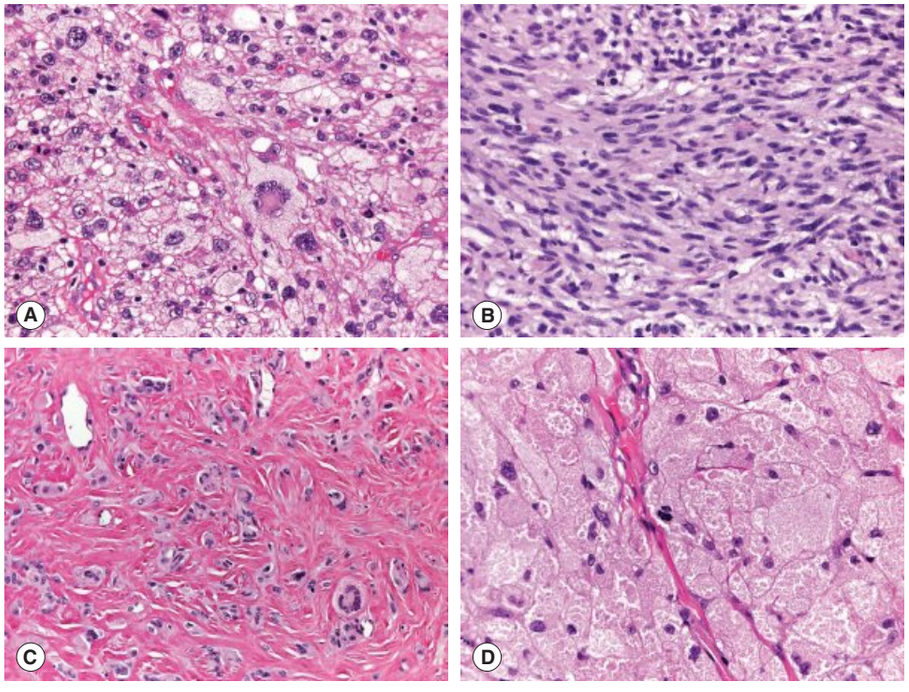


Fig. 116.31 Atypical fibroxanthoma (AFX) – four different histopathologic variants. A "Conventional" AFX with multiple "Touton-like" giant cells and marked pleomorphism. **B** Spindle cell variant characterized by a proliferation of spindle cells with only minimal pleomorphism. **C** Keloidal variant characterized by pleomorphic tumor cells embedded in a desmoplastic stroma. **D** Granular cell variant characterized by granular cytoplasm of the neoplastic cells, resembling a granular cell tumor. *Courtesy Lorenzo Cerroni, MD.*

rate of 25%–30% and a metastatic rate of 10%[92]. Progressive metastatic disease may occur[92].

DERMATOFIBROSARCOMA PROTUBERANS

Clinical Features

Dermatofibrosarcoma protuberans (DFSP) is a locally aggressive sarcoma of intermediate malignancy that favors young to middle-aged adults. Lesions that are present at birth or with an onset during childhood have also been reported. DFSP occurs on the trunk in 50%–60% of patients, the proximal extremities in 20%–30%, and the head and neck in 10%–15%. There is a predilection for the shoulder or pelvic region. Initially, a slowly growing, asymptomatic, skin-colored, indurated plaque is seen that eventually develops violaceous to red–brown nodules measuring from one to several centimeters in diameter (Fig. 116.32)[100]. On palpation, the lesion is firm and attached to the subcutaneous tissue. There are reports of accelerated growth during pregnancy[101].

The early plaque stage may be misdiagnosed as a benign tumor and incompletely excised. Moreover, superficial samples may not yield diagnostic material. Congenital and childhood-onset DFSP may have an atrophic appearance and/or hypopigmented to blue–red color, with the latter potentially leading to misdiagnosis as a vascular malformation or tumor. Multiple DFSPs have been observed in children with adenosine deaminase-deficient severe combined immunodeficiency[102].



Fig. 116.32 Dermatofibrosarcoma protuberans. A broad, pink–brown, multinodular, firm plaque on the back.

Pathology

Early plaque lesions are characterized by a flat surface and low cellularity and are comprised of slender spindle-shaped cells arranged as long fascicles parallel to the skin surface. The cells are scattered between thin collagen fibers and infiltrate thick collagen bundles which appear cellular and wavy. Nuclear atypia is minimal and mitotic figures are rare. Adnexal structures are infiltrated and obliterated. The spindle cells infiltrate into the subcutaneous tissue, very often in a multilayered pattern (Fig. 116.33A)[103].

In the nodular stage, the tumor becomes more cellular, with the cells arranged as short fascicles in a "storiform" arrangement (Fig. 116.33B). The cells infiltrate the subcutaneous tissue in a "honeycomb" pattern. Nuclei are hyperchromatic, and mitotic figures are easily identified. The nodules may develop myxomatous areas, characterized by more rounded to stellate cells in a highly vascular myxomatous stroma. Fibrosarcomatous areas are highly cellular, with intersecting fascicles in a "herringbone" pattern, with increased cytologic atypia and frequent mitoses.

Less than 5% of DFSPs contain melanin-producing cells with melanocyte or melanocyte-schwannian differentiation, and they are referred to as Bednar tumors[104].

In plaque-stage tumors, the spindle-shaped cells are strongly positive for CD34 (Fig. 116.33C)[10,105,106]. The reaction is stronger within the plaque areas than in the nodular foci[107]. The general immunostaining pattern of DFSP – CD34-positive, factor XIIIa-negative – serves to distinguish it from large and/or highly cellular dermatofibromas.

Unique cytogenetic abnormalities have been reported, such as reciprocal t(17;22) translocations (see below) and supernumerary ring chromosomes containing sequences from chromosomes 17 and 22[108]. Overexpression of *p53* has been found within the fibrosarcomatous areas of DFSP that have higher proliferative activity and aneuploidy[109].

The pathologic differential diagnosis of the plaque stage of DFSP includes atrophic dermatofibroma, dermatomyofibroma, fibroblastic connective tissue nevus, and neurofibroma. For the nodular stage, it includes deep dermatofibroma extending to the subcutaneous tissue, fibrosarcoma, and malignant peripheral nerve sheath tumor. The clinicopathologic criteria for CD34$^+$ plaque-like dermal fibroma (medallion-like dermal dendrocyte hamartoma) and superficial, mostly dermal DFSP overlap. However, the former does *not* have an unbalanced reciprocal

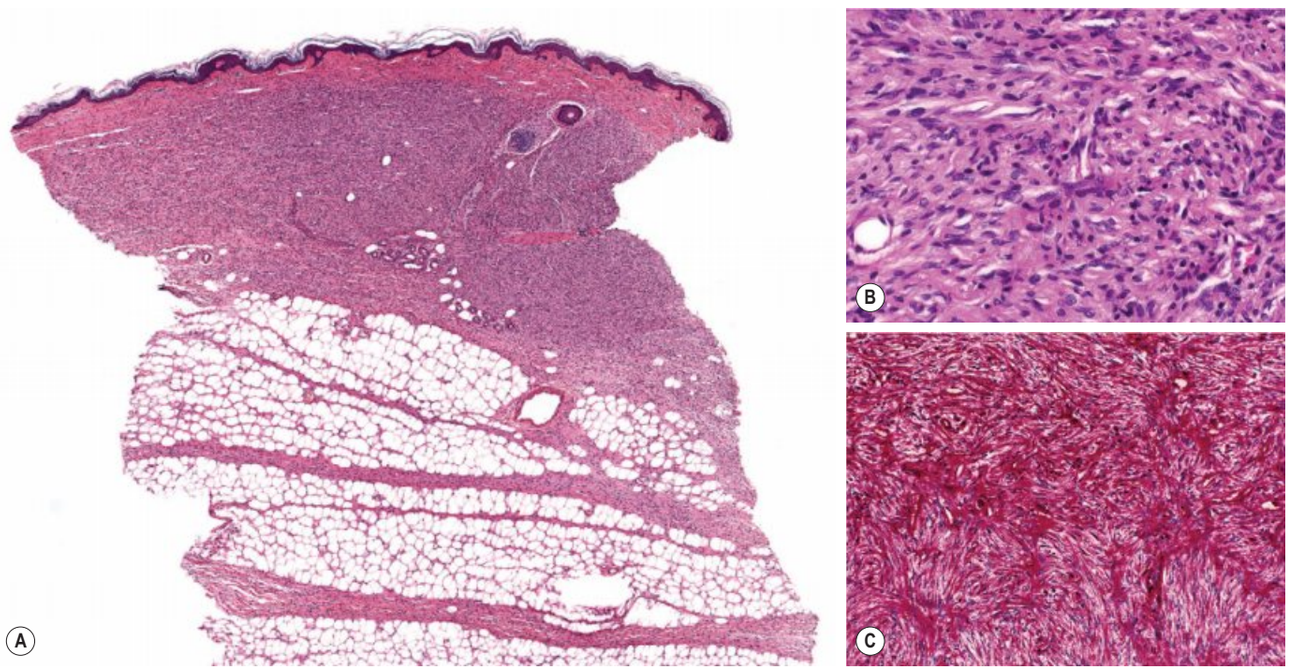


Fig. 116.33 Dermatofibrosarcoma protuberans. A Characteristic multilayered pattern of infiltration into the subcutaneous tissue. Note storiform pattern (**B**) and positivity for CD34 (**C**). *Courtesy Lorenzo Cerroni, MD.*

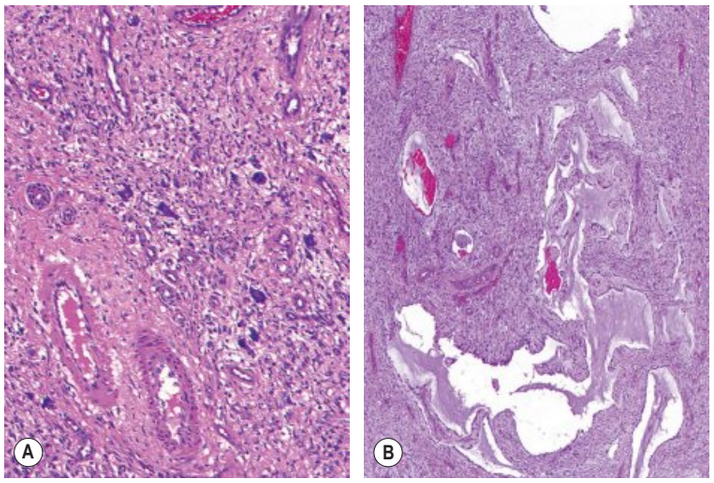


Fig. 116.34 Giant cell fibroblastoma. This variant of DFSP has a biphasic architecture consisting of: (**A**) foci of giant tumor cells with atypical nuclei; and (**B**) areas with pseudovascular or "angiectoid" spaces. Often the areas with atypical tumor cells and lacunar spaces are situated close to one another.

t(17;22) translocation[110] and it usually has a cellular, band-like, CD34$^+$ fibroblastic proliferation within the papillary and adjacent upper reticular dermis. For DFSP and its simulators, incisional biopsy specimens, including ample subcutaneous tissue, are optimal for diagnosis.

Molecular diagnostics utilizing FISH, RT-PCR or NGS can facilitate precise diagnosis via detection of the *COL1A1-PDGFB* gene fusion found in the majority of DFSPs (see Table 116.3). Rarely, alternative fusions involving *PDGFD* (*COL6A3-PDGFD*; *EMILIN2-PDGFD*) are identified[111,112]. In fibrosarcomatous DFSP, alterations in the PDGFRB/AKT/mTOR pathway have been reported[113].

Treatment

Complete surgical excision, including Mohs micrographic surgery, is the standard treatment for DFSP[114]. This tumor is characterized by its local invasion and tendency to recur. In rare cases, recurrent tumors with fibrosarcomatous areas have metastasized to the lungs[115]. Because the translocation (17;22) places the platelet-derived growth factor (PDGF) subunit B gene under the control of the collagen 1A1 promoter, imatinib (which targets the PDGF receptor [as well as other proteins with tyrosine kinase activity, e.g. KIT and BCR-ABL]) was tried in patients with DFSP. It is currently FDA-approved for adults with unresectable, recurrent, and/or metastatic DFSP. In a recent systematic review of relevant studies (2002–2017) in which imatinib was administered for metastatic or locally advanced DFSP, there was a complete response, partial response, or stable disease in 5%, 55%, and 28% of patients, respectively[116]. Either dosage (400 or 800 mg/day) led to similar results. Tumor progression occurred in 9% of patients, with severe adverse side effects in 15%[116].

GIANT CELL FIBROBLASTOMA

Clinical Features

Giant cell fibroblastoma is a rare, locally aggressive, histologic variant of DFSP[90]. It presents as a solitary, slow-growing, asymptomatic, skin-colored nodule involving the neck, trunk, or groin. In approximately half of patients, a protuberant or polypoid configuration is seen. Giant cell fibroblastoma usually appears during early childhood, with a strong predilection for boys[117].

Pathology

This lesion is composed of diffusely infiltrating sheets of spindle-shaped fibroblasts and multinucleated cells with hyperchromatic nuclei within a slightly myxoid matrix (Fig. 116.34A). Irregular "angiectoid" or pseudovascular spaces lined by multinucleated giant cells are present throughout the tumor (Fig. 116.34B). These giant cells do not react with markers for endothelial differentiation but do react with anti-CD34 antibodies[118]. Molecular studies have shown that giant cell fibroblastoma and DFSP share the same t(17;22) chromosomal translocation which places the PDGF subunit B gene under the control of the promoter of the collagen 1A1 gene[119]. Accordingly, in the most recent WHO classification of tumors of soft tissue and bone, giant cell fibroblastoma is considered to be closely related to DFSP[90,120].

MALIGNANT TUMORS WITH FIBROBLASTIC AND MYOFIBROBLASTIC DIFFERENTIATION		
Type of sarcoma	**Genetic abnormalities**	**Comments**
Adult-type fibrosarcoma	*STRN3-NTRK3* fusion	Often diagnosed after excluding synovial sarcoma, solitary fibrous tumor, MPNST
Congenital or infantile fibrosarcoma*	*ETV6-NTRK3* fusion; other *NTRK*-related fusions	
Low-grade fibromyxoid sarcoma (hyalinizing spindle cell tumor with giant rosettes)	*FUS-CREB3L2*; *FUS-CREB3L1*; *EWSR1-CREB3L1* fusions	IHC: expression of MUC4
Myxofibrosarcoma	Complex karyotype	Diagnosis based upon morphology
Myxoinflammatory fibroblastic sarcoma	Reciprocal t(1;10) (p22;q24) translocations; *BRAF*-related fusions; *VGLL3* gene amplification	
Sclerosing epithelioid fibrosarcoma	*FUS-CREB3L2*; *FUS-CREB3L1*; *EWSR1-CREB3L1* fusions	IHC: expression of MUC4
*Locally aggressive but overall favorable outcome[122].		

Table 116.4 Malignant tumors with fibroblastic and myofibroblastic differentiation. *CREB3L1*, cAMP responsive element binding protein 3 like 1; *CREB3L2*, CREB3 like 2; *ETV6*, ETS variant transcription factor 6; *EWSR1*, EWS RNA binding protein 1; *FUS*, FUS RNA binding protein; IHC, immunohistochemistry; MPNST, malignant peripheral nerve sheath tumor; MUC4, mucin 4, cell surface associated; *NTRK3*, neurotrophic receptor tyrosine kinase 3; *VGLL3*, vestigial like family member 3.

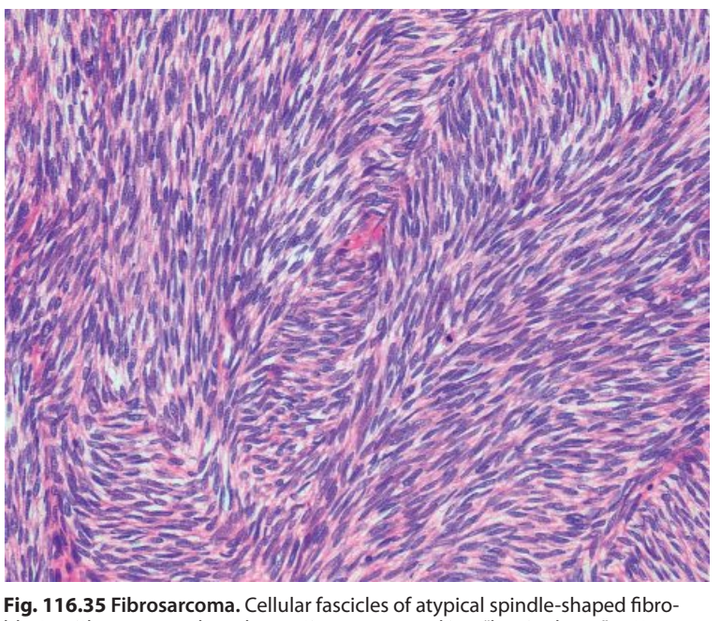


Fig. 116.35 Fibrosarcoma. Cellular fascicles of atypical spindle-shaped fibroblasts with coarse nuclear chromatin are arranged in a "herringbone" pattern.

Treatment

This tumor is regarded as being of intermediate biologic behavior, with a significant risk of local recurrence if incompletely excised[117]. Metastases have not been reported[90].

FIBROSARCOMA

Clinical Features

Previously, the term "fibrosarcoma" encompassed a heterogeneous group of high-grade and low-grade soft tissue tumors. Nowadays, specific tumor entities within the group of fibroblastic and myofibroblastic soft tissue sarcomas can be identified via molecular diagnostics (Table 116.4)[121].

Classic fibrosarcomas usually affect middle-aged adults. The most common location is the lower extremities, followed by the upper extremities, trunk, and head and neck region. This is a neoplasm predominantly of the deep soft tissues, with secondary involvement of the overlying subcutis and skin. Fibrosarcoma is a slowly growing tumor that measures from 1 to 10 cm in diameter and is usually diagnosed when it becomes a palpable painful nodule or plaque[123]. They may appear in old burn scars and in areas of prior irradiation[124].

Pathology

The tumor is composed of a proliferation of atypical spindle-shaped cells arranged as intersecting fascicles in a "herringbone" pattern (Fig. 116.35). There are thin collagen bundles between the cells which have scanty cytoplasm and elongated hyperchromatic nuclei. Mitotic figures are easily identified and myxomatous foci may be present. A sclerosing epithelioid variant that simulates an infiltrating carcinoma has been described[125]. High-grade fibrosarcomas are characterized by increased cellularity with more atypical nuclei, a higher mitotic rate, foci of necrosis, and a less distinct "herringbone" pattern.

Treatment

The traditional treatment for fibrosarcoma is wide excision. When wide free margins cannot be achieved, adjuvant radiation therapy and amputation are additional options. In high-grade fibrosarcomas, neoadjuvant or adjuvant systemic chemotherapy is given. Hematogenous metastases to the lung, and less often to the bones, develop in patients with high-grade or poorly differentiated fibrosarcomas. The overall 5-year survival rate is ~40%[123]. In tumors with *NTRK* fusions, targeted therapy with pan-tropomyosin receptor kinase (TRK) inhibitors (e.g. larotrectinib, entrectinib) has shown encouraging results[126,127].

EPITHELIOID SARCOMA

Synonyms/variants: ■ Classic or conventional – distal type
■ Proximal – large-cell type

Clinical Features

In the 5th edition of the WHO classification of soft tissue and bone tumors, epithelioid sarcomas are classified within the tumor group with uncertain differentiation. Two clinicopathologic subtypes of epithelioid sarcoma are recognized: (1) the *conventional or classic ("distal") form*, characterized by its proclivity for acral sites and a pseudogranulomatous growth pattern; and (2) the *proximal-type ("large-cell") variant* that usually arises more proximally or on the trunk and is composed of nests and sheets of large epithelioid cells[90,128]. Classic epithelioid sarcomas present as a slow-growing, firm, subcutaneous nodule of the distal extremities, usually the hands and fingers. There may be associated ulceration if the tumor involves the dermis. Advanced metastatic disease can present as a linear arrangement of widely spaced, ulcerated nodules extending from distal to proximal sites on affected extremities, with intervening tumor-free skin. If there is involvement of a large nerve, associated pain, paresthesias, and muscle wasting can occur[129].

The majority of patients are between 20 and 40 years of age, and men are affected twice as often as women. Hand and finger lesions may resemble the localized type of tenosynovial giant cell tumor (giant cell tumor of tendon sheath), fibroma of tendon sheath, nodular fasciitis, subcutaneous granuloma annulare, rheumatoid nodule, or ganglion cyst. Penile lesions can mimic Peyronie disease[129].

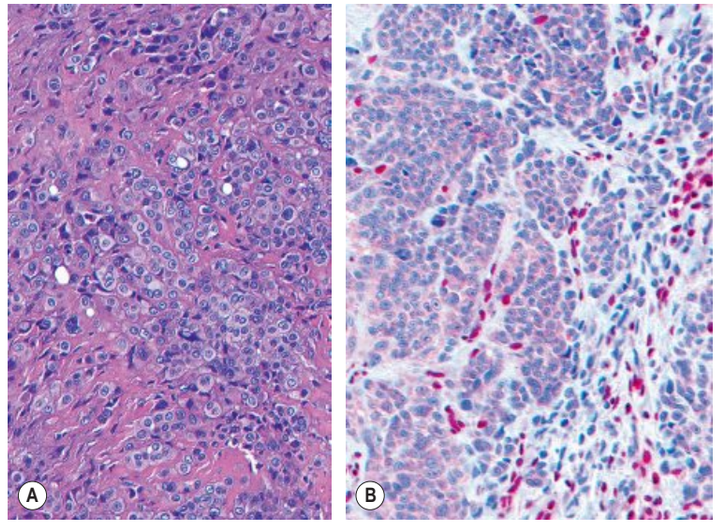


Fig. 116.36 Epithelioid sarcoma. A Large epithelioid tumor cells with ample cytoplasm may imitate a granulomatous or epithelial growth pattern. **B** The nuclei of these tumor cells are INI1-negative, which is an important diagnostic feature. Note the adjacent INI1-positive lymphocyte nuclei.

Pathology

In *classic "distal" epithelioid sarcoma*, there is a nodular proliferation of spindle-shaped to round or epithelioid/polygonal cells with abundant eosinophilic cytoplasm and small uniform nuclei without prominent nucleoli (Fig. 116.36A). Epithelioid tumor cells are usually seen centrally, with a gradual transition to a spindle cell morphology towards the periphery[128]. When present, cytoplasmic vacuoles may mimic vascular tumors. Within larger tumor nodules, zones of central necrosis surrounded by palisaded tumor cells can be seen as well as a mixed chronic inflammatory cell infiltrate.

Proximal-type epithelioid sarcoma has a multinodular, sheet-like growth pattern and is composed of large epithelioid (carcinoma-like) cells that have enlarged vesicular nuclei with prominent nucleoli and abundant eosinophilic cytoplasm. A rhabdoid morphology is more commonly observed in this variant. While necrosis can be seen, a pseudogranulomatous morphology is more typical of the classic form (see above).

Both subtypes of epithelioid sarcoma demonstrate an infiltrative growth pattern and these tumors are frequently associated with fascia, periosteum, tendons, and nerves. The tumor cells are typically positive for keratins, EMA, and CD34 while negative for S100, HMB45, and CD31. ERG expression has been reported in up to two-thirds of tumors.

Epithelioid sarcomas have distinct genetic alterations of 22q11–12, including mutations, deletions, and other alterations of the tumor suppressor gene *SMARCB1/INI1* (see Table 116.3)[90]. Therefore, loss of INI1 expression by immunohistochemistry is characteristic of both conventional and proximal-type epithelioid sarcoma[130] (Fig. 116.36B).

Treatment

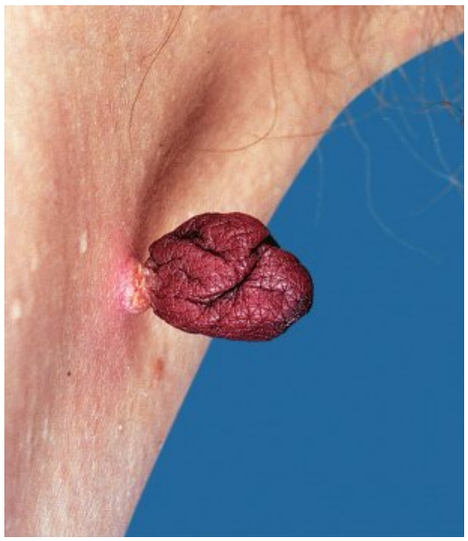
Both subtypes typically demonstrate an infiltrating growth pattern along tendons, nerves and fascia, with skip lesions commonly observed in classic "distal" epithelioid sarcomas. Although earlier therapeutic approaches involved radical surgery, including amputation, there has been a movement toward more conservative surgery with adjuvant radiation therapy[131]. Epithelioid sarcoma, especially the proximal ("large-cell") type, is an aggressive tumor with a high local recurrence rate. For all epithelioid sarcoma variants, 5- and 10-year overall survival rates are 60%–80% and 40%–60%, respectively[90,129,132]. Metastases develop in 40%–50% of patients, usually after repeated recurrences, and frequently involve the lung and regional lymph nodes. For metastatic or locally advanced epithelioid sarcoma with INI1 loss, tazemetostat, an oral inhibitor of the methyltransferase enzyme EZH2, improved disease outcome[133].

Additional figures, references and table on The dermal dendrocyte hamartomas, available in our eBook (see inside front cover for access code).

REFERENCES

1. Banik R, Lubach D. Skin tags: localization and frequencies according to sex and age. *Dermatologica*. 1987;174:180–183.
2. Gould BE, Ellison RC, Greene HL, Bernhard JD. Lack of association between skin tags and colon polyps in a primary care setting. *Arch Intern Med*. 1988;148:1799–1800.
3. Kahana M, Grossman E, Feinstein A, et al. Skin tags: a cutaneous marker for diabetes mellitus. *Acta Derm Venereol*. 1987;67:175–177.
4. De la Torre C, Ocampo C, Doval IG, et al. Acrochordons are not a component of the Birt-Hogg-Dube syndrome: does this syndrome exist? Case reports and review of the literature. *Am J Dermatopathol*. 1999;21:369–374.
5. Meigel WN, Ackerman AB. Fibrous papule of the face. *Am J Dermatopathol*. 1979;1:329–340.
6. Rehbein HM. Pearly penile papules: incidence. *Cutis*. 1977;19:54–57.
7. Schaffer JV, Gohara MA, McNiff JM, et al. Multiple facial angiofibromas: a cutaneous manifestation of Birt-Hogg-Dubé syndrome. *J Am Acad Dermatol*. 2005;53(Suppl. 1):S108–S111.
8. Yazici AC, Baz K, Ikizoglu G, et al. Familial eruptive dermatofibromas in atopic dermatitis. *J Eur Acad Dermatol Venereol*. 2006;20:90–92.
9. Goette DK, Helwig EB. Basal cell carcinomas and basal cell carcinoma-like changes overlying dermatofibromas. *Arch Dermatol*. 1975;111:589–592.
10. Abenoza P, Lillemoe T. CD34 and factor XIIIa in the differential diagnosis of dermatofibroma and dermatofibrosarcoma protuberans. *Am J Dermatopathol*. 1993;15:429–434.
11. Cerio R, Spaull J, Oliver GF, Wilson Jones E. A study of factor XIIIa and MAC 387 immunolabeling in normal and pathological skin. *Am J Dermatopathol*. 1990;12:221–233.
12. Reid MB, Gray C, Fear JD, Bird CC. Immunohistological demonstration of factors XIIIa and XIIIs in reactive and neoplastic fibroblastic and fibrohistiocytic lesions. *Histopathology*. 1986;10:1171–1178.
13. Vanni R, Fletcher CD, Sciot R, et al. Cytogenetic evidence of clonality in benign fibrous histiocytoma: a report of the CHAMP study group. *Histopathology*. 2000;37:212–217.
14. Chen TC, Kuo T, Chan HL. Dermatofibroma is a clonal proliferative disease. *J Cutan Pathol*. 2000;27:36–39.
15. Calonje E. Is cutaneous benign fibrous histiocytoma (dermatofibroma) a reactive inflammatory process or a neoplasm? *Histopathology*. 2000;37:278–280.
16. Lodewick E, Avermaete A, Blom WAM, et al. Fatal case of metastatic cellular fibrous histiocytoma: case report and review of literature. *Am J Dermatopathol*. 2014;36:e156–e162.
17. Yann CJ, Saggini A, Doyle LA, et al. DNA copy number changes in tumors within the spectrum of cellular, atypical, and metastasizing fibrous histiocytoma. *J Am Acad Dermatol*. 2014;71:256–263.
18. Dickson BC, Swanson D, Charames GS, et al. Epithelioid fibrous histiocytoma: molecular characterization of *ALK* fusion partners in 23 cases. *Modern Pathol*. 2018;31:753–762.
19. Supsrisunjai C, Hsu CK, Michael M, et al. Coagulation factor XIII-a subunit missense mutation in the pathobiology of autosomal dominant multiple dermatofibromas. *J Invest Dermatol*. 2020;140:624–635.e7.
20. Cooper PH, Mackel SE. Acquired fibrokeratoma of the heel. *Arch Dermatol*. 1985;121:386–388.
21. Kint A, Baran R, De Keyser H. Acquired (digital) fibrokeratoma. *J Am Acad Dermatol*. 1985;12:816–821.
22. Kint A, Baran R. Histopathologic study of Koenen tumors. Are they different from acquired digital fibrokeratoma? *J Am Acad Dermatol*. 1988;18:369–372.
23. Fetsch JF, Laskin WB, Miettinen M. Superficial acral fibromyxoma: a clinicopathologic and immunohistochemical analysis of 37 cases of a distinctive soft tissue tumor with a predilection for the fingers and toes. *Hum Pathol*. 2001;32:704–714.
24. Hollmann TJ, Bovée JV, Fletcher CD. Digital fibromyxoma (superficial acral fibromyxoma): a detailed characterization of 124 cases. *Am J Surg Pathol*. 2012;36:789–798.
25. Ashby-Richardson H, Rogers GS, Stadecker MJ. Superficial acral fibromyxoma: an overview. *Arch Pathol Lab Med*. 2011;135:1064–1066.
26. Kazakov DV, Mentzel T, Burg G, Kempf W. Superficial acral fibromyxoma: report of two cases. *Dermatology*. 2002;205:285–288.
27. Carranza C, Molina-Ruiz AM, Pérez de la Fuente T, et al. Subungual acral fibromyxoma involving the bone: a mimicker of malignancy. *Am J Dermatopathol*. 2015;37:555–559.
28. Al-Daraji WI, Miettinen M. Superficial acral fibromyxoma: a clinicopathological analysis of 32 tumors including 4 in the heel. *J Cutan Pathol*. 2008;35:1020–1026.
29. Agaimy A, Michal M, Giedl J, et al. Superficial acral fibromyxoma: clinicopathological, immunohistochemical, and molecular study of 11 cases highlighting frequent Rb1 loss/deletions. *Hum Pathol*. 2017;60:192–198.
30. Rapini RP, Golitz LE. Sclerotic fibromas of the skin. *J Am Acad Dermatol*. 1989;20:266–271.
31. Hanft VN, Shea CR, McNutt NS, et al. Expression of CD34 in sclerotic ("plywood") fibromas. *Am J Dermatopathol*. 2000;22:17–21.
32. Kamino H, Lee JY, Berke A. Pleomorphic fibroma of the skin: a benign neoplasm with cytologic atypia. A clinicopathologic study of eight cases. *Am J Surg Pathol*. 1989;13:107–113.
33. Rudolph P, Schubert C, Zelger BG, et al. Differential expression of CD34 and Ki-Mlp in pleomorphic fibroma and dermatofibroma with monster cells. *Am J Dermatopathol*. 1999;21:414–419.
34. Wilson Jones E, Cerio R, Smith NP. Multinucleate cell angiohistiocytoma: an acquired vascular anomaly to be distinguished from Kaposi's sarcoma. *Br J Dermatol*. 1990;122:651–663.
35. Chang SN, Kim HS, Kim SC, Yang WI. Generalized multinucleate cell angiohistiocytoma. *J Am Acad Dermatol*. 1996;35:320–322.
36. Hugel H. Plaque-like dermal fibromatosis/dermatomyofibroma. *Hautarzt*. 1991;42:223–226.
37. Kamino H, Reddy VB, Gero M, Greco MA. Dermatomyofibroma. A benign cutaneous, plaque-like proliferation of fibroblasts and myofibroblasts in young adults. *J Cutan Pathol*. 1992;19:85–93.
38. Mentzel T, Kutzner H. Dermatomyofibroma: clinicopathologic and immunohistochemical analysis of 56 cases and reappraisal of a rare and distinct cutaneous neoplasm. *Am J Dermatopathol*. 2009;31:44–49.
39. Rao AS, Vigorita VJ. Pigmented villonodular synovitis (giant-cell tumor of the tendon sheath and synovial membrane). A review of eighty-one cases. *J Bone Joint Surg Am*. 1984;66:76–94.
40. Panagopoulos I, Brandal P, Gorunova L, et al. Novel CSF1-S100A10 fusion gene and CSF1 transcript identified by RNA sequencing in tenosynovial giant cell tumors. *Int J Oncol*. 2014;44:1425–1432.
41. Möller E, Mandahl N, Mertens F, Panagopoulos I. Molecular identification of COL6A3-CSF1 fusion transcript in tenosynovial giant cell tumors. *Genes Chromosomes Cancer*. 2008;47:21–25.
42. Nishido J. Updates on the cytogenetics and molecular cytogenetics of benign and intermediate soft tissue tumors. *Oncol Lett*. 2013;5:12–18.
43. Chung EB, Enzinger FM. Fibroma of tendon sheath. *Cancer*. 1979;44:1945–1954.
44. Carter JM, Wang X, Dong J, et al. USP6 genetic rearrangements in cellular fibroma of tendon sheath. *Mod Pathol*. 2016;29:865–869.
45. Satti MB. Tendon sheath tumours: a pathological study of the relationship between giant cell tumour and fibroma of tendon sheath. *Histopathology*. 1992;20:213–220.
46. Erickson-Johnson MR, Chou MM, Evers BR, et al. Nodular fasciitis: a novel model of transient neoplasia induced by MYH9-USP6 gene fusion. *Lab Invest*. 2011;91:1427–1433.
47. Sarangarajan R, Dehner LP. Cranial and extracranial fasciitis of childhood: a clinicopathologic and immunohistochemical study. *Hum Pathol*. 1999;30:87–92.
48. Price SK, Kahn LB, Saxe N. Dermal and intravascular fasciitis. Unusual variants of nodular fasciitis. *Am J Dermatopathol*. 1993;15:539–543.
49. Hussein MR. Cranial fasciitis of childhood: a case report and review of literature. *J Cutan Pathol*. 2008;35:212–214.
50. de Feraudy S, Fletcher CD. Intradermal nodular fasciitis: a rare lesion analyzed in a series of 24 cases. *Am J Surg Pathol*. 2010;34:1377–1381.
51. Montgomery EA, Meis JM. Nodular fasciitis. Its morphologic spectrum and immunohistochemical profile. *Am J Surg Pathol*. 1991;15:942–948.
52. Amary MF, Ye H, Berisha F, et al. Detection of USP6 gene rearrangement in nodular fasciitis: an important diagnostic tool. *Virchows Arch*. 2013;463:97–98.
53. Bernstein KE, Lattes R. Nodular (pseudosarcomatous) fasciitis, a nonrecurrent lesion: clinicopathologic study of 134 cases. *Cancer*. 1982;49:1668–1678.
54. Hellemans J, Preobrazhenska O, Willaert A, et al. Loss-of-function mutations in *LEMD3* result in osteopoikilosis, Buschke-Ollendorff syndrome and melorheostosis. *Nat Genet*. 2004;36:1213–1218.
55. de Feraudy S, Fletcher CDM. Fibroblastic connective tissue nevus. A rare cutaneous lesion analyzed in a series of 25 cases. *Am J Surg Pathol*. 2012;36:1509–1515.
56. Viale G, Doglioni C, Iuzzolino P, et al. Infantile digital fibromatosis-like tumour (inclusion body fibromatosis) of adulthood: report of two cases with ultrastructural and immunocytochemical findings. *Histopathology*. 1988;12:415–424.
57. Niamba P, Léauté-Labrèze C, Boralevi F. Further documentation of spontaneous regression of infantile digital fibromatosis. *Pediatr Dermatol*. 2007;24:280–284.
58. Laskin WB, Mettinen M, Fetsch JF. Infantile digital fibroma/fibromatosis: a clinicopathologic and immunohistochemical study of 69 tumors from 57 patients with long-term follow-up. *Am J Surg Pathol*. 2009;33:1–13.
59. Stanford D, Rogers M. Dermatological presentations of infantile myofibromatosis: a review of 27 cases. *Australas J Dermatol*. 2000;41:156–161.
60. Beham A, Badve S, Suster S, Fletcher CD. Solitary myofibroma in adults: clinicopathological analysis of a series. *Histopathology*. 1993;22:335–341.
61. Agaimy A, Bieg M, Michal M, et al. Recurrent somatic PDGFRB mutations in sporadic infantile/solitary adult myofibromas but not in angioleiomyomas and myopericytomas. *Am J Surg Pathol*. 2017;41:195–203.
62. Wu D, Wang S, Oliveira DV, et al. The infantile myofibromatosis NOTCH3 L1519P mutation leads to hyperactivated ligand-independent Notch signaling and increased PDGFRB expression. *Dis Model Mech*. 2021;14: dmm046300.
63. Suurmeijer AJ, Dickson BC, Swanson D, et al. Novel SRF-ICA1L fusions in cellular myoid neoplasms with potential for malignant behavior. *Am J Surg Pathol*. 2020;44:55–60.
64. Dachy G, de Krijger RR, Fraitag S, et al. Association of PDGFRB mutations with pediatric myofibroma and myofibromatosis. *JAMA Dermatol*. 2019;155:946–950.
65. Fukasawa Y, Ishikura H, Takada A, et al. Massive apoptosis in infantile myofibromatosis. A putative mechanism of tumor regression. *Am J Pathol*. 1994;144:480–485.
66. Smith KJ, Skelton HG, Barrett TL, et al. Cutaneous myofibroma. *Mod Pathol*. 1989;2:603–609.
67. Kutzner H, Hügel H, Rütten A, Braun M. Acquired benign myofibroma of the skin (adult myofibroma). *Hautarzt*. 1993;44:561–568.
68. Requena L, Kutzner H, Hügel H, et al. Cutaneous adult myofibroma: a vascular neoplasm. *J Cutan Pathol*. 1996;23:445–457.
69. Mentzel T, Dei Tos AP, Sapi Z, Kutzner H. Myopericytoma of skin and soft tissues: clinicopathologic and immunohistochemical study of 54 cases. *Am J Surg Pathol*. 2006;30:104–113.
70. Hung YP, Fletcher CDM. Myopericytomatosis: clinicopathologic analysis of 11 cases with molecular identification of recurrent PDGFRB alterations in myopericytomatosis and myopericytoma. *Am J Surg Pathol*. 2017;8: 1034–1044.
71. Fetsch JF, Miettinen M. Calcifying aponeurotic fibroma: a clinicopathologic study of 22 cases arising in uncommon sites. *Hum Pathol*. 1998;29:1504–1510.
72. Puls F, Hofvander J, Magnusson L, et al. FN1-EGF gene fusions are recurrent in calcifying aponeurotic fibroma. *J Pathol*. 2016;238:502–507.
73. Paller AS, Gonzalez-Crussi F, Sherman JO. Fibrous hamartoma of infancy. Eight additional cases and a review of the literature. *Arch Dermatol*. 1989;125:88–91.
74. Popek EJ, Montgomery EA, Fourcroy JL. Fibrous hamartoma of infancy in the genital region: findings in 15 cases. *J Urol*. 1994;152:990–993.
75. Yoon TY, Kim JW. Fibrous hamartoma of infancy manifesting as multiple nodules with hypertrichosis. *J Dermatol*. 2006;33:427–429.
76. Sotelo-Avila C, Bale PM. Subdermal fibrous hamartoma of infancy: pathology of 40 cases and differential diagnosis. *Pediatr Pathol*. 1994;14:39–52.
77. Al-Ibraheemi A, Martinez A, Weiss SW, et al. Fibrous hamartoma of infancy: a clinicopathologic study of 145 cases, including 2 with sarcomatous features. *Mod Pathol*. 2017;30:474–485.
78. Allen PW. The fibromatoses: a clinicopathologic classification based on 140 cases. *Am J Surg Pathol*. 1977;1:255–270.
79. Beltraminelli H, Itin P. Pachydermodactyly – just a sign of emotional distress. *Eur J Dermatol*. 2009;19:5–13.
80. Crago AM, Chmielecki J, Rosenberg M, et al. Near universal detection of alterations in CTNNB1 and Wnt pathway regulators in desmoid-type fibromatosis by whole-exome sequencing and genomic analysis. *Genes Chromosomes Cancer*. 2015;54:606–615.

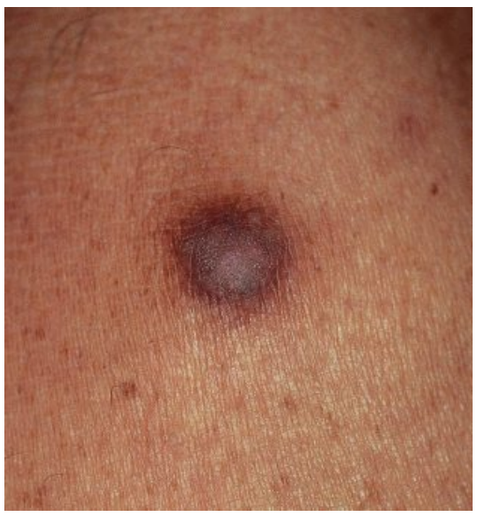
81. Carlson JW, Fletcher CD. Immunohistochemistry for beta-catenin in the differential diagnosis of spindle cell lesions: analysis of a series and review of the literature. *Histopathology*. 2007;51:509–514.
82. De Wever I, Dal Cin P, Fletcher CDM, et al. Cytogenetic, clinical and morphologic correlations in 78 cases of fibromatosis: a report from the CHAMP study group. *Mod Pathol*. 2000;13:1080–1085.
83. Desai SS, Hentz VR. The treatment of Dupuytren disease. *J Hand Surg Am*. 2011;36:936–942.
84. Gelbard MK, Dorey F, James K. The natural history of Peyronie's disease. *J Urol*. 1990;144:1376–1379.
85. Kasper B, !Baumgarten C, Garcia J et al. An update on the management of sporadic desmoid-type fibromatosis: a European Consensus Initiative between Sarcoma PAtients EuroNet (SPAEN) and European Organization for Research and Treatment of Cancer (EORTC)/Soft Tissue and Bone Sarcoma Group (STBSG). Ann Oncol 2017;10:2399–408.
86. Enzinger FM, Zhang RY. Plexiform fibrohistiocytic tumor presenting in children and young adults. An analysis of 65 cases. *Am J Surg Pathol*. 1988;12:818–826.
87. Jaffer S, Ambrosini-Spaltro A, Mancini AM, et al. Neurothekeoma and plexiform fibrohistiocytic tumor: mere histologic resemblance or histogenetic relationship? *Am J Surg Pathol*. 2009;33:905–913.
88. Moosavi C, Jha P, Fanburg-Smith JC. An update on plexiform fibrohistiocytic tumor and addition of 66 new cases from the Armed Forces Institute of Pathology, in honor of Franz M. Enzinger, MD. *Ann Diagn Pathol*. 2007;11:313–319.
89. Fretzin DF, Helwig EB. Atypical fibroxanthoma of the skin. A clinicopathologic study of 140 cases. *Cancer*. 1973;31:1541–1552.
90. WHO Classification of Tumours Editorial Board, editors. *WHO Classification of Tumours - Soft Tissue and Bone Tumours*. Lyon: International Agency for Research on Cancer; 2020.
91. Brenn T. Pleomorphic dermal neoplasms: a review. *Adv Anat Pathol*. 2014;21:108–130.
92. Miller K, Goodlad JR, Brenn T. Pleomorphic dermal sarcoma: adverse histologic features predict aggressive behavior and allow distinction form atypical fibroxanthoma. *Am J Surg Pathol*. 2012;36:1317–1326.
93. Ferrara N, Baldi G, Di Marino MP, et al. Atypical fibroxanthoma with osteoclast-like multinucleated giant cells. *In Vivo*. 2000;14:105–107.
94. Calonje E, Wadden C, Wilson-Jones E, et al. Spindle-cell non-pleomorphic atypical fibroxanthoma: analysis of a series and delineation of a distinctive variant. *Histopathol*. 1993;22:247–254.
95. Crowson AN, Carlson-Sweet K, Macinnis C, et al. Clear cell atypical fibroxanthoma: a clinicopathologic study. *J Cutan Pathol*. 2002;29:374–381.
96. Thum C, Husain EA, Mulholland K, et al. Atypical fibroxanthoma with pseudoangiomatousfeatures: a histological and immunohistochemical mimic of cutaneous angiosarcoma. *Ann Diagn Pathol*. 2013;17:502–507.
97. Kim J, McNiff JM. Keloidal atypical fibroxanthoma: a case series. *J Cutan Pathol*. 2009;36:535–539.
98. Rudisaile SN, Hurt MA, Santa Cruz DJ. Granular cell atypical fibroxanthoma. *J Cutan Pathol*. 2005;32:314–317.
99. Mirza B, Weedon D. Atypical fibroxanthoma of the skin: a clinicopathological study of 89 cases. *Australas J Dermatol*. 2005;46:235–238.
100. Taylor HB, Helwig EB. Dermatofibrosarcoma protuberans: a study of 115 cases. *Cancer*. 1962;15: 717–725.
101. Parlette LE, Smith CK, Germain LM, et al. Accelerated growth of dermatofibrosarcoma protuberans during pregnancy. *J Am Acad Dermatol*. 1999;41:778–783.
102. Kesserwan C, Sokolic R, Cowen EW, et al. Multicentric dermatofibrosarcoma protuberans in patients with adenosine deaminase-deficient severe combined immune deficiency. *J Allergy Clin Immunol*. 2012;129:762–769.
103. Kamino H, Jacobson M. Dermatofibroma extending into the subcutaneous tissue. Differential diagnosis from dermatofibrosarcoma protuberans. *Am J Surg Pathol*. 1990;14:1156–1164.
104. Ding JA, Hashimoto H, Sugimoto T, et al. Bednar tumor (pigmented dermatofibrosarcoma protuberans). An analysis of six cases. *Acta Pathol Jpn*. 1990;40: 744–754.
105. Aiba S, Tabata N, Ishii H, et al. Dermatofibrosarcoma protuberans is a unique fibrohistiocytic tumour expressing CD34. *Br J Dermatol*. 1992;127:79–84.
106. Kutzner H. Expression of the human progenitor cell antigen CD34 (HPCA-1) distinguishes dermatofibrosarcoma protuberans from fibrous histiocytoma in formalin-fixed, paraffin-embedded tissue. *J Am Acad Dermatol*. 1993;28:613–617.
107. Kamino H, Burchette J, Garcia J. Immunostaining for CD34 in plaque and nodular areas of dermatofibrosarcoma protuberans. *J Cutan Pathol*. 1992;19:530.
108. Pedeutour F, Simon MP, Minoletti F, et al. Translocation, t(17;22)(q22;q13), in dermatofibrosarcoma protuberans: a new tumor-associated chromosome rearrangement. *Cytogenet Cell Genet*. 1996;72:171–174.
109. Hisaoka M, Okamoto S, Morimitsu Y, et al. Dermatofibrosarcoma protuberans with fibrosarcomatous areas. Molecular abnormalities of the p53 pathway in fibrosarcomatous transformation of dermatofibrosarcoma protuberans. *Virchows Arch*. 1998;433:323–329.
110. Kutzner H, Mentzel T, Palmedo G, et al. Plaque-like CD34-positive dermal fibroma ("medallion-like dermal dendrocyte hamartoma"). Clinicopathologic, immunohistochemical, and molecular analysis of 5 cases emphasizing its distinction from superficial, plaque-like dermatofibrosarcoma protuberans. *Am J Surg Pathol*. 2010;34:190–201.
111. Dadone-Montaudié B, Alberti L, Duc A, et al. Alternative PDGFD rearrangements in dermatofibrosarcomas protuberans without PDGFB fusions. *Mod Pathol*. 2018;31:1683–1693.
112. Dickson BC, Hornick JL, Fletcher CDM, et al. Dermatofibrosarcoma protuberans with a novel COL6A3-PDGFD fusion gene and apparent predilection for breast. *Genes Chromosomes Cancer*. 2018;57:437–445.
113. Hiraki-Hotokebuchi Y, Yamada Y, Kohashi K, et al. Alteration of PDGFRβ-Akt-mTOR pathway signaling in fibrosarcomatous transformation of dermatofibrosarcoma protuberans. *Hum Pathol*. 2017;67:60–68.
114. Gloster Jr HM, Harris KR, Roenigk RK. A comparison between Mohs micrographic surgery and wide surgical excision for the treatment of dermatofibrosarcoma protuberans. *J Am Acad Dermatol*. 1996;35:82–87.
115. Mentzel T, Beham A, Katenkamp D, et al. Fibrosarcomatous ("high-grade") dermatofibrosarcoma protuberans: clinicopathologic and immunohistochemical study of a series of 41 cases with emphasis on prognostic significance. *Am J Surg Pathol*. 1998;22:576–587.
116. Navarrete-Dechent C, Mori S, Barker CA, et al. Imatinib treatment for locally advanced or metastatic dermatofibrosarcoma protuberans. *JAMA Dermatol*. 155:361–369.
117. Jha P, Moosavi C, Fanburg-Smith JC. Giant cell fibroblastoma: an update and addition of 86 new cases from the Armed Forces Institute of Pathology, in honor of Dr. Franz M Enzinger. *Ann Diagn Pathol*. 2007;11:81–88.
118. Harvell JD, Kilpatrick SE, White WL. Histogenetic relations between giant cell fibroblastoma and dermatofibrosarcoma protuberans. CD34 staining showing the spectrum and a simulator. *Am J Dermatopathol*. 1998;20:339–345.
119. Simon MR, Pedeutour F, Sirvent N, et al. Deregulation of the platelet-derived growth factor B-chain gene via fusion with collagen gene *COL1A1* in dermatofibrosarcoma protuberans and giant-cell fibroblastoma. *Nat Genet*. 1997;15:95–98.
120. Shmookler BM, Enzinger FM, Weiss SW. Giant cell fibroblastoma. A juvenile form of dermatofibrosarcoma protuberans. *Cancer*. 1989;64:2154–2161.
121. Yamazaki F, Nakatani F, Asano N, et al. Novel NTRK3 fusions in fibrosarcomas of adults. *Am J Surg Pathol*. 2019;43:523–530.
122. Soule EH, Pritchard DJ. Fibrosarcoma in infants and children: a review of 110 cases. *Cancer*. 1977;40: 1711–1721.
123. Scott SM, Reiman HM, Pritchard DJ, Ilstrup DM. Soft tissue fibrosarcoma. A clinicopathologic study of 132 cases. *Cancer*. 1989;64:925–931.
124. Wiklund TA, Blomqvist CP, Raty J, et al. Postirradiation sarcoma. Analysis of a nationwide cancer registry material. *Cancer*. 1991;68:524–531.
125. Meis-Kindblom JM, Kindblom LG, Enzinger FM. Sclerosing epithelioid fibrosarcoma. A variant of fibrosarcoma simulating carcinoma. *Am J Surg Pathol*. 1995;19:979–993.
126. Doebele RC, Drilon A, Paz-Ares L, et al. Entrectinib in patients with advanced or metastatic NTRK fusion-positive solid tumours: integrated analysis of three phase 1–2 trials. *Lancet Oncol*. 2020;21:271–282.
127. Laetsch TW, DuBois SG, Mascarenhas L, et al. Larotrectinib for paediatric solid tumours harbouring NTRK gene fusions: phase 1 results from a multicentre, open-label, phase 1/2 study. *Lancet Oncol*. 2018;19:705–714.
128. Guillou L, Wadden C, Coindre JM, et al. "Proximal-type" epithelioid sarcoma, a distinctive aggressive neoplasm showing rhabdoid features. Clinicopathologic, immunohistochemical, and ultrastructural study of a series. *Am J Surg Pathol*. 1997;21:130–146.
129. Chase DR, Enzinger FM. Epithelioid sarcoma. Diagnosis, prognostic indicators, and treatment. *Am J Surg Pathol*. 1985;9:241–263.
130. Hornick JL, Dal Cin P, Fletcher CD. Loss of INI1 expression is characteristic for both conventional and proximal-type epithelioid sarcoma. *Am J Surg Pathol*. 2009;33:542–550.
131. Callister MD, Bailo MT, Pisters PW, et al. Epithelioid sarcoma: results of conservative surgery and radiotherapy. *Int J Radiat Oncol Biol Phys*. 2001;51:384–391.
132. Evans HL, Baer SC. Epithelioid sarcoma: a clinicopathologic and prognostic study of 26 cases. *Semin Diagn Pathol*. 1993;10:286–291.
133. Gounder M, Schöffski P, Jones RL, et al. Tazemetostat in advanced epithelioid sarcoma with loss of INI1/SMARCB1: an international, open-label, phase 2 basket study. *Lancet Oncol*. 2020;11:1423–1432.



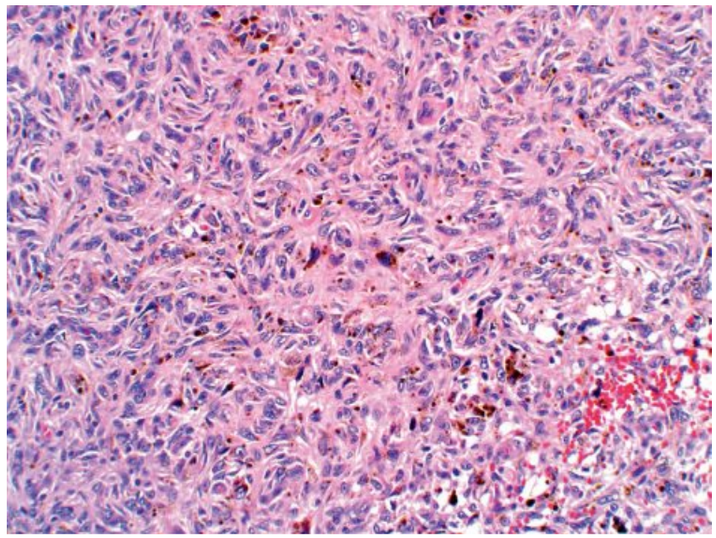
eFig. 116.1 Infarcted skin tag. A pedunculated dark-red papule in the axilla.



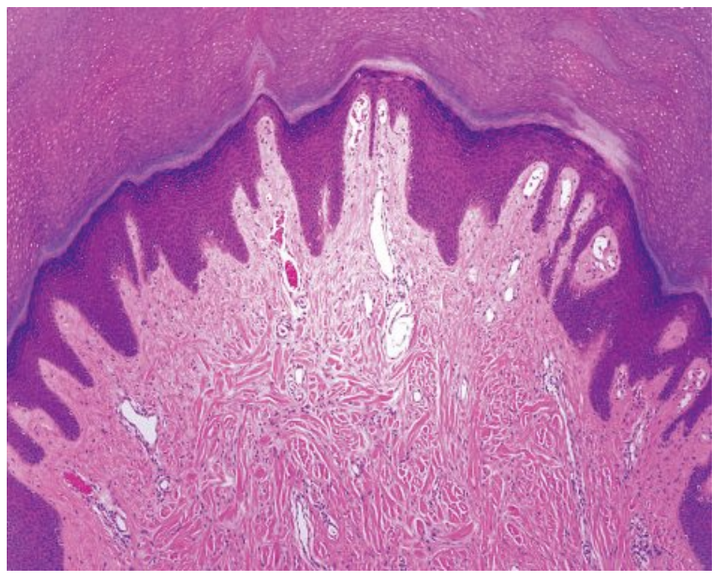
eFig. 116.2 Facial angiofibromas of tuberous sclerosis. There are multiple firm papules on the nose and cheek.



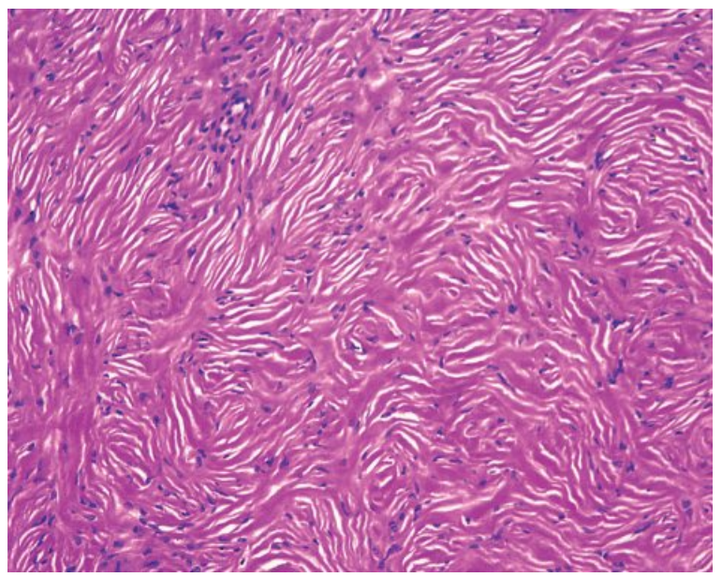
eFig. 116.3 Dermatofibroma. Hyperpigmented firm papule on the lower extremity. *Courtesy Jean L. Bolognia, MD.*



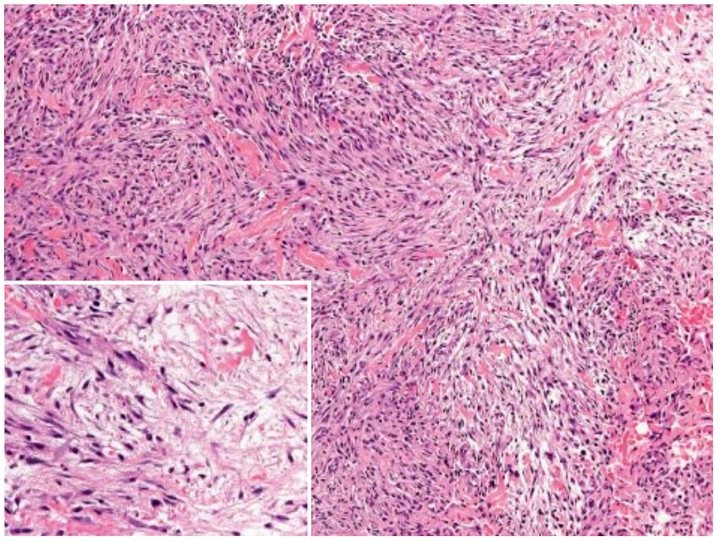
eFig. 116.4 Dermatofibroma, sclerosing hemangioma pattern. In addition to plump fibroblasts and blood vessels, there are extravasated red blood cells and abundant hemosiderin pigment. *Courtesy Hideko Kamino, MD.*



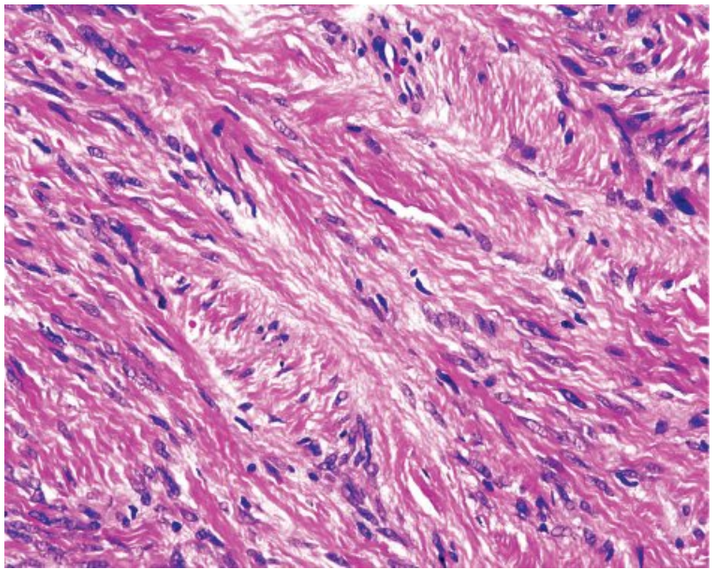
eFig. 116.5 Acral fibrokeratoma. There is a digitated fibrovascular core with vertically arranged collagen bundles lined by epidermal hyperplasia. Note the thick stratum corneum. *Courtesy Hideko Kamino, MD.*



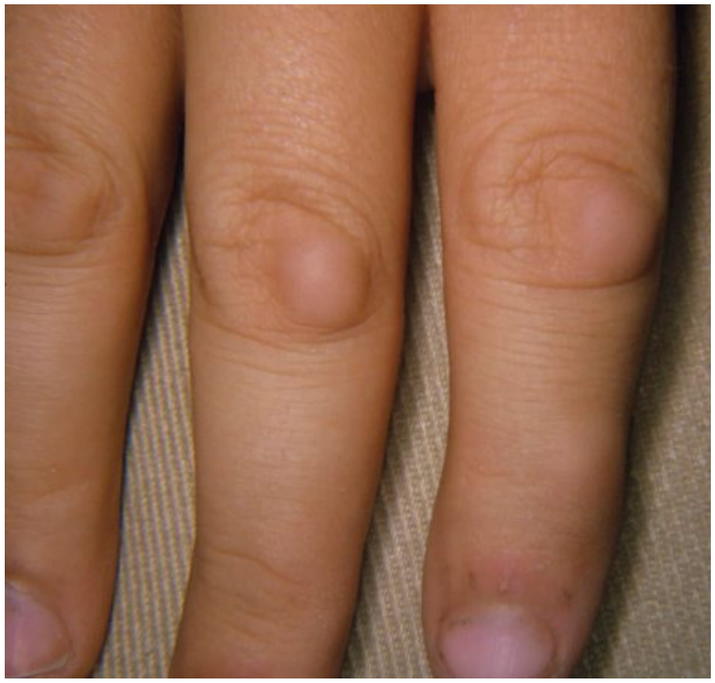
eFig. 116.6 Sclerotic fibroma. The collagen bundles in this hypocellular tumor are arranged in short parallel bundles, leading to a laminated or "plywood" appearance. *Courtesy Hideko Kamino, MD.*



eFig. 116.7 Nodular fasciitis. Proliferation of spindle-shaped and plump fibroblasts arranged in a haphazard array with focally myxoid stroma. The plump and spindle-shaped fibroblasts within the myxoid stroma have a vague "tissue culture-like" appearance (inset). *Courtesy Lorenzo Cerroni, MD.*



eFig. 116.8 Fibromatosis. Slender spindle-shaped fibroblasts and collagen strands are arranged in broad sweeping fascicles. *Courtesy Hideko Kamino, MD.*



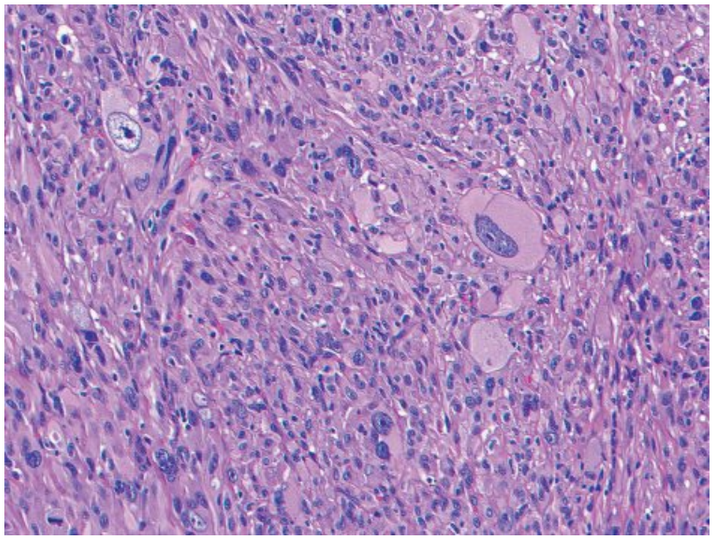
eFig. 116.9 Knuckle pads. Skin-colored papules overlying the medial distal interphalangeal joints. There is a reduction in surface skin lines.



eFig. 116.10 Atypical fibroxanthoma. A purplish exophytic nodule on the lateral cheek of an elderly man.



eFig. 116.11 Atypical fibroxanthoma. A red, dome-shaped nodule on the nose of an elderly man. *Courtesy Lorenzo Cerroni, MD.*



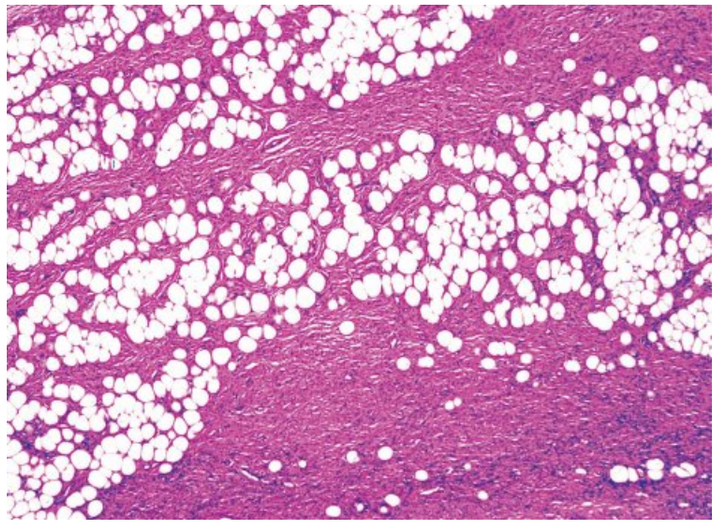
eFig. 116.12 Atypical fibroxanthoma. A markedly sarcomatous tumor pattern with tumor cells of various sizes and shapes that have hyperchromatic and pleomorphic nuclei. While an identical pattern may be encountered in pleomorphic dermal sarcoma/undifferentiated pleomorphic sarcoma of skin, deep subcutaneous invasion, necrosis, and/or lymphovascular or perineural invasion points to the latter.



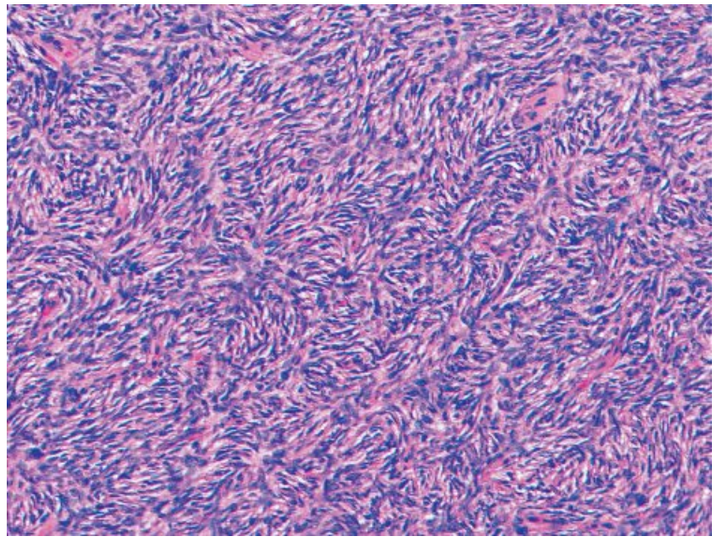
eFig. 116.13 Atrophic dermatofibrosarcoma protuberans (DFSP) in a boy with adenosine deaminase-associated severe combined immunodeficiency (ADA-SCID). Brown plaque with central elevation overlying the clavicle. The patient had two additional DFSP tumors with a similar appearance. *Courtesy Edward Cowen, MD.*



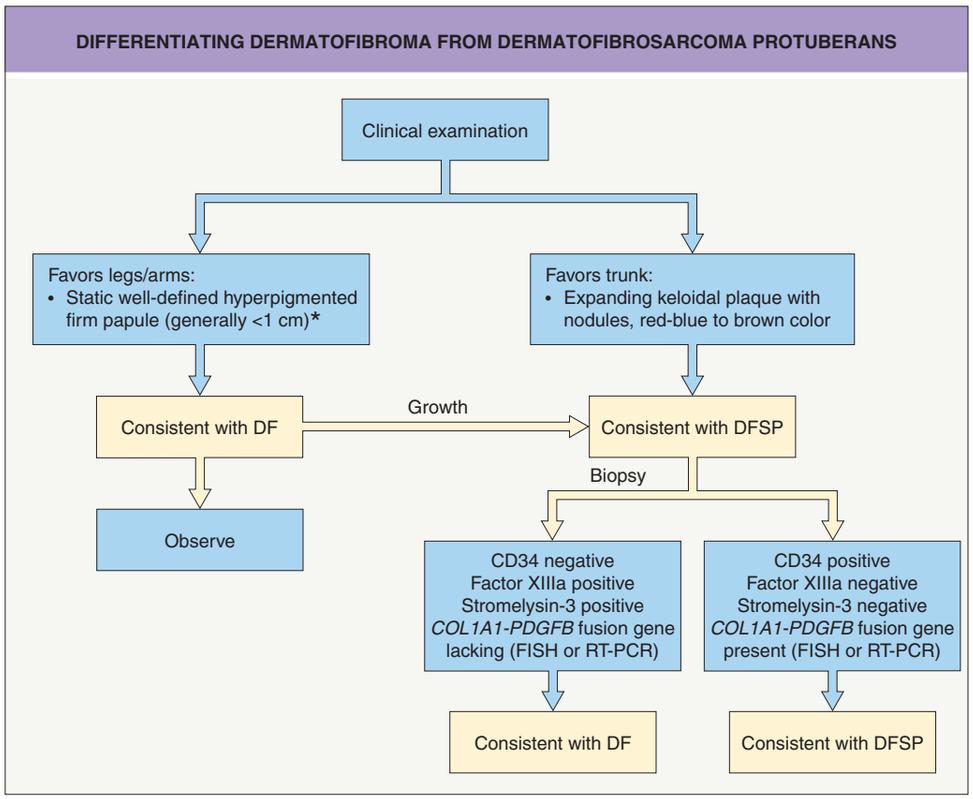
eFig. 116.14 Dermatofibrosarcoma protuberans. A broad red–brown plaque on the abdomen, with a superimposed nodule.



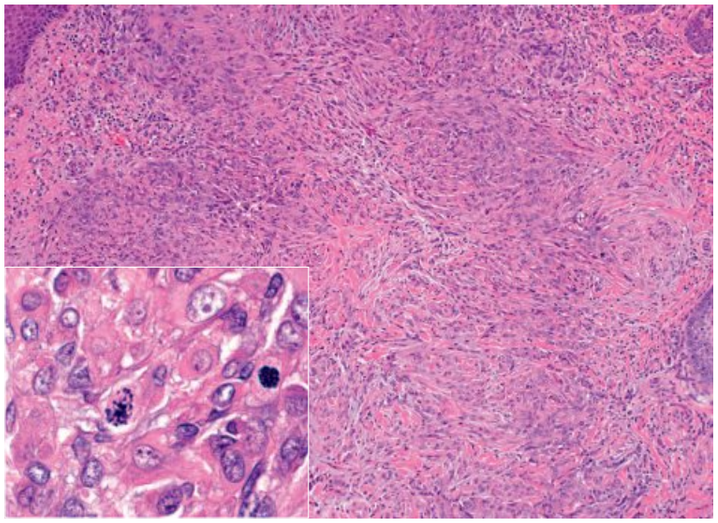
eFig. 116.15 Dermatofibrosarcoma protuberans. At the base of the tumor, the neoplastic cells infiltrate the subcutaneous tissue to produce a honeycomb pattern. *Courtesy Hideko Kamino, MD.*



eFig. 116.16 Dermatofibrosarcoma protuberans. The spindle-shaped cells are arranged in a "storiform" pattern.



eFig. 116.17 Differentiating dermatofibroma (DF) from dermatofibrosarcoma protuberans (DFSP). At the periphery of dermatofibromas, there may be an increased number of $CD34^{+}$ cells, most likely representing pre-existing dendritic cells that were displaced by the cells of the dermatofibroma. *In patients with skin phototype I, it may be pink in color. FISH, fluorescent *in situ* hybridization; RT-PCR, reverse transcription polymerase chain reaction.



eFig. 116.18 Epithelioid sarcoma. Palisading of atypical epithelioid cells. Pleomorphism and mitoses are present (inset). *Courtesy Lorenzo Cerroni, MD.*

THE DERMAL DENDROCYTE HAMARTOMAS					
	Epidemiology*	**Most common site**	**Clinical presentation**	**Pathology**	**Immunophenotype**
Fat-storing hamartoma of dermal dendrocytes	Congenital 1 pt (male)	Lumbar‡	Single, reddish-brown plaque with nodularity	Lipidized histiocytes between collagen bundles within reticular dermis	+ Factor XIIIa (CD34 was not performed)
Dermal dendrocyte hamartoma with stubby white hair	Congenital 1 pt (female)	Back‡	Single, soft, red nodule with short white hairs	Spindle cells	+ CD34; – factor XIIIa
Congenital CD34+ granular cell dendrocytosis	Congenital 1 pt (male)	Face and extremities‡	Numerous skin-colored papules and plaques	"Granular cells" interstitially arranged, primarily within superficial dermis	+ CD34; – factor XIIIa
CD34+ plaque-like dermal fibroma	Congenital or acquired	Trunk, proximal extremities	Flat, round plaque 2-5 cm in diameter	Band-like proliferation of spindle cells in the superficial dermis	+ CD34; – factor XIIIa
Fibroblastic connective tissue nevus	Mostly children; F > M	Trunk > head & neck > extremities	Tan–brown to tan–white, smooth, firm nodule	Proliferation of bland intradermal fibroblastic/myofibroblastic cells	+ CD34; – factor XIIIa in two-thirds of analyzed cases

*To date.
†May require analysis for the COL1A1-PDGFB fusion gene (e.g. via fluorescence in situ hybridization [FISH]) to exclude an atrophic dermatofibrosarcoma protuberans, which can have similar clinicopathologic features (see text).
‡Based on only one reported patient.

eTable 116.1 The dermal dendrocyte hamartomas.

E-REFERENCES

e1. Yang P, Hirose T, Hasegawa T, et al. Aneurysmal fibrous histiocytoma of the skin. A histological, immunohistochemical, and ultrastructural study. *Am J Dermatopathol*. 1995;17:179–184.
e2. Fukamizu H, Oku T, Inoue K, et al. Atypical ("pseudosarcomatous") cutaneous histiocytoma. *J Cutan Pathol*. 1983;10:327–333.
e3. Leyva WH, Santa Cruz DJ. Atypical cutaneous fibrous histiocytoma. *Am J Dermatopathol*. 1986;8:467–471.
e4. Tamada S, Ackerman AB. Dermatofibroma with monster cells. *Am J Dermatopathol*. 1987;9:380–387.
e5. Kaddu S, McMenamin ME, Fletcher CD. Atypical fibrous histiocytoma of the skin: clinicopathologic analysis of 59 cases with evidence of infrequent metastasis. *Am J Surg Pathol*. 2002;26:35–46.
e6. Doyle LA, Fletcher CD. Metastasizing "benign" cutaneous fibrous histiocytoma: a clinicopathologic analysis of 16 cases. *Am J Surg Pathol*. 2013;37:484–495.
e7. Mentzel T, Wiesner T, Cerroni L, et al. Malignant dermatofibroma: clinicopathological, immunohistochemical, and molecular analysis of seven cases. *Mod Pathol*. 2013;26:256–267.
e8. Wilson Jones E, Cerio R, Smith NP. Epithelioid cell histiocytoma: a new entity. *Br J Dermatol*. 1989;120:185–195.
e9. Dezfoulian B, Nikkels AF, Pierard-Franchimont C, Pierard GE. Epithelioid cell histiocytoma: a report of two cases. *Dermatology*. 1995;190:349–350.
e10. Mentzel T, Kutzner H, Rütten A, Hügel H. Benign fibrous histiocytoma (dermatofibroma) of the face: clinicopathologic and immunohistochemical study of 34 cases associated with an aggressive clinical course. *Am J Dermatopathol*. 2001;23:419–426.
e11. Iwata J, Fletcher CD. Lipidized fibrous histiocytoma: clinicopathologic analysis of 22 cases. *Am J Dermatopathol*. 2000;22:126–134.

117 Smooth Muscle, Adipose, and Cartilage Neoplasms

Steven Kaddu

Chapter Contents

Leiomyoma 2116
Leiomyosarcoma 2119
Smooth Muscle Hamartoma 2121
Lipoma 2122
Angiolipoma 2124
Spindle Cell/Pleomorphic Lipoma 2124
Hibernoma 2125
Nevus Lipomatosus Superficialis 2126
Lipoblastoma/Lipoblastomatosis 2127
Atypical Lipomatous Tumor/Liposarcoma 2127
Extraskeletal Chondroma 2129

INTRODUCTION

Smooth muscle, adipose, and cartilage neoplasms arising in the skin and subcutis comprise a wide spectrum of benign and malignant neoplasms that show myocyte, adipocyte, and chondrocyte differentiation, respectively. Tumors of fat, especially lipomas, occur most commonly. These neoplasms often present as solitary lesions with significant overlap in clinical appearance. In addition, the clinical differential diagnosis can be rather broad (Fig. 117.1). As with other cutaneous tumors, multiple lesions raise the possibility of an inherited disease (e.g. hereditary leiomyomatosis and renal cell cancer).

In this group of neoplasms, the histopathologic diagnosis is established primarily on the basis of characteristic morphologic features, including architecture and cytomorphology, as well as identification of the predominant direction and level of differentiation (Fig. 117.2). Determination of whether a tumor is benign or malignant also requires assessment of features such as circumscription and if atypia and increased mitotic activity are present. Great care is necessary when applying traditional morphologic criteria for malignancy to cutaneous mesenchymal neoplasms because some clinically less aggressive tumors may exhibit prominent atypical features. In other words, aggressive behavior is not always predictable based solely on morphologic findings. For several of these neoplasms, immunohistochemical studies provide helpful diagnostic information (Table 117.1). Cytogenetic analysis and molecular studies are increasingly being used for diagnosis and classification of many soft tissue tumors as there can be relatively histiotype-specific molecular features (see below).

A number of tumor-related and patient-related factors may influence the choice of treatment, including tumor type and size, anatomic location, patient's life expectancy, presence of comorbidities, and cosmetic concerns. For the majority of solitary, benign, or relatively non-aggressive malignant neoplasms, excisional surgery with clear margins is the treatment of choice. However, removal of a benign tumor is often done at the patient's request rather than for medical reasons. Other modalities, e.g. cryotherapy, laser ablation (multiple leiomyomas), liposuction (large lipomas), may be preferable in certain patients. For more aggressive malignant tumors, the therapeutic goal is complete eradication, via either wide local excision or Mohs micrographic surgery, while trying to preserve normal function and avoiding mutilating surgery. As expected, the most significant predictor of recurrences is surgical margin status. In some dermal sarcomas, extension into the subcutis represents a negative prognostic factor.

TUMORS OF SMOOTH MUSCLE

Leiomyoma

Synonyms: ■ Superficial leiomyoma ■ Leiomyoma cutis ■ Superficial benign smooth muscle tumor

Key features

- Three distinct variants: piloleiomyoma, genital leiomyoma, and angioleiomyoma
- A solitary or multiple clustered (piloleiomyomas) papules or nodules in an adult
- Piloleiomyomas and angioleiomyomas may be painful
- Multiple piloleiomyomas may be a manifestation of hereditary leiomyomatosis and renal cell cancer (Reed syndrome)
- Smooth muscle cells (myocytes) are fusiform cells with centrally located, cigar-shaped nuclei

Introduction

Superficial (cutaneous) leiomyomas represent benign smooth muscle tumors that can arise from: (1) arrector pili muscles; (2) the dartoic, vulvar, or mammary smooth muscles; or (3) the muscles enveloping dermal blood vessels. Thus, they are subclassified into piloleiomyomas (solitary or multiple), leiomyomas of the external genitalia, and angioleiomyomas. Some authors categorize vulvar and scrotal leiomyomas separately, based upon distinctive clinical and histologic features[1].

History

In an early review article, Arthur Purdy Stout[2] cites an 1854 publication of Rudolf Virchow as the first case report of multiple leiomyomas involving the skin near the areola in a 32-year-old man.

Epidemiology

Cutaneous leiomyomas are relatively uncommon neoplasms, but their exact incidence is not known[3]. Angioleiomyomas appear to be more common than piloleiomyomas[4], with genital leiomyomas being the least common variant.

Pathogenesis

The exact pathogenesis of superficial leiomyomas has yet to be determined. Piloleiomyomas are thought to arise from the smooth muscle cells within the arrector pili muscle of the folliculosebaceous unit. Leiomyomas of the external genitalia are probably derived from the network of smooth muscles in the external genitalia (e.g. scrotum, vulva) and areolae. Angioleiomyomas are believed to originate from the smooth muscle within the walls of arteries and veins. However, there is a morphologic spectrum that encompasses angioleiomyoma and myopericytoma. Angioleiomyomas may exhibit cytogenetic abnormalities including monosomy of chromosome 13 and loss of 6p, 21q, and 13q, as well as *NOTCH2* rearrangement.

Multiple piloleiomyomas may occur sporadically or they may be inherited in an autosomal dominant manner (with variable penetrance) as a component of hereditary leiomyomatosis and renal cell cancer (HLRCC), also referred to as Reed syndrome, in which patients have multiple cutaneous leiomyomas and uterine leiomyomatosis as well as renal cell cancer[5,6] (Table 117.2). Affected individuals are heterozygous for germline loss-of-function mutations in the fumarate hydratase gene

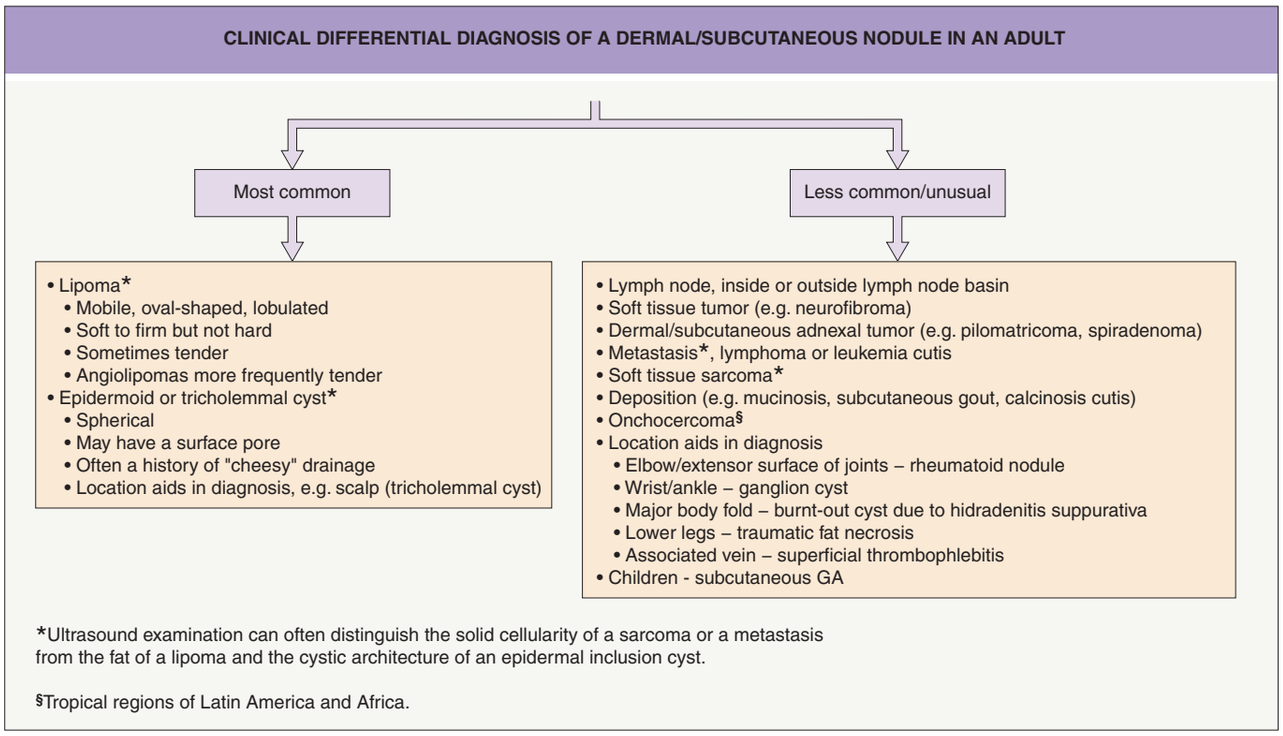


Fig. 117.1 Clinical differential diagnosis of a dermal/subcutaneous nodule in an adult. GA, granuloma annulare.

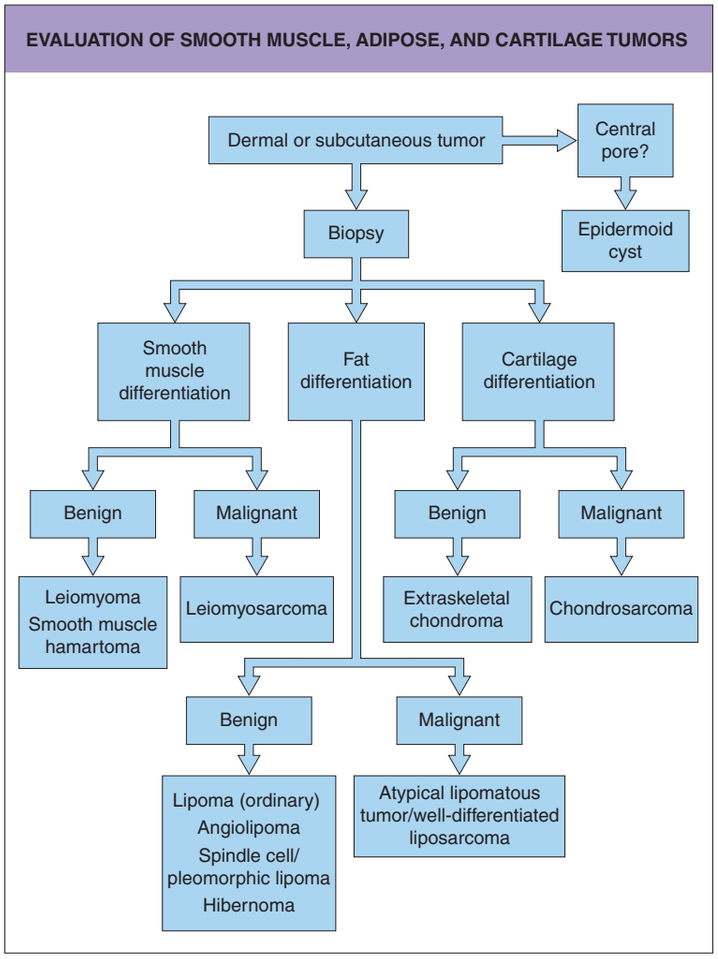


Fig. 117.2 Evaluation of smooth muscle, adipose, and cartilage tumors.

(*FH*). Although the molecular basis of HLRCC is known, how this translates into smooth muscle tumors is not understood.

Multifocal subcutaneous leiomyomas arising in the setting of immunodeficiency, including HIV infection, may be associated with Epstein–Barr virus infection.

Clinical features

Piloleiomyomas can be solitary or multiple, and in an occasional patient may even number in the hundreds. They present as firm, reddish-brown to skin-colored papules or nodules. Solitary piloleiomyomas develop primarily during adulthood and there is an approximately equal sex distribution[7]; rare congenital or pediatric cases have been reported. When multiple, the distribution pattern is most often clustered (Fig. 117.3), linear, or along the lines of Blaschko, but widespread lesions are observed occasionally. Most piloleiomyomas measure 1–2 cm in diameter, and they usually develop on the extremities and trunk (especially the shoulder), with solitary lesions favoring the limbs and multiple lesions the trunk[7]. Piloleiomyomas are often associated with spontaneous or induced pain, e.g. following cold exposure, but the explanation is still unclear[7].

Genital leiomyomas are most often solitary and painless. They can develop on the vulva, penis, scrotum, nipple, or areola and usually measure less than 2 cm in diameter. Occasionally, lesions are pedunculated.

Angioleiomyomas most commonly present as a solitary, firm subcutaneous nodule on the lower extremity. They often develop in women during the fourth to sixth decades of life[4]. Approximately 50% of angioleiomyomas are painful.

Pathology

Piloleiomyomas are typically centered within the reticular dermis, with focal extension into the subcutaneous fat in some cases. They are composed of interlacing fascicles of relatively bland smooth muscle cells (myocytes), which peripherally tend to ramify between surrounding dermal collagen bundles (Fig. 117.4); often there is a close relationship to hair follicles[4]. Occasionally, the overlying epidermis is hyperplastic. Smooth muscle cells have abundant brightly eosinophilic cytoplasm and blunt-ended, cigar-shaped nuclei.

Mitotic figures are rare. In the presence of bland cytology, one or two morphologically normal mitotic figures per 10 high-power fields may be seen, which does not signify aggressive behavior. Cases with

IMMUNOHISTOCHEMISTRY OF SELECTED SMOOTH MUSCLE, ADIPOSE, AND CARTILAGE NEOPLASMS		
Neoplasm	**Cell type(s)**	**Stain(s)**
Leiomyoma	Myocytes	• Smooth muscle actin (SMA) + [more sensitive], desmin + [more specific] • If diagnostic dilemma, h-caldesmon +, calponin +, muscle actin (HHF35) +, smooth muscle myosin (SMM) +
Leiomyosarcoma	Myocytes	• SMA +, desmin + (may be –) • If diagnostic dilemma, h-caldesmon +, calponin +, muscle actin (HHF35) +, SMM + • Pitfall: cytokeratin + (some cases)
Lipoma	Adipocytes	• S100 + • Adipophilin –
Angiolipoma	Adipocytes, endothelial cells	• S100 + (adipocytes) • CD34 +, CD31 + (vascular component)
Spindle cell/pleomorphic lipoma	Spindle and multinucleated giant cells, adipocytes	• CD34 + (spindle and multinucleated giant cells) • S100 + (adipocytes)
Hibernoma	Adipocytes, spindle cells	• S100 +, CD31 + (adipocytes) • CD34 + (spindle cells)
Lipoblastoma/ lipoblastomatosis	Adipocytes	• S100 +
Atypical lipomatous tumor/liposarcoma	Adipocytes, adipoblasts	• MDM2, CDK4 and p16 staining depends upon histologic subtype (see Table 117.4 & Fig. 117.19) • CD10 + in ~20%
Extraskeletal chondroma	Chondrocytes	• S100 +

Table 117.1 Immunohistochemistry of selected smooth muscle, adipose, and cartilage neoplasms. When the neoplasm is easily recognizable, e.g. lipoma, immunohistochemical staining is not routinely done. Myofibroblasts can be SMA +, SMM +, and calponin +; fibroblasts can be SMA +. CDK4, cyclin-dependent kinase 4 (cell cycle regulation); h, high molecular weight; MDM2 (binds p53).

CLINICAL FEATURES OF HEREDITARY LEIOMYOMATOSIS AND RENAL CELL CANCER (REED SYNDROME)	
Genetic aspects	• Autosomal dominant • Mutations in the gene on chromosome 1q42.3-43 that encodes fumarate hydratase, an enzyme in the mitochondrial Krebs cycle
Clinical features	• Cutaneous leiomyomas: multiple painful, grouped, skin-colored to red–brown papules appear during the second to fourth decades • Uterine leiomyomas: >90% of affected women; menorrhagia and pelvic pressure or pain • Renal cell carcinoma: 10%–15% of patients with syndrome; most commonly type 2 papillary renal cell carcinomas that are often early-onset and aggressive (metastases in >50% of patients); less often tubulo-papillary or collecting duct carcinomas
Screening of individuals with multiple cutaneous leiomyomas	• Abdominal and pelvic ultrasound (or CT scan) • Complete history and physical examination, including pelvic examination in women • Immunohistochemistry of cutaneous leiomyomas: (1) negative staining for fumarate hydratase (in one series, 83% sensitivity and 75% specificity was found[9]); and (2) intracellular accumulation of S-(2-succino)-cysteine • Genetic testing for heterozygous pathogenic variant in the fumarate hydratase gene (*FH*; 70%–90% detected by sequence analysis) • If pathogenic *FH* variant not detected, can measure fumarate hydratase activity (will be ≤60%)
Patients with confirmed syndrome	• Complete history and physical examination yearly, including pelvic examination in women • Yearly abdominal MRI (if baseline or follow-up scan normal) • If renal lesion detected, then CT scan and renal ultrasound performed; PET-CT scan can be done • Complete physical examination (including pelvic examination in women) of first-degree family members and other family members as indicated; abdominal and pelvic ultrasound as indicated
Establishing diagnosis: heterozygous pathogenic variant in *FH* (rarely not detected). Clinical criteria: major criterion is multiple cutaneous leiomyomas (at least 1 confirmed histologically); minor criteria are: (1) severely symptomatic uterine leiomyomas before age 40; (2) type 2 papillary renal cell carcinoma before age 40; and (3) first-degree relative who meets one of these aforementioned criteria. Diagnosis is strongly suspected if major criterion met or ≥2 minor criteria present.	

Table 117.2 Clinical features of hereditary leiomyomatosis and renal cell cancer (Reed syndrome). CT, computed tomography; MRI, magnetic resonance imaging; PET, positron emission tomography.

nuclear pleomorphism and atypical nuclei, but without mitotic activity (symplastic leiomyomas), have also been described[8].

In leiomyomas, smooth muscle differentiation is usually obvious in H&E-stained sections, but sometimes special stains for smooth muscle cells are utilized. Tumor cells consistently stain positively for both smooth muscle actin (SMA) and desmin, with other useful markers listed in Table 117.1. In HLRCC, there is often negative immunohistochemical staining for fumarate hydratase in the cutaneous leiomyomas (in one series, 83% sensitivity/75% specificity[9]). Intracellular accumulation of S-(2-succino)-cysteine in uterine leiomyomas may suggest fumarate hydratase aberration but this is not specific for HLRCC[10]. In contrast to uterine leiomyomas, cutaneous leiomyomas do not express receptors for estrogen or progesterone[11].

Genital leiomyomas of the scrotum or vulva tend to be larger and better circumscribed than piloleiomyomas. Scrotal leiomyomas are usually homogeneous spindle cell tumors, while vulvar lesions may demonstrate an epithelioid cytology, myxoid changes, and/or hyalinization[1]. Leiomyomas of the nipple closely resemble piloleiomyomas.

Angioleiomyomas are usually well-circumscribed tumors centered within the superficial subcutis (Fig. 117.5). They are composed of bland smooth muscle cells compactly arranged into bundles and whorls around thick-walled vascular channels[4]. Degenerative changes including hyalinization, focal thrombosis, myxoid changes, dystrophic calcification, pyknotic nuclear atypia, and fat foci may be present. Tumors composed of a proliferation of blood vessels, smooth muscle cells, and adipose tissue are termed angiomyolipomas or angiolipoleiomyomas.

Differential diagnosis

For single lesions, the clinical appearance is nonspecific and the differential diagnosis includes a wide range of entities that can present as solitary dermal nodules, including dermatofibromas. When a lesion is painful or there is a clustering of multiple red–brown papulonodules, the diagnosis may be strongly suspected prior to biopsy.

Histopathologically, leiomyomas need to be distinguished from other spindle cell tumors with fibrohistiocytic or peripheral nerve sheath differentiation.



Fig. 117.3 Clustered piloleiomyomas on the back. The trunk is a common location for multiple piloleiomyomas. Patients with this clinical presentation need to be evaluated for the possibility of hereditary leiomyomatosis and renal cell cancer (Reed syndrome; see Table 117.2). *Courtesy Julie V. Schaffer, MD.*

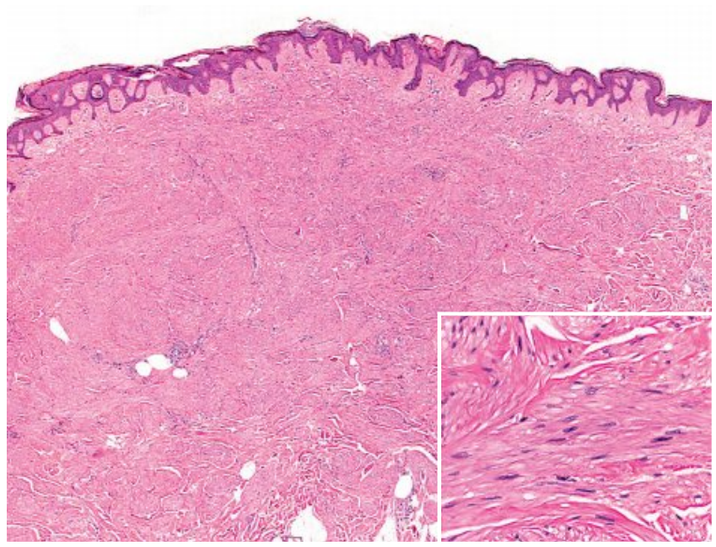


Fig. 117.4 Piloleiomyoma. Bundles of myocytes within the dermis are arranged in interdigitating fascicles. Inset, the myocytes have eosinophilic cytoplasm and elongated or cigar-shaped nuclei.

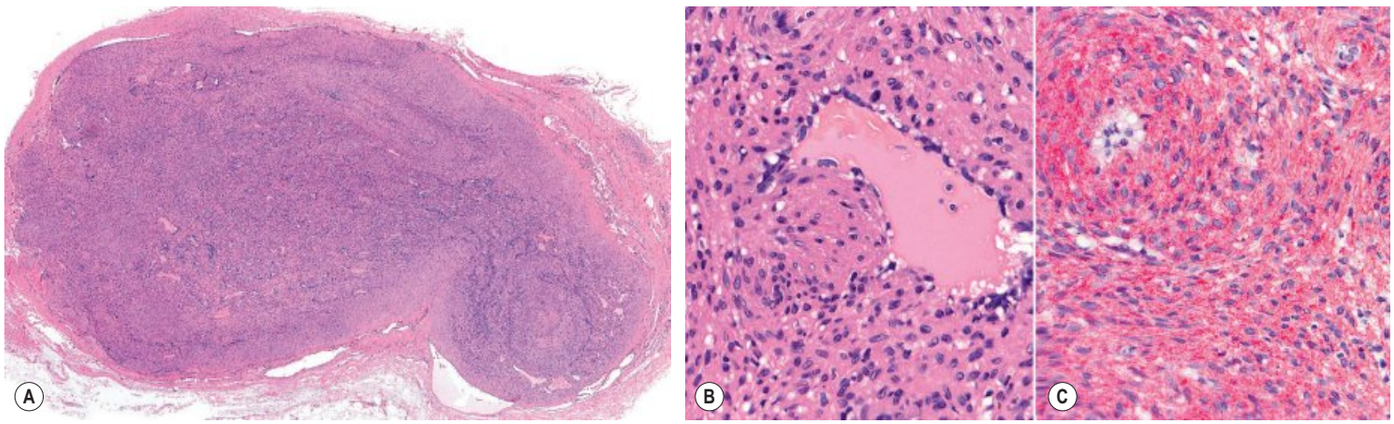


Fig. 117.5 Angioleiomyoma. A Angioleiomyomas are well circumscribed and often located in the deep dermis, extending into the subcutis. **B** At higher magnification, thick-walled vessels are surrounded by aggregates of smooth muscle cells and stain positively for smooth muscle actin (**C**).

Treatment

Simple excision is usually curative for solitary or limited tumors. For those tumors that are not amenable to surgery because of their number or location, treatment with gabapentin, medications that reduce smooth muscle contraction (e.g. nifedipine, nitroglycerin, doxazosin), cryotherapy, or CO_2 laser ablation may provide relief from pain[12,13].

Leiomyosarcoma

Synonyms: ■ Atypical intradermal smooth muscle neoplasm ■ Piloleiomyosarcoma ■ Superficial leiomyosarcoma ■ Superficial malignant smooth muscle tumor

Key features

- Malignant smooth muscle neoplasm
- Occurs primarily in adults >50 years of age
- Most commonly located on the extremities, in particular the lower leg
- *Dermal* leiomyosarcomas are typically cured by simple excision and rarely metastasize; *subcutaneous* leiomyosarcomas require wide excision and have a 25%–40% risk of metastasis

Introduction

For management and prognostic reasons, it is important to differentiate between "superficial leiomyosarcomas" that are limited to the dermis and lesions that primarily arise in or extensively involve the subcutis. The former have a favorable prognosis and can recur, but very rarely metastasize. Subcutaneous leiomyosarcomas, in contrast, metastasize in ~25%–40% of cases[14,15]. To emphasize this distinction, the term *atypical intradermal smooth muscle neoplasm* has been suggested for dermal lesions (rather than leiomyosarcoma).

Epidemiology

Cutaneous and subcutaneous leiomyosarcomas are rare neoplasms, comprising only 4%–6.5% of soft tissue sarcomas[16,17].

Pathogenesis

Dermal leiomyosarcomas are thought to arise from either arrector pili or genital smooth muscles. Subcutaneous leiomyosarcomas probably originate from vascular smooth muscle. Predispositions include Li–Fraumeni syndrome due to *TP53* mutations, retinoblastoma (RB) inactivation due to *RB1* or *CDKN2A* ($p14^{ARF}$) mutations or deletions (see Fig. 107.4), and Epstein–Barr viral infection in the setting of immunosuppression. Anecdotal reports describe a rare association with trauma and radiation[17,18].

Clinical features

Cutaneous and subcutaneous leiomyosarcomas classically present as a solitary, firm, skin-colored to red–brown nodule or plaque. Dermal



Fig. 117.6 Leiomyosarcoma. Two red–brown tumor nodules on the lower extremity. *Courtesy Lorenzo Cerroni, MD.*

tumors range from 0.5 to 4 cm in diameter[19], while subcutaneous lesions tend to be larger. Sometimes the tumors are painful or become ulcerated. Leiomyosarcomas favor the extremities, in particular the lower leg of older adults (Fig. 117.6)[4,19,20]. There is a slight male preponderance[4]. Patients with multiple tumors should be evaluated to exclude the possibility of metastases due to a primary retroperitoneal or visceral leiomyosarcoma.

Pathology

The histopathologic features of leiomyosarcomas span a morphologic continuum that, at the well-differentiated end, demonstrates an overlap with leiomyomas, while poorly differentiated lesions closely resemble atypical fibroxanthomas or "malignant fibrous histiocytomas"[21]. Leiomyosarcomas of moderate differentiation are comprised of cells that cytologically resemble normal smooth muscle cells. However, compared to leiomyomas, malignant smooth muscle tumors are more cellular, exhibit cytologic atypia, and contain easily identifiable mitotic figures (Fig. 117.7). At least focally, the spindle cells are arranged in fascicles. Cytologically, poorly differentiated leiomyosarcomas may resemble myofibroblastic or fibrohistiocytic tumors. Notably, the degree of differentiation may vary within a single tumor. Rarely, the cells have an epithelioid appearance[22].

A definitive diagnosis of leiomyosarcoma often requires adjuvant special stains and/or immunohistochemical studies to support the cell lineage. Leiomyosarcomas consistently stain positive for SMA and desmin. Of the two markers, SMA is more sensitive and desmin is somewhat more specific; additional useful markers are listed in Table 117.1. By definition, dermal leiomyosarcomas (atypical intradermal smooth muscle neoplasms) are superficial malignant neoplasms with at least 90% of the tumor confined to the dermis[23]. They are usually poorly circumscribed and are composed of spindle cells; the latter are focally arranged in fascicles that infiltrate between adjacent collagen bundles. In comparison, subcutaneous leiomyosarcomas tend to be better circumscribed and may be surrounded by a pseudocapsule of compressed tissue.

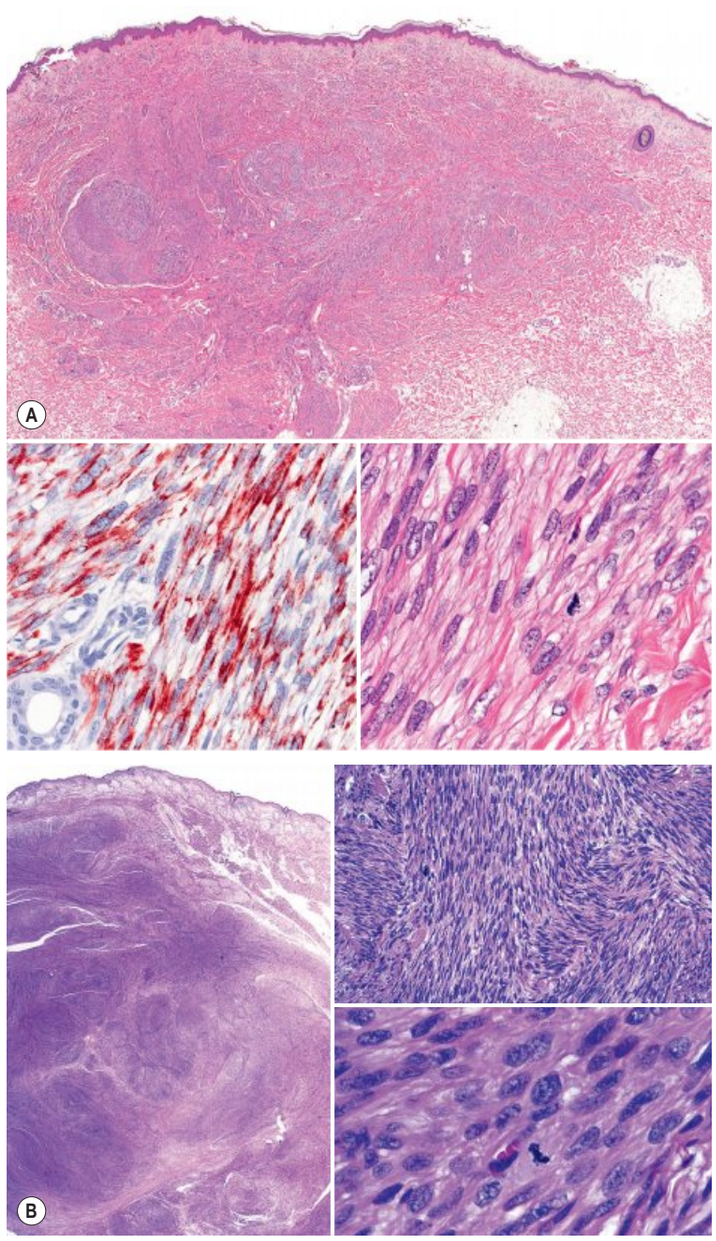


Fig. 117.7 Leiomyosarcoma – dermal versus subcutaneous. A In the superficial leiomyosarcoma, the tumor bundles are confined to the dermis, with the spindled cells staining positively for desmin and exhibiting slight nuclear pleomorphism; a mitotic figure is also seen. **B** A large tumor, composed of interdigitating fascicles, extends from the upper reticular dermis deep into the subcutis; at higher magnification, nuclei are pleomorphic and hyperchromatic. Mitotic figures are numerous and easily identified.

Differential diagnosis

Because the clinical features are not unique, the differential diagnosis includes a number of tumors that can present as solitary plaques, e.g. dermatofibrosarcoma protuberans, or firm nodules (see Fig. 117.1).

The histopathologic differential diagnosis usually raises two problems: the differentiation of leiomyosarcoma from leiomyoma and its delineation from other spindle cell neoplasms. Traditionally, the number of mitotic figures is used as the most reliable diagnostic criterion when trying to predict clinical behavior. In the presence of cytologic atypia, a mitotic rate of one or more mitotic figures per high-power field is generally considered to be indicative of malignancy[16]. It is important to remember, however, that the prognosis of leiomyosarcomas appears to depend more on the depth of involvement (dermal vs subcutaneous), and the extent of mitotic activity is probably more important in subcutaneous lesions. Necrosis and angiolymphatic invasion are generally not useful in predicting prognosis for patients with dermal and subcutaneous leiomyosarcomas.

The distinction of leiomyosarcoma from other dermal spindle cell neoplasms nearly always requires immunophenotyping. This is best approached by using a panel of antibodies that examine the neoplasm for its line of differentiation (Table 117.3). A standard panel consists of antibodies to SMA, desmin, cytokeratin, S100 protein, and CD68. Leiomyosarcoma will usually be SMA-positive and desmin-positive, but negative for keratin, S100 protein, and CD68.

Treatment

Wide excision with meticulous examination of all surgical margins is crucial in order to prevent recurrence. Recurrent tumors tend to infiltrate more deeply, and they are often less well differentiated. In addition, they are more difficult to treat and carry a higher risk of metastasis. Several authors have reported successful treatment with Mohs micrographic surgery[17], allowing for complete margin control.

Complete surgical excision of a primary dermal leiomyosarcoma can be curative. Local recurrences, due to incompletely excised tumors, are

IMMUNOHISTOCHEMICAL FINDINGS IN LEIOMYOSARCOMA RELATIVE TO OTHER SPINDLE CELL TUMORS					
	Leiomyosarcoma	**SCC**	**Melanoma**	**Nerve sheath tumors**	**AFX/PDS**
Actin	+	–	–	–	–/+
Desmin	+/–	–	–	–	–
Cytokeratin	–/+	+	–	–	–
S100 protein	–/+	–	+	+	–/+
CD68	–	–	–/+	–	+/–
h-Caldesmon	+/–	–	–	–	–
CD10	+/–	+/–	–/+	+/–	+

Table 117.3 Immunohistochemical findings in leiomyosarcoma relative to other spindle cell tumors. +, positive in >90% of cases; –, negative in >90% of cases; +/–, positive in 50%–75% of cases; –/+, usually negative but expression may be observed in up to 25% of anomalous cases. AFX, atypical fibroxanthoma; h, high molecular weight; PDS, pleomorphic dermal sarcoma; SCC, spindle cell squamous carcinoma. CD10 is also known as CALLA, common acute lymphocytic leukemia antigen; CD68 is a glycoprotein expressed by monocytes and macrophages; h-caldesmon is a calmodulin binding protein that inhibits ATPase activity of myosin.

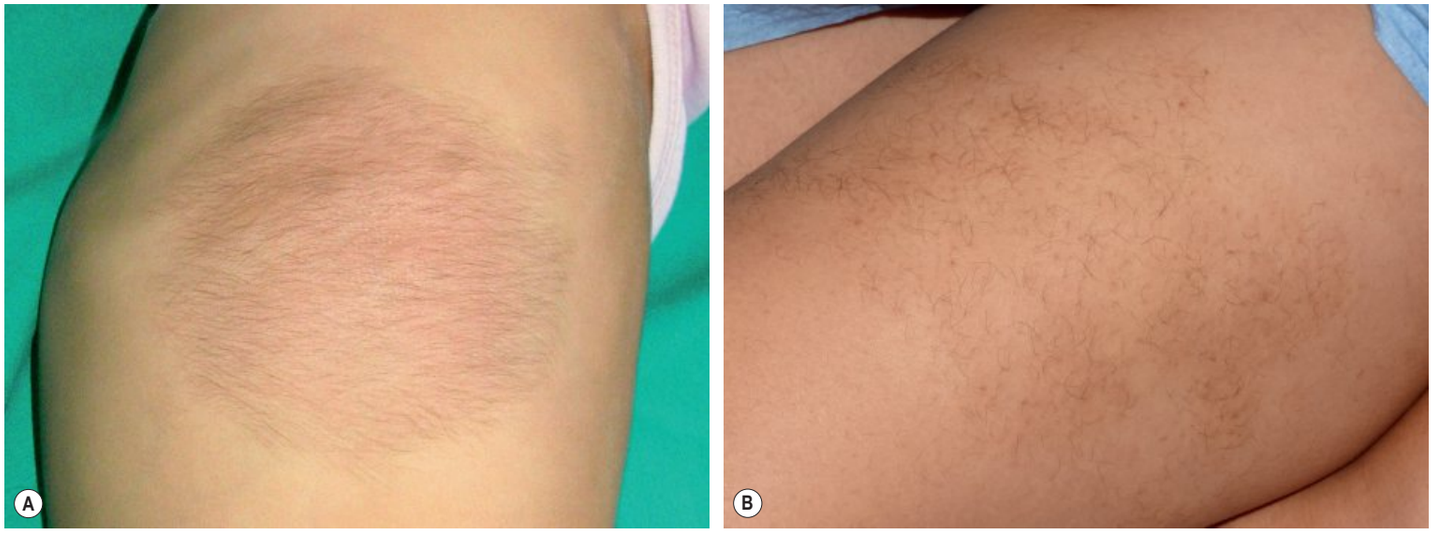


Fig. 117.8 Smooth muscle hamartoma. A A hyperpigmented plaque with hypertrichosis that can be misdiagnosed clinically as a congenital melanocytic nevus or less often a neurofibroma. **B** Sometimes the hamartoma has a broken-up appearance and there is overlap with Becker melanosis (nevus) both clinically and histologically. *A, Courtesy Antonio Torello, MD; B, Courtesy Julie V. Schaffer, MD.*

unusual and metastases rarely, if ever, develop. As noted previously, some authors have even suggested using the term "atypical intradermal smooth muscle neoplasm" rather than leiomyosarcoma[24].

Subcutaneous leiomyosarcomas metastasize in 25%–40% of patients. The risk of metastasis appears to be related to size, as metastasis is unlikely in tumors <5 cm in diameter. Metastatic spread occurs hematogenously to the lung and, less often, other visceral organs, or via the lymphatics to regional lymph nodes[18,23].

Smooth Muscle Hamartoma

Key features

- Congenital or acquired skin-colored to hyperpigmented plaque on the trunk or proximal extremities
- Commonly exhibit follicular prominence and/or hypertrichosis
- Clinical and histopathologic overlap with Becker melanosis (nevus)

Introduction

Hamartoma is derived from the Greek word *hamartia*, which means "fault", "defect", or "flaw", and *oma* (tumor). Hamartomas are defined as lesions that are: (1) most commonly present at birth, but can also be acquired; and (2) are composed of aberrant mature or nearly mature structures. The term hamartoma is synonymous with "nevus", for example, nevus sebaceus, apocrine nevus, eccrine nevus. A smooth muscle hamartoma may be congenital or acquired and may be associated with Becker melanosis (nevus).

History

The first description of a smooth muscle hamartoma is attributed to Stokes in 1923[25].

Epidemiology

The estimated incidence ranges from 1 : 1000 to 1 : 27 000 live births.

Clinical features

Smooth muscle hamartomas not associated with Becker melanosis (nevus) present as firm, skin-colored or hyperpigmented plaques, most commonly located on the trunk, buttocks, or proximal extremities (Fig. 117.8). Surface changes may be present in the form of small follicular papules or hypertrichosis. Lesions with hypertrichosis and hyperpigmentation overlap with Becker melanosis (see Ch. 112). These hamartomas are most often solitary, but may be multiple. Extensive lesions can present as large areas of hypertrichotic skin with dimpling (accentuated upon exposure to cold) and/or folding, and generalized involvement may produce a "Michelin tire baby" phenotype (see Table 97.7)[26]. Rubbing of the plaque may result in a pseudo-Darier sign, consisting of transient induration of the affected area.

Pathology

Well-defined and thickened bundles of smooth muscle are haphazardly distributed throughout the dermis. Connections with hair follicles may

be present. The epidermis is often acanthotic and has hyperpigmentation of the basal layer.

Differential diagnosis

Clinically and histologically, smooth muscle hamartomas demonstrate overlap with Becker melanosis, and the two lesions possibly represent a spectrum of phenotypic expression of the same process. Leiomyomas usually present as papulonodules rather than plaques. Histologically, the smooth muscle fibers in a piloleiomyoma aggregate to form dermal tumors with irregular margins, but they are not haphazardly scattered throughout the dermis as in a smooth muscle hamartoma.

Treatment

Therapy may be indicated for cosmetic reasons. A small lesion may be amenable to excision. Treatment of Becker melanosis with lasers that target melanin (e.g. Q-switched ruby laser) lead to modest, if any, improvement[27]. Photoepilation of pigmented hairs via laser therapy is usually more successful (see Ch. 137).

TUMORS OF FAT

Lipoma

Key features

- Common benign tumor of mature fat
- Asymptomatic, soft to rubbery, subcutaneous nodule arising at any site but rare on the hands and feet
- Multiple lipomas are seen in familial multiple lipomatosis, Madelung disease, adiposis dolorosa, Gardner syndrome, PTEN hamartoma tumor syndrome, and Proteus syndrome

Introduction

(Ordinary) lipomas are benign tumors composed of mature adipocytes. They are among the most common neoplasms in humans, and they represent the most common mesenchymal neoplasm[28]. Lipomas are often solitary, but 5%–10% of patients have multiple lipomas, usually in the setting of a lipomatosis or less often a multisystem syndrome.

Epidemiology

Lipomas develop at any age, but they usually become clinically apparent between the fourth and sixth decades of life. Most studies report the incidence of lipomas to be slightly higher in men than in women[28].

Pathogenesis

Little is known about the pathogenesis of lipomas. Of note, the incidence of lipomas is increased in overweight individuals, diabetics, and patients with elevated serum cholesterol[28]. In familial multiple lipomatosis, there is clearly a genetic component. In approximately two-thirds of patients, clonal chromosomal aberrations are present (Table 117.4).

Clinical features

Classically, lipomas present as solitary, painless, soft (to rubbery), mobile, subcutaneous nodules, with a normal overlying epidermis[4]. They are often oval in shape and may feel multilobular. Most lipomas measure a few centimeters in diameter, but occasionally reach over 10 cm in size. Although lipomas may develop within any fatty tissue, sites of predilection are the neck, proximal extremities, forearms, and buttocks; lipomas also occur on the trunk, but are very rarely seen on the hands and feet. They present primarily in adults over the age of 30 years.

Lipomas usually exhibit an initial slow growth phase, then remain stable in size with no tendency to involute. The rate of growth may accelerate during periods of weight gain, but weight loss, even when extreme, does not seem to affect their size. Weight loss, however, may result in lipomas becoming more clinically apparent.

Multiple lipomas may be observed in patients with a lipomatosis or in the setting of a multisystem syndrome, such as Proteus syndrome.

Infiltrating or diffuse lipomatosis is characterized by non-encapsulated mature fat infiltrating subcutaneous tissue, muscle, skin, and, at times, even fascia and bone. This entity usually occurs before 30 years of age and is rarely congenital. Diffuse lipomatosis has been described

ADIPOSE NEOPLASMS – CYTOGENETIC ABNORMALITIES, IMMUNOHISTOCHEMICAL STAINING, AND FISH

Neoplasm	Cytogenetic abnormalities	IHC staining (%)		FISH*	
		MDM2	CDK4	MDM2	CDK4
Lipoma	12q13–15 structural rearrangements (usually translocations) 6p21–33 structural rearrangement of band 13q deletions Supernumerary ring chromosomes	0–4	0–2	–	–
Angiolipoma	Rarely rearrangements of chromosome 13 Activating *PIK3CA* mutations (see text)	0	0	–	–
Spindle cell/pleomorphic lipoma	13q (partial loss, monosomy) 16q (partial loss, monosomy)	0–25	0–6	–	–
Hibernoma	11q13–21; 10q22 (rearrangements)	0	0	NA	NA
Lipoblastoma/lipoblastomatosis	8q11–13 (rearrangements)† Polysomy 8†	0	0	NA	NA
Liposarcomas					
Atypical lipomatous tumor/well-differentiated liposarcoma (see Fig. 117.19C)	12q13–15 amplification in the form of supernumerary ring and giant chromosomes 12q15–24 duplications	**45–100**	**85–90**	**90–100**	**75–100**
Dedifferentiated liposarcoma	12q13–15 amplification in the form of supernumerary ring chromosomes (this region contains *MDM2*, *CDK4*, *HMGA2*, and *SAS*)	**55–95**	**90–100**	**100**	**100**
Myxoid or round cell liposarcoma	12;16 translocations – lead to FUS–DDIT3 fusion oncoprotein	0–4	0–4	20	NA
Pleomorphic liposarcoma	Variable and complex	0	0	NA	NA

*To detect gene amplification; quantitative PCR can also be done and similar results are obtained for atypical lipomatous tumors and dedifferentiated liposarcomas.
†Leads to overexpression of *PLAGI* which is located on 8q12.

Table 117.4 Adipose neoplasms – cytogenetic abnormalities, immunohistochemical staining, and fluorescent *in situ* hybridization (FISH). Both atypical lipomatous tumors and dedifferentiated liposarcomas also stain positively for p16 (>80%). CDK4, cyclin-dependent kinase 4 (cell cycle regulation); DDIT3, DNA-damage-inducible transcript 3; FUS (RNA binding protein); HMGA2 (transcription factor); IHC, immunohistochemical; MDM2 (binds p53); PLAG1, pleomorphic adenoma gene 1 (transcription factor); NA, not available; SAS, member transmembrane 4 superfamily. More common findings by IHC and FISH are in **bold**. *Adapted from http://surgpathcriteria.stanford.edu.*



Fig. 117.9 Familial multiple lipomatosis. Several discrete lipomas are present on the forearm.



Fig. 117.10 Benign symmetric lipomatosis (Madelung disease). Large symmetric fatty deposits in the supraclavicular region, lateral chest, and abdomen.

in association with tuberous sclerosis (see Ch. 61) and paralytic poliomyelitis[29–31]. The lower extremities are most commonly affected, but involvement of the head, neck, face, and upper extremities have all been reported. Pelvic involvement may lead to urinary tract, intestinal, and even vena caval obstruction[32].

Familial multiple lipomatosis is also known as familial multiple lipomas, multiple circumscribed lipomas, hereditary multiple lipomas, and discrete lipomatosis. This disorder is characterized by multiple lipomas occurring in several members of one kindred. The tumors are discrete, mobile, and surrounded by a capsule, as opposed to the diffuse and infiltrative tumor growth observed in benign symmetric lipomatosis (Madelung disease)[33]. Favored sites include, but are not limited to, forearms and thighs (Fig. 117.9). The neck and shoulders are generally spared.

Proteus syndrome is a complex sporadic disorder due to mosaicism for an activating mutation in the *AKT1* oncogene. It is characterized by asymmetric, disproportionate (i.e. progressive and distorting) overgrowth of multiple tissues and multiple hamartomatous malformations (see Ch. 62)[34]. The tissue overgrowth tends to plateau after adolescence.

Lipomatosis arising in the setting of Proteus syndrome is associated with overgrowth of multiple tissues in a mosaic pattern, and this can lead to partial gigantism of the head or limbs, vascular malformations, and skeletal deformities as well as areas of lipohypoplasia (see Table 104.5)[35]. Connective tissue nevi (particularly cerebriform lesions on the palms and soles) and epidermal nevi are also commonly observed in these patients.

The PIK3CA (phosphatidylinositol-4,5-bisphosphate 3-kinase catalytic subunit alpha)-related overgrowth spectrum includes: (1) **hemihyperplasia–multiple lipomatosis** which is characterized by multiple lipomas in association with asymmetric (but non-progressive and non-distorting) overgrowth, mild macrodactyly, capillary malformations, and thickened plantar skin with prominent creases; and (2) **CLOVES syndrome** which is characterized by *c*ongenital *l*ipomatous *o*vergrowth (typically not progressive), *v*ascular malformations, *e*pidermal nevi, and *s*keletal/*s*pinal abnormalities (see Table 104.5). Other individuals with Proteus-like features have a germline mutation in *PTEN* plus a postzygotic "second hit" in affected tissues and this results in *s*egmental *o*vergrowth, *l*ipomatosis, *a*rteriovenous *m*alformations, and *e*pidermal *n*evi (**SOLAMEN**)[36].

Benign symmetric lipomatosis is also known as Madelung disease in the American literature[37], benign symmetric lipomatosis of Launois–Bensaude in the European literature[38], and multiple symmetric lipomatosis in OMIM. It consists of extensive symmetric fat deposits in the head, neck, and shoulder girdle area (Fig. 117.10). When the mediastinum is involved, complications related to a space-occupying mass may ensue. Most patients are men, and a high percentage suffer from alcoholism; this may account for several disorders reported in association with benign symmetric lipomatosis, such as peripheral neuropathy, squamous cell carcinomas of the head and neck, and macrocytic anemia.

Pathogenic variants in *MT-TK*, which encodes mitochondrial tRNA lysine, have been described in a subset of patients with benign symmetric lipomatosis. When patients have additional findings such as partial lipoatrophy, myopathy, and hypertriglyceridemia, the possibility of mutations in *LIPE* (lipase E, hormone sensitive type; see Ch. 101) or *MFN2* (mitofusin 2, a mitochondrial protein) can be considered. In one family, heterozygosity for a pathogenic variant in *CAPSL* was observed, with its protein product, calcyphosine-like, hypothesized to play a role in adipogenesis.

Multiple painful lipomas are present primarily on the arms, trunk, and in the periarticular soft tissue in **adiposis dolorosa (Dercum disease**). This disease most commonly affects premenopausal women, and it is associated with weakness and psychiatric symptoms such as depression[39]. Pain is intermittent, but it may be debilitating, necessitating sophisticated pain management. Pain is caused by lipomas compressing adjacent nerves.

In addition, lipomas may be part of **Gardner syndrome**. This syndrome consists of polyposis of the colon (eventuating in colonic carcinoma unless there is surgical intervention), odontomas, multiple epidermoid cysts (often with foci of matrical differentiation), osteomas, leiomyomas, and desmoid fibromatosis (see Ch. 63). Retinal pigment epithelial hamartomas (RPEH) represent an early characteristic finding in Gardner syndrome. Mutations in *APC* are responsible for this syndrome as well as familial adenomatous polyposis.

Multiple lipomas are also seen in **Bannayan–Riley–Ruvalcaba syndrome** and **Cowden syndrome**, autosomal dominantly inherited hamartoma syndromes due to mutations in the tumor suppressor gene *PTEN*[40,41]. As outlined in Table 63.3, these two disorders have overlapping features and exist along a disease spectrum[30]. Nowadays they are referred to as the PTEN hamartoma tumor syndrome.

Pathology

Lipomas are composed of a uniform population of mature fat cells with small, uniform, and eccentric nuclei (Fig. 117.11). The fat cells are arranged in lobules with capillaries scattered throughout the lesion. Mitotic figures are absent. Microscopically, lipomas may be indistinguishable from mature adipose tissue. Some lipomas contain lipocytes with intranuclear vacuoles that need to be distinguished from lipoblasts. Fibrolipoma and myxolipoma represent lipomas with an admixture of significant amounts of fibrous tissue and myxoid stroma, respectively. Occasionally, foci of cartilaginous tissue and osseous metaplasia may be present. Secondary changes, due primarily to trauma, include focal fat necrosis and/or aggregates of foamy macrophages.

Differential diagnosis

An epidermoid cyst without a pore is the most common entity in the clinical differential diagnosis, including for subfrontalis lipomas of the

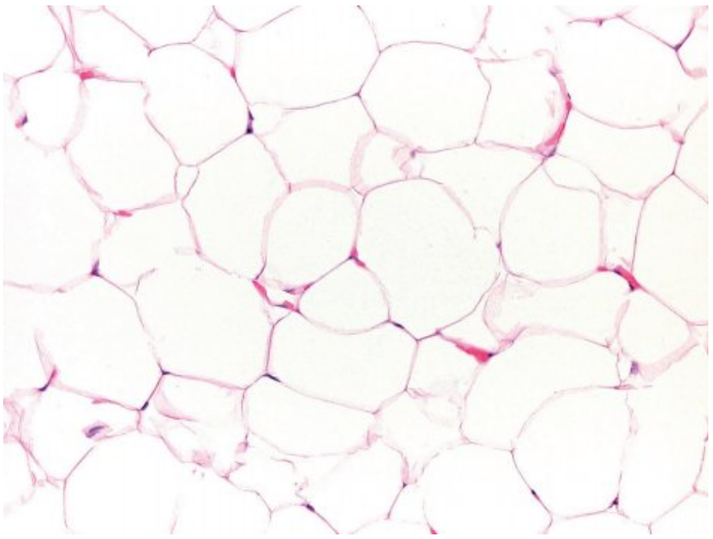


Fig. 117.11 Lipoma (ordinary). A uniform population of mature adipocytes with small and eccentric nuclei is seen.

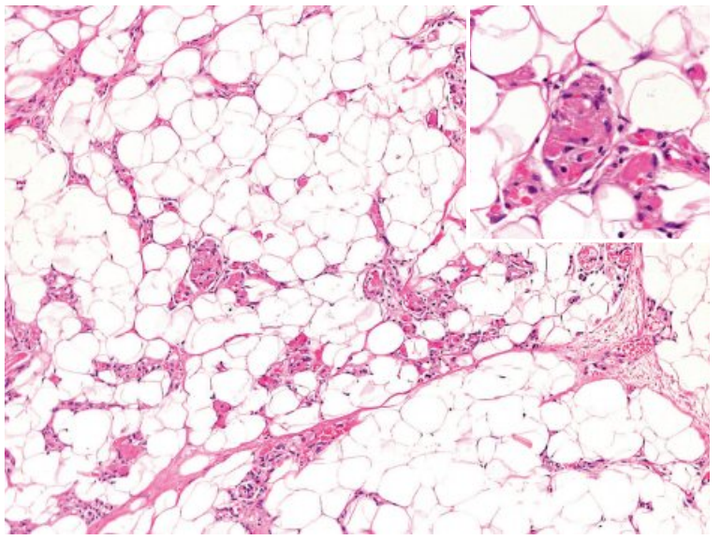


Fig. 117.12 Angiolipoma. Mature fat is admixed with a variable number of small blood vessels. Occasionally, the vessels are occluded by fibrin thrombi (inset).

forehead. An ultrasound examination can be done to distinguish between these two entities (see Fig. 117.1). As lipomas are histologically indistinguishable from normal fat, a definitive diagnosis may not be possible if the specimen is too small to demonstrate the overall architecture.

Treatment

Small solitary lipomas are usually cured by simple excision. Local recurrence after excision is more common with larger-sized lipomas. Larger lesions, or systemic lipomatoses, may be amenable to liposuction (see Ch. 156).

Angiolipoma

Key features

- Soft subcutaneous nodule, usually less than 2 cm in diameter
- Typically located on the forearms of young adults
- More often painful than are ordinary lipomas
- Well-circumscribed lesion composed of mature fat cells intermingled with small, focally thrombosed vessels

Introduction

Angiolipomas are benign subcutaneous tumors composed of mature fat and a vascular component.

Epidemiology

Patients with angiolipomas are typically young adults in their late teens or early twenties; ~5% of cases are familial.

Pathogenesis

The pathogenesis of angiolipomas is not known. A small number of cases are familial, thus suggesting a genetic component. Unlike lipomas, hibernomas, and many other fatty tumors, angiolipomas usually have a normal karyotype. Rarely, rearrangements of chromosome 13 have been observed. In one study of 18 angiolipomas, activating mutations in *PIK3CA* were identified in the majority (78%) of the tumors, with each having the same mutation [c.1634A>C (p.E545A)] within exon 9[42]. These findings suggest that activation of the PI3K/AKT pathway may play a key role in the formation of angiolipomas.

Clinical features

Angiolipomas usually measure <2 cm in diameter and are clinically similar to ordinary lipomas. However, they may be painful. In approximately two-thirds of patients, the tumors are found on the forearms. Less common sites are the trunk and upper arms. An estimated two-thirds of patients have multiple tumors[28].

Pathology

Mature adipose tissue is admixed with a variable number of small vessels (Fig. 117.12). Occasional blood vessels are occluded by fibrin thrombi. A cellular variant is characterized by dense cellular angiomatous tissue with a prominent number of spindle cells. Mast cells are more numerous than in ordinary lipomas, and older lesions may contain areas of fibrosis.

Differential diagnosis

Clinically, angiolipomas cannot be reliably distinguished from other benign fatty tumors, although the presence of pain may be a clue. The histopathologic differential diagnosis includes an ordinary lipoma, but no lower threshold exists for the minimal number of vessels required to warrant the diagnosis of angiolipoma. The identification of thrombosed vessels may be helpful in this situation, as they are usually not seen in ordinary lipomas. Highly vascular or cellular angiolipomas may be difficult to distinguish from Kaposi sarcoma, spindle cell lipoma, and spindle cell hemangioendothelioma.

Treatment

Surgical excision is curative and, to date, no malignant transformation has been reported. Angiolipomas tend to be more circumscribed than ordinary lipomas and are therefore more readily excised *in toto*.

Spindle Cell/Pleomorphic Lipoma

Key features

- Solitary, subcutaneous nodule on the upper back of middle-aged to older men
- Histologic triad of spindle cells, mature fat cells, and strands of dense collagen
- Pleomorphic lipomas also contain an admixture of floret-like cells

Introduction

Spindle cell and pleomorphic lipomas represent a group of histologically distinct tumors composed of mature fat cells, a population of spindle cells, and strands of dense collagen. Pleomorphic lipomas also contain an admixture of bizarre, often multinucleated cells ("floret-like cells"). Not only do spindle cell and pleomorphic lipomas share common karyotypic abnormalities (see Table 117.4), but tumors with intermediate histopathologic features (between classic spindle cell lipoma and pleomorphic lipoma) are sometimes observed. Spindle cell/pleomorphic lipomas usually develop on the posterior neck, upper back, and shoulders of middle-aged and older men, and their clinical appearance is similar to other fatty tumors.

History
Spindle cell lipoma was first described by Enzinger and Harvey in 1975[43].

Epidemiology
Although these tumors have occasionally been reported in women and young men, the vast majority of spindle cell and pleomorphic lipomas have been observed in middle-aged to older men[43].

Pathogenesis
The pathogenesis of spindle cell and pleomorphic lipomas is unknown. Only a small fraction of cases occurs in a familial setting. The spindle cells in spindle cell and pleomorphic lipomas probably represent undifferentiated mesenchymal cells. Partial loss or monosomy of 13q or 16q are the most common clonal chromosomal abnormalities. Of note, the deletions of 13q tend to cluster within the 13q14 region, where *RB1* resides.

Clinical features
A spindle cell/pleomorphic lipoma presents as a solitary, slowly growing, mobile and painless subcutaneous nodule without epidermal changes. These lipomas most commonly develop on the posterior neck, upper back, and shoulders, but can also occur in other sites including the breast, upper aerodigestive tract, and orbit[28,44]. Multiple spindle cell lipomas and familial cases are rare.

Pathology
Histopathologically, the diagnosis of *spindle cell lipoma* requires the presence of three components, admixed in varying proportions: (1) mature fat cells; (2) small, uniform spindle cells; and (3) strands of dense, eosinophilic ("ropey") collagen[45] (Fig. 117.13). In some tumors, variable myxoid areas are seen, whereas in others, spindle cells may predominate; mature fat cells may even be inconspicuous or absent. The spindle cells have bland, uniform nuclei, and pale eosinophilic "bipolar" cytoplasm. Other possible histologic features include a plexiform pattern, foci with nuclear palisading, cleft-like spaces, and numerous mast cells.

Pleomorphic lipomas are characterized by the presence of mature adipocytes admixed with a variable number of bizarre, multinucleated cells ("floret-like cells"), and occasional lipoblasts (Fig. 117.14). By immunohistochemistry, the spindle cells in both spindle cell and pleomorphic lipomas are CD34-positive and rarely S100-positive. In some tumors, demonstration of loss of the *RB1* locus via molecular diagnostics may help to confirm the diagnosis.

Differential diagnosis
Clinically, spindle cell/pleomorphic lipomas are indistinguishable from other benign superficial lipomatous tumors, with anatomic location being the most characteristic finding. The histopathologic appearance is diagnostic, but problems may arise when the spindle cell population is predominant. In the latter situation, immunophenotyping may be helpful. The major entities in the differential diagnosis are nodular fasciitis (actin-positive, CD34-negative) and neurofibroma or schwannoma (both S100-positive).

Treatment
In general, surgical excision is curative; recurrences are rare.

Hibernoma

Synonyms: ■ Lipoma of immature adipose tissue ■ Lipoma of embryonic fat ■ Fetal lipoma

Key features
- Rare benign fatty tumor derived from brown fat
- Except for a larger average size, clinically indistinguishable from a lipoma
- The most common locations are the interscapular area, thighs, neck, and chest

Introduction
A hibernoma is a rare benign tumor that is derived from brown fat. Brown fat is prominent in hibernating animals, but it is also found in humans. Brown fat first appears in the human fetus and persists into childhood. In children, brown fat is most prominent in the interscapular area, neck, mediastinum, anterior abdominal wall, and around some of the intraperitoneal and retroperitoneal organs. Brown fat gradually disappears with increasing age, and, in adults, it only persists in the neck and around the kidneys, adrenal glands, and the aorta. The main function of brown fat is heat production.

History
This neoplasm was first described in 1906 by Merkel[46] as a pseudo-lipoma of the breast. The term hibernoma was first introduced by Gery in 1914[47].

Epidemiology
Hibernomas occur primarily in adults. Individuals who develop these tumors are younger than patients with ordinary lipomas and are typically in their thirties. In a series of 170 hibernomas, patient ages ranged from 2 to 75 years, with a mean age of 38 years. The series included nine children[48].

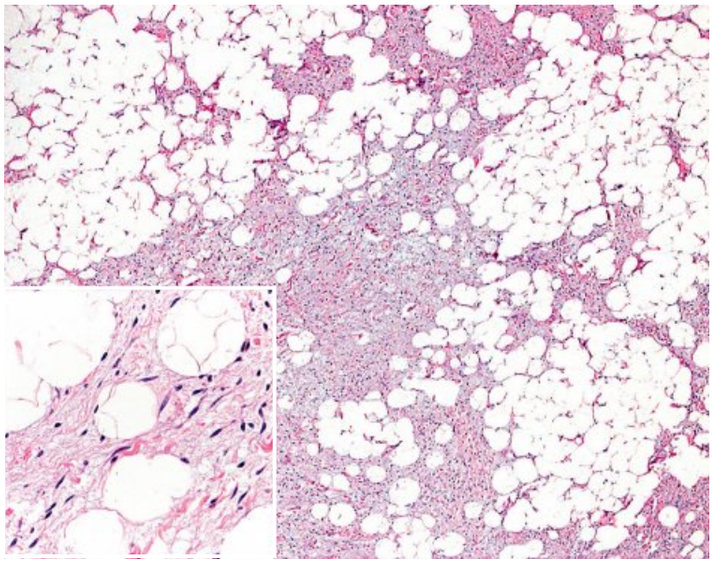


Fig. 117.13 Spindle cell lipoma. Areas of spindle cells are admixed with mature fat cells. The spindle cells are small, uniform, bland, and have inconspicuous cytoplasm (inset).

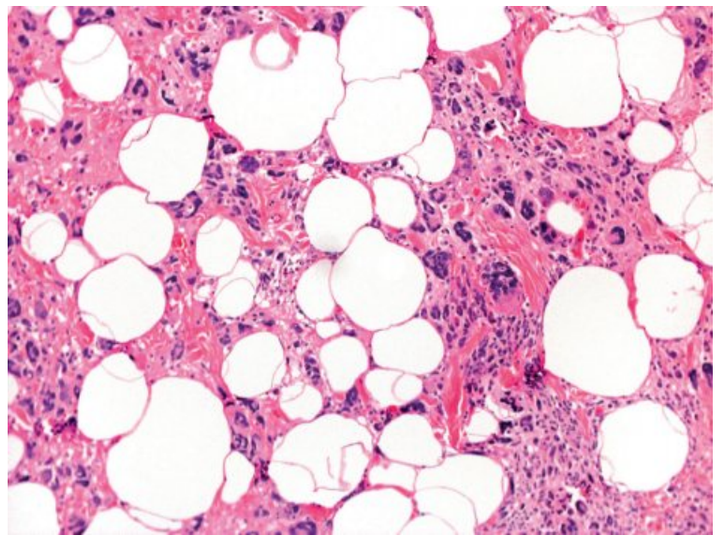


Fig. 117.14 Pleomorphic lipoma. Numerous floret-like multinucleate cells are present in this tumor. Sometimes only a few floret-like multinucleate cells are seen and the majority of cells are mature adipocytes.

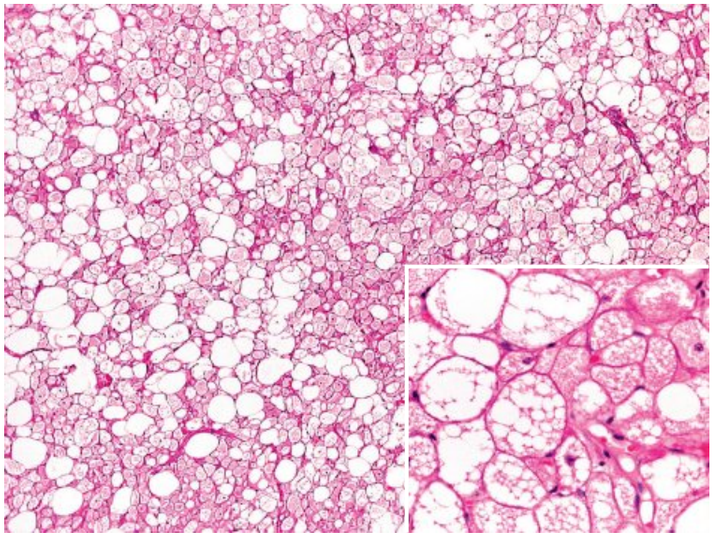


Fig. 117.15 Hibernoma. Irregular aggregates of large cells with abundant cytoplasm. Inset, the cytoplasm of hibernoma cells ranges from multivacuolated to granular (due to multiple tiny vacuoles).

Pathogenesis

Little is known about the pathogenesis of hibernoma. Characteristic clonal chromosomal abnormalities consist of structural rearrangements of 11q13–21.

Clinical features

Hibernomas are slow-growing tumors located in the subcutis or, occasionally, within skeletal muscle. They are clinically indistinguishable from ordinary lipomas, and the most common locations are the upper trunk (interscapular area, shoulder, chest), neck, extremities, and abdominal cavity/retroperitoneum. Hibernomas can measure up to 25 cm in diameter (average size, 10 cm)[5].

Pathology

On cut sections, hibernomas have a characteristic tan to deep red–brown color. Histologic examination shows pronounced lobulation. Highly vascular interlobular septa surround individual lobules. Common to hibernomas are the characteristic brown fat cells with a small central nucleus and multivacuolated to granular eosinophilic cytoplasm (Fig. 117.15). The cellular membrane is distinct. These typical hibernoma cells are admixed with variable numbers of mature fat cells and pale multivacuolated cells. Rarely, myxoid, lipoma-like, or spindle cell variants may be observed[48,49]. Adipocytes stain positively for CD31 and this can aid in establishing the diagnosis (see Table 117.1).

Differential diagnosis

Except for a larger average size, hibernomas are clinically indistinguishable from lipomas. However, their histopathologic features are characteristic.

Treatment

Surgical excision is curative. In a clinicopathologic study of 66 cases, none recurred after complete excision[48].

Nevus Lipomatosus Superficialis

Synonym: ■ Nevus lipomatosis of Hoffman and Zurhelle

Key features

- Hamartoma present at birth or becomes apparent within the first two decades of life
- Grouped soft papulonodules, usually on the hips and upper thighs
- Mature fat cells in the dermis are the defining histopathologic feature



Fig. 117.16 Nevus lipomatosus superficialis. A This hamartoma is characterized by grouped, soft, pedunculated, skin-colored tumors. **B** Histopathologically, irregular aggregates of mature fat cells ectopically located in the dermis are the characteristic feature.

Introduction

Nevus lipomatosus superficialis is a connective tissue nevus or hamartoma that is characterized by grouped soft papulonodules. It is most commonly located on the buttocks or upper thighs.

History

Nevus lipomatosus was first described by Hoffman and Zurhelle in 1921.

Epidemiology

This rare hamartoma is present at birth or becomes apparent during the first two decades of life, and no sex preference has been observed.

Pathogenesis

While the pathogenesis is unknown, there is speculation that precursor cells around dermal blood vessels give rise to mature fat cells in a mosaic pattern.

Clinical features

Nevus lipomatosus superficialis consists of soft, clustered papulonodules that are present at birth, or appear during childhood or adolescence. An initial presentation in adults has been described. The lesions consist of soft, yellow to skin-colored papules or nodules that are clustered, do not cross the midline, and may follow the lines of Blaschko (Fig. 117.16A).

Individual lesions may be sessile or pedunculated, and they have a smooth or cerebriform surface. The pelvic girdle area and upper thighs are the most common locations.

Pathology
The defining histopathologic feature consists of mature fat cells ectopically located within the dermis (Fig. 117.16B). Skin appendages are not displaced.

Differential diagnosis
A solitary acquired papilloma that contains fat cells but no adnexal structures within the dermis is a variant of a skin tag known as a lipofibroma, not a nevus lipomatosus superficialis. The congenital circumferential folds of excess skin in patients with the "Michelin tire baby" phenotype can have the histologic findings of nevus lipomatosus superficialis (see Table 97.7)[50]. In focal dermal hypoplasia (Goltz syndrome), the dermis is either absent and completely replaced by fat cells, or significantly thinned. Adnexal structures are missing. Clinically, agminated neurofibromas may be mistaken for nevus lipomatosus.

Treatment
Most lesions are amenable to excision.

Lipoblastoma/Lipoblastomatosis

Synonym: ■ Embryonic lipoma

Key features
- Benign neoplasm of immature fat cells that arises primarily on the extremities of children
- The circumscribed form is termed lipoblastoma, and the diffuse form is termed lipoblastomatosis
- Histopathologically, indistinguishable from myxoid liposarcoma

Introduction
This is a rare variant of lipoma, and it represents a benign tumor of immature fat cells that occurs almost exclusively in children. When circumscribed, this neoplasm is termed lipoblastoma, and when diffuse, it is known as lipoblastomatosis.

History
The term lipoblastoma was coined by Vellios and colleagues in 1958 when they reported a case of lipoblastomatosis.

Epidemiology
Lipoblastoma and lipoblastomatosis are tumors of infancy. Occasionally, these neoplasms are described in older children, or even teenagers, but the majority occur before the age of 3 years. Congenital tumors have been observed. Boys are affected twice as often as girls.

Pathogenesis
Lipoblastomas are neoplasms of immature (embryonic) white fat, and they probably represent residual areas of immature fat. The latter is suggested by sequential biopsies showing maturation to mature fat and by the almost exclusive occurrence in infancy and childhood. Lipoblastomas commonly display structural alterations, i.e. translocations, inversions, insertions or rings, of 8q11–q13 which lead to rearrangement of *PLAG1*, a finding that argues for a clonal neoplasm.

Clinical features
Most tumors are circumscribed and limited to the subcutis, and hence represent lipoblastomas. They occur primarily on the extremities and less often in the head and neck region or on the trunk. These superficial lesions clinically simulate ordinary lipomas, presenting as slow-growing, soft, mobile, painless nodules, measuring 3–5 cm in diameter.

Lipoblastomatosis affects the deeper soft tissue and often diffusely infiltrates adjacent skeletal muscle. This process can occur in the mediastinum, mesentery, and retroperitoneum. Rare tumors weigh up to 1 kg. Depending on the location, the tumor may result in symptoms of local obstruction or compression.

Pathology
Grossly, lipoblastomas are paler than ordinary lipomas, and they have a myxoid quality. Histologically, it is a lobulated neoplasm. The stroma is often myxoid, contains a plexiform vascular network, and is divided into lobules by connective tissue septa. Deep-seated tumors often lack the lobulation, and they may grow in a diffuse pattern. The tumors are composed of fat cells spanning the range of maturation from immature stellate and spindled mesenchymal cells, to lipoblasts with a single cytoplasmic vacuole that indents a peripherally located nucleus, to small and mature adipocytes. Lipoblastomas are paucicellular, cytologically bland, and lack mitotic activity. Serial biopsies of a lipoblastoma may show gradual maturation to a mature fatty tumor. The adipocytes in lipoblastomas stain positively for S100, CD56, and CD34. Molecular demonstration of *PLAG1* rearrangements may be helpful in confirming the diagnosis.

Differential diagnosis
Histopathologically, lipoblastoma and myxoid liposarcoma may be indistinguishable. Clinical parameters that aid in the differential diagnosis are the age of the patient and the location of the tumor. Myxoid liposarcomas almost always develop in individuals older than 20 years of age, and they are located in the deep soft tissue, rather than the subcutis. Nevertheless, in a child, an immature fat tumor that contains areas of marked cellularity, loss of lobulation, and mitotic figures should raise concern for a myxoid liposarcoma.

Treatment
Lipoblastoma, if treated with complete excision, rarely recurs. Unusual cases of spontaneous resolution without treatment exist[51]. In a series of 14 patients with lipoblastomas/lipoblastomatosis, 22% recurred after excision[52]. Wide excision is the therapy of choice for the diffuse form of the disease.

Atypical Lipomatous Tumor/Liposarcoma

Synonym: ■ Atypical lipoma

Key features
- Sarcoma of deep soft tissue that is only rarely limited to the skin
- Five major histologic subtypes, ranging from locally aggressive tumors without metastatic potential to malignant neoplasms with a significant risk of metastatic dissemination
- Cutaneous involvement may represent superficial extension of a deeply situated tumor
- Tumors confined to the skin ("primary cutaneous liposarcoma") usually have a good prognosis

Introduction
Liposarcoma is the second most common soft tissue sarcoma after malignant fibrous histiocytoma. Five histopathologic subtypes are recognized by the World Health Organization (WHO), with important prognostic, cytogenetic, molecular, and epidemiologic differences. The biologic behavior of the subtypes ranges from locally aggressive tumors without metastatic potential to highly malignant neoplasms with a significant risk of systemic spread. There is considerable controversy among soft tissue pathologists regarding the nomenclature of this tumor when it is confined to the skin. Some experts prefer the term atypical lipomatous tumor for all liposarcomas in the subcutis, because these tumors recur but have virtually no metastatic potential[53,54]. Others prefer to retain the term liposarcoma because histologically and cytogenetically these tumors are the same, regardless of location, and also because these tumors carry a small risk for dedifferentiation, which confers metastatic potential[55].

Epidemiology
The annual incidence of all types of soft tissue liposarcoma is estimated at 2.5 per million, based on a Swedish study. The average age at presentation is 50 years. Rare cases arise in children older than 10 years of age, but virtually never in children younger than 10 years of age.



Fig. 117.17 Liposarcoma. Note the large mass in the right buttock. *Courtesy Ronald P. Rapini, MD.*

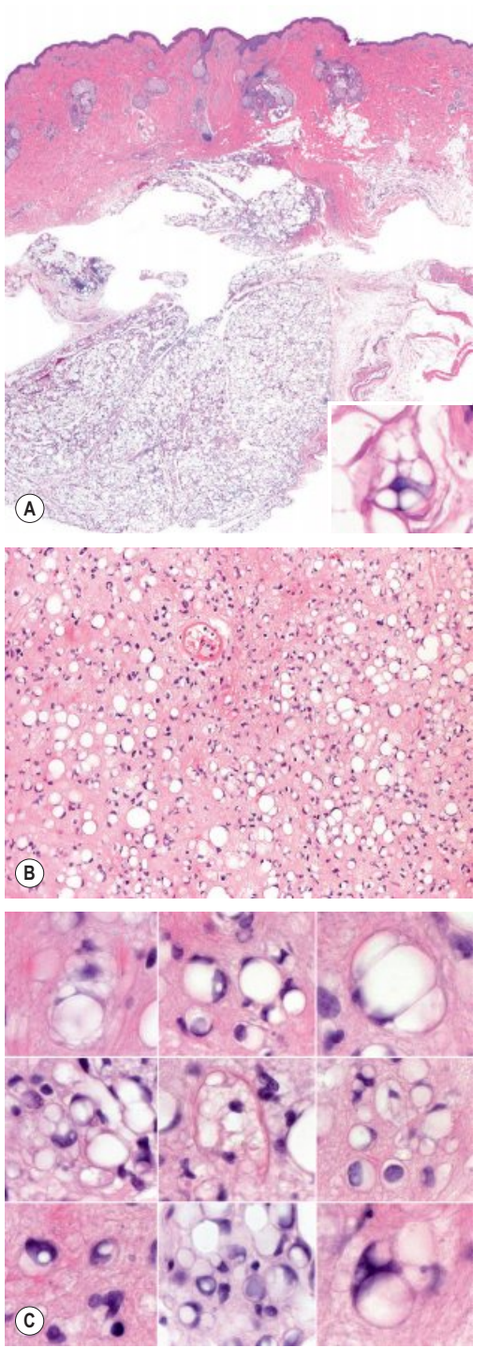


Fig. 117.18 Atypical lipomatous tumor/well-differentiated liposarcoma vs dedifferentiated liposarcoma. A In an atypical lipomatous tumor, irregular aggregates of "hypercellular" fat tissue are seen as are lipoblasts. Lipoblasts are immature fat cells with a hyperchromatic nucleus that is scalloped by cytoplasmic fat vacuoles (inset). Their presence is mandatory for a diagnosis of atypical lipomatous tumor or liposarcoma. **B** In this dedifferentiated liposarcoma, lipocytes and lipoblasts are dispersed in a collagenous stroma and do not form well-differentiated structures. **C** Panel demonstrating the varied morphologic appearances of lipoblasts.

Pathogenesis

It appears that liposarcomas arise *de novo*, rather than from pre-existing lipomas. Chromosomal anomalies differ, depending upon the particular subtype (see Table 117.4). In well-differentiated and dedifferentiated liposarcomas, there is amplification of genes in the 12q13–15 region that are involved in cell cycle regulation (see Fig. 107.4), and this amplification can be detected via fluorescent *in situ* hybridization (FISH). In myxoid or round cell liposarcomas, 12;16 translocations lead to a FUS–DDIT3 fusion oncoprotein.

Clinical features

Liposarcoma is a tumor primarily of the deep soft tissue of the extremities and retroperitoneum. Legs and buttocks are more frequently affected than the upper extremities (Fig. 117.17). It originates in, and is limited to, the dermis or subcutis only in exceptional circumstances[56,57]. Primary cutaneous liposarcomas are described as dome-shaped or polypoid, and they measure between 1 and 20 cm[57]. If a liposarcoma presents in the subcutis, this will often be due to direct extension from an underlying sarcoma of the deep soft tissue.

Tumors limited to the dermis or subcutis can recur, but they do not metastasize or cause patient death. Liposarcomas of the deep soft tissue and retroperitoneum are malignant neoplasms, capable of recurrence, metastasis, and causing patient death. The prognosis depends on the location, degree of differentiation, and the histopathologic subtype.

Pathology

The *sine qua non* for the diagnosis of liposarcoma is the presence of lipoblasts. Lipoblasts are immature fat cells, characterized by a hyperchromatic nucleus that is indented or scalloped by cytoplasmic fat vacuoles (Fig. 117.18). However, the lipoblasts need to be present in the appropriate histopathologic context, as they are not specific for liposarcomas, but can also be found in lipoblastomas and pleomorphic lipomas, or can closely resemble histiocytes found in fat necrosis or fat atrophy.

The histopathologic appearance is highly variable and depends on the particular subtype (Fig. 117.19A,B). A **well-differentiated** liposarcoma (atypical lipomatous tumor) consists of mature fat with a variable number of lipoblasts and cells with hyperchromatic nuclei. **Myxoid** liposarcoma resembles immature fat and can be histologically indistinguishable from a lipoblastoma. Small and uniformly bland spindle cells are set in a myxoid matrix with plexiform vessels. In the more cellular areas, myxoid liposarcoma merges with **round cell** liposarcoma, which is characterized by sheets of primitive round cells. Several classification schemes recognize round cell liposarcoma as a part of the spectrum of myxoid liposarcoma. **Pleomorphic** liposarcoma is the least common subtype; it exhibits an extreme degree of nuclear pleomorphism and resembles a malignant fibrous histiocytoma[58,59]. **Dedifferentiated** liposarcoma is a biphasic tumor comprised of areas of well-differentiated liposarcoma/atypical lipomatous tumor and areas of a non-lipogenic sarcoma.

Given the correlation of molecular findings with liposarcoma subtype (see Table 117.4), chromosomal analysis, immunohistochemistry (CDK4, MDM2, adipophilin)[60], and FISH (*CDK4*, *MDM2*) can assist in diagnosis and classification (Fig. 117.19C).

Differential diagnosis

Liposarcomas of the skin and superficial subcutaneous tissue are exceedingly rare, and they should be diagnosed only after histopathologic mimics, metastases, and direct extension from a deep soft tissue sarcoma have been excluded. In addition, these tumors need to be distinguished from a spindle cell/pleomorphic lipoma, a benign lipomatous tumor that commonly arises on the upper back and posterior neck of older men and is characterized histopathologically by the presence of a variable number of floret-like cells and occasional lipoblasts, admixed with mature adipocytes.

Myxoid liposarcoma can be histologically indistinguishable from lipoblastoma and lipoblastomatosis. This differential diagnosis relies on clinical parameters and is discussed above under lipoblastoma. Of note, silicone granulomas may occasionally mimic liposarcoma histologically.

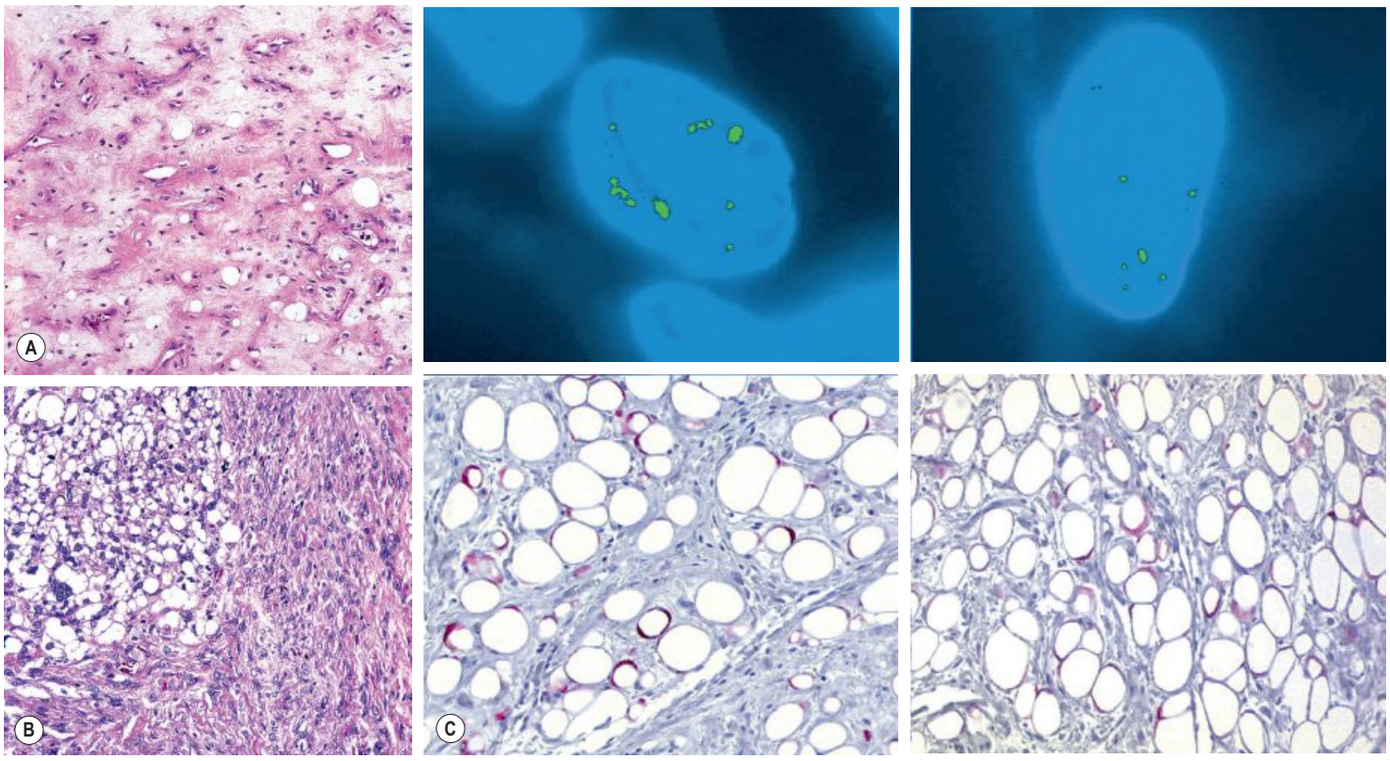


Fig. 117.19 The varied histopathologic features of liposarcoma. A Myxoid liposarcoma – without the clinical context, this tumor can be indistinguishable from lipoblastoma. Bland spindle cells occur in a myxoid matrix with plexiform vessels. **B** Pleomorphic liposarcoma – anaplastic and cellular neoplasm. Lipoblasts may be difficult to find. **C** Demonstration of *MDM2* amplification (left) and *CDK4* amplification (right) via fluorescent *in situ* hybridization (FISH; top) as well as increased protein expression via immunohistochemistry (bottom) can assist in the diagnosis of a well-differentiated liposarcoma (atypical lipomatous tumor). *C, Courtesy Heinz Kutzner, MD.*

Treatment

Wide excision is the treatment of choice. Tumors limited to the dermis and subcutis may be treated by dermatologists. The treatment of most liposarcomas, however, will require an oncologic soft tissue surgeon. It is not uncommon for liposarcomas to have a multinodular growth pattern and extend into muscle and fascial planes. Excision needs to be carefully planned using MRI and other radiographic information.

TUMORS OF CARTILAGE

Extraskeletal Chondroma

Synonym: ■ Chondroma of soft parts

Key features

- Rare benign tumor of mature cartilage
- Most commonly located near the small joints of the hands and feet

Introduction

Cartilage can be found in the skin as a result of metaplasia, as a component of chondroid syringomas, and as the exclusive component of extraskeletal chondromas. By definition, extraskeletal chondromas are not attached to bone and occur outside the synovial space. With the exception of two clinical series[61,62], most of the experience with extraskeletal chondromas is in the form of case reports.

Epidemiology

Extraskeletal chondromas are rare tumors that occur in children as well as adults, but most patients are beyond their third decade.

Clinical features

Extraskeletal chondromas present as solitary painless nodules on the hands and feet, most often the fingers. They grow slowly and are often associated with tendons. Rare locations include the trunk, head, neck, oropharynx, and larynx.

Pathology

On gross examination, chondromas are sharply circumscribed and often lobulated. Most measure less than 2 cm, but larger lesions can occur. Histopathologically, they consist of hyaline cartilage that may be admixed with variable amounts of fibrous tissue or myxoid stroma. The cartilage may compose only a small portion of the tumor. Calcification is common, and lesional cells are S100-positive.

Differential diagnosis

Synovial chondromatosis consists of multiple, discrete, osteocartilaginous nodules and favors the large joints, such as the knee, hip, and elbow. Histologic differentiation of extraskeletal chondromas from grade I chondrosarcoma or myxoid chondrosarcoma may be difficult, but chondrosarcomas rarely affect the hands and feet, and they are in continuity with bone and cartilage.

Treatment

Local excision is usually curative. Up to 20% of extraskeletal chondromas may recur.

Acknowledgment

The author wishes to thank the late Sabine Kohler, MD, for her valuable contribution to this chapter in the previous editions.

Additional figures available in our eBook (see inside front cover for access code).

REFERENCES

1. Newman PL, Fletcher CD. Smooth muscle tumours of the external genitalia: clinicopathological analysis of a series. *Histopathology*. 1991;18:523–529.
2. Stout AP. Solitary cutaneous and subcutaneous leiomyoma. *Am J Cancer*. 1937;29:435–469.
3. Orellana-Diaz O, Hernandez-Perez E. Leiomyoma cutis and leiomyosarcoma: a 10-year study and a short review. *J Dermatol Surg Oncol*. 1983;9:283–287.
4. Fletcher CDM. Soft tissue tumors. In: Fletcher CDM, ed. *Diagnostic Histopathology of Tumors*. 3rd ed. Philadelphia: Churchill Livingstone; 2007:1527–1593.
5. Badeloe S, Frank J. Clinical and molecular genetic aspects of hereditary multiple cutaneous leiomyomatosis. *Eur J Dermatol*. 2009;19:545–551.
6. Muller M, Ferlicot S, Guillaud-Bataille M, et al. Reassessing the clinical spectrum associated with hereditary leiomyomatosis and renal cell carcinoma syndrome in French FH mutation carriers. *Clin Genet*. 2017;92:606–615.
7. Raj S, Calonje E, Kraus M, et al. Cutaneous pilar leiomyoma: clinicopathologic analysis of 53 lesions in 45 patients. *Am J Dermatopathol*. 1997;19:2–9.
8. Mahalingam M, Goldberg LJ. Atypical pilar leiomyoma: cutaneous counterpart of uterine symplastic leiomyoma? *Am J Dermatopathol*. 2001;23:299–303.
9. Llamas-Velasco M, Requena L, Kutzner H, et al. Fumarate hydratase immunohistochemical staining may help to identify patients with multiple cutaneous and uterine leiomyomatosis (MCUL) and hereditary leiomyomatosis and renal cell cancer (HLRCC) syndrome. *J Cutan Pathol*. 2014;41:859–865.
10. Reyes C, Karamurzin Y, Frizzell N, et al. Uterine smooth muscle tumors with features suggesting fumarate hydratase aberration: detailed morphologic analysis and correlation with S-(2-succino)-cysteine immunohistochemistry. *Mod Pathol*. 2014;27:1020–1027.
11. McGinley KM, Bryant S, Kattine AA, et al. Cutaneous leiomyomas lack estrogen and progesterone receptor immunoreactivity. *J Cutan Pathol*. 1997;24:241–245.
12. Thompson Jr. JA. Therapy for painful cutaneous leiomyomas. *J Am Acad Dermatol*. 1985;13:865–867.
13. Christenson LJ, Smith K, Arpey CJ. Treatment of multiple cutaneous leiomyomas with CO_2 laser ablation. *Dermatol Surg*. 2000;26:319–322.
14. Svarvar C, Bohling T, Berlin O, et al. Clinical course of nonvisceral soft tissue leiomyosarcoma in 225 patients from the Scandinavian Sarcoma Group. *Cancer*. 2007;109:282–291.
15. Hornick JL, Fletcher CD. Criteria for malignancy in nonvisceral smooth muscle tumors. *Ann Diagn Pathol*. 2003;7:60–66.
16. Fields JP, Helwig EB. Leiomyosarcoma of the skin and subcutaneous tissue. *Cancer*. 1981;47:156–169.
17. Bernstein SC, Roenigk RK. Leiomyosarcoma of the skin. Treatment of 34 cases. *Dermatol Surg*. 1996;22:631–635.
18. Weiss SW, Goldblum JR. Leiomyosarcoma. In: Weiss SW, ed. *Soft Tissue Tumors*. 4th ed. St Louis: Mosby; 2001:727–748.
19. Massi D, Franchi A, Alos L, et al. Primary cutaneous leiomyosarcoma: clinicopathological analysis of 36 cases. *Histopathology*. 2010;56:251–262.
20. Kaddu S, Beham A, Cerroni L, et al. Cutaneous leiomyosarcoma. *Am J Surg Pathol*. 1997;21:979–987.
21. Suster S. Epithelioid leiomyosarcoma of the skin and subcutaneous tissue. Clinicopathologic, immunohistochemical, and ultrastructural study of five cases. *Am J Surg Pathol*. 1994;18:232–240.
22. Brenn T. Pleomorphic dermal neoplasms: a review. *Adv Anat Pathol*. 2014;21:108–130.
23. Kempson RL, Fletcher CDM, Evans HL, et al. Smooth muscle tumors. In: Rosai J, Sobin LH, eds. *Tumors of Soft Tissues*. Washington, DC: Armed Forces Institute of Pathology; 2001:239–256.
24. Kraft S, Fletcher CD. Atypical intradermal smooth muscle neoplasms: clinicopathologic analysis of 84 cases and a reappraisal of cutaneous "leiomyosarcoma". *Am J Surg Pathol*. 2011;35:599–607.
25. Stokes JH. Nevus pilaris with hyperplasia of no-striated muscle. *Arch Dermatol Syph*. 1923;7:479–481.
26. Glover MT, Malone M, Atherton DJ. Michelin-tire baby syndrome resulting from diffuse smooth muscle hamartoma. *Pediatr Dermatol*. 1989;6:329–331.
27. Nanni CA, Alster TS. Treatment of a Becker's nevus using a 694-nm long-pulsed ruby laser. *Dermatol Surg*. 1998;24:1032–1034.
28. Weiss SW, Goldblum JR. Benign lipomatous tumors. In: Weiss SW, ed. *Soft Tissue Tumors*. 4th ed. St. Louis: Mosby; 2001:571–639.
29. Karademir M, Kocak M, Usal A, et al. A case of infiltrating lipomatosis with diffuse, symmetrical distribution. *Br J Clin Pract*. 1990;44:728–730.
30. Klein JA, Barr RJ. Diffuse lipomatosis and tuberous sclerosis. *Arch Dermatol*. 1986;122:1298–1302.
31. Kindblom LG, Moller-Nielsen J. Diffuse lipomatosis in the leg after poliomyelitis. *Acta Pathol Microbiol Scand [A]*. 1975;83:339–344.
32. Klein FA, Smith MJ, Kasenetz I. Pelvic lipomatosis: 35-year experience. *J Urol*. 1988;139:998–1001.
33. Leffell DJ, Braverman IM. Familial multiple lipomatosis. Report of a case and a review of the literature. *J Am Acad Dermatol*. 1986;15:275–279.
34. Biesecker LG, Happle R, Mulliken JB, et al. Proteus syndrome: diagnostic criteria, differential diagnosis, and patient evaluation. *Am J Med Genet*. 1999;84:389–395.
35. Biesecker LG. The multifaceted challenges of Proteus syndrome. *JAMA*. 2001;285:2240–2243.
36. Zhou X, Hampel H, Thiele H, et al. Association of germline mutation in the PTEN tumour suppressor gene and Proteus and Proteus-like syndromes. *Lancet*. 2001;358:210–211.
37. Enzi G. Multiple symmetric lipomatosis: an updated clinical report. *Medicine (Baltimore)*. 1984;63:56–64.
38. Ruzicka T, Vieluf D, Landthaler M, et al. Benign symmetric lipomatosis Launois-Bensaude. Report of ten cases and review of the literature. *J Am Acad Dermatol*. 1987;17:663–674.
39. Reece PH, Wyatt M, O'Flynn P. Dercum's disease (adiposis dolorosa). *J Laryngol Otol*. 1999;113:174–176.
40. Bannayan GA. Lipomatosis, angiomatosis, and macrencephalia. A previously undescribed congenital syndrome. *Arch Pathol*. 1971;92:1–5.
41. Wanner M, Celebi JT, Peacocke M. Identification of a PTEN mutation in a family with Cowden syndrome and Bannayan-Zonana syndrome. *J Am Acad Dermatol*. 2001;44:183–187.
42. Saggini A, Santonja C, Nájera L, et al. Frequent activating PIK3CA mutations in sporadic angiolipoma. *J Cutan Pathol*. 2021;48:211–216.
43. Enzinger FM, Harvey DA. Spindle cell lipoma. *Cancer*. 1975;36:1852–1859.
44. Creytens D, van Gorp J, Savola S, et al. Atypical spindle cell lipoma: a clinicopathologic, immunohistochemical, and molecular study emphasizing its relationship to classical spindle cell lipoma. *Virchows Arch*. 2014;465:97–108.
45. Kempson RL, Fletcher CDM, Evans HJ, et al. Lipomatous tumors. In: Rosai J, Sobin LH, eds. *Tumors of Soft Tissues*. Washington, DC: Armed Forces Institute of Pathology; 2001:187–238.
46. Merkel H. On a pseudolipoma of the breast (peculiar fat tumor). *Beitr Pathol Anat*. 1906;39:152–157.
47. Gery L. Discussions. *Bull Mem Soc Anat (Paris)*. 1914:111–112.
48. Furlong MA, Fanburg-Smith JC, Miettinen M. The morphologic spectrum of hibernoma: a clinicopathologic study of 170 cases. *Am J Surg Pathol*. 2001;25:809–814.
49. Moretti VM, Brooks JS, Lackman RD. Spindle-cell hibernoma: a clinicopathologic comparison of this new variant. *Orthopedics*. 2010;33:52–55.
50. Ross CM. Generalized folded skin with an underlying lipomatous nevus. "The Michelin Tire baby." *Arch Dermatol*. 1969;100:320–323.
51. Mognato G, Cecchetto G, Carli M, et al. Is surgical treatment of lipoblastoma always necessary? *J Pediatr Surg*. 2000;35:1511–1513.
52. Mentzel T, Calonje E, Fletcher CD. Lipoblastoma and lipoblastomatosis: a clinicopathological study of 14 cases. *Histopathology*. 1993;23:527–533.
53. Azumi N, Curtis J, Kempson RL, et al. Atypical and malignant neoplasms showing lipomatous differentiation. A study of 111 cases. *Am J Surg Pathol*. 1987;11:161–183.
54. Evans HL, Soule EH, Winkelmann RK. Atypical lipoma, atypical intramuscular lipoma, and well differentiated retroperitoneal liposarcoma: a reappraisal of 30 cases formerly classified as well differentiated liposarcoma. *Cancer*. 1979;43:574–584.
55. Weiss SW, Rao VK. Well-differentiated liposarcoma (atypical lipoma) of deep soft tissue of the extremities, retroperitoneum, and miscellaneous sites. A follow-up study of 92 cases with analysis of the incidence of "dedifferentiation". *Am J Surg Pathol*. 1992;16:1051–1058.
56. Yoshikawa H, Ueda T, Mori S, et al. Dedifferentiated liposarcoma of the subcutis. *Am J Surg Pathol*. 1996;20:1525–1530.
57. Dei Tos AP, Mentzel T, Fletcher CD. Primary liposarcoma of the skin: a rare neoplasm with unusual high grade features. *Am J Dermatopathol*. 1998;20:332–338.
58. Gardner JM, Dandekar M, Thomas D, et al. Cutaneous and subcutaneous pleomorphic liposarcoma: a clinicopathologic study of 29 cases with evaluation of MDM2 gene amplification in 26. *Am J Surg Pathol*. 2012;36:1047–1051.
59. Al-Zaid T, Frieling G, Rosenthal S. Dermal pleomorphic liposarcoma resembling pleomorphic fibroma: report of a case and review of the literature. *J Cutan Pathol*. 2013;40:734–739.
60. Ramírez-Bellver JL, López J, Macías E, et al. Primary dermal pleomorphic liposarcoma: utility of adipophilin and MDM2/CDK4 immunostainings. *J Cutan Pathol*. 2017;44:283–288.
61. Dahlin DC, Salvador AH. Cartilaginous tumors of the soft tissues of the hands and feet. *Mayo Clin Proc*. 1974;49:721–726.
62. Chung EB, Enzinger FM. Chondroma of soft parts. *Cancer*. 1978;41:1414–1424.



eFig. 117.1 Clustered piloleiomyomas on the back. The trunk is a common location for multiple piloleiomyomas. Patients with this clinical presentation need to be evaluated for the possibility of hereditary leiomyomatosis and renal cell cancer (Reed syndrome; see Table 117.2).



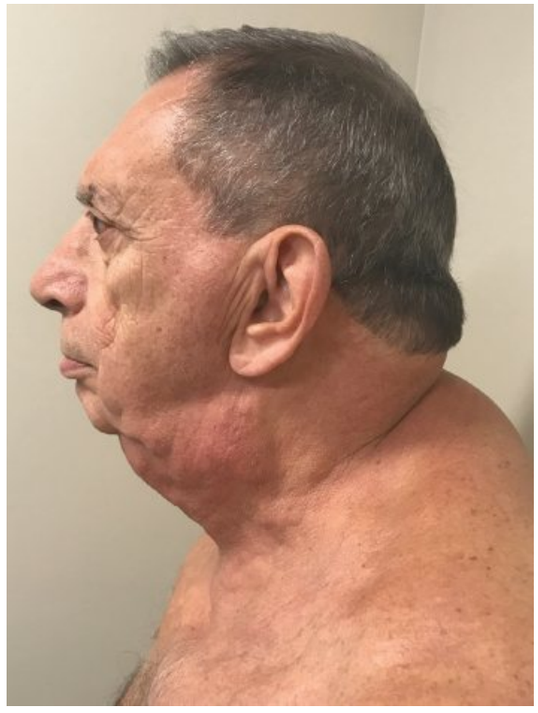
eFig. 117.2 Clustered piloleiomyomas on the back. The patient had hereditary leiomyomatosis and renal cell cancer (Reed syndrome).



eFig. 117.3 Smooth muscle hamartoma. This infant presented with a firm plaque on the thigh. *Courtesy Ronald P. Rapini, MD.*



eFig. 117.4 Smooth muscle hamartoma. Circumscribed congenital hypertrichosis in association with a skin-colored plaque. *Courtesy Karynne O. Duncan, MD.*



eFig. 117.5 Benign symmetric lipomatosis (Madelung disease). Diffuse symmetric fat deposits within the neck and upper trunk. *Courtesy Carolyn Carroll, MD.*

118 Mastocytosis

Michael D. Tharp

Key features

- Mastocytosis can develop from birth to adulthood and may involve only the skin (most children and some adults) or multiple organs such as the bone marrow, liver, spleen, and/or lymph nodes (primarily adults)
- Childhood disease is more common and often presents with one or more tan to pink–brown or brown papules or plaques (maculopapular mastocytosis) that frequently resolve by adolescence
- Mastocytomas are thicker plaques or nodules that are few in number and occur primarily in children
- Adults with mastocytosis often have cutaneous lesions; when present, they typically appear as small red–brown macules or papules ("urticaria pigmentosa") and tend to be associated with milder disease
- Adult mastocytosis persists throughout life
- Stroking of mastocytosis lesions often leads to urtication (Darier sign), which is more pronounced in children due to a higher density of mast cells
- Activating mutations in codon 816 of *KIT* are detected in the majority of adults and ~40% of children with mastocytosis; extracellular domain mutations occur more often in childhood-onset than in adult-onset disease
- Patients may have accompanying symptoms of mast cell mediator release such as pruritus, flushing, headaches, abdominal pain, diarrhea, and syncope
- Treatment is primarily directed at controlling symptoms in patients with limited disease and inhibiting activating *KIT* mutations in those with more advanced disease

INTRODUCTION

Mastocytosis represents a spectrum of clinical disorders with a common phenotype of tissue mast cell hyperplasia that can involve the skin, bone marrow, and other organs. Despite significant advances in understanding the pathogenesis of mastocytosis, explanations for the differences in clinical presentations and course between childhood-onset and adult-onset disease are still needed (Fig. 118.1). Childhood mastocytosis has an excellent prognosis, with ~50%–70% of affected children experiencing resolution by adolescence. In contrast, adult-onset mastocytosis typically has a chronic course and is more often associated with extracutaneous involvement and systemic symptoms[1]. Therapy for mastocytosis usually centers on inhibiting the effects of secreted mast cell mediators[2–4], with tyrosine kinase inhibitors such as midostaurin, avapritinib, and imatinib representing options in patients with more advanced systemic disease[5–8]. Cytoreductive therapies (e.g. cladribine) and rarely hematopoietic stem cell transplantation may also be utilized in advanced systemic disease[4].

HISTORY

The original description of mastocytosis was by Nettleship and Tay, who told of a 2-year-old girl with hyperpigmented papules that spontaneously urticated[9]. Eight years later, in 1877, Paul Ehrlich formally discovered the mast cell. The next year, Sangster suggested the name "urticaria pigmentosa". Unna was the first to demonstrate that mast cells were responsible for the cutaneous findings in mastocytosis patients[10].

EPIDEMIOLOGY

Mastocytosis can be present at birth or develop any time thereafter, including into late adulthood. Childhood-onset mastocytosis is defined as presenting prior to puberty. In a pediatric series (n=101), cutaneous mastocytosis appeared by ages 6 months and 2 years in 73% and 97% of children, respectively[11]. Adult-onset mastocytosis most often develops in the third or fourth decade of life, has no sex preference, and occurs in all races[12,13].

While most individuals with mastocytosis have no family history of the disorder, there have been over 70 familial cases reported, including at least 15 sets of monozygotic twins; however, twin pairs discordant for the disease have also been described. Mastocytosis has been documented in three generations of a single kindred[14,15].

PATHOGENESIS

Mast cells are derived from pluripotent $CD34^+$ precursors in the bone marrow that then circulate in the peripheral blood as agranular, monocytic-appearing cells. After migrating into tissues, these immature mast cells assume their typical granular morphology (see Ch. 18). Circulating mast cell precursors express CD34, the tyrosine kinase receptor KIT (CD117), and IgG receptors (FcγRII), but not high-affinity IgE receptors (FcεRI)[16]. The KIT receptor is expressed on mast cells, melanocytes, primitive hematopoietic stem cells, primordial germ cells, and interstitial cells of Cajal. Activation of KIT by its ligand (stem cell factor [SCF]) induces mast cell growth and maturation, and it extends cell survival by preventing apoptosis. Membrane-bound and soluble forms of SCF exist, and both induce KIT activation. SCF is produced by bone marrow stromal cells, fibroblasts, keratinocytes, endothelial cells, and reproductive Sertoli and granulosa cells. Peripheral blood mast cell precursors cultured in the presence of SCF and other cytokines (e.g. interleukin [IL]-3, -4, -6, -9) become $KIT^+/CD34^-/Fc\gamma RII^-/Fc\varepsilon RI^+$ and develop characteristic cytoplasmic mast cell granules, as seen in mature tissue mast cells[16,17].

Alterations in KIT structure and activity are central to the pathogenesis of mastocytosis. *Somatic* activating mutations in *KIT* involving codon 816 represent the most common genetic abnormality in patients with sporadic mastocytosis. The result is a substitution of the amino acid aspartic acid (D) with valine (V), i.e. D816V, or less commonly another amino acid (Fig. 118.2). These mutations lead to constitutive, ligand-independent activation of the receptor. Less common activating mutations and a rare dominant inactivating mutation have also been identified in children and adults with mastocytosis (see Fig. 118.2). In addition, rare *germline* mutations have been reported[15,18–20].

In a study in which the entire *KIT* sequence was analyzed in skin biopsy specimens from 50 children (ages 0–16 years) with primarily maculopapular mastocytosis, codon 816 mutations were found in 42% and other activating mutations in 44% of the patients[18]. However, the mechanism by which childhood disease often resolves spontaneously, despite the presence of underlying somatic *KIT* mutations, remains unknown[14,18].

In a transgenic mouse model of mastocytosis in which human activated *KIT* (D816V) was expressed, only 8 of 28 genetically identical animals developed clinical features of mastocytosis, ranging from indolent mast cell hyperplasia to an invasive mast cell tumor[21]. In another model utilizing the homologous mouse *Kit* D814V, results ranged from advanced mast cell disease when this mutation appeared in undifferentiated bone marrow progenitors to variable mast cell tumors/skin disease when *Kit* D814V was only expressed in committed mast cell progenitors or mature mast cells[22]. The diverse phenotypic expression of gain-of-function *KIT* mutations, along with the lack of *KIT* mutations in some patients and families with mastocytosis, points to

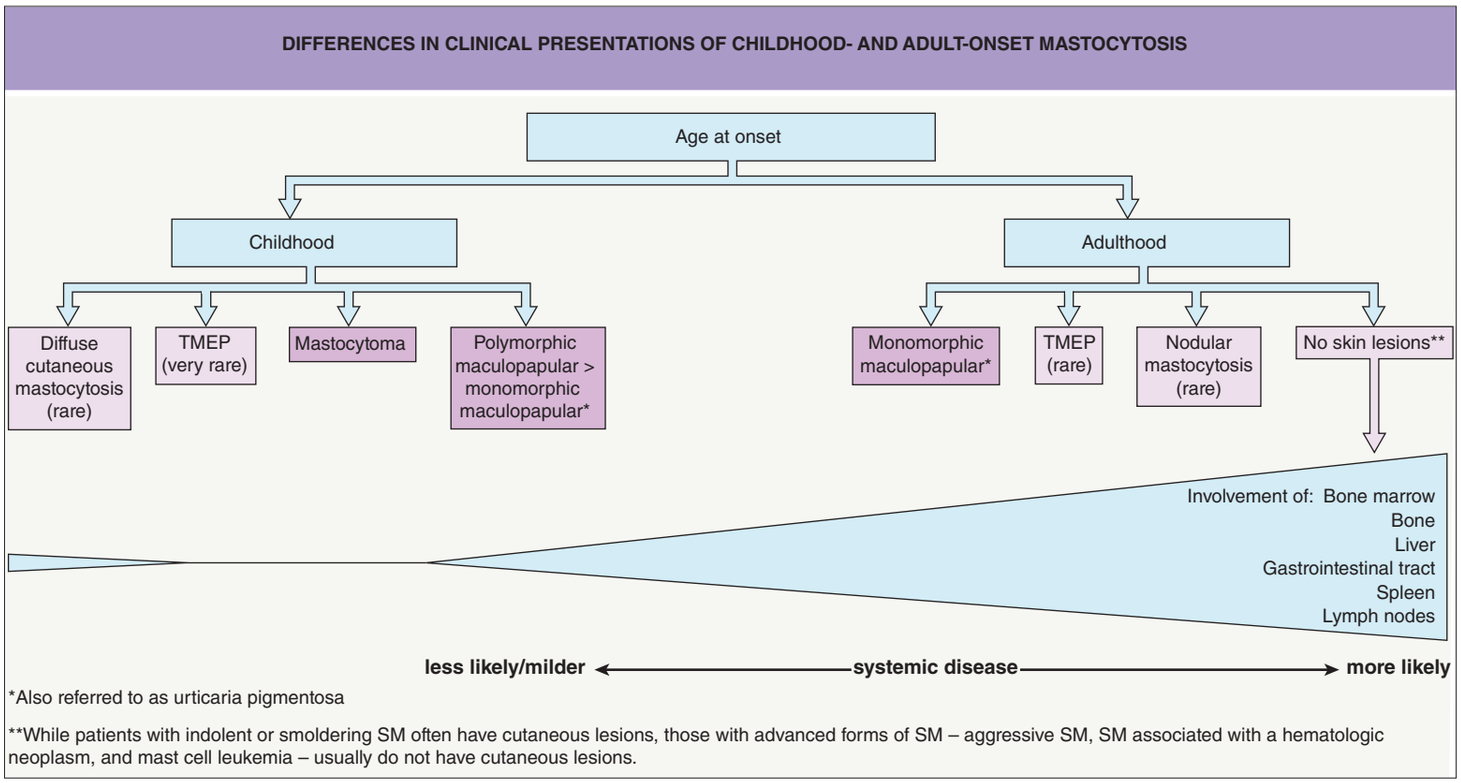


Fig. 118.1 Clinical presentations of childhood and adult-onset mastocytosis. The darker boxes represent the most common forms. Based upon the WHO classification scheme (see Tables 118.1 & 118.2), most children and a small proportion of adults have isolated cutaneous mastocytosis. Most adults with skin lesions have indolent systemic mastocytosis (SM), while those with advanced forms of SM usually do not have cutaneous involvement. In general, children have a benign course with a tendency for spontaneous remission. SM, systemic mastocytosis; TMEP, telangiectasis macularis eruptive perstans.

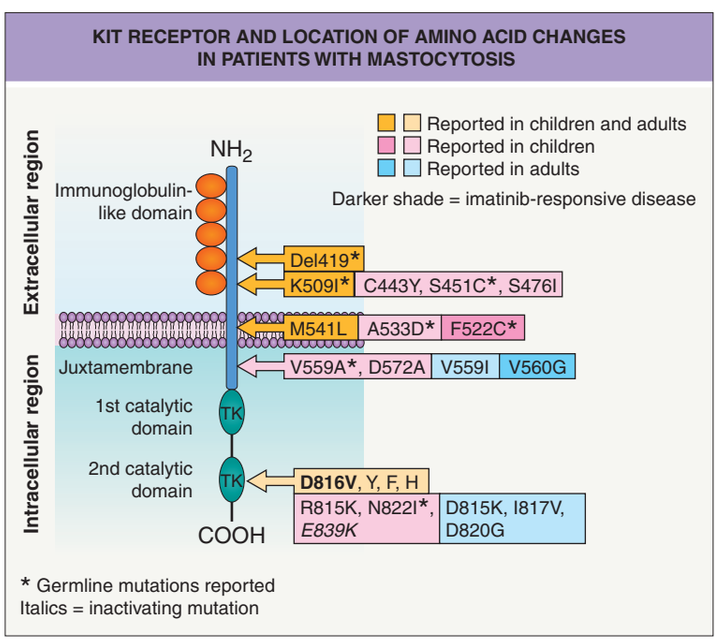


Fig. 118.2 KIT receptor and location of amino acid changes (due to *KIT* mutations) in pediatric and adult patients with mastocytosis. For example, D816V means that a mutation in codon 816 resulted from valine (V) being replaced by aspartic acid (D). The plasma membrane-bound KIT receptor is composed of three distinct regions: (1) the extracellular region (five immunoglobulin-like repeats [orange]); (2) the transmembrane region; and (3) the intracellular region (two tyrosine kinase domains [green]). The most common site for activating mutations is exon 17, which contains codon 816. The result is constitutive ligand-independent activation of the receptor. TK, tyrosine kinase domain (one binds ATP and the other has phosphotransferase activity).

additional pathogenic factors in mastocytosis. Indeed, in adult patients with advanced systemic mastocytosis, somatic mutations have been identified in *KIT* plus a variety of other genes such as *TET2, ASXL1, JAK2, SRSF2, RUNX1*, and *CBL*, which encode *Tet* methylcytosine dioxygenase *2*, *a*dditional *s*ex combs *l*ike *1*, transcriptional regulator, *J*anus *k*inase *2*, *s*erine and arginine *r*ich *s*plicing *f*actor *2*, runt related transcription factor 1, and *Cbl* proto-oncogene, respectively[23,24].

CLINICAL FEATURES

Signs and Symptoms

Many children and adults with cutaneous mastocytosis have few, if any, symptoms. When symptoms do occur, they are due to the diverse physiologic effects of secreted mast cell mediators, such as histamine, eicosanoids, and cytokines (Fig. 118.3). These complaints and findings may range from pruritus and flushing to abdominal pain and diarrhea to palpitations, dizziness, and syncope. Of interest is the relative absence of pulmonary symptoms in mastocytosis. Complaints of fever, night sweats, malaise, weight loss, bone pain, epigastric distress, and problems with mentation (cognitive disorganization) often signal the presence of systemic disease. There are even rare reports of deaths in children and adults in association with extensive mast cell mediator release[2,13,14].

Symptoms of mastocytosis can be exacerbated by exercise, heat, friction, or other trauma to skin lesions. In addition, alcohol, narcotics, salicylates and other nonsteroidal anti-inflammatory drugs (NSAIDs), polymyxin B, and anticholinergic medications have been implicated in precipitating symptoms of mastocytosis. Some systemic anesthetic agents may potentially induce anaphylaxis (see below)[12].

Cutaneous Lesions

Childhood-onset mastocytosis, which almost always affects the skin, has three major clinical presentations: (1) solitary or few (≤3) lesions, referred to as "mastocytomas": 15%–50% of patients; (2) multiple

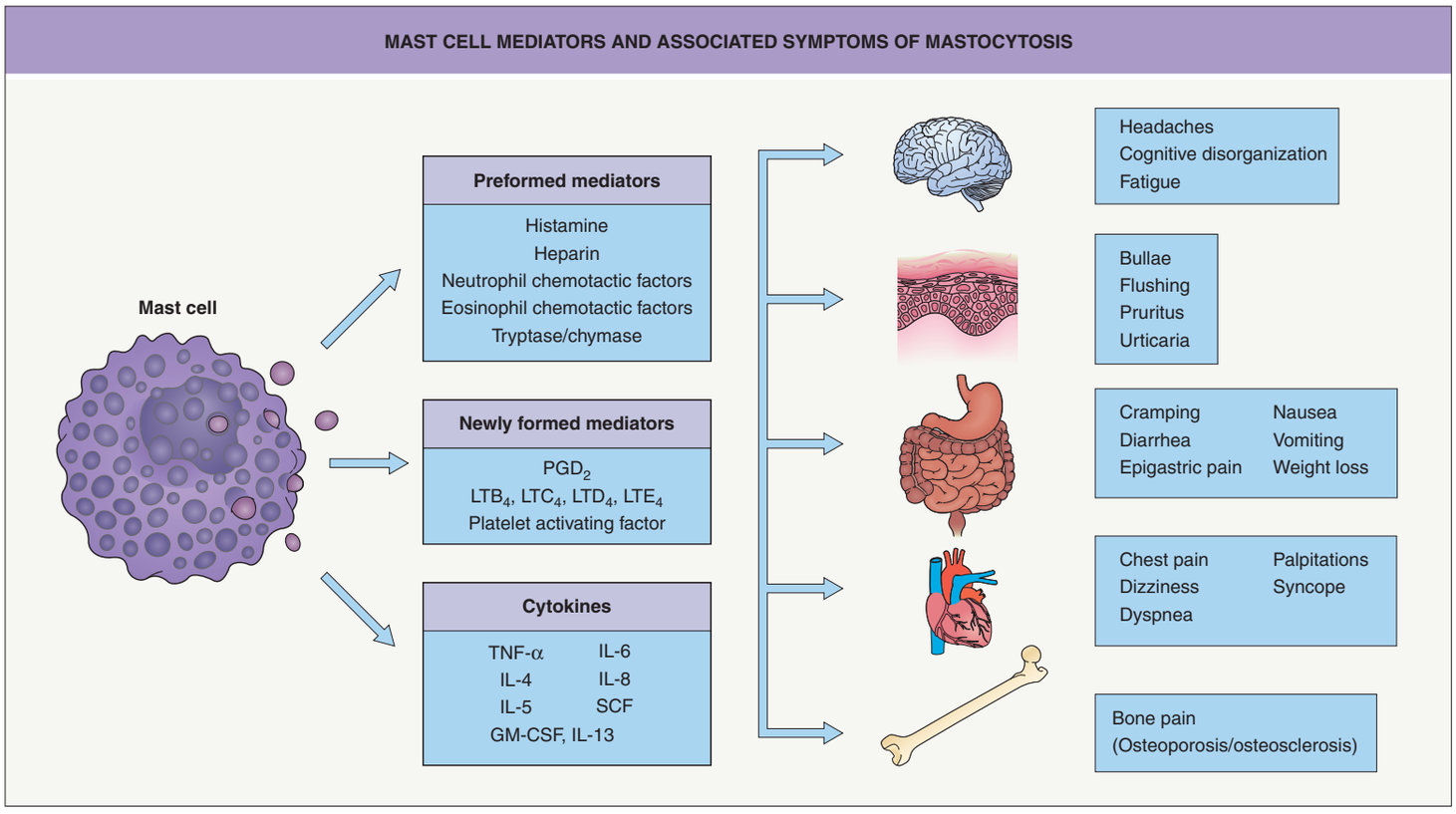


Fig. 118.3 Mast cell mediators and associated symptoms of mastocytosis. GM-CSF, granulocyte–macrophage colony-stimulating factor; IL, interleukins; LT, leukotrienes; PGD_2, prostaglandin D_2; SCF, stem cell factor; TNF, tumor necrosis factor.

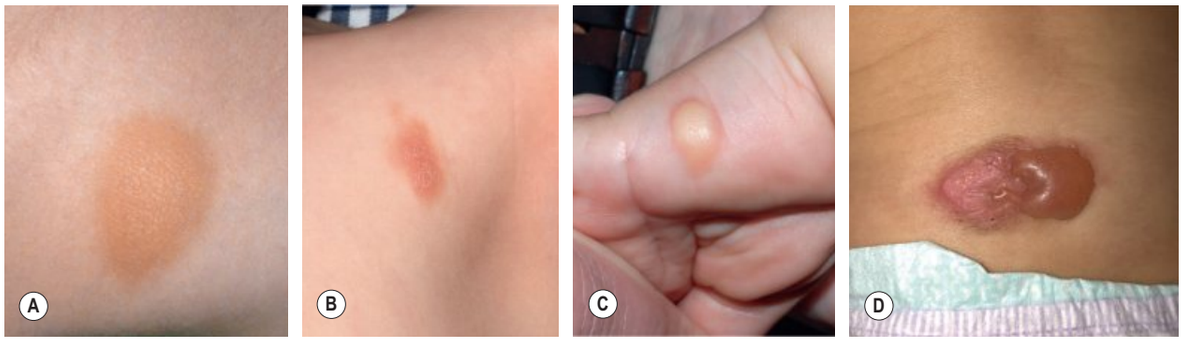


Fig. 118.4 Mastocytomas in young children. Tan (**A**) and pink–tan (**B**) plaques with a leathery surface. **C** Swelling and a subtle rim of erythema resulting from urtication of a yellowish nodule on the wrist. **D** Bullae formation within a pink–brown plaque on the back. *A, Courtesy Antonio Torrelo, MD; B–D Courtesy Julie V. Schaffer, MD.*

(<10 to >100) lesions, referred to as "maculopapular" mastocytosis: 45%–75% of patients; and (3) diffuse cutaneous involvement: <5%–10% of patients. A mastocytoma appears as a tan or yellow–tan to brown nodule or plaque, which may be only slightly elevated and typically has a leathery texture (Fig. 118.4). These lesions can be congenital or become evident during infancy, and they favor the distal extremities[11,12,14]. Bullae may arise within a mastocytoma, leading to misdiagnoses such as bullous impetigo.

Children with multiple lesions of mastocytosis most often present with *large, polymorphic* yellow–tan to pink–brown or brown plaques and nodules, which are frequently admixed with smaller lesions (Fig. 118.5D–F). This cutaneous variant is associated with an earlier onset during infancy and is more likely to spontaneously resolve[14,25]. Less often, only *small, monomorphic* tan to reddish-brown macules or papules are evident (Fig. 118.5A,B), similar to the typical urticaria pigmentosa presentation in adults (see below)[14]. Multiple lesions favor the trunk and classically spare the central face, palms, and soles.

Diffuse cutaneous mastocytosis presents within the first few months of life as thickened skin with a leathery texture and variable hyperpigmentation in a generalized distribution (Fig. 118.6); however, systemic disease is typically absent and spontaneous resolution usually occurs[26]. This term should be reserved for diffuse skin involvement rather than the confluence of individual lesions. Less common presentations of mastocytosis in children include ill-defined tan or telangiectatic patches; small, firm brown nodules; and yellowish patches with superimposed doughy papules ("xanthelasmoid" mastocytosis)[12].

Blistering following urtication is common in infants and young children with mastocytosis, especially those with large, thick lesions or the diffuse form. The latter patients may present with extensive bullae and erosions (see Fig. 118.6; see Ch. 34). The tendency to blister usually remits by 3 to 5 years of age, and it is believed to result from the release of mast cell serine proteases[14,17].

The most common cutaneous lesions of *adult-onset mastocytosis* are small (<1 cm), monomorphic, reddish-brown macules and papules (Fig. 118.7). This pattern is now referred to as maculopapular but the term urticaria pigmentosa is still commonly employed. In patients with skin type I, the macules and papules may appear pink to red in color. Lesions are most numerous on the trunk and proximal extremities and appear less frequently on the face, distal extremities, or palms and soles. Individual lesions can resolve, but the total number usually increases over time. Close inspection reveals variable hyperpigmentation and fine telangiectasias. These lesions are most often associated with indolent systemic mastocytosis[1,12] (see below).

Less commonly, yellow–tan to red–brown or violaceous nodules or papulonodules develop, representing a hallmark of indolent disease (see below)[12,27]. Severe infiltrative mastocytosis may progress to diffuse thickening of the skin, especially in flexural sites; facial involvement may acquire a leonine appearance. A rare form of cutaneous mastocytosis



Fig. 118.5 Maculopapular cutaneous mastocytosis in children. Patients can present with variable numbers and sizes of papules, which may be scattered (**A**), clustered (**B**), or nearly confluent (**C**), as well as predominantly plaques (**D, E**) or papulonodules (**F**). As in solitary lesions, the degree of associated hyperpigmentation can vary. Note the Darier sign (**C**, **D**). *A, C, Courtesy Antonio Torrelo, MD; B, D, E Courtesy Julie V. Schaffer, MD.*



Fig. 118.6 Diffuse cutaneous mastocytosis and blistering in infants. Diffusely infiltrated skin with multiple erosions and a leathery texture that may be subtle (**A**) or striking (**B**). This appearance has been compared to pigskin. **C** Spontaneous blister superimposed on a plaque. *A, Courtesy Antonio Torrelo, MD.*

is telangiectasia macularis eruptiva perstans (TMEP), which is characterized by macules and patches composed of telangiectasias without significant hyperpigmentation (Fig. 118.8). Mastocytomas are extremely rare in adults[1,12].

Formation of an urticaria-like wheal upon firmly stroking or rubbing of skin lesions (Darier sign) results from release of mast cell mediators and is indicative of the diagnosis (Fig. 118.9). Darier sign is readily demonstrated in pediatric patients, especially with nodular lesions, and if vigorously induced may precipitate systemic symptoms[11,14]. This sign tends to be more subtle in typical adult mastocytosis lesions and TMEP. These differences reflect lesional mast cell density, which is higher in mastocytomas and childhood maculopapular mastocytosis than in adult-onset cutaneous mastocytosis[28]. Dermographism may also be observed in the uninvolved skin of pediatric and adult mastocytosis patients[1,14,28].

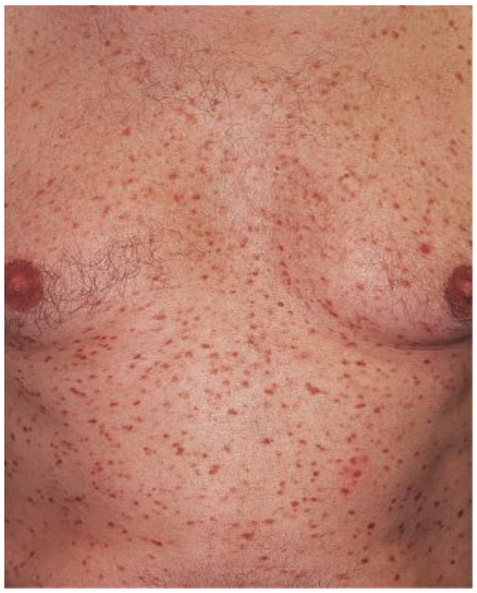


Fig. 118.7 Adult maculopapular mastocytosis ("urticaria pigmentosa"). Numerous reddish-brown macules and papules.



Fig. 118.8 Telangiectasia macularis eruptiva perstans. Multiple lesions composed of telangiectasias are present.

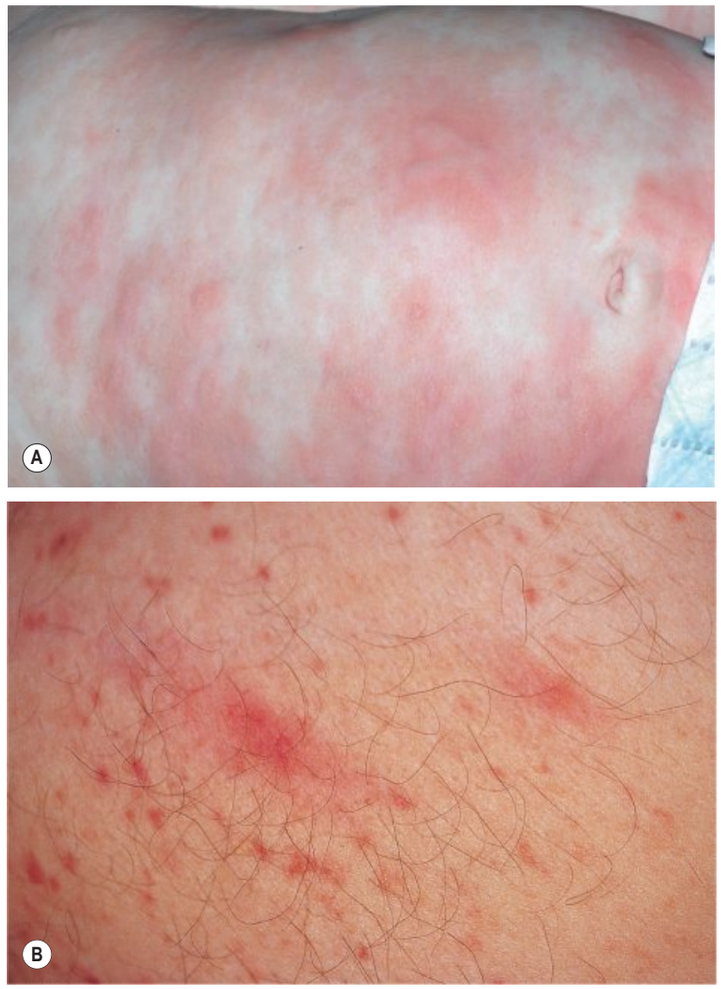


Fig. 118.9 Darier sign in mastocytosis. A An infant with extensive cutaneous involvement. **B** An adult with macular and papular lesions. *A, Courtesy Julie V. Schaffer, MD; B, Courtesy Thomas Horn, MD.*

Systemic Manifestations

Skeletal lesions frequently occur in adult patients with mastocytosis but are rare in children (see Fig. 118.1)[11,14]. Bone involvement can be associated with skeletal pain. In one study of 142 adults with mastocytosis, 40% had skeletal involvement, with a similar frequency in those with childhood-onset and adult-onset disease[29]. Bony lesions may appear as radio-opacities, radiolucencies, or a mixture of the two. The skull, spine, and pelvis are most commonly involved. In an earlier study of 58 adult systemic mastocytosis patients, 57% had diffuse bone involvement, whereas only 2% had focal lesions. Demineralization was the most common change in patients with diffuse skeletal disease, followed by osteosclerosis and mixed lesions of osteosclerosis and osteoporosis[30]. Osteoporosis is more prevalent in men with mastocytosis and may be the presenting manifestation of the disease[30,31].

Undecalcified iliac crest biopsies from adult mastocytosis patients have demonstrated increased numbers of mast cells and evidence of enhanced cortical and trabecular bone turnover. These observations led to the hypothesis that mast cells and their mediators are directly responsible for the associated skeletal changes. For example, mast cell-derived heparin and SCF have been implicated in promoting osteoporosis via stimulation of osteoclastic activity. Osteoclasts have been shown to express KIT receptors on their surface and to be activated by SCF. Mast cell histamine, however, is also capable of promoting bone sclerosis through activation of fibroblasts, and mast cell-derived IL-6 appears to induce both bone resorptive and fibrotic activities[30,32].

The **bone marrow** is involved in nearly all adult patients with systemic mastocytosis. In general, a bone marrow biopsy appears to be more reliable than an aspirate for identifying abnormal mast cell morphology and distribution[33]. Multifocal mast cell aggregates are typically located in perivascular and paratrabecular locations. Bone marrow involvement is relatively uncommon in children with mastocytosis, and bone marrow biopsy is not routinely recommended[14,34].

Splenomegaly is relatively common in patients with advanced systemic mastocytosis but rare in those with indolent systemic disease[35,36]. Increased numbers of mast cells and eosinophils are frequently observed in the spleen, as are various degrees of fibrosis and hematopoiesis. In general, **lymph node** enlargement is uncommon in mastocytosis patients but it does occur in those with more advanced systemic disease. Among 58 systemic mastocytosis patients, 26% had peripheral lymphadenopathy, whereas 19% had central nodal disease[37]. Histologically, early involvement of lymph nodes often consists of only clusters of mast cells, while in more advanced disease, mast cell infiltrates involve the paracortex and are often accompanied by eosinophils[37,38].

Gastrointestinal (GI) symptoms such as abdominal pain, diarrhea, nausea and vomiting resulting from mast cell mediator release may occur spontaneously or be precipitated by alcohol, aspirin, NSAIDs, or certain foods[36,39]. Approximately 25% of patients with isolated cutaneous disease and 70% of those with systemic mastocytosis report GI symptoms[39]. Diarrhea in patients with mastocytosis is usually episodic; it can result from malabsorption, increased motility, and/or acid hypersecretion, with the former due to mast cell infiltration and the latter two symptoms likely related to the release of mast cell histamine and prostaglandins. Patients with systemic mastocytosis are at increased risk of gastritis and peptic ulcers, which occasionally lead to

GI hemorrhage. A number of radiographic changes in the GI tract have been described, including urticaria-like lesions and thickened gastric, duodenal and jejunal folds, as well as mucosal nodules and/or peptic ulcers. Biopsies of mucosal nodules have demonstrated numerous mast cells with varying numbers of eosinophils[40]. Gastrointestinal stromal tumors (GISTs) frequently have underlying *somatic* activating KIT mutations and are occasionally seen together with cutaneous mastocytosis in families with *germline* activating *KIT* mutations (see Fig. 118.2)[41]. **Hepatomegaly** most commonly occurs in advanced systemic mastocytosis and is not always associated with abnormal liver function tests[35,36].

A mixed organic **brain** syndrome with a constellation of symptoms – including irritability, fatigue, headache, poor attention span and motivation, limited short-term memory, inability to work effectively, and difficulty in interacting with other people – has been described in patients with mastocytosis. It has been hypothesized that these symptoms may be secondary to mast cell mediators. Electroencephalographic studies in these patients range from normal to changes consistent with a toxic or metabolic process[42].

Classification of Mastocytosis

The World Health Organization (WHO) classification scheme for mastocytosis was proposed in 2001 and then modified in 2008 and 2016 (Table 118.1)[36]. *Cutaneous mastocytosis* represents the largest group and includes nearly all affected children and some adults. Childhood-onset mastocytosis resolves by adolescence in ~50%–70% of patients, with persistence into adulthood in the remainder[13,14]. The WHO has also established criteria for the diagnosis of *systemic mastocytosis* (SM; Table 118.2)[36]. From a dermatologic perspective, appreciation of indolent and smoldering SM is important as these patients frequently have cutaneous lesions.

Although patients with *indolent systemic mastocytosis* (ISM) have detectable mast cell infiltrates in multiple organs (e.g. bone marrow, liver, spleen, lymph nodes), organ impairment is generally absent and there are few, if any, systemic symptoms. Patients with ISM frequently have slightly increased numbers of spindle-shaped, hypogranulated bone marrow mast cells (BMMCs) that express CD25 ± CD2, which are not expressed in normal BMMCs. CD25 appears to be the most reliable marker for BMMCs with gain-of-function *KIT* mutations in exon 17 (see Fig. 118.2)[33,36]. Progression of ISM to more severe forms of SM appears to be unusual. In a study of 145 adults with ISM, the cumulative probabilities of disease progression to more advanced SM at 10 and 25 years were 1.7% and 8.4%, respectively[43].

Compared to individuals with ISM, patients with the *smoldering SM* (SSM) have increased disease burden manifesting as "B" findings – e.g. hepatosplenomegaly, lymphadenopathy, serum tryptase levels >200 ng/ml (see Table 118.2) – and are more likely to be anemic and an older age. The overall prognosis for SSM patients is less favorable than ISM due to an increased risk for developing more advanced systemic disease[43–46].

SM with an associated hematologic neoplasm (SM-AHN) does not usually present with cutaneous lesions, but affected individuals may have "B" and "C" findings (see Table 118.2). In some patients, the hematologic neoplasm precedes the development of SM. The overall prognosis of SM-AHN patients depends upon the severity of the hematologic disease[44,45].

Patients with *aggressive SM* (ASM) have "C" findings with organ dysfunction secondary to mast cell infiltrates, notably in the liver (e.g. ascites, portal hypertension), bone (pain, pathologic fractures), gastrointestinal tract (malabsorption), and spleen (hypersplenism) (see Table 118.2). They also may develop cytopenias, leukocytoses (eosinophilia, basophilia, monocytosis), and/or thrombocytosis as a reflection of abnormal myelopoiesis. Serum tryptase levels are often elevated, reflecting a significantly increased total body mast cell burden. The overall prognosis appears to depend upon the response to treatment (Fig. 118.10)[33,44,45].

Mast cell leukemia (MCL) is rare and is divided into acute and chronic forms. Diagnosis requires ≥10% mast cells among nucleated peripheral blood cells and ≥20% atypical mast cells in the bone marrow[1,36,44]. However, because mature mast cells are rarely observed in the blood

WHO 2016 CLASSIFICATION OF MASTOCYTOSIS
Cutaneous mastocytosis (CM)
• Maculopapular CM (urticaria pigmentosa) • Diffuse CM • Mastocytoma of skin (cutaneous mastocytoma)
Systemic mastocytosis (SM)
• Indolent SM* • Smoldering SM* • SM with an associated hematologic (non-mast cell lineage) neoplasm • Aggressive SM • Mast cell leukemia
Mast cell sarcoma
*Forms of SM most likely to have cutaneous involvement; see Table 118.2 for defining criteria.

Table 118.1 WHO 2016 classification of mastocytosis.

WHO CRITERIA FOR THE DIAGNOSIS OF SYSTEMIC MASTOCYTOSIS AND RELATED B & C FINDINGS
WHO criteria for systemic mastocytosis (SM)
Major criterion
Multifocal, dense infiltrates of MCs (aggregates of ≥15 MCs) in BM biopsies and/or in sections of other extracutaneous organ(s)
Minor criteria
• In BM smears, >25% of all MCs are atypical – *or* – >25% of MCs are spindle-shaped in infiltrates within extracutaneous organ(s) • *KIT* point mutation at codon 816 in the BM or another extracutaneous organ • MCs in BM, blood, or another extracutaneous organ express CD2 and/or CD25 • Baseline serum tryptase level >20 ng/ml (if there is an unrelated myeloid neoplasm, this is not valid as an SM criterion)
SM diagnosis requires either the major criterion plus 1 minor criterion or 3 minor criteria
Criteria for B and C findings in patients with SM
B findings: indicate a high burden of MCs and/or expansion of the neoplastic process into multiple hematopoietic lineages, without impairment of organ function
• MC infiltration of the BM >30% and basal serum tryptase level >200 ng/ml • Hypercellular BM with loss of fat cells, discrete signs of dysmyelopoiesis without substantial cytopenias, or WHO criteria for a myelodysplastic syndrome or myeloproliferative neoplasm • Organomegaly: palpable hepatomegaly with normal liver function, palpable splenomegaly without hypersplenism, and/or lymphadenopathy on palpation or imaging (>2 cm)
C findings: indicate organ damage produced by mast cell infiltration (should be confirmed on biopsy if possible)
• Cytopenia(s) caused by MCs: absolute neutrophil count <1000/mcl, hemoglobin <10 g/dl, or platelet count <100 000/mcl • Hepatomegaly with abnormal liver function, ascites, and/or portal hypertension • Splenomegaly with associated hypersplenism • Skeletal osteolytic lesions with pathologic fractures (fractures from osteoporosis alone is not a C finding) • Malabsorption with hypoalbuminemia and weight loss due to gastrointestinal MCs
*In SM patients with <2 B findings and no C findings, the diagnosis is **indolent SM**.* *When ≥2 B findings but no C findings are present, the diagnosis is **smoldering SM**.* *When ≥1 C findings (± B findings) are present, the diagnosis is either **aggressive SM** (<20% MCs in BM smears) or **MC leukemia** (≥20% MCs in BM smears)*

Table 118.2 WHO criteria for the diagnosis of systemic mastocytosis (SM) and related B & C findings. BM, bone marrow; MC, mast cell.

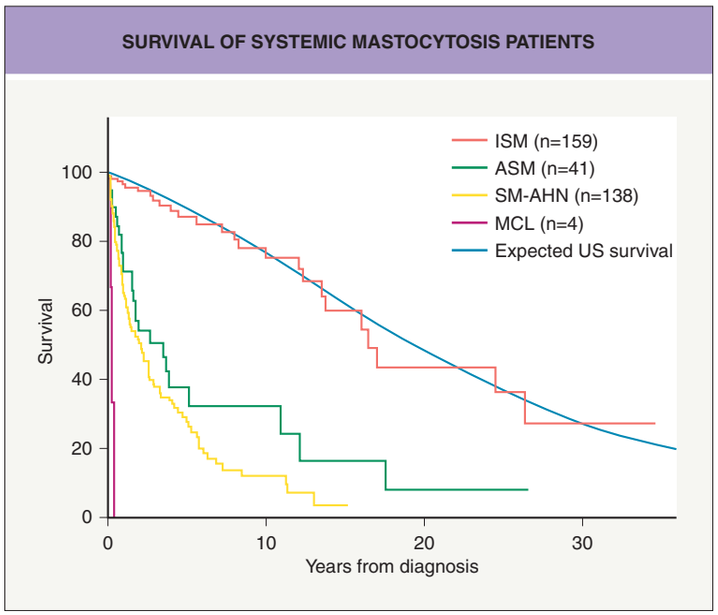


Fig. 118.10 Survival of patients with systemic mastocytosis (SM). The life expectancy of patients with indolent SM (ISM) was not significantly different from the age- and sex-matched US population from the appropriate time period, and leukemic transformation rarely occurred. Based upon these data, the authors recommended that, in general, therapy for ISM should be symptom-directed. ASM, aggressive SM; SM-AHN, SM with associated hematologic neoplasm; MCL, mast cell leukemia. *From Lim K-H, Tefferi A, Lasho TL, et al. Systemic mastocytosis in 342 consecutive adults: survival studies and prognostic factors. Blood 2009;113:5727–36.*

of normal individuals, their presence should raise the suspicion of an "aleukemic" form of MCL in which patients have fewer circulating mast cells[47]. Most MCL patients do not have cutaneous lesions, but those with an acute onset frequently exhibit "B" and "C" findings. Multi-organ failure, including of the bone marrow, often occurs over weeks to a few months in the acute form, with an expected survival of a year or less from the time of diagnosis[44,45]. Chronic MCL, however, has a more indolent course and survival is similar to SSM[47].

The presence of mutations in *KIT* and other genes may also have clinical implications in patients with mastocytosis. Advanced forms of mastocytosis are associated with gain-of-function *KIT* mutations in not only BMMC progenitors but also bone marrow mesenchymal stem cells, leading to involvement of lymphocytic or myeloid cell lineages[22,23,33,48]. In a study of 39 SM patients with a *KIT* D816V mutation, additional mutations in genes such as *TET2, SRSF2, ASXL1, RUNX1*, and *CBL* were found in 25% of those with ISM/SSM and 89% of those with more advanced forms of SM. These additional mutations were associated with decreased overall survival[24]. In contrast, patients with familial disease often lack *KIT* mutations in codons 815 and 816; their overall prognosis appears to be good but is less well defined[15,49].

An approach to the initial evaluation of a patient with cutaneous mastocytosis is presented in Fig. 118.11. A thorough history is crucial, with inquiries into the duration and progression as well as factors that provoke symptoms. For *childhood-onset* mastocytosis, the diagnosis is usually established clinically by recognition of characteristic skin lesions with a positive Darier sign (see Fig. 118.9). If the diagnosis is in doubt, confirmation can be achieved via a skin biopsy. No further testing is indicated for most children. However, additional evaluation should be performed in children who develop severe mast cell mediator-related symptoms or have evidence of hepatosplenomegaly, with the latter representing a marker of systemic involvement[14,50] (see Fig. 118.11).

Dermatologists have an opportunity to make the initial diagnosis of mastocytosis in adults who have cutaneous involvement, which can be confirmed by a skin biopsy demonstrating increased numbers of mast cells and/or the presence of an activating *KIT* mutation. Most of these patients have ISM, with fewer individuals having isolated cutaneous disease. For adults with skin lesions of mastocytosis, a baseline CBC with differential, serum tryptase level, liver function tests (LFTs), and DEXA scan of the lumbar spine and femur should be performed (see Fig. 118.11).

Recent guidelines from the American Initiative in Mast Cell Diseases (AIM) and European Competence Network on Mastocytosis (ECNM) recommend complete staging including a bone marrow biopsy in all adult mastocytosis patients to assist with prognostication[1,33,44,51]. However, other clinicians (including the author) do not believe that a bone marrow biopsy is required in adults with cutaneous lesions who have a normal or slightly elevated serum tryptase level[4] as well as a normal CBC and normal LFTs[50]. Of note, there is agreement that a bone marrow biopsy is indicated in those who have B or C findings (see Table 118.2)[1,44,50,51]. Detection of the *KIT* D816V mutation in the peripheral blood can help to determine the likelihood of SM and follow disease progression over time[52,53]. A provisional diagnosis of "mastocytosis in the skin" is given to adults with skin lesions of mastocytosis in whom a bone marrow biopsy has not been performed, and a scoring system has been developed to assess the risk of SM in these individuals[51,54] (see Fig. 118.11).

PATHOLOGY

Direct Studies

The diagnosis of mastocytosis is established by the presence of characteristic mast cells in one or more organs. For patients with cutaneous lesions, an increased number of mast cells can be demonstrated in a biopsy of lesional skin (Fig. 118.12). Eosinophils may be found within the dermis; hyperpigmentation of the basal layer of the epidermis with a few melanophages in the upper dermis is a common finding. Special stains, such as toluidine blue, Leder, and Giemsa, or monoclonal antibodies that recognize CD117 (KIT) or tryptase are helpful in identifying tissue mast cells[1] (Fig. 118.13).

Mast cell densities in childhood maculopapular mastocytosis and mastocytomas are 40-fold and 150-fold higher than in normal skin, respectively, and are therefore relatively easy to identify. In comparison, the density is ~30% lower in adults[28]. For nodular, papular, and macular lesions (including TMEP) of mastocytosis, mast cells have been quantified using a morphometric technique and shown to have densities of 63.2% (± 8.2% SEM), 16.1% (± 4.8% SEM), and 3.5% (± 1.8% SEM), respectively, compared to 0.4% (± 0.1% SEM) in normal skin[28]. In childhood mastocytosis, mast cells in lesional skin typically have a round or cuboidal shape, whereas they tend to appear fusiform or dendritic in adults. *KIT* mutations can often be detected in lesional skin and may help to confirm the diagnosis[18].

Biopsies of normal-appearing skin from patients with mastocytosis have normal concentrations of mast cells and thus are not useful for diagnosis[28]. A biopsy of the GI tract or bone marrow may be indicated in patients with mast cell mediator-related symptoms who lack skin lesions. Increased mast cell numbers in association with variable numbers of eosinophils can be observed in GI biopsies[1,33,39,50]. The bone marrow of patients with systemic disease frequently shows multifocal, spindle-shaped mast cells that express CD25 ± CD2. The detection of >25% atypical mast cells in extracutaneous tissues and the expression of CD25 and/or CD2 represent minor WHO diagnostic criteria for SM (see Table 118.2). Although coexpression of CD30 in BMMCs was initially reported to predict more advanced mastocytosis, a study of 142 patients demonstrated similar CD30 positivity across all systemic mastocytosis subgroups[55]. Because mast cells may appear hypogranular in tissues of patients with systemic disease, the combination of monoclonal antibodies against CD117 (KIT) and tryptase may be useful for their identification[36,56].

Indirect Studies

Detection of circulating mast cell mediators and/or their metabolites can offer indirect evidence of mastocytosis. Two forms (α and β) of mast cell tryptase have been identified[1,57]. Serum α-tryptase levels are elevated in patients with SM, regardless of whether or not they are experiencing acute symptoms, and therefore may be useful in assessing total body mast cell burden. However, β-tryptase is often detected both in mastocytosis patients and in patients *without* mastocytosis who are experiencing anaphylactic symptoms. Total (α and β) serum tryptase levels correlate with the extent of mast cell disease. In one study, half of those patients with total serum tryptase levels between 20 and 75 ng/ml had evidence of SM, whereas all patients

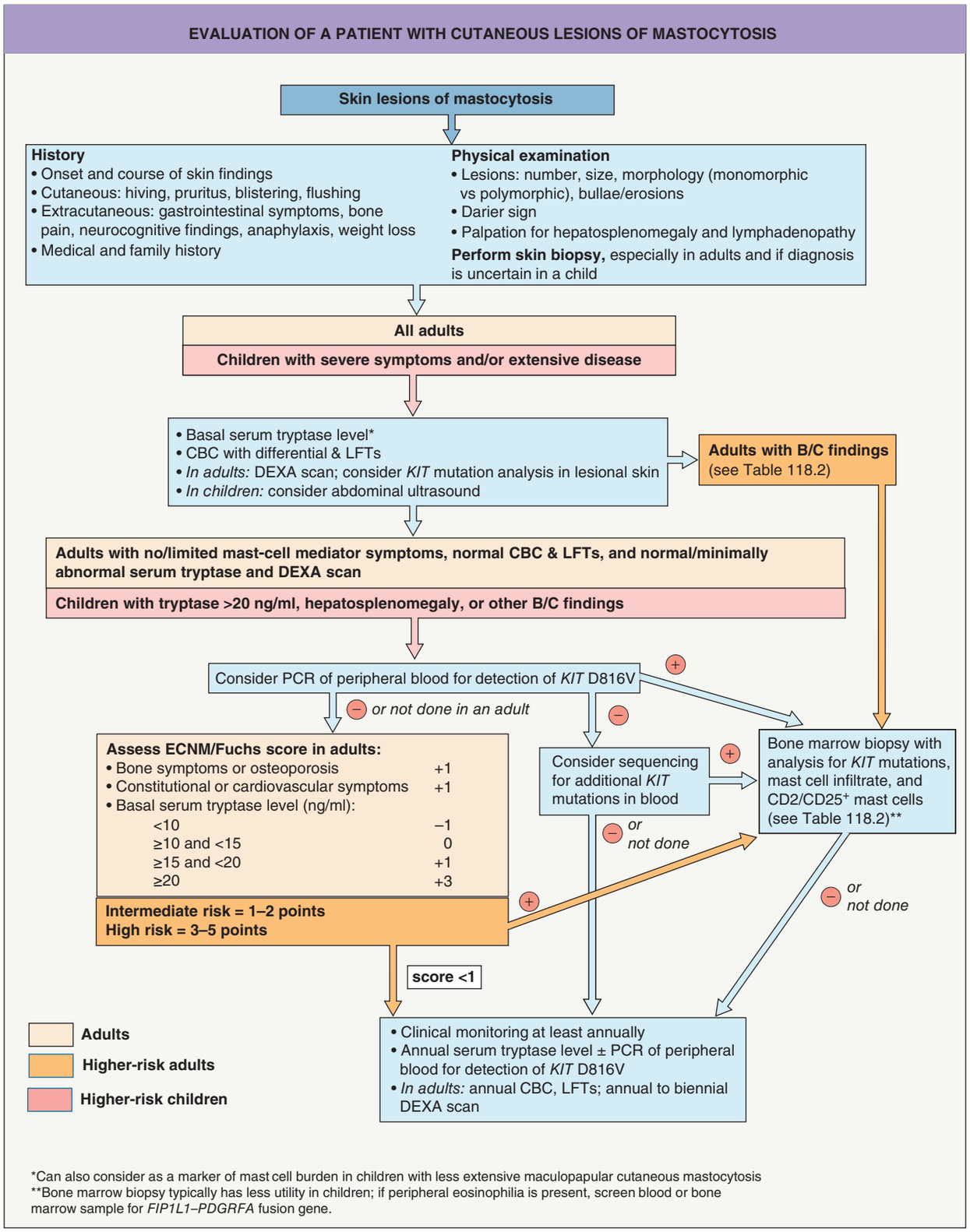


Fig. 118.11 Evaluation of a patient with cutaneous lesions of mastocytosis. Diagnosis of mastocytosis in the skin requires one major criterion – clinically typical skin lesions associated with the Darier sign – plus one minor criterion. The minor criteria are: (1) increased number of mast cells in lesional skin; and (2) detection of an activating *KIT* mutation in lesional skin. Additional investigations can be performed as directed by extracutaneous findings.

with levels >75 ng/ml had systemic involvement[5,57]. Of note, a total serum tryptase level >20 ng/ml represents one of the minor criteria for SM (see Table 118.2)[36].

Urinary excretion of histamine, MeImAA (1,4-methylimidazole acetic acid [histamine's major metabolite that is more persistently elevated]), and PGD_2M (major prostaglandin D_2 metabolite) are historical markers of mastocytosis disease that have low sensitivity and specificity. Plasma levels of IL-6 are also elevated in patients with mastocytosis, correlating with severity of bone marrow pathology, organomegaly, and extent of skin involvement[58].

DIFFERENTIAL DIAGNOSIS

The lesions of childhood and adult mastocytosis are so characteristic that they are only occasionally confused with other skin disorders. Mastocytomas may be misdiagnosed as café-au-lait macules, arthropod bites, Spitz or congenital melanocytic nevi, pseudolymphomas, or juvenile xanthogranulomas[11,14,49]. Childhood maculopapular lesions that spontaneously urticate may be mistaken for urticaria but are distinguished by the associated hyperpigmentation. The differential diagnosis for blisters due to mastocytosis in children may include bullous

arthropod bites, bullous impetigo, herpes simplex viral infection, linear IgA bullous dermatosis and, less often, other autoimmune bullous dermatoses. Infants with diffuse cutaneous mastocytosis can develop widespread blisters, which may be mistaken for epidermolysis bullosa or toxic epidermal necrolysis. Demonstration of increased mast cells in either the blister fluid or a skin biopsy helps to establish the diagnosis of mastocytosis. Nodular scabies in children has occasionally been misdiagnosed as mastocytosis.

The smaller maculopapular lesions typical of adult mastocytosis may at first glance appear as lentigines or melanocytic nevi, but mastocytosis lesions usually have associated erythema[56]. The differential diagnosis of TMEP includes other telangiectatic conditions, but some hyperpigmented maculopapular lesions are often evident. Lastly, if mast cells are not readily detected due to the presence of other leukocytes within the dermis, the patient may be misdiagnosed as having a histiocytic disorder or vasculitis[59].

Mast cell activation syndrome (MCAS) is characterized by symptoms of mast cell mediator release, but unlike mastocytosis there is no evidence of mast cell proliferation or persistent skin lesions. Serum tryptase levels may be slightly elevated in MCAS, and treatment with antihistamines, leukotriene inhibitors, and/or omalizumab is often of benefit[2,3]. Of note, the term mast cell activation *disorders* is sometimes used to encompass the various forms of mastocytosis and MCAS[60].

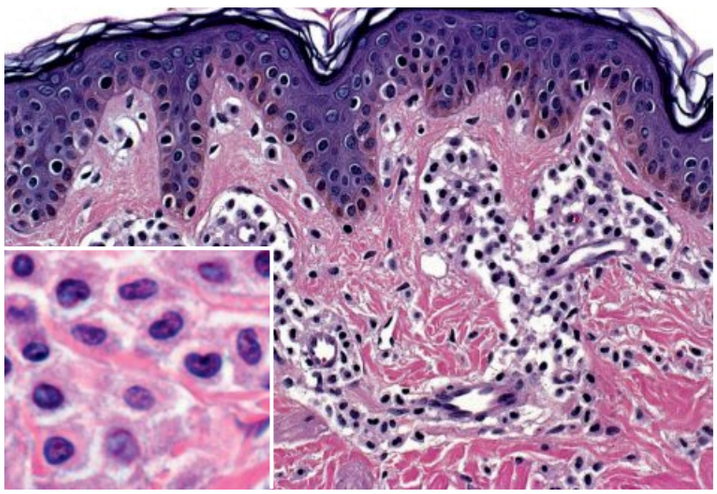


Fig. 118.12 Cutaneous mastocytosis – histologic features. Mast cells within the dermis have a rounded or cuboidal appearance. Granules are seen within the amphophilic cytoplasm (inset). *Courtesy Lorenzo Cerroni, MD.*

TREATMENT

Treatment of patients with mastocytosis is directed primarily at alleviating symptoms, since there is no cure for this disorder. Many patients with cutaneous mastocytosis and ISM have few, if any, symptoms and therefore require little or no therapy. Mastocytosis patients should be provided with information on environmental triggers (e.g. friction, heat) and potential mast cell degranulating agents (Table 118.3)[61]. Systemic anesthetic agents that have been directly or indirectly implicated in precipitating anaphylactoid reactions in mastocytosis patients are also listed in Table 118.3. In contrast, local injections of lidocaine can be used safely in these patients. It has been recommended that mastocytosis patients undergoing general anesthesia be monitored postoperatively for at least 24 hours, since delayed anaphylaxis can occur[62,63].

Antihistamines are often helpful in controlling the symptoms associated with mastocytosis[36,44]. The second-generation antihistamines cetirizine, loratadine, and fexofenadine are preferred because they have longer half-lives and more specific antagonism of the H1 receptor (see Table 18.5). Use of multiple agents and higher than standard doses are often required for symptom control. For example, the author recommends fexofenadine 360 mg in the morning and up to 40 mg of cetirizine at night for control of histamine-related symptoms in adults. In some instances, the addition of an H2 antagonist (e.g. cimetidine, famotidine, nizatidine) may prove beneficial, especially in patients with gastric acid hypersecretion[44].

Oral **cromolyn** sodium (disodium cromoglycate; 400–800 mg/day), a mast cell stabilizer with poor oral absorption, may alleviate GI manifestations and (to a lesser degree) cutaneous and CNS symptoms associated with mastocytosis. Use of topical cromolyn for cutaneous mastocytosis has also been described but has limited efficacy.

Narrowband ultraviolet B or psoralen plus UVA (PUVA) **phototherapy** administered up to four times a week may help to control pruritus and cutaneous whealing in patients with mastocytosis. While this treatment can reduce skin mast cell histamine content, it does not eliminate the mast cell infiltrates[59,64].

Potent topical **corticosteroids**, especially under occlusion for 6 weeks or more, may eliminate pruritus and cutaneous whealing as well as reduce the number of lesional skin mast cells, but this can also lead to skin atrophy[65]. Intralesional injections of triamcinolone acetonide have also been successful in clearing cutaneous mast cell infiltrates. In SM patients, relief of cutaneous and GI symptoms with prednisone alone or in combination with cyclosporine has been described[66]. However, if possible, systemic corticosteroids should be avoided due to the risk of worsening associated osteoporosis. Mastocytosis patients with decreased bone density may benefit from treatment with bisphosphonates or denosumab, a RANK ligand inhibitor[30].

Some patients with severe mastocytosis experience recurrent, life-threatening episodes of hypotension following mast cell mediator release, and therefore should be provided with a premeasured **epinephrine** (adrenaline) preparation (e.g. EpiPen®, Auvi-Q®) for

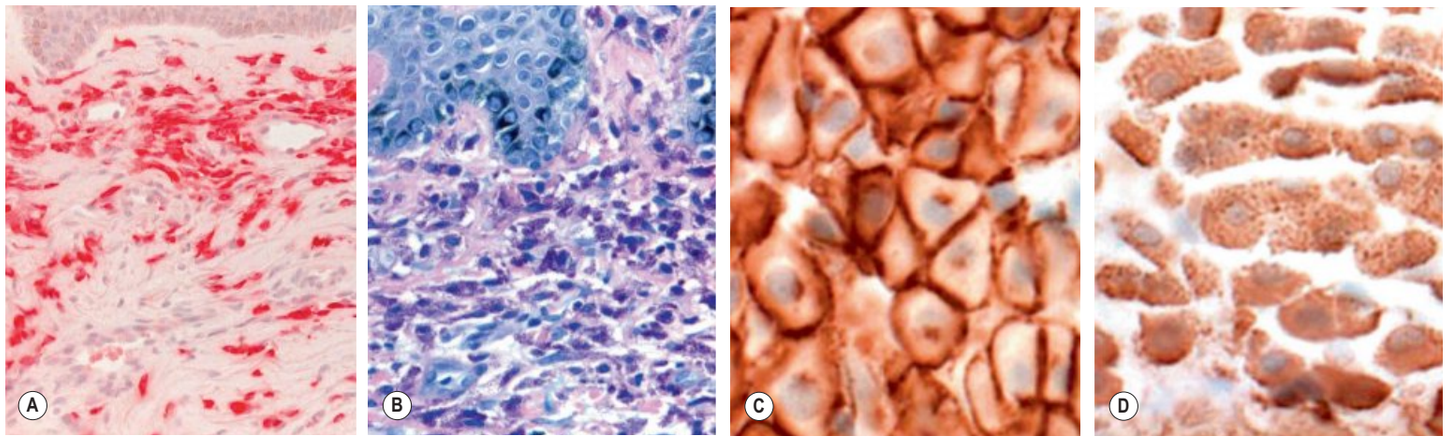


Fig. 118.13 Special stains to detect dermal mast cells. A The Leder method utilizes naphthol AS-D chloroacetate esterase and the mast cell granules appear red. **B** With the Giemsa stain, the mast cell granules stain metachromatically purple. Immunohistochemical staining with monoclonal antibodies that recognize CD117/KIT receptor (**C**) or tryptase (**D**) can also be employed. *A, B, Courtesy Lorenzo Cerroni, MD; C, D, Courtesy Antonio Subtil, MD.*

THERAPEUTIC LADDER FOR MASTOCYTOSIS
Avoidance of relevant mast cell stimuli
Physical
Friction Exercise Heat (e.g. hot bath) or cold (e.g. swimming)
Dietary
Hot beverages Spicy foods Alcohol
Medications
Aspirin Nonsteroidal anti-inflammatory drugs Narcotics (e.g. morphine, codeine) Anticholinergics (e.g. scopolamine) Dextromethorphan (a cough suppressant) Polymyxin B sulfate Some systemic anesthetics, including lidocaine*, d-tubocurarine, metocurine, etomidate, thiopental, succinylcholine hydrochloride (suxamethonium chloride), enflurane, isoflurane (see text for alternatives) Iodine-based radiographic dyes Dextran (in some IV solutions)
Local therapy for symptom control
Potent and superpotent topical corticosteroids, including under occlusion (2) Topical calcineurin inhibitors (3) Intralesional corticosteroids (3) Hydrocolloid dressing (for mastocytoma; 3)
Systemic therapy for symptom control
Oral antihistamines (1) Oral cromolyn sodium (1) Omalizumab (2) Oral PUVA [psoralens plus ultraviolet A] (2) Narrowband ultraviolet B (3) Oral corticosteroids (3) UVA1 (3) Pre-measured epinephrine with auto-injector (EpiPen®, Auvi-Q®) (3)
Systemic therapy for advanced mastocytosis
Midostaurin (2) Avapritinib (2) Imatinib mesylate (non-codon 816 *KIT* mutation; 1) Cladribine (2) Interferon-α-2b (2; limited success) Hematopoietic stem cell transplantation (2)
*Local lidocaine injections are safe; although no large case series exist, systemic anesthetics that have been safely administered to patients with mastocytosis include fentanyl, midazolam, propofol, sufentanil, remifentanil, ketamine, desflurane, sevoflurane, cisatracurium, pancuronium, and vecuronium bromide.

Table 118.3 Therapeutic ladder for mastocytosis. Clinically relevant triggers for mast cell degranulation vary substantially among mastocytosis patients; avoidance of environmental and dietary exposures as well as medications should be approached on an individual basis, considering the patient's previous experiences[61]. Additional tyrosine kinase inhibitors under investigation for the treatment of systemic mastocytosis include repretinib and (for patients with non-codon 816 KIT mutations) masitinib. Key to evidence-based support: (1) prospective controlled trial; (2) retrospective study or large case series; (3) small case series or individual case reports.

emergency use. In some instances, these patients may experience additional similar attacks within hours of the initial event; prednisone 20–40 mg/day for 2–4 days may suppress these recurrent reactions[36,44].

Omalizumab, a humanized murine monoclonal antibody to IgE approved for the treatment of asthma and chronic spontaneous urticaria, has been reported to control symptoms in patients with mastocytosis who are resistant to antihistamine therapy. In a series of 40 adults with cutaneous mastocytosis or ISM, omalizumab (150–300 mg every 2 weeks) induced a >50% reduction in mast cell mediator-related symptoms in 22 patients (55%), with a median time to response of 2 months[2]. In this and most other reports, omalizumab reduced symptoms, but not serum tryptase levels or skin lesions, in mastocytosis patients[2]. However, a 50%–90% reduction in maculopapular lesions was reported in two mastocytosis patients treated with omalizumab (300 mg monthly) for 5–7 months[3]. At present, omalizumab's mechanism of action in mastocytosis remains unclear[2,3].

Multitargeted **tyrosine kinase inhibitors** are capable of limiting proliferation and promoting apoptosis of D816V-expressing mast cells. Among such agents, midostaurin and avapritinib are FDA-approved for the treatment of aggressive SM (including ASM, SM-AHN, and MCL), with overall response rates of ≥60% and ≥75%, respectively, and a median survival of ~30–40 months for midostaurin in this patient group[6,67]. Imatinib mesylate is a tyrosine kinase inhibitor that blocks KIT and PDGF receptors, as well as the BCR-ABL oncoprotein associated with chronic myelogenous leukemia. However, the active site for imatinib within the KIT receptor is proximal to the location affected by the common codon 816 mutations (see Fig. 118.2). The resulting amino acid substitutions impede the binding of imatinib to KIT and thereby negate its potential therapeutic effect[5]. On the other hand, imatinib may alleviate the signs and symptoms of mastocytosis in patients with other *KIT* mutations (e.g. del419, K509I, F522C, V560G; see Fig. 118.2)[5,44,49,67] as well as in those with wild type *KIT* or a myeloproliferative disorder associated with the *FIP1L1–PDGFRA* fusion gene[68]. Other genes mutated in SM and their respective pathways may serve as potential therapeutic targets in the future.

Among chemotherapeutic agents, intravenous cladribine has the most evidence of efficacy in reducing skin lesions and BMMCs in patients with advanced SM, including those with the D816 *KIT* mutation[4,44]. However, a recent registry-based analysis found significantly longer overall and disease-free survival of patients with advanced SM treated with midostaurin compared to those who received cladribine[7]. For patients with SM-AHN, chemotherapy should be directed at the associated hematologic disorder[36,44].

Local radiation therapy with ~20–40 Gy over a 7- to 14-day period may benefit patients with pain due to bone involvement[69]. Splenectomy can be helpful in mastocytosis patients with hypersplenism who experience significant cytopenias and may improve survival in patients with aggressive disease[44,70]. Interferon α-2b has been used with limited success in patients with aggressive forms of mastocytosis[71], and non-myeloablative allogeneic hematopoietic stem cell transplantation has been performed with variable benefit in patients with life-threatening SM[72].

Additional figures available in our eBook (see inside front cover for access code).

REFERENCES

1. Akin C, Valent P. Diagnostic criteria and classification of mastocytosis in 2014. *Immunol Allergy Clin North Am*. 2014;34:207–218.
2. Lemal R, Gouquet G, Terriou L, et al. Omalizumab therapy for mast cell mediator symptoms in patients with ISM, CM, MMAS and MCAS. *J Allergy Clin Immunol*. 2019;7:2387–2396.
3. Hinojosa T, Lewis DJ, Vangipuram R, et al. The efficacy of omalizumab in cutaneous mastocytosis: a case series. *Dermatol Ther*. 2019;32:e12848.
4. Tefferi A, Li CY, Butterfield JH, Hoagland HC. Treatment of systemic mast-cell disease with cladribine. *N Engl J Med*. 2001;344:307–309.
5. Vega-Ruiz A, Cortes JE, Sever M, et al. Phase II study of imatinib mesylate as therapy for patients with systemic mastocytosis. *Leuk Res*. 2009;33:1481–1484.
6. Gotlib J, Kluin-Nelemans HC, George TI, et al. Efficacy and safety of midostaurin in advanced SM. *N Engl J Med*. 2016;374:2530–2541.
7. Lübke J, Schwaab J, Naumann N, et al. Superior efficacy of midostaurin over cladribine in advanced systemic mastocytosis: a registry-based analysis. *J Clin Oncol*. 2022;40:1783–1794.
8. Robinson WA, Quiery AT, Drummond MW. Safety and efficacy of avapritinib in advanced systemic mastocytosis: the phase 1 EXPLORER trial. *Nat Med*. 2021;27:2183–2191.
9. Nettleship ETW. Rare forms of urticaria. *Br Med J*. 1869;2:323–324.

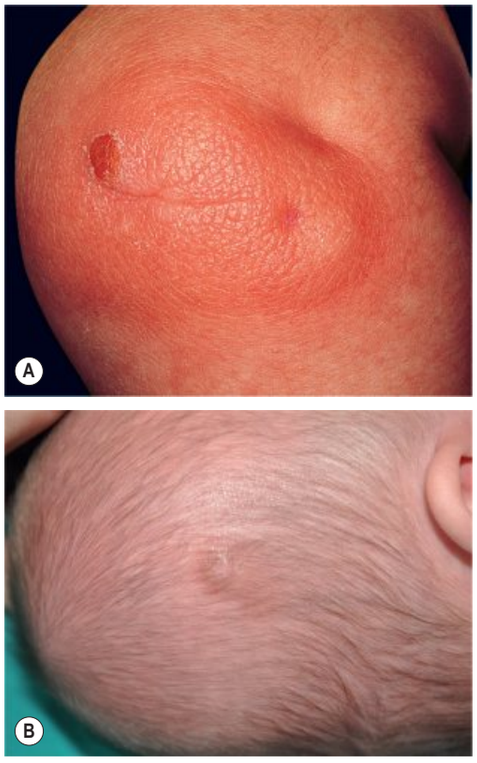
10. Sangster A. An anomalous mottled rash accompanied by pruritus, factitious urticaria and pigmentation. Urticaria pigmentosa? *Trans Clin Soc*. 1878;11:161–163.
11. Lange M, Niedoszytko M, Renke J, et al. Clinical aspects of paediatric mastocytosis: a review of 101 cases. *J Eur Acad Dermatol Venereol*. 2013;27:97–102.
12. Hartmann K, Escribano L, Grattan C, et al. Cutaneous manifestations in patients with mastocytosis: consensus report of the European Competence Network on Mastocytosis; the American Academy of Allergy, Asthma & Immunology; and the European Academy of Allergology and Clinical Immunology. *J Allergy Clin Immunol*. 2016;137:35–45.
13. Caplan RM. The natural course of urticaria pigmentosa. Analysis and follow-up of 112 cases. *Arch Dermatol*. 1963;87:146–157.
14. Klabiber M, Kumar S, Irani AM. Mastocytosis in children. *Cur Allergy Asthma Rep*. 2017;17:80–88.
15. Longley BJ Jr, Metcalfe DD, Tharp M, et al. Activating and dominant inactivating c-KIT catalytic domain mutations in distinct clinical forms of human mastocytosis. *Proc Natl Acad Sci USA*. 1999;96:1609–1614.
16. Rottem M, Okada T, Goff JP, Metcalfe DD. Mast cells cultured from the peripheral blood of normal donors and patients with mastocytosis originate from a CD34+/Fc epsilon RI- cell population. *Blood*. 1994;84:2489–2496.
17. Longley BJ, Tyrrell L, Ma Y, et al. Chymase cleavage of stem cell factor yields a bioactive, soluble product. *Proc Natl Acad Sci USA*. 1997;94:9017–9021.
18. Bodemer C, Hermine O, Palmerini F, et al. Pediatric mastocytosis is a clonal disease associated with D816V and other activating c-KIT mutations. *J Invest Dermatol*. 2010;130:80.
19. Chan EC, Bai Y, Kirshenbaum AS, et al. Mastocytosis associated with a rare germline KIT K509I mutation displays a well-differentiated mast cell phenotype. *J Allergy Clin Immunol*. 2014;134:178–187.
20. Yang Y, Letard S, Borge L, et al. Pediatric mastocytosis-associated KIT extracellular domain mutations exhibit different functional and signaling properties compared with KIT-phosphotransferase domain mutations. *Blood*. 2010;116:1114–1123.
21. Zappulla JP, Dubreuil P, Desbois S, et al. Mastocytosis in mice expressing human Kit receptor with the activating Asp816Val mutation. *J Exp Med*. 2005;202:1635–1641.
22. Gerbaulet A, Wickenhauser C, Scholten J, et al. Mast cell hyperplasia, B cell malignancy and intestinal inflammation in mice with conditional expression of a constitutively active kit. *Blood*. 2011;117:2012–2021.
23. Damaj G, Joris M, Chandesris O, et al. ASXL1 but not TET2 mutations adversely impact overall survival of patients suffering SM with associated clonal hematologic non-mast-cell diseases. *PLoS ONE*. 2014;9:e85362.
24. Schwaab J, Schnittger S, Sotlar K, et al. Comprehensive mutational profiling in advanced systemic mastocytosis. *Blood*. 2013;122:2460–2466.
25. Wiechers T, Rabenhorst A, Schick T, et al. Large maculopapular cutaneous lesions are associated with favorable outcome in childhood-onset mastocytosis. *J Allergy Clin Immunol*. 2015;136:1581–1590.
26. Lange M, Niedoszytko M, Nedoszytko B, et al. Diffuse cutaneous mastocytosis: analysis of 10 cases and a brief review of the literature. *J Eur Acad Dermatol Venereol*. 2012;26:1565–1571.
27. Kasprowicz S, Chan IJ, Wall DJ, Tharp MD. Nodular mastocytosis. *J Am Acad Dermatol*. 2006;55:347–349.
28. Kasper CS, Tharp MD. Quantification of cutaneous mast cells using morphometric point counting and a conjugated avidin stain. *J Am Acad Dermatol*. 1987;16:326–331.
29. Lanternier F, Cohen-Akenine A, Palmerini F, et al. Phenotypic and genotypic characteristics of mastocytosis according to the age of onset. *PLoS ONE*. 2008;3:e1906.
30. Orsolini G, Viapiana O, Rossini M, et al. Bone disease in mastocytosis. *Immunol Allergy Clin N Am*. 2018;38:443–454.
31. Travis WD, Li CY, Bergstralh EJ, et al. Systemic mast cell disease. Analysis of 58 cases and literature review. *Medicine (Baltimore)*. 1988;67:345–368.
32. Linkhart TA, Linkhart SG, MacCharles DC, et al. Interleukin-6 messenger RNA expression and interleukin-6 protein secretion in cells isolated from normal human bone: regulation by interleukin-1. *J Bone Miner Res*. 1991;6:1285–1294.
33. Radia DH, Green H, Oni C, et al. The clinical and pathological panoply of SM. *Br J Haematol*. 2020;188:623–640.
34. Parker RI. Hematologic aspects of mastocytosis: I: Bone marrow pathology in adult and pediatric systemic mast cell disease. *J Invest Dermatol*. 1991;96:47S–51S.
35. Metcalfe DD. The liver, spleen, and lymph nodes in mastocytosis. *J Invest Dermatol*. 1991;96:45S–46S. discussion 46S, 60S–65S.
36. Valent P, Akin C, Metcalfe DD. Mastocytosis: 2016 updated WHO classification and novel emerging treatment concepts. *Blood*. 2017;129:1420–1427.
37. Travis WD, Li CY. Pathology of the lymph node and spleen in systemic mast cell disease. *Mod Pathol*. 1988;1:4–14.
38. Teodosio C, Mayado A, Sánchez-Muñoz L, et al. The immunophenotype of mast cells and its utility in the diagnostic work-up of SM. *J Leukoc Biol*. 2015;97:49–59.
39. Doyle LA, Sepehr GJ, Hamilton MJ, et al. A clinicopathologic study of 24 cases of systemic mastocytosis involving the gastrointestinal tract and assessment of mucosal mast cell density in irritable bowel syndrome and asymptomatic patients. *Am J Surg Pathol*. 2014;38:832–843.
40. Sokol H, Georgin-Lavialle S, Canioni D, et al. Gastrointestinal manifestations in mastocytosis: a study of 83 patients. *J Allergy Clin Immunol*. 2013;132:866–873. e1–3.
41. Hartmann K, Wardelmann E, Ma Y, et al. Novel germline mutation of KIT associated with familial gastrointestinal stromal tumors and mastocytosis. *Gastroenterology*. 2005;129:1042–1046.
42. Rogers MP, Bloomingdale K, Murawski BJ, et al. Mixed organic brain syndrome as a manifestation of SM. *Psychosom Med*. 1986;48:437–447.
43. Escribano L, Alvarez-Twose I, Sanchez-Munoz L, et al. Prognosis in adult indolent systemic mastocytosis: a long-term study of the Spanish Network on Mastocytosis in a series of 145 patients. *J Allergy Clin Immunol*. 2009;124:514–521.
44. Pardanani A. Systemic mastocytosis in adults: 2021 update on diagnosis, risk stratification and management. *Am J Hematol*. 2021;96:508–525.
45. Lim KH, Tefferi A, Lasho TL, et al. SM in 342 consecutive adults: survival studies and prognostic factors. *Blood*. 2009;113:5727–5736.
46. Pardanani A, Lim KH, ZLasho TL, et al. WHO subvariants of indolent mastocytosis. Clincial details and prognostic evaluation in 159 consecutive adults. *Blood*. 2010;115:150–151.
47. Valent P, Sotlar K, Sperr WR, et al. Chronic mast cell leukemia; a novel leukemia-variant with distinct morphological and clinical features. *Leuk Res*. 2015;39:1–5.
48. Garcia-Montero AC, Jara-Acevedo M, Alvarez-Twose I, et al. KIT D816V-mutated bone marrow mesenchymal stem cells in indolent SM are associated with disease progression. *Blood*. 2016;127:761–768.
49. Zhang LY, Smith ML, Schultheis B, et al. A novel K509I mutation of KIT identified in familial mastocytosis-in vitro and in vivo responsiveness to imatinib therapy. *Leuk Res*. 2006;30:373–378.
50. Greenberger PA, Metcalfe DD. Controversies in allergy: is a bone marrow biopsy optional or essential in the evaluation of the patient with a suspected mast cell disorder? *J Allergy Clin Immunol*. 2019;7:1134–1138.
51. Valent P, Hartmann K, Schwaab J, et al. Personalized management strategies in mast cell disorders: ECNM-AIM user's guide for daily clinical practice. *J Allergy Clin Immunol Pract*. 2022;10:1999–2012.e6.
52. Hoermann G, Sotlar K, Jawhar M, et al. Standards of genetic testing in the diagnosis and prognostication of systemic mastocytosis in 2022: recommendations of the EU-US Cooperative Group. *J Allergy Clin Immunol Pract*. 2022;10:1953–1963.
53. Carter M, Bai Y, Ruiz Esteves K, et al. Detection of KIT D816V in peripheral blood of children with manifestations of cutaneous mastocytosis suggests systemic disease. *Br J Haematol*. 2018;183:775.
54. Fuchs D, Kilbertus A, Kofler K, et al. Scoring the risk of having systemic mastocytosis in adult patients with mastocytosis in the skin. *J Allergy Clin Immunol Pract*. 2021;9:1705–1712.e4.
55. Morgado JM, Perbellini O, Johnson RC, et al. CD30 expression by bone marrow mast cells from different diagnostic variants of SM. *Histopathology*. 2013;63:780–787.
56. Lee HW, Jeong YI, Choi JC, et al. Two cases of telangiectasia macularis eruptiva perstans demonstrated by immunohistochemistry for c-kit (CD 117). *J Dermatol*. 2005;32:817–820.
57. Schwartz LB, Sakai K, Bradford TR, et al. The alpha form of human tryptase is the predominant type present in blood at baseline in normal subjects and is elevated in those with systemic mastocytosis. *J Clin Invest*. 1995;96:2702–2710.
58. Theoharides TC, Boucher W, Spear K. Serum interleukin-6 reflects disease severity and osteoporosis in mastocytosis patients. *Int Arch Allergy Immunol*. 2002;128:344–350.
59. Brazzelli V, Grassi S, Merante S, et al. Narrow-band UVB phototherapy and psoralen-ultraviolet A photochemotherapy in the treatment of cutaneous mastocytosis: a study in 20 patients. *Photodermatol Photoimmunol Photomed*. 2016;32:238–246.
60. Frieri M, Patel R, Celestin J. Mast cell activation syndrome: a review. *Curr Allergy Asthma Rep*. 2013;13:27–32.
61. Adverse reactions to drugs and biologics in patients with clonal mast cell disorders: a group report of the Mast Cells Disorder Committee, American Academy of Allergy and Immunology. *J Allergy Clin Immunol*. 2019;143:880–93.
62. Borgeat A, Ruetsch YA. Anesthesia in a patient with malignant SM using a total intravenous anesthetic technique. *Anesth Analg*. 1998;86:442–444.
63. Konrad FM, Schroeder TH. Anaesthesia in patients with mastocytosis. *Acta Anaesthesiol Scand*. 2009;53:270–271.
64. Kolde G, Frosch PJ, Czarnetzki BM. Response of cutaneous mast cells to PUVA in patients with urticaria pigmentosa: histomorphometric, ultrastructural, and biochemical investigations. *J Invest Dermatol*. 1984;83:175–178.
65. Barton J, Lavker RM, Schechter NM, Lazarus GS. Treatment of urticaria pigmentosa with corticosteroids. *Arch Dermatol*. 1985;121:1516–1523.
66. Kurosawa M, Amano H, Kanbe N, et al. Response to cyclosporin and low-dose methylprednisolone in aggressive SM. *J Allergy Clin Immunol*. 1999;103:S412–S420.
67. Piris-Villaespesa M, Alvarez-Twose I. Systemic mastocytosis: following the tyrosine kinase inhibitor roadmap. *Front Pharmacol*. 2020;11:e443.
68. Pardanani A, Ketterling RP, Brockman SR, et al. CHIC2 deletion, a surrogate for FIP1L1-PDGFRA fusion, occurs in systemic mastocyosis associated with eosinophilia and predicts response to imatinib mesylate therapy. *Blood*. 2003;102:3093–3096.
69. Johnstone PA, Mican JM, Metcalfe DD, et al. Radiotherapy of refractory bone pain due to systemic mast cell disease. *Am J Clin Oncol*. 1994;17:328–330.
70. Friedman B, Darling G, Norton J, et al. Splenectomy in the management of systemic mast cell disease. *Surgery*. 1990;107:94–100.
71. Butterfield JH. Response of severe SM to interferon alpha. *Br J Dermatol*. 1998;138:489–495.
72. Ustun C, Reiter A, Scott BL, et al. Hematopoietic stem-cell transplantation for advanced SM. *J Clin Oncol*. 2014;32:3264–3274.



eFig. 118.1 Mastocytoma with blistering and erosion. *Courtesy Julie V. Schaffer, MD.*

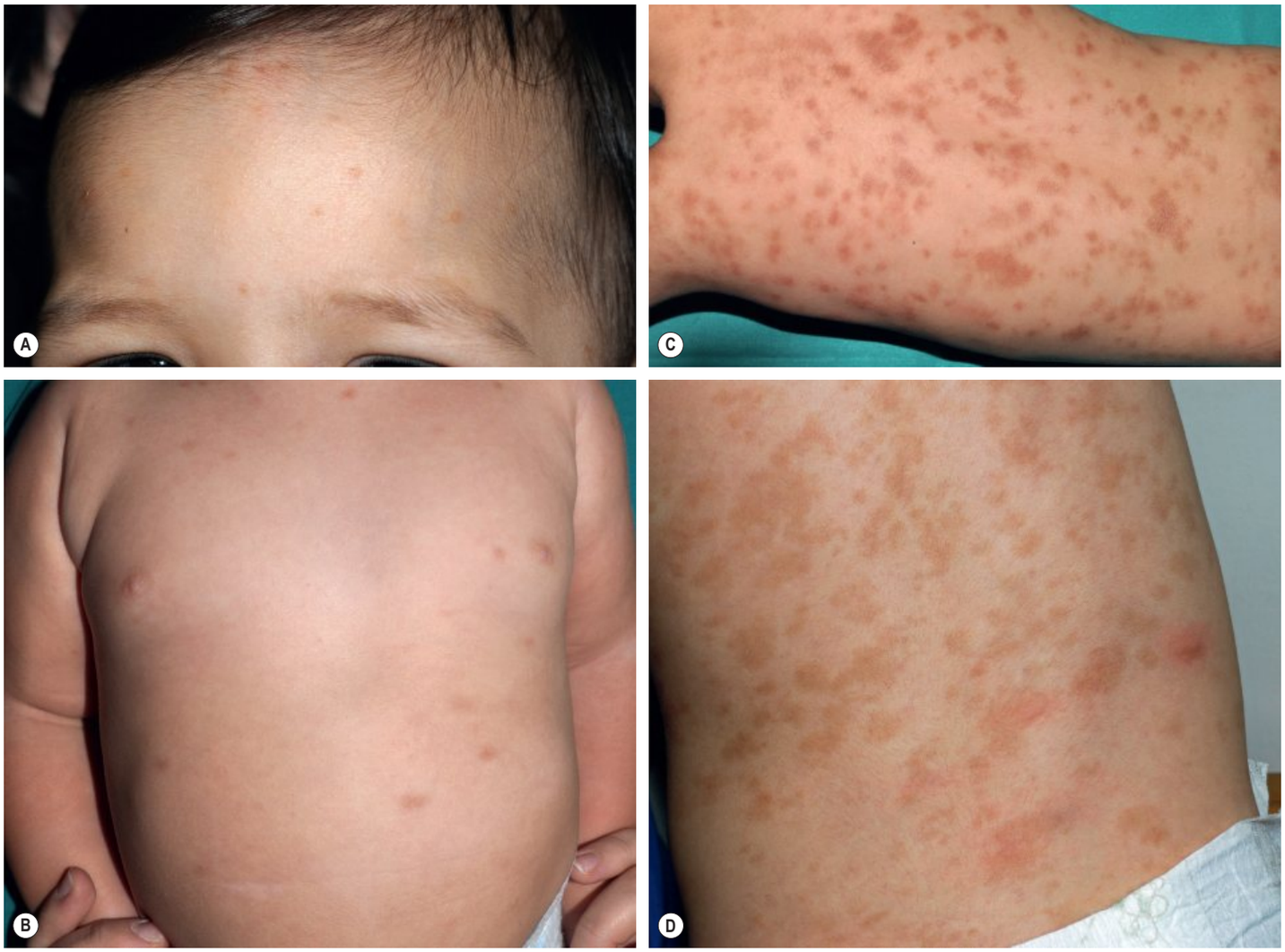


eFig. 118.3 Mastocytoma with bulla formation. *Courtesy Theodore Zaki, MD.*





eFig. 118.2 Mastocytomas in infants. A Note the leathery appearance of the skin and erosions. **B** Subtle tan papule on the scalp. **C** Darker brown plaque. *B, Courtesy Antonio Torrelo, MD; C, Courtesy Joyce Rico, MD.*



eFig. 118.4 Maculopapular cutaneous mastocytosis in children. A–D Variable numbers of tan to brown macules, papules, and plaques are evident, with monomorphous (**A**) or polymorphous (**B–D**) lesions. *B, C, Courtesy Antonio Torrelo, MD; D, Courtesy Julie V. Schaffer, MD.*



eFig. 118.5 Diffuse cutaneous mastocytosis. Leathery, infiltrated skin with multiple erosions.



eFig. 118.6 Diffuse cutaneous mastocytosis. Thickened skin with a leathery texture in a generalized distribution, with multiple superimposed vesicles and erosions. *Courtesy Julie V. Schaffer, MD.*





eFig. 118.7 Adult maculopapular mastocytosis ("urticaria pigmentosa"). Multiple small (**A**) and (**B**) larger, confluent red–brown papules and plaques.



eFig. 118.8 Adult maculopapular mastocytosis ("urticaria pigmentosa"). Numerous reddish-brown macules and papules that were present on the extremities and the trunk. The patient had a normal serum tryptase level. *Courtesy Jonathan S. Leventhal, MD.*

119 B Cell Lymphomas of the Skin

Lorenzo Cerroni and Isabella Fried

Synonyms: ■ Cutaneous B cell lymphomas ■ *S*kin-*a*ssociated *l*ymphoid *t*issue (SALT)-related B cell lymphomas

Key features

- Cutaneous B cell lymphomas represent a group of lymphomas whose primary site is the skin; they are derived from B lymphocytes in different stages of differentiation. The skin can also be the site of secondary involvement by extracutaneous (usually nodal) B cell lymphomas
- Most primary cutaneous B cell lymphomas (>80%) are low-grade malignancies, and they are characterized by indolent behavior and a good prognosis
- Precise classification can be achieved only after a complete synthesis of clinical, histopathologic, immunophenotypic, and molecular features. The WHO-EORTC and ICC classifications provide the basis for a consistent classification of patients
- Treatment options for low-grade types include primarily "watchful waiting", intralesional corticosteroids and local radiotherapy; when solitary lesions are present, surgical excision is an option. Systemic or intralesional anti-CD20 antibody may be used in some patients, while systemic chemotherapy is only required in patients with high-grade tumors

CLASSIFICATION OF B CELL LYMPHOMAS WITH PRIMARY CUTANEOUS MANIFESTATIONS	
WHO-EORTC 2018	**ICC 2022**
• Primary cutaneous follicle center lymphoma	• Primary cutaneous follicle center lymphoma
• Primary cutaneous marginal zone B cell lymphoma*	• Primary cutaneous marginal zone lymphoproliferative disorder
• Primary cutaneous diffuse large B cell lymphoma, leg type	• Primary cutaneous diffuse large B cell lymphoma, leg type
• Primary cutaneous diffuse large B cell lymphoma, other	• Diffuse large B cell lymphoma, NOS
• EBV^+ mucocutaneous ulcer (provisional)	• EBV^+ mucocutaneous ulcer
• Intravascular diffuse large B cell lymphoma	• Intravascular diffuse large B cell lymphoma
*Includes cases previously designated as primary cutaneous immunocytoma and primary cutaneous plasmacytoma.	

Table 119.1 Classification of B cell lymphomas with primary cutaneous manifestations – WHO-EORTC 2018 and ICC 2022. EBV, Epstein–Barr virus; ICC, International Consensus Classification; NOS, not otherwise specified.

INTRODUCTION

Although B cell lymphomas represent the majority of non-Hodgkin lymphomas (NHLs) arising within *lymph nodes*, they represent a minority of the NHLs whose primary site is the *skin*. In the classification of cutaneous lymphomas published by the World Health Organization (WHO) and the European Organization for Research and Treatment of Cancer (EORTC) Cutaneous Lymphoma Project Group (Table 119.1), B cell lymphomas represented ~25% of all cutaneous lymphomas[1]. The WHO-EORTC classifications of 2005 and 2018 have been integrated with only minor changes into the International Consensus Classification (ICC) of Mature Lymphoid Neoplasms published in 2022 (see Table 119.1)[2,3].

Primary cutaneous lymphomas are defined as *malignant lymphomas confined to the skin at presentation after complete staging procedures*[1,4]. In general, most patients with primary cutaneous B cell lymphoma (pCBCL) are diagnosed by dermatologists, as extracutaneous symptoms and signs are observed only very rarely at the onset of the disease. Consequently, dermatologists should be conversant with the clinicopathologic features of this group of diseases, in order to be able to establish the diagnosis in its early stages. Additionally, as aggressive treatment modalities are needed only in selected cases, these patients should be managed primarily by dermatologists with special expertise in cutaneous lymphomas.

HISTORY

In the past, cutaneous B cell lymphomas were thought to be invariably secondary, that is, due to dissemination of extracutaneous (usually nodal) B cell lymphomas to the skin. In the 1980s, it was recognized that B cell lymphomas whose primary site is the skin, i.e. pCBCLs, represent a distinct group of extranodal lymphomas[4]. The widespread use of immunohistochemical and molecular genetic techniques that can establish clonality, in particular the detection of rearrangements of immunoglobulin genes by PCR (utilizing routine biopsy samples), has shown that some of the cases previously classified as cutaneous B cell pseudolymphomas harbor a monoclonal population of lymphocytes, thus representing low-grade malignant B cell lymphomas of the skin[4,5].

EPIDEMIOLOGY

For the past several decades, the incidence of pCBCL had been rising, but now appears to have stabilized[6]. pCBCLs may occur more frequently in specific regions of the world. For example, analysis of data from four academic centers in the US showed that they represented only 4.5% of all the cases of primary cutaneous lymphoma registered in those centers[7]. In contrast, pCBCL represented ~25% of all the cases of primary cutaneous lymphoma in the Dutch and Austrian registries for cutaneous lymphomas[1].

Regional variations have also been observed with regard to the incidence of specific types of pCBCL. In the two largest series published to date, the relative frequencies of follicle center lymphoma and marginal zone lymphoma varied considerably. Follicle center lymphoma represented 71% of all pCBCLs in the Netherlands, but only 41% in Graz; conversely, marginal zone lymphoproliferative disorder (at that time classified as lymphoma) represented 42% of all cases of pCBCL in Graz, but only 10% in the Netherlands. On the other hand, the relative frequency of the third most common type of pCBCL, the diffuse large B cell lymphoma, leg type, was similar in the two series (~15%), indicating that, in these two series, differences in the relative frequencies were confined to B cell lymphomas characterized by an indolent behavior. This suggests that these variations may be due, at least in part, to a different classification of patients in different centers.

In addition to differences in diagnostic and classification standards, true regional variations in the incidence of special types of pCBCL may be due to the presence of different etiologic factors. For example, the association between pCBCL and infection with specific *Borrelia* subspecies in endemic areas has been known for many years (see below and Ch. 74). This association may explain, in part, regional differences in the incidence of pCBCLs, but the relatively low percentage of such cases (even in countries with endemic *Borrelia* infections) suggests that other etiologies are also involved in regional variations.

pCBCL affects adults of both sexes. With the exception of precursor B lymphoblastic lymphoma/leukemia (which only rarely represents an example of true pCBCL), CBCLs are uncommon in children and adolescents.

ETIOLOGY AND PATHOGENESIS

The pathogenesis of pCBCL is unknown. In contrast to the many nodal B cell lymphomas that have been linked to specific genetic alterations (e.g. nodal follicular lymphomas and interchromosomal 14;18 translocations), there are relatively limited data on the specific genetic features of pCBCLs, especially for low-grade subtypes (for details see below).

Some similarities to the clinicopathologic features observed in B cell lymphomas arising in the gastric mucosa (so-called *mucosa-associated lymphoid tissue* [MALT] lymphomas) led to the hypothesis that pCBCLs are caused by longstanding antigenic stimulation, possibly due to chronic infection with specific microorganisms. In fact, it has been long established that MALT lymphomas originating in the stomach are linked to chronic antigenic stimulation due to infection with *Helicobacter pylori*. As previously mentioned, *Borrelia* spp. are thought to play an etiologic role in a minority of cases of pCBCL, particularly in Europe. In patients from a region in Austria with endemic *Borrelia* infections, specific DNA sequences of *Borrelia* were detected in 18% of all cases of pCBCL[8]; similar findings have been reported from Scotland[9].

At present, no other microorganism has been convincingly linked to the development of pCBCL. However, it should be noted that pCBCLs have been described in immunosuppressed patients, including those with AIDS and solid organ transplant recipients, and reversible pCBCLs have been observed in patients undergoing therapy with methotrexate (in particular those with rheumatoid arthritis), thus suggesting that immune dysregulation may play a role in the development of this disease[10–12].

CLINICAL FEATURES

In the WHO-EORTC 2018 and ICC 2022 classification schemes, pCBCLs have been divided into five major types (see Table 119.1)[1,3]. Follicle center lymphoma and marginal zone B cell lymphoproliferative disorder are characterized by an indolent clinical behavior, whereas diffuse large B cell lymphoma, leg type, and intravascular diffuse large B cell lymphoma have an aggressive clinical behavior. A further type, Epstein–Barr virus (EBV)-positive mucocutaneous ulcer, is characterized by an indolent behavior. It must be emphasized that, in addition to pCBCLs, the skin can be a site of secondary involvement for practically all types of extracutaneous (usually nodal) B cell lymphomas and leukemias. Complete staging should be performed in all patients with a confirmed diagnosis of high-grade B cell lymphoma involving the skin. This includes a complete blood examination, flow cytometry of peripheral blood, CT examination of the chest, abdomen and pelvis, and, if possible, positron emission tomography (PET)[13]. On the other hand, cutaneous low-grade B cell lymphomas without extracutaneous symptoms are only rarely upstaged by CT of the chest, abdomen and pelvis, functional imaging (PET-CT scan), or bone marrow biopsy[13]. Thus, extensive radiologic imaging and bone marrow biopsy is viewed as superfluous in the staging and follow-up of patients with indolent types of pCBCL confined to the skin[13,14]. A recommended staging evaluation for patients with CBCL is summarized in Table 119.2.

Primary Cutaneous Follicle Center Lymphoma

*P*rimary *c*utaneous *f*ollicle *c*enter *l*ymphoma (PCFCL) is defined as a neoplastic proliferation of germinal center cells confined to the skin. It represents a common subtype of pCBCL.

Clinically, patients present with solitary or grouped, pink- to plum-colored papules, plaques or tumors, which, especially on the trunk, can be surrounded by patches of erythema (Fig. 119.1 & 119.2)[15]. The term *Crosti's lymphoma* has been used to denote those patients with a peripheral patch of erythema. Ulceration is uncommon. Occasionally patients present with miliary and/or agminated small papules that can have an acneiform appearance[16]. Preferential locations are the scalp and forehead or the back. The skin lesions are usually asymptomatic, and, as a rule, B symptoms (i.e. fever, night sweats, weight loss) are rare. The serum level of lactate dehydrogenase (LDH), which is a powerful prognostic factor in systemic lymphomas, is within normal limits.

The prognosis is favorable[1,17]. Recurrences are observed in up to 50% of patients, but dissemination to lymph nodes or internal organs is rare.

RECOMMENDED STAGING INVESTIGATIONS FOR PATIENTS WITH A CONFIRMED DIAGNOSIS OF B CELL LYMPHOMA INVOLVING THE SKIN

Type of cutaneous lymphoma	Low-grade (without extracutaneous symptoms)	High-grade
History and physical examination		
• Presence/absence of "B" symptoms, including fever, night sweats, weight loss, malaise	√	√
• Complete lymph node examination	√	√
• Palpation of abdomen for hepatosplenomegaly	√	√
• Examination of oral cavity	√	√
• History of organ transplantation and/or other immune suppression (e.g. HIV, iatrogenic, congenital)	√	√
Laboratory studies		
• Complete blood count with differential and platelet count	√	√
• Comprehensive serum chemistries including LDH	√	√
• Flow cytometry of peripheral blood mononuclear cells	√ (optional)	√
Imaging studies		
• Ultrasound of abdomen and superficial lymph nodes as screening prior to PET-CT or CT scan	√	√
• Whole-body PET-CT scan or CT scan if PET-CT not available	√*	√
Additional studies as clinically indicated		
• Bone marrow biopsy	√*,†	√
• Excisional biopsy of enlarged lymph nodes or other suspicious lesions	√*	√
• PCR analysis for *Borrelia* spp. DNA in patients from endemic areas (Europe) or travelers to endemic areas	√	√

*Only if suspicion for extracutaneous lymphoma.
†In the US, often replaced by flow cytometry plus PET-CT.

Table 119.2 Recommended staging investigations for patients with a confirmed diagnosis of B cell lymphoma involving the skin. CT, computed tomography; HIV, human immunodeficiency virus; LDH, lactate dehydrogenase; PCR, polymerase chain reaction; PET, positron emission tomography.



Fig. 119.1 Cutaneous follicle center lymphoma. Prominent pale pink nodule of the lateral eyebrow. The nodule is accompanied by infiltrated darker pink plaques on the forehead.



Fig. 119.2 Cutaneous follicle center lymphoma. Large nodule on the upper back. Note the surrounding erythematous papules, patches, and plaques (Crosti's lymphoma).



Fig. 119.3 Cutaneous marginal zone B cell lymphoproliferative disorder. Well-circumscribed, erythematous nodule on the back that was firm to palpation (inset).

Primary Cutaneous Marginal Zone B Cell Lymphoproliferative Disorder

*P*rimary *c*utaneous *m*arginal *z*one B cell *l*ymphoproliferative *d*isorder (PCMZLD) has been recognized as a distinct variant of low-grade malignant pCBCL[5,18]. In the ICC classification of 2022 it is no longer grouped with other marginal zone lymphomas of mucosa-associated lymphoid tissue, and it has been downgraded to a lymphoproliferative disorder rather than a true lymphoma[3]. It is still listed as a lymphoma in the 5th edition of the WHO classification[18a]. Of note, cases classified in the past as *primary cutaneous immunocytoma* or *primary cutaneous plasmacytoma* represent examples of PCMZLD with prominent lymphoplasmacytic or plasmacytic differentiation, respectively, and the terms cutaneous immunocytoma and cutaneous plasmacytoma are not used in the WHO-EORTC and ICC 2022 classification schemes[1–3].

Clinically, patients present with recurrent pink–violet to red–brown papules, plaques, and nodules that favor the extremities (upper > lower) or trunk (Fig. 119.3 & 119.4). Generalized lesions can be observed in a small number of patients. Ulceration rarely occurs and skin lesions are usually asymptomatic. As a rule, B symptoms (i.e. fever, night sweats, weight loss) are not present. The serum level of LDH is within normal limits. In some instances, resolution of lesions may be accompanied by secondary anetoderma due to loss of elastic fibers in the area of the tumor infiltrate.

The prognosis of PCMZLD is excellent. In a study of 32 patients with PCMZLD, none of them developed lymph node or internal involvement during a mean follow-up of more than 4 years[5].

Of note, PCMZLD can arise in areas affected by acrodermatitis chronica atrophicans and it may be linked to infection by *Borrelia* spp. more frequently than are other types of pCBCL, particularly in Europe[8].



Fig. 119.4 Cutaneous marginal zone B cell lymphoproliferative disorder. Two thick pink–violet plaques on the foot, one of which has a flat surface. Molecular analysis revealed *Borrelia* DNA within the infiltrate. In the past, these tumors, which demonstrated prominent lymphoplasmacytic differentiation histologically, were classified as cutaneous immunocytomas.

Primary Cutaneous Diffuse Large B Cell Lymphoma, Leg Type

Primary cutaneous *d*iffuse *l*arge *B c*ell *l*ymphoma, *l*eg *t*ype (DLBCLLT), represents a form of pCBCL that is characterized by a predominance of large round cells (centroblasts, immunoblasts) positive for Bcl-2, MUM-1 (*mu*ltiple *m*yeloma oncogene *1* or interferon regulatory factor 4 [expressed by post germinal center B cells and plasma cells]), and FOX-P1[1]. It occurs almost exclusively in elderly patients, predominantly women.

Clinically, patients present with solitary or clustered, erythematous to red–brown nodules, located primarily on the distal aspect of one leg (Fig. 119.5). In some patients, lesions may arise on both lower extremities contemporaneously or within a short interval of time. Ulceration may also occur. Small erythematous papules can be seen adjacent to larger nodules. It must be emphasized that in ~20% of patients, tumors with similar morphologic and phenotypic features can arise in areas other than the lower extremities, but the designation DLBCLLT is still applied[19].

The prognosis of DLBCLLT is less favorable than that of other types of pCBCL, with an estimated disease-specific 5-year survival rate of 50%–60%[1].

It must be stressed that some patients with *nodal* large B cell lymphoma can present with secondary cutaneous lesions located exclusively on the legs, underlying the need for complete staging investigations before a diagnosis of DLBCLLT can be established. PET scans are superior to CT studies for discovering evidence of systemic disease.

Intravascular Diffuse Large B Cell Lymphoma

*Intrav*ascular *d*iffuse *l*arge *B c*ell *l*ymphoma (IVDLBCL) is a rare malignant proliferation of large B lymphocytes within blood vessels[4]. Most patients have a B cell phenotype, but a T cell variant has been reported. In occasional patients, the skin may be the only affected site, although more often there is systemic involvement (including the CNS) from the onset. Clinically, patients present with indurated, erythematous or violaceous patches and plaques, preferentially located on the trunk and thighs and often with prominent telangiectasias. The clinical appearance is not typical of cutaneous lymphoma, and it may sometimes suggest a diagnosis of panniculitis or vascular tumors. Interestingly, in several patients, IVDLBCL was observed to be confined to cherry angioma lesions. The prognosis of IVDLBCL is poor, and the disease usually runs an aggressive course[20].



Fig. 119.5 Cutaneous diffuse large B cell lymphoma, leg type. On both lower legs, multiple violet–brown nodules as well as a large flat tumor.

Precursor B Lymphoblastic Lymphoma/Leukemia

B cell lymphoblastic lymphomas/leukemias are malignant proliferations of precursor B lymphocytes. Reports of patients whose primary site is the skin have been rare. It should be emphasized, however, that all patients should be assumed to have, and treated for, systemic disease, even in the absence of documented systemic involvement at the time of presentation.

In contrast to the other cutaneous B cell lymphomas, this disease shows a clear-cut predilection for children and young adults[21]. Clinically, patients present with solitary large erythematous tumors, commonly located on the head and neck. Patients with primary skin disease often have asymptomatic lesions of a few weeks' duration. Those with secondary skin lesions may have systemic symptoms, e.g. weight loss, fever, fatigue, night sweats. The serum level of LDH is often elevated, reflecting the aggressive, and often systemic, nature of the disease. The disease is highly aggressive, and the prognosis of untreated patients is poor.

Other Cutaneous B Cell Lymphomas

Rare cases of pCBCL do not fit within the subtypes reviewed above. In the ICC 2022 classification, these patients are divided amongst several categories, including (but not limited to) large B cell lymphomas arising in the setting of immune suppression, plasmablastic lymphoma, and diffuse large B cell lymphoma, not otherwise specified (NOS)[2,3]. Plasmablastic lymphoma is a rare lymphoma that usually arises within the oral cavity in patients with severe immunosuppression, especially HIV-related[4], but can also be observed in immunocompetent patients. It is often associated with infection by EBV.

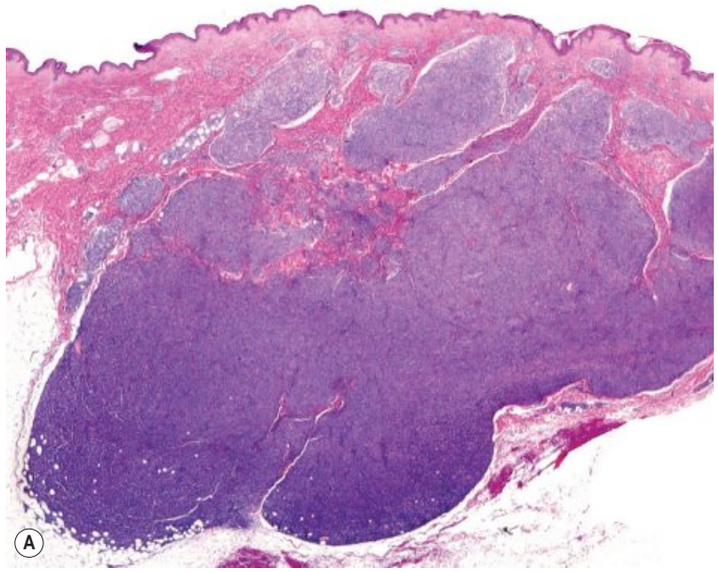
EBV-positive mucocutaneous ulcer is a low-grade B cell malignancy that usually arises within the context of immune senescence or in immunocompromised hosts. It most commonly presents as ulcers of the oral mucosa.

PATHOLOGY

In addition to routine histology and immunohistochemical phenotyping, which when combined are sufficient for the diagnosis of most cases of pCBCL, molecular investigations are becoming increasingly important for precise stratification of patients with aggressive B cell lymphomas.

Primary Cutaneous Follicle Center Lymphoma

In PCFCL, nodular or diffuse infiltrates are seen within the entire dermis, often extending into the subcutaneous fat (Fig. 119.6A)[4]. The epidermis is usually spared. A clear-cut follicular pattern with formation of neoplastic germinal centers was observed in only a minority of cases (25%) in the series from Graz (Fig. 119.7)[17]. However, a higher percentage of cases may show at least some follicular architecture. In those with a follicular pattern, the neoplastic follicles show morphologic features of malignancy, including the presence of a reduced or absent mantle zone, the lack of tingible body macrophages, and a monomorphism of the follicles – so-called "dark" and "clear" areas are no longer recognizable (see Fig. 119.7 [inset])[17].



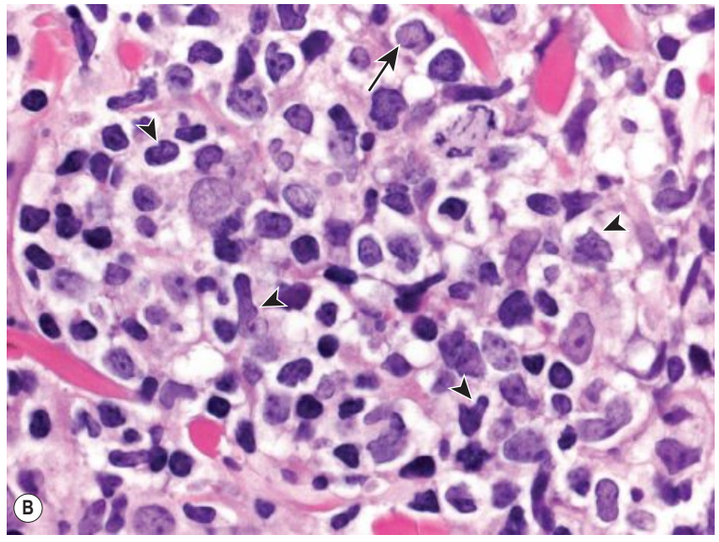


Fig. 119.6 Cutaneous follicle center lymphoma, diffuse type. A Diffuse infiltrate *without* a follicular pattern. **B** Centroblasts (arrow) and medium- and large-sized centrocytes (cleaved cells; arrowheads) predominate.

In both the follicular and diffuse variants, centrocytes (small to large, cleaved follicle center cells) predominate within the neoplastic infiltrate (Fig. 119.6B) and are admixed with a variable number of centroblasts (large, non-cleaved follicle center cells with prominent nucleoli), immunoblasts, small lymphocytes, histiocytes, and, in some cases, eosinophils and plasma cells. In contrast to nodal FCLs, grading is not used for the classification of PCFCL. On a cytomorphologic basis, some cases of PCFCL with a diffuse pattern of growth and a predominance of large centrocytes have the appearance of a large cell lymphoma, but the prognosis of these cases is similar to that of lesions without the large cell morphology[1,19]. Patients with a monotonous proliferation of centroblasts and/or immunoblasts should be classified as having diffuse large B cell lymphoma. An accompanying infiltrate of small T lymphocytes and histiocytes/macrophages is usually present, and, in some instances, these cells can be predominant. In rare cases, a population of monoclonal

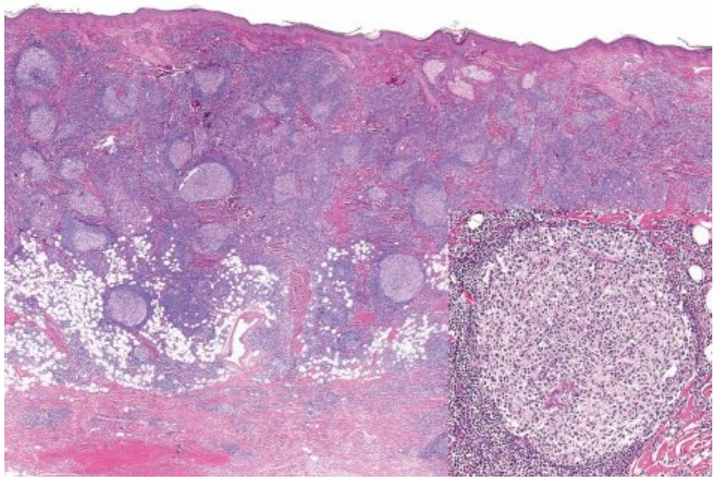


Fig. 119.7 Cutaneous follicle center lymphoma, follicular type. Neoplastic follicles with a monomorphous morphology (lack of polarization) within the entire dermis and superficial subcutis. Note the absence of dark and clear areas within the central portion of the follicle (inset).

plasma cells belonging to the neoplastic clone can be observed, representing a pitfall in the differential diagnosis with PCMZLD[21a,21b].

In addition to cases characterized by numerous large cells, morphologic variants of PCFCL include those with a predominant spindle cell morphology, which can simulate sarcomas or other spindle cell tumors histopathologically, thus representing a diagnostic pitfall[22]. Lesions in which a few B cell blasts are admixed with numerous T lymphocytes have been classified as "T cell/histiocyte-rich B cell lymphomas", and in the skin probably represent another rare morphologic variant of PCFCL[4]. Of note, when there is nodal involvement with this latter morphologic variant, it is classified as a large B cell lymphoma.

The tumor cells express B cell-associated antigens (CD20, CD79a, PAX-5); they are $CD5^-$ and $CD43^-$ (see Table 0.13 for the specificities of CD markers). When follicles are present, they are characterized by an irregular network of $CD21^+$ follicular dendritic cells. Bcl-6 (a marker of germinal center cells and other lymphoid cells) is positive in virtually all cases, irrespective of the pattern of growth. In most cases with a follicular growth pattern, and in a minority of those with a diffuse growth pattern, neoplastic cells also stain positively for CD10. The presence of small clusters of $Bcl\text{-}6^+$ cells outside the follicles is considered strongly suggestive of a diagnosis of PCFCL[16]. Of note, Bcl-6 is also expressed by a subset of T lymphocytes (follicular T helper lymphocytes), but these cells are never arranged within clusters in cases of PCFCL.

In the vast majority of cases, staining for the protein product of *BCL-2* (Bcl-2) yields negative results within neoplastic follicles, representing a major difference from follicular lymphomas arising within lymph nodes[23]. Positivity for Bcl-2 by >75% neoplastic lymphocytes has been related to a higher rate of cutaneous recurrence[23a]. A useful, though somewhat counterintuitive, distinguishing immunohistochemical feature is the *lower* degree of proliferative activity within *malignant* follicles as detected by the anti-Ki-67 antibody (expressed by proliferating cells), in contrast to the *strong* Ki-67-positivity in *reactive* follicles[17]. In cases with large cell morphology (predominance of large cleaved cells), immunohistochemical staining for MUM-1 is either negative or is positive in a minority of neoplastic cells (in contrast to strong expression of MUM-1 by DLBCLLT; see below)[1,19]. The interchromosomal 14;18 translocation, typically found in *nodal* follicular lymphomas, is present in a minority of PCFCLs[23]. Therefore, the presence of the 14;18 translocation and/or expression of Bcl-2 should raise suspicion that the patient has a systemic lymphoma involving the skin. Analysis of the genes that encode the joining segment (J_H) and other regions of the immunoglobulin heavy chain (IGH) reveals the presence of a monoclonal rearrangement in the majority of patients (60%–70%). When gene expression in PCFCLs was analyzed via cDNA microarrays, a *germinal center cell signature pattern* was observed.

Analysis of morphologic, immunohistochemical, and molecular data suggests that follicular lymphomas originating in the lymph nodes and the skin, although characterized by a similar morphologic pattern, have different pathogenic mechanisms.

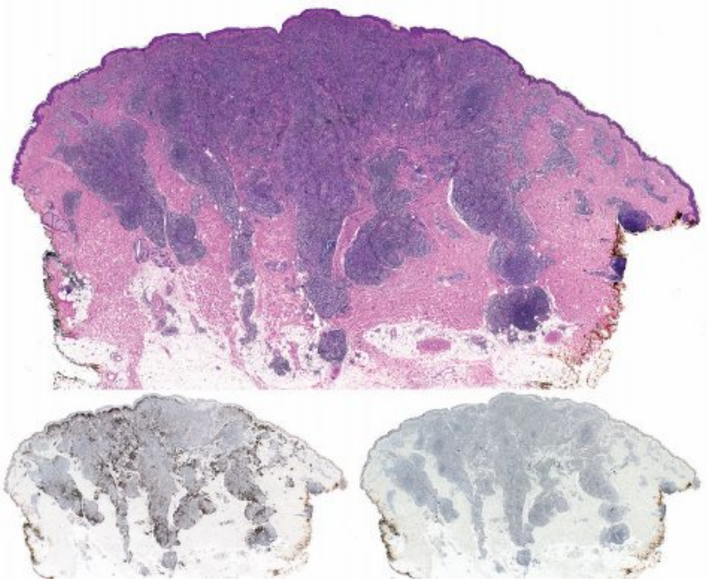


Fig. 119.8 Cutaneous marginal zone B cell lymphoproliferative disorder. Nodular lymphoid infiltrate within the entire dermis. Monotypic expression of kappa immunoglobulin light chain (left inset) with negativity for lambda light chain (right inset).

Primary Cutaneous Marginal Zone B Cell Lymphoproliferative Disorder

Histology of PCMZLD shows a patchy, nodular, or diffuse infiltrate involving the dermis and subcutaneous fat. The epidermis is spared. A characteristic pattern can be observed at scanning magnification (Fig. 119.8): nodular infiltrates (sometimes containing reactive germinal centers) are surrounded by a pale-staining population of small- to medium-sized cells with indented nuclei, inconspicuous nucleoli, and abundant pale cytoplasm – variously described as marginal zone cells, centrocyte-like cells, or monocytoid B cells (Fig. 119.9A)[4,5]. In addition, plasma cells (at the margins of the infiltrate), lymphoplasmacytoid cells, small lymphocytes, and occasional large blasts are observed. Eosinophils are also a common finding. In some patients, there may be a granulomatous reaction with epithelioid and giant cells. Cases with a predominance of lymphoplasmacytoid lymphocytes were once classified as cutaneous immunocytomas, but are now considered variants of PCMZLD. PAS-positive intranuclear inclusions (Dutcher bodies) are sometimes observed and represent a valuable clue to the diagnosis (Fig. 119.9B). Occasionally, the predominant cell type is a plasma cell (Fig. 119.9C), and although such cases used to be classified as primary cutaneous plasmacytomas, they are now also considered to be variants of PCMZLD[1]. Finally, rare cases are characterized by the predominance of large blastoid cells resembling plasmablasts (Fig. 119.9D)[24]. Solitary cutaneous nodular amyloidosis (cutaneous amyloidoma) harboring a small monoclonal population of plasma cells may represent a peculiar, rare variant of PCMZLD[25].

The centrocyte-like cells stain positively for CD20, CD79a, Fc receptor-like 4 (FCRL4/IRTA1)[26], and Bcl-2; they are negative for CD5, CD10, and Bcl-6. In the overwhelming majority of cases, intracytoplasmic monotypic expression of immunoglobulin light chains (either κ or λ, but not both) can be observed (see Fig. 119.8; Fig. 119.10). The monoclonal population of B lymphocytes is often characteristically arranged at the periphery of the cellular aggregates. Staining for proliferation markers also shows increased positivity at the periphery of the nodules (as well as in reactive germinal centers). IgG4 expression is observed in less than half of cases with plasmacytic differentiation but is not associated with systemic IgG4-related disease[27]. Monoclonal rearrangement of *IGH* can be detected in the majority of cases (60%–80%).

PCMZLDs express class-switched immunoglobulins, e.g. the same clone can switch from IgM to IgG or IgA[28]. Although the B lymphocyte changes antibody production from one class to another, the cell retains affinity for the same antigen. PCMZLD are also characterized

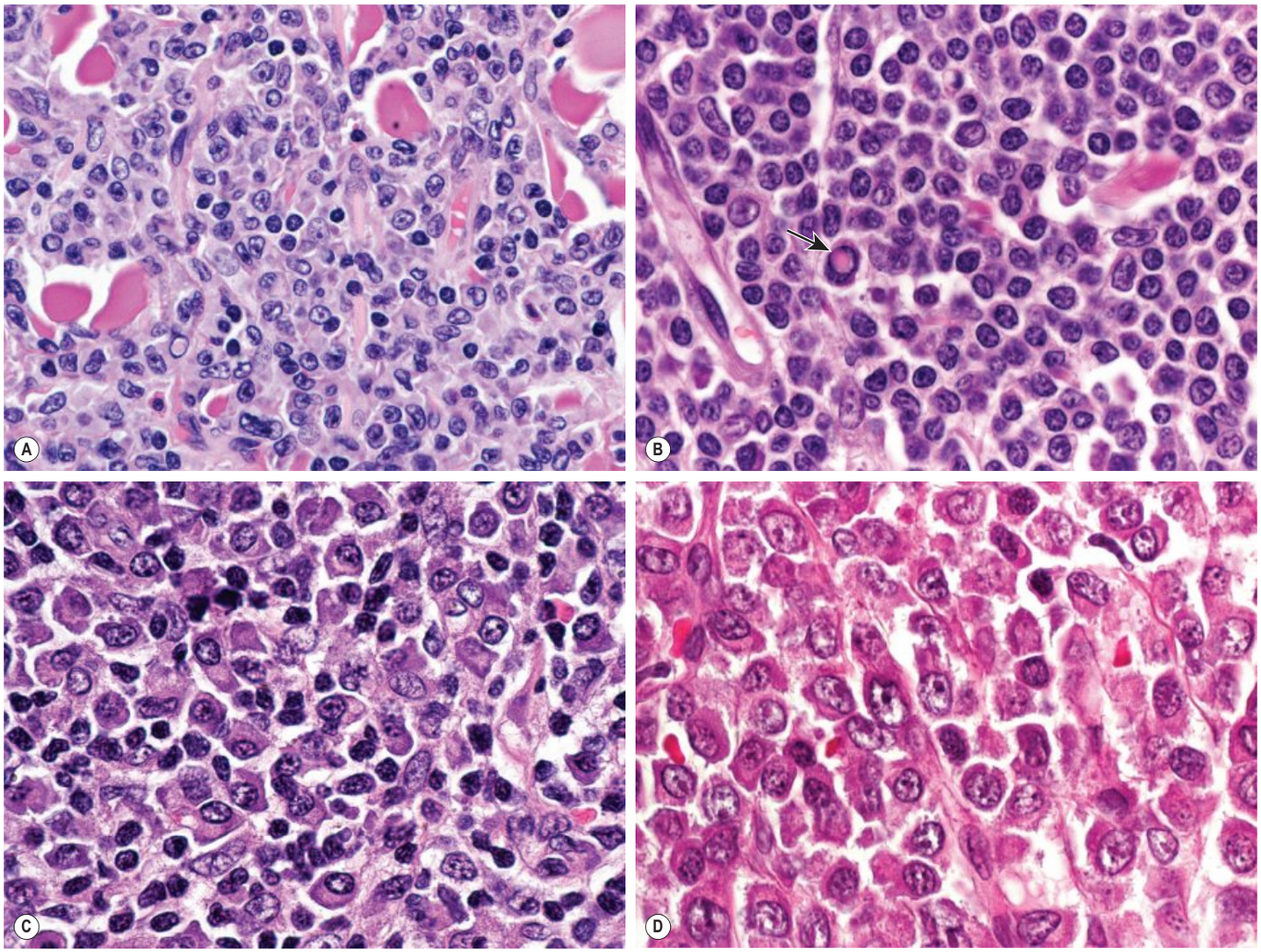


Fig. 119.9 Cutaneous marginal zone B cell lymphoproliferative disorder – spectrum of cell types. A Admixture of marginal zone cells, plasmacytoid cells, and plasma cells. **B** Predominance of lymphoplasmacytoid cells (formerly classified as cutaneous immunocytoma; note an intranuclear eosinophilic inclusion [Dutcher body, arrow]). **C** Predominance of plasma cells (formerly classified as cutaneous plasmacytoma). **D** Predominance of large blastoid cells similar to plasmablasts.

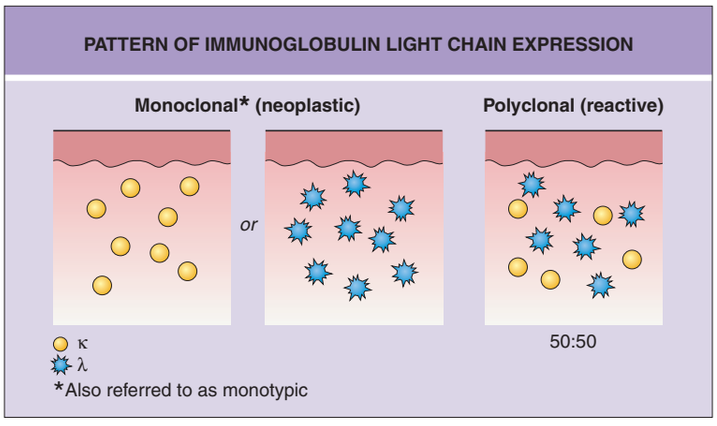


Fig. 119.10 Pattern of immunoglobulin light chain expression. Detection of monoclonal expression of immunoglobulin light chains (κ or λ) is a key diagnostic feature for primary cutaneous marginal zone B cell lymphoproliferative disorder. Monoclonality is defined as a >10/1 ratio.

by aberrant somatic hypermutations allowing binding to different antigens[29]. A minority of PCMZLD express IgM (non-switched cases), but this is associated with a higher frequency of extracutaneous dissemination.

A particular translocation, t(14;18)(q32;21), that involves *IGH* and *MALT1* has been detected in a subset of PCMZLD (~30%) as well as MALT lymphomas arising in organs other than the skin. In gene expression studies utilizing cDNA microarrays, PCMZLDs had a *plasma cell signature pattern*. Other genetic aberrations include trisomy 3 (with upregulation of *FOXP1*) and rarely an 11;18 or a 3;14 translocation[30]. However, in more than 50% of patients, no molecular abnormalities have been found.

Primary Cutaneous Diffuse Large B Cell Lymphoma, Leg Type

In DLBCLLT, a dense diffuse infiltrate is seen within the dermis and subcutis. The infiltrate usually involves the entire papillary dermis extending to the dermal–epidermal junction. Involvement of the epidermis by clusters of large atypical cells, simulating the Pautrier microabscesses found in cutaneous T cell lymphoma, can be observed in some cases (B cell epidermotropism), representing a potential diagnostic pitfall[4]. The neoplastic infiltrate consists predominantly of immunoblasts (large round cells with abundant cytoplasm and prominent nucleoli) and centroblasts (Fig. 119.11). Of note, cases of pCBCLs with a predominance of large cleaved cells (i.e. large centrocytes) are classified among the PCFCLs (see above)[1]. Reactive small lymphocytes are usually few in number, and mitoses are frequent. The common finding of immunoglobulin gene hypermutations is evidence that DLBCLLT is a large cell lymphoma, representing post germinal center lymphocytes that originated from lymphocytes of the germinal center.

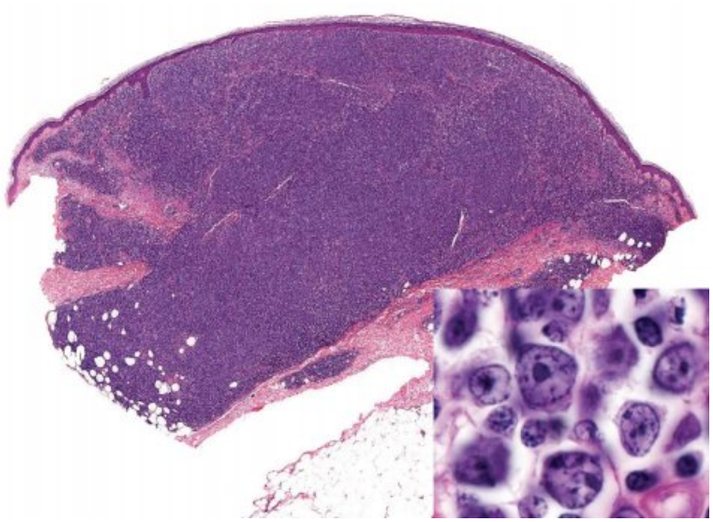


Fig. 119.11 Cutaneous diffuse large B cell lymphoma, leg type. Within the entire dermis, there is a dense, diffuse lymphoid infiltrate. Large cells with a round morphology (mainly immunoblasts) predominate (inset).

Neoplastic cells are positive for B cell markers (CD20, CD79a, PAX-5, IgM), but there can be (partial) loss of antigen expression. Bcl-2, MUM-1 (see above), FOX-P1, and MYC are expressed by neoplastic cells in most patients[1,19,31]. These markers are useful in the differential diagnosis of DLBCLLT from PCFCL, diffuse type; in the latter, Bcl-2, MUM-1, and FOX-P1 are usually either negative or expressed by a small minority of cells (Fig. 119.12). The tumors demonstrate monoclonal rearrangement of *IGH*. The interchromosomal 14;18 translocation is not present. An algorithmic approach to the diagnosis of cutaneous diffuse large B cell lymphomas is provided in Fig. 119.13. The differential expression of lymphoid markers in various types of diffuse large B cell lymphoma with cutaneous involvement is summarized in Table 119.3.

Rare cases of otherwise typical cutaneous DLBCLLT show expression of CD30 by neoplastic cells[19]. In nodal diffuse large B cell lymphomas, CD30 expression was associated with a better prognosis, but data on DLBCLLT are lacking. Hypermethylation of the genes that encode p15 and/or p16 (*CDKN2B*, *CDKN2A*), resulting in decreased expression of these proteins, has been observed in some patients. 9p21 deletions, possibly leading to loss-of-function of *CDKN2A*, are associated with a worse prognosis. A worse prognosis has also been noted in patients whose tumors have *MYD88* mutations.

In *nodal* diffuse large B cell lymphomas that have a rearrangement of *MYC* associated with additional rearrangements in *BCL-2* and/or *BCL-6* ("double-hit" or "triple-hit" lymphomas) have a worse prognosis. A poor prognosis is also associated with expression of the respective proteins as detected by immunohistochemistry ("double expression" or "triple expression" patterns). Data regarding primary cutaneous B cell lymphomas are still fragmentary, but it appears that *MYC* rearrangements are more common than in B cell lymphomas at extracutaneous sites, whereas double-hits are very rare and do not affect prognosis[32,33]. Expression of MYC, Bcl-2 and Bcl-6 is common in primary cutaneous lymphomas, but the prognostic value of "double expression", if any, is still unclear[32,33]. While the cut-off values for determining positivity of Bcl-2 and MYC expression within cells lack uniformity, currently accepted cut-off points are 50% for Bcl-2 and 40% for MYC.

Genetic data obtained by FISH or microarray chip technologies have confirmed that DLBCLLTs show clear molecular differences from PCFCL, diffuse type, confirming the need of classifying these cases separately[34]. The molecular profile of DLBCLLT is similar to that observed in diffuse large B cell lymphomas of the lymph nodes, with the *signature pattern of an activated B lymphocyte*[35].

Intravascular Diffuse Large B Cell Lymphoma

IVDLBCL is characterized by a proliferation of large atypical lymphocytes that fills dilated blood vessels within the dermis and subcutaneous tissues (Fig. 119.14). The malignant cells are large with scanty cytoplasm and often have prominent nucleoli. They are positive for B cell-associated markers as well as for Bcl-2, MUM-1, and FOX-P1. Staining with endothelial cell-related antibodies (e.g. CD31, CD34) highlights the characteristic intravascular location of the cells. Molecular analysis shows monoclonal rearrangement of *IGH*. The genetic profile is similar to that observed in diffuse large B cell lymphomas – activated B cell type.

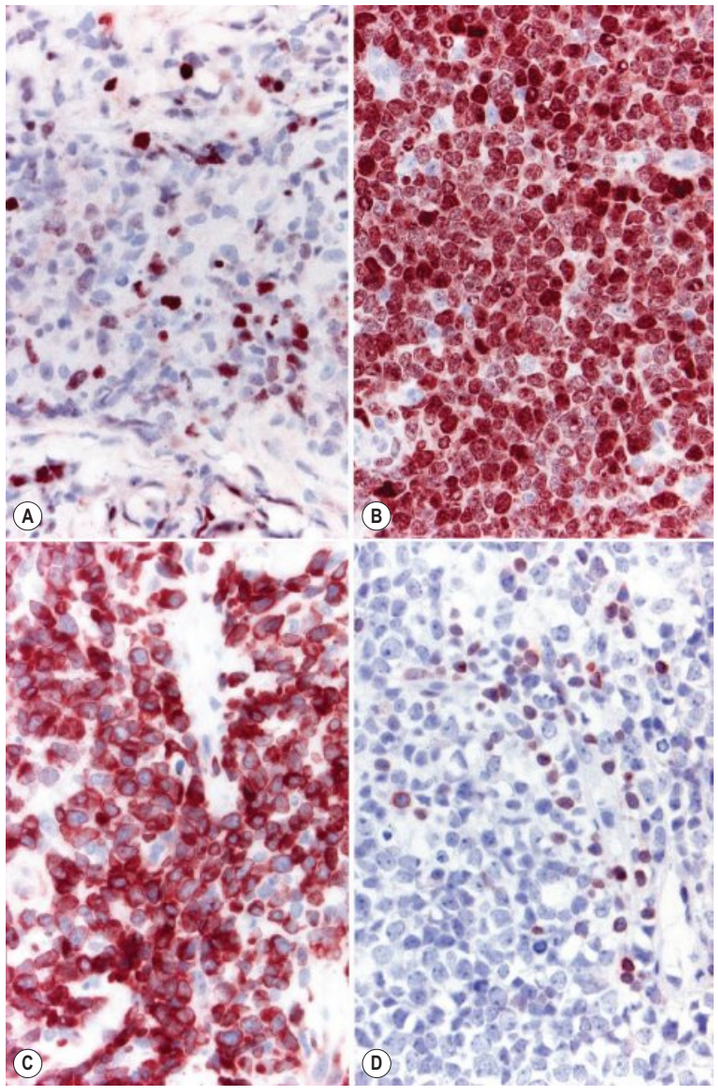


Fig. 119.12 Immunohistochemical staining with anti-Bcl-2 and anti-MUM-1 antibodies. Staining with anti-Bcl-2 antibody shows negativity (except for reactive small lymphocytes) in follicle center lymphoma, diffuse type (**A**) and positivity of most tumor cells in diffuse large B cell lymphoma, leg type (**B**). Anti-MUM-1 antibody stains virtually all the tumor cells in primary cutaneous diffuse large B cell lymphoma, leg type (**C**) while only a minority of cells are positive in primary cutaneous follicle center lymphoma, diffuse type (**D**).

Precursor B Lymphoblastic Lymphoma/Leukemia

Histologically, precursor B lymphoblastic lymphoma/leukemia shows a monomorphous proliferation of medium-sized cells with scanty cytoplasm and round or convoluted nuclei with fine chromatin (Fig. 119.15). A "starry sky" pattern is commonly seen at low power, due to the presence of macrophages with inclusion bodies ("tingible bodies"). Another characteristic feature is the arrangement of neoplastic cells in a "mosaic-stone" pattern. Mitoses and necrotic cells are abundant. It must be stressed that histologic features alone do not allow differentiation of lymphoblastic lymphomas of B cell phenotype from those of T cell lineage. Immunohistology demonstrates positive staining for TdT (terminal deoxynucleotidyl transferase; present on precursor

T and B cells), PAX-5, CD10, and the cytoplasmic μ-chain of immunoglobulins, and in most cases, CD20 and CD79a. CD20 is negative in the pre-pre-B cell variant, which is CD34$^+$. Molecular analyses usually show a monoclonal rearrangement of *IGH* and a polyclonal pattern for T cell receptor genes (*TCR*), but a lack of rearrangement of *IGH* or monoclonal rearrangement of both *TCR* and *IGH* may be observed.

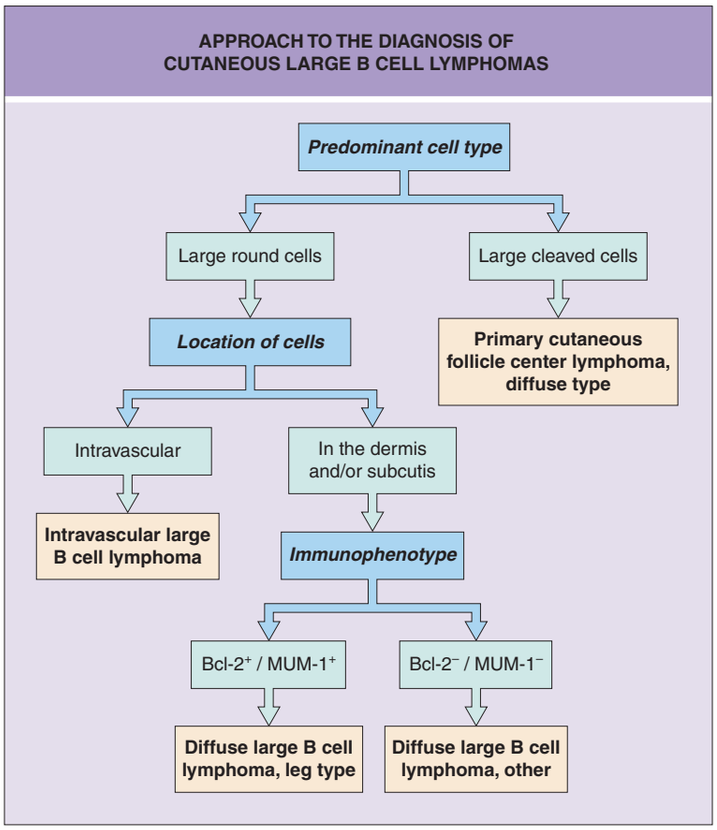


Fig. 119.13 Approach to the diagnosis of cutaneous large B cell lymphomas. In most patients with primary cutaneous diffuse large B cell lymphoma, leg type, the neoplastic cells strongly express MUM-1 and FOX-P1 (as well as Bcl-2), whereas in primary cutaneous follicle center lymphoma, diffuse type, these stains are usually either negative or expressed by a small minority of cells (see Fig. 119.12).

Other Cutaneous B Cell Lymphomas

EBV$^+$ mucocutaneous ulcer is characterized by the presence of atypical cells positive for CD30 and PAX5 within a polymorphous background, mimicking the features observed in Hodgkin lymphoma. EBV is detected within the atypical cells, but positivity is also observed in small lymphocytes, representing a clue for differentiation from true Hodgkin lymphoma (where EBV-positivity is limited to large, atypical cells)[36]. In addition, clinical features of the two entities are completely different.

Plasmablastic lymphoma is characterized by a proliferation of plasmablasts with large eccentric nuclei, abundant cytoplasm, and prominent nucleoli. While the tumor cells may appear lymphoid, they stain like plasma cells. They are positive for CD38, CD138 and MUM-1, but negative for CD20; they express monotypic immunoglobulin light chains. *In situ* hybridization for EBV (EBER-1) is positive in the vast majority of cases.

DIFFERENTIAL DIAGNOSIS

Although differential diagnoses of pCBCLs vary according to the type of lymphoma, in general they include inflammatory processes that may simulate malignant lymphomas clinically and/or histopathologically, referred to as cutaneous lymphoid hyperplasia, lymphocytoma cutis or "pseudolymphoma" (see Ch. 121). It must be emphasized that a definitive diagnosis of pCBCL can be reached only after careful examination of the clinical, histopathologic, immunophenotypic and molecular features; in some cases, only repeated examination of the patient and sequential biopsy specimens will allow the correct classification[4]. A schematic diagram with examples of the use of immunohistochemical stains and PCR in the differential diagnosis of pCBCLs is presented in Figure 119.16.

Patients for whom no definitive diagnosis can be established at the time of presentation should provisionally be classified as having "cutaneous atypical lymphoid proliferation of B cell lineage", and they should be re-examined at regular intervals[4]. A complete staging investigation does not belong in the diagnostic evaluation of these patients; that is, patients without a definitive diagnosis of CBCL should not be screened for extracutaneous disease until the diagnosis is established with certainty[4]. In contrast, once the diagnosis of CBCL has been established, complete staging is mandatory, as clinicopathologic features alone do not allow for the differentiation of primary from secondary cutaneous B cell lymphomas (see Table 119.2). A diagnostic algorithm for evaluation of patients at first presentation is provided in Figure 119.17.

In the following section, the major differential diagnoses of each of the main types of pCBCL are outlined separately, as they differ according to the lymphoma type.

IMMUNOHISTOCHEMICAL MARKER EXPRESSION IN PRIMARY AND SECONDARY CUTANEOUS LARGE B CELL LYMPHOMAS WITH OVERLAP IN ROUTINE HISTOPATHOLOGIC FINDINGS

	Immunohistochemical marker expression							
	Bcl-2	**Bcl-6**	**CD10**	**CD5**	**MUM-1**	**Cyclin D1**	**TdT**	**EBER-1**
Primary cutaneous lymphomas								
Follicle center lymphoma, diffuse	−	+	+/−	−	−	−	−	−
Marginal zone lymphoma, blastoid	+	−	−	−	−	−	−	−
Diffuse large B cell lymphoma, leg type	+	+/−	−	−	+	−	−	−
Systemic lymphomas with secondary skin involvement								
EBV$^+$ DLBCL	+/−	−/+	−/+	−	+	−	−	+
Nodal DLBCL	+	+/−	+/−	−/+	+/−	−	−	−
Mantle cell lymphoma, blastic	+	−/+	−	+	−/+	+	−	−
CLL/SLL → Richter syndrome	+/−	−	−	+	−	−	−	−
Burkitt lymphoma	−	+	+	−	−	−	−	+
B lymphoblastic lymphoma	+	−	+	−	−	−	+	−

+/−, majority of cases positive; −/+, majority of cases negative.

Table 119.3 Immunohistochemical marker expression in primary and secondary cutaneous large B cell lymphomas with overlap in routine histopathologic findings. As to be expected, there can be phenotypic overlap amongst these entities. All stain positively for CD20. The most helpful stains are shaded. CLL/SLL, B cell chronic lymphocytic leukemia/small lymphocytic lymphoma; DLBCL, diffuse large B cell lymphoma; EBV, Epstein–Barr virus.

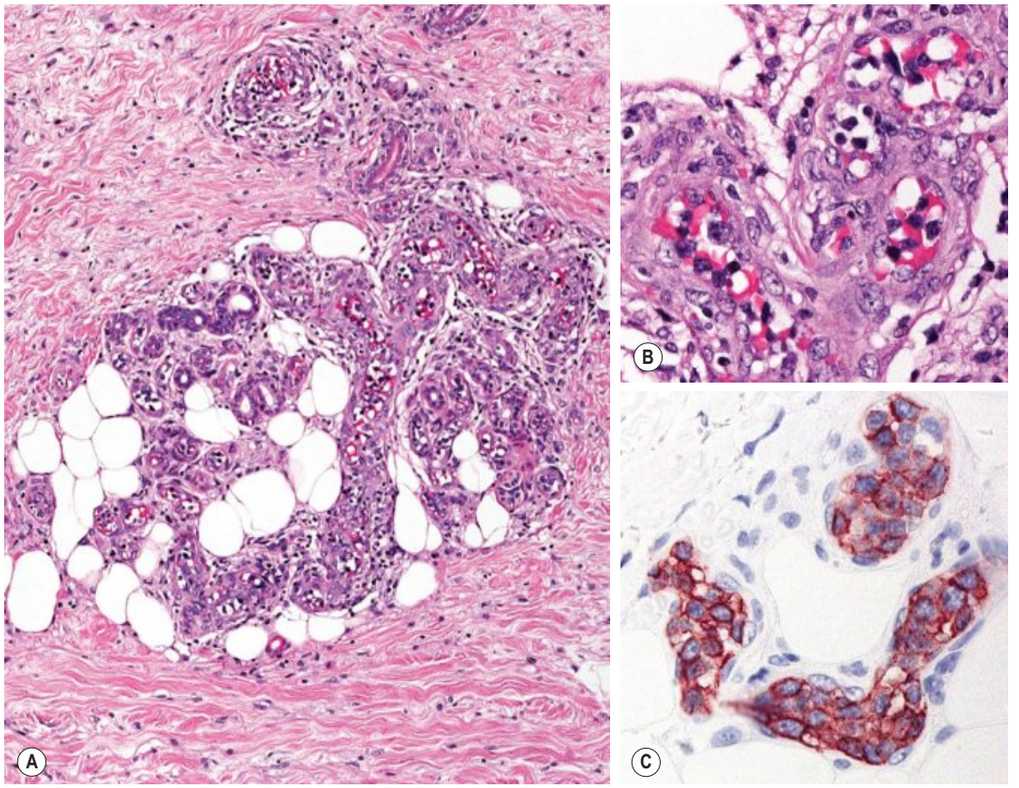


Fig. 119.14 Cutaneous diffuse intravascular large B cell lymphoma – histopathologic features. A Dermal cluster of several small blood vessels filled with large, atypical lymphocytes (**B**) which are positive for CD20 (**C**).

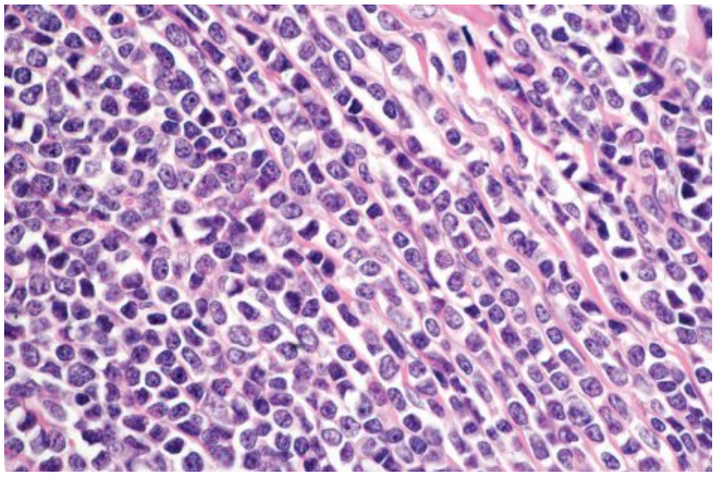


Fig. 119.15 Precursor B lymphoblastic lymphoma/leukemia. Medium-sized blasts with the characteristic "mosaic-stone" linear arrangement.

PCFCL with a follicular pattern of growth should be differentiated from B cell pseudolymphomas with prominent germinal centers, such as *Borrelia*-induced lymphocytoma cutis (cutaneous lymphoid hyperplasia)[17,37]. Lymphocytoma cutis can be triggered by a number of stimuli, including arthropod bites, vaccinations, tattoos and drugs, and it has a predilection for particular body sites such as the earlobes, nipples, and scrotum[37]. Clinically, lesions are usually solitary and relatively small. Although histologically a follicular pattern is almost always observed, germinal centers in lymphocytoma cutis are reactive, and they are accompanied by inflammatory infiltrates with small lymphocytes, plasma cells, and often eosinophils[4,37]. The germinal centers in *Borrelia*-induced lymphocytoma cutis are often devoid of a clear-cut mantle, but they are characterized by the presence of many tingible body macrophages, "clear" and "dark" areas, and a normal (high) proliferation rate[37].

Rare cases of cutaneous PCMZLD can have a prominent presence of reactive germinal centers, and they should be differentiated from the follicular type of PCFCL. In these cases, so-called follicular colonization by neoplastic marginal zone cells can indeed cause significant problems in histopathologic differential diagnosis, similar to what happens in B cell lymphomas of the MALT type. However, the overall architecture of the infiltrate, the presence of a population of monoclonal plasma cells belonging to the neoplastic clone, and the negativity of neoplastic cells for CD10 and Bcl-6 usually allow the diagnosis of cutaneous PCMZLD to be established.

As mentioned previously, secondary cutaneous involvement by primary extracutaneous follicular lymphomas has morphologic and phenotypic features similar or identical to those observed in primary cutaneous B cell lymphoma, except for the usual positivity of neoplastic cells for Bcl-2 in secondary cutaneous lesions. Consequently, the occurrence of a cutaneous follicular lymphoma with clear-cut positivity for Bcl-2 within neoplastic follicles should be considered as a hint (although exceptions can be encountered) for the diagnosis of secondary skin lesions of nodal lymphoma.

The differential diagnosis of **PCMZLD** consists primarily of reactive processes and other types of low-grade pCBCL. Benign, reactive processes do not have monotypic restriction of immunoglobulin light chain expression, in contrast to what is observed in the great majority of cases of PCMZLD. PCFCL, diffuse type, can be differentiated from PCMZLD by the architectural pattern and cytomorphology, with the former being characterized by a diffuse infiltrate of B lymphocytes with a predominance of centrocytes and centroblasts. Moreover, in contrast to PCMZLD, neoplastic cells in PCFCL express Bcl-6.

PCMZLD should also be distinguished from secondary cutaneous lesions of B cell chronic lymphocytic leukemia (B-CLL), a condition in which neoplastic B lymphocytes display positivity for CD20, CD23 and CD43, and usually for CD5. Helpful diagnostic features are: (1) the absence, in B-CLL, of plasma cells belonging to the neoplastic clone; and (2) the positivity for CD5 observed in most cases of cutaneous B-CLL, but practically never in PCMZLD. $CD20^+/CD5^+$ infiltrates are also seen in secondary skin involvement from mantle cell lymphoma, but in contrast to CLL, mantle cell lymphoma is usually positive for cyclin D1 and negative for CD23 (rare cases of mantle cell lymphoma that are negative for cyclin D1 are positive for SOX11).

PCMZLD with prominent plasma cell differentiation must be differentiated from reactive plasma cell proliferations and from inflammatory pseudotumors (plasma cell granulomas). In reactive conditions, plasma cells are not atypical, and they display a polyclonal pattern of immunoglobulin light chain expression. Besides inflammatory pseudotumors,

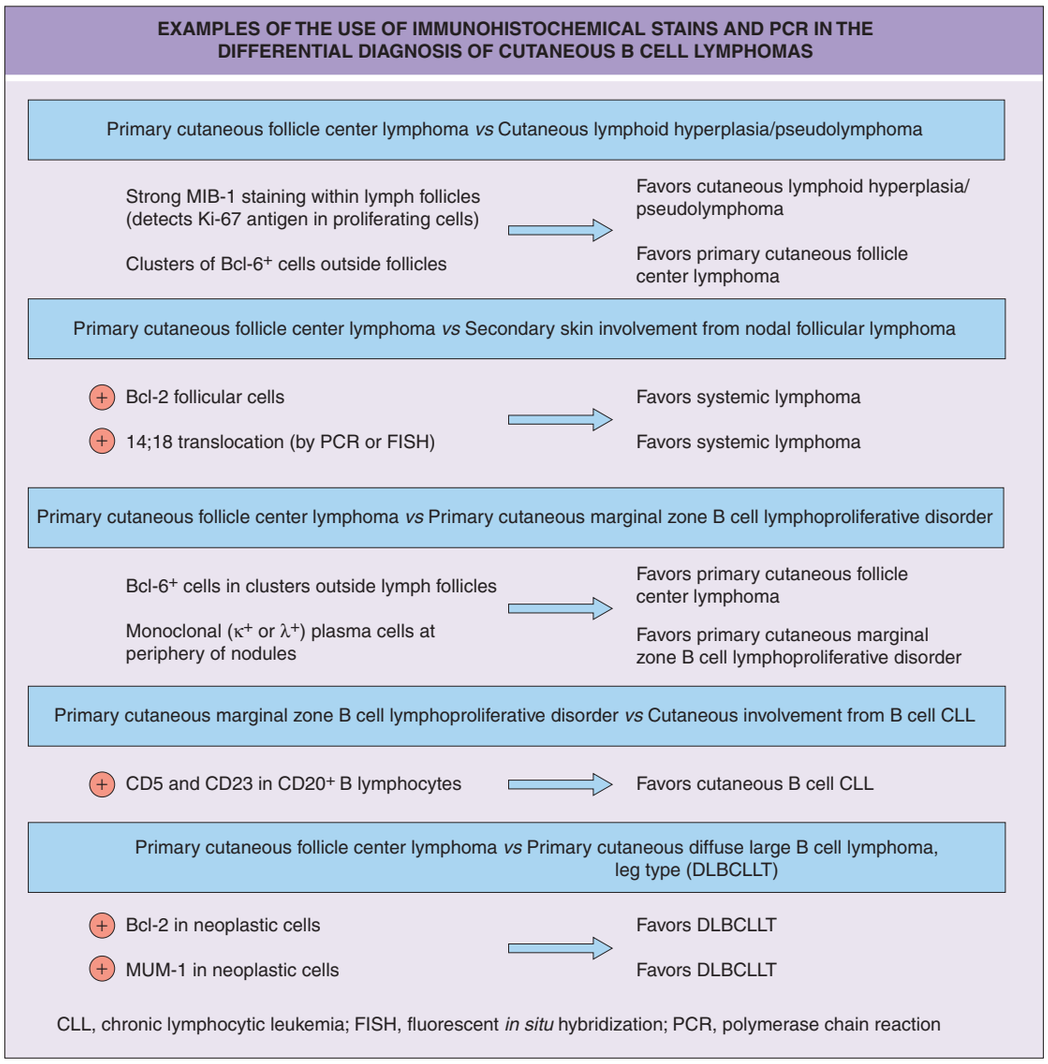


Fig. 119.16 Examples of the use of immunohistochemical stains and PCR in the differential diagnosis of cutaneous B cell lymphomas. This represents a simplification and is intended to assist dermatologists in their interpretation of pathology reports. $CD20^+/CD5^+$ infiltrates are also seen in secondary skin involvement from mantle cell lymphoma, but in contrast to CLL, mantle cell lymphoma is also positive for cyclin D1 and negative for CD23 (see Table 119.3).

reactive skin diseases with a predominance of plasma cells are very rare, with the exception of lesions arising on mucosal surfaces, spirochetal infections (e.g. syphilis, pinta, yaws, acrodermatitis chronica atrophicans), and cutaneous and systemic plasmacytosis. The latter disorder usually displays a polyclonal pattern of immunoglobulin light chain expression, but rarely monoclonality has been reported[38]. A silver stain (e.g. Warthin–Starry) or immunohistochemical staining for *Treponema pallidum* can help to highlight the microorganisms in cases of syphilis (see Fig. 0.33). The rare entity *pretibial lymphoplasmacytic plaque in children* is characterized by a polyclonal pattern of the plasma cells.

DLBCLLT must be differentiated from a number of entities, including cutaneous involvement from systemic lymphomas as well as specific infiltrates of acute myelogenous leukemia and non-lymphoid tumors (e.g. solid organ metastases; see Ch. 122). The clinicopathologic pattern together with phenotypic and molecular features allow correct classification of these lesions in most instances. In order to avoid diagnostic errors, detailed immunophenotyping is mandatory in all cases of cutaneous lymphoma, especially in those showing medium- to large-sized cell morphology.

The differential diagnosis of **IVDLBCL** is not a problem in typical cases. The large number of atypical cells within *blood vessels* is pathognomonic of this condition. Distinction between T and B cell types cannot be achieved on morphologic grounds alone. Rare cases of intralymphatic anaplastic large T cell lymphoma (ALCL) are characterized by a proliferation of neoplastic $CD30^+$ T cells within *lymphatic vessels*. This disorder represents a variant of ALCL and has similar phenotypic and prognostic features[39]. IVDLBCL should also be distinguished from reactive disorders characterized by an intravascular proliferation of atypical cells, in particular intralymphatic histiocytosis (IH) and benign intralymphatic proliferation of T cell lymphoid blasts (BIPTCLB). IH occurs in association with systemic disorders such as rheumatoid arthritis as well as metallic orthopedic implants. Within the dermis, *lymphatic vessels* that stain positively for podoplanin contain intraluminal collections of histiocytes ($CD68^+$, $CD20^-$, $CD3^-$). Of note, focal areas of IH can be an incidental finding. BIPTCLB is a rare entity observed in a wide range of cutaneous and extracutaneous disorders from pyogenic granuloma to appendicitis. As in IH, the *lymphatic vessels* are affected.

Cases of **precursor B lymphoblastic lymphoma/leukemia** should be differentiated from other cutaneous lymphomas/leukemias and from non-lymphoid tumors such as Ewing sarcoma, Merkel cell carcinoma, and small cell lung carcinoma. Positivity for TdT represents the most important immunohistochemical feature for the diagnosis of cutaneous lymphoblastic lymphoma. Histologic features of cutaneous lesions do not allow the differentiation of T cell from B cell lymphoblastic lymphomas, thus emphasizing the importance of complete immunophenotypic and genotypic analyses.

In immunosuppressed patients, the possibility of post-transplant lymphoproliferative disorder should be considered (Table 119.4).

TREATMENT

The most appropriate treatment modality for patients with a pCBCL is selected after exact classification of the lymphoma, analysis of results of staging investigations, and consideration of the overall condition of the patient[4]. Those patients with secondary cutaneous lesions of extracutaneous B cell lymphoma should be treated in a hemato-oncologic, not dermatologic, setting[4].

Before reviewing the major therapeutic strategies, it must be emphasized that many patients with low-grade pCBCL can be managed

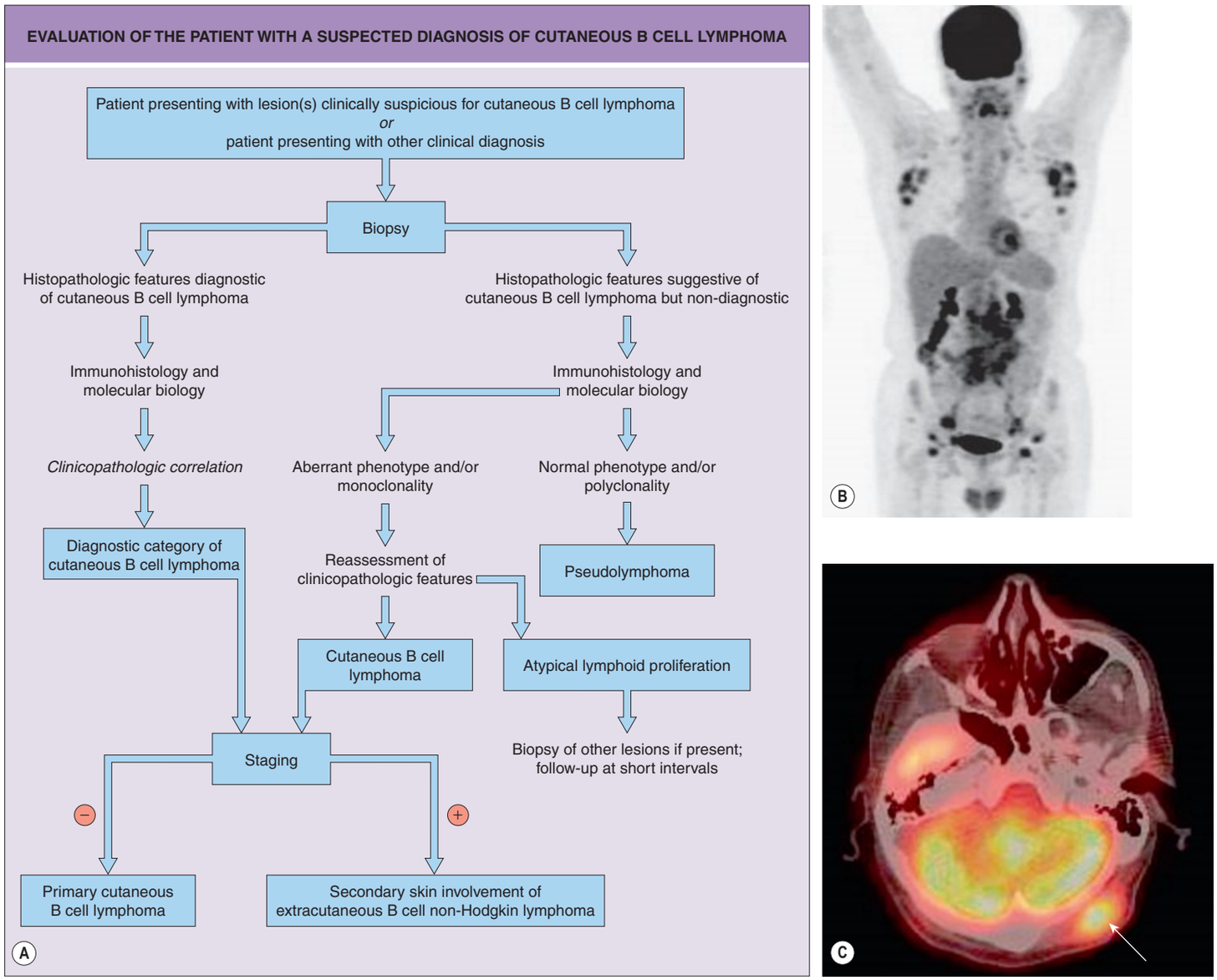


Fig. 119.17 Evaluation of the patient with a suspected diagnosis of cutaneous B cell lymphoma. A Algorithm outlining approach to the patient. **B, C** Positron emission tomography (PET) scans in a 66-year-old patient with stage IV B cell non-Hodgkin lymphoma. He had a 1-year history of a cutaneous nodule of the scalp that was originally diagnosed as an epidermoid inclusion cyst. Biopsy of the nodule showed a diffuse large B cell lymphoma ($CD10^+$, $CD20^+$, variably $Bcl\text{-}2^+$, $MUM\text{-}1^-$) and a PET-CT scan was performed for staging. There is evidence of widespread disease involving multiple lymph node basins in the dedicated (MIP) image (**B**) as well as a scalp lesion in a PET-CT fusion image (**C**; arrow). *B,C, Courtesy Dennis Cooper, MD.*

POST-TRANSPLANT LYMPHOPROLIFERATIVE DISORDERS
• Arise in the setting of immunosuppression
• Most commonly seen in solid organ transplant recipients, but can also affect other chronically immunosuppressed hosts (e.g. patient with rheumatoid arthritis receiving chronic methotrexate, HIV-positive patient)
• Patients most commonly present with extranodal disease, often involving the transplanted organ
• Other common sites of involvement include the GI tract and skin
• In the skin, polymorphic or monomorphic infiltrates are seen with the latter having similar clinicopathologic findings as conventional cutaneous B and NK/T cell lymphomas
• The abnormal lymphocytes are often EBV-positive, especially if B cells
• Initial therapeutic intervention is reduction of immunosuppression
• If persistent disease, appropriate treatment is administered depending on cell type

Table 119.4 Post-transplant lymphoproliferative disorders. EBV, Epstein–Barr virus; GI, gastrointestinal.

conservatively with a so-called watchful-waiting strategy, similar to what is often adopted for indolent B cell lymphomas and leukemias at extracutaneous sites[4,40]. Follow-up examinations in these patients should be performed at least every 6 months or at the onset of new lesions and/or new symptoms, in order to treat the patient as soon as it is necessary. Many patients managed conservatively with a watchful-waiting strategy experience a prolonged course and long survival, and they do not need aggressive treatment. For cosmesis and sometimes psychological benefit, intralesional triamcinolone can be injected into the papulonodules.

Most patients with pCBCLs that are low-grade (PCFCL, PCMZLD) and who have a solitary or few lesions can be treated by local radiotherapy, simple surgical excision, or surgical excision followed by radiotherapy of the surgical field[4,40]. It has been reported that recurrences are less frequently seen in patients treated by radiotherapy with wide margins (about 10–20 cm beyond clinically apparent lesions); this approach seems to be justified for so-called Crosti's lymphoma, a type of PCFCL arising on the back, in which erythematous nodules, papules, and patches surrounding the tumor represent specific infiltrates that can extend far beyond the main bulk of the lesion[41]. Radiotherapy with wide margins, however, does not seem to be justified for lesions other

than Crosti's lymphoma, as margins of about 3–5 cm usually suffice (depending on the size of the lesion). Surgical excision with narrow margins is a valuable therapeutic modality for patients with solitary well-circumscribed lesions and in the authors' opinion represents the treatment of choice for PCMZLD. In these patients, relapse rates do not seem to be higher than in patients treated with more time-intensive modalities such as local radiotherapy.

A few reports have appeared in which low-grade pCBCLs were treated with systemic antibiotics, achieving a complete resolution in at least a percentage of the patients[42]. This type of treatment is conceptually analogous to that adopted for *Helicobacter pylori*-associated MALT lymphomas of the stomach, which in their early stages can be cured by eradication of *H. pylori* infection. Complete response to antibiotic therapy has been observed in some patients with *Borrelia*-associated pCBCL. Although not yet corroborated by adequate data, antibiotic treatment of patients with pCBCLs should be considered before more aggressive therapeutic options are employed, particularly in European countries endemic for *Borrelia* infections. It is important to treat patients at the onset of the disease, because, in later stages, lesions may no longer be sensitive to systemic antibiotics. PCR analysis of *Borrelia* DNA is a rapid test that should be performed in all patients with pCBCL from European endemic areas, in order to identify those who would more likely benefit from early antibiotic treatment.

Another treatment modality for low-grade pCBCL is subcutaneous or intralesional interferon, particularly interferon-α-2a. Although some favorable results have been reported, it appears that treatment with interferon is associated with a complete response in about 50% of patients. Therapy with interferon (or intralesional triamcinolone) should be considered for patients presenting with multiple lesions at different body sites, such that local radiotherapy becomes difficult to administer.

Intralesional or systemic injection of anti-CD20 monoclonal antibody (rituximab) has been used to induce tumor reduction in patients with indolent pCBCLs[43,44]. Intralesional administration should be considered in patients presenting with a few, localized lesions. Therapy with intravenous rituximab represents a valid alternative to established treatments, especially in patients who present with disseminated skin lesions or relapse after radiotherapy. Rituximab can also be administered in combination with other treatment modalities for pCBCLs with more aggressive behavior (e.g. DLBCLLT). Additional monoclonal antibodies, bispecific T-cell engaging antibodies (e.g. mosunetuzumab), and small-molecule inhibitors (e.g. ibrutinib, lenalidomide) are also employed for aggressive B-cell lymphomas.

Patients with DLBCLLT and a limited number of patients with disseminated lesions of PCFCL, diffuse type, need more aggressive treatment modalities (e.g. systemic chemotherapy plus rituximab)[40,45]. The regimen used most frequently is cyclophosphamide, doxorubicin, vincristine and prednisone (CHOP) plus rituximab, and it represents the standard of care for DLBCLLT. In the absence of signs of transformation into high-grade lymphoma, aggressive treatment is not indicated in patients with PCMZLD. In the setting of significant comorbidities, rituximab alone or in combination with local radiotherapy may be administered. For relapsed DLBCLLT, CAR-T cell therapy is increasingly being used, especially when recurrence occurs within one year of primary therapy. In the setting of longer remissions, salvage chemotherapy followed by autologous HSCT is an option.

Systemic chemotherapy plus rituximab is the treatment of choice for patients with IVDLBCL, regardless of results of staging investigations. As with DLBCLLT, the addition of rituximab to anthracycline-based chemotherapy significantly improves outcome[45]. Finally, patients with precursor B lymphoblastic lymphoma/leukemia should be treated as B cell acute lymphoblastic leukemia by a hematologist.

PLASMA CELL DYSCRASIAS, INCLUDING MULTIPLE MYELOMA

A plasma cell dyscrasia represents a clonal proliferation of plasma cells and it can lead to a monoclonal gammopathy composed of intact immunoglobulins, isolated light chains (15% of patients) or, rarely, isolated heavy chains. The term plasma cell dyscrasia encompasses a number of entities, including monoclonal gammopathy of undetermined significance (MGUS; serum paraprotein <3 g/dl), smoldering/asymptomatic myeloma, and active/symptomatic myeloma, as well as light and heavy chain deposition diseases and systemic amyloidosis (AL). While proliferations of plasma cells within the skin are rare, an understanding of the spectrum and natural history of plasma cell dyscrasias is important for dermatologists given the number of cutaneous disorders associated with monoclonal gammopathies (Table 119.5; Fig. 119.18).

CUTANEOUS CONDITIONS ASSOCIATED WITH MONOCLONAL GAMMOPATHY
Proliferation of lymphoplasmacytic cells in the skin
• Extramedullary cutaneous plasmacytoma*
• Cutaneous Waldenström macroglobulinemia†
Deposition of the monoclonal protein in the skin, by definition
• Primary systemic amyloidosis (light chains)
• Cryoglobulinemic occlusive vasculopathy (type I cryoglobulins‡)
• Hyperkeratotic spicules (follicular > non-follicular)
• Crystal-storing histiocytosis
• Crystalglobulinemia
• IgM storage papules (cutaneous macroglobulinosis)†
• Subepidermal bullous dermatosis associated with IgM gammopathy†
Deposition of the monoclonal protein in the skin frequently observed
• Plasma cell dyscrasia-associated acquired cutis laxa, acral or generalized (amyloid and/or IgG)
• Plasma cell dyscrasia-associated reactive angioendotheliomatosis (type I cryoglobulins or amyloid)
Almost always associated with monoclonal gammopathy
• Scleromyxedema
• POEMS syndrome¶
• AESOP syndrome – *a*denopathy and *e*xtensive skin patch *o*verlying a *p*lasmacytoma; may coexist with POEMS syndrome¶
• TEMPI syndrome – *t*elangiectasias, *e*levated erythropoietin and erythrocytosis, *m*onoclonal gammopathy, *p*erinephric fluid collection, and *i*ntrapulmonary shunting
• Schnitzler syndrome†
• Necrobiotic xanthogranuloma
Frequently associated with monoclonal gammopathy
• Normolipemic plane xanthoma
• Scleredema (type 2)
• Angioedema secondary to acquired C1 esterase inhibitor deficiency
• Idiopathic systemic capillary leak syndrome (Clarkson syndrome)
Significant association with monoclonal gammopathy, primarily IgA (at least 15% of cases)
• Erythema elevatum diutinum
• Subcorneal pustular dermatosis (SPD) and SPD-type IgA pemphigus
• Pyoderma gangrenosum
• Neutrophilic papular xanthoma
Occasionally associated with monoclonal gammopathy
• Sweet syndrome
• Cutaneous small vessel vasculitis‡, including adult IgA vasculitis with monoclonal IgA gammopathy
• Xanthoma disseminatum
• Epidermolysis bullosa acquisita
• Paraneoplastic pemphigus
• Atypical scleroderma§
*In the current IC 2022 classification (see Table 119.1), primary cutaneous plasmacytoma is classified as primary cutaneous marginal zone B cell lymphoproliferative disorder.
†IgM monoclonal gammopathy is present by definition; in Schnitzler syndrome, IgG gammopathy has occasionally been observed; Waldenström macroglobulinemia is due to a lymphoplasmacytic lymphoma.
‡Cryoglobulinemic vasculitis can occur secondary to type II cryoglobulins.
¶Polyneuropathy (P), organomegaly (O), endocrinopathy (E), M-protein (M), skin changes (S; see Ch. 53 for list of skin changes); diagnosis requires monoclonal plasmaproliferative disorder & neuropathy + one other major criterion (sclerotic bone lesions, Castleman disease, increased serum VEGF levels) and one minor criterion (extravascular volume overload, papilledema, O, E, S, thrombocytosis/polycythemia).
§Possible association; sclerodermoid changes can also occur in the setting of primary systemic amyloidosis.

Table 119.5 Cutaneous conditions associated with monoclonal gammopathy. In some entities, there is a predominance of one type of immunoglobulin light chain, e.g. λ in scleromyxedema, κ in necrobiotic xanthogranuloma.



Fig. 119.18 Disorders associated with a monoclonal gammopathy. Subcorneal pustular dermatosis characterized by superficial vesiculopustules arising within a background of erythema; the patient had an IgA kappa monoclonal gammopathy. The clinical differential diagnosis includes IgA pemphigus. *Courtesy Karynne O. Duncan, MD.*

The diagnosis of symptomatic myeloma has recently been broadened from the need for disease-related CRAB (*c*alcium elevation, *r*enal insufficiency, *a*nemia and/or *b*one lesions [osteolytic > osteosclerotic]) to include patients with ≥60% bone marrow plasmacytosis, >1 lytic lesion on total body MRI (or PET-CT), or a ratio of involved : uninvolved free light chains of ≥100 : 1.

Of note, the level of circulating monoclonal protein associated with several of the skin disorders listed in Table 119.5 may be so low as to fall below the detection limit of a serum protein electrophoresis or an IgA paraprotein may not be detected because it falls within and is obscured by the β band. As a result, the more sensitive serum immunofixation electrophoresis (IFE) is required to detect an intact immunoglobulin (e.g. IgG, IgA) paraprotein.

In diagnosing patients with systemic amyloidosis whose cutaneous amyloid deposits are composed of light chains, the serum free light chain (SFLC) ratio is much more sensitive than even the serum IFE. In addition, because light chains are rapidly excreted into the urine, a urine IFE in addition to SFLC assay is necessary to exclude a light chain-producing plasma cell dyscrasia.

Histopathology

In specific skin lesions (see Table 119.5), diffuse infiltration of the dermis by atypical plasma cells or lymphoplasmacytoid cells is present, usually with several mitoses. Multinucleated plasma cells may be found. The infiltrating cells can be difficult to recognize as plasma cells, and CD45 and CD20 are negative in the vast majority of cases. Neoplastic plasma cells can be stained with CD38 and CD138, and they express monotypic immunoglobulins. Intracytoplasmic eosinophilic inclusions (Russell bodies) are often present; the cells are called Mott cells when these bodies form grape-like clusters. PAS-positive eosinophilic inclusions in the nucleus (Dutcher bodies) can also be observed. These are thought to be immunoglobulin or glycoprotein accumulations, and they can be found in other neoplastic conditions in which plasma cells are prevalent (e.g. plasma cell-rich PCMZLD; see Fig. 119.9B).

Differential Diagnosis

The differential diagnosis of PCMZLD with prominent plasma cell differentiation (formerly called cutaneous plasmacytoma) is discussed above. Cutaneous Waldenström macroglobulinemia has histologic features similar to PCMZLD with prominent lymphoplasmacytic differentiation (formerly called cutaneous immunocytoma)[46], except that direct immunofluorescence demonstrates monoclonal IgM within and around the infiltrating cells. Immunofixation electrophoresis of the serum detects the circulating monoclonal protein as IgM.

CUTANEOUS AND SYSTEMIC PLASMACYTOSIS

In cutaneous and systemic plasmacytosis, an entity most commonly seen in Asians, red–brown to violet–brown papules or nodules favor the back but can be widely disseminated[38]. Patients with the systemic form also have lymphadenopathy and occasionally have involvement of the lung, liver, spleen, or kidneys. The associated hypergammaglobulinemia is polyclonal as are the infiltrating plasma cells. Histologically, there are variably large aggregates of polyclonal plasma cells in the dermis, usually admixed with an inflammatory infiltrate and sometimes with reactive germinal centers[38]. The findings may overlap with those of plasma cell-rich Castleman disease.

Additional figures available in our eBook (see inside front cover for access code).

REFERENCES

1. Willemze R, Cerroni L, Kempf W, et al. The 2018 update of the WHO-EORTC classification for primary cutaneous lymphomas. *Blood*. 2019;133:1703–1714.
2. Swerdlow SH, Campo E, Harris NL, eds. *WHO Classification of Tumours of Haematopoietic and Lymphoid Tissues*. Lyon: IARC Press; 2008.
3. Campo E, Jaffe ES, Cook JR, et al. The International Consensus Classification of Mature Lymphoid Neoplasms: a report from the Clinical Advisory Committee. *Blood*. 2022:140:1229–1253.
4. Cerroni L. *Skin Lymphoma – The Illustrated Guide*. 5th ed. Oxford: Wiley-Blackwell; 2020.
5. Cerroni L, Signoretti S, Höfler G, et al. Primary cutaneous marginal zone B-cell lymphoma: a recently described entity of low-grade malignant cutaneous B-cell lymphoma. *Am J Surg Pathol*. 1997;21:1307–1315.
6. Korgavkar K, Weinstock MA. Changing incidence trends of cutaneous B-cell lymphoma. *J Invest Dermatol*. 2014;134:840–842.
7. Zackheim HS, Vonderheid EC, Ramsay DL, et al. Relative frequency of various forms of primary cutaneous lymphomas. *J Am Acad Dermatol*. 2000;43:793–796.
8. Cerroni L, Zöchling N, Pütz B, Kerl H. Infection by *Borrelia burgdorferi* and cutaneous B-cell lymphoma. *J Cutan Pathol*. 1997;24:457–461.
9. Goodlad JR, Davidson MM, Hollowood K, et al. Primary cutaneous B-cell lymphoma and *Borrelia burgdorferi* infection in patients from the highlands of Scotland. *Am J Surg Pathol*. 2000;24:1279–1285.
10. Seçkin D, Barete S, Euvrard S, et al. Primary cutaneous posttransplant lymphoproliferative disorders in solid organ transplant recipients: a multicenter European case series. *Am J Transplant*. 2013;13:2146–2153.
11. Beylot-Barry M, Vergier B, Masquelier B, et al. The spectrum of cutaneous lymphomas in HIV infection. A study of 21 cases. *Am J Surg Pathol*. 1999;23:1208–1216.
12. Koens L, Senff NJ, Vermeer MH, et al. Methotrexate-associated B-cell lymphoproliferative disorders presenting in the skin: a clinicopathologic and immunophenotypical study of 10 cases. *Am J Surg Pathol*. 2014;38:999–1006.
13. Vachhani P, Neppalli VT, Cancino CJ, et al. Radiological imaging and bone marrow biopsy in staging of cutaneous B-cell lymphoma. *Br J Haematol*. 2019;184:674–676.
14. Terhorst D, Mestel DS, Humme D, et al. Evaluation of different methods in the follow-up of patients with indolent types of primary cutaneous lymphomas. *Br J Dermatol*. 2012;166:1295–1300.
15. Berti E, Alessi E, Caputo R, et al. Reticulohistiocytoma of the dorsum. *J Am Acad Dermatol*. 1988;19:259–272.
16. Massone C, Fink-Puches R, Laimer M, et al. Miliary and agminated-type primary cutaneous follicle center lymphoma: report of 18 cases. *J Am Acad Dermatol*. 2011;65:749–755.
17. Cerroni L, Arzberger E, Pütz B, et al. Primary cutaneous follicle center cell lymphoma with follicular growth pattern. *Blood*. 2000;95:3922–3928.
18. Bailey EM, Ferry JA, Harris NL, et al. Marginal zone lymphoma (low-grade B-cell lymphoma of mucosa-associated lymphoid tissue type) of skin and subcutaneous tissue. A study of 15 patients. *Am J Surg Pathol*. 1996;20:1011–1023.

18a. Falini B, Martino G, Lazzi S, et al. A comparison of the International Consensus and 5th World Health Organization classifications of mature B-cell lymphomas. *Leukemia*. 2023;37(1):18–34.

19. Kodama K, Massone C, Chott A, et al. Primary cutaneous large B-cell lymphomas: clinicopathologic features, classification, and prognostic factors in a large series of patients. *Blood*. 2005;106:2491–2497.
20. Fonkem E, Lok E, Robison D, et al. The natural history of intravascular lymphomatosis. *Cancer Med*. 2014;3:1010–1024.
21. Lee WJ, Moon HR, Won CH, et al. Precursor B- or T-lymphoblastic lymphoma presenting with cutaneous

involvement: a series of 13 cases including 7 cases of cutaneous T-lymphoblastic lymphoma. *J Am Acad Dermatol*. 2014;70:318–325.

21a. Skala SL, Harms PW, Fullen DR, et al. Cutaneous follicle center lymphomas with plasmacytic differentiation. *J Cutan Pathol*. 2021;48:632–636.

21b. Kelley JT, Brown NA, Hristov AC, Bresler SC. Primary cutaneous follicle center lymphoma with extensive plasmacytic differentiation and t(14;18) in both the lymphoid and plasma cell components. *J Cutan Pathol*. 2021;48:969–974.

22. Yann CJ, Cerroni L, LeBoit PE. Cutaneous spindle-cell B-cell lymphomas. Most are neoplasms of follicular center cell origin. *Am J Surg Pathol*. 2015;39:737–743.

23. Cerroni L, Volkenandt M, Rieger E, et al. Bcl-2 protein expression and correlation with the inter-chromosomal 14;18 translocation in cutaneous lymphomas and pseudolymphomas. *J Invest Dermatol*. 1994;102:231–235.

23a. Pileri A, Grandi V, Agostinelli C, et al. BCL-2 expression in primary cutaneous follicle center lymphoma is associated with a higher risk of cutaneous relapses: a study of 126 cases. *J Eur Acad Dermatol Venereol*. 2022;36:e811–e813.

24. Magro CM, Yang A, Fraga G. Blastic marginal zone lymphoma: a clinical and pathological study of 8 cases and review of the literature. *Am J Dermatopathol*. 2013;35:319–326.

25. Walsh NM, Lano IM, Green P, et al. AL Amyloidoma of the skin/subcutis: cutaneous amyloidosis, plasma cell dyscrasia or a manifestation of primary cutaneous marginal zone lymphoma? *Am J Surg Pathol*. 2017;41:1069–1076.

26. Ikeda JI, Kohara M, Tsuruta Y, et al. Immunohistochemical analysis of the novel marginal zone B-cell marker IRTA1 in malignant lymphoma. *Hum Pathol*. 2017;59:70–79.

27. Brenner I, Roth S, Puppe B, et al. Primary cutaneous marginal zone lymphomas with plasmacytic differentiation show frequent IgG4 expression. *Mod Pathol*. 2013;26:1568–1576.

28. van Maldegem F, van Dijk R, Wormhoudt TAM, et al. The majority of cutaneous marginal zone B-cell lymphomas expresses class-switched immunoglobulins and develops in a T-helper type 2 inflammatory environment. *Blood*. 2008;112:3355–3361.

29. Deutsch AJA, Frühwirth M, Aigelsreiter A, et al. Primary cutaneous marginal zone B-cell lymphomas are targeted by aberrant somatic hypermutation. *J Invest Dermatol*. 2009;129:476–479.

30. Rinaldi A, Mian M, Chigrinova E, et al. Genome-wide DNA profiling of marginal zone lymphomas identifies subtype-specific lesions with an impact on the clinical outcome. *Blood*. 2011;117:1595–1604.

31. Lucioni M, Berti E, Arcaini L, et al. Primary cutaneous B-cell lymphoma other than marginal zone: clinicopathologic analysis of 161 cases: comparison with current classification and definition of prognostic markers. *Cancer Med*. 2016;5:2740–2755.

32. Schrader AMR, Jansen PM, Vermeer MH, et al. High incidence and clinical significance of MYC rearrangements in primary cutaneous diffuse large B-cell lymphoma, leg type. *Am J Surg Pathol*. 2018;42:1488–1494.

33. Menguy S, Frison E, Prochazkova-Carlotti M, et al. Double-hit or dual expression of MYC and BCL2 in primary cutaneous large B-cell lymphomas. *Mod Pathol*. 2018;31:1332–1342.

34. Hoefnagel JJ, Dijkman R, Basso K, et al. Distinct types of primary cutaneous large B-cell lymphoma identified by gene expression profiling. *Blood*. 2005;105:3671–3678.

35. Pham-Ledard A, Prochazkova-Carlotti M, Andrique L, et al. Multiple genetic alterations in primary cutaneous large B-cell lymphoma, leg type support a common lymphomagenesis with activated B-cell-like diffuse large B-cell lymphoma. *Mod Pathol*. 2014;27:402–411.

36. Prieto-Torres L, Eraña I, Gil-Redondo R, et al. The spectrum of EBV-positive mucocutaneous ulcer: a study of 9 cases. *Am J Surg Pathol*. 2019;43:201–210.

37. Colli C, Leinweber B, Müllegger R, et al. *Borrelia burgdorferi*-associated lymphocytoma cutis: clinicopathologic, immunophenotypic, and molecular study of 106 cases. *J Cutan Pathol*. 2004;31:232–240.

38. Honda R, Cerroni L, Tanikawa A, et al. Cutaneous plasmacytosis: report of 6 cases with or without systemic involvement. *J Am Acad Dermatol*. 2013;68:978–985.

39. Ferrara G, Ena L, Cota C, Cerroni L. Intralymphatic spread is a common finding in cutaneous CD30+ lymphoproliferative disorders. *Am J Surg Pathol*. 2015;39:1511–1517.

40. Hristov AC, Tejasvi T, Wilcox RA. Cutaneous B-cell lymphomas: 2021 update on diagnosis, risk-stratification, and management. *Am J Hematol*. 2020; 95:1209–1213.

41. Gulia A, Saggini A, Wiesner T, et al. Clinicopathologic features of early lesions of primary cutaneous follicle center lymphoma, diffuse type: implications for early diagnosis and treatment. *J Am Acad Dermatol*. 2011;65:991–1000.

42. Kiesewetter B, Raderer M. Antibiotic therapy in nongastrointestinal MALT lymphoma: a review of the literature. *Blood*. 2013;122:1350–1357.

43. Muniesa C, Domingo-Domenech E, Fornons-Servent R, et al. Systemic rituximab for the treatment of the indolent forms of primary cutaneous B-cell lymphomas: data from the Spanish Primary Cutaneous Lymphoma Registry. *J Am Acad Dermatol*. 2020;83:1535–1538.

44. Brandenburg A, Humme D, Terhorst D, et al. Long-term outcome of intravenous therapy with rituximab in patients with primary cutaneous B-cell lymphomas. *Br J Dermatol*. 2013;169:1126–1132.

45. Ferreri AJM, Dognini GP, Bairey O, et al. The addition of rituximab to anthracycline-based chemotherapy significantly improves outcome in "Western" patients with intravascular large B-cell lymphoma. *Br J Haematol*. 2008;143:253–257.

46. Spicknall KE, Dubas LE, Mutasim DF. Cutaneous macroglobulinosis with monotypic plasma cells: a specific manifestation of Waldenström macroglobulinemia. *J Cutan Pathol*. 2013;40:440–444.



eFig. 119.1 Cutaneous follicle center lymphoma. Prominent pink–violet nodule on the lateral forehead with a few telangiectasias. The nodule is surrounded by papules and large infiltrated plaques.



eFig. 119.2 Cutaneous follicle center lymphoma. Large ulcerated tumors on the scalp surrounded by infiltrated erythematous nodules and plaques.



eFig. 119.3 Cutaneous follicle center lymphoma. Large ulcerated tumor on the back. Note surrounding erythematous papules, patches, and plaques (Crosti's lymphoma).



eFig. 119.4 Cutaneous marginal zone B cell lymphoproliferative disorder. Two well-circumscribed, erythematous nodules on the shoulder.



eFig. 119.5 Cutaneous marginal zone B cell lymphoproliferative disorder. Dome-shaped erythematous nodule with smooth surface. The surrounding area shows features of acrodermatitis chronica atrophicans. This tumor, which demonstrated prominent lymphoplasmacytic differentiation histologically, would have been classified as cutaneous immunocytoma in the past.



eFig. 119.6 Cutaneous diffuse large B cell lymphoma, leg type. Multiple red–brown tumors on the lower leg.



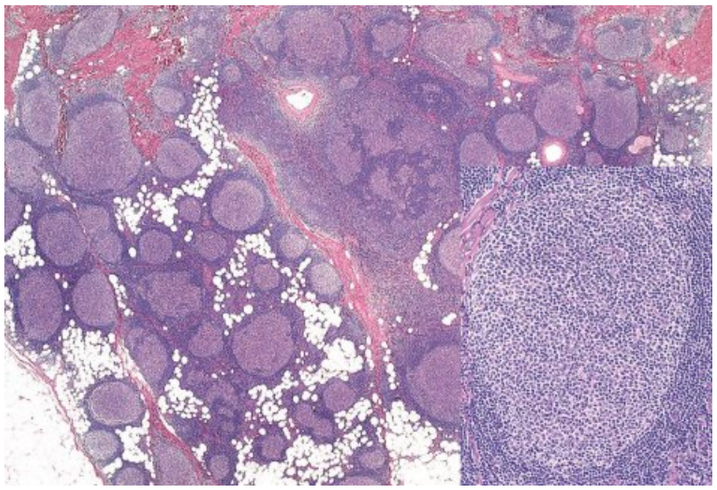
eFig. 119.8 Cutaneous diffuse large B cell lymphoma, leg type. Multiple red–brown papulonodules and a tumor on the lower leg.



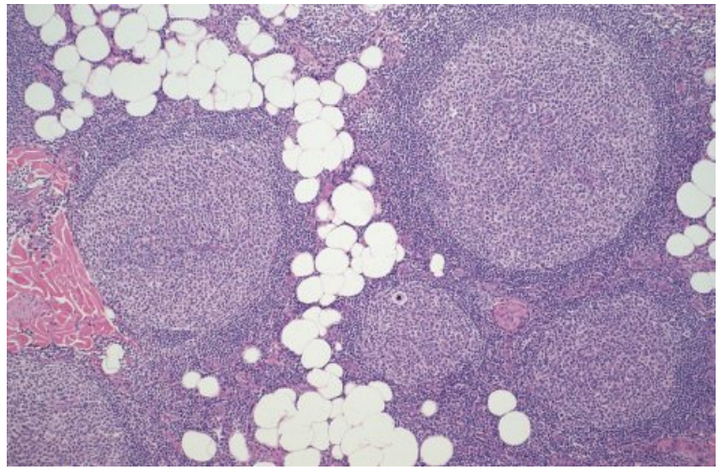
eFig. 119.7 Cutaneous diffuse large B cell lymphoma, leg type. Multiple coalescing red–brown papulonodules and plaques on the lower leg.



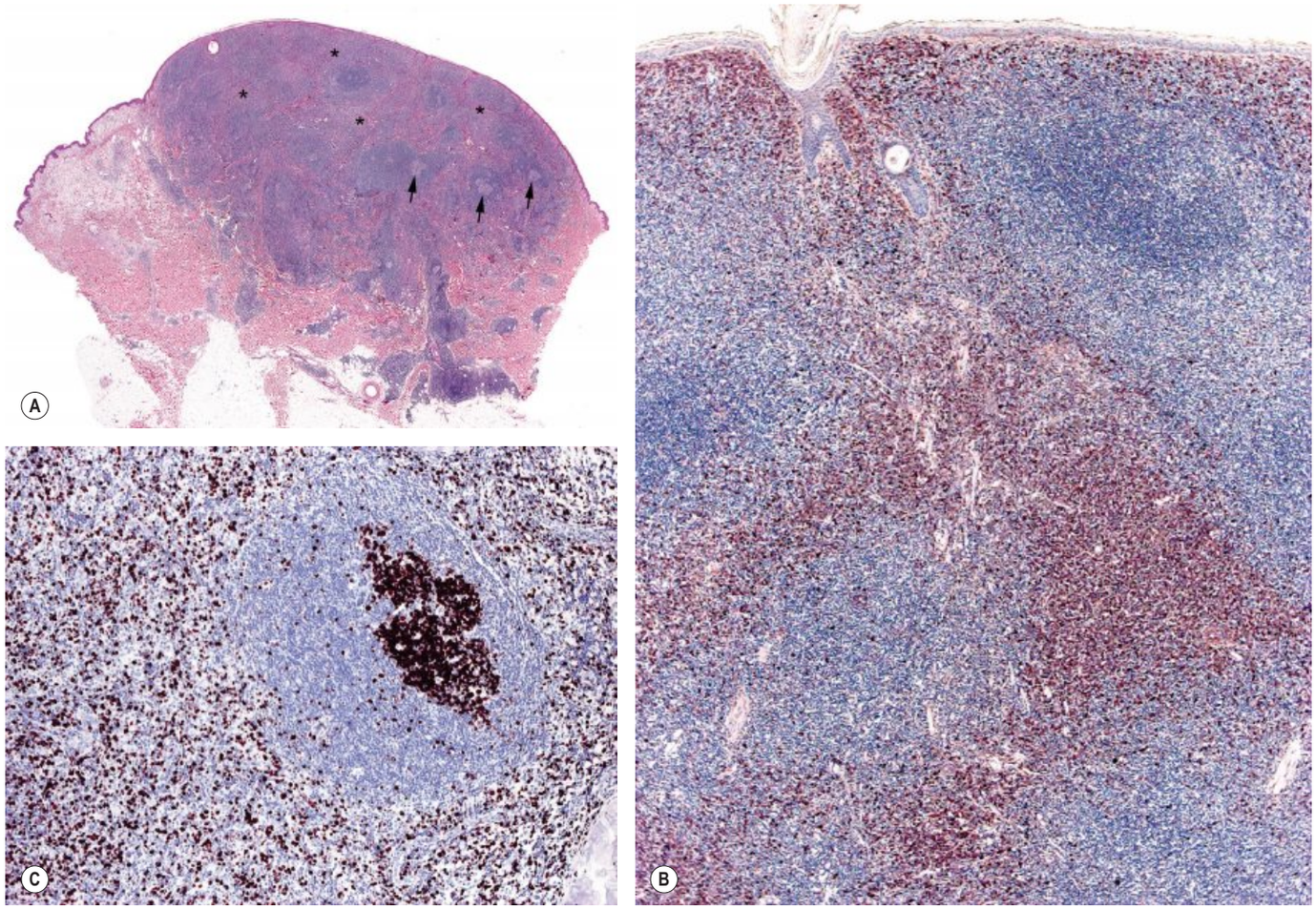
eFig. 119.9 Precursor B lymphoblastic lymphoma/leukemia. Large erythematous tumor on the face of a small child.



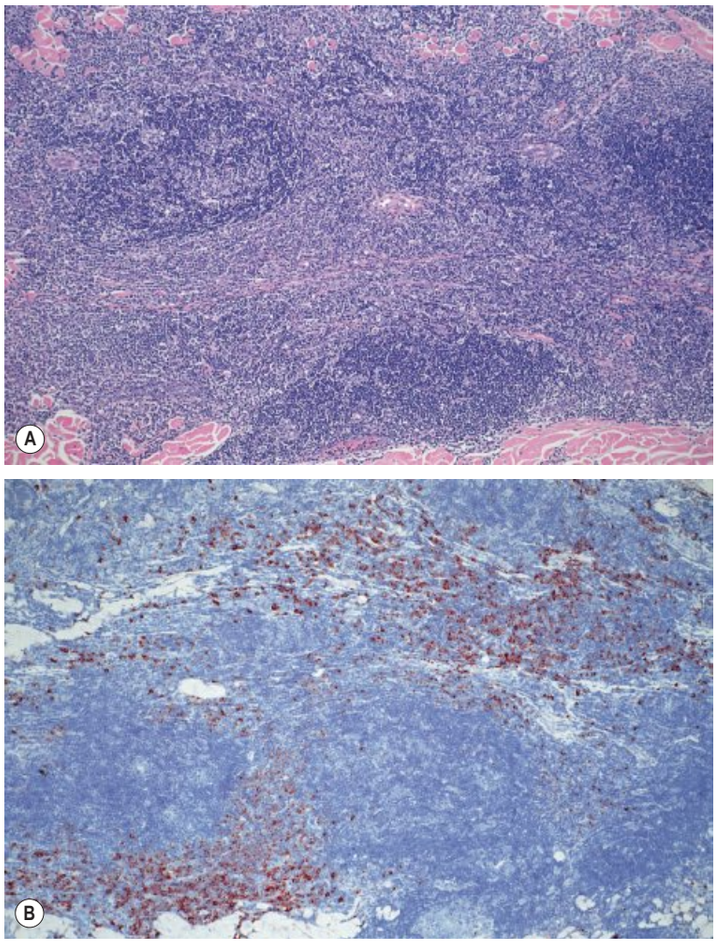
eFig. 119.10 Cutaneous follicle center lymphoma, follicular type. Neoplastic follicles with a monomorphous morphology (lack of polarization). Note the absence of dark and clear areas within the central portion of the follicle (inset).



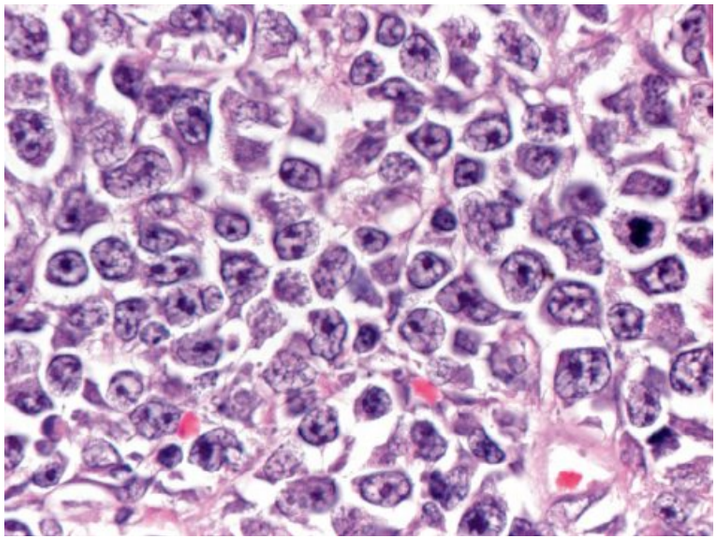
eFig. 119.11 Cutaneous follicle center lymphoma, follicular type. Neoplastic follicles with monomorphous morphology.



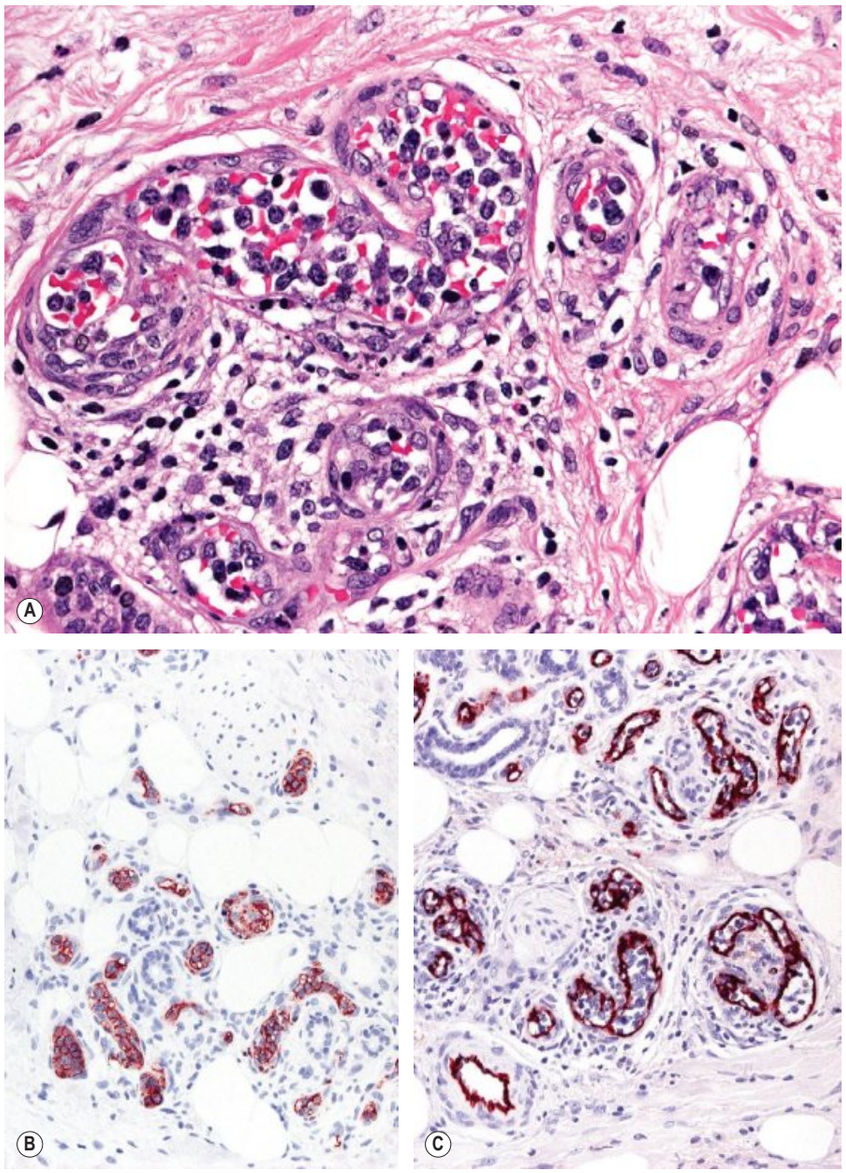
eFig. 119.12 Cutaneous marginal zone B cell lymphoproliferative disorder. A Small nodules of *reactive* lymphocytes (dark areas), some of which have reactive germinal centers (arrows). The nodules are surrounded by *neoplastic* marginal zone cells, lymphoplasmacytoid cells, and plasma cells (clear areas [*]). **B** Monotypic expression of λ immunoglobulin light chain within the neoplastic population of cells (in the clear areas). **C** MIB-1 staining shows marked proliferation within a germinal center in a reactive lymphoid follicle and increased proliferation of neoplastic cells in the perifollicular area.



eFig. 119.13 Cutaneous marginal zone B cell lymphoproliferative disorder.
A Small nodules of reactive lymphocytes (dark areas) surrounded by neoplastic marginal zone cells, lymphoplasmacytoid cells and plasma cells (clear areas).
B Monotypic expression of λ immunoglobulin light chain within the neoplastic population of cells.



eFig. 119.14 Cutaneous diffuse large B cell lymphoma, leg type. Large cells with a round morphology (mainly immunoblasts) predominate.



eFig. 119.15 Cutaneous diffuse intravascular large B cell lymphoma. A Intravascular proliferation of medium- to large-sized atypical lymphocytes. **B** Positive immunohistochemical staining of neoplastic cells for CD20. **C** Intravascular location of neoplastic cells highlighted by staining for endothelial cells (CD31).



eFig. 119.16 Follicular spicules in a patient with multiple myeloma. *Courtesy Irwin Braverman, MD.*



eFig. 119.17 Plasmacytosis – cutaneous involvement. Multiple violet–brown oval-shaped plaques on the back. *Courtesy Boni Elewski, MD.*

120 Cutaneous T Cell Lymphoma

Rein Willemze and Werner Kempf

Chapter Contents

Mycosis Fungoides 2159
Variants of Mycosis Fungoides 2164
Sézary Syndrome 2166
Adult T Cell Leukemia/Lymphoma 2168
Primary Cutaneous CD30-Positive Lymphoproliferative Disorders 2168
Subcutaneous Panniculitis-Like T Cell Lymphoma 2171
Extranodal NK/T Cell Lymphoma, Nasal Type 2172
Primary Cutaneous Aggressive Epidermotropic CD8-Positive Cytotoxic T Cell Lymphoma 2173
Primary Cutaneous Acral CD8-Positive T Cell Lymphoma 2173
Primary Cutaneous Gamma/Delta T Cell Lymphoma 2174
Primary Cutaneous CD4-Positive Small/Medium T Cell Lymphoproliferative Disorder 2174
Primary Cutaneous Peripheral T Cell Lymphoma, NOS 2174

INTRODUCTION

The term cutaneous T cell lymphoma (CTCL) describes a heterogeneous group of neoplasms of skin-homing T cells that show considerable variation in clinical presentation, histologic appearance, immunophenotype, and prognosis. CTCLs represent ~75%–80% of all primary cutaneous lymphomas, whereas primary cutaneous B cell lymphomas (CBCLs) account for ~20%–25%[1]. For many years, mycosis fungoides (MF) and Sézary syndrome (SS) were the only known types of CTCL. Over the past three decades, based on a combination of clinical, histologic and immunophenotypic criteria, new types of CTCL and CBCL have been defined and new classifications for the group of primary cutaneous lymphomas have been formulated[1–3,3a,3b]. A major advantage in the management of primary cutaneous lymphomas compared with lymphomas arising at other sites is that the former can be seen and can be biopsied easily, giving the dermatologist the unique opportunity to correlate the clinical appearance and clinical behavior with histologic, immunophenotypic, and genetic aspects of these conditions. Hence, the dermatologist can play a key role in the diagnosis, classification, and treatment of these diseases.

HISTORY

In 1806, a French physician, Jean Louis Alibert, was the first to describe a patient with MF. This case was designated *pian fungoïde* in his atlas, but in 1835 it was renamed *mycosis fungoïde* because of the resemblance of some skin tumors to mushrooms. In 1870, Bazin described the natural progression from a nonspecific premycotic phase to plaque lesions and finally to tumors, which probably represents one of the first descriptions of the "multistep model" in the development of a malignancy. In 1885, Vidal and Brocq used the term "mycosis fungoides d'emblée" for patients presenting with skin tumors not preceded by patches or plaques. It has now become clear that such cases mostly represent another type of CTCL. The erythrodermic form of MF was described in 1892 by Besnier and Hallopeau. These early descriptions of the major clinical forms of MF were followed by descriptions of Sézary syndrome by Sézary and Bouvrain in 1938, pagetoid reticulosis by Woringer and Kolopp in 1939, and lymphomatoid papulosis (LyP) by Macaulay in 1968.

Thus, in the early 1970s, MF and some related conditions were the only types of cutaneous lymphoma that had been rather well described. Reports on cutaneous lymphomas other than MF/SS, commonly designated in the past as malignant reticulosis or reticulum cell sarcoma, were few. Moreover, they were firmly believed to represent skin manifestations of a systemic lymphoma and treated as such.

The CTCL Concept

In 1968, Lutzner and Jordan described the ultrastructural features of the circulating atypical cells in SS. Characteristically, the nuclei of these cells had deep and narrow indentations, giving them a cerebriform appearance. Three years later, similar cells were found in the skin and lymph nodes of patients with MF. In 1975, based on the observation that the neoplastic cells in MF, SS, and related conditions not only had the same morphology but also a common T cell phenotype, the term "CTCL" was suggested for this group of diseases. Within a short time, this term gained wide acceptance, particularly in the US. The introduction of the CTCL concept can be considered as a landmark in the history of this group of diseases. However, a major disadvantage has been that in many subsequent studies, distinction was no longer made between MF, SS, and other T cell neoplasms, entities which may vary considerably in clinical presentation and clinical behavior.

The Concept of Primary Cutaneous Lymphomas

At about the same time that the CTCL concept was introduced, several European groups started to classify cutaneous lymphomas according to the criteria of the Kiel classification, a system used by hematopathologists for the categorization of nodal lymphomas. It was then determined that many types of CBCL and CTCL (other than classic MF and SS) can present in the skin without any evidence of extracutaneous disease at the time of diagnosis. It appeared that these primary cutaneous lymphomas often have a completely different clinical behavior and prognosis when compared to morphologically similar lymphomas arising within lymph nodes, and therefore require different types of treatment[2]. In addition, differences in the presence of specific chromosomal translocations and in the expression of oncogenes, viral sequences or antigens (e.g. EBV), and adhesion receptors involved in tissue-related lymphocyte homing were found.

Such differences underscored that primary cutaneous lymphomas represent a distinct group and may explain, at least in part, their different clinical behavior. For instance, the observation that the neoplastic T cells in most CTCLs express cutaneous lymphocyte antigen (CLA) and the CC-chemokine receptors 4 (CCR4) and 10 (CCR10) indicates that they are the neoplastic counterparts of normal skin-homing T cells, and this explains why these CTCLs present in the skin. Perhaps most importantly, it appeared that different types of CTCL and CBCL with different clinical behaviors and different therapeutic requirements may have an identical histologic appearance. This implies that histologic features should always be combined with clinical and immunophenotypic data before a definite diagnosis (classification) is made.

Such an approach resulted in the delineation of several new types of CTCL and CBCL, and it formed the basis of the European Organization for Research and Treatment of Cancer (EORTC) classification for primary cutaneous lymphomas[2].

EORTC, WHO, and WHO-EORTC Classification Schemes

The EORTC classification scheme was the first one that was specifically designed for the group of primary cutaneous lymphomas. It contained

WHO-EORTC CLASSIFICATION FOR CUTANEOUS T-CELL LYMPHOMAS – 2018 UPDATE		
WHO-EORTC classification	**Frequency (%)***	**5-year survival rate (%)***
Indolent clinical behavior		
Mycosis fungoides (MF)	52	88
Mycosis fungoides variants		
• Folliculotropic MF	7	75
• Pagetoid reticulosis	<1	100
• Granulomatous slack skin	<1	100
Primary cutaneous CD30-positive lymphoproliferative disorders		
• Primary cutaneous anaplastic large cell lymphoma (C-ALCL)	10	95
• Lymphomatoid papulosis (LyP)	16	99
Subcutaneous panniculitis-like T cell lymphoma (SPTCL)	1	87
Primary cutaneous CD4-positive small/medium T cell lymphoproliferative disorder†	8	100
Primary cutaneous acral CD8-positive T cell lymphoproliferative disorder§,†	<1	100
Aggressive clinical behaviour		
Sézary syndrome (SS)	3	36
Adult T-cell leukemia/lymphoma (ATLL)	<1	NDA
Extranodal NK/T-cell lymphoma, nasal type	1	16
Primary cutaneous aggressive epidermotropic CD8-positive cytotoxic T cell lymphoma†	<1	31
Primary cutaneous gamma/delta T cell lymphoma (PCGD-TCL)	<1	11
Primary cutaneous peripheral T cell lymphoma (PTCL), NOS	3	15

*Based on data included in Dutch and Austrian cutaneous lymphoma registries between 2002 and 2017[1].
†While listed as provisional entities in the 2018 WHO-EORTC classification, included as distinct entities in the 5th edition of the WHO classification of haematolymphoid tumours and the 2022 ICC classification of mature lymphoid neoplasms[3a,3b].
§In the 5th edition of the WHO classification reclassified as lymphoproliferative disorder rather than lymphoma[3a].

Table 120.1 WHO-EORTC classification for cutaneous T cell lymphomas – 2018 update[1]. NDA, no data available; NOS, not otherwise specified.

a limited number of well-defined types of CTCL and CBCL, and a distinction was made between cutaneous lymphomas with indolent, intermediate, or aggressive clinical behavior. By including well-defined and recognizable disease entities, this classification provided the clinician with detailed information on staging, preferred mode of treatment, clinical behavior and prognosis, serving as a useful guide for optimal management and treatment.

Collaboration between the EORTC and the World Health Organization (WHO) groups resulted in the publication of the WHO-EORTC consensus classification for primary cutaneous lymphomas in 2005 and its update in 2018[1]. In this 2018 update, the terminology and definitions of the different types of CTCL are identical to those in the 2016 revision of the WHO classification[3]. In the 2023 WHO classification (5th revision) as well as in the 2022 International Consensus Classification (ICC) of mature lymphoid neoplasms, only minor changes have been introduced, namely, primary cutaneous acral CD8-positive T cell lymphoma has been listed as a lymphoproliferative disorder rather than a lymphoma[3a,3b]. The frequency and survival of patients with the different types of CTCL recognized in the updated 2018 WHO-EORTC classification are presented in Table 120.1. Following a description of practical guidelines for diagnosis, classification, and staging, relevant features of the different types of CTCL included in this classification are presented.

PRACTICAL GUIDELINES FOR DIAGNOSIS, CLASSIFICATION AND STAGING OF CTCL

Diagnosis

The first step in the evaluation of a patient suspected of having CTCL is to decide if it represents a lymphoma or a benign condition. Skin biopsies – preferably deep punch biopsies 4–6 mm wide or an excisional or incisional biopsy from the most representative skin lesions – should be performed. In the US, broad shave (tangential) biopsies are also done for suspected patch/plaque stage MF.

Since prior treatment with topical corticosteroids or phototherapy (narrowband UVB, PUVA) may change the original histology profoundly, biopsies from untreated skin lesions are preferred. Even if an adequate biopsy specimen is obtained, a definite diagnosis is not always possible. First, several types of CTCL, such as MF, are often preceded for years by skin lesions that are neither clinically nor histologically diagnostic. The gradual progression from this prediagnostic phase to overt lymphoma explains why it has always been so difficult to reach a consensus on the minimal histologic criteria needed for an unequivocal diagnosis of MF[4]. In most cases, repeated biopsies, when appropriate, will ultimately result in the correct diagnosis.

Secondly, atypical T cell infiltrates are found not only in CTCL but also in reactive conditions, e.g. lymphomatoid drug eruptions (T cell pseudolymphomas). Therefore, a definite diagnosis should always be based on a combination of clinical, histologic and, in most cases, immunophenotypic criteria, and it may be supplemented with the results of gene rearrangement analysis.

Immunophenotyping

Immunohistochemical studies on paraffin sections using antibodies reactive with cell-surface or cytoplasmic molecules are extremely important in the diagnosis and classification of cutaneous lymphomas. By using a panel of such antibodies (see Ch. 0), distinction can be made between neoplasms of T cell, B cell, NK cell, and myeloid or monocytic origin. Within the group of CTCLs, such studies have contributed to the delineation of new subtypes and provided important diagnostic and prognostic criteria.

With respect to the diagnosis of CTCL, demonstration of an aberrant phenotype, i.e. loss of one or more T cell-associated antigens, such as CD2, CD3, CD4 or CD5, by the neoplastic T cells, can be considered as an important additional criterion in establishing a definite diagnosis of CTCL[4]. However, loss of CD7 expression, which may be caused by chronic T cell stimulation and is commonly observed in benign dermatoses, is a less reliable marker.

T Cell Receptor Gene Rearrangement Analysis

T cell receptor (TCR) gene rearrangement analysis, utilizing a standardized assay (e.g. BIOMED-2), may provide useful information for the diagnosis and staging of malignant lymphomas[5]. However, caution is warranted in interpreting the results of such analyses. Clonal T cell populations have been detected not only in skin lesions, lymph nodes, and peripheral blood of patients with CTCL and in cases of chronic dermatitis preceding MF ("clonal dermatitis"), but also in skin lesions of patients with apparently benign conditions, such as pityriasis lichenoides et varioliformis acuta, lichen planus, lichen sclerosus, and some pseudolymphomas[5].

Demonstration of clonal T cell populations can therefore not be used as an absolute criterion of malignancy, but should always be considered in conjunction with clinical and histologic features, which together remain the "gold standard". If the clinical and histologic findings are not consistent, and an aberrant phenotype is not detected, a definite diagnosis of CTCL should not be made.

High-throughput sequencing (HTS) of TCR genes, most commonly the TCRβ gene, was more recently introduced as a novel technique. It provides detailed information on the number of distinct T cell clones present within a sample as well as their relative frequency[6]. HTS-TCR is a much more sensitive technique for the early diagnosis of CTCL and allows tracking of specific T cell clones over time and following treatment. In addition, HTS-TCR can be performed on multiple tissues, e.g. skin and peripheral blood. Studies suggest that a tumor clone frequency >25% in lesional skin of early stage MF is associated with reduced survival[7].

DIFFERENTIAL DIAGNOSIS OF COMMON HISTOLOGIC PATTERNS IN CUTANEOUS T CELL LYMPHOMA		
Histologic category	**Differential diagnosis**	**Diagnostic criteria/clues**
Epidermotropic CTCL (simulating or consistent with plaque stage MF)	Mycosis fungoides (MF)	• Characteristic patches and plaques • Most atypical cells within the epidermis (basal layer)
	Pagetoid reticulosis	• Solitary plaque, commonly on distal extremities • Neoplastic cells confined mostly to an often acanthotic epidermis • Often $CD8^+$ phenotype; CD30 expression common
	Lymphomatoid papulosis (LyP), type B or type D	• Recurrent, self-healing papular eruption • Sometimes extension of infiltrate into lower dermis • In some cases, admixture with large atypical cells as in type A LyP (mixed type A and B) • LyP type B is $CD4^+$; type D is $CD8^+$
	Primary cutaneous aggressive epidermotropic CD8-positive cytotoxic T cell lymphoma	• Infiltrated plaques, but often eruptive nodules and tumors with ulceration • Intraepidermal accumulation of medium-sized pleomorphic T cells or small blast cells; no typical cerebriform appearance • Phenotype: $CD8^+$, TIA-1^+, granzyme B^+, $CD45RA^+$, $CD7^{-/+}$
	Sézary syndrome	• Often more monotonous infiltrate histologically • Erythroderma • Peripheral blood involvement • Same T cell clone in the skin and blood
	Adult T cell leukemia/lymphoma	• Often clinically and histologically identical to MF • Check HTLV-1 status in patients from endemic areas
CTCL with diffuse pleomorphic infiltrates ($CD30^-$) (simulation or consistent with tumor stage MF; few $CD30^+$ tumor cells may be present)	Tumor stage MF	• Concurrent patches and plaques • Variable numbers of small, medium-sized, and/or large cerebriform T cells and/or blast cells • Variable admixture with inflammatory cells
	Primary cutaneous peripheral T cell lymphoma, NOS	• Histologically, often indistinguishable from MF with large cell transformation • No prior or concurrent patches and plaques
	Primary cutaneous CD4-positive small/medium T cell lymphoproliferative disorder (and/or nodular pseudo-T cell lymphoma [see text])	• Presents as solitary plaque or tumor (2–3 cm) • No prior or concurrent patches and plaques • Scattered medium-sized to large pleomorphic T cells (<30% of cells; express PD-1) • Many admixed $CD8^+$ T cells, B cells, and histiocytes • No aberrant phenotype (i.e. no "marker loss") • Clonal T cell population in most cases
CD30-positive CTCL (see Fig. 120.11)	Lymphomatoid papulosis, type A/C	• Recurrent self-healing papules and nodules • Histologic spectrum (from typical LyP to identical to C-ALCL)
	Primary cutaneous anaplastic large cell lymphoma (C-ALCL)	• Generally, solitary or localized nodules or tumors • No evidence of prior or concurrent MF or another type of CTCL • No extracutaneous disease (staging negative) • Histologic spectrum (from typical C-ALCL to similar to LyP) • Phenotype: CLA^+, EMA^-, ALK^-; common loss of pan-T cell markers
	Systemic ALCL with secondary skin involvement	• Prior or concurrent extracutaneous involvement (exception: involvement of one regional lymph node basin which has same prognosis as C-ALCL) • Often generalized skin lesions • Phenotype: CLA^-, EMA^+, ALK^+ (mainly in pediatric subgroup)
	MF with large cell transformation	• Histologically, an admixture with typical cerebriform cells, but sometimes indistinguishable from C-ALCL • Prior or concurrent patches and plaques
CTCL with subcutaneous involvement	Subcutaneous panniculitis-like T cell lymphoma	• Infiltrates confined to subcutis • Characteristic rimming of individual fat cells by neoplastic T cells • Deeply seated nodules and plaques, mainly involving the legs and trunk • Characteristic $CD3^+$, $CD4^-$, $CD8^+$, $CD56^-$, $\beta F1^+$ T cell phenotype
	Other types of CTCL	• Subcutaneous infiltrates represent extension from dermal infiltrates • For specific features: see text

Table 120.2 Differential diagnosis of common histologic patterns in cutaneous T cell lymphoma (CTCL). ALK, anaplastic lymphoma kinase; βF1, positivity reflects α/β T cell origin; CLA, cutaneous lymphocyte antigen; C-ALCL, cutaneous anaplastic large cell lymphoma; EMA, epithelial membrane antigen; PD-1, programmed death-1 (CD279); TIA, T cell restricted intracellular antigen.

Classification

Once a diagnosis of CTCL has been made, the type of CTCL should be determined. As noted previously, the histologic diagnosis is not the final diagnosis, which means that CTCL cannot be classified on the basis of histologic criteria alone. For instance, in the case of a skin biopsy showing a dermal infiltrate which is composed predominantly of CD30-positive large anaplastic or pleomorphic T cells, the *histologic diagnosis* will be (CD30-positive) anaplastic large cell lymphoma (ALCL). However, depending upon the clinical presentation, the *definite diagnosis* may be: a primary cutaneous ALCL; cutaneous involvement of a systemic ALCL; large cell transformation of MF with expression of CD30; or LyP (in cases of recurrent self-healing papules). Obviously, each of these conditions requires a different approach in terms of staging and treatment.

In Table 120.2, the differential diagnosis of four histologic categories has been elaborated. This histologic subdivision into epidermotropic CTCL, CTCL with diffuse pleomorphic infiltrates, CD30-positive CTCL, and subcutaneous CTCL is neither complete nor meant as an alternative classification. It is only presented as an illustration of how histology should be combined with clinical and immunophenotypic data to arrive at a definite diagnosis.

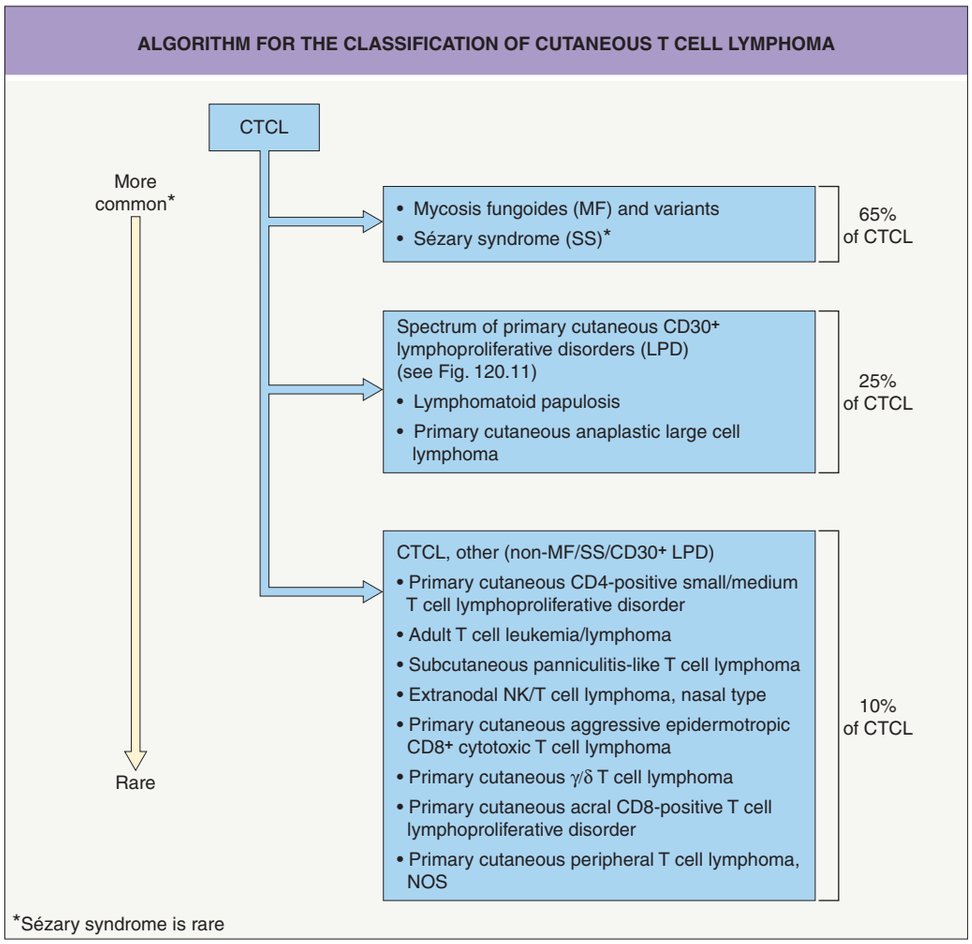


Fig. 120.1 Algorithm for the classification of cutaneous T cell lymphoma (CTCL). NOS, not otherwise specified. See also Table 120.1. *Adapted from Willemze R, Beljaards RC, Meijer CJLM. Classification of primary cutaneous T-cell lymphoma. Histopathology 1994;24:405–15.*

Practical Guidelines

For those not regularly involved in the diagnosis and classification of CTCL and perhaps confused by the many different types of CTCL, a stepwise approach, as presented in Fig. 120.1, may serve as a practical guide.

Step one: Based on a combination of clinical, histologic, and immunophenotypic criteria, distinction is first made between classic MF, MF variants, and SS on the one hand *and* CTCL other than these conditions on the other. The rationale for this first step is that dermatologists are familiar with the former set of conditions, which comprise ~65% of CTCLs, and these lymphomas require a different clinical approach in terms of staging and therapy compared to the other forms of CTCL.

Step two: The second category to be considered is the group of *primary* cutaneous CD30-positive lymphoproliferative disorders. It implies that evaluation of skin biopsies from patients with (suspected) CTCL should always include CD30 immunostaining. This group includes cases of cutaneous ALCL (C-ALCL) and LyP, which together represent the second most common group of CTCL (see Table 120.1). Patients within this spectrum of disease generally have an excellent prognosis, and most individuals can be managed easily by dermatologists.

Step three: With the first two steps, ~90% of CTCL will be classified correctly. The remaining group (10% of patients) contains rare types of CTCL, including those that usually have an indolent clinical behavior (subcutaneous panniculitis-like T cell lymphoma, primary cutaneous CD4-positive small/medium T cell lymphoproliferative disorder, and primary cutaneous acral CD8-positive T cell lymphoproliferative disorder) as well as ones with an aggressive clinical behavior (extranodal NK/T cell lymphoma, nasal type, primary cutaneous gamma/delta T cell lymphoma, and primary cutaneous aggressive epidermotropic CD8-positive cytotoxic T cell lymphoma) (see Table 120.1). The term primary cutaneous peripheral T cell lymphoma (PTCL), not otherwise specified (NOS) is employed for the remaining cases that do not fit into any of the aforementioned entities. It should be emphasized that because of overlapping clinicopathologic features and highly aberrant phenotypes, distinction between different types of aggressive CTCL is sometimes very difficult.

Staging

Apart from CTCL, a term preferably used only for *primary* CTCL, systemic T cell lymphomas frequently present or relapse in the skin. Adequate staging procedures are required to differentiate between CTCL and these systemic lymphomas secondarily involving the skin. The extent of staging procedures is dependent on the type of (suspected) CTCL, and in the case of classic MF, on the clinical stage of the disease[8]. In cases of early patch/plaque stage MF, pagetoid reticulosis, unequivocal cases of LyP, and probably typical cases of primary cutaneous CD4-positive small/medium T cell lymphoproliferative disorder and primary cutaneous acral CD8-positive T cell lymphoproliferative disorder, staging procedures are generally not mandatory. In cases of suspected SS, adequate staging with special emphasis on assessment of peripheral blood involvement by cytology, immunophenotyping (flow cytometry), and TCR gene rearrangement analysis is essential. In all other types of CTCL, routine hematologic staging, including complete and differential blood cell counts, a serum chemistry panel, computed tomographic (CT) scans and/or positron emission tomography (PET) of the chest and abdomen, and in most cases bone marrow sampling, are required[9].

MYCOSIS FUNGOIDES

Definition

Mycosis fungoides (MF) represents the most common type of CTCL and accounts for ~50% of all primary cutaneous lymphomas (see Table 120.1). The term MF should be restricted to the classic "Alibert–Bazin" type characterized by the typical evolution of patches, plaques, and tumors, or for clinicopathologic variants showing a similar clinical course.

Epidemiology

MF has an incidence of about 0.4 per 100 000 inhabitants per year in the US[10]. MF typically affects older adults (median age at diagnosis: 55–60 years), but it may occur in children and adolescents as well. Men are affected more often than women, with a male-to-female ratio of 1.6–2.0 : 1.

Pathogenesis

The etiology and the pathogenetic mechanisms involved in the development and stepwise progression of MF are largely unknown. Genetic, environmental, and immunologic factors have all been considered.

Genetic factors

Lymphomagenesis is considered to be a multifactorial process, in which a stepwise accumulation of genetic abnormalities may result in clonal proliferation, malignant transformation, and ultimately, progressive and widely disseminated disease. Although the successive clinical steps of tumor progression were described more than a century ago, the molecular events underlying the different steps of tumor progression have not been fully identified. In gene expression studies of early stage MF, an overexpression of the transcription factor TOX and PDCD1 (PD-1) was observed and noted to be a useful diagnostic marker[11]. Advanced stages of MF usually have complex karyotypes with somatic copy-number variants constituting the vast majority of all driver mutations[12].

In tumor stage MF, integrated whole-genome sequencing and RNA sequencing have shown rearrangements in multiple genes involved in transcriptional regulation and signal transduction. Deletions of *HNRNPK* and *SOCS1*, which encode signaling inhibitors of the JAK-STAT pathway, were the most frequent genetic alterations in MF after deletion of *CDKN2A*[13]. Deletion or inactivation of *CDKN2A* has been associated with a shorter survival in patients with tumor stage MF while deletion of *HNRNPK* and *SOCS1* may contribute to constitutive activation of STAT3.

Staphylococcus aureus and its toxins can also activate STAT3 signaling and increase expression of the interleukin-2 receptor (IL-2R) in tumor cells and nonmalignant T cells, thereby stimulating proliferation of tumor cells in CTCL[14]. Aggressive antibiotic treatment can effectively eradicate this stimulus, normalize the tumor microenvironment, inhibit STAT3 signaling and cellular proliferation within lesional skin, and provide significant clinical improvement in MF and Sézary syndrome[14]. *Staphylococcus aureus* α-toxin also blocks $CD8^+$ T cell-mediated killing of malignant T cells, allowing immune evasion and continued proliferation[15].

Environmental factors

Persistent antigenic stimulation has been demonstrated to play a crucial role in the development of various malignant lymphomas, including *m*ucosa-*a*ssociated *l*ymphoid *t*issue (MALT) lymphomas (*Helicobacter pylori* infection), CBCL (*Borrelia burgdorferi* infection), and enteropathy-type T cell lymphoma (celiac disease). In MF, persistent antigenic stimulation has also been proposed as an initial event, but the nature of the antigen(s) involved is unknown. Large case–control studies have suggested a relationship with industrial or environmental exposures, but their role in the development of MF remains controversial[16]. Whereas the etiologic roles of human T cell leukemia virus 1 (human T cell lymphotropic virus 1; HTLV-1) in adult T cell leukemia/lymphoma and EBV in nasal NK/T cell lymphoma have been firmly established, conclusive evidence for a primary etiologic role of these and other viruses in MF is lacking.

Immunologic factors

$CD8^+$ cytotoxic T cells (CTL) are thought to play a crucial role in the antitumor response in MF. A relationship between high percentages of $CD8^+$ CTL in the dermal infiltrates and improved survival has been described[17]. These $CD8^+$ T cells exert their antitumor effect both by a direct cytotoxic effect and by the production of cytokines, particularly interferon (IFN)-γ. They can mediate tumor cell lysis via exocytosis of cytotoxic granules containing perforin, granzymes, and T cell-restricted intracellular antigen (TIA-1), and by expression of Fas ligand (FasL), which interacts with Fas (CD95; APO-1) on the neoplastic T cells. Both pathways ultimately lead to activation of caspase 3 and tumor cell death. Loss of Fas expression or function by the neoplastic T cells is one of the many mechanisms by which tumor cells can escape from an effective antitumor response[18].

In most patients, the neoplastic T cells in SS and tumor stage MF are derived from $CD4^+$ T cells with a Th2 cytokine profile (production of IL-4, IL-5, and IL-10), whereas the cytotoxic T cells are the main producers of IFN-γ, which plays an important role in augmenting T cell- and NK cell-mediated killing. In accordance with this concept, a gradual shift from a predominantly type 1 cytokine profile in MF patches and plaques to a predominantly type 2 cytokine profile in MF tumors has been suggested. Increased levels of Th2 cytokines may impair the Th1 cell-mediated antitumor response and contribute to the immunosuppression seen in patients with advanced MF[19].

Clinical Features

Characteristically, patients with classic MF progress from patch stage to plaque stage and finally to tumor stage disease, and they have a protracted clinical course over years or even decades. Before a definite diagnosis is made, patients generally have many years of nonspecific eczematous or psoriasiform skin lesions and non-diagnostic biopsies. The median duration from onset of skin lesions to the diagnosis of MF is 4–6 years, but it may vary from several months to more than five decades[20].

Early patch stage MF is characterized by the presence of variably sized erythematous, finely scaling lesions, which may be mildly pruritic (Fig. 120.2A). These early lesions may show variable degrees of atrophy, and a poikilodermatous variant consisting of patches with mottled hyper- and hypopigmentation, atrophy, and telangiectasia has been described (formerly called poikiloderma vasculare atrophicans). Generalized hypopigmented lesions may be observed in patients with



Fig. 120.2 Mycosis fungoides, limited patch/plaque stage disease (stage 1A). A Patches on the buttocks involving less than 10% of the skin surface. **B** Few atypical T cells in the basal layer of the epidermis. Immunohistochemical staining for CD3 more clearly demonstrates many atypical lymphocytes in a characteristic linear configuration along the epidermal basal layer (inset).

darkly pigmented skin (Fig. 120.3), and this is also a common presentation of juvenile-onset MF.

The initial skin lesions have a predilection for the buttocks and other covered sites of the trunk and limbs. With progression, more infiltrated reddish-brown, scaling plaques develop, which gradually enlarge and may have an annular, polycyclic, or typical horseshoe-shaped configuration (Fig. 120.4A). It should be stressed that many patients never progress beyond the plaque stage of the disease. However, a minority of patients may develop nodules or tumors. These patients with tumor stage MF characteristically show a combination of patches, plaques, and tumors (Fig. 120.5A); the latter often show ulceration.

If only skin tumors are present without preceding or concurrent patches or plaques, a diagnosis of MF is highly unlikely and another type of CTCL should be considered. The risk of developing extracutaneous disease correlates with the extent and type of skin lesions. It is exceedingly rare in patients with limited patch/plaque stage disease, relatively uncommon in patients with generalized plaques, and most likely in patients with skin tumors or erythroderma[20]. Initially extracutaneous dissemination most often involves the regional lymph nodes draining areas of extensive skin involvement. Visceral involvement may develop subsequently and can involve any organ. The bone marrow is rarely involved.

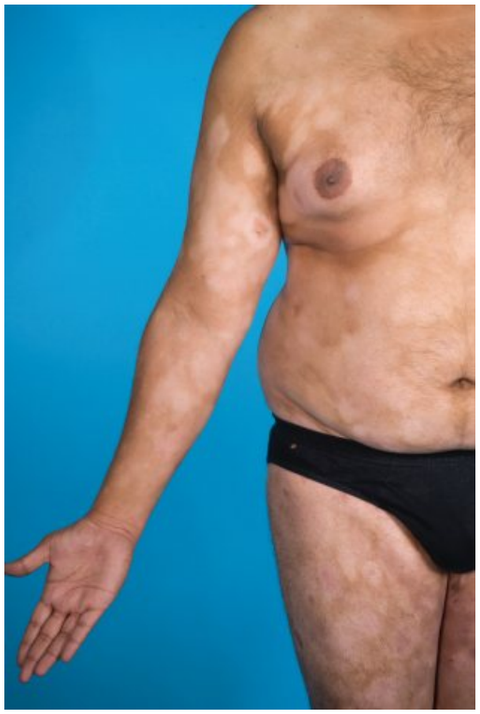


Fig. 120.3 Hypopigmented mycosis fungoides (stage 1B). Generalized hypopigmented lesions as well as pink to pink–brown plaques.

Pathology

Early *patch* lesions in MF show superficial band-like or lichenoid infiltrates, consisting primarily of lymphocytes. Atypical cells, with small to medium-sized, highly convoluted (cerebriform) and sometimes hyperchromatic nuclei, are few in number and are mostly confined to the epidermis (epidermotropism). These lymphocytes characteristically colonize the basal layer of the epidermis as single cells surrounded by vacuolated halos, often in a linear configuration[4] (Fig. 120.2B).

In *plaques*, epidermotropism is generally more pronounced (Fig. 120.4B). The presence of intraepidermal nests of atypical cells (referred to as Pautrier microabscesses, although the initial description was by Darier) is a highly characteristic feature, but is observed in only a minority of cases. The epidermis may show acanthosis and elongated rete ridges, but spongiosis is generally mild or absent. The dermal infiltrates are also more pronounced, and they may contain a higher number of atypical cells with cerebriform nuclei and occasional blast cells, as well as admixed eosinophils and plasma cells. Rarely, a predominantly interstitial infiltrate that may resemble morphea is observed (interstitial MF).

With progression to *tumor* stage MF, the dermal infiltrates can involve the entire dermis and extend into the subcutaneous tissue. Epidermotropism may no longer be present. The tumor cells increase in number and size, showing variable proportions of small, medium-sized, or large cells with cerebriform nuclei, blast cells with prominent nuclei, and intermediate forms (Fig. 120.5B). *Large cell transformation*, defined by the presence of CD30-negative or CD30-positive large cells exceeding 25% of the infiltrate or forming microscopic nodules, may occur and is generally associated with a poor prognosis. However, within this group, CD30-positive patients have a much better prognosis than CD30-negative patients[21].

Immunophenotype

The neoplastic cells in MF have a mature $CD3^+$, $CD4^+$, $CD45RO^+$, $CD8^-$ memory T cell phenotype. In a minority of patients with otherwise classic MF, a $CD3^+$, $CD4^-$, $CD8^+$ mature T cell phenotype or more rarely a γ/δ T cell phenotype ($\beta F1^-$, $TCR\gamma/\delta^+$, $CD3^+$, $CD4^-$, $CD8^+$) may be seen[22,23]. These patients have the same clinical behavior and prognosis as $CD4^+$ cases and should not be considered separately. Demonstration of an aberrant phenotype (e.g. loss of pan-T cell antigens such as CD2, CD3, and CD5) is an important adjunct in the diagnosis of MF, but is uncommon in the early stages of MF. A $CD8^+$ T cell phenotype is more common in pediatric MF and in some variants of MF including hypopigmented, hyperpigmented, or poikilodermatous MF.

Differential Diagnosis

Regarding the differential diagnosis of MF, three categories should be considered. The first category contains a diverse group of benign

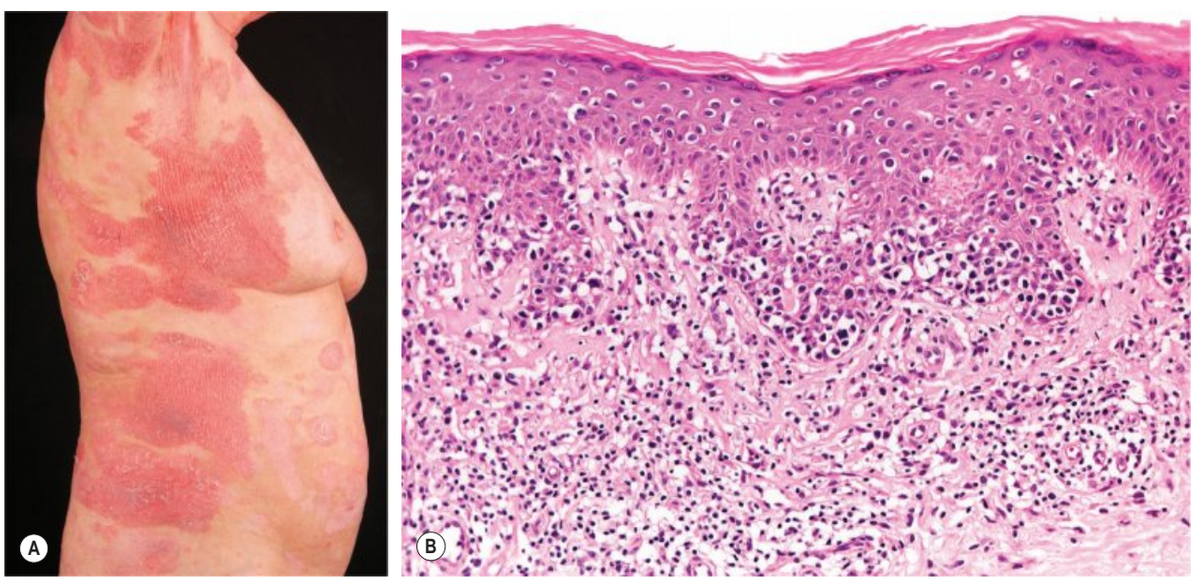


Fig. 120.4 Mycosis fungoides, generalized patch/plaque stage disease (stage 1B). A Extensive patches and plaques with scale involving more than 10% of the skin surface. **B** Epidermotropism with the formation of small nests of atypical cells (Pautrier microabscesses). The majority of the dermal infiltrate is composed of small reactive lymphocytes. *A, Courtesy Lorenzo Cerroni, MD.*

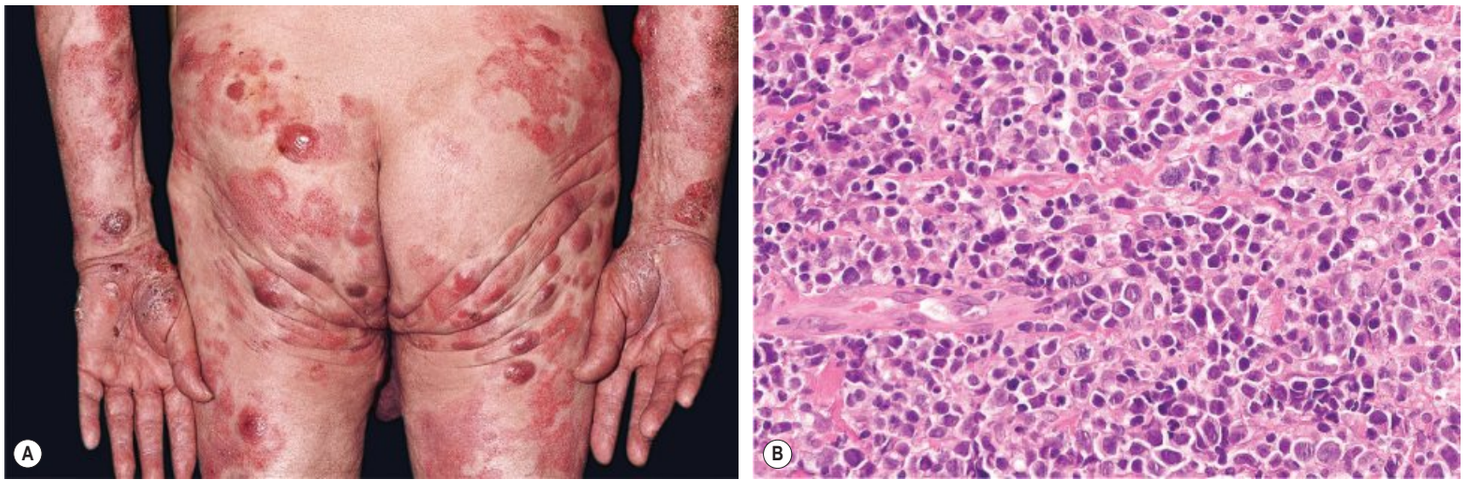


Fig. 120.5 Mycosis fungoides, tumor stage. A Multiple skin tumors in combination with typical patches and plaques. **B.** Diffuse dermal infiltrates of medium-sized to large neoplastic T cells.

dermatoses, which early MF may resemble clinically, and it includes several types of eczema, psoriasis, superficial fungal infections, and drug reactions. These specific diagnoses can generally be excluded by histologic and other standard dermatologic examinations. This category may also include patients with *large plaque parapsoriasis* (parapsoriasis en plaque) who show slightly scaly, sometimes atrophic, erythematous patches or plaques, which are commonly located on the trunk and buttocks (see Ch. 9). Whereas large plaque parapsoriasis cannot be distinguished clinically from early patch or plaque stage MF, the histologic features are often not consistent with MF. Long-term follow-up studies have documented progression of large plaque parapsoriasis to overt MF in ~10% of cases. However, one prevailing opinion is that large plaque parapsoriasis should be considered a form of MF, rather than a potential precursor of MF, but the authors feel there is no consensus. There is more consensus that small plaque parapsoriasis does not represent MF.

A second category includes several benign conditions with histologic features highly suggestive of MF. Examples of these are lymphomatoid contact dermatitis, lymphomatoid drug reactions, and actinic reticuloid. Apart from subtle histologic differences (e.g. the predominance of atypical T cells in the dermal infiltrates rather than in the epidermis), careful evaluation of the clinical features, which are generally not consistent with MF, often results in a correct diagnosis.

The third category includes other types of (epidermotropic) CTCL, which may resemble MF histologically. Diagnostic features of these entities are presented in Table 120.2.

Staging Systems and Staging Procedures

Staging patients with MF and SS is important, since it determines management and treatment and has prognostic significance. In 2007, a revised clinical staging system for MF and SS was proposed, which is based on the TNM (tumor–node–metastasis) classification system and takes into account the type and extent of skin lesions (T1–4) as well as the presence or absence of nodal (N0–3), visceral (M0–1), and peripheral blood involvement (B0–2)[8] (Table 120.3 & 120.4).

Evaluation of patients suspected of having MF should include a thorough physical examination with special attention to the type and extent of skin lesions and the presence of palpable lymph nodes, as well as skin biopsies, complete blood counts, and serum chemistries. Enlarged lymph nodes should be biopsied. Histologically, distinction can be made between lymph nodes showing dermatopathic lymphadenopathy without involvement by MF (N1), dermatopathic lymphadenopathy with early MF involvement (N2), and lymph nodes showing effacement of the normal lymph node architecture by neoplastic T cells (N3). The prognostic significance of such a subdivision has been well established.

No further examinations are recommended for patients with stage IA–B disease. CT or PET-CT scans of the chest and abdomen are recommended in patients in whom extracutaneous disease is suspected, but they are less useful in patients with limited patches and/or plaques without lymphadenopathy. Examination of other organs, including the bone marrow, should only be performed if clinically indicated.

TNMB CLASSIFICATION OF MYCOSIS FUNGOIDES AND SÉZARY SYNDROME	
T (skin)	
T_1	Limited patch/plaque (involving <10% of total skin surface)
T_2	Generalized patch/plaque (involving ≥10% of total skin surface)
T_3	Tumor(s)
T_4	Erythroderma
N (lymph node)	
N_0	No enlarged lymph nodes
N_1	Enlarged lymph nodes, histologically uninvolved
N_2	Enlarged lymph nodes, histologically involved (nodal architecture uneffaced)
N_3	Enlarged lymph nodes, histologically involved (nodal architecture [partially] effaced)
Nx	Clinically abnormal lymph nodes; no histologic confirmation
M (viscera)	
M_0	No visceral involvement
M_1	Visceral involvement
B (blood)	
B_0	Absence of significant blood involvement: <5% of peripheral blood lymphocytes are atypical (Sézary) cells
B_1	Low blood tumor burden: >5% of peripheral blood lymphocytes are atypical (Sézary) cells, but does not meet the criteria for B_2 (B_{1a}: clone negative; B_{1b}: clone positive)
B_2	High blood tumor burden: clone positive *plus* either ≥1000/mcl Sézary cells – *or* – CD4/CD8 ratio >10, $CD4^+CD7^-$ cells ≥40%, or $CD4^+CD26^-$ cells ≥30%)

Table 120.3 TNMB classification of mycosis fungoides and Sézary syndrome.

Treatment

The choice of an initial treatment in MF depends on the stage of the disease and the general condition and age of the patient[24,25]. Given the chronic and recurrent nature of MF, treatment should be aimed at improving symptoms while limiting toxicity. Following the traditional "stage-based" approach, skin-directed therapies are preferred in the

CLINICAL STAGING SYSTEM FOR MYCOSIS FUNGOIDES AND SÉZARY SYNDROME				
Clinical stage				
IA	T_1	N_0	M_0	$B_{0–1}$
IB	T_2	N_0	M_0	$B_{0–1}$
IIA	$T_{1–2}$	$N_{1–2}$	M_0	$B_{0–1}$
IIB	T_3	$N_{0–1}$	M_0	$B_{0–1}$
III	T_4	$N_{0–2}$	M_0	$B_{0–1}$
IVA_1	$T_{1–4}$	$N_{0–2}$	M_0	B_2
IVA_2	$T_{1–4}$	N_3	M_0	$B_{0–2}$
IVB	$T_{1–4}$	$N_{0–3}$	M_1	$B_{0–2}$

Table 120.4 Clinical staging system for mycosis fungoides and Sézary syndrome. The shaded boxes highlight the required features for the three subdivisions of stage IV disease.

early stages of MF (stages IA–IIA) and even in patients with limited tumor stage MF (IIB) (Table 120.5). These skin-directed therapies include topical or intralesional corticosteroids, topical cytotoxic agents (e.g. mechlorethamine [nitrogen mustard]), phototherapy, and radiotherapy. In patients with stage IA disease even expectant management with active surveillance can be considered. The efficacy of skin-directed therapies in MF is explained by the preferential localization of the neoplastic skin-homing T cells to the epidermis and superficial dermis. Systemic multi-agent chemotherapy is not useful in these early stages, since it does not improve survival and is associated with considerable morbidity.

In patients with refractory or progressive skin disease, skin-directed therapies can be combined with IFN-α or systemic retinoids. Alternatively, novel agents such as denileukin diftitox, mogamulizumab, or *h*istone *deac*etylase *i*nhibitors (HDACi) such as vorinostat and romidepsin can be used, before systemic chemotherapy is considered. HDACi and denileukin diftitox have been approved by the FDA for patients with relapsed and refractory CTCL, but they have not been registered for CTCL in Europe. While denileukin diftitox was withdrawn from the market in 2014, a revised version is currently under investigation. In general, systemic chemotherapy is only indicated in advanced stages when there is nodal or visceral involvement or in patients with rapidly progressive tumors unresponsive to less aggressive therapies.

TREATMENT OF MYCOSIS FUNGOIDES
Premycotic phase
• Topical or intralesional corticosteroids; narrowband UVB*
• If former not effective, PUVA*
Stage IA–IIA (patches/plaques)
• PUVA*; HN2 (see Ch. 129)
• Narrowband UVB* (if only patches)
• Topical corticosteroids, topical retinoids†, or topical imiquimod (if only limited patches/thin plaques as second-line therapy)
• Local radiotherapy (if single lesion)
• TSEB (if generalized thick plaques)
Stage IIB (skin tumors)
• PUVA or HN2 + local radiotherapy (if only a few tumors)
• TSEB (followed by skin-directed therapies)
• Relapse: PUVA + IFN-α; PUVA + retinoids (acitretin; oral bexarotene‡); second-line therapy: HDACi (romidepsin, vorinostat)‡
• Add local radiotherapy (if persistent tumors); consider second course of TSEB (10–20 Gy)
Stage III (erythroderma)
• ECP; if not effective, add IFN-α and/or systemic retinoids
• Low-dose methotrexate
• Add skin-directed therapies (PUVA; HN2; local radiotherapy), if necessary
• Second-line therapy: oral bexarotene‡; HDACi‡; low-dose alemtuzumab
Stage IV (nodal, visceral involvement)
• Brentuximab vedotin
• Gemcitabine
• Liposomal doxorubicin
• Pralatrexate
• Multi-agent chemotherapy (e.g. CHOP) (becoming historical)
• Mogamulizumab¶,§
• Add skin-directed therapies (PUVA; HN2), if necessary
• Allogeneic hematopoietic stem cell transplantation (utilizing reduced-intensity conditioning regimens)
*Address UV-shielded areas (e.g. upper inner thighs) via positioning.
†Bexarotene 1% gel (FDA approved for CTCL), tazarotene 0.1% gel, alitretinoin 0.1% gel.
‡Efficacy compared to traditional treatments yet to be determined.
¶Most effective in patients with blood involvement (B2).
§Do not administer if considering allogeneic hematopoietic stem cell transplantation as can worsen graft versus host disease.

Table 120.5 Treatment of mycosis fungoides. Topical bis-chloronitrosourea (BCNU; carmustine) is rarely used nowadays. Anti-PD-1 antibodies have been used to treat Sézary syndrome in the setting of PD-1 positivity and anti-staphylococcal antibiotics may lead to improvement. Use of dupilumab has been reported to lead to worsening of disease. CHOP, cyclophosphamide, hydroxydaunomycin (doxorubicin), Oncovin® (vincristine) and prednisone; ECP, extracorporeal photopheresis; HDACi, histone deacetylase inhibitors; HN2, topical mechlorethamine (nitrogen mustard); IFN, interferon; TSEB, total skin electron beam.

Skin-directed therapies

Topical corticosteroids

In many MF patients with only patches and thin plaques, application of topical corticosteroids is effective in controlling disease activity. In patients with limited patch/plaque stage disease (mainly patches), complete remissions in up to 60% of patients have been reported. In more advanced stages, they continue to be an important adjuvant therapy.

Topical chemotherapy

Topical application of mechlorethamine has proven to be an effective treatment for early stage MF. Mechlorethamine, either dissolved in water or compounded in an ointment- or gel-based preparation (see Ch. 129), results in complete remissions in approximately 60%–80% of patients with stage IA–B disease. Side effects include skin irritation, allergic contact dermatitis, and an increased risk for the development of skin cancer related to long-term use.

Radiotherapy

Total skin electron beam irradiation (TSEB) with an energy of 4–6 MeV is a highly effective treatment in patients with skin-limited MF (see Ch. 139). The total dose is traditionally 36 Gy administered in fractions of 1.5–2 Gy over an 8- to 10-week period. Recently, lower total doses (10–12 Gy) have been employed, with the advantages of a shorter duration of treatment, fewer side effects, and opportunity for re-treatment. TSEB is most effective in patients with stage IA–B disease, with complete response rates of >80%. However, in most centers, such patients are treated with phototherapy or topical chemotherapy. TSEB is particularly useful in patients with tumor stage MF, where complete response rates of ~40% have been reported. Side effects are generally mild and include erythema, scaling, and temporary loss of hair, nails, and sweat gland function.

Local radiotherapy with X-ray or preferably electron beam may be considered for single tumors in patients with plaque stage disease, either in combination with other modalities (e.g. PUVA) as an alternative to TSEB, or for new tumors following TSEB. A dose of ≥8 Gy suffices. In patients with unilesional MF, local radiotherapy may be curative.

Phototherapy

Several types of phototherapy can be used in the treatment of MF, in particular PUVA therapy and narrowband UVB therapy (Ch. 134). Extracorporeal photopheresis (ECP) may be effective in patients with erythrodermic MF (see the section on Sézary syndrome).

PUVA treatment has become a standard therapy for the early stages of MF. In patients with stages IA–IIA, complete response rates of 80%–90% have been reported. In many centers, maintenance PUVA therapy (every 2 to 4 weeks) is given to prolong remission. Although sustained complete remissions have been reported, most patients will relapse after cessation of PUVA therapy or during maintenance treatment. Recurrent or persistent lesions particularly favor UV-shielded areas, such as the inner thighs and

the gluteal cleft. In tumor stage MF, PUVA therapy alone is unlikely to result in complete responses, but favorable results may be achieved when combined with systemic retinoids, IFN-α, or radiotherapy.

In patients with only patches, *narrowband UVB* therapy (311 nm) represents first-line therapy.

Systemic therapies (other than chemotherapy)

Interferons

The most commonly prescribed biological response modifier has been interferon-alpha (IFN-α). In most centers, IFN-α is administered subcutaneously in doses of 3 to 9 million units three times a week. Side effects include flu-like symptoms, hair loss, nausea, depression, and bone marrow suppression and although they are generally mild and reversible, dose reductions are commonplace. The overall response rate of IFN-α, when used as a single agent, is ~50%, with 17% representing complete remissions. The combination of PUVA and IFN-α appears to produce higher response rates than PUVA alone, and this combination may also be considered in patients with early tumor stage disease, when PUVA therapy alone is insufficient.

Retinoids

When used as a single agent, the overall and complete response rates of several first- and second-generation oral retinoids (isotretinoin, acitretin) and a novel RXR-selective retinoid (bexarotene) are roughly similar to those of IFN-α. A combination of retinoids (including bexarotene) plus PUVA (RePUVA) produces response rates similar to those of PUVA alone, although patients treated with RePUVA require fewer treatments and a lower cumulative UVA dose. In many centers, bexarotene has replaced the earlier-generation retinoids (see Table 126.4), but comparative studies have never been performed. In patients with patches or thin plaques, topical retinoids (bexarotene 1% gel [FDA approved for CTCL], tazarotene 0.1% gel, alitretinoin 0.1% gel) may be considered, but skin irritation is a limiting factor.

Denileukin diftitox

Denileukin diftitox is a fusion protein, in which diphtheria toxin is linked to IL-2. It binds to the high-affinity IL-2 receptor expressed by the neoplastic T cells in MF, and internalization of the toxin results in inhibition of protein synthesis and cell death. Overall and complete clinical response rates are ~30% and 10%, respectively. Denileukin diftitox can have substantial side effects, including capillary leak syndrome, fever, and fluid retention. A revised version is currently under investigation (see above).

Histone deacetylase inhibitors

HDACi, such as vorinostat and romidepsin, represent a novel class of drugs used in cancer therapy. Inhibition of the enzyme HDAC affects the expression of many genes (and their protein products) that are involved in cellular proliferation, differentiation, migration, and apoptosis. Studies of both vorinostat and romidepsin report overall response rates of ~35% in patients with MF and SS, but complete responses are rare. The most common side effects are fatigue, gastrointestinal symptoms, and reversible thrombocytopenia. It remains to be determined which patients are most likely to benefit from this therapy.

Mogamulizumab

Discussed in SS treatment section.

Systemic chemotherapy

In patients with advanced and refractory disease, gemcitabine or liposomal doxorubicin may be considered, but responses are generally short-lived. More recently, high response rates have been reported with brentuximab vedotin (an anti-CD30 monoclonal antibody coupled to the anti-tubulin agent monomethyl auristatin E) in patients with advanced, CD30-expressing MF/SS[26]. Systemic multi-agent chemotherapy should only be used in patients with unequivocal lymph node or visceral involvement, or in patients with progressive skin tumors that have failed to respond to other therapies. In many centers, the standard treatment in such cases was the administration of six cycles of CHOP (*c*yclophosphamide, *h*ydroxydaunomycin [doxorubicin], *O*ncovin® [vincristine] and *p*rednisone). However, with this and other combination regimens, high response rates can be achieved for extracutaneous involvement, but as with single-agent chemotherapy, the responses are generally short-lived. Moreover, concurrent patches and plaques are often less responsive, and may require additional treatment with PUVA or mechlorethamine.

In young patients with refractory, progressive MF and SS, an allogeneic hematopoietic stem cell transplantation (HSCT) may be considered. Using reduced-intensity conditioning regimens, durable responses have been reported, but the optimal conditioning regimen and optimal timing for the transplant are still a matter of debate[27]. Prior to transplantation, patients may benefit from tumor debulking via TSEB or brentuximab vedotin[24]. Results with autologous HSCT in MF and SS have been disappointing, suggesting the need for a graft-versus-tumor response.

Prognosis

The prognosis of patients with MF is dependent on the stage, and in particular the type and extent of skin lesions and the presence of extracutaneous disease[20]. Patients with limited patch/plaque stage MF have a similar long-term life expectancy as an age-, sex-, and race-matched control population. The disease-related 10-year survival is 96% for stage IA, 77%–83% for stage IB, 42% for stage IIB, but only 20% for stage IV[20]. Patients usually die of systemic involvement or infections.

VARIANTS OF MYCOSIS FUNGOIDES

Apart from the classic Alibert–Bazin type of MF, many clinical and/or histologic variants have been reported. Clinical variants, such as bullous and hyper- or hypopigmented MF, have clinical behavior similar to that of classic MF, and they are therefore not considered separately. In contrast, folliculotropic MF, pagetoid reticulosis, and granulomatous slack skin have distinctive clinicopathologic features, clinical behavior and/or prognosis, and therefore they have been included as distinct variants or subtypes of MF in the WHO-EORTC classification scheme.

Folliculotropic MF

Synonyms: ■ Adnexotropic (folliculotropic and syringotropic) MF ■ Folliculocentric MF ■ Pilotropic MF ■ MF-associated follicular mucinosis

Definition

Folliculotropic MF is a distinct variant of MF characterized by the presence of folliculotropic infiltrates, often with sparing of the epidermis and preferential involvement of the head and neck region. Most cases show mucinous degeneration of the hair follicles (follicular mucinosis; Ch. 46) and are traditionally designated as MF-associated follicular mucinosis. Similar cases, but without follicular mucinosis, have been reported as pilotropic MF. Compared with classic MF, folliculotropic MF was previously said to have a worse prognosis. However, when more recent studies defined subgroups of early and advanced folliculotropic MF, the prognosis was similar to early and advanced stage classic MF[28,29].

Epidemiology

This variant is found in ~10%–20% of MF patients. It occurs mostly in adults, but may occasionally affect children and adolescents. Men are affected more often than women.

Clinical features

Patients may present with (grouped) follicular papules, acneiform lesions, indurated plaques, and sometimes tumors, which preferentially involve and are most pronounced in the head and neck area (see Fig. 36.15C). Infiltrated plaques in the eyebrow region with concurrent alopecia are a common and highly characteristic finding (Fig. 120.6A). Some patients may have keratosis pilaris-like lesions located primarily on the trunk and extremities and they are often associated with alopecia. Rarely, patients present with either a solitary cutaneous lesion (solitary or unilesional folliculotropic MF) or erythroderma. Sometimes a prominent feature is eruptive small cysts and comedones (comedonal MF; see Fig. 36.15D). Pruritus is often more severe than in classic MF and may represent a reliable parameter of disease activity. Secondary bacterial infections are frequently observed.

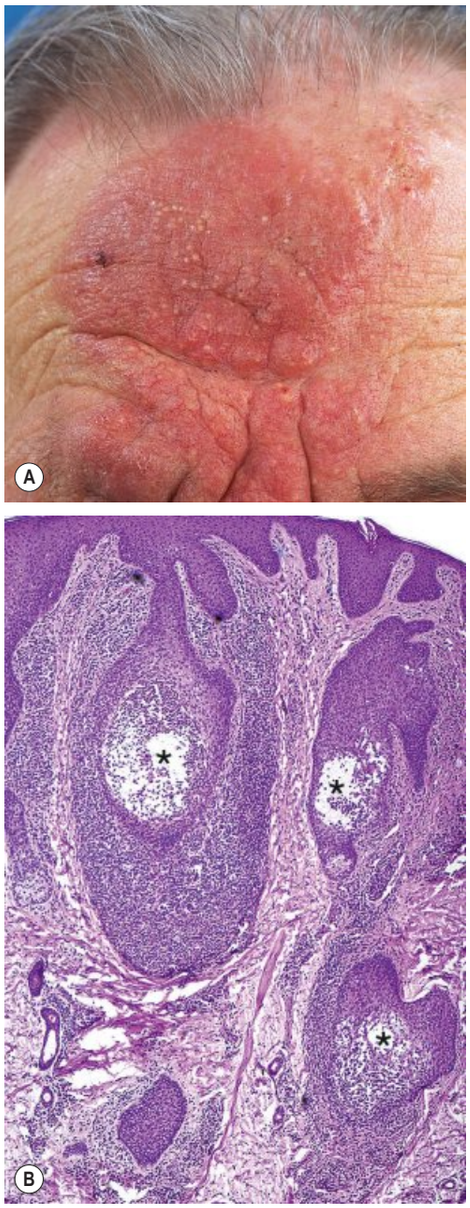


Fig. 120.6 Folliculotropic mycosis fungoides. A Infiltrated plaques on the forehead and eyebrow with concurrent hair loss. **B** Characteristic perifollicular infiltrates with extensive follicular mucinosis (asterisks). Note absence of epidermotropism.

Pathology

There are perifollicular infiltrates, with variable infiltration of the follicular epithelium by small, medium-sized, or sometimes large T cells with cerebriform and hyperchromatic nuclei[30]. Infiltration of the interfollicular epidermis, characteristic of early stage classic MF, is uncommon; i.e. folliculotropism rather than epidermotropism is seen (Fig. 120.6B). Although mucinous degeneration of the follicular epithelium (follicular mucinosis), which can be visualized by Alcian blue or colloidal iron staining is often present, cases without follicular mucinosis have been described. Infiltration of the follicular epithelium may be accompanied by infiltration of the eccrine sweat glands (syringotropism), a combination that is often referred to as adnexotropic MF.

In early stage lesions such as patches with follicular prominence and acneiform or keratosis pilaris-like lesions, the perifollicular infiltrates are generally sparse and contain variable numbers of small reactive T cells, histiocytes, and occasional eosinophils, in addition to atypical T cells. The perifollicular infiltrates in plaques or tumors are more dense and more diffuse and may contain an increasing number of blast cells. There is often a considerable admixture with eosinophils, and especially if there is secondary bacterial infection, plasma cells. If the hair follicle epithelium is destroyed, a granulomatous reaction can be observed. Large cell transformation has been reported in >20% of folliculotropic MF cases and is more common than in classic MF[28]. As a result, an admixture of CD30-positive blast cells with $CD3^+$, $CD4^+$, $CD8^-$ neoplastic T cells (most common phenotype as in classic MF) is often observed.

Differential diagnosis

The distinctive clinical and histologic features should facilitate an early and correct diagnosis. However, because of the preferential involvement of the head and neck area, the absence of patches and plaques on the trunk and buttocks, and particularly because of the absence of epidermotropic atypical T cells, the diagnosis of MF or CTCL is often not considered and is misinterpreted as seborrheic dermatitis or atopic dermatitis. Clinicopathologic correlation is also required to differentiate folliculotropic MF from other types of CTCL. The relationship between folliculotropic MF and the so-called benign or idiopathic form of follicular mucinosis (alopecia mucinosa) resembles the relationship between classic MF and "parapsoriasis". In the case of persistent generalized lesions of the idiopathic form, patients should be monitored regularly, since progression into overt folliculotropic MF has been reported. The unilesional form of follicular mucinosis occurs more often in children and does not progress to MF.

Treatment

Recognition of indolent and aggressive subgroups of folliculotropic MF is important as it supports a stepwise, stage-adapted therapeutic approach, similar to early and advanced stage classic MF[31]. Patients with early stage disease may do quite well with non-aggressive skin-directed therapies, such as topical corticosteroids, PUVA, or topical mechlorethamine. In patients with unresponsive disease, treatment options include PUVA plus local radiotherapy, IFN-α or retinoids, systemic retinoids alone, or TSEB. For those rare patients with a solitary plaque or tumor, local radiotherapy is the preferred mode of treatment.

Pagetoid Reticulosis

Synonyms: ■ Woringer–Kolopp disease ■ Unilesional MF

Definition

This is a rare variant of MF, characterized by the presence of localized patches or plaques with an intraepidermal proliferation of neoplastic T cells. The term pagetoid reticulosis should only be used for the localized type (Woringer–Kolopp type) and not for the disseminated type (Ketron–Goodman type). Nowadays, patients with generalized disease would most likely be classified as having primary cutaneous aggressive epidermotropic CD8-positive cytotoxic T cell lymphoma, primary cutaneous gamma/delta T cell lymphoma, or tumor stage MF[1].

Epidemiology

Pagetoid reticulosis is extremely rare, and it accounts for fewer than 1% of CTCL cases. It mostly affects adults.

Clinical features

Patients present with a solitary, slowly progressive psoriasiform or hyperkeratotic patch or plaque. It usually develops on an extremity, in particular the hand or foot (Fig. 120.7A). In contrast to classic MF, extracutaneous dissemination or disease-related deaths have not been reported.

Pathology

The typical histologic picture consists of a hyperplastic epidermis with marked infiltration by large atypical pagetoid cells, arranged singly or in nests or clusters (Fig. 120.7B). The atypical cells have medium-sized or large, sometimes hyperchromatic and cerebriform nuclei and abundant, vacuolated cytoplasm. The superficial dermis may have an infiltrate of mostly small lymphocytes, but rarely contains neoplastic T cells.

Immunophenotype

The neoplastic T cells may show either a $CD3^+$, $CD4^+$, $CD8^-$ or a $CD3^+$, $CD4^-$, $CD8^+$ phenotype. CD30 is often expressed[32].

Differential diagnosis

Pagetoid reticulosis should be differentiated from other types of epidermotropic CTCL, such as MF, LyP type B, LyP type D, and primary cutaneous aggressive epidermotropic CD8-positive cytotoxic T cell lymphoma (see Table 120.2). Useful criteria for pagetoid reticulosis include the characteristic clinical presentation and the often strictly epidermal localization of the neoplastic T cells.

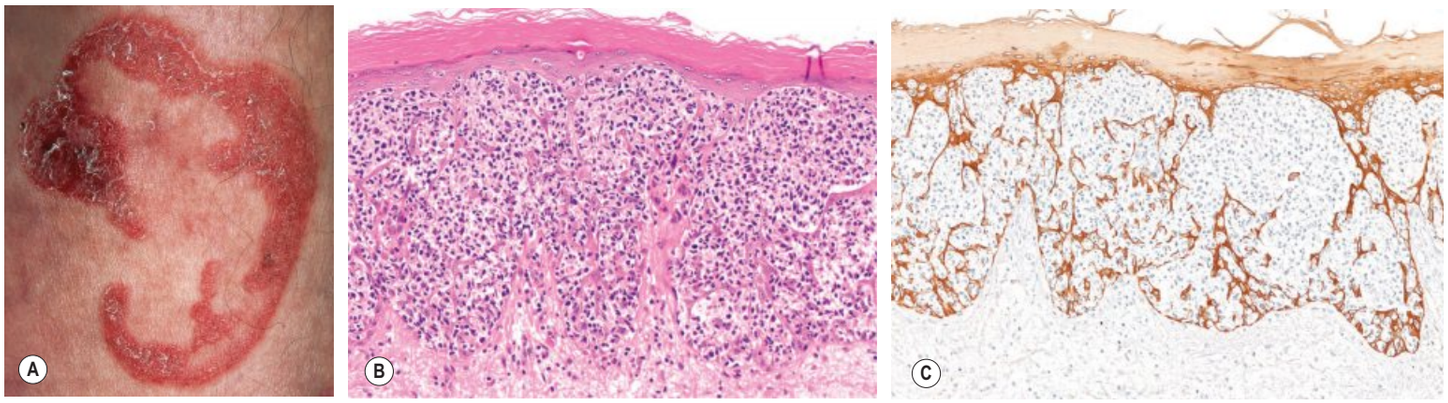


Fig. 120.7 Pagetoid reticulosis. A Solitary plaque on the left upper leg. **B** Purely intraepidermal proliferation of atypical T cells. **C** Immunohistochemical staining for keratin shows almost complete replacement of the epidermis by atypical T cells.

Treatment

The preferred mode of treatment is radiotherapy or surgical excision.

Granulomatous Slack Skin

Definition

This is an extraordinarily rare type of CTCL characterized by the slow development of folds of lax skin and a granulomatous infiltrate with clonal T cells.

Epidemiology

It is an extremely rare type of CTCL, with ~60 cases reported. It typically affects adolescents and adults, and mostly occurs in men.

Clinical features

This condition is characterized by circumscribed areas of pendulous lax skin with a predilection for the axilla and groin (Fig. 120.8A). In approximately one-third of the reported patients, an association with Hodgkin lymphoma was observed. Most patients have an indolent clinical course.

Pathology

Fully developed lesions show dense granulomatous dermal infiltrates that contain atypical T cells with cerebriform nuclei, macrophages, and often many multinucleated giant cells; destruction of elastic tissue and elastophagocytosis by the multinucleated cells is also seen (Fig. 120.8B). Phagocytized lymphocytes are usually present within the cytoplasm of some of the multinucleated histiocytic giant cells. The epidermis may be infiltrated by small atypical T cells with cerebriform nuclei, as in classic MF. The atypical T cells have a $CD3^+$, $CD4^+$, $CD8^-$ phenotype. A large study noted overlapping histologic features between granulomatous slack skin and granulomatous MF[33].

Treatment

Radiotherapy may be effective, but experience is still limited. Rapid recurrences after surgical excision have been reported.



Fig. 120.8 Granulomatous slack skin. A Pendulous fold of atrophic lax skin in the right inguinal area. **B** Multinucleated giant cells with intracellular leukocytes, surrounded by a dense leukocytic infiltrate. Inset: Elastic tissue stain showing a multinucleated giant cell containing an elastic fiber (elastophagocytosis).

SÉZARY SYNDROME

Definition

Sézary syndrome (SS) is defined historically by the triad of erythroderma, generalized lymphadenopathy, and the presence of neoplastic T cells (Sézary cells) in the skin, lymph nodes, and peripheral blood (see Table 120.4). Criteria for the diagnosis of SS include demonstration of a T cell clone in the peripheral blood (preferably the same T cell clone as in the skin), in combination with either an absolute Sézary cell count ≥1000 cells/mcl or immunophenotypic abnormalities including an expanded $CD4^+$ T cell population resulting in a CD4/CD8 ratio >10, $CD4^+CD7^-$ cells ≥40%, or $CD4^+CD26^-$ cells ≥30%[1]. While SS is often designated as a leukemic phase or variant of MF, more recent studies have revealed major genomic and phenotypic differences between these two entities, suggesting that SS and MF should be considered as separate lymphomas arising from distinct functional T cell subsets[34,35].

Epidemiology

SS is a rare disease accounting for <5% of all CTCL (see Table 120.1). It occurs exclusively in adults.

Clinical Features

SS is characterized by erythroderma, which may be associated with marked exfoliation, edema, and lichenification; it is intensely pruritic (Fig. 120.9A). Lymphadenopathy, alopecia, onychodystrophy, and palmoplantar hyperkeratosis are common findings. The overt clinical picture may be preceded by a non-diagnostic dermatitis. The prognosis is generally poor, with an overall 5-year survival of ~35%. Most patients die of opportunistic infections due to immunosuppression.

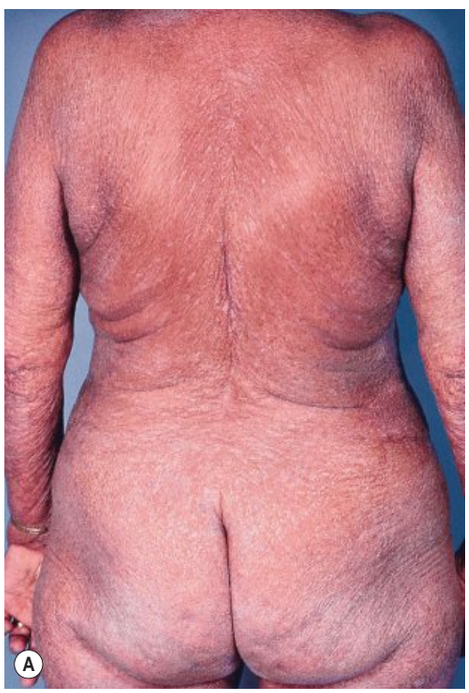
Pathology

The histologic features in SS may be similar to those in MF. However, the cellular infiltrates in SS are more often monotonous, and epidermotropism may be absent. In up to one-third of skin biopsies from patients with otherwise classic SS, the histologic findings may be nonspecific. Involved lymph nodes characteristically show a dense, monotonous infiltrate of Sézary cells with effacement of the normal lymph node architecture. The bone marrow may be involved, but the infiltrates are often sparse and mainly interstitial. The neoplastic T cells have a $CD3^+$, $CD4^+$, $CD8^-$ phenotype, characteristically lack CD7 and CD26 expression, and express programmed death-1 (PD-1; CD279) in almost all cases[5,36] (Fig. 120.9B).

Pathogenesis

The pathogenesis of SS is unknown. Conclusive evidence of an etiologic role for HTLV-1 is lacking. Previous studies suggested that the neoplastic $CD4^+$ T cells in SS patients were derived from central memory T cells and the neoplastic cells in MF from effector memory T cells. However, more recent studies found that Sézary cells may also be derived from other T cell subsets[35,36]. In addition, tumor cell populations in individual SS patients had a high degree of single-cell heterogeneity, and these distinct subpopulations of malignant T cells may differ in their sensitivity to treatments[37].

Studies of genetic alterations in SS have shown extensive genetic instability and complex structural and numerical alterations. Chromosomal aberrations include *deletions* involving chromosomes 10q22–25 (harbors *PTEN*) and 17p12–13 (includes *TP53*) and *gains* involving chromosomes 8q22–24 (includes *MYC*), 10p11.2, and 17q22–25[34,38]. Gene expression studies found increased expression of *PLS3* (T-plastin), *TWIST1*, *DNM3*, *EPH4* and *CD158k/KIR3DL2*, which might serve as diagnostic markers[5,36]. With next generation sequencing, alterations in genes that play a role in T cell activation, NF-κB and JAK-STAT signaling, apoptosis control, chromatin remodeling, and DNA damage response were identified[12].



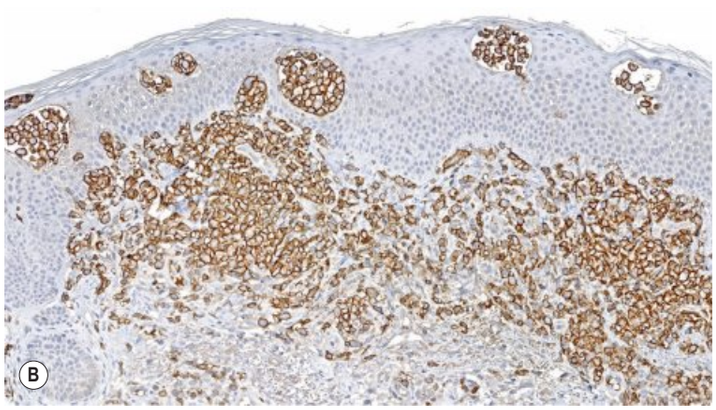


Fig. 120.9 Sézary syndrome. A Erythroderma with diffuse scaling. **B** Strong expression of PD-1 by neoplastic T cells within the dermal infiltrate and Pautrier microabscesses.

Differential Diagnosis

Differentiation between SS and non-neoplastic forms of erythroderma may be extremely difficult. The differential diagnosis includes erythroderma secondary to psoriasis, atopic dermatitis, or other forms of dermatitis, pityriasis rubra pilaris, and drug reactions as well as idiopathic erythroderma (see Ch. 10). Demonstration of an identical T cell clone in skin and peripheral blood is an important diagnostic criterion favoring SS. New biomarkers supporting a diagnosis of SS include PD-1 (CD279), TOX, and KIRDL2 (CD158k)[4,36]. Demonstration of a predominant $CD3^+$, $CD4^-$, $CD8^+$ T cell population in the skin and peripheral blood is highly suggestive of actinic reticuloid (see Ch. 87).

Treatment

Being a systemic disease (leukemia) by definition, systemic treatment is required. Skin-directed therapies like PUVA or potent topical corticosteroids may be used as adjuvant therapy. Extracorporeal photopheresis (ECP), either alone or in combination with other treatment modalities, has been suggested as the treatment of choice in SS and erythrodermic MF, with overall response rates of 30%–80%, and complete response rates of 14%–25%[24,25]. This great variation in response rates may reflect differences in patient selection and/or concurrent therapies. The suggested superiority of ECP over traditional low-dose chemotherapy regimens has not yet been substantiated by randomized controlled trials. Beneficial effects have also been reported with IFN-α (either alone or in combination with PUVA therapy) as well as prolonged treatment with methotrexate, but complete responses are uncommon.

Low-dose alemtuzumab (10 mg SC thrice weekly for 12 weeks), single-agent chemotherapy (gemcitabine, liposomal doxorubicin), or multi-agent chemotherapy (CHOP or CHOP-like regimens) have been recommended as second-line treatments for SS, but responses are generally short-lived[25]. Allogeneic HSCT may have curative potential, even in patients with advanced disease (see MF treatment). The monoclonal antibody mogamulizumab targets the CC chemokine receptor 4 (CCR4), which is consistently expressed on malignant T cells in MF/SS as well as on Th2, Th17, and regulatory T cells, resulting in their destruction via antibody-dependent cellular cytotoxicity. While mogamulizumab has shown significant clinical efficacy in both MF and SS, it is most effective in patients with blood involvement[39]. Patients may develop a mogamulizumab-associated rash (MAR) that often favors the head and neck and may mimic MF[39a]. Clinical presentation is variable and may include folliculotropic MF-like scalp lesions with alopecia, photodistributed dermatitis, a morbilliform eruption, and erythroderma. Histologically, psoriasiform, spongiotic, lichenoid, and/or granulomatous patterns can be seen. Demonstration of an inverted or normalized CD4:CD8 ratio of intraepidermal T cells and an absence of clonal T cells may be useful criteria for differentiating MAR from recurrent MF/SS. Treatment options include high potency topical corticosteroids, systemic corticosteroids, and/or methotrexate; increasing the dosing interval or discontinuation of mogamulizumab may be considered[39b].

ADULT T CELL LEUKEMIA/LYMPHOMA

Definition

Adult T cell leukemia/lymphoma (ATLL) is a type of T cell neoplasm etiologically associated with HTLV-1. Skin lesions are generally a manifestation of widely disseminated disease. However, a slowly progressive form that sometimes has only cutaneous lesions has been described (smoldering variant)[40].

Epidemiology

ATLL is endemic in areas with a high prevalence of HTLV-1 in the population, such as southwestern Japan, the Caribbean Islands, and parts of Central Africa. In addition, a high prevalence is seen in Jewish individuals whose ancestors were from Mashhad, Iran. However, only a minority of seropositive patients eventually develop ATLL. The disease occurs in adults, and men are affected more frequently than women. Vertical transmission is more common than horizontal transmission.

Clinical Features

Most patients present with acute ATLL characterized by the presence of leukemia, lymphadenopathy, organomegaly, hypercalcemia, and frequently skin lesions (Fig. 120.10); it has a poor prognosis. Chronic and smoldering variants often present with patches, plaques, and papular skin lesions, which may closely resemble MF, and circulating neoplastic T cells are few or absent. Such cases have a more protracted clinical course, but progression to a high-grade malignant disseminated form of the disease may occur.

Pathology

Skin lesions demonstrate a superficial or more diffuse infiltration of small, medium-sized, or large pleomorphic T cells, which often display marked epidermotropism. The histologic picture may be indistinguishable from MF. Skin lesions in the smoldering type may have sparse dermal infiltrates with only slightly atypical cells. The neoplastic T cells express a $CD3^+$, $CD4^+$, $CD8^-$, $CD25^+$ phenotype, and – as in SS – strongly express PD-1.

Differential Diagnosis

Differentiation between chronic or smoldering variants of ATLL and MF may be extremely difficult, particularly in endemic areas. In such cases, a definite diagnosis of ATLL requires demonstration of clonally integrated HTLV-1. Some patients have a preceding history of HTLV-1-associated infective dermatitis (see Ch. 13).

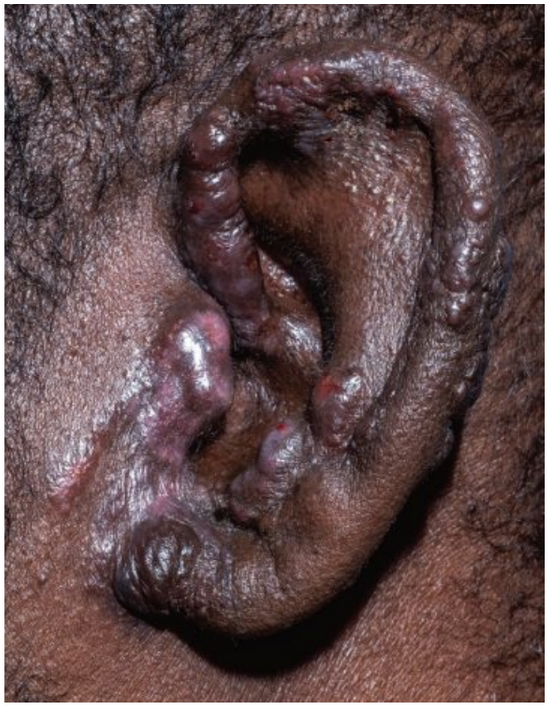


Fig. 120.10 Adult T cell leukemia/lymphoma (ATLL). Multiple papulonodules, a few of which are eroded, of the external ear. *Courtesy Edward Cowen, MD.*

Treatment

ATLL may be treated with a combination of zidovudine and IFN-α, but in most cases, systemic chemotherapy is required[41]. In Japan, mogamulizumab (anti-CCR4) is approved for treating ATLL. For chronic and smoldering disease mainly affecting the skin, skin-directed therapies as in MF are preferred.

PRIMARY CUTANEOUS CD30-POSITIVE LYMPHOPROLIFERATIVE DISORDERS

Primary cutaneous CD30-positive lymphoproliferative disorders represent the second most common group of CTCL, accounting for ~25% of CTCL (see Table 120.1). This group includes primary cutaneous anaplastic large cell lymphoma (C-ALCL), lymphomatoid papulosis (LyP), and borderline cases. C-ALCL and LyP have overlapping clinical, histologic, and immunophenotypic features and form a spectrum of disease (Fig. 120.11). Thus, histologic criteria alone are often insufficient to distinguish between the two ends of the spectrum. In the end, the clinical appearance and course are used as decisive criteria for the definite diagnosis and choice of treatment. The term "borderline case" refers to patients in whom, despite careful clinicopathologic correlation, a definite distinction between C-ALCL and LyP cannot be made. Longitudinal clinical evaluation will generally disclose whether the patient has C-ALCL or LyP[42].

Guidelines for the diagnosis and treatment of primary cutaneous CD30-positive lymphoproliferations are provided in Fig. 120.11.

Primary Cutaneous Anaplastic Large Cell Lymphoma

Definition

Primary cutaneous anaplastic large cell lymphoma (C-ALCL) is composed of large cells with an anaplastic, pleomorphic, or immunoblastic cytomorphology and expression of the CD30 antigen by the majority (>75%) of tumor cells. Patients should not have clinical evidence of or a history of MF. In such individuals, a diagnosis of tumor stage MF with large cell transformation is more likely.

Epidemiology

These lymphomas account for ~10% of all CTCLs (see Table 120.1). They predominantly affect adults and are rare in children or adolescents. The male-to-female ratio is approximately 2:1.

Clinical features

Most patients present with solitary or localized nodules or tumors (sometimes papules) that often develop ulceration (Fig. 120.12A). Multifocal lesions are seen in about 15% of patients. The skin lesions may show partial or complete spontaneous regression, as in LyP. These lymphomas frequently relapse in the skin. Extracutaneous dissemination occurs in 10%–15% of patients, and it mainly involves the regional lymph nodes. The prognosis is usually favorable, with a 10-year disease-related survival exceeding 85%[43,44]. However, patients who present with extensive skin lesions on the leg have a reduced survival rate[43].

Pathology

Histologically, these lymphomas show diffuse non-epidermotropic infiltrates with cohesive sheets of large CD30-positive tumor cells (Fig. 120.12B). In most cases, the tumor cells have the characteristic morphology of anaplastic cells, with round, oval or irregularly shaped nuclei, prominent (eosinophilic) nucleoli, and abundant cytoplasm. Less commonly (20%–25%), tumor cells have a pleomorphic, immunoblastic, or Reed–Sternberg cell-like appearance. The mitotic index is generally high. Reactive lymphocytes are often present at the periphery of the tumor.

Ulcerating lesions may show LyP-like histology with an abundant inflammatory infiltrate of reactive T cells, histiocytes, eosinophils, neutrophils, and relatively few CD30-positive cells. In such cases, epidermal hyperplasia may be prominent at the edge of the ulceration.

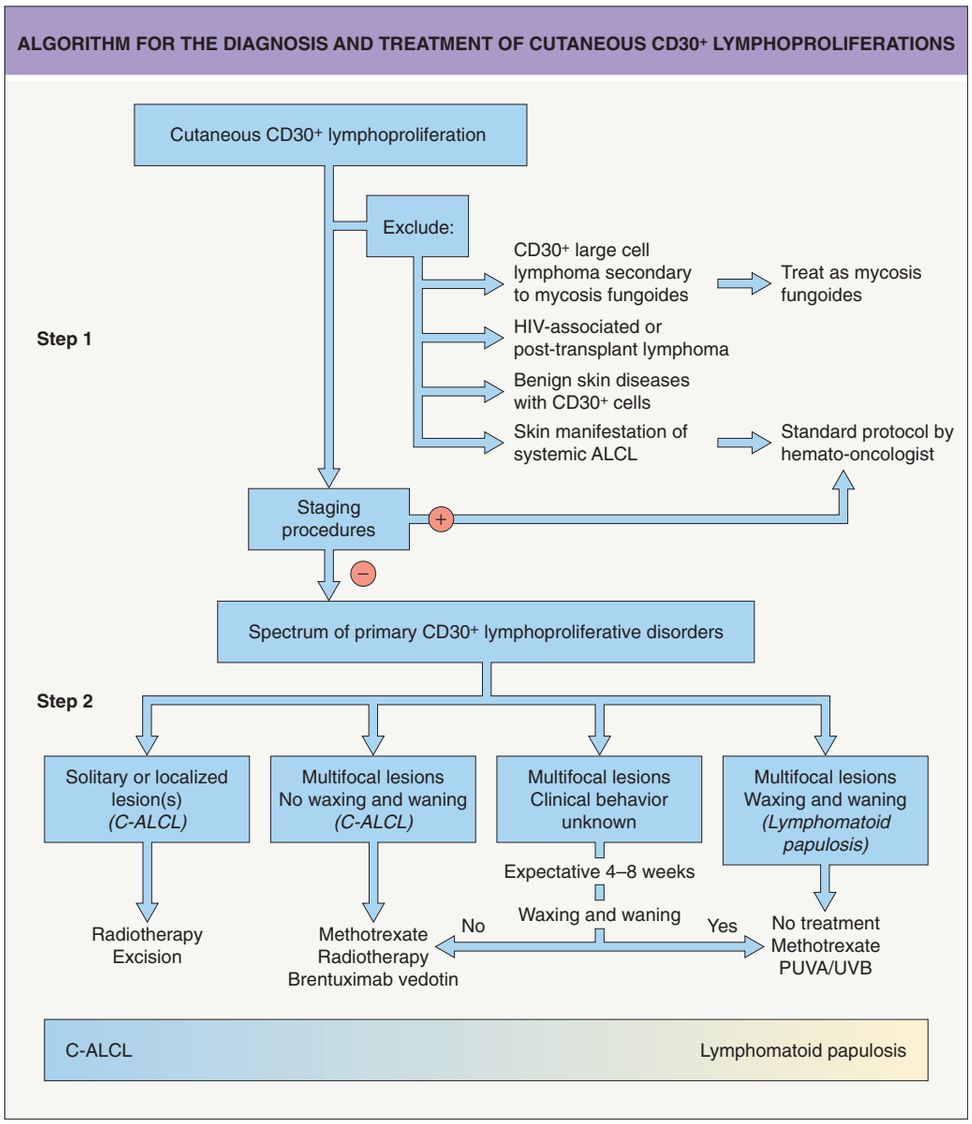


Fig. 120.11 Algorithm for the diagnosis and treatment of primary cutaneous CD30-positive lymphoproliferations. Cases previously designated as regressing atypical histiocytosis, as well as rare cases of primary cutaneous Hodgkin lymphoma with an indolent clinical course, also belong to this spectrum. Of note, there are reports of ALCL developing in patients with breast implants. C-ALCL, cutaneous anaplastic large cell lymphoma. *From reference* 42.

Intralymphatic complexes of tumor cells are common, and purely intralymphatic cases of C-ALCL have been observed[45].

Immunophenotype

The neoplastic cells often express a CD4+ T cell phenotype with variable loss of CD2, CD5, and/or CD3. Some cases (<5%) have a CD8+ T cell phenotype. *CD30 must be expressed by the majority of neoplastic cells*. Expression of cytotoxic proteins (granzyme B, TIA-1, perforin) is noted in ~70% of cases, while MUM1/IRF4 (multiple myeloma oncogene 1/interferon regulatory factor 4) is expressed in almost all cases[45]. Unlike systemic ALCL, most C-ALCLs express CLA (cutaneous lymphocyte antigen), but do not express EMA (epithelial membrane antigen) or ALK (anaplastic lymphoma kinase); the latter is indicative of a t(2;5) chromosomal translocation.

Genetic features

The t(2;5) *translocation*, which is found predominantly in systemic ALCL in children, is not present in the vast majority of C-ALCLs. However, unusual cases of ALK+ C-ALCL have been reported, both in children and in adults, including cases with: (1) strong nuclear and cytoplasmic staining characteristic of the t(2;5) chromosomal translocation; or (2) expression of cytoplasmic ALK protein, indicative of a variant translocation[46,47]. While many of these patients had an excellent prognosis, rapid progression to systemic ALCL has been reported. *Rearrangements* of the *DUSP22-IRF4* locus on chromosome 6p25.3 are found in ~25% of C-ALCLs and in a small subset of LyP, but do not have prognostic significance[48].

Rearrangements of *TP63* on chromosome 3q28 are associated with poor survival in ALK-negative systemic ALCL, but are not or only rarely found in C-ALCL. A novel recurrent *NPM1-TYK2 gene fusion*, resulting in constitutive STAT signaling, has been described in both C-ALCL and LyP. In addition, *TYK2* breaks were found in 15% of primary cutaneous CD30+ T cell lymphoproliferative disorders[49].

Frequent *chromosomal aberrations*, found in almost half of the patients with C-ALCL, are gains of 7q31 and losses on 6q16–21 and 13q34[50]. In contrast to tumor stage MF and PTCL, NOS, loss of 9p21.3 is rarely observed in C-ALCL. Gene expression profiling has demonstrated high expression of skin-homing chemokine receptor genes *CCR10* and *CCR8* in C-ALCL, which may explain its affinity for the skin and low incidence of dissemination to extracutaneous sites[50].

Treatment

Radiotherapy or surgical excision is first-line therapy in patients presenting with a solitary or a few localized nodules or tumors[25,51]. However, if a solitary lesion disappears spontaneously, no further therapy is required. Patients presenting with multifocal skin lesions can be treated with radiotherapy (if there are only a few lesions) or low-dose methotrexate as in LyP. Brentuximab vedotin has shown high response rates in patients with primary cutaneous CD30-positive lymphoproliferations and is used to treat multifocal skin lesions refractory to conventional therapies as well as extracutaneous disease[25,26]. Multiagent chemotherapy is only indicated for extracutaneous disease beyond locoregional lymph nodes and those rare patients with rapidly progressive skin disease unresponsive to brentuximab vedotin.

Lymphomatoid Papulosis

Definition

Lymphomatoid papulosis (LyP) is defined as a chronic, recurrent, self-healing papulonecrotic or papulonodular skin disease with histologic



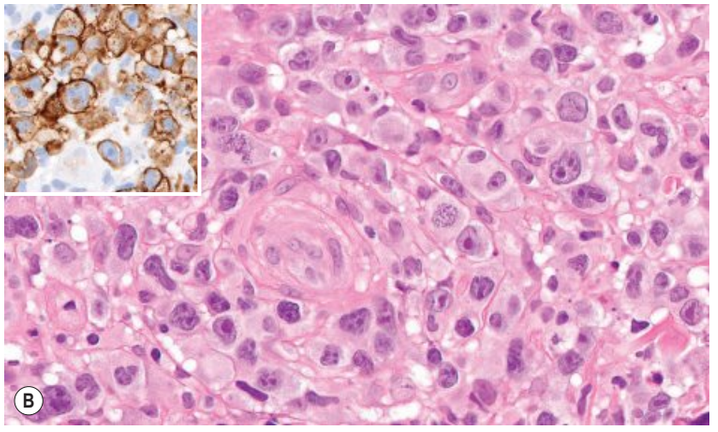


Fig. 120.12 Primary cutaneous anaplastic large cell lymphoma. **A** Characteristic clinical presentation with a solitary tumor. **B** Detail of dermal infiltrate showing cohesive clusters of large (CD30-positive [inset]) anaplastic cells with pronounced eosinophilic nucleoli and abundant cytoplasm.



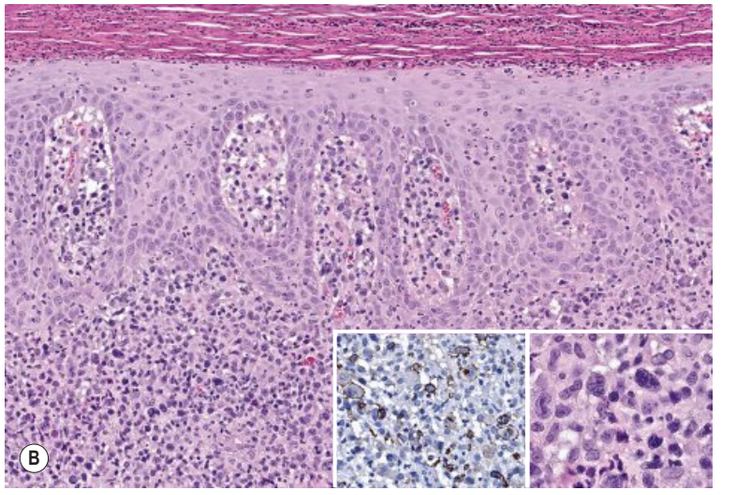


Fig. 120.13 Lymphomatoid papulosis (LyP). **A** Clinical presentation with papulonecrotic skin lesions at different stages of evolution. **B** Dense dermal infiltrate with scattered large anaplastic cells that have prominent nucleoli and abundant cytoplasm (right inset). Note the sprinkling of neutrophils within the epidermis. Immunohistochemical stain of type A LyP demonstrates scattered large $CD30^+$ cells (left inset).

features suggestive of a (CD30-positive) malignant lymphoma. Since the introduction of the term LyP in 1968 by Macaulay, there has been continued discussion as to whether LyP is a malignant, premalignant, or benign condition. Because of the overlapping clinical and histologic features between LyP and C-ALCL, including the presence of an aberrant T cell phenotype, the presence of clonally rearranged TCR genes in 60%–70% of the patients, and the presence of identical T cell clones in LyP lesions and associated lymphoma lesions, LyP is best regarded as a low-grade variant of CTCL.

Pathogenesis

The initiating event in LyP is unknown. Several authors have suggested a viral etiology. However, studies searching for an etiologic role for HTLV-1, EBV, and other herpes viruses, including herpes simplex virus types 1 and type 2 and human herpesvirus-6, have been consistently negative. The mechanisms involved in the spontaneous disappearance of skin lesions, or in the tumor progression observed in some patients with LyP, have not yet been identified. It has been suggested that interactions between CD30 and its ligand (CD30L) may contribute to apoptosis of the neoplastic T cells and the subsequent regression of the skin lesions, but the exact mechanism is as yet unknown[45,49].

Epidemiology

LyP accounts for ~15% of all CTCL (see Table 120.1). It may occur at any age. The youngest patient reported to date was 8 months old, and the oldest was 92 years of age. In large series, the average age of onset is 45 years[52]. The male-to-female ratio is approximately 1.5:1.

Clinical features

The typical skin lesions in LyP are red–brown papules and nodules that may develop central hemorrhage, necrosis, and crusting; they subsequently disappear spontaneously within 3 to 12 weeks. Characteristically, skin lesions in different stages of evolution coexist (Fig. 120.13A). The papulonodules may leave transient hypopigmented or hyperpigmented macules and occasionally, superficial atrophic (varioliform) scars, or they may disappear without ulceration or sequelae. The number of lesions varies from several to more than one hundred. Lesions may be localized, sometimes clustered within rather well-defined areas, or generalized. The predominant sites of involvement are the trunk and limbs, and very rarely, concurrent intraoral lesions are present. The eruption is generally asymptomatic.

The duration of the disease ranges from several months to more than 40 years. In up to 20% of patients, LyP may be preceded by, associated with, or followed by another type of cutaneous or systemic lymphoma, generally MF or C-ALCL[52]. However, the prognosis is usually excellent. In a study of 504 patients with LyP, only 14 patients (3%) developed a systemic lymphoma, and only five patients (1%) died of systemic disease over a median follow-up period of 120 months[52]. Risk factors for the development of a systemic lymphoma are unknown.

Pathology

The histologic picture of LyP is extremely variable, which in part correlates with the age of the sampled skin lesion (Fig. 120.13B). In addition, several histologic types of LyP have been described (Table 120.6), with LyP type A being the classic and most common type of LyP (>75%)[42]. It should be noted that different types of LyP may occur in different but

LYMPHOMATOID PAPULOSIS (LyP) – HISTOLOGIC SUBTYPES AND THEIR DIFFERENTIAL DIAGNOSES		
LyP type	**Characteristic histologic features**	**Primary differential diagnosis**
Type A	Wedge-shaped infiltrate with scattered or small clusters of large, atypical, sometimes multinucleated or Reed–Sternberg-like, $CD30^+$ T cells The T cells are within an extensive inflammatory infiltrate composed of small lymphocytes, histiocytes, neutrophils, and/or eosinophils Neutrophils may be scattered within the epidermis	C-ALCL Tumor stage MF Hodgkin lymphoma
Type B	Epidermotropic, with a superficial perivascular to band-like and sometimes wedge-shaped infiltrate of small to medium-sized, atypical $CD4^+$, $CD30^+$ T cells	Patch/plaque stage MF
Type C	Diffuse infiltrates or large clusters of large $CD30^+$ T cells, with relatively few admixed inflammatory cells	C-ALCL Transformed MF ($CD30^+$)
Type D	Marked epidermotropism of atypical, small to medium-sized, $CD8^+$, $CD30^+$ pleomorphic T cells Necrotic keratinocytes may be present	Primary cutaneous aggressive epidermotropic $CD8^+$ cytotoxic T cell lymphoma Pityriasis lichenoides et varioliformis acuta
Type E	Prominent angioinvasion and angiodestruction by medium-sized $CD8^+$, $CD30^+$ pleomorphic T cells Vascular occlusion and/or thrombi; hemorrhage, extensive necrosis, and ulceration	Extranodal NK/T cell lymphoma
Type F	Perifollicular infiltrates with variable degree of folliculotropism of atypical $CD30^+$ T cells	Folliculotropic MF
DUSP-IRF4 type*	Extensive epidermotropism by weakly $CD30^+$ small to medium-sized T cells with cerebriform nuclei Strongly $CD30^+$ medium-sized to large blast cells in the dermis	Transformed MF C-ALCL
*Chromosomal rearrangements involving the *DUSP-IRF4* locus on 6p25.3; localized skin lesions in older individuals.		

Table 120.6 Lymphomatoid papulosis (LyP) – histologic subtypes and their differential diagnoses. C-ALCL, cutaneous anaplastic large cell lymphoma; MF, mycosis fungoides. *Adapted from Kempf W. A new era for cutaneous CD30-positive T-cell lymphoproliferative disorders. Semin Diagn Pathol 2017;34:22–35.*

concurrent lesions, and that a single LyP lesion may show histologic features of different subtypes of LyP. Knowledge of the variable histologic presentations of LyP is more important for pathologists than for clinicians as the subtype has no therapeutic or prognostic implications.

Differential diagnosis

LyP is often diagnosed clinically as more common entities. Small recurrent LyP lesions on the trunk are frequently misinterpreted as folliculitis or arthropod bites for years, and notably, $CD30^+$ cells can be observed in many benign conditions, including various viral infections, arthropod bite reactions, scabies, atopic dermatitis, and drug reactions[45]. On the other hand, because of the presence of multifocal skin lesions with the histologic features of CD30-positive CTCL, LyP patients are regularly treated unnecessarily with multi-agent chemotherapy by physicians not familiar with this condition. Obviously, when the clinical features are taken into account, differentiation between LyP and the malignant lymphomas it may resemble histologically is not difficult.

Because of the clinical similarities between LyP and pityriasis lichenoides, a relationship between the two conditions was initially suggested. More recently, clonal T cell populations have been demonstrated in skin biopsies of both conditions. However, pityriasis lichenoides occurs more often in younger patients, is often relatively short-lived, does not develop nodular lesions, and rarely, if ever, progresses to a lymphoma. Histologically, the diseases are usually easily distinguished, and CD30-positive blast cells are generally not seen in pityriasis lichenoides, but in rare cases differentiation may be challenging[45] (see Ch. 9).

Treatment

The treatment of patients with LyP is unsatisfactory[51]. Topical or systemic corticosteroids and antibiotics are not effective. Aggressive treatment modalities such as systemic chemotherapy or TSEB irradiation may produce complete remissions, but after discontinuation of therapy, the LyP lesions generally reappear within weeks or months, and the disease follows its natural course. Since a curative therapy is not available and none of the available treatment modalities affects the natural course of the disease, the short-term benefits of active treatment should be balanced carefully against potential side effects[42,51].

In patients with relatively few non-scarring lesions, expectant management is reasonable. When there are cosmetically disturbing lesions (e.g. scarring or many papulonodules), low-dose oral methotrexate (5–20 mg/week) is the most effective therapy for reducing the number of skin lesions. PUVA therapy is also effective, but is less attractive if maintenance treatment is required. When larger skin tumors develop in the course of LyP, they can be observed for a period of 4 to 12 weeks for the possibility of spontaneous remission. If spontaneous resolution does not occur, such lesions can be excised or treated with radiotherapy. Because of the potential risk for developing a systemic lymphoma, long-term follow-up is required in all patients with LyP.

COMPARISON OF SUBCUTANEOUS PANNICULITIS-LIKE T CELL LYMPHOMA AND PRIMARY CUTANEOUS GAMMA/DELTA T CELL LYMPHOMA WITH SUBCUTANEOUS INVOLVEMENT		
	SPTCL	**PCGD-TCL with subcutaneous involvement**
Phenotype	α/β T cell phenotype	γ/δ T cell phenotype
T cell receptor	$\beta F1^+$, $TCR\gamma/\delta1^-$	$\beta F1^-$, $TCR\gamma/\delta1^+$
T cell phenotype	$CD3^+$, $CD4^-$, $CD8^+$	$CD3^+$, $CD4^-$, $CD8^-$
Coexpression of CD56	Absent	Common
Architecture	Subcutaneous	Subcutaneous and epidermal/dermal
Clinical features	Nodules and plaques Rarely ulceration	Nodules and plaques Ulceration common
Hemophagocytic lymphohistiocytosis (HLH)*	Uncommon	Common
Survival (5-year)	>80%	<10%
Treatment	Systemic corticosteroids	Systemic chemotherapy
*Presence significantly decreases 5-year survival rate.		

Table 120.7 Comparison of subcutaneous panniculitis-like T cell lymphoma (SPTCL) and primary cutaneous gamma/delta T cell lymphoma (PCGD-TCL) with subcutaneous involvement[53]. Hemophagocytic lymphohistiocytosis has also been referred to as hemophagocytic syndrome. βF1, positivity reflects α/β T cell origin; TCR, T cell receptor.

SUBCUTANEOUS PANNICULITIS-LIKE T CELL LYMPHOMA

Definition

Subcutaneous panniculitis-like T cell lymphoma (SPTCL) is a cytotoxic T cell lymphoma composed of α/β TCR-positive T cells that preferentially infiltrate subcutaneous tissue[1,3]. In past classifications, cases with subcutaneous involvement and a γ/δ T cell phenotype were included in this group. However, patients with a γ/δ T cell phenotype have different clinicopathologic features and usually a much more aggressive clinical course compared to those with an α/β T cell phenotype. Therefore, the

former were reclassified as having primary cutaneous gamma/delta T cell lymphoma (PCGD-TCL) (Table 120.7).

Epidemiology

SPTCL is a rare condition, accounting for <1% of all CTCL. It may occur in adults as well as in young children, and both sexes are equally affected.

Clinical Features

Patients generally present with a solitary or multiple nodules or deeply seated plaques with a diameter varying from 1 to 20 cm. The skin lesions involve primarily the extremities and the trunk and less commonly the face; when the nodules and plaques resolve, they may be replaced by areas of lipoatrophy (Fig. 120.14A). Ulceration is uncommon. Systemic symptoms such as fever, fatigue, and weight loss may be present in over half of the patients. Laboratory abnormalities including cytopenias and elevated liver function tests are common, but a frank hemophagocytic lymphohistiocytosis (HLH) is observed in only ~15% of patients[53]. Dissemination to extracutaneous sites is rare and while hepatosplenomegaly may be seen, it is generally not due to lymphomatous involvement.

SPTCL may be preceded for years or decades by a seemingly benign panniculitis. Up to 20% of patients have an associated autoimmune disease, most commonly systemic lupus erythematosus. Recent studies have suggested overlapping features between SPTCL and lupus profundus[54]. SPTCL has a favorable prognosis with a 5-year overall survival of ~80%[53]. However, the presence of HLH is associated with a more unfavorable prognosis.

Pathology

Subcutaneous infiltrates simulating a lobular panniculitis are seen in SPTCL. Small, medium-sized, or sometimes large pleomorphic T cells with hyperchromatic nuclei are present and are often admixed with many macrophages. The overlying epidermis and dermis are typically uninvolved. Rimming of individual fat cells by neoplastic T cells is a helpful, although not entirely specific, diagnostic feature (Fig. 120.14B). Necrosis, karyorrhexis, and cytophagocytosis are common findings. In contrast to lupus panniculitis, clusters of B cells, plasma cells, and plasmacytoid dendritic cells are not present.

Immunophenotype

These lymphomas have a TCRα/β$^+$, CD3$^+$, CD4$^-$, CD8$^+$ T cell phenotype, with expression of cytotoxic proteins. The neoplastic T cells express βF1, but are negative for TCRγ/δ and CD56, facilitating differentiation from PCGD-TCL with subcutaneous involvement and panniculitis-like lesions (see Table 120.7). CD30 is rarely, if ever, expressed.

Genetic Features

Recently, germline mutations in *HAVCR2* that lead to loss-of-function of TIM3 (T cell immunoglobulin mucin 3) were reported in 60%–85% of SPTCL patients[55]. TIM3 deficiency can lead to activation of macrophages and T cells, and patients can develop HLH.

Treatment

While doxorubicin-based chemotherapy has traditionally been used, more conservative immunosuppressive regimens (e.g. prednisone, cyclosporine, methotrexate) are often effective and should be considered as first-line therapy in patients with SPTCL without associated HLH. In patients presenting with a solitary lesion, local radiotherapy may be effective[25,53]. Ruxolitinib has been reported to successfully treat HLH in patients with germline mutations in *HAVCR2*.

EXTRANODAL NK/T CELL LYMPHOMA, NASAL TYPE

Extranodal NK/T cell lymphoma, nasal type is an EBV-positive lymphoma with an NK cell, or more rarely a cytotoxic T cell, phenotype and aggressive clinical behavior. It occurs more commonly in Asia and Central and South America and is very rare in Western countries[1,3]. The skin is the second most common site of involvement after the nasal cavity/nasopharynx, and some patients have only cutaneous lesions[56].

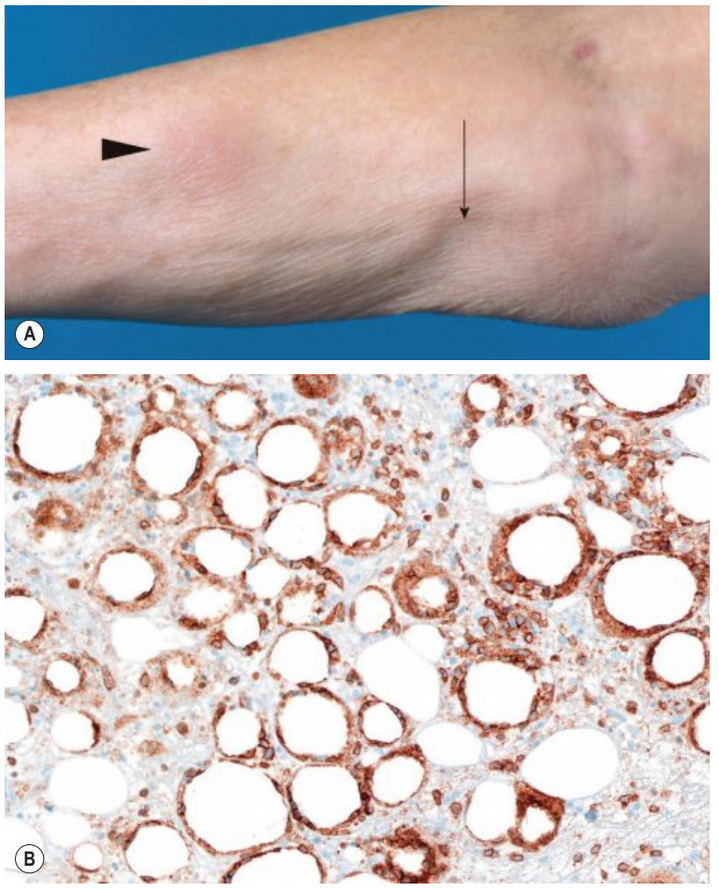


Fig. 120.14 Subcutaneous panniculitis-like T cell lymphoma (SPTCL). A Pink nodular skin lesions (arrowhead) as well as an area of lipoatrophy (arrow) at the site of a resolved nodule. **B** Subcutaneous infiltration with rimming of CD8-positive neoplastic T cells around adipocytes.

This lymphoma affects primarily adults, with a predominance of men. The typical presentation is multiple plaques or tumors on the trunk and extremities or, in the case of nasal NK/T cell lymphoma, a midfacial destructive tumor (Fig. 120.15). Of note, the latter was previously referred to as lethal midline granuloma. Ulceration is common.

Histologically, there are dense infiltrates involving the dermis and often the subcutis. Prominent angiocentricity and angiodestruction are often accompanied by extensive necrosis. Cell size ranges from small to large, but most cases consist of medium-sized cells with irregular or oval nuclei, moderately dense chromatin, and pale cytoplasm. In some cases, a heavy inflammatory infiltrate of small lymphocytes, histiocytes, plasma cells, and eosinophils can be seen. The TCR usually has a germline configuration, but can be clonally rearranged in the rare T cell-derived cases. The neoplastic cells express CD2, CD56, cytoplasmic CD3ε, and cytotoxic proteins (TIA-1, granzyme B, perforin), but they lack surface CD3. Detection of EBV by *in situ* hybridization and expression of cytotoxic proteins is required for diagnosis.

These lymphomas have an aggressive clinical behavior and are often resistant to chemotherapy. Combined modality treatment including L-asparaginase (the SMILE regimen) is the preferred mode of treatment[57]. In rare cases with small solitary lesions, radiotherapy alone can be considered[25,58].

Hydroa Vacciniforme-Like Lymphoproliferative Disorder

The updated WHO-EORTC classification contains a new section entitled chronic active EBV infection. It includes hydroa vacciniforme-like lymphoproliferative disorder (HV-like LPD) and hypersensitivity reactions to mosquito bites[1,3]. HV-like LPD is used as an encompassing term for cases previously referred to as HV, intermediate forms, and HV-like T cell lymphoma; however, there is some controversy regarding the relationship between the two ends of this spectrum[59].



Fig. 120.15 Extranodal NK/T cell lymphoma, nasal type. A Ulcerated plaques and papulonodules. **B** Ulceration of the hard palate. *Courtesy Luis Requena, MD.*

These disorders occur primarily in children and adolescents from Asia or in indigenous populations from Latin America. Clinically, classic HV presents with a papulovesicular eruption in sun-exposed sites, in particular the face, earlobes, and dorsal hands (see Fig. 87.9). There is often seasonal activity, but no systemic symptoms. In more severe cases, there is involvement of both sun-exposed and non-sun-exposed areas as well as facial swelling (see Fig. 87.10). Extensive ulceration is common and systemic symptoms such as fever, wasting, lymphadenopathy, and hepatosplenomegaly may be present. The clinical course is variable and patients may have recurrent skin lesions for many years before progression to systemic lymphoma.

PRIMARY CUTANEOUS AGGRESSIVE EPIDERMOTROPIC CD8-POSITIVE CYTOTOXIC T CELL LYMPHOMA

These tumors are characterized by a proliferation of epidermotropic CD8-positive cytotoxic T cells and an aggressive clinical behavior[60,61]. Differentiation from other types of CTCL expressing a CD8-positive cytotoxic T cell phenotype, including primary cutaneous acral CD8-positive T cell lymphoproliferative disorder, pagetoid reticulosis, and rare cases of MF, LyP, and C-ALCL, is based on the clinical presentation and clinical behavior. In the latter conditions, no differences in clinical presentation or prognosis are observed between $CD4^+$ and $CD8^+$ cases.

Clinically, these lymphomas are characterized by the presence of localized or disseminated eruptive papules, nodules, and tumors with central ulceration and necrosis *or* by superficial, hyperkeratotic patches and plaques (Fig. 120.16). They may disseminate to other visceral sites (lung, testis, central nervous system, oral mucosa), but lymph nodes are often spared. The median survival is 12 months, but some patients have a prodromal phase of chronic patches prior to the development of aggressive ulcerative lesions[62].

Histologically, these lymphomas show strongly epidermotropic, band-like to diffuse infiltrates of small, medium-sized, or large pleomorphic T cells with a $CD3^+$, $CD4^-$, $CD8^+$, $CD7^{-/+}$, $CD45RA^+$, granzyme B^+, perforin$^+$, TIA-1^+ phenotype[57,61]. The epidermis may be acanthotic or atrophic, and there may be necrotic keratinocytes, ulceration and variable spongiosis, sometimes with blister formation. Invasion and destruction of cutaneous adnexal structures are commonly seen. Angiocentricity and angioinvasion may be present.

These lymphomas run an aggressive clinical course and their response to systemic chemotherapy is often short-lived. Allogeneic HSCT should be considered in selected patients[62].



Fig. 120.16 Primary cutaneous aggressive epidermotropic CD8-positive cytotoxic T cell lymphoma. Generalized skin tumors with central ulceration. Previously, such cases were designated as disseminated pagetoid reticulosis (Ketron–Goodman type).

PRIMARY CUTANEOUS ACRAL CD8-POSITIVE T CELL LYMPHOPROLIFERATIVE DISORDER

In the 2018 updated WHO-EORTC classification, primary cutaneous acral CD8-positive T cell lymphoma was included as a provisional entity characterized by a diffuse infiltrate of clonal atypical medium-sized $CD8^+$ cytotoxic T cells. Although the histologic features suggest an aggressive lymphoma, there is usually a solitary skin lesion in an acral location that has an indolent clinical behavior[1,3,63]. As a result, in the 5th edition of the WHO Classification of Haematolymphoid Tumours, this condition has been reclassified as primary cutaneous acral CD8-positive T cell lymphoproliferative disorder[3a].

Patients typically present with a solitary, slowly enlarging papule or nodule. The most common site is the ear, but papulonodules can develop in other acral sites including the nose and the foot[63,64].

Histologically, there is a diffuse proliferation of monomorphic medium-sized atypical T cells throughout the dermis, often extending into the subcutaneous fat. The epidermis is generally spared and separated from the dermal infiltrate by a clear grenz zone. The atypical cells have a $CD3^+$, $CD4^-$, $CD8^+$, $CD30^-$ T cell phenotype with variable loss of T cell antigens (CD2, CD5, CD7). They are also positive for TIA-1, but unlike other types of $CD8^+$ CTCL, are negative for other cytotoxic proteins (granzyme B, perforin). Positive CD68 staining often has a Golgi dot-like pattern. In almost all cases, the proliferation rate as assessed by Ki-67 is very low (<10%).

The prognosis is excellent and in typical cases staging is not recommended. Surgical excision and radiotherapy represent treatment options. Cutaneous relapses may occur, but dissemination to extracutaneous sites is exceptional[65].

PRIMARY CUTANEOUS GAMMA/DELTA T CELL LYMPHOMA

Primary cutaneous gamma/delta T cell lymphoma (PCGD-TCL) is a lymphoma composed of a clonal proliferation of mature, activated gamma/delta T cells with a cytotoxic phenotype. This group includes cases previously known as SPTCL with a gamma/delta T cell phenotype. PCGD-TCL should be differentiated from SPTCL, other types of aggressive cytotoxic cutaneous T/NK cell lymphomas, and tumor stage MF, but this may prove extremely difficult and requires integration of clinical, histologic, phenotypic, and molecular genetic data (see Tables 120.2 and 120.7). It should be noted that TCRγ/δ expression is not only found in PCGD-TCL, but has also been reported in other types of CTCL, including rare cases of otherwise classic MF and LyP[22,23].

PCGD-TCL generally presents with disseminated plaques and/or ulceronecrotic nodules or tumors, particularly on the extremities, but other sites may be affected[53,66] (Fig. 120.17). Involvement of mucosal and other extranodal sites is frequently observed, but involvement of lymph nodes, spleen, or bone marrow is uncommon. In patients with panniculitis-like tumors, HLH may occur.

Histologically, three major patterns of involvement can be seen: epidermotropic, dermal, and/or subcutaneous. The epidermal pattern can vary from mild epidermotropism to a marked pagetoid reticulosis-like infiltrate. Rimming of fat cells may be observed when there is subcutaneous involvement, similar to SPTCL. Angiocentricity and angiodestruction are commonly seen. The neoplastic cells are generally medium to large in size with coarsely clumped chromatin, and they have a $TCR\gamma/\delta^+$, $TCR\alpha/\beta$ $(\beta F1)^-$, $CD3^+$, $CD2^+$, $CD4^-$, $CD5^-$, $CD7^{+/-}$, $CD8^-$, $CD56^+$ phenotype with strong expression of cytotoxic proteins.

Most patients have aggressive, often rapidly fatal disease, which is resistant to multi-agent chemotherapy. Patients with subcutaneous fat involvement may have a worse prognosis in comparison to patients with epidermal or dermal disease only[66]. There are, however, reports of patients with an indolent clinical course[67].

PRIMARY CUTANEOUS CD4-POSITIVE SMALL/MEDIUM T CELL LYMPHOPROLIFERATIVE DISORDER

In the 2005 WHO-EORTC classification, primary cutaneous CD4-positive small/medium T cell *lymphoma* was included as a provisional entity characterized by a solitary skin lesion (without prior or concurrent patches or plaques typical of MF) and a predominance of small to medium-sized $CD4^+$ pleomorphic T cells histologically. These cases also had the same benign clinical course as well as clinical, histopathologic, and immunophenotypic features as the entity previously referred to as *nodular cutaneous pseudo-T cell lymphoma*. Therefore, it is highly uncertain if these lesions represent a frank malignancy[68,69]. As a result, in the 2018 WHO-EORTC classification, the term "primary cutaneous CD4-positive small/medium T cell *lymphoproliferative disorder*" rather than lymphoma was assigned[1,3].

Characteristically, patients present with a solitary plaque or tumor, generally on the face, the neck, or the upper trunk[68,69]. Histologically, lesions show dense, diffuse, or nodular infiltrates within the dermis with a tendency to infiltrate the subcutis. Epidermotropism may be present focally. There is a predominance of small/medium-sized $CD3^+$, $CD4^+$, $CD8^-$, $CD30^-$ pleomorphic T cells. A small proportion (<30%) of large pleomorphic cells may be present. A variable proportion of atypical $CD4^+$ T cells, either scattered or forming small clusters, consistently express follicular helper T cell markers – programmed death-1 (PD-1; CD279), ICOS, BCL6, and CXCL13[69,70]. The proliferation rate as assessed by Ki-67 is generally low. Almost all cases show a considerable admixture with reactive $CD8^+$ T cells, $CD20^+$ B cells, plasma cells, and histiocytes, including multinucleated giant cells.

Patients have an excellent prognosis and in typical cases staging procedures are not required. Skin lesions that don't resolve spontaneously after skin biopsy should be treated. First-line therapies are intralesional corticosteroids and surgical excision; only by exception is radiotherapy used[68,69].

Rare patients who present with generalized skin lesions, large and rapidly growing tumors, >30% large pleomorphic T cells, and/or a high proliferative fraction do not belong in this category[71]. Such cases usually have a more aggressive clinical course and should be classified as primary cutaneous peripheral T cell lymphoma, NOS (see below).

PRIMARY CUTANEOUS PERIPHERAL T CELL LYMPHOMA, NOS

The designation "primary cutaneous peripheral T cell lymphoma (PTCL), NOS (not otherwise specified)" is used for CTCLs that do not fit into any of the better-defined subtypes outlined in Table 120.1. It is therefore a diagnosis of exclusion. Clinically, these patients present with solitary or localized, but more frequently generalized, nodules or tumors[72] (Fig. 120.18).



Fig. 120.17 Primary cutaneous gamma/delta T cell lymphoma. Multiple plaques and nodules of the upper inner arm, several of which are ulcerated. *Courtesy Jake Wang, MD.*



Fig. 120.18 Primary cutaneous peripheral T cell lymphoma, NOS. Rapidly growing nodules and tumors. Note: the skin lesions in the left upper corner do not represent patches, but rather deep plaques present for 2 weeks.

Histologically, there are nodular or diffuse infiltrates with variable numbers of medium-sized to large pleomorphic or immunoblast-like T cells. Epidermotropism is generally mild or absent. Most cases have an aberrant $CD4^+$ T cell phenotype with variable loss of pan-T cell antigens. CD30 staining is negative or restricted to a few scattered tumor cells. Rare cases may show coexpression of CD56.

Patients should be treated with systemic chemotherapy, but the prognosis is generally poor, with a 5-year survival of <20%[72]. Enrollment in clinical trials, including with JAK1-specifiic inhibitors, should also be considered.

Additional figures available in our eBook (see inside front cover for access code).

REFERENCES

1. Willemze R, Cerroni L, Kempf W, et al. The 2018 update of the WHO-EORTC classification for primary cutaneous lymphomas. *Blood*. 2019;133:1703–1714.
2. Willemze R, Kerl H, Sterry W, et al. EORTC classification for primary cutaneous lymphomas: a proposal from the Cutaneous Lymphoma Study Group of the European Organization for Research and Treatment of Cancer. *Blood*. 1997;90:354–371.
3. Swerdlow SH, Campo E, Harris NL, et al. *World Health Organization Classification of Tumours of Hematopoietic and Lymphoid Tissue*. Revised 4th edition. Lyon: IARC Press; 2017.

3a. Alaggio R, Amador C, Anagnostopoulos I, et al. The 5th edition of the World Health Organization Classification of Haematolymphoid Tumours: Lymphoid Neoplasms. *Leukemia*. 2022;36:1720-1748.

3b. Campo E, Jaffe ES, Cook JR, et al. The International Consensus Classification of Mature Lymphoid Neoplasms: a report from the Clinical Advisory Committee. *Blood*. 2022;140:1229-1253.

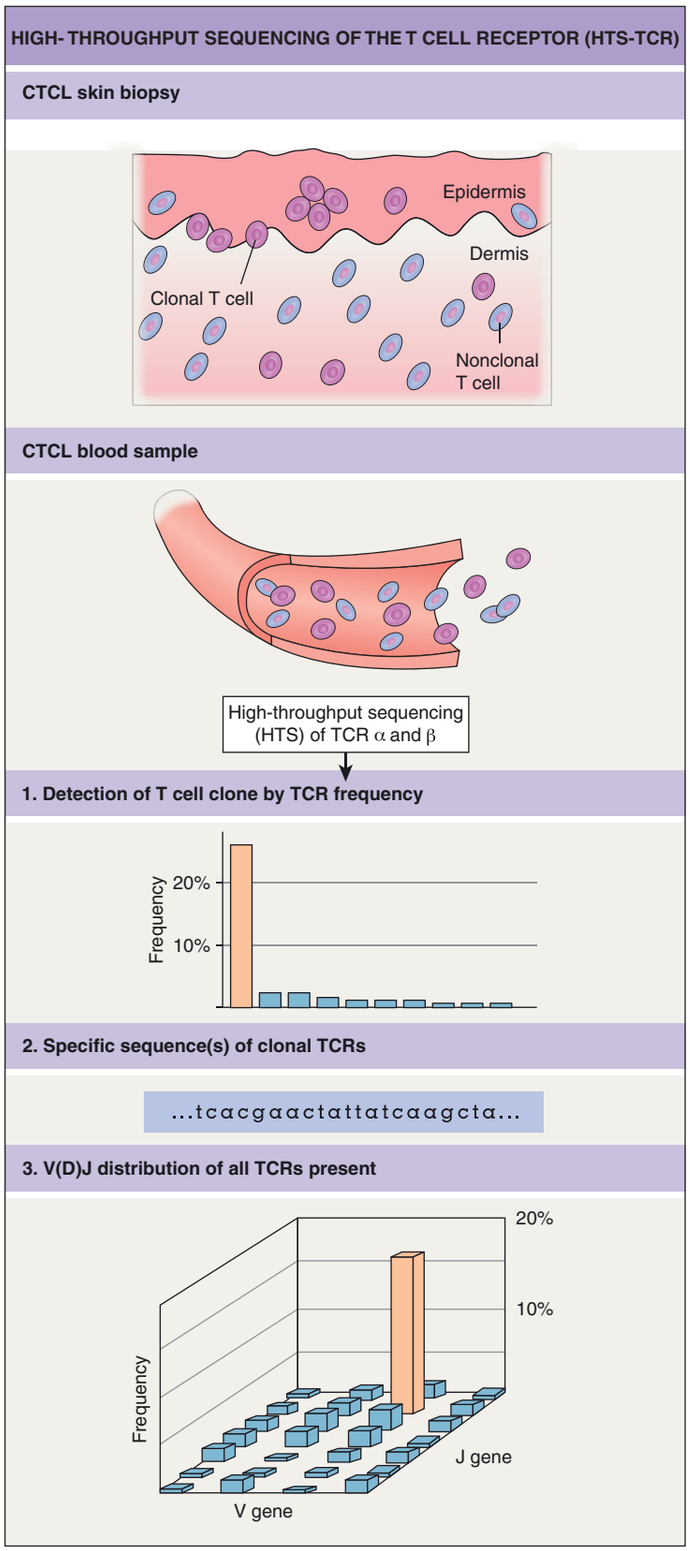
4. Pimpinelli N, Olsen EA, Santucci M, et al. Defining early mycosis fungoides. *J Am Acad Dermatol*. 2005;53:1053–1063.
5. Walia R, Yeung CCS. An update on molecular biology of cutaneous T cell lymphoma. *Front Oncol*. 2020;9:1558.
6. Kirsch IR, Watanabe R, O'Malley JT, et al. TCR sequencing facilitates diagnosis and identifies mature T cells as the cell of origin of CTCL. *Sci Transl Med*. 2015;7308ra158.
7. de Masson A, O'Malley JT, Elco CP, et al. High-throughput sequencing of the T cell receptor β gene identifies aggressive early-stage mycosis fungoides. *Sci Transl Med*. 2018;100eaar5894.
8. Olsen E, Vonderheid E, Pimpinelli N, et al. Revisions to the staging and classification of mycosis fungoides and Sezary syndrome: a proposal of the International Society for Cutaneous Lymphomas (ISCL) and the cutaneous lymphoma task force of the European Organization of Research and Treatment of Cancer (EORTC). *Blood*. 2007;110:1713–1722.
9. Kim YH, Willemze R, Pimpinelli N, et al. TNM classification system for primary cutaneous lymphomas other than mycosis fungoides and Sezary syndrome: a proposal of the International Society for Cutaneous Lymphomas (ISCL) and the Cutaneous Lymphoma Task Force of the European Organization of Research and Treatment of Cancer (EORTC). *Blood*. 2007;110:479–484.
10. Korgavkar K, Xiong M, Weinstock M. Changing incidence trends of cutaneous T-cell lymphoma. *JAMA Dermatol*. 2013;149:1295–1299.
11. Zhang Y, Wang Y, Yu R, et al. Molecular markers of early-stage mycosis fungoides. *J Invest Dermatol*. 2012;132:1698–1706.
12. Choi J, Goh G, Walradt T, et al. Genomic landscape of cutaneous T cell lymphoma. *Nat Genet*. 2015;47:1011–1019.
13. Bastidas Torres AN, Cats D, Mei H, et al. Genomic analysis reveals recurrent deletion of JAK-STAT signaling inhibitors HNRNPK and SOCS1 in mycosis fungoides. *Genes Chromosomes Cancer*. 2018;57:653–664.
14. Lindahl LM, Willerslev-Olsen A, Gjerdrum LMR, et al. Antibiotics inhibit tumor and disease activity in cutaneous T-cell lymphoma. *Blood*. 2019;134:1072–1083.
15. Blümel E, Munir Ahmad S, Nastasi C, et al. *Staphylococcus aureus* alpha-toxin inhibits CD8+ T cell-mediated killing of cancer cells in cutaneous T-cell lymphoma. *Oncoimmunology*. 2020;9:1751561.
16. Aschebrook-Kilfoy B, Cocco P, La VC, et al. Medical history, lifestyle, family history, and occupational risk factors for mycosis fungoides and Sézary syndrome: the InterLymph Non-Hodgkin Lymphoma Subtypes Project. *J Natl Cancer Inst Monogr*. 2014;2014:98–105.
17. Vermeer MH, van Doorn R, Dukers D, et al. CD8+ T cells in cutaneous T-cell lymphoma: expression of cytotoxic proteins, Fas Ligand, and killing inhibitory receptors and their relationship with clinical behavior. *J Clin Oncol*. 2001;19:4322–4329.
18. Stutz N, Johnson RD, Wood GS. The Fas apoptotic pathway in cutaneous T-cell lymphomas: frequent expression of phenotypes associated with resistance to apoptosis. *J Am Acad Dermatol*. 2012;671327.e1–10.
19. Kim EJ, Hess S, Richardson SK, et al. Immunopathogenesis and therapy of cutaneous T cell lymphoma. *J Clin Invest*. 2005;115:798–812.
20. Agar NS, Wedgeworth E, Crichton S, et al. Survival outcomes and prognostic factors in mycosis fungoides/Sezary syndrome: validation of the revised International Society for Cutaneous Lymphomas/European Organisation for Research and Treatment of Cancer staging proposal. *J Clin Oncol*. 2010;28:4730–4739.
21. Benner MF, Jansen PM, Vermeer MH, Willemze R. Prognostic factors in transformed mycosis fungoides: a retrospective analysis of 100 cases. *Blood*. 2012;119:1643–1649.
22. Massone C, Crisman G, Kerl H, Cerroni L. The prognosis of early mycosis fungoides is not influenced by phenotype and T-cell clonality. *Br J Dermatol*. 2008;159:881–886.
23. Rodriguez-Pinilla SM, Ortiz-Romero PL, Monsalvez V, et al. TCR-gamma expression in primary cutaneous T-cell lymphomas. *Am J Surg Pathol*. 2013;37:375–384.
24. Trautinger F, Eder J, Assaf C, et al. EORTC consensus recommendations for the treatment of mycosis fungoides/Sezary syndrome – Update 2017. *Eur J Cancer*. 2017;77:57–74.
25. Willemze R, Hodak E, Zinzani PL, Specht L, Ladetto M. Primary cutaneous lymphomas: ESMO Clinical Practice Guidelines for diagnosis, treatment and follow-up. *Ann Oncol*. 2018;29:iv30–iv40.
26. Prince HM, Kim YH, Horwitz SM, et al. Brentuximab vedotin or physician's choice in CD30-positive cutaneous T-cell lymphoma (ALCANZA): an international, open-label, randomised, phase 3, multicentre trial. *Lancet*. 2017;390:555–566.
27. Iqbal M, Reljic T, Ayala E, et al. Efficacy of allogeneic hematopoietic cell transplantation in cutaneous T cell lymphoma: results of a systematic review and meta-analysis. *Biol Blood Marrow Transplant*. 2020;26:76–82.
28. van Santen S, Roach RE, van Doorn R, et al. Clinical staging and prognostic factors in folliculotropic mycosis fungoides. *JAMA Dermatol*. 2016;152:992–1000.
29. Hodak E, Amitay-Laish I, Atzmony L, et al. New insights into folliculotropic mycosis fungoides (FMF): a single-center experience. *J Am Acad Dermatol*. 2016;75:347–355.
30. Gerami P, Guitart J. The spectrum of histopathologic and immunohistochemical findings in folliculotropic mycosis fungoides. *Am J Surg Pathol*. 2007;31:1430–1438.
31. van Santen S, van Doorn R, Neelis KJ, et al. Recommendations for treatment in folliculotropic mycosis fungoides: report of the Dutch Cutaneous Lymphoma Group. *Br J Dermatol*. 2017;177:223–228.
32. Haghighi B, Smoller BR, LeBoit PE, et al. Pagetoid reticulosis (Woringer-Kolopp disease): an immunophenotypic, molecular, and clinicopathologic study. *Mod Pathol*. 2000;13:502–510.
33. Kempf W, Ostheeren-Michaelis S, Paulli M, et al. Granulomatous mycosis fungoides and granulomatous slack skin: a multicenter study of the Cutaneous Lymphoma Histopathology Task Force Group of the European Organization for Research and Treatment of Cancer (EORTC). *Arch Dermatol*. 2008;144:1609–1617.
34. van Doorn R, van Kester MS, Dijkman R, et al. Oncogenomic analysis of mycosis fungoides reveals major differences with Sezary syndrome. *Blood*. 2009;113:127–136.
35. Campbell JJ, Clark RA, Watanabe R, Kupper TS. Sezary syndrome and mycosis fungoides arise from distinct T-cell subsets: a biologic rationale for their distinct clinical behaviors. *Blood*. 2010;116:767–771.
36. Nicolay JP, Felcht M, Schledzewski K, et al. Sézary syndrome: old enigmas, new targets. *J Dtsch Dermatol Ges*. 2016;14:256–264.
37. Buus TB, Willerslev-Olsen A, Fredholm S, et al. Single-cell heterogeneity in Sézary syndrome. *Blood Adv*. 2018;2:2115–2126.
38. Chevret E, Merlio JP. Sézary syndrome: translating genetic diversity into personalized medicine. *J Invest Dermatol*. 2016;136:1319–1324.
39. Kim YH, Bagot M, Pinter-Brown L, et al. Mogamulizumab versus vorinostat in previously treated cutaneous T-cell lymphoma (MAVORIC): an international, open-label, randomised, controlled phase 3 trial. *Lancet Oncol*. 2018;19:1192–1204.

39a. Hirotsu KE, Neal TM, Khodadoust MS, et al. Clinical characterization of mogamulizumab-associated rash during treatment of mycosis fungoides or Sézary syndrome. *JAMA Dermatol*. 2021;157:700–707.

39b. Musiek ACM, Rieger KE, Bagot M, et al. Dermatologic events associated with the anti-CCR4 antibody mogamulizumab: characterization and management. *Dermatol Ther (Heidelb)*. 2022;12:29–40.

40. Tokura Y, Sawada Y, Shimauchi T. Skin manifestations of adult T-cell leukemia/lymphoma: clinical, cytological and immunological features. *J Dermatol*. 2014;41:19–25.
41. Cook LB, Fuji S, Hermine O, et al. Revised Adult T-Cell Leukemia-Lymphoma International Consensus Meeting Report. *J Clin Oncol*. 2019;37:677–687.
42. Bekkenk MW, Geelen FA, van Voorst Vader PC, et al. Primary and secondary cutaneous CD30(+) lymphoproliferative disorders: a report from the Dutch Cutaneous Lymphoma Group on the long-term follow-up data of 219 patients and guidelines for diagnosis and treatment. *Blood*. 2000;95:3653–3661.
43. Benner MF, Willemze R. Applicability and prognostic value of the new TNM classification system in 135 patients with primary cutaneous anaplastic large cell lymphoma. *Arch Dermatol*. 2009;145:1399–1404.
44. Fernández-de-Misa R, Hernández-Machín B, Combalía A, et al. Prognostic factors in patients with primary cutaneous anaplastic large cell lymphoma: a multicentric, retrospective analysis of the Spanish Group of Cutaneous Lymphoma. *J Eur Acad Dermatol Venereol*. 2020;34:762–768.
45. Kempf W. A new era for cutaneous CD30-positive T-cell lymphoproliferative disorders. *Semin Diagn Pathol*. 2017;34:22–35.
46. Oschlies I, Lisfeld J, Lamant L, et al. ALK-positive anaplastic large cell lymphoma limited to the skin: clinical, histopathological and molecular analysis of 6 pediatric cases. A report from the ALCL99 study. *Haematologica*. 2013;98:50–56.
47. Melchers RC, Willemze R, van de Loo M, et al. Clinical, histologic, and molecular characteristics of anaplastic lymphoma kinase-positive primary cutaneous anaplastic large cell lymphoma. *Am J Surg Pathol*. 2020;44:776–781.
48. Wada DA, Law ME, Hsi ED, et al. Specificity of IRF4 translocations for primary cutaneous anaplastic large cell lymphoma: a multicenter study of 204 skin biopsies. *Mod Pathol*. 2011;24:596–605.
49. Prieto-Torres L, Rodriguez-Pinilla SM, Onaindia A, et al. CD30-positive primary cutaneous lymphoproliferative disorders: molecular alterations and targeted therapies. *Haematologica*. 2019;104:226–235.
50. van Kester MS, Tensen CP, Vermeer MH, et al. Cutaneous anaplastic large cell lymphoma and peripheral T-cell lymphoma NOS show distinct chromosomal alterations and differential expression of chemokine receptors and apoptosis regulators. *J Invest Dermatol*. 2010;130:563–575.
51. Kempf W, Pfaltz K, Vermeer MH, et al. EORTC, ISCL, and USCLC consensus recommendations for the treatment of primary cutaneous CD30-positive lymphoproliferative disorders: lymphomatoid papulosis and primary cutaneous anaplastic large-cell lymphoma. *Blood*. 2011;118:4024–4035.
52. Melchers RC, Willemze R, Bekkenk MW, et al. Frequency and prognosis of associated malignancies in 504 patients with lymphomatoid papulosis. *J Eur Acad Dermatol Venereol*. 2020;34:260–266.
53. Willemze R, Jansen PM, Cerroni L, et al. Subcutaneous panniculitis-like T-cell lymphoma: definition, classification, and prognostic factors: an EORTC Cutaneous Lymphoma Group Study of 83 cases. *Blood*. 2008;111:838–845.

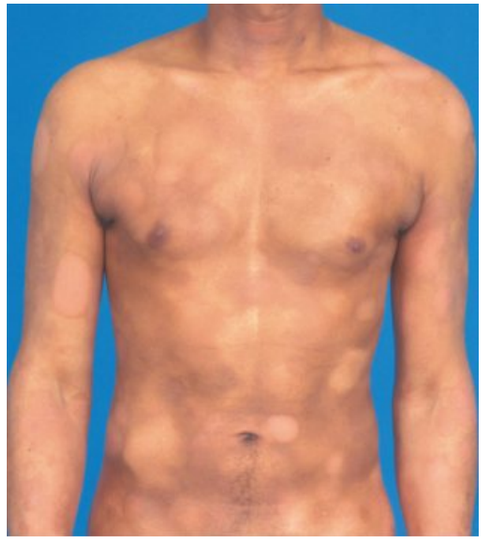
54. Bosisio F, Boi S, Caputo V, et al. Lobular panniculitic infiltrates with overlapping histopathologic features of lupus panniculitis (lupus profundus) and subcutaneous T-cell lymphoma: a conceptual and practical dilemma. *Am J Surg Pathol*. 2015;39:206–211.
55. Gayden T, Sepulveda FE, Khuong-Quang DA, et al. Germline HAVCR2 mutations altering TIM-3 characterize subcutaneous panniculitis-like T cell lymphomas with hemophagocytic lymphohistiocytic syndrome. *Nat Genet*. 2018;50:1650–1657. Erratum in: Nat Genet 2019;51:196.
56. Geller S, Myskowski PL, Pulitzer M. NK/T-cell lymphoma, nasal type, γδ T-cell lymphoma, and CD8-positive epidermotropic T-cell lymphoma-clinical and histopathologic features, differential diagnosis, and treatment. *Semin Cutan Med Surg*. 2018;37:30–38.
57. Yamaguchi M, Kwong YL, Kim WS, et al. Phase II study of SMILE chemotherapy for newly diagnosed stage IV, relapsed, or refractory extranodal natural killer (NK)/T-cell lymphoma, nasal type: the NK-Cell Tumor Study Group study. *J Clin Oncol*. 2011;29:4410–4416.
58. Li YX, Yao B, Jin J, et al. Radiotherapy as primary treatment for stage IE and IIE nasal natural killer/T-cell lymphoma. *J Clin Oncol*. 2006;24:181–189.
59. Gru AA, Jaffe ES. Cutaneous EBV-related lymphoproliferative disorders. *Semin Diagn Pathol*. 2017;34:60–75.
60. Berti E, Tomasini D, Vermeer MH, et al. Primary cutaneous CD8-positive epidermotropic cytotoxic T cell lymphomas. A distinct clinicopathological entity with an aggressive clinical behavior. *Am J Pathol*. 1999;155:483–492.
61. Robson A, Assaf C, Bagot M, et al. Aggressive epidermotropic cutaneous CD8+ lymphoma: a cutaneous lymphoma with distinct clinical and pathological features. Report of an EORTC Cutaneous Lymphoma Task Force Workshop. *Histopathology*. 2015;67:425–441.
62. Guitart J, Martinez-Escala ME, Subtil A, et al. Primary cutaneous aggressive epidermotropic cytotoxic T-cell lymphomas: reappraisal of a provisional entity in the 2016 WHO classification of cutaneous lymphomas. *Mod Pathol*. 2017;30:761–772.
63. Petrella T, Maubec E, Cornillet-Lefebvre P, et al. Indolent CD8-positive lymphoid proliferation of the ear: a distinct primary cutaneous T-cell lymphoma? *Am J Surg Pathol*. 2007;31:1887–1892.
64. Greenblatt D, Ally M, Child F, et al. Indolent CD8(+) lymphoid proliferation of acral sites: a clinicopathologic study of six patients with some atypical features. *J Cutan Pathol*. 2013;40:248–258.
65. Alberti-Violetti S, Fanoni D, Provasi M, et al. Primary cutaneous acral CD8 positive T-cell lymphoma with extra-cutaneous involvement: a long-standing case with an unexpected progression. *J Cutan Pathol*. 2017;44:964–968.
66. Merrill ED, Agbay R, Miranda RN, et al. Primary cutaneous T-cell lymphomas showing gamma-delta (γδ) phenotype and predominantly epidermotropic pattern are clinicopathologically distinct from classic primary cutaneous γδ T-cell lymphomas. *Am J Surg Pathol*. 2017;41:204–215.
67. Guitart J, Weisenburger DD, Subtil A, et al. Cutaneous γδ T-cell lymphomas: a spectrum of presentations with overlap with other cytotoxic lymphomas. *Am J Surg Pathol*. 2012;36:1656–1665.
68. Beltraminelli H, Leinweber B, Kerl H, Cerroni L. Primary cutaneous CD4+ small-/medium-sized pleomorphic T-cell lymphoma: a cutaneous nodular proliferation of pleomorphic T lymphocytes of undetermined significance? A study of 136 cases. *Am J Dermatopathol*. 2009;31:317–322.
69. Cetinozman F, Jansen PM, Willemze R. Expression of programmed death-1 in primary cutaneous CD4-positive small/medium-sized pleomorphic T-cell lymphoma, cutaneous pseudo-T-cell lymphoma, and other types of cutaneous T-cell lymphoma. *Am J Surg Pathol*. 2012;36:109–116.
70. Rodriguez Pinilla SM, Roncador G, Rodriguez-Peralto JL, et al. Primary cutaneous CD4+ small/medium-sized pleomorphic T-cell lymphoma expresses follicular T-cell markers. *Am J Surg Pathol*. 2009;33:81–90.
71. Garcia-Herrera A, Colomo L, Camos M, et al. Primary cutaneous small/medium CD4+ T-cell lymphomas: a heterogeneous group of tumors with different clinicopathologic features and outcome. *J Clin Oncol*. 2008;26:3364–3371.
72. Bekkenk MW, Vermeer MH, Jansen PM, et al. Peripheral T-cell lymphomas unspecified presenting in the skin: analysis of prognostic factors in a group of 82 patients. *Blood*. 2003;102:2213–2219.



eFig. 120.1 High-throughput sequencing of the T cell receptor (HTS-TCR). In a patient with CTCL, DNA is isolated from lesional skin or blood and subjected to HTS-TCR. 1. HTS-TCR identifies an expanded population of clonal malignant T cells within lesional skin and/or the blood. 2. DNA sequencing of clonal TCRs in performed. 3. The relative frequencies of different V(D)J clones is shown; the presence of a dominant clone is confirmed by finding of a single high column (peach) on the background of several flatter columns (blue). *From Weed J, Girardi M. The difficult—and often delayed—diagnosis of CTCL. Sci Transl Med 2015;7:308fs41.*



eFig. 120.2 Mycosis fungoides, generalized patch/plaque stage disease (stage 1B). Extensive patches and plaques involving more than 10% of the skin surface.



eFig. 120.3 Mycosis fungoides (stage 1B). Generalized hypopigmented lesions as well as pink-colored plaques.



eFig. 120.4 Mycosis fungoides (stage 1B) in an adult. Generalized hypopigmented lesions of varying sizes as well as hyperpigmented and pink-colored plaques. *Courtesy Kalman Watsky, MD.*



eFig. 120.5 Hypopigmented mycosis fungoides in a 12-year-old girl with phototype V skin. *Courtesy Kalman Watsky, MD.*



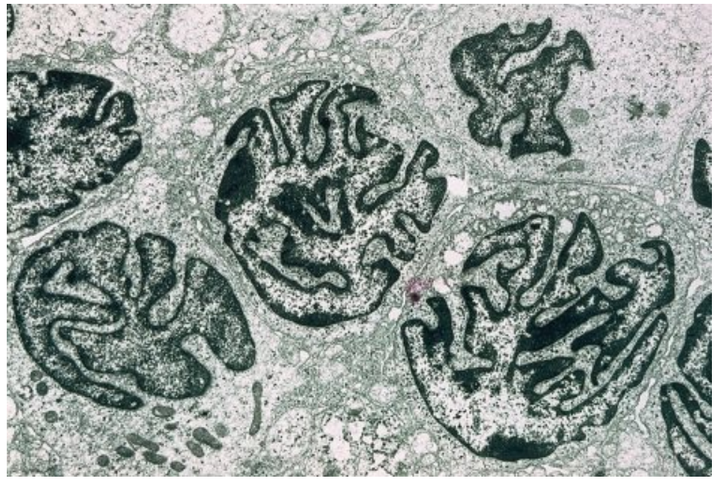
eFig. 120.6 Erythrodermic mycosis fungoides with large cell (CD30-positive) transformation. Multiple nodules, several of which are ulcerated, as well as erythematous plaques and a background of diffuse erythema. *Courtesy Anna Eisenstein, MD.*



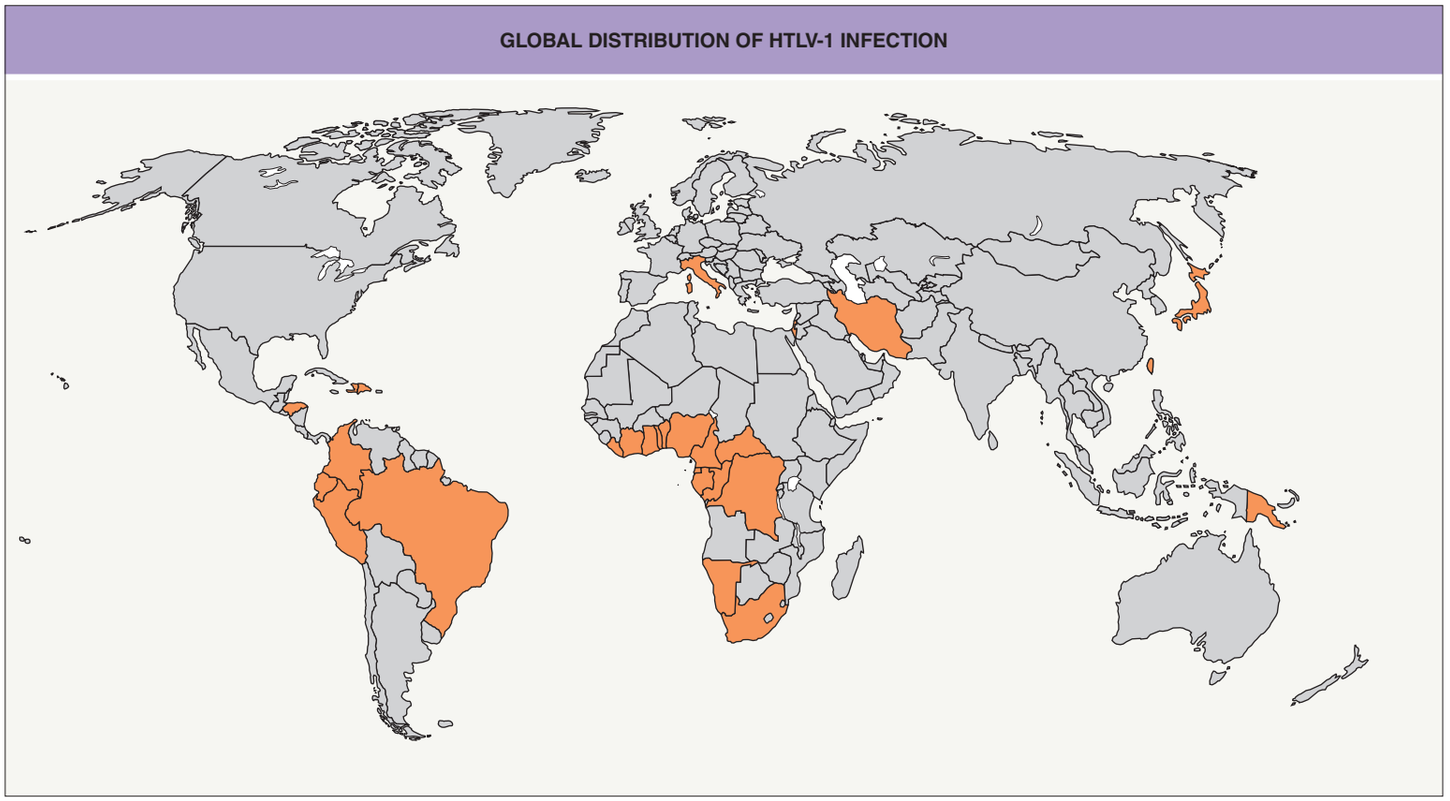
eFig. 120.7 Mycosis fungoides with large cell (CD30-positive) transformation. A Prior to matched unrelated allogeneic hematopoietic stem cell transplant (HSCT). **B** Three months following HSCT. *Courtesy Dennis Cooper, MD.*



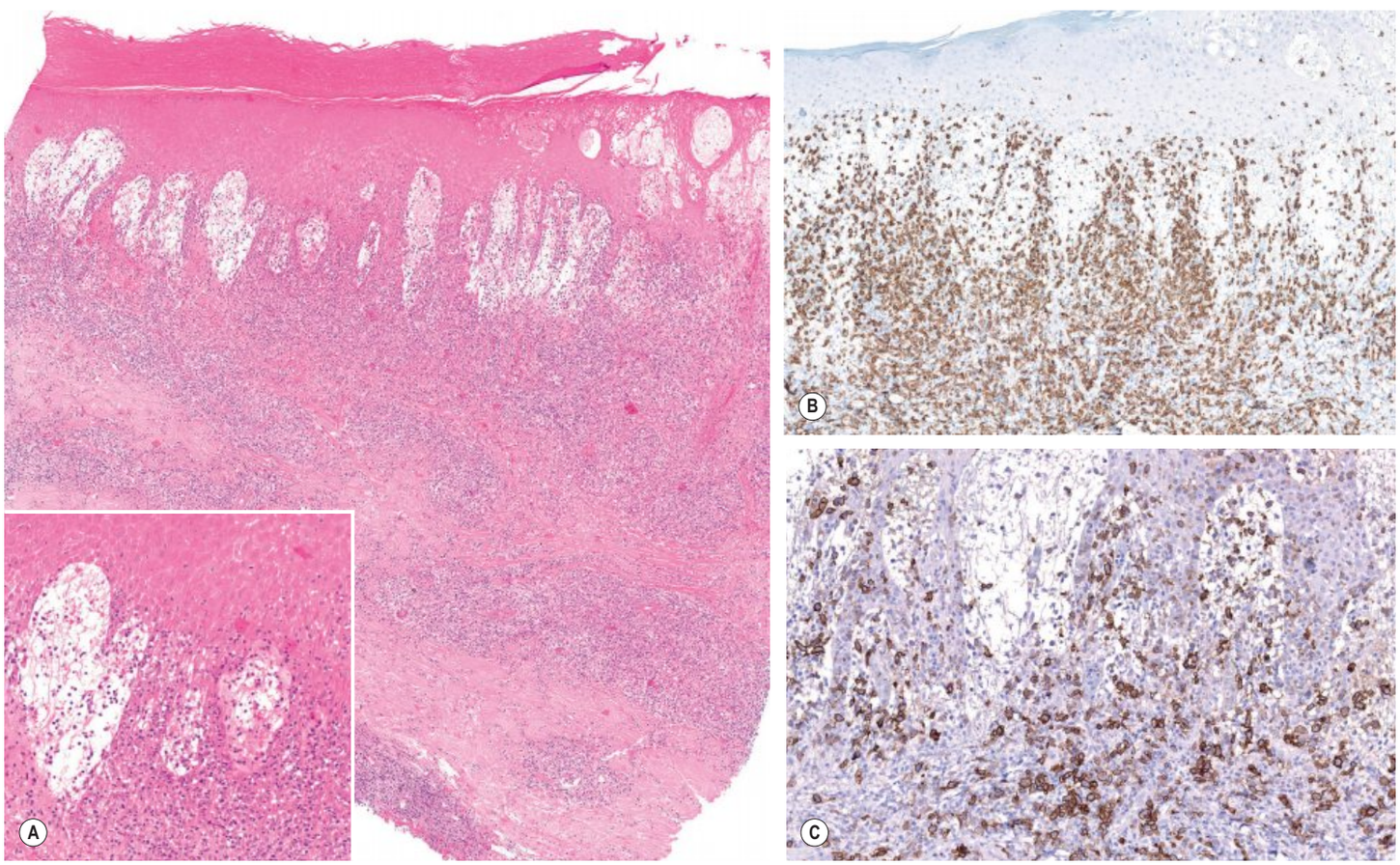
eFig. 120.8 Folliculotropic mycosis fungoides. Acneiform lesions and cysts in the face.



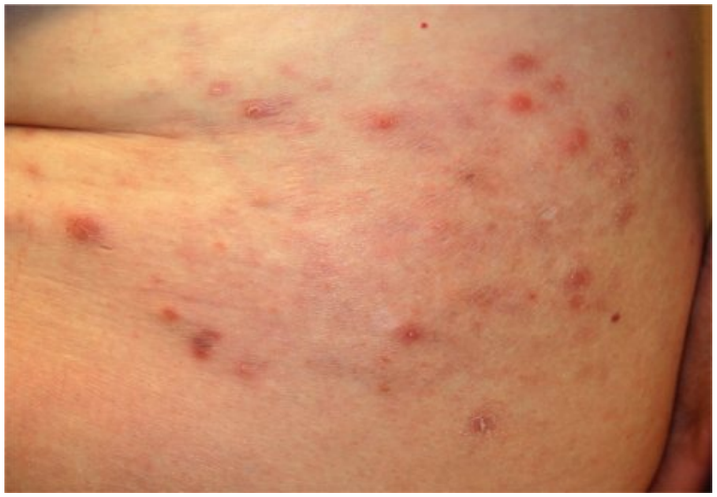
eFig. 120.9 Sézary syndrome. Electron photomicrograph of a skin biopsy showing characteristic Sézary cells.



eFig. 120.10 Map of the global distribution of HTLV-1 infection. Countries with a prevalence of HTLV-1 infection of 1%–5% are shaded orange. *From clinicalgate.com/human-immunodeficiency-virus-disease-aids-and-related-disorders/*.



eFig. 120.11 Lymphomatoid papulosis, type D. A Prominent epithelial hyperplasia with focal vesiculation and subepidermal edema as well as dense lymphoid infiltrates within the dermis. Note several epidermotropic lymphocytes (inset). **B** Strong expression of CD8. **C** Many cells, including intraepidermal ones, express CD30.



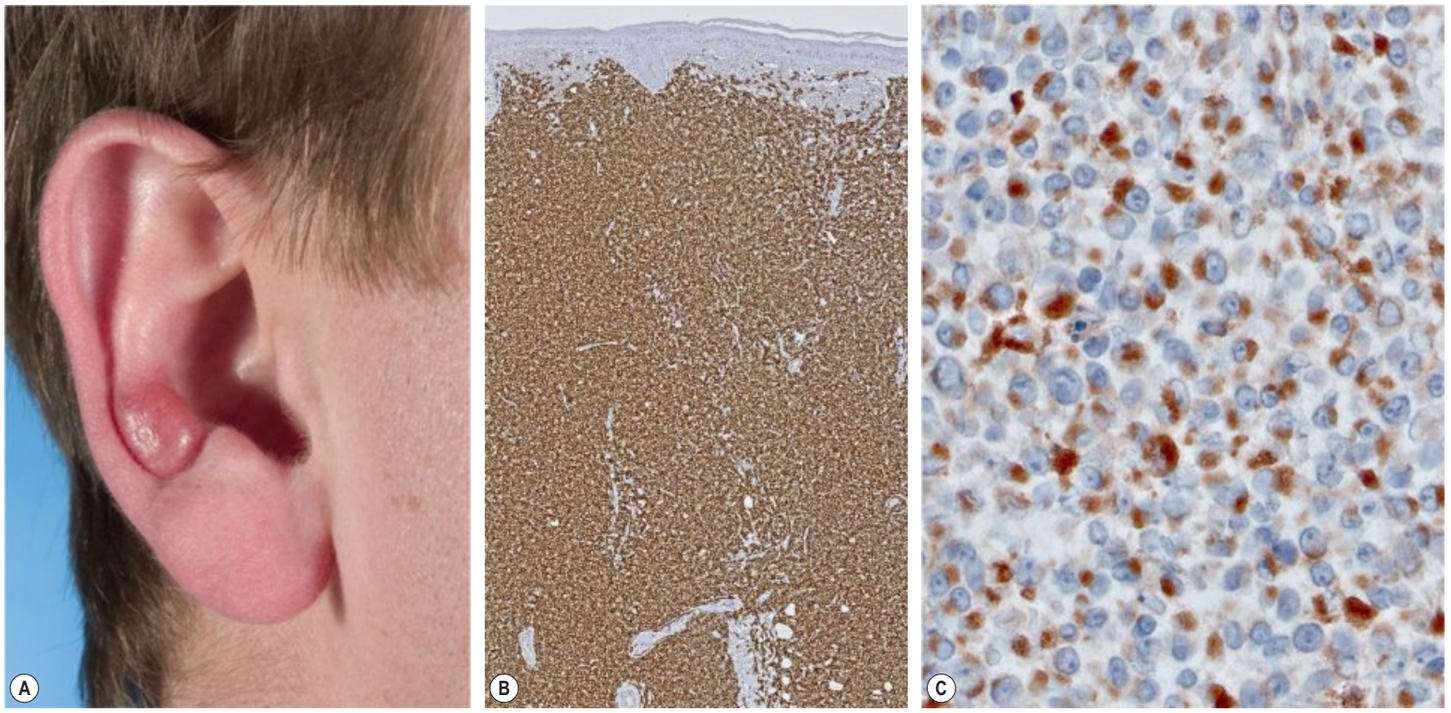
eFig. 120.12 Agminated lymphomatoid papulosis. Cluster of pink papules at the periphery of a thin, broken-up erythematous plaque.



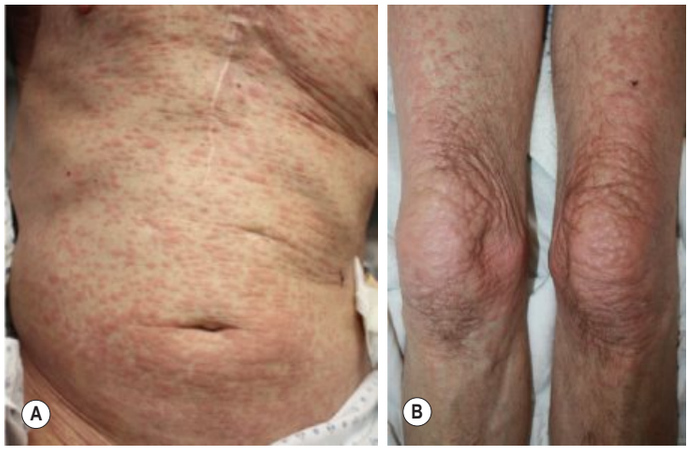
eFig. 120.13 Nasal NK/T cell lymphoma. An extensive ulceronecrotic nasal mass, previously referred to as lethal midline granuloma.



eFig. 120.14 Extranodal NK/T cell lymphoma, nasal type. The patient had an active Epstein–Barr viral infection. *Courtesy Adriana Gamarra, MD.*



eFig. 120.15 Primary cutaneous CD8-positive acral T cell lymphoma. A Pink papulonodule on the right ear. **B** A diffuse infiltrate of atypical $CD8^+$ T cells throughout the dermis. **C** CD68 staining shows a dot-like staining.



eFig. 120.16 Cutaneous involvement in a patient with peripheral T cell lymphoma. Numerous firm pink papules (**A**) and nodules (**B**), some of which have become confluent.

Other Lymphoproliferative and Myeloproliferative Diseases

121

Cesare Massone, Harry L. Winfield and Bruce R. Smoller

Chapter Contents

Benign Lymphocytic Infiltrates *2177*
Cutaneous Extramedullary Hematopoiesis *2181*
Malignant Hematopoietic Infiltrates *2182*

BENIGN LYMPHOCYTIC INFILTRATES

Lymphocytic Infiltrate of Jessner

Synonyms: ■ Lymphocytic infiltrate of Jessner–Kanof ■ Benign lymphocytic infiltrate of the skin ■ Jessner lymphocytic infiltrate of the skin ■ Jessner lymphocytic infiltration of the skin ■ Jessner–Kanof lymphocytic infiltration of the skin

Key features

- Erythematous papules, plaques, and less commonly nodules
- Most common on the head, neck, and back
- Dermal infiltrate of lymphocytes without epidermal involvement

History

Lymphocytic infiltrate of Jessner (LIJ) was initially described in 1953 by Jessner and Kanof[1] as circinate papules on the face, surrounding a central area of clearing.

Epidemiology

This entity occurs primarily in middle-aged adults. There is no sex predilection.

Pathogenesis

Benign lymphocytic infiltrate of the skin remains a controversial entity[2]. Several authors believe it is a variant of cutaneous lupus erythematosus (primarily LE tumidus), an opinion shared by the authors of this chapter. Rare cases of drug-induced disease (e.g. angiotensin-converting enzyme [ACE] inhibitors, glatiramer acetate, targeted immunomodulators ["biologics"]) have been described[3,4] as have familial cases[5].

Clinical features

Cutaneous lesions appear primarily on the head, neck, and back as one or several asymptomatic, erythematous papules, plaques, and less commonly nodules, with an absence of secondary epidermal changes such as scale (Fig. 121.1). Annular plaques with central clearing are commonly observed and individual lesions last several weeks to months. There are no associated systemic manifestations. Although spontaneous resolution occurs, recurrences are common.

Pathology

The epidermis is unremarkable, with little evidence of interface dermatitis. There is a superficial and deep, primarily perivascular, lymphocytic infiltrate that may surround hair follicles (Fig. 121.2). A mild increase in dermal mucin may be seen. Because some cases may be misinterpreted morphologically as a cutaneous lymphoproliferative disorder, detailed immunophenotypic studies and clinicopathological correlation are required[6]. By immunohistochemistry, a mixed T cell infiltrate with a predominance of $CD8^+$ lymphocytes is observed, admixed with variably large clusters of $CD123^+$ plasmacytoid dendritic cells. The distribution of plasmacytoid dendritic cells is identical to that seen in LE tumidus, further supporting a close relationship[7].

Differential diagnosis

The differential diagnosis includes the plaque form of polymorphic light eruption, LE tumidus, cutaneous lymphoid hyperplasia (pseudolymphoma), reticular erythematous mucinosis, and cutaneous lymphoma (Fig. 121.3). Subacute cutaneous LE and discoid LE are distinguished by the presence



Fig. 121.1 Lymphocytic infiltrate of Jessner. A Annular erythematous plaque on the cheek. **B** On the central back, pink papules and plaques due to confluence of papules (inset). On palpation, the lesions feel infiltrated. *B, Courtesy Lorenzo Cerroni, MD.*

of secondary changes, including scale, central hypopigmentation, and follicular plugging, along with interface changes histologically. Because in LE tumidus interface changes are sparse, if present at all, distinction from LIJ is impossible when there is increase in dermal mucin. Reticular erythematous mucinosis, which is considered by some as synonymous with LE tumidus, has abundant dermal mucin.

Polymorphic light eruption is associated with sun exposure and usually has a self-limited clinical course. Histologically, papillary dermal edema is often seen and usually there are no clusters of $CD123^+$ plasmacytoid dendritic cells. For some patients, phototesting may provide additional helpful information (see Fig. 121.3).

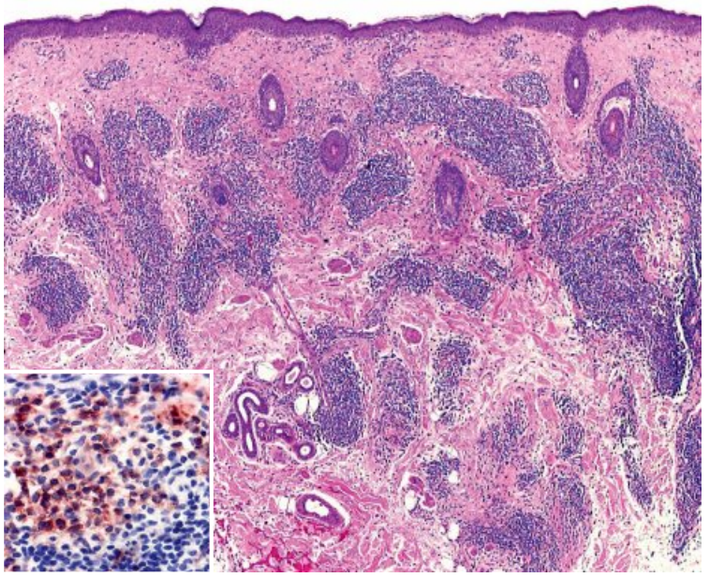


Fig. 121.2 Lymphocytic infiltrate of Jessner. A superficial and deep perivascular infiltrate without an interface component is characteristic. $CD123^+$ plasmacytoid dendritic cells are present within the infiltrate (inset).

Cutaneous lymphomas can have significant clinical and histopathologic overlap with LIJ. If the dermal lymphocytic infiltrate is extensive, immunophenotypic analyses allow distinction between the two entities (see Chs. 119 & 120). Although individual lesions of borderline lepromatous leprosy may resemble LIJ, these patients have a greater number of widespread lesions and bacilli are detected within the dermis by special stains (see Table 75.2).

Treatment

The cutaneous manifestations of LIJ may resolve spontaneously within months to years, without scarring. Oral antibiotics and topical or intralesional corticosteroids have been used with limited success. Up to 50% of patients may improve with hydroxychloroquine. In general, the disorder is resistant to radiation therapy. A crossover study of oral thalidomide (100 mg/day) versus placebo in 25 patients resulted in a clinical response of 76% for thalidomide and 16% for placebo. In isolated case reports, improvement following pulsed dye (595 nm) laser treatment or chemotherapy (for an unrelated malignancy) has been described[8].

Cutaneous Lymphoid Hyperplasia (Pseudolymphoma of the Skin)

Synonyms: ■ Lymphocytoma cutis ■ Lymphadenosis benigna cutis (LABC) ■ Spiegler–Fendt sarcoid ■ Miliary lymphocytoma

Key features

- Often an isolated, firm, erythematous to violaceous nodule or plaque that measures 1–3 cm in diameter
- Most common on the face and upper trunk
- Mixed dermal infiltrate of lymphocytes, plasma cells, and eosinophils; reactive germinal centers
- Polyclonal inflammatory infiltrate

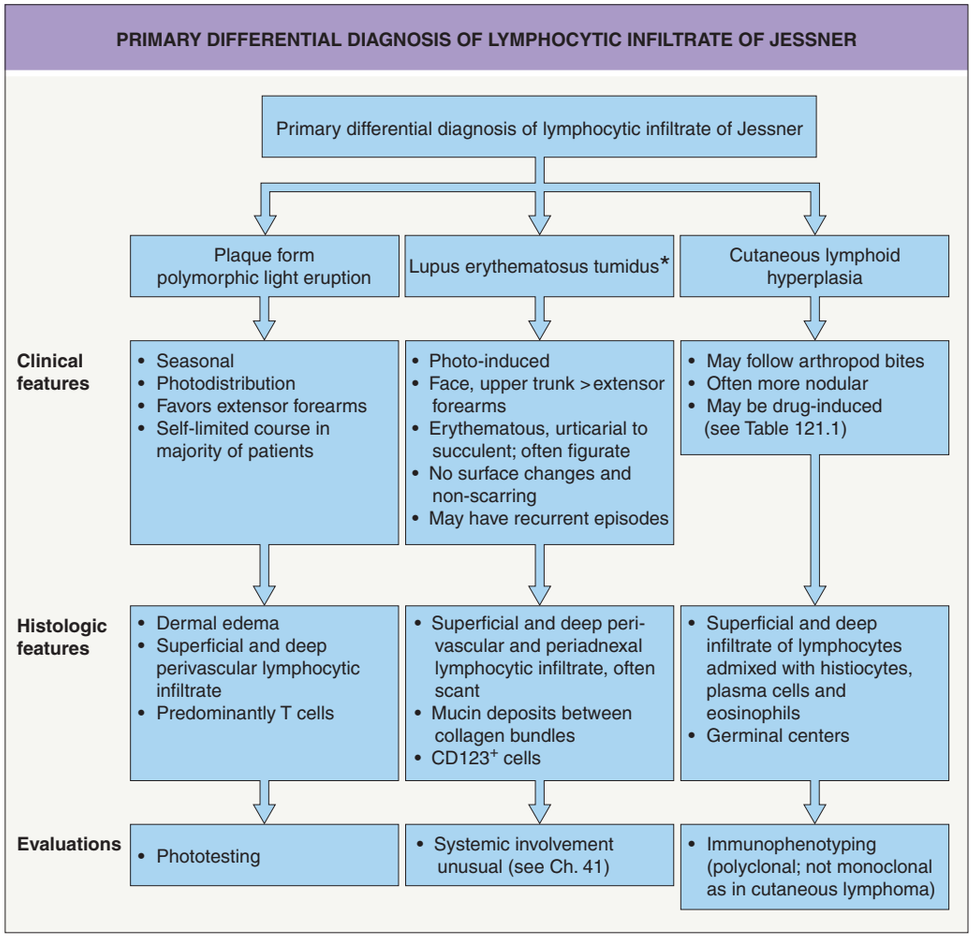


Fig. 121.3 Primary differential diagnosis of lymphocytic infiltrate of Jessner. Reticular erythematous mucinosis (REM) can also be considered in the differential diagnosis; histologically, abundant dermal mucin is observed. *Several authors consider lymphocytic infiltrate of Jessner, LE tumidus, and REM to be similar entities along a clinical spectrum. The differential diagnosis also includes cutaneous T and B cell lymphomas.

History

Cutaneous lymphoid hyperplasia (pseudolymphoma) was first reported by Spiegler in 1894. He described patients who presented with clinical features of a malignant neoplasm but experienced a benign clinical course. Although a characteristic feature is the resemblance to cutaneous lymphoma, there is a spectrum of clinical and histologic findings, reflecting its heterogeneous nature[9].

Epidemiology

Precise data regarding incidence, prevalence, and geographic distribution are lacking. Both children and adults can be affected.

Pathogenesis

Cutaneous lymphoid hyperplasia (CLH) does not represent a single disease, but rather reflects an exaggerated local immunologic reaction to a stimulus, often unrecognized. The possibility of a hapten-driven immunologic response to cells damaged by a direct toxic effect of stimuli has been suggested[10]. Inciting agents include arthropod bites (including ticks and mites), tattoos, metal implants, contact allergens, vaccinations, and medications (Table 121.1)[9–12]. In addition, several infections such as herpes zoster and in Europe Lyme borreliosis have been associated with CLH[9,13,14].

MEDICATIONS ASSOCIATED WITH CUTANEOUS LYMPHOID HYPERPLASIA (PSEUDOLYMPHOMA)	
Anticonvulsants	*Carbamazepine, phenobarbital, phenytoin, ethosuximide, lamotrigine, valproic acid*, ethotoin, *gabapentin*
Antiarrhythmics	*Mexiletine*, procainamide
Antibiotics	*Trimethoprim–sulfamethoxazole, cefixime*, cefuroxime*, nitrofurantoin*, clarithromycin*, vancomycin, rifampin, levofloxacin*
Antidepressants	*Amitriptyline*, desipramine, *fluoxetine*, clompramine, lithium, *sertraline*
Antihistamines	*Cimetidine, ranitidine*, nizatidine, doxepin
Antihypertensives (including diuretics)	*Atenolol*, *captopril*, lisinopril, *diltiazem*, *amlodipine*, *furosemide*, amiloride, losartan, valsartan, clonidine patch, metoprolol
Antineoplastic agents	*Imatinib*, fluorouracil, *gemcitabine*, oxaliplatin, tamoxifen, leucovorin, *ipilimumab, nivolumab*
Antipsychotics	*Chlorpromazine*, perphenazine, thioridazine
Lipid-lowering agents	Gemfibrozil, lovastatin
Nonsteroidal anti-inflammatory drugs (NSAIDs)	*Aspirin*, *ibuprofen*, *naproxen*, *diclofenac*, indomethacin, ketoprofen, sulindac, diflunisal, oxaprozin, nabumetone
Rheumatologic agents	*Allopurinol*, *dapsone*, *sulfasalazine*, methotrexate, gold, D-penicillamine
Sedatives	Benzodiazepines
Steroid hormones	Estrogen, progesterone
Stimulants	Methylphenidate
Targeted immunomodulators ("biologics")	Adalimumab, etanercept, infliximab, secukinumab, tocilizumab
Vaccines*	Hepatitis A, hepatitis B, influenza, quadrivalent HPV, tetanus, varicella–zoster, SARS-CoV-2, early summer meningoencephalitis, GM-CSF-producing tumor cell vaccine, hyposensitization injections
Miscellaneous	Aldesleukin (interleukin-2), bromocriptine, cyclosporine, glatiramer acetate, interferon-alpha, zoledronic acid; black cohosh
*Often aluminum-adsorbed or aluminum-containing.	

Table 121.1 Medications associated with cutaneous lymphoid hyperplasia (pseudolymphoma). For patients with the drug reaction with eosinophilia and systemic symptoms (DRESS)/drug-induced hypersensitivity syndrome (DIHS) who have atypical lymphocytes in the blood and skin, the term pseudolymphoma is sometimes applied; however, although this is a separate entity (see Ch. 21), there is overlap. The drugs in *italics* have also been reported to cause DRESS/DIHS. GM-CSF, granulocyte-macrophage colony-stimulating factor; HPV, human papilloma virus. *Adapted from references 9, 10, and 13.*

Clinical features

CLH usually presents as a single, 1–3 cm, firm, erythematous to violaceous plaque or nodule located on the head, neck, or upper extremities (Fig. 121.4A). That said, presentations can vary from multiple clustered papules to larger panniculitis-like nodules (Fig. 121.4B)[9]. The vast majority of lesions lack surface changes such as scale.

Pathology

The histopathological features are variable and the pattern may resemble either a low-grade B cell lymphoma (follicle center lymphoma, marginal zone lymphoma) or a T cell lymphoma, in particular mycosis fungoides, lymphomatoid papulosis (LyP), cutaneous anaplastic large cell lymphoma (cALCL), or subcutaneous panniculitis-like T cell lymphoma[9,13].

In CLH with *B cell predominance*, there is typically a superficial and deep nodular or diffuse infiltrate of lymphocytes, admixed with histiocytes and occasional plasma cells and eosinophils. In florid cases, germinal centers with prominent tingible-body macrophages may be observed (Fig. 121.5). Distinction from follicle center lymphoma can be made on routine histologic sections or with the addition of immunohistochemical stains (Table 121.2). Clonality, based upon IgH gene rearrangements or restricted κ or λ expression, is usually not seen

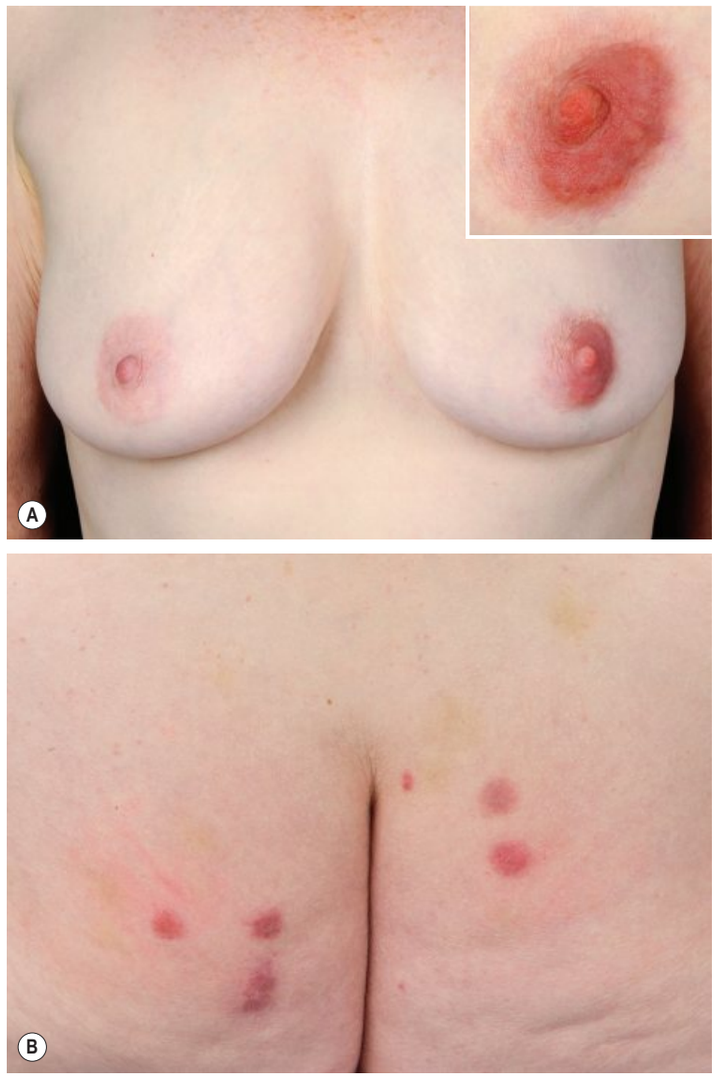


Fig. 121.4 Cutaneous lymphoid hyperplasia (pseudolymphoma) – clinical presentations. A Oval erythematous infiltrated plaque involving the lateral areola and nipple (inset) which was *Borrelia burgdorferi*-associated. **B**. Several pink and pink–violet papules on the buttocks at the sites of arthropod bites. *Courtesy Lorenzo Cerroni, MD.*

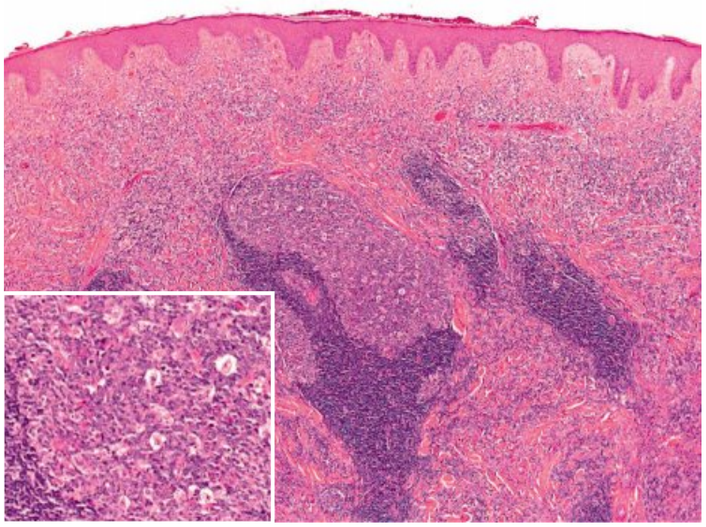


Fig. 121.5 Cutaneous lymphoid hyperplasia (pseudolymphoma) – histopathologic features. Lymphoid cells are seen throughout the dermis in a nodular and diffuse pattern. There is germinal center formation and tingible-body macrophages are present within the germinal centers (inset). The patient had *Borrelia burgdorferi*-associated lymphocytoma cutis. *Courtesy Lorenzo Cerroni, MD.*

MICROSCOPIC DIFFERENCES BETWEEN CUTANEOUS LYMPHOID HYPERPLASIA (PSEUDOLYMPHOMA) AND PRIMARY CUTANEOUS FOLLICLE CENTER LYMPHOMA	
Cutaneous lymphoid hyperplasia (pseudolymphoma)	**Primary cutaneous follicle center lymphoma**
Histologic features	
Mixed cellular infiltrate, including eosinophils and plasma cells	Predominantly lymphocytic infiltrate (eosinophils and plasma cells present in some cases)
Reactive germinal centers	Neoplastic germinal centers
Mantle zone present	No or reduced mantle zone
Tingible-body macrophages present	No tingible-body macrophages
Polarization of follicles with light and dark areas	Monomorphous appearance of follicles without polarization
Immunophenotypic features	
T and B lymphocytes	Predominance of B lymphocytes ($CD20^+$)
Bcl-6^+ cells restricted to lymph follicles	Clusters of Bcl-6^+ cells outside of lymph follicles
Bcl-2 positivity only on T lymphocytes	Bcl-2 positivity on neoplastic B cells (small minority of cases)
High proliferation of germinal centers	Reduced proliferation of germinal centers
Ig genes: polyclonal pattern	Ig genes: monoclonal rearrangement, restricted light chain expression

Table 121.2 Microscopic differences between cutaneous lymphoid hyperplasia (pseudolymphoma) and primary cutaneous follicle center lymphoma. Ig, immunoglobulin.

in pseudolymphomas (see Fig. 119.10)[9,14]. PCR analysis for *Borrelia burgdorferi* DNA is positive in *Borrelia*-associated lymphocytoma cutis and pseudolymphomatous acrodermatitis chronica atrophicans[9,14].

In *T cell-predominant* infiltrates, $CD4^+$ T helper lymphocytes are commonly observed within the dermis, admixed with a minority of $CD8^+$ cytotoxic/suppressor T cells. An accompanying population of B lymphocytes is usually present. A mycosis fungoides-like pattern is most often encountered in drug-induced pseudolymphomas (see Table 121.1). Histologically, epidermotropism, spongiosis, vacuolar degeneration of the basal layer, papillary dermal edema, and red cell extravasation may be seen. Prominent papillary dermal fibrosis, which can be seen in mycosis fungoides, is absent, but T cell clonality may be present.

$CD30^+$ pseudolymphomas include persistent arthropod bite reactions, drug reactions, and the atypical lymphoid infiltrates associated with cutaneous poxvirus infections (e.g. molluscum contagiosum, orf). Additional findings related to the underlying disorder can aid in diagnosis, and there is polyclonal rearrangement of the TCR genes[9,13].

Differential diagnosis

Pseudolymphomas may be difficult to differentiate from *cutaneous lymphomas* (see Pathology section). Although the presence of clonality may aid in distinguishing reactive from neoplastic processes, it should not be used alone to establish malignancy. In addition to clinicopathologic correlation, longitudinal evaluation plays a key role in making this distinction.

Acral pseudolymphomatous angiokeratoma of children (APACHE), originally thought to represent a vascular nevus, is now categorized as a pseudolymphoma. In contrast to other pseudolymphomas, it favors the extremities of children between the ages of 2 and 16 years, usually presenting as a unilateral grouping of small, red to violet, "angiomatous" papules. Histologically, there is a dermal infiltrate of lymphocytes, histiocytes, and plasma cells accompanied by prominently thickened capillaries[9].

Kikuchi–Fujimoto disease, also known as histiocytic necrotizing lymphadenitis, is an idiopathic systemic inflammatory disease most commonly seen in young adult women. It is associated with a variety of viral and bacterial infections (e.g. Epstein–Barr virus, cytomegalovirus) as well as autoimmune diseases (e.g. systemic LE). In addition to fever, malaise, weight loss, and gastrointestinal symptoms, patients develop cervical lymphadenopathy. Histologically, involved lymph nodes show infiltration of plasmacytoid dendritic cells in the paracortical area and later histiocytes and necrosis in the absence of an identifiable pathogen. Cutaneous findings, present in 40% of patients, include acneiform eruptions, urticaria, ulcers, and indurated erythematous plaques. Histologically, dense superficial and deep perivascular lymphohistiocytic infiltrates with nuclear debris (in the absence of neutrophils) are seen; interface changes are commonly present[15,16].

In *"pseudolymphomatous folliculitis"*, there is typically a solitary facial nodule that is due to a predominantly perifollicular and periadnexal dermal infiltrate. It is unclear whether these cases really represent an entity or, as the authors of this chapter believe, a mixture of different reactive conditions. The infiltrate is typically mixed with a predominance of T or B cells that may have cellular atypia; granulomas are variably present[17,18]. There is irregular hyperplasia and distortion of the follicular epithelium, with blurring of the dermal–epidermal junction, and infiltrates of $CD1a^+$/$S100^+$ mononuclear cells surround and infiltrate these distorted follicles. This entity should be distinguished from primary cutaneous $CD4^+$ small/medium-sized pleomorphic T cell lymphoproliferative disorder, which is characterized by more pronounced pleomorphism of the cells[17–19]. Distinction from pilotropic mycosis fungoides is based on the presence of a mixed infiltrate of T and B lymphocytes as well as absent or minimal folliculotropism in pseudolymphomatous folliculitis.

Cutaneous and systemic plasmacytosis is a benign condition of unknown etiology observed primarily in Asians, especially those of Japanese ancestry. It is characterized by multiple, reddish-brown, infiltrated maculopapules and plaques, most often on the trunk. Histopathologically, variably dense superficial and deep perivascular infiltrates composed predominantly of mature polyclonal plasma cells are seen[9,20,21]. The plasmacytosis may be accompanied by anemia, B symptoms, and hypergammaglobulinemia, as well as lymphadenopathy, hepatosplenomegaly, interstitial pneumonia, and mesangial proliferative glomerulonephritis. A reactive dysfunction of plasma cells triggered by various stimuli has been postulated[22]. As in Castleman disease, there is an elevation in circulating/tissue IL-6, but in the absence of HHV-8 infection[9,20,21].

Intralymphatic histiocytosis (formerly intravascular histiocytosis) has been observed most often in patients with rheumatoid arthritis or metallic orthopedic implants[23]. It has also been reported in association with severe osteoarthritis, solid organ malignancies (e.g. breast cancer), lymphedema, and various skin disorders (e.g. Morbihan disease, granulomatous cheilitis, healing cellulitis). Clinically, intralymphatic histiocytosis usually presents with poorly defined erythematous plaques that may have a reticular pattern (Fig. 121.6A). The lesions can co-localize anatomically with underlying disorders or implants. Histologically, collections of epithelioid histiocytes are seen within dilated lymphatic

vessels – findings that resemble intravascular large cell lymphoma (Fig. 121.6B)[9,23]. The histiocytes are CD68$^+$, S100$^-$, and CD1a$^-$; the endothelial cells express D2-40. Intralymphatic histiocytosis can be differentiated from reactive angioendotheliomatosis and other intravascular proliferations via immunohistology[9,23].

Additional examples of pseudolymphoma are outlined in Table 121.3.

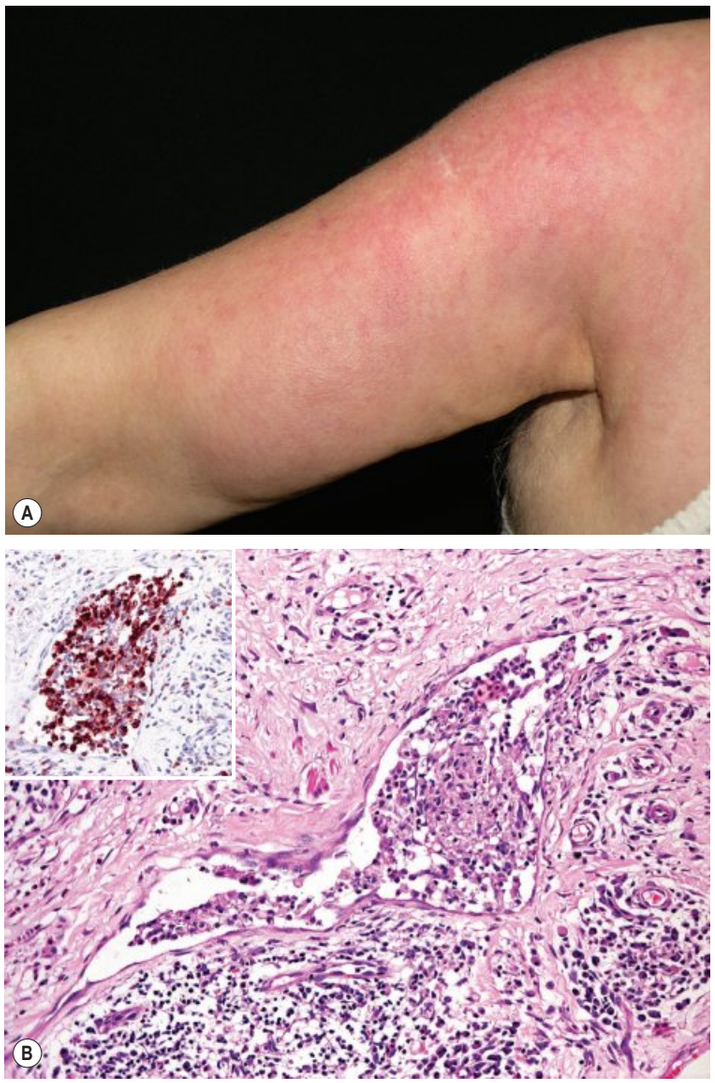


Fig. 121.6 Intralymphatic histiocytosis. A Reticulated erythematous plaque of the upper arm and shoulder in a patient with rheumatoid arthritis. **B** Dilated dermal lymphatic vessel filled with histiocytes, admixed with some leukocytes, and surrounded by a lymphoplasmacytic perivascular infiltrate; note CD68 positivity of the histiocytes (inset). *A, Courtesy Luis Requena, MD; B, Courtesy Lorenzo Cerroni, MD.*

Treatment

CLH is a benign, reactive condition and it should be treated conservatively. Spontaneous resolution may occur without scarring, and performance of a biopsy, even if partial, can be followed by spontaneous regression. Medication-associated CLH usually resolves after drug discontinuation[12]. Topical and intralesional corticosteroids or topical tacrolimus may lead to improvement. For persistent lesions, simple excision, cryosurgery, laser ablation, photodynamic therapy, phototherapy, and radiation therapy are other options. Hydroxychloroquine, thalidomide, and intralesional or intravenous rituximab have also been reported as successful therapies[17,24]. For *Borrelia*-associated pseudolymphoma, appropriate antibiotics are administered (see Ch. 19).

CUTANEOUS EXTRAMEDULLARY HEMATOPOIESIS

Key features

- Evidence of bone marrow dysfunction
- Most common associations are TORCH (*t*oxoplasmosis, *o*ther agents, *r*ubella, *c*ytomegalovirus and *h*erpes simplex virus) infections in neonates and myelofibrosis in adults
- Widely disseminated erythematous to violaceous papules and nodules, with neonatal form referred to as "blueberry muffin baby"
- Diffuse dermal infiltrate of immature erythrocytes, leukocytes, and megakaryocytes

Epidemiology

Cutaneous extramedullary hematopoiesis (CEMH) is a reflection of bone marrow dysfunction and is most commonly seen in neonates following congenital infections. It may also occur in adults with myelodysplasia or myeloproliferative neoplasms (myelofibrosis, polycythemia vera, essential thrombocythemia)[9], as well as following splenectomy for myeloproliferative neoplasms. A very rare association is primary hypertrophic osteoarthropathy[25].

Pathogenesis

CEMH occurs normally during early embryogenesis and abates prior to birth. Thereafter, it occurs only as a secondary phenomenon in response to altered bone marrow function. Dermal hematopoiesis reflects an expansion of follicular, dermal, or circulating hematopoietic stem cells and is probably induced by cytokines (e.g. IL-3, G-CSF, TGF-β)[25]. Rarely, in otherwise healthy individuals, primary cutaneous neoplasms such as pilomatricomas, nevus sebaceus, hemangiomas, and pyogenic granulomas may be associated with localized CEMH[9,25,26].

Clinical Features

The clinical presentation consists of erythematous to violaceous papules and nodules which may ulcerate. When widely disseminated in

ENTITIES THAT CAN MIMIC CUTANEOUS T AND B CELL LYMPHOMAS		
More common	**Uncommon**	**Rare**
• Persistent arthropod bites, scabies • *Borrelia* infections, in particular lymphocytoma cutis and acrodermatitis chronica atrophicans (Europe) • CD30$^+$ reactive lymphoid infiltrates in the context of cutaneous infections (e.g. herpes simplex, herpes zoster, molluscum contagiosum) • Drug eruptions (lichenoid, lymphomatoid) (see Table 121.1) • Lichenoid (lymphomatoid) keratosis • Pseudolymphomatous infiltrates in cutaneous lupus erythematosus • Lichen sclerosus of genital skin	• Lymphomatoid contact dermatitis • Pigmented purpura, lichenoid variant • Pityriasis lichenoides (acute or chronic forms) • Pseudolymphomatous atopic dermatitis • Pseudolymphomatous folliculitis • Pseudolymphomatous reactions to tattoo pigments • Syphilis, primary and secondary	• Actinic reticuloid • APACHE (acral pseudolymphomatous angiokeratoma of children) • Cutaneous IgG4-related disease* • Cutaneous plasmacytosis • Hydroa vacciniforme • Intralymphatic histiocytosis • Kikuchi–Fujimoto disease • Lobular panniculitis in children with congenital immunodeficiencies • Pseudolymphomatous reactions to vaccinations • Vitiligo (inflammatory stage)
*Increased IgG4-positive plasma calls and sclerotic stroma; can also be seen in granuloma faciale-like lesions.		

Table 121.3 Entities that can mimic cutaneous T and B cell lymphomas. These entities are sometimes referred to as pseudolymphomas. For details see reference 9.

neonates, it leads to the classic "blueberry muffin baby" (Fig. 121.7)[25]. This can be seen in association with congenital viral infections and prenatal anemias (Table 121.4). Dermal hematopoiesis is most often seen with rubella and cytomegalovirus, and serologic titers for TORCH infections can aid in diagnosis.

Pathology

CEMH is characterized by a dermal infiltrate of immature white and red blood cell precursors (erythroblasts) and megakaryocytes, centered around vessels of the superficial vascular plexus. It may also extend into the deeper reticular dermis and exhibit a diffuse pattern. All three hematopoietic cell lines are present in varying ratios, depending upon the underlying disease process.

Differential Diagnosis

The clinical differential diagnosis in neonates is outlined in Table 121.4 and in adults the possibility of leukemia cutis needs to be considered. Histologically, the differential diagnosis is limited. Distinguishing CEMH from disseminated congenital leukemia cutis and neonatal neuroblastoma is important. Whereas all three hematopoietic cell lines (erythrocytes, leukocytes, and megakaryocytes) are represented in CEMH, there is an atypical, monomorphous infiltrate of immature leukocytes in leukemia cutis.



Fig. 121.7 Extramedullary hematopoiesis. "Blueberry muffin baby" secondary to congenital rubella. *Courtesy Eugene Mirrer, MD.*

DIFFERENTIAL DIAGNOSIS OF "BLUEBERRY MUFFIN BABY"
Disseminated extramedullary hematopoiesis

• Congenital TORCH infections
  • Toxoplasmosis
  • Other – coxsackievirus, parvovirus
  • Rubella
  • Cytomegalovirus
• Severe hemolytic anemias
  • Congenital spherocytosis
  • Rhesus hemolytic disease
  • ABO incompatibility
• Other causes of severe anemia
  • Twin–twin transfusion
  • Chronic fetomaternal hemorrhage
  • Severe internal bleeding (e.g. intracranial)
  • Congenital leukemia or myelodysplasia
• Aicardi–Goutières syndrome

Neoplastic infiltration
• Congenital leukemia cutis, transient myeloproliferative disorder • Neonatal neuroblastoma, peripheral primitive neuroectodermal tumor • Congenital Langerhans cell histiocytosis, disseminated xanthogranulomas (early lesions), hemophagocytic lymphohistiocytosis • Congenital alveolar rhabdomyosarcoma • Infantile myofibromatosis • Multifocal infantile hemangiomas, other vascular lesions (e.g. multifocal lymphangioendotheliomatosis, glomuvenous malformations)

Table 121.4 Differential diagnosis of "blueberry muffin baby". TORCH, toxoplasmosis, other agents, rubella, cytomegalovirus, and herpes simplex virus.

Treatment

Treatment of the underlying bone marrow dysfunction results in reversal of the cutaneous process. Spontaneous resolution can occur with some viral infections.

MALIGNANT HEMATOPOIETIC INFILTRATES

Leukemia Cutis

Key features

- Pink to red–brown or purple papules and nodules; hemorrhagic ulcers
- Diffuse dermal infiltrate of neoplastic leukocytes
- Monomorphic immature precursor cells in some types

Epidemiology

Multiple types of leukemia exist, each with its own epidemiologic characteristics. Acute lymphoblastic leukemia (ALL) tends to be a neoplasm of childhood. Acute myelogenous leukemia (AML) and chronic myelogenous leukemia (CML) occur primarily in adults, and chronic lymphocytic leukemia (CLL) and hairy cell leukemia are most common in elderly patients[28,29]. Development of CML-associated leukemia cutis can be a harbinger of blast transformation[9], while the development of leukemia cutis in a patient with myelodysplastic syndrome (MDS) points to progression to AML[27]. In some patients with MDS, cutaneous lesions with an accumulation of benign-appearing dendritic and myeloid cells and a chronic course have been described. Leukemia cutis is most commonly seen in patients with *NPM1*-mutated AML and less often in CLL[9,28,29a,29b].

Pathogenesis

Specific chromosomal abnormalities are associated with particular subtypes of leukemia. The Philadelphia chromosome, the primary diagnostic feature of CML, represents a translocation between chromosomes 9 and 22 [t(9;22)]. This translocation results in fusion of the two genes *BCR* and *ABL*, with constitutive activation of the tyrosine kinase activity of the fusion oncoprotein. It is this kinase activity that is selectively inhibited by imatinib mesylate (Gleevec®). Additionally, 95% of patients with promyelocytic leukemia have a t(15;17) translocation, which leads to abnormal expression of a fusion retinoic acid receptor that is the target of all-*trans* retinoic acid therapy.

A variety of non-random chromosomal abnormalities exists in ALL and AML that can influence prognosis, and in AML mutations in particular genes can be favorable (e.g. *CEBPA*) or unfavorable (e.g. *FLT3*-ITD)[29a,29b]. *NPM1* is the most frequently mutated gene in patients with AML and normal cytogenetics; as noted previously, *NPM1*-mutated AML is the subtype most commonly associated with leukemia cutis[29a,29b]. Table 121.5 outlines the relationship between specific abnormalities and prognosis in CLL[28,29].

RELATIONSHIP BETWEEN SPECIFIC MOLECULAR ABNORMALITIES AND PROGNOSIS IN CHRONIC LYMPHOCYTIC LEUKEMIA	
Molecular abnormalities	**Prognosis**
Chromosomal	
13q deletion	Favorable
Trisomy 12	Intermediate
11q deletion	Poor
17p deletion	Poor
Genetic mutations	
TP53	Poorest
Other	
Unmutated *IGHV* genes	Poor

Table 121.5 Relationship between specific molecular abnormalities and prognosis in chronic lymphocytic leukemia. *TP53* is located on chromosome 17p and 17p deletions often involve *TP53*. *IGHV*, immunoglobulin heavy chain variable region gene.

Clinical features

Leukemia can lead to nonspecific reactive skin lesions (Table 121.6) or specific infiltrates. The latter most commonly present as multiple, generalized or localized, firm papules and nodules that vary in color from pink to red–brown to purple. The papulonodules often become hemorrhagic and thrombocytopenia usually plays a role in this associated hemorrhage. Ulcerative and rarely bullous lesions occur. Leukemia cutis can develop in any location, but the head, neck, and trunk are most commonly involved (Fig. 121.8A). Leukemic infiltrates may arise at sites of trauma or scars.

Rarely, myelogenous leukemias may present with dermal or subcutaneous nodules known as myeloid sarcomas or chloromas. These skin lesions may precede the development of systemic leukemia by months.

"INFLAMMATORY" DISORDERS ASSOCIATED WITH LEUKEMIAS AND MYELODYSPLASTIC SYNDROMES

Cutaneous disorder	Associated leukemias and MDS
Neutrophilic dermatoses	
Sweet syndrome, including histiocytoid variant*	AML > MDS, CML, hairy cell leukemia, CNL > ALL, CLL
Pyoderma gangrenosum†	AML, MDS, CML, hairy cell leukemia > ALL, CLL
Neutrophilic eccrine hidradenitis	AML ≫ ALL, CML, CLL
Reactive erythemas	
Eosinophilic dermatosis of hematologic malignancy (including exaggerated reactions to arthropod bites)	CLL >>> AML, CML
Erythroderma	CLL‡
Facial erythema and edema	T cell prolymphocytic leukemia
Vasculitis	
Polyarteritis nodosa	Hairy cell leukemia ≫ CMML, MDS
Vasculitis (small vessel/ leukocytoclastic)	Hairy cell leukemia, CLL > AMML, ALL, MDS
Erythema elevatum diutinum	Hairy cell leukemia, CLL
Panniculitis	
Erythema nodosum¶	AML, CML, CMML
Other panniculitides§	Hairy cell leukemia, AML, CMML
Other	
Urticaria	CLL, hairy cell leukemia
Erythema multiforme‖	CLL
Paraneoplastic pemphigus	CLL
Recalcitrant adult-onset eczema	CLL (T cell)
Acral ischemia with lividity	CML#
Reactive granulomatous dermatitis including interstitial granulomatosis dermatitis, sarcoidal, GA-like	MDS
Pernio	CMML

*Histiocytoid variant linked to hematologic malignancies and MDS.
†Especially bullous.
‡Many probably represented Sézary syndrome.
¶Isolated case reports; may occur concomitantly with Sweet syndrome and some cases better classified as subcutaneous Sweet syndrome.
§Sweet syndrome may have a subcutaneous component.
‖May have represented paraneoplastic pemphigus.
#Leukostasis/hyperleukocytosis syndrome.

Table 121.6 "Inflammatory" disorders associated with leukemias and myelodysplastic syndromes[18–21]. Most patients with CML who develop vitiligo-like changes are receiving imatinib. Infiltrates of leukemic cells (CLL > AML) may be seen in post-herpes zoster scars (see Table 80.7). ALL, acute lymphoblastic leukemia; AML, acute myelogenous leukemia; AMML, acute myelomonocytic leukemia; CLL, chronic lymphocytic leukemia; CML, chronic myelogenous leukemia; CMML, chronic myelomonocytic leukemia; CNL, chronic neutrophilic leukemia; GA, granuloma annulare; MDS, myelodysplastic syndrome.

Gingival hyperplasia, secondary to leukemic infiltrates, favors acute monocytic or acute myelomonocytic leukemia, especially those with *NPM1* mutations.

In one series, cutaneous eruptions of leukemia accounted for 30% of all skin biopsy specimens in patients with leukemia[30]. Other diagnoses included GVHD, drug eruptions, infectious processes, purpura, and small vessel vasculitis. In most patients with acute leukemia, cutaneous lesions are present at the time of diagnosis or recurrence, but occasionally, skin involvement precedes the appearance of leukemia in the peripheral smear ("aleukemic" leukemia cutis). Rarely, leukemia cutis predates apparent bone marrow involvement by months or even years.

Of note, asymptomatic dermal leukemic infiltrates of CLL may be evident in biopsy specimens of primary cutaneous neoplasms (e.g. squamous cell carcinoma) and inflammatory or infectious disorders such as herpes simplex and herpes zoster viral infections. This phenomenon indicates that these neoplastic cells retain the capability to respond to chemotactic stimuli and migrate into tissues (inflammatory oncotaxis)[31,32].

The characteristics of the different forms of leukemia cutis are summarized in Table 121.7.

Pathology

Histologic features of leukemia cutis vary with the type of leukemia. The neoplastic infiltrates may be perivascular, interstitial, nodular, and/or diffuse; occasionally, they densely surround the eccrine glands[30–32]. Diagnosis is more difficult when the perivascular and periadnexal infiltrates are sparse and mimic inflammatory disorders[32].

AML represents a neoplastic proliferation of immature myeloid cells and encompasses multiple subtypes[29a,29b]. In general, the neoplastic cells recapitulate myeloid precursor cells in their immature stages of development (Fig. 121.8B). In many cases, cytoplasmic granules can be found. The most common forms of AML that involve the skin and present *de novo* (without previous evidence of systemic disease) are the more differentiated subtypes – acute myelomonocytic and acute monocytic leukemia. Immunohistochemically, the infiltrates of AML are positive for myeloid markers such as myeloperoxidase, CD33, CD34, and CD68 and are usually negative for CD123[9,29a,29b].

In CML, there is a range of myeloid precursors, including promyelocytes, metamyelocytes, bands, and mature neutrophils. Although cutaneous lesions of CML are rare, they are typically seen in patients with chronic myelomonocytic leukemia and are associated with blast transformation and a poor prognosis[9,29a,29b].

ALL represents a clonal expansion of immature lymphocytes, most commonly of B cell lineage and less commonly T cell lineage. Rarely, cytoplasmic granularity may be present, and this corresponds with a precursor B cell immunophenotype. Cells of ALL may be difficult to identify in skin biopsy specimens and immunostaining for terminal deoxytransferase may prove helpful[9,28,29].

Cutaneous CLL is characterized by a dense infiltrate of uniform-appearing, small, round lymphocytes of B cell lineage (Fig. 121.9). The cells appear mature, but the monomorphous nature and paucity of other cell types within the infiltrate suggest a leukemic infiltrate. The lymphocytes often surround adnexal and vascular structures. Immunohistochemically, CLL shows positivity for LEF1, CD5 (variable), CD20, and CD23[9,28,31,33].

Differential diagnosis

The clinical differential diagnosis includes cutaneous lymphoma, cutaneous lymphoid hyperplasia, infectious emboli, vasculitis, panniculitis, and drug eruptions. The histologic differential diagnosis of leukemia cutis depends upon the type of leukemia present. Distinguishing some cases of leukemia cutis from lymphomas involving the skin can be difficult. For myeloid leukemias, the differential diagnosis includes mainly extramedullary hematopoiesis (see above), diffuse large cell lymphomas, and histiocytoid Sweet syndrome. Of note, in some cases of histiocytoid Sweet syndrome[34] neoplastic cells of AML may be present within the infiltrate[35].

Treatment

No specific treatment for leukemia cutis currently exists. The cutaneous eruptions typically resolve following successful treatment of the leukemia.

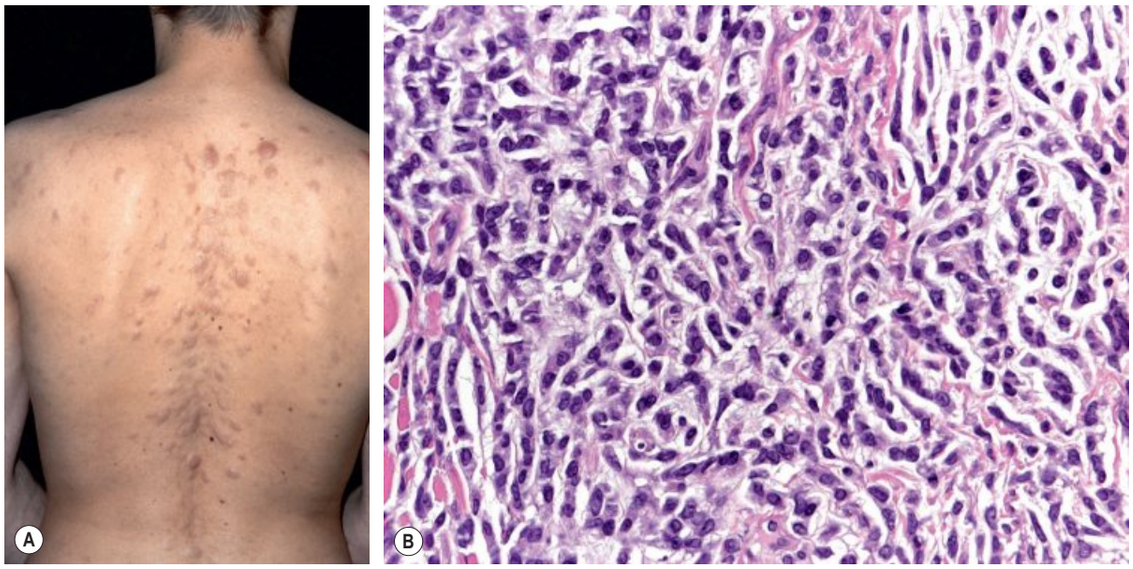


Fig. 121.8 Leukemia cutis. A Numerous violet–brown papules and plaques on the back of a patient with acute myelogenous leukemia. **B** Histologically, an infiltrate of atypical monocytoid cells characterized by nuclear pleomorphism and relatively abundant cytoplasm is seen.

CHARACTERISTICS OF DIFFERENT TYPES OF LEUKEMIA CUTIS				
Type of leukemia	**ALL**	**CLL**	**AML**	**CML**
Characteristic age	Between 2 and 5 years of age	Late 7th decade or older	Variable, most commonly 7th decade	Variable, most commonly after 50 years of age
Presenting anatomic site	Predominantly head and neck	Generalized; may appear at sites of infection (e.g. herpes zoster) or neoplasms (e.g. SCC)	Generalized	Variable
Clinical course	Aggressive	Indolent	Aggressive	Intermediate*
Subtype of leukemia/ immunophenotype	• 85%: B cell ALL ($CD19^+$, TdT^+, $CD20^+$, $CD5^+$, $CD10^+$, $CD22^+$, $CD79a^+$, $PAX\text{-}5^+$) • 15%: T cell ALL (TdT^+, $CD1a^+$, $CD2^+$, $CD3c^+$, $CD4^+$, $CD5^+$, $CD7^+$, $CD8^+$)	• B cell type ($CD5^+$, $CD23^+$, $LEF1^+$, $CD20^+$)	• $CD33^+$, $CD34^+$, myeloperoxidase$^+$ > $CD13^+$, $CD68^+$ • Markers may not be present if undifferentiated	• Most commonly, CMML • Cutaneous involvement associated with blast transformation
Incidence of cutaneous involvement	• Rare	• Not infrequent • Usually an incidental finding in biopsy specimens†	• More common with *NPM1*-mutated AML • May be presenting sign	• Rare
Time of presentation	• Late	• Late	• Early or late • May be the first sign of recurrence after treatment	• Late
Clinical appearance‡	• Large, non-ulcerated tumors • Nonspecific papulonodules	• Nonspecific papulonodules	• Nonspecific papulonodules	• Nonspecific papulonodules

*When acceleration or blast transformation occurs, becomes aggressive.
†Including primary cutaneous neoplasms (e.g. SCC), inflammatory disorders, and infectious diseases (see text).
‡Less common presentations reviewed in the text.

Table 121.7 Characteristics of different types of leukemia cutis. ALL, acute lymphoblastic leukemia; AML, acute myelogenous leukemia; CLL, chronic lymphocytic leukemia; CML, chronic myelogenous leukemia; CMML, chronic myelomonocytic leukemia; SCC, squamous cell carcinoma; TdT, terminal deoxytransferase.

Cutaneous Hodgkin Lymphoma

Synonyms: ■ Cutaneous Hodgkin disease ■ Cutaneous Hodgkin's disease

Key features

- Advanced stage in most patients with skin involvement
- Dermal nodules and plaques, sometimes ulcerated
- Dense dermal infiltrate with lymphocytes and eosinophils
- Atypical cells (lacunar cells, Reed–Sternberg cells)

History

In 1832, Thomas Hodgkin described a series of patients with lymphadenopathy, splenomegaly, and weight loss, all of whom died of their disease. Wilks reported a subsequent series of patients in 1885, and designated the illness Hodgkin's disease.

Epidemiology

Cutaneous involvement by Hodgkin lymphoma (HL) is rare[9,36–38]. In one large study, only 0.5% of patients with HL had cutaneous involvement[38], primarily in the setting of advanced disease and serving as a marker of poor prognosis. The existence of true primary cutaneous HL is debatable[9].

The incidence of HL peaks during early adulthood, with a second, smaller peak in the sixth decade. Of note, compared to the general population, mycosis fungoides and LyP occur at higher rates in patients with HL[37,39]. This reflects the increased incidence of non-Hodgkin lymphomas in general in HL patients. The underlying reason for this phenomenon is not known.

Pathogenesis

Approximately 30% of patients with classic HL (see below) have Epstein–Barr virus (EBV) DNA within the pathognomonic Reed–Sternberg tumor cells. The precise role of EBV in HL pathogenesis is not known[40]. In classic HL, the Reed–Sternberg cells represent the malignant population and are usually derived from B cell lymphocytes.

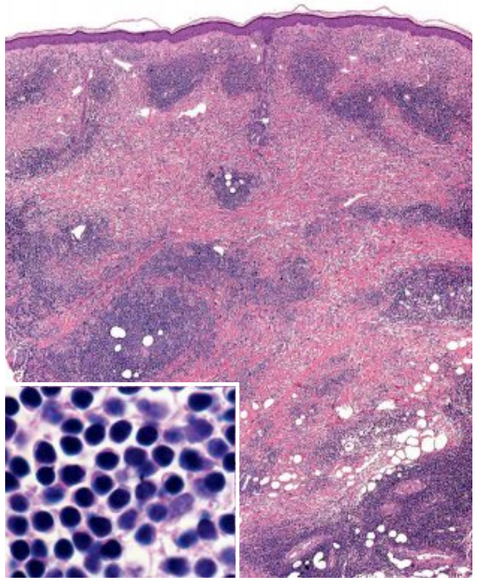


Fig. 121.9 Chronic lymphocytic leukemia (CLL). Nodular-diffuse infiltrates of lymphocytes are present within the entire dermis and superficial subcutis. The cells in CLL are small, monomorphous, hyperchromatic lymphocytes that lack significant cytologic atypia (inset). *Courtesy Lorenzo Cerroni, MD.*



Fig. 121.10 Blastic plasmacytoid dendritic cell neoplasm. Multiple firm violaceous nodules and plaques on the back. The scale-crust is at the site of a previous biopsy. *Courtesy Lorenzo Cerroni, MD.*

Clinical features

Classic HL includes the nodular sclerosing (most common), mixed cellularity, and lymphocyte-depleted forms of the disease, and it is characterized histologically by the presence of Reed–Sternberg cells. A small minority of patients have a non-classic, more indolent form of the disease, referred to as nodular lymphocyte-predominant HL.

Cutaneous involvement usually consists of multiple papulonodules or plaques in a patient with known, advanced disease. The trunk is the most common site of involvement[38], and lesions often appear in sites distal to affected lymph nodes. Lymphadenopathy, splenomegaly, and constitutional symptoms (e.g. fevers, chills, night sweats) are additional signs and symptoms.

In 20%–50% of patients with HL, paraneoplastic cutaneous disorders can develop. These include primary pruritus, acquired ichthyosis, persistent dermatitis, widespread eczema craquelé, hyperpigmentation, and occasionally, erythema nodosum[37].

Pathology

The histologic features of cutaneous HL are similar to those of affected lymph nodes. A nodular or diffuse dermal infiltrate consisting of lymphocytes admixed with eosinophils and plasma cells is present; epidermotropism is not seen. Depending upon the histologic subtype, Reed–Sternberg cells (or mononuclear variants) and lacunar cells may be present. The latter, most common in the nodular sclerosing subtype of HL, are large cells with abundant eosinophilic cytoplasm. The retraction of this cytoplasm from adjacent cells during fixation gives rise to a giant cell residing within a clear space. Areas of dermal sclerosis may be seen and extension into the subcutaneous fat is common.

Reed–Sternberg cells express CD30, fascin, and CD15, but not CD45RB (leukocyte common antigen) or CD20. They are positive for PAX-5, MUM-1, and in ~30% of cases, EBV (EBER-1). The background infiltrate of lymphocytes is composed predominantly of T cells[32]. In non-classic lymphocyte-predominant HL, the malignant cells stain positively for CD20[9,29].

Differential diagnosis

The histologic differential diagnosis of HL includes cALCL and LyP, both of which have cells that stain positively for CD30 (see Ch. 120). Clinicopathologic correlation is important in differentiating between these entities. Both LyP and cALCL can present with variably ulcerated papules and nodules, but patients with LyP do not have evidence of systemic involvement and crops of their lesions appear and then spontaneously resolve. Sheets of atypical $CD30^+$ cells are usually seen in cALCL, and the cells in LyP and most cases of cALCL do not stain positively for CD15 or PAX-5[9].

Treatment

Patients with stage IV HL, who may have secondary cutaneous disease, have a cure rate of ~70%–80% following combination chemotherapy. Treatments for recurrent disease include salvage chemotherapy, autologous HSCT, and anti-CD30 (brentuximab) and anti-PD-1 antibodies[41].

Blastic Plasmacytoid Dendritic Cell Neoplasm

Synonyms: ■ $CD4^+/CD56^+$ hematodermic neoplasm ■ Blastic NK cell lymphoma

Key features

- Single to multiple, non-tender papules, nodules, and plaques that can resemble bruises
- At initial presentation, skin is the most common site of involvement
- Dense perivascular infiltrate of uniformly atypical, medium-sized mononuclear cells
- Immunohistochemical profile: $CD123^+$, $CD4^+$, $CD56^+$, $TCF4^+$
- T cell receptor (TCR) and IgH gene rearrangements are not present
- Predictable good initial response to chemotherapy, but relapses common and poor survival

History and epidemiology

In 1994, blastic plasmacytoid dendritic cell neoplasm (BPDCN) was described by Adachi et al.[42] as a $CD4^+/CD56^+$ lymphoma presenting predominantly in the skin. Initially classified as blastic NK cell lymphoma due to its CD56 expression, this rare tumor was subsequently reclassified, first as a hematodermic neoplasm and then as a neoplasm of plasmacytoid dendritic cells[43]. Currently, BPCDN is listed as a myeloid-related specific entity in both the 2022 International Consensus Classification of Myeloid Neoplasms and in the recent WHO classification of Myeloid and Histiocytic/Dendritic Neoplasms[29a,29b,44].

BPDCN is a disease of adults, usually those >50 years of age, but pediatric cases have been reported. The male-to-female ratio is 3:1.

Pathogenesis

BPDCN represents a malignant proliferation of plasmacytoid dendritic cells. These cells produce large amounts of type I interferons (IFN), specifically IFN-α, and they express several Toll-like receptors (e.g. TLR7, TLR9), making them critical in the defense against viruses and other pathogens[29a,29b,45].

Clinical features

Clinically, BPDCN presents as solitary or multiple, non-tender, variably pruritic, erythematous to violaceous papules, plaques, or nodules that can resemble bruises (Fig. 121.10). Ulceration is uncommon. In most patients, the skin is the presenting site of involvement. However, further evaluation usually reveals subclinical regional lymph node, peripheral

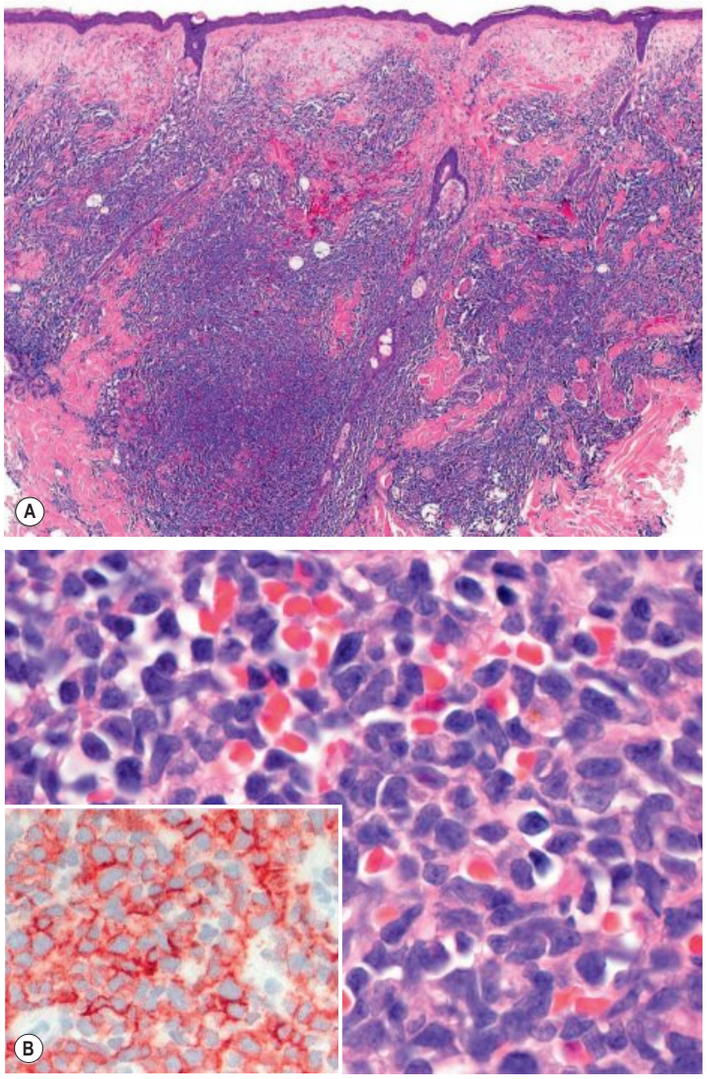


Fig. 121.11 Blastic plasmacytoid dendritic cell neoplasm. A Dense diffuse infiltrates of monomorphous blastoid cells within the entire dermis, with a grenz zone below the epidermis. **B** Diffuse infiltrate of medium-sized blastoid mononuclear cells admixed with extravasated erythrocytes; positive immunohistochemical staining for CD56 (inset). *Courtesy Lorenzo Cerroni, MD.*

blood, and bone marrow involvement in the majority of patients. Those individuals with initial negative staging eventually develop hematologic involvement. Symptoms of fevers, chills, night sweats, or weight loss are uncommon at presentation but may develop with disease progression.

Pathology

A diffuse dermal infiltrate of monotonous, atypical, medium-sized mononuclear cells is seen (Fig. 121.11A). These cells have fine blastic chromatin, indistinct nucleoli, and scant agranular eosinophilic cytoplasm. Intratumoral hemorrhage is common. In early lesions, the infiltrate may be perivascular and periadnexal. A grenz zone is almost always present and the infiltrate commonly extends into the subcutis[9,46,47].

Immunohistochemical studies are necessary to establish the diagnosis. The cells are $CD4^+$, $CD56^+$, $CD123^+$, $TCL1^+$, $CD2AP^+$, $BDCA2^+$/$CD303^+$, $TCF4^+$, myeloperoxidase$^-$, and EBV^- (Fig. 121.11B). TdT is variably positive. Although there are descriptions of aberrant $CD4^-$, $CD56^-$, or $CD123^-$ cases, diagnostic immunophenotypic criteria have been established[9,28,29a,29b,46,48].

The tumor cells have germline configurations of Ig (H and L) and TCR genes, i.e. lack rearrangement. Abnormalities of several chromosomes, including regions that contain genes involved in cell cycle regulation, have been reported[43,49–51].

Differential diagnosis

The differential diagnosis includes AML and other cutaneous lymphomas. BPDCN, however, lacks IgH and TCR gene rearrangements and has a characteristic immunohistochemical profile (see above). There are subtypes of AML that may express CD4, CD56, and CD123, but expression of TCL1, BDCA2/CD303, TCF4, and CD2-associated protein (CD2AP) points to the diagnosis of BPDCN[9,52]. Of note, there are reports of patients with BPDCN developing AML[29a,29b,44].

Treatment

Initial treatment of BPDCN originally consisted of multidrug chemotherapeutic regimens. Although response rates were high (up to 80%), invariably patients relapsed followed by progression, with one year being the median overall survival. Currently, tagraxofusp (an anti-CD123 fusion protein composed of recombinant IL-3 fused to truncated diphtheria toxin) is the recommended first-line therapy for BPDCN. Depending upon duration of response, which is yet to be determined, it may serve as a bridge to allogeneic HSCT[53,54].

Angioimmunoblastic T Cell Lymphoma

Synonyms:
- Angioimmunoblastic lymphadenopathy
- Angioimmunoblastic lymphadenopathy with dysproteinemia

Key features

- Constitutional symptoms (fever, sweats, weight loss)
- Variable cutaneous manifestations, including morbilliform eruption, urticaria, and rarely, erythroderma
- Polyclonal gammopathy, autoantibodies, autoimmune hemolytic anemia, immune thrombocytopenia, and peripheral eosinophilia
- Generalized lymphadenopathy, hepatosplenomegaly, and pleural effusions
- Most commonly, a superficial perivascular infiltrate within the dermis with eosinophils, but not atypia of the lymphocytes

History

This disease was initially described in 1974 as angioimmunoblastic lymphadenopathy with dysproteinemia, and its features included generalized lymphadenopathy, hepatosplenomegaly, polyclonal hypergammaglobulinemia, and a hemolytic anemia[55,56].

Epidemiology

Angioimmunoblastic T cell lymphoma (AITL) is a relatively rare disease of the middle-aged and elderly, with a nearly equal incidence in men and women[56]. It represents the second most common subtype of peripheral T cell lymphoma (PTCL; see Ch. 120)[28,56].

Pathogenesis

AITL was originally considered to be an atypical reactive process or an abnormal immunologic reaction, until next-generation sequencing identified recurrent mutations in several genes (e.g. *DNMT3A*, *TET2*, *IDH2*, *RHOA*) within neoplastic T cells[57]. In addition, EBV is often present in non-neoplastic B cells[28,29], thus explaining the occasional development of B cell lymphomas in these patients. Currently, in the 5th edition of the WHO classification of hematolymphoid neoplasms and in the 2022 International Consensus Classification of mature lymphoid neoplasms, it is considered to be a subtype of follicular helper T-cell lymphoma[28,29].

Clinical features

Patients with AITL usually present at an advanced stage with fever, weight loss, night sweats, generalized lymphadenopathy, and hepatosplenomegaly[28,29,56,57]. Approximately one-half of the patients have cutaneous manifestations. The most common presentation is a widespread morbilliform eruption that resembles a viral exanthem. Other cutaneous findings include petechiae (often associated with thrombocytopenia), urticaria, purpura, papulonodules, and rarely, erythroderma[57–59]. EBV positivity has been reported to be more common in those with papulonodules as opposed to other cutaneous manifestations[59]. As with HD, generalized pruritus may be a presenting symptom[57].

Patients can develop a host of autoimmune diseases including rheumatoid arthritis, vasculitis, and the entities listed in key features. In addition hypergammaglobulinemia, multiple autoantibodies, and

peripheral eosinophilia, laboratory abnormalities include lymphopenia, elevated LDH, and cold agglutinins[28,29,55–57]. AITL has an aggressive behavior, with a median survival of <3 years[28,29,56,57]. Both circulating EBV DNA copy number and EBV positivity within skin lesions are considered negative prognostic markers[59].

Pathology

In the skin, the histopathologic features vary, with five patterns described to date. These include: (1) a superficial perivascular infiltrate composed of plasma cells, eosinophils, and lymphocytes that lack atypia (most common pattern); (2) a sparse perivascular infiltrate with atypical lymphocytes; (3) a dense superficial and deep infiltrate of pleomorphic lymphocytes; (4) a vasculitis, with or without atypical lymphocytes; and (5) necrotizing granulomas[28,29,56,57]. A presentation with necrotizing granulomas resembling an infectious process has been reported[58]. Similar to involved lymph nodes, the skin may have increased numbers of venules with a prominent endothelial lining ("high endothelial venules").

By immunohistochemistry, the neoplastic cellular phenotype corresponds to T follicular helper cells ($CD3^+$, $CD4^+$, $CD8^-$, $CD10^+$, PD-1^+, $ICOS^+$, Bcl-6^+, chemokine ligand $CXCL13^+$) plus clusters of $CD21^+$ follicular dendritic cells[60]. As noted previously, EBV-encoded RNA (EBER) is often detected within non-neoplastic B cells but not in the neoplastic T cells[29,59], and EBER-1^+ B cells more commonly accompany dense, superficial and deep infiltrates of pleomorphic, large-sized atypical lymphocytes[59].

Molecular analysis demonstrates a monoclonal TCR rearrangement and usually a polyclonal immunoglobulin pattern[29]. The most common chromosomal abnormalities are trisomy 3 and tristomy 5[61].

Differential diagnosis

The morbilliform nature of the eruption belies its malignant nature. Consequently, confusion with a drug eruption or viral exanthem is common. As cutaneous histologic changes are subtle, a specific diagnosis often cannot be rendered. Differentiation from other cutaneous lymphomas with a T follicular helper cell phenotype may be very difficult, and the diagnosis of cutaneous AITL can only be established in patients with proven extracutaneous AITL.

Treatment

The majority of patients present with stage III–IV disease[56,57] and treatment options include multidrug chemotherapeutic regimens (e.g. cyclophosphamide, doxorubicin, vincristine, and prednisone [CHOP]) versus CHOP plus brentuximab vedotin in those who have any evidence of CD30 expression in tumor cells. This may be followed by autologous HSCT. In patients with relapsed or refractory disease and a good performance status, allogeneic HSCT can be performed. Gentler palliative options include epigenetic modifiers such as histone deacetylase (HDAC) inhibitors (e.g. romidepsin) and possibly phosphoinositide-3-kinase inhibitors[56].

Lymphomatoid Granulomatosis

Key features

- EBV-driven angiocentric/destructive lymphoproliferative disorder
- Presents with cough, dyspnea, chest pain, and constitutional symptoms
- Cavitary pulmonary nodules on chest radiograph
- Nodular or ulcerative cutaneous lesions in 25%–50% of patients

History

Lymphomatoid granulomatosis (LG) was first described in 1972 as a pulmonary angiitis/granulomatosis that mimicked granulomatosis with polyangiitis. Initially thought to represent a reactive process, subsequent studies demonstrated a malignant clonal B cell population admixed with an abundant, polyclonal, reactive T cell population[28,29].

Epidemiology

LG is a rare disease of adults, usually presenting in the fifth to sixth decade of life. The male-to-female ratio is approximately 2:1. The disease can affect children, most commonly in the setting of immunodeficiency syndromes[28,29,62].

Pathogenesis

The pathogenesis of LG is often related to EBV infection, occasionally in combination with immunosuppression. Factors associated with LG include use of immunosuppressive medications (e.g. azathioprine, methotrexate, imatinib), HIV infection, Wiskott–Aldrich syndrome, X-linked lymphoproliferative syndrome, and additional lymphoproliferative disorders[28,29]. In the WHO classification of hematopoietic tumors, LG is categorized as an angiocentric/angiodestructive lymphoproliferative disease with variable histological grades[28,29].

Clinical features

Patients with LG present with symptoms related to pulmonary involvement, such as cough, dyspnea, and chest pain. Constitutional symptoms include fever, weight loss, malaise, arthralgias, and myalgias. Cutaneous lesions develop in 25%–50% of patients and usually present as nodules or ulcerated plaques (Fig. 121.12). Rarely, LG may present as a maculopapular exanthem. The kidney, brain, and gastrointestinal tract may be affected. In contrast to angioimmunoblastic T cell lymphoma, the lymph nodes and spleen are rarely involved.

Pathology

In LG, there are three histopathologic grades: (1) *grade 1* – polymorphous lymphoid infiltrate without cytologic atypia, along with a few large cells, and few cells are positive for EBV-encoded RNA 1 (EBER-1) and latent membrane protein via *in situ* hybridization and immunohistochemistry, respectively; (2) *grade 2* – polymorphous inflammatory background with scattered large cells and more abundant EBER-1^+ cells; and (3) *grade 3* – sheets of large B cells and numerous EBER-1^+ cells predominate over the inflammatory background. The amount of necrosis increases with the grade and angiocentricity/angiodestruction is consistently present. Granulomatous changes are often present. The neoplastic cells stain positively for CD20 and CD79a, and in most high-grade lesions there is a monoclonal rearrangement of the J_H genes[9,28,29].

Differential diagnosis

The clinical differential diagnosis includes various forms of cutaneous lymphoma, as well as infectious and inflammatory disorders (e.g. medium-sized vessel vasculitis, pyoderma gangrenosum). The histopathologic differential diagnosis is broad and encompasses most of the lymphoproliferative disorders mentioned above, including B cell and T cell lymphomas. Other disorders with histologic evidence of granulomatosis include granulomatosis with polyangiitis, sarcoidosis, and infectious processes. Diagnosis is based upon histopathologic findings plus immunohistochemical and molecular analyses. Because the existence



Fig. 121.12 Lymphomatoid granulomatosis. Ulcerated violaceous plaque in the popliteal fossa. *Courtesy Jean L. Bolognia, MD.*

of skin-limited disease without pulmonary involvement is debatable, such a diagnosis requires compelling evidence.

Treatment

LG follows an aggressive course, with the 5-year mortality ranging from 60% to 90%. For higher-grade disease, treatment commonly involves multidrug chemotherapy and/or rituximab (anti-CD20 monoclonal antibody), and, for grade 1 disease, IFN-α. Reversal of exogenous immunosuppression may also lead to clinical improvement[28,29].

Additional figures available in our eBook (see inside front cover for access code).

REFERENCES

1. Jessner M, Kanof NB. Lymphocytic infiltration of the skin. *Arch Dermatol*. 1953;68:447–449.
2. Toonstra J, Wildschut A, Boer J, et al. Jessner's lymphocytic infiltration of the skin. A clinical study of 100 patients. *Arch Dermatol*. 1989;125:1525–1530.
3. Noider S, Casper C, Kuhn A, et al. Jessner-Kanof lymphocytic infiltration of the skin associated with glatiramer acetate. *Mult Scler*. 2005;11:245–248.
4. Guarneri C, Lentini M, Polimeni G, et al. Ustekinumab-induced drug eruption resembling lymphocytic infiltration (of Jessner-Kanof) and lupus erythematosus tumidus. *Br J Clin Pharmacol*. 2016;81:792–794.
5. Dippel E, Poenitz N, Klemke CD, et al. Familial lymphocytic infiltration of the skin: histochemical and molecular analysis in three brothers. *Dermatology*. 2002;204:12–16.
6. Pereira A, Ferrara G, Calamaro P, et al. The histopathological spectrum of pseudolymphomatous infiltrates in cutaneous lupus erythematosus. *Am J Dermatopathol*. 2018;40:247–253.
7. Tomasini D, Mentzel T, Hantschke M, et al. Plasmacytoid dendritic cells: an overview of their presence and distribution in different inflammatory skin diseases, with special emphasis on Jessner's lymphocytic infiltrate of the skin and cutaneous lupus erythematosus. *J Cutan Pathol*. 2010;37:1132–1139.
8. Borges da Costa J, Boixeda P, et al. Pulsed-dye laser treatment of Jessner lymphocytic infiltration of the skin. *J Eur Acad Dermatol Venereol*. 2008;23:595–596.
9. Cerroni L. *Skin Lymphoma – The Illustrated Guide*. 5th ed. London: Wiley Blackwell; 2020.
10. Albrecht J, Fine LA, Piette W. Drug-associated lymphoma and pseudolymphoma: recognition and management. *Dermatol Clin*. 2007;25:233–244.
11. Shear NH. *Litt's Drug Eruption and Reaction Manual*. 26th ed. Boca Raton: CRC Press; 2019.
12. Magro CM, Daniels BH, Crowson AN. Drug induced pseudolymphoma. *Semin Diagn Pathol*. 2018;35:247–259.
13. Werner B, Massone C, Kerl H, et al. Large CD30-positive cells in benign, atypical lymphoid infiltrates of the skin. *J Cutan Pathol*. 2008;35:1100–1107.
14. Leinweber B, Colli C, Chott A, et al. Differential diagnosis of cutaneous infiltrates of B lymphocytes with follicular growth pattern. *Am J Dermatopathol*. 2004;26:4–13.
15. Atwater AR, Longley BJ, Aughenbaugh WD. Kikuchi's disease: case report and systematic review of cutaneous and histopathologic presentations. *J Am Acad Dermatol*. 2008;59:130–136.
16. Paradela S, Lorenzo J, Martinez-Gomez W, et al. Interface dermatitis in skin lesions of Kikuchi-Fujimoto's disease: a histopathological marker of evolution into systemic lupus erythematosus? *Lupus*. 2008;17:1127–1135.
17. Balode D, Beļajeva L, Ruesseler V, et al. Diagnostic challenges and treatment options for cutaneous T cell pseudolymphoma: a case study with rituximab treatment. *Am J Case Rep*. 2020;21:e919616.
18. Kazakov DV, Belousova IE, Kacerovska D, et al. Hyperplasia of hair follicles and other adnexal structures in cutaneous lymphoproliferative disorders: a study of 53 cases, including so-called pseudolymphomatous folliculitis and overt lymphomas. *Am J Surg Pathol*. 2008;32:1468–1478.
19. Willemze R, Cerroni L, Kempf W, et al. The 2018 update of the WHO-EORTC classification for primary cutaneous lymphomas. *Blood*. 2019;133:1703–1714. [correction appears in *Blood*. 2019;134:1112].
20. Yashiro A, Sawada T, Shimamoto M. A kind of plasmacytosis: primary cutaneous plasmacytoma? Jpn. *J Dermatol*. 1976;86:910.
21. Honda R, Cerroni L, Tanikawa A, et al. Cutaneous plasmacytosis: report of 6 cases with or without systemic involvement. *J Am Acad Dermatol*. 2013;68:978–985.
22. Kato K, Satoh T, Tanaka-Fujimoto T, et al. IgG4-positive cells in skin lesions of cutaneous and systemic plasmacytosis. *Eur J Dermatol*. 2013;23:255–256.
23. Vilas Boas P, Cerroni L, Requena L. Intravascular cutaneous disorders. A clinicopathologic review. *Am J Dermatopathol*. 2021;43:119–136.
24. Miguel D, Peckruhn M, Elsner P. Treatment of cutaneous pseudolymphoma: a systematic review. *Acta Derm Venereol*. 2018;98:310–317.
25. Khalil S, Ariel Gru A, Saavedra AP. Cutaneous extramedullary haematopoiesis: implications in human disease and treatment. *Exp Dermatol*. 2019;28:1201–1209.
26. Vega Harring SM, Niyaz M, Okada S, Kudo M. Extramedullary hematopoiesis in a pyogenic granuloma: a case report and review. *J Cutan Pathol*. 2004;31:555–557.
27. Longacre TA, Smoller BR. Leukemia cutis. Analysis of 50 biopsy-proven cases with an emphasis on occurrence in myelodysplastic syndromes. *Am J Clin Pathol*. 1993;100:276–284.
28. Campo E, Jaffe ES, Cook JR, et al. The International Consensus Classification of Mature Lymphoid Neoplasms: a report from the Clinical Advisory Committee. *Blood*. 2022;140:1229–1253.
29. Alaggio R, Amador C, Anagnostopoulos I, et al. The 5th edition of the World Health Organization Classification of Haematolymphoid Tumours: Lymphoid Neoplasms. *Leukemia*. 2022;36:1720–1748.

29a. Khoury JD, Solary E, Abla O, et al. The 5th edition of the World Health Organization Classification of Haematolymphoid Tumours: Myeloid and Histiocytic/Dendritic Neoplasms. *Leukemia*. 2022;36:1703–1719.

29b. Arber DA, Orazi A, Hasserjian RP, et al. International Consensus Classification of Myeloid Neoplasms and Acute Leukemias: integrating morphologic, clinical, and genomic data. *Blood*. 2022;140:1200–1228.

30. Desch JK, Smoller BR. The spectrum of cutaneous disease in leukemias. *J Cutan Pathol*. 1993;20:407–410.
31. Cerroni L, Zenahlik P, Höfler G, et al. Specific cutaneous infiltrates of B-cell chronic lymphocytic leukemia. A clinicopathologic and prognostic study of 42 patients. *Am J Surg Pathol*. 1996;20:1000–1010.
32. Martínez-Escanamé M, Zuriel D, Tee SI, et al. Cutaneous infiltrates of acute myelogenous leukemia simulating inflammatory dermatoses. *Am J Dermatopathol*. 2013;35:419–424.
33. Plaza JA, Comfere NI, Gibson LE, et al. Unusual cutaneous manifestations of B-cell chronic lymphocytic leukemia. *J Am Acad Dermatol*. 2009;60:772–780.
34. Alegría-Landa V, Rodríguez-Pinilla SM, Santos-Briz A, et al. Clinicopathologic, immunohistochemical, and molecular features of histiocytoid Sweet syndrome. *JAMA Dermatol*. 2017;153:651–659.
35. Kakaletsis N, Kaiafa G, Savopoulos C, et al. Initially lymphocytic Sweet's syndrome in male patients with myelodysplasia: a distinguished clinicopathological entity? Case report and systematic review of the literature. *Acta Haematol*. 2014;132:220–225.
36. Introcaso CE, Kantor J, Porter DL, Junkins-Hopkins JM. Cutaneous Hodgkin's disease. *J Am Acad Dermatol*. 2008;58:295–298.
37. Rubenstein M, Duvic M. Cutaneous manifestations of Hodgkin's disease. *Int J Dermatol*. 2006;45:251–256.
38. Huong G, Olson LC, Rippis GE, Magro CM. An index case of cutaneous Hodgkin lymphoma and review of the literature. *Am J Dermatopathol*. 2016;38:739–743.
39. Kadin ME, Drews R, Samel A, et al. Hodgkin's lymphoma of T cell type: clonal association with a CD30+ cutaneous lymphoma. *Hum Pathol*. 2001;32:1269–1272.
40. Vasef MA, Kamel OW, Chen Y-Y, et al. Detection of Epstein-Barr virus in multiple sites involved by Hodgkin's disease. *Am J Pathol*. 1995;147:1408–1415.
41. Connors JM, Cozen W, Steidl C, et al. Hodgkin lymphoma. *Nat Rev Dis Primers*. 2020;6:61.
42. Adachi M, Maeda K, Takekawa M, et al. High expression of CD56 (N-CAM) in a patient with cutaneous CD4-positive lymphoma. *Am J Hematol*. 1994;47:278–282.
43. Petrella T, Dalac S, Maynadié M, et al. CD4+ CD56+ cutaneous neoplasms: a distinct hematological entity? Groupe Français d'Etude des Lymphomes Cutanés (GFELC). *Am J Surg Pathol*. 1999;23:137–146.
44. Sapienza MR, Pileri A, Derenzini E, et al. Blastic plasmacytoid dendritic cell neoplasm: state of the art and prospects. *Cancers (Basel)*. 2019;11:595.
45. Laribi K, Denizon N, Besançon A, et al. Blastic plasmacytoid dendritic cell neoplasm: from origin of the cell to targeted therapies. *Biol Blood Marrow Transplant*. 2016;22:135–167.
46. Cota C, Vale E, Viana I, et al. Cutaneous manifestations of blastic plasmacytoid dendritic cell neoplasm – morphologic and phenotypic variability in a series of 33 patients. *Am J Surg Pathol*. 2010;34:75–87.
47. Massone C, Chott A, Metze D, et al. Subcutaneous, blastic natural killer (NK), NK/T-cell, and other cytotoxic lymphomas of the skin: a morphologic, immunophenotypic, and molecular study of 50 patients. *Am J Surg Pathol*. 2004;28:719–735.
48. Ascani S, Massone C, Ferrara G, et al. CD4-negative variant of CD4+/CD56+ hematodermic neoplasm: description of three cases. *J Cutan Pathol*. 2008;35:911–915.
49. Wiesner T, Obenauf AC, Cota C, et al. Alterations of the cell-cycle inhibitors p27(KIP1) and p16(INK4a) are frequent in blastic plasmacytoid dendritic cell neoplasms. *J Invest Dermatol*. 2010;130:1152–1157.
50. Pagano L, Valentini CG, Grammatico S, Pulsoni A. Blastic plasmacytoid dendritic cell neoplasm: diagnostic criteria and therapeutical approaches. *Br J Haematol*. 2016;174:188–202.
51. Sapienza MR, Fuligni F, Agostinelli C, et al. Molecular profiling of blastic plasmacytoid dendritic cell neoplasm reveals a unique pattern and suggests selective sensitivity to NF-κB pathway inhibition. *Leukemia*. 2014;28:1606–1616.
52. Marafioti T, Paterson JC, Ballabio E, et al. Novel markers of normal and neoplastic human plasmacytoid dendritic cells. *Blood*. 2008;111:3778–3792.
53. Pemmaraju N, Lane AA, Sweet KL, et al. Tagraxofusp in blastic plasmacytoid dendritic-cell neoplasm. *N Engl J Med*. 2019;380:1628–1637.
54. Massone C, Raiola AM, Dominietto A, et al. Blastic plasmacytoid dendritic cell neoplasm: underlining the importance of an early diagnosis and the use of tagraxofusp therapy before wide dissemination. *Australas J Dermatol*. 2021;62:e316–e318.
55. Frizzera G, Moran EM, Rappaport H. Angioimmunoblastic lymphadenopathy with dysproteinemia. *Lancet*. 1974;1:1070–1073.
56. Moskowitz AJ. Practical treatment approach for angioimmunoblastic T-cell lymphoma. *J Oncol Pract*. 2019;15:137–143.
57. Piris MA, Rodriguez-Pinilla SM, Santonja C, et al. Update on peripheral T-cell lymphomas with T-helper phenotype: are there too many subtypes? *Semin Diagn Pathol*. 2020;37:24–31.
58. Jayaraman AG, Cassarino D, Advani R, et al. Cutaneous involvement by angioimmunoblastic T-cell lymphoma: a unique histologic presentation, mimicking an infectious etiology. *J Cutan Pathol*. 2006;33:6–11.
59. Lee WJ, Won KH, Choi JW, et al. Cutaneous angioimmunoblastic T-cell lymphoma: Epstein-Barr virus positivity and its effects on clinicopathologic features. *J Am Acad Dermatol*. 2019;81:989–997.
60. Yu H, Shahsafaei A, Dorfman DM. Germinal-center T-helper-cell markers PD-1 and CXCL13 are both expressed by neoplastic cells in angioimmunoblastic T-cell lymphoma. *Am J Clin Pathol*. 2009;131:33–41.
61. Lunning MA, Vose JM. Angioimmunoblastic T-cell lymphoma: the many-faced lymphoma. *Blood*. 2017;129:1095–1102.
62. Beaty MW, Toro J, Sorbara L, et al. Cutaneous lymphomatoid granulomatosis: correlation of clinical and biologic features. *Am J Surg Pathol*. 2001;25:1111–1120.



eFig. 121.1 Lymphocytic infiltrate of Jessner. Pink, arciform plaques on the mid back. On palpation, the lesions feel infiltrated. *Courtesy Lorenzo Cerroni, MD.*



eFig. 121.2 Lymphocytic infiltrate of Jessner. Pink plaques on the cheek composed of confluent papules. Note that one plaque is arciform. *Courtesy Lorenzo Cerroni, MD.*



eFig. 121.3 Lymphocytic infiltrate of Jessner. Infiltrated pink papules and plaques of the central back. Note the annular and arciform configuration (inset). *Courtesy Lorenzo Cerroni, MD.*



eFig. 121.4 Cutaneous lymphoid hyperplasia (lymphocytoma cutis). A Violet papulonodules on the helix and lobe of the ear (unknown etiology). **B** Multiple red–brown to violet papules at the sites of *Hirudo medicinalis* (medicinal leech) application. *B, Courtesy Josef Smolle, MD.*





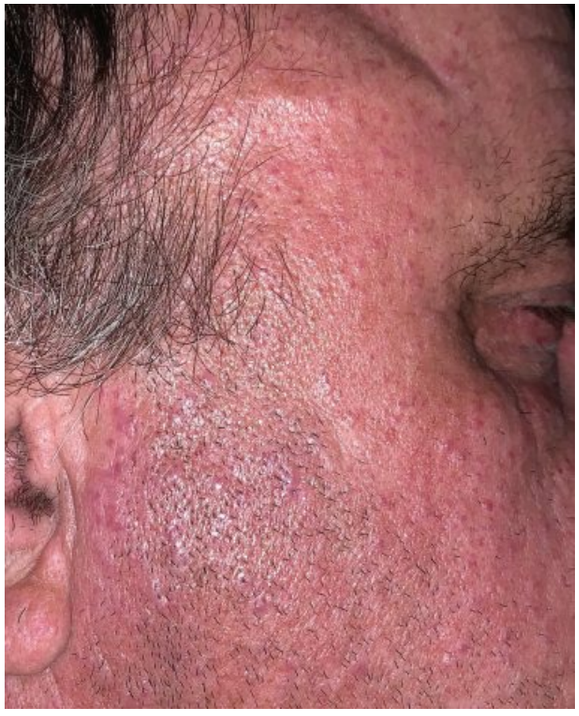
eFig. 121.5 Cutaneous lymphoid hyperplasia (pseudolymphoma) – clinical presentations. **A** Pink nodule on and adjacent to the areola in an Austrian woman with *Borrelia burgdorferi*-associated lymphocytoma cutis. **B** Multiple red–brown to violet papules at the sites of *Hirudo medicinalis* (medicinal leech) application. *Courtesy Lorenzo Cerroni, MD.*



eFig. 121.7 Extramedullary hematopoiesis. "Blueberry muffin baby" secondary to congenital rubella. *Courtesy James Graham, MD.*



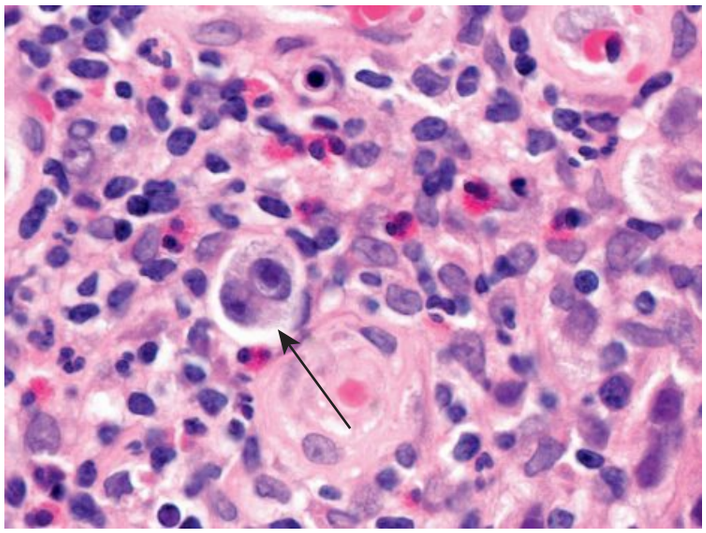
eFig. 121.8 Leukemia cutis. Multiple red–brown papules and plaques in a patient with hairy cell leukemia.



eFig. 121.6 Miliarial-type perifollicular B cell cutaneous lymphoid hyperplasia (pseudolymphoma). This is an unusual variant that presents as numerous violaceous perifollicular papules in the head and neck region. *Courtesy Karynne O. Duncan, MD.*



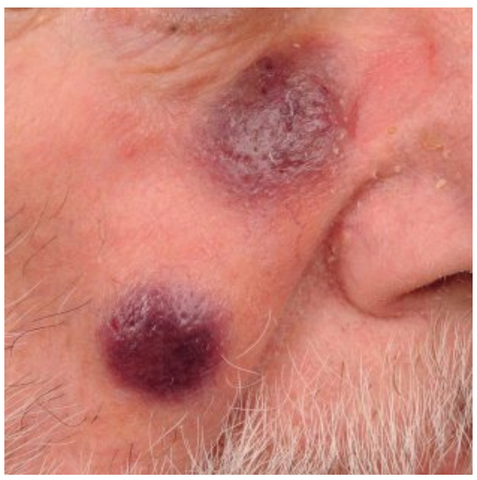
eFig. 121.9 Cutaneous Hodgkin lymphoma. Pink to red–brown papulonodules within a thin erythematous plaque; note the larger tumor on the hip. *Courtesy Lorenzo Cerroni, MD.*



eFig. 121.10 Cutaneous Hodgkin lymphoma. Polymorphic infiltrate with lymphocytes, eosinophils, histiocytes, and a Reed–Sternberg cell (arrow). *Courtesy Lorenzo Cerroni, MD.*



eFig. 121.11 Cutaneous Hodgkin lymphoma. Large dull pink–brown plaque with central clearing is noted on the lower abdomen. The small ulceration represents the site of a previous skin biopsy.



eFig. 121.12 Blastic plasmacytoid dendritic cell neoplasm. Two firm violaceous nodules on the cheek. *Courtesy Lorenzo Cerroni, MD.*



eFig. 121.13 Retiform purpura due to microvascular occlusion in a patient with advanced myelofibrosis. There are hemorrhagic bullae within the retiform purpura. *Courtesy Jonathan S. Leventhal, MD and Lauren Levy, MD.*

Cutaneous Metastases 122

Christine J. Ko and Jennifer M. McNiff

Key features

- Cutaneous metastases are uncommon and rarely may be the presenting sign of an internal malignancy
- In general, cutaneous metastases are associated with a poor prognosis
- In women, breast carcinoma and melanoma are the malignancies that most frequently metastasize to the skin
- In men, melanoma and carcinomas of the head and neck, lung, and colon are the malignancies that most frequently metastasize to the skin
- Among common malignancies, breast carcinoma is the most likely to metastasize to the skin
- The most common clinical presentation for a cutaneous metastasis is a firm, painless, erythematous nodule
- Cutaneous metastases may arise in the anatomic vicinity of the primary cancer
- Cutaneous metastases typically have histologic features similar to, but not necessarily identical to, those of the primary malignancy
- Treatments include excision, chemotherapy, immunotherapy, and radiotherapy; the latter is often administered for palliation

INTRODUCTION

Given their prognostic implications, cutaneous metastases represent an important dermatologic entity. The skin is not a particularly common site for metastatic spread, and because the clinical appearance of cutaneous metastases can mimic more common disorders, e.g. epidermoid cysts (inflamed and non-inflamed; Fig. 122.1), lipomas, cellulitis, there may be a delay in diagnosis. This is especially true when the primary malignancy is occult. An understanding of the clinical spectrum as well as advances in histological assessment of skin metastases is vital to establishing the correct diagnosis.



Fig. 122.1 Cutaneous metastasis of small cell lung carcinoma. A skin-colored nodule on the neck that resembles an epidermoid cyst or lipoma. *Courtesy Ian Odell, MD, PhD.*

EPIDEMIOLOGY

Depending upon the series, cutaneous metastases occur in 1% to 10% of patients with metastatic disease (to any organ)[1]. Although uncommon, their recognition is important because they can be the first sign of metastatic disease and, as a result, have profound prognostic implications. The proportion of patients with metastatic disease who have cutaneous metastases depends upon the particular malignancy, e.g. the highest incidence is in individuals with metastatic melanoma, where up to 45% of patients can develop skin metastases (Table 122.1)[1]. Sex-specific cancer rates also influence the frequency of the various types of cutaneous metastases. In women, skin metastases are most often due to breast carcinoma (70%) and melanoma (12%), followed by carcinomas originating from the ovary, head and neck, and lung[1]. In men with skin metastases, the most common underlying malignancies are melanoma (32%), followed by carcinomas of the head and neck (16%), lung (12%), and colon (11%).

The overall prevalence of a cancer is also an important determinant. For instance, although skin metastases develop in only 2.5% of patients with metastatic lung cancer, they account for 12% of all cutaneous metastases in men due to the high prevalence of lung cancer[1] (Fig. 122.2).

CUTANEOUS METASTASES IN PATIENTS WITH METASTATIC CANCER

Primary malignancy	Percentage of all patients with cutaneous metastases*	Percentage of all patients *with metastatic disease* who developed cutaneous metastases*
Breast	50	30
Melanoma	18	45
SCC (head and neck)†	7	13
Lung	5	2.5
Unknown	4.5	7.5
Colon/rectum	4	4.5
Ovary	2.5	4
Urinary bladder	1.5	8
Endocrine glands	1	12.5
Esophagus	1	8.5
Gallbladder/bile ducts	<1	5.5
Liver	<1	5
Kidney	<1	4.5
Stomach	<1	2
Pancreas	<1	2
Uterine cervix	<1	1
Prostate	<1	<1
Testes	<1	<1

*The percentages are for men and women combined.
†Larynx, oropharynx, nasal sinuses.

Table 122.1 Cutaneous metastases in patients with metastatic cancer. Rates of metastatic spread do vary depending upon the series. *Adapted from Lookingbill DP, Spangler N, Helm KF. Cutaneous metastases in patients with metastatic carcinoma: a retrospective study of 4020 patients. J Am Acad Dermatol 1993;29:228–36.*

Similarly, the age of the patient plays a role, with rhabdomyosarcoma and neuroblastoma responsible for the majority of cutaneous metastases seen in children[2,3].

Cutaneous metastases develop an average of 36 months (range, 1 to 177 months) after the initial diagnosis of the primary malignancy[2,4]. Unfortunately, the vast majority (~95%) of patients with cutaneous metastases have advanced, stage III or IV disease. Rarely, cutaneous metastases can be the presenting sign of an internal malignancy (<1% of all new cancer diagnoses).

PATHOGENESIS

In 1889, Dr Stephen Paget espoused the "seed and soil" hypothesis as the paradigm of metastatic disease – a malignancy must develop the capability to dissociate from its native environment, survive during transit, and then propagate in a new milieu. This process includes detachment, intravasation, circulation, stasis, extravasation, and finally proliferation[5,6]. It is estimated that ≤0.01% of tumor cells shed into the vasculature form metastatic foci at distant sites[7].

The ability of a malignancy to acquire metastatic potential is thought to occur via one of two mechanisms[8]. In the clonal expansion or linear progression model, selective growth advantages are acquired during the course of tumor development. Over time, subpopulations of cells acquire genetic characteristics that enable them to dissociate and then propagate in distant tissues. In this model, metastatic foci have similar phenotypes and genotypes to the original tumor. Alternatively, in the variant or parallel progression model, rare, highly aggressive stem cell-like clones with high metastatic potential exist within the tumor and can cause dissemination at any point during tumorigenesis.

It is generally accepted that certain cancers tend to metastasize to distinct tissues. The mechanism by which they choose their final destination is related to hemostatic forces and surface protein expression patterns. When tumor emboli lodge in the first vascular bed they encounter, adhesion molecule interactions (e.g. integrins) facilitate extravasation and account for the commonly noted involvement of regional nodal basins. Yet, certain cancers have an affinity for specific tissues that are not anatomically convenient, such as prostate cancer spreading to bone and ocular melanoma metastasizing to the liver[3]. Adhesion molecule expression seems likely to influence this tissue-specific homing of metastases. However, these mechanisms may be attenuated in highly aggressive, undifferentiated tumors that display a more random distribution of metastases.

CLINICAL FEATURES

The clinical characteristics of cutaneous metastasis can provide important clues. When a patient with a known history of cancer presents with an extremely firm and rapidly growing erythematous nodule or an eruption of multiple skin nodules in close proximity to the primary tumor (Table 122.2), the diagnosis of cutaneous metastasis is relatively straightforward. However, the skin lesions may grow more slowly, and while metastases typically appear within several years of the diagnosis of the primary malignancy, they can present decades later.

The color of cutaneous metastases varies, from skin-colored to pink–red to blue–black, with the latter most commonly observed in metastatic melanoma (Fig. 122.3). In general, dermal and subcutaneous metastases are firmer on palpation than lipomas or epidermoid and tricholemmal (pilar) cysts. Cutaneous metastases can arise from hematogenous or lymphatic spread as well as direct extension. In the case of the latter two scenarios, as stated previously, proximity of the

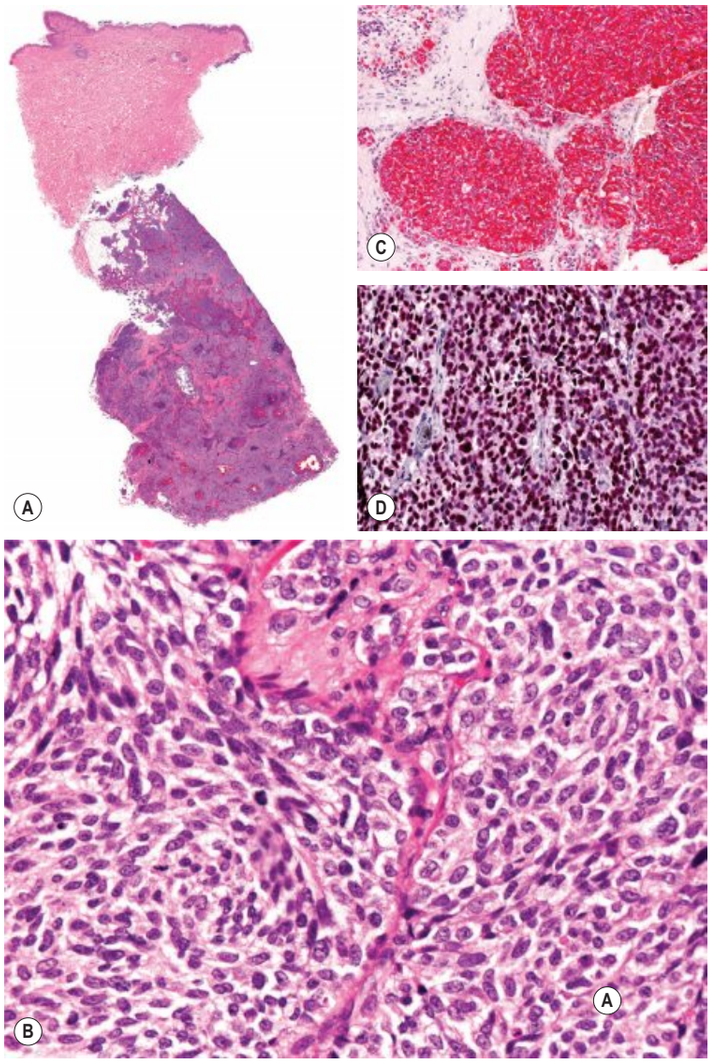


Fig. 122.2 Subcutaneous metastasis of small cell lung carcinoma. A Note sparing of the dermis. **B** Higher magnification demonstrating clusters of basaloid cells. **C** The tumor cells stain positively for CK7. **D** The tumor cells also stain positively for TTF-1 (thyroid transcription factor-1). *Courtesy Lorenzo Cerroni, MD.*

ANATOMIC LOCATIONS OF CUTANEOUS METASTASES			
Anatomic site	**Primary malignancy (men)**	**Primary malignancy (women)**	**Comments**
Scalp	Lung, renal	Breast	Can lead to alopecia ("alopecia neoplastica"; Fig. 122.3A)
Head & neck	SCC of the head & neck*, lung	Breast	Eyelid metastases from breast carcinoma have been reported; breast & lung metastases can lead to a "clown nose"
Upper extremities	Lung, renal, colon	Breast	Uncommon site in men and usually occurs late during disease
Back	Lung	Breast	20% of BSA, but site of 8% of metastases
Chest	Lung	Breast	
Abdomen	Colon, lung, stomach	Colon, ovary, breast	Sister Mary Joseph nodule (Fig. 122.4): most commonly gastric, colon, ovarian, or pancreatic cancers
Pelvis	Colon	Colon, ovary	Site of 8% of cutaneous metastases
Lower extremities	Melanoma > lung, renal	Melanoma > lung, renal	Uncommon site: 36% of BSA but site of only 4% of metastases

*e.g. larynx, oropharynx, nasal sinuses.

Table 122.2 Anatomic locations of cutaneous metastases. The trunk is the most common site (~55% of metastases) and the scalp is the site of ~15% of metastases[1]. BSA, body surface area; SCC, squamous cell carcinoma.
Adapted from Klein CA. Parallel progression of primary tumours and metastases. Nat Rev Cancer 2009;9:302–12.

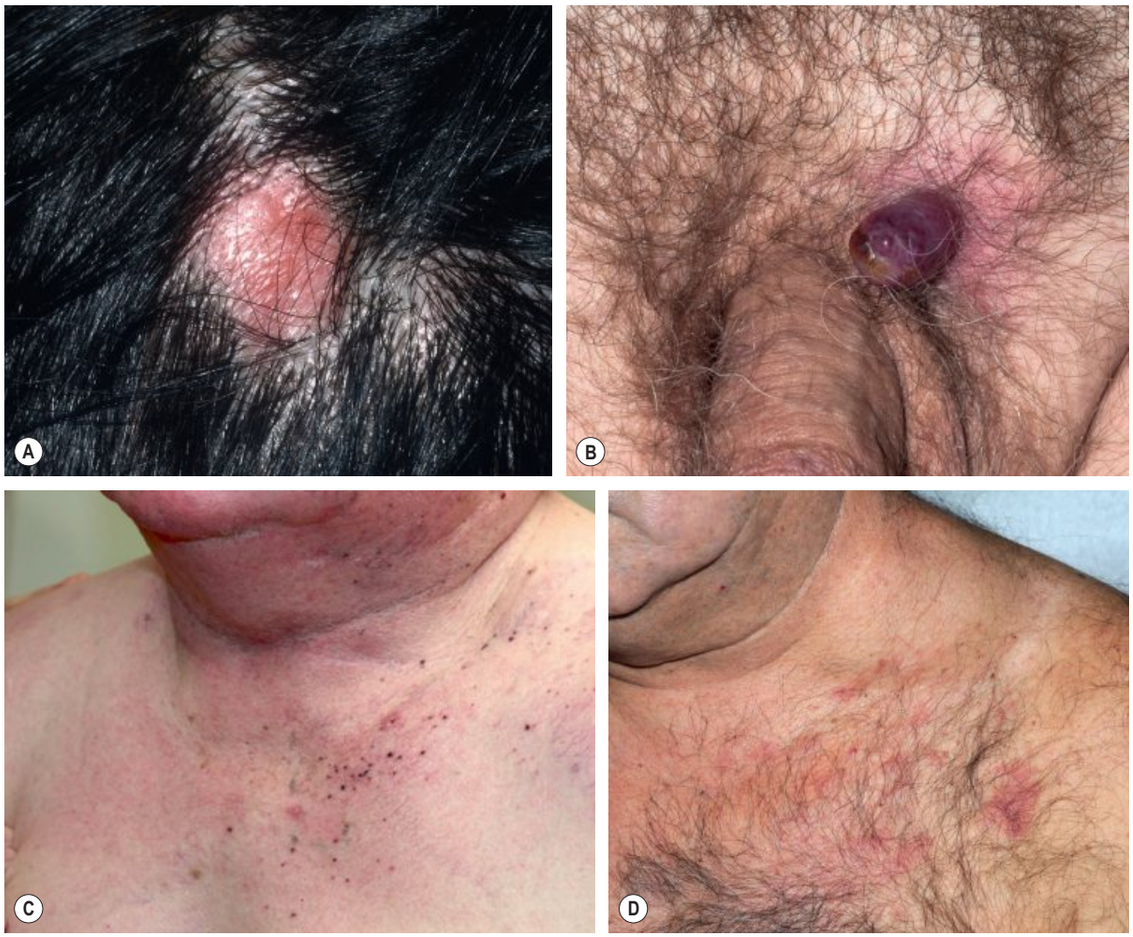


Fig. 122.3 Cutaneous metastases. **A** Pink nodule on the scalp with associated alopecia due to a metastasis from lung carcinoma (alopecia neoplastica). **B** Red–purple eroded nodule due to a metastasis from renal cell carcinoma; such lesions may be confused with vascular tumors. **C** Multiple small dark purple to black papules on the left neck and chest due to metastatic melanoma. **D** Pink papules and plaques on the chest due to metastases from adenocarcinoma of the colon. The patient was referred for treatment of dermatitis. *A, Courtesy Lorenzo Cerroni, MD; B, Courtesy Edward Cowen, MD; C, Courtesy Chris Bunick, MD; D, Courtesy Kalman Watsky, MD.*



Fig. 122.4 Cutaneous metastasis of colon carcinoma. An umbilical Sister Mary Joseph nodule presenting as a pink plaque with scale-crust. *Courtesy Stuart Lessin, MD.*

metastasis to the primary malignancy serves as a diagnostic clue. An example of lymphatic spread is in-transit metastases of melanoma while direct extension is most commonly observed with breast carcinoma and squamous cell carcinoma of the head and neck.

There are additional examples of anatomic localization, including the predilection of gastrointestinal malignancies to metastasize to the periumbilical region, referred to as a Sister Mary Joseph nodule (Fig. 122.4). Occasionally, implantation of tumor occurs at the time of a surgical procedure, e.g. chest tube placement for a malignant pleural effusion due to lung cancer. Although the distribution of cutaneous metastases is usually more random in the case of hematogenous spread, the scalp can be a preferred site for some malignancies, e.g. renal cell carcinoma.

Of all the carcinomas that metastasize to the skin, breast cancer may be the one with the widest range of clinical presentations (Table 122.3), varying from papulonodules to patches of erythema mimicking erysipelas (inflammatory carcinoma) to woody induration with a *peau d'orange* appearance (Fig. 122.5). The latter is often referred to as "*en cuirasse*" due to its clinical resemblance to the leather armor of a soldier (*cuirassier*)[1]. In addition, intravascular metastases can lead to erythematous papules that may resemble vascular proliferations, including the angiosarcomas that can follow breast irradiation (see Ch. 114).

Less common presentations include the dermatitis-like appearance of Paget disease, both mammary and extramammary (see Table 122.3). Metastases of renal cell carcinoma can resemble pyogenic granulomas, including a tendency to bleed (see Fig. 122.3B). Rarely, intravascular metastases lead to a reticulated vascular pattern that is reflective of a vaso-occlusive process or the cutaneous metastases assume an unusual distribution pattern, e.g. zosteriform.

In addition to metastases from solid organs, leukemias and systemic lymphomas can also involve the skin (see Chs. 119–121). The lesions are often pink–violet to red–brown papulonodules and therefore may be clinically indistinguishable from cutaneous metastases due to solid organ malignancies. Skin involvement by leukemia or lymphoma is classically not referred to as "metastases".

PATHOLOGY

Adenocarcinoma, squamous cell carcinoma (SCC), and melanoma represent the three major categories of cutaneous metastases (Table 122.4). In broad terms, these metastatic tumors generally lack an epidermal connection or involvement, are situated in the dermis or subcutis, and are composed of nodules, nests, or cords of atypical cells with mitoses (Table 122.5). However, it is important to note that occasionally there are primary "dermal" nodular melanomas[9], and primary cutaneous spindle cell SCCs often lack a prominent epidermal component. In addition, cutaneous metastases of both melanoma and



Fig. 122.5 Various presentations of cutaneous metastases of breast carcinoma. A Eroded erythematous nodules in the axilla. **B** Inflammatory form (carcinoma erysipeloides) with patches of erythema that may initially be misdiagnosed as infectious cellulitis. **C** Primarily *en cuirasse* form with obvious induration and *peau d'orange* appearance in addition to papulonodules. **D** Mixed pattern – reticulated erythema of carcinoma erysipeloides as well as *peau d'orange* appearance near the areola. *A, D, Courtesy Stuart Lessin, MD.*

CLINICAL PRESENTATIONS OF CUTANEOUS METASTASES AND HISTOLOGIC CORRELATES			
Type	**Clinical description**	**Histology**	**Associated primary malignancy**
Dermal or subcutaneous nodules	Small miliary lesions to large tumors; single or multiple	Tumor cells infiltrating among collagen bundles or replacing dermis; grenz zone often present	Most common presentation; any type
Inflammatory carcinoma (carcinoma erysipeloides)	Erythematous patch with spreading border; resembles erysipelas	Tumor cells within dilated lymphatic vessels	Breast ≫ lung, ovary, prostate, GI, others
En cuirasse	Morpheaform or sclerodermoid, depending upon extent; indurated with *peau d'orange* appearance	Fibrosis with infiltrating tumor cells	Breast ≫ lung, GI, kidney, others
Carcinoma telangiectodes	Red–violet papules; purpuric patches with telangiectasias	Tumor cells within superficial blood vessels and RBC sludging	Breast
Paget disease*	Patches extending from the nipple and areola that resemble dermatitis	Large, atypical epithelial cells with abundant pale cytoplasm arranged in solitary units and small nests within all layers of the epidermis	Breast
Alopecia neoplastica	Nodules or plaques on the scalp in association with alopecia	Cords of tumor cells between collagen bundles	Breast > lung (Fig. 122.3A), renal, others
Pyogenic granuloma-like	Rapidly growing nodule resembling a vascular tumor (particularly a pyogenic granuloma)	Neoplastic cells in cords and lobules admixed with prominent hemorrhage and "pseudovascular" spaces	Renal clear cell carcinoma (Fig. 122.3B), hepatocellular carcinoma > others

*Lesions of extramammary Paget disease share similar histopathologic features with those of Paget disease of the breast, but usually represent (>75% of patients) primary cutaneous adenocarcinomas (see Ch. 73); an underlying visceral malignancy is most likely when there is perianal involvement.

Table 122.3 Clinical presentations of cutaneous metastases and histologic correlates. An individual patient can have an admixture of the various types. Occasionally, cutaneous metastases have a zosteriform distribution pattern and clinically they can resemble dermatoses, including eczema, vasculitis, and erythema annulare centrifugum. Obviously, they can also mimic cutaneous tumors, including non-melanoma skin cancers, epidermoid or pilar cysts, lipomas, granular cell tumors, or angiosarcoma[4]. GI, gastrointestinal; RBC, red blood cell.

PATHOLOGIC FINDINGS IN CUTANEOUS METASTASES			
Malignancy	**Possible histological clues**	**Immunohistochemical markers**	**Comments**
Adenocarcinomas – CEA positive and typically negative for p40/p63, CK5/6, D2–40 (podoplanin)			
Breast	Single filing or cords of cells (lobular CA); tumor cells form glandular structures (ductal CA); signet ring cells	CK7, ER/PR, mammoglobulin, gross cystic disease fluid protein-15 (GCDFP-15), GATA3	Breast CA can be ER/PR-negative; GCDFP-15 positivity also seen in cutaneous adnexal and salivary gland tumors; occasionally, ER/PR positivity in some primary cutaneous adnexal carcinomas
Colon	Columnar cells with basally oriented nuclei and intracytoplasmic mucin production; gland formation; "dirty" necrosis	CK20, CDX2, villin, SATB2	Mucinous CA can develop from other tissues (lung, ovary, uterine cervix) and rarely can be primary cutaneous
Non-small cell lung, adenocarcinoma		CK7, TTF-1, napsin A	Non-small cell lung CA can be TTF-1-negative; TTF-1 positivity not limited to lung or thyroid CA
Ovarian	Psammoma bodies can be seen in papillary serous CA	CA125, CK7, ER/PR, mesothelin, WT-1 (serous CA), PAX8	Mucinous ovarian CA may closely resemble other types of mucinous CA
Prostate		PSA, PSAP, NKX3.1	High-grade CA may lose glandular differentiation as well as PSA & PSAP expression
Pancreatobiliary		CK7, CK20, CA19.9, CA125	CA19.9 is not specific for pancreatobiliary tumors
Gastric	Signet ring cells (signet ring type)	CK7, CK20, lysozyme, CDX2, CDH17	Non-signet ring cell type gastric CA may not have distinct morphology; signet ring cell CA is not limited to the stomach (e.g. can be seen in breast CA)
Thyroid	Thyroid follicle formation (follicular CA); papillary structure, psammoma bodies (papillary CA)	TTF-1, thyroglobulin, napsin A	High-grade tumors (insular CA, anaplastic CA) may lose characteristic thyroid gland morphology
Squamous cell carcinoma – islands of keratin-producing epithelial cells that stain positively for cytokeratins (e.g. CK5/6, CK903, MNF116) and p40/p63			
Melanoma – stains positively for S100, SOX10, HMB45, MITF, MelanA (MART-1); see Ch. 113			
Merkel cell carcinoma – stains positively for CK20, SATB, and in a majority of cases, Merkel cell polyomavirus; see Ch. 115			
Neuroendocrine (non-Merkel cell carcinoma)			
Small cell carcinoma (including lung)	Nuclear molding, scant cytoplasm, indistinct nucleoli	Keratins, INSM1, TTF-1, CD56, neuron-specific enolase, chromogranin, synaptophysin; negative for CK20	Some small cell CAs, including lung, may not express neuroendocrine markers
Neuroendocrine tumor, including carcinoid tumor and atypical carcinoid tumor	Nests of cells with neuroendocrine morphology	Neuroendocrine markers (INSM1, CD56, chromogranin); medullary thyroid CA: calcitonin and TTF-1	Poorly preserved tissue may resemble lymphoma, carcinoma or small cell CA
Other			
Renal (clear cell)	Clear cytoplasm, highly vascular	Co-expression of EMA and vimentin, PAX8, CD10, RCC-Ma, napsin A	Renal cell CA can be composed of other cell types (e.g. granular or spindle)
Bladder and urothelial	Medium-sized tumor cells arranged in nests or sheets	p40/p63, CK5/6, CK7, CK20, GATA3; uroplakin II	May resemble high-grade cutaneous adnexal CA

Table 122.4 Pathologic findings in cutaneous metastases. p40/p63 negativity favors metastases, but it may be negative in some cutaneous adnexal carcinomas, particularly mucinous eccrine carcinoma. CA, carcinoma; CDH17, cadherin 17; CDX2, homeobox protein CDX2; CEA, carcinoembryonic antigen; CK, cytokeratin; EMA, epithelial membrane antigen; ER, estrogen receptor; GATA3, a transcription factor that regulates mammary epithelial differentiation; INSM1, insulinoma-associated protein 1; MITF, microphthalmia transcription factor; MNF116, pankeratin marker; NKX3.1, NK3 homeobox 1; PAX8, paired box 8; PR, progesterone receptor; PSA, prostate-specific antigen; PSAP, prostatic-specific acid phosphatase; RCC-Ma, renal cell carcinoma marker – detects a renal tubule antigen (highly specific); SATB2, special AT-rich sequence-binding protein 2/SATB homeobox 2; SCC, squamous cell carcinoma; SOX-10, SRY-box transcription factor 10; TTF-1, thyroid transcription factor 1; WT-1, product of Wilms tumor gene.

HISTOLOGIC CLUES TO THE DIAGNOSIS OF CUTANEOUS METASTASES
Well-circumscribed, usually symmetric, dermal or subcutaneous nodules of atypical cells with numerous mitoses and without connection to the epidermis (rarely cutaneous metastases are epidermotropic)
Presence of atypical cells within lymphatic vessels (differential diagnosis: intravascular lymphoma [neoplastic cells found in blood, not lymphatic, vessels], intravascular angiosarcoma [neoplastic cells in blood or lymphatic vessels], intralymphatic histiocytosis, intralymphatic cutaneous anaplastic large cell lymphoma, benign intralymphatic proliferation of T cell lymphoid blasts, Merkel cell carcinoma [neoplastic cells usually in lymphatic vessels, rarely in blood vessels])
Atypical cells arranged in lines within the dermis (differential diagnosis: myelogenous leukemia)
Presence of necrosis *en masse* at the center of a nodule of atypical cells (differential diagnosis: some lymphomas, some primary cutaneous adnexal carcinomas)

Table 122.5 Histologic clues to the diagnosis of cutaneous metastases.

SCC (cutaneous, oropharyngeal, or solid organ) may show significant epidermal involvement so that distinction from a synchronous or metachronous primary skin tumor can be difficult. Four primary histopathologic patterns of cutaneous metastases are: (1) nodular; (2) diffuse, including infiltrative; (3) intravascular, including intralymphatic; and (4) epidermotropic (Fig. 122.6).

The following can serve as histologic clues to the diagnosis of cutaneous metastases, in addition to those outlined in Table 122.5: (1) atypical single cells infiltrating through collagen bundles (breast carcinoma[10]; see Fig. 122.6B); (2) clear cells plus abundant hemorrhage (renal cell carcinoma; Fig. 122.7); (3) "dirty" necrosis within glandular structures (colon carcinoma); (4) formation of colloid within

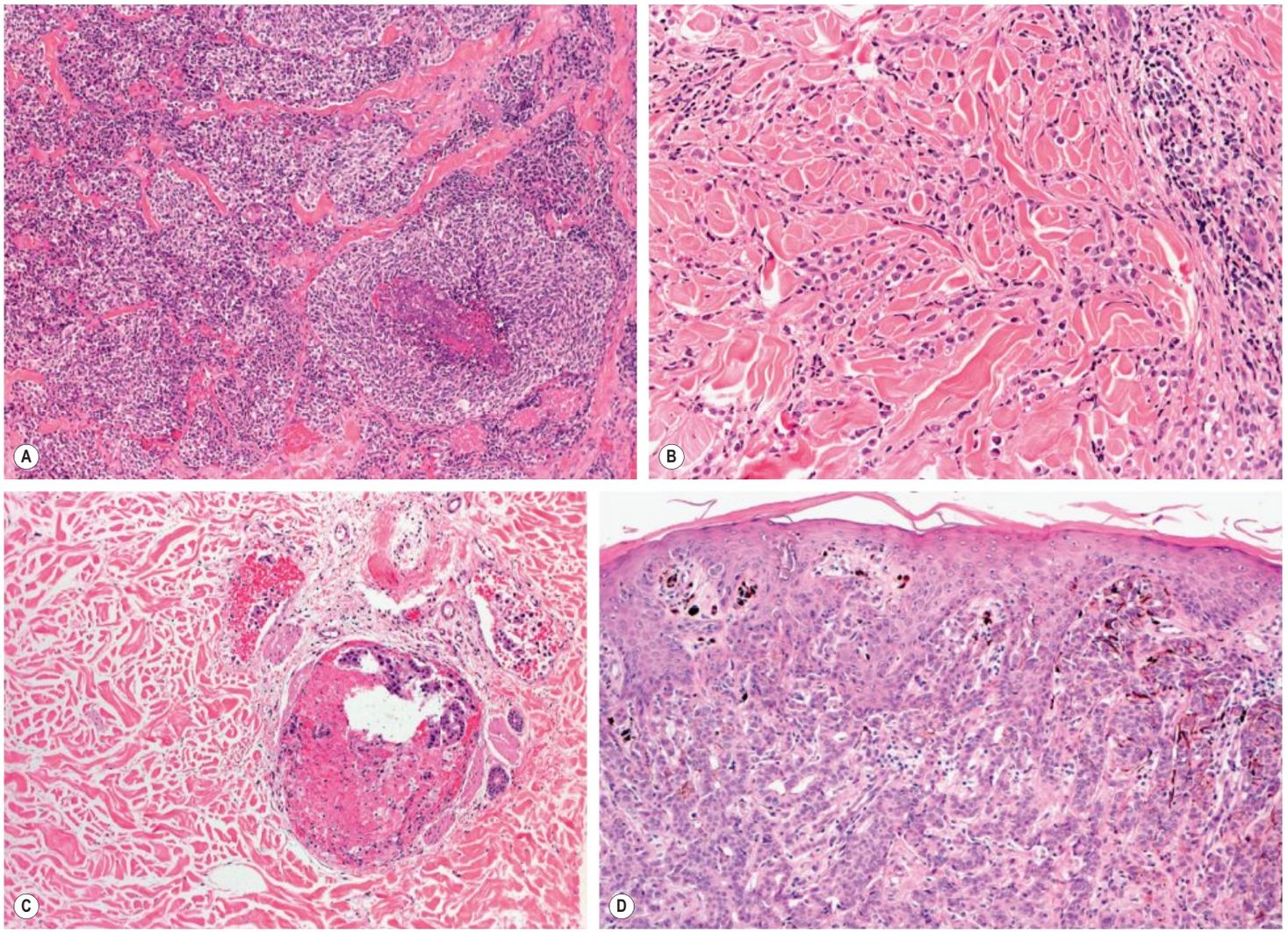


Fig. 122.6 Major patterns of cutaneous metastases. A Nodular pattern with focal, prominent necrosis in a cutaneous metastasis of small cell lung carcinoma. **B** Diffuse pattern with linear arrays of single cells in a metastasis of breast carcinoma. **C** Intralymphatic pattern in a metastatic breast carcinoma; tumor cells are confined to dilated lymphatic vessels. **D** Epidermotropic pattern in a metastasis of breast carcinoma; tumor cells are in both the dermis and the epidermis. The presence of focal pigmentation and melanocyte hyperplasia could lead to the misdiagnosis of a melanocytic tumor. *Courtesy Lorenzo Cerroni, MD.*

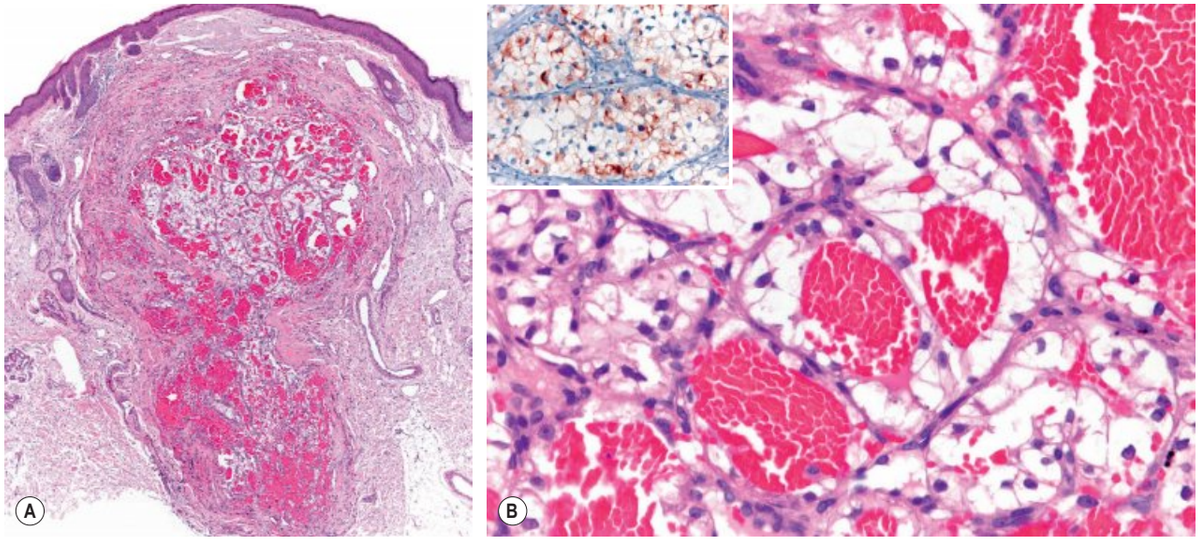


Fig. 122.7 Histopathologic features of cutaneous metastasis from clear cell renal cell carcinoma. A Vertically oriented hemorrhagic tumor within the dermis resembling an angiomatous tumor. **B** Tumor cells with clear cytoplasm arranged as fine trabecular structures and lobules surrounding hemorrhagic areas. The lack of prominent atypia can be misleading and lead to the erroneous diagnosis of hemangioma. Positive immunohistochemical staining with RCC-Ma (renal cell carcinoma marker), a monoclonal antibody directed against a proximal tubule antigen, labels clear cell renal cell carcinoma (inset). *Courtesy Lorenzo Cerroni, MD.*

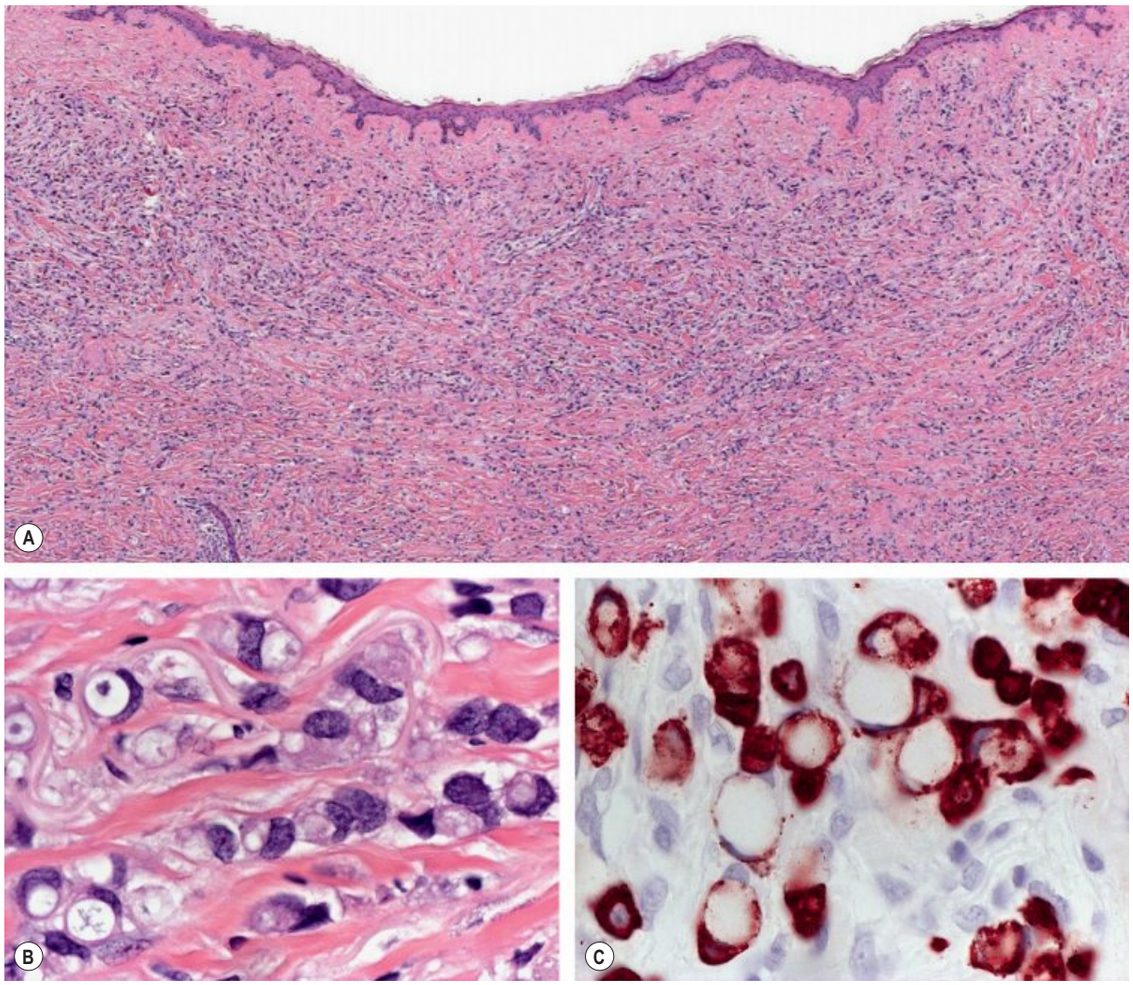


Fig. 122.8 Histopathologic features of cutaneous metastases of signet ring adenocarcinoma of the breast (A, B) and stomach (C). A Diffuse infiltration of neoplastic cells throughout the entire dermis. **B** Detail of neoplastic cells with signet ring cell morphology due to intracellular mucin accumulation. **C** Signet ring cells are not unique to breast carcinoma and may be observed in primary cutaneous carcinomas (e.g. histiocytoid carcinoma of the eyelid), non-epithelial neoplasms (e.g. melanoma), and a variety of adenocarcinomas, particularly those from the gastrointestinal tract. A cytokeratin (pan-CK) stain in this metastatic signet ring cell carcinoma of the stomach highlights the peculiar morphology of the cells, with intracellular mucin pressing the nuclei and distorting them, thus conferring the characteristic shape similar to that of a signet ring. *Courtesy Lorenzo Cerroni, MD.*

lumina (thyroid carcinoma); (5) psammoma bodies (thyroid or ovarian carcinoma); and (6) signet ring cells (gastric or breast carcinoma; Fig. 122.8)[11]. In addition to melanoma and SCC (see above), epidermotropism can occasionally be seen in cutaneous metastases from other malignancies, in particular breast carcinoma, and less often carcinomas of the prostate, colon, larynx, penis, or vagina[11]. Rarely, epidermotropic metastases, especially from breast carcinoma, may contain pigment and even an intratumoral increase in melanocytes, leading to the misdiagnosis of a melanocytic tumor (see Fig. 122.6D). When there is intravascular involvement, this may be confused with benign entities such as intralymphatic histiocytosis (Fig. 122.9).

Complete evaluation of a cutaneous metastasis often requires the use of a panel of histochemical stains (Fig. 122.10; see Table 122.4)[12]. While such stains are not a substitute for a detailed history and physical examination plus diagnostic imaging and biopsy of the primary tumor[12], the resulting information does provide direction and may circumvent the need for a more invasive biopsy of another tissue. In order to distinguish between a primary cutaneous tumor (usually an adnexal carcinoma) and a cutaneous metastasis (especially of adenocarcinoma), immunostains, in particular p40/p63, CK5/6 and D2–40 (podoplanin), can prove helpful[13–15]. Primary cutaneous tumors are typically positive for some or all these markers and metastases lack staining. Important exceptions are p63-positivity in some metastatic adenocarcinomas (breast, urothelial, and lung) and an absence of p63 staining in some primary cutaneous adnexal carcinomas.

In the case of cutaneous metastases from adenocarcinomas, various combinations of CK7 and CK20 expression can provide useful information (see Fig. 122.10)[15]. This panel is also employed to evaluate extramammary Paget disease, in which CK20 positivity points to a secondary form of the disease that is originating from a visceral malignancy (see Fig. 73.16).

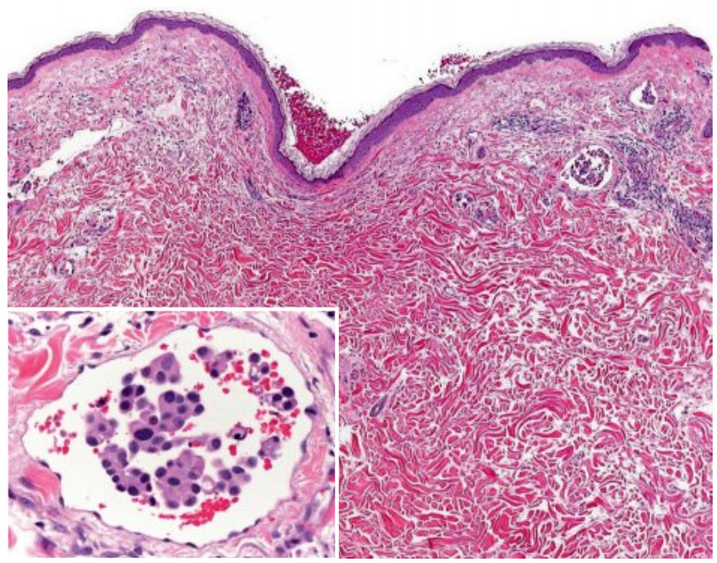


Fig. 122.9 Histopathologic features of cutaneous metastasis of urothelial micropapillary bladder carcinoma. Complexes of neoplastic cells within dilated lymphatic spaces in the dermis. Detail of a lymphatic space with intravascular tumor complexes admixed with erythrocytes (inset). Neoplastic urothelial (transitional) cells exhibit round–ovoid nuclei and abundant eosinophilic cytoplasm, and they form small rosette-like aggregates. These histopathologic features may simulate a benign condition, namely, intralymphatic histiocytosis. *Courtesy Lorenzo Cerroni, MD.*

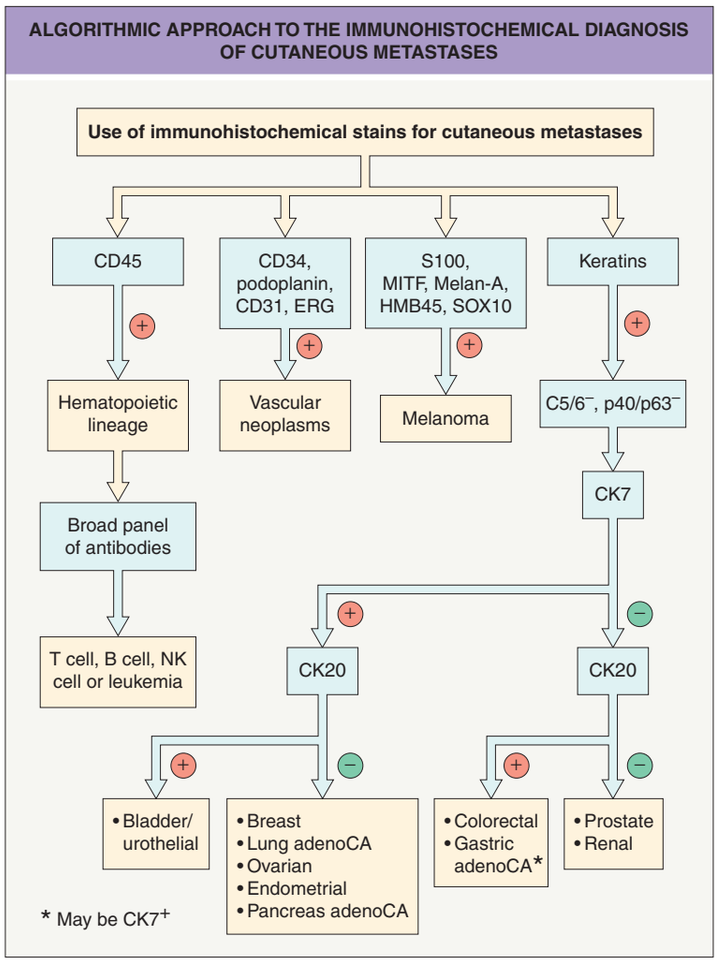


Fig. 122.10 Algorithmic approach to the immunohistochemical diagnosis of cutaneous metastases. The main differential diagnosis of metastatic adenocarcinoma is a primary cutaneous adnexal tumor (generally CK5/6$^+$, p40$^+$/p63$^+$). For tumors not clearly classifiable as a primary skin tumor, clinical history and directed immunohistochemical stains can be key to confirming the diagnosis. adenoCA, adenocarcinoma. *Adapted from Handa U, Kundu R, Dimri K. Cutaneous metastasis: a study of 138 cases diagnosed by fine-needle aspiration cytology. Acta Cytol 2017;61:47–54; Saeed S, Keehn CA, Morgan MB. Cutaneous metastasis: a clinical, pathological, and immunohistochemical appraisal. J Cutan Pathol 2004;31:419–30.*

Certain organ-restricted markers may also be useful including: CD10, RCC, and PAX8 (positive in renal and ovarian tumors); thyroid-specific transcription factor-1 (TTF-1) (thyroid, lung; see Fig. 122.2); thyroglobulin (thyroid); prostate specific antigen (PSA) and NKX3.1 (prostate); CDX2, CDH17, and SATB2 (gastrointestinal); Hep Par1 and arginase-1 (hepatocellular carcinoma); and CD56 and insulinoma-associated protein 1 (INSM1) (neuroendocrine) (see Table 122.4). In cutaneous metastases of SCC, staining for pankeratins and EMA may be positive, but this information is not helpful in determining the site of the primary SCC.

In addition to the histologic examination of conventional skin biopsies, cutaneous metastases can be sampled via fine-needle aspiration cytology[16].

TREATMENT AND PROGNOSIS

Typically, cutaneous metastases are a harbinger of late-stage or progressive disease and as such portend a poor prognosis. The average survival time following the initial diagnosis of cutaneous metastasis is 7.5 months[17] and half of patients expire within the first 6 months[18]. Whether the patient has a known or unknown primary malignancy, the development of cutaneous metastases calls for a multidisciplinary approach, including medical and surgical oncologists, radiation oncologists, and mental health care providers when appropriate. Localized treatment of cutaneous metastases can be undertaken for functional, palliative, or cosmetic indications. When feasible, surgical excision is performed; however, radiation and focal chemotherapeutics or immunotherapies can be considered on a case-by-case basis. Systemic therapies are indicated for immuno- or chemotherapy-responsive tumors. When malodorous, topical metronidazole solution (supplied for intravenous use) can be applied via cotton gauze or pump spray once to twice daily or crushed metronidazole tablets can be sprinkled onto the tumor twice daily.

Additional figures available in our eBook (see inside front cover for access code).

REFERENCES

1. Lookingbill DP, Spangler N, Helm KF. Cutaneous metastases in patients with metastatic carcinoma: a retrospective study of 4020 patients. *J Am Acad Dermatol*. 1993;29:228–236.
2. Nashan D, Lucas Muller M, Braun-Falco M, et al. Cutaneous metastases of visceral tumors: a review. *J Cancer Res Clin Oncol*. 2009;135:1–14.
3. Schwartz RA. Cutaneous metastatic disease. *J Am Acad Dermatol*. 1995;33:161–182.
4. Sariya D, Ruth K, Adams-McDonnell R, et al. Clinicopathologic correlation of cutaneous metastases: experience from a cancer center. *Arch Dermatol*. 2008;144:1155–1162.
5. Brodland DG, Zitelli JA. Mechanisms of metastasis. *J Am Acad Dermatol*. 1992;27:1–10.
6. Brodland DG. The life of a skin cancer. *Mayo Clin Proc*. 1997;72:475–478.
7. Morgan-Parkes JH. Metastases: mechanisms, pathways, and cascades. *Adv Clin Med*. 1995;164:1075–1082.
8. Klein CA. Parallel progression of primary tumours and metastases. *Nat Rev Cancer*. 2009;9:302–312.
9. Swetter SM, Ecker PM, Johnson DL, Harvell JD. Primary dermal melanoma. A distinct subtype of melanoma. *Arch Dermatol*. 2004;140:99–103.
10. McKee PH. Cutaneous metastases. *J Cutan Pathol*. 1985;12:239–250.
11. Schwartz RA. Histopathologic aspects of cutaneous metastatic disease. *J Am Acad Dermatol*. 1995;33:649–657.
12. Bellizzi AM. An algorithmic immunohistochemical approach to define tumor type and assign site of origin. *Adv Anat Pathol*. 2020;27:114–163.
13. Mahalingam M, Nguyen LP, Richards JE, et al. The diagnostic utility of immunohistochemistry in distinguishing primary skin adnexal carcinomas from metastatic adenocarcinom to skin: an immunohistochemical reappraisal using cytokeratin 15, nestin, p63, D2-40, and calretinin. *Mod Pathol*. 2010;23:713–719.
14. Lee JJ, Mochel MC, Piris A, et al. p40 exhibits better specificity than p63 in distinguishing primary skin adnexal carcinomas from cutaneous metastases. *Hum Pathol*. 2014;45:1078–1083.
15. Chu P, Wu E, Weiss LM. Cytokeratin 7 and cytokeratin 20 expression in epithelial neoplasms: a survey of 435 cases. *Mod Pathol*. 2000;13:962–972.
16. Handa U, Kundu R, Dimri K. Cutaneous metastasis: a study of 138 cases diagnosed by fine-needle aspiration cytology. *Acta Cytol*. 2017;61:47–54.
17. Saeed S, Keehn CA, Morgan MB. Cutaneous metastasis: a clinical, pathological, and immunohistochemical appraisal. *J Cutan Pathol*. 2004;31:419–430.
18. Schoenlaub P, Sarraux A, Grosshans E, et al. Survival after cutaneous metastasis: a study of 200 cases. *Ann Dermatol Venereol*. 2001;128:1310–1315.



eFig. 122.1 Melanoma metastases. Cluster of firm blue and skin-colored nodules in the axilla.



eFig. 122.2 Metastases of melanoma. Multiple pink firm papules on the leg.



eFig. 122.3 Metastasis of renal cell carcinoma (alopecia neoplastica). The scalp is a preferred site for cutaneous metastases of renal cell carcinoma.



eFig. 122.4 Metastasis of signet ring adenocarcinoma (alopecia neoplastica). A firm lobulated pink plaque on the scalp. *Courtesy Nour Kibbi, MD.*



eFig. 122.5 Scalp metastases of breast carcinoma. Note the lack of terminal hairs within the pink plaques. *Courtesy Jonathan Leventhal, MD.*



eFig. 122.6 Metastasis of renal cell carcinoma. Pink–violet firm papule with telangiectasias on the scalp. *Courtesy Jonathan Leventhal, MD.*



eFig. 122.8 Metastasis of signet ring adenocarcinoma (unknown primary). Firm pink plaque with telangiectasias on the chest. *Courtesy Nour Kibbi, MD.*



eFig. 122.7 Multiple metastases of colon carcinoma along the surgical excision scar. *Courtesy Jonathan Leventhal, MD.*



eFig. 122.9 Metastasis of breast carcinoma. The large, ulcerated, red–purple nodule was very firm to palpation. *Courtesy Jeffrey M. Cohen, MD.*

Public Health and Dermatology 123

Eric J. Yang, Eleni Linos and Abrar A. Qureshi

INTRODUCTION

As a dermatologist walks into the examination room of the patient in Fig. 123.1, several diagnostic possibilities likely come to mind. The patient's history, additional physical findings, and other clues help narrow the differential diagnosis. In this case, knowing the patient's history of atopic dermatitis lends context to the appearance of monomorphous punched-out erosions and allows one to arrive at the diagnosis of eczema herpeticum. Therefore, awareness of the epidemiology of a disease, how it is distributed within populations, and the factors that influence its distribution can assist in establishing a diagnosis[1–3].

Considering the high or increasing prevalence of many skin conditions, dermatologists have the potential to play an important role in public health research and policy. This chapter highlights the relevance of dermatologic conditions to public health, the impact epidemiology can have on a dermatology practice, and major types of public health studies, as well as research design concepts and terminology used in epidemiology.

THE PUBLIC HEALTH IMPORTANCE OF DERMATOLOGY

Skin conditions are a major cause of morbidity worldwide. Based on analysis of global burden of disease data[4], skin diseases accounted for over 41 million disability-adjusted life years (DALYs) lost in 2013 and ranked as the fourth most common cause of non-fatal disease burden (Table 123.1). In the US, dermatology accounts for 4% of *all* outpatient visits, representing the third most common subspecialty ambulatory visit (after ophthalmology and orthopedics). In addition, ~5%–8% of primary care and 4% of emergency department visits are primarily for dermatologic conditions, with the most common outpatient diagnoses including eczema, skin infections, benign neoplasms, acne, psoriasis, and skin cancer[5–7]. Notably, in 2010, the symptom of itch accounted for 1% of all outpatient visits in the US[8].

Not only are dermatologic conditions common, but some are rising in incidence. For example, the incidence of melanoma increased by ~3% per year in the US from 1981 to 2005, and then at a lower rate of ~1% per year from 2005 to 2019[9]; these increases have included all tumor thickness groups, although mortality has overall been stable, with improvement more recently, especially in women and younger individuals[10]. In addition, many countries have experienced an increase in the frequency of keratinocyte carcinomas, i.e. basal cell carcinomas (BCCs) and squamous cell carcinomas (SCCs)[11–15]. Indoor tanning is associated with an increased risk of skin cancer and has reached alarming rates among youth, with indoor tanning exposure in nearly 20% of adolescents in the US, Canada, and Northern and Western Europe[16].

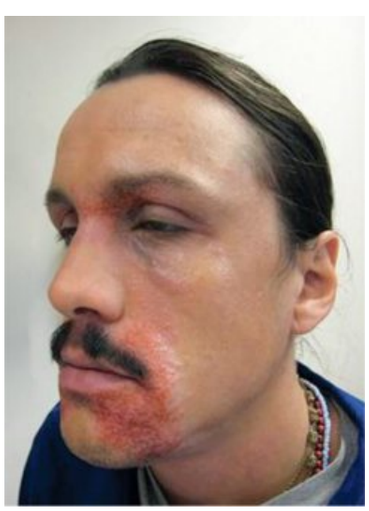


Fig. 123.1 Eczema herpeticum: diagnosis facilitated by knowledge of epidemiology. Grouped vesicles and punched-out erosions are evident. Based on this information alone, eczema herpeticum is in the differential diagnosis. However, awareness of the patient's history of atopic dermatitis, in combination with knowledge regarding the epidemiology of eczema herpeticum, allows for greater certainty in establishing the diagnosis.

Ensuring the health of Lesbian, Gay, Bisexual and Transgender (LGBT) persons is important for all physicians, including dermatologists. Recognition and treatment of sexually transmitted infections such as HIV and syphilis is essential, with the associated cutaneous manifestations often alerting one to the diagnosis[17] (see Chs. 78 and 82). In addition, high rates of skin cancer are a concern for gay men, based upon reports of six-fold higher rates of tanning bed use and over double the rates of skin cancer as compared to heterosexual men[18]. Cutaneous carcinomas are also more common and more aggressive in HIV-infected individuals.

Dermatologic care for transgender patients receiving gender-affirming hormonal and surgical treatments may include therapy for acne vulgaris and androgenetic alopecia exacerbated by testosterone treatment, terminal hair removal, and use of neurotoxin and dermal fillers to feminize or masculinize the face. Dermatologists must continue to address deficits in cultural competence related to transgender patients; an example would be recent modifications to make the FDA-mandated iPledge risk mitigation program more inclusive of transgender patients[19]. As emerging data suggest continued health disparities amongst the LGBT community, there is a greater need for healthcare providers who are culturally competent in LGBT health as well as more research on how to evaluate and address the existing disparities. Important considerations on the approach to caring for LGBT patients are outlined in Table 123.2.

ROLE OF EPIDEMIOLOGY IN DERMATOLOGY

Epidemiologic studies have yielded information on the etiology, risk factors, natural history, prognosis, incidence, prevalence, and effective treatments of dermatologic diseases. The impact that epidemiologic data can have on patient care and systems-based practice in dermatology is outlined in Table 123.3.

OBSERVATIONAL STUDIES

Participants in observational studies are observed and certain outcomes are measured, without external manipulation or an attempt to affect the outcome.

Descriptive Studies

Many of the studies currently being done in dermatology are descriptive. These include case reports and case series. A *case report* is a detailed description of an individual patient's demographics, clinical presentation, diagnosis, treatment, and disease course. A *case series* reports on some aspect(s) of a disease, diagnostic procedure, or treatment in a group of patients with common characteristics[20]. Case reports and series are useful for determining the manifestations of rare conditions, reporting the preliminary outcomes of experimental therapies, and generating hypotheses for larger studies. A major limitation of case series is the lack of a control group (Table 123.4)[20,21], although previous data (e.g. on the prevalence of risk factors in the general population) can sometimes be utilized for comparison.

An example of a valuable case series is the description of scalp involvement in patients with dermatomyositis by Kasteler and Callen[22]. Fourteen of the 17 patients with dermatomyositis who were

DISABILITY-ADJUSTED LIFE YEAR (DALY) RATES FOR ALL SKIN CONDITIONS COMBINED (2013)	
DALY rate/ 100 000 individuals	**Region**
<500	Central Asia
500–600	Central Europe, Eastern Europe, Central Latin America, East Asia, North Africa, Middle East
600–700	South Asia, Sub-Saharan Africa
700–800	High-income North America, Western Europe, Southern Latin America
>800	Australasia, Oceania

Table 123.1 Disability-adjusted life year (DALY) rates for all skin conditions combined (2013). Data from reference 4.

APPROACHES TO CARE FOR LESBIAN, GAY, BISEXUAL AND TRANSGENDER (LGBT) PATIENTS	
Goal	**Actions**
Create a safe and welcoming environment	• Display inclusive images in the office and waiting areas • Train staff on LGBT cultural competence and establish a zero-tolerance policy for discrimination • Include LGBT-specific demographic options on medical intake forms • Provide gender-neutral restrooms; allow patients to use the restroom of their choice • Recognize health disparities including health risk factors, barriers to care, discrimination, and minority stress
Use inclusive and patient-centered language	• Ask patients how they would like to be addressed • Ask which pronouns the patient prefers and use the patient's preferred terminology • Ask for clarification from the patient when needed • Apologize for errors when appropriate • Respect the patient's support system
Elicit sexual history when clinically appropriate	• Normalize sexual history taking in the context of medical care • Ask if the patient is sexually active; if they have sex with men, women, or both • Ask about which body parts the patient uses to have sexual intercourse • Ask about plans to become pregnant and/or contraceptive measures • Ask about methods of protection from HIV and other STDs • Ask transgender patients about completed/planned gender-affirming medical or surgical treatments

Table 123.2 Approaches to care for Lesbian, Gay, Bisexual and Transgender (LGBT) patients[19]. HIV, human immunodeficiency virus; STDs, sexually transmitted diseases.

seen in the authors' practice over a 5-year period had scalp involvement, manifesting as atrophic, erythematous, scaly plaques. Five of the 14 affected individuals had previously been diagnosed with scalp psoriasis or seborrheic dermatitis. This study helped raise awareness of scalp involvement as a manifestation of dermatomyositis.

Using Epidemiology to Identify the Cause of Disease

Case–control, cohort, and cross-sectional studies are often performed to help elucidate the etiology and risk factors of a disease (see Table 123.4). These methods involve studying a disease of interest (e.g. cutaneous SCC) and an exposure that is suspected of being a risk factor for the disease (e.g. ultraviolet [UV] radiation), so that the study participants can be categorized as having the disease or not and as being exposed to the potential risk factor or not (Table 123.5).

USES FOR EPIDEMIOLOGY IN DERMATOLOGY
Epidemiology applied at the patient care level
• Provide context to assist with diagnosis • Give guidance to patients on avoiding triggers and modifiable risk factors for their disease • Provide evidence for management strategies • Prevent associated comorbidities for patients and their families through early screening
Epidemiology applied at the systems level
• Raise awareness of the burden and distribution of skin disease in the community • Allow for appropriate allocation of resources for common and emerging conditions • Determine changing and future healthcare needs • Affect public policy

Table 123.3 Uses for epidemiology in dermatology.

Case–control study

A case–control study identifies a group of individuals with a disease, as well as a comparison group without the disease from the same population. The study design retrospectively evaluates the level of exposure in the disease group (cases), as compared to that in the group without disease (controls). To ensure that those with disease and without are comparable, both types of participants should be sampled from a single population and data collected in the same way for each group[23]. In addition, cases and controls should be matched on possible confounding factors; for example, if there is a 60-year-old female case, then a 60-year-old female control from the same general population would be selected.

A *confounder* is an extraneous variable that is associated with both the exposure and the disease being studied; it could therefore account for a part or all of the relationship between the exposure and disease. Although the confounder may be a contributing factor to the disease, it is not caused by the exposure and thus is not along the "causal pathway" between the exposure and disease[1,2] (Fig. 123.2). Age and sex are examples of possible confounders. These and other characteristics that may be associated with both the exposure and the disease should also be recorded and placed in the statistical model. If an association remains after accounting for confounders, it is more likely to be a true one.

In a case–control study, one can calculate the odds of having had the exposure among those with disease (a/c), as compared to the odds of having had the exposure among those without disease (b/d) (see Table 123.5). The association measure used for case–control studies is an *odds ratio* (OR), which equals (a/c)/(b/d) or ad/bc. An OR = 1 denotes a null association, whereas an OR statistically significantly greater or less than 1 indicates a positive or negative association, respectively. An OR is different from a *relative risk* (RR), the rate of disease among those exposed divided by that among those unexposed, (a/a+b)/(c/c+d) (see Cohort study section below). While the RR cannot be directly calculated from a case–control study, the OR approximates the RR when the disease is rare.

One of the major advantages of a case–control study is that it can yield information on a disease with many possible predictors, yet use only a limited number of participants. Therefore, it is well-suited for the investigation of rare conditions. Also, these studies are relatively inexpensive and time-efficient. One of the disadvantages of a case–control study is that it is not clear if the exposure preceded the disease, so causality cannot be established. In addition, this type of study has several potential biases. *Sampling bias* can occur when cases and controls are collected separately and may not be comparable. Because of the retrospective ascertainment of exposure, *recall bias* can occur; for example, those with disease may recall the exposure with greater detail because they have been contemplating the potential causes of their condition. Of note, a case–control study does not yield information on the incidence or prevalence of a disease.

An example of a case–control study is that by Picard et al.[24], which examined the association between psoriasis (here the "exposure") and coronary artery disease. They compared the prevalence of psoriasis in

STUDY TYPES AND THEIR CHARACTERISTICS						
Type of study	**Study group**	**Control group**	**Association measure frequently used**	**Advantages**	**Limitations**	**Level of evidence for whether a therapy is efficacious***
Case series	Persons with disease	None	Varies (e.g. percentile)	• Describes rare conditions and therapies	• No control group, no information on background level of exposure for comparison	4
Case–control	Persons with disease	Persons without disease	OR (approximates the RR in rare diseases)	• Can study rare diseases • Short duration, inexpensive, small size	• Potential for bias and confounding because sampling two different populations • Does not establish causal relationship • Limited to one disease	3
Cohort	Persons exposed	Persons not exposed	RR or absolute risk†	• Causal inference • Can evaluate a number of diseases • Yields incidence of disease • Can study rare exposures	• Often requires a large sample size • Less feasible for rare diseases	2‡
Cross-sectional	Persons with disease or exposed	Either of the above	OR or relative prevalence	• Can study several exposures and diseases • Relatively short duration • Yields *disease and exposure prevalence*	• Does not establish causality • Less feasible for rare diseases	2‡
Randomized controlled trials (RCTs)	Persons randomized to treatment	Persons randomized to control	Varies (e.g. RR or percentiles)	• Ability to demonstrate causality • Randomization and blinding help to decrease bias or confounding	• Expensive • Can expose participants to potential harm • Answers a narrow clinical question	1

*The level of evidence for a therapeutic efficacy has a scale of 1–5, 1 being the best. Expert opinions represent level 5. The level of evidence for therapeutic efficacy for a systematic review depends on the types of studies it reviews. A systematic review of RCTs with good homogeneity ranks above an individual RCT.
†***Absolute risk reduction*** is the incidence rate of disease in the exposed group subtracted by that of the unexposed group. This is affected by the rate of disease in the population; the greater the prevalence of disease, the higher the absolute risk reduction. The reciprocal of absolute risk reduction is the ***number needed to treat*** to avoid one person getting the disease.
‡In general, a cohort study (2b) is ranked as better than a cross-sectional study (2c).

Table 123.4 Study types and their characteristics[2,21,23]**.** OR odds ratio; RR, relative risk.

CATEGORIZATION OF STUDY PARTICIPANTS, BASED ON THEIR DISEASE AND EXPOSURE		
	Disease (e.g. cutaneous SCC)	**No disease (e.g. no cutaneous SCC)**
Exposed (e.g. high-dose UV)	a	b
Non-exposed (e.g. no high-dose UV)	c	d

Table 123.5 Categorization of study participants, based on their disease and exposure. An odds ratio (OR) = (a/c)/(b/d) whereas relative risk (RR) = (a/a+b)/(c/c+d). SCC, squamous cell carcinoma; UV, ultraviolet radiation.

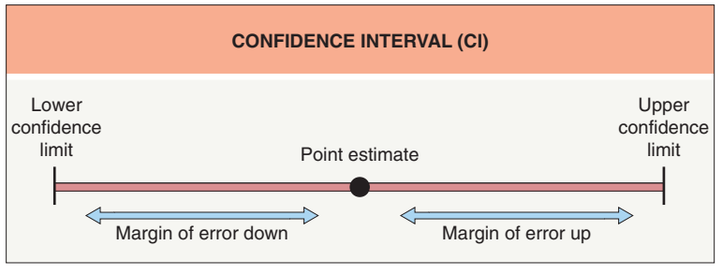


Fig. 123.3 Confidence interval (CI). A confidence interval derived from a valid analysis will, over unlimited repetitions of the study, contain the true parameter 95% of the time.

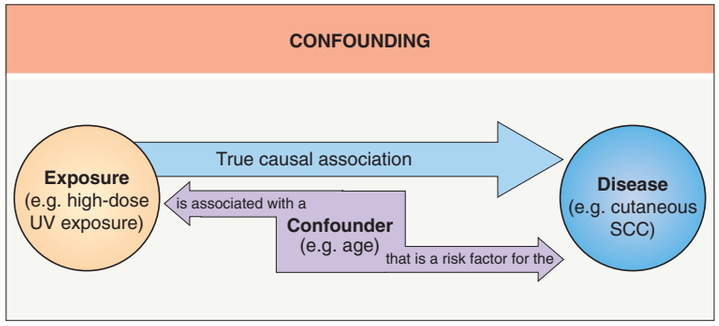


Fig. 123.2 Confounding. The blue arrow represents a true association, in this case a causal one. The purple arrow does not represent a true association, but one found because of confounding. SCC, squamous cell carcinoma; UV, ultraviolet radiation.

case patients referred to a cardiologist for coronary artery disease (CAD; confirmed by angiography) to that in age- and sex-matched control patients without CAD (lack of history or symptoms; no Q wave on electrocardiogram) who were referred to a surgeon for a non-cardiovascular condition. The investigators found that psoriasis was present in 8.0% of cases and 3.4% of controls, with an OR of 2.64 (95% confidence interval [CI], 1.42–4.88). In other words, those with CAD had 2.64 times greater odds of having psoriasis, when compared to those without CAD. The 95% CI does not include 1, signifying that the OR is statistically significant (Fig. 123.3). However, upon adjusting for potentially confounding cardiovascular risk factors in multivariate analysis, the OR decreased to 1.84 (95% CI, 0.99–3.40), which includes 1 and is therefore only of borderline significance.

Cohort study

A cohort study recruits its participants from the general population, and those recruited must be without the disease of interest. Using the example given in Table 123.5, all participants would need to be

SCC-free at the onset of the study. They are then categorized as having or not having high-dose UV exposure and are followed over time. At the end of the study, one can calculate the rate of cutaneous SCC among those with high-dose UV exposure (a/a+b) and compare it to the rate of SCC among those without high-dose UV exposure (c/c+d). Therefore, a cohort study compares the incidence of disease between those exposed and not exposed to particular risk factor(s). This is usually expressed in terms of a RR (see definition above). Similar to an OR, a RR of 1 represents a null association, whereas a RR statistically significantly greater or less than 1 indicates a positive or negative association, respectively. A cohort study can be done prospectively, allowing for more control over measuring outcomes (preferred particularly for fatal diseases), or retrospectively, which is less expensive and requires less time.

One of the advantages of a cohort study is that it can determine the *incidence* of a disease, which is the number of new cases divided by the total number of people at risk in a particular population (e.g. participants in the study) over a specified time period (e.g. length of study)[1]. It also gives information on the natural history of a disease, since it captures data from the time of disease onset. Another advantage is that a cohort study establishes temporality, as the exposure precedes the outcome, and therefore allows for causal inference between the exposure and disease. The disadvantages are that a cohort study often requires a large sample size and is less feasible for rare outcomes.

A cohort study by Zhang et al.[25] looked at the association between tanning bed use and development of skin cancers. Their study population included >70 000 female nurses who were followed between 1989 and 2009. After adjusting for possible confounders (e.g. age, skin type, sun exposure, UV index at place of residence), they found that for an incremental increase of 4 sessions/year in mean use of tanning beds prior to age 35 years, the RR of developing BCC was 1.15 (95% CI, 1.11 to 1.19). Thus, the use of tanning beds a mean of 4 or 8 times per year resulted in a ~15% or ~30% higher risk of BCC, respectively, compared to not using tanning beds. This demonstrates a "dose response" effect, i.e. women who used tanning beds more often had a higher skin cancer risk. Furthermore, the authors noted that women exposed to tanning beds in their teenage or college years were at higher risk than those exposed later in life.

Effect modification or *interaction* occurs when the association between the exposure and disease varies across levels of a variable (e.g. age; Fig. 123.4). Therefore, the exposure and effect modifier have an interdependent role in their effect on the disease. When this happens, the association between exposure and disease should be displayed at various levels or strata of the effect modifier[1,2].

Cross-sectional study

A cross-sectional study is similar to a cohort study, except that the initial population does not need to be free of the disease of interest and both the exposure and disease are measured at a single time point, without a follow-up period. It yields information on the *prevalence* of disease, which is the number of affected individuals divided by the number of people in the population at risk (e.g. total number of study participants), at a given time. It allows one to study the association between exposure and disease, but it does not provide information about which preceded the other. Cross-sectional study results are often expressed in terms of ORs or *relative prevalence*, which compares the prevalence rate of a disease among those exposed to that among the unexposed. While mathematically it is represented by (a/a+b)/(c/c+d) (see Table 123.5), here a/a+b and c/c+d are prevalence rates, rather than incidence rates, as in a cohort study.

The advantages of a cross-sectional study are that it is relatively fast, inexpensive, and does not require follow-up. It is the only epidemiologic study that gives the prevalence of a disease, exposure, or other risk factor. One of its weaknesses is that it does not demonstrate temporality, and so it cannot establish a causal relationship between the exposure and disease. Also, it is not practical for rare diseases or rare exposures, which would require a very large study population.

An example of a cross-sectional study is one by Love et al.[26], which used a national database representative of the non-institutionalized civilian US population, the National Health and Nutrition Examination Survey. It found that the prevalence of metabolic syndrome was 40% among psoriasis cases, compared to 23% among controls. After adjusting for age, sex, race/ethnicity, smoking status, and C-reactive protein levels, the OR for the association between psoriasis and metabolic syndrome was 1.96 (95% CI 1.01–3.77). Therefore, patients with psoriasis had a 1.96 times or 96% greater odds of having metabolic syndrome, as compared to those without psoriasis.

ASSESSING THE EFFICACY OF A PREVENTIVE OR THERAPEUTIC INTERVENTION

Clinical Trials

Unlike observational studies, clinical trials involve an intervention. In a randomized controlled trial (RCT), participants are randomized to receive the intervention versus a placebo or an alternative therapy. Participants can be blinded to their group, as can the observers (double-blinded). The participants are followed for a given period of time, during which disease outcomes and safety are measured. Table 123.6 presents the four phases for testing of new drug therapies. *Intention-to-treat analysis* is then performed, which classifies participants into the intervention group that they were assigned through randomization, rather than the actual intervention that they received; variation can arise if participants crossed over into the other intervention group because of non-compliance, side effects, or other reasons. This preserves the randomization of the study design. However, an analysis taking into account the actual intervention received is done as well, for comparison. The outcome measures for a RCT vary according to the outcome of interest (e.g. relative risk, percentile improvement comparison across groups, prognosis measures; Table 123.7). The concept of statistical significance is applied to assess whether the differences in outcome occurred by chance or likely represent a true effect of the intervention.

The major advantage of a controlled trial is its ability to demonstrate causality (Table 123.8). Randomization can eliminate confounding effects and blinding can eliminate bias. The disadvantages are that controlled trials are relatively expensive, can expose participants to potential harm, and answer a narrow clinical question. Therefore, RCTs are often reserved for well-developed research questions that

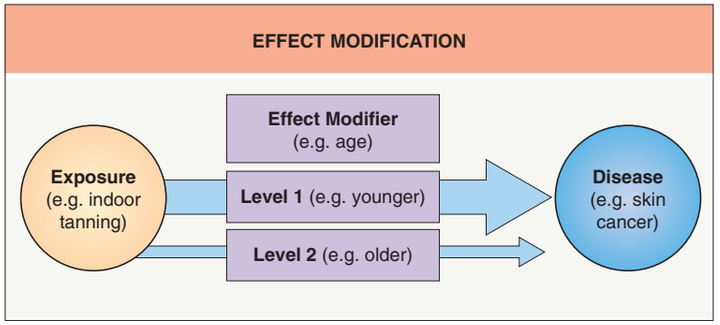


Fig. 123.4 Effect modification. The blue arrow represents a true association, in this case a causal one; the thicker it is, the stronger the association. If a variable causes effect modification, the strength of the association between exposure and disease varies across levels of the effect modifier. In some cases, there may not be an association for a given level of the effect modifier. Age is an effect modifier for many conditions. Interaction represents a similar concept that occurs when the exposure and another variable are interdependent in their effect on disease. MI, myocardial infarction.

THE FOUR PHASES OF TESTING A NEW DRUG	
Phase I	An unblinded, uncontrolled study that involves a few volunteers and focuses on a drug's safety and pharmacologic profile
Phase II	A small, randomized trial that tests for efficacy as well as relative safety
Phase III	A larger, randomized trial that tests for effectiveness and safety
If the drug passes phase III, it can be approved by the FDA	
Phase IV	A trial or observational study used for post-marketing surveillance to assess the rate of serious side effects and evaluate for additional therapeutic uses

Table 123.6 The four phases of testing a new drug[2,23]. FDA, Food and Drug Administration.

FIVE WAYS OF EXPRESSING PROGNOSIS AND SURVIVAL DATA	
Case-fatality rate	The number who died from the disease of interest divided by the number of those with the disease; used more for short-term acute conditions
Five-year survival	The percentage of patients who are alive 5 years after diagnosis or after treatment begins; often used in evaluating cancer research
Observed survival rate	Expressed in probability of survival each year of the study (e.g. a life table) or based on the time interval from baseline to when a study participant dies (e.g. a Kaplan–Meier plot)
Median survival rate	The length of time at which half of the study population survives; can be useful for diseases with extremes in survival
Relative survival rate	The observed survival in those with the disease divided by expected survival if the disease were absent

Table 123.7 Five ways of expressing prognosis and survival data. Considering that there are some dermatologic conditions that are fatal, being aware of survival measures is useful.

FACTORS THAT STRENGTHEN CAUSAL INFERENCE
Evidence of temporality – the exposure preceded the disease or outcome
Consistent across other studies and reproducible
A strong association (e.g. the further the RR or OR is from 1), given that it is statistically significant in a well-powered study
A dose–response relationship – the greater the exposure, the greater the risk of disease
Cessation of the exposure is associated with *decreased risk of disease*
Biological plausibility and *consistency with other scientific knowledge* – there is a mechanism linking the exposure to the disease that makes sense

Table 123.8 Factors that strengthen causal inference. A well-designed randomized controlled trial provides the best evidence for establishing causality. Cohort studies can infer causality, as the exposure precedes the disease in these studies[2,23]. OR, odds ratio; RR, relative risk.

are based on previous evidence from smaller or observational studies. Generally, participants in clinical trials should be easy to recruit as well as reasonably likely to benefit and unlikely to be harmed from the intervention; participants with a high level of adherence to the treatment and follow-up plan are also desirable. The design of the intervention should balance efficacy and safety, with interim monitoring during the trial to ensure that participants are not exposed to a harmful intervention, denied a beneficial intervention, or continued in a trial that cannot answer the question it was intended to answer. Whenever possible, trials should include comparison with placebo. When comparing active treatments in an equivalence or superiority trial, comparison with the gold-standard treatment for the patient population being studied can maximize the relevance to clinical practice. A well-designed blinded RCT is thought of as the gold standard for study design[21] (see Table 123.4).

An example of an RCT is assessment of the efficacy and safety of etanercept in children and adolescents with moderate to severe plaque psoriasis by Paller et al.[27]. It involved randomizing 211 pediatric patients (4 to 17 years of age) with psoriasis to a double-blinded trial of once-weekly subcutaneous injections of etanercept or placebo, for 12 weeks. The primary endpoint was ≥75% improvement from baseline in the psoriasis area and severity index (PASI 75). The patients randomized to receive etanercept were significantly more likely to achieve a PASI 75 (57%) than those receiving placebo (11%) ($P < 0.001$). The authors were able to conclude that etanercept significantly reduced disease severity in children and adolescents with moderate to severe plaque psoriasis.

Systematic Reviews

A systematic review identifies completed studies that address a specific research question and then aggregates and statistically analyzes the results across studies, to arrive at a conclusion about a body of research[1]. Although traditionally applied to RCTs, systematic reviews can also draw data from observational studies. A systematic review should have a written protocol addressing the research question it seeks to answer, utilize comprehensive and unbiased methods for identifying studies, and clearly describe the statistical aspects of the review, i.e. meta-analysis. It should also include a summary estimate of effect plus CI based on the findings of all eligible studies (see Fig. 123.3). In addition, it should have an assessment of heterogeneity across the studies used, to indicate the degree of variability in the findings in different studies. It should address publication bias by taking into account unpublished studies, as positive studies are more likely to get published. It also usually includes subgroup analyses based on additional measures done by some or all of the studies that are supplemental to the main research question. If any of the design decisions were questionable or arbitrary, analyses should be done to assess how sensitive the findings of the meta-analysis are to decisions taken in designing particular studies or inclusion of certain studies. Here, the less sensitive the study the better. The characteristics and the findings of individual studies should be displayed clearly in tables and figures to allow the reader to visualize the data and not rely solely on the conclusions of the meta-analysis[2,23].

The advantage of a systematic review is that it enables the integration of the results of multiple studies, allowing for greater power. While it is often time-consuming, it does not require significant financial resources. In addition, the results are sometimes used to develop practice guidelines. However, a systematic review is only as valuable as the quality of the studies upon which it is based. Caution must be exercised in interpreting systematic reviews, with recognition that they may not take into account unpublished studies, the quality of all of the studies may not be equal, studies may not be comparable (e.g. different outcome measures), and adjusting for biases can be a formidable task. In addition, having a single estimate of risk based on those from several studies may give a false sense of certainty regarding the magnitude of the risk[2,23]. A systematic review of RCTs that have homogeneous results gets the highest ranking of all study types[21] (see Table 123.4), but the level of evidence is considerably lower for systematic reviews limited by the factors discussed above.

The Cochrane Skin Group, which stems from the larger Cochrane Collaboration Group that reviews a variety of healthcare studies, is dedicated to the production of systematic reviews on dermatologic topics[28]. An example of a systematic review is that by Wehner et al.[16], which utilized available studies to summarize the effects of indoor tanning on risk of BCC and cutaneous SCC. The authors searched large databases (e.g. PubMed, Embase, Web of Science) and extracted data from the 12 studies (all observational) that met their inclusion criteria, with assessment of methodologic quality, heterogeneity, and publication bias through established methods. They found summary RRs of 1.29 (95% CI, 1.08–1.53) for BCC and 1.67 (95% CI, 1.29–2.17) for SCC in individuals who reported ever using a tanning bed compared to those who never used tanning beds[16]. By applying these summary RRs to the prevalence of indoor tanning in the US, they calculated the population attributable risk fraction of indoor tanning to be 8.2% for SCC and 3.7% for BCC.

GENETIC EPIDEMIOLOGY

When considering the etiology of a disease, it is important to account for genetic susceptibility as well as environmental factors. Because of advances in molecular and genetic techniques, epidemiologic studies have expanded to include use of biologic samples. Upon completion of the Human Genome Project in 2003 and the International HapMap Project in 2005, researchers were able to use a technique known as the genome-wide association study (GWAS). This method examines the association between disease and single nucleotide polymorphisms (SNPs), markers for groups of DNA variation inherited together in blocks (haplotypes). Findings from these studies can be used to investigate the molecular pathways of disease. One can look for associations in a hypothesis-driven or non-hypothesis-driven manner.

A study by Petukhova et al.[29] illustrates the use of GWAS techniques to explore the pathogenesis of alopecia areata (AA). Using genetic samples from 1054 cases and 3278 controls, they identified 139 SNPs significantly associated with AA ($P \leq 5 \times 10^{-7}$). They found an association between these SNPs and the genomic regions containing several genes that control the activation of T cells and cytokine production.

The results of the study implicated both innate and acquired immunity in the pathogenesis of AA and suggested potential autoimmune mechanisms for this condition.

HEALTH SERVICES RESEARCH

The field of health services research applies techniques of epidemiologic investigation to assess the association between health services provided in the community and disease outcomes. Outcomes for this kind of research include traditional endpoints such as mortality and morbidity, as well as others such as usage and access, patient satisfaction, quality of life, and disability measures. In addition to the *efficacy* of an intervention in an ideal, controlled environment, it is important to assess *effectiveness* in real life situations (e.g. with factors that decrease adherence; Table 123.9) and *efficiency* (e.g. cost : benefit ratio).

ADHERENCE IN DERMATOLOGIC CARE: OBSTACLES AND POTENTIAL SOLUTIONS

Obstacles	Potential solutions
Lack of understanding of the disease process or frustration with previous treatment failures	• Increased education for patients/families, including in-office discussion, written materials, online resources, and disease support groups • Express empathy and recognition of the disease's impact on the patient's life
Lack of understanding of the treatment regimen	• Provide a written treatment plan tailored to individual patient needs • Give specifics, e.g. where to apply topical medications and how much to use • Avoid complex regimens in patients who are less motivated or less medically sophisticated
Treatment too time-consuming	• Simplified regimens, e.g. once daily administration when possible, combination products
Products are difficult, bothersome, or unpleasant to use	• For topical medications, choose a vehicle that is easy to apply and readily absorbed • Tailor the vehicle or method of administration to the patient's preferences, e.g. less greasy for teens, less burning for young children
Concern about or occurrence of side effects	• Ask about and address specific concerns, e.g. steroid phobia, desire for "natural" products • Provide anticipatory guidance on potential side effects and how to prevent or improve them, e.g. taking an oral medication with food/water, moisturizer use, and dose adjustments
Giving up because expect immediate/rapid results	• Inform patients/families of the expected time course of improvement
Don't receive or forget to use the medication	• Anticipate potential issues with receiving the medication, e.g. need for prior authorization, problems with insurance coverage, or lack of immediate availability at the pharmacy • Prescribe an adequate amount of the medication • Plan a follow-up call or text, especially within the week after starting treatment • Discuss making the medicine part of a daily routine (e.g. brushing teeth) and putting it in a visible/accessible location • Reminder systems utilizing charts/calendars, electronic devices, or help from family members • Schedule follow-up appointments sooner/more frequently • Have patients/families bring their bottles/tubes to the visit or check electronic medical record to see if refills obtained • Ask specifically about how often medications are used

Table 123.9 Adherence in dermatologic care: obstacles and potential solutions.

HEALTH POLICY IMPLICATIONS OF RESEARCH

The ultimate goal of medical research is to benefit patients. The appropriate application of research findings to healthcare policy and practice is a critical component of medical advances. The international "choosing wisely" campaign is a physician-led, patient-focused initiative with the goal of utilizing evidence-based medicine to improve quality of care and reduce the unnecessary and potentially harmful use of tests, procedures, and treatments. Patient-centered communication and shared decision-making have also been highlighted as top priorities in cancer care. For example, overdiagnosis of asymptomatic BCCs in patients near the end of life may lead to anxiety and intensive treatments with harms that outweigh the benefits, whereas an individualized approach that incorporates the patient's input and overall prognosis can optimize their overall well-being[30].

Quality-of-Life Measures

Quality of life (QOL) has been defined by the World Health Organization (WHO) as "the individuals' perception of their position in life, in the context of the cultural and value systems in which they live and in relation to their goals, expectations, standards, and concerns". QOL is an important outcome measure for dermatologic conditions because, while many conditions are not fatal, they can cause significant morbidity leading to decreased QOL. Patients may place different weights on various QOL measures depending on their personal values, background, and education. Therefore, development of a QOL measure that is valid can be challenging. The most commonly used QOL instrument in dermatology is the Dermatology Life Quality Index (DLQI), which has been employed for numerous conditions. It is a self-administered, 10-item questionnaire about patients' perceptions of the impact of their skin disease over the last week[31]. The DLQI has been validated for dermatology patients aged ≥16 years, with good-to-excellent internal consistency, high test–retest reliability, and results that correlate with those of other QOL instruments (although less so for mental and emotional aspects)[32]. Another commonly used, validated dermatologic QOL instrument is Skindex, which is available in 29- and 16-item versions with separate scores for symptoms, emotions, and functioning[33,34].

IMPORTANT CONCEPTS WHEN DESIGNING AND REVIEWING A STUDY

Research Question and Design

There are important concepts to consider when planning research or interpreting published literature. These concepts apply to both observational studies and clinical trials (Table 123.10). First, it is important to be aware of the study design needed to best answer the research question of interest. Furthermore, one must recognize the questions that a particular study design can and cannot answer; for example, a case–control study cannot determine causality.

Methods

When considering study methodology, it is important to recognize the importance of a control group and to understand random (due to chance) and systematic errors that may affect the study. *Systematic errors* are due to bias, "sources of variation that distort the study findings in one direction"[23]. The opposite of systematic errors is validity. Several types of bias that can occur in epidemiologic studies are described in Table 123.11. Some studies are particularly prone to certain types of bias. For example, retrospective studies are especially susceptible to recall bias, a type of information bias (see section on Case–control study). An effort should be made in the study design to decrease systematic errors.

The baseline patient characteristics, exposures, other risk factors, and disease characteristics should be measured reliably and accurately (Fig. 123.5). Information on validity (accuracy) is often expressed using sensitivity and specificity or predictive values. *Sensitivity* represents the likelihood of testing positive for someone who has the disease (a/a+c) (Table 123.12). *Specificity* is the likelihood of testing negative for someone who does not have the disease (d/b+d). These measures yield

IMPORTANT CONSIDERATIONS WHEN REVIEWING A STUDY	
Research question and study design	• Given the study design, what are the questions it can and cannot answer? (See Table 123.4)
Methods	• ***Is there a control group?*** • Was an effort made to decrease systematic errors? • Were exposure and disease measured reliably and accurately? • ***Were potential confounders included in the statistical model examining the association between exposure and disease?*** • Were tests done looking for effect modification or interaction between the exposure and other study variables? (See Fig. 123.4)
Results	• Are baseline characteristics significantly different across exposure groups? If so, were these variables adjusted for in the statistical model? • ***Was the correct outcome measure for a given study design used?*** • Is the association statistically significant? (e.g. P value <0.05 or a 95% CI that does not include 1, in the case of a ratio) • Did the study have enough power, usually referring to number of participants, to detect statistical significance?
Conclusions	• ***How strong is the evidence for a causal association?*** (See Table 123.8) • Could a type I error have occurred (false-positive)? • Could a type II error have occurred (false-negative)? • ***What conclusions can be drawn given the type of the study design, its strengths and limitations, including biases?*** (See Table 123.4) • How generalizable are the findings? • Was the study industry-sponsored? • Do the authors have significant conflicts of interest? • Are the findings compelling enough to affect current clinical practice and the direction of future research?

Table 123.10 Important considerations when reviewing a study. Common pitfalls are in ***bold italics***. CI, confidence interval; OR, odds ratio[2,23].

TYPES OF ERRORS AND BIAS	
Type of error	**Example**
Random errors	
Systematic errors	
• *Ascertainment bias:* all of those who are supposed to be represented in a population are not represented	Study enrolling patients from a dermatology clinic only includes those who have access to care
• *Selection bias:* participants are selected differently across exposure or disease categories	Study enrolling patients with bullous pemphigoid from inpatient settings may select for higher disease severity
• *Misclassification bias:* participants are wrongfully thought to belong to one category of exposure or disease, when they actually belong to another	Patients with self-reported eczema may not actually have atopic dermatitis
• *Information bias:* inaccuracies in collection of data regarding the exposure or disease (e.g. *recall bias*)	Patients diagnosed with melanoma may be more likely to recall sunburns and UV exposure in childhood than patients without skin cancer history

Table 123.11 Types of errors and bias. There are two types of errors: random (due to chance) and systematic. UV, ultraviolet.

information on how well we are able to identify those who have or do not have the disease, when we test the general population. A different perspective on the validity of a test is gained through measuring predictive value. This allows us to inform individual patients about what their test results mean. The *positive predictive value* is the likelihood of having the disease when testing positive (a/a+b). The *negative predictive value* is the likelihood of not having the disease when testing negative (d/c+d).

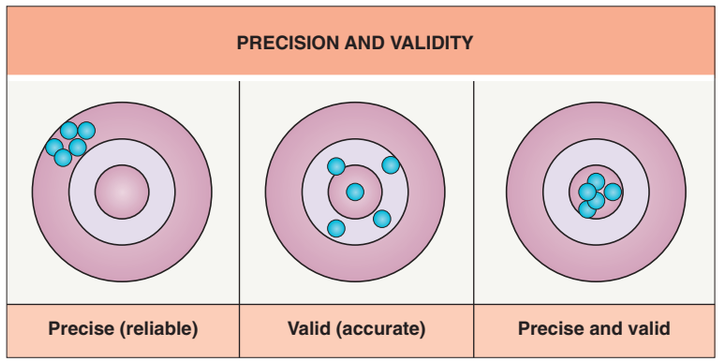


Fig. 123.5 Precision and validity. Precision (reliability) is the relative lack of random error, and validity (accuracy) is the relative lack of systematic error. *From Porta M. Dictionary of Epidemiology, 5th edn. Cary, NC: Oxford University Press, 2008:2. © 2008. Oxford University Press. All rights reserved.*

CONCEPTS OF SENSITIVITY, SPECIFICITY, POSITIVE PREDICTIVE VALUE, AND NEGATIVE PREDICTIVE VALUE			
Result of screening test	**True condition (as determined by gold standard)**		
	Disease	**No disease**	
Positive	a (true positives)	b (false positives)	Positive predictive value = a/a+b (increases with increased disease prevalence)
Negative	c (false negatives)	d (true negatives)	Negative predictive value = d/c+d (decreases with increased disease prevalence)
	Sensitivity = a/a+c	Specificity = d/b+d	

Table 123.12 Concepts of sensitivity, specificity, positive predictive value, and negative predictive value.

Predictive values depend on the prevalence of a disease – the higher the prevalence, the higher the positive predictive value and the lower the negative predictive value.

Statistical methods should include adjustments for potential confounders including when examining the association between exposure and disease (see Fig. 123.2). If not adjusted for, confounders may lead to a false association between an exposure and a disease. When analyzing disease outcome, it is also important to test for effect modification of the exposure by other study variables suspected of playing an interdependent role with the exposure (see Fig. 123.4). If there is a significant effect modification variable for an association, then the association measure should be presented for different levels of the effect modification variable.

Results

In analyzing results, it is important to assess whether baseline characteristics significantly differ across both exposure and outcome groups. If this occurs, such potential confounders need to be placed in the statistical model addressing the association between the exposure and disease so that they may be adjusted for. Next, the correct outcome measure must be reported for a given study design, e.g. OR for a case–control study. *Statistical significance* is typically demonstrated by a P value ≤0.05 and/or by a 95% CI that does not include 1 within the interval for measures that represent a ratio (zero for measures that represent a difference). A *95% CI* that shows significance indicates that there is 95% confidence that the association is not due to chance alone (see Fig. 123.3). Whether the study was sufficiently powered to detect a statistically significant difference should also be determined. *Power* is affected by the number of participants. When planning a study, performance of a power calculation assists the investigator in including enough participants to detect a statistically significant difference between study groups if it exists. The

variables included in the calculation vary according to study design, but they always include the expected magnitude of the association being measured, desired level of significance, and sample size.

Conclusions

In drawing conclusions about the results, the factors that support causality for the association in question should be determined (see Table 123.8). If statistical significance is found, one needs to determine whether the association makes biological and clinical sense. If it does not make sense, a *type I error* may have occurred, where a statistically significant association is found when one does not truly exist (false positive). The more statistical tests that are performed for a study, the more likely a statistically significant association will be found based on chance alone. In studies utilizing large databases where many comparisons are made, the false discovery rate increases and statistical methods (e.g. the Benjamini–Hochberg procedure) should be used to adjust P values in order to mitigate the risk of type I errors[35]. Alternatively, if an association is not found when one would be expected, a *type II error* may have occurred, where no statistical significance is found when one truly exists (false negative). This can be caused by a study not having enough power.

The conclusions that can be drawn given the type of study design must be recognized, taking into account the strengths and limitations, including potential biases. In extrapolating the results, the *generalizability* of the study must also be considered. This pertains to how applicable the results are to the greater population and groups that did not participate in the study. It should also be noted if a trial was industry-sponsored. Lastly, it is important to consider the implications of the study on current clinical practices and the direction of future research.

Strengthening the Reporting of Observational Studies in Epidemiology (STROBE) and the Consolidated Standards for Reporting Trials (CONSORT)

There is a need to ensure appropriate reporting of findings from dermatologic studies. Langan et al.[36] found that dermatologic papers infrequently reported sample size calculations, missing data, losses to follow-up, and statistical methods. Ubriani et al.[37] noted that in 2004–2005 only 20%–49% of articles published in three prominent dermatology journals reported the design of their study in the title or abstract of the paper.

In order to improve the quality of reporting of observational studies in medical research, criteria for reporting have been suggested in the form of the Strengthening the Reporting of Observational Studies in Epidemiology (STROBE) checklist. Items critical for inclusion include the design of the study in the title or abstract and an informative summary of what was done in the abstract. The methods section should describe: (1) eligibility criteria, sources, and selection methods for participants; (2) methods of follow-up, matching criteria (if applicable), and numbers of exposed/unexposed individuals; (3) all outcomes, exposures, predictors, potential confounders, and effect modifiers, as well as diagnostic criteria; (4) all statistical methods (including those dealing with confounding), examination of subgroups and interactions, how missing data and losses to follow-up were addressed, and any sensitivity analysis[38]. The Consolidated Standards for Reporting Trials (CONSORT) statement is a similar initiative for improving the quality of reporting for RCTs. This 25-item checklist emphasizes reporting how the trial was designed, analyzed, and interpreted. It also includes a flow diagram that displays the progress of all participants through the trial[39].

OPPORTUNITIES FOR RESEARCH IN DERMATO-EPIDEMIOLOGY

While each of the study types discussed above provides valuable information, there is a relative paucity of studies that include a control group or a large study population in dermatologic research. Considering the high prevalence of many skin conditions and the rising incidence of diseases such as melanoma, the field of dermatology is likely to play a bigger role in public health research in the future. Therefore, it is important for dermatologists to understand epidemiologic and clinical research techniques, and to advocate for the inclusion of dermatology-related questions in local, state, and national surveys, allowing for larger epidemiologic studies to be conducted.

Associations of dermatologic conditions with comorbid diseases have become increasingly well characterized, and the implications of skin disease treatment on population health are now being explored. For example, patients with psoriasis have an increased risk of metabolic syndrome, myocardial infarction, and stroke; studies are now evaluating the effect of psoriasis treatment on coronary artery disease and other cardiovascular risk markers[40]. Further research may help clarify the role of dermatologic care in improving the overall health of the population.

Multiple sources of data can be analyzed for information on skin conditions, including national databases and disease registries. Other opportunities for epidemiologic research include conducting systematic reviews, participating in multicenter clinical trials, and utilization of molecular technologies (e.g. genomics, proteomics). Dermatologists interested in gaining greater experience in epidemiologic research may consider enrolling in public health classes, connecting with mentors in the field, or getting involved with communities of researchers in this area. Multiple funding sources are currently available for dermato-epidemiology research, including those from dermatologic societies or foundations and national grants. As dermatologists become more active in these arenas, patients will be more likely to reap the benefits of research in dermato-epidemiology.

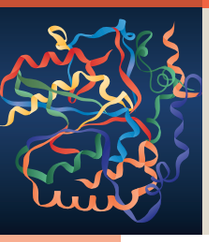
Acknowledgment

The authors wish to thank Ken Katz, MD, MSc, MSCE for his valuable contribution to this chapter.

REFERENCES

1. Porta MI. *Dictionary of Epidemiology*. 5th ed. Cary, NC: Oxford University Press; 2008.
2. Gordis L. *Epidemiology*. 4th ed. Philadelphia: Elsevier/Saunders; 2009.
3. Barzilai DA, Freiman A, Dellavalle RP, et al. Dermatoepidemiology. *J Am Acad Dermatol*. 2005;52:559–573.
4. Karimkhani C, Dellavalle RP, Coffeng LE, et al. Global skin disease morbidity and mortality: an update from the Global Burden of Disease Study 2013. *JAMA Dermatol*. 2017;153:406–412.
5. Feldman SR, Fleischer Jr AB, McConnell RC. Most common dermatologic problems identified by internists, 1990–1994. *Arch Intern Med*. 1998;158:726–730.
6. Kerr OA, Tidman MJ, Walker JJ, et al. The profile of dermatological problems in primary care. *Clin Exp Dermatol*. 2010;35:380–383.
7. Centers for Disease Control and Prevention. National Ambulatory Medical Care Survey: 2008 Summary Tables. <https://www.cdc.gov/nchs/ahcd/web_tables.htm>.
8. Shive M, Linos E, Berger T, et al. Itch as a patient-reported symptom in ambulatory care visits in the United States. *J Am Acad Dermatol*. 2013;69:550–556.
9. Howlader N, Noone AM, Krapcho M, et al., editors. *SEER Cancer Statistics Review, 1975–2019*. Bethesda, MD: National Cancer Institute; 2022.
10. Shaikh WR, Dusza SW, Weinstock MA, et al. Melanoma Thickness and Survival Trends in the United States, 1989 to 2009. *J Natl Cancer Inst*. 2015;108djv294.
11. Brewster DH, Bhatti LA, Inglis JH, et al. Recent trends in incidence of nonmelanoma skin cancers in the East of Scotland, 1992–2003. *Br J Dermatol*. 2007;156:1295–1300.
12. Birch-Johansen F, Jensen A, Mortensen L, et al. Trends in the incidence of nonmelanoma skin cancer in Denmark 1978–2007: rapid incidence increase among young Danish women. *Int J Cancer*. 2010;127:2190–2198.
13. Holterhues C, Vries E, Louwman MW, et al. Incidence and trends of cutaneous malignancies in the Netherlands, 1989–2005. *J Invest Dermatol*. 2010;130:1807–1812.
14. Lomas A, Leonardi-Bee J, Bath-Hextall F. A systematic review of worldwide incidence of nonmelanoma skin cancer. *Br J Dermatol*. 2012;166:1069–1080.
15. Rogers HW, Weinstock MA, Feldman SR, et al. Incidence estimate of nonmelanoma skin cancer (keratinocyte carcinomas) in the US population, 2012. *JAMA Dermatol*. 2015;151:1081–1086.
16. Wehner MR, Shive ML, Chren MM, et al. Indoor tanning and non-melanoma skin cancer: systematic review and meta-analysis. *BMJ*. 2012;345:e5909.
17. Katz KA, Furnish TJ. Dermatology-related epidemiologic and clinical concerns of men who have sex with men, women who have sex with women, and transgender individuals. *Arch Dermatol*. 2005;141:1303–1310.
18. Mansh M, Katz KA, Linos E, et al. Association of skin cancer and indoor tanning in sexual minority men and women. *JAMA Dermatol*. 2015;151:1308–1316.
19. Yeung H, Luk KM, Chen SC, et al. Dermatologic care for lesbian, gay, bisexual, and transgender persons: terminology, demographics, health disparities,

and approaches to care. *J Am Acad Dermatol*. 2019;80:581–589.
20. Nijsten T, Stern RS. How epidemiology has contributed to a better understanding of skin disease. *J Invest Dermatol*. 2012;132:994–1002.
21. OCEBM Levels of Evidence Working Group. The Oxford 2011 Levels of Evidence. Oxford Centre for Evidence-Based Medicine. <www.cebm.net/index.aspx?o=5653>.
22. Kasteler JS, Callen JP. Scalp involvement in dermatomyositis. Often overlooked or misdiagnosed. *JAMA*. 1994;272:1939–1941.
23. Hulley SB, Cummings SR, Browner WS, et al. *Designing Clinical Research*. 2nd ed. Philadelphia: Wolters Kluwer Health/Lippincott Williams & Wilkins; 2001.
24. Picard D, Bénichou J, Sin C, et al. Increased prevalence of psoriasis in patients with coronary artery disease: results from a case–control study. *Br J Dermatol*. 2014;171:580–587.
25. Zhang M, Qureshi AA, Geller AC, et al. Use of tanning beds and incidence of skin cancer. *J Clin Oncol*. 2012;30:1588–1593.
26. Love TJ, Qureshi AA, Karlson EW, et al. Prevalence of the metabolic syndrome in psoriasis: results from the National Health and Nutrition Examination Survey, 2003–2006. *Arch Dermatol*. 2011;147:419–424.
27. Paller AS, Siegfried EC, Langley RG, et al. Etanercept Pediatric Psoriasis Study Group. Etanercept treatment for children and adolescents with plaque psoriasis. *N Engl J Med*. 2008;358:241–251.
28. Collier A, Johnson KR, Delamere F, et al. The Cochrane Skin Group: promoting the best evidence. *J Cutan Med Surg*. 2005;9:324–331.
29. Petukhova L, Duvic M, Hordinsky M, et al. Genome-wide association study in alopecia areata implicates both innate and adaptive immunity. *Nature*. 2010;466:113–117.
30. Linos E, Schroeder SA, Chren MM. Potential overdiagnosis of basal cell carcinoma in older patients with limited life expectancy. *JAMA*. 2014;312:997–998.
31. Basra MKA, Fenech R, Gatt RM, et al. The Dermatology Life Quality Index 1994–2007: a comprehensive review of validation data and clinical results. *Br J Dermatol*. 2008;159:997–1035.
32. Both H, Essink-Bot ML, Busschbach J, Nijsten T. Critical review of generic and dermatology-specific health-related quality of life instruments. *J Invest Dermatol*. 2007;127:2726–2739.
33. Chren MM, Lasek RJ, Quinn LM, Covinsky KE. Convergent and discriminant validity of a generic and a disease-specific instrument to measure quality of life in patients with skin disease. *J Invest Dermatol*. 1997;108:103–107.
34. Chren MM, Lasek RJ, Sahay AP, Sands LP. Measurement properties of Skindex-16, a brief quality-of-life measure for patients with skin diseases. *J Cutan Med Surg*. 2001;5:105–110.
35. Elston DM. Data dredging and false discovery. *J Am Acad Dermatol*. 2020;82:1301–1302.
36. Langan S, Schmitt J, Coenraads PJ, et al. European Dermato-Epidemiology Network (EDEN). The reporting of observational research studies in dermatology journals: a literature-based study. *Arch Dermatol*. 2010;146:534–541.
37. Ubriani R, Smith N, Katz KA. Reporting of study design in titles and abstracts of articles published in clinically oriented dermatology journals. *Br J Dermatol*. 2007;156:557–559.
38. von Elm E, Altman DG, Egger M, et al. The Strengthening the Reporting of Observational Studies in Epidemiology (STROBE) statement: guidelines for reporting observational studies. *Epidemiology*. 2007;18:800–804.
39. Altman DG, Schulz KF, Moher D, et al. The revised CONSORT statement for reporting randomized trials: explanation and elaboration. *Ann Intern Med*. 2001;134:663–694.
40. Elnabawi YA, Dey AK, Goyal A, et al. Coronary artery plaque characteristics and treatment with biologic therapy in severe psoriasis: results from a prospective observational study. *Cardiovasc Res*. 2019;115:721–728.



124-1 Skin Barrier

Matthias Schmuth, Jason Meyer, Gopinathan K. Menon, Kenneth R. Feingold, Theodora M. Mauro and Peter M. Elias

Chapter Contents

Structural Basis for the Permeability Barrier 2206
Stratum Corneum Formation and Organization 2206
Epidermal Metabolism and the Skin Barrier 2208
Cutaneous Diseases and Barrier Dysfunction 2209
Treatment of Skin Barrier Dysfunction 2210

STRUCTURAL BASIS FOR THE PERMEABILITY BARRIER

The skin provides the largest interface between the human body and the external environment[1,2]. Therefore, one of its most important functions is to prevent ingress of potentially harmful exogenous substances (outside-in barrier). However, because desiccation is incompatible with life (inside-out barrier requirement), the skin must also prevent excessive loss of water and other bodily constituents[3]. Tight junctions not only play an important role in directly blocking passage of some molecules – they also direct epidermal differentiation and formation of the lipid barrier[4,5]. Of note, the tight junction barrier develops before the lipid barrier, both in a fetal rat model and in human epidermal equivalents (HEE), with tight junction expression receding as the lipid barrier develops[6].

The skin's remarkable barrier properties are sustained in large part by epidermal homeostasis[1,2], which insures that the generation of corneocytes and lipids is optimized in order to support this function[7]. The corneocytes within the stratum corneum are composed primarily of keratin filaments encased in a cornified envelope (CE), and they have been likened to "bricks". Corneocytes are further surrounded by a cornified lipid envelope (CLE) and an extracellular milieu of lipids organized as multiple lamellar bilayers, analogous to "mortar" (Fig. 124.1)[8].

At the stratum granulosum–stratum corneum interface, keratinocytes contain abundant filament aggregating protein (filaggrin), which also plays a role in barrier function. Filaggrin has a predominance of arginine over lysine residues and is found within liquid-like keratohyalin condensates. As a result of their phase separation- and pH-driven assembly and disassembly during keratinocyte terminal differentiation, these membrane-less structures become osmotically active amino acids. The latter undergo deamination regulated by changes in environmental humidity[9].

As they differentiate, keratinocytes accumulate lipid-containing lamellar bodies, i.e. tubuloreticular structures, whose secreted contents play a key role in the formation of the stratum corneum (see Fig. 124.1). These extracellular structured lipids will comprise ~10% of the volume of the stratum corneum[10]. They prevent excessive loss of body water and likewise block entry of exogenous compounds, including most topically applied drugs (except for those that are lipid-soluble and of low molecular weight).

STRATUM CORNEUM FORMATION AND ORGANIZATION

The formation of the stratum corneum barrier involves various cellular organelles within differentiating keratinocytes as well as degradation of the nucleus. The resulting flattened corneocytes along with an extracellular milieu of lipids are structurally organized as "bricks and mortar" (see Fig. 124.1; Table 124.1)[3]. For most of the skin surface in humans, the stratum corneum is typically comprised of about 20 corneocyte cell layers, which differ in their thickness, packing of keratin filaments, filaggrin content and number of corneodesmosomes, depending on body site[8]. Corneocytes are reinforced by a highly resilient sheath of multiple proteins, cross-linked into the CE, while the cell interior is packed with keratin filaments embedded in a matrix composed primarily of filaggrin and its breakdown products. Some of these breakdown products serve as "natural moisturizing factor" while others have antimicrobial properties[11].

At the stratum granulosum–stratum corneum interface, lamellar body contents are secreted, fused end-to-end, and progressively elongated into lamellar membrane sheets[12,13], a sequence requiring the action of a battery of lipolytic "processing" enzymes (see below) (Fig. 124.2). Glucosylceramide-based bilayers with cubic-like symmetry are organized within the extracellular spaces into ceramide-based lamellar membranes that surround the corneocytes[14] (lipid processing). Variations in the number of lamellar membranes (which determines lipid weight %), membrane substructure, and/or lipid composition provide the structural and biochemical basis for site-related variations in permeability[15].

The volume of the extracellular lipid-enriched matrix of the stratum corneum includes the structures that limit transdermal delivery of hydrophilic drugs as well as the so-called stratum corneum "reservoir"[16]. Within this reservoir, lipid-soluble drugs (e.g. topical corticosteroids) can accumulate and be slowly released. Of note, its volume can vary dramatically. For example, at baseline, these domains account for ~10% of stratum corneum volume, but with hydration or the inspissation of topical agents, they can account for up to 50% of stratum corneum volume.

The exceptionally low permeability of normal stratum corneum to water-soluble drugs is the consequence of several characteristics of the lipid-enriched extracellular matrix (Table 124.2)[14]. Moreover, not only the paired-bilayer arrangement of extracellular lipids, but also their hydrophobicity and the composition and distribution of the three key species (ceramides, cholesterol and free fatty acids) in a critical (1 : 1 : 1) molar ratio, are further characteristics that provide for optimal barrier function.

Ceramides account for ~50% of the total stratum corneum lipid mass and are crucial for the lamellar organization of the stratum corneum barrier[17]. Of the nine ceramide species, acylceramides or ceramides 1, 4, and 7 (which contain ω-hydroxy-linked essential fatty acids in an ester linkage) are epidermis-unique compounds, known to be important for barrier function[12]. Keratinocytes also synthesize triglycerides, with the final step in the pathway catalyzed by diacylglycerol transferase (DGAT). Lipases and acyltransferases then break down the triglycerides, thereby releasing fatty acids that serve as building blocks for ceramides and acylceramides. The latter are both essential for lamellar bilayer and CLE formation.

Free fatty acids, which consist predominantly of very-long-chain, saturated species with ≥18 carbon atoms, and *cholesterol* each account for 10%–15% of stratum corneum lipids. A subset of fatty acids contains linoleic acid thus providing an explanation for the abnormal extracellular matrix observed in essential fatty acid deficiency. Cholesterol promotes the intermixing of different lipid species and regulates its "phase" behavior[18]. A decrease in the concentration of any of these critical lipid species alters their molar ratio within lamellar membranes which then compromises barrier integrity and function.

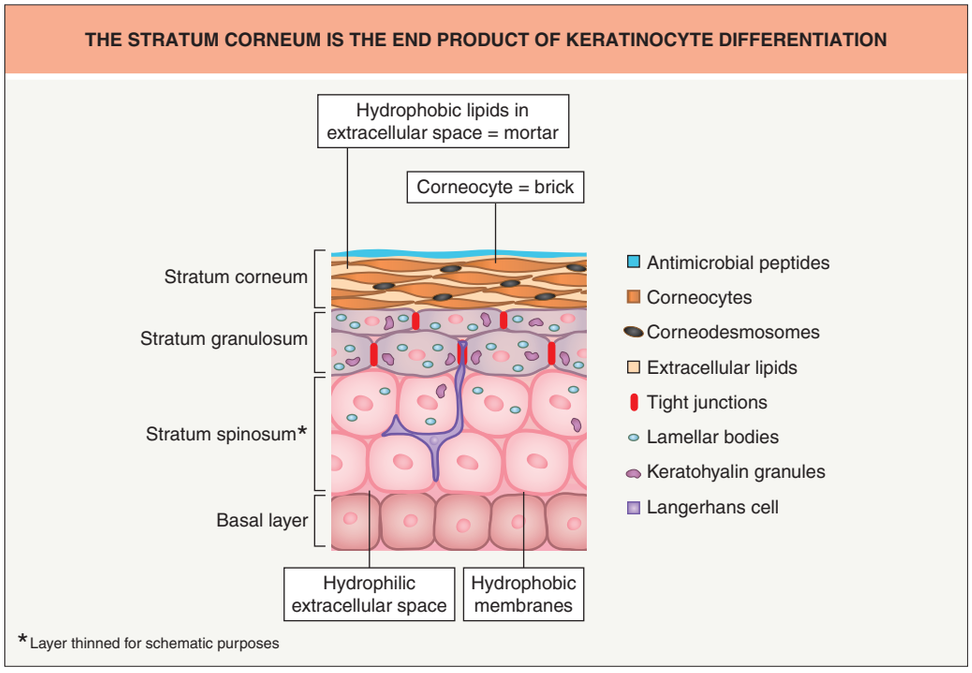


Fig. 124.1 The stratum corneum is the end product of keratinocyte differentiation. In a vectorial process, keratinocytes differentiate while moving outward from the basal to the outer epidermal layer, forming lipid-enriched lamellar bodies and tight junctions within the granular layer. The skin barrier is intimately linked with the innate immune system, e.g. antimicrobial peptide production, Langerhans cell activation. The stratum corneum barrier is a unique two-compartment system, analogous to a brick wall. Whereas lipids are sequestered extracellularly within the stratum corneum, the corneocytes are lipid-depleted but protein-enriched.

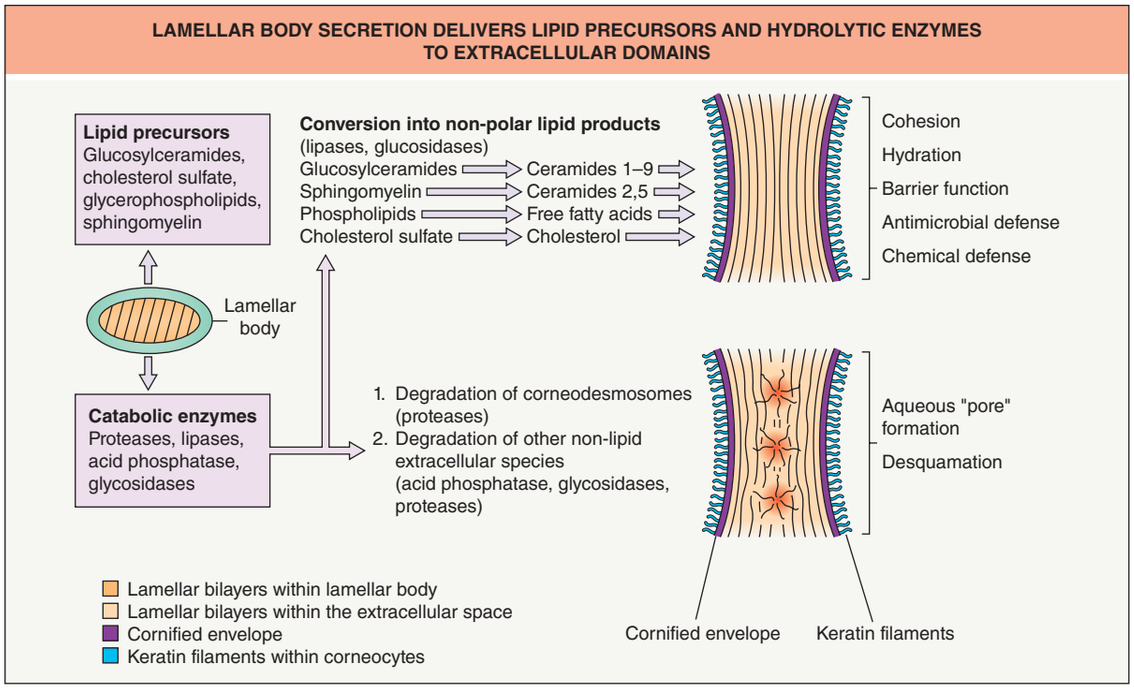


Fig. 124.2 Lamellar body secretion delivers lipid precursors and hydrolytic enzymes to extracellular domains. These organelles also release antimicrobial peptides, including human β-defensin 2 and LL-37 (the carboxy-terminal fragment of human cathelicidin). As a result, the antimicrobial barrier is intimately linked to the permeability barrier. In atopic dermatitis, for example, there is both an impaired permeability barrier and reduced expression of antimicrobial peptides, explaining in part the predisposition to colonization with *Staphylococcus aureus*. Reduced conversion of cholesterol sulfate to cholesterol via steroid sulfatase and sphingomyelin to ceramide via sphingomyelinase leads to X-linked ichthyosis and Niemann–Pick disease, respectively.

FEATURES OF THE STRATUM CORNEUM

- Primary barrier to water-soluble drug absorption into skin and maintaining skin hydration
- Two-compartment organization: “bricks and mortar”
- Microheterogeneity within extracellular spaces: “There’s more to the mortar than lipid”
- Persistent metabolic activity: dynamic changes in cytosol, cornified envelope, and interstices from inner to outer stratum corneum
- Homeostatic links to the nucleated cell layers: barrier function regulates epidermal DNA and lipid synthesis
- Pathophysiologic links to deeper skin layers: barrier abrogation and/or epidermal injury initiates epidermal hyperplasia and inflammation
- Stratum corneum as a biosensor: changes in external humidity alone regulate proteolysis of filaggrin, epidermal DNA and lipid synthesis, and initiation of inflammation

Table 124.1 Features of the stratum corneum.

FACTORS AFFECTING HOW STRATUM CORNEUM LIPIDS MEDIATE BARRIER FUNCTION

- Predominantly extracellular localization
- Amount of lipid (lipid weight %)
- Elongated, tortuous pathway: increases diffusion length
- Organization into lamellar membrane structures
- Hydrophobic composition: absence of polar lipids and presence of very long-chain saturated fatty acids
- Correct molar ratio: approximately 1 : 1 : 1 of three key lipids: ceramides, cholesterol, and free fatty acids
- Unique molecular structures (e.g. acylceramides)

Table 124.2 Factors affecting how stratum corneum lipids mediate barrier function.

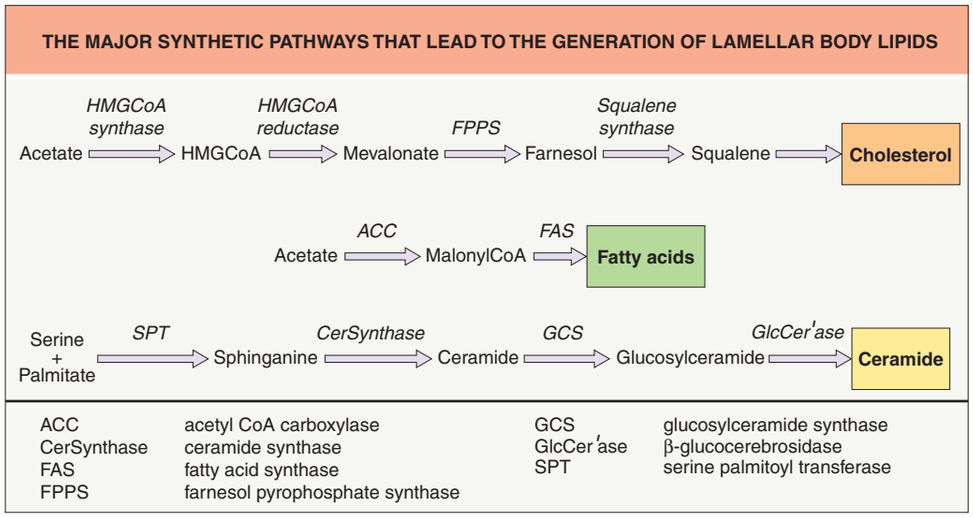


Fig. 124.3 The major synthetic pathways that lead to the generation of lamellar body lipids. The key enzymes in each pathway are shown. Applications of specific, conduritol-type inhibitors of β-glucocerebrosidase to intact skin lead to a progressive abnormality in barrier function. In both a transgenic murine model of Gaucher disease (GD) (produced by targeted disruption of the β-glucocerebrosidase gene) and in the severe, type 2 neuronopathic form of GD, infants present with a barrier abnormality. This is attributable to accumulation of glucosylceramides, depletion of ceramides, and persistence of immature lamellar bodies within the interstices of the stratum corneum.

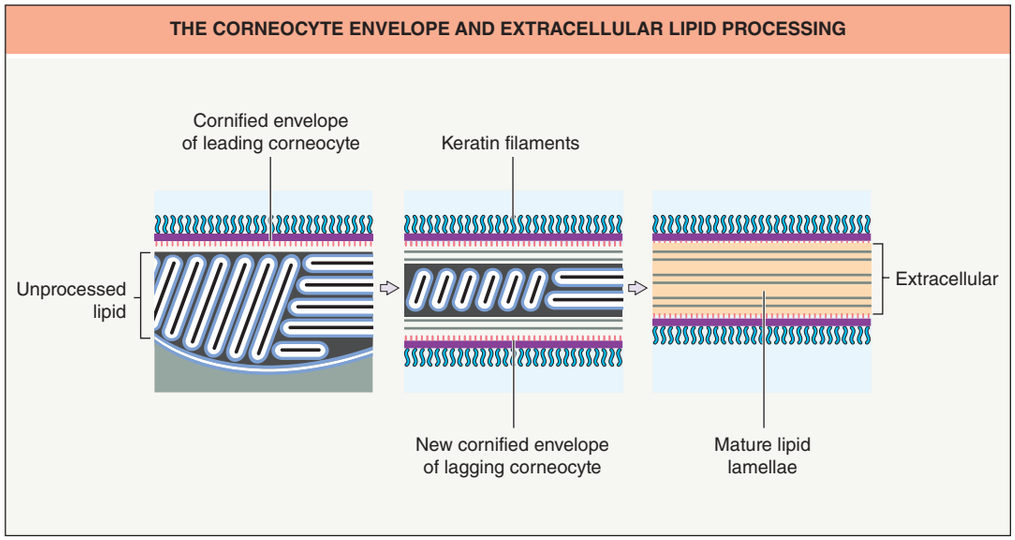


Fig. 124.4 The corneocyte envelope (CE) and extracellular lipid processing. After secretion of lamellar body contents into the extracellular space, lipolytic enzymes remove polar headgroups (indicated by blue outlines) to generate neutral lipids. These lipids align along the structured, hydrophobic template provided by the CE of the leading corneocyte, resulting in the formation of stacked, mature lipid lamellae. Meanwhile, transglutaminase 1 generates the CE on the lagging corneocyte, and ALOX12B, ALOXE3 and SDR9C7 catalyze oxidation reactions that precede anchoring and immobilization of the corneocyte lipid envelope (CLE; pink hatch marks) onto the CE. Dysfunction of these enzymes is seen in autosomal recessive congenital ichthyoses.

EPIDERMAL METABOLISM AND THE SKIN BARRIER

Biosynthetic Activities

Epidermal differentiation is a vectorial process that is accompanied by dramatic changes in lipid composition, including loss of triglycerides and phospholipids with the concomitant emergence of ceramides, cholesterol, and free fatty acids in the stratum corneum (see Fig. 124.2). Although epidermal lipid synthesis is both highly active and largely autonomous from systemic influences, it can be regulated by external influences, i.e. changes in the status of the permeability barrier[19]. Acute perturbations of the permeability barrier by environmental factors stimulate a characteristic recovery sequence that leads to restoration of normal function over about 72 hours in young skin (the cutaneous stress test)[20]. This metabolic sequence includes a rapid increase in cholesterol, free fatty acid, glucosylceramide, and ceramide synthesis that is restricted to the underlying epidermis; this is attributable to a prior increase in mRNA and enzyme activity/mass for each of the key synthetic enzymes (Fig. 124.3). Synthesis of each of these key lipids is required for normal barrier homeostasis, particularly in the context of barrier repair[12,19].

Lamellar Body Secretion

The unique two-compartment organization of the stratum corneum is attributable to the secretion of lamellar body-derived lipids and co-localized hydrolases at the stratum granulosum–stratum corneum interface[12]. Under basal conditions, lamellar body secretion is slow, but sufficient to provide for barrier integrity. Following acute barrier disruption, calcium is lost from the outer epidermis and much of the preformed pool of lamellar bodies in the outermost cells of the stratum granulosum is quickly secreted[20–22]. Calcium (Ca^{2+}) is an important regulator of lamellar body secretion, with the normally high levels of Ca^{2+} within the stratum granulosum restricting lamellar body secretion to low, maintenance levels[23,23a].

Extracellular Processing

Extrusion of the polar lipid contents of lamellar bodies at the stratum granulosum–stratum corneum interface is followed by the processing of those lipids into more hydrophobic species that form mature lamellar membranes (Fig. 124.4). The extracellular hydrolysis of glucosylceramides, phospholipids, and cholesterol sulfate due to the co-secretion of a set of hydrolytic enzymes results in the accumulation of their non-polar derivatives – ceramides, free fatty acids, and cholesterol within the stratum corneum interstices (see Fig. 124.2). Concurrently, the plasma membrane is replaced by the CE/CLE complex via the activity of transglutaminase 1 and lipoxidases, which catalyze cross-linking of the CE and CLE, respectively[24]. The CLE provides a highly structured, hydrophobic monolayer of protein-bound ω-OH-acylceramides, upon which processed lipids are organized into elongated mature lipid lamellae.

Extracellular processing of *glucosylceramides* by β-glucocerebrosidase plays a key role in barrier homeostasis (see legend to Fig. 124.3).

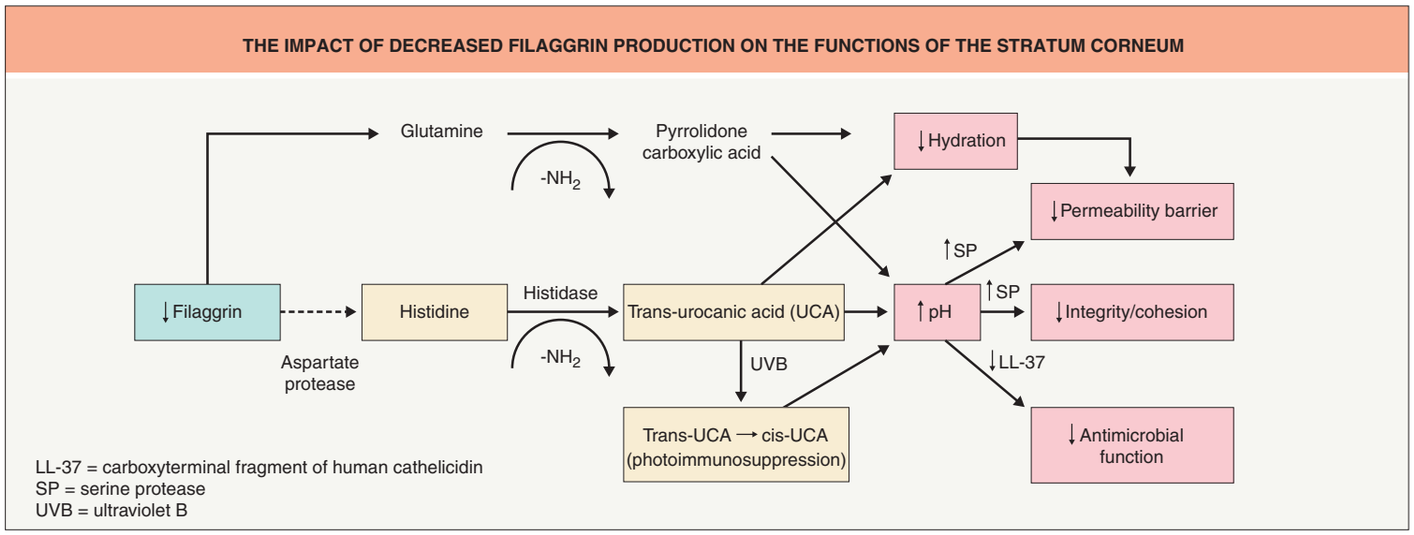


Fig. 124.5 The impact of decreased filaggrin production on the functions of the stratum corneum.

In addition, *phospholipid* hydrolysis, catalyzed by one or more secretory phospholipases (e.g. $sPLA_2$), generates a family of nonessential free fatty acids, which are also required for barrier homeostasis[25]. *Sphingomyelin* hydrolysis by acidic sphingomyelinase generates two of the nine ceramides required for normal barrier homeostasis (see Fig. 124.2). Sphingomyelinase is upregulated during epidermal injury, during which ceramide generation contributes to barrier recovery[26] as well as inflammation via its role as a second messenger in TNF receptor signaling[27]. The resultant epidermal disease represents an example of outside-in pathogenesis.

Finally, *cholesterol sulfate* is desulfated during passage from the inner to the outer stratum corneum[28]. Both cholesterol sulfate and its processing enzyme, steroid sulfatase, are concentrated in membrane domains of the stratum corneum. Of note, the content of cholesterol sulfate in these sites is increased by ~10-fold in X-linked ichthyosis (see Ch. 57). Excessive cholesterol sulfate increases the permeability of lamellar membranes, which together with decreased cholesterol content, lead to barrier dysfunction in X-linked ichthyosis[28] (see Fig. 124.2).

In addition to lipid precursors and lipolytic enzymes, lamellar bodies contain proteases and antiproteases that orchestrate the orderly digestion of corneodesmosomes, allowing corneocyte shedding or *desquamation*. By controlling the thickness of the stratum corneum, the rate of desquamation has a major impact on the barrier properties of skin. For example, while stratum corneum from palmoplantar skin is more permeable than in other sites, it is much thicker and therefore has a longer lag time for the penetration of topically applied drugs[1]. When stratum corneum permeability is increased in the setting of skin diseases such as psoriasis[29] and inherited ichthyoses[30], associated scale (due to abnormal desquamation and a thickened stratum corneum) provides partial compensation by mitigating barrier dysfunction.

Lamellar bodies also deliver antimicrobial peptides, including human β-defensin 2 and LL-37 (the carboxy-terminal fragment of human cathelicidin). In addition, corneocyte-derived peptide fragments[31], sebaceous gland-derived fatty acids, and free long-chain bases derived from ceramides exhibit antimicrobial activity[32]. Antimicrobial peptide levels and permeability barrier function are interdependent[33]. For example, topical agents that improve the skin barrier simultaneously enhance antimicrobial peptide production[34]. Emerging evidence supports a crosstalk between host immune effectors and cutaneous microorganism communities, i.e. the skin microbiome[35].

Acidification

The stratum corneum surface has an acidic pH ("acid mantle") which develops progressively within the extracellular space (whereas the interior of the corneocytes remains neutral). This pH gradient reflects an ~100-fold increase in the concentration of protons and forms over a span of ~10 microns[36]. Several processes contribute to the formation of the pH gradient: (1) extraepidermal mechanisms, including surface deposits of eccrine gland- and sebaceous gland-derived products as well as metabolites of microbial metabolism; (2) endogenous catabolic processes, e.g. phospholipid-to-free fatty acid hydrolysis, deamination of histidine to urocanic acid; and/or (3) local efflux of protons within the lower stratum corneum by sodium-proton antiporters [NHE_1] located in the apical plasma membrane of outer granular cells[36].

Because key extracellular processing enzymes, including β-glucocerebrosidase and acidic sphingomyelinase, exhibit optimal activity at an acidic pH, an acid mantle is critical for barrier generation. Loss of the pH gradient, leading to neutralization of the stratum corneum, is a common feature of skin diseases such as atopic dermatitis[37], in which it is thought to contribute to the pathogenesis of barrier dysfunction.

CUTANEOUS DISEASES AND BARRIER DYSFUNCTION

Abnormalities of the skin barrier are observed in both common and rare skin diseases. Causes of barrier dysfunction include (but are not limited to): mechanical trauma, exposure to detergents or solvents, seborrhea, prolonged water exposure, ultraviolet radiation, infection, inflammatory dermatoses, certain drugs, and genetic mutations and polymorphisms. Low humidity downregulates barrier competence while cold temperatures impair permeability barrier homeostasis[38]. Many disorders of cornification, including the ichthyoses, are due to pathogenic variants in genes that encode key components of the skin barrier, such as keratin and enzymes involved in extracellular lipid synthesis, among others[39].

Mutations and genetic polymorphisms in barrier-related genes also contribute to the pathogenesis of more common skin diseases, e.g. filaggrin in atopic dermatitis (see Ch. 12)[40,41] or cornified envelope proteins LCE3B and LCE3C in psoriasis[42]. Figure 124.5 depicts the impact of reduced filaggrin production on various functions of the stratum corneum. Aging skin also displays barrier abnormalities and increased susceptibility to xerotic eczema and pruritus due to age-associated declines in CE proteins and stratum corneum lipid content as well as elevated skin surface pH[43,44].

Barrier dysfunction induces a wide range of cellular responses in epidermal keratinocytes. Beyond controlling barrier recovery, they also affect epidermal proliferation (important in wound healing) and inflammation (outside-in link between barrier and inflammation)[45]. The latter is characterized by the production and release of epidermal cytokines involved in both innate immunity (e.g. TNF, IL-1α) and leukocyte recruitment and activation (e.g. IL-17, IL-22). When epidermal inflammation occurs on a large scale, it can have a local as well as a systemic impact via circulating cytokines[46,47]. This may explain in part the association between skin diseases with barrier dysfunction and disorders such as cardiovascular disease[46].

Inflammation can also initiate barrier dysfunction (inside-out link between inflammation and barrier) via two major mechanisms: (1) disruption of epidermal integrity (e.g. spongiotic, vesiculobullous, or ulcerative diseases), with defects in or loss of the stratum corneum; and (2) permeabilization of the stratum corneum interstices via changes in the lipid membranes. The first mechanism is relatively well characterized[48], with structural defects in the stratum corneum a rather straightforward explanation for impaired barrier function. The second mechanism typically involves a pronounced disorganization of stratum corneum lipid lamellae, as for example in psoriasis[47]. Psoriatic scale contains immature CEs[49,50] and CLEs (as assessed by covalently bound lipid composition) that make them fragile and less hydrophobic[51] than normal corneocytes, which could explain the failure to properly organize extracellular lipids into barrier-providing mature lipid lamellae. There are also changes in the composition of the extracellular lipids in some inflammatory skin diseases, particularly in the chain length of ceramides and fatty acids[52], which correlate with alterations in the lateral packing of lipid membranes and increased permeability. How inflammation induces these changes is an area of active investigation since the role of several inflammatory cytokines (e.g. IL-1, TNF) on epidermal homeostasis and barrier function remains unclear[53]. Finally, psychological stress disrupts permeability barrier homeostasis, impairs stratum corneum cohesion[54], and compromises epidermal innate immunity by increasing endogenous glucocorticoids[55,56].

TREATMENT OF SKIN BARRIER DYSFUNCTION

Therapies for barrier dysfunction are still limited. Semi-occlusive emollients, especially petrolatum[57], reduce transepidermal water loss, although less effectively than native stratum corneum lipids[58]. Impermeable and vapor-permeable dressings can provide nearly complete occlusion and are as effective as potent topical corticosteroids in the treatment of psoriasis[59], but are normally limited to small treatment areas. Moreover, these treatments are no substitute for the stratum corneum as a microbial barrier – they are applied on top of (superficial to) the microbiome, thereby providing an underlying moist environment that facilitates microbial growth and enhanced penetration. This explains why emollients and occlusive dressings increase the risk of skin infections[60]. Of note, topical probiotics can have beneficial effects on skin barrier homeostasis[61].

Targeted therapy of barrier dysfunction must address the underlying cause. While inflammation can be treated with anti-inflammatory and immunomodulatory drugs, a new class of therapeutic agents that addresses defects in lipid metabolism is emerging. For example, porokeratosis and CHILD syndrome, both resulting from defects in cholesterol synthesis, have been reported to improve following application of cholesterol plus lovastatin (the latter blocks accumulation of pathogenic lipid precursors)[62,63]. Ceramide-based, triple-lipid mixtures are employed to address defective barrier function. Increasing knowledge about the pathophysiology of skin barrier-driven diseases should offer major opportunities for novel therapies.

REFERENCES

1. Scheuplein RJ, Blank IH. Permeability of the skin. *Physiol Rev*. 1971;51:702–747.
2. Elias PM, Friend DS. The permeability barrier in mammalian epidermis. *J Cell Biol*. 1975;65:180–191.
3. Kubo A, Ishizaki I, Kubo A, et al. The stratum corneum comprises three layers with distinct metal-ion barrier properties. *Sci Rep*. 2013;3:1731.
4. Furuse M, Hata M, Furuse K, et al. Claudin-based tight junctions are crucial for the mammalian epidermal barrier: a lesson from claudin-1-deficient mice. *J Cell Biol*. 2002;156:1099–1111.
5. Kirschner N, Rosenthal R, Gunzel D, et al. Tight junctions and differentiation–a chicken or the egg question? *Exp Dermatol*. 2012;21:171–175.
6. Celli A, Zhai Y, Jiang YJ, et al. Tight junction properties change during epidermis development. *Exp Dermatol*. 2012;21:798–801.
7. Kalinin AE, Kajava AV, Steiner PM. Epithelial barrier function: assembly and structural features of the cornified cell envelope. *Bioessays*. 2002;24:789–800.
8. Elias PM, McNutt NS, Friend DS. Membrane alterations during cornification of mammalian squamous epithelia: a freeze-fracture, tracer, and thin-section study. *Anat Rec*. 1977;189:577–594.
9. Quiroz FE, Fiore VF, Levorse J, et al. Liquid-liquid phase separation drives skin barrier formation. *Science*. 2020;367:6483:eaax9554.
10. Lin T-K, Crumrine D, Ackerman LD, et al. Cellular changes that accompany shedding of human corneocytes. *J Invest Dermatol*. 2012;132:2430–2439.
11. Rawlings AV, Scott IR, Harding CR, Bowser PA. Stratum corneum moisturization at the molecular level. *J Invest Dermatol*. 1994;103:731–741.
12. Elias PM, Menon GK. Structural and lipid biochemical correlates of the epidermal permeability barrier. *Adv Lipid Res*. 1991;24:1–26.
13. Lampe MA, Burlingame AL, Whitney J, et al. Human stratum corneum lipids: characterization and regional variations. *J Lipid Res*. 1983;24:120–130.
14. Narangifard A, Wennberg CL, den Hollander L. Molecular reorganization during the formation of the human skin barrier studied in situ. *J Invest Dermatol*. 2021;141:1243–1253.
15. Potts RO, Francoeur ML. The influence of stratum corneum morphology on water permeability. *J Invest Dermatol*. 1991;96:495–499.
16. Rougier A, Dupuis D, Lotte C, et al. In vivo correlation between stratum corneum reservoir function and percutaneous absorption. *J Invest Dermatol*. 1983;81:275–278.
17. Bouwstra JA, Gooris GS, Cheng K, et al. Phase behavior of isolated skin lipids. *J Lipid Res*. 1996;37:999–1011.
18. Wertz PW, Downing DT. Ceramides of pig epidermis: structure determination. *J Lipid Res*. 1983;24:759–765.
19. Norlen L, Nicander I, Lundh Rozell B, et al. Inter- and intra-individual differences in human stratum corneum lipid content related to physical parameters of skin barrier function in vivo. *J Invest Dermatol*. 1999;112:72–77.
20. Schmuth M, Feingold KR, Elias PM. Stress test of the skin: the cutaneous permeability barrier treadmill. *Exp Dermatol*. 2020;29:112–113.
21. Feingold KR. The regulation and role of epidermal lipid synthesis. *Adv Lipid Res*. 1991;24:57–82.
22. Menon GK, Feingold KR, Elias PM. Lamellar body secretory response to barrier disruption. *J Invest Dermatol*. 1992;98:279–289.
23. Lee SH, Elias PM, Proksch E, et al. Calcium and potassium are important regulators of barrier homeostasis in murine epidermis. *J Clin Invest*. 1992;89:530–538.

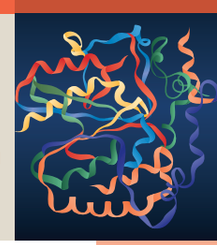
23a. Celli A, Crumrine D, Meyer JM, Mauro TM. Endoplasmic reticulum calcium regulates epidermal barrier response and desmosomal structure . *J Invest Dermatol*. 2016;136:1840–7.

24. Wertz PW. Lipid metabolic events underlying the formation of the corneocyte lipid envelope. *Skin Pharmacol Physiol*. 2021;34:38–50.
25. Mao-Qiang M, Feingold KR, Jain M, Elias PM. Extracellular processing of phospholipids is required for permeability barrier homeostasis. *J Lipid Res*. 1995;36:1925–1935.
26. Schmuth M, Man MQ, Weber F, et al. Permeability barrier disorder in Niemann-Pick disease: sphingomyelin-ceramide processing required for normal barrier homeostasis. *J Invest Dermatol*. 2000;115:459–466.
27. Jensen JM, Schütze S, Förl M, et al. Roles for tumor necrosis factor receptor p55 and sphingomyelinase in repairing the cutaneous permeability barrier. *J Clin Invest*. 1999;104:1761–1770.
28. Zettersten E, Man MQ, Sato J, et al. Recessive x-linked ichthyosis: role of cholesterol-sulfate accumulation in the barrier abnormality. *J Invest Dermatol*. 1998;111:784–790.
29. Motta S, Monti M, Sesana S, et al. Abnormality of water barrier function in psoriasis. Role of ceramide fractions. *Arch Dermatol*. 1994;13:452–456.
30. Erickson TR, Murphrey MB, Abu-Zayed H, et al. Transepidermal water loss in the orphan forms of ichthyosis. *Pediatric Dermatol*. 2020;37:771–773.
31. Latendorf T, Gerstel U, Wu Z, et al. Cationic intrinsically disordered antimicrobial peptides (CIDAMPs) represent a new paradigm of innate defense with a potential for novel anti-infectives. *Sci Rep*. 2019;9:3331.
32. Wertz PW. Lipids and the permeability and antimicrobial barriers of the skin. *J Lipids*. 2018;2:2018.
33. Aberg KM, Man M-Q, Gallo RL, et al. Co-regulation and interdependence of the mammalian epidermal permeability and antimicrobial barriers. *J Invest Dermatol*. 2008;128:917–925.
34. Grether-Beck S, Felsner I, Brenden H, et al. Urea uptake enhances barrier function and antimicrobial defense in humans by regulating epidermal gene expression. *J Invest Dermatol*. 2012;132:1561–1572.
35. Byrd A, Belkaid Y, Segre JA. The human skin microbiome. *Nat Rev Microbiol*. 2018;16:143–155.
36. Behne MJ, Meyer JW, Hanson KM, et al. NHE1 regulates the stratum corneum permeability barrier homeostasis. Microenvironment acidification assessed with fluorescence lifetime imaging. *J Biol Chem*. 2002;277:47399–47406.
37. Danby SG, Cork MJ. pH in Atopic dermatitis. *Curr Probl Dermatol*. 2018;54:95–107.
38. Halkier-Sorensen L. Occupational skin diseases. *Contact Derm*. 1996;35(1 Suppl):1–120.
39. Schmuth M, Martinz V, Janecke AR, et al. Inherited ichthyoses/generalized Mendelian disorders of cornification. *Eur J Hum Genet*. 2013;21:123–133.
40. Sandilands A, Terron-Kwiatkowski A, Hull PR, et al. Comprehensive analysis of the gene encoding filaggrin uncovers prevalent and rare mutations in ichthyosis vulgaris and atopic eczema. *Nat Genet*. 2007;39:650–654.
41. Pellerin L, Henry J, Hsu CY, et al. Defects of filaggrin-like proteins in both lesional and nonlesional atopic skin. *J Allergy Clin Immunol*. 2013;131:1094–1102.
42. de Cid R, Riveira-Munoz E, Zeeuwen PL, et al. Deletion of the late cornified envelope LCE3B and LCE3C genes as a susceptibility factor for psoriasis. *Nat Genet*. 2009;41:211–215.
43. Wang Z, Man M-Q, Li T, et al. Aging-associated alterations in epidermal function and their clinical significance. *Aging*. 2020;12:5551–5565.
44. Choi E-H, Man M-Q, Xu P, et al. Stratum corneum acidification is impaired in moderately aged human and murine skin. *J Invest Dermatol*. 2007;127:2847–2856.

45. Sextius P, Marionnet C, Bon FX, et al. Large scale study of epidermal recovery after stratum corneum removal: dynamics of genomic response. *Exp Dermatol*. 2010;19:259–268.
46. Hu L, Mauro TM, Dang E, et al. Epidermal dysfunction leads to an age-associated increase in levels of serum inflammatory cytokines. *J Invest Dermatol*. 2017;137:1277–1285.
47. Ye L, Mauro TM, Dang E, et al. Topical applications of an emollient reduce circulation pro-inflammatory cytokine levels in chronically aged humans: a pilot clinical study. *J Eur Acad Dermatol Venereol*. 2019;33:2197–2201.
48. Gunathilake R, Schmuth M, Scharschmidt TC, et al. Epidermal barrier dysfunction in non-atopic HIV: evidence for an "inside-to-outside" pathogenesis. *J Invest Dermatol*. 2010;13:1185–1188.
49. Michel S, Schmidt R, Shroot B, et al. Morphological and biochemical characterization of the cornified envelopes from human epidermal keratinocytes of different origin. *J Invest Dermatol*. 1988;91:11–15.
50. Ishida Yamamoto A, Eady RA, Watt FM, et al. Immunoelectron microscopic analysis of cornified cell envelope formation in normal and psoriatic epidermis. *J Histochem Catochem*. 1996;44:167–175.
51. Hirao T, Terui T, Takeuchi I, et al. Ratio of immature cornified envelopes does not correlate with parakeratosis in inflammatory skin disorders. *Exp Dermatol*. 2003;12:591–601.
52. Mojumdar EH, Kariman Z, van Kerckhove L, et al. The role of ceramide chain length distribution on the barrier properties of the skin lipid membranes. *Biochem Biophys Acta*. 2014;1838:2473–2483.
53. Man MQ, Wood L, Elias PM, Feingold KR. Cutaneous barrier repair and pathophysiology following barrier disruption in IL-1 and TNF type I receptor deficient mice. *Exp Dermatol*. 1999;8:261–266.
54. Choi EH, Brown BE, Crumrine D, et al. Mechanisms by which psychologic stress alters cutaneous permeability barrier homeostasis and stratum corneum integrity. *J Invest Dermatol*. 2005;124:587–595.
55. Denda M, Tsuchiya T, Elias P, et al. Stress alters cutaneous permeability barrier homeostasis. *Am J Physiol Regul Integr Comp Physiol*. 2000;278:R367–R372.
56. Choi E-H, Brown BE, Crumrine D, et al. Mechanisms by which psychologic stress alters cutaneous permeability barrier homeostasis and stratum corneum integrity. *J Invest Dermatol*. 2005;124:587–595.
57. Dempski RE, De Marco JD, Marcus AD. An in vitro study of the relative moisture occlusive properties of several topical vehicles and Saran Wrap. *J Invest Dermatol*. 1965;44:361–363.
58. Smith WP, Christensen MS, Nacht S, et al. Effect of lipids on the aggregation and permeability of human stratum corneum. *J Invest Dermatol*. 1982;78:7–11.
59. Griffiths CE, Tranfaglia MG, Kang S. Prolonged occlusion in the treatment of psoriasis: a clinical and immunohistologic study. *J Am Acad Dermatol*. 1995;32:618–622.
60. Cleminson J, McGuire W. Topical emollient for preventing infection in preterm infants. *Cochrane Database Syst Rev*. 2016:29.
61. Gueniche A, Genyacoub J, Philippe D, et al. Lactobacillus paracasei CNCM I-2116 (ST11) inhibits substance P-induced skin inflammation and accelerates skin barrier function recovery in vitro. *Eur J Dermatol*. 2010;20:731–737.
62. Paller AS, van Steensel MAM, Rodriguez-Martin M, et al. Pathogenesis-based therapy reverses cutaneous abnormalities in an inherited disorder of distal cholesterol metabolism. *J Invest Dermatol*. 2011;131:2242–2248.
63. Atzmony L, Lim YH, Hamilton C, et al. Topical cholesterol/lovastatin for the treatment of porokeratosis: a pathogenesis-directed therapy. *J Am Acad Dermatol*. 2020;82:123–131.

Transdermal and Topical Drug Delivery

124-2



Mark R. Prausnitz

Chapter Contents

Parameters Affecting Skin Permeability *2211*
Strategies to Enhance Transdermal Drug Delivery *2213*

PARAMETERS AFFECTING SKIN PERMEABILITY

The skin is an attractive site for drug delivery, whether for *topical delivery* to locally treat cutaneous conditions or for *transdermal delivery* into the systemic circulation via absorption through the skin for other indications[64,65]. However, normal skin provides a significant barrier to drug absorption, whereas diseased skin can provide a lesser or greater barrier, depending on its associated epidermal changes[66]. While the most straightforward method of circumventing the stratum corneum barrier is an intradermal needle injection (e.g. the Mantoux technique)[67], this is often not practical for patients to perform on a routine basis.

Understanding the parameters that affect the permeability of this barrier is essential for achieving successful drug therapy via the skin without intradermal or subcutaneous injections. While local cutaneous effects are generally achieved by dissolving or suspending the drug in a vehicle that is applied topically as a semi-solid formulation (e.g. cream or ointment)[68], administration of systemic therapy via the skin is typically accomplished through the use of a patch. In either situation, drug is supplied at the surface of the skin for diffusion across the stratum corneum, with the goal of reaching therapeutic targets within the skin and/or systemic uptake via superficial dermal capillaries.

Parameters Controlling Absorption

Conventional transdermal drug delivery is a passive process governed by Fick's law, that is, the rate of absorption or flux (J) of any substance across a barrier is proportional to its concentration difference across that barrier[69,70]. For topically applied *drugs*, the concentration difference can be simplified as the concentration of drug in the vehicle, C_v, and the proportionality constant relating flux to concentration is the permeability coefficient, K_p (Eq. 1). K_p is composed of factors that relate to both drug and barrier, as well as their interaction. These factors are: D, the drug diffusion coefficient; K_m, the drug partition coefficient; and L, the length of the diffusion pathway across stratum corneum (Eq. 2). Thus, four factors control the kinetics of percutaneous drug absorption (Eq. 2); however, it is of great practical importance that two of the four (C_v, K_m) are highly dependent on one additional factor, the vehicle in which the drug is supplied to the skin.

$$J = K_p C_v \tag{1}$$

$$J = \left(\frac{DK_m}{L}\right) C_v \tag{2}$$

Role of the Vehicle

The vehicle is an important link between drug potency and therapeutic effectiveness, since extensive pharmaceutical research has shown that the composition of the vehicle can profoundly influence the rate and extent of absorption (bioavailability). As illustrated by the potency ranking scale for topical corticosteroids[71], the same drug appears

EFFECT OF VEHICLE ON CORTICOSTEROID POTENCY			
Corticosteroid*	**Potency class**	**Corticosteroid***	**Potency class**
Betamethasone dipropionate		**Fluocinonide**	
• Diprolene ointment 0.05%	1	• Lidex ointment 0.05%	2
• Diprolene gel 0.05%	1	• Lidex cream 0.05%	2
• Diprolene cream AF 0.05%	2	• Lidex gel 0.05%	2
• Diprosone ointment 0.05%	2	• Lidex solution 0.05%	2
• Diprosone cream 0.05%	3	• Lidex E cream 0.05%	3
• Diprosone lotion 0.05%	5		
Clobetasol propionate		**Triamcinolone acetonide**	
• Temovate ointment 0.05%	1	• Aristocort A ointment 0.1%	3
• Temovate cream 0.05%	1	• Kenalog cream 0.1%	4
• Temovate gel 0.05%	1	• Kenalog lotion 0.1%	5
• Temovate E cream 0.05%	1	• Aristocort cream 0.1%	6
• Olux foam 0.05%	1		
• Temovate Scalp Application 0.05%	2		
*Generic name in header, followed by trade names.			

Table 124.3 Effect of vehicle on corticosteroid potency. In this table, the potency class ranges from 1 (highest potency) to 6 (lowest potency).

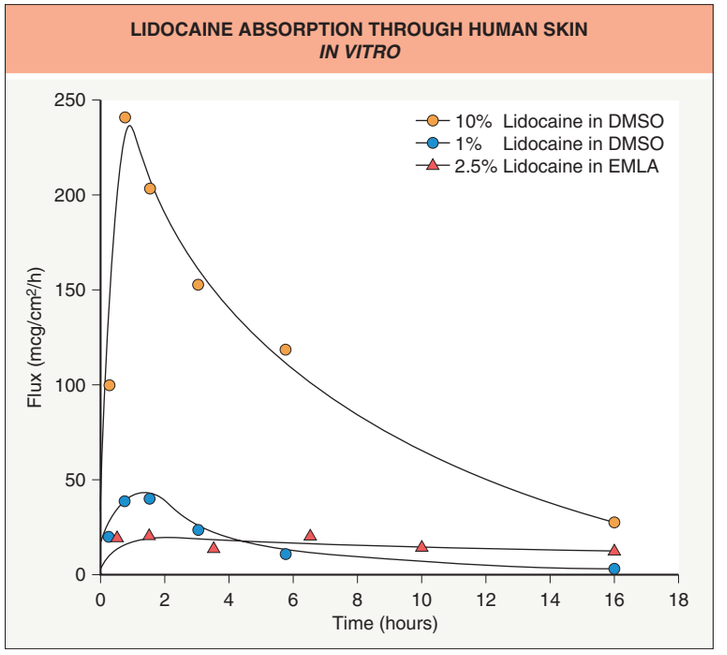


Fig. 124.6 Lidocaine absorption through human skin *in vitro*. Incorporation of DMSO as a co-solvent with ethanol results in both increased drug solubility (C_v) and partitioning (K_m). At 10% drug concentration, the maximum flux in the presence of DMSO is 10-fold greater than that achieved in an emulsion formulation without DMSO (eutectic mixture of lidocaine 2.5% and prilocaine 2.5% [EMLA]). At 1% drug concentration in DMSO, the maximum flux is two-fold greater than 2.5% drug in EMLA. *Reproduced from Mallory SB, et al. Topical lidocaine for anesthesia in patients undergoing pulsed dye laser treatment for vascular malformations. Pediatr Dermatol 1993;10:370–5.*

in different potency classes when formulated in different vehicles (Table 124.3). It was once axiomatic that ointments were more potent than creams. Though true for the early corticosteroid products, it is no longer generally applicable. Greater understanding of the science underlying topical formulations has allowed creams, gels, solutions, and foams to be specifically formulated equipotent to ointments (see Table 124.3).

In the rational design of dermatologic vehicles that maximize bioavailability, two factors are of critical importance: (1) solubilizing the drug in the vehicle (C_v); and (2) maximizing movement (partitioning) of drug from vehicle to stratum corneum (K_m). The partition coefficient describes the ability of a drug to escape from the vehicle and move into the outermost layer of the stratum corneum. It is defined as the equilibrium solubility of drug in the stratum corneum (sc) relative to its solubility in the vehicle ($K_m = C_{sc}/C_v$).

Drug Concentration

The driving force for percutaneous absorption is the concentration of *soluble* drug in the vehicle. Many older topical drug products were marketed with the expectation that higher concentrations were more potent. Although true for some products such as tretinoin gels and creams (0.01%–0.1%), in which the drug is completely solubilized at all concentrations, for others it is not the case. Hydrocortisone 1% and 2.5% in a cream formulation have been shown to be of equal potency, as have triamcinolone acetonide 0.025%, 0.1% and 0.5% creams[71]. One of the major advances in formulating glucocorticoids, as first shown with fluocinonide, came when it was discovered that the addition of propylene glycol to the vehicle could completely solubilize the drug, leading to corticosteroid products with greater potency.

Newer products are now tested during the development process to ensure that increased drug concentration results in increased bioavailability. However, excess non-dissolved drug can sometimes be advantageous, especially in transdermal patches worn for prolonged periods of time (e.g. up to a week). In this situation, as dissolved drug is absorbed into the body, non-dissolved drug can then become dissolved in order to maintain an equilibrium, thereby maintaining a constant dissolved drug concentration over time and providing a constant rate of delivery[72].

Partition Coefficient

In general, topically applied drugs are poorly absorbed because only a small fraction partitions into the stratum corneum. Most of the drug remains on the skin surface, subject to loss from a multitude of factors (exfoliation, sweating, wash-off, rub-off, adsorption onto clothing, and chemical or photochemical degradation). Even 10–12 hours following application, a drug that has not been lost by exfoliation or rub-off remains largely on the skin surface, and it is easily removed by a simple soap and water wash[73]. In the case of patches worn for several days, as much as half of the original amount of drug may still be present in the patch when it is removed, and this can pose a safety hazard upon disposal, especially with potentially dangerous drugs such as fentanyl[74].

A number of physical and chemical factors can improve partitioning. Hydration of the skin due to occlusion, either from a topical formulation or a patch, expands the reservoir volume available to drugs within the stratum corneum; this can increase absorption by as much as five- to ten-fold[75]. Common excipients such as ethanol and propylene glycol can also alter barrier structure so as to increase partitioning[76]. In addition, many excipients have good solvent properties and, as a result, positively affect C_v as well as K_m. The use of high concentrations of propylene glycol to maximize bioavailability has become pervasive among the super- and high-potency corticosteroids, but at a price. Adverse events such as burning and stinging are common when such preparations are applied to fissured or eroded skin, and contact dermatitis may occur.

A number of other compounds have been identified as enhancers. Dimethylsulfoxide (DMSO), the archetypical enhancer, exemplifies the effects that can be achieved (Fig. 124.6). As with ethanol and propylene glycol, both C_v and K_m are affected. Because DMSO is a superb solvent, higher drug concentrations can be achieved than with other solvents. In addition, DMSO expands the stratum corneum barrier, permitting increased drug uptake and possibly an increased rate of diffusion (D) through the barrier. However, the use of powerful enhancers such as DMSO is constrained by excessive skin irritation or toxicity[77].

Regional Variation

All body sites are not equally permeable[78]. Variations in stratum corneum thickness and lipid composition, the number of sebaceous glands, and hydration status can all affect absorption. Current data and clinical experience suggest that one can crudely rank regional permeability as follows: scrotum >> face/scalp > trunk/extremities > palm/sole >> nail.

STRATEGIES TO ENHANCE TRANSDERMAL DRUG DELIVERY

Despite the significant permeability barrier of the stratum corneum, drug delivery via the skin is a very attractive option and is widely employed for both local and systemic therapy (Table 124.4; Fig. 124.7)[64,65]. Topical treatment of cutaneous disorders obviously targets the site of disease, thereby minimizing adverse side effects elsewhere within the body. Delivery of systemic therapies via the skin avoids degradation of the medication within the gastrointestinal tract and from first-pass metabolism by the liver, both of which are associated with oral administration of drugs, in addition to evading the pain and safety issues associated with injections. Transdermal delivery of drugs, especially via long-acting patches, enables infrequent dosing and maintenance of steady-state drug levels.

Many dermatologic medications can be applied topically to the skin because the required dosage is often exceedingly small and therefore they can be effective even in the setting of highly inefficient absorption. In addition, a number of skin disorders are associated with compromised barrier function, which leads to an enhanced drug uptake in sites of involvement[79].

In contrast, systemic drug delivery via the skin typically requires administration of larger doses through normal skin. As a result, at the time of writing, fewer than two dozen drugs have been FDA-approved for transdermal administration. The drugs contained within these patches share several characteristics – they are low-molecular-weight (<400 Da), lipophilic (octanol–water partition coefficient up to 10 000), and relatively low-dose (typically <10 mg per day)[80] (Table 124.5).

Significant efforts have been expended on the development of new approaches to enhance transdermal drug delivery and thereby increase the number of drugs administered via this route (Fig. 124.8). These strategies can be broadly subdivided into chemical and physical approaches (Table 124.6).

TRANSDERMAL DRUG DELIVERY: THEORETICAL ADVANTAGES
• Drug delivery targeted to skin, i.e. for dermatologic indications • Improved patient adherence to therapy • Improved efficacy, i.e. continuous release • Reduced toxicity: (a) no "peaks" and (b) lower total absorbed dose • Bypass hepatic first-pass metabolism • Avoid local gastrointestinal side effects/metabolism • Decreased dosing frequency • Avoid painful injections • Reduced costs to patient due to decreased: (a) total dose and (b) dosing frequency (increased efficiency)

Table 124.4 Transdermal drug delivery: theoretical advantages.

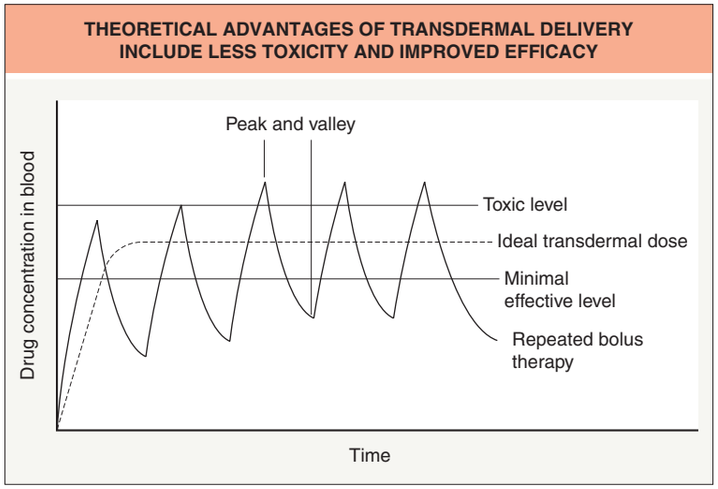


Fig. 124.7 Theoretical advantages of transdermal delivery include less toxicity and improved efficacy. This is due to a reduction in the "peaks" and "valleys" associated with repeated bolus therapy.

Chemical Enhancement

Chemical enhancers include compounds that interact with the lipid matrix of the stratum corneum to alter its nanostructure and thereby increase permeability[64,65,76]. The major advantages of chemical enhancers are that they are typically low cost, can be incorporated into a conventional patch or topical formulation, and do not require the complexity of a battery-powered device. The primary disadvantage of chemical enhancers is that they are often associated with skin irritation or toxicity when present at high concentrations and with long exposure times[77]. Thus, chemical enhancers have been employed principally to increase permeability to compounds that already cross the skin reasonably well, but they have generally been unable to significantly impact delivery of new classes of molecules (e.g. highly water-soluble drugs) or macromolecules such as proteins, gene-based medicines, and vaccines.

CONVENTIONAL TRANSDERMAL DRUG DELIVERY UTILIZING PATCHES
Ideal drug characteristics
• Low dosage (<10 mg/day) • Low molecular weight (<400 Da) • Moderately lipophilic
Examples of drugs available in transdermal patches
Buprenorphine, capsaicin, clonidine, estradiol, ethinyl estradiol, fentanyl, granisetron, glyceryl trinitrate (nitroglycerin), levonorgestrel, lidocaine, methylphenidate, methyl salicylate, nicotine, norelgestromin, norethindrone acetate, oxybutynin, rivastigmine, rotigotine, scopolamine, selegiline, sumatriptan, testosterone

Table 124.5 Conventional transdermal drug delivery utilizing patches.

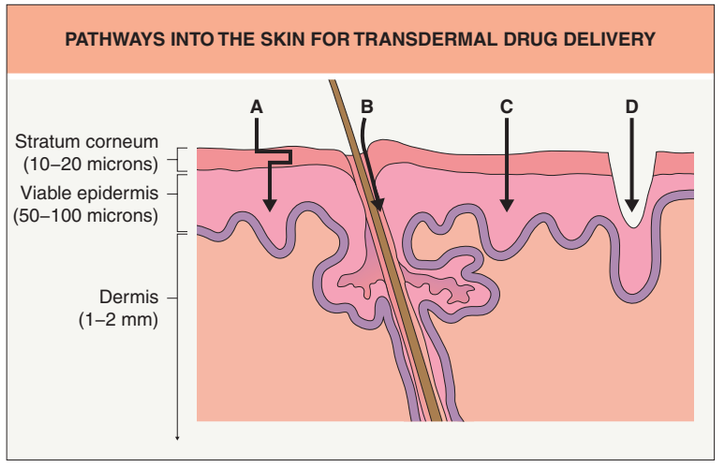


Fig. 124.8 Pathways into the skin for transdermal drug delivery. A Transdermal transport via a tortuous pathway largely within extracellular lipids. This pathway is utilized during drug absorption in association with chemical and some physical enhancers. **B** Transport through hair follicles and sweat ducts can be enhanced by iontophoresis and certain particulate formulations. **C** Transport directly across the stratum corneum is enabled by electroporation. **D** Stripping, ablation, abrasion, fractional photothermolysis, microneedles, and STAR particles remove or puncture stratum corneum to make micron-scale (or larger) pathways into the skin. *Reproduced with permission from Prausnitz MR, et al. Current status and future potential of transdermal drug delivery. Nat Rev Drug Discov 2004;3:115–24.*

STRATEGIES TO ENHANCE TRANSDERMAL DRUG DELIVERY	
Chemical	
• Ionic liquids • Liposomes/nanoparticles • Peptides	• Solvents • Surfactants/detergents • Water
Physical	
• Electroporation • Fractional photothermolysis • Iontophoresis • Mechanical abrasion • Microneedles	• STAR particles • Stripping • Thermal ablation • Ultrasound (cavitational) • Ultrasound (thermal)

Table 124.6 Strategies to enhance transdermal drug delivery. STAR particles, star-shaped particles.

The most common chemical enhancer is *water*, which leads to hydration of the stratum corneum when it accumulates during prolonged occlusion; the occlusion can result from a topical formulation or a patch[75]. Following 24–48 hours of occlusion, corneocytes swell, the intercellular spaces become distended, and the lacunar network becomes dilated. Distention of lacunae is thought to eventually lead to connections within an otherwise discontinuous system, creating "pores" in the stratum corneum interstices through which polar and non-polar substances can penetrate more readily.

Solvents, such as ethanol, methanol, chloroform and acetone, as well as *detergents* can extract barrier lipids and/or disrupt their bilayer structures, which then permeabilizes the stratum corneum[76,77]. Morphologic changes in human stratum corneum following exposure to solvents include phase separation and disruption of lamellar bilayers[81], in addition to the creation of defects in corneocyte membranes (with detergents). Moreover, *surfactants*, such as sodium dodecyl (lauryl) sulfate, and vehicles (e.g. propylene glycol) extract lipids and create extensive expansion of pre-existing lacunar domains. Furthermore, solvent-based penetration enhancers, such as azone, sulfoxides, urea and free fatty acids, not only extract extracellular lipids, but they also alter stratum corneum lipid organization (phase behavior), thereby increasing transdermal delivery and expanding intercellular domains (Fig. 124.9; see Fig. 124.6). More recent work suggests that combinations of particular chemical enhancers that adhere to specific, narrow-range compositions can be especially effective[82]. Topical medications have also been formulated as *ionic liquids*, which are drug salts paired with counterions that enable the drug to be in liquid form without the need for a solvent[83]. Certain peptides, such as polyarginine[84] and magainin[85], are believed to disrupt or penetrate stratum corneum lipids and thereby also increase transdermal drug delivery.

Finally, *liposomes* and *nanoparticles* represent additional "chemical" methods frequently employed to enhance delivery into the skin, especially in the case of cosmetics and moisturizers[86]. While intact liposomes typically do not penetrate the stratum corneum[87], they can be used to increase effective drug solubility in a vehicle (C_v) and facilitate partitioning into the skin (K_m). When nanoparticles contain drugs, this can result in an increase in drug concentrations on the skin surface, thereby increasing drug delivery into the skin, and, in some cases, nanoparticles enable slow release of drugs over time[88].

Physical Enhancement

There are a number of physical methods to increase drug delivery via the skin, many of which require the use of devices and some of which hold the promise to significantly expand the spectrum of drugs that can be administered transdermally to include water-soluble molecules and macromolecules[89,90].

Stripping is a simple technique used in research protocols to remove stratum corneum by sequential application of adhesive tape or cyanoacrylate glue[91]. Tape stripping removes both corneocytes and extracellular lipids, thereby reducing the elongated path length that drugs otherwise need to traverse, and it mechanically disrupts lamellar bilayers, even in the retained lower stratum corneum layers. Barrier disruption of human skin requires multiple strippings, which can lead to inflammation. More strippings are required to disrupt the barrier in subjects with skin phototypes V and VI (darkly pigmented) than with phototypes I and II (lightly pigmented)[92].



Fig. 124.9 Lipophilic agents (e.g. *n*-butanol) penetrate across the stratum corneum via the intercellular spaces. Note huge volume expansion of extracellular domains in this electron photomicrograph, representing the putative stratum corneum reservoir. *Method: n*-butanol precipitation *in situ* with osmium vapors. C, corneocyte.

Iontophoresis and electroporation represent electrically assisted, physical approaches to enhance delivery of drugs/macromolecules across the stratum corneum[93]. *Iontophoresis* uses low currents applied for minutes to hours from an externally placed electrode (with the same charge as the drug) in order to drive these molecules across the stratum corneum, primarily by electrophoresis[94]. As the rate of drug delivery is generally proportional to the applied current, iontophoresis offers an opportunity for programmable drug delivery, especially with the more recent development of miniaturized microprocessor systems. Clinically, iontophoresis has been employed to deliver: fentanyl and lidocaine for pain relief[95], pilocarpine to induce sweating (as a diagnostic test)[96], tap water to treat hyperhidrosis[97], and sumatriptan for migraine relief. Reverse iontophoresis has been used to extract glucose from the skin as a means of monitoring glucose levels in diabetic patients[98].

Electroporation (electropermeabilization) utilizes very short (microsecond to millisecond) and relatively high voltage (~100 V) electrical pulses to induce structural rearrangement of stratum corneum lipids, leading to pore formation[99,100]. Although currently at the research stage with regard to transdermal delivery, electroporation is being used to drive chemotherapeutic agents into superficial skin tumors by applying surface or penetrating electrodes[101].

While *ultrasound* is widely and safely employed in both medical diagnostics and physical therapy, this technology can also be used to enhance transdermal delivery. When ultrasound is utilized in a manner that resembles medical imaging, it is not very effective at increasing skin permeability. However, ultrasound administered in the context of heating deep tissues (as is done during physical therapy) has been shown to increase drug penetration into the skin, and this technique is actually used to increase local delivery of anti-inflammatory agents at the time of physical therapy[102]. With still different settings (in particular low frequencies such as <1 MHz), ultrasound can generate bubble activity, referred to as "*cavitation*", that can create microscopic defects in stratum corneum structure[103]. Cavitational ultrasound of the skin has been approved as a pretreatment prior to the application of lidocaine as a means of accelerating local anesthesia. In a related approach, pulsed laser beams have also been used to generate photomechanical shockwaves at the skin surface, which also increase skin permeability[104].

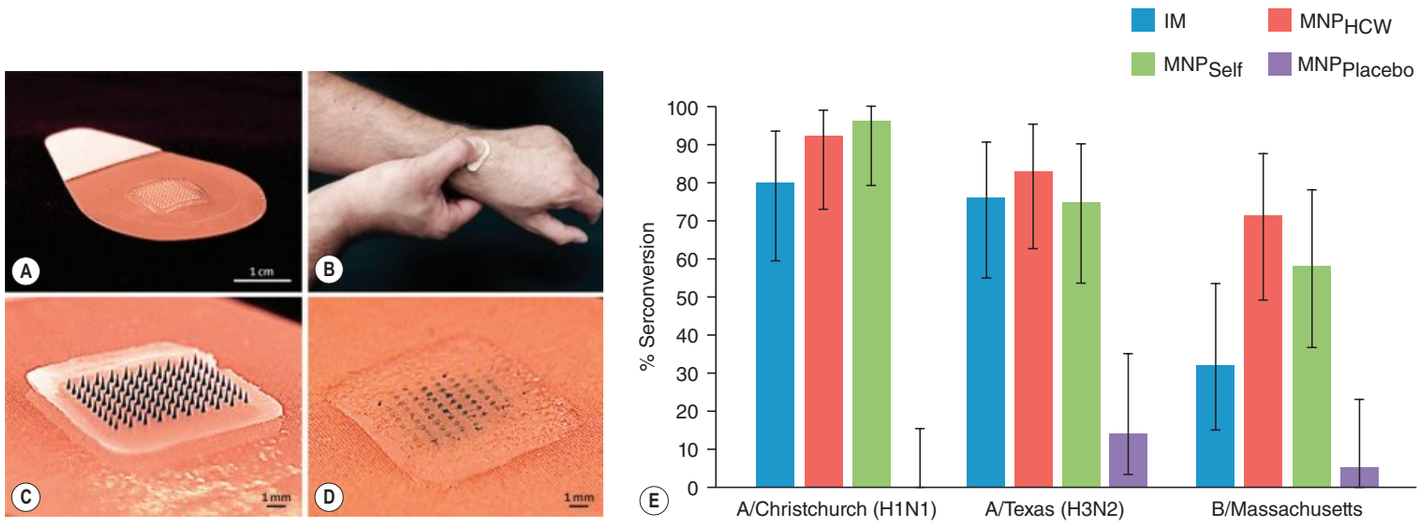


Fig. 124.10 Influenza vaccination of human subjects using a microneedle patch. A Microneedle patch. **B** Microneedle patch manually applied to the skin. Magnified view of 10 × 10 array of microneedles shown **C** before and **D** after application to skin. **E** Seroconversion against three influenza virus strains measured 28 days after influenza vaccination by intramuscular injection (IM) or microneedle patch (MNP$_{HCW}$) administered by a health care worker, microneedle patch self-administered by study subjects (MNP$_{self}$) and placebo microneedle patch containing no vaccine (MNP$_{placebo}$). *Reproduced with permission from Rouphael NG, et al. The safety, immunogenicity, and acceptability of inactivated influenza vaccine delivered by microneedle patch (TIV-MNP 2015): a randomised, partly blinded, placebo-controlled, phase 1 trial. Lancet 2017;390:649–58.*

In addition to the methods described above that disrupt stratum corneum structure on a nanometer scale, there are methods for producing micron-scale holes across the stratum corneum. This enables delivery of much larger molecules with much greater fluxes into the skin. With *thermal ablation*, microsecond- to millisecond-long pulses of heat are applied utilizing electrical filaments, radiofrequency electrodes, or lasers which lead to micropores in the stratum corneum[105,106]. Because the pulses are so short, there is not enough time for heat to propagate deeply into the tissue, thereby localizing the ablation to the epidermis and minimizing pain; these latter effects have been demonstrated in clinical trials. An at least partial removal of the stratum corneum and an increase in skin permeability can be accomplished via sandpaper abrasion and microdermabrasion[107,108]. *Fractional photothermolysis* has also been used to create micron-scale holes in the skin (Chs. 136 & 137), as a means of enhancing delivery of several topical agents, including lidocaine, 5-aminolevulinic acid, and 5-fluorouracil[109].

Finally, *microneedles* represent another micron-scale approach to drug delivery via the skin and this technique has received significant attention in recent years[110]. Microneedles typically measure 0.2–1 mm in length; they can be solid or hollow and are manufactured by microfabrication tools adapted from those developed for the microelectronics industry. In clinical trials, *solid microneedles* have been used to punch microscopic holes into the skin prior to the application of drug-loaded patches such as those containing naltrexone[111]. Drug-coated solid microneedles, designed to undergo dissolution upon insertion into the skin, have also been tested, and the efficacy of zolmitriptan delivered in this manner for the treatment of migraine headaches has been demonstrated[112]. Fully water-soluble microneedles that encapsulate pharmaceutical compounds have also been developed, in particular for simplified vaccinations via patches that generate no sharps waste (Fig. 124.10)[113].

Microneedle technology has gained widespread use in the field of cosmetic dermatology. Initially, microneedles in a roller format were used to produce microinjuries to the skin in order to induce collagen formation and reduce the appearance of wrinkles[114]. More recently, water-soluble microneedles composed of hyaluronic acid have been employed for at-home delivery of dermal filler. Various microneedle designs have also been used to administer bioactive agents into the skin with claimed beneficial properties.

Hollow microneedles have been designed to enable simple and reliable intradermal injections. Clinical trials in patients with diabetes have shown accelerated pharmacokinetics of insulin after microneedle injections into the skin, when compared to conventional subcutaneous infusions[115]. Influenza vaccine that is approved for injection into the skin using a microneedle demonstrated increased immunogenicity in the elderly and a lower dose was effective in non-elderly adults[116]. This increased effectiveness of the vaccine is due to the highly immunoresponsive environment in the skin compared to muscle, the conventional site of vaccination.

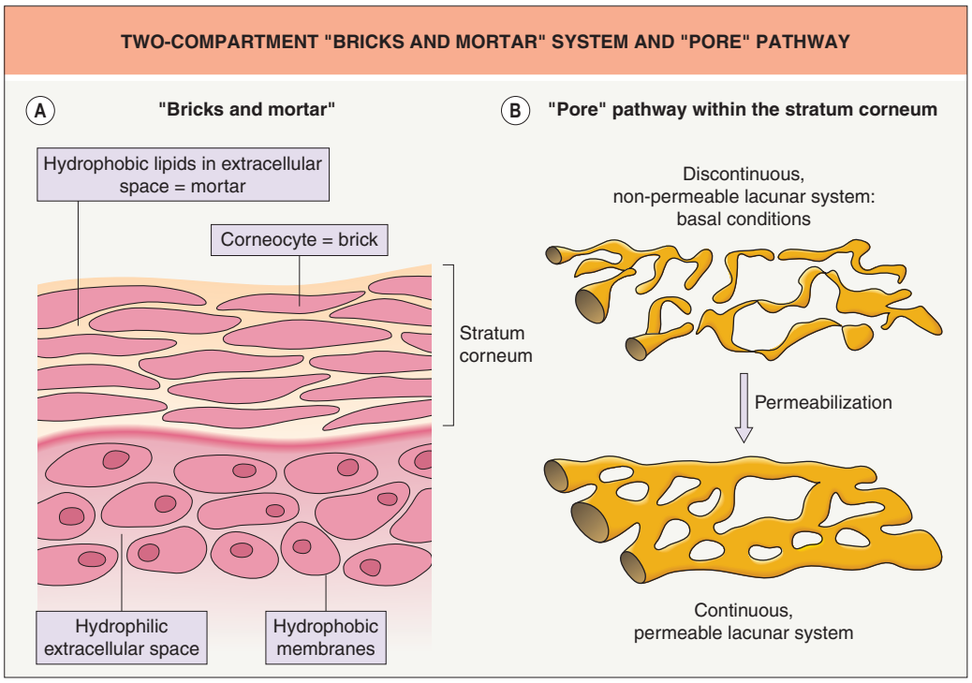
A more recently developed microneedle technology is called *STAR particles*, which enable microneedle-based delivery over large areas of skin[117]. These millimeter-sized particles have sub-millimeter microneedles protruding from their surface. When mixed with a topical formulation and rubbed onto the skin, the STAR particles create microscopic pores that enable increased absorption of water-soluble drugs and macromolecules.

Additional figures available in our eBook (see inside front cover for access code).

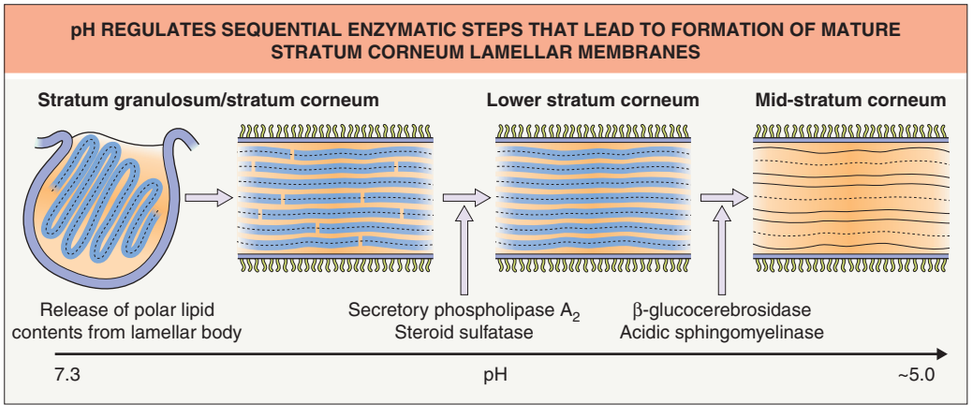
REFERENCES

64. Prausnitz MR, Langer R. Transdermal drug delivery. *Nat Biotechnol*. 2008;26:1261–1268.
65. Pastore MN, Kalia YN, Horstmann M, Roberts MS. Transdermal patches: history, development and pharmacology. *Br J Pharmacol*. 2015;172:2179–2209.
66. Bucks DAW. Permeability through diseased and damaged skin. In: Walters K, Roberts M, eds. *Dermatologic, Cosmeceutic and Cosmetic Development*. New York: Informa Healthcare; 2008:157–167.
67. Flynn PM, Shenep JL, Mao L, et al. Influence of needle gauge in Mantoux skin testing. *Chest*. 1994;106:1463–1465.
68. Weiss SC. Conventional topical delivery systems. *Dermatol Ther*. 2011;24:471–476.
69. Mitragotri S, Anissimov YG, Bunge AL, et al. Mathematical models of skin permeability: an overview. *Int J Pharm*. 2011;418:115–129.
70. Franz TJ. Kinetics of cutaneous drug penetration. *Int J Dermatol*. 1983;22:499–505.
71. Stoughton RB. Vasoconstrictor assay: specific applications. In: Maibach HI, Surber C, eds. *Topical Corticosteroids*. Basel: Karger; 1992:42–53.
72. Gupta SK, Southam M, Gale R, Hwang SS. System functionality and physicochemical model of fentanyl transdermal system. *J Pain Symptom Manage*. 1992;7(3 Suppl.):S17–S26.
73. Franz TJ, Lehman PA. Percutaneous absorption of sulconazole nitrate in man. *J Pharm Sci*. 1988;77:489–491.

74. US Food and Drug Administration. *Guidance for Industry. Residual Drug in Transdermal and Related Drug Delivery Systems*. Silver Spring, MD: Center for Drug Evaluation and Research (CDER); August 2011.
75. Van Den Merwe E, Ackermann C. Physical changes in hydrated skin. *Int J Cosmet Sci*. 1987;9:237–247.
76. Lane ME. Skin penetration enhancers. *Int J Pharm*. 2013;447:12–21.
77. Karande P, Jain A, Ergun K, et al. Design principles of chemical penetration enhancers for transdermal drug delivery. *Proc Natl Acad Sci USA*. 2005;102:4688–4693.
78. Wester RC, Maibach HI. Regional variation in percutaneous absorption. In: Bronaugh RL, Maibach HI, eds. *Percutaneous Absorption: Drugs, Cosmetics, Mechanisms, Methodology*. New York: Marcel Dekker; 1999:107–116.
79. Bucks DAW. Permeability through diseased and damaged skin. In: Walters K, Roberts M, eds. *Dermatologic, Cosmeceutic and Cosmetic Development*. New York: Informa Healthcare; 2008:157–167.
80. Choy YB, Prausnitz MR. The rule of five for non-oral routes of drug delivery: ophthalmic, inhalation and transdermal. *Pharm Res*. 2011;28:943–948.
81. Menon GK, Lee SH, Roberts MS. Ultrastructural effects of some solvents and vehicles on the stratum corneum and other skin components: evidence for an "extended mosaic-partitioning model of the skin barrier". In: Robert MS, Walters KA, eds. *Dermal Absorption and Toxicity Assessment*. New York: Marcel Dekker; 1998:727–751.
82. Karande P, Jain A, Mitragotri S. Discovery of transdermal penetration enhancers by high-throughput screening. *Nat Biotechnol*. 2004;22:192–197.
83. Shamshina JL, Barber PS, Rogers RD. Ionic liquids in drug delivery. Expert Opin Drug Deliv. 2013;10:1367–1381.
84. Rothbard JB, Garlington S, Lin Q, et al. Conjugation of arginine oligomers to cyclosporin A facilitates topical delivery and inhibition of inflammation. *Nat Med*. 2000;6:1253–1257.
85. Kim YC, Ludovice PJ, Prausnitz MR. Transdermal delivery enhanced by magainin pore-forming peptide. *J Control Release*. 2007;122:375–383.
86. Chacko IA, Ghate VM, Dsouza L, Lewis SA. Lipid vesicles: a versatile drug delivery platform for dermal and transdermal applications. *Colloids Surf B Biointerfaces*. 2020;195:111262.
87. Lasch J, Laub R, Wohlrab W. How deep do intact liposomes penetrate into human skin? *J Contr Rel*. 1992;18:55–58.
88. Yu YQ, Yang X, Wu XF, Fan YB. Enhancing permeation of drug molecules across the skin via delivery in nanocarriers: novel strategies for effective transdermal applications. *Front Bioeng Biotechnol*. 2021;9:646554.
89. Arora A, Prausnitz MR, Mitragotri S. Micro-scale devices for transdermal drug delivery. *Int J Pharm*. 2008;364:227–236.
90. Banga AK. *Transdermal and Intradermal Delivery of Therapeutic Agents: Application of Physical Technologies*. Boca Raton, FL: CRC Press; 2011.
91. Spruit D, Malten KE. The regeneration rate of the water vapour loss of heavily damaged skin. *Dermatologica*. 1966;132:115–123.
92. Reed JT, Ghadially R, Elias PM. Skin type, but neither race nor gender, influence epidermal permeability barrier function. *Arch Dermatol*. 1995;131: 1134–1138.
93. Banga AK. *Electrically-Assisted Transdermal and Topical Drug Delivery*. London: Taylor & Francis; 1998.
94. Wang Y, Zeng L, Song W, Liu J. Influencing factors and drug application of iontophoresis in transdermal drug delivery: an overview of recent progress. *Drug Deliv Transl Res*. 2022;12(1):15–26.
95. Mayes S, Ferrone M. Fentanyl HCl patient-controlled iontophoretic transdermal system for the management of acute postoperative pain. *Ann Pharmacother*. 2006;40:2178–2186.
96. Beauchamp M, Lands LC. Sweat-testing: a review of current technical requirements. *Pediatr Pulmonol*. 2005;39:507–511.
97. Kreyden OP. Iontophoresis for palmoplantar hyperhidrosis. *J Cosmet Dermatol*. 2004;3:211–214.
98. Tamada J, Garg S, Jovanovic L, et al. Noninvasive glucose monitoring: comprehensive clinical results. Cygnus Research Team. *JAMA*. 1999;282:1839–1844.
99. Prausnitz MR, Bose VG, Langer R, Weaver JC. Electroporation of mammalian skin: a mechanism to enhance transdermal drug delivery. *Proc Natl Acad Sci USA*. 1993;90:10504–10508.
100. Denet AR, Vanbever R, Preat V. Skin electroporation for transdermal and topical delivery. *Adv Drug Deliv Rev*. 2004;56:659–674.
101. Yarmush ML, Golberg A, Serša G, et al. Electroporation-based technologies for medicine: principles, applications, and challenges. *Annu Rev Biomed Eng*. 2014;16:295–320.
102. Machet L, Boucaud A. Phonophoresis: efficiency, mechanisms and skin tolerance. *Int J Pharm*. 2002;243:1–15.
103. Polat BE, Hart D, Langer R, Blankschtein D. Ultrasound-mediated transdermal drug delivery: mechanisms, scope, and emerging trends. *J Control Release*. 2011;152:330–348.
104. Doukas AG, Kollias N. Transdermal drug delivery with a pressure wave. *Adv Drug Deliv Rev*. 2004;56:559–579.
105. Levin G, Gershonowitz A, Sacks H, et al. Transdermal delivery of human growth hormone through RF-microchannels. *Pharm Res*. 2005;22:550–555.
106. Bramson J, Dayball K, Evelegh C, et al. Enabling topical immunization via microporation: a novel method for pain-free and needle-free delivery of adenovirus-based vaccines. *Gene Ther*. 2003;10:251–260.
107. Glenn GM, Flyer DC, Ellingsworth LR, et al. Transcutaneous immunization with heat-labile enterotoxin: development of a needle-free vaccine patch. *Expert Rev Vaccines*. 2007;6:809–819.
108. Andrews S, Lee JW, Choi SO, Prausnitz MR. Transdermal insulin delivery using microdermabrasion. *Pharm Res*. 2011;28:2110–2118.
109. Wenande E, Anderson RR, Haedersdal M. Fundamentals of fractional laser-assisted drug delivery: an in-depth guide to experimental methodology and data interpretation. *Adv Drug Deliv Rev*. 2020;153:169–184.
110. Prausnitz MR. Engineering microneedle patches for vaccination and drug delivery to skin. *Annu Rev Chem Biomol Eng*. 2017;8:177–200.
111. Wermeling DP, Banks SL, Hudson DA, et al. Microneedles permit transdermal delivery of a skin-impermeant medication to humans. *Proc Natl Acad Sci USA*. 2008;105:2058–2063.
112. Tepper SJ, Dodick DW, Schmidt PC, Kellerman DJ. Efficacy of ADAM zolmitriptan for the acute treatment of difficult-to-treat migraine headaches. *Headache*. 2019;59:509–517.
113. Rouphael NG, Paine M, Mosley R, et al. TIV-MNP 2015 Study Group. The safety, immunogenicity, and acceptability of inactivated influenza vaccine delivered by microneedle patch (TIV-MNP 2015): a randomised, partly blinded, placebo-controlled, phase 1 trial. *Lancet*. 2017;390:649–658.
114. McCrudden MT, McAlister E, Courtenay AJ, et al. Microneedle applications in improving skin appearance. *Exp Dermatol*. 2015;24:561–566.
115. Pettis RJ, Ginsberg B, Hirsch L, et al. Intradermal microneedle delivery of insulin lispro achieves faster insulin absorption and insulin action than subcutaneous injection. *Diabetes Technol Ther*. 2011;13:435–442.
116. Atmar RL, Patel SM, Keitel WA. Intanza®: a new intradermal vaccine for seasonal influenza. *Expert Rev Vaccines*. 2010;9:1399–1409.
117. Tadros AR, Romanyuk A, Miller IC, et al. STAR particles for enhanced topical drug and vaccine delivery. *Nat Med*. 2020;26:341–347.



eFig. 124.1 Two-compartment "bricks and mortar" system and "pore" pathway. A The stratum corneum is a unique two-compartment system, analogous to a brick wall. Whereas lipids are sequestered extracellularly within the stratum corneum, the corneocyte is lipid-depleted but protein-enriched. **B** The degradation of corneodesmosomes results in discontinuous lacunar domains, which represent the likely aqueous "pore" pathway. These lacunae can enlarge and extend, forming a continuous but collapsible network under certain conditions, e.g. occlusion, prolonged hydration, sonophoresis.



eFig. 124.2 pH regulates sequential enzymatic steps that lead to formation of mature stratum corneum lamellar membranes. The process begins at the stratum granulosum–stratum corneum interface. Of note, in atopic dermatitis, a higher pH is observed.

Glucocorticoids 125

Courtney R. Schadt and Scott M. Jackson

Key features

- Glucocorticoids continue to be among the most commonly prescribed anti-inflammatory agents in dermatology and all of medicine, with a large number of disorders responding to these drugs
- Proper use of systemic glucocorticoids requires a working knowledge of the hypothalamic–pituitary–adrenal (HPA) axis
- Proper use of topical and intralesional glucocorticoids requires awareness of their various formulations and potencies
- Glucocorticoids have a broad range of potential adverse effects that can be minimized by a variety of strategies
- Clinical usage guidelines facilitate proper dosing and administration of glucocorticoids for both short- and long-term therapy

INTRODUCTION

The Nobel Prize in Medicine was awarded in 1950 to Hench and associates[1] for their initial work on the beneficial effects and toxicities of corticosteroids for rheumatic disorders. In 1951, Sulzberger and colleagues[2] first reported the use of systemic cortisone and adrenocorticotropic hormone (ACTH) as therapies for inflammatory skin diseases. One year later, Sulzberger and Witten successfully treated eczematous eruptions with topical hydrocortisone. A novel method of high-dose glucocorticoid therapy was introduced to dermatology in 1982 by Johnson and Lazarus[3], who used pulse intravenous therapy for pyoderma gangrenosum. During the past 40 years, a variety of other anti-inflammatory/immunomodulatory drugs have been developed, allowing for a "steroid-sparing" effect and minimization of risks from long-term therapy with systemic glucocorticoids.

PHARMACOLOGY AND MECHANISM OF ACTION

Structure and Metabolism

All steroids, including glucocorticoids, have the basic four-ring structure of cholesterol, with three hexane rings and one pentane ring. Fig. 125.1 shows the chemical structure of hydrocortisone (cortisol). Modifications in the basic four-ring structure of glucocorticoids result in systemic agents that have different potencies, mineralocorticoid effects, durations of action (biologic half-life), and metabolism; these agents are commonly referred to as corticosteroids, and this term is used elsewhere in the book. Table 125.1 lists the key pharmacologic properties of the major systemic agents used today. Similar changes in the basic structure of the glucocorticoid molecule have resulted in various topical agents with differing solubilities, lipophilic properties, degrees of percutaneous absorption, and glucocorticoid receptor-binding activities. Table 14.11 defines glucocorticoid structural classes relevant for allergic reactions and cross-reactivity among agents.

When examining the chemical structure of glucocorticoids, it is important to recognize that active agents such as hydrocortisone (see Fig. 125.1) have a hydroxyl group at the 11 position. The corresponding inactive drug, cortisone, has a ketone group at the 11 position and must undergo hepatic conversion to hydrocortisone for biologic activity. The same is true for prednisone, which must undergo the identical 11-hydroxylation by the liver to produce an active agent, prednisolone. Since conversion of the inactive drug to its active analogue is impaired in patients who have severe hepatic disease, it is best to treat such individuals with a medication such as prednisolone that does not require metabolic alteration to be of therapeutic benefit[4].

In addition to indicating equivalent glucocorticoid doses in milligrams, Table 125.1 shows that these agents differ in their relative mineralocorticoid as well as glucocorticoid potencies. Cortisone and hydrocortisone have fairly significant mineralocorticoid potency, whereas prednisone and prednisolone have slight mineralocorticoid effects. A drug that has no mineralocorticoid activity, such as methylprednisolone, would be most appropriate in situations where mineralocorticoid effects must be avoided[4].

Plasma half-lives of the various systemic glucocorticoids vary from about 1 to 5 hours, as seen in Table 125.1. However, the plasma half-life is a poor indicator of the duration of action (biologic activity) of each drug. Duration of biologic effect is best assessed by the period of suppression of ACTH secretion from the pituitary gland after the administration of a single dose of a particular glucocorticoid. As indicated in Table 125.1, short-acting glucocorticoids have an effect for 8–12 hours, intermediate-acting agents for 24–36 hours, and long-acting agents for more than 48 hours. Duration of biologic activity is a critical factor in choosing a glucocorticoid for alternate-day therapy. Intermediate-acting agents should be used for this purpose, with long-acting agents avoided because there would be no period for recovery of the hypothalamic–pituitary–adrenal (HPA) axis (see below)[4].

Absorption and Distribution

Oral glucocorticoids are absorbed in the jejunum, with peak plasma levels occurring 30–90 minutes after intake. Administration of these drugs with food may delay absorption but does not decrease the amount absorbed.

Once glucocorticoids reach the plasma, the primary carrier protein is corticosteroid-binding globulin (CBG), also known as transcortin. Most endogenous cortisol is bound to CBG, and low doses of exogenous glucocorticoids are primarily bound by this high-affinity, but low-capacity, carrier system. With higher glucocorticoid doses, some binding also occurs to albumin in a low-affinity fashion, but with a greater capacity because of the larger amount of albumin in plasma. The avidity with which exogenous glucocorticoids bind to these two carrier proteins is less than that of endogenous cortisol. As exogenous glucocorticoids fill CBG binding sites, an increase in low-affinity binding to albumin leads to a greater fraction of free (unbound) glucocorticoid. This free fraction is biologically active, entering cells and mediating glucocorticoid effects[5]. Disorders that result in decreased binding proteins in the plasma, such as hepatic or renal disease, increase the free fraction of exogenous glucocorticoids and thereby augment the therapeutic effects and toxicities of these drugs.

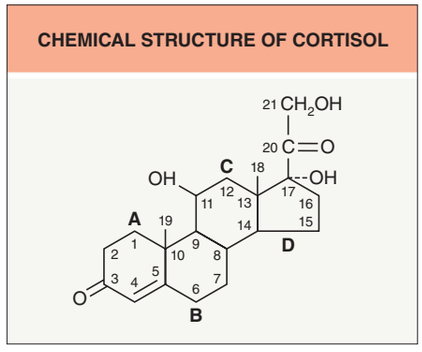


Fig. 125.1 Chemical structure of cortisol (hydrocortisone). Note the hydroxyl group at the 11 position.

PHARMACOLOGY OF SYSTEMIC GLUCOCORTICOIDS (GCs)					
	Equivalent GC *dose* (mg)	**GC *potency* (relative)**	**Mineralocorticoid potency (relative)**	**Duration of action (hours)***	**Plasma half-life (minutes)**
Short-acting					
Cortisone	25	0.8	1.0	8–12	60
Hydrocortisone	20	1	0.8	8–12	90
Intermediate-acting					
Prednisone	5	4	0.25	24–36	60
Prednisolone	5	4	0.25	24–36	200
Methylprednisolone	4	5	0	24–36	180
Triamcinolone	4	5	0	24–36	300
Long-acting					
Dexamethasone	0.75	25–30	0	36–54	200
Betamethasone	0.6	30–35	0	36–54	200

*Differs for intramuscular administration (see text).

Table 125.1 Pharmacology of systemic glucocorticoids (GCs). These agents are commonly referred to as corticosteroids, and this term is used elsewhere in the book.

The Hypothalamic–Pituitary–Adrenal (HPA) Axis

A working knowledge of the normal function of the HPA axis is required to understand glucocorticoid physiology. The hypothalamus produces corticotropin-releasing hormone, which is released in small pulses into the pituitary circulation. The anterior pituitary responds to corticotropin-releasing hormone with synthesis of ACTH and its subsequent pulsatile secretion into the peripheral circulation. ACTH is the hormone that stimulates the middle layer of the adrenal cortex to generate and release cortisol. Under basal conditions, the adrenals produce ~20–30 mg of cortisol (equivalent to 5–7.5 mg of prednisone) per day in an adult, but this may increase up to 10-fold under times of maximal stress. ACTH also has some role in stimulating adrenal androgen production, but it is not significantly involved in the production of the major mineralocorticoid, aldosterone. The major mineralocorticoid control mechanisms are the renin–angiotensin system and serum potassium levels.

There are three main control mechanisms for endogenous cortisol secretion[6]. The first is a negative feedback effect by plasma cortisol, which inhibits the secretion of corticotropin-releasing hormone and ACTH by the hypothalamus and pituitary, respectively. The second method of regulation is the pulsatile secretion of ACTH, which is based on a circadian cycle, with increasing pulses beginning several hours after the onset of sleep and reaching a maximum shortly before waking. From these ACTH pulses, the peak release of cortisol in a typical sleep cycle is at about 6–8 a.m. With other sleep cycles, the circadian pattern will adjust so that peak cortisol levels occur just prior to waking. The third form of control of endogenous cortisol production comes from neural effects on the HPA axis in response to various emotional or physical stresses. These neural stimuli include catecholamine production from the brainstem, corticotropin-releasing hormone from sites other than the hypothalamus, and vasopressin.

Molecular Mechanisms

As depicted in Fig. 125.2, the glucocorticoid free (unbound) fraction enters cells and exerts its effects by binding to a cytoplasmic glucocorticoid receptor, which is within a protein complex that includes heat shock proteins[5]. Binding of glucocorticoids to this receptor leads to their translocation into the nucleus and eventual release from the protein complex. In the nucleus, the glucocorticoid receptor forms a dimer that binds to glucocorticoid response elements in the promoter region of certain genes (see Fig. 125.2). Approximately 10–100 genes in each cell are regulated directly by glucocorticoids[7]. This binding affects the rate of transcription, inducing or (less often) repressing specific messenger RNA production and protein synthesis.

The glucocorticoid receptor also interacts with other transcription factors that have a central role in the inflammatory response as well as their coactivator molecules, such as cAMP response element binding protein (CREB)-binding protein. Nuclear factor-κB (NF-κB) is an important transcription factor that induces the expression of many genes that play a significant role in chronic inflammation, encoding various cytokines, adhesion molecules, inflammatory enzymes, and growth factors. By indirectly and directly inhibiting NF-κB, the glucocorticoid receptor can dramatically reduce the inflammatory process (see Fig. 125.2)[5]. The glucocorticoid receptor also has an inhibitory effect on activator protein 1 (AP-1), a heterodimeric transcription factor composed of proteins such as c-jun, c-fos, and activating transcription factor; this likewise controls expression of growth factor and cytokine genes. The key cytokines and other proinflammatory molecules that are inhibited by glucocorticoids and the effects of these drugs on inflammatory cells are summarized in Table 125.2[8,9].

CLINICAL INDICATIONS, DOSAGES, HPA-AXIS SUPPRESSION, TAPERING, AND CONTRAINDICATIONS

Table 125.3 lists major categories of dermatologic disease where systemic glucocorticoids are used. There are many more skin conditions for which topical and intralesional glucocorticoids can be helpful, such as eczematous and papulosquamous disorders and other localized inflammatory processes.

Oral Therapy

Dermatologists use glucocorticoids for short periods to treat acute conditions such as extensive allergic contact dermatitis and other acute eczematous disorders. Therapy is considered short-term if it is administered for ~3 weeks or less. If a skin disease requires a longer course of therapy (months to years), the addition of a glucocorticoid-sparing agent should be considered to assist in reducing the dosage and duration of glucocorticoid therapy. An oral agent with an intermediate duration of action, such as prednisone, is usually given in a single early-morning dose to achieve the least HPA axis suppression. In some severe acute dermatoses, the dose can be divided and administered twice daily for better initial control (versus more frequent intravenous administration), but conversion to a single early-morning dose should occur as soon as possible. Split-dose therapy results in parallel increases in efficacy and toxicity. The total number of milligrams given daily as a split dose is considered to be biologically equivalent to a slightly higher single morning dose. The daily dose of prednisone varies depending on the severity of the dermatosis, but for most moderate conditions, a common initial dose is 40–60 mg/day in average-weight adults or ~1 mg/kg/day in children.

Prednisone is often the intermediate-acting glucocorticoid of choice for both short- and long-term therapy. It is inexpensive and available

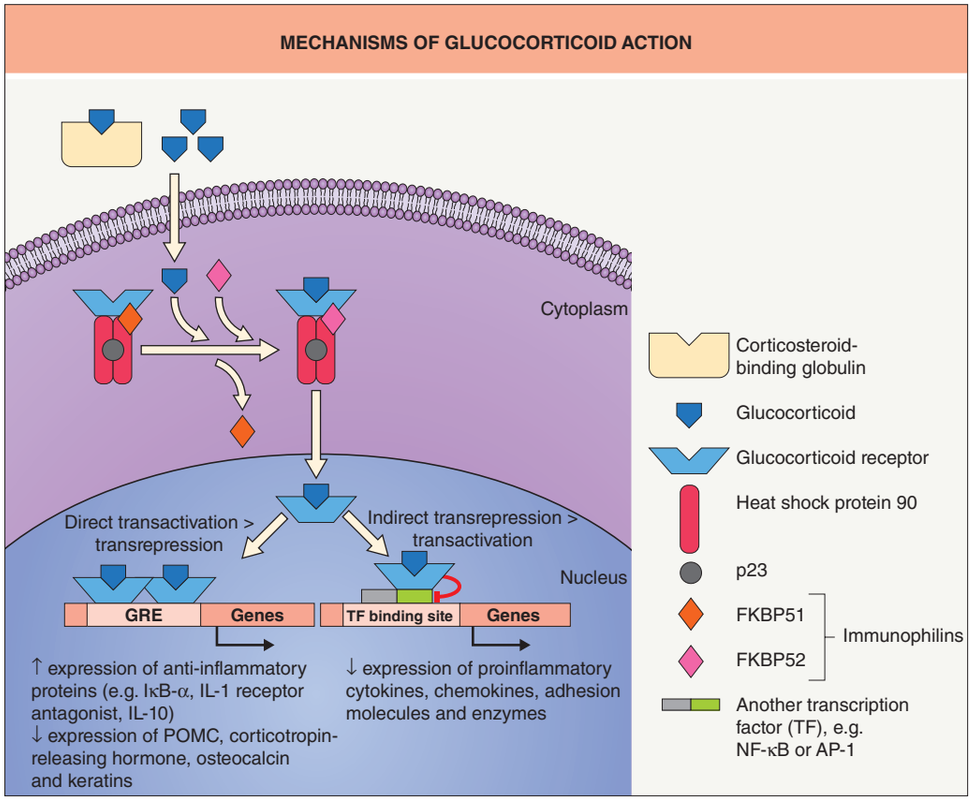


Fig. 125.2 Mechanisms of glucocorticoid action. "Free" glucocorticoid enters the cell and binds to the glucocorticoid receptor, which forms a complex that includes the 90 kDa heat shock protein and an immunophilin, FK506-binding protein 51 (FKBP51) in the cytoplasm. After glucocorticoid binding, FKBP52 replaces FKBP51 and facilitates nuclear translocation. In the nucleus, ligand-bound glucocorticoid receptor homodimers directly bind to glucocorticoid response elements (GREs) in the promoter regions of target genes, which leads to activation or (less often) repression of transcription. Glucocorticoid receptor monomers can also indirectly affect gene expression by interacting with and inhibiting other transcription factors such as nuclear factor-κB (NF-κB) or activator protein 1 (AP-1), resulting in decreased transcription of proinflammatory genes. IL, interleukin; IκB-α, inhibitor κB-α; POMC, proopiomelanocortin.

ANTI-INFLAMMATORY EFFECTS OF GLUCOCORTICOIDS
Decreased production of cytokines and other proinflammatory molecules
• Tumor necrosis factor • Granulocyte–macrophage colony-stimulating factor • Interleukin (IL)-1, IL-2, IL-6, and IL-8 • Intercellular adhesion molecule (ICAM)-1, E-selectin • Leukotrienes and prostaglandins (due to decreased phospholipase A_2 and cyclooxygenase activity)
Effects on inflammatory cells

• Neutrophils
  • Increased release from the bone marrow, resulting in neutrophilia due to a larger circulating pool
  • Decreased infiltration into sites of inflammation due to reduced expression of endothelial adhesion molecules and chemoattractants
  • Decreased apoptosis
  • Milder effects on phagocytosis and bactericidal function
• Lymphocytes
  • Redistribution of T cells to lymphoid depots, resulting in transient lymphopenia
  • Decreased activation and proliferation of effector (helper > cytotoxic) T cells, related to decreased IL-2 signaling and antigen presentation
  • Decreased B cell function and antibody production (at high doses)
  • Increased apoptosis
  • Increased regulatory T cell function
• Eosinophils
  • Decreased release from bone marrow and recruitment to sites of inflammation
  • Increased apoptosis
• Monocytes/macrophages
  • Decreased production, differentiation, and antigen presentation
• Mast cells
  • Decreased maturation, cytokine production, high-affinity IgE receptor (FcεRI) expression, and mediator release
• Erythrocytes
  • Decreased destruction due to reduced autohemolysis and erythrophagocytosis

Table 125.2 Anti-inflammatory effects of glucocorticoids.

MAJOR USES OF SYSTEMIC GLUCOCORTICOIDS IN DERMATOLOGY	
Severe dermatitis	
• Contact dermatitis (various forms) • Acute exacerbations of atopic dermatitis (risk rebound flare upon discontinuation)	• Photodermatitis • Exfoliative erythrodermas
Bullous dermatoses	
• Pemphigus (all forms) • Bullous pemphigoid • Mucous membrane (cicatricial) pemphigoid	• Linear IgA bullous dermatosis • Epidermolysis bullosa acquisita • Gestational pemphigoid • Erythema multiforme (major)
Vasculitis	
• Cutaneous (various types)	• Systemic (various types)
Autoimmune connective tissue diseases	
• Lupus erythematosus • Dermatomyositis • Systemic sclerosis (selected patients) • Eosinophilic fasciitis	• Morphea (severe generalized and linear variants) • Mixed connective tissue disease • Relapsing polychondritis
Neutrophilic dermatoses	
• Sweet syndrome (acute febrile neutrophilic dermatosis)	• Pyoderma gangrenosum • Behçet disease
Other disorders	
• Sarcoidosis • Lichen planus • Panniculitis (some types) • Urticaria/angioedema (acutely)	• Drug reaction with eosinophilia and systemic symptoms (DRESS) • Arthropod bites/stings

Table 125.3 Major uses of systemic glucocorticoids in dermatology.

ALTERNATE-MORNING GLUCOCORTICOID THERAPY

• "Off" days allow recovery of hypothalamic–pituitary–adrenal (HPA) axis
• Decreases risks of:
  • Growth suppression
  • Myopathy
  • Hypertension
  • Opportunistic infections
  • Electrolyte imbalances (e.g. hypokalemia, hypocalcemia)
• Does *not* substantially alter risks of osteoporosis or cataracts
• Fluctuations in glucose levels can make diabetes mellitus more difficult to manage

Table 125.4 Alternate-morning glucocorticoid therapy.

in many dosage forms[6]. Methylprednisolone can be used if there is a need to avoid any mineralocorticoid effects. Intermediate-acting drugs such as prednisone and methylprednisolone are also utilized for alternate-morning therapy, which allows the HPA axis to recover in the last 12 hours of the off-day of therapy. Other advantages of alternate-morning glucocorticoid therapy are listed in Table 125.4. Two important side effects of long-term glucocorticoid therapy that are not minimized by alternate-morning dosing are osteoporosis and cataracts (see below).

Intramuscular Therapy

Dermatologists occasionally use intramuscular administration of glucocorticoids for control of acute dermatoses[10]. Although some acute dermatoses respond very well to intramuscular glucocorticoid therapy, serious conditions such as pemphigus vulgaris or systemic lupus erythematosus (SLE) are best treated by other routes of systemic administration because of the initial need for higher daily doses and the requirement for more control over dosage changes. Advantages of intramuscular glucocorticoid therapy include guaranteed compliance due to physician administration and an assured steady release of glucocorticoids from the injected depot preparation. Critics of intramuscular therapy stress that oral morning doses are more physiologic, are absorbed more predictably, allow more precise tapering, and can be administered on alternate-morning schedules to decrease HPA axis suppression. There is also the possibility of lipoatrophy or a sterile abscess at an injection site, especially with triamcinolone, if the injection is not given deeply enough into the muscle. Intramuscular agents such as betamethasone and dexamethasone, which have a duration of action of less than 1 week, may be preferred in self-limited dermatoses. Longer-acting intramuscular agents that produce effects for about 3 weeks, such as triamcinolone acetonide and methylprednisolone acetate, should not be given more than about four to six times per year. The physician might be lulled into thinking that therapy is intermittent and relatively safe, while in fact it is continuous for ≥3 weeks per injection, necessitating time for HPA axis recovery.

Intravenous and Pulse Therapy

Intravenous doses of glucocorticoids may be necessary in life-threatening dermatologic conditions. A total daily dose of 2 mg/kg or more of methylprednisolone is given initially in divided doses every 6–8 hours in these acute and critical situations. Another method of dosing glucocorticoids in severe dermatologic disease is intravenous pulse therapy[11]. With this method, methylprednisolone is given intravenously in doses of 0.5–1 g over 2 hours daily for 1–5 days. This therapy was formerly given in an inpatient setting with cardiac monitoring because arrhythmias and rare cases of sudden death are possible if rapid administration results in acute electrolyte shifts. However, coadministration of potassium helps to avoid this problem, and slow infusion of the methylprednisolone over 2 hours usually prevents cardiac effects, allowing use of this therapy in an outpatient setting. Pulse therapy allows for a dramatic acute effect in severe dermatoses and is usually followed by maintenance therapy with oral glucocorticoids.

Topical Therapy

For topical glucocorticoid therapy, there are many different medications available in a wide range of potencies and a variety of vehicles. Topical glucocorticoids have been categorized by the WHO into four major potency groups that span seven classes, ranging from the ultra high potency agents in class 1 to the very low potency agents in class 7. These classes have been developed based on vasoconstrictor assays and double-blind clinical studies. Investigators graded the intensity of cutaneous vasoconstriction within normal skin of control subjects after overnight application of various agents and found significant correlation between degree of vasoconstriction and clinical efficacy (response of psoriatic lesions treated for 2–3 weeks)[12]. A list of topical preparations in each class is shown in Table 125.5. The vehicle can greatly influence the percutaneous absorption and therapeutic efficacy of a particular glucocorticoid. In some instances, brand-name and generic formulations of the same agent, concentration, and vehicle type may have different potencies (see Table 124.3). Limited insurance coverage and generic substitutions may result in patients receiving a different formulation than was intended by the clinician, with potential consequences on the effectiveness of therapy.

An ointment formulation is often more potent than the same molecule in a cream or lotion base because occlusive vehicles enhance percutaneous absorption through increased hydration of the stratum corneum. Gel preparations also tend to be readily absorbed. In selecting a topical glucocorticoid preparation for clinical use, one must first choose the desired potency based on the type, location, thickness, and extent of lesions. Next, one must select the proper vehicle based on the need for hydration or a drying effect, location on the body, and potential for irritation or sensitization by components of the vehicle. Lotions are elegant for the face, creams rub in well, ointments are advantageous for dry lesions, and gels or foams are more useful in hairy areas or for a drying effect (see Fig. 129.3). For the face and body folds, high potency glucocorticoid preparations should be avoided if possible due to the risks of skin atrophy in both locations and steroid rosacea/perioral dermatitis on the face. "Pulse dosing" (e.g. twice daily on the weekends only) may reduce the risk of epidermal atrophy with more potent glucocorticoids. Beyond decreasing the potency or the frequency of application of a topical glucocorticoid, it is not certain that any other modification reduces the risk of cutaneous atrophy or steroid rosacea/perioral dermatitis.

Certain topical glucocorticoids such as mometasone furoate and fluticasone propionate have low percutaneous absorption and are rapidly metabolized in the liver, minimizing their systemic bioavailability[13]. The latter agent is also highly lipophilic and has high affinity for the glucocorticoid receptor without significant binding to androgen, progesterone, estrogen, or mineralocorticoid receptors.

Commonly prescribed ophthalmic glucocorticoid preparations are listed in Table 125.6.

Intralesional Therapy

For many localized disorders, especially when topical therapy is not beneficial and systemic therapy is best avoided, intralesional glucocorticoid therapy can be very effective. A triamcinolone acetonide suspension is diluted to the desired concentration, which depends on the condition and the location to be treated; it is then injected in small amounts into the lesion(s), usually with a 30-gauge needle. With thick dermal lesions such as keloids, concentrations as high as 20–40 mg/ml of triamcinolone may be injected, as the desired result is to decrease the excessive connective tissue. However, with other disorders, atrophy of the dermis or fat can occur as a side effect, and a more dilute concentration (as low as 2 mg/ml of triamcinolone acetonide) should be used. This method of administration allows the clinician to bypass the barrier of a thickened stratum corneum and/or to treat a dermal or perifollicular inflammatory process (e.g. granuloma annulare, nodulocystic acne, alopecia areata) directly with higher concentrations of glucocorticoid at the site of the pathology, reducing the risk of epidermal atrophy.

HPA Axis Suppression

Exogenous glucocorticoids can induce a secondary type of adrenal insufficiency that is related to both the dose and duration of treatment. Adrenal suppression usually occurs after 4 weeks of systemic treatment with doses just above physiologic levels and earlier with higher doses[14]. This effect is lessened by administering the glucocorticoid in a single morning dose and decreased even more by using an intermediate-acting agent on alternate mornings.

POTENCY RANKING OF SOME COMMONLY USED TOPICAL GLUCOCORTICOIDS		
WHO potency group	**Class**	**Topical glucocorticoid agent and formulation**
Ultra high (super-potent)	1	Betamethasone dipropionate ointment* and gel* 0.05% Clobetasol propionate ointment, cream, gel, lotion, foam, solution ("scalp application")†, spray, and shampoo 0.05% Desoximetasone spray 0.25% Diflorasone diacetate ointment* 0.05% Fluocinonide cream 0.1% Flurandrenolide tape 4 mcg/cm^2 Halobetasol propionate ointment, cream, lotion, and foam 0.05%
High	2	Amcinonide ointment 0.1% Betamethasone dipropionate ointment, cream*, and lotion* 0.05% Clobetasol propionate cream 0.025% Desoximetasone cream, ointment 0.25% or gel 0.05% Diflorasone diacetate cream* and ointment 0.05% Fluocinonide cream, ointment, gel, and solution 0.05% Halcinonide cream, ointment, and solution 0.1% Halobetasol propionate lotion 0.01% Mometasone furoate ointment 0.1% Triamcinolone acetonide ointment 0.5%
	3	Amcinonide cream and lotion 0.1% Betamethasone dipropionate cream, lotion‡, and spray¶ 0.05% Betamethasone valerate ointment 0.1% and foam 0.12%¶ Diflorasone diacetate cream 0.05% Fluticasone propionate ointment 0.005% Triamcinolone acetonide ointment 0.1% or cream 0.5%
Moderate (medium)	4	Betamethasone valerate foam 0.12%¶ Desoximetasone cream 0.05% Fluocinolone acetonide ointment 0.025% Flurandrenolide ointment 0.05% Hydrocortisone valerate ointment 0.2% Mometasone furoate cream and lotion 0.1% Triamcinolone acetonide cream and ointment (Kenalog®) 0.1% or spray 0.2%
	5	Betamethasone dipropionate lotion 0.05%‡ Betamethasone valerate cream and lotion 0.1% Clocortolone pivalate cream 0.1% Fluocinolone acetonide cream 0.025% or oil and shampoo 0.01% Fluticasone propionate cream and lotion 0.05% Flurandrenolide cream and lotion 0.05% Hydrocortisone butyrate cream, ointment, lotion, and solution 0.1% Hydrocortisone probutate cream 0.1% Hydrocortisone valerate cream 0.2% Prednicarbate cream and ointment 0.1% Triamcinolone acetonide ointment 0.025% or lotion 0.1%
Low	6	Alclometasone dipropionate cream and ointment 0.05% Betamethasone valerate lotion 0.05% Desonide cream, gel, ointment, lotion, and foam 0.05% Fluocinolone acetonide cream and solution 0.01% Triamcinolone acetonide cream and lotion 0.025%
	7	Dexamethasone sodium phosphate cream 0.1% Hydrocortisone (acetate) cream, ointment, gel, lotion, and solution 0.5%–2.5% Methylprednisolone acetate cream 0.25%

*Optimized vehicle.
†In some classifications, class 2.
‡Depending upon classification, class 3 or class 5.
¶Depending upon classification, class 3 or class 4.

Table 125.5 Potency ranking of some commonly used topical glucocorticoids. Note different concentrations for betamethasone valerate, clobetasol, desoximetasone, fluocinolone, halobetasol, and triamcinolone acetonide,

The entire HPA axis is affected by exogenous glucocorticoids. The hypothalamus is the first to be suppressed and the quickest to recover, whereas the adrenals are the last of the three glands to be suppressed and the slowest to recover. After high-dose therapy for months to years, ACTH levels may not return to normal for several months. Full recovery of the adrenal glands with normal serum cortisol levels may take even longer, sometimes up to 1 year[6]. There can be altered stress responsiveness in situations such as infection or surgery. Symptoms of weakness, fatigue, anorexia, nausea, and fever may occur, and patients may even rarely develop hypotension or shock. Small doses of intravenous glucocorticoids may be needed prior to physically stressful situations such as major surgical procedures. Minor surgical procedures under local anesthesia do not require replacement therapy. Endocrinologic consultation should be obtained if the rare addisonian crisis occurs.

Even in the absence of overt adrenal insufficiency, a *glucocorticoid withdrawal syndrome* presenting with arthralgias, myalgias, headache, mood changes, fatigue, nausea, and decreased appetite can also occur upon rapid tapering of long-term glucocorticoid therapy. Low intracellular glucocorticoid levels are thought to be the cause, and a return to previous doses with slower tapering alleviates this syndrome.

With regard to HPA axis suppression, the primary screening test for basal function of the entire axis is the morning serum cortisol level. The morning glucocorticoid dose should be omitted on the day the

OPHTHALMIC GLUCOCORTICOIDS
Maximum strength
Loteprednol suspension 0.5% Prednisolone suspension and solution 1% Rimexolone suspension 1%
Moderate strength
Fluorometholone ointment 0.1% and suspension 0.1% or 0.25% Loteprednol suspension 0.2% Prednisolone suspension and solution 0.125%
Lower strength
Betamethasone solution 0.1%* Dexamethasone ointment 0.05%, suspension and solution 0.1% Difluprednate emulsion 0.05% Medrysone suspension 1%
*Not available in the US.

Table 125.6 Ophthalmic glucocorticoids.

cortisol level is checked between 6 and 8 a.m. Impaired basal HPA axis function is suggested by serum cortisol levels below 10 mcg/dl. Adrenal function alone can be tested by using the more specific ACTH stimulation test, in which serum cortisol levels are measured at baseline and then 30 and/or 60 minutes after intravenous or intramuscular administration of 250 mcg (standard-dose test; can be adjusted for weight in young children) or 1 mcg (low-dose test, which may be more sensitive) of ACTH (cosyntropin)[15]. If it is necessary to test stress responsiveness of the HPA axis or the adrenal glands in greater detail, endocrinologic consultation should be obtained for the ACTH stimulation test or for other evaluations including the corticotropin-releasing factor test, the insulin hypoglycemia test, or the metyrapone test.

Tapering Systemic Glucocorticoids

There is a paucity of high-quality studies examining systemic glucocorticoid tapering regimens for chronic medical conditions, including dermatologic diseases[14]. Some endocrinologic organizations advise tapering following oral administration of: (1) 40 mg of prednisone or the equivalent daily for more than one week; (2) any glucocorticoid dose daily for more than three weeks; (3) repeated glucocorticoid doses in the evenings; and (4) a glucocorticoid course within one year of stopping long-term therapy or in patients with other risks factors for adrenal insufficiency[14]. However, there is little evidence supporting these recommendations. As noted above, oral glucocorticoids should be taken as a single dose in the morning when possible to reduce the risk of adrenal insufficiency[16]. If the disease flares during the taper, the last glucocorticoid dose at which the condition was controlled should be resumed, with subsequent slower dose reduction.

Other factors that may impact the glucocorticoid regimen include the severity and chronicity of the underlying skin disease, time of onset of effectiveness of a coadministered steroid-sparing agent, and the patient's age and comorbidities (e.g. diabetes mellitus, psychiatric disease, hypertension, osteoporosis). Acute skin conditions (e.g. allergic contact dermatitis) of moderate severity can generally be treated with a 2- to 3-week glucocorticoid course. However, more serious chronic skin conditions, such as pyoderma gangrenosum, SLE, dermatomyositis, and vasculitis typically require longer courses with slow tapering over 6–8 or more weeks. As the dose of prednisone is decreased, the taper should be slowed.

In general, a course of systemic glucocorticoids longer than 3–4 weeks can be tapered as follows, with close monitoring of disease activity: prednisone (or equivalent) >40 mg/day – decrease by 5–10 mg weekly; 20–40 mg/day – decrease by 5 mg weekly; 10–20 mg/day – decrease by 2.5 mg weekly; and 5–10 mg/day – decrease by 1 mg every 2–3 weeks. Another method of glucocorticoid dosage tapering is to convert from daily to alternate-day therapy once the prednisone dose is about 20–30 mg/day[4]. The simplest way to convert is to multiply the previous daily dose by 2–2.5 times for the on-day dose, and taper therapy rapidly on the off-day. An alternative method is to increase the on-day dose by 5 mg increments and decrease the off-day dose by a similar amount, until therapy is eventually doubled on the on-day and stopped on the off-day. Finally, simultaneous tapering and alternate-morning conversion can be accomplished by decreasing the dose by 5 mg on the alternate morning, with the patient eventually taking the same dose every other morning as they were taking daily.

SIDE EFFECTS OF SHORT-TERM SYSTEMIC GLUCOCORTICOID THERAPY
• Mood changes, anxiety, insomnia • Gastrointestinal intolerance (e.g. nausea, vomiting) • Hyperglycemia • Fluid/sodium retention • Increased appetite, weight gain • Acneiform eruptions • Increased infections • Amenorrhea • Muscular weakness, muscle effects • Impaired wound healing

Table 125.7 Side effects of short-term systemic glucocorticoid therapy.

Contraindications

There are several contraindications to systemic or local glucocorticoid therapy[6]. Herpes simplex keratitis is considered a contraindication to local glucocorticoid treatment of the eye, whereas active tuberculosis and systemic fungal infections are usually considered as contraindications to systemic glucocorticoid therapy. Previous history of hypersensitivity to an intravenous preparation, which is rare, should preclude further use of that particular drug. Relative contraindications to systemic glucocorticoid therapy include active peptic ulcer disease, severe depression or psychosis, and an extensive chronic dermatosis (e.g. psoriasis) likely to flare after rapid glucocorticoid taper. In such situations, systemic glucocorticoid treatment should be used only when the benefits clearly outweigh the risks.

MAJOR SIDE EFFECTS

Short-term glucocorticoid therapy is usually extremely safe for self-limited and acute dermatoses. When side effects do occur with short courses of systemic therapy, those listed in Table 125.7 are most common. With long-term systemic glucocorticoid therapy at supraphysiologic doses, there is an increased incidence of more serious effects. Table 125.8 lists the major categories of complications and major adverse effects in each category. Most of these side effects are dose-related. As shown in Table 125.9, some patients have a higher risk of side effects from glucocorticoids[6]. The following discussion highlights selected toxicities of glucocorticoid therapy.

Osteoporosis

Osteoporosis is one of the most prevalent side effects in patients receiving long-term systemic glucocorticoid therapy. Without preventative measures, osteoporosis develops in 30%–50% of all patients treated chronically with glucocorticoids[17]. A rapid decline in bone mineral density occurs within the first 3 months of usage, and the rate of loss peaks at 6 months[18]. Postmenopausal White women are at highest risk for complications such as fractures, because they have the lowest bone mass before beginning therapy. The greatest amount of bone loss is usually observed in young men, because they have the highest pretreatment bone mass. The development of osteopenia and osteoporosis is not avoided by alternate-morning treatment schedules.

Trabecular bone, which is present in the axial skeleton (vertebrae, ribs), has a metabolic turnover rate eight times that of cortical bone (long bones), making trabecular bone much more prone to demineralization[19]. Although many patients with osteoporosis have no symptoms, more advanced disease can produce bone pain, fractures, and vertebral collapse. The mechanism of glucocorticoid-induced bone loss includes both direct and indirect effects[20]. Glucocorticoids *directly* reduce the proliferation and function of osteoblasts, increase apoptosis of osteoblasts, and promote proliferation of osteoclasts. They act *indirectly* by increasing urinary calcium excretion and reducing intestinal absorption of calcium. This decreases serum calcium and stimulates parathyroid hormone release, which drives osteoclasts to resorb bone.

MAJOR SIDE EFFECTS OF LONG-TERM SYSTEMIC GLUCOCORTICOID THERAPY	
Musculoskeletal	
Osteoporosis	Muscle atrophy
Osteonecrosis (e.g. hip)	Myopathy
Growth retardation	
Ophthalmologic	
Cataracts	Hemorrhage
Glaucoma	Exophthalmos
Infection	
Gastrointestinal	
Nausea, vomiting	Intestinal perforation
Gastroesophageal reflux	Pancreatitis
Peptic ulcer disease	Esophagitis (reflux or candidal)
Metabolic	
Hyperglycemia	Hypocalcemia
Hyperlipidemia	Hypokalemic alkalosis
Obesity	
Cardiovascular	
Hypertension	Atherosclerosis
Peripheral edema	
Gynecologic, obstetric	
Amenorrhea	Fetal effects (rare adrenal insufficiency; cleft palate in animal studies)
Hematologic, cellular	
Leukocytosis	Eosinopenia
Lymphopenia	Immunosuppression with increased risk of infections
Nervous system	
Mood, personality changes	Pseudotumor cerebri
Psychiatric problems, psychosis	Peripheral neuropathy
Seizures	Epidural lipomatosis
Cutaneous	
Atrophy, striae, telangiectasia	Hirsutism
Vascular fragility, purpura	Infections
Acne, acneiform eruptions	
Hypothalamic–pituitary–adrenal (HPA) axis	
Suppression	Adrenal (addisonian) crisis
Withdrawal syndrome	

Table 125.8 Major side effects of long-term systemic glucocorticoid therapy.

PATIENTS AT HIGHER RISK FOR TOXICITY FROM GLUCOCORTICOID THERAPY	
Patient group	**Concerns**
Female patients	• Slower metabolism/clearance of GCs due to estrogen • Lower baseline bone density • Often given a higher dose per kg when not adjusted based on weight
Postmenopausal women, elderly patients	• Increased risk of osteoporosis, especially if limited physical activity
Pediatric patients	• Temporary retardation of growth • Increased likelihood of striae distensae in adolescents
Patients with SLE, dermato/polymyositis or rheumatoid arthritis	• Long-term use associated with a higher risk of aseptic necrosis of bone, muscle atrophy or osteoporosis, respectively
Patients with hepatic disease (e.g. secondary to alcoholism)	• Decreased metabolism of GCs and lipids, leading to high serum triglyceride levels
Patients with hypoalbuminemia	• Increased free fraction of GCs results in greater side effects
Patients who smoke and/or have high alcohol intake	• Increased risk of osteoporosis and peptic ulcer disease

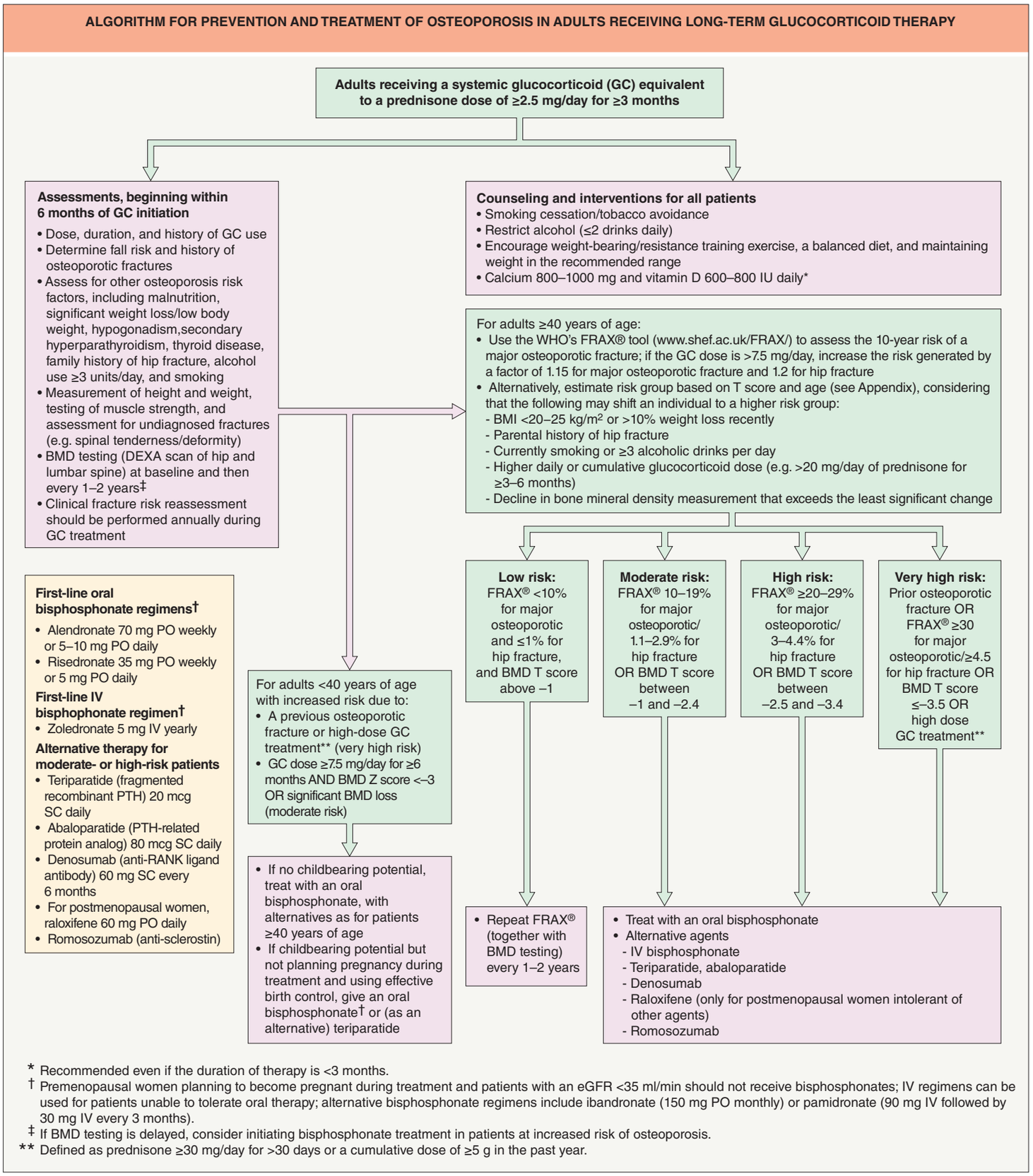
Table 125.9 Patients at higher risk for toxicity from glucocorticoid (GC) therapy. SLE, systemic lupus erythematosus.



Fig. 125.3 Radiograph of the spine showing severe demineralization. This is indicative of advanced osteoporosis.

Although routine radiographs can detect vertebral compression fractures, these plain X-ray studies are not sensitive enough to detect osteoporosis until 20%–60% of bone mass is lost (Fig. 125.3). Currently, the best measurement of osteoporosis is quantification of bone mineral density with dual-energy X-ray absorptiometry (DEXA), which is preferred because of its sensitivity, reproducibility, and low radiation exposure. Ideally, patients on long-term glucocorticoids should have a baseline DEXA examination of the hip and lumbar spine, with a repeat study performed every 1–3 years at the same sites. In densitometry reports, T scores are used to connote a standard deviation from the mean of a healthy control population. Osteopenia is defined as a T score between −1 and −2.5 standard deviations below the mean, with a T score less than −2.5 (i.e. −2.6 or below) defining osteoporosis[17]. For patients beginning long-term glucocorticoid therapy, risk factors for decreased bone density should be assessed and guidelines for the prevention and treatment of osteoporosis followed (Fig. 125.4)[18,21]. Endocrinologic consultation should be obtained in patients who develop significant osteopenia or osteoporosis. Further information on recommended regimens for osteoporosis prevention and treatment in patients receiving long-term glucocorticoid therapy is provided in Fig. 125.4[22].

In general, experts agree that patients with a history of low-impact fractures and adults with moderate to high fracture risk, especially postmenopausal women and men ≥50–65 years of age, should begin concomitant *bisphosphonate* therapy when initiating a glucocorticoid treatment course lasting ≥3 months (see Fig. 125.4). Since the largest reduction in bone mass occurs during the first 6 months of glucocorticoid therapy, it is important to initiate this and other preventative measures promptly[18]. Alendronate and risedronate are first-line oral agents given daily or weekly. They should be taken on an empty stomach, only with water, upon arising in the morning; patients should remain upright for at least 30–60 minutes after administration. Although generally well tolerated, gastrointestinal side effects can occur and, if severe, may necessitate changing to a different agent. Intravenous bisphosphonates such as zoledronate 4–5 mg IV once yearly or pamidronate 30 mg IV



* Recommended even if the duration of therapy is <3 months.
† Premenopausal women planning to become pregnant during treatment and patients with an eGFR <35 ml/min should not receive bisphosphonates; IV regimens can be used for patients unable to tolerate oral therapy; alternative bisphosphonate regimens include ibandronate (150 mg PO monthly) or pamidronate (90 mg IV followed by 30 mg IV every 3 months).
‡ If BMD testing is delayed, consider initiating bisphosphonate treatment in patients at increased risk of osteoporosis.
** Defined as prednisone ≥30 mg/day for >30 days or a cumulative dose of ≥5 g in the past year.

Fig. 125.4 Algorithm for prevention and treatment of osteoporosis in adults receiving long-term glucocorticoid therapy. Based on the American College of Rheumatology 2023 recommendations (www.rheumatology.org/glucocorticoid-induced-osteoporosis-guideline). Recommendations for children receiving glucocorticoid therapy for ≥3 months include: (1) clinical fracture risk assessment within 6 months of beginning therapy and then annually; (2) for those 4–17 years of age, calcium 1 g and vitamin D 600 IU daily; and (3) for those with history of an osteoporotic fracture and a glucocorticoid dose of ≥0.1 mg/kg/day, treatment with an oral bisphosphonate. Androgen-deprivation therapy in men and (especially in women) rheumatoid arthritis represent additional risk factors for osteoporosis. BMD, bone mineral density; BMI, body mass index; DEXA, dual-energy X-ray absorptiometry; IV, intravenously; PO, per os; PTH, parathyroid hormone; SC, subcutaneously.

every 3 months are alternatives. Osteonecrosis of the jaw represents a potential complication of bisphosphonate therapy, occurring most often with high-dose intravenous administration in patients with an underlying malignancy (e.g. multiple myeloma) and occasionally in association with invasive dental work[23]. Several case reports and small series have described atypical fractures of the subtrochanteric or diaphyseal femur in patients receiving long-term bisphosphonate therapy, but larger studies have demonstrated a very low absolute risk[23,24]. All bisphosphonates, especially those with long half-lives (e.g. ibandronate), should be avoided in premenopausal women who might become pregnant, as these agents cross the placenta and produce teratogenicity, including fetal skeletal abnormalities. Furthermore, bisphosphonates should not be administered to patients with an estimated glomerular filtration rate (eGFR) of <35 ml/minute.

Several other agents that can reduce bone resorption or increase bone formation represent options to prevent and treat glucocorticoid-induced osteoporosis in high-risk patients or those who do not tolerate bisphosphonates. *Teriparatide* (a fragment of human parathyroid hormone [PTH]) and *abaloparatide* (a PTH-related protein analogue) are additional options that increase bone formation. *Denosumab* is a monoclonal antibody directed against RANKL (receptor activator of NF-κB ligand) that blocks osteoclast maturation and thereby leads to decreased bone resorption. It is not cleared by the kidney and can be used in patients with eGFR <35 ml/minute. Potential side effects include hypocalcemia, dermatitis, osteonecrosis of the jaw, increased risk of infections, and fetal harm. *Raloxifene* is a selective estrogen receptor modulator (SERM) with less anti-resorptive potency than bisphosphonates; it represents an alternative for selected postmenopausal women (e.g. those with a high risk of invasive breast cancer), but increased risk of cardiovascular disease and thrombosis limit its use. Of note, estrogen/progestin therapy is no longer a first-line treatment for osteoporosis in postmenopausal women due to increased risk of breast cancer, stroke, myocardial infarction, and venous thromboembolism[25]. *Romosozumab*, a monoclonal antibody that increases bone density by targeting sclerostin, is likewise not a first-line agent due to the associated risk of cardiovascular disease and thrombosis. Because discontinuation of denosumab, teriparatide, abaloparatide, or romosozumab may lead to rapid bone loss and increased fracture risk, sequential therapy with a bisphosphonate for at least one year is recommended.

Osteonecrosis

Osteonecrosis (also known as aseptic necrosis or avascular necrosis) has numerous causes, and it is an uncommon but serious complication of glucocorticoid treatment[26]. Additional risk factors include physical trauma, sickle cell disease, alcohol abuse, cigarette smoking, HIV infection, and elevated serum triglycerides. The incidence of glucocorticoid-related osteonecrosis is higher in renal transplant recipients and patients with SLE, altered lipid metabolism, fatty degeneration of the liver, or alcoholism.

Localized bone pain during activity is the usual initial symptom of osteonecrosis, with the pain eventually occurring at rest and requiring analgesics for relief. The proximal femur is the most common site, although the distal femur or humeral head may be affected. Most patients who develop osteonecrosis while on glucocorticoids have been treated for at least 6–12 months, paralleling the time needed to induce changes in bone marrow fat deposition.

The mechanism of this condition is not completely understood, although intraosseous hypertension secondary to fat cell enlargement may compromise terminal arterioles at certain sites. Some investigators believe that fat emboli can originate from fatty deposits in the liver or from serum triglycerides, whereas others believe that only bone-derived fat emboli produce arterial occlusion with subsequent infarction.

Signs of osteonecrosis may not be evident on standard X-rays for as long as 6 months after bone pain begins (Fig. 125.5A). Therefore, early MRI, the most specific and sensitive radiologic examination, is recommended for confirmation of diagnosis (Fig. 125.5B). Initial medical treatment is conservative and consists of trauma prevention, rest, and modified weight bearing with the use of crutches[27]. More advanced cases in young patients may require hip salvaging procedures such as core decompression to reduce intraosseous pressure, vascularized fibular grafting, or electric stimulation. Eventual total joint arthroplasty is often unavoidable.

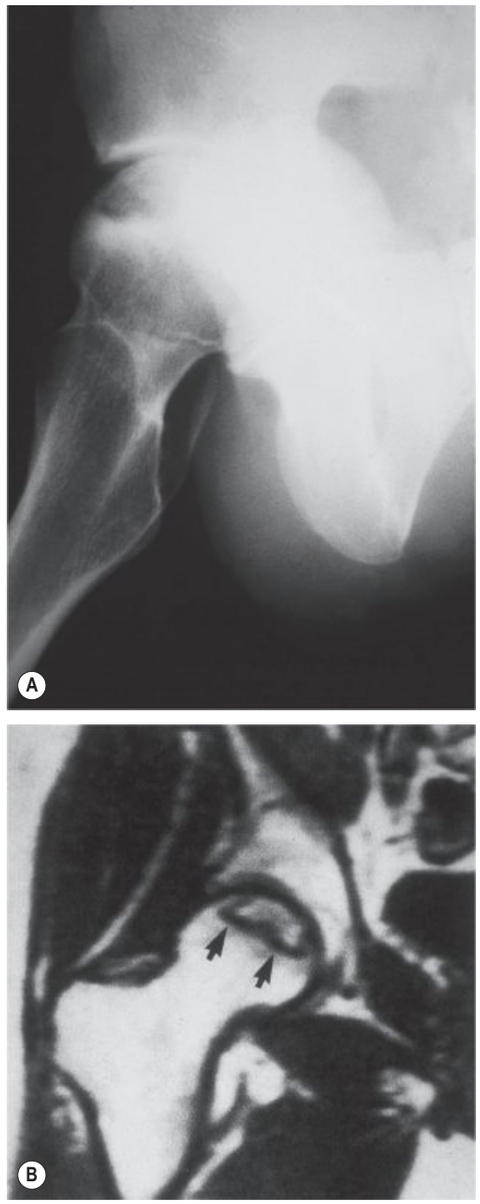


Fig. 125.5 Osteonecrosis of the femoral head. **A** Radiograph fails to demonstrate early stages of osteonecrosis. **B** In contrast, osteonecrosis is clearly evident on an MRI of the hip in the same patient (arrows).

Growth Suppression

The doses of systemic glucocorticoids required to produce growth suppression are not much higher than physiologic doses. Alternate-morning therapy can minimize this effect but does not eliminate it completely[28]. Glucocorticoid therapy via inhalants or extensive, chronic use of topical agents may also rarely produce growth suppression. Once the glucocorticoid therapy is discontinued, there is often a compensatory growth spurt with normal development of height. If chronic glucocorticoid therapy is given just before or during early puberty, the expected pubertal growth spurt is often delayed; with continued glucocorticoid administration, compensatory growth may occasionally be prevented by epiphyseal closure.

Glucocorticoids can suppress growth by several mechanisms, including interference with nitrogen and mineral retention; inhibition of collagen and protein matrix synthesis; and decreased release and signaling of growth hormone[28]. Growth monitoring should be done every 3–6 months, and growth hormone therapy may be considered in certain situations to restore linear growth and reverse other catabolic effects.

Myopathy

Myopathy is an uncommon complication of glucocorticoid therapy. The classic (chronic) form presents as painless, symmetrical proximal muscle weakness, most often of the lower extremities. It typically begins

FEATURES THAT DISTINGUISH GLUCOCORTICOID (GC)-RELATED MYOPATHY FROM MYOSITIS		
Feature	**Glucocorticoid-related myopathy**	**Myositis**
Clinical setting	• More likely with a high GC dose • Improves within 3–4 weeks when the GC dose is decreased	• Less likely with a high GC dose • Worsens when the GC dose is decreased
Clinical presentation	• Weakness, usually without myalgias	• Weakness, often associated with myalgias
Laboratory findings	• Usually normal serum creatine kinase • Elevated urine creatine*, which decreases as the GC dose is decreased	• Elevated serum creatine kinase • Elevated urine creatine*, which increases as the GC dose is decreased
EMG findings	• Normal	• Abnormal
MRI findings	• Signs of muscle atrophy	• Signs of muscle inflammation/edema
Muscle biopsy findings	• Atrophy	• Inflammation and necrosis

*Percent creatinuria can be calculated as creatine (mg) / [creatine + creatinine (mg)] in a 24-hour urine sample; however, elevated levels (>10%) are not specific to myopathy.

Table 125.10 Features that distinguish glucocorticoid (GC)-related myopathy from myositis. The myopathy is also referred to as corticosteroid-induced myopathy or simply steroid myopathy. EMG, electromyography; MRI, magnetic resonance imaging.

many weeks to months after systemic therapy is initiated, usually in patients treated with doses equivalent to >40 mg/day of prednisone. Although possibly more common with fluorinated glucocorticoids (e.g. dexamethasone, betamethasone, triamcinolone), the condition can occur with any agent[29]. Alternate-morning therapy might decrease its incidence. Diagnosis of myopathy may be difficult, as serum muscle enzyme levels and electromyographic studies tend to be normal. Muscle biopsy findings are relatively nonspecific, with variable muscle fiber diameters and atrophy of type II fibers but no substantial inflammation or necrosis. Increased urinary creatine excretion can be a clue to the diagnosis. Gradual reduction of the glucocorticoid dose along with physical therapy is useful in managing this complication, although muscle function may not return to normal for many months.

With inflammatory muscle diseases such as dermatomyositis, the glucocorticoids used to treat the disorder may actually increase the tendency for muscle atrophy. Steroid-sparing agents are often utilized after initial control with glucocorticoids, especially if glucocorticoid tapering is not occurring at an acceptable rate[4] (see Ch. 42). Findings that help to distinguish glucocorticoid-related myopathy from myositis are presented in Table 125.10.

Cataracts

The cumulative dosage and duration of therapy are the most important factors in the development of posterior subcapsular cataracts in patients receiving systemic glucocorticoid therapy. This adverse effect has been noted in patients receiving as little as 10 mg/day of prednisone for 1 year. Cataract development is not reduced by alternate-morning schedules, although patients on continuous therapy are at higher risk than those receiving intermittent treatment. While there may be some individual susceptibility factors, children are at greatest risk, developing cataracts with lower doses and shorter treatment durations compared to adults. Cataracts that occur as a manifestation of atopic keratoconjunctivitis in patients with atopic dermatitis are often anterior subcapsular lesions, but cataracts may also occur in a posterior location and be indistinguishable from those associated with glucocorticoids.

Ophthalmologic examinations are recommended every 6–12 months for patients on long-term systemic glucocorticoid therapy. Progression of cataracts can still occur despite decreasing or discontinuing glucocorticoid therapy, but discontinuing the glucocorticoids occasionally deters further cataract formation or reverses lens opacification[30].

Metabolic Effects

Glucocorticoids produce *hyperglycemia* by affecting glucose metabolism through enhanced hepatic gluconeogenesis and decreased peripheral insulin-mediated glucose uptake. Relative insulin resistance is produced by decreasing the affinity of cellular receptors for insulin. Although worsening of pre-existing or subclinical glucose intolerance is common, new-onset diabetes mellitus usually occurs only with high-dose therapy, and ketoacidosis is rare. Most patients will revert to their prior glucose status within a few months of discontinuing glucocorticoid therapy. Blood glucose levels should be assessed periodically during high-dose or long-term glucocorticoid therapy. Diabetic patients require closer monitoring, and they may need to be switched from oral antidiabetic agents to insulin or given higher insulin doses due to glucocorticoid-induced insulin resistance. Alternate-morning glucocorticoid schedules are usually not possible in diabetic patients because of the resulting fluctuations in insulin requirements.

Hyperlipidemia is a common side effect of glucocorticoid therapy, especially in patients with prior lipid abnormalities. Elevation of triglycerides is most frequently observed, but elevations of high- or low-density lipoproteins occur in some patients. The mechanism of hypertriglyceridemia is likely related to relative insulin insufficiency. A diet low in saturated fat and calories should be instituted in patients on long-term glucocorticoids.

Chronic glucocorticoid therapy often leads to weight gain with central redistribution of fat, including the classic "buffalo hump" and "moon facies". Other potential metabolic effects include hypokalemic alkalosis associated with high-dose therapy, especially with agents that have a substantial mineralocorticoid effect, and uncommonly the development of hypocalcemia, which may rarely lead to tetany in children on high-dose therapy. Potassium supplementation may be necessary, and adequate calcium intake is mandatory.

Cardiovascular Effects

Although the majority of patients with endogenous glucocorticoid excess (Cushing syndrome) have hypertension, administration of exogenous glucocorticoids produces hypertension in only about 20% of patients, because of the lower mineralocorticoid effect of these agents. Glucocorticoid therapy-associated hypertension is more common in patients with pre-existing hypertension or decreased renal function, in the elderly, and when glucocorticoids with greater mineralocorticoid activity are used[27]. Because glucocorticoids rarely affect blood pressure during the first 2 weeks of therapy, short courses of glucocorticoids in hypertensive patients almost never produce problems. When such patients receive long-term therapy, sodium restriction is important along with the possible institution of a thiazide diuretic. Alternate-morning therapy may reduce blood pressure elevation. The pathogenesis of glucocorticoid-induced hypertension is not totally understood, but it is likely related to vasoconstriction from potentiation of catecholamines and inhibition of vasodilators; sodium retention related to mineralocorticoid activity; and intravascular volume expansion.

Accelerated atherosclerosis occasionally develops in association with long-term systemic glucocorticoid therapy, especially in patients with SLE, rheumatoid arthritis, and renal transplants. This adverse effect has also been observed in children treated with glucocorticoids, and it has long been noted in patients with Cushing syndrome from chronic endogenous glucocorticoid excess. Instances of thromboembolic complications and atrioventricular conduction problems have also been reported with glucocorticoid therapy.

Gastrointestinal Effects

The relationship between systemic glucocorticoid therapy and peptic ulcer disease (PUD) is controversial, with varying results in different published case series. There does seem to be an increased incidence of PUD in patients (such as those with rheumatoid arthritis) treated concomitantly with glucocorticoids and NSAIDs or aspirin[31]. Other additive risk factors include smoking, alcohol use, and a history of PUD. When PUD occurs in patients receiving glucocorticoids, it is more likely to be gastric than duodenal, with milder pain symptoms and a greater chance of a major complication such as hemorrhage or perforation. This is related to the tendency of glucocorticoids to mask

signs and symptoms of inflammation and to inhibit wound healing. A possible mechanism of ulceration in these situations is decreased mucus production and mucosal cell renewal. The administration of oral glucocorticoids with food, as well as the use of H2 receptor antagonists or proton pump inhibitors in higher-risk settings, decreases the likelihood of PUD in patients on glucocorticoids.

Glucocorticoid-related nausea, vomiting, and gastroesophageal reflux are also minimized by administration with food and/or taking acid-suppressing medications. Candidal esophagitis, which can occur in patients with an erosive oral mucosal disease such as pemphigus vulgaris, requires treatment with oral antifungals (e.g. fluconazole). Other gastrointestinal side effects of glucocorticoids include pancreatitis in association with hypertriglyceridemia, fatty liver changes, and (rarely) intestinal perforation.

Infection

Patients receiving systemic glucocorticoids have an increased susceptibility to many bacterial, viral, fungal, and parasitic infections. Cutaneous staphylococcal and superficial fungal infections are common. Fever and signs of inflammation may be masked in patients taking glucocorticoids, making early recognition of infection difficult. Alternate-morning therapy and doses equivalent to <10 mg/day of prednisone reduce the chance of opportunistic infection.

Reactivation of tuberculosis represents a potential concern in patients on chronic glucocorticoid therapy. In addition to assessing risk of exposure, a tuberculosis history should be taken and, if negative or uncertain, a tuberculin skin test or interferon-γ release assay performed prior to beginning therapy. A chest radiograph should be obtained for patients with a positive tuberculin reaction (≥5 mm of induration in individuals receiving the equivalent of ≥15 mg/day of prednisone for a month or more) or interferon-γ release assay, a history of tuberculosis, or other risk factors (e.g. pre-existing immunosuppression). A 9-month course of isoniazid is recommended for those with an untreated latent tuberculosis infection.

An increased risk of *Pneumocystis jirovecii* pneumonia has been observed in patients receiving glucocorticoid therapy at a dose equivalent to ≥20 mg/day of prednisone for longer than a month who also have another cause of immunocompromise. Susceptible individuals include those with systemic inflammatory disorders such as granulomatosis with polyangiitis or SLE, especially if they are receiving additional immunosuppressive agents and/or have complications such as pulmonary disease or lymphopenia[32]. These high-risk patients should receive prophylaxis, typically with trimethoprim–sulfamethoxazole (TMP-SMX; e.g. one double-strength tablet three times weekly or daily)[33]. While HIV-positive patients with $CD4^+$ counts <200/mm^3 routinely receive TMP-SMX prophylaxis, it should also be considered in HIV-positive individuals with $CD4^+$ counts >200/mm^3 who are receiving systemic glucocorticoid therapy.

Patients receiving chronic glucocorticoid therapy at supraphysiologic doses may have inadequate antibody responses to immunizations. Live-virus vaccines (see Table 128.8) should not be given to children or adults during or (if treated for ≥2 weeks) within a month after discontinuing glucocorticoid therapy at a dose equivalent to ≥20 mg/day of prednisone or ≥2 mg/kg/day in children weighing <10 kg[34].

Obstetric and Gynecologic Effects

An increased incidence of cleft palate has been noted in rodents exposed to very large doses of glucocorticoids early in gestation; therefore, the safety of glucocorticoids during the first trimester of pregnancy has been debated. However, clinical experience and several clinical trials have shown minimal effects in the offspring of women treated with glucocorticoids during pregnancy[35] (see Ch. 27). Only small amounts of prednisone reach the fetus in an active form, because a placental enzyme, 11-hydroxysteroid dehydrogenase type 2, inactivates most prednisolone crossing into the fetal circulation. This enzyme has a limited ability to metabolize fluorinated glucocorticoids (e.g. betamethasone, dexamethasone), so greater amounts of these agents reach the fetus. Pregnant patients on glucocorticoids do have a slightly increased risk of both hypertension, which might account for smaller fetal gestational size, and gestational glucose intolerance, which is relatively common with moderate to high glucocorticoid doses. When large glucocorticoid doses are used near the time of delivery, fetal HPA axis suppression occasionally occurs, resulting in a pseudo-addisonian neonate. Even though glucocorticoids are secreted into breast milk, the American Academy of Pediatrics has determined that prednisone therapy is compatible with breastfeeding; if possible, nursing should be delayed for ~4 hours after prednisone administration.

In non-pregnant women, amenorrhea may occur from systemic therapy with glucocorticoids, most frequently with intramuscular injections. To prevent unnecessary concern, premenopausal women receiving systemic glucocorticoids should be alerted to this possibility. Decreased sperm counts have also been reported in men receiving systemic glucocorticoids.

Nervous System Effects

The potentially misleading term "steroid psychosis" has been utilized for the broad spectrum of neuropsychiatric effects of systemic glucocorticoids. Glucocorticoids can impact behavior, affect, and cognition in multiple ways, with only a small portion of affected individuals experiencing delusions or other psychotic symptoms[36]. Mood changes range from euphoria, irritability, and mania to hopelessness and depression. Attention, memory, psychomotor speed, and sleep may also be affected. Depression tends to develop with longer-term glucocorticoid use, while manic symptoms are more often associated with short-term or pulsed administration[36].

Neuropsychiatric effects most frequently occur in patients receiving doses >40 mg/day of prednisone or the equivalent and arise within the first few weeks of therapy[36,37]. However, symptoms can also develop upon glucocorticoid tapering. Blood–brain barrier damage and hypoalbuminemia increase the likelihood of neuropsychiatric complications; other possible risk factors include female sex, older age, use of a longer-acting glucocorticoid, and a previous primary psychiatric condition or neuropsychiatric reaction to glucocorticoids[36].

To manage neuropsychiatric complications, the glucocorticoid should be discontinued or tapered to ≤40 mg/day prednisone or the equivalent if possible. Consultation with a psychiatrist may be necessary. Low-dose olanzapine can be helpful in the treatment of both psychotic and affective symptoms[36].

Pseudotumor cerebri is another possible complication of high-dose or long-term glucocorticoid therapy and presents with headache, nausea, vomiting, visual changes, and papilledema. It typically develops after rapid tapering or discontinuation of the glucocorticoid, so returning to a higher dose followed by more gradual tapering is recommended. Although the condition is reversible, there is potential for visual loss.

Seizures occur uncommonly, primarily affecting seizure-prone patients on high glucocorticoid doses. Other infrequent neurologic complications include electroencephalographic changes, enhancement of tremor, peripheral neuropathy, and epidural lipomatosis.

Cutaneous Effects

Patients receiving systemic glucocorticoids can develop a broad range of cutaneous effects, many of which are similar to those associated with endogenous Cushing syndrome. These include purpura, telangiectasias, atrophy, striae (Fig. 125.6), pseudoscars, acneiform or rosacea-like eruptions, and facial plethora. In one study, almost half of patients developed skin changes after 3 months of treatment with a mean prednisone dosage of 30 mg/day[38]. Localized development of telangiectasias, atrophy, and hypopigmentation can also result from chronic use of topical glucocorticoids, especially long-term daily application of potent agents or use under occlusion, and from intralesional glucocorticoid therapy (Figs. 125.7 & 125.8). Intralesional administration occasionally leads to these findings in a linear pattern along pathways of lymphatic drainage (see Fig. 66.28).

Systemic glucocorticoid-induced acne or folliculitis characteristically presents with monomorphic papulopustules on the chest and back (Fig. 125.9). Acne vulgaris itself is also frequently worsened by continuous glucocorticoid therapy, although inflammatory and cystic acne lesions may be temporarily improved by very short intermittent courses of systemic glucocorticoids, or by intralesional injections of cysts (see Ch. 36). An acneiform or rosacea-like perioral, perinasal, or periorbital eruption can also occur secondary to use of inhaled glucocorticoids or application of topical glucocorticoids (especially more potent agents) to



Fig. 125.6 Extensive striae in a patient on chronic oral prednisone therapy. *Courtesy Julie V. Schaffer, MD.*

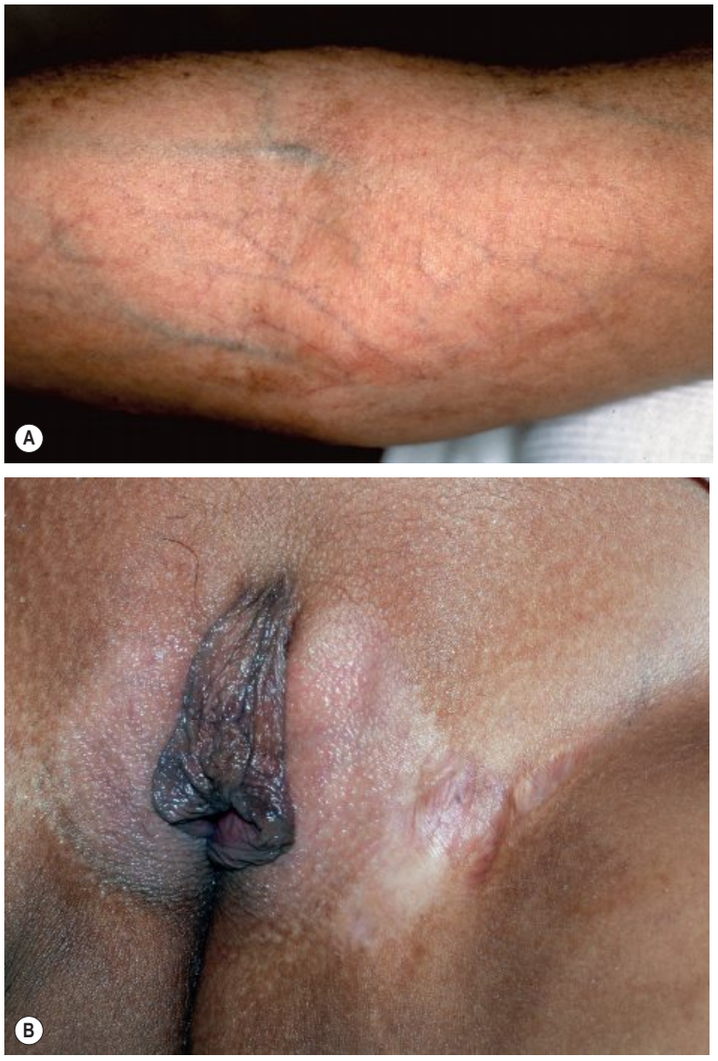


Fig. 125.7 Cutaneous atrophy due to chronic daily application of topical glucocorticoids. A Note the prominent vascular pattern on the arm. **B** This 10-year-old girl's seborrheic dermatitis had been treated with a mid-potency topical glucocorticoid on a daily basis for several years, resulting in striae and hypopigmentation. *B, Courtesy Julie V. Schaffer, MD.*

the face (Fig. 125.10). In addition, long-term continuous use of potent topical glucocorticoids on the face or in the groin can lead to erythema, edema, papulopustules, and a burning sensation upon their discontinuation, referred to as "topical steroid addiction" in social media[39].



Fig. 125.8 Local side effects of intralesional glucocorticoids. Telangiectasias, dermal and subcutaneous atrophy, and yellow–white deposits of triamcinolone acetonide (arrow). *Courtesy Jean L. Bolognia, MD.*



Fig. 125.9 Systemic glucocorticoid-induced acne. Note the monomorphic pink papulopustules in a characteristic location on the upper trunk.

Other cutaneous effects from systemic glucocorticoids include acanthosis nigricans, telogen effluvium, hirsutism, and hypertrichosis. Localized hypertrichosis can also develop in areas of topical glucocorticoid application. In addition, systemic and topical glucocorticoid therapy may impair wound healing by inhibiting fibroblast function and collagen production. This can result in decreased angiogenesis, extrafibrillar matrix ("ground substance") production, and wound re-epithelialization[4].

INTERACTIONS AND DOSE ALTERATIONS

Considerations regarding interactions between glucocorticoids and other medications as well as medical conditions that may require alteration of the glucocorticoid regimen are presented in Table 125.11.

Acknowledgment

The authors wish to acknowledge the late Lee T Nesbitt Jr, MD, for his valuable contribution to this chapter in the previous editions.

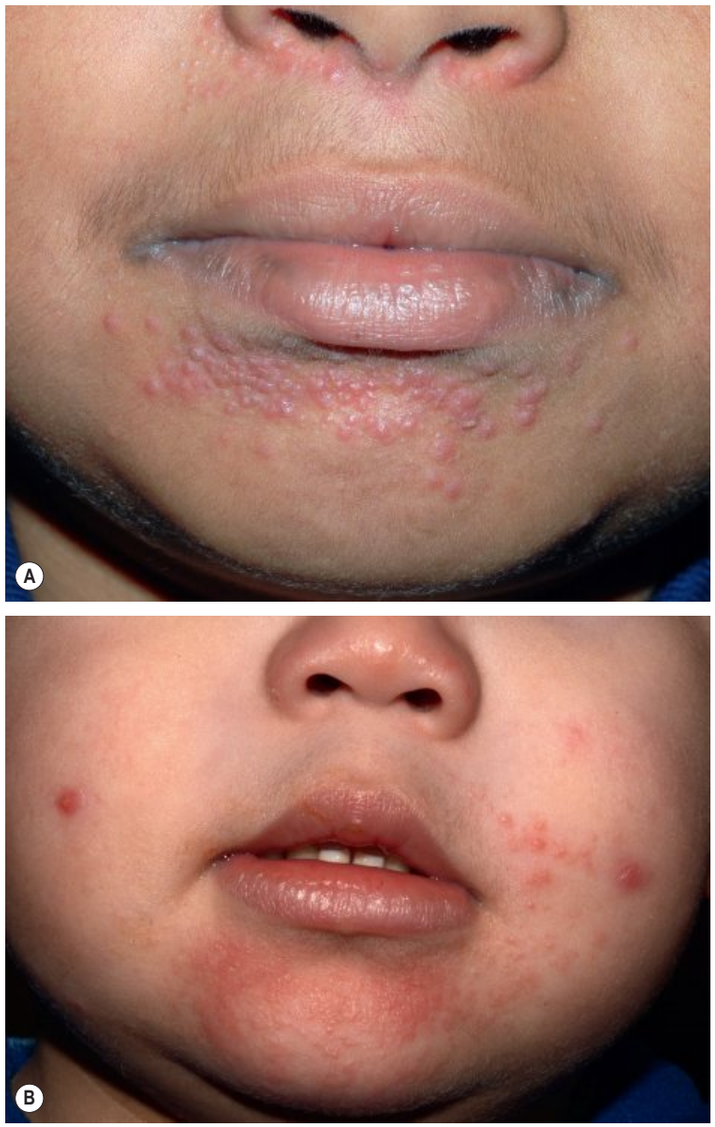


Fig. 125.10 Topical and inhaled glucocorticoid-induced perioral eruptions. Monomorphic small pink papules coalescing around the nose and mouth that resulted from application of a mid-potency topical glucocorticoid (**A**) and administration of an inhaled glucocorticoid for asthma via a face mask (**B**). Note the two additional larger papulopustules in **B**. *Courtesy Julie V. Schaffer, MD.*

GLUCOCORTICOID (GC) THERAPY: DOSING AND SIDE-EFFECT CONSIDERATIONS RELATED TO DRUG INTERACTONS AND MEDICAL CONDITIONS	
Increased dose of GC required	Induction of cytochrome P450 metabolism* (particularly CYP3A4; see Table 131.8) • Phenytoin • Phenobarbital • Rifampin Decreased GI absorption, increased hepatic clearance, and lower prednisolone : prednisone ratio • Hyperthyroidism
Decreased dose of GC required	Inhibition of cytochrome P450 metabolism (particularly CYP3A4; see Table 131.8) • Ketoconazole > other azole antifungals • Erythromycin > clarithromycin Altered protein binding and decreased hepatic metabolism (e.g. via competitive inhibition) • Estrogens/oral contraceptives Increased free (unbound) fraction of GC • Hypoalbuminemia Renal function impaired Liver function impaired†
Specific side effect potentiated	Risk of GI side effects/peptic ulcer disease • NSAIDs Risk of infections • Other immunosuppressive agents Risk of hypokalemia • Potassium-depleting diuretics • Amphotericin B
Decreased levels/ increased dose requirements of other drugs	• Insulin, oral hypoglycemic agents (due to GC-related insulin resistance) • Isoniazid • Salicylates • Warfarin (variable; GC can also increase vascular fragility)
Increased levels/ decreased dose requirements of other drugs	• β-carotene • Cyclosporine

*Of note, dexamethasone itself may act as a CYP3A4 inducer.
†In patients with severe hepatic disease, conversion of prednisone to its active form (prednisolone) may be decreased.

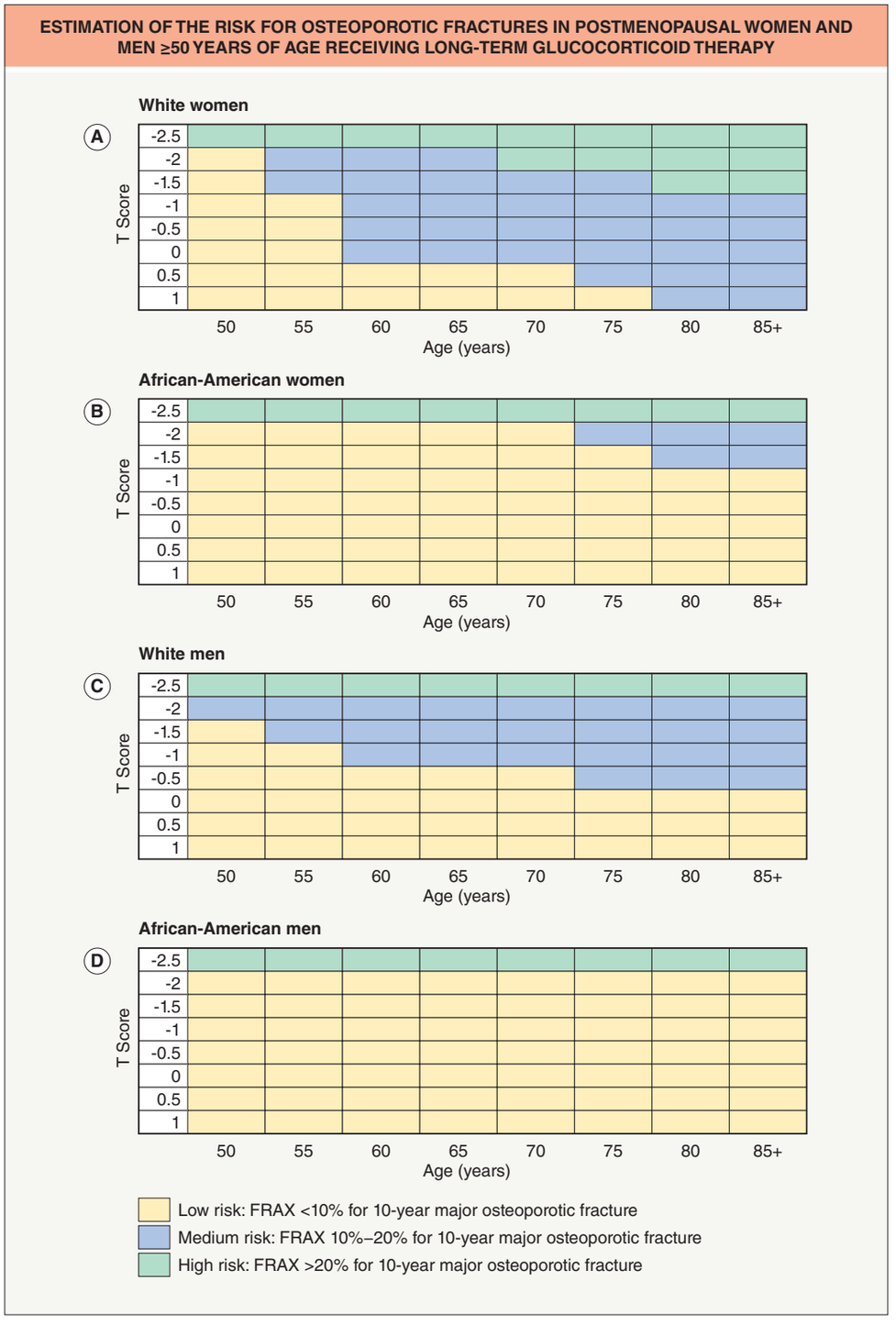
Table 125.11 Glucocorticoid (GC) therapy: dosing and side-effect considerations related to drug interactions and medical conditions. GI, gastrointestinal; NSAIDs, nonsteroidal anti-inflammatory drugs.

Additional figures available in our eBook (see inside front cover for access code).

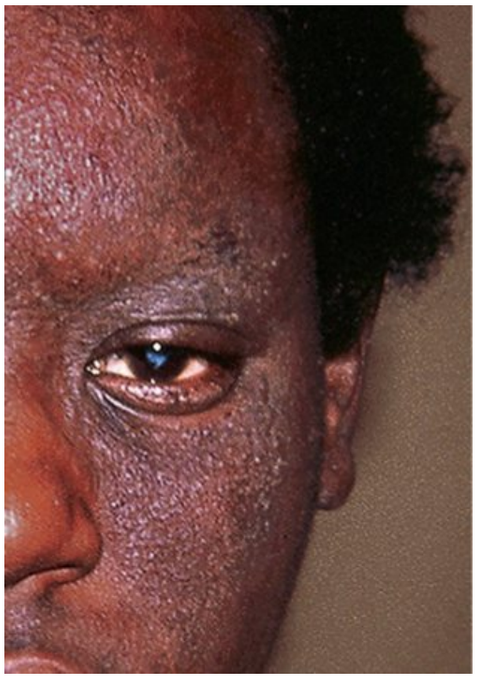
REFERENCES

1. Hench PS, Kendall EC, Slocumb CH, et al. Effects of cortisone acetate and pituitary ACTH on rheumatoid arthritis, rheumatic fever, and certain other conditions. Study in clinical physiology. *Arch Intern Med*. 1950;85:545–666.
2. Sulzberger MB, Witten VH, Yaffe SN. Cortisone acetate administered orally in dermatologic therapy. *AMA Arch Dermatol Syphilol*. 1951;64:573–578.
3. Johnson RB, Lazarus GS. Pulse therapy: therapeutic efficacy in the treatment of pyoderma gangrenosum. *Arch Dermatol*. 1982;118:76–84.
4. Jackson SM, Gilchrist HM, Nesbitt LT. Update on the dermatologic use of systemic glucocorticosteroids. *Dermatol Ther*. 2007;4:187–205.
5. Rhen T, Cidlowki JA. Antiinflammatory action of glucocorticoids—new mechanisms for old drugs. *N Engl J Med*. 2005;353:1711–1723.
6. Wolverton SE. Systemic corticosteroids. In: Wolverton SE, ed. *Comprehensive Dermatologic Drug Therapy*. 3rd ed. Philadelphia: WB Saunders; 2013:143–168.
7. Fauci AS, Dale DC, Balow JE. Glucocorticosteroid therapy: mechanisms of action and clinical considerations. *Ann Intern Med*. 1976;84:304–315.
8. Boumpas DT, Chrousos GP, Wilder RL, et al. Glucocorticoid therapy for immune-mediated diseases: basic and clinical correlates. *Ann Intern Med*. 1993;119:1198–1208.
9. Barnes PJ. Corticosteroid effects on cell signaling. *Eur Respir J*. 2006;27:413–426.
10. Robins DN. Intramuscular triamcinolone: a safe, effective and underutilized dermatologic therapy. *J Drugs Dermatol*. 2009;8:580–585.
11. Baethge BA, Lidsky MD, Goldberg JW. A study of adverse effects of high-dose intravenous (pulse) methylprednisolone therapy in patients with rheumatic disease. *Ann Pharmacother*. 1992;26:316–320.
12. Comell RC, Stoughton RB. Correlation of the vasoconstrictor assay and clinical activity. *Arch Dermatol*. 1985;121:63–67.
13. Chu AC, Munn S. Fluticasone propionate in the treatment of inflammatory dermatoses. *Br J Clin Pract*. 1995;49:131–133.
14. Joseph RM, Hunter AL, Ray DW, et al. Systemic glucocorticoid therapy and adrenal insufficiency in adults: a systematic review. *Semin Arthritis Rheum*. 2016;46:133–141.
15. Kazlauskaite R, Evans AT, Villabona CV, et al. Corticotropin tests for hypothalamic-pituitary-adrenal insufficiency: a metaanalysis. *J Clin Endocrinol Metab*. 2008;93:4245–4253.
16. Richter B, Neises G, Clar C. Glucorticoid withdrawal schemes in chronical medical disorders: a systematic review. *Endrinol Metab Clin N Am*. 2002;31:751–778.
17. Iqbal MM. Osteoporosis: epidemiology, diagnosis and treatment. *South Med J*. 2000;93:2–18.
18. Lane NE, Lukert B. The science and therapy of glucocorticoid-induced bone loss. *Endocrinol Metab Clin North Am*. 1998;27:465–483.
19. Grossman JM, Gordon R, Ranganath VK, et al. American College of Rheumatology 2010 recommendations for the prevention and treatment of glucocorticoid-induced osteoporosis. *Arthritis Care Res*. 2010;62:1515–1526.
20. Summey BT, et al. Glucocorticoid-induced bone loss in dermatologic patients: an update. *Arch Dermatol*. 2006;142:82–90.
21. Qaseem A, Snow V, Shekelle P, et al. Pharmacologic treatment of low bone density or osteoporosis to

prevent fractures: a clinical practice guideline from the American College of Physicians. *Ann Intern Med*. 2008;149:404–415.
22. Buckley L, Guyatt G, Fink HA, et al. American College of Rheumatology guideline for the prevention and treatment of glucocorticoid-induced osteoporosis. *Arthritis Care Res*. 2017;69:1521–1537.
23. Khosla S, Bilezikian JP, Dempster DW, et al. Benefits and risks of bisphosphonate therapy for osteoporosis. *J Clin Endocrinol Metab*. 2012;97:2272–2282.
24. Park-Wyllie LY, Mamdani MM, Juurlink DN, et al. Bisphosphonate use and the risk of subtrochanteric or femoral shaft fractures in older women. *JAMA*. 2011;305:783–789.
25. Cauley JA, Robbins J, Chen Z, et al. Effects of estrogen plus progestin on risk of fracture and bone mineral density: Women's Health Initiative randomized trial. *JAMA*. 2003;290:1729–1738.
26. Mankin HJ. Nontraumatic necrosis of bone (osteonecrosis). *N Engl J Med*. 1992;326:1473–1479.
27. Whitworth JA. Mechanisms of glucocorticoid-induced hypertension. *Kidney Int*. 1987;31:1213–1224.
28. Allen DB. Growth suppression by glucocorticoid therapy. *Endocrinol Metab Clin North Am*. 1996;25:699–717.
29. Lacomis D, Samuels MA. Adverse neurologic effects of glucocorticosteroids. *J Gen Intern Med*. 1991;6:367–377.
30. Renfro L, Snow JS. Ocular effects of topical and systemic steroids. *Dermatol Clin*. 1992;10:505–512.
31. Piper JM, Ray WA, Daugherty JR, Griffin MR. Corticosteroid use and peptic ulcer disease: role of nonsteroidal anti-inflammatory drugs. *Ann Intern Med*. 1991;114:735–740.
32. Gerhart JL, Kalaaji AN. Development of Pneumocystis carinii pneumonia in patients with immunobullous and connective tissue disease receiving immunosuppressive medications. *J Am Acad Dermatol*. 2010;62:957–961.
33. Green H, Paul M, Vidal L, Leibovici L. Prophylaxis of Pneumocystis pneumonia in immunocompromised non-HIV-infected patients: systematic review and meta-analysis of randomized controlled trials. *Mayo Clin Proc*. 2007;82:1052–1059.
34. Kimberlin DW, ed. *Red Book: Report of the Committee on Infectious Diseases*. 30th ed. Elk Grove Village, IL: American Academy of Pediatrics; 2015:78.
35. Reed BR. Pregnancy, drugs, and the dermatologist. *Curr Prob Dermatol*. 1994;6:33–54.
36. Dubovsky AN, Arvikar S, Stern TA, Axelrod L. The neuropsychiatric complications of glucocorticoid use: steroid psychosis revisited. *Psychosomatics*. 2012;53:103–115.
37. West S, Kenedi C. Strategies to prevent the neuropsychiatric side-effects of corticosteroids: a case report and review of the literature. *Curr Opin Organ Transplant*. 2014;19:201–208.
38. Fardet L, Flahault A, Kettaneh A, et al. Corticosteroid-induced clinical adverse events: frequency, risk factors, and patient's opinion. *Br J Dermatol*. 2007;157:142–148.
39. Hajar T, Leshem YA, Hanifin JM, et al. A systematic review of topical corticosteroid withdrawal ("steroid addiction") in patients with atopic dermatitis and other dermatoses. *J Am Acad Dermatol*. 2015;72:541–549.



Appendix. Estimation of the risk for osteoporotic fractures in postmenopausal women and men ≥50 years of age receiving long-term glucocorticoid therapy. The presence of additional risk factors (see Fig. 125.4) may shift an individual to a higher risk group.



eFig. 125.1 A 12-year-old girl treated intermittently with systemic glucocorticoids for severe atopic dermatitis. Note lens opacity of the left eye, due to development of a cataract.



eFig. 125.2 Topical glucocorticoid-induced perioral eruptions. These monomorphic hypopigmented (**A**) and erythematous rosacea-like (**B**) papules resulted from the application of mid-potency topical glucocorticoids. *B, Courtesy Kalman Watsky, MD*.



eFig. 125.3 Striae in a patient on chronic prednisone therapy.

126 Retinoids

Jean-Hilaire Saurat and Olivier Sorg

Key features

- Retinoids are structural and functional analogues of vitamin A that exert multiple effects on cellular differentiation and proliferation, the immune system, and embryonic development
- Retinoic acid receptors (RARs) and retinoid X receptors (RXRs) are ligand-dependent transcription factors belonging to the steroid–thyroid hormone nuclear receptor superfamily
- *Topical* retinoids are used to treat a number of conditions including acne, photoaging, and psoriasis; the limiting factor is dose-related skin irritation, and teratogenicity risk is very low to non-existent
- *Oral* retinoids are the most effective drugs available for severe acne (isotretinoin) and many disorders of cornification (acitretin and isotretinoin). They are also helpful in the management of psoriasis, especially pustular and erythrodermic forms (acitretin > isotretinoin), pityriasis rubra pilaris (acitretin and isotretinoin), cutaneous T cell lymphoma (bexarotene), and chronic hand eczema (alitretinoin)
- Systemic retinoid therapy requires careful patient selection and monitoring due to associated teratogenicity and other potential toxicities; laboratory abnormalities (e.g. hypertriglyceridemia, elevated transaminases); ocular, musculoskeletal, and (primarily for bexarotene) endocrinological or hematologic adverse effects

INTRODUCTION

Vitamin A (retinol) and related compounds with either structural (retinol derivative) or functional (vitamin A activity) similarities are known as retinoids (Fig. 126.1). The importance of retinoids in cutaneous biology was first appreciated early in the twentieth century by Wolbach, who observed that vitamin A-deficient animals manifested altered keratinization, such as epidermal hyperkeratosis and squamous metaplasia of mucous membranes. The anti-keratinizing properties of vitamin A led von Stuettgen and Bollag to administer topical and systemic retinoids to treat disorders of cornification. In initial clinical trials with oral vitamin A, tolerable doses were ineffective but higher, potentially effective doses were too toxic. Because of this narrow therapeutic window, a program was launched to engineer synthetic retinoids with higher therapeutic activity and lower toxicity. Parallel to efforts with systemic agents, a growing interest in topical retinoids emerged.

All-*trans*-retinoic acid (a*t*-RA; tretinoin), a naturally occurring metabolite of retinol (see Fig. 126.1), was the first retinoid to be synthesized. Orally, it did not have significant advantages over vitamin A, and, as a result, the primary dermatologic focus became its topical use, especially for acne vulgaris and photoaging.

Initially synthesized in 1955, 13-*cis*-retinoic acid (13-*cis*-RA; isotretinoin) was first studied clinically almost two decades later. Its use was delayed by concerns regarding its teratogenicity, which were amplified because of the thalidomide tragedy. Results of isotretinoin treatment of psoriasis were equivocal, and etretinate was subsequently found to be more effective. In the mid to late 1970s, Peck and colleagues described the effectiveness of oral isotretinoin in the treatment of lamellar ichthyosis and other disorders of cornification as well as its ability to produce complete responses with prolonged remissions in patients with treatment-resistant nodulocystic acne[1,2]. Topical isotretinoin has also been formulated and has efficacy similar to that of topical tretinoin for acne. In 1999, the US Food and Drug Administration (FDA) approved 9-*cis*-retinoic acid (9-*cis*-RA; alitretinoin) 0.1% gel for the topical treatment of cutaneous Kaposi sarcoma. To date, oral alitretinoin has been approved outside of the US to treat severe, recalcitrant hand eczema.

In 1972, Bollag developed two aromatic retinoids: etretinate and its free acid metabolite, acitretin. Both had a therapeutic index ten times more favorable than that of tretinoin in the chemically induced rodent papilloma test model. Etretinate and acitretin represent second-generation retinoids, and their development constituted a breakthrough in the systemic treatment of psoriasis and disorders of cornification.

A major advance in understanding the molecular pharmacologic features and mechanisms of action of retinoids came with the discovery of nuclear receptors known as retinoic acid receptors (RARs) and retinoid X receptors (RXRs). This allowed the development of new retinoids that target specific retinoid receptors. FDA-approved third- and fourth-generation retinoids include topical adapalene (acne), topical tazarotene (psoriasis and acne), topical trifarotene (acne), and oral as well as topical bexarotene (cutaneous T cell lymphoma [CTCL]). Lastly, topical precursors of retinoic acid such as retinyl esters, retinol and retinaldehyde are included in cosmeceutical products.

MECHANISM OF ACTION

Retinoids are involved in the regulation of diverse biologic functions (Table 126.1). They can: (1) affect cellular growth, differentiation and morphogenesis; (2) inhibit tumor promotion and malignant cell growth; (3) exert immunomodulatory actions; and (4) alter cellular cohesiveness[3].

Vitamin A Metabolism

Vitamin A (retinol) must be acquired through the diet as retinyl esters and provitamin A carotenoids; of the latter, β-carotene is particularly efficient in its ability to be converted to vitamin A. Within the intestinal lumen, retinyl esters are hydrolyzed to retinol, which is then absorbed and stored in the liver in the ester form (especially retinyl palmitate; Fig. 126.2). Retinol and its esters represent the main dietary source, as well as transport and storage form, of vitamin A. Once inside the bloodstream, after release of the retinyl ester (storage form) from the liver, retinol is transported bound to a complex of retinol-binding protein (RBP) and transthyretin. The uptake of retinol from the RBP–transthyretin complex to target cells is mediated by STRA6 (stimulated by retinoic acid 6), a dimeric transmembrane protein that acts as an RBP–retinol receptor[4,5] (see Fig. 126.2).

The cellular pathway leading to conversion of retinol to a*t*-RA, the biologically active ligand that binds to nuclear RARs, consists of a two-step process. Retinol (vitamin A alcohol) is first reversibly oxidized to retinaldehyde (vitamin A aldehyde), which is then irreversibly converted to retinoic acid (vitamin A acid). Cellular RBP (CRBP-I) facilitates these enzymatic reactions by delivering retinol to appropriate enzymes (see Fig. 126.2).

Two additional intracellular carriers, cellular retinoic acid-binding proteins (CRABP-I and CRABP-II), are thought to transport retinoic acid to the nucleus and buffer the level of free a*t*-RA in the cell. The latter is accomplished by sequestering a*t*-RA and by promoting metabolism of a*t*-RA by cytochrome P450 enzymes belonging to the CYP26 family (e.g. CYP26A1). CRABP-I regulates the metabolic fate of its ligands by directly affecting the activities of RA-metabolizing cytochrome P450 enzymes, while CRABP-II markedly stimulates the RA-induced transcriptional activity of RAR through protein–protein interactions[6].

Intracellularly, retinoic acid is found in both all-*trans* and 9-*cis* configurations (see Fig. 126.2). Physiologically, a*t*-RA (tretinoin) is the predominant retinoic acid form, and only a small fraction is isomerized (enzymatically or non-enzymatically) into 13-*cis*-RA (isotretinoin) or converted to polar metabolites with unknown biologic activity. a*t*-RA is the primary active ligand that binds to the three known nuclear RARs,

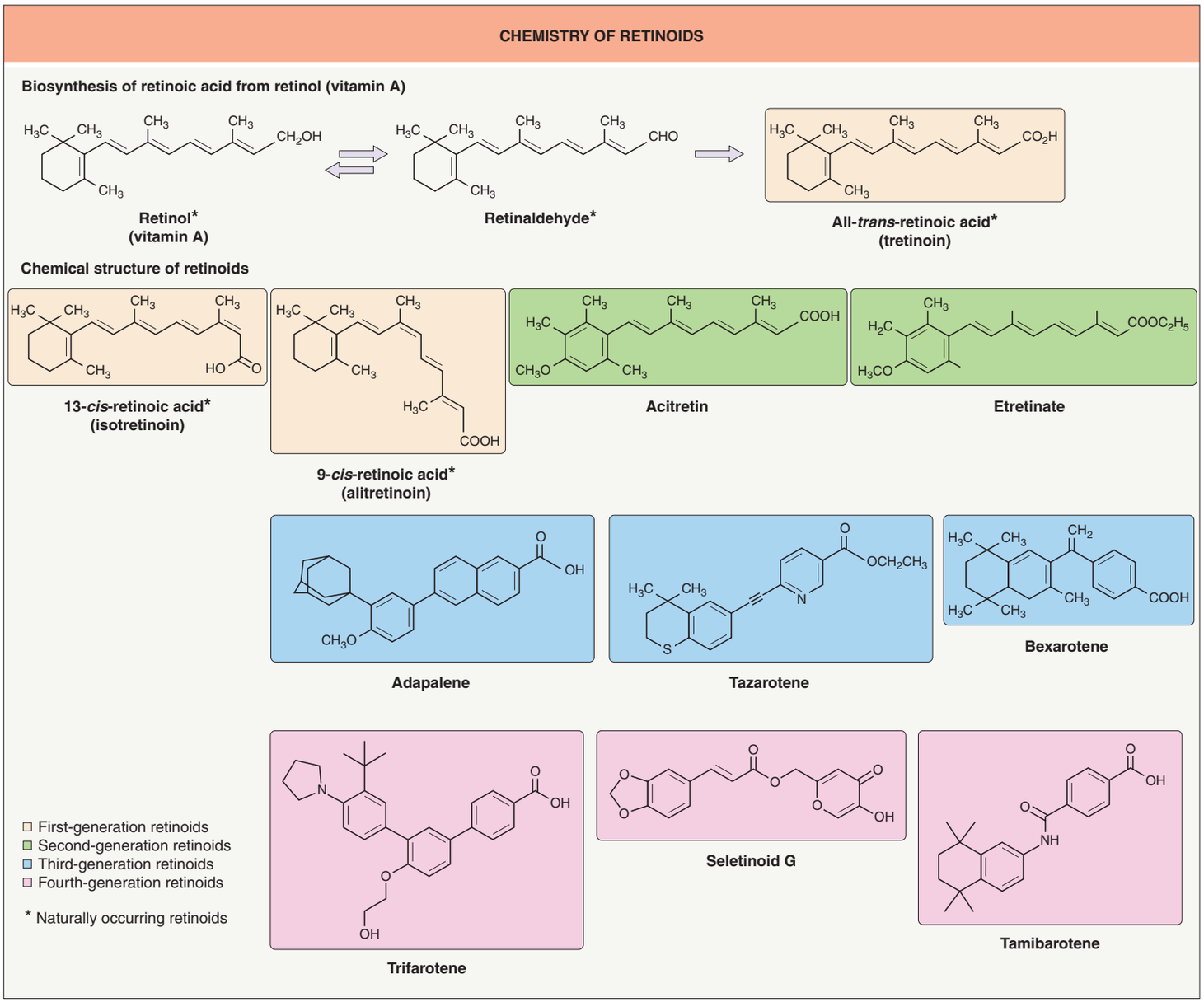


Fig. 126.1 Chemical structure of natural and synthetic retinoids. Motretinide is an additional second-generation retinoid.

BIOLOGIC FUNCTIONS OF RETINOIDS
Functions of vitamin A (retinol)*
• Embryonic growth • Morphogenesis • Differentiation and maintenance of epithelial tissues • Reproduction (retinol) • Visual function (retinaldehyde)
Biologic effects of retinoids
• Modulation of proliferation and differentiation • Anti-keratinization • Alteration of cellular cohesiveness • Anti-acne and anti-seborrheic effects • Immunologic and anti-inflammatory effects • Tumor prevention and therapy • Induction of apoptosis • Effects on extracellular matrix components
*Retinoic acid can substitute for retinol with regard to growth, morphogenesis, and epithelial differentiation; it cannot substitute completely for retinol in reproductive function, nor can it replace retinaldehyde in the visual system.

Table 126.1 Biologic functions of retinoids.

which mediate, at least in part, the molecular and cellular effects of retinoic acid. Although the biosynthesis of 9-*cis*-RA (alitretinoin) is not well-defined, it might be produced from all-*trans*-retinol via 9-*cis*-retinol and 9-*cis*-retinaldehyde.

Retinoid Receptors

Retinoids exert most of their physiologic effects on DNA transcription by binding to two distinct families of nuclear receptors, RARs and RXRs (see Fig. 126.2). These receptor families belong to a superfamily of nuclear receptors that act as ligand-activated transcription factors and include the steroid, vitamin D_3, and thyroid hormone receptors as well as peroxisome proliferator-activated receptors (PPARs). The RAR and RXR receptor families each contain three receptor isotypes (α, β and γ) encoded by different genes. *at*-RA (tretinoin) binds only to RARs, whereas 9-*cis*-RA (alitretinoin) binds both to RARs and RXRs (Table 126.2).

RARs function as heterodimers with RXRs, whereas RXRs may also act as homodimers or participate in the formation of heterodimers with a variety of other nuclear receptors, including vitamin D_3, thyroid hormone, and PPARs. Such heterodimers provide a mechanism for cross-talk between nuclear hormone signaling pathways.

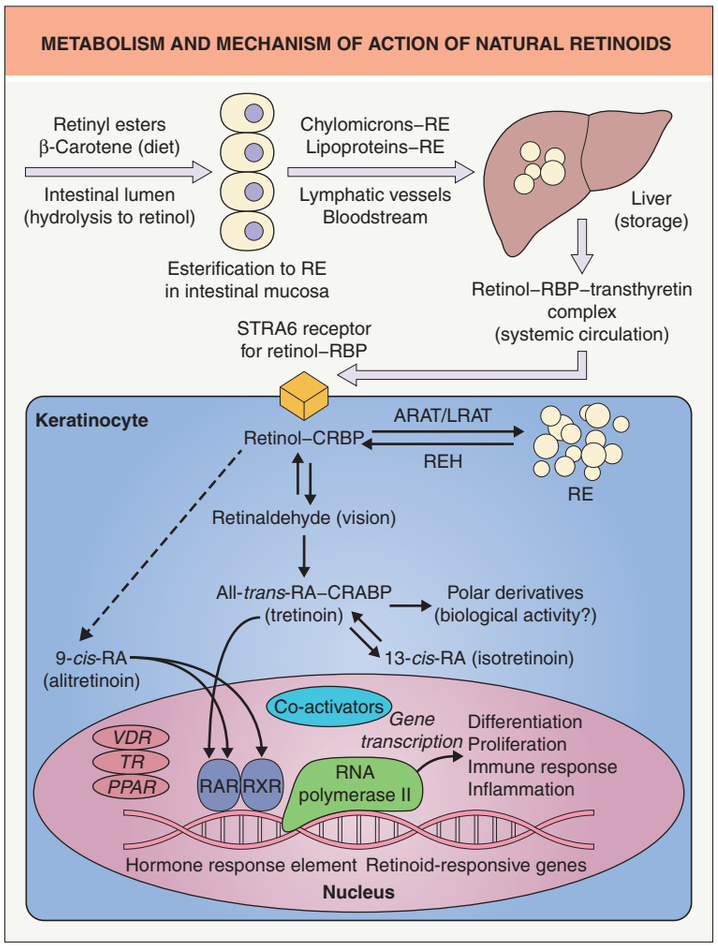


Fig. 126.2 Metabolism and mechanism of action of natural retinoids. ARAT, acyl-CoA:retinol acyl transferase; CRABP, cellular retinoic acid-binding protein; CRBP, cellular retinol-binding protein; LRAT, lecithin:retinol acyl transferase; PPAR, peroxisome proliferator-activated receptor; RA, retinoic acid; RAR, retinoic acid receptor; RBP, retinol-binding protein; RE, retinyl esters; REH, retinyl ester hydrolase; RXR, retinoid X receptor; STRA6, stimulated by retinoic acid 6; TR, thyroid receptor; VDR, vitamin D_3 receptor.

Dimers of retinoid receptors (RAR/RXR or RXR/RXR) are localized to the nucleus and bind, even in the unliganded state, to specific DNA regulatory sequences called retinoid hormone response elements (RAREs) in the promoter regions of retinoid-responsive genes (see Fig. 126.2). Unliganded receptors bind to co-repressor molecules and repress transcription. However, when the receptor binds its ligand, it undergoes a conformational change resulting in the release of co-repressors and recruitment of co-activators. These molecules include histone acetylases that change the conformation of chromatin and allow access to DNA by transcriptional machinery. The retinoid–receptor complex thereby modulates the transcription of specific sets of genes, and it is likely that many of the differentiation-inducing actions of retinoids are mediated by this mechanism.

In addition to *direct upregulation* of gene transcription via binding of retinoid–receptor complexes to RAREs, retinoids can have *indirect* effects on gene transcription that result from the *downregulation* of genes that do not contain RAREs in their promoter region. The retinoid–receptor complex is thought to antagonize transcription factors such as activator protein-1 (AP1) and nuclear factor-interleukin-6 (NF-IL6) by competing for the same set of required co-activator proteins, thereby leading to decreased expression of AP1 and NF-IL6-responsive genes; expression of the latter genes promotes cellular proliferation and inflammation. The antiproliferative and anti-inflammatory actions of retinoids are believed to be mediated by this type of indirect negative gene regulation. In particular, retinoic acid has important roles in inhibiting IL-6-driven induction of proinflammatory Th17 cells and in promoting differentiation of anti-inflammatory regulatory T cells (see Ch. 4). The anti-inflammatory effects of *at*-RA (tretinoin) have also been associated with its ability to regulate the expression and activation of Toll-like receptors (TLRs), especially TLR2. The biologic relevance of non-genomic effects of retinoids (e.g. cross-talk with extracellular protein/peptide signals acting via membrane receptors with downstream phosphorylation) remains under investigation.

The existence of several types and varied distributions of receptors, dimers, hormone response elements, and regulatory proteins shows that retinoid action is mediated via multiple pathways and results in a complex process of activation or inhibition of a large set of coordinately regulated genes. However, the exact mechanism of retinoid action in many dermatologic conditions is still unknown, and, so far, the nuclear receptor concept does not fully explain the biologic diversity of retinoid effects.

Retinoids in the Skin

Vitamin A and its bioactive metabolites play a major role in promoting the keratinocyte differentiation that occurs from the epidermal basal layer to the stratum corneum[7]. Retinyl esters and retinol are the major retinoids found in the skin, with the former reaching a concentration of >1000 pmol/g in the epidermis. Epidermal retinoids can absorb UVB radiation and have ~2%–3% of the UVB-filtering capacity of the melanin in phototype II/III skin[7,8]. The UVB absorption process results in dramatic depletion of epidermal retinoids[9], which can be prevented by application of topical retinoids[10]. Nutritional deficiency, aging, and oxidative stress can also lead to lowered retinoid levels in the skin[7]. There has been ongoing debate regarding possible generation of reactive oxygen species upon the interaction of UVA radiation with retinyl esters (e.g. retinyl palmitate) present in cosmetics and sunscreens, but the theoretical potential for photocarcinogenicity has not been shown to be clinically relevant.

Synthetic Retinoids

There are now four generations of retinoids (see Fig. 126.1). The *first-generation* non-aromatic retinoids (tretinoin, isotretinoin, alitretinoin) are synthesized by chemically modifying the polar end group and the polyene side chain of vitamin A. *Second-generation* mono-aromatic retinoids (etretinate, acitretin, motretinide) are formed by replacing the cyclic moiety of vitamin A with different substituted and unsubstituted ring systems. *Third-generation* polyaromatic retinoids (adapalene, bexarotene, tazarotene), called arotinoids, are produced by cyclization of the polyene side chain. *Fourth-generation* polyaromatic retinoids (trifarotene, seletinoid G, tamibarotene) were designed to have increased selectivity of binding.

Commercially available retinoids differ not only in their spectrum of clinical efficacy but also in their observed toxicity and pharmacokinetics. Each retinoid should be investigated as a unique drug, and the lack of disease response to one retinoid does not necessarily signify unresponsiveness to other retinoids.

The oral bioavailability of retinoids is considerably enhanced when administrated with food, especially with a fatty meal, due to their lipophilic properties. More recently, a lidose–isotretinoin formulation with enhanced absorption when taken without food was developed. Retinoid metabolism is predominantly hepatic; it involves oxidation and chain shortening to biologically inactive and polar metabolites, facilitating biliary and/or renal elimination. The oxidative metabolism is induced by the retinoids themselves and possibly also by other agents known to stimulate hepatic cytochrome P450 isoforms. Table 126.2 summarizes the key pharmacologic features and nuclear binding profiles of retinoids used in dermatology.

First-generation retinoids

Tretinoin (all-*trans*-retinoic acid)

Tretinoin, the predominant physiologic form of retinoic acid, was the first topical retinoid to be utilized for the treatment of acne and photoaging. It binds to cellular retinoic acid-binding proteins (CRABPs) and non-selectively to nuclear RARs (see above), resulting in modulation of keratinocyte proliferation and differentiation, inflammation, and extracellular matrix production. Because the standard tretinoin formulation is photolabile, night-time application is recommended to prevent degradation.

KEY PHARMACOLOGIC FEATURES AND NUCLEAR BINDING PROFILES OF RETINOIDS											
Retinoid	**Type**	**Systemic absorption or bioavailability* (% dose)**	**Elimination half-life**	**Metabolism**	**Excretion**	**Nuclear receptor binding affinity**					
						RAR			RXR		
						α	β	γ	α	β	γ
Topical retinoids*											
Tretinoin† (all-*trans*-retinoic acid)	Natural (1st generation)	<2% in normal skin	Normally present in the skin	Isomerization to 13-*cis*-RA (epidermis)	Desquamation, biliary	+	+	+	–	–	–
Alitretinoin (9-*cis*-retinoic acid)	Natural (1st generation)	Minimal	Normally present in the skin	Main metabolite: 4-oxo-9-*cis*-RA	Desquamation, biliary	+	+	+	+	+	+
Adapalene	3rd generation	Minimal	Unknown	Minimal biotransformation due to chemical rigidity	Desquamation, biliary	±	+	+	–	–	–
Tazarotene	3rd generation	<1%–6% in normal skin	16 hours (tazarotenic acid)	Rapid (within 20 minutes) ester hydrolysis within the skin to form its active metabolite, tazarotenic acid; excreted metabolites: sulfoxides, sulfones	Desquamation, renal (within 3 days), biliary (within 7 days)	±	+	+	–	–	–
Trifarotene	4th generation	≤10 pmol/L	2–9 hours	Hepatic	Biliary	–	–	+	–	–	–
Systemic retinoids											
Tretinoin†	Natural (1st generation)	50%	1 hour	Hepatic; main metabolites: *cis*- and *trans*-4-oxo derivatives	Biliary, renal	+	+	+	–	–	–
Isotretinoin (13-*cis*-RA)	Natural (1st generation)	25%	20 hours	Hepatic, endogenous concentration reached within 2 weeks; main metabolite: 4-oxo-isotretinoin	Biliary, renal	–	–	–	–	–	–
Alitretinoin	Natural (1st generation)	Unknown	2–10 hours	Hepatic; main metabolite: 4-oxo-alitretinoin	Renal, biliary	+	+	+	+	+	+
Acitretin (and etretinate)	2nd generation	60%	2 days	Hepatic, re-esterification to etretinate indirectly increased by alcohol consumption; main metabolite: *cis*-acitretin	Biliary, renal	+‡	+‡	+‡	–	–	–
Bexarotene¶	3rd generation	Unknown	7–9 hours	Hepatic	Biliary	–	–	–	+	+	+
Tamibarotene	4th generation	NA	2–3 hours	Hepatic	NA	+	+	–	±	±	±

*Topical formulations have limited propensity for distribution to systemic tissues; oral bioavailability is highly variable and increases when administered with food.
†Also binds the cellular retinoic acid-binding protein (CRABP).
‡Activate RARs despite binding poorly to them.
¶Also available in a topical form.

Table 126.2 Key pharmacologic features and nuclear binding profile of retinoids. NA, not available; RA, retinoic acid; RAR, retinoic acid receptor; RXR, retinoid X receptor.

Isotretinoin (13-*cis*-retinoic acid)

Isotretinoin is a naturally occurring retinoid resulting from the metabolism of vitamin A (see Fig. 126.2)[11]. 13-*cis*-RA and a*t*-RA are two physiologically interconvertible isomers that differ in their elimination half-lives: approximately 20 hours and 1 hour, respectively. Isotretinoin undergoes first-pass metabolism in the liver and subsequent enterohepatic recycling. In plasma, more than 99% of isotretinoin is protein-bound, mainly to albumin. There is neither liver nor adipose tissue storage, in contrast to vitamin A. The major metabolite of isotretinoin, 4-oxo-isotretinoin, is produced by oxidation. Isotretinoin and its metabolites are excreted in the urine and feces. After discontinuation of isotretinoin, *physiologic* concentrations of the drug and its major metabolites are reached within 2 weeks, ranging from 2 days for a*t*-RA to 10 days for 4-oxo-isotretinoin. Therefore, 1 month of post-therapy contraception provides an adequate safety margin to avoid teratogenicity.

Among natural and synthetic retinoids, only oral isotretinoin and its 4-oxo-isotretinoin metabolite significantly suppress sebum production, which explains their dramatic effects on acne. Isotretinoin-induced seboatrophy is unlikely to be RAR/RXR-mediated since isotretinoin has no clear affinity for any known retinoid receptor[12], and potent RAR/RXR ligands such as tretinoin and alitretinoin do not lead to seboatrophy. The mechanism of isotretinoin-induced seboatrophy is thought to involve sebocyte apoptosis[13], but inhibition of either sebocyte progenitor differentiation or the genes encoding sebogenic enzymes represent two other possible pathomechanisms.

Alitretinoin (9-*cis*-retinoic acid)

Alitretinoin is a naturally occurring pan-agonist retinoid that binds to both RARs and RXRs[14], representing the endogenous ligand for the latter. Topical alitretinoin 0.1% gel is FDA-approved for the treatment of cutaneous Kaposi sarcoma, and oral alitretinoin therapy is currently utilized outside the US for refractory chronic hand eczema. The absorption of oral alitretinoin from the gastrointestinal tract is variable and dose-proportional over the therapeutic range of 10–30 mg daily; the absolute bioavailability of alitretinoin has not been determined. Alitretinoin is metabolized via oxidation by CYP3A4 enzymes of the liver into 4-oxo-alitretinoin, and both the parent drug and its metabolite also undergo isomerization into a*t*-RA and 4-oxo-a*t*-RA, respectively. Elimination is primarily renal, with the half-life of unchanged alitretinoin ranging between 2 and 10 hours. Alitretinoin concentrations return to normal within 1–3 days after treatment cessation.

The mechanism of action of alitretinoin in chronic hand eczema is unknown, although downregulated expression of RARs and RXRs in lesional skin was recently described[15]. Alitretinoin has immunomodulatory and anti-inflammatory effects that include suppressing the expansion of cytokine-activated leukocyte subsets and antigen-presenting cells.

Second-generation retinoids

Acitretin

Acitretin is the major metabolite and the pharmacologically active form of etretinate[16]. Although acitretin and etretinate are equally effective, acitretin has much more rapid elimination. Etretinate is approximately 50 times more lipophilic than acitretin and binds strongly to plasma proteins, particularly lipoproteins and albumin. Etretinate is stored in adipose tissue (including subcutaneous fat), from which it is released slowly, with a long terminal half-life of up to 120 days. Under identical conditions, acitretin carries a negatively charged group that makes it much less lipophilic than etretinate. As a result, acitretin does not accumulate in adipose tissue and is eliminated from the body more rapidly, with a half-life of 2 days.

The major serious adverse effect of oral retinoids is teratogenicity, and, therefore, the length of time that these drugs are present in the body is of great importance. Re-esterification of acitretin to etretinate may occur when acitretin is taken simultaneously with alcohol[17,18]. This finding prompted the manufacturer to extend the time of contraception for female patients with childbearing potential taking acitretin to 2 years after its discontinuation, as it is for etretinate. The FDA advises a contraceptive period of at least 3 years for acitretin, based on the pharmacokinetics of acitretin and etretinate observed in clinical trials and on previous safety experience with etretinate. However, acitretin retains its shorter half-life in women who strictly avoid alcohol during treatment and for 2 months thereafter.[16] Because of its improved risk–benefit ratio, acitretin was approved by the FDA in 1996 as a substitute for etretinate, which is no longer commercially available[16].

Acitretin's mechanism of action is still not clearly understood. Paradoxically, it activates all three RAR subtypes despite binding poorly to them. Evidence supports a normalization of differentiation and proliferation as well as a modification of inflammatory responses and neutrophil function.

Third-generation retinoids

Adapalene

Adapalene is a photostable, rigid, and highly lipophilic synthetic retinoid with higher affinity for RAR-β/γ than for RAR-α. Since RAR-β is not expressed in keratinocytes, RAR-γ is the primary target receptor for adapalene in the epidermis. Adapalene does not bind to cellular retinoic acid-binding proteins (CRABPs) but does induce expression of CRABP-II. Its lipophilic properties may contribute to better pilosebaceous uptake and anti-acne activity. Given its negligible transdermal absorption, the teratogenic risks of topical adapalene appear to be minimal. Adapalene affects the cellular differentiation, keratinization, and inflammatory processes that are abnormal in acne. Although adapalene has not been shown to be sebostatic *in vivo* in humans, it was found to inhibit triacylglycerol biosynthesis and lipid droplet accumulation *in vitro* in hamster sebocytes[19].

Tazarotene

Tazarotene is a prodrug that is rapidly converted by cutaneous esterases to its free carboxylic acid (tazarotenic acid), which is the active metabolite. It has a higher affinity for RAR-β/γ than RAR-α and no affinity for RXR[20]. Because of its rapid metabolism, systemic exposure is low. Tazarotene appears to modulate the pathogenesis of psoriasis by regulating expression of retinoid responsive genes, including those involved in cell proliferation, cell differentiation, and inflammation[21].

Bexarotene

Bexarotene, an RXR-selective retinoid (rexinoid), is FDA-approved in oral (1999) and topical (2000) forms for treatment of CTCL. This compound is about 100-fold more potent at binding to RXRs than to RARs. In plasma, bexarotene is highly bound (>99%) to various proteins that have yet to be characterized. Bexarotene has a clearance profile similar to that of isotretinoin, with a terminal half-life of between 7 and 9 hours[22]. Bexarotene is metabolized by CYP3A4 and generates its own oxidative metabolites via hepatic CYP3A4 induction. Neither bexarotene nor its metabolites are excreted in the urine; their elimination is thought to occur primarily via the hepatobiliary system[22]. The exact mechanism of action of bexarotene in CTCL is still unknown, but it probably acts through regulation of cellular differentiation and proliferation, as well as via induction of apoptosis[23].

Fourth-generation retinoids

Trifarotene

Trifarotene, a fourth-generation retinoid with 20-fold higher affinity for RAR-γ than RAR-α/β, was FDA-approved in 2019 as a topical acne treatment for individuals ≥9 years of age[24]. This agent was designed to be stable in keratinocytes but rapidly metabolized in hepatic microsomes, thereby minimizing systemic drug levels. In addition to effects on known retinoid-mediated pathways, gene expression profiling has shown that trifarotene modulates proteolysis, reduces intercellular adhesion, and activates transporters involved in skin hydration[25].

Retinoic acid metabolism blocking agents

*R*etinoic *a*cid *m*etabolism *b*locking *a*gents (RAMBAs) inhibit catabolism of *a*t-RA by P450 enzymes in the CYP26 family, thereby raising the intracellular levels of endogenous *a*t-RA in the skin and other targeted tissues[26]. This limits systemic exposure and the potential for toxicity, and *a*t-RA levels return to the physiologic range within 24 hours of discontinuing these medications. Liarozole, an imidazole derivative without antifungal properties, is a RAMBA with low isoenzyme specificity that also inhibits P450-mediated pathways of steroid biosynthesis whereas talarozole, a triazole derivative, is a more selective and highly active CYP26 enzyme inhibitor. DX314, a CYP26B1-selective RAMBA that may protect epidermal barrier integrity, is also under investigation[27]. Liarozole has been granted orphan drug status for congenital ichthyosis by the European Commission and the FDA. In a randomized, placebo-controlled phase II/III trial in 64 patients with moderate-to-severe lamellar ichthyosis, a 41%–50% response rate was observed in patients receiving liarozole, compared to 11% with placebo, with borderline statistical significance ($p=0.056$)[26].

INDICATIONS (TABLE 126.3)

Topical Retinoids

The most important element in topical retinoid therapy is patient education. Local skin irritation can be expected, and noticeable beneficial effects often take weeks or months to appear. Administration of topical retinoids should be titrated depending on cutaneous irritation, which may mean decreasing the concentration or the frequency of application. It is generally wise to begin with a low-strength formulation and then increase the concentration as tolerance builds. Another tactic is to start by applying a given concentration every other day. Daytime moisturizers with sunscreen are important components of any topical retinoid regimen.

Acne

Topical retinoids, of which tretinoin is the prototype, are mainstays in the treatment of comedonal and inflammatory acne vulgaris[28]. The primary mode of action in acne is thought to be the normalization of differentiation and proliferation of the follicular epithelium (see Ch. 36), which leads to the loosening and unseating of microcomedones, thereby preventing obstruction of the pilosebaceous unit. In addition, topical retinoids may have anti-inflammatory activity. The mechanism of action of topical isotretinoin (not available in the US) is similar to that of topical tretinoin because of intraepithelial isomerization of isotretinoin to tretinoin (see Fig. 126.2). In contrast to oral isotretinoin, topical isotretinoin fails to suppress sebum production; it is less irritating and probably also somewhat less effective than tretinoin. The topical synthetic retinoids adapalene, tazarotene, and trifarotene have comparable or (for adapalene) improved tolerability while maintaining efficacy similar to that of topical tretinoin[29,30].

Topical retinoids should be applied to the entire face or all acne-prone areas once a day as tolerated, with tretinoin applied in the evening to prevent inactivation by UV light. Application of these medications to dry skin may reduce skin irritation by minimizing dermal absorption. Patients should be advised that beneficial effects do not typically become evident for 6–8 weeks or longer. An apparent exacerbation may occur during the first month of therapy, representing the externalization of deeper-seated acne lesions as the follicular epithelium is loosening. With the exception of mild, primarily comedonal acne, topical retinoids are typically used concomitantly with benzoyl peroxide products and antibiotics (oral or topical) that target *Cutibacterium acnes* and inflammatory processes that contribute to acne (see Ch. 36).

CLINICAL INDICATIONS FOR RETINOIDS IN DERMATOLOGY		
Topical retinoids		
FDA-approved indications	Acne vulgaris (tretinoin, adapalene, tazarotene, trifarotene) Photoaging, e.g. fine facial wrinkling, mottled pigmentation, facial roughness (tretinoin, tazarotene) Psoriasis, <20% of body surface area (tazarotene*) Cutaneous T cell lymphoma (bexarotene) Kaposi sarcoma (alitretinoin)	
Selected non-FDA-approved indications	Some disorders of cornification (ichthyoses) Darier disease Pityriasis rubra pilaris Rosacea Pigmentary disorders, e.g. melasma, postinflammatory hyperpigmentation Lentigines Actinic keratoses Striae Wound healing Lichen planus (oral and cutaneous) Verrucae planae (flat warts) Corticosteroid-induced atrophy Therapy and prevention of skin cancer (basal cell carcinoma; xeroderma pigmentosum)	
Systemic retinoids		
FDA-approved indications	Psoriasis (acitretin)	Pustular psoriasis (localized and von Zumbusch) Erythrodermic psoriasis Severe and recalcitrant plaque-type psoriasis*
	Acne (isotretinoin)	Nodulocystic acne Recalcitrant acne with tendency for scarring
	Cutaneous T cell lymphoma (bexarotene)	Resistant to at least one systemic therapy
Selected non-FDA-approved indications	Rosacea and acne-related disorders	Hidradenitis suppurativa Eosinophilic pustular folliculitis (Ofuji disease) AIDS-associated eosinophilic folliculitis Pyoderma faciale (rosacea fulminans) Acne with solid facial edema Dissecting cellulitis of the scalp
	Disorders of cornification and related conditions	Ichthyoses, various forms (see Ch. 57) Darier disease Keratoderma Papillon–Lefèvre syndrome
	Inflammatory disorders	Chronic hand eczema (alitretinoin, acitretin) Pityriasis rubra pilaris Lupus erythematosus Lichen planus
	Chemoprophylaxis of neoplastic processes	Xeroderma pigmentosum Basal cell nevus syndrome Skin cancer in solid organ transplant patients
	Treatment of neoplastic processes	Epithelial precancerous conditions Basal cell carcinoma Advanced squamous cell carcinoma Keratoacanthoma (including those induced by BRAF inhibitors and immune checkpoint inhibitors) Kaposi sarcoma Sebaceous hyperplasia Muir–Torre syndrome Leukoplakia Langerhans cell histiocytosis
	Miscellaneous conditions	Atrophoderma vermiculatum Ulerythema ophryogenes Confluent and reticulated papillomatosis Bazex syndrome (paraneoplastic acrokeratosis) Follicular mucinosis Sarcoidosis Granuloma annulare Lichen sclerosus (genital or extragenital) Subcorneal pustular dermatosis Graft-versus-host disease Verruca vulgaris, condyloma

*Combination therapy, e.g. with a topical corticosteroid or photo(chemo)therapy, is often required.

Table 126.3 Clinical indications for retinoids in dermatology. Of note, the oral form of tretinoin (all-*trans*-retinoic acid; *at*-RA) is FDA-approved for the treatment of acute promyelocytic leukemia (APL). Tamibarotene, a fourth-generation retinoid, is currently approved in Japan for the treatment of APL.

Psoriasis

Topical application of tretinoin or isotretinoin has limited efficacy in psoriasis. Although topical tazarotene was shown to be effective in treating mild to moderate plaque-type psoriasis affecting ≤20% of the body surface area, irritation limits its use as monotherapy. A combination of tazarotene and a mid- to high-potency topical corticosteroid can improve efficacy and reduce the likelihood of both irritation and corticosteroid-induced atrophy.

Photoaging

Several controlled studies have demonstrated that topical retinoids, including tretinoin and tazarotene creams, can improve fine wrinkling and lighten uneven pigmentation[31]. It generally takes 3–6 months of daily application to see significant clinical improvement. Cutaneous irritation is usually the limiting factor. Retinaldehyde was found to be as effective as tretinoin in treating photodamage in less extensive trials[32], and it had a better tolerance profile that may reflect more controlled delivery of retinoic acid to target cells. Seletinoid G, a fourth-generation polyaromatic retinoid with RAR-γ selectivity designed to produce less skin irritation, is under investigation as a treatment for photoaging.[33]

Photoaging is the consequence of UVR-induced damage to the skin, which is characterized by decreased vitamin A content[7] as well as lower expression of RXR-α and RAR-γ (the major retinoid receptors in keratinocytes)[34] in the acute setting and then later by upregulation of AP1-driven matrix metalloproteinases (MMPs). Topical retinoids promote cellular differentiation and extracellular matrix synthesis, including an increase in hyaluronic acid via a CD44-mediated mechanism in addition to decreased MMP production[35]. Histologic findings after repeated topical application of tretinoin include compaction of the stratum corneum, epidermal hyperplasia (acanthosis), correction of atypia (e.g. actinic keratoses), dispersion of melanin granules, increased dermal collagen synthesis, and angiogenesis. These findings explain reported observations of smoother skin, a rosy glow, decreased blotchy pigmentation, and diminished fine lines and wrinkles following topical retinoid treatment[36].

Other indications

Other FDA-approved indications for topical retinoids include alitretinoin 0.1% gel for cutaneous Kaposi sarcoma and bexarotene 1% gel for CTCL[37]. There are also numerous "off-label" uses for topical retinoids (see Table 126.3).

Systemic Retinoids

Psoriasis

Several randomized, controlled, multicenter trials have been performed to ascertain the efficacy of acitretin in plaque-type and pustular psoriasis, with similar results to prior studies of etretinate[38]. Guidelines for use of acitretin in psoriasis are summarized in Tables 8.13 and 8.14. The best results have been obtained in acral or generalized (von Zumbusch) pustular psoriasis, in which acitretin is considered to be a first-line therapy. The various forms of pustular psoriasis, as well as erythrodermic psoriasis, tend to clear relatively rapidly with acitretin monotherapy. Rebound does not usually occur after stopping treatment, and reintroduction produces a beneficial response.

Plaque-type psoriasis responds variably to acitretin. Although complete clearance of plaques is achieved in only about 30% of treated patients, substantial improvement is obtained in an additional 50%. The mean decrease in the Psoriasis Area and Severity Index (PASI) score is ~60%–70%, depending on the dosage and duration of treatment. Many of the plaques may remain, but they are thinner with less scale and erythema.

An initial worsening with increased erythema and/or extent of involvement of plaque-type psoriasis may occur within a few days of starting acitretin therapy at a dosage of 0.5–1 mg/kg per day (~25–70 mg/day in adults). Utilization of a lower dose (10 mg/day) initially, followed by a progressive increase, helps to avoid this complication.

Total clearance of psoriatic plaques usually requires that oral retinoids be combined with other treatments such as topical corticosteroids, topical vitamin D derivatives, anthralin (dithranol), or photo(chemo) therapy (narrowband UVB or psoralen plus UVA [PUVA])[39,40]. The "Re-PUVA" combination, in which retinoids are given for 14 days before starting PUVA, can produce an accelerated response rate and resolution of lesions that would not clear with a retinoid or PUVA alone (Fig. 126.3). The cumulative UVA exposure required to produce a remission is also significantly lower with Re-PUVA, reducing the risk of UVA-induced carcinogenesis. Oral retinoids can also be combined with bath PUVA. Lastly, the combination of acitretin with UVB phototherapy has been shown to be more effective than retinoid or UVB phototherapy alone in patients with psoriasis[41,42].

Isotretinoin is less effective than acitretin for psoriasis, although some efficacy has been shown in combination with PUVA[43]. Isotretinoin is still occasionally used in women of childbearing age with psoriasis who need a systemic retinoid to avoid the long post-acitretin contraception period.

Acne

The introduction of oral isotretinoin was a key advance in acne therapy and it still remains the most effective medication. With the possible exception of hormonal acne, isotretinoin has been shown to induce long-term remissions and even "cure" acne. It is the only medication that affects, albeit not to the same degree or permanently, all the major etiologic factors implicated in acne: sebum production, comedogenesis, and colonization with *C. acnes* (Fig. 126.4; see Ch. 36). Among natural and synthetic retinoids studied in humans, only isotretinoin has been found to suppress sebum production (see above).

In the early 1980s, oral isotretinoin use was restricted to patients suffering from severe nodulocystic acne. With increasing experience, however, its use has been extended to patients with less severe disease who have responded unsatisfactorily to conventional therapies such as topical retinoids plus oral antibiotics. Patients with moderate acne that shows signs of scarring also represent candidates for oral isotretinoin therapy.

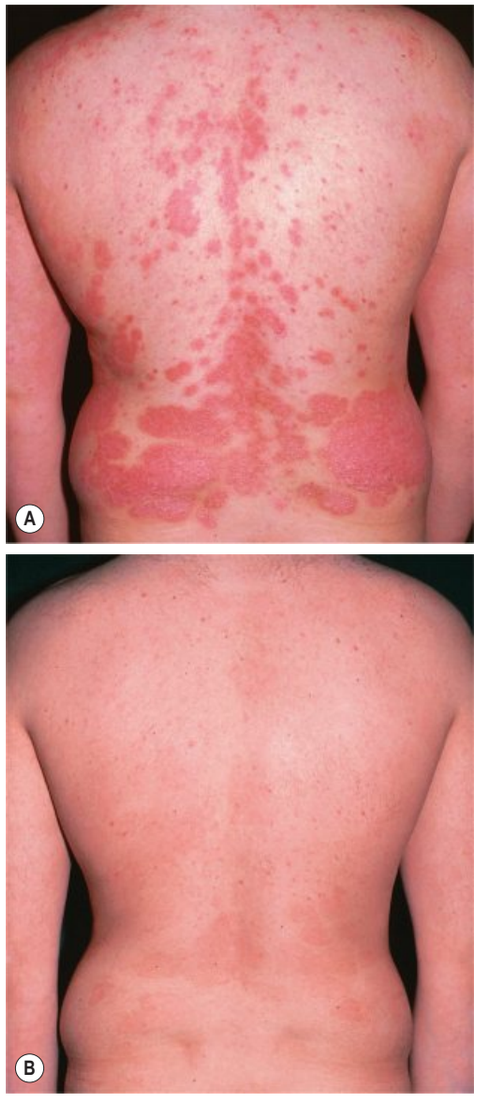


Fig. 126.3 Chronic plaque-type psoriasis. Before (**A**) and after (**B**) treatment with a combination of acitretin and PUVA.



Fig. 126.4 Severe acne vulgaris. Before (**A**) and after (**B**) treatment with oral isotretinoin. *Courtesy Ángela Hernández-Martín, MD.*

Acne morbidity extends beyond the aesthetics of physical appearance. Psychosocial consequences of acne range from depression and anxiety to interpersonal and work-related difficulties. Quality-of-life studies have shown that isotretinoin treatment significantly improves sociability and self-esteem.

It was initially considered that optimal benefit would be achieved with an isotretinoin dose of 1 mg/kg per day. However, this can induce undesirable dose-dependent effects, and similar short-term therapeutic results have been obtained with doses below 0.5 mg/kg per day. In order to avoid the higher incidence of relapses associated with lower-dose isotretinoin, treatment can be continued for a longer period of time in order to reach a critical cumulative dose threshold. The cumulative dose was first recognized to be important in isotretinoin therapy for acne by Harms et al. in 1989[44]; it refers to the total amount of oral isotretinoin taken by the patient over the entire course, divided by the body weight (mg/kg body weight). For example, a patient weighing 50 kg and receiving 25 mg/day of isotretinoin for 100 days would have received a cumulative dose of 50 mg/kg (25 mg × 100 = 2500 mg, divided by 50 kg = 50 mg/kg). Data from several studies indicated that post-therapy relapse is minimized by a treatment course amounting to a total of at least 120 mg/kg, with minimal further therapeutic gain beyond about 150 mg/kg[45]. However, a 6-month course of low-dose isotretinoin (20 mg/day; mean cumulative dose = 70 mg/kg) was also found to be effective in the treatment of moderate acne, with a low incidence of severe side effects and a reduced cost compared with higher doses[46].

A lag period of 1–3 months may occur before the onset of the therapeutic effect. Approximately one-third of patients with acne require a second course of isotretinoin therapy, either for persistent disease or for relapse. A major predictive factor for resistance to isotretinoin treatment is closed comedonal and microcystic acne. Hyperandrogenemia due to ovarian or adrenal dysfunction should be excluded in women with a history of acne that is either refractory to isotretinoin or has relapsed following appropriate courses of isotretinoin.

A flare of disease during the first few weeks of treatment, sometimes with an acne fulminans-like presentation and subsequent evolution of acne cysts into lesions resembling pyogenic granulomas, is occasionally observed with isotretinoin treatment (see Fig. 36.17). The incidence of this side effect may be reduced by using lower doses of isotretinoin during the first 3–4 weeks of therapy[47]. Because oral isotretinoin is a potent teratogen, prevention of pregnancy in female patients with childbearing potential is critical, with a need for continuous effective contraception from 1 month prior to initiating therapy until 1 month after the last dose (see below)[47].

Isotretinoin has a more limited effect on hidradenitis suppurativa and dissecting cellulitis of the scalp, which can occur together with acne conglobata as components of the follicular occlusion tetrad[48]. Some clinicians recommend oral isotretinoin during the weeks or months preceding surgery for hidradenitis suppurativa, and sometimes also during the postoperative period, while others avoid isotretinoin perioperatively because of reports of enhanced scarring (see below).

Cutaneous T cell lymphoma

Isotretinoin and acitretin are somewhat effective and are considered to be of equal potency in the treatment of mycosis fungoides (MF). Retinoids can be used in combination with PUVA, interferon, or systemic chemotherapy (see Ch. 120). Despite initial improvement of the various stages of MF, it is often impossible to maintain remissions with these retinoids as monotherapy.

Both oral and topical bexarotene can produce clinical responses in CTCL. Two multicenter clinical trials of oral bexarotene were conducted in patients with stage I–IIA (early) disease (n = 58) or stage IIB–IVB (advanced) disease (n = 94)[23]. Patients in the early-stage study randomly assigned to a low-dose arm of 6.5 mg/m^2 per day had a 20% response rate, in contrast to 54% and 67% for patients receiving starting doses of 300 mg/m^2 per day and 650 mg/m^2 per day (then decreased to 500 mg/m^2 per day), respectively[41]. However, dose-dependent toxicity was a significant problem. Response rates were ~50% for the patients with advanced CTCL, who all received doses of 300–650 mg/m^2 per day[23,37].

Bexarotene is FDA-approved as oral therapy for CTCL that has been refractory to at least one systemic agent, and as a topical gel formulation for refractory early-stage CTCL. Given the high incidence of side effects, in particular hyperlipidemia (see below), a commonly recommended starting dose for oral bexarotene is 150 mg/m^2 per day (Table 126.4). Combination therapies utilizing bexarotene together with PUVA, narrowband UVB, methotrexate, interferon-α, or denileukin diftitox have also been evaluated in clinical trials and case series[49].

Chronic hand eczema

In a randomized, double-blind, placebo-controlled, multicenter study, 1032 adults with severe chronic hand eczema were treated with 30 mg or 10 mg of oral alitretinoin versus placebo once daily for 12–24 weeks. Responses, defined as clear or almost clear hands, were achieved in 48%, 28%, and 17% of the patients in the three groups, respectively. Treatment was well tolerated, with dose-dependent adverse events including headache, mucocutaneous side effects, hyperlipidemia, and hypothyroidism. Improvement typically began to develop after ~4 weeks of treatment, and the median time to relapse, defined as recurrence of 75% of initial signs and symptoms, was 6 months in the absence of any further therapy[50]. Oral alitretinoin (currently not available in the US) therefore represents a therapeutic option for adults with severe, recalcitrant chronic hand eczema, with the possibility of using intermittent courses to induce intermediate-term remissions[51].

Other "off-label" clinical uses

The multiple effects of retinoids explain their role in treating a broad spectrum of cutaneous diseases. Although many skin disorders respond to retinoids (see Table 126.3), benefit has been established in controlled studies for relatively few conditions.

Ichthyosis

Acitretin and isotretinoin can be of benefit in patients with non-syndromic autosomal recessive congenital ichthyoses (Fig. 126.5; see Ch. 57)[52]. Good results have also been observed in patients with X-linked recessive ichthyosis and ichthyosis vulgaris; however, these diseases tend to be less severe and do not usually require systemic retinoid therapy. Given the lifelong duration of heritable ichthyoses, intermittent retinoid courses are sometimes prescribed.

Darier disease

Severe forms of Darier disease are often treated with systemic retinoids. Therapy should be started with a low dose (e.g. acitretin 10 mg/day,

APPROACH TO ORAL BEXAROTENE THERAPY FOR CUTANEOUS T-CELL LYMPHOMA			
	Bexarotene administration	**Monitoring**	**Management of side effects**
Prior to treatment		Baseline CBC, basic metabolic panel, hepatic panel, TSH, free T4, fasting lipid panel, CK Determine if patient takes medications that inhibit or induce CYP3A4 (see Ch. 131)	Dietary and lifestyle modifications to minimize risk of hyperlipidemia If pre-existing laboratory abnormalities, administer: • Levothyroxine to achieve normal free T4 levels • A fibrate (e.g. fenofibrate)* to achieve triglyceride level <200 mg/dl and HDL level >50 mg/dl • A statin† to achieve LDL level <160 mg/dl
Day –7			Start fibrate (e.g. fenofibrate 145–200 mg daily)*
Day 0	Start bexarotene 150 mg/m^2 daily		Start levothyroxine 0.05 mg daily
Days 7 to 28		Free T4‡ & fasting lipid panel every 1–2 weeks	Adjust levothyroxine and fibrate doses and/or add statin† as required to keep laboratory values in target ranges above
Day 28¶	Increase to bexarotene 300 mg/m^2 daily		
Day 29 onward	Adjust bexarotene dose as needed depending on disease response	Free T4‡ & fasting lipid panel • Every 1–2 weeks until in target range and after subsequent dose changes • Otherwise every 1–2 months CBC every 1–2 months	As above; a triglyceride level <400 mg/dl may be a more realistic target for some patients

*Reduce dose for patients with decreased creatinine clearance; because gemfibrozil raises bexarotene levels, these medications should ***not*** be administered concomitantly.
†Niacin represents another option for patients with combined hyperlipidemia; patients receiving a fibrate and statin concomitantly may be at increased risk of rhabdomyolysis.
‡Monitor free T4 as indicator of hypothyroidism; bexarotene lowers TSH levels (central hypothyroidism).
¶May increase dose as early as day 14 or, if more time is required to normalize lipid and free T4 levels, after day 28.

Table 126.4 Approach to initiating oral bexarotene therapy for cutaneous T cell lymphoma. CBC, complete blood count; CK, creatine kinase; HDL, high-density lipoprotein; LDL, low-density lipoprotein; T4, thyroxine; TSH, thyroid-stimulating hormone.

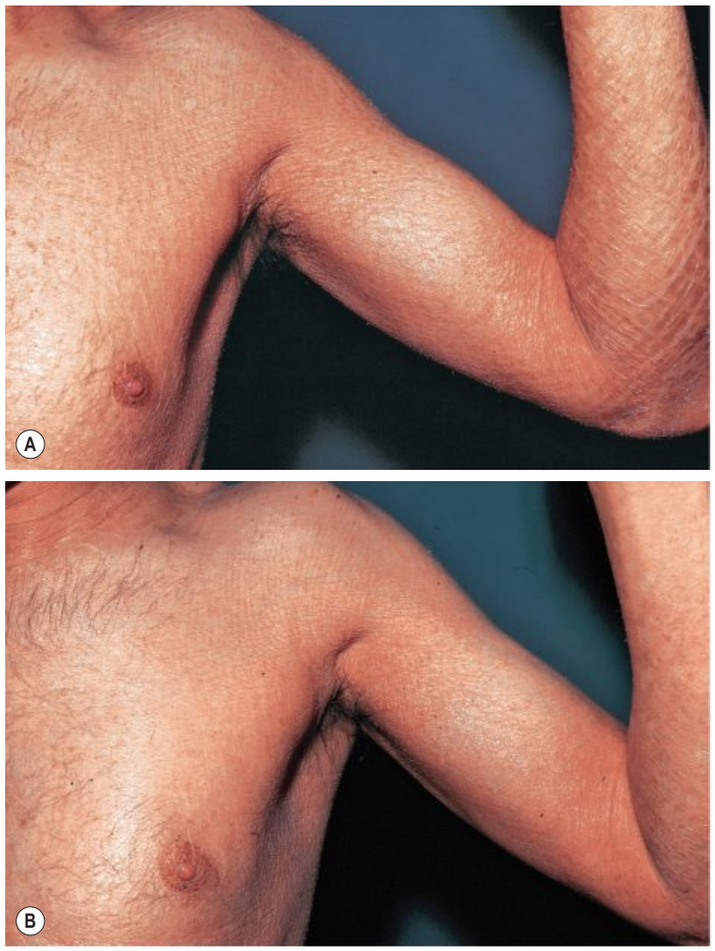


Fig. 126.5 Lamellar ichthyosis. Before (**A**) and after (**B**) treatment with acitretin.

isotretinoin 20 mg/day) in order to prevent an initial exacerbation of the disease; 20 mg/day of acitretin is usually sufficient for significant improvement.

Pityriasis rubra pilaris

Treatment with an oral retinoid (acitretin, isotretinoin, or alitretinoin) can lead to clearance of pityriasis rubra pilaris (PRP) (Fig. 126.6; see Ch. 9). In extensive cases, concomitant use of methotrexate may be advantageous, but with attention to possible liver toxicity.[53]

Rosacea

In severe or treatment-resistant rosacea, isotretinoin typically has a greater effect on inflammatory lesions than on vascular manifestations[54]. A low daily dose (10 mg) is often sufficient, although higher-dose acne vulgaris regimens are sometimes used for severe disease.

Premalignant and malignant skin lesions

Acitretin has been shown to be effective in the treatment of premalignant skin lesions, including human papillomavirus-induced neoplasia and actinic keratoses. In patients with basal cell nevus syndrome and xeroderma pigmentosum as well as solid organ transplant recipients, it may reduce the development of keratinocyte carcinomas (see Ch. 108). A prospective, open, randomized crossover study demonstrated that acitretin (25 mg/day for 12 months) prevented the development of squamous cell carcinoma in renal transplant recipients[55].

Lupus erythematosus

Both isotretinoin and acitretin have been used successfully in patients with various forms of lupus erythematosus (LE), including hypertrophic LE.[56] Recommended doses range from 0.2–1.0 mg/kg/day. Recurrence after completion of treatment is a limiting factor. Comparable therapeutic efficacy has been observed for acitretin and hydroxychloroquine in chronic and subacute cutaneous LE[57].

DOSAGE

The different formulations, strengths, and standard dosage ranges of topical and systemic retinoids currently available for use in dermatology are outlined in Table 126.5.

CONTRAINDICATIONS

Topical Retinoids

Topical retinoids should be avoided during pregnancy and nursing, due primarily to medicolegal issues raised by the teratogenicity of



Fig. 126.6 Pityriasis rubra pilaris. Before (**A**) and after (**B**) treatment with acitretin.

oral retinoids. Use of irritating topical products (e.g. abrasive cleansers, astringents) and hair removal via waxing should be avoided in areas being treated with a topical retinoid.

Systemic Retinoids

The absolute contraindications are pregnancy, women contemplating becoming pregnant or non-compliant with contraception, breastfeeding, and hypersensitivity to medication components. Relative contraindications include moderate to severe hypercholesterolemia or hypertriglyceridemia, significant hepatic dysfunction (especially for bexarotene), hypothyroidism (especially for bexarotene and alitretinoin), suicidal ideation, and pseudotumor cerebri. Patients should be advised not to take vitamin A supplements in excess.

MAJOR SIDE EFFECTS

Topical Retinoids

By far the most common side effect of topical retinoids is skin irritation characterized by erythema and peeling (Table 126.6). "Retinoid dermatitis" typically occurs during the first month of treatment and tends

ADVERSE EFFECTS OF TOPICAL RETINOIDS	
Skin irritation (retinoid dermatitis)	Erythema Peeling, scaling Dryness Burning Pruritus Photosensitivity
Uncommon	Hypo- or hyperpigmentation Ectropion Allergic contact dermatitis Sticky skin

Table 126.6 Adverse effects of topical retinoids.

FORMULATIONS OF TOPICAL AND SYSTEMIC RETINOIDS				
Retinoid	**Route**	**Formulations**	**Standard dosage range**	**Major indications**
Retinol	Topical	Various (0.15%, 0.3%)		Cosmeceutical products
Retinaldehyde	Topical	Various (0.05%–0.1%)		
Tretinoin†	Topical	Gel, cream, solution (0.1%, 0.08%, 0.06%, 0.05%, 0.04%, 0.025%, 0.02%, 0.01%)		Acne vulgaris Photoaging
	Oral	10 mg capsules	45 mg/m^2/day	Acute promyelocytic leukemia
Tazarotene‡	Topical	Gel, cream, lotion, foam (0.045%, 0.05%, 0.1%)		Acne vulgaris Plaque-type psoriasis Photoaging
Adapalene¶	Topical	Gel, cream, lotion (0.1%, 0.3%)		Acne vulgaris
Trifarotene	Topical	Cream (0.005%)		Acne vulgaris
Isotretinoin	Topical§	Gel (0.05%)		Acne vulgaris*
	Oral	8, 10, 16, 20, 24, 25, 30, 35, 40 mg capsules	0.5–2 mg/kg/day	Severe, recalcitrant acne; related dermatoses*
Acitretin	Oral	10, 17.5, 22.5, 25 mg capsules	25–50 mg/day	Psoriasis Disorders of cornification*
Bexarotene	Topical	Gel (1%)		Cutaneous T cell lymphoma
	Oral	75 mg capsules	300 mg/m^2/day	
Alitretinoin	Topical	Gel (0.1%)		Kaposi sarcoma
	Oral§	10, 30 mg capsules	10–30 mg/day	Chronic hand eczema*

*Not an FDA-approved indication.
†Tretinoin is also available in combination with clindamycin phosphate 1.2% for acne or with fluocinolone acetonide 0.01% plus hydroquinone 4% for melasma.
‡Tazarotene 0.045% is also available in combination with halobetasol propionate 0.01% for plaque psoriasis.
¶Adapalene 0.1% is available over the counter and adapalene 0.1% and 0.3% are also available in combination with benzoyl peroxide 2.5% for acne.
§Currently not available in the US.

Table 126.5 Formulations of topical and systemic retinoids. Systemic retinoids are teratogenic and therefore contraindicated during pregnancy. Although topical retinoids have very low levels of systemic absorption, their use during pregnancy is not recommended and per the FDA, topical tazarotene and bexarotene are contraindicated during pregnancy. Topical tretinoin may be oxidized and inactivated by benzoyl peroxide, so it is recommended that these medications be applied at different times.

to recede thereafter. It usually responds to a temporary reduction in the frequency, amount, or duration (e.g. "short contact" therapy) of retinoid application and to the use of moisturizers. Desquamation and peeling correspond to the hyperproliferative response of the epidermis to tretinoin mediated by RARs, but the erythema does not seem to be receptor-mediated. The perioral area of the face is most sensitive to peeling, and retinoid use in this region can be limited or avoided.

Although no photoallergic or phototoxic reactions have been proven for topical retinoids, some patients note a decreased tolerance to UVR. Erythema tends to develop shortly after sun exposure and is often accompanied by a sensation of heat, raising the question of involvement of infrared irradiation. The potential for teratogenicity from use of topical retinoids is very low to non-existent. Systemic absorption of topically applied retinoids has been inconsequential in both animal and human studies[58–60], and there is no evidence that topical application of tretinoin during pregnancy causes congenital disorders. Temporary worsening of acne may occur within the first weeks of therapy. Uncommon side effects include transient hypo- or hyperpigmentation, koebnerization of psoriasis (especially with tazarotene), allergic contact dermatitis, and rarely ectropion. Of note, topical retinoids have been used to treat ectropion in patients with ichthyosis.

Systemic Retinoids

Teratogenicity is the most concerning adverse effect of oral retinoids (Table 126.7). The side-effect profile of systemic retinoids (Table 126.8) resembles the toxic effects of vitamin A or hypervitaminosis A syndrome. Acute retinoid toxicity can include mucocutaneous (most common) and laboratory abnormalities, while chronic retinoid toxicity may occasionally produce bony changes.

Teratogenicity

Systemic retinoids are potent teratogens, and fetal deformities are the major concern in treating fertile women with oral retinoids. So far, with regard to teratogenicity, no safe minimal dose during pregnancy has been established. The defects seen in retinoid embryopathy can include craniofacial (microtia/anotia, micrognathia), cardiovascular, thymic, and central nervous system (CNS; hydrocephalus, microcephaly) abnormalities (see Table 126.7)[58,61]. These malformations may lead to spontaneous abortion, premature birth, or fetal death. The putative mechanism involves toxic effects on neural crest cells, particularly with exposure during the fourth week of gestation. No typical retinoid embryopathy malformations have been reported in pregnancies where only the male partner was taking acitretin or isotretinoin at the time of conception. Although it is often recommended that men who are actively trying to father children avoid systemic retinoid therapy due to

RETINOID EMBRYOPATHY
Craniofacial
• Atresia of the ear canal, microtia, anotia • Microphthalmia • Asymmetry of the face • Cleft palate • Micrognathia
Cardiovascular (especially conotruncal and aortic arch defects)
• Transposition of the great vessels • Tetralogy of Fallot • Truncus arteriosus • Supracristal ventricular septal defect • Interrupted aortic arch • Retroesophageal right subclavian artery • Hypoplastic aorta
Central nervous system
• Hydrocephalus • Microcephaly • Cortical agenesis • Cerebellar hypoplasia • Mental retardation • Difficulty with visual motor integration
Third and fourth pharyngeal pouches
• Thymic hypoplasia • Parathyroid hypoplasia
Other
• Limb anomalies • Anal and vaginal atresia

Table 126.7 Retinoid embryopathy.

ADVERSE EFFECTS OF SYSTEMIC RETINOIDS	
Acute effects	
Mucocutaneous	Xerosis with pruritus* Cheilitis* Dry mucosa*: mouth, nose (epistaxis), eyes (see below) Skin fragility* Retinoid dermatitis (see Table 126.6)* Palmoplantar peeling* Photosensitivity Sticky sensation (palms, soles) Granulation tissue with pyogenic granuloma-like lesions (e.g. at sites of acne cysts, periungual) Intertriginous erosions with exuberant granulation tissue Nail fragility with softening, onycholysis, paronychia Facial swelling *Staphylococcus aureus* infection Telogen effluvium, hair thinning
Ocular	Xerophthalmia* Blepharoconjunctivitis Reduced night vision Blurred vision, photophobia, keratitis, corneal ulceration (rare)
Systemic	Myalgias Arthralgias Anorexia, nausea, diarrhea, abdominal pain Headache, pseudotumor cerebri (rare) Fatigue, lethargy, irritability Depression, suicidal ideation (rare and controversial) Toxic hepatitis (rare) Clinical signs of hypothyroidism (with bexarotene*) Pancreatitis secondary to hypertriglyceridemia (rare) Hyperuricemia with gout (rare)
Laboratory	Elevated liver function tests (usually transient, minor): AST, ALT, alkaline phosphatase, LDH, bilirubin Hyperlipidemia: hypertriglyceridemia*; increased cholesterol, VLDL and LDL; decreased HDL Decreased free thyroxine (T4) (with bexarotene*) Elevated creatine kinase Leukopenia (with bexarotene) Agranulocytosis (with bexarotene) Thrombocytosis, thrombocytopenia Hypercalcemia (rare)
Chronic effects	
Mucocutaneous	Alopecia (rare) Dry eyes, corneal opacities (rare)
Systemic	DISH syndrome-like bone changes Osteophyte and bony bridge formation, especially of vertebrae (rarely clinically significant at dosages for acne) Anterior > posterior spinal ligament calcification Extraspinal tendon and ligament calcification Osteoporotic changes in long bones (rare, with possible exception of long-term etretinate) Premature epiphyseal closure (rare) Periosteal thickening Myopathy (rare)
*Common adverse effects.	

Table 126.8 Adverse effects of systemic retinoids. See Table 126.7 for teratogenicity. ALT, alanine aminotransferase; AST, aspartate aminotransferase; DISH, diffuse idiopathic skeletal hyperostosis; HDL, high-density lipoprotein; LDH, lactate dehydrogenase; LDL, low-density lipoprotein; VLDL, very-low-density lipoprotein.

the presence of the drug in semen, only ~0.0001%–0.0005% of a typical oral dose would be delivered to a female partner (https://dailymed.nlm.nih.gov/).

In the US, physicians, patients (female or, to prevent sharing of medication, male), and pharmacies must register with a pregnancy risk reduction program (iPLEDGE™) in order for isotretinoin to be prescribed. The program requires female patients with childbearing potential to review an educational booklet, receive monthly counseling, take monthly comprehension and pregnancy tests (as well as two pregnancy tests prior to instituting therapy), and pledge to use two forms of effective contraception (or abstinence) continuously for 1 month before, during, and for 1 month after isotretinoin treatment[62,63]. Patients taking systemic retinoids should not donate blood while on therapy and for 1 month or 3 years after the last dose of isotretinoin or acitretin, respectively.

Skin and mucous membrane adverse effects

Dose-dependent mucocutaneous toxicity is the most commonly observed side effect of oral retinoids, and it reflects decreased production of sebum, reduced stratum corneum thickness, and altered skin barrier function (Fig. 126.7). Dry lips or cheilitis is the earliest and the most frequent finding (Fig. 126.8). Dryness of the mouth, nasal mucosa (associated with fragility and epistaxis), and eyes (see below) are other potential manifestations.

Xerosis of the skin and associated pruritus, peeling (especially of the palms and soles), and fissuring (particularly of the fingertips) are frequent side effects. Exacerbations of atopic dermatitis may occur. Photosensitivity is occasionally observed, in particular with isotretinoin, and probably reflects a reduction in the thickness of the stratum corneum. *Staphylococcus aureus* colonization correlates with isotretinoin-induced reduction in sebum production and may lead to cutaneous infections. Diffuse hair loss due to telogen effluvium is a relatively common complaint, although objective alopecia tends to occur only at high dosage levels. Effects on the nail apparatus can include thinning, fragility, and shedding of the nail plate as well as paronychia-like changes with periungual granulation tissue that can resemble pyogenic granulomas.



Fig. 126.7 Retinoid dermatitis. Xerosis, peeling, and erythema of the face in a patient treated with oral isotretinoin.



Fig. 126.8 Cheilitis in an isotretinoin-treated patient.

Mucocutaneous side-effect profiles vary among the systemic retinoids. Isotretinoin causes more mucosal dryness, and acitretin has been associated with higher incidences of alopecia and palmoplantar peeling, whereas bexarotene induces milder mucocutaneous and ocular side effects than other oral retinoids. Delayed wound healing and abnormal scarring during isotretinoin therapy have been described, and it has traditionally been suggested that elective procedures be postponed until 6–12 months after discontinuing isotretinoin when possible. However, recent systematic reviews and consensus recommendations do not support delaying most surgical and cosmetic procedures in patients currently receiving or who have recently completed isotretinoin therapy, with the exception of fully ablative laser treatments and mechanical dermabrasion[64]. Medium-depth and deep chemical peels are also often delayed.

Common laboratory abnormalities

Dyslipidemia

Hypertriglyceridemia is the most frequently observed systemic effect of retinoid therapy. Isotretinoin and etretinate/acitretin elevate triglycerides in 25%–50% and cholesterol in 20%–30% of treated patients[65], whereas bexarotene elevates triglycerides and cholesterol in ~80% and ~50% of patients, respectively[23]. A concomitant increase in total and low-density lipoprotein (LDL) cholesterol is frequently observed. In cases of severe retinoid-induced hypertriglyceridemia, eruptive xanthomas and acute hemorrhagic pancreatitis may occur. A higher incidence of acute hemorrhagic pancreatitis has been encountered in patients taking bexarotene, as compared to first- or second-generation retinoids.

Baseline fasting serum lipid levels should be obtained before initiating bexarotene therapy and every 1–2 weeks during therapy until levels become stable (generally in 4–8 weeks). For other oral retinoids, monitoring of lipid levels (together with liver function tests) is typically performed monthly for the first 2 months and then at 3-month intervals if baseline lipid levels are normal, there are no increases in dosage, and risk factors (obesity, high alcohol intake, diabetes) are absent. Less frequent monitoring (e.g. at baseline and after 2 months of treatment if results are normal) has been recommended for low-risk adolescents and young adults receiving isotretinoin for acne or ichthyosis, with subsequent testing every 6–12 months for ichthyosis patients on long-term treatment[52,66]. Discontinuation of therapy is suggested if fasting triglycerides reach 800 mg/dl (8 g/L). Less severe increases may be treated by dose reduction, withdrawing therapy until normalization of serum lipids occurs, and changes in diet or lifestyle. In some instances, lipid-lowering agents may be indicated. Coadministration of bexarotene with a statin (e.g. atorvastatin) for hypercholesterolemia and/or fenofibrate for hypertriglyceridemia is recommended to treat retinoid-induced hyperlipidemia and to lower the risk of pancreatitis[16,67]. Some authors recommend starting all patients on fenofibrate 7 days before initiating bexarotene treatment[37].

The effects of retinoid-induced hyperlipidemia during long-term therapy on the development of atherosclerotic cardiovascular disease is unknown. Retinoids are thought to cause hyperlipidemia by interfering with lipid clearance. Bexarotene increases the expression of apolipoprotein C-III, which prevents the uptake of lipids from very-low-density lipoproteins (VLDL) into cells.

Liver effects

Transient elevations in serum transaminases occur in ~20% of patients treated with acitretin and much less frequently in those receiving isotretinoin or bexarotene therapy. Circulating levels of alkaline phosphatase, lactic dehydrogenase, and bilirubin may also occasionally become elevated during retinoid therapy. Liver function test abnormalities are typically mild, usually developing between 2 and 8 weeks after starting therapy and then returning to normal within another 2–4 weeks despite continued therapy. Severe or persistent hepatotoxic reactions occur in <1% of patients. Acitretin therapy elicited no biopsy-proven hepatotoxicity in a 2-year prospective study, thus suggesting that periodic liver biopsy is not necessary[68]. No studies have specifically evaluated the use of retinoids in patients with hepatic insufficiency. However, since retinoids are metabolized by hepatic cytochrome P450 isoenzymes

(e.g. CYP3A4) and undergo partial biliary elimination, significant hepatic insufficiency is likely to interfere with drug elimination. Transaminase elevations to greater than three times the upper limit of normal should prompt discontinuation of retinoid therapy. Other causes of hepatic dysfunction should be excluded.

Other systemic adverse effects

Ophthalmologic effects

The most common ocular retinoid effects are dryness and irritation. Xerophthalmia due to decreased Meibomian gland secretions may prohibit the use of contact lenses and can lead to blepharoconjunctivitis, keratitis, or corneal opacities (especially with isotretinoin). Alterations in visual function, mainly nyctalopia (reduced night vision), excessive glare sensitivity, and changes in color perception, have also been reported[69]. Competitive inhibition of ocular retinol dehydrogenase by retinoids, resulting in decreased rhodopsin formation, may be the cause of nyctalopia.

Bone effects

Bone pain can occur in retinoid-treated patients without objective evidence of any abnormalities and without sequelae. Several reports have also implicated therapy with oral retinoids, including etretinate and isotretinoin, in the formation of diffuse hyperostoses of the spine (diffuse idiopathic skeletal hyperostosis [DISH] syndrome-like changes) as well as calcification of tendons and ligaments, particularly in the ankles[70]. These changes are thought to be related to the dose and duration of retinoid treatment[52], with specific findings including anterior spinal ligament calcification, osteophyte ("spur") formation, extraspinal calcifications, and bony bridges, but not narrowing of the disk space. Of note, many of the bone changes observed are common in the general population (especially in adults) and not clinically significant. Prospective studies have shown that the likely potential effect of retinoids is to worsen pre-existing skeletal overgrowth rather than to induce *de novo* changes.

Osteoporosis has been observed with hypervitaminosis A and after long-term therapy with etretinate but not with acitretin or isotretinoin. Several investigations in patients receiving a standard isotretinoin course for acne (~1 mg/kg/day for 5–6 months), including an open-label trial in 217 adolescents and three controlled studies in adolescents (n = 21; n = 358) and young adults (n=36), showed no significant changes in bone mineral density[71,72]. Likewise, a study of 30 adults found no association between acitretin therapy (median duration, 3.6 years) for chronic dermatoses and risk of osteopenia or osteoporosis. Although there are rare reports of premature epiphyseal closure in children treated with oral retinoids (e.g. >1 mg/kg/day for ≥4–6 years)[52], this has not been observed in acne treatment studies. A baseline radiographic survey or bone density evaluation is not required prior to administering an oral retinoid, although monitoring high-risk patients who require prolonged high-dose therapy may be useful.

Muscle effects

Although muscular pain and cramps can occur in patients taking acitretin, these symptoms are more common with higher doses of isotretinoin therapy, especially in individuals involved in vigorous physical activity. Occasionally, elevated creatine kinase levels may be observed. Increased muscle tone as well as axial muscle rigidity and myopathy have been reported in patients receiving etretinate and acitretin therapy, respectively.

Central nervous system and psychiatric effects

Although individual signs of increased intracranial pressure, such as headache, nausea and vomiting, are occasionally observed in patients taking a systemic retinoid, the complete pseudotumor cerebri syndrome with papilledema and blurred vision is very rare[73]. Concomitant use of other drugs associated with intracranial hypertension (e.g. tetracyclines) is considered a risk factor for developing pseudotumor cerebri and should therefore be avoided[74]. Examination for papilledema should be performed immediately when a patient receiving retinoid therapy complains of a persistent headache, especially if it is accompanied by visual changes, nausea or vomiting, or when pseudotumor cerebri is otherwise suspected.

Although there have been anecdotal reports of depression, psychosis, and suicide attempts in acne patients taking isotretinoin, a causal link has not been established. Multiple prospective and population-based studies as well as case–control, prescription sequence symmetry, and meta-analyses have failed to find an increased risk of depression or suicidal behavior associated with isotretinoin therapy for acne[75–77]. In contrast, several studies and meta-analyses actually noted a significant *decrease* in depressive symptoms in individuals treated with isotretinoin compared to baseline or a control group receiving other acne therapies[75–77], while one small case-crossover study showed a positive correlation between recent exposure to isotretinoin and diagnosis of depression in patients with acne. Acne patients should be informed of possible associations between isotretinoin and psychiatric issues prior to initiating this treatment and monitored for depressive symptoms or suicidal ideation during therapy.

Hypothyroidism

Clinical and biochemical central hypothyroidism occurred in 40% of patients in CTCL trials with bexarotene and was rapidly and completely reversible with cessation of therapy[23,78]. Dose-dependent decreases in serum thyroid-stimulating hormone (TSH) levels were also noted in clinical trials of alitretinoin. This effect is probably mediated via suppressed secretion of the β-subunit of TSH by the thyrotrope cells of the anterior pituitary, which express RXR-γ. Free T4 levels should be monitored before and during bexarotene and alitretinoin therapy and normalized with thyroid hormone replacement as necessary[37].

Hematologic effects

A high incidence (~30%) of dose-related leukopenia was reported in studies of bexarotene for CTCL, occurring as early as 2–4 weeks and characterized by a decrease in neutrophils rather than lymphocytes[23]. Hematologic abnormalities are much less common with other retinoids, but monitoring the complete blood count in HIV-infected patients is warranted.

Gastrointestinal effects

Uncommon nonspecific gastrointestinal complaints have been reported in association with retinoid therapy. Although there have been case reports of isotretinoin administration preceding the onset of inflammatory bowel disease (IBD) and one study showed an association between previous isotretinoin use and the development of ulcerative colitis, a cause-and-effect relationship has not been established. Several large population-based studies found that patients with IBD were no more likely to have used isotretinoin prior to diagnosis than matched controls[79,80], and a meta-analysis concluded that isotretinoin use does not increase the risk of IBD overall or ulcerative colitis specifically[79]. Potential confounding effects of severe inflammatory acne itself and treatment with oral antibiotics may also contribute to an apparent association between isotretinoin and IBD.

Renal effects

Renal toxicity is not characteristic of retinoid therapy. Isotretinoin has been safely administered to patients with end-stage kidney disease who were undergoing hemodialysis. Renal function should be monitored in patients with a history of kidney disease.

Summary

Most adverse effects associated with retinoids are preventable or manageable through proper patient selection, diligent monitoring, and dose adjustments (or occasionally discontinuation of treatment) as indicated.

INTERACTIONS

Concurrent use of systemic retinoids with alcohol or other medications having similar side effects may increase the incidence of adverse events. The following should be avoided or used with caution:

- tetracycline, doxycycline, minocycline (may increase intracranial pressure)
- alcohol (increased conversion of acitretin to etretinate and hepatotoxicity)
- methotrexate (synergistic liver toxicity with retinoids; however, combination may be used with caution in patients with PRP or severe psoriasis)
- vitamin A supplements (risk of hypervitaminosis A).

Retinoid drug levels and resultant potential for toxicity may increase with CYP3A4 inhibitors such as azoles and macrolides. In contrast, medications and herbal supplements including antituberculous drugs (e.g. rifampin), anticonvulsants (e.g. phenytoin, carbamazepine), and St. John's wort may decrease the drug levels of retinoids via CYP3A4 induction (see Table 131.8). Retinoids may also increase the drug levels of cyclosporine via competition for CYP3A4 metabolism[16]. Concomitant administration of bexarotene and gemfibrozil results in a substantial increase in plasma concentrations of bexarotene, at least partially because of cytochrome P450 CYP3A4 inhibition that is induced by gemfibrozil. Concomitant administration of fenofibrate (for hypertriglyceridemia) or atorvastatin (for hypercholesterolemia) does not affect bexarotene plasma levels and, therefore, can be utilized together with bexarotene (see Table 126.4).

In rare instances, patients with diabetes mellitus may have more difficult glucose control while taking a retinoid; however, the causal relationship remains uncertain. Acitretin has been shown to possibly reduce the efficacy of progestin-only contraceptives. Also, unprotected UVR exposure or photosensitizing medications should be avoided because of the potential for increased photosensitivity related to retinoid therapy. Since retinoids act through nuclear receptor dimers, cross-talk with other nuclear receptors may provide synergistic effects: for example, interactions between RXR and vitamin D receptor (VDR) positively influence the action of vitamin D_3, and cross-talk with PPAR and its ligands is under investigation.

USE IN PREGNANCY AND LACTATION

All systemic retinoids are teratogenic and are absolutely contraindicated during pregnancy and lactation (formerly FDA category X). As discussed above, pregnancy testing is necessary for female patients of childbearing potential before instituting oral retinoid therapy (two tests required in the US for isotretinoin) and then at regular intervals (e.g. monthly for isotretinoin) during its administration. Adequate contraception for at least 1 month before initiation and throughout the treatment course is also mandatory in this patient group. Acitretin requires contraception for 3 years (US) or 2 years (Europe) after cessation of therapy, whereas isotretinoin, bexarotene, and alitretinoin require contraception for just 1 month after cessation of therapy.

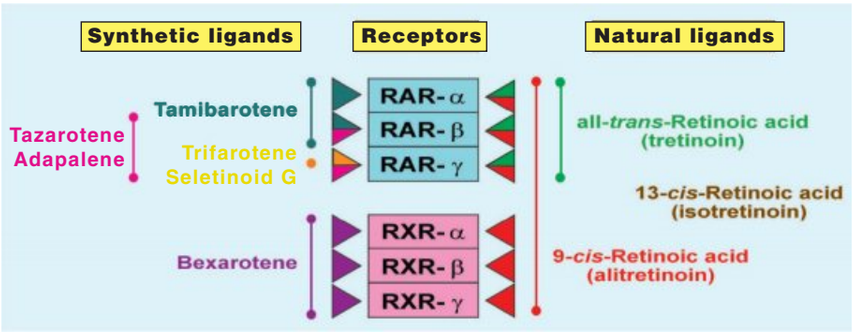
Although no evidence exists for teratogenicity of topical retinoids in humans, they are nevertheless not recommended for use during pregnancy. Since no dermatologic condition that is known to be responsive to topical retinoids is life-threatening to the mother or fetus, it is wiser to postpone treatment until after delivery, primarily for medicolegal reasons rather than scientific data in the opinion of the authors. As it is not known whether topical retinoids pass into the breast milk, topical retinoid use is generally not recommended during breastfeeding.

Additional figures available in our eBook (see inside front cover for access code).

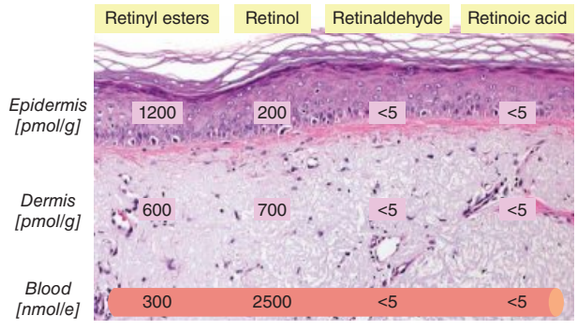
REFERENCES

1. Peck GL, Olsen TG, Yoder FW, et al. Prolonged remissions of cystic and conglobate acne with 13-cis-retinoic acid. *N Engl J Med*. 1979;300:329–333.
2. Peck GL, Yoder FW. Treatment of lamellar ichthyosis and other keratinising dermatoses with an oral synthetic retinoid. *Lancet*. 1976;2:1172–1174.
3. Brun PJ, Yang KJ, Lee SA, et al. Retinoids: potent regulators of metabolism. *Biofactors*. 2013;39:151–163.
4. Chen Y, Clarke OB, Kim J, et al. Structure of the STRA6 receptor for retinol uptake. *Science*. 2016;353:aad8266.
5. Kawaguchi R, Yu J, Honda J, et al. A membrane receptor for retinol binding protein mediates cellular uptake of vitamin A. *Science*. 2007;315:820–825.
6. Wei LN. Cellular retinoic acid binding proteins: genomic and non-genomic functions and their regulation. *Subcell Biochem*. 2016;81:163–178.
7. Sorg O, Saurat JH. Topical retinoids in skin ageing: a focused update with reference to sun induced epidermal vitamin A deficiency. *Dermatology*. 2014;228:314–325.
8. Sorg O, Tran C, Carraux P, et al. Spectral properties of topical retinoids prevent DNA damage and apoptosis after acute UVB exposure in hairless mice. *Photochem Photobiol*. 2005;81:830–836.
9. Sorg O, Tran C, Carraux P, et al. Retinol and retinyl ester epidermal pools are not identically sensitive to UVB irradiation and antioxidant protective effect. *Dermatology*. 1999;199:302–307.
10. Tran C, Sorg O, Carraux P, et al. Topical delivery of retinoids counteracts the UVB-induced epidermal vitamin A depletion in hairless mouse. *Photochem Photobiol*. 2001;73:425–431.
11. Wiegand UW, Chou RC. Pharmacokinetics of oral isotretinoin. *J Am Acad Dermatol*. 1998;39:S8–S12.
12. Torma H. Interaction of isotretinoin with endogenous retinoids. *J Am Acad Dermatol*. 2001;45:S143–S149.
13. Nelson AM, Zhao W, Gilliland KL, et al. Neutrophil gelatinase-associated lipocalin mediates 13-cis retinoic acid-induced apoptosis of human sebaceous gland cells. *J Clin Invest*. 2008;118:1468–1478.
14. Kane MA. Analysis, occurrence, and function of 9-cis-retinoic acid. *Biochim Biophys Acta*. 2012;1821:10–20.
15. Nada HR, Rashed LA, Elantably DMM, El Sharkawy DA. Expression of retinoid receptors in hand eczema. *Int J Dermatol*. 2020;59:576–581.
16. Wiegand UW, Chou RC. Pharmacokinetics of acitretin and etretinate. *J Am Acad Dermatol*. 1998;39:S25–S33.
17. Chou RC, Wyss R, Huselton CA, Wiegand UW. A potentially new metabolic pathway: ethyl esterification of acitretin. *Xenobiotica*. 1992;22:993–1002.
18. Gronhoj Larsen F, Steinkjer B, Jakobsen P, et al. Acitretin is converted to etretinate only during concomitant alcohol intake. *Br J Dermatol*. 2000;143:1164–1169.
19. Sato T, Akimoto N, Kitamura K, et al. Adapalene suppresses sebum accumulation via the inhibition of triacylglycerol biosynthesis and perilipin expression in differentiated hamster sebocytes in vitro. *J Dermatol Sci*. 2013;70:204–210.
20. Gaikwad J, Sharma S, Hatware KV. Review on characteristics and analytical methods of tazarotene: an update. *Crit Rev Anal Chem*. 2020;50:90–96.
21. Duvic M. Tazarotene: a review of its pharmacological profile and potential for clinical use in psoriasis. *Expert Opin Investig Drugs*. 1997;6:1537–1551.
22. Querfeld C, Nagelli LV, Rosen ST, et al. Bexarotene in the treatment of cutaneous T-cell lymphoma. *Expert Opin Pharmacother*. 2006;7:907–915.
23. Quereux G, Saint-Jean M, Peuvrel L, et al. Bexarotene in cutaneous T-cell lymphoma: third retrospective study of long-term cohort and review of the literature. *Expert Opin Pharmacother*. 2013;14:1711–1721.
24. JAMA. Trifarotene (Aklief)—a new topical retinoid for acne. *JAMA*. 2020;323:1310–1311.
25. Aubert J, Piwnica D, Bertino B, et al. Nonclinical and human pharmacology of the potent and selective topical retinoic acid receptor-gamma agonist trifarotene. *Br J Dermatol*. 2018;179:442–456.
26. Vahlquist A, Blockhuys S, Steijlen P, et al. Oral liarozole in the treatment of patients with moderate/severe lamellar ichthyosis: results of a randomized, double-blind, multinational, placebo-controlled phase II/III trial. *Br J Dermatol*. 2014;170:173–181.
27. Veit JGS, De Glas V, Balau B, et al. Characterization of CYP26B1-selective inhibitor, DX314, as a potential therapeutic for keratinization disorders. *J Invest Dermatol*. 2021;141:72–83.
28. Valente Duarte de Sousa IC. Novel pharmacological approaches for the treatment of acne vulgaris. *Expert Opin Investig Drugs*. 2014;23:1389–1410.
29. Cunliffe WJ, Caputo R, Dreno B, et al. Clinical efficacy and safety comparison of adapalene gel and tretinoin gel in the treatment of acne vulgaris: Europe and U.S. multicenter trials. *J Am Acad Dermatol*. 1997;36:S126–S134.
30. Gregoriou S, Kritsotaki E, Katoulis A, Rigopoulos D. Use of tazarotene foam for the treatment of acne vulgaris. *Clin Cosmet Investig Dermatol*. 2014;7:165–170.
31. Darlenski R, Surber C, Fluhr JW. Topical retinoids in the management of photodamaged skin: from theory to evidence-based practical approach. *Br J Dermatol*. 2010;163:1157–1165.
32. Creidi P, Vienne MP, Ochonisky S, et al. Profilometric evaluation of photodamage after topical retinaldehyde and retinoic acid treatment. *J Am Acad Dermatol*. 1998;39:960–965.
33. Lee ES, Ahn Y, Bae IH, et al. Synthetic retinoid seletinoid G improves skin barrier function through wound healing and collagen realignment in human skin equivalents. *Int J Mol Sci*. 2020;21:3198.
34. Wang Z, Boudjelal M, Kang S, et al. Ultraviolet irradiation of human skin causes functional vitamin A deficiency, preventable by all-*trans* retinoic acid pre-treatment. *Nat Med*. 1999;5:418–422.
35. Kaya G, Grand D, Hotz R, et al. Upregulation of CD44 and hyaluronate synthase by topical retinoids in mouse skin. *J Invest Dermatol*. 2005;124:284–287.
36. Mukherjee S, Date A, Patravale V, et al. Retinoids in the treatment of skin aging: an overview of clinical efficacy and safety. *Clin Interv Aging*. 2006;1:327–348.
37. Gniadecki R, Assaf C, Bagot M, et al. The optimal use of bexarotene in cutaneous T-cell lymphoma. *Br J Dermatol*. 2007;157:433–440.
38. Ortiz NE, Nijhawan RI, Weinberg JM. Acitretin. *Dermatol Ther*. 2013;26:390–399.
39. Yamauchi PS, Rizk D, Lowe NJ. Retinoid therapy for psoriasis. *Dermatol Clin*. 2004;22:467–476, x.
40. Racz E, Prens EP. Phototherapy and photochemotherapy for psoriasis. *Dermatol Clin*. 2015;33:79–89.
41. Lebwohl M. Acitretin in combination with UVB or PUVA. *J Am Acad Dermatol*. 1999;41:S22–S24.
42. Saurat JH, Geiger JM, Amblard P, et al. Randomized double-blind multicenter study comparing acitretin-PUVA, etretinate-PUVA and placebo-PUVA in the treatment of severe psoriasis. *Dermatologica*. 1988;177:218–224.
43. Saurat JH. Systemic retinoids. What's new? *Dermatol Clin*. 1998;16:331–340.
44. Harms M, Duvanel T, Williamson C, et al. Isotretinoin for acne: should we consider the total cumulative dose? In: Marks R, Plewig G, eds. *Acne and Related Disorders*. London: Martin Dunitz; 1989:203–206.
45. Rademaker M. Isotretinoin: dose, duration and relapse. What does 30 years of usage tell us? *Australas J Dermatol*. 2013;54:157–162.
46. Amichai B, Shemer A, Grunwald MH. Low-dose isotretinoin in the treatment of acne vulgaris. *J Am Acad Dermatol*. 2006;54:644–646.
47. Dessinioti C, Zouboulis CC, Bettoli V, Rigopoulos D. Comparison of guidelines and consensus articles on the management of patients with acne with oral isotretinoin. *J Eur Acad Dermatol Venereol*. 2020;34:2229–2240.
48. Blok JL, van Hattem S, Jonkman MF, Horvath B. Systemic therapy with immunosuppressive agents and retinoids in hidradenitis suppurativa: a systematic review. *Br J Dermatol*. 2013;168:243–252.
49. Valipour A, Jager M, Wu P, et al. Interventions for mycosis fungoides. *Cochrane Database Syst Rev*. 2020;7:CD008946.
50. Ruzicka T, Lynde CW, Jemec GB, et al. Efficacy and safety of oral alitretinoin (9-cis retinoic acid) in patients with severe chronic hand eczema refractory to topical corticosteroids: results of a randomized, double-blind, placebo-controlled, multicentre trial. *Br J Dermatol*. 2008;158:808–817.

51. Blair HA, Scott LJ. Alitretinoin: a review in severe chronic hand eczema. *Drugs*. 2016;76:1271–1279.
52. Zaenglein AL, Levy ML, Stefanko NS, et al. Consensus recommendations for the use of retinoids in ichthyosis and other disorders of cornification in children and adolescents. *Pediatr Dermatol*. 2021;38:164–180.
53. Kromer C, Sabat R, Celis D, Mossner R. Systemic therapies of pityriasis rubra pilaris: a systematic review. *J Dtsch Dermatol Ges*. 2019;17:243–259.
54. Sbidian E, Vicaut E, Chidiack H, et al. A randomized-controlled trial of oral low-dose isotretinoin for difficult-to-treat papulopustular rosacea. *J Invest Dermatol*. 2016;136:1124–1129.
55. George R, Weightman W, Russ GR, et al. Acitretin for chemoprevention of non-melanoma skin cancers in renal transplant recipients. *Australas J Dermatol*. 2002;43:269–273.
56. Nutan F, Ortega-Loayza AG. Cutaneous lupus: a brief review of old and new medical therapeutic options. *J Investig Dermatol Symp Proc*. 2017;18:S64–S68.
57. Ruzicka T, Sommerburg C, Goerz G, et al. Treatment of cutaneous lupus erythematosus with acitretin and hydroxychloroquine. *Br J Dermatol*. 1992;127:513–518.
58. Jick H. Retinoids and teratogenicity. *J Am Acad Dermatol*. 1998;39:S118–S122.
59. Nohynek GJ, Meuling WJ, Vaes WH, et al. Repeated topical treatment, in contrast to single oral doses, with Vitamin A-containing preparations does not affect plasma concentrations of retinol, retinyl esters or retinoic acids in female subjects of child-bearing age. *Toxicol Lett*. 2006;163:65–76.
60. Panchaud A, Csajka C, Merlob P, et al. Pregnancy outcome following exposure to topical retinoids: a multicenter prospective study. *J Clin Pharmacol*. 2012;52:1844–1851.
61. Lammer EJ, Chen DT, Hoar RM, et al. Retinoic acid embryopathy. *N Engl J Med*. 1985;313:837–841.
62. Lam C, Zaenglein AL. Contraceptive use in acne. *Clin Dermatol*. 2014;32:502–515.
63. Werner CA, Papic MJ, Ferris LK, et al. Women's experiences with isotretinoin risk reduction counseling. *JAMA Dermatol*. 2014;150:366–371.
64. Spring LK, Krakowski AC, Alam M, et al. Isotretinoin and timing of procedural interventions: a systematic review with consensus recommendations. *JAMA Dermatol*. 2017;153:802–809.
65. Stoll D, Binnert C, Mooser V, Tappy L. Short-term administration of isotretinoin elevates plasma triglyceride concentrations without affecting insulin sensitivity in healthy humans. *Metabolism*. 2004;53:4–10.
66. Hansen TJ, Lucking S, Miller JJ, et al. Standardized laboratory monitoring with use of isotretinoin in acne. *JAm Acad Dermatol*. 2016;75:323–328.
67. Talpur R, Ward S, Apisarnthanarax N, et al. Optimizing bexarotene therapy for cutaneous T-cell lymphoma. *J Am Acad Dermatol*. 2002;47:672–684.
68. Roenigk Jr HH, Callen JP, Guzzo CA, et al. Effects of acitretin on the liver. *J Am Acad Dermatol*. 1999;41:584–588.
69. Safran AB, Haliaoua B, Roth A, Saurat JH. Ocular side-effects of oral treatment with retinoids. In: JH S, ed. *Retinoids: 10 Years On*. Basel: Karger; 1991:315–326.
70. Carey BM, Parkin GJ, Cunliffe WJ, Pritlove J. Skeletal toxicity with isotretinoin therapy: a clinico-radiological evaluation. *Br J Dermatol*. 1988;119:609–614.
71. DiGiovanna JJ, Langman CB, Tschen EH, et al. Effect of a single course of isotretinoin therapy on bone mineral density in adolescent patients with severe, recalcitrant, nodular acne. *J Am Acad Dermatol*. 2004;51:709–717.
72. Hoover KB, Miller CG, Galante NC, Langman CB. A double-blind, randomized, Phase III, multicenter study in 358 pediatric subjects receiving isotretinoin therapy demonstrates no effect on pediatric bone mineral density. *Osteoporos Int*. 2015;26:2441–2447.
73. Sarkar S, Das K, Roychoudhury S, Shrimal A. Pseudotumor cerebri in a child treated with acitretin: a rare occurrence. *Indian J Pharmacol*. 2013;45:89–90.
74. Lee AG. Pseudotumor cerebri after treatment with tetracycline and isotretinoin for acne. *Cutis*. 1995;55:165–168.
75. Bigby M. Does isotretinoin increase the risk of depression? *Arch Dermatol*. 2008;144:1197–1199, discussion 234–5.
76. Huang YC, Cheng YC. Isotretinoin treatment for acne and risk of depression: a systematic review and meta-analysis. *J Am Acad Dermatol*. 2017;76:1068–1076.e9.
77. Marqueling AL, Zane LT. Depression and suicidal behavior in acne patients treated with isotretinoin: a systematic review. *Semin Cutan Med Surg*. 2007;26:210–220.
78. Sherman SI, Gopal J, Haugen BR, et al. Central hypothyroidism associated with retinoid X receptor-selective ligands. *N Eng J Med*. 1999;340:1075–1079.
79. Lee SY, Jamal MM, Nguyen ET, et al. Does exposure to isotretinoin increase the risk for the development of inflammatory bowel disease? A meta-analysis. *Eur J Gastroenterol Hepatol*. 2016;28:210–216.
80. Racine A, Cuerq A, Bijon A, et al. Isotretinoin and risk of inflammatory bowel disease: a French nationwide study. *Am J Gastroenterol*. 2014;109:563–569.



eFig. 126.1 Binding properties of natural and synthetic retinoids on nuclear retinoid receptors.



eFig. 126.2 Mean physiologic concentrations of natural retinoids in the skin and blood. Vitamin A (retinol) is found in the skin mainly esterified to fatty acids, whereas unesterified retinol is the major circulating form.



eFig. 126.3 Osteophytes and bony ridges without narrowing of the disk spaces in an acne patient treated with a prolonged (several-year) course of isotretinoin.



eFig. 126.4 Severe acne vulgaris. Before (**A**) and after (**B**) treatment with oral isotretinoin.

127 Antimicrobial Drugs

Ashley N. Millard-Garcia, Alexandra Cameli Carley, Erik J. Stratman, Jack L. Lesher Jr and R. Carol McConnell

Key features

- Bacterial, fungal, and viral infections of the skin and soft tissue are very common
- Selection of the appropriate treatment depends on the infecting microorganism, the site and extent of the infection, and patient characteristics (e.g. age, pregnancy/lactation, comorbid medical conditions)
- Physicians must be aware of the drug interactions and potential adverse effects of antimicrobial medications

ANTIBACTERIAL AGENTS

INTRODUCTION

With hundreds of antibiotics now available, physicians have abundant therapeutic options, which can potentially be confusing and overwhelming. Selection of the most appropriate antibiotic depends upon identification of the infecting microorganism and its sensitivity to antimicrobial agents. When possible and practical, a culture should be obtained prior to starting therapy.

In acutely ill patients, empiric therapy with broad-spectrum antibiotics may initially be necessary. Knowledge of local bacterial resistance patterns should guide antibiotic selection. Once the microbe is identified, preferably along with antibiotic sensitivities, medications can be adjusted accordingly. Indiscriminate use of broad-spectrum antibiotics leads to development of resistant bacteria. The site and extent of the infection; the side effect profiles and costs of possible medication choices; and patient characteristics, including age and medical comorbidities (e.g. impaired renal or hepatic function) as well as pregnancy and lactation status, also influence drug selection.

Antibacterial drugs are characterized as either bacteriostatic or bactericidal (Table 127.1). Bacteriostatic drugs inhibit growth and replication of bacteria and limit spread of infection, allowing the immune system to eliminate the pathogen. Bactericidal agents kill bacteria directly.

BACTERIOSTATIC VERSUS BACTERICIDAL DRUGS

Bacteriostatic	Bactericidal
Chloramphenicol	Aminoglycosides
Clindamycin	Bacitracin
Erythromycin	Carbapenems
Oxazolidinones	Monobactams
Sulfonamides	Nitroimidazoles
Tetracyclines	Penicillins
Trimethoprim	Polymyxin B
	Quinolones
	Vancomycin
	Lipoglycopeptides

Table 127.1 Bacteriostatic versus bactericidal drugs. Clindamycin may be either bacteriostatic or bactericidal depending on the susceptibility of the infecting organism and the concentration achieved at the site of infection. Factors such as the infecting organism and growth conditions can also affect whether other drugs are bacteriostatic or bactericidal.

TOPICAL ANTIBACTERIAL AGENTS

Introduction

Topical antibacterials are used to treat acne vulgaris, rosacea, and superficial bacterial infections and to prevent infection after surgery or injuries. Topical antibacterials are applied directly to the affected skin and thus deliver a high concentration of the medication locally with little chance of adverse systemic effects. However, their utility is limited to localized superficial conditions.

Topical Antibacterial Agents Used to Treat Acne Vulgaris and Rosacea

Table 127.2 lists topical antibiotics commonly used to treat inflammatory acne vulgaris and rosacea, with contributions from their anti-inflammatory as well as antibacterial effects.

Mechanisms of action

Azelaic acid is a dicarboxylic acid derivative with activity against *Cutibacterium acnes* (formerly *Propionibacterium acnes*) and *Staphylococcus epidermidis*. It is usually bacteriostatic but can be bactericidal in high concentrations. Its activity may be due to inhibition of microbial cellular protein synthesis. Azelaic acid also has anticomedonal effects by normalizing keratinization. It thins the stratum corneum, decreases the number and size of keratohyalin granules, and reduces the amount and distribution of filaggrin in the epidermis. Azelaic acid has antiproliferative effects against hyperactive and abnormal melanocytes, but it rarely causes hypo- or depigmentation of normally pigmented skin (see Table 127.2).

Benzoyl peroxide is bacteriostatic against *C. acnes*. Once absorbed by the skin, it is converted to benzoic acid. Its effects are believed to be due to oxidation of bacterial proteins by reactive oxygen species, which are released when the drug is decomposed by cysteine in the skin. Daily use of 10% benzoyl peroxide for 2 weeks decreases free fatty acids by 50% and *C. acnes* by 98%, which is comparable to results obtained after use of topical antibiotics for 4 weeks[1]. Benzoyl peroxide also has keratolytic and desquamative effects.

Clindamycin is a semisynthetic lincosamide antibiotic that inhibits protein synthesis by binding to the bacterial 50 S ribosomal subunit. It is active against Gram-positive cocci and anaerobes including staphylococci, streptococci, *C. acnes*, *Corynebacterium* spp., *Clostridium* spp., and *Gardnerella vaginalis*. Clindamycin may be either bacteriostatic or bactericidal, depending on the susceptibility of the infecting organism and the concentration achieved at the site of infection.

Erythromycin is a macrolide antibiotic that also inhibits protein synthesis by binding to the bacterial 50 S ribosomal subunit. It is active against Gram-positive cocci including group A β-hemolytic streptococci and *Staphylococcus aureus*, as well as some Gram-negative bacilli. Erythromycin has additional anti-inflammatory properties (see Macrolides below).

Tetracycline (topical formulation not available in the US; used to treat acne and superficial skin infections) and *minocycline* are tetracycline-class antibiotics that inhibit the bacterial 30 S ribosomal subunit and have anti-inflammatory as well as bacteriostatic effects (see Tetracyclines below). Minocycline's lipophilicity allows it to achieve high concentrations in the sebaceous follicle, and *C. acnes* has a low propensity for developing minocycline resistance[2].

Sodium sulfacetamide is a sulfonamide whose bacteriostatic effects involve disruption of folic acid synthesis (see Fig. 127.6). It is active against several Gram-positive and Gram-negative organisms. Some topical preparations combine sodium sulfacetamide with sulfur, which acts as a keratolytic as well as antimicrobial agent (see Ch. 129).

Metronidazole is a nitroimidazole with antioxidant and anti-inflammatory as well as antimicrobial effects against anaerobic bacteria. DNA strand breaking is its presumed mechanism of action.

TOPICAL ANTIBACTERIALS USED FOR ACNE VULGARIS AND ROSACEA					
Generic name	**Selected trade name(s)®**	**Formulations**	**Dosing frequency**	**Considered safe to use during pregnancy***	**Side effects**
Azelaic acid	Azelex, Cutacelan, Finacea, Finevin, Skinoderm, Skinoren	20% cream, 15% gel	BID		Pruritus, burning/stinging, dryness, peeling; rarely hypo-/depigmentation, hypertrichosis, allergic contact dermatitis, keratosis pilaris, exacerbation of recurrent herpes labialis
Benzoyl peroxide	Acne-Aid, Benoxyl, Benzac, Benzagel, BenzaShave, BenzEFoam, Brevoxyl, Clearasil, Dermoxyl, Desquam-X, Oxy, NeoBenz, PanOxyl, Persa-Gel, Triaz, Zapzyt	2.5%–10% lotion, cream, gel, foam, solution, stick, cleansing bar, cleansing lotion, cloths, pads, mask, shaving cream	Daily–TID; mask qwk	√*	Irritation, allergic contact dermatitis; occasionally blistering, crusting, severe erythema & edema; bleaches hair and colored fabrics
Clindamycin	Basocin, Cleocin T, Clinac, Clinda-Derm, Clindagel, Clindets, Cutaclin, Dalacin, Dalagis, Eurocin-A, Evoclin	1% gel, lotion, solution, foam, pledgets; 2% vaginal cream	BID	√	Gram-negative folliculitis, bacterial resistance; possible rare pseudomembranous colitis (risk from topical use is likely not clinically significant[56])
Erythromycin	Akne-Mycin, A/T/S, Emgel, Erycette, Eryderm, Erygel, Erymax, Ery-Sol, Erythra-Derm, ETS, Ilotycin, Sans-Acne, Staticin, Theramycin Z, T-Stat, Zineryt	1.5% or 2% solution; 2% pledgets, gel, ointment	BID	√	Eye irritation, skin tenderness, Gram-negative folliculitis, bacterial resistance; rarely generalized urticarial reactions
Minocycline	Amzeeq, Zilexi	1.5% or 4% foam	Daily		Erythema, dryness, pruritus, water-soluble yellow discoloration
Sodium sulfacetamide	Klaron, Mexar, Ovace, Seb-Prev, Sebizon *With 5% sulfur:* Avar Cleanser, Clarifoam, Clenia, Novacet, Plexion, Prascion, Rosac, Rosaderm, Rosanil, Rosula, Sulfacet-R, Sulfatol, SulZee, Sumaxin, Suphera, Topisulf, Zetacet	10% lotion, cream, suspension, foam, wash/cleanser, cleansing cloths	BID		Dryness, pruritus; may cross-react in patients allergic to related oral medications
Metronidazole	MetroGel, MetroCream, MetroLotion, Noritate	0.75% or 1% gel, cream, lotion	Daily–BID	√	Watery eyes, metallic taste in the mouth, nausea, numbness and paresthesias have been reported with topical use[19]; may cross-react in patients allergic to the oral form
Dapsone	Aczone	5% gel 7.5% gel	BID Daily		Dryness, peeling, erythema; in patients with G6PD deficiency, occasional drop in hemoglobin level and rarely methemoglobinemia; concurrent use with benzoyl peroxide may cause temporary local yellow–orange skin discoloration
Benzoyl peroxide/ erythromycin	Benzamycin	5%/3% gel	BID	√*	See above
Benzoyl peroxide/ clindamycin	Acanya, Benzaclin, Duac, Neuac, Z-Clinz	2.5%–10%/1% gel	BID	√*	See above
Benzoyl peroxide/ adapalene	Epiduo, Epiduo Forte	2.5/0.1%–0.3% gel	Daily		See above
Clindamycin phosphate/tretinoin	Veltin, Ziana	1.2/0.025% gel	Daily		See above

*Formerly FDA pregnancy category B, with the exception of products containing benzoyl peroxide, which were category C but have only ~2% systemic absorption.

Table 127.2 Topical antibacterials used for acne vulgaris and rosacea. Erythromycin has also been combined with zinc acetate (e.g. Zyneret® lotion or solution; not available in the US), as has benzoyl peroxide with zinc lactate (e.g. Triaz® products); zinc has possible antiandrogenic activity and may suppress sebum production. BID, twice daily; qwk, weekly; TID, three times daily.

Dapsone is a sulfone drug whose antimicrobial effects include inhibition of dihydropteroate synthase and prevention of bacterial folic acid synthesis. It also has anti-inflammatory effects that target neutrophils, inhibiting their chemotaxis and decreasing myeloperoxidase activity.

Indications

Azelaic acid, benzoyl peroxide, clindamycin, erythromycin, minocycline, sodium sulfacetamide, and dapsone are used topically for mild to moderate inflammatory acne vulgaris and rosacea. Studies have shown

that combining erythromycin or clindamycin with benzoyl peroxide is more effective for the treatment of acne than either of the former agents alone; clindamycin plus benzoyl peroxide is also more effective than benzoyl peroxide alone[3]. These synergistic combinations may slow the development of antibiotic resistance, which is a significant issue with erythromycin, clindamycin, and tetracycline.

Azelaic acid may also be useful for melasma and other forms of hyperpigmentation. Topical clindamycin and erythromycin can treat superficial bacterial infections of the skin, whereas topical clindamycin and metronidazole are both indicated for bacterial vaginosis.

Dosages

Topical antibacterial agents are usually used once or twice a day (see Table 127.2). A small amount of medication is applied in a thin layer onto clean, dry skin. Benzoyl peroxide cleansing bars and washes are used one to three times a day. Benzoyl peroxide shave cream is used like other shaving creams, and the mask is applied in a thin layer once a week, left on for 15 to 25 minutes, and then rinsed off.

Contraindications

The chief contraindication for these medications is a history of hypersensitivity to any component of the formulation. Azelaic acid, sodium sulfacetamide, erythromycin, and clindamycin preparations may contain propylene glycol, which can be a sensitizer. Topical clindamycin should be used with caution in patients with a history of inflammatory bowel disease or antibiotic-associated colitis.

Major side effects

Adverse reactions to topical antibacterial agents used to treat acne vulgaris and rosacea are usually mild and transient. Stinging is especially common with alcohol-containing solutions and pledgets. Table 127.2 lists side effects of individual drugs.

Interactions

Simultaneous application of more than one topical medication can increase or decrease the effect of one or both of the medications. Benzoyl peroxide may increase irritant effects of other topical acne medications, and it can decrease the activity of tretinoin when applied together. A temporary yellow–orange staining of the skin and hair occasionally occurs with concomitant use of topical dapsone and benzoyl peroxide.

Pregnancy and lactation

Formal studies on the use of most topical antibacterial agents during pregnancy and breastfeeding are lacking, but significant exposure to the fetus or nursing infant is not expected. In general, topical antibiotics are considered safe during pregnancy and lactation[4].

Topical Antibacterial Agents Used to Treat Superficial Infections

Table 127.3 lists antibacterial agents commonly used to prevent and treat superficial skin infections.

Mechanisms of action

The mechanisms of action of the topical antibacterial agents used to treat superficial infections are listed in Table 127.3.

Mupirocin (pseudomonic acid A) is derived from *Pseudomonas fluorescens*. It is clinically active against staphylococci; groups A, B, C, and G streptococci; and some Gram-negative aerobic bacteria. It is usually bacteriostatic but may be bactericidal at high concentrations.

Retapamulin is in the pleuromutilin class, derived from fermentation of a mushroom, *Clitopilus passeckerianus*. It has activity against *Streptococcus pyogenes* and *S. aureus*[5].

Ozenoxacin is a quinolone antibiotic active against Gram-positive organisms including *S. aureus* and *Str. pyogenes*[5].

Neomycin and *gentamicin* are aminoglycoside antibiotics. Neomycin is bactericidal against Gram-positive and Gram-negative bacteria including *S. aureus, Escherichia coli, Haemophilus influenzae, Proteus* spp., and *Serratia* spp. It is generally not effective against *Pseudomonas aeruginosa*. Gentamicin is effective against sensitive strains of group A β-hemolytic and α-hemolytic streptococci, *S. aureus* (coagulase-positive, coagulase-negative, and some penicillinase-producing strains), and Gram-negative bacteria including *P. aeruginosa, Aerobacter aerogenes, E. coli, Proteus vulgaris*, and *Klebsiella pneumoniae*.

Bacitracin is a cyclic polypeptide antibiotic that has a thiazolidine ring and peptide side chains. Bacitracin is active against Gram-positive organisms such as staphylococci, streptococci, corynebacteria, and clostridia.

Polymyxin B is a cyclic lipopeptide antibiotic that is rapidly bactericidal for various Gram-negative organisms, including *P. aeruginosa, E. coli, K. pneumoniae, Enterobacter aerogenes, H. influenzae, Proteus mirabilis*, and *Serratia marcescens*. It is not active against Gram-positive organisms.

TOPICAL ANTIBACTERIAL AGENTS USED FOR SUPERFICIAL SKIN INFECTIONS

Generic name	Trade name(s)®	Formulations (OTC/Rx)	Dosing frequency	Considered safe to use during pregnancy*	Class – mechanism of action
Mupirocin	Bactoderm, Bactroban, Centany, Eismycin	2% ointment or cream (Rx)	TID	√ (topical antibiotic of choice during pregnancy)	Monoxycarbolic acid – inhibits protein synthesis by reversibly binding to bacterial isoleucyl transfer RNA synthetase
Retapamulin	Altabax	1% ointment (Rx)	BID	√	Pleuromutilin – inhibits protein synthesis by interacting with the L3 protein on the bacterial 50S ribosomal subunit
Ozenoxacin	Xepi	1% cream (Rx)	BID		Quinolone – disrupts bacterial replication through inhibition of DNA gyrase and topoisomerase IV
Neomycin	Myciguent	0.5% ointment or cream (OTC)	Daily–TID		Aminoglycoside – inhibits protein synthesis by binding to the bacterial 30S ribosomal subunit; may also inhibit bacterial DNA polymerase
Gentamicin	Garamycin, Gentamar, G-Myticin	0.1% ointment or cream (Rx)	TID–4 times daily		
Bacitracin	Baciguent	400–500 units per gram ointment (OTC)	TID		Cyclic polypeptide – inhibits bacterial cell wall synthesis by forming a complex with C55-phenol pyrophosphate in the bacterial cell wall
Polymyxin B	Polysporin ointment = bacitracin + polymyxin B Neosporin ointment = bacitracin, polymyxin B + neomycin Neosporin cream = polymyxin B + neomycin only	5000–10 000 units per gram ointment (OTC)	Daily–TID		Cyclic lipopeptide – interacts with the phospholipids of bacterial cell membranes, increasing their cellular permeability

*Formerly FDA pregnancy category B.

Table 127.3 Topical antibacterial agents used for superficial skin infections. BID, twice daily; OTC, over-the-counter; Rx, prescription; TID, three times daily.

Indications

Mupirocin, retapamulin, ozenoxacin, gentamicin, neomycin, bacitracin, and combination products containing polymyxin B are utilized for the treatment and prevention of superficial bacterial skin infections. The intranasal preparation made with the calcium salt of mupirocin is indicated for the eradication of nasopharyngeal carriage of *S. aureus*. Studies implicating nasal staphylococci as a potential source for wound infections and bacteremia suggest that intranasal application of mupirocin may decrease the incidence of infections in susceptible individuals (e.g. those with recurrent staphylococcal infections)[6]. Decolonization of known *S. aureus* carriers with the use of mupirocin nasal ointment and chlorhexidine body wash for five days prior to Mohs micrographic surgery may reduce the risk of surgical site infection and be more effective than oral antibiotic prophylaxis on the day of surgery[7].

Mupirocin has been shown to be as effective as systemic antibiotics for localized impetigo due to *Str. pyogenes* or *S. aureus* in patients ≥2 months of age[8]. Retapamulin and ozenoxacin are also indicated for the topical treatment of impetigo due to *Str. pyogenes* or *S. aureus* in patients ≥9 and ≥2 months of age, respectively. Although retapamulin is FDA-approved for infections with methicillin-sensitive *S. aureus* (MSSA) only, rates of retapamulin resistance in methicillin-resistant *S. aureus* (MRSA) isolates are low[5].

Dosages

Table 127.3 outlines the formulations and dosing for the antibacterial agents used for the treatment of superficial skin infections. Intranasal mupirocin is applied into the nares two to four times a day for 5 to 14 days.

Contraindications

As with all topical medications, the main contraindication is a history of hypersensitivity to any component of the formulation.

Major side effects

Potential side effects of *mupirocin* include burning, stinging, pain, and pruritus, as well as erythema, edema, increased exudate, allergic contact dermatitis, headache, and nausea. Use of nasal mupirocin is occasionally associated with headaches, rhinitis, respiratory tract congestion, pharyngitis, dysgeusia, burning, stinging, and cough. Use of mupirocin on extensive areas of skin with decreased barrier function has been reported to cause renal toxicity from systemic absorption of polyethylene glycol. *Retapamulin* can cause application site irritation and pruritus.

Side effects of *neomycin* include allergic contact dermatitis in 5% to 15% of patients[9], in particular when neomycin is applied to cutaneous ulcerations and/or areas of chronic stasis dermatitis. The most common symptoms are pruritus, erythema, and edema. In the setting of impaired renal function, there is an increased risk of side effects related to systemic absorption; caution should also be exercised if the medication is used over extensive areas. Irreversible ototoxicity and renal failure have been reported with the use of topical neomycin on open wounds[10]. Neomycin may also cause mast cell degranulation and histamine release[1].

Possible side effects of *gentamicin* include erythema, pruritus, edema, and photosensitization. There is a risk of producing gentamicin-resistant strains of *Pseudomonas* when this agent is applied to heavily colonized skin (e.g. leg ulcers).

Adverse effects of *bacitracin* include irritant and allergic contact dermatitis. Chronic stasis dermatitis predisposes to the latter. Anaphylaxis has been reported in patients with a history of multiple previous exposures when bacitracin was applied to open wounds.

There are few side effects from *polymyxin B*. Contact sensitization has been reported. Of note, some cross-reactivity exists between bacitracin and polymyxin B because they are both derived from *Bacillus* species.

Interactions

There are no known significant drug interactions with the topical antibiotics used for superficial skin infections.

Pregnancy and lactation

In general, topical antibiotics are considered safe during pregnancy and lactation[4]. Neither topical nor nasal mupirocin has been specifically studied in pregnant women. However, mupirocin has not been shown to cause birth defects or other problems in animal studies and there is very little systemic absorption of topically applied mupirocin, making it the topical antibiotic of choice during pregnancy[11].



Fig. 127.1 Localized argyria. Gray discoloration due to application of silver sulfadiazine cream.

Other Topical Antibacterial Agents

Fusidic acid is a fusidane antibiotic isolated from the fungus *Fusidium coccineum*. It is not approved in the US but is used in Europe and Canada for mild to moderately severe cutaneous infections, external eye infections, and eradication of nasopharyngeal carriage of *S. aureus*. It is available as a 2% cream, ointment, or impregnated gauze applied three times daily. It has a steroid-like structure but no steroid effects[12]. Fusidic acid inhibits bacterial protein synthesis by interfering with elongation factor G. It is active against Gram-positive bacteria, especially *S. aureus*. This medication has a bacteriologic efficacy comparable to that of mupirocin or retapamulin for impetigo and may be more cost-effective[12,13]. When combined with topical corticosteroids, it is useful in treating atopic dermatitis with superimposed staphylococcal infection[12]; it is also effective for erythrasma[14]. Fusidic acid has few adverse effects, although allergic contact dermatitis has been reported.

Iodoquinol is a halogenated oxyquinoline with antibacterial and antifungal activity. Its mechanism of action is unknown. Commercially available combination products containing 1% iodoquinol plus 1%–2% hydrocortisone are applied three to four times a day for superficial bacterial and fungal skin infections. Topical iodoquinol (1%) preparations have a high iodine content, and data on their safety during pregnancy is lacking. A related medication, topical clioquinol (iodochlorhydroxyquin), is used primarily for the treatment of superficial fungal infections (see below).

Mafenide acetate cream, a sulfonamide, is applied once or twice daily for thermal burns. It has antibacterial and antifungal activity. The most common side effect is burning; urticaria or facial edema can also occur. Rarely, mafenide acetate may cause bone marrow suppression or lead to hemolytic anemia in patients with G6PD deficiency. It should be used with caution in patients with renal or pulmonary disease due to its potential to cause metabolic acidosis. Furthermore, mafenide acetate may cause intense pain upon application and can be associated with *Candida* superinfection.

Silver sulfadiazine is a 1% cream applied once to twice daily for thermal burns. It interacts with bacterial cell walls and membranes, resulting in broad antimicrobial effects. Silver sulfadiazine may interfere with the activity of topical proteolytic enzymes. It is contraindicated in patients with a history of sulfonamide hypersensitivity and should be used with caution in patients with G6PD deficiency (due to risk of hemolysis), renal or hepatic impairment, and porphyria. Localized argyria due to deposits of silver in the dermis can also occur (Fig. 127.1).

SYSTEMIC ANTIBACTERIAL AGENTS

Systemic antibacterial agents have the potential to cause a wide range of adverse effects and to have significant interactions with other systemic medications. For example, rifampin may reduce the efficacy

SITES OF ACTION OF DIFFERENT CLASSES OF SYSTEMIC ANTIBACTERIAL DRUGS	
Site of action	**Drug class(es)**
Cell wall	Penicillins Cephalosporins Carbapenems Monobactams Vancomycin Lipoglycopeptides β-lactamase inhibitors
Cell membrane	Daptomycin Oritavancin, telavancin
Inhibit nucleic acid synthesis	Sulfonamides Trimethoprim
DNA gyrase	Quinolones
DNA strand breakage	Nitroimidazoles (e.g. metronidazole)
Ribosomal subunit	Aminoglycosides – 30S Tetracyclines – 30S Glycylcycline (tigecycline) – 30S Chloramphenicol – 50S Clindamycin – 50S Macrolides – 50S Oxazolidinones – 50S Streptogramins (quinupristin/dalfopristin) – 50S

Table 127.4 Sites of action of different classes of systemic antibacterial drugs.

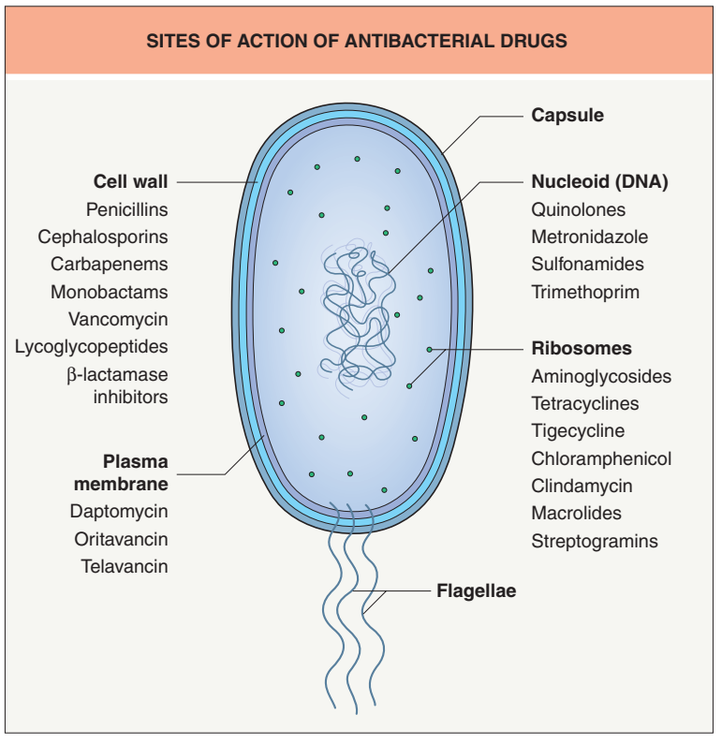


Fig. 127.2 Sites of action of antibacterial drugs. This figure illustrates a prototypical bacterial cell. Each class of antibacterial drug exerts its effect on a particular component of the cell.

of oral contraceptives. Bacteriostatic antibacterial agents can decrease the efficacy of bactericidal antibacterial agents, because the latter target actively dividing cells. In addition, use of systemic antibacterial agents can lead to the development of bacterial resistance. The mechanisms of action of the major classes of antibacterial drugs are listed in Table 127.4 and illustrated in Fig. 127.2. Systemic antibiotics may be used perioperatively by dermatologic surgeons to prevent surgical site infections in high-risk situations such as procedures involving the lower extremity or groin, wedge excisions on the lip or ear, skin flaps on the nose, and skin grafts. Antibiotic prophylaxis is also recommended in patients at high risk for infective endocarditis or hematogenous infection of a total joint replacement who have surgery involving the oral mucosa or infected skin (see Ch. 151)[15].

Penicillins

Mechanism of action

Penicillins are β-lactam antibiotics that exert bactericidal effects by binding and inactivating penicillin-binding proteins in bacterial cell walls. They inhibit bacterial cell wall synthesis by blocking transpeptidase cross-linking of peptidoglycan chains (Fig. 127.3).

The natural penicillins (penicillin G and penicillin V) are active against Gram-positive and Gram-negative cocci, most Gram-positive bacilli, and spirochetes. Penicillinase-resistant penicillins (methicillin, nafcillin, and dicloxacillin), referred to as anti-staphylococcal penicillins, have greater efficacy against *S. aureus*. Aminopenicillins (ampicillin, amoxicillin) have an extended spectrum to include *H. influenzae*, *E. coli*, *Salmonella* and *Shigella* spp., and some other Gram-negative bacteria, but not *Pseudomonas* spp. Antipseudomonal penicillins (e.g. piperacillin, azlocillin) cover *P. aeruginosa* and depending upon the particular drug, *B. fragilis* and *Klebsiella* spp. However, in general, this group of penicillins has been replaced by cefepime and when anaerobe coverage is desired, the carbapenem meropenem. Addition of the β-lactamase inhibitors clavulanic acid, sulbactam, tazobactam, avibactam, and durlobactam extends the spectrum of penicillins to include staphylococci and other β-lactamase-producing bacteria (Fig. 127.4).

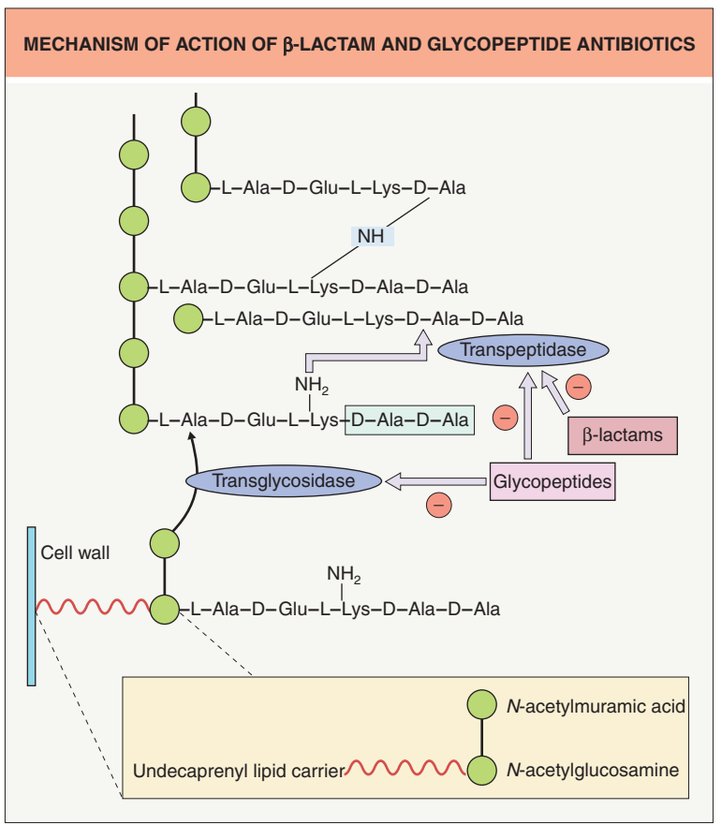


Fig. 127.3 Mechanism of action of β-lactam and glycopeptide antibiotics. Simplified schematic of mechanisms of action of β-lactam antibiotics (penicillins, cephalosporins) and glycopeptides (e.g. vancomycin, dalbavancin) in interfering with enzymatic steps in bacterial cell wall (peptidoglycan) synthesis.

Indications

Penicillins are used for syphilis and streptococcal skin infections, such as erysipelas, as well as other cutaneous infections such as erysipeloid. Amoxicillin with clavulanic acid is the drug of choice for cat, dog, and human bites. It is useful also for acute paronychia. The penicillinase-resistant penicillins, e.g. dicloxacillin, are used for suspected MSSA skin infections such as impetigo, folliculitis, and non-purulent cellulitis; however, sensitivity testing should be obtained when MRSA is a clinical concern (see Ch. 74). Amoxicillin may be used for Lyme disease when doxycycline is contraindicated.

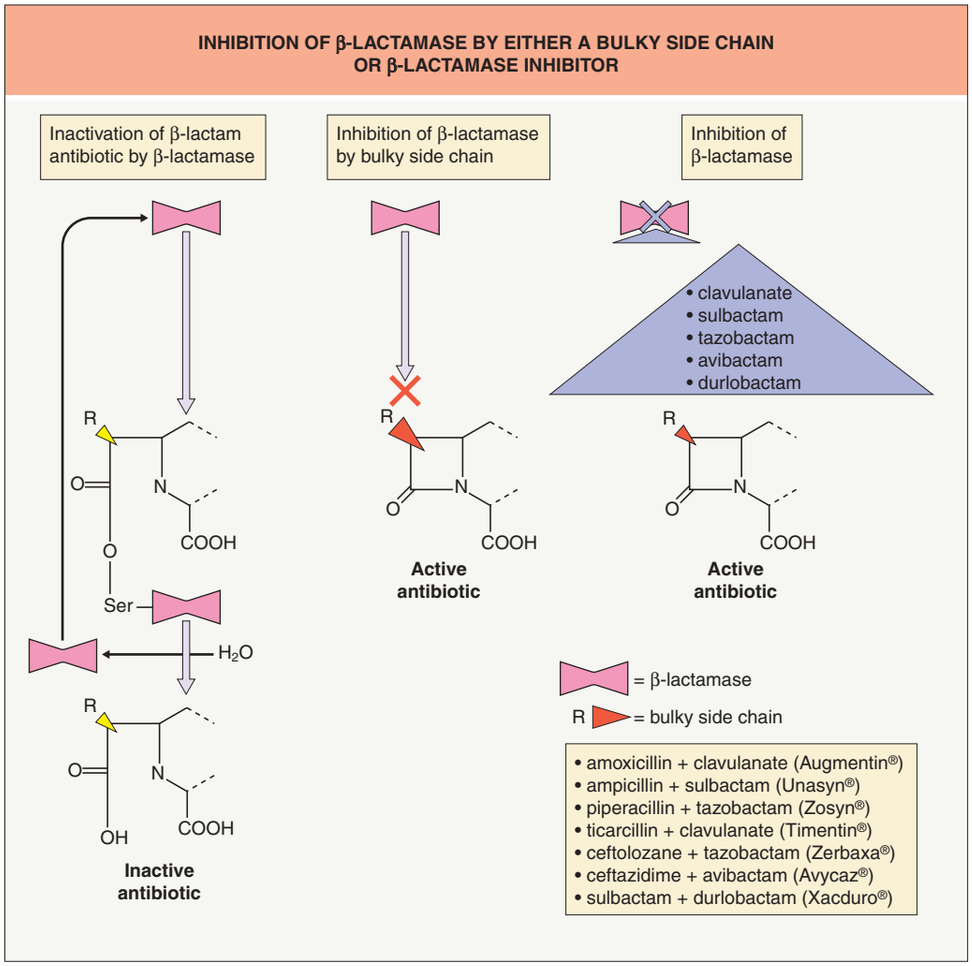


Fig. 127.4 Inhibition of β-lactamase by either a bulky side chain or β-lactamase inhibitor. Placement of a bulky side chain on the penicillin molecule (e.g. methicillin, nafcillin, dicloxacillin) can inhibit bacterial β-lactamase, as can the combination of a penicillin with a β-lactamase inhibitor (e.g. clavulanic acid, sulbactam, tazobactam). The latter group of drugs has no inherent antibacterial activity. Inhibition of β-lactamase allows the antibiotic to remain active and inhibit bacterial transpeptidase.

Dosages

The pediatric and adult dosages of commonly used penicillins are listed in Table 127.5. Amoxicillin and amoxicillin with clavulanic acid should be taken with food. Other penicillins should be taken on an empty stomach.

Contraindications

Penicillins are contraindicated in patients with known immediate-type (IgE-mediated) hypersensitivity to any penicillin, such as a history of penicillin-associated urticaria, angioedema, or anaphylaxis. However, only 10%–20% of patients who report a history of allergy to penicillins have an allergy identified upon skin testing[16]. Among patients allergic to penicillin, ~2%–15% are allergic to cephalosporins and <1% to carbapenems through cross-reactivity[17].

Skin testing for penicillin allergy utilizes: (1) the major allergen benzylpenicilloyl polylysine; (2) the minor allergens benzylpenicillin G, benzylpenicilloate, and penicilloyl propylamine; and (3) negative (saline) and positive (histamine) controls. Either epicutaneous (prick) or intradermal testing may be performed, usually by an allergist. Antihistamines should be avoided prior to testing. Patients who have had a life-threatening reaction to penicillin should be tested with 100-fold dilutions of the allergens before being tested with full-strength allergens in a monitored setting where treatment for anaphylaxis is available.

Patients who report a history of penicillin allergy but are skin-test-negative to all major and minor allergenic determinants can use penicillin in a monitored setting. Skin-test-positive patients may be desensitized orally or intravenously in a hospital setting over ~4 hours. Rarely, serious IgE-mediated allergic reactions can occur. Blood tests can also be used to detect specific IgE directed against penicillin, but this method is less sensitive and informative than skin tests.

Major side effects

Drugs in the penicillin group cause hypersensitivity reactions characterized by urticaria, flushing, and pruritus in 5%–15% of patients. In severe cases, anaphylaxis, shock, and even death may occur. In addition, penicillins can cause morbilliform and other exanthematous eruptions (Fig. 127.5A), which may be associated with fever and eosinophilia. Serum sickness-like reactions, Stevens–Johnson syndrome (SJS), toxic epidermal necrolysis (TEN), and pustular eruptions such as acute generalized exanthematous pustulosis (AGEP) develop less often. These drugs also occasionally lead to autoimmune phenomena, including hemolytic anemia or vasculitis. Of note, ampicillin and amoxicillin almost invariably cause a generalized morbilliform eruption in patients with infectious mononucleosis; this reaction is also more likely in patients with chronic lymphocytic leukemia and those taking concomitant allopurinol.

Penicillins can induce acute interstitial nephritis characterized by proteinuria, hematuria, renal casts, eosinophilia, eosinophiluria, fever, and declining renal function. Prolonged use of penicillins may lead to reversible neutropenia, anemia, agranulocytosis, and platelet dysfunction. Penicillins can cause diarrhea, pseudomembranous colitis, and hepatic dysfunction. Treatment with penicillins is associated with oral or vaginal overgrowth of *Candida* spp. in ~10% of patients.

ORAL DOSAGES OF COMMONLY USED PENICILLINS

Generic name	Pediatric oral dosage	Adult oral dosage
Penicillin V potassium	25–50 mg/kg/day divided q6–8 h	250–500 mg 4 times daily
Dicloxacillin	12.5–50 mg/kg/day divided q6 h	125–500 mg 4 times daily
Ampicillin	50–100 mg/kg/day divided q6 h	250–500 mg 4 times daily
Amoxicillin	25–50 mg/kg/day divided q8 h or q12 h	250–500 mg BID
Amoxicillin/clavulanate	20–40 mg/kg/day (of amoxicillin) divided q8 h or q12 h*	500–875 mg BID

*Do not double the dose of clavulanate if you double the amoxicillin dose, as this causes excessive clavulanate dosage and increased risk of gastrointestinal side effects like diarrhea.

Table 127.5 Oral dosages of commonly used penicillins. BID, twice daily; h, hours; q, every.

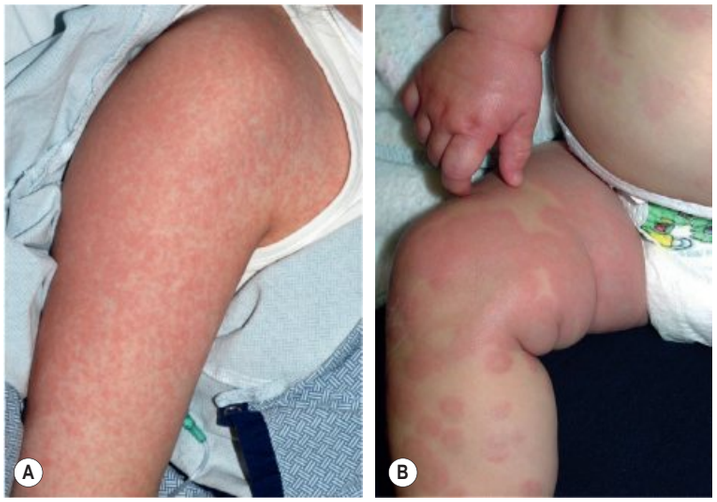


Fig. 127.5 Drug eruptions secondary to β-lactam antibiotics. A Morbilliform exanthem due to amoxicillin. **B** Serum sickness-like reaction presenting with coalescing annular erythematous plaques in an infant treated with cefaclor. Note the dusky centers of some lesions. *A, Courtesy Julie V. Schaffer, MD.*

Interactions

Because probenecid blocks the secretion of penicillins in the distal renal tubules, concomitant administration of these two drugs increases the serum levels and duration of action of the penicillins. When amoxicillin or ampicillin is used concomitantly with allopurinol, there is an increased risk of morbilliform drug eruption, and when tetracyclines are used together with penicillins, the bactericidal effect of penicillins is decreased.

Pregnancy and lactation

Penicillins are generally safe during pregnancy and in nursing mothers.

Cephalosporins

Mechanism of action

Like the penicillins, the cephalosporins are bactericidal β-lactam antibiotics that bind to penicillin-binding proteins and interfere with bacterial cell wall synthesis (Table 127.6). First-generation cephalosporins are very effective against Gram-positive organisms (staphylococci and streptococci) and less effective against Gram-negative organisms; however, they are active against *E. coli, Klebsiella*, and *Proteus* spp. Second-generation cephalosporins are equally effective against Gram-positive and Gram-negative bacteria. Their spectrum includes all of the organisms covered by first-generation cephalosporins plus *Enterobacter* spp., *Neisseria gonorrhea*, and *H. influenzae*. Third-generation cephalosporins are more effective against Gram-negative bacteria than Gram-positive bacteria. Fourth-generation cephalosporins have an extended spectrum against Gram-negative (including *Enterobacter* and *Klebsiella* spp.) and Gram-positive organisms, but have minimal resistance to β-lactamase. Fifth-generation cephalosporins (e.g. ceftaroline) have activity against *S. aureus* including MRSA, *Str. pyogenes*, *Str. agalactiae*, *Str. pneumoniae*, *H. influenzae*, *E. coli*, and *Klebsiella*. Cephamycins, β-lactam antibiotics very similar to cephalosporins, are resistant to β-lactamase and have a broad spectrum, including *E. coli, Klebsiella*, *Proteus*, *Serratia*, and *Bacteroides* spp.

Indications

Cephalosporins are useful in staphylococcal and streptococcal skin and soft tissue infections. A first-generation agent such as cephalexin or cefadroxil is the cephalosporin of choice in uncomplicated skin infections such as impetigo, staphylococcal folliculitis, erysipelas, cellulitis, and ecthyma. However, with the exception of fifth generation agents (e.g. ceftaroline), MRSA is resistant to cephalosporins.

Dosages

See Table 127.7 for dosages of the more commonly used cephalosporins.

DIFFERENT CLASSES OF CEPHALOSPORINS AND ROUTES OF ADMINISTRATION

Generic name	Trade name(s)®	Route(s) of administration
First generation		
Cefadroxil	Duracef, Ultracef	po
Cefazolin	Ancef, Kefzol, Zolicef	im, iv
Cephalexin	Keflex, Keftab, Biocef	po
Cephalothin*	Keflin, Seffin	im, iv
Cephapirin*	Cefadyl	im, iv
Cephradine*	Velosef, Anspor	po, im, iv
Second generation		
Cefaclor	Ceclor, Ceclor CD	po
Cefamandole*	Mandol	im, iv
Cefmetazole*	Zefazone	iv
Cefonicid*	Monocid	im, iv
Cefprozil	Cefzil	po
Cefuroxime sodium	Zinacef, Kefurox	im, iv
Cefuroxime axetil	Ceftin	po
Loracarbef (a carbacephem)*	Lorabid	po
Third generation		
Cefdinir	Omnicef	po
Cefditoren	Spectracef	po
Cefixime	Suprax	po
Cefoperazone*	Cefobid	im, iv
Cefotaxime	Claforan	im, iv
Cefpodoxime proxetil	Vantin	po
Ceftazidime	Ceptaz, Fortaz, Tazidime, Tazicef	im, iv
Ceftibuten	Cedax	po
Ceftizoxime	Cefizox	im, iv
Ceftriaxone	Rocephin	im, iv
Fourth generation		
Cefepime	Maxipime	im, iv
Fifth generation		
Ceftaroline	Teflaro	iv
Ceftolozane	Zerbaxa (with tazobactam)	iv
Ceftobiprole*	Zevtera, Mabelio	iv
Cephamycins†		
Cefoxitin	Mefoxin	im, iv
Cefotetan	Cefotan	im, iv
Siderophore cephalosporin‡		
Cefiderocol	Fetroja	iv

*Not currently available in the US.
†Sometimes grouped with second-generation cephalosporins.
‡Only active against aerobic Gram-negative bacilli.

Table 127.6 Different classes of cephalosporins and routes of administration. im, intramuscularly; iv, intravenously; po, orally.

Contraindications

Cephalosporins are contraindicated in patients with a history of an immediate-type (IgE-mediated) hypersensitivity to this class of drugs. Approximately 10%–15% of adults and 2% of children allergic to penicillins have cross-reactivity to cephalosporins[17].

DOSAGES OF COMMONLY PRESCRIBED CEPHALOSPORINS		
Generic name	**Pediatric dosage**	**Adult dosage**
Cephalexin	25–100 mg/kg/day divided q6 h or q12 h	250–500 mg 4 times daily
Cefadroxil	30 mg/kg/day divided q12 h	1–2 g daily
Cefaclor	40 mg/kg/day divided q8 h or q12 h	250–500 mg TID
Cefprozil	30 mg/kg/day divided q12 h	250–500 mg daily
Cefuroxime axetil	20–30 mg/kg/day divided q12 h	250–500 mg BID
Cefpodoxime proxetil	10 mg/kg/day divided q12 h	100–400 mg BID
Ceftibuten	9 mg/kg/day divided q24 h	400 mg daily
Cefixime	8 mg/kg/day divided q12 h or q24 h	200 mg BID or 400 mg daily
Ceftriaxone	50 mg/kg im × 1 (max 1 g)	1–4 g im daily; 250 mg im × 1 for uncomplicated gonorrhea
Cefdinir	14 mg/kg/day divided q12 h or q24 h	300 mg BID or 600 mg daily

Table 127.7 Dosages of commonly prescribed cephalosporins. Administration is oral unless otherwise noted. BID, twice daily; h, hours; im, intramuscularly; q, every; TID, three times daily.

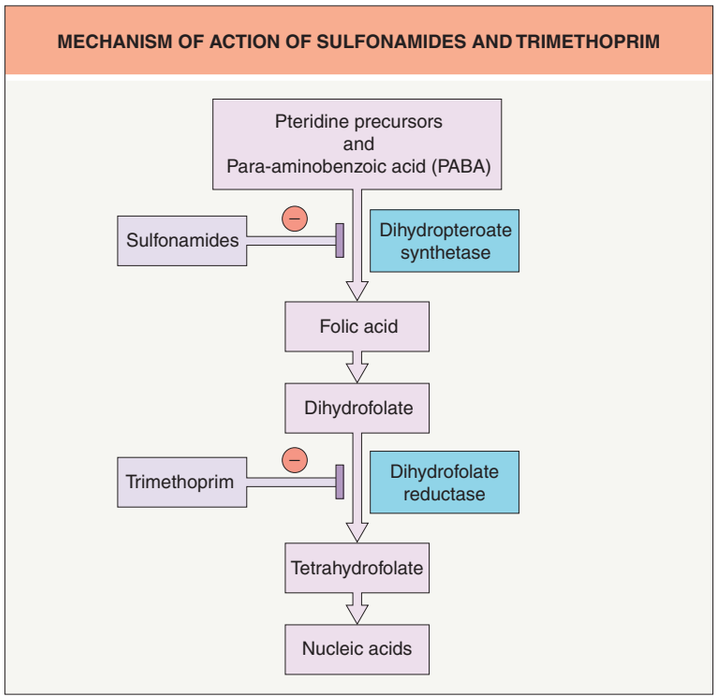


Fig. 127.6 Mechanism of action of sulfonamides and trimethoprim. Sulfonamides inhibit the conversion of pteridine precursors and PABA to folic acid by dihydropteroate synthetase. Trimethoprim inhibits the conversion of dihydrofolate to tetrahydrofolate by dihydrofolate reductase. The end result of both actions is inhibition of bacterial nucleic acid synthesis.

Major side effects

Cutaneous reactions are similar to those seen with the penicillins, including morbilliform eruptions, urticaria, anaphylaxis, and AGEP. Cefaclor is associated with a significantly higher rate of serum sickness-like reactions in children compared to other cephalosporins and other antibiotic classes (Fig. 127.5B)[18]. Cephalosporins may also lead to neutropenia, thrombocytopenia, and Coombs-positive hemolytic anemia, especially in the setting of renal insufficiency. They can cause diarrhea, nausea, and pseudomembranous colitis. Certain cephalosporins/cephamycins with a methylthiotetrazole side group (e.g. cefotetan, cefoperazone, cefamandole) can cause a disulfiram-like effect when alcohol is ingested concomitantly and have anti-vitamin K effects leading to an enhanced risk of bleeding.

Cephalosporins (particularly cefepime) can cause toxic-metabolic encephalopathy. It manifests as seizures, myoclonus, confusion and, less frequently, psychosis 1–10 days after medication initiation[19]. Risk factors include elevated plasma drug levels, renal insufficiency, and pre-existing CNS impairment[19].

Interactions

Administration of oral cephalosporins together with aminoglycosides can increase the likelihood of nephrotoxicity. Probenecid may decrease renal clearance of cephalosporins. Antacids, didanosine, and proton pump inhibitors may decrease absorption of some oral cephalosporins (e.g. cefuroxime).

Pregnancy and lactation

Cephalosporins have not shown adverse effects during pregnancy or lactation and are considered compatible with breastfeeding[4,20].

Sulfonamides and Co-trimoxazole

Mechanism of action

Sulfamethoxazole, *sulfasalazine*, and *sulfisoxazole* are sulfonamides that compete with para-aminobenzoic acid (PABA) to be the substrate for dihydropteroate synthetase (Fig. 127.6). Dihydropteroate synthetase catalyzes the reaction that combines pteridine precursors with PABA to make folic acid. Thus, sulfonamides prevent the synthesis of bacterial folic acid, an essential cofactor for bacterial nucleic acid synthesis. They have a bacteriostatic effect against Gram-positive bacteria (especially *S. aureus*), Gram-negative bacteria, *Chlamydia*, and *Nocardia* spp.

Co-trimoxazole is a synergistic combination of sulfamethoxazole and trimethoprim. It blocks two consecutive steps in the biosynthesis of bacterial nucleic acids (see Fig. 127.6). The sulfonamide inhibits dihydropteroate synthetase and trimethoprim blocks the action of dihydrofolate reductase, which normally converts dihydrofolate to tetrahydrofolate (the active form of folic acid). This combination may be bactericidal or bacteriostatic depending on the drug concentration and the susceptibility of the infecting organism. It is active against most Gram-positive and Gram-negative organisms.

Indications

Co-trimoxazole is used for furuncles or purulent cellulitis suspected to be due to MRSA, inflammatory acne vulgaris recalcitrant to other antibacterial agents, and granuloma inguinale. Other indications for co-trimoxazole include respiratory tract, prostate, urinary tract, and gastrointestinal infections. It is utilized to treat *Pneumocystis jirovecii* pneumonia and as *P. jirovecii* prophylaxis in patients who are immunosuppressed due to systemic medications or HIV infections. Systemic sulfonamides are also used for *Chlamydia* conjunctivitis and *Nocardia* infections. Sulfasalazine is commonly prescribed for ulcerative colitis and psoriatic arthritis.

Dosages

One double-strength capsule of co-trimoxazole contains 160 mg of trimethoprim and 800 mg of sulfamethoxazole (Septra DS®, Bactrim DS®), and in adults this is given twice a day; for *Pneumocystis* prophylaxis, it is taken thrice weekly. In children, the dose is 8–12 mg/kg/day of trimethoprim and 40–60 mg/kg/day of sulfamethoxazole, divided into two doses. Oral sulfadiazine and sulfisoxazole are typically dosed at 2–4 g/day in adults or 75–150 mg/kg/day in children, divided every 4–8 hours.

Contraindications

The sulfonamides and co-trimoxazole are contraindicated in patients with a history of hypersensitivity to this class of medications. Sulfonamides are contraindicated in the third trimester of pregnancy and in lactating patients (see below). They are also contraindicated in patients with porphyria. Sulfonamides can precipitate an acute attack of pseudoporphyria or true porphyria, possibly by increasing levels of porphyrins via hepatocellular damage, stimulating cytochrome P450 activity, or inhibiting other liver enzymes. Co-trimoxazole is contraindicated in patients with megaloblastic anemia, folate deficiency, or G6PD deficiency. It should be used cautiously in patients with impaired hepatic or renal function and in individuals with bone marrow suppression.

Major side effects

The sulfonamides and co-trimoxazole may cause fixed drug or morbilliform eruptions, urticaria, angioedema, photosensitivity, SJS, TEN, exfoliative erythroderma, and vasculitis. Additional uncommon cutaneous side effects include AGEP, Sweet syndrome, linear IgA bullous dermatosis, erythema nodosum, and radiation recall. In HIV-infected patients, these drugs are especially common causes of cutaneous eruptions. Non-cutaneous side effects include hemolytic anemia in the setting of G6PD deficiency, agranulocytosis, thrombocytopenia, eosinophilia, methemoglobinemia, nephrotoxicity, hepatotoxicity, neurotoxicity, and kernicterus in newborns. Co-trimoxazole may also cause nausea, vomiting, glossitis, and stomatitis, as well as dizziness and headaches. Trimethoprim (alone or in combination with sulfamethoxazole) can induce folate deficiency with megaloblastic anemia, leukopenia, and granulocytopenia. It can also cause thrombocytopenia. Administration of folinic acid, which does not impair antibacterial activity because it does not enter bacteria, can reverse the sequelae of folate deficiency.

Interactions

Sulfonamides decrease protein binding and renal clearance of methotrexate, and both agents (as well as the trimethoprim in co-trimoxazole) inhibit folic acid metabolism; these mechanisms can lead to potentially life-threatening methotrexate-induced myelosuppression and other toxicities such as mucositis. The sulfonamides and co-trimoxazole can potentiate the effects of oral hypoglycemics and the anticoagulant effect of warfarin. They should not be used in patients on methenamine for urinary tract infections. Monoamine oxidase (MAO) inhibitors and probenecid may increase sulfonamide adverse effects through altered hepatic metabolism and renal clearance, respectively.

Pregnancy and lactation

Co-trimoxazole should be avoided during pregnancy and lactation as well as for the first 2 months of life. The sulfonamides and co-trimoxazole may cause fetal harm due to their inhibition of folic acid during the first two trimesters; they also result in increased risk of kernicterus during the third trimester. Systemic sulfonamides are excreted in breast milk and may cause hepatic toxicity, anemia, and other adverse effects in nursing infants.

Macrolides

Mechanism of action

Macrolides are bacteriostatic and inhibit bacterial protein synthesis by binding to the 50S ribosomal subunit. Erythromycin is effective against Gram-positive and Gram-negative cocci, most Gram-positive bacilli, and spirochetes. Clarithromycin has an expanded spectrum that includes *H. influenzae* and *Moraxella catarrhalis*. Azithromycin also covers *H. influenzae*. Clarithromycin and azithromycin are both effective against atypical mycobacteria, *Treponema pallidum*, and *Borrelia burgdorferi*; however, they are not first-line agents for infections with the latter two organisms.

Macrolides also have anti-inflammatory effects, including inhibiting production of proinflammatory cytokines (e.g. interleukin [IL]-8, tumor necrosis factor [TNF]), reducing expression of matrix metalloproteinases, and decreasing leukocyte migration and adhesion.

Indications

Macrolides are commonly used for staphylococcal and streptococcal skin infections in patients allergic to penicillins. However, there are regions where a significant percentage of *S. aureus* isolates are erythromycin-resistant, and occasionally *Str. pyogenes* is resistant to erythromycin. Other dermatologic applications of erythromycin and azithromycin include inflammatory acne or rosacea, erythrasma, pitted keratolysis, bacillary angiomatosis, and cat scratch disease. These agents can also be used for the acute and chronic forms of pityriasis lichenoides. In addition, macrolides are indicated for several sexually transmitted diseases, including chancroid, lymphogranuloma venereum, chlamydia, and granuloma inguinale. Macrolides are employed for non-tuberculous mycobacterial infections and a variety of bacterial respiratory infections, including pharyngitis, mycoplasmal pneumonia, Legionnaires disease, diphtheria, and pertussis.

Dosages

Table 127.8 outlines the dosages for commonly prescribed macrolides. Erythromycin base should be taken on an empty stomach; other formulations should be taken with food.

Contraindications

Macrolides are contraindicated in patients with a history of hypersensitivity or hepatic impairment related to this drug class. These agents should be used with caution in those with QT prolongation, electrolyte abnormalities (e.g. hypokalemia, hypomagnesemia), hepatic dysfunction, or renal dysfunction.

Major side effects

The use of erythromycin may be limited by gastrointestinal side effects (e.g. nausea, vomiting, abdominal cramping), whereas azithromycin has improved gastrointestinal tolerance. Erythromycin estolate can cause intrahepatic cholestasis in adults, and this risk increases during pregnancy. Less common side effects include stomatitis, jaundice, transient deafness, and cardiac arrhythmias. Although hypersensitivity reactions to macrolides are uncommon, AGEP may occur. Urticaria, SJS, TEN, and vasculitis are unusual complications.

Interactions

Macrolides have numerous significant drug interactions. Due to CYP3A4 inhibition (see Ch. 131), macrolides (clarithromycin and erythromycin > azithromycin) increase the risk of *torsades de pointes* when used with grepafloxacin, sparfloxacin, terfenadine, astemizole, or cisapride; all of the latter drugs have been removed from the US

DOSAGES OF COMMONLY USED MACROLIDES

Generic name	Oral pediatric dosage	Oral adult dosage
Azithromycin	Bacterial infections: 10 mg/kg (max 500 mg) on day 1, then 5 mg/kg (max 250 mg) daily on days 2–5 Acne vulgaris, rosacea, or pityriasis lichenoides: 5–10 mg/kg thrice weekly	Bacterial infections: 500 mg on day 1, then 250 mg daily on days 2–5 (Zithromax® "Z-pack") Chancroid: 1 g once Acne vulgaris, rosacea, or pityriasis lichenoides: 250–500 mg thrice weekly
Clarithromycin	15 mg/kg daily divided q12 h Maximum 1 g/day Adjust for decreased renal function	250–500 mg BID Adjust for decreased renal function
Erythromycin base	30–50 mg/kg daily divided q6–8 h Maximum 2 g/day	250–500 mg 4 times daily or 333 mg TID or 500 mg BID
Erythromycin estolate	20–50 mg/kg daily divided q6–12 h Maximum 2 g/day	250–500 mg BID–4 times daily
Erythromycin ethyl succinate	20–50 mg/kg daily divided q8–12 h Maximum 2 g/day	400 mg 4 times daily
Erythromycin stearate	20–50 mg/kg daily divided q6 h	250–500 mg BID–4 times daily

Table 127.8 Dosages of commonly used macrolides. BID, twice daily; h, hours; q, every.

and most worldwide markets because of this cardiac risk. By the same mechanism, macrolides increase serum levels and potential toxicity of anticonvulsants, benzodiazepines, buspirone, corticosteroids, warfarin, HMG-CoA reductase inhibitors, colchicine, oral contraceptives, cyclosporine, tacrolimus, disopyramide, felodipine, and ergot alkaloids. Macrolides can increase serum levels of theophylline by inhibiting CYP1A2, leading to cardiac arrhythmias. Macrolides may also increase digoxin levels by altering gut flora, which metabolize digoxin.

Clarithromycin administered in conjunction with calcium channel blockers increases the risk of bradycardia and hypotension. Erythromycin used concomitantly with lovastatin has been reported to cause rhabdomyolysis. Macrolides may interfere with the effectiveness of chloramphenicol or clindamycin (see below), and antacids can decrease the absorption of azithromycin. Clarithromycin levels may be increased when this drug is administered with fluconazole, hexobarbital, alfentanil, disopyramide, or bromocriptine.

Pregnancy and lactation

Erythromycin (with the exception of erythromycin estolate) and azithromycin are generally considered safe during pregnancy, whereas clarithromycin is not recommended due to adverse fetal effects in animal studies. Erythromycin estolate is contraindicated in pregnancy due to the risk of maternal cholestatic hepatitis. This may represent a hypersensitivity reaction to the estolate component, and it can be accompanied by rash, fever, leukocytosis, and eosinophilia in addition to findings related to liver disease (e.g. nausea, vomiting, abdominal pain, jaundice, liver enzyme abnormalities). An increased risk of infantile hypertrophic pyloric stenosis has been described when: (1) mothers received oral macrolides during late pregnancy or while breastfeeding in the neonatal period; and (2) infants received macrolides during the first two weeks of life[4].

Tetracyclines

Mechanism of action

Tetracyclines (Table 127.9) inhibit bacterial protein synthesis by binding to the 30 S ribosomal subunit. They are mainly bacteriostatic but may be bactericidal at high concentrations. Tetracyclines are active against many bacteria, including MRSA, *Rickettsia*, *Chlamydia*, and *Mycoplasma* spp. However, they are not active against *Proteus* spp. or *P. aeruginosa*. Tetracyclines also have anti-inflammatory effects, such as inhibition of matrix metalloproteinase activity, leukocyte chemotaxis, and production of proinflammatory cytokines (e.g. TNF, IL-1β).

Indications

Tetracyclines are indicated for acne vulgaris, rosacea, and periorificial dermatitis. They are first-line treatments for rickettsial infections (e.g. Rocky Mountain spotted fever, rickettsialpox, typhus, Q fever, trench fever), Lyme disease, and ehrlichiosis. These agents are used in syphilis (in penicillin-allergic patients), granuloma inguinale, chlamydial infections (including lymphogranuloma venereum and psittacosis), actinomycosis, brucellosis, mycoplasmal pneumonia, and cholera. Tetracyclines are also useful for treating skin infections due to MRSA (e.g. furuncles, purulent cellulitis) as well as MSSA, *Vibrio vulnificus*, and *Mycobacterium marinum*. In addition, tetracyclines are employed for pityriasis lichenoides and in conjunction with nicotinamide for bullous pemphigoid.

Dosages

Doxycycline, minocycline, and sarecycline may be taken with or without food. To decrease the likelihood of esophagitis, the pills should not be "dry swallowed" and should be taken at least half an hour prior to bedtime. Table 127.9 lists the dosages of commonly prescribed tetracyclines.

DOSAGES AND ROUTES OF ADMINISTRATION OF THE TETRACYCLINES

Generic name	Trade name(s)®	Routes of administration	Adult dosage	Dose adjustment for renal impairment
Demeclocycline	Declomycin, Declostatin, Ledermycin	po	300 mg q12 h	Decrease dose and/or increase interval
Doxycycline hyclate	Vibramycin, Vibra-Tabs, Doxy-Caps, Acticlate, Atridox	po	50–100 mg daily–q12 h; 150 mg daily	None
	Periostat		20 mg q12 h (sub-antimicrobial)	
Doxycycline hyclate delayed release	Doryx, Doxteric	po	50–200 mg daily	None
Doxycycline monohydrate	Monodox, Adoxa, Doxyhexal	po	50–100 mg daily–q12 h	None
Doxycycline monohydrate immediate and delayed release	Oracea	po	40 mg daily	Dose adjustment may be considered (per package insert)
Minocycline	Minocin, Dynacin, Vectrin	po	50–100 mg daily–q12 h	Decrease dose and/or increase interval; for CrCl <80 ml/min, do not exceed 200 mg daily
Minocycline extended release	Solodyn	po	45–135 mg daily	Decrease dose and/or increase interval
Oxytetracycline	Terramycin	po, im	250–500 mg q6 h	Decrease dose and/or increase interval
Tetracycline	Panmycin, Sumycin	po,	250–1500 mg/day divided into 2–4 doses	Decrease dose and/or increase interval*
Sarecycline	Seysara	po	60–150 mg daily	No dose adjustment for renal impairment; not studied in end-stage renal disease
Omadacycline	Nuzyra	po, iv	Skin infections: 450 mg po daily on days 1 and 2, then 300 mg po daily; 200 mg iv on day 1, then either 100 mg iv or 300 mg po daily	No dose adjustment, including in end-stage renal disease

*Recommended interval adjustments for dose of 250–500 mg (originally given q6 to q12 h), based on CrCl: if 50–80 ml/min, administer q8 to q12 h; if 10–50 ml/min, administer q12 h to daily; if <10 ml/min, administer daily.

Table 127.9 Dosages and routes of administration of the tetracyclines. Sarecycline is approved for the treatment of moderate to severe, non-nodular, inflammatory acne vulgaris in patients ≥9 years of age but has not been evaluated for the treatment of infections. Omadacycline is indicated for the treatment of community-acquired bacterial pneumonia and bacterial skin infections in adults. CrCl, creatinine clearance; h, hours; im, intramuscularly; iv, intravenously; min, minute; po, orally; q, every.

Contraindications

Tetracyclines should not be administered for a duration >21 days in patients <8 years of age (to avoid tooth discoloration) or in pregnant women (see below). All tetracyclines except doxycycline and omadacycline should be dose-adjusted in patients with renal impairment (see Table 127.9). Sarecycline has not been studied in the setting of end-stage renal disease or severe hepatic impairment.

Major side effects

Common side effects of tetracyclines include gastrointestinal upset, vaginal candidiasis, and phototoxicity (especially doxycycline). Minocycline does not typically lead to overt phototoxicity but may cause diffuse "muddy brown" hyperpigmentation that is accentuated in sun-exposed areas, as well as bluish discoloration of scars (including those due to acne) and normal skin (in particular on the shins) (Fig. 127.7; see Table 67.5). Gray to blue–gray discoloration of the oral mucosa, sclerae, nails, and teeth (including occasional tooth discoloration in adults) can also occur, as can black pigmentation of the thyroid gland. Deposition of tetracyclines in the teeth and bones occurs in children, causing discoloration and hypoplasia of the teeth (deciduous and permanent) and occasionally temporarily stunting growth. Dizziness is another potential side effect of minocycline.

Tetracyclines (especially minocycline) can cause allergic reactions, including urticaria and a minocycline "hypersensitivity syndrome" (drug reaction with eosinophilia and systemic symptoms [DRESS]; see Ch. 21) that often includes pneumonitis as well as hepatitis; these reactions may occur more frequently in Black patients[21]. Tetracyclines have also been associated with serum sickness-like reactions, esophageal ulcerations, infectious enterocolitis, blood dyscrasias, idiopathic intracranial hypertension (risk of which may be increased when given together with a systemic retinoid), nephrotoxicity, nephrogenic diabetes insipidus, and hepatitis. Minocycline use has been linked to a variety of autoimmune conditions, including drug-induced lupus, polyarteritis nodosa, polyarthritis, antiphospholipid antibody syndrome, and autoimmune hepatitis. These autoimmune reactions often develop after a year or more of therapy, and affected individuals frequently have anti-neutrophil cytoplasmic antibodies (ANCA), usually with perinuclear staining and myeloperoxidase specificity, as well as anti-nuclear antibodies (ANA)[22].

Additional adverse effects of omadacycline include infusion site reactions, hypertension, insomnia, and increased mortality compared to moxifloxacin (2% vs 1%) in patients treated for community-acquired bacterial pneumonia.

Interactions

Food decreases the absorption of tetracycline and omadacycline by about 50%. Patients should not eat or drink (other than water) for 2 hours before or 1 hour after taking tetracycline, or for 4 hours before and 2 hours (4 hours

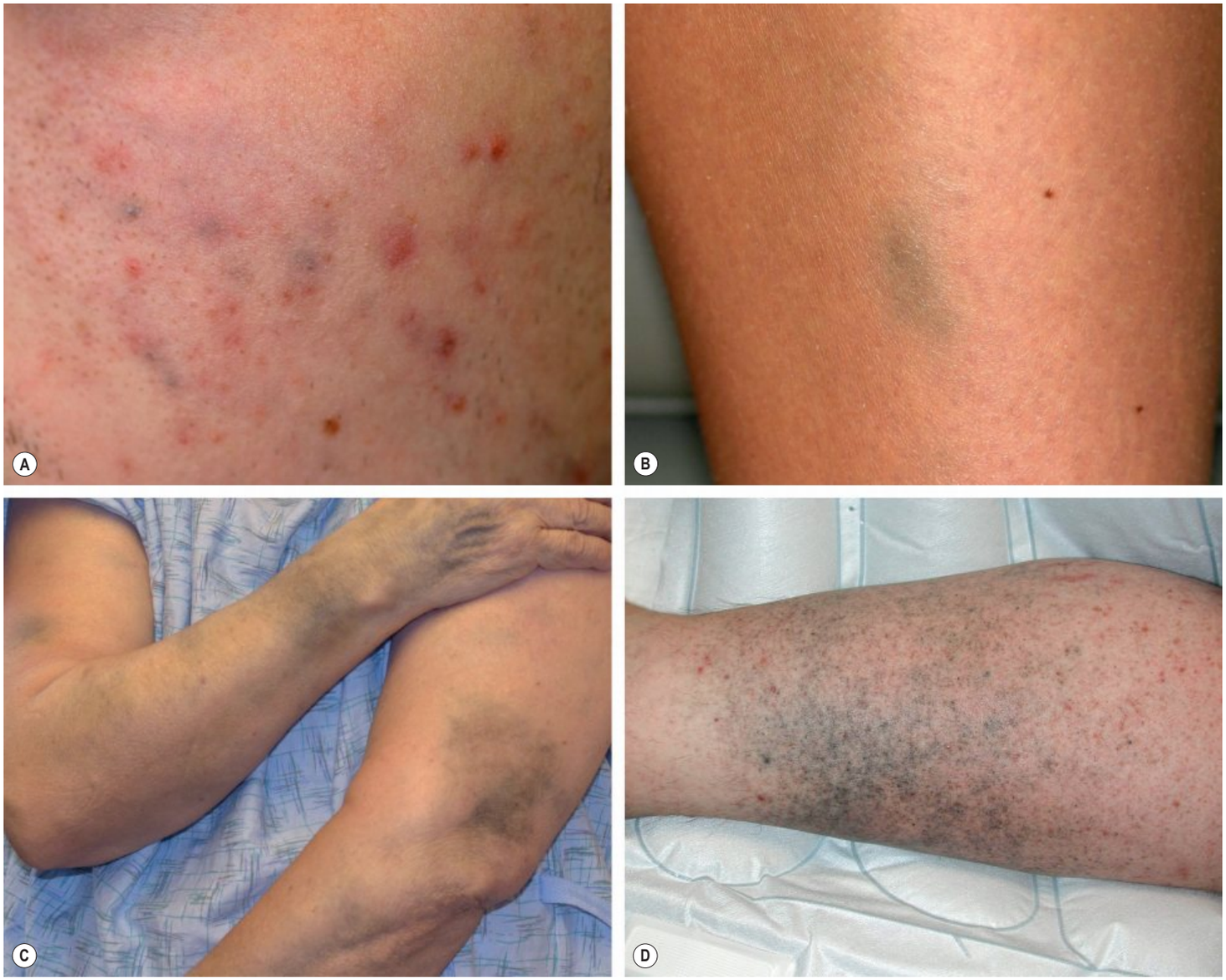


Fig. 127.7 Minocycline pigmentation. Blue–gray discoloration of acne scars (**A**) and in previously normal skin, including a subtle solitary patch on the shin (**B**) as well as more extensive macules and patches (**C, D**). Involvement of the shins and arms may be misdiagnosed as ecchymoses.

for dairy products, antacids, and multivitamins) after taking omadacycline. Minocycline, doxycycline, and sarecycline may be taken with food to avoid gastrointestinal upset. Absorption of tetracyclines is impaired by polyvalent cations such as calcium, aluminum, magnesium, iron, zinc, and bismuth. Thus, absorption of tetracyclines can be inhibited by antacids, some laxatives, medications containing magnesium (e.g. quinapril), dietary supplements, and dairy products (the latter primarily for tetracycline and omadacycline). Antacids, H2 blockers, and proton pump inhibitors can also decrease tetracycline absorption by increasing stomach pH. Tetracyclines increase the serum levels and potential toxicity of digoxin, lithium and warfarin, and they can reduce insulin requirements. Barbiturates, phenytoin, and carbamazepine decrease the half-life of doxycycline. As noted above, bacteriostatic tetracyclines may interfere with the effectiveness of bactericidal penicillins, and coadministration of tetracyclines and oral retinoids may increase the risk of idiopathic intracranial hypertension.

Pregnancy and lactation

Systemic tetracyclines should not be used during pregnancy or lactation. These drugs cross the placenta and are excreted in breast milk, potentially leading to staining of the deciduous teeth, enamel hypoplasia, and impaired skeletal growth in developing fetuses and nursing infants.

Clindamycin

Mechanism of action

Clindamycin is a lincosamide that suppresses bacterial protein synthesis by binding to the bacterial 50S ribosomal subunit. It is active against Gram-positive cocci, including *S. aureus*, *Streptococcus pneumoniae*, *Str. pyogenes*, *Str. viridans*, and anaerobic streptococci. It is not active against enterococci. Clindamycin is also active against anaerobes, including peptostreptococci, peptococci, *Bacteroides* spp., and fusobacteria.

Indications

Clindamycin may be used for anaerobic abscesses, chlamydial infections, and bacterial vaginosis. Clindamycin can be effective in skin infections caused by MRSA as well as MSSA or *Str. pyogenes*, including impetigo, cellulitis, folliculitis, furunculosis, and ecthyma. It may also be useful in necrotizing fasciitis and (considering its inhibition of protein production) toxin-mediated conditions such as staphylococcal scalded skin and toxic shock syndromes. Of note, staphylococci and β-hemolytic streptococci that are sensitive to clindamycin but resistant to erythromycin on initial susceptibility testing should be evaluated with the D (double-disk diffusion)-test for inducible clindamycin resistance. This occurs in bacteria that carry the *erm* gene which encodes erythromycin ribosomal methylase; when expression of this protein is induced (e.g. by erythromycin) or becomes constitutive (selected for during clindamycin therapy), it modifies the bacterial ribosome and results in resistance to both macrolides and lincosamides (see Ch. 74).

Dosages

Clindamycin is formulated for oral, intravenous, and intramuscular administration. It is typically dosed from 150–450 mg 3–4 times daily in adults, and 8–25 mg/kg/day divided into 3–4 doses in children.

Contraindications

Clindamycin is contraindicated in patients with hypersensitivity to the drug and in patients with colitis.

Major side effects

Clindamycin carries a relatively high risk of pseudomembranous colitis, with reported rates from 0.01% to 10%[23]. It occasionally increases serum levels of liver enzymes. Clindamycin may also cause hypersensitivity reactions (especially in HIV-positive patients), transient neutropenia, thrombocytopenia, eosinophilia, and possibly neuromuscular blockade. SJS and TEN are rare side effects.

Interactions

Clindamycin binds at or near the sites of binding of erythromycin and chloramphenicol. These drugs should not be used concomitantly. It may potentiate the neuromuscular effect of botulinum toxin or neuromuscular blockers.

Pregnancy and lactation

There are no known adverse effects of systemic clindamycin on the developing fetus[4]. In rat and mouse studies, oral and subcutaneous clindamycin have not been shown to cause birth defects. Although clindamycin is generally considered to be compatible with breastfeeding[4,20], it may modify the bowel flora of nursing infants and can potentially interfere with the interpretation of bacterial culture results obtained in a febrile nursing infant.

Quinolones

Mechanism of action

Quinolones are rapidly bactericidal by inhibiting two bacterial type II topoisomerases, DNA gyrase and topoisomerase IV. They are active against Gram-negative aerobes, staphylococci, and streptococci, but not against anaerobes.

Table 127.10 lists the drugs in this class.

Indications

Quinolones are indicated for sinusitis, acute exacerbations of chronic bronchitis, community acquired pneumonia, urinary tract infections, gastrointestinal infections, chlamydia, osteomyelitis, and some skin and soft tissue infections.

Second-generation quinolones (e.g. ciprofloxacin, ofloxacin, norfloxacin) have good coverage of Gram-negative rods and some Gram-positive coverage, and they are the most potent antipseudomonal quinolones. Third-generation quinolones (e.g. levofloxacin) are broad spectrum, with coverage of Gram-negative rods and greater Gram-positive cocci coverage, especially of *Streptococcus* spp. Fourth-generation quinolones (e.g. moxifloxacin, gemifloxacin) are very broad spectrum, with coverage of Gram-negative rods, Gram-positive cocci, anaerobes, and atypical bacteria. They have minimal antipseudomonal activity but cover *Streptococcus* spp. and *S. aureus*; however, quinolone resistance to the latter organism can develop rapidly. A newer quinolone, delafloxacin, has activity against MRSA and is approved for bacterial skin infections as well as community-acquired bacterial pneumonia.

Dosages

Ciprofloxacin and levofloxacin are dosed at 250 to 750 mg twice a day. Quinolone doses must be adjusted for renal impairment. Although quinolone use in pediatric patients is generally avoided unless there is no safe and effective alternative[24] (see below), ciprofloxacin 20–40 mg/kg/day in two divided doses has been administered to children.

QUINOLONES			
Generic name	**Trade name(s)®**	**Generation**	**Routes of administration**
Alatrofloxacin*	Trovan IV	4th	iv, im
Ciprofloxacin	Cipro	2nd	po, iv
Delafloxacin	Baxdela		po, iv
Enoxacin*	Penetrex	2nd	po
Gatifloxacin*	Tequin	4th	po, iv
Gemifloxacin	Factive	4th	po
Levofloxacin	Levaquin	3rd	po, iv
Lomefloxacin*	Maxaquin	2nd	po
Moxifloxacin	Avelox	4th	po
Norfloxacin*	Chibroxin, Noroxin	2nd	po
Ofloxacin	Floxin	2nd	po, iv
Sparfloxacin*	Zagam	3rd	po
Trovafloxacin*	Trovan	4th	po, iv

*Withdrawn from US market.

Table 127.10 Quinolones. im, intramuscularly; iv, intravenously; po, orally.

Contraindications

Quinolones are contraindicated in patients with QT prolongation or hypokalemia as well as in those with a history of hypersensitivity to this drug class. Quinolones are also avoided, if possible, during pregnancy and in patients under 18 years of age because of a potential risk of arthropathy and tendinopathy (see below).

Major side effects

In studies involving juvenile animals, quinolones have been shown to damage cartilage in weight-bearing joints. However, quinolones have been used to treat children with cystic fibrosis, and a systematic literature review found that joint changes (most often arthralgias or stiffness) were reversible and affected <1.5% (232/16 184) of pediatric patients treated with ciprofloxacin[24]. Quinolones may cause gastrointestinal upset, changes in taste, abnormal liver function tests, phototoxicity, nephrotoxicity, headache, dizziness, lightheadedness, drowsiness and, rarely, increased intracranial pressure and seizures. Rupture of tendons, in particular the Achilles tendon, is occasionally observed. Exacerbation of myasthenia gravis has also been described, and gatifloxacin has been associated with dysglycemia.

Interactions

Cations (e.g. calcium, aluminum, magnesium, iron, and zinc salts), antacids, and sucralfate prevent absorption of quinolones. Quinolones increase serum levels and potential toxicities of caffeine, theophylline, and aminophylline due to CYP1A2 inhibition. They may also increase serum levels of warfarin. Use of quinolones in combination with cyclosporine may increase serum creatinine levels in renal transplant patients. Quinolones can also increase circulating levels of procainamide by decreasing its renal clearance.

Quinolones should be used with caution in patients who are taking antiarrhythmics, erythromycin, antipsychotics, tricyclic antidepressants, or other drugs that can cause QT prolongation or lower the seizure threshold. Quinolones may also increase seizure risk if administered with NSAIDs. Use of gatifloxacin, or to a lesser degree other quinolones, in combination with sulfonylureas increases the risk of hypoglycemia, especially in elderly patients.

Pregnancy and lactation

Quinolones should be avoided during pregnancy or nursing because of the arthropathy identified in animal studies.

Metronidazole

Mechanism of action

Metronidazole is an nitroimidazole. Its mechanism of action is thought to be due to DNA strand breaking.

Indications

In addition to its antiprotozoal actions, metronidazole has activity against anaerobic cocci (including *Peptococcus* and *Peptostreptococcus* spp.), anaerobic Gram-negative bacilli (including *Bacteroides* and *Fusobacterium* spp.), and anaerobic Gram-positive bacilli (including *Clostridium* spp.). It is indicated for trichomoniasis, amebiasis, and anaerobic bacterial infections. Metronidazole has been utilized for skin and soft tissue infections; oral and dental infections; intra-abdominal, pelvic and brain abscesses; anaerobic pulmonary infections; and osteomyelitis. It is used in combination with a broad-spectrum β-lactamase inhibitor–penicillin combination to treat Fournier gangrene. Metronidazole is also used to treat giardiasis, New World mucocutaneous leishmaniasis, and bacterial vaginosis. Another nitroimidazole, *secnidazole*, was recently approved for the treatment of bacterial vaginosis and trichomoniasis via a single oral dose (2 g) in patients ≥12 years of age.

Dosages

Metronidazole is available for oral and intravenous administration. For bacterial infections, it is given as 500 mg orally every 6 to 8 hours for 7 to 14 days. For bacterial vaginosis or trichomoniasis, a single 2 g dose is given or 500 mg may be taken twice a day for 7 days. The pediatric dose is 30 mg/kg/day in divided doses every 6 hours.

Contraindications

Metronidazole is contraindicated in patients with prior hypersensitivity to the drug. It should be used with caution in patients with impaired liver function.

Major side effects

Metronidazole can cause a morbilliform or pityriasis rosea-like eruption, pruritus, fever, gastrointestinal disturbances, a metallic taste, and xerostomia. Other potential adverse effects include thrombophlebitis, transient leukopenia, dark urine, and neurologic symptoms (e.g. headache, confusion, syncope, seizures, sensory neuropathy).

Interactions

Metronidazole increases circulating levels of cyclosporine, tacrolimus, and phenytoin; it may increase the anticoagulant effect of warfarin. Metronidazole can cause a disulfiram-like reaction when combined with ethanol or protease inhibitors, and administration of metronidazole with disulfiram may precipitate psychosis. Metronidazole may increase the risk of neuropathy due to reverse transcriptase inhibitors.

Pregnancy and lactation

Although metronidazole crosses the placenta, multiple cross-sectional and cohort studies in pregnant women have shown no teratogenicity or mutagenic effects on the developing human fetus. The CDC therefore no longer recommends that metronidazole be avoided during the first trimester of pregnancy. Metronidazole is secreted in breast milk, but reported series have not shown adverse effects in exposed nursing infants. Its use is thought to be compatible with breastfeeding[4,20], although some clinicians recommend deferring nursing for 24 hours following treatment with a single 2 g dose.

Other Antibacterial Agents Used in Gram-Positive Skin Infections

In addition to vancomycin, *linezolid* and *tedizolid* (oxazolidinones), *quinupristin/dalfopristin* (streptogramins), and *tigecycline* (a glycylcycline) can be used to treat serious streptococcal and staphylococcal skin infections, including MRSA (Table 127.11). These three latter antibiotic classes inhibit bacterial protein synthesis (see Table 127.4). *Vancomycin*, a cyclic glycopeptide, and related lipoglycopeptides (e.g. *dalbavancin*, *oritavancin*, *telavancin*) bind to peptidoglycan and thereby inhibit bacterial cell wall synthesis (see Fig. 127.3); in addition, oritavancin and telavancin disrupt bacterial membrane integrity. *Daptomycin*, a cyclic lipopeptide used for complicated skin infections, also kills bacteria by its effects on cell membranes, resulting in depolarization that inhibits protein and nucleic acid synthesis. Table 127.11 outlines the indications, dosages, and side effects of these antibacterial agents.

Dapsone

The oral form of dapsone, a sulfone drug that is used in combination therapy for leprosy and for the treatment of neutrophilic dermatoses, is discussed in Chapters 31 and 130.

ANTIFUNGAL AND ANTIVIRAL AGENTS

ANTIFUNGAL AGENTS

Localized superficial dermatophytoses usually respond to topical antifungal agents (Table 127.12), which rarely have serious side effects. Several of these products are available without a prescription. Fungal infections of the hair and nails as well as systemic mycoses generally require systemic antifungal medications. In addition, fungal skin infections in patients who are immunocompromised, have extensive areas of involvement, or fail to respond to topical therapy may need systemic treatment.

Mechanisms of Action

The mechanisms of action of antifungal agents are outlined in Table 127.13 and illustrated in Figures 127.8 and 127.9. Most azoles

OTHER ANTIBACTERIAL AGENTS USED IN GRAM-POSITIVE SKIN INFECTIONS					
Generic name	**Trade name(s)®**	**Formulations**	**Indications and dosing**	**Data on use during pregnancy***	**Major side effects**
Oxazolidinones					
Linezolid	Zyvox	600 mg tablet 100 mg/5 ml oral suspension iv	Skin infections (e.g. with MRSA): 10 mg/kg up to 400–600 mg po or (if complicated) iv q12 h† × 7–14 days Adjust dose for renal impairment	Potential fetal risk based on animal studies	Headache, insomnia, diarrhea (occasionally due to *Clostridium difficile*), nausea/vomiting, bone marrow suppression (thrombocytopenia > anemia or leukopenia; especially if treated >14 days), neuropathy (peripheral or optic; primarily if treated >28 days), pancreatitis, elevated transaminase levels, lactic acidosis (rare), serotonin syndrome (when taken concurrently with other MAOIs, SSRIs or tricyclics), hypertension (when taken with α-agonist drugs)
Tedizolid	Sivextro	200 mg tablet iv	Acute Gram-positive skin infections in adults: 200 mg po or iv q24 h × 6 days	Potential fetal risk based on animal studies	Headache, nausea/vomiting, diarrhea (occasionally due to *Clostridium difficile*), dizziness, bone marrow suppression (anemia or thrombocytopenia > neutropenia), neuropathy (peripheral or optic); drug interactions potentially leading to serotonin syndrome or hypertension (see linezolid above)
Glycopeptides‡					
Vancomycin	Vancocin	iv¶	Serious infections due to MRSA or other Gram-positive bacteria: 500 mg iv q6 h or 1 g q12 h in adults; 10 mg/kg iv q6 h in children Adjust dose for renal impairment	Animal studies have not shown fetal risk	Nephrotoxicity (increased risk if given together with aminoglycosides or other nephrotoxic drugs), infusion site reactions, hypotension and vancomycin flushing syndrome, ototoxicity, neutropenia, nausea/vomiting, diarrhea (occasionally due to *C. difficile*); occasionally other drug eruptions, including linear IgA bullous dermatosis
Lipoglycopeptides					
Telavancin	Vibativ	iv	Complicated skin infections due to MRSA or other Gram-positive bacteria: 10 mg/kg iv q24 h × 7–14 days Adjust dose for renal impairment	Potential fetal risk based on animal studies	Nephrotoxicity, infusion site reactions, flushing syndrome, QT prolongation, headache, insomnia, foamy urine, dysgeusia, nausea/vomiting, diarrhea (occasionally due to *C. difficile*)
Oritavancin	Orbactiv	iv	Acute Gram-positive skin infections in adults: 1200 mg iv as *single dose*	Animal studies have not shown fetal risk	Headache, nausea/vomiting, diarrhea (occasionally due to *C. difficile*), pruritus, infusion site reactions, flushing syndrome, dizziness, tachycardia, elevated hepatic transaminases; abscesses and osteomyelitis, perhaps due to incomplete bacterial clearance; falsely elevates aPTT for 120 hours (iv unfractionated heparin is contraindicated during this period) and PT/INR for 12 hours; may increase warfarin levels
Dalbavancin	Dalvance	iv	Acute Gram-positive skin infections in adults: 1500 mg iv as single dose, or 1000 mg iv on day 1 + 500 mg iv on day 8 Adjust dose for renal impairment	Animal studies have not shown fetal risk	Headache, nausea/vomiting, diarrhea (occasionally due to *C. difficile*), pruritus, flushing syndrome, elevated hepatic transaminases
Lipopeptides					
Daptomycin	Cubicin	iv	Complicated Gram-positive skin infections: 4 mg/kg iv q24 h × 7–14 days Adjust dose for renal or hepatic impairment	Animal studies have not shown fetal risk	Constipation, diarrhea, nausea/vomiting, headache, insomnia, morbilliform eruptions, infusion site reactions, elevated transaminase and creatine kinase levels, myopathy (at higher doses), nephrotoxicity, eosinophilic pneumonia (rare)
Others					
Quinupristin/dalfopristin	Synercid	iv	Serious skin infections due to *S. aureus* or *Str. pyogenes*: 7.5 mg/kg iv q12 h	Animal studies have not shown fetal risk	Hyperbilirubinemia, infusion site reactions, arthralgias/myalgias, headache, nausea/vomiting, diarrhea (occasionally due to *C. difficile*)
Tigecycline	Tygacil	iv	Complicated skin infections: 50 mg iv q12 h × 5–14 days Adjust dose for hepatic impairment	Fetal risk (inhibition of bone growth, tooth discoloration) with use in 2nd and 3rd trimesters based on animal studies	Nausea/vomiting, diarrhea (occasionally due to *C. difficile*), abdominal pain, headache, infusion site reactions, tooth discoloration (if age <8 years), anaphylaxis/hypersensitivity§, photosensitivity, pancreatitis, hepatic dysfunction, pseudotumor cerebri; black box warning for increased all-cause mortality; use only if no alternatives are available

*These medications should only be used during pregnancy if the potential maternal benefits outweigh the fetal risks; there are no adequate human studies on the use of these agents during pregnancy.
†Every 8 hours for children with complicated infections or who are <5 years of age.
‡Additional glycopeptide antibiotics not available in the US include teicoplanin.
¶Oral capsules and solution with minimal systemic absorption are also available to treat *C. difficile*-associated diarrhea and staphylococcal enterocolitis.
§Cross-reacts with tetracyclines.

Table 127.11 Other antibacterial agents used in Gram-positive skin infections. aPTT, activated partial thromboplastin time; INR, international normalized ratio; MAOI, monoamine oxidase inhibitor; MRSA, methicillin-resistant *Staphylococcus aureus*; PT, prothrombin time; SSRI, selective serotonin reuptake inhibitor. h, hours; iv, intravenous(ly); po, orally; q, every.

TOPICAL ANTIFUNGAL AGENTS				
Generic name	**Trade name(s)®**	**Formulation(s)**	**Considered safe to use during pregnancy***	**OTC/Rx**
Imidazoles				
Butoconazole	Femstat-3, Gynazole-1, Mycelex-3	2% vaginal cream		OTC
Clotrimazole	Canesten, Clotrimaderm, Cruex, Desenex AF, FemCare, Gyne-Lotrimin, Lotrimin AF, Mycelex, Myclo, Myclo-Gyne, Neo-Zol	1% lotion, solution, cream, aerosol solution, lozenges, troches, powder	√	OTC, Rx
Econazole	Spectazole, Ecostatin	1% cream, lotion, spray		Rx
Efinaconazole	Jublia	10% topical solution		Rx
Ketoconazole	Nizoral, Nizoral AD shampoo, Extina, Xolegel	2% cream, gel, foam; 1% and 2% shampoo		OTC, Rx
Luliconazole	Luzu	1% cream		Rx
Miconazole	Femizol-M, Micatin, Micozole, Monistat, Monistat-Derm, Triple Paste AF, Vusion, Zeasorb AF	2% cream, lotion, powder, aerosol powder, aerosol solution; 0.25% ointment (with zinc oxide)		OTC, Rx
Oxiconazole	Myfungar, Oceral, Oceral GB, Okinazole, Oxistat, Oxizole	1% cream, lotion	√	Rx
Sertaconazole	Ertaczo	2% cream		Rx
Sulconazole	Exelderm, Sulcosyn	1% cream, solution		Rx
Terconazole	Fungistat 3 or 5, Terazol 3 or 7, Tercospor	0.4% and 0.8% vaginal cream, 80 mg vaginal suppositories		Rx
Tioconazole	GyneCure, Trosyd AF, Trosyd J, Vagistat 1	20% nail lacquer, 6.5% vaginal cream, ointment		OTC
Allylamines				
Naftifine	Naftin	1% cream and gel, 2% gel	√	Rx
Terbinafine	Lamisil, Lamifen	1% cream, solution, aerosol solution	√	OTC
Benzylamine				
Butenafine	Mentax, Lotrimin Ultra	1% cream		OTC, Rx
Polyenes				
Nystatin	Acronistina, Barstatin, Bio-Statin, Candio, Canstat, Kandistatin, Korostatin, Lystin, Micostatin, Moronal, Mycostatin, Mycostatine, Mykinac, Mytrex, Nadostine, Nilstat, Nyaderm, Nystacid, Nystan, Nystex, Nystop, O-V Statin, Pedi-Dri	100 000 USP units/g cream, ointment, powder, oral suspension, lozenges (pastilles), vaginal tablets	√ (for pastilles)	Rx
Amphotericin B†	Fungizone	3% cream, ointment, lotion	√	Rx
Others				
Ciclopirox olamine	Batrafen, Batrafen Nail Lacquer, Brumixol, Ciclochem, Fungowas, Loprox, Miclast, Micoxolamina, Mycoster, Nail Batrafen, Penlac, Primax	0.77% and 1% cream, gel, lotion, solution, 8% nail lacquer	√	Rx
Tavaborole	Kerydin	5% solution		Rx
Tolnaftate	Aftate, Equate, Genaspore, NP-27, Pitrex, Tinactin, Ting	1% cream, gel, powder, solution, aerosol liquid, aerosol powder		OTC
Undecylenic acid	Caldesene, Cruex, Decylenes, Gordochom	20% cream, 25% ointment, solution, 15% powder, aerosol foam, aerosol powder		OTC
Clioquinol†	Vioform HC, Lococorten-Vioform	3% clioquinol with 1% hydrocortisone or 0.02% flumethasone in a cream or ointment		–
Iodoquinol (iodochlorhydroxyquin)‡	Alcortin, Vytone	1% iodoquinol with 2% hydrocortisone gel		Rx

*Formerly FDA pregnancy category B. However, topical administration of all the listed agents typically results in minimal systemic absorption.
†Not currently available in the US.
‡A synthetic hydroxyquinoline with both antifungal and antibacterial effects.

Table 127.12 Topical antifungal agents. Topical agents with antifungal activity not listed in this table include Whitfield's ointment (benzoic acid and salicylic acid), selenium sulfide, sodium thiosulfate, salicylic acid plus sulfur, zinc pyrithione, haloprogin, mafenide, amorolfine, propylene glycol and benzoyl peroxide. OTC, over the counter; Rx, prescription.

are fungistatic, although some are fungicidal at high concentrations. Allylamines, benzylamines, and ciclopirox olamine have both fungistatic and fungicidal effects. The polyene antifungal agents – nystatin and amphotericin B – are fungistatic at low concentrations and fungicidal at high concentrations. Amphotericin B is available in three lipid formulations (liposomal, lipid complex, and cholesteryl complex [colloidal dispersion]) that are less nephrotoxic but more expensive than the conventional form of this agent.

MECHANISM OF ACTION OF ANTIFUNGAL DRUGS	
Drug class(es)	**Mechanism of action**
Allylamines Benzylamines Tolnaftate (a thiocarbamate)	Interferes with cell membrane synthesis via inhibition of squalene epoxidase, which is required for lanosterol formation; the resultant accumulation of intracellular squalene is fungicidal
Ciclopirox olamine (a hydroxypyridone)	Chelates polyvalent cations (e.g. Fe^{3+}) that have important functions in fungal cytochromes, catalases, and peroxidases; it thereby inhibits respiration, blocks transport of amino acids and alters cell membrane permeability
Echinocandins Ibrexafungerp (a triterpenoid)	Interfere with cell wall synthesis/permeability via inhibition of β-(1,3)-D-glucan synthesis
Flucytosine	Cytosine analogue that interferes with DNA synthesis
Griseofulvin	Disrupts mitotic spindle by interacting with microtubules, thereby inhibiting mitosis in dermatophytes
Imidazoles Triazoles	Interfere with cell membrane synthesis via inhibition of the fungal cytochrome P450-dependent 14-α-demethylase, which normally converts lanosterol to 14-demethyl lanosterol; this leads to accumulation of toxic 14-α-methyl sterols and prevents synthesis of ergosterol, which is required for structural integrity of the fungal cell membrane; these drugs may also impair fungal triglyceride/phospholipid synthesis and inhibit fungal oxidative/peroxidase enzymes (resulting in accumulation of toxic levels of hydrogen peroxide)
Polyenes	Bind irreversibly to cell membrane sterols (e.g. ergosterol) and increase membrane permeability
Selenium sulfide	Antimitotic properties; reduces cellular adhesion in the stratum corneum, facilitating shedding of fungi
Tavaborole (an oxaborole)	Blocks fungal protein synthesis via inhibition of the fungal leucyl-transfer ribonucleic acid (tRNA) synthetase

Table 127.13 Mechanism of action of antifungal drugs. In addition to antifungal effects, these agents have anti-inflammatory properties (see text).

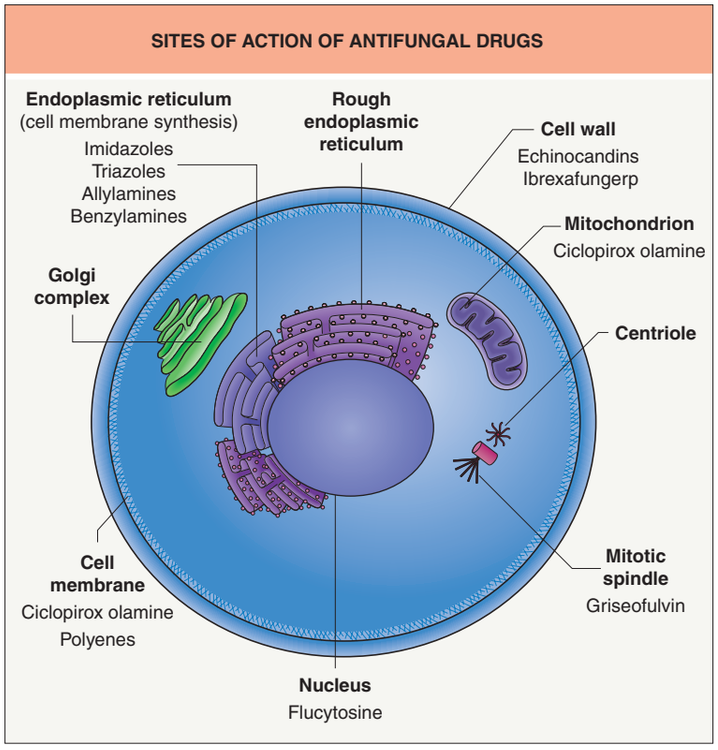


Fig. 127.8 Sites of action of antifungal drugs. Of note, ciclopirox olamine has more than one site of action. In addition, tavaborole inhibits a fungal aminoacyl-tRNA synthetase.

The aforementioned classes of antifungal agents all have anti-inflammatory effects. For example, naftifine inhibits chemotaxis and the production of reactive oxygen intermediates by neutrophils. Azoles inhibit neutrophil chemotaxis, calmodulin activity, synthesis of leukotrienes and prostaglandins, and histamine release from mast cells. Ketoconazole has anti-inflammatory activity comparable to that of hydrocortisone[25]. Ciclopirox olamine is also anti-inflammatory due to its inhibition of prostaglandin and leukotriene synthesis.

Griseofulvin is fungistatic against *Trichophyton*, *Microsporum*, and *Epidermophyton* spp. It is not active against yeast (including *Malassezia* and *Cryptococcus* spp.), dimorphic fungi, or the fungi that cause chromomycosis.

Indications

Topical antifungal agents

Topical azoles are indicated for tinea corporis, tinea pedis, tinea cruris, tinea (pityriasis) versicolor, and mucocutaneous candidiasis. In addition, *efinaconazole* 10% solution has been approved for the topical treatment of onychomycosis due to *Trichophyton rubrum* and *T. mentagrophytes*, with a combined clinical and mycologic cure rate of 15%–20% after daily application for 48 weeks. Of the topical azoles, oxiconazole and sulconazole have relatively weak activity against *Candida* spp. Butoconazole, clotrimazole, econazole, miconazole, terconazole, and tioconazole are available in vaginal preparations to treat *Candida* vaginitis. *Ketoconazole* is additionally indicated for seborrheic dermatitis. Topical antifungal therapy for limited tinea versicolor may have equivalent or better efficacy than oral therapy, with fewer side effects[26].

Topical allylamines and *benzylamines* are indicated for tinea pedis, tinea cruris, and tinea corporis. *In vitro*, butenafine and terbinafine have been shown to be 10 to 100 times and 2 to 30 times more effective than azole antifungals against common dermatophytes, respectively[27,28]. Clinical trials have shown that terbinafine, butenafine, and naftifine were superior to azole antifungals for tinea pedis, with significantly higher mycologic cure rates a month after stopping treatment and lower clinical relapse rates[27,29]. Butenafine 1% cream applied daily for 2 weeks for tinea cruris resulted in a 62% combined clinical and mycologic cure rate 4 weeks after the end of treatment[30]. *Topical terbinafine* and *butenafine* are also indicated for *Candida* infections, although they have relatively weak anti-*Candida* action compared to the topical azoles. In some geographic regions (e.g. India), isolates of *Trichophyton* with increasing resistance to terbinafine have been observed due to mutations in the gene that encodes squalene epoxidase[31].

Of the two topical polyenes, only *nystatin* is commonly used. It is indicated for mucocutaneous *Candida* infections. Polyenes are not effective against dermatophytes[32]. Nystatin is not well absorbed when taken orally. However, this fact may be used to an advantage in treating anogenital candidiasis and candidal diaper dermatitis.

Ciclopirox olamine is active against dermatophytes, *Malassezia* spp., *Candida*, actinomycetes, molds, and Gram-positive and Gram-negative bacteria. It is indicated for tinea corporis, tinea pedis, tinea cruris, onychomycosis, tinea versicolor, mucocutaneous candidiasis, and seborrheic dermatitis. *In vitro*, it is less potent against dermatophytes than the allylamine and benzylamine antifungals, but more potent than azole antifungals. However, it is more effective than the azoles, allylamines, or benzylamines against *Candida*.

Tavaborole 5% solution is an oxaborole approved to treat toenail onychomycosis caused by *T. rubrum* and *T. mentagrophytes*. The combined clinical and mycologic cure rate is 6%–10% following daily application for 48 weeks.

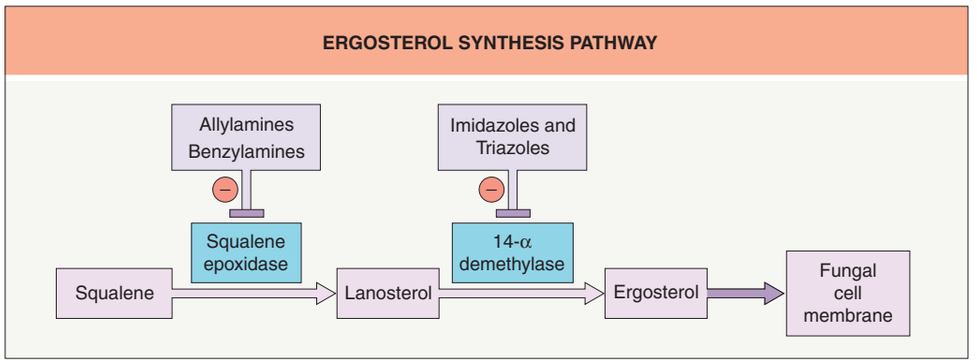


Fig. 127.9 Ergosterol synthesis pathway. Squalene is converted to lanosterol by squalene epoxidase. This enzyme is inhibited by the allylamine and benzylamine antifungals. 14-α demethylase converts lanosterol to ergosterol. Imidazole and triazole antifungals inhibit this conversion.

INDICATIONS FOR SYSTEMIC ANTIFUNGAL AGENTS

Generic name	Antifungal spectra	Indications
Terbinafine	*Epidermophyton floccosum*, *Trichophyton mentagrophytes*, *T. rubrum*, *T. tonsurans*	Onychomycosis Superficial fungal infections: widespread, severe, or resistant to topical antifungals*
Itraconazole	Dermatophytes, yeasts (*Candida*, *Pityrosporum* spp.), dimorphic fungi, some molds	Blastomycosis, histoplasmosis, and aspergillosis (oral and intravenous); onychomycosis (oral); oropharyngeal and esophageal candidiasis (solution) Superficial fungal infections: widespread, severe, or resistant to topical antifungals*
Fluconazole	*Candida* spp., *T. tonsurans*, *T. rubrum*, *Microsporum canis*	Oropharyngeal, esophageal, vaginal, and systemic candidiasis Cryptococcal meningitis Superficial fungal infections resistant to topical antifungals*
Voriconazole	*Aspergillus*, *Candida*, *Fusarium*, *Scedosporium* spp.	Invasive aspergillosis (superior to amphotericin B), disseminated or esophageal candidiasis, serious infections caused by *Fusarium* and *Scedosporium apiospermum*
Posaconazole	*Candida*, *Aspergillus*, *Cryptococcus*, *Fusarium*, *Zygomycetes* spp.	Prevention of invasive aspergillosis and *Candida* infections in immunosuppressed hosts Treatment of oropharyngeal candidiasis, especially if resistant to other azoles
Isavuconazonium sulfate (isavuconazole)	*Candida, Aspergillus, and Cryptococcus* spp.; Zygomycetes; dimorphic fungi	Invasive aspergillosis and mucormycosis
Oteseconazole	*Candida* spp.	Recurrent vulvovaginal candidiasis
Griseofulvin	*Trichophyton*, *Microsporum*, *Epidermophyton* spp. (no activity against *Candida* or *Malassezia* spp.)	Tinea capitis and onychomycosis Superficial fungal infections: widespread, severe or resistant to topical antifungals
Amphotericin B	*Candida* spp., *Cryptococcus neoformans*, dimorphic fungi (*Histoplasma capsulatum*, *Coccidioides immitis*, *Blastomyces dermatitidis*), *Aspergillus* spp.	Severe fungal infections including disseminated systemic candidiasis, cryptococcal meningitis, blastomycosis, disseminated histoplasmosis, extracutaneous sporotrichosis, coccidioidomycosis, paracoccidioidomycosis, mucormycosis, and aspergillosis
Flucytosine	*Candida*, *Cryptococcus*, *Aspergillus* spp., agents of chromomycosis	Second-line or combination therapy for severe fungal infections including candidiasis, cryptococcosis, aspergillosis, and chromomycosis
Caspofungin acetate†	*Aspergillus fumigatus*, *A. flavus*, *A. terrus*, *Candida* spp.	Invasive aspergillosis in patients refractory to or intolerant of other antifungals, candidemia, esophageal candidiasis
Micafungin†	*Candida*, *Aspergillus* spp.	Prophylaxis for *Candida* infections in hematopoietic stem cell transplant patients, esophageal candidiasis
Anidulafungin†	*Candida*, *Aspergillus* spp.	Candidemia, esophageal candidiasis, intra-abdominal *Candida* infections and peritonitis
Ibrexafungerp	*Candida*, *Aspergillus* spp.	Vulvovaginal candidiasis
Ketoconazole	Most dermatophytes, *Candida* spp., dimorphic fungi	Systemic fungal infections in patients who have failed or are intolerant to other therapies: histoplasmosis, coccidioidomycosis, blastomycosis

*Resistant superficial fungal infections treated by systemic terbinafine and azole antifungals include tinea corporis, tinea cruris and tinea pedis. The azoles are also used for tinea versicolor.
†Members of the echinocandin class of antifungal drugs.

Table 127.14 Indications for systemic antifungal agents. Fosravuconazole is approved in Japan for the treatment of onychomycosis. The use of flucytosine is declining, but it is still given in certain situations.

Tolnaftate, *undecylenic acid*, and *clioquinol* are indicated for dermatophyte infections, but they are less efficacious than the aforementioned topical agents; tolnaftate is also effective for *Malassezia* infections.

Systemic antifungal agents

Indications for systemic antifungal agents are outlined in Table 127.14. *Griseofulvin* is classically the drug of choice for treating dermatophyte infections resistant to topical therapy in children. Mycologic cure rates are usually 80% to 95%. *Terbinafine*, *itraconazole*, and *fluconazole* are also effective in treating superficial dermatophyte infections of the skin, hair, and nails in adults and children. Terbinafine therapy for onychomycosis results in a mycologic cure rate of ~70% for the toenails and 80% for fingernails, but there are significant recurrence rates, especially for toenails. Itraconazole, used continuously or in a pulse regimen, produces

similar mycologic cure rates. Terbinafine has been shown to have a higher combined clinical and mycologic cure rate than itraconazole (38% vs 23%, $p=0.004$) after 12 weeks of continuous oral therapy for toenail onychomycosis[33]. Fluconazole is generally the drug of choice for systemic candidiasis. However, fungemia due to azole-resistant *Candida* can occur. Because fluconazole is relatively hydrophilic compared to other systemic azole antifungal drugs, it is distributed to the cerebrospinal fluid and can be used to treat fungal meningitis. *Oteseconazole* is FDA approved for the treatment of recurrent vulvovaginal candidiasis in women who do not have reproductive potential. *Ibrexafungerp* is also approved for the treatment and prevention of recurrences of vulvovaginal candidiasis in women and post-menarchal girls.

DOSING OF TERBINAFINE	
Oral tablets	
Adults	250 mg daily
Children over 2 years old and under 20 kg	62.5 mg daily
Children over 2 years old and 20–40 kg	125 mg daily
Children over 2 years old and over 40 kg	250 mg daily

Table 127.15 Dosing of terbinafine. Terbinafine comes in 250 mg tablets. 125 mg or 187.5 mg packets of granules were previously available; dosage was weight-based and the granules were taken after sprinkling on a non-acidic, non-fruity, soft food.

Dosages

Topical antifungal agents

Topical antifungal agents are generally applied twice a day until resolution of clinical signs and symptoms, usually for 1 to 4 weeks. Occlusion is not required. Shampoos are typically used every 3 to 4 days and are left in place for 5 minutes before rinsing. *Nystatin* oral suspension is held in the mouth for as long as possible before swallowing or expectorating, repeated four times daily. There is essentially no systemic absorption. Nystatin pastilles are allowed to dissolve slowly in the mouth four to five times a day for up to 14 days. *Ciclopirox olamine* nail lacquer is applied daily for 1 week and then removed with alcohol; this cycle is repeated for 48 weeks. *Efinaconazole* and *tavaborole* solutions are also applied daily for 48 weeks but do not require periodic removal. Each of these drugs can have some efficacy when applied over cosmetic nail polish, with an increase to twice daily use recommended for ciclopirox olamine.

Systemic antifungal agents

A typical treatment course of oral *terbinafine* is 12 weeks for toenail onychomycosis, 6 weeks for fingernail onychomycosis, and 2 weeks for superficial tinea infections resistant to topical antifungal agents. For tinea capitis, terbinafine is given continuously for 3–6 weeks. Dosages for adults and children are shown in Table 127.15.

Due to potential toxicity, oral *ketoconazole* is no longer routinely utilized for fungal infections of the skin or nails, including candidiasis and dermatophyte infections. Its use should be restricted to treatment of endemic mycoses (e.g. blastomycosis, coccidioidomycosis) in patients who have failed or are intolerant of other therapies.

Itraconazole oral solution should be taken on an empty stomach, whereas the capsules should be taken with a full meal to enhance absorption. Pediatric dosing is 3 to 5 mg/kg daily. Doses over 200 mg should be divided into two doses per day. For tinea capitis in children, itraconazole may be given continuously for 2 to 4 weeks or as 1- to 3-week-long pulses with 3 weeks without drug in between each pulse. Adult oral dosages for various indications are outlined in Table 127.16. Treatment of oropharyngeal and esophageal candidiasis is for at least 3 weeks and should be continued for at least 2 weeks after symptoms resolve. Itraconazole solution is swished in the mouth, 10 mg at a time, for several seconds and then swallowed.

Table 127.17 outlines the oral dosing of *fluconazole*. Unlike itraconazole, fluconazole is not dependent on a low gastric pH for absorption.

Voriconazole is used to treat serious fungal infections in patients ≥2 years of age. The recommended dose for adults is 4 mg/kg intravenously every 12 hours (following two loading doses of 6 mg/kg 12 hours apart) or 200 mg orally every 12 hours. For children ages ≤11 years or those 12–14 years weighing <50 kg, the usual dose is 8 mg/kg intravenously every 12 hours (following two loading doses of 9 mg/kg 12 hours apart) or 8 mg/kg (maximum 350 mg) orally every 12 hours. Dose adjustments should be made in patients with hepatic dysfunction, and oral administration is preferred in patients with renal impairment to avoid accumulation of the intravenous vehicle. In immunocompromised patients, such as recipients of hematopoietic stem cell transplants, the prophylactic regimen is typically the same oral dose used for treatment twice daily.

Posaconazole is available as 100 mg delayed-release (DR) tablets and a 40 mg/ml suspension, both taken with food and approved for patients ≥13 years of age. Intravenous administration is also approved for adults. For prophylaxis of invasive fungal infections in immunocompromised patients, the oral dosage is 200 mg three times daily of the suspension, or 300 mg twice daily on the first day and then 300 mg daily of the DR tablets. For oropharyngeal candidiasis, the oral suspension is given as 100 mg twice daily on the first day and then 100 mg daily for 13 days. In cases refractory to fluconazole or itraconazole, the dose is increased to 400 mg orally twice daily, and the duration of treatment varies according to the response[34]. Because of fewer cutaneous side effects (see Table 127.19), posaconazole is often preferred over voriconazole, but its greater cost can limit access.

ADULT DOSING OF ORAL ITRACONAZOLE	
Indication	**Adult dosage**
Tinea versicolor	200 mg po daily for 5–7 days
Tinea corporis, tinea cruris	100 mg po daily for 2 weeks – *or* – 200 mg po daily for 1 week
Tinea pedis	100 mg po daily for 2 weeks – *or* – 200 mg po daily for 1 week
Blastomycosis, histoplasmosis	200 mg po daily May increase by 100 mg increments to a maximum of 400 mg po daily for at least 3 months
Cutaneous sporotrichosis	200 mg po daily for 3–6 months or until 2–4 weeks after all lesions have resolved
Aspergillosis	200–400 mg po daily for at least 3 months May give loading dose of 200 mg TID for first 3 days in life-threatening conditions
Onychomycosis of toenails	200 mg po daily for 12 weeks – *or* – 200 mg po BID for 1 week, then 3 weeks without treatment, repeated twice more for a total of three pulses of therapy
Onychomycosis of fingernails	200 mg po daily for 6 weeks – *or* – 200 mg po BID for 1 week, then 3 weeks without treatment, then 200 mg po BID for 1 week (2 pulses)
Oropharyngeal candidiasis	Swish and swallow 200 mg daily for 1–2 weeks
Oropharyngeal candidiasis refractory to fluconazole	Swish and swallow 100 mg BID
Esophageal candidiasis	Swish and swallow 100–200 mg daily

Table 127.16 Adult dosing of oral itraconazole. Itraconazole is available in 100 mg capsules and a 10 mg/ml cherry-caramel-flavored solution. The safety of itraconazole in children has not been specifically studied. Children 3 to 16 years old have been treated for systemic fungal infections with itraconazole capsules or solution, typically at a dose of 5 mg/kg/day, without any problems. Animal studies have shown teratogenicity at high doses, causing skeletal defects in rats. Of note, itraconazole oral solution contains the excipient hydroxypropyl-β-cyclodextrin, which produced pancreatic adenocarcinomas in rats (but not mice) when given for extended periods. BID, twice daily; po, orally; TID, three times daily.

Isavuconazonium sulfate (prodrug of isavuconazole) is approved for treatment of invasive aspergillosis and mucormycosis in adults. It is available in 74.5 and 186 mg capsules as well as in a solution for intravenous administration, both given as a loading dose of 372 mg (equivalent to 200 mg of isavuconazole) every 8 hours for 6 doses, followed by 372 mg once daily starting 12–24 hours after the last loading dose.

Oteseconazole is available in 150 mg capsules and can be administered alone or in conjunction with initial fluconazole therapy for recurrent vulvovaginal candidiasis. In the oteseconazole-only regimen, 600 mg is

DOSING OF ORAL FLUCONAZOLE		
Indication	**Pediatric dosage**	**Adult dosage**
Tinea versicolor		400 mg once *or* 300 mg once, with possible second dose in 1 week, depending on clinical response
Tinea corporis, tinea cruris	6 mg/kg qwk for 2–4 weeks	50–100 mg daily *or* 150 mg qwk for 2–4 weeks
Tinea pedis	6 mg/kg qwk for 2–6 weeks	150–450 mg qwk for 2–6 weeks
Tinea capitis	6 mg/kg/day for 3–6 weeks	6 mg/kg/day for 3–6 weeks
Onychomycosis	6 mg/kg qwk for 3–4 months (fingernails) or 5–7 months (toenails), or until nails are clear	150–450 mg qwk for 6 months (fingernails) or 9 months (toenails), or until nails are clear
Oropharyngeal candidiasis	6 mg/kg on day 1 then 3 mg/kg q24–72 h for 14 days*	200 mg on day 1 then 100 mg daily for at least 2 weeks
Vaginal candidiasis		150 mg once
Esophageal candidiasis	6 mg/kg on day 1 then 3–12 mg/kg q24–72 h for 21 days*	200 mg on day 1 then 100 mg daily for at least 3 weeks Treat for at least 2 weeks after symptoms resolve
Systemic candidiasis	6–12 mg/kg q24–72 h for 28 days*	800 mg on day 1 then up to 400 mg daily
Prophylaxis of candidiasis in bone marrow transplantation	10–12 mg/kg q24 h (maximum 600 mg/day)	400 mg daily
Cryptococcal meningitis (following induction therapy, typically with a lipid formulation of amphotericin B + flucytosine for ≥2 weeks)	Consolidation: 10–12 mg/kg daily for 8 weeks Maintenance: 6 mg/kg daily for 6–12 months	Consolidation: 400 mg daily for 8 weeks Maintenance: 200 mg daily for 6–12 months
Prevention of relapse of cryptococcal meningitis in HIV patients		200 mg daily
*If the patient is less than 14 days old, dosing is every 24–72 h. If the patient is over 14 days old, dosing is every 24 h.		

Table 127.17 Dosing of oral fluconazole. Fluconazole is available as 50 mg, 100 mg, 150 mg, and 200 mg tablets and as an orange-flavored suspension in 10 mg/ml and 40 mg/ml strengths. Since oral fluconazole is highly bioavailable, intravenous therapy is only required for patients who are unable to take oral medications, expected to have poor gastrointestinal absorption, or severely ill. h, hours; q, every; qwk, weekly.

taken on day 1, then 450 mg on day 2, and then 150 mg weekly for 11 weeks beginning on day 14. Alternatively, fluconazole 150 mg can be given on days 1, 4, and 7, followed by oteseconazole 150 mg daily for 7 days and then weekly for 11 weeks beginning on day 28.

Ibrexafungerp is also available in 150 mg capsules. A 300 mg dose is administered twice, approximately 12 hours apart; this can be done once for treatment of vulvovaginal candidiasis and/or monthly for six months for prevention of recurrences.

Dosages for *griseofulvin* are shown in Table 127.18. In the US, increasing doses have been required for the treatment of tinea capitis due to *Trichophyton tonsurans*. The long duration of therapy required with griseofulvin is a disadvantage and contributes to non-compliance. Absorption of griseofulvin is improved when it is administered with fatty foods. Drug particle size reduction through micronization and ultra-micronization has also significantly enhanced oral absorption.

Dosing of intravenous *amphotericin B* varies depending upon the formulation of the medication (e.g. 0.75–1 mg/kg/day of conventional amphotericin B versus 3–5 mg/kg/day of lipid formulations). In adults, flucytosine is given at a dose of 150 mg/kg orally daily, divided into four doses. Taking the medicine over 15 minutes decreases associated nausea. Doses of both drugs should be adjusted in patients with renal insufficiency.

Caspofungin acetate is given by slow intravenous infusion over 1 hour. For treatment of *Aspergillus* infections, 70 mg is administered on day 1 and 50–70 mg daily thereafter. Caspofungin must not be mixed with solutions containing dextrose, and patients with moderate hepatic insufficiency should receive 35 mg daily after the 70 mg loading dose. This drug has not been adequately studied in children.

Micafungin is also only available in an intravenous form. For esophageal candidiasis, it is administered as 150 mg intravenously daily. In hematopoietic stem cell transplant patients, as prophylaxis for *Candida* infections, it may be given at a dose of 50 mg intravenously daily. *Anidulafungin* is available in an intravenous form for *Candida* infections as well. In candidemia, the dose is 100 mg intravenously daily after a loading dose of 200 mg; treatment should continue until 2 weeks after the most recent positive blood culture. For esophageal candidiasis, the dose is 50 mg daily after an initial loading dose of 100 mg.

ORAL DOSING OF GRISEOFULVIN			
Generic name	**Adult**		**Pediatric (over 2 years of age)**
	Tinea corporis, cruris	**Tinea pedis, manuum, unguium, capitis**	
Griseofulvin microsize* (125 mg/5 ml suspension; 250 and 500 mg tablets)	500–1000 mg daily	750–1500 mg daily	15–20 mg/kg daily (usual maximum 1 g); use higher range of 20–25 mg/kg daily for tinea capitis
Griseofulvin ultramicrosize* (125 and 250 mg tablets)	375–500 mg daily	500–750 mg daily	10–15 mg/kg/day (maximum usually 750 mg/day)
Duration of treatment			
2–4 weeks for tinea corporis 6–12 weeks for tinea capitis 4–6 weeks for tinea pedis 4 months or until nails are clear for fingernail onychomycosis† 6 months or until nails are clear for toenail onychomycosis†			
*To increase absorption, griseofulvin should be taken with a fatty meal. †No longer commonly used for this indication; may require a longer duration of treatment.			

Table 127.18 Oral dosing of griseofulvin.

Contraindications

Topical and systemic antifungals are contraindicated in patients with hypersensitivity to the agent or any of the formulation components. Because of the potential for severe hepatotoxicity and QT prolongation, use of *ketoconazole* should be restricted to systemic fungal infections in patients who have failed or are intolerant to other therapies. Systemic antifungals are contraindicated in patients who are taking other drugs

that may cause potentially serious interactions (see below). *Itraconazole* is contraindicated in patients with left-sided heart disease, and its use for onychomycosis should be avoided in pregnant or lactating patients. Ketoconazole and itraconazole may not be absorbed in patients with achlorhydria. *Fluconazole* absorption, however, is not dependent on a low gastric pH. *Griseofulvin* is contraindicated in patients with acute intermittent porphyria, variegate porphyria, porphyria cutanea tarda, or liver failure; it should not be given to pregnant women (see below). Both *oteseconazole* and *ibrexafungerp* are contraindicated during pregnancy; the latter drug is also contraindicated in all women of reproductive potential and during lactation (see below). All systemic antifungal agents should be used with caution in patients with liver or kidney disease. Flucytosine should be used with caution in patients with bone marrow suppression.



Fig. 127.10 Accelerated photoaging due to chronic voriconazole therapy. Note the solar lentigines in this young man with chronic granulomatous disease. *Courtesy Edward Cowen, MD.*

Major Side Effects

The most common side effect of topical antifungal drugs is local skin irritation, which may be more severe with occlusion. Clinical manifestations include burning, stinging, pruritus, erythema, edema, peeling, blistering, and allergic contact dermatitis. *Clioquinol* can cause discoloration of clothes, skin, hair, and nails.

Oral *terbinafine* may cause a morbilliform eruption and, less commonly, urticaria, pruritus, alopecia, or dermatitis. Additional cutaneous reactions include SJS, TEN, AGEP, flares of pustular or other forms of psoriasis, and subacute cutaneous lupus erythematosus. Non-cutaneous side effects of terbinafine include gastrointestinal disturbances, elevated liver enzymes, headaches, taste and visual disturbances, transient decreases in absolute lymphocyte count, and, rarely, neutropenia in immunosuppressed patients. This drug should be used with caution in patients with liver or kidney disease. It is recommended that liver enzyme tests be performed at baseline, although the utility of monitoring asymptomatic patients during therapy has been questioned[35]. The side effects of the *systemic azole antifungals* are listed in Table 127.19. Side effects of *ibrexafungerp* include diarrhea, nausea/vomiting, abdominal pain, headache, and dizziness.

Griseofulvin infrequently causes adverse effects, most commonly headache and gastrointestinal disturbances. Less often, it leads to cutaneous side effects such as fixed drug eruptions, photosensitivity, petechiae, pruritus, exfoliative dermatitis, urticaria/angioedema, and serum sickness-like reactions. It can also precipitate or exacerbate lupus erythematosus or porphyria. Griseofulvin has occasionally been associated with enuresis, proteinuria, increased urinary frequency, arthralgias, fever, neurologic side effects (confusion, blurred vision, vertigo, depression, nightmares, insomnia, ataxia, paresthesias), syncope, epistaxis, estrogen-like effects, sore throat, hepatotoxicity, and leukopenia.

SIDE EFFECTS OF SYSTEMIC AZOLE ANTIFUNGAL AGENTS	
Generic name	**Side effects**
Itraconazole	• Morbilliform eruption, pruritus, urticaria, alopecia, Stevens–Johnson syndrome (rarely); parenteral administration may result in infusion site reactions • Anorexia, nausea, vomiting, abdominal pain, hepatic dysfunction • Fatigue, headaches, dizziness • Fever, edema, hypokalemia, neutropenia (rarely) • Rarely causes congestive heart failure, pulmonary edema, anaphylaxis, peripheral neuropathy
Fluconazole	• Morbilliform eruption, exfoliative dermatitis (rarely) • Nausea, vomiting, abdominal pain, diarrhea, hepatotoxicity • Headache
Posaconazole	• QT prolongation • Hepatitis • Diarrhea, nausea, vomiting, fever, headache, hypokalemia, neutropenia • Avoid if moderate or severe renal impairment
Voriconazole	• Phototoxicity; this can lead to pseudoporphyria and (with chronic use) accelerated photoaging (Fig. 127.10), aggressive or multifocal cutaneous squamous cell carcinomas (especially in the setting of immunosuppression), and melanoma • Visual disturbances (e.g. blurred vision, altered color perception, photophobia), headache, hallucinations • Nausea, vomiting, diarrhea, abdominal pain, hepatotoxicity • Fever, peripheral edema • QT prolongation
Isavuconazonium sulfate (isavuconazole)	• Nausea, vomiting, diarrhea, hepatic dysfunction • Headache • Hypokalemia • Dyspnea, cough • Peripheral edema
Oteseconazole	• Headache • Nausea
Ketoconazole (FDA has advised against prescribing unless failure of other therapies for systemic fungal infections)	• FDA black box warnings: serious hepatotoxicity, QT prolongation and drug interactions leading to QT prolongation • Nausea, vomiting, abdominal pain • Anaphylaxis, urticaria, pruritus • Adrenocortical insufficiency (at doses ≥400 mg daily), decreased testosterone production

Table 127.19 Side effects of systemic azole antifungal agents.

Amphotericin B commonly causes fever, chills, nausea, and vomiting. Less often, it causes anorexia, diarrhea, orthostatic hypotension, hypertension, tachycardia, dyspnea, headache and skin eruptions, including exanthems, exfoliative dermatitis, fixed drug eruptions, flushing, urticaria, and infusion site reactions. Amphotericin B can also produce hypokalemia, thrombocytopenia, and renal toxicity characterized by increased BUN and creatinine; unusual side effects include seizures, arrhythmias, agranulocytosis, liver failure, and anaphylaxis.

Flucytosine can cause neurologic side effects (headaches, fatigue, vertigo, ataxia, paresthesias, confusion, hallucinations), gastrointestinal disturbances (nausea, vomiting, abdominal pain, diarrhea), hypokalemia, and hypoglycemia. Serious potential side effects include cardiac and respiratory arrest, renal failure, cytopenias, gastrointestinal bleeding, and colitis.

Caspofungin acetate may cause headaches, nausea, vomiting, fever, phlebitis, flushing, facial swelling, urticaria, other rashes, pruritus, infusion reactions, and anaphylaxis. Laboratory abnormalities that have been observed include increased alkaline phosphatase, hypokalemia, eosinophilia, proteinuria, and hematuria. *Micafungin* may uncommonly cause anaphylaxis, liver or kidney dysfunction, thrombophlebitis, and hemolytic anemia. It can also result in headaches, nausea, rigors, leukopenia, rashes, and injection site reactions. *Anidulafungin* may cause liver toxicity, diarrhea, hypokalemia, and infusion reactions.

Interactions

Systemic *terbinafine* inhibits the cytochrome P450 isoform CYP2D6. As such, it may increase serum levels and toxic effects of other drugs metabolized by this pathway, including β-blockers, tricyclic antidepressants, selective serotonin reuptake inhibitors (SSRIs), MAO inhibitors, and type B and class IC antiarrhythmics. Terbinafine increases cyclosporine clearance by 15% and decreases caffeine clearance by 19%. It also decreases the efficacy of codeine. Terbinafine used with thioridazine may cause prolonged QT intervals and arrhythmias. Whereas cimetidine increases terbinafine levels, rifampin decreases terbinafine levels by doubling its rate of clearance.

Azole antifungal drugs exert their therapeutic effect by inhibiting cytochrome P450 enzymes (see Table 127.13 and Ch. 131). Cytochrome P450 enzymes play a major role in transforming lipophilic drugs to more easily excreted metabolites. Inhibition of this enzyme family is the cause of many of the azole antifungals' drug–drug interactions. These interactions, which have resulted in black box warnings by the US FDA, are listed in Table 127.20.

Ibrexafungerp is a substrate of CYP3A. As a result, CYP3A inhibitors (e.g. azole antifungals) increase exposure and CYP3A inducers (e.g. rifampin, phenytoin) reduce exposure to ibrexafungerp.

Griseofulvin may decrease the levels and efficacy of warfarin and salicylates. Barbiturates may decrease griseofulvin efficacy by decreasing its absorption. Griseofulvin potentiates the effect of alcohol or may induce a disulfiram-like reaction. It also increases estrogen-metabolizing liver enzymes, which may make oral contraceptives less effective or cause menstrual irregularities.

Systemic corticosteroids, loop diuretics, and thiazide diuretics increase the risk of developing hypokalemia due to *amphotericin B*. Antipsychotics used concomitantly with amphotericin B may cause QT prolongation and cardiac arrhythmias. Nephrotoxic drugs such as

SELECTED DRUG INTERACTIONS OF SYSTEMIC AZOLE ANTIFUNGAL AGENTS

Interacting drug	Result	Azoles involved
Astemizole, terfenadine, cisapride (banned or restricted)	Arrhythmia, torsade de pointes	K, It, F, V, P, Is
Warfarin	Increased warfarin levels	K, It, F, V, P
Cyclosporine, tacrolimus, sirolimus	Increased levels of interacting drug, nephrotoxicity, neurotoxicity, hypertension	K, It, V, P, Is > F
Mycophenolate mofetil (MMF)	Increased MMF levels	Is
Rifampin, rifamycin, rifabutin	Decreased plasma levels of azole antifungals (K also decreases absorption of rifamycin)	K, It, F, V, P, Is
Phenytoin	Phenytoin causes decreased levels of Is, It, K, and P; F and P cause increased levels of phenytoin	K, It, F, V, P, Is
Sildenafil (Viagra®), tadalafil (Cialis®)	Increased levels of interacting drug	K, It, F, V, P, Is
Oral hypoglycemics	Hypoglycemia	K, It, F, V, P, Is, O
Oral contraceptives	Increased levels of estrogens & progestins; effects on contraception debated	K, It, F, V, Is, O
Antacids, H2 antihistamines, proton pump inhibitors, anticholinergics, didanosine	Decreased gastrointestinal absorption of azole antifungals Administration of omeprazole with V or Is causes increased levels of both drugs	K, Is, It, V, Is
Benzodiazepines	Excessive sedation	K, It, F, V, P, Is
Indinavir	Increased indinavir levels	K, P
Corticosteroids	Increased corticosteroid levels	K, P
Digoxin	Increased digoxin levels	It, F, V, P, Is
HMG-CoA reductase inhibitors/"statins" (e.g. atorvastatin, simvastatin)	Increased statin levels; rhabdomyolysis, myopathy	It, V, P, Is, O
Dihydropyridine calcium channel blockers	Edema	It, V, P, Is
Phenobarbital, carbamazepine, isoniazid, nevirapine	Decreased levels of azole antifungals; increased carbamazepine and nevirapine levels with P	It, V, P, Is
Pimozide, buspirone, quinidine, vincristine	Increased levels of interacting drug	It, V, P, Is
Thiazide diuretics (e.g. HCTZ)	Increased levels of F	F
Theophylline, nucleoside analogues	Increased levels of interacting drug	F, V, P
Ritonavir, lopinavir	Increased levels of interacting drug	It, K, P, Is
Ergotamine, dihydroergotamine	Increased levels of interacting drug	K, It, F, V, P, Is

Table 127.20 Selected drug interactions of systemic azole antifungal agents. Oteseconazole is an inhibitor of the breast cancer resistance protein (BCRP) and can lead to increased levels of BCRP substrates, which include mitoxantrone, methotrexate, topotecan, irinotecan, tyrosine kinase inhibitors (e.g. imatinib, gefitinib), statins, prazosin, glyburide, nitrofurantoin, dipyridamole, statins, and cimetidine. K, ketoconazole; It, itraconazole; F, fluconazole; V, voriconazole, P, posaconazole; Is, isavuconazonium sulfate (isavuconazole); O, oteseconazole.

cisplatin, flucytosine, gentamicin, and vancomycin can compound the nephrotoxicity of amphotericin B. Amphotericin may increase digoxin levels. Cisplatin used in conjunction with *flucytosine* increases the risk for nephrotoxicity and bone marrow suppression.

Caspofungin acetate does not affect the cytochrome P450 system. It does decrease tacrolimus levels, and cyclosporine increases caspofungin levels. Phenytoin, rifampin, dexamethasone, carbamazepine, and several antiretroviral drugs (efavirenz, nelfinavir, nevirapine) can decrease caspofungin levels.

Pregnancy and Lactation

Topical antifungal agents

Topical imidazoles, nystatin, ciclopirox olamine, tolnaftate, and undecylenic acid have not been shown to cause adverse fetal effects when used during pregnancy. Although a small amount of ciclopirox olamine is absorbed through the skin, animal studies involving mice, rats, rabbits, and monkeys showed no harm to the fetus at doses 10 times higher than the topical human dose. In general, topical antifungals are thought to be compatible with breastfeeding[4,20]. Topical oxiconazole is excreted in breast milk, but it is not known whether other topical imidazoles, nystatin, and ciclopirox olamine pass into breast milk.

Systemic antifungal agents

Systemic antifungal drugs should not be used to treat onychomycosis if the patient is pregnant or contemplating pregnancy. During pregnancy, they should be reserved for serious fungal infections and used only if the benefit outweighs the risk. Although animal studies of oral *terbinafine* have shown no adverse effects during pregnancy, there are no adequate studies in pregnant women. Orally administered terbinafine is secreted in breast milk and is not recommended for use in nursing mothers.

There are no adequate human studies of the effects of azole antifungals during pregnancy or nursing. The risk of fetal abnormalities is increased with exposure to *fluconazole*, *ketoconazole*, *itraconazole*, and *voriconazole* in the first trimester[4]. Of note, a single 150 mg dose of fluconazole has not been associated with fetal malformations, but it may increase the risk of miscarriage. *Itraconazole* is excreted in human milk and should be avoided in lactating patients. *Fluconazole* is excreted in breast milk, but the level of exposure is substantially lower than doses given safely to neonates[4,20]. Due to ocular abnormalities in exposed animal fetuses, *oteseconazole* is contraindicated in women of reproductive potential as well as during pregnancy and lactation.

Ibrexafungerp is also contraindicated during pregnancy due to fetal malformations in animal studies, and women of reproductive potential are advised to use effective contraception during treatment and for four days after the last dose. There are no human or animal data on the presence of ibrexafungerp in milk or its effects during nursing.

Griseofulvin has been associated with fetal abnormalities in rats and dogs. Rare cases of conjoined twins have been reported in women taking griseofulvin in the first trimester of pregnancy. Patients should avoid pregnancy during treatment with griseofulvin and for at least 1 month after its discontinuation[36].

ANTIVIRAL AGENTS

This section reviews antiviral agents used for infections with herpes simplex virus (HSV), varicella–zoster virus (VZV), and cytomegalovirus (CMV). Table 127.21 lists the topical antiherpetic antiviral medications. Antiretroviral medications are addressed in Chapter 78.

Mechanisms of Action

Fig. 127.11 illustrates the mechanism of action of antiherpetic drugs utilized for HSV and VZV infections.

Valacyclovir is the prodrug of acyclovir. It is almost completely converted to acyclovir by valacyclovir hydrolase while passing through the gastrointestinal tract and liver. It has an oral bioavailability approximately three times greater than that of acyclovir (55% vs 15%–30%) and more convenient dosing.

Penciclovir is an acyclic guanosine analogue with a mechanism of action similar to acyclovir. It reaches higher intracellular concentrations and has a longer intracellular half-life than acyclovir (2.3–3 hours vs 1.3–1.5 hours). However, it is less potent because it does not cause chain termination of viral DNA, and it has a poor oral bioavailability. For these reasons, this medication is only available in topical form. *Famciclovir* is the prodrug of penciclovir. The bioavailability of famciclovir is about 77%. Like valacyclovir, it is converted to its active form in the gastrointestinal tract and liver. *In vitro* studies show that penciclovir is at least as effective as acyclovir against HSV-1 and HSV-2[37].

Docosanol, also known as behenyl alcohol, is a saturated 22-carbon aliphatic alcohol that exhibits antiviral activity against several lipid-enveloped viruses, including HSV. After the virus has attached to the host cell, n-docosanol prevents the fusion of the HSV envelope with the plasma membrane of uninfected cells.

Indications

Topical antiviral agents

Topical acyclovir 5% ointment is indicated for the initial episode of genital herpes. It decreases the duration of viral shedding from 7 days to 4 days[38]. In some studies, it has also been shown to be effective in recurrent genital herpes[39]. Acyclovir 5% cream and an acyclovir 5% plus hydrocortisone 1% combination cream are indicated for recurrent orolabial herpes in immunocompetent individuals ages ≥12 years and ≥6 years, respectively; mean healing times are shortened by ~0.5 days

TOPICAL ANTIHERPETIC ANTIVIRAL AGENTS

Generic name	Selected trade name(s)®	Formulations (OTC/Rx)	Considered safe to use during pregnancy*	Dosage	Side effects
Acyclovir	Acic, Aciclosina, Acivir, Aclovir, Acyclo-V, Acyvir, Cicloferon, Cicloviral, Clinovir, Cusiviral, Cyclivex, Cyclovir, Deherp, Entir, Herpex, Lovir, Oppvir, Poviral, Supraviran, Vicorax, Virex, Virless, Zevin, Zoter, Zovir, Zovirax With 1% hydrocortisone: Xerese Buccal tablet: Sitavig	5% ointment, cream; 50 g mucoadhesive buccal tablet (Rx)	√	q3 h, 6 times/day for 7 days In Canada: 4–6 times/day for up to 10 days With hydrocortisone: 5 times/day for 5 days Buccal tablet: single application	Burning, stinging, discomfort; less often, pruritus, erythema, edema, or mucosal irritation (when applied to genital lesions)
Penciclovir	Denavir, Vectavir	1% cream (Rx)	√	q2 h while awake (≥6 times/day) for 4 days	Burning, stinging, discomfort; less often, erythema or decreased sensation (particularly to touch); occasionally, headache and dysgeusia
Docosanol	Abreva	10% cream (OTC)	√	5 times/day until resolved	Burning, pruritus, xerosis, erythema, edema, acne

*Former FDA pregnancy category B.

Table 127.21 Topical antiherpetic antiviral agents. OTC, over the counter; Rx, prescription.

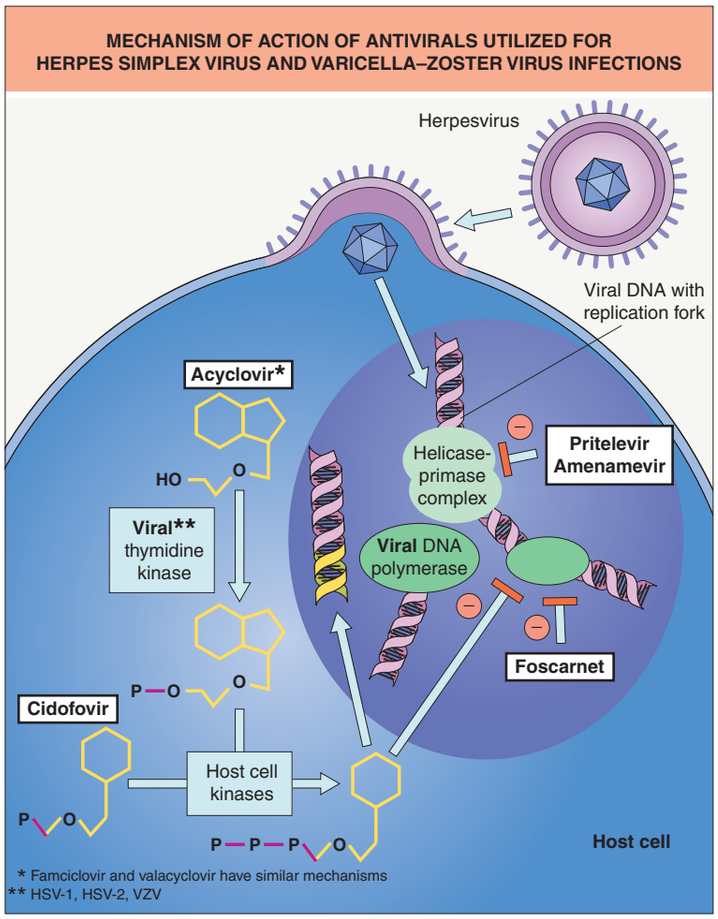


Fig. 127.11 Mechanism of action of antivirals utilized for herpes simplex virus (HSV) and varicella–zoster virus (VZV) infections. Acyclovir is a synthetic purine nucleoside analogue (similar in chemical structure to deoxyguanosine) that has a high affinity for HSV-1, HSV-2, and VZV thymidine kinase, which phosphorylates and activates the drug. Human cellular guanylate kinase then phosphorylates acyclovir twice, to transform it into acyclovir triphosphate, which blocks viral DNA synthesis by competitively inhibiting and inactivating viral DNA polymerase and by becoming irreversibly incorporated into the viral DNA chain, causing DNA chain termination. Valacyclovir, penciclovir, and famciclovir have similar mechanisms of action. Cidofovir is an acyclic nucleoside phosphate analogue of deoxycytosine monophosphate that does not require viral thymidine kinase to become activated, but otherwise also has a similar mechanism. Foscarnet, an inorganic pyrophosphate analogue, selectively inhibits viral DNA polymerase by blocking its pyrophosphate binding sites. Helicase-primase inhibitors (pritelivir, amenamevir) block DNA unwinding at the replication fork and synthesis of primers during viral replication. Pritelivir is being investigated as a treatment for acyclovir-resistant mucocutaneous HSV infections in immunocompromised hosts, and amenamevir is approved in Japan for the treatment of herpes zoster.

for acyclovir alone and 1.5 days for the combination. Although acyclovir ointment is also indicated for limited, non-life-threatening mucocutaneous herpes simplex infections in immunocompromised individuals, these patients often require systemic therapy.

Penciclovir is active against HSV-1, HSV-2, VZV, and EBV. Penciclovir 1% cream is indicated for treatment of recurrent orolabial herpes simplex infections in immunocompetent patients ≥12 years of age. Compared to placebo, topical penciclovir shortens healing time by ~0.5 days and decreases pain and viral shedding in herpes labialis[40]. *Docosanol* is available in the US as a non-prescription topical treatment for recurrent orolabial herpes in patients ≥12 years of age, shortening healing time by almost 1 day.

Systemic antiviral agents

Oral acyclovir and valacyclovir are indicated for initial and recurrent episodes of genital herpes, herpes simplex suppression, varicella (acyclovir for both children and adults, valacyclovir for children), and herpes zoster; valacyclovir and a single-dose acyclovir mucoadhesive buccal tablet are also indicated for recurrent orolabial herpes.

COMPARATIVE SUSCEPTIBILITY OF HERPESVIRUSES TO ANTIVIRAL DRUGS

Antiviral drug	Viral susceptibility				Main target organisms
	HSV-1	HSV-2	VZV	CMV	
Acyclovir, valacyclovir	+++	+++	++	–	HSV-1, HSV-2, VZV
Cidofovir	+	+	++	+++	CMV, resistant HSV
Famciclovir	+++	+++	++	–	HSV-1, HSV-2, VZV
Foscarnet	++	++	+	++	CMV, resistant HSV, VZV
Ganciclovir, valganciclovir	+	+	+	+++	CMV
Letermovir	–	–	–	+++	CMV
Maribavir	–	–	–	+++	CMV

Table 127.22 Comparative susceptibility of herpesviruses to antiviral drugs. CMV, cytomegalovirus; HSV, herpes simplex virus; VZV, varicella–zoster virus.

Intravenous acyclovir is used for HSV and VZV infections in immunocompromised patients, neonatal HSV infection, and other severe or disseminated HSV and VZV infections. Off-label uses of acyclovir and valacyclovir include prevention of recurrent herpes-associated erythema multiforme and treatment of eczema herpeticum, primary herpes gingivostomatitis, and herpetic whitlow. *Famciclovir* is indicated for herpes zoster, recurrent genital and orolabial herpes, and herpes suppression in immunocompetent adults as well as recurrent herpes simplex infections in HIV-infected adults.

Acyclovir, valacyclovir, and famciclovir are considered equivalent in safety and efficacy (time to healing, duration of pain, and viral shedding) for initial episodes of genital herpes[41]. Famciclovir and valacyclovir have the advantage of greater oral bioavailability and more convenient dosing. Valacyclovir is at least as effective as acyclovir in decreasing the duration of pain in herpes zoster[42]. Table 127.22 lists the relative susceptibilities of herpesviruses to the antiviral drugs.

Dosages

Antiviral therapy (topical or systemic) should be started as soon as possible after the onset of signs and symptoms. A glove or applicator should be used to apply topical antivirals to prevent autoinoculation of the finger. Table 127.21 details the dosing regimens of the *topical* antiviral drugs. Table 127.23 lists the available formulations of *systemic* antiviral medications. Table 80.4 outlines the dosages of the systemic antiherpetic medications for their various indications. Intravenous, rather than oral, treatment may be required in severely immunosuppressed patients, patients who cannot take medications orally, and those who cannot be relied upon to take the medication correctly[43].

The majority of people who are seropositive for HSV-2 are asymptomatic[44], and it is thought that asymptomatic viral shedding leads to most transmission of genital herpes. The physician must decide whether to treat on an episodic basis or in a continuous suppressive fashion. Factors that influence this decision include the number of outbreaks per year, the severity of outbreaks, a lack of prodromal symptoms, and an HSV-seronegative sexual partner[43]. Suppression with acyclovir 400 mg twice daily can decrease recurrences by 80%–90% and asymptomatic shedding by 95%[45]. A year-long, double-blind, placebo-controlled study demonstrated that 1 g of valacyclovir taken daily reduced recurrence rates by 78%[46]. In addition, a multicenter, randomized, placebo-controlled study showed that daily valacyclovir significantly lowered the risk of transmission of genital herpes in heterosexual, immunocompetent, monogamous, HSV-2 discordant couples[47].

Acyclovir, valacyclovir, and famciclovir are all effective against herpes labialis when used intermittently or suppressively, and they are all effective in treating herpes zoster. Treatment of varicella in healthy children is controversial, but it does not alter antibody production at 28 days or at 1 year[48]. Oral therapy is recommended for healthy adolescents and adults as well as children with chronic skin or lung disease or on long-term salicylates; intravenous administration is indicated for immunocompromised individuals, including those receiving chronic systemic corticosteroid therapy.

FORMULATIONS OF SYSTEMIC ANTIVIRAL DRUGS	
Antiviral drug	**Available formulations**
Acyclovir	200 mg capsules; 400 mg and 800 mg tablets; iv solution; 200 mg/5 ml banana-flavored suspension
Valacyclovir	500 mg and 1000 mg tablets*
Famciclovir	125 mg, 250 mg, and 500 mg tablets
Ganciclovir	250 mg and 500 mg capsules; iv solution
Valganciclovir	450 mg tablets; 50 mg/ml oral solution
Letermovir	240 mg, 480 mg tablets; iv solution
Maribavir	200 mg tablets
*Pharmacies can compound valacyclovir tablets into an oral suspension (25 or 50 mg/ml).	

Table 127.23 Formulations of systemic antiviral drugs. iv, intravenous.

Contraindications

As with other medications, antiviral agents are contraindicated in patients with hypersensitivity to the drug or any components of the formulation. Systemic antivirals need to be dose-adjusted for patients with impaired renal function (see Table 80.5); renal function should be monitored in patients taking nephrotoxic medications. Thrombotic thrombocytopenic purpura and hemolytic uremic syndrome have been reported in immunocompromised patients receiving valacyclovir.

Major Side Effects

Table 127.21 lists the side effects of *topical* antiviral agents, which have limited systemic absorption, and Table 127.24 lists the side effects of *systemic* antiherpetic medications.

Interactions

No clinically important drug interactions with *topical* antivirals have been identified. Table 127.25 lists the interactions of the *systemic* antiviral agents with other medications.

Pregnancy and Lactation

Topical antiviral agents

There are no adequate studies of topical antiviral agents in pregnant or lactating women. Small amounts of topical acyclovir are absorbed through the skin and mucous membranes. Topical docosanol has not been shown to cause birth defects or other problems in animal studies using rats or rabbits. Although it is not known if topically applied antivirals pass into breast milk, to date, no problems in nursing infants due to these agents have been reported.

Systemic antiviral agents

Systemic acyclovir, valacyclovir, and famciclovir have not been shown to be teratogenic in animal studies and historically were FDA pregnancy category B. Acyclovir is traditionally the drug of choice for genital herpes in pregnant women because of its long history of safe use. Varicella in pregnant women should be treated with acyclovir due to the high risk of maternal mortality from varicella pneumonia as well as fetal death or premature delivery[49]. It is not known, however, whether acyclovir prevents congenital varicella syndrome. Acyclovir is excreted in breast milk; acyclovir and valacyclovir are considered to be compatible with breastfeeding, and they are preferred over famciclovir during lactation[20].

Other Antiviral Agents

Herpes infection resistant to commonly used drugs is a problem in immunocompromised patients. Foscarnet and cidofovir are two alternative treatments in this situation (see Table 127.22 and Fig. 127.11).

Foscarnet is an intravenous antiviral used for cytomegalovirus (CMV) retinitis or CMV skin infections in patients with HIV as well as for acyclovir-resistant herpes simplex infections. Foscarnet is an inorganic pyrophosphate analogue that selectively inhibits viral DNA polymerase by blocking its pyrophosphate binding sites, preventing cleavage of pyrophosphate from deoxyadenosine triphosphate. Foscarnet does not require phosphorylation to be activated, and thus it circumvents the commonest mode of viral resistance involving viral thymidine kinase (see Fig. 127.11). Foscarnet is active against all herpesviruses. Side effects of the intravenous form include nephrotoxicity, anemia, erosive penile lesions, thrombophlebitis, seizures, gastrointestinal disturbances, and changes in serum calcium, magnesium, and phosphate levels.

Cidofovir is an acyclic nucleoside phosphate analogue of deoxycytosine monophosphate. It inhibits viral DNA polymerase and causes DNA chain termination. It differs from acyclovir and penciclovir in that

SIDE EFFECTS OF SYSTEMIC ANTIVIRAL AGENTS COMMONLY USED IN DERMATOLOGY	
Acyclovir and valacyclovir	• Cutaneous: morbilliform eruption, Stevens–Johnson syndrome, injection site reaction, urticaria, angioedema • Gastrointestinal: nausea, vomiting, diarrhea, abdominal pain • Hematologic: aplastic anemia, leukopenia, thrombocytopenia • Neurologic: headaches, vertigo, lethargy, confusion, hallucinations, depression, seizures, encephalopathy, coma (CNS disturbances more likely in elderly patients) • Cardiovascular: hypertension, tachycardia, anaphylaxis • Other: malaise, arthralgia, myalgia, dyspnea, dysmenorrhea • Reversible crystalluria-induced nephropathy with intravenous acyclovir (typically in patients with pre-existing renal dysfunction or dehydration) • Thrombotic thrombocytopenic purpura or hemolytic uremic syndrome in immunocompromised patients with valacyclovir
Famciclovir	• Pruritus, paresthesias, headache, fatigue, nausea, vomiting, diarrhea, and flatulence

Table 127.24 Side effects of systemic antiviral agents commonly used in dermatology.

DRUG INTERACTIONS OF SYSTEMIC ANTIVIRAL AGENTS COMMONLY USED IN DERMATOLOGY	
Interacting drug	**Result**
Amphotericin	Increases serum acyclovir level
Cimetidine	Decreases rate of conversion of valacyclovir to acyclovir Increases serum levels of acyclovir and valacyclovir
Digoxin	Famciclovir increases digoxin levels
Glyburide with metformin (Glucovance®)	Acyclovir or valacyclovir may cause lactic acidosis in patients with decreased renal function
Interferon	May worsen potential neurotoxicity of acyclovir
Intrathecal methotrexate	May worsen potential neurotoxicity of acyclovir
Nephrotoxic drugs (i.e. cisplatin)	Acyclovir increases risk of nephrotoxicity
Probenecid	Decreases rate of conversion of valacyclovir to acyclovir Increases serum levels of acyclovir and valacyclovir
Theophylline	Acyclovir causes decreased metabolism and increased serum levels of theophylline Theophylline increases serum levels of acyclovir and valacyclovir
Zidovudine	Increases serum levels of acyclovir and valacyclovir

Table 127.25 Drug interactions of systemic antiviral agents commonly used in dermatology.

it does not require viral thymidine kinase to become activated. It is also used for CMV retinitis in patients with HIV. Cidofovir is currently available in intravenous form only, and side effects include nephrotoxicity, iritis, neutropenia, metabolic acidosis, and gastrointestinal disturbances. However, a compounded topical form has been used with some success for herpes simplex resistant to acyclovir, molluscum contagiosum, condyloma acuminata, verruca vulgaris, and viral-associated trichodysplasia spinulosa[50]. *In vitro*, cidofovir is active against DNA viruses including mpox, variola, and vaccinia.

Ganciclovir (oral and intravenous) and its prodrug *valganciclovir* (oral) are deoxynucleotide analogue CMV DNA polymerase inhibitors that are approved for the treatment of CMV retinitis in patients with HIV and prevention of CMV disease in transplant recipients. Side effects include diarrhea, nausea/vomiting, cytopenias, and impaired renal function.

Maribavir, an inhibitor of the CMV UL97 protein kinase, is an oral medication that is approved for patients ≥12 years of age with post-transplant CMV infections that fail to respond to other medications. Side effects include taste disturbance, nausea/vomiting, diarrhea, and fatigue.

Letermovir is an inhibitor of the CMV DNA terminase complex, which is necessary for the packaging and processing of CMV viral DNA. Available in oral and IV formulations, it is currently approved for prophylaxis against CMV disease in adult CMV-seropositive allogeneic hematopoietic stem cell transplant recipients[51]. Uncommon side effects include nausea/vomiting, abdominal pain, diarrhea, peripheral edema, cough, headache, fatigue, cardiac adverse events (tachycardia, atrial fibrillation), and rarely hypersensitivity reactions.

Drugs such as pritelivir and amenamevir that target the HSV helicase–primase complex (composed of three proteins that unravel DNA) have been shown to be effective *in vitro* as well as in animal models (see Fig. 127.11)[52]. In randomized controlled trials (RCTs), adults with a history of genital herpes due to HSV-2 who received pritelivir had significantly fewer days with genital lesions and decreased HSV shedding compared to those who received placebo[53,54]. Pritelivir received FDA Breakthrough Therapy designation in 2020 and is being investigated for acyclovir-resistant mucocutaneous HSV infections in immunocompromised hosts. Amenamevir is approved in Japan for the treatment of herpes zoster, and in a Japanese RCT, 7-day courses of amenamevir and valacyclovir had similar efficacy and safety for the treatment of herpes zoster in immunocompetent patients[55].

Additional figures available in our eBook (see inside front cover for access code).

REFERENCES

1. Tunkel AR. Topical antibacterials. In: Mandell GL, Bennett JE, Dolin R, eds. *Mandell, Douglas, and Bennett's Principles and Practice of Infectious Disease*. 5th ed. Philadelphia: Churchill Livingstone; 2000:428–435.
2. Martins AM, Marto JM, Johnson JL, Graber EM. A review of systemic minocycline side effects and topical minocycline as a safer alternative for treating acne and rosacea. *Antibiotics (Basel)*. 2021;10:757.
3. Harkaway KS, McGinley KJ, Foglia AN, et al. Antibiotic resistance patterns in coagulase-negative staphylococci after treatment with topical erythromycin, benzoyl peroxide, and combination therapy. *Br J Dermatol*. 1992;126:586–590.
4. Murase JE, Heller MM, Butler DC. Safety of dermatologic medications in pregnancy and lactation: Part I. Pregnancy. *J Am Acad Dermatol*. 2014;70(401):e1–e14.
5. Schachner LA, Andriessen A, Benjamin LT, et al. Do antimicrobial resistance patterns matter? An algorithm for the treatment of patients with impetigo. *J Drugs Dermatol*. 2021;20:134–142.
6. von Eiff C, Becker K, Machka K, et al. Nasal carriage as a source of *Staphylococcus aureus* bacteremia. *N Engl J Med*. 2001;344:11–16.
7. Cherian P, Gunson T, Borchard K, et al. Oral antibiotics versus topical decolonization to prevent surgical site infection after Mohs micrographic surgery – a randomized, controlled trial. *Dermatol Surg*. 2013;39:1486–1493.
8. Leyden JJ. Review of mupirocin ointment in the treatment of impetigo. *Clin Pediatr*. 1992;31:549–553.
9. McEvoy GK, ed. *American Hospital Formulary Service (AHFS) Drug Information*. Bethesda: American Society of Health-System Pharmacists; 2001:539–541. 3322–4.
10. Manuel MA, Kurtz Saiphoo CS, Nedzelski JM. Nephrotoxicity and ototoxicity following irrigation of wounds with neomycin. *Can J Surg*. 1979;22:274–277.
11. Koh YP, Tian EA, Oon HH. New changes in pregnancy and lactation labelling: review of dermatologic drugs. *Int J Womens Dermatol*. 2019;5:216–226.
12. Wilkinson JD. Fusidic acid in dermatology. *Br J Dermatol*. 1998;139(Suppl. 53):37–40.
13. Oranje AP, Chosidow O, Sacchidanand S, et al. Topical retapamulin ointment, 1%, versus sodium fusidate ointment, 2%, for impetigo: a randomized, observer-blinded, noninferiority study. *Dermatology*. 2007;215:331–340.
14. Hamann K, Thorn P. Systemic or local treatment of erythrasma? A comparison between erythromycin tablets and fucidin cream in general practice. *Scand J Prim Health Care*. 1991;9:35–39.
15. Wright TI, Baddour LM, Berbari EF, et al. Antibiotic prophylaxis in dermatologic surgery: advisory statement 2008. *J Am Acad Dermatol*. 2008;59:464–473.
16. Salkind AR, Cuddy PG, Foxworth JW. Is this patient allergic to penicillin? An evidence-based analysis of the likelihood of penicillin allergy. *JAMA*. 2001;285:2498–2505.
17. Anderson JA. Antibiotic drug allergy in children. *Curr Opin Pediatr*. 1994;6:656–660.
18. Ibia EO, Schwartz RH, Wiedermann BL. Antibiotic rashes in children. A survey in a private practice setting. *Arch Dermatol*. 2000;136:849–854.
19. Triplett JD, Lawn ND, Chan J, Dunne JW. Cephalosporin-related neurotoxicity: metabolic encephalopathy or non-convulsive status epilepticus? *J Clin Neurosci*. 2019;67:163–166.
20. Butler DC, Heller MM, Murase JE. Safety of dermatologic medications in pregnancy and lactation: Part II. Lactation. *J Am Acad Dermatol*. 2014;70(417):e1–e10.
21. Le Cleach L, Bocquet H, Roujeau JC. Reactions and interactions of some commonly used systemic drugs in dermatology. *Dermatol Clin*. 1998;16:421–429.
22. El-Hallak M, Giani T, Yeniay BS, et al. Chronic minocycline-induced autoimmunity in children. *J Pediatr*. 2008;153:314–319.
23. Bartlett JG. Anti-anaerobic antibacterial agents. *Lancet*. 1982;2:478–481.
24. Adefurin A, Sammons H, Jacqz-Aigrain E, et al. Ciprofloxacin safety in paediatrics: a systematic review. *Arch Dis Child*. 2011;96:874–880.
25. van Cutsem J, van Gerven F, Cauwenbergh G, et al. The anti-inflammatory effects of ketoconazole. A comparative study with hydrocortisone acetate in a model using living and killed *Staphylococcus aureus* on the skin of guinea-pigs. *J Am Acad Dermatol*. 1991;25:257–261.
26. Stratman EJ. Failure to use available evidence to guide tinea versicolor treatment: comment on "pityriasis versicolor". *Arch Dermatol*. 2010;146:1140.
27. Arika T, Yokoo M, Yamaguchi H. Topical treatment with butenafine significantly lowers relapse rate in an interdigital tinea pedis model in guinea pigs. *Antimicrob Agents Chemother*. 1992;36:2523–2525.
28. Shadomy S, Wang H, Shadomy HJ. Further in vitro studies with oxiconazole nitrate. *Diagn Microbiol Infect Dis*. 1988;9:231–237.
29. Ablon G, Rosen T, Spedale J. Comparative efficacy of naftifine, oxiconazole, and terbinafine in short-term treatment of tinea pedis. *Int J Dermatol*. 1996;35:591–593.
30. Lesher JL Jr, Babel DE, Stewart DM, et al. Butenafine 1% cream in the treatment of tinea cruris: a multicenter, vehicle-controlled, double-blind trial. *J Am Acad Dermatol*. 1997;36:S20–S24.
31. Burmester A, Hipler UC, Hensche R, Elsner P, Wiegand C. Point mutations in the squalene epoxidase gene of Indian ITS genotype VIII T. mentagrophytes identified after DNA isolation from infected scales. *Med Mycol Case Rep*. 2019;26:23–34.
32. Lesher JL Jr, Smith JG Jr. Antifungal agents in dermatology. *J Am Acad Dermatol*. 1987;17:383–394.
33. De Backer M, De Vroey C, Lesaffre E, et al. Twelve weeks of continuous oral therapy for toenail onychomycosis caused by dermatophytes: double-blind comparative trial of terbinafine 250 mg/day versus itraconazole 200 mg/day. *J Am Acad Dermatol*. 1998;38:S57–S63.
34. Cornely OA, Maertens J, Winston DJ, et al. Posaconazole vs. fluconazole or itraconazole prophylaxis in patients with neutropenia. *N Engl J Med*. 2007;356:348–359.
35. Stolmeier DA, Stratman HB, McIntee TJ, Stratman EJ. Utility of laboratory test result monitoring in patients taking oral terbinafine or griseofulvin for dermatophyte infections. *JAMA Dermatol*. 2018;154:1409–1416.
36. Smith EB. The treatment of dermatophytosis: safety considerations. *J Am Acad Dermatol*. 2000;43:S113–S119.
37. Bacon TH, Howard BA, Spender LC, Boyd MR. Activity of penciclovir in antiviral assays against herpes simplex virus. *J Antimicrob Chemother*. 1996;37:303–313.
38. Corey L, Nahmias AJ, Guinan ME, et al. A trial of topical acyclovir in genital herpes simplex virus infections. *N Engl J Med*. 1982;306:1313–1319.
39. Fiddian AP, Kinghorn GR, Goldmeier D, et al. Topical acyclovir in the treatment of genital herpes: a comparison with systemic therapy. *J Antimicrob Chemother*. 1983;12:67–77.
40. Spruance SL, Rea TL, Thoming C, et al. Penciclovir cream for the treatment of herpes simplex labialis. *JAMA*. 1997;277:1374–1379.
41. Loveless M, Sacks SL, Harris JRW. Famciclovir in the management of first-episode genital herpes. *Infect Dis Clin Pract*. 1997;6:S12–S16.
42. Herne K, Cirelli R, Lee P, Tyring SK. Antiviral therapy of acute herpes zoster in older patients. *Drugs Aging*. 1996;8:97–112.
43. Chang YC, Madkan ZK, Sra K, et al. Systemic antiviral agents. In: Wolverton SE, ed. *Comprehensive Dermatologic Drug Therapy*. 2nd ed. Philadelphia: Saunders; 2007:101–112.
44. Centers for Disease Control and Protection (CDC). Seroprevalence of herpes simplex virus type 2 among persons aged 14–49 years – United States, 2005–2008. *MMWR Morb Mortal Wkly Rep*. 2010;59:456–459.
45. Wald A, Zeh J, Barnum G, et al. Suppression of subclinical shedding of herpes simplex virus type 2 with acyclovir. *Ann Intern Med*. 1996;124:8–15.
46. Reitano M, Tyring S, Lang W, et al. Valacyclovir for the suppression of recurrent genital herpes simplex virus infection: a large-scale dose range-finding study. *J Infect Dis*. 1998;178:603–610.
47. Corey L, Wald A, Patel R, et al. Once-daily valacyclovir to reduce the risk of transmission of genital herpes. *N Engl J Med*. 2004;350:11–20.
48. Englund JA, Arvin AM, Balfour Jr. HH. Acyclovir treatment for varicella does not lower gpl and IE-62 (p170) antibody responses to varicella-zoster virus in normal children. *J Clin Microbiol*. 1990;28:2327–2330.
49. Mutalik S, Gupte A, Gupte S. Oral acyclovir therapy for varicella in pregnancy. *Int J Dermatol*. 1997;36:49–51.
50. Zabawski Jr EJ, Cockerell CJ. Topical and intralesional cidofovir: a review of pharmacology and therapeutic effects. *J Am Acad Dermatol*. 1998;39:741–745.

51. Marty FM, Ljungman P, Chemaly RF, et al. Letermovir prophylaxis for cytomegalovirus infection in hematopoietic-cell transplantation. *N Engl J Med*. 2017;377:2433–2444.
52. Crumpacker CS, Schaffer PA. New anti-HSV therapeutics target helicase-primase complex. *Nat Med*. 2002;8:327–328.
53. Wald A, Corey L, Timmler B, et al. Helicase-primase inhibitor pritelivir for HSV-2 infection. *N Engl J Med*. 2014;370:201–210.
54. Wald A, Timmler B, Magaret A, et al. Effect of pritelivir compared with valacyclovir on genital HSV-2 shedding in patients with frequent recurrences: a randomized clinical trial. *JAMA*. 2016;316:2495–2503.
55. Kawashima M, Nemoto O, Honda M, et al. Amenamevir, a novel helicase-primase inhibitor, for treatment of herpes zoster: a randomized, double-blind, valaciclovir-controlled phase 3 study. *J Dermatol*. 2017;44:1219–1227.
56. van Hoogdalem EJ. Transdermal absorption of topical anti-acne agents in man; review of clinical pharmacokinetic data. *J Eur Acad Dermatol Venerol*. 1998;11:S13–S19.



eFig. 127.1 Allergic contact dermatitis secondary to a topical antibiotic.



eFig. 127.2 Drug-induced subacute cutaneous lupus erythematosus secondary to oral terbinafine.

128 Systemic Immunomodulators

J. Mark Jackson and Jeffrey P. Callen

Chapter Contents

Interferons 2272
Granulocyte–Macrophage and Granulocyte Colony-Stimulating Factors (GM-CSF and G-CSF) 2272
Targeted Immune Modulators 2272
Tumor Necrosis Factor Inhibitors 2273
Interleukin-12/23 and Interleukin-23 Inhibitors 2280
Interleukin-17 Inhibitors 2281
Spesolimab-sbzo 2282
Interleukin-4/13 Receptor and Interleukin-13 Inhibitors 2283
Interleukin-1 Inhibitors 2283
Rituximab 2284
Omalizumab 2285
Janus Kinase (JAK) Inhibitors 2285
Targeted Immune Modulators Under Investigation and Other Targeted Therapies 2287
Intravenous Immune Globulin (IVIg) 2287

INTERFERONS

Interferons (IFNs) are a family of secretory glycoproteins produced by most eukaryotic cells in response to a variety of viral and non-viral stimuli. IFNs display antiviral activity and have immunoregulatory and antiproliferative effects. IFN does not inactivate viruses directly but rather renders cells resistant to viruses.

There are three antigenically distinct IFNs, originally described as leukocyte (α), fibroblast (β), and immune (γ)[1] (Table 128.1). IFN-α and IFN-β are type I interferons, whereas IFN-γ represents a type II interferon. Of note, a targeted immune modulator that inhibits the type I interferon receptor is approved as treatment for systemic lupus erythematosus. IFNs must be injected intralesionally or administered parenterally due to the large size of the protein. IFN-α-2a and IFN-α-2b are the agents most frequently used for cutaneous diseases. The dermatologic uses, side effects, and interactions of IFNs are outlined in Table 128.2.

INTERFERONS				
Generic name	**Trade name®**	**Route**	**Half-life**	**Peak effect**
Interferon-α-2a	Roferon-A	sc	5.1 h	3.8–7.3 h
Interferon-α-2a	Pegasys*	sc	160 h	72–96 h
Interferon-α-2b	Intron A Rebetrol when combined with ribavirin	iv, il, im, sc	2–3 h	30 min (iv) 3–12 h (im, sc)
Interferon-α-2b	PegIntron* Besremi*	sc sc	40 h 160 h	15–44 h 48–120 h
Interferon-α-N3	Alferon N	il	2–3 h	3–12 h
Interferon-β-1a	Avonex	im	10 h	3–15 h
	Rebif Plegridy*	sc sc, im	69 h 78 h	16 h 6–12 h
Interferon-β-1b	Betaseron Extavia	sc sc	4.3 h 4.3 h	1–8 h 6–12 h
Interferon-γ-1b	Actimmune	sc	5.9 h	4.7 h

*Pegylated forms in which polyethylene glycol (PEG) side chains were added to increase the half-life.

Table 128.1 Interferons. Dermatologic FDA-approved indications include condyloma acuminata (IFN-α-2b), melanoma (IFN-α-2b), and AIDS-associated Kaposi sarcoma (IFN-α-2a and IFN-α-2b). h, hours; il, intralesional; im, intramuscular; iv, intravenous; sc, subcutaneous.

GRANULOCYTE–MACROPHAGE AND GRANULOCYTE COLONY-STIMULATING FACTORS (GM-CSF AND G-CSF)

The indications and side effects of granulocyte–macrophage and granulocyte colony-stimulating factors (GM-CSF and G-CSF) are outlined in Table 128.3.

TARGETED IMMUNE MODULATORS

Key features

- Dermatologic indications for tumor necrosis factor (TNF) inhibitors such as etanercept, adalimumab, and infliximab include psoriasis and hidradenitis suppurativa
- Several agents that block interleukin (IL)-12 and/or IL-23 signaling, which is important for the Th17 immune response, are approved for the treatment of psoriasis. Ustekinumab binds to the p40 subunit shared by these cytokines, whereas guselkumab, risankizumab, and tildrakizumab bind to the p19 subunit of IL-23
- The IL-17 inhibitors secukinumab, ixekizumab, and brodalumab are approved for the treatment of psoriasis
- The IL-36 receptor antagonist spesolimab is approved for the treatment of generalized pustular psoriasis
- Agents that block IL-4 and/or IL-13 signaling are approved for the treatment of atopic dermatitis. Dupilumab binds to the IL-4 receptor α subunit shared by these cytokines, whereas tralokinumab and lebrikizumab bind to IL-13
- The IL-1 antagonists anakinra, canakinumab, and rilonacept are used to treat several autoinflammatory diseases, including cryopyrin-associated periodic syndromes and deficiency of the IL-1 receptor antagonist (DIRA)
- Rituximab blocks CD20 on B cells and is approved for the treatment of B cell lymphoma, pemphigus vulgaris, granulomatosis with polyangiitis, and microscopic polyangiitis
- Omalizumab binds to the IgE receptor on mast cells and is approved for the treatment of chronic spontaneous urticaria
- Oral Janus kinase (JAK) inhibitors are approved for the treatment of atopic dermatitis (upadacitinib and abrocitinib), alopecia areata (baricitinib and ritlecitinib), and graft-versus-host disease (ruxolitinib)

Introduction

Advances in molecular technology have enabled the development of drugs that target specific proteins involved in disease pathogenesis. This has resulted in effective therapies for a variety of immune-mediated skin disorders, including psoriasis, atopic dermatitis, hidradenitis suppurativa, pemphigus vulgaris, urticaria, alopecia areata, and cutaneous B cell lymphoma as well as the cutaneous manifestations of

DERMATOLOGIC USES, SIDE EFFECTS, AND INTERACTIONS OF INTERFERONS
FDA-approved indications
Condyloma acuminata (α) AIDS-associated Kaposi sarcoma (α) Melanoma (adjuvant) (α) Chronic granulomatous disease (γ)
Selected off-label dermatologic uses
Neoplasms
Basal cell carcinoma (α) Actinic keratoses (α) Squamous cell carcinoma (α) Giant condyloma of Buschke–Lowenstein (α) Cutaneous T cell lymphoma (α, β, γ) Granulomatous slack skin (α, γ) Infantile hemangioma (α) Tufted angioma (α)
Infections
Verrucae vulgaris (α, β, γ) Epidermodysplasia verruciformis (α) Herpes zoster (α) Herpes simplex (α) Necrolytic acral erythema (with hepatitis C) (α) Leishmaniasis (γ) Leprosy (γ) *Mycobacterium avium* complex infections (γ)
Inflammatory/other
Atopic dermatitis (γ) Keloids (α, γ) Behçet disease (α) Systemic sclerosis (γ) Scleromyxedema (α)
Side effects
• ***Systemic:*** flu-like symptoms (fever, chills, headache, myalgias, arthralgias), hypotension, tachycardia, arrhythmias, rhabdomyolysis, gastrointestinal symptoms (nausea, vomiting, diarrhea), hepatitis, bone marrow suppression (high-dose therapy), thyroiditis (hepatitis C patients) • ***Cutaneous:*** necrosis at injection site (IFN-β-1b for multiple sclerosis; Fig. 128.1), psoriasis (Fig. 128.2), vitiligo, alopecia areata
Interactions
• Decreased clearance of aminophylline; increased risk of renal failure when used with interleukin-2; additive effects with other myelosuppressive or neurotoxic medications
Pregnancy
• Animal studies have shown an increased risk of abortion at high doses; no adequate studies in pregnant women

Table 128.2 Dermatologic uses, side effects, and interactions of interferons. *Adapted from Wolverton SE. Comprehensive Dermatologic Drug Therapy, 3rd edition. Philadelphia: WB Saunders, 2012.*

GRANULOCYTE–MACROPHAGE AND GRANULOCYTE COLONY-STIMULATING FACTORS (GM-CSF & G-CSF)
Properties
These glycoproteins regulate the survival, proliferation, differentiation, and functional activation of hematopoietic cells
Uses
• Treatment of neutropenia in settings of myelosuppressive chemotherapy and hematopoietic stem cell transplantation • Other forms of neutropenia (e.g. associated with AIDS, WHIM syndrome, or dyskeratosis congenita) • Mobilization of peripheral blood progenitor cells • In dermatology, both have been studied as promoters of wound healing, and GM-CSF has been investigated as a component of melanoma vaccine therapy
Side effects
GM-CSF
• ***Systemic:*** fever, myalgias, bone pain; occasionally flares of autoimmune disease • ***Cutaneous:*** morbilliform eruption (within 24–48 hours of administration; mixed infiltrate with granulocytes/macrophages); pustular or urticarial injection site reactions (Fig. 128.3); Sweet syndrome, small vessel vasculitis, urticarial plaques with tense bullae, epidermolysis bullosa acquisita
G-CSF
• ***Systemic:*** bone pain (transient, mild "dull ache"; 20% of recipients); occasionally, elevated serum uric acid, LDH, or alkaline phosphatase • ***Cutaneous:*** Sweet syndrome (within 1–2 weeks of administration); injection site reactions, pyoderma gangrenosum, small vessel vasculitis, folliculitis; histologically, the infiltrate is composed of neutrophils, eosinophils and large histiocytes with cytologic atypia and many mitotic figures
Interactions
Additive effects with other drugs that cause neutrophilia, e.g. corticosteroids, lithium
Pregnancy and lactation
Animal reproduction studies have shown adverse fetal effects, but no adequate studies in pregnant women; unknown if excreted in breast milk

Table 128.3 Granulocyte–macrophage and granulocyte colony stimulating factors (GM-CSF & G-CSF). LDH, lactate dehydrogenase; WHIM, warts, hypogammaglobulinemia, infections, and myelokathexis.

systemic conditions such as Crohn disease, sarcoidosis, and vasculitis. These drugs, which are referred to as "biologic" agents, work via mechanisms that include altering T cell activation and differentiation into Th1, Th2, or Th17 cells; blocking cytokines, their receptors, or their intracellular signaling mechanisms; and eliminating pathogenic B cells.

The nomenclature utilized for targeted immune modulators is summarized in Table 128.4. In general, antibodies and fusion proteins represent large molecules that require parenteral administration.

Tumor Necrosis Factor Inhibitors

The FDA has approved multiple tumor necrosis factor (TNF; previously known as TNF-α) inhibitors: etanercept (Enbrel®), etanercept-szzs (Erelzi™), etanercept-ykro (Eticovo™), infliximab (Remicade®), infliximab-abda (Renflexis®), infliximab-axxq (Avsola™), infliximab-dyyb (Inflectra®), infliximab-qbtx (Ixifi™), adalimumab (Humira®), adalimumab-aacf (Idacio®), adalimumab-aaty (Yuflyma®),



Fig. 128.1 Postinflammatory hyperpigmentation and ulceration at sites of interferon-β-1b injection in a woman with multiple sclerosis. *Courtesy Jean L. Bolognia, MD.*

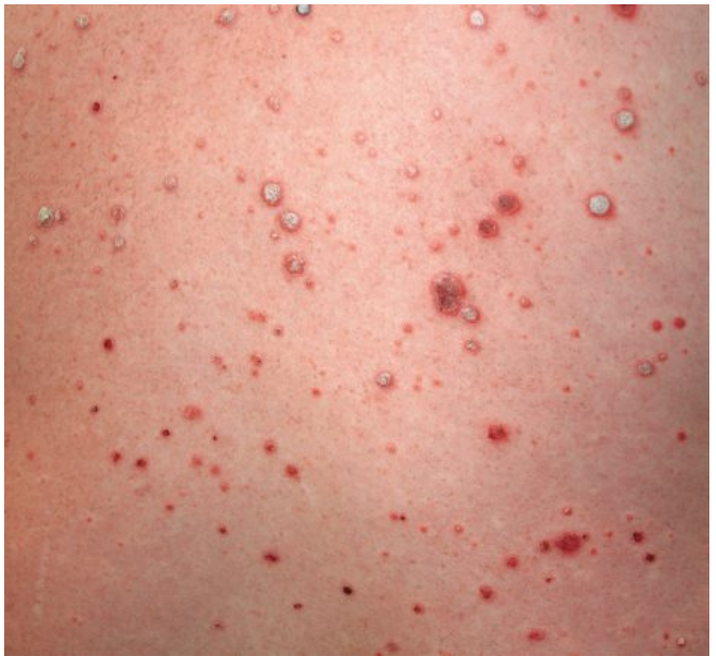


Fig. 128.2 Interferon-induced flare of psoriasis.



Fig. 128.3 Erythematous edematous plaque at the site of GM-CSF injection.

NOMENCLATURE FOR MONOCLONAL ANTIBODIES AND FUSION PROTEINS						
Prefix	**Sub-stem A: *target* system [previous nomenclature system]**		**Sub-stem B: *source* system**		**Suffix**	
Variable "Peg-" can be used if pegylated (or can add pegol as a second word)	-anibi-	Angiogenesis	-a-	Rat	-mab	Immunoglobulin variable domain
	-b(a)- [-ba(c)-]	Bacterial	-e-	Hamster		
	-f(u)- [-fung-]	Fungal	-i-	Primate	-cept	Receptor (takes the place of a variable domain)
	-k(i)- [-ki(n)-]	Interleukin	-o-	Mouse		
	-l(i)- [-li(m)-]	Immunomodulating	-u-	Human	-nib	Tyrosine kinase inhibitor
	-n(e)- [-ne(u)(r)-]	Nervous system	-xi-	Chimeric†		
	-tox(a)-	Toxin*	-zu-	Humanized‡		
	-t(u)-	Tumor				
	-v(i)-	Viral				

*If conjugated to (rather than directed at) a toxin, the suffix -tox can be used in a second word.
†Contains contiguous *foreign*-derived amino acids comprising the *entire variable* region (both heavy and light chains), linked to a constant region of human origin.
‡Has segments of foreign-derived amino acids *interspersed* with human-derived amino acids in the *variable* region, linked to a constant region of human origin.

Table 128.4 Nomenclature for monoclonal antibodies and fusion proteins. For example, ada-lim-u-mab, inf-li-xi-mab and certo-li-zu-mab pegol are immunomodulating immunoglobulins that are human, chimeric, and humanized, respectively.

adalimumab-adaz (Hyrimoz®), adalimumab-adbm (Cyltezo®), adalimumab-afzb (Abrilada®), adalimumab-aqvh (Yusimry™), adalimumab-atto (Amjevita®), adalimumab-bwwd (Hadlima®), adalimumab-fkjp (Hulio™), golimumab (Simponi®), and certolizumab pegol (Cimzia®). A review of their mechanisms of action, major side effects, contraindications, and use in pregnancy is followed by a discussion of issues that relate specifically to individual drugs.

Mechanism of action

Infliximab, adalimumab, golimumab, and certolizumab pegol are monoclonal antibodies, while etanercept is a dimeric fusion protein composed of the extracellular portions of two p75 TNF receptors linked to the Fc portion of IgG1 (Fig. 128.4). Although all four monoclonal antibodies target human TNF, infliximab is chimeric (human–mouse) IgG1, adalimumab and golimumab are human recombinant IgG1, and certolizumab pegol is a humanized pegylated Fab fragment (see Table 128.4).

All of the TNF inhibitors bind to soluble TNF and block its ability to activate TNF receptors (Fig. 128.4). By interacting with membrane-bound TNF, the IgG1 monoclonal antibodies can also activate complement-dependent cytotoxicity and induce cellular apoptosis[2]. This capacity to destroy TNF-producing cells may explain the greater efficacy of these monoclonal antibodies compared to etanercept in the treatment of granulomatous conditions as well as the potentially higher risk of infections associated with their use. In addition to the anti-inflammatory effects of TNF inhibitors (see Fig. 8.1B), blocking TNF signaling may have an impact on the neuroendocrine system[3].

Contraindications

Each TNF inhibitor is contraindicated in patients with known hypersensitivity to that particular medication, and infliximab is contraindicated in those with an allergy to murine proteins. These agents should be avoided in patients with significant active infection, malignancy, congestive heart failure (especially if unstable), multiple sclerosis, or other demyelinating diseases[4,5] (see Table 8.19).

Major side effects (Table 128.5)

Infections

Disseminated and/or opportunistic infections such as histoplasmosis, coccidioidomycosis, listeriosis, and *Pneumocystis jirovecii* pneumonia may occur in patients treated with TNF inhibitors[6]. An increased risk of symptomatic mycobacterial infections (Fig. 128.5), including

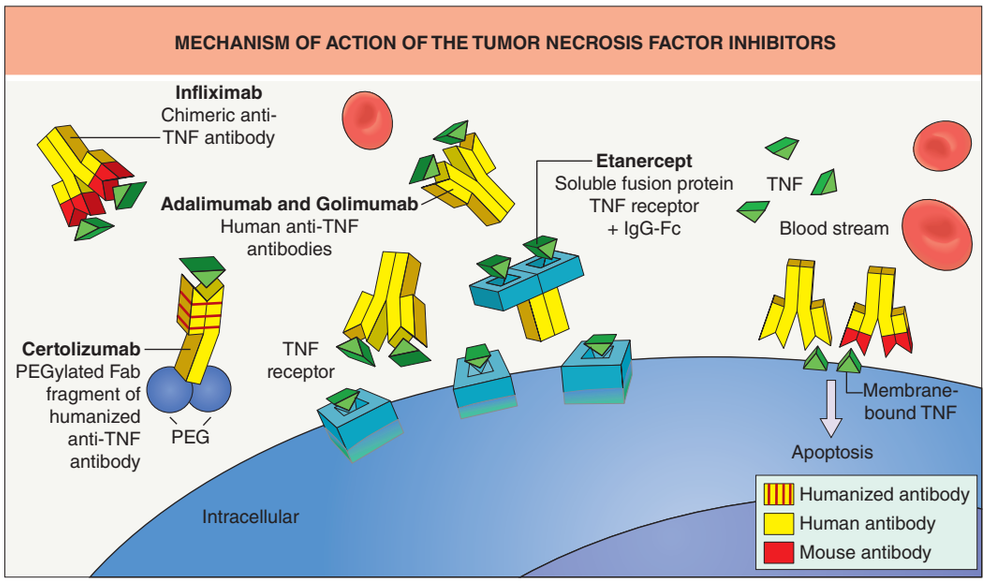


Fig. 128.4 Mechanism of action of the tumor necrosis factor (TNF) inhibitors.

FDA WARNINGS AND PRECAUTIONS FOR TARGETED IMMUNE MODULATORS WITH DERMATOLOGIC INDICATIONS
TNF inhibitors: adalimumab, certolizumab, etanercept, golimumab, infliximab

• Increased risk of serious infections, including tuberculosis, bacterial sepsis, systemic fungal infections (e.g. histoplasmosis), and infections due to opportunistic pathogens
• Risk of hepatitis B virus reactivation
• Malignancies (especially lymphomas) have been reported in patients receiving these agents, including children and adolescents
  • For *infliximab*, lymphomas are seen more often than in the general population and fatal hepatosplenic T cell lymphomas have developed in patients with inflammatory bowel disease who were also receiving azathioprine or 6-mercaptopurine
  • An increased risk of non-melanoma skin cancer and melanoma has been observed in patients with rheumatoid arthritis treated with TNF inhibitors
• Congestive heart failure (exacerbation or new onset) has been observed
• Demyelinating disease (exacerbation or new onset) has been observed
• Anaphylaxis or severe allergic reactions can occur, including serum sickness-like reactions to *infliximab*
• Other potential adverse events include autoimmune hepatitis, cytopenias, and a lupus-like syndrome; see Table 128.7 for additional cutaneous side effects

Ustekinumab

• Serious infections have been observed; may increase the risk of infection and reactivation of latent infections
  • Patients genetically deficient in IL-12/IL-23 have an increased risk of severe infections with mycobacteria and *Salmonella*
  • BCG vaccination should not be given in the year prior to initiation or the year following completion of ustekinumab therapy
• Could potentially increase the risk of malignancies
• Hypersensitivity reactions (e.g. angioedema, anaphylaxis) and pneumonitis have been reported
• Reversible posterior leukoencephalopathy syndrome has been reported

IL-23 inhibitors: guselkumab, risankizumab, tildrakizumab
• May increase the risk of infections including tuberculosis • Hypersensitivity reactions have been reported
IL-17 inhibitors: ixekizumab, secukinumab, brodalumab
• Serious infections have been observed; may increase the risk of infection and reactivation of latent infections   • Patients genetically deficient in IL-17 are prone to chronic mucocutaneous candidiasis • New onset and exacerbation of inflammatory bowel disease have occurred • Hypersensitivity reactions (e.g. angioedema, anaphylaxis) can develop • For *brodalumab*: suicidal ideation and behavior, including complete suicides, have occurred
IL-4/13 receptor and IL-13 inhibitors: dupilumab, tralokinumab
• Hypersensitivity reactions can occur • Conjunctivitis and keratitis may develop • May potentially affect the immune response to helminth infections
IL-1 inhibitors: anakinra, canakinumab, rilonacept
• Increased risk of serious infections • Coadministration with TNF inhibitors is not recommended • Hypersensitivity reactions (e.g. angioedema, anaphylaxis) can develop
Spesolimab
• May increase the risk of infections • Hypersensitivity and infusion-related reactions may develop, including drug reaction with eosinophilia and systemic symptoms

Table 128.5 US Food and Drug Administration (FDA) warnings and precautions for targeted immune modulators with dermatologic indications.

FDA WARNINGS AND PRECAUTIONS FOR TARGETED IMMUNE MODULATORS WITH DERMATOLOGIC INDICATIONS
Rituximab
• Severe infusion reactions can occur   • 80% of fatal reactions occur with the first infusion • Tumor lysis syndrome can develop in lymphoma patients, especially those with a high tumor burden, and lead to acute renal failure • Progressive multifocal leukoencephalopathy has been reported • Serious infections (bacterial, fungal, or viral) up to 1 year after completing therapy and reactivation of viral infections may occur, especially hepatitis B virus reactivation with fulminant hepatitis • Cardiac arrhythmias and angina can occur and may be life-threatening • Bowel obstruction and perforation have been described • Stevens–Johnson syndrome/toxic epidermal necrolysis and onset of paraneoplastic pemphigus have been described • Late-onset neutropenia (≥4 weeks after infusion) develops in a subset of patients • Decreased antibody responses to immunization, including COVID mRNA vaccines, has been noted • B cell lymphopenia can occur in infants exposed to rituximab *in utero*
Omalizumab
• Administer only in a healthcare setting prepared to manage anaphylaxis, which can be life-threatening, and observe patients for an appropriate period after administration • Patients can develop serum sickness-like reactions with fever, arthralgias, and an urticarial eruption • Malignancies have been observed in clinical studies of asthma patients, although a meta-analysis did not find an increased risk of malignancy • Do not abruptly discontinue corticosteroids upon initiation of omalizumab therapy
JAK inhibitors: abrocitinib, baricitinib, deucravacitinib, ritlecitinib, ruxolitinib, tofacitinib, upadacitinib
• Increased risk of bacterial, mycobacterial, invasive fungal and viral infections, including tuberculosis, herpes zoster, hepatitis B, and infections due to opportunistic pathogens • Laboratory monitoring is recommended due to potential changes in lymphocytes, neutrophils, hemoglobin, platelets (especially with abrocitinib, ritlecitinib, and ruxolitinib), liver enzymes, and lipids • Increased risk of major adverse cardiac events (MACE) and all-cause mortality in rheumatoid arthritis patients ≥50 years of age with at least one cardiovascular risk factor treated with *tofacitinib* compared with those treated with TNF inhibitors • Higher rate of malignancies (in particular lymphomas and lung cancers) in rheumatoid arthritis patients treated with *tofacitinib* compared with those treated with TNF inhibitors • Thrombosis (e.g. deep venous thrombosis, pulmonary embolism, arterial thrombosis) has occurred • Gastrointestinal perforations have been reported in patients treated with *baricitinib, tofacitinib, and upadacitinib* • Progressive multifocal leukoencephalopathy has been reported in a patient treated with *ruxolitinib* • Hypersensitivity reactions (e.g. angioedema, anaphylaxis) can develop • May cause fetal harm based on animal studies

Table 128.5 US Food and Drug Administration (FDA) warnings and precautions for targeted immune modulators with dermatologic indications. Live vaccines (see Table 128.8) should not be given to patients receiving these medications. BCG, bacillus Calmette–Guérin; IL, interleukin; JAK, Janus kinase; LE, lupus erythematosus; TNF, tumor necrosis factor.



Fig. 128.5 Atypical mycobacterial infection complicating adalimumab therapy. This patient was being treated for Crohn disease.

reactivation of latent tuberculosis, has also been observed in patients treated with these agents. However, most of the studies evaluating the risk of infection associated with the use of TNF inhibitors have been in patients with rheumatoid arthritis or inflammatory bowel disease, who often concomitantly receive additional immunosuppressive agents such as prednisone and methotrexate. The actual risk of infections is likely lower in patients receiving a TNF inhibitor as monotherapy. For example, a meta-analysis of 20 randomized controlled trials (RCTs; total n=6810) of TNF inhibitor therapy for psoriasis or psoriatic arthritis over rather limited periods of 12–30 weeks found no association between the use of these agents and the risk of infection (overall or serious) when adjusted for different follow-up times in treatment and control groups[7].

Recommended monitoring for dermatologic patients receiving TNF inhibitors is outlined in Table 128.6. A purified protein derivative (PPD) skin test, IFN-γ release assay (e.g. QuantiFERON® TB Gold Plus, T-SPOT®.TB), and/or chest X-ray (e.g. if immunosuppression or history of tuberculosis) is required at baseline and is typically, especially if risk factors, repeated annually during therapy. Patients with untreated or inadequately treated latent tuberculosis should receive antituberculous therapy prior to treatment with a TNF inhibitor. Reactivation of hepatitis B virus has also been observed in patients who are chronic hepatitis B carriers (i.e. hepatitis B surface antigen positive) while receiving a TNF inhibitor, so patients should be evaluated for hepatitis B virus infection prior to therapy. TNF inhibitors do not generally appear to have an adverse effect on viral load or hepatitis activity in psoriasis patients with chronic hepatitis C virus infection[8].

Risk of malignancy

The potential of TNF inhibitors to increase the risk of malignancy is controversial and may be dependent upon the disease being treated. TNF inhibitor therapy in patients with rheumatoid arthritis has been associated with an approximately threefold increase in the risk of lymphoma and malignancy in general[9,10]; however, this patient group is known to have a heightened susceptibility to lymphoma and often receives additional immunosuppressive agents. Most studies have not demonstrated an increase in the risk of other internal malignancies in patients treated with TNF inhibitors[11]. Keratinocyte carcinomas and melanoma may be more frequent in patients with rheumatoid arthritis who are treated with TNF inhibitors than those who do not receive

RECOMMENDED EVALUATION FOR PATIENTS RECEIVING TARGETED IMMUNE MODULATORS FOR DERMATOLOGIC DISORDERS	
Baseline history and physical examination	

• Complete medical history, including prior/current medications, vaccinations*, and allergies
• Complete physical examination
• Pay particular attention to history, risk, symptoms, and signs of:
  • Tuberculosis and other chronic as well as acute infections
  • Malignancy
  • For *TNF inhibitors*: congestive heart failure, demyelinating diseases (e.g. multiple sclerosis)
  • For *brodalumab*: depression, suicidal ideation/behavior
  • For *IL-17 inhibitors*: Crohn disease and ulcerative colitis
  • For *rituximab*: arrhythmias
  • For *JAK inhibitors*: risk factors for thrombosis and intestinal perforation (e.g. diverticulitis)
• Pregnancy status	

Laboratory testing	
Prior to treatment	***During treatment***

• PPD†/interferon-γ release assay‡ and/or (e.g. if immunosuppression or history of tuberculosis) chest X-ray
• CBC and CMP
• Hepatitis B and C virus serologic profiles
• Consider HIV testing
• For *JAK inhibitors*: also lipid profile
	• Annual PPD†/interferon-γ release assay‡ and/or chest X-ray
	• CBC and CMP as noted below or clinically indicated
	  • For *anakinra*: CBC monthly for 3 months and then every three months
	  • For *JAK inhibitors*: CBC, CMP, and lipid profile within 1–2 months and then every 3 months

*Recommended vaccines should be administered prior to initiation of therapy, with live vaccines (see Table 128.8) given at least 2–4 weeks prior to starting the medication; the bacillus Calmette–Guérin (BCG) vaccine should not be given in the year prior to beginning or the year after completing ustekinumab therapy. †≥5 mm of induration should be considered as positive. ‡e.g. QuantiFERON® TB Gold Plus or T-SPOT®.TB.	

Table 128.6 Recommended evaluation for patients receiving targeted immune modulators for dermatologic disorders. Table 8.19 provides guidance for the selection of systemic therapies in psoriasis patients with comorbidities. CBC, complete blood count with differential; CMP, comprehensive metabolic panel (includes liver function tests); IL, interleukin; JAK, Janus kinase; PPD, purified protein derivative skin test; TNF, tumor necrosis factor.

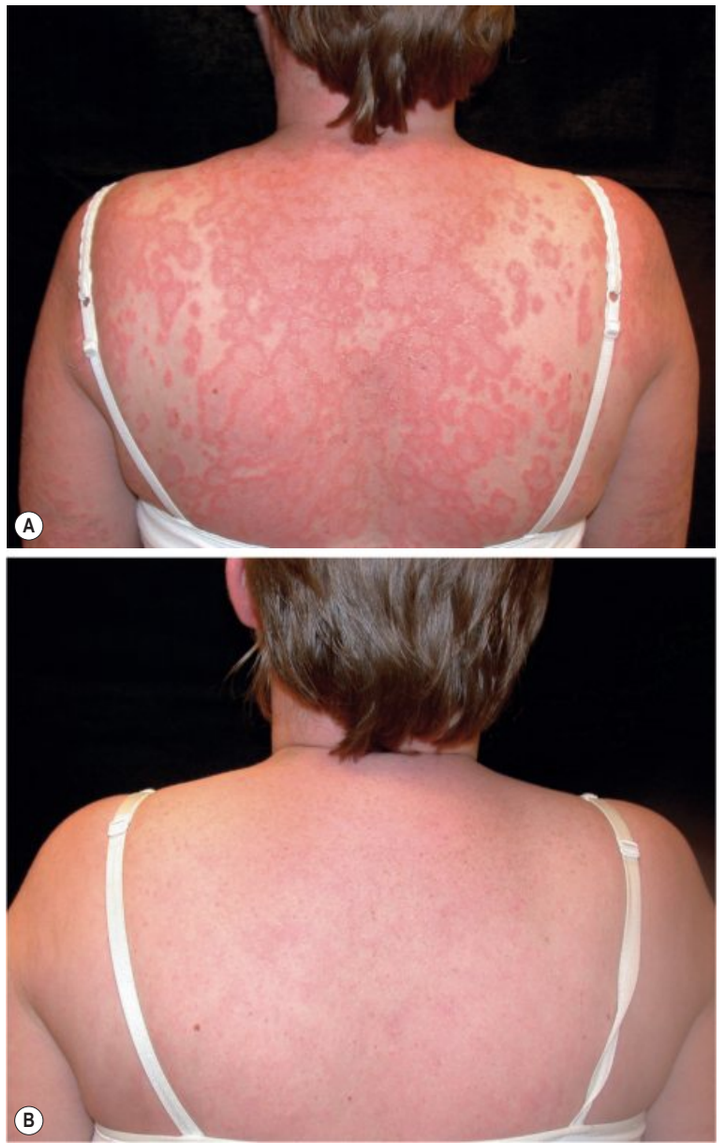


Fig. 128.6 Excellent clinical response to etanercept. Subacute cutaneous lupus erythematosus, before (**A**) and after (**B**) administration of etanercept.

these agents[12]. A meta-analysis of 20 RCTs (total n=6810) of TNF inhibitor therapy for psoriasis or psoriatic arthritis over rather limited periods of 12–30 weeks found no significant association with development of malignancy[13].

Adolescents and young adults with inflammatory bowel disease who receive infliximab and concomitant azathioprine or 6-mercaptopurine appear to have an increased risk of a rare, aggressive hepatosplenic T cell lymphoma. In an analysis of 48 malignancies in children and adolescents treated with TNF inhibitors that were reported to the FDA[14], it was noted that half were lymphomas, almost two-thirds were in patients taking infliximab, and 88% of the patients were concomitantly receiving another immunosuppressive agent. Although the incidence of malignancy was higher than the background rate in the general pediatric population, the potential role of other medications as well as the underlying disorders, primarily inflammatory bowel disease and juvenile idiopathic arthritis (JIA), precluded establishing a causal relationship with TNF inhibitor therapy.

Autoimmunity

Treatment with TNF inhibitors is associated with an increased likelihood of developing anti-nuclear and anti-dsDNA antibodies. Signs and symptoms of cutaneous and systemic lupus erythematosus (SLE) occasionally arise in patients receiving TNF inhibitors, but in general resolve upon cessation of treatment[15–17]. Conversely, several small case series have reported marked improvement of subacute cutaneous lupus erythematosus by etanercept[18,19] (Fig. 128.6). It is not necessary to evaluate patients for autoantibodies before or during therapy with TNF inhibitors. However, the development of anti-nuclear antibodies may be linked to loss of TNF inhibitor efficacy[20].

Demyelinating diseases

Although etanercept was originally utilized as a therapy for multiple sclerosis, new onset or exacerbation of multiple sclerosis or other demyelinating diseases represents a potential complication of TNF inhibitor treatment[4]. In some patients, symptoms of multiple sclerosis have abated despite continued therapy. It seems reasonable to avoid using TNF inhibitors in patients with a history of multiple sclerosis or other demyelinating diseases.

Congestive heart failure

There have been reports of congestive heart failure worsening or developing in patients receiving TNF inhibitors. As a result, it is recommended that therapy with TNF inhibitors be avoided in patients with unstable cardiac disease.

Cutaneous reactions

A variety of adverse skin reactions to TNF inhibitors have been described (Table 128.7). A new onset of psoriasis or a psoriasiform eruption occurs in ~5%–10% of patients with no previous history of psoriasis, often manifesting in adults as palmoplantar pustulosis (Fig. 128.7); in children, lesions tend to involve the scalp and ears[21–23]. Patients can also develop eczematous eruptions, which presumably reflect a shift towards Th1-mediated inflammation. Cutaneous small vessel vasculitis and reactive granulomatous dermatitis (RGD) have also been reported in patients undergoing TNF inhibitor therapy[24], but a subset of

CUTANEOUS SIDE EFFECTS OF TARGETED IMMUNE MODULATORS
Injectable agents
• Injection site reactions, e.g. erythema/edema, occasionally small vessel vasculitis; "recall" reactions at previous sites
Tumor necrosis factor inhibitors
• New-onset psoriasis, especially palmoplantar pustulosis • Interstitial granulomatous dermatitis and other granulomatous eruptions • Cutaneous small vessel vasculitis • Eczematous eruptions • Lichenoid dermatitis • Lupus-like syndrome-associated malar rash or discoid lesions • Other types of cutaneous lupus, e.g. SCLE, chilblain lupus
Interleukin-12/23, -23, and -17 inhibitors
• New-onset psoriasis, including palmoplantar pustulosis • Eczematous eruptions • Lichenoid dermatitis (primarily IL-17 inhibitors) • Granulomatous eruptions • Neutrophilic dermatoses (e.g. pyoderma gangrenosum) • Cutaneous small vessel vasculitis • Cutaneous lupus erythematosus (e.g. SCLE, discoid) • Vitiligo, alopecia areata, autoimmune bullous dermatoses • Hypertrichosis (IL-17 inhibitors)
Dupilumab
• Facial ± neck erythema or dermatitis • Psoriasis and psoriasiform eruptions • Lichen planus and lichenoid eruptions • Eosinophilic granulomatosis with polyangiitis • Alopecia areata, vitiligo • Unmasking of cutaneous T-cell lymphoma
JAK inhibitors
• Acne, papulopustular eruptions • Granulomatous dermatitis • Cutaneous small vessel vasculitis • SCLE • Lymphomatoid papulosis • Extensive cutaneous HPV infection, disseminated molluscum contagiosum • Keratinocyte and Merkel cell carcinomas

Table 128.7 Cutaneous side effects of targeted immune modulators. Allergic reactions manifesting with urticaria and angioedema can also occur with most agents. HPV, human papillomavirus; SCLE, subacute cutaneous lupus erythematosus; SJS, Stevens–Johnson syndrome.

these patients have rheumatoid arthritis, which itself can be associated with vasculitis and RGD (see Ch. 93)[25]. Additional cutaneous reactions that have been described in patients receiving TNF inhibitors include lichenoid dermatitis and other granulomatous conditions[26].

Vaccination

Live vaccines are contraindicated in patients receiving TNF inhibitors (Table 128.8). The effectiveness of vaccines in patients receiving these agents is unknown, but an immune response to influenza and pneumococcal vaccines has been documented[27]. It is recommended that patients (especially children) be brought up to date with all immunizations prior to initiating treatment with TNF inhibitors.

Use in pregnancy

In animal studies, TNF inhibitors have not shown evidence of harm to the fetus, but adequate studies in pregnant women have not been conducted[28]. Because IgG antibodies cross the placenta, their administration during late pregnancy could potentially increase risk of infection in the infant. Of note, pegylated certolizumab represents an exception as it has minimal placental transfer. Although TNF inhibitors are present in human milk, systemic exposure in a breastfed infant is expected to be low due to minimal oral absorption.

Etanercept

Etanercept (Enbrel®) and its biosimilars are fusion proteins consisting of the extracellular domain of the TNF receptor fused with the Fc portion of human IgG1[29].





Fig. 128.7 Psoriasiform reactions to tumor necrosis factor inhibitors. A Palmoplantar pustulosis that developed as a complication of infliximab. **B** Eruption of plaque psoriasis in a patient receiving infliximab therapy. The patient had received infliximab for GVHD of the gastrointestinal tract.

VACCINES THAT CONTAIN LIVE ATTENUATED VIRUSES OR BACTERIA
Adenovirus Bacillus Calmette–Guérin (BCG) Cholera, *oral form in the US* Herpes zoster, *live attenuated form (Zostavax®)** Influenza (including H1N1), *intranasal form* Measles, mumps, and rubella Rotavirus Polio, *oral form* Typhoid, *oral form* Vaccinia (smallpox vaccine) Varicella Yellow fever
*No longer available in the US, where a recombinant herpes zoster vaccine (Shingrix®) is administered.

Table 128.8 Vaccines that contain live attenuated viruses or bacteria.

Indications

Etanercept has been approved for the treatment of moderate to severe plaque psoriasis in adults since 2004 and in children ages 4–17 years since 2016. Depending on the regimen (see below), ~30%–60% and ~15%–25% of patients achieve a 75% and 90% improvement in their Psoriasis Area and Severity Index (PASI) score, respectively[30]. Other approved indications for etanercept include rheumatoid arthritis, psoriatic arthritis, and ankylosing spondylitis in adults as well as JIA in children ≥2 years of age.

Etanercept has been used to treat a variety of other mucocutaneous disorders, including toxic epidermal necrolysis, hidradenitis suppurativa, dermatomyositis, cutaneous lupus erythematosus, lichen planus, autoimmune bullous diseases (especially mucous membrane [cicatricial] pemphigoid), neutrophilic dermatoses (including pyoderma gangrenosum), multicentric reticulohistiocytosis, relapsing polychondritis, and GVHD[18,31,32]. Although successful treatment of sarcoidosis has been described in case reports and small series, etanercept therapy failed to improve systemic manifestations of sarcoidosis in RCTs[33].

Dosages
The approved dose for moderate to severe plaque psoriasis is 50 mg twice weekly for the first 3 months, followed by 50 mg weekly. Etanercept is available in 25 and 50 mg prefilled syringes, 50 mg autoinjectors, and 25 mg multiple-use vials. The recommended dose for pediatric psoriasis is 0.8 mg/kg (maximum 50 mg) weekly.

Specific side effects
Side effects shared with other TNF inhibitors are discussed above and summarized in Tables 128.5 and 128.7. Injection site reactions are the most common side effect of etanercept (Fig. 128.8) but in general are mild to moderate and diminish in frequency after the first month of treatment. Erythema, pruritus, pain, and swelling have been described, and "recall" reactions at sites of previous injections have been reported. These reactions do not progress to anaphylaxis.

Interactions
The concomitant use of etanercept and methotrexate is approved for the treatment of rheumatoid arthritis and psoriatic arthritis. Due to the potential for increased immunosuppression, combination of etanercept with other targeted immune modulators should generally be avoided. A study of anakinra plus etanercept for patients with rheumatoid arthritis found no increase in efficacy but a substantial increase in the frequency of infection[34]. Etanercept has been used together with narrowband UVB without an increase in adverse events[35].

Infliximab
Infliximab and its biosimilars are chimeric human–mouse monoclonal IgG1 antibodies, and their target is human TNF[36].

Indications
Infliximab is approved for the treatment of adults with chronic severe plaque psoriasis. Compared with the other TNF inhibitors, its onset of action tends to be faster and a higher proportion of patients (~75%–85% and ~50%–65%) achieve a 75% and 90% reduction in the PASI score, respectively[37]. Infliximab is also approved for the treatment of adults with psoriatic arthritis, Crohn disease (including associated fistulas), ulcerative colitis, rheumatoid arthritis, and ankylosing spondylitis, as well as children ≥6 years of age with Crohn disease and ulcerative colitis. Infliximab appears to be useful for pyoderma gangrenosum, whether or not it is associated with inflammatory bowel disease[38]. It has been effective as a treatment for sarcoidosis, granulomatous cheilitis, Behçet disease, various vasculitides, pityriasis rubra pilaris, reactive arthritis, subcorneal pustular dermatosis, hidradenitis suppurativa, GVHD, Sjögren syndrome, and multicentric reticulohistiocytosis[39].



Fig. 128.8 Etanercept injection site reaction. Similar reactions occur with nearly all subcutaneously injected biologic therapies.

Dosages
In patients with plaque psoriasis, the typical infliximab regimen is 5 mg/kg administered by slow intravenous infusion at 0, 2, and 6 weeks, and then every 8 weeks. However, doses ranging from 3 to 10 mg/kg have been utilized, and the frequency of administration as well as the dose can be adjusted when the response is inadequate. For Crohn disease, rheumatoid arthritis, and psoriatic arthritis, it is approved for concomitant administration with methotrexate, azathioprine, or low-dose prednisone. Loss of efficacy over time may be related to the development of neutralizing anti-chimeric antibodies and has been associated with the presence of anti-nuclear antibodies[40,41]; the concurrent administration of low-dose weekly methotrexate may help to prevent the formation of anti-chimeric antibodies.

Specific side effects
Side effects shared with other TNF inhibitors are discussed above and summarized in Tables 128.5 and 128.7. Infusion-related reactions are the most commonly reported side effect of infliximab, occurring in ~15% of patients. The incidence of severe reactions, in particular anaphylaxis, is ~1%. Associated symptoms include fever, chills, pruritus, urticaria, chest pain, hypotension, hypertension, and shortness of breath. Infusion reaction risk has been linked to the presence of human anti-chimeric antibodies. Risk of reactions may be lessened by a slower infusion rate or concomitant use of methotrexate, azathioprine, or corticosteroids.

Interactions
Infliximab should not be administered together with other targeted immune modulators due to the potential for additive immunosuppression; concomitant use with anakinra or abatacept has been associated with the development of severe infections.

Adalimumab
Adalimumab (Humira®) and its biosimilars are human recombinant IgG1 monoclonal antibodies with specificity for human TNF[42].

Indications
Adalimumab is approved for the treatment of moderate to severe plaque psoriasis in adults; ~65%–75% and ~40%–45% of patients achieve a 75% and 90% improvement in their PASI score, respectively[36]. It is also approved for the treatment of moderate to severe hidradenitis suppurativa in patients ≥12 years of age, with ~40%–60% of these individuals achieving a 50% reduction in the abscess/inflammatory nodule count with no increase in the draining fistula count[43]. Additional approved indications include psoriatic arthritis, rheumatoid arthritis, ankylosing spondylitis, uveitis, and Crohn disease in adults as well as JIA and Crohn disease in children ≥2 years and ≥6 years of age, respectively. There have also been reports of successful adalimumab therapy for pustular psoriasis[44], sarcoidosis, pyoderma gangrenosum, Behçet disease, other neutrophilic dermatoses, and dermatomyositis.

Dosages
Adalimumab is supplied in 10–80 mg prefilled syringes as well as 40 and 80 mg autoinjectors; it is administered subcutaneously. For the treatment of psoriasis in adults, a loading dose of 80 mg is typically given, followed by 40 mg on day 8 and then 40 mg every other week. The approved regimen for hidradenitis suppurativa in adults and adolescents weighing ≥60 kg is a loading dose of 160 mg, 80 mg on day 15, and then either 40 mg weekly or 80 mg every other week starting on day 29. For adolescent HS patients weighing 30–59 kg, a loading dose of 80 mg is followed by 40 mg every other week starting on day 8. Loss of efficacy of adalimumab over time related to the production of anti-adalimumab antibodies can occur and may be prevented by the concurrent administration of low-dose weekly methotrexate; loss of efficacy has also been associated with the development of anti-nuclear antibodies[20].

The concomitant use of adalimumab and methotrexate is approved for the treatment of psoriatic arthritis, rheumatoid arthritis, and JIA.

Side effects

Side effects shared with other TNF inhibitors, including risk of infection with mycobacteria (see Fig. 128.5) and fungi, are discussed above and summarized in Tables 128.5 and 128.7[45].

Interactions

The concomitant administration of other targeted immune modulators with adalimumab may increase the risk of infection and should be avoided[46].

Golimumab

Golimumab (Simponi®, Simponi ARIA®) is a human recombinant IgG1 monoclonal antibody with specificity for human TNF[42]. It is approved for the treatment of psoriatic arthritis, rheumatoid arthritis, ankylosing spondylitis, polyarticular JIA, and ulcerative colitis; it can be administered together with methotrexate. Golimumab may also be useful in the treatment of other conditions that respond to TNF inhibitors. For psoriatic arthritis, it is administered as a 50 mg subcutaneous injection (prefilled syringe or autoinjector) monthly in adults or via a 2 mg/kg intravenous infusion at weeks 0 and 4, and then every 8 weeks, in patients ≥2 years of age[47].

Certolizumab pegol

Certolizumab pegol (Cimzia®) is a pegylated Fab fragment of a humanized monoclonal antibody with specificity for human TNF. It is approved for the treatment of psoriasis in adults, with ~60%–75% and ~35%–50% of patients achieving a 75% and 90% improvement in their PASI score, respectively[48]. Certolizumab is also approved for psoriatic arthritis, rheumatoid arthritis, and Crohn disease. It is supplied in a 200 mg prefilled syringe and administered subcutaneously. For psoriasis, 400 mg is given every 2 weeks, with an option of switching to a 200 mg dose after 4 weeks in patients weighing ≤90 kg.

Interleukin-12/23 and Interleukin-23 Inhibitors

Ustekinumab (Stelara®) is a monoclonal antibody that targets both IL-12 and IL-23. Monoclonal antibodies that target IL-23 alone include guselkumab (Tremfya®), risankizumab (Skyrizi®), tildrakizumab (Ilumya®), and mirikizumab (approved in Japan). A review of their mechanisms of action as well as shared contraindications, side effects, interactions, and use in pregnancy is followed by a discussion of issues that relate specifically to individual FDA-approved drugs.

Mechanism of action

Ustekinumab binds to the p40 subunit that is shared by the heterodimeric IL-12 and IL-23 cytokines, whereas guselkumab, risankizumab, tildrakizumab, and mirikizumab target the p19 subunit that is specific to IL-23 (Fig. 128.9D). IL-12 has a critical role in the development of Th1 cells and NK cell activation, whereas IL-23 is necessary for the generation of Th17 cells (see Fig. 4.9).

Contraindications

Ustekinumab and IL-23 inhibitors are contraindicated in patients with known hypersensitivity to these agents, and they should be avoided in patients with serious active infections or malignancies.

Side effects (see Table 128.5)

The most common adverse events in clinical trials of ustekinumab and IL-23 inhibitors were upper respiratory tract infections. Injection site reactions occurred in <5% of patients, and dermatophyte infections were observed in ~1% of patients treated with guselkumab or risankizumab. Hypersensitivity reactions have also been reported, including anaphylaxis, angioedema, and urticaria.

Assessment for tuberculosis is recommended at baseline and, depending on risk factors, repeated annually during therapy (see Table 128.6). Patients with untreated latent tuberculosis should receive antituberculous therapy prior to beginning treatment. In patients treated with IL-23 inhibitors, preservation of IL-12 activity and the resultant Th1 response is thought to result in less risk of infection with *Mycobacterium* spp. and other intracellular pathogens.

Interactions

Live vaccines should be avoided (see Table 128.8), and patients (especially children) should be brought up to date with immunizations prior to initiating treatment. Other targeted immune modulators should not be administered together with ustekinumab and IL-23 inhibitors. The concomitant administration of other immunosuppressive agents might increase the risk of infection.

Use in pregnancy

Animal reproduction studies have not shown adverse fetal effects, with the exception of increased fetal loss in pregnant monkeys who received high doses of risankizumab. There are no adequate studies in pregnant women. Safety during lactation is unknown.

Ustekinumab

Ustekinumab (Stelara®) is a human IgG1 monoclonal antibody that binds with high affinity and specificity to the p40 subunit shared by the heterodimeric IL-12 and IL-23 cytokines (see Fig. 128.9D).

Indications

Ustekinumab is approved for the treatment of moderate to severe plaque psoriasis and psoriatic arthritis in adults and children ≥6 years of age, with ~65%–80% and ~40%–55% of patients achieving a 75% and 90% improvement in their PASI scores, respectively[49]. Ustekinumab is also approved for adults with Crohn disease and ulcerative colitis. In addition, there are reports of its benefit in the treatment of other dermatologic conditions, such as hidradenitis suppurativa and pyoderma gangrenosum.

Dosages

For the treatment of psoriasis in adults and children weighing 60–100 kg, ustekinumab is administered as a subcutaneous injection of 45 mg, with the dose increased to 90 mg for patients weighing >100 kg; 0.75 mg/kg is administered to children weighing <60 kg. It is given at weeks 0 and 4, and then every 12 weeks. Ustekinumab is available as a 45 or 90 mg prefilled syringe, a 45 mg single-dose vial, and a solution for intravenous infusion in patients with Crohn disease. Measurement of serum levels of ustekinumab and anti-ustekinumab antibodies is commercially available and may be of utility in patients with a suboptimal therapeutic response.

Specific side effects

Side effects shared with IL-23 inhibitors are discussed above. Ustekinumab is associated with a potential risk of severe and disseminated infections with mycobacteria and *Salmonella*, which also occur in patients with genetic deficiencies in the IL-12/IL-23 signaling pathway (see Fig. 60.2). An increase in candidal infections has been observed in patients with Crohn disease. A possible excess of major adverse cardiovascular events (MACEs) such as myocardial infarction or stroke was noted in patients who received anti-IL-12/23 therapy in individual clinical trials, but meta-analyses and a 5-year follow-up study did not find a significant increase in the risk of MACEs[50–52]. Although the effects of IL-12/23 inhibitors on vascular inflammation and thrombosis, especially early in the course of therapy, remain to be determined, cardiovascular risk factors should be assessed prior to initiating treatment. Other potential severe side effects of ustekinumab are listed in Table 128.5. Retiform purpura progressing to cutaneous necrosis on the leg was reported in a patient treated with ustekinumab[53].

Guselkumab

Guselkumab (Tremfya®) is a human IgG1 monoclonal antibody that binds with high affinity and specificity to the p19 subunit of IL-23. It is approved for the treatment of adults with moderate to severe plaque psoriasis or psoriatic arthritis, with ~85% and ~65%–70% of psoriasis patients achieving a 75% and 90% improvement in their PASI score, respectively. Guselkumab is supplied in a 100 mg prefilled syringe or autoinjector that is administered subcutaneously at weeks 0 and 4, and then every 8 weeks.

Tildrakizumab

Tildrakizumab (Ilumya®) is a humanized IgG1 monoclonal antibody that specifically binds to the p19 subunit of IL-23. It is approved for the treatment of moderate to severe plaque psoriasis in adults, with ~65%

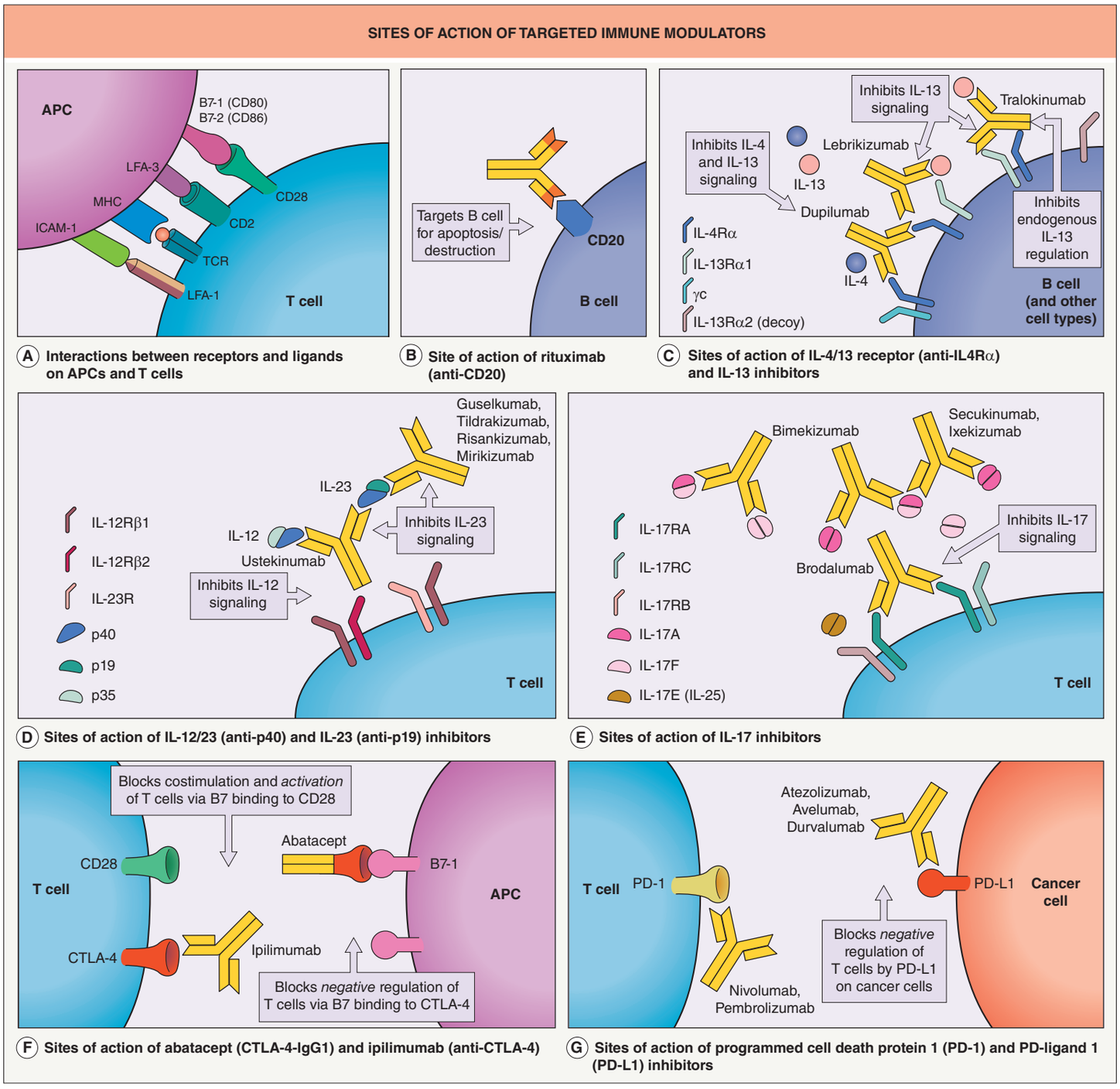


Fig. 128.9 Sites of action of targeted immune modulators. A Activation of T cells requires two signals. The first occurs when the major histocompatibility complex antigen interacts with the T cell receptor (TCR). A second costimulatory signal is required for T cell activation to occur. **B** Site of action of rituximab. **C** Sites of action of IL-4/13 receptor (anti-IL4Rα) and IL-13 inhibitors. **D** Sites of action of IL-12/23 (anti-p40) and IL-23 (anti-p19) inhibitors. **E** Sites of action of IL-17 inhibitors. **F** Sites of action of abatacept and ipilimumab. **G** Sites of action of programmed cell death protein 1 (PD-1) and PD-ligand 1 (PD-L1) inhibitors. APC, antigen-presenting cell; CTLA-4, cytotoxic T lymphocyte antigen 4; ICAM, intercellular adhesion molecule; IL, interleukin; LFA, lymphocyte function antigen; MHC, major histocompatibility complex; R, receptor.

and ~40% of patients achieving a 75% and 90% improvement in their PASI score, respectively. Tildrakizumab is supplied in a 100 mg prefilled syringe that is administered subcutaneously at weeks 0 and 4, and then every 12 weeks.

Risankizumab

Risankizumab (Skyrizi®) is a humanized IgG1 monoclonal antibody that binds with high affinity and specificity to the p19 subunit of IL-23. It is approved for the treatment of moderate to severe psoriasis, psoriatic arthritis, and Crohn disease in adults. Approximately 90% and 75% of psoriasis patients achieve a 75% and 90% improvement in their PASI score, respectively. Risankizumab is supplied in a 150 mg prefilled syringe or autoinjector that is administered subcutaneously at weeks 0 and 4, and then every 12 weeks.

Interleukin-17 Inhibitors

Currently, three IL-17 inhibitors are approved for the treatment of psoriasis: ixekizumab (Taltz®) and secukinumab (Cosentyx®), which target IL-17A, and brodalumab (Siliq™), which blocks the IL-17 receptor A (Fig. 128.9E). Bimekizumab (Bimzelx®), which targets both IL-17A and IL-17F, is approved in Europe, Canada, and Japan. A review of their

shared contraindications, major side effects, interactions, and use in pregnancy is followed by a discussion of issues that relate specifically to individual drugs.

Contraindications

Each IL-17 inhibitor is contraindicated in patients with a known hypersensitivity to that particular agent or components of its formulation. These medications should be used with caution in patients with chronic/recurrent infections or inflammatory bowel disease, with Crohn disease representing a contraindication for brodalumab (see below). Administration of an IL-17 inhibitor should be avoided or discontinued in patients with a serious active infection.

Major side effects

The most common adverse events in clinical trials of IL-17 inhibitors were nasopharyngitis/upper respiratory tract infections and (for ixekizumab) injection-site reactions[54–56]. Hypersensitivity reactions have also been reported, including anaphylaxis, angioedema, and urticaria. Mucocutaneous candidiasis, most often oral or vulvovaginal, develops in ~5% of patients[55,57]; this reflects the important role of IL-17 in defense against *Candida* (see Fig. 60.2)[58]. These infections are typically mild or moderate and resolve with standard treatment[55]. Neutropenia (<1500 cells/mm^3) occurs in ~1%–2% of patients, which is similar to the frequency in patients receiving etanercept[54,56]. Assessment for tuberculosis is required at baseline and, depending on risk factors, repeated annually during therapy (see Table 128.6). Patients with untreated or inadequately treated latent tuberculosis should receive antituberculous therapy prior to beginning treatment.

In 0.1%–0.5% of patients receiving IL-17 inhibitors, a new onset or exacerbation of Crohn disease or ulcerative colitis has been reported. An increased risk of adverse cardiovascular events was not observed in clinical trials. Cutaneous reactions that have been described in patients receiving IL-17 inhibitors are listed in Table 128.7.

Interactions

Live vaccines should be avoided (see Table 128.8), and patients (especially children) should be brought up to date with immunizations prior to initiating treatment. To avert a potential increased risk of infection, other targeted immune modulators should not be coadministered with IL-17 inhibitors.

Use in pregnancy

There are no adequate studies on IL-17 inhibitor use in pregnant women, although human IgG is known to cross the placenta. No evidence of harm to the fetus was observed in pregnant monkeys receiving up to 19–30 times the maximum recommended human doses of ixekizumab, secukinumab, and brodalumab; however, there were a few deaths of newborn monkeys in the ixekizumab group. Safety during lactation is unknown.

Ixekizumab

Mechanism of action

Ixekizumab (Taltz®) is a humanized IgG4 monoclonal antibody that binds and inhibits IL-17A, resulting in neutralization of IL-17A homodimers and IL-17A/F heterodimers (see Fig. 128.9E). In its hinge region, there is substitution of proline for serine which prevents the formation of half-antibodies (half-mers) that can undergo Fab-arm exchange with endogenous human IgG4.

Indications

Ixekizumab is approved for the treatment of moderate to severe plaque psoriasis in patients ≥6 years of age, with ~90% and ~70%–75% of patients achieving a 75% and 90% improvement in their PASI score, respectively, within 12 weeks of beginning treatment[54]. Ixekizumab is also indicated for the treatment of psoriatic arthritis and ankylosing spondylitis in adults.

Dosages

Ixekizumab is administered as a subcutaneous injection (prefilled syringe or autoinjector), with a loading dose of 160 mg followed by 80 mg every 2 weeks for 12 weeks and then every 4 weeks. Pediatric dosing is based on body weight: 160 mg loading and then 80 mg every 4 weeks if >50 kg; 80 mg loading and then 40 mg every 4 weeks if 25–50 kg; and 40 mg loading and then 20 mg every 4 weeks if <25 kg. It is supplied in 80 mg prefilled syringes and autoinjectors; currently 20 and 40 mg doses must be prepared and administered by a healthcare professional.

Secukinumab

Mechanism of action

Secukinumab (Cosentyx®) is a human IgG1κ monoclonal antibody that binds with high affinity and selectivity to IL-17A (see Fig. 128.9E).

Indications

Secukinumab is approved for moderate to severe plaque psoriasis in patients ≥6 years of age. Approximately 75%–85% and 65%–75% of adults treated with the 300 mg and 150 mg doses, respectively, achieve a 75% improvement in their PASI score, with ~65% of those who received 300 mg reaching 90% improvement by week 12[59]. Secukinumab is also approved for psoriatic arthritis in patients ≥2 years of age, enthesitis-related arthritis in patients ≥4 years of age, and ankylosing spondylitis in adults.

Dosages

Secukinumab is administered as a subcutaneous injection at weeks 0, 1, 2, 3, and 4; thereafter, it is given every 4 weeks. The standard dose for psoriasis in adults is 300 mg; doses of 150 mg and 75 mg are given to children weighing ≥50 kg (or selected adults weighing <90 kg) and <50 kg, respectively. It is available in prefilled syringes (75, 150, and 300 mg) and autoinjectors (150 and 300 mg).

Brodalumab

Mechanism of action

Brodalumab (Siliq™) is a human IgG2κ monoclonal antibody that selectively binds the IL-17 receptor A, inhibiting its interactions with IL-17A/F and IL-17E (also known as IL-25) (see Fig. 128.9E).

Indications

Brodalumab is approved for the treatment of moderate to severe plaque psoriasis in adults who have failed or become unresponsive to other systemic therapies. Approximately 80%–90% and 65%–75% of patients achieve a 75% and 90% reduction in their PASI score, respectively[57].

Dosages

Brodalumab is available in prefilled syringes and administered as a 210 mg subcutaneous injection every 2 weeks.

Additional contraindications and major side effects

Contraindications and major side effects shared with other IL-17 inhibitors are described above. Brodalumab is contraindicated in patients with Crohn disease. Suicidal ideation and completed suicides occurred during clinical trials of brodalumab[60]. As a result, this medication is only available through a restricted Risk Evaluation and Mitigation Strategy (REMS) program, which requires provider and pharmacy certification as well as a patient–prescriber agreement form.

Spesolimab-sbzo

Spesolimab-sbzo (Spevigo®) is a humanized IgG1 monoclonal antibody that binds to the IL-36 receptor, preventing downstream proinflammatory signaling. It is approved for the treatment of generalized pustular psoriasis flares in adults. A single 900 mg intravenous infusion is administered, which leads to a lack of visible pustules after 1 week in >50% of patients[61]; a repeat dose may be given 1 week later in patients without an inadequate response.

Contraindications

Spesolimab is contraindicated in patients with a history of hypersensitivity to this agent and should be avoided in patients with serious active infections.

Major side effects

The most common adverse reactions are asthenia and fatigue, nausea and vomiting, infection, headache, and pruritus. Hypersensitivity and

infusion-related reactions have occurred, including drug hypersensitivity with eosinophilia and systemic symptoms (DRESS). Assessment for tuberculosis is recommended prior to initiating treatment (see Table 128.5).

Interactions

Live vaccines are contraindicated and the response to vaccines may be muted (see Table 128.8).

Use in pregnancy

There are no adequate studies of spesolimab in pregnant women, and animal reproduction studies have not shown harm to the fetus. Its safety during lactation is unknown.

Interleukin-4/13 Receptor and Interleukin-13 Inhibitors

Dupilumab (Dupixent®) is a monoclonal antibody that targets the receptor which binds both IL-4 and IL-13. Monoclonal antibodies that target IL-13 include tralokinumab (Adbry™) and lebrikizumab (currently under FDA review for atopic dermatitis). A review of the mechanisms of action as well as shared contraindications, side effects, interactions, and use in pregnancy of these agents is followed by a discussion of issues that relate specifically to individual FDA-approved drugs.

Mechanisms of action

Dupilumab is a human IgG4 monoclonal antibody that specifically binds to the IL-4Rα subunit of the heterodimeric IL-4 and IL-13 receptor (Fig. 128.9C). This blocks signaling by these cytokines and the resultant Th2-mediated inflammation. Tralokinumab (Adbry™) is a human IgG4 monoclonal antibody that binds to IL-13, blocking its interaction with the IL-13Rα1 subunit of the IL-4/-13 receptor as well as IL-13Rα2, a decoy receptor. Lebrikizumab is a humanized IgG4 monoclonal antibody that also binds to soluble IL-13 but blocks its interaction with the IL-4Rα subunit, preventing heterodimerization with IL-13Rα1.

Contraindications

These agents are contraindicated in patients with known sensitivity to the drug or components of its formulation. Administration should be avoided or discontinued in patients with a serious active helminth infection.

Major side effects

The most common side effects are injection site reactions and conjunctivitis (see Table 128.5), with each occurring in ~10% of patients. Conjunctivitis typically develops in the first weeks to months of treatment, and manifestations of ocular surface disease may also include dry eyes, blepharitis, keratitis, eyelid dermatitis, and palpebral edema[62] (Fig. 128.10). Warm compresses, lubricant eye drops (i.e. artificial tears), and antihistamine/mast cell stabilizer eye drops (e.g. ketotifen) are often recommended for initial management; corticosteroid, cyclosporine, or lifitegrast eye drops and tacrolimus ointment represent additional treatment options.

Interactions

Live vaccines should be avoided (see Table 128.8), and patients (especially children) should be brought up to date with all immunizations prior to initiating treatment.

Use in pregnancy

There are no available data on use in pregnant women, although human IgG is known to cross the placenta. No evidence of fetal harm was observed in animal studies. Safety during lactation is unknown.

Dupilumab

Indications

Dupilumab is approved for the treatment of patients ≥6 months of age with moderate to severe atopic dermatitis that is not adequately controlled with topical therapy. It is also approved for prurigo nodularis in adults. Approximately 40%–50% of adolescents and adults treated with dupilumab alone and ~60%–70% of children or adults treated with dupilumab plus topical corticosteroids achieve a 75% improvement in their Eczema Area and Severity Index (EASI) score[63]. Non-dermatologic indications for dupilumab include asthma in patients ≥6 years of age, eosinophilic esophagitis in patients ≥12 years of age, and chronic rhinosinusitis with nasal polyposis in adults.



Fig. 128.10 Conjunctivitis and ectropion requiring surgical repair associated with dupilumab therapy for atopic dermatitis. The patient's facial and eyelid dermatitis flared on dupilumab. Of note, the conjunctivitis and ectropion recurred after rechallenge with dupilumab. *Courtesy Jonathan S. Leventhal, MD.*

Dosages

Administration via subcutaneous injection depends on age and weight: a 600 mg loading dose and then 300 mg every *2 weeks* in adults and children weighing ≥60 kg; a 400 mg loading dose and then 200 mg every *2 weeks* in children weighing 30–59 kg; a 600 mg loading dose and then 300 mg every *4 weeks* in children ≥6 years of age weighing 15–29 kg; 300 mg every *4 weeks* in children ≤5 years of age weighing 15–29 kg; and 200 mg every *4 weeks* in children ≤5 years of age weighing 5–14 kg. It is available in prefilled syringes (100, 200, and 300 mg) and autoinjectors (200 and 300 mg).

Specific side effects

In addition to the side effects noted above, facial ± neck erythema or dermatitis may develop in association with dupilumab therapy, with potential contributing factors including rosacea/demodicosis, allergic contact dermatitis, and *Malassezia*-related dermatitis[64]. Depending on the suspected etiology, treatment options include topical corticosteroids, topical calcineurin inhibitors, and topical or oral (e.g. itraconazole) antifungal agents. Dupilumab-associated psoriasis/psoriasiform eruptions, lichen planus/lichenoid eruptions, and eosinophilic granulomatosis with polyangiitis have also been reported.

Tralokinumab

Tralokinumab (Adbry™) is approved for the treatment of adults with moderate to severe atopic dermatitis that is not adequately controlled with topical therapy. Monotherapy and combination therapy with topical corticosteroids result in ~30% and 55% of patients achieving a 75% improvement in their EASI score, respectively[65,66]. A loading dose of 600 mg is followed by 300 mg every 2 weeks; a decrease in frequency to every 4 weeks may be considered in patients with clear or almost clear skin after 16 weeks of treatment. It is supplied in a 150 mg prefilled syringe.

Interleukin-1 Inhibitors

Currently, there are three approved IL-1 antagonists: anakinra, canakinumab, and rilonacept. Dermatologic uses of these medications include treatment of cryopyrin-associated periodic syndrome (CAPS) and the pustular eruptions and bone lesions (e.g. osteomyelitis) of the autosomal recessive *d*eficiency of the *I*L-1 *r*eceptor *a*ntagonist (DIRA) (see Tables 45.2 & 45.7). CAPS represents a spectrum of autosomal dominant disorders featuring urticarial lesions and variable extracutaneous manifestations associated with gain-of-function mutations in the

gene that encodes cryopyrin, a protein that functions in an "inflammasome" complex that releases IL-1β (see Fig. 4.2). A review of these agents' shared contraindications, major side effects, and interactions is followed by a discussion of issues that relate specifically to individual drugs.

Contraindications

Each IL-1 antagonist is contraindicated in patients with a known hypersensitivity to that particular agent or components of its formulation. Administration should not be initiated in patients with active infections, and discontinuation should be considered if a serious infection develops.

Major side effects

Adverse effects include an increased risk of serious infections, flu-like symptoms, and injection site reactions (see Table 128.5). Assessment for tuberculosis is required at baseline and typically repeated annually during therapy. Patients with untreated latent tuberculosis should receive antituberculous therapy prior to beginning treatment.

Interactions

Other immunosuppressive agents, particularly TNF inhibitors, should not be coadministered with IL-1 antagonists[34]. Live vaccines should also be avoided (see Table 128.8), and it is unknown whether vaccines have a full effect.

Anakinra

Mechanism of action

Anakinra (Kineret®) is a recombinant, non-glycosylated human IL-1 receptor antagonist. The drug binds to IL-1 type 1 receptors and thereby acts as a competitive inhibitor of IL-1, downregulating its inflammatory effects (see Fig. 45.13).

Indications

Anakinra is approved for the treatment of rheumatoid arthritis in adults as well as CAPS, in particular NOMID, in both children and adults[67,68] (see Table 45.2). In addition, anakinra has been reported to aid in the control of DIRA (see above and Table 45.7), generalized pustular psoriasis/deficiency of the IL-36 receptor antagonist (DITRA), SAPHO syndrome, Schnitzler syndrome, hidradenitis suppurativa, pyoderma gangrenosum, and *p*yogenic *a*rthritis–*p*yoderma gangrenosum–*a*cne (PAPA) syndrome[69–71].

Dosages

Anakinra is administered via *daily* subcutaneous injection at a dose of 100 mg in adults with rheumatoid arthritis and a starting dose of 1–2 mg/kg in children with NOMID, followed by titration to a maximum dose of 8 mg/kg daily as needed to control active inflammation. It is available in 100 mg graduated prefilled syringes.

Additional contraindications

In addition to the shared contraindications for IL-1 antagonists noted above, anakinra should be used with caution in patients with renal impairment; every other day administration is recommended for NOMID patients with a creatinine clearance <30 mL/min.

Additional major side effects

In addition to infections, neutropenia and thrombocytopenia represent potentially serious reactions. Complete blood counts should be performed monthly for 3 months and then quarterly (see Table 128.6). Injection site reactions are usually mild and tend to abate with continued therapy.

Use in pregnancy

In animal studies, anakinra has not shown evidence of harm to the fetus. Adequate studies in pregnant women have not been conducted, and its safety during lactation is unknown.

Canakinumab

Mechanism of action

Canakinumab (Ilaris®) is a human IgG1κ monoclonal antibody that binds and neutralizes IL-1β (see Fig. 45.13).

Indications

Canakinumab is approved for the treatment of the following conditions: CAPS in patients ≥4 years of age (see above and Table 45.2); TNF receptor-associated periodic syndrome (TRAPS), hyperimmunoglobulinemia D syndrome (HIDS), and familial Mediterranean fever (FMF) in adult and pediatric patients (see Table 45.2); and systemic JIA in patients ≥2 years of age. Canakinumab has also been successfully used to treat DIRA, generalized pustular psoriasis, Schnitzler syndrome, hidradenitis suppurativa, pyoderma gangrenosum, and PAPA syndrome[70,72,73].

Dosages

Canakinumab is given every 4–8 weeks as a subcutaneous injection of 150–300 mg in patients who weigh >40 kg and 2–4 mg/kg in patients who weigh 15–40 kg. In general, the doses are lower and the drug is administered less frequently in patients with CAPS as compared to those with TRAPS, HIDS, or FMF. It is available in 150 mg single-dose vials.

Use in pregnancy

Canakinumab has been associated with delayed skeletal development in animal reproduction studies. Adequate studies in pregnant women have not been conducted, and it should be used with caution in nursing women[74].

Rilonacept

Mechanism of action

Rilonacept (Arcalyst®) is a dimeric fusion protein composed of the extracellular portion of the IL-1 receptor and the Fc portion of IgG1. It blocks IL-1β signaling by acting as a soluble decoy receptor, preventing interaction of IL-1β with cell surface receptors (see Fig. 45.13). Rilonacept has less affinity for IL-1α and the IL-1 receptor antagonist.

Indications

Rilonacept is approved for the treatment of CAPS in patients ≥12 years of age. It has also been reported to be of benefit in patients with Schnitzler syndrome.

Dosages

Rilonacept is administered via subcutaneous injection, with a loading dose of 320 mg in adults or 4.4 mg/kg in pediatric patients, followed by weekly injections of 160 mg or 2.2 mg/kg.

Use in pregnancy

Rilonacept has been associated with minor skeletal anomalies in animal reproduction studies. Adequate studies in pregnant women have not been conducted, and it should be used with caution in nursing women.

Rituximab

Rituximab (Rituxan®) and its biosimilars are chimeric monoclonal antibodies directed against the CD20 antigen present on the surface of mature B cells[75].

Mechanism of action

Rituximab binds to CD20 on the surface of mature B cells and causes apoptosis of these cells (see Fig. 128.9B). It targets and selectively depletes $CD20^+$ B cells without affecting stem cells or existing plasma cells. Possible mechanisms of cell lysis include complement-dependent cytotoxicity and antibody-dependent cell-mediated cytotoxicity. In patients with pemphigus vulgaris, downregulation of desmoglein-3-specific $CD4^+$ T cells as well as depletion of B cells and decreased anti-desmoglein-3 antibody levels has been observed[76].

Indications

Rituximab is approved for the treatment of the following disorders: pemphigus vulgaris, B cell non-Hodgkin lymphoma (NHL), chronic lymphocytic leukemia, and rheumatoid arthritis in adults; granulomatosis with polyangiitis and microscopic polyangiitis in patients ≥2 years of age; and mature B cell NHL and mature B cell acute leukemia in children ≥6 months of age[77,78]. It has been successfully used to treat primary cutaneous B cell lymphoma[79]. In addition to its approved indications, rituximab has demonstrated efficacy in other autoimmune

bullous dermatoses (e.g. bullous pemphigoid, mucous membrane pemphigoid[80], paraneoplastic pemphigus), SLE, cutaneous lupus erythematosus[81], dermatomyositis[82], chronic GVHD[83], cryoglobulinemic vasculitis, and other forms of cutaneous small vessel vasculitis[84].

Dosages

The dosing regimen for pemphigus vulgaris is 1 g administered intravenously at weeks 0 and 2, followed by 500 mg at 12 months and then every 6 months. For lymphomas, rituximab 375 mg/m^2 is given intravenously weekly for 48 weeks. Rituximab is approved for concomitant use with methotrexate in patients with rheumatoid arthritis, and with chemotherapy in patients with B cell lymphoma. Efficacy may be reduced in patients who develop anti-rituximab antibodies[85].

Contraindications

Rituximab is contraindicated in patients allergic to the drug or its components, hepatitis B carriers, and patients with cardiac arrhythmias, angina pectoris, a high tumor burden, or active infection.

Major side effects (see Table 128.5)

In clinical trials, the most common adverse events were infusion reactions and infections, with no significant change in average immunoglobulin levels. Deaths within 24 hours of rituximab infusion have been attributed to reaction-related sequelae including hypoxia, acute respiratory distress syndrome, myocardial infarction, ventricular fibrillation, and cardiogenic shock. Approximately 80% of these deaths occurred in association with the first infusion. Acute kidney failure requiring dialysis has occurred in the setting of tumor lysis syndrome following treatment with rituximab, with instances of fatal outcome. Severe mucocutaneous reactions, including Stevens–Johnson syndrome/toxic epidermal necrolysis, have occasionally been noted in patients given rituximab. Rarely patients have developed paraneoplastic pemphigus during treatment, but it is not clear whether this phenomenon is drug-related or disease-related.

Hypogammaglobulinemia and late-onset neutropenia (≥4 weeks after infusion) develop in ~1%–30% of patients, with incidence related to factors such as age and the underlying disease (more frequent with hematologic disorders than pemphigus). Progressive multifocal leukoencephalopathy and hepatitis B virus activation potentially leading to fulminant hepatitis have also been reported.

Interactions

Live vaccines are contraindicated and the response to vaccines may be muted, as recently witnessed with COVID mRNA vaccines (see Table 128.8). Combination with other targeted immune modulators, particularly natalizumab, may increase the risk of infection. Combination with cisplatin increases the risk of nephrotoxicity.

Use in pregnancy

There are no adequate studies of rituximab in pregnant women, and its safety during lactation is unknown. B cell lymphopenia can occur in infants exposed to rituximab *in utero*.

Omalizumab

Omalizumab (Xolair®) is a recombinant humanized monoclonal antibody that targets IgE.

Mechanism of action

Omalizumab is a humanized IgG1 monoclonal antibody that selectively binds to and decreases serum levels of free human IgE. It also downregulates the number of high-affinity IgE receptors on mast cells, basophils, and dendritic cells[86,87]. These two mechanisms limit the release of inflammatory mediators and, via its effects on dendritic cells, decrease antigen presentation to T cells.

Indications

Omalizumab is approved for the treatment of patients ≥12 years of age with chronic spontaneous urticaria (CSU), patients ≥6 years of age with asthma, and adults with chronic rhinosinusitis with nasal polyps[88,89]. In addition, it has variable utility in the treatment of atopic dermatitis[90], eosinophilic granulomatosis with polyangiitis, bullous pemphigoid, and mastocytosis.

Dosages

Omalizumab is administered as a subcutaneous injection of 150 or 300 mg every 4 weeks for CSU, with dosing independent of serum IgE level or body weight. Patients with asthma receive 75–375 mg every 2–4 weeks, with dosing determined by the baseline serum total IgE level and body weight.

Contraindications

There are no contraindications other than previous hypersensitivity to omalizumab.

Major side effects (see Table 128.5)

The most common serious adverse event is anaphylaxis, which occurs in 0.1%–0.2% of asthma patients and has rarely been reported in CSU patients. A possible increased overall risk of malignancy was noted in clinical trials in asthma patients – 0.5% with omalizumab vs 0.2% with placebo; however, subsequent larger longitudinal studies failed to demonstrate an increased risk of malignancy[91]. Injection site reactions occur in 10%–15% of patients.

Interactions

No specific interactions with other medications have been noted.

Use in pregnancy

Omalizumab has not shown evidence of fetal harm in animal studies, and adequate studies in pregnant women have not been conducted. It is excreted into the breast milk of monkeys, and caution is advised when administering it to nursing women.

Janus Kinase (JAK) Inhibitors

Oral Janus kinase (JAK) inhibitors include abrocitinib (Cibinqo™), baricitinib (Olumiant®), deucravacitinib (Sotyktu™), ritlecitinib (Litfulo™), ruxolitinib (Jakafi®), tofacitinib (Xeljanz®), and upadacitinib (Rinvoq®). These agents are currently approved for the treatment of dermatologic disorders including atopic dermatitis, psoriasis, alopecia areata, and graft-versus-host disease. Other skin conditions for which successful oral JAK inhibitor therapy has been reported include dermatomyositis, STAT1-related chronic mucocutaneous candidiasis, and interferonopathies (see Table 45.7). A review of the mechanism of action, contraindications, side effects, and use in pregnancy of JAK inhibitors is followed by a discussion of indications, dosing, and interactions of individual FDA-approved drugs. *Topical* JAK inhibitors such as ruxolitinib 1.5% cream (Opzelura™), which is approved for the treatment of atopic dermatitis and vitiligo, are discussed in Chapter 129.

Mechanism of action

There are four known JAK enzymes: JAK1, JAK2, JAK3, and tyrosine kinase 2 (TYK2). These tyrosine kinases are expressed primarily in hematopoietic cells and play a key role in the transduction of cytokine-mediated signals, with the latter leading to activated transcription of inflammatory proteins (Fig. 128.11). Examples of JAK-dependent cytokines include: IFN-γ – JAK1/2; IL-2, IL-4 – JAK1/3; IFN-α/β – JAK1/TYK2; and IL-12/23 – JAK2/TYK2. These cytokines are implicated in the pathogenesis of inflammatory and autoimmune skin diseases such as atopic dermatitis, psoriasis, alopecia areata, and vitiligo[92].

Contraindications

Use of JAK inhibitors should be avoided in patients with a serious active infection, thrombotic disorders, severe hepatic impairment, lymphopenia (<500 cells/mm^3), neutropenia (<1000 cells/mm^3), anemia (hemoglobin <8–9 g/dL), or (especially with abrocitinib and ruxolitinib) thrombocytopenia (<50 000 cells/mm^3). Caution is advised in patients at increased risk of gastrointestinal perforation, especially when considering treatment with baricitinib, tofacitinib, or upadacitinib.

Major side effects

Serious bacterial, mycobacterial, invasive fungal, viral (e.g. human papillomavirus, herpes zoster, herpes simplex virus; Fig. 128.12), and other opportunistic infections have occurred in patients receiving JAK inhibitors. Assessment for tuberculosis at baseline and monitoring during therapy is required. Patients with untreated latent tuberculosis should receive antituberculous therapy before beginning treatment.

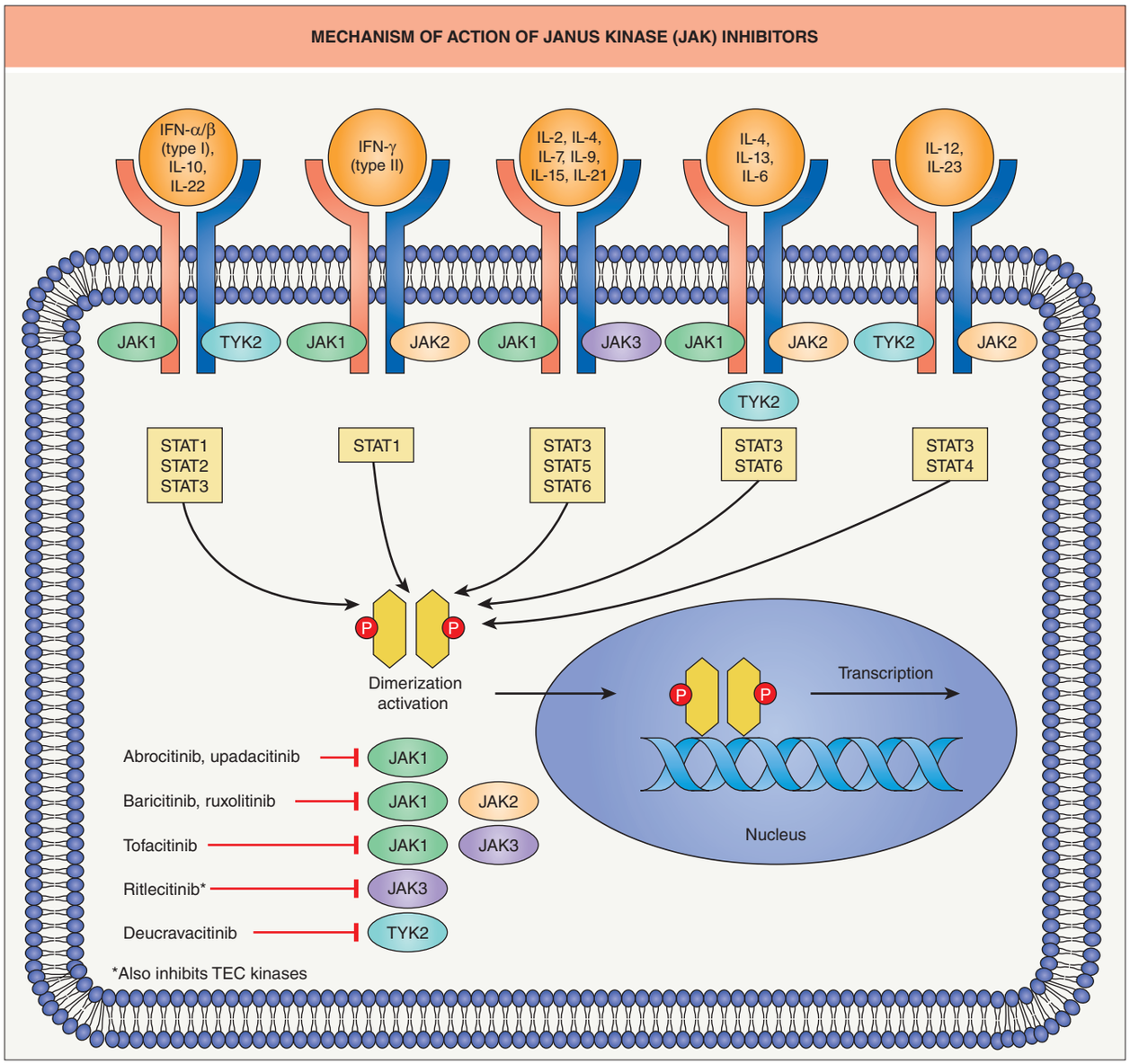


Fig. 128.11 Mechanism of action of Janus kinase (JAK) inhibitors. Different combinations of receptor-associated JAKs and STAT (signal transducer and activator of transcription) proteins transduce cytokine signals. Upon phosphorylation by JAKs, the STATs dimerize, translocate to the nucleus, and activate target genes. IL, interleukin; IFN, interferon.



Fig. 128.12 Eczema herpeticum. Vesicular facial eruption in patient on oral ruxolitinib for chronic graft-versus-host disease. Note the central delling. *Courtesy Edward Cowen, MD.*

Neutropenia, lymphopenia, anemia, thrombocytopenia (primarily for abrocitinib and ruxolitinib), hyperlipidemia, and elevated liver enzyme levels have been observed in patients treated with JAK inhibitors. Monitoring of the complete blood count (CBC), liver enzyme levels, and lipid profile at baseline, in 1–2 months, and every 3 months thereafter during therapy is recommended (see Table 128.6).

Additional adverse effects of JAK inhibitors include acne, thrombosis, major cardiovascular events, and gastrointestinal perforation (primarily for baricitinib, tofacitinib, and upadacitinib). Although an RCT found a higher rate of malignancies in rheumatoid arthritis patients treated with tofacitinib as compared to those who received TNF inhibitors, meta-analyses have not shown an increased risk of malignancy after a mean follow-up time of ~300 person-months when tofacitinib was compared to placebo or other therapies in patients with RA[93]. Keratinocyte and Merkel cell carcinomas have occurred in patients treated with JAK inhibitors. Progressive multifocal leukoencephalopathy (PML) has been observed in patients treated with ruxolitinib for myelofibrosis. Consultation with an oncologist should be considered when planning JAK inhibitor therapy in patients with a recent history of malignancy.

Interactions

Oral JAK inhibitors should not be administered to patients receiving other targeted immune modulators or immunosuppressive agents such as cyclosporine due to an increased risk of infection. Live vaccines are contraindicated and the response to vaccines may be impaired. It is recommended that patients be brought up to date with all immunizations prior to initiating treatment with a JAK inhibitor.

Use in pregnancy

High doses of JAK inhibitors have been associated with reduced fetal body weight, increased fetal mortality, and skeletal malformations in

animal reproduction studies. Adequate studies in pregnant women have not been conducted, and use in nursing mothers is not recommended.

Abrocitinib

The Janus kinase 1 (JAK1)-selective inhibitor abrocitinib (Cibinqo™) is approved for the treatment of refractory, moderate to severe **atopic dermatitis** in patients ≥12 years of age, with ~40%–60% (higher response rates with higher doses) of patients achieving a 75% improvement in the EASI score. The initial dose of abrocitinib for atopic dermatitis is 100 mg daily, which can be increased to 200 mg daily if an adequate response is not achieved after 12 weeks of treatment. Coadministration of abrocitinib with antiplatelet drugs (with the exception of low-dose aspirin) can increase the risk of bleeding and is contraindicated during the first 3 months of treatment. Coadministration with P-glycoprotein substrates (e.g. digoxin) can also increase plasma concentrations of the latter.

Baricitinib

The JAK1/2 inhibitor baricitinib (Olumiant®) is approved for the treatment of adults with severe **alopecia areata** (≥50% scalp hair loss), with ~15%–25% and ~30%–40% of patients who received a daily dose of 2 or 4 mg, respectively, for 36 weeks achieving ≥80% scalp coverage[94]. Baricitinib is also approved for adults with rheumatoid arthritis. The usual baricitinib starting dose for patients with alopecia areata is 2 mg daily, with 4 mg daily recommended for those who fail to respond to this dose or have nearly complete/complete hair loss; the dose can be decreased to 2 mg daily when an adequate response is achieved. Inhibitors of organic anion transporter 3 (OAT3; e.g. probenecid) can increase the blood levels of baricitinib.

Deucravacitinib

Deucravacitinib (Sotyktu™) is a TYK2 inhibitor approved for adults with moderate to severe **plaque psoriasis**, with ~50%–60% and ~30%–40% of patients achieving a 75% and 90% improvement in their PASI score, respectively. The dose is 6 mg daily. Increased serum creatine phosphokinase levels were noted in ~3% of patients in clinical trials.

Ritlecitinib

The JAK3 and TEC kinase inhibitor ritlecinib (Litfulo™) is approved for the treatment of severe **alopecia areata** in individuals ≥12 years of age, with ~25% of patients who received a daily dose of 50 mg for 24 weeks achieving ≥80% scalp coverage[94a]. Treatment should not be initiated in patients with a platelet count <100 000/mm^3 or absolute lymphocyte count <500/mm^3.

Ruxolitinib

The JAK1/2 inhibitor ruxolitinib (Jakafi®) is approved for patients ≥12 years of age with acute or chronic **graft-versus-host disease** (GVHD) as well as adults with polycythemia vera and myelofibrosis. The starting doses of ruxolitinib for acute and chronic GVHD are 5 and 10 mg twice daily, respectively. In a study of 12 adults with moderate to severe alopecia areata, 75% had >50% improvement in their Severity of Alopecia Tool (SALT) score after treatment with ruxolitinib 20 mg twice daily for 3–6 months, but hair loss recurred upon its discontinuation[95]. Fluconazole and strong inhibitors of CYP3A4 (e.g. itraconazole) increase blood levels of ruxolitinib and so avoidance or dose modification of these inhibitors is required.

Tofacitinib

The JAK1/3 inhibitor tofacitinib (Xeljanz®) is FDA-approved for children ≥2 years of age with polyarticular idiopathic arthritis as well as adults with rheumatoid arthritis, psoriatic arthritis, ankylosing spondylitis, and ulcerative colitis. In an open-label study of 66 adults with severe alopecia areata treated with tofacitinib 5 mg twice daily for 3 months, 32% had >50% improvement in their SALT score; however, drug cessation led to disease relapse in a median of 8 weeks[96]. Fluconazole and strong inhibitors of CYP3A4 (e.g. itraconazole) increase blood levels of tofacitinib and require dose modifications.

Upadacitinib

The JAK1-selective inhibitor upadacitinib (Rinvoq®) is approved for the treatment of refractory, moderate to severe **atopic dermatitis** in patients ≥12 years of age, with ~65%–75% of patients achieving a 75% improvement in the EASI score. Upadacitinib is also approved for adults with psoriatic arthritis, rheumatoid arthritis, ankylosing spondylitis, ulcerative colitis, and Crohn disease. The initial dose of upadacitinib for atopic dermatitis is 15 mg daily, which can be increased to 30 mg daily in patients who do not have an adequate response. Strong inhibitors of CYP3A4 (e.g. itraconazole) increase blood levels of upadacitinib and require dose modifications.

Targeted Immune Modulators Under Investigation and Other Targeted Therapies

Development of targeted immune modulators for use in dermatology continues. Table 128.9 is a partial listing of the drugs that are currently under investigation for dermatologic disorders. Additional drugs that are being developed for non-cutaneous inflammatory diseases might be effective for skin disorders (Table 128.10).

INTRAVENOUS IMMUNE GLOBULIN (IVIg)

Key features

- IVIg is useful for inflammatory disorders, including some cutaneous diseases
- Doses for inflammatory disorders are empiric, but have generally been 2 g/kg/month for chronic diseases, and 3 g/kg total for acute conditions
- There are only a few skin disorders for which there is a high level of evidence indicating effectiveness of IVIg

IVIg is a sterile solution of globulins extracted from pooled plasma donated by 100 000–200 000 individuals per production cycle. Processing results in a product that is predominantly IgG, having eliminated all but trace amounts of IgA and other soluble immunologically active particles. It has a half-life of 3 to 5 weeks.

TARGETED IMMUNE MODULATORS FOR UNDER DEVELOPMENT FOR DERMATOLOGIC INDICATIONS

Name	Mechanism of action (disease)	Phase
Injectable agents under development		
Amlitelimab	OX40 ligand inhibitor (atopic dermatitis)	II
Cendakimab	IL-13 inhibitor (atopic dermatitis)	II
Eblasakimab	IL-13 receptor α1 inhibitor (atopic dermatitis)	II
Gumokinab	IL-17A inhibitor (psoriasis)	
IBI112	IL-23 inhibitor (psoriasis)	II
IMO-8400	TLR7/8/9 antagonist (psoriasis)	II
Imsidolimab	IL-36 receptor (generalized pustular psoriasis)	III
Izokibep	IL-17A inhibitor (hidradenitis suppurativa, psoriasis)	II
Neihulizumab	P selectin glycoprotein ligand 1 (PSGL-1) inhibitor (GVHD)	II
Nemolizumab	IL-31 receptor A inhibitor (prurigo nodularis)	III
Rocatinlimab	OX40 inhibitor (atopic dermatitis)	III
Vixarelimab	Oncostatin M receptor β inhibitor (prurigo nodularis)	II
Vunakizumab	IL-17A inhibitor (psoriasis)	III
Oral agents under development		
Jaktinib	JAK1/2 inhibitor (psoriasis, alopecia areata)	II
Piclidenoson	Adenosine A3 receptor inhibitor (psoriasis)	III
PN-235	IL-23 receptor inhibitor (psoriasis)	II
RIST4721	CXCR2 inhibitor (palmoplantar pustulosis)	II

Table 128.9 Targeted immune modulators for psoriasis under development. IL, interleukin; JAK, Janus kinase.

OTHER TARGETED ("BIOLOGIC") AGENTS USED IN MEDICINE		
Drug (Trade name®)	**Target**	**Selected FDA-approved indications**
Abatacept (Orencia)	B7–1 (CD80)	Rheumatoid arthritis, juvenile idiopathic arthritis, adult psoriatic arthritis
Abciximab (ReoPro)	Glycoprotein IIb/IIIa	Cardiovascular disease
Aducanumab (Aduhelm)	Amyloid beta	Alzheimer disease
Alemtuzumab (Campath)	CD52	B cell CLL
Alirocumab (Praluent)	PCSK9	Hypercholesterolemia
Amivantamab (Rybrevant)	EGF, MET	Non-small cell lung cancer
Anifrolumab (Saphnelo)	Type I interferon receptor	Systemic lupus erythematosus
Ansuvimab (Ebanga)	Ebola	Ebola
Atezolizumab (Tecentriq)	PD-L1	Urothelial cancer, non-small cell lung cancer, breast cancer, hepatocellular cancer
Atoltivimab, maftivimab, odesivimab (Inmazeb)	Ebola	Ebola
Avelumab (Bavencio)	PD-L1	Metastatic Merkel cell carcinoma, urothelial carcinoma, renal cell carcinoma
Basiliximab (Simulect)	IL-2 receptor α (CD25)	Solid organ transplantation; off-label use for GVHD
Belimumab (Benlysta)	B lymphocyte stimulator	Systemic lupus erythematosus (LE); off-label use for cutaneous LE
Benralizumab (Fasenra)	IL-5 receptor α	Asthma
Bevacizumab (Avastin)	VEGF	Colorectal cancer, non-squamous/non-small cell lung cancer, other malignancies
Bezlotoxumab (Zinplava)	*Clostridium difficile* toxins	*C. difficile* diarrhea
Blinatumomab (Blincyto)	CD19 & CD3 (BiTE)	B cell ALL
Brentuximab vedotin (Adcetris)	CD30	Anaplastic large cell and Hodgkin lymphomas, peripheral T cell lymphoma, refractory mycosis fungoides
Brolucizumab (Beovu; intravitreal agent)	VEGF	Age-related macular degeneration
Burosumab (Crysvita)	FGF23	X-linked hypophosphatemia
Caplacizumab (Cablivi)	Von Willebrand factor	Thrombotic thrombocytopenic purpura
Cemiplimab (Libtayo)	PD-1	Cutaneous SCC and basal cell carcinoma
Cetuximab (Erbitux; IgG1)	EGFR	Head and neck SCC, colorectal cancer
Crizanlizumab (Adakveo)	P-selectin	Sickle cell disease
Daratumumab (Darzalex)	CD38	Multiple myeloma
Denosumab (Prolia, Xgeva)	RANK ligand	Osteoporosis, bone metastases
Dinutuximab (Unituxin)	Glycolipid GD2	Neuroblastoma
Dostarlimab (Jemperli)	PD-1	Endometrial cancer
Durvalumab (Imfinzi)	PD-L1	Advanced/metastatic urothelial carcinoma, lung cancer
Eculizumab (Soliris)	Complement component 5	Paroxysmal nocturnal hemoglobinuria, atypical hemolytic uremic syndrome, generalized myasthenia gravis, neuromyelitis optica spectrum disorder
Elotuzumab (Empliciti)	SLAMF7 (CD319)	Multiple myeloma
Emapalumab (Gamifant)	Interferon-δ	Hemophagocytic lymphohistiocytosis
Emicizumab (Hemlibra)	Factors IXa and X	Hemophilia A
Enfortumab vedotin (Padcev)	Nectin-4	Bladder cancer
Epcoritamab (Epkinly)	CD20 & CD3 (BiTE)	Diffuse large B cell lymphoma
Eptinezumab (Vyepti)	CGRP	Migraine
Erenumab (Aimovig)	CGRP	Migraine
Evinacumab (Evkeeza)	ANGPTL3	Familial hypercholesterolemia
Evolocumab (Repatha)	PCSK9	Hyperlipidemia
Faricimab (Vabysmo; intravitreal agent)	VEGF, Ang-2	Neovascular age-related macular degeneration
Fremanezumab (Ajovy)	CGRP	Migraine
Galcanezumab (Emgality)	CGRP	Migraine
Glofitamab (Columvi)	CD20 & CD3 (BiTE)	Diffuse large B cell lymphoma
Ibalizumab (Trogarzo)	CD4	Human immunodeficiency virus infection
Ibritumomab tiuxetan (Zevalin)*	CD20	Non-Hodgkin lymphoma
Inebilizumab (Uplizna)	CD19	Neuromyelitis optica
Ipilimumab (Yervoy)	CTLA-4 (CD152)	Unresectable/metastatic melanoma or adjuvant treatment of melanoma with lymph node involvement (Fig. 128.9F), other cancers

Table 128.10 Other targeted ("biologic") agents used in medicine.

OTHER TARGETED ("BIOLOGIC") AGENTS USED IN MEDICINE		
Drug (Trade name®)	**Target**	**Selected FDA-approved indications**
Isatuximab (Sarclisa)	CD38	Multiple myeloma
Lanadelumab (Takhzyro)	Kallikrein	Hereditary angioedema
Lecanemab (Leqembi)	Amyloid beta	Alzheimer disease
Loncastuximab tesirine (Zynlonta)	CD19	Large B cell lymphoma
Margetuximab (Margenza)	HER2	$HER2^+$ breast cancer
Mepolizumab (Nucala)	IL-5	Asthma
Mirvetuximab soravtansine (Elahere)	Folate receptor alpha (plus microtubule inhibitor)	Ovarian cancer
Mogamulizumab (Poteligeo)	CCR4	Non-Hodgkin lymphoma, cutaneous T-cell lymphoma
Mosunetuzumab (Lunsumio)	CD20 & CD3 (BiTE)	Follicular lymphoma
Muromonab (Orthoclone OKT3)	CD3	Acute allograft rejection (renal, cardiac, hepatic)
Natalizumab (Tysabri)	α-4 integrin	Multiple sclerosis, Crohn disease
Naxitamab (Danyelza)	GD2	Neuroblastoma
Necitumumab (Portrazza)	EGFR	Advanced squamous non-small cell lung cancer
Nirsevimab (Beyfortus)	RSV	RSV disease
Nivolumab (Opdivo)	PD-1	Unresectable/metastatic melanoma, squamous cell head/neck cancer, non-small cell lung cancer, other malignancies
Nivolumab plus relatlimab (Opdualag)	PD-1 and LAG-3	Unresectable/metastatic melanoma
Obiltoxaximab (Anthim)	*Bacillus anthracis* spores	Anthrax
Obinutuzumab (Gazyva)	CD20	CLL, follicular lymphoma
Ocrelizumab (Ocrevus)	CD20	Multiple sclerosis
Ofatumumab (Arzerra, Kesimpta)	CD20	B cell CLL, multiple sclerosis
Olaratumab (Lartruvo)	Platelet-derived growth factor receptor-α	Soft tissue sarcoma
Palivizumab (Synagis)	Respiratory syncytial virus (RSV)	RSV infections
Panitumumab (Vectibix)	EGFR	Metastatic colorectal cancer
Pembrolizumab (Keytruda)	PD-1	Unresectable/metastatic melanoma, Merkel cell carcinoma, squamous cell head/neck cancer, non-small cell lung cancer, other malignancies
Pertuzumab (Perjeta)**	HER2	$HER2^+$ breast cancer
Polatuzumab vedotin (Polivy)	CD79b	Diffuse large B cell lymphoma
Ramucirumab (Cyramza)	VEGFR2	Advanced gastric carcinoma; metastatic colorectal and non-small cell lung cancers
Ranibizumab (Lucentis; intravitreal agent)	VEGF	Age-related macular degeneration, diabetic retinopathy/macular edema
Raxibacumab	*Bacillus anthracis* spores	Anthrax
Ravulizumab (Ultomiris)	C5	Paroxysmal nocturnal hemoglobinuria
Reslizumab (Cinqair)	IL-5	Asthma
Retifanlimab (Zynyz)	PD-1	Metastatic/recurrent advanced Merkel cell carcinoma
Romosozumab (Evenity)	Sclerostin	Osteoporosis
Rozanolixizumab (Rystiggo)	Neonatal Fc receptor	Myasthenia gravis
Sacituzumab govitecan (Trodelvy)	Trop-2	Breast cancer
Sarilumab (Kevzara)	IL-6 receptor	Rheumatoid arthritis
Satralizumab (Enspryng)	IL-6 receptor	Neuromyelitis optica
Siltuximab (Sylvant)	IL-6	Multicentric Castleman disease
Sutimlimab (Enjaymo)	C1s	Cold agglutinin disease
Tafasitamab (Monjuvi)	CD19	Large B cell lymphoma
Talquetamab (Talvey)	GPRC5D & CD3 (BiTE)	Multiple myeloma
Tebentafusp (Kimmtrak)	gp100 & HLA-directed CD3 (BiTE)	Uveal melanoma
Teclistamab (Tecvayli)	BCMA & CD3 (BiTE)	Multiple myeloma
Teprotumumab (Tepezza)	IGF-1R	Thyroid eye disease
Teplizumab (Tzield)	CD3	Type 1 diabetes mellitus
Tezepelumab (Tezspire)	TSLP	Asthma

Table 128.10 Other targeted ("biologic") agents used in medicine.

Continued

OTHER TARGETED ("BIOLOGIC") AGENTS USED IN MEDICINE		
Drug (Trade name®)	**Target**	**Selected FDA-approved indications**
Tisotumab vedotin (Tivdak)	Tissue factor	Cervical cancer
Tocilizumab (atlizumab; Actemra)	IL-6 receptor	Rheumatoid arthritis, juvenile idiopathic arthritis, giant cell arteritis
Trastuzumab (Herceptin)**	HER2	HER2-overexpressing breast and metastatic gastric cancers
Tremelimumab (Imjudo)	CTLA-4	Hepatocellular carcinoma
Ublituximab (Briumvi)	CD20	Multiple sclerosis
Tyrosine kinase inhibitors (see Table 21.16)		
Abemaciclib (Verzenio)	CDK4/6	Advanced/metastatic breast cancer
Acalabrutinib (Calquence)	Bruton tyrosine kinase	Mantle cell lymphoma
Adagrasib (Krazati)	KRAS with G12C mutation	Non-small cell lung cancer
Afatinib (Gilotrif)	EGFR, HER2	Non-small cell lung cancer
Alectinib (Alecensa)	ALK	ALK^+ non-small cell lung cancer
Alpelisib (Piqray)	PI3K	Breast cancer
Asciminib (Scemblix)	Abl	CML
Avapritinib (Ayvakit)	KIT, PDGFR	Gastrointestinal stromal tumor
Axitinib (Inlyta)	VEGFR1-3, KIT, PDGFR	Renal cell cancer
Binimetinib (Mektovi)	MEK	Unresectable/metastatic melanoma (in combination with encorafenib)
Bosutinib (Bosulif)	Abl, Src	CML
Brigatinib (Alunbrig)	ALK, EGFR	ALK^+ non-small cell lung cancer
Cabozantinib (Cometriq)	VEGFR2, MET	Metastatic medullary thyroid cancer, renal cell carcinoma, hepatocellular carcinoma
Capmatinib (Tabrecta)	MET	Non-small cell lung cancer
Ceritinib (Zykadia)	ALK	ALK^+ non-small cell lung cancer
Cobimetinib (Cotellic)	MEK1/2	Unresectable/metastatic melanoma (in combination with vemurafenib)
Copanlisib (Aliqopa)	PI3K	Follicular lymphoma
Crizotinib (Xalkori)	ALK	ALK^+ non-small cell lung cancer
Dabrafenib (Tafinlar)	BRAF serine/threonine kinase with V600E/K mutation	Unresectable/metastatic melanoma with the BRAF V600E/K mutation
Dacomitinib (Vizimpro)	EGFR	Non-small cell lung cancer
Dasatinib (Sprycel)	KIT, Abl	CML, Philadelphia chromosome-positive ALL
Duvelisib (Copiktra)	PI3K	CLL, small lymphocytic lymphoma, follicular lymphoma
Encorafenib (Braftovi)	BRAF serine/threonine kinase with V600E/K mutation	Unresectable/metastatic melanoma with the BRAF V600E/K mutation
Entrectinib (Rozlytrek)	TRKs, ROS1, ALK	Non-small cell lung cancer, solid tumors with NTRK gene fusion
Erdafitinib (Balversa)	FGFR1/2/3/4, RET, PDGFR	Bladder cancer
Erlotinib (Tarceva)	EGFR	Non-small cell lung and pancreatic cancer
Fedratinib (Inrebic)	JAK2	Myelofibrosis
Fostamatinib (Tavalisse)	SYK	Immune thrombocytopenia
Futibatinib (Lytgobi)	FGFR2	Cholangiocarcinoma
Gefitinib (Iressa)	EGFR	Non-small cell lung cancer
Gilteritinib (Xospata)	FLT3	AML
Ibrutinib (Imbruvica)	Bruton tyrosine kinase	Mantle cell lymphoma, Waldenstrom macroglobulinemia, marginal zone lymphoma, chronic GVHD
Infigratinib (Truseltiq)	FGFR1/2/3	Cholangiocarcinoma
Imatinib (Gleevec, Glivec)	KIT, Abl, PDGFR	CML, ALL, myelodysplastic/myeloproliferative diseases, GIST, DFSP (see Ch. 116), systemic mastocytosis (see Ch. 118), hypereosinophilic syndrome (see Fig. 26.6); off-label use for sclerodermatous conditions (e.g. morphea, chronic GVHD)
Inotuzumab ozogamicin (Besponsa)	CD22	ALL
Lapatinib (Tykerb, Tycerb)	EGFR, HER2	Metastatic breast cancer
Larotrectinib (Vitrakvi)	TRKs	Solid tumors with NTRK gene fusion
Leniolisib (Joenja)	PI3Kδ	Activated phosphoinositide 3-kinase delta (PI3Kδ) syndrome

Table 128.10 Other targeted ("biologic") agents used in medicine.

OTHER TARGETED ("BIOLOGIC") AGENTS USED IN MEDICINE		
Drug (Trade name®)	**Target**	**Selected FDA-approved indications**
Lenvatinib (Lenvima)	VEGFR1–3	Thyroid cancer, renal cell cancer, hepatocellular cancer, endometrial cancer
Lorlatinib (Lorbrena)	ALK, ROS1	Non-small cell lung cancer
Mobocertinib (Exkivity)	EGFR	Non-small cell lung cancer
Neratinib (Nerlynx)	EGFR, HER2/4	$HER2^+$ breast cancer
Nilotinib (Tasigna)	KIT, Abl, PDGFR	CML
Niraparib (Zejula)	PARP	Ovarian, fallopian tube, and peritoneal cancers
Obinutuzumab (Gazyva)	CD20	CLL, follicular lymphoma
Osimertinib (Tagrisso)	EGFR	Non-small cell lung cancer
Pacritinib (Vonjo)	JAK2, FLT3	Myelofibrosis
Pazopanib (Votrient)	VEGFR1-3, PDGFR, KIT	Renal cell carcinoma, soft tissue sarcoma
Palbociclib (Ibrance)	CDK4/6	Advanced/metastatic breast cancer
Pexidartinib (Turalio)	CSF1R, KIT, FLT3	Giant cell tumor
Pemigatinib (Pemazyre)	FGFR2	Cholangiocarcinoma
Pirtobrutinib (Jaypirca)	Bruton tyrosine kinase	Mantle cell lymphoma
Ponatinib (Iclusig)	Abl, VEGFR, PDGFR, FGFR, KIT, others	CML, Philadelphia chromosome-positive ALL
Pralsetinib (Gavreto)	RET	Non-small cell lung cancer, thyroid cancer
Quizartinib (Vanflyta)	FLT3, KIT, PDGFRs, others	AML
Regorafenib (Stivarga)	VEGFR2, TIE2, others	Advanced/metastatic colorectal cancer, GIST, hepatocellular cancer
Ribociclib (Kisqali)	CDK4/6	Advanced/metastatic breast cancer
Ripretinib (Qinlock)	KIT, PDGFR	Gastrointestinal stromal tumor
Selpercatinib (Retevmo)	RET	Non-small cell lung cancer, thyroid cancer
Selumetinib (Koselugo)	MEK1/2	Plexiform neurofibromas in neurofibromatosis type 1
Sorafenib (Nexavar)	VEGFR1&2, PDGFR, BRAF	Renal cell, hepatocellular, and thyroid carcinomas
Sotorasib (Lumakras)	KRAS with G12C mutation	Non-small cell lung cancer
Sunitinib (Sutent)	VEGFR1&2, PDGFR, KIT, FLT3	Renal cell carcinoma, GIST, pancreatic neuroendocrine tumors
Tepotinib (Tepmetko)	MET	Non-small cell lung cancer
Tivozanib (Fotivda)	VEGF	Renal cell carcinoma
Trametinib (Mekinist)	MEK1/2	Unresectable/metastatic melanoma (in combination with dabrafenib), anaplastic thyroid cancer, non-small cell lung cancer
Tucatinib (Tukysa)	HER2	$HER2^+$ breast cancer
Umbralisib (Ukoniq)	PI3Kδ, CK1ε	Marginal zone lymphoma, follicular lymphoma
Vandetanib (Caprelsa)	VEGFR, EGFR, RET	Metastatic medullary thyroid cancer
Vemurafenib (Zelboraf)	BRAF serine/threonine kinase with V600E mutation	Unresectable or metastatic melanoma with the BRAF V600E mutation, Erdheim–Chester disease
Zanubrutinib (Brukinsa)	Bruton tyrosine kinase	Mantle cell lymphoma, CLL
Hedgehog pathway inhibitor		
Sonidegib (Odomzo)	Smoothened receptor	Advanced recurrent or unresectable basal cell carcinoma
Vismodegib (Erivedge)	Smoothened receptor	Unresectable or metastatic basal cell carcinoma

*Radioactive forms are used, with ibritumomab tiuxetan conjugated to yttrium-90 or indium-111.
**Conjugated forms include ado-trastuzumab emtansine (Kadcyla), fam-trastuzumab deruxtecan (Enhertu), and pertuzumab/trastuzumab/hyaluronidase (Phesgo).

Table 128.10 Other targeted ("biologic") agents used in medicine. ALL, acute lymphoblastic leukemia; AML, acute myelogenous leukemia; ANGPTL3, angiopoietin-like protein 3; ATLL, adult T cell leukemia–lymphoma; BCMA, B cell maturation antigen; BiTE, bi-specific T-cell engager; CDK, cyclin-dependent kinase; CLL, chronic lymphocytic leukemia; CK1, casein kinase 1; CGRP, calcitonin gene-related peptide; CML, chronic myelogenous leukemia; CSF1R, colony-stimulating factor-1 receptor; CTLA-4, cytotoxic T lymphocyte antigen-4; DFSP, dermatofibrosarcoma protuberans; EGFR, epidermal growth factor receptor; FGFR2, fibroblast growth factor receptor 2; FLT3, FMS-like tyrosine kinase 3; GIST, gastrointestinal stromal tumors; GPRC5D, G-protein coupled receptor family C group 5 member D; GVHD, graft-versus-host disease; IGF-1R, insulin-like growth factor 1 receptor; IL, interleukin; LAG-3, lymphocyte activation gene 3; MEK, mitogen-activated protein kinase kinase; MET, mesenchymal–epithelial transition; PCSK9, proprotein convertase subtilisin/kexin type 9; PD-1, programmed cell death protein 1; PD-L1, programmed cell death ligand 1; PDGFR, platelet-derived growth factor receptor; PI3K, phosphoinositide 3-kinase; RANK, receptor activator of nuclear factor κB; SCC, squamous cell carcinoma; TRK, tropomyosin receptor kinase; TSLP, thymic stromal lymphopoietin; VEGF, vascular endothelial growth factor; VEGFR, VEGF receptor.

IVIg is used in the treatment of immunodeficiency syndromes, hypogammaglobulinemia (e.g. due to myeloma), inflammatory disorders, and infectious diseases[97]. It is occasionally administered as prophylaxis to susceptible individuals exposed to particular infectious agents, such as nonimmune, immunocompromised patients exposed to varicella–zoster virus. Clinical studies, most of which were uncontrolled, and anecdotal reports suggest that IVIg is useful for some cutaneous conditions[98–100] (Table 128.11), but randomized clinical trials, barring those for dermatomyositis, are lacking.

USES OF IVIg IN DERMATOLOGY			
Indication	**Summary of evidence**	**Dosing**	**Comments**
Dermatomyositis	Benefit established	2 g/kg (over 2 days) Initially given every month, maintenance schedule individualized	Beneficial in patients intolerant of prednisone or immunosuppressives
Kawasaki disease	Benefit established	2 g/kg (over 6–12 hours)	
Toxic epidermal necrolysis	Case series, anecdotal evidence	1 g/kg/day for 3 days	Benefit controversial
Pemphigus variants	Case series, anecdotal evidence	2 g/kg (over 2–3 days) Initially given every month, maintenance schedule individualized	Adjunctive or second-line therapy
Bullous pemphigoid	Case series, anecdotal evidence	2 g/kg (over 2–3 days) Initially given every month, maintenance schedule individualized	Adjunctive or second-line therapy
Mucous membrane (cicatricial) pemphigoid	Case series, anecdotal evidence	2–3 g/kg (over 3 days) Initially given every 2–6 weeks, maintenance schedule individualized	Adjunctive or second-line therapy
Epidermolysis bullosa acquisita	Anecdotal evidence	2 g/kg (over 2–3 days) Initially given every month, maintenance schedule individualized	Adjunctive or second-line therapy
Necrotizing fasciitis	Uncertain benefit	2 g/kg (over 6–12 hours); repeat 1–2 g/kg in 2–5 days if disease progresses	Adjunctive for progressive disease
Pyoderma gangrenosum	Uncertain benefit	2 g/kg (over 2 days) Initially given every month, maintenance schedule individualized	May be considered
Atopic dermatitis	Uncertain benefit (inconsistent results in controlled studies)	2 g/kg (over 1–2 days) Monthly	

Table 128.11 Uses of IVIg in dermatology. *Adapted from Mydlarski PR, Mittman N, Shear NH. Intravenous immunoglobulin: use in dermatology. Skin Therapy Lett 2004;9:1–6.*

SELECTED PREPARATIONS OF IVIg THAT ARE AVAILABLE IN THE US				
	Gammagard®S/D	**Privigen®**	**Gamunex®-C**	**Carimune® NF**
Form	Lyophilized	Liquid	Liquid	Lyophilized
Concentration	5% (also 10%)	10%	10%	3%–12%
Maximum infusion rate	4.0 mL/kg/h	4.8 mL/kg/h	4.8 mL/kg/h	2.5 mL/kg/h
Time to infuse 70 g	5.3 h	2 h	2 h	6.6 h
pH	6.8	4.8	4.25	6.4–6.8
Osmolarity (mOsm/L)	636	320	260	192–1074
Sugar content	2% glucose	None	None	1.67 g sucrose/g of protein
Sodium content	0.85%	Trace	Trace	<20 mg/g of protein
IgA (mcg/mL)	<2.2	<25	46	720

Table 128.12 Selected preparations of IVIg that are available in the US. Subcutaneous immunoglobulin preparations are also available. Information on additional products is provided at: https://primaryimmune.org/publication/characteristics-ig-products-used-treat-pi-licensed-use-us.

Mechanism of Action

The immunomodulatory effects of IVIg may be exerted through one or more of the following mechanisms: (1) functional blockade of Fc receptors; (2) inhibition of complement-mediated damage; (3) alteration of cytokine and cytokine antagonist profiles; (4) reduction of circulating antibodies via anti-idiotype antibodies; and (5) neutralization of toxins that trigger autoantibody production[97,101]. In toxic epidermal necrolysis, IVIg is believed to block Fas (CD95)-mediated keratinocyte death by inhibiting Fas–Fas ligand interactions (see Ch. 20).

Indications

IVIg is approved for treatment of primary and secondary immunodeficiency diseases. Table 128.11 lists dermatologic disorders for which IVIg represents a therapeutic option.

Dosages

At least nine different preparations of IVIg are available in the US[102]. The products differ in their sugar content, sodium content, osmolarity, pH, and IgA levels (Table 128.12). The doses recommended vary depending upon the disease state being treated (see Table 128.11).

Contraindications

Preparations containing IgA are contraindicated in patients with a history of hypersensitivity to IVIg, the presence of anti-IgA antibodies, or a profound IgA deficiency; the latter may be associated with the development of anti-IgA antibodies and a risk of anaphylaxis.

Major Side Effects

Major toxicity includes the potential for anaphylaxis, aseptic meningitis, thromboembolic events, hyperviscosity syndromes, dyshidrotic eczema (pompholyx; Fig. 128.13), cardiac collapse, and pulmonary edema. These risks vary with the preparation selected and the patient being treated. For example, renal failure represents a potential complication of sucrose-containing products, which can lead to "osmotic nephrosis". Pretreatment with acetaminophen and diphenhydramine may lessen infusion reactions, and decreasing the rapidity of the infusion lessens



Fig. 128.13 New-onset dyshidrotic eczema in an adult receiving monthly IVIg.
Courtesy Jean L. Bolognia, MD.

the risk of thromboembolic events, aseptic meningitis, and renal or cardiovascular events.

Interactions

Individuals receiving IVIg may have a suboptimal response to vaccination with live viruses.

Use in Pregnancy

There does not appear to be an excessive risk in pregnancy or lactation associated with the use of IVIg.

Additional tables on Mechanisms of action for interferons, Interpretation of hepatitis B and C serologic test results, and Examples of biosimilars of monoclonal antibodies used in dermatology, available in our eBook (see inside front cover for access code).

REFERENCES

1. Havell EA, Berman B, Ogburn CA, et al. Two antigenically distinct species of human interferon. *Proc Natl Acad Sci USA*. 1975;72:2185–2187.
2. Mitoma H, Horiuchi T, Tsukamoto H, et al. Mechanisms for cytotoxic effects of anti-tumor necrosis factor agents on transmembrane tumor necrosis factor alpha-expressing cells: comparison among infliximab, etanercept, and adalimumab. *Arthritis Rheum*. 2008;58:1248–1257.
3. Straub RH, Härle P, Sarzi-Puttini P, Cutolo M. Tumor necrosis factor-neutralizing therapies improve altered hormone axes. An alternative mode of anti-inflammatory action. *Arthritis Rheum*. 2006;54:2039–2046.
4. Mohan N, Edwards ET, Cupps TR, et al. Demyelination occurring during anti-tumor necrosis factor alpha therapy for inflammatory arthritides. *Arthritis Rheum*. 2001;44:2862–2869.
5. Behnam SM, Behnam SE, Koo JY. TNF-alpha inhibitors and congestive heart failure. *Skinmed*. 2005;4:363–368.
6. Bergstrom L, Yocum DE, Ampel NM, et al. Increased risk of coccidioidomycosis in patients treated with tumor necrosis factor alpha antagonists. *Arthritis Rheum*. 2004;50:1959–1966.
7. Dommasch ED, Abuabara K, Shin DB, et al. The risk of infection and malignancy with tumor necrosis factor antagonists in adults with psoriatic disease: a systematic review and meta-analysis of randomized controlled trials. *J Am Acad Dermatol*. 2011;64:1035–1050.
8. Peterson JR, Hsu FC, Simkin PA, Wener MH. Effect of tumour necrosis factor alpha antagonists on serum transaminases and viraemia in patients with rheumatoid arthritis and chronic hepatitis C infection. *Ann Rheum Dis*. 2003;62:1078–1082.
9. Wolfe F, Michaud K. Lymphoma in rheumatoid arthritis: the effect of methotrexate and anti-tumor necrosis factor therapy in 18,572 patients. *Arthritis Rheum*. 2004;50:1740–1751.
10. Bongartz T, Sutton AJ, Sweeting MJ, et al. Anti-TNF antibody therapy in rheumatoid arthritis and the risk of serious infections and malignancies: systematic review and meta-analysis of rare harmful effects in randomized controlled trials. *JAMA*. 2006;295:2275–2285.
11. Lebwohl M, Blum R, Berkowitz E, et al. No evidence for increased risk of cutaneous squamous cell carcinoma in patients with rheumatoid arthritis receiving etanercept for up to 5 years. *Arch Dermatol*. 2005;141:861–864.
12. Mariette X, Matucci-Cerinic M, Pavelka K, et al. Malignancies associated with tumor necrosis factor inhibitors in registries and prospective observational studies: a systematic review and meta-analysis. *Ann Rheum Dis*. 2011;70:1895–1904.
13. Dommasch ED, Abuabara K, Shin DB, et al. The risk of infection and malignancy with tumor necrosis factor antagonists in adults with psoriatic disease: a systematic review and meta-analysis of randomized controlled trials. *J Am Acad Dermatol*. 2011;64:1035–1050.
14. Diak P, Siegel J, La Grenade L, et al. Tumor necrosis factor alpha blockers and malignancy in children: forty-eight cases reported to the Food and Drug Administration. *Arthritis Rheum*. 2010;62:2517–2524.
15. Shakoor N, Michalska M, Harris CA, Block JA. Drug-induced systemic lupus erythematosus associated with etanercept. *Lancet*. 2002;359:579–580.
16. Wetter DA, Davis MD. Lupus-like syndrome attributable to anti-tumor necrosis factor alpha therapy in 14 patients during an 8-year period at Mayo Clinic. *Mayo Clin Proc*. 2009;84:979–984.
17. Comby E, Tanaff P, Mariotte D, et al. Evolution of antinuclear antibodies and clinical patterns in patients with active rheumatoid arthritis with long term infliximab therapy. *J Rheumatol*. 2006;33:24–30.
18. Norman R, Greenberg RG, Jackson JM. Case reports of etanercept in inflammatory dermatoses. *J Am Acad Dermatol*. 2006;54(Suppl. 2):S139–142.
19. Fautrel B, Foltz B, Frances C, et al. Regression of subacute cutaneous lupus erythematosus in a patient with rheumatoid arthritis treated with a biologic tumor necrosis factor alpha-blocking agent: comment on the article by Pisetsky and the letter from Aringer et al. *Arthritis Rheum*. 2002;46:1408–1409.
20. Pink AE, Fonia A, Allen MH, et al. Antinuclear antibodies associate with loss of response to anti-TNF alpha therapy in psoriasis – a retrospective, observational study. *Br J Dermatol*. 2010;162:780–785.
21. Kary S, Worm M, Audring H, et al. New onset or exacerbation of psoriatic skin lesions in patients with definite rheumatoid arthritis receiving tumour necrosis factor alpha antagonists. *Ann Rheum Dis*. 2006;65:405–407.
22. Murphy MJ, Cohen JM, Vesely MD, et al. Paradoxical eruptions to targeted therapies in dermatology: a systematic review and analysis. *J Am Acad Dermatol*. 2022;86:1080–1091.
23. Cyrenne BM, Parpia AS, Sibbald C. Paradoxical psoriasis in pediatric patients: a systematic review. *Pediatr Dermatol*. 2021;38:1086–1093.
24. Mohan N, Edwards ET, Cupps TR, et al. Leukocytoclastic vasculitis associated with tumor necrosis factor-alpha blocking agents. *J Rheumatol*. 2004;31:1955–1958.
25. Deng A, Harvey V, Sina B, et al. Interstitial granulomatous dermatitis associated with the use of tumor necrosis factor alpha inhibitors. *Arch Dermatol*. 2006;142:198–202.
26. Aikaterini-Evaggelia M, Athina M, Dessinioti C, et al. Cutaneous side effects of anti-tumor necrosis factor biologic therapy: a clinical review. *J Am Acad Dermatol*. 2009;61:486–504.
27. Fomin I, Caspi D, Levy V, et al. Vaccination against influenza in rheumatoid arthritis: the effect of disease modifying drugs, including TNF alpha blockers. *Ann Rheum Dis*. 2006;65:191–194.
28. Diav-Citrin O, Otcheretianski-Volodarsky A, Shechtman S, Ornoy A. Pregnancy outcome following gestational exposure to TNF-alpha-inhibitors: a prospective, comparative, observational study. *Reprod Toxicol*. 2014;43:78–84.
29. Mease PJ, Goffe BS, Metz J, et al. Etanercept in the treatment of psoriatic arthritis and psoriasis: a randomized trial. *Lancet*. 2000;356:385–390.
30. Paller AS, Siegfried EC, Langley RG, et al. Etanercept treatment for children and adolescents with plaque psoriasis. *N Engl J Med*. 2008;358:241–251.
31. Alexis AF, Strober BE. Off-label dermatologic uses of anti-TNF-α therapies. *J Cutan Med Surg*. 2005;9:296–302.
32. Sand FL, Thomsen SF. Off-label use of TNF-alpha inhibitors in a dermatological university department: retrospective evaluation of 118 patients. *Dermatol Ther*. 2015;28:158–165.
33. Baughman RP, Lower EE, Bradley DA, et al. Etanercept for refractory ocular sarcoidosis: results of a double-blind randomized trial. *Chest*. 2005;128:1062–1067.
34. Genovese MC, Cohen S, Moreland L, et al. Combination therapy with etanercept and anakinra in the treatment of patients with rheumatoid arthritis who have been treated successfully with methotrexate. *Arthritis Rheum*. 2004;50:412–419.
35. Gambichler T, Tigges C, Scola N, et al. Etanercept plus narrowband ultraviolet B phototherapy of psoriasis is more effective than etanercept monotherapy at 6 weeks. *Br J Dermatol*. 2011;164:1383–1386.
36. Brimhall AK, King LN, Licciardone JC, et al. Safety and efficacy of alefacept, efalizumab, etanercept and infliximab in treating moderate to severe plaque psoriasis: a meta-analysis of randomized controlled trials. *Br J Dermatol*. 2008;159:274–285.
37. Chaudhari U, Romano P, Mulcahy LD, et al. Efficacy and safety of infliximab monotherapy for plaque-type psoriasis: a randomized trial. *Lancet*. 2001;357:1842–1846.
38. Brooklyn TN, Dunnill MG, Shetty A, et al. Infliximab for the treatment of pyoderma gangrenosum: a randomized, double-blind, placebo controlled trial. *Gut*. 2006;55:505–509.
39. Scheinfeld N. Off-label uses and side effects of infliximab. *J Drugs Dermatol*. 2004;3:273–284.
40. Baert F, Noman M, Vermeire S, et al. Influence of immunogenicity on the long-term efficacy of infliximab in Crohn's disease. *N Engl J Med*. 2003;348:601–608.
41. Miele E, Markowitz JE, Mamula P, Baldassano RN. Human antichimeric antibody in children and young adults with inflammatory bowel disease receiving infliximab. *J Pediatr Gastroenterol Nutr*. 2004;38:502–508.
42. Mease PJ. Adalimumab: an anti-TNF agent for the treatment of psoriatic arthritis. *Expert Opin Biol Ther*. 2005;5:1491–1504.
43. Kimball AB, Okun MM, Williams DA, et al. Two phase 3 trials of adalimumab for hidradenitis suppurativa. *N Engl J Med*. 2016;375:422–434.
44. Callen JP, Jackson JH. Adalimumab effectively controlled recalcitrant generalized pustular psoriasis in an adolescent. *J Dermatolog Treat*. 2005;16:350–352.
45. Leonardi C, Papp K, Strober B, et al. The long-term safety of adalimumab treatment in moderate to severe psoriasis: a comprehensive analysis of all adalimumab exposure in all clinical trials. *Am J Clin Dermatol*. 2011;12:321–337.
46. Vogelzang EH, Kneepkens EL, Nurmohamed MT, et al. Anti-adalimumab antibodies and adalimumab concentrations in psoriatic arthritis; an association with disease activity at 28 and 52 weeks of follow-up. *Ann Rheum Dis*. 2014;73:2178–2182.
47. Kavanaugh A, van der Heijde D, McInnes IB, et al. Golimumab in psoriatic arthritis: one-year clinical efficacy, radiographic, and safety results from a phase III, randomized, placebo-controlled trial. *Arthritis Rheum*. 2012;64:2504–2517.
48. Gottlieb AB, Blauvelt A, Thaçi D, et al. Certolizumab pegol for the treatment of chronic plaque psoriasis: results through 48 weeks from 2 phase 3, multicenter, randomized, double-blinded, placebo-controlled studies (CIMPASI-1 and CIMPASI-2). *J Am Acad Dermatol*. 2018;79:302–314. e6.
49. Papp KA, Langley RG, Lebwohl M, et al. Efficacy and safety of ustekinumab, a human interleukin-12/23 monoclonal antibody, in patients with psoriasis: 52-week results from a randomised, double-blind, placebo-controlled trial (PHOENIX 2). *Lancet*. 2008;371:1675–1684.

50. Ryan C, Leonardi CL, Krueger JG, et al. Association between biologic therapies for chronic plaque psoriasis and cardiovascular events: a meta-analysis of randomized controlled trials. *JAMA*. 2011;306:864–871.
51. Rungapiromnan W, Yiu ZZ, Warren RB, et al. Impact of biologic therapies on risk of major adverse cardiovascular events in patients with psoriasis: systematic review and meta-analysis of randomized controlled trials. *Br J Dermatol*. 2017;176:890–901.
52. Langley RG, Lebwohl M, Krueger GG, et al. The PHOENIX 2 Investigators. Long-term efficacy and safety of ustekinumab, with and without dosing adjustment, in patients with moderate-to-severe psoriasis: results from the PHOENIX 2 study through 5 years of follow-up. *Br J Dermatol*. 2015;172:1371–1383.
53. Lipsker D, Lutz D. Cutaneous infarction under IL12/23 p40 inhibition: a cautionary tale. *Arch Dermatol*. 2011;147:1344.
54. Gordon KB, Blauvelt A, Papp KA, et al. UNCOVER-1 Study Group; UNCOVER-2 Study Group; UNCOVER-3 Study Group. Phase 3 trials of ixekizumab in moderate-to-severe plaque psoriasis. *N Engl J Med*. 2016;375:345–356.
55. Gómez-García F, Epstein D, Isla-Tejera B, et al. Short-term efficacy and safety of new biological agents targeting the interleukin-23-T helper 17 pathway for moderate-to-severe plaque psoriasis: a systematic review and network meta-analysis. *Br J Dermatol*. 2017;176:594–603.
56. van de Kerkhof PC, Griffiths CE, Reich K, et al. Secukinumab long-term safety experience: a pooled analysis of 10 phase II and III clinical studies in patients with moderate to severe plaque psoriasis. *J Am Acad Dermatol*. 2016;75:83–98. e4.
57. Lebwohl M, Strober B, Menter A, et al. Phase 3 studies comparing brodalumab with ustekinumab in psoriasis. *N Engl J Med*. 2015;373:1318–1328.
58. Gaffen SL, Hernández-Santos N, Peterson AC. IL-17 signaling in host defense against Candida albicans. *Immunol Res*. 2011;50:181–187.
59. Langley RG, Elewski BE, Lebwohl M, et al. ERASURE Study Group. FIXTURE Study Group. Secukinumab in plaque psoriasis–results of two phase 3 trials. *N Engl J Med*. 2014;371:326–338.
60. Papp KA, Leonardi C, Menter A, et al. Brodalumab, an anti-interleukin-17-receptor antibody for psoriasis. *N Engl J Med*. 2012;366:1181–1189.
61. Bachelez H, Choon SE, Marrakchi S, et al. Trial of spesolimab for generalized pustular psoriasis. *N Engl J Med*. 2021;385:2431–2440.
62. Fachler T, Shreberk-Hassidim R, Molho-Pessach V. Dupilumab-induced ocular surface disease: a systematic review. *J Am Acad Dermatol*. 2022;86:486–487.
63. Simpson EL, Bieber T, Guttman-Yassky E, et al. SOLO 1 and SOLO 2 Investigators. Two phase 3 trials of dupilumab versus placebo in atopic dermatitis. *N Engl J Med*. 2016;375:2335–2348.
64. Jo CE, Finstad A, Georgakopoulos JR, et al. Facial and neck erythema associated with dupilumab treatment: a systematic review. *J Am Acad Dermatol*. 2021;84:1339–1347.
65. Silverberg JI, Toth D, Bieber T, et al. Tralokinumab plus topical corticosteroids for the treatment of moderate-to-severe atopic dermatitis: results from the double-blind, randomized, multicentre, placebo-controlled phase III ECZTRA 3 trial. *Br J Dermatol*. 2021;184:450–463.
66. Wollenberg A, Blauvelt A, Guttman-Yassky E, et al. Tralokinumab for moderate-to-severe atopic dermatitis: results from two 52-week, randomized, double-blind, multicentre, placebo-controlled phase III trials (ECZTRA 1 and ECZTRA 2). *Br J Dermatol*. 2021;184:437–449.
67. Furst DE. Anakinra: review of recombinant human interleukin-1-receptor antagonist in the treatment of rheumatoid arthritis. *Clin Ther*. 2004;26:1960–1975.
68. Goldbach-Mansky R, Dailey NJ, Canna SW, et al. Neonatal-onset multisystem inflammatory disease responsive to interleukin-1beta inhibition. *N Engl J Med*. 2006;355:581–592.
69. Crouch R, Akhras V, Sarkany R. Schnitzler's syndrome: successful treatment with anakinra. *Australas J Dermatol*. 2007;48:178–181.
70. Skendros P, Papagoras C, Lefaki I, et al. Successful response in a case of severe pustular psoriasis after interleukin-1β inhibition. *Br J Dermatol*. 2017;176:212–215.
71. Tzanetakou V, Kanni T, Giatrakou S, et al. Safety and efficacy of anakinra in severe hidradenitis suppurativa: a randomized clinical trial. *JAMA Dermatol*. 2016;152:52–59.
72. Kolios AG, Maul JT, Meier B, et al. Canakinumab in adults with steroid-refractory pyoderma gangrenosum. *Br J Dermatol*. 2015;173:1216–1223.
73. Krause K, Tsianakas A, Wagner N, et al. Efficacy and safety of canakinumab in Schnitzler syndrome: a multicenter randomized placebo-controlled study. *J Allergy Clin Immunol*. 2017;139:1311–1320.
74. Lachmann HJ, Kone-Paut I, Kuemmerle-Deschner JB, et al. Use of canakinumab in the cryopyrin-associated periodic syndrome. *N Engl J Med*. 2009;360:2416–2425.
75. Scheinfeld N. A review of rituximab in cutaneous medicine. *Dermatol Online J*. 2006;12:3.
76. Zambruno G, Borradori L. Rituximab immunotherapy in pemphigus: therapeutic effects beyond B-cell depletion. *J Invest Dermatol*. 2008;128:2745–2747.
77. Anonymous. Rituximab (Rituxan) for rheumatoid arthritis. *Med Lett Drugs Ther*. 2006;48:34–35.
78. Kanwar AJ, Vinay K, Sawatkar GU, et al. Clinical and immunological outcomes of high- and low-dose rituximab treatments in patients with pemphigus: a randomized, comparative, observer-blinded study. *Br J Dermatol*. 2014;170:1341–1349.
79. Bonnekoh B, Schulz M, Franke I, Gollnick H. Complete remission of primary cutaneous B-cell lymphoma of the lower leg by first-line monotherapy with the CD20-antibody rituximab. *J Cancer Res Clin Oncol*. 2002;128:161–166.
80. Heelan K, Walsh S, Shear NH. Treatment of mucous membrane pemphigoid with rituximab. *J Am Acad Dermatol*. 2013;69:310–311.
81. Anolik JH, Aringer M. New treatments for SLE: cell-depleting and anti-cytokine therapies. *Best Pract Res Clin Rheumatol*. 2005;19:859–878.
82. Levine TD. Rituximab in the treatment of dermatomyositis: an open-label pilot study. *Arthritis Rheum*. 2005;52:601–607.
83. Cutler C, Miklos D, Haesook T, et al. Rituximab for steroid-refractory chronic graft-versus-host disease. *Blood*. 2006;108:756–762.
84. Chung L, Funke AA, Chakravarty EF, et al. Successful use of rituximab for cutaneous vasculitis. *Arch Dermatol*. 2006;142:1407–1410.
85. Schmidt E, Hennig K, Mengede C, et al. Immunogenicity of rituximab in patients with severe pemphigus. *Clin Immunol*. 2009;132:334–341.
86. Holgate S, Casale T, Wenzel S, et al. The anti-inflammatory effects of omalizumab confirm the central role of IgE in allergic inflammation. *J Allergy Clin Immunol*. 2005;115:459–465.
87. Beck LA, Saini S. Wanted: a study with omalizumab to determine the role of IgE-mediated pathways in atopic dermatitis. *J Am Acad Dermatol*. 2006;55:540–541.
88. Saini S, et al. A randomized, placebo-controlled, dose-ranging study of single-dose omalizumab in patients with H1-antihistamine–refractory chronic idiopathic urticaria. *J Allergy Clin Immunol*. 2011;128:567–573.
89. Kaplan AP, Joseph K, Maykut RJ, et al. Treatment of chronic autoimmune urticaria with omalizumab. *J Allergy Clin Immunol*. 2008;122:569–573.
90. Hotze M, Baurecht H, Rodríguez E, et al. Increased efficacy of omalizumab in atopic dermatitis patients with wild-type filaggrin status and higher serum levels of phosphatidylcholines. *Allergy*. 2014;69:132–135.
91. Long A, Rahmaoui A, Rothman KJ, et al. Incidence of malignancy in patients with moderate-to-severe asthma treated with or without omalizumab. *J Allergy Clin Immunol*. 2014;134:560–567.
92. Shreberk-Hassidim R, Ramot Y, Zlotogorski A. Janus kinase inhibitors in dermatology: a systematic review. *J Am Acad Dermatol*. 2017;76:745–753. e19.
93. Bezzio C, Vernero M, Ribaldone DG, et al. Cancer risk in patients treated with the JAK inhibitor tofacitinib: systematic review and meta-analysis. *Cancers (Basel)*. 2023;15:2197.
94. King B, Ohyama M, Kwon O, et al. Two phase 3 trials of baricitinib for alopecia areata. *N Engl J Med*. 2022;386:1687–1699.

94a. King B, Zhang X, Harcha WG, et al. Efficacy and safety of ritlecitinib in adults and adolescents with alopecia areata: a randomised, double-blind, multicentre, phase 2b-3 trial. *Lancet*. 2023;401:1518–1529.

95. Mackay-Wiggan J, Jabbari A, Nguyen N, et al. Oral ruxolitinib induces hair regrowth in patients with moderate-to-severe alopecia areata. *JCI Insight*. 2016;1:e89790.
96. Kennedy Crispin M, Ko JM, Craiglow BG, et al. Safety and efficacy of the JAK inhibitor tofacitinib citrate in patients with alopecia areata. *JCI Insight*. 2016;1:e89776.
97. Mydlarski PR, Mittman N, Shear NH. Intravenous immunoglobulin: use in dermatology. *Skin Therapy Lett*. 2004;9:1–6.
98. French LT, Trent JT, Kerdel FA. Use of intravenous immunoglobulin in toxic epidermal necrolysis and Stevens-Johnson syndrome: our current understanding. *Int Immunopharmacol*. 2006;6:543–549.
99. Dalakas MC. The role of high-dose immune globulin in the treatment of dermatomyositis. *Int Immunopharmacol*. 2006;6:550–556.
100. Ahmed AR. Use of intravenous immunoglobulin therapy in autoimmune blistering diseases. *Int Immunopharmacol*. 2006;6:557–578.
101. Bayary J, Dasgupta S, Misra N, et al. Intravenous immunoglobulin in autoimmune disorders: an insight into the immunoregulatory mechanisms. *Int Immunopharmacol*. 2006;6:528–534.
102. Siegel J. Safety considerations in IGIV utilization. *Int Immunopharmacol*. 2006;6:523–527.

MECHANISMS OF ACTION FOR INTERFERONS	
Cellular mechanism	**Clinical effect**
Induction of 2′-5′-oligoadenylate synthetase Induction of ribonuclease Induction of protein kinase P1	Antiviral
Induction of 2′-5′-oligoadenylate synthetase Inhibition of various growth factors Enhanced *TP53* tumor suppressor gene expression Downregulation of *MYC*, *FOX*, and certain *RAS* oncogenes	Antiproliferative
Induction of class I & II MHC antigens Increased number of natural killer (NK) cells Inhibit production of Th2 cytokines such as IL-4 and IL-5	Immunoregulatory

eTable 128.1 Mechanisms of action for interferons. IL, interleukin; MHC, major histocompatibility complex. *Courtesy Brian Berman, MD, Tami De Araujo, MD, and Mark Lebwohl, MD.*

INTERPRETATION OF HEPATITIS B AND C SEROLOGIC TEST RESULTS					
Hepatitis B (HBV)					
	HBsAg	**Anti-HBs Ab***	**Anti-HBc Ab***	**IgM Anti-HBc Ab**	**Comments**
Susceptible	–	–	–		
Immune/natural infection	–	+	+		Can reactivate with immunosuppressive therapy†; consider serial measurement of HBV DNA
Immune/Hep B vaccine	–	+	–		
Acutely infected	+	–	+	+	Measure HBV DNA; treat with antiviral agent (e.g. tenofovir, entecavir, telbivudine) prior to immunosuppressive therapy
Chronically infected	+	–	+	–	See Acutely infected
Resolved infection > false-positive anti-HBc Ab, "low level" chronic infection, resolving acute infection	–	–	+		With exception of false-positive anti-HBc Ab, can reactivate with immunosuppressive therapy†; measure HBV DNA
Hepatitis C (HCV)					
	Anti-HCV Ab‡		**HCV RNA**		**Comments**
Current HCV infection	+		detected		Treat with antiviral agents (e.g. sofosbuvir + ledipasvir)
No current HCV infection	+		–		Can reactivate with immunosuppressive therapy¶; consider serial measurement of HCV RNA

*IgG Ab.
†Includes TNF inhibitors, rituximab, chemotherapy.
‡If anti-HCV Ab present, then presumptive HCV infection (current or past that has resolved) and need to test for HCV RNA.
¶Includes rituximab, chemotherapy; TNF inhibitors have been used safely.

eTable 128.2 Interpretation of hepatitis B and C serologic test results. Shading emphasizes need to treat prior to instituting immunosuppressive therapy. *Courtesy Jean L. Bolognia, MD.*

EXAMPLES OF BIOSIMILARS OF MONOCLONAL ANTIBODIES USED IN DERMATOLOGY	
Generic name	**Trade name (manufacturer)**
Adalimumab	**Humira® (AbbVie)**
Adalimumab-aacf	Idacio® (Fresenius Kabi)
Adalimumab-aaty	Yuflyma® (Celltrion)
Adalimumab-adaz	Hyrimoz® (Sandoz)
Adalimumaba-adbm	Cyltezo® (Boehringer Ingelheim)
Adalimumab-afzb	Abrilada® (Pfizer)
Adalimumab-aqvh	Yusimry™ (Coherus BioSciences)
Adalimumab-atto	Amjevita® (Amjen)
Adalimumab-bwwd	Hadlima® (Samsung Bioepis)
Adalimumab-fkjp	Hulio™ (Mylan)
Etanercept	**Enbrel®** (Amgen)
Etanercept-szzs	Erelzi™ (Sandoz)
Etanercept-ykro	Eticovo™ (Samsung Bioepis)
Infliximab	**Remicade®** (Jannsen)
Infliximab-abda	Renflexis® (Pfizer)
Ifliximab-axxq	Avsola™ (Amgen)
Infliximab-dyyb	Inflectra® (Pfizer)
Infliximab-qbtx	Ixifi™ (Pfizer)
Rituximab	**Rituxan®** (Genentech)
rituximab-abbs	Truxima® (Celltrion)
rituximab-arrx	Riabni™ (Amgen)
rituximab-pvvr	Ruxience® (Pfizer)

eTable 128.3 Examples of biosimilars of monoclonal antibodies used in dermatology

129 Other Topical Medications

Mark Marchitto, Matthew Fox, Yolanda R. Helfrich and Sewon Kang

Chapter Contents

General Principles of Topical Therapy 2295
Antipruritic Agents 2296
Keratolytics and Humectants 2296
Skin-Lightening Agents 2297
Agents that Affect Hair Growth 2298
Immunomodulatory Agents 2300
Chemotherapeutic Agents 2303
Vitamin D Analogues 2304
Miscellaneous Agents 2305

Key features

- Absorption of topical medications depends upon several factors, including cutaneous barrier function, the anatomic site, the active agent, and characteristics of the vehicle
- In neonates, there is a greater risk of systemic toxicity with use of topical medications
- Combination or rotational therapy using topical agents may result in increased efficacy and decreased risk of side effects

INTRODUCTION

Topical medications are fundamental in the armamentarium of dermatologic therapeutics, offering the ability to deliver treatment directly to the skin while limiting systemic side effects. However, topical therapy can be time-consuming and messy, and it may not be practical for generalized skin disorders or effective for conditions with deeper involvement. Choosing an appropriate topical regimen requires consideration of the disease process and involved site(s) as well as the vehicle, application strategy, and duration of use of the selected agent. This chapter reviews general principles of topical therapy and topical medications not discussed elsewhere in the textbook. Table 129.1 lists topical medications covered in other chapters.

GENERAL PRINCIPLES OF TOPICAL THERAPY

Topical formulations consist of an active ingredient in a non-active base (vehicle). To be effective, topical medications must gain entry into the skin and reach the desired target site, e.g. the epidermis below the stratum corneum or the dermis, in adequate concentrations. Successful topical therapy therefore requires percutaneous absorption, which depends upon factors related to the skin being treated as well as the agent and its vehicle (Table 129.2). The role of the stratum corneum in skin barrier function, including percutaneous absorption of medications, is discussed in Chapter 124.

Quantity of Application

In general, topical medications should be applied to the skin as a thin layer. A thicker layer of medication does not result in enhanced penetration or additional therapeutic benefit. One gram of cream covers a ~10 cm × 10 cm area of skin, and the same amount of ointment spreads nearly 10% further.

TOPICAL MEDICATIONS DISCUSSED IN OTHER CHAPTERS	
Topical medications	**Chapter(s)**
Chapters on medical therapy or cosmetics	
Glucocorticoids	125
Retinoids	126
Antimicrobials (antibacterials, antifungals, antivirals)	127
Sunscreens	132
Anesthetics	143
Cosmeceuticals	153
Chemical peel agents	154
Other chapters	
Clascoterone for acne	36
Brimonidine and oxymetazoline for facial erythema in rosacea	37
Aluminum chloride and topical anticholinergic agents for hyperhidrosis	39
Topical immunotherapy for alopecia areata (with squaric acid dibutyl ester or diphencyprone)	69
Sinecatechins for anogenital warts	79
Antiparasitic agents (including treatments for infestations)	83, 84
Insect repellents	85
Topical β-blockers (e.g. timolol) for infantile hemangiomas	103
Wound healing agents	105, 141
Tirbanibulin for actinic keratoses	109
Hemostatic agents	151

Table 129.1 Topical medications discussed in other chapters.

FACTORS THAT AFFECT PERCUTANEOUS ABSORPTION
Characteristics of the patient/skin

• Patient age
  • Suboptimal skin barrier function in neonates, especially if premature (see Table 129.4)
• Diseases, physical injuries, or chemical exposures that disrupt skin barrier function (e.g. Netherton syndrome)
• A thicker stratum corneum decreases absorption
• Skin hydration and/or occlusion increase absorption (e.g. in a skin fold)
• Anatomic location (approximate ratio of absorption compared to the forearm)
  • *Higher absorption:* scrotum (40), face (10), axilla (4), scalp (3)
  • *Intermediate absorption*: trunk (1.5), arm (1)
  • *Lower absorption*: palm (0.8), ankle (0.4), sole (0.1)

Properties of the medication/its application

• Drug/prodrug properties that increase absorption
  • Smaller molecular size and/or lower frictional coefficient
  • Increased lipophilicity
  • Increased concentration and/or solubility
• Vehicle composition
• Application under occlusion increases absorption (e.g. ointment, occlusive dressing)

Table 129.2 Factors that affect percutaneous absorption.

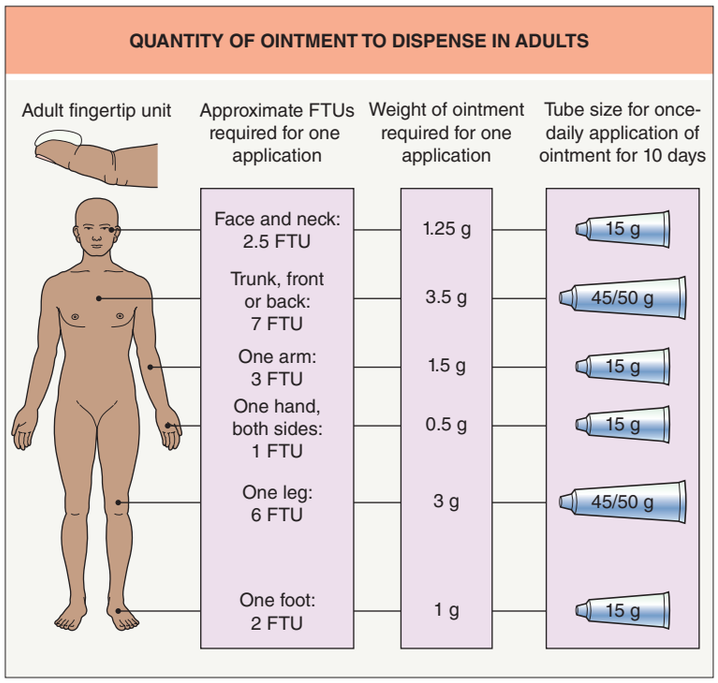
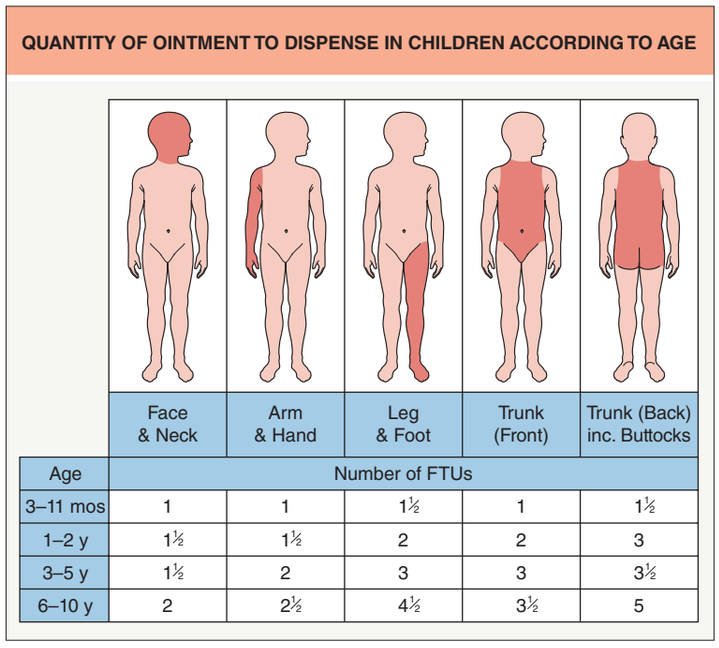


Fig. 129.1 Quantity of ointment to dispense in adults. FTU, fingertip unit. *Redrawn from Long CC, Finlay AY. The finger-tip unit – a new practical measure. Clin Exp Dermatol 1991;16:444–7.*



Age	Face & Neck	Arm & Hand	Leg & Foot	Trunk (Front)	Trunk (Back) inc. Buttocks
	Number of FTUs				
3–11 mos	1	1	1½	1	1½
1–2 y	1½	1½	2	2	3
3–5 y	1½	2	3	3	3½
6–10 y	2	2½	4½	3½	5

Fig. 129.2 Quantity of ointment to dispense in children, according to age. FTU, fingertip unit (in an adult). *Redrawn from Long CC, Mills CM, Finlay AY. A practical guide to topical therapy in children. Br J Dermatol 1998;138:293–6.*

A practical guide to quantifying the amount of ointment necessary to treat different areas of the body is the "fingertip unit" (FTU), which represents the amount of ointment dispensed from a 5 mm-diameter nozzle that extends from the distal crease to the tip of the index finger in an adult[1]. One FTU is equal to ~0.5 g, and the quantities required to treat various areas of the body in adults and children are presented in Figs. 129.1 and 129.2. The appropriate amount to treat the entire body of an adult man is ~20 g, therefore requiring ~250 g per week if applied twice daily. Because ~0.5 FTU (0.25 g) can treat an area equivalent to one side of an extended ("flat") hand, estimating the number of "flat hand areas" of affected skin assists in determining the amount of medication needed. For example, four "flat hand areas" would require 1 g per application and ~15 g per week if applied twice daily.

Formulations and Vehicles

A classification of topical formulations and clinical guidelines for vehicle selection are presented in Fig. 129.3. A discussion of how vehicles affect drug delivery is found in Chapter 124.

Topical Therapy During Pregnancy and Lactation

The decision to use topical medications during pregnancy and lactation should be based on the potential risk of the medication and the extent to which the condition affects the health of the woman. Use of the following topical medications during pregnancy (not a comprehensive list) is generally contraindicated: podophyllin, anthralin, lindane, chemotherapeutics (e.g. carmustine, mechlorethamine hydrochloride [nitrogen mustard], 5-fluorouracil), tazarotene, and peels with phenol or salicylic acid. In 2015, the US Food and Drug Administration (FDA) replaced pregnancy risk categories with narrative sections addressing pregnancy and lactation, which include risk summaries as well as information on pregnancy exposure registries, clinical considerations, and available data. Table 129.3 lists topical medications with minimal risk during pregnancy and lactation.

Topical Therapy in Neonates

Although the stratum corneum provides competent skin barrier function in full-term newborns under basal conditions (see Ch. 2), it undergoes structural and functional maturation during the first few weeks to months of life. Several factors result in an increased risk of systemic toxicity from topically applied medications during the neonatal period (the first 30 days of life) (Table 129.4). Systemic toxicity has been reported in neonates exposed to topical corticosteroids, salicylic acid, lindane, hexachlorophene, chlorhexidine, and propylene glycol (Table 129.5).

Combination and Rotational Topical Therapy

The advantages of using a single topical agent include improved compliance and sometimes lower cost. However, combination or rotational therapy may be employed to provide additive/synergistic effects via different mechanisms of action or to decrease potential side effects by reducing exposure to one or both agents, especially if they have different adverse-effect profiles. Examples of this strategy for topical therapy include various combinations of benzoyl peroxide, retinoids, and antibiotics to treat acne; use of a corticosteroid together with a vitamin D analogue or tazarotene to treat psoriasis; and rotating use of a corticosteroid and calcineurin inhibitor to treat atopic dermatitis.

ANTIPRURITIC AGENTS

Pruritus involves multiple components of the nervous system, including skin surface receptors, peripheral (especially unmyelinated C fibers) and central nerves, and specific brain regions (see Ch. 5). Treatment of the associated dermatologic condition, e.g. by applying topical corticosteroids to inflamed skin and moisturization of dry skin, or the underlying systemic cause remains the most effective method of alleviating itch. Topical antipruritic agents may help reduce the urge to scratch, potentially improving the efficacy of skin disease-specific therapies. Mechanisms of action of topical antipruritics include substituting a different sensation for itching, anesthetizing cutaneous nerve endings, and blocking molecular mediators of pruritus[2]. Unfortunately, a relative lack of comparative studies has made antipruritics difficult to evaluate. Commonly used agents are outlined in Table 129.6 (also see Table 5.5).

KERATOLYTICS AND HUMECTANTS

Keratolytic agents reduce the thickness of the stratum corneum via elimination of squames. This can be beneficial in diseases characterized by reduced desquamation or accelerated epidermal proliferation.

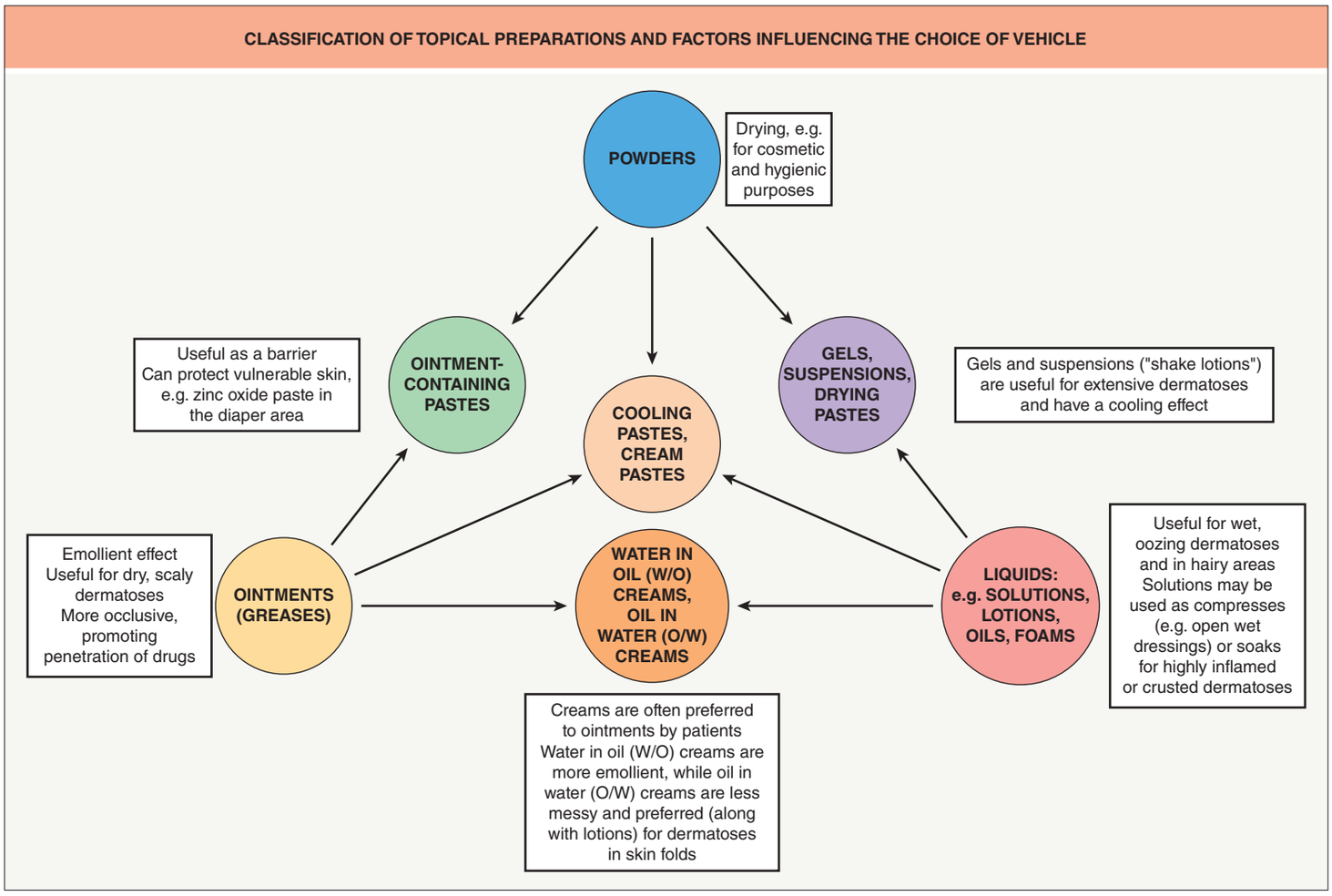


Fig. 129.3 Classification of topical preparations and factors influencing the choice of vehicle. Monophasic preparations are in primary colors. Diphasic preparations, which represent a combination of two monophasic preparations, are in secondary colors. Cooling pastes and cream pastes are triphasic preparations. Ointments, creams, gels, and pastes (highly concentrated suspensions) are semi-solids. Creams and lotions may be emulsions, i.e. contain mixtures of ≥2 liquids that are normally immiscible, brought together by emulsifiers. Foams and aerosol sprays represent liquids with pressurized gaseous propellants, and paints are alcohol-based solutions. Preparations containing alcohol or salicylic acid can lead to stinging and burning when applied to fissured or eroded skin. Vehicles may also contain preservatives, absorption promoters, and fragrances. *Adapted from Polano MK. Principles of formulation. Topical Skin Therapeutics. New York: Churchill Livingstone; 1984.*

Keratolytics and humectants are reviewed in Table 129.7, and their use in cosmeceutical products and chemical peels is discussed in Chapters 153 and 154.

SKIN-LIGHTENING AGENTS

Hydroquinone

Introduction, dosages, and indications

Hydroquinone (1,4-dihydroxybenzene) is used to treat melasma and other disorders of hyperpigmentation (see Ch. 67)[3]. In the US, 2% formulations are available over the counter, while 3% solution and 4% cream or gel require a prescription. Although twice-daily application is commonly recommended, irritant contact dermatitis can limit frequency of application. Some products contain hydroquinone combined with a sunscreen or with tretinoin (0.05%–0.1%) and a class 5–7 corticosteroid[4].

Mechanism of action

Hydroquinone reduces skin pigmentation by competing with tyrosine as a substrate for tyrosinase (the initial enzyme in melanin biosynthesis; see Ch. 65) and via selective damage to melanosomes and melanocytes via production of reactive oxygen radicals[3].

Side effects

Irritant or (less often) allergic contact dermatitis can develop. Exogenous ochronosis occasionally occurs with prolonged use of higher concentrations of hydroquinone. A variety of neoplasms have been noted to develop in rodents that received large systemic doses of the medication, but the relevance to topical therapy in humans has not been determined[3]. Concern regarding potential adverse effects related to misuse of hydroquinone led to its removal from Japanese and European markets.

Use in pregnancy

Animal reproduction studies have not consistently shown adverse fetal effects, and there are no adequate studies in pregnant women. Because of the potential for substantial systemic absorption (~30%–50%), it is recommended that hydroquinone use be avoided during pregnancy.

Monobenzyl Ether of Hydroquinone

Monobenzyl ether of hydroquinone (MBEH) 20% is infrequently used to depigment remaining uninvolved skin in patients with extensive, treatment-resistant vitiligo so as to achieve a uniform appearance (see Ch. 66). It is thought to act via competitive inhibition of tyrosinase and free radical-mediated damage of melanocytes. Depigmentation is typically long-lasting, but repigmentation (especially in a perifollicular distribution) can occur following sun exposure. Both irritant and allergic contact dermatitis are possible side effects[5].

Mequinol

Mequinol (4-hydroxyanisole) is a skin-lightening agent. A solution composed of mequinol 2% and tretinoin 0.01% is FDA-approved for

TOPICAL MEDICATIONS WITH MINIMAL RISK DURING PREGNANCY AND LACTATION	
Pregnancy	**Lactation**
Azelaic acid	Acyclovir
Ciclopirox	Bacitracin
Clindamycin	Benzoyl peroxide
Clotrimazole	Butoconazole
Erythromycin	Calcipotriene
Metronidazole*	Ciclopirox
Mupirocin	Clotrimazole
Naftifine	Erythromycin
Nystatin†	Hydroquinone
Oxiconazole	Ketoconazole
Permethrin	Metronidazole
Retapamulin	Mupirocin
Terbinafine	Nystatin
	Oxiconazole
	Terbinafine

*The CDC no longer recommends avoidance of oral metronidazole during the first trimester.
†Intravaginal topical application not advised close to term because of risk of contamination if membranes have ruptured; pregnancy category A for pastilles.

Table 129.3 Topical medications with minimal risk during pregnancy and lactation. Minimal risk refers to medications where there is no evidence of fetal risk in humans based on data from human or (if no adequate human data) animal studies. The medications listed were previously designated as FDA pregnancy category B.

FACTORS THAT INCREASE THE RISK OF SYSTEMIC TOXICITY FROM TOPICAL MEDICATIONS IN NEONATES
• Increased ratio of surface area to body weight (fourfold greater than in adults)
• Suboptimal epidermal barrier function due to the neonatal stratum corneum being on average ~30% thinner and having a higher pH (neutral instead of acidic), less hydration, and smaller corneocytes (reflecting more rapid cell turnover)
• Decreased hepatic metabolism of drugs
• Decreased renal excretion of drugs
• Increased distribution of drug, including into the CNS due to a more permeable blood–brain barrier
• Decreased plasma protein binding

Table 129.4 Factors that increase the risk of systemic toxicity from topical medications in neonates.

POTENTIAL SYSTEMIC SIDE EFFECTS OF TOPICAL MEDICATIONS	
Medication	**Systemic side effect**
Androgens	Virilization in women, children*, and fetuses
Boric acid	Generalized erythema, fever, vomiting, mental status change
Calcipotriene (calcipotriol)	Hypercalcemia, hypercalciuria
Carmustine (BCNU)	Bone marrow suppression
Chlorhexidine	Nausea, signs of ethanol intoxication
Clindamycin	Diarrhea, pseudomembranous colitis (controversial)
Corticosteroids	Iatrogenic Cushing syndrome, inhibition of hypothalamic–pituitary axis
Dimethylsulfoxide	Nausea, abdominal pain
Epinephrine (adrenaline)	Tachycardia
Estrogens	Pseudoprecocious puberty, gynecomastia, hypogonadism in men
Gentamicin	Ototoxicity
Hexachlorophene	Neurotoxicity, coma, death
Iodine	Hypothyroidism
Lidocaine and other topical anesthetics	With overdose (>5 mg/kg of lidocaine absorbed): *early/lower levels* – paresthesias (e.g. perioral tingling), tinnitus, dysgeusia (e.g. metallic taste), lightheadedness, tremors; *late/higher levels* – seizures, hypotension, arrhythmias, cardiopulmonary arrest (see Ch. 143)
Lindane	CNS toxicity
Malathion	CNS toxicity, hyperglycemia
Mechlorethamine (nitrogen mustard)	Myelosuppression
Mercury	CNS and renal toxicity, acrodynia
Minoxidil	Cardiac toxicity
Neomycin	Ototoxicity, nephrotoxicity
Phenol	Cardiac arrhythmia, death
Podophyllin	Gastrointestinal (nausea, vomiting), neurologic (mental status changes, peripheral polyneuropathy) and hematologic (thrombocytopenia, leukopenia) effects
Prilocaine–lidocaine (EMLA®)	Methemoglobinemia (perioral/acral cyanosis, vascular "mottling") related to prilocaine; see lidocaine above
Propylene glycol	Hyperosmolality, with or without lactic acidosis
Salicylic acid	Tinnitus (early sign), gastrointestinal symptoms (e.g. nausea, vomiting), CNS toxicity (e.g. confusion, delirium, seizures), metabolic acidosis with respiratory compensation (i.e. tachypnea), hypoglycemia, coma, death
Silver (silver nitrate, silver sulfadiazine)	Leukopenia, argyria

*May occur from passive transfer of paternal topical testosterone.

Table 129.5 Potential systemic side effects of topical medications. For most, the risk of these side effects is either theoretical or exists only in instances where the medication is applied to neonates or in quantities greatly exceeding normal exposure. CNS, central nervous system.

treatment of solar lentigines (formerly pregnancy category X). However, the latter product is no longer commercially available in the US. Mequinol is a substrate of tyrosinase and may serve as a competitive inhibitor of melanin biosynthesis[3].

AGENTS THAT AFFECT HAIR GROWTH

Both unwanted excessive hair and hair loss are common dermatologic complaints. Minoxidil, bimatoprost, and eflornithine are reviewed here, and topical immunotherapy with diphencyprone (DPCP) or squaric acid dibutyl ester (SADBE) for alopecia areata is covered in Chapter 69. The use of anthralin for alopecia areata is discussed below.

Minoxidil

Introduction, dosages, and indications

Originally developed as an antihypertensive agent, minoxidil has been known for decades to promote hair growth. Available in 2% and 5% solutions and a 5% foam, topical minoxidil is FDA-approved for the treatment of androgenetic alopecia in both men and women (see Ch. 69). It is also used for other forms of hair loss, including alopecia areata. Minoxidil is typically applied once or twice daily to the scalp[6].

Mechanism of action

Minoxidil causes premature termination of the telogen phase, lengthens the anagen phase, and can increase follicle size, particularly

TOPICAL AGENTS USED TO ALLEVIATE PRURITUS			
Agent	**Classification/derivation**	**Mechanism of action**	**Uses and side effects**
Pramoxine 1% (gel, lotion); in combination with 0.5%–2.5% hydrocortisone in lotion, cream, ointment, or foam	Ester anesthetic	Blocks transmission of sensory nerve impulses; hypoalgesic effect on cold pain, but not heat pain[90]; duration of effect is 2–4 hours	• Beneficial for uremic pruritus[91] and histamine-induced itch; uses include pruritus ani, notalgia paresthetica, and nonspecific mild pruritus • Allergic contact dermatitis is extremely uncommon
Menthol (up to 16% in a variety of lotions, creams, ointments, and gels)	Cyclic terpene alcohol derived from plants in the *Mentha* genus	Activates TRPM8 cation channels, which also respond to cold thermal stimuli[92,93]; possible central itch modulation via Aδ fiber and/or κ-opioid receptor activation[94]	• Provides a cooling sensation • Inconsistent antipruritic results in controlled studies • Irritation, especially of inflamed or eroded skin; rare allergic contact dermatitis
Phenol	Originally a distillation product of coal tar	Thought to act directly on cold receptors	• Cooling and antipruritic effects; found in throat sprays and lozenges • Should not be used in pregnant women or infants <6 months of age • Irritation, especially of inflamed or eroded skin
Camphor (0.25%–0.5%; various preparations)	Ketone originally derived from the camphor laurel tree (*Cinnamomum camphora*)	Local anesthetic effect	• Cooling sensation may relieve mild pruritus • Irritation, especially of inflamed or eroded skin
Capsaicin (0.025%–0.1% cream, lotion, gel, or stick; 0.025%, 8% patch)	Natural alkaloid; derived from Solanaceae family members, including hot chili peppers of the *Capsicum* genus	Activates the TRPV1 vanilloid receptor, which also responds to temperatures >43°C (109°F); repeated release of substance P from C neurons eventually leads to depletion of this neuropeptide (and reduced transmission of heat, pain, and itch)[95]	• Applied three to five times daily or via a single 1-hour application of the 8% patch • Initially evokes a sensation of warmth/burning[96], with onset of the therapeutic effect ~1 week after initiation • Transdermal patch is FDA-approved for treatment of postherpetic neuralgia • Uses include notalgia paresthetica, brachioradial pruritus, renal pruritus, prurigo nodularis, psoriatic pruritus, and itch associated with a burning sensation • Burning, stinging, and/or erythema at the application site occur in >50% of patients[97] • Hand washing after application helps to prevent contact with (and irritation of) non-affected skin, eyes, and other mucosal surfaces • Animal reproduction studies have not shown adverse fetal effects; no adequate studies in pregnant women
Doxepin 5% cream	Tricyclic compound	Potent histamine antagonist (H1 and H2); sedation via anticholinergic properties	• Applied four times daily for up to 7 days • Shown to relieve pruritus in patients with atopic dermatitis, lichen simplex chronicus, and nummular eczema[98,99] • Drowsiness due to systemic absorption occurs in ~25% of patients[100] • Occasionally irritant or (less often) allergic contact dermatitis; systemic contact dermatitis with subsequent administration of oral doxepin has been described • Contraindicated in patients with untreated narrow angle glaucoma or urinary retention and those receiving MAO inhibitors • Animal reproduction studies have not shown adverse fetal effects, and no adequate studies in pregnant women; use during lactation is not recommended
Diphenhydramine (2% cream, lotion, gel, or spray)	Antihistamine	H1 histamine antagonist; localized anesthetic effect via blockage of sodium channels	• Use is *not recommended* due to lack of efficacy as an antipruritic agent and potency as a topical sensitizer, which can lead to allergic contact dermatitis

Table 129.6 Topical agents used to alleviate pruritus. Calamine lotion is listed in Table 129.11. MAO, monoamine oxidase; TRPM8, transient receptor potential melastatin 8; TRPV1, transient receptor potential vanilloid 1.

of miniaturized follicles[6,7]. Stimulation of vascular endothelial growth factor and prostaglandin synthesis may also play a role[7]. Although oral minoxidil relaxes vascular smooth muscle by opening ATP-dependent potassium channels, this mechanism has not been definitively linked to stimulation of hair growth[7].

Side effects

While generally well-tolerated, topical minoxidil can cause dryness, irritation, and (uncommonly) allergic contact dermatitis; components of the solution formulation, in particular propylene glycol, may be responsible for these side effects. Topical minoxidil can also lead to unwanted hair growth at adjacent sites inadvertently exposed to medication (e.g. the face or ears). Systemic side effects such as headache and peripheral edema are occasionally observed.

Use in pregnancy

Animal reproduction studies with *oral* minoxidil have shown adverse effects with regard to ability to conceive and survival of offspring, but there are no adequate studies in pregnant women.

Bimatoprost

Introduction, dosages, and indications

Bimatoprost is a synthetic prostaglandin $F_{2\alpha}$ analogue that was initially utilized for the treatment of glaucoma. Following observations of thickening and elongation of the eyelashes in glaucoma patients treated with bimatoprost 0.03% ophthalmic solution (Fig. 129.4), this agent was explored as a treatment for eyelash hypotrichosis and, in 2008, FDA-approved for this indication. When bimatoprost is applied nightly to the skin of the

TOPICAL KERATOLYTICS AND HUMECTANTS				
Agent	**Dosage**	**Mechanism of action**	**Indications**	**Side effects**
Keratolytics				
Salicylic acid (2-hydroxybenzoic acid)	0.5%–40% lotion, ointment, gel, foam, solution, shampoo, cleanser, pad, plaster; OTC or prescription	Alters corneocyte adhesion, likely via disruption of desmosomal proteins; possible mild anti-inflammatory effects	0.5%–2%: comedolytic for acne 2%–10%: hyperkeratotic dermatoses 10%–40%: corns, calluses, verrucae, focal hyperkeratosis; increases penetration of other topical agents 20%–30%: chemical peels	Irritation, burning, peeling, erosions (depending on the site and concentration); allergic contact dermatitis (uncommon); systemic absorption from extensive application, especially in neonates/infants, can lead to salicylism (see Table 129.5)
α-hydroxy acids: glycolic, lactic > mandelic, tartaric, malic, and citric acids	Various concentrations and pH levels; cleanser, shampoo, lotion, cream, gel, solution, mask	Diminish strength of intercellular bonding, thereby weakening corneocyte cohesion and leading to exfoliation; act at lower, newly forming levels of the stratum corneum; higher concentrations may have dermal effects (e.g. thickening)	Xerosis, ichthyoses, other hyperkeratotic dermatoses, acne, rosacea, photoaging; chemical peels	Irritation and burning, especially when applied to inflamed or eroded/fissured skin
Humectants				
Propylene glycol	10%–70%* solution or gel	Humectant, occlusive, and keratolytic agent*	Ichthyoses, keratodermas, other hyperkeratotic dermatoses	Irritation, burning
Urea	10%–50% cream, lotion, solution, gel, or foam; OTC or prescription (higher concentrations)	Due to its hygroscopic properties; absorption of water into the stratum corneum results in increased hydration, desquamation of corneocytes, enhanced barrier function, and decreased sensitizing effects of topical irritants	Xerosis, hyperkeratotic dermatoses (e.g. keratoderma climactericum, ichthyosis, psoriasis), nail avulsion; increases penetration of other topical medications	Irritation and burning, especially when applied to inflamed or eroded/fissured skin
*Often employed at lower concentrations as a preservative and penetration enhancer in vehicles.				

Table 129.7 Topical keratolytics and humectants[101–108]. Considering the low systemic absorption with topical application, use of these agents to a limited area is considered to be safe during pregnancy. Use of these agents in cosmeceutical products and chemical peels is discussed in Chapters 153 and 154, respectively.



Fig. 129.4 Unilateral trichomegaly. Bimatoprost ophthalmic solution (0.03%) was applied to one eye to treat glaucoma. *Courtesy Jean L. Bolognia, MD.*

upper eyelid margin, increased eyelash length, fullness, and darkness are noted within 16 weeks in ~75% of patients[8–11]; upon discontinuation of treatment, return toward baseline typically begins within 4 weeks.

Bimatoprost was also found to improve eyebrow hypotrichosis in a randomized, vehicle controlled trial[12]. Its potential utility for various forms of scalp alopecia (e.g. androgenetic) has also been investigated.

Mechanism of action

In animal studies, bimatoprost and other prostaglandin $F_{2\alpha}$ analogues (e.g. latanoprost) prolonged the anagen phase, increased the proportion of anagen follicles, and enlarged the dermal papilla and hair bulb during early anagen[13].

Side effects

Bimatoprost ophthalmic solution can cause pruritus and irritation of the eye, conjunctival hyperemia, and hyperpigmentation of the eyelid skin and iris, with the latter likely to be permanent[8,12]. Decreased intraocular pressure may occur but is generally not of clinical significance.

Use in pregnancy

Animal reproduction studies with high *oral* doses of bimatoprost have shown risk of spontaneous abortion and other adverse outcomes (e.g. early delivery), but systemic absorption is limited with topical use; there are no adequate studies in pregnant women.

Eflornithine

Eflornithine 13.9% cream is FDA-approved for the treatment of excessive and unwanted facial hair in women; it was discontinued by the original manufacturer in 2023. It irreversibly inhibits ornithine decarboxylase in the skin, leading to decreased polyamine synthesis and arrest of follicular matrix cell proliferation[14]. Twice-daily application for 24 weeks has been shown to significantly decrease facial hair[14], and use of eflornithine together with laser hair removal may result in more rapid and complete reduction in facial hair than laser treatment alone[15]. Eflornithine is usually well tolerated, with occasional burning or acneiform eruptions at sites of application[14]. Adverse fetal effects have been observed in animal reproduction studies when there was ingestion of eflornithine from topical application sites.

IMMUNOMODULATORY AGENTS

Imiquimod

Introduction, dosages, and indications

Imiquimod stimulates innate and adaptive immune response pathways, resulting in antiviral, antitumor, and immunoregulatory properties. Commercially available as 2.5%, 3.75%, and 5% creams, it

is FDA-approved for the treatment of: (1) anogenital warts[16]; (2) actinic keratoses (AKs) on the face or scalp[17,18]; and (3) superficial basal cell carcinoma (BCC) measuring up to 2 cm in diameter on the trunk, neck, or extremities (excluding the hands and feet)[19]. Off-label cutaneous uses with variable efficacy include treatment of common warts[20], Bowen disease (squamous cell carcinoma *in situ*)[21], nodular BCC, lentigo maligna, melanoma metastases, T cell lymphoma, Paget disease, and leishmaniasis as well as prevention of keloid recurrence following surgical excision[22–24]. Although imiquimod has been utilized to treat molluscum contagiosum, unpublished randomized controlled trials (RCTs) showed no difference in its efficacy compared to that of placebo[25].

FDA-approved regimens for imiquimod application are as follows: (1) *for anogenital warts* – 5% cream three times weekly for up to 16 weeks, or 3.75% cream daily for up to 8 weeks (~50% and ~30% clearance, respectively); (2) *for AKs* – 5% cream twice weekly for 16 weeks, or 2.5%–3.75% cream daily for two 2-week cycles separated by 2 weeks without treatment (~50% and ~35% clearance, respectively); and (3) *for superficial BCC* – 5% cream five times weekly for 6 weeks (~75% clearance). The frequency of application and duration of therapy for off-label uses vary.

Mechanism of action

The mechanism of action is depicted in Fig. 129.5[26]. In animal models, imiquimod's antiviral and antitumor activity is explained at least in part by the effects of IFN-α[27].

Side effects

The most common adverse reactions to imiquimod cream are erythema, edema, scaling, erosion, and ulceration at the site of application (Figs. 129.6 & 129.7). These reactions tend to be more intense and frequent in patients with actinic damage. Development of erosive pustular dermatosis of the scalp has been associated with the use of imiquimod for AKs of the scalp[28], and reactions with histologic findings mimicking those of lupus erythematosus have been described. Flu-like symptoms such as fatigue, fever, headache, diarrhea, and myalgias occur in ~1%–2% of patients, but systemic immune alterations have not been described.

Use in pregnancy

Animal reproduction studies with *systemic* imiquimod administration have shown adverse fetal effects, but percutaneous absorption of imiquimod cream is minimal. There are no adequate studies in pregnant women.

Topical Calcineurin Inhibitors (TCIs)

Introduction, dosages, and indications

Tacrolimus ointment and pimecrolimus cream are anti-inflammatory agents that allow treatment of eczematous and other inflammatory dermatoses without the side effects of topical corticosteroids. Tacrolimus 0.1% and 0.03% ointments are indicated for treatment of "moderate to severe" atopic dermatitis in patients ≥16 and ≥2 years of age, respectively, while pimecrolimus 1% cream is indicated for treatment of "mild to moderate" atopic dermatitis in individuals ≥2 years of age. Pimecrolimus has also been studied extensively in infants 3–23 months of age, and the American Academy of Dermatology's current guidelines recommend off-label use of pimecrolimus 1% cream and tacrolimus 0.03% ointment for children <2 years of age with mild to severe atopic dermatitis[29].

TCIs are also frequently used to treat other inflammatory skin conditions, especially when there is facial (including the eyelids) and intertriginous involvement. Examples include eczematous and seborrheic dermatitis as well as psoriasis, lichen planus (oral and genital), vitiligo, pyoderma gangrenosum, perioral dermatitis, granulomatous rosacea, cutaneous Crohn disease, lichen sclerosus, and cutaneous lesions of dermatomyositis, lupus erythematosus, and chronic graft-versus-host disease (GVHD)[30].

Mechanism of action

The mechanism of action is depicted in Fig. 129.8.

Contraindications

The TCI labels were revised in 2006 to include a boxed warning regarding a theoretical concern for risk of malignancy. However, there has been no short-term or long-term (>20 years) evidence of

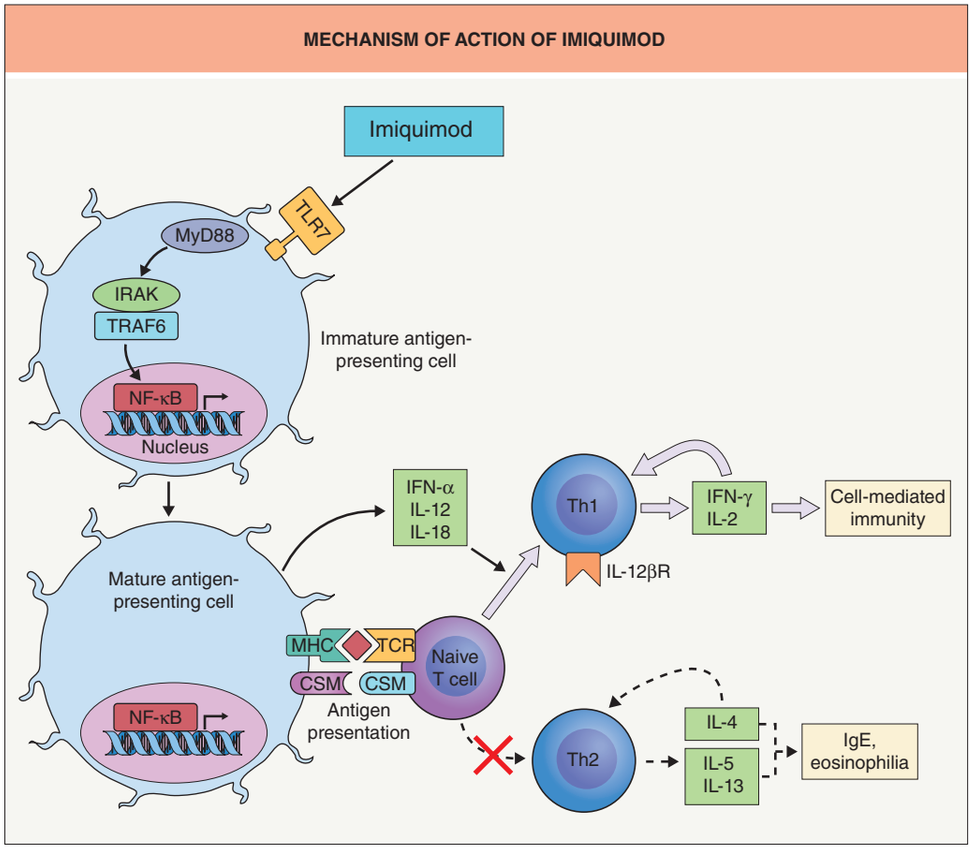


Fig. 129.5 Mechanism of action of imiquimod. Binding of imiquimod to Toll-like receptor 7 (TLR7) on antigen-presenting cells (e.g. Langerhans cells, other dendritic cells, macrophages) leads to interaction of the cytoplasmic portion of the receptor with MyD88. This facilitates association of MyD88 with interleukin (IL)-1 receptor-associated kinase (IRAK), which in turn activates TNF receptor-activated 6 (TRAF6) and ultimately results in stimulation of nuclear factor-κB-mediated signaling. Imiquimod thereby promotes antigen-presenting cell maturation and secretion of interferon (IFN)-α, IL-12, IL-18, and other cytokines, which induce IFN-γ production by naive T cells and result in enhancement of cell-mediated immunity via a Th1-type response. CSM, costimulatory molecule; MHC, major histocompatibility complex; TCR, T cell receptor.



Fig. 129.6 Reaction to topical imiquimod treatment of an actinic keratosis. **A** Inflammation and erosions developed after application of imiquimod to an actinic keratosis and actinically damaged skin. **B** Following discontinuation of imiquimod, the inflammation subsided and the actinic keratosis had cleared. Note the residual hypopigmentation. *Courtesy J. Mark Jackson, MD and Jeffrey P. Callen, MD.*



Fig. 129.7 Inflammation at the site of application of imiquimod to an amelanotic lentigo maligna. The patient had residual disease despite multiple surgical procedures including skin graft placement. The inflammation did not occur until the tenth month of application. Three years later, the lesion recurred, but only within the graft. *Courtesy Jean L. Bolognia, MD.*

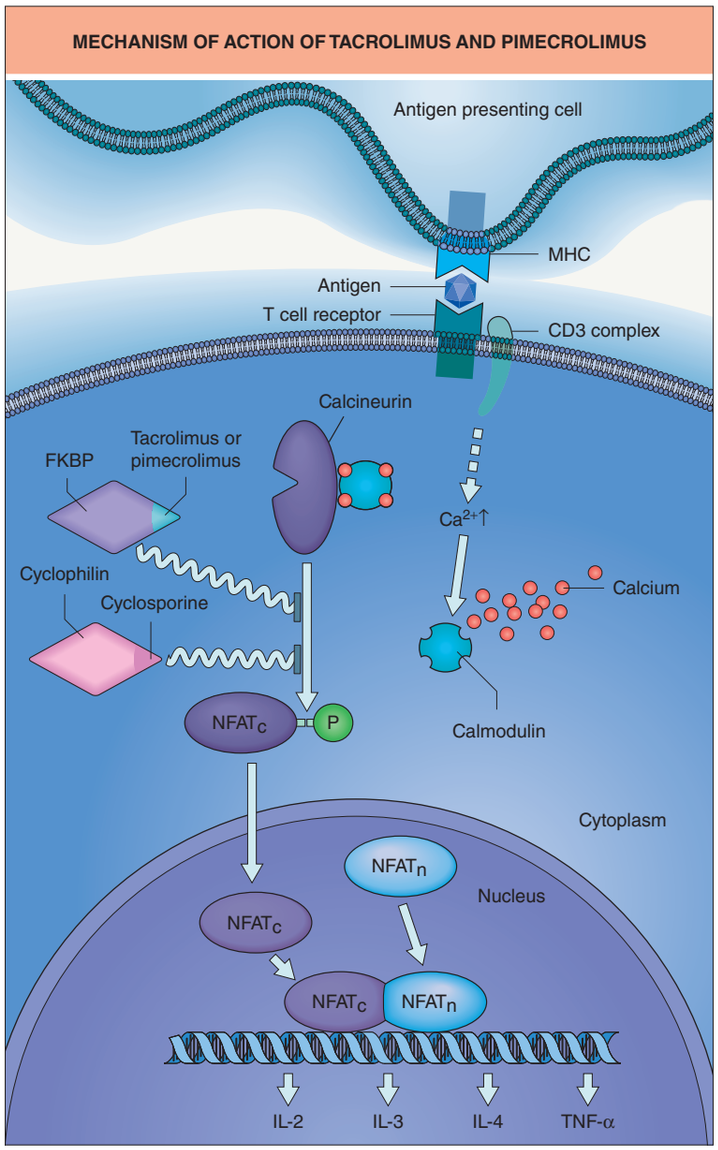


Fig. 129.8 Mechanism of action of tacrolimus and pimecrolimus. Both tacrolimus and pimecrolimus bind to the FK506-binding protein (FKBP), forming complexes that inhibit calcineurin[89]. Calcineurin normally dephosphorylates the cytoplasmic subunit of nuclear factor of activated T cells (NFAT), which then translocates to the nucleus and forms a complex that promotes transcription of proinflammatory cytokines, including the T cell mitogen IL-2. *From Nghiem P, Pearson G, Langley RG. Tacrolimus and pimecrolimus: from clever prokaryotes to inhibiting calcineurin and treating atopic dermatitis. J Am Acad Dermatol 2002:46:228–41.*

systemic immunosuppression or an increased risk for malignancy in clinical studies, systematic reviews, or post-marketing surveillance of either medication[31–34]. A task force of international experts concluded that the boxed warning is not justified and recommended its removal[33].

Because TCIs shorten the time to skin tumor formation in animal photocarcinogenicity studies, the package inserts recommend that patients minimize or avoid natural or artificial sunlight exposure. TCIs generally have negligible systemic absorption even with use on extensive areas of dermatitis, although low systemic levels have been observed following application to ulcers or eroded mucosal surfaces[35,36]. A rare exception is patients with Netherton syndrome, who have significant absorption of topical tacrolimus (but less so for pimecrolimus) that necessitates monitoring of blood levels or avoidance of TCI therapy[32,37].

Major side effects

Burning, stinging, or a sensation of warmth at sites of application are the most common side effects of TCIs. A local flushing reaction in association with alcohol consumption can also occur. There are scattered reports of allergic contact dermatitis and a rosacea-like granulomatous reaction on the face due to topical tacrolimus. *Staphylococcus aureus* colonization of the skin is actually reduced in atopic dermatitis patients treated with TCIs.

Use in pregnancy

Animal studies with *systemically* administered tacrolimus indicate harmful fetal effects only at doses that are toxic to the mother. There are no adequate studies in pregnant women.

Topical Janus Kinase (JAK) Inhibitors

Introduction, dosages, and indications

Janus kinase (JAK) inhibitors function by impeding proinflammatory cytokine-mediated signaling via the JAK-signal transducer and activator of transcription (STAT) pathway (see Ch. 128)[38]. Ruxolitinib 1.5% cream, a JAK1/2-selective inhibitor, is FDA-approved for the treatment of mild to moderate atopic dermatitis (short-term or non-continuous chronic use) and vitiligo in patients ≥12 years of age. Clear/almost clear skin and a ≥2-grade improvement were achieved by ~50% of individuals with mild to moderate atopic dermatitis treated with ruxolitinib 1.5% cream twice daily for 8 weeks[39], and >75% improvement of facial vitiligo was seen in ~30% of patients treated twice daily for 24 weeks[40].

Delgocitinib 0.25% or 0.5% ointment represents a pan-JAK inhibitor that is approved in Japan for the treatment of atopic dermatitis in adult and pediatric patients[41]. Tofacitinib 2% cream, a JAK1/3 inhibitor, has also demonstrated efficacy for atopic dermatitis in a randomized controlled study[42]. Additional dermatologic conditions for which topical JAK inhibitors have shown benefit include hand eczema, psoriasis, cutaneous lupus erythematosus, and alopecia areata[43–46].

Mechanism of action

The mechanism of action of JAK inhibitors is depicted in Fig. 128.11.

Major side effects

The most common side effects of topical JAK inhibitors include pruritus, erythema, and acne at application sites. However, the JAK inhibitor class-wide black box warning notes potential increased risks of serious infection, death, cancer, cardiovascular events, and thrombosis (see Ch. 128).

Use in pregnancy

Animal reproduction studies with high *oral* doses of tofacitinib and ruxolitinib have shown harmful fetal effects. There are no adequate studies in pregnant women.

Topical Phosphodiesterase-4 Inhibitors

Phosphodiesterase-4 (PDE-4) inhibitors function by inhibiting the degradation of cyclic AMP, which leads to decreased production of proinflammatory cytokines such as tumor necrosis factor (TNF), interferon-γ, and interleukins (ILs)-2, -4, -12, -23, and -31 (see Fig. 130.4). Crisaborole 2% ointment is a PDE-4 inhibitor that is FDA-approved for the treatment of mild to moderate AD in patients ≥3 months of age, with ~30% of these patients achieving clear/almost clear skin with a ≥2-grade improvement after 4 weeks of twice daily treatment[47]. Another PDE-4 inhibitor, roflumilast 0.3% cream, was recently FDA-approved for the treatment of plaque psoriasis (including in intertriginous sites) in patients ≥12 years of age; ~40% of such individuals achieved clear/almost clear skin with a ≥2-grade improvement after 8 weeks of once daily treatment[48]. The most common side effect of these medications is stinging or burning in the area of application. In animal reproduction studies, *oral* administration of crisaborole has not shown adverse fetal effects, but high *oral* doses of rofluminast have resulted in fetal harm. There are no adequate studies in pregnant women.

Aryl Hydrocarbon Receptor Agonists

Tapinarof is an aryl hydrocarbon receptor agonist that decreases expression of IL-17 and increases production of skin-barrier proteins such as filaggrin and loricrin as well as antioxidant enzymes. Tapinarof 1% cream is FDA-approved for the treatment of plaque psoriasis in adults, with ~40% of these patients achieving clear or almost clear skin after 12 weeks of once daily treatment[49]. Topical tapinarof is currently under investigation as a treatment for atopic dermatitis. The most common side effects include folliculitis and contact dermatitis. Animal reproduction studies have not shown harmful fetal effects, and there are no adequate studies in pregnant women.

CHEMOTHERAPEUTIC AGENTS

5-Fluorouracil

Mechanism of action

5-Fluorouracil (5-FU) is a pyrimidine analogue that interferes with DNA synthesis by irreversibly inhibiting thymidylate synthetase, which prevents cellular proliferation and results in cell death, preferentially affecting rapidly dividing cells[50]. It is also incorporated into DNA and RNA, leading to DNA breakage and decreased protein synthesis, and it disrupts the exosome complex that degrades RNA.

Indications and dosages

Topical 5-FU is used primarily to treat AKs[51], especially when there are numerous lesions, and sites of severe actinic damage without clinically evident AK lesions. In a randomized controlled trial, a ≥75% reduction in the number of AKs in a 25–100 cm^2 area on the head 12 months after completing therapy was achieved by a higher proportion of patients treated with 5-FU 5% cream (75%) than those who received imiquimod 5% cream (54%), methyl aminolevulinate photodynamic therapy (38%), or ingenol mebutate 0.015% gel (29%)[52]. 5-FU is less effective for hypertrophic AKs, owing to decreased percutaneous absorption through the thickened stratum corneum. Additional dermatologic applications of topical 5-FU include treatment of actinic cheilitis, SCC *in situ* (Bowen disease), superficial BCC, cutaneous and genital warts, porokeratoses, nail psoriasis, and extramammary Paget disease[51]; in addition, intralesional 5-FU may be of benefit for keloids. Topical 5-FU can also improve the appearance of photoaged skin via epidermal injury and subsequent dermal remodeling, similar to that seen following laser therapy[53].

5-FU is available as a cream (0.5%, 1%, and 5%) and solution (2% and 5%). Regimens vary depending on the concentration and vehicle as well as the indication and anatomic location. For example, duration of treatment is usually longer on the extremities than on the face. 5-FU is typically applied once or twice daily for 2 to 6 weeks. Pretreatment with a topical retinoid for 2 weeks can increase efficacy on the extremities and trunk. Application of topical calcipotriene (calcipotriol) 0.005% ointment together with 5-FU 5% cream (e.g. both twice daily for 4 days) induces thymic stromal lymphopoietin (TSLP) production and optimizes $CD4^+$ T cell-mediated immunity, resulting in a synergistic effect against AKs[54]. An office-based technique utilized for severely photodamaged extremities is weekly application of 5-FU (~10–20 g/extremity) that is then occluded by a zinc oxide-impregnated wrap.

Side effects

During treatment of AKs and photodamage, the skin progresses through stages of erythema (sometimes painful and associated with edema), crusted erosions, and re-epithelialization. The principal side effects are related to this localized inflammatory response (Fig. 129.9), which is occasionally followed by residual pigmentary changes. A mid-potency topical corticosteroid can be applied for symptomatic relief once peak inflammation has been attained. Systemic adverse events are rare, and systemic levels of 5-FU after topical application are very low[51].

Contraindications and use in pregnancy

Use of 5-FU is contraindicated in patients with a history of hypersensitivity to this agent and those with dihydropyrimidine dehydrogenase deficiency. 5-FU is potentially teratogenic (formerly pregnancy category X), and its use during pregnancy and lactation is contraindicated.

Mechlorethamine Hydrochloride

Introduction, dosages, and indications

Mechlorethamine hydrochloride (HCl), a form of nitrogen mustard, was introduced in 1959 and is used to treat limited or generalized patch/plaque-stage mycosis fungoides (MF). Concentrations ranging from 10 to 40 mg/dl (0.01%–0.04% w/w) can be compounded in an ointment or (less often) aqueous solution. Mechlorethamine 0.016% w/w gel is FDA-approved for stage 1 A/1B MF. Topical mechlorethamine



Fig. 129.9 Reactions to topical 5-fluorouracil. **A** Inflammation with erythema and crusting at sites of actinic keratoses on the forehead. **B** More severe inflammatory response with diffuse erythema and crusting in a patient treated for actinic keratoses. **C** Inflammation of actinic keratoses and areas of photodamage. **D** Large red–purple patches at sites of application on the upper chest in a patient with severe photodamage. *D, Courtesy Jean L. Bolognia, MD.*

is typically applied daily to affected areas until clearance is achieved, which typically takes 10–12 months with an ointment, 1–4 months with a solution, and 6–12 months with the gel[55]. Less often the entire body is treated, excluding the genitalia and applying sparingly to the skin folds.

Older studies suggested that treatment with mechlorethamine ointment or solution could result in a complete response (CR) rate of ~35%–75% in patients with patch/plaque-stage MF[56]. However, in a more recent 12-month randomized trial, the CR rate was 14% for 0.02% gel and 12% for an Aquaphor®-based 0.02% ointment; response rates rose to 59% and 48%, respectively, when partial responses were included[57].

Mechanism of action

Mechlorethamine is an alkylating agent (i.e. donates alkyl groups to DNA), with cytotoxicity that preferentially affects rapidly dividing cells. Immunostimulatory effects have also been postulated to have a role in treatment of patients with MF[56].

Side effects

Irritant and/or allergic contact dermatitis occurs in at least half of patients and may result in interruption of treatment. However, irritant reactions may improve with continued use, and patients can be desensitized if necessary. Other potential side effects include pruritus, xerosis, bacterial skin infections, vesiculation, ulceration, hyperpigmentation, urticaria, anaphylaxis, and (with prolonged use) development of SCC[56].

Use in pregnancy

Mechlorethamine can cause adverse fetal effects, and its use during pregnancy or lactation is contraindicated.

Carmustine

Introduction, dosages, and indications

Topical nitrosoureas have been utilized in the treatment of MF since 1972[58], but their use is declining. Carmustine (1,3-bis [2-chloroethyl]-1-nitrosourea; BCNU) currently represents a second- or third-line therapeutic option for MF, due to the potential for hematologic complications secondary to systemic absorption. It is available as an aqueous solution and ointment. Carmustine is applied once or twice daily until clearance of the treated areas occurs, which typically requires 1–4 months with the aqueous solution and 6–12 months with the ointment. A complete response is achieved in 85% of patients with limited patch/plaque-type disease (T1) and ~50% of those with generalized patch/plaque-type disease (T2)[56,59].

Mechanism of action

Carmustine is a nitrosourea alkylating agent that produces alkylation and subsequent cross-linking of DNA, thereby disrupting DNA synthesis and resulting in cytotoxicity that preferentially affects dividing cells[56].

Side effects

Erythema, tenderness, bullae, and persistent telangiectasias can develop at application sites[56]. Allergic contact dermatitis occurs less frequently than with mechlorethamine. However, higher levels of systemic absorption (5%–30% of the administered dose) can lead to side effects such as mild to moderate myelosuppression[60].

Use in pregnancy

Carmustine can cause adverse fetal effects, and its use during pregnancy or lactation is contraindicated.

VITAMIN D ANALOGUES

Mechanism of action

The skin serves as both a site of vitamin D biosynthesis (see Fig. 51.11) and a target organ for its ultimate activity. The cutaneous effects of 1,25-dihydroxyvitamin D_3 (calcitriol, the active form of vitamin D) include inhibiting proliferation and promoting differentiation of keratinocytes, as well as decreasing production of inflammatory mediators such as IL-2, IL-6, IL-8, interferon-γ, and chemokines[61]. Vitamin D exerts its regulatory functions by binding to vitamin D receptors (VDRs) on keratinocytes, melanocytes, Langerhans cells, macrophages, T cells, and fibroblasts.

Topical agents and their indications

Several topical vitamin D analogues are available for clinical use: calcipotriene, calcitriol, tacalcitol, and maxacalcitol; their formulations and dosing are outlined in Table 129.8. The primary indication for these agents is the treatment of psoriasis[62–66], but they have been used to treat other skin conditions such as vitiligo, morphea, ichthyoses, and Hailey–Hailey disease. Application of a vitamin D analogue in combination with a high-potency topical corticosteroid in patients with psoriasis can have greater efficacy and more rapid onset of action than either agent alone, as well as less irritation than the vitamin D analogue alone[63]. Additive benefits can also occur when vitamin D analogues are used together with acitretin, cyclosporine, or phototherapy for psoriasis or with phototherapy for vitiligo; the vitamin D analogue should be applied after phototherapy sessions to avoid degradation by UV light.

Side effects

The most common side effects are irritation, burning, and stinging at the application site, which limits use of vitamin D analogues on the face and in intertriginous areas. Allergic contact dermatitis has been described with calcipotriene. The systemic effects of vitamin D and its analogues include releasing calcium from the bone, increasing renal tubular reabsorption and intestinal absorption of calcium, and decreasing parathyroid hormone release. Use of excessive amounts of topical vitamin D analogues can lead to hypercalcemia and hypercalciuria. Parathyroid hormone levels should be monitored if use exceeds recommended amounts (see Table 129.8). Patients with renal disease and those receiving medications that can increase the serum calcium level (e.g. thiazide diuretics, high doses of oral vitamin D) may be at increased risk of developing hypercalcemia.

Use in pregnancy

Animal reproduction studies with *systemically* administered calcipotriene and calcitriol have demonstrated fetal skeletal abnormalities. There are no adequate studies in pregnant women.

MISCELLANEOUS AGENTS

Topical Sirolimus (Rapamycin)

Introduction, dosages, and indications

Sirolimus (rapamycin) is a *m*ammalian (*m*echanistic) *t*arget of *r*apamycin (mTOR) inhibitor with antiproliferative and immunomodulatory effects. Uses of *systemic* sirolimus include rejection prophylaxis and probable reduction of cutaneous SCC risk in solid organ transplant recipients; prophylaxis and treatment of GVHD; and treatment of lymphangioleiomyomatosis and other tumors associated with tuberous sclerosis complex (TSC; see Ch. 61), Kaposi sarcoma, kaposiform hemangioendothelioma, and lymphatic malformations[67]. *Topical* sirolimus has been utilized to treat angiofibromas, other TSC-related skin lesions, superficial lymphatic malformations, port-wine birthmarks (together with pulsed dye laser therapy), psoriasis, epidermal and sebaceous nevi, acanthosis nigricans, and confluent and reticulated papillomatosis (CARP)[68–77]. Sirolimus 0.2% gel is FDA-approved for the treatment of facial angiofibromas in patients ≥6 years of age with TSC. Application of sirolimus 0.1%–1% ointment, gel, cream, or solution (e.g. Rapamune® 1 mg/ml [0.1%]) once or twice daily to the facial angiofibromas of TSC usually leads to flattening and reduced erythema within 3 months, with better results in children than adults[69–74].

TOPICAL VITAMIN D_3 AND ITS ANALOGUES

Agent	Available formulations	Maximum weekly dose
Calcipotriene (calcipotriol) 0.005% (50 mcg/g)	Cream, ointment, solution, foam; combined with betamethasone dipropionate 0.064% in an ointment, suspension, and foam	100 g
Calcitriol [1,25$(OH)_2D_3$] 3 mcg/g	Ointment	200 g
Tacalcitol [1,24$(OH)_2D_3$] 4 mcg/g*	Ointment, lotion	70 g
Maxacalcitol 25 mcg/g*	Ointment, lotion	70 g

*Not available in the US.

Table 129.8 Topical vitamin D_3 and its analogues. These agents are typically applied twice daily. In general, treatment of >30% of the body surface area is not recommended. Calcipotriene is the US Adopted Name (USAN) and calcipotriol is the International Nonproprietary Name (INN).

Mechanism of action

Sirolimus binds to the FK506 binding protein FKBP12, forming a complex that inhibits mTOR (see Fig. 61.12). This leads to reduced proliferation and protein synthesis of T lymphocytes and other immune cells as well as decreased vascular endothelial growth factor (VEGF) production.

Side effects

Local skin irritation is more common with a gel or solution formulation than with an ointment[69,70]. Little to no systemic absorption has been observed with topical therapy[70–74].

Use in pregnancy

Animal reproduction studies with *oral* sirolimus have demonstrated adverse fetal effects. There are no adequate studies in pregnant women.

Diclofenac Sodium

Diclofenac sodium 3% in a gel vehicle containing hyaluronic acid is FDA-approved for treatment of AKs. This NSAID inhibits cyclooxygenase (COX)-2 and (to a lesser degree) COX-1. Its mechanism of action against AKs is thought to involve induction of apoptosis, alteration of cellular proliferation, and inhibition of angiogenesis. Twice-daily application for 60–90 days results in AK clearance rates of up to 30%–50%, with potential side effects including irritant, allergic, and photoallergic contact dermatitis. Animal reproduction studies have failed to demonstrate fetal risk, and there are no adequate studies in pregnant women.

Ingenol Mebutate

Ingenol mebutate, a diterpene ester from the *Euphorbia peplus* plant, was FDA-approved as a topical treatment for AKs[78–80]. However, this medication has been withdrawn from the market in the US and Europe due to its association with an increased risk of keratinocyte carcinoma. Application of ingenol mebutate 0.015% or 0.05% gel to areas with AKs on the face/scalp or trunk/extremities, respectively, once daily for 2–3 consecutive days led to a clearance rate of ~40%. This agent induces cell death in proliferating keratinocytes via disruption of the plasma membrane and mitochondria; it also triggers an inflammatory response that eradicates residual tumor cells[78–80]. Erythema, scaling, and crusting develop in most patients[78]; less frequently, swelling, vesiculation, ulceration, and dyspigmentation occur. Animal reproduction studies have demonstrated adverse fetal effects, and there are no adequate studies in pregnant women.

Tar

Introduction and indications

Topical tar has served as a skin-directed therapy for >2000 years, since the Greek physician Dioscorides applied "asphalt" to manage several cutaneous diseases[81]. Among the various types of tar (e.g. wood, bituminous [shale], petroleum, coal), coal tar is most often used as a dermatologic treatment. Currently, tar is utilized primarily in the management of psoriasis and several forms of dermatitis (e.g. seborrheic, nummular, atopic, hand), most commonly in conjunction with other therapeutic modalities. The classic Goeckerman regimen employs topical tar in combination with UVB radiation for the treatment of psoriasis[82].

Dosages

Coal tar in concentrations of 0.5% to 10% is available and can be compounded in a broad range of vehicles, including ointment, lotion, gel, foam, solution, oil, shampoo, and soap. *Liquor carbonis detergens* is a distillate of crude coal tar that is typically used in concentrations of 3%–10%.

Mechanism of action

Coal tar is thought to suppress DNA synthesis, which may lead to normalization of epidermal differentiation in conditions such as psoriasis[81]. It appears to have anti-inflammatory, antimicrobial, and antipruritic effects. In animal studies, tar has been found to decrease sebum secretion. Coal tar (but not other forms of tar) has a photosensitizing effect in the 330–550 nm range of the UVA and visible light spectra[81].

Side effects

The unpleasant odor, messiness, and staining potential of topical tar limit its use. Acneiform eruptions, folliculitis, and irritant contact dermatitis (including pustules within plaques of psoriasis) may occur at application sites, and "tar smarts" can develop following exposure to UVA radiation. Ever since Sir Percivall Pott described an increased risk of scrotal cancer in chimney sweepers in 1775, tar has been implicated as a potential carcinogen[81]. However, the evidence that topical tar formulations used in the treatment of skin disease result in an increased risk of skin cancer is inconclusive.

Use in pregnancy

Animal reproduction studies have shown adverse fetal effects, and there are no adequate studies in pregnant women. Use in the first trimester is not recommended.

Anthralin

Introduction, dosages, and indications

Anthralin, the synthetic form of the chrysarobin found in the bark of the South American araroba tree, has been used to treat dermatologic conditions for >80 years[83]. It is available in 0.5% and 1% creams. Although no longer commonly used for psoriasis, short-contact anthralin therapy, with gradual increases in the application time ± concentration, continues to be employed to treat alopecia areata via induction of an irritant effect (Table 129.9)[83].

Mechanism of action

Anthralin induces a brisk inflammatory response at sites of application, which may result from generation of extracellular oxygen free radicals[83]. Inhibition of mitochondrial respiration and cell growth are thought to reduce keratinocyte proliferation and lead to antipsoriatic effects.

Side effects

Use of anthralin is limited by irritation at application sites (depending on the concentration and contact time) and staining of skin, clothing, and household items (e.g. bed sheets, furniture). Staining and irritation can be ameliorated by application of triethanolamine 10% cream to treatment sites after removal of the anthralin-containing product.

SAMPLE PROTOCOL FOR SHORT-CONTACT ANTHRALIN THERAPY FOR ALOPECIA AREATA
• Anthralin 0.5% cream is applied sparingly to affected areas of the scalp daily, followed by washing with shampoo/soap and water • An initial application time of 10 minutes is increased in 10-minute increments every 4–5 days until slight irritation (e.g. erythema, scaling, pruritus) occurs • If excessive irritation develops, treatment is withheld for several days and resumed at the last tolerated application time • If there is no irritation with a 60-minute contact time, 1% anthralin is applied for 10 minutes and application times increased as above • If there is no irritation with 1% anthralin applied for 60 minutes, overnight application is considered • Initial responses are typically seen within 12 weeks; cosmetically acceptable responses require a mean of 24 weeks
Additional information
• Brownish staining of treated areas of the scalp and hair is expected • To prevent staining of clothing, bedding, and furniture, patients should wash their hands thoroughly after applying anthralin and avoid touching fabrics with their scalp until it has been washed off • Avoid getting anthralin into the eyes; do not apply to eyelids or eyelashes • Special care should be taken in sensitive areas (areas of scalp near the ears, eyebrows)

Table 129.9 Sample protocol for short-contact anthralin therapy for alopecia areata. *Courtesy Julie V. Schaffer, MD and Jean L. Bolognia, MD.*

Use in pregnancy

There are no adequate studies in animals or pregnant women.

Podophyllin and Podophyllotoxin

Introduction, dosages, and indications

Podophyllin resin is a crude extract from the May apple plant (*Podophyllum peltatum* or *Podophyllum emodi*) that has been employed for decades to treat condylomata acuminata. However, the concentration of its most active ingredient is not standardized in the 10%–25% solutions that are applied in the physician's office weekly and washed off 1 to 4 hours later[84]. In contrast, podophyllotoxin is available in a stable and standardized 0.5% solution and gel as well as a 0.15% cream. These compounds lack the mutagens that are found in podophyllin and can be applied by the patient, usually twice daily for three consecutive days each week for 4–6 weeks. Reported clearance rates for condylomata acuminata range from 30%–60% with podophyllin and from 45%–75% with podophyllotoxin[84].

Mechanism of action

Podophyllin and podophyllotoxin act by arresting mitosis through reversible binding to tubulin.

Side effects

Common adverse effects associated with both podophyllin and podophyllotoxin include burning, erythema, and skin breakdown at application sites. The extent of irritation may be reduced by application of petrolatum to unaffected surrounding skin. Because of its percutaneous absorption, application of large amounts of podophyllin can result in systemic toxicity (see Table 129.5).

Use in pregnancy

Use of podophyllin during pregnancy is contraindicated due to its teratogenic effects. However, a study of pregnant women treated with podophyllotoxin did not show an increased risk of adverse fetal outcomes.

Cantharidin

Introduction, dosages, and indications

Cantharidin is a vesicant derived from "blister beetles" in the Coleoptera order and Meloidae family. It has been used since the 1950s to treat warts and molluscum contagiosum (MC). Although cantharidin met the safety requirements outlined by the Food, Drug, and Cosmetic Act of 1938, it lost its FDA approval in 1962 when its manufacturers failed to submit required efficacy data[85]. A 0.7% concentration of cantharidin is available in a film-forming solution. VP-102, a drug-delivery device containing cantharidin 0.7% plus gentian violet, was FDA approved for the in-office treatment of MC in 2023. This formulation, was shown in randomized controlled studies to result in complete MC clearance in ~50% of patients treated at 3-week intervals for 12 weeks[86]. Another formulation that is primarily used for warts combines 1% cantharidin with 2% podophyllin and 30% salicylic acid.

A thin film of cantharidin is typically applied to lesions in the office. Occlusion may be used after drying, especially for treatment of warts. The residual film is washed off thoroughly with soap and water or rubbing alcohol by the patient (or a parent) 2 to 6 hours after application, or in 24 hours for VP-102. Blisters typically form over the next 12–24 hours, followed by superficial erosions; healing of treated areas (with temporary residual erythema) occurs over a period of 4–7 days[85]. Benefits of cantharidin use include painless application (particularly advantageous in young children) and a lack of scarring.

Mechanism of action

Cantharidin acts via release of neutral serine proteases that cause desmosomal plaque degeneration, leading to detachment of desmosomes from

tonofilaments; resultant acantholysis is intraepidermal and therefore non-scarring[85].

Side effects

The blisters and erosions that form after cantharidin treatment can be painful or pruritic, and postinflammatory hypopigmentation may take several months to resolve. Use of cantharidin to treat warts occasionally results in a "doughnut wart" due to clearance in the center but not at the periphery of the lesion. Cantharidin poisoning has been described following ingestion, with sequelae including blistering and erosions in the mouth and gastrointestinal tract as well as dysuria, hematuria, and renal failure. Standard in-office application of cantharidin, however, does not generally cause systemic effects.

Sulfur

Introduction

Sulfur, a yellow non-metallic element, has been employed as a treatment for seborrheic dermatitis, rosacea, acne, tinea versicolor, and scabies. Sulfur is typically used in concentrations of 2%–10%, often in combination with a second agent, e.g. 2% sulfur plus 2% salicylic acid in shampoos (for seborrheic dermatitis) or 5% sulfur plus 10% sodium sulfacetamide in a cream, suspension, or gel (for rosacea, acne, and seborrheic dermatitis; see Ch. 127). Application of 5%–10% sulfur ointment to the entire body for 2–3 consecutive nights represents a classic scabies treatment; however, it is inferior to topical permethrin therapy.

Mechanism of action

Sulfur has antibacterial, antifungal, and keratolytic properties.

Side effects

An offensive odor similar to that of rotten eggs limits the use of sulfur in the absence of masking fragrances. Side effects are generally mild and include dryness and pruritus.

Contraindications

Topical sulfur is contraindicated in patients with a sensitivity to sulfur.

Use in pregnancy

Topical sulfur (5%–10%) has been used to treat scabies in young infants and pregnant or lactating women, but safety data are lacking.

Azelaic Acid

Introduction and indications

Azelaic acid, a naturally occurring dicarboxylic acid, is used in the treatment of rosacea, acne, melasma, and postinflammatory hyperpigmentation.

Mechanism of action

Azelaic acid inhibits the production of free radical oxygen by neutrophils. This reduces oxidative tissue injury at sites of inflammation and decreases melanin production. Studies have also demonstrated selective cytotoxic and antiproliferative effects on hyperactive and abnormally proliferating melanocytes, with little effect on normal melanocytes. It may act as a competitive inhibitor of tyrosinase, further explaining its skin-lightening effects[87,88]. In addition, azelaic acid has antimicrobial activity against *Cutibacterium* (formerly *Propionibacterium*) *acnes* and *Staphylococcus epidermidis* as well as moderate anticomedogenic properties via modification of epidermal keratinization.

Dosages

Azelaic acid, which is applied twice daily, is available by prescription in a 20% cream and 15% gel as well as in 10%–14% over-the-counter formulations.

Side effects

Azelaic acid may cause mild to moderate irritant contact dermatitis (e.g. dryness, peeling, erythema), which often subsides after 2 to 4 weeks of treatment.

Use in pregnancy

Azelaic acid is considered safe to use during pregnancy.

Topical Immunotherapy

A sample protocol for topical immunotherapy with squaric acid dibutyl ester (SADBE) for cutaneous warts is outlined in Table 129.10, and use of SADBE or diphencyprone for alopecia areata is discussed in Chapter 69.

The Old and the New

Topical agents of historical interest are presented in Table 129.11. Many newer barrier-repair creams and moisturizers have purported benefit in

SAMPLE PROTOCOL FOR TOPICAL IMMUNOTHERAPY WITH SQUARIC ACID DIBUTYL ESTER FOR CUTANEOUS WARTS
• Sensitize with a 2% SADBE solution in acetone applied to a small (e.g. 2 cm × 2 cm) area on the inner aspect of the upper arm or medial thigh; cover with a dressing and do not wash for 24 hours • After 1 week (2 weeks if the initial reaction was severe), apply 0.2% SADBE solution to non-facial warts; cover with a light dressing and wash after 12–24 hours • Apply approximately twice weekly to warts; can increase or decrease the length of time between treatments depending on the duration of the reaction, with repeat application once the erythematous/eczematous reaction has subsided • If there is no inflammation or response of the warts after 2–4 weeks, increase the concentration to 0.5% (and subsequently to 1% and 2% as needed); decrease concentration (e.g. from 0.2% to 0.1%) and/or amount applied if excessive inflammation, e.g. more than mild erythema and pruritus • Responses are usually seen within 3 months, with complete clearance in 60%–80% of patients after a mean of 6–8 weeks
Additional information
• The acetone solution should be applied using a cotton-tip applicator • SADBE should be refrigerated and protected from light • Side effects include severe or widespread eczematous reactions (which can be treated with topical or, if required, systemic corticosteroids), lymphadenopathy, and postinflammatory pigment alterations (especially in patients with darkly pigmented skin)

Table 129.10 Sample protocol for topical immunotherapy with squaric acid dibutyl ester (SADBE) for cutaneous warts. This is not an FDA-approved medication.

TRADITIONAL TOPICAL MEDICATIONS		
Agent	**Components**	**Classic uses**
1-2-3 paste	Burow's solution, petrolatum, zinc oxide	In the diaper area as a protective barrier to treat and prevent irritant dermatitis Hand eczema, erosions, ulcerations
Aqueous silver nitrate 10% solution*	Silver nitrate	Small recalcitrant ulcerations Excess granulation tissue, bleeding – silver nitrate applicators ("sticks")
Black cat*	Acetone, collodion, crude coal tar	Psoriasis, lichen simplex chronicus, nummular eczema, hypertrophic lichen planus
Burow's solution	Aluminum acetate	Weeping, macerated, and/or infectious skin conditions, especially in intertriginous and acral sites (e.g. acute allergic contact dermatitis, tinea pedis/cruris, candidiasis)

Table 129.11 Traditional topical medications.

Continued

TRADITIONAL TOPICAL MEDICATIONS		
Agent	**Components**	**Classic uses**
Calamine lotion	Zinc oxide, ferric oxide, glycerin, bentonite magma, calcium hydroxide solution (lime water)	Acute and subacute pruritic dermatoses, especially acute allergic contact dermatitis
Castellani paint (carbol fuchsin)	Phenol, resorcinol, basic fuchsin (without the latter in colorless version)	Fissures, primarily on digits in the setting of chronic hand dermatitis Cutaneous candidiasis, tinea pedis/cruris, pustular dermatoses of the hands and feet
Chrysarobin*	Chrysarobin, chloroform	Chronic paronychia
Fluffy tannic acid powder*	Fluffy tannic acid, bentonite, kaolin	Hyperhidrosis, contact dermatitis of the hands/feet
Gentian violet solution	Gentian violet	Candidiasis, tinea pedis/cruris
P&S® liquid	Mineral oil, glycerin, phenol	Psoriasis/sebopsoriasis with excessive hyperkeratosis (especially of the scalp)
Potassium permanganate	$KMnO_4$	Weeping, macerated, and/or infectious skin conditions, especially in intertriginous and acral sites (e.g. tinea cruris/pedis, candidiasis)
Schamberg lotion*	Menthol, phenol, zinc oxide, calcium hydroxide solution, olive oil	Acute and subacute pruritic dermatoses
Whitfield ointment	Benzoic acid (6%), salicylic acid (3%)	Tinea pedis
*Primarily of historical interest.		

Table 129.11 Traditional topical medications.

EXAMPLES OF NEWER PRESCRIPTION BARRIER-REPAIR/ MOISTURIZING AGENTS	
Agent	**Active ingredients**
Atopiclair®/Pruclair™ cream	Glycyrrhetinic acid (licorice root), *Vitis vinifera* (grape vine) extract, *Butyrospermum parkii* (shea butter), hyaluronic acid, telmesteine
Eletone® cream	70% oil (mineral oil, white petrolatum) dispersed in 30% water
EpiCeram® emulsion	3:1:1 molar ratio of ceramide, cholesterol and free fatty acids (e.g. capric, linoleic, palmitic acids)
Hylatopic® (Plus) emollient foam cream, and lotion	*Theobroma grandiflorum* seed butter, hyaluronic acid, ceramide (latter in "Plus" version)
MimyX®/PruMyx™ cream	Palmitamide monoethanolamine, palm glycerides, hydrogenated lecithin, squalane, olive oil
Neosalus® foam	Dimethicone, stearic acid
Promiseb™ cream	Glycyrrhetinic acid, *Vitis vinifera* extract, *Butyrospermum parkii*, piroctone olamine, hydrogenated castor oil, telmesteine
Tetrix™ cream	Aluminum magnesium hydroxide stearate, cyclomethicone, dimethicone, hexyl laurate

Table 129.12 Examples of prescription barrier-repair/moisturizing agents. These agents are FDA-approved as "medical devices" and available by prescription. Over-the-counter barrier-repair moisturizers containing ceramides or "pseudoceramides" and filaggrin breakdown products are also available.

the management of various dermatoses, such as atopic dermatitis and irritant contact dermatitis; examples of these agents and their active ingredients are listed in Table 129.12.

Additional figures and table available in our eBook (see inside front cover for access code).

REFERENCES

1. Long CC, Finlay AY. The finger-tip unit–a new practical measure. *Clin Exp Dermatol*. 1991;16:444–447.
2. Hercogova J. Topical anti-itch therapy. *Dermatol Ther*. 2005;18:341–343.
3. Draelos ZD. Skin lightening preparations and the hydroquinone controversy. *Dermatol Ther*. 2007;20:308–313.
4. Torok HM, Jones T, Rich P, et al. Hydroquinone 4%, tretinoin 0.05%, fluocinolone acetonide 0.01%: a safe and efficacious 12-month treatment for melasma. *Cutis*. 2005;75:57–62.
5. Dorsey CS. Dermatitic and pigmentary reactions to monobenzyl ether of hydroquinone: report of two cases. *Arch Dermatol*. 1960;81:245–248.
6. Price VH. Treatment of hair loss. *N Engl J Med*. 1999;341:964–973.
7. Messenger AG, Rundegren J. Minoxidil: mechanisms of action on hair growth. *Br J Dermatol*. 2004;150:186–194.
8. Smith S, Fagien S, Whitcup SM, et al. Eyelash growth in subjects treated with bimatoprost: a multicenter, randomized, double-masked, vehicle-controlled, parallel-group study. *J Am Acad Dermatol*. 2012;66:801–806.
9. Yoelin S, Walt JG, Earl M. Safety, effectiveness, and subjective experience with topical bimatoprost 0.03% for eyelash growth. *Dermatol Surg*. 2010;36:638–649.
10. Tosti A, Pazzaglia M, Voudouris S, Tosti G. Hypertrichosis of the eyelashes caused by bimatoprost. *J Am Acad Dermatol*. 2004;51:S149–S150.
11. Schweiger ES, Pinchover L, Bernstein RM. Topical bimatoprost for the treatment of eyebrow hypotrichosis. *J Drugs Dermatol*. 2012;11:106–108.
12. Beer KR, Julius H, Dunn M, Wilson F. Treatment of eyebrow hypotrichosis using bimatoprost: a randomized, double-blind, vehicle-controlled pilot study. *Dermatol Surg*. 2013;39:1079–1087.
13. Cohen JL. Enhancing the growth of natural eyelashes: the mechanism of bimatoprost-induced eyelash growth. *Dermatol Surg*. 2010;36:1361–1371.
14. Wolf Jr JE, Shander D, Huber F, et al. Randomized, double-blind clinical evaluation of the efficacy and safety of topical eflornithine HCl 13.9% cream in the treatment of women with facial hair. *Int J Dermatol*. 2007;46:94–98.
15. Hamzavi I, Tan E, Shapiro J, Lui H. A randomized bilateral vehicle-controlled study of eflornithine cream combined with laser treatment versus laser treatment alone for facial hirsutism in women. *J Am Acad Dermatol*. 2007;57:54–59.
16. Centers for Disease Control and Prevention, Workowski KA, Berman SM. Sexually transmitted diseases treatment guidelines, 2006. *MMWR Recomm Rep*. 2006;55:1–94.
17. Hadley G, Derry S, Moore RA. Imiquimod for actinic keratosis: systematic review and meta-analysis. *J Invest Dermatol*. 2006;126:1251–1255.
18. Swanson N, Abramovits W, Berman B, et al. Imiquimod 2.5% and 3.75% for the treatment of actinic keratoses: results of two placebo-controlled studies of daily application to the face and balding scalp for two 2-week cycles. *J Am Acad Dermatol*. 2010;62:582–590.
19. Ceilley RI, Del Rosso JQ. Current modalities and new advances in the treatment of basal cell carcinoma. *Int J Dermatol*. 2006;45:489–498.
20. Weisshaar E, Gollnick H. Potentiating effect of imiquimod in the treatment of verrucae vulgares in immunocompromised patients. *Acta Derm Venereol*. 2000;80:306–307.

21. Patel GK, Goodwin R, Chawla M, et al. Imiquimod 5% cream monotherapy for cutaneous squamous cell carcinoma in situ (Bowen's disease): a randomized, double-blind, placebo-controlled trial. *J Am Acad Dermatol*. 2006;54:1025–1032.
22. Berman B, Kaufman J. Pilot study of the effect of postoperative imiquimod 5% cream on the recurrence rate of excised keloids. *J Am Acad Dermatol*. 2002;47:S209–S211.
23. Cacao FM, Tanaka V, Messina MC. Failure of imiquimod 5% cream to prevent recurrence of surgically excised trunk keloids. *Dermatol Surg*. 2009;35:629–633.
24. Berman B, Harrison-Balestra C, Perez OA, et al. Treatment of keloid scars post-shave excision with imiquimod 5% cream: a prospective, double-blind, placebo-controlled pilot study. *J Drugs Dermatol*. 2009;8:455–458.
25. Katz KA. Imiquimod is not an effective drug for molluscum contagiosum. *Lancet Infect Dis*. 2014;14:372–373.
26. Desai T, Chen CL, Desai A, Kirby W. Basic pharmacology of topical imiquimod, 5-fluorouracil, and diclofenac for the dermatologic surgeon. *Dermatol Surg*. 2012;38:97–103.
27. Imbertson LM, Beaurline JM, Couture AM, et al. Cytokine induction in hairless mouse and rat skin after topical application of the immune response modifiers imiquimod and S-28463. *J Invest Dermatol*. 1998;110:734–739.
28. Vaccaro M, Barbuzza O, Guarneri B. Erosive pustular dermatosis of the scalp following treatment with topical imiquimod for actinic keratosis. *Arch Dermatol*. 2009;145:1340–1341.
29. Eichenfield LF, Tom WL, Berger TG, et al. Guidelines of care for the management of atopic dermatitis: section 2. Management and treatment of atopic dermatitis with topical therapies. *J Am Acad Dermatol*. 2014;71:116–132.
30. Carroll CL, Fleischer AB. Jr. Tacrolimus ointment: the treatment of atopic dermatitis and other inflammatory cutaneous disease. *Expert Opin Pharmacother*. 2004;5:2127–2137.
31. Callen J, Chamlin S, Eichenfield LF, et al. A systematic review of the safety of topical therapies for atopic dermatitis. *Br J Dermatol*. 2007;156:203–221.
32. Tennis P, Gelfand JM, Rothman KJ. Evaluation of cancer risk related to atopic dermatitis and use of topical calcineurin inhibitors. *Br J Dermatol*. 2011;165:465–473.
33. Luger T, Boguniewicz M, Carr W, et al. Pimecrolimus in atopic dermatitis: consensus on safety and the need to allow use in infants. *Pediatr Allergy Immunol*. 2015;26:306–315.
34. Legendre L, Barnetche T, Mazereeuw-Hautier J, et al. Risk of lymphoma in patients with atopic dermatitis and the role of topical treatment: a systematic review and meta-analysis. *J Am Acad Dermatol*. 2015;72:992–1002.
35. Thomson MA, Hamburger J, Stewart DG, Lewis HM. Treatment of erosive oral lichen planus with topical tacrolimus. *J Dermatolog Treat*. 2004;15:308–314.
36. Remitz A, Reitamo S. Long-term safety of tacrolimus ointment in atopic dermatitis. *Expert Opin Drug Saf*. 2009;8:501–506.
37. Yan AC, Honig PJ, Ming ME, et al. The safety and efficacy of pimecrolimus, 1%, cream for the treatment of Netherton syndrome: results from an exploratory study. *Arch Dermatol*. 2010;146:57–62.
38. Damsky W, King BA. JAK inhibitors in dermatology: the promise of a new drug class. *J Am Acad Dermatol*. 2017;76:736–744.
39. Papp K, Szepietowski JC, Kircik L, et al. Efficacy and safety of ruxolitinib cream for the treatment of atopic dermatitis: results from 2 phase 3, randomized, double-blind studies. *J Am Acad Dermatol*. 2021;85:863–872.
40. Rosmarin D, Passeron T, Pandya AG, et al. Two Phase 3, randomized, controlled trials of ruxolitinib cream for vitiligo. *N Engl J Med*. 2022;387:1445–1455.
41. Nakagawa H, Nemoto O, Igarashi A, et al. Delgocitinib ointment, a topical Janus kinase inhibitor, in adult patients with moderate to severe atopic dermatitis: a phase 3, randomized, double-blind, vehicle-controlled study and an open-label, long-term extension study. *J Am Acad Dermatol*. 2020;82:823–831.
42. Bissonnette R, Papp KA, Poulin Y, et al. Topical tofacitinib for atopic dermatitis: a phase IIa randomized trial. *Br J Dermatol*. 2016;175:902–911.
43. Liu LY, Craiglow BG, King BA. Tofacitinib 2% ointment, a topical Janus kinase inhibitor, for the treatment of alopecia areata: a pilot study of 10 patients. *J Am Acad Dermatol*. 2018;78:403–404.
44. Papp KA, Bissonnette R, Gooderham M, et al. Treatment of plaque psoriasis with an ointment formulation of the Janus kinase inhibitor, tofacitinib: a Phase 2b randomized clinical trial. *BMC Dermatol*. 2016;16:15.
45. Bayart CB, DeNiro KL, Brichta L, et al. Topical Janus kinase inhibitors for the treatment of pediatric alopecia areata. *J Am Acad Dermatol*. 2017;77:167–170.
46. Worm M, Bauer A, Elsner P, Mahler V, Molin S, Nielsen TSS. Efficacy and safety of topical delgocitinib in patients with chronic hand eczema: data from a randomized, double-blind, vehicle-controlled phase IIa study. *Br J Dermatol*. 2020;182:1103–1110.
47. Paller AS, Tom WL, Lebwohl MG, et al. Efficacy and safety of crisaborole ointment, a novel, nonsteroidal phosphodiesterase 4 (PDE4) inhibitor for the topical treatment of atopic dermatitis (AD) in children and adults. *J Am Acad Dermatol*. 2016;75:494–503.e4.
48. Lebwohl MG, Kircik LH, Moore AY, et al. Effect of roflumilast cream vs vehicle cream on chronic plaque psoriasis: the DERMIS-1 and DERMIS-2 randomized clinical trials. *JAMA*. 2022;328:1073–1084.
49. Lebwohl MG, Stein Gold L, et al. Phase 3 trials of tapinarof cream for plaque psoriasis. *N Engl J Med*. 2021;385:2219–2229.
50. Longley DB, Harkin DP, Johnston PG. 5-fluorouracil: mechanisms of action and clinical strategies. *Nat Rev Cancer*. 2003;3:330–338.
51. Tsai EY, Zackheim H, Kim YH. Topical and intralesional chemotherapeutic agents. In: Wolverton SE, ed. *Comprehensive Dermatologic Drug Therapy*. 2nd ed. Philadelphia: Saunders; 2007.
52. Jansen MHE, Kessels JPHM, Nelemans PJ, et al. Randomized trial of four treatment approaches for actinic keratosis. *N Engl J Med*. 2019;380:935–946.
53. Sachs DL, Kang S, Hammerberg C, et al. Topical fluorouracil for actinic keratoses and photoaging: a clinical and molecular analysis. *Arch Dermatol*. 2009;145:659–666.
54. Cunningham TJ, Tabacchi M, Eliane JP, et al. Randomized trial of calcipotriol combined with 5-fluorouracil for skin cancer precursor immunotherapy. *J Clin Invest*. 2017;127:106–116.
55. Talpur R, Venkatarajan S, Duvic M. Mechlorethamine gel for the topical treatment of stage IA and IB mycosis fungoides-type cutaneous T-cell lymphoma. *Expert Rev Clin Pharmacol*. 2014;7:591–597.
56. Berthelot C, Rivera A, Duvic M. Skin directed therapy for mycosis fungoides: a review. *J Drugs Dermatol*. 2008;7:655–666.
57. Lessin SR, Duvic M, Guitart J, et al. Topical chemotherapy in cutaneous T-cell lymphoma: positive results of a randomized, controlled, multicenter trial testing the efficacy and safety of a novel mechlorethamine, 0.02%, gel in mycosis fungoides. *JAMA Dermatol*. 2013;149:25–32.
58. Zackheim HS. Treatment of mycosis fungoides with topical nitrosourea compounds. *Arch Dermatol*. 1972;106:177–182.
59. Zackheim HS, Epstein Jr EH, Crain WR. Topical carmustine (BCNU) for cutaneous T cell lymphoma: a 15-year experience in 143 patients. *J Am Acad Dermatol*. 1990;22:802–810.
60. Zackheim HS, Feldmann RJ, Lindsay C, Maibach HI. Percutaneous absorption of 1,3-bis (2-chloroethyl)-l-nitrosourea (BCNU, carmustine) in mycosis fungoides. *Br J Dermatol*. 1977;97:65–67.
61. Helfrich YSD, Kang S. Topical vitamin D_3. In: Wolverton SE, ed. *Comprehensive Drug Therapy*. 2nd ed. Philadelphia: Saunders; 2007.
62. Ashcroft DM, Po AL, Williams HC, Griffiths CE. Systematic review of comparative efficacy and tolerability of calcipotriol in treating chronic plaque psoriasis. *BMJ*. 2000;320:963–967.
63. Lebwohl M, Siskin SB, Epinette W, et al. A multicenter trial of calcipotriene ointment and halobetasol ointment compared with either agent alone for the treatment of psoriasis. *J Am Acad Dermatol*. 1996;35:268–269.
64. Kircik L. Efficacy and safety of topical calcitriol 3 microg/g ointment, a new topical therapy for chronic plaque psoriasis. *J Drugs Dermatol*. 2009;8:s9–s16.
65. Lebwohl M, Menter A, Weiss J, et al. Calcitriol 3 microg/g ointment in the management of mild to moderate plaque type psoriasis: results from 2 placebo-controlled, multicenter, randomized double-blind, clinical studies. *J Drugs Dermatol*. 2007;6:428–435.
66. Veien NK, Bjerke JR, Rossmann-Ringdahl I, Jakobsen HB. Once daily treatment of psoriasis with tacalcitol compared with twice daily treatment with calcipotriol. A double-blind trial. *Br J Dermatol*. 1997;137:581–586.
67. Paghdal KV, Schwartz RA. Sirolimus (rapamycin): from the soil of Easter Island to a bright future. *J Am Acad Dermatol*. 2007;57:1046–1050.
68. Ormerod AD, Shah SA, Copeland P, et al. Treatment of psoriasis with topical sirolimus: preclinical development and a randomized, double-blind trial. *Br J Dermatol*. 2005;152:758–764.
69. Tu J, Foster RS, Bint LJ, Halbert AR. Topical rapamycin for angiofibromas in paediatric patients with tuberous sclerosis: follow up of a pilot study and promising future directions. *Australas J Dermatol*. 2014;55:63–69.
70. Haemel AK, O'Brian AL, Teng JM. Topical rapamycin: a novel approach to facial angiofibromas in tuberous sclerosis. *Arch Dermatol*. 2010;146:715–718.
71. Foster RS, Bint LJ, Halbert AR. Topical 0.1% rapamycin for angiofibromas in paediatric patients with tuberous sclerosis: a pilot study of four patients. *Australas J Dermatol*. 2012;53:52–56.
72. DeKlotz CM, Ogram AE, Singh S, et al. Dramatic improvement of facial angiofibromas in tuberous sclerosis with topical rapamycin: optimizing a treatment protocol. *Arch Dermatol*. 2011;147:1116–1117.
73. Mutizwa MM, Berk DR, Anadkat MJ. Treatment of facial angiofibromas with topical application of oral rapamycin solution (1mgmL(-1)) in two patients with tuberous sclerosis. *Br J Dermatol*. 2011;165:922–923.
74. Wataya-Kaneda M, Nakamura A, Tanaka M, et al. Efficacy and safety of topical sirolimus therapy for facial angiofibromas in the tuberous sclerosis complex: a randomized clinical trial. *JAMA Dermatol*. 2017;153:39–48.
75. Marqués L, Núñez-Córdoba JM, Aguado L, et al. Topical rapamycin combined with pulsed dye laser in the treatment of capillary vascular malformations in Sturge-Weber syndrome: phase II, randomized, double-blind, intraindividual placebo-controlled clinical trial. *J Am Acad Dermatol*. 2015;72:151–158.
76. Kurtyka DJ, Burke KT, DeKlotz CMC. Use of topical sirolimus (Rapamycin) for treating confluent and reticulated papillomatosis. *JAMA Dermatol*. 2021;157:121–123.
77. Coerdt KM, Todd SP, DeKlotz CMC. Topical rapamycin for acanthosis nigricans in the Fitzpatrick IV/V adolescent population. *Pediatr Dermatol*. 2021;38:296–298.
78. Anderson L, Schmieder GJ, Werschler WP, et al. Randomized, double-blind, double-dummy, vehicle-controlled study of ingenol mebutate gel 0.025% and 0.05% for actinic keratosis. *J Am Acad Dermatol*. 2009;60:934–943.
79. Ogbourne SM, Suhrbier A, Jones B, et al. Antitumor activity of 3-ingenyl angelate: plasma membrane and mitochondrial disruption and necrotic cell death. *Cancer Res*. 2004;64:2833–2839.
80. Berman B, Goldenberg G, Hanke CW, et al. Efficacy and safety of ingenol mebutate 0.015% gel after cryosurgery of actinic keratosis: 12-month results. *J Drugs Dermatol*. 2014;13:741–747.
81. Paghdal KV, Schwartz RA. Topical tar: back to the future. *J Am Acad Dermatol*. 2009;61:294–302.
82. Goeckerman WH. Treatment of psoriasis. Continued observations on the use of crude coal tar and ultraviolet light. *Arch Dermatol Syph*. 1931;24:446–450.
83. Harris DR. Old wine in new bottles: the revival of anthralin. *Cutis*. 1998;62:201–203.
84. Rivera A, Tyring SK. Therapy of cutaneous human Papillomavirus infections. *Dermatol Ther*. 2004;17:441–448.
85. Moed L, Shwayder TA, Chang MW. Cantharidin revisited: a blistering defense of an ancient medicine. *Arch Dermatol*. 2001;137:1357–1360.
86. Eichenfield LF, McFalda W, Brabec B, et al. Safety and efficacy of VP-102, a proprietary, drug-device combination product containing cantharidin, 0.7% (w/v), in children and adults with molluscum contagiosum: two phase 3 randomized clinical trials. *JAMA Dermatol*. 2020;156:1315–1323.
87. Gillbro JM, Olsson MJ. The melanogenesis and mechanisms of skin-lightening agents–existing and new approaches. *Int J Cosmet Sci*. 2011;33:210–221.
88. Roos TC, Alam M, Roos S, et al. Pharmacotherapy of ectoparasitic infections. *Drugs*. 2001;61:1067–1088.
89. Stuetz A, Baumann K, Grassberger M, et al. Discovery of topical calcineurin inhibitors and pharmacological profile of pimecrolimus. *Int Arch Allergy Immunol*. 2006;141:199–212.
90. Yosipovitch G, Maibach HI. Effect of topical pramoxine on experimentally induced pruritus in humans. *J Am Acad Dermatol*. 1997;37:278–280.
91. Young TA, Patel TS, Camacho F, et al. A pramoxine-based anti-itch lotion is more effective than a control lotion for the treatment of uremic pruritus in adult hemodialysis patients. *J Dermatolog Treat*. 2009;20:76–81.
92. McKemy DD, Neuhausser WM, Julius D. Identification of a cold receptor reveals a general role for TRP channels in thermosensation. *Nature*. 2002;416:52–58.
93. Peier AM, Moqrich A, Hergarden AC, et al. A TRP channel that senses cold stimuli and menthol. *Cell*. 2002;108:705–715.

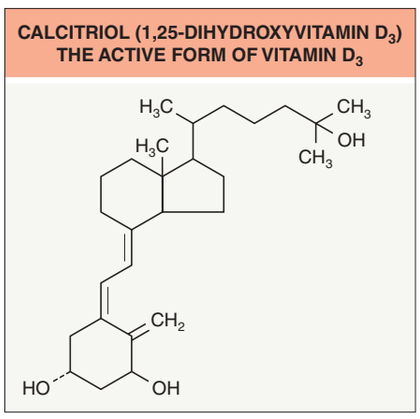
94. Patel T, Ishiuji Y, Yosipovitch G. Menthol: a refreshing look at this ancient compound. *J Am Acad Dermatol*. 2007;57:873–878.
95. Lynn B. Capsaicin: actions on nociceptive C-fibres and therapeutic potential. *Pain*. 1990;41:61–69.
96. Caterina MJ, Schumacher MA, Tominaga M, et al. The capsaicin receptor: a heat-activated ion channel in the pain pathway. *Nature*. 1997;389:816–824.
97. Mason L, Moore RA, Derry S, et al. Systematic review of topical capsaicin for the treatment of chronic pain. *BMJ*. 2004;328:991.
98. Drake LA, Millikan LE. The antipruritic effect of 5% doxepin cream in patients with eczematous dermatitis Doxepin Study Group. *Arch Dermatol*. 1995;131:1403–1408.
99. Drake LA, Fallon JD, Sober A. Relief of pruritus in patients with atopic dermatitis after treatment with topical doxepin cream. The Doxepin Study Group. *J Am Acad Dermatol*. 1994;31:613–616.
100. Taylor JS, Praditsuwan P, Handel D, Kuffner G. Allergic contact dermatitis from doxepin cream. One-year patch test clinic experience. *Arch Dermatol*. 1996;132:515–518.
101. Loden M. Urea-containing moisturizers influence barrier properties of normal skin. *Arch Dermatol Res*. 1996;288:103–107.
102. Hellgren L, Larsson K. On the effect of urea on human epidermis. *Dermatologica*. 1974;149:289–293.
103. Hessel A, Cruz-Ramon JC. Agents used for treatment of hyperkeratosis. In: Wolverton SE, ed. *Comprehensive Drug Therapy*. 2nd ed. Philadelphia: Saunders; 2007.
104. Lin AN, Nakatsui T. Salicylic acid revisited. *Int J Dermatol*. 1998;37:335–342.
105. Imayama S, Ueda S, Isoda M. Histologic changes in the skin of hairless mice following peeling with salicylic acid. *Arch Dermatol*. 2000;136:1390–1395.
106. Van Scott EJ, Yu RJ. Hyperkeratinization, corneocyte cohesion, and alpha hydroxy acids. *J Am Acad Dermatol*. 1984;11:867–879.
107. Smith WP. Epidermal and dermal effects of topical lactic acid. *J Am Acad Dermatol*. 1996;35:388–391.
108. Van Scott EJ, Yu RJ. Control of keratinization with alpha-hydroxy acids and related compounds. I. Topical treatment of ichthyotic disorders. *Arch Dermatol*. 1974;110:586–590.



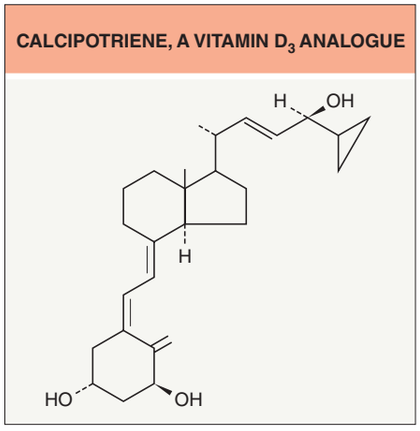
eFig. 129.1 An adult fingertip unit.



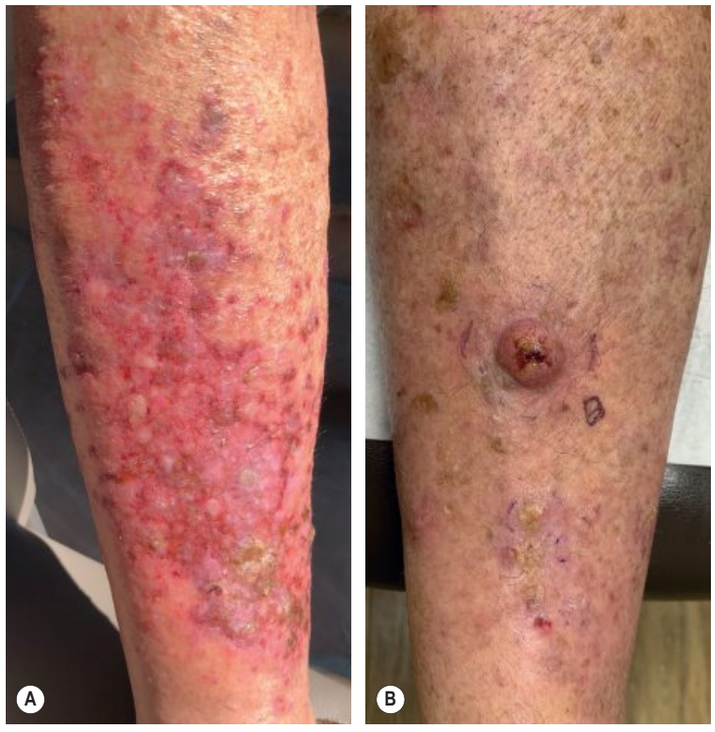
eFig. 129.4 Exuberant inflammatory reaction following topical application of imiquimod to a lentigo maligna (melanoma *in situ*). The site had been pretreated for two weeks with 0.1% tazarotene cream. *Courtesy Lauren Daman, MD.*



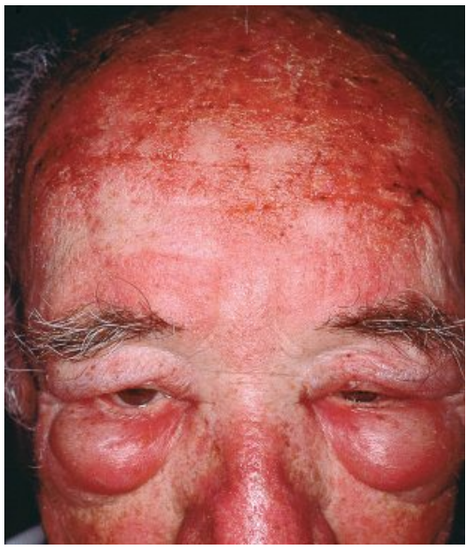
eFig. 129.2 Calcitriol (1,25-dihydroxyvitamin D_3), the active form of vitamin D_3.



eFig. 129.3 Calcipotriene (calcipotriol), a vitamin D_3 analogue.



eFig. 129.5 Atypical squamous proliferations (ASPs) following topical imiquimod therapy. A Treatment of actinic keratoses on the shin of a woman with topical imiquimod (thrice weekly for three weeks) led to an exuberant inflammatory response that included eruptive ASPs. **B** While there was clearance of the inflammatory response and the majority of the ASPs after two weeks of topical corticosteroids, a KA-type of SCC developed requiring surgical removal. *Courtesy Karynne O. Duncan, MD.*



eFig. 129.6 Reactions to topical 5-fluorouracil. Note the erythema and crusting in areas of solar damage, as well as periorbital edema.

TRADITIONAL FDA CLASSIFICATION SYSTEM OF PHARMACEUTICAL PREGNANCY CATEGORIES	
Category	**Description**
A	Controlled studies show no risk. Adequate well-controlled studies in pregnant women have failed to demonstrate risk to the fetus.
B	No evidence of risk in humans. Either animal studies show risk, but human studies do not; or, if no adequate human studies have been done, animal findings are negative.
C	Risk cannot be ruled out. Human studies are lacking, and animal studies are either positive for fetal risk or lacking as well. However, potential benefits may justify the potential risk.
D	Positive evidence for risk. Human studies, or investigational or post-marketing data, show risk to fetus. Nevertheless, potential benefits may outweigh potential risk.
X	Contraindicated in pregnancy. Studies in animals or humans, or investigational or post-marketing reports, have shown fetal risk, which clearly outweighs any possible benefit to the patient.

eTable 129.1 Traditional FDA classification system of pharmaceutical pregnancy categories. In 2015, the FDA replaced these pregnancy risk categories with narrative sections addressing pregnancy and lactation, which include risk summaries as well as information on pregnancy exposure registries, clinical considerations, and available data. The new format is used for prescription drugs approved from June 30, 2015 onward and is being phased in for other drugs approved since 2001. FDA, Food and Drug Administration.

Other Systemic Drugs 130

Mary P. Maiberger, Julia R. Nunley and Stephen E. Wolverton

Chapter Contents

Antimalarials 2313
Apremilast 2316
Azathioprine 2317
Bleomycin 2319
Clofazimine 2319
Colchicine 2319
Cyclophosphamide 2319
Cyclosporine 2320
Dapsone 2321
Hydroxyurea 2322
Leukotriene (LT) Inhibitors 2322
Methotrexate 2323
Mycophenolate Mofetil and Mycophenolate Sodium 2325
Saturated Solution of Potassium Iodide (SSKI) 2326
Sirolimus (Rapamycin) and Tacrolimus 2326
Thalidomide and Lenalidomide 2326

INTRODUCTION

This chapter is designed to be a broad overview of selected systemic therapies for dermatologic diseases. It provides an historical perspective for each drug, a discussion of its mechanism of action and side effects, and touches on indications and clinical use. This information should serve as a starting point, allowing the reader to readily compare and contrast treatment options. It is not a substitute for the in-depth knowledge and experience necessary to implement these therapies, nor is it a complete library of systemic drugs used in dermatology. Several systemic medications are reviewed in other chapters (Table 130.1) and not discussed here.

Systemic drugs discussed in this chapter may be subdivided into broad categories, such as immunosuppressive/anti-inflammatory, cytotoxic, and antiproliferative (Table 130.2). Drugs in a single category act in a relatively similar fashion and generally have similar important side effects. For example, immunosuppressive drugs suppress the body's ability to recognize or eliminate infections and neoplastic cells. Patients may be at increased risk for opportunistic infections and selected lymphoproliferative malignancies as well as squamous cell carcinomas. Given this increased risk for infection, patients with either an active infection or one that may reactivate (e.g. latent tuberculosis, hepatitis B viral infection) should be cautiously given these drugs, with prior (when possible) or concomitant administration of antimicrobial or antiviral medications.

Most of the drugs discussed herein lack Food and Drug Administration (FDA) approval for dermatologic indications. However, in most instances, their use is based on the mechanism of action of the drug and the presumed pathogenesis of the disease, combined with published case series, case reports, and a limited number of clinical trials.

When choosing therapy for a patient, certain broad general principles apply. First, the physician should be aware of all common therapeutic modalities available that are likely to yield optimal results. Certain systemic medications will not be utilized frequently enough for a given clinician to become comfortable with their use; therefore, patients requiring more specialized drugs should be referred to colleagues experienced with their use. Patients should be advised of all reasonable therapeutic choices as well as the risk–benefit profile of each modality. Non-compliance is a relative contraindication for all medications discussed in this chapter.

Prior to initiation of several of these medications, based upon potential side effects, the patient should have a complete history and physical examination, with specific emphasis on organ systems that may be affected by the particular drug. Tuberculin skin testing and/or interferon-gamma release assays (IGRAs; e.g. QuantiFERON-TB Gold Plus, T-SPOT.*TB*) should be performed prior to using immunosuppressive medications, specifically corticosteroids (particularly when a prolonged course is anticipated) and systemic immunomodulators ("biologics"; see Ch. 128). Consultation with appropriate generalists or specialists in selected situations may be required prior to initiating therapy as well as for periodic screening for treatment complications. Table 130.3 outlines suggested monitoring guidelines for systemic medications discussed in this chapter. Some tests may need to be performed more frequently in high-risk patients or in patients with abnormal results. Additionally, each outpatient visit should include an appropriate review of systems and physical examination.

The use of each drug during pregnancy and lactation is reviewed. Wherever possible, this has been referenced with the eleventh edition of *Drugs in Pregnancy and Lactation* by Briggs and colleagues. Additionally, in 2015, under the Pregnancy and Lactation Labeling Rule (PLLR), the FDA abolished the letter rating system for drug safety in pregnant women and during lactation; the letters have been replaced by narrative-based labeling with three subsections: (1) pregnancy; (2) lactation; and (3) females and males of reproductive potential[1]. In general, one should be circumspect in prescribing systemic medications to those with childbearing potential. It is not adequate to merely ask patients if they are utilizing birth control; each patient must be made acutely aware of the risks associated with medication use during pregnancy and risks of continuing therapy if one becomes pregnant.

SYSTEMIC MEDICATIONS COVERED IN OTHER CHAPTERS	
Antihistamines	Ch. 18
Antimicrobials	Ch. 127
Cytokines, including G-CSF, GM-CSF, interferons	Ch. 128
Glucocorticosteroids	Ch. 125
Interleukin (IL)-1 and IL-1R antagonists, including anakinra, canakinumab, rilonacept	Chs. 45 & 128
Intravenous immunoglobulin (IVIg)	Ch. 128
Ivermectin	Ch. 84
JAK inhibitors, e.g. tofacitinib	Ch. 128
Psoralens	Ch. 134
Psychotropic agents, including pimozide, atypical antipsychotic agents	Ch. 7
Retinoids, including acitretin, bexarotene, isotretinoin	Chs. 8, 36, & 126
Spironolactone	Ch. 36
Systemic immunomodulators, including rituximab, TNF inhibitors, IL-12/23, IL-23, IL-17 inhibitors	Ch. 128

Table 130.1 Systemic medications covered in other chapters. IL-1R, interleukin-1 receptor; G-CSF, granulocyte colony-stimulating factor; GM-CSF, granulocyte–macrophage colony-stimulating factor; JAK, Janus kinase.

CATEGORIES OF SYSTEMIC DRUGS USED IN DERMATOLOGY BASED UPON MECHANISM OF ACTION			
Immunosuppressive/Anti-inflammatory	**Cytotoxic**	**Antiproliferative**	**Miscellaneous**
Apremilast Azathioprine Mycophenolate mofetil Cyclosporine Lenalidomide Tacrolimus Thalidomide	Cyclophosphamide Bleomycin	Methotrexate* Hydroxyurea	Dapsone Antimalarials Saturated solution of potassium iodide (SSKI)
*Also immunosuppressive/anti-inflammatory.			

Table 130.2 Categories of systemic drugs used in dermatology based upon mechanism of action.

MONITORING GUIDELINES FOR SYSTEMIC MEDICATIONS			
Drug	**Initial screening**	**Follow-up monitoring**	**Special considerations**
Antimalarials	***Ocular***: During the first year, a baseline examination* to exclude pre-existing maculopathy ***Laboratory***: CBC CMP G6PD (selected cases) ECG (at-risk patients)**	***Ocular***: After 5 years of continuous use with appropriate doses, annual screening* (unless high-risk patient or symptoms develop[5]; see Table 130.4) ***Laboratory***: Periodic CBC and CMP	• G6PD testing before antimalarial therapy is controversial and is probably most important with the use of primaquine • Urine or serum porphyrins should be measured when porphyria is clinically suspected • Retinopathy risk is greatest for those on treatment for at least 5 years (especially with chloroquine) and if maximum daily safe maintenance dose has been exceeded
Azathioprine	CBC CMP UA Consider pregnancy test for women of childbearing potential TPMT level, if available Tuberculosis screening† (should be considered depending on clinical situation)	CBC every 2 weeks for 2 months, then every 2–3 months if stable LFTs every 2 weeks for 2 months, then every 2–3 months if stable	• 25% dose reduction is necessary if GFR 10–50 ml/min; 50% dose reduction if GFR <10 ml/min • Frequency of laboratory studies is based on baseline TPMT determination (see Table 130.6); if TPMT is not known, hematologic parameters should be more closely monitored • Discontinue therapy, at least temporarily, if WBC declines to <3500–4000 cells/mm^3 or if hemoglobin <10 g/dl • Yearly skin examination and age-appropriate cancer screening, including yearly gynecologic examination in women
Cyclophosphamide	CBC CMP UA Pregnancy test for women of childbearing potential	CBC every week for 2–3 months, then every 2 weeks if stable. After 3–6 months, may decrease to every 3 months if stable UA every week for 2–3 months, then every 2 weeks if stable. After 3–6 months may decrease to every 3 months if stable CMP monthly for 3–6 months, then every 3 months if stable	• Discontinue temporarily or lower dose if WBC declines to <3500–4000 cells/mm^3 or PLT count to <100 000 cells/mm^3 • Stop treatment if red blood cells appear in urine; refer to urologist if hematuria persists • Yearly physical examination and CBC as well as age-appropriate cancer screening
Cyclosporine	At least 2 baseline blood pressure readings At least 2 baseline serum creatinine levels CMP (must include BUN, magnesium, potassium and uric acid) CBC UA with microscopic examination Fasting lipid profile (TG, cholesterol, HDL)	CBC at 1 month, then every 2–4 months CMP (must include BUN, creatinine, uric acid, potassium, magnesium) every 2 weeks for 1–2 months, then monthly or every 3 months if stable UA with microscopic examination every month if abnormal; otherwise yearly Fasting lipid panel every 2–4 weeks for 1–2 months, then every 3 months if stable	• Blood pressure must be monitored every 2 weeks for first 3 months and then monthly if stable • Lower dose by 25%–50% if serum creatinine remains elevated (over 2 weeks) by >25% of baseline • Lower dose by 25%–50%, or discontinue, if at any time serum creatinine is elevated by ≥50% of baseline • Consider creatinine clearance if >6 months of therapy • Skin examination at least yearly and age-appropriate cancer screening • Consider trough whole drug cyclosporine level if non-compliance, poor absorption or drug interactions are suspected
Dapsone	CBC CMP UA G6PD level Genetic screen for HLA-B*13:01 for at-risk populations (e.g. Chinese)	CBC every 2 weeks for 2 months, then every 3–4 months; after 9–12 months of therapy, for patients on lower doses with stable normal laboratory values, consider twice-yearly testing Reticulocyte count if anemia develops CMP every 3–4 months UA every 3–4 months	• Each visit should include an assessment of peripheral motor function and an assessment for the signs and symptoms of methemoglobinemia and peripheral neuropathy (e.g. motor strength, reflexes) • Methemoglobin level if clinically indicated • Increase monitoring frequency when dose is increased

Table 130.3 Monitoring guidelines for systemic medications, as recommended by the authors.

MONITORING GUIDELINES FOR SYSTEMIC MEDICATIONS			
Drug	**Initial screening**	**Follow-up monitoring**	**Special considerations**
Methotrexate	CBC CMP Pregnancy test for women of childbearing potential Baseline panel of biochemical markers (see Fig. 130.7) Serologic tests for hepatitis A, B, and C viruses Tuberculosis screening† (should be considered depending on clinical situation) HIV testing if indicated	CBC and LFTs after initial test dose of 2.5–5 mg in higher risk patients CBC and LFTs 1–3 weeks after initiation and after each dose escalation, then monthly for 2–4 months, and then every 3–4 months, if stable BUN and serum creatinine every 6–12 months Yearly panel of biochemical markers Depending upon biochemical markers and risk factors for hepatotoxicity, yearly GI consult +/– VCTE (see Fig. 130.7)	• See Fig. 130.7[36] • Elevation of LFTs <3× upper limit of normal, repeat in 2–4 weeks • Elevation of LFTs ≥3× upper limit of normal, reduce dose or discontinue, closely monitor, repeat in 2–4 wks • Persistent elevation of LFTs during a 12-month period or a decline in serum albumin below the normal range in a patient with normal nutritional status, GI consult and consideration of liver biopsy • Consider creatinine clearance, especially in elderly patients
Mycophenolate mofetil	CBC CMP Pregnancy test for women of childbearing potential Serologic tests for hepatitis B and C virus Tuberculosis screening† HIV testing	CBC every 2 weeks for 2–3 months, then monthly for first year CMP after 1 month and then every 3–4 months	• Discontinue or decrease dose if WBC declines to <3500–4000 cells/mm^3
Thalidomide and lenalidomide	CBC CMP TSH Pregnancy test in women of childbearing potential Subjective review of sensory and motor neurologic function and neurologic examination (thalidomide > lenalidomide) Assessment of risk of arterial and venous thromboembolism (lenalidomide, thalidomide if combined with dexamethasone)	Consider CBC and LFTs every 2–3 months (recommend monthly for lenalidomide) Pregnancy test every week for 4 weeks, then monthly for women of childbearing potential with regular menses, or every 2 weeks for those with irregular menses and as clinically indicated Neurologic examination monthly for 3 months, then every 1–6 months Monitor for signs of venous or arterial thromboembolism	***Thalidomide:*** • Measurements of sensory nerve action potential amplitudes (SNAP), if indicated by history prior to therapy • Consider SNAP measurements every 6 months, or as indicated ***Lenalidomide:*** • Thromboprophylaxis may be recommended based upon underlying risk factors

*Automated visual fields and spectral domain optical coherence tomography (SD-OCT).
**Individuals with known cardiac disease including arrhythmias as well as those receiving other drugs that prolong the QT/QTc interval.
†Tuberculin skin testing (purified protein derivative [PPD]) or interferon-gamma release assay such as the QuantiFERON®-TB Gold Plus test.

Table 130.3 Monitoring guidelines for systemic medications, as recommended by the authors. Before using any of these medications, the risk–benefit profiles and adverse effects should be thoroughly discussed with each patient. More frequent monitoring is needed in high-risk patients, when results are abnormal, or when increasing doses. BUN, blood urea nitrogen; CBC, complete blood count with differential and platelet count; CMP, comprehensive metabolic panel (includes liver function tests); ECG, electrocardiogram; G6PD, glucose-6-phosphate dehydrogenase; GFR, glomerular filtration rate; GI, gastroenterology; HDL, high-density lipoproteins; HLA, human leukocyte antigen; LFTs, liver function tests; TG, triglycerides; TPMT, thiopurine methyltransferase; UA, urinalysis; VCTE, vibration-controlled transient elastography; WBC, white blood count.

Family planning consultation and communication with the patient's obstetrician or primary care physician can prove helpful.

Several of the medications reviewed in this chapter, including mycophenolate mofetil, thalidomide, and lenalidomide, are subject to FDA-mandated Risk Evaluation and Mitigation Strategies (REMS). In addition to medication guides for patients, there are educational programs for health care providers and restrictive computerized programs to ensure compliance and safe medication use, especially as it pertains to pregnancy.

Lastly, several drugs discussed herein have parenteral formulations. Clinicians who administer parenteral medications in the ambulatory setting should be current in Advanced Cardiac Life Support (ACLS) training and keep emergency resuscitation supplies available.

ANTIMALARIALS

Quinine and its derivatives have been used since the 1600s to treat malaria. Quinine, derived from the bark of the cinchona tree in South America, was first used in dermatology by Payne in 1894 to treat discoid lesions in patients with lupus erythematosus (LE). The most common antimalarials are hydroxychloroquine (Plaquenil®), chloroquine (Aralen®), and quinacrine; currently the latter, which can lead to yellow skin discoloration, has limited availability in the US and will not be discussed in detail (see Ch. 41).

The antimalarials are absorbed extensively into tissues and slowly released, leading to a half-life of 40–50 days. A steady state is achieved slowly, and it may take 3–4 months to see adequate clinical effects. Hydroxychloroquine is catabolized into two metabolites, desethylhydroxychloroquine and desethylchloroquine. Chloroquine is only metabolized into the latter. The initial metabolites undergo further change into the primary amine form. Overall, 50% of each drug undergoes renal excretion[2].

Mechanism of Action

The mechanisms of action of antimalarials are complex and incompletely understood. Known endpoints include the following: stabilization of lysosomes within injured cells; inhibition of antigen presentation, cell-mediated immunity, and the synthesis of proinflammatory cytokines; and antithrombotic/antiplatelet effects[3]. The photoprotective effect attributed to the antimalarials may result from their anti-inflammatory properties[3].

Dosages

Most conditions will respond to dosages between 200 and 400 mg/day of hydroxychloroquine or 250 mg/day of chloroquine, with a maximum safe chronic dose (from an ocular standpoint) being 5 mg/kg/day and 2.3 mg/kg/day, respectively, utilizing *real* body weight. After a suitable therapeutic response has been achieved, the response may be maintained with hydroxychloroquine 100–200 mg daily. If available, quinacrine (100 mg/day) can be added to 200 mg twice daily of hydroxychloroquine, to maximize the clinical benefit without increasing the

risk of ocular toxicity. Lower doses of chloroquine (125 mg twice weekly) or hydroxychloroquine (100 mg three times weekly) must be used in patients with porphyria cutanea tarda, in order to minimize the risk of a toxic reaction (e.g. hepatotoxicity) in addition to a marked increase in urinary uroporphyrin output and flare of cutaneous disease (Fig. 130.1).

If no response is noted after 3–4 months, the specific antimalarial has failed and should be discontinued; however, a different antimalarial can be tried. In patients with porphyria cutanea tarda the antimalarial can be slowly increased to daily dosing if necessary and if laboratory monitoring of transaminases allows.

Monitoring guidelines are outlined in Table 130.3 and in the next section.

Major Side Effects

Antimalarials are highly concentrated in the iris and choroid, reaching levels 480 000 times that of plasma[4]. However, irreversible retinopathy rarely occurs when dosages remain within the recommended range and patients are monitored by an ophthalmologist experienced with the ocular effects of antimalarials. As noted in Table 130.4, the risk of retinopathy is much less with hydroxychloroquine than with chloroquine.

Because of the risk of dose-related ocular toxicity, referral to an ophthalmologist for evaluation is required. The American Academy of Ophthalmology (AAO) guidelines recommend that a baseline examination be performed within the first year of antimalarial use. With the exception of higher risk individuals (e.g. the elderly, history of maculopathy, renal or hepatic dysfunction) and those patients with symptoms, annual screening is performed after five years of continuous use (see Table 130.4)[5,6]. Of note, more recent data regarding long-term usage suggest a significant potential for retinopathy after 10 years of continuous therapy[7].

Up to one-third of patients who receive antimalarials for over 4 months will develop a blue–gray to black hyperpigmentation on their shins (Fig. 130.2), face, palate, and/or nail beds (Table 130.5). The discoloration fades after cessation of therapy but may take months to years to resolve completely. Reversible bleaching of the hair roots (achromotrichia) occurs in up to 10% of patients, presumably due to interference with melanosomal function. Another 10%–20% may develop an exanthem, ranging from urticaria to lichenoid reactions to exfoliative erythroderma (Fig. 130.3). Of interest, morbilliform and urticarial exanthems have been observed with greater frequency in individuals with dermatomyositis as compared to those with LE.



Fig. 130.1 Hydroxychloroquine-induced porphyria cutanea tarda (PCT). While low doses of antimalarials (e.g. 100–200 mg of hydroxychloroquine 2–3 times per week) can be used in the management of PCT, higher doses, such as those used to treat cutaneous LE, can lead to flares of PCT. This patient developed skin fragility and bullous lesions six weeks after beginning hydroxychloroquine for rheumatoid arthritis. The eruption resolved with discontinuation of the medication.

RISK FACTORS AND TYPES OF RETINOPATHY ASSOCIATED WITH ANTIMALARIAL THERAPY

	Hydroxychloroquine	Chloroquine
Risk factors		
Dosing risk		
Daily dose	>400 mg/day (>5 mg/kg/day, based upon *real* body weight)	>250 mg/d (>2.3 mg/kg/day based upon *real* body weight)
Total cumulative dose	>1000 g	>460 g
Other risk factors		
Ocular	History of retinopathy or maculopathy	History of retinopathy or maculopathy
Systemic	Renal or hepatic dysfunction Use of tamoxifen and aromatase inhibitors	Renal or hepatic dysfunction
Age	Elderly	Elderly
Types of retinopathy		
Reversible ocular toxicity: • Corneal deposits leading to blurred vision, halos of colors around lights • Loss of accommodation/diplopia • Premaculopathy: no visual symptoms or loss of visual acuity, central and paracentral scotomata	Observed in 5% of patients Often reversible with discontinuation of therapy	Observed in 90% of patients Often reversible with discontinuation of therapy
Irreversible ocular toxicity (true retinopathy): • "Bull's eye" pigment deposition • Central scotomata • Changes in visual acuity	Incidence of 0.5% after 6 years of treatment If develops, suspend treatment	Incidence can reach 1% after 5 years of treatment If develops, suspend treatment

Table 130.4 Risk factors and types of retinopathy associated with antimalarial therapy. The ocular examination should include white 10-2 threshold testing (automated visual field testing) plus one or more of the following, if available: spectral domain optical coherence tomography to detect early thinning of photoreceptors in retina, multifocal electroretinogram, or fundus autofluorescence. Adapted from references 2, 5, 6, and 49.

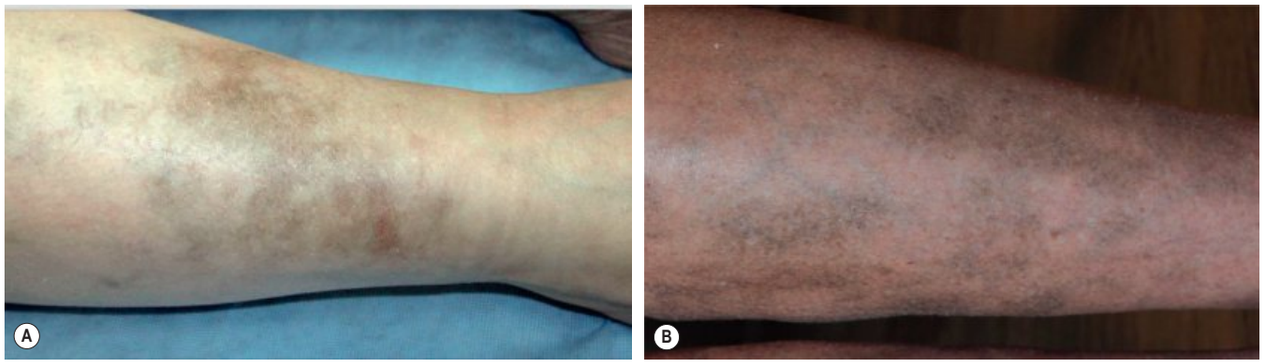


Fig. 130.2 Discoloration of the shins due to antimalarial drugs. A Areas of blue-gray to brown discoloration due to chloroquine. **B** Scattered brown to brown-gray patches due to hydroxychloroquine. *B, Courtesy Kalman Watsky, MD.*

SIDE EFFECTS OF SYSTEMIC DRUGS USED IN DERMATOLOGY			
Drug	**Common**	**Uncommon**	**Rare**
Antimalarials	***Derm***: blue–gray to black discoloration; yellowing from quinacrine	***Derm***: bleaching of hair roots, exanthem (e.g. urticarial, lichenoid) ***GI***: nausea, vomiting, elevated liver enzymes ***Neuro***: irritability, nervousness	***Heme***: pancytopenia, hemolysis (G6PD-deficient, primarily with non-dermatologic antimalarials) ***Ophtho***: reversible (early) and irreversible retinopathy, vision changes (see Table 130.4)
Apremilast	***GI:*** nausea, diarrhea ***ENT:*** nasopharyngitis ***Metabolic:*** weight loss	***Neuro:*** headaches	***Psych:*** depression and suicidal ideation
Azathioprine	***Derm***: keratinocyte carcinomas ***Heme***: leukopenia, thrombocytopenia, immunosuppression	***GI***: nausea, vomiting ***ID***: opportunistic infections	***Heme***: pancytopenia ***GI***: pancreatitis, hepatitis ***Malignancy***: lymphoma, cutaneous and gynecologic SCC Hypersensitivity syndrome
Cyclophosphamide	***GI***: nausea, vomiting ***GU***: sterility (higher doses or long-term administration) ***Heme***: leukopenia	***Derm***: diffuse hyperpigmentation, nail pigmentation, alopecia ***GU***: dysuria, hemorrhagic cystitis, amenorrhea, azoospermia, sterility (with lower doses) ***Heme***: anemia, thrombocytopenia ***ID***: opportunistic infections	***GI***: hemorrhagic colitis, hepatotoxicity ***Heme***: aplastic anemia ***Malignancy***: bladder (esp. chronic oral administration), lymphoma, acute leukemia ***Pulmonary***: pneumonitis, interstitial fibrosis Anaphylaxis
Cyclosporine	***Cardiac***: hypertension ***Derm***: keratinocyte carcinomas ***GU***: renal dysfunction* ***Metabolic***: hyperlipidemia ***Neuro***: headache, tremor	***Derm***: hypertrichosis, gingival hyperplasia, sebaceous hyperplasia, acneiform eruption, epidermoid cysts ***GI***: nausea, diarrhea ***Neuro***: paresthesia, hyperesthesia ***Metabolic***: hyperkalemia†, hypomagnesemia, hyperuricemia	***Derm***: trichodysplasia spinulosa/viral-associated trichodysplasia (see Ch. 81) ***ID***: infections (unless combined with other immunosuppressives) ***Musculoskeletal***: myalgias, myositis ***GI***: hepatotoxicity ***Malignancy***: lymphoma ***Pulmonary***: dyspnea, bronchospasm
Dapsone	***Heme***: hemolysis, methemoglobinemia	***GI***: dyspepsia, anorexia	***Heme***: agranulocytosis ***Neuro***: peripheral neuropathy Dapsone hypersensitivity syndrome
Hydroxyurea	***Heme***: anemia, megaloblastic changes	***Derm***: leg ulcers, alopecia ***Heme***: leukopenia	***Derm***: hyperpigmentation, dermatomyositis-like lesions, keratinocyte carcinomas ***GI***: hepatitis ***GU***: renal dysfunction ***Heme***: thrombocytopenia ***Malignancies***: acute leukemia
Methotrexate	***Heme***: leukopenia	***Derm***: photosensitivity, alopecia, oral ulcers ***GI***: elevated liver enzymes, nausea, vomiting, anorexia, cirrhosis ***Heme***: thrombocytopenia	***Derm***: necrosis of psoriatic plaques, accelerated rheumatoid (cutaneous) nodulosis ***Heme***: pancytopenia, lymphoproliferative disorder (primarily in patients with RA) ***ID***: infections ***Pulmonary***: pneumonitis, fibrosis
Mycophenolate mofetil	***GI***: diarrhea, cramps, nausea, vomiting	***Heme***: anemia, leukopenia, thrombocytopenia ***ID***: opportunistic infections	***Derm***: oral aphthae (especially in organ transplant patients) ***GU***: dysuria, sterile pyuria ***Neuro***: insomnia, dizziness, tinnitus
Saturated solution of potassium iodide (SSKI)	***Derm***: acneiform eruption ***GI***: nausea, vomiting, diarrhea, abdominal pain ***Metabolic***: reversible hypothyroidism	***Derm***: iododerma ***Metabolic***: hyperkalemia	***Cardiac***: CHF, pulmonary edema ***Derm***: flare of dermatitis herpetiformis ***GI***: salivary gland enlargement ***Metabolic***: irreversible hyperthyroidism, goiter, "iodism" Hypersensitivity reactions
Tacrolimus	***Cardiac***: hypertension ***Derm***: keratinocyte carcinomas ***GU***: renal dysfunction* ***Neuro***: paresthesias	***Derm:*** alopecia ***ID***: infections ***Metabolic***: hyperkalemia†, hypomagnesemia	***Derm:*** trichodysplasia spinulosa/viral-associated trichodysplasia (see Ch. 81) ***Metabolic***: diabetes mellitus, hyperuricemia ***Malignancy***: lymphoma
Thalidomide and lenalidomide	***Derm***: xerosis, pruritus ***GI***: constipation ***Neuro***: peripheral neuropathy (thalidomide > lenalidomide), sedation ***Ob/Gyn***: fetal abnormalities, amenorrhea ***Heme***: neutropenia and thrombocytopenia (more common with lenalidomide)	***Cardiac***: peripheral edema ***Endo***: hyper- and hypothyroidism ***GI***: xerostomia, increased appetite ***Gyn***: primary ovarian failure ***Heme***: thromboses (esp. in combination with corticosteroids) ***Psych***: headache, mood changes	***Derm***: exfoliative erythroderma, TEN ***Heme***: leukopenia Hypersensitivity reaction (in HIV+ patients receiving thalidomide)

*Not permanent during short-term treatment if guidelines are followed.
†Especially when used in conjunction with angiotensin converting enzyme (ACE) inhibitors.

Table 130.5 Side effects of systemic drugs used in dermatology. CHF, congestive heart failure; Derm, dermatologic; G6PD, glucose-6-phosphate dehydrogenase; Endo, endocrine; ENT, ear, nose and throat; esp., especially; GI, gastrointestinal; GU, genitourinary; Gyn, gynecologic; Heme, hematologic; ID, infectious diseases; Neuro, neurologic; Ob/Gyn, obstetrical/gynecologic; Ophtho, ophthalmologic; Psych, psychiatric; RA, rheumatoid arthritis; SCC, squamous cell carcinoma; TEN, toxic epidermal necrolysis.



Fig. 130.3 Drug reaction with eosinophilia and systemic symptoms (DRESS) secondary to hydroxychloroquine. The individual lesions were edematous and became confluent. *Courtesy Jean L. Bolognia, MD.*

Antimalarials have been reported to worsen psoriasis in some patients, even though in the past they were commonly used to treat psoriatic arthritis. Psoriatic patients traveling to malaria-endemic areas may take these drugs prophylactically.

Laboratory abnormalities do not commonly occur, but it is the practice of the authors to monitor patients as outlined in Table 130.3. An overdose of antimalarials can be fatal, and although pediatric usage is safe and effective, patients should be warned to keep the drug out of the reach of small children.

Indications

The most common dermatologic use for antimalarials is as first-line systemic therapy for cutaneous LE, after topical or intralesional corticosteroids. Antimalarials are especially useful in patients with widespread discoid lesions and in those with the annular or papulosquamous lesions of subacute cutaneous LE (SCLE). Antimalarial use has also been credited with fewer thromboembolic events in patients with systemic LE (SLE)[3]. Additional cutaneous disorders that may respond to antimalarial therapy include lichen planus, dermatomyositis, and polymorphous light eruption[8].

Contraindications

The only true contraindication is hypersensitivity to the drug. Caution should be used in patients with severe blood dyscrasias or hepatic disorders because bone marrow suppression and hepatitis can occasionally occur. Should ophthalmologic changes of pre-maculopathy develop, an alternative medication should be considered. Ocular changes at this stage are potentially reversible but could progress if the drug were continued. With the exception of halofantrine, antimalarial medications that prolong the QT/QTc interval have a low risk of cardiotoxicity. In patients with known cardiac disease including arrhythmias as well as those receiving other drugs that prolong the QT/QTc interval, consultation with a cardiologist is recommended.

Use in Pregnancy and Lactation

Chloroquine is thought to be safe for treatment and prophylaxis of malaria during pregnancy; however, there have been anecdotal reports of an increase in birth defects in pregnant women being treated for SLE. Hydroxychloroquine is thought to be safer during pregnancy. Although excreted into breast milk, standard doses of either drug are not harmful to breastfed infants and are approved by the American Academy of Pediatrics for use during lactation[9].

Drug Interactions

Cimetidine may increase circulating levels of antimalarials, and antimalarials may increase digoxin levels. Kaolin and magnesium trisilicate, over-the-counter gastrointestinal drugs, decrease absorption of antimalarials. The most significant potential interaction is the additive risk of retinal toxicity when chloroquine and hydroxychloroquine are used concomitantly. Combined therapy consisting of chloroquine or hydroxychloroquine plus quinacrine is acceptable. As noted previously, assessment is required when antimalarials are coadministered with other medications that prolong the QT/QTc interval (e.g. azithromycin).

In patients with LE, cigarette smoking has been associated with decreased efficacy of antimalarials. It is unknown whether this represents a "drug–drug" interaction, decreased compliance (as a manifestation of high-risk behavior), or an unrecognized interplay. Suspected noncompliance can be confirmed by measuring serum levels of hydroxychloroquine.

APREMILAST

A novel, small-molecule inhibitor of phosphodiesterase 4, apremilast (Otezla®) works intracellularly to reduce the production of proinflammatory mediators and increase those that are anti-inflammatory (see below). When administered orally, apremilast is 70%–75% bioavailable, with peak plasma concentrations observed at ~2.5 hours. Nearly 70% of the drug is bound to plasma proteins, and it is metabolized by cytochrome P450 (CYP) enzymes, predominately CYP3A4 (see Ch. 131); this is followed by glucuronidation and non-CYP-mediated hydrolysis. Apremilast has a terminal elimination half-life of 6–9 hours and is excreted in the urine and feces.

Mechanism of Action

Apremilast inhibits phosphodiesterase 4, which is an intracellular enzyme that degrades cAMP and represents the predominant phosphodiesterase in keratinocytes, dendritic cells, monocytes, and neutrophils. Increasing intracellular cAMP levels activates protein kinase A, leading to enhanced expression of several transcription factors including *c*AMP-*r*esponse *e*lement *b*inding protein (CREB), while inhibiting others such as nuclear factor kappa B (NF-κB). By inhibiting phosphodiesterase 4 and increasing intracellular cAMP levels, apremilast has multiple downstream effects: it decreases the production of inflammatory mediators such as TNF, IFN-γ, and interleukins (IL)-2, -12, and -23; it increases the production of anti-inflammatory mediators including IL-10; and it inhibits natural killer responses (Fig. 130.4)[10].

Dosages

The recommended dosage for psoriatic arthritis and psoriasis is 30 mg twice daily. In order to reduce gastrointestinal symptoms, an upward titration of the dose by 10 mg/day is recommended, starting with an initial dose of 10 mg/day. Apremilast is available in 10, 20, and 30 mg tablets. For individuals with severe renal impairment, the recommended maximum daily dose is 30 mg; there is no dosing adjustment for hepatic impairment.

Major Side Effects

The most common side effects are gastrointestinal, especially nausea and diarrhea, which are most evident during the first 15 days of administration and gradually resolve over several weeks. Headache and nasopharyngitis are additional potential side effects. Because depression, including suicidal ideation, can be observed in up to 1% of patients, patients with a history of depression should be monitored closely. Loss of ~5%–10% of body weight occurs in ~10% of patients. No laboratory monitoring is recommended, but serial measurements of weight can be considered.

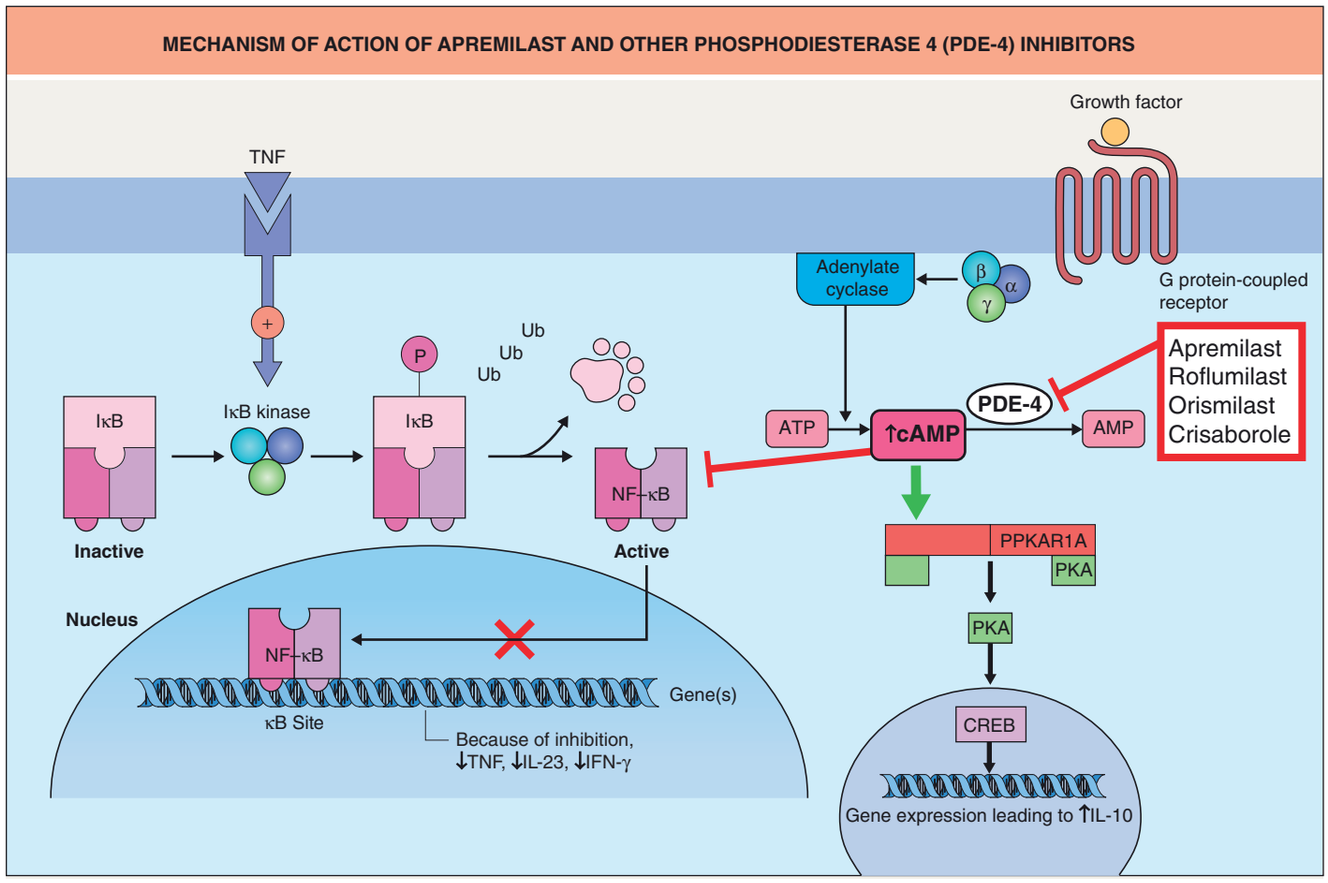


Fig. 130.4 Mechanism of action of apremilast and other phosphodiesterase 4 (PDE-4) inhibitors. Inhibition of phosphodiesterase 4 (PDE-4) results in increased intracellular cAMP levels. This leads to activation of protein kinase A (PKA), which in turn phosphorylates the transcription factor *c*AMP *r*esponse element *b*inding protein (CREB). Binding of CREB acts to increase the expression of anti-inflammatory mediators, e.g. interleukin (IL)-10. Increased intracellular cAMP levels also inhibit nuclear factor kappa B (NF-κB) leading to decreased expression of inflammatory mediators, e.g. tumor necrosis factor-alpha (TNF-α), IL-23, interferon-γ (IFN-γ). NEMO is another name for the gamma subunit of IκB kinase. ATP, adenosine triphosphate; α, α subunit of the stimulatory G protein; Ub, ubiquitin. *Adapted from Schafer P. Apremilast – mechanism of action and application to psoriasis and psoriatic arthritis. Biochem Pharmacol 2012;83:1583–90.*

Indications

Apremilast is FDA-approved for adult patients with active psoriatic arthritis and moderate to severe plaque psoriasis. The ESTEEM trial reported that a significantly greater proportion of patients receiving apremilast (30 mg BID) achieved Psoriasis Area and Severity Index (PASI)-75 (33.1%) and PASI-50 (58.7%) at week 16 compared with placebo (5.3% and 17.0%); quality of life measures and nail and scalp psoriasis were similarly improved[11,12]. It is also approved for the treatment of oral ulcers associated with Behçet disease and is currently being investigated for other inflammatory skin diseases including lichen planus, hidradenitis suppurativa, granulomatous dermatoses, discoid LE, and atopic dermatitis.

Contraindications

Apremilast is contraindicated in patients with known hypersensitivity to the drug or its components. Dosing should be adjusted for renal failure (see above). Relative contraindications include a history of depression or suicidal ideation.

Use in Pregnancy and Lactation

Because well-controlled studies of pregnant women receiving apremilast have not been conducted, incidences of malformations and fetal loss are currently not known. In studies in monkeys, administration of apremilast during organogenesis resulted in dose-related increases in abortion/embryo-fetal death at dose exposures of 2.1× MRHD (maximum recommended human therapeutic dose) and no adverse effects at exposure of 1.4×. Although it is not known whether apremilast or its metabolites are present in human milk, the drug was detected in the milk of lactating mice[1]. Fertility studies in male mice detected no adverse effects; in female mice, estrous cycles were prolonged (at higher doses) and those mice that became pregnant had an increased incidence of early postimplantation loss[1].

Drug Interactions

Coadministration of apremilast with potent CYP450 inducers including rifampin, phenobarbital, carbamazepine, and phenytoin may significantly diminish apremilast levels and should be avoided (see Ch. 131).

AZATHIOPRINE

Azathioprine was developed in 1959 from its parent drug 6-mercaptopurine (6-MP). After its anti-inflammatory and immunosuppressive effects were noted, dermatologists began to utilize azathioprine for the treatment of inflammatory diseases. With its moderately potent immunosuppressive and anti-inflammatory effects, azathioprine has a reasonable risk–benefit profile. However, it should be reserved for serious, life-threatening or recalcitrant dermatoses after other therapies have failed.

Azathioprine (Imuran®, Azasan®, Azamun™) has an 88% bioavailability. Immediately after absorption, it is converted to 6-MP and subsequently processed through three different, competing pathways (Fig. 130.5). When 6-MP is catabolized via two of these metabolic pathways, by either xanthine oxidase or thiopurine methyltransferase (TPMT), inactive metabolites result. Active metabolites, such as the purine analogue thioguanine monophosphate and others, are produced from the third and only anabolic pathway via hypoxanthine-guanine phosphoribosyl transferase (HGPRT)[13]. Should either the xanthine oxidase or TPMT catabolic pathway be blocked, more 6-MP will be shunted through the anabolic HGPRT pathway, leading to more active metabolites; excessive immunosuppression and pancytopenia may result[13].

The TPMT pathway is important because enzyme activity varies based upon genetic polymorphisms[14], and evaluating enzyme activity helps to guide dosing parameters. When TPMT activity within red blood cells (RBCs) is measured, which mirrors systemic activity, three subsets are identified – high, intermediate, and low activity (Table 130.6). Azathioprine should be avoided in patients with *low* activity because of the risk of accumulating metabolites which could increase the risk of severe myelosuppression. Underdosing is possible in those with *high* enzyme levels and the dosage may need to be titrated upwards. Although TPMT activity may vary somewhat between different laboratories and within different batches of the same test kit, knowledge of baseline TPMT activity is clinically useful in most patients.

Ethnic variations at the *TPMT* locus have also been described, with certain mutations unique to particular ethnic groups[14]. However, given the diversity of ethnicities, one should not profile a specific group as a means of predicting TPMT activity. Rather, the functional enzyme assay should be utilized prior to initiating azathioprine.

Although decreased xanthine oxidase activity is rarely due to genetic polymorphisms, this enzyme is inhibited by the medications allopurinol and febuxostat (see Fig. 130.5). Azathioprine dosage should be decreased by 75% in patients receiving allopurinol or febuxostat.

Mechanism of Action

6-Thioguanine, the active metabolite of azathioprine, is a purine analogue similar in structure to both adenine and guanine. Instead of an amino or hydroxyl group, it contains a thiol moiety. Incorporation of 6-thioguanine into DNA and RNA inhibits purine metabolism and cell division. 6-Thioguanine has other activities which are not well understood, such as suppression of T cell function and B cell antibody production[15]. It also decreases the number of Langerhans cells in the skin and inhibits their ability to present antigens[16].

Dosages

Available in 25, 50, 75, and 100 mg tablets, *empiric* dosing is generally started at 50 mg/day and increased to a maximum of 2.5 mg/kg/day according to clinical efficacy and careful monitoring. Maximum doses based on baseline TPMT determination are outlined in Table 130.6. In either case, renal insufficiency dictates dose reduction (see Table 130.3). Baseline evaluation should include a complete medication history because of adverse effects when azathioprine is used concomitantly with allopurinol, febuxostat, captopril, or warfarin (see below). Monitoring guidelines are outlined in Table 130.3.

Major Side Effects

Major side effects are related to the immunosuppressive effects of azathioprine (see Table 130.5). Pancytopenia occurs rarely, particularly when doses are based on TPMT activity. Patients may be at increased risk for malignancies, especially lymphoproliferative disorders and squamous cell carcinomas of the skin and female genitourinary tract, and should be monitored accordingly. Factors influencing a patient's malignancy risk include degree and duration of immunosuppression, skin phototype, and existing comorbidities.

Azathioprine may rarely cause a life-threatening hypersensitivity reaction. It most commonly develops during the first month of therapy and when there is concurrent use of either cyclosporine or methotrexate. The cutaneous eruption is typically morbilliform with areas of confluence. Other components of the syndrome include fever, respiratory and gastrointestinal distress, hepatotoxicity, and possible cardiovascular collapse. This hypersensitivity reaction represents an absolute contraindication as re-exposure may lead to cardiovascular collapse. Azathioprine can also induce the triad of pancreatitis, polyarthritis, and panniculitis, referred to as PPP syndrome.

Indications

Although azathioprine has FDA approval for non-dermatologic uses only, dermatologists have been using this drug for decades to treat severe dermatologic conditions, most often as a corticosteroid-sparing agent in the treatment of immunobullous diseases, chronic actinic dermatitis, and various subtypes of cutaneous vasculitis[15,17]. It is inexpensive and has moderate immunosuppressive and anti-inflammatory effects. Clinical benefit of the drug may not be apparent until it has been administered for at least 4 to 6 weeks.

DOSING OF AZATHIOPRINE AS DETERMINED BY BASELINE THIOPURINE METHYLTRANSFERASE (TPMT) ACTIVITY	
TPMT activity (U/ml)	**Maximum dose of azathioprine (AZA)**
Low: <6.3	AZA contraindicated
Intermediate: 6.3–15	Up to 1 mg/kg/day
High: 15.1–26.4	Up to 2–2.5 mg/kg/day

Table 130.6 Dosing of azathioprine as determined by baseline thiopurine methyltransferase (TPMT) activity. Doses are based upon *actual* weight. U, units. Adapted from reference 13.

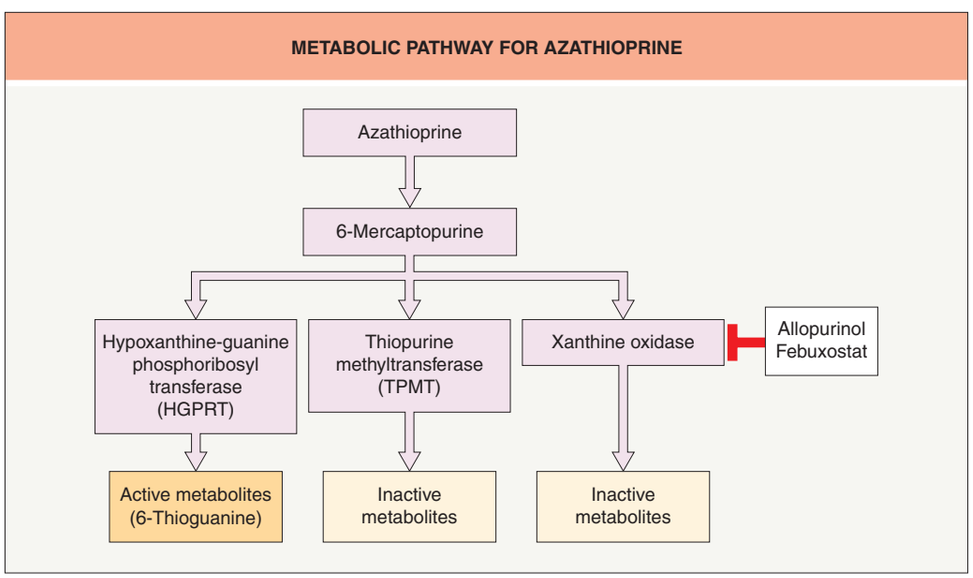


Fig. 130.5 Metabolic pathway for azathioprine. Either decreased activity of TPMT or inhibition of xanthine oxidase by allopurinol or febuxostat can lead to shunting of 6-mercaptopurine to the HGPRT pathway. As a result of this shunting, there is an increase in active metabolites and an increased risk of toxicity. Azathioprine dosage should be decreased by 75% in patients receiving allopurinol or febuxostat. *Adapted from Wolverton SE. Comprehensive Dermatologic Drug Therapy, 4th edn. Philadelphia: Saunders, 2020.*

Contraindications

Absolute contraindications to azathioprine therapy include history of a hypersensitivity reaction, as re-challenge may prove fatal. Active serious infections and pregnancy are relative contraindications. Concomitant use of allopurinol or febuxostat requires dose reduction of azathioprine (see above) or selection of an alternative medication.

Use in Pregnancy and Lactation

Azathioprine may be associated with preterm delivery, low-birth-weight infants, sporadic anomalies, and hematologic toxicities. Even though it is considered relatively safe for use in transplant patients who become pregnant, for dermatologic purposes it should not be prescribed during pregnancy. Azathioprine may be compatible with breastfeeding, but it is recommended that patients wait for four hours after medication ingestion to initiate breastfeeding and to monitor complete blood counts in breastfed infants. There is no recommendation for male patients to discontinue azathioprine when trying to conceive with their partner; data regarding effects on female fertility are limited[1].

Drug Interactions

Inhibition of xanthine oxidase by allopurinol or febuxostat (see Fig. 130.5) increases the risk of pancytopenia in azathioprine-treated patients. Captopril may increase the risk of leukopenia. Azathioprine can decrease the effectiveness of warfarin and pancuronium, necessitating larger doses of these drugs. Since azathioprine may decrease the effectiveness of intrauterine contraceptive devices, alternative birth control methods should be employed.

BLEOMYCIN

The dosage, uses, and side effects are outlined in Table 130.7.

CLOFAZIMINE

The dosage, uses, and side effects are outlined in Table 130.8.

COLCHICINE

The dosage, uses, and side effects are outlined in Table 130.9.

CYCLOPHOSPHAMIDE

Cyclophosphamide (Cytoxan®) was derived from mechlorethamine (nitrogen mustard) in 1958; the latter was combined with phosphoric acid in an effort to make an inert drug capable of entering and releasing active mechlorethamine within target cells[18]. It has ~75% oral bioavailability, peaks in the plasma at about 1 hour, and crosses the blood–brain barrier. Cyclophosphamide itself is inactive, but it is metabolized by CYP enzymes into the active metabolite 4-hydroxy-cyclophosphamide (nornitrogen mustard; $t_{1/2}$ = 3.3 hours), which may then be converted into the other active metabolite phosphoramide mustard ($t_{1/2}$ = 9 hours). Metabolites are excreted primarily via the kidney (50%). The inactive metabolite acrolein is believed to cause hemorrhagic cystitis and associated transitional cell carcinoma of the bladder[19].

BLEOMYCIN
Source: *Streptomyces verticillus* **Mechanism of action**: inhibits DNA synthesis in infected keratinocytes, but no direct effect on the human papillomavirus **Dermatologic use**: intralesional treatment of therapy-resistant verrucae vulgaris; 65%–80% of lesions clear after 1 to 2 injections **Dosage**: 0.1 to 0.3 ml of 1 U/ml (of saline) injected into targeted lesions, with maximum total dose per treatment = 2 ml; repeated every 3 to 6 weeks until resolution; given its rapid degradation and expense, newly constituted solution should be divided into glass vials and can be stored at 2–8°C for ~3 months **Side effects of intralesional administration**: injection is extremely painful (local or regional anesthesia may be required); pain and burning postinjection for 2–3 days; Raynaud phenomenon occasionally; nail dystrophy; flagellate dermatitis (above recommended total dose); no systemic toxicity with recommended total dose **Contraindications:** pregnancy, immunosuppression, vascular compromise **Pregnancy and lactation**: not recommended; formerly pregnancy prescribing category D

Table 130.7 Bleomycin. Case reports of its use for keloids, hypertrophic scars, keratinocyte carcinomas, and vascular tumors (e.g. hemangiomas).

Mechanism of Action

Cyclophosphamide is an alkylating agent that functions in a cell cycle-independent fashion. Although its major effect is suppression of B cell function, it also suppresses T cell function (especially of regulatory

CLOFAZIMINE
Drug properties: riminophenazine dye (red color) **Mechanism of action**: disrupts cell membranes (activation of phospholipase A_2 leads to generation of membrane-destabilizing lysophospholipids); enhances superoxide production; inhibits neutrophil motility and lymphocyte proliferation **Dermatologic use**: treatment of multibacillary Hansen disease (leprosy), other infections (mycobacterial, malacoplakia, rhinoscleroma), and inflammatory skin diseases including neutrophilic dermatoses (pyoderma gangrenosum, Sweet syndrome), granuloma faciale, orofacial granulomatosis, erythema dyschromicum perstans, and discoid LE **Dosage**: 50–400 mg orally daily*; avoid long-term administration of >200 mg daily; see Table 75.5 for leprosy regimens **Side effects**: discoloration of skin† (red to red–brown diffusely, bluish to violet–brown in lesional sites), cornea/conjunctiva, and body fluids (urine, sweat, tears); xerosis/ichthyosis; gastrointestinal symptoms (abdominal pain, nausea, vomiting, diarrhea); ocular irritation; elevated hepatic enzymes; crystal deposition-related enteropathy (rarely); cardiac arrhythmias (rarely; associated with electrolyte disturbances) **Monitoring guidelines**: baseline electrolyte panel; periodic LFTs if daily doses >100 mg; periodic evaluation for GI side effects and skin discoloration **Contraindications**: prior hypersensitivity reaction **Pregnancy and lactation**: for dermatologic disorders, should be avoided during pregnancy and lactation (concentrated in breast milk) *Larger doses are usually divided into two to four times daily. †Due to deposits of drug within fat and macrophages.

Table 130.8 Clofazimine. LE, lupus erythematosus; LFTs, liver function tests.

COLCHICINE
Source: alkaloid from *Colchicum autumnale* (autumn crocus) **Mechanism of action**: prevents microtubule assembly, resulting in mitotic arrest at metaphase and inhibition of cellular motility; decreases neutrophil chemotaxis, adhesion, and degranulation **Dermatologic use**: treatment of neutrophilic dermatoses (Behçet disease, Sweet syndrome), cutaneous small vessel vasculitis, neutrophil-rich autoimmune bullous diseases (EBA, linear IgA bullous dermatosis), and aphthous stomatitis **Dosage**: 0.5 or 0.6 mg orally two to three times daily; drug must be shielded from light (degraded by UVR) **Side effects**: commonly, gastrointestinal symptoms (diarrhea, abdominal pain, nausea, vomiting; dose-related); occasionally, alopecia, peripheral neuropathy, myopathy, and bone marrow suppression (with prolonged therapy*); multiorgan failure with acute overdose† **Monitoring guidelines**: baseline CBC, CMP, and UA; repeat CBC monthly for first several months then every 3–6 months **Contraindications**: prior hypersensitivity reaction; severe renal, hepatic, gastrointestinal, or cardiac disease; blood dyscrasias **Pregnancy and lactation**: for dermatologic disorders, should be avoided during pregnancy; excreted in breast milk, but use during lactation allowed per AAP recommendations *Particularly in patients with renal insufficiency. †A toxic epidermal necrolysis-like reaction has been described.

Table 130.9 Colchicine. In patients with renal or hepatic impairment on colchicine, P-glycoprotein and strong CYP3A4 inhibitors should be avoided. AAP, American Academy of Pediatrics; CBC, complete blood count with differential and platelet count; CMP, comprehensive metabolic panel (includes liver function tests); EBA, epidermolysis bullosa acquisita; UA, urinalysis; UVR, ultraviolet radiation.

T cells). Clearly, the T cell effects are greatest if the drug is given prior to antigen presentation. Cyclophosphamide crosses the nuclear membrane, covalently binds with DNA, and inhibits the synthesis of guanine, cytosine, and adenine. Cytotoxicity occurs by several mechanisms: (1) DNA cross-linking with various proteins or other DNA strands; (2) G-C → A-T substitution; and (3) depurination resulting in chain scission. These mechanisms can overwhelm the DNA repair mechanisms, inducing cell death[18].

Dosages

Cyclophosphamide is available in 25 and 50 mg tablets. Doses range from 1 to 3 mg/kg/day, either as a single morning dose or in equally divided doses. Dermatologic diseases seldom require more than 2 to 2.5 mg/kg/day of cyclophosphamide. Dose reduction is necessary in patients with hepatic or renal dysfunction. Because of the risk of hemorrhagic cystitis, patients should be advised to always consume plenty of fluids. A monthly intravenous infusion (pulse) of 500 to 1000 mg has been used to treat a number of rheumatologic disorders, including severe SLE. Nowadays, monthly IV administration is favored over chronic daily use because of a reduced risk of side effects including bladder toxicity.

Prior to prescribing cyclophosphamide, patients should have a documented white blood count (WBC) of >4500/mm^3 and a granulocyte count of >1500/mm^3. If the counts are lower and there is no alternative drug, then consultation with a hematologist is recommended. Laboratory monitoring guidelines are outlined in Table 130.3. Of note, it is not necessary to induce significant myelosuppression in order to achieve immunosuppression[19].

Major Side Effects

The most common side effects from cyclophosphamide treatment are hematologic and gastrointestinal (see Table 130.5). Dermatologic side effects include anagen effluvium (5%–30%, typically reversible), pigmented bands of the teeth (irreversible), diffuse cutaneous hyperpigmentation, transverse ridging and hyperpigmentation of nails, acral erythema, and, rarely, Stevens–Johnson syndrome. Up to 40% of patients have hemorrhagic cystitis, presumably from the acrolein metabolite, which is associated with a 10-fold increase in the risk for transitional cell carcinoma of the bladder. This risk is greater in patients who receive chronic "low-dose" cyclophosphamide (as traditionally given for dermatologic diseases) than in those exposed to brief courses of high-dose pulse therapy (as given for systemic lymphomas and SLE). Immunosuppression is significant, especially in patients concomitantly receiving systemic corticosteroid therapy. Infection and malignancy risks are real with appropriate monitoring recommended. Long-term or high-dose therapy may be associated with infertility in either sex[15].

Indications

Although cyclophosphamide is only FDA-approved for use in advanced mycosis fungoides and hematopoietic malignancies, it can be useful in treating a variety of severe cutaneous diseases. Cyclophosphamide has been regularly used to treat systemic vasculitides, in particular granulomatosis with polyangiitis and severe eosinophilic granulomatosis with polyangiitis, while it represents second-line therapy for polyarteritis nodosa and microscopic polyangiitis[19]. In the future, administration of rituximab or avacopan may lead to a reduction in its use for ANCA-related vasculitides. Cyclophosphamide can also be employed as a corticosteroid-sparing agent in a variety of severe mucocutaneous diseases or as monotherapy after corticosteroids are discontinued. In particular, cyclophosphamide plus corticosteroids can be used to treat mucous membrane (cicatricial) pemphigoid, especially when there is rapidly progressive or severe ocular involvement.

Contraindications

Absolute contraindications are pregnancy, lactation, depressed bone marrow function, and hypersensitivity to the drug. Cyclophosphamide-allergic patients may have cross-reactions with chlorambucil or mechlorethamine. Relative contraindications include active infections and significantly impaired hepatic or renal function.

Use in Pregnancy and Lactation

Cyclophosphamide is a first-trimester teratogen and is immunosuppressive in breastfed infants. It should not be used during pregnancy or lactation[9]. There is a high rate of permanent azoospermia; therefore cryopreservation of sperm may be necessary before treatment[1]. The risk of infertility in females is related to cumulative dose and patient age[1]; consultation with a reproductive endocrinologist prior to initiating therapy is recommended to discuss oocyte, embryo, and ovarian tissue cryopreservation.

Drug Interactions

Allopurinol, cimetidine, and chloramphenicol may elevate cyclophosphamide drug levels and produce toxicity (via CYP450 interactions), whereas barbiturates may enhance conversion to inactive metabolites. Digoxin absorption may be decreased. Cyclophosphamide may enhance the effect of succinylcholine, increase the cardiotoxicity of doxorubicin, and cause additive immunosuppressive and carcinogenic effects with other immunosuppressive drugs. Unpredictable effects can be seen when used with the inhalation anesthetics halothane and nitrous oxide.

CYCLOSPORINE

Cyclosporine, a cyclic peptide of 11 amino acids, was isolated from the soil fungus *Tolypocladium inflatum* in 1970 and was found to have clinical immunosuppressive effects in 1976. In 1979, during a rheumatoid arthritis trial, it was discovered that cyclosporine improved cutaneous psoriasis in patients with psoriatic arthritis. Two forms are available, the original preparation (Sandimmune®) and a predigested microemulsion (Neoral®) that is more completely and consistently absorbed. The latter is available as capsules (25 and 100 mg) or as an oral solution (100 mg/ml)[20]. The solution can be mixed in orange juice or apple juice, but grapefruit juice should be avoided because it alters cyclosporine's metabolism (see Fig. 131.4).

Bioavailability of the microemulsion is not known, but it yields 40%–106% higher peak blood levels than the original formulation. Cyclosporine is both metabolized by the CYP3A4 pathway and is a CYP3A4 inhibitor; primary excretion is via bile and feces. Only 6% of cyclosporine is excreted unchanged in the urine. Drug levels (11-hour trough level) can be measured but the therapeutic range is relatively wide; determinations are helpful when drug–drug interactions or non-compliance are a concern.

Mechanism of Action

T cell receptor activation causes release of intracellular calcium that in turn binds calmodulin and activates calcineurin (see Ch. 129). This calcineurin complex dephosphorylates the nuclear factor of activated T cells ($NFAT_c$) which is present within the cytoplasm, allowing it to migrate into the nucleus and bind with its intranuclear counterpart $NFAT_n$. This complex is a transcription factor for inflammatory cytokines such as IL-2. IL-2 receptors are also upregulated as a result of this process.

Cyclosporine binds to cyclophilin, a member of the family of intracytoplasmic proteins called immunophilins. This complex blocks the dephosphorylation of $NFAT_c$ and the subsequent upregulation of IL-2 and IL-2 receptors, resulting in a reduction of $CD4^+$ and $CD8^+$ (cytotoxic) T cells in the epidermis[15,20].

Dosages

Cyclosporine is best used on a short-term basis (<6–12 months) to control flares of psoriasis relatively quickly and to provide an alternative to the patient's current regimen (see Ch. 8). However, safety has been documented in psoriasis patients receiving therapy for up to 2 years[21]. It is reasonable to use cyclosporine as sequential therapy with acitretin, methotrexate, or other systemic agents such as systemic immunomodulators ("biologics"). After psoriasis clearance has been initiated by cyclosporine, the alternative medicine may be started and advanced to the therapeutic dose. At the same time, cyclosporine may be weaned by 1 mg/kg/day each month until the patient is maintained on the

alternate systemic agent. Historically, the maximum dermatologic dose for cyclosporine is 5 mg/kg/day, although a maximum dose of 4 mg/kg/day of the microemulsion formulation should be considered, given its greater bioavailability. The dose for obese patients is based on ideal body weight.

For psoriasis patients with a severe flare or recalcitrant disease, cyclosporine may be initiated at the maximum dosage until significant disease resolution occurs. The dose is then tapered by 1 mg/kg/day every 2 weeks until the minimum effective maintenance dose is determined. For most patients with more moderate disease, therapy should be initiated at 2.5 mg/kg/day and increased by 0.5 to 1 mg/kg/day every other week until clinical improvement is seen or a maximum dose of 4–5 mg/kg/day (depending upon the formulation) is reached. If no improvement is observed after 3 months at maximum dose, therapy has failed and should be discontinued[22,23].

Patients must be adequately monitored for the development of hypertension and laboratory abnormalities as outlined in Table 130.3. If the serum creatinine rises by >25% over baseline, the value should be rechecked within 2 weeks. If it returns to <25% over baseline, therapy can be continued at the current dose. However, if the elevation persists at that level, the dose should be decreased by 25%–50% for 1 month and then the serum creatinine rechecked. If it is still >25% above baseline, therapy should be discontinued until the serum creatinine is within 10% of the baseline value. At that time, restarting therapy may be considered, but at a significantly lower dose.

Major Side Effects

Cyclosporine is associated with a wide variety of adverse effects, including hypertension, renal dysfunction, hyperlipidemia, hyperkalemia, hyperuricemia, hypomagnesemia, hypertrichosis, and gingival hyperplasia (see Table 130.5). Most of the side effects associated with short-term therapy are reversible upon discontinuation of the drug. A quarter of all psoriasis patients on cyclosporine will develop hypertension, which is usually mild and manageable; calcium channel blockers of the dihydropyridine class are the recommended first-line antihypertensive agents. A direct vasoconstrictive effect of cyclosporine on the kidney vasculature is responsible for the development of hypertension short-term[24]. Hypertension due to cyclosporine is both time- and dose-related.

Modern, conservative dosing guidelines have prevented significant kidney damage in the vast majority of patients on short-term therapy. However, renal interstitial fibrosis has been demonstrated histologically even in the absence of abnormal laboratory tests in patients on appropriate dosing and monitoring regimens. Renal biopsy specimens from patients on long-term treatment demonstrate irreversible changes including renal tubular atrophy, arteriolar hyalinosis, glomerular obsolescence, and interstitial fibrosis[25,26]. In fact, all patients on cyclosporine for >2 years were shown to have some of these abnormalities.

Although transplant recipients on high doses and prolonged courses of cyclosporine have an increased risk of certain malignancies (e.g. lymphoma, cutaneous squamous cell carcinoma), patients with skin diseases on cyclosporine for less than 2 years and on lower "dermatologic" doses have not been observed to have a similar risk.

Indications

Cyclosporine can be beneficial for patients with psoriasis who have failed or cannot tolerate other therapies and for those with widespread, inflammatory disease. In fact, cyclosporine has FDA approval for three "types" of psoriasis: (1) severe; (2) recalcitrant; and (3) disabling. Patients with plaque-type psoriasis may also benefit from cyclosporine in rotating or sequential regimens with other modalities.

The use of cyclosporine in atopic dermatitis has been examined, and a high percentage of patients improve with therapy; unfortunately, most relapse within 4 weeks of discontinuation. Cyclosporine efficacy has been established in patients with severe pyoderma gangrenosum; however, some clinicians prefer cyclosporine for idiopathic pyoderma gangrenosum only, arguing that when there is a known underlying cause, therapy is best aimed at the latter (e.g. inflammatory bowel disease, myelodysplasia). Very short-term cyclosporine has been used for Stevens–Johnson syndrome and toxic epidermal necrolysis as well as other severe cutaneous adverse reactions such as DRESS (drug reaction with eosinophilia and systemic symptoms) and AGEP (acute generalized exanthematous pustulosis) with promising results[27]. Most other uses of cyclosporine are based upon anecdotal evidence[28].

Contraindications

Absolute contraindications include significant renal impairment, uncontrolled hypertension, and hypersensitivity to cyclosporine. Relative contraindications include age <18 years or >64 years, controlled hypertension, and medication usage that may interfere with cyclosporine metabolism or worsen renal function. Caution is necessary if used in patients with significant infections, recent live-virus vaccinations (see Table 128.9) or immunodeficiency syndromes, or in combination with methotrexate, phototherapy, or other immunosuppressive drugs.

Use in Pregnancy and Lactation

Cyclosporine is not associated with an increased risk of major fetal malformations when compared to the general population[1]. Use during pregnancy should be considered only in exceptional patients for whom the potential benefits dramatically outweigh the risks, with close monitoring of maternal blood pressure and renal function[1]. Cyclosporine is excreted into breast milk and should not be used during lactation, due to risks of immunosuppression and possible carcinogenesis in the breastfed infant[9]. There is no recommendation for male patients to discontinue cyclosporine while trying to conceive with their partner and limited data are available regarding impact on female fertility[1].

Drug Interactions

Drugs that interact with cyclosporine are discussed in Chapter 131. The clinician should review the patient's medication list for potential interactions using the following guidelines. In general, drugs that inhibit the CYP3A4 pathway will increase cyclosporine levels, while inducers of the 3A4 pathway will decrease the effectiveness of cyclosporine, due to lower serum levels. Some drugs will potentiate renal toxicity, such as nonsteroidal anti-inflammatory drugs (NSAIDs), aminoglycosides, amphotericin B, and miscellaneous antibiotics (vancomycin, trimethoprim–sulfamethoxazole). Cyclosporine will reduce the renal clearance of digoxin, lovastatin, and prednisolone. Increased risk of hyperkalemia occurs with concurrent use of angiotensin-converting enzyme (ACE) inhibitors, potassium supplements, and potassium-sparing diuretics.

DAPSONE

Dapsone is a sulfone drug, and sulfones are related to the sulfonamide family. Sulfonamides were initially derived from coal tar in the early 1900s for use as fabric dyes. Medically, they were first demonstrated to be effective against streptococcal infections. Synthesized in 1908, dapsone was shown to be effective against tuberculosis and Hansen disease (leprosy). During the first half of the twentieth century, the related drugs sulfapyridine and sulfoxone were used to treat dermatitis herpetiformis (DH). However, since 1953, dapsone (the parent compound of sulfoxone) has been the mainstay of treatment for DH. Due to its activity in neutrophil-mediated dermatoses, dapsone has also proven useful in the treatment of several forms of autoimmune bullous diseases and vasculitis syndromes.

Dapsone is 80% orally bioavailable, peaks in the serum between 2 and 6 hours post-administration and has a half-life of 24–30 hours. Being highly lipophilic, it has excellent cell penetration. Dapsone and its major metabolite monoacetyldapsone are strongly protein-bound and undergo enterohepatic recirculation. Thus, dapsone may be found in the bloodstream up to 1 month following a single dose[29].

Dapsone is metabolized by *N*-acetylation and *N*-hydroxylation in the liver[29,30]. Acetylation yields monoacetyldapsone, which is then de-acetylated to dapsone, yielding an equilibrium between dapsone and monoacetyldapsone. Hydroxylation via CYP enzymes produces *N*-hydroxy-dapsone, the metabolite which is believed to be responsible for the majority of dapsone side effects. Both dapsone and *N*-hydroxy-dapsone undergo glucuronidation in the liver, which results in more water-soluble compounds that are rapidly excreted in the urine[29].

Mechanism of Action

Dapsone is clinically most useful in the treatment of dermatologic diseases involving neutrophilic infiltrates. Researchers have demonstrated that dapsone inhibits neutrophil myeloperoxidase, thus reducing damage from the neutrophil respiratory burst mediated by this enzyme. Furthermore, dapsone has been shown to inhibit neutrophil chemotaxis to *N*-formyl-methionyl-leucyl-phenylalanine (fMLP) and to interfere with the CD11b/CD18-mediated neutrophil binding that induces chemoattractant signal transduction. IgA adherence is also inhibited. It is of clinical interest that dapsone also inhibits eosinophil myeloperoxidase activity, and thus may be efficacious in diseases in which eosinophils have a central role in pathogenesis, such as eosinophilic cellulitis[30].

Dosages

Dapsone is available in 25 and 100 mg tablets. The initial dose is often 50 mg/day in a single dose. Most conditions require 50–200 mg/day for adequate control of symptoms; rarely are dosages up to 300 mg/day required. In those with DH who respond to dapsone, rapid resolution of symptoms (within 48 hours) is usually noted; conversely, symptoms flare relatively rapidly after discontinuing therapy. Patients must be strictly warned against self-adjustment of the dosage, due to dose-dependent side effects.

Because of potential adverse effects, any cardiopulmonary or neurologic symptoms should be assessed prior to therapy. Documentation of peripheral motor nerve function may occasionally be necessary before or during therapy. Table 130.3 outlines monitoring guidelines for therapy. The clinician must be aware of all signs and symptoms associated with methemoglobinemia and peripheral neuropathy to ensure proper monitoring.

Major Side Effects

Serious systemic side effects of dapsone may be idiosyncratic or pharmacologic. The pharmacologic and dose-dependent adverse effects include methemoglobinemia and hemolytic anemia (see Table 130.5). Agranulocytosis, peripheral motor neuropathy, and dapsone hypersensitivity are idiosyncratic reactions; however, patients on higher daily doses or long-term therapy may be more likely to develop a peripheral motor neuropathy. Although rare, dapsone hypersensitivity syndrome may be fatal. Patients present with fever, hepatitis, and a generalized cutaneous eruption. Cutaneous reactions range from an exanthematous eruption to toxic epidermal necrolysis (TEN). Liver failure has occurred in patients with the dapsone hypersensitivity syndrome[31], and hypothyroidism may develop following resolution of the acute eruption. Thus, there is significant overlap with DRESS/DIHS (drug reaction with eosinophilia and systemic symptoms/drug-induced hypersensitivity syndrome). In particular, HLA-B*13:01 has been associated with dapsone-related DRESS in Chinese populations and its incidence can be reduced via screening prior to therapy[32].

Indications

Dapsone works well in a number of neutrophilic dermatoses and immunobullous diseases. Although only FDA-approved for DH, dapsone is very useful in linear IgA bullous dermatosis, bullous eruption of SLE, erythema elevatum diutinum, mucous membrane (cicatricial) pemphigoid, and perhaps cutaneous small vessel vasculitis[29,30]. It is also a key component of combination therapy for Hansen disease.

Contraindications

The absolute contraindication to dapsone therapy is prior hypersensitivity to dapsone. Relative contraindications include a low glucose-6-phosphate dehydrogenase (G6PD) level, significant cardiopulmonary disease, and allergy to sulfonamide antibiotics (because of possible cross-reactivity). In patients with low G6PD levels, there is an increased risk for oxidative stress of the dapsone metabolites on RBCs. Those with significant cardiopulmonary disease may not tolerate the methemoglobinemia and hemolysis induced by dapsone.

Use in Pregnancy and Lactation

Dapsone does not appear to present a major risk to the fetus; however, it should only be used during pregnancy if the benefits clearly outweigh the risks. There have been publications reporting its use in pregnant patients with Hansen disease. Dapsone is found in breast milk and can cause hemolytic anemia in breastfed infants; however, it is approved by the American Academy of Pediatrics for use during lactation when required, as in patients with Hansen disease[9].

Drug Interactions

Drugs that may increase dapsone levels (and side effects) are probenecid (via decreased renal clearance), trimethoprim, and other folate antagonists such as methotrexate. Sulfonamides and hydroxychloroquine increase the oxidative stress on RBCs and may worsen hemolysis. Dapsone levels may be reduced by activated charcoal, para-aminobenzoic acid (PABA), and rifampin. Although cimetidine can increase absolute levels of dapsone, the former leads to a reduction in the more toxic hydroxylamine metabolite, and thus the end result is a lower level of methemoglobin.

HYDROXYUREA

The dosage, uses, and side effects are outlined in Table 130.10.

LEUKOTRIENE (LT) INHIBITORS

Initially identified as the slow-reacting substance of anaphylaxis, leukotrienes play a key role in systemic and cutaneous inflammatory reactions[33]. Primarily used for the treatment of asthma, leukotriene inhibitors have been explored in a myriad of dermatologic conditions, including atopic dermatitis, urticaria, autoimmune bullous diseases, and Sjögren–Larsson syndrome[33]. These inhibitors include montelukast

HYDROXYUREA
Formulation: Hydrea®; 100% bioavailable; renal excretion: 80%; accumulates preferentially in leukocytes > erythrocytes; can cross blood–brain barrier
Mechanism of action: inhibits M_2 subunit of ribonucleotide reductase thereby blocking DNA synthesis; cells are arrested in G_2 phase and unable to repair UV- and ionizing radiation-induced damage; also causes gene hypomethylation, inducing differentiation and normalization of psoriatic skin; resistance may arise via increased levels of ribonucleotide reductase or alteration of the enzyme
Dermatologic use: maintenance therapy of psoriasis after control with another drug or phototherapy, but ineffective in psoriatic arthritis; lymphocytic hypereosinophilic syndrome unresponsive to corticosteroids
Dosage: 20–30 mg/kg/day in divided doses, with a maximum of 2 g/day; average dose: 1–2 g/day
Side effects: megaloblastosis (all patients), with 10%–35% developing anemia (see Table 130.5); rarely, leukopenia, thrombocytopenia, or transient reversible hepatitis with an acute "flu-like" syndrome; ulcers of the distal lower extremity (Fig. 130.6A); diffuse cutaneous hyperpigmentation and mucosal pigmentation (Fig. 130.6B); dermatomyositis-like eruption on dorsal hands, keratinocyte carcinomas
Monitoring guidelines: baseline CBC, CMP, UA, and pregnancy test for women of childbearing potential then CBC weekly until stable and then monthly; CMP and UA monthly until stable then every 3–6 months; a drop in HGB of 1–2 g should be expected; discontinue hydroxyurea if: HGB declines by more than 3 g, WBC drops to <3500–4000 cell/mm^3, or PLT to <100 000/mm^3
Contraindications: *absolute* – hypersensitivity to drug; *relative* – blood dyscrasias; infections; cardiac, renal, or pulmonary disease; unstable/fulminant psoriasis; concomitant use of cytarabine
Pregnancy and lactation: known teratogen; not to be used during pregnancy or lactation. Potentially irreversible decreased sperm motility and spermatogenesis in male fertility studies; limited data on impact on female fertility[1]

Table 130.10 Hydroxyurea. CBC, complete blood count with differential and platelet count; CMP, comprehensive metabolic panel (includes liver function tests); HGB, hemoglobin; UA, urinalysis; WBC, white blood count.



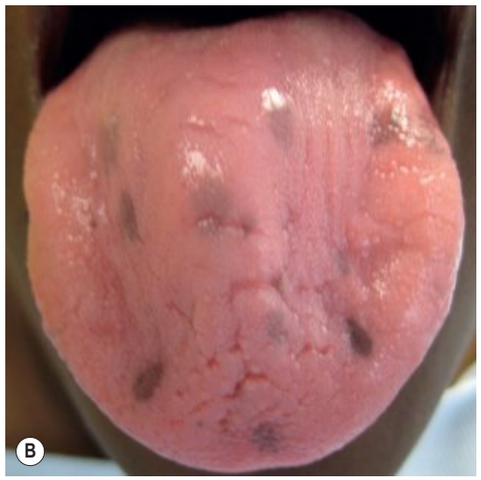


Fig. 130.6 Hydroxyurea-induced mucocutaneous changes. A Lower extremity ulcerations. **B** Hyperpigmentation of the oral mucosa. *B, Courtesy Brian Horvath, MD.*

(Singulair®), zafirlukast (Accolate®), and pranlukast (Ultair®), which block LTC_4, LTD_4 and LTE_4, as well as zileuton (Zyflo CR®) which inhibits 5-lipoxygenase (Table 130.11)[33].

LEUKOTRIENE INHIBITORS
Mechanisms of action: antagonists of cysteinyl leukotriene receptors (block LTC_4, LTD_4 & LTE_4 binding) – montelukast (Singulair®), pranlukast (Ultair®), zafirlukast (Accolate®); inhibitor of 5-lipoxygenase – zileuton (Zyflo CR®)
Dermatologic uses: limited evidence for atopic dermatitis, autoimmune bullous diseases, urticaria, Sjögren–Larsson syndrome; primary use is asthma
Dosages*: montelukast – 10 mg [adults], 5 mg [children 6–14 years]; pranlukast – 225 mg BID [adults], 7 mg/kg/day [children]; zafirlukast – 20 mg BID [adults & adolescents], 10 mg BID [5–12 years] on empty stomach; zileuton – 1200 mg BID [adults & adolescents] with meals
Side effects: indigestion, nausea, myalgias, headaches, hepatitis; montelukast, pranlukast, and zafirlukast have been associated with the development of eosinophilia and eosinophilic granulomatosis with polyangiitis (Churg–Strauss syndrome), usually in the setting of a taper of corticosteroids
Contraindications: prior hypersensitivity reaction to drug; significant liver disease
Monitoring guidelines: zafirlukast – LFTs every 2–3 months; zileuton – baseline LFTs, monthly LFTs for 2–3 months and then every 2–3 months
Pregnancy and lactation: montelukast and zafirlukast most likely compatible; zileuton limited data so harm cannot be assessed
Drug interactions: zileuton may increase circulating levels of propranolol, theophylline, terfenadine, or warfarin; zafirlukast may increase circulating levels of warfarin; aspirin or erythromycin may decrease plasma level of zafirlukast; phenobarbital may reduce levels of montelukast
*Oral.

Table 130.11 Leukotriene inhibitors. LFTs, liver function tests.

METHOTREXATE

The effectiveness of the folic acid analogue methotrexate (MTX) in psoriasis was noted in the early 1950s, but remained without FDA approval until the 1960s. MTX is not difficult to use and oral administration achieves reliable blood levels unaffected by food intake. MTX is widely distributed throughout the body but penetrates the blood–brain barrier poorly.

Within 1 hour of ingestion, distribution and active cellular uptake is complete. Plasma MTX is 50% protein-bound, and irreversibly bound to dihydrofolate reductase, the enzyme it inhibits. By 4 hours, the kidneys have excreted the plasma portion of the drug[34]. Over the next 10–27 hours, the drug is slowly released from body tissues.

Mechanism of Action

Dihydrofolate reductase (DHFR) converts dihydrofolate to tetrahydrofolate (fully reduced folic acid; see Fig. 127.6), which is a necessary cofactor in the synthesis of thymidylate and purine nucleotides, which, in turn, are required for DNA/RNA synthesis. MTX competitively inhibits DHFR, although this inhibition can be at least partially reduced by concomitant folic acid administration. MTX also exerts partially reversible inhibition downstream on thymidylate synthetase, inhibiting cell division during the S phase[15].

Although originally believed to suppress keratinocyte proliferation, it is more likely that MTX inhibits DNA synthesis in immunologically active cells. MTX decreases inflammation through other mechanisms as well. For example, by inhibiting aminoimidocarboxyamido-ribonucleotide transformylase, MTX increases local tissue concentrations of the potent anti-inflammatory mediator adenosine. By inhibiting methionine synthase, MTX reduces production of the proinflammatory mediator S-adenyl methionine[35].

Dosages

MTX is administered as a once-weekly dose of up to 30 mg for dermatologic and rheumatologic diseases. Oncologists may prescribe 20–40 mg/m^2 every 1 to 4 weeks with folinic acid rescue. Historically, MTX was administered in three doses over 24 hours (8 a.m. and 8 p.m. day 1, and 8 a.m. day 2). There were theoretical advantages for the divided dosing regimen from a cell cycle kinetics standpoint. However, since the clinical result is the same, a single dose, which is easier and less confusing (for the patient and the pharmacist), is currently recommended. The patient should be admonished to adhere to the dosing schedule religiously, as more frequent dosing is much more likely to produce major hematologic complications and potentially an increased risk of liver fibrosis. Because absorption of oral MTX in doses >15 mg may be impaired, the weekly dose can be split into two administrations in patients requiring higher doses. Parenteral administration (intramuscular or subcutaneous) is available for patients who cannot tolerate oral MTX and has also been advocated by some clinicians for use in erythrodermic patients who may have decreased gastrointestinal absorption or when compliance is an issue. Also, in addition to a lower incidence of gastrointestinal side effects, subcutaneous MTX may be more efficacious. Use of intralesional MTX is reviewed in Chapter 108.

Available in 2.5 mg tablets, therapy may begin with a test dose of 2.5–5 mg followed one week later by a CBC with platelet count and hepatic profile. This test dose may be considered in higher risk patients (e.g. reduced renal function, hyperlipidemia, potential drug–drug interactions)[36]. In low-risk patients, treatment may be started at 10 to 15 mg weekly and gradually increased by 2.5 to 5 mg every 2–4 weeks until satisfactory results are obtained with minimal toxicity. For parenteral administration, both prefilled syringes (7.5, 10, 15, 20, 25 mg) and a 2 ml vial (25 mg/ml) are available.

Laboratory monitoring – CBC with platelet count and hepatic profile – can be done 1–3 weeks after initiation and following each dose escalation (see Table 130.3). Once disease control has been attained for at least 1–2 months, the MTX can be tapered by 2.5 mg every 1–2 weeks to the lowest dose that still maintains disease control. The usual weekly dose for psoriasis is 10–15 mg, although doses up to 25 mg per week are not uncommonly used, except in patients with renal insufficiency.

RISK FACTORS FOR DEVELOPING HEPATIC TOXICITY FROM METHOTREXATE
• Persistent abnormal liver function tests
• History of liver disease, including chronic hepatitis B or C viral infections
• Previous or concurrent excessive alcohol intake
• Family history of inheritable liver disease
• Diabetes mellitus
• Obesity
• Hyperlipidemia
• History of significant exposure to hepatotoxic drugs or chemicals
• Lack of folate supplementation

Table 130.12 Risk factors for developing hepatic toxicity from methotrexate. Adapted from reference 33.

Major Side Effects

The most important side effects of MTX include pancytopenia and hepatotoxicity (see Table 130.5). Pancytopenia typically develops early, compared to hepatic fibrosis and cirrhosis, which may take years to develop and are related to higher cumulative doses. Risk factors for hepatotoxicity are well established (Table 130.12). Before prescribing MTX, references discussing this issue in detail should be reviewed[34] and consultation with a hepatologist considered for patients with risk factors.

While the gold standard for detection of hepatic fibrosis remains liver biopsy, this invasive procedure harbors risks and is no longer routinely performed prior to initiating MTX (see Table 130.3). Both a panel of serum biomarkers and imaging studies can be performed to assess liver fibrosis (Table 130.13)[36,38]. Screening algorithms for assessing methotrexate hepatotoxicity have also been developed (Fig. 130.7) and take into account whether patients have risk factors for hepatotoxicity (see Table 130.12).

Photosensitivity may occur with MTX and patients should take appropriate sun precautions (see Ch. 21)[15]. Gastrointestinal intolerance is often abated with concomitant folic acid therapy (1–5 mg orally daily, based on symptoms). Other MTX-induced side effects include accelerated rheumatoid (cutaneous) nodulosis and reversible lymphoproliferative disorders. When used in very high doses, MTX may cause reversible oligospermia[34].

Drug Indications

MTX has FDA approval for use in psoriasis; however, it is used primarily for those individuals with severe, debilitating, or recalcitrant disease. Other disorders that respond to MTX include dermatomyositis and lymphomatoid papulosis. Of note, pityriasis rubra pilaris commonly requires up to twice the typical psoriasis dose, whereas PLEVA often responds to small MTX doses (2.5–5 mg/week). Methotrexate can also be used as a "steroid-sparing" agent, and in the elderly, monotherapy with weekly MTX is an option for the treatment of bullous pemphigoid.

Contraindications

Absolute contraindications to MTX are pregnancy and lactation. Relative contraindications include significant liver disease, elevated liver enzymes, and excessive alcohol intake. The presence of active infection or immunodeficiency, and the desire for imminent pregnancy are relative contraindications to MTX therapy. Caution is indicated and significant dose reduction necessary if used in patients with decreased renal function. In the elderly, serum creatinine levels may be deceptively low and not reflect true renal function.

Use in Pregnancy and Lactation

MTX is an abortifacient and teratogen and should not be used during pregnancy. The American Academy of Pediatrics considers MTX to be contraindicated in breastfeeding owing to concerns of immune suppression, growth retardation, and carcinogenesis[9]. Both female and male patients should discontinue MTX for at least three months before attempting to conceive[1].

SELECTED METHODS OF MONITORING FOR HEPATIC FIBROSIS	
Biochemical markers (+/– age, sex)	
Benefits: only requires serum sample; good inter-laboratory reproducibility	
Limitations: most panels primarily validated for hepatitis B or C viral infections, alcoholic liver disease, and/or NASH; interpretation of results may require critical analysis to avoid false positives or negatives (e.g. Gilbert disease, chronic hemolysis)	
Test	**Methodology**
FibroTest™*	Measurement of α_2-macroglobulin, haptoglobin, apolipoprotein A_1, GGT, and total bilirubin; computational formula includes age and sex
FibroSure™*	Measurement of α_2-macroglobulin, haptoglobin, apolipoprotein A_1, ALT, AST, GGT, total bilirubin, cholesterol, TTG, and glucose; formula includes age, sex, height, and weight
FibroMeter™*	Measurement of α_2-macroglobulin, ALT, AST, GGT, prothrombin index, urea, and platelet count; formula includes age and sex
Fibrosis-4 (Fib-4) index	Measurement of ALT, AST, and platelet count; formula includes age
PROMETHEUS® Fibrospect II®	Measurement of α_2-macroglobulin, hyaluronic acid, and TIMP-1
Type III procollagen peptide (PIIINP)†	Serum marker of collagen turnover, but active PSA may falsely elevate level
Imaging	
Vibration-controlled transient elastography (VCTE; FibroScan®)	• Assesses liver stiffness by measuring low-frequency elastic shear waves propagating through the liver • Validated bedside test with high sensitivity and high negative predictive value for liver fibrosis and good reproducibility • Less reliable in patients with higher BMI (≥30–40)
Magnetic resonance elastography	• Modified-contrast method to image the propagation characteristics of shear waves in the entire liver • Can be used in obese patients or patients with ascites, but more costly than VCTE
Liver biopsy	• Histopathologic assessment of degree of fibrosis, but there can be sampling error • More costly invasive procedure with risk of hemorrhage; risk percutaneous > transjugular • Considered gold standard
*Tests available in major commercial laboratories in US. †Not commercially available in US.	

Table 130.13 Methods of monitoring for hepatic fibrosis. If liver function tests, biochemical markers, or imaging assays indicate abnormalities, consultation with a gastroenterologist is recommended. ALT, alanine aminotransferase; AST, aspartate aminotransferase; BMI, body mass index; GGT, γ-glutamyl transpeptidase; NASH, nonalcoholic steatohepatitis; PIIIP N-P, amino-terminal propeptide of type III procollagen; PSA, psoriatic arthritis; TIMP-1, tissue inhibitor of metalloproteinase 1; TTG, triglycerides. Adapted from references 36 and 37.

Drug Interactions

Drugs that elevate MTX blood levels include NSAIDs, salicylates, sulfonamides, chloramphenicol, phenothiazines, phenytoin, and tetracyclines. Dipyridamole and probenecid increase intracellular accumulation of MTX. Trimethoprim, sulfonamides, and dapsone also inhibit the folate metabolic pathway (see Ch. 127) and markedly increase the risk for pancytopenia with concomitant use. However, the combination of MTX with reduced doses of trimethoprim–sulfamethoxazole used for *Pneumocystis jirovecii* pneumonia (PCP) prophylaxis was reported to be well tolerated[39]. Systemic retinoids and alcohol may cause synergistic liver damage in combination with MTX.

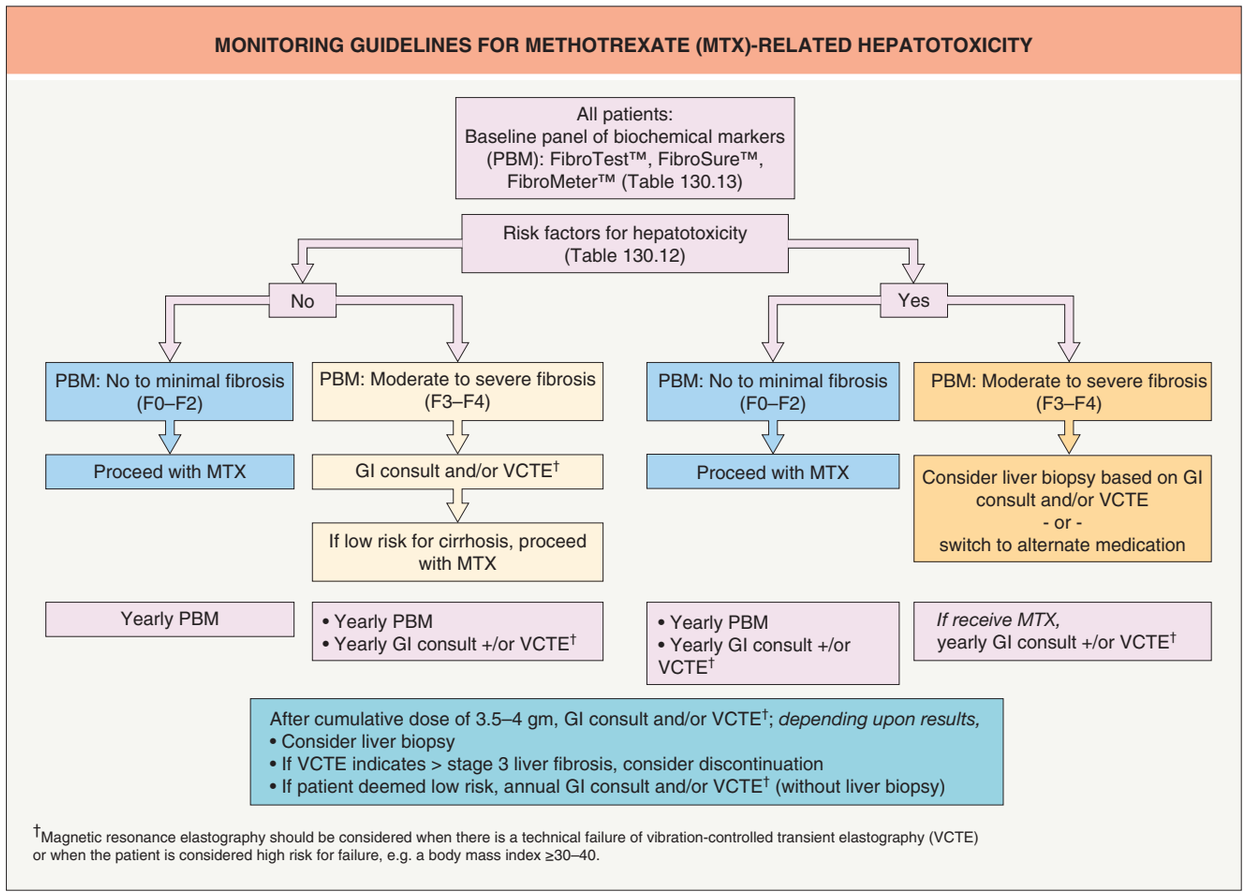


Fig. 130.7 Monitoring guidelines for methotrexate-related hepatotoxicity. GI, gastroenterology; VCTE, vibration-controlled transient elastography. *Adapted from Menter A, Gelfand JM, Connor C, et al. Joint American Academy of Dermatology-National Psoriasis Foundation guidelines of care for the management of psoriasis with systemic nonbiologic therapies. J Am Acad Dermatol 2020;82:1445–86.*

MYCOPHENOLATE MOFETIL AND MYCOPHENOLATE SODIUM

Mycophenolic acid (MPA) was used to treat various forms of psoriasis beginning in the 1970s. Its use declined steadily until the early 1990s, when a more bioavailable and safer formulation, mycophenolate mofetil (CellCept®), became commercially available. Initially inactivated during first-pass glucuronidation in the liver (into the phenolic glucuronide of MPA, MPAG), MPA is then reactivated in the epidermis and gastrointestinal tract by β-glucuronidase (see Fig. 131.1). Mycophenolate mofetil has greater bioavailability than MPA, undergoes complete presystemic conversion to MPA after ingestion, and then follows the same inactivation/activation cycle[40]. Mycophenolate mofetil is 94% bioavailable. MPA is 97% and MPAG 82% albumin-bound. Over 90% of the drug is excreted in the urine, mainly as MPAG. Renal insufficiency can increase plasma concentrations up to sixfold[19]. Enrollment in the REMS program for MPA preparations (see Introduction) is recommended but not yet FDA-mandated. It provides education on pregnancy planning and prevention (www.mycophenolaterems.com).

Mechanism of Action

MPA selectively and non-competitively inhibits the enzyme inosine monophosphate dehydrogenase (IMPDH), preventing conversion of inosine- and xanthine-5-phosphate to guanosine-5-phosphate. This blocks *de novo* synthesis of guanine nucleotides and their subsequent incorporation into DNA (Fig. 130.8). DNA synthesis in T and B lymphocytes is preferentially inhibited because these cells lack the purine salvage pathway and are dependent on *de novo* purine synthesis. MPA decreases immunoglobulin levels and delayed-type hypersensitivity responses by inhibiting proliferative responses to mitogenic and allospecific stimulation; MPA also suppresses antibody formation by B lymphocytes.

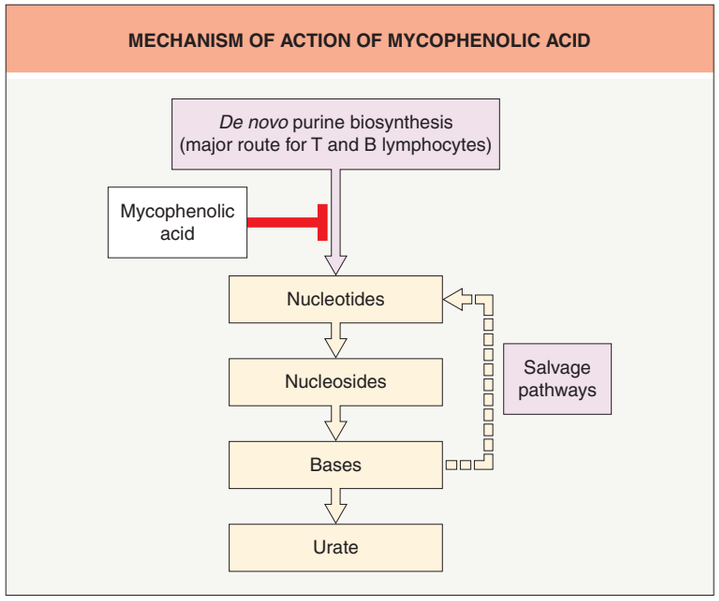


Fig. 130.8 Mechanism of action of mycophenolic acid. While most nucleated cells utilize salvage pathways, T and B lymphocytes must rely primarily on the *de novo* pathway for purine biosynthesis. Mycophenolic acid, the active drug form of the prodrug mycophenolate mofetil, inhibits inosine monophosphate dehydrogenase, an enzyme in the *de novo* pathway of purine biosynthesis. *Adapted from Wolverton SE. Comprehensive Dermatologic Drug Therapy, 4th edn. Philadelphia: Saunders, 2020.*

Dosages

Mycophenolate mofetil (CellCept®) is available in 250 mg capsules, 500 mg tablets, and a 200 mg/ml solution. For dermatologic diseases, best results are obtained with doses of 2000–3000 mg daily, in divided doses.

A newer enteric-coated formulation, mycophenolate sodium (Myfortic®), is also available in 360 mg and 720 mg tablets. Therapeutic equivalence has been documented by comparing enteric-coated mycophenolate sodium (720 mg twice daily) with mycophenolate mofetil (1000 mg twice daily).

Major Side Effects

The most common side effects of mycophenolate mofetil are gastrointestinal, including nausea, vomiting, diarrhea, abdominal cramps, and tenderness (see Table 130.5). Cutaneous side effects are rare. Significant hematologic and hepatic toxicity occur uncommonly. In 2008, the FDA released a safety report regarding a potential association (in transplant patients) between mycophenolate mofetil and the development of progressive multifocal leukoencephalopathy. Although rare, and cause-and-effect remains speculative, patients should be monitored accordingly[41]. Monitoring guidelines are outlined in Table 130.3. For a WBC <3500–4000 cells/mm^3, the dosage should be reduced or therapy discontinued[40].

Indications

Mycophenolate mofetil is currently FDA-approved for renal allograft rejection only. However, it is quite useful in the treatment of autoimmune bullous diseases, severe forms of atopic dermatitis, cutaneous LE, dermatomyositis, and refractory pyoderma gangrenosum. Mycophenolate mofetil is generally used in conjunction with other immunosuppressive drugs, most commonly as a "steroid-sparing" agent.

Contraindications

Absolute contraindications to mycophenolate mofetil use are pregnancy and allergy to MPA. Relative contraindications include lactation, as MPA is partially excreted in breast milk. Peptic ulcer disease and hepatic, renal, or cardiopulmonary disease are also relative contraindications. As noted previously, renal insufficiency can increase plasma concentrations up to sixfold[19].

Use in Pregnancy and Lactation

Human data suggest that mycophenolate mofetil may cause birth defects, with a characteristic phenotype of cleft lip and palate, microtia with atresia of the external auditory canal, micrognathia, and hypertelorism[42]. Additional data suggest that defect severity may be dependent on dose and duration of therapy as well as timing during pregnancy[43]. Based on the MPA REMS, a pregnancy test must be done immediately before starting an MPA preparation as well as 8–10 days later and at routine follow-up visits. Mycophenolate mofetil is contraindicated during lactation, due to potential immunosuppression. Due to the risk of teratogenicity, male and female patients are advised to discontinue the medication for three months and six weeks, respectively, before attempting to conceive. There are limited data regarding its impact on female fertility[1].

Drug Interactions

Drugs that alter the enterohepatic recirculation or gastrointestinal absorption of mycophenolate mofetil, such as cholestyramine, iron, or aluminum and magnesium hydroxides, may decrease the effectiveness of mycophenolate mofetil (see Ch. 131). Plasma levels of both acyclovir and mycophenolate mofetil are elevated when used concomitantly.

SATURATED SOLUTION OF POTASSIUM IODIDE (SSKI)

The dosage, uses, and side effects are outlined in Table 130.14.

SATURATED SOLUTION OF POTASSIUM IODIDE (SSKI)
Formulation: saturated solution; rapid absorption and wide distribution in thyroid and salivary glands, choroid plexus, and placenta; primarily renal excretion
Mechanism of action: speculative; possible immune modulator; suppresses neutrophil migration and toxicity
Dermatologic use: erythema nodosum; cutaneous and lymphocutaneous sporotrichosis (not systemic); neutrophilic dermatoses; other granulomatous diseases
Dosage: concentration = 1000 mg/ml of saturated solution*; inflammatory diseases: initial dose = 150–300 mg three times per day, then increased weekly until clinical response; sporotrichosis: initial dose = 600 mg three times per day, then increased (maximum = 6 g/day if tolerated) for a total of 6–10 weeks
Side effects: short-term – GI (see Table 130.5), acneiform eruption, reversible hypothyroidism > iododerma, hyperkalemia; long-term – "iodism" with burning mouth, metallic taste, sore teeth and gums, severe headache
Monitoring guidelines: baseline TFTs, including TSH and T_4; pregnancy test in women of childbearing potential; repeat TSH one month after therapy or if symptoms of hypothyroidism develop
Contraindications: hypersensitivity reaction to iodides; thyroid, renal, or cardiac disease; Addison disease (risk of hyperkalemia)
Pregnancy and lactation: avoid during pregnancy; fetal goiter and hypothyroidism known risks; compatible with breastfeeding per AAP
Drug interactions: risk of hyperkalemia with ACE inhibitors, potassium-sparing diuretics, and potassium-containing medications; increased risk of hypothyroidism with concomitant use of amiodarone, lithium, phenazone, and possibly sulfones
*See Table 100.6 for drops (gtt) to mg conversion.

Table 130.14 Saturated solution of potassium iodide (SSKI). AAP, American Academy of Pediatrics; GI, gastrointestinal; TFTs, thyroid function tests; TSH, thyroid stimulating hormone.

SIROLIMUS (RAPAMYCIN) AND TACROLIMUS

The dosage, uses, and side effects are outlined in Table 130.15.

THALIDOMIDE AND LENALIDOMIDE

Few drugs have garnered such notoriety as has thalidomide. Originally introduced in Europe during the 1950s as a sedative/hypnotic, it was commonly used to control morning sickness during pregnancy and thus was prescribed to thousands of pregnant women with tragic results. By 1961, thalidomide was withdrawn worldwide after being linked to thousands of babies born with phocomelia (severe underdevelopment of the extremities)[44]. At the time of withdrawal, thalidomide had never received FDA approval for use in the US. Renewed interest in the drug ensued in the mid-1960s with reports that thalidomide provided significant relief from symptoms of erythema nodosum leprosum (ENL). Thalidomide (Thalomid®) received FDA approval for treatment of ENL in 1997 and has since been successfully employed for various inflammatory skin conditions. Lenalidomide (Revlimid®), a second-generation thalidomide analogue, has been used to treat skin disorders such as refractory cutaneous LE since its release in 2006.

In the US, both the prescribing physician and the dispensing pharmacist must be enrolled in the FDA-mandated THALOMID REMS® program (www.thalomidrems.com) or REVLIMID REMS® program (www.revlimidrems.com). Standardized informed consent forms, patient education packets, and monitoring requirements are included in these programs.

Thalidomide is a lipophilic, non-polar piperidine-dione that is poorly absorbed and highly protein-bound. Peak plasma levels are attained 2–6 hours after ingestion and absorption is not affected by food intake. The half-life of thalidomide is 9 hours. Although the major degradative pathway is non-enzymatic hydrolysis, the drug is also metabolized by CYP enzymes. The precise method of excretion is unknown but non-renal[45].

Both thalidomide and lenalidomide possess immunomodulatory, antiangiogenic, and antitumor properties. Lenalidomide produces a greater effect on T cells as well as IL-2 and IFN-γ production compared to thalidomide. There is a minimal risk of neuropathy with lenalidomide, and sedation and constipation are much less common[46].

SIROLIMUS (RAPAMYCIN) AND TACROLIMUS
Sirolimus (rapamycin)
Drug properties: macrocyclic lactone antibiotic **Mechanism of action**: mTOR (*m*echanistic [or *m*ammalian] *t*arget *o*f *r*apamycin) inhibitor; first binds FK-binding protein 12 (FKBP12) then protein pair binds mTOR complex 1 (mTORC1); blocks T lymphocyte proliferation; inhibits cell proliferation and angiogenesis (Akt pathway) **Dermatologic use**: Kaposiform hemangioendothelioma or tufted angioma with Kasabach–Merritt phenomenon, lymphatic malformations; GVHD – prophylaxis, acute, and chronic; post-transplant Kaposi sarcoma, keratinocyte carcinomas, and lymphoproliferative disorder (substitute immunosuppressant); topical formulations – facial angiofibromas and ungual fibromas in tuberous sclerosis complex, lymphatic and vascular malformations, perhaps hyperkeratotic disorders (e.g. epidermal nevi, acanthosis nigricans) **Dosage**: in children, initially, 0.8 mg/m^2 twice daily, then titrated to obtain trough level of 5–15 ng/ml in children; in adults, loading dose of 6 mg followed by maintenance dose of 2 mg daily, with dose adjusted based upon trough levels; compounded topical formulations usually 1% cream or ointment, but varies from 0.1%–1%; 0.1% oral solution used topically
Tacrolimus
Drug properties: macrolide lactone antibiotic **Mechanism of action**: calcineurin inhibitor (see Ch. 128); inhibits production of cytokines such as IL-8 **Dermatologic use**: GVHD – prophylaxis, acute, and chronic; pyoderma gangrenosum; sarcoidosis; recalcitrant psoriasis **Dosage**: 1–2 mg orally twice daily (blood level 5–10 ng/ml)
Sirolimus and tacrolimus
Side effects: immunosuppression, hypertension, diabetes mellitus (tacro > CSA), renal dysfunction (tacro > siro), hyperlipidemia, posterior reversible encephalopathy syndrome (PRES; tacro > CSA or siro); *tacrolimus:* hyperkalemia (esp. in conjunction with ACE inhibitors). For mucocutaneous side effects, see Table 21.17. **Monitoring guidelines**: see those for CSA (see Table 130.3); lower dose or discontinue treatment if serum creatinine rises by >30% of baseline **Contraindications**: uncontrolled hypertension, significant renal impairment, prior hypersensitivity reaction to drug; see contraindications for cyclosporine; *tacrolimus*: for parenteral administration, allergy to HCO-60 (polyoxyl 60 hydrogenated castor oil that is used as a surfactant) **Pregnancy and lactation**: for dermatologic disorders, should be avoided during pregnancy and lactation (concentrated in breast milk) **Drug interactions**: other renal-toxic drugs

Table 130.15 Sirolimus (rapamycin; Rapamune®) and tacrolimus (Prograf®). There is significantly less hypertrichosis as compared to cyclosporine. Everolimus is an immunosuppressant with a mechanism of action similar to sirolimus that also has anti-tumor effects (e.g. tuberous sclerosis complex-associated tumors, Kaposi sarcoma); additional side effects include mucositis, diarrhea, and pulmonary toxicity. ACE, angiotensin converting enzyme; CSA, cyclosporine; siro, sirolimus; tacro, tacrolimus.

Mechanism of Action

The precise mechanism of actions of thalidomide and lenalidomide are unknown. However, the anti-inflammatory and immunomodulatory effects on dermatologic diseases are thought to be largely through inhibition of TNF release and activity.

Dosages

A major emphasis of the THALOMID REMS® and REVLAMID REMS® programs is pregnancy prevention. Prior to therapy, women of childbearing potential must be on birth control for 1 month and have a negative serum pregnancy test within 24 hours of the first dose. If initial history or physical examination indicates peripheral nervous system disease, neurologic consultation should be sought. Monitoring guidelines are listed in Table 130.3.

Thalidomide is available in 50, 100, 150 and 200 mg capsules. Dosing regimens will vary according to the particular disease and severity. Used in combination with anti-leprosy chemotherapy, the dose for ENL ranges from 100 to 400 mg/day (see package insert for details). Dosages for HIV-associated oral aphthae and neutrophilic dermatoses are generally 100 mg/day. Sedation is the most common dose-limiting side effect, being fairly common at even 50 mg/day. Lenalidomide is available in 2.5, 5, 10, 15, 20, and 25 mg capsules. Dosages to treat skin diseases typically range from 5 to 10 mg daily.

Patients with recalcitrant discoid or SCLE lesions experience 75%–90% clearance rates with thalidomide (Fig. 130.9). The initial dose of 50–100 mg/day is subsequently tapered to 25–50 mg/day after a clinical effect is seen, usually within 2 weeks. Acute cutaneous lesions of SLE have up to a 90% resolution rate, but require higher doses and longer treatment periods before results are noted. For some patients, intermittent courses of thalidomide (for 2–3 months) can be used to clear lesions, with antimalarials given concomitantly and as maintenance therapy.

Major Side Effects

A single dose of *thalidomide* during the first 21–36 days of gestation yields a 100% incidence of birth defects (see Table 130.5). Sedation is by far the most common adverse side effect and may necessitate night-time dosing and gradual titration of the dose. Constipation is also common. Permanent nerve damage (primarily sensory neuropathy) can develop and is more common with long-term therapy. Measurements of sensory nerve action potential amplitudes (SNAP) may be indicated before and/or during therapy. Amenorrhea and primary ovarian failure may occur.

Severe leukopenia, exfoliative erythroderma, and TEN are rare consequences of thalidomide treatment. A hypersensitivity reaction specific to HIV-positive patients has been described. Common dermatologic side effects include brittle fingernails, xerosis, pruritus, and red palms. Peripheral edema can develop occasionally. Vascular thromboses are unusual unless the patient is receiving concomitant corticosteroids.



Fig. 130.9 Improvement of discoid lupus erythematosus with thalidomide. A Baseline. **B** Following therapy with a marked reduction in erythema and scale-crust. *Courtesy Jeffrey Callen, MD.*

In addition to teratogenicity, *lenalidomide* can cause significant neutropenia and thrombocytopenia, requiring close monitoring as outlined in Table 130.3. Hepatotoxicity has also been observed. While neuropathy is typically not seen with lenalidomide, venous and arterial thromboembolism can occur, consisting predominately of deep venous thrombosis and pulmonary embolus. Thromboprophylaxis is recommended with the choice (e.g. low-dose ASA, directly acting oral anticoagulant) based upon the patient's risk factors. Severe drug eruptions including Stevens–Johnson syndrome have also been reported.

Indications

Thalidomide is FDA-approved and 99% effective for ENL (type II leprosy reaction) although it has no effect on type I leprosy reactions. A variety of off-label uses of thalidomide have emerged over the years including cutaneous LE (see above), prurigo nodularis, actinic prurigo, and aphthous stomatitis[47,48]. Although HIV-associated mucosal ulceration, as well as aphthae associated with neutrophilic dermatoses (including Behçet disease), respond rapidly to thalidomide, ulcerations relapse quickly when the drug is discontinued. Curiously, the highest rate of peripheral neuropathy has been observed in prurigo nodularis patients[47].

Lenalidomide is currently FDA approved for follicular or mantle cell lymphoma, multiple myeloma, and deletion 5q myelodysplastic syndrome. Taking advantage of the reduced risk of neuropathy, lenalidomide has been used to treat a similar group of skin diseases as thalidomide including severe refractory cutaneous LE, chronic actinic dermatitis, and prurigo nodularis[48]. Because of its association with a monoclonal gammopathy, lenalidomide has also been used to treat scleromyxedema.

Contraindications

Absolute contraindications to thalidomide and lenalidomide therapy include sensitivity to the drug, pregnancy and, for thalidomide, a pre-existing peripheral neuropathy. Women of childbearing potential must agree to use highly effective methods of birth control with both thalidomide and lenalidomide (e.g. two reliable forms of contraception simultaneously). Men taking these medications who have female partners of childbearing potential must wear condoms (even if they have had a vasectomy) while their partners use an additional form of birth control (either oral or barrier). Relative contraindications for both medications include significant hepatic or renal disease, a history of neurologic disease, congestive heart failure, hypertension, constipation, and hypothyroidism. In patients with a predisposing condition (e.g. antiphospholipid antibodies, myeloma), there can be an increased risk of thromboses, especially with lenalidomide. Individuals receiving antimalarials should continue to do so, because these drugs have been reported to inhibit platelet aggregation and adhesion.

Use in Pregnancy and Lactation

Thalidomide and lenalidomide should not be used in pregnant women[9]. It is also wise to avoid both drugs in nursing mothers. There are limited data regarding male fertility, but animal studies have reported testicular degeneration. To date, no adverse effects have been observed in animal studies of female fertility[1].

Drug Interactions

Thalidomide may amplify the sedative effects of alcohol, barbiturates, chlorpromazine, and reserpine. Any drug that significantly induces the CYP3A4 enzymes may decrease the effectiveness of hormonal contraception, increasing the potential of pregnancy and, thus, teratogenicity. Lenalidomide may increase the level of digoxin, thus monitoring of plasma levels is recommended. Patients receiving concomitant prothrombotic agents, e.g. estrogen, IVIg, erythropoietin, along with lenalidomide may have an increased risk of thromboembolism.

Additional figures and tables on Select cutaneous disorders that can be treated with specific systemic drugs, and Methotrexate – counseling for patients of childbearing potential, available in our eBook (see inside front cover for access code).

REFERENCES

1. Koh YP, Tian EA, Oon HH. New changes in pregnancy and lactation labelling: review of dermatologic drugs. *Int J Womens Dermatol*. 2019;5:216–226.
2. Callen JP, Rosenbach M, Camisa C. Antimalarial agents. In: Wolverton SE, ed. *Comprehensive Dermatologic Drug Therapy*. 4th ed. Philadelphia: WB: Saunders; 2020:234–244.
3. Wozniacka A, Carter A, McCauliffe DP. Antimalarials in cutaneous lupus erythematosus: mechanisms of therapeutic benefit. *Lupus*. 2002;11:71–81.
4. Weiss JS. Antimalarial medications in dermatology. *Dermatol Clin*. 1991;9:377–385.
5. Marmor MF, Kellner U, Lai TYY, et al. Recommendations on screening for chloroquine and hydroxychloroquine retinopathy (2016 revision). *Ophthalmology*. 2016;123:1386–1394.
6. Mavrikakis I, Sfikakis PP, Mavrikakis E, et al. The incidence of irreversible retinal toxicity in patients treated with hydroxychloroquine: a reappraisal. *Ophthalmology*. 2003;110:1321–1326.
7. Melles RB, Marmor MF. The risk of toxic retinopathy in patients on long-term hydroxychloroquine therapy. *JAMA Ophthalmol*. 2014;132:1453–1460.
8. Kalia S, Dutz JP. New concepts in antimalarial use and mode of action in dermatology. *Dermatol Ther*. 2007;20:160–174.
9. Briggs GG, Freeman RK, Towers C, Forinash A. *Drugs in Pregnancy and Lactation*. 11th ed. Philadelphia: Lippincott Williams & Wilkins; 2017.
10. Schafer P. Apremilast mechanism of action and application to psoriasis and psoriatic arthritis. *Biochem Pharmacol*. 2012;83:1583–1590.
11. Papp K, Reich K, Leonardi CL, et al. Apremilast, an oral phosphodiesterase 4 (PDE4) inhibitor, in patients with moderate to severe plaque psoriasis: results of a phase III, randomized, controlled trial (Efficacy and Safety Trial Evaluating the Effects of Apremilast in Psoriasis [ESTEEM] 1). *J Am Acad Dermatol*. 2015;73:37–49.
12. Rich P, Gooderham M, Bachelez H, et al. Apremilast, an oral phosphodiesterase 4 inhibitor, in patients with difficult-to-treat nail and scalp psoriasis: results of 2 phase III randomized, controlled trials (ESTEEM 1 and ESTEEM 2). *J Am Acad Dermatol*. 2016;74:134–142.
13. Grove D, Rahnama-Moghadam S. Azathioprine. In: Wolverton SE, ed. *Comprehensive Dermatologic Drug Therapy*. 4th ed. Philadelphia: WB: Saunders; 2020:169–177.
14. Patel A, Swerlick R, McCall C. Azathioprine in dermatology: the past, the present, and the future. *J Am Acad Dermatol*. 2006;55:369–389.
15. Stern DK, Tripp JM, Ho VC, Lebwohl M. The use of systemic immune moderators in dermatology: an update. *Dermatol Clin*. 2005;23:259–300.
16. Liu H, Wong C. In vitro immunosuppressive effects of methotrexate and azathioprine on Langerhans cells. *Arch Dermatol*. 1997;289:94–97.
17. Wise M, Callen JP. Azathioprine: a guide for the management of dermatology patients. *Dermatol Ther*. 2007;20:206–215.
18. Ahmed AR, Hombal SM. Cyclophosphamide, a review on relevant pharmacology and clinical uses. *J Am Acad Dermatol*. 1984;11:1115–1126.
19. High WA. Cytotoxic agents. In: Wolverton SE, ed. *Comprehensive Dermatologic Drug Therapy*. 4th ed. Philadelphia: WB: Saunders; 2020:209–221.
20. Sekhon S, Bhutani T, Koo JYM. Cyclosporine. In: Wolverton SE, ed. *Comprehensive Dermatologic Drug Therapy*. 4th ed. Philadelphia: WB: Saunders; 2020:187–199.
21. Dutz JP, Ho VC. Immunosuppressive agents in dermatology, an update. *Dermatol Ther*. 1998;16:235–251.
22. Koo J, Lee J. Cyclosporine, what clinicians need to know. *Psoriasis*. 1995;13:897–907.
23. Amor KT, Ryan C, Menter A. The use of cyclosporine in dermatology Part I and II. *J Am Acad Dermatol*. 2010;63:925–972.
24. Grossman RM, Chevret S, Abi-Rached J, et al. Long-term safety of cyclosporin in the treatment of psoriasis. *Arch Dermatol*. 1996;132:623–629.
25. Zachariae H. Renal toxicity of long-term cyclosporin. *Scand J Rheumatol*. 1999;28:65–68.
26. Luke RG. Mechanism of cyclosporine-induced hypertension. *Am J Hypertension*. 1991;4:468–471.
27. Zimmermann S, Sekula P, Venhoff M, et al. Systemic immunomodulating therapies for Stevens-Johnson syndrome and toxic epidermal necrolysis: a systematic review and meta-analysis. *JAMA Dermatol*. 2017;153:514–522.
28. Madan V, Griffiths CEM. Systemic ciclosporin and tacrolimus in dermatology. *Dermatol Ther*. 2007;20:239–250.
29. Wolf R, Tuzun B, Tuzun Y. Dapsone: unapproved uses or indications. *Clin Dermatol*. 2000;18:37–53.
30. Bhatia SM, Hall RP. Dapsone. In: Wolverton SE, ed. *Comprehensive Dermatologic Drug Therapy*. 4th ed. Philadelphia: WB: Saunders; 2020:222–233.
31. Coleman MD. Dapsone: modes of action, toxicity and possible strategies for increasing patient tolerance. *Br J Dermatol*. 1993;129:507–513.
32. Tangamornsuksan W, Lohitnavy M. Association between HLA-B*1301 and dapsone-induced cutaneous adverse drug reactions: a systematic review and meta-analysis. *JAMA Dermatol*. 2018;154:441–446.
33. Wedi B, Kapp A. Pathophysiological role of leukotrienes in dermatologic diseases: potential therapeutic implications. *Biodrugs*. 2001;15:729–743.
34. Bangert CA, Costner MI. Methotrexate in dermatology. *Dermatol Ther*. 2007;20:216–228.
35. Olsen EA. The mechanism of action of methotrexate. *Rheum Dis Clin North Am*. 1997;23:739–755.
36. Menter A, Gelfand JM, Connor C, et al. Joint American Academy of Dermatology-National Psoriasis Foundation guidelines of care for the management of psoriasis with systemic nonbiologic therapies. *J Am Acad Dermatol*. 2020;82:1445–1486.

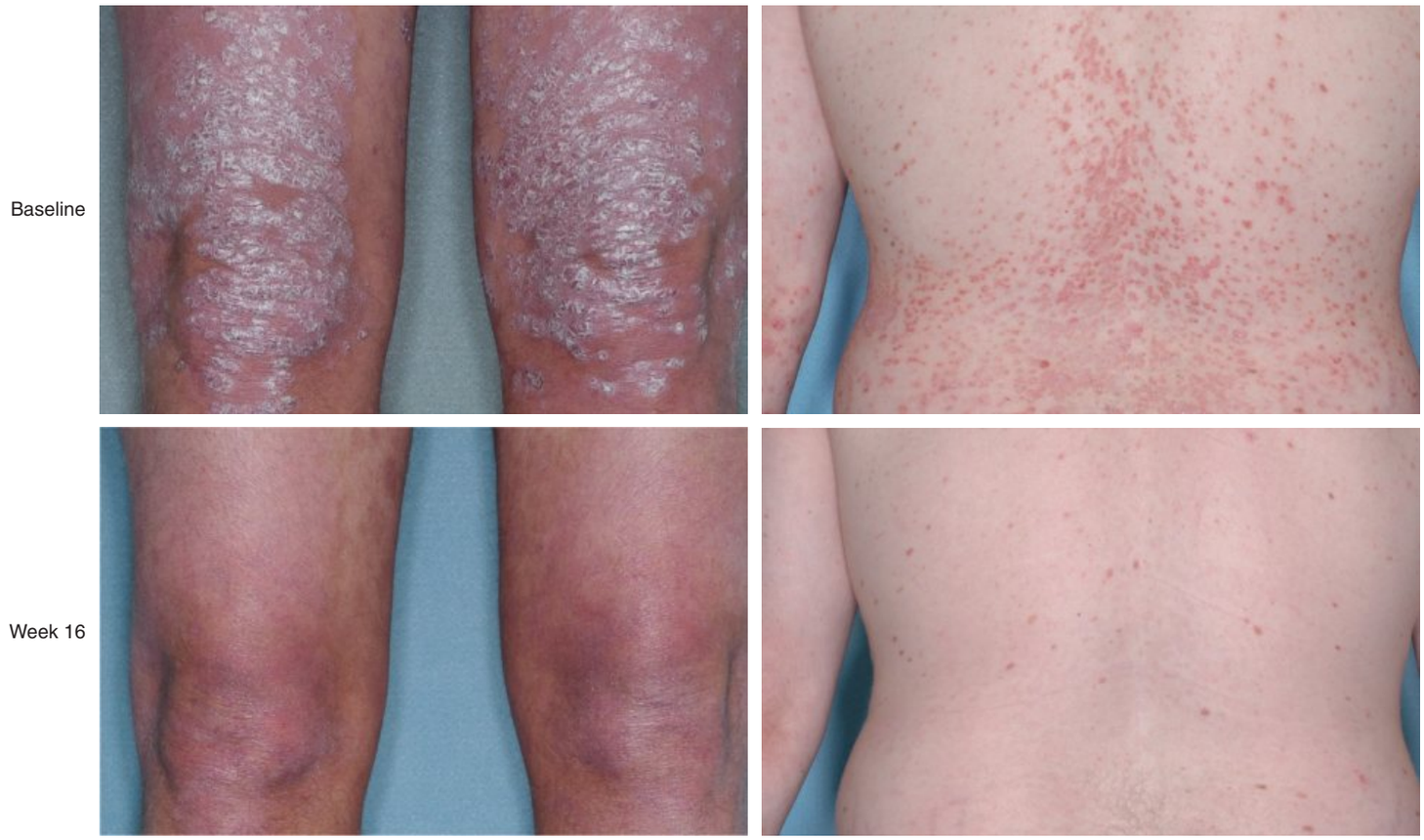
37. Bauer B, Chyou P, Stratman EJ, Green C. Noninvasive testing for nonalcoholic steatohepatitis and hepatic fibrosis in patients with psoriasis receiving long-term methotrexate sodium therapy. *JAMA Dermato*. 2017;153:977–982.
38. Schmeltzer PA, Talwalkar JA. Noninvasive tools to assess hepatic fibrosis: ready for prime time? *Gastroenterol Clin North Am*. 2011;40:507–521.
39. Havele SA, Ellis A, Chaitoff A, et al. Safety of trimethoprim-sulfamethoxazole for *Pneumocystis jirovecii* pneumonia prophylaxis in patients taking methotrexate. *J Am Acad Dermatol*. 2021;84:166–168.
40. Orvis AK, Wesson SK, Breza Jr TS, et al. Mycophenolate mofetil in dermatology. *J Am Acad Dermatol*. 2009;60:183–199.
41. Neff RT, Hurst FP, Falta EM, et al. Progressive multifocal leukoencephalopathy and use of mycophenolate mofetil after kidney transplantation. *Transplantation*. 2008;86:1474–1478.
42. Perez-Aytes A, Ledo A, Boso V, et al. In utero exposure to mycophenolate mofetil: a characteristic phenotype? *Am J Med Genet A*. 2008;146A:1–7.
43. Ang GS, Simpson SA, Reddy AR. Mycophenolate mofetil embryopathy may be dose and timing dependent. *Am J Med Genet A*. 2008;146A:1963–1966.
44. Powell RJ, Gardner-Medwin JMM. Guideline for the clinical use and dispensing of thalidomide. *Postgrad Med J*. 1994;70:901–904.
45. Davis LS, Owen CE. Miscellaneous systemic drugs. In: Wolverton SE, ed. *Comprehensive Dermatologic Drug Therapy*. 4th ed. Philadelphia: WB: Saunders; 2020:446–463.
46. Kotla V, Goel S, Nischal S, et al. Mechanism of action of lenalidomide in hematological malignancies. *J Hematol Oncol*. 2009;2:36.
47. Faver IR, Guerra SG, Su WP, el-Azhary R. Thalidomide for dermatology: a review of clinical uses and adverse effects. *Int J Dermatol*. 2005;44:61–67.
48. Nahmias Z, Nambudiri VE, Vleugels RA. Thalidomide and lenalidomide for the treatment of refractory dermatologic conditions. *J Am Acad Dermatol*. 2016;75:210–212.
49. Rodriguez-Caruncho R, Bielsa Marsol I. Antimalarials in dermatology: mechanism of action, indications, and side effects. *Actas Dermosifiliogr*. 2014;105:243–252.



eFig 130.1 Generalized lichenoid drug eruption due to hydroxychloroquine. There is significant postinflammatory hyperpigmentation.



eFig. 130.2 Pustular psoriasis induced by hydroxychloroquine. Pink plaques studded with pustules with desquamation on the thigh are seen.



eFig. 130.3 Response of plaque psoriasis to apremilast. *Courtesy J. Mark Jackson, MD.*



eFig. 130.4 Azathioprine hypersensitivity reaction. Pink to red macules, papules and areas of confluence are seen. *Courtesy Kalman Watsky, MD.*



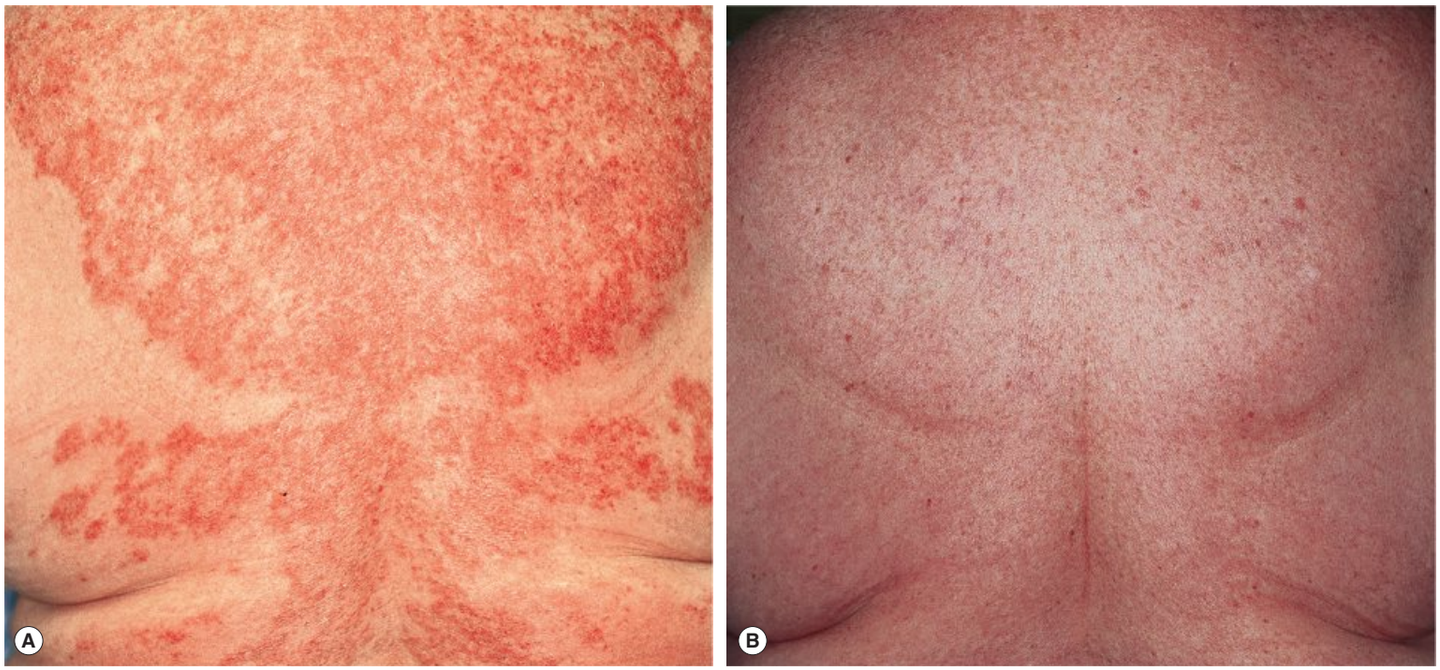
eFig. 130.5 Eruptive sebaceous hyperplasia in a patient receiving cyclosporine. *Courtesy Department of Dermatology, Medical University of Graz.*



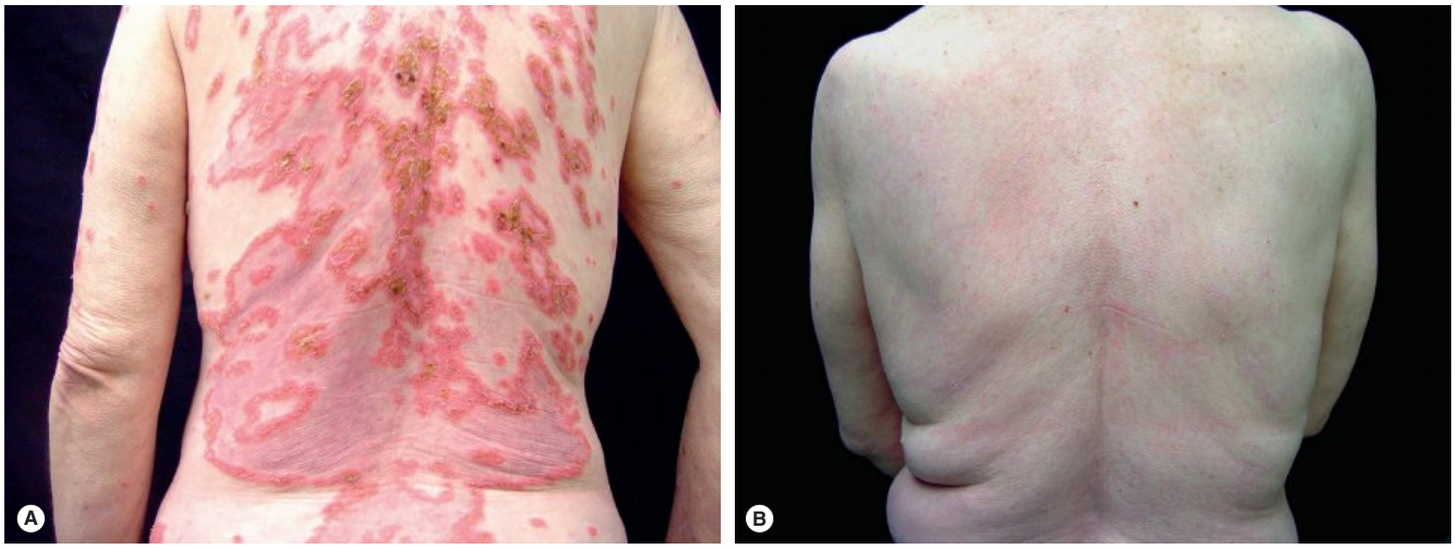
eFig. 130.6 Ulceration of the lateral malleolus in a patient receiving hydroxyurea. *Courtesy Karynne O. Duncan, MD.*



eFig. 130.7 Viral-associated trichodysplasia in a renal transplant recipient receiving tacrolimus, mycophenolate mofetil, and prednisone. Numerous skin- to pink-colored folliculocentric papules, many with central spiny excrescences, developed on the nose and cheeks. This disorder is most commonly seen in the setting of immunosuppression due to systemic calcineurin inhibitors. *Courtesy Mark Kirchhof, MD, and Sheila Au, MD.*



eFig. 130.8 Effect of thalidomide on subacute cutaneous lupus erythematosus. A The patient's disease was not controlled despite prednisone (60 mg/day), hydroxychloroquine (600 mg/day), and isotretinoin (60 mg/day), all for at least 2 months. **B** Thalidomide (50–100 mg/day) was begun and the lesions resolved over 6 to 8 weeks. *Courtesy Jean L. Bolognia, MD.*



eFig 130.9 Improvement of extensive subacute cutaneous lupus erythematosus with thalidomide. A Baseline. **B** Complete clearing over a year later. *Courtesy Jeffrey Callen, MD.*

SELECT CUTANEOUS DISORDERS THAT CAN BE TREATED WITH SPECIFIC SYSTEMIC DRUGS									
Antimalarials	**Azathioprine**	**CTX**	**Cyclosporine**	**Dapsone**	**Methotrexate**	**MMF**	**SSKI**	**Thalidomide**	**Lenalidomide**
• Antiphospholipid antibody syndrome • Cutaneous LE including DLE*, SCLE, lupus tumidus, lupus panniculitis • Dermatomyositis† • GVHD (chronic) • Lichen planus and its variants, e.g. lichen planopilaris • Livedoid vasculopathy • Morphea • Polymorphic light eruption • Porphyria cutanea tarda‡ • Sarcoidosis	• Atopic dermatitis • Behçet disease • Bullous pemphigoid • Chronic actinic dermatitis • Dermatomyositis • Mucous membrane (cicatricial) pemphigoid • Oral lichen planus • Pemphigus	• Cutaneous T cell lymphoma* • Mucous membrane (cicatricial) pemphigoid • Pemphigus • Systemic LE (renal) • Systemic sclerosis (pulmonary) • Systemic vasculitides, including granulomatosis with polyangiitis, polyarteritis nodosa, eosinophilic granulomatosis with polyangiitis	• Atopic dermatitis • Behçet disease • Chronic actinic dermatitis • Dermatomyositis (pulmonary) • GVHD (acute) • Psoriasis* • Pyoderma gangrenosum • Sweet syndrome • Stevens–Johnson syndrome/ toxic epidermal necrolysis • Urticaria (chronic)	• Behçet disease (aphthous stomatitis)* • Bullous eruption of SLE • Cutaneous small vessel vasculitis • Dermatitis herpetiformis* • Erythema elevatum diutinum • Hansen disease (leprosy) • Lichen planus • Linear IgA bullous dermatosis • Mucous membrane (cicatricial) pemphigoid • Sweet syndrome • Urticaria (chronic)	• Atopic dermatitis • Bullous pemphigoid • Cutaneous T cell lymphoma • Cutaneous LE • Dermatomyositis • Langerhans cell histiocytosis • Lichen planus • Lymphomatoid papulosis • Palmoplantar pustulosis • Pityriasis rubra pilaris • Pityriasis lichenoides et varioliformis acuta • Psoriasis* • Systemic sclerosis	• Atopic dermatitis • Bullous pemphigoid • Cutaneous LE • Dermatomyositis • GVHD (acute and chronic) • Lichen planus • Ocular mucous membrane (cicatricial) pemphigoid • Pemphigus • Systemic sclerosis (pulmonary) • Urticaria (chronic)	• Erythema nodosum • Sporotrichosis	• Actinic prurigo • Aphthous stomatitis • Behçet disease • Erythema nodosum leprosum • GVHD (chronic) • Prurigo nodularis • Subacute cutaneous and discoid LE • Sweet syndrome	• Chronic actinic dermatitis • Cutaneous LE • Dermatomyositis • Prurigo nodularis

*FDA-approved dermatologic conditions.
†Cutaneous drug reactions more common than in other autoimmune connective tissue diseases.
‡Low-dose.

eTable 130.1 Select cutaneous disorders that can be treated with specific systemic drugs. Their use is based on double-blind controlled trials or large clinical series if these studies exist. CTX, cyclophosphamide; DLE, discoid LE; GVHD, graft-versus-host disease; LE, lupus erythematosus; MMF, mycophenolate mofetil; SCLE, subacute cutaneous LE; SLE, systemic LE; SSKI, saturated solution of potassium iodide.

METHOTREXATE (MTX) – COUNSELING FOR PATIENTS OF CHILDBEARING POTENTIAL
Female
• Should not become pregnant while receiving MTX • MTX can cause birth defects and abortions • Must use highly effective means of contraception (e.g. OCPs; IUD; condom + spermicide) • After discontinuing MTX, wait three months before attempting to become pregnant[1]
Male
• May lead to low sperm counts • Drug is present in semen • Must use highly effective means of contraception (e.g. OCPs, IUD [female partner]; condom + spermicide) • After discontinuing MTX, wait three months before trying to conceive with their partner

eTable 130.2 Methotrexate (MTX) – counseling for patients of childbearing potential. This drug was formerly pregnancy category X. IUD, intrauterine device; MTX, methotrexate; OCPs, oral contraceptive pills.

131 Drug Interactions

Lukas Koch, Birger Kränke, Lori E. Shapiro, Sandra R. Knowles and Neil H. Shear

Chapter Contents

Putting Interactions into Perspective 2330
Assessment of Risk in the Clinical Outcome of Drug Interactions . 2330
Levels of Evidence 2331
Absorption 2331
Distribution 2333
Drug Biotransformation 2334
The Confusing World of Drug Interactions. 2335
How to Minimize the Risk of Drug–Drug Interactions. 2337

INTRODUCTION

There are two concerns in drug safety: drug reactions and drug interactions. When multiple medications are prescribed, drug interactions become an important safety and efficacy consideration for patients and physicians alike. Non-prescription drugs, in addition to herbal supplements and alternative medicines as well as foods (such as grapefruit juice), may also be implicated in interactions with drug therapy.[1]

It is difficult to obtain precise rates of incidence and prevalence, as specific diagnostic codes for drug interactions are lacking[1a]. This may be due to the fact that interactions can affect multiple processes by which drugs are absorbed, distributed, bound by plasma proteins, metabolized, and excreted, i.e. pharmacokinetic drug interactions. The drug interaction prevalence rate for hospitalized patients is about 1.1%[2], but differs considerably amongst medical disciplines[3]. Every second dermatologic inpatient has a potential risk for relevant drug interactions[4], but one has to keep in mind that *potential* drug interactions far outnumber *actual* drug interactions[3].

Although it is impossible to remember all potential drug interactions, knowledge of the interactive properties of drugs can help reduce the risk of serious adverse outcomes. Moreover, it is the responsibility of physicians to counsel patients regarding drug interactions[5]. Unfortunately, even when serious new drug interactions are recognized and reported, physicians, pharmacists, and patients are often unaware that there is a risk[6].

PUTTING INTERACTIONS INTO PERSPECTIVE

While most drugs are associated with interactions, many do not produce significant outcomes[7]. In fact, not all listed or reported drug interactions are actually clinically significant. Whereas some have little clinical relevance, others are clearly defined as contraindications on the basis of substantiation of risk, potential severity, and frequency of occurrence. Still others can be successfully managed by dosage adjustment and monitoring. In other words, prescribing drugs with the potential for a deleterious interaction increases the risk of, but need not lead to, an adverse outcome.

In one study that examined the occurrence of drug interactions, based upon adverse events reported during large clinical trials[8], the authors concluded that serious adverse drug reactions (ADRs) secondary to drug–drug interactions were infrequent; however, drug–drug interactions that involved selected drugs with a narrow therapeutic index (which elicited life-threatening undesired effects) did occur. Drug–drug interactions are the most common cause of medication errors in high-income countries, with a prevalence of 20%–40%, especially due to polypharmacy in the elderly[9]. Thus, for most drug interactions, it is necessary to assess each patient situation individually.

ASSESSMENT OF RISK IN THE CLINICAL OUTCOME OF DRUG INTERACTIONS

The clinical importance of specific drug interactions is often either over- or underestimated, as these assessments are based primarily on clinical experience in using a particular drug combination[10]. The clinical outcome of most drug interactions is highly situational, as most patients who receive drugs with the potential for interactions do not develop adverse effects. Emphasis should be placed on those factors that increase or decrease the risk to a given patient.

In order to prevent or detect drug interactions, the physician needs to identify risk factors in each individual patient. That said, some patient groups are more likely than others to develop adverse events caused by drug interactions. Identified risk factors are listed in Table 131.1.

The *elderly* frequently experience drug interactions because of the physiologic changes that accompany the aging process and the types of drugs that older patients tend to receive[11]. Polypharmacy, which is common in the elderly, makes them particularly susceptible. In addition, medications may impair pathways of drug elimination by interfering with drug metabolism, thereby increasing the likelihood of adverse drug reactions. Alterations due to advanced age, including changes in drug–protein binding and drug distribution within tissue, may also promote drug interactions. Of note, most adverse metabolic drug interactions occur when an inhibitor or inducer is begun in a patient who previously had stable levels of a substrate drug.

HIV-infected patients also have a high rate of adverse drug reactions. In some instances, this may relate to phenotypic changes in drug metabolism, which can vary with progression of the underlying HIV infection[12]. The latter can alter enzyme function, with resultant changes in drug metabolism and a higher rate of adverse reactions in these patients. A helpful website that provides up-to-date information regarding drug interactions in HIV-infected patients is hosted by the University of Liverpool (www.hiv-druginteractions.org)[13].

A major source of interindividual differences in drug metabolism is *genetic polymorphisms*, which are inherited and can result in significant variations in the activity of drug-metabolizing enzymes. For example, the genes encoding cytochrome P450 (CYP) isoforms are highly polymorphic (see Table 131.13). In some cases, it is actually possible and useful to determine an individual's genotype[14]. Further details on genetic polymorphisms are discussed later in the chapter.

Interactions with other drugs can predispose a patient to the development of certain types of ADR. For example, coadministration of valproic acid increases the risk of severe cutaneous adverse reactions to lamotrigine[15], and allopurinol increases the risk of exanthematous eruptions to antibiotics such as amoxicillin. A disease state itself may directly affect the likelihood of an ADR. For example, active infection with Epstein–Barr virus or cytomegalovirus also increases the risk of exanthematous eruptions to amoxicillin and ampicillin. The disease state may also dictate the way in which a drug is prescribed, and this can subsequently affect the outcome. When a drug has more than one therapeutic action, an interacting drug may affect the action of the initial drug when it is used to treat one disease but not when it is used to treat another disease.

An example of intrinsic effects of disease states would be when epinephrine (adrenaline) is given to patients receiving non-cardioselective β-adrenergic blockers such as propranolol (but who do not have anaphylaxis), and this results in hypertension. In contrast, the same β-blockers inhibit the pressor response to epinephrine when the latter is given to patients with anaphylaxis[16].

An example of a dose-dependent drug interaction is the concomitant use of nonsteroidal anti-inflammatory drugs (NSAIDs) and methotrexate. Available evidence indicates that the risk of this combination

PATIENT RISK FACTORS FOR DRUG INTERACTIONS
• Multiple medications, i.e. polypharmacy
• Demographic risk factors
• Female sex
• Extremes of age – very young and elderly
• Major organ dysfunction, especially in the setting of multiple medical problems
• Liver dysfunction
• Renal insufficiency*
• Congestive heart failure
• Metabolic and endocrine risk factors
• Obesity
• Hypothyroidism
• Hypoproteinemia
• Pharmacogenetic risk factors
• Slow acetylator phenotype
• Reduced thiopurine methyltransferase (TPMT) activity
• Reduced glucose-6-phosphate dehydrogenase (G6PD) activity
• Other genetic polymorphisms (see text and Table 131.13)
• Other medical issues
• Hypothermia
• Hypotension
• Dehydration
*May be underestimated in elderly patients.

Table 131.1 Patient risk factors for drug interactions[11].

is considerably greater in patients receiving high-dose methotrexate as cancer chemotherapy than it is in patients receiving lower weekly dosages for psoriasis[17]. This is because the distribution of the drug is not very important mechanistically in determining drug interactions, but changes in drug elimination are. When larger doses of methotrexate (as used in cancer therapy) are given in combination with an NSAID, reduced drug elimination via the kidneys becomes an important issue, increasing the risk of methotrexate toxicity. However, in patients with impaired renal function, the addition of an NSAID to the lower doses used by dermatologists for psoriasis or as a steroid-sparing agent can also be associated with an increased risk of methotrexate toxicity due to the NSAID's effect on renal elimination.

Sex-related differences in pharmacokinetics may cause variations in drug bioavailability, distribution, metabolism (e.g. CYP2D6), and clearance[18]. The effect of obesity on metabolism is also cytochrome-specific. For example, obesity decreases the activity of CYP3A4 and increases the activity of CYP2E1[19].

Certain medications are clearly more likely to be involved in drug interactions. More specifically, clinically significant interactions occur more frequently with drugs that have a narrow margin of safety, i.e. a narrow therapeutic window. Drugs with the potential for such serious interactions include warfarin and cyclosporine. When prescribing a new medication that could potentially interact with warfarin, it is prudent to have the patient's international normalized ratio (INR) measured within 2–3 days of administration of the new drug.

Medication-related factors that contribute to clinical risk include the dose, route of administration and duration of administration of the *precipitant drug* (the drug that causes the interaction) as well as the sequence of administration of the interacting drugs. Most metabolic drug interactions are dose-related. That is, as the dose of the precipitant drug is increased, the magnitude of its effect on the *object drug* tends to increase. Thus, the **dose** of the precipitant drug is often an important determinant of risk. However, the dose of the object drug may also affect the risk of an adverse drug interaction. For example, a patient who takes small doses of an object drug with serum concentrations at the lower end of the target range is at a lesser risk when an enzyme-inhibiting precipitant drug is added, than would be a patient taking large doses of the same object drug. Lastly, the bioavailability of either drug may have an impact. The **route of administration** is a significant risk factor for some non-metabolic drug interactions, such as when one drug binds to another in the gastrointestinal (GI) tract. However, the route of administration can also be important for metabolic drug interactions, especially when the drug undergoes extensive first-pass metabolism in the gut wall and liver by CYP3A4 or P-glycoprotein (see below). Most drug interactions also have a typical **time course** over which the effects develop. For example, giving rifampin, a typical inducer of CYP3A4, for only a few days is unlikely to have much effect on substrates of CYP3A4, as induction of an enzyme takes weeks to occur.

In summary, there is pharmacodynamic and pharmacokinetic variability between people, as well as host variability in terms of disease state. Overall, this variability contributes to confusion, as tables and lists that outline potentially interacting medications vary amongst different sources. One reason is that various levels of evidence exist for many of these drugs in terms of their ability to contribute to/cause drug interactions. This is outlined in more detail in the next section.

LEVELS OF EVIDENCE

Drug interaction literature is often confusing due to poorly substantiated claims. This confusion occurs as a result of inaccurate or cursory evaluations of published cases or inappropriate extrapolations from the literature. Metabolic drug interactions are a major source of potential clinical problems, but their investigation during drug development is often incomplete. *In vitro* studies give very accurate data on the interactions of drugs with selective CYP isozymes, but their interpretation in the clinical context is difficult. Although *in vitro* systems have been developed to test the effects of certain drugs on the metabolism of other drugs, these systems may not accurately predict the effect in patients receiving drugs with complex metabolism. In addition, problems with the detection of adverse events after a drug has been released arise mainly because such events are rare. It takes a surveillance system with a high degree of sensitivity to detect such problems[20].

Furthermore, most *in vivo* and *in vitro* studies of drug interactions evaluate two-drug regimens, and the results may not apply to the multidrug regimens used clinically. This is especially true for a regimen consisting of three or more drugs with opposing effects on CYP3A4 metabolism. The lack of studies of multiple drug interactions provides little assistance to the prescribing physician, who is left to rely on adverse events or treatment failure to demonstrate whether an interaction has occurred. In addition, the design of *in vivo* studies is sometimes poor (choice of prototype substrate, doses, schedule of administration, number of volunteers), with the risk of minimizing the real potential for interaction. To link *in vitro* and *in vivo* studies, several authors have suggested using extrapolation techniques, based on the comparison of *in vitro* inhibition data with the active *in vivo* concentrations of the inhibitor. However, the lack of knowledge with regard to one or several important parameters, such as the role of metabolites and intrahepatocyte accumulation, often limits the ability to make safe and accurate predictions.

The uncertainty and inaccuracy of predicting the extent and duration of *in vivo* drug interactions currently stems from a lack of definitive models by which to assess likely substrate and inhibitor concentrations at the active site of metabolism. Additional issues contributing to the uncertainty of predicting drug interactions include assumptions of the contribution of presystemic drug extraction and the effect of inhibitors on the processes involved. Therefore, these methods are useful for complementing *in vivo* studies and helping to design clinically relevant *in vivo* studies, but in the near future they will not totally replace *in vivo* investigations.

ABSORPTION

Interactions that alter the absorption of drugs often lead to dramatic changes in plasma drug concentrations. Drug interactions within the GI tract can result in decreased absorption. This reduces the bioavailability or the amount of drug available to the systemic circulation and results in subtherapeutic serum concentrations. The underlying mechanisms of most drug interactions that alter GI absorption involve: (1) the formation of drug complexes that reduce absorption; (2) alterations in gastric pH; and/or (3) changes in GI motility that alter transit time[9].

Common drugs that form complexes with other drugs include antacids, sucralfate, and bile acid sequestrants (e.g. cholestyramine, colestipol, colesevelam) (Table 131.2). A significant interaction occurs between multivalent cations – such as calcium (e.g. within milk products), aluminum, iron, and magnesium – and tetracyclines or

DRUG INTERACTIONS THAT REDUCE THE EFFICACY OF SUBSTRATES			
Mechanism	**Substrate/ parent drug**	**Concomitant drugs**	**Time course**
Reduced GI absorption	Itraconazole (encapsulated) Ketoconazole‡ Posaconazole	Antacids* H_2 antihistamines Proton pump inhibitors Sucralfate	Rapid
	Fluoroquinolones	Antacids* Iron Sucralfate	
	Tetracycline Bisphosphonates	Divalent cations Calcium Magnesium Iron	
	Mycophenolate mofetil	Iron Antacids*	
Induction of CYP3A4†	Calcineurin inhibitors Cyclosporine Tacrolimus Oral contraceptives Corticosteroids Dexamethasone Methylprednisolone Prednisone Warfarin	Anticonvulsants Carbamazepine Phenobarbital Phenytoin Antituberculous agents Isoniazid Rifampin Dexamethasone Griseofulvin	1–2 weeks
Antagonistic effects	Epinephrine	β-Blockers	
	Cyproheptadine	SSRI antidepressants Fluoxetine Paroxetine	

*Often contain aluminum hydroxide, magnesium hydroxide, and/or calcium carbonate.
†Also A5, A7.
‡Has been withdrawn by the European Medicines Agency and per the US FDA, it is no longer indicated for *Candida* or dermatophyte infections or as first-line therapy for chromomycosis or dimorphic fungal infections.

Table 131.2 Drug interactions that reduce the efficacy of substrates. In addition, bile acid sequestrants (e.g. cholestyramine, colestipol, colesevelam) dramatically reduce GI absorption of furosemide and thiazide diuretics. GI, gastrointestinal; SSRI, selective serotonin reuptake inhibitors.

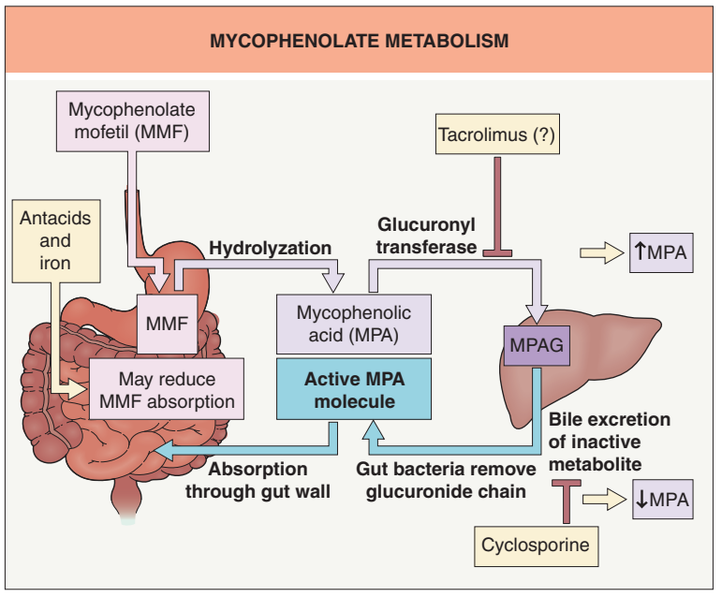


Fig. 131.1 Mycophenolate metabolism. Mycophenolate is hydrolyzed to mycophenolic acid (MPA). Following glucuronidation in the liver, inactive MPA glucuronide (MPAG) is excreted into the gut via bile acid secretion. In the gut, bacteria remove the glucuronide chain to produce MPA, the active molecule, which is then reabsorbed through the gut wall. Cyclosporine impairs MPA enterohepatic recirculation by inhibiting biliary excretion of MPAG (thereby *decreasing* MPA levels), whereas tacrolimus may inhibit UDP-glucuronyl transferase (thereby *increasing* MPA levels).

fluoroquinolone antibiotics. For example, there is an 85% reduction in the absorption of ciprofloxacin when ingested 5–10 minutes after a dose of an aluminum hydroxide/magnesium hydroxide antacid[21]. These interactions can be easily avoided by administering the fluoroquinolone at least 2 hours before or 6 hours after the antacid or multivalent cations. Alendronate, as well as other bisphosphonates prescribed for the prevention and treatment of osteoporosis, form complexes with cations and several other drugs, thereby further decreasing their already low oral absorption. However, once weekly dosing reduces the opportunity for bisphosphonate-related interactions. When mycophenolate mofetil and iron preparations were administered concomitantly, a significant decrease in mycophenolate mofetil absorption was observed (Fig. 131.1)[22].

Drugs that increase gastric pH, such as proton pump inhibitors, antacids and H_2 antihistamines, may reduce the absorption of drugs such as encapsulated itraconazole and posaconazole, which are best absorbed in an acidic environment[23]. Although itraconazole is best absorbed when the gastric pH is low, its administration with food is more important for achieving high plasma concentrations[24]. Of note, the absorption of fluconazole is unaffected by variations in gastric pH. Similarly, the coadministration of drugs that can increase gastric pH (see above) with atazanavir and raltegravir is not recommended. Drugs that affect GI motility, such as anticholinergic agents, may decrease the rate of absorption but not the extent of absorption. An overall reduction in drug absorption has more clinical significance[25].

Some drugs may interfere with the enterohepatic recirculation of a substrate drug. When the substrate is excreted into the GI tract, a second drug can bind to it and prevent its reabsorption back into the systemic circulation. The bound substrate drug is excreted in the feces, thereby effectively shortening its half-life. An example of this is the concurrent administration of warfarin and bile acid sequestrants (e.g. cholestyramine, colestipol, colesevelam) in which the half-life of warfarin is shortened.

P-glycoprotein (PGP)

Membrane-bound transport systems may also determine drug disposition[26]. These transporters are found in multiple tissues and actively pump drug molecules either out of cells (efflux) or into cells (uptake). PGP is an ATP-dependent plasma membrane glycoprotein belonging to the superfamily of ATP-binding cassette transporters that functions primarily as an efflux pump (Fig. 131.2)[27]. Other transporters include the organic anion and organic cation transporters. In humans, the multidrug resistance (MDR) genes, including *MDR1*, encode membrane glycoproteins that function as drug transporters and hence affect both drug absorption and elimination.

High levels of PGP are found in superficial columnar epithelial cells of the small intestine, the apical surface of epithelial cells in the proximal tubules of the kidney, and in the biliary canalicular membrane of hepatocytes. PGP is also detected in high concentrations in the endothelial cells of the capillaries of the blood–brain barrier, testes, uterus and placenta. An understanding of the physiologic regulation of these transporter proteins is key to designing strategies for improving the therapeutic efficacy of drugs that serve as their substrates (Table 131.3).

These membrane-bound transport systems seem to have developed as a mechanism for protecting the body from harmful substances. It appears that PGP acts as a pump whereby the efflux of drugs from the cell membrane or cytoplasm is powered by the energy from ATP hydrolysis. For example, the aminoglycoside antibiotics amikacin and tobramycin are not effectively delivered orally, perhaps because of active efflux from the brush border cells of the small intestine by the PGP pump. The most remarkable property of PGP is its ability to transport a diverse array of compounds that do not appear to share obvious structural characteristics. The range of substrates, inhibitors, and inducers of PGP is vast and expanding (Tables 131.3 & 131.4). Examples of inducers of PGP include dexamethasone, doxorubicin, phenobarbital, rifampin, trazodone, and St. John's wort.

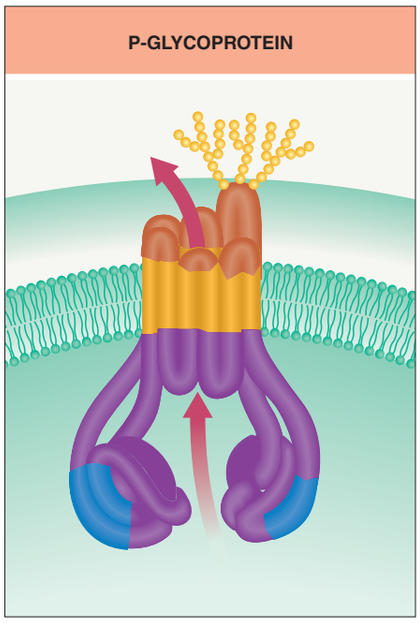


Fig. 131.2 P-glycoprotein. This is an ATP-dependent plasma membrane glycoprotein that functions as a drug transporter and hence affects both drug absorption and elimination.
Courtesy Ian Worpole.

INHIBITORS OF P-GLYCOPROTEIN		
Antimicrobials	**Psychotropic agents**	**Cardiac agents**
Clarithromycin	Amitriptyline	Amiodarone
Erythromycin	Chlorpromazine	Carvedilol
Itraconazole	Desipramine	Diltiazem
Ivermectin	Disulfiram	Dipyridamole
Ketoconazole	Doxepin	Felodipine
Mefloquine	Fluphenazine	Nicardipine
Ofloxacin	Haloperidol	Nifedipine
Posaconazole	Imipramine	Propranolol
Rifampin	**Steroid hormones**	Verapamil
Voriconazole	Progesterone	**Miscellaneous**
Immunosuppressives	Testosterone	Grapefruit juice
Cyclosporine		Orange juice isoflavones
Tacrolimus		Ritonavir
		Tamoxifen

Table 131.4 Inhibitors of P-glycoprotein.

P-GLYCOPROTEIN SUBSTRATES		
Antimicrobials	**HIV protease inhibitors**	**Cardiac agents**
Ciprofloxacin	Indinavir	Amiodarone
Erythromycin	Nelfinavir	Atorvastatin
Ivermectin	Ritonavir	Dabigatran
Other quinolones	Saquinavir	Digoxin
Rifampin	**Immunosuppressives**	Diltiazem
Anticancer agents	Cyclosporine	Lovastatin
Actinomycin D	Dexamethasone	Nadolol
Daunorubicin	Tacrolimus	Pravastatin
Docetaxel	**Rheumatologic agents**	Propranolol
Doxorubicin	Colchicine	Quinidine
Etoposide	Methotrexate	Timolol
Mitomycin C	Quinine	Verapamil
Paclitaxel	**Antiemetics**	**Miscellaneous**
Vinblastine	Domperidone	Cimetidine
Vincristine	Ondansetron	Lidocaine
		Loperamide

Table 131.3 P-glycoprotein substrates.

Because PGP blocks absorption in the gut, these glycoproteins should be considered part of the "first-pass effect". In fact, PGP can "set up" or act as "gatekeepers" for later cytochrome P450 actions. Although the inhibition and induction of intestinal CYP3A enzymes from metabolic processes result in direct changes in drug absorption, the inhibition and induction of PGP primarily affect the rate of drug absorption[28]. If one drug is a substrate of both PGP and CYP3A4 (which are found in close proximity in the intestinal wall), and a second drug is added that is an inhibitor of both PGP and CYP3A4 (e.g. erythromycin, ketoconazole), then a greater amount of the first drug will be absorbed. Because CYP3A4 is inhibited, higher levels of *unmetabolized* drug will enter the blood. The effect of PGP blockade is to "open the gates" so that the later actions of CYP3A4 inhibition will be increased.

PGP is an important component of the blood–brain barrier and an active PGP will prevent drugs from entering the brain. It has been suggested that the reason newer antihistamines do not cause sedation is that PGP activity acts as a barrier to CNS penetration. This would suggest that PGP inhibitors (see Table 131.4) could interact with and allow increased cerebral concentrations of these antihistamines, with an attendant increase in sedation[29].

Evidence also suggests that intestinal PGP plays a significant role in the first-pass elimination of cyclosporine, probably by being a rate-limiting step in absorption. Intestinal CYP3A4 is thought to play a lesser role[30]. However, the overlap of tissue distribution and substrate specificity of CYP3A4 and PGP in the intestinal wall makes it difficult to define the precise mechanisms of some drug interactions and to predict the plasma concentrations of certain drug combinations. Moreover, the involvement of CYP3A4 and PGP in drug interactions is not always complementary.

DISTRIBUTION

Drugs that are highly protein-bound (>90%) may cause interactions based on alterations in distribution. When one drug displaces another from plasma protein-binding sites, the free serum concentration of the displaced drug is increased, and its pharmacologic effect increases. However, the unbound fraction of the drug is not only more available to sites of action but is also more readily eliminated. Any enhanced pharmacologic effect occurs only transiently because of a compensatory increase in elimination, and the *effect of displacement interactions is then negligible*. Therefore, interactions involving drug displacement from binding proteins tend to be self-limiting[31]. Typically, the pharmacologic activity of the displaced drug is increased for a few days. This is followed by a return of the pharmacologic response back to the previous unbound serum concentration, even if the concomitant therapy is continued. Therefore, it is safe to say that if a patient does not manifest an adverse event from the combination therapy in the first week or so of administration, an adverse event probably will not occur.

In practice, protein-binding displacement interactions do not produce clinically significant changes in drug response unless the drug also has a limited distribution in the body, is slowly eliminated, or has a low therapeutic index[25]. For this reason, protein-binding displacement interactions may assume greater importance when the displacing drug also reduces the elimination of the substrate drug. Good examples of this principle are the interactions between NSAIDs and methotrexate (Table 131.5).

Medications that are most susceptible to interactions based on changes in drug distribution involving displacement from binding proteins include warfarin, sulfonamides, and phenytoin[11].

DRUG INTERACTIONS THAT INCREASE RISK OF SUBSTRATE DRUG TOXICITY			
Mechanism	**Substrate**	**Interactive drugs**	**Time course**
Competitive inhibition of CYP3A4*	Cyclosporine Everolimus Sirolimus Tacrolimus Dapsone H1 antihistamines Macrolides Erythromycin HMG-CoA reductase inhibitors Lovastatin Simvastatin Metoprolol Midazolam Phenytoin Pimozide Quinidine Triazolam Warfarin	Antidepressants Fluoxetine Nefazodone Azole antifungals Itraconazole Ketoconazole† Posaconazole Voriconazole Fluconazole (high doses) Grapefruit juice HIV-1 protease inhibitors Indinavir Ritonavir Macrolides Clarithromycin Erythromycin Quinine Diltiazem Cimetidine	Rapid
Reduced metabolic clearance	Azathioprine Methotrexate	Allopurinol Febuxostat Salicylates	Rapid Variable
Displacement from plasma proteins	Methotrexate	NSAIDs Salicylates Sulfonamides	Rapid
Reduced renal elimination	Methotrexate	NSAIDs Penicillins Probenecid Salicylates Sulfonamides	Rapid
Synergy	Methotrexate Retinoids Acitretin Isotretinoin Serotonin reuptake inhibitors	Retinoids Acitretin Isotretinoin Sulfonamides Tetracyclines Alcohol Monoamine oxidase inhibitors	Variable Variable Variable

*Also A5 and A7.
†Has been withdrawn by the European Medicines Agency and per the US FDA, it is no longer indicated for *Candida* or dermatophyte infections or as first-line therapy for chromomycosis or dimorphic fungal infections.

Table 131.5 Drug interactions that increase risk of substrate drug toxicity[1,57]. Sulfonamides are inhibitors of anionic tubular secretion of methotrexate. NSAIDs, nonsteroidal anti-inflammatory drugs.

DRUG BIOTRANSFORMATION

Cytochrome P450 Enzymes

After their administration, drugs are metabolized through a series of reactions to enhance their hydrophilicity and to facilitate excretion. These drug biotransformation reactions are broadly grouped into two phases, I and II. *Phase I* reactions involve intramolecular changes such as oxidation, reduction, and hydrolysis that make the drug more polar and therefore more readily eliminated. *Phase II* reactions are conjugation reactions in which an endogenous substance combines with the functional group derived from phase I reactions to produce a highly polar drug conjugate that can be even more readily eliminated. These reactions involve glucuronidation and sulfation.

The cytochrome P450 (CYP) enzymes are the major drug-metabolizing enzymes (Fig. 131.3). They are present in the endoplasmic reticulum of many cells, but their highest concentrations are found in hepatocytes. CYP enzymes are also present in the crypt cells of the GI tract, with the highest concentrations found in the enterocytes at the tips of the villi; their presence accounts for the first-pass metabolism of many drugs. These heme-containing proteins are encoded by a gene superfamily, with the encoded isoforms exhibiting distinct but overlapping substrate specificities and isoform-specific regulatory and pharmacogenetic properties[32]. The nomenclature employs a three-tier classification consisting of the family (40% homology in amino acid sequence), the subfamily (~75% homology), and the individual protein (e.g. CYP2D6).

An increased understanding of CYP drug metabolism has solved much of the mystery behind drug interactions. While there are ~60 genes that encode CYP isoforms, over 90% of drug oxidation can be attributed to six main cytochromes: CYP1A2, 2C9, 2C19, 2D6, 2E1 and 3A4[33] (see Fig. 131.3); with regard to systemic dermatologic therapies, CYP3A subfamily is the most important[34]. The metabolism of a drug by a specific isoenzyme indicates that it is a substrate for that enzyme. *Whether enzyme inhibition or induction occurs is an entirely separate issue*. Many drugs serve only as substrates and produce no significant enzyme inhibition or induction. It is entirely possible for a drug to be a substrate for one enzyme and inhibit or induce another enzyme that is not involved with its own metabolism. Therefore, drug interactions are more aptly termed drug–protein–drug (food) interactions. These are affected by: genetics (polymorphic genes cause particular enzymes to be less effective, 2D6 being an example); drugs (a drug may inhibit or induce a cytochrome, or interfere in the chemical pathway of another drug, e.g. itraconazole reduces cyclosporine metabolism by inhibiting CYP3A4); chemicals (dioxin is an inducer of CYP3A4 while a food such as grapefruit juice is an inhibitor of CYP3A4); and the environment

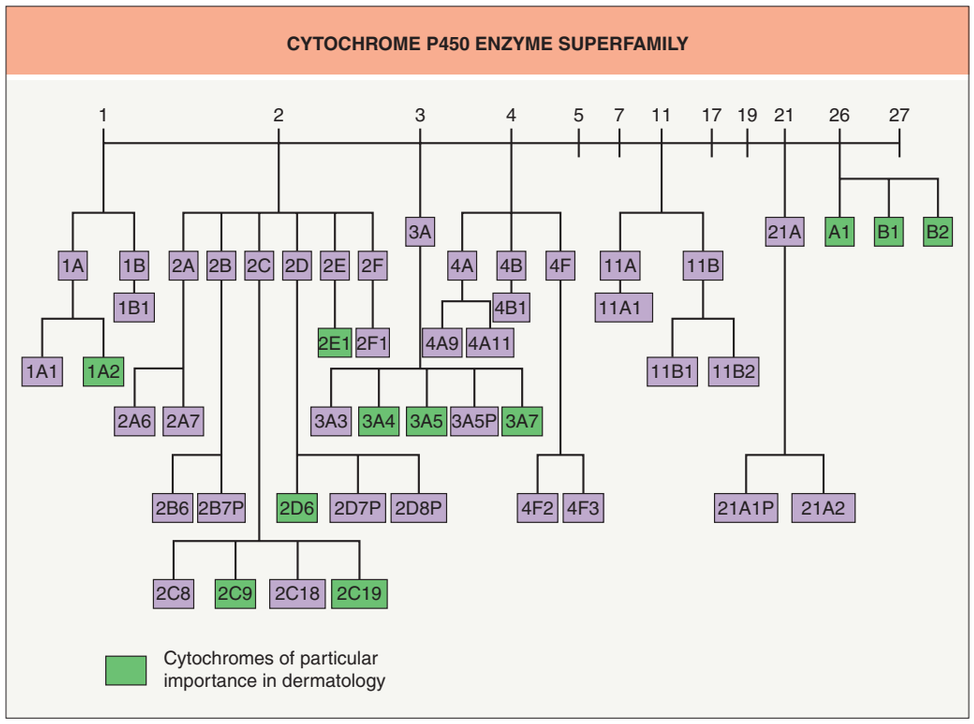


Fig. 131.3 Cytochrome P450 enzyme superfamily.

INFLUENCES ON CYTOCHROME P450 ACTIVITY					
	Cytochrome P450 activity				
	1A2	**2C**	**2D6**	**2E1**	**3A4**
Nutrition	↑			↑ (obesity ↑)	↓ (obesity ↓)
Smoking	↑				
Alcohol				↑	
Drugs	↑ or ↓	↑ or ↓	↑ or ↓		↑ or ↓
Environmental factors	↑			↑	↑
Genetics		↑ or ↓	+		

Table 131.6 Influences on cytochrome P450 activity.

(cigarette smoke is an inducer of CYP1A2). Deciding what is clinically relevant is a challenging, relatively new field of investigation.

Drug metabolism is investigated even before human exposure. With recombinant human CYP enzymes, it is possible to determine the metabolic pathways, potential genetic polymorphisms, ability to induce or inhibit drug metabolism, and possible drug interactions. Although there are limitations to the information gleaned from *in vitro* studies, nonetheless this information can be used to guide more expensive *in vivo* studies.

However, using *in vitro* tests that focus on cytochrome enzymes alone to predict clinical interactions may not always be reliable for a variety of reasons. First, it is not always possible to know the therapeutic concentration of a new drug and its primary metabolites in specific tissues[26]. Second, there are a large number of pathways and interactions, and it is impossible to test them all even in an *in vitro* system. Third, the demonstration of an *in vitro* effect does not tell physicians whether that effect is likely to occur in clinical practice, i.e. the clinical significance of an *in vitro* interaction is unknown. Fourth, the underlying disease state may contribute to the development of a drug interaction and this would be unaccounted for by *in vitro* studies alone. Until clinical data demonstrate the presence or absence of a clinically significant interaction, dosage adjustments based on *in vitro* tests are premature.

THE CONFUSING WORLD OF DRUG INTERACTIONS

Why does it take so long to learn about interactions? Some drugs come to market and their various interactions are not realized for several years[35]. One reason is that drugs are prescribed on the basis of indications that may have their own adverse effects on patient outcome. In addition, studies in healthy volunteers are not sufficient to determine the contribution of underlying diseases to the development of interactions. The latter are affected by genetics, drugs, chemicals, the underlying health status of the patient, the therapeutic index of the drug affected by the interaction, dose-related factors, the duration of coadministration, the time course of the interaction, whether active metabolites are involved, and the environment (Table 131.6). Furthermore, the multiple metabolic pathways of some drugs can make it difficult to predict the outcome of drug interactions. However, the risk of a specific drug to have a significant drug–drug interaction is usually lower when it is metabolized by multiple CYP enzymes.

Metabolism

The most clinically relevant drug interactions are those caused by alterations in drug metabolism, and CYP isoenzymes are the key players in drug metabolism. Members of the CYP3A subfamily are the most abundant of the human *hepatic* cytochromes and account for up to 70% of *GI* cytochromes. This subfamily contains the major metabolizing isoforms for many of the drugs prescribed by dermatologists (Tables 131.2, 131.5, 131.7 & 131.8; Fig. 131.4). CYP3A4 in particular has a pivotal role in xenobiotic metabolism and has been estimated to be involved in the metabolism of ~50% of the drugs in clinical use[33]. Although the most important isoform is 3A4, there is close structural homology to 3A5 and 3A7, and so these three isoforms are grouped together. Of note, CYP3A4 is also located in the placenta, uterus, kidney, lung, and fetus.

There is significant interindividual variability in the metabolic activity of CYP3A4. The extent of variability may be as much as 20-fold and the individual level of CYP3A4 activity probably has clinical relevance. Obesity also plays a role in drug metabolism in an enzyme-specific way[19] as it decreases isoform 3A4 metabolism (see Table 131.6), and more than a third of Americans are obese.

The successful application of information regarding CYP in order to prevent drug interactions and improve the therapeutic risk/benefit ratio can occur only if we know which enzyme is responsible for the metabolism of a particular drug. Drug interactions are also made more predictable by determining which compounds induce and inhibit which specific P450 enzymes. While knowing all of the major enzyme substrates, inhibitors, and inducers is a formidable task, Tables 131.7 to 131.10[36,37] are intended to summarize large amounts of this information.

SUBSTRATES OF CYP3A4,5,7		
Antiarrhythmics	**Cancer chemotherapy**	**Protease inhibitors**
Amiodarone	Busulfan	Indinavir
Lidocaine	Cyclophosphamide	Nelfinavir
Propafenone	Docetaxel	Ritonavir
Quinidine	Doxorubicin	Saquinavir
Anticonvulsants	Etoposide	**Miscellaneous**
Carbamazepine	Ifosfamide	Acetaminophen
Ethosuximide	Paclitaxel	Clarithromycin
Antidepressants	Tamoxifen	Codeine
Amitriptyline	Vinblastine	Colchicine
Doxepin	Vincristine	Dabrafenib
Imipramine	**HMG-CoA reductase inhibitors**	Enalapril
Sertraline	Atorvastatin	Encorafenib
Antihistamines	Lovastatin	Erythromycin
Loratadine	Simvastatin	Estrogens
Benzodiazepines	**Immunosuppressive drugs**	Flutamide
Alprazolam	Apremilast	Losartan
Diazepam	Corticosteroids	Montelukast
Midazolam	Cyclophosphamide	Omeprazole
Triazolam	Cyclosporine	Oral contraceptives
Calcium channel blockers	Dapsone	Pimozide
Amlodipine	Everolimus	Retinoic acid
Diltiazem	Sirolimus	Rifabutin
Felodipine	Tacrolimus	Rifampin
Isradipine		Sildenafil
Nifedipine		Theophylline
Verapamil		Vemurafenib
		Warfarin
		Zileuton

Table 131.7 Substrates of CYP3A4,5,7[36].

CYP3A4 INHIBITORS AND INDUCERS	
Inhibitors	**Inducers**
Antibiotics	***Anticonvulsants***
Ciprofloxacin	***Carbamazepine***
Clarithromycin	Ethosuximide
Erythromycin	Oxcarbazepine
Norfloxacin	Phenobarbital
Troleandomycin	***Phenytoin***
Antifungals (azoles)	Primidone
Fluconazole	***Antiretrovirals***
Itraconazole	Efavirenz
Ketoconazole*	Nevirapine
Posaconazole	Ritonavir
Voriconazole	***Antituberculous agents***
Antiretrovirals	Rifabutin
Amprenavir	***Rifampin***
Atazanavir	***Miscellaneous***
Boceprevir	Bexarotene
Delavirdine	Bosentan
Indinavir	Dabrafenib
Nelfinavir	Dexamethasone
Ritonavir	Griseofulvin
Saquinavir	Pioglitazone
Calcium channel blockers	***St John's wort***
Diltiazem	Troglitazone
Nifedipine	Vemurafenib
Verapamil	
SSRIs	
Fluoxetine	
Fluvoxamine	
Nefazodone	
Sertraline	
Others	
Amiodarone	
Antiprogestins	
Cannabinoids	
Cyclosporine	
Dronedarone	
Cimetidine	
Grapefruit juice	
Imatinib	
Interferon-gamma	
Quinine	
Tacrolimus	
Tamoxifen	
Zafirlukast	

*Has been withdrawn by the European Medicines Agency and per the US FDA, it is no longer indicated for *Candida* or dermatophyte infections or as first-line therapy for chromomycosis or dimorphic fungal infections.

Table 131.8 CYP3A4 inhibitors and inducers[36]. For the treatment of SARS-CoV-2, ritonavir is combined with nirmatrelvir and increases levels of nirmatrelvir. Drugs in ***bold italics*** are particularly potent inhibitors. SSRI, selective serotonin reuptake inhibitors.

Cytochrome induction

The effect of induction is to increase the amount of P450 present and to accelerate the oxidation and clearance of a drug. The onset and offset of enzyme induction are *gradual* because the induction phase depends on the accumulation of the particular inducing agent and the subsequent synthesis of new enzyme. The offset depends on elimination of the inducer and decay of the increased enzyme levels.

The most common enzyme inducers are aromatic anticonvulsants (phenobarbital, phenytoin, carbamazepine), rifampin, and other antituberculous drugs (see Tables 131.2, 131.8 & 131.9). Inducers may enhance parent drug metabolism, so that therapeutic efficacy is actually reduced if the parent drug is the active moiety (Fig. 131.5). Alternatively, inducers may enhance the metabolism of a substrate to active metabolites, with the potential for exaggerated toxicity.

Drug interactions involving enzyme induction are not as common as inhibition-based drug interactions but may be equally profound and clinically significant.

Cytochrome inhibition

Inhibition of drug metabolism is the most important mechanism for drug interactions because it can lead to an increase in plasma drug concentration, enhanced drug response, and toxicity. In contrast to the time course seen with enzyme induction, inhibition of drug metabolism begins within the first one or two doses of the inhibitor and is maximal when a steady-state concentration of the inhibitor is achieved. Therefore, the time course for inhibitory actions is usually in terms of *days* not weeks.

Inhibitory interactions can be either competitive or non-competitive. An example of *competitive* inhibition involves the tight binding of inhibitors such as macrolides, cimetidine, and ketoconazole to the heme moiety of the cytochrome P450 isozyme. As long as the inhibitor occupies this specific site of the CYP, the substrate cannot be biotransformed. As the concentration of the inhibiting drug increases, the degree of saturation of the isoenzyme increases. When the enzyme system is saturated, further metabolic activity by that enzyme system is limited. At that point, a patient becomes the equivalent of a poor metabolizer and concentrations of co-prescribed medications begin to rise. The extent of inhibition of one drug by another depends on the affinity each compound has for the CYP isoform. In addition to the concentration of substrate required to saturate the system and the half-life of the inhibitor drug, competitive inhibition clearly depends on the affinity of the substrate for the enzyme being inhibited. The onset and offset of enzyme inhibition are dependent on the time to steady state and the half-life of the inhibitor.

The significance of an elevated plasma level of a particular drug is determined largely by the therapeutic margin of the drug. Therefore, when considering the potential clinical relevance of an interaction, one must exercise more caution with drugs that have a narrow therapeutic range. *Non-competitive* inhibition is less common and occurs when the enzyme is destroyed, inactivated, or changed by the inhibitor such that it can no longer metabolize the original substrate.

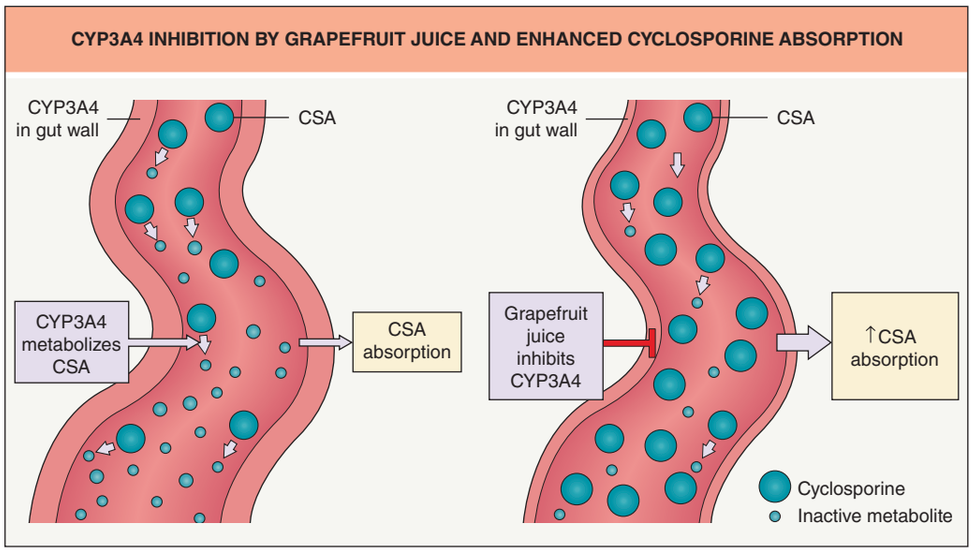


Fig. 131.4 CYP3A4 inhibition by grapefruit juice and enhanced cyclosporine absorption. CSA, cyclosporine.

DRUG-METABOLIZING ENZYMES CYP1A2, 2C9 AND 2C19: SELECTED SUBSTRATES, INHIBITORS AND INDUCERS

Isozyme	Substrate	Inhibitors	Inducers
CYP1A2	Amitriptyline Caffeine Clomipramine Clozapine Desipramine Fluvoxamine Haloperidol Imipramine Propranolol Tacrine Theophylline Warfarin Zileuton Zolmitriptan	Cimetidine ***Ciprofloxacin*** Clarithromycin ***Erythromycin*** ***Fluvoxamine*** Ketoconazole ***Norfloxacin*** ***Paroxetine*** Terbinafine Ticlopidine	Barbiturates Brussels sprouts Cabbage Carbamazepine Charbroiled foods Cigarette smoking Omeprazole Phenobarbital Phenytoin Rifampin Ritonavir
CYP2C9	Abrocitinib Diclofenac Fluoxetine Fluvastatin Ibuprofen Losartan Montelukast Phenytoin Piroxicam Sulfonamides Tricyclic antidepressants Valproic acid Warfarin Zafirlukast	***Amiodarone*** ***Cimetidine*** Clopidogrel ***Fluconazole**** Fluvoxamine Imatinib Ketoconazole Leflunomide Omeprazole Sulfonamides Trimethoprim Voriconazole Zafirlukast	Barbiturates Carbamazepine Dabrafenib Ethanol Griseofulvin Rifampin St John's wort
CYP2C19	Abrocitinib Citalopram Cyclophosphamide Clopidogrel Diazepam Hexobarbital Imipramine Indomethacin Lansoprazole Nelfinavir Nilutamide Omeprazole Pantoprazole Progesterone Proguanil Teniposide Warfarin	Cimetidine Felbamate ***Fluconazole**** ***Fluoxetine*** ***Fluvoxamine*** Indomethacin Ketoconazole Lansoprazole Modafinil Omeprazole Paroxetine ***Ticlopidine*** Topiramate Voriconazole	Carbamazepine Efavirenz Norethindrone Prednisone Ritonavir ***Rifampin*** St John's wort

*In particular high-dose.

Table 131.9 Drug-metabolizing enzymes CYP1A2, 2C9, and 2C19: selected substrates, inhibitors, and inducers[36,37]. Drugs in ***bold italics*** are particularly potent inhibitors.

SUBSTRATES AND INHIBITORS OF CYP2D6

Substrates of CYP2D6		Inhibitors of CYP2D6
Antiarrhythmics	***Antidepressants***	Amiodarone Amitriptyline ***Bupropion*** Celecoxib Chlorpheniramine Cimetidine Clomipramine ***Delavirdine*** Desipramine Diphenhydramine Donepezil Doxepin ***Fluoxetine*** Fluphenazine Haloperidol Hydroxychloroquine Imatinib Imipramine ***Lopinavir*** ***Methotrimeprazine*** Moclobemide Nortriptyline ***Paroxetine*** Pimozide Propafenone ***Quinidine*** Ranitidine ***Ritonavir*** Sertraline (weak) ***Terbinafine*** ***Thioridazine*** Ticlopidine ***Tipranavir*** Venlafaxine (weak)
Encainide Flecainide Mexiletine Propafenone	Amitriptyline Clomipramine *N*-desmethylclomipramine Desipramine Fluoxetine Imipramine Maprotiline Mianserin Norfluoxetine Nortriptyline Paroxetine Trazodone* Trimipramine Venlafaxine	
Antipsychotics	***Miscellaneous***	
Aripiprazole Clozapine Haloperidol Perphenazine Risperidone Thioridazine Zuclopenthixol	Captopril Codeine Dextromethorphan Diphenhydramine Domperidone Donepezil Ethylmorphine 4-Hydroamphetamine Oxycodone Phenformin Tramadol	
β-Blockers		
Alprenolol Bufuralol Metoprolol Propranolol Timolol		

*Applies to metabolite rather than the parent drug.

Table 131.10 Substrates and inhibitors of CYP2D6[36,37]. Drugs in ***bold italics*** are particularly potent inhibitors.

HOW TO MINIMIZE THE RISK OF DRUG–DRUG INTERACTIONS

One commonly perpetuated myth is that all drugs in a given class are equally susceptible or contributory to drug interactions. Understanding the differences between drugs in a particular class with regard to potential for drug interactions is clinically relevant. Specific drugs, from a given class of drugs associated with interactions, may have little or no clinical potential for drug interactions and are therefore safer choices (Table 131.11).

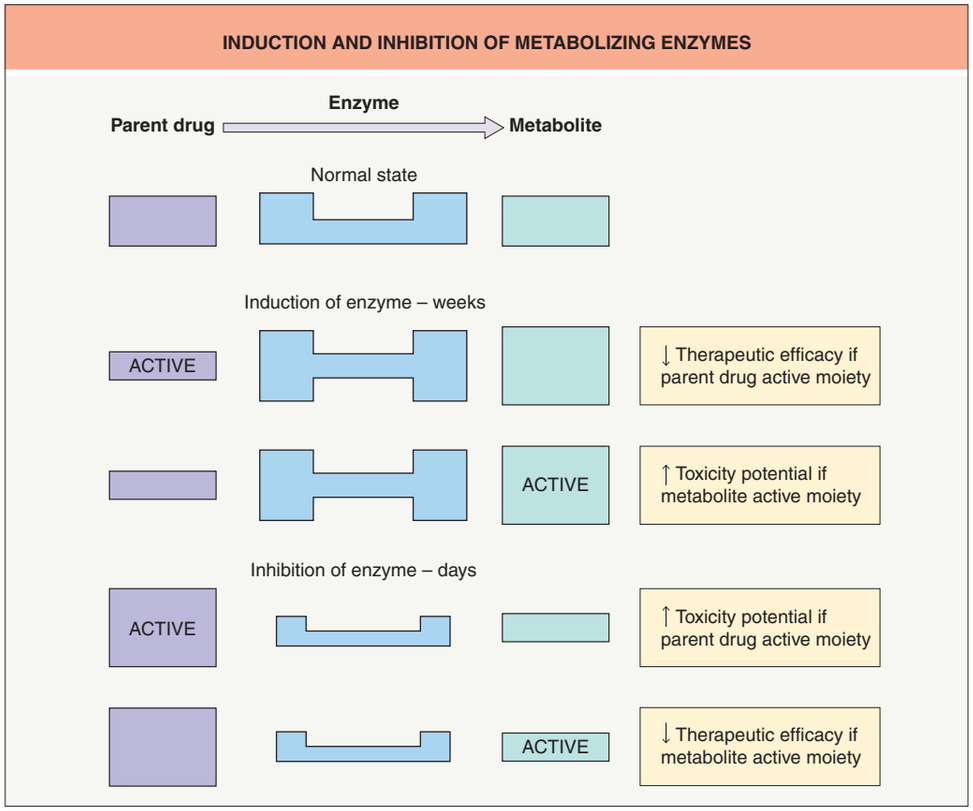


Fig. 131.5 Induction and inhibition of metabolizing enzymes. Induction of an enzyme takes 1–2 weeks to occur while inhibition can occur rapidly within days.

Various drug classes commonly encountered by dermatologists will be discussed, with emphasis on important interactions and ways to minimize risks by appropriate drug choices within a given drug class.

Allylamine Antifungals

Terbinafine is an orally active allylamine antifungal used in the treatment of dermatophytoses. Reports suggest some degree of significant inhibition of CYP2D6 and CYP1A2 by terbinafine[38]. There are four principal levels of activity of CYP2D6 in the general population: poor metabolizers (PM), intermediate metabolizers (IM), extensive metabolizers (EM), and ultrarapid metabolizers. The EM status is by far the most common and is considered "normal". Approximately 7.5% of White individuals and <2% of Asians and African-Americans are poor metabolizers. Inhibition of CYP2D6 by terbinafine would make individuals who have active enzyme (extensive metabolizers) into poor metabolizers, and this effect could possibly last for weeks after discontinuing terbinafine. This can cause two problems: there may be an accumulation of the parent drug (substrate), and this can result in dose-dependent drug toxicity, or there can be reduced formation of active metabolites, and this can result in loss of efficacy (see Fig. 131.5)[39].

Terbinafine appears to be a potent inhibitor of CYP2D6, and so clinicians should be aware of potential interactions (see Table 131.10). The area of greatest concern, because of possible severity and common use, would be bradycardia from excess *β-blockade* (e.g. propranolol) or from the accumulation of *donepezil* (used to treat Alzheimer disease)[40]. Codeine or tramadol could lose their analgesic effect, as active metabolites are not formed when CYP2D6 activity is low[39].

Azole Antifungals

The triazoles itraconazole and posaconazole as well as the imidazole ketoconazole require an acid milieu for absorption; therefore, concomitant *antacids*, *H_2 blockers*, *proton pump inhibitors*, and *sucralfate* significantly reduce absorption (see Table 131.2). The administration of these agents with carbonated cola beverages will acidify (pH <3) the stomach, thereby improving absorption of the antifungal drug. Fluconazole and voriconazole are alternatives for patients in whom drugs that reduce gastric acidity are required, as these antifungal medications do not rely on an acid milieu for absorption.

Among the systemic azole antifungals, itraconazole, voriconazole, posaconazole, and ketoconazole are CYP3A4 inhibitors that are able to

DRUGS AND FOODS WITH DIFFERING POTENTIAL FOR DRUG–DRUG INTERACTIONS BASED ON METABOLISM

Drug/food class	More potential for interaction	Less potential for interaction
ACE inhibitors and angiotensin II receptor blockers (ARBs)	NSAIDs	Acetaminophen Celecoxib
Antifungals	Azoles and triazoles (CYP3A4 inhibition)	Terbinafine
Calcium channel blockers	Diltiazem Nicardipine Verapamil	Amlodipine Nifedipine
Macrolides	Clarithromycin Erythromycin	Azithromycin
Quinolones	Ciprofloxacin Enoxacin	Levofloxacin Lomefloxacin Ofloxacin
H_2 blockers	Cimetidine	Famotidine Nizatidine Ranitidine
Protease inhibitors	Ritonavir (most potent) Indinavir	Saquinavir Nelfinavir
HMG-CoA reductase inhibitors	Simvastatin Lovastatin	Pravastatin Fluvastatin Rosuvastatin
Citrus fruit juice	Grapefruit juice	Orange juice

Table 131.11 Drugs and foods with differing potential for drug–drug interactions based on metabolism. ACE, angiotensin-converting enzyme; NSAIDs, nonsteroidal anti-inflammatory drugs.

induce drug–drug interactions[41]. Many substrates are metabolized via these enzymes (see Tables 131.2, 131.5, 131.7), and moderate to severe drug interactions have been observed with several substrates, including *cyclosporine*, *warfarin*, *sirolimus*, and *everolimus*. Itraconazole is contraindicated when the patient is also receiving the following CYP3A substrate drugs: *triazolam*, *oral midazolam*, *lovastatin*, *simvastatin*, *quinidine*, or *pimozide*. Caution has been suggested with *cyclosporine, warfarin, digoxin*, and *atorvastatin*. Significant effects on the metabolism of fluvastatin or pravastatin by itraconazole do not appear to occur[42] (see Table 131.11). Fluconazole inhibition of CYP3A4 is dose-related: 100 mg/day usually has little effect on CYP3A4, but inhibition can occur at daily doses of 200–400 mg (or more), depending upon the substrate.

When the azole antifungals are administered with *cyclosporine*, concentrations of the latter are increased, requiring careful monitoring of cyclosporine levels. Similarly, frequent monitoring of the INR is required for patients on *warfarin* who require therapy with an azole antifungal. The azole antifungals reportedly increase the anticoagulant effects of warfarin by two- to threefold.

Azole antifungals also interfere with the metabolism of benzodiazepines such as *triazolam* and *midazolam*, leading to increased levels and sedation. There is also decreased metabolism of some of the HMG-CoA reductase inhibitors, e.g. *lovastatin* and *simvastatin*, leading to increased levels, as well as to rhabdomyolysis. Additional drugs whose metabolism is decreased by azoles include *tacrolimus, indinavir*, and *calcium channel blockers*. Peripheral edema due to an interaction between nifedipine and itraconazole has been reported. It was suspected that itraconazole inhibited the metabolism of this calcium channel blocker, resulting in an increased serum nifedipine concentration and leg edema. This hypothesis was confirmed by obtaining serum levels of nifedipine, itraconazole, and hydroxyitraconazole (the active metabolite of itraconazole) before and after the administration of itraconazole[43]. The authors recommended that patients receiving both azole or triazole antifungals and calcium channel blockers should be monitored for side effects such as leg edema and, more importantly, hypotension, because of the increased serum concentration of the calcium channel blocker.

Fluconazole, but not itraconazole, interacts with the angiotensin II receptor blocker *losartan*, but not valsartan or irbesartan. Fluconazole inhibits losartan's metabolism to the active metabolite E-3174[44]. The clinical significance of this interaction remains unclear, but the possibility of a reduced therapeutic effect of losartan should be borne in mind. *Phenytoin* is a substrate of CYP2C9, and concurrent fluconazole use at bedtime has resulted in several cases of phenytoin toxicity[45].

In contrast to the azole antifungals, terbinafine is an allylamine that does not inhibit CYP3A4[46]. This antifungal may be a viable therapeutic option in patients on concomitant therapy with a high likelihood of drug interactions with the azoles (see above).

Azathioprine

Azathioprine is metabolized to 6-mercaptopurine (6-MP) and there are three subsequent pathways for the metabolism of 6-MP. Both thiopurine methyltransferase (TPMT) and xanthine oxidase metabolize 6-MP to inactive metabolites, whereas hypoxanthine–guanine phosphoribosyltransferase (HGPRT) metabolizes 6-MP to active purine analogues, in particular 6-thioguanine (see Fig. 130.5). *Allopurinol* and *febuxostat* inhibit the metabolism of 6-MP via xanthine oxidase; this leads to increased levels of 6-MP (plus active purine analogues via HGPRT) and, as a result, increased antimetabolite effects and associated toxicity including pancytopenia. Combining either azathioprine or 6-MP with allopurinol or febuxostat should be avoided. If either allopurinol or febuxostat must be prescribed, an alternate immunosuppressant should be selected.

Colchicine

Colchicine is a substrate of PGP and concurrent use of PGP inhibitors has resulted in severe colchicine toxicity. It is also a substrate for CYP3A4, so inhibitors of this enzyme may result in increased plasma concentrations of colchicine. Given the possibility of fatal colchicine toxicity, few situations would warrant the concomitant use of colchicine with a *CYP3A4 or PGP inhibitor* (see Tables 131.4 & 131.8). However, if this combination must be prescribed, careful monitoring for colchicine toxicity (diarrhea, abdominal pain, fever, muscle pain or weakness, paresthesias) should be performed. If toxicity is suspected, both drugs must be discontinued immediately. Of note, grapefruit juice is an inhibitor of both PGP and CYP3A4, and colchicine toxicity has been reported with the intake of large amounts of grapefruit juice.

Cyclosporine/Everolimus/Sirolimus/Tacrolimus

Numerous drug interactions with cyclosporine have surfaced that are associated with its metabolism and presystemic metabolism (both by the CYP3A4 enzyme and by PGP), in the liver and intestine, respectively. It is thought that this GI tract metabolism may explain its erratic absorption. *Diltiazem* can decrease cyclosporine dosing by as much as 30%[47], while effects with *grapefruit juice* have been variable.

Other drugs that alter cyclosporine concentrations via cytochrome 3A4 inhibition include other calcium channel inhibitors (*verapamil*, *nifedipine*), triazoles and imidazoles (*fluconazole*, *itraconazole*, *posaconazole*, *ketoconazole*), macrolides (*erythromycin*, *clarithromycin*), and *tacrolimus*. Conversely, isoform 3A4 inducers, such as *rifampin*, *phenytoin*, *carbamazepine* and *phenobarbital*, decrease cyclosporine concentrations. Decreased cyclosporine levels have also been observed with coadministration of *trioglitazone* or *ticlopidine*[48]. More recently, acute kidney injury due to interaction of cyclosporine with methyl-1-testosterone has been reported, highlighting the danger of anabolic steroids purchased online as "supplements"[49]. Cyclosporine trough levels, as well as signs of toxicity versus adequate immunosuppressive response, should be monitored when any of these drugs are combined with cyclosporine.

Grapefruit Juice

Grapefruit juice interactions are of potential clinical relevance for a wide range of drugs. The mechanisms of grapefruit juice interactions are exclusively pharmacokinetic in nature. The effect is mediated mainly by the suppression of CYP3A4 and PGP in the small intestinal wall by either fresh or frozen grapefruit juice[50] (see Fig. 131.4). This results in a diminished first-pass metabolism, with higher bioavailability and increased maximal plasma concentrations of substrates of this enzyme and/or transporter. The effect is most pronounced in drugs with high first-pass degradation, such as *felodipine*, *nifedipine*, *saquinavir*, *cyclosporine*, *midazolam*, *triazolam*, *terazosin*, *ethinylestradiol*, *17β-estradiol*, *prednisone*, and the HMG-CoA reductase inhibitors *lovastatin* and *simvastatin*[51,52]. In the case of cyclosporine, for example, inhibition of its metabolism by grapefruit juice can lead to increased immunosuppression and toxicity.

It is not yet clear which component in grapefruit juice is to blame. Psoralen, mainly a bergamottin compound, is thought to be the major inhibitor, with a minor role attributable to flavonoids such as naringenin and quercetin[53]. Even a change in the brand or batch of grapefruit juice may influence the grapefruit juice/drug interaction to an unpredictable degree, as grapefruit juice is a natural product that is not standardized in composition. Similar interactions have not been seen with other citrus fruit juices, such as orange juice. Lack of 6,7-dihydroxybergamottin in orange juice probably accounts for the absence of inhibitory effects[54]. However, isoflavones in orange juice may mediate this food's inhibitory effect on PGP.

In general, it is recommended that patients refrain from ingesting grapefruit juice when taking a drug that is extensively metabolized, unless a lack of interaction has been documented. Orange juice is a good alternative (see Table 131.11). Another option is ingestion of the grapefruit juice an hour before or two hours after drug ingestion.

Herbal Remedies

Herbal medicines (see Ch. 133) have become a popular form of therapy. They are perceived to be "natural" by the public and thus harmless. Although many current therapeutic agents (e.g. digitalis, atropine, vincristine) have been derived from plants, little is known about the relative safety of current herbal therapies compared with prescription drugs, and even less is known when the two are co-consumed. Because of under-reporting, our present knowledge represents the tip of the iceberg. It is estimated that 80% of the world's population relies primarily on traditional medicines utilizing plant extracts or their active ingredients.

The interactions of phytomedicines with prescription medications are under-researched[55]. Of note, medications with a narrow therapeutic

index or potential life-threatening toxicity, such as cardiovascular drugs (e.g. amiodarone), immunosuppressants (e.g. everolimus, cyclosporine, sirolimus), NSAIDs (including aspirin), opioids (e.g. fentanyl, oxycodone), and warfarin are considered to be at increased risk for significant drug–herb interactions[56]. Because herbs are not sold as drugs, no proof of efficacy or warnings about side effects are required. Moreover, herbal medications are not standardized so different herbal brands have varying amounts of active ingredients and therefore may interact differently with other medications. Even different lots of the same brand may vary considerably. Also, not all, or even any, additional ingredients may be listed on the label[57].

When a drug is prescribed, the quality and dosage of the substance are assured. No such quality control exists for herbal preparations. Contamination, mislabeling, and misidentification of herbs are known problems. Some patients do not know even what they are taking, as they may purchase a product whose ingredients are listed in a foreign language only. In sum, it is important to educate patients to inform their healthcare providers of all alternative medications.

A study in 12 healthy volunteers examined the effect of the ingestion of *St John's wort* on cytochrome activity[58]. Short-term administration (less than two weeks) of St John's wort had no effect on CYP activity, whereas long-term St John's wort administration resulted in a significant and selective induction of CYP3A activity in the intestinal wall. St John's wort did not alter the activity of CYP2C9, CYP1A2, or CYP2D6. Reduced therapeutic efficacy of drugs metabolized by CYP3A should be anticipated during long-term administration of St John's wort.

See Table 131.12 for some important drug interactions between herbal medicines and dermatologic therapies.

HERBAL REMEDIES/PRESCRIPTION DRUG INTERACTIONS		
Herbal remedy	**Side effects/ contraindications**	**Drug interaction**
Berberine (Goldenseal)	Nervousness, confusion, nausea, tremors	Increases concentration of dextromethorphan via 2D6 inhibition
Coenzyme Q10[57]	Reduced efficacy of warfarin	Warfarin
Ginseng[75]	Can reduce the anticoagulant response of warfarin	Warfarin
Kava	CNS depressant	Alcohol, barbiturates, benzodiazepines, opiates
Licorice (*Glycyrrhiza glabra* or *uralensis*)	Contraindicated if hypertension, diabetes mellitus, hypokalemia, hepatic or renal disease	Cyclosporine, digoxin, prednisone, thiazides
Purple coneflower (*Echinacea angustifolia* or *purpurea*)	Recurrent erythema nodosum Caution in patients with HIV, autoimmune CTD, TB, MS, or ragweed/ sunflower allergies	Immunomodulators and cyclosporine, methotrexate, corticosteroids
Ginkgo (*Ginkgo biloba*), garlic, ginger[76]	Can cause spontaneous bleeding	Can potentiate aspirin, digoxin, NSAIDs, warfarin, heparin
St. John's wort[57] (oral) (inducer of CYP2C19, CYP3A4 & P-glycoprotein)	Photosensitivity Erectile dysfunction	Cyclosporine, digoxin, nevirapine, oral contraceptives, erlotinib, imatinib Reduced activity of macrolides, finasteride, dutasteride Reduced plasma concentrations of fexofenadine, voriconazole (>50%)
Valerian	CNS depressant	Alcohol, barbiturates, benzodiazepines, opiates
Zemaphyte (Chinese herbal therapy)	Diarrhea, transaminitis/ reversible acute hepatitis/fatal hepatic necrosis, reversible dilated cardiomyopathy, worsening of atopic dermatitis, urticaria	Methotrexate

Table 131.12 Herbal remedies/prescription drug interactions. CNS, central nervous system; CTD, connective tissue disease; MS, multiple sclerosis; TB, tuberculosis.

HMG-CoA Reductase Inhibitors

Although dermatologists may not prescribe these lipid-lowering agents, their use by family physicians and specialists is so widespread that it is fairly common to encounter patients who are taking this class of drugs. To date, all reports of significantly increased rates of myalgias from combination therapy with a "statin" plus certain other drugs involve simvastatin or lovastatin. Notably, these are the statins with the highest known metabolic dependency on the CYP3A4 pathway for elimination[59]. Fluvastatin is metabolized via CYP2C9 and therefore is not expected to interact with CYP3A4 inhibitors, but may interact with 2C9 inhibitors. Pravastatin is not metabolized by CYP3A4, nor is it cleared by PGP to a clinically significant degree[60].

Kinase Inhibitors

Kinase inhibitors represent an expanding class of drugs that has played an important role in the treatment of a wide range of malignancies including melanoma. More recently, kinase inhibitors have been used to treat inflammatory skin disorders including psoriasis and atopic dermatitis. With regard to drug–drug interactions, the most relevant kinase inhibitors for dermatologists are BRAF/MEK and Janus kinase (JAK) inhibitors.

The selective BRAF inhibitors dabrafenib, encorafenib, and vemurafenib are substrates of CYP3A4. Concomitant use of strong inducers or inhibitors of these enzymes (see Table 131.8) should be avoided or used with caution, as they could significantly alter drug levels of these BRAF inhibitors. Furthermore, dabrafenib is a substrate of CYP2C8 and a potent inducer of a variety of CYP enzymes and transporter proteins, leading to a potential risk for significant drug–drug interactions. For example, the coadministration of dabrafenib and immunosuppressive drugs (*everolimus*, *tacrolimus*) may require dosage adjustment to avoid graft rejection[61].

With regard to the JAK inhibitor baricitinib, its concentration may become elevated in the setting of concomitant therapy with probenecid due to the latter's inhibition of organic anion transporter 3[62].

Macrolide Antibiotics

When a macrolide is required in a patient who is receiving systemic *tacrolimus*, azithromycin should be used (rather than erythromycin or clarithromycin) because this does not produce significant inhibition of CYP3A4[63]. When erythromycin is prescribed to a patient on long-term *warfarin*, there is a risk of increased plasma warfarin levels, with increased anticoagulation and hemorrhage. This occurs because tacrolimus and warfarin are CYP3A4 substrates and erythromycin is a potent inhibitor. The coadministration of erythromycin plus *azole antifungals* leads to an increased risk for prolonged QT interval and torsades de pointes.

Erythromycin also inhibits the metabolism of *sildenafil*, resulting in a significant increase in serum levels of sildenafil[64]. If concurrent administration is unavoidable, reduced doses of sildenafil and *tadalafil* are recommended. In addition, an interaction between erythromycin and *carbamazepine* has been well established[65]. Erythromycin significantly inhibits hepatic metabolism of carbamazepine; the interaction is highly predictable, develops with rapid onset, and may also occur with clarithromycin or troleandomycin[65]. Concurrent use should therefore be avoided.

Quinolone Antibiotics

In the GI tract, all fluoroquinolones interact with multivalent cation-containing products, and the bioavailability of the quinolone can be reduced by up to 50% when coadministered with *iron* compounds

PHARMACOGENETICS – IMPACT OF POLYMORPHISMS ON DRUG METABOLISM		
Cytochrome P450 (CYP) isoenzyme	**Frequency of poor metabolizers**	**Examples of drugs affected**
CYP2C9	6%–8%	Glyburide, warfarin, phenytoin
CYP2C19	3%–5% of White individuals 12%–23% of Asians	Diazepam, omeprazole, pantoprazole
CYP2D6	6%–10% of White individuals 3%–6% of Mexican-Americans 2%–5% of African-Americans 1% of Asians	Codeine, imipramine, propafenone, metoprolol
CYP3A5	90%–95% of White individuals 70%–75% of Asians 30%–35% of African-Americans	Numerous (~50% of drugs are metabolized by CYP3A4/5)

Table 131.13 Pharmacogenetics – impact of polymorphisms on drug metabolism.

(ciprofloxacin and moxifloxacin are more affected than levofloxacin or gemifloxacin). There is also a significant decrease in the bioavailability of quinolones when given with *sucralfate*[65], and antibiotic treatment failure has been documented. If sucralfate cannot be discontinued, the quinolone should be taken 2–6 hours before the sucralfate. Similar decreases in bioavailability occur when a quinolone is given concurrently with an *antacid*[65]. The antacid should therefore be taken 6 hours prior to or 2 hours after the antibiotic.

Sparfloxacin is associated with cardiac manifestations in the form of QTc prolongation and it has a high phototoxicity potential. While moxifloxacin can prolong the QT interval, it does not alter the QT dispersion (QT dispersion is thought to be a more sensitive predictor of the risk of torsades de pointes). As such, the increased risk of torsades de pointes attributable to moxifloxacin is questionable[66]. Levofloxacin has no QT prolongation and a very low phototoxic potential, making it one of the safest fluoroquinolones in terms of drug interactions[67]. An enhanced anticoagulant effect of *warfarin* has been reported after coadministration with norfloxacin, ciprofloxacin, ofloxacin, or enoxacin[48].

Pimozide

Pimozide is a neuroleptic that may be used for psychogenic dermatologic problems such as delusions of parasitosis. While newer drugs may replace pimozide (see Ch. 7), as long as it is still being prescribed, dermatologists must be aware of its drug–drug interactions. Based upon case reports, pimozide may lead to prolongation of the QT interval and cardiac arrhythmias. Patients who are at risk of ventricular arrhythmias because of a prolonged QT interval or electrolyte disturbances, or who take other drugs that affect the QT interval, should use pimozide with caution. Pimozide is oxidized by two CYP isoforms, CYP3A4 and CYP1A2, with the former representing the responsible isoform at therapeutically relevant pimozide concentrations[68]. Adding a CYP3A4 inhibitor such as *clarithromycin*, *erythromycin*, or an *azole antifungal* may increase the risk of toxicity. A baseline assessment of the QT interval and reassessment 6 hours after a pimozide dose may be helpful in patients at risk who require pimozide.

Pharmacogenetics – Role of Polymorphisms

Cytochrome P450 enzymes

The genes encoding the CYP isoenzymes are highly polymorphic, and, as a result, the individuals within a general population have different levels of enzyme activity due to the presence of variant alleles. People with genetically determined low levels of activity are referred to as *poor* metabolizers. Those who have a functional enzyme are known as *extensive* metabolizers. There are yet others who have more than the usual complement of functional genes and more than the usual amounts of certain enzymes, and they are referred to as *ultrarapid* metabolizers. Still others have partially functional enzymes and are *slower* metabolizers than normal (*intermediate* metabolizers). Poor metabolizers may have a larger response and be at greater risk of toxicity than extensive metabolizers for drugs that are highly dependent on clearance to an inactive metabolite by the particular isoform[69]. On the other hand, ultrarapid metabolizers might not reach therapeutically active plasma concentrations of certain drugs, thereby not achieving the anticipated desired effect.

CYP enzymes that exhibit genetic polymorphisms include CYP1A2, CYP2C9, CYP2C19, CYP2D6, CYP2E1, and CYP3A5 (Table 131.13). However, provocation tests are not routinely employed in clinical practice and unfortunately there are no clinical parameters that are useful in predicting the metabolizing status of a given individual. Molecular analysis of the genes that encode the key CYP isoenzymes can be performed, i.e. testing is commercially available, but this is also not routinely done.

Other drug-metabolizing enzymes

Pharmacogenetic variation can also occur in other drug-metabolizing enzymes. Pertinent to dermatologists, the enzyme thiopurine methyltransferase (TPMT) is important in the metabolism of azathioprine and 6-mercaptopurine to non-toxic metabolites. There is a 0.3% rate of homozygous deficiency of this enzyme, putting these patients at significant risk for toxicity, especially myelosuppression[70]. Conversely, 88% of the population is homozygous for the active TPMT enzyme and may therefore require doses greater than the recommended daily dose of azathioprine (1–2 mg/kg/day) to achieve therapeutic success. Determination of the patient's TPMT level provides *a priori* information that allows the individualization of azathioprine dosing, thereby minimizing toxicity and maximizing efficacy.

Drug–Cytokine Interactions

Cytochrome P450 drug metabolism can be altered by certain proinflammatory cytokines, such as interleukin (IL)-6, IL-1, and tumor necrosis factor (TNF)[71]. These cytokines can cause a reduction in CYP3A function and they are released during periods of stress, trauma or infection, as well as administered as immunomodulators, in particular IL-2[72].

Drug–Virus Interactions

Human herpes virus (HHV) 6/7

The pathogenesis of drug reaction with eosinophilia and systemic symptoms (DRESS)/drug-induced hypersensitivity syndrome (DIHS) is a complex adverse reaction to medications. It is thought to involve: (1) genetic factors, including deficiencies of detoxifying enzymes and associations with specific HLA haplotypes such as HLA-B*57-01/abacavir and HLA-B*58-01/allopurinol (see Table 21.3); (2) virus-drug interactions, in particular HHV-6 reactivation; (3) drug-induced immunosuppression followed by an inflammatory immune recovery syndrome; and (4) drug-specific T cells, with the latter having been isolated from the blood and skin in lamotrigine- and carbamazepine-induced DRESS.

Human immunodeficiency virus (HIV)

A helpful website that contains current information regarding drug interactions in patients receiving antiretroviral medications is www.hiv-druginteractions.org[13]. For example, the coadministration of pimozide with most of the protease inhibitors or delavirdine is contraindicated because of the risk of inducing ventricular arrhythmias. In addition, there are reports of adrenal suppression and iatrogenic Cushing syndrome when patients on ritonavir-based antiretroviral therapy received inhaled, intra-articular, and even topical corticosteroids[73]. Moreover, recreational and illicit drug use may cause drug-drug interactions with antiretroviral medications[73a].

Hepatitis C virus

With respect to drug interactions, multi-drug direct-acting antiviral regimens, such as elbasvir/grazoprevir, sofosbuvir/velpatasvir, sofosbuvir/velpatasvir/voxilaprevir, and glecaprevir/pibrentasvir, are safely administered[73b]. However, interactions with other drugs do exist, e.g., plasma concentrations of glecaprevir/pibrentasvir can be decreased by inducers of PGP and CYP3A. A useful website for screening potential interactions is www.hep-druginteractions.org[73c].

CONCLUSION

Dealing with drug interactions is a challenge in clinical practice. Although no one can be expected to know all drug interactions, useful resources are available. One of the best pocket reference guides is *The Top 100 Drug Interactions* by Hansten and Horn (www.hansten-andhorn.com)[57]. This handbook is concise, up-to-date and, unlike most desk references, it is not limited by class-related statements that may falsely and unnecessarily restrict therapeutic options. A helpful website that contains comprehensive information regarding drug interactions related to CYP isoenzymes is The Flockhart Table™ (drug-interactions.medicine.iu.edu)[74].

More research during the early stages of drug development is required to identify new interactions, define mechanisms of older interactions, and examine the safety of new drugs from classes that are known to cause interactions. We also need more sensitive post-marketing surveillance tools to identify important drug interactions that become evident over time in diseased hosts and that were not seen in pre-marketing studies of healthy volunteers. Physicians need better tools, but, in the meantime, understanding the nuances of the cytochrome P450s will help take the fear out of prescribing.

Because the best evidence for clinically relevant drug interactions comes from case reports, prescribing physicians can have a major impact. Observations of drug interactions should be confirmed, if possible, by serum drug concentrations. Then they should be reported to regulatory bodies and submitted to journals. By understanding the mechanisms behind drug interactions and staying alert for toxicities, we can help make drug therapy safer and reduce the fear of drug interactions.

REFERENCES

1. Hadeler EK, Maderal AD. Drug interactions of natural supplements in dermatology: a review. *Int J Dermatol*. 2021;60:1183–1189.

1a. Weideman RA, McKinney WP, Bernstein IH. Predictors of potential drug interactions. *Hosp Pharm*. 1998;33:835–840.

2. Dechanont S, Maphanta S, Butthum B, Kongkaew C. Hospital admissions/visits associated with drug-drug interactions: a systematic review and meta-analysis. *Pharmacoepidemiol Drug Saf*. 2014;23:489–497.

3. Magro L, Morreti U, Leone R. Epidemiology and characteristics of adverse drug reactions caused by drug-drug interactions. *Expert Opin Drug Saf*. 2012;11:83–94.

4. Koch L, Kränke B, Aberer W. Potential drug-drug interactions and adverse drug reactions in dermatological inpatients. *J Dtsch Dermatol Ges*. 2016;14:1122–1129.

5. Hoey J. Drug interactions: who warns the patients? [editorial]. *CMAJ*. 1999;161:117.

6. Smalley W, Shatin D, Wysowski DK, et al. Contraindicated use of cisapride: impact of Food and Drug Administration regulatory action. *JAMA*. 2000;284:3036–3039.

7. Shapiro LE, Shear NH. Drug interactions/P450. *Curr Probl Dermatol*. 2001;13:141–152.

8. du Souich P. In human therapy, is the drug-drug interaction or the adverse drug reaction the issue? *Can J Clin Pharmacol*. 2001;8:153–161.

9. Palleria C, Di Paolo A, Giofre C, et al. Pharmacokinetic drug-drug interactions and their implication in clinical management. *J Res Med Sci*. 2013;18:601–610.

10. Hansten PD, Horn JR. *Drug Interactions Analysis and Management*. St Louis, MO: Facts & Comparisons (Wolters Kluwer Health); 2007.

11. Montamat SC, Cusack BJ, Vestal RE. Management of drug therapy in the elderly. *N Engl J Med*. 1989;321:303–309.

12. Devanathan AS, Anderson DJC, Cottrell ML, et al. Contemporary drug-drug interactions in HIV treatment. *Clin Pharmacol Ther*. 2019;105:1362–1377.

13. University of Liverpool. Interaction checker. <www.hiv-druginteractions.org>; 2022.

14. Samer CF, Ing Lorenzini K, Rollason V, et al. Applications of CYP450 testing in the clinical setting. *Mol Diagn Ther*. 2013;17:165–184.

15. Sullivan JR, Watson A. Lamotrigine-induced toxic epidermal necrolysis treated with intravenous cyclosporine: a discussion of pathogenesis and immunosuppressive management. *Australas J Dermatol*. 1996;37:208–212.

16. Toogood J. Beta blocker therapy and the risk of anaphylaxis. *CMAJ*. 1987;136:929–933.

17. Tugwell P, Bennett K, Bell M, Gent M. Methotrexate in rheumatoid arthritis: indications, contraindications, efficacy and safety. *Ann Intern Med*. 1987;107:358–366.

18. Schwartz JB. The influence of sex on pharmacokinetics. *Clin Pharmacokinet*. 2003;42:107–121.

19. Kotlyar M, Carson SW. Effects of obesity on the cytochrome P450 enzyme system. *Int J Clin Pharmacol Ther*. 1999;39:8–19.

20. Hoey J. Postmarketing drug surveillance: what it would take to make it work. *CMAJ*. 2001;165:1293.

21. Marchbanks C. Drug-drug interactions with fluoroquinolones. *Pharmacotherapy*. 1993;13:23–25.

22. Morii M, Ueno K, Ogawa A, et al. Impairment of mycophenolate mofetil absorption by iron ion. *Clin Pharmacol Ther*. 2000;68:613–616.

23. Bodey GP. Azole antifungal drugs. *Clin Infect Dis*. 1992;14:5161–5169.

24. Zimmermann T, Yeates RA, Laufen H, et al. Influence of concomitant food intake on the oral absorption of two triazole antifungal agents, itraconazole and fluconazole. *Eur J Clin Pharmacol*. 1994;46:147–150.

25. Hansten PD. Drug interactions. *Drug Interactions Newsletter*. 1996:893–906.

26. Anonymous. Drug interactions. *Med Lett Drugs Ther*. 1999;41:61–62.

27. Preiss R. P-glycoprotein and related transporters. *Int J Clin Pharmacol Ther*. 1998;36:3–8.

28. Benet LZ, Izumi T, Zhang Y, et al. Intestinal MDR transport proteins and P-450 enzymes as barriers to oral delivery. *J Control Release*. 1999;62:25–31.

29. Chishty M, Reichel A, Siva J, et al. Affinity for the P-glycoprotein efflux pump at the blood-brain barrier may explain the lack of CNS side-effects of modern antihistamines. *J Drug Target*. 2001;9:223–228.

30. Lown KS, Mao RR, Leichtman AB, et al. Role of intestinal p-glycoprotein (mdr1) in interpatient variation in the oral bioavailability of cyclosporine. *Clin Pharmacol Ther*. 1997;62:248–260.

31. Shapiro LE, Singer MI, Shear NH. Pharmacokinetic mechanisms of drug-drug and drug-food interactions in dermatology. *Curr Opin Dermatol*. 1997;4:25–31.

32. Birkett DJ, Mackenqie PI, Veronese ME, et al. In vitro approaches can predict human drug metabolism. *Trends Pharmacol Sci*. 1993;14:292–294.

33. Wienkers LC, Heath TG. Predicting in vivo drug interactions from in vitro drug discovery data. *Nat Rev Drug Discov*. 2005;4:825–833.

34. Coondoo A, Chattopadhyay C. Drug interactions in dermatology: what the dermatologist should know. *Indian J Dermatol*. 2013;58:249–254.

35. Giacomini KM, Krauss RM, Roden DM, et al. When good drugs go bad. *Nature*. 2007;446:975–977.

36. Michalets E. Update: clinically significant cytochrome P450 drug interactions. *Pharmacotherapy*. 1998;18:84–112.

37. Rendic S, Di Carlo FJ. Human cytochrome P450 enzymes. *Drug Metab Rev*. 1997;29:413–580.

38. Abdel Rahman SM, Gotschall RR, Kaufmann RE, et al. Investigation of terbinafine as a CP2D6 inhibitor *in vivo*. *Clin Pharmacol Ther*. 1999;65:465–472.

39. Wormhoudt LW, Commandeur JN, Vermeulen NP. Genetic polymorphism of human *N*-acetyltransferase, cytochrome P450, glutathione-S-transferase, and epoxide hydrolase enzymes: relevance to xenobiotic metabolism and toxicity. *Crit Rev Toxicol*. 1999;29:59–124.

40. Barner EL, Gray SL. Donepezil use in Alzheimer disease. *Ann Pharmacother*. 1999;32:70–77.

41. Page RL, Mueller SW, Levi ME, et al. Pharmacokinetic drug-drug interactions between calcineurin inhibitors and proliferation signals inhibitors with anti-microbial agents: implications for therapeutic drug monitoring. *J Heart Lung Transplant*. 2011;30:124–135.

42. Kellick KA, Bottorff M, Toth PP. A clinician´s guide to statin drug-drug interactions. *J Clin Lipidol*. 2014;8:30–46.

43. Tailor S, Gupta A, Walder S, Shear N. Peripheral edema due to nifedipine-itraconazole interaction: a case report. *Arch Dermatol*. 1996;132:350–352.

44. Kaukonen KM, Olkkola KT, Neuvonen PJ. Fluconazole but not itraconazole decreased the metabolism of losartan to E-3174. *Eur J Clin Pharmacol*. 1998;53:445–449.

45. Cadle RM, Zenon III GJ, Rodriguez-Bvarradas MC, et al. Fluconazole induced symptomatic phenytoin toxicity. *Ann Pharmacother*. 1994;28:292–295.

46. Gupta AK, Katz HI, Shear NH. Drug interactions with itraconazole, fluconazole and terbinafine and their management. *J Am Acad Dermatol*. 1999;41:237–248.

47. Shennib H, Auger JL. Diltiazem improves cyclosporine dosage in cystic fibrosis lung transplant recipients. *J Heart Lung Transplant*. 1994;10:292–296.

48. Tatro DS, ed. *Drug Interaction Facts*. St Louis: Facts & Comparisons; 1999. xxi–xxvii, 39–40, 720a–b, 2406–42.

49. Al-Niaimi F, Lyon CC. Acute kidney injury due to interaction of methyl-1-testosterone with ciclosporin metabolism in a patient with severe atopic dermatitis. *Dermatol Ther (Heidelb)*. 2013;3:211–214.

50. Fuhr U. Drug interactions with grapefruit juice. *Drug Saf*. 1998;18:251–272.

51. Roller L. Drugs and grapefruit juice [letter]. *Clin Pharmacol Ther*. 1998;63:87–88.

52. Kantola T, Kivisto KT, Neuvonen PJ. Grapefruit juice greatly increases serum concentrations of lovastatin and lovastatin acid. *Clin Pharmacol Ther*. 1998;63:397–402.

53. Schmiedlin-Ren P, Edwards DJ, Fitzsimmons ME, et al. Mechanisms of enhanced oral availability of CYP3A4 substrates by grapefruit juice constituents. Decreased enterocyte CYP3A4 concentration and mechanism-based inactivation by furanocoumarins. *Drug Metab Dispos*. 1997;25:1228–1233.

54. Edwards DJ, Bellevue FH, Woster PM. Identification of 6,7-dihydroxybergamottin, a cytochrome P450 inhibitor, in grapefruit juice. *Drug Metab Dispos*. 1996;24:1287–1290.

55. Ernst E. Harmless herbs? A review of the recent literature. *Am J Med*. 1998;104:170–178.

56. Mouly S, Lloret-Linares C, Sellier PO, et al. Is the clinical relevance of drug-food and drug-herb interactions limited to grapefruit juice and Saint-John's Wort? *Pharmacol Res*. 2017;118:82–92.

57. Hansten P, Horn J. *The Top 100 Drug Interactions: A Guide to Patient Management*. Edmonds, WA: H&H Publications; 2013:1–193.

58. Wang Z, Gorski JC, Hamman MA, et al. The effects of St John's wort (*Hypericum perforatum*) on human cytochrome P450 activity. *Clin Pharmacol Ther*. 2001;70:317–326.

59. Bottorf MB. Distinct drug-interaction profiles for statins. *Am J Health Syst Pharm*. 1999;56:1019–1020.

60. Ford NE, Sonnichsen DS. Clinically significant cytochrome P450 drug interactions – a comment. *Pharmacotherapy*. 1998;18:890–891.

61. Levavasseur M, Darras S, Mortier L, et al. Drug interaction between dabrafenib and immunosuppressive drugs: about one case. *Melanoma Res*. 2016;26:532–534.

62. Posada MM, Cannady EA, Payne CD, et al. Prediction of transporter-mediated drug-drug interactions for baricitinib. *Clin Transl Sci*. 2017;10:509–519.

63. McKindley D, Dufresne R. Current knowledge of the cytochrome p-450 isozyme system: can we predict clinically important drug interactions? *Med Health*. 1998;81:38–42.

64. Hansten PD, Horn JR. *Drug Interactions: Hansten and Horn's Guide to Patient Management*. ebook: <www.hanstenandhorn.com>.

65. Tatro DS, ed. *Drug Interaction Facts*. St Louis: Facts & Comparisons; 1998:91–92, 609a–10, 685d–g, 714a–b.

66. Tsikouris JP, Peeters MJ, Cox CD, et al. Effects of three fluoroquinolones on QT analysis after standard treatment courses. *Ann Noninvasive Electrocardiol*. 2006;11:52–56.

67. Lode H. Evidence of different profiles of side effects and drug-drug interactions among the quinolones – the pharmacokinetic standpoint. *Chemotherapy*. 2001;47(Suppl. 3):24–31. 44–8.

68. Desta Z, Kerbusch T, Soukhova N, et al. Identification and characterization of human cytochrome P450 isoforms interacting with pimozide. *J Pharmacol Exp Ther*. 1998;285:428–437.
69. Daly AK. Molecular basis of polymorphic drug metabolism. *J Mol Med*. 1995;73:539–553.
70. Snow J, Gibson L. A pharmacogenetic basis for the safe and effective use of azathioprine and other thiopurine drugs in dermatologic patients. *J Am Acad Dermatol*. 1995;32:114–116.
71. Prandota J. Important role of proinflammatory cytokines/other endogenous substances in drug-induced hepatotoxicity: depression of drug metabolism during infections/inflammation states, and genetic polymorphisms of drug-metabolizing enzymes/cytokines may markedly contribute to this pathology. *Am J Ther*. 2005;12:254–261.
72. Schwartz DH, Merigan TC. Interleukin-2 in the treatment of HIV disease. *Biotherapy*. 1990;2:119–136.
73. Tseng A, Foisy M. Important drug-drug interactions in HIV-infected persons on antiretroviral therapy: an update on new interactions between HIV and non-HIV drugs. *Curr Infect Dis Rep*. 2012;14:67–82.
73a. Funke B, Spinner CD, Esser S, et al. High prevalence of recreational and illicit drug use in German people living with HIV with a potential for drug-drug interactions with antiretroviral therapy. *Int J STD AIDS*. 2021;32:75–82.
73b. Gao LH, Nie QH, Zhao XT. Drug-drug interactions of newly approved direct-acting antiviral agents in patients with hepatitis C. *Int J Gen med*. 2021;14:289–301.
73c. University of Liverpool. Interaction checker. <www.hepdruginsteractions.org>; 2023.
74. Flockhart DA. *Drug Interactions: Cytochrome P450 Drug Interaction Table*. Indiana University School of Medicine; 2007. <https://drug-interactions.medicine.iu.edu>.
75. Yuan CS, Wei G, Dey L, et al. Brief communication: American ginseng reduces warfarin's effect in healthy patients. A randomized controlled trial. *Ann Intern Med*. 2004;141:23–27.
76. Matthews Jr. MK. Association of ginkgo biloba with intracerebral hemorrhage. *Neurology*. 1998;50:1933–1934.

132 Sunscreens and Photoprotection

Brandon L. Adler and Vincent A. DeLeo

Chapter Contents

Sunscreen Regulation 2345
Mechanisms of Sunscreen Action 2345
Active Ingredients in Sunscreens 2346
Sunscreen Benefits 2348
Sunscreen Safety 2350
Photoprotective Clothing 2351
Photoprotection Strategies and Sunscreen Recommendations . 2352

Key features

- Modern sunscreens were first developed during the 1940s with the primary aim of preventing sunburn. Today, sunscreens are also used to prevent other aspects of photodamage, including carcinogenesis and photoaging
- The active ingredients in sunscreens include: (1) soluble organic filters, i.e. "chemical" compounds, that absorb UV radiation; and (2) insoluble metal oxide filters, i.e. "physical" agents, that both absorb and scatter UV radiation
- The ability of sunscreens to prevent actinic keratoses and cutaneous squamous cell carcinoma has been demonstrated in human studies, and there is growing evidence that they can also prevent photoaging and cutaneous melanoma
- Following topical application, common organic filters are absorbed systemically at levels that exceed the FDA threshold requiring additional safety studies; however, to date there has been no evidence of harm related to their use
- Established side effects from sunscreens include irritation (which is common) and allergy (which is rare)
- In the laboratory, exposure to oxybenzone was found to be associated with coral bleaching; as a result, some localities have passed legislation prohibiting the sale of oxybenzone-containing sunscreens
- Photoprotection and sun avoidance may lead to a decrease in vitamin D levels in some individuals; optimum vitamin D levels can be achieved with a balanced diet and oral supplementation

INTRODUCTION AND HISTORY

Sun Exposure

Evidence exists that even ancient civilizations sought protection from the damaging effects of the sun. The concept of excessive sun exposure as unhealthy or at least cosmetically unacceptable eventually spread to Northern Europe, especially among the aristocracy, and continued into the nineteenth century until the period of the Industrial Revolution. In 1890, Palm noted that children in urban slums of England had rickets whereas those in similar housing conditions in sunny India did not, and linked the lack of sun to the development of rickets[1]. Physicians then began to treat such children with artificial UV radiation. At the same time, Finsen began to treat a number of other diseases, including cutaneous tuberculosis and, interestingly, lupus erythematosus, with artificial light; he was awarded the Nobel Prize for this work in 1903. At the turn of the twentieth century, the image of tanned skin as aesthetically pleasing began to emerge. The French fashion designer Coco Chanel is often credited with developing the concept of tanned skin as beautiful that still persists today. Indeed, for decades consumers applied various oils to the skin and used metal reflectors to enhance tanning. However, the twentieth century also saw the recognition of sunburn as an effect of UVB, the discovery of UVB-specific DNA mutations, and establishment of UVB as a complete carcinogen.

During the 1990s, dermatologists and other healthcare professionals made serious efforts to educate consumers regarding the damaging effects of excessive sun exposure as well as exposure to artificial tanning devices. Despite these efforts, recent studies show that while understanding of the adverse effects of exposure has increased, there has been very little positive change in behavior. This is especially true for adolescents and young adults, who continue to suffer sunburns and who continue to seek tans through natural and artificial exposure. For example, a systematic review in 2014 reported the prevalence of exposure to indoor tanning in the US, Europe, and Australia to be 36% for adults, 55% for university students, and 19% for adolescents[2]. Even in children and adolescents with a parental history of melanoma, sun protection was noted to be suboptimal[3], and some studies have found that sunscreen usage has actually been declining[4,5].

Sunscreens

Sunscreens attenuate UV wavelengths which would otherwise interact with molecules in the skin (chromophores) to generate photochemical reactions, leading to photobiologic change. These preparations are usually combinations of active filters that absorb or scatter incident radiation, and they are dispersed in a variety of topical vehicles. The active ingredients are not meant to be absorbed in any large quantity into the living epidermis, dermis, or general circulation.

In 1928, the first modern sunscreen, a product containing benzyl salicylate and benzyl cinnamate, was introduced in the US. However, widespread use of sunscreens did not occur until World War II, when the US military provided preparations containing red petrolatum to prevent sunburn in troops stationed in sunny areas. After the war, there was an increased interest in UV-absorbing chemicals, and para-aminobenzoic acid (PABA), patented in 1943, was the first of these to gain widespread usage. It was not until the mid-1970s that sunscreens gained a degree of consumer acceptance.

While solar radiation reaching the surface of the earth and human skin includes ultraviolet, visible, and infrared rays (see Fig. 134.1), the initial sunscreens were formulated primarily to prevent sunburn and therefore contained primarily UVB-absorbing agents (Fig. 132.1). As scientific evidence grew documenting the deleterious effects of longer-wavelength UVA radiation and as manufacturers strove to develop higher levels of protection against burning, agents with absorption in the longer wavelengths (e.g. benzophenones) were combined with UVB absorbers. The inorganic sunscreens (e.g. titanium dioxide) were used from the early days of sunscreen manufacturing, but because of large particle size, were not cosmetically acceptable in high concentrations. Newer technology allowed for micronization of such particles, with an increase in transparency and therefore greater cosmetic acceptability. More recently, chemical agents with greater UVA absorption have been introduced (see below) and are gaining in popularity.

Today, a wide array of sunscreen-containing preparations, including foundations, moisturizers, and lipsticks, are commercially available. Another improvement in sunscreen products has been the development of agents with increased substantivity. Such agents, usually marketed as "sports" products, have bases which persist on the stratum corneum for longer than do the usual bases, allowing for vigorous outdoor activity, sweating, and even swimming with retained photoprotection.

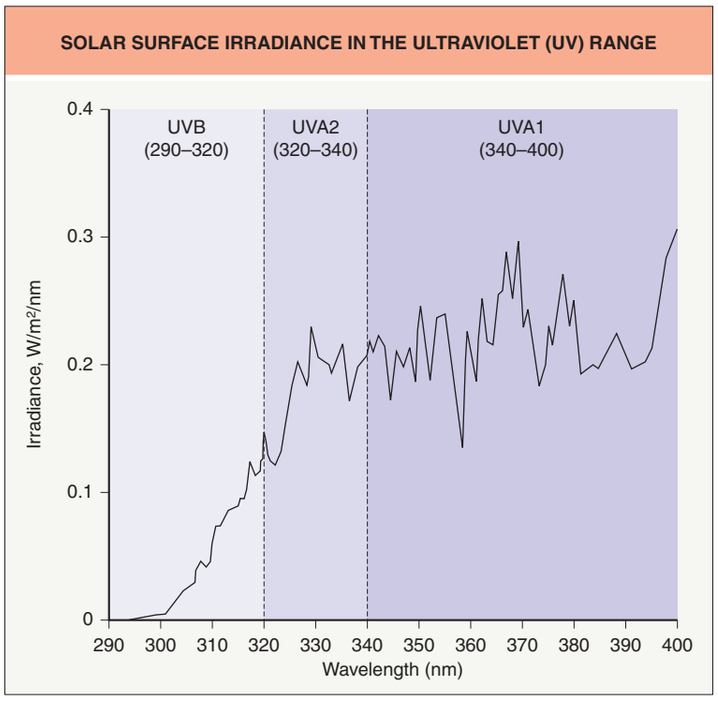


Fig. 132.1 Solar surface irradiance in the UV range. Note that the defined boundary between UVB and UVA differs between the International Commission on Illumination (315 nm) and the FDA (320 nm). *Courtesy Mark Naylor, MD.*

SUNSCREEN REGULATION

Globally, the manufacturing and regulation of sunscreens vary, including efficacy testing and labeling (Table 132.1). Since sunscreens alter the structure or function of skin, they are considered over-the-counter (OTC) drugs in the US and are regulated by the Food and Drug Administration (FDA). FDA regulations include the maximum concentration of active ingredients, safety labeling, and the methodology for determining the sun protection factor (SPF).

Sun Protection Factor (SPF)

Sunscreen efficacy is assessed based upon its SPF, which is determined by cutaneous phototesting utilizing artificial sunlight (Table 132.2). The methodology for measuring SPF, which predominantly represents UVB protection, has been standardized. If properly tested and applied, a product with an SPF of 15 would allow 15 times as much time in the sun with the same resultant level of erythema as without the product in a given individual (by attenuating 93.3% of the UV reaching the skin). Similarly, an SPF 50 product would allow 50 times as much exposure with the same result (via 98% UV blockage). Since the SPF is calculated as a ratio, the theoretical percentage of UV filtering basically levels off at SPF 30 and above (Fig. 132.2).

Testing for UVA Protection

Since scientists became aware of the damage that can be caused by photons longer than 315–320 nm, many attempts have been made to develop a standard method of testing for protecting against long-wave or UVA radiation. Because there is no easily reproducible cutaneous biologic endpoint that is relatively specific for UVA radiation (as erythema is for UVB), photobiologists have suggested a number of assays, including both *in vivo* and *in vitro* methodologies, to determine the UVA protection factor (UVA-PF).

The most commonly utilized human skin-based assays include immediate pigment darkening (IPD) and persistent pigment darkening (PPD), each with endpoints that measure a different aspect of the skin's tanning response to UVA radiation. The former, as discussed in Chapter 86, is dependent upon radiation-induced darkening of pre-existing melanin, while the latter is a more complex response which involves *de novo* synthesis and transfer of melanin. Both endpoints can be produced with relatively small amounts of UVA radiation, making them reasonable for human phototesting. In Japan, the assay for PPD is favored[6].

The most commonly accepted *in vitro* method for assessing UVA protection is the critical wavelength (CW) determination, which is utilized in the European Union, Australia, and the US. This is a relatively simple assay in which the sunscreen is dissolved in solvent and the absorption spectrum is determined by a spectrophotometer. The CW for the product represents the wavelength at which the *cumulative* absorption of solar-simulated radiation above 290 nm is 90%[7] (Fig. 132.3).

Evolution of FDA Sunscreen Standards

In 1999, the FDA published sunscreen regulations for 16 approved active ingredients that included: (1) limiting the maximum allowable SPF value on the label; and (2) changing the terminology for rating substantivity. As a result, manufacturers had to limit their labeling and marketing of efficacy claims regarding protection from sunburn. Methods for testing and labeling UVA protection were not addressed.

Based upon additional input from industry, dermatologists, and photobiologists, the FDA published its Final Rule for "Labeling and Effectiveness Testing: Sunscreen Drug Products for Over-the-Counter Human Use" in 2011. The major label on each product consisted of the SPF value and, if efficacy in the UVA range was deemed sufficient, the term "Broad Spectrum". UVA testing was limited to an *in vitro* CW determination (see Fig. 132.3 & Table 132.1), with a CW ≥370 nm meriting the broad spectrum designation. Substantivity ratings were limited to "Water Resistant (40)" and "Water Resistant (80)", with the number reflecting minutes. The maximum SPF was capped at 50+.

In 2019, the FDA released a proposed rule for a final sunscreen monograph, notable for its provisions regarding evaluation of safety data (Table 132.3). In order to determine that an active ingredient is *g*enerally *r*ecognized *a*s *s*afe and *e*ffective (GRASE), there is a requirement to conduct trials under maximal usage conditions to assess systemic absorption of active ingredients. If an appropriately conducted maximal usage trial detects a steady-state plasma level >0.5 ng/ml, further studies of carcinogenicity as well as reproductive and developmental toxicity may be required. Each of the 16 approved active ingredients was assigned to one of three categories (see Table 132.3): (1) GRASE; (2) not GRASE; or (3) insufficient data to support positive GRASE determination. Currently, the only GRASE ingredients are inorganic zinc oxide and titanium dioxide. The two non-GRASE ingredients, PABA and trolamine salicylate, are no longer marketed in the US. For the remaining 12 organic UV filters, while additional safety data are needed, this does not imply that they are unsafe.

The 2019 proposal also raised the maximum labeled SPF value from 50+ to 60+ (Table 132.4). To ensure sufficient UVA protection, broad spectrum sunscreens would need to possess a UVA1/UV ratio of ≥0.7 in addition to the CW ≥370 nm required in the 2011 monograph (see Fig. 132.3). Updated labeling requirements are designed to make it easier for consumers to locate a sunscreen's active ingredients.

Per the Sunscreen Innovation Act (SIA; 2014), the FDA was required to issue a final sunscreen monograph by November 2019, but the deadline was postponed. Under the 2020 CARES Act, the OTC monograph process was to be reformed. In September 2021, the FDA released a proposed final order for sunscreens that was not substantially different from the 2019 proposal, but it was intended to aid in the transition to the new processes created by the CARES Act[7a].

An additional issue in the US has been the limited number of active sunscreen ingredients approved by the FDA. A process for approval of new sunscreen agents, termed the Time and Extent Application (TEA), is available; studies of efficacy and safety conducted outside of the US are accepted in the application. The SIA mandates timelines for regulatory review of novel sunscreens, especially those that are already marketed in other countries. Nonetheless, to date, the FDA has not approved a new active sunscreen ingredient since 1999.

MECHANISMS OF SUNSCREEN ACTION

When applied properly, sunscreens form a film or coating on the surface of the stratum corneum that attenuates or "filters out" radiation that would otherwise reach the living epidermis and dermis. The active

GLOBAL COMPARISON OF EFFICACY TESTING AND LABELING OF SUNSCREENS					
	US	**Canada**	**European Union**	**Australia, New Zealand**	**Japan**
Regulatory category	Drugs	Drugs	Cosmetics	Drugs	Cosmetics
No. of allowed ingredients	16	20	30	30	34
Ultraviolet B					
Efficacy testing	SPF	SPF	SPF	SPF	SPF
Label descriptors	None	Medium to very high	Low to very high	Low to very high	None
Highest SPF allowed	50+	50+	50+	50+	50+
Ultraviolet A					
Efficacy testing					
• CW ≥370 nm	√	√	√	√	• UVA-PF (*in vitro*) • PPD • PA system
• UVA-PF (*in vitro*) to SPF ratio ≥0.33		√	√	√	
• PPD (*in vivo*) to SPF ratio ≥0.33		√			
Label descriptors	Broad spectrum	Broad spectrum	UVA seal	Broad spectrum	PA+ (2–4), PA++ (4–8), PA+++ (8–16), or PA++++ (>16)

Table 132.1 Global comparison of efficacy testing and labeling of sunscreens. The ratio of ≥0.33 for UVA efficacy means that protection in the UVA range must be at least one-third as great as in the UVB range (SPF). The UVA protection factor (UVA-PF) is calculated from the measured *in vitro* transmittance after irradiation and is weighted with the persistent pigment darkening (PPD) action spectrum and with the "standard" output spectrum of a UVA-filtered solar simulator. CW, critical wavelength; PA, protection grade of UVA; SPF, sun protection factor.

DETERMINATION OF THE SUN PROTECTION FACTOR (SPF)

- 10 human subjects
- Skin type I or II
- Irradiation: light source which mimics solar spectrum
- Procedure: determine minimal erythema dose (MED) in sunscreen-protected* and unprotected skin
- $\text{SPF} = \frac{\text{MED protected}}{\text{MED unprotected}}$
- To test substantivity – after application and before MED testing:
  - Water resistant (40): 2 × 20-min water immersions (whirlpool bath)†
  - Water resistant (80): 4 × 20-min water immersions (whirlpool bath)†

*Sunscreen product applied at 2 mg/cm^2.
†Air drying in between immersions.

Table 132.2 Determination of the sun protection factor (SPF).

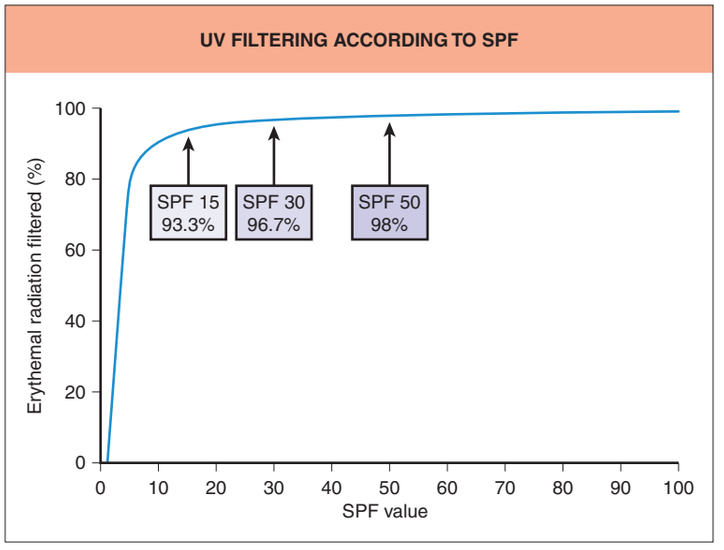


Fig. 132.2 Relationship between sun protection factor (SPF) and the amount of UV radiation that is filtered by a sunscreen. The percentage of UV blockage basically levels off above SPF 30.

agents in sunscreen products do this by either absorbing or scattering photons before they penetrate the skin surface. Nowadays, many sunscreen products contain combinations of agents that work by one or both mechanisms. Active sunscreen ingredients have conventionally been divided into so-called organic "chemical" agents which are water- or oil-soluble and function through photon absorption *versus* inorganic metal oxide "physical" agents which are insoluble and scatter light energy. However, there are limitations and exceptions to this seemingly clear-cut distinction.

When organic sunscreen agents absorb radiation, they are initially raised to a higher-energy, excited molecular state. Upon reverting to their ground state, this stored energy is usually dissipated in the form of heat, which is barely perceptible and non-damaging to the skin. However, some sunscreen agents, once excited, can undergo photochemical reactions with other sunscreen components (e.g. ecamsule), resulting in loss of their photoprotective efficacy. As a result, such agents (particularly avobenzone) lack photostability, i.e. they are deemed to be photolabile. In order to preserve efficacy, sunscreen agents such as avobenzone are combined with photostabilizers (e.g. salicylates, octocrylene).

In the past, opaque topical sun protection products consisting of insoluble metal oxide filters were considered "sunblockers", but since 1999 the FDA has not considered the concept of achieving complete blockage via topical photoprotection to be valid. Whereas *absorption* of solar radiation is directly related to *chemical structure*, optical *physical scattering* (and reflection) by inorganic agents is based primarily on *particle size*. Because sunscreens formulated with large-particle inorganic agents are cosmetically unacceptable due to their opaque appearance, particles are now micronized and the resultant products are significantly less visible. However, there is evidence that within the UV spectrum these inorganic agents such as particulate titanium dioxide, especially when micronized, also exhibit significant direct photon absorption that may be more important than their photon scattering effects[8].

ACTIVE INGREDIENTS IN SUNSCREENS

Currently, most sunscreens contain a combination of two or more agents in order to achieve broad spectrum protection. Fig. 132.4 lists, according to type of activity and spectrum of protection, the active agents currently used in sunscreens[9].

Organic (Soluble) Filters

Para-aminobenzoic acid and derivatives

PABA and its derivatives, including padimate O (octyl dimethyl PABA), are highly effective UVB absorbers. PABA is no longer marketed in the US, due in part to safety concerns.

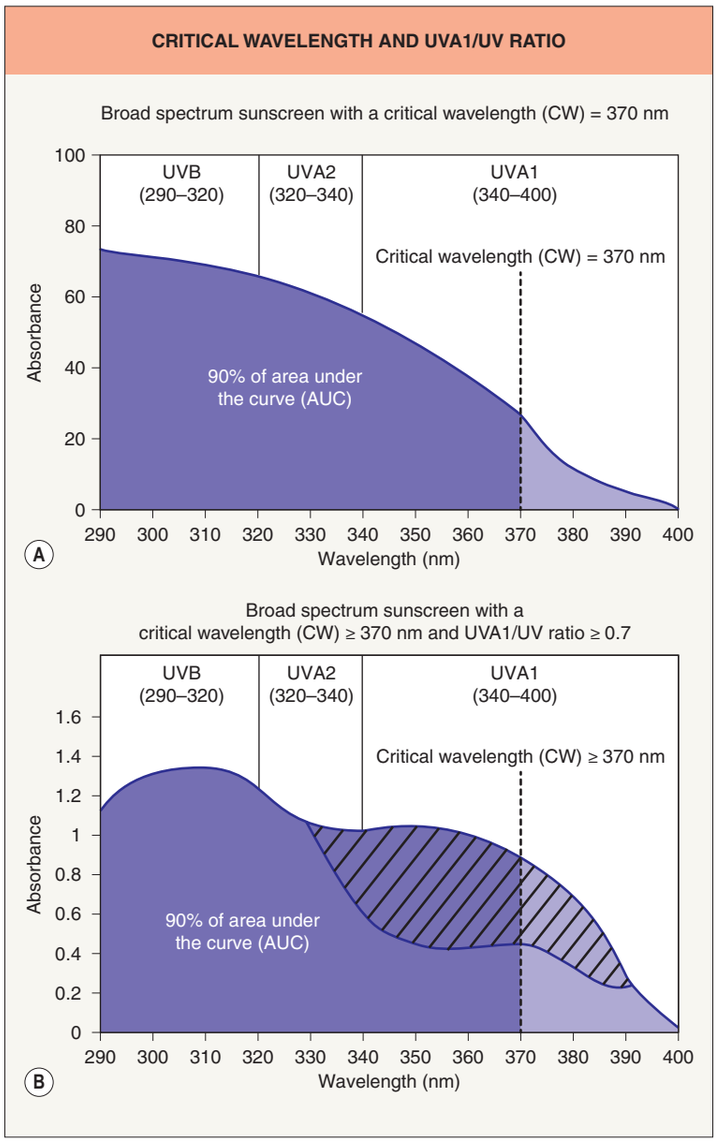


Fig. 132.3 Critical wavelength and UVA1/UV ratio. Critical wavelength (CW) represents the wavelength at which 90% of solar-simulated radiation above 290 nm is cumulatively absorbed by the sunscreen. **A** A broad spectrum sunscreen with CW = 370 nm. **B** A broad spectrum sunscreen with both a CW ≥370 nm and a UVA1/UV ratio of ≥0.7. The area with parallel lines represents the absorption needed for a sunscreen to have a UVA1/UV ratio of ≥0.7. *Adapted from Diffey BL, Tanner PR, Matts PJ, et al. In vitro assessment of the broad spectrum ultraviolet protection of sunscreen products. J Am Acad Dermatol 2000;43:1024–35 and the Federal Register 2019;84:6204–75.*

Cinnamates

Octyl methoxycinnamate (octinoxate) is a good UVB absorber but is not as potent as PABA and its esters. Presently, it is one of the most common sunscreen ingredients in the US.

Salicylates

The salicylates are relatively weak UVB absorbers but have the ability to stabilize other agents, thereby preventing photodegradation. Consequently, they are used in combination with other organic filters and include octisalate, homosalate, and trolamine salicylate. The latter is no longer included in US sunscreens, due in part to safety issues.

Benzophenones

Benzophenones are good UVA absorbers, although their effectiveness is primarily in the UVA2 range. Oxybenzone is the most commonly used agent in this group and actually affords both UVB and UVA protection. Sulisobenzone and dioxybenzone have similar protective spectra but are infrequently utilized.

Other organic filters

Octocrylene is a commonly used UVB filter which is primarily employed to stabilize photolabile agents. *Ensulizole* is likewise a photostable UVB absorber. *Avobenzone* is an excellent UVA filter with absorption well into the UVA1 range, but is very photolabile. It is therefore combined with other agents which assist in stabilizing its protective ability. *Menthyl anthranilate* is a UVA filter with a maximum absorption in the UVA2 range, but its efficacy is relatively weak. *Ecamsule* has maximum absorption at 345 nm, but was FDA-approved for use in only a single line of commercial products.

Agents currently awaiting approval in the US include amiloxate (UVB), enzacamene (4-methyl-benzylidene camphor; UVB), ethylhexyl triazone (UVB), iscotrizinol (UVB and UVA), drometrizole trisiloxane (UVB and UVA), bisoctrizole (UVB and UVA), and bemotrizinol (UVA) (see Fig. 132.4).

Inorganic (Insoluble) Filters

The two major inorganic sunscreens are titanium dioxide and zinc oxide. These inorganic compounds are the sole sunscreens in so-called "chemical-free" products but they are also combined with organic filters. Micronized zinc oxide appears to have better activity in the UVA1 range than does titanium dioxide at comparable concentrations[10]. With the advent of nanotechnology (see below), smaller particles of inorganic agents can be incorporated into sunscreen products.

Other Photoprotective Agents

Dihydroxyacetone is the compound most commonly used in sunless tanners. This agent, which when applied is colorless, binds to and

FDA PROPOSED ORDER (2021) FOR GRASE STATUS OF SUNSCREEN ACTIVE INGREDIENTS AND DOSAGE FORMS			
	GRASE	**Not GRASE**	**Insufficient data to support positive GRASE determination**
Active sunscreen ingredients	Zinc oxide Titanium dioxide	Para-aminobenzoic acid* Trolamine salicylate*	Avobenzone, cinoxate, dioxybenzone, ensulizole, homosalate, meradimate, octinoxate, octisalate, octocrylene, oxybenzone, padimate O, sulisobenzone
Dosage forms†	Lotions, creams, ointments, oils, gels, butters, pastes, sticks, sprays‡	Sunscreen–insect repellent combinations¶	Powders

*Not currently marketed in the US.
†Wipes, towelettes, body washes, shampoos, and other dosage forms are categorized as "new drugs" because the FDA has not yet received enough information about their efficacy and safety.
‡Sprays are approved as GRASE subject to testing, including particle size restrictions to avoid inhalation toxicity; flammability testing; and related safety labeling requirements.
¶Data suggest that combining some sunscreen active ingredients with some insecticides may increase absorption of one or both components. CDC recommends that if applying both a sunscreen and an insect repellent, apply the sunscreen first and then the insect repellent.

Table 132.3 FDA proposed order (2021) for GRASE status of sunscreen active ingredients and dosage forms. Each of the 16 approved active ingredients was assigned to one of three categories: (1) GRASE (*g*enerally *r*ecognized as *s*afe and *e*ffective); (2) not GRASE; or (3) insufficient data to support positive GRASE determination. For the third group, the FDA requires additional information to determine whether or not sunscreens with these ingredients and dosage forms are GRASE. Of note, this does not mean that the FDA has concluded that these ingredients and dosage forms are unsafe. *Adapted from US Food and Drug Administration. Proposed Order (OTC000008): Amending Over-the-Counter (OTC) Monograph M020: Sunscreen Drug Products for OTC Human Use. 2021. https://dps-admin.fda.gov/omuf/omuf/sites/omuf/files/primary-documents/2022-09/Proposed%20Administrative%20Order%20OTC000008_Amending%20M020_Sunscreen_Signed24Sept2021.pdf.*

FDA PROPOSED ORDER ON SUNSCREENS (2021) – ULTRAVIOLET B (UVB) AND ULTRAVIOLET A (UVA) PROTECTION AND LABELING REQUIREMENTS
Ultraviolet B (UVB) protection
• Raise the maximum proposed labeled SPF from 50+ to 60+ • Allow marketing on sunscreen products formulated up to an SPF of 80
Ultraviolet A (UVA) protection

• Require any sunscreen with SPF 15 or higher to be BROAD SPECTRUM
• Requirement for all BROAD SPECTRUM sunscreens with an SPF ≥15: as the SPF increases, so too does the magnitude of protection against UVA
• Require that BROAD SPECTRUM sunscreens provide adequate protection against UVA
  • UV absorbance critical wavelength of ≥370 nm (90% of the area under the curve [AUC])
  • UVA1/UV ratio of ≥0.7

Substantivity*
• WATER RESISTANT (40 minutes) or WATER RESISTANT (80 minutes) • The following designations are prohibited: "WATERPROOF", "SUNBLOCK", "ALL DAY PROTECTION", or "SWEAT PROOF"
Additional labeling
• Include an alphabetical listing of active ingredients on the front of the packaging • If the SPF of the sunscreen is <15, then it must have the following Skin Cancer/Skin Aging Alert: "Spending time in the sun increases your risk of skin cancer and early skin aging. This product has been shown only to help prevent sunburn, not skin cancer or early skin aging" • Require font and placement changes to ensure the terms SPF, BROAD SPECTRUM, and WATER RESISTANT are obvious on the label • Optional: If a sunscreen has an SPF ≥15 *and* is BROAD SPECTRUM, then can state that the product can help to reduce the risk of skin cancer and the risk of early skin aging, when used regularly and as directed in combination with other sun protection measures
*These changes were proposed and implemented in the 2011 FDA final rule for "Labeling and Effectiveness Testing: Sunscreen Drug Products for Over-the-Counter Human Use"

Table 132.4 FDA proposed order on sunscreens (2021) – ultraviolet B (UVB) and ultraviolet A (UVA) protection and labeling requirements. Active ingredient safety nd dosage forms are addressed in Table 132.3. For an explanation of critical wavelength and UVA1/UV ratio, see text and Fig. 132.3. SPF, sun protection factor. *Adapted from US Food and Drug Administration. Proposed Order (OTC000008): Amending Over-the-Counter (OTC) Monograph M020: Sunscreen Drug Products for OTC Human Use. 2021. https://dps-admin.fda.gov/omuf/omuf/sites/omuf/files/primary-documents/2022-09/Proposed%20Administrative%20Order%20OTC000008_Amending%20M020_Sunscreen_Signed24Sept2021.pdf.*

"stains" the stratum corneum to produce a tanned appearance. Although it has a very low SPF, it does offer some protection from long-wave radiation (even into the visible range). Iron oxide offers protection across the UV spectrum and into the visible range, and is used as a colorant in some products (e.g. tinted sunscreens)[11].

Other "active" ingredients have been added to sunscreens, with claims of increasing efficacy of the finished products[9]. The most popular of these are antioxidants, including vitamins E and C and green tea polyphenols, some of which have decreased UV-induced damage in *in vitro* and *in vivo* assays[11a]. However, factors including chemical structure, concentration, and stability in a finished product cannot be determined from package labels, so at this point there are no accepted standards whereby clinicians and consumers can judge efficacy.

SUNSCREEN BENEFITS

An effective sunscreen should protect against sunburn, carcinogenesis, photoaging, photoimmune suppression, and photosensitivity. Efficacy of a given sunscreen product is usually assumed if the combined absorption spectra of the agents in a product match the action spectrum of a given adverse event. The action spectra for the adverse effects of sun exposure are listed in Table 132.5. There is abundant evidence that sunburn, photoaging, keratinocyte carcinoma induction, and photoimmune suppression are all most efficiently produced by UVB radiation. However, studies have shown that for some of these events, UVA also plays a greater or lesser role. For example, UVB is about 1000 times as effective at inducing erythema in human skin as is UVA. On the other hand, photoaging was originally thought to be primarily due to UVB radiation, but UVA penetrates more deeply into the dermis and is likely to have an important role in this process. Similarly, although most studies (in a number of model systems) demonstrated that the maximally effective radiation for inducing photoimmune suppression is in the UVB range, sunscreens providing only UVB protection were not totally effective in blocking this effect[12].

With regard to cutaneous squamous cell carcinoma (SCC), epidemiologic and animal studies, combined with the identification of UVB and UVA "signature" mutations in human SCCs, strongly support causation primarily by UVB, but UVA may also play a role[13]. Most evidence also supports the role of UVB in basal cell carcinoma (BCC) induction, but the action spectrum for melanoma remains controversial. Still, UVB seems the most likely culprit. For example, in transgenic mice in which melanocytes are aberrantly located in the epidermis, a single erythemal (burning) dose to neonatal mice greatly enhanced melanoma formation[14].

It must also be remembered that even though UVA may be less effective at inducing a given event in the skin when compared to UVB, there is 10 to 20 times more UVA than UVB in sunlight. In terms of the relative UV doses received by the skin, this ratio is even higher when an individual wears a UVB-protective sunscreen, especially if the SPF is ≥8; this allows a person to stay in the sun longer and results in relatively higher levels of UVA absorption[15]. Therefore, the use of broad spectrum sunscreens should be a goal of any photoprotection strategy.

Although the effectiveness of the protection of a given product might be predicted from a comparison of the action spectrum (see Table 132.5) versus the absorption spectrum (see Fig. 132.4), the most valid measures of efficacy are prospective studies in human subjects. However, for skin cancer and photoaging, such studies are difficult to conduct because these photobiologic processes have such a long latency period. Animal models can be utilized, as has often been done for photoaging and SCC induction, but their availability has been quite limited for BCC (e.g. mice with only one normal allele for *Ptch*) and melanoma (e.g. opossums). Another approach has been to employ assays that measure the effect of sunscreens on biologic endpoints known to be important pathophysiologic precursors, but before the development of recognizable lesions. Examples would be studying the effects of sunscreens on the development of actinic keratoses or assaying for DNA damage or mutated genes in human skin[15].

Much of the information on sunscreen efficacy is based on retrospective case–control studies. Because of the lower level of validity of these studies, the variability of study design, and especially inherent recall bias, many such studies arrive at conflicting results.

Sunburn

Myriad unpublished SPF studies performed during the pre-marketing testing of sunscreens attest to their ability to prevent sunburn. However, controlled human studies in "real world" settings have found that sunscreen usage does not always prevent sunburn[16]. The major reason for this discrepancy is that individuals actually do not apply sunscreens at the same surface density as is utilized in controlled SPF testing, i.e. 2 mg/cm^2. Some studies have shown that most sunscreen users apply only 20%–50% of that quantity[17]. This means that the SPF is correspondingly reduced, i.e. applying only one-half of the standard amount of an SPF 15 product may result in protection comparable to a product with an SPF of 7.5 or even less[17]. The proper quantity of sunscreen to cover the skin of an adult is ~30–45 ml or 2–3 tablespoons. Strategies to improve compliance include applying the product twice to gain the proper surface density, which also reduces the occurrence of "skip" areas, or to use a product with twice the SPF as desired[18,19]. A recent randomized, double-blind trial demonstrated significantly greater sunburn protection with SPF100+ sunscreen compared to SPF50+ sunscreen during five days under actual use conditions[20].

Photoaging

In an actinic keratosis study, a significant reduction in dermal elastosis was noted with daily sunscreen use over a 2-year period[21]. A shorter-term study found that sunscreens with broad spectrum coverage that extended significantly into the UVA spectrum prevented many biochemical measures of sun damage (from solar-simulated radiation) in human volunteers[22]. More recently, 903 Australian

ACTIVE COMPONENTS OF SUNSCREENS

	Absorption			
	UVB	UVA2	UVA1	Visible
	290–320 nm	320–340 nm	340–400 nm	400–700 nm
Organic, soluble, "chemical absorbers"				
PABA derivatives				
PABA (para-aminobenzoic acid) [no longer marketed in the US]	■			
Padimate O (octyl dimethyl PABA)	■			
Cinnamates				
Octyl methoxycinnamate (Octinoxate, Parsol MCX)	■			
Cinoxate	■			
Amiloxate*	■			
Salicylates				
Octisalate (octyl salicylate)	■			
Homosalate (homomethyl salicylate)	■			
Trolamine salicylate [no longer marketed in the US]	■			
Benzophenones				
Dioxybenzone (benzophenone-8)	■	▒		
Oxybenzone (benzophenone-3)	■	■		
Sulisobenzone (benzophenone-4)		■	▒	
Others				
Octocrylene	■			
Ensulizole (phenylbenzimidazole sulfonic acid)	■			
Enzacamene (4-methyl-benzylidene camphor [4-MBC], Eusolex 6300, Neo Heliopan® MBC)*	■			
Ethylhexyl triazone [octyl triazone] (Uvinal® T 150)*	■			
Iscotrizinol (diethylhexyl butamido triazone, Uvasorb® HEB)*	■	■		
Drometrizole trisiloxane (Mexoryl™ XL)*	■	■	■	
Bisoctrizole (methylene-bis-benzotriazolyl tetramethylbutylphenol, Tinosorb® M)*	■	■	■	
Menthyl anthranilate (meradimate)		■		
Avobenzone (butyl methoxydibenzoyl methane, Parsol 1789)		■	■	
Ecamsule (terephthalylidene dicamphor sulfonic acid, Mexoryl™ SX)**		■	■	
Bemotrizinol (bis-ethylhexyloxyphenol methoxyphenyl triazine, Tinosorb® S)*		■	■	
Diethylamino hydroxybenzoyl hexyl benzoate (Uvinul® A Plus)*		■	■	
Bisdisulizole (Neo Heliopan® AP)*		■	■	
Inorganic, insoluble, "physical blockers"* **				
Titanium dioxide	■	■	▒	▒
Zinc oxide	■	■	■	▒
Other agents (not considered active screens)				
Dihydroxyacetone	▒	▒	▒	▒
Iron oxide	▒	▒	▒	▒

*Currently not FDA-approved. **This agent was approved for use by the FDA in a single line of commercial products under an Individual New Drug (IND) process. ***Depending on particle size, with micronized particles shifting protection toward UVA2; inorganic filters, especially when micronized, have been shown to function primarily by photon absorption rather than by scattering in the UV range[8] .

Fig. 132.4 Active components of sunscreens. Lighter colored bars represent variable efficacy. "Boosters" that are not UV filters are also added to sunscreen products, e.g. tiny spheres that scatter incoming radiation and agents that increase the spread of the sunscreen on the skin.

adults were studied for a period of 4.5 years. Half were instructed to use sunscreen daily while the remainder were allowed discretionary use of sunscreens. At the conclusion of the study, the daily sunscreen group showed no detectable increase in photoaging whereas skin aging was 24% higher in the discretionary group[23].

Photoimmunologic Suppression

Immune suppression by UV radiation was first reported in animal studies which showed that mice could no longer reject UV-induced skin tumors if they had been irradiated with non-tumorigenic doses of UV before transplantation of the tumors. This immunosuppressive

ACTION SPECTRA FOR PHOTODAMAGE				
Effect	Spectrum of light			Type of evidence
	UVB	UVA	Visible	
Sunburn	++++	+		1
Photoaging	++++	++	?	3,4
Squamous cell carcinoma	++++	+		2,3,4
Basal cell carcinoma	+++	+		2,4
Cutaneous melanoma	++	+		3,4
Photoimmune suppression	++++	++		1,3,4
Photosensitivity	+	+++	+	1 (varies with disease)

Table 132.5 Action spectra for photodamage (relative values). 1, human studies; 2, epidemiologic studies; 3, animal studies; 4, *in vitro* studies of associated biologic endpoints.

effect of UV has been shown to affect delayed-type hypersensitivity and contact sensitivity as well as tumor rejection and it occurs in humans as well as animals[24,25]. While the responsible action spectrum has been shown to be predominantly in the UVB range, in experimental studies UVB sunscreens have not always afforded protection against immune suppression[26]. In an elegantly designed study in a large number of human volunteers, Kelly and colleagues[27] reported that sunscreen did offer some protection against immune suppression but the level of protection was not as great as for sunburn. The researchers quantified photoprotection from immune suppression as the immune protective factor (IPF) and compared the IPF with the erythema protection factor (EPF), a measure similar to SPF. In their study, the IPF was only 4.9, while the EPF was 14.2. The authors postulated that this difference was due to UVA radiation not blocked by the applied sunscreen[27]. Some investigators concerned about the effect of photoimmune suppression on various aspects of human health have suggested that sunscreens should be tested and labeled for IPF as well as SPF, although its clinical relevance is not directly apparent.

Actinic Keratoses and Keratinocyte Skin Cancer

Because of the long latency period for the development of SCC and BCC, the first two prospective studies in humans examining the effect of sunscreen on cancer prevention tracked actinic keratoses, precursors of SCC, as surrogates for SCC development. In a group of 53 individuals with a previous history of actinic keratoses, an SPF 29 sunscreen was applied daily over a 2-year period[28]; the sunscreen-treated group had significantly fewer actinic keratoses over the 2-year period compared with the placebo group. The difference between the two groups with regard to skin cancers was not significant, probably due to the relatively short duration of the trial.

During a single Australian summer, 588 individuals (>40 years of age) were randomized to daily application of an SPF 17 sunscreen versus vehicle cream[29]. A significant reduction in the number of actinic keratoses in the sunscreen-treated group was observed. Several years later, a prospective Australian study compared an active intervention group, in which SPF 17 sunscreen was supplied and its daily use encouraged, against the background rate of sunscreen use in the general population[30]. The number of SCCs was found to be significantly less in the sunscreen-treated group, but there was no difference in the number of BCCs between the two groups. From clinical observations regarding anatomic distribution, the relationship between UV radiation and BCC is known to be more complex than with SCC.

In a prospective trial involving 120 solid organ transplant recipients (all of whom received education regarding sun protection), 60 individuals were given free broad spectrum sunscreen to apply daily to the head and neck, forearms, and hands[31]. Over a period of 24 months in which an average of 5.6 applications per week was recorded, significantly fewer *new* actinic keratoses and SCCs developed in the sunscreen group as compared to the control group. While the baseline actinic keratosis count was equal in the two groups, there was also a significant overall reduction in the number of actinic keratoses and fewer invasive SCCs in the sunscreen group. The reduction in BCCs was not statistically significant.

Cutaneous Melanoma

Developing sunscreen efficacy studies for decreasing the risk of melanoma is difficult and some might not consider them to be ethical. As with SCC and actinic keratoses, a number of researchers have used the development of melanocytic nevi in children as a surrogate marker for melanoma risk. The number of nevi has been related not only to sun exposure in children, but also to an enhanced risk for melanoma[32]. In several retrospective epidemiologic studies, researchers have actually reported that children who used sunscreens had an increased number of nevi[33]. However, in the only prospective controlled study published to date, it was demonstrated that sunscreens could suppress the development of melanocytic nevi[34]. This latter study was conducted over a 3-year period with an SPF 30 sunscreen in a total of 485 Canadian schoolchildren 6 to 9 years of age.

Retrospective case–control studies of melanoma patients have produced conflicting results with regard to sunscreen usage and the risk of developing melanoma. Some of these studies showed a decreased risk, while others actually showed an increased risk. Meta-analyses of the published studies by two different groups concluded that sunscreen usage did not increase the risk of developing melanoma, but the analyses could not confirm a protective effect from using sunscreen[35,36].

This dichotomy of results has led to a significant controversy concerning the use of sunscreens. The controversy is based on two different but related lines of reasoning. The first relates to the action spectrum for induction of melanoma. If in fact the action spectrum for melanoma is in the UVA range (as suggested by studies in fish but not other animal models), then wearing sunscreens with UVB protection will allow individuals to stay in the sun longer and receive larger doses of UVA, thereby increasing their risk of developing melanoma. The second theory is based on the concept that sunscreen usage decreases vitamin D levels in humans. Because vitamin D has been shown to reduce proliferation and increase differentiation of various normal and tumor cells, low vitamin D levels might increase the risk of developing some cancers, including melanoma[37].

However, in a prospective study, 1621 Australians (ages 25–75 years) were randomly assigned to daily or discretionary sunscreen application to the head and arms (in combination with 30 mg β-carotene or placebo supplements) for a period of 4 years[38]. They were then followed for another 10 years, and over that time period, 11 new primary cutaneous melanomas were identified in the daily sunscreen group and 22 in the discretionary group. This represented a reduction in the observed rate in the former group (hazard ratio [HR], 0.50; 95% CI, 0.24 to 1.02; $p = 0.05$); the reduction in invasive melanomas was more substantial: 3 in the daily group versus 11 in the discretionary group.

Photosensitivity Disorders (see Ch. 87)

Some of these reactions are caused by UVB radiation, but the majority of affected individuals react to UVA and/or visible light. Therefore, they require photoprotection with agents that absorb or reflect longer wavelengths and a small number of studies have confirmed the efficacy of such agents[37]. Currently, the most protective formulations appear to be avobenzone- and ecamsule-containing products[39]. Other useful agents include inorganic titanium and zinc oxides and benzophenones. The self-tanners containing dihydroxyacetone in combination with regular sunscreen usage may offer some benefit and iron oxide-containing products may also be helpful. In general, conventional sunscreens are of limited value in patients with cutaneous porphyria because the Soret band includes the violet–blue visible range (see Ch. 49).

SUNSCREEN SAFETY

Sunscreens have been utilized for decades with an excellent safety record, but usage patterns and recommendations have evolved significantly over time. In the past, sunscreens were primarily applied intermittently during times of intense sun exposure; however, as knowledge of their protective effects grew, this led to the current recommendation for daily use. Sunscreens are also incorporated into a broad array of personal care products. In the 2003–2004 National Health and

Nutrition Examination Survey, high exposure to organic UV filters was demonstrated in that oxybenzone was detected in 96.8% of urine samples[40].

The major established adverse effects of sunscreens are minor skin irritation, which is common, and allergic contact dermatitis, which is rare[41]. These reactions are often due to ingredients in the base of the product, such as fragrance or preservatives. Between 1999 and 2009, the organic compounds most often responsible for the rare instances of allergy or photoallergy in North America were oxybenzone and avobenzone[41a]. However, in Europe there has been an increasing number of reports of contact allergy and photocontact allergy to octocrylene. One speculation is that this is due to the use of topical NSAIDs (particularly ketoprofen) which cross-react with octocrylene and benzophenones[42].

Concerns have been raised, especially in the lay press, suggesting that some sunscreen agents are mutagenic or carcinogenic or have adverse hormonal effects in various *in vitro* and animal studies[43]. These concerns relate primarily to retinyl palmitate, benzophenones, and nanoparticle titanium and zinc oxides. Although retinoids are known to be anticarcinogenic, there is evidence that *retinyl palmitate*, when used as an additive in sunscreens and other personal care products, may absorb radiation and could theoretically lead to photodamage. *Nanoparticles* of titanium and zinc oxides could theoretically cause toxicity if they were to penetrate into the dermis, but studies show that such penetration does not occur in normal human epidermis (but can occur via hair follicles)[44]. While nanosized metal oxides may generate reactive oxygen species (ROS) when exposed to UV light, potential toxicity from ROS production is minimized by coating the particles with compounds such as silica or aluminum oxide. Finally, in animal studies, *benzophenones* were found to have estrogen-like effects and there is a single study in which decreased fecundity was reported in men with high exposure to these agents[45].

In 2019–2020, the FDA published two randomized trials assessing plasma concentrations of organic UV filters under maximal use conditions. In the initial pilot study of 24 participants, sunscreens containing avobenzone, oxybenzone, octocrylene, and ecamsule were applied at 2 mg/cm^2 to 75% BSA four times daily for four days[46]. Plasma concentrations of all four filters were >0.5 ng/ml after four applications on day 1. The expanded follow-up study included 48 volunteers who applied sunscreens with six active ingredients (avobenzone, oxybenzone, octocrylene, homosalate, octisalate, and octinoxate), again at 2 mg/cm^2 to 75% BSA, but with a modified dosing protocol of one application on the first day followed by four times daily on days 2–4[47]. All six filters reached systemic concentrations above the threshold following only one application.

The clinical effects of systemic absorption of organic UV filters are presently unknown. At the time of writing, no available data suggest that any organic filters need to be avoided for safety reasons. While ongoing evaluation of sunscreen safety is appropriate, physicians should stress that the overall risk–benefit analysis favors sunscreens as safe and a necessary component of a preventive health strategy. Concerned patients may use physical blockers containing zinc and titanium oxides, acknowledging that a possible association of sunscreen use with frontal fibrosing alopecia has been reported in observational studies, but there is a lack of causal evidence to date to support the relationship[48].

In 2021, a private laboratory undertook a study to examine 293 batches of sunscreens and after-sun products from multiple manufacturers for the presence of benzene, a known carcinogen. Benzene was identified at concentrations >2 ppm (the maximum concentration allowed by the FDA when use is unavoidable) in 4.7% of the products, primarily spray and gel formulations. This was followed by manufacturer recalls[48a].

Environmental Effects

Questions have also been raised as to the possible environmental impact of ubiquitous sunscreen use[49]. Organic UV filters are detectable in surface water throughout the world, even reaching the Arctic[50]. A major concern is that organic filters, in particular oxybenzone, may promote bleaching of coral reefs. Bleaching represents a response to environmental stressors in which corals expel symbiotic algae and turn white; coral death may follow.

A 2016 study reported an association between oxybenzone exposure and coral bleaching under laboratory conditions, as well as *in vitro* toxicity to coral cells[51]. The possibility of conversion of oxybenzone to phototoxic glucoside conjugates by sea anemones and corals has been raised[51a]. However, limited conclusions can be drawn from these results, which may not accurately reflect real-world exposure conditions[52]. Perhaps more importantly, coral bleaching is thought to be primarily driven by climate change, among other factors unrelated to sunscreen[41]. Nonetheless, this study influenced legislation passed in Hawaii and other localities prohibiting sale and distribution of sunscreens containing oxybenzone and octinoxate. In 2021, the FDA published a notice of intent to prepare an environmental impact statement for oxybenzone and octinoxate under the National Environmental Policy Act. While awaiting more definitive data, conscious consumers should be directed to use inorganic filters, which pose fewer environmental concerns.

Sunscreen and Vitamin D Status

Some researchers believe that sunscreens may actually be deleterious to health by blocking the production of vitamin D. The first step in the production of this important nutrient is the photochemical conversion within the epidermis of 7-dehydrocholesterol to previtamin D_3 by UVB radiation (see Fig. 51.11). Sunscreens that are effective at filtering UVB photons can result in decreased levels of vitamin D. However, the majority of human studies that measured serum vitamin D levels in sunscreen users (as compared to non-users) found that the levels, though reduced, remained within the normal range[53]. In addition, studies have shown that darkly pigmented individuals, women, and in the wintertime individuals who live in northerly climes all have reduced levels[54].

Recently, scientists in the fields of nutrition and bone metabolism have presented data suggesting that individuals who have serum vitamin D levels in the low normal range may actually have insufficient vitamin D for optimum health. Some of these studies suggest that not only do these low normal or "insufficient" levels of vitamin D adversely affect good musculoskeletal health, but they may also increase the risk of cancer, immune dysfunction, and a broad range of other diseases[55]. A recent systematic review found an association between vitamin D deficiency (<20 ng/ml) and greater Breslow depth and higher mortality rate in patients with melanoma, but causality has not been established[56].

Controversy has arisen in part because scientists cannot agree on what constitutes the "normal" range for serum 25-OH vitamin D levels and similarly cannot agree on the minimum recommended daily intake for the vitamin. Although vitamin D can be obtained from foods such as fish oils, in developed countries the more common sources are vitamin D-fortified milk and milk products, as well as vitamin supplements. In 2010, the Institute of Medicine issued a consensus statement regarding the recommended dietary allowance for vitamin D – 600 IU per day, except for those over 70 years of age in whom 800 IU per day was recommended. Unfortunately, the tanning salon industry continues to promote the concept that UV light exposure and tanning represent the optimum way to assure healthy vitamin D metabolism[57].

PHOTOPROTECTIVE CLOTHING

The broad range of textiles used in the manufacture of clothing results in highly variable degrees of sun protection. While other countries have mandated the testing required for the labeling of textiles claiming to be photoprotective, no US governmental agencies have regulatory control of such testing. However, the Federal Trade Commission does have the authority to regulate advertising claims regarding the sun protection of textiles.

The European Committee for Standardization published the methodology for determining the UV Protection Factor (UPF). It is based upon *in vitro* spectrophotometric measurements and standards whereby apparel textiles with a UPF >40 (similar to SPF) are labeled "UPF 40+". In addition, UVA transmission needs to be <5%[58]. In the US, textile industry organizations have developed a similar system that covers both UVB and UVA protection. Labeling includes the UPF plus a descriptor, from Good UV Protection (UPF 15–24) to Excellent UV Protection (UPF 40–50+); ratings <15 are not allowed[59].

Important factors that determine the protection afforded by a given textile include fabric porosity, type, color, weight, and thickness as well as the addition of absorbers. In the absence of UPF ratings, porosity is probably the most important factor, with the tighter the weave the greater the protection[60].

PHOTOPROTECTION STRATEGIES AND SUNSCREEN RECOMMENDATIONS

There is ever-increasing evidence that although the public is aware of the damaging effects of sun exposure, there does not seem to be a significant degree of alteration in behavior. Thinking of sunscreens as "the last line of defense" against UV damage to the skin emphasizes the importance of wearing hats and tightly woven clothing and seeking shade when considering the overall approach to sun safety (Table 132.6).

Special Populations

Sunscreens are not approved for use in infants younger than 6 months of age. Concerned parents can therefore limit their infant's time in the sun and use protective clothing. In older children, there is the possibility of using only inorganic filters, e.g. titanium and zinc oxides, in non-nanoparticle formulations. The same can be recommended for concerned pregnant women. In the future, formulations may use nanoparticles that are bioadhesive such that they stay on the skin surface and do not enter hair follicles.

GUIDELINES FOR PHOTOPROTECTION
• Avoid direct sun exposure between 10 AM and 4 PM whenever possible
• Seek the shade to shelter you from direct sun exposure
• Wear protective clothing, hats, and sunglasses whenever possible
• Apply sunscreen to all exposed skin when you will be outdoors
• Use a sunscreen with an SPF 30 or greater that is labeled as BROAD SPECTRUM
• Use up to 1 to 2 ounces of sunscreen to cover exposed skin (in an adult)
• Apply the sunscreen 15 minutes before sun exposure
• Use a water resistant sunscreen if you are going to swim or perspire heavily
• Re-apply sunscreen every 2 hours or after swimming or excessive sweating

Table 132.6 Guidelines for photoprotection. SPF, sun protection factor.

Additional figure available in our eBook (see inside front cover for access code).

REFERENCES

1. Giacomoni PU. Sunprotection: historical perspective. In: Shaath NA, ed. *Sunscreens: Regulations and Commercial Development*. 3rd ed. Boca Raton, FL: Taylor & Francis; 2005:71–81.
2. Wehner MR, Chren MM, Nameth D, et al. International prevalence of indoor tanning: a systematic review and meta-analysis. *JAMA Dermatol*. 2014;150:390–400.
3. Glenn BA, Lin T, Chang LC, et al. Sun protection practices and sun exposure among children with a parental history of melanoma. *Cancer Epidemiol Biomarkers Prev*. 2015;24:169–177.
4. Basch CH, Basch CE, Rajan S, et al. Use of sunscreen and indoor tanning devices among a nationally representative sample of high school students, 2001–2011. *Prev Chronic Dis*. 2014;11:E144.
5. Jones SE, Saraiya M, Miyamoto J, et al. Trends in sunscreen use among U.S. high school students: 1999–2009. *J Adolesc Health*. 2012;50:304–307.
6. Moyal D, Chardon A, Kollias N. UVA protection efficacy of sunscreens can be determined by the persistent pigment darkening (PPD) method (part 1): calibration of the method. *Photodermatol Photoimmunol Photomed*. 2000;16:245–249.
7. Diffey BL, Tanner PR, Matts PJ, et al. In vitro assessment of the broad spectrum ultraviolet protection of sunscreen products. *J Am Acad Dermatol*. 2000;43:1024–1035.

7a. Lim HW, Mohammad TF, Wang SQ. Food and Drug Administration's proposed sunscreen final administrative order: How does it affect sunscreens in the United States? *J Am Acad Dermatol*. 2022;86:e83–e84.

8. Cole C, Shyr T, Ou-Yang H. Metal oxide sunscreens protect skin by absorption, not by reflection or scattering. *Photodermatol Photoimmunol Photomed*. 2016;32:5–10.
9. Kullavanijaya P, Lim HW. Photoprotection. *J Am Acad Dermatol*. 2005;52:938–958.
10. Pinnell SR, Fairhurst D, Gillies R, et al. Microfine zinc oxide is a superior sunscreen ingredient to microfine titanium dioxide. *Dermatol Surg*. 2000;26:309–314.
11. Lyons AB, Trullas C, Kohli I, et al. Photoprotection beyond ultraviolet radiation: a review of tinted sunscreens. *J Am Acad Dermatol*. 2021;84:1393–1397.

11a. Chen L, Hu JY, Wang SQ. The role of antioxidants in photoprotection: a critical review. *J Am Acad Dermatol*. 2012;67:1013–24.

12. Young AR. Are broad-spectrum sunscreens necessary for immunoprotection? *J Invest Dermatol*. 2003;121:ix–x.
13. Agar NS, Halliday GM, Barnetson RS, et al. The basal layer in human squamous tumors harbors more UVA than UVB fingerprint mutations: a role for UVA in human skin carcinogenesis. *Proc Natl Acad Sci USA*. 2004;101:4954–4959.
14. Zaidi MR, Day C-P, Merlino G. From UVs to metastases: modeling melanoma initiation and progression in the mouse. *J Invest Dermatol*. 2008;128:2381–2391.
15. Fourtanier A. Mexoryl SX protects against solar-simulated photocarcinogenesis in mice. *Photodermatol Photoimmunol Photomed*. 1996;64:688–693.
16. Wright MW, Wright ST, Wagner RF. Mechanisms of sunscreen failure. *J Am Acad Dermatol*. 2001;44:781–784.
17. Petersen B, Wulf HC. Application of sunscreen – theory and reality. *Photodermatol Photoimmunol Photomed*. 2014;30:96–101.
18. Diffey BL. When should sunscreens be reapplied? *J Am Acad Dermatol*. 2001;45:882–885.
19. Teramura T, Mizuno M, Asano H, et al. Relationship between sun-protection factor and application thickness in high-performance sunscreen: double application of sunscreen is recommended. *Clin Exp Dermatol*. 2012;37:904–908.
20. Kohli I, Nicholson CL, Williams JD, et al. Greater efficacy of SPF 100+ sunscreen compared with SPF 50+ in sunburn prevention during 5 consecutive days of sunlight exposure: a randomized, double-blind clinical trial. *J Am Acad Dermatol*. 2020;82:869–877.
21. Boyd AS, Naylor M, Cameron GS, et al. The effects of chronic sunscreen use on the histologic changes of dermatoheliosis. *J Am Acad Dermatol*. 1995;33:941–946.
22. Stenberg C, Larko O. Sunscreen application and its importance for the sun protection factor. *Arch Dermatol*. 1985;121:1400–1402.
23. Hughes MC, Williams GM, Baker P, Green AC. Sunscreen and prevention of skin aging: a randomized trial. *Ann Intern Med*. 2013;158:781–790.
24. Ullrich SE. Photoimmune suppression and photocarcinogenesis. *Front Biosci*. 2002;17:d684–d703.
25. Hanneman KK, Cooper KD, Baron ED. Ultraviolet immunosuppression: mechanisms and consequences. *Dermatol Clin*. 2006;24:19–25.
26. Baron ED, Fourtanier A, Compan D, et al. High ultraviolet A protection affords greater immune protection confirming that ultraviolet A contributes to photoimmunosuppression in humans. *J Invest Dermatol*. 2003;121:869–875.
27. Kelly DA, Seed PT, Young AR, et al. A commercial sunscreen's protection against ultraviolet radiation-induced immunosuppression is more than 50% lower than protection against sunburn in humans. *J Invest Dermatol*. 2003;120:65–71.
28. Naylor MF, Boyd A, Smith DW, et al. High sun protection factor (SPF) sunscreens in the suppression of actinic neoplasia. *Arch Dermatol*. 1995;131:170–175.
29. Thompson SC, Jolley D, Marks R. Reduction of solar keratoses by regular sunscreen use. *N Engl J Med*. 1993;329:1147–1151.
30. Green A, Williams G, Neale R, et al. Daily sunscreen application and betacarotene supplementation in prevention of basal-cell and squamous-cell carcinomas of the skin: a randomised controlled trial. *Lancet*. 1999;354:723–729.
31. Ulrich C, Jurgensen JS, Degen A, et al. Prevention of non-melanoma skin cancer in organ transplant patients by regular use of a sunscreen: a 24 months, prospective, case-control study. *Br J Dermatol*. 2009;161(Suppl. 3):78–84.
32. Azizi E, Iscovich J, Pavlotsky F, et al. Use of sunscreen is linked with elevated naevi counts in Israeli school children and adolescents. *Melanoma Res*. 2000;10:491–498.
33. Autier P, Dor JF, Severi G. More about sunscreen use, wearing clothes, and number of nevi in 6 to 7 year old European children. *J Natl Cancer Inst*. 1999;91:1165–1166.
34. Gallagher RP, Rivers JK, Lee TK, et al. Broad-spectrum sunscreen use and the development of new nevi in white children: a randomized controlled trial. *JAMA*. 2000;283:2955–2960.
35. Bastuji-Garin S, Diepgen TL. Cutaneous malignant melanoma, sun exposure, and sunscreen use: epidemiological evidence. *Br J Dermatol*. 2002;146(Suppl. 61):24–30.
36. Huncharek M, Kupelnick B. Use of topical sunscreens and the risk of malignant melanoma: a meta-analysis of 9067 patients from 11 case control studies. *Am J Public Health*. 2003;93:11–12.
37. Eide MJ, Weinstock MA. Public health challenges in sun protection. *Dermatol Clin*. 2006;24:119–124.
38. Green AC, Williams GM, Logan V, Strutton GM. Reduced melanoma after regular sunscreen use: randomized trial follow-up. *J Clin Oncol*. 2011;29:257–263.
39. DeLeo V. Sunscreen use in photodermatoses. *Dermatol Clin*. 2006;24:27–33.
40. Calafat AM, Wong LY, Ye X, et al. Concentrations of the sunscreen agent benzophenone-3 in residents of the United States: National Health and Nutrition Examination Survey 2003--2004. *Environ Health Perspect*. 2008;116:893–897.
41. DeLeo VA. Photocontact dermatitis. *Dermatol Ther*. 2004;17:279–288.

41a. DeLeo VA, Adler BL, Warshaw EM, et al. Photopatch test results of the North American Contact Dermatitis Group, 1999-2009. *Photodermatol Photoimmunol Photomed*. 2022;38:288–291.

42. de Groot AC, Roberts DW. Contact and photocontact allergy to octocrylene: a review. *Contact Dermatitis*. 2014;70:193–204.
43. Adler BL, DeLeo VA. Sunscreen safety: a review of recent studies on humans and the environment. *Curr Dermatol Rep*. 2020;9:1–9.
44. Mohammed YH, Holmes A, Haridass IN, et al. Support for the safe use of zinc oxide nanoparticle sunscreens: lack of skin penetration or cellular toxicity after repeated application in volunteers. *J Invest Dermatol*. 2019;139:308–315.
45. Buck Louis GM, Kannan K, Sapra KJ, et al. Urinary concentrations of benzophenone-type ultraviolet radiation filters and couples' fecundity. *Am J Epidemiol*. 2014;180:1168–1175.
46. Matta MK, Zusterzeel R, Pilli NR, et al. Effect of sunscreen application under maximal use conditions on plasma concentration of sunscreen active ingredients: a randomized clinical trial. *JAMA*. 2019;321:2082–2091.
47. Matta MK, Florian J, Zusterzeel R, et al. Effect of sunscreen application on plasma concentration of sunscreen active ingredients: a randomized clinical trial. *JAMA*. 2020;323:256–267.
48. Robinson G, McMichael A, Wang SQ, et al. Sunscreen and frontal fibrosing alopecia: a review. *J Am Acad Dermatol*. 2020;82:723–728.

48a. Hudspeth A, Zenzola N, Kucera K, et al. Independent sun care product screening for benzene contamination. *Environ Health Perspect*. 2022;130:37701.

49. Schneider SL, Lim HW. Review of environmental effects of oxybenzone and other sunscreen active ingredients. *J Am Acad Dermatol*. 2019;80:266–271.

50. Tsui MM, Leung HW, Wai TC, et al. Occurrence, distribution and ecological risk assessment of multiple classes of UV filters in surface waters from different countries. *Water Res*. 2014;67:55–65.
51. Downs CA, Kramarsky-Winter E, Segal R, et al. Toxicopathological effects of the sunscreen UV filter, oxybenzone (benzophenone-3), on coral planulae and cultured primary cells and its environmental contamination in Hawaii and the U.S. Virgin Islands. *Arch Environ Contam Toxicol*. 2016;70:265–288.
51a. Vuckovic K, Tinoco AI, Ling L, et al. Conversion of oxybenzone sunscreen to phototoxic glucoside conjugates by sea anemones and corals. *Science*. 2022;376:644–648.
52. Mitchelmore CL, Burns EE, Conway A, et al. A critical review of organic ultraviolet filter exposure, hazard, and risk to corals. *Environ Toxicol Chem*. 2021;40:967–988.
53. Passeron T, Bouillon R, Callender V, et al. Sunscreen photoprotection and vitamin D status. *Br J Dermatol*. 2019;181:916–931.
54. Nesby-O'Dell S, Scanlon KS, Cogswell ME, et al. Hypovitaminosis D prevalence and determinants among African American and white women of reproductive age: third National Health and Nutrition Examination Survey, 1988–1994. *Am J Clin Nutr*. 2002;76:187–192.
55. Pludowski P, Holick MF, Pilz S, et al. Vitamin D effects on musculoskeletal health, immunity, autoimmunity, cardiovascular disease, cancer, fertility, pregnancy, dementia and mortality: a review of recent evidence. *Autoimmun Rev*. 2013;12:976–989.
56. Tsai TY, Kuo CY, Huang YC. The association between serum vitamin D level and risk and prognosis of melanoma: a systematic review and meta-analysis. *J Eur Acad Dermatol Venereol*. 2020;34:1722–1729.
57. Madigan LM, Lim HW. Tanning beds: impact on health, and recent regulations. *Clin Dermatol*. 2016;34:640–648.
58. Gambichler T, Laperre J, Hoffman K. The European standard for sun-protective clothing: EN 13758. *J Eur Acad Dermatol Venereol*. 2006;20:125–130.
59. Hatch KL. American standards for UV-protective textiles. *Recent Results Cancer Res*. 2002;160:42–47.
60. Hoffman K, Laperre J, Avermaete A, et al. Defined UV protection by apparel textiles. *Arch Dermatol*. 2001;137:1089–1094.



eFig. 132.1 Lack of sunburn in areas of sunscreen application on the back.
Peripheral edge represents outline of fingers. *Courtesy Kalman Watsky, MD.*

133 Complementary and Alternative Medicine

Apple Bodemer, Raja Sivamani and Peter Lio

Chapter Contents

Natural Products – Medical Applications 2354
Cannabinoids 2357
Diet-Based Therapies 2358
Traditional Chinese Medicine 2358
Homeopathy 2359
Aromatherapy 2359
Mind–Body Medicine 2359
Ayurveda 2360

Key features

- Globally, complementary and alternative medicine (CAM) is commonly utilized by patients with skin disease
- CAM encompasses a diverse group of therapies and systems, many without strong evidence of efficacy
- Among dermatology patients, the most popular forms of CAM include herbals, dietary supplements, homeopathy, and acupuncture
- Scientific research regarding CAM is ongoing, with results varying from promising to demonstrating minimal, if any, benefit

INTRODUCTION

Complementary and alternative medicine (CAM) represents a diverse set of healthcare systems, practices, and treatments that are grouped together because they are not considered part of conventional medicine (Table 133.1). More specifically, "complementary medicine" can be defined as non-mainstream modalities or approaches used *in conjunction with* conventional medicine, while "alternative medicine" typically refers to the use of non-mainstream approaches *in place of* a conventional treatment. Integrative medicine seeks to blend CAM with more conventional therapies and implies assimilation of healing practices from multiple traditions and cultures.

Multiple studies suggest that from 35% to 70% of patients with skin disease have used CAM[1]. In the US, there tends to be a greater use of CAM in women, adults 30 to 69 years of age, those with higher levels of education, and former smokers[2]. CAM utilization also correlates with the number of health conditions, number of doctor visits during the past year, and hospitalization within the past year. The overwhelming majority of CAM users in high-income countries, including those with dermatologic disorders, use CAM to complement conventional medicine rather than as a complete alternative[2]. Interestingly, individuals with skin conditions are more likely to use CAM than the general population, making this topic particularly relevant to dermatologists[3].

In this chapter, a number of the major alternative or complementary systems and therapies employed for dermatologic conditions are reviewed. In order to maximize utility, we have focused on treatments with at least some supportive evidence of efficacy (Table 133.2).

NATURAL PRODUCTS – MEDICAL APPLICATIONS

Conventional dermatology uses many products of herbal origin, including podophyllin, psoralens, oatmeal, and pyrethrins; such accepted treatments are discussed elsewhere in this textbook. This section limits its discussion to botanicals, insect-based products, and dietary supplements that may be less well known to clinicians, but nonetheless are used by patients to treat skin ailments. Side effects are also reviewed (Table 133.3; Fig. 133.1).

Aloe Vera

Aloe vera (*Aloe barbadensis*) is applied topically to treat a number of afflictions including thermal burns, ulcers, chronic wounds, and mild cutaneous infections. It has also been used successfully to treat psoriasis[4]. Aloe gel is the clear viscous material found in the inner part of the leaf of the aloe plant and is the most common component used to treat skin conditions. A yellowish layer called aloin can be found just under the skin of the aloe leaf. It contains latex and can cause allergic reactions in susceptible individuals. When applied to the skin, aloe gel's anti-inflammatory effects are thought to be due to a reduction in levels of thromboxane A2, thromboxane B2, and prostaglandin 2[5]. Although generally well tolerated, aloe vera gel may cause an allergic contact dermatitis.

Capsaicin

Capsaicin is found in hot peppers (*Capsicum*), and it is a mixture of vanillyl amides of isodecenoic acid. Topical capsaicin is used for postherpetic neuralgia, notalgia paresthetica, diabetic neuropathy, complex regional pain syndrome, and hemodialysis-related pruritus. By binding to the vanilloid receptor-1 on pain fibers, capsaicin stimulates the release and eventual depletion of the neurotransmitter substance P. Prolonged exposure leads to deactivation of these neurons[6]. While there is some concern that systemically administered capsaicin is associated with an increase in carcinogenesis, this has not been found in studies of topical capsaicin[7]. Topical capsaicin is considered safe enough to appear in multiple over-the-counter (OTC) preparations; however, the associated stinging and burning sensations can be very unpleasant, especially when applied to fissured or denuded skin and should be used with caution.

Chamomile

Chamomile (*Matricaria recutita*; *Chamaemelum nobile)* is one of the earliest and most widely used medicinal plants. It has been employed for a variety of conditions, including mucocutaneous inflammation, as well as promotion of wound healing. Chamomile is traditionally used for dermatitis and may be applied topically or ingested as a tea. When applied topically, it has been shown to be beneficial in atopic dermatitis and nonspecific skin irritation. Chamomile contains terpenoids and flavonoids that inhibit cyclooxygenase and lipoxygenase as well as regulate T-helper-cell (Th2) activation and histamine release[8]. Chamomile is a member of the ragweed family and has the potential to induce allergic contact dermatitis in addition to contact urticaria.

Colloidal Oatmeal

For decades, colloidal oatmeal has been used for its calming and soothing effects on the skin. Many OTC products are derived from whole oat kernels ground into a fine powder and then combined with emollients to create various preparations from bath powders to moisturizing creams[8]. Colloidal oatmeal is one of the few natural ingredients approved by the US Food and Drug Administration (FDA) to treat multiple skin conditions, including allergic contact dermatitis to poison ivy, irritant diaper dermatitis, and eczema[9].

The therapeutic properties of oats are thought to derive from their diverse chemical composition. Firstly, oats have a high concentration

CLASSIFICATION OF COMPLEMENTARY AND ALTERNATIVE MEDICINE (CAM)		
Biologically-based practices	Dietary supplements	Vitamins Minerals Fatty acids Amino acids Prebiotics, probiotics
	Herbal products	
	Diet-based therapies	Vegan Macrobiotic Vegetarian Paleo
Alternative medicine systems	Ayurveda Homeopathy Naturopathy	
	Traditional healers	Shaman
	Traditional Chinese medicine	Acupuncture Acupressure Moxibustion or cupping Chinese herbs
Mind–body medicine	Meditation Biofeedback Hypnotherapy Guided imagery Breath work Prayer and spirituality	
	Creative outlets	Music therapy Art therapy Dance therapy
Manipulative and body-based practices	Massage Chiropractic Reflexology Alexander technique Feldenkrais method Rolfing Osteopathy Tai chi	
Energy medicine	Reiki Therapeutic touch Craniosacral Qi gong Magnetic therapy Light therapy	

Table 133.1 Classification of complementary and alternative medicine (CAM). Based on classifications from the National Center for Complementary and Alternative Medicine (National Institutes of Health).

of starches which explains their water-holding capacity that contributes to skin barrier protection. Secondly, high concentrations of phenols provide antioxidant and anti-inflammatory properties. For example, *in vitro*, oat extracts decreased the concentrations of the proinflammatory cytokine IL-8 as well as NF-κB[9]. Lastly, its cleansing activity is thought to be due to the saponins present in the grain. Products that contain colloidal oatmeal tend to have very low allergenicity[10].

Escharotics

Escharotics include zinc chloride, bloodroot (*Sanguinaria canadensis*), and goldenseal (*Hydrastis canadensis*). These agents are caustic and can produce pain and necrotic crusts with subsequent scarring. In the past, escharotics were used topically to treat skin cancers and played a role in the fixed-tissue technique initially used in Mohs micrographic surgery, but they have since been replaced with more predictable and reliable methods.

Escharotics are commercially available as herbal supplements and are often marketed as "highly successful treatments for skin cancer"[11]. One of the greatest concerns regarding these unregulated and unsubstantiated claims, aside from inadequate treatment, is partial treatment leading to clinical but not histologic clearance and subsequently a more advanced recurrence. In an illustrative case report, after an escharotic was used to treat a basal cell carcinoma (BCC), the patient determined that it was cured. However, the tumor was still present, recurred underneath the scar, and ultimately led to metastasis[11]. These botanicals are neither safe nor effective for the treatment of skin cancers, and their use should be discouraged.

SELECTED TYPES OF COMPLEMENTARY AND ALTERNATIVE MEDICINE (CAM) WITH PROMISING EVIDENCE FOR TREATING DERMATOLOGIC DISEASES		
Skin disease	**Type of CAM**	**Comments**
Acne	• Tea tree oil (topical)	• Safe and effective; some risk for ACD or ICD
	• Dietary modification (avoiding dairy and high-glycemic foods)	• Probably decreases inflammation; adherence may be challenging
Atopic dermatitis	• Sunflower seed oil	• Enhances barrier function and may reduce pruritus
	• Coconut oil	• Antibacterial and moisturizing effects
	• Acupuncture/ acupressure	• May modestly reduce pruritus; can be expensive to see practitioner
Hidradenitis suppurativa	• Dietary modification (avoiding dairy and high-glycemic foods) • Weight reduction (via hypocaloric diet*)	• May reduce potential triggers • Reduces mechanical stress, improves insulin resistance
	• Zinc, riboflavin, vitamin D supplementation (oral)	• Zinc gluconate (90 mg daily), riboflavin (3 mg TID), and vitamin D repletion may lead to improvement
Psoriasis	• Indigo naturalis	• Anti-inflammatory effects on skin and nails; stains fabric
	• Curcumin (topical and oral)	• May have anti-inflammatory effects; color and odor can be offensive
	• Dietary modification (weight reduction via hypocaloric diet) for overweight or obese individuals	• Reduction in adipose tissue may lead to a decrease in inflammatory cytokines
Seborrheic dermatitis	• Tea tree oil (topical)	• Appears modestly effective; ACD or ICD may occur
Urticaria	• Vitamin D supplementation (oral)	• May help certain subset of population; safe
	• Acupuncture	• Multiple possible mechanisms; can be expensive to see practitioner
Verrucae	• Garlic (topical)	• Effective irritant and antiviral; unpleasant smell and ICD may deter its use
	• Zinc supplementation (oral)	• Results of clinical studies appear to be better than clinical experience; gastrointestinal upset fairly common
	• Propolis (oral)	• May be immunomodulatory; bee allergy is contraindication

*And/or bariatric surgery.

Table 133.2 Selected types of complementary and alternative medicine (CAM) with promising evidence for treating dermatologic diseases. ACD, allergic contact dermatitis; ICD, irritant contact dermatitis; TID, three times daily.

Feverfew

Feverfew (*Tanacetum parthenium*) is a flowering plant from the daisy family. Originally named for its fever-reducing properties, it is also used

DIETARY SUPPLEMENTS THAT INHIBIT PLATELET FUNCTION OR ENHANCE ANTICOAGULATION		
Effect	**Dietary supplements**	
Inhibits platelet aggregation	• Borage seed oil* • Bromelain (bromelin) • Clove • Feverfew • Garlic • Ginger • Ginseng	• Green tea • Huang qi • Kava kava • Onion • Salicylic acids† • Turmeric • Vitex
Inhibits platelet aggregation and adhesion	• Fish oil • Vitamin E	
Inhibits platelet activating factor	• Gingko	
Vitamin K antagonists: • Inhibit hepatic synthesis of vitamin K-dependent coagulation factors II, VI, IX, and X as well as proteins C and S • Potentiate effect of warfarin	Coumarin-containing compounds: • Arnica • Anise • Asafoetida • Alfalfa • Bilberry • Celery • Chamomile • Fenugreek • Goldenseal	• Horse chestnut • Horseradish • Licorice • Parsley • Passionflower • Quassia • Red clover • Rue
*Contains alpha-linoleic acid. †Includes meadowsweet and willow bark; inhibits platelet synthesis of thromboxane A2.		

Table 133.3 Dietary supplements that inhibit platelet function or enhance anticoagulation. *Adapted from Reddy KK, Grossman L, Rogers GS. Common complementary and alternative therapies with potential use in dermatologic surgery: risks and benefits. J Am Acad Dermatol 2013;68;e127–35.*



Fig. 133.1 Phototoxic reaction to herbal tea. *Courtesy Josef Smolle, MD.*

to treat headaches, arthritis, and digestive disorders. Use of topical feverfew had been limited by the presence of irritating parthenolides in the plant, but an industry-patented process now allows for removal of these irritants[12]. Feverfew possesses antioxidant and anti-inflammatory properties; it is thought to inhibit proinflammatory mediators released from macrophages and to reduce neutrophil chemotaxis[8]. It has also been shown to protect DNA against oxidative damage and appears to reduce UV radiation-induced DNA damage[13]. Dermatologic applications include treatment of irritated sensitive skin, facial erythema, and tactile roughness.

Green and Black Tea

The tea plant (*Camellia sinensis*) has been cultivated in Asia for thousands of years. Green tea is made from unfermented tea leaves and can be ingested or applied topically. It contains the highest concentration of polyphenol antioxidants of any tea, save perhaps for white tea, which is the least processed of all teas. Both topical and oral green tea can protect against inflammation, ultraviolet light-induced photodamage, chemical carcinogenesis, and photocarcinogenesis[14]. Topical green tea has been shown to decrease sebum production and may be beneficial in patients with acne[15]. While green tea is very safe both topically and systemically, topical application of a 2% preparation did lead to limited mild pruritus or stinging in 10%–15% of individuals, but this resolved within a few days despite continued use[15].

Black tea, the fully oxidized version of the same plant, was shown to be effective by day 3 when used as a compress to treat facial dermatitis in 22 adults ($p = 0.00004$), with no side effects reported[16].

Honey

In addition to fructose and glucose, honey also contains numerous proteins, amino acids, vitamins, enzymes, and minerals. While honey is used to treat a wide variety of conditions, it is most commonly applied to wounds to enhance healing. The latter effect is thought to be due to its antimicrobial properties and the enzymatic release of hydrogen peroxide. Honey has been shown to inhibit a wide variety of pathogens, e.g. *Staphylococcus aureus* (including MRSA), *Escherichia coli*, *Pseudomonas aeruginosa*, *Acinetobacterium baumannii*[17]. It has also led to improvement of several dermatitides (seborrheic, atopic, diaper), psoriasis, pityriasis (tinea) versicolor, and herpetic ulcers[17].

Active components of various honey formulations have been identified, e.g. methylglyoxal in manuka honey[18], and then associated with therapeutic benefits. Medical-grade honeys are now available by prescription, suggesting that honey may be entering the realm of conventional medicine. Although an allergic contact dermatitis to honey has been observed (probably related to propolis), there have been no reports of significant adverse events and topical application of honey is thought to be well tolerated[5].

Horse Chestnut Seed Extract

Oral horse chestnut seed extract (HCSE) (*Aesculus hippocastanum* L.) is used to treat chronic venous insufficiency. In controlled studies, there was a decrease in leg volume, calf and ankle circumferences, and pain, with an efficacy equivalent to that of grade II compression stockings[19]. HCSE contains *escin* (a triterpene saponin), which inhibits the release of elastase and hyaluronidase from leukocytes, thus preventing proteoglycan degradation and vascular leakage. Natural horse chestnut seeds are poisonous and need to be processed to remove *esculin*, a toxic component. Side effects of esculin include hepatotoxicity, renal toxicity, anaphylaxis, and possible potentiation of anticoagulation. Of note, drug interactions may limit the use of oral HCSE in patients receiving anticoagulants, aspirin, nonsteroidal anti-inflammatory drugs (NSAIDs), insulin, oral hypoglycemic agents, or other supplements that affect serum glucose levels[20].

Indigo Naturalis

Indigo naturalis is derived from the *Strobilanthes formosanus* plant and provides a well-known name for a dark blue color. Topical indigo naturalis has been observed to improve plaque psoriasis[4] as well as nail psoriasis in children[21]. The latter may be explained by an inhibition of epidermal keratinocyte proliferation by indirubin, an active component of indigo naturalis. Indirubin has been shown to down-regulate CDC25B expression, which is known to play an important role in the hyperproliferation of epidermal keratinocytes[22]. Tryptanthrin, another compound present in indigo naturalis, has been shown to inhibit production of interferon-γ, decrease levels of IL-17 and IL-6[23], and inhibit TNF. While oral indigo can cause hepatotoxicity, topical indigo is generally well tolerated. Mild pruritus has been reported and since indigo is a blue dye, staining of clothing and skin can occur.

Licorice Root

Licorice root (*Glycyrrhiza inflata*; *Glycyrrhiza glabra*) has long been considered a natural remedy. *Glycyrrhiza glabra* contains glabridin and *Glycyrrhiza inflata* contains licochalcone A, both of which have anti-irritant and anti-inflammatory properties[8]. Additionally, licorice extracts have been shown to have anti-elastase and anti-tyrosinase activity making them attractive ingredients in anti-aging products[24]. Licorice can be used to treat rosacea and dermatitis and is found in OTC preparations that target sensitive skin[25]. Licorice also contains glycyrrhizin, a substance that, if ingested in high doses, can cause hypokalemia, arrhythmias, hypertension, and/or congestive heart failure; de-glycyrrhizinated licorice (DGL) is available and may be preferable when administering licorice systemically.

Marigold

Marigold (*Calendula officinalis)* is a flower native to northern Mediterranean countries. Topically, marigold is most commonly used to treat dermatitis, but has been employed for wounds, ulcers, thermal burns, and herpes zoster. There is also evidence to support the use of calendula ointment to reduce radiation-induced skin toxicity[26]. Marigold contains flavonoids, triterpene saponins, and carotenoids which confer anti-inflammatory, antimicrobial, and immunomodulating properties. In animal studies, an increase in glycoproteins and collagen was observed in wound sites treated with topical marigold. There are rare reports of allergic contact dermatitis to *Calendula*, but it is generally well tolerated[6].

Menthol

Menthol is a naturally occurring plant compound that is used in multiple products including pharmaceuticals, pesticides, and flavoring agents. Topical preparations that contain menthol are used for their antipruritic, analgesic, and cooling properties. Menthol is thought to act through the cation channel TRPM8, a member of the TRP (transient receptor potential) family of ion channels, which is also activated by cold. However, the precise mechanism by which menthol suppresses pruritus is unclear. In addition to affecting sensory pathways, menthol exhibits antibacterial and antifungal activity[27].

Prebiotics, Probiotics, and Postbiotics

Prebiotics are non-digestible compounds in food that encourage the growth of certain desirable types of bacteria within the intestine. *Probiotics* are live microorganisms that are ingested or applied in an attempt to alter the resident flora into a more beneficial balance. In the gut, the microflora has been shown to influence gene expression and differentiation of cells involved in the immune system. These gut microbes can influence systemic inflammation and have even been found to impact the skin barrier[28]. *Postbiotics* are byproducts of probiotics that have bioactivity. Probiotics can be ingested in a tablet form or as a component of foodstuffs such as yogurt, miso, and tempeh.

Patients with eczema have been shown to have abnormal gastrointestinal flora and may have increased inflammation and intestinal permeability. Probiotics decrease intestinal inflammation and permeability, and may alter antigen presentation in a beneficial way. However, the results of clinical trials have been mixed and outstanding questions remain, including the ideal patient, the type and dosage of the probiotics, and the timing and frequency of administration[29]. Patients with acne appear to have a deficiency in short-chain fatty acid-producing bacteria in their gut microbiome. Thus far, pilot studies are promising for the use of oral probiotics in acne but expanded clinical studies are needed. More recently, a meta-analysis found that probiotics improved the efficacy of immune checkpoint inhibitors in cancer patients[29a].

Side effects of probiotics usually consist of mild gastrointestinal symptoms. While there are case reports of sepsis thought to be due to probiotics, the overwhelming body of evidence suggests that they are safe even in critically ill patients[30]. Nonetheless, before recommending probiotic supplementation in immunocompromised patients, it would be wise to carefully weigh potential benefits.

Tea Tree Oil

Tea tree oil is an essential oil from the leaves of the native Australian tree, *Melaleuca alternifolia*. The indigenous people of Australia use tea tree oil from crushed leaves as a traditional remedy to treat wounds and skin infections. It has been shown to have activity against a wide variety of bacteria, fungi, and even viruses and protozoa. Tea tree oil is commonly used as a topical antimicrobial agent and has shown efficacy in treating acne as well as fungal and bacterial infections of the skin, mucosae, and nails. The antiseptic properties of tea tree oil are thought in part to be due to disruption of bacterial membranes[31].

Tea tree oil can be very irritating and is a cause of allergic and irritant contact dermatitis. In general, it should be diluted before direct application to the skin, with concentrations of up to 10% not resulting in significant reactions[31]. In patients with onychomycosis, tea tree oil may be safely applied directly to nails.

Prepubertal gynecomastia, which was self-limited and not associated with hormonal abnormalities, developed in a boy who used a shampoo containing lavender and tea tree oil. *In vitro*, both of these essential oils can have mild estrogenic and anti-androgenic effects[32]. There are a few additional reports of essential oil-related gynecomastia, but their incorporation into numerous OTC personal care products (as a denominator) needs to be kept in mind. In a recent exchange, authors of a case study of lavender-associated prepubertal gynecomastia concluded: "It is true you cannot establish causality based on 4 case studies, but…there is value to pursuing this question in epidemiologic studies"[33].

Turmeric

Turmeric is the ground root of *Curcuma longa* and its active compound is curcumin. Curcumin is the yellow pigment that gives turmeric, curry, and yellow mustard their color, and it has been used for centuries in cooking and cosmetics. Turmeric has antimicrobial, antioxidant, anti-inflammatory, and anticancer activities[34]. It inhibits lipoxygenase and cyclooxygenase, thereby reducing levels of leukotrienes, thromboxanes, and prostaglandins. While data are limited, there are studies looking at the use of turmeric and curcumin in acne, alopecia, atopic dermatitis, oral lichen planus, photoaging, pruritus, psoriasis, radiodermatitis, and vitiligo. Oral turmeric is very safe even at high doses. Topical turmeric has been evaluated for psoriasis and wound healing[25], but color and odor can be limiting.

Vitex (Chasteberry)

An extract of vitex dried fruit (*Vitex agnus-castus*) has been used to treat menstrual cycle disorders. As a corollary, oral vitex has also been used to improve hormonal acne in women, with the German Commission E recommending 40 mg of the extract daily for acne[35]. It is thought to help reduce levels of luteinizing hormone, prolactin, fasting insulin, and testosterone, thereby improving hormonal acne. Potential adverse effects include headache, nausea, gastrointestinal disturbance, abnormal menstruation, and rash; these are typically mild and reversible. Theoretically, vitex could interfere with medications that affect dopamine pathways[36]. Given the hormonal effects of oral vitex, it should not be used by pregnant or nursing women[5].

CANNABINOIDS

There has been increasing interest in cannabinoids, the group of compounds that act on cannabinoid receptors and are often associated with *Cannabis sativa* or *Cannabis indica*. Within the field of dermatology, these compounds are of interest due to their potential antipruritic, anti-inflammatory, and anti-nociceptive properties, all of which do not require any psychoactive aspects of the plant[37]. While there is promise for both topical and oral application of a range of compounds including cannabidiol (CBD), N-palmitoylethanolamide (PEA), and even whole plant extracts, there is surprisingly little clinical evidence for any of these, let alone approved formulations that have been tested in a rigorous fashion. In fact, a recent review identified only 8 clinical studies of cannabinoids for dermatologic conditions, with 7 focused on atopic dermatitis, eczema, or pruritus[37]. Of these, 6 reported improvement based upon at least some metrics, while in the second

largest study of this group, a topical PEA-containing product led to no significant differences in chronic pruritus.

There is a need for high-quality trials to evaluate efficacy and safety of particular products, as it is simply not appropriate to generalize results about an ingredient or individual compound given all the complex variables involved: formulation, route of administration, dosage, and frequency of use.

DIET-BASED THERAPIES

Skin disorders are well represented in the long and complex history of the therapeutic use of "fad diets"[38]. Over the past several decades, there has been renewed interest in employing dietary modifications to influence cutaneous diseases. Obesity is thought to contribute to a proinflammatory state and there is some evidence that weight loss is beneficial in *psoriasis*[39]. In a subset of patients, a gluten-free diet may also improve psoriasis[40]. Dairy and high-glycemic foods may be contributing factors for *acne*, and avoiding these foods appears to significantly reduce acne severity[38].

Although dietary avoidance of certain allergens can be helpful in patients with systemic contact dermatitis, the story is much more complex in the case of atopic dermatitis. There is widespread belief outside the conventional medical community that foods are the "root cause" of atopic dermatitis, and while it is a compelling idea, there is limited evidence to support this theory[41]. Some support exists for avoiding known allergens (specifically eggs)[42], especially in infants. Overall, excluding foods in patients without specific allergies appears to have an insignificant effect[43]. Severe nutritional deficiencies and even kwashiorkor have been reported in infants on restrictive diets, underscoring the fact that there is risk associated with pronounced dietary modifications.

TRADITIONAL CHINESE MEDICINE

With a history spanning over 2000 years, traditional Chinese medicine (TCM) is a sophisticated system that encompasses health and disease. Diagnostic evaluation includes parameters such as pulse rate and appearance of the tongue as well as an assessment of tendencies and habits. An individualized TCM diagnosis is then rendered that is usually quite different from a conventional Western diagnosis. For example, patients sharing the Western diagnosis "acne" would not necessarily all be treated in the same manner because their underlying diagnoses could be vastly different, necessitating different approaches.

TCM encompasses a multitude of treatment modalities, including herbal medicine, acupuncture, massage, exercise, and dietary and lifestyle modifications (Table 133.4). For health to occur, balance and harmony must be achieved between two opposing and complementary forces, Yin and Yang. Additionally, normal flow patterns of *qi*, or life-force, are essential for health. Restoration of flow is the goal of therapy, often via acupuncture, moxibustion, and massage.

TRADITIONAL CHINESE MEDICINE (TCM) TREATMENT MODALITIES	
Modality	**Delivery methods/related modalities**
Herbal medicine	Decoctions – water is used to simmer herbs, then the decanted fluid is taken in divided doses
	Topical poultices
	Essential oils
	Lotions, creams, ointments
	Tablets, capsules
Acupuncture	Needles – stainless steel (most common), gold, silver
	Moxibustion
	Cupping, coining, rubbing
	Acupressure
	Electroacupuncture
	Auricular acupuncture
	Laser acupuncture
	Medicamentous acupuncture
	Magnet therapy
Therapeutic exercise	Tai ji (tai chi), qi gong (chi gong)
Massage therapy	Tui na, acupressure

Table 133.4 Traditional Chinese medicine (TCM) treatment modalities.
Courtesy Amy Geng and Raymond G. Dufresne, Jr.

Treatment of Dermatologic Diseases

TCM has been employed for a number of dermatologic conditions. While a complete discussion is beyond the scope of this chapter, the next sections highlight some of the evidence for its use in atopic dermatitis and psoriasis.

Atopic dermatitis

A Cochrane systematic review analyzed 28 studies of Chinese *herbal preparations* for atopic dermatitis, both ingested and applied topically. They found that in most of the studies reviewed, Chinese herbal therapy was superior to placebo in terms of reducing eczema severity and decreasing pruritus[44]. Nonetheless, the authors concluded that there is still insufficient evidence for efficacy as the quality of the studies was low. Even with the inclusion of additional studies, a similar conclusion was reached several years later – high quality randomized controlled trials were needed[45].

Herbal preparations are generally considered safe; side effects are rare and usually mild when they do occur. However, in addition to associated allergic reactions and photosensitivity, herbs may have pharmacologic effects and interact with other medications. They may also be adulterated with corticosteroids and contain arsenic or mercury[46].

Acupuncture has been used anecdotally for a variety of skin conditions, including atopic dermatitis, lichen planus, psoriasis, alopecia areata, and verrucae[47]. More support exists for the use of acupuncture for alleviation of symptoms associated with dermatologic disorders, such as pain or pruritus. A pilot study demonstrated decreased pruritus in patients with atopic dermatitis after applying acupressure to a single point on the arm[48]. Acupuncture and acupressure may work via so-called "gate control" and/or by stimulating release of neuroactive substances including endorphins and enkephalins. By altering the release of neurotransmitters, acupuncture may exert anti-inflammatory and immunomodulatory effects.

Side effects of acupuncture include pruritus, petechiae, ecchymoses and subcutaneous hematomas, but are fairly rare. Infection and pneumothorax have also been reported.

Psoriasis

TCM *herbs* with anti-inflammatory effects, in particular indigo naturalis, *Tripterygium wilfordii*, *Tripterygium hypoglaucum* and *Camptotheca acuminata*, are used to treat psoriasis. In a study of 801 psoriatic patients, over half responded to a decoction of five herbs (*Rhizoma sparganii*, *Rhizoma zedoariae*, *Herba serissae*, *Boswellia* resin, and *Commiphora myrrha*)[49]. Herbs that contain furocoumarins, such as *Radix angelicae dahuricae*, have been used in conjunction with UVA phototherapy for a psoralen-like effect. Psoriasis clearance rates were similar for *Radix angelicae dahuricae* plus UVA versus PUVA (with 8-MOP), with fewer side effects. As with other botanicals, TCM herbs have biologically active components, and they may have serious side effects. TCM should be administered under the supervision of a licensed practitioner.

Acupuncture has not been well studied in psoriasis, but there are several reports of plaques appearing at sites of acupuncture needle insertions due to Koebner phenomenon[50].

Moxibustion, Cupping and Other Treatment Modalities

Moxibustion is the practice of burning dried moxa (*Artemisia vulgaris*), arranged in small cone-shaped piles, over acupuncture points. Side effects include first- and second-degree burns.

Cupping is another method used to stimulate acupuncture points. It is accomplished by igniting alcohol-soaked cotton, placing the burning cotton in a jar, and placing the jar on the skin. A vacuum is created, and circular areas of erythema and ecchymosis may result (Fig. 133.2). Nowadays, some practitioners use a vacuum device that negates the risk of fire.



Fig. 133.2 Cupping. A Well-demarcated circular areas that are pink–purple and yellow in color and contain petechiae. **B** Circular purpura due to cupping done to relieve the pain that preceded the appearance of cutaneous lesions of herpes zoster. *A, Courtesy Donald J. Baker, MD; B, Courtesy Kalman Watsky, MD.*



Fig. 133.3 Linear ecchymoses on the back due to coining. *Courtesy Amy Geng and Raymond G. Dufresne, Jr.*

Skin scraping, also known as *coining* or spooning, is commonly practiced in Southeast Asia to improve circulation. A tool is used to rub skin that has been treated with oil; symmetric, linear ecchymoses may result (Fig. 133.3).

Any patient with cutaneous lesions in patterns suggestive of external causes should be asked about traditional medicine before accusations of abuse arise.

HOMEOPATHY

Homeopathy is a system of healing founded in Germany at the end of the 18th century. It is composed of two theories: (1) "like cures like" – the suggestion that a disease can be cured by a substance that produces similar symptoms in people who do not have the disease; and (2) "law of minimum dose" – the concept that the *lower* the dose of the medication, the greater the efficacy of the medication[51]. Homeopathic remedies come from substances that are derived from plants, minerals or animals, many of which are considered toxic in their crude form. Serial dilutions and "succussion" – a process by which a solution is violently shaken a given number of times between dilutions – create the final product. Homeopathic remedies are often prepared as sugar pellets to be placed under the tongue, but they may also be formulated as ointments, gels, drops, or creams. The FDA regulates homeopathic remedies, but unlike traditional medications, it does not evaluate them for safety and effectiveness.

In dermatology, homeopathy is most often used for the treatment of atopic dermatitis and psoriasis[52]. In general, there is little evidence to support the effectiveness of homeopathic therapies for skin disease[53], and some evidence from controlled clinical studies suggest that homeopathy is actually *ineffective* for eczema[54].

While many homeopathic remedies are highly diluted, some products sold or labeled as homeopathic may not be diluted sufficiently and may still contain active ingredients. Like any drug or dietary supplement that contains active compounds, these homeopathic remedies may cause side effects (e.g. allergic reactions, intoxications) or drug interactions[51].

AROMATHERAPY

During the early part of the 20th century, while studying the effects of essential oils on different disease states, the French chemist René-Maurice Gattefossé coined the term "aromatherapy". The latter represents the therapeutic use of aromatic essential oils which can be made from any plant part, including leaves, stems, flowers, fruits, or roots. Essential oils are typically obtained via steam distillation or by cold pressing the plant.

Essential oils contain a mixture of various organic compounds, in particular alcohols, aldehydes, esters, ketones, terpenes, lactones, aromatic aldehydes, and phenols. Oils high in ketones are used for their wound healing properties, whereas oils high in alcohols are used for their antimicrobial properties. There is evidence that essential oils, when applied topically, can enter the bloodstream[55].

In aromatherapy, essential oils may be used externally or internally. The most common routes of administration are inhalation and massage, but compresses, creams, gels, sprays, and baths are also employed. Aromatherapy may be used directly to treat dermatologic conditions, or indirectly to treat the anxiety or other symptoms associated with cutaneous disorders. Aromatherapy has been used to treat many conditions including acne, alopecia areata, pruritus, and scarring as well as for analgesia and wound healing.

Tea tree oil (*Melaleuca alternifolia*) is one of the most commonly employed essential oils in aromatherapy of skin conditions. A single-blind trial in acne patients found similar efficacies for tea tree oil 5% gel and benzoyl peroxide 5% lotion; tea tree oil had a slower onset of action but fewer side effects. In a randomized, controlled, double-blind trial for alopecia areata, an aromatherapy essential oil blend of thyme, rosemary, lavender, and cedarwood led to significantly greater improvement than did the placebo (44% vs 15%)[56].

It is important to note that essential oils have biologically active components and may be toxic. For example, oils with high concentrations of aldehydes and phenols may cause skin irritation. Phototoxicity can occur with oils derived from citrus plants due to the presence of psoralens or furocoumarins. Essential oils containing high concentrations of ketones should be used cautiously in pregnant women and infants, and a number of essential oils can cause allergic or irritant contact dermatitis (Table 133.5)[55].

MIND–BODY MEDICINE

Mind–body medicine encompasses a wide range of therapeutic modalities that emphasize the complex interactions involving the brain, the body, and behavior and the ways in which emotional, mental, social,

ESSENTIAL OILS ASSOCIATED WITH ALLERGIC AND/OR IRRITANT CONTACT DERMATITIS			
Bergamot	Grape seed	Lemongrass	Rose
Cinnamal	Jasmine	Neroli	Rosemary
Clove	Laurel	Orange	Sandalwood
Frankincense	Lavender	Peppermint	Yarrow
Geraniol	Lemon	Propolis	Ylang ylang

Table 133.5 Essential oils associated with allergic and/or irritant contact dermatitis. *Adapted from Trattner A, David M, Lazarov A. Occupational contact dermatitis due to essential oils. Contact Dermatitis 2008;58:282–4 and Bleasel N, Tate B, Rademaker M. Allergic contact dermatitis following exposure to essential oils. Australas J Dermatol 2002;43:211–3.*

spiritual, experiential, and behavioral factors can affect health. Mind–body practices include meditation, hypnosis, yoga, tai chi, qi gong, biofeedback, and cognitive behavioral therapies (see Table 133.1).

Because multiple skin disorders have significant psychological or behavioral components, stress and emotion can have a substantial impact on the skin. Acne, rosacea, alopecia areata, atopic dermatitis, seborrheic dermatitis, dyshidrotic eczema, psoriasis, herpes simplex viral infections, and pruritus are among the dermatologic diseases that have been linked to emotional triggers and stress (Table 133.6). Psychotropic drugs (e.g. antidepressants, antipsychotics, anxiolytics, sedatives) are often used to treat psychocutaneous disorders such as dermatitis artefacta, trichotillomania, and acne excoriée (see Ch. 7), and they are occasionally used when there is a significant psychological component to other chronic skin diseases. In the same way that these pharmacologic interventions may be helpful, there may be a role for mind–body modalities to help modulate the underlying stress response associated with these conditions.

Mindfulness and meditation are two of the most popular mind–body practices. While there are many different approaches to meditation, the specific type of mindfulness practice or meditation appears not to matter – it is the consistency of the practice that provides the benefit. Meditation has been shown to be helpful in treating acne, eczema, urticaria, hyperhidrosis, and psoriasis[57].

Webster's Dictionary defines biofeedback as: "the technique of making unconscious or involuntary bodily processes (such as heartbeats or brain waves) perceptible to the senses…in order to manipulate them by conscious mental control". During a biofeedback session, sensors are attached to the participant in order to detect immediate changes in physiologic functions such as heart rate, breathing, and brain activity. It has been found to have some effectiveness in treating rosacea, eczema, acne, psoriasis, and urticaria[58]. Biofeedback can be particularly helpful for people who are data-driven and respond well to immediate feedback.

Hypnosis has been used successfully for atopic dermatitis, alopecia areata, acne excoriée, herpes simplex viral infections, neurodermatitis, pruritus, verrucae, and psoriasis[59]. Mind–body modalities have also been shown to be useful preoperatively and during dermatologic procedures (e.g. cutaneous surgery). Slower breathing, biofeedback, guided imagery, hypnosis, and music can help calm and balance the patient's autonomic nervous system[60].

Mind–body medicine remains an active area of research. The hypothalamic–pituitary–adrenal (HPA) axis and autonomic nervous system (ANS) affect immunity and endocrine function via their regulation of glucocorticoid and catecholamine production, respectively. Therefore, psychological and behavioral interventions that affect the activity of the HPA axis and ANS have the potential to positively impact or treat disease. The skin itself produces enough hormones, neurotransmitters, neuropeptides, and functional receptors to form complete cutaneous neuroendocrine axes. These include cutaneous equivalents of: (1) the HPA axis; (2) the cholinergic system; (3) the catecholaminergic system; (4) the serotoninergic/melatoninergic system; (5) steroidogenic pathways; and (6) the pituitary–thyroid axis. These local neuroendocrine systems are used by the skin to preserve homeostasis[61].

Mind–body modalities have minimal side effects because neither physical nor chemical agents are used. However, they could trigger negative reactions in individuals with mental health disorders such as post-traumatic stress disorder (PTSD), schizophrenia, paranoia, or anxiety. Those who are at risk should work with experienced practitioners[62].

DERMATOLOGICAL CONDITIONS ASSOCIATED WITH PSYCHO-EMOTIONAL FACTORS	
Dermatological conditions with psycho-emotional component	
• Atopic dermatitis • Contact dermatitis • Dyshidrotic eczema • Lichen simplex chronicus • Nummular dermatitis • Pruritus (sine materia) • Urticaria • Psoriasis • Seborrheic dermatitis • Lichen planus • Vitiligo	• Telogen effluvium • Alopecia areata • Median nail dystrophy • Acne vulgaris • Rosacea • Perioral dermatitis • Hyperhidrosis • Verrucae • Herpes simplex viral infection • Gardner–Diamond syndrome
Psychocutaneous disorders	
• Dermatitis artefacta • Excoriation (skin-picking) disorder • Acne excoriée • Trichotillomania • Onychotillomania • Delusional infestation • Body dysmorphic disorder	• Somatic symptom disorder • Illness anxiety disorder • Dermatologic phobias • Venereophobia • Oncophobia • Bromidrosiphobia • Glossodynia* • Vulvodynia*
*Following exclusion of underlying medical etiologies.	

Table 133.6 Dermatological conditions associated with psycho-emotional factors. *Adapted with permission from Panconesi E, Gallassi F, Sarti MG, Bellini MA. Biofeedback, cognitive-behavioral methods, hypnosis: 'alternative psychotherapy'? Clin Dermatol 1998;15:709–10.*

AYURVEDA

Ayurveda originated in India more than 3000 years ago and still plays a prominent role in healthcare in India today. Typically, Ayurvedic medicine employs the use of herbal compounds, diet and lifestyle changes, and oil massages. The cornerstone of this modality is to determine an individual's profile and set of imbalances; once established, it becomes the foundation for clinical treatment decisions. To determine a person's constitution, an Ayurvedic practitioner describes bodily functions through the use of three descriptive units known as *doshas*.

The three doshas are *vata*, *pitta*, and *kapha*. *Vata* refers to motion such as the movement of blood, the motion of water in transepidermal water loss, or the motion of the body in general. When out of balance, *vata* leads to dryness, scaling, and loss of tissue as is seen in atopic dermatitis or in photoaging. *Pitta* refers to the metabolic processes in the body such as enzymatic activities and, when out of balance, represents inflammation in the body. Any disease such as acne, psoriasis, atopic dermatitis, or rosacea that has an inflammatory component has a pitta imbalance. *Kapha* refers to structure and substance, e.g. the level of cutaneous hydration, the presence of collagen, the strength and structure of hair. When out of balance, *kapha* leads to overproduction of substance and fibrosis as is seen in hypertrophic scars, systemic sclerosis, and scleredema.

Illness in Ayurveda is defined as an imbalance of the normal ratios of *doshas*, with therapies aimed at correcting this imbalance through the use of diet, mind–body techniques, and herbal formulations. Although there have been few clinical trials on the use of Ayurvedic medicine for dermatologic diseases, several reports suggest that topical and oral curcumin are efficacious in psoriasis. Members of the ginger family, which includes *Curcuma longa* (see above), are common ingredients in Ayurvedic medications. Curcumin is thought to down-regulate kinases in patients with psoriasis[1].

Ayurveda has a rich history of utilizing dietary restriction in skin diseases but also utilizes a variety of herbal formulations with the potential for interaction with conventional medicines. Ayurvedic herbal products are regulated as dietary supplements rather than as drugs and it is imperative to assess the safety testing of herbs. While there is concern for the possibility of heavy metal contamination in herbs, many companies now perform a battery of third-party tests to ensure that herbs are within regulatory limits.

CONCLUSION

Although for many dermatologic diseases high-quality evidence to support the use of CAM is lacking, it is still important for dermatologists to recognize and acknowledge the widespread use of CAM by patients. While it is essential to be aware of potential side effects and drug–drug interactions, it is equally important to appreciate cultural differences when caring for patients.

Additional figure available in our eBook (see inside front cover for access code).

REFERENCES

1. Bhuchar S, Katta R, Wolf J. Complementary and alternative medicine in dermatology: an overview of selected modalities for the practicing dermatologist. *Am J Clin Dermatol*. 2012;13:311–317.
2. Barnes PM, Bloom B, Nahin RL. Complementary and alternative medicine use among adults and children: United States, 2007. *Natl Health Stat Report*. 2008;12:1–23.
3. Smith N, Shin DB, Brauer JA, et al. Use of complementary and alternative medicine among adults with skin disease: results from a national survey. *J Am Acad Dermatol*. 2009;60:419–425.
4. Deng S, May BH, Zhang AL, et al. Plant extracts for the topical management of psoriasis: a systematic review and meta-analysis. *Br J Dermatol*. 2013;169:769–782.
5. Bedi MK, Shenefelt PD. Herbal therapy in dermatology. *Arch Dermatol*. 2002;138:232–242.
6. Derry S, Sven-Rice A, Cole P, et al. Topical capsaicin (high concentration) for chronic neuropathic pain in adults. *Cochrane Database Syst Rev*. 2013(2). CD007393.
7. Bode AM, Dong Z. The two faces of capsaicin. *Cancer Res*. 2011;71:2809–2814.
8. Emer J, Waldorf H, Berson D. Botanicals and anti-inflammatories: natural ingredients for rosacea. *Semin Cutan Med Surg*. 2011;30:148–155.
9. Reynertson KA, Garay M, Nebus J, et al. Anti-inflammatory activities of colloidal oatmeal (Avena sativa) contribute to the effectiveness of oats in treatment of itch associated with dry, irritated skin. *J Drugs Dermatol*. 2015;14:43–48.
10. Criquet M, Roure R, Dayan L, et al. Safety and efficacy of personal care products containing colloidal oatmeal. *Clin Cosmet Investig Dermatol*. 2012;5:183–193.
11. McDaniel S, Goldman GD. Consequences of using escharotic agents as primary treatment for nonmelanoma skin cancer. *Arch Dermatol*. 2002;138:1593–1596.
12. Bowe WP. Cosmetic benefits of natural ingredients: mushrooms, feverfew, tea, and wheat complex. *J Drugs Dermatol*. 2013;12:s133–s136.
13. Rodriguez KJ, Wong HK, Oddos T, et al. A purified feverfew extract protects from oxidative damage by inducing DNA repair in skin cells via a PI3-kinase-dependent Nrf2/ARE pathway. *J Dermatol Sci*. 2013;72:304–310.
14. Draelos ZD. The art and science of new advances in cosmeceuticals. *Clin Plast Surg*. 2011;38:397–407.
15. Saric S, Notay M, Sivamani RK. Green tea and other tea polyphenols: effects on sebum production and acne vulgaris. *Antioxidants (Basel)*. 2016;6:2.
16. Witte M, Krause L, Zillikens D, Shimanovich I. Black tea dressings–a rapidly effective treatment for facial dermatitis. *J Dermatolog Treat*. 2019;30:785–789.
17. McLoone P, Oluwadun A, Warnock M, Fyfe L. Honey: a therapeutic agent for disorders of the skin. *Cent Asian J Glob Health*. 2016;5:241.
18. Burlando B, Cornara L. Honey in dermatology and skin care: a review. *J Cosmet Dermatol*. 2013;12:306–313.
19. Underland V, Sæterdal I, Nilsen ES. Cochrane summary of findings: horse chestnut seed extract for chronic venous insufficiency. *Glob Adv Health Med*. 2012;1:122–123.
20. Pittler MH, Ernst E. Horse chestnut seed extract for chronic venous insufficiency. *Cochrane Database Syst Rev*. 2012;(11):CD003230.
21. Liang C-Y, Lin T-Y, Lin Y-K. Successful treatment of pediatric nail psoriasis with periodic pustular eruption using topical indigo naturalis oil extract. *Pediatr Dermatol*. 2013;30:117–119.
22. Hsieh W-L, Lin Y-K, Tsai C-N, et al. Indirubin, an acting component of indigo naturalis, inhibits EGFR activation and EGF-induced CDC25B gene expression in epidermal keratinocytes. *J Dermatol Sci*. 2012;67:140–146.
23. Cheng HM, Wu YC, Wang Q, et al. IL-17 targeting mechanism of indigo naturalis as a topical agent in moderate psoriasis. *BMC Complement Altern Med*. 2017;17:439–449.
24. Ciganović P, Jakimiuk K, Tomczyk M, Zovko Končić M. Glycerolic licorice extracts as active cosmeceutical ingredients: extraction optimization, chemical characterization, and biological activity. *Antioxidants (Basel)*. 2019;8:445–458.
25. Wu J. Anti-inflammatory ingredients. *J Drugs Dermatol*. 2008;7:s13–s16.
26. Kumar S, Juresic E, Barton M, Shafiq J. Management of skin toxicity during radiation therapy: a review of the evidence. *J Med Imaging Radiat Oncol*. 2010;54:264–279.
27. Patel T, Ishiuji Y, Yosipovitch G. Menthol: a refreshing look at this ancient compound. *J Am Acad Dermatol*. 2007;57:873–878.
28. Kober MM, Bowe WP. The effect of probiotics on immune regulation, acne, and photoaging. *Int J Womens Dermatol*. 2015;1:85–89.
29. Huang R, Ning H, Shen M, et al. Probiotics for the treatment of atopic dermatitis in children: a systematic review and meta-analysis of randomized controlled trials. *Frontiers in cellular and infection microbiology*. 2017;7:392–402.

29a. Zhang L, Jin Q, Kuang T, et al. The correlation between probiotic use and outcomes of cancer patients treated with immune checkpoint inhibitors. *Front Pharmacol*. 2022;13:937874.

30. Doron S, Snydman DR. Risk and safety of probiotics. *Clin Infect Dis*. 2015;60 Suppl 2(Suppl 2):S129–S134.
31. Carson CF, Hammer KA, Riley TV. Melaleuca alternifolia (tea tree) oil: a review of antimicrobial and other medicinal properties. *Clin Microbiol Rev*. 2006;19:50–62.
32. Henley DV, Lipson N, Korach KS, Bloch CA. Prepubertal gynecomastia linked to lavender and tea tree oils. *N Engl J Med*. 2007;356:479–485.
33. Ramsey JT, Diaz A, Naidu A, Korach KS. Response to letter to the editor: "Lavender products associated with premature thelarche and prepubertal gynecomastia: case reports and endocrine disrupting chemicals activities". *J Clin Endocrinol Metab*. 2020;105:e3500–e3501.
34. Nguyen TA, Friedman AJ. Curcumin: a novel treatment for skin-related disorders. *J Drugs Dermatol*. 2013;12:1131–1137.
35. Nasri H, Bahmani M, Shahinfard N, et al. Medicinal plants for the treatment of acne vulgaris: a review of recent evidences. *Jundishapur J Microbiol*. 2015;8:e25580.
36. Daniele C, Thompson Coon J, Pittler MH, et al. *Vitex agnus castus*: a systematic review of adverse events. *Database of Abstracts of Reviews of Effects (DARE): Quality-assessed Reviews [Internet]*. York (UK): Centre for Reviews and Dissemination (UK); 2005.
37. Nickles MA, Lio PA. Cannabinoids in dermatology: hope or hype? *Cannabis Cannabinoid Res*. 2020;5:279–282.
38. Katta R, Desai SP. Diet and dermatology: the role of dietary intervention in skin disease. *J Clin Aesthet Dermatol*. 2014;7:46–51.
39. Debbaneh M, Millsop JW, Bhatia BK, et al. Diet and psoriasis, part I: impact of weight loss interventions. *J Am Acad Dermatol*. 2014;71:133–140.
40. Bhatia BK, Millsop JW, Debbaneh M, et al. Diet and psoriasis, part II: celiac disease and role of a gluten-free diet. *J Am Acad Dermatol*. 2014;71:350–358.
41. Gelmetti C. Diet and atopic dermatitis. *J Eur Acad Dermatol Venereol*. 2000;14:439–440.
42. Mohajeri S, Newman SA. Review of evidence for dietary influences on atopic dermatitis. *Skin Therapy Lett*. 2014;19:5–7.
43. Lim NR, Lohman ME, Lio PA. The role of elimination diets in atopic dermatitis: a comprehensive review. *Pediatr Dermatol*. 2017;34:516–527.
44. Gu S, Yang AWH, Xue CCL, et al. Chinese herbal medicine for atopic eczema. *Cochrane Database Syst Rev*. 2013;(9):CD008642.
45. Gu SX, Zhang AL, Coyle ME, et al. Chinese herbal medicine for atopic eczema: an overview of clinical evidence. *J Dermatolog Treat*. 2017;28:246–250.
46. Ernst E. Adverse effects of herbal drugs in dermatology. *Br J Dermatol*. 2000;143:923–929.
47. Chen C-J, Yu H-S. Acupuncture, electrostimulation, and reflex therapy in dermatology. *Dermatol Ther*. 2003;16:87–92.
48. Lee KC, Keyes A, Hensley JR, et al. Effectiveness of acupressure on pruritus and lichenification associated with atopic dermatitis: a pilot trial. *Acupunct Med*. 2012;30:8–11.
49. Koo J, Desai R. Traditional Chinese medicine in dermatology. *Dermatol Ther*. 2003;16:98–105.
50. Wu JJ, Caperton C. Images in clinical medicine. Psoriasis flare from Koebner's phenomenon after acupuncture. *N Engl J Med*. 2013;368:1635.
51. National Center for Complementary and Integrative Health. Homeopathy: what you need to know. <http://www.nccih.nih.gov/health/homeopathy>; 2021.
52. Smolle J. Homeopathy in dermatology. *Dermatol Ther*. 2003;16:93–97.
53. Simonart T, Kabagabo C, De Maertelaer V. Homoeopathic remedies in dermatology: a systematic review of controlled clinical trials. *Br J Dermatol*. 2011;165:897–905.
54. Ernst E. Homeopathy for eczema: a systematic review of controlled clinical trials. *Br J Dermatol*. 2012;166:1170–1172.
55. Stevensen CJ. Aromatherapy in dermatology. *Clin Dermatol*. 1998;16:689–694.
56. Hay IC, Jamieson M, Ormerod AD. Randomized trial of aromatherapy. Successful treatment for alopecia areata. *Arch Dermatol*. 1998;134:1349–1352.
57. Kabat-Zinn J, Wheeler E, Light T, Skillings A. Influence of a mindfulness meditation-based stress reduction intervention on rates of skin clearing in patients with moderate to severe psoriasis undergoing phototherapy (UVB) and photochemotherapy (PUVA). *Psychosom Med*. 1998;60:625–632.
58. Bilkis MR, Mark KA. Mind-body medicine. Practical applications in dermatology. *Arch Dermatol*. 1998;134:1437–1441.
59. Shenefelt PD. Hypnosis in dermatology. *Arch Dermatol*. 2000;136:393–399.
60. Shenefelt PD. Relaxation strategies for patients during dermatologic surgery. *J Drugs Dermatol*. 2010;9:795–799.
61. Slominski A. Neuroendocrine system of the skin. *Dermatology*. 2005;211:199–208.
62. Boyd JE, Lanius RA, McKinnon MC. Mindfulness-based treatments for posttraumatic stress disorder: a review of the treatment literature and neurobiological evidence. *J Psychiatry Neurosci*. 2018;43:7–25.



eFig. 133.1 Flagellate mushroom dermatitis (shiitake mushroom dermatitis) due to ingestion of mushroom extract as a supplement. Scratching leads to long, flagellate streaks which may be followed by hyperpigmentation or brown discoloration. *Courtesy Melissa Atkinson, PA*.

134 Ultraviolet Therapy

Herbert Hönigsmann† and Thomas Schwarz

Chapter Contents

Phototherapy with UVB 2362
Phototherapy with the 308 nm Excimer Laser or Lamp 2367
Phototherapy with UVA1 2367
Photochemotherapy with Psoralens (PUVA) 2367
Extracorporeal Photochemotherapy (Photopheresis) 2376

Key features

- Phototherapy represents the use of ultraviolet (UV) radiation for the treatment of skin diseases
- Currently, phototherapy encompasses irradiation with broadband UVB (290–320 nm), narrowband UVB (311–313 nm), 308 nm excimer laser, UVA1 (340–400 nm), UVA (320–400 nm) plus psoralens (PUVA) or alone, and extracorporeal photochemotherapy (photopheresis)
- Therapeutic success depends upon proper selection of the phototherapy modality for a given disease
- Proper dosimetry is required to avoid acute side effects such as a sunburn reaction, blistering, and burning sensations
- The risk of skin carcinogenesis represents the major long-term side effect of phototherapy; with the exception of PUVA, the magnitude of this risk is not yet clearly delineated

INTRODUCTION

Over the past half-century, phototherapy has greatly influenced treatment concepts in dermatology. Studies focusing on the effects of electromagnetic radiation (Fig. 134.1) on the skin have induced fruitful collaborations between basic scientists and clinicians.

Although ultraviolet (UV) radiation had been used for decades in the management of common skin diseases such as psoriasis and atopic dermatitis, the introduction of PUVA in the mid-1970s sparked a whole new series of discoveries, including high-intensity UV sources and selective spectra in the UVB and UVA range, e.g. narrowband UVB (311–313 nm) and UVA1 (340–400 nm).

PHOTOTHERAPY WITH UVB

Historical Aspects

To date, the only dermatologist to be awarded a Nobel Prize in medicine was Dr Niels Finsen in 1903. The award recognized his demonstration of the beneficial effect of UV radiation on lupus vulgaris, and he eventually became known as the "father of photomedicine". The combination of topical crude coal tar followed by UV irradiation for the treatment of psoriasis was introduced by Goeckerman in 1925 and became a standard therapy for psoriasis for half a century, particularly in the US. In the 1970s, it was observed that broadband (BB) UVB radiation alone, if given in doses that produce a slight erythema, could clear the milder forms of psoriasis, particularly the guttate type. In the 1980s, the discovery that the combination of psoralens with UVA (PUVA) exerts potent anti-inflammatory effects opened a new era of phototherapy. A further major advance was the development of fluorescent bulbs that emitted narrowband (NB) UVB radiation at 311–313 nm in the mid-1980s. This narrow spectrum is superior in clearing psoriasis and thus represents the most effective and most frequently used UVB phototherapy for psoriasis; it is also beneficial for a variety of other dermatoses that were previously treated with PUVA (see below).

Principles and Mechanisms

UVB phototherapy refers to the use of artificial UVB radiation without the addition of exogenous photosensitizers. The radiation is absorbed by endogenous chromophores, and photochemical reactions involving these UV-absorbing biomolecules mediate a variety of biologic effects, ultimately leading to the therapeutic effects. The most important chromophore for UVB is nuclear DNA. Absorption of UV by nucleotides causes the formation of DNA photoproducts, primarily pyrimidine dimers (see Ch. 86)[1].

UVB exposure reduces DNA synthesis and thus is used to suppress the accelerated DNA synthesis found in psoriatic epidermal cells. UVB also induces the expression of the tumor suppressor gene *TP53*, and this can lead to either cell cycle arrest (allowing time for DNA repair) or apoptosis of keratinocytes ("sunburn cells") if the DNA damage is too severe to be repaired. Through these mechanisms, p53 prevents photocarcinogenesis.

In addition to its effect on the cell cycle, UV induces the release of prostaglandins and cytokines. Interleukin (IL)-6 and IL-1, for example, seem to play important roles in producing the systemic symptoms of UV phototoxicity (sunburn) and immune suppression, respectively[1]. There is also increasing evidence that UV radiation can affect, in addition to DNA, extranuclear molecular targets located in the cytoplasm and cell membrane. These targets include cell surface receptors, kinases, phosphatases, and transcription factors. It was shown that nuclear and cytoplasmic/membrane effects are not mutually exclusive – rather they independently contribute to the multiple biologic effects of UVB.

Many of the therapeutic effects of UVB may be due to its immunosuppressive properties which have been linked to the formation of pyrimidine dimers. UV radiation suppresses contact allergy, delayed-type hypersensitivity, and immune surveillance against UV-induced keratinocyte carcinomas in mice. Of note, Langerhans cells are very sensitive to UVB, which alters their antigen-presenting function. Keratinocytes also secrete soluble mediators such as IL-1 and IL-6, prostaglandin E_2, and TNF in response to UVB, which by themselves can alter the immune response. Therapeutic UVB suppresses the type 1 (proinflammatory) axis as defined by IL-12, interferon (IFN)-γ, and IL-8, and can selectively reduce proinflammatory cytokine production by individual T cells[1].

The interplay of the various photobiological pathways is far from being completely understood. In psoriasis, both epidermal keratinocytes and cutaneous lymphocytes may be targeted by UVB. Immune suppression, alteration of cytokine expression, and cell cycle arrest may all contribute to the suppression of disease activity in psoriatic plaques[2]. In addition, a subset of T cells, Th17 cells, which seem to play a central role in the immunopathogenesis of psoriasis, are also downregulated by UVB[3]. More recently, evidence was presented that keratinocyte apoptosis may be a key mechanism in the clearance of psoriatic plaques[4].

Action Spectrum and Radiation Sources

Parrish and Jaenicke[5] demonstrated that for antipsoriatic activity, 304 and 313 nm were the optimally effective wavelengths (Fig. 134.2), even at suberythemogenic doses. Erythemogenic UVA doses are also therapeutically effective, but 1000 times higher fluences are needed

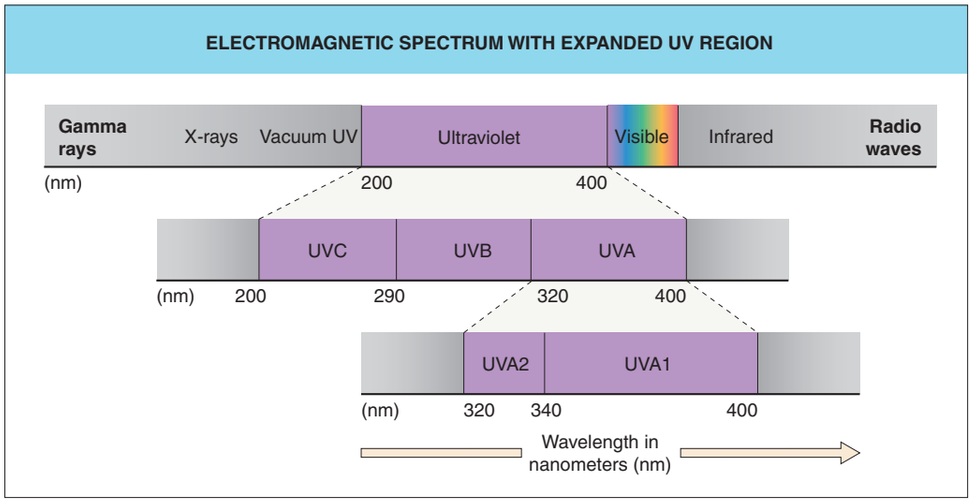


Fig. 134.1 Electromagnetic spectrum with expanded UV region.

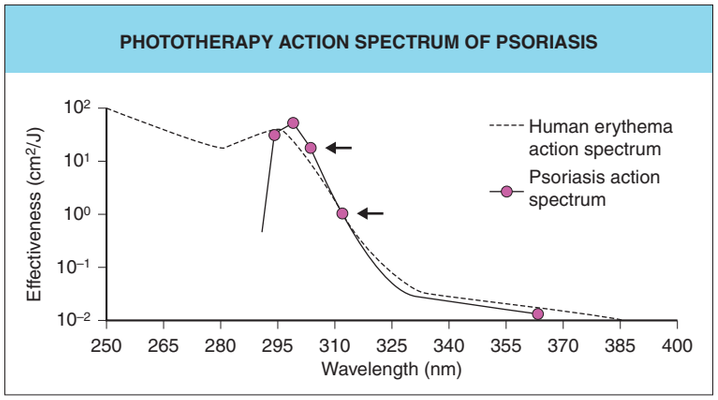


Fig. 134.2 Phototherapy action spectrum of psoriasis. The phototherapy action spectrum of psoriasis is plotted as the reciprocal of the lowest effective daily dose to clearing versus wavelength. Circles represent the reciprocal of the lowest effective daily dose for wavelengths that cleared psoriasis (295, 300, 304, 313, 365 nm); the arrows point to the wavelengths that were optimally effective (304, 313 nm). Presently, narrowband UVB sources that emit wavelengths between 311 and 313 nm are available. *Adapted from Parrish JA, Jaenicke KF. Action spectrum for phototherapy of psoriasis. J Invest Dermatol 1981;76:359–62.*

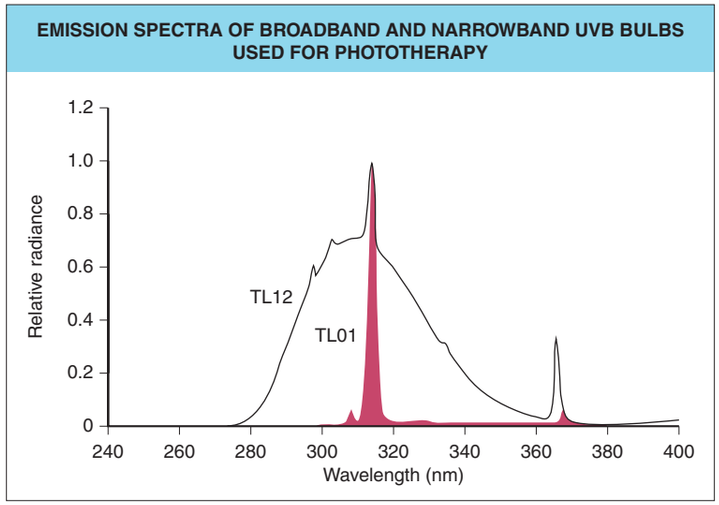


Fig. 134.3 Emission spectra of broadband and narrowband UVB bulbs used for phototherapy. Philips TL12, broadband UVB bulb; Philips TL01, narrowband UVB bulb.

(as compared with UVB) which practically speaking is not feasible. The addition of UVA also does not enhance the therapeutic efficacy of UVB in psoriasis (unlike atopic dermatitis). The Philips TL01 fluorescent lamp that emits NB-UVB (311–313 nm) was introduced to optimally meet the requirements for antipsoriatic activity (Fig. 134.3).

Devices that contain UV radiation-emitting bulbs are available in a wide range of sizes and designs including enclosed whole-body cabinets, portable flat panels, and hand-held units. When reliable patients live far distances from physician-supervised phototherapy centers or for other reasons are unable to schedule multiple treatments per week, UVB units designed for home use can be utilized. Practical guidelines for home phototherapy have been published[6].

Exposure to natural sunlight is called heliotherapy. Natural sunlight contains sufficient UVB radiation such that it is sometimes used to treat photoresponsive dermatoses. However, due to variables that affect UVB irradiance, including time of day, cloud cover, season, altitude and latitude, appropriate exposure times cannot be standardized. As a result, there is a greater probability of sunburn and an inadequate therapeutic response.

Treatment Protocols

Over the past several years, a number of dermatologic societies have published guidelines for utilizing phototherapy. They all provide more or less similar recommendations with some slight variations which are due to national differences in the health care system, reimbursement, legal requirements, availability/approval of alternative therapies, and of course traditions regarding prescribing practices. Table 134.1 lists some of the available guidelines. Most of these guidelines are updated regularly and are made available through online sources.

Before starting phototherapy, determination of the patient's UV sensitivity via phototesting is frequently recommended, since skin typing by history alone does not always reflect the actual sensitivity of a particular individual. However, phototesting is not mandatory for the experienced therapist and, for practical reasons, is often not done. Testing is performed by exposing four to six small template areas (e.g. 1 cm diameter circles or squares) of usually non-sun-exposed skin (lower back, buttocks) to an incremental series of UVB doses. In successive test sites, the incremental increases can be fixed (e.g. 10 or 20 mJ/cm^2) or proportional (e.g. 40% higher). An example is given in Table 134.2. Note that the actual doses delivered as specified in fluence units (mJ/cm^2) strongly depend on the type of UVB unit; for example, NB-UVB is much less erythemogenic than BB-UVB and consequently higher numerical doses are required.

The minimal erythema dose (MED) is defined as the lowest dose that causes a minimally perceptible erythema reaction at 24 hours after irradiation. Sunbathing or exposure to tanning lamps should be avoided before phototesting. It is crucial to document the type of lamp used for the MED determination, since the values obtained with broadband and narrowband sources differ by up to ten-fold (see Table 134.2).

Despite continued discussion as to whether visual assessment of the MED is the optimal method for establishing the initial UVB dose, it

EXAMPLES OF NATIONAL PHOTOTHERAPY GUIDELINES
Dosimetry
Moseley H, Allan D, Amatiello H, et al. Guidelines on the measurement of ultraviolet radiation in ultraviolet phototherapy: report issued by the British Association of Dermatologists and British Photodermatology Group 2015. Br J Dermatol 2015;173:333–50.
Ultraviolet B
Ibbotson SH, Bilsland D, Cox NH, et al. An update and guidance on narrowband ultraviolet B phototherapy: a British Photodermatology Group Workshop Report. Br J Dermatol 2004;151:283–97. Mehta D, Lim HW. Ultraviolet B phototherapy for psoriasis: review of practical guidelines. Am J Clin Dermatol 2016;17:125–33. Elmets CA, Lim HW, Stoff B, et al. Joint American Academy of Dermatology-National Psoriasis Foundation guidelines of care for the management and treatment of psoriasis with phototherapy. J Am Acad Dermatol 2019;81:775–804.* Mohammad TF, Al-Jamal M, Hamzavi IH, et al. The Vitiligo Working Group recommendations for narrowband ultraviolet B light phototherapy treatment of vitiligo. J Am Acad Dermatol 2017;76:879–88.
Psoralens plus UVA (PUVA) and/or UVA1
Ling TC, Clayton TH, Crawley J, et al. British Association of Dermatologists and British Photodermatology Group guidelines for the safe and effective use of psoralen-ultraviolet A therapy 2015. Br J Dermatol 2016;174:24–55. Herzinger T, Berneburg M, Ghoreschi K, et al. S1-Guidelines on UV photo-therapy and photochemotherapy. J Dtsch Dermatol Ges 2016;14:853-76.† Halpern SM, Anstey AV, Dawe RS, et al. Guidelines for topical PUVA: a report of a workshop of the British photodermatology group. Br J Dermatol 2000;142:22–31.
Cutaneous T cell lymphoma (CTCL)
Olsen EA, Hodak E, Anderson T, et al. Guidelines for phototherapy of mycosis fungoides and Sézary syndrome: a consensus statement of the United States Cutaneous Lymphoma Consortium. J Am Acad Dermatol 2016;74:27–58.
Photopheresis
Knobler R, Arenberger P, Arun A, et al. European dermatology forum – updated guidelines on the use of extracorporeal photophoresis 2020 – part 1. J Eur Acad Dermatol Venereol 2020;34:2693–716. Knobler R, Arenberger P, Arun A, et al. European dermatology forum – updated guidelines on the use of extracorporeal photophoresis 2020 – part 2. J Eur Acad Dermatol Venereol 2020;35:27–49.
*Also reviews PUVA and excimer laser. †Also reviews UVB.

Table 134.1 Examples of national phototherapy guidelines.

RECOMMENDED EXPOSURE DOSES (FLUENCES) FOR MED PHOTOTESTING TO BROADBAND AND NARROWBAND UVB SOURCES (mJ/cm^2)						
Broadband UVB	20	40	60	80	100	120
Narrowband UVB	200	400	600	800	1000	1200

$$\text{Time (sec)} = \frac{\text{Fluence (delivered dose of UV in mJ/cm}^2\text{ [UVB] or J/cm}^2\text{ [UVA])}}{\text{Irradiance (measured UV intensity expressed in mW/cm}^2\text{ [UVB] or W/cm}^2\text{ [UVA])}}$$

Table 134.2 Recommended exposure doses (fluences) for minimal erythema dose (MED) phototesting to broadband and narrowband UVB sources (mJ/cm^2). 1 watt (W) = 1 joule (J) of energy per second.

is an easily performed procedure that does not require any specialized equipment. An initial therapeutic UVB dose equal to 70% of the MED is typically recommended. Subsequent treatments are given two to five times weekly. Since UVB erythema peaks within 24 hours after exposure, doses may be increased with each successive treatment. However, if treatments are given five times weekly, the doses should be increased every other treatment. The rate of increase depends on treatment frequency and the response to the preceding UVB exposure. The objective of the dose increments is to achieve a minimally perceptible erythema as a clinical indicator of optimal dosimetry. For example, with thrice-weekly exposures, doses are increased by a maximum of 40% if no erythema appears, and by a maximum of 20% upon development of slight erythema. If mild erythema persists, the dose should be maintained. With daily exposures, these rates are no more than 30%, 15% and 0%, respectively. If more intensive or painful erythema develops, irradiations are stopped until the symptoms disappear. Treatment is then continued until complete remission is achieved or no further improvement can be obtained with continued phototherapy (Fig. 134.4).

Whether maintenance treatment leads to a more prolonged remission time is still a matter of debate, since minimal precise data are available. In cutaneous T cell lymphoma (CTCL), most therapists perform maintenance treatment for several months to a year. For psoriasis, some centers use a 2-month maintenance phase with twice-weekly exposures for 1 month and once-weekly exposures for another month. The last effective UVB dose is given throughout the maintenance phase. If relapses occur during the maintenance phase, treatment frequency and UVB dose are again increased until clearing. Of note, there was some evidence in a randomized study that maintenance NB-UVB may lead to longer remission times in plaque-type psoriasis[7].

Phototherapy for Psoriasis

Guttate psoriasis and minimally elevated lesions of psoriasis respond most favorably and rapidly to BB-UVB, while chronic, plaque-type psoriasis is more resistant. In terms of clearing efficiency and duration of remission, BB-UVB is inferior to both NB-UVB and PUVA. As a result, in many countries, NB-UVB has largely replaced conventional BB-UVB phototherapy. Based on several publications, NB-UVB phototherapy appears to be somewhat less effective than PUVA.

In addition to the treatment protocols mentioned above, other regimens may be used. Some schedules utilize skin type-dependent starting doses and fixed increments regardless of skin reaction. Sometimes, the patient's extremities (in particular the lower extremities which tend to respond more slowly) can be exposed to higher doses than the trunk.

Adjunctive topical agents and combination therapies are often used to improve efficacy and reduce the cumulative UVB dose, with the ultimate aim of minimizing the risk of long-term side effects. Narrowband UVB has been successfully combined with therapies such as anthralin and vitamin D analogues. The use of bland emollients before UVB treatment is laborious and time-consuming, and in our experience does not dramatically increase treatment efficacy. The concurrent use of topical corticosteroids may reduce remission times and thus is discouraged by some dermatologists.

Systemic drugs such as retinoids increase efficacy, particularly in patients with chronic plaque-type psoriasis[8,9]. In addition, retinoids may reduce the carcinogenic potential of UVB phototherapy. There have been open-label studies and small comparison studies regarding the efficacy of combining UVB phototherapy with systemic immunomodulators ("biologics")[10,11]. To date, there have been no large-scale studies, and long-term data, including remission times, are unavailable.

Phototherapy for Cutaneous T Cell Lymphoma, in Particular Mycosis Fungoides

For early stages (IA, IB, and IIA) of mycosis fungoides (MF), conventional treatment strategies include topical corticosteroids, UV radiation, topical retinoids (e.g. bexarotene), and topical cytotoxic agents (e.g. mechlorethamine [nitrogen mustard]). More advanced stages are treated with various combinations that include total body electron beam radiation therapy (see Ch. 139), local radiotherapy, systemic retinoids, PUVA, systemic chemotherapy (e.g. gemcitabine), and immunomodulators (e.g. brentuximab vedotin, mogamulizumab, IFN) (see Table 120.5), but none of these regimens have been demonstrated to induce permanent remission.

Lesions of MF frequently occur in non-sun-exposed areas of the body, and patients with early stage MF often benefit from exposure to natural sunlight. Response to phototherapy is related to the type (i.e. patch stage MF does better than the plaque type) but not the extent of skin involvement. In a more recent study, prolonged maintenance therapy (up to 30 months) resulted in a relapse-free period of 26 ± 10 months[12].

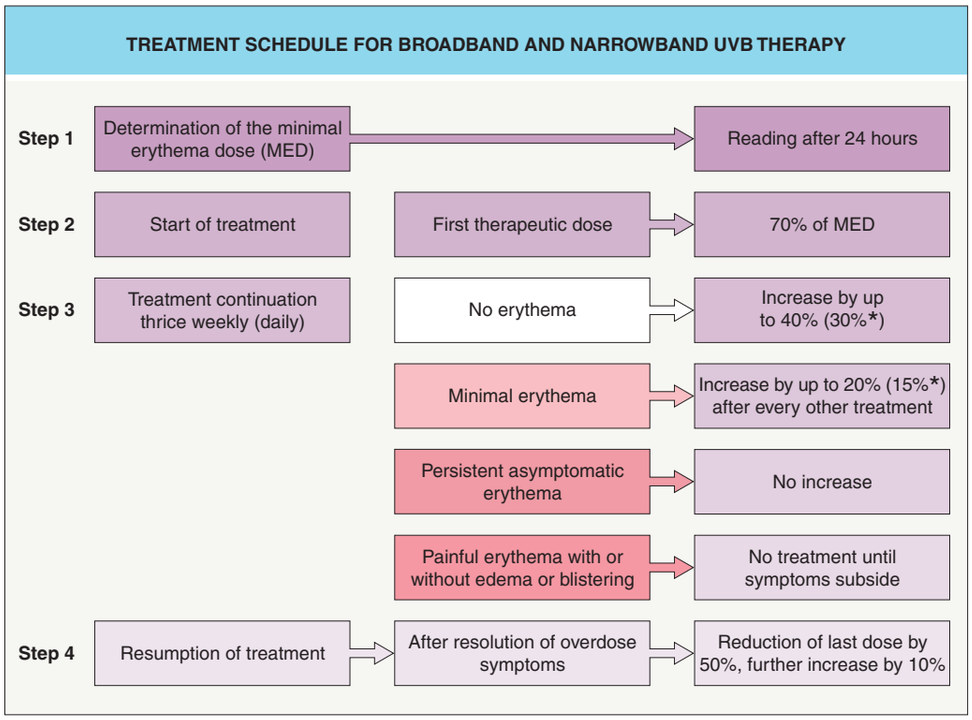


Fig. 134.4 Treatment schedule for broadband and narrowband UVB therapy. *If treatments are given five times per week or daily.

The proposed mechanisms for UVB phototherapy of MF include impairment of epidermal Langerhans cell function and alterations in cytokine production and adhesion molecule expression by keratinocytes[13]. Moreover, NB-UVB can induce apoptosis of T lymphocytes, which may more specifically contribute to the beneficial effect of this light source[14].

UVB phototherapy is clearly less efficient than PUVA, and the duration of treatment in the clearing and maintenance phases is longer and thus requires higher patient compliance. Whether patients would benefit from adding UVA, as is sometimes recommended, remains questionable. Likewise, NB-UVB and BB-UVB therapy have not been compared in MF. It is possible that combining a systemic retinoid (e.g. bexarotene) with NB-UVB may increase efficacy. Lastly, a pilot study documented the efficacy of medium- to high-dose UVA1 therapy (see below) in patients with stage IA and IB MF. However, there is no evidence that UVA1 is superior to PUVA and no long-term follow-up is available.

Phototherapy for Vitiligo

Many patients observe follicular repigmentation in areas of vitiligo following sun exposure. Because of seasonal and weather-dependent variations in sunlight intensity in moderate climates, exposure to natural sunlight is often not a practical option for inducing repigmentation. In the past, PUVA was most frequently used for the treatment of vitiligo, but exposure to artificial UVB irradiation, in particular NB-UVB, can also provide an acceptable therapeutic effect, if given for a sufficiently long period. Although the action spectrum for phototherapy of vitiligo is not known, NB-UVB has clearly become quite popular in recent years. In comparison studies of NB-UVB with PUVA, NB-UVB was as effective as PUVA but had fewer side effects (Fig. 134.5). Also, in a randomized double-blind trial of non-segmental vitiligo, NB-UVB therapy was superior to oral PUVA therapy and the color match of repigmented skin was considered to be better in the patients treated with NB-UVB[15]. UVA alone is of limited benefit.

Since intense erythema may induce the Koebner phenomenon and worsening of the disease, it is necessary to stay within a dose range that induces minimally perceptible erythema. Therefore, initial assessment of the MED in a vitiliginous area that is normally not sun-exposed (e.g. buttocks, lower back, abdomen) is recommended. The UVB doses have to be increased more carefully than in other disorders, because of the increased photosensitivity of depigmented skin.

The initial exposure is 70% of the MED in lesional skin, and subsequent doses are chosen according to the response in vitiligo areas, i.e. the goal is to induce a barely perceptible erythema that has a light pink color. The presence or absence of faint erythema is the only useful parameter for determining dosage increments. The dose should not be increased more than once weekly by 5%–20% of the preceding dose. Despite the lack of pigment, vitiliginous skin does develop photoadaptation, probably as a

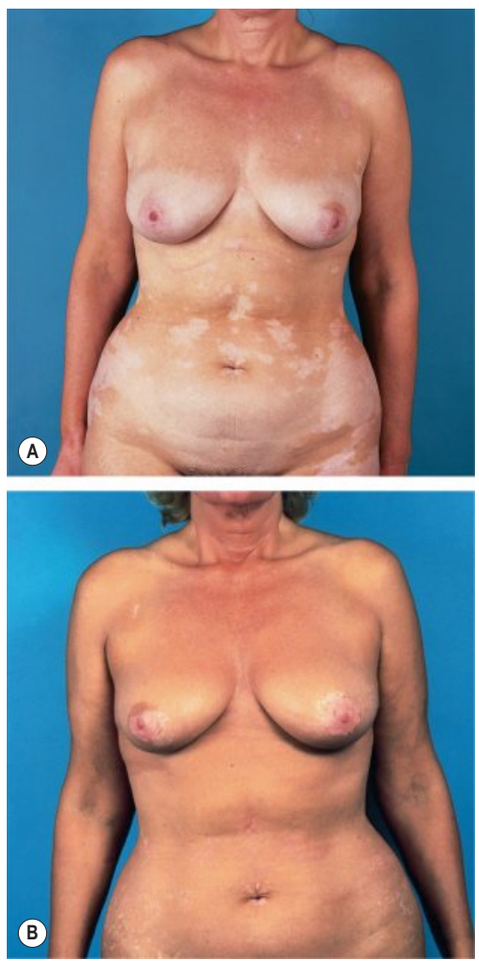


Fig. 134.5 Narrowband UVB phototherapy for vitiligo. A Before treatment. **B** After 10 months of treatment (twice weekly). Note the persistence of depigmentation of the areolae, an area which is particularly resistant to treatment.

result of epidermal hyperplasia and thickening of the stratum corneum. In contrast to previous assumptions, the risk of developing keratinocyte carcinoma is not enhanced in vitiliginous areas. Usually, a maximum dose will be reached during the first couple of months which is then used throughout the entire treatment period. Most commonly, two to three treatments per week are given. Although few controlled studies are available for any particular phototherapy regimen to be preferred over another, consensus recommendations are available[16].

More recently, the combination of an afamelanotide implant plus NB-UVB phototherapy resulted in clinically apparent, statistically significant superior and faster repigmentation compared with NB-UVB monotherapy. Afamelanotide is an analogue of α-melanocyte stimulating hormone that can induce diffuse hyperpigmentation of the skin, especially in sun-exposed sites. Of note, the response was more noticeable in patients with skin phototypes IV to VI[17]. Enhanced repigmentation with a combination of NB-UVB plus topical 1.5% ruxolitinib cream twice daily has also been reported[17a].

Phototherapy for Atopic Dermatitis

Broadband UVB (BB-UVB) phototherapy

Based on the empirical experience that sun exposure is beneficial for patients with atopic dermatitis, BB-UVB has been used to treat atopic dermatitis since the late 1970s.

UVA/UVB phototherapy

Subsequent studies suggested that a combination of UVA plus UVB irradiation (UVA/UVB therapy) is superior to conventional BB-UVB, conventional UVA, or low-dose UVA1 therapy in the management of chronic, moderate atopic dermatitis. A paired-comparison study demonstrated statistically significant differences in favor of UVA/UVB therapy, compared with BB-UVB therapy[18].

Narrowband UVB (NB-UVB) phototherapy

Earlier studies showed that NB-UVB irradiation not only improved the total clinical score, but also substantially reduced the need for topical corticosteroids. These beneficial effects were still present in the majority of patients 6 months after cessation of phototherapy. Narrowband UVB therapy has also been used successfully in conjunction with UVA1 therapy. However, due to the lack of baseline data on the duration and severity of atopic dermatitis, a final conclusion on preference of phototherapy in the acute or chronic phases cannot be drawn from available studies[19].

Phototherapy for Photodermatoses

In the majority of patients, polymorphous light eruption (PMLE) gradually abates with continual outdoor light exposure. For patients prone to PMLE, NB-UVB phototherapy can be used prophylactically to induce "hardening" of the skin before a vacation to a sunny climate or during the springtime (see Ch. 87). Two to three treatments per week for a total of 12–15 sessions are typically administered prior to an anticipated increase in exposure to sunlight. Despite using reduced UVB doses (as compared to those for psoriasis), this phototherapy regimen can induce a transient photoeruption; the latter usually responds to topical corticosteroids and smaller incremental increases in subsequent UVB doses. The precise mechanisms by which phototherapy induces adaptation to sunlight are not known, but may include thickening of the stratum corneum and modulation of cutaneous immune functions. This phenomenon is not due to hyperpigmentation, as was previously thought – patients with skin phototype I respond equally well to NB-UVB as other skin phototypes.

Narrowband UVB phototherapy has also been shown to be capable of inducing "hardening" in patients with erythropoietic protoporphyria, actinic prurigo, and solar urticaria[20]. For solar urticaria, however, the UVA rush hardening regimen appears to be preferable, since effective protection can be achieved within a few days with this protocol[21].

Phototherapy for Pityriasis Lichenoides

Both pityriasis lichenoides acuta and chronica can have a prolonged course and be rather resistant to therapy. As sunlight may lead to some improvement, UVB phototherapy has also been associated with some success. However, PUVA seems to be more effective (see below), especially in the acute form of the disease (perhaps because of the deeper extension of the dermal inflammatory infiltrate). Although some authors have recommended PUVA as the treatment of choice for the acute form[22], PUVA may be reserved for cases of pityriasis lichenoides chronica that are UVB-resistant.

Phototherapy for Seborrheic Dermatitis

Facial and truncal seborrheic dermatitis generally improves during the summer and "sunny" vacations. Accordingly, UV radiation also seems to have a beneficial effect on this condition. However, flares of dermatitis may occasionally occur. In an open prospective study, NB-UVB was found to be an effective treatment in severe cases[23]. Nonetheless, because topical therapies lead to improvement of seborrheic dermatitis in the majority of patients, phototherapy does not represent a first-line treatment.

Phototherapy for Pruritus

Both NB- and BB-UVB therapy can be of benefit in various forms of pruritus, particularly those associated with diabetes and renal or hepatic disorders, as well as in idiopathic pruritus. However, in patients with cholestatic pruritus, remissions are relatively short-lived. In a case series, NB-UVB led to improvement of uremic pruritus[24].

Side Effects of Phototherapy With UVB

Short-term side effects include erythema (Fig. 134.6), xerosis accompanied by pruritus, occasional blistering, and an increased frequency of recurrent herpes simplex viral infections. Painful erythema resulting from overexposure is treated with topical corticosteroids. Systemic nonsteroidal anti-inflammatory drugs and corticosteroids can prove useful in severe cases if administered early.

Long-term side effects include photoaging and carcinogenesis. Although UVB is a known carcinogen, its carcinogenic potential seems to be much lower than that of PUVA. In a British study involving 3867 patients who had been treated with NB-UVB, no significant association between NB-UVB treatment and basal cell carcinoma (BCC), squamous cell carcinoma (SCC), or melanoma was found[25]. There was a small increase in BCCs amongst those patients who had also been previously treated with PUVA. To determine the true carcinogenic risk of NB-UVB phototherapy, additional longitudinal studies are essential.



Fig. 134.6 Target-like appearance of psoriatic lesions secondary to phototoxicity due to UVB. Annular erythema is separated from the psoriatic plaques by Woronoff's ring.

PHOTOTHERAPY WITH THE 308 NM EXCIMER LASER OR LAMP

With the 308 nm excimer laser, monochromatic UVB radiation can be delivered to specific sites of affected skin at higher fluences than are typically administered with whole-body exposure. Clinical use of this laser for plaque-type psoriasis was first reported in 1997[26] and it is FDA-approved for this indication. Possible advantages are the lower number of treatments that may be necessary to induce clearing as well as the ability to selectively target affected skin with a reduced cumulative dose, thus perhaps reducing the long-term risk of carcinogenicity[27]. However, widespread psoriasis generally cannot be treated with this modality because the spot size is limited to just a few square centimeters.

Clearly, the excimer laser is most suitable for patients with stubborn plaques unresponsive to other treatments and/or those with difficult-to-treat localized areas such as the palms, soles, knees, and elbows. Whether it really represents a therapeutic advancement still remains to be determined by larger and longer-term studies, particularly in view of the high costs of laser treatments. However, both non-laser excimer lamps and hand-held targeted UV devices are less expensive and appear to be similarly effective[27].

Based upon case series, targeted phototherapy with the excimer laser or excimer lamp may also serve as a treatment modality for the management of stable vitiligo[28] as well as a variety of chronic inflammatory localized dermatoses such as granuloma annulare, lichen planus, lichen simplex chronicus, and alopecia areata[29].

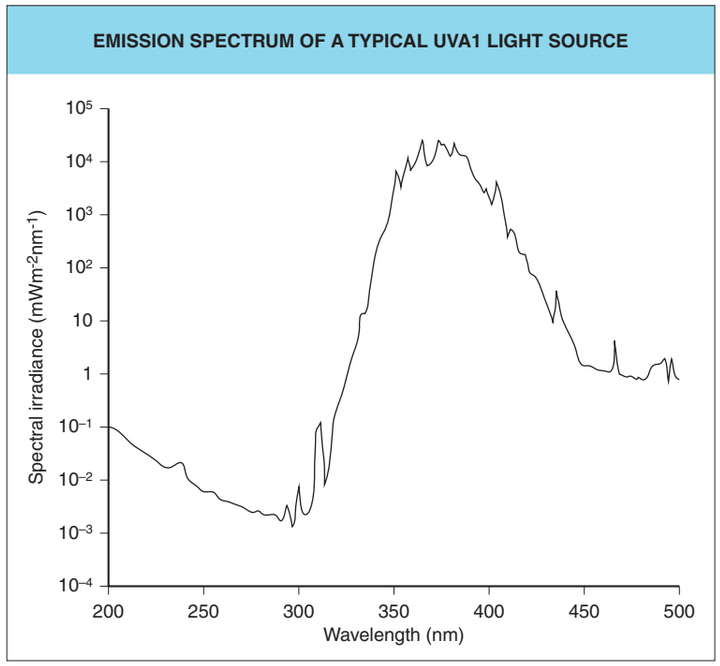


Fig. 134.7 Emission spectrum of a typical UVA1 light source (filtered metal halide lamp).

PHOTOTHERAPY WITH UVA1

The UVA spectrum (320–400 nm) has been arbitrarily subdivided into two parts: UVA1 (340–400 nm) and UVA2 (320–340 nm) (see Fig. 134.1). The main reason for this subdivision was the observation that UVA2 resembled UVB in its ability to induce erythema, immunomodulation, and photocarcinogenesis. Because of its longer wavelength, UVA1 radiation penetrates more deeply into the skin than UVA2 (see Ch. 86), and thus it affects not only epidermal structures, but also mid and deep dermal components, especially blood vessels. Since the skin is a large organ, exposure of circulating immune cells to UVA1 irradiation may have significant systemic ramifications. In particular, its ability to induce T lymphocyte apoptosis is likely to be relevant in the treatment of atopic dermatitis. UVA1 irradiation may also reduce the number of Langerhans cells and mast cells in the dermis in atopic dermatitis and cutaneous mastocytosis. In addition, it has been shown that increased collagenase expression in treated lesions of localized scleroderma (morphea) accompanies improvement with UVA1 irradiation. Perhaps the efficacy of UVA1 in localized scleroderma, and in other sclerosing conditions, is in part due to this action.

UVA1 phototherapy has been investigated as a safer alternative to PUVA for treating chronic conditions. Its major disadvantages are the higher fluences (e.g. 30–130 J/cm^2 per session) and therefore exposure times that are required as well as the higher costs for the lamps. To date, most of the UVA1 studies have been performed in Europe, where efficient sources of UVA1 radiation are more widely available (Fig. 134.7).

UVA1 can have a therapeutic effect on atopic dermatitis[30,31] (Fig. 134.8). It seems to be more effective than UVA/UVB therapy, at least for severe exacerbations of atopic dermatitis. If used as a monotherapy, medium and high daily doses are better than low doses. When UVA1 and NB-UVB were compared for the treatment of atopic dermatitis, they seemed to be equally effective[32]. However, as noted previously, there is currently no consensus as to the preferred type of UV phototherapy for atopic dermatitis[19].

UVA1 therapy has been reported to be beneficial in several other dermatoses[33], in particular sclerosing dermatoses[34], acute GVHD, and chronic sclerodermoid GVHD[35,36]. UVA1 has also been used to treat urticaria pigmentosa[33] and MF[37]. However, its efficacy, especially for the latter indication, requires confirmation in larger patient series.

Side Effects of Phototherapy with UVA1

The adverse effects of UVA1 are less severe than those of UVB and UVA2, although the high fluences usually induce marked tanning, especially in more darkly pigmented individuals. Until more is known about UVA1 therapy, its use (especially with high doses such as 130 J/cm^2) should be limited to treating diseases with periods of severe, acute exacerbations, and in general, one treatment cycle should not exceed 15–20 successively administered exposures and should not be repeated more than once a year. A European prospective longitudinal study has been initiated to monitor patients treated with UVA1 phototherapy for the development of skin cancer and photoaging. An increased expression of *TP53* and a slight increase in Bcl-2 protein expression in keratinocytes were found in human skin after UVA1 irradiation (even with suberythemogenic doses), suggesting that UVA1 may cause DNA damage[38]. In addition, UVA1 induced pro-mutagenic cyclobutane pyrimidine dimers and oxidative DNA damage (at both the genomic and nucleotide resolution level) in normal human skin fibroblasts[39]. Of note, in the years since the widespread use of UVA1 phototherapy in Europe began in 1992, no serious negative side effects in humans have been reported.

PHOTOCHEMOTHERAPY WITH PSORALENS (PUVA)

Psoralen photochemotherapy (PUVA) combines the use of psoralens (P) and long-wave UV radiation (UVA). This combination results in a therapeutically beneficial phototoxic effect, which is not produced by either of the components alone. Psoralens can be administered orally or applied topically in the form of solutions, creams, or baths with subsequent UVA exposure.

Historical Aspects

Topical exposure to extracts, seeds, or parts of plants (e.g. *Ammi majus*, *Psoralea corylifolia*) that contain natural psoralens, followed by exposure to sunlight, was used as a remedy for vitiligo for thousands of years in ancient Egypt and India[40]. In 1974, it was shown that the oral ingestion of 8-methoxypsoralen (8-MOP) and subsequent exposure to a new, high-intensity, artificial UVA radiation source was highly effective for the treatment of psoriasis[41]. This was followed by recognition of its therapeutic effect for multiple skin disorders (Table 134.3). Over the past decade, the use of PUVA has decreased significantly, due in part to the increased risk of developing keratinocyte carcinomas and melanoma, especially with prolonged use in fair-skinned individuals, in addition to the effectiveness of NB-UVB and especially systemic

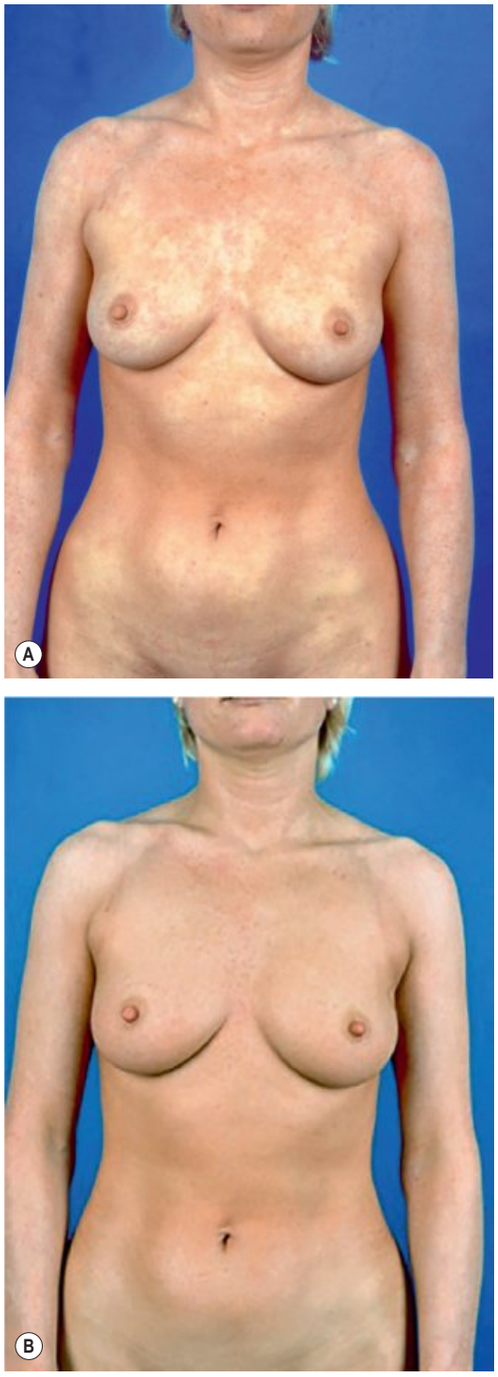


Fig. 134.8 UVA1 phototherapy of atopic dermatitis (split-body comparison). **A** Before treatment. **B** After treatment (15 exposures) with high-dose (130 J/cm^2, left side) *versus* medium-dose (65 J/cm^2, right side) UVA1 phototherapy. Note that there is no difference in the therapeutic result.

PUVA-RESPONSIVE DISEASES	
Therapy of disease	**Prevention of disease**
Psoriasis	Polymorphic light eruption†
Palmoplantar pustulosis	Solar urticaria†
Atopic dermatitis	Chronic actinic dermatitis*,†
Mycosis fungoides (stages IA, IB, IIA)	Hydroa vacciniforme*,†
Vitiligo	
Generalized lichen planus	
Urticaria pigmentosa	
Cutaneous GVHD	
Generalized granuloma annulare	
Prurigo nodularis	
Pityriasis lichenoides (acute and chronic)*	
Lymphomatoid papulosis*	
Pityriasis rubra pilaris*,†	
Pigmented purpuric dermatoses*	
Langerhans cell histiocytosis*	
Localized scleroderma*	

*Experience is limited to a small number of patients.
†These diseases may flare prior to therapeutic response.

Table 134.3 PUVA-responsive diseases. GVHD, graft-versus-host disease.

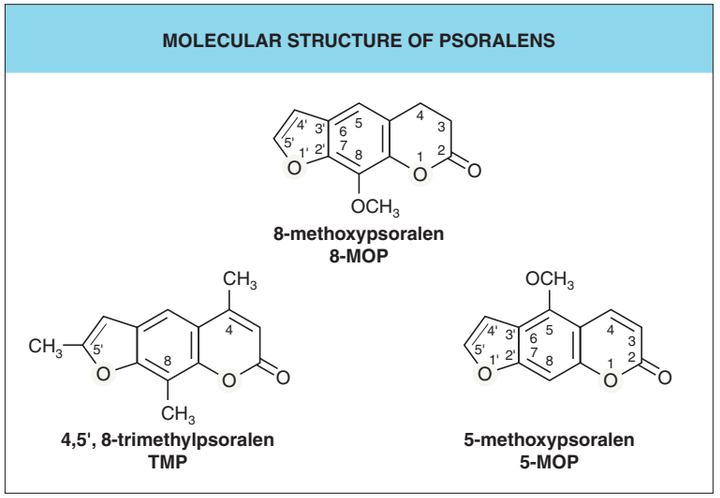


Fig. 134.9 Molecular structure of psoralens.

immunomodulators ("biologics") in psoriasis. Even though PUVA often represents a second-line form of phototherapy, it is essential that dermatologists become familiar with treatment regimens, potential side effects, and indications, in particular since it is still the (see meta-analysis below) therapy of choice in early stage mycosis fungoides.

Psoralens

Psoralens are naturally occurring linear furocoumarins that are found in a large number of plants, and there are several synthetic psoralen compounds. For oral and topical (bath, cream) PUVA, mainly 8-MOP (methoxsalen) is used; it is of plant origin but also available as a synthetic drug. The synthetic compound, 4,5′,8-trimethylpsoralen (TMP, trioxsalen), is less phototoxic than 8-MOP after oral administration, but more phototoxic when delivered via bath-water. TMP had been used primarily in Scandinavia for bath PUVA. 5-Methoxypsoralen (5-MOP, bergapten) is also therapeutically effective when given orally; it is less erythemogenic and is not associated with gastrointestinal intolerance (Fig. 134.9). In some European countries, it was routinely used for PUVA, but it is no longer commercially available. Oral preparations of 8-MOP contain crystals, micronized crystals, or solubilized psoralens in a gel matrix. The latter liquid preparation induces earlier, higher, and more reproducible peak plasma levels than the crystalline preparations.

The steps between the ingestion of a psoralen and its arrival in the skin include disintegration and dissolution of the drug, absorption, first-pass effect, blood transport, and tissue distribution. The absorption rate of a psoralen from the gut depends on the physicochemical properties of the molecule, the rate of dissolution, the galenic characteristics of the preparation, and the fat content of concomitantly ingested food. Peak serum levels are usually reliably and predictably achieved by liquid preparations, whereas wide time variability occurs with crystalline formulations. Before reaching the skin via the circulation, psoralens are metabolized during their passage through the liver. Plasma levels of 8-MOP administered orally at different doses show a strong non-linearity, indicating a saturable first-pass effect. Thus, small differences in the ingested doses and absorption rates of psoralens lead to large differences in plasma levels. As a practical consequence, small amounts of the drug are almost completely metabolized by the liver during the first pass and therefore may be therapeutically inactive.

8-MOP serum levels show a wide range of inter-individual differences. Even on different occasions in the same patient, serum levels may differ; however, the levels are usually sufficiently constant to provide for relatively reproducible therapeutic results. This unpredictable pharmacokinetic behavior is probably due to inter- and intra-individual variations in intestinal absorption, first-pass effect, blood distribution in the body, and metabolism and elimination of the drug.

For a given patient, serum levels of 8-MOP correspond fairly well with skin reactivity, with the peak of skin phototoxicity coinciding with peak serum levels. A correlation between 8-MOP serum levels and epidermal concentrations does exist. Whether there is a significant correlation between maximum psoralen blood concentrations and the minimal phototoxicity dose (MPD) remains equivocal.

The pharmacokinetics of topical 8-MOP depend on the mode of application. 8-MOP administered topically as a 0.15% emulsion or solution has been shown to result in plasma levels comparable to those obtained by oral delivery, when large areas of the body are treated. In contrast, due to the much lower concentrations that are typically used, plasma levels following bath-PUVA treatment of almost the entire body surface are very low. Bath-water-delivered psoralens are readily absorbed into the skin, but promptly eliminated without cutaneous accumulation[2].

Psoralen photochemistry

Psoralens react with DNA in three steps. First, in the absence of UV radiation, the psoralen intercalates into the DNA double strand. Via a photochemical reaction, absorption of photons in the UVA range results in the formation of a 3,4- or 4′,5′-cyclobutane monoadduct with pyrimidine bases of native DNA. The 4′,5′ monoadducts can absorb a second photon and this reaction leads to the formation of an interstrand cross-link of the double helix with the 5,6 double bond of the pyrimidine base of the opposite strand (Fig. 134.10).

UVA-activated psoralens can also react with molecular oxygen. The reactive oxygen species formed by this reaction cause cell membrane damage by lipid peroxidation and may activate the cyclooxygenase and arachidonic acid metabolic pathways.

The cross-linking of psoralens with epidermal DNA inhibits DNA replication and causes cell cycle arrest. Although not proven, it is generally assumed that this effect may be the therapeutic mechanism in psoriasis. Psoralen photosensitization also causes an alteration in the expression of cytokines and cytokine receptors. However, DNA cross-linking does not appear to be a prerequisite for all the therapeutic effects of PUVA, and the successful treatment of other skin diseases is unlikely to be due directly to this molecular reaction. Psoralens also interact with RNA, proteins, and other cellular components and indirectly modify proteins and lipids via singlet oxygen-mediated reactions or by generating free radicals[42,43].

PUVA can reverse the pathologically altered patterns of keratinocyte differentiation markers and reduce the number of proliferating epidermal cells. Infiltrating lymphocytes are strongly suppressed by PUVA, with variable effects on different T cell subsets. PUVA is far more potent in inducing apoptosis in lymphocytes than in keratinocytes[1], which may

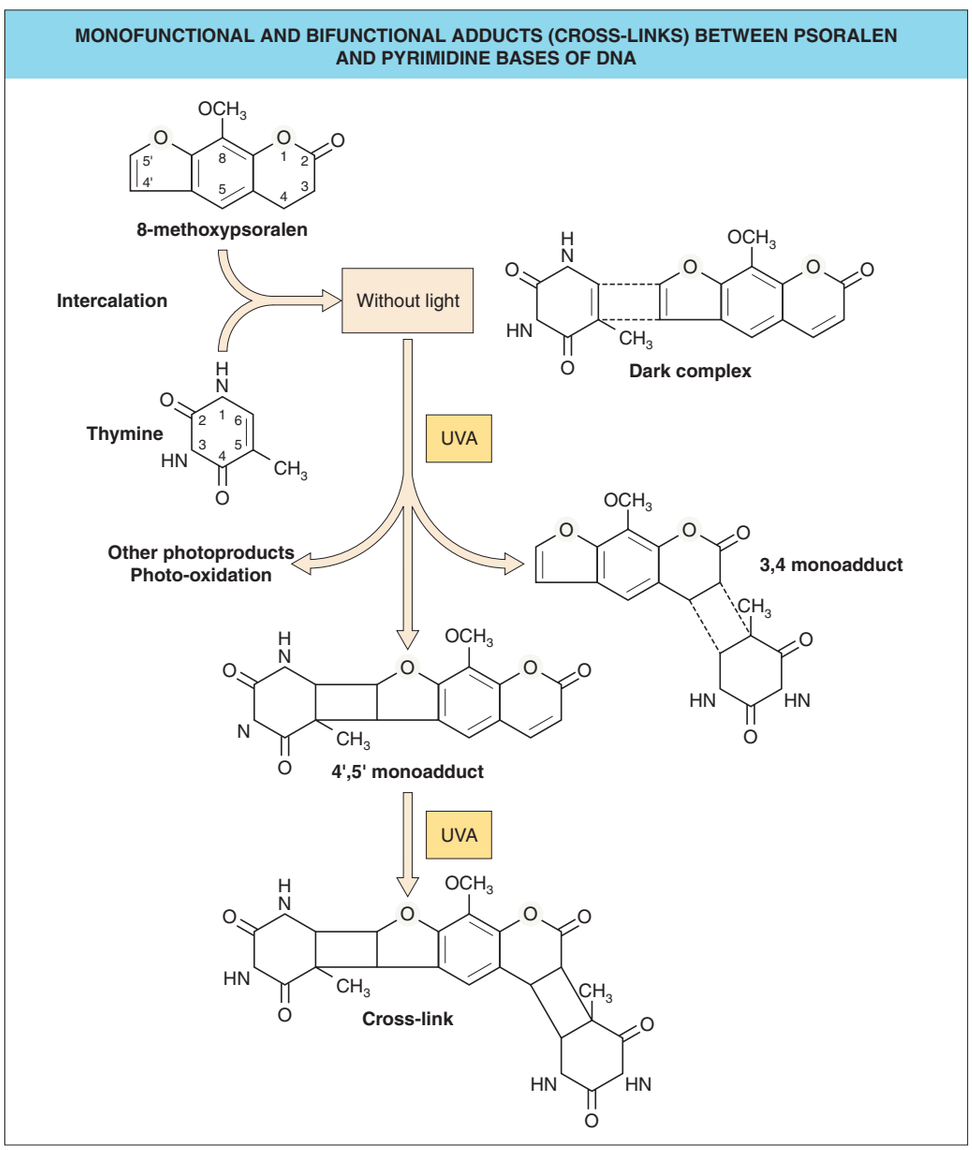


Fig. 134.10 Monofunctional and bifunctional adducts (cross-links) between psoralen and pyrimidine bases of DNA.

explain its efficacy in CTCL as well as in inflammatory skin diseases. Although much is known about pathways and mechanisms in psoralen photosensitization, the interactions and relative contributions to the clearing of a specific disease are not well understood.

Psoralens also stimulate melanogenesis. This involves the photoconjugation of psoralens to DNA in melanocytes, followed by mitosis and subsequent proliferation of melanocytes, increased formation and melanization of melanosomes, enhanced transfer of melanosomes to keratinocytes, and increased synthesis of tyrosinase via stimulation of cAMP activity (see Ch. 65).

Action Spectrum and Light Sources

The action spectrum for 8-MOP-induced delayed erythema has its maximum activity in the 330–335 nm range and the antipsoriatic activity of 8-MOP (plus UVA) appears to parallel this erythema action spectrum[44]. Conventional therapeutic UVA fluorescent tubes and broad-spectrum metal halide lamps, which are filtered in the UVB and UVC range, effectively cover the psoralen action spectrum. The typical fluorescent UVA lamp used for PUVA therapy peaks at 352 nm and emits ~0.5% in the UVB range (Fig. 134.11). Major advantages of mercury halide units are the stability of output and their high irradiance, enabling shorter treatment times.

UVA doses are given in J/cm^2, instead of mJ/cm^2 used for UVB, and are usually measured with a photometer with a maximum sensitivity at 350–360 nm. Within the phototherapy cabinet, the irradiance must be relatively uniform to ensure that the dose does not vary at different anatomic sites. UVB emission should be kept low enough to avoid erythemogenic UVB doses so that sufficient UVA is absorbed to activate the psoralen photosensitivity reaction.

Photobiologic Effects of PUVA

PUVA treatment produces an inflammatory response that manifests as delayed phototoxic erythema. The reaction depends on the dose of drug, the dose of UVA, and the individual's sensitivity (skin type). More recently, it was shown that changes in 8-MOP dose had no detectable effect on the maximum slope of the PUVA erythema dose–response curve. Thus, 8-MOP dose changes within individuals, over a narrow but clinically relevant range, appear to significantly alter the threshold response to PUVA erythema but not the rate of increase in erythema with increasing UVA dose[45].

The time course for PUVA erythema differs markedly from sunburn or UVB erythema; the latter appears after 4–6 hours and peaks 12–24 hours after exposure to UVB. PUVA erythema does not occur before 24–36 hours and it peaks at 72–96 hours or even later after exposure. It has a shallower dose–response curve than UVB erythema (by a factor of ~2) and this difference is maintained even at the time of maximum erythema[46]. PUVA erythema persists for longer periods of time (lasting up to more than 1 week) and it consists of a deeper red, even a violaceous, hue. Severe reactions may lead to blistering and to superficial skin necrosis. Overdoses of PUVA are frequently followed by edema, intense pruritus, and sometimes by a peculiar stinging sensation in the affected skin area. At present, erythema is the only clinical parameter that allows for an assessment of the magnitude of the PUVA reaction and then determination of UVA dose adjustments[2].

Pigmentation, the second important effect of PUVA, may develop without clinically evident erythema, especially when oral TMP is used. In normal skin, PUVA pigmentation peaks about 7 days after exposure and may last from several weeks to months. As with sun-induced tanning, the individual's ability to tan is genetically determined, but the dose–response curve is much steeper. A few PUVA exposures result in a much deeper tan than that produced by multiple exposures to solar radiation. When administering PUVA therapy for inflammatory and neoplastic disorders, an important strategy is to produce a clinical response prior to the induction of significant pigmentation.

Treatment Protocols

Oral PUVA

For oral PUVA, the general approach is to keep the dose of psoralen, as well as the interval between drug intake and UVA exposure, constant, and to vary the UVA dose according to the patient's sensitivity. A dosage of 8-MOP of 0.6 to 0.8 mg/kg body weight is administered orally 1–3 hours before exposure, depending on the absorption characteristics of the particular drug formulation (see above).

The initial UVA doses are selected either by skin phototyping[8,47] or by determining the minimal phototoxicity dose (MPD)[48]. In the US, skin reactivity to solar radiation is evaluated and patients are classified based on a skin phototype scheme according to their sunburn and tanning history. Therapeutic doses of UVA are then given according to an empirical scheme based on this classification[8,45] (Table 134.4). In Europe, until recently, the most widely used approach consisted of MPD determination analogous to MED determination. The MPD is defined as the minimal dose of UVA (following psoralen ingestion) that produces a barely perceptible, but well-defined, erythema. The doses range from 0.5 to 5 J/cm^2 if oral 8-MOP is used. Erythema readings are performed 72 to 96 hours after irradiation, when the phototoxicity reaction usually peaks. As with the MED, the MPD is determined on previously non-sun-exposed skin (lower back or buttocks). Since determining the MPD is rather time-consuming and can take up to a week to perform, it has been abandoned for practical reasons in most European phototherapy centers and replaced by phototyping. In several phototherapy guidelines, MPD testing is still recommended but not considered to be mandatory.

Oral PUVA should not be used in patients with hepatitis because a slower metabolism of psoralens may prolong photosensitivity. Impaired renal function may also reduce psoralen excretion.

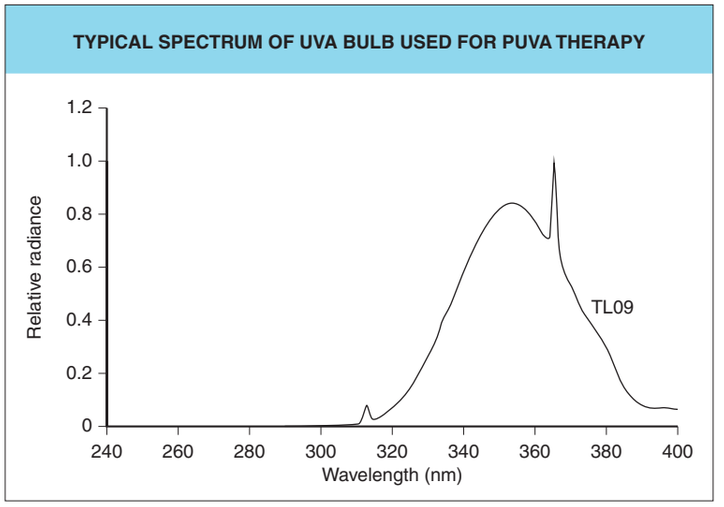


Fig. 134.11 Typical spectrum of a UVA bulb (Philips TL09) used for PUVA therapy.

SKIN PHOTOTYPES AND INITIAL DOSE OF UVA FOR PUVA THERAPY

Skin phototype*	Skin reaction	Recommended initial dose (J/cm^2)
I†	Always burns, never tans	0.25–0.5
II	Always burns, but sometimes tans	0.5–1.0
III	Sometimes burns, but always tans	1.5
IV	Never burns, always tans	2.0
V‡	Moderately pigmented skin	2.5
VI	Darkly pigmented skin	3.0

*Types I–IV are determined by history; types V and VI by physical examination (skin color).
†Patients with erythrodermic psoriasis are to be classified as skin phototype I for determination of UVA dosage.
‡Patients with this phototype should be classified into a lower skin phototype category if the sunburning history so indicates.

Table 134.4 Skin phototypes and initial dose of UVA for PUVA therapy. These irradiation doses are based upon an oral 8-MOP dose of 0.6–0.8 mg/kg.

Bath PUVA

Bath-water delivery of psoralens has become increasingly popular because it provides uniform drug distribution over the skin surface, very low psoralen plasma levels, and a rapid elimination of free psoralens from the skin, thereby reducing the period of photosensitivity. Due to the absence of systemic photosensitization, bath-water delivery of 8-MOP circumvents gastrointestinal side effects and potential ocular effects. Skin psoralen levels are highly reproducible and photosensitivity lasts no more than 2 hours. However, peak erythema is delayed as compared to the oral route; therefore erythema readings should be performed 96 to 120 hours after irradiation, which is the major reason why MPD determination has been replaced by phototyping in most phototherapy centers. The higher incidence of unwanted phototoxicity can be prevented by a lower starting dose and more cautious dosimetry during the initial treatment phase.

Originally, bath PUVA was performed with TMP, but 8-MOP is now being used as well. Bath PUVA consists of 15–20 minutes of whole body (or hand and foot) immersion in solutions of 0.5–5.0 mg of 8-MOP per liter of bath water. Irradiation has to be performed immediately thereafter, as photosensitivity decreases rather rapidly. However, one must take into account that, unlike with oral PUVA, the phototoxic threshold *declines* early on during treatment (this may be due to persistent psoralen adducts)[2]. Thus, at the onset, dose increments should be done more cautiously.

Topical PUVA

Application of 8-MOP (0.1%–0.01%) in creams, ointments, or lotions, followed by UVA irradiation, is effective but has several disadvantages. The non-uniform distribution on the skin surface may produce unpredictable phototoxic erythema reactions, and inadvertent application to surrounding uninvolved skin can lead to cosmetically unacceptable hyperpigmentation. Furthermore, if numerous lesions are present, the application is laborious and time-consuming, and the treatment does not prevent the development of new active lesions in previously unaffected, untreated areas. Finally, extensive application ("paint" PUVA) of a 0.15% 8-MOP emulsion was found to cause plasma levels comparable to those detected with oral ingestion. Therefore, topical PUVA utilizing psoralen creams, ointments, or lotions is now reserved primarily for dermatoses of the palms and soles.

Initial Treatment (Clearing) Phase

The initial treatment phase is defined as the treatment period until clearing of the disease is achieved; repeated exposures are required, with gradual dose increments as pigmentation develops. Doses that are too low frequently result in failure of treatment, except in those diseases in which induction of pigmentation is the desired objective. In most dermatoses amenable to PUVA, the frequency of treatments should be reduced after satisfactory control of the disease.

If MPD testing is performed, a safe initial therapeutic dose for oral PUVA is 50%–70% of the MPD. For bath PUVA, it is advisable to start at only 30% of the MPD, because photosensitivity is up to 10 times higher than with oral PUVA (Fig. 134.12). As noted previously, nowadays, most centers start with doses based on the patient's skin phototype.

Irradiations are given two to four times weekly. Dose increments are performed no more often than twice a week (at least 72 hours apart) and never during the first week of treatment (if initial dose is based on MPD), in order to avoid an accumulation of delayed cutaneous phototoxicity. Although not necessary for therapeutic success, a minimally perceptible erythema is considered a clinical indicator of adequate dosimetry. There exists no rigid scheme for dose increments; the major parameter for dose adjustments should be the clinical response of the disease. It is essential to note that with bath PUVA, the MPD can even decrease during the first days after initiation of treatment by up to 50%, but then increase at later stages. This may be due to persistent psoralen adducts which are converted into cross-links upon subsequent exposures.

In the absence of erythema, the UVA dose can be increased safely by 30% in both oral PUVA and bath PUVA (see Fig. 134.12). However, because of erythema formation and/or an adequate treatment response, some patients will not require dose adjustments over prolonged periods of time.

Maintenance Phase

The purpose of maintenance therapy is to prolong the duration of clinical remission. In the original European regimen, maintenance therapy consisted of one month of twice-weekly treatments utilizing the final UVA dose administered during the clearing phase, followed by another month of once-weekly exposures. However, results of a more recent study indicated that short-term maintenance therapy was not

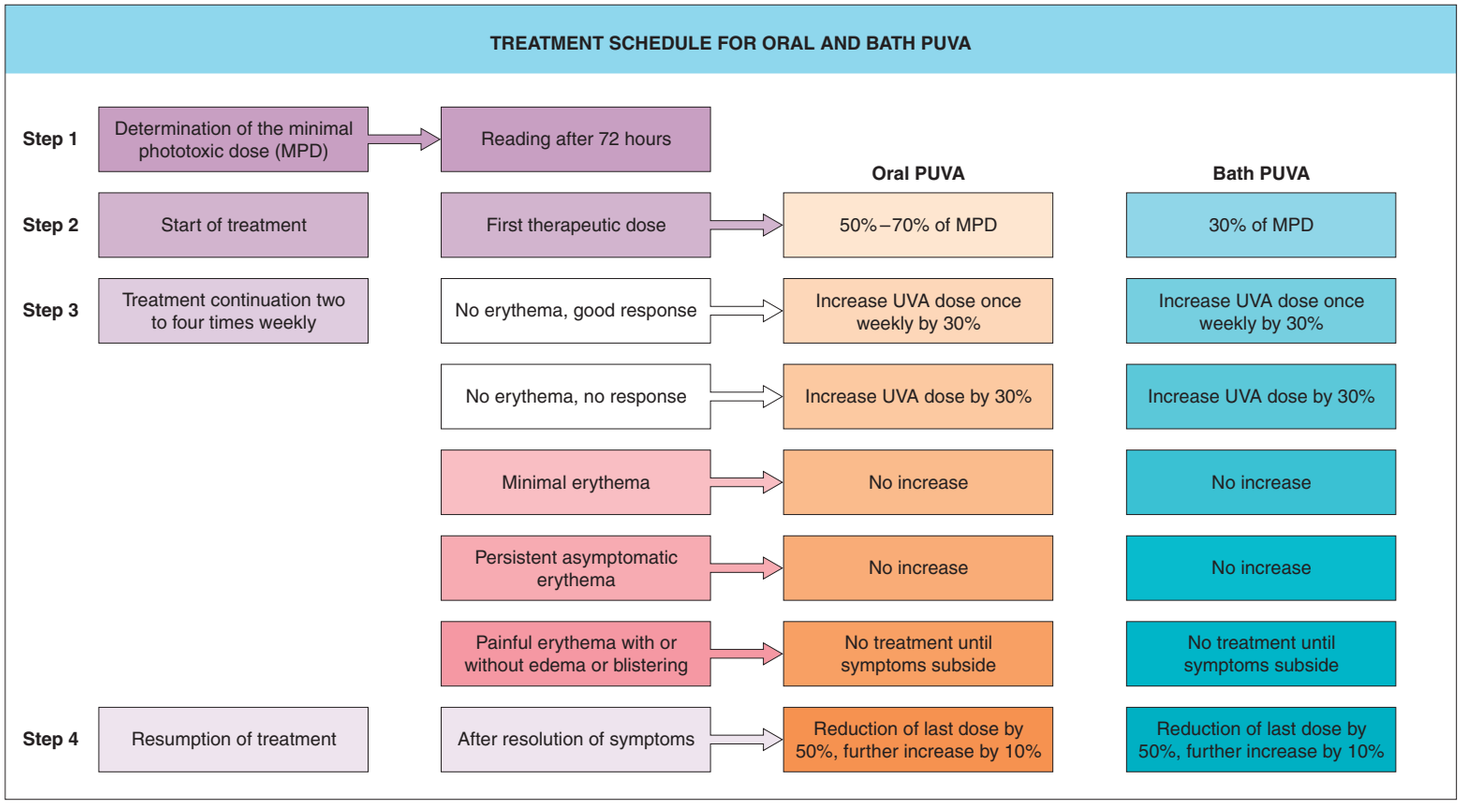


Fig. 134.12 Treatment schedule for oral and bath PUVA.

effective in preventing early relapses of psoriasis[49]. For MF, many institutions recommend some form of permanent maintenance therapy, but there is a lack of prospective studies to validate this recommendation. Perhaps a once-monthly treatment would be a feasible compromise.

Mild relapses during the maintenance phase are handled by temporarily increasing the frequency of treatments; in the case of a severe relapse, the original clearing phase schedule must be resumed until clearing is once again achieved. A disadvantage of maintenance therapy for patients in remission is the potential to overtreat the patient and to increase the potential for long-term toxicity that is related to the total cumulative dose of PUVA.

PUVA for Psoriasis

Basically, all types of psoriasis respond to PUVA (Fig. 134.13), although the management of erythrodermic or generalized pustular psoriasis is more difficult[2]. Both the US and the European regimens have proven to be highly efficient and therefore have remained in use, although with the advent of systemic immunomodulators ("biologics"; see Ch. 128), phototherapy for all types of psoriasis has lessened.

Three studies have compared bath-water delivery of 8-MOP with oral administration[50–52]. In two reports, initial doses were determined by skin phototyping and treatments were given two to three times weekly. Dosage increments were made with every treatment in the first study[50], whereas smaller increments were performed every third treatment in the second[51]. Patients in the third study were treated according to the guidelines of the standard European regimen for oral PUVA; this group had the lowest incidence of treatment failures and overdose episodes[52]. Relative to the results obtained with oral PUVA, bath PUVA showed equal clearing rates with lower numbers of exposures. The greater therapeutic efficacy could be due to a higher penetration of psoralens through the abnormal stratum corneum overlying psoriatic plaques as compared with healthy perilesional skin where phototoxicity is monitored during the therapy. The incidence of erythema and pruritus was similar or lower with bath PUVA as compared to oral therapy. In all the investigations, episodes of systemic intolerance such as nausea and vomiting were recorded only with oral PUVA[2].

PUVA alone can produce a definite remission in many cases of psoriasis, but a considerable number of patients require combination therapy (see below).



Fig. 134.13 PUVA treatment for psoriasis (four times weekly). A Before treatment. **B** After 6 weeks of treatment.

Combination Treatments

Topical combination

As with UVB phototherapy, PUVA can be combined with other treatment modalities to improve efficacy and to reduce potential side effects[2]. Topical adjuvant therapies include corticosteroids, anthralin, tar, and vitamin D analogues (see Chs. 125 & 129). However, some patients are reluctant to "retry" topical agents that previously proved unsuccessful when used alone.

Methotrexate, cyclosporine, systemic immunomodulators ("biologics")

The combination of PUVA and methotrexate (MTX) during the clearing phase reduces the duration of treatment, number of exposures, and cumulative UVA dose, and it is also effective in clearing patients unresponsive to PUVA or UVB alone[53]. To date, no increased risk of keratinocyte carcinomas has been reported for this combination. In contrast, cyclosporine plus PUVA has been clearly shown to dramatically enhance cutaneous carcinogenesis. Thus, this latter combination should be categorically discouraged[53], including the use of cyclosporine subsequent to PUVA therapy. Presently, there are no studies evaluating the safety and efficacy of biologics plus PUVA.

Retinoids

The combination of PUVA with systemic retinoids (RePUVA) is one of the most potent therapeutic regimens for psoriasis. The therapeutic efficacy of PUVA therapy is significantly enhanced upon combination with oral retinoids (acitretin [0.5–0.75 mg/kg] or isotretinoin [0.75–1 mg/kg]) that are administered daily for 5–10 days before PUVA is started, with the combination continued throughout the clearing phase. RePUVA reportedly can reduce the number of exposures by one-third and the total cumulative UVA dose by more than one-half. RePUVA can also clear "poor PUVA responders"[2].

The underlying mechanism of the synergistic action of retinoids plus PUVA may be a reduction in the inflammatory infiltrate and an accelerated desquamation of the psoriatic plaques, thereby optimizing the optical properties of the skin. In theory, retinoids may also reduce the long-term carcinogenic risk of PUVA by reducing the number of exposures and providing chemoprevention against skin cancers. Some evidence for this was presented in a study where patients with psoriasis treated with PUVA in combination with systemic retinoids showed a reduced risk of SCC but not a significantly altered incidence of BCC[54].

Short-term side effects of retinoids are completely reversible upon discontinuation, and long-term toxicity is not relevant because of the limited duration of their use (until clear). The potential teratogenicity of retinoids represents a serious concern. For women of childbearing age, the use of isotretinoin is an option, because contraception is only necessary for 1–2 months after discontinuation of therapy, as opposed to acitretin, which requires two subsequent years of contraception[2].

PUVA for Cutaneous T Cell Lymphoma, in Particular Mycosis Fungoides

Based on the empirical beneficial effect of natural sunlight on early stage MF, Gilchrest et al.[55] first reported the successful use of PUVA for MF. Patients with unsatisfactory responses to other therapies and histologically confirmed plaque or tumor stage MF or the erythrodermic form of CTCL were subjected to PUVA. Complete clearing was observed, except

in those areas that were shielded from UVA exposures, thus excluding the possibility of spontaneous remission. This also indicated that the therapeutic effect of PUVA was local rather than systemic.

Numerous studies followed which addressed the rates of initial response and average duration of remission in relation to the stage of MF, the efficacy of PUVA compared with other established treatment options, the efficacy of combination treatments, the mechanisms responsible for the therapeutic effects, and the risk of short- and long-term side effects[2].

Treatment schedules and dosimetry in the photochemotherapy of MF are essentially the same as for psoriasis, consisting of three phases – clearing, maintenance, and follow-up. Some authors suggest that remission should be confirmed by histologic examination of previously involved areas. In some institutions, maintenance therapy includes two exposures per week for one month and one exposure per week for another month. If still in remission, therapy is discontinued and the patient is monitored monthly and then bimonthly. If a relapse occurs, the patient is again treated with three or four PUVA exposures per week until complete clearing. However, other investigators advocate permanent maintenance treatment consisting of treatments once monthly or every other month, as it appears that PUVA treatment is not curative. Since the course of MF varies considerably from patient to patient, the final answer remains to be determined.

Clinical experience indicates that patients benefit most from individualized schedules. For example, a recent study described the administration of a low frequency regimen (2×/week) for early MF (stage IA–IIA)[56]. Oral PUVA was administered for up to 24 weeks in 27 patients; 19 complete and 8 partial remissions were observed and the average cumulative UVA dose was rather low (78.5 J/cm^2). Eleven of the 19 patients with a complete remission underwent maintenance therapy (14 exposures over 9 months), with 7 of those still in remission after one year. In comparison, 7 of 8 patients who did not receive maintenance therapy experienced a relapse.

Several studies involving large patient cohorts have provided information on the initial response rates of PUVA treatment in relation to disease stage. Overall, the best initial complete response rates were obtained for stages IA (~90%), IB (~76%) and IIA (~78%), as compared to stages IIB and III (~60%). There was some heterogeneity in results and the use of different treatment protocols, psoralen preparations, and light sources may have contributed to this finding. Only a few patients with stage IV disease have been treated with PUVA monotherapy, because, in this stage, PUVA is generally considered to be only a palliative or adjunctive therapy. Relapses usually respond to PUVA in the same manner as the initial response. Clinical remissions appear to be directly related to phototoxic destruction of the malignant infiltrate. Thus, complete clearing may be induced when the cells are confined to the epidermis and the superficial dermis and do not exceed the depth of UVA penetration into the skin. Patients with tumor stage MF exhibit a high rate of early recurrences, which require permanent maintenance treatment; often only the combination of PUVA with local radiotherapy and/or systemic chemo-immunotherapy can result in complete tumor resolution.

In summary, the data thus far indicate that PUVA is an excellent treatment option for early stage (IA–IIA) CTCL (Fig. 134.14). High rates of complete clearing can be achieved and a substantial percentage of patients remain free of disease for many years. In a meta-analysis of seven studies that compared PUVA versus NB-UVB for the treatment of early MF (IA–IIA), 778 patients (527 PUVA, 251 NB-UVB) were analyzed[57]. Complete remission was achieved in 74% of the patients in the PUVA group and 62% in the NB-UVB group; the remission-free interval ranged from 10 to 45 months (mean 33 months) in the PUVA group compared to 5 to 24 months (mean 15 months) in the NB-UVB group. The significantly longer remissions rates may be one of the reasons why in some treatment guidelines PUVA is regarded as the therapy of choice in early stage MF[58].

In advanced stages (IIB–IVB) of MF, PUVA is not sufficient as monotherapy, but as an adjunctive treatment it can reduce the tumor burden in the skin and can improve the quality of life for patients. Presently, no therapeutic regimen is known to arrest eventual progression of advanced stages of MF to tumor formation, dissemination, and a fatal outcome. Prolonged remissions have been observed with combinations of PUVA plus systemic retinoids (e.g. bexarotene[59]) or IFN-α-2a[60,61]. Possible long-term side effects related to frequent PUVA treatments are probably less meaningful for patients with CTCL compared with patients who have benign disorders.



Fig. 134.14 PUVA treatment for cutaneous T cell lymphoma (mycosis fungoides). A Before treatment. **B** After 12 weeks of treatment that was four times weekly.

While PUVA therapy is very effective in inducing remission as long as the lymphoma is confined to the skin, the impact of this therapy on the natural course of CTCL and on patient survival is not yet determined.

PUVA for Vitiligo

As mentioned previously, vitiligo was the first disease treated with an ancient form of psoralen photochemotherapy in India and Egypt. PUVA in its modern form stimulates melanogenesis as well as melanocyte

proliferation and migration, and it reconstitutes the normal skin color in more than 50% of vitiligo patients.

Treatment protocols and results

Nowadays, oral 8-MOP is the photosensitizer most frequently used, followed by exposure to sunlight or artificial UVA radiation. In the past, if sunlight were the radiation source, oral TMP was the preferred photosensitizer due to its weaker phototoxicity. To induce repigmentation, patients need constant long-term therapy. It is crucial that the patient understands that PUVA, like other vitiligo therapies, may require months or even years to achieve a satisfactory result. Overly optimistic prognoses regarding therapeutic efficacy and length of time to produce adequate repigmentation should be avoided. The patients must also be aware that the treatments stimulate the pigmentation of normal skin, which will intensify the contrast between normal and vitiliginous skin.

Treatments should be given at least twice a week, but not more than three times, with at least one day between treatments. If there is no response after 4–5 months or ~30–40 treatments, PUVA should be terminated. Responsiveness is defined as development of multiple perifollicular macules of repigmentation, or, in the case of small (<2 cm) lesions, contraction in size. If treatment is discontinued, reversal of acquired repigmentation may occur unless the lesion has completely repigmented. Completely repigmented areas can be stable for a decade or more without relapse.

Photochemotherapy with topical 8-MOP can be used in patients with small lesions (<5% total body surface area) or in children in whom one may hesitate to use systemic PUVA. The therapy must be done in an office setting, since home treatment involves a high risk of severe phototoxic side effects. Topical 8-MOP preparations (0.0005%–0.005% 8-MOP in a cream or ointment base) are applied evenly on the treatment area 30 minutes prior to irradiation. Exposure times (beginning at $\leq 0.25\,J/cm^2$) are increased weekly in increments of $0.25\,J/cm^2$ unless marked erythema occurs. Once- to twice-weekly treatments are recommended. With topical PUVA, the vehicle plays a major role in delivery and resulting cutaneous psoralen levels. Solutions should be avoided as they can "run", producing hyperpigmented streaks. Application of sunscreen to the surrounding uninvolved skin prior to application of the topical psoralen can reduce hyperpigmented rims.

Patient selection appears to be critically important. For oral PUVA, the patients should be ages 10–12 years or older, and for all forms, they must be available for 12–24 months of continuous therapy. Lips, distal dorsal hands, fingers and toes, palms, soles, and nipples are very refractory to treatment, as are large areas with only white hairs. Patients need to be made aware of this fact.

Stable disease, i.e. nonprogressive for at least 6 months to a year, is usually easier to treat. On average, a complete treatment regimen consists of at least 150 exposures. However, because of the different response rates in different body areas, total repigmentation is only rarely achieved, and ~30% of patients do not respond at all, despite months of therapy. As mentioned above, in a trial involving patients with non-segmental vitiligo, NB-UVB therapy resulted in a better color match when compared to oral PUVA[15]. As a result, the use of NB-UVB has increased while PUVA therapy for vitiligo has waned in most phototherapy centers.

PUVA for Atopic Dermatitis (See Ch. 12)

Many patients with moderate, severe, and even erythrodermic forms of atopic eczema can benefit from PUVA therapy[53]. The treatment guidelines are essentially the same as for psoriasis, but patients may develop a temporary flare of their dermatitis during the initial treatment phase. Also, atopic dermatitis is more difficult to treat than psoriasis and quite often a higher number of treatments is required. Although atopic dermatitis may be cleared by PUVA, recurrence rates are high and rapid, requiring frequent maintenance exposures. However, in young patients, long-term maintenance therapy should be avoided. A combination of PUVA with topical corticosteroids appears to be superior to PUVA alone in maintaining remissions, and in a more recent study involving patients with severe atopic dermatitis, PUVA provided better short- and long-term responses than did medium-dose UVA1. These latter results require further confirmation. Due to the introduction of systemic immunomodulators such as dupilumab to treat moderate-to-severe atopic dermatitis, the importance of PUVA as a therapeutic approach will likely decrease in the future.

PUVA for Lichen Planus (See Ch. 11)

In generalized lichen planus, PUVA can provide an effective alternative to systemic corticosteroids. Studies have pointed to an overall response rate between 50% and 90%, suggesting that lichen planus is less responsive than psoriasis to PUVA. In addition, more treatment sessions and higher cumulative UVA doses were generally necessary for complete remission and not all patients responded satisfactorily. Marked postinflammatory hyperpigmentation may impair the final cosmetic result. An exacerbation during PUVA treatment has been reported in a few patients. Bath PUVA also works in lichen planus, and a combined RePUVA regimen (as is used for psoriasis) may accelerate clearing in disseminated and particularly keratotic forms of lichen planus. Compared to NB-UVB, oral PUVA led to a better initial clinical response rate, but both were effective treatments and produced similar long-term outcomes[62].

PUVA for Graft-Versus-Host Disease (see Ch. 52)

Due to clinical and histologic similarities between idiopathic lichen planus and lichenoid GVHD, PUVA treatment was evaluated for the latter[63]. Beneficial effects were observed in patients who had not responded to conventional immunosuppressive therapy alone. PUVA can also improve acute GVHD[64]. Results of PUVA therapy for scleroderma-like variants of cutaneous GVHD are controversial[65]. In our experience, the more localized and circumscribed morpheaform lesions appear to respond to PUVA fairly rapidly, with softening of the associated sclerosis. However, the more advanced and widespread sclerodermoid form hardly responds to PUVA.

In contrast to other conditions, PUVA may exert not only local but also systemic effects, since improvement of mucosal erosions was observed during treatment of chronic lichenoid GVHD with PUVA, but this could have also been coincidental. Apparently, there is no improvement of GVHD of other organs, e.g. liver and gut. Of note, deterioration of liver GVHD has not been reported thus far. This is important, since psoralens are metabolized by the liver.

The therapeutic regimen used for the treatment of chronic GVHD is basically the same as for psoriasis. UVA doses should not be increased too aggressively, in order to avoid erythema and possible (re)activation of GVHD. The UVA dosage is increased by no more than $0.5\,J/cm^2$ every second to fourth exposure and patients are treated three to four times weekly. After clearing of skin lesions, exposures are reduced according to the maintenance schedule outlined for psoriasis.

There may be a slight overall increased risk of cutaneous malignancies in hematopoietic stem cell recipients, but much less than in solid organ transplant patients who receive long-term immunosuppression. If patients are receiving long-term prophylactic treatment with voriconazole, switching to posaconazole should be considered in order to reduce possible enhancement of SCC formation.

PUVA for Urticaria Pigmentosa (See Ch. 118)

PUVA causes a temporary involution of cutaneous mastocytosis[66,67]. The treatment results in loss of Darier's sign, relief of itching, and flattening and sometimes disappearance of cutaneous macules and papules. Surprisingly, even systemic symptoms such as histamine-induced migraines and flushing fade gradually as treatment is continued[66]. In most patients, the clinical manifestations recur several months after discontinuation of PUVA. The recurrences respond as well as the original lesions, and clearing of signs and symptoms can again be achieved. In children, PUVA is also often helpful, and appears to be justified in widespread, disabling mastocytosis. To avoid sudden mediator release from mast cells, a PUVA regimen of gradually increasing doses, especially during the initial phase, seems advisable, although the therapy should otherwise be undertaken according to the usual guidelines.

PUVA for Miscellaneous Dermatoses

Both acute and chronic pityriasis lichenoides[22] respond to photochemotherapy and favorable results have been reported for lymphomatoid papulosis[22,68]. Nevertheless, the experience with these conditions is limited to anecdotal cases. In pityriasis rubra pilaris, the results are

quite inconsistent. Some patients seem to respond well[22], while others may flare and some require combination treatment with retinoids or methotrexate. Generalized granuloma annulare has been reported to clear completely, but long-term maintenance treatment was required to maintain remissions[69]. There were initial reports of both topical and systemic PUVA leading to regrowth of hair in patients with alopecia areata in whom exposures were localized to the alopecia areas. The number of treatments required for regrowth varied widely, and circumscribed lesions responded better than did total alopecia. However, follow-up studies of larger patient groups concluded that PUVA is generally not effective in alopecia areata[70,71], which is in accordance with our own experience. Localized scleroderma and pansclerotic morphea have been successfully treated with bath PUVA and oral PUVA[72].

PUVA for Photodermatoses

Tolerance to sunlight can be induced in several photodermatoses with NB-UVB (see above) or PUVA[73]. Although NB-UVB is tried first due to safety concerns, PUVA represents a very effective preventive treatment for polymorphous light eruption (PMLE; via hardening)[74]. In ~70% of patients with this condition, a 3- to 4-week course of PUVA suffices to suppress the disease upon subsequent exposure to sunlight. PUVA induces pigmentation rapidly and intensively at relatively low (suberythemogenic) UVA doses that usually remain well below the threshold doses for eliciting the PMLE. About 10% of the patients develop typical lesions during the initial phase of PUVA, and as with UVB phototherapy, interventions include interruption of treatment, reduction in the UVA dose, and application of topical corticosteroids.

The therapeutic value of preventive photochemotherapy for PMLE has to be balanced against its potential long-term side effects. Given the fact that very few treatments and low cumulative UVA doses (ranging from 15 to 40 J/cm^2 per treatment course, depending on skin type and photosensitizer) are required for photoprotection and that PMLE can severely restrict outdoor activities, PUVA treatment of PMLE is justified when other preventive measures (e.g. sunscreens, NB-UVB) fail[74].

There is also some experience with PUVA prophylaxis of other photodermatoses. In solar urticaria, PUVA therapy is an effective preventive treatment and is certainly better than antihistamines[75]. Sensitivity to sunlight can be decreased by 10-fold or more after a single treatment course. The suppressive effect may last throughout the summer, depending on regularly repeated sunlight exposures. Problems may occur during the first several PUVA exposures, since in some patients the urticaria threshold dose appears to be lower than their MPD. In these cases, stepwise UVA irradiation of single quadrants of the body a few hours before each PUVA treatment has proven useful[75]. PUVA is then administered during the refractory period. Of note, UVA rush hardening appears to be equally effective as PUVA, with the advantage of inducing the hardening effect and providing protection within a few days[21].

Successful photochemotherapy has also been reported in occasional patients with chronic actinic dermatitis and hydroa vacciniforme[76].

Side Effects and Long-Term Hazards of PUVA

As discussed above, oral 8-MOP has a high incidence of nausea (30% of patients) and vomiting (10% of patients), and this may occasionally require discontinuation of the medication. These side effects are more common with liquid than with crystalline preparations, probably because of higher psoralen serum levels.

The short-term side effects of the combined action of psoralens plus UVA radiation consist of redness, swelling, and occasionally blister formation as can be seen with excessive sunburns. Generalized pruritus or tingling sensations may herald phototoxic side effects. When large areas of skin are affected, systemic symptoms of excess phototoxicity such as fever and general malaise may occur. Nonsteroidal anti-inflammatory drugs and topical and systemic corticosteroids may be required to alleviate these symptoms, but they have to be given early. Because of high epidermal psoralen concentrations, such overdosage phenomena are more common after topical psoralen application. Accumulation of phototoxic effects after several consecutive UVA exposures is also more common with topical PUVA.

Some patients experience persistent pruritus during PUVA treatment, particularly after slight UVA overdosage, and in rare cases, a stinging pain may develop in circumscribed areas. PUVA-induced skin pain unrelated to actual phototoxic burns occurs rarely, but it may necessitate discontinuation of treatment. The mechanism is unknown and the symptoms are unresponsive to antihistamines. Usually, these complaints subside slowly upon continuation of treatment.

Ophthalmologic effects

Eye protection is mandatory during UVA exposure, and UVA-opaque glasses are required for ambient exposure until the evening of the treatment day. UVA penetrates into the ocular lens and potentially could induce cataracts by forming psoralen-protein photoproducts. The higher permeability of the ocular lens at a younger age led to the relative contraindication of oral PUVA in children younger than 12 years of age. Despite the experimental data indicating a risk of premature cataract formation, clinical evaluation has shown no increase in lens opacities even in patients who neglected to practice careful eye protection[77]. Obviously, there is no risk with topical or bath PUVA.

Laboratory data

Because psoralens can cause liver damage in laboratory animals when given in excessive doses, concern was expressed in the past regarding possible hepatotoxic effects in humans. Several large-scale studies demonstrated no significant abnormal laboratory findings in patients receiving PUVA over prolonged periods of time[47,48]. In particular, serial laboratory examinations performed over a period of several years have not revealed any substantial evidence for an impairment of hepatic function. Liver biopsies after 1 year of therapy did not show signs of hepatotoxicity. Anecdotal case reports of hepatitis during PUVA treatment were most likely unrelated to therapy. Several large-scale studies have negated a possible relationship between PUVA therapy and the occurrence of anti-nuclear antibodies[78].

Potential long-term risks of PUVA

Repeated phototoxic injury to the skin can be expected to result in cumulative actinic damage regardless of whether it is induced by sunlight, artificial UV radiation, or PUVA. Although the precise action spectrum of actinic damage has not been determined, epidermal changes are attributed to UVB and dermal changes more to UVA, because the latter penetrates more deeply into the skin. Thus, chronic exposure to PUVA may produce changes in the skin that generally resemble those known as dermatoheliosis and may add to the injury induced by sunlight. High cumulative doses of whole body UVB or PUVA result in pigmentary changes, xerosis, loss of elasticity, wrinkle formation, and actinic keratoses. Additionally, PUVA may induce profuse formation of dark stellate lentigines (Fig. 134.15), termed PUVA lentiginosis[48]. These lentigines result from repeated and prolonged treatment and are commonly associated with high cumulative doses of UVA and a high number of treatments. So far, no increased risk of cutaneous melanoma

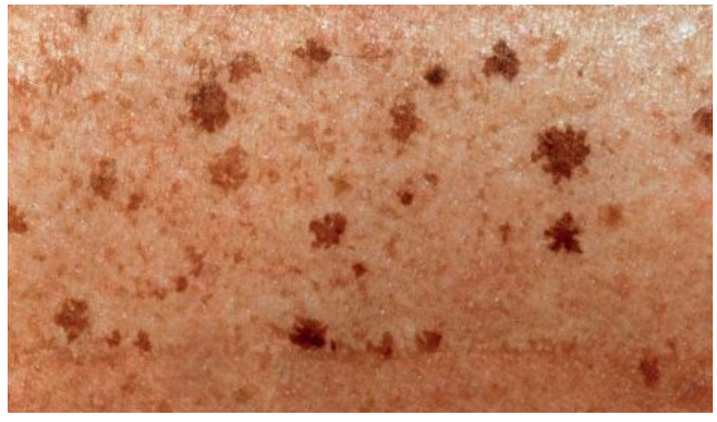


Fig. 134.15 PUVA lentigines. These develop after repeated PUVA treatments over several years and usually within a background of photodamaged skin.

associated with these lentigines has been recorded, but the cosmetic effect may be quite disturbing.

The major concern with prolonged and repeated phototherapeutic regimens is photocarcinogenesis. Therefore, from the onset, PUVA-treated patients were carefully monitored for the development of precursors and malignant skin tumors. Almost all data were obtained from psoriatics, since they represent the largest group of patients receiving PUVA.

The risk is certainly related to DNA damage, but PUVA-induced immunosuppression may play a role as well. In PUVA patients, the risk of SCC, but not of BCC, is significantly increased in comparison with matched controls, and the magnitude of the increase appears to be dose-dependent[79]. However, there is uncertainty regarding PUVA being the sole factor; many of the affected patients had previous exposure to excessive sunlight and to treatments with carcinogenic potential, including arsenic, UVB, and antimetabolite therapy[80]. Specifically, high levels of UVB exposure appear to increase the risk of keratinocyte carcinomas in PUVA-treated patients[81]. Of note, in non-White individuals who received long-term oral PUVA therapy, an increased risk of skin cancers was not observed[82]. In a more recent update from the original PUVA study, exposure to <150 PUVA treatments had, at most, modest effects on SCC risk and even high-dose exposure to PUVA did not greatly increase BCC risk[83].

According to a single study, the genitalia of male patients previously treated with tar and UVB appeared to be particularly susceptible to the carcinogenic effects of PUVA[84], but the risk seemed not to be increased if there had only been exposure to PUVA[85]. In a retrospective study from France comprised of 5400 patients treated between 1978 and 1998, no case of genital skin cancer was found, despite the fact that the genital area had not been protected during UVA exposure, raising the question as to whether genital shielding is absolutely necessary[86]. No increased risk of cutaneous carcinoma has so far been reported for patients treated with PUVA for vitiligo.

Only a few anecdotal cases of cutaneous melanoma have been described in long-term PUVA-treated psoriatics, and, to date, with one exception, no increased risk of melanoma has been observed in any reported large-scale study. However, Stern et al.[87] reported on the cohort of 1380 patients enrolled in the PUVA Follow-up Study (16-center study), and since 1975, 23 patients had developed 26 invasive or *in situ* cutaneous melanomas. Beginning 15 years after the initial exposure to PUVA, an increased risk of melanoma was observed in their cohort of PUVA-treated patients. However, the lead author concluded that perhaps PUVA has been judged unfairly. Its long-term risks have been subject to much greater scrutiny than the risks of other therapies utilized for severe psoriasis, such as methotrexate and particularly immunosuppressive therapies such as cyclosporine (CSA). Notably, several other US studies, as well as European studies, have not observed an increased risk of melanoma in patients treated with PUVA[88,89].

An increased risk of cutaneous SCC has been observed in solid organ transplant recipients who have received long-term CSA and in patients who have received CSA subsequent to PUVA therapy[90]. UVA-sparing, aggressive regimens without prolonged maintenance therapy may be safer than continuous non-aggressive regimens (see Table 134.4).

In a study of 944 Swedish and Finnish patients[91], bath PUVA with TMP appeared to have no relevant risk of carcinogenesis. In addition, no association between cutaneous carcinoma and 8-MOP bath PUVA was found in 158 Finnish psoriatic patients[92]. Perhaps related to lower cumulative UVA doses, these data on the long-term safety of bath PUVA are encouraging, but no premature conclusions should be drawn[93].

UVB and PUVA in HIV-Infected Patients

Treatment of psoriasis with oral PUVA has not induced progression of HIV disease nor was there an increase in side effects. The conclusion is that PUVA may be safe for HIV-infected patients with psoriasis. Theoretical modeling of UVB- and PUVA-induced HIV promoter activation in human skin indicated that UVB was more likely than PUVA to activate viral transcription *in vivo*. Although further studies are needed to unequivocally establish the safety of both UVB and PUVA phototherapy in HIV-associated psoriasis, the benefits are considerable, particularly in those with severe psoriasis[94].

EXTRACORPOREAL PHOTOCHEMOTHERAPY (PHOTOPHERESIS)

Extracorporeal photochemotherapy (photopheresis, ECP) was introduced in the early 1980s for the palliative treatment of erythrodermic CTCL[95]. Efficacy was observed in several uncontrolled clinical trials, and it was FDA-approved as a device in 1988 for the treatment of this disease. In 1994, at the International Consensus Conference on Staging and Treatment Recommendations for CTCL, ECP was recommended as the first line of treatment for patients with erythrodermic CTCL[96]. However, not all authorities agree (see Ch. 120).

Attempts to better characterize those CTCL patients who are more likely to respond to ECP revealed the following:

- There seems to be a significant linear association between response and CD4:CD8 ratio. Patients with a ratio <10 are more likely to respond than are patients with a ratio >10.
- There is a marginally significant linear association between response and LDH level. Patients whose LDH is not elevated at the start of treatment tend to have a better response to ECP compared to patients with an elevated LDH[97].

ECP has also been advocated for the treatment of chronic cutaneous GVHD as well as acute GVHD[98,99].

Treatment Protocols

The ECP procedure involves the passage of blood from an arm vein through a photopheresis machine and then back to the patient. Within the machine, a discontinuous flow cell separator harvests peripheral blood mononuclear cells (PBMC) within a buffy coat collection. The red cell fraction is returned to the patient without further treatment. 8-MOP solution is administered directly into the collection of the PBMC, thereby avoiding 8-MOP-induced nausea. The collection of PBMC is then exposed to 2 J/cm^2 of UVA and reinfused into the patient. This treatment is typically repeated on two successive days with 2- to 4-week intervals.

Mechanism of Action

Despite the fact that ECP has been in use for over 40 years, the mode of action still remains enigmatic. It was postulated that the response of CTCL to ECP is due to the induction of an immune response against the malignant cells. More recent experimental results suggest that infusion of autologous haptenated cells, in which apoptosis was induced by 8-MOP/UVA, induces immunologic tolerance. The nature of this tolerance is due primarily to regulatory T cells, because transfer in an animal model conferred similar protection. The demonstration of the induction of regulatory T cells may explain why, in humans, ECP exerts a beneficial effect in a wide variety of diseases which would be amenable to such activity. The generation of antigen-specific regulatory T cells may explain why generalized immunosuppression has not been noted with ECP[100,101]. Monocyte-derived immature dendritic cells may play a role as well.

Side Effects

Side effects of ECP are uncommon and consist of episodes of hypotension and vasovagal reflex due to volume shifts during treatments; the latter usually do not interfere with the treatment.

Other Indications

A number of studies have been performed in order to evaluate the efficacy of ECP in inflammatory diseases other than CTCL and chronic GVHD where autoreactive T cells play a key role. Uncontrolled clinical trials have revealed variable success in selected entities such as atopic dermatitis, systemic sclerosis, pemphigus vulgaris, and systemic lupus erythematosus[102].

REFERENCES

1. Weichenthal M, Schwarz T. Phototherapy. How does UV work? *Photodermatol Photoimmunol Photomed*. 2005;21:260–266.
2. Hönigsmann H. Phototherapy for psoriasis. *Clin Exp Dermatol*. 2001;26:343–350.
3. Nickoloff BJ. Cracking the cytokine code in psoriasis. *Nat Med*. 2007;13:242–244.
4. Weatherhead SC, Farr PM, Jamieson D, et al. Keratinocyte apoptosis in epidermal remodeling and clearance of psoriasis induced by UV radiation. *J Invest Dermatol*. 2011;131:1916–1926.
5. Parrish JA, Jaenicke KF. Action spectrum for phototherapy of psoriasis. *J Invest Dermatol*. 1981;76:359–362.
6. Anderson KL, Feldman SR. A guide to prescribing home phototherapy for patients with psoriasis: the appropriate patient, the type of unit, the treatment regimen, and the potential obstacles. *J Am Acad Dermatol*. 2015;72:868–878.
7. Boztepe G, Karaduman A, Sahin S, et al. The effect of maintenance narrow-band ultraviolet B therapy on the duration of remission for psoriasis: a prospective randomized clinical trial. *Int J Dermatol*. 2006;45:245–250.
8. Menter A, Korman NJ, Elmets CA, et al. Guidelines of care for the management of psoriasis and psoriatic arthritis. Section 5. Guidelines of care for the treatment of psoriasis with phototherapy and photochemotherapy. *J Am Acad Dermatol*. 2010;62:114–135.
9. Pathirana D, Ormerod AD, Saiag P, et al. European S3-guidelines on the systemic treatment of psoriasis vulgaris. *J Eur Acad Dermatol Venereol*. 2009;23(Suppl. 2):1–70.
10. Wolf P, Hofer A, Legat FJ, et al. Treatment with 311-nm ultraviolet B accelerates and improves the clearance of psoriatic lesions in patients treated with etanercept. *Br J Dermatol*. 2009;160:186–189.
11. Calzavara-Pinton PG, Sala R, Arisi M, et al. Synergism between narrowband ultraviolet B phototherapy and etanercept for the treatment of plaque-type psoriasis. *Br J Dermatol*. 2013;169:130–136.
12. Boztepe G, Sahin S, Ayhan M, et al. Narrowband ultraviolet B phototherapy to clear and maintain clearance in patients with mycosis fungoides. *J Am Acad Dermatol*. 2005;53:242–246.
13. Volc-Platzer B, Hönigsmann H. Photoimmunology of PUVA and UVB therapy. In: Krutmann J, Elmets CA, eds. *Photoimmunology*. Oxford: Blackwell Science; 1995:265–273.
14. Ozawa M, Ferenczi K, Kikuchi T, et al. 312-nanometer ultraviolet B light (narrow-band UVB) induces apoptosis of T cells within psoriatic lesions. *J Exp Med*. 1999;189:711–718.
15. Yones SS, Palmer RA, Garibaldinos TM, Hawk JLM. Randomized double-blind trial of treatment of vitiligo. *Arch Dermatol*. 2007;143:578–584.
16. Mohammad TF, Al-Jamal M, Hamzavi IH, et al. The Vitiligo Working Group recommendations for narrowband ultraviolet B light phototherapy treatment of vitiligo. *J Am Acad Dermatol*. 2017;76:879–888.
17. Lim HW, Grimes PE, Agbai O, et al. Afamelanotide and narrowband UV-B phototherapy for the treatment of vitiligo: a randomized multicenter trial. *JAMA Dermatol*. 2015;151:42–50.

17a. Pandya AG, Harris JE, Lebwohl M, et al. Addition of narrow-band UVB phototherapy to ruxolitinib cream in patients with vitiligo. *J Invest Dermatol*. 2022;142:3332–3335.

18. Jekler J, Larkö O. Phototherapy for atopic dermatitis with ultraviolet A (UVA), low-dose UVB and combined UVA and UVB: two paired comparison studies. *Photodermatol Photoimmunol Photomed*. 1991;8:151–156.
19. Garritsen FM, Brouwer MW, Limpens J, Spuls PI. Photo(chemo)therapy in the management of atopic dermatitis: an updated systematic review with implications for practice and research. *Br J Dermatol*. 2014;170:501–513.
20. Collins P, Ferguson J. Narrow-band UVB (TL-01) phototherapy: an effective preventative treatment for the photodermatoses. *Br J Dermatol*. 1995;132:956–963.
21. Beissert S, Ständer H, Schwarz T. UVA rush hardening for the treatment of solar urticaria. *J Am Acad Dermatol*. 2000;42:1030–1032.
22. Honig B, Morison WL, Karp D. Photochemotherapy beyond psoriasis. *J Am Acad Dermatol*. 1994;31:775–790.
23. Pirkhammer D, Seeber A, Hönigsmann H, Tanew A. Narrow-band ultraviolet B (TL-01) phototherapy is an effective and safe treatment option for patients with severe seborrhoeic dermatitis. *Br J Dermatol*. 2000;143:964–968.
24. Ada S, Seçkin D, Budakoğlu I, Ozdemir FN. Treatment of uremic pruritus with narrowband ultraviolet B phototherapy: an open pilot study. *J Am Acad Dermatol*. 2005;53:149–151.
25. Hearn RM, Kerr AC, Rahim KF, et al. Incidence of skin cancers in 3867 patients treated with narrow-band ultraviolet B phototherapy. *Br J Dermatol*. 2008;159:931–935.
26. Bónis B, Kemény L, Dobozy A, et al. 308-nm UVB excimer laser for psoriasis. *Lancet*. 1997;350:1522.
27. Köllner K, Wimmershoff MB, Hintz C, et al. Comparison of the 308-nm excimer laser and a 308-nm excimer lamp with 311-nm narrowband ultraviolet B in the treatment of psoriasis. *Br J Dermatol*. 2005;152:750–754.
28. Nicolaidou E, Antoniou C, Stratigos A, Katsambas AD. Narrowband ultraviolet B phototherapy and 308-nm excimer laser in the treatment of vitiligo: a review. *J Am Acad Dermatol*. 2009;60:470–477.
29. Aubin F, Vigan M, Puzenat E, et al. Evaluation of a novel 308-nm monochromatic excimer light delivery system in dermatology: a pilot study in different chronic localized dermatoses. *Br J Dermatol*. 2005;152:99–103.
30. Krutmann J, Diepgen TL, Luger TA, et al. High-dose UVA1 therapy for atopic dermatitis: results of a multicenter trial. *J Am Acad Dermatol*. 1998;38:589–593.
31. Tzaneva S, Seeber A, Schwaiger M, et al. High-dose versus medium-dose UVA1 phototherapy for patients with severe, generalized atopic dermatitis. *J Am Acad Dermatol*. 2001;45:503–507.
32. Majoie IM, Oldhoff JM, van Weelden H, et al. Narrowband ultraviolet B and medium-dose ultraviolet A1 are equally effective in the treatment of moderate to severe atopic dermatitis. *J Am Acad Dermatol*. 2009;60:77–84.
33. Tuchinda C, Kerr HA, Taylor CR, et al. UVA1 phototherapy for cutaneous diseases: an experience of 92 cases in the United States. *Photodermatol Photoimmunol Photomed*. 2006;22:247–253.
34. Andres C, Kollmar A, Mempel M, et al. Successful ultraviolet A1 phototherapy in the treatment of localized scleroderma: a retrospective and prospective study. *Br J Dermatol*. 2010;162:445–447.
35. Ständer H, Schiller M, Schwarz T. UVA1-therapy for treatment of sclerodermic graft-versus-host-disease of the skin. *J Am Acad Dermatol*. 2002;46:799–800.
36. Wetzig T, Sticherling M, Simon JC, et al. Medium dose long-wavelength ultraviolet A (UVA1) phototherapy for the treatment of acute and chronic graft-versus-host disease of the skin. *Bone Marrow Transplant*. 2005;35:515–519.
37. Zane C, Leali C, Airò P, et al. 'High-dose' UVA1 therapy of widespread plaque-type, nodular, and erythrodermic mycosis fungoides. *J Am Acad Dermatol*. 2001;44:629–633.
38. Edström DW, Porwit A, Ros A-M. Effects on human skin of repetitive ultraviolet-A1 (UVA1) irradiation and visible light. *Photodermatol Photoimmunol Photomed*. 2001;17:66–70.
39. Besaratinia A, Synold TW, Chen HH, et al. DNA lesions induced by UV A1 and B radiation in human cells: comparative analyses in the overall genome and in the *p53* tumor suppressor gene. *Proc Natl Acad Sci USA*. 2005;102:10058–10063.
40. Pathak MA, Fitzpatrick TB. The evolution of photochemotherapy with psoralens and UVA (PUVA): 2000 BC to 1992 AD. *J Photochem Photobiol B*. 1992;14:3–22.
41. Parrish JA, Fitzpatrick TB, Tanenbaum L, Pathak MA. Photochemotherapy of psoriasis with oral methoxsalen and long wave ultraviolet light. *N Engl J Med*. 1974;291:1207–1211.
42. Caffieri S, Zarebska Z, Dall'Acqua F. Psoralen photosensitization: damages to nucleic acid and membrane lipid components. *Acta Biochim Pol*. 1996;43:241–246.
43. Averbeck D. Recent advances in psoralen phototoxicity mechanism. *Photochem Photobiol*. 1989;50:859–882.
44. Brücke J, Tanew A, Ortel B, Hönigsmann H. Relative efficacy of 335 and 365 nm radiation in photochemotherapy of psoriasis. *Br J Dermatol*. 1991;124:372–374.
45. Ibbotson SH, Dawe RS, Farr PM. The effect of methoxsalen dose on ultraviolet-A-induced erythema. *J Invest Dermatol*. 2001;116:813–815.
46. Ibbotson SH, Farr PM. The time-course of psoralen ultraviolet A (PUVA) erythema. *J Invest Dermatol*. 1999;113:346–350.
47. Melski JW, Tanenbaum L, Parrish JA, et al. Oral methoxsalen photochemotherapy for the treatment of psoriasis: a cooperative clinical trial. *J Invest Dermatol*. 1977;68:328–335.
48. Henseler T, Wolff K, Hönigsmann H, et al. Oral 8-methoxypsoralen photochemotherapy of psoriasis. The European PUVA study: a cooperative study among 18 European centres. *Lancet*. 1981;1:853–857.
49. Radakovic S, Seeber A, Hönigsmann H, Tanew A. Failure of short-term psoralen and ultraviolet A light maintenance treatment to prevent early relapse in patients with chronic recurring plaque-type psoriasis. *Photodermatol Photoimmunol Photomed*. 2009;25:90–93.
50. Lowe NJ, Weingarten D, Bourget T, Moy LS. PUVA therapy for psoriasis: comparison of oral and bath-water delivery of 8-methoxypsoralen. *J Am Acad Dermatol*. 1986;14:754–760.
51. Collins P, Rogers S. Bath-water compared with oral delivery of 8-methoxypsoralen PUVA therapy for chronic plaque psoriasis. *Br J Dermatol*. 1992;127:392–395.
52. Calzavara-Pinton PG, Ortel B, Hönigsmann H, et al. Safety and effectiveness of an aggressive and individualized bath-PUVA regimen in the treatment of psoriasis. *Dermatology*. 1994;189:256–259.
53. Morison WL. Phototherapy and photochemotherapy. *Adv Dermatol*. 1992;7:255–270.
54. Nijsten TE, Stern RS. Oral retinoid use reduces cutaneous squamous cell carcinoma risk in patients with psoriasis treated with psoralen-UVA: a nested cohort study. *J Am Acad Dermatol*. 2003;49:644–650.
55. Gilchrest BA, Parrish JA, Tanenbaum L, et al. Oral methoxsalen photochemotherapy of mycosis fungoides. *Cancer*. 1976;38:683–689.
56. Vieyra-Garcia P, Fink-Puches R, Porkert S, et al. Evaluation of low-dose, low-frequency oral psoralen-UV-A treatment with or without maintenance on early-stage mycosis fungoides: a randomized clinical trial. *JAMA Dermatol*. 2019;155:538–547.
57. Phan K, Ramachandran V, Fassihi H, Sebaratnam DF. Comparison of narrowband UV-B with psoralen-UV-A phototherapy for patients with early-stage mycosis fungoides: a systematic review and meta-analysis. *JAMA Dermatol*. 2019;155:335–341.
58. Trautinger F, Eder J, Assaf C, et al. European Organisation for Research and Treatment of Cancer consensus recommendations for the treatment of mycosis fungoides/Sézary syndrome - Update 2017. *Eur J Cancer*. 2017;77:57–74.
59. Zhang C, Duvic M. Treatment of cutaneous T-cell lymphoma with retinoids. *Dermatol Ther*. 2006;19:264–271.
60. Stadler R. Optimal combination with PUVA: rationale and clinical trial update. *Oncology (Williston Park)*. 2007;21:29–32.
61. Stadler R, Otte HG, Luger T, et al. Prospective randomized multicenter clinical trial on the use of interferon-α-2a plus acitretin versus interferon-α-2a plus PUVA in patients with cutaneous T-cell lymphoma stages I and II. *Blood*. 1998;92:3578–3581.
62. Wackernagel A, Legat FJ, Hofer A, et al. Psoralen plus UVA vs. UVB-311 nm for the treatment of lichen planus. *Photodermatol Photoimmunol Photomed*. 2007;23:15–19.
63. Volc-Platzer B, Hönigsmann H, Hinterberger W, Wolff K. Photochemotherapy improves chronic cutaneous graft-versus-host disease. *J Am Acad Dermatol*. 1990;23:220–228.
64. Kunz M, Wilhelm S, Freund M, et al. Treatment of severe erythrodermic acute graft-versus-host disease with photochemotherapy. *Br J Dermatol*. 2001;144:901–902.
65. Ziemer M. Graft-versus-host disease of the skin and adjacent mucous membranes. *J Dtsch Dermatol Ges*. 2013;11:477–495.
66. Christophers E, Hönigsmann H, Wolff K, Langner A. PUVA-treatment of urticaria pigmentosa. *Br J Dermatol*. 1978;98:701–702.
67. Kolde G, Frosch PJ, Czarnetzki BM. Response of cutaneous mast cells to PUVA in patients with urticaria pigmentosa: histomorphometric, ultrastructural, and biochemical investigations. *J Invest Dermatol*. 1984;83:175–178.
68. Christensen HK, Thomsen K, Vejlsgaard GL. Lymphomatoid papulosis: a follow-up study of 41 patients. *Semin Dermatol*. 1994;13:197–201.
69. Browne F, Turner D, Goulden V. Psoralen and ultraviolet A in the treatment of granuloma annulare. *Photodermatol Photoimmunol Photomed*. 2011;27:81–84.
70. Healy E, Rogers S. PUVA treatment for alopecia areata – does it work? A retrospective review of 102 cases. *Br J Dermatol*. 1993;129:42–44.

71. Taylor CR, Hawk JL. PUVA treatment of alopecia areata partialis, totalis and universalis: audit of 10 years' experience at St. John's Institute of Dermatology. *Br J Dermatol*. 1995;133:914–918.
72. Usmani N, Murphy A, Veale D, et al. Photochemotherapy for localized morphoea: effect on clinical and molecular markers. *Clin Exp Dermatol*. 2008;33:698–704.
73. Hönigsmann H. Mechanisms of phototherapy and photochemotherapy for photodermatoses. *Dermatol Ther*. 2003;16:23–27.
74. Hönigsmann H. Polymorphous light eruption. *Photodermatol Photoimmunol Photomed*. 2008;24:155–161.
75. Roelandts R. Diagnosis and treatment of solar urticaria. *Dermatol Ther*. 2003;16:52–56.
76. Roelandts R. Phototherapy of photodermatoses. *J Dermatolog Treat*. 2002;13:157–160.
77. Malanos D, Stern RS. Psoralen plus ultraviolet A does not increase the risk of cataracts: a 25-year prospective study. *J Am Acad Dermatol*. 2007;57:231–237.
78. Calzavara-Pinton PG, Franceschini F, Rastrelli M, et al. Antinuclear antibodies are not induced by PUVA treatment with uncomplicated psoriasis. *J Am Acad Dermatol*. 1994;30:955–958.
79. Henseler T, Christophers E, Hönigsmann H, Wolff K. Skin tumors in the European PUVA study. Eight year follow-up of 1643 patients treated with PUVA for psoriasis. *J Am Acad Dermatol*. 1987;16:108–116.
80. Stern RS, Liebman EJ, Vakeva L. Oral psoralen and ultraviolet-A light (PUVA) treatment of psoriasis and persistent risk of nonmelanoma skin cancer. PUVA Follow-up Study. *J Natl Cancer Inst*. 1998;90:1278–1284.
81. Lim JL, Stern RS. High levels of ultraviolet B exposure increase the risk of non-melanoma skin cancer in psoralen and ultraviolet A-treated patients. *J Invest Dermatol*. 2005;124:505–513.
82. Murase JE, Lee EE, Koo J. Effect of ethnicity on the risk of developing nonmelanoma skin cancer following long-term PUVA therapy. *Int J Dermatol*. 2005;44:1016–1021.
83. Stern RS. PUVA Follow-Up Study. The risk of squamous cell and basal cell cancer associated with psoralen and ultraviolet A therapy: a 30-year prospective study. *J Am Acad Dermatol*. 2012;66:553–562.
84. Stern RS. Genital tumors among men with psoriasis exposed to psoralens and ultraviolet A radiation (PUVA) and ultraviolet B radiation. *N Engl J Med*. 1990;322:1093–1097.
85. Wolff K, Hönigsmann H. Genital carcinomas in psoriasis patients treated with photochemotherapy. *Lancet*. 1991;337:439.
86. Aubin F, Puzenat E, Arveux P, et al. Genital squamous cell carcinoma in men treated by photochemotherapy. A cancer registry-based study from 1978 to 1998. *Br J Dermatol*. 2001;144:1204–1206.
87. Stern RS. PUVA Follow up Study. The risk of melanoma in association with long-term exposure to PUVA. *J Am Acad Dermatol*. 2001;44:755–761.
88. Forman AB, Roenigk Jr HH, Caro WA, Magid ML. Long-term follow-up of skin cancer in the PUVA-48 cooperative study. *Arch Dermatol*. 1989;125:515–519.
89. Chuang TY, Heinrich LA, Schultz MD, et al. PUVA and skin cancer: a historical cohort study on 492 patients. *J Am Acad Dermatol*. 1992;26:173–177.
90. Marcil I, Stern RS. Squamous-cell cancer of the skin in patients given PUVA and ciclosporin: nested cohort crossover study. *Lancet*. 2001;358:1042–1045.
91. Hannuksela-Svahn A, Sigurgeirsson B, Pukkala E, et al. Trioxsalen bath PUVA did not increase the risk of squamous cell skin carcinoma and cutaneous malignant melanoma in a joint analysis of 944 Swedish and Finnish patients with psoriasis. *Br J Dermatol*. 1999;141:497–501.
92. Hannuksela-Svahn A, Pukkala E, Koulu L, et al. Cancer incidence among Finnish psoriasis patients treated with 8-methoxypsoralen bath PUVA. *J Am Acad Dermatol*. 1999;40:694–696.
93. Morison WL, Baughman RD, Day RM, et al. Consensus workshop on the toxic effects of long-term PUVA therapy. *Arch Dermatol*. 1998;134:595–598.
94. Menon K, Van Voorhees AS, Bebo Jr BF, et al. Psoriasis in patients with HIV infection: from the Medical Board of the National Psoriasis Foundation. *J Am Acad Dermatol*. 2010;62:291–299.
95. Edelson R, Berger C, Gasparro F, et al. Treatment of cutaneous T-cell lymphoma by extracorporeal photochemotherapy. Preliminary results. *N Engl J Med*. 1987;316:297–303.
96. Trautinger F, Knobler R, Willemze R, et al. EORTC consensus recommendations for the treatment of mycosis fungoides/Sézary syndrome. *Eur J Cancer*. 2006;42:1014–1030.
97. Knobler E, Warmuth I, Cocco C, et al. Extracorporeal photochemotherapy – the Columbia Presbyterian experience. *Photodermatol Photoimmunol Photomed*. 2002;18:232–237.
98. Greinix HT, Volc-Platzer B, Rabitsch W, et al. Successful use of extracorporeal photochemotherapy in the treatment of severe acute and chronic graft-versus-host disease. *Blood*. 1998;92:3098–3104.
99. Greinix HT, Worel N, Just U, Knobler R. Extracorporeal photopheresis in acute and chronic graft-versus-host disease. *Transfus Apher Sci*. 2014;50:349–357.
100. Maeda A, Schwarz A, Kernebeck K, et al. Intravenous infusion of syngeneic apoptotic cells by photopheresis induces antigen-specific regulatory T cells. *J Immunol*. 2005;174:5968–5976.
101. Maeda A, Schwarz A, Bullinger A, et al. Experimental extracorporeal photopheresis inhibits the sensitization and effector phases of contact hypersensitivity via two mechanisms: generation of IL-10 and induction of regulatory T cells. *J Immunol*. 2008;181:5956–5962.
102. Knobler R, Barr ML, Couriel DR, et al. Extracorporeal photopheresis: past, present, and future. *J Am Acad Dermatol*. 2009;61:652–665.

Photodynamic Therapy 135

Harvey Lui and Sunil Kalia

Chapter Contents

History and Development 2379
Photodynamic Therapy (PDT) – Photochemistry, Photobiology, and Mechanism of Action 2379
Components of PDT 2382
Dermatologic Applications 2384
Adverse Effects and Complications of PDT 2386
Practice and Techniques 2388
Future Directions 2388

Synonym: ■ Photoradiation therapy

Key features

- Photodynamic therapy (PDT) is an established, light-based therapeutic option for actinic keratoses (AKs) and superficial keratinocyte cancers, with an expanding range of applications including acne, photoaging, cutaneous infections, and vascular anomalies
- The photodynamic effect is due to photochemical reactions that generate singlet oxygen and it requires three components: photosensitizing molecules, photoactivating wavelengths of light, and tissue oxygen
- Singlet oxygen is highly reactive and initiates a series of cellular and tissue reactions that culminate in necrosis, apoptosis, and/or antimicrobial effects; host immunologic responses to singlet oxygen-altered tissue may also contribute to the overall clinical effect
- For cutaneous indications, the current standard technique is topical application of pro-photosensitizers (e.g. aminolevulinic acid and its derivatives) that are metabolized *in situ*, i.e. within the skin, to photoactive protoporphyrin IX
- Non-coherent artificial light (blue or red), daylight, or other light sources can be used to illuminate the skin and energize the photosensitizer

INTRODUCTION

Photodynamic therapy (PDT) requires the sequential administration of a photosensitizing agent that is then activated by light in order to generate singlet oxygen within biologic tissues (Fig. 135.1). Singlet oxygen is a highly reactive form of oxygen that can induce cellular necrosis and/or apoptosis while modulating a variety of biologic processes. During the latter part of the twentieth century, PDT was synonymous with the use of *systemic* photosensitizers in combination with red *laser* light to treat cancers. However, in dermatology, the practice of PDT has evolved into applying a *topical* photosensitizer precursor locally to the skin and then illuminating the treatment site(s) with artificial visible light or natural daylight.

HISTORY AND DEVELOPMENT

The photodynamic effect was originally studied in the early 1900s by a medical student who noted that cultures of *Paramecium* would die only if exposed to both an organic dye (acridine) and visible light. His professor discovered the oxygen-dependence of this effect and coined the term "photodynamic action" to describe the phenomenon. In humans, hematoporphyrin was subsequently shown by Meyer Betz to induce profound and persistent generalized photosensitivity, including when he self-injected this agent. In addition to its fluorescent properties when illuminated with a Wood's lamp, hematoporphyrin was shown to localize to neoplastic tissue and then induce tumor involution when exposed to visible light.

The modern era of clinical PDT began in the 1970s when Dougherty and colleagues combined systemically administered *hematoporphyrin derivative* with visible light to treat cutaneous and subcutaneous malignancies in humans; they also confirmed the role of singlet oxygen[1]. With the advent of lasers and fiberoptic endoscopes, the use of PDT was extended to carcinomas of the lung, bladder, and esophagus. Hematoporphyrin derivative and its subsequent porphyrin-based congeners require intravenous administration, and they induce marked generalized cutaneous photosensitivity that can last for days to weeks, necessitating strict avoidance of outdoor and bright indoor light.

Because they are relatively large molecules, porphyrins are poorly absorbed through the skin. The key breakthrough in developing PDT as a practical dermatologic therapeutic modality can be attributed to the Canadian team of Kennedy and Pottier. In the 1980s, they noted that the topical application of a naturally occurring porphyrin precursor, 5-aminolevulinic acid (ALA), as a prodrug could photosensitize the skin by inducing *local intracutaneous* production of protoporphyrin IX (PpIX; see Fig. 135.1). Their successful treatment of keratinocyte cancers[2] using topical ALA plus broadband red light abrogated the two major disadvantages associated with the use of systemic porphyrin photosensitizers (see above).

The elegance of using topical ALA for PDT lies in how it takes advantage of the endogenous porphyrin biosynthetic pathway (which is present in all nucleated cells) to generate PpIX from ALA. The simplicity of this approach greatly facilitated clinical PDT research, culminating in the FDA approval of topical ALA plus blue fluorescent light for the treatment of actinic keratoses (AKs) in 1999. Five years later, topical methyl aminolevulinate (mALA), an esterified derivative of ALA, in combination with red light-emitting diode (LED) light was approved in several countries for dermatologic PDT. It was subsequently shown that natural daylight could safely and effectively activate ALA for skin-based PDT[3].

PDT – PHOTOCHEMISTRY, PHOTOBIOLOGY, AND MECHANISM OF ACTION

PDT is somewhat analogous to PUVA (psoralen plus UVA light) therapy to the extent that both treatment modalities involve the administration of photosensitizers followed by exposure to specific wavelengths of light. Mechanistically, they involve exogenously derived photosensitizers that transfer photon energy from light to drive specific photochemical reactions within the skin. Nevertheless, there are important differences between PDT and PUVA (Table 135.1), the most fundamental of which is that, by definition, PDT generates singlet oxygen, which in turn is biologically active.

PDT Photochemistry

The transduction of energy from light to tissue can be illustrated diagrammatically by considering the resting and excited states of the molecules involved in photochemical reactions (Fig. 135.2). The photosensitizer is present within the target tissue in its ground, lower-energy resting state. Its efficiency as a chromophore for absorbing light energy

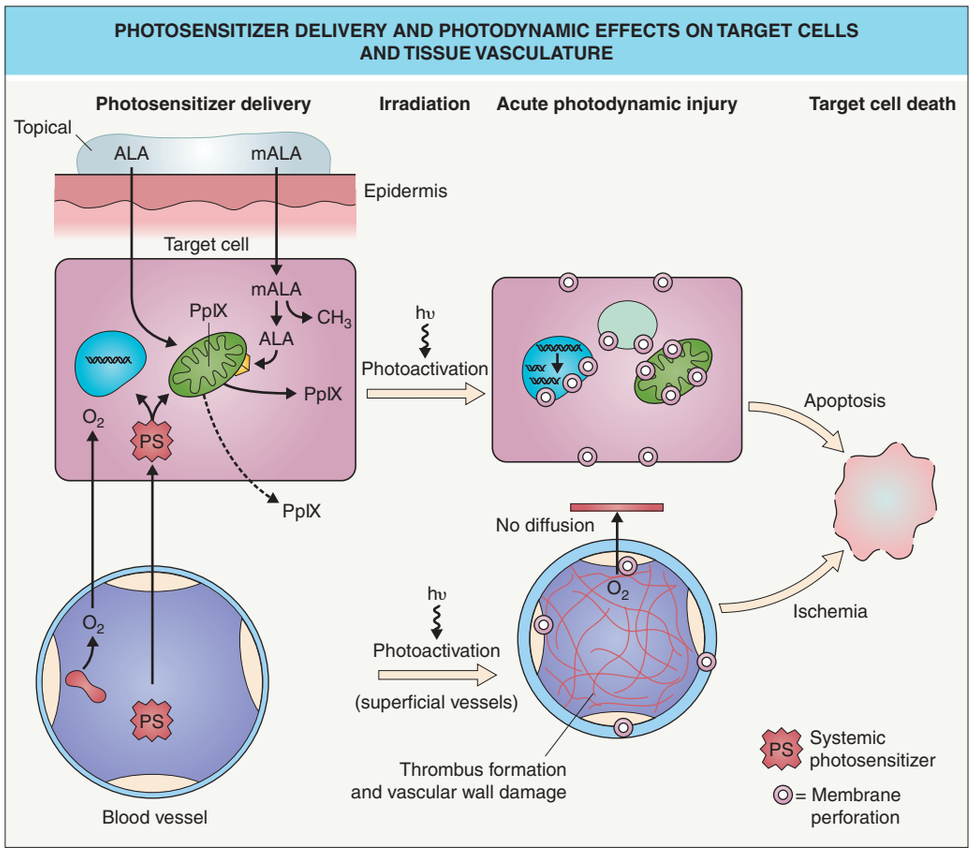


Fig. 135.1 Photosensitizer delivery and photodynamic effects on target cells and tissue vasculature. Topical photosensitizers 5-aminolevulinic acid (ALA) and methyl aminolevulinate (methyl-esterified ALA; mALA) diffuse through the stratum corneum into target epithelial cells; if systemic photosensitizers are used, they arrive through the bloodstream. Oxygen is delivered via erythrocyte circulation. ALA derived from any source is converted to protoporphyrin IX (PpIX) within mitochondria. PpIX then leaks from the mitochondria to other cellular structures. After there has been sufficient time for photosensitizer partitioning to subcellular structures, target tissue is irradiated with photoactivating light. During acute photodynamic injury, plasma and nuclear membranes lose integrity. Acute photodynamic injury within cutaneous endothelial cells leads to thrombus formation and vascular collapse. Target cell and tissue oxygen delivery cease. Both direct apoptosis and ischemic necrosis contribute to irreversible target cell injury and death.

PHOTODYNAMIC THERAPY VERSUS PUVA THERAPY

Features	PDT	PUVA
Routes of administration of photosensitizer	Topical Systemic (IV)	Topical Systemic (PO)
Photosensitizer	ALA or mALA (as prodrugs)	8-methoxypsoralen
Active form of photosensitizer	PpIX	8-methoxypsoralen
Photosensitizer activation	Visible light	Ultraviolet A
Photochemical reaction	Type II: converts O_2 to singlet O_2	Type I: covalent adducts between psoralen and DNA; non-oxygen-dependent
Relationship with skin cancer	Treats keratinocyte carcinomas	Carcinogenic
Effects of long-term use	Generally safe, can be used to treat photoaging	Skin cancer, photoaging

Table 135.1 Photodynamic therapy (PDT) versus PUVA (psoralen plus UVA light) therapy. ALA, 5-aminolevulinic acid; IV, intravenously; mALA, methyl aminolevulinate; PO, orally; PpIX, protoporphyrin IX.

is related to its absorption spectrum (Fig. 135.3). If light of an appropriate wavelength reaches the photosensitizer within tissue, photon absorption occurs and the photosensitizer is excited to a higher-energy "singlet" state. This excited singlet is short-lived, lasting nanoseconds, and then undergoes intersystem crossing to a more stable "triplet" state, which has a lifetime on the order of microseconds. The "triplet" photosensitizer can in turn transfer its stored energy to molecular oxygen, yielding singlet oxygen ($^1O_2$), and, as a result, returns to its resting ground state. Photochemical reactions that are mediated by oxygen are referred to as type II photochemical or photosensitized reactions. The singlet oxygen thus generated reacts with a variety of cellular biomolecules, including lipids, proteins, and nucleic acids.

Singlet oxygen is by no means the only active intermediate generated by the excited triplet photosensitizer; a variety of additional reactive oxygen species are also generated from molecular oxygen and undoubtedly contribute to the overall biologic effect. Being highly reactive, singlet oxygen and its related oxygen species can also chemically inactivate the photosensitizer itself by a process known as *photobleaching*, which also destroys its fluorescence properties (Fig. 135.4). This is one way by which the light exposure during PDT automatically self-limits or shuts down the overall process.

Light within the visible spectrum is typically used for PDT. This is because ultraviolet light is carcinogenic and has limited tissue penetration, while infrared radiation (>850 nm) has minimal absorption by ALA.

When PDT photosensitizers are excited to their singlet states following light absorption, they can alternatively return to their ground state via the emission of photons (see Fig. 135.2). This "re-emission" of light by the photosensitizer is termed fluorescence and the latter property permits, with Wood's lamp illumination, direct visualization of photosensitizer accumulation within tissue as well as its subsequent depletion as a result of photobleaching following therapeutic light exposure (see Fig. 135.4).

Photobiologic Mechanisms of Action

Although the precise and most relevant molecular sequence of reactions initiated by singlet oxygen has not been determined, oxidative damage (including to cellular membranes) is known to trigger cellular injury and apoptosis. For a given PDT clinical effect or indication, the specific mechanism of action depends on the target tissue, the photosensitizer and its delivery route, subcellular photosensitizer localization, and the overall drug–light dose delivered. For example, when topical ALA is applied to an epidermal neoplasm such as a superficial basal cell carcinoma (BCC), PpIX accumulates within the tumor cells themselves, with direct cytotoxicity upon light activation (see Fig. 135.1). In contrast, systemic photosensitizers are known to preferentially localize to the vascular bed of tumors. Light activation then leads to vascular collapse and ischemic tumor necrosis.

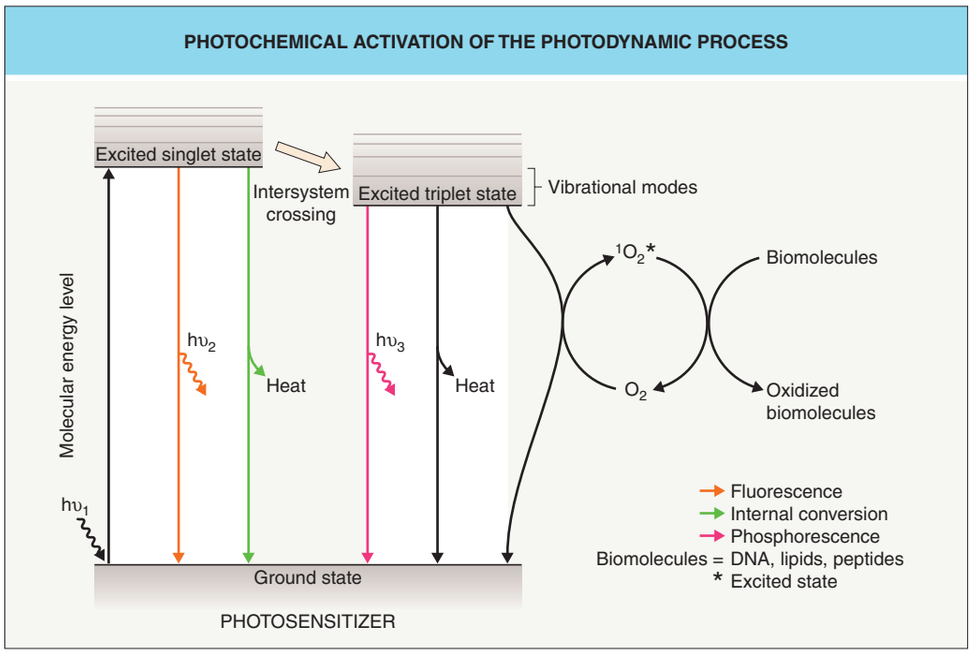


Fig. 135.2 Photochemical activation of the photodynamic process and the generation of reactive singlet oxygen: the Jablonski energy state diagram. The photosensitizer is delivered to or generated within the target tissue in its ground, lower-energy resting state. If light of an appropriate wavelength is used to irradiate the photosensitizer within tissue, photon absorption occurs and the photosensitizer is excited to a higher-energy "singlet" state. The excited singlet is short-lived, lasting nanoseconds, and then undergoes intersystem crossing to a more stable "triplet" state which has a lifetime on the order of microseconds. The "triplet" photosensitizer species can transfer its energy to molecular oxygen, yielding singlet oxygen ($^1O_2$) and as a result, returns to its resting ground state. See PDT Photochemistry section for additional details.

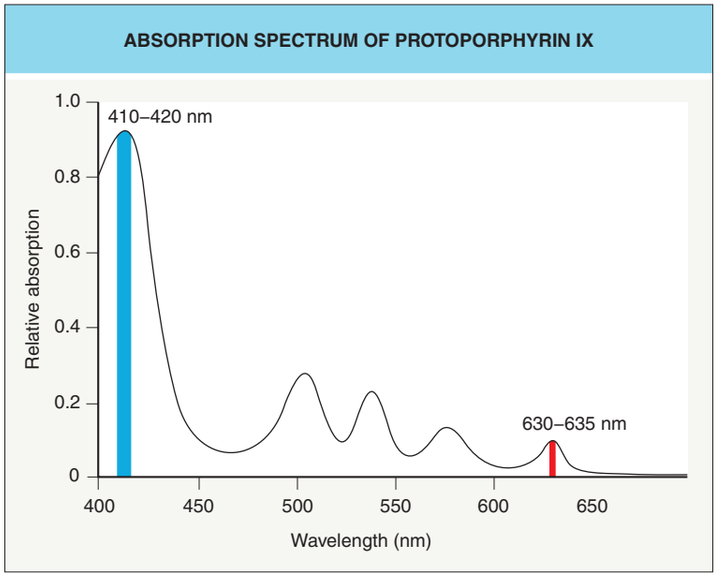


Fig. 135.3 Absorption spectrum of protoporphyrin IX (PpIX). The absorption spectrum depicts the efficiency of absorption of light as a function of wavelength. It reveals the major absorption (photoactivation) peaks of PpIX. Blue (410–420 nm) or red (630 nm) wavelengths are typically used to activate PpIX with artificial light; when daylight is used, the other PpIX absorption peaks are also activated.

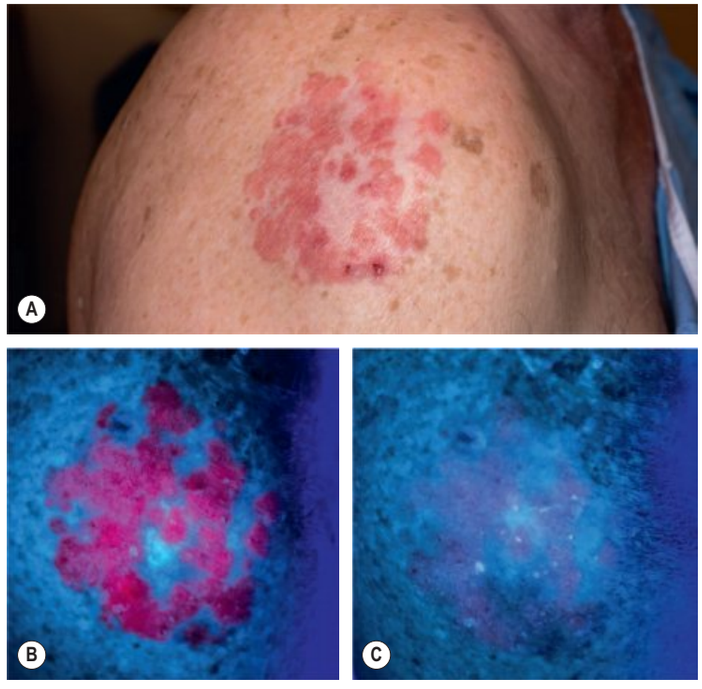


Fig. 135.4 Fluorescence of intratumor protoporphyrin IX (PpIX) when illuminated by a Wood's lamp (365 nm). A Large superficial basal cell carcinoma (BCC) of the shoulder. **B** Following application of topical methyl aminolevulinate (mALA) for 3 hours under occlusion, the BCC demonstrates selective pink-red fluorescence due to accumulation of PpIX. **C** Immediately following exposure to red light from an LED (light-emitting diode), the fluorescence almost disappears due to photobleaching.

At a high drug–light dose combination, greater levels of singlet oxygen are generated during PDT, leading to necrotic tissue damage. With lower levels of drug and/or light, damage is more limited, with predominantly apoptotic changes within cells. Because PDT is oxygen-dependent, larger targeted tumors, which can be relatively hypoxic, may be more resistant to the desired therapeutic effect.

Tissues exposed to PDT can become inflamed as a result of normal host responses to injury as well as activation of specific immunologic reactions. However, the types of immunologic reactions vary depending upon the target and mode of PDT delivery. In animal models of contact hypersensitivity, PDT suppresses local and systemic immune responses in addition to reducing epidermal Langerhans cells[4]. There is also evidence that the photosensitizers used in PDT can target activated T cells[5], providing a rationale for using PDT to treat inflammatory dermatoses or mycosis fungoides. Microbes, including viruses, bacteria, fungi and parasites, may be susceptible to singlet oxygen, and there are clinical studies attesting to the potential utility of PDT in the treatment of skin infections.

PDT Selectivity

PDT was initially conceived and developed as a method for targeted tumor destruction. Several findings help to explain this selectivity (Table 135.2). In neoplasms, where cellular metabolism is higher than normal, local factors such as enhanced perfusion, vascular and lymphatic hyperpermeability, pH, and lipoprotein receptors on target cells may lead to preferential accumulation and retention of photosensitizers within the tumor. For topical PDT, the specific site of drug application is set by the physician, thereby delimiting the area of photosensitization and treatment. Inherent differences in the permeability of skin lesions such as BCCs and AKs facilitate the selective uptake of topical ALA-like prodrugs into diseased skin.

THERAPEUTIC SELECTIVITY DURING PHOTODYNAMIC THERAPY	
Photosensitizer effects	**Light effects**
• Selective photosensitizer retention • Selective photosensitizer biodistribution and uptake • Ability to confine the area of topical photosensitizer application to lesion(s) • Incubation time of topical photosensitzer	• Spatial confinement of light exposure to the target area • Wavelength dependence for light penetration into skin • Photobleaching of photosensitizer

Table 135.2 Therapeutic selectivity during photodynamic therapy (PDT).

Selectivity is also achieved by determining the manner in which PDT light is delivered (see Table 135.2). This involves aiming the activation light at just the specific skin target (plus a limited margin of adjacent normal-appearing skin). Most clinical photosensitizers, and porphyrins in particular, exhibit multiple absorption maxima across the visible spectrum (see Fig. 135.3). Because light penetration within tissue is wavelength-dependent, the use of shorter wavelengths, i.e. blue light, will primarily limit the PDT effect to the epidermis, whereas red light will induce deeper biologic and clinical effects.

Photosensitizer localization within the skin can be readily visualized because PDT photosensitizers usually have high fluorescence quantum yields that are apparent with Wood's light examination (see Fig. 135.4). However, the intensity of this fluorescence does not necessarily correlate with the ensuing PDT reaction or ultimate clinical outcome. Following the therapeutic light exposure stage, the phenomenon of photobleaching can be confirmed visually by the absence or marked reduction of fluorescence.

Advantages and Limitations of PDT

Advantages of PDT include its relative conceptual simplicity as well as the accessibility of the skin to direct application of photosensitizing drugs and activating light. PDT photosensitizers typically have minimal dark toxicity (i.e. negligible toxicity in the absence of light) and are therefore relatively safe. PDT can also be used in patients with a variety of comorbidities, including those who are anticoagulated. PDT treatments can be repeated and there are minimal long-term side effects. Additionally, it has the advantage of being a physician-supervised therapy, which limits the effects of low adherence as can be the case with at-home topical treatments.

Nonetheless, PDT is far from a perfect therapeutic modality as it has inherent limitations. Topical photosensitization is limited by drug penetration into the epidermis and dermis, while the depth of penetration of visible light is also limited when exposure is via surface illumination. Thus, PDT is primarily useful for treating cutaneous tumors or diseases that are relatively superficial.

The multiplicity of potential drug and light dose combinations and permutations makes it complicated to determine the optimal conditions necessary for effective and safe PDT. Moreover, the literature is replete with a wide array of different reported parameters, making it difficult to standardize treatment regimens and compare clinical efficacy, even for the same indication. The commercially recommended treatment parameters are based on strict clinical trial protocols and do not provide much flexibility in terms of dosing. From the patient perspective, intraoperative local pain at the site of light exposure can be intense and even intolerable, and for many patients this represents the most significant disincentive for repeat treatments. Commercially available PDT systems (i.e. photosensitizers and artificial light sources) incur significant cost, thereby posing a practical barrier to accessing a treatment that is fundamentally based on a naturally occurring compound combined with visible light. Natural daylight activation of photosensitizers can partially circumvent the costs, pain, and apparent complexity of administering PDT.

COMPONENTS OF PDT

A range of photosensitizers have been developed and evaluated along with a multiplicity of different light sources and delivery systems (Table 135.3). The two basic pro-photosensitizers that are utilized are ALA and mALA. They were originally used with either artificial blue or red light devices. Additional light sources have been adopted and include natural daylight and investigative garments that incorporate low irradiance light-emitting diodes and are placed over the skin.

Photosensitizers

Although topical and systemic photosensitizers based on the full porphyrin structure have been developed and evaluated, to date none have become practical, either on a clinical or commercial level, for dermatologic use. Thus, for practical purposes, topical PDT relies primarily on the "ALA prodrug" approach.

ALA and mALA represent topical prodrugs that are converted within the skin into PpIX. A familiarity with porphyrinogenesis in mammalians aids in understanding the pharmacology of ALA and its congeners. ALA (5-aminolevulinic acid, δ-aminolevulinic acid) is synthesized in all nucleated cells, and it is an intermediate compound in the heme biosynthetic pathway (see Fig. 49.1); ALA synthase catalyzes the formation of ALA from succinyl-CoA and glycine. The latter reaction represents the rate-limiting step in this pathway and is inhibited by heme. When pharmacologic quantities of ALA are supplied to cells as in PDT, this regulatory step is bypassed, leading to an intracellular accumulation of PpIX, which is photodynamically active. Of note, PpIX is synthesized within mitochondria (see Fig. 135.1) and then diffuses to cellular membrane systems such as the endoplasmic reticulum and the plasma membrane.

Unlike fully formed porphyrin molecules that are relatively large, ALA is small and readily crosses the cutaneous permeability barrier via active transport mechanisms. Within the skin, the absorbed ALA induces porphyrinogenesis, thereby inducing "porphyria" at the cellular level. In some PDT applications, the skin is first prepared by gentle curettage to remove excess surface scale and crust or to remove the stratum corneum; this preparatory step can promote topical drug absorption. Within the skin, PpIX accumulates in the epidermis and sebaceous glands due to its lipophilicity.

The carboxyl moiety of ALA can be esterified by a variety of side chains, the simplest of which results in mALA. Substituted ALA congeners are absorbed into the skin by passive and active mechanisms different from those of ALA. Upon their uptake into cells, these substituents are hydrolyzed to yield free ALA (see Fig. 135.1). Both ALA and mALA are considered prodrugs or pro-photosensitizers since the skin cells themselves generate the active photosensitizer PpIX following application of these exogenous compounds.

ALA has been compounded in a variety of different vehicles for topical application and, in North America, it is currently commercially available in 10% and 20% preparations. The FDA-approved indication for ALA is treatment of AKs, although multiple off-label uses have been explored and described (Table 135.4). An incubation time allows ALA to be absorbed and converted to PpIX. When utilizing artificial light with ALA, many clinicians typically use a shorter incubation period of 1–4 hours, instead of the recommended 14–18 hours employed in the original controlled clinical trials. Pretreatment with microneedling or ablative fractional laser therapy can allow for even shorter incubation times while retaining similar efficacy in reducing AKs[6].

Mechanistically, mALA is similar in principle to ALA; it is available in a 16.8% cream formulation that must be refrigerated. The recommendation is to apply mALA for 3–4 hours under occlusion prior to exposure to red light from an LED device. It has been used for multiple different skin diseases, but depending upon the country, the approved indications include treatment of AKs and/or superficial keratinocyte carcinomas (see Table 135.4). Currently, mALA is not commercially available in the US.

Newer ALA formulations have recently been developed, including a nanoemulsion gel and an ALA-impregnated adhesive topical patch, with the latter not requiring pretreatment with curettage (see Table 135.3)[7].

Light Sources

Choosing a light source for PDT depends fundamentally on three considerations. First, the spectral output of the light should include a waveband that corresponds to one or more of the peaks in the absorption spectrum of the photosensitizer (see Fig. 135.3). Next, the desired depth of effect determines which photosensitizer absorption peak should be chosen. For PpIX, red light activation will provide a deeper clinical effect as compared to blue light. Finally, the surface area to be treated must be considered. For example, while lasers can provide precise irradiation, they may be less practical when treating broader, extensive surfaces.

COMPARISON OF ARTIFICIAL LIGHT-ACTIVATED PDT, DAYLIGHT-ACTIVATED PDT, AND ALTERNATIVE TECHNIQUES FOR PDT			
Feature	**Artificial light-activated PDT**	**Daylight-activated PDT (D-PDT)**	**Technique variations of PDT (off-label)**
Lesion preparation	• Curettage	• Application of sunscreen (15 min prior) • Curettage	• Topical keratolytics (e.g. retinoids, salicylic acid, α-hydroxy acids) • Tape stripping • Microdermabrasion • Fractional CO_2 laser • Fractional Er:YAG laser • Microneedling • Elevation of skin temperature
Drug delivery	• Topical	• Topical	• Topical • Intralesional • Intravenous • Iontophoresis • Ultrasound-assisted
Photosensitizer	• ALA 20% hydroalcoholic solution (Levulan®)* • mALA 16.8% cream (Metvixia®)*,†,‡ • ALA 10% gel (Ameluz®)*,† • ALA-impregnated patch (Alacare®)†,‡	• mALA 16.8% cream (Metvixia®) • Use of other photosensitizers for D-PDT is possible but off-label; limited published evidence	• Various other photosensitizers
Incubation time before light exposure	• ALA solution: 1–4 h (FDA-approved for 14–18 h for face and scalp, 3 hours for upper extremities; no occlusion)* • mALA: 3–4 h, under occlusion*,†,‡ • ALA gel: 3 h, under occlusion*,† • ALA patch: 8 mg/4 cm^2 apply plaster for 4 h†,‡	• Maximum 30 min, no occlusion	• Variable
Light activation	• ALA solution: blue fluorescent light (417 nm peak emission, 10 J/cm^2 [Blu-U®])* • mALA: red LED light (630 nm peak emission, 37 J/cm^2 [Aktilite®])*,†,‡ • ALA gel: red LED light (635 nm peak emission, 37 J/cm^2 [BF-RhodoLED®])*,† • 5-ALA patch: red LED light	• Daylight exposure for 2 h†	**Light sources:** • Other LED lamps • Lasers (e.g. copper vapor, KTP, pulsed dye) • Intense pulsed light • Wearable low-irradiance light source (Ambulite®) • Incandescent lamp (e.g. slide projector) • Arc lamp • Metal halide lamp • Fiberoptic probes **Light delivery:** • Fractionated (i.e. repeat) light doses within the same PDT session may enhance the effect
Pain	• Mild to severe (depending on incubation period)	• Minimal to low	• Variable

*FDA-approved; Metvixia® and Aktilite® were approved by the FDA, but are currently unavailable commercially in the US.
†Approved in multiple European countries.
‡Approved in the UK and Australia.

Table 135.3 Comparison of artificial light-activated PDT, daylight-activated PDT, and alternative techniques for PDT. ALA, 5-aminolevulinic acid; BCC, basal cell carcinoma; LED, light-emitting diode; mALA, methyl aminolevulinate.

Artificial light sources (conventional PDT)

The use of artificial lamps can be referred to as "conventional PDT". Light-emitting diodes (LEDs) and blue fluorescent lamps have been the most commonly employed and approved artificial light sources for PDT (see Table 135.3). In general, these commercial devices are relatively simple to use and can be powered by standard electrical outlets.

Off-label light sources have also been used for PDT. Lasers (e.g. copper vapor, KTP, pulsed dye) may be as effective as non-coherent artificial lights for PDT[8]. However, they are significantly more expensive, more complex to operate, and less studied. Intense pulsed light (IPL) has also been used as an artificial light source for PDT[9]. Adhesive light-emitting patches[10] and fabric garments with incorporated lights[11] have been designed to be worn by patients, and because they operate at low irradiances, there may be less pain associated with these devices.

Natural outdoor light (daylight PDT; D-PDT)

Studies have shown that natural outdoor light may be used for "daylight PDT (D-PDT)". Drug activation occurs because this light includes all the appropriate activating wavelengths. The main apprehension with daylight activation is the inability to precisely control the light dose delivered to the skin, with the possibility of phototoxicity from overexposure or lack of efficacy due to underexposure. However, randomized controlled trials have demonstrated both safety and efficacy of daylight-activated PDT (DA-PDT). Specifically, non-inferiority for effective treatment of AKs and superiority in degree of associated pain were demonstrated in a split-face trial of daylight- versus red light-activated PDT[3].

Although not yet FDA-approved, D-PDT has several practical and safety advantages. There is no requirement for a specific topical drug incubation time since patients are typically exposed to outdoor light immediately after drug application. Patient self-exposure to ambient outdoor light eliminates the requirement for staff to operate a specialized device and, perhaps most importantly, the level of PDT-related pain is much reduced with D-PDT. Published measurements of daylight doses in various cities can help clinicians identify months in which there is sufficient outdoor light to effectively administer D-PDT in their locale[12,13]. As a general rule, if the latitude is <45° (as in most of the US, southern Europe, South America, and Australia), PDT can be done year-round depending on weather conditions[14]. At higher latitudes in the northern hemisphere, it might be preferable to avoid daylight PDT from October to April. Of note, direct sunlight exposure to the skin is not necessary for daylight PDT. Lastly, non-mineral, untinted sunscreens applied to provide daylight UV protection do not interfere with the absorption of visible light by PpIX.

Light delivery

Regardless of the specific light source, the PDT light dose is measured and delivered in a manner analogous to conventional phototherapy. The ***irradiance*** of the light source is specified in units of W/cm^2, which represents the power density per unit area. Irradiance depends on the light source itself, and it can vary based on the lamp's age, overall operating conditions, and the distance from the lamp to the skin target. For D-PDT, irradiance is affected by geographic location, season, time

PHOTODYNAMIC THERAPY – DERMATOLOGIC APPLICATIONS	
FDA-approved indications	
Actinic keratoses of the face and scalp (ALA solution/blue light or ALA gel/red light) Actinic keratoses of the upper extremities (ALA solution/blue light)	
Off-label* applications with controlled studies demonstrating efficacy	
Actinic keratoses (including D-PDT and PDT of sites other than the face, scalp, and upper extremities) Superficial basal cell carcinoma Squamous cell carcinoma *in situ* (Bowen disease) Prevention of keratinocyte carcinomas	Acne Photoaging Verrucae vulgares Condylomata acuminata Leishmaniasis
Off-label applications for which PDT is *not* considered first-line therapy	
Actinic cheilitis Porokeratosis Sebaceous hyperplasia Nodular basal cell carcinoma Extramammary Paget disease Cutaneous metastases Capillary malformations (port-wine birthmarks)	Rosacea Psoriasis Hidradenitis suppurativa Necrobiosis lipoidica Chronic ulcers Superficial fungal infections
Diseases for which PDT is *not* generally recommended	
High-risk basal cell carcinoma Invasive squamous cell carcinoma	Melanoma
*Per the FDA.	

Table 135.4 Photodynamic therapy (PDT) – dermatologic applications. ALA, 5-aminolevulinic acid; D-PDT, daylight-activated photodynamic therapy; mALA, methyl aminolevulinate.

of day, cloud coverage, humidity, and air pollutants. The light dose used to activate the photosensitizer is also known as the ***fluence*** and is measured in J/cm^2. The ***exposure time*** in seconds required to deliver a specified fluence can be determined from the formula:

$$\text{exposure time (seconds)} = \frac{\text{fluence (J/cm}^2\text{)}}{\text{irradiance (W/cm}^2\text{)}}$$

PDT Dosimetry

Although PDT is deceptively simple in concept, there are multiple considerations when determining the appropriate doses of photosensitizer and light. Current clinical PDT dosing guidelines have been determined by systematic as well as semi-empiric clinical investigations; nevertheless, they are based on several basic concepts unique to PDT. The net production of singlet oxygen depends on both the amount of photosensitizer and the fluence of light delivered to the target. A certain degree of reciprocity (i.e. inverse relationship) exists between these two components, in that a high photosensitizer level combined with a low fluence can in theory produce an equivalent amount of singlet oxygen as a low concentration of photosensitizer activated by a high fluence.

Another important limit to the principle of drug–light dose reciprocity relates to the irradiance of the activating light. At very high irradiances, there is significant heat production due to both non-radiative photosensitizer absorption/relaxation and nonspecific light absorption by other tissue chromophores. This leads to photothermal effects superimposed on the PDT process itself. At lower irradiances, however, there is evidence that the pain associated with PDT might be reduced[15]. In D-PDT, the reduced pain may be due to the lower irradiance and longer gradual exposure to natural outdoor light as compared to artificial lamps (i.e. hours versus minutes).

An interesting and useful variation in light delivery is to fractionate the total light dose into a series of two or more separate exposures, each punctuated by defined pauses. The potential net effect of fractionating the light dose is to achieve a greater overall PDT effect without applying more drug[16,17]. Mechanistically, there are several reasons why this can happen. During PDT, molecular oxygen is consumed, and a pause in light exposure allows oxygen to be replenished via vascular reperfusion and diffusion. Likewise, this pause may also allow more PpIX photosensitizer to be synthesized *de novo* from the residual ALA that may still be present within viable skin cells; unlike PpIX, ALA itself does not undergo photobleaching.

Other factors that can influence the PDT effect include the duration of incubation between drug application and light exposure. A longer incubation interval for topical ALA or mALA leads to greater accumulation of active photosensitizer in the skin prior to light exposure. With D-PDT, the incubation period is intentionally minimal since patients are typically instructed to go outdoors immediately after the topical agent is applied. In this way, PpIX is gradually activated as soon as it is synthesized in the skin, which is another reason why there is less overall treatment pain with D-PDT.

DERMATOLOGIC APPLICATIONS

PDT agents can photosensitize neoplastic, inflamed, and vascular tissues, modulate immunologic processes, localize to the pilosebaceous unit, and induce lethal damage to microbes. To date, good-quality clinical evidence outside of cutaneous oncology is limited; for the most part, non-oncologic uses of PDT are off-label or investigational. Dermatologic applications for PDT are summarized in Table 135.4.

Oncologic

PDT is an accepted and approved treatment for AKs. There are also multiple controlled trials on the use of topical PDT for superficial carcinomas such as superficial BCC and Bowen disease (squamous cell carcinoma *in situ*) with licensed approvals varying according to country. PDT is not indicated for cutaneous melanoma.

Based on biophysical considerations alone, AKs can be treated with either blue or red light, whereas red light should be used for superficial keratinocyte carcinomas because of its deeper tissue penetration. Multiple studies have documented that cosmesis following PDT can be superior to that following conventional therapies[18]. PDT may be particularly practical and well suited for patients with multiple synchronous AKs or larger, superficial keratinocyte carcinomas, as well as those with evidence of field cancerization. A single PDT session may be sufficient for AKs, with retreatment if required, whereas at least two separate PDT sessions are usually recommended for the treatment of superficial BCC and Bowen disease.

Actinic keratoses

Clinical trials have demonstrated that up to 90% of face and scalp AKs can be cleared with topical PDT (Fig. 135.5), with a one-year sustained clearance of ~80%[19]. ALA and mALA appear to have similar clearance rates[20]. The PDT clearance rate is superior when compared to cryotherapy, 50% trichloroacetic acid, topical diclofenac, and CO_2 laser[21–24], but less effective than topical 5% 5-fluorouracil; it is comparable to topical imiquimod for AKs on the head[25]. PDT combined with imiquimod is more effective than either treatment alone[26], and fractionation of light exposures is associated with improved outcomes[17].

On acral sites, cryotherapy may perform better than PDT (88% vs 78% clearance in one study)[27], which in turn may clear more lesions than imiquimod (58% vs 37%)[28]. Patients also report higher satisfaction with PDT than with imiquimod[29]. Resistance to PDT may be explained by the hyperkeratotic nature of AKs in acral sites, thus making them more difficult to eradicate due to drug and light penetration issues. Consequently, prior to PDT, gentle curettage debridement of scale is often recommended. Several other methods for lesion preparation to enhance PDT efficacy have been described (see Table 135.3). For hypertrophic AKs, multiple treatment sessions may be required to achieve a satisfactory overall result. PDT can also be used in combination or sequentially with other topical treatments for AKs.

In solid organ transplant recipients, the response rate to PDT appears to be lower than in immunocompetent patients (48% vs 72%)[30]. This supports a role for immune activation as part of the mechanism of action of PDT. That said, possibly due to its major effect being direct cytotoxicity, PDT has been shown to be superior to topical 5-fluorouracil or imiquimod for clearance of AKs in transplant recipients[31].

Daylight treatment of AKs has been studied extensively. In randomized controlled trials, mALA D-PDT for AKs was as effective, less painful, and scored higher for patient satisfaction compared to red LED-activated mALA PDT[3,32]. In general, two hours of daylight exposure are sufficient to deliver an effective light dose throughout the year at latitudes <45° (see above regarding higher latitudes)[14,33]. As expected, mALA D-PDT clears



Fig. 135.5 Photodynamic therapy (PDT) of facial actinic keratoses and photoaging. A Pretreatment. **B** Following 3 monthly PDT sessions utilizing topical methyl aminolevulinate (mALA), clearing of actinic keratoses and a smoother, more even skin surface texture and color. *Courtesy Luis Torezan, MD.*



Fig. 135.6 Photodynamic therapy (PDT) of a large superficial basal cell carcinoma (BCC). A Superficial BCC measuring 11.5 by 9 cm on the upper abdomen. **B** Six months following 6 sessions of PDT using topical methyl aminolevulinate (mALA) followed by irradiation with red light from an LED (light-emitting diode), there is complete clinical clearing (closer view).

thin AKs more readily than hypertrophic AKs[34]. D-PDT with either mALA or ALA nanoemulsion gel have been used successfully to treat AKs[35].

Actinic cheilitis represents a useful potential PDT application since alternative treatment approaches such as surgical vermilionectomy or laser vaporization are more complicated and have associated morbidities[36].

Basal cell carcinomas (BCCs)

Superficial BCCs respond well to PDT, with an expected primary clearance rate of 92%–97% at 12 weeks and 9% recurrence rate at 12 months (Fig. 135.6)[37,38]. Although less effective than surgery, PDT has the advantage of improved cosmetic outcome over both surgery and cryotherapy. Longer term follow-up with a two-session protocol found that the 5-year response rate for imiquimod (80%) was superior to either 5-fluorouracil (70%) or PDT (63%) for clearance of superficial BCCs[39]. More than one session of PDT is recommended to treat a given BCC and two separate illuminations per treatment session (fractionation) increases the long-term clearance rate[16].

Nodular BCCs do not appear to be as well suited to PDT in that lower and variable response rates of 35%–90% have been observed[40]. This type of BCC is best treated surgically when possible. Similarly, difficult-to-treat BCCs (e.g. high risk areas of the face, recurrent, sclerosing type) are probably best treated by Mohs micrographic surgery because of the importance of achieving deep margin control. Multiple superficial BCCs arising in the context of cancer-prone genodermatoses such as basal cell nevus syndrome are a good indication for PDT since multiple lesions can be treated during one session and multiple surgeries thereby minimized[41].

D-PDT has also been studied for the treatment of superficial and nodular BCCs, with ~75% of lesions treated with two sessions having a complete response at 12 months[42]. Because daylight activation of photosensitizers may be due predominantly to the superficially penetrating blue wavelengths within natural outdoor light[13], it is not yet known if daylight is a sufficiently effective light source for treating BCCs.

Squamous cell carcinomas (SCCs)

Bowen disease is confined, by definition, to atypical keratinocytes that span the entire epidermis, and is thus eminently within the therapeutic range of PDT. Many PDT experts consider Bowen disease to be an ideal application since PDT can be used to treat multiple lesions as well as large, extensive plaques. A PDT clearance rate for Bowen disease of ~90% can be achieved with a 2-year sustained clearance rate of ~70%[43]. For clearance of Bowen disease, PDT outperforms topical 5-fluorouracil, imiquimod, and cryotherapy[44,45]. Bowen disease of the anogenital region and lower extremity can also be an appropriate target for PDT. In the case of lower extremity Bowen disease, a single session of ablative fractional laser-assisted PDT demonstrated superior long-term efficacy compared to two standard mALA sessions, with a 5-year clearance rate of 85%[46]. In this setting, the fractional laser is not used for photosensitizer activation, but rather for treatment site preparation prior to topical drug application (see Ch. 136). PDT is not recommended for recurrent Bowen disease or microinvasive or invasive SCC[43].

PDT photochemoprevention of AKs and keratinocyte carcinomas

PDT is an effective intervention for managing field cancerization beyond just clearing visible AKs. There is increasing evidence that skin sites treated with topical PDT may develop new lesions at a slower rate, raising the possibility of a photodynamic prevention effect[47]. Photochemoprevention with PDT may prove especially beneficial in reducing the incidence of AKs and SCCs in solid organ transplant recipients, particularly when periodic "maintenance" PDT is performed[48].

Extramammary Paget disease

Treatment of *in situ* extramammary Paget disease is complicated given the difficult anatomic locations of these lesions, the high recurrence rate due to unpredictable subclinical and adnexal extension, and significant

morbidity. Although PDT is a potential treatment that would allow anatomic preservation, variable success has been reported; the absence of conclusive evidence precludes its recommendation as first-line therapy.

Other neoplasms

Because activated and malignant T cells can be selectively sensitized by exogenous ALA, PDT has been used to treat the mycosis fungoides form of cutaneous T cell lymphoma[49]. Patch- or plaque-stage lesions may be more responsive than tumor-stage mycosis fungoides. While PDT's historical roots in dermatology lie in its initial use during the 1970s to treat intracutaneous metastases[1], it is now widely accepted that PDT is far more appropriate for treating superficial carcinomas rather than advanced disease.

Non-Oncologic PDT Applications

Acneiform disorders

Not only did early studies demonstrate that exogenous ALA could induce PpIX formation within the skin, they also noted the preferential accumulation of active photosensitizer and selective phototoxicity within the pilosebaceous unit. In addition, singlet oxygen exerts antibacterial and anti-inflammatory effects. These effects, in addition to antibiotic resistance and the challenges surrounding the use of oral isotretinoin, have provided an impetus to developing PDT regimens for acne. A reduction in inflammatory acne lesions of 60%–70% was reported with both ALA and mALA PDT, with the two photosensitizers producing similar effects. Use of higher red light fluences and longer incubation times are associated with longer remission, but also with more pain and local reactions[50] (Fig. 135.7). Currently, there is no consensus as to the optimum PDT parameters for treating acne.

It should be noted that *Cutibacterium* (formerly *Propionibacterium*) *acnes* produces cutaneous porphyrins, which can be readily demonstrated with Wood's lamp examination of any sebaceous-dense area, including normal skin. Exposure to high-intensity blue light alone, in the absence of any exogenous PDT prodrug, can lead to clinical improvement of inflammatory acne lesions.

PDT has also been used to treat other acneiform disorders. It was superior to topical 1% clindamycin for the treatment of perioral dermatitis in a small split-face trial[51]. Rosacea and hidradenitis suppurativa represent other diseases for which PDT was reported as being useful[52,53]. In patients with rosacea, ALA-PDT reduced papulopustular lesions as well as flushing, pruritus, burning, and prickling sensations.



Fig. 135.7 Use of photodynamic therapy (PDT) for moderate but recalcitrant acne vulgaris. This patient declined the use of oral isotretinoin and had failed therapy with topical agents and oral antibiotics. **A** Baseline. **B** Three days after PDT utilizing topical 20% 5-aminolevulinic acid (ALA; 3 hours incubation) followed by irradiation with red light from an LED (light-emitting diode; 630 nm; 37 J/cm^2; 70 mW/cm^2); intense inflammation and pustulation is limited to treated sites. **C** Two months after single treatment session.

Photoaging

When used to treat AKs and keratinocyte carcinomas, PDT is thought to produce cosmetically favorable results, including improvement of sun-damaged skin. Well-designed trials directly comparing PDT to non-PDT treatments in which photoaging is the primary focus are sparse relative to the extent that this treatment approach is promoted and used in clinical practice (see Fig. 135.5). A randomized trial of repetitive D-PDT to prevent AKs found a significant reduction in fine lines, pigmentation, skin roughness, and erythema[54]. Optimal PDT parameters for treatment of photoaging have not yet been determined. Histologically, PDT appears to increase collagen deposition and decrease elastosis[55].

Cutaneous infections

There are several mechanisms by which PDT can treat infectious diseases. Singlet oxygen may directly destroy microbes or it may activate host immunologic reactions against the microorganisms. In addition, PDT can induce necrosis of infected tissue, for example, in the treatment of verrucae or condylomata. Conditions that have been shown, in controlled trials, to improve with PDT include verrucae vulgares[56], condylomata acuminata[57], and leishmaniasis[58]. The emergence of drug-resistant bacteria plus the need for better antibiotic stewardship have also motivated investigations into employing PDT for bacterial skin infections and colonized chronic leg ulcers[59]. In addition, PDT has been used on superficial fungal infections such as tinea pedis and onychomycosis.

Vascular anomalies

Systemic photosensitizers are biodistributed via the peripheral circulation and it stands to reason that intravascular drug activation with light would be useful in inducing the involution of abnormal vascular structures. Vascular malformations such as port-wine birthmarks have been shown to respond to systemic PDT with results that appear to be at least equivalent to those achieved with conventional pulsed dye laser therapy[60]. Experience with this technique is largely from China, where hematoporphyrin-type preparations are used systemically. Topical ALA/pulsed dye laser-activated PDT has also been described[61], taking advantage of combined photodynamic and photothermal effects.

ADVERSE EFFECTS AND COMPLICATIONS OF PDT

Neither PDT photosensitizers nor artificial visible light ordinarily possess significant inherent toxicity, and the adverse effects related to PDT are largely an extension of the photochemical and photobiologic reactions that are generated by reactive oxygen moieties. Interestingly, erythropoietic protoporphyria and X-linked dominant protoporphyria could be considered possible toxicity models for ALA and its congeners since they result in constitutive overaccumulation of PpIX.

Photosensitivity

With topical PDT, photosensitivity manifests as varying degrees of local erythema, edema, and/or blistering of any exposed site, with subjective symptoms of pain or a burning sensation. Conventional chemical sunscreens, even those with a high sun protection factor, are not useful in managing local photosensitivity since the action spectrum extends throughout the visible spectrum, which is not blocked by these sunscreens.

Pain

The incubation period, which follows application of the topical photosensitizer, is generally uneventful, but within seconds to minutes of illumination of the skin with artificial light, patients will often experience a range and series of unpleasant sensations at the site of light exposure. Various terms are relayed by patients to describe these sensations, including pain, warmth, burning, stinging, smarting, and

stabbing. The intensity will usually build with time and there can be spread of the discomfort beyond the actual treatment field. Studies of factors associated with this pain have found inconsistent associations, including older age, treatment of AKs or well-innervated areas like the face and scalp, size of the treatment area, skin phototypes I–II, use of ALA as the photosensitizer, and intensity of ALA-induced fluorescence[62].

The rate of light delivery can influence the degree of pain, with lower irradiances being more tolerable[15]. In D-PDT, a lower irradiance is used for photosensitizer activation and this technique is associated with significantly less pain[3]. Other potential strategies for modifying irradiance include increasing the distance from the light source and the use of low-irradiance, portable LED sources[10,11]. Sometimes, temporary interruption of the artificial light exposure will allow the pain to dissipate temporarily.

A variety of practical strategies have been designed to manage the pain of PDT (Table 135.5). Of note, topical anesthesia with eutectic

STEPS IN ADMINISTERING TOPICAL PHOTODYNAMIC THERAPY AND PRACTICAL CONSIDERATIONS
Preoperative phase

• Confirm that the patient is a good candidate for PDT: appropriate indication, assess comorbidities; consider PDT especially in the setting of:
  • Field cancerization
  • Multiple synchronous or metachronous superficial tumors
  • Skin cancer-prone genodermatosis
  • Solid organ transplant recipient
• Select treatment site(s) and confirm diagnosis by histologic examination if necessary
• Exclude contraindications: porphyria, photosensitivity disorder, pregnancy, photosensitizer hypersensitivity
• Provide patient with counseling and education in terms of expectations and precautions
• Determine the photosensitizer, light source, and treatment parameters that will be employed
• Determine the number of PDT sessions to be given, the number of light exposures per session (fractionation), and the time interval; for keratinocyte carcinomas, two separate PDT sessions one week apart are recommended
• Check weather report (temperature, precipitation) if daylight-activating PDT is to be used

Intraoperative phase
Topical drug application
• Confirm treatment site(s) • Consider degreasing the treatment surface with topical acetone or by microdermabrasion • Apply chemical sunscreen to all exposed skin (daylight-activating PDT only) • Prepare treatment site(s): most commonly by gentle curettage of excess stratum corneum or scale-crust if appropriate; consider using microneedling or fractional laser • Apply topical photosensitizer to the target treatment site(s); occlusion and coverage by opaque material are optional • Incubate the photosensitizer according to the indication, specific prodrug, and light source to be used
Light administration/drug activation

• Non-coherent artificial light activation
  • Remove any residual topical medication prior to light exposure
  • Confirm the presence of PpIX fluorescence by Wood's lamp examination (optional)
  • Provide protective eyewear to patient and staff
  • Position patient and lamp(s) for uniform exposure and patient comfort
  • Confirm light dose to be given, and then initiate light exposure (typically 5–15 minutes depending on the light source); a healthcare professional can assist with pain management during the light exposure if necessary (see below)
• Daylight (outdoor) activation
  • Confirm the field area to be exposed to daylight
  • Provide timer and monitor treatment duration during light exposure (~2 hours)
  • Periodically verify tolerance of treatment with patient
  • Cleanse treatment area upon return to the clinic to remove any residual topical photosensitizer
• At the completion of the light exposure, confirm photobleaching of PpIX by Wood's lamp examination (optional)

Pain management during light exposure

• Assemble tools and devices for pain control
• The physical presence of a healthcare professional is very important for providing reassurance and monitoring; verbal reassurance and distraction, especially during artificial light-activated PDT
• Reinforce to the patient that the sensation of pain indicates that the appropriate PDT reactions are occurring
• Additional specific strategies for managing pain may include:
  • Applying an ice cube or ice pack near the treatment site
  • Spraying cold water over the treatment site
  • Providing a fan that can be held by the patient
  • Directing forced cold air toward the treatment site
  • Interrupting the light exposure temporarily
  • Infiltration, nerve block, or tumescent local anesthesia
  • Hypnosis
  • Nitrous oxide/oxygen mixture inhalation
  • Transcutaneous nerve stimulation

Postoperative phase
• Reduce swelling by using ice packs • Prescribe oral analgesics to be taken if necessary • Recommend avoidance of sun exposure and bright indoor light for 48 hours • Arrange follow-up, including next PDT session if appropriate; for keratinocyte carcinomas, a repeat course/cycle of PDT may be appropriate 2–3 months after the first course/cycle if there is clinical evidence of residual disease • If lesion recurs despite multiple treatment cycles, consider alternate treatment (e.g. surgery, radiotherapy)

Table 135.5 Steps in administering topical photodynamic therapy (PDT) and practical considerations. ALA, 5-aminolevulinic acid; LED, light-emitting diode; mALA, methyl aminolevulinate; PpIX, protoporphyrin IX.

mixture of lidocaine 2.5% and prilocaine 2.5% (EMLA®), morphine gel, tetracaine gel, or capsaicin cream is generally ineffective. Moreover, in one trial, there was no difference between placebo and oxycodone plus acetaminophen in time to pain onset and level of pain[63]. Scalp nerve blocks appear superior to intravenous analgesics and forced cold air[64]. For some patients, the pain can be so intense that they will not be willing to undergo any more than one treatment session.

Inflammation

At the end of the light exposure, the treated site will usually exhibit an immediate wheal and flare reaction. Over the next 24–48 hours, localized phototoxicity may manifest as edema, induration, urticaria, purpura, pustules, and blistering, along with exudation and crusting (Fig. 135.8). Depending on the indication and the PDT drug–light dose, frank tissue necrosis may supervene accompanied by erosions and ulceration. Local reactions can evolve over the ensuing 1–4 weeks and any wounds will heal by second intention.

For the treatment of AKs, cutaneous application of mALA for 30 minutes (rather than the recommended 3 hours) and/or pretreatment with superpotent topical corticosteroids led to reduced cutaneous inflammation but equivalent efficacy[65]. D-PDT typically generates local reactions that are milder and of shorter duration.

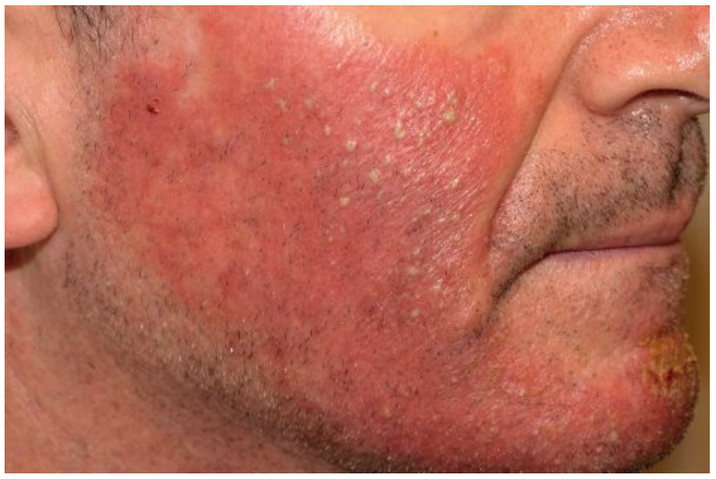


Fig. 135.8 Erythema, edema, and multiple pustules 4 days after photodynamic therapy (PDT) for actinic keratoses. Topical 20% 5-aminolevulinic acid (ALA) was followed by irradiation with red light from an LED (light-emitting diode).

Photosensitizer Allergy

Multiple case reports have documented contact hypersensitivity to mALA. In a controlled trial, contact sensitization to mALA was observed in as many as 35% of patients who had *previously* undergone five or more mALA-based PDT sessions; only 1.7% of the control subjects who had not previously undergone PDT demonstrated sensitization[66].

Rare, Unusual or Controversial Reactions

Exceptionally, PDT has been reported to precipitate herpes simplex reactivation[67], facial nerve palsy, hypertensive crisis, alopecia, localized bullous pemphigoid, pityriasis rubra pilaris, erosive pustular dermatosis of the scalp, and transient memory impairment. Cases of keratinocyte carcinomas recurring with more aggressive histology[68], arising *de novo*[69], or progressing within PDT fields have been reported; melanomas have also been reported following PDT, but the significance of these findings is difficult to interpret in the absence of control data.

PRACTICE AND TECHNIQUES

The practical administration of PDT requires attention to a number of details during the preoperative, intraoperative, and postoperative stages (see Table 135.5). Although the commercial PDT systems for dermatology come with officially recommended and approved protocols, the practice of PDT is not uncommonly off-label, both in terms of indications and specific procedural steps guided by the individual practitioner's experience and empiric preferences. One round of topical drug plus light (administered as a single exposure or as multiple fractionated exposures) can be considered a single PDT session. A "course" or "cycle" of PDT may involve one or more individual PDT sessions separated by a set time interval. What should not be underestimated is the time and staffing necessary to provide appropriate patient counseling and education as well as intraoperative support and supervision during the light exposure phase. Consensus recommendations and guidelines from various expert groups and dermatologic societies have been published to guide the use of PDT[13,70,71].

FUTURE DIRECTIONS

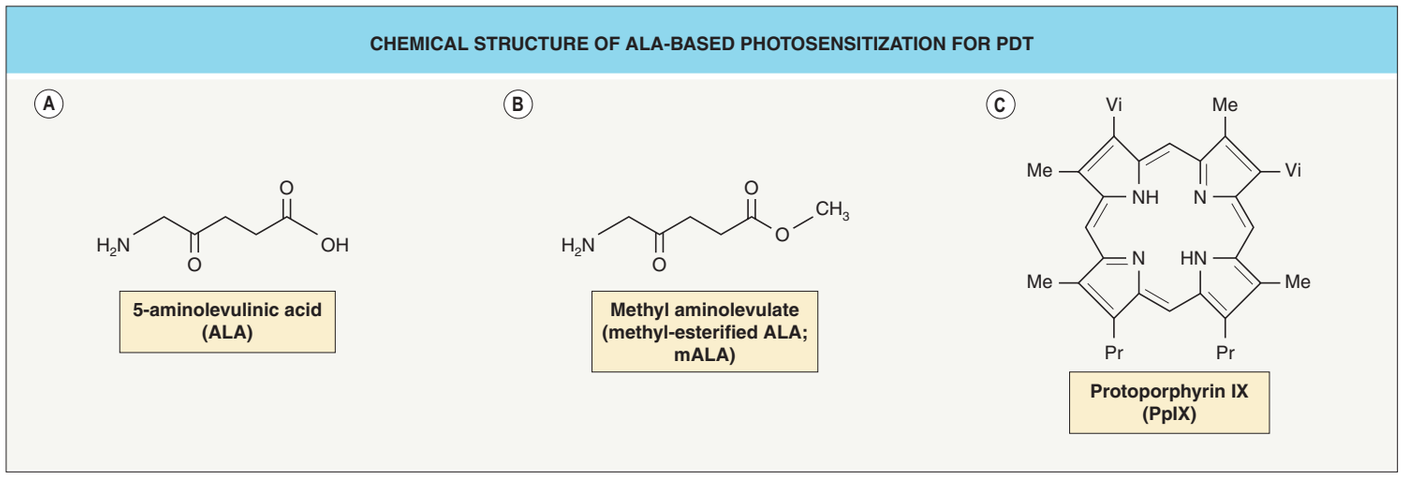
Controlled trials and cumulative clinical experience continue to redefine the spectrum of PDT applications. On the horizon are new photosensitizers and novel ways of delivering ALA. Knowledge gained from D-PDT, including less associated pain, has led to investigations in which low irradiance LED sources are used instead of conventional light sources. Advances in PDT have been accompanied by progress in imaging techniques such as confocal reflectance microscopy. Combination of the two in the future could lead to noninvasive diagnosis and delineation of cutaneous carcinomas as well as treatment and long-term evaluation.

Additional figures available in our eBook (see inside front cover for access code).

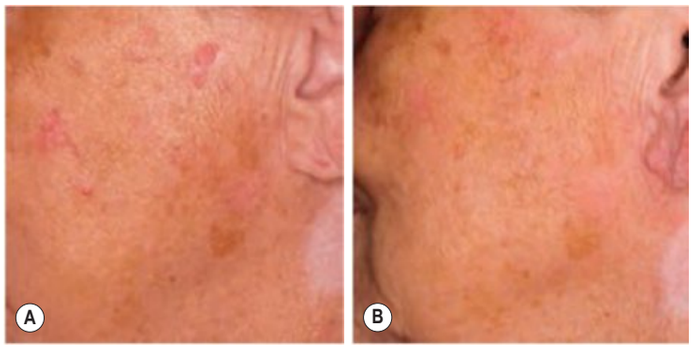
REFERENCES

1. Dougherty TJ, Kaufman JE, Goldfarb A, et al. Photoradiation therapy for the treatment of malignant tumors. *Cancer Res*. 1978;38:2628–2635.
2. Kennedy JC, Pottier RH, Pross DC. Photodynamic therapy with endogenous protoporphyrin IX: basic principles and present clinical experience. *J Photochem Photobiol B*. 1990;6:143–148.
3. Rubel DM, Spelman L, Murrell DF, et al. Daylight photodynamic therapy with methyl aminolevulinate cream as a convenient, similarly effective, nearly painless alternative to conventional photodynamic therapy in actinic keratosis treatment: a randomized controlled trial. *Br J Dermatol*. 2014;171:1164–1171.
4. Hayami J, Okamoto H, Sugihara A, Horio T. Immunosuppressive effects of photodynamic therapy by topical aminolevulinic acid. *J Dermatol*. 2007;34:320–327.
5. Bissonnette R, Tremblay JF, Juzenas P, et al. Systemic photodynamic therapy with aminolevulinic acid induces apoptosis in lesional T lymphocytes of psoriatic plaques. *J Invest Dermatol*. 2002;119:77–83.
6. Petukhova TA, Hassoun LA, Foolad N, et al. Effect of expedited microneedle-assisted photodynamic therapy for field treatment of actinic keratoses: a randomized clinical trial. *JAMA Dermatol*. 2017;153:637–643.
7. Szeimies RM, Stockfleth E, Popp G, et al. Long-term follow-up of photodynamic therapy with a self-adhesive 5-aminolaevulinic acid patch: 12 months data. *Br J Dermatol*. 2010;162:410–414.
8. Kim BS, Kim JY, Song CH, et al. Light-emitting diode laser versus pulsed dye laser-assisted photodynamic therapy in the treatment of actinic keratosis and Bowen's disease. *Dermatol Surg*. 2012;38:151–153.
9. Hasegawa T, Suga Y, Mizuno Y, et al. Efficacy of photodynamic therapy with topical 5-aminolevulinic acid using intense pulsed light for Bowen's disease. *J Dermatol*. 2010;37:623–628.
10. Ibbotson SH, Ferguson J. Ambulatory photodynamic therapy using low irradiance inorganic light-emitting diodes for the treatment of non-melanoma skin cancer: an open study. *Photodermatol Photoimmunol Photomed*. 2012;28:235–239.
11. Vicentini C, Vignion-Dewalle AS, Thecua E, et al. Photodynamic therapy for actinic keratosis of the forehead and scalp: a randomized, controlled, phase II clinical study evaluating the noninferiority of a new protocol involving irradiation with a light-emitting, fabric-based device (the Flexitheralight protocol) compared with the conventional protocol involving irradiation with the Aktilite CL 128 lamp. *Br J Dermatol*. 2019;180:765–773.
12. Wiegell SR, Fabricius S, Heydenreich J, et al. Weather conditions and daylight-mediated photodynamic therapy: protoporphyrin IX-weighted daylight doses measured in six geographical locations. *Br J Dermatol*. 2013;168:186–191.
13. Wiegell SR, Wulf HC, Szeimies RM, et al. Daylight photodynamic therapy for actinic keratosis: an international consensus: International Society for Photodynamic Therapy in Dermatology. *J Eur Acad Dermatol Venereol*. 2012;26:673–679.
14. Wulf HC. Photodynamic therapy in daylight for actinic keratoses. *JAMA Dermatol*. 2016;152:631–632.
15. Cottrell WJ, Paquette AD, Keymel KR, et al. Irradiance-dependent photobleaching and pain in delta-aminolevulinic acid-photodynamic therapy of superficial basal cell carcinomas. *Clin Cancer Res*. 2008;14(14):4475–4483.
16. de Vijlder HC, Sterenborg H, Neumann HAM, et al. Light fractionation significantly improves the response

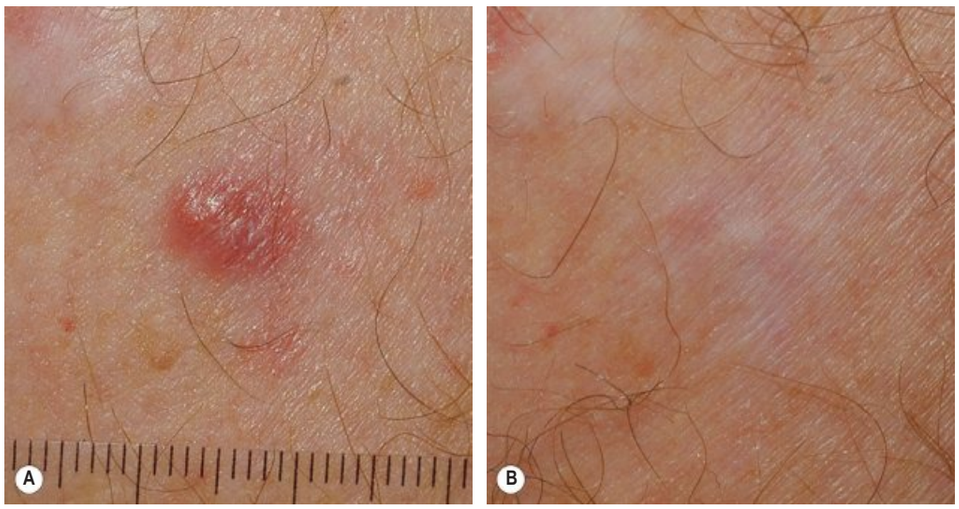
of superficial basal cell carcinoma to aminolaevulinic acid photodynamic therapy: five-year follow-up of a randomized, prospective trial. *Acta Derm Venereol*. 2012;92:641–647.
17. Sotiriou E, Apalla Z, Chovarda E, et al. Single vs. fractionated photodynamic therapy for face and scalp actinic keratoses: a randomized, intraindividual comparison trial with 12-month follow-up. *J Eur Acad Dermatol Venereol*. 2012;26:36–40.
18. Morton C, Campbell S, Gupta G, et al. Intraindividual, right-left comparison of topical methyl aminolaevulinate-photodynamic therapy and cryotherapy in subjects with actinic keratoses: a multicentre, randomized controlled study. *Br J Dermatol*. 2006;155:1029–1036.
19. Morton CA, Szeimies RM, Sidoroff A, Braathen LR. European guidelines for topical photodynamic therapy part 1: treatment delivery and current indications actinic keratoses, Bowen's disease, basal cell carcinoma. *J Eur Acad Dermatol Venereol*. 2013;27:536–544.
20. Ko DY, Kim KH, Song KH. Comparative study of photodynamic therapy with topical methyl aminolevulinate versus 5-aminolevulinic acid for facial actinic keratosis with long-term follow-up. *Ann Dermatol*. 2014;26:321–331.
21. Patel G, Armstrong AW, Eisen DB. Efficacy of photodynamic therapy vs other interventions in randomized clinical trials for the treatment of actinic keratoses: a systematic review and meta-analysis. *JAMA Dermatol*. 2014;150:1281–1288.
22. Nuzzo SD, Cortelazzi C, Boccaletti V, et al. Comparative study of trichloroacetic acid versus photodynamic therapy with topical 5-aminolevulinic acid for actinic keratosis of the scalp. *Photodermatol Photoimmunol Photomed*. 2015;31:233–238.
23. Zane C, Facchinetti E, Rossi MT, et al. A randomized clinical trial of photodynamic therapy with methyl aminolaevulinate vs. diclofenac 3% plus hyaluronic acid gel for the treatment of multiple actinic keratoses of the face and scalp. *Br J Dermatol*. 2014;170:1143–1150.
24. Scola N, Terras S, Georgas D, et al. A randomized, half-side comparative study of aminolaevulinate photodynamic therapy vs. CO2 laser ablation in immunocompetent patients with multiple actinic keratoses. *Br J Dermatol*. 2012;167:1366–1373.
25. Jansen MHE, Kessels JPHM, Nelemans PJ, et al. Randomized trial of four treatment approaches for actinic keratosis. *N Engl J Med*. 2019;380:935–946.
26. Serra-Guillen C, Nagore E, Hueso L, et al. A randomized pilot comparative study of topical methyl aminolevulinate photodynamic therapy versus imiquimod 5% versus sequential application of both therapies in immunocompetent patients with actinic keratosis: clinical and histologic outcomes. *J Am Acad Dermatol*. 2012;66:E131–E137.
27. Kaufmann R, Spelman L, Weightman W, et al. Multicentre intraindividual randomized trial of topical methyl aminolaevulinate-photodynamic therapy vs. cryotherapy for multiple actinic keratoses on the extremities. *Br J Dermatol*. 2008;158:994–999.
28. Sotiriou E, Apalla Z, Maliamani F, et al. Intraindividual, right-left comparison of topical 5-aminolevulinic acid photodynamic therapy vs. 5% imiquimod cream for actinic keratoses on the upper extremities. *J Eur Acad Dermatol Venereol*. 2009;23:1061–1065.
29. Serra-Guillen C, Nagore E, Hueso L, et al. A randomized comparative study of tolerance and satisfaction in the treatment of actinic keratosis of the face and scalp between 5% imiquimod cream and photodynamic therapy with methyl aminolaevulinate. *Br J Dermatol*. 2011;164:429–433.
30. Dragieva G, Prinz BM, Hafner J, et al. A randomized controlled clinical trial of topical photodynamic therapy with methyl aminolaevulinate in the treatment of actinic keratoses in transplant recipients. *Br J Dermatol*. 2004;151:196–200.
31. Togsverd-Bo K, Halldin C, Sandberg C, et al. Photodynamic therapy is more effective than imiquimod for actinic keratosis in organ transplant recipients: a randomized intraindividual controlled trial. *Br J Dermatol*. 2018;178:903–909.
32. Wiegell SR, Haedersdal M, Philipsen PA, et al. Continuous activation of PpIX by daylight is as effective as and less painful than conventional photodynamic therapy for actinic keratoses; a randomized, controlled, single-blinded study. *Br J Dermatol*. 2008;158:740–746.
33. Wiegell SR, Fabricius S, Stender IM, et al. A randomized, multicentre study of directed daylight exposure times of 11/2 vs. 21/2 h in daylight-mediated photodynamic therapy with methyl aminolaevulinate in patients with multiple thin actinic keratoses of the face and scalp. *Br J Dermatol*. 2011;164:1083–1090.
34. Wiegell SR, Fabricius S, Gniadecka M, et al. Daylight-mediated photodynamic therapy of moderate to thick actinic keratoses of the face and scalp: a randomized multicentre study. *Br J Dermatol*. 2012;166:1327–1332.
35. Räsänen JE, Neittaanmäki N, Ylitalo L, et al. 5-aminolaevulinic acid nanoemulsion is more effective than methyl-5-aminolaevulinate in daylight photodynamic therapy for actinic keratosis: a nonsponsored randomized double-blind multicentre trial. *Br J Dermatol*. 2019;181:265–274.
36. Sotiriou E, Apalla Z, Chovarda E, et al. Photodynamic therapy with 5-aminolevulinic acid in actinic cheilitis: an 18-month clinical and histological follow-up. *J Eur Acad Dermatol Venereol*. 2010;24:916–920.
37. Szeimies RM, Ibbotson S, Murrell DF, et al. A clinical study comparing methyl aminolevulinate photodynamic therapy and surgery in small superficial basal cell carcinoma (8-20 mm), with a 12-month follow-up. *J Eur Acad Dermatol Venereol*. 2008;22:1302–1311.
38. Basset-Seguin N, Ibbotson SH, Emtestam L, et al. Topical methyl aminolaevulinate photodynamic therapy versus cryotherapy for superficial basal cell carcinoma: a 5 year randomized trial. *Eur J Dermatol*. 2008;18:547–553.
39. Jansen MHE, Mosterd K, Arits AHMM, et al. Five-year results of a randomized controlled trial comparing effectiveness of photodynamic therapy, topical imiquimod, and topical 5-fluorouracil in patients with superficial basal cell carcinoma. *J Invest Dermatol*. 2018;138:527–533.
40. Roozeboom MH, Aardoom MA, Nelemans PJ, et al. Fractionated 5-aminolevulinic acid photodynamic therapy after partial debulking versus surgical excision for nodular basal cell carcinoma: a randomized controlled trial with at least 5-year follow-up. *J Am Acad Dermatol*. 2013;69:280–287.
41. Pauwels C, Mazereeuw-Hautier J, Basset-Seguin N, et al. Topical methyl aminolevulinate photodynamic therapy for management of basal cell carcinomas in patients with basal cell nevus syndrome improves patient's satisfaction and reduces the need for surgical procedures. *J Eur Acad Dermatol Venereol*. 2011;25:861–864.
42. Wiegell SR, Skodt V, Wulf HC. Daylight-mediated photodynamic therapy of basal cell carcinomas – an explorative study. *J Eur Acad Dermatol Venereol*. 2014;28:169–175.
43. Calzavara-Pinton PG, Venturini M, Sala R, et al. Methylaminolaevulinate-based photodynamic therapy of Bowen's disease and squamous cell carcinoma. *Br J Dermatol*. 2008;159:137–144.
44. Salim A, Leman JA, McColl JH, et al. Randomized comparison of photodynamic therapy with topical 5-fluorouracil in Bowen's disease. *Br J Dermatol*. 2003;148:539–543.
45. Morton C, Horn M, Leman J, et al. Comparison of topical methyl aminolevulinate photodynamic therapy with cryotherapy or Fluorouracil for treatment of squamous cell carcinoma in situ: results of a multicenter randomized trial. *Arch Dermatol*. 2006;142:729–735.
46. Kim HJ, Song KH. Ablative fractional laser-assisted photodynamic therapy provides superior long-term efficacy compared with standard methyl aminolevulinate photodynamic therapy for lower extremity Bowen disease. *J Am Acad Dermatol*. 2018;79:860–868.
47. Apalla Z, Sotiriou E, Chovarda E, et al. Skin cancer: preventive photodynamic therapy in patients with face and scalp cancerization. A randomized placebo-controlled study. *Br J Dermatol*. 2010;162:171–175.
48. Togsverd-Bo K, Omland SH, Wulf HC, et al. Primary prevention of skin dysplasia in renal transplant recipients with photodynamic therapy: a randomized controlled trial. *Am J Transplant*. 2015;15:2986–2990.
49. Quereux G, Brocard A, Saint-Jean M, et al. Photodynamic therapy with methyl-aminolevulinic acid for pauci-lesional mycosis fungoides: a prospective open study and review of the literature. *J Am Acad Dermatol*. 2013;69:890–897.
50. Sakamoto FH, Torezan L, Anderson RR. Photodynamic therapy for acne vulgaris: a critical review from basics to clinical practice: part II. Understanding parameters for acne treatment with photodynamic therapy. *J Am Acad Dermatol*. 2010;63:195–211. quiz 211–2.
51. Richey DF, Hopson B. Photodynamic therapy for perioral dermatitis. *J Drugs Dermatol*. 2006;5:12–16.
52. Fan L, Yin R, Lan T, et al. Photodynamic therapy for rosacea in Chinese patients. *Photodiagnosis Photodyn Ther*. 2018;24:82–87.
53. Schweiger ES, Riddle CC, Aires DJ. Treatment of hidradenitis suppurativa by photodynamic therapy with aminolevulinic acid: preliminary results. *J Drugs Dermatol*. 2011;10:381–386.
54. Karrer S, Szeimies RM, Philipp-Dormston WG, et al. Repetitive daylight photodynamic therapy versus cryosurgery for prevention of actinic keratoses in photodamaged facial skin: a prospective, randomized controlled multicentre two-armed study. *Acta Derm Venereol*. 2021;101:adv00355.
55. Szeimies RM, Torezan L, Niwa A, et al. Clinical, histopathological and immunohistochemical assessment of human skin field cancerization before and after photodynamic therapy. *Br J Dermatol*. 2012;167:150–159.
56. Stender IM, Na R, Fogh H, et al. Photodynamic therapy with 5-aminolaevulinic acid or placebo for recalcitrant foot and hand warts: randomised double-blind trial. *Lancet*. 2000;355:963–966.
57. Ying ZL, Li XJ, Dang H. 5-aminolevulinic acid-based photodynamic therapy for the treatment of condylomata acuminata in Chinese patients: a meta-analysis. *Photodermatol Photoimmunol Photomed*. 2013;29:149–159.
58. Asilian A, Davami M. Comparison between the efficacy of photodynamic therapy and topical paromomycin in the treatment of Old World cutaneous leishmaniasis: a placebo-controlled, randomized clinical trial. *Clin Exp Dermatol*. 2006;31:634–637.
59. Morley S, Griffiths J, Philips G, et al. Phase IIa randomized, placebo-controlled study of antimicrobial photodynamic therapy in bacterially colonized, chronic leg ulcers and diabetic foot ulcers: a new approach to antimicrobial therapy. *Br J Dermatol*. 2013;168:617–624.
60. Gao K, Huang Z, Yuan KH, et al. Side-by-side comparison of photodynamic therapy and pulsed-dye laser treatment of port-wine stain birthmarks. *Br J Dermatol*. 2013;168:1040–1046.
61. Liu SX, Yang CJ, Yang S, et al. Topical application of 5-aminolevulinic acid followed by 595-nm pulsed dye laser irradiation for the treatment of recalcitrant port-wine stains: a primary study. *J Cosmet Laser Ther*. 2012;14:189–192.
62. Fink C, Enk A, Gholam P. Photodynamic therapy – aspects of pain management. *J Dtsch Dermatol Ges*. 2015;13:15–22.
63. Huang N, Zeng J, Liang J, et al. A randomized, double-blind, placebo-controlled study of oral oxycodone plus acetaminophen for the treatment of pain in photodynamic therapy on port wine stains. *Photodiagnosis Photodyn Ther*. 2014;11:134–140.
64. Klein A, Karrer S, Horner C, et al. Comparing cold-air analgesia, systemically administered analgesia and scalp nerve blocks for pain management during photodynamic therapy for actinic keratosis of the scalp presenting as field cancerization: a randomized controlled trial. *Br J Dermatol*. 2015;173:192–200.
65. Wiegell SR, Petersen B, Wulf HC. Pulse photodynamic therapy reduces inflammation without compromising efficacy in the treatment of multiple mild actinic keratoses of the face and scalp: a randomized clinical trial. *Br J Dermatol*. 2016;174:979–984.
66. Korshoj S, Solvsten H, Erlandsen M, Sommerlund M. Frequency of sensitization to methyl aminolaevulinate after photodynamic therapy. *Contact Dermatitis*. 2009;60:320–324.
67. Nobbe S, Trueb RM, French LE, Hofbauer GFL. Herpes simplex virus reactivation as a complication of photodynamic therapy. *Photodermatol Photoimmunol Photomed*. 2011;27:51–52.
68. Fiechter S, Skaria A, Nievergelt H, et al. Facial basal cell carcinomas recurring after photodynamic therapy: a retrospective analysis of histological subtypes. *Dermatology*. 2012;224:346–351.
69. Calista D. Development of squamous cell carcinoma after photodynamic therapy with methyl aminoleuvulinate. *Br J Dermatol*. 2014;171:905–908.
70. Braathen LR, Szeimies RM, Basset-Seguin N, et al. International Society for Photodynamic Therapy in Dermatology. Guidelines on the use of photodynamic therapy for nonmelanoma skin cancer: an international consensus. International Society for Photodynamic Therapy in Dermatology, 2005. *J Am Acad Dermatol*. 2007;56:125–143.
71. Eisen DB, Asgari MM, Bennett DD, et al. Guidelines of care for the management of actinic keratosis. *J Am Acad Dermatol*. 2021;85:e209–e233.



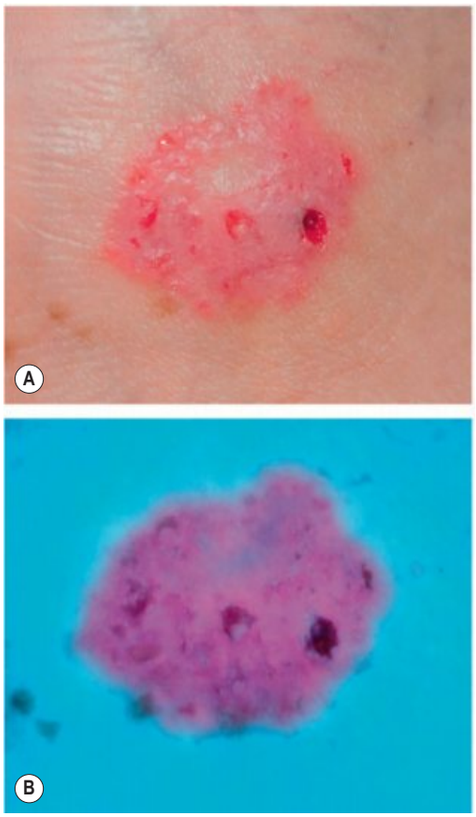
eFig. 135.1 Chemical structure of ALA-based photosensitization for PDT. A 5-aminolevulinic acid (ALA). **B** Methyl aminolevulinate (methyl-esterified ALA; mALA). **C** Protoporphyrin IX (PpIX). Me, methyl; Pr, propionic acid; Vi, vinyl.



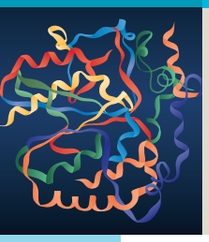
eFig. 135.2 Photodynamic therapy (PDT) of facial actinic keratoses. A Pre-treatment. **B** Three months following PDT utilizing topical methyl aminolevulinate (mALA; 3 hours under occlusion) plus irradiation with red light from an LED (light-emitting diode), resulting in clearing of lesions.



eFig. 135.3 Photodynamic therapy (PDT) of a superficial basal cell carcinoma (BCC). A Superficial BCC prior to treatment. **B** Two years following PDT utilizing topical methyl aminolevulinate (mALA; 3 hours under occlusion) plus irradiation with red light from an LED (light-emitting diode; 37 J/cm^2), with complete clinical resolution.



eFig. 135.4 Fluorescence of intratumor protoporphyrin IX (PpIX) when illuminated by a Wood's lamp (365 nm). A Superficial basal cell carcinoma (BCC). **B** Following application of topical methyl aminolevulinate (mALA) for 3 hours under occlusion, the BCC demonstrates selective pink–red fluorescence due to accumulation of PpIX.



136 Lasers and Other Energy-Based Technologies – Principles and Skin Interactions

Fernanda H. Sakamoto, Mathew M. Avram and R. Rox Anderson

Chapter Contents

Lasers 2390
Skin Optics 2390
Thermal Interactions 2392
Selective Photothermolysis 2393
Photomechanical Effects 2393
Cooling for Skin Protection 2393
Applications of Laser Principles 2393
Principles of Laser Safety 2397
Non-Laser Energy Sources 2397
Future Directions 2398

Acronym: ■ LASER – light amplification by stimulated emission of radiation

Key features

- Laser surgery works via precise tissue heating when optical energy is absorbed within the skin
- Heat is created exactly where light is absorbed by molecules called chromophores
- The major chromophores for visible and near-infrared light are melanin and hemoglobins; water and fat are major mid- and far-infrared chromophores
- Red and near-infrared wavelengths are deeply penetrating
- Wavelength(s) of lasers or intense pulsed light (IPL) sources are often matched for absorption by chromophores in skin targets such as blood vessels, hair follicles, melanin-containing cells, tattoo ink, or tissue layers
- Selective heating and damage of targets can occur when a pulse of selectively absorbed light is delivered faster than the targets can cool by heat conduction
- The time for a tissue target to cool is its thermal relaxation time, equal in seconds to approximately the square of the target size in millimeters
- Very short (nanosecond) laser pulses, produced by Q-switched lasers, and picosecond laser pulses can precisely damage small targets such as individual melanocytes and tattoo ink particles
- Millisecond lasers and IPL sources selectively affect multicellular targets such as blood vessels, hair follicles, and tissue layers
- Fractional laser treatments create an array of microscopic thermal injury zones
- Radiofrequency electrical current, traditionally used for skin surgery, has been re-configured for a esthetic applications
- High-intensity, focused ultrasound can heat a precise focus within or below the skin
- By crystallizing lipids, controlled cooling (cryolipolysis) can reduce localized subcutaneous fat
- Laser microscopy of intact living skin is an emerging diagnostic tool

INTRODUCTION

The last century took us from Einstein's insight into the quantum nature of light, to the invention of the ruby laser in 1960, to the wide spectrum of lasers available today. In particular, the principle of selective photothermolysis guided the development of pulsed lasers that target specific skin structures such as blood vessels, melanosomes, tattoo ink, and hair follicles. Flashlamps, also called intense pulsed light (IPL) sources, can mimic these lasers to some extent. In contrast, fractional photothermolysis uses thousands of microscopic zones of thermal injury to stimulate skin remodeling. Additional energy-based technologies include focused ultrasound, radiofrequency electric current, pulsed electromagnetic field therapy, and controlled skin cooling. The field of energy-based treatments is dynamic, and a steady source of innovation.

LASERS

LASER is an acronym for *l*ight *a*mplification by *s*timulated *e*mission of *r*adiation. It is a physical process that can be explained by Einstein's principles of electromagnetic radiation[1]. The quantum unit of electromagnetic energy is a photon, and stimulated emission occurs when one photon stimulates an excited atom to emit a second, identical photon. The idea of lasers was envisioned by Charles Townes and colleagues[2], and in 1960 the first laser, utilizing a flashlamp-excited ruby crystal, was introduced[3]. Soon thereafter, Leon Goldman[4] initiated dermatologic applications of laser technology.

All lasers have four essential components (Fig. 136.1): (1) a gas, liquid, or solid medium that can be excited to generate light (Table 136.1); (2) a source of "pump" energy for exciting the medium; (3) mirrors at the end(s) which form an optical cavity that favors the amplification process; and (4) a delivery system. Light is amplified as it travels back and forth between the laser's mirrors thereby generating a very high intensity laser beam.

Laser light has several properties that are different from other light sources. *Monochromaticity* refers to emission of a well-defined wavelength, rather than a band of wavelengths. *Coherence* describes light waves that travel in phase, both in time and space, similar to a column of soldiers marching in step. *Collimation* refers to a very parallel beam of light. Coherence and collimation allow lasers to be focused to very small spot sizes (see Fig. 136.1).

Lasers may emit a continuous beam or pulses of light, with nearly all dermatologic lasers currently in use emitting pulsed light. Q-switched lasers produce short pulses at very high peak power. "Q" refers to a quality factor for light traveling across the laser cavity, which can be changed suddenly, i.e. "switched", to produce a short, intense burst of light. Dermatologic Q-switched lasers are designed to produce pulses of ~1–100 nanoseconds, with fluence (the energy delivered per unit area) typically in the 2–10 J/cm^2 range. These short, high-power pulses are particularly useful for selective removal of tattoos and pigmented lesions while limiting thermal damage to surrounding tissues[5]. The repetition rate for pulsed lasers is expressed in hertz (Hz). Of note, some lasers emit a rapid train of low-energy pulses that behave surgically like continuous-wave lasers and are called quasicontinuous.

SKIN OPTICS

At the skin surface, 4%–7% of light of all wavelengths is **reflected** because of the change in refractive index between air (n=0) and stratum corneum (n=1.45)[6]. This is termed Fresnel reflectance because it follows Fresnel's equations relating reflectance to the angle of incidence, plane of polarization, and refractive index[7]. The remaining 93%–96% of incident light enters the skin, where it is **scattered** and/or **absorbed** (Fig. 136.2). Scattering occurs when photons "bounce" off particles and

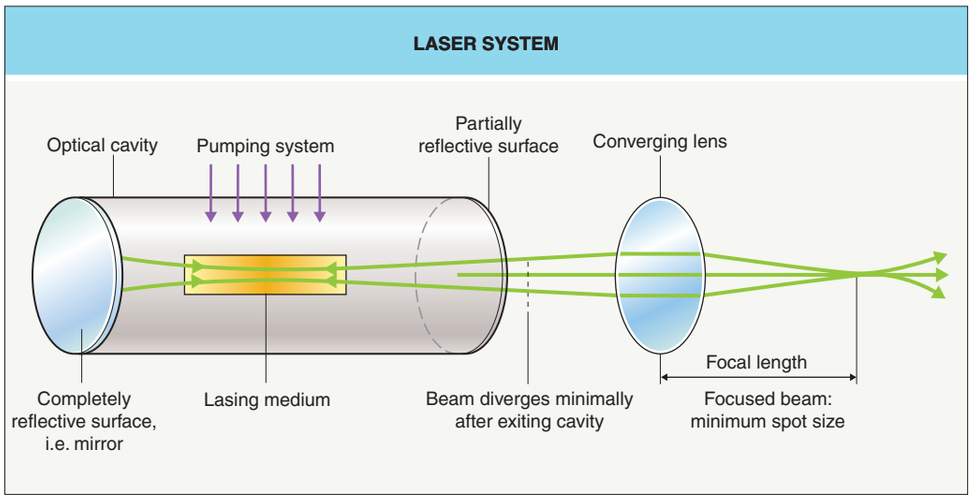


Fig. 136.1 Laser system. The pumping system stimulates the lasing medium to emit photons. The mirrors at the ends of the cavity reflect this light back and forth along one axis, leading to amplification of the stimulated emission process; one of the mirrors is only partially reflective, allowing the laser light to exit. Lasers produce beams of light with low divergence (spread) that are close to being collimated (i.e. parallel light waves). This then allows the beam to be tightly focused by a converging lens or mirror as focusing is required to produce a specific spot size.

TYPES OF LASER MEDIA

Gas	Liquid	Solid
Argon Carbon dioxide Copper vapor Helium–neon Krypton Xenon chloride*	Rhodamine dye dissolved in organic solvent†	Crystal • Alexandrite • Erbium-doped yttrium aluminum garnet (YAG) • Holmium-doped YAG • Neodymium-doped YAG • Potassium titanyl phosphate • Ruby Semiconductor • Diode (e.g. aluminum gallium arsenide)

*In excimer lasers.
†In pulsed dye lasers.

Table 136.1 Types of laser media. Lasers are often named for the medium contained within their optical cavity.

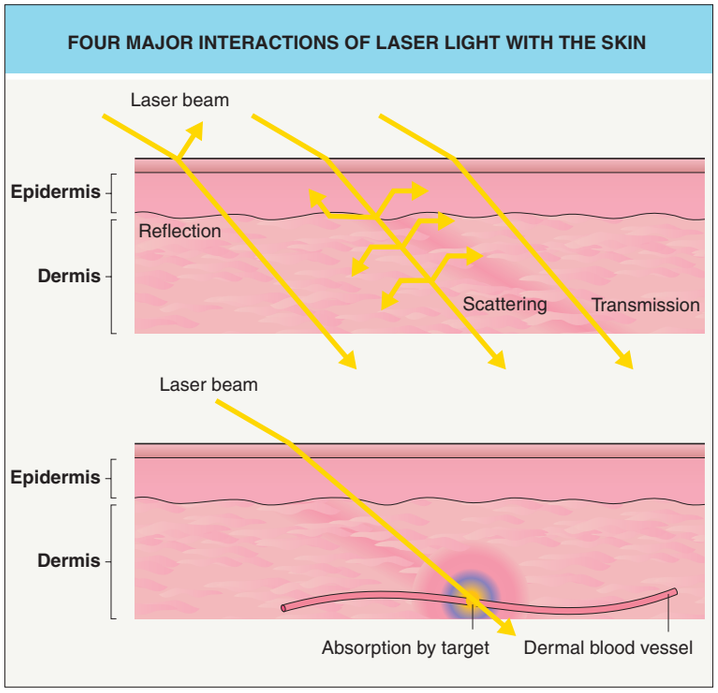


Fig. 136.2 Four major interactions of laser light with the skin. These are reflection, scattering, transmission, and absorption.

fibers within the skin, leading to diffusion of the incoming beam of light and limiting its depth of penetration. The *absorption coefficient* of any material is defined as the probability per unit path length that a photon at a particular wavelength will be absorbed, and it depends

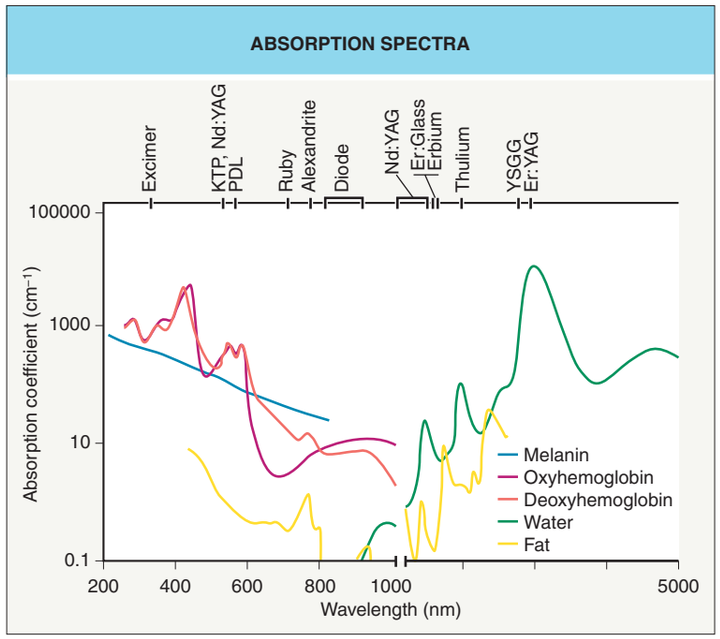


Fig. 136.3 Absorption spectra. The heterogeneous absorption spectra of chromophores allow selective photothermolysis to work. Er, erbium; KTP, potassium titanyl phosphate; Nd, neodymium-doped; YAG, yttrium aluminum garnet; PDL, pulsed dye laser; YSGG, yttrium scandium gallium garnet.

on the concentration of chromophores (absorbing molecules) present. After the energy of the photon is absorbed by the chromophore, heat or photochemical reactions lead to tissue effects.

The four primary skin chromophores are water, lipids, hemoglobin, and melanin (Fig. 136.3). Chromophores exhibit characteristic bands of absorption at certain wavelengths. It is this fact that allows for the delineation of specific targets for different laser wavelengths. While melanin absorbs broadly across the visible and ultraviolet (UV) spectrum, oxyhemoglobin and reduced hemoglobin in blood exhibit strong bands in the UV, blue, green, and yellow regions. Water and lipids have strong absorption in the infrared (IR) region (Fig. 136.4).

Optical properties of the epidermis and dermis are different. In pigmented epidermis, melanin absorption is usually the dominant process over the majority of the optical spectrum (200–1000 nm) (see Fig. 136.3). In the dermis, there is strong, wavelength-dependent scattering by collagen fibers, which attenuates penetration of light. This scattering varies inversely with wavelength. In general, between 280 and 1300 nm, the depth of penetration increases with wavelength (Fig. 136.5). Beyond 1300 nm, penetration decreases due to the absorption of light by water. The most deeply penetrating wavelengths are 650–1200 nm, while the least penetrating wavelengths are within the UV and IR regions.

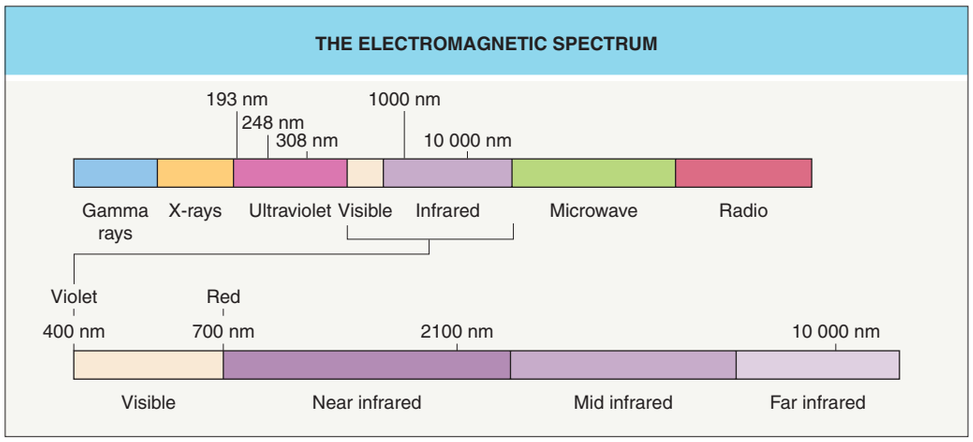


Fig. 136.4 The electromagnetic spectrum. The visible component is only a small portion of the spectrum.

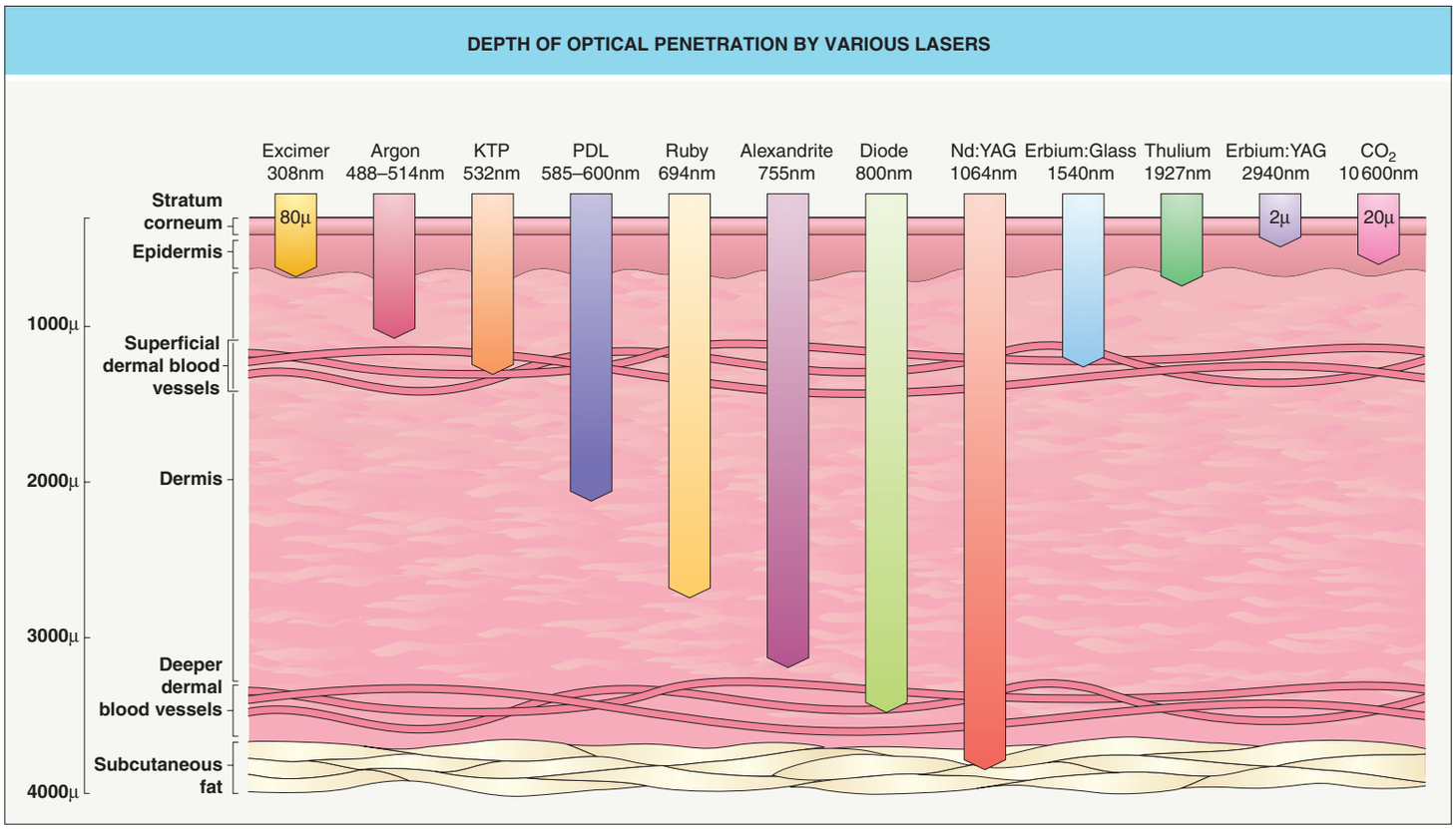


Fig. 136.5 Depth of optical penetration by various lasers. Optical penetration of about 50% of the light. It should be noted that the treatment depth can greatly exceed the optical penetration depth for ablative lasers. For example, the depth of optical penetration for CO_2 lasers is only ~20 microns, but fractional CO_2 lasers can vaporize nearly full-thickness microchannels through the dermis. KTP, potassium titanyl phosphate; μ, microns; Nd, neodymium; PDL, pulsed dye laser; YAG, yttrium aluminum garnet.

THERMAL INTERACTIONS

Most laser interactions involve heat. As temperature is raised, essential macromolecules are denatured including proteins, DNA, RNA, and cell membranes, leading to loss of function. Thermal coagulation yields cell necrosis and, if widespread, a burn. Laser skin surgery requires precise control over the placement and amount of heat-induced injury.

Most human cells can easily withstand temperatures up to 40°C. Cellular survival is dependent upon both exposure time and temperature. In most organisms, exposure to sub-lethal heat induces a cellular reaction termed the heat shock response. Normal protein synthesis is replaced by synthesis of proteins called heat shock proteins; the latter confer some resistance to thermal injury[8]. Laser-induced thermal injury is well described by an Arrhenius model[9] – the rate of denaturation is exponentially related to temperature. Thus, accumulation of denatured material rises exponentially with temperature and proportionally with time[10]. Near a critical temperature (which is different for different tissues), rapid coagulation occurs; this is what accounts for the well-defined histologic boundaries of dermal coagulation in laser and other burn injuries. In the dermis, type I collagen plays a primary role in thermal coagulation, whereas elastin is extremely thermally stable and can survive boiling without apparent injury. Fibrillar type I dermal collagen has a sharp melting and shrinkage transition at 60–70°C. At or above this temperature range, scarring becomes more likely. Selective photothermolysis permits selected heating of targets within the dermis, such as blood vessels or hair follicles, with preservation of dermis between targets. However, even with selective photothermolysis, there is an absolute need to keep the bulk skin temperature well below ~60–70°C. Clinically, immediate skin responses can indicate localized thermal damage or excessive and non-selective unwanted damage[11,12].

When laser light, intense pulsed light (IPL), radiofrequency (RF), ultrasound, or other form of energy is absorbed by tissue, heat is produced locally which immediately begins to diffuse into the surrounding tissue.

PULSE DURATIONS AND TARGETS OF SELECTIVE PHOTOTHERMOLYSIS			
Chromophore	**Diameter**	**TRT**	**Typical laser pulse duration**
Tattoo ink particle	0.01–0.5 micron	100 ps–250 ns	300 ps–50 ns
Melanosome	0.5 micron	250 ns	10–100 ns
PWB vessels	30–100 microns	1–10 ms	0.4–20 ms
Terminal hair follicle	300 microns	100 ms	3–100 ms
Leg vein	1 mm	1 s	0.1 s

Table 136.2 Pulse durations and targets of selective photothermolysis. m, milli; n, nano; p, pico; s, second; PWB, port-wine birthmark; TRT, thermal relaxation time.

Heat diffusion via conduction is also called thermal relaxation. *Thermal relaxation time* (TRT) is defined, for a given tissue structure, as the time required for the heated tissue to cool halfway towards its initial temperature. The key to clean ablation of tissue is to ablate it quickly, before much heat is conducted into surrounding tissue[13].

SELECTIVE PHOTOTHERMOLYSIS

The concept of selective photothermolysis[14] first arose to guide the design of a laser for treating pediatric port-wine birthmarks. Selective, localized heating (with focal destruction of "target" structures) is achieved by a combination of selective light absorption and a *pulse duration shorter than or approximately equal to the TRT of the targets*. Choice of wavelength(s) must correspond to absorption by chromophores within the skin targets. The wavelength must also penetrate to the anatomic depth of the skin targets.

The TRT of a target is proportional to the square of its size (Table 136.2). Thus, for a given material and shape, an object half the size will cool in one-quarter of the time. For most tissue structures, TRT (in seconds) is approximately equal to the square of the target dimension (in millimeters). Shape also affects TRT, and for a given thickness, planes cool faster than spheres. In general, the optimal pulse duration for *selective photothermolysis* is approximately equal to the TRT. Selective photothermolysis typically utilizes pulsed (rather than continuous) sources[15]. Blood vessels encompass a wide range of TRTs, including capillaries (tens of microseconds), large venules of adult port-wine birthmarks (up to tens of milliseconds), and telangiectasias and leg veins (hundreds of milliseconds). Small, pigmented targets (e.g. melanosomes within melanocytes in a nevus of Ota, tattoo ink particles within fibroblasts) are best treated with short (sub-microsecond) pulses, while larger pigmented targets (e.g. hair follicles) have longer TRTs and are best treated with longer (millisecond) pulses[16].

The potential for targeting intracellular particles and structures is increasing as lasers with even shorter pulses, e.g. picosecond (10^{-12} second) or femtosecond (10^{-15} second), are becoming available for medical use. At the extremely high intensity of femtosecond lasers, molecules can simultaneously absorb more than one photon, which opens the door to very precise sub-surface tissue cutting without thermal damage, as well as UV-like photochemistry triggered deep within the tissue. Femtosecond lasers are already in use for precise cornea surgery.

PHOTOMECHANICAL EFFECTS

Pulsed lasers can also cause mechanical effects[17]. Sudden heating induces thermal expansion with consequent acoustic and/or shock waves that can rupture or increase permeability of cell membranes. Cavitation, the violent formation and collapse of steam bubbles, may also occur. Examples of mechanical injury are purpura due to vessel rupture from pulsed dye lasers emitting pulses less than ~10 milliseconds[18], and tattoo ink particle fracture from lasers emitting picosecond pulses.

A number of parameters control laser–tissue effects, including wavelength, fluence, irradiance, spot size, and pulse duration (Table 136.3). With smaller spot sizes, scattering leads to a greater loss of photons from the beam as it penetrates the skin, as compared to larger spot sizes. The greatest effective penetration depth into skin occurs with the combination of a penetrating wavelength (600–1300 nm; see Fig. 136.5) and a large spot size.

USEFUL LASER TERMS		
Term	**Definition**	**Unit**
Energy	Fundamental unit of work	Joules (J)
Power	Rate at which energy is delivered	Watts (W)
Fluence	Amount of energy delivered per unit area	J/cm^2
Irradiance	Power delivered per unit area	W/cm^2
Pulse duration (pulse width)	Laser exposure duration	Seconds (s)
Spot size	Diameter of the laser beam on the skin surface	mm
Chromophore	Medium that absorbs light	
Thermal relaxation time	Time required for heated tissue to lose 50% of its heat through diffusion	Seconds (s)

Table 136.3 Useful laser terms.

COOLING FOR SKIN PROTECTION

Epidermal melanin is an undesired chromophore when treating dermal targets. Epidermal damage can be minimized through the use of skin cooling, which is especially important with darkly pigmented skin. All cooling methods extract heat at the skin surface via a cooling agent (gas, liquid, or solid). For dynamic cryogen spray cooling, a very cold *liquid* fluorocarbon is sprayed onto the skin. *Solid* contact cooling typically consists of a cold sapphire window held against the skin, through which laser or IPL energy is delivered. Cold *air or* cold *gels* can also be used for skin cooling.

The terms precooling, parallel cooling, and postcooling refer to cooling before, during, and after the laser exposure, respectively[19]. For pulse durations shorter than ~5 milliseconds (e.g. from many pulsed dye and all Q-switched lasers), there is not enough time for parallel cooling to extract much heat, but precooling provides some protection. For short-pulsed lasers, cryogen spray cooling represents the most aggressive and effective form of precooling. Parallel cooling is effective for pulses longer than ~5 milliseconds. Bulk skin cooling before and after laser treatments (e.g. with ice or cold air) is useful for minimizing pain, erythema, and edema[16].

APPLICATIONS OF LASER PRINCIPLES

Currently available medical lasers are outlined in Table 136.4 and their applications are discussed in Chapter 137.

Ablative (Vaporizing) Skin Resurfacing

The ablative lasers are far-IR CO_2 (10 600 nm) or erbium (Er:YAG: 2940 nm) devices which emit wavelengths strongly absorbed by water. Pulsed and/or scanned focused beams are used to precisely vaporize superficial tissue, causing a "plume" of material leaving the skin. Most of the heat is removed during vaporization, but a thin layer of residual thermal damage remains that is useful for hemostasis. Laser resurfacing is very useful for treating photoaging, scars, and lesions such as epidermal nevi and seborrheic keratoses. Resurfacing removes the old epidermis and stimulates contraction and remodeling of the dermis for many months after treatment. Being a controlled partial-thickness burn, meticulous technique and wound care are important in order to avoid infection and other complications. Scarring, transient hyperpigmentation, delayed-onset permanent hypopigmentation, prolonged erythema, and bacterial, viral, and fungal infections have been reported after laser resurfacing[20].

Interactions During Treatment of Vascular Lesions

Oxyhemoglobin has an absorption band at 577 nm, within the yellow spectrum (see Fig. 136.3). Yellow, flashlamp-pumped *pulsed dye lasers* (PDLs) that emit 0.45 to 40 millisecond pulses of 585–600 nm light are therefore frequently used to treat microvascular lesions; 532 nm green lasers and some IPLs represent alternatives. Most port-wine birthmarks require six or more treatments in order to achieve stable improvement, and only a minority can be fully removed. Treatment is more effective before 6 months of age, and resistance may be due in part to vessels deeper than 1.5 mm (see Fig. 136.5). For the treatment of deeper vessels,

LASERS IN MEDICINE							
Laser	**Wavelength (nm)**	**Mode**	**Average power (W)**	**Average energy per pulse (J)**	**Pulse duration (sec)**	**Pulse rep. rate (Hz)**	**Target chromophore**
Excimer (ArF)	193	Pulsed	10	0.1	10^{-8}	100	Proteins
Excimer (XeCl)	308	Pulsed	10	0.1	10^{-7}	100	Proteins
Argon	488, 514	CW	1–10				Hemoglobins, melanin
Copper vapor	511, 578	Quasi-CW	1–10	10^{-3}	10^{-8}	2×10^{3}	Hemoglobins, melanin
KTP	532	Quasi-CW	1–10	10^{-4}	10^{-8}	104	Hemoglobins, melanin
Q-switched, frequency-doubled Nd:YAG	532	Pulsed (ns)	1–3	0.2^{-1}	10^{-8}	5–10	Melanin, red tattoos
Pulsed dye	585–600	Pulsed	10	5	$(0.45–40) \times 10^{-3}$	2	Hemoglobins
Argon dye	630	CW	0.5–2				Photosensitizing drugs
Ruby	694	Pulsed	30	30	10^{-3}	1	Melanin
Q-switched ruby	694	Pulsed (ns)	2	2	3×10^{-8}	1	Melanin, black and green tattoos
Alexandrite	755	Pulsed	30	30	10^{-3}	1	Melanin, deoxyhemoglobin
Q-switched alexandrite	755	Pulsed	5	0.5–5	10^{-7}	1–10	Melanin, black and green tattoos
Picosecond alexandrite	755	Pulsed	2	0.5	7.5×10^{-10}	1–10	Melanin, black and green tattoos
Diode (AlGaAs)	~800	CW/pulsed	5–3000	5–100	$(5–400) \times 10^{-3}$	1–2	Melanin, hemoglobins
Nd:YAG	1064	CW	10–100				Hemoglobins
Q-switched Nd:YAG	1064	Pulsed (ns)	5–10	1	10^{-8}	5–10	Black tattoos
Long-pulsed Nd:YAG	1064	Pulsed	1–50	1–50	$(1–200) \times 10^{-3}$	0–10	Hemoglobins, melanin
Picosecond Nd:YAG	1064*	Pulsed	5	0.5	4×10^{-10}	1–10	Melanin, black and red tattoos
Long-pulsed Nd:YAG	1320	Pulsed	1–50	1–50	$(1–200) \times 10^{-3}$	0–10	Water
Diode	1450	Pulsed	10–15	10–15	0.15–0.25	1	Water
Erbium:glass	1540	Pulsed	10	5	1×10^{-3}	2	Water
Fiber or Diode	1726	Pulsed	~70 ~40	~7 ~2	0.05–0.1	10	Sebum lipids
Holmium:YAG	2000	Pulsed	5–100	0.2–5	10^{-3}	10–20	Water
Erbium:YAG	2940	Pulsed	10–20	0.1–3	$(3–100) \times 10^{-4}$	5–100	Water
Carbon dioxide	10600	CW/pulsed	1–500	0.05–0.5	10^{-5}–10^{-3}	10^{2}–10^{4}	Water

*Also 532 nm.

Table 136.4 Lasers in medicine. AlGaAs, aluminum gallium arsenide; ArF, argon fluoride; CW, continuous wave; KTP, potassium titanyl phosphate; Nd, neodymium; ns, nanosecond; XeCl, xenon chloride; YAG, yttrium aluminum garnet.

high-fluence, millisecond-domain *alexandrite* lasers (755 nm) can be employed and they are particularly effective for treating hypertrophic and/or PDL-resistant vascular lesions. Given the absorption band of reduced hemoglobin at 760 nm, alexandrite lasers are also useful for treating venous malformations, labial venous lakes, and hypertrophic port-wine birthmarks. Other lasers with wavelengths in the near-IR range (e.g. 980 nm and 810 nm diode lasers) have been utilized to target larger, deeper vessels (e.g. venous malformations).

Currently, the 585–600 nm flashlamp-pumped PDL is a standard treatment for cutaneous microvascular lesions including port-wine birthmarks, telangiectasias, erythematous scars, and when indicated, hemangiomas. The treatment fluence is decreased for more darkly pigmented skin. The principal side effect is purpura, which is dependent on pulse duration, fluence, and spot size[21]. Purpura is the result of microvascular hemorrhage, subsequent thrombosis, and delayed appearance of vasculitis. When the pulse duration exceeds ~20 milliseconds, there is little or no immediate purpura because cavitation and vessel rupture are avoided. It should be noted, however, that even when no immediate post-treatment purpura is observed, delayed purpura can still occur due to a phase of vasculitis several days after treatment[22]. *Potassium titanyl phosphate* (KTP) lasers, with a wavelength of 532 nm and variable pulse durations in the millisecond domain, are also used to treat vascular lesions. In general, there is less resultant purpura than with PDLs (see Fig. 137.2). When combined with parallel skin cooling windows, these lasers can be very versatile.

Filtered xenon flashlamps, which emit a wide range of wavelengths, serve as sources of IPL. Compared with most vascular lasers, IPL is less selective and less powerful but is still useful for selective photothermolysis of telangiectasias and poikiloderma. IPL sources typically deliver a large, uniform, rectangular exposure spot. For removal of lentigines, the telangiectasias of rosacea and poikiloderma of Civatte, or dark terminal hairs in fair-skinned individuals, IPL provides a good alternative to lasers. However, for treatment of entities that require very short pulses, e.g. tattoos or nevus of Ota, IPL should not be used.

Interactions During Treatment of Pigmented Lesions and Tattoos

Melanosomes are melanin-containing organelles that range from ~0.3–1 micron in size, and they can act as a primary target for selective photothermolysis of pigmented lesions[23]. Melanin has a broad absorption spectrum (see Fig. 136.3), which lends itself to possible targeting by a wide range of lasers[24]. Choice of treatment wavelength is based on avoiding absorption by other chromophores and on matching the depth of light penetration to the depth of the lesion. In general, red and near-IR lasers are the most selective and penetrating devices for pigment cell targeting. The TRT of melanosomes is about 70–250 nanoseconds[14], making Q-switched lasers an excellent choice for targeting melanosomes. When the fluence threshold for melanosome disruption is reached, the melanin-containing cell dies, and Q-switched lasers are able to selectively target individual pigmented cells. If the goal is to also remove adjacent, non-pigmented cells (e.g. during hair removal), millisecond pulses are used in order to allow heat transfer from pigmented to adjacent non-pigmented cells.

Treatment of tattoos with Q-switched nanosecond or picosecond lasers fragments the ink particles and selectively kills pigment-containing cells, with resultant ink particle release. Subsequent removal



Fig. 136.6 Histologic findings following ablative fractional photothermolysis. A microthermal zone (MTZ) of injury (arrow) is apparent after use of a CO_2 laser (10 600 nm) at 100 mJ/pulse. E, epidermis; D, dermis. *Courtesy Wellman Center for Photomedicine, Massachusetts General Hospital, Harvard Medical School.*

of tattoo ink particles can occur via an epidermal crust and/or lymphatic transport while some particles are rephagocytosed by dermal cells[25]. Of note, different laser wavelengths are needed for different ink colors (see Table 136.4). Picosecond (10^{-12} sec) laser pulses have long been known to be more effective than nanosecond pulses for pulverizing tattoo ink particles[26] and are now commercially available[27]. With shorter pulse durations, photoacoustic effects may be greater and photothermal effects reduced, providing a possible explanation for less inflammation and less postinflammatory hyperpigmentation.

Q-switched ruby and *alexandrite* lasers are very useful for epidermal and dermal pigmented lesions (e.g. lentigines, nevus of Ota) as well as for black and green tattoos (see Ch. 137). Café-au-lait macules and melanocytic nevi may respond to treatment with Q-switched ruby lasers (or, for nevi, long-pulsed ruby lasers that target nests of melanocytes), but recurrences are common and residual dermal melanocytes remain in laser-treated nevi[28,29]. Laser treatment of congenital melanocytic nevi is usually considered when surgical options are limited. However, laser removal of acquired melanocytic nevi is quite controversial given the potential risk for partial removal of a subtle early melanoma. Of note, postinflammatory hyperpigmentation and melasma respond poorly to laser treatment[30].

The *Q-switched Nd:YAG* laser emits at 1064 nm, with typical pulse durations of 10 nanoseconds. Its primary use is in the treatment of black tattoos and dermal melanocytoses such as nevus of Ota in highly pigmented skin. Frequency-doubling to produce 532 nm visible green light is generally available in the same device, which can effectively remove epidermal melanin pigment as well as red tattoos.

Interactions During Hair Removal

Permanent reduction of pigmented hairs is currently the most popular medical laser procedure. By damaging stem cells in the outer root sheath and/or dermal papilla, high-energy, millisecond-domain pulses at wavelengths in the red to near-IR region of the spectrum are highly effective. *Ruby*, *alexandrite*, *diode*, and *Nd:YAG* lasers are all used for this purpose, and IPL sources are also effective. However, due to the paucity of melanin, none of these devices work well for blonde or white hair. Since light must first travel through the pigmented epidermis to reach hair follicles, skin cooling is essential for safe permanent reduction of hair in individuals with darkly pigmented skin. The primary mechanism for *temporary* hair loss is induction of catagen, which can occur at low fluences whereas higher fluences produce enough follicular injury to cause permanent miniaturization or degeneration of terminal hair follicles. Low-energy IPL devices and an 810 nm diode laser source intended for home use are also available[31]. For unknown reasons, paradoxical hypertrichosis due to stimulation of a vellus-to-terminal hair transition can occur after laser or IPL treatments, particularly on the face of Mediterranean women.

Non-Ablative Skin Rejuvenation

Non-ablative facial rejuvenation for the treatment of fine lines and non-dynamic rhytides uses mid-IR lasers (e.g. 1320 nm Nd:YAG, 1450 nm diode, 1540 nm erbium:glass) whose wavelengths are weakly absorbed by water. These lasers work via thermal effects on the dermis, presumably stimulating a wound healing response. Responses to non-ablative rejuvenation are usually gradual and subtle, and well-controlled studies are lacking.

Fractional Photothermolysis

Fractional photothermolysis (FP) represents a treatment strategy in which numerous small zones of thermal injury are created (Fig. 136.6), stimulating turnover and remodeling of both the epidermis and dermis[32]. *Non-ablative* FP uses focused, mid-IR, laser microbeams to create a pixelated pattern of microscopic columns of thermal damage, called microthermal treatment zones (MTZs). Typically, ~1 million MTZs are placed per full-face treatment. Density (percentage of skin treated) and depth of thermal damage are separately controlled. The energy delivered per MTZ accurately controls the depth of treatment which is typically up to ~2 mm, i.e. well into the reticular dermis. In general, the depth of thermal damage should correlate with the depth of skin pathology being treated, e.g. a greater depth for hypertrophic scars than for atrophic scars[33].

Tissue spared around each MTZ initiates rapid repair and stimulates remodeling. Desquamation of the epidermal portion of each MTZ removes some basal layer pigment and a small amount of papillary dermal debris. Non-ablative FP has been reported to improve several skin conditions including scars, fine rhytides, telangiectasias, dermatoheliosis, and poikiloderma. There are a myriad of commercially available non-ablative, as well as ablative, FP devices (see Ch. 137).

Ablative FP uses carbon dioxide or erbium (Er:YAG) lasers to vaporize many small vertical channels that can extend deeply into the skin. Because remodeling is provided by tissue between the columns of ablation, the depth of ablation can be far deeper than with traditional ablative resurfacing procedures. Care must be taken to avoid scarring, especially in areas where thin skin has limited adnexal structures such as the infraorbital and neck regions. By creating deep channels into the dermis, ablative FP is also an effective mechanism for enhancing topical drug delivery (see below)[34–37].

Clinical applications of fractional lasers include treatment of photoaging, striae distensae, poikiloderma, and scars. Ablative FP has been shown to significantly improve the elasticity and appearance of hypertrophic traumatic or burn scars[38–40]. The mechanisms by which microscale burns within the narrow, deep, FP-induced laser wounds lead to improvement of scars from thermal burns remain largely unknown.

Ablative fractional lasers have been shown to increase topical drug absorption by orders of magnitude, especially for large molecules that are typically excluded from the skin. However, to date, large-scale dose-response and pharmacokinetic data are generally lacking. Nonetheless, laser-assisted drug delivery (LADD) has been broadly utilized as an off-label indication[40a]. Drugs that are cleared for injection or parenteral use are generally safer for LADD than are topical medications, as the latter include vehicles, solvents, or stabilizers that are not intended for entry into the skin[40b]. Further developments will hopefully lead to a reduction in both time for drug metabolism (e.g. topical anesthetics, topical prodrug photosensitizers for photodynamic therapy) and systemic side effects[40a].

Laser-Induced Optical Breakdown (Plasma Formation)

The term plasma is used to describe matter where electrons are stripped away from atoms and molecules, producing free electrons and ions. Natural examples of plasma include lightning, the sun, and a candle flame. The high intensity of a focused, pulsed laser can cause plasma formation. Laser-induced plasmas are commonly used for intraocular surgery, but cutaneous applications have recently been introduced. For example, as a treatment for epidermal pigmented lesions or photoaging, a lens array can be used to focus a picosecond pulsed laser so that it can induce optical breakdown within the epidermis[41,42].

Interactions During Laser Targeting of Lipids and Sebaceous Glands

Lipids absorb near-infrared wavelengths around 915, 1210, 1726, and 2300 nm[43,44]. Despite the depth of subcutaneous fat and sebaceous glands, controlled skin cooling allows selective photothermolysis of these lipid-rich structures[44]. That is, by extracting heat at the skin surface, deeply penetrating wavelengths absorbed by lipids can be used to selectively heat sebaceous glands or subcutaneous fat. Recently, 1726 nm laser devices have been approved to treat mild to severe acne in the US and Europe, with a reported clearance of 40–80% of inflammatory acne for up to 2 years, depending on the device.

Alternatively, for skin structures that lack specific natural chromophores, use of exogenous nanoparticles or microparticles can allow "customized" targeting. For example, in order to target sebaceous follicles, gold microparticles tailored to absorb near-infrared wavelengths have been introduced for acne treatment[45–47]. These particles absorb light very strongly by creating surface plasmon resonance; the latter occurs when the frequency of incoming light matches the frequency for electric currents to resonate in the particle. The particles are forcefully massaged into sebaceous follicles before laser treatment.

Laser-Based Diagnostics

Laser technology has been instrumental in the development of biological microscopy and tissue imaging. Optical coherence tomography (OCT) uses near-IR, low-coherence light for high-resolution cross-sectional imaging of body tissues. OCT is now a standard procedure in ophthalmology and is employed in high-resolution coronary artery imaging. Its use in dermatology is rapidly emerging.

Laser confocal microscopy captures light scattered or emitted from a thin plane "section" inside skin and can be used to delineate tumor margins. Reflectance confocal microscopy is able to view the skin *in vivo* with histology-like resolution down to a depth of ~0.3 mm, whereas OCT is capable of imaging the skin to a depth of ~2 mm. Because histochemical stains are not used, both confocal microscopy and OCT of skin tumors reveal useful diagnostic features that are different from those of conventional histopathology. While confocal microscopy is limited to imaging small areas, OCT generally does not have that limitation. The field of *in vivo* microscopy continues to rapidly advance.

PRINCIPLES OF LASER SAFETY
Potential eye injuries (patients and dermatologists)
Blindness occurs rapidly and painlessly
• Blindness can occur even if only 1% of the beam is reflected into the eye from shiny metal, glass, or plastic surfaces • Highest risk of eye injury and blindness with near-infrared lasers such as Q-switched lasers • Lasers and IPL sources used for hair removal can target the retina and uveal tract • Anterior eye injury from lasers or IPL sources usually occurs with treatment of the lower eyebrow or vascular lesions near the eye (without an eye shield properly in place) • An opaque laser eye shield covering the patient's cornea will not prevent damage if the laser or IPL directly impacts exposed sclera • Long-pulse, near-infrared laser light can penetrate through the eyelid to damage the eye
Prevention of eye injuries
Proper use of laser-protective eyewear (including eye shields)
• Wrap-around glasses and goggles are rated by optical density (OD) at specific wavelengths (corresponding to various lasers): OD=log (1/T), where T is transmittance of light through the eyewear; OD=6 implies transmittance through the goggles is 10^{-6} • After determining wavelength of laser, check goggles for required OD and wavelength ranges of protection (printed directly on eyewear) • For dermatological lasers, proper protection is an OD ≥4 at the wavelength of the laser being used • Color of the goggles is not an indication of protection
Fire hazards
• Drapes, clothing, dry hair, and plastic materials, including endotracheal tubes, can be ignited, especially when oxygen is in use • Greatest risk is with the CO_2 and erbium:YAG lasers used for skin resurfacing and ablative fractional treatments
Prevention of fires
• Remember to place the laser in STANDBY mode when not actually treating the patient • Avoid inadvertently activating the laser foot-switch • Moisten any hair near the treatment field; remove mascara and eye makeup when working around eyelids • Alcohol, acetone or other flammable skin-cleaning solutions must be allowed to completely dry before laser use • Reduce intraoperative oxygen concentration to <40% • A fire extinguisher and water should be readily available
Possible cutaneous burns
• Can occur with essentially all dermatologic laser, IPL, RF, or therapeutic ultrasound devices • Primarily due to improper device, dosimetry, and/or treatment technique
Prevention of cutaneous burns
• Knowledge and careful observation of specific clinical endpoint responses for a particular laser–lesion combination
Inhalation of laser-generated "plume" materials
• Particularly with resurfacing or vaporization of hair during its removal; the latter can release irritating sulfur and other oxides
Prevention of laser "plume" biohazards
• Smoke evacuator and good ventilation are most effective measures • Sub-micrometer surgical filter masks provide some protection when worn properly • Q-switched lasers capture particulate material in plastic cones

Table 136.5 Principles of laser safety. IPL, intense pulsed light; RF, radiofrequency.

PRINCIPLES OF LASER SAFETY

The principles of laser safety are outlined in Table 136.5[48,49].

NON-LASER ENERGY SOURCES

Flashlamps (Intense Pulsed Light)

Filtered xenon flashlamps, also referred to as intense pulsed light (IPL) sources, are used for non-ablative skin rejuvenation, pigmented hair removal, and the treatment of vascular and pigmented lesions. By utilizing filters, different wavelength bands can be chosen, which are delivered in millisecond-domain pulses. Compared with lasers, IPL devices are generally less target-selective, as they emit a wider range of wavelengths and are unable to deliver the very short pulses needed for selective photothermolysis of very small targets such as tattoo ink particles or the melanin-containing cells of nevus of Ota. Attempts to remove tattoos with IPL are inappropriate (despite advertising or FDA approvals to the contrary), as this often leads to burns and/or scarring. In a side-by-side comparative study, IPL was inferior to the PDL for the treatment of port-wine birthmarks. Despite limitations, IPL devices are very versatile and can successfully treat epidermal pigmented lesions, poikiloderma, and telangiectasias.

Photobiomodulation (PBM, also called Low Level Light Therapy; LLLT)

Over the past 50 years, lasers and light-emitting diode (LED) sources have been used for a wide variety of "biostimulation" treatments, mainly outside the US. Of note, moderate irradiances at wavelengths absorbed by cytochromes have long been reported to modulate metabolism in mammals. The FDA mandate to balance risks and benefits is such that devices posing no known risk are sometimes cleared for sale with little or no evidence of efficacy, and many sources sold for PBM do not have specific indications. The FDA has cleared low-power red lasers and/or LEDs (continuous, mW power, 630–800 nm wavelength) for treatment of carpal tunnel syndrome and for stimulating hair growth in patients with androgenetic alopecia, based on evidence from clinical trials[50,51]. Although the latter have shown a statistically significant increase in terminal hair counts relative to placebo, the clinical significance remains to be determined, and the combination of PBM with medical or surgical treatments for hair loss remains largely untested. Nonetheless, scientific and clinical evidence has been mounting in support of PBM having *bona fide* photobiologic effects mediated via mitochondrial activity. Mitochondrial signaling pathways affected by light include those that are redox-sensitive, ATP- and cyclic AMP-dependent, and/or regulated by nitric oxide[52].

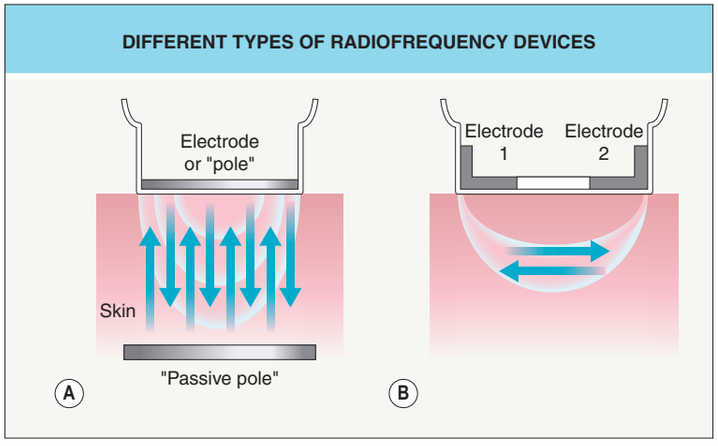


Fig. 136.7 Different types of radiofrequency (RF) devices. A A monopolar RF device has one pole located on the treatment handpiece, while the other (if present at all) is a larger "passive" electrode placed remotely on the patient's body. **B** A bipolar RF device has both poles located within the treatment handpiece and current flows between the electrodes, often in a banana-shaped pattern.

Radiofrequency

Radiofrequency (RF) describes a rapidly alternating electric current that locally heats tissue, based on both local current density and electrical impedance of the tissue. The energy deposited at a certain site is proportional to the local tissue impedance multiplied by the square of the local current density. As the name implies, RF generators operate at frequencies similar to radio bands. The current is delivered from one or more electrodes held in contact or close proximity to the skin. The number of treatment electrodes defines an RF device as monopolar, bipolar, or multipolar. In monopolar RF devices, one pole is located on the treatment handpiece, while the other (if present at all) is a large "passive" electrode placed remotely on the patient's body (Fig. 136.7A). Bipolar and multipolar RF devices have multiple active electrodes that are held against the skin, and current flows between them (Fig. 136.7B). Because electrode size and spacing have a strong influence, the pattern and depth of heating can be adjusted to some extent. Invasive RF needles are also available, which produce a fractional pattern of deep thermal injury.

Unlike most lasers and IPL sources, there is little or no intrinsic selectivity to the deposition of energy from an RF source. The single relevant exception is lipid-rich tissue such as subcutaneous fat, which has substantially higher electrical impedance due to its lower water content. A large RF electrode configured to deliver a current path through subcutaneous fat could, in theory, preferentially heat fibrous septae. This is because the septae carry a higher current density than the fat lobules which surround them. Following large-electrode, monopolar or bipolar RF, cellulite improvement has been described by several authors, but the apparent improvement in appearance does not correspond to fat destruction[53].

While many monopolar and bipolar RF devices have been described for skin "tightening" as well as removal of cellulite or fat, the quality of clinical study-based evidence is generally poor. The RF devices intended for "tightening" are designed to produce partial denaturation of type I collagen, which occurs at temperatures above ~60°C and leads to some immediate tissue contraction and subsequent new collagen synthesis[54]. Because improper electrode contact with skin is a common cause of injury (e.g. burns), some devices have integrated skin cooling systems and/or sensors that monitor proper electrode–skin contact.

At high frequencies, RF can also be transmitted across a dielectric (insulating) material, similar to radio transmissions through air. RF transmission to the skin from an emitting electrode is called capacitive coupling. At the high frequencies utilized with capacitive coupling, a combination of induced current and rotational oscillations in water molecules produces tissue heating[55]. The combination of a bipolar RF device with infrared light sources has been used to treat photoaging and to induce skin tightening[56]. More recently, multiple skin-penetrating RF microneedles have been applied in an array (i.e. a "fractional" fashion) to treat acne scars, photoaging, and striae distensae, as well as for other applications (e.g. skin tightening)[57–60]; however, most of the clinical studies are small with limited follow-up times.

High-Intensity Focused Electromagnetic (HIFEM)

In HIFEM treatments, there is application of low-frequency magnetic field pulses (3–30 Hz) using a non-contact device. The magnetic pulses induce electric currents in tissue that can stimulate action potentials, producing muscle contraction[61]. This therapeutic modality has been used for decades in sports medicine, and nowadays dermatologists are also offering HIFEM treatments for muscle toning and body contouring. Intense exercise or induced muscle contraction can reduce intramuscular fat, but (despite claims) reduction of subcutaneous fat via HIFEM treatments has not yet been proven[62].

Nano-Pulse Stimulation (NPS)

NPS consists of applying high-voltage, nanosecond electrical pulses that are delivered by parallel rows of microneedles inserted into tissue. The electrical pulses porate cellular and organelle membranes, leading to increased intracellular calcium, disruption of ATP production, and consequent cell apoptosis[63,64]. NPS has been investigated for the treatment of seborrheic keratoses[65], sebaceous hyperplasia[66], and viral warts[67], but the potential for causing useful selective and/or sublethal cellular responses remains unclear.

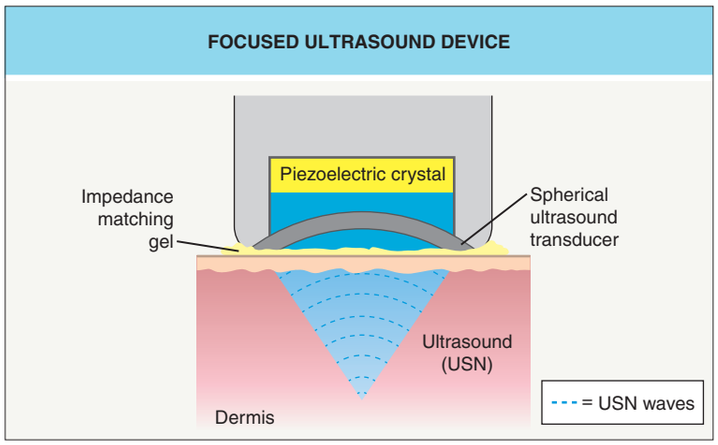


Fig. 136.8 Focused ultrasound device. The ultrasound waves are generated by a piezoelectric crystal. After passing through a spherical ultrasound transducer, they are focused deeper within the skin.

Ultrasound

High-frequency acoustic waves are routinely used for diagnostic medical imaging, at frequencies from ~20 kHz to 10 MHz. Ultrasound is an oscillating pressure (stress) wave that propagates at the speed of sound[68,69], with minimal scattering in soft tissues. This minimal scattering allows the ultrasound waves to be focused deeply within most soft tissues. Intensity is concentrated near the focal point, to the extent that tissue damage can occur by one or more of three mechanisms – heating, cavitation, or shock waves. *Heating* is favored at high ultrasound frequencies while *cavitation* (a rapidly expanding gas bubble) is favored at low ultrasound frequencies; *shock waves* are high pressure, supersonic pressure waves that can be very destructive. Therapeutically, focused ultrasound can be used to destroy targets, such as renal calculi by shock waves, tumors by heating, and thrombi by cavitation, in addition to dermatologic applications. The attenuation (absorption) of ultrasound is greater at higher frequencies, and different materials have different attenuation coefficients[69].

Focused, pulsed ultrasound devices capable of locally destroying subcutaneous abdominal fat have been FDA-cleared for waist circumference reduction (see Ch. 156). In addition, a non-invasive, focused ultrasound device, operating at MHz frequencies, has been FDA-cleared for brow lifts. This device focuses millisecond-domain pulses at the level of the deep dermis and/or superficial fascia, up to a depth of ~4.5 mm (Fig. 136.8). A small focal zone of thermal damage is produced with each pulse, sufficient to achieve tissue contraction at the focus. The treatment transducer is also used for imaging, in order to verify positioning and treatment at the proper tissue plane. This represented the first combined diagnostic and therapeutic ultrasound device for dermatologic use.

Cryolipolysis

Cryolipolysis describes a process in which lipid-rich cells are preferentially affected by cold. Because lipids crystallize at temperatures well above the freezing point of tissue water, lipid-rich cells, including adipocytes and sebocytes, suffer stress and undergo apoptosis (see Ch. 156). Following deep cooling, cold panniculitis occurs (see Ch. 100)[70], eventuating in selective loss of subcutaneous fat tissue[71,72]. Prolonged hypoesthesia is a common side effect when cryolipolysis is employed to remove unwanted subcutaneous fat; the proposed underlying mechanism is damage to the lipid-rich myelin sheaths that surround cutaneous sensory nerves. However, this effect has recently been recognized as a potential treatment for cutaneous pain and pruritus[73].

FUTURE DIRECTIONS

In vivo optical image-guided laser surgery for cutaneous malignancies would be a welcome advance[74]. Currently, dermatologists use histology-guided Mohs micrographic surgery, primarily for the removal of non-life-threatening tumors. Development of a rapid, image-guided version of Mohs micrographic surgery would represent a valuable and improved approach.

Use of Raman spectroscopy to detect inelastic light scattering from molecular vibration modes can provide a "fingerprint" image of a desired molecule, thus allowing precise *in vivo* analysis of the skin[75,76]. It may even be possible to manipulate immunologic responses, e.g. inducing tolerance, preventing inflammation; experimentally, lasers have been used to enhance the immune response to vaccines by increasing antigen-presenting cells[77].

An injectable version of cryolipolysis has been developed that utilizes ice slurries, similar in concept to a physiologic daiquiri. Injected ice slurry has been shown to produce neural selective cryoneurolysis[78] and fat reduction[79]. The same innovation may be useful as a treatment for sleep apnea[80].

A potential improvement in fractional lasers would be the ability to guide the laser microbeam based on skin imaging. For example, the precise texture of the skin could potentially be rewritten by image-guided laser ablation, similar in principle to the precise laser surgery performed to correct refractive power of the cornea.

Fractional lasers can destroy or remove nearly half of the tissue of the skin, followed by rapid healing without a scar, a capability unmatched by any classical surgical tool. However, it is clearly the microscale pattern of injury – not the laser *per se* – that underlies the skin's tolerance to fractional laser treatment. As a result, the general concept of fractional photothermolysis has spawned various other techniques. For example, in patients with photoaging, mechanical removal of full-thickness micro-columns of skin tissue via coring needles has recently been shown to produce similar esthetic results as fractional laser treatment, again with rapid and scar-free healing. Recently, a micro-coring device was FDA-approved for the treatment of lower face photoaging and laxity. Fractional coring needles can also be used to obtain full-thickness skin tissue for grafting, and recently such needle harvesting has been shown to greatly reduce donor site morbidity[81–84].

Lasers and energy-based technologies will forever be an innovative, changing, and integral part of dermatology.

REFERENCES

1. Einstein A. Zur Quantentheorie der Strahlung. *Physiol Z*. 1917;18:121–128.
2. Malt RA, Townes CH. Optical masers in biology and medicine. *N Engl J Med*. 1963;269:1417–1421.
3. Maiman TH. Stimulated optical radiation in ruby. *Nature*. 1960;187:493–494.
4. Goldman L, Blaney DJ, Kindel DJ, Frank EK. Effect of the laser beam on the skin: preliminary report. *J Invest Dermatol*. 1963;40:121–122.
5. Raulin C, Schonermark MP, Greve B, Werner S. Q-switched ruby laser treatment of tattoos and benign pigmented skin lesions: a critical review. *Ann Plast Surg*. 1998;41:555–565.
6. Anderson RR, Parrish JA. The optics of human skin. *J Invest Dermatol*. 1981;77:13–19.
7. Anderson RR. Polarized light examination and photography of the skin. *Arch Dermatol*. 1991;127:1000–1005.
8. Polla BS, Anderson RR. Thermal injury by laser pulses: protection by heat shock despite failure to induce heat-shock response. *Lasers Surg Med*. 1987;7:398–404.
9. Henriques FC. Studies of thermal injury. *Arch Pathol*. 1947;43:489–502.
10. Welch AJ. The thermal response of laser irradiated tissue. *IEEE J Quant Electron*. 1984;20:1471–1481.
11. Wanner M, Sakamoto FH, Avram MM, et al. Immediate skin responses to laser and light treatments: therapeutic endpoints: how to obtain efficacy. *J Am Acad Dermatol*. 2016;74:821–833.
12. Wanner M, Sakamoto FH, Avram MM, Anderson RR. Immediate skin responses to laser and light treatments: warning endpoints: how to avoid side effects. *J Am Acad Dermatol*. 2016;74:807–819.
13. Hruza GJ, Geronemus RG, Dover JS, Arndt KA. Lasers in dermatology–1993. *Arch Dermatol*. 1993;129:1026–1035.
14. Anderson RR, Parrish JA. Selective photothermolysis: precise microsurgery by selective absorption of pulsed radiation. *Science*. 1983;220:524–527.
15. Anderson RR. Laser-tissue interactions. In: Goldman MP, ed. *Cutaneous Laser Surgery*. St Louis: Mosby; 1994:1–17.
16. Anderson RR. Lasers in dermatology – a critical update. *J Dermatol*. 2000;27:700–705.
17. Watanabe S, Flotte TJ, McAuliffe DJ, Jacques SL. Putative photoacoustic damage in skin induced by pulsed ArF excimer laser. *J Invest Dermatol*. 1988;90:761–766.
18. Garden JM, Tan OT, Kerschmann R, et al. Effect of dye laser pulse duration on selective cutaneous vascular injury. *J Invest Dermatol*. 1986;87:653–657.
19. Zenzie HH, Altshuler GB, Smirnov MZ, Anderson RR. Evaluation of cooling methods for laser dermatology. *Lasers Surg Med*. 2000;26:130–144.
20. Nanni CA, Alster TS. Complications of carbon dioxide laser resurfacing. An evaluation of 500 patients. *Dermatol Surg*. 1998;24:315–320.
21. Lanigan SW. Patient-reported morbidity following flashlamp-pumped pulsed tunable dye laser treatment of port wine stains. *Br J Dermatol*. 1995;133:423–425.
22. Waner M, Dinehart SM, Wilson MB, Flock ST. A comparison of copper vapor and flashlamp pumped dye lasers in the treatment of facial telangiectasia. *J Dermatol Surg Oncol*. 1993;19:992–998.
23. Polla LL, Margolis RJ, Dover JS, et al. Melanosomes are a primary target of Q-switched ruby laser irradiation in guinea pig skin. *J Invest Dermatol*. 1987;89:281–286.
24. Murphy GF, Shepard RS, Paul BS, et al. Organelle-specific injury to melanin-containing cells in human skin by pulsed laser irradiation. *Lab Invest*. 1983;49:680–685.

25. Taylor CR, Anderson RR, Gange RW, et al. Light and electron microscopic analysis of tattoos treated by Q-switched ruby laser. *J Invest Dermatol*. 1991;97:131–136.
26. Izikson L, Farinelli W, Sakamoto F, et al. Safety and effectiveness of black tattoo clearance in a pig model after a single treatment with a novel 758 nm 500 picosecond laser: a pilot study. *Lasers Surg Med*. 2010;42:640–646.
27. Ross V, Naseef G, Lin G, et al. Comparison of responses of tattoos to picosecond and nanosecond Q-switched neodymium: YAG lasers. *Arch Dermatol*. 1998;134:167–171.
28. Goldberg DJ. Benign pigmented lesions of the skin. Treatment with the Q-switched ruby laser. *J Dermatol Surg Oncol*. 1993;19:376–379.
29. Grossman MC, Anderson RR, Farinelli W, et al. Treatment of cafe au lait macules with lasers. A clinicopathologic correlation. *Arch Dermatol*. 1995;131:1416–1420.
30. Taylor CR, Anderson RR. Ineffective treatment of refractory melasma and postinflammatory hyperpigmentation by Q-switched ruby laser. *J Dermatol Surg Oncol*. 1994;20:592–597.
31. Wheeland RG. Simulated consumer use of a battery-powered, hand-held, portable diode laser (810 nm) for hair removal: a safety, efficacy and ease-of-use study. *Lasers Surg Med*. 2007;39:476–493.
32. Manstein D, Herron GS, Sink RK, et al. Fractional photothermolysis: a new concept for cutaneous remodeling using microscopic patterns of thermal injury. *Lasers Surg Med*. 2004;34:426–438.
33. Anderson RR, Donelan MB, Hivnor C, et al. Laser treatment of traumatic scars with an emphasis on ablative fractional laser resurfacing: consensus report. *JAMA Dermatol*. 2014;150:187–193.
34. Haak CS, Bhayana B, Farinelli WA, et al. The impact of treatment density and molecular weight for fractional laser-assisted drug delivery. *J Control Release*. 2012;163:335–341.
35. Haak CS, Farinelli WA, Tam J, et al. Fractional laser-assisted delivery of methyl aminolevulinate: impact of laser channel depth and incubation time. *Lasers Surg Med*. 2012;44:787–795.
36. Haedersdal M, Katsnelson J, Sakamoto FH, et al. Enhanced uptake and photoactivation of topical methyl aminolevulinate after fractional CO2 laser pretreatment. *Lasers Surg Med*. 2011;43:804–813.
37. Haedersdal M, Sakamoto FH, Farinelli WA, et al. Fractional CO(2) laser-assisted drug delivery. *Lasers Surg Med*. 2010;42:113–122.
38. Waibel J, Beer K. Fractional laser resurfacing for thermal burns. *J Drugs Dermatol*. 2008;7:59–61.
39. Anderson RR, Donelan MB, Hivnor C, et al. Laser treatment of traumatic scars with an emphasis on ablative fractional laser resurfacing: consensus report. *JAMA Dermatol*. 2014;150:187–193.
40. Seago M, Shumaker PR, Spring LK, et al. Laser treatment of traumatic scars and contractures: 2020 International Consensus Recommendations. *Lasers Surg Med*. 2020;52:96–116.
40a. Haedersdal M, Sakamoto FH, Farinelli WA, et al. Pretreatment with ablative fractional laser changes kinetics and biodistribution of topical 5-aminolevulinic acid (ALA) and methyl aminolevulinate (MAL). *Lasers Surg Med*. 2014;46:462–9.
40b. Labadie JG, Ibrahim SA, Worley B, et al. Evidence-based clinical practice guidelines for laser-assisted drug delivery. *JAMA Dermatol*. 2022;158:1193–1201.
41. Tanghetti EA. The histology of skin treated with a picosecond alexandrite laser and a fractional lens array. *Lasers Surg Med*. 2016;48:646–652.
42. Balu M, Lentsch G, Korta DZ, et al. In vivo multiphoton-microscopy of picosecond-laser-induced optical breakdown in human skin. *Lasers Surg Med*. 2017;49:555–562.
43. Anderson RR, Farinelli W, Laubach H, et al. Selective photothermolysis of lipid-rich tissues: a free electron laser study. *Lasers Surg Med*. 2006;38:913–919.
44. Sakamoto FH, Doukas AG, Farinelli WA, et al. Selective photothermolysis to target sebaceous glands: theoretical estimation of parameters and preliminary results using a free electron laser. *Lasers Surg Med*. 2012;44:175–183.
45. Paithankar DY, Sakamoto FH, Farinelli WA, et al. Acne treatment based on selective photothermolysis of sebaceous follicles with topically delivered light-absorbing gold microparticles. *J Invest Dermatol*. 2015;135:1727–1734.
46. Fuchs CSK, Bay C, Adatto M, et al. Acne treatment with light absorbing gold microparticles and optical pulses: an open-label European multi-centered study in moderate to moderately severe acne vulgaris patients. *Lasers Surg Med*. 2019;51:686–693.
47. Fuchs CSK, Ortner VK, Mogensen M, et al. Transfollicular delivery of gold microparticles in healthy skin and acne vulgaris, assessed by in vivo reflectance confocal microscopy and optical coherence tomography. *Lasers Surg Med*. 2019 https://doi.org/10.1002/lsm.23076.
48. Hammes S, Augustin A, Raulin C, et al. Pupil damage after periorbital laser treatment of a port-wine stain. *Arch Dermatol*. 2007;143:392–394.
49. Chuang GS, Farinelli W, Christiani DC, et al. Gaseous and particulate content of laser hair removal plume. *JAMA Dermatol*. 2016;152:1320–1326.
50. Leavitt M, Charles G, Heyman E, Michaels D. HairMax LaserComb laser phototherapy device in the treatment of male androgenetic alopecia: a randomized, double-blind, sham device-controlled, multicentre trial. *Clin Drug Investig*. 2009;29:283–292.
51. Kim H, Choi JW, Kim JY, et al. Low-level light therapy for androgenetic alopecia: a 24-week, randomized, double-blind, sham device-controlled multicenter trial. *Dermatol Surg*. 2013;39:1177–1183.
52. Borutaite V, Budriunaite A, Brown GC. Reversal of nitric oxide-, peroxynitrite- and S-nitrosothiol-induced inhibition of mitochondrial respiration or complex I activity by light and thiols. *Biochim Biophys Acta*. 2000;1459:405–412.
53. Emilia del Pino M, Rosado RH, Azuela A, et al. Effect of controlled volumetric tissue heating with radio-frequency on cellulite and the subcutaneous tissue of the buttocks and thighs. *J Drugs Dermatol*. 2006;5:714–722.
54. Arnoczky SP, Aksan A. Thermal modification of connective tissues: basic science considerations and clinical implications. *J Am Acad Orthop Surg*. 2000;8:305–313.
55. Goldberg DJ, Fazeli A, Berlin AL. Clinical, laboratory, and MRI analysis of cellulite treatment with a unipolar radiofrequency device. *Dermatol Surg*. 2008;34:204–209.
56. Yu CS, Yeung CK, Shek SY, et al. Combined infrared light and bipolar radiofrequency for skin tightening in Asians. *Lasers Surg Med*. 2007;39:471–475.
57. Bhargava S, Cunha PR, Lee J, Kroumpouzos G. Acne scarring management: systematic review and evaluation of the evidence. *Am J Clin Dermatol*. 2018;19:459–477.
58. Gold M, Taylor M, Rothaus K, Tanaka Y. Non-insulated smooth motion, micro-needles RF fractional treatment for wrinkle reduction and lifting of the lower face: international study. *Lasers Surg Med*. 2016;48:727–733.
59. Kleidona IA, Karypidis D, Lowe N, et al. Fractional radiofrequency in the treatment of skin aging: an evidence-based treatment protocol. *J Cosmet Laser Ther*. 2020;22:9–25.
60. Lu H, Guo J, Hong X, et al. Comparative effectiveness of different therapies for treating striae distensae: a systematic review and network meta-analysis. *Medicine (Baltimore)*. 2020;99:e22256.
61. Goldberg DJ, Enright KM, Goldfarb R, et al. The role and clinical benefits of high-intensity focused electromagnetic devices for non-invasive lipolysis and beyond: a narrative review and position paper. *J Cosmet Dermatol*. 2021;20:2096–2101.
62. Zachary CB, Burns AJ, Pham LD, Jimenez Lozano JN. Clinical study demonstrates that electromagnetic muscle stimulation does not cause injury to fat cells. *Lasers Surg Med*. 2021;53:70–78.
63. Vernier PT, Sun Y, Marcu L, et al. Calcium bursts induced by nanosecond electric pulses. *Biochem Biophys Res Commun*. 2003;310:286–295.
64. Kaufman D, Martinez M, Jauregui L, et al. A dose-response study of a novel method of selective tissue modification of cellular structures in the skin with nanosecond pulsed electric fields. *Lasers Surg Med*. 2020;52:315–322.
65. Hruza GJ, Zelickson BD, Selim MM, et al. Safety and efficacy of nanosecond pulsed electric field treatment of seborrheic keratoses. *Dermatol Surg*. 2019;46:1183–1189.
66. Munavalli GS, Zelickson BD, Selim MM, et al. Safety and efficacy of nanosecond pulsed electric field treatment of sebaceous gland hyperplasia. *Dermatol Surg*. 2019;46:803–809.
67. Nuccitelli R, LaTowsky BM, Lain E, et al. Safety and efficacy of nano-pulse stimulation treatment of non-genital, cutaneous warts (verrucae). *Lasers Surg Med*. 2021;53:1301–1306.
68. Carstensen EL, Miller MW, Linke CA. Biological effects of ultrasound. *J Bio Physics*. 1974;2:179–192.
69. Ziskin MC. Fundamental physics of ultrasound and its propagation in tissue. *Radiographics*. 1993;13:705–709.
70. Epstein Jr EH, Oren ME. Popsicle panniculitis. *N Engl J Med*. 1970;282:966–967.
71. Manstein D, Laubach H, Watanabe K, et al. Selective cryolysis: a novel method of non-invasive fat removal. *Lasers Surg Med*. 2008;40:595–604.
72. Zelickson B, Egbert BM, Preciado J, et al. Cryolipolysis for noninvasive fat cell destruction: initial results from a pig model. *Dermatol Surg*. 2009;35:1462–1470.
73. Garibyan L, Cornelissen L, Sipprell W, et al. Transient alterations of cutaneous sensory nerve function by noninvasive cryolipolysis. *J Invest Dermatol*. 2015;135:2623–2631.
74. Suter MJ, Gora MJ, Lauwers GY, et al. Esophageal-guided biopsy with volumetric laser endomicroscopy and laser cautery marking: a pilot clinical study. *Gastrointest Endosc*. 2014;79:886–896.
75. Austin LA, Osseiran S, Evans CL. Raman technologies in cancer diagnostics. *Analyst*. 2016;141:476–503.
76. Jalian HR, Tam J, Vuong LN, et al. Selective cryolysis of sebaceous glands. *J Invest Dermatol*. 2015;135:2173–2180.
77. Chen X, Kim P, Farinelli B, et al. A novel laser vaccine adjuvant increases the motility of antigen presenting cells. *PLoS ONE*. 2010;5:e13776.
78. Garibyan L, Moradi Tuchayi S, Wang Y, et al. Neural selective cryoneurolysis with ice slurry injection in a rat model. *Anesthesiology*. 2020;133:185–194.
79. Garibyan L, Moradi Tuchayi S, Javorsky E, et al. Subcutaneous fat reduction with injected ice slurry. *Plast Reconstr Surg*. 2020;145:725e–733ee.
80. Moradi Tuchayi S, Tam J, Wojtkiewicz GR, et al. Injectable slurry for selective destruction of neck adipose tissue in New Zealand obese mouse model. *Sleep Breath*. 2020;24:1715–1718.
81. Tam J, Wang Y, Farinelli WA, et al. Fractional skin harvesting: autologous skin grafting without donor-site morbidity. *Plast Reconstr Surg Glob Open*. 2013;1:e47.
82. Pozner JN, Kilmer SL, Geronemus RG, et al. A novel microcoring technology for scarless skin removal: summary of three prospective clinical trials. *Plast Reconstr Surg Glob Open*. 2021;9:e3905.
83. Russe E, Purschke M, Farinelli WA, et al. Micro-fractional, directional skin tightening: a porcine model. *Lasers Surg Med*. 2016;48:264–269.
84. Russe E, Purschke M, Limpiangkanan W, et al. Significant skin-tightening by closure of fractional ablative laser holes. *Lasers Surg Med*. 2018;50:64–69.

137 Lasers and Other Energy-Based Therapies

Christopher B. Zachary, Kristen M. Kelly and Erica G. Baugh

Chapter Contents

Types of Lasers and Intense Pulsed Light 2400
Ablative Lasers: Carbon Dioxide and Er:Yag 2402
Fractionated Lasers 2403
Treatment of Chronic Photodamage 2406
Treatment of Vascular Lesions 2406
Treatment of Melanin-Containing Lesions 2411
Hair Removal 2413
Treatment of Scars 2414
Treatment of Striae Distensae 2415
Treatment of Cellulite 2415
Treatment of Tattoos 2415
Treatment of Psoriasis and Vitiligo 2416
Pre- and Postoperative Considerations, Side Effects, and Complications 2416
Radiofrequency and Ultrasound 2418
Microwaves 2418
Home-Based Lasers 2419
Emerging Technologies 2419

INTRODUCTION

This chapter considers laser and light applications for both medical and aesthetic purposes as related to the skin. Anderson and Parrish developed the concept of selective photothermolysis[1] whereby laser energy could be used for targeted destruction of skin components (see Ch. 136). Their 1983 treatise continues to support our understanding of laser–tissue interactions and still drives new therapeutic applications of lasers in dermatology. Given the multiplicity of lasers available (Fig. 137.1), the laser surgeon must understand the capabilities and limitations of each device so that the appropriate system can be selected and the parameters tailored to treat the intended target. Safe and effective laser therapy is achieved when the operator understands the nature of the target, its location within the skin, and the potential collateral damage. Other energy-based devices, such as those that utilize radiofrequency waves, intense focused ultrasound, or microwaves, are also discussed.

TYPES OF LASERS AND INTENSE PULSED LIGHT

The earliest lasers used by dermatologists were applied to vascular lesions and consisted of continuous or quasi-continuous wave lasers, which emitted a constant beam of light. These included argon (488, 514 nm), argon pumped tunable dye (488–638 nm), copper vapor and copper bromide (511 nm, 578 nm), potassium titanyl phosphate (KTP, 532 nm), and krypton (568 nm) lasers. Although these lasers had wavelengths that corresponded to the hemoglobin absorption spectrum, the nature of their continuous beams generally induced nonspecific thermal damage to surrounding structures, leading to scarring and dyschromia. The root of the problem, a mismatch between the laser pulse duration and the thermal relaxation time of the target tissue (see Ch. 136), was effectively resolved once it was understood that laser pulse duration should approximately match the thermal relaxation time of the targeted tissue.

Pulsed Dye Laser

The pulsed dye laser (PDL) is considered to be the laser of choice for the treatment of various cutaneous vascular lesions, especially facial telangiectasias, port-wine birthmarks (PWBs), superficial hemangiomas, poikiloderma of Civatte, and erythematotelangiectatic rosacea[2]. Hypertrophic and keloidal scars, psoriasis, and warts are also amenable to treatment with PDL. While the initial PDL systems emitted 577 nm yellow light, slightly longer wavelength PDL devices (585 or 595 nm) were subsequently adopted to allow deeper tissue penetration of up to 1.2 mm.

The choice of appropriate PDL parameters affects tissue response, in terms of both efficacy and appearance. Short pulse durations (0.45–3 millisecond [ms]) cause a purpuric reaction related to intravascular coagulation or vessel leakage (Fig. 137.2C,D). While very effective for telangiectasias, the bruised appearance is not cosmetically acceptable to many patients. Although slightly less effective, longer pulse durations (6–10 ms) with multiple passes or "pulse stacking", consisting of application of a rapid succession of pulses to a particular location with cooling to achieve "purpura-free" treatments, is quite effective and less noticeable.

Epidermal protection during laser treatments, including those with PDL, is critical. Cooling helps to reduce blistering, crusting, and subsequent dyspigmentation, i.e. hypo- and hyperpigmentation. The most common cooling strategies are contact cooling, forced cold air, and cryogen spray. The Syneron-Candela PDL systems incorporate cryogen spray cooling (Dynamic Cooling Device™) which is deployed immediately before the light pulse, while Cynosure systems use forced cold air. In addition to protecting the epidermis from non-selective thermal damage, cooling allows for the use of higher fluences, with improved efficacy.

KTP Laser (Frequency-Doubled Nd:YAG Laser)

KTP 532 nm laser light is produced by passing 1064 nm light from an Nd:YAG (neodymium–yttrium–aluminum–garnet) laser through a potassium titanyl phosphate (KTP) crystal, which effectively halves the wavelength and doubles the frequency. Since this wavelength closely corresponds to the first absorption peak of hemoglobin at 542 nm, the KTP laser can be used to effectively treat some vascular lesions (e.g. telangiectasias) in a purpura-free manner (Fig. 137.2A,B). In addition, this laser is a popular device for the removal of lentigines and other epidermal pigmented lesions. While this laser is best employed in patients with skin phototypes I–III, it can used in darker skin phototypes (IV–VI) for unique applications, such as dermatosis papulosa nigra.

Nd:YAG Laser

The deeply penetrating Nd:YAG 1064 nm laser has significantly less hemoglobin absorption than the wavelengths of the PDL or KTP lasers. However, its absorption by melanin is also very limited. The latter property theoretically enhances the safety profile of the 1064 nm laser in patients with darker phototypes. This laser can be used to treat deeper vascular lesions and spider veins up to 3 mm diameter[3]. Because of its poor coefficient of absorption by hemoglobin, much higher fluences are required to produce transmural heating of blood vessels. As a consequence of the higher fluences and longer pulse widths, this wavelength has a narrow window of safety, with a significant potential for volumetric heating and collateral damage; in addition, it tends to be quite painful. Cooling is critical for epidermal protection and pain control, as well as to reduce the risk of scarring from nonspecific thermal injury. Nd:YAG lasers should be used with extra caution when treating vascular lesions.

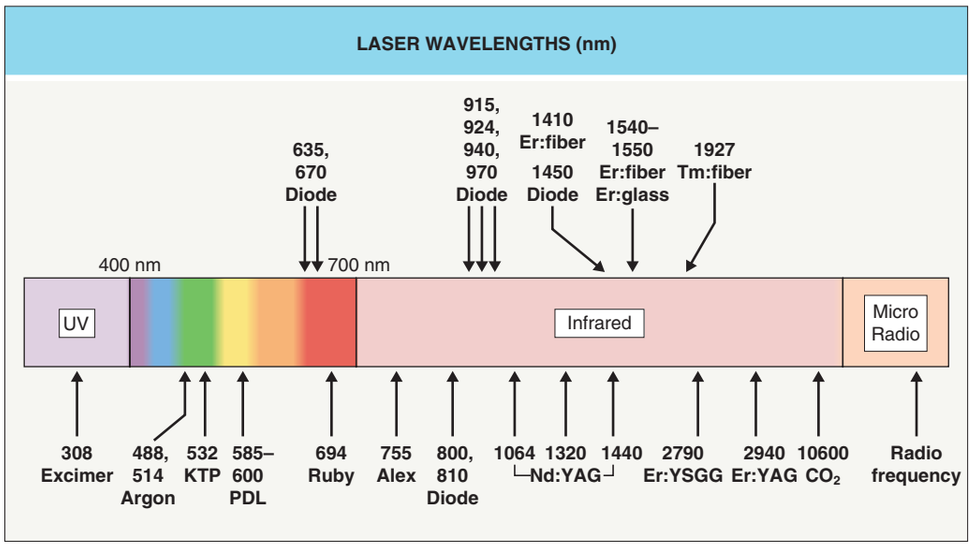


Fig. 137.1 Laser wavelengths (nm). Laser wavelengths lie predominantly within the ultraviolet, visible and infrared portions of the electromagnetic spectrum. Alex, alexandrite; Er, erbium; KTP, potassium titanyl phosphate; Micro, microwaves; Nd, neodymium; PDL, pulsed dye laser; Radio, radio waves; Tm, thulium; UV, ultraviolet; YAG, yttrium–aluminum–garnet; YSGG, yttrium–scandium–gallium–garnet.

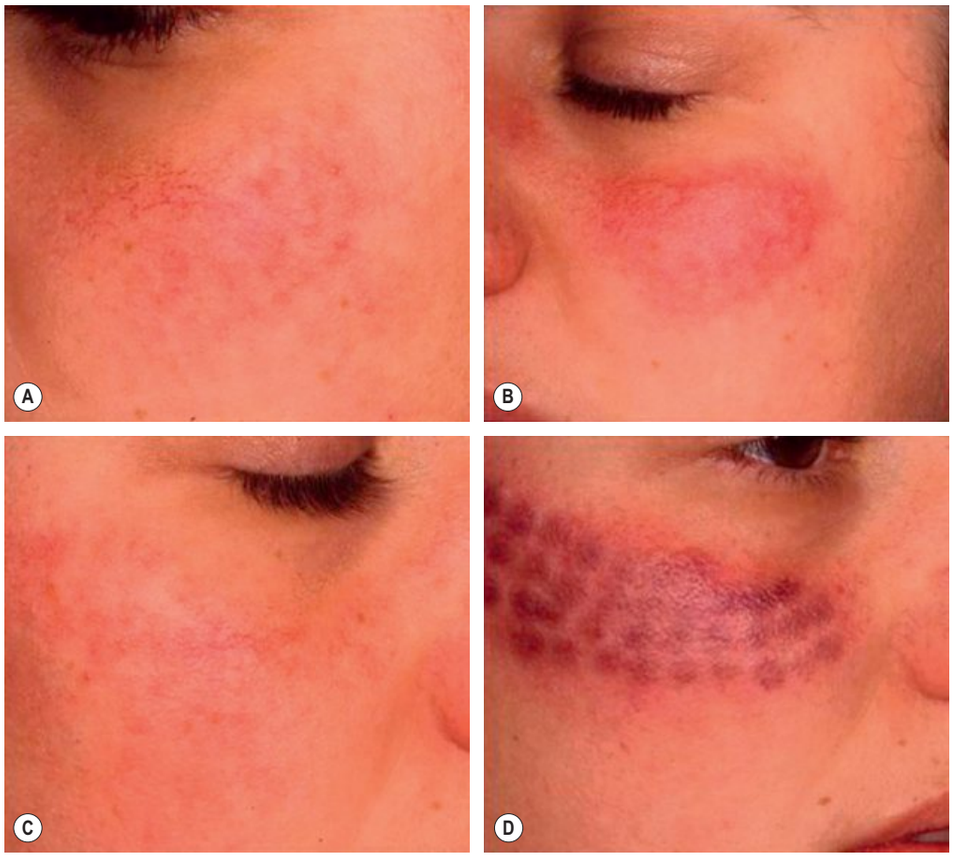


Fig. 137.2 Treatment of facial telangiectasias – potassium titanyl phosphate (KTP) laser versus pulsed dye laser (PDL). A, C Before treatment. Mild erythema follows KTP therapy (**B**) compared to circles of purpura after PDL (**D**).

Intense Pulsed Light

Intense pulsed light (IPL) systems emit filtered polychromatic light with wavelengths ranging from visible to near infrared (500–1200 nm). Sophisticated filtering and pulsing systems prevent unwanted wavelengths from damaging the skin, thus making this device more selective and quite versatile. Integrated skin cooling is a useful feature present in some devices, and it can be employed to provide epidermal protection, while at the same time allowing greater fluences to reach deeper targets. IPL systems can be used to treat a number of conditions, including rosacea, PWBs, hemangiomas, poikiloderma of Civatte and lentigines, as well as provide overall photorejuvenation.

Cold ultrasound gel or aloe vera gel should be applied both to protect the epidermis from excessive heat and to reduce the difference in refractive indexes between air and skin, thereby allowing better penetration and absorption of light. In addition, the gel enhances gliding of the handpiece from one location to the next.

Despite these measures, thermal injury to the epidermis can still occur, leading to blistering, scarring, and permanent pigmentary alterations. This is generally operator-dependent, with a greater risk when treating patients with a tan or darker skin phototypes (Fig. 137.3). IPL is most commonly used for patients with phototypes I–III with chronic photodamage or for hair removal. For treatment of patients with more darkly pigmented skin, longer wavelength filters or lower fluences plus longer pulse widths can be used (Fig. 137.4). Filters can also be used for other specific indications, e.g. treatment of vascular lesions.

The authors' preferred technique is to deliver multiple passes to a particular treatment area, with each subsequent pass oriented at



Fig. 137.3 Dyspigmentation with potential for scarring due to inappropriate intense pulsed light (IPL) treatments. Bands of hypopigmentation on the face (**A**) and arms (**B**) in two patients with darker skin phototypes.

a different angle. This allows for uniform, consistent coverage and prevents zebra-like pigmentary irregularities and skip areas. If double or triple pulses are utilized in any one area, adequate time for epidermal cooling should be allowed between passes. The observable endpoints of IPL treatment are darkening of lentigines (see Fig. 137.4B) and either a disappearance or intravascular coagulation of telangiectasias in the treated areas.

As with any of these devices, the initial pulses should be assessed in terms of the tissue response. Potential problems that should be avoided include excessive blanching, bruising, and production of the Nikolsky sign or other signs of excessive non-selective heating. If cooling is being used, it should be assessed for efficacy. Additionally, care must be taken to avoid inadvertent photoepilation of eyebrows, and in men, bearded skin.

ABLATIVE LASERS: CARBON DIOXIDE AND ER:YAG

Both the CO_2 (10 600 nm) and Er:YAG (2940 nm) lasers have wavelengths in the infrared portion of the electromagnetic spectrum (see Fig. 137.1), with the major chromophore being water. Based upon the energy absorbed per volumetric unit, the minimum fluence necessary for the CO_2 laser to produce tissue ablation has been calculated to be 5 J/cm^2. Below this fluence, tissue is not vaporized, rather it is coagulated. However, both vaporization and coagulation are useful in the treatment of skin disease, and these wavelengths can be manipulated to achieve an appropriate balance of the two. When using these resurfacing lasers, the photothermal coagulative effect is responsible for hemostasis, collagen rejuvenation, skin tightening, and, by extension, many of the complications such as scarring that can be seen with these devices.

To achieve selective photothermolysis of the skin with the CO_2 laser, it has been suggested that the ideal pulse duration is ≤1 ms. The development of high-powered, short-pulsed CO_2 lasers (as compared to their continuous wave predecessors) has allowed for more selective control of tissue vaporization and thermal injury. The first pass of the high-energy, short-pulsed CO_2 laser induces localized tissue vaporization with surrounding coagulation/desiccation. Since this residual carbonized tissue acts as a heat sink, subsequent CO_2 laser pulses tend to vaporize less and heat more, causing non-selective damage. Thus, second and subsequent passes should only be applied after removal of the desiccated "charred" material at the surface of the skin[4,5].

The Er:YAG laser emits light at 2940 nm, with water affinity being nearly 15 times greater than that of the CO_2 laser. This allows the Er:YAG laser to vaporize tissue more efficiently, leaving only a small residue of coagulated tissue. As a consequence of the limited photothermal effects, hemostasis and collagen contraction are significantly reduced with Er:YAG lasers. Sub-ablative coagulation settings, achieved by lengthening the laser pulse duration, have been incorporated into newer modulated Er:YAG laser systems (e.g. Sciton®), inducing more hemostasis and resulting in better tissue contraction. While pure Er:YAG lasers demonstrated only modest tissue tightening as compared to CO_2 lasers, modulated Er:YAG systems have produced comparable resurfacing results[5]. It is critical that the laser surgeon be constantly aware of the depth of vaporization.

The fully ablative CO_2 and long-pulsed Er:YAG lasers remain the gold standard for photorejuvenation, wrinkle reduction, and skin tightening. To date, nothing can beat the results obtained by an experienced laser surgeon using one of these lasers. Specifically, even deep, coarse and fixed perioral and periorbital rhytides can be significantly diminished or eliminated (Fig. 137.5)[4]. Redundant skin is tightened by thermal coagulation, collagen contraction, and associated fibroplasia. However, this dramatic improvement comes at the expense of slow healing. A split-face study of Er:YAG and CO_2 laser resurfacing demonstrated this duality; the side treated with the CO_2 laser had 63% improvement with 7.7 days of crusting, compared to the Er:YAG laser-treated side which had 48% improvement with an average of 3.4 days of crusting[6].

In general, more significant clinical improvement has gone hand in hand with more thermal damage, leading to more discomfort, more extensive wound care, and longer healing times. Additional side effects include persistent erythema for 3+ months, risk of scarring, a 15% chance of delayed-onset permanent hypopigmentation, and a line of demarcation between treated and untreated areas. All patients with actinic bronzing will note an improvement or lightening of their skin pigmentation in the treated areas. To avoid any demarcation lines in these regions, it is prudent to treat entire anatomic areas. This is particularly true for skin phototypes I and II. Skin phototypes IV–VI tend not to have actinic bronzing and hence focal or geographic areas can be treated.

Treatment of acne scarring is a common indication for ablative lasers. Elevated or distensible acne scars are most amenable to resurfacing, compared to icepick and non-distensible scars, which are often resistant[7]. Focal ablation has been effectively used for resurfacing benign epidermal tumors and proliferations such as seborrheic keratoses, epidermal nevi, and verrucae; actinic keratoses and actinic cheilitis can also be significantly improved[8]. Additionally, benign hyperplasia or neoplasms with an elevated component can be "debulked", e.g. rhinophyma, lymphangioma, adnexal tumors (including syringomas and angiofibromas; Fig. 137.6), and xanthomas. Based upon more limited experience and case reports, effective treatment of balanitis xerotica obliterans, porokeratosis, keratoderma, chondrodermatitis nodularis helicis, and Hailey–Hailey disease has been observed. Other possible indications for both the CO_2 and Er:YAG lasers include treatment of hidradenomas, colloid milium, eruptive hair cysts, and onychodystrophy.



Fig. 137.4 Intense pulsed light (IPL) treatment of lentigines in a patient with Fitzpatrick phototype IV skin. Because of the more darkly pigmented skin, lower energy and a longer pulse duration were carefully employed. **A** Before treatment. **B** Lentigines are appropriately slightly darker immediately following IPL. **C** Dry crusting of the skin 3 days postoperatively. **D** Excellent improvement of facial lentigines at 10 days.

Among the most significant risks with ablative resurfacing is infection, whether by bacteria, viruses, or fungi. Specifically, and especially if the treated region involves perioral skin or adjacent areas, antiviral medications (e.g. valacyclovir, famciclovir) should be initiated prophylactically the day prior to, or at least the morning of, the procedure and continued for 15 days. This is true even in the absence of prior herpetic infection so as to prevent the possibility of a generalized herpetic infection in the denuded skin. Antibiotic coverage, especially against staphylococci, may be prudent, but is much debated. Antifungal prophylaxis with fluconazole (a single-dose 200 mg tablet) given during the early postoperative period has been demonstrated to prevent candidal infection and may promote re-epithelialization.

FRACTIONATED LASERS

Traditional laser resurfacing yielded impressive facial photorejuvenation and significant tissue tightening. However, these outcomes were often at the cost of delayed healing, persistent redness and swelling, infection, unpredictable pigmentary changes (hypo- or hyperpigmentation), and scarring. In 2004, fractionated photothermolysis (FP) was introduced (Table 137.1). The development of fractionated lasers has changed the way laser surgeons practice. One can be aggressive in terms of depth and density, and yet relatively safe in terms of patient downtime, postoperative recovery, and complications. In contrast to traditional lasers where the spot size of the device defined the smallest treatment unit on the skin, hundreds of controlled microscopic zones of coagulative or ablative injury are delivered to the skin with each scan or stamp of the fractional device[9]. These areas of microscopic thermal injury are defined as microscopic treatment zones (MTZs; also referred to as microthermal zones). While MTZs appear to be minute dots on the skin, they actually represent exact columns or cylinders of epidermal and dermal thermal damage (see Fig. 136.6)[10]. MTZs are deliberate and calibrated such that the resultant depth, width, and density are defined. Each microdot or cylinder of damage is surrounded by normal unaffected skin, which acts as a reservoir for healing and enables these micro-wounds to resolve quickly with minimal discomfort (Fig. 137.7). Histologically, the healing wounds appear as microscopic epidermal necrotic debris (MENDs); the latter are composed of fragmented and damaged skin components, including epidermis, dermis, melanin, and elastin[11]. The skin surface heals within 7 days with extrusion of the MENDs.

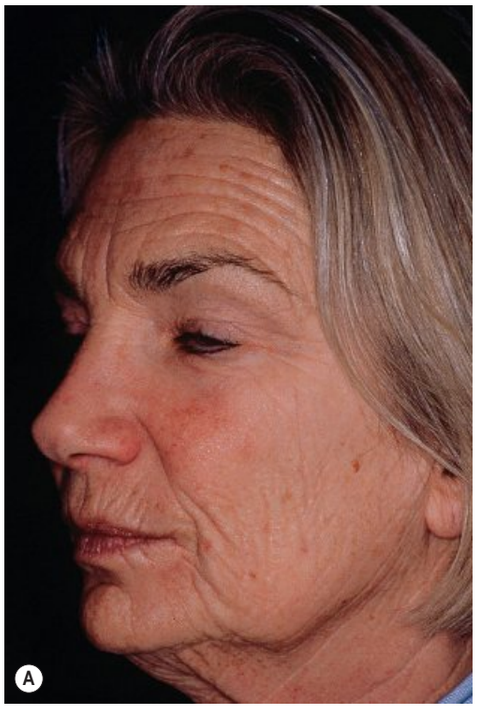
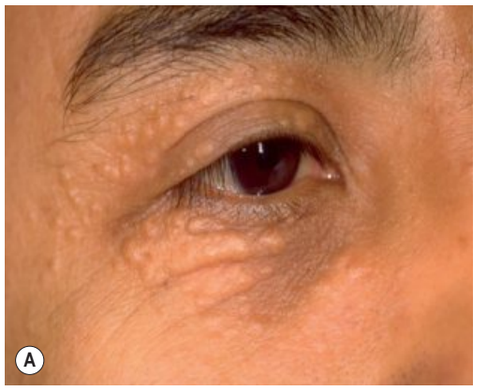




Fig. 137.5 Ablative CO_2 laser resurfacing. **A** Before treatment. **B** One year after resurfacing. *Courtesy Jeffrey Dover, MD, and Kenneth Arndt, MD.*



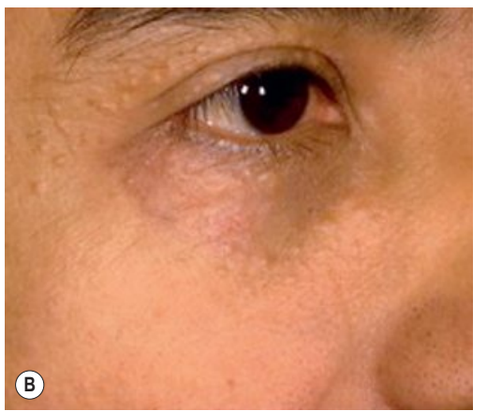


Fig. 137.6 Treatment of syringomas with ablative erbium:YAG laser. A Before treatment. **B** Three months following treatment: note the difference between the treated lower eyelid and the untreated upper eyelid.

Non-Ablative Fractional Photothermolysis

The first system to be cleared for clinical use was the Fraxel® SR750 (Reliant Technologies), which is a 1550 nm erbium-doped fiber fractionated laser that targets water as its chromophore. The laser handpiece employs a scanning system allowing for uniform deposition of MTZs. The second-generation system (Fraxel® DUAL) includes both 1550 nm and 1927 nm wavelengths. This is a major development as it increases the versatility of this device. The 1550 nm wavelength allows for adjustment of the MTZ energies up to 70 mJ with a depth of injury down to 1500 microns and treatment densities of 5%–50% (Video 137.1). The depth of these MTZs is an operator-dependent parameter and can be adjusted to match the thickness of skin or entity being treated. The 1927 nm wavelength provides a more superficial non-ablative impact in which the depth is non-linear. This wavelength is very useful for patients with photodamage and fine lines. It can be used in skin phototypes III and IV (especially Asians) with very little postinflammatory hyperpigmentation. Some like this device for the treatment of melasma, alone or in combination with nanosecond or picosecond lasers and topical agents. These two wavelengths (1550 and 1927 nm) can be used in combination in the same treatment session.

Collagen remodeling is induced with this fractionated heating of the skin. The very nature of fractional photothermolysis (FP) allows for the safe application of incredibly high fluences to narrow tissue columns, which if applied to confluent areas would certainly cause delayed healing and tissue scarring.

New indications and applications for this novel technology continue to evolve and include patients with chronic photodamage, skin laxity, rhytides, striae, and multiple types of scarring, including acne, hypopigmented, traumatic, and surgical scars (Fig. 137.8). One of the first clinical applications of FP was treatment of facial melasma. While initial studies were promising with near-complete clearance of melasma after a few treatments, this early exuberance has been tempered by a more considered and lengthy assessment of response, with the tendency of melasma to recur.

Ablative Fractional Photothermolysis

Following the success of fractionated *non-ablative* rejuvenation came the development of fractionated *ablative* rejuvenation. The first commercially available system was the Fraxel re:pair laser, originally manufactured by Reliant Technologies. This scanning fractionated CO_2 laser has the ability to place 2000 microablative MTZs per second. Indeed, many other companies have produced their own fractionated ablative devices using CO_2, Er:YAG, and Er:YSGG (yttrium–scandium–gallium–garnet) wavelengths (see Table 137.1). As an example, the re:pair® system creates MTZs ~120–150 microns wide and 200–1500 microns in depth. The speed of delivery corresponds to the speed at which the operator moves the handpiece over the skin. The fluence of each laser microbeam can be adjusted up to 70 mJ/MTZ by the operator and the density ranges from 10% to 70% of the skin surface. UltraPulse® DeepFX™ (Lumenis), an equivalent system that utilizes a galvanic scanner, creates a pattern of MTZs, each of which is 110 microns wide and 50–4000 microns deep (depending on parameters chosen)[12]. Because this greater depth of microablative channels approximates the depth of thicker scars, this system may be of greater benefit when treating such scars.

EXAMPLES OF FRACTIONATED LASER AND RADIOFREQUENCY DEVICES*				
Laser type	**Wavelength (nm)**	**Laser name™,® (examples)**	**Energy of MTZ (per micropulse)**	**MTZ depth (microns)**
Laser – ablative				
Rolling scanner				
CO_2	10 600	Fraxel re:pair	5–70 mJ/MTZ	200–1500
Stamping scanner				
CO_2	10 600	UltraPulse Deep FX	2.5–50 mJ/MTZ	50–4000
CO_2	10 600	CO2RE	1–90 mJ/MTZ	750
Er:YSGG	2790	Pearl Fractional	60–320 mJ/MTZ	1000
Er:YAG	2940	Lux 2940	≤15 mJ/MTZ	50–300
Er:YAG	2940	Pixel	14–27 mJ/MTZ	30–70
Er:YAG	2940	ProFractional	≤400 J/cm^2	1000
Laser – non-ablative				
Rolling scanner				
Erbium fiber	1550	Fraxel re:store	4–70 mJ/MTZ	500–1400
Erbium/thulium fiber	1550/1927	Fraxel DUAL	4–70 mJ/MTZ	500–1400/200
Erbium fiber	1410	Fraxel re:fine	5–20 mJ/MTZ	650
Stamping scanner				
Diode/bipolar RF	915 and bipolar RF	Matrix IR	≤70 J/cm^2	500
Nd:YAG	1440 ± 1320	Affirm	8–12 mJ/MTZ	200–300
Er:Glass	1540	Fractional 1540	15–50 mJ/MTZ	125–850
Er:Glass	1540	Mosaic	5–40 mJ/MTZ	1000
Er:Glass	1540	Matisse	≤250 J/cm^2	30–150
Radiofrequency (RF) – ablative and non-ablative				
Ablative, invasive	RF – unipolar	Pixel RF	Up to 300 W	100–150 mm (80–120 mm diameter)
Nonablative	RF – unipolar, insulated microneedles	INFINI	Up to 50 W	0.5–3.5 mm (49 or 16 microneedles)
		Fractora	≤62 mJ/pin	Up to 1 mm (20 or 60 pin tip)
		Profound	Temperature controlled	2–3 mm (7 pairs of microneedles)
	RF – monopolar or bipolar	INTRAcel	Temperature/impedance controlled	0.5–2 mm (49 microneedles)

*A partial list.

Table 137.1 Examples of fractionated laser and radiofrequency devices. CO_2, carbon dioxide; Er, erbium; Er:YAG, erbium-doped yttrium–aluminum–garnet; J, joule; mJ, millijoule; MTZ, microthermal zone or microscopic treatment zone; Nd, neodymium; RF, radiofrequency; Er:YSGG, erbium:yttrium–scandium–gallium–garnet; W, watts.

The fractional devices, both ablative and non-ablative, have been used for traditional resurfacing indications such as improvement of rhytides and acne scarring (Fig. 137.9). Initial studies utilizing re:store® for the treatment of periorbital rhytides showed mild improvement in 12% of patients, noticeable improvement in 30%, and moderate to significant improvement in 54% after one to four treatments[13]. Settings for pulse energy and treatment density should be tailored for the individual patient. Collective experience has also shown that fine to moderate rhytides respond more favorably than do deeper rhytides, and less dramatic improvement should be expected compared to fully ablative resurfacing[14].

When used for acne scarring, fractional deep dermal ablation (FDDA™) treatment has demonstrated significant efficacy. In a study of 30 patients with moderate to severe acne scarring who underwent one to three treatments[15], mild to moderate overall improvement was noted with energies ranging from 20 to 100 mJ and densities of 600–1600 MTZ/cm^2. A fractionated ablative depth of 1.5 mm or greater will likely induce optimal outcomes when treating acne scarring. The concept that a high density of fractional injury always provides better outcomes has recently been challenged, with some evidence that a low-to-medium density is as good or better. Although some patients may initially view multiple treatments as inconvenient, the benefits of rapid skin healing (within 5–7 days) and remarkably little postoperative discomfort compared to traditional laser resurfacing are distinct advantages (see Fig. 137.7).

Ablative FP offers the opportunity for relatively safe treatment of anatomic regions that were notoriously difficult to rejuvenate with conventional ablative resurfacing. Areas such as the neck and upper chest can now be more easily treated, albeit at reduced energy and density. Another advantage of fractionated systems is the ability to safely treat all skin phototypes, including patients with darkly pigmented skin (Fig. 137.10).

Evidence that fractionated laser therapies induce neocollagenesis is supported histologically. Increased expression of collagen remodeling markers such as heat shock proteins (47, 70 and 72), collagen III, proliferating cell nuclear antigen, and α-smooth muscle actin have been demonstrated within treatment areas[16,17]. In addition to inducing neocollagenesis, ablative fractionated systems induce *volumetric tissue reduction* and dermal plumping[17,18]. Taken collectively, the vaporization volume of millions of tiny-diameter cylinders of skin adds up. A standard aggressive fractionated CO_2 laser treatment can remove 5–7 cm^3 from the skin of the face[19]. The original hope was that this volumetric tissue reduction would result in impressive skin tightening. In practice, every one of these tiny holes is actually repaired with new collagen and elastin, leading to improvement in color, texture and tone, but with less skin tightening than anticipated. However, periodic treatments will improve skin laxity and could possibly prevent or delay the need for future facelift procedures.

Fractionated lasers represent a major therapeutic advance in the treatment of surgical, traumatic, and burn scars. Documented



Fig. 137.7 Improvement of depressed acne scarring following treatment with fractionated CO_2 laser (Fraxel re:pair®). A Preoperatively. **B, C** Intraoperatively, pin-point bleeding from microscopic treatment zones (MTZs; also referred to as microthermal zones) is observed. **D** Four days postoperatively. **E** One month postoperatively.

improvement in overall appearance, texture, mobility, and symptoms such as pain and itch has been well described[20]. The traditional approach was to allow scars to mature for 1–2 years prior to any intervention, but this has been demonstrated to be incorrect. Early intervention, even at the time of suture removal, can hasten healing and reduce ultimate disfigurement. A combination approach consisting of PDL, fractionated lasers (ablative or non-ablative), and/or radiofreqency microneedling (± intralesional corticosteroids or 5-fluorouracil) is likely to improve the appearance of scars[21] (see below).

Fractionated Laser Assisted Drug Delivery

Significant advances have been made in fractionated laser assisted drug delivery by disrupting the barrier function of the stratum corneum[22]. Both ablative and non-ablative lasers can dramatically increase the uptake of any topical agent. Understanding the relation of depth of fractionated ablation, the associated collar of spongy coagulation inside each channel, the density of laser channels, and the hydrophilic/lipophilic nature of the topical medications are all important.

The MTZs function as channels through which even large-sized molecules may be delivered to essentially any depth within the skin. Studies have been conducted utilizing a diverse array of therapeutic agents including anesthetics, chemotherapeutic drugs, corticosteroids, and stem cells[23,24]. Fractionated delivery of topical aminolevulinic acid (ALA) for photodynamic therapy (PDT) in areas such as the extremities can dramatically improve drug absorption and efficacy.

TREATMENT OF CHRONIC PHOTODAMAGE

While we are blessed by the sun in terms of "the good outside", chronic sun exposure wreaks havoc with our skin, inducing lentigines, telangiectasias, rhytides, and cutaneous carcinomas. Although successful laser treatment of lentigines and telangiectasias is possible based upon specific wavelengths (see above), there is a less well understood improvement that comes from nonspecific heating of the dermis, which induces the production of new collagen and elastin.

It has been said that twice yearly treatments with IPL could maintain a youthful appearance. In a study of 135 patients with poikiloderma of Civatte, IPL treatment of the neck and/or upper chest led to >75% clearance of telangiectasias and hyperpigmentation after a mean of three treatments[25]. While the emitted light is broad, IPL filters allow for more targeted treatments. It has been postulated that the shorter wavelengths are responsible for the improvement in pigmentation and telangiectasias, while the longer wavelengths are responsible for collagen remodeling via thermal effects on tissue water[26]. However, many wavelengths are absorbed by dermal water and their impact is likely the cause of improved appearance, particularly after repeated treatments.

While the ablative lasers can produce dramatic improvement in skin laxity and photodamage, their short-term side effects of discomfort, oozing, edema, persistent erythema, and extended healing time, plus the potential risks for infection, scarring, and delayed-onset hypopigmentation have led to a shift toward non-ablative laser therapies. "Subsurface remodeling" secondary to dermal wound healing responses can be seen in patients treated by IPL, PDL, and a number of other lasers. The long-pulsed PDL can be used with a multiple-pass technique for photorejuvenation. It is worthy to note that both the 585 nm and 595 nm PDLs have received FDA clearance for treatment of periocular wrinkling. While collagen remodeling has been demonstrated histologically, clinical improvement of wrinkles is variable and modest.

In addition to specifically improving pigmentation, KTP and Nd:YAG lasers have also been shown to cause a 20%–40% improvement in texture and a 20%–30% improvement in rhytides[27]. Lastly, laser surgeons must appreciate the science behind the energy delivery, rather than base assumptions on exaggerated claims by device manufacturers. No one laser or wavelength meets all of the objectives required for skin rejuvenation.

TREATMENT OF VASCULAR LESIONS

The target chromophore in vascular lesions is hemoglobin, in particular oxyhemoglobin, with absorption peaks at 418, 542 and 577 nm (see Fig. 136.3). While the primary target is hemoglobin, the structurally complex nature of the skin does not allow for simplistic "targeting". Factors such as blood vessel depth, vessel diameter, and skin phototype are also highly relevant considerations when treating vascular lesions. An equally important consideration is the structures that the laser surgeon wishes to avoid, e.g. the epidermis and hair follicles.



Fig. 137.8 Non-ablative fractionated laser therapy for scar remodeling. **A** Patient at presentation with traumatic hypertrophic and fibrotic scarring. **B** After three treatments with Fraxel re:store®. **C** Marked improvement of scarring after five treatments performed over 6 months.

The most commonly used devices for the treatment of vascular lesions include IPL and the 532 nm KTP, 595 nm PDL, and 1064 nm Nd:YAG lasers. Other systems such as the 755 nm alexandrite and the 800 nm and 940 nm diode lasers also play an important role in the treatment of vascular lesions (Table 137.2).

Clinical improvement is best achieved by photothermal vascular damage[28]. As the pulse width approximates or slightly exceeds the thermal relaxation time of the target vessel, photothermal damage results. This induces *intravascular* thrombosis or vessel rupture and subsequent collagenous fibrosis of the blood vessel wall and adjacent tissues[28]. These changes result in vessel disappearance or an immediate purpuric reaction (see Fig. 137.2D). Given the unwanted cosmetic appearance of the latter, which can last for 2 weeks, longer pulse widths (>6 ms) are often used, as they produce gentler heating of the target vessel and avoid bruising altogether. However, some degree of intravascular thrombosis may be a prerequisite for clinical improvement and resolution of vascular lesions, as is the case in port-wine birthmarks (PWBs).

Port-Wine Birthmarks (PWBs)

One of the first clinical applications of laser therapy was treatment of congenital vascular lesions, namely PWBs. PWBs are capillary malformations that involve primarily the mid to superficial dermis; they occur in 0.3%–0.5% of newborns and initially present as pink to red patches. These vascular anomalies are cosmetically and psychologically problematic and are frequently located on the face. When PWBs are bilateral and/or involve the "forehead area", there is a higher risk of Sturge–Weber syndrome[29], with somatic activating mutations in *GNAQ* found in both Sturge–Weber syndrome and non-syndromic PWBs[30] (see Ch. 104). PWBs located on the extremities may be a sign of Klippel–Trenaunay or Parkes Weber syndrome, with associated tissue hypertrophy and additional vascular malformations (venous, lymphatic, arteriovenous) present.

An early treatment of PWBs utilized the continuous wave argon laser (488 and 514 nm). Despite the wavelength's relative specificity for its vascular target, this laser caused marked scarring in up to a third of patients due to nonspecific thermal injury. The latter occurred because the pulse duration of ~200 ms dramatically exceeded the thermal relaxation time of the PWB vessels (~1–10 ms)[31]. A therapeutic paradigm shift then occurred based upon the concept of selective photothermolysis, leading to the development of the PDL which was specifically designed to treat PWBs.

While the early PDLs emitted a 577 nm wavelength, the current PDL systems deliver 585 and 595 nm wavelengths, allowing targeted delivery of laser energy deeper into the skin with increased efficacy. These longer wavelengths are less well absorbed by hemoglobin, but they penetrate slightly deeper into the skin[32]. The addition of epidermal cooling has allowed the use of higher energy fluences and treatment of all skin

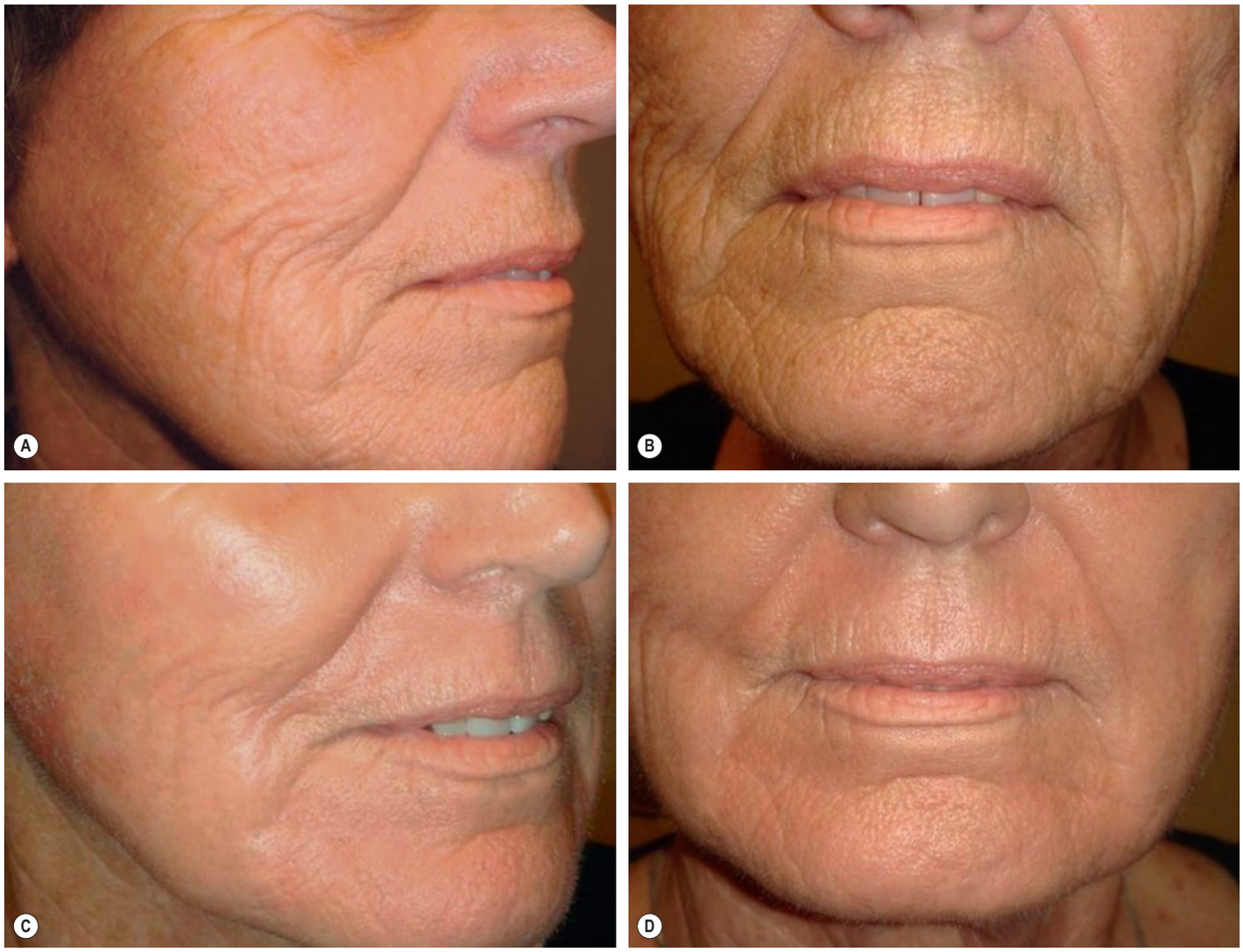


Fig. 137.9 Fractionated CO_2 laser (Fraxel re:pair®) resurfacing. A, B Coarse rhytides and solar elastosis. **C, D** Significant improvement in color, texture, tone, and wrinkling following one treatment. Mild residual erythema and edema persist at 1 month.



Fig. 137.10 Treatment of acne scarring with fractionated CO_2 laser (Fraxel re:pair®) in a patient with skin phototype IV. A Before treatment. **B** Three months after treatment, visible postinflammatory hyperpigmentation is seen. **C** Ten months postoperatively, there is improvement in postinflammatory hyperpigmentation. **D** One year postoperatively, improvement in acne scarring is noted.

phototypes, although darker skin phototypes are still more challenging. Commonly used settings range from energy fluences of 4–15 J/cm^2 with pulse widths of 1.5–10 ms and a 7–12 mm spot size.

For both technical and psychological reasons, early treatment of PWBs is recommended. The dilated and ectatic vessels of PWBs are neither proliferative nor do they self-involute. Their total surface area becomes larger in proportion to the growth of the child. Soft tissue hypertrophy and nodules may develop over time and the color can darken to deep red or purple. When these changes occur, treatment becomes more challenging and often requires the use of lasers with longer wavelengths, along with higher energy fluences and longer pulse durations, in order to effectively treat the deeper and thicker vessels. From a psychological standpoint, PWBs have been shown to impact social and cognitive development during childhood and can have lasting repercussions on adult social relationships[33]. In addition, early treatment permits shorter treatment sessions (as the lesions are smaller) and may allow resolution of the capillary malformation prior to the child starting school when social interactions increase. Laser treatment in children younger than 6 months of age has been demonstrated to be safe and effective[34].

LASERS AND OTHER DEVICES USED FOR THE TREATMENT OF VASCULAR LESIONS					
Laser/device	**Wavelength (nm)**	**Fluence (J/cm²)**	**Pulse duration (ms)**	**Target structure**	**Applications**
Skin-surface application					
Variable-pulsed KTP laser	532	Up to 40	1–100	Telangiectasia, venulectasia	Facial telangiectasias, erythematotelangiectatic rosacea, cherry angiomas, leg telangiectasias, venous malformations
Pulsed dye laser	585, 590, 595, 600	Up to 40	0.45–40	Telangiectasia	Port-wine birthmarks, erythematotelangiectatic rosacea, facial and leg telangiectasias, cherry angiomas, spider angiomas, venous lakes, infantile hemangiomas, hypertrophic scars, striae rubrae, verrucae
Long-pulsed alexandrite laser	755	Up to 100	3–100	Venulectasia, telangiectasia	Leg telangiectasias ("spider veins"), venous malformations, port-wine birthmarks
Diode laser	800, 810, 840, 940, 980	10–100	5–400	Venulectasia, telangiectasia	Leg venulectasias and telangiectasias ("spider veins"), blue reticular veins, venous malformations
Long-pulsed Nd:YAG laser	1064	5–900	0.25–500	Venulectasia, telangiectasia	Leg venulectasias and telangiectasias ("spider veins"), blue reticular veins, facial telangiectasias, venous lakes, venous malformations
Intense pulsed light	400–1200	10–80	2–200	Telangiectasia, venulectasia	Erythematotelangiectatic rosacea, leg telangiectasias ("spider veins")
Endovascular application					
Diode lasers	810, 940			Varicose veins	Saphenous vein insufficiency
Nd:YAG laser	1320			Varicose veins	Saphenous vein insufficiency
Radiofrequency energy source	Radiofrequency			Varicose veins	Saphenous vein insufficiency

Table 137.2 Lasers and other devices used for the treatment of vascular lesions. For details on endovascular applications, see Chapter 155. ms, millisecond.

While 70% of PWBs will have good or very good improvement following treatment (Fig. 137.11), a minority (<10%) will have very modest or no improvement. The degree of PWB clearance is dependent on several factors including the size of the lesion and its anatomic location[35]. For example, centrally located facial lesions (i.e. medial cheeks, upper lip, and nose) tend to be more treatment-resistant as compared to lesions located in the periorbital region or on the forehead, lateral cheeks, or chin. Likewise, PWBs on distal extremities are more treatment-resistant and require a more aggressive approach. Although a remarkable response can be obtained after one laser treatment, treatment of PWBs typically requires multiple (10 or more) sessions.

Given that PWBs are composed of various-sized blood vessels, each with its own requisite treatment parameters, the PDL may prove inadequate in eliminating the entire capillary malformation. A poor response may be related to poor laser penetration, a mismatch of parameters to vessel size, inadequate vascular heating, or scarce or poor chromophore uptake[36]. Given the limitations of the PDL, resistant components of PWBs can be treated with the alexandrite laser or IPL.

Infantile Hemangiomas

Representing the most common tumor of infancy, hemangiomas have a predilection for the head and neck region (60%), followed by the trunk and the extremities. They are present in 1%–2% of neonates and there is a higher incidence in premature infants. These tumors classically grow rapidly within the first few weeks of life. Infantile hemangiomas may have both superficial and deep components, with the superficial portions appearing red and the deeper components appearing blue. They can be categorized as focal or segmental (see Ch. 103). Their natural maturation involves a proliferative phase, a static phase, and an involutional phase. Although hemangiomas can regress leaving the affected skin with normal texture and color, many heal with hyper- or hypopigmentation and atrophy or fibrofatty change (see Fig. 103.9).

Treatment of infantile hemangiomas, if any, should be tailored to the specific lesion, with consideration of its location, size, proliferative rate, and whether it is likely to produce a functional or anatomic deficit. Currently, oral β-blockers, most commonly propranolol, are a mainstay of therapy for infantile hemangiomas that threaten vital functions, are potentially disfiguring, or have severe ulceration[37]. Other therapeutic options include monitoring, topical timolol (for thin lesions), corticosteroids (topical, intralesional or systemic), laser therapy, and less often surgical excision.

Although the role of laser therapy in the treatment of infantile hemangiomas is still controversial[38], in some studies PDL has been shown to slow progression, decrease time to involution, and promote healing of ulcerated lesions[39]. A retrospective study of 90 patients with infantile hemangiomas treated with PDL demonstrated a significant improvement in color and decrease in thickness in 81% and 64% of patients, respectively[40]. Combining systemic β-blockers with laser therapy may lead to a more rapid response and enhanced resolution; for example, in one retrospective study of infants with segmental facial hemangiomas treated concurrently or sequentially (propranolol followed by PDL), there was more complete clearance over a shorter time period following concurrent or sequential therapy (3 and 6 months, respectively) compared to propranolol alone (almost 10 months)[41].

Epidermal protection is critical in the treatment of infantile hemangiomas. Ulceration, scarring, and pigmentary changes can occur if the epidermis is not adequately protected via cooling or if excessive energies are employed.

Telangiectasias

Patients frequently present with facial telangiectasias and they are often associated with chronic photodamage and rosacea. Telangiectasias can also occur on the face and elsewhere in the setting of liver disease, autoimmune connective tissue diseases, surgical scars, and the overuse of topical corticosteroids. Facial telangiectasias are typically located on the nose, cheeks and chin; they measure 0.1–1.0 mm in diameter and are commonly treated with PDL, KTP laser, or IPL. When the PDL is used with short pulse durations, significant clearance can be achieved, albeit with significant bruising (see Fig. 137.2D). Clearance of facial vessels can be achieved with *non-purpuric energy fluences* or treatments that employ energy fluences ranging from 6 to 8.5 J/cm² with longer pulse durations (6–20 ms) and 7–12 mm spot sizes. At these settings, multiple passes and/or cautious pulse-stacking techniques (see above) are typically employed to improve efficacy. Multiple treatment sessions may be required. These techniques can also benefit patients with recurring flushing and central facial erythema (Fig. 137.12).

Treatment of telangiectasias with the KTP laser induces little or no bruising compared to the PDL (see Fig. 137.2), but edema can occur.



Fig. 137.11 Treatment of a port-wine birthmark with the pulsed dye laser (PDL). A Before treatment. **B** Purpuric response immediately after treatment with the PDL (585 nm, 0.45 ms). **C** Six weeks after the fourth treatment. *Courtesy Jeffrey Dover, MD, and Kenneth Arndt, MD.*

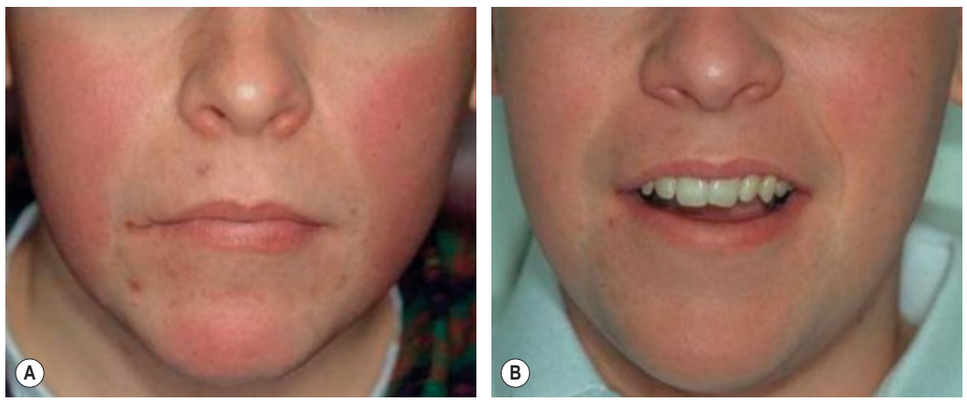


Fig. 137.12 Erythematotelangiectatic rosacea. A Before treatment. **B** Improvement of facial erythema and flushing two months following pulsed dye laser therapy.

Larger-caliber, darker, and deeper facial vessels can be effectively treated with the Nd:YAG laser, particularly in dark-skinned patients. However, to compensate for the diminished absorption of 1064 nm light by hemoglobin (nearly 10-fold less compared with 595 nm light), an increased fluence is required, making vigorous cooling necessary both for epidermal protection and to reduce patient discomfort. Even with these measures, there is a risk of scarring when the long-pulsed Nd:YAG laser is used to target blood vessels. Finally, IPL is commonly employed for purpura-free treatment of facial telangiectasias utilizing a 550 or 560 nm cut-off filter. The treatment endpoint for telangiectasias is vessel spasm or change in the vessel color to a duskier appearance.

Poikiloderma of Civatte

Poikiloderma of Civatte is a hallmark reflection of photodamage and involves the lateral aspects of the cheeks, neck, and upper chest. While a prominent component is telangiectasias, there is also epidermal atrophy and actinic dyspigmentation. Comprehensive treatment requires consideration of each component. Options include IPL, PDL, and KTP laser; newer devices such as the fractionated ablative and non-ablative lasers can also be used. When there is insufficient overlap of adjacent PDL pulses, a persistent "honeycomb-like" appearance may occur, with circles of improvement in color, texture, and tone surrounded by a network of relatively untreated skin (Fig. 137.13). This mottled look can require multiple treatments to eradicate.

Since IPL can favorably improve both dyspigmentation and telangiectasias, this system is perhaps more ideally suited to treat poikiloderma of Civatte. Several studies have reported 50%–75% improvement in both the vascular component and the actinic dyspigmentation, with a low side-effect profile[25]. The pertinent short-term side effects are transient erythema and intentional darkening of lentigines, which all disappear in about a week. Although "footprinting" is possible with IPL, it is far less common than with PDL, given the larger size of the crystal IPL handpiece.



Fig. 137.13 "Footprinting" on the cheek of a young girl following pulsed dye laser therapy of a port-wine birthmark. There is a honeycomb-like appearance due to circles of improvement surrounded by a network of relatively untreated skin.

Additionally, use of a multiple-pass technique applied in different orientations tends to minimize this unintended "footprint" consequence.

Telangiectasias and Venulectasias of the Leg ("Spider" Leg Veins)

"Spider veins" of the legs are a common cosmetic problem for which patients seek treatment. These telangiectasias and venulectasias are red and blue in color, measure 0.2 to 2 mm in diameter, and develop in dependent areas, predominantly the legs. While a number of spider veins appear independently of deeper vascular disorders, a surprisingly high percentage can be improved by treating deeper underlying venous disease. While the superficial venous system is located in the skin, subcutaneous tissue, and superficial fascia, the deep venous system is located within underlying muscle, with the two plexuses interconnected

by perforating veins (see Fig. 155.1)[42]. Whether as a consequence of age, hormonal or genetic factors, or from trauma to the vessel wall, venous valvular incompetence produces increased hydrostatic pressure and ultimately vessel dilation (see Fig. 105.2).

Whereas facial telangiectasias are generally superficial, small in caliber, and have normal hydrostatic pressures, leg veins are larger in diameter, thicker in caliber, and are situated more deeply within the skin. Additionally, as in any treatment site, there is heterogeneity in the size, color, and caliber of ectasias. These properties make treatment of leg veins even more challenging. Sclerotherapy is the first-line therapy for telangiectasias of the lower extremities (see Ch. 155). Laser treatment represents a viable option in a minority of patients such as those with needle phobias, telangiectatic matting[43], or a history of adverse reactions to sclerosing agents (see Table 137.2). The PDL and KTP lasers can be used to treat small-caliber, pink and red blood vessels which are too fine to cannulate with sclerotherapy needles, e.g. the telangiectatic matting that can be a consequence of prior sclerotherapy.

Given that leg veins are heterogeneous in their color, size, caliber and depth, and that many result from venous valvular incompetence, duplex ultrasonography can assist in determining the most appropriate treatment strategy. Combination therapy using endovenous lasers, ambulatory phlebectomy, and sclerotherapy may represent the best approach for long-term, successful treatment of lower extremity ectasias (see Ch. 155). Synergistic improvement may be achieved when these treatments are used in combination.

Pyogenic Granulomas

Pyogenic granulomas (PGs) are idiopathic, abruptly appearing, vascular neoplasms that tend to grow rapidly and bleed easily. Over half of these lesions recur after electrocoagulation, presumably because such desiccative treatments fail to ablate the deeper vascular components[44]. Both the argon and CO_2 lasers have been used to treat these neoplasms. More specific targeting of the vascular nature of PGs has been attempted with the PDL, whether used directly on the lesion or in combination with glass slide diascopy to blanch out superficial components. Higher success rates may be achieved with antecedent removal of the papular component (by shave or electrodesiccation techniques) prior to PDL targeting of the more deeply situated vessels. While shave removal followed by desiccation is still the first-line treatment for most patients, less scarring is noted with the PDL, when used either with modest energy fluences (1.5 ms pulses) *without cooling* or multiple stacked pulses (5–10 ms) *with cooling*.

Venous Lakes and Cherry Angiomas

Venous lakes are commonly seen on the lips or ears as gray–blue to purple compressible papulonodules representing dilated venules within the superficial dermis. These lesions are brought to the attention of dermatologists because of cosmetic concerns or a history of periodic bleeding. Traditionally, electrocoagulation has been used, but scarring and recurrence are common. IPL and PDL can be used but often light penetration is not deep enough. Longer wavelength devices including alexandrite laser or Nd:YAG laser may improve resolution.

Cherry angiomas, which vary in color from bright red to purple, are also benign lesions of cosmetic concern (see Ch. 114). Optimal treatment is by PDL or KTP lasers, although some clinicians still use more traditional technology such as electrocoagulation.

Verrucae

Verruca vulgaris is caused by the human papillomavirus, which induces epidermal hyperplasia and neovascularization in affected skin. The use of lasers is said to be based on the principle of targeting their vascular component, which is evident histologically as dilated blood vessels within the dermal papillae. Use of the PDL has been shown to induce intravascular thrombosis and vessel wall necrosis in patients with verrucae[45]. However, the nonspecific heat effect from lasers is likely the main mechanism underlying wart clearance with laser therapy. "Laserthermia" of warts, particularly with the Nd:YAG laser, has produced clearance in 75% of patients[46]. The mechanism may involve coagulation of epidermal proteins and blood vessels, with stimulation of a reactive inflammatory response. Although a similar tissue response is likely caused by CO_2 laser ablation of verrucae, response rates have been more variable, ranging from 30% to 80%[47]. Most notably, scarring and onychodystrophy can result from treatment of periungual verrucae with such ablative laser therapies[48].

A notable lack of bleeding and scarring makes the PDL laser a favorable choice. Given the limited penetration of the PDL, hyperkeratotic portions of the wart are first pared down. If bleeding occurs, hemostasis should be achieved, being careful to avoid application of flammable topical agents to the treatment area. Then, the lesions are treated until a dusky gray color is seen. However, rather high fluences are utilized, making this treatment quite painful, especially on the fingers. Depending upon the pain tolerance of the patient, digital nerve blocks may be needed. This procedure can be repeated every 2–4 weeks until clinical resolution.

While laser therapy for verrucae is not exclusively beneficial, it does supplement the dermatologist's armamentarium in the treatment of these recalcitrant lesions.

Pain Considerations

PDL treatment can be associated with significant discomfort and has been typically described as a "hot rubber band" snapping on the skin. Whereas this procedure is generally well tolerated by adults, children may require anesthesia. When local anesthesia is chosen (most often for localized lesions), agents that blanch the vasculature and decrease the hemoglobin target need to be avoided. In addition, topical anesthetics should not be applied to ulcerated lesions and dosing recommendations need to be followed (see Tables 143.4 & 143.5). Larger vascular anomalies in children may require injected local or general anesthesia. KTP laser therapy is associated with fleeting stinging as the laser is applied onto the skin. IPL treatments can be performed with or without topical anesthesia. Forced cold air or ice chilling is an effective method for reducing discomfort and protecting the epidermis at the same time, but associated vasoconstriction decreases the vascular target. Vibration distraction (gate theory) can also be effective. Nerve blocks are simple and effective for digital procedures.

TREATMENT OF MELANIN-CONTAINING LESIONS

Ephelides and Lentigines

Since melanin has a broad absorption spectrum (see Fig. 136.3), many lasers can be used to treat melanin-containing lesions. At the lower end of the therapeutic window, the penetration of green lasers is limited to the superficial papillary dermis. These lasers are best utilized for epidermal pigmented lesions. Thus, the frequency-doubled Nd:YAG (532 nm) laser, either Q-switched or normal mode, effectively treats lentigines and ephelides in most skin phototypes with limited recurrence[49]. Of note, in patients with a history of systemic gold therapy, Q-switched lasers will likely induce permanent darkening of the skin; such exposure needs to be determined prior to treatment. Additional lasers, e.g. the 800 nm diode, as well as IPL can also be used to treat epidermal pigmented lesions (Table 137.3). While the PDL is most commonly used for vascular lesions, 595 nm light is also well absorbed by melanin and can be used to treat pigmented lesions. By incorporating compression, the vascular component of the skin is blanched out and melanin-containing lesions can be targeted.

In general, the Q-switched ruby and alexandrite lasers are more effective when treating more deeply situated pigmented lesions (e.g. nevus of Ota), as these wavelengths have an increased depth of penetration. Q-switched ruby (694 nm) laser light is better absorbed by melanin than is alexandrite (755 nm) laser light, which might be an advantage in lighter-skinned individuals, but problematic in darker-skinned patients, given the increased likelihood of nonspecific heating of normal epidermal melanin. Q-switched Nd:YAG laser light is much less well absorbed by melanin and reaches more deeply into the skin; therefore, it is primarily used to treat dermal pigmented lesions.

For the treatment of lentigines, ephelides, and café-au-lait macules as well as nevus of Ota, understanding these profiles allows one to choose the optimal device. The clinical response of pigmented lesions to Q-switched lasers is determined by where the pigment is located (epidermal, dermal or mixed) and whether it is intracellular or extracellular, as well as the composition of the pigment (usually melanin)[50].

LASERS AND OTHER LIGHT-BASED DEVICES USED FOR THE TREATMENT OF PIGMENTED LESIONS				
Laser/device	**Wavelength (nm)**	**Fluence (J/cm^2)**	**Pulse duration**	**Applications**
Q-switched lasers (*highly pigment-specific*)				
Q-switched Nd:YAG, frequency-doubled	532	0.4–6	5–10 ns/ps	Lentigines
Q-switched ruby	694	3–12	20–40 ns	Lentigines, nevi*
Q-switched alexandrite	755	1–12	50–100 ns/ps	Lentigines, nevi*
Q-switched Nd:YAG	1064	3–12	5–10 ns/ps	Nevi*
IPL, long-pulsed lasers, and PDL with compression (*less pigment-specific*)				
Intense pulsed light (IPL)	500–1200	Up to 30	5–10 ms	Lentigines, nevi*
Diode	800	5–50	5–100 ms	Lentigines, nevi*
Nd:YAG	1064	Up to 300	1–100 ms	Nevi*
PDL with compression	595	3–5	0.45–1.5 ms	Lentigines
Long-pulsed alexandrite	755	25–50	0.5–300 ms	Lentigines, nevi*
*Treatment of pigmented melanocytic nevi (especially acquired lesions) is controversial.				

Table 137.3 Lasers and other light-based devices used for the treatment of pigmented lesions. Q-switched lasers are most effective for treating pigmented lesions due to their very short pulse durations, which effectively target the melanosome. In addition to the lasers listed above, pigment non-selective ablative lasers, such as CO_2 (10 600 nm) and erbium:YAG (Er:YAG; 2940 nm), can remove superficial pigmented lesions via nonspecific destruction. Parameters are dependent upon skin phototype, skin cooling technology and morphologic features; a test site is recommended when there are concerns regarding unwanted side effects such as hypopigmentation.

Benign Melanocytic Nevi

Laser removal of acquired and congenital nevi is controversial since no specimen is available for tissue diagnosis and margin assessment. Furthermore, the future biologic behavior of laser-resistant cells and the effect (if any) of laser thermal injury on these cells is unknown. Patients with atypical pigmented lesions should be examined carefully and regularly, preferably with total body imaging. Laser treatment of melanocytic lesions should only be considered for clinically banal lesions in patients with no personal or family history of melanoma.

Both acquired and congenital melanocytic nevi have been treated with Q-switched ruby, alexandrite, and Nd:YAG lasers[51]. The 694 and 755 nm devices can improve the appearance of acquired junctional melanocytic nevi without scarring. In general, smaller and thinner lesions are typically more treatment-sensitive. While congenital nevi can be lightened, complete eradication is much more difficult and recurrence is common. Laser therapy decreases the number of pigmented nevus cells in the papillary dermis, but is unlikely to affect deeper seated, non-pigmented cells that are closely associated with adnexal structures. This has been demonstrated histologically as persistent nests of nevus cells in the mid papillary and deeper dermis at depths of 0.16–0.44 mm. Deeper components of these nevi located within muscle or under fascia will also remain unaffected by laser surgery.

The normal mode (non-Q-switched), long-pulsed ruby and alexandrite lasers have also been used to treat acquired nevi. Some clinical lightening observed has been attributed to fibroplasia of the dermis overlying the residual nevus cells. Although fibroplasia may be cosmetically useful, this change potentially hides early signs of malignant transformation and might cause a delay in diagnosis. Therefore, patients who have any melanocytic nevi treated with lasers should understand that they need to report subsequent changes in color, shape, or size. Clinicians should remember that early cutaneous melanoma can have a subtle clinical appearance and they should have a low threshold for biopsy.

Café-au-Lait Macules and Nevus Spilus

Café-au-lait macules (CALM) are tan–brown patches, which histologically correspond to hypermelanosis of the basal melanocytes and keratinocytes. While these lesions can be seen in genodermatoses such as neurofibromatosis and McCune–Albright syndrome (see Ch. 61), they are typically isolated benign lesions. Cosmetic improvement can be achieved with the Q-switched ruby, alexandrite, and KTP lasers. However, CALM can be resistant to laser therapy, and they are prone to a high rate of recurrence. Use of the long-pulsed alexandrite laser has been reported to have a lower incidence of recurrence[52].

Nevus spilus consists of multiple lentigines and/or melanocytic nevi superimposed on a background CALM. Although the treatment of these lesions is very similar to that of CALM, these are typically more resistant and require multiple sessions. They may respond to normal-mode laser wavelengths or IPL. Rarely, malignant transformation has been described in nevus spilus, and thus caution is advised when treating with laser or light therapy.

Nevus of Ota and Nevus of Ito

Clinically, nevus of Ota and nevus of Ito appear as blue–gray patches and histologically, spindled pigment-producing melanocytes are present in the papillary dermis. These entities differ only in their anatomic location. Nevus of Ota involves the face (primarily V1/V2 distribution), while nevus of Ito corresponds to the distribution of the posterior supraclavicular and lateral brachial nerves. Both have been successfully treated with Q-switched ruby, alexandrite, and Nd:YAG lasers[53]. Generally, high energy fluences are required, with multiple treatments spaced at least 6 weeks apart. A drawback of the Q-switched ruby laser is the tendency for hypopigmentation, which is a consequence of increased absorption by normal epidermal melanin. Hypopigmentation is observed less often with Q-switched alexandrite lasers (755 nm), which also achieve deeper penetration into the dermis.

Near-infrared lasers, namely the Q-switched Nd:YAG (1064 nm), have even deeper penetration into the skin but are less well absorbed by melanin. Although these characteristics appear to negate each other, they allow for safer use in patients with darker skin and also allow for clearance of more deeply seated pigment. When in a sacral location, circumscribed dermal melanocytosis (Mongolian spot) spontaneously lightens in 95% of individuals by age 10 years. More persistent extra-sacral lesions can be treated with Q-switched lasers.

Blue nevi share some histologic features with nevi of Ota and Ito but are well-circumscribed gray–blue to blue–black papules (common) and plaques (cellular). As such, laser treatment of these lesions is similar to that of nevi of Ota and Ito. While blue nevi are clinically benign, rare malignant transformation has been reported in cellular blue nevi. In addition, the clinical differential diagnosis of blue nevi may include cutaneous melanoma and thus dermoscopy can provide useful information.

Melasma

Melasma is a complex and therapeutically challenging disorder with both intrinsic (e.g. genetic, hormonal) and extrinsic (e.g. ultraviolet light) factors (see Ch. 67). It most commonly involves the face and presents as tan to dark brown patches with sparing of photoprotected sites. Medical and procedural therapeutic strategies include sun avoidance, sunblocks, topical retinoids, hydroquinone, tranexamic acid, chemical peels, and laser therapy. While treatment regimens boast varying degrees of improvement, recurrence is the norm despite recommended measures such as strict sun protection.

Clinically, melasma is often categorized by distribution pattern and location of excess melanin. In epidermal melasma, melanin is localized to the basal and suprabasal epidermal layers and in dermal melasma, melanin is deposited within melanophages. The mixed variant includes features of both epidermal and dermal types. Although these subtypes are said to be distinguishable by Wood's lamp illumination, which accentuates epidermal pigmentation, histologic and confocal microscopy studies have shown an admixture of both types within a

single lesion. Of note, dermal deposits of melanin respond poorly to commonly prescribed topical therapeutic agents.

Since melasma is a disorder of hyperpigmentation due to increased melanin within epidermal melanocytes and dermal melanophages, it may seem intuitive that melasma should respond favorably to Q-switched lasers. However, this assumption has been demonstrated to be less than accurate. Although the melanophages present in dermal melasma can be selectively damaged by Q-switched lasers, the subsequent epidermal response frequently induces an inflammatory process that perpetuates or aggravates the problem[54]. Attempts at improving melasma by superficial laser resurfacing with Er:YAG may lead to temporary improvement, only to be followed by problematic postinflammatory hyperpigmentation.

Non-ablative, fractionated laser systems (see below) may also lead to improvement of melasma, but as with other therapies, recurrences are common and there is the potential for a deterioration in appearance. A preliminary case report described significant clinical improvement of treatment-resistant facial melasma after two treatments[55], with a subsequent study demonstrating that 60% of patients with skin phototypes III–V achieved 75%–100% improvement[56]. Although the precise explanation for how the photothermal energy improves melasma is not clear, the clinical improvements may be the direct consequence of increased hydroquinone absorption into the epidermis and dermis with the beneficial effect on dermal melanophages via microscopic channels.

Despite the multiple options described above, melasma remains a difficult-to-treat disorder, and regimens of topical retinoids, bleaching agents, and diligent sun protection remain the mainstay of therapy.

Becker Melanosis (Nevus)

Becker melanosis is a hamartoma that typically presents during childhood or early adolescence as light to dark-brown patches or plaques on the shoulder, upper back, or lateral arm (see Ch. 112). It is associated with variable amounts of hypertrichosis as well as a smooth muscle hamartoma. Because melanin is located in both the epidermis and the dermal follicular matrix, treatment of Becker melanosis may require targeting both of these components. The basal layer melanin component requires nanosecond range pulse durations, and successful lightening has been accomplished with Q-switched ruby and alexandrite lasers[57]. In contrast, the follicular melanin responds more favorably to the ms pulse durations that characterize photoepilation systems. While these simplistic distinctions allow for methodical treatment, Becker melanosis is typically somewhat resistant to therapy. Often, cosmetic improvement is more reasonably and realistically approached with the objective of photoepilation alone, as opposed to comprehensive eradication of the hamartoma.

Postinflammatory Hyperpigmentation and Drug-Induced Discoloration

Postinflammatory hyperpigmentation (PIH) is a common side effect of many dermatologic procedures, both medical and cosmetic. For patients with darker skin phototypes, PIH should be anticipated and a treatment plan promptly initiated. Common topical therapies include corticosteroids, retinoids, and bleaching creams. A newer treatment strategy is the use of fractionated photothermolysis with a low density and low to moderate energy. The fine columns (referred to as microthermal or microablative zones; see below) can be generated at a desired depth, allowing for drug delivery and increased penetration of therapeutic topical agents into the skin. For treatment-resistant patients, Q-switched ruby, alexandrite, and Nd:YAG lasers have been used to expedite resolution of PIH. However, since PIH can be caused by these devices, circumspection is appropriate.

As opposed to PIH, which is due to excess melanin, discoloration that results from sclerotherapy is a consequence of vessel destruction, erythrocyte extravasation, and interstitial hemosiderin deposition. The Q-switched ruby laser has been used successfully to treat this common sequela from sclerotherapy, with a reported 92% improvement rate[58], but the success rate is quite variable.

Drug-induced hyperpigmentation or discoloration represents deposition of drug metabolites, iron, melanin, or a combination of these components in the dermis and/or epidermis (see Table 67.5). The resultant color depends on the initiating medication and can range from blue–gray or brown to yellow or red. Use of Q-switched ruby, alexandrite, and 1064 nm Nd:YAG lasers has led to improvement of minocycline-, amiodarone-, imipramine- and silver (argyria)-induced hyperpigmentation or discoloration.

HAIR REMOVAL

Hair removal is one of the most commonly performed laser procedures. According to the American Society for Dermatologic Surgery, there were 385 000 laser hair removal procedures completed in 2018 alone[59]. While the distribution, density, and color of hair is related to sex and genetic background, the acceptability and desirability of hair are often related to societal and cultural norms. Markedly excessive hair can be a marker for an underlying endocrinopathy or a medication side effect and a possible etiology should be investigated prior to photoepilation (see Ch. 70). While most patients who undergo photoepilation have the cosmetic objective of decreasing unwanted hair, there are several medical applications of laser hair removal, such as treatment of pseudofolliculitis barbae or folliculitis decalvans.

Although the patient's ultimate desire may be to achieve total hairlessness in an anatomic region, complete eradication of hair is often an unattainable objective. Realistic expectations are key and the laser surgeon should clearly and specifically communicate these objectives to the patient. For some patients with particularly coarse, dense unwanted hair, a successful outcome might be a transition to finer, lighter hair. Potential side effects should be reviewed, including pigmentary changes (hyper- or hypopigmentation), erythema, edema, discomfort, and very rarely, scarring.

Photoepilation is based on selectively delivering energy to both pigmented and non-pigmented structures within the hair follicle. Thermal energy delivered to the melanin-rich hair shaft and hair bulb matrix will destroy surrounding follicle structures while minimizing non-selective injury to the surrounding tissues. Often, non-pigmented structures near the follicle are targeted, such as the follicular stem cells that line the outer root sheath and actually reside quite far from the pigmented hair shaft (see Ch. 68)[60]. Three mechanisms have been proposed to explain hair follicle destruction. These include: (1) photothermal injury to the follicle via direct heating of the follicle; (2) photomechanical injury by induction of shock waves and violent cavitation; and (3) photochemical injury by production of toxic intermediaries such as singlet oxygen or free radicals[61]. Heat-induced change of the follicular structures and immediate surrounding tissues can result in transient growth arrest via induction of catagen or permanent hair removal via follicular fibrosis.

Although the absorption of melanin corresponds to wavelengths from 400 to 1200 nm, the best lasers for photoepilation have wavelengths of 600 to 1100 nm, a range where there is more selective absorption by melanin and the light penetrates relatively deeply into the skin. Given this relatively broad therapeutic spectrum, many laser systems have been utilized, including the ruby (694 nm), alexandrite (755 nm), diode (800–810 nm), and Nd:YAG (1064 nm) lasers, in addition to a variety of IPL systems with different cut-off filters. The optimal wavelength is probably in the ruby laser range (694 nm), but longer pulsing beyond 3 to 4 ms is problematic, which has led to the utilization of alternative wavelengths. However, the safety and efficacy of laser hair removal is dependent on the operator's sophisticated knowledge regarding the practical application of laser–tissue interactions and the principles of selective photothermolysis. From a practical perspective, this entails accurate selection of the laser system, the optimal pulse duration, and the appropriate fluence to achieve hair removal while protecting the epidermis and minimizing non-selective dermal heat injury. Inappropriate selection can result in permanent scarring and dyspigmentation.

Selection of the appropriate pulse duration is critical for effective photoepilation. As the thermal relaxation time of a hair follicle is ~10–30 ms, the pulse duration should be adjusted to match these parameters. However, extension of the pulse duration beyond the thermal relaxation time of the follicular unit promotes delivery of thermal damage to the surrounding non-pigmented stem cells and should induce more consistent follicular destruction[60]. Coarser, thicker, and darker hairs may have relatively longer thermal relaxation times compared to thinner, finer hairs[61]. The ideal patient for hair removal is one with lighter skin (phototypes I–III) and dark brown to black hair (Fig. 137.14).

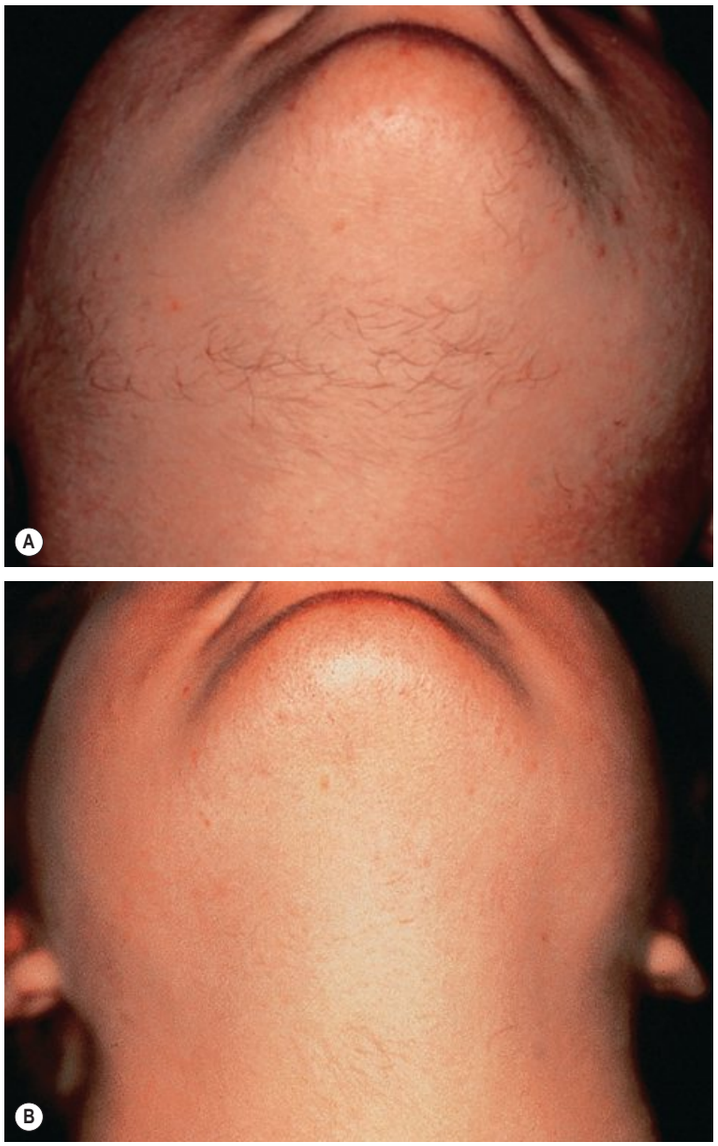


Fig. 137.14 Laser hair removal. A Before treatment. **B** Two years after three long-pulsed diode laser treatments; there is almost complete and long-term hair growth reduction. *Courtesy Jeffrey Dover, MD, and Kenneth Arndt, MD.*

In general, higher energy fluences achieve greater hair reduction. However, since overzealous energy fluences might induce excessive collateral heat, a conservative selection of parameters is recommended. Typical danger zones are the chin and lip (where there is a greater density of hair follicles) as well as pigmented genital or inguinal skin. Energy fluence can be titrated up, if necessary, with each treatment as hair becomes less dense but tissue endpoints should be carefully monitored to avoid adverse effects. Parameters are not interchangeable between devices, even those with the same laser or IPL wavelength. It is incumbent on the operator to know how to operate each system that he or she employs.

Laser hair removal in patients with darker skin can be more problematic as epidermal melanin competes with the follicular target. For patients with skin phototypes IV–VI, the long-pulsed Nd:YAG laser is generally regarded as the safest system. However, the most common criticism of the long-pulsed Nd:YAG laser is the associated pain.

Appropriate cooling of the epidermis is critical with hair removal devices. Cooling can be applied immediately prior to (pre-cooling), during (parallel cooling), or after laser pulsing (post-cooling). Aside from protecting the epidermis from excessive heat, contact cooling handpieces allow compression of the skin and facilitate delivery of more laser energy to the targeted hair follicles.

Although commercial laser and IPL companies might argue otherwise, no system is inherently superior for photoepilation. In general, lighter skin phototypes (I–III) respond better to treatment with the 755 nm alexandrite or the 800 nm diode laser, while darker skin phototypes (IV–VI) respond better to treatment with the 1064 nm Nd:YAG laser. Most studies have shown comparable efficacy rates when sufficient energy fluence is used and multiple treatments are performed. Regardless of the laser or IPL system utilized, serial treatments are required for significant, long-term hair reduction. Typically, three to ten treatments are recommended, delivered at 4- to 8-week intervals, depending on anatomic location, skin phototype, and hair regrowth. Response rates of 70%–90% hair reduction at 6-month follow-up have been reported[62]. Long-term efficacy of laser hair removal correlates with higher concentrations of eumelanin[63]. Recent attempts have been made to treat non-pigmented, gray or white hair, but so far there is little evidence of benefit.

Paradoxical hypertrichosis following the use of hair removal devices is a well-documented side effect of photoepilation. This has generally been described in patients with Mediterranean, Hispanic or Asian backgrounds, skin phototypes III or IV, and dark lanugo hair. Of note, it can occur with any of the laser or IPL hair removal systems. Initial reports suggested that affected patients should be evaluated for hyperandrogenemia, but paradoxical hypertrichosis occurs more commonly than does hyperandrogenemia[64]. The largest retrospective analysis to date of 750 patients found that the overall incidence of paradoxical hypertrichosis was 4.5% (although it is likely higher), and the hypertrichosis occurred most often on the face and neck of patients with skin phototypes III and IV. These authors postulated that the hair induction occurred at the borders of the treated areas, perhaps because of sub-therapeutic energy fluences during laser therapy and local inflammatory responses following photoepilation[65]. While paradoxical hypertrichosis can be difficult to treat, in one author's experience (CBZ), treatment with the nanosecond Q-switched Nd:YAG (1064 nm) laser can provide at least temporary improvement. It has been suggested that application of ice to the perimeter of the treatment area and use of the highest tolerated energy fluence may minimize this side effect.

Proper pre-treatment preparation of the skin prior to photoepilation allows for optimal treatment results. Failure to recognize the need to avoid treating suntanned skin has resulted in numerous burns, scars, and permanent pigmentary changes. In sunny climates, patients should be advised to apply broad-spectrum high SPF sunscreens for weeks prior to laser therapy and to avoid tanning both before and after photoepilation, in order to prevent PIH. Secondly, patients should avoid plucking, waxing, threading, and electrolysis prior to laser treatment as these will remove the target chromophore. Patients can be advised that shaving or depilatory creams are acceptable. Finally, given that photoepilation is often associated with some degree of discomfort, topical anesthetics can be applied prior to treatment. While increasing patient comfort during the procedure is an important objective, several deaths have been reported with misuse of strong topical anesthetics applied to large areas under occlusion in unsupervised situations.

During the procedure, the laser surgeon should constantly assess the skin's reaction to the laser energy and adjust parameters, if necessary. The operator should expect to observe perifollicular erythema and focal edema, indicating proper parameter selection. Skin changes to avoid are charring, blistering, crusting, or ulceration of the skin; these reflect dermal heat injury and are a marker of an energy fluence that is too high. In severe cases this may result in dermal necrosis and marked scarring.

TREATMENT OF SCARS

Laser therapy, particularly fractional laser resurfacing, has become an increasingly valuable tool for the treatment of burn and traumatic scars. It may also have the potential to improve the wound healing process and mitigate scar formation when employed prior to surgical incision[66]. When selecting specific laser treatment modalities, important characteristics to consider are scar type (hypertrophic, flat, atrophic, contracted, distensible, icepick), location on the body, erythema, dyschromia (hyperpigmented, hypopigmented), and thickness. In addition, individuals with darker skin phototypes are more susceptible to PIH. When determining settings for laser treatment depth[20], scar thickness has historically been estimated by palpation, but recently optical coherence tomography (OCT) was shown to have

greater accuracy[67]. Laser penetration should be proportional to, but not exceed, the thickness of the scar[20], with optimal laser penetration between 50%–75% of scar depth[68].

For traumatic scars characterized primarily by erythema, vascular lasers are used to target oxyhemoglobin within the scar's microvasculature[69]. PDL at low fluence settings and short pulse width is most commonly used, with treatments every 1 or 2 months until goals are reached[20]. If multiple devices are to be used during a scar treatment session, it is important to treat the erythematous element first, to avoid erythema or blood created by the other procedures being targeted by the vascular laser[69]. In patients with skin phototypes I–IV, PDL can be especially effective in improving the quality and cosmetic appearance of surgical scars when instituted early, i.e. from the day of suture removal[69].

Scar texture and dyspigmentation can be addressed with fractional laser resurfacing. For hypertrophic and contracted scars, ablative fractional lasers are the most effective treatment, as they induce robust tissue remodeling and improvement in symptoms and cosmesis can be seen within days to weeks[20]. Burn scars are most effectively treated with at least three rounds of the ablative fractional CO_2 laser at 4- to 6-week intervals[70]; low densities are recommended[71]. Hypertrophic or keloidal surgical scars respond well to intralesional injections of triamcinolone acetonide ± 5-fluorouracil after ablative fractional resurfacing[69]. Since atrophic scars reflect collagen destruction, both ablative and non-ablative fractional lasers are employed as they induce neocollagenesis and remodeling within atrophic areas. Similar results are observed, but non-ablative fractional lasers are better tolerated[20] and safer in skin phototypes IV–VI[71]. Fractional laser resurfacing may begin once the scar has stable epidermal coverage, with a minimum interval of 1 to 3 months between treatments until the desired improvement or a therapeutic plateau is reached[20].

Scar hyperpigmentation is most commonly due to deposition of melanin via a poorly understood mechanism. Hyperpigmentation refractory to traditional topical therapy may be treated with Q-switched lasers (694, 755, and 1064 nm) or non-ablative fractional resurfacing. Because darker skin phototypes are more susceptible to PIH with high-density non-ablative fractional resurfacing, lower densities are preferable. Hypopigmented scars are more difficult to treat, although they do show modest improvement in color and texture with ablative and non-ablative fractional resurfacing, especially when supplemented with prostaglandin analogues[72]. For example, the erbium-doped 1550 nm fractionated laser combined with topical bimatoprost and tretinoin have been shown to induce repigmentation in atrophic, hypopigmented surgical scars[69].

TREATMENT OF STRIAE DISTENSAE

Striae distensae are common after pregnancy, growth spurts in adolescence, or rapid weight gain. Histologically, there is thinning of the epidermis and atrophy of the dermis. In their early inflammatory stages, they often appear pink to purple in color and are called striae rubrae. The latter mature and take on a more pallid color and then are termed striae albae (see Ch. 99).

Although treatment of striae is not medically necessary, many patients seek cosmetic improvement. Several lasers, including PDL, 308 nm excimer, fully ablative, ablative fractional, non-ablative fractional (1450/1550 nm), and Q-switched or low-fluence, long-pulsed Nd:YAG (1064 nm) lasers, as well as IPL, have been used with varying degrees of success with regard to the color and texture of striae[73]. More targeted studies have correlated clinical improvement with increased elastin remodeling or formation. Fractionated photothermolysis has been shown to improve atrophic scars[4], and in a pilot study of striae in patients with skin phototypes IV–VI, epidermal thickening and remodeling of collagen and elastin fibers was observed after 1550 nm fractionated photothermolysis[74]. In spite of some wistful reports, the results of striae treatment with lasers have been quite disappointing.

TREATMENT OF CELLULITE

The treatment of cellulite is covered in Chapter 156, including the use of the minimally invasive 1440-nm side-firing laser, Rapid Acoustic Pulse™ technology, and vacuum-assisted subcision.

TREATMENT OF TATTOOS

A tattoo represents the presence of exogenous pigmented material in the skin. Although the most common purpose for tattooing is artistic and cosmetic, it has also been utilized in the medical field, in particular as radiation port markers. Additionally, tattoo pigment composed of lead, carbon, asphalt, gunpowder, or coal can be introduced explosively or traumatically. Once embedded, the exogenous pigment is taken up predominantly by dermal macrophages. These pigment particles measure from 2 to 400 nm, but generally average ~40 nm in diameter. Tattoo removal is a common patient request. Prior to advancements in laser technology, removal was frequently associated with disfiguring scarring. With the evolution of the Q-switched nanosecond and picosecond lasers, pigment eradication can now be more safely achieved, with less scarring and/or pigmentary changes.

Q-switched lasers are characterized by having extremely short pulses, which induce photomechanical and photoacoustic laser–tissue interactions. The immediate local exponential increase in temperature to 200–300°C causes dramatic expansion of organelles such as lysosomes within macrophages, followed by their equally catastrophic contraction/collapse, leading to *cavitation* of the tattoo-bearing macrophages. The exceptionally short pulse duration limits the thermal damage to just the macrophage.

Clinically, the laser tissue reaction is seen as immediate epidermal whitening, which is essentially nitrogen vapor within the epidermis and immediately adjacent to the tattoo pigment particles in the dermis (Fig. 137.15). Mechanical damage results in cell membrane rupture and the release of exogenous pigment into the extracellular space. Some of this released pigment departs the skin and drains via the lymphatics to local lymph nodes, while the remainder is simply re-phagocytosed. In addition, there is fragmentation of tattoo ink particles and this changes their optical properties and/or allows easier reuptake by macrophages followed by removal from the site.

More recently, Q-switched pulsed lasers in the shorter picosecond domain (1 trillionth of a second or 10^{-12} seconds) have been developed and they are said to be more effective in removing ultrasmall tattoo particles with extremely short thermal relaxation times[75]. Compared to Q-switched nanosecond lasers, picosecond devices have been shown to clear tattoos with fewer treatment sessions and may be more effective for blue and green tattoo pigments[75]. However, this is not always the case and traditional nanosecond lasers are still a good option for many tattoos.

Selection of the appropriate Q-switched laser is determined by the colors of tattoo pigment to be targeted (Fig. 137.16). Based on "complementary matching" of tattoo pigment, green tattoo pigment is most



Fig. 137.15 Immediate tissue whitening following treatment of a tattoo with the Q-switched alexandrite laser. *Courtesy Roy Grekin, MD.*

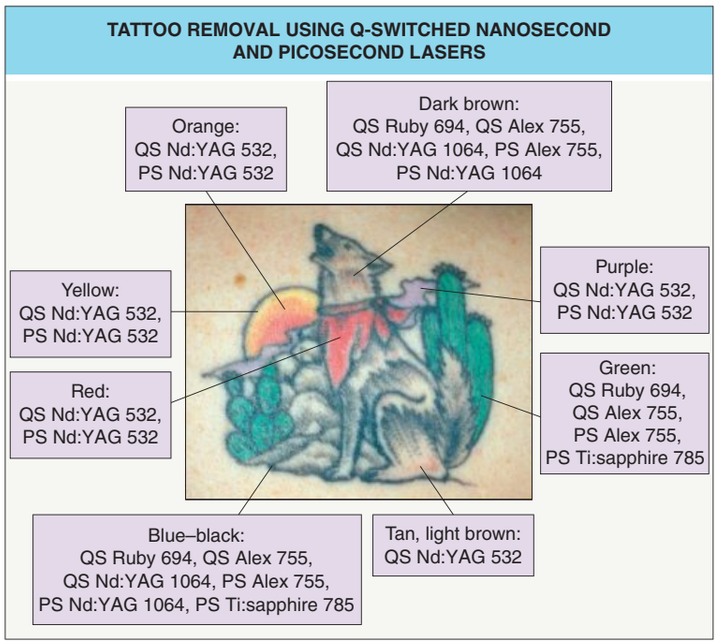


Fig. 137.16 Tattoo removal using Q-switched nanosecond and picosecond lasers. The Q-switched (QS) Nd:YAG (532 nm) laser can be used to try to remove red, orange, yellow, purple, and tan/light brown pigments. The QS alexandrite (Alex; 755 nm) and QS ruby (694 nm) lasers can be employed to remove green tattoo ink, while the QS Alex, QS ruby and QS Nd:YAG (1064 nm) lasers can remove blue–black and dark brown tattoo ink. The picosecond (PS) Alex 755 and PS Nd:YAG 1064 can remove blue, black and dark brown tattoo ink; the former can also remove green tattoo ink. The PS Nd:YAG 532 can remove red, orange, yellow and purple tattoo ink. The PS titanium (Ti):sapphire 785 nm laser is used to remove green and blue tattoo ink. See Table 137.4 for details. *Courtesy Jean L. Bolognia, MD.*

effectively removed by a red laser (694 nm), and red tattoo pigment is best removed with a green laser (532 nm). Blue and black pigments are removed with all three lasers – ruby, alexandrite, and Nd:YAG (Table 137.4). More difficult to remove are yellow and orange pigments, as these are not well absorbed by currently commercially available Q-switched laser light.

Despite all the advances in laser therapy, total eradication of tattoos can prove frustratingly difficult. One additional refinement is the so-called "R20" technique consisting of four repeated treatments (at 20-minute intervals) during the same treatment session. The 20-minute delay allows the laser-induced epidermal gas bubbles to disappear after which the treatment is repeated[76]. A further refinement is the use of topical perfluorodecalin (PFD), which immediately removes nitrogen gas bubbles, allowing for shorter time intervals[77]. The latest solution in this regard is the use of Rapid Acoustic Pulse™ (RAP™, Soliton, Inc.) technology which uses high energy tuned shockwaves to clear the epidermal and intradermal vacuolar whitening rapidly enabling multiple laser passes in a single office laser tattoo removal session[78].

Amateur tattoos often incorporate blue–black pigments that are carbon-based, such as India ink. Given that these tattoos have only a few colors and lower ink density, coupled with the observation that they may be placed at variable depths (primarily superficially) in the skin, amateur tattoos are relatively easy to remove. Professional tattoo artists incorporate a wider spectrum of colors and deposit the pigments within the deep papillary and superficial reticular dermis. Hence, removal can be problematic, even with the best devices.

Complications of tattoo removal include both hyper- and hypopigmentation. While hypopigmentation can be observed with the ruby and alexandrite lasers, hyperpigmentation commonly occurs in patients with more darkly pigmented skin. It has often been said that Q-switched lasers remove tattoo pigment without scarring. While this is often true, there can be significant textural changes after multiple treatments with high energy fluence devices. Additionally, inflammatory reactions to tattoo ink have been reported, including eczematous, granulomatous, and lichenoid reactions. When systemic reactions occur after laser treatment, they are the consequence of mobilized antigens.

Paradoxical darkening of skin-colored tattoo ink is a common phenomenon following treatment with any of the Q-switched lasers. This unfortunate event happens immediately after a single laser pulse and is caused by a shift from an oxidized state to a reduced state in the tattoo pigment. This was classically reported as darkening of red "lip liner" to dark brown or black pigment as the ferric oxide tattoo was reduced to ferrous oxide (Fig. 137.17). Similar color changes can be seen in tattoos with titanium dioxide, a common agent used to lighten tattoo pigments; when a Q-switched laser is applied to titanium, it can change from white to blue–black. Although this problematic side effect can be improved via continued treatment with any of the Q-switched lasers, a test spot is wise with such tattoos, particularly on the face.

TREATMENT OF PSORIASIS AND VITILIGO

Psoriasis affects nearly 2% of the US population and often commits patients to a lifetime of treatment. The range of therapies includes topical corticosteroids and vitamin D_3 analogues, systemic retinoids, methotrexate, phototherapy, and targeted immunomodulators ("biologic agents"; see Ch. 8). Despite the variety of treatment options available, some psoriatic plaques are recalcitrant. Application of laser therapy may represent a novel approach to resistant lesions, particularly those in "problem areas" such as the scalp and intertriginous zones. The most commonly used laser for psoriasis is the 308 nm XeCl excimer laser. As a localized narrowband UVB therapy, the excimer laser has been demonstrated to clear psoriatic plaques by impeding epidermal cell proliferation and perhaps inducing localized immunosuppression. Compared to conventional UVB phototherapy, treatment with the excimer laser cleared psoriatic plaques two times faster and with lower cumulative UVB doses[79]. Additionally, PDL has been used to treat psoriasis by targeting the underlying abnormal vasculature. While both systems are beneficial, the excimer laser has been shown to yield more favorable improvement[80].

The excimer laser has also been shown to produce impressive improvement of vitiliginous skin when used as adjuvant therapy, especially when combined with topical tacrolimus[81]. Lastly, the excimer laser has been used to repigment, at least temporarily, some of the patients who developed delayed-onset permanent hypopigmentation following standard CO_2 or Er:YAG laser resurfacing procedures.

PRE- AND POSTOPERATIVE CONSIDERATIONS, SIDE EFFECTS, AND COMPLICATIONS

Preoperative Considerations

Prior to any laser procedure (especially ablative), an appropriate medical history should be obtained, including allergies and medications. Physicians should specifically elicit any history of prior cosmetic procedures. Patients with a history of autoimmune connective tissue disease, diabetes mellitus, or drug, alcohol, or tobacco abuse should be treated cautiously, as wound healing may be impaired. Q-switched lasers are contraindicated in patients with a history of prior systemic gold therapy. Individuals with a personal or family history of vitiligo should probably not be treated with certain devices, as vitiligo could be incited or worsened (Koebner phenomenon).

During the consultation, the patient and laser surgeon must mutually identify the problem(s) to be treated and establish reasonable expectations for improvement. Whereas one ablative fractionated procedure may achieve marked improvement in rhytides and acne scarring, three to six treatments may be required with a non-ablative system if little "downtime" is required. Potential risks of laser therapy are reviewed, which may include scarring, blistering, infection, hyper- or hypopigmentation, and milia/acne formation. If an ablative fractional laser treatment is planned, then there should be a thorough discussion of postoperative wound care (see below).

Anesthesia and Eye Protection

Both ablative and non-ablative fractional resurfacing can be quite painful without appropriate anesthesia, particularly when using high energies with a high density. Application of topical anesthetics in a lipophilic ointment base or under occlusion for ~1 hour after thorough

TATTOO PIGMENTS, LASERS USED FOR THEIR REMOVAL, AND POTENTIAL COMPLICATIONS			
Color/etiology	**Pigment**	**Lasers**	**Complications**
Traumatic	Lead, dirt, gunpowder, other	QS ruby, QS alexandrite, QS Nd:YAG (1064)	Hypopigmentation, micro-explosions (gunpowder)
Amateur black	India ink, carbon	QS ruby, QS alexandrite, QS Nd:YAG (1064), PS alexandrite, PS Nd:YAG (1064)	Hypopigmentation
Professional black	Carbon, iron oxide, logwood extract	QS ruby, QS alexandrite, QS Nd:YAG (1064), PS alexandrite, PS Nd:YAG (1064), PS Ti:sapphire (785)	Hypopigmentation
Blue	Cobalt aluminate (azure blue)	QS ruby, QS alexandrite, QS Nd:YAG (1064), PS alexandrite, PS Nd:YAG (1064), PS Ti:sapphire (785)	Hypopigmentation
Green	Chromium oxide (casalis green), hydrated chromium sesquioxide (guignet green), malachite green, lead chromate, ferro-ferric cyanide, curcumin green, phthalocyanine dyes (copper salts with yellow coal tar dyes)	QS ruby, QS alexandrite, PS alexandrite, PS Ti:sapphire (785)	Hypopigmentation, allergic reactions (chromium)
Red	Mercury sulfide (cinnabar), cadmium selenide (cadmium red), sienna (red ochre; ferric hydrate and ferric sulfate), azo dyes	QS Nd:YAG (532), PS Nd:YAG (532)	Hypopigmentation, tattoo ink darkening, allergic reactions (mercury sulfide, cadmium, azo dyes)
Yellow	Cadmium sulfide (cadmium yellow), ochre, curcumin yellow	QS Nd:YAG (532), PS Nd:YAG (532)	Hypopigmentation, tattoo ink darkening, allergic reactions (cadmium)
Brown	Ochre	*Tan/light brown*: QS Nd:YAG (532) *Dark brown*: QS ruby, QS alexandrite, QS Nd:YAG (1064), PS alexandrite, PS Nd:YAG (1064)	Hypopigmentation, tattoo ink darkening
Violet	Manganese violet	QS Nd:YAG (532), PS Nd:YAG (532)	Hypopigmentation, tattoo ink darkening
White	Titanium dioxide, zinc oxide	QS Nd:YAG (532)	Hypopigmentation, tattoo ink darkening
Skin colored	Iron oxides	QS Nd:YAG (532)	Hypopigmentation, tattoo ink darkening

Table 137.4 Tattoo pigments, lasers used for their removal, and potential complications. Hyperpigmentation and textural changes also occasionally occur as complications. Hypo- and hyperpigmentation are more common in individuals with highly pigmented skin, and they are best treated with the Q-switched (QS) Nd:YAG (1064) laser to reduce this risk. PS, picosecond; Ti, titanium.

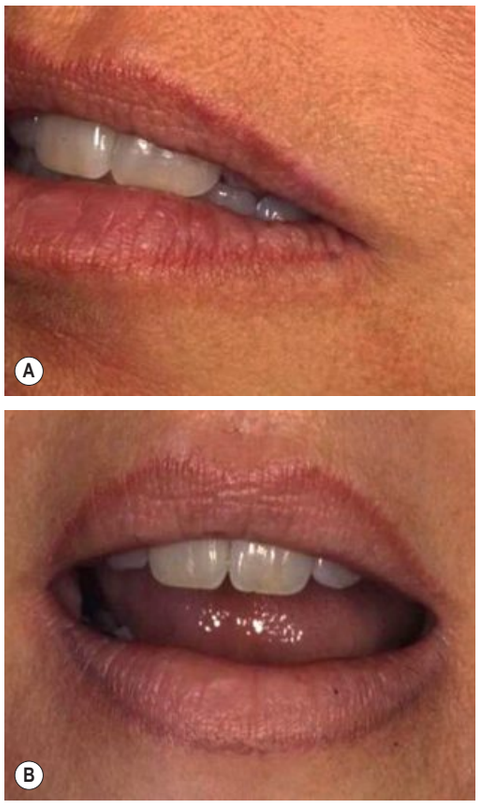


Fig. 137.17 Paradoxical tattoo darkening reaction following Q-switched laser removal of pink tattoo at the lip margin. **A** Before treatment. **B** Immediately after treatment.

skin cleansing is a simple and effective method for increasing patient comfort. Cooling strategies such as forced cold air or contact cooling can enhance patient tolerance. For more aggressive ablative procedures, supplementary anesthesia with nerve blocks, tumescent anesthesia, nitrous oxide (Pro-Nox™, Clarion Medical Technologies), systemic narcotics, or anxiolytics are often used.

Ocular injury can occur without appropriate wavelength-specific eye protection during laser procedures. An outline of safety precautions is provided in Table 136.5.

Post-therapy Considerations, Side Effects, and Complications

Following ablative fractional resurfacing, punctate bleeding and serosanguineous drainage are normal side effects (see Fig. 137.7), which dry into a thin keratinous crust within 24–48 hours. Patients are encouraged to minimize this crusting and aid in its exfoliation by applying dilute vinegar–water soaks to the treated sites every couple of hours. This is followed by a thin coat of white petrolatum ointment or generous amounts of a bland moisturizing cream until re-epithelization is completed.

Edema and erythema of treated skin is observed following both ablative and non-ablative fractionated therapies, but these side effects are much more pronounced after ablative procedures[82]. Topical application of a potent corticosteroid (e.g. fluocinonide ointment) immediately following the procedure can reduce these side effects. Non-ablative FP typically requires little or no "downtime" for healing, and the edema and erythema resolve within 24–48 hours. For ablative FP, the erythema dramatically improves within 1 week, but mild erythema and edema can persist for 3–6 weeks. Most patients are able to return to their normal activities, including work, and to apply makeup around 7 days following ablative FP. Well-documented side effects of generalized and

persistent erythema or delayed hypopigmentation that are seen with traditional resurfacing have been reported only rarely with fractionated lasers. Additionally, lines of demarcation are easily avoided by feathering the transitional skin between treated and untreated regions with near-minimal fluence and density settings.

Because only minute areas of damage are induced and the skin heals rapidly, fractionated ablative systems offer an unparalleled safety margin as compared to traditional ablative lasers. However, infection is still the most significant complication and can lead to permanent scarring. It is advised that all patients begin oral antiviral therapy the day prior to, or the morning of, the procedure. They should also have easy access to postoperative skin evaluations, especially if fever, pain, angular erythema, or pustular discharge is noted. Use of oral antibiotics and antifungal agents can be decided on a case-by-case basis.

Although scarring is an infrequent event, recent case reports have alerted laser surgeons to be cautious in "underprivileged" areas such as the neck and chest which are relatively devoid of adnexal structures[83]. Whereas skin on the cheek with its thicker dermis and abundant sebaceous glands can tolerate high energies and up to 70% ablation for certain indications, more modest energy and significantly less ablation density should be employed on thinner, finer, and less privileged areas.

Another noteworthy consideration for minimizing the risk of scarring is avoidance of immediate and direct scanned overlap of treatment areas. Use of a non-overlapping technique allows the treated skin sufficient time to cool before the application of the subsequent pass. This prevents bulk heating, a likely cause of scarring when it has occurred with fractional laser therapy. While ancillary cooling is not necessary, forced cold air is recommended as it facilitates heat dissipation, minimizes the potential for non-selective heat injury, and makes the procedure more comfortable. Where there is plume, smoke evacuation devices should be used.

PIH is a near certain side effect when treating darker skin phototypes. This predictable event can be mitigated with early application of 4% hydroquinone cream, starting shortly after non-ablative procedures. For those who have undergone ablative FP, this topical treatment can be started once the serosanguineous discharge of the immediate postoperative period has ceased. Patients with a prior history of melasma or other pigmentary disorders might be pretreated with topical hydroquinone prior to the procedure.

RADIOFREQUENCY AND ULTRASOUND

Skin Tightening

Monopolar radiofrequency (RF) energy generates dermal heat in a manner which is directly related to tissue impedance. The first commercially available monopolar RF device was ThermaCool TC™ (Thermage®) which delivered high-frequency RF energy to the skin via a thin, coupling electrode handpiece with active cooling. *In vivo* studies demonstrated that RF energy produced collagen contraction after disrupting hydrogen bonds within the collagen triple-helix structure[84].

After RF tissue tightening received FDA clearance for periorbital rhytide reduction in 2002, it was more widely used on the face and neck for improvement of skin laxity. A split-face study demonstrated average brow elevation of 2–4 mm, superior palpebral crease elevation of 1.9 mm, and reduction of jowl surface area by 22%[84]. Although other early studies reported similar conclusions, results in clinical practice were far more variable and unpredictable, and the treatments were associated with significant patient discomfort[85]. Aside from transient erythema and edema, irregular depressions ("mattress-top" irregularities) were seen, which were attributed to excessive treatment (outside the recommended parameters) causing localized fat atrophy. New algorithms and devices were developed, which increased both the reproducibility of the results and patient comfort. They included the use of: (1) lower energies over a larger tip in a multiple-pass technique[13]; (2) a transcutaneous electrical nerve stimulation (TENS)-like interruption of RF energy interspersed with hot/cold skin stimulation; (3) vibration (acting on the gate theory of pain); (4) a modulated RF profile; and (5) more distributive electrodes. In 2017, RF technology received FDA clearance for non-invasive smoothing of skin on the face, around the eyes, and body.

Bipolar RF devices create localized heat by conducting current between the two electrodes on the skin surface (see Fig. 136.7). Studies purport to have shown a 25%–50% improvement in wrinkles, skin smoothness, and texture[13]. There are reasons to believe that the bipolar devices are not as efficient as monopolar devices in their ability to tighten tissue or create new collagen.

Ultrasound (US) has emerged as a recognized technique for non-invasive tissue tightening. The primary mechanism is the absorption of either very brief focused or much longer diffuse acoustic energy. US is colorblind and thus can be used on all skin phototypes.

Ultherapy™ (Merz) utilizes *high intensity focused ultrasound* (HIFU) and has been cleared by the FDA for improvement in the appearance of the face, neck, and décolletage. Depth-specific transducers induce ms pulses of focal injury within the skin without damage to the epidermis. Use of a prototype device led to significant skin tightening, with a 1 mm eyebrow lift in >75% of treated subjects[86]. In cadaveric skin, damage was noted at a depth of 4.2 mm, including damage to the superficial muscular aponeurotic system (SMAS)[87]. This targeted approach was met with significant enthusiasm, and a number of investigators have observed good clinical improvement. However, some clinicians still remain highly skeptical about the long-term benefits. Side effects include focal bruising and pain, reported by 25% and ≤55% of patients, respectively.

SofWave™ (SofWave Medical Ltd) provides more *diffuse US* with mid-dermal heating to 60–70°C, maximally targeting a depth of 1.5 mm for 5 seconds without damage to the underlying structures including bone, nerves, fat, and blood vessels. This device has no disposables, no moving parts, and no optics. The parallel delivery of more diffuse ultrasound beams, integrated cooling, and a large contact area allow for less discomfort and faster treatments. Patients should understand that these devices are no replacement for surgical skin tightening and may take multiple treatments to achieve the desired outcome.

Radiofrequency Microneedling Devices

Radiofrequency (RF) microneedling devices have made major inroads into traditional methods for skin rejuvenation. A plethora of such devices have been FDA cleared and are used for rejuvenation, "tightening", and improvement in scarring. Some are monopolar, while others are bipolar; electrodes are either insulated or non-insulated (see Table 137.1). The original device, Profound® RF (Candela), was shown to induce new collagen and elastin within the mid dermis, leading to improvement in facial and extrafacial skin laxity. However, the procedure is quite uncomfortable, requiring topical anesthetic, nerve blocks, and possibly nitrous oxide and parenteral pain control.

In general, RF microneedling is performed 4–6 times at one-month intervals using only topical anesthesia. The needle density and length are sufficient to provide both superficial and deep controlled thermal injury (see Table 137.1). Given the relatively low cost of device acquisition, low patient downtime and lack of PIH, this device has become quite popular among aesthetic surgeons and the spa industry.

Use of microneedling devices without RF may improve acne scarring, but there remains little evidence to support touted skin tightening benefits. The addition of RF and/or the immediate use of topical agents may provide real benefits.

MICROWAVES

In the electromagnetic spectrum, microwaves lie between infrared light and radio waves. Microwaves can heat substances via a process called dielectric heating. The latter occurs when energy causes a rotation of dipole molecules. Because it is an ion, water has a high dipole moment whereas fat has a low dipole moment. As a result, there is less absorption in the subcutaneous layer and selectivity for the dermis. Furthermore, application of concurrent cooling protects the upper dermis and selectively heats the deeper dermis.

Dielectric heating by microwaves was found to induce both eccrine and apocrine sweat gland thermolysis with relative selectivity. This discovery led to the first commercially available therapeutic microwave device – miraDry® (Miramar Labs). Studies have shown that 90% of patients had at least a 50% reduction in sweating, and ~80% maintained this reduction at 12 months[88]. All subjects experienced transient swelling, discomfort, and/or numbness within the treatment area, with a few patients noting longer-lasting side effects including altered sensation in or around the treatment site, papulonodules in the axillae, and hair loss[89].

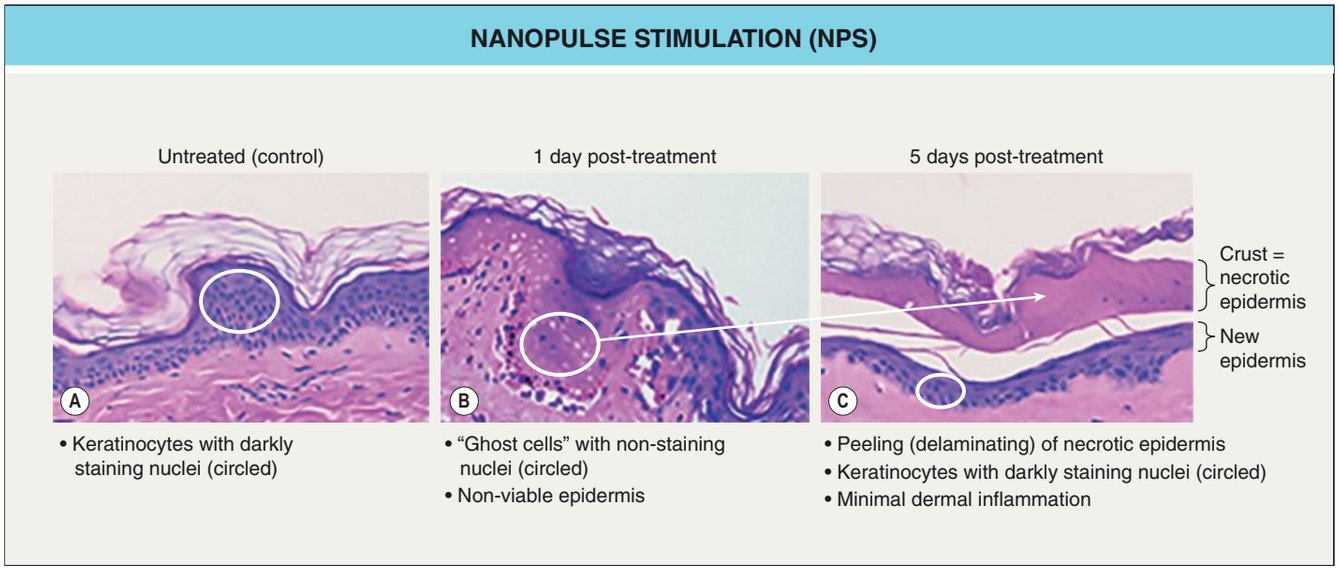


Fig. 137.18 Nanopulse stimulation (NPS). Cellular apoptotic death. **A** Abdominal skin, untreated. **B** Abdominal skin, 1 day after NPS treatment. **C** Abdominal skin, 5 days post NPS treatment. *From Kaufman D, Martinez M, Jauregui L, et al. A dose-response study of a novel method of selective tissue modification of cellular structures in the skin with nanosecond pulsed electric fields. Lasers Surg Med 2020;52:315–22.*

HOME-BASED LASERS

The notion that home-based laser and light devices might someday replace office-based treatments has not caused many physicians to lose sleep. In practice, however, there are some devices that can efficiently remove hair, reduce the signs of photodamage, induce a degree of skin tightening, and improve acne. That said, there is an even larger number of devices that are totally ineffective. In general, those devices that are effective and designed by highly skilled engineers are rather expensive, while the ineffective devices are relatively cheap and therefore appealing to the consumer. Potential economic rewards have driven some companies to manufacture devices which are so ineffective that they are awarded FDA clearance by virtue of their safety alone.

Although little peer-reviewed literature is available, one well-controlled, office-based study demonstrated that nearly all of the patients were able to correctly administer their own treatments. Additionally, the observed side effects of hyper- and hypopigmentation, crusting, and blistering were transient and had resolved by the conclusion of the study[90]. Use of these devices on darker skin phototypes and tanned skin is clearly contraindicated. The patients need to assume a high degree of responsibility with these devices. There will be complications, but we should not underestimate the ability of the public to use (or abuse) these devices.

EMERGING TECHNOLOGIES

To prevent and control acne via sebaceous gland suppression, gold-coated silica microparticles can be excited with commonly available lasers at a low energy fluence[91]. Localized damage can be achieved with minimal injury to surrounding structures. Sebacia Microparticles (Sebacia, Inc.) is the first such commercially available product. In addition, when sebum was compared to water, a wavelength of 1726 nm was found to have a small but significant absorption differential. Use of a "sebum laser" led to focal damage of sebaceous glands with sparing of surrounding structures and was reported to prevent and treat acne.

Nano-Pulse Stimulation™ (NPS™) technology (Pulse Biosciences, Inc.) utilizes non-thermal energy and has a unique mechanism of action that targets only cellular morphology while sparing the non-cellular stroma (Fig. 137.18)[92,93]. Ultrafast (nanosecond) electrical energy pulses are delivered via microneedle arrays. In clinical trials, NPS has been used to treat common warts, seborrheic keratoses, sebaceous hyperplasia, and superficial basal cell carcinomas, with a reportedly low incidence of hyper- or hypopigmentation and rarely scarring. Regulated cell death has also been observed in malignant tumor-bearing animals as has a secondary immune response that leads to rejection of re-introduced malignant cells of the same lineage[94].

CONCLUSIONS

Increasingly, we are asking the question, "Lasers: what's the truth?" This reality check is necessary so that we start to ask the right questions and are critically aware of the answers. Laser engineers are very insightful and they can provide us with semi-intelligent laser, light, and other energy systems that can more precisely target the correct structures and induce appropriate healing responses. We should celebrate the enormous energy that goes into newer and more sophisticated devices, just as we should criticize and reject devices which underperform and overpromise. Those of us who are involved in new technology development know that, just around the corner, advances are going to bring us smarter, cheaper, more durable, more tunable devices. Total internal reflection of spontaneous emission of radiation (TRASER) devices, which are neither lasers nor IPL, are more efficient than lasers and are tunable. Our hope is that as new technologies come online, there will be a continued attempt to answer the ongoing tough questions pertaining to both surgical and medical dermatology.

Additional figures and video available in our eBook (see inside front cover for access code).

REFERENCES

1. Anderson RR, Parrish JA. Selective photothermolysis: precise microsurgery by selective absorption of pulsed radiation. *Science*. 1983;220:524–527.
2. Alexiades-Armenakas MR, Dover JS, Arndt KA. The spectrum of laser skin resurfacing: nonablative, fractional, and ablative laser resurfacing. *J Am Acad Dermatol*. 2008;58:719–737. quiz 738–40.
3. Levy JL, Elbahr C, Jouve E, Mordon S. Comparison and sequential study of long pulsed Nd:YAG 1,064 nm laser and sclerotherapy in leg telangiectasias treatment. *Lasers Surg Med*. 2004;34:273–276.
4. Alster TS, Garg S. Treatment of facial rhytides with a high-energy pulsed carbon dioxide laser. *Plast Reconstr Surg*. 1996;98:791–794.
5. Zachary CB. Modulating the Er: YAG laser. *Lasers Surg Med*. 2000;26:223–226.
6. Newman JB, Lord JL, Ash K, McDaniel DH. Variable pulse erbium: YAG laser skin resurfacing of perioral rhytides and side-by-side comparison with carbon dioxide laser. *Lasers Surg Med*. 2000;26:208–214.
7. Jacob CI, Dover JS, Kaminer MS. Acne scarring: a classification system and review of treatment options. *J Am Acad Dermatol*. 2001;45:109–117.
8. Johnson TM, Sebastien TS, Lowe L, Nelson BR. Carbon dioxide laser treatment of actinic cheilitis: clinicohistopathologic correlation to determine the optimal depth of destruction. *J Am Acad Dermatol*. 1992;27:737–740.

9. Manstein D, Herron GS, Sink RK, et al. Fractional photothermolysis: a new concept for cutaneous remodeling using microscopic patterns of thermal injury. *Lasers Surg Med*. 2004;34:426–438.
10. Laubach HJ, Tannous Z, Anderson RR, Manstein D. Skin responses to fractional photothermolysis. *Lasers Surg Med*. 2006;38:142–149.
11. Hantash BM, Bedi VP, Sudireddy V, et al. Laser-induced transepidermal elimination of dermal content by fractional photothermolysis. *J Biomed Opt*. 2006;11:041115.
12. Ross EV. Nonablative laser rejuvenation in men. *Dermatol Ther*. 2007;20:414–429.
13. Sadick NS, Trelles MA. Nonablative wrinkle treatment of the face and neck using a combined diode laser and radiofrequency technology. *Dermatol Surg*. 2005;31:1695–1699.
14. Geronemus RG. Fractional photothermolysis: current and future applications. *Lasers Surg Med*. 2006;38:169–176.
15. Walgrave SE, Ortiz AE, MacFalls HT, et al. Evaluation of a novel fractional resurfacing device for treatment of acne scarring. *Lasers Surg Med*. 2009;41:122–127.
16. Jih MH, Kimyai-Asadi A. Fractional photothermolysis: a review and update. *Semin Cutan Med Surg*. 2008;27:63–71.
17. Hantash BM, Bedi VP, Kapadia B, et al. In vivo histological evaluation of a novel ablative fractional resurfacing device. *Lasers Surg Med*. 2007;39:96–107.
18. Hantash BM, Bedi VP, Chan KF, Zachary CB. Ex vivo histological characterization of a novel ablative fractional resurfacing device. *Lasers Surg Med*. 2007;39:87–95.
19. Rahman Z, MacFalls H, Jiang K, et al. Fractional deep dermal ablation induces tissue tightening. *Lasers Surg Med*. 2009;41:78–86.
20. Anderson RR, Donelan MB, Hivnor C, et al. Laser treatment of traumatic scars with an emphasis on ablative fractional laser resurfacing: consensus report. *JAMA Dermatol*. 2014;150:187–193.
21. Karmisholt KE, Banzhaf CA, Glud M, et al. Laser treatments in early wound healing improve scar appearance: a randomized split-wound trial with nonablative fractional laser exposures vs. untreated controls. *Br J Dermatol*. 2018;179:1307–1314.
22. Wenande E, Olesen UH, Nielsen MM, et al. Fractional laser-assisted topical delivery leads to enhanced, accelerated and deeper cutaneous 5-fluorouracil uptake. Expert Opinion. *Drug Delivery*. 2017;14:307–317.
23. Sklar LR, Burnett CT, Waibel JS, et al. Laser assisted drug delivery: a review of an evolving technology. *Lasers Surg Med*. 2014;46:249–262.
24. Waibel JS, Rudnick A, Shagalov DR, Nicolazzo DM. Update of ablative fractionated lasers to enhance cutaneous topical drug delivery. *Adv Ther*. 2017;34:1840–1849.
25. Weiss RA, Goldman MP, Weiss MA. Treatment of poikiloderma of Civatte with an intense pulsed light source. *Dermatol Surg*. 2000;26:823–827; discussion 828.
26. Hardaway CA, Ross EV, Paithankar DY. Non-ablative cutaneous remodeling with a 1.45 µm mid-infrared diode laser: phase II. *J Cosmetic Laser Therapy*. 2002;4:9–14.
27. Hardaway CA, Ross EV. Nonablative laser skin remodeling. *Dermatologic Clin*. 2002;20:97.
28. Garden JM, Tan OT, Kerschmann R, et al. Effect of dye laser pulse duration on selective cutaneous vascular injury. *J Invest Dermatol*. 1986;87:653–657.
29. Waelchli R, Aylett S, Robinson K, et al. New vascular classification of port-wine stains: improving prediction of Sturge–Weber risk. *Br J Dermatol*. 2014;171:861–867.
30. Shirley MD, Tang H, Gallione CJ, et al. Sturge–Weber syndrome and port-wine stains caused by somatic mutation in GNAQ. *N Engl J Med*. 2013;368:1971–1979.
31. Dierickx C, Goldman MP, Fitzpatrick RE. Laser treatment of erythematous/hypertrophic and pigmented scars in 26 patients. *Plast Reconstr Surg*. 1995;95:84–90; discussion 91–2.
32. Tan OT, Morrison P, Kurban AK. 585 nm for the treatment of port-wine stains. *Plast Reconstr Surg*. 1990;86:1112–1117.
33. Lanigan SW, Cotterill JA. Psychological disabilities amongst patients with port wine stains. *Br J Dermatol*. 1989;121:209–215.
34. Chapas AM, Eickhorst K, Geronemus RG. Efficacy of early treatment of facial port wine stains in newborns: a review of 49 cases. *Lasers Surg Med*. 2007;39:563–568.
35. Renfro L, Geronemus RG. Anatomical differences of port-wine stains in response to treatment with the pulsed dye laser. *Arch Dermatol*. 1993;129:182–188.
36. Waner M, Suen JY. *Hemangiomas and Vascular Malformations of the Head and Neck*. Wilmington, DE: Wiley Liss; 1999.
37. Léauté-Labrèze C, Dumas de la Roque E, Hubiche T, et al. Propranolol for severe hemangiomas of infancy. *N Engl J Med*. 2008;358:2649–2651.
38. Garden JM, Bakus AD, Paller AS. Treatment of cutaneous hemangiomas by the flashlamp-pumped pulsed dye laser: prospective analysis. *J Pediatr*. 1992;120:555–560.
39. Kim HJ, Colombo M, Frieden IJ. Ulcerated hemangiomas: clinical characteristics and response to therapy. *J Am Acad Dermatol*. 2001;44:962–972.
40. Rizzo C, Brightman L, Chapas AM, et al. Outcomes of childhood hemangiomas treated with the pulsed-dye laser with dynamic cooling: a retrospective chart analysis. *Dermatol Surg*. 2009;35:1947–1954.
41. Reddy KK, Blei F, Brauer JA, et al. Retrospective study of the treatment of infantile hemangiomas using a combination of propranolol and pulsed dye laser. *Dermatol Surg*. 2013;39:923–933.
42. Friedmann DP, Liolios AM, Goldman MP. An update on the treatment of lower extremity veins. *Curr Dermatol Reports*. 2014;3:113–121.
43. Kauvar AN, Khrom T. Laser treatment of leg veins. *Semin Cutan Med Surg*. 2005;24:184–192.
44. Patrice SJ, Wiss K, Mulliken JB. Pyogenic granuloma (lobular capillary hemangioma): a clinicopathologic study of 178 cases. *Pediatr Dermatol*. 1991;8:267–276.
45. Tan O, Hurwitz R, Stafford T. Pulsed dye laser treatment of recalcitrant verrucae: a preliminary report. *Lasers Surg Med*. 1993;13:127–137.
46. Pfau A, Abd-el-Raheem TA, Bäumler W, et al. Nd:YAG laser hyperthermia in the treatment of recalcitrant verrucae vulgares (Regensburg's technique) *Acta Derm Venereol*. 741994212–214.
47. Street ML, Roenigk RK. Recalcitrant periungual verrucae: the role of carbon dioxide laser vaporization. *J Am Acad Dermatol*. 1990;23:115–120.
48. Logan RA, Zachary CB. Outcome of carbon dioxide laser therapy for persistent cutaneous viral warts. *Br J Dermatol*. 1989;121:99–105.
49. Rashid T, Hussain I, Haider M, Haroon TS. Laser therapy of freckles and lentigines with quasi-continuous, frequency-doubled, Nd:YAG (532 nm) laser in Fitzpatrick skin type IV: a 24-month follow-up. *J Cosmet Laser Ther*. 2002;4:81–85.
50. Dierickx C. IL-37 Lasers in pigmentary disorders. *Pigment Cell Res*. 2003;16:590.
51. Grevelink JM, van Leeuwen RL, Anderson RR, Byers HR. Clinical and histological responses of congenital melanocytic nevi after single treatment with Q-switched lasers. *Arch Dermatol*. 1997;133:349–353.
52. Railan D, Kilmer S. Treatment of benign pigmented cutaneous lesions. *Cutaneous Cosmetic Laser Surg*. 2006:93–108.
53. Chan HH, Leung RS, Ying SY, et al. A retrospective analysis of complications in the treatment of nevus of Ota with the Q-switched alexandrite and Q-switched Nd:YAG lasers. *Dermatol Surg*. 2000;26:1000–1006.
54. Taylor CR, Anderson RR. Ineffective treatment of refractory melasma and postinflammatory hyperpigmentation by Q-switched ruby laser. *J Dermatol Surg Oncol*. 1994;20:592–597.
55. Tannous ZS, Astner S. Utilizing fractional resurfacing in the treatment of therapy-resistant melasma. *J Cosmetic Laser Ther*. 2005;7:39–43.
56. Rokhsar CK, Fitzpatrick RE. The treatment of melasma with fractional photothermolysis: a pilot study. *Dermatol Surg*. 2005;31:1645–1650.
57. Raulin C, Schönermark MP, Greve B, Werner S. Q-switched ruby laser treatment of tattoos and benign pigmented skin lesions: a critical review. *Ann Plast Surg*. 1998;41:555–565.
58. Tafazzoli A, Rostan EF, Goldman MP. Q-switched ruby laser treatment for postsclerotherapy hyperpigmentation. *Dermatol Surg*. 2000;26:653–656.
59. American Society for Dermatologic Surgery (ASDS). Survey on Dermatologic Procedures. <https://www.asds.net/portals/0/PDF/procedures-survey-results-infographic-2018.pdf>; 2018.
60. Dierickx CC. Hair removal by lasers and intense pulsed light sources. *Dermatol Clin*. 2002;20:135–146.
61. Dierickx C. Laser-assisted hair removal: state of the art. *Dermatol Ther*. 2000;13:80–89.
62. Lepselter J, Elman M. Biological and clinical aspects in laser hair removal. *J Dermatol Treat*. 2004;15:72–83.
63. Liew SH, Ladhani K, Grobbelaar AO, et al. Ruby laser-assisted hair removal success in relation to anatomic factors and melanin content of hair follicles. *Plast Reconstr Surg*. 1999;103:1736–1743.
64. Moreno-Arias G, Castelo-Branco C, Ferrando J. Paradoxical effect after IPL photoepilation. *Dermatol Surg*. 2002;28:1013–1016; discussion 1016.
65. Kontoes P, Vlachos S, Konstantinos M, et al. Hair induction after laser-assisted hair removal and its treatment. *J Am Acad Dermatol*. 2006;54:64–67.
66. Friedman O, Gofstein D, Arad E, et al. Laser pretreatment for the attenuation of planned surgical scars: a randomized self-controlled hemi-scar pilot study. *J Plast Reconstr Aesthet Surg*. 2020;73:893–898.
67. Waibel JS, Rudnick AC, Wulkan AJ, Holmes JD. The diagnostic role of optical coherence tomography (OCT) in measuring the depth of burn and traumatic scars for more accurate laser dosimetry: pilot study. *J Drugs Dermatol*. 2016;15:1375–1380.
68. Issler-Fisher AC, Fisher OM, Haertsch P, et al. Ablative fractional resurfacing with laser-facilitated steroid delivery for burn scar management: does the depth of laser penetration matter? *Lasers Surg Med*. 2020;52:149–158.
69. Eilers Jr. RE, Ross EV, Cohen JL, Ortiz AE. A combination approach to surgical scars. *Dermatol Surg*. 2016;42(Suppl 2):S150–S156.
70. Douglas H, Lynch J, Harms KA, et al. Carbon dioxide laser treatment in burn-related scarring: a prospective randomised controlled trial. *J Plast Reconstr Aesthet Surg*. 2019;72:863–870.
71. Seago M, Shumaker PR, Spring LK, et al. Laser Treatment of Traumatic Scars and Contractures: 2020 International Consensus Recommendations. *Lasers Surg Med*. 2020;52:96–116.
72. Kauvar ANB, Kubicki SL, Suggs AK, Friedman PM. Laser therapy of traumatic and surgical scars and an algorithm for their treatment. *Lasers Surg Med*. 2020;52:125–136.
73. Lokhande AJ, Mysore V. Striae distensae treatment review and update. *Indian Dermatol Online J*. 2019;10:380–395.
74. Kim BJ, Lee DH, Kim MN, et al. Fractional photothermolysis for the treatment of striae distensae in Asian skin. *Am J Clin Dermatol*. 2008;9:33–37.
75. Izikson L, Farinelli W, Sakamoto F, et al. Safety and effectiveness of black tattoo clearance in a pig model after a single treatment with a novel 758 nm 500 picosecond laser: a pilot study. *Lasers Surg Med*. 2010;42:640–646.
76. Kossida T, Rigopoulos D, Katsambas A, Anderson RR. Optimal tattoo removal in a single laser session based on the method of repeated exposures. *J Am Acad Dermatol*. 2012;66:271–277.
77. Reddy KK, Brauer JA, Anolik R, et al. Topical perfluorodecalin resolves immediate whitening reactions and allows rapid effective multiple pass treatment of tattoos. *Lasers Surg Med*. 2013;45:76–80.
78. Kaminer MS, Capelli CC, Sadeghpour M, et al. Increased tattoo fading in a single laser tattoo removal session enabled by a rapid acoustic pulse device: a prospective clinical trial. *Lasers Surg Med*. 2020;52:70–76.
79. Bónis B, Kemény L, Dobozy A, et al. 308 nm UVB excimer laser for psoriasis. *Lancet*. 1997;350:1522.
80. Taibjee SM, Cheung ST, Laube S, Lanigan SW. Controlled study of excimer and pulsed dye lasers in the treatment of psoriasis. *Br J Dermatol*. 2005;153:960–966.
81. Passeron T, Ostovari N, Zakaria W, et al. Topical tacrolimus and the 308-nm excimer laser: a synergistic combination for the treatment of vitiligo. *Arch Dermatol*. 2004;140:1065–1069.
82. Fisher GH, Geronemus RG. Short-term side effects of fractional photothermolysis. *Dermatol Surg*. 2005;31:1245–1249.
83. Fife DJ, Fitzpatrick RE, Zachary CB. Complications of fractional CO_2 laser resurfacing: four cases. *Lasers Surg Med*. 2009;41:179–184.
84. Zelickson BD, Kist D, Bernstein E, et al. Histological and ultrastructural evaluation of the effects of a radio-frequency-based nonablative dermal remodeling device: a pilot study. *Arch Dermatol*. 2004;140:204–209.
85. Jacobson LG, Alexiades-Armenakas M, Bernstein L, Geronemus RG. Treatment of nasolabial folds and jowls with a noninvasive radiofrequency device. *Arch Dermatol*. 2003;139:1371–1372.
86. Alam M, White LE, Martin N, et al. Ultrasound tightening of facial and neck skin: a rater-blinded prospective cohort study. *J Am Acad Dermatol*. 2010;62:262–269.
87. Laubach HJ, Makin IR, Barthe PG, et al. Intense focused ultrasound: evaluation of a new treatment modality for precise microcoagulation within the skin. *Dermatol Surg*. 2008;34:727–734.
88. Glaser DA, Coleman 3rd WP, Fan LK, et al. A randomized, blinded clinical evaluation of a novel microwave device for treating axillary hyperhidrosis: the dermatologic

reduction in underarm perspiration study. *Dermatol Surg*. 2012;38:185–191.
89. Lupin M, Hong HC, O'Shaughnessy KF. Long-term efficacy and quality of life assessment for treatment of axillary hyperhidrosis with a microwave device. *Dermatol Surg*. 2014;40:805–807.
90. Rohrer TE, Chatrath V, Yamauchi P, Lask G. Can patients treat themselves with a small novel light based hair removal system? *Lasers Surg Med*. 2003;33:25–29.
91. Munavalli G, Blomgren R, Kauvar A, et al. Selective photothermolysis of sebaceous glands for treatment of acne: efficient delivery of gold coated microparticles as chromophores into the sebaceous glands with ultrasound, a human histology study. *Lasers Surg Med*. 2014;46:3–4.
92. Kaufman D, Martinez M, Jauregui L, et al. A dose-response study of a novel method of selective tissue modification of cellular structures in the skin with nanosecond pulsed electric fields. *Lasers Surg Med*. 2020;52:315–322.
93. Newman J, Jauregui L, Knape WA, et al. A dose-response study of nanosecond electric energy pulses on facial skin. *J Cosmetic Laser Ther*. 2020;22:195–199.
94. Nuccitelli R. Application of pulsed electric fields to cancer therapy. *Bioelectricity*. 2019;1:30–34.



eFig. 137.1 Lentigines. Before (**A**) and 6 weeks after (**B**) a single Q-switched ruby laser treatment. There is lightening of the treated lesions, but an additional treatment is required to achieve full fading.



eFig. 137.2 Photodamage treated with fractionated ablative CO_2 laser. **A** Preoperative. **B** Characteristic pin-point bleeding from microscopic treatment zones (MTZ; also referred to as microthermal zones) immediately following laser therapy. **C** Improvement of lentigines, solar elastosis and fine static rhytides 3 months postoperatively.

138 Cryosurgery

Paola Pasquali

Key features

- A minimally invasive surgical technique that utilizes subzero temperatures to destroy benign, premalignant, and malignant lesions
- Compared to standard excisional surgery, cryosurgery requires less time to perform but healing time is often more prolonged as it occurs via second intention
- Damage to surrounding structures is predictable and can be limited, with the preserved underlying stroma providing a structural framework for wound repair
- The preferred and most commonly used cryogen is liquid nitrogen due to its very low boiling point (−196 C) which allows for freezing of skin lesions at temperatures needed for their destruction; this includes malignant cells which require freezing temperatures of at least −50 C
- Cryosurgery often leads to an excellent cosmetic result, but in patients with darker skin phototypes, hypopigmentation due to destruction of melanocytes can occur

HISTORICAL BACKGROUND

Reducing the temperature of the skin was initially done to provide anesthesia or lessen inflammation. With the advent of potent cryogens, selective destruction of tissue became possible. James M. Arnott is credited with first describing the use of controlled freezing in the 1800s to destroy tumors[1]. Liquefied oxygen and carbon monoxide preceded the introduction of liquid nitrogen (LN) by Carl von Linde. By 1898, James Dewar had developed a flask that permitted storage and transportation of LN thereby rendering LN accessible to physicians.

In 1899, Archibald Campbell White reported on the successful treatment of multiple benign and malignant skin conditions with liquefied air applied via an adapted bottle; the latter could be considered the prototype of modern hand-held units. Herman V. Allington then described how LN-saturated cotton swabs could be used to treat various skin conditions. In 1961, the neurosurgeon Irving S. Cooper, together with Arnold Lee, developed the first cryosurgical probe. Increased use of LN for medical purposes followed the design of safe portable hand-held units.

PRINCIPLES OF CRYOSURGERY AND CRYOBIOLOGY

Cryosurgery is defined as a surgical procedure that utilizes very low temperatures to destroy living tissue. The term *cryotherapy* should be reserved for when living tissue is exposed to cold in order to induce physiological changes but not tissue destruction. *Cryobiology* represents the study of the effects of low temperatures on living tissues.

Heat transfers from hot to cold[2], and the larger the temperature difference between a cryogen and its target tissue, the faster the heat transfer. The ideal cryogen has the lowest possible temperature and is capable of producing the parameters necessary to destroy both benign and malignant cells; for the latter, the tissue temperature needs to be below −50°C. The most commonly used cryogen is LN which boils at −196°C (77°K; −321°F). LN is relatively safe to handle, non-toxic, and commercially available. For the treatment of actinic keratoses (AKs) and cutaneous carcinomas, LN is the recommended cryogen whereas for benign lesions, cryogens with higher boiling points (e.g. liquid nitrous oxide [−88°C], carbon dioxide gas [−78°C], other compressed organic gases [−55 to −75°C]) can also be employed.

The mechanisms of injury in cryosurgery can be attributed to both direct and indirect effects (Table 138.1). Such events are the result of fast freezing followed by slow thawing, i.e. a freeze–thaw cycle. Repeated freeze–thaw cycles increase the destructive effects of cryosurgery. The material interposed between the cryogen and the lesion to be treated is also a determinant of the speed of freezing. *Air* is a poor conductor of cold such that the greater the distance between the skin lesion and the source of the cryogen, the lesser the freezing. *Water* is a better conductor than air (e.g. a presoaked verruca freezes faster), and *ice* is better than water as in the intra- and extracellular ice crystals present after the first freeze–thaw cycle. Finally, *metal* is an excellent conductor explaining the deep and fast freezing of tissue that results from frozen metal probes placed in direct contact with the skin[3].

Different cells and tissues have different sensitivities to cold. The lethal temperature for melanocytes is around −4°C, while that for keratinocytes is −35°C. Keratinocyte cancer cells require around −50°C, sarcoma cells −60°C, and vascular endothelium −15°C to −40°C. Of note, cartilage and bone are quite resistant to freezing.

Cryoimmunology

Cryoimmunology is the study of the innate and humoral immune responses to antigens derived from frozen skin lesions. Development of newer immunologic assays has made it possible to measure such responses, which can be either immunostimulatory or immunosuppressive[4].

One major difference between conventional excisional surgery and cryosurgery is that the latter leaves the tumor "*in situ*". At the center of the frozen lesion, there will be necrosis due to direct cellular damage (see Table 138.1), leading to release of tumor-specific antigens capable of stimulating an immune response. Once the innate immune system is activated, antigen-presenting cells (APCs) engulf tumor fragments and present processed antigens to T cells, initiating both T and B cell immune responses (see Ch. 4). At the periphery, the temperatures are higher and therefore sublethal, with the cells undergoing apoptosis rather than necrosis. This leads to "silent cell death" associated with minimal inflammation (see Table 138.1)[4].

The response to cryosurgery can be enhanced by the addition of adjuvants[5]. These include agents that augment ice injury (e.g. glycine), inducers of apoptosis (e.g. topical 5-fluorouracil)[6], and immunomodulators (e.g. topical imiquimod). Such combinations have been termed *immunocryosurgery*, with promising results having been published[7]. However, further studies are needed to better understand the underlying mechanisms of cryoimmunology, define the ideal parameters for tumor destruction, and determine the precise interactions between cryosurgery and potential adjuvants.

INSTRUMENTS AND TECHNIQUES

Cryosurgical techniques can be subdivided into several types (Table 138.2):

- ***Open*** (***spray***, ***open-spray***; Fig. 138.1A). This is the most frequently used technique. The instrument consists of a metal container with spraying tips or openings through which the cryogen is released. This technique is suitable for lesions that are flat or elevated as well as benign or malignant; the key factor is achieving the correct freezing temperature. Larger openings deliver more LN and freeze tissue faster, so they are ideal for larger, bulky lesions. Smaller openings freeze tissue slower and allow for a more precise freezing. Therefore, they are ideal for small benign lesions, such as lentigines or seborrheic keratoses.

CRYOSURGERY – MECHANISMS OF INJURY				
Type of injury	**Type of cell death**	**Phase**	**Location**	**Type of response**
Direct injury	Necrosis: direct freezing of water leads to extracellular then intracellular ice crystal formation with edema and cellular lysis Temperature required: –20°C for most cells –50°C or lower for malignant cells	Freeze period	Center of treated lesion	Inflammation: +++ Short-lived, nonspecific innate immune response
Vascular injury	Ischemia due to secondary damage of vascular endothelium	Thawing(~1 hour after freezing)	Periphery of treated lesion and normal surrounding skin	Inflammation: +/++
Apoptosis	Occurs at sublethal temperatures, e.g. approx. –20°C for malignant cells	4–8 hours after thawing	Periphery of treated lesion	Inflammation: –/+
Immunologic	Antigens released from damaged cells lead to immune response	Late event	Lymph nodes	Adaptive immune response

Table 138.1 Cryosurgery – mechanisms of injury.

CRYOSURGICAL TECHNIQUES						
Technique		**Common uses**			**Advantages**	**Disadvantages**
Type	**Synonym**	**B**	**PM**	**M**		
Open	Spray Open-spray	√	√	√	Any size or surface	For small lesions, care should be taken regarding normal surrounding skin Not appropriate for pedunculated lesions
Semi-open	Confined spray Cone Confined	√			Relative sparing of normal surrounding skin	Appropriate size of cone required
Semi-closed	Chamber			√	Deep and fast freezing	Indicated for cutaneous malignanciesAppropriate size of chamber required
Closed	Contact Probe Cryoprobe	√		√	Deep and fast freezing	Appropriate size and shape of probe required
Tweezers	Cryotweezers	√			Spares normal surrounding skin Pedunculated lesions	Limited to superficial lesions
Intralesional	–	√		√	Freezing occurs from the center of the lesion	Invasive
Dipstick	Cotton-tipped applicator	√			May be less frightening for children	Variability in amount of LN within cotton tip Loss of temperature control Dripping of LN may lead to unintended sites of freezing

Table 138.2 Cryosurgical techniques. B, benign lesions; LN, liquid nitrogen; M, malignant lesions; PM, premalignant lesions.

- ***Semi-open*** (***confined spray***, ***cone***, ***confined***; Fig. 138.1B). This refers to the use of a polycarbonate plate with holes, neoprene cones, or otoscope specula to restrict sprayed LN to a limited area. All of these items are composed of non-conducting materials. Freezing is faster than with the open technique as the LN is confined to the lesion. As splattering of LN is avoided and normal surrounding tissue is spared, it tends to be less painful.
- ***Semi-closed*** (***chamber***; Fig. 138.1C). One end of a metal cone is attached to the cryogen unit while the rubber-protected distal end is held firmly against the skin. This system generates potent and deep freezing and should be reserved for skin cancers and cutaneous metastases.
- ***Closed*** (***probe***, ***contact***, ***cryoprobe***; Fig. 138.1D,E). The cryogen is delivered via a closed system, i.e. from the unit through metal probes in contact with the skin; the remaining cryogen exits by way of a rubber releasing hose. Probes come in different shapes and diameters. To ensure homogeneous freezing, they need to be applied to flat tumor surfaces. In addition, when treating hemangiomas, the probe should be applied with pressure in order to "press out" the blood and lower the final temperature. For delicate procedures, such as freezing cysts near the eye, ultrasound gel or water can be placed on the skin under the probe.
- ***Tweezers*** (Fig. 138.1F). A previously frozen Teflon® forceps is used to grasp pedunculated lesions. The freezing front is then allowed to advance just to the skin surface. This is an ideal technique for filiform lesions, with sparing of normal surrounding skin as well as minimization of post-treatment hypo- or hyperpigmentation.
- ***Intralesional*** (Fig. 138.1G). While originally developed for keloids, this technique consists of passing a thick needle through the tumor. One end of the needle is attached to the cryogen unit (screwed on or via a Luer lock), while the other end that has exited the skin allows for LN release. It can be used for large nodular tumors where freezing originating from the center of the mass provides an advantage. It is ideal for preserving surrounding tissue.
- ***Dipstick*** (Fig. 138.1H). A LN-saturated, cotton-tipped applicator is placed directly onto the lesion. This technique is still used by some physicians for verrucae and solar lentigines.

PREOPERATIVE CONSIDERATIONS

Patients need to be aware of the relative advantages and disadvantages of cryosurgery compared to other therapies (Table 138.3). A disadvantage is the longer healing times (e.g. ~2–3 weeks for the trunk and arms, >1 month for the legs) while an advantage is the lack of preoperative requirements such that cryosurgery can be performed at the time of the initial office visit. In addition, the need for postoperative

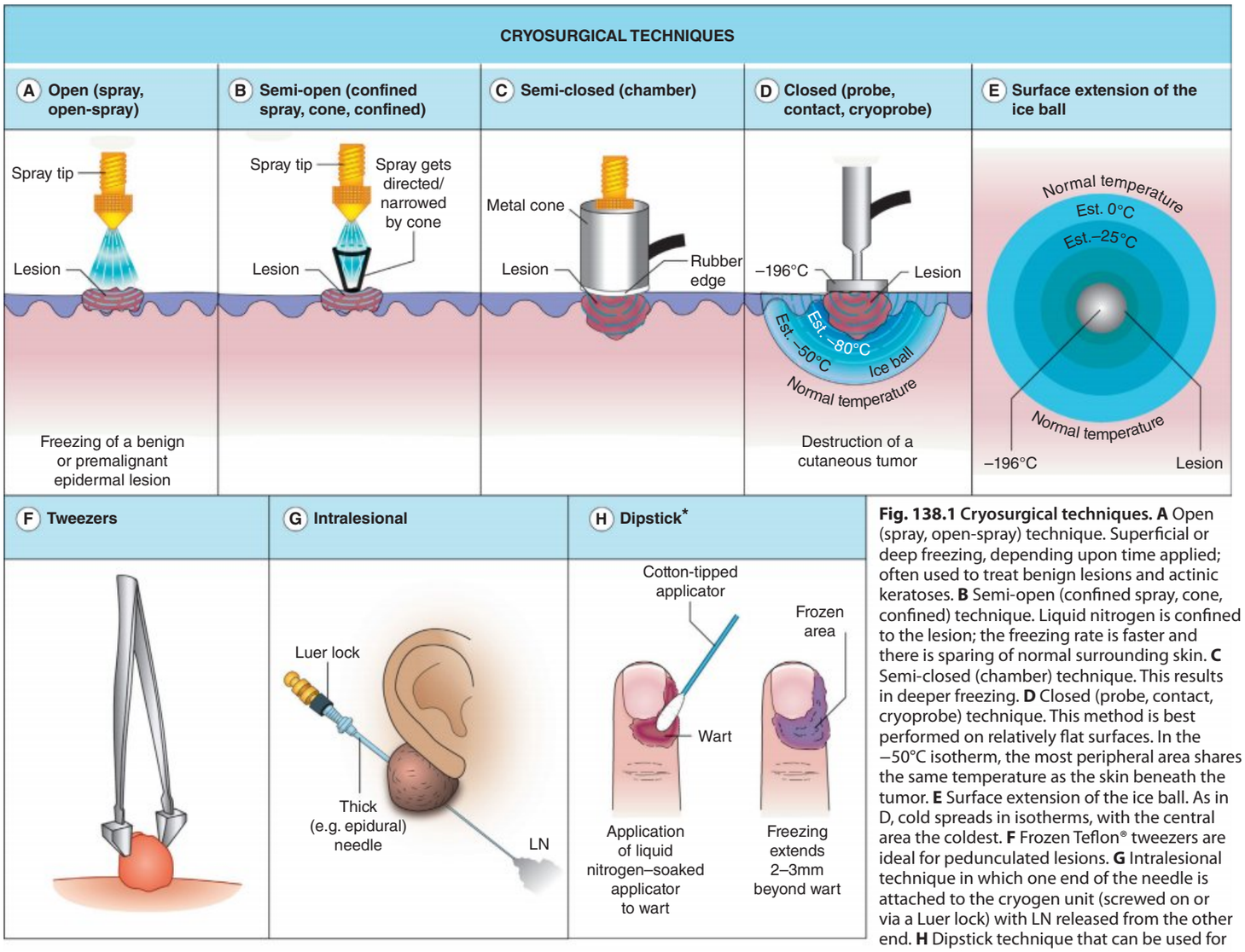


Fig. 138.1 Cryosurgical techniques. A Open (spray, open-spray) technique. Superficial or deep freezing, depending upon time applied; often used to treat benign lesions and actinic keratoses. **B** Semi-open (confined spray, cone, confined) technique. Liquid nitrogen is confined to the lesion; the freezing rate is faster and there is sparing of normal surrounding skin. **C** Semi-closed (chamber) technique. This results in deeper freezing. **D** Closed (probe, contact, cryoprobe) technique. This method is best performed on relatively flat surfaces. In the −50°C isotherm, the most peripheral area shares the same temperature as the skin beneath the tumor. **E** Surface extension of the ice ball. As in D, cold spreads in isotherms, with the central area the coldest. **F** Frozen Teflon® tweezers are ideal for pedunculated lesions. **G** Intralesional technique in which one end of the needle is attached to the cryogen unit (screwed on or via a Luer lock) with LN released from the other end. **H** Dipstick technique that can be used for verrucae. *Not recommended by the author due to the disadvantages listed in Table 138.2.

CRYOSURGERY – ADVANTAGES AND DISADVANTAGES	
Advantages	**Disadvantages**
• Safe and relatively simple procedure • Quick, low-cost procedure • Low-cost equipment (compared to other surgical modalities) • Can be done in the outpatient setting and in nursing homes • Versatility – treatment of a variety of conditions • Treatment of any area of the body, including earlobes, eyelids, nasal alae • Ideal for patients with multiple lesions, allergies to local anesthetics, fear of undergoing surgery, or significant surgical risk due to comorbidities • Minimal, if any, work or sports restrictions • Safe during pregnancy • Excellent cosmetic results	• Longer healing time with deep freezing procedures as second intention healing is required • Contraindicated in patients with cold-triggered conditions or cold-sensitive patients • Hypo- or hyperpigmentation, especially in darker skin phototypes • At free margins, scarring can lead to retraction (e.g. ectropion) • Possible alopecia following deep freezing of hair-bearing areas • Caution required when treating sites with underlying superficial nerves • Not recommended for convex areas, e.g. cheeks • In patients with rosacea, disappearance of erythema at treatment sites can lead to a Swiss cheese-like appearance

Table 138.3 Cryosurgery – advantages and disadvantages. See Table 138.8 for additional details.

care and potential side effects should be reviewed. Contraindications include cold urticaria, cold intolerance, cryoglobulinemia, and other cold-triggered conditions.

For certain clinical situations, skin preparation can improve the effectiveness of cryosurgery. Examples include: (1) removal of excess keratin (a poor conductor of cold) from verrucae via curettage, paring, or application of salicylic or lactic acid for 10–15 days prior to cryosurgery; (2) application of imiquimod to condylomata acuminata; and (3) pretreatment with topical 5-fluorouracil cream[8], diclofenac sodium gel[9], ingenol mebutate gel[10], imiquimod, or retinoic acid cream or gel[11] to remove atrophic and mildly keratotic AKs, with the remaining hyperkeratotic AKs then treated with cryosurgery.

Cryoanesthesia

Cryogens applied for just a few seconds can be used as an anesthetic, e.g. prior to needle insertion or incision and drainage of an inflamed epidermoid cyst. This technique is helpful in needle-phobic patients and can also be used prior to removal of benign lesions (Fig. 138.2)[12].

TREATMENT

Cryosurgery should not be performed without first establishing the correct diagnosis via clinical examination, dermoscopy, and/or histologic examination. The appropriate technique is then chosen (see Table 138.2).

Benign Lesions

Table 138.4 outlines benign conditions that are amenable to cryosurgical management[13]. For some, such as verrucae, it is a first-line option. The open (spray) technique is used for most benign lesions, including verrucae and acne cysts, while the semi-open technique or cryotweezers may be preferred for filiform warts and acrochordons (Video 138.1). The closed (contact, probe) technique can be employed for small adnexal cysts, pseudocysts (e.g. mucoceles), and sebaceous hyperplasia[14] as well as for vascular lesions (e.g. hemangiomas, spider telangiectasias, pyogenic granulomas) (Fig. 138.3). A single freeze–thaw cycle is usually sufficient for benign lesions and cryogens other than LN can be used (see above). Whenever using the spray technique, the use of small diameter apertures and intermittent spraying leads to a more delicate spray and less damage to normal surrounding skin.

For verrucae, removal of excess keratin and moistening of the lesion can improve the effectiveness of cryosurgery (see above). When removing verrucae and seborrheic keratoses, the freezing front should extend a few millimeters beyond the clinical margin to avoid a doughnut wart or residual lesion. If the closed or contact technique is used to treat hemangiomas and other vascular lesions, it is best to prefreeze the probe to prevent it from sticking to the skin surface and to press firmly (see Fig. 138.3). These recommendations are reflected in the PPPP rule: probe • pressure • prefreezing • patience. If the probe does become frozen to the skin lesion, simply allow for thawing before removing the probe. This approach is also recommended for mucosal lesions. Mucoceles may be drained prior to treatment with the closed technique.

Lentigines are lightened with a brief 3- to 4-second freeze and either the open spray or the dipstick technique can be employed. For keloids, the open spray technique – either alone or immediately prior to corticosteroid injection – or the intralesional technique is preferred. In darker skin phototypes, the anticipated cryosurgical technique may initially be performed in a test site that is in a cosmetically insensitive ("hidden") location. The site is then examined for hypo- or hyperpigmentation prior to cryosurgery in other locations.

Premalignant Lesions, Including Actinic Keratoses

Cryosurgery is a very effective therapeutic option for AKs and other premalignant conditions (Fig. 138.4)[15,16]. One 20- to 40-second freeze–thaw cycle is usually sufficient for a 1 cm lesion. The surface temperature reaches −15° to −20°C and, once frozen, the lesion can be grasped between two fingers (Fig. 138.5). Initial freezing should be in the center of the AK, with the freezing front then spreading laterally ~2–3 mm

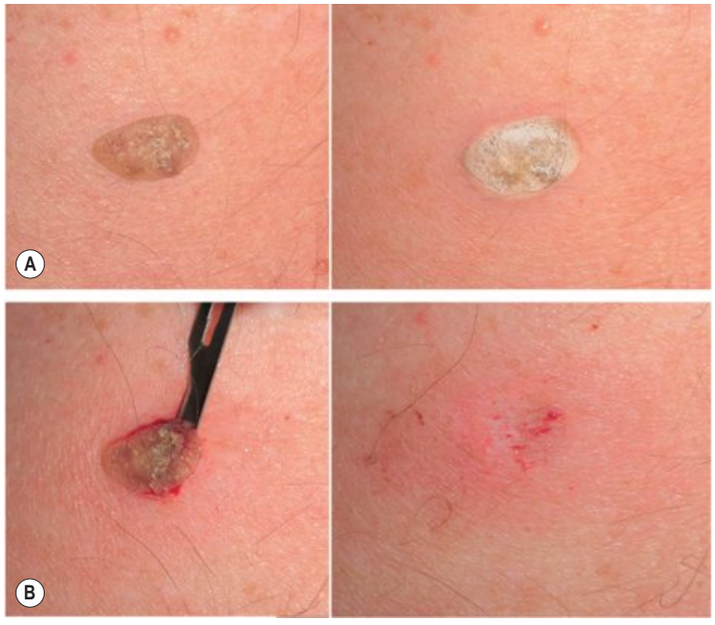


Fig. 138.2 Shave removal of a seborrheic keratosis following the use of liquid nitrogen as an anesthetic. A A seborrheic keratosis (SK) is frozen with a 2–3 mm margin. **B** Once the tissue starts thawing, a swift stroke with a curette or scalpel will make the SK "pop out". A hemostatic solution (aluminum chloride) is applied before complete thawing.

BENIGN CONDITIONS AMENABLE TO CRYOSURGERY	
• Acne cysts	• Lentigo
• Acne keloidalis nuchae	• Lichen sclerosus (of vulva)
• Acne vulgaris	• Lymphangioma
• Acquired perforating disorder	• Cutaneous lymphoid hyperplasia (lymphocytoma cutis)
• Acrochordons	• Molluscum contagiosum
• Angiofibroma	• Mucocele
• Angiokeratomas, including of Fordyce	• Myxoid cyst
• Cherry angioma	• Nevoid hyperkeratosis of the nipple
• Chondrodermatitis nodularis helicis	• Orf
• Chromoblastomycosis	• Pearly penile papules
• Clear cell acanthoma	• Porokeratosis
• Condyloma acuminatum	• Prurigo nodularis
• Dermatofibroma	• Pyogenic granuloma
• Discoid lupus erythematosus	• Rhinophyma
• Eccrine poroma	• Rosacea
• Elastosis perforans serpiginosa	• Sarcoidosis
• Epidermal nevus	• Sebaceous hyperplasia
• Erosive adenomatosis of the nipple	• Seborrheic keratosis
• Folliculitis keloidalis	• Syringocystadenoma papilliferum
• Granuloma annulare	• Syringoma
• Granuloma faciale	• Trichiasis
• Hemangioma	• Trichoepithelioma
• Herpes simplex	• Venous lake
• Keloid	• Verruca vulgaris
• Leishmaniasis	• Xanthoma

Table 138.4 List of benign lesions reported to be amenable to cryosurgical treatment. *Courtesy Emanuel G. Kuflik, MD.*

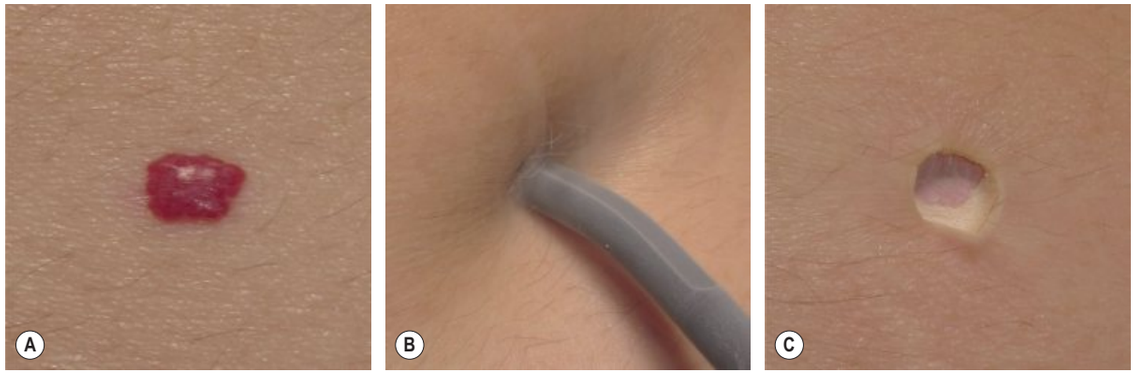


Fig. 138.3 Removal of a cherry angioma via the closed (probe, contact, cryoprobe) technique. A Prior to treatment. **B** A previously frozen probe is pressed into the lesion. **C** The frozen angioma and a transient depression can be seen.

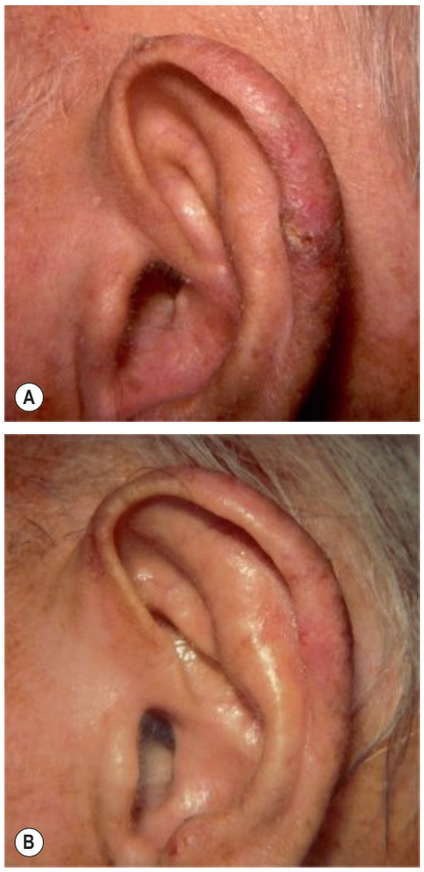


Fig. 138.4 Actinic keratosis treated with the open-spray technique. A Prior to treatment. **B** Three weeks later. *Courtesy Emanuel G. Kuflik, MD.*

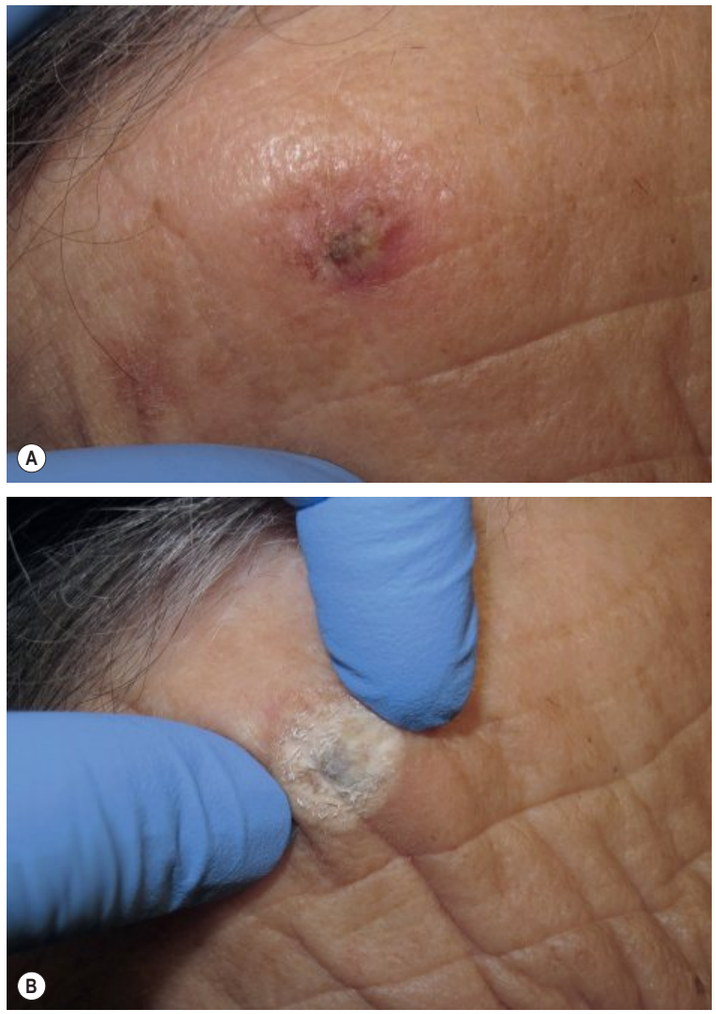


Fig. 138.5 Cryosurgery of a hypertrophic actinic keratosis. A Prior to treatment. **B** The open-spray technique should produce a block of frozen tissue that can be grabbed with both fingers; the surface temperature is approximately −15°C.

beyond the clinical margin. Some clinicians treat each lesion with two 15-sec freeze–thaw cycles. Recurrences should be assessed to determine if a squamous cell carcinoma needs to be excluded.

Within areas of significant cutaneous photodamage, there are rarely single AKs but rather multiple AKs as well as subclinical epidermal dysplasia. This is often referred to as "field cancerization" and is best treated by a combination of cryosurgery plus a topical agent (e.g. 5-fluorouracil, imiquimod) or photodynamic therapy. The latter are used to treat subclinical disease and thin lesions while cryosurgery is used to treat thicker keratotic AKs. It is more logical to first treat the field and then use cryosurgery for residual lesions[17].

Cryopeeling refers to the treatment of large areas of photodamaged skin, i.e. field treatment via cryosurgery. The areas of involvement are superficially frozen for 5–10 seconds, and given the associated pain, it is best to apply a topical anesthetic before and immediately after the procedure (see Ch. 143). Individual thicker lesions can be treated at the same time with a longer freeze time (see above)[18]. The freeze time for actinic cheilitis ranges from 10 to 20 seconds.

Cutaneous Malignancies

Cryosurgery is a reasonable alternative for the treatment of skin cancer (Table 138.5), but the lesions and techniques need to be carefully selected[19,20]. Because a double freeze–thaw cycle is more destructive, it is the recommended cryosurgical procedure for skin cancer. Except for very small lesions, local anesthesia is administered. In addition, since keratin is a poor conductor of cold, removal of excess keratin via curettage or paring will assist in reaching the correct freezing temperature at the base of the tumor, thus improving effectiveness[21].

The most commonly used techniques are open (spray) and closed (contact, probe); the closed technique is preferred as it leads to deeper and faster freezing (see Table 138.2). However, it is important to use a probe that corresponds to the size and shape of the tumor to assure complete apposition. The presence of air pockets ("interphase") between the probe and the tumor surface can prevent achievement of the desired final temperature. If the open (spray) technique is chosen, the freezing

CUTANEOUS MALIGNANCIES AMENABLE TO CRYOSURGERY		
Type	**Cryosurgery**	
	Amenable	**Not recommended**
Bowen disease, keratoacanthoma	All	–
Basal cell carcinoma	Especially useful for superficial lesions Tumors with well-defined borders	Morpheaform, infiltrative, and/or recurrent tumors Tumors with ill-defined margins or perineural invasion
Squamous cell carcinoma	Especially useful for superficial lesions Tumors with well-defined borders	Poorly differentiated, infiltrative, and/or recurrent tumors Tumors with ill-defined margins or perineural invasion
Lentigo maligna	Selected cases (e.g. elderly, mutilating surgery required)	
Kaposi sarcoma	Selected lesions that have not responded to other therapies	Avoid plantar surface
Melanoma	As palliation	

Table 138.5 Cutaneous malignancies amenable to cryosurgery.

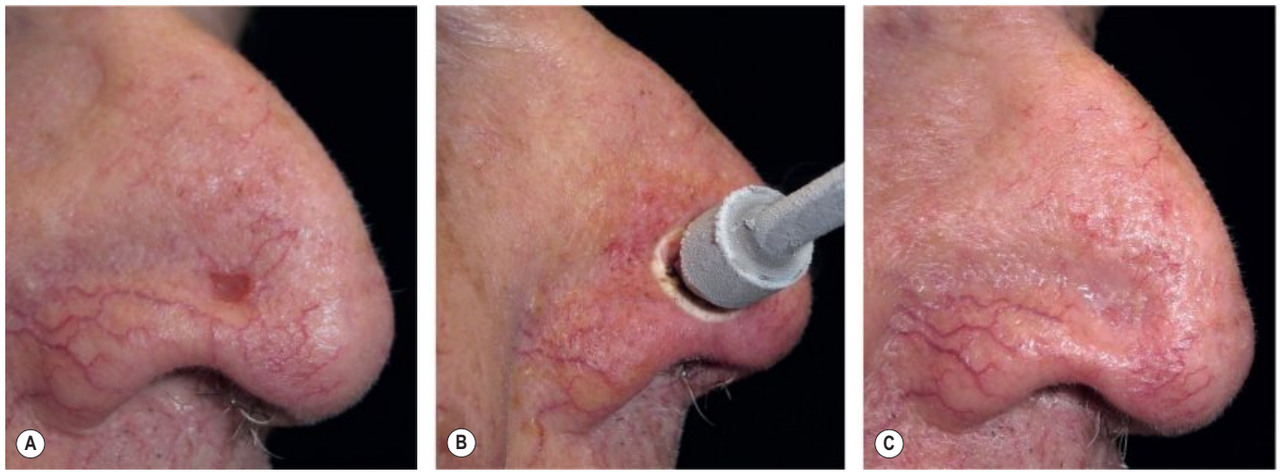


Fig. 138.6 Treatment of a basal cell carcinoma on the nose with the closed (probe, contact, cryoprobe) technique. A Prior to treatment. **B** An appropriately sized frozen cryoprobe is pressed against the tumor; a double freeze–thaw cycle is performed. **C** Healing is nearly complete a few weeks later.

should begin in the center of the tumor followed by lateral spread of the freeze front to 5 mm beyond the clinical margin of the tumor. A similar margin should be obtained with the closed technique.

Because cold advances as isotherms (see Fig. 138.1D,E), temperatures should be measured at the external margin. The temperature can be monitored by measuring (via an infrared thermometer) the surface temperature at the external margin and thereby inferring the temperature at the base of the tumor. More recently, high frequency ultrasound (HFUS; ~22 MHz) has been employed to determine the width, depth, and shape of tumors, thereby providing very useful information for selecting the optimal cryosurgical technique. For example, when basal cell carcinomas (BCCs) are thin, they can be safely treated with either the spray or the probe technique whereas for deeper nodular BCCs, the probe technique is preferred (Fig. 138.6; Video 138.2).

HFUS can also be used to monitor the freezing procedure. An initial black area is seen when the tumor is completely frozen. Re-appearance of the tumor is indicative of thawing, which first occurs at its surface and is last seen at the tumor base. By combining this information with measurement of the temperature[22] at the outer edge of the frozen tumor, the temperature at the base of the tumor can be implied[23].

For patients with multiple BCCs, dermoscopic diagnosis and HFUS of each lesion can be followed by a double freeze–thaw cycle, all in one treatment session. BCCs in several sites, including the nose, ears[24], and eyelids, have been treated successfully with cryosurgery[25]. Immunocryosurgery, consisting of a 5-week course of topical imiquimod with a double freeze–thaw cycle at week two, has also been utilized for skin cancer (Fig. 138.7). Lastly, melanocytes are known to be very sensitive to cold and cryosurgery is an option for selected cases of lentigo maligna (Fig. 138.8)[26,27]. However, it is important to ensure that melanocytes within the follicular epithelium are destroyed. Of note, cryosurgery has also been used, in combination with imiquimod, as treatment for locoregional cutaneous metastases of melanoma[28].



Fig. 138.7 Treatment of a large, ill-defined, postauricular basal cell carcinoma with immunocryosurgery. A Prior to treatment. **B** Eight months later, following a 5-week course of topical imiquimod with a double freeze–thaw cycle at week two.

Palliative Treatment

Cryosurgery has long been used for palliative (compassionate) treatment of skin cancer (Table 138.6)[29]. Detailed discussion with the patient and/or family/caretakers should be undertaken before instituting palliative treatment. The goal is to reduce pain, bleeding, infection, tissue destruction, foul smell, and/or tumoral masses that cause personal and social rejection. Palliative cryosurgery can improve quality of life in individuals with inoperable tumors or in those who reject conventional therapies or are poor surgical candidates due to underlying medical conditions.

Large tumoral masses can be treated by either: (1) the segmental technique; or (2) the fractional technique. In the *segmental* technique, the tumor is divided by imaginary lines into portions. Each segment is treated independently, allowing the freezing fronts to overlap. The aim is to avoid excessive freezing in the center of the tumor prior to the freeze front reaching the periphery. In the *fractional* technique, the center of the tumor is treated and then allowed to heal[30]. As the central



Fig. 138.8 A lentigo maligna on the forehead of a 72-year-old man. A The lesion measures 3.1 × 2.5 cm. **B** Cryosurgery to the entire lesion. Note the wide lateral spread of freeze. **C** The healed cryosurgical site 5 months after treatment. *Courtesy Emanuel G. Kuflik, MD.*

INDICATIONS FOR PALLIATIVE CRYOSURGERY
• Medical comorbidities that lead to significant surgical risk (e.g. cardiac, pulmonary, coagulopathy) • Bedridden patients • Failure of other treatment options • Patient has declined other treatment modalities, e.g. due to possibly disfiguring surgery, transportation issues for radiotherapy • The procedure improves the patient's quality of life or the caregiver's management, e.g. reducing pain, foul smell, bleeding • Mental illness that makes other procedures difficult to accomplish

Table 138.6 Indications for palliative cryosurgery.

scar contracts, it reduces the tumor diameter and residual disease can then be treated. In some patients, repeated treatment of the central tumor is performed to further reduce tumor burden.

The open (spray) technique is most commonly employed, especially in tumors with an irregular surface or in patients with a bleeding diathesis in whom curettage should be avoided. The closed (probe) technique, although ideal for skin cancer treatment, requires probes whose size appropriately matches that of the tumor, and since these tumors are usually very large, proper probes can be difficult to obtain. The semi-closed (chamber) technique, which is very destructive, is ideal for cutaneous metastases as long as the tumor fits inside the chamber. For very large tumors, the intralesional technique is an option.

EXPECTED POSTOPERATIVE EVENTS AND CARE

Compared to conventional excisional surgery, cryosurgery can be performed more rapidly but since healing is by second intention, healing time is prolonged. The latter is especially true for the lower extremities. The expected course and postoperative care are outlined in Table 138.7. Degree of edema will be determined by the depth of the freeze as well as the anatomic location, e.g. cryosurgery of eyelid lesions often leads to more edema (even with light freezing) than does a deep freeze on the arm. Patients with cold sensitivity can also develop more edema after cryosurgery.

For lesions that develop a large bulla, the fluid is often drained to decrease pressure and possibly hasten healing; the blister roof is usually left intact to serve as a biologic dressing although the recommendation of some cryosurgeons is to remove it, especially for verrucae to minimize risk of reimplantation. A gauze dressing can be placed if there is significant oozing and application of a bland topical ointment such as petrolatum enhances second intention healing. Eschars due to cryonecrosis, a later event when deep freezing is performed, should be debrided to facilitate healing.

CRYOSURGERY – POSTOPERATIVE CARE AND EXPECTED SIDE EFFECTS			
Expected side effect	**Time of appearance**	**Duration**	**Postoperative care/Treatment**
Exudation	Hours to days post procedure	Depends on depth of freezing	Wash with soap and water For deep freezing procedures, a bland ointment such as petrolatum can be applied
Pain	During the procedure and a few seconds afterwards (during thawing)	Short-lived	Usually well tolerated In sensitive patients or with deep freezing procedures, use local anesthesia
Urticarial reaction	Immediate	Minutes	None
Edema	A few minutes (sensitive areas) to 12–24 hours post procedure	Depending on the depth and site, a few days to a week Longer duration on the face	No treatment is effective
Vesicle/bulla	Minutes to 24 hours post procedure	Days	Fluid allowed to drain spontaneously or drained by the patient or surgeon
Eschar formation	After a week	Days or weeks	Can be debrided with scissors Care should be taken in vascular lesions

Table 138.7 Cryosurgery – postoperative care and expected side effects.

COMPLICATIONS

As with any surgical procedure, there is the possibility of complications. It is important to distinguish between a severe expected event and a complication, a distinction that is not always obvious. For example, treatment of a tumor in the periorbital region can lead to substantial edema such that the eyelids are swollen shut for several days, and while annoying, this would not be considered a complication. Table 138.8 outlines some of the possible complications of cryosurgery and helpful interventions.

FUTURE TRENDS (IMAGING TECHNOLOGY FOR MONITORING CRYOSURGICAL OUTCOME)

Cryosurgery is now, and will be in the future, a readily available, simple, and cost-effective surgical procedure. As the number of cutaneous

COMPLICATIONS OF CRYOSURGERY	
Complication	**Treatment**
Inadvertent freeze of patient or medical personnel from LN released from vent	Usually none (superficial injury)
LN insufflation (when spray freezing a previously curetted lesion)	None (reabsorbs spontaneously)
Bleeding after removal of eschar that was protecting an underlying vessel	Hemostasis, from simple pressure to electrocoagulation and rarely ligation of bleeding vessel
Pain (after a few days or weeks)	Topical, or occasionally oral, antibiotics if due to infection (most common cause)
Hypo- or hyperpigmentation	If secondary to superficial freezing, it usually improves spontaneously over time With deep freezing procedures, hypopigmentation can be permanent and treatment-resistant
Pseudoepitheliomatous hyperplasia	No treatment required as it resolves over time
Milia	Extraction (occasionally occurs with deep freezing procedures)
Scar retraction/notching	Permanent as due to tissue destruction from the tumor and its treatment; reconstructive surgery is an option
Alopecia	Can be permanent following deep freezing procedures in hair-bearing sites
Atrophic/depressed scar	Usually improves with time, but is sometimes permanent, especially following deep freezing procedures

Table 138.8 Complications of cryosurgery. LN, liquid nitrogen.

malignancies increases worldwide with many amenable to minimally invasive techniques, principles and proper techniques become an essential component of the scope of practice of dermatology and should be familiar to all dermatologists. Cryosurgery will clearly benefit from the newer non-invasive imaging techniques (e.g. dermoscopy, HFUS, confocal microscopy[31], optical coherence tomography[32]) that assist in diagnosis and provide information on the depth, volume, and histology of cutaneous tumors. In addition, these techniques can improve margin control while the effects of freezing can be visualized *in situ*. Non-invasive devices that measure skin temperature should also provide valuable information that can be used to standardize cryosurgical procedures.

Additional figures available in our eBook (see inside front cover for access code).

REFERENCES

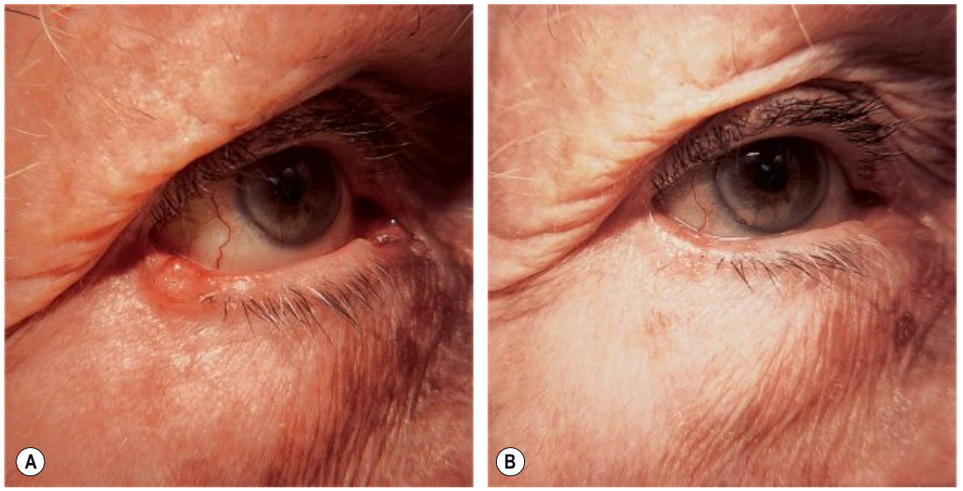
1. Cooper SM, Dawber RP. The history of cryosurgery. *J R Soc Med*. 2001;94:196–201.
2. Stańczyk M, Telega JJ. Thermal problems in biomechanics–a review. Part III. Cryosurgery, cryopreservation and cryotherapy. *Acta Bioeng Biomech*. 2003;5:3–22.
3. Gage AA, Baust JM, Baust JG. Experimental cryosurgery investigations in vivo. *Cryobiology*. 2009;59:229–243.
4. Sabel MS. Cryo-immunology: a review of the literature and proposed mechanisms for stimulatory versus suppressive immune responses. *Cryobiology*. 2009;58:1–11.
5. Goel R, Anderson K, Slaton J, et al. Adjuvant approaches to enhance cryosurgery. *J Biomech Eng*. 2009;131:074003.
6. Clarke DM, Baust JM, Van Buskirk RG, Baust JG. Chemo-cryo combination therapy: an adjunctive model for the treatment of prostate cancer. *Cryobiology*. 2001;42:274–285.
7. Gaitanis G, Bassukas ID. Immunocryosurgery for non-superficial basal cell carcinoma: a prospective, open-label phase III study for tumours ≤2 cm in diameter. *Acta Derm Venereol*. 2014;94:38–44.
8. Jorizzo J, Weiss J, Furst K, et al. Effect of a 1-week treatment with 0.5% topical fluorouracil on occurrence of actinic keratosis after cryosurgery: a randomized, vehicle-controlled clinical trial. *Arch Dermatol*. 2004;140:813–816.
9. Mastrolonardo M. Topical diclofenac 3% gel plus cryotherapy for treatment of multiple and recurrent actinic keratoses. *Clin Exp Dermatol*. 2009;34:33–35.
10. Berman B, Goldenberg G, Hanke CW, et al. Efficacy and safety of ingenol mebutate 0.015% gel after cryosurgery of actinic keratosis: 12-month results. *J Drugs Dermatol*. 2014;13:741–747.
11. Ianhez M, Fleury Jr LF, Miot HA, Bagatin E. Retinoids for prevention and treatment of actinic keratosis. *An Bras Dermatol*. 2013;88:585–593.
12. Pasquali P, Freites-Martinez A, Fortuño-Mar A. Cryobiopsy: an alternative technique to conventional shave biopsy. *J Am Acad Dermatol*. 2015;73:867–868.
13. Andrews MD. Cryosurgery for common skin conditions. *Am Fam Physician*. 2004;69:2365–2372.
14. Ataş H, Gönül M. Evaluation of the efficacy of cryosurgery in patients with sebaceous hyperplasia of the face. *J Cutan Med Surg*. 2017;21:202–206.
15. Ianhez M, Miot HA, Bagatin E. Liquid nitrogen for the treatment of actinic keratosis: a longitudinal assessment. *Br J Dermatol*. 2014;170:1114–1121.
16. Zane C, Facchinetti E, Rossi MT, et al. Cryotherapy is preferable to ablative CO2 laser for the treatment of isolated actinic keratoses of the face and scalp: a randomized clinical trial. *Br J Dermatol*. 2014;170:1114–1121.
17. Pasquali P, Segurado-Miravalles G, Baldi A, et al. Monitoring sequential treatment of actinic keratosis using post-processed images: ingenol mebutate and cryosurgery. *Photodermatol Photoimmunol Photomed*. 2019;35:447–448.
18. Chiarello SE. Cryopeeling (extensive cryosurgery) for treatment of actinic keratoses: an update and comparison. *Dermatol Surg*. 2000;26:728–732.
19. Kuflik EG. Cryosurgery for skin cancer: 30-year experience and cure rates. *Dermatol Surg*. 2004;30:297–300.
20. Bernardeau K, Derancourt C, Cambie M, et al. Cryosurgery of basal cell carcinoma: a study of 358 patients. *Ann Dermatol Venereol*. 2000;127:175–179.
21. Samain A, Boullié MC, Duval-Modeste AB, Joly P. Cryosurgery and curettage-cryosurgery for basal cell carcinomas of the mid-face. *J Eur Acad Dermatol Venereol*. 2015;29:1291–1296.
22. Goldberg LH, Kaplan B, Vergilis-Kalner I, Landau J. Liquid nitrogen: temperature control in the treatment of actinic keratosis. *Dermatol Surg*. 2010;36:1956–1961.
23. Pasquali P. High-frequency ultrasound (HFUS) in the management of skin cancer treated with cryosurgery. In: Pasquali P, ed. *Cryosurgery. A Practical Manual*. Berlin: Springer-Verlag; 2015:159–171.
24. Nordin P, Stenquist B. Five-year results of curettage-cryosurgery for 100 consecutive auricular non-melanoma skin cancers. *J Laryngol Otol*. 2002;116:893–898.
25. Lindgren G, Larkö O. Cryosurgery of eyelid basal cell carcinomas including 781 cases treated over 30 years. *Acta Ophthalmol*. 2014;92:787–792.
26. McLeod M, Choudhary S, Giannakakis G, Nouri K. Surgical treatments for lentigo maligna: a review. *Dermatol Surg*. 2011;37:1210–1228.
27. Bassukas ID, Gamvroulia C, Zioga A, et al. Cryosurgery during topical imiquimod: a successful combination modality for lentigo maligna. *Int J Dermatol*. 2008;47:519–521.
28. Rivas-Tolosa N, Ortiz-Brugués A, Toledo-Pastrana T, et al. Local cryosurgery and imiquimod: a successful combination for the treatment of locoregional cutaneous metastasis of melanoma: a case series. *J Dermatol*. 2016;43:553–556.
29. Kuflik EG. Cryosurgery for palliation. *J Dermatol Surg Oncol*. 1985;11:867–869.
30. Gonçalves JC. Fractional cryosurgery for skin cancer. *Dermatol Surg*. 2009;35:1788–1796.
31. Pasquali P, Segurado-Miravalles G, Freites-Martínez A, et al. Cryosurgical management of basal cell carcinoma: in vivo follow-up using reflectance confocal microscopy. *Int J Dermatol*. 2019;58:e30–e32.
32. Themstrup L, Banzhaf C, Mogensen M, Jemec GB. Cryosurgery treatment of actinic keratoses monitored by optical coherence tomography: a pilot study. *Dermatology*. 2012;225:242–247.



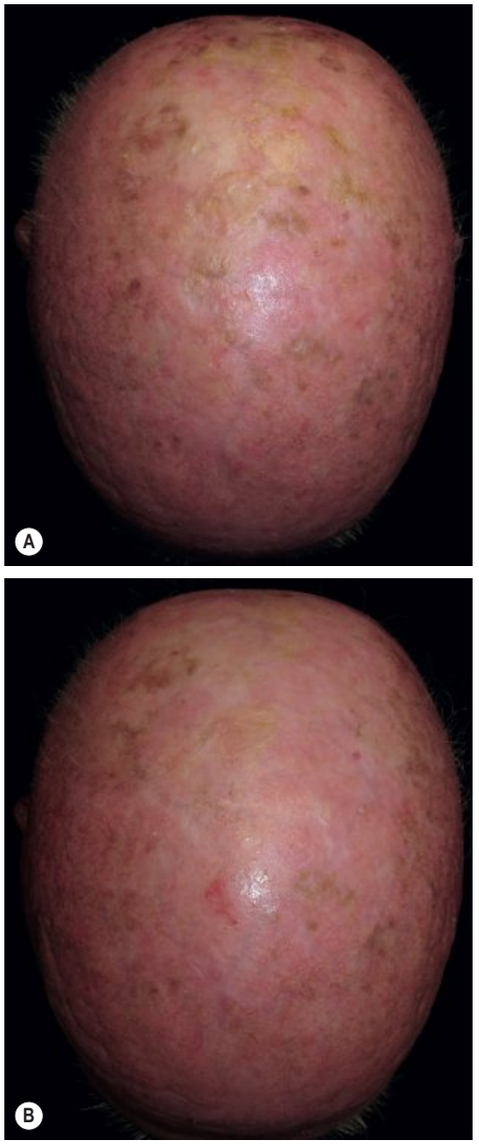
eFig. 138.1 Shave removal of a cutaneous horn following use of liquid nitrogen as an anesthetic. A Cutaneous horn of the lower eyelid. **B** Brief superficial freeze (5–7 seconds). **C** Shave removal with a scalpel. **D** Aluminum chloride solution (hemostatic agent) was applied prior to the onset of bleeding. No pain was felt by the patient.



eFig. 138.2 Squamous cell carcinoma on the cheek of an 83-year-old disabled woman. A The lesion measured 6×4.5 cm. **B** Prior to cryosurgery, the tumor was shaved flush with the surrounding skin in order to assure proper probe apposition. **C** Two years post cryosurgery, there is a hypopigmented scar without evidence of tumor recurrence.



eFig. 138.3 Basal cell carcinoma on the right lower eyelid margin. A Papular lesion with telangiectasias on the eyelid margin of an 82-year-old woman. **B** The healed cryosurgical site 6 months after treatment. Excellent cosmetic result; note loss of cilia. *Courtesy Emanuel G. Kuflik, MD.*



eFig. 138.4 Cryopeeling. Liquid nitrogen is sprayed for a few seconds onto the entire area of photodamaged skin utilizing an acne aperture; the latter is an aperture that emits a soft, vaporized spray. Topical anesthesia is applied one hour before and immediately after freezing the skin. **A** Prior to treatment. **B** After a single treatment.

139 Radiotherapy

Melissa Rasar Young, Michael J. Veness and Shawn W. Richards

Chapter Contents

Basics of Radiotherapy 2430
Radiotherapy of Benign Skin Disorders 2433
Radiotherapy of *In Situ* Cutaneous Malignancies 2433
Radiotherapy of Invasive Carcinomas, Sarcomas, and Lymphomas 2434
Palliation 2437
Reactions and Complications 2438
Future Trends 2440

Synonyms: ■ Radiation therapy ■ X-ray therapy ■ Radiation treatment

Key features

- Radiotherapy is an important modality in the treatment of patients with skin malignancies
- Radiotherapy may reduce morbidity (as compared to surgery), decrease the risk of recurrent disease, and even be life-saving
- Although most patients with skin cancer are adequately treated by modalities other than radiotherapy, there are factors that may favor its recommendation (e.g. comorbidities, location)
- Modern radiotherapy has an established role as a definitive, adjuvant, or palliative treatment
- Treating benign skin disease with radiotherapy must always be carefully considered in light of the risk of radiation-induced malignancy, especially in younger patients

BASICS OF RADIOTHERAPY

Indications

In dermatology, the primary role of radiotherapy is to treat basal cell carcinoma (BCC) and cutaneous squamous cell carcinoma (SCC; see Ch. 108)[1]. It is also used to treat less common, but potentially aggressive, cutaneous malignancies and, occasionally, benign diseases. The former include Merkel cell carcinoma, Kaposi sarcoma (AIDS- and non-AIDS-related), angiosarcoma, adnexal carcinoma, lymphoma, and lentigo maligna.

While the majority of skin cancers are amenable to excision or other treatment modalities (e.g. electrodesiccation and curettage) which are often more cost-effective, there are clinical settings where radiotherapy is favored. For example, *definitive* radiotherapy is often recommended when the outcome (functional and/or cosmetic) is likely to be better with radiotherapy than with surgery, especially in the situation where the clinician is constrained by the site or size of the tumor. Likewise, elderly patients with advanced lesions for whom complex surgery is best avoided are also excellent candidates for radiotherapy. The aim of *adjuvant* radiotherapy is to reduce the risk of recurrence, whereas *palliative* radiotherapy plays an important role in patients with advanced and/or incurable disease.

Mechanism of Action

X-rays are a powerful form of ionizing electromagnetic radiation and the lethal damage they produce within double-stranded DNA represents the basis for radiation therapy[2]. When X-rays (often referred to as photons) are absorbed by biological matter, an electron may be ejected from an atom with the local release of large amounts of energy resulting in DNA damage. Rapidly dividing cells, i.e. malignant cells, are more susceptible to lethal injury and mitotic death. Although normal adjacent tissues maintain mechanisms for repair following sublethal damage, there are limitations as to the dose of ionizing radiation normal tissue can tolerate, beyond which late reactions arise (see below). A therapeutic ratio is achieved when radiation is delivered in small divided doses (fractions), which allows time for repair of sublethal DNA damage in normal tissues without compromising tumor destruction.

Treatment Machines

In the modern era of radiation oncology, high-energy megavoltage (MV) photons (6–25 MV) are generated by a linear accelerator (LINAC) located within a heavily shielded concrete bunker. One of the advantages of megavoltage radiotherapy is its ability to treat deep-seated internal malignancies with relative skin sparing. However, in general, when treating cutaneous lesions, deep beam penetration and skin sparing are not desirable. Less penetrating modalities that avoid skin sparing, such as *low-energy* kilovoltage (kV) photons (50–300 kVp) supplied by a *superficial/orthovoltage* machine, superficial brachytherapy or electron beam therapy, are preferred modalities for cutaneous lesions. With these therapies, tissue penetration is measured in millimeters to centimeters and there is less normal tissue exposure. Radiotherapy modalities are summarized in Table 139.1.

Terminology

The International Unit of radiotherapy is a Gray (Gy)[3]. One Gy is equivalent to 100 cGy or 100 rads (in the older terminology). A fraction of radiotherapy refers to the dose delivered in one treatment. Treatments are typically delivered on a daily (Monday to Friday) basis. The daily outpatient treatments are only minutes in duration and treatment regimens usually consist of 10 to 30 weekday visits.

Radiotherapy Doses

Typical fractionation protocols for small SCCs and BCCs consist of 40 Gy in 10 (4 Gy) fractions or 50 Gy in 20 (2.5 Gy) fractions. Hypofractionation refers to the delivery of larger doses per fraction (4–7 Gy); typically a lower total dose is then delivered based upon the biological effective dose (BED; Table 139.2). The latter is calculated based upon a 2 Gy per fraction equivalent that is required to eradicate a tumor[4]. This calculation provides an explanation for commonly prescribed schedules: 45 Gy in 15 (3 Gy) fractions, 40 Gy in 10 (4 Gy) fractions, and 35 Gy in 5 (7 Gy) fractions.

For BCCs and SCCs, there is not a marked dose–response such that local control is similar whether a patient receives 40 Gy in 10 fractions (47 Gy BED) or 50 Gy in 20 fractions (52 Gy BED). When the tumors are larger or more infiltrative, better local control is achieved with a BED of around 60 Gy. However, late effects increase as the total dose and dose per fraction increase and it is these late effects that will impact cosmesis and late tissue damage (e.g. fibrosis, atrophy, ulceration due to necrosis).

Radiation Modalities

Low-energy photons (superficial and orthovoltage)

Superficial and orthovoltage radiotherapy are two modalities that: (1) utilize low-energy photons; (2) lack skin-sparing properties; and

RADIOTHERAPY MODALITIES AND PHYSICAL AND TECHNICAL PARAMETERS					
Modality	**Radiation type**	**Energy**	**Tumor target thickness**	**Bolus**	**Shielded room**
Superficial radiotherapy	X-ray photons	30–150 kV	< 0.5 cm	No	Yes
Orthovoltage radiotherapy	X-ray photons	100–300 kV	< 1 cm	No	Yes
Electron beam therapy	Electrons	6–15 MeV	Up to 3 cm	Yes	Yes
LINAC	X-ray photons	6–15 MV	Variable	Yes	Yes
Radioisotope brachytherapy	Ir-192, gamma photons	380 keV	< 0.5–1 cm	No	Yes
Electronic brachytherapy	X-ray photons	50–70 kV	< 3–4 mm	No	No

Table 139.1 Radiotherapy modalities and physical and technical parameters. k, kilo; Ke, kiloelectron; LINAC, linear accelerator; M, mega; Me, megaelectron; V, volts.

SUGGESTED DOSE FRACTIONATION SCHEDULES FOR BASAL CELL CARCINOMAS AND CUTANEOUS SQUAMOUS CELL CARCINOMAS		
Dose fractionation schedule	**Indication**	**Biological effective dose (BED)***
Single 8–20 Gy fraction	Elderly, infirm (palliation)	
35 Gy in 7 fractions of 5 Gy	Elderly, medical comorbidity	44 Gy
40 Gy in 10 fractions of 4 Gy	Older, otherwise well	47 Gy
45 Gy in 15 fractions of 3 Gy	Older, otherwise well	49 Gy
50 Gy in 20 fractions of 2.5 Gy	Younger and/or lesion <2–3 cm	52 Gy
60 Gy in 30 fractions of 2 Gy	Younger and/or large lesion	60 Gy
*Calculated by converting to 2 Gy/fraction using the linear quadratic equation.		

Table 139.2 Suggested dose fractionation schedules for basal cell carcinomas (BCCs) and cutaneous squamous cell carcinomas (SCCs).

(3) have source-to-surface distances (SSD) ranging from 10 to 60 cm. The qualities and "hardness" of superficial/orthovoltage photon beams are determined by the placement of filters within the radiation beam[5]. "Half value layer" (HVL) is an important concept in radiation physics and it refers to the thickness of an absorbent filter (often copper [Cu] or aluminum [Al]) that is required to reduce the beam intensity by 50%. These filters serve to remove the softer photon component and improve the penetration quality of the beam. The following are two examples of the influence of filters: a typical 100 kVp superficial photon beam with an HVL of 7 mm of Al delivers 100% of a prescribed dose to the surface, 85% at 5 mm, and 70% at 10 mm whereas a 250 kVp orthovoltage beam with an HVL of 2.5 mm of Cu delivers 95% of prescribed dose at 5 mm and 90% at 10 mm. In summary, different photon beam energies will have unique HVLs that result in varied beam qualities and dose penetration.

Superficial radiotherapy

Office-based superficial radiotherapy was once the standard modality by which dermatologists treated skin cancer[6]. Typical machines delivered photons of 30–150 kVp with a depth dose suitable for most patients with cutaneous malignancies <5 mm in depth[7]. Over time, the high cost of radiotherapy machines and increased enthusiasm and training in dermatologic surgery led to a significant decline in office-based radiotherapy. More recently, introduction of superficial radiation therapy (SRT) machines has led to renewed interest in office-based radiotherapy for BCCs and cutaneous SCCs.

Orthovoltage radiotherapy

Orthovoltage units utilize higher energy photons of 150–300 kVp, and because of greater prescribed dose depths, are utilized for lesions >5 mm in depth. Some clinicians estimate tumor thickness and then choose an appropriate beam energy and HVL that will achieve 90%–95% of the prescribed dose at the depth of the tumor. However, this latter approach requires an accurate estimate of tumor thickness.

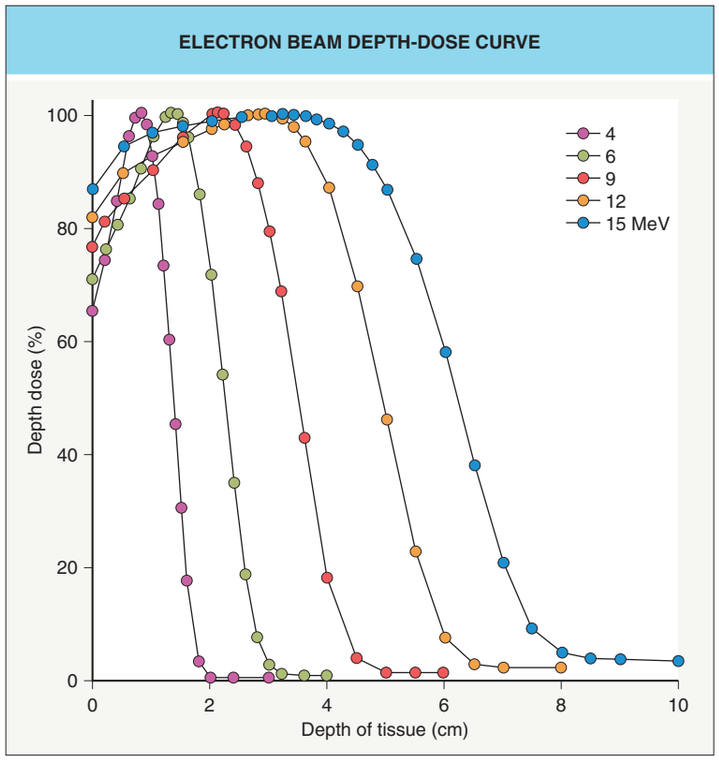


Fig. 139.1 Electron beam depth-dose curve. Electrons offer the advantage of a rapid linear decline in dose beyond a well-defined tissue depth that is a function of the selected beam energy. *Courtesy Lynn Wilson, MD.*

An important consideration when delivering orthovoltage radiotherapy is the generation of a photoelectric effect due to a higher energy range when compared to low-energy photons. A consequence of this photoelectric effect is the delivery of a higher dose of radiation to underlying bone or cartilage. The latter does not occur with electrons (see below) or low-energy photons (see above). As a result, some clinicians use this as a justification for the use of electrons when treating lesions near bone or cartilage, although supportive clinical data are limited.

Electron beam therapy

A linear accelerator can generate electrons which can be utilized in a variety of treatment settings. Unlike X-rays, electrons are particulate radiation with a negative charge. Low-energy electrons (6–8 MeV [megaelectron volts]) offer an alternative to low-energy photons when treating cutaneous tumors, but the former do have some disadvantages[8]. For example, electron beams are relatively skin-sparing (Fig. 139.1), and, as a result, a tissue equivalent bolus needs to be placed on the skin surface (Fig. 139.2). Also, utilizing electron beams for small treatment fields (<4 cm^2) may result in tumor underdosing at the deepest extent of the tumor.

Electrons offer the advantage of a rapid linear decline in dose beyond a well-defined tissue depth that is a function of the selected beam energy

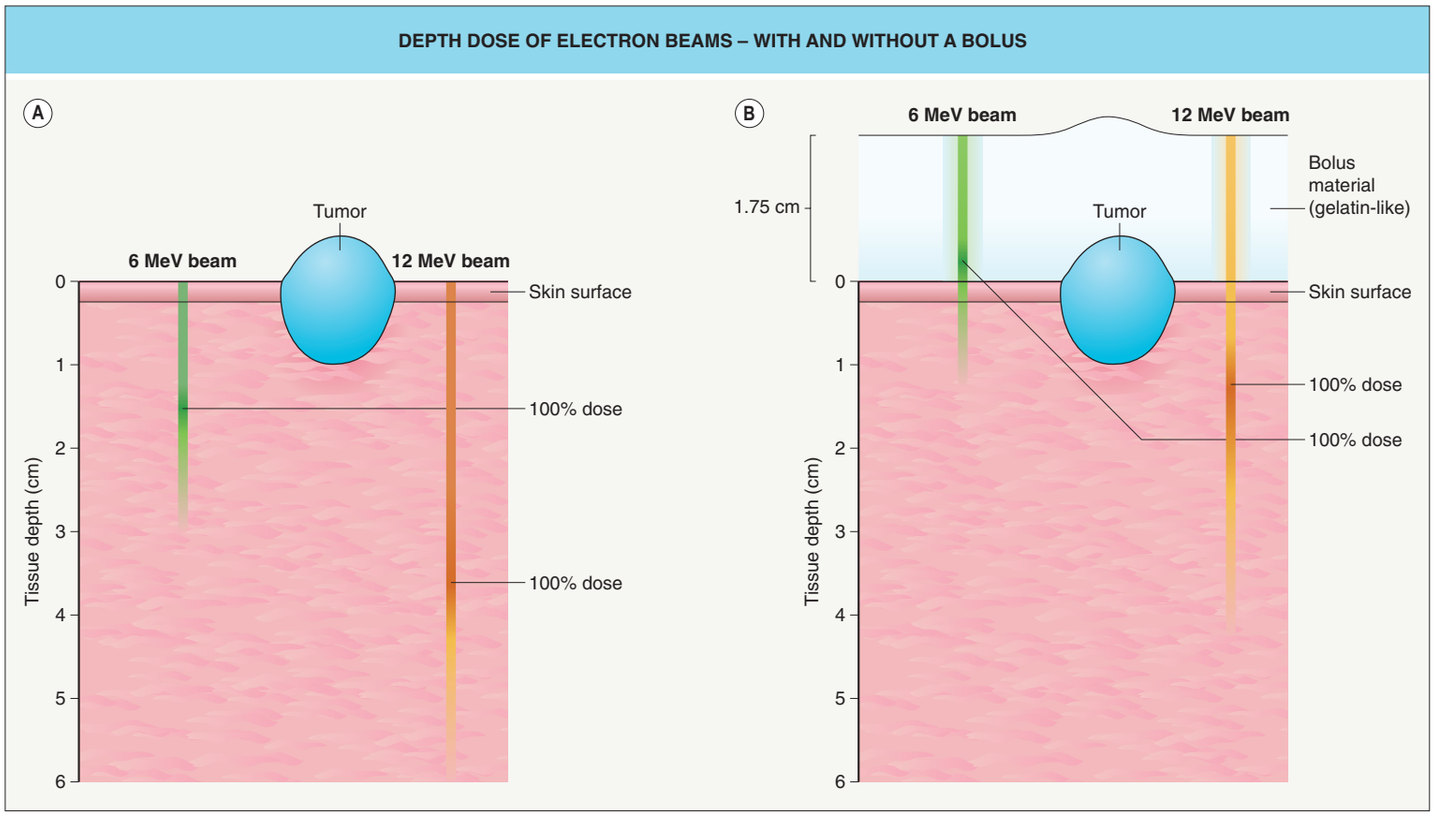


Fig. 139.2 Depth dose of electron beams – with and without a bolus. A Beams with a dose of 6 MeV and 12 MeV. **B** Demonstration of the bolus effect whereby a more appropriate dose of radiation is obtained at the skin surface. Bolus material needs to be tissue equivalent and maintain a constant thickness; its composition varies from paraffin wax to thermoplastics (e.g. Aquaplast®). *Courtesy Lynn Wilson, MD.*

(see Fig. 139.1). For example, a 6 MeV electron beam provides some of its dose (~70%–75%) at the surface, but deposits 100% of the specified dose at a depth of ~1.5 cm. Using a higher-energy beam will result in deposition of a higher percentage of the dose at the skin surface (see Fig. 139.1), but with a higher dose to subcutaneous tissues as well as the skin surface (see Fig. 139.2A). On the other hand, if a tissue equivalent bolus of 1 cm is applied in conjunction with a 6 MeV beam, close to 100% of the desired dose will be obtained at the skin surface (see Fig. 139.2B). In other words, the dose will be brought 1 cm closer to the skin surface, further minimizing the dose to underlying structures.

Tumors treated with electrons require 10–20 mm margins due to a wider penumbra (dose drop-off at the field edge). Electrons also have a lower relative biological effectiveness (RBE) in comparison to photons, leading some clinicians to recommend a 10%–15% increase in total dose to compensate. It is important to appreciate the intricacies of using electron beam therapy, in particular the limitations of dose delivery with small fields. This requires careful attention to the margin and dose distribution at the edge of the radiation field when treating small cutaneous malignancies.

Brachytherapy

Radioisotope brachytherapy

Radioisotope brachytherapy represents radiotherapy that is delivered by the direct application of a radioactive source near or inside involved tissues. Most centers utilize a high dose-rate (HDR) system that delivers more than 12 Gy/hr, with Ir-192 being the most commonly used isotope. Treatments are delivered by the placement of surface applicators onto the skin at the site of the tumor. The radioactive source is often delivered to the applicators via a remotely controlled machine in a dedicated shielded HDR suite. Applicator selection varies depending on the location and surface contours of the target area, e.g. conical surface applicators for flat surfaces, flexible mesh style "flap" applicators for molding onto curved surfaces. When treating deeper tumors, interstitial catheters may be surgically placed within the target tissue.

The dose "fall-off" is steep with brachytherapy, providing an excellent opportunity to spare adjacent normal tissue which is not easily achieved with photon- or electron-based treatments. Per American Brachytherapy Society (ABS) consensus guidelines, HDR skin brachytherapy represents a standard of care option for appropriately selected patients with keratinocyte carcinomas[9]. Because HDR delivery systems require Nuclear Regulatory Commission (NRC) oversight, special shielded vaults, and careful security and safety protocols, radioisotope brachytherapy is performed by a radiation oncologist in a controlled setting.

Electronic brachytherapy

A newer, non-isotope-generated form of brachytherapy, referred to as electronic (surface) brachytherapy, utilizes a miniature electronic X-ray source instead of a radioactive source. The currently available systems operate in the 50–70 kVp energy range, require little shielding, and are considered more portable. Electronic brachytherapy systems are not subject to NRC oversight, but may need to adhere to local regulations[10]. Similar to radioisotope brachytherapy, a steep dose fall-off allows for sparing of adjacent organs and tissues. However, there are some concerns as to tissue dose calculations as well as the potential for different radiobiological effectiveness due to the photons' low energy. Therefore, consensus guidelines for calculating tissue dosages are yet to be finalized[10,11].

As with radioisotope brachytherapy, suitable lesions need to be superficial (<3–4 mm in depth) and well-defined. While data are emerging regarding the safety and efficacy of electronic brachytherapy for the treatment of keratinocyte carcinomas, given the lack of both long-term follow-up and a consensus regarding dosimetric properties of this modality, the ABS does not advise its use outside of prospective or registry trials[10].

Advantages of Radiotherapy

Radiotherapy offers the advantage of a non-surgical approach, thereby avoiding surgical morbidity, scarring, and the need for reconstruction. In situations where reconstruction with grafts or flaps is required, improved cosmesis may result from radiotherapy[12]. Radiotherapy fields can also be tailored with generous margins in order to encompass "at-risk" areas

(e.g. possible sites of clinically inapparent tumor extensions) that, if surgically approached, would require involved and complex surgery. In addition, standard oncologic excision margins in certain sites are often difficult to achieve without causing surgical morbidity; such sites include the midface triangle, i.e. the periorbital region (especially the medial canthus), the lower eyelid, nose (especially the ala nasi and nasal tip), nasolabial fold, lip, and chin.

Disadvantages of Radiotherapy

Radiotherapy does have its disadvantages; in particular, most patients require a protracted course of treatment compared to what is often a simple outpatient excision. Patients should also be informed that because of the risk of serious late effects such as soft tissue and cartilage necrosis, a second course of definitive radiotherapy cannot be delivered to the same site. In addition, the reduced "quality" of irradiated skin may make subsequent surgery difficult if the tumor recurs or persists following radiation therapy. Over time, irradiated skin may also develop dyspigmentation, telangiectasias, and a shiny appearance. Lastly, individuals with xeroderma pigmentosum or basal cell nevus syndrome should not be irradiated owing to their marked predisposition for developing multiple and recurrent skin cancers, often at a young age.

Tumors that have deeply invaded cartilage or bone often do better with a combination of excision plus adjuvant radiotherapy, although definitive radiotherapy still remains an option. Radiotherapy of lesions located on the foot, anterior lower leg, or dorsum of the hand, although not contraindicated, should be avoided if possible; lesions in such sites are best treated with excision. Unfortunately, radiotherapy to poorly vascularized tissue is often associated with poor healing, thus irradiation of skin cancers arising in sites of chronic ulceration, trauma, or thermal burns should be avoided, if possible. In addition, patients with systemic sclerosis and other causes of cutaneous fibrosis may experience severe fibrotic reactions following radiotherapy.

Radiotherapy has a very small (~1 in 1000) risk of causing a radiation-induced in-field malignancy (often soft tissue/bone sarcoma) 10–15 or more years after exposure. However, these data were obtained from studies involving many different malignancies treated by various techniques and dosing schedules. It is likely that with modern radiotherapeutic techniques as well as the smaller volumes being irradiated when treating skin cancers, a figure of 1 in 1000 represents an overestimate of the real risk. Nonetheless, for younger patients (<50–60 years of age), this is an important issue and patients need to be informed of the potential 5-10X greater risk of a second malignancy within the treatment field when compared to individuals not receiving radiotherapy[12a].

RADIOTHERAPY OF BENIGN SKIN DISORDERS

Background

The role of radiotherapy in treating benign cutaneous disorders has markedly diminished over the past several decades. It is no longer ethical to offer radiotherapy as a treatment for acne, warts, hirsutism, or tinea capitis. The role of radiotherapy in treating inflammatory skin conditions (e.g. dermatitis, psoriasis, lichen planus) is historical due to efficacious alternative treatments (e.g. corticosteroids, phototherapy, systemic immunomodulators), and the risk of exposing patients to ionizing radiation. Superficial radiotherapy has occasionally been used to treat recalcitrant Hailey-Hailey disease.

Keloids

Recurrent keloids, often refractory to re-excision and intralesional corticosteroid injections, can have significant cosmetic, functional, and psychologic sequelae for patients. The addition of low-dose (12–20 Gy) adjuvant radiotherapy delivered in three to five fractions, beginning within 24–48 hours following surgery, can markedly and safely reduce the incidence of recurrence[13]. A recent dose-response study involving 250 keloids concluded that 20 Gy delivered in 5 fractions was the optimal postoperative regimen, when balancing relapse rate (2%) against adverse effects[14]. A common site for keloids is the earlobe and patients can be treated with low-energy photons plus lead shielding of surrounding tissues. Young patients with keloids of the lower anterior neck (in close proximity to the thyroid gland) should not be irradiated.

Cutaneous Lymphoid Hyperplasia (Cutaneous Pseudolymphoma)

Cutaneous lymphoid hyperplasia (cutaneous pseudolymphoma) often arises on the face (see Ch. 121). When lesions fail to respond to intralesional corticosteroids, low-dose fractionated radiotherapy utilizing low-energy photons (10–15 Gy in five fractions) is an efficacious treatment option with minimal, if any, side effects.

RADIOTHERAPY OF *IN SITU* CUTANEOUS MALIGNANCIES

Squamous Cell Carcinoma *In Situ* (Bowen Disease)

Radiotherapy can be used, albeit infrequently, to treat SCC *in situ*. The malignancy is limited to the epidermis and its appendages, arises more commonly in sun-exposed sites, and usually presents as a slowly growing, scaly, erythematous plaque. A biopsy is important to exclude the possibility of eczema or psoriasis. Only a small minority (<5%) become invasive SCCs, although this may be higher (10%–30%) in genital lesions such as erythroplasia of Queyrat. Patients are treated with 40–50 Gy in 10–20 fractions using superficial low-energy photons (110–150 kVp), with reported local five-year cure rates of 98%–100%[15].

Patients with widespread actinic keratoses have been treated with radiotherapy under special circumstances. Given that other very effective therapies are readily available (see Ch. 108), radiotherapy should not be considered a first-line treatment modality.

Lentigo Maligna

Lentigo maligna (melanoma *in situ* arising within photodamaged skin) often presents as a longstanding and large-sized hyperpigmented patch on the face of elderly patients (see Ch. 113). The size and location often preclude simple excision, and radiotherapy remains a well-established, evidenced-based option with excellent five-year cure rates of 90%–95%[16] (Fig. 139.3). Reported doses range from 35 to 100 Gy administered in 5–10 fractions, i.e. large doses per fraction. However, dose fractionation schedules of 40–50 Gy in 10–20 fractions would also be efficacious[17]. Field margins of 1–1.5 cm are recommended, demarcated by Wood's lamp examination or confocal microscopy (if available), and treating to a depth of at least 5 mm.



Fig. 139.3 Lentigo maligna (melanoma *in situ*). A An 82-year-old man with a lentigo maligna on his right cheek. **B** Three months after superficial radiotherapy (45 Gy in 15 daily fractions, 120 kVp, HVL 4.2 mm Al).

RADIOTHERAPY OF INVASIVE CARCINOMAS, SARCOMAS, AND LYMPHOMAS

Basal Cell Carcinoma

Definitive radiotherapy

BCCs – in particular primary tumors <2 cm in diameter – can be treated with a number of therapeutic modalities. However, there is a paucity of randomized controlled trials comparing these different modalities. In a Cochrane Review focusing on BCCs, the authors analyzed the published results of seven different treatment categories[18]. Although they suggested the need for further research, surgery and radiotherapy appeared to be the two most efficacious modalities, with surgery probably leading to the lowest recurrence rates[18]. Of note, Mohs micrographic surgery is said to result in some of the highest long-term cure rates[19].

While local control rates (90%–95%) for either excision or radiotherapy are probably similar, management decisions are often based on other factors (Table 139.3). For example, radiotherapy would be favored in an elderly patient with a BCC located on the nasal tip or nasal alae (Fig. 139.4). In the locations outlined in Table 139.3, excision followed by primary closure is often difficult to accomplish and grafts or flaps are frequently required if surgical excision is chosen (Fig. 139.5). In addition, achieving negative deep margins via excision may be difficult in these locations. Although larger lesions (>20 mm) can still be eradicated via definitive radiotherapy (see below), with increasing size and depth of invasion, local control rates decrease. Therefore, surgery combined with adjuvant radiotherapy is often recommended to try to achieve better local control.

PATIENT FACTORS AND TUMOR CHARACTERISTICS THAT FAVOR RADIOTHERAPY	
Patient factors	Older age (>70 years)
	Patient preference (avoidance of surgery)
	Receiving medications that affect coagulation and platelet function
	Significant medical comorbidities
Tumor characteristics	Site: Ala nasi, nasal tip, nasal bridge, lower eyelid, medial canthus, helix
	Size/depth: Extensive and superficial
	Stage: Locally advanced requiring complex surgery

Table 139.3 Patient factors and tumor characteristics that favor radiotherapy. Many of these indications are relative.

Superficial BCCs that involve large areas are also treated with radiotherapy (Fig. 139.6), although alternatives such as photodynamic therapy, electrodesiccation and curettage, and topical imiquimod are reasonable options. It is important to note that tumors can take many weeks to completely regress after radiotherapy and, therefore, early re-biopsy is not recommended. Dose fractionation schedules vary and are determined by patient and tumor factors (see below).

Adjuvant (postoperative) radiotherapy

A recommendation for radiotherapy is often made in the setting of incomplete excision of a BCC. A positive deep margin is always a concern, especially when a local flap has been used for reconstruction, because deep recurrences can be difficult to detect. In particular, undetected deep recurrences of tumors located within the midface and periorbital regions may be associated with significant local morbidity. It is accepted that at least 20%–30% of incompletely excised BCCs will

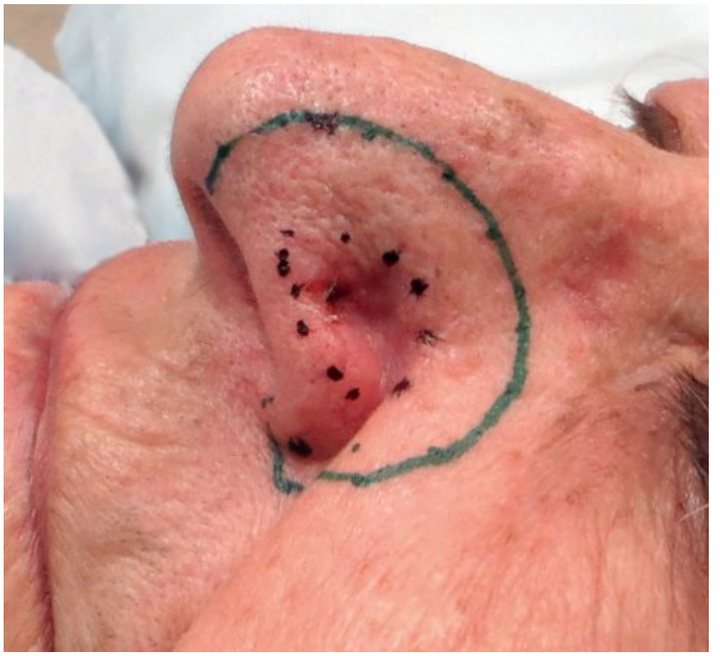


Fig. 139.4 Superficial basal cell carcinoma (BCC). A 78-year-old woman with a 1.5 cm BCC on the left ala nasi. The tumor was treated with definitive radiotherapy using superficial energy photons (45 Gy in 15 daily fractions, 100 kVp, HVL 7 mm Al). Note the 1 cm field margin to encompass subclinical extension of this poorly defined BCC.

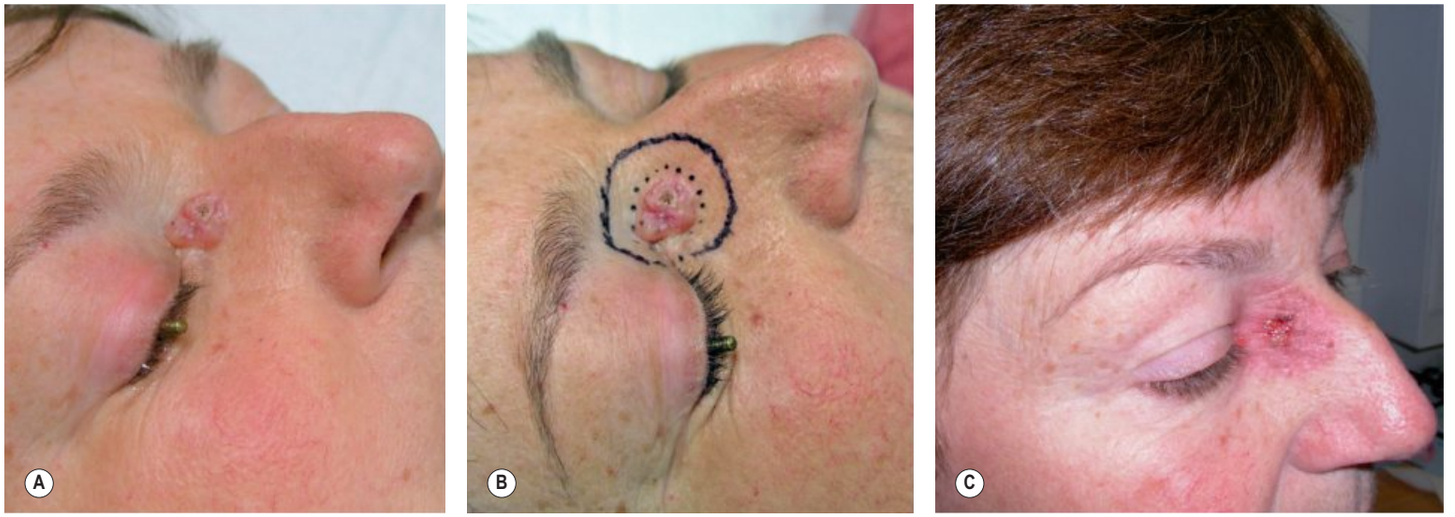


Fig. 139.5 Nodular basal cell carcinoma. A A 56-year-old woman with a 1.5 cm nodular basal cell carcinoma of the right medial canthus. The patient received 55 Gy in 25 daily fractions using orthovoltage energy photons (250 kVp, HVL 2.5 mm Cu) following pre-treatment insertion of an internal eye shield. **B** A 10 mm radiotherapy field margin has been placed around the patient's tumor so as to encompass both macroscopic disease and possible surrounding microscopic (subclinical) spread. **C** At completion of radiotherapy, the tumor has regressed markedly. Note the confluent erythema demarcating the treatment field.



Fig. 139.6 Extensive basal cell carcinoma. **A** An elderly woman with a large basal cell carcinoma occupying much of the left temple region. **B** Three months after 40 Gy in 10 daily fractions using superficial energy photons (100 kVp, HVL 7 mm Al).

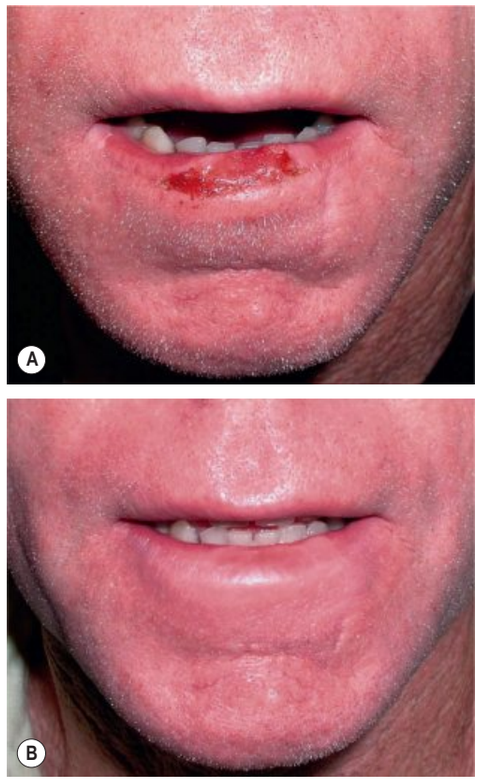


Fig. 139.7 Squamous cell carcinoma. **A** A 55-year-old man with a squamous cell carcinoma occupying most of his mid lower vermilion lip. The patient decided to undergo definitive radiotherapy and received 55 Gy in 25 daily fractions using orthovoltage energy photons (250 kVp, HVL 2.5 mm Cu) and had an oral cavity lead shield fitted to protect his teeth and mandible. **B** Four months after radiotherapy, he is disease-free and has experienced an excellent cosmetic result.

recur. In one study, 69 of 100 patients with incompletely excised BCCs had residual tumor identified histologically at the time of re-excision[20]. While re-excision is favored when there is a positive margin, sometimes the anatomic site precludes safe re-excision (e.g. the periosteum of the nose) and thus adjuvant radiotherapy is an option.

The aim of adjuvant radiotherapy is to reduce the incidence of local recurrence by eradicating residual microscopic BCC. In a Canadian trial, the addition of adjuvant radiotherapy improved the 5-year local control rate from 61% to 91%[21]. Because the majority of recurrences were successfully salvaged via surgery, the 10-year local control rates were similar (92% vs 90%).

Squamous Cell Carcinoma

Definitive radiotherapy

The approach to treating patients with cutaneous SCC is influenced by the small risk (<5%)[22] of metastatic spread to regional lymph nodes and the need to achieve local control. Of note, some patients can be considered as having high-risk SCC when certain unfavorable features are present; these include recurrent tumor, diameter >2 cm, thickness >2 mm, invasion beyond fat, high-grade (i.e. poorly differentiated) histology, perineural invasion, ear or non-hair-bearing lip as the primary site, and immunosuppressed host. These SCCs have a greater risk of developing recurrence and metastatic nodal disease[23].

In general, high-risk patients should have lesions excised with wider margins and be followed closely for at least 5 years[24]. However, depending upon the circumstances, some patients are treated with definitive (or adjuvant) radiotherapy. Definitive radiotherapy of cutaneous SCC is an excellent treatment option, especially in the clinical settings outlined in Table 139.3. For example, multiple medical comorbidities may preclude patients from having extensive surgery. In addition, for sites such as the lower lip, radiotherapy can result in excellent maintenance of function (even with more extensive tumors; Fig. 139.7), as well as cure rates comparable to surgery (see section on lip SCC)[25].

To date, there is no consensus as to which high-risk patients should be offered elective treatment (e.g. surgical, radiotherapy) of regional lymph nodes. Future sentinel lymph node biopsy (SLNB) studies may help resolve this issue. Compared to CT and MRI, SLNB is more sensitive at detecting occult nodal metastases, but its impact on overall survival needs to be determined. In a meta-analysis of studies in which patients with high-risk SCCs underwent SLNB, a positive SLN was observed in 12.3% of patients, all of whom had SCCs >2 cm in diameter[26].

The currently recommended margins for the surgical excision of SCC are 4–6 mm, with wider margins for high-risk tumors[27]. For the latter, Mohs micrographic surgery or wide local excision under general anesthesia may be utilized. In a study of cutaneous SCCs, 95% of tumors <2 cm in diameter had negative margins if excised with a 4 mm margin as did 95% of tumors >2 cm when excised with a 6 mm margin[28]. It is generally not appropriate to merely observe an incompletely excised SCC. Recurrent SCCs are associated with a lower control rate and a higher incidence of regional metastases, when compared to previously untreated SCCs[29].

Adjuvant (postoperative) radiotherapy

Adjuvant radiotherapy is an option when excision of an SCC is incomplete and re-excision is not advisable. In addition, it is considered when there are high-risk features such as perineural invasion, an immunocompromised host, and an anatomic site that has a high risk of recurrence. Special clinical situations are outlined below.

Keratoacanthomas

A keratoacanthoma (KA) typically presents as a rapidly enlarging papulonodule with a central keratin plug. Difficulty often arises in distinguishing these tumors histologically from well-differentiated SCCs, and many authorities consider most KAs to be a well-differentiated variant of SCC. Although KAs can regress spontaneously, a significant number become large and unsightly with destruction of underlying tissue. If surgery is not considered, radiotherapy consisting of 25 Gy in 5 fractions can lead to durable regression. If the diagnosis of KA versus well-differentiated SCC is uncertain, a dose fractionation schedule appropriate for an SCC should be prescribed.

Special clinical situations

SCC of the lip

In regions of the world that have a high incidence of keratinocyte carcinomas (e.g. Australia), SCC of the lip is considered a skin cancer, not an oral cancer[25]. Compared to oral SCC, there is a lower propensity for spread to regional nodes. Nearly all lesions arise on the lower lip, usually as a consequence of chronic sun exposure.

For SCCs of the lip, the outcome with surgery versus radiotherapy is similar. The laxity of the lip means that wedge excision (± vermilionectomy) is the procedure of choice, with primary closure often possible. When >30%–50% of the lip is involved, excision with appropriate margins is usually not achievable without risking function (e.g.

oral competency). Complex reconstruction is an option (see Ch. 147), but insensate tissue may be needed for reconstruction and this can have an impact on function. Therefore, radiotherapy is an excellent treatment option for SCC of the lip. The lower lip lends itself very well to treatment with orthovoltage photons following insertion of a 3 mm intraoral lead shield to protect the mandible and teeth (see Fig. 139.7). Doses are similar to those for any other equivalent-sized SCC, with a recommended total dose of 50–55 Gy in 20–25 fractions[30].

Lymph node metastases of SCC

Patients with metastatic SCC involving regional lymph nodes (usually of the head and neck) are best referred to a multidisciplinary cancer service[31]. Parotid lymph nodes represent a common site for metastases from a previously treated scalp, forehead, or ear SCC; in such cases, surgery (parotidectomy ± neck dissection) is required.

To improve locoregional control, adjuvant radiotherapy is nearly always recommended in patients with nodal metastases, as the risk of nodal relapse remains high despite surgery. Even patients with multiple unfavorable features (e.g. involvement of multiple nodes, extranodal spread, close margins) can still expect a 5-year disease-free survival of 70%–75% with the combination of surgery plus adjuvant radiotherapy[32].

Perineural invasion of SCC and BCC

Perineural invasion is an uncommon but serious consequence of SCC and, to a lesser extent, BCC[33]. Up to 2% and 5% of excised BCCs and SCCs, respectively, are noted to have incidental perineural invasion, with a minority of patients presenting clinically with neurologic signs (e.g. motor deficit) or symptoms. Formication (sensation of ants crawling) may herald the diagnosis of perineural invasion, but dysesthesias, paresthesias, numbness, and pain are all suggestive symptoms. The diagnosis is frequently delayed because perineural invasion is often not suspected.

A consensus is lacking regarding the most appropriate treatment following the diagnosis of perineural invasion and no universally accepted guidelines exist[33]. After surgical excision, consideration is given to adjuvant radiotherapy, with some centers factoring in whether there is invasion of small-caliber (<0.1 mm) versus large-caliber (≥0.1 mm) nerves[34]. If perineural invasion is limited to small-caliber nerves, some institutions favor observation.

Radiotherapy alone is often recommended for those with advanced disease extending into the cranial cavity. As expected, prognosis is poor once signs (e.g. craniopathies) or symptoms develop. When periorbital SCCs, especially those in the supraorbital area, are associated with perineural invasion, adjuvant radiotherapy should be considered[34]. In some circumstances, additional surgery may be undertaken to explore and dissect out potentially involved nerves. Alternatively, radiotherapy, often requiring multi-field megavoltage photons to treat neural pathways to the brainstem as well as first echelon lymph nodes, can be recommended[33–35]. While radiotherapy (e.g. 50–70 Gy; 2 Gy/fraction) has the advantage of avoiding surgery, there is some risk of late radiation damage to orbital and CNS structures. The utilization of very conformal, volume-based, intensity-modulated radiotherapy (IMRT) allows for safer delivery of radiation to important CNS structures[35].

Immunosuppressed hosts

Solid organ transplant recipients and individuals with chronic lymphocytic leukemia[36], especially those undergoing therapy (e.g. fludarabine, alemtuzumab), have a significantly increased risk of developing cutaneous SCCs, including aggressive and metastatic SCCs. The role of reduction of immunosuppression and chemoprophylaxis with retinoids is discussed in Chapter 108.

The basic tenets of obtaining adequate surgical margins and examining for perineural invasion are of particular importance in this group of patients. Whilst prophylactic treatment to regional lymph nodes is not recommended, adjuvant radiotherapy to incompletely excised tumors or those with significant perineural invasion should be strongly considered. Transplant patients usually tolerate radiotherapy well, with no greater degree of acute toxicity[37].

Dose fractionation schedules and fields

An appropriate dose fractionation schedule depends upon both patient and tumor factors[38]. However, decisions should not be based on age alone, as the presence or absence of relevant comorbidities must also be considered. As a generalization, smaller lesions (2–3 cm) in older patients (>70 years of age) are adequately treated by using 40–45 Gy in 10–15 daily fractions, resulting in acceptable local control and cosmesis (see Table 139.2). Elderly or infirm patients may be best served by prescribing single large fractions (see palliation below) or just three to five fractions. For larger invasive lesions (>3–4 cm) and/or younger patients, a lower fraction size (2–2.5 Gy) and total doses of 50–60 Gy are recommended so as to optimize local control and produce acceptable late effects. Some clinicians administer a higher dose for cutaneous SCCs than for equivalent-sized BCCs. However, the data to support this practice are conflicting, and, in the opinion of the authors, this is not required. Also, the dose for different subtypes or grades of BCC or SCC does not need to vary nor does the dose prescribed in the adjuvant setting.

A field margin of 5–10 mm beyond macroscopic disease or a surgical site is usually adequate (see Fig. 139.5B). For a small, well-defined BCC, a 5 mm field margin is adequate if superficial photons are used. For SCCs and infiltrative BCCs, a wider margin of 10–15 mm is required in order to encompass surrounding subclinical spread. Ideally, adjuvant treatment should start within 6–7 weeks of excision. While some clinicians are reluctant to administer radiotherapy to a grafted site, it is uncommon for a healed skin graft to be lost because of radiotherapy[39].

Merkel Cell Carcinoma

Merkel cell carcinoma is a primary cutaneous neuroendocrine (small cell) carcinoma that most often arises in the head and neck region (see Ch. 115)[40]. These tumors often lack diagnostic clinical features but usually have grown rapidly. Merkel cell carcinomas are aggressive, having a high propensity for locoregional relapse and distant spread, and patients need to be appropriately evaluated prior to instituting therapy.

Currently, wide local excision of the primary lesion with margins of at least 15–20 mm or Mohs micrographic surgery is recommended. Guidelines also advocate sentinel lymph node biopsy (SLNB) if the draining lymph nodes are not palpable (see Fig. 115.19); assessment of the regional lymph nodes is a critical component of management[41]. When adjuvant locoregional radiotherapy is administered, there is evidence that extensive local surgery may not necessarily lead to a better outcome[42]. In patients considered medically or technically inoperable, radiotherapy alone (50–60 Gy in 20–33 fractions) can result in excellent in-field control in most patients (75%–80%), with death usually from distant relapse[43].

Adjuvant locoregional radiotherapy improves recurrence rates and disease-free survival[44,45] and is recommended unless the patient has a low-risk Merkel cell carcinoma (primary ≤1 cm, no lymphovascular invasion histologically, negative margins, SLNB negative, and immunocompetent host). Treatment should include the excision site, in-transit tissue (because of the risk of in-transit metastases), and the draining lymph node basin (Fig. 139.8). Adjuvant radiotherapy of in-transit tissue does vary, from most frequently performed in the head and neck region to not performed in the distal extremities. In an attempt to reduce the risk of locoregional relapse (which can occur in 40%–50% of patients treated with surgery alone), a typical dose fractionation schedule would be 50 Gy in 20–25 daily fractions[46]. Palliative radiotherapy and immunotherapy or chemotherapy can be offered to patients with advanced or metastatic disease.

Angiosarcoma

Most angiosarcomas present as violaceous plaques on the scalp and face of older adults (see Ch. 114). These tumors often extend well beyond the clinically apparent margins[47] and locally extensive disease is usually present at the time of diagnosis. Unfortunately, excision alone is usually followed by local recurrences because of the multicentric and insidious nature of this tumor. Relapses can occur at the periphery of treated sites as well as regionally.

Angiosarcomas tend to be radio-responsive and therefore can be treated with radiotherapy. Patients with limited and operable disease may undergo excision followed by *adjuvant* radiotherapy. Alternatively, *definitive* radiotherapy is also an option, with a reasonable likelihood of obtaining in-field control[48]. In the case of scalp involvement, a

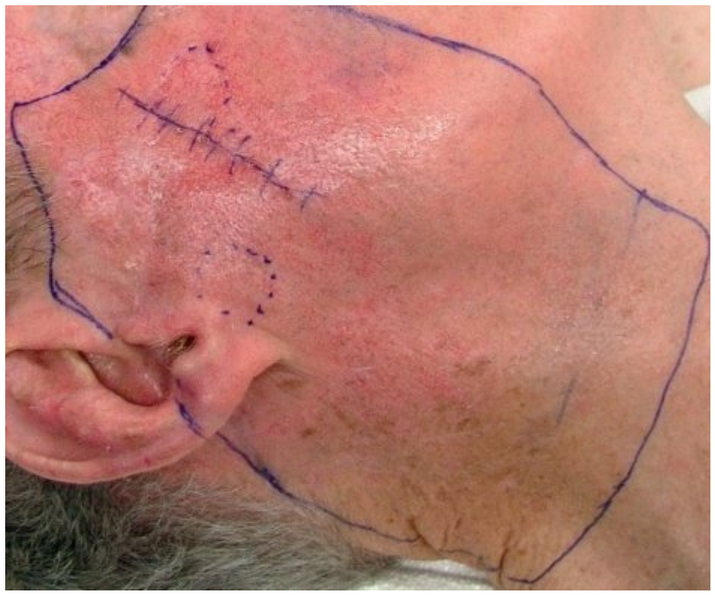


Fig. 139.8 Merkel cell carcinoma. Following local surgical excision, this 68-year-old man underwent wide-field radiotherapy (9 MeV electron beam with a tissue equivalent bolus, 55 Gy in 25 daily fractions); the field encompassed the primary excision site, in-transit tissue, and non-palpable regional draining nodes of the parotid and upper neck. The obvious pre-auricular lymph node (circled) contained biopsy-proven, low-grade parotid tumor which was treated concurrently with radiotherapy.

technique can be used that encompasses the entire scalp and combines matching photon and electron fields[47]. Other options include multiple static electron fields or electron arcs. Lastly, various combinations of medications (e.g. paclitaxel, propranolol, pazopanib, carotuximab, erbulin mesylate) have been administered in patients with recurrent disease.

Kaposi Sarcoma

Kaposi sarcoma (KS) is a type of spindle cell malignancy that arises from the vascular endothelium, usually presenting as violaceous papules and plaques (see Ch. 114). Classic KS favors the legs of elderly men of Mediterranean or Jewish origin[49], whereas AIDS-associated KS has a more widespread distribution pattern, including the oral cavity (see Ch. 78).

While the role of radiotherapy for AIDS-related KS has markedly diminished with the advent of antiretroviral therapy, it is a radioresponsive tumor and various dose fractionation schedules have been used to effectively treat cutaneous lesions. Regimens range from a single 8 Gy irradiation to 30–40 Gy in 10–20 daily fractions[50]. Because patients often develop acute painful reactions from radiotherapy to the oral cavity and the plantar surface, they should undergo radiotherapy to only one foot at a time.

Classic KS usually has a long and indolent clinical course. Patients with localized resectable tumors that are symptomatic may undergo excision. Radiotherapy is also an effective modality for palliating areas of symptomatic disease. Single small doses of 8–12 Gy are reported to result in symptom relief and tumor reduction in most patients; however, in some circumstances, higher, more-fractionated doses may be considered to sites of limited disease. Occasionally, there is a sense of chasing the disease, as lesions gradually appear at the periphery of irradiated sites. For patients with widespread disease, total skin electron beam therapy (see below) has been utilized.

Cutaneous Lymphomas

Cutaneous lymphomas are exquisitely radiosensitive. However, except for primary cutaneous B cell lymphoma (see Ch. 119) and selected patients with cutaneous T cell lymphoma (CTCL; see Ch. 120), the role of radiotherapy is essentially palliative. Patients with sites of symptomatic local disease (lymph nodes, dermal nodules and plaques, ulcers) can be palliated with doses of 12–30 Gy, often requiring orthovoltage or megavoltage energy photons. In the indolent forms of primary cutaneous B cell lymphoma, local radiotherapy with doses of 36–40 Gy may be curative[51].

Total skin electron beam therapy

Selected patients with mycosis fungoides (MF) and Sézary syndrome may be treated with total skin electron beam therapy (TSEBT). This treatment, which is complex and usually delivered by specialized centers of radiation oncology, has particular advantages. They include comprehensive coverage of the entire skin surface and an acceptable toxicity profile, in addition to the option of repeating TSEBT if other treatments fail. Historically, TSEBT consisted of 36 Gy administered over 9 weeks, but in recent trials, 12 Gy over 3 weeks provided excellent response rates (~90%)[52,53]. Although TSEBT can be offered to patients with all stages of disease, it is usually reserved for more advanced stages (IIB, III, IV) and/or disease that has failed to respond to less aggressive therapies (e.g. phototherapy, topical alkylating agents, oral retinoids).

Treatment consists of a 4–6 MeV beam (see Fig. 139.1) with patients often treated in the standing position at a distance of 7 meters from the linear accelerator. Irradiation is administered four days per week[54]. X-ray contamination is less than 2% of the dose. Each week, the entire skin surface receives two cycles of treatment and a total of 2 Gy is given to the entire skin surface during each cycle. The perineum, plantar surface, and scalp receive supplemental "boosts", as these areas are not adequately treated with the patient in the standing position. Lead contact lenses are used to shield the eyes, and depending upon the total anticipated dose, the hands and feet can also be shielded for a portion of the cycle. Patients with tumor stage disease often receive supplemental boosts via orthovoltage or electrons at the completion of TSEBT.

As there is no significant dose of radiation to the bone marrow or viscera, patients receiving TSEBT do not typically have systemic sequelae (e.g. cytopenias, nausea, vomiting, diarrhea), although patients can develop erythema, blisters, and/or skin pain[55]. Alopecia, dyspigmentation, and hypohidrosis are often seen as well and can be permanent with higher-dose regimens. A repeat course of TSEBT may be given months to years later for those who develop recurrent treatment-resistant disease. The most suitable candidates for repeat TSEBT are individuals with longer intervals between courses (>6 months) and those who had a longer disease-free interval following the first course.

Adnexal Carcinomas

Adnexal (appendageal) carcinomas, such as microcystic adnexal carcinoma and sebaceous, eccrine, or apocrine carcinoma, are rare and therefore any treatment approach needs to be individualized (Ch. 111). Many of these tumors are aggressive in nature, with a propensity to develop regional and distant metastases. While patients with operable cancers should have them excised with appropriate margins, inoperable lesions may respond to radiotherapy[56]. Adjuvant radiotherapy may also be recommended in the setting of incomplete excision. Doses similar to those employed for equivalent keratinocyte carcinomas should be administered (see Table 139.2).

PALLIATION

Locally Advanced Tumors

Occasionally, elderly, debilitated, or mentally ill patients present with advanced and neglected skin cancers, which, though not curable, can be palliated. Such tumors are often painful, bleeding, and infected, causing problems for both the patient and the caregiver. With the addition of a bolus (see Fig. 139.2), single large fractions of 8–20 Gy can be given quickly (within minutes) using megavoltage photons. Uncooperative patients may require mild sedation prior to treatment. These large single fractions are well tolerated with minimal toxicity. Alternative regimens include multiple, medium-sized fractions given once or twice a week (e.g. 8 Gy × 3). In elderly patients who are otherwise well, higher total dose fractionation schedules such as 35 Gy in 5–7 fractions or 40 Gy in 10 fractions (Fig. 139.9) may be more appropriate and can be considered more aggressive in intent. These are often given as two or three fractions per week.



Fig. 139.9 Metastatic squamous cell carcinoma involving the parotid lymph nodes. A An 85-year-old man with advanced and inoperable SCC of his right parotid lymph nodes. **B** Following a two-week course of palliative radiotherapy (40 Gy in 10 daily fractions using 12 MeV electrons plus a tissue equivalent bolus), he experienced a complete clinical response.

Metastases

Dermal-based metastases occur most frequently in patients with lung and breast cancer, and, in general, are associated with a poor prognosis (see Ch. 122). Both in-transit metastases and distant dermal metastases can develop in patients with cutaneous SCC, Merkel cell carcinoma, and melanoma. Cutaneous metastases may also present as rapidly enlarging subcutaneous masses with intact overlying skin.

Ulceration and bleeding are complications of cutaneous metastases that respond to palliative radiotherapy. Orthovoltage photons or megavoltage photons (with a bolus) administered as a single 8 Gy fraction or as 20 Gy in five fractions are effective regimens. Metastatic deposits elsewhere (e.g. skeletal) are also palliated with a similar dose fractionation schedule.

REACTIONS AND COMPLICATIONS

Acute Reactions (Acute Radiodermatitis)

Acute morbidity from skin-directed radiotherapy is usually minimal (in-field cutaneous erythema and desquamation) and limited to the irradiated area (Table 139.4). Systemic side effects such as fatigue, nausea, and vomiting do not occur.

Daily washing with water (± mild soap or soap-free cleansers) is recommended while receiving radiotherapy, including non-skin-directed. Use of prophylactic topical corticosteroids (e.g. mometasone) may reduce the severity of acute radiodermatitis and improve comfort and pruritus[57]. Given the limited time period of application, cutaneous atrophy is usually not an issue. No particular dressing has proven to be superior[58].

Most patients can expect to have local discomfort and moist desquamation by the conclusion of radiation therapy (Fig. 139.10), which then lasts for a few weeks. Hemorrhagic crusting can also develop and re-epithelialization usually occurs by week 3 or 4 following completion of radiotherapy. Delayed healing (beyond 6–8 weeks) is uncommon, as is associated soft tissue infection.

In-field radiation *recall* can occur following administration of antineoplastic drugs, including chemotherapeutic agents (e.g. anthracyclines, taxanes, antimetabolites; see Table 21.15), immunotherapies, and targeted therapies (e.g. inhibitors of EGFR, mTOR, and BRAF). Rarely, it develops following other medications or vaccines (e.g. SARS-CoV-2). Radiation *enhancement* characterized by higher grade, in-field skin toxicity and mucositis can also occur, including with the concurrent use of epidermal growth factor receptor inhibitors (EGFRi)[59]. This may be complicated by secondary staphylococcal infections.

RADIOTHERAPY REACTIONS AND COMPLICATIONS	
	Reaction or complication
Acute radiodermatitis	Grade 1: faint erythema or dry desquamation
	Grade 2: moderate to brisk erythema, moderate edema, moist desquamation confined to skin folds
	Grade 3: moist desquamation in areas other than skin folds, bleeding induced by minor trauma or abrasion
	Grade 4: life-threatening consequences, skin necrosis or ulceration of full-thickness dermis, spontaneous bleeding from involved skin, skin graft indicated
Late effects*	Hypo- or hyperpigmentation†
	Telangiectasia†
	Epidermal atrophy† and fragility
	Permanent epilation/alopecia, sweat gland atrophy
	Subdermal fibrosis and contracture (e.g. breast contracture)
	Necrosis of soft tissue, cartilage and/or bone
	Atypical vascular proliferation
	Benign tumors – eccrine poromas (also referred to as eccrine poromatosis)
	Radiation-induced malignancy‡ – SCC, BCC, angiosarcoma, osteosarcoma, pleomorphic undifferentiated sarcoma (previously referred to as malignant fibrous histiocytoma), and other soft tissue sarcomas

*Many late effects are uncommon.
†Components of poikiloderma; a TP53 haplotype containing two variant alleles was associated with almost a twofold increase in risk for telangiectasia. Variants in *TP53* may therefore modify the risk of late skin toxicity after radiotherapy.
‡Many reports have been in patients whose dose fractionation schedules and techniques are now historical in nature.

Table 139.4 Radiotherapy reactions and complications. BCC, basal cell carcinoma; SCC, squamous cell carcinoma.

Late Reactions

The late effects of radiotherapy (e.g. telangiectasia, epidermal atrophy, dyspigmentation, fibrosis; see Table 139.4 & Fig. 139.10) often appear months to years later. They are more likely to appear with continued unprotected sun exposure, when a large dose per fraction (>3–4 Gy) was delivered, if the total dose was >55 Gy, and when large fields were irradiated. Chronic non-healing, radiation-induced ulcers represent poorly vascularized tissue that requires the importation of well-vascularized tissue to enable healing. The latter usually consists of local skin flaps or sometimes staged skin–muscle or axial pedicle flaps of non-irradiated tissue; grafts do not take well on irradiated tissue due to the poor vascular bed.

In a review of over 400 patients treated with radiotherapy, 92% were considered to have a good or excellent cosmetic result[60]. However, 36% of those receiving >60 Gy in ≤2 Gy fractions had only a fair (16%) or poor (20%) cosmetic result. Smaller treatment fields (2–3 cm) tolerate hypofractionation better than do larger areas, but, even so, if cosmesis is an important consideration, larger fractions should be avoided. Patients should also be warned of the small risk (<5%) of late soft tissue and cartilage necrosis, which are related to larger tumor size and larger doses per fraction.

Younger Patients

When irradiating younger patients, better long-term cosmetic results are more likely if a low dose per fraction (2 Gy/fraction) is administered. A typical dose for a small BCC would be 50–54 Gy delivered in



Fig. 139.10 Acute and chronic cutaneous side effects of radiation therapy. A Confluent moist desquamation and marked edema in a patient near completion of radiotherapy for a squamous cell carcinoma with neurotropism (grade 2 acute radiodermatitis). **B** Confluent moist desquamation and superficial ulcerations on the breast after three weeks of radiotherapy for breast cancer (grade 3). **C** Dry desquamation of the neck several weeks following radiation therapy for a pharyngeal squamous cell carcinoma (grade 1). **D** Development of morphea and lichen sclerosus within irradiated skin; note the purpura that accompanies lichen sclerosus. **E** Permanent scarring alopecia and telangiectasias of the occipital scalp after radiotherapy for anaplastic cerebellar astrocytoma. **F** In-field telangiectasias; note the square distribution pattern. *A, F, Courtesy Jean L. Bolognia, MD; B, D, E, Courtesy Jonathan Leventhal, MD.*

DISEASES INDUCED BY RADIATION THERAPY
Disease not confined to the sites of irradiation
• Autoimmune bullous diseases (bullous pemphigoid, pemphigus foliaceus, pemphigus vulgaris, paraneoplastic pemphigus) • Eosinophilic, polymorphic, and pruritic eruption associated with radiotherapy (EPPER) syndrome • Erythema multiforme, including EMPACT syndrome* • Herpes zoster
Disease limited to sites of irradiation
• Autoimmune bullous diseases (bullous pemphigoid, pemphigus vulgaris) • Atypical vascular proliferation, angiosarcoma** • Comedonal acne, folliculitis • Digitate keratosis (also referred to as postirradiation minute digitate hyperkeratosis) • Erythema multiforme, including EMPACT syndrome* • Graft-versus-host disease • Grover disease (transient acantholytic dermatosis) • Lichen planus • Lichen sclerosus • Morphea (localized scleroderma) • Postirradiation pseudosclerodermatous panniculitis (also referred to as sclerosing postirradiation panniculitis) • Psoriasis† • Radiation recall, radiation enhancement (see Tables 21.15 & 21.16) • Urticaria pigmentosa • Vitiligo
Lesions that spare irradiation sites
• Exanthematous drug eruption
*EMPACT begins in the site(s) of radiation but then may generalize. **In or near irradiation site. †May generalize.

Table 139.5 Diseases induced by radiation therapy. Neoplasms are listed in Table 139.4. EMPACT, erythema multiforme associated with phenytoin and cranial radiation therapy.

25–27 daily fractions[61]. However, even with this dose fractionation schedule, patients can still expect some degree of in-field hypopigmentation and telangiectasia; the latter can be addressed via pulsed dye laser treatment and camouflaging cosmetics (see Ch. 153). Other options, therefore, should be considered prior to recommending radiotherapy to younger patients. The risk of a radiotherapy-induced in-field malignancy arising decades after high-dose, therapeutic, skin-directed radiotherapy is rare and poorly documented in the literature (see Table 139.4).

Cutaneous Diseases Induced by Radiation Therapy

Table 139.5 outlines the cutaneous disorders that are induced by radiotherapy, with some occurring outside the field of radiation[62] as well as others limited to the site of irradiation.

FUTURE TRENDS

Modern radiotherapy has entered a new and exciting era. Accurate conformal radiotherapy is being delivered via sophisticated three-dimensional CT-based planning and treatment systems. Intensity-modulated radiotherapy (IMRT)[63] is allowing tumor doses to escalate and normal tissue doses to decrease. The integration of MRI and functional imaging such as positron emission tomography (PET) into planning systems further enhances the accurate delivery of radiotherapy as may reflectance confocal microscopy.

Additional figures and table on Treatment of acute radiodermatitis, available in our eBook (see inside front cover for access code).

REFERENCES

1. Mendenhall WM, Amdur RJ, Hinerman RW, et al. Radiotherapy for cutaneous squamous and basal cell carcinomas of the head and neck. *Laryngoscope*. 2009;119:1994–1999.
2. Withers HR. Biological basis of radiation therapy for cancer. *Lancet*. 1992;339:156–163.
3. Goldschmidt H, Breneman JC, Breneman DL. Ionizing radiation therapy in dermatology. *J Am Acad Dermatol*. 1994;30:157–182.
4. Silva JJ, Tsang RW, Panzarella T, et al. Results of radiotherapy for epithelial skin cancer of the pinna: the Princess Margaret Hospital experience, 1982–1993. *Int J Radiat Oncol Biol Phys*. 2000;47:451–459.
5. Khan FM. Quality of x-ray beams. In: Khan FM, ed. *The Physics of Radiation Therapy*. 1st ed. Baltimore: Williams & Wilkins; 1984:110–120.
6. Hernández-Machin B, Borrego L, Gil-Garcia M, Hernández BH. Office-based radiation therapy for cutaneous carcinoma: evaluation of 710 treatments. *Int J Dermatol*. 2007;46:453–459.
7. Pashazadeh A, Boese A, Friebe M. Radiation therapy techniques in the treatment of skin cancer: an overview of the current status and outlook. *J Dermatolog Treat*. 2019;8:831–839.
8. van Hezewijk M, Creutzberg CL, Putter H, et al. Efficacy of a hypofractionated schedule in electron beam radiotherapy for epithelial skin cancer: analysis of 434 cases. *Radiother Oncol*. 2010;95:245–249.
9. Shah C, Ouhib Z, Kamrava M, et al. ABS Consensus Statement: The American Brachytherapy Society consensus statement for skin brachytherapy. *Brachytherapy*. 2020;19:415–426.
10. Tom MC, Hepel JT, Patel R, et al. Special Section on Intraoperative Radiation Therapy and Eclectronic Brachytherapy. The American Brachytherapy Society consensus statement for electronic brachytherapy. *Brachytherapy*. 2019;18:292–298.
11. Ouhib Z, Kasper M, Calatayud JP, et al. Aspects of dosimetry and clinical practice of skin brachytherapy: The American Brachytherapy Society working group report. *Brachytherapy*. 2015;14:840–858.
12. Alam M, Nanda S, Mittal B, et al. The use of brachytherapy in the treatment of nonmelanoma skin cancer: a review. *J Am Acad Dermatol*. 2011;65:377–388.

12a. Berrington de Gonzalez A, Gilbert E, Curtis R, et al. Second solid cancers after radiation therapy: a systematic review of the epidemiologic studies of the radiation dose-response relationship. *Int J Radiat Oncol Biol Phys*. 2013;86:224–233.

13. Huang Q, Veness M, Richards S. The role of adjuvant radiotherapy in recurrent keloids. *Australas J Dermatol*. 2004;45:162–166.
14. Renz P, Hasan S, Gresswell S, et al. Dose effect in adjuvant radiation therapy for the treatment of resected keloids. *Int J Radiation Oncol Biol Phys*. 2018;102:149–154.
15. Lukas-Vanderspek LA, Pond GR, Wells W, Tsang RW. Radiation therapy for Bowen's disease of the skin. *Int J Radiat Oncol Biol Phys*. 2005;63:505–510.
16. Fogarty GB, Hong A, Scolyer RA, et al. Radiotherapy for lentigo maligna: a literature review and recommendations for treatment. *Br J Dermatol*. 2014;170:52–58.
17. Huynh NT, Veness MJ. Radiotherapy for lentigo maligna. *Arch Dermatol*. 2002;138:981–982.
18. Bath-Hextall FJ, Perkins W, Bong J, Williams HC. Interventions for basal cell carcinoma of the skin. *Cochrane Database Syst Rev*. 2007;1:CD003412.
19. Rowe DE, Carroll RJ, Day Jr CL. Long-term recurrence rates in previously untreated (primary) basal cell carcinoma: implications for patient follow-up. *J Dermatol Surg Oncol*. 1989;15:315–328.
20. Palmer VM, Wilson PR. Incompletely excised basal cell carcinoma: residual tumor rates at Mohs re-excision. *Dermatol Surg*. 2013;39:706–718.
21. Liu FF, Maki E, Warde P, et al. A management approach to incompletely excised basal cell carcinomas of the skin. *Int J Radiat Oncol Biol Phys*. 1991;20:423–428.
22. Stevens JS, Murad F, Smile TD, et al. Validation of the 2022 National Comprehensive Cancer Network risk stratification for cutaneous squamous cell carcinoma. *JAMA Dermatol*. 2023;159:728–735.
23. Ruiz ES, Karia PS, Besaw R, Schmults CD. Performance of the American Joint Committee on Cancer Staging Manual, 8th Edition vs the Brigham and Women's Hospital Tumor Classification System for cutaneous squamous cell carcinoma. *JAMA Dermatol*. 2019;155:819–825.
24. Motley R, Kersey P, Lawrence C. Multiprofessional guidelines for the management of the patient with primary cutaneous squamous cell carcinoma. *Br J Dermatol*. 2002;146:18–25.
25. Najim M, Cross S, Gebski V, et al. Early-stage squamous cell carcinoma of the lip: the Australian experience and the benefits of radiotherapy in improving outcome in high-risk patients after resection. *Head Neck*. 2012;35:1426–1430.
26. Schmitt AR, Brewer JD, Bordeaux JS, Baum CL. Staging for cutaneous squamous cell carcinoma as a predictor of sentinel lymph node biopsy results: meta-analysis of American Joint Committee on Cancer criteria and a proposed alternative system. *J Am Acad Dermatol*. 2014;150:19–24.
27. Dessinioti C, Stratigos AJ. Overview of guideline recommendations for the management of high-risk and advanced cutaneous squamous cell carcinoma. *J Eur Acad Dermatol Venereol*. 2022;36(Suppl1):11–18.
28. Brodland DG, Zitelli JA. Surgical margins for excision of primary cutaneous squamous cell carcinoma. *J Am Acad Dermatol*. 1992;27:241–248.
29. Kwan W, Wilson D, Moravan V. Radiotherapy for locally advanced basal cell and squamous cell carcinomas of the skin. *Int J Radiat Oncol Biol Phys*. 2004;60:406–411.
30. Babington S, Veness MJ, Cakir B, et al. Squamous cell carcinoma of the lip: is there a role for adjuvant radiotherapy in improving local control following incomplete or inadequate excision? *ANZ J Surg*. 2003;73:621–625.
31. Veness MJ, Porceddu S, Palme CE, Morgan GJ. Cutaneous head and neck squamous cell carcinoma metastatic to parotid and cervical lymph nodes. *Head Neck*. 2007;29:621–631.
32. Wang JT, Palme CE, Morgan GJ, et al. Predictors of outcome in patients with metastatic cutaneous head and neck squamous cell carcinoma involving cervical lymph nodes: improved survival with the addition of adjuvant radiotherapy. *Head Neck*. 2012;34:1524–1528.
33. Buchanan L, De'Ambrosis B, De'Ambrosis K, et al. Defining incidental perineural invasion: the need for a national registry. *Australas J Dermatol*. 2014;55:107–110.
34. Geist DE, Garcia-Moliner M, Fitzek MM. Perineural invasion of cutaneous squamous cell carcinoma and basal cell carcinoma: raising awareness and optimizing treatment. *Dermatol Surg*. 2008;34:1642–1651.
35. Mendenhall WM, Ferlito A, Takes RP, et al. Cutaneous head and neck basal and squamous cell carcinomas with perineural invasion. *Oral Oncol*. 2012;48:918–922.
36. Tomaszewski JM, Gavriel H, Link E, et al. Aggressive behavior of cutaneous squamous cell carcinoma in patients with chronic lymphocytic leukemia. *Laryngoscope*. 2014;124:2043–2048.
37. Veness MJ, Harris D. Role of radiotherapy in the management of organ transplant recipients diagnosed with non-melanoma skin cancers. *Australas Radiol*. 2006;51:12–20.
38. Likhacheva A, Awan M, Barker CA, et al. Definitive and postoperative radiation therapy for basal and squamous cell cancers of the skin: an ASTRO clinical practice guideline. *Pract Radiat Oncol*. 2020;10:8–20.
39. Bui DT, Chunilal A, Mehrara BJ, et al. Outcome of split-thickness skin grafts after external beam radiotherapy. *Ann Plast Surg*. 2004;52:551–557.
40. Veness MJ, Palme CE, Morgan GJ. Merkel cell carcinoma: a review of management. *Curr Opin Otolaryngol Head Neck Surg*. 2008;16:170–174.
41. Howle J, Hughes M, Gebski V, Veness MJ. Merkel cell carcinoma: an Australian perspective and the importance of addressing the regional lymph nodes in clinically node-negative patients. *J Am Acad Dermatol*. 2012;67:33–40.
42. Hruby G, Scolyer RA, Thompson JF, et al. The important role of radiation treatment in the management of Merkel cell carcinoma. *Br J Dermatol*. 2013;169:975–982.
43. Veness M, Foote M, Gebski V, Poulsen M. The role of radiotherapy alone in patients with Merkel cell carcinoma: reporting the Australian experience of 43 patients. *Int J Radiat Oncol Biol Phys*. 2010;78:703–709.
44. Veness MJ, Perera L, McCourt J, et al. Merkel cell carcinoma: improved outcome with adjuvant radiotherapy. *ANZ J Surg*. 2005;75:275–281.
45. Clark JC, Veness MJ, Gilbert R, et al. Merkel cell carcinoma of the head and neck: is adjuvant radiotherapy necessary? *Head Neck*. 2007;29:249–257.
46. Foote M, Harvey J, Porceddu S, et al. Effect of radiotherapy dose and volume on relapse in Merkel cell cancer of the skin. *Int J Radiat Oncol Biol Phys*. 2010;77:677–684.
47. Veness M, Cooper S. Treatment of cutaneous angiosarcomas of the head and neck. *Australas Radiol*. 1995;39:277–281.
48. Spratt DE, Gordon-Spratt EA, Romanyshyn JC, et al. Radiation therapy in treatment of cutaneous angiosarcoma of the head and neck. *World J Surg Med Rad Oncol*. 2013;2:6–18.
49. Caccialanza M, Marca S, Piccinno R, Eulisse G. Radiotherapy of classic and human immunodeficiency virus-related Kaposi's sarcoma: results in 1482 lesions. *J Eur Acad Dermatol Venereol*. 2008;22:297–302.
50. Lukawska J, Cottrill C, Bower M. The changing role of radiotherapy in AIDS-related malignancies. *Clin Oncol*. 2003;15:2–6.
51. Smith BD, Glusac EJ, McNiff JM, et al. Primary cutaneous B-cell lymphoma treated with radiotherapy: a comparison of the European Organization for Research

and Treatment of Cancer and the WHO classification systems. *J Clin Oncol*. 2004;22:634–639.
52. Jones GW, Kacinski BM, Wilson LD, et al. Total skin electron radiation in the management of mycosis fungoides: consensus of the European Organization for Research and Treatment of Cancer (EORTC) Cutaneous Lymphoma Project Group. *J Am Acad Dermatol*. 2002;47:364–370.
53. Hoppe RT, Harrison C, Tavallaee M, et al. Low-dose total skin electron beam therapy as an effective modality to reduce disease burden in patients with mycosis fungoides: results of a pooled analysis from 3 Phase-II clinical trials. *J Am Acad Deramatol*. 2015;72:286–292.
54. Wilson LD. Delivery and sequelae of total skin electron beam therapy. *Arch Dermatol*. 2003;139:812–813.
55. Lloyd S, Chen Z, Foss FM, et al. Acute toxicity and risk of infection during total skin electron beam therapy for mycosis fungoides. *J Am Acad Dermatol*. 2013;69:537–543.
56. Dowd M, Kumar RJ, Sharma R, Mural R. Diagnosis and management of sebaceous carcinoma: an Australian experience. *ANZ J Surg*. 2008;78:158–163.
57. Wong RK, Bensadoun RJ, Boers-Doets CB, et al. Clinical practice guidelines for the prevention and treatment of acute and late radiation reactions from the MASCC Skin Toxicity Study Group. *Support Care Cancer*. 2013;21:2933–2948.
58. Chan RJ, Larsen E, Chan P. Re-examining the evidence in radiation dermatitis management literature: an overview and a critical appraisal of systematic reviews. *Int J Radiat Oncol Biol Phys*. 2012;84:e357–e362.
59. Pryor DI, Porceddu SV, Burmeister BH, et al. Enhanced toxicity with concurrent cetuximab and radiotherapy in head and neck cancer. *Radiother Oncol*. 2009;90:172–176.
60. Locke J, Karimpour S, Young G, et al. Radiotherapy for epithelial skin cancers. *Int J Radiat Oncol Biol Phys*. 2001;51:748–755.
61. Huynh NT, Veness MJ. Basal cell carcinoma of the lip treated with radiotherapy. *Australas J Dermatol*. 2002;43:15–19.
62. Veness MJ, Dwyer P. Erythema multiforme-like reaction associated with radiotherapy. *Australas Radiol*. 1996;40:334–337.
63. Kramkimel N, Dendale R, Bolle S, et al. Management of advanced non-melanoma skin cancers using helical tomotherapy. *J Eur Acad Dermatol Venereol*. 2014;28:641–650.



eFig. 139.1 Nodular basal cell carcinoma. A A 72-year-old woman with a 1 cm nodular basal cell carcinoma on the right ala nasi. **B** Four months after superficial radiotherapy (45 Gy in 15 daily fractions, 100 kVp, HVL 7 mm Al).



eFig. 139.2 Acute and chronic cutaneous side effects of radiation therapy. A Stevens–Johnson syndrome localized to multiple radiation ports in a patient receiving phenobarbital. **B** Dry desquamation and erythema of the neck 10 days following radiation therapy for a pharyngeal Hodgkin lymphoma. **C** In-field hypo- and hyperpigmentation 10 years after radiotherapy for a basal cell carcinoma. **D** In-field poikiloderma, fibrosis and ulceration; nowadays, this is seen much less often. **E** Spindle cell carcinoma within a radiation port. Note the background poikiloderma. *A, Reprinted with permission from Duncan KO, Tigelaar RE, Bolognia JL. J Am Acad Dermatol 1999;40:493–6; B, Courtesy Louis A. Fragola, Jr, MD; E, Courtesy Robert Hartman, MD.*

TREATMENT OF ACUTE RADIODERMATITIS	
Grade(s)	**Treatment**
1	• Continue RT • Mid-potency topical corticosteroid cream BID up to 2 weeks after treatment completed (often initiated on day 1 of RT as prophylaxis)
2/3	• Consider putting RT on hold/removal of bolus per physician discretion • Bacterial cultures of moist areas • Topical antibiotics (e.g. mupirocin, silver sulfadiazine) • Biologic dressings (e.g. hydrogel, hydrocolloid) • Continue topical corticosteroids to areas outside of moist desquamation and surrounding skin • Pain management
4	• Hold RT • Consult wound management specialist

eTable 139.1 Treatment of acute radiodermatitis. For clinical grading, see Table 139.4. BID, twice daily; RT, radiation therapy.

140 Electrosurgery

Sheldon V. Pollack

Chapter Contents

Indications/Contraindications 2444
Preoperative History and Considerations 2444
Description of Techniques 2445
Variations/Unusual Situations 2447
Postoperative Care 2448
Complications 2448
Electroepilation 2449
Iontophoresis 2449
Future Trends 2449

Synonym: ■ Radiosurgery (historical)

Key features

- Electrosurgery encompasses a group of procedures by which tissue is removed or destroyed through the application of electrical energy
- True ***electrocautery*** uses direct current to create a red-hot tip, which can be safer for patients with pacemakers and implantable cardioverter-defibrillators
- In modern electrosurgery, high-frequency alternating current is converted to heat within the treated tissues as a result of resistance to its passage
- ***Electrodesiccation*** is superficial ablation by touching the tissue with a monoterminal device
- ***Electrofulguration*** is superficial ablation via the use of a monoterminal device whose electrode is held at a slight distance from the tissue, allowing a spark to jump to the tissue
- ***Electrocoagulation*** uses a biterminal device for deeper coagulation
- ***Electrosection*** uses a biterminal device to cut while achieving hemostasis by mild lateral heat spread
- In order to minimize adverse sequelae, lateral heat spread should be kept to a minimum by using the appropriate waveform, power setting, and electrode size

INTRODUCTION AND BACKGROUND

Definition

Modern electrosurgery encompasses a group of techniques by which high-frequency alternating electrical current is applied to living tissues in order to achieve superficial coagulation, deep coagulation, or cutting of the skin. Since living tissue is a poor conductor of electricity, the flow of electrical current is hampered and builds up at the site of application. This resistance to the flow of electricity results in its conversion to heat. The use of different varieties of electrosurgical current, each characterized by a distinctive waveform, results in unique biologic outcomes, including desiccation, coagulation, or section of treated skin.

Electrocautery

The forerunner of modern electrosurgery was electrocautery (from Greek *kauterion*, branding iron)[1]. In electrocautery, invented in 1875, a metal wire is heated by resistance to the flow of direct current electricity, as in an electric toaster. Hemostasis (even in a wet field) can be obtained with electrocautery, but the resulting third-degree burn may result in prolonged healing times and may cause inferior cosmetic outcomes.

Of note, electrocautery, with its hot element (Fig. 140.1), is different from modern electrosurgery, in which high-frequency alternating current is applied via an unheated electrode. Electrocautery units are of value for providing hemostasis for surgical patients with implantable cardioverter-defibrillators (ICDs) because external electromagnetic fields may compromise the function of these devices; with modern-era permanent pacemakers the latter is primarily a concern when electrosurgery is performed within 5 cm of the device[2]. A number of electrocautery units are currently produced; among them is the Geiger TCU Thermal Cautery Unit. Disposable battery-powered electrocautery instruments are also available, but the desired temperature can diminish during contact with tissue.

Historical Aspects

Although used by most dermatologists on a daily basis, high-frequency electrosurgery could not have been developed if several major advances in the knowledge of electricity had not occurred. In order for alternating current electricity to be utilized for medical purposes, it was necessary for high-frequency currents to be produced. A generator that could provide such current was developed in 1889 by Thompson, who noted heat in his wrists when current was passed through his hands when immersed in saline solution[3]. Experiments conducted by Jacques Arsène d'Arsonval in 1891 established that the application, in human subjects, of electric currents with frequencies greater than 10 000 cycles per second (10 KHz) failed to cause neuromuscular stimulation and the associated tetanic response[4,5]. Also in the 1890s, Oudin, following some modifications to d'Arsonval's equipment, was able to generate a spray of sparks that caused superficial tissue destruction.

At the turn of the twentieth century, Rivière conceived the notion of using very small treatment electrodes in order to concentrate the current density. This would enable one to treat a skin lesion with an electric spark[6]. Walter de Keating-Hart and Pozzi[7] in 1907 introduced the term "fulguration" (from Latin *fulgur*, lightning), referring to the superficial carbonization that resulted when the spark from the Oudin coil was used to treat skin. They claimed that this modality was ideal for treating skin cancer and that the spark could selectively destroy tumor cells by interfering with their source of nutrition.

In 1909, Doyen[8] introduced the term "electrocoagulation" (from Latin *coagulare*, to curdle) to describe a different form of electrosurgery in which tissue was touched directly with the treatment electrode and an indifferent electrode was added to the circuit. The indifferent electrode allowed for direct removal of the electricity entering the patient and caused the latter to flow back into the electrosurgical device. By removing this static energy build-up, shocks were avoided in surgeons and other bystanders. The amperage was effectively increased while the "recycling" of electrical current allowed for lower voltages to be utilized. The current produced with this biterminal arrangement penetrated more deeply than fulguration and directly coagulated tissues rather than causing only surface carbonization. Doyen claimed that this more deeply penetrating current was more likely to be effective in the destruction of tumor cells.

William Clark, in 1911, reported on the use of an electrosurgical output that caused dehydration of tissue without carbonization at the surface[9]. He substituted a multiple spark gap for the usual single one

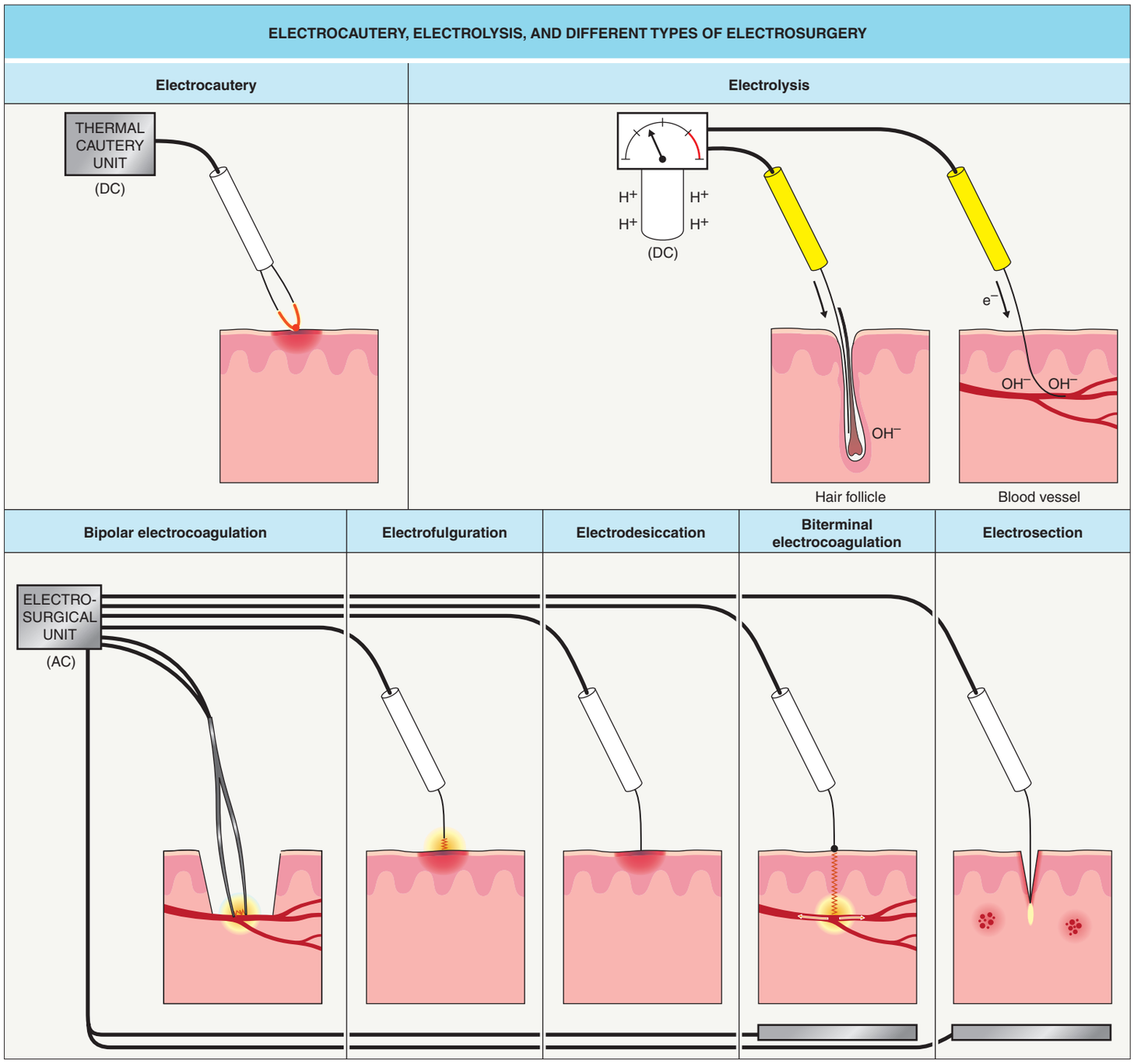


Fig. 140.1 Electrocautery, electrolysis, and different types of electrosurgery. AC, alternating current; DC, direct current; e^-, electron; H^+, proton; OH^-, hydroxide ion.

in a monoterminal Oudin current generator. This provided a smoother current that resulted in the production of fine sparks as opposed to the long, thick sparks seen with electrofulguration. Clark used the term "desiccation" (from Latin *desiccare*, to dry out) to describe this action.

The next major event in the development of electrosurgery came in 1923 when Dr George A. Wyeth, a noted tumor surgeon, used electrosurgery for cutting tissues[10]. His apparatus, which he termed an "endotherm knife" (Greek *endo*, within; *thérmē*, heat), used a thermionic vacuum tube instead of a spark gap[11]. Wyeth called the technique "electrothermic endothermy". He believed that the technique was particularly applicable to tumor surgery since it sealed off not only the smaller blood vessels but also the lymphatics that might otherwise provide for dissemination of metastatic disease.

A Harvard physicist, William Bovie, PhD, probably made the most important contribution to the development of electrosurgery. With financial assistance from the Liebel-Flarsheim Company of Cincinnati, he built an operating room electrosurgical device that offered both coagulating and cutting currents[12]. Dr Harvey Cushing, a distinguished neurosurgeon, became quite interested in these techniques and, with Bovie at the controls, began using electrosurgery for controlling bleeding and cutting through tissues during surgical procedures at Peter Bent Brigham Hospital in 1926. Dr Cushing's favorable impressions of electrosurgery assured acceptance of this technique by the surgical world. The subsequent impact of Bovie's machine upon medicine was so great that the word "bovie" is still often used generically as a noun to refer to an electrosurgical apparatus or even as a verb to describe the act of performing electrosurgery[13].

Electrosurgical Devices and Outputs

The circuitries of all electrosurgical instruments share certain design features necessary for production of suitable electrical outputs for electrosurgery. Standard household current first passes through a transformer which alters the voltage, providing the levels and characteristics

APPLICATIONS OF DIFFERENT WAVEFORMS IN ELECTROSURGERY

60 Hz Alternating current		Unaltered sine wave	
Spark gap circuit			
Modality	**Electrode configuration**		**Waveform**
Electrodesiccation	Monoterminal	Markedly damped	
Electrofulguration	Monoterminal	Markedly damped	
Electrocoagulation	Biterminal	Moderately damped	
Electronic circuit			
Modality	**Electrode configuration**		**Waveform**
Electrocoagulation	Biterminal	Partially rectified	
Electrosection, with coagulation	Biterminal	Fully rectified	
Electrosection, pure cutting	Biterminal	Fully rectified, filtered	

Fig. 140.2 Applications of different waveforms in electrosurgery.

required for the instrument's various circuit functions. The current next travels through an oscillating circuit that may employ a spark gap, a thermionic vacuum tube, or solid-state transistors to increase electrical frequency. Finally, this altered electrical energy is delivered to the treatment electrode.

Each electrosurgical current produces its own unique wavy pattern of current flow, or *waveform*. The latter may be either *damped* or *undamped*, depending on the type of oscillating circuit used. In general, damped waveforms provide electrodesiccation and electrofulguration, whereas the application of moderately damped and undamped currents results in electrocoagulation and cutting currents, respectively (Fig. 140.2). The spark gap generator produces a damped wave, consisting of bursts of energy in which successive wave amplitudes gradually return to zero. This occurs due to the resistance to energy flow presented by the gap.

Use of a thermionic tube results in a more uniform output. The valve tube circuit is able to neutralize the internal resistance responsible for the damping effect seen in the spark gap circuit, and the amplitude of output therefore remains unchanged. Depending on the circuitry used, the output can be moderately damped (partially rectified) or slightly damped (fully rectified). A filtered, fully rectified output is essentially continuous and uniform, similar to an undamped wave. The different types of waveforms each result in different biologic outcomes and are, therefore, used for different electrosurgical procedures[14,15].

Terminology: Monopolar, Bipolar, Monoterminal, and Biterminal

The terms *monopolar* and *bipolar* denote the number of tissue contacting tips at the end of the surgical electrode. When the surgical electrode has only one tip projecting from its end, it is a monopolar electrode. If it has two tips, it is a bipolar electrode. Therefore, an electrosurgical forceps (that plugs into two ports on the electrosurgical device) is considered to be bipolar, as opposed to a pointed electrode, which is monopolar (and plugs into one port on the device).

Monoterminal refers to the use of a treatment electrode without an indifferent or dispersive electrode ("ground plate"). *Biterminal* denotes that both treatment and indifferent electrodes are used (see Fig. 140.1). Such is the case with electrocoagulation and electrosection, in which use of the indifferent plate, although not *technically* necessary for the machine to work, will definitely enhance the efficiency of the electrosurgical apparatus. In biterminal electrosurgical applications, there is "recycling" of the energy that comes out of the treatment electrode, passes through the patient and is then removed from the patient via the indifferent electrode. Electrodesiccation and its variant, electrofulguration, are monoterminal procedures in which the indifferent electrode serves no purpose and, in most instances, is not even connected to the patient.

A simple way to visualize this is to think of the wires coming out of the machine as terminals. If only one wire (the handpiece for the electrode) is attached to the machine, then the application is monoterminal in nature. If, in addition, a "ground plate" is used, requiring a second wire to be attached to the machine, then the procedure is biterminal (see Fig. 140.6).

When a ball electrode is used to electrocoagulate a bleeding vessel, one is using biterminal, monopolar electrosurgery. In the case of bipolar forceps in which the electrode is connected to both the active and the dispersive electrode termini, we are using a bipolar modality.

INDICATIONS/CONTRAINDICATIONS

The simplest way to think of electrosurgical applications in the clinical setting is to consider the three major capabilities of electrosurgery units. These include superficial tissue destruction (electrodesiccation), deep tissue destruction (electrocoagulation), and cutting (electrosection)[16,17]. Destruction or excision of skin lesions by electrosurgery should be accomplished with the smallest possible amount of damage to normal tissues. Whether electrosurgery, cryosurgery or ablative laser surgery is used, the greater the penetration of the destructive modality into the skin, the greater the likelihood that unacceptable scarring will result. Because the destructive effects of electrocoagulation extend more deeply than those of electrodesiccation, the clinician must consider the histologic characteristics of the lesion to be treated when selecting the appropriate current. A partial list of dermatologic conditions that are commonly treated by each electrosurgical modality is found in Table 140.1.

There are no absolute contraindications to the use of electrosurgery, but precautions should be taken during the treatment of patients with cardiac implantable electronic devices (see Variations/Unusual Situations, below).

PREOPERATIVE HISTORY AND CONSIDERATIONS

The preoperative assessment of patients undergoing electrosurgery should concentrate on potential hazards to either the patient or the treatment team. A patient history of previous allergic reactions to skin cleansers, anesthetics, or postoperative topicals and dressings should be sought. Electrosurgery should be used with care in patients with cardiac implantable electronic devices.

Smoke evacuation equipment should always be available to safely remove the smoke plume when extensive electrosurgery, particularly electrosection, is performed. In such procedures, the operator and assistants should wear masks and use eye protection to prevent exposure to smoke-borne microbes and noxious particles. Gloves should always be worn when electrosurgical procedures are performed.

Preparatory to electrosurgery, the lesion and surrounding skin should be cleansed with a non-alcoholic skin cleanser such as chlorhexidine or povidone iodine. There is a potential for alcohol to ignite with electrosurgery, so it should be avoided or allowed to thoroughly dry prior to therapy.

Local anesthesia, usually via 1% lidocaine with epinephrine (adrenaline), is almost always used when performing electrosurgery. The usual exception is in the treatment of small facial telangiectasias, in which anesthesia is omitted. Local infiltration is most often used for anesthetizing localized superficial lesions, whereas field blocks and/or nerve blocks should be considered when performing larger electrosurgical procedures such as rhinophyma repair. When a local anesthetic is used prior to treatment of a dome-shaped lesion, such as a large angioma, it is helpful to massage the swollen anesthetized treatment site prior to electrosurgery, in order to flatten it. This prevents the development of a depressed scar subsequent to the procedure.

Prior to activating the electrosurgery unit, the operator should determine that the appropriate current and power settings for the

COMMON DERMATOLOGIC INDICATIONS FOR ELECTROSURGERY
Electrofulguration/electrodesiccation (superficial skin ablation)
Acrochordon
Actinic keratosis
Angioma (small)
Dermatosis papulosa nigra
Epidermal nevus
Hemostasis (capillary bleeding)
Lentigo
Seborrheic keratosis
Verruca plana
Electrocoagulation (deep skin ablation)
Angiofibroma
Angioma (large)
Basal cell carcinoma
Bowen disease (squamous cell carcinoma *in situ*)
Hemostasis (arterial bleeding)
Hirsutism (electroepilation)
Ingrown toenail matrixectomy
Banal melanocytic nevi
Sebaceous hyperplasia
Squamous cell carcinoma
Syringoma
Telangiectasia
Trichoepithelioma
Verruca vulgaris (all locations)*
Electrosection (skin incision/excision)
Acne keloidalis nuchae
Blepharoplasty incision
Debulking procedures
Rhinophyma repair
Rhytidectomy incisions and undermining
Scar revision
Shave removal of benign skin lesions (e.g. fibromas, melanocytic nevi)
Skin flap incisions and undermining
Skin resurfacing
Surgical excision of malignant or benign skin lesions
*Some clinicians use electrodesiccation and curettage.

Table 140.1 Common dermatologic indications for electrosurgery.

particular procedure have been selected, that the dispersive electrode has been properly placed, and that the correct treatment electrode has been chosen. Disposable sleeves that slip over the handle of the wand and disposable electrode tips are often utilized. It is unacceptable to use the same electrode tip on multiple patients without sterilization, erroneously assuming that heat will destroy pathogens.

DESCRIPTION OF TECHNIQUES

Electrodesiccation and Electrofulguration

For very superficial lesions, such as those involving only the epidermis, electrosurgical destruction by *electrodesiccation* can be achieved with little, if any, scarring. The markedly damped, high-voltage current generated by spark gap electrosurgical units causes superficial tissue damage by dehydration of the treatment site. It is delivered in a monoterminal (concentrative) fashion (see Fig. 140.1). If the electrode is held at a slight distance from the tissue, a spark is formed between the electrode and the tissue. This technique, termed *electrofulguration*, achieves very superficial destruction because the surface carbonization it produces insulates the underlying tissues from thermal heat spread.

Dermatologists who employ a Hyfrecator® or similar device often utilize this type of waveform. As the surface becomes charred by sparking at the surface, it is common for blood to appear in droplets that penetrate through the surface char. This is because the electrical current does not penetrate deeply enough to seal nearby blood vessels. Therefore, when surgical excision is undertaken, electrocoagulation is a better current to employ in order to provide hemostasis (see below). However, for treatment of small very superficial epidermal lesions, electrofulguration should be considered the waveform of choice. For example, it is very effective for the treatment of dermatosis papulosa nigra.

Electrodesiccation is the method of choice when superficial tissue destruction is desired. For example, it is ideal for treatment of epidermal lesions such as seborrheic or actinic keratoses (Fig. 140.3), acrochordons, verrucae planae, or small epidermal nevi. Hemostasis of mild capillary bleeding can also be achieved by use of electrodesiccation. A standard technique for treating keratoses by this method is to move the electrode slowly across the surface of the lesion (for small lesions) or to insert it directly into the lesion (for larger lesions), while applying current at a low power setting. After a few seconds, the lesion bubbles as the epidermis separates from the underlying dermis. It can then be easily removed with a curette or simply by rubbing a piece of gauze across the treatment site. The clinical endpoint in treating epidermal lesions is punctate bleeding, which is controlled with pressure, by spot electrocoagulation, or by topical hemostatic agents such as aluminum chloride. More profuse bleeding indicates probable damage to the dermis, with a greater likelihood of subsequent scarring. Extremely small superficial lesions can be treated by electrofulguration, which causes the least amount of damage to adjacent tissues.

Electrocoagulation

In electrocoagulation, a moderately damped current is applied in a *biterminal* manner (both concentrative and dispersive electrodes are used). This current is of higher amperage and lower voltage than that utilized for electrodesiccation. Because this type of current penetrates more deeply, it has the potential for greater tissue destruction.

Electrocoagulation is particularly useful for deep tissue destruction and surgical hemostasis. It is our preferred modality for treating small and uncomplicated primary basal cell and squamous cell carcinomas, as well as other lesions such as trichoepitheliomas, which extend into the dermis. Much of the literature refers to "curettage and electrodesiccation (C&E)" or "electrodesiccation and curettage (ED&C)", but, in fact, electrocoagulation may be the preferred electrosurgical waveform for all but the most superficial tissue destruction.

When performed properly, electrosurgery plus curettage yields cure rates of 90%–95% for uncomplicated basal cell carcinomas and superficial squamous cell carcinomas, making it an efficient, cost-effective treatment. Thorough curettage is likely the key element affecting success. Initially, a large curette (4–6 mm) is used to debulk the tumor, followed by a smaller curette (2 mm). The curette should be scraped across the surface of the treatment site in every direction, from superior to inferior, inferior to superior, left to right and right to left, using fairly firm downward pressure. In this way, all tumor extensions are eradicated.

After thorough curettage, the electrode is brought into direct contact with the tissue to be treated and is moved slowly around the periphery and across the curetted portion of the lesion, which eventually becomes charred. A curette may then be used to gently remove the charred tissue. For treatment of skin cancers, this procedure is repeated two or more times in an attempt to remove any small tumor extensions (Fig. 140.4). During the last curettage, a very small curette (1 mm) may be used to remove the final tiny "roots" of the tumor. Scarring must be expected with this procedure, and wounds following curettage and electrosurgery are allowed to heal by second intention.

Electrocoagulation is also effective for treatment of superficial telangiectasias (Fig. 140.5), unwanted hair (electroepilation), and ingrown toenails (electrosurgical matrixectomy). Hemostasis using electrocoagulation can be achieved by either monopolar or bipolar means. Because the electrosurgical energy may be transmitted for several millimeters along the vessel wall, it is important to use the minimum effective exposure time and power setting in order to prevent delayed bleeding from damaged vessels. We often use monopolar electrocoagulation, in which the electrode is touched directly to the bleeding vessel. Coagulation can also be achieved by touching the electrode to a hemostat that has been clamped on the severed vessel. In bipolar electrocoagulation (Fig. 140.6), a bipolar forceps is used to provide more directed pinpoint hemostasis. Electrocoagulation current delivered in this manner causes less adjacent tissue damage but requires a dry operative field to be effective.

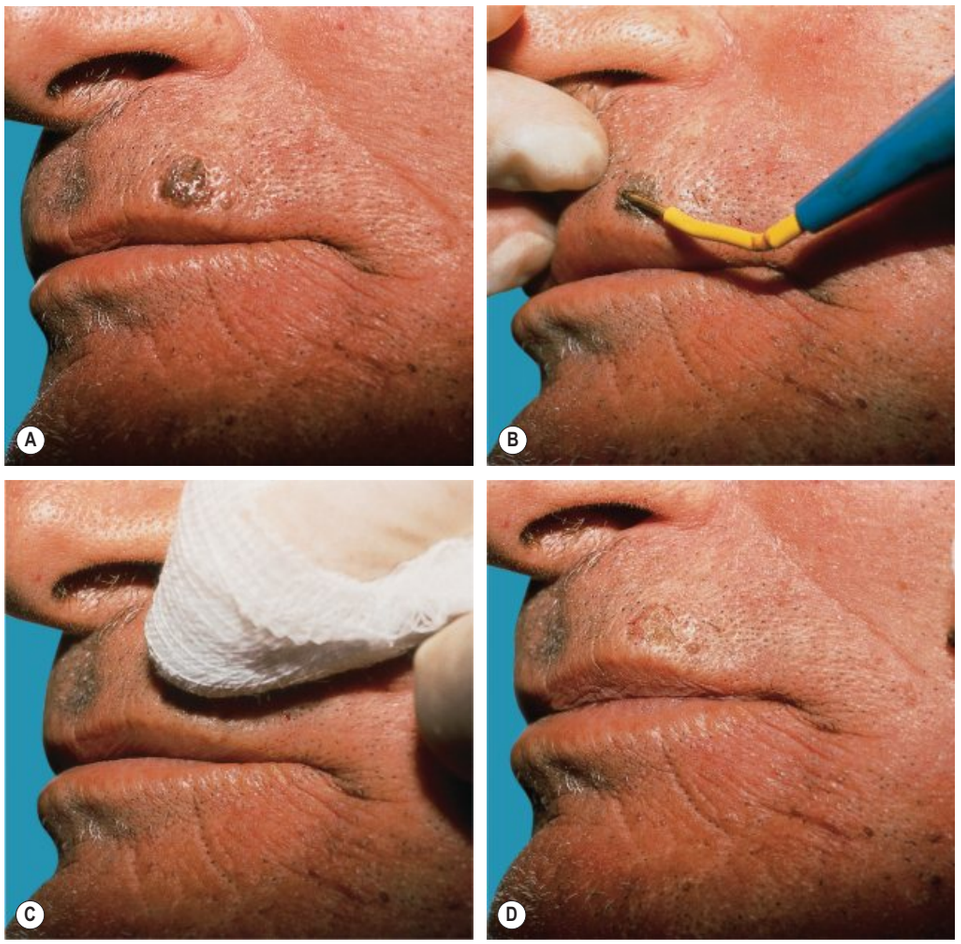


Fig. 140.3 Seborrheic keratosis on the upper lip. A Given its epidermal location, electrosurgical destruction should employ a current that provides the most superficial type of tissue damage. **B** Under local anesthesia, the lesion is treated by electrodesiccation. Delivery of current is stopped when the lesion begins to "bubble". **C** In lieu of a curette, a gauze pad is useful for removing charred tissue after desiccation of superficial lesions. **D** There is minimal bleeding, indicating that damage did not penetrate deeply into the dermis.



Fig. 140.4 Basal cell carcinoma on the right deltoid area, treated by curettage and electrosurgery. A Nodular basal cell carcinoma preoperatively after injection of local anesthesia. **B** The tumor is curetted to debulk all friable tissue. **C** Further curettage, often with a smaller-diameter curette, should proceed in all directions to remove small extensions of tumor. **D** Following thorough curettage, the surface and periphery of the wound are treated by electrocoagulation current to stop bleeding and potentially remove further tumor. **E** Final wound – curettage and electrosurgery have been repeated twice more, until all friable tissue has been removed. Healing occurs over 4–6 weeks, depending upon the site.

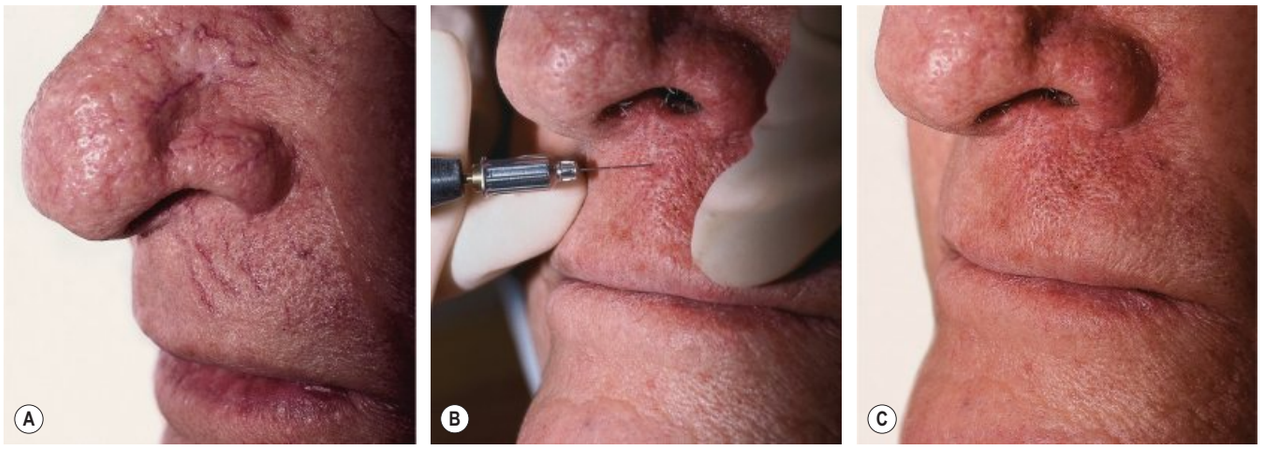


Fig. 140.5 Telangiectasias on nose and upper lip being treated by fine-needle electrocoagulation. A Preoperative photograph shows linear telangiectasias on the nose and upper lip. **B** The electrode consists of a hub adapter with a 30-gauge metal-hubbed needle attached. The machine is energized at a low power setting and the electrode momentarily touches the skin surface, along the length of the vessel being treated, at 3 to 4 mm intervals. The patient experiences some discomfort during the procedure, but this is usually tolerable. **C** The same patient immediately after treatment. This technique is usually performed quickly without anesthesia.

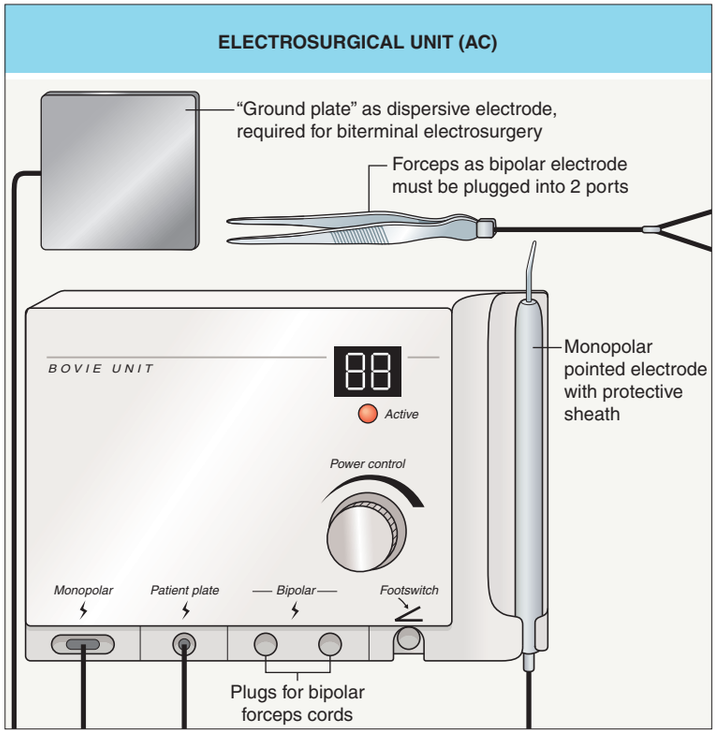


Fig. 140.6 Electrosurgical unit (AC) with attached electrosurgery pencil. The monopolar pencil is used for electrodesiccation and electrofulguration. When used with the grounding plate, it is utilized in a biterminal mode for electrocoagulation. Alternatively, the unit can be used with the bipolar forceps to provide pinpoint electrocoagulation for hemostasis. Bipolar electrocoagulation is also recommended for use in patients with cardiac implantable electronic devices. AC, alternating current.

Electrosection (Cutting)

Electrosection involves the biterminal application of a slightly damped current. The current, of low voltage and high amperage, causes minimal lateral heat spread and tissue damage, and it has the additional advantage of simultaneously achieving hemostasis and cutting. "Pure" cutting can be obtained using a true undamped tube current, which provides the least amount of lateral heat spread and causes vaporization of tissue without hemostasis. Such current has been suggested by Chiarello[18] to be useful in debulking large skin cancers, contouring surrounding skin following shave excisions, scar revision following skin flaps and grafts, and rhinophyma repair. When electrosection is performed using a filtered, fully rectified current, subsequent spot electrocoagulation can be achieved by changing to the electrocoagulation current.

Electrosection can be used to perform rapid and effortless excisions or incisions. Virtually no manual pressure by the operator is required. Electrodes configured as loops, triangles, or diamonds can be used for quick removal of skin tags, papillomas, intradermal nevi, and other exophytic skin lesions. A straight, narrow electrode is most often used to incise the skin and is applied to the tissue in brisk, continuous paintbrush-like strokes. The difference between electrosection and scalpel excision is immediately apparent to the first-time user of electrosection. At the appropriate power setting, the electrode passes smoothly through the tissue like a "hot knife through butter". If perceptible sparking occurs during incision, the power setting is too high; if the electrode "drags", the power setting is too low.

Slightly damped currents cause some charring at the margins of the excised tissue. Therefore, when a specimen suitable for histopathologic analysis is required, the filtered current (see Fig. 140.2) should be used because it does not create significant electrosurgical artifact. It is recommended that the new initiate to electrosection develops technical skills and concepts by practicing on beefsteak before utilizing this technique in the clinical arena.

The major advantage of electrosection over scalpel surgery is that when a blended cutting and coagulating current is utilized, hemostasis is achieved immediately as the incision is made. However, larger blood vessels (>2 mm) require additional spot electrocoagulation at the completion of the excision. Another drawback is that vaporization of the tissue generates a smoke plume, which can be unpleasant for both the patient and the operator and may contain potentially infectious viral particles (see below). Consequently, effective smoke evacuation equipment should be available during such procedures.

Electrosection is extremely useful for achieving relatively bloodless excision of large, bulky lesions, such as acne keloidalis nuchae and rhinophyma (Fig. 140.7), in which the surgical defect is allowed to heal by second intention. Electrosurgical excision followed by primary closure can also be undertaken with no impairment of wound healing, as compared with conventional scalpel surgery. This modality has been used, without complication, to create skin flaps and perform cosmetic facial surgery, including blepharoplasty and rhytidectomy, with excellent outcomes.

VARIATIONS/UNUSUAL SITUATIONS

Cardiac Implantable Electronic Devices

The use of electrosurgery in patients with cardiac implantable electronic devices raises the question of whether the flow of electrical energy during electrosurgery might interfere with the function of these devices[19]. Although modern permanent pacemakers and ICDs have improved shielding technology to guard them from the influence of

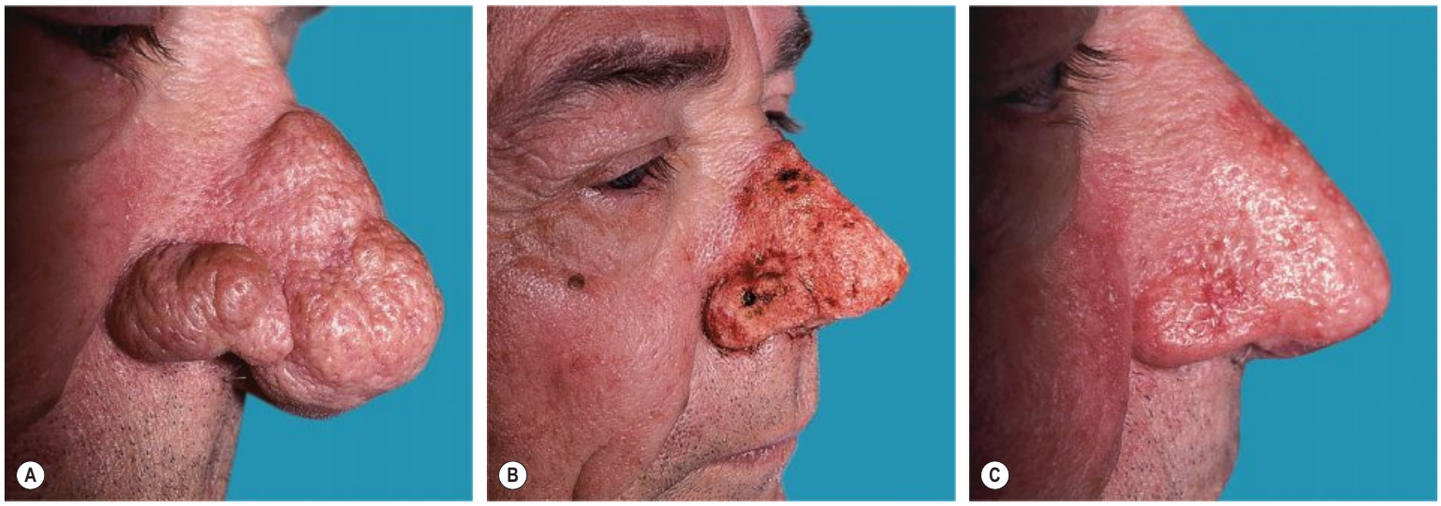


Fig. 140.7 Rhinophyma. A Moderately severe rhinophyma in a middle-aged man. **B** Immediately after electrosurgical planing of excess sebaceous glands. Care is taken to perform subtotal removal as very aggressive therapy can result in significant scarring and possible deformity caused by scar contracture. **C** Four weeks later, healing with good cosmetic outcome is noted. During healing, the wound is kept moist with an ointment (e.g. petrolatum) and semi-occlusive dressings.

external electromagnetic currents, prudence requires that a modicum of precaution be taken. If used indiscriminately in these patients, electrosurgery can occasionally trigger skipped beats, reprogramming of a pacemaker, firing of an ICD, asystole, or bradycardia.

Routine precautions recommended when using electrosurgery in patients with cardiac implantable electronic devices include: (1) utilize short bursts of energy that are less than 5 seconds in duration; (2) keep power settings as low as possible; (3) avoid the use of cutting current; and (4) avoid use on the skin around the device. Although recommended in the literature, most dermatologists do not follow specific precautions such as intraoperative monitoring, preoperative cardiology consultation, or postoperative evaluation of the cardiac device by a cardiologist. This may be due to the fact that to date there have been no reported cases of interference with a pacemaker or ICD in a dermatologic setting. Also, at least one article suggests that practical experience of complications due to electrosurgical interference is rare among dermatologic surgeons[20].

There is less risk of potential side effects when the electrosurgical current is confined to a very small area, as is the case when bipolar forceps are used as electrodes. A way to virtually eliminate such risk in very unstable cardiac patients or those with ICDs is to use true electrocautery, rather than other forms of electrosurgery[21]. Although use of this modality may cause more of a burn injury than is seen with true electrosurgery, there is no flow of current to cause electrical interference. In a survey of Mohs surgeons, 34% used electrocautery and 19% used bipolar forceps in patients with pacemakers or ICDs. Among this group, there was only one reported case of interference in one of the electrocautery patients. However, since there is no current flow in true electrocautery, this was likely an error in reporting.

It is the author's belief that the use of either electrocautery or bipolar forceps as electrodes in patients with cardiac implantable electronic devices will eliminate the need for intraoperative monitoring, preoperative cardiology consultation, or postoperative evaluation by a cardiologist in the majority of patients.

POSTOPERATIVE CARE

Standard postoperative wound management, incorporating an ointment (e.g. petrolatum) and/or semi-occlusive dressings, is followed. For superficial skin ablations, such as those following electrodesiccation or electrofulguration, twice-daily application of an ointment such as petrolatum is generally all that is required. An adhesive plaster may be used if the area is prone to rubbing. An eschar forms within a few days and separates in about 10 days. For deeper wounds, in which healing can take 2–4 weeks (or longer on the lower extremities), once- or twice-daily application of an ointment (e.g. petrolatum) followed by an adhesive plaster is recommended. For larger wounds, such as those following rhinophyma repair, Telfa™ sheets are cut to size to cover the defect and kept in place with semi-occlusive paper tape (e.g. Micropore™, 3M Corporation).

COMPLICATIONS

Patients should be warned of the possibility of delayed bleeding and should be reassured that it can, in the vast majority of cases, be controlled by 20–30 minutes of *constant* direct pressure over the wound. Trips to the local emergency room to stop postoperative bleeding are unusual but can occur. Patients should also be advised that for ablative procedures including electrocoagulation, scarring, in the form of a hypopigmented area, may occur.

Other potential hazards of electrosurgery are briefly discussed below.

Fire

There is a risk of fire or explosion if electrosurgical procedures are conducted in the presence of alcohol, oxygen, or bowel gases (methane). Care should be taken to be certain that the operative site is free of alcohol residue, i.e. confirm any alcohol-containing skin preparation has completely dried before proceeding with electrosurgery. Of note, aluminum chloride solutions used for hemostasis can contain over 90% alcohol (v/v). Oxygen is usually not a problem except in the operating room setting. Bowel gases are highly flammable! Use care in the perianal region.

Thermoelectric Burns

Although modern generators are isolated from earth, and are often equipped with sophisticated monitoring systems, current can still be diverted away from the return electrode and cause an accidental burn at the point at which it leaves the patient's body. Alternative pathways occur when the current is diverted from the return electrode and finds an alternative path to return to the generator. When the point of contact between the patient and the grounded object is small, even a relatively low-power current can generate sufficient current density to cause a burn. Grounded objects may include metal parts of the operating table, table accessories, or ECG electrodes. This problem is reduced, but not eliminated, by the use of isolated electrosurgical units, which have little or no connection to the ground.

Microorganism Transmission

The potential exists for transmission of microorganisms either via the electrode[22,23] or via smoke plume inhalation. Neither possibility has been investigated in sufficient depth to yield conclusive results. Practitioners should minimize the risk of possible electrode transmission by using

disposable or sterilized electrodes. Adapters are available that allow disposable metal hypodermic needles to be used as electrodes.

Surgical Smoke

During surgical procedures using a laser or electrosurgical unit, the thermal destruction of tissue creates a smoke by-product. Research studies have confirmed that this smoke plume can contain toxic gases and vapors such as benzene, hydrogen cyanide and formaldehyde, bioaerosols, dead and live cellular material (including blood fragments)[24], and viruses[25]. At high concentrations, the smoke causes ocular and upper respiratory tract irritation in healthcare personnel and creates visual problems for the surgeon. The smoke has unpleasant odors and has been shown to have mutagenic potential[26].

Research by the National Institute for Occupational Safety and Health (NIOSH) has shown that airborne contaminants generated by these surgical devices can be effectively controlled by appropriate ventilation using a portable smoke evacuation system. Smoke evacuators contain a suction unit (vacuum pump), filter, hose, and an inlet nozzle. The smoke evacuator should have high efficiency in airborne particle reduction and should be used in accordance with the manufacturer's recommendations to achieve maximum efficiency. A capture velocity of approximately 100–150 feet per minute at the inlet nozzle is generally recommended. It is also important to choose a filter that is effective in collecting the contaminants. A high-efficiency particulate air (HEPA) filter or equivalent is recommended for trapping particulates. Various filtering and cleaning processes also exist which remove or inactivate airborne gases and vapors. The different filters and absorbers used in smoke evacuators require monitoring and replacement on a regular basis and are considered a possible biohazard requiring proper disposal.

The smoke evacuator hose inlet nozzle must be kept within 2 inches of the surgical site to effectively capture airborne contaminants generated by these surgical devices. The smoke evacuator should be activated at all times when airborne particles are produced during an electrosurgical procedure that generates a significant smoke plume. After each procedure, all tubing distal to the filter must be considered infectious waste and be disposed of appropriately. The filters themselves may be used for the cumulative time specified by the manufacturer before replacement.

ELECTROEPILATION

Electroepilation is the use of electricity for the permanent removal of hair[27]. It predated the development of laser hair removal and is still used, in a variety of forms, by aestheticians and electrologists. The word *electrolysis*, which is used by most people as a generic term to mean the electrical destruction of hair, is technically the use of direct (galvanic) current for hair removal. Hair destruction with an alternating current occurs as a result of the accumulation of heat in the vicinity of the hair bulb and is designated *thermolysis*.

Electrolysis vs Thermolysis

Electrolysis uses direct current to create a destructive chemical reaction at the hair root. The negative electrode (anode) is inserted into the hair follicle (see Fig. 140.1). The positive electrode (cathode) is a moistened pad held in the patient's hand. When direct current is applied, a chemical reaction at the tip of the anode causes the production of sodium hydroxide. The latter acts as a caustic and destroys the hair root. This process may take from 30 to 60 seconds to occur, so pure "galvanic electrolysis" is a tedious procedure to perform. Of note, electrolysis can also be used to treat small telangiectasias (see Fig. 140.1).

Thermolysis relies on heat to cause hair destruction. A high-frequency (13.56 MHz) alternating current is used. As the current passes through tissue, it encounters resistance, causing the current to stall and convert to heat. Current can be applied by the "slow" (manual) technique or the "flash" technique. Lower heat is used over 3–10 seconds in the slow technique. Gentle traction of the hair allows the operator to determine when destruction is complete. The flash technique uses higher heat, delivered by a preset mechanical timer (<1 second). Several such pulses may be required to cause hair root destruction. Theoretically, the flash technique is less painful.

The technique for needle insertion is the same as for electrolysis. A patient hand-held electrode is not required since the patient is not included in the electrical circuit. The speed of thermolysis allows for treatment of much larger areas over a shorter time period. For this reason, it has replaced galvanic electrolysis as the preferred manner of electroepilation. The *blend* is a form of electroepilation that takes advantage of attributes of both electrolysis and thermolysis, by blending the two types of current in one machine. The blend is slower than thermolysis, but may offer some advantages in rate of hair root destruction, particularly for coarser hairs.

Side Effects

Thermolysis and the blend are more painful than classic galvanic electrolysis and the risk of scarring and hair regrowth may be higher. However, highly motivated patients generally tolerate the pain and are treated with 30- to 60-minute sessions once or twice weekly. The use of topical anesthetics under occlusion for 1–2 hours pretreatment decreases the pain in some patients. Scarring is a real risk and is operator-dependent. Generally, when this occurs, it presents as punctate or ice pick-like depressed scars. In some patients, small hypertrophic papules may appear.

Hair regrowth has been reported in the range of 15% to 50%, and this is also technique-dependent. Regrowth may be related, in part, to the hair cycle. Hairs treated while in telogen phase may not experience root destruction. Some electrologists recommend shaving 2 days prior to treatment so that only actively growing hairs will be apparent.

Varying degrees of erythema and edema may be present shortly after the procedure. Postinflammatory hypo- and hyperpigmentation have been reported. The theoretical risk of infections, both local and systemic, exists, but proper skin cleansing helps prevent this problem. Some patients have a higher propensity for developing post-treatment folliculitis and it is recommended that they cleanse with an antibacterial cleanser (e.g. chlorhexidine), before and after treatment. Disposable needles are the norm in the practice of permanent hair removal.

IONTOPHORESIS

In some patients, tap or deionized water iontophoresis can be used successfully to treat localized hyperhidrosis of the palms, soles, or axillae. In this technique, direct electrical current is passed through the treatment site while the patient is in contact with an aqueous ionic solution. The electric current introduces ions from the solution into the patient's skin and appears to inhibit sweating by occluding the eccrine ducts at the level of the stratum corneum[28].

A battery-powered unit for home use (Drionic®) is available. It is more effective for treatment of palmoplantar hyperhidrosis than for axillary hyperhidrosis. Cessation of sweating usually requires treatment of each palm or sole with 20 mA of current for 30 minutes daily. The recent use of botulinum toxin type A injections for hyperhidrosis has provided many hyperhidrosis sufferers with a more efficient and longer-lasting treatment modality, albeit at greater expense.

FUTURE TRENDS

Interest and innovation in electrosurgery have actually increased over the past three decades, since continuous wave CO_2 laser systems were introduced. Practitioners came to realize that superficial ablation, deep ablation, and tissue incision with immediate hemostasis were available through electrosurgery without the need for expensive laser systems. As examples, specially adapted electrosurgery equipment that utilizes electricity to remove the epidermis and upper dermis for facial skin resurfacing has been introduced[29] as has the use of electrosurgical cutting current (Ellman® Surgitron®) to resurface surgical scars. The latest electrosurgical development is use of a standard radiosurgery device (Surgitron® Dual RF™) for non-ablative tightening of skin laxity[30]. Radiofrequency current produces heat because of resistance in the dermis and subcutaneous tissue. When heated, collagen fibrils will denature and contract, presumably leading to the observed tissue tightening.

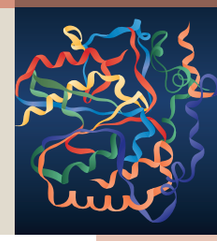
REFERENCES

1. Blankenship ML. Physical modalities. Electrosurgery, electrocautery and electrolysis. *Int J Dermatol*. 1979;18:443–452.
2. Weyer C, Siegle RJ, Girard G, Eng P. Investigation of hyfrecators and their *in vitro* interference with implantable cardiac devices. *Dermatol Surg*. 2012;38:1843–1848.
3. Mitchell JP, Lumb GN. Principles of surgical diathermy and its limitations. *Br J Surg*. 1962;50:314–320.
4. d'Arsonval A. Action physiologique des courants alternatifs. *Soc Biol*. 1891;43:283–286.
5. d'Arsonval A. Action physiologique des courants alternatifs à grande fréquence. *Arch Physiol Norm Path*. 1893;5:401–408.
6. Rivière AJ. Action des courants de haute fréquence et des effleuves du résonateur Oudin sur certaines tumeurs malignes. *J Med Intern*. 1900;4:776–777.
7. Pozzi M. Remarques sur la fulguration. *Bull Assoc Franc Cancer*. 1909;2:64–69.
8. Doyen D. Sur la destruction des tumeurs cancéreuses accessibles par la méthode de la voltaisation bipolaire et de l'électro-coagulation thermique. *Arch Elec Med Exp Clin*. 1909;17:791–795.
9. Clark WL. Oscillatory desiccation in the treatment of accessible malignant growths and minor surgical conditions: a new electrical effect. *J Adv Therap*. 1911;29:169–183.
10. Wyeth GA. Endothermy, surgical adjunct in accessible malignancy and precancerous conditions. *Surg Gynec Obstet*. 1923;36:711–714.
11. Wyeth GA. The endotherm. *Am J Electrotherapeut Radiol*. 1924;42:186–187.
12. Cushing H. Electro-surgery as an aid to the removal of intracranial tumors, with a preliminary note on a new surgical-current generator by WT Bovie, PhD. *Surg Gynec Obstet*. 1928;47:751–752.
13. Goldwyn RM. Bovie: the man and the machine. *Ann Plast Surg*. 1979;2:135–153.
14. Taheri A, Mansoori P, Sandoval LF, et al. Electrosurgery: part I. Basics and principles. *J Am Acad Dermatol*. 2014;70:591.e1–14.
15. Taheri A, Mansoori P, Sandoval LF, et al. Electrosurgery: part II. Technology, applications, and safety of electrosurgical devices. *J Am Acad Dermatol*. 2014;70:607.e1–12.
16. Pollack SV. *Electrosurgery of the Skin*. New York: Churchill Livingstone; 1991.
17. Sebben JE. *Cutaneous Electrosurgery*. Chicago: Year Book Medical Publishers; 1989.
18. Chiarello S. Controlled vaporization of tumor tissue utilizing radio frequency cutting current through a blunt hockey stick scalpel or radio frequency knife. *Dermatol Surg*. 1998;24:158–160.
19. Riordan AT, Gamache C, Fosko SW. Electrosurgery and cardiac devices. *J Am Acad Dermatol*. 1997;37:250–255.
20. El-Gamal HM, Dufresne Jr RG, Saddler K. Electrosurgery, pacemakers and ICDs: a survey of precautions and complications experienced by cutaneous surgeons. *Dermatol Surg*. 2001;27:385–390.
21. Wilson JH, Lattner S, Jacob R, Stewart R. Electrocautery does not interfere with the function of the automatic implantable cardioverter defibrillator. *Ann Thorac Surg*. 1991;51:225–226.
22. Sherertz EF, Davis GL, Rice RW, et al. Transfer of hepatitis B virus by contaminated reusable needle electrodes after electrodesiccation in simulated use. *J Am Acad Dermatol*. 1986;15:1242–1246.
23. Bennett RG, Kraffert CA. Bacterial transference during electrodesiccation and electrocoagulation. *Arch Dermatol*. 1990;126:751–755.
24. Berberian BJ, Burnett JW. The potential role of common dermatologic practice techniques in transmitting disease. *J Am Acad Dermatol*. 1986;15:1057–1058.
25. Sawchuck WS, Weber PJ, Lowy DR, et al. Infectious papillomavirus in the vapor of warts treated with carbon dioxide laser or electrocoagulation: detection and protection. *J Am Acad Dermatol*. 1989;21:41–49.
26. Tomita Y, Mihashi S, Nagata K, et al. Mutagenicity of smoke condensates induced by CO_2-laser irradiation and electrocauterization. *Mutat Res*. 1981;89:145–149.
27. Pollack SV, Grekin RC. Electrosurgery and electroepilation. In: Roenigk RK, Roenigk HH, eds. *Dermatologic Surgery: Principles and Practice*. 2nd ed. New York: Marcel Dekker; 1996:219–231.
28. Sato K, Timm DE, Sato F, et al. Generation and transit pathway of H^+ is critical for inhibition of palmar sweating by iontophoresis in water. *J Appl Physiol*. 1993;75:2258–2264.
29. Grekin RC, Tope WD, Yarborough Jr JM, et al. Electrosurgical facial resurfacing: a prospective multicenter study of efficacy and safety. *Arch Dermatol*. 2000;136:1309–1316.
30. Rusciani A, Curinga G, Menichini G, et al. Nonsurgical tightening of skin laxity: a new radiofrequency approach. *J Drugs Dermatol*. 2007;6:381–386.

Biology of Wound Healing

141

Sabine A. Eming



Chapter Contents

Mechanisms of Tissue Repair and Regeneration are Evolutionarily Conserved *2451*
Impact of Wound Depth on Wound Healing *2452*
Skin Repair – Cellular and Molecular Aspects *2453*
Impaired Wound Healing – Risk Factors *2460*
Therapeutic Options for Chronic Wounds *2460*
Future Directions. *2461*

Key features

- Wound healing is a complex and dynamic biologic process, with consecutive cascades consisting of early-stage coagulation and inflammation, intermediate tissue formation and proliferation, and late-stage resolution and tissue remodeling
- Effective wound healing requires spatial and temporal synchronization of cell–cell and cell–matrix interactions as well as an interplay of nutrients, metabolites, and cytokines
- Extracellular matrix proteins are multifunctional molecules that bind directly to cell surface receptors (e.g. integrins); in addition to tissue stability and dynamics, matrix proteins influence cellular growth factor signaling (e.g. VEGF, TGF-β)
- In children and adults, cutaneous wound healing represents a *reparative* process that can lead to fibrosis (scar), whereas injured fetal tissue can heal without fibrosis, in a process resembling *regeneration*
- Several medical disorders (e.g. venous hypertension, atherosclerosis, diabetes mellitus, autoimmune inflammatory diseases) as well as local (e.g. pressure, infection) and systemic (e.g. aging) factors are associated with chronic non-healing wounds

INTRODUCTION

Restoration of skin integrity and homeostasis following injury is a fundamental process that ensures survival. The primary goal of the wound healing response is to promptly re-establish a functional skin barrier. Ideally, the wound healing response would lead to complete regeneration of skin tissue and its adnexal structures, with complete restoration of original skin function and morphology. Unfortunately, precise replication of the latter is often not the final result of wound repair and the quality of newly formed skin tissue varies considerably. Beyond age, a multitude of local and systemic factors impact the outcome of the wound healing response (Table 141.1).

Regeneration Versus Repair

In children and adults, the cutaneous wound healing response characteristically replaces damaged tissue with fibrosis, leading to scar formation. In addition, adnexal structures (e.g. hair follicles, sweat and sebaceous glands), as well as the components and architecture of the dermal extracellular matrix, may fail to regenerate. This can result in a loss of normal skin function and impaired morphology. Because this type of wound healing is not ideal, it is referred to as a *reparative process*. In contrast, during embryogenesis injured fetal skin can heal completely without fibrosis, a process that resembles *regeneration*[1].

The underlying mechanisms that determine whether tissue regeneration versus tissue repair will occur remain a mystery. It is not clear whether the loss of regenerative capacity after birth is due to systemic factors or an intrinsic incapability of cells to form competent stem cells. New insights will hopefully come from experimental studies in model organisms (e.g. amphibians, fish) that retain throughout their adult life the capability to regenerate tissues after injury as well as from studies of wound repair in fetal skin[2]. In the future, these insights may lead to methods for transforming repair into regeneration and may provide novel therapies that allow wound healing with minimal scarring.

Effect of Immune Response on Wound Healing

The immune system, including both innate and adaptive immune responses, plays a critical role in wound healing. By influencing multiple repair mechanisms (e.g. angiogenesis, fibroplasia, connective tissue deposition, epithelialization), inflammation has an impact on all stages of the repair response and ultimately on the extent of scarring (Fig. 141.1). In several models, there appears to be an inverse correlation between the appropriateness of the inflammatory immune response and the ability to undergo regeneration, with inappropriate immune reactions leading to tissue damage and impairment of tissue repair. However, this paradigm has recently been challenged by studies in which inflammatory signals were found to be crucial for promoting timely repair and inducing fundamental processes involved in regeneration[3]. Interestingly, these findings emerged from well-established models within the field of tissue regeneration (e.g. heart regeneration in mice) and not immunology[4,5].

MECHANISMS OF TISSUE REPAIR AND REGENERATION ARE EVOLUTIONARILY CONSERVED

Amphibians

Among vertebrates, amphibians and fish are exceptional in their capacity to regenerate anatomically complete and fully functional tissues and organs during adulthood. In particular, urodele amphibians (newts and salamanders) can regenerate a range of organs and tissues[2,6]. Cellular and molecular studies have focused primarily on limb regeneration after amputation and in adult salamanders, the immediate influx of macrophages after tissue damage (preceding blastema formation) was found to be an essential component of regeneration[7]. In axolotl, dedifferentiation of connective tissue cells (e.g. fibroblasts) enables successful regeneration, while in frogs intrinsic restrictions that impede dedifferentiation of connective tissue cells prevent regeneration[8].

Zebrafish

Zebrafish also represent a valuable model for the study of regeneration. Adult zebrafish maintain regenerative capacity, not only after caudal fin amputation but also following skin injury[9]. Interestingly, infiltration of myeloid inflammatory cells occurs during both fin and skin regeneration, suggesting that in principle regeneration can occur in the presence of inflammatory signals. Thus, by examining skin wound healing in zebrafish it may be possible to distinguish between beneficial and harmful inflammatory mediators and how they influence scar formation.

Mammals

The effects of inflammation on regeneration and repair have also been studied in mammals, primarily in mice, but also in humans. In addition

LOCAL AND SYSTEMIC FACTORS THAT CONTRIBUTE TO THE QUALITY OF THE WOUND HEALING RESPONSE
Characteristics of the damaged tissue/organ
• Tissue architecture • Resident and recruited cell types • Transcriptional networks • Regenerative capacity
Characteristics of the type of tissue damage
• Mechanical, ultraviolet, chemical, microbial • Extent and severity of the injury
Wound microenvironment
• Perturbed tissue architecture • Altered cell–cell and cell–matrix interactions • Tissue oxygenation • Microbial contamination
Systemic factors
• Genetic background • Age • Obesity, diabetes mellitus, peripheral arterial disease • Autoimmune connective tissue diseases (e.g. systemic sclerosis, rheumatoid arthritis) • Medications (e.g. corticosteroids, angiogenesis inhibitors such as bevacizumab) • Diet, nutritional status • Smoking

Table 141.1 Local and systemic factors that contribute to the quality of the wound healing response.

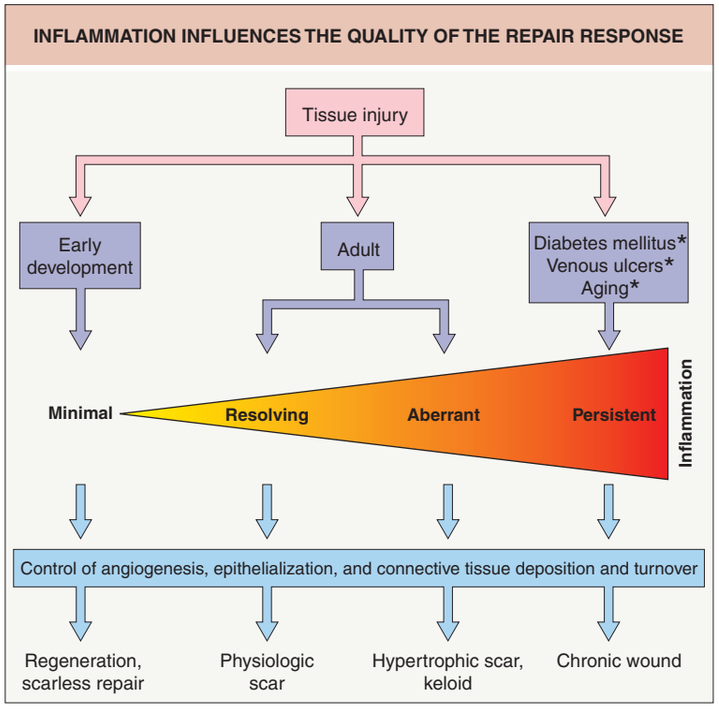


Fig. 141.1 Inflammation influences the quality of the repair response. Modulation of the local immune response at the site of injury can influence repair mechanisms and the quality of tissue restoration. *The underlying etiology of chronic, non-healing ulcers is multifactorial and it includes hypoxia due to vascular disease or sustained pressure and infection, as well as persistent inflammation (see Ch. 105).

to transgenic mouse models, refined mouse models that allow inducible and time-restricted depletion of specific immune cells have unraveled critical functions of individual immune cell lineages in skin repair. For example, in addition to the central role macrophages play in clearing cell detritus and microorganisms, they exert distinct functions during the different phases of repair[10]. In particular, macrophages recruited immediately after injury are essential for inducing vascular sprouts and angiogenesis[11]. Once the wound begins to contract, focal adhesion kinase/extracellular signal-regulated kinase (FAK-ERK) is activated within fibroblasts, leading to the release of chemokine ligand 2 (CCL2), one of the major chemokines known to drive monocyte/macrophage recruitment[12]. Thus, a close interaction between macrophages and fibroblasts is envisioned.

In the presence of a functional immune system, higher vertebrates, including rodents and humans, can undergo post-amputation fingertip regeneration[13,14]. Previously it was thought that the blastema, an undifferentiated pluripotent cell population that is thought to arise from mature cells via dedifferentiation, was responsible for mouse distal digit regeneration. However, genetic fate mapping and clonal analysis of individual cells revealed that rather than pluripotent blastema cells a wide range of lineage-restricted tissue stem/progenitor cells contribute to the restoration of the mouse distal digit[14]. In humans, conservatively managed amputation injuries in children (but not adults) can be followed by restoration of the contour, fingerprints, and normal sensation and function of the digit with minimal scarring[15]. While the molecular mechanisms underlying this phenomenon are not yet understood, investigation of conserved mechanisms in more easily trackable non-human models will hopefully allow extrapolation to humans.

Clinical Implications

The underlying etiology of chronic, non-healing ulcers is multifactorial (see Ch. 105). It includes hypoxia due to vascular disease or sustained pressure, infection, and persistent inflammation[16]. How inflammation impairs healing is still not well understood, but increased protease activity (e.g. metalloproteinases [MMPs], serine proteinases) and generation of reactive oxygen species are thought to play a major role. Unraveling the underlying molecular pathophysiology of chronic wounds in humans will clearly involve studies of both regeneration and repair.

IMPACT OF WOUND DEPTH ON WOUND HEALING

In clinical practice, skin wounds are often categorized according to their depth (Fig. 141.2). Defects that affect only the epidermis (or a portion of the epidermis) are referred to as *erosions*. When the wound extends into the dermis, it is termed an *ulceration*. In *"partial-thickness"* wounds, the epidermis and papillary dermis are missing, with the ulcer extending into the mid dermis, but the adnexal structures remain. *Full-thickness* wounds, on the other hand, involve the entire dermis and extend into the subcutaneous fat. As a result, adnexal structures are lost as a source of keratinocytes for re-epithelialization.

The depth of a skin injury affects the capacity of the skin to repair or regenerate (see Fig. 141.2). When erosions heal, there is regeneration of the entire epidermis without scarring. Ulcerations, however, heal via a reparative process and are associated with scar formation. In partial-thickness wounds, the preserved adnexal structures serve as a source of epithelial cells to repopulate the epidermis. Epithelia from these structures, as well as from the wound edge, migrate across the wound surface to provide coverage. In contrast, re-epithelialization can only occur from the wound edges in full-thickness wounds because adnexal structures are lost.

Healing of full-thickness wounds includes, to some extent, contraction whereas in partial-thickness wounds contraction is minimal. Contraction may be mediated by mechanical or biologic factors, e.g. the differentiation of fibroblasts into myofibroblasts. More recent studies in mice suggest that the contributions of different stem cell sources for wound fibroblasts may determine the outcome of the repair response. These include a superficial cell population that is critical for hair development and a deeper cell population that forms the lower dermis and may provide a source of locally derived wound fibroblasts that can develop into myofibroblasts[17]. Human dermal fibroblasts in the papillary versus reticular dermis differ in their sphingolipid content and as a result, FGF receptor signaling promotes a proliferative lipotype versus a fibrogenic lipotype, respectively[18].

During contraction, the wound area decreases via centripetal movement of *pre-existing* tissue, not the formation of new tissue. Unfortunately, contraction of wounds may result in cosmetically disfiguring contractures. However, the contraction of wounds occurs in

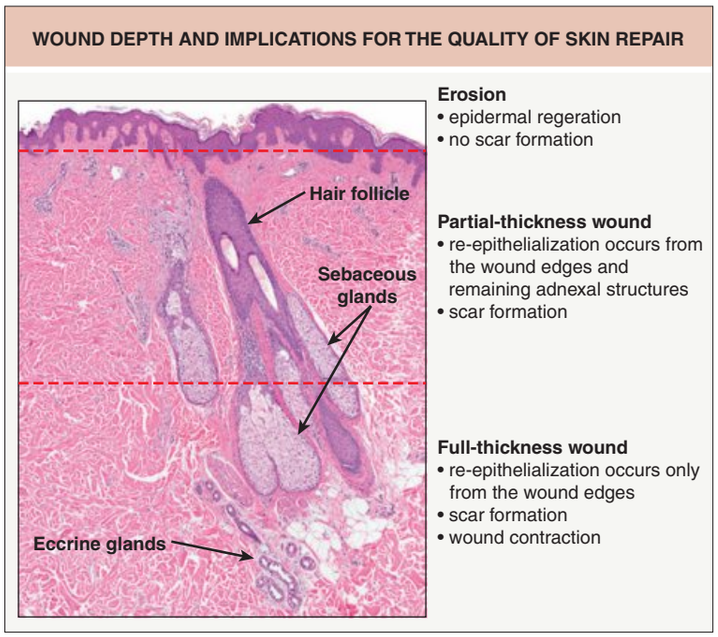


Fig. 141.2 Wound depth and implications for the quality of skin repair. The depth of skin injury determines the ability of the skin to repair versus regenerate. The red dashed lines indicate the levels of injury: injury limited to the epidermis has the capability for regeneration, while injuries to the dermis heal with scar formation. If adnexal structures are present, they contribute to re-epithelialization and faster wound closure. If these structures are lost, epithelia can only migrate from the wound edges and complete restoration of the epidermis will require a longer time period.

predictable directions (in relation to "skin tension lines"), and in order to direct the contracture, surgical incisions should be placed parallel to these skin tension lines whenever possible. Also, an argument in favor of using full-thickness skin grafts is to prevent wound contraction and subsequent contracture (see Ch. 148).

Primary Versus Second Intention Healing

When an acute wound (e.g. a surgical excision) is allowed to heal on its own, this is termed *second intention healing* (see Ch. 146). In *primary intention healing*, wound closure is accomplished by approximating the wound edges, e.g. side-to-side closures, flaps, grafts. *Tertiary intention healing* refers to wounds that are closed with the goal of primary intention healing, but dehiscence occurs, and the wound is then allowed to heal by second intention. In second intention healing, the time interval until complete re-epithelialization depends on several factors including wound depth, anatomic location (e.g. facial wounds heal faster than acral wounds), secondary infection, vascular supply, geometric shape (a more narrow diameter will heal faster), age, and systemic disorders (e.g. diabetes mellitus).

For smaller wounds, especially those that are partial-thickness, primary and second intention healing can produce similar cosmetic results. Once wounds have a diameter >8 mm, primary intention healing leads to better cosmetic results. The decision to choose primary versus second intention wound healing depends on several factors including the patient's overall medical status and cosmetic concerns as well as the depth, size, and location of the defect, in particular whether it is located on a convex or concave surface. In addition to comorbidities such as atherosclerosis, venous hypertension and diabetes mellitus, the risk of infection (which may be increased in open wounds) and the patient's preference also influence the decision.

SKIN REPAIR – CELLULAR AND MOLECULAR ASPECTS

In most mammalian organ systems, the repair response involves a complex and dynamic interplay of numerous cell types, including cells that reside within the tissue (e.g. keratinocytes, endothelial cells, fibroblasts) and hematopoietic cells, either tissue-resident or recruited to the site of tissue damage. For simplicity, three sequential phases of wound healing have been delineated: Inflammation, Proliferation, and Remodeling (Fig. 141.3)[19].

The Phases of Wound Healing

Tissue injury causes leakage of blood constituents into the wound site and the release of vasoactive factors, resulting in the activation of the clotting cascade and resultant hemostasis. Clotted blood forms a matrix that allows for cell adhesion and migration. Not only do platelets trapped within the clot play an important role in hemostasis, they also provide a rich source of growth factors (e.g. PDGF) and proinflammatory cytokines that mediate the recruitment of inflammatory cells and fibroblasts into the wound.

The *inflammatory phase* of repair is characterized by chemoattraction and local activation of innate immune functions, both of which lead to an early influx of polymorphonuclear leukocytes (PMNs; neutrophils). This is followed by invasion of blood monocytes, which differentiate into tissue macrophages[10,11]. While one function of the inflammatory infiltrate is to combat invading microbes, another equally important function is the release of cytokines and growth factors (e.g. IL-1, IL-6, vascular endothelial growth factor [VEGF], tumor necrosis factor [TNF], TGF-β; Table 141.2), which are critical for initiating the proliferative phase of skin repair.

During the *proliferative phase*, granulation tissue is newly formed and consists primarily of invading macrophages, fibroblasts, and endothelial cells (as vessel precursors). This granulation tissue serves to cover and fill the wound area. Fibrin, fibronectin, vitronectin, type III collagen, and tenascin are important components of the provisional extracellular wound matrix that facilitate cell adhesion, migration, and proliferation. At the wound edge, epidermal–mesenchymal interactions stimulate keratinocyte proliferation and migration, leading to re-epithelialization[20].

Once epithelialization is complete, cell proliferation and neovascularization cease, scar tissue forms, and the wound enters the *remodeling* (*maturation*) *phase*, which lasts for several months. The remodeling phase is characterized by a balance between the synthesis of new components of the scar matrix and their degradation by proteases. This balance determines whether the scar will eventually be normal or abnormal (e.g. atrophic scars, hypertrophic scars, keloids). The mechanisms underlying granulation tissue regression and its transformation into scar tissue are largely unknown. Typically, there is also regression of vascular structures, transformation of fibroblasts into myofibroblasts, substitution of the provisional extracellular matrix (ECM) with a permanent collagenous matrix, and a final resolution of the inflammatory response.

However, if the inflammatory response persists, a disturbed healing response may lead to chronic skin ulcers (see Fig. 141.3). Although the mechanisms that direct resolution of the inflammatory response are not well understood, recent studies in patients and in experimental models have found that transitioning from early proinflammatory macrophages to resolving late-stage macrophages is a pivotal component of wound healing[11,21,22]. In addition, resolution involves increased production of anti-inflammatory mediators, active suppression of proinflammatory factors, normalization of microvascular permeability, clearance of inflammatory cells, and epithelialization.

Cellular Components

Keratinocytes

Within hours after injury, keratinocytes at the wound edge are activated and undergo fundamental phenotypic and functional changes that are required to re-epithelialize the wound bed (Fig. 141.4). To initiate migration, keratinocytes need to modify their junctions and adhesion molecules: hemidesmosomes become detached and collagen-binding receptors are replaced by integrins that allow keratinocytes to adhere to the newly formed provisional wound matrix. In addition, keratinocytes begin to proliferate as they reduce their production of proteins normally expressed by differentiated stratified epidermis, in particular specific keratins (see Ch. 56). During wound healing, a classic marker of activated keratinocytes is the expression of keratins associated with proliferation such as keratins 6 (K6) and K16. The cytoskeletal changes

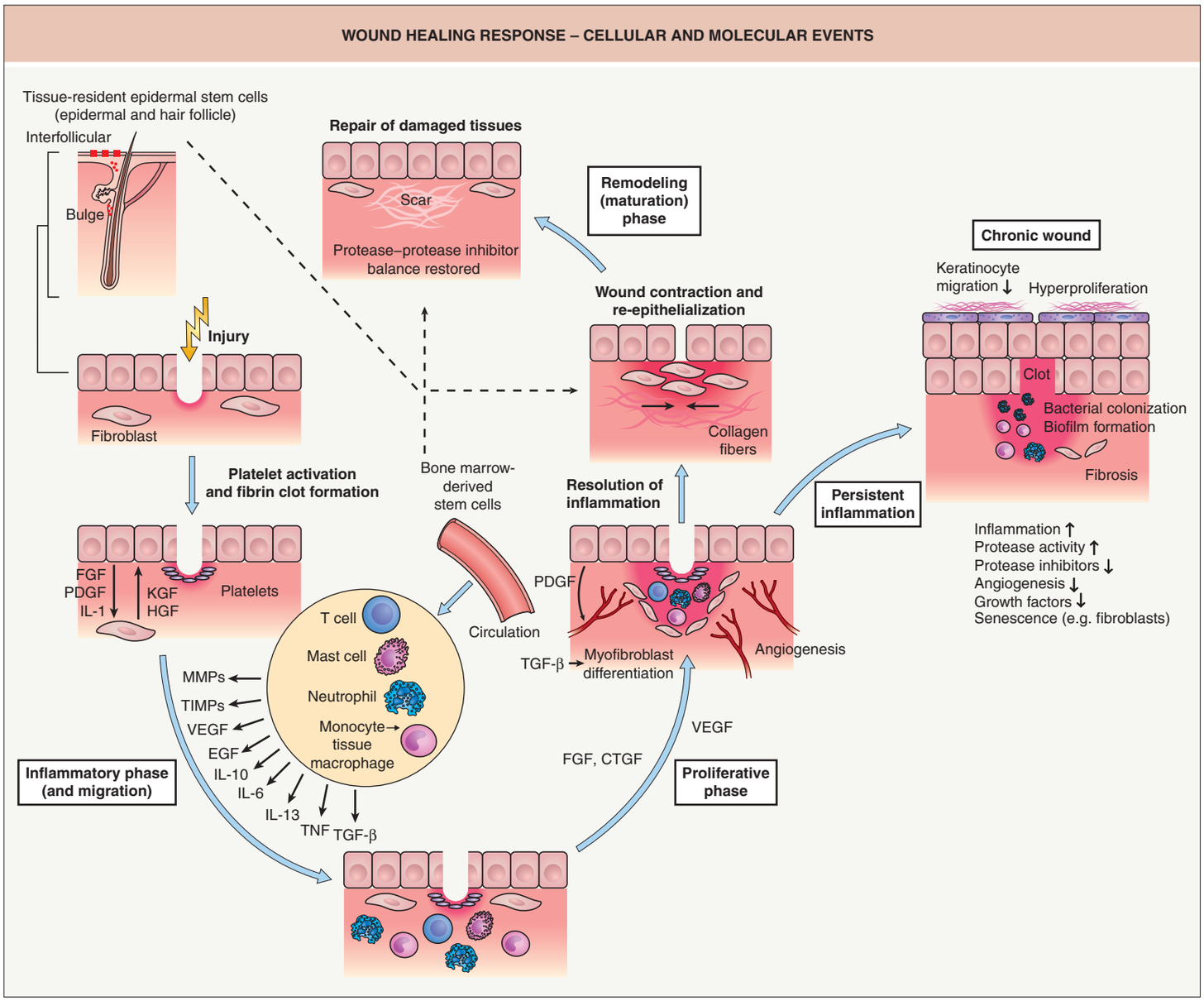


Fig. 141.3 Wound healing response – cellular and molecular events. Leakage of blood constituents and vasoactive factors into the wound site leads to hemostasis. The fibrin clot consists of platelets as well as extracellular matrix molecules (e.g. fibronectin, vitronectin) which facilitate the infiltration and migration of cells. Influx of different subsets of leukocytes characterizes the *inflammatory phase* of repair. These cells release angiogenic growth factors and proinflammatory cytokines, which then induce the recruitment of additional inflammatory cells, fibroblasts, and endothelial cells into the wound site. During the *proliferative phase* in which there is formation of granulation tissue, activated macrophages, endothelial cells, and fibroblasts form a functional unit essential for efficient blood vessel growth. Transformation of granulation tissue and provisional wound matrix into scar tissue occurs during the *remodeling phase* and this is characterized by a decrease in inflammation and regression of vascular structures. Lastly, stem cells that are intrinsic to the skin (e.g. epidermal stem cells) as well as circulating stem cells contribute to the repair response. If the inflammatory response persists, a disturbed healing response may ensue leading to chronic skin ulceration. The microenvironment of chronic ulcers is characterized by multiple hostile factors including increased protease activity, proinflammatory factors, senescent cells, fibrosis, and impaired cellular migration. CTGF, connective tissue growth factor; EGF, epidermal growth factor; FGF, fibroblast growth factor; HGF, hepatocyte growth factor; IL, interleukin; KGF, keratinocyte growth factor; MMPs, matrix metalloproteinases; PDGF, platelet-derived growth factor; TGF, transforming growth factor; TIMPs, tissue inhibitors of metalloproteinases; TNF, tumor necrosis factor; VEGF, vascular endothelial growth factor. *Adapted from Wynn TA. Common and unique mechanisms regulate fibrosis in various fibroproliferative diseases. J Clin Invest 2007;117:524–9.*

associated with keratinocyte activation provide plasticity and flexibility, while maintaining resilience of the intracellular scaffold that is important for migration[23]. Many of the growth factors active during wound healing, such as keratinocyte growth factor (KGF) or hepatocyte growth factor (HGF), are potential regulators of these processes. These growth factors can be synthesized either by activated keratinocytes (and act in an autocrine loop) or by cells present in the dermis, in particular fibroblasts, and then they act in a paracrine fashion[24].

As the stratified epithelium consists of keratinocytes committed to multiple stages of differentiation, it is important to know which keratinocytes can be activated for regeneration. Experimental data from mice expressing a transgene within defined keratinocyte subpopulations revealed that interfollicular epidermal stem cells, transient amplifying cells, and early differentiated cells have the ability to form a fully differentiated epidermis[25]. These data suggest that primarily skin stem cells and transient amplifying cells contribute to wound healing and that keratinocytes become irreversibly committed to the differentiation process relatively quickly and then respond poorly to activating signals. Once keratinocytes process profilaggrin into filaggrin, they undergo specific changes that mark late terminal differentiation, which seemingly demarcates the final "line of regenerative potency" within the differentiating keratinocyte population (see Fig. 141.4)[26].

Studies in mice that focused on the contribution of stem cells to the formation of a new epidermis after injury concluded that multiple

GROWTH FACTORS INVOLVED IN WOUND HEALING			
Growth factor	**Abbreviation**	**Source**	**Functions**
Platelet-derived growth factor	PDGF	Platelets, keratinocytes, fibroblasts, endothelial cells, perivascular cells	Fibroblast proliferation, chemotaxis & collagen metabolism; angiogenesis
Transforming growth factor-β	TGF-β	Platelets, keratinocytes, fibroblasts, endothelial cells, macrophages	Fibroblast proliferation, chemotaxis & collagen metabolism; angiogenesis; immunomodulation
Transforming growth factor-α	TGF-α	Platelets, keratinocytes	Keratinocyte proliferation & migration
Epidermal growth factor	EGF	Platelets	Keratinocyte proliferation & migration
Interleukins	IL-1, IL-10	Leukocytes, keratinocytes	Fibroblast proliferation; proinflammatory (IL-1); anti-inflammatory (IL-10)
Tumor necrosis factor	TNF	Leukocytes, keratinocytes	Promotes inflammation
Connective tissue growth factor	CTGF	Fibroblasts, endothelial cells	Fibroblast proliferation, chemotaxis & collagen metabolism
Fibroblast growth factor	FGF	Keratinocytes, macrophages	Fibroblast & epithelial cell proliferation; matrix deposition, wound contraction; angiogenesis
Keratinocyte growth factor	KGF	Fibroblasts	Keratinocyte proliferation
Insulin-like growth factor 1	IGF-1	Fibroblasts	Keratinocyte proliferation & differentiation
Hepatocyte growth factor	HGF	Fibroblasts, macrophages	Keratinocyte proliferation
Vascular endothelial growth factor	VEGF	Platelets, keratinocytes, macrophages, neutrophils	Angiogenesis; vascular permeability; macrophage chemotaxis

Table 141.2 Growth factors involved in wound healing.

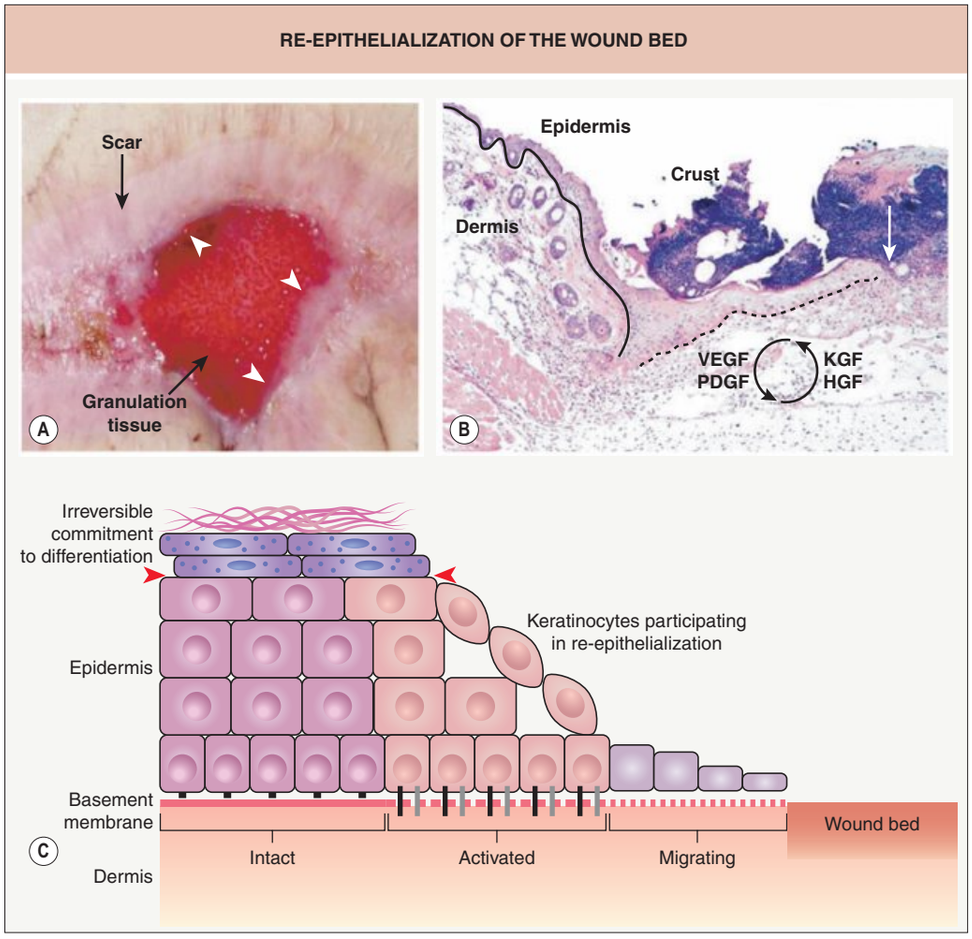


Fig. 141.4 Re-epithelialization of the wound bed. **A** Clinical appearance of a re-epithelializing wound; arrowheads indicate the epithelial wound edge. **B** Histology of the wound edge demonstrating the migration of keratinocytes over the wound bed; this process is in part regulated by growth factors synthesized by fibroblasts such as keratinocyte growth factor (KGF) and hepatocyte growth factor (HGF). The white arrow indicates the tip of the epithelial tongue, the black dashed line indicates activated and migrating epithelium, and the black solid line indicates intact epithelium. **C** Epithelial cells present at the wound edge undergo marked morphologic and functional alterations. They lose their contacts with neighboring cells and the underlying extracellular matrix, then proliferate and migrate toward the center of the wound. The red arrowheads demarcate the terminally differentiated cells that are irreversibly committed.

populations of stem cells reside within different locations of the epidermis and skin appendages. Under normal homeostatic conditions, stem cells residing in different locations maintain the differentiated lineages specific to those locations, i.e. hair follicle stem cells (HFSCs) maintain the hair lineages, sebaceous gland stem cells produce differentiated sebocytes, and stem cells within the interfollicular epidermis (IFE) give rise to the outermost barrier layers of the epidermis[27]. Although in principle cells from all stem cell populations are capable of participating in epithelialization after a cutaneous injury, their specific contributions vary[27,28]. The current view is that stem cells from the interfollicular epidermis as well as cells that lie within the lower bulge area (region of the hair follicle defined as the attachment site of the arrector pili muscle) and above the bulge (the isthmus) contribute long-lasting progeny during re-epithelialization, whereas cells located in the bulge play a minor role[27–29]. These findings are supported by studies in which epidermal wound repair still occurred despite the absence of

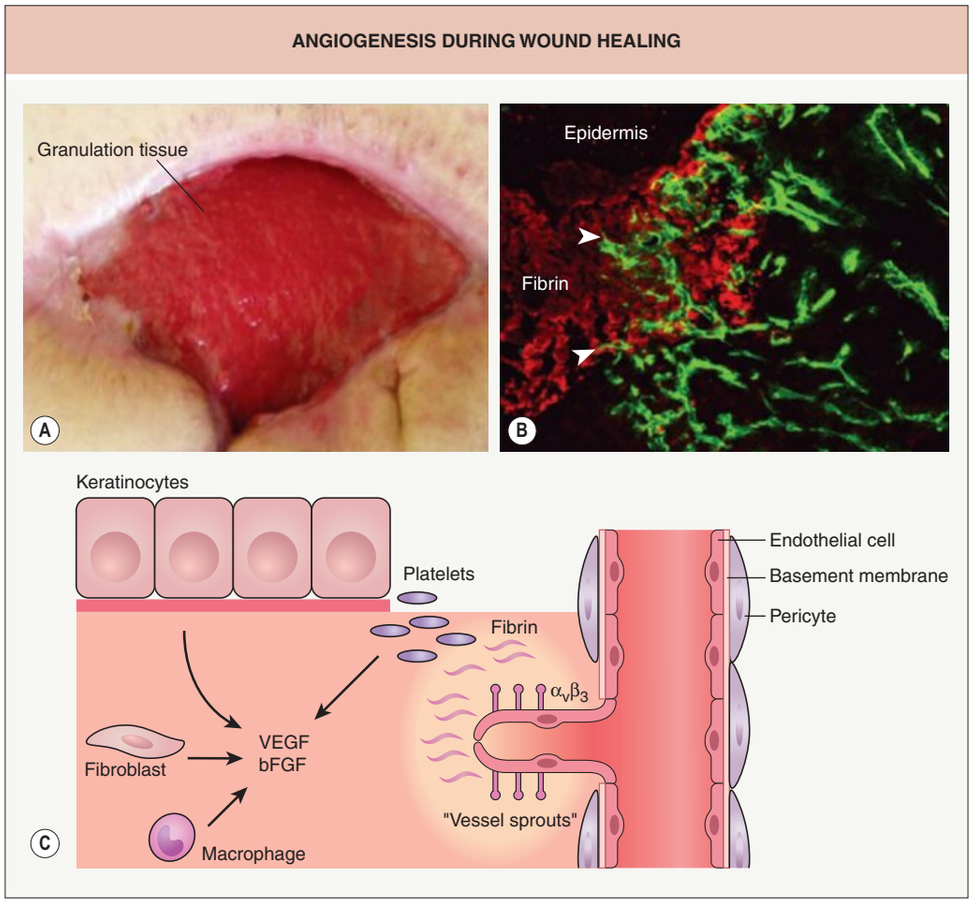


Fig. 141.5 Angiogenesis during wound healing. **A** Clinical appearance of a highly vascularized wound bed. **B** Immunohistochemical staining demonstrating endothelial invasion ($CD31^+$ [green]) into a fibrin matrix (red); white arrowheads indicate sprouting capillaries. **C** Capillary sprouts invade the fibrin/fibronectin-rich provisional wound matrix and within a few days they organize into a microvascular network throughout the granulation tissue. The process is regulated by dynamic interactions amongst endothelial cells, growth factors (e.g. VEGF, bFGF), and the extracellular matrix. In particular, the $\alpha_v\beta_3$ integrin appears to be required for endothelial cell attachment and wound angiogenesis. bFGF, basic fibroblast growth factor; VEGF, vascular endothelial growth factor.

hair follicles in mutant mice. Nonetheless, an acceleration of epidermal wound healing has been observed during the growth phase of the hair cycle. Collectively, these findings help to explain how depth of injury affects a wound's capability to repair and to re-epithelialize.

Endothelial cells

Activated and proliferating endothelial cells that form blood vessels normally express $\alpha_v\beta_3$ integrins and are major contributors to angiogenesis, which is a vital component of wound healing (Fig. 141.5)[30]. New blood vessels ensure the delivery of nutrients to meet the increased metabolic requirements of wound tissue and they help to reverse the hypoxic and acidotic milieu[31]. Neoangiogenesis in wounds occurs via both *angiogenesis* (sprouting of capillaries from existing blood vessels) and *vasculogenesis* (mobilization of bone marrow-derived endothelial progenitor cells; see Ch. 102). This is a highly complex process – it requires dynamic, temporally and spatially regulated interactions amongst endothelial cells, soluble angiogenic growth factors, and ECM molecules. In addition, wound angiogenesis is, at least in part, induced by the innate immune response. Immediately after injury, different subsets of leukocytes, especially macrophages, are attracted to the wound site where they release multiple pro-angiogenic mediators (e.g. VEGF-A, IL-6, IL-8, TNF) that trigger and sustain the angiogenic response[11,22].

During neoangiogenesis, degradation of the surrounding ECM occurs via MMPs and serine and cysteine proteases[32], with new vessels sprouting from existing vessels and growing along a growth factor gradient determined primarily by VEGF. Importantly, as shown for VEGF-A, the time of action, cellular source, and concentration of a given cytokine determine whether it activates, terminates, or inhibits angiogenesis. The delayed healing response observed in patients receiving anti-VEGF-A agents (e.g. bevacizumab) highlights the critical role VEGF-A plays in angiogenesis during tissue repair[33]. Of note, both the ECM (often via integrins) and growth factor concentrations provide signals that balance the formation of new blood vessels and the prevention of aberrant angiogenesis.

Genetically engineered mice have also provided evidence that wound angiogenesis requires dynamic interactions amongst endothelial cells, pro- and anti-angiogenic growth factors, and the ECM environment[30]. For example, basement membrane proteins provide essential information for the organization and orientation of endothelial cells. Anchoring of endothelial cells to this dense polymer layer is crucial for the proper function of blood vessels, and removal of major components of the basement membrane leads to leakiness of blood vessels. A vital role for these components (laminins, nidogens, types III and IV collagens, heparin sulfate proteoglycans) is reflected in genetic disorders such as the vascular form of Ehlers–Danlos syndrome, in which reduced or abnormal type III collagen fibers are associated with vascular fragility.

Leukocytes and platelets

The inflammatory response in normal wound healing is characterized by spatially and temporally changing patterns of various leukocyte subsets. The well-defined chronology of these events appears essential for optimal repair.

Platelets and polymorphonuclear leukocytes

Immediately after injury, extravasated blood components form a hemostatic blood clot (Fig. 141.6). Platelets then aggregate within the clot and release a wide spectrum of factors that amplify the aggregation response, trigger the coagulation cascade, and act as chemoattractants for cells involved in the inflammatory phase.

Within a few hours following the injury, polymorphonuclear leukocytes (PMNs; neutrophils) transmigrate across the endothelial cell wall of capillaries. Upon activation, neutrophils release proinflammatory cytokines including IL-8 and TNF as well as the chemokines growth-related oncogene-α (GRO-α) and monocyte chemoattractant protein-1 (MCP-1)[34,35]. This leads to expression of adhesion molecules (selectins, ICAM, VCAM) that are essential for leukocyte adhesion and diapedesis (see Fig. 141.6 and Ch. 102)[36]. Neutrophils can further amplify their own recruitment via IL-8 and GRO-α.

Bacterial products such as lipopolysaccharides and formyl-methionyl peptides, which accumulate within infected wounds, can accelerate directed neutrophil locomotion. In addition to controlling infectious agents, recruited neutrophils play a major role in the debridement of devitalized tissue. To accomplish these tasks, they release a large variety of

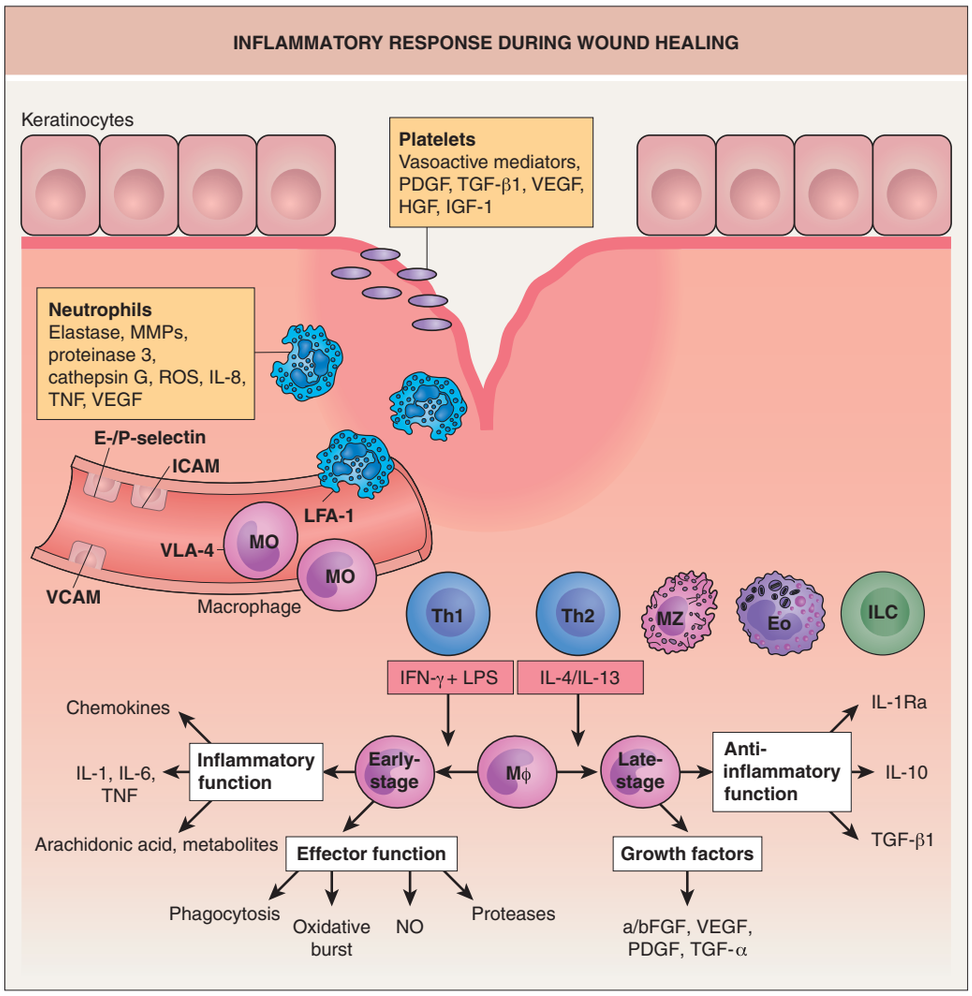


Fig. 141.6 Inflammatory response during wound healing. During normal wound healing, the inflammatory response is characterized by spatially and temporally changing patterns of leukocyte subsets. A well-defined chronology and interplay is essential for optimal repair. Within a few hours after injury, neutrophils transmigrate across the endothelial cell wall of blood capillaries; recruited neutrophils begin to debride devitalized tissue and attack infectious agents by releasing a number of antimicrobial molecules, proteases, and cytokines. Shortly after the neutrophils appear, monocytes migrate from the blood vessels into the dermis, become activated within the wound environment, and then transform into tissue macrophages. In addition to functioning as antigen-presenting cells and phagocytes, macrophages are thought to play an integral role in wound healing due to their release of numerous growth factors. Their morphologic and functional heterogeneity is a reflection of factors released by other cells, e.g. T cells or mast cells, present in the wound environment. Eo, eosinophil; FGF, fibroblast growth factor; HGF, hepatocyte growth factor; ICAM, intercellular adhesion molecule; IFN, interferon; IGF, insulin-like growth factor; IL, interleukin; IL-1Ra, interleukin-1 receptor antagonist; ILC, innate lymphoid cell; LFA-1, lymphocyte function-associated antigen 1; LPS, lipopolysaccharide; MMPs, matrix metalloproteinases; MO, monocyte; Mϕ, macrophage; MZ, mast cell; NO, nitric oxide; PDGF, platelet-derived growth factor; ROS, reactive oxygen species; TGF, transforming growth factor; TNF, tumor necrosis factor; VCAM, vascular cell adhesion molecule; VEGF, vascular endothelial growth factor; VLA-4, very late antigen-4.

highly active antimicrobial substances (reactive oxygen species, cationic peptides, eicosanoids) and proteases (elastase, cathepsin G, proteinase 3, urokinase-type plasminogen activator). However, uncontrolled release of these factors can cause severe damage to the tissues of the host[16,36]. The important role of neutrophils in phagocytosis and debridement is underlined by the observation that patients with defined deficiencies in PMN function, such as the leukocyte-adhesion deficiency syndrome 1 (LAD1)[37] or attenuated PMN actin polymerization[38], in which neutrophil locomotion is impaired, also display impaired wound healing.

Blood monocytes and tissue macrophages

The attraction of blood monocytes into the wound site occurs via chemotactic factors including growth factors, proinflammatory cytokines, and chemokines. Examples of the latter are macrophage inflammatory protein 1α (MIP-1α), MCP-1, RANTES, and fractalkine[34]. Within the wound, the major sources of chemoattractants include platelets trapped in the fibrin clot, hyperproliferative keratinocytes at the wound edges, fibroblasts, and various subsets of leukocytes including macrophages. When monocytes extravasate from the blood vessel, they become activated and differentiate into mature tissue macrophages.

Macrophages have a variety of functions during wound healing[10,11,22]. While their role as antigen-presenting cells may be less important in this setting (e.g. RAG1 knockout mice lacking mature T cells have normal wound healing)[39], they are important phagocytes. Macrophages are also a major source of growth factors, such as TGF-β, TNF, PDGF, bFGF, Relm, and VEGF. These factors critically regulate angiogenesis, keratinocyte motility, the recruitment and activation of immune cells, and the synthesis of ECM molecules.

The central role that macrophages play in wound healing was established over 30 years ago. In rats, a significant delay in wound healing was observed when antisera was used to deplete macrophages[40]. More recent studies have supported and extended these observations[10,11,22]. For example, ICAM-1-deficient mice, P- and E-selectin-double-deficient mice, and mice deficient in β-1,4-galactosyltransferase (which glycosylates P- and E-selectins) all have profound delays in wound closure (see Fig. 141.6); this delay is associated with a significantly reduced infiltration of macrophages. These studies demonstrate the importance of cell adhesion molecules in regulating blood monocyte recruitment and infiltration into the wound site.

Differentiation of monocytes into tissue macrophages involves profound changes in gene expression and cellular function. This activation is directed by mediators present in the microenvironment and is thought to be crucial for the proper adaptation of macrophage functions to the specific requirements of the wound site[41]. Macrophages sense their microenvironment via numerous cell surface receptors, including Toll-like receptors, complement receptors, Fc receptors, and cytokine receptors[42].

One model of tissue macrophage activation is based on the observation that macrophages acquire distinct states of activation (see Fig. 141.6)[38]. Traditionally it was thought that macrophages at one end of the spectrum exhibited proinflammatory activities such as the production of IL-1 and nitric oxide (NO). This led to promotion of type I immune responses and eradication of invading microorganisms, and these cells were termed *M1* or *"classically activated"* macrophages. At the other end of the spectrum, the macrophages had a rather non-inflammatory phenotype, produced IL-10, and were hyporesponsive to proinflammatory stimuli. These cells were involved in debris scavenging, tissue remodeling, resolving inflammation, and promoting repair and were termed *M2* or *"alternatively activated"* macrophages. However, recent studies have challenged this model by demonstrating that the phenotypes of activated macrophages are much more complex. For example, injury-associated macrophages displayed substantial heterogeneity across activation patterns and metabolic signatures that critically affected the outcome of the healing response[22].

Studies in mice and humans have shown that early and late wound stages are characterized by specifically activated *early-stage inflammatory* macrophages and *late-stage non-inflammatory* macrophages, respectively (see Fig. 141.6)[7]. Cells associated with different stages

are characterized by distinct gene expression profiles[22,43]. Early-stage wound macrophage activation is mediated by cytokines, in particular interferon-γ (IFN-γ), followed by Toll-like receptor (TLR)-mediated triggers such as lipopolysaccharide signaling via TLR4. Key mediators of late-stage macrophage activation are IL-4 and IL-13, acting through the common receptor chain IL-4Rα.

T cells

During the tissue remodeling phase, when wound closure is complete and local infections have been overcome, cells of the *adaptive* immune response, in particular T cells, are the most frequent leukocyte subset in human skin wounds[44]. $CD4^+$ T cells can differentiate into different subsets, e.g. Th1 and Th2 cells (see Ch. 4), thereby influencing the wound microenvironment by secreting distinct cytokine profiles (see Fig. 141.6)[45]. Th1 cells are a primary source of IFN-γ, while Th2 cells are the major source of IL-4 and IL-13. These cytokines have a major effect on the state of macrophage activation. Thus, even though they are not mandatory for wound healing, $CD4^+$ T cell cytokines influence two important components of wound healing: macrophage function and angiogenesis. However, additional investigations are needed to understand why wound healing appears to be unaffected in T cell-deficient mice (e.g. RAG1 knockout mice).

Mast cells

Mast cells are a hematopoietic cell population that normally resides in skin and mucous membranes. They are an important source of a number of mediators such as prostaglandins and biogenic amines as well as pro- and anti-inflammatory cytokines (e.g. TNF, IL-8) that strongly influence inflammation, tissue modulation, and vascular modeling. However, almost entirely normal wound healing was observed in mice genetically depleted of mast cells, suggesting that mast cells may only play a fine-tuning role during wound repair[46].

Fibroblasts

Connective tissue, including the dermis, is usually composed of large amounts of ECM in which a small number of relatively quiescent fibroblasts are embedded. During development, fibroblasts establish a "resting" tension by actively synthesizing and cross-linking fibrillar ECM proteins such as collagen and elastin (see Ch. 95). This establishes the shape of the skin and ensures that the skin retains its shape in response to mechanical stress.

During tissue repair, fibroblasts next to the site of injury become activated, reconstitute new ECM, and restore proper matrix tension. To achieve these goals, fibroblasts acquire smooth muscle cell-like features including contractile stress fibers and *de novo* expression of α-smooth muscle actin (α-SMA), thus differentiating into myofibroblasts (Fig. 141.7)[43]. The transition of fibroblasts into myofibroblasts depends on the concerted action of both cytokines and ECM proteins, in particular TGF-β1 and the cellular fibronectin splice variant ED-A, respectively[47]. Acquisition and maintenance of the myofibroblast phenotype also depend on mechanical tension, which is regulated by the interaction between the rigidity of the ECM and the contractile activity of its cells. Rho-ROCK signaling serves as an important integrator of profibrotic pathways and it can be activated by integrin signaling in a FAK-dependent manner or by TGF-β and Engrailed 1 (EN1)[48].

After wound closure, apoptosis of myofibroblasts or reverse differentiation into fibroblasts normally occurs. However, abnormal persistence of myofibroblasts has been observed in hypertrophic scars and keloids (see Fig. 141.7). Determining how the perception of mechanical signals translates into myofibroblast differentiation may lead to therapeutic strategies for exaggerated scarring[49,50].

Stem cells

Stem cells are defined as cells that have self-renewing capabilities and can differentiate into multiple cell lineages (see Ch. 2). *Embryonic stem cells* are derived from mammalian embryos in the blastocyst stage and have the ability to generate any terminally differentiated cell in the body. *Adult stem cells* – previously thought to be restricted to their tissue of origin – can be reprogrammed to differentiate into various cell types and to replenish damaged tissues, including muscle, liver, and skin[51]. During wound healing, tissue-resident stem cells (e.g. epidermal stem cells, hair follicle stem cells, mesenchymal stem cells) as well as stem cells recruited from the bloodstream can participate in the repair process (see Fig. 141.3)[27,51].

To date, the best-studied model of adult stem cells is the hematopoietic system, in which long-term self-renewal is achieved solely by specific and rare hematopoietic stem cells (HSC). These cells reside within the bone marrow niche and can give rise to all blood cell lineages. In addition to hematopoietic progenitors, other cells with stem cell-like qualities, such as mesenchymal stem cells (MSCs) and multipotent adult progenitor cells (MAPC), have been cultured from human and murine bone marrow[52].

MSCs were first isolated from bone marrow and later from various tissues including adipose, pancreas, skeletal muscle, neural tissue, and skin. After appropriate stimulation, these cells differentiate into mature committed cells. In animal studies, they migrated from their bone marrow niche to injury sites and differentiated appropriately, e.g. into endothelial, neural, or cardiac tissues. Within injured murine skin, differentiation into fibroblasts, endothelial cells, and keratinocytes was observed[53]. However, the percentage of MSCs recruited into small cutaneous wounds in mice appears to be low[47]. Nonetheless, there is significant therapeutic interest in delivering stem or progenitor cells to skin wounds to promote repair or optimize the quality of the repair response (see below)[51,52,54].

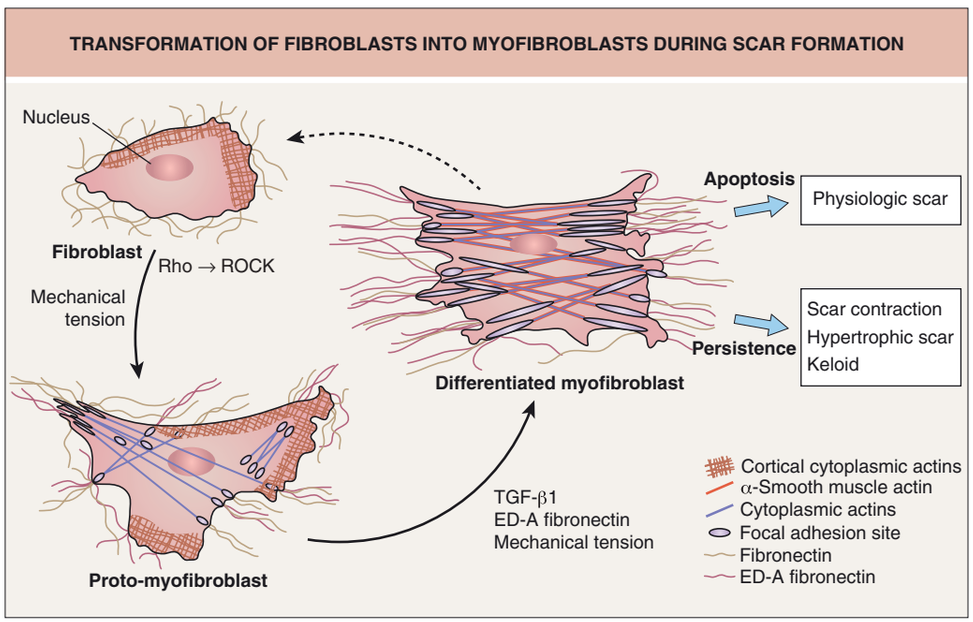


Fig. 141.7 Transformation of fibroblasts into myofibroblasts during scar formation. Fibroblasts undergo a series of phenotypic and functional changes during granulation tissue formation and then scar formation. This process has beneficial (e.g. release of growth factors[76], regeneration of adipocytes[77]) as well as harmful (e.g. fibrogenesis) effects. Under mechanical stress, fibroblasts differentiate into proto-myofibroblasts which are characterized by the expression of a fibronectin variant ED-A; the latter, in combination with TGF-β1, promotes the differentiation of proto-myofibroblasts into myofibroblasts. The Rho/ROCK signaling pathway also plays an important role. Typically, myofibroblasts express α-smooth muscle actin (SMA) and can generate potent contractile forces. The persistence of myofibroblasts within the scar may lead to disabling scar contraction. *From Tomasek JJ, Gabbiani G, Hinz B, et al. Myofibroblasts and mechano-regulation of connective tissue remodelling. Nat Rev Mol Cell Biol 2002;3:349–63.*

Growth Factors and Their Receptors

In addition to cell–matrix interactions (see below), all stages of the repair process are influenced by a complex network of soluble peptide growth factors, chemokines, and hormones as well as their receptors (see Figs. 141.3, 141.5 & 141.6)[55]. Major growth factor families that contribute significantly to the wound healing process include PDGF, FGF, VEGF, and TGF-β (see Table 141.2). These growth factors are synthesized and secreted by various cell types involved in the wound healing process, including keratinocytes, fibroblasts, vascular endothelial cells, platelets, and inflammatory cells. Growth factors may act on the producer cell (*autocrine* stimulation), an adjacent cell (*paracrine* stimulation), or distant cells (*endocrine* stimulation)[55]. Following binding of growth factors to their respective receptors, complex signaling cascades result in cellular functions crucial for wound healing, including cellular proliferation and migration[56].

Extracellular Matrix

Although the ECM was long viewed as an inert scaffold upon which cells were arranged, it has been redefined as a dynamic, mobile, and flexible structure that plays a key role in regulating cellular behavior. Genetically modified mice have greatly accelerated our understanding of the multifunctionality of the ECM in both developmental and regenerative processes[57].

During the three phases of wound healing, the components of the ECM continuously change in order to support wound phase-specific repair mechanisms. In the inflammatory phase, the initial wound matrix (consisting primarily of blood constituents such as fibrin and fibronectin) provides a substrate for migration and in-growth of various cell types, including macrophages and fibroblasts (Fig. 141.8). During the proliferative phase, granulation tissue is formed and components of the provisional matrix (e.g. vitronectin, tenascin) facilitate cell adhesion, migration, and proliferation (see Fig. 141.3). In the remodeling phase, the provisional matrix matures and is replaced by type I collagen which increases the tensile strength of the wound.

Matrix molecules can regulate cellular functions via interaction with specific transmembrane receptors on the cell surface (e.g. integrins; see below) or they can bind growth factors, e.g. TGF-β. For example, in Marfan syndrome, the reduction in fibrillin-1 synthesis leads to decreased levels of extracellular fibrillin-rich microfibrils, which normally act as a reservoir for TGF-β (see Fig. 95.6). Thus, mutations affecting a component of the ECM can give rise to a phenotype that reflects disturbances in TGF-β signaling[58].

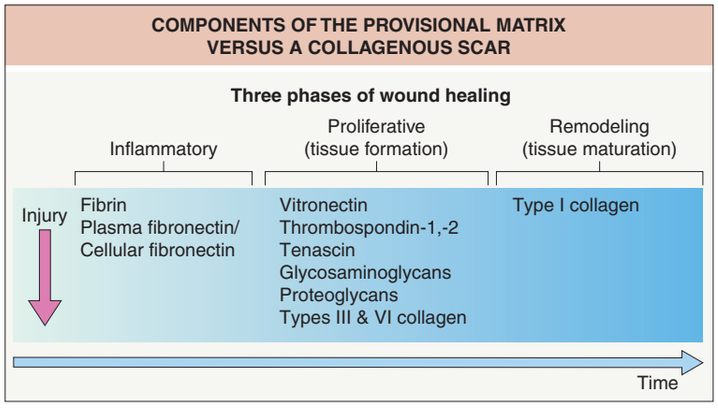


Fig. 141.8 Components of the provisional matrix versus a collagenous scar. The first extracellular matrix to be deposited within the wound space and surrounding tissue is the fibrin clot. Leukocytes, fibroblasts, and endothelial cells invade the fibrin clot, which is then lysed. These cells begin to deposit a network of ECM components, including fibronectin, vitronectin, tenascin, and type III collagen. Following complete re-epithelialization, fibroblasts start to deposit a stable matrix composed of type I collagen. Thus the wound evolves from an initial plasma-derived provisional matrix to an *in situ* cell-derived provisional matrix and finally to a mechanically stable collagen matrix. Examples of glycosaminoglycans are hyaluronic acid, chondroitin-4-sulfate, and dermatan sulfate, while examples of proteoglycans are decorin, biglycan, versican, and syndecan (see Ch. 95).

Integrins

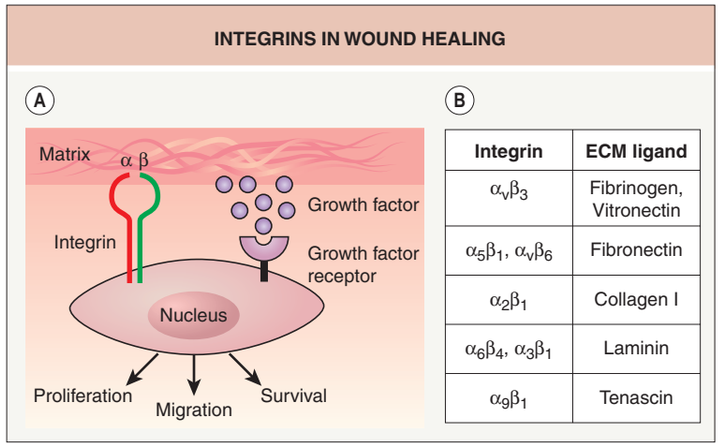
Integrins are transmembrane receptors on the cell surface that recognize and bind to ECM proteins. They are heterodimers composed of α-subunits and β-subunits. Eighteen α-subunits and eight β-subunits can assemble in 24 different combinations, with overlapping substrate specificity and cell type-specific expression patterns[59]. For example, integrins containing β1 or β3 chains are ECM receptors, whereas those containing β2 chains are leukocyte cell–cell receptors. The composition of integrins expressed by a particular cell determines to which ECM components that cell can bind. For example, $\alpha_9\beta_1$ binds to tenascin and $\alpha_V\beta_6$ to fibronectin (Fig. 141.9).

Upon binding of an integrin to its ligand, the integrin may change its configuration and transform into an activated state[60]. This can trigger a signaling cascade within the cell that leads to alterations in gene expression as well as a change in the integrin's binding characteristics. Integrin-mediated signaling is also influenced by the binding of growth factors and cytokines to their respective receptors, along with various levels of cross-talk (see Fig. 141.9). For example, $\alpha_V\beta_3$ binding in conjunction with VEGF-A binding to its receptor leads to synergistic downstream effects which regulate endothelial cell function. Thus, it is well established that integrins are more than just simple receptors mediating the physical attachment of cells to their environment.

Proteases (Proteinases)

Proteases are enzymes that cleave peptide bonds at specific sites along polypeptides. They can be classified into distinct groups based upon the biochemical mechanisms responsible for their catalytic activities[61]. Proteases are crucial for tissue remodeling, which is a fundamental process in all stages of wound repair, i.e. they are active during inflammation, angiogenesis, and re-epithelialization. For skin repair, the most important proteases are serine proteases and metalloproteinases. In addition to matrix degradation, these proteases are crucial for growth factor activation and they exert antimicrobial activities. However, to protect tissues from excessive and uncontrolled proteolytic degradation, protease activity has to be tightly regulated by protease inhibitors. An imbalance with high levels of proteases and low levels of protease inhibitors is a major contributor to chronic, non-healing skin ulcers (see Fig. 141.3)[16,62].

Serine proteases have a catalytically essential serine residue in their active site. Neutrophils and macrophages are an important source of serine proteases, which includes neutrophil elastase, cathepsin G, and proteinase 3. Furthermore, plasmin and its activators, tissue-type plasminogen activator (tPA) and urokinase-type plasminogen activator (uPA), are serine proteases that are fundamental for wound repair. In addition to dissolving the fibrin clot, the plasmin-related proteases are involved in activating matrix metalloproteinases (MMPs) and numerous growth factors.



Integrin	ECM ligand
$\alpha_v\beta_3$	Fibrinogen, Vitronectin
$\alpha_5\beta_1$, $\alpha_v\beta_6$	Fibronectin
$\alpha_2\beta_1$	Collagen I
$\alpha_6\beta_4$, $\alpha_3\beta_1$	Laminin
$\alpha_9\beta_1$	Tenascin

Fig. 141.9 Integrins that play a role in wound healing. A Integrins are transmembrane receptors that recognize and bind to extracellular matrix (ECM) proteins. They are heterodimers composed of one α-subunit and one β-subunit. Integrins allow cells to attach to the ECM and they interact with growth factor receptors, ultimately controlling cellular functions essential for wound healing. **B** The composition of integrins expressed by a cell determines the ECM components to which that cell can bind.

The major *ser*ine *p*rotease *in*hibitors (SERPINs; e.g. α_1-antichymotrypsin) and α_2-macroglobulins are synthesized by hepatocytes and released into the plasma. In contrast, *s*ecretory *l*eukocyte *p*rotease *i*nhibitor (SLPI) and elafin are synthesized locally by keratinocytes. Plasminogen activator inhibitors (PAIs) are the major inhibitors of uPA and are produced by endothelial cells.

The family of MMPs shares a common domain structure and includes collagenases, gelatinases, and stromelysins. Collectively, they are capable of degrading all the components of the ECM. At least 28 members of the human MMP family have been identified and are differentially expressed by diverse cell types[63]. MMPs can be subdivided into several groups based upon substrate specificity, and they are inhibited by *t*issue *i*nhibitors of *m*etallo*p*roteinases (TIMPs) which are synthesized by connective tissue cells and leukocytes.

IMPAIRED WOUND HEALING – RISK FACTORS

The complex network of cell–cell and cell–matrix interactions leading to wound healing can be disturbed. This may result in either a delayed healing response and ultimately a chronic wound or excessive scarring as in hypertrophic scars or keloids. Dysfunctional wound healing represents a major clinical and socioeconomic problem, and the development of effective therapies is essential.

Impaired healing can be classified according to whether it results from systemic factors or the local microenvironment (see Table 141.1)[16]. A chronic wound is a symptom of an underlying disease rather than a disease entity. The most common systemic factors influencing wound repair are venous insufficiency, advanced age, atherosclerosis, and diabetes mellitus-associated microangiopathy (see Fig. 105.1); less commonly vasculitis, hypercoagulability, malnutrition, and concomitant therapies (e.g. hydroxyurea, immunosuppressives) play a role. Local factors include inadequate blood supply, necrotic tissue, increased proteolytic activity, mechanical irritation, pressure, bacterial components, local toxins, and growth factor deficiency (Table 141.3). Each of these factors has to be critically considered when assessing factors responsible for impaired healing and when outlining a treatment regimen for a non-healing wound.

Wound Healing and Aging

The prevalence of chronic wounds increases with age[64], as does the prevalence of venous hypertension, peripheral artery disease, and diabetes mellitus. Aging can be regarded as an accumulation of molecular changes that leads to functional failure in different tissues, including impaired wound healing. Aging may be triggered by two principal mechanisms: telomere shortening (see Fig. 67.22) and DNA damage. Telomere shortening or dysfunction leads to instability of chromosomes. A functional link between age-dependent telomere shortening and impaired wound healing has been demonstrated in telomerase-deficient mice (telomerase is an enzyme that prevents telomere shortening)[65]. How telomere shortening translates into impaired cell function during the healing response is not understood. Patients with Werner syndrome have impaired DNA repair and also develop chronic skin ulcers. Furthermore, mice with increased activation of the transcription factor p53 within the epidermis develop an early aging phenotype of their skin with impaired wound healing[66].

THERAPEUTIC OPTIONS FOR CHRONIC WOUNDS

Wound Dressings

A large variety of wound dressings is currently available, with recommendations for specific dressings based on the characteristics of the wound (see Ch. 145). Clinical experience, rather than controlled trials, forms the basis of many of these recommendations. There is still no consensus on the mechanisms of action, but most dressings are thought to support wound healing by acting as a barrier between the wound and the environment, by preventing drying of the tissue[67], or by allowing autolytic debridement. Only a few dressings appear to be able to interfere with cellular and molecular mechanisms of the wound microenvironment or to counteract mechanisms that are detrimental to repair, e.g. elevated protease activity or increased inflammation (see Fig. 141.3). Of note, controlled trials have shown the benefit of compression therapy in the case of venous ulcers.

COMMON ENVIRONMENTAL FEATURES OF ACUTE VERSUS CHRONIC SKIN WOUNDS IN HUMANS, IRRESPECTIVE OF UNDERLYING SYSTEMIC DISEASE

Acute wounds (healing)	Chronic wounds (non-healing)
Limited tissue damage	Sustained tissue damage
Injury induces cascade of successive phases of hemostasis, inflammation, proliferation, and scar formation	Uncontrolled activation of multiple repair phases
Healing cascade is transient and self-limiting	Continuous cell activation
Dynamic process	"Deadlocked" processes
Limited inflammatory response	• Deregulated and persistent inflammation with multiple sequelae: abundant proinflammatory mediators; increased protease activity; and degradation of critical growth factors and ECM molecules • Proteolytic cleavage of growth factors and ECM results in fragments with new functions
Controlled cellular proliferation	Sustained cellular proliferation
Cellular migration	Disturbed cellular migration
Controlled angiogenesis	• Altered vascular function, vascular leakage, and reduced angiogenesis • Excessive tissue fibrosis results in deregulation of cellular and ECM function as well as mechanotransduction
Normal epidermal–dermal interactions	• Disturbed epidermal–dermal interactions due to an absent epidermis • Exhaustion of stem cells • Increase in necrotic and apoptotic cells • Increase in senescent cells, e.g. fibroblasts • Increased bacterial load and formation of biofilms • Eventually malignant transformation can occur

Table 141.3 Common environmental features of acute versus chronic skin wounds in humans, irrespective of underlying systemic disease. Although many chronic skin wounds result from a combination of underlying systemic diseases that prevent healing (see Ch. 105), it remains unresolved as to what extent the pathophysiology of the local microenvironment overlaps with that of the different underlying systemic diseases. ECM, extracellular matrix.

Growth Factors

Growth factors are essential regulators of cellular function during repair. Experimental studies have shown that the topical application of specific growth factors can modify and probably even accelerate wound repair[56,68]. Based on these observations, clinical trials to determine whether tissues with inherently poor or pathologically altered healing potential could benefit from therapeutic growth factor interventions have been conducted. PDGF-BB was the first and, to date, only approved recombinant growth factor for the topical treatment of diabetic foot ulcers, but due to limited efficacy, its use in daily clinical practice is limited (see Ch. 105).

The limited success of clinical trials with growth factors underscores an important aspect of the growth factor/tissue repair paradigm: the effective delivery of growth factors to the wound site. The latter is biologically and biochemically complex, and in settings such as a chronic or infected wound, the environment is hostile to repair. Current drug delivery strategies suffer from the inherent loss of drug activity due to the combined effects of physical inhibition and proteolytic degradation. While this loss of activity may be one reason for the limited success of clinical studies and delivery of growth factors via genetically modified cells could represent a better approach, a major remaining factor is poor blood supply.

Cell- and Tissue-Based Therapies

When skin defects are too large to heal by second intention, skin grafts and cell-based treatments can be used to cover the wound and replace the defect. Split-thickness skin grafts are commonly used to treat acute surgical or chronic wounds (see Ch. 148). In addition, "pinch" grafts, which are 2–5 mm superficial skin biopsies often obtained from the anterolateral thigh, can be placed dermis-down in a clean wound bed.

To aid in the healing of acute surgical or chronic wounds as well as extensive thermal burns, efforts have been made to develop skin substitutes that have properties similar to native skin[69,70]. Both autologous and allogeneic components have been incorporated into bioengineered human skin equivalents (see Ch. 145). Clinical studies have demonstrated a beneficial effect on chronic wounds refractory to conventional therapy, but these skin substitutes tend to be expensive and grafted cells are eventually lost.

FUTURE DIRECTIONS

Currently limitations in the treatment of chronic wounds are partly due to an incomplete understanding of the molecular mechanisms hindering repair and a lack of animal models that reflect the complex multifactorial nature of chronic ulcers. In addition, clinical research is often hampered by a heterogeneous patient population with a range of comorbidities. The success of innovative therapies will depend on comprehensive knowledge of the underlying pathomechanisms and correction of pathogenic factors, with advances in molecular diagnostics and material sciences playing a key role[16,68].

Stem Cells

Recent advances in stem cell biology may provide novel treatment strategies for acute and chronic wounds (Fig. 141.10)[27]. There is great interest in delivering stem or progenitor cells, either applied topically or via stimulation of their recruitment from the circulation into the wound site. Preliminary work suggests that topically applied autologous bone marrow-derived cells promote the healing of treatment-resistant chronic wounds[69]. Furthermore, recruitment of $CD34^+$ cells from the circulation has shown promise in ischemic limbs[70]. Adipose tissue also serves as a reliable source of mesenchymal stromal/stem cells. Lastly, advances in induced pluripotent stem cell (iPSC) technology and gene editing of somatic cells hold great promise for improving the skin's regenerative capacity[71]. However, stem cell therapy still poses many questions regarding potential side effects and stem cell survival and differentiation within the hostile "chronic wound" environment.

Molecular Modeling of Growth Factors

Advances in biomaterial science and protein engineering are expected to contribute to the development of novel therapies for tissue repair. For example, the creation of protease-resistant growth factors might circumvent the imbalance in proteolytic activity that is characteristic of chronic wounds[72]. When growth factors were engineered to have enhanced binding to ECM molecules, they demonstrated augmented biologic properties associated with tissue repair[73]. This approach not only utilizes the ECM as a carrier, but it also mimics the natural interactions between growth factors and the ECM, which appears to be crucial for the physiologic actions of growth factors.

Biomaterials and Tissue Engineering

Currently, collagen- or fibrin-based products are the most commonly employed biomaterials for guiding tissue regeneration. They are used as carriers for transplanted cells, as acellular scaffolds, or as an immediate coverage for large trauma- or disease-associated skin defects[68]. However, their mechanisms of healing action remain speculative and well-controlled clinical trials are needed.

Preclinical studies of various synthetic materials are underway in which three-dimensional extracellular microenvironments are being used to mimic natural extracellular matrices[73]. For example, bioactive components, including heparin, cyclic Arg-Gly-Asp (RGD) adhesion peptides, and growth factors, have been integrated into polyethylene glycol (PEG)-based hydrogel matrices. Clinical studies will need to establish the physiologic relevance of these synthetic materials and their ability to encourage new tissue growth within wounds.

Wound Metabolism

Wound healing represents a metabolically demanding process and during the healing response cells have to adapt to their different metabolic requirements. In general, the resulting metabolites are regarded as waste products and cellular metabolism is viewed as necessary for controlling energy homeostasis. However, there is emerging evidence that metabolites have critical signaling functions and cellular metabolism is tightly linked to the orchestration of cell activation and function[74]. Enhanced understanding of how cell-intrinsic and -extrinsic metabolic changes are linked to wound healing will be important in the future as this could lead to the development of new diagnostic and therapeutic approaches that enforce endogenous repair mechanisms and normalize pathologic healing conditions[74].

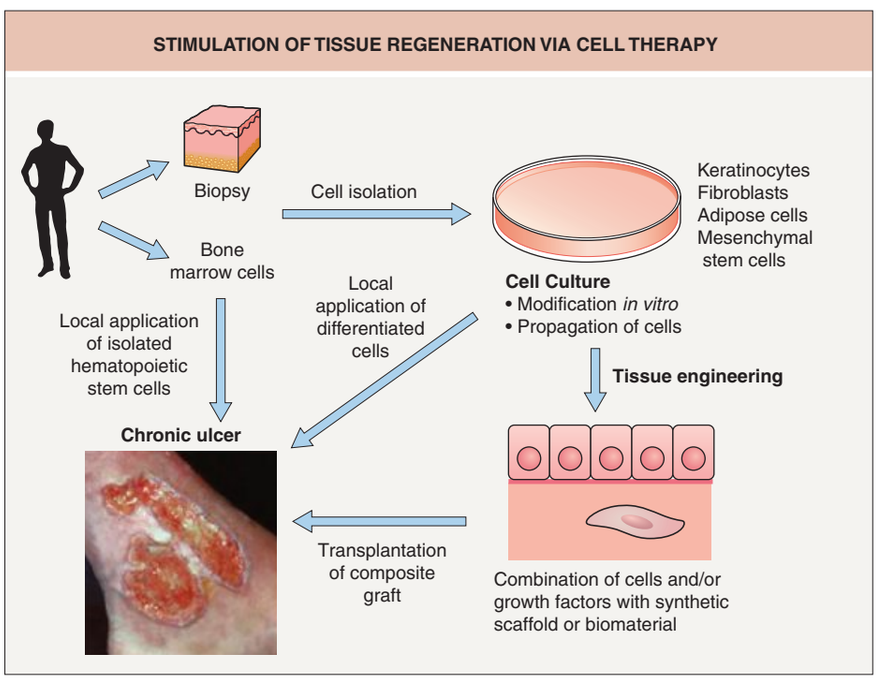


Fig. 141.10 Stimulation of tissue regeneration via cell therapy. Wounding stimulates the engraftment of bone marrow-derived stem/progenitor cells to the skin and induces bone marrow-derived cells to incorporate into skin structures. Therefore, bone marrow might provide a valuable source of stem cells for skin repair. Furthermore, differentiated cells can be isolated from skin biopsies, propagated and/or genetically modified *in vitro*, and either applied directly to the wound bed or combined with biologic/synthetic biomaterials to be applied as composite skin graft.

Advances in Systemic Drug Development

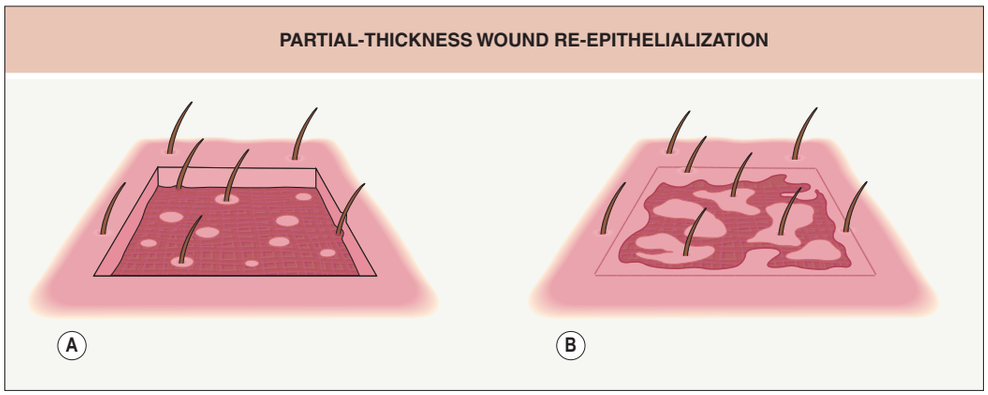
Chronic wounds and excessive tissue fibrosis are often symptoms of an underlying systemic disorder (e.g. vasculitis, pyoderma gangrenosum) or predisposing condition (e.g. older age). Over the past decade, there have been significant drug developments as well as an escalation in drug repurposing of immunomodulators (e.g. biologics, small molecules) and anti-aging medications (e.g. metformin, mTOR inhibitors). In other words, the efficacy of drugs that target a single cytokine or signaling pathway in several different organs (e.g. joints, gut, skin) has stimulated a shift from organ-based to molecular-based disease concepts[75]. Importantly, impaired cutaneous wound healing associated with inflammatory systemic disorders (e.g. vasculitic ulcers in rheumatoid arthritis, pyoderma gangrenosum) has been found to improve with cytokine-specific therapeutic strategies[16,75]. It is therefore likely that in the future patients with impaired wound healing will indirectly benefit from advances in drug development where the intended disease indications did not include enhanced wound healing.

Additional figures and tables on Chemical mediators of inflammation that play a role in wound healing and Different types of matrix metalloproteinases involved in wound repair, available in our eBook (see inside front cover for access code).

REFERENCES

1. Larson BJ, Longaker MT, Lorenz HP. Scarless fetal wound healing: a basic science review. *Plast Reconstr Surg*. 2010;126:1172–1180.
2. Goldman JA, Poss KD. Gene regulatory programmes of tissue regeneration. *Nat Rev Genet*. 2020;21:511–525.
3. Medzhitov R. The spectrum of inflammatory responses. *Science*. 2021;374:1070–1075.
4. Lavine KJ, Epelman S, Uchida K, et al. Distinct macrophage lineages contribute to disparate patterns of cardiac recovery and remodeling in the neonatal and adult heart. *Proc Natl Acad Sci*. 2014;111:16029–16034.
5. Shiraishi M, Shintani Y, Shintani Y, et al. Alternatively activated macrophages determine repair of the infarcted adult murine heart. *J Clin Invest*. 2016;126:2151–2166.
6. Eming SA, Hammerschmidt M, Krieg T. Interrelation of immunity and tissue repair or regeneration. *Semin Cell Dev Biol*. 2009;20:517–527.
7. Godwin JW, Pinto AR, Rosenthal NA, et al. Macrophages are required for adult salamander limb regeneration. *Proc Natl Acad Sci USA*. 2013;110:9415–9420.
8. Lin TY, Gerber T, Taniguchi-Sugiura Y, et al. Fibroblast dedifferentiation as a determinant of successful regeneration. *Dev Cell*. 2021;56:1541–1551. e6.
9. Richardson R, Slanchev K, Kraus C, et al. Adult zebrafish as a model system for cutaneous wound-healing research. *J Invest Dermatol*. 2013;133:1655–1665.
10. Lucas T, Waisman A, Ranjan R, et al. Differential roles of macrophages in diverse phases of skin repair. *J Immunol*. 2010;184:3964–3977.
11. Willenborg S, Lucas T, van Loo G, et al. CCR2 recruits an inflammatory macrophage subpopulation critical for angiogenesis in tissue repair. *Blood*. 2012;120:613–625.
12. Wong VW, Rustad KC, Akaishi S, et al. Focal adhesion kinase links mechanical force to skin fibrosis via inflammatory signaling. *Nat Med*. 2011;18:148–152.
13. Neufel DA, Zhao W. Bone regrowth after digit tip amputation in mice is equivalent in adults and neonates. *Wound Repair Regen*. 1995;3:461–466.
14. Rinkevich Y, Lindau P, Ueno H. Germ-layer and lineage-restricted stem/progenitors regenerate the mouse digit tip. *Nature*. 2011;476:409–413.
15. Lee LP, Lau PY, Chan CW. A simple and efficient treatment for fingertip injuries. *J Hand Surg*. 1995;20:63–71.
16. Eming SA, Martin P, Tomic-Canic M. Wound repair and regeneration: mechanisms, signaling, and translation. *Sci Transl Med*. 2014;6:265sr6.
17. Plikus MV, Wang X, Sinha S. Fibroblasts: origins, definitions, and functions in health and disease. *Cell*. 2021;184:3852–3872.
18. Capolupo L, Khven I, Lederer AR, et al. Sphingolipids control dermal fibroblast heterogeneity. *Science*. 2022;376:eabh1623.
19. Rodrigues M, Kosaric N, Bonham CA, et al. Wound healing: a cellular perspective. *Physiol Rev*. 2019;99:665–706.
20. Werner S, Krieg T, Smola H. Keratinocyte-fibroblast interactions in wound healing. *J Invest Dermatol*. 2007;127:998–1008.
21. Cox N, Pokrovskii M, Vicario R, Geissmann F, et al. Origins, biology, and diseases of tissue macrophages. *Annu Rev Immunol*. 2021;39:313–344.
22. Willenborg S, Sanin DE, Jais A, et al. Mitochondrial metabolism coordinates stage-specific repair processes in macrophages during wound healing. *Cell Metab*. 2021;S1550-4131:00482–00484.
23. Coulombe PA. Wound epithelialization: accelerating the pace of discovery. *J Invest Dermatol*. 2003;121:219–230.
24. Szabowski A, Maas-Szabowski N, Andrecht S, et al. c-Jun and JunB antagonistically control cytokine-regulated mesenchymal-epidermal interaction in skin. *Cell*. 2000;103:745–755.
25. Li A, Pouliot N, Redvers R, Kaur P. Extensive tissue-regenerative capacity of neonatal human keratinocyte stem cells and their progeny. *J Clin Invest*. 2004;113:390–400.
26. Morasso MI, Tomic-Canic M. Epidermal stem cells: the cradle of epidermal determination, differentiation and wound healing. *Biol Cell*. 2005;97:173–183.
27. Fuchs E, Blau HM. Tissue stem cells: architects of their niches. *Cell Stem Cell*. 2020;27:532–556.
28. Ito M, Liu Y, Yang Z, et al. Stem cells in the hair follicle bulge contribute to wound repair but not to homeostasis of the epidermis. *Nat Med*. 2005;11:1351–1354.
29. Mascré G, Dekoninck S, Drogat B, et al. Distinct contribution of stem and progenitor cells to epidermal maintenance. *Nature*. 2012;489:257–262.
30. Eming SA, Brachvogel B, Odorisio T, Koch M. Regulation of angiogenesis: wound healing as a model. *Prog Histochem Cytochem*. 2007;42:115–170.
31. Schiffmann LM, Werthenbach JP, Heintges-Kleinhofer F, et al. Mitochondrial respiration controls neoangiogenesis during wound healing and tumour growth. *Nat Commun*. 2020;11:3653.
32. Roy R, Zhang B, Moses MA. Making the cut: protease-mediated regulation of angiogenesis. *Exp Cell Res*. 2006;312:608–622.
33. Chen HX, Cleck JN. Adverse effects of anticancer agents that target the VEGF pathway. *Nat Rev Clin Oncol*. 2009;6:465–477.
34. Gillitzer R, Goebeler M. Chemokines in cutaneous wound healing. *J Leukoc Biol*. 2001;69:513–521.
35. Nathan C. Neutrophils and immunity: challenges and opportunities. *Nat Rev Immunol*. 2006;6:173–182.
36. Henson PM, Vandivier RW. The matrix degrades, neutrophils invade. *Nat Med*. 2006;12:280–281.
37. Kuijpers TW, Van Lier RA, Hamann D, et al. LAD1/variant. A novel immunodeficiency syndrome characterized by dysfunctional beta2 integrins. *J Clin Invest*. 1997;100:1725–1733.
38. Roos D, Kuijpers TW, Mascart-Lemone F, et al. A novel syndrome of severe neutrophil dysfunction: unresponsiveness confined to chemotaxis-induced functions. *Blood*. 1993;81:2735–2743.
39. Gawronska-Kozak B, Bogacki M, Rim JS, et al. Scarless skin repair in immunodeficient mice. *Wound Repair Regen*. 2006;14:265–276.
40. Leibovich SJ, Ross R. The role of the macrophage in wound repair. *Am J Pathol*. 1975;78:71–100.
41. Gordon S. Alternative activation of macrophages. *Nature*. 2003;3:23–35.
42. Karin M, Lawrence T, Nizet V. Innate immunity gone awry: linking microbial infections to chronic inflammation and cancer. *Cell*. 2006;124:823–835.
43. Askenase MH, Goods BA, Beatty HE, et al. Longitudinal transcriptomics define the stages of myeloid activation in the living human brain after intracerebral hemorrhage. *Sci Immunol*. 2021;6:eabd6279.
44. Fishel RS, Barbul A, Beschorner WE, et al. Lymphocyte participation in wound healing: morphologic assessment using monoclonal antibodies. *Ann Surg*. 1987;206:25–29.
45. Park JE, Barbul A. Understanding of the role of immune regulation in wound healing. *Am J Surg*. 2004;187:11S–16S.
46. Willenborg S, Eckes B, Brinckmann J, et al. Genetic ablation of mast cells redefines the role of mast cells in skin wound healing and bleomycin-induced fibrosis. *J Invest Dermatol*. 2014;134:2005–2015.
47. Hinz B. Formation and function of the myofibroblast during tissue repair. *J Invest Dermatol*. 2007;127:526–537.
48. Györfi A-H, Matei A-E, Fuchs M, et al. Engrailed 1 coordinates cytoskeletal reorganization to induce myofibroblast differentiation. *J Exp Med*. 2021;218:e20201916.
49. Tomasek JJ, Gabbiani G, Hinz B, et al. Myofibroblasts and mechano-regulation of connective tissue remodelling. *Nat Rev Mol Cell Biol*. 2002;3:349–363.
50. Bayat A, McGrouther DA, Ferguson MW. Skin scarring. *BMJ*. 2003;326:88–92.
51. Kørbling M, Estrov Z. Adult stem cells for tissue repair – a new therapeutic concept? *N Engl J Med*. 2003;349:570–582.
52. Badiavas EV, Abedi M, Butmarc J, et al. Participation of bone marrow derived cells in cutaneous wound healing. *J Cell Physiol*. 2003;196:245–250.
53. Krause DS, Theise ND, Collector MI, et al. Multi-organ, multi-lineage engraftment by a single bone marrow-derived stem cell. *Cell*. 2001;105:369–377.
54. Cha J, Falanga V. Stem cells in cutaneous wound healing. *Clin Dermatol*. 2007;25:73–78.
55. Werner S, Grose R. Regulation of wound healing by growth factors and cytokines. *Physiol Rev*. 2003;83:835–870.
56. Schäfer M, Werner S. Transcriptional control of wound repair. *Annu Rev Cell Dev Biol*. 2007;23:69–92.
57. Aszódi A, Legate KR, Nakchbandi I, Fässler R. What mouse mutants teach us about extracellular matrix function. *Annu Rev Cell Dev Biol*. 2006;22:591–621.
58. Habashi JP, Judge DP, Holm TM, et al. Losartan, an AT1 antagonist, prevents aortic aneurysm in a mouse model of Marfan syndrome. *Science*. 2006;312:117–121.
59. Hynes RO. Integrins: bidirectional, allosteric signaling machines. *Cell*. 2002;110:673–687.
60. Legate KR, Wickström SA, Fässler R. Genetic and cell biological analysis of integrin outside-in signaling. *Genes Dev*. 2009;23:397–418.
61. Barrick B, Campbell EJ, Owen CA. Leukocyte proteinases in wound healing: roles in physiologic and pathologic processes. *Wound Repair Regen*. 1999;7:410–422.
62. Weiss SJ. Tissue destruction by neutrophils. *N Engl J Med*. 1989;320:365–376.
63. Chen P, Parks WC. Role of matrix metalloproteinases in epithelial migration. *J Cell Biochem*. 2009;108:1233–1243.
64. Ding X, Kakanj P, Leptin M, Eming SA. Regulation of the wound healing response during aging. *J Invest Dermatol*. 2021;141:1063–1070.
65. Rudolph KL, Chang S, Lee HW, et al. Longevity, stress response, and cancer in aging telomerase-deficient mice. *Cell*. 1999;96:701–712.
66. Gannon HS, Donehower LA, Lyle S, Jones SN. Mdm2-p53 signaling regulates epidermal stem cell senescence and premature aging phenotypes in mouse skin. *Dev Biol*. 2011;353:1–9.
67. Singer A, Dagum AB. Current management of acute cutaneous wounds. *N Engl J Med*. 2008;359:1037–1046.
68. Rennert RC, Rodrigues M, Wong VW, et al. Biological therapies for the treatment of cutaneous wounds: phase III and launched therapies. *Expert Opin Biol Ther*. 2013;13:1523–1541.
69. Otero-Viñas M, Falanga V. Mesenchymal stem cells in chronic wounds: the spectrum from basic to advanced therapy. *Adv Wound Care (New Rochelle)*. 2016;5:149–163.
70. Kawamura A, Horie T, Tsuda I, et al. Clinical study of therapeutic angiogenesis by autologous peripheral blood stem cell (PBSC) transplantation in 92 patients with critically ischemic limbs. *J Artif Organs*. 2006;9:226–233.
71. Bilousova G, Roop DR. Induced pluripotent stem cells in dermatology: potentials, advances, and limitations. *Cold Spring Harb Perspect Med*. 2014;4:a015164.

72. Roth D, Piekarek M, Paulsson M, et al. Plasmin modulates vascular endothelial growth factor-A-mediated angiogenesis during wound repair. *Am J Pathol*. 2006;168:670–684.
73. Lutolf MP, Hubbell JA. Synthetic biomaterials as instructive extracellular microenvironments for morphogenesis in tissue engineering. *Nat Biotechnol*. 2005;23:47–55.
74. Eming SA, Murray PJ, Pearce EJ, et al. Metabolic orchestration of the wound healing response. *Cell Metab*. 2021;33:1726–1743.
75. Schett G, McInnes IB, Neurath MF. Reframing immune-mediated inflammatory diseases through signature cytokine hubs. *N Engl J Med*. 2021;385:628–639.
76. Demaria M, Ohtani N, Youssef SA, et al. An essential role for senescent cells in optimal wound healing through secretion of PDGF-AA. *Dev Cell*. 2014;31:722–733.
77. Plikus MV, Guerrero-Juarez CF, Ito M, et al. Regeneration of fat cells from myofibroblasts during wound healing. *Science*. 2017;355:748–752.



eFig. 141.1 Partial-thickness wound re-epithelialization. A The red area is the wound bed and the pink areas within the wound bed represent remaining adnexal structures; the latter serve as a source of keratinocytes. **B** Over a period of several days after wounding, cells migrate from both the wound edges and the adnexal structures, eventually leading to re-epithelialization. *Courtesy Robert S. Kirsner, MD.*



eFig. 141.2 Tertiary intention healing. A Dehiscence of a surgical excision that was closed primarily. **B** Same wound 1 month later, following second intention healing. *Courtesy Robert S. Kirsner, MD.*

DIFFERENT TYPES OF MATRIX METALLOPROTEINASES INVOLVED IN WOUND REPAIR	
Enzyme	**MMP number**
Collagenase-1	MMP-1
Collagenase-2	MMP-8
Collagenase-3	MMP-13
Collagenase-4	MMP-18
Stromelysin-1	MMP-3
Stromelysin-2	MMP-10
Stromelysin-3	MMP-11
Gelatinase-A	MMP-2
Gelatinase-B	MMP-9
Matrilysin	MMP-7
Macrophage metalloproteinase (elastase)	MMP-12
MT1-MMP	MMP-14

eTable 141.2 Different types of matrix metalloproteinases (MMPs) involved in wound repair. MT1, membrane-type 1.

CHEMICAL MEDIATORS OF INFLAMMATION THAT PLAY A ROLE IN WOUND HEALING	
Chemical mediator	**Action**
Histamine	Increased vascular permeability
Serotonin	Stimulation of fibroblast proliferation Cross-linking of collagen molecules
Kinins	Increased vascular permeability
Prostaglandins	Increased vascular permeability
	Sensitize pain receptors
	Increased synthesis of GAGs
Complement	Increased vascular permeability
	Increased phagocytosis
	Enhanced bacterial lysis
	Mast cell and basophil activation

eTable 141.1 Chemical mediators of inflammation that play a role in wound healing. GAGs, glycosaminoglycans.

142 Surgical Anatomy of the Head and Neck

Franklin P. Flowers, Charya B. Goldsmith and Matthew Steadmon

Chapter Contents

Topographic Anatomy of the Head and Neck 2464
Skin Tension Lines 2465
Cosmetic Subunits 2467
Free Margins 2467
The Superficial Musculoaponeurotic System 2469
Muscles of Facial Expression 2471
Vascular Anatomy 2473
The Facial Nerve 2474
Sensory Innervation of the Head and Neck 2476
Lymphatic Drainage of the Head and Neck 2477

Key features

- The muscles of facial expression all arise from the second branchial arch, are concentrated in the central facial region, and receive their motor innervation from the facial nerve (cranial nerve VII)
- The superficial musculoaponeurotic system (SMAS) is a fibromuscular layer that ensheathes and connects the facial muscles and plays an intricate role in coordinating facial expressions
- The SMAS can be utilized as a guide to dissection, tissue mobilization, and closure, thereby minimizing trauma to neurovascular tissues
- The three branches of the trigeminal nerve (cranial nerve V) provide sensory innervation to the face, while various branches of the cervical plexus provide sensory innervation to the neck, parts of the ear, and posterior scalp
- Familiarity with the muscular and neurovascular structures of the head and neck region allows the surgeon to properly approach the "danger zones", e.g. Erb's point in the neck, the temporal nerve as it crosses the zygomatic arch, and the marginal mandibular nerve at the jawline just anterior to the masseter muscle
- The rich and anastomosing vascular supply of the face and scalp, derived from both the external and internal carotid arteries, explains the excellent healing potential and viability of local flaps and grafts in this region
- Cosmetic subunits and the junction lines separating them should be considered when planning excisions, repairs, and cosmetic procedures of the head and neck

The dermatologic surgeon must have a comprehensive knowledge of regional anatomy in order to obtain acceptable operative results. Proper tissue movement on the face and neck is essential for obtaining closures that are under minimal tension without cosmetic distortion or functional loss of vital structures. In addition to reducing postoperative morbidity, a fundamental appreciation for the macromechanics of the head and neck leads to preservation of tissue viability as well as sensory and motor innervation[1,2]. The fascial planes, vascular supply, innervation, and cosmetic subunits of the face must be considered when planning a surgical or cosmetic procedure. In order to accurately and thoroughly counsel patients regarding procedural risks and benefits, the surgeon must have a thorough appreciation of head and neck anatomy.

TOPOGRAPHIC ANATOMY OF THE HEAD AND NECK

It is possible to pinpoint underlying anatomic structures of the head and neck by observing surface anatomy. The bony structure of the face serves as a simple anatomic framework (Fig. 142.1). The supraorbital ridges are formed by the frontal bone and are more prominent in men. The supraorbital foramen transmits the supraorbital nerve (from the ophthalmic division of the trigeminal nerve) and its associated artery and vein. This foramen is palpable on the bony supraorbital ridge at the vertical midpupillary line. This line lies approximately one fingerbreadth lateral to the lateral nasal root or 2.5 cm lateral of the midline on the face (Fig. 142.2). Other important foramina lie in this midpupillary line and transmit important neurovascular bundles. The infraorbital foramen is located 1 cm below the infraorbital rim in the midpupillary line. It transmits the infraorbital nerve (from the maxillary division of the trigeminal nerve) and its associated artery and vein. The mental foramen lies in the same vertical line in the midportion of the mandible. The mental neurovascular bundle emerges here as a terminal sensory branch of the mandibular division of the trigeminal nerve.

The anterior border of the temporalis muscle can be palpated in the temporal fossa above the zygomatic bone. The latter bone forms the malar eminence of the cheek. The buccal fat pad provides fullness to the cheek; elderly or cachectic patients often have very prominent zygomatic arches. These arches form the widest points on the face and serve as the point of attachment for several muscles of facial expression and for the masseter muscle. The masseter muscle spans the zygomatic arch and mandibular ramus, serving as a muscle of mastication innervated by a motor branch of the trigeminal nerve (see below). This muscle is easily palpated by clenching the jaw.

The parotid gland lies beneath the subcutaneous fat of the lateral cheek and is invested by parotid fascia. The superficial lobe of the parotid covers the posterior half of the masseter muscle and extends from the preauricular sulcus to the angle of the mandible. The deep lobe lies on the medial side of the ramus of the mandible and is connected to the superficial lobe by an isthmus. The superficial temporal artery and vein, as well as branches of the facial nerve (which provides motor innervation to the muscles of facial expression), course through the parotid gland in channels between glandular tissue[3]. The duct of the parotid gland (Stensen's duct) travels across the anterior surface of the masseter muscle (Fig. 142.3). After crossing the muscle surface, the duct penetrates deeper to pierce the buccinator muscle and eventually drains into the mouth at the level of the second upper molar. It can be palpated as a "cord" crossing a clenched masseter muscle. If the duct is transected, a chronic draining fistula will form, requiring corrective surgical intervention. Stensen's duct can be identified topographically by drawing a line between the tragus and the midportion of the cutaneous upper lip. The duct traverses the masseter muscle at the middle one-third of this line (see Fig. 142.3).

Several structures of importance can be located by observing the surface anatomy of the neck. The sternocleidomastoid muscle is comprised of two heads originating from the sternum and the medial one-third of the clavicle. It inserts onto the outer surface of the mastoid process and nuchal ridge, dividing the neck into anterior and posterior triangles. A dermatologic surgeon should be familiar with the anatomic structures that lie within each of these topographic triangles. Although the sternocleidomastoid muscle covers and protects most of the major anatomic structures in the neck, the external jugular vein traverses its surface with many cutaneous sensory nerves of the cervical plexus (Fig. 142.4). In addition, the posterior triangle of the neck contains trunks of the brachial and cervical plexus as well as the spinal accessory

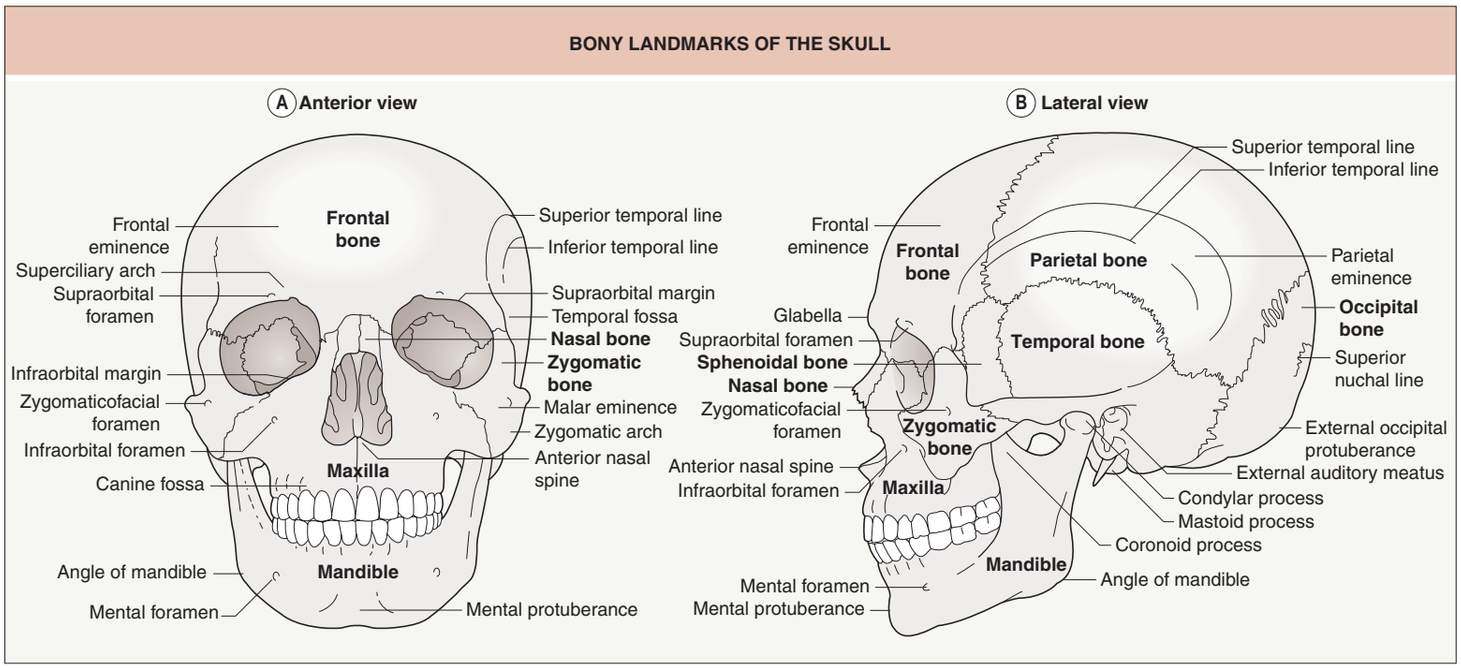


Fig. 142.1 Bony landmarks of the skull. A Anterior view. **B** Lateral view.

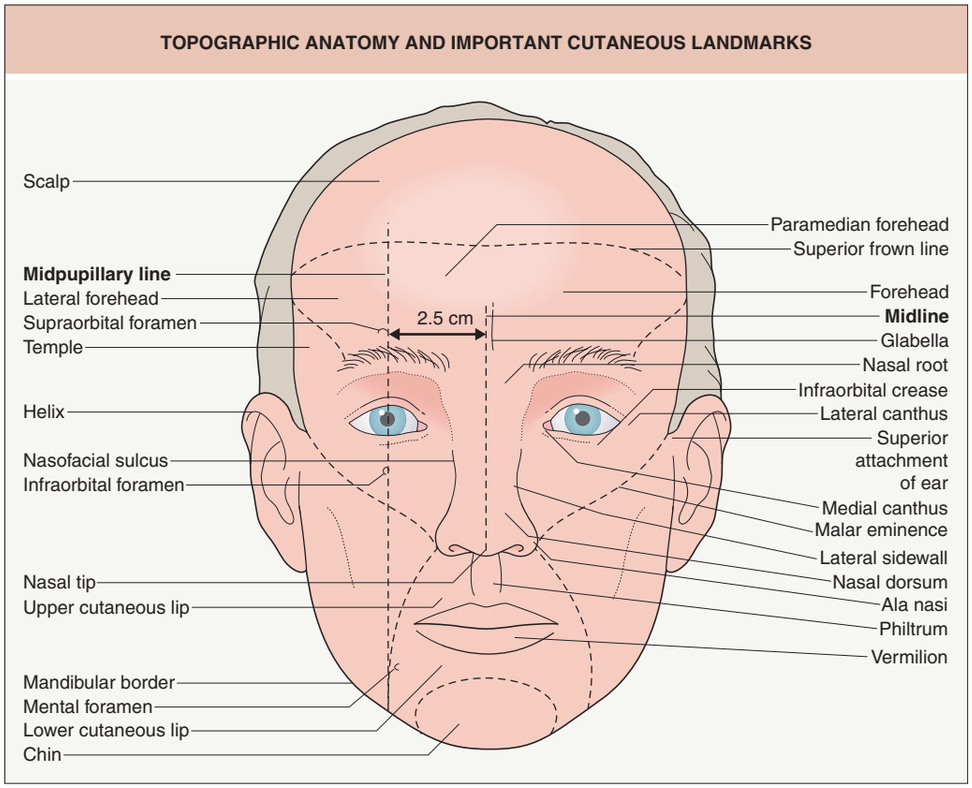


Fig. 142.2 Topographic anatomy and important cutaneous landmarks.

nerve (cranial nerve XI). Cranial nerve XI innervates the trapezius muscle of the back. It may be damaged when operating in the posterior triangle. This may result in chronic shoulder and neck pain, shoulder drop and trapezius atrophy, "winged" scapula, arm paresthesias, and the inability to abduct the arm greater than 80°.

Erb's point designates the area where the cervical plexus emerges from the posterior margin of the sternocleidomastoid muscle (see Figs. 142.4 & 151.6). The spinal accessory nerve also courses through this area on its way to the trapezius muscle (see Fig. 142.4). This surgical danger zone can be visualized by drawing a line connecting the angle of the jaw to the mastoid process. In an adult, a perpendicular line dropped 6 cm from the midpoint of this connector will intersect the posterior border of the sternocleidomastoid where the spinal accessory nerve and cervical plexus emerge[4]. Extreme caution is warranted when dissecting around these anatomic structures, in order to avoid loss of innervation to the trapezius muscle.

SKIN TENSION LINES

Collagen and elastin afford flexibility and extensibility to the skin, and derangements of their architecture or abundance contribute to the aging process. Wrinkles (rhytides) develop over time in predictable areas on

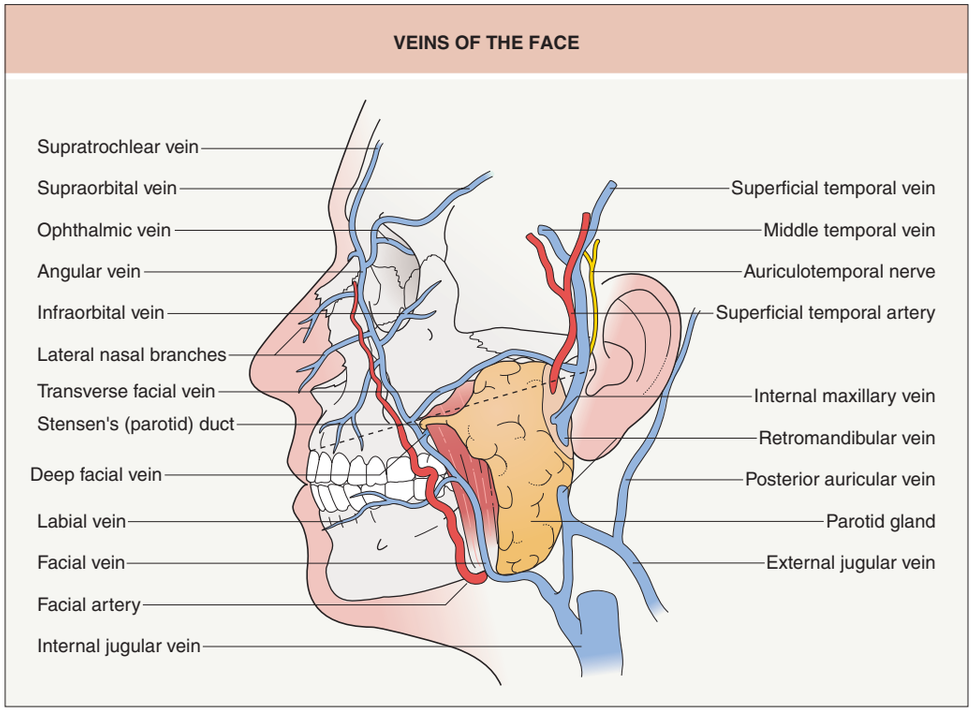


Fig. 142.3 Veins of the face. Stensen's duct can be identified topographically by drawing a line between the tragus and midportion of the cutaneous upper lip (dotted line). It can be palpated as a cord at the middle third of this line.

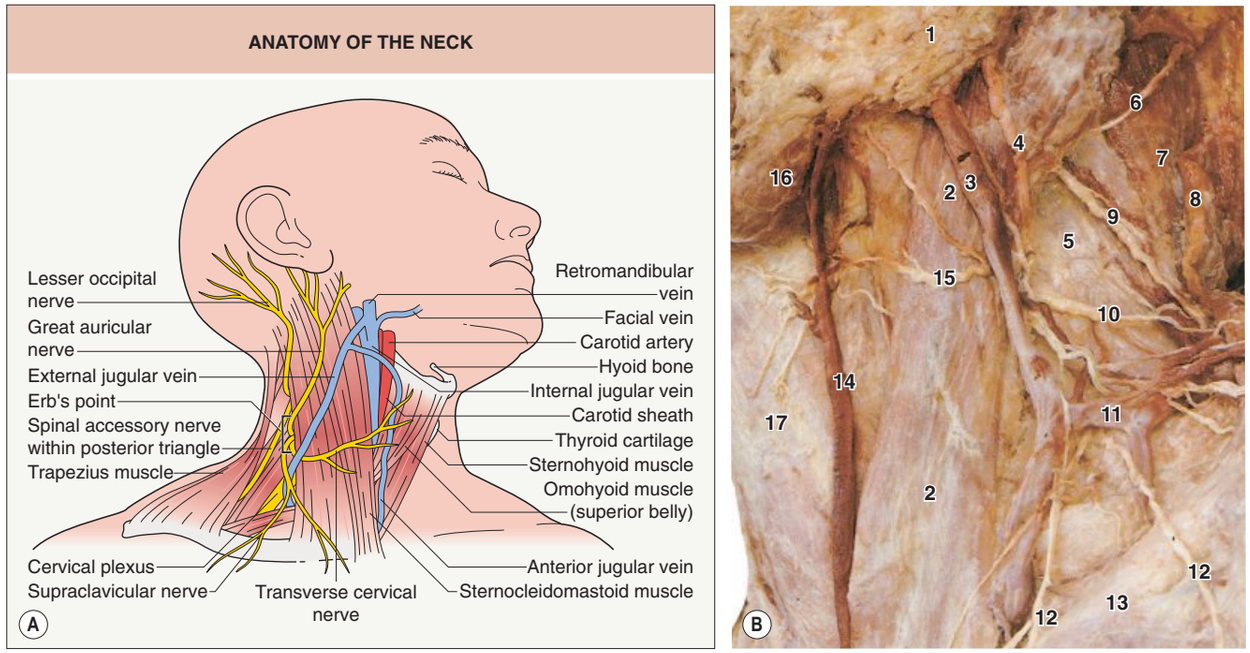


Fig. 142.4 Anatomy of the neck. A The sternocleidomastoid muscle (SCM) divides the neck into anterior and posterior triangles; Erb's point designates the area where the cervical plexus emerges from the posterior margin of the SCM. **B** The platysma was removed completely and the investing layer of deep cervical fascia was removed only from the posterior triangle. The following structures are identified: 1, parotid gland; 2, sternocleidomastoid muscle; 3, external jugular vein; 4, great auricular nerve; 5, prevertebral fascia overlying levator scapulae muscle; 6, lesser occipital nerve; 7, splenius capitis muscle; 8, trapezius muscle; 9, spinal accessory nerve; 10, cervical nerves to the trapezius; 11, superficial cervical vein; 12, supraclavicular nerves; 13, clavicle; 14, anterior jugular vein; 15, transverse cervical nerve; 16, submandibular gland; and 17, investing layer of deep cervical fascia. *B, From Logan B, Reynolds P, Rice S, Hutchings R. McMinn's Color Atlas of Head and Neck Anatomy. 5th ed. Neck superficial dissection II. London: Elsevier; 2017.*

the face. The fine wrinkles seen on an aged face may be referred to as the skin tension lines (Fig. 142.5); on the body, skin tension lines are an important consideration when designing surgical excisions (Fig. 142.6). Many environmental and intrinsic factors, such as ultraviolet exposure, smoking, underlying facial muscles, etc., contribute to the appearance of the expressive human face. A thorough understanding of the derivation and implications of skin tension lines is essential to successful dermatologic surgery.

Continuous tension is exerted on the skin of the head and neck by the muscles of facial expression. A complicated network composed of muscles, elastin, fibrous septae of collagen, and fascial planes contributes to this stress, which eventually results in sagging, wrinkling, and redundant skin. Collagen is flexible but much less extensible than elastic fibers. The resistance to tensile forces by collagen promotes a "youthful" appearance. Over time, the prolonged tension exerted on the skin from many factors forces collagen fibrils to accommodate by way of elongation. Eventually, aged skin manifests the consequences of persistent skin tension. The collagenous tissue becomes increasingly intertwined, diminished in volume, and permanently elongated. This causes the accentuation of skin tension lines[4].

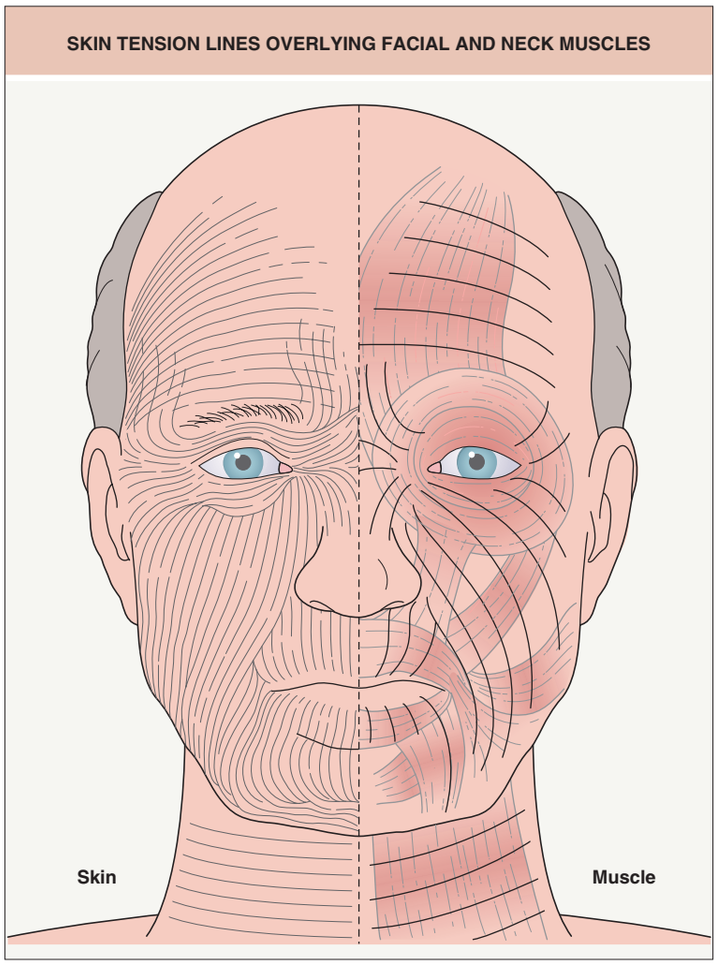


Fig. 142.5 Skin tension lines overlying facial and neck muscles. Note that wrinkles are often directed perpendicularly to the underlying muscle fibers of facial expression.

Elastic fibers promote extensibility (i.e. the ability of skin to stretch) and elasticity (i.e. the skin's capacity to restore its original shape after physical stress). They contribute to the skin tension lines by promoting vector distribution of tension along fascial planes. The elastic properties of the skin explain the phenomenon whereby round surgical wounds relax into an axis parallel to the patient's wrinkles. Tension vectors are increased parallel to the skin tension lines and are diminished perpendicular to them; therefore, the linear appearance of wrinkles is often directed perpendicularly to the underlying muscle fibers of facial expression (see Fig. 142.5). The continuous tension exerted on the overlying skin by these muscles challenges the competency of elastic tissue and collagen. They induce this geometric linearity via fibrous connections to the dermis via the SMAS. For example, the forehead undergoes transverse wrinkling due to contractions of the frontalis muscle, whose fibers run in a cephalocaudad direction. Periocular rhytides are often radially oriented due to underlying contraction of the orbicularis oculi. Similarly, perioral wrinkling occurs under the influence of the concentric orbicularis oris muscle, which induces a radial arrangement of skin tension lines. The procerus muscle causes transverse nasal root lines, and vertical glabellar lines are determined by the corrugator supercilii muscles (Fig. 142.7).

Knowledge of these functional anatomic principles is necessary in surgical and cosmetic dermatology. For example, the successful use of botulinum toxin for the diminution of rhytides requires an understanding of the anatomic relationships between various muscle groups and their influence on the skin tension lines. Proper surgical technique entails placement of incision lines parallel to the skin tension lines in order to achieve excellent cosmesis. It is helpful to determine and even sketch the patient's skin tension lines with a surgical marking pen. This will help orient the axis of incision and guide the closure parallel to, and preferably "buried" within, individual lines of tension.

COSMETIC SUBUNITS

Cosmetic units (i.e. aesthetic, topographic, or regional units) represent the major structural areas of the face that are separated by contour or junctional lines or boundaries (Fig. 142.8). Units are designated based upon their similarity in topographic anatomy, texture and color, solar exposure, hair density, and sebaceous features. The forehead, temples, eyelids, nose, cheeks, upper and lower lips, chin, and ears represent the major cosmetic subunits of the face. Within each division, smaller units are designated that further guide surgical closures. The junctional or contour lines between cosmetic units serve as excellent locations to place incisions and hide surgical scars. They include the hairline, alar and nasolabial creases, eyebrows, the philtrum, the labiomental crease, and the upper and lower vermilion–cutaneous interfaces (see Figs. 142.2 & 142.12).

In general, defects should be repaired with tissue from within the same cosmetic unit in order to preserve topographic consistency and to match skin color and texture. If this cannot be achieved, it is reasonable to utilize tissue from an adjacent aesthetic unit, which will most closely match the skin of the recipient cosmetic unit. The goal is to optimize the match in skin texture, color, actinic damage, and thickness. Scars that cross aesthetic units and boundary lines are obvious and often cosmetically unacceptable. A primary goal of cutaneous surgery is to "respect" the cosmetic subunits.

An appreciation for cosmetic units and contour lines also helps the surgeon determine areas of "recruitable" tissue for closures. Redundant or freely mobile skin can be mobilized from the preauricular folds, neck, nasolabial folds, temple, glabella, the lower and lateral cheeks, and the "jowls"[5]. The potential for such tissue recruitment depends on the patient's age, degree of actinic damage, and skin elasticity. Areas of redundancy or high elasticity may serve as excellent donor sites within or adjacent to the cosmetic subunit which contains a given surgical defect. For example, cheek advancement flaps and temple to lateral forehead advancement and rotation flaps are frequently used for defect repairs.

The forehead unit can be divided into the glabella, temple, and supra-eyebrow aesthetic subunits. The transverse creases of this region serve as excellent sites to place cosmetically acceptable incisional scars. The eyelids represent a major cosmetic subunit of the face whose subdivisions correspond to portions of the orbicularis oculi muscles[6] (Fig. 142.9). The inferior pretarsal portion of the upper eyelid is relatively fixed, while the preseptal unit becomes increasingly redundant with age. Over time, progressive laxity of the preseptal unit can cause functional visual impairment in some patients. It is the preseptal unit of the palpebral portion of the lid that is reduced in a blepharoplasty. The infraorbital crease lies between the lower eyelid and the upper cheek.

Nasal cosmetic subunits include the alar groove (which defines the ala nasi) and the columella, which extends from the nasal tip to the junction with the upper cutaneous lip. The root, dorsum, lateral sidewalls, soft triangles, and nasal tip are important landmarks that pose a significant challenge in dermatologic surgery (Fig. 142.10). The nasal tip unit forms the shape of a chevron or heart due to the anatomy of the nasal cartilage (Fig. 142.11). When possible, surgical defects should be contained within the boundaries of a given nasal subunit in order to produce acceptable cosmesis[7].

The philtrum is located above the upper vermilion lip and extends superiorly to the columella of the nose (Fig. 142.12). Because it is a midline structure, even minimal anatomic distortion results in a poor cosmetic outcome. The vermilion lip extends from the vermilion lip–cutaneous junction to the mucous membrane junction. It is a modified epithelium that usually does not contain adnexal structures or salivary glands. Approximation of the vermilion border is crucial to maintaining facial symmetry. The melolabial or nasolabial crease serves as a useful landmark that separates the cheek from the mouth and chin aesthetic units. It is an ideal place to hide suture lines and often serves as a generous donor site for repairs.

The external ear (auricle or pinna) consists of a single cartilaginous plate that results in the complex curves and folds of the ear (Fig. 142.13). The skin is loose on the posterior portion but tightly adherent on the anterior surface.

FREE MARGINS

Free margins of the face are anatomic structures that are in some way discontinuous with adjacent skin. They include the lips, helices, eyelids,

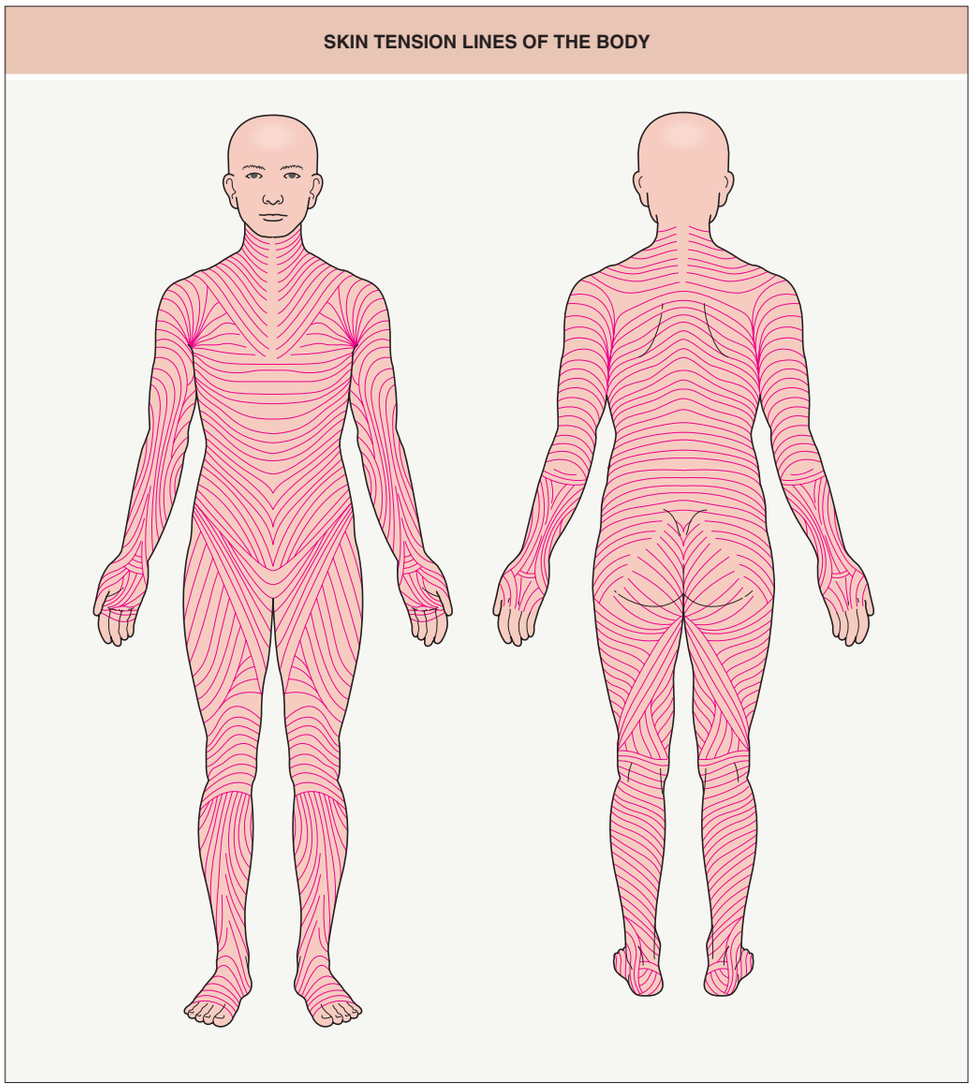


Fig. 142.6 Skin tension lines of the body. See Fig. 142.5 for the skin tension lines of the face and neck.

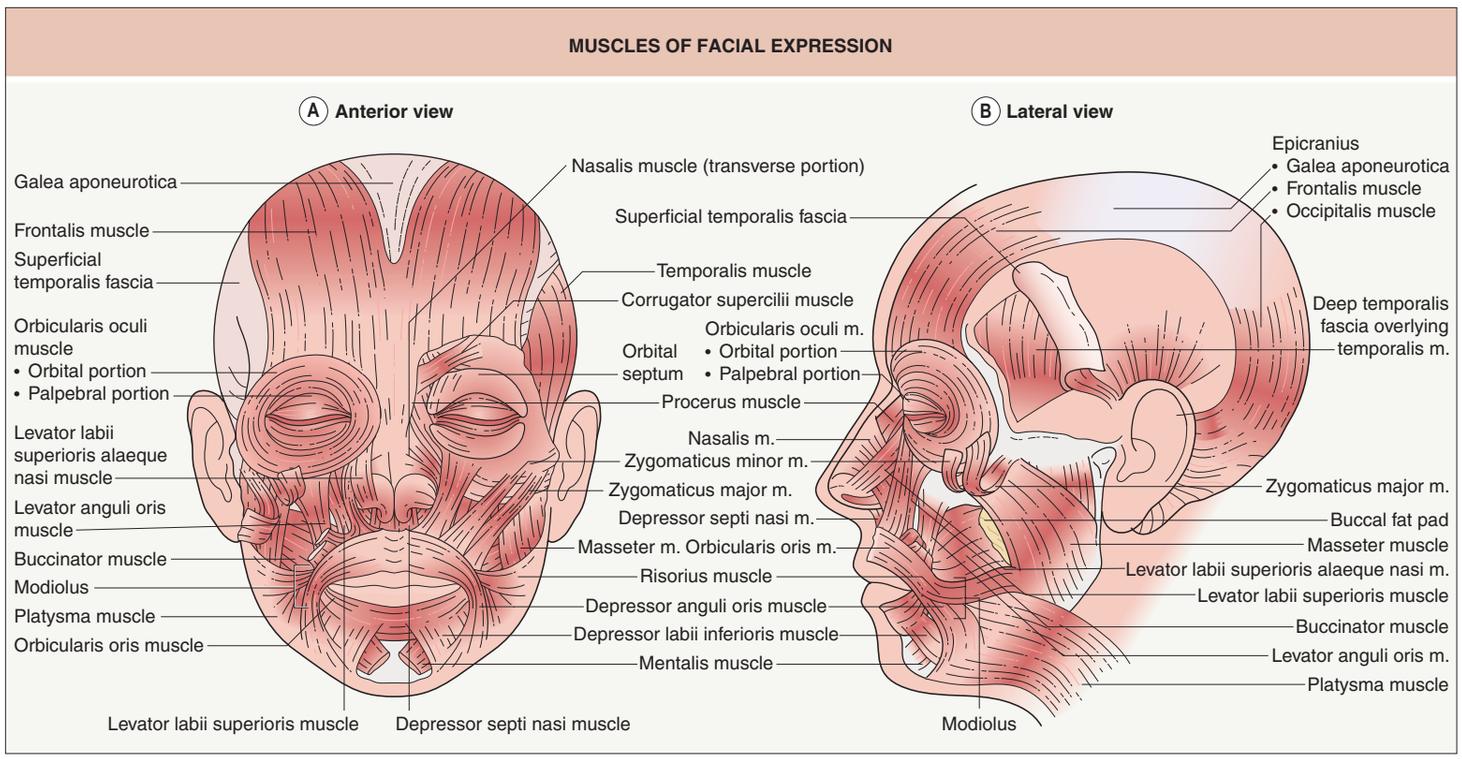


Fig. 142.7 Muscles of facial expression. A Anterior view. **B** Lateral view. The transverse portion of the nasalis muscle is identified. m, muscle.

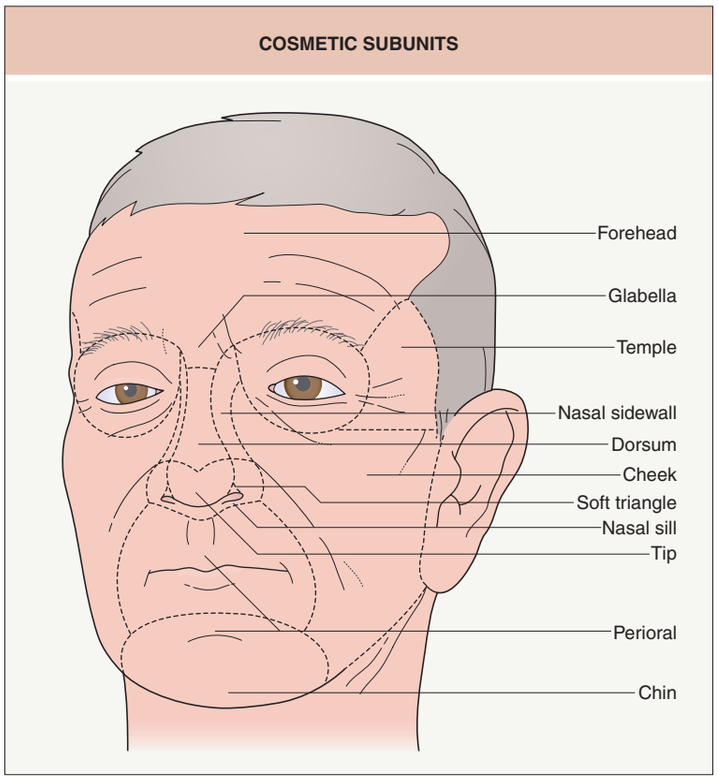


Fig. 142.8 Cosmetic subunits.

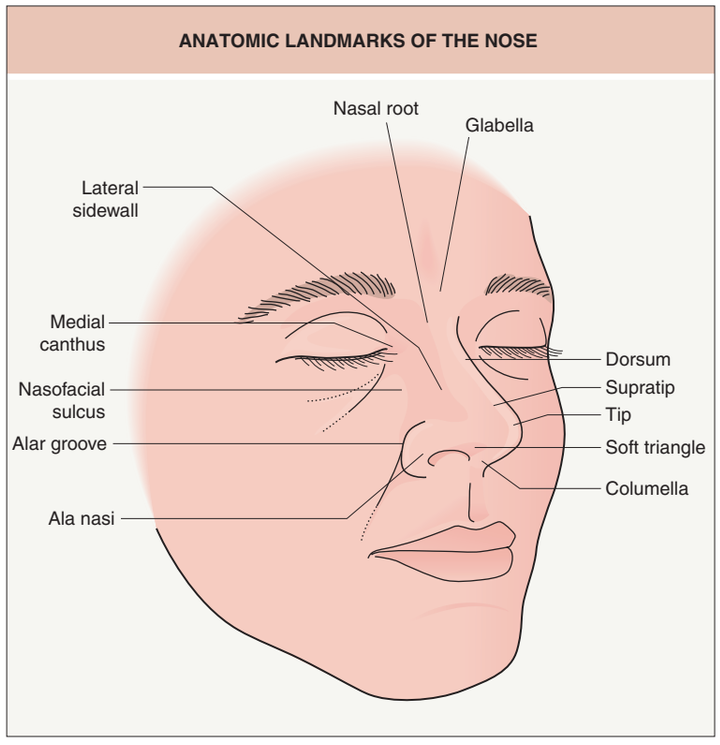


Fig. 142.10 Anatomic landmarks of the nose.

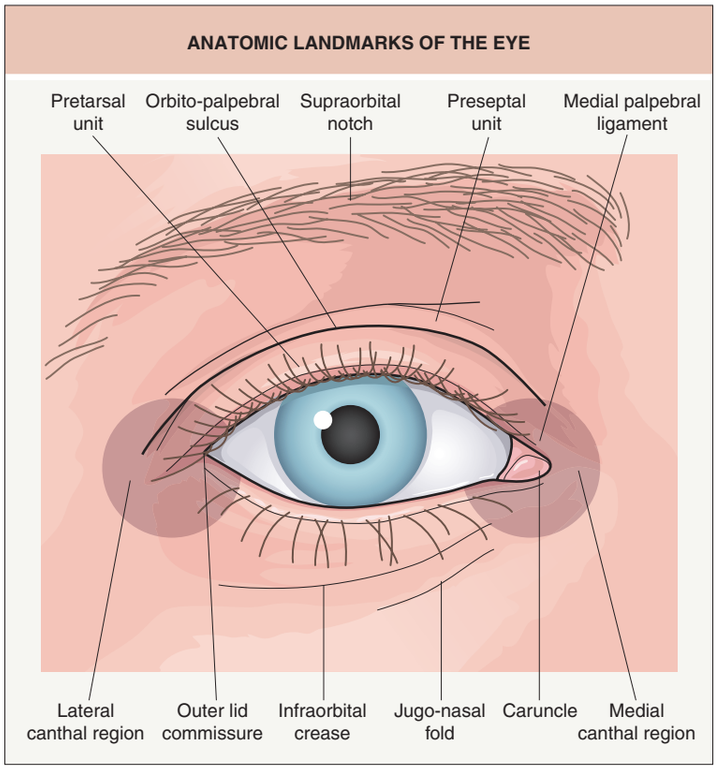


Fig. 142.9 Anatomic landmarks of the right eye.

and nostrils. These areas deserve special attention from the dermatologic surgeon because they do not have evenly distributed tension vectors. This characteristic makes the free margins especially vulnerable to any iatrogenic directional pull. Surgical closures, wound healing, and scar contraction can cause these free margins to lose their cosmetic or functional integrity. Ectropion (eyelid eversion) or eclabium (lip eversion) may ensue. Primary elliptical closures that are parallel to a free margin and second intention healing are not frequently used in these areas.

The opposing force inflicted upon a free margin depends on closure axis orientation, flap or graft design, and the tensile strength and elasticity of the skin. Aged skin is often less able to resist directional vectors. The lower eyelid often becomes especially lax with cumulative actinic damage and age. The "pinch" or "snap" test can be used in free margin evaluation by gently pulling the lower lid away from the eye. Upon release, a competent lower lid should assume its original shape against the globe, while a lax lid will regain its configuration slowly[4]. Instruct the patient to open his or her mouth and gaze upwards while simulating closure options under the eye. This generates the maximum intraoperative tension on the lower eyelid and can help to estimate the risk for distortion of this free margin. No more than 2 mm of inferior pull or "drag" on the lower eyelid can generally be tolerated during cutaneous surgical repairs. Any additional inferior tension puts the patient at high risk for ectropion[8].

Maintenance of cosmesis and function of the lip vermilion is of utmost importance. Elliptical closures often create drag on these free margins, but careful redirection of tension vectors may allow simple closures here. Flaps that can be performed in this area are reviewed in Chapter 147. Although the helical rims are free margins, they are far more "forgiving" than the aforementioned sites. Second intention healing and axial elliptical closures can achieve excellent results on the ear. The tissue is easily dissected and the posterior auricular skin provides excellent mobility. Most patients have some ear asymmetry at baseline, thus making this free margin less cosmetically sensitive.

The nasal tip, alae, and adjacent lateral sidewall require special consideration due to their classification as "free margins" and the underlying cartilage framework that prevents significant tissue mobility. Elevation and distortion of the nasal rim may occur if second intention healing or simple primary closure is attempted (see Fig. 148.9). Full-thickness skin grafts and transposition or rotation flaps from adjacent areas are particularly appealing repairs in this cosmetically sensitive area[9].

THE SUPERFICIAL MUSCULOAPONEUROTIC SYSTEM

The superficial musculoaponeurotic system (SMAS) or superficial fascia of the head and neck region plays an intricate role in coordinating and exaggerating facial expressions. It is a fibromuscular layer that ensheathes and connects the facial muscles. When the regional muscles contract, their impulse is distributed by the SMAS via fibrous

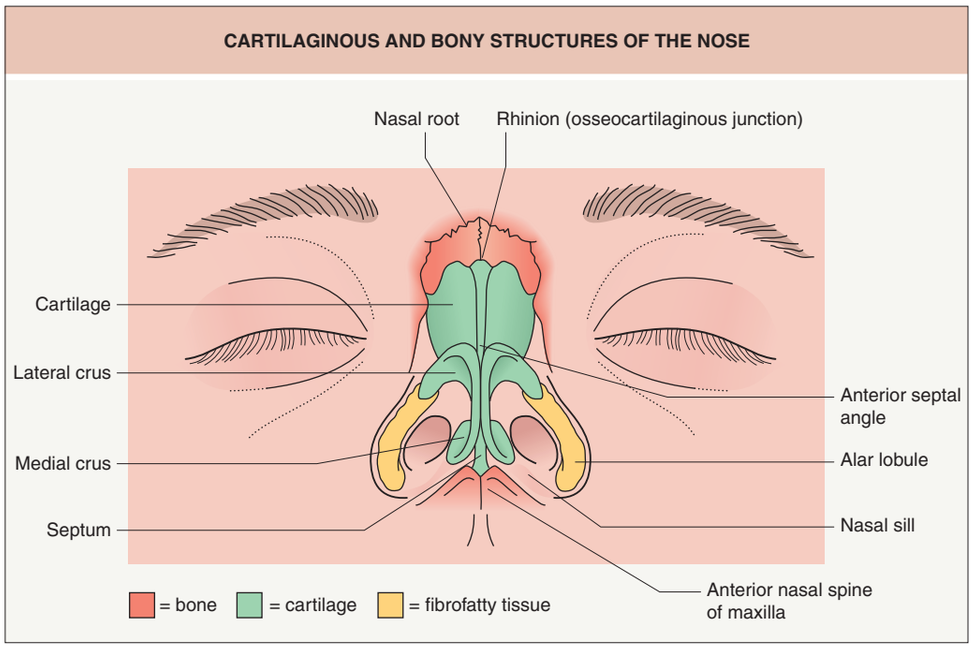


Fig. 142.11 Cartilaginous and bony structures of the nose.

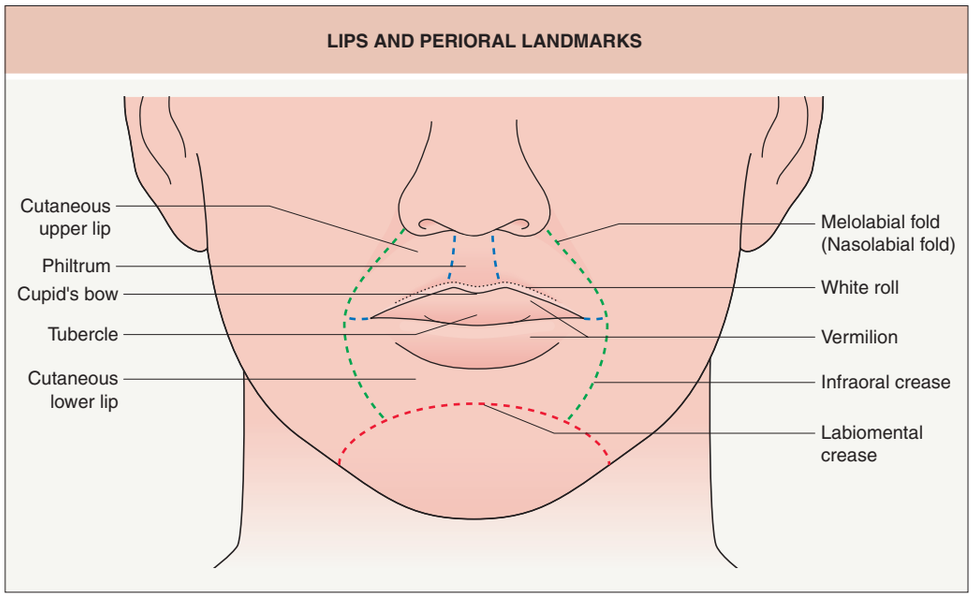


Fig. 142.12 Lips and perioral landmarks.

connections to the skin and other muscle groups. This contributes to organized movements, symmetry in facial expression, and the appearance of skin tension lines. In certain areas where facial musculature is absent, the SMAS layers form a thick, inelastic membrane. These regions are clinically identifiable as the galea aponeurotica of the scalp and the superficial temporalis fascia. Major anatomic structures predictably course in and around the superficial fascia. The dermatologic surgeon can maximize this relatively avascular dissection plane and minimize trauma to important neurovascular structures by using the SMAS as a guide to dissection, tissue mobilization, and closure. Rejuvenation procedures such as facelifts rely on the redistribution and manipulation or plication of the head and neck SMAS.

The deep fascia of the face covers bone, cartilage, muscles of mastication, and visceral structures. It is a continuous sheath, forming periosteum, perichondrium, temporalis muscle fascia, and the parotid–masseteric fascia[1]. This fascia is resistant to stretch and particularly impedes tissue movement on the scalp. Plication or suspension sutures are often used to "tack" overlying structures to the deeper fascia in order to secure tissue and redirect tension vectors.

The SMAS of the cheek is located between the skin and the deeper muscles of mastication. By mobilizing the preauricular SMAS plane, the anterolateral neck and lower cheek below the zygomatic arch can be repositioned as a whole. The SMAS of the cheek is continuous with the orbicularis oculi muscle of the lower eyelid and has several bony attachments in the periocular region[10]. Note that the SMAS of the upper face is discontinuous with the SMAS below the zygoma. This separation is due to different embryologic development patterns of the upper and lower facial muscle groups. The galea aponeurotica of the scalp and the fascia of the superficial temporalis muscle split to envelop the frontalis muscle of the forehead and the occipitalis muscle of the posterior scalp. This superior SMAS terminates 1 cm below the zygomatic arch.

The parotid gland, Stensen's duct, and emerging branches of the facial nerve lie on the deep masseteric fascia. They are covered by thin fibrotic platysma remnants called the parotid fascia, which is covered by the SMAS. The aponeurotic investiture of the central face is thin and often indistinct. The intrinsic nasal muscles and lip elevators and depressors are essentially devoid of superficial fascial interconnections. This makes dissection in this area challenging, because the planes are often difficult to establish and many important anatomic structures are under threat of compromise.

Large sensory nerves and axial blood vessels that supply the face ascend to lie within the SMAS or between the SMAS and subcutaneous fat (Fig. 142.14). Motor nerves run deep to the SMAS and penetrate the muscles of facial expression from their undersurface. Knowledge

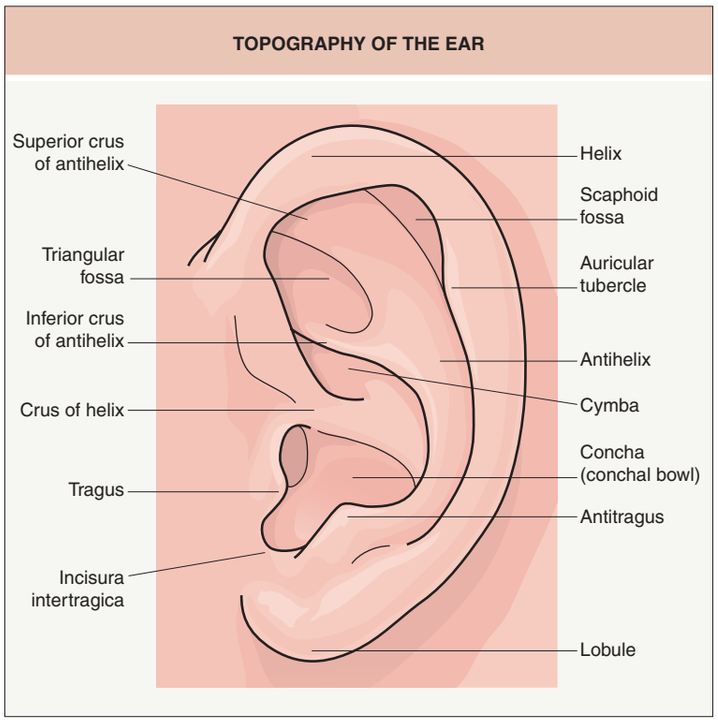


Fig. 142.13 Topography of the ear.

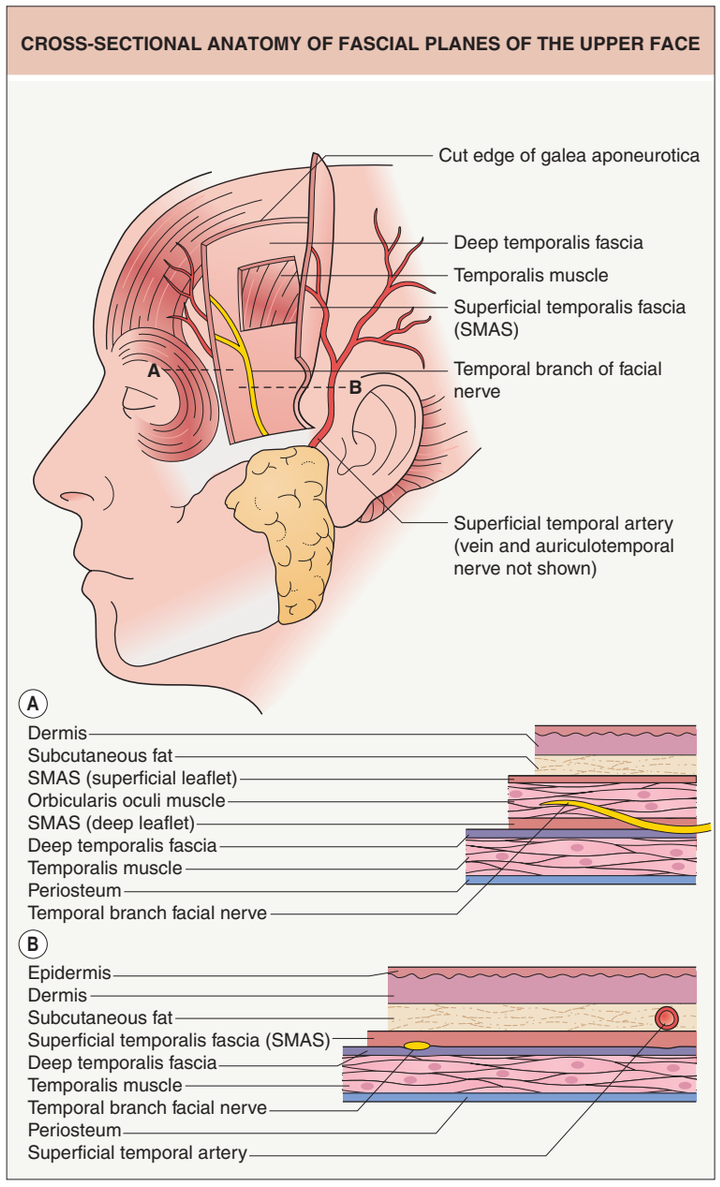


Fig. 142.14 Cross-sectional anatomy of fascial planes of the upper face. SMAS, superficial musculoaponeurotic system.

of these anatomic relationships assists the surgeon in establishing a relatively avascular and safe plane of dissection. Blunt dissection of the scalp SMAS separates the galea aponeurotica from the skull periosteum, the superficial temporalis fascia from the deep temporalis fascia, and the subfrontalis SMAS from the forehead periosteum. This is called the subgaleal plane, and it is the ideal avascular dissection plane for scalp surgery. Beware of the supraorbital/supratrochlear neurovascular bundles above the eyebrows when dissecting to the deep galea, as these can be damaged as they exit their respective foramina. In the SMAS–parotid fascial plane of the cheek, the buccal and zygomatic branches of the facial nerve are endangered due to thin protective aponeurotic tissue in this area. The superficial temporal vessels and auriculotemporal nerve course within the superficial temporalis fascia above the zygomatic arch, then assume a superficial plane in the subcutaneous fat.

Surgical undermining and dissection should maximize the horizontal planes provided by the superficial fascial network of the head and neck. Undermining in the subcutaneous fat of the face below the subdermal plexus minimizes the risk to motor nerves, but remember that sensory branches and blood vessels course through this area. There is sparse subcutaneous fat on the dorsal nose, forehead, upper lip, and eyelid. With the exception of the forehead where dissection is usually in the subgaleal plane, the ideal dissection plane in these regions lies just superficial to the thin investing fascia (SMAS) covering the regional muscles of facial expression[11].

In short, the SMAS acts as a unifying infrastructure to the head and neck that creates an anatomic plane for identification and protection of key structures. Knowledge of neurovascular anatomy with respect to the superficial investing fascia will promote effective surgical dissection and closures that minimize functional compromise and maximize cosmesis.

MUSCLES OF FACIAL EXPRESSION

The muscles of facial expression arise from the second branchial arch, are innervated by the facial nerve (cranial nerve VII), and are concentrated in the central facial region. They insert into overlying skin and other local muscle groups and contribute to the relaxed skin tension lines of this region. Fluidity of facial movements is orchestrated by their interaction with the SMAS. A surgeon must have detailed knowledge of these muscles and the potential consequences of disrupting their innervation (Table 142.1).

The epicranius or occipitofrontalis muscle of the scalp has an anterior and posterior region connected by the galea aponeurotica (see Fig. 142.7).

Contraction of these muscles allows the skin to slide over the scalp. However, humans no longer have voluntary control of the posterior muscle group, which is innervated by the posterior auricular branch of the facial nerve. The *frontalis* muscle, a member of the epicranius complex, begins at the anterior hairline and inserts into the forehead and eyebrow skin. It also connects with the procerus, orbicularis oculi, and corrugator supercilii muscles. Midline vertical forehead skin tension lines occur due to variation in distance between the left and right frontalis bellies. Horizontal skin tension lines occur perpendicular to the frontalis contractile orientation (see Fig. 142.5).

The small *periauricular* muscles, also referred to as the temporoparietalis group, arise from the superficial temporalis fascia and the lateral galea. They help draw back the temporal skin and are innervated by the posterior ramus of the temporal branch of the facial nerve. The *orbicularis oculi* muscle complex is the major group that acts on the eyelid and periorbital skin. It inserts into the medial and lateral canthal tendons and encircles the eye region. Its palpebral portion has a preseptal component overlying the orbital septum and a pretarsal portion overlying the tarsal plate of the eyelid. The orbicularis oculi is intertwined with the procerus, corrugator supercilii, and frontalis muscles and attaches to the superficial temporalis fascia at its lateral border[12].

The *corrugator supercilii* muscle is located over the medial upper orbital rim. It contributes to a "scowling" facial expression by drawing

MUSCLES OF FACIAL EXPRESSION INNERVATED VIA CRANIAL NERVE VII (THE FACIAL NERVE)			
Muscle	**Innervation – facial nerve branch(es)**	**Functions**	**Ipsilateral complications from functional loss**
Frontalis	Temporal	• Raises eyebrows • Aids in opening eyes widely (in conjunction with orbicularis oculi)	• Flattening of horizontal forehead tension lines • Inability to raise lowered/"droopy" eyebrow • May be unable to open eyes widely • Only 15% of patients have cross-innervation*
Corrugator supercilii	Temporal	• Draws brows medially & downward (scowl expression)	• Difficulty scowling/furrowing brow • Rarely occurs due to cross-innervation†
Orbicularis oculi – upper portion	Temporal	• Closes upper eyelids • Voluntary tight closure (orbital component) • Gentle eye closure & blinking (palpebral component) • Aids in tear extraction (palpebral component)	• Difficulty with eye closure • Rarely occurs due to cross-innervation†
Auricular – anterior and superior (also referred to as temporoparietalis)	Temporal	• Draws back temporal skin	
Auricular – posterior	Posterior auricular	• Draws back temporal skin	
Orbicularis oculi – lower portion	Zygomatic	• Closes lower eyelids • Tight and gentle eye closures – similar to upper portion (see above) • Aids in tear extraction	• Difficulty with tight eyelid closure • Lower eyelid droop • Complete loss uncommon due to cross-innervation by temporal branch
Nasalis – alar portion	Zygomatic	• Facilitates alar flaring & compression	
Procerus	Zygomatic	• Causes foreshortening of the nose & "bunny" lines (with nasalis)	
Levator anguli oris	Zygomatic and buccal	• Elevates & retracts mouth angles	• Difficulty smiling • Difficulty with lip seal
Zygomaticus major	Zygomatic and buccal	• Elevates & retracts mouth angles	• Difficulty smiling • Difficulty with lip seal
Buccinator	Buccal	• Pursing of lips • Apposition of cheeks to teeth & gingivae • Prevents cheek overextension during high intraoral pressure	• Inability to whistle • Food accumulates between teeth & buccal mucosa with chewing
Depressor septi nasi	Buccal	• Pulls columella down toward lip	
Nasalis – transverse portion	Buccal	• Facilitates alar flaring & compression	
Zygomaticus minor	Buccal	• Elevates & retracts mouth angles	• May have an effect on smiling expression
Levator labii superioris	Buccal	• Elevates upper lip	
Risorius	Buccal and/or marginal mandibular	• Elevates & retracts mouth angles	• Asymmetric "crooked" smile at rest
Orbicularis oris	Buccal and marginal mandibular	• Pursing & puckering of lips • Apposition of corners of the mouth • Pulls lips against teeth & gingivae	• Difficulty with feeding • Drooling • Muffled speech • Inability to enunciate the letters M, V, F, P, or O
Depressor anguli oris	Marginal mandibular	• Depresses & retracts lip	• Inability to smile‡
Depressor labii inferioris	Marginal mandibular	• Depresses & retracts lip	• Inability to smile‡
Mentalis	Marginal mandibular	• Depresses & retracts lip • Elevates chin • Protrudes lower lip • Dimpling of chin	• Inability to smile‡
Platysma	Marginal mandibular and cervical	• Minor role in retracting mouth angles	

*By the zygomatic branch of the facial nerve.
†By other motor nerves.
‡Normal at rest, but asymmetric expression when smiling.

Table 142.1 Muscles of facial expression innervated via cranial nerve VII (the facial nerve)[4]. Due to a high degree of anastomoses, damage to the zygomatic or buccal branches is often temporary and less debilitating than a similar injury to the temporal branch.

the eyebrows medially and downward. It interdigitates with and is covered by the frontalis and orbicularis oculi muscles. The vertical and oblique skin tension lines of the glabella are caused by contraction of this muscle. The *procerus* muscle overlies the nasal bone and attaches to the nasal root skin. It is responsible for "bunny lines", i.e. skin tension lines exaggerated by wrinkling up the nose. Adjacent to the procerus is the *nasalis* muscle, which courses across the nasal dorsum. Inferiorly, the *depressor septi nasi* muscle, which lies deep to the orbicularis oris, pulls the columella down toward the lip and can form a transverse skin tension line across the philtrum.

An intricate network of interdigitating agonist and antagonist muscle groups contributes to lip movements and oral expression. Lip elevators, depressors, and retractors assist the sphincteric *orbicularis oris* muscle in lip movement. The orbicularis oris muscle is unique in that it has no

bony or cartilaginous attachment. Facial arteries and veins are covered and protected from damage by the lip elevator muscles. The quadratus labii superioris muscle group is comprised of several lip elevators. The *levator anguli oris* and *risorius* muscles are mouth angle retractors and elevators. The *zygomaticus major* muscle travels from the zygoma downward and diagonally to the upper corner of the mouth, where it contributes to the nasolabial fold. *Zygomaticus* major and *minor* muscles are the main contributors to smile formation. The risorius muscle also contributes to a smiling facial expression. The modiolus platform is formed by the convergence of fibers from the orbicularis oris and lip elevators and depressors. It is located 1 cm lateral to the mouth angle and accounts for cheek "dimples" in some patients. It works in synergy with the perioral muscles to facilitate speech enunciation.

The *buccinator* muscle constitutes a large area of the cheek as it courses from the posterior maxillary area to the upper medial surface of the mandible, where it interdigitates with the orbicularis oris. The facial vascular bundle crosses its surface. The parotid duct and transverse facial artery run parallel to each other as the duct pierces the buccinator to enter the mouth at the second maxillary molar. The *depressor anguli oris* (triangularis), *depressor labii inferioris* (quadratus), and the *mentalis* muscles are lip depressors and retractors that antagonize the superior perioral muscle groups. The mentalis muscle has bellies with variable proximities to each other, and a patient with a chin "dimple" or "cleft chin" has a larger distance between mentalis muscle bellies. This is a normal anatomic variant.

The *platysma* muscle runs from the superficial fascia of the chest across the anterior and lateral neck over the mandible to intercalate with the lower lip depressors and retractors. It is continuous with the superficial fascia or SMAS of the lower face. The platysma muscle provides only a thin protective cover to the anterior facial vascular bundle and mandibular branch of the trigeminal nerve.

VASCULAR ANATOMY

The internal carotid artery supplies the eyelids, upper nose and nasal dorsum, forehead, and scalp via sub-branches of its ophthalmic branch. The ophthalmic artery arises behind the eye and branches into the orbital and ocular group. The ocular group supplies the eye itself and its associated muscles. The orbital group includes the supraorbital, supratrochlear, dorsal nasal, and anterior ethmoidal arteries (Fig. 142.15). The supraorbital artery exits the orbit through the supraorbital foramen alongside the supraorbital nerve and perforates the frontalis muscle to ultimately course in the subcutaneous tissue of the forehead and scalp. The supratrochlear artery exits the medial orbit and courses medial to the supraorbital artery to supply the nasal root and the low midline forehead. This artery serves as the axial blood supply for the midline forehead flap often used to repair nasal defects. The success of this flap depends upon isolation and preservation of the supratrochlear artery. The anterior ethmoidal artery exits the nasal passage at the interface of the nasal bone and nasal cartilage to provide arterial supply to the nasal dorsum. The dorsal nasal artery and supratrochlear artery are two of the terminal branches of the ophthalmic artery. The dorsal nasal artery supplies the dorsal nose and crosses the midline over the nasal root to anastomose with the contralateral angular artery. Knowledge of the ophthalmic artery and its branches is of particular importance when planning cosmetic filler injection. Because of their proximal connections, the orbital group of vessels represents a potential site for embolus introduction into the central retinal artery that can lead to complications including blindness (see Fig. 142.15)[13].

While the internal carotid artery contributes to some areas of the scalp and upper face, the external carotid artery supplies most of the face. The facial artery branches off from the external carotid artery and courses deep to the mandible up through or behind the submandibular salivary gland. It passes over the mandible onto the face and can be palpated anterior to the masseter muscle. Its tortuous course maintains a diagonal and superior direction passing alongside the nose and terminating at the medial canthus where it anastomoses with the dorsal nasal artery. The platysma and risorius muscles protect the facial artery near the mandible. As the vessel traverses up the face, it becomes covered by the zygomaticus muscles of the midface and the orbicularis oculi as it nears the medial canthus.

The facial artery gives rise to the inferior and superior labial arteries that course horizontally below and above the lips, respectively. These arteries are found deep to the orbicularis oris in the submucosal plane, but can course more superficially into the submucosa of the lip in elderly patients. After forming the superior labial branch, the facial artery becomes known as the angular artery (Fig. 142.16). At its endpoint near the medial canthal tendon, the angular (or facial) artery anastomoses with the dorsal nasal branch of the ophthalmic artery. Since the ophthalmic artery is a branch of the internal carotid system, this anastomosis joins the internal and external carotid arterial systems. During most of their course, the facial artery and vein are covered by the superficial muscles of facial expression. The facial artery also anastomoses with branches of the internal maxillary (the infraorbital branch)

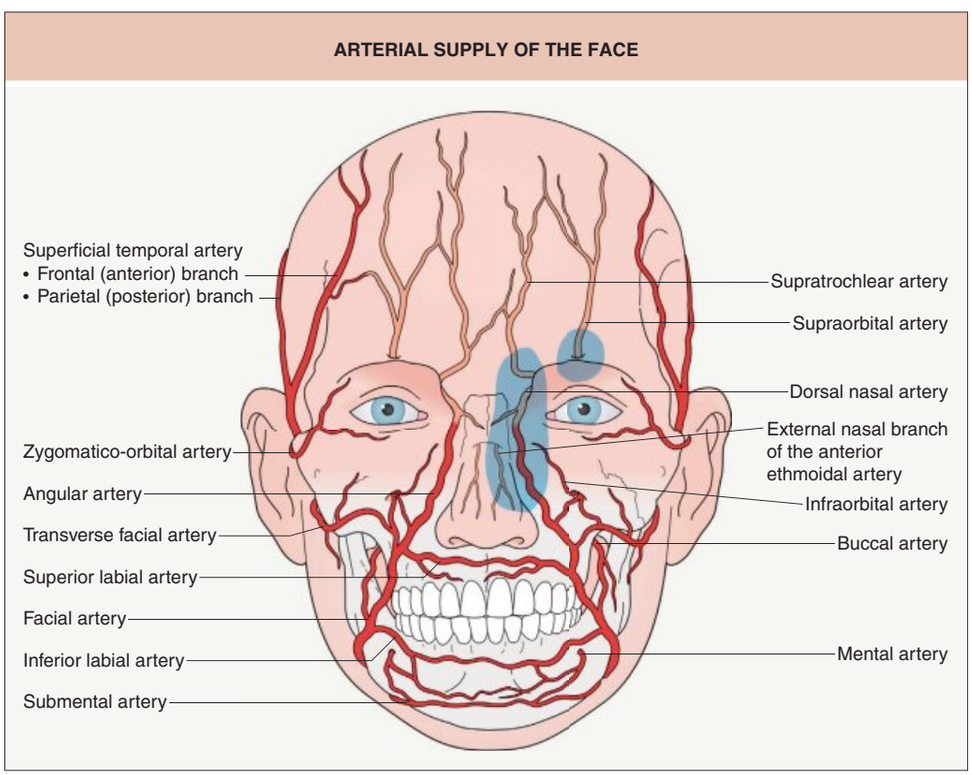


Fig. 142.15 Arterial supply of the face. Light pink designates arteries derived from the internal carotid artery; dark pink, from the external carotid artery. Blue highlighted areas denote high risk for filler injection.

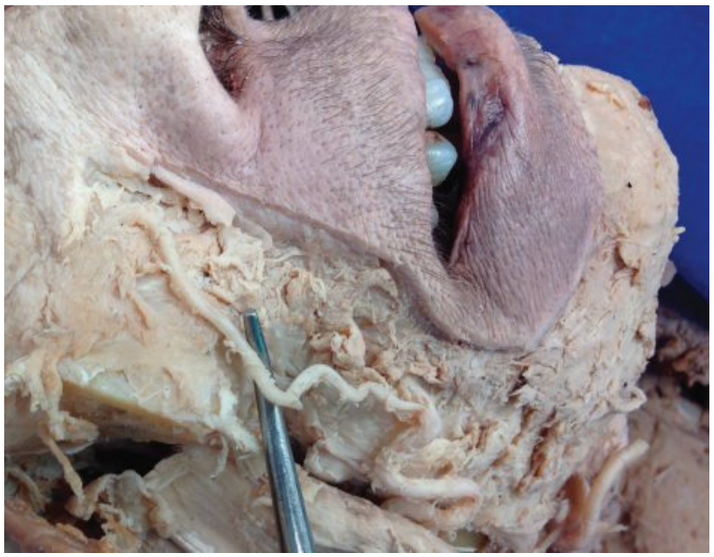


Fig. 142.16 The angular artery. After forming the superior labial branch, the facial artery becomes known as the angular artery.

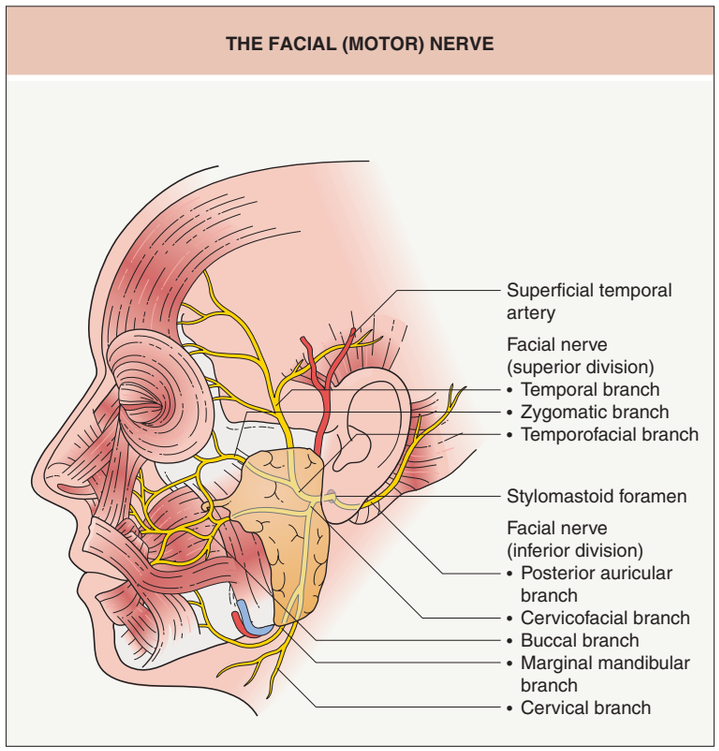


Fig. 142.17 The facial (motor) nerve.

and superficial temporal (transverse facial) arterial trees. This allows excellent blood supply to the facial skin even if distal arterial branches are cut or tied off during surgery. The high density of arterial supply to the head and neck accounts for its excellent healing potential and viability of local flaps and grafts.

The lateral face, scalp, and forehead are primarily supplied by the superficial temporal artery and its branches. This artery arises in the superficial lobe of the parotid gland as the terminal branch of the external carotid artery. It courses superficially to the main facial nerve trunks, then gives off the transverse facial artery before exiting the parotid gland superficially. The transverse facial artery runs parallel to and 2 cm below the zygomatic arch[4]. The superficial temporal artery exits the parotid and enters the subcutaneous fat in the preauricular crease, where it assumes an ascending vertical course over the zygomatic arch (see Fig. 142.14). It can be easily palpated just medial to the upper tragus of the ear. It runs alongside and superficial to the auriculotemporal nerve within, then above, the SMAS layer of the temple and lateral forehead. The most superficial portion of the superficial temporal artery is often visible in aged patients within the subdermal fat above the galea aponeurotica as it courses cephalad above and anterior to the ear. Here it forms the frontal (anterior) and parietal (posterior) arterial branches that originate just above the uppermost attached portion of the ear (see Fig. 142.15). The forehead, eyebrows, and lateral scalp receive their arterial supply from these branches of the superficial temporal artery. There are many anastomoses on the scalp between the bilateral superficial temporal arteries. Because of this rich supply chain, the entire scalp tissue remains viable even if one of these arteries is occluded. This rich anastomotic network also explains why scalp surgery can be a bloody process. Surgical dissection at the level of the galea aponeurotica may serve to avoid transection of the copious subdermal vascular supply.

Most of the arteries of the face run anterior to and parallel with their corresponding veins (see Fig. 142.3). The veins lack valves and therefore permit two-way flow of venous blood. The facial vein connects to the deep facial vein as it drains the cheek. The deep facial vein parallels the internal maxillary artery and anastomoses with the pterygoid venous plexus medial to the upper mandibular ramus. The facial vein crosses over the submandibular gland, while its corresponding artery passes beneath. It then drains into the internal jugular vein, which connects with the external jugular vein via the retromandibular vein. The facial vein can communicate with the cavernous sinus of the brain via the ophthalmic vein or the pterygoid plexus. The paranasal area and upper lip are the regions drained by this network. This interface may permit skin or wound infections to gain access to the cavernous sinus of the brain from the draining facial or ophthalmic veins, with potentially devastating consequences.

Arterial blood supply to the face is delivered by a rich subdermal plexus that is fed by larger perforating arteries. Wound healing and flap success depend on maximal blood supply to the area. Axial flaps, such as the paramedian forehead flap, incorporate a named subcutaneous artery (e.g. the supratrochlear artery) into their design. Random pattern flaps are maintained by the subdermal arterial plexus and do not rely on a single feeder artery to maintain blood flow. The anastomotic vascular network permits facial arteries to be clamped or tied off during surgery without compromising tissue viability. Nearby ipsilateral or contralateral anastomotic arterial branches can often compensate for any loss in local blood supply.

THE FACIAL NERVE

The muscles of facial expression are innervated by the facial nerve, or cranial nerve VII. Upon exiting the skull at the stylomastoid foramen near the level of the earlobe, the facial nerve immediately gives off the posterior auricular branch, which provides motor innervation to the occipitalis and posterior auricular muscles (Fig. 142.17). The remainder of the nerve trunk enters the parotid gland and bifurcates into the lower cervicofacial and the horizontally oriented temporofacial branches. The temporal, zygomatic, buccal, marginal mandibular, and cervical branches arise from these two major rami of the facial nerve. If a line is drawn from the superior border of the tragus to the angle of the mandible, the entrance site of the facial nerve trunk into the parotid gland lies at the midpoint.

After coursing through glandular parotid tissue, branches of the facial nerve travel between the SMAS and the deep fascia before penetrating the lateral underside of the facial muscles. There is significant variability in the course and arborization of this nerve from patient to patient. Cranial nerve VII has two major roots, the smaller of which, via the chorda tympani branch, provides taste sensation to the anterior two-thirds of the tongue; the chorda tympani nerve travels with the lingual nerve (cranial nerve V_3) to the tongue. Sensory innervation to a portion of the external auditory meatus, soft palate, and pharynx is also derived from this small facial nerve root. The submaxillary, submandibular, and lacrimal glands contain parasympathetic fibers of the facial nerve that have secretory effects. In addition to the muscles of facial expression (see Table 142.1), the buccinator, stapedius, posterior belly of the digastric, stylohyoid, and platysma muscles are all innervated by branches of the facial nerve.

While the facial nerve trunk is well protected in adults at its exit from the skull by the mastoid process, tympanic ring, and mandibular

ramus, the surgeon must beware when performing procedures in this anatomic region in children. Because the mastoid process is not fully developed until age five, the main facial nerve trunk lies in a superficial subcutaneous plane behind the earlobe and may be damaged in superficial cutaneous procedures[14]. The major facial nerve branches on the cheek are protected only by a small amount of parotid tissue (superficial lobe), parotid fascia, and subcutaneous fat (Fig. 142.18). If a surgical procedure requires violation of the parotid fascia, meticulous dissection is necessary to avoid major facial nerve damage and subsequent functional disability. Of note, the motor nerves of the face course deeper than the sensory nerves or axial vasculature.



Fig. 142.18 Branches of the facial nerve. Following dissection of the parotid gland, multiple branches are visible; those lifted by the dissecting probe include (from top to bottom): temporal, zygomatic (2 branches), and buccal.

Temporal Branch

The temporal branch of the facial nerve provides motor innervation to the frontalis, upper orbicularis oculi, and corrugator supercilii muscles. It usually has three to five rami that originate over the middle third of the zygomatic arch for a combined approximately 2.5 cm "danger" zone in this area (Table 142.2; see Fig. 151.6). As the most anterior branch of the temporal nerve crosses over the zygomatic arch, it is almost always located, at a minimum, 2 cm posterior to the orbital rim[15]. The most posterior ramus of the temporal branch can be topographically located on the temple 1 cm anterior to a vertical line drawn from the anterior insertion of the ear to the scalp. This posterior ramus runs anterior to the superficial temporal artery and vein. The dermatologic surgeon must exercise caution when working in this area as the superficially located temporal branch is at highest risk for injury within this zone[16].

The temporal branch of the facial nerve courses between the superficial and deep temporalis fascia, penetrating the underside of the frontalis muscle from its lateral edges (see Fig. 142.17). The superficial temporal artery and vein as well as the auriculotemporal sensory nerve run posterior to but more superficially than the temporal nerve branch (see Fig. 142.3). This neurovascular bundle lies in the subcutaneous fat overlying the SMAS of the temple and lateral forehead region. Remember that once the temporal nerve reaches the lateral underbelly of its ipsilateral target muscles, it is most protected. In order to avoid damaging this facial nerve branch, the surgeon should either remain superficial to the SMAS (i.e. the superficial temporalis fascia) or dissect in the subgaleal plane from the medial to lateral forehead. Similar to the other facial nerve divisions, the greatest potential for nerve damage lies in the lateral regions of the face. The central face has many nerve arborizations and protective muscles that usually afford minimal risk for facial motor nerve damage.

Damage to a ramus of the temporal branch of the facial nerve can result in notable cosmetic and functional loss. The temporal branch consists of long, usually singular, and often superficially coursing rami that have few arborizations or cross-innervations. These characteristics make nerve damage and permanent sequelae more likely when cutaneous procedures are performed in the lateral forehead and temporal regions. Even though the upper orbicularis oculi and corrugator supercilii muscles are innervated by the temporal branch, minimal functional or cosmetic compromise occurs, due to cross-innervation by other motor nerves. However, only 15% of patients will have any cross-innervation to the frontalis muscle by the more inferior zygomatic branch of the facial nerve. Such arborization permits retention of some functional mobility of the frontalis should the temporal branch be sacrificed. For the other 85% of patients, violation of the temporal nerve results in motor denervation and the inability to raise a now lowered or "droopy"

SURGICAL DANGER ZONES OF THE HEAD AND NECK

Danger zone	Nerve(s)	Function	Location most susceptible to injury	Injury/deficit
Erb's point	• Spinal accessory • Cervical plexus (lesser occipital, great auricular, transverse cervical, supraclavicular nerves)	• Motor innervation to the trapezius (spinal accessory) • Sensory innervation (cervical plexus)	Draw a line connecting the angle of the mandible to the mastoid process, *then* from the midpoint of this line draw a 6 cm vertical line; the intersection of the lowermost point of the vertical line and the posterior border of the sternocleidomastoid muscle identifies Erb's point	• Inability to elevate the shoulder or abduct the arm >80° • Winged scapula • Loss of sensation to areas of the head/neck
Temple	Temporal branch (facial)	• Motor innervation to the frontalis, orbicularis oculi, corrugator supercilii, and anterior and superior auricular muscles	Draw 2 lines to delineate the zone*: (1) from the inferior earlobe to the lateral edge of the eyebrow; and (2) from the tragus to just above and lateral to the highest forehead crease	• Inability to elevate ipsilateral frontalis muscle • Flattening of forehead tension lines • Brow ptosis
Mandible at the site of the facial artery	Marginal mandibular branch (facial)	• Motor innervation to the orbicularis oris, risorius, and depressors of the lower lip (depressor anguli oris, depressor labii inferioris, and mentalis) muscles	Exits the inferior portion of the parotid gland, then courses over the mandible anterior to the facial artery; it is located 1–2 cm above the inferior border of the mandible	• Inability to smile/ipsilateral crooked smile • Drooling

*In this area, the temporal nerve is protected only by skin, subcutaneous fat, and a thin layer of SMAS.

Table 142.2 Surgical danger zones of the head and neck. See Fig. 151.6 which also includes the buccal branch of the facial nerve, but the latter is rather deep in the cheek and much less at risk.

eyebrow[4] (see Fig. 151.7). Flattening of the forehead with diminished visibility of wrinkles and skin tension lines on the ipsilateral side is easily noted. The functional loss of the frontalis muscle significantly hampers a patient's ability to communicate non-verbally via facial expression and may have devastating psychosocial consequences. Over time, the inability to raise one's eyebrow can lead to eyebrow and eyelid ptosis and upper visual field compromise as muscular disuse atrophy progresses. Unilateral brow lifts and blepharoplasty may be necessary if the temporal nerve branch is permanently damaged.

Zygomatic and Buccal Branches

The **zygomatic** branch of the facial nerve provides motor innervation to the lower orbicularis oculi, procerus, mouth elevator, and nasal muscles (see Fig. 142.17). Its fibers course horizontally and upwards after emerging from the parotid gland as the second division of the facial nerve (see Fig. 142.18). There is marked variability in the innervation it provides to these muscles; thereby, damage to this nerve branch can have unpredictable outcomes. Generally, injury to the zygomatic branch results in decreased orbicularis oculi function and a diminished ability to close the ipsilateral eyelid tightly. The orbicularis oculi is also innervated in its supraorbital aspect by the temporal branch of the facial nerve. Therefore, complete loss of circumferential periocular motor function is highly unlikely. Other effects may include dysfunction of nasal muscles and lip elevators.

The **buccal** branch is the third division of the facial nerve, and it courses inferiorly to the zygomatic branch in a downward direction on the cheek (see Fig. 142.17). It innervates the orbicularis oris, zygomaticus major and minor, lip elevator, buccinator, and nasal muscles to a variable extent. Damage to this nerve causes buccinator dysfunction that results in accumulation of food between the teeth and the buccal mucosa with chewing, as well as an ipsilateral crooked smile at rest. Approximately 80% of patients have anastomoses between the fibers of the zygomatic and buccal branches[17]. Each branch has two points of arborization, with the first occurring 2 cm anterior to the anterior edge of the parotid gland and the second usually occurring under the modiolus 1 cm lateral to the oral commissure at the anterior aspect of the buccal fat pad. Here the nerves may be damaged due to their superficial anatomy, protected only by the thin fascia of the SMAS, an often underdeveloped risorius muscle, and the subcutaneous fat. At the first branching site near the parotid, the zygomatic and buccal nerves lie between the masseter muscle and the posterior side of the buccal fat pad.

Although damage to the zygomatic or buccal branches of the facial nerve may occur during surgical procedures, subsequent motor dysfunction is often temporary and far less debilitating than a similar injury to the temporal nerve. The high degree of anastomoses between the zygomatic and buccal branches minimizes functional damage and promotes nerve recovery after trauma. Partial paralysis of the perioral muscles may occur, causing variable symptomatic defects in facial expression, including a diminished ability or unilateral defect in forming a smile or pucker, lip pursing, and lip seal formation. Drooling, food accumulation between the cheeks and gingivae, and muffled speech may occur secondary to buccal or zygomatic nerve damage. Orbicularis oculi defects have already been discussed and include lower eyelid droop, which can lead to chronic conjunctivitis, sicca symptoms, and ectropion. Difficulty wrinkling up the nose and inability to flare the nostrils may also occur with zygomatic or buccal branch trauma. Fortunately, most of these symptoms resolve within 6 months due to the extensive ramification and cross-innervation of these branches of the facial nerve.

Marginal Mandibular Branch

The orbicularis oris, mentalis, and lip depressor muscles are innervated by the marginal mandibular branch of the facial nerve. The nerve courses along the angle of the mandible below the parotid gland and continues up over the mandibular body anterior to the facial artery, which can be palpated easily as it courses over the medial mandible (see Fig. 142.17). The marginal mandibular nerve is very susceptible to damage due to its superficial location over the bony edge of the jaw, where it is covered only by fascia and an often unpredictably thin or poorly developed platysma muscle. This facial nerve branch is often composed of only one ramus. The marginal mandibular nerve "communicates" with the buccal branch of the facial nerve in only 10% of patients; therefore, damage to the marginal mandibular nerve can lead to permanent disfiguring and functional defects in facial expression[4]. Normal symmetric facial expression and function of the mouth depends upon the equal and opposite effects exerted by the lip depressors and elevators in conjunction with the orbicularis oris muscle. Characteristically, a patient with marginal mandibular nerve damage cannot form a symmetric smile. There is inability to pull the ipsilateral lower lip downward and laterally or evert the corresponding vermilion border. The end result is a "crooked" smile. The defect is appreciated upon smiling, but is not as apparent when the patient is at rest.

Cervical Branch

The cervical branch of the facial nerve innervates the platysma muscle. This muscle receives nerve fibers from the marginal mandibular nerve as well. Damage incurred to the cervical branch rarely causes functional or cosmetic defects.

SENSORY INNERVATION OF THE HEAD AND NECK

The trigeminal nerve, or cranial nerve V, provides the primary sensory innervation to the face, while the upper cervical nerves (C2, C3) provide sensory supply to the neck, part of the ear, and posterior scalp (Fig. 142.19). The facial, glossopharyngeal, and vagus nerves provide a small portion of sensory innervation to the ear[18]. The trigeminal nerve is the largest cranial nerve. It has motor (to the muscles of mastication), sensory, and parasympathetic functions, supplying secretory fibers (originating from the facial and glossopharyngeal nerves) to the lacrimal and parotid glands. The sensory branches of the trigeminal nerve course more superficially than the trunk of the facial nerve and are therefore readily subject to damage during surgical procedures. Fortunately, most resulting sensory dysfunction is not debilitating or permanent. Transmedian re-innervation after unilateral trigeminal root transection has been demonstrated. This is due to collateral sprouting of sensory nerves from the contralateral trigeminal nerve root[19]. The sensory nerves exist in the superficial plane between the subcutaneous fat and

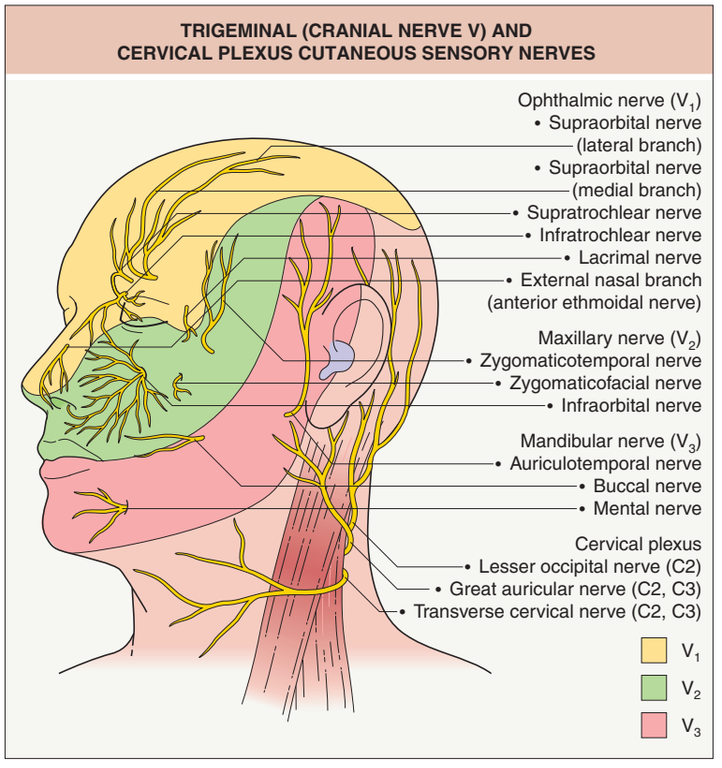


Fig. 142.19 Trigeminal (cranial nerve V) and cervical plexus cutaneous sensory nerves. The concha and external auditory canal are variably innervated by branches of the vagus (cranial nerve X), facial (VII), and auriculotemporal nerves (purple–gray). The upper cervical nerves (C2, C3) also provide sensory innervation to part of the ear as well as to the neck and posterior scalp.

the SMAS and often run together with arteries and veins in neurovascular bundles. Knowledge of the sites where the major branches of sensory nerves emerge from the skull assists the surgeon in performing regional nerve blocks that facilitate facial surgery and improve patient comfort (see Ch. 143).

The trigeminal nerve is divided into three main branches: ophthalmic (V_1), maxillary (V_2), and mandibular (V_3) (see Fig. 142.19). The smallest, uppermost sensory branch is the **ophthalmic** division, which gives off three branches (nasociliary, frontal, and lacrimal nerves) before exiting the orbit. Sensory fibers to the sinuses and upper nasal septal mucosa, as well as secretory parasympathetic fibers to the lacrimal gland (that originate from the facial nerve), are also provided by the ophthalmic branch of the trigeminal nerve. The nasociliary branch gives rise to the infratrochlear nerve and the external branch of the anterior ethmoidal nerve. Sensory innervation to the root of the nose and part of the medial canthus is supplied by the infratrochlear nerve. The nasal dorsum, tip, supratip, and columella derive cutaneous innervation from the external nasal branch of the anterior ethmoidal nerve, which emerges between the upper nasal cartilage and nasal bones. Nerve blocks for the nose rely on knowledge of these anatomic relationships among the sensory nerves. The nasociliary branch also supplies the corneal surface via the ciliary nerve. If an episode of herpes zoster involves the nasal tip, then close ophthalmologic follow-up is warranted due to presumed corneal involvement.

The frontal nerve branch of the ophthalmic division forms the supratrochlear and supraorbital nerves. The exit route (supratrochlear ridge) of the supratrochlear nerve lies 1 cm lateral to the midline on the supraorbital ridge. This branch of the frontal nerve provides sensory innervation to the medial upper eyelid, medial forehead, and frontal scalp. The supraorbital foramen (through which emerges the supraorbital neurovascular bundle) lies 2.5 cm lateral to the midline on the supraorbital ridge (see Fig. 142.2). After penetrating the frontalis muscle to emerge above the frontalis SMAS, the supraorbital nerve provides cutaneous sensation to the forehead, scalp, and upper eyelid. A small lacrimal nerve branch of the ophthalmic division of cranial nerve V innervates the lateral eyelid skin and lies near the upper lateral orbital rim. Frontal nerve blocks, and specifically the supratrochlear and supraorbital block, offer quick and effective anesthesia for surgical procedures of the forehead.

The **maxillary** branch (V_2) of the trigeminal nerve forms the infraorbital, zygomaticofacial, and zygomaticotemporal cutaneous sensory branches (see Fig. 142.19). The infraorbital foramen lies 2.5 cm lateral to midline and 1 cm inferior to the infraorbital rim, in the same vertical line as the supraorbital and mental foramina. The infraorbital neurovascular bundle emerges here to provide significant sensory innervation to the medial cheek, upper lip, nasal sidewall and ala, and the lower eyelid. Infraorbital nerve blocks offer simple and effective anesthesia for much of the cheek, lower eyelid, upper lip, and nose. Lateral to the infraorbital foramen, the zygomaticofacial nerve emerges to innervate the skin of the malar eminence. Cutaneous innervation of the temple and supratemporal scalp region is provided by a third branch of the maxillary division, the zygomaticotemporal nerve. It emerges from the lateral orbital margin at the zygomatic bone. The superior alveolar and palatine nerves are deeper branches of V_2 that provide sensory innervation to the upper teeth, palate, nasal mucosa, and gingiva.

The **mandibular** branch (V_3) is the largest division of the trigeminal nerve and the only one to carry both cutaneous sensory and motor fibers. It supplies cutaneous sensory innervation to the face as well as motor innervation to the muscles of mastication[20]. The auriculotemporal, buccal, and inferior alveolar nerves represent the three main cutaneous branches of V_3. The auriculotemporal nerve emerges from behind the neck of the mandible to course just deep to the superficial temporal artery from the superior margin of the parotid gland in the preauricular sulcus up towards the lateral scalp (see Fig. 142.19). It provides sensory innervation to the external ear and auditory canal, temple, temporoparietal scalp, temporomandibular joint, and tympanic membrane. It also carries parasympathetic secretory fibers to the parotid gland.

The buccal nerve supplies sensory innervation to the cheek, buccal mucosa, and gingiva. It runs deep to the parotid gland over the pterygoid muscle to the upper surface of the buccinator, which it pierces to reach the overlying skin. Because the terminal branches of the buccal nerve are small and numerous, regional buccal nerve block techniques are not feasible anesthetic options. The inferior alveolar branch of V_3 innervates the mandibular teeth as it courses through the mandibular sulcus. Its terminal branch forms the mental nerve, which emerges from the mental foramen in the same topographic line as the supraorbital and infraorbital neurovascular bundles (i.e. 2.5 cm lateral to the midline). The mental vein, artery, and nerve emerge from the mental foramen below the lower second premolar. The lingual nerve supplies sensory innervation to the anterior two-thirds of the tongue, the floor of the mouth, and the lower gingivae. It arises from V_3 and courses parallel and superior to the inferior alveolar nerve.

The cervical plexus is a network of arborizing and anastomosing nerve branches of the ventral rami of the four most superior cervical nerves. It emerges from the mid-posterior margin of the sternocleidomastoid (SCM) muscle at Erb's point to give off three branches, designated as C2, C3, and C4. C2 and C3 compose the great auricular nerve, which runs from the posterior edge of the SCM towards the earlobe in the same plane and path as the external jugular vein (see Figs. 142.4 & 142.19). It innervates the skin of the lateral neck, angle of the jaw, and part of the auricular and postauricular skin.

The lesser occipital nerve (C2) emerges from the same point at the SCM and assumes a course parallel to the SCM upward to innervate the skin of the neck, posterior ear, and postauricular scalp. The transverse cervical nerve (C2 and C3) likewise emerges from behind the SCM and arcs anteriorly around and across the SCM in a transverse direction. Its many terminal branches supply the skin of the anterior neck. The supraclavicular nerve (C3 and C4) emerges from the same point at the SCM posterior margin, then courses inferiorly until it reaches the supraclavicular region, where it terminates, and provides sensory innervation to the anterior chest and shoulder skin (see Fig. 142.4).

Perineural invasion of cutaneous tumors may be encountered by the clinician. Patients are often asymptomatic from dermal nerve twig infiltration by tumor cells, with the diagnosis made only by histopathologic tissue examination. However, some patients may experience sensory abnormalities and, rarely, motor dysfunction. Most of these scenarios occur in the setting of SCC (incidence rates range from 3% to 14%) with <1% of BCCs showing any histologic evidence of perineural spread[17]. Knowledge of the neuroanatomy of the head and neck assists the surgeon in planning adjuvant therapy for patients with nerve involvement.

LYMPHATIC DRAINAGE OF THE HEAD AND NECK

Melanomas, SCCs, Merkel cell carcinomas, and other cutaneous neoplasms may spread via the lymphatics to regional lymph nodes. It is important for the clinician to have a thorough understanding of the lymphatic drainage of the head and neck (Fig. 142.20), as well as the remainder of the body, in order to appropriately stage and manage patients. Before any surgical endeavor is undertaken for a malignancy

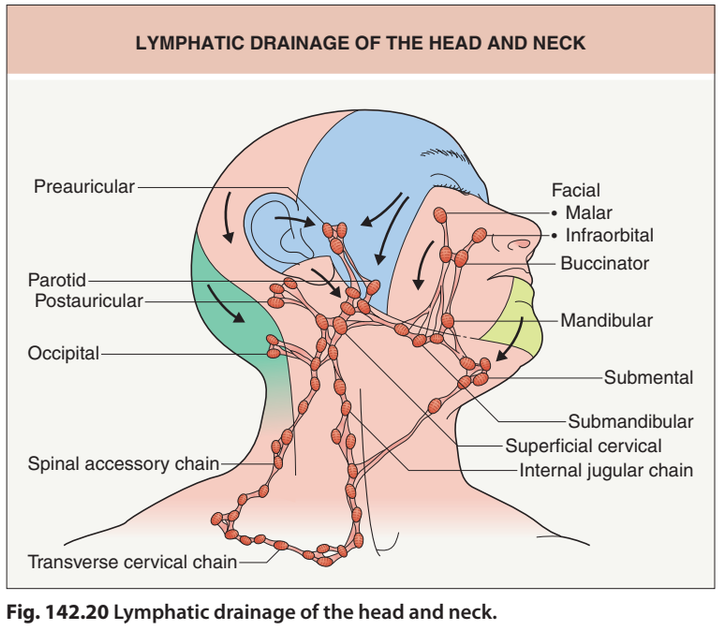


Fig. 142.20 Lymphatic drainage of the head and neck.

with metastatic potential, palpation of regional lymph nodes and basins should be performed. Head and neck cancers usually spread to adjacent lymph nodes in a diagonal direction from cephalad to caudad (see Fig. 142.20). There is a large degree of variability in drainage pathways, but the anatomic location of individual lymph nodes is more consistent from patient to patient. Cutaneous malignancies that breach the papillary dermis may spread from small lymph capillaries to progressively larger and deeper lymphatic trunks in the area. Lymph channels often course along the same directional pathway as the head and neck veins. They are more numerous and often more superficial than the corresponding veins and lie predominantly between the superficial and deep fascial layers.

Important primary lymphatic drainage patterns of the head and neck region include the following: parotid nodes, which often collect from the forehead, temple, and eyelids (upper lateral face); submandibular nodes, from the lower and medial face; and submental nodes, from the central lower lip and chin. Lateral cervical nodes are the common subsequent lymph collection site from these areas.

Parotid nodes may be extraglandular or intraglandular. The extraglandular channels are invested within the parotid sheath. Two-thirds of all individuals will also have one to three pretragal and infra-auricular lymph nodes that are considered part of the parotid node basin[4]. These pre- and infra-auricular nodes drain the ear, the lateral lower cheek, the frontolateral scalp, and the forehead, as well as the nasal root. Drainage of the parotid unit may then follow the external or internal jugular vein in the jugular lymph node chain; therefore, palpation for nodes from the site of the cutaneous lesion to the supraclavicular and even axillary nodal basins is recommended.

Submandibular nodes should be examined as the patient relaxes the neck muscles and tilts the chin down. This nodal group drains the gingival and mucous membranes, lower eyelids, anterior two-thirds of the tongue, lips, nose, and medial cheeks. The submental nodes (up to eight) of the neck lie beneath the platysma and drain the anterior third of the tongue and floor of the mouth, in addition to the lower middle lip, chin, and medial lower cheeks. They are best examined by elevating the chin and asking the patient to engage the platysma. Submental nodes frequently drain bilaterally or contralaterally and empty into the submandibular basin or directly into the internal jugular lymphatic chain. Note that up to one-quarter of healthy individuals have small (less than 1 cm), non-fixed, palpable submental nodes[4].

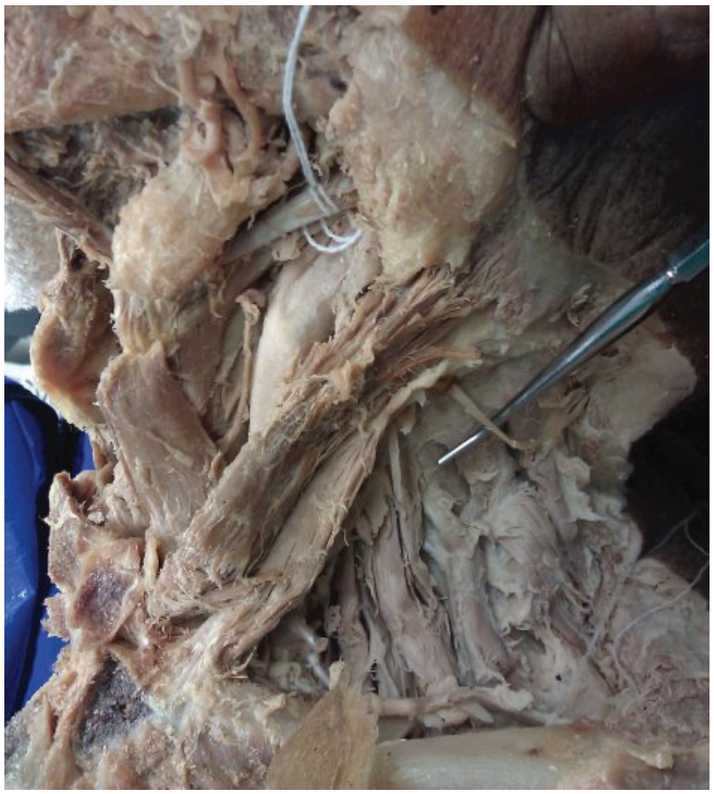
The superficial lateral cervical nodes are adjacent to the infra-auricular parotid nodes and lie near the high external jugular vein. Use the sternocleidomastoid muscle as a landmark to palpate these nodes (up to four) over its cephalad portion. Deeper lateral cervical nodes include the spinal accessory, internal jugular, and transverse cervical chains, which form a triangle on the neck. The internal jugular chain is the main lymphatic collection trunk of the head and neck and may contain up to 25 lymph nodes in each patient. The internal jugular chain on the right often drains into the subclavian vein, whereas the left-sided lymphatic chain empties into the thoracic duct. These nodes can be palpated by rolling two fingers over the area of the carotid triangle.

Acute or chronic lymphedema may ensue after transection of larger lymphatic channels or nodes, or even after disruption of smaller channels in areas (e.g. infraorbital) with limited or vulnerable lymphatic drainage. Adequate drainage can be achieved by orienting flaps in the same direction as lymphatic patterns. The surgeon must be mindful of the variability in drainage patterns and sites and the fact that malignancies do not respect the midline. Since cross-communication between lymphatics may result in contralateral drainage, bilateral examination for lymphadenopathy should be undertaken before a neoplasm is excised.

Additional figures and table, Sensory innervation of the head and neck, available in our eBook (see inside front cover for access code).

REFERENCES

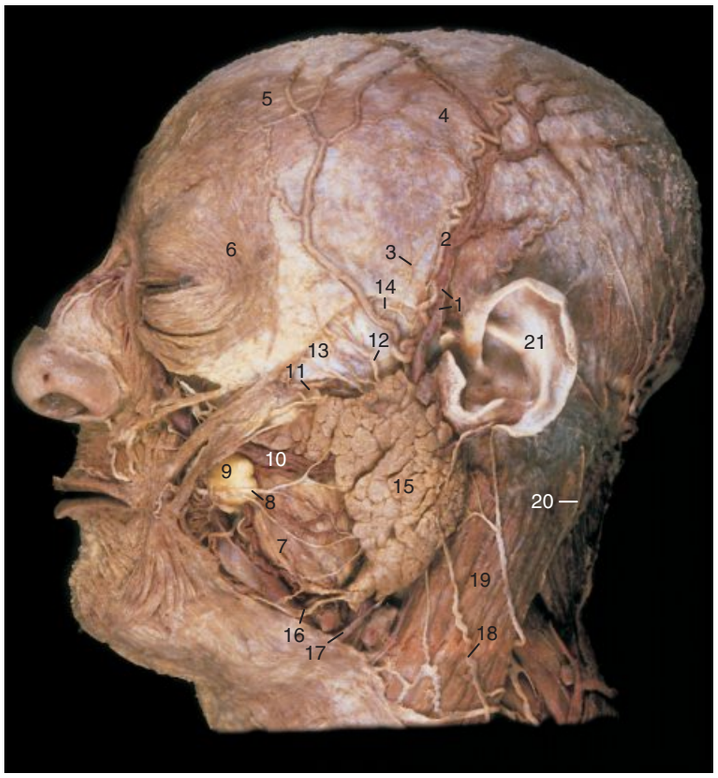
1. Dzubow LM. Tissue movement – a macrobiomechanical approach. *J Dermatol Surg Oncol*. 1989;15:389–399.
2. Dzubow LM. *Facial Flaps: Biomechanics and Regional Application*. Norwalk: Appleton & Lange; 1990.
3. Robinson JK, Sengelmann RD, Hanke CW, Siegel DM. *Surgery of the Skin: Procedural Dermatology*. St Louis: Mosby; 2005.
4. Salasche SJ, Bernstein G, Senkarik M. *Surgical Anatomy of the Skin*. Norwalk: Appleton & Lange; 1988.
5. Summers BK, Siegle RJ. Facial cutaneous reconstructive surgery: general aesthetic principles. *J Am Acad Dermatol*. 1993;29:669–681.
6. Zide BM, Jelks GW. *Surgical Anatomy of the Orbit*. New York: Raven Press; 1985.
7. Stegman SJ, Tromovitch TA, Glogau RG. *Cosmetic Dermatologic Surgery*. 2nd ed. St Louis: Mosby; 1990.
8. Larrabee WF, Makielski KH. *Surgical Anatomy of the Face*. New York: Raven Press; 1993.
9. Tromovitch TA, Stegman SJ, Glogau RG. *Flaps and Grafts in Dermatologic Surgery*. Chicago: Year Book; 1989.
10. Gosain AK, Yousif NJ, Madiedo G, et al. Surgical anatomy of the SMAS: a reinvestigation. *Plast Reconstr Surg*. 1993;92:1254–1265.
11. Burger GC, Menick FJ. *Aesthetic Reconstruction of the Nose*. St Louis: Mosby; 1994.
12. Harvey DT, Taylor SR, Itani KM, Loewinger RJ. Mohs micrographic surgery of the eyelid: an overview of anatomy, pathophysiology, and reconstruction options. *Dermatol Surg*. 2013;39:673–697.
13. Carruthers JD, Fagien S, Rohrich RJ, et al. Blindness caused by cosmetic filler injection: a review of cause and therapy. *Plast Reconstr Surg*. 2014;134:1197–1201.
14. Myckatyn TM, Mackinnon SE. A review of facial nerve anatomy. *Semin Plast Surg*. 2004;18:5–11.
15. Prendergast PM. Anatomy of the face and neck. In: Shiffman MA, Di Giuseppe A, eds. *Cosmetic Surgery*. Berlin: Springer; 2013:29–46.
16. Brown SM, Oliphant T, Langtry J. Motor nerves of the head and neck that are susceptible to damage during dermatological surgery. *Clin Exp Dermatol*. 2014;39:677–682.
17. Carlson KC, Roenigk RK. Know your anatomy: perineural involvement of basal and squamous cell carcinoma on the face. *J Dermatol Surg Oncol*. 1990;16:827–833.
18. Drake RL. *Gray's Atlas of Anatomy*. Churchill Livingstone; 2007.
19. Robinson PP. Recession of sensory loss from the midline following trigeminal sensory root section: collateral sprouting from the normal side? *Brain Res*. 1983;259:177–180.
20. Leach BC, Kulbersh JS, Day TA, Cook J. Cranial neuropathy as a presenting sign of recurrent aggressive skin cancer. *Dermatol Surg*. 2008;34:483–497.



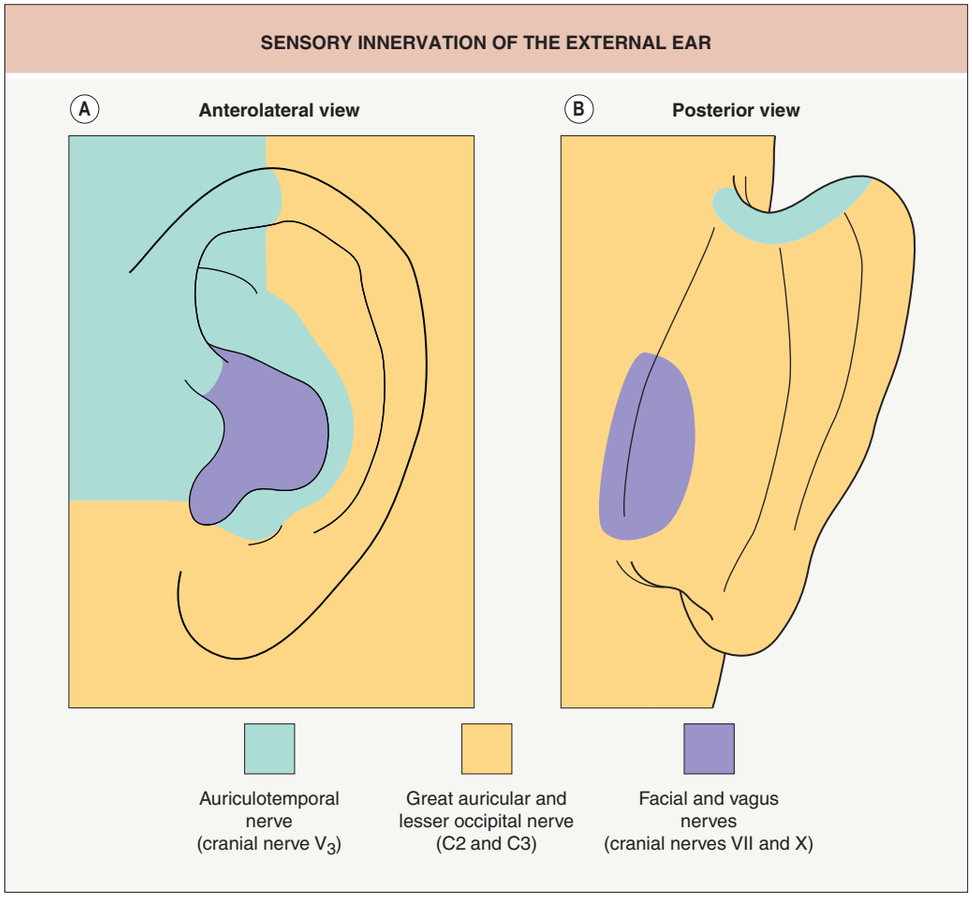
eFig. 142.1 Location of the spinal accessory nerve (cranial nerve XI) within the posterior triangle of the neck. The spinal accessory nerve (lifted by the dissecting probe) traverses behind the sternocleidomastoid muscle towards the trapezius muscle.



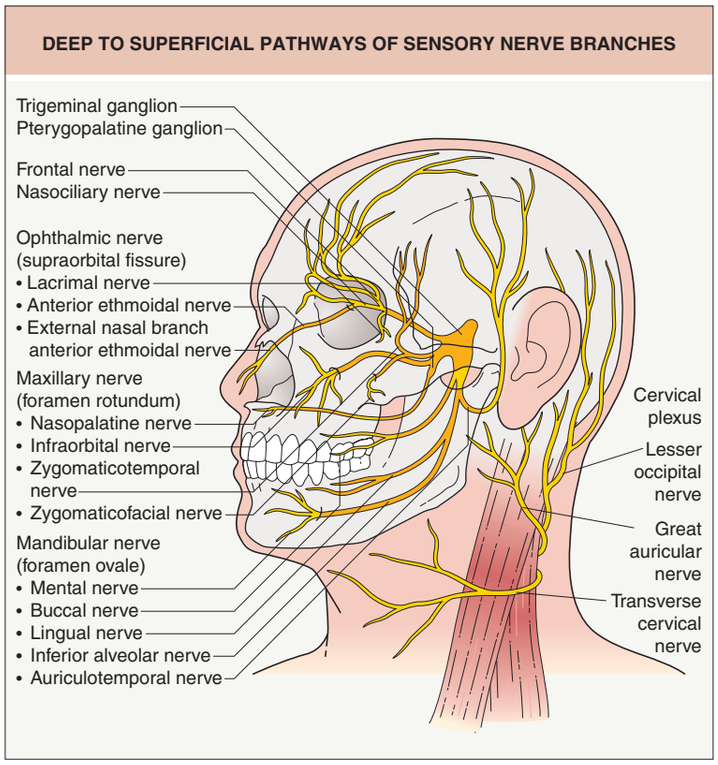
eFig. 142.2 Facial artery and other anatomic structures of the lower face and neck. The facial artery (6) is seen passing behind the submandibular gland and then over the mandible in a location anterior to the masseter. The following structures are identified: 1, masseter muscle; 2, marginal mandibular branch of facial nerve; 3, parotid gland; 4, cervical branch of facial nerve; 5, jugulodigastric lymph nodes; 6, facial artery; 7, hypoglossal nerve; 8, facial vein; 9, posterior branch of retromandibular vein; 10, sternocleidomastoid muscle (SCM); 11, great auricular nerve; 12, external jugular vein; 13, transverse cervical nerve; 14, spinal accessory nerve; 15, clavicular head of SCM; 16, sternal head of SCM; 17, common carotid artery; 18, internal carotid artery; 19, external carotid artery; 20, submandibular gland; 21, body of mandible; and 22, buccal fat pad. *From Logan B, Reynolds P, Rice S, Hutchings R: McMinn's Color Atlas of Head and Neck Anatomy. 5th ed. Neck superficial dissection III. London: Elsevier; 2017.*



eFig. 142.3 Branches of the facial nerve. The following structures are identified: 1, auriculotemporal nerve; 2, superficial temporal artery; 3, zygomaticotemporal nerve; 4, galea aponeurotica; 5, frontalis muscle; 6, orbicularis oculi muscle; 7, masseter muscle; 8, buccal branches of facial nerve; 9, buccal fat pad; 10, parotid duct; 11, transverse facial artery; 12, zygomatic branch of facial nerve; 13, zygomatic arch; 14, temporal branch of facial nerve; 15, parotid gland; 16, marginal mandibular branch of facial nerve; 17, cervical branch of facial nerve; 18, great auricular nerve; 19, sternocleidomastoid muscle; 20, lesser occipital nerve; and 21, cartilage of pinna. *From Logan B, Reynolds P, Rice S, Hutchings R: McMinn's Color Atlas of Head and Neck Anatomy. 5th ed. Face superficial dissection B. London: Elsevier; 2017.*



eFig. 142.4 Sensory innervation of the external ear. **A** Anterolateral view. **B** Posterior view.



eFig. 142.5 Deep to superficial pathways of sensory nerve branches.

SENSORY INNERVATION OF THE HEAD AND NECK

- **Trigeminal nerve**
  - Ophthalmic branch (V_1)
    - Nasociliary – anterior nasal septum, nasal wall, cornea, iris, ethmoid/sphenoid sinuses
    - Infratrochlear – root of nose, medial canthus
    - Anterior ethmoidal (external nasal branch) – nasal dorsum, tip, supratip, columella
    - Ciliary – corneal surface
    - Frontal
      - Supratrochlear – medial upper eyelid, medial forehead, frontal scalp
      - Supraorbital – forehead, scalp, upper eyelid
    - Lacrimal – lateral eyelid
  - Maxillary branch (V_2)
    - Infraorbital – medial cheek, upper lip, nasal sidewall and ala, lower eyelid
    - Zygomaticofacial – malar eminence
    - Zygomaticotemporal – temple, supratemporal scalp
    - Superior alveolar and palatine – upper teeth, palate, nasal mucosa, gingiva
  - Mandibular branch (V_3)
    - Auriculotemporal – external anterior ear and external auditory canal, temple, temporoparietal scalp, temporomandibular joint, tympanic membrane
    - Buccal – cheek, buccal mucosa, gingiva
    - Inferior alveolar – mandibular teeth; chin and lower lip (mental nerve)
    - Lingual – anterior two-thirds of tongue, floor of mouth, lower gingivae
- **Vagus nerve** (X) – external auditory canal, concha, postauricular sulcus
- **Facial nerve** (VII) – external auditory canal, postauricular sulcus
- **Great auricular nerve** (C2, C3) – lateral neck, angle of the jaw, posterior and inferior ear, portions of the helical rim, postauricular scalp
- **Facial nerve (VII)** – external auditory canal, concha, postauricular sulcus
- **Vagus nerves** – external auditory canal, concha, postauricular sulcus
- **Lesser occipital nerve** (C2) – neck, postauricular scalp
- **Transverse cervical nerve** (C2, C3) – anterior neck
- **Supraclavicular nerve** (C3, C4) – anterior chest, shoulder

eTable 142.1 Sensory innervation of the head and neck.

143 Anesthesia

George J. Hruza

Key features

- Local anesthetics are classified into two groups – amides and esters – depending upon the linkage in their intermediate chain
- "Anesthetic allergies" vary from palpitations secondary to epinephrine and vasovagal reactions, to urticaria and anaphylaxis from preservatives or the local anesthetic (especially esters)
- Additives to the local anesthetic include epinephrine, sodium bicarbonate, and hyaluronidase
- Nerve blocks are particularly helpful when performing procedures on the face, digits, and palmoplantar surfaces

INTRODUCTION

Effective anesthesia is an essential component of dermatologic surgery, and almost all dermatologic surgical procedures can be performed under local anesthesia. Local anesthetics have been in use since the 1880s with the introduction of cocaine hydrochloride, which was extracted from the leaves of the South American bush *Erythroxylon coca*[1]. This was followed by procaine in 1904, tetracaine in 1930, and lidocaine, the first amide local anesthetic, was introduced in 1943[1]. The introduction of lidocaine was a major breakthrough because lidocaine is far less likely to cause an allergic reaction than the ester-type anesthetics that preceded it.

Local anesthesia has several advantages over general anesthesia, including reduced morbidity (especially in poor-risk patients), reduced cost, reduced procedure time, and faster recovery. The main disadvantages are some limitation on the extent of a procedure and the possibility of greater patient discomfort from the injections. Knowledge of the physiology, dosage, side effects, and proper "painless" local anesthesia technique are essential for performing dermatologic surgery and to keep patients safe and satisfied[2].

DISCUSSION

Physiology and Structure

Local anesthetics act by blocking sodium channels in the axon cell membrane, and this prevents sodium from entering the nerve cell. The nerve cell is not depolarized and consequently the action potential is blocked. The cationic form of the anesthetic appears to bind to the inner pore of voltage-gated sodium channels, possibly leading to both narrowing of the pore lumen (steric block) and creation of an electrostatic barrier to permeation[3]. Smaller unmyelinated C-type nerve fibers that conduct pain sensation are blocked more quickly and easily than intermediate fibers that also carry sensations of heat and cold. The myelinated A-type fibers that carry pressure sensation and motor fibers are blocked last. Clinically, this is evident when an area seems fully anesthetized for scalpel surgery, but the patient still feels the pressure of the surgeon's fingers at the surgical site.

All local anesthetics consist of three parts (Fig. 143.1):

- a secondary or tertiary amine end
- an aromatic end
- an intermediate connecting chain that contains an ester or amide.

The aromatic portion is hydrophobic and lipophilic. This is essential to allow the anesthetic to diffuse through nerve cell membranes. The amine portion is hydrophilic and is responsible for the anesthetic's water solubility, which is important for preparing, storing, and administering the anesthetic[3].

Local anesthetics are weak organic bases, which, to be water-soluble and injectable, require the addition of a hydrochloride salt. In aqueous solution, the salt equilibrates between the ionized and non-ionized form. The ionized form is water-soluble, allowing injection into and diffusion through tissue. However, it is the non-ionized, lipid-soluble base that can diffuse into the nerve cell membrane. Within the sodium channel's inner pore, it is the ionized cation that is responsible for blocking nerve conduction (see above)[3].

The dissociation constant (pKa) of each anesthetic determines the proportion of the anesthetic base and its cation at a given pH. The pKa of all local anesthetics is higher than physiologic pH. For most local anesthetics at a pH of 7.4, 80% or more is in the cationic ionized form. Alkalinization of the anesthetic solution, as is done with the addition of sodium bicarbonate, will speed its onset of action as more of the anesthetic will be in the non-ionized form. However, if the pH is raised too much, the anesthetic may precipitate out of solution. Anesthetic sensitivity to pH also helps explain why infected tissue is difficult to effectively anesthetize[4]. The inflammatory response surrounding the infection acidifies the site (reduces the pH), which reduces the proportion of the anesthetic in the non-ionized, lipid-soluble form.

Pharmacology

Local anesthetics are classified into two groups, depending on the linkage in the intermediate chain (Table 143.1). Amide anesthetics have an amide linkage and ester anesthetics have an ester linkage (Fig. 143.1). They differ in how they are metabolized and in the risk of sensitization. Ester anesthetics are hydrolyzed by plasma pseudocholinesterase, and the metabolites are excreted by the kidneys. Patients with a deficiency of functional pseudocholinesterase, who are often diagnosed after prolonged paralysis following administration of standard doses of succinylcholine, are at an increased risk of ester anesthetic toxicity. The metabolite para-aminobenzoic acid (PABA) is responsible for the allergic reactions seen with ester anesthetics. Amide anesthetics are metabolized by the hepatic microsomal cytochrome P450 enzyme system, and the metabolites are excreted by the kidneys. Patients with severe liver disease may be at increased risk of amide anesthetic toxicity.

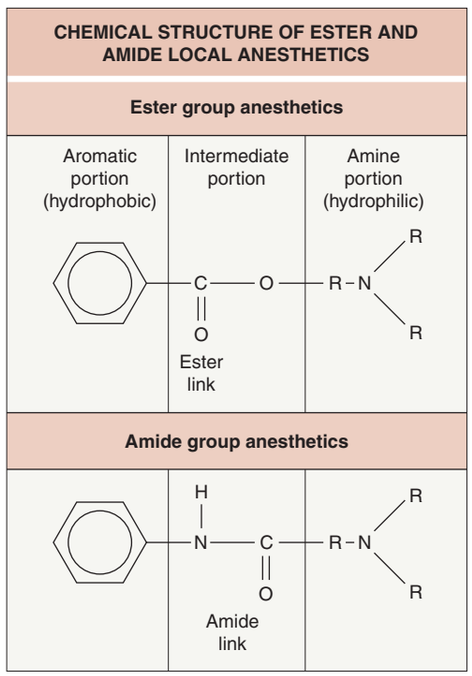


Fig. 143.1 Chemical structure of the ester and amide group local anesthetics. The aromatic (hydrophobic and lipophilic) end is joined to the amine (hydrophilic) end with an ester or amide linkage.

LOCAL ANESTHETICS FOR INFILTRATIVE AND NERVE BLOCK ANESTHESIA					
Generic name	**Trade name®**	**Onset (min)**	**Duration plain (h)**	**Maximum dose plain (mg for 70 kg person)**	**Maximum dose with epinephrine (mg for 70 kg person)**
Amides					
Articaine	Septocaine	2–4	0.5–2	350	500
Bupivacaine hydrochloride	Marcaine	5–8	2–4	175	225
Etidocaine	Duranest	3–5	3–5	300	400
Levobupivacaine hydrochloride	Chirocaine	2–10	2–4	150	Not available
Lidocaine	Xylocaine	Rapid	0.5–2	350	500 (3500 dilute)
Mepivacaine	Carbocaine	3–20	0.5–2	300	500
Prilocaine hydrochloride	Citanest	5–6	0.5–2	400	600
Ropivacaine*	Naropin	1–15	2–6	200	Not available
Esters					
Chloroprocaine hydrochloride	Nesacaine	5–6	0.5–2	800	1000
Procaine	Novocaine	5	1–1.5	500	600
Tetracaine	Pontocaine	7	2–3	100	Not available
*Addition of epinephrine has no effect on onset or duration of action of ropivacaine.					

Table 143.1 Local anesthetics for infiltrative and nerve block anesthesia. In clinical practice, the duration of anesthesia appears to be less than stated, especially for head and neck areas. Addition of epinephrine prolongs anesthesia by a factor of two. 1% lidocaine solution = 10 mg/ml.

Local anesthetics differ in the speed of onset, duration of action, and potency, depending on each compound's intrinsic chemical characteristics (Table 143.1). A low pKa leads to rapid onset of anesthesia, as more of the anesthetic will be in the non-ionized form. Greater lipid solubility is associated with higher anesthetic potency, as the compound penetrates the nerve cell membrane more easily. Duration of action is determined by the strength of anesthetic binding to the sodium channel pore.

For pregnant women, the local anesthetic of choice is lidocaine. It is historically classified as FDA pregnancy category B, which means that, in animal studies, no teratogenic effects have been documented. Studies in pregnant women who received lidocaine during the first trimester of pregnancy have shown no increase in anatomic abnormalities in the newborns. However, it is recommended that lidocaine, as with all other pharmacologic agents, be used cautiously during the first 4 months of pregnancy, when maximum organogenesis takes place. Lidocaine crosses the placenta into the fetus. Lidocaine can be safely used in nursing mothers with the realization that some of the anesthetic may be excreted in the mother's milk.

Lidocaine can be safely used in children, but the maximum recommended dosage should be adjusted downward based on the child's weight and age. Care must be taken in premature infants due to cardiovascular effects. Parabens, used as preservatives, are bound to albumin. In a jaundiced newborn, they could displace bilirubin from the albumin, worsening the hyperbilirubinemia[5]. For this reason, only paraben-free anesthetics should be used in newborns.

Additions to Local Anesthetics

Epinephrine

All local anesthetics, except for cocaine hydrochloride, relax vascular smooth muscle, which results in vasodilation. This causes increased bleeding at the operative site and reduced duration of anesthetic action as the anesthetic is rapidly removed from the surgical site via the dilated blood vessels. The addition of epinephrine (adrenaline) has the beneficial effect of constricting blood vessels, which prolongs the duration of anesthesia 100% to 200% by slowing removal of the anesthetic from the surgical site. Also, there is reduced intraoperative bleeding due to the vasoconstriction. The addition of epinephrine provides more effective anesthesia by decreasing the volume of anesthetic needed. The reduced absorption rate decreases anesthetic toxicity and allows larger doses to be used safely. The vasoconstrictive effect of epinephrine, manifested by skin blanching, takes about 15 minutes to fully develop. While they usually coincide, blanching does not always denote the anesthetized area.

Epinephrine is premixed with local anesthetics at a concentration of 1 : 100 000 or 1 : 200 000. However, concentrations as low as 1 : 1 000 000 achieve effective vasoconstriction, while concentrations >1 : 100 000 are associated with a greater risk of side effects. The concentration used in a given patient should be individualized. Patients who have relative contraindications to epinephrine should receive lower concentrations, while highly vascular areas such as the scalp should receive higher concentrations. At an epinephrine concentration of 1 : 100 000, the maximum dosage used is determined by the anesthetic with which the epinephrine is premixed (Table 143.1).

Epinephrine is a strong β- and α-agonist and, as such, it must be used cautiously in patients with altered β- and α-receptors. Absolute contraindications to the use of epinephrine include hyperthyroidism and pheochromocytoma. Patients taking β-blockers, monoamine oxidase inhibitors, tricyclic antidepressants, and phenothiazines are more sensitive to epinephrine. Therefore, epinephrine should be used with caution, with the dose and concentration reduced accordingly. In patients taking β-blockers, severe hypertension developing after injection of epinephrine-containing anesthetics has been reported[6]. This is probably due to unopposed α-adrenergic activity with its associated vasoconstriction. Fortunately, this reaction seems to be quite rare[7], and mainly occurs when higher doses are used. Patients with severe hypertension or with severe cardiovascular disease (especially coronary artery disease) may have their underlying disease exacerbated if large amounts of epinephrine are administered with the local anesthetic. High doses of epinephrine can induce labor. However, the low doses of epinephrine used in cutaneous surgery can be safely used during pregnancy. Epinephrine use in the periorbital area in patients with narrow angle glaucoma should be avoided, as it may aggravate the patient's glaucoma.

The use of epinephrine on digits has been controversial. Historically, epinephrine was not used on digits for fear of causing vasoconstriction that might result in digital necrosis. More recent studies have not demonstrated any increased risk from epinephrine in digital anesthesia. It appears that most cases of digital necrosis occurred due to vessel compression from too much anesthetic volume being injected (tamponade), constricting circumferential dressings, tourniquets, postoperative hot soaks (possibly due to heat-induced edema), infection, use of vasoconstrictive anesthetics such as cocaine hydrochloride, or non-standard mixing of lidocaine with epinephrine[8]. There is no evidence of digital necrosis due solely to commercially available lidocaine with epinephrine[8]. However, epinephrine is contraindicated for digital anesthesia in patients with peripheral artery disease. We have found that combining lidocaine with dilute epinephrine (1 : 500 000) and small volumes provides safe digital anesthesia. Ring blocks of the digit should be avoided.

Self-limited systemic side effects of epinephrine include palpitations, anxiety, fear, diaphoresis, headache, tremor, weakness, tachycardia, and elevated blood pressure. These signs and symptoms can be seen on occasion even with normal doses used for skin surgery, but they usually resolve within a few minutes (Table 143.2). They are more commonly seen when injecting highly vascular areas, especially the face and scalp. Skin necrosis from vasoconstriction is an extremely rare complication of epinephrine injection and would be an issue only in patients with severe vascular compromise at the injection site.

Serious side effects of epinephrine injection include cardiac arrhythmias (e.g. ventricular tachycardia, ventricular fibrillation), cardiac arrest, and cerebral hemorrhage. None of these should be expected to occur at the doses used for skin surgery. However, it is prudent to limit the total dose injected in patients with severe cardiac disease.

Epinephrine is stable only in an acidic environment. Therefore, when epinephrine is premixed with local anesthetics, the pH is lowered into the 3.5 to 5.5 range with the addition of acidic preservatives such as sodium metabisulfite to stabilize the epinephrine. This acidic solution not only is more painful at the time of injection[9], but also slows the onset of anesthetic action, as less anesthetic is in the non-ionized form. By preparing the mixture fresh daily and using it by the end of the day, the mixture has a higher pH, which is less painful. Adding 0.5 ml epinephrine (1 : 1000) to 50 ml plain lidocaine will give a final concentration of 1 : 100 000 epinephrine. Alternatively, the lidocaine with epinephrine can be neutralized with sodium bicarbonate (see below).

Sodium bicarbonate

Injecting the standard mixture of lidocaine with epinephrine at a pH of 3.5 to 5.5 is quite painful, with significant stinging due to the acidic pH. The pH can be neutralized with the addition of sodium bicarbonate. Adding one part of 8.4% sodium bicarbonate to ten parts lidocaine with epinephrine will bring the pH into a more physiologic 7 to 8 range. This mixture significantly reduces the pain of anesthetic injection[9,10]. Both components can be drawn up into the syringe, immediately before injection. Alternatively, 5 ml sodium bicarbonate (8.4%) can be added to a 50 ml bottle of lidocaine with epinephrine. As the epinephrine activity is lost at a rate of 25% per week in an alkaline or neutral environment, the mixture should be labeled with the date prepared, kept refrigerated, and used within about 1 week. There is evolving FDA and United States Pharmacopeia (USP) <https://www.usp.org/compounding/general-chapter-797> guidance that requires any buffered local anesthetic (in office "compounding") to be used within 4 hours of preparation. As state boards of pharmacy adopt this guidance, physicians in those states will be required to comply. Several dermatology societies are developing a USP monograph to extend the time that buffered lidocaine can be used after preparation.

Hyaluronidase

Hyaluronidase (derived from bovine testicular hyaluronidase) depolymerizes hyaluronic acid, which breaks up ground substance, allowing anesthetics to diffuse further away from the injection point. In addition, there is less distortion of the injected structures[11]. The greater diffusion of anesthetic may decrease its duration of action. Hyaluronidase is most useful for periorbital surgery and to increase the rate of successful nerve blocks. It is prepared by adding 150 units (U) to 30 ml of local anesthetic. Allergic reactions to hyaluronidase are rare, but they can occur. Some surgeons recommend an intradermal skin test before using hyaluronidase. In addition, the preparation may contain thimerosal preservative, which can cause contact dermatitis.

Anesthetic Mixtures

In an attempt to take advantage of different anesthetic properties, some surgeons combine two local anesthetics in one syringe. For example, a combination of lidocaine, for its rapid onset of action, with bupivacaine hydrochloride, for its longer duration of action, is often used. However, a study looking at such combinations has found that these mixtures do not live up to their promise. The mixture seems to take on the properties of one of the components to the exclusion of the other[12]. Therefore, most surgeons will inject the rapid-onset anesthetic first and the longer-acting anesthetic later, to minimize the pain of injection and maximize the duration of action.

Side Effects

Vasovagal reactions

By far the most common side effect of local anesthetic injection is a vasovagal reaction, in which the vagus nerve discharges due to patient anxiety, resulting in an increase in parasympathetic tone (Table 143.2). Vasovagal reactions are manifested by dizziness, diaphoresis, syncope, bradycardia, and hypotension. Placing the patient in the Trendelenburg position will rapidly relieve the patient's symptoms. A cold towel on the forehead can also be helpful. Oxygen, fluids, atropine, or epinephrine are usually not necessary. To avoid significant vasovagal reactions, patients should have local anesthetic infiltrated in the recumbent position.

Allergic reactions

The most important side effect of local anesthetics is the development of allergic reactions. The allergy is usually a type I IgE-mediated reaction manifested by urticaria, angioedema, bronchospasm, and, on rare occasions, anaphylaxis with associated hypotension and tachycardia (Table 143.2). Most true local anesthetic allergies have been reported with ester anesthetics; amide anesthetics are implicated only very rarely. Preservatives added to multidose vials, especially methylparaben and sodium metabisulfite, have frequently been shown to be the cause of "local anesthetic" allergy[13].

There is some allergy cross-reactivity amongst the various ester anesthetics and amongst the amide anesthetics, but there is no cross-reactivity between the ester and amide anesthetic classes. It is PABA

DIFFERENTIAL DIAGNOSIS OF LOCAL ANESTHETIC SYSTEMIC REACTIONS

Diagnosis	Pulse rate	Blood pressure	Signs and symptoms	Emergency management
Vasovagal reaction	Low	Low	Excess parasympathetic tone; diaphoresis, hyperventilation, nausea	Trendelenburg position, cold compress, reassurance
Epinephrine reaction	High	High	Excess α- and β-adrenergic receptor stimulation; palpitations	Reassurance (usually resolves within minutes), phentolamine, propranolol
Anaphylactic reaction	High	Low	Peripheral vasodilation with reactive tachycardia; stridor, bronchospasm, urticaria, angioedema	Epinephrine 1 : 1000 0.3 ml subcutaneous, antihistamines, corticosteroids, fluids, oxygen, airway maintenance
Lidocaine overdose				
1–6 mcg/ml	Normal	Normal	Circumoral and digital paresthesias, restlessness, drowsiness, euphoria, lightheadedness	Observation
6–9 mcg/ml	Normal	Normal	Nausea, vomiting, muscle twitching, tremors, blurred vision, tinnitus, dysgeusia (e.g. metallic taste), confusion, excitement, psychosis	Diazepam, airway maintenance
9–12 mcg/ml	Low	Low	Seizures, cardiopulmonary depression, arrhythmia	Respiratory support
>12 mcg/ml	Severely low	Severely low	Coma, cardiopulmonary arrest	Cardiopulmonary resuscitation and life support

Table 143.2 Differential diagnosis of local anesthetic systemic reactions. In case of systemic reactions during or after local anesthetic injections, hemodynamic signs are helpful in determining the cause of the reaction.

(the metabolite of ester anesthetics) that is thought to be responsible for ester anesthetic allergic reactions. Ester anesthetics can also cause type IV delayed hypersensitivity reactions and cross-react with several contact sensitizers, including PABA, para-amino salicylic acid, and para-phenylenediamine (PPD).

Patients who present with a history of "local anesthetic" allergy need to be questioned in detail about the "allergy" with a review of relevant medical records whenever possible. Often, the "allergy" is a result of a vasovagal reaction or epinephrine sensitivity. If the reaction seems to represent a true allergic reaction and the offending anesthetic is known (usually an ester), using an anesthetic from the other class (usually an amide) in a preservative-free solution is a reasonable option. Skin testing, by an allergist, may be warranted if the offending agent is not certain[14]. The testing should include pinprick followed by intradermal tests of an ester anesthetic, an amide anesthetic, methylparaben, and sodium metabisulfite. Alternatively, for small procedures, adequate anesthesia can be obtained with intradermal injection of 1% diphenhydramine solution. Epinephrine may be added to counteract vasodilation caused by diphenhydramine, to enhance the anesthetic effect, and to reduce systemic antihistamine symptoms[15]. Intradermal normal saline with benzyl alcohol preservative will achieve very brief anesthesia through pressure effects on cutaneous nerve endings and the anesthetic properties of the benzyl alcohol preservative. It can be used for very short procedures such as a shave biopsy[16].

Limited allergic reactions can be managed with oral antihistamines and prednisone. However, patients developing bronchospasm, angioedema, or hemodynamic compromise require immediate emergency management including subcutaneous epinephrine, bronchodilators, parenteral antihistamines, corticosteroids, intravenous fluids, and oxygen (Table 143.2).

Local side effects

Bruising and edema are frequently seen after local anesthetic infiltration, especially in the periorbital area. Periorbital edema will often develop after surgery on the forehead and frontal scalp. Transient motor nerve paralysis is sometimes seen. This may be delayed for some time after the sensory nerves have become anesthetized, because of the large myelinated nerve fibers involved. The paralysis may persist for several hours after the sensory nerves have returned to normal. Informing the patient when a motor nerve has been affected by the anesthetic will eliminate distressed patient telephone calls. Prolonged sensory nerve paresthesia may develop if a sensory nerve is injured due to intraneural injection. This is most commonly seen after nerve blocks. It can be minimized by avoiding intraneural injections and by using small-gauge needles for injection.

Overdosage

If the local anesthetic dosage administered is kept within recommended ranges, clinical symptoms of local anesthetic overdose are unlikely to be encountered. Maximum recommended dosages of *lidocaine* are 5 mg/kg plain (i.e. with no epinephrine), 7 mg/kg if with epinephrine and at standard (1%–2%) concentrations, and 35–50 mg/kg for tumescent lidocaine anesthesia consisting of dilute 0.05%–0.1% lidocaine with 1 : 1 000 000 epinephrine (Table 143.1)[17,18].

The symptoms of local anesthetic overdose are directly related to its serum blood level, with worsening CNS and cardiovascular signs and symptoms as the level increases (Table 143.2). CNS symptoms start with circumoral and digital numbness and tingling, followed by lightheadedness, tinnitus, visual disturbances, slurred speech, muscle twitching, and, finally, seizures and coma. Cardiovascular and pulmonary symptoms develop at significantly higher doses than do early CNS symptoms and include hypotension, arrhythmias, respiratory depression, and cardiac arrest.

When lidocaine is administered, there are over 150 potential drug–drug interactions. Most are minor or only relevant when large doses of lidocaine are used. Patients receiving medications that inhibit the liver's cytochrome P450 system (e.g. erythromycin, ketoconazole, itraconazole; see Ch. 131), and therefore inhibit lidocaine metabolism, can exhibit signs of lidocaine overdose at lower doses. With large doses of lidocaine, patients taking class I and III antiarrhythmic drugs (e.g. amiodarone) are at increased risk of cardiac arrhythmias and those taking CNS depressants (e.g. opiates) are at increased risk of CNS toxicity.

Bupivacaine hydrochloride has a greater risk of cardiac toxicity than lidocaine. *Prilocaine hydrochloride* metabolizes to ortho-toluidine, which is an oxidizing agent capable of converting hemoglobin to methemoglobin. This can become significant with large doses of more than 500 mg. *Benzocaine* has also been implicated in causing methemoglobinemia when used on mucosal surfaces[19]. The treatment of methemoglobinemia is methylene blue infusion.

Topical Anesthetics

Skin

Historically, the only anesthetic used for topical anesthesia of keratinized skin was benzocaine, which is an ester anesthetic. Anesthesia was generally effective only when applied to traumatized skin. Little, if any, anesthesia was achieved in intact normal skin. Of greater concern was the high rate of allergic contact dermatitis seen with benzocaine.

There are now several topical anesthetics that achieve moderate superficial anesthesia of intact skin (Table 143.3). EMLA® is available in a cream formulation or as a disc. It is a eutectic mixture of 2.5% lidocaine and 2.5% prilocaine hydrochloride. EMLA® is able to achieve superficial anesthesia, with the degree of anesthesia related to the amount and duration of application before surgery. The cream is applied as a thick layer under occlusion at least 1 hour before the procedure while the disc itself provides occlusion. It is especially useful for reducing the pain of non-ablative laser procedures and to reduce the pain of local anesthetic or other injections. Some dermatologists who perform CO_2 laser ablative resurfacing solely under EMLA® anesthesia prepare the skin with vigorous degreasing followed by two applications of EMLA® 1 hour apart under occlusion. Additional EMLA® is applied to the skin after the first pass with the laser has removed the epidermis.

EMLA® appears to be safe, but some caution is advised when using large amounts on skin with a damaged skin barrier and in infants who might be susceptible to methemoglobinemia from too much prilocaine hydrochloride absorption. For recommended applications in children, see Table 143.4. It should not be used in patients with G6PD deficiency. EMLA® often blanches the skin after application, followed by vasodilation 30–60 minutes after its removal. The vasodilation is usually of no clinical significance, but there are reports of petechiae and purpura developing at the site of EMLA® application. Additional reported side effects include occasional burning and irritation, chemical injury to the eye, contact urticaria, and allergic contact dermatitis, with the latter two reactions most often due to the prilocaine component.

Other preparations that have been optimized for epidermal penetration include: LMX®, containing 4% or 5% lidocaine (Table 143.5); Topicaine®, containing 4% lidocaine; 4% tetracaine gel; 30%–40% lidocaine in acid mantle cream; and various other compounded mixtures of lidocaine, benzocaine, and tetracaine (Table 143.3). Due to safety issues reported with compounded medications (see below), the FDA has severely restricted access to compounded topical anesthetics.

In a comparison study, EMLA® and LMX® 4% were found to achieve superior anesthesia to tetracaine 4% gel, which was superior to Betacaine LA®, which was superior to control[20]. According to the manufacturer, LMX® does not require occlusion to be effective. A comparison of EMLA® under occlusion and LMX® unoccluded found that LMX® achieved equivalent anesthesia to EMLA® after less than one-third of application time[21]. None of the topical anesthetics have any significant effectiveness for palmar or plantar surfaces.

Pliaglis® is a 7% lidocaine/7% tetracaine preparation that, when cold, is a cream, but when placed on the skin and exposed to air it becomes a flexible membrane. Once anesthesia has been achieved (after about 30 minutes), the membrane can be peeled off prior to the procedure. This product is useful for laser procedures[22]. The anesthetic level is equivalent to that of the other topical anesthetics.

Iontophoresis of 1%–4% lidocaine with epinephrine can enhance the depth and effectiveness of topical anesthesia. It is practical only for rather small areas, but anesthesia can be achieved within a few minutes with a 1 mA current. The main drawback is the additional equipment and supplies needed. Ultrasound or warm steaming of the skin also enhances the effect of topical anesthetics, probably by enhancing anesthetic penetration. In addition, fractionated ablative lasers and skin microneedling devices have been shown to enhance penetration of topical anesthetics, leading to improved local anesthesia[23]. When performing multi-pass laser treatments of large areas, these techniques may reduce the need for injectable anesthetics.

TOPICAL ANESTHETICS FOR MUCOUS MEMBRANE AND INTACT SKIN ANESTHESIA				
Generic name	**Trade name®**	**Concentration (%)**	**Type**	**Primary use**
Benzocaine	Americaine otic	20	Ester	Tympanic membrane
Benzocaine gel, liquid, spray	HurriCaine	20	Ester	Mucous membranes
Benzocaine/tetracaine/butamben (butyl aminobenzoate) gel, liquid, spray	Cetacaine, Exactacain		Esters	Mucous membranes
Benzocaine/lidocaine/tetracaine	compounded	Various	Ester/amide/ester	Intact skin
Cocaine hydrochloride nasal solution	Goprelto, Numbrino	2–10	Ester	Nasal mucosa
Dibucaine (cinchocaine)	Nupercainal	1	Amide	Mucous membranes
Lidocaine cream	LMX	4–5	Amide	Intact skin (4%); anorectal (5%)
Lidocaine gel	Topicaine 4	4	Amide	Intact skin
Lidocaine solution	Xylocaine	2–5	Amide	Mucous membranes
Lidocaine in acid mantle cream	compounded	30–40	Amide	Intact skin
Lidocaine/prilocaine eutectic mix [cream or disc]	EMLA	2.5/2.5	Amides	Intact skin
Lidocaine/prilocaine cream	Lidopril	2.5/2.5	Amides	Intact skin
Lidocaine/tetracaine peel	Pliaglis	7/7	Amide/ester	Intact skin
Lidocaine/tetracaine patch	Synera	7/7	Amide/ester	Intact skin
Proparacaine (proxymetacaine) ophthalmic solution	Alcaine	0.5	Ester	Conjunctiva
Tetracaine gel	Tetracaine gel	4	Ester	Intact skin
Tetracaine ophthalmic solution	Pontocaine	0.5	Ester	Conjunctiva

Table 143.3 Topical anesthetics for mucous membrane and intact skin anesthesia. Anesthetics for topical skin anesthesia require application 0.5–2 hours prior to surgery under occlusion for maximal effect. Benzocaine is a potent topical sensitizer.

MAXIMUM RECOMMENDED EMLA® APPLICATION IN CHILDREN				
Age	**Weight (kg)**	**Maximum total dose of cream (g)**	**Maximum area (cm^2)**	**Maximum time (hours)**
<3 months	<5	1	10	1
3–12 months	5–10	2	20	4
1–6 years	10–20	10	100	4
7–12 years	>20	20	200	4

Table 143.4 Maximum recommended application of eutectic mix of lidocaine 2.5%/prilocaine 2.5% (EMLA®) in children. Because of the prilocaine, the product should not be used in: (1) premature neonates with a gestational age <37 weeks because of increased risk of methemoglobinemia due to immature reductase pathways; and (2) young children (especially those <1 year of age) receiving medications that may increase the risk of methemoglobinemia (e.g. acetaminophen, antimalarials, dapsone, nitrofurantoin, nitroglycerin, phenobarbital, phenytoin, sulfonamides).

MAXIMUM RECOMMENDED LIDOCAINE 4% LIPOSOMAL CREAM (LMX4®) APPLICATION IN CHILDREN			
Age	**Weight (kg)**	**Maximum area**	**Maximum time (hours)**
<12 months	<10	100 cm^2 (4 × 4 in)	1
1–6 years	10–20	200 cm^2 (5.5 × 5.5 in)	2
7–12 years	>20	600 cm^2 (9 × 9 in)	2*

*0.072 mg 4% lidocaine absorption/cm^2/h × 600 cm^2 × 2 h = 86 mg (≤4 mg/kg).

Table 143.5 Maximum recommended lidocaine 4% liposomal cream (LMX4®) application in children. Cream should be applied to intact skin, with or without occlusion. Currently not FDA approved for children <2 years of age, so its application in that age group represents an off-label use. *Courtesy Julie V. Schaffer, MD.*

Topical skin anesthetics are useful for primarily non-invasive laser, intense pulsed light, and other energy-based therapies (see Ch. 137). They are very helpful in reducing the pain of needle insertion as well as some of the pain of injection when injecting local anesthetics, botulinum toxin, or filler materials such as the various hyaluronic acid-based filler materials that, due to their acidity, sting on injection. Of note, filler materials are now frequently premixed with lidocaine to reduce the pain of their injection (see Table 158.4). However, anesthesia is too unpredictable to use topical skin anesthetics even for minor surgical procedures such as skin biopsies, curettage, or electrodesiccation.

The various preparations have different recommendations regarding times of application and need for occlusion. However, for maximal effectiveness, the anesthetic should be applied as a thick layer under occlusion to the proposed treatment area for at least 1 hour. Caution should be exercised when large areas are to be anesthetized, especially when using compounded mixtures with high lidocaine concentrations, as several deaths have been reported in patients applying compounded topical anesthetics under occlusion to their entire lower extremities.

Mucous membranes

Topical anesthetics for mucous membranes are far more effective than skin anesthetics, as the stratum corneum barrier is absent (Table 143.3). One to two drops of 0.5% tetracaine into each eye achieves complete conjunctival anesthesia after a few seconds of stinging. This allows for insertion of eye shields or painless injection through the conjunctiva. Proparacaine (proxymetacaine) hydrochloride is an equally effective alternative conjunctival anesthetic that has less associated stinging sensations.

A 2%–10% solution of cocaine hydrochloride is the topical anesthetic of choice for intranasal anesthesia because of its excellent vasoconstrictive and hemostatic properties. However, onerous record-keeping requirements make it relatively impractical for in-office use. Due to its significant cardiac stimulatory effects, cocaine hydrochloride should be used with caution in patients with significant heart disease.

Oral and anal mucosa can be effectively anesthetized within a couple of minutes with 2%–4% lidocaine jelly or viscous lidocaine as well as various benzocaine-containing preparations. Topical intraoral anesthesia is especially helpful in reducing the pain of nerve block injections done via the intraoral route.

Cryoanesthesia

Rapid cooling of the skin surface is used routinely for many non-ablative laser procedures. The anesthesia is achieved with one of the following: a short burst of cryogen sprayed onto the skin surface (Dynamic Cooling

COMPRESSED AIR DELIVERY SYSTEMS FOR LIDOCAINE					
Generic name	**Delivery system**	**Trade name®**	**Amount/concentration**	**Type**	**Primary use**
Lidocaine HCl monohydrate powder	Pressurized helium	Zingo	0.5 mg (pre-filled)	Amide	Intact skin
Lidocaine buffered powder	Compressed carbon dioxide	J-tip	1% or 2%	Amide	Intact skin

Table 143.6 Compressed air delivery systems for lidocaine. Lidocaine is delivered into the dermis.

Device™); a cold glass window placed directly onto the site being treated (contact cooling); an iced gel placed on the surface being treated (passive cooling); or −5°C refrigerated air blown onto the skin surface with a coupling gel in place (Cryo 5™). All of these methods cool the skin to reduce pain of laser treatment and to protect the epidermis from laser-induced heat injury.

Cryoanesthesia can also be helpful in skin surgery. Dermabrasion can be done entirely under cryoanesthesia by freezing the skin with a cryogen spray before dermabrading. Unfortunately, the most effective and safe cryogen sprays (Frigiderm®, Fluro-Ethyl®) contain chlorofluorocarbons that are harmful to the ozone layer, and their manufacture has been discontinued. Ethyl chloride spray can, through evaporative cooling, achieve brief anesthesia to reduce the pain of needle insertion. An ice cube or −5°C forced air cooling (see above) will likewise numb the skin just long enough to reduce the pain of needle insertion. We have found forced air cooling helpful in reducing the pain of palmar and finger injections of botulinum toxin A for hyperhidrosis. However, if the cold air is aimed directly onto the needle, the liquid within the needle may freeze momentarily, making it seem that the needle is clogged. Moving the cold air blower away from the needle for 5 to 10 seconds will permit the contents of the needle to thaw out, allowing injection to continue.

Anesthetic Injection Techniques

Local infiltration

The great majority of dermatologic surgical procedures are done under anesthesia achieved with local infiltration. There are several maneuvers that can significantly reduce the pain of injection[24]. The pain of needle insertion is reduced by reassurance, verbal distraction, and mechanical distraction such as a pinch at the site of injection. Mechanical distraction works via the gate theory of pain. The pinching stimulates cutaneous nerves, making them somewhat refractory to the immediately following pinprick sensation from needle insertion. A very useful adjunct, which also takes advantage of the gate theory of pain, is the use of vibration at or immediately proximal to the injection site. This is very useful when injecting anesthetic in very anxious or young patients and has made it feasible for us to eliminate the need for nerve block anesthesia when injecting botulinum toxin A into the palms and soles in many patients. Care must be taken when applying a vibrator to the injection site, as the needle may move unpredictably across the skin surface due to the vibration before being inserted into the skin. Small 30-gauge needles that are inserted quickly further reduce pain. Slow, timid needle insertion is felt more by the patient than a quick needle insertion. Topical anesthesia, as noted above, can almost completely eliminate the pain of needle insertion.

The actual injection of the anesthetic causes a significant stinging sensation that is usually far more painful than the needle insertion. Buffering the anesthetic to a physiologic pH and using an anesthetic that has been warmed to body temperature will reduce the stinging sensation[9,10,25]. Injecting the anesthetic as slowly as practical will reduce the pain from tissue distention by the anesthetic fluid, and this also allows the injection of additional anesthetic to be done through an already numb area. Additional sticks should be made through an already numb area, and the injection should start on the side that the sensory innervation is coming from and proceed distally. Using the smallest practical syringe size, usually 1 or 3 ml, will allow for low pressures of injection, which are less painful. Subcutaneous anesthetic injection is less painful than intradermal injection, but the onset of anesthesia is slower and of shorter duration. We usually start by creating a small intradermal wheal, followed by subcutaneous injection, and finishing with intradermal injection at the incision line to enhance anesthesia and hemostasis.

TUMESCENT ANESTHESIA FORMULA	
Ingredient	**Quantity (ml)**
Lidocaine 1%	50–100
Epinephrine (1 : 1000)	1
Sodium bicarbonate 8.4%	10
Hyaluronidase 150 U/ml	6 (optional)
Triamcinolone acetonide 40 mg/ml	0.25 (optional)
Normal saline 0.9%	900–950

Table 143.7 Tumescent anesthesia formula. For tumescent anesthesia, a final concentration of 0.05% to 0.1% lidocaine with 1 : 1 000 000 epinephrine is prepared. Hyaluronidase may be added to enhance diffusion and corticosteroids may be added to reduce inflammation, edema, and possibly fibrosis.

There are also compressed air delivery systems for administering lidocaine into the dermis and they may be useful in children (Table 143.6).

Field block anesthesia

Field block anesthesia involves injecting a ring of anesthetic around the proposed surgical site. It is useful for anesthetizing large areas while conserving the amount of anesthetic used and minimizing distortion of the surgical site. Injecting a ring of anesthesia around a cyst will avoid puncturing the cyst. Ring block anesthesia is practical only in areas where innervation arrives horizontally through the skin, such as is seen on the scalp, rather than vertically from deeper tissues, as is seen on the eyelid. A ring block may achieve anesthesia, but there will be no hemostasis at the incision site. Therefore, the addition of intradermal anesthetic with epinephrine at the proposed incision site is recommended. The most frequent use of ring block anesthesia is on the scalp, nose (for rhinophyma repair), ear pinna, and on the trunk and extremities (where the injection is started as a ring block but often finished with infiltration inside the ring block).

Tumescent anesthesia

Tumescent anesthesia involves the subcutaneous infiltration of large amounts of dilute 0.05%–0.1% lidocaine with 1 : 1 000 000 epinephrine (Table 143.7). It has been used most extensively for liposuction under local anesthesia (see Ch. 156), ambulatory phlebectomy, hair transplantation, and dermabrasion. The anesthetic is infiltrated with the help of a pump, with the injection carried out through long 18- to 20-gauge 3.5 inch (8.9 cm) spinal needles or specially designed multiport cannulas. The infiltration is started slowly with small needles and then gradually speeded up utilizing spinal needles and finally infiltration cannulas. Infiltration of the deep subcutaneous plane is done first, followed by the superficial fat compartment. The solution is injected until firm tumescence of the tissue has been achieved. Anesthesia and epinephrine-induced hemostasis develop within about 20 minutes and last for several hours, which is significantly longer than the duration of anesthesia achieved with conventional concentrations of lidocaine with epinephrine. In the subcutaneous fat, dilute lidocaine is absorbed at a much slower rate than standard lidocaine concentrations. Doses as high as 35–50 mg/kg lidocaine have been found to be safe when used in tumescent anesthesia[17,18].

Nerve Block Techniques

Nerve blocks are an effective and efficient way to anesthetize large areas using the least amount of anesthetic, minimizing both patient discomfort and distortion of the operative site. When injecting in the

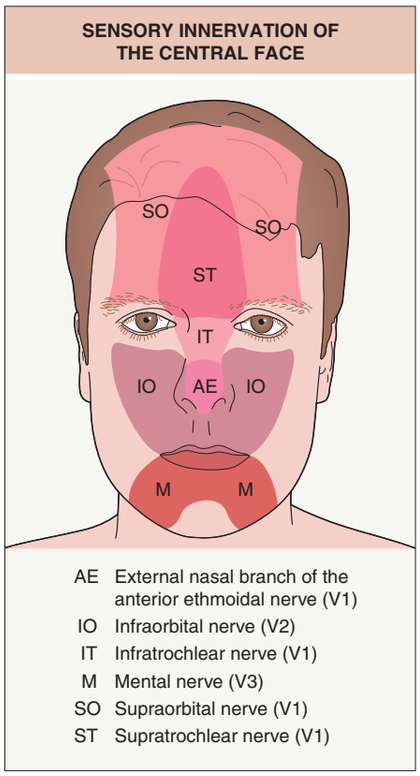


Fig. 143.2 Sensory innervation of the central face.

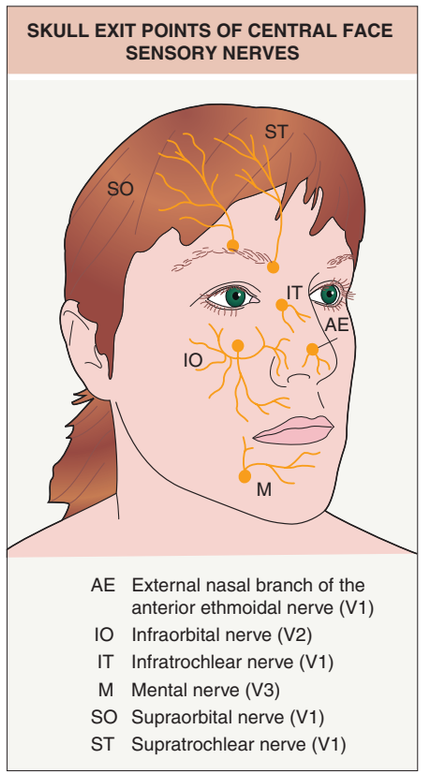


Fig. 143.3 Skull exit points of central face sensory nerves.

region of a nerve, care must be taken not to inject the accompanying blood vessels. Using larger, 25- to 27-gauge needles allows one to draw back to make sure that the needle is not intravascular. To reduce pain of injection, an intradermal wheal using a 30-gauge needle should be placed first. The aim of nerve block injections is to deposit the anesthetic near, but not into the nerve, as intraneural injection may cause nerve injury and subsequent dysesthesia. Insertion of the needle into a nerve is usually felt by the patient as a sharp pain radiating along the nerve. If this happens, the needle should be pulled back and repositioned slightly. Intra-foramina injections should also be avoided to minimize risk of nerve injury. With proper placement, most nerves can be blocked with a 1–2 ml injection. The addition of hyaluronidase will enhance diffusion of the anesthetic and increase the rate of nerve block "take".

For most nerve blocks, 1% lidocaine with epinephrine and sodium bicarbonate is used. If prolonged anesthesia is desired, 0.25% bupivacaine hydrochloride with epinephrine can be added. As the sensory nerves are large and myelinated, anesthetic effect may take 10 to 20 minutes to develop[26]. Using 2% lidocaine may increase success of the nerve block. Articaine 4% with or without epinephrine supplied in dental carpules seems to be especially effective for relatively painless facial nerve blocks, with very small volumes (often <0.2 ml/injection site) of anesthetic needed for effective anesthesia. This seems to be due to its more effective diffusion from the site of injection compared to lidocaine. Some surgeons omit epinephrine from the nerve block anesthetic as it is not needed for vasoconstriction at the site of the nerve. We use it as part of our anesthetic mix to prolong the duration of the nerve block. Once a nerve has been effectively blocked, local infiltration of lidocaine with epinephrine along the proposed incision line to achieve local vasoconstriction may be helpful in reducing bleeding.

Facial nerve blocks

The forehead and frontal scalp above the eyebrows are innervated by the *supraorbital nerve* (Fig. 143.2), which exits the skull through the supraorbital foramen at or immediately above the orbital rim in the midpupillary line (Fig. 143.3). The notch can often be palpated on the patient. Approximately 1 ml of anesthetic is infiltrated through a 0.5 inch (1.3 cm) needle inserted perpendicularly into the skin immediately superficial to the periosteum at the orbital rim in the midpupillary line (Fig. 143.4). The *supratrochlear nerve* innervates the midforehead, glabella, and frontal scalp (Fig. 143.2). It exits the skull at the upper



Fig. 143.4 Locations of needle insertions for central face nerve blocks. From superior to inferior, the supraorbital, infraorbital, and mental nerves are marked with an "x" and the supratrochlear, infratrochlear, and external nasal nerves are marked with a rectangle.

medial portion of the orbit (Fig. 143.3). Injecting 1 ml of anesthetic immediately superficial to the periosteum at the superomedial orbital rim at the junction of the glabella and eyebrow will block the supratrochlear nerve (Fig. 143.4). To achieve complete forehead and frontal scalp anesthesia requires extending a line of anesthetic injected into the subcutaneous plane laterally from the supraorbital nerve to the region immediately superior and posterior to the attachment of the ear pinna. This will block the auriculotemporal nerve and greater auricular nerve branches that innervate the forehead, temple, and frontal scalp (see Ch. 142).

The *infraorbital nerve* exits the skull through the infraorbital foramen (Fig. 143.3) and innervates the medial cheek, upper lip, and nasal ala (Fig. 143.2). With a 1 inch (2.5 cm) needle inserted perpendicularly to

the skin, 2 ml of anesthetic is injected approximately 1 cm inferior to the orbital rim in the midpupillary line, immediately superficial to the maxillary bone periosteum (Fig. 143.4). A less painful and more reliable alternative is to block the infraorbital nerve through the intraoral approach. The needle is inserted between the first and second premolars (bicuspids), moving cephalad parallel to the periosteum until the horizontal portion of the maxillary bone is reached (Fig. 143.5). The needle is pulled back slightly and the anesthetic is injected. The pain of needle insertion can be lessened by applying a topical anesthetic to the mucosa a couple of minutes prior to injection. The *infratrochlear nerve*, which innervates the lateral and dorsal nose (Fig. 143.2), can be blocked by injecting anesthetic superficial to the periosteum at the inferomedial orbital rim at the superior end of the nose–cheek concavity (Fig. 143.4). The nasal tip receives innervation from the external nasal branch of the *anterior ethmoidal nerve* (Fig. 143.2), which emerges at the nasal cartilage and bone junction slightly lateral from the midline (Fig. 143.3). Perichondrial infiltration of anesthetic at this spot will anesthetize the nasal tip (Fig. 143.4). To complete nasal anesthesia, a few drops of anesthetic at the base of the columella may be needed as well.

The lower lip and portions of the chin are innervated by the *mental nerve* (Fig. 143.2), which exits the mandible through the mental foramen in the midpupillary line (Fig. 143.3). A 0.5 inch (1.3 cm) needle is inserted perpendicular to the skin to the level of the periosteum in the midpupillary line halfway cephalad along the mandible, and 1 ml of anesthetic is injected to block the mental nerve (Fig. 143.4). The intraoral route is less painful and more reliable. The needle is inserted between the first and second premolars (bicuspids) caudally along the periosteum to a halfway point down the mandible (Fig. 143.6).

Digital nerve blocks

Nerve blocks for the fingers and toes are technically very similar. There are two options to anesthetize a digit. The technique most commonly used by dermatologists blocks the sensory nerves coursing laterally along the digit. A 0.5 inch (1.3 cm) needle is inserted perpendicular to the digit near its base in the horizontal plane until the bone is touched. At this point, the needle is withdrawn slightly, positioned dorsally and anesthetic is injected. Next, the needle is positioned ventrally and additional anesthetic is injected. This process is repeated on the other side of the digit. This block can be done without epinephrine or with dilute 1 : 500 000 epinephrine, and small volumes (usually <1.5 ml) should be injected to minimize the risk of ischemic injury from mechanical circumferential compression of the blood supply to the digit. However, as noted previously, there is no documented risk of ischemic injury from standard 1 : 100 000 epinephrine concentrations when used for digital anesthesia in patients without significant peripheral vascular compromise (as long as the injected anesthetic volume is limited).

Alternatively, the digit can be blocked at the level of the metacarpal or metatarsal bone. A 1.5 inch (3.8 cm) needle is inserted dorsally between the metacarpal/metatarsal bones, and anesthetic is infiltrated as the needle is advanced ventrally, with most of the anesthetic injected just dorsal to the palmar/plantar skin. This injection will block the metacarpal/metatarsal nerve, which travels immediately superficial to the flexor retinaculum. The process is repeated on the other side of the metacarpal/metatarsal bone of the digit being anesthetized. The advantage of this block is that there is less risk of compression injury than can occur with the more commonly performed digital block.

Penile nerve block

The dorsal nerve of the penis is a branch of the pudendal nerve. It divides into major anterior (dorsal) and minor posterior (ventral) branches at the base of the penis. By injecting a ring of anesthesia without epinephrine or with 1 : 500 000 epinephrine in the subcutaneous plane around the base of the penis, most of the penis will be anesthetized. The only areas that may require additional anesthetic infiltration will be the periurethral region of the glans and, sometimes, the ventral glans and frenulum.

Hand nerve block

With the popularity of botulinum toxin A for palmar and plantar hyperhidrosis, a method to anesthetize the palmar surface is necessary. Topical anesthetics are ineffective on palmoplantar skin, and local anesthetic injections into the palms and soles are very painful. Nerve block of the median nerve will anesthetize the palmar surface of the first three and a half fingers plus two-thirds of the palmar surface (Fig. 143.7). Block of the ulnar nerve will anesthetize the rest of the fingers and palm (Fig. 143.7). The median nerve lies in the carpal tunnel, deep to the palmaris longus tendon and between the flexor digitorum superficialis and flexor carpi radialis tendons. By apposing the thumb and fifth finger with the wrist slightly flexed, the palmaris longus tendon will become apparent. A 0.5–1 inch (1.3–2.5 cm) needle is inserted at the first (proximal) wrist crease, immediately medial (ulnar) to the palmaris longus tendon (Fig. 143.8). It is then advanced deep into the



Fig. 143.5 Intraoral route for infraorbital nerve block. The needle is inserted cephalad between the premolar (bicuspid) teeth in the midpupillary line.



Fig. 143.6 Intraoral route for mental nerve block. The needle is inserted caudally between the premolar (bicuspid) teeth in the midpupillary line.

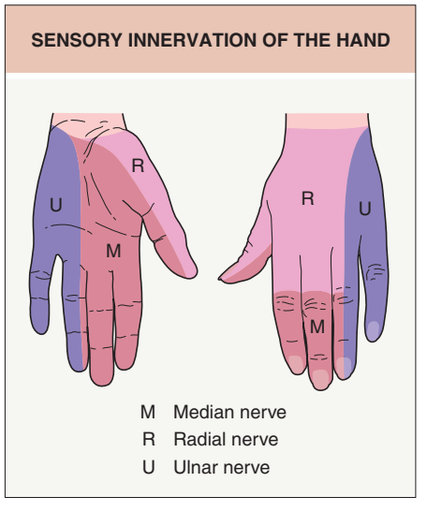


Fig. 143.7 Sensory innervation of the palmar surface and dorsal surface of the right hand.

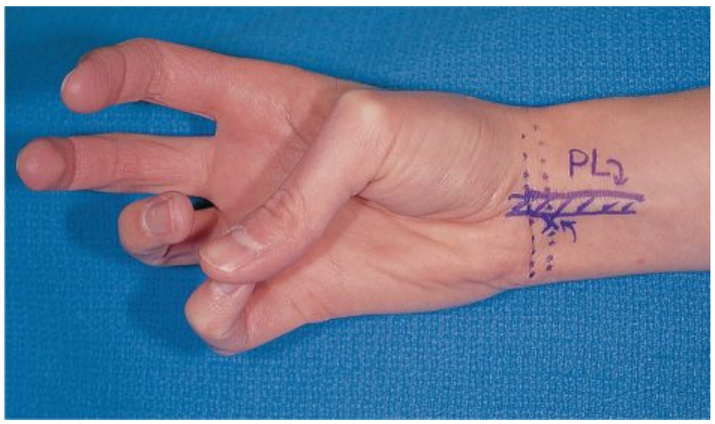


Fig. 143.8 Cutaneous markers for the median nerve location at the wrist. Note thumb and little finger apposition and wrist flexion to visualize the palmaris longus (PL) tendon. X, needle entry point.

carpal tunnel and a few milliliters of anesthetic are injected. A slight "popping" or reduction in resistance can be felt as the needle enters the carpal tunnel.

The ulnar nerve is most easily blocked at the elbow where it travels between the olecranon process and the epicondyle of the humerus. The ulnar nerve is the "funny bone". The patient's arm is flexed, and the needle is inserted between the bones with several milliliters of anesthetic injected.

An alternative is to have an anesthesiologist perform a Bier block, in which the blood is pushed out of the arm with a compressive bandage, a tourniquet is applied, and dilute lidocaine is injected intravenously. Anesthesia of the hand will develop in 5 to 10 minutes and last for about 1 hour. Once the procedure is complete, the tourniquet is gradually released and the anesthetic is released into the general circulation. Therefore, the dose administered should be monitored to keep it at a safe level.

Foot nerve block

Anesthesia of the plantar surface requires nerve blocks of the posterior tibial nerve, which innervates the heel and middle of the sole of the foot; the sural nerve, which innervates the fifth toe and the lateral side of the sole of the foot; the superficial peroneal nerve, which innervates the skin of the toes; the saphenous nerve, which innervates the instep; and the deep peroneal nerve, which innervates the skin between the first and second toes (Fig. 143.9). Before starting injections around the ankle, the area should be thoroughly prepped with antiseptic to minimize the risk of infection.

The patient is placed in the prone position. The posterior tibial artery is palpated or located using a Doppler ultrasound probe, and a 1.5 inch (3.8 cm) needle is directed anteriorly and laterally, immediately lateral to the arterial pulse, until the bone is touched. The needle is pulled back slightly, and several milliliters of anesthetic are injected in the groove between the medial malleolus and the Achilles tendon (Fig. 143.10). The sural nerve is blocked by injecting anesthetic in the groove between the lateral malleolus and Achilles tendon in an identical fashion to the tibial nerve injection (Fig. 143.10).

With the patient in the supine position, the saphenous and superficial peroneal nerves are blocked by infiltrating anesthetic subcutaneously from malleolus to malleolus along the dorsum of the foot (Fig. 143.11). The deep peroneal nerve is blocked by inserting a 1.5 inch (3.8 cm) needle lateral to the extensor hallucis longus tendon (toward the middle of the foot) down to the bone (Fig. 143.11). Next, the needle is pulled back slightly, and several milliliters of anesthetic are injected. The tendon is identified by having the patient dorsiflex his or her great toe against resistance. Alternatively, local anesthetic can be infiltrated between the first and second toes for easier and more expeditious anesthesia.

Higher Levels of Anesthesia

In anxious patients, or when relatively large areas are to be anesthetized, oral or sublingual anxiolytics such as triazolam (Halcion®) 0.25–0.5 mg or zolpidem tartrate (Ambien®) 5–10 mg will reduce anxiety and may even generate a certain degree of amnesia for the procedure. Diazepam (Valium®) 5–10 mg is useful for longer procedures due to its longer duration of action, but it does not produce amnesia for the procedure. The addition of a narcotic analgesic such as oxycodone (10 mg)/acetaminophen (325 mg) orally (Percocet®) or meperidine hydrochloride (Demerol®) 50 mg intramuscularly will act synergistically with the anxiolytics to achieve a greater degree of sedation as well as reducing the pain of local anesthetic infiltration. We find these useful for longer procedures done under tumescent anesthesia. Of course, consent for the procedure has to be obtained before taking any of these medications and patients must have someone else take them home after the procedure.

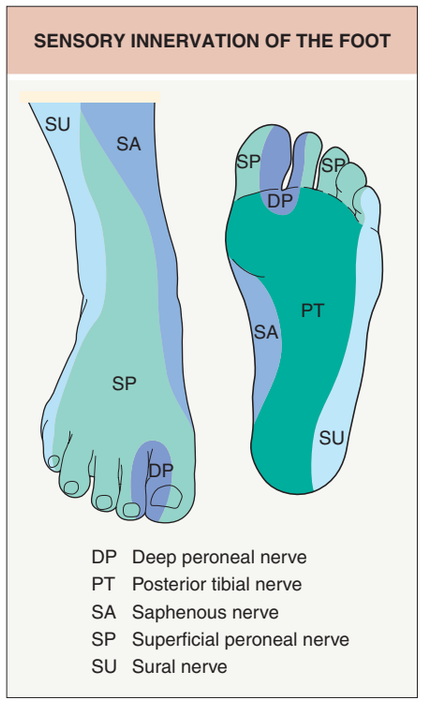


Fig. 143.9 Sensory innervation of the dorsal surface and plantar surface of the right foot.

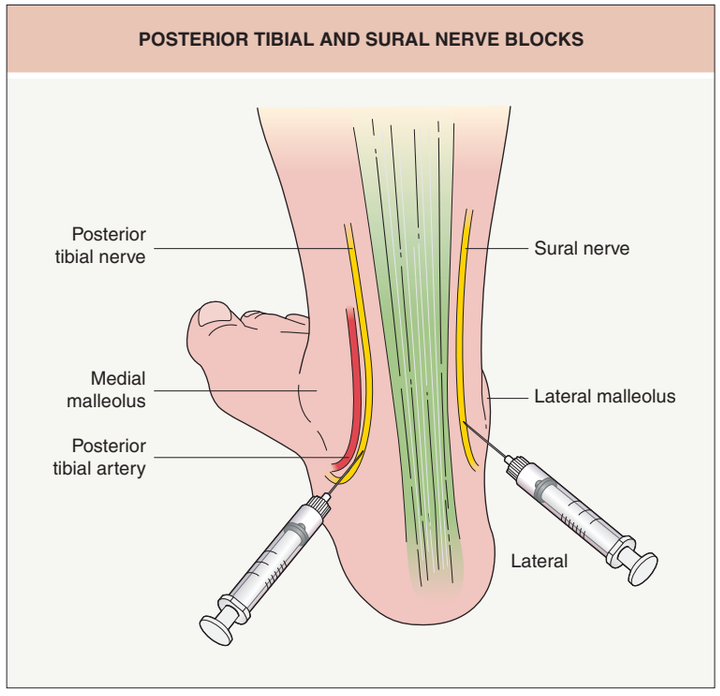


Fig. 143.10 Posterior tibial and sural nerve blocks.

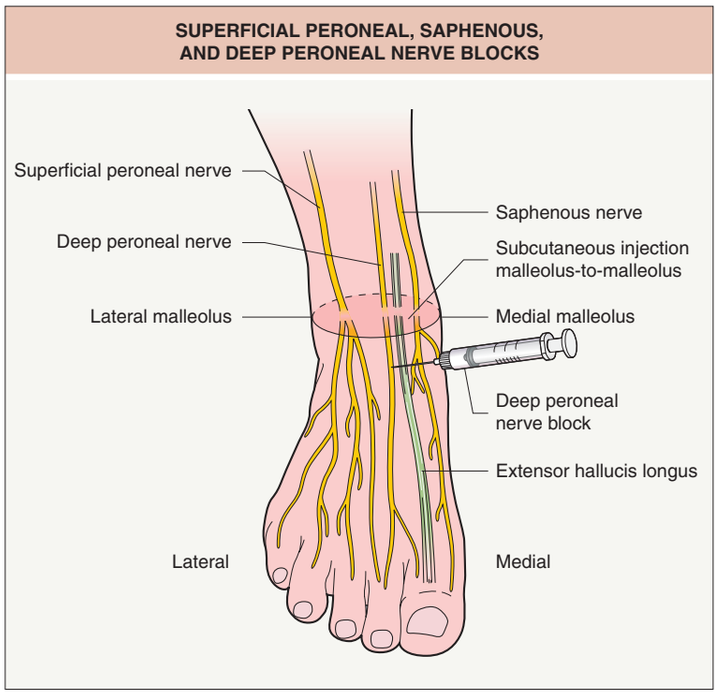


Fig. 143.11 Superficial peroneal, saphenous, and deep peroneal nerve blocks. Great toe dorsiflexion aids in visualizing the extensor hallucis longus tendon.

Credentialing for higher levels of anesthesia may be regulated by state or national (outside the US) medical licensure authorities and hospitals, and the physician must be in full compliance with the rules in his or her particular state or country. Most of the regulations require procedures done under general anesthesia or with intravenous sedation to be done in an ambulatory surgery center or hospital with a supervising anesthesiologist. Higher levels of anesthesia involving the use of intravenous medications such as midazolam hydrochloride (Versed®) and fentanyl should be done in a monitored environment with appropriate resuscitative equipment readily available. Nitrous oxide administration is a useful form of moderate analgesia, with the degree depending on the concentration administered. At a 20% concentration, the analgesia is equivalent to giving a narcotic analgesic. At an 80% concentration, most patients will become unconscious. The advantage of nitrous oxide is the rapid reversal of anesthetic effect as soon as the gas is turned off. With proper training, nitrous oxide can be safely administered in the office, as it has been done for many years in many dental offices. An easier version of nitrous oxide analgesia, Pro-Nox™ (Clarion Medical Technologies), delivers a fixed ratio of 50% nitrous oxide and 50% oxygen. The patient holds the mouthpiece and controls how much they inhale, remaining conscious throughout the procedure[27]. General inhalation anesthesia or deep intravenous sedation with propofol should generally be performed by anesthesiologists.

REFERENCES

1. Wildsmith JAW, Strichartz GR. Local anaesthetic drugs – an historical perspective. *Br J Anaesth*. 1984;56:937–939.
2. Kouba DJ, LoPiccolo MC, Alam M, et al. Guidelines for the use of local anesthesia in office-based dermatologic surgery. *J Am Acad Dermatol*. 2016;74:1201–1219.
3. McNulty MM, Edgerton GB, Shah RD, et al. Charge at the lidocaine binding site residue Phe-1759 affects permeation in human cardiac voltage-gated sodium channels. *J Physiol*. 2007;581:741–755.
4. Bieter RN. Applied pharmacology of local anesthetics. *Am J Surg*. 1936;34:500–510.
5. Rasmussen LF, Ahlfors CE, Wennberg RP. The effect of paraben preservatives on albumin binding of bilirubin. *J Pediatr*. 1976;89:475–478.
6. Foster CA, Aston SJ. Propranolol-epinephrine interaction: a potential disaster. *Plast Reconstr Surg*. 1983;72:74–78.
7. Dzubow LM. The interaction between propranolol and epinephrine as observed in patients undergoing Mohs surgery. *J Am Acad Dermatol*. 1986;15:71–75.
8. Krunic AL, Wang LC, Soltani K, et al. Digital anesthesia with epinephrine: an old myth revisited. *J Am Acad Dermatol*. 2004;51:755–759.
9. Stewart JH, Chinn SE, Cole GW, Klein JA. Neutralized lidocaine with epinephrine for local anesthesia – II. *J Dermatol Surg Oncol*. 1990;16:842–845.
10. Stewart JH, Cole GW, Klein JA. Neutralized lidocaine with epinephrine for local anesthesia. *J Dermatol Surg Oncol*. 1989;15:1081–1083.
11. Lewis-Smith PA. Adjunctive use of hyaluronidase in local anaesthesia. *Br J Plast Surg*. 1986;39:554–558.
12. Galindo A, Witcher T. Mixtures of local anesthetics: bupivacaine-chloroprocaine. *Anesth Analg*. 1980;59:683–685.
13. Nagel JE, Fuscaldo JT, Fireman P. Paraben allergy. *JAMA*. 1977;237:1594–1595.
14. Glinert RJ, Zachary CB. Local anesthetic allergy. Its recognition and avoidance. *J Dermatol Surg Oncol*. 1991;17:491–496.
15. Roberts EW, Loveless H. The utilization of diphenhydramine for production of local anesthesia: report of a case. *Tex Dent J*. 1979;97:13–15.
16. Wiener SG. Injectable sodium chloride as a local anesthetic for skin surgery. *Cutis*. 1979;23:342–343.
17. Lillis PJ. Liposuction surgery under local anesthesia: limited blood loss and minimal lidocaine absorption. *J Dermatol Surg Oncol*. 1988;14:1145–1148.
18. Klein JA. Tumescent technique for regional anesthesia permits lidocaine doses of 35 mg/kg for liposuction. *J Dermatol Surg Oncol*. 1990;16:248–263.
19. Kane GC, Hoehn SM, Behrenbeck TR, Mulvagh SL. Benzocaine-induced methemoglobinemia based on the Mayo Clinic experience from 28 478 transesophageal echocardiograms: incidence, outcomes, and predisposing factors. *Arch Intern Med*. 2007;167:1977–1982.
20. Friedman PM, Fogelman JP, Nouri K, et al. Comparative study of the efficacy of four topical anesthetics. *Dermatol Surg*. 1999;25:950–954.
21. Altman DA, Gildenberg SR. High-energy pulsed light source hair removal device used to evaluate the onset of action of a new topical anesthetic. *Dermatol Surg*. 1999;25:816–818.
22. Alster TS. The lidocaine/tetracaine peel: a novel topical anesthetic for dermatologic procedures in adult patients. *Dermatol Surg*. 2007;33:1073–1081.
23. Oni G, Rasko Y, Kenkel J. Topical lidocaine enhanced by laser pretreatment: a safe and effective method of analgesia for facial rejuvenation. *Aesthet Surg J*. 2013;33:854–861.
24. Arndt KA, Burton C, Noe JM. Minimizing the pain of local anesthesia. *Plast Reconstr Surg*. 1983;72:676–679.
25. Bainbridge LC. Comparison of room temperature and body temperature local anaesthetic solutions. *Br J Plast Surg*. 1991;44:147–148.
26. Grekin RC, Auletta MJ. Local anesthesia in dermatologic surgery. *J Am Acad Dermatol*. 1988;19:599–614.
27. Lin MJ, Dubin DP, Khorasani H. Nitrous oxide reduces pain associated with local anesthetic injections. 2019;23:602–607.

Wound Closure Materials and Instruments

144

Todd V. Cartee and Christie R. Travelute

Key features

- The characteristics ascribed to a suture include:
  - capillarity
  - USP size
  - coefficient of friction
  - plasticity
  - tensile strength
  - physical configuration
  - elasticity
  - memory
  - pliability
  - tissue reactivity
- Sutures used to approximate the dermis and deeper tissue layers are generally absorbable, while percutaneous sutures can be either absorbable or nonabsorbable
- The most commonly employed needle in dermatologic surgery is a 3/8 circle that is triangular in shape, with a reverse cutting surface
- Needle holders with small smooth jaws accommodate finer needles and those with large serrated jaws are best for larger needles
- The major types of scissors used in dermatologic surgery are Gradle, tissue, undermining, serrated, suture-cutting, and bandage-cutting

INTRODUCTION

As dermatologic surgery continues to expand as a specialty, so does the variety of materials and instruments that are available to facilitate the ever-growing complexity of tissue excision and repair that are encountered during its practice. A thorough working knowledge of these tools is essential and allows the physician to optimize the cosmetic and functional outcome for a given procedure. For example, the suture material and surgical instruments for a melanoma excision on the back will vary greatly from those chosen for a blepharoplasty. This chapter will review the wound closure materials and surgical instruments of the greatest value to the dermatologic surgeon. Helpful hints and model surgical tray setups are included to assist in the preparation for dermatologic surgery in specific anatomic locations.

DISCUSSION

Sutures

Since prehistoric times, humans have been using various materials to close skin wounds. The first known reference appears in the Edwin Smith Papyrus (c. 1600 BCE)[1]. Although the precise suture material was not described, examination of artifacts from that time period suggests that it was most likely linen. Hippocrates has been credited with being the first to use the term "suture" in reference to sewing human tissue in 400 BCE.

Over the centuries, suture materials that have been employed include cotton, leather, flax, insect mandibles, horse and even human hair[2–8]. Ancient Roman physicians would braid the hair of gladiators tightly to close their scalp wounds and by doing this, these innovative surgeons demonstrated the understanding that sutures can produce immediate hemostasis in addition to wound edge approximation.

The ideal suture, were it to exist, would handle easily, hold a secure knot, and have high tensile strength. It would neither cause inflammation nor promote infection, and it would gradually dissolve, thereby obviating the need for suture removal. Unfortunately, the perfect suture material does not exist. However, the ever-widening array of choices available to the dermatologic surgeon and a knowledge of each suture's individual characteristics increases the likelihood of choosing the best possible materials for each surgical situation.

Suture materials are divided into two categories: (1) absorbable; and (2) non-absorbable. Studies of wound-healing by Levenson et al.[9] have shown that during the first 1–2 weeks after surgery, the intrinsic tensile strength of the wound is ~7%–10% of native bursting pressure. At 5 weeks, the intrinsic tensile strength is ~60%, and, in general, after 1 month, dehiscence is unlikely with normal activity. During this time period, absorbable buried dermal sutures are utilized to alleviate tension and maintain wound edge approximation. Transepidermal, non-absorbable sutures are non-tension-bearing, but allow for fine adjustments of the epidermal edges.

The characteristic attributes ascribed to a suture are defined and standardized by the United States Pharmacopeia (USP) as follows:

- Two **physical configurations** exist: monofilament and multifilament. Multifilament suture can be spun, twisted, or braided. Braiding serves to increase pliability, strength, knot security and handling[10], but may abrade or shear tissue. Braiding also potentially increases the risk of infection by allowing bacteria to become entrapped within filament strands[11]. Monofilament sutures have a low coefficient of friction and slide easily through tissue (see below)[12]. Their drawback is that they are traditionally stiffer than braided suture and may have decreased knot security, requiring additional throws to ensure that the knot is secure.
- **Capillarity** is defined as the ability of a suture to absorb and transfer fluid. Multifilament sutures have greater capillarity than monofilament.
- The **USP size** of a suture is determined by the diameter needed to achieve a given tensile strength, and this is expressed in multiples of zeros; the smaller the cross-sectional diameter of the suture, the more zeros. For example, 7–0 polyglactin 910 (Vicryl®, Polysorb®) is a much finer suture than 3–0 polyglactin 910. The actual diameter of a given USP size varies depending upon the composition of the suture, with a 4–0 surgical gut being a larger-diameter suture than 4–0 polypropylene because polypropylene is innately stronger. In general, the smallest suture that will provide adequate tensile strength for the indicated repair should be utilized.
- **Elasticity** refers to the ability of a suture to regain its original length after being stretched. An elastic suture, such as polybutester, allows for tissue swelling and then maintains tension on the wound edges after the edema has resolved.
- The **coefficient of friction** determines the ease with which a suture will pull through tissue. A suture with a low friction coefficient, such as polypropylene, slides easily through tissue. For this reason, polypropylene is commonly used for the running subcuticular suture (see Ch. 146). Knot strength is directly proportional to the friction coefficient of the suture material. The more slippery the suture material, the more likely it is that the resulting knot will unravel. Hence, when suturing with polypropylene, it is prudent to place several additional throws for each knot.
- **Memory** is defined as a suture's tendency to retain its natural configuration and is determined by the elasticity and plasticity of the suture material. Memory is a useful property for maintaining closure during the postoperative period. High-memory sutures, such as nylon, are widely used for surface approximation. Drawbacks of high-memory sutures are that they do not handle very easily and have a relatively low knot strength. As with sutures that have a low coefficient of friction, a few extra throws may be helpful to ensure a secure knot. Suture material with low memory, such as silk, is easy to handle and rarely becomes untied.
- **Plasticity** is the ability of the suture to be molded or retain its new length and form as well as tensile strength after it has been stretched. This is an important characteristic for a suture material that is to be used in situations with tissue edema.

Sutures with plasticity, such as polypropylene, will stretch to accommodate edema and not cut into tissue[13].

- **Pliability** refers to how easily the suture can be bent. Braided suture materials, such as silk, are the most pliable, and they are capable of being tied readily into a knot.
- The **tensile strength** of a suture is determined by the force required to snap it divided by the cross-sectional diameter of the suture. In general, synthetic materials are stronger than natural materials. A suture that has been knotted has approximately one-third the tensile strength of the same material unknotted[14].
- **Tissue reactivity** is the degree of foreign body inflammatory response evoked by a suture when placed into a wound. In general, natural materials (such as surgical gut) are degraded by proteolytic enzymes and cause a far greater inflammatory response than do synthetic materials (such as poliglecaprone 25) which are absorbed by hydrolysis[12,15].

Types of Suture Material

Sutures are characterized as absorbable or non-absorbable based upon their ability to be enzymatically digested or hydrolyzed. Most absorbable sutures lose the majority of their tensile strength long before they are fully absorbed. Sutures that are absorbable do not require removal. In contrast, non-absorbable sutures are resistant to hydrolysis and enzymatic degradation. Non-absorbable sutures such as nylon and polypropylene are usually used as surface or cutaneous sutures, and they are routinely removed 5–14 days after surgery (earlier on the face and later on the trunk and extremities).

Absorbable sutures

The most commonly used absorbable sutures are described below and summarized in Table 144.1[16].

Surgical gut

Surgical gut (catgut), one of the first sutures ever mass-produced, is composed of 97%–98% purified collagen fibers derived from bovine or ovine intestine. It is a natural tan fiber that is packaged wet in alcohol and dries quickly when exposed to air. Plain surgical gut is not commonly used nowadays because of high tissue reactivity and slow digestion but rapid loss of tensile strength. Specifically, when used as a buried suture, plain gut loses its tensile strength within 7 to 10 days but requires 60 to 70 days for complete digestion[17].

Chromic gut is plain gut that has been processed with chromium salts to increase its resistance to enzymatic degradation and decrease its tissue reactivity. The tensile strength of chromic gut typically lasts for 10 to 14 days. Chromic gut is still widely used for suturing of mucosal surfaces.

Fast-absorbing gut is plain gut that has been heated to begin breakdown of the collagenous material within the suture prior to use. It maintains its tensile strength for 5 to 7 days[18]. Fast-absorbing gut has become popular for suturing skin grafts and for placing surface sutures in wounds that are well approximated by buried sutures. No increase in wound infections has been observed in comparative studies, and this suture is convenient for the surgeon and the patient because it does not require removal[18,19]. However, its relatively high coefficient of friction leads to noticeable tissue drag when suturing skin. This disadvantage

COMMONLY USED ABSORBABLE SUTURES

Suture	Configuration	Tensile strength	Ease of handling	Knot security*	Tissue reactivity	Uses
Surgical gut (plain)	Virtually monofilament	Poor at 7–10 days	Fair	Poor	Moderate	Rarely used nowadays in skin
Surgical gut (chromic)	Virtually monofilament	Poor at 21–28 days	Poor	Poor	Less than plain	Skin grafts, surface sutures for mucosae
Surgical gut (fast-absorbing)	Virtually monofilament	50% at 5–7 days	Fair	Poor	Low	Skin grafts, epidermal closure
Polyglycolic acid (Dexon®)	Braided†	20% at 21 days	Good	Good	Low	Subcutaneous closure, vessel ligature
Polyglactin 910 (Vicryl®, Polysorb®)	Braided†	75% at 14 days 50% at 21 days 25% at 28 days	Good	Good	Low	Subcutaneous closure, vessel ligature
Polydioxanone (PDS II®)	Monofilament	wks / 4/0 and smaller / 3/0 and larger 2 / 60% / 80% 4 / 40% / 70% 6 / 35% / 60%	Poor	Moderate	Low	Subcutaneous closure (high-tension areas)
Polyglyconate (Maxon®)	Monofilament	80% at 14 days 60% at 28 days	Fair	Good	Low	Subcutaneous closure (high-tension areas)
Poliglecaprone 25 (Monocryl®)	Monofilament	50%–60% at 7 days 20%–30% at 14 days 0% at 21 days	Fair	Moderate	Minimal	Subcutaneous closure (avoid if high-tension site)
Glycomer 631 (Biosyn®)	Monofilament	75% at 14 days 40% at 21 days	Fair	Moderate	Minimal	Subcutaneous closure; similar to poliglecaprone 25 plus an additional week of tensile strength
Polyglytone 6211 (Caprosyn®)	Monofilament	20% at 10 days	Fair	Moderate	Minimal	Subcutaneous closure; more rapid absorption than poliglecaprone 25

*Directly proportional to the friction coefficient and indirectly proportional to memory.
†Multifilament.

Table 144.1 Commonly used absorbable sutures. wks, weeks. *Adapted from Garrett AB. Wound closure materials. In: Wheeland R (ed). Cutaneous Surgery. Philadelphia: WB Saunders, 1994:199–205.*

can be ameliorated by the addition of a thin layer of petrolatum ointment[20] (known as "greasing the gut").

Polyglycolic acid

Polyglycolic acid (Dexon®), introduced in 1970, was the first synthetic absorbable suture and its reduced tissue reactivity and predictable absorption profile represented a vast improvement over surgical gut[21]. It is a braided glycolic acid polymer with easy handling qualities, and it maintains 20% of its tensile strength at 3 weeks. Polyglycolic acid suture is available plain or coated with poloxamer 188. This lubricant coating allows the suture to pass more easily through tissue and makes it more pliable, which facilitates knot tying.

Polyglactin 910

Polyglactin 910 (Vicryl®, Polysorb®), a synthetic, braided copolymer of glycolide and L-lactide, was first introduced in 1974 and supplanted polyglycolic acid as the most popular buried absorbable suture in cutaneous surgery[22]. The water-repelling properties of lactide delay penetration of water and delay the loss of tensile strength. Polyglactin 910 maintains 75% of its tensile strength at 2 weeks and 50% at 3 weeks. Although stronger than polyglycolic acid, polyglactin 910 absorption is generally complete by 90 days, whereas polyglycolic acid is usually still being absorbed at 120 days[23].

Polyglactin 910 is available either undyed or dyed violet. Although the violet color usually dissipates, some surgeons avoid the dyed form because occasionally it may be visible when embedded in the skin[24]. Polyglactin 910 comes coated with a mixture of polyglactin 370 and calcium stearate that serves as a lubricant, facilitating the passage of the suture through tissue. Polyglactin 910 is immensely popular due to its easy handling characteristics and because it holds knots well and does not tear tissue.

Although polyglactin 910 is traditionally used as an absorbable dermal suture, it may be used safely for wound edge approximation as a running cutaneous suture and removed in 5–14 days[25]. This method still requires suture removal, but the use of a single suture for both the dermal and surface wound closure results in a 50% savings in suture cost per reconstruction. In the authors' experience, polyglactin 910 is also an excellent choice for the vermilion lip as it does not irritate the opposing mucosal surfaces and leads to much less inflammation than silk.

Polyglactin 910 is also available in a partially hydrolyzed form (Vicryl Rapide®), which is useful as a percutaneous suture that does not need to be removed as it spontaneously dislodges in 7–14 days. This suture is indicated for wound edge approximation where only 1–2 weeks of support will be needed and suture removal may be painful or is inconvenient.

Polydioxanone

Polydioxanone (PDS II®) is a monofilament polymer made from the polyester poly (*p*-dioxanone). The primary advantage of polydioxanone over polyglycolic acid and polyglactin 910 is prolonged tensile strength[26]. It maintains ~70% of its tensile strength at 2 weeks and 50% at 4 weeks. Traces of buried polydioxanone are present in 6-month histologic preparations[27]. Polydioxanone is employed in high-tension areas, such as the proximal extremities and trunk. When compared with polyglycolic acid in closure of skin wounds under tension, polydioxanone was associated with less scar spread and a lower incidence of hypertrophic scar formation[28].

Similar to polyglycolic acid and polyglactin 910, polydioxanone has minimal tissue reactivity[26] although it is slightly higher than poliglecaprone 25 in a murine model[27]. As a monofilament suture, it retains packaging memory[27] and can be relatively stiff and difficult to tie[29]. However, polydioxanone glides through tissue easily[27].

Polyglyconate

Polyglyconate (Maxon®), a copolymer of glycolic acid and trimethylene carbonate, is also an absorbable monofilament suture. Its overall properties and indications are similar to polydioxanone. It maintains 80% of its tensile strength at 2 weeks and 60% at 4 weeks[30], with complete absorption occurring via hydrolysis by ~180 days. Despite this prolonged absorption, there is minimal tissue reactivity. Polyglyconate may be most useful for large surgical procedures on the trunk or extremities that are under substantial tension and require prolonged, suture-based approximation during healing.

Poliglecaprone 25

Poliglecaprone 25 (Monocryl®) is an absorbable monofilament suture consisting of a copolymer of glycolide and ε-caprolactone. It exhibits very high *initial* tensile strength, but this declines rapidly in the early postoperative period with ~50%–60% of its tensile strength at 1 week, only 20%–30% at 2 weeks (undyed), and essentially 0% at 21 days[31]. This absorption profile limits its use in areas where prolonged dermal support is desired. Complete absorption occurs at ~90 days[27].

Poliglecaprone 25 offers supple handling and minimal tissue reactivity, which led to a lower incidence of hypertrophic scarring when compared to partially hydrolyzed polyglactin 910 (Vicryl Rapide®) for skin approximation in a breast reduction scar model[32]. Furthermore, poliglecaprone 25 demonstrates better knot tying and security than other commonly used absorbable monofilament suture materials[27]. Because poliglecaprone 25 induces less inflammation than polyglactin 910 and glides easily through tissue, for many dermatologic surgeons it has become the absorbable suture of choice for low tension closures in the head and neck region. In a randomized study of deep dermal sutures for repair of Mohs defects, a statistically higher rate of suture extrusion occurred with polyglactin 910 (11%) versus poliglecaprone 25 (3%), but there was no difference in ultimate cosmesis[33].

Its minimal tissue reactivity permits the use of poliglecaprone 25 for epidermal approximation (with removal at 5–14 days), thereby eliminating the need for separate dermal and surface sutures. A randomized, blinded, split-scar study comparing running 5–0 poliglecaprone 25 versus 6–0 polypropylene for facial surface closures found no significant differences in cosmetic outcome at 1 week or 4 months[34]. Poliglecaprone 25 can also achieve epidermal approximation as a running subcuticular suture that does not require removal[35].

Glycomer 631 and polyglytone 6211

Glycomer 631 (Biosyn®) and polyglytone 6211 (Caprosyn®) are absorbable monofilament sutures with comparable physical characteristics to poliglecaprone 25. Complete absorption of glycomer 631 occurs between 90 and 110 days, with low tissue reactivity. Polyglytone 6211, introduced in 2002, was designed to offer the most rapid absorption profile within this class of suture (20% tensile strength at 10 days; complete absorption at 56 days). This property was postulated to underpin its reported low rate of suture extrusion[36].

Non-absorbable sutures

The most commonly used non-absorbable sutures are described below and summarized in Table 144.2[16].

Silk

Silk is a braided, natural suture. It represents the gold standard for ease of handling, knot formation and knot stability, by which newer synthetic sutures are measured. Because braided silk is very soft and pliable, it is commonly used on mucosal surfaces and in intertriginous regions. Despite these advantages, there are major drawbacks to its use in cutaneous surgery. Silk has a low tensile strength, its braided configuration produces a high coefficient of friction, and the high capillarity increases the risk of infection. In fact, the presence of one braided silk suture in a contaminated wound was shown to increase the virulence of staphylococci by 10 000-fold[37]. As an organic, foreign protein (fibroin) made by the silkworm, silk has very high tissue reactivity.

Nylon

Nylon (Ethilon®, Dermalon®), a monofilament polymerized polyamide, was the first synthetic non-absorbable suture to become commercially available. Because of its low cost, high tensile strength and low tissue reactivity, nylon is the most commonly used non-absorbable suture in dermatologic surgery[38,39]. It is also available as a braided suture (Surgilon®, Nurolon®) which handles more easily but is more expensive.

Nylon's elasticity allows it to expand and contract with transient wound edema but its stiffness and memory lead to decreased knot security[39]. In practice, this can be easily counteracted by firmly setting knots and increasing the number of knot throws. This monofilament is available as clear or dyed in a black or green color. The green suture can be helpful when working in dark hair-bearing areas.

Traditionally, nylon is placed as a cutaneous suture but clear nylon may be used as a tension-bearing deep suture that is not removed.

COMMONLY USED NON-ABSORBABLE SUTURES						
Suture	**Configuration**	**Tensile strength**	**Ease of handling**	**Knot security***	**Tissue reactivity**	**Uses**
Silk	Braided†	No decrease in 365 days	Gold standard	Good	Moderate	Mucosal surfaces
Nylon:						
Ethilon®	Monofilament	Decreases 20% per year	Good to fair	Poor	Low	Epidermal closure
Dermalon®	Monofilament	Good	Good to fair	Poor		
Surgilon®	Braided†	Good	Good	Fair		
Nurolon®	Braided†	Good	Good	Fair		
Polypropylene (Prolene®, Surgilene®, Surgipro®)	Monofilament	Extended	Good to fair	Poor	Minimal	Running subcuticular suture
Polyester (Dacron®, Mersilene®, Ethibond®)	Braided†	Indefinite	Very good	Good (coating decreases)	Minimal	Mucosal surfaces
Polybutester (Novafil®)	Monofilament	Extended	Good to fair	Poor	Low	Epidermal closure

*Directly proportional to the friction coefficient and indirectly proportional to memory.
†Multifilament.

Table 144.2 Commonly used non-absorbable sutures. *Adapted from Garrett AB. Wound closure materials. In: Wheeland R (ed). Cutaneous Surgery. Philadelphia: WB Saunders, 1994:199–205.*

It can be very useful when approximating the orbicularis oris muscle in a lip wedge repair or tacking tissue to the periosteum in situations where prolonged wound strength is desired.

Polypropylene

Polypropylene (Prolene®, Surgilene®, Surgipro®) is a monofilament polymer of propylene. It is an inert plastic that has minimal tissue reactivity. The major advantage of this suture is its low coefficient of friction, which allows for a gentle, smooth pull through tissue[40]. Even after extended periods of time, it can be withdrawn easily without disrupting the wound (Fig. 144.1). This characteristic makes it a good choice for the running subcuticular suture. Polypropylene also has high plasticity and stretches with tissue swelling, thus reducing the likelihood of postoperative track marks[13,39]. Disadvantages of this suture are its memory (which compromises knot security) and increased cost compared to nylon. It is available in clear and dyed blue forms. Similar to nylon, polypropylene may be used as a subcutaneous suture in areas of high tension to provide prolonged support.



Fig. 144.1 Polypropylene suture. The blue color of the polypropylene suture is visible under the skin one year after its placement as a running subcuticular closure; the patient had neglected to return for suture removal. The suture was easily removed even after one year given its very low coefficient of friction and minimal tissue adherence.

Polyester

Polyester sutures (Dacron®, Mersilene®, Ethibond®) are braided, multifilament sutures with high tensile strength, very good handling, and low tissue reactivity. Ethibond® comes coated with polybutilate, which decreases its drag through tissue (decreased friction coefficient). Similar to polyglactin 910, polyester sutures are of great assistance for approximation of mucosal tissues, particularly the vermilion lip. They combine the soft feel of silk with a lack of tissue reactivity.

Polybutester

Polybutester (Novafil®) is a monofilament suture of polyglycol terephthalate and polybutylene terephthalates. Its major advantages are good handling, low coefficient of friction, high elasticity, and low tissue reactivity[41].

Suture Selection

In general, a surgeon should select the smallest suture that will provide adequate strength for a given closure (Table 144.3). For facial repairs under low tension, 4–0 or 5–0 polyglactin 910 or poliglecaprone 25 are common absorbable sutures, and 5–0 or 6–0 nylon, polypropylene or fast-absorbing gut are typical cutaneous sutures. Poliglecaprone 25 is popular as a dermal suture due to its relatively fast absorption and reduced rate of suture extrusion. Polypropylene (removed at 7–14 days) or poliglecaprone 25 (buried and left in place) are the most commonly used sutures for running subcuticular closures. Polyglactin 910 (buried and left in place) may also be employed as a subcuticular suture despite concerns over tissue reactivity with such superficial placement. Indeed, in a randomized controlled trial (RCT), polyglactin 910 resulted in better scar appearance than polypropylene removed at 14 days[42].

For larger truncal defects, 3–0 or 4–0 polyglactin 910 or poliglecaprone 25 for buried sutures and 3–0 or 4–0 nylon for superficial closure are good choices. Alternatively, running subcuticular closures are particularly valuable on the trunk and extremity to eliminate the possibility of suture track marks[43], which are common in these locations. Polydioxanone and polyglyconate offer the most prolonged dermal support and are a consideration for wounds under significant tension, while poliglecaprone 25's rapid loss of tensile strength makes it a poor choice for such closures. An alternative to traditional sutures are skin staples. They offer a quick, strong method for surface closure of large scalp and truncal defects[44].

Fast-absorbing gut (5–0 or 6–0) is a convenient suture for skin grafts and for any head and neck reconstructions that are well approximated with buried sutures. While some surgeons are concerned that fast-absorbing gut's relatively higher tissue reactivity might increase early peri-incisional erythema and suture track marks, this has not been the

COMMONLY UTILIZED SUTURES BY SITE			
Site	**Deep suture**	**Surface suture**	**Other suture**
Face	4–0/5–0 polyglactin 910 or poliglecaprone 25	(1) 5–0/6–0 nylon or polypropylene (2) 6–0 fast-absorbing gut or partially hydrolyzed polyglactin 910	
Neck and distal extremities	4–0 polyglactin 910 or poliglecaprone 25	(1) 4–0/5–0 nylon or polypropylene (2) 4–0/5–0 poliglecaprone 25 running subcuticular	
Trunk, proximal extremities, and scalp	3–0/4–0 polyglactin 910 (any) or poliglecaprone 25 (low tension) or polydiaxonone (high tension)	(1) 3–0/4–0 nylon or polypropylene (2) 4–0/5–0 poliglecaprone 25 running subcuticular	
Mucosa	None	(1) 5–0 silk (2) 5–0 polyester or 5–0/6–0 polyglactin 910	
Vascular ligature			3–0/4–0 polyglactin 910

Table 144.3 Commonly utilized sutures by site. In practice, there is considerable variation, depending upon the preference of the surgeon and the characteristics of the wound, and this table reflects the bias of the authors and editors. For surface sutures: (1) = option if sutures are to be removed and (2) = option if sutures are left in place.

authors' experience. An RCT comparing 5–0 fast-absorbing gut and 5–0 polypropylene did find a small, but statistically significant, difference in cosmetic outcome that favored polypropylene; no difference in erythema was observed[45]. Another properly powered RCT focusing on facial skin closures found no difference in cosmetic outcomes between 5–0 and 6–0 fast-absorbing gut[46]. However, this study did not include repairs on the nose, lip, or eyelid.

Cyanoacrylate tissue adhesives (e.g. 2-octyl-cyanoacrylate [Dermabond®], a blend of 2-octyl-cyanoacrylate and *n*-butyl-cyanoacrylate [GluSeal®, LiquiBand®]) offer a practical and rapid alternative method of epidermal closure for wounds that are well-approximated with deep sutures[47,48]. Wound closure tapes offer a non-traumatic alternative to epidermal sutures, and they are useful when applied to healing wounds following suture or staple removal. Additionally, they can be used over a running subcuticular suture at the time of surgery, relieving tension on the wound edges and providing a cosmetic, convenient alternative to a daily dressing change[49]. Maloney and colleagues[50] demonstrated that the optimal application of wound closure tapes is in a parallel non-overlapping pattern, following complete coating of the skin surface with liquid gum mastic adhesive. MicroMend® is a wound closure device that mimics a butterfly closure and can be removed by the patient. It consists of two arrays of microstaples anchored onto the skin and connected by a bridge. Although this device is an efficient alternative to sutures, studies are needed to determine its value compared to other wound closure options.

Complications

Suture-related complications are generally associated with placement technique, e.g. tied too tightly with strangulation of the tissue, tied too loosely and not approximating the wound edges well, or placed too superficially and extruding through the suture line. However, suture materials can also create complications due to their inherent properties. Some suture material, such as surgical gut and silk, are quite inflammatory. Synthetic absorbable sutures, such as polyglactin 910 and poliglecaprone 25, generally create little tissue reaction, but occasionally they may cause a granulomatous foreign body reaction (see Fig. 151.18).

Patients can develop a sterile pustule or suture abscess with associated inflammation ranging from mild to marked with focal ulceration (Fig. 144.2). These reactions can be distressing, especially if the patient has not been warned of the possibility that they may occur. In patients receiving anticoagulants, the reaction may be hemorrhagic rather than purulent (see Fig. 144.2C,D). Rarely, they may become secondarily infected, and those reactions that are particularly purulent or exudative should be cultured for bacteria. Deep sutures may also extrude or "spit," sometimes creating a sinus track within the skin.

Removal of the offending suture is the basic treatment for both suture abscess and suture extrusion. If it is readily accessible, the suture should be grasped with a smooth forceps and snipped. A comedone extractor may help to express a suture that is slightly embedded; otherwise, the intact skin overlying the suture may need to be nicked with a #11 blade and then gently probed with a tissue forceps. Antibiotics are rarely necessary. Removing the foreign suture material is usually sufficient to resolve the reaction.

Needles

The ideal needle is sharp and strong, and closely matches the suture diameter. The needle should be strong enough to hold its shape and retain its sharpness, pass after pass. The best needles are made of high-quality stainless steel, and the size and shape of the needle should be selected to correspond to the thickness and toughness of the tissue to be sutured.

There are several major brands of suture materials and each manufacturer uses a different needle nomenclature (Fig. 144.3). Most manufacturers, however, provide needle comparison reference guides. In general, the needle is the most expensive component of the needle/suture and the latter is the most expensive disposable used in dermatologic surgery.

A needle is composed of three parts: the shank, the body and the point (Fig. 144.4)[51]. In dermatologic surgery, most needles have a swaged shank with a hollow proximal end into which the suture is inserted and then crimped. The suture track is determined by the size of the needle shank, not the suture size. The body of the needle can be straight, 1/4 circle, 3/8 circle, 1/2 circle, or 5/8 circle (Fig. 144.5). The most common shape used in skin surgery is the 3/8 circle. Alternatively, 1/2 circle needles are valuable for suturing in tight spaces such as placing deep dermal sutures within small (<1 cm) nasal and eyelid defects or fitting multiple buried sutures into high tension wounds on the back or scalp. For the former, the authors use the P-2 needle[52] and for the latter, find the RB-1 taper point needle an excellent choice.

The most common needle used in cutaneous surgery is the triangular, reverse-cutting type (see Fig. 144.4). Triangular "cutting" needles pass through dense tissues more easily than round taper point needles. The *conventional cutting* needle has its sharp edge on the inside arc of the needle while the sharp edge of the *reverse cutting* needle faces outward. Reverse cutting needles are preferred as they minimize the risk of tearing through the wound edge during suture placement. Taper point needles do not pierce dense tissue easily, but they are less likely to tear delicate tissues such as nasal mucosa.

For the majority of wound closures on the face, the Ethicon P ("plastic") and PS ("plastic skin") or an equivalent series are adequate and economical (see Fig. 144.3). The PS-2 and P-3 needles are particularly suited to dermatologic surgery. They are reverse cutting and their tips are electropolished for added sharpness. The PC ("precision cosmetic") series represents Ethicon's superior skin surgery needles, and they can be used for fine, delicate work. These needles have the sharpest tips and have flattened bodies for better grasping and needle strength. If wound edges are fragile, one must exercise some caution when using PC needles with conventional cutting points. The PC-1 needle is a very fine, sharp, 13 mm needle ideal for delicate facial repairs and is the only PC needle attached to fast-absorbing gut.

The FS ("for skin") and equivalent series of needles are not finely honed, and they are less sharp and less expensive. These needles are adequate for skin surgery on the trunk or extremities. SC-1 is a 13 mm straight needle that the authors believe facilitates full-thickness through and through quilting sutures placed to conform flaps and grafts to the topography of the ear[53].

The number after the series designation denotes the needle size. Most needles are drawn to size on the package (Fig. 144.6). The smallest needle/suture unit that will provide adequate tensile strength for a



Fig. 144.2 Suture reactions. A Mild reaction at the superior edge of the wound (arrow). **B** Moderate reaction with two pustules and an inflammatory rim. **C, D** Hemorrhagic suture abscess in a patient on warfarin and appearance following incision (#11 blade) and drainage of small coagulum. **E** Severe inflammatory reaction leading to several focal ulcerations. **F** Severe ulcerative and granulomatous suture reaction, with visible polyglactin 910 suture material (arrows).

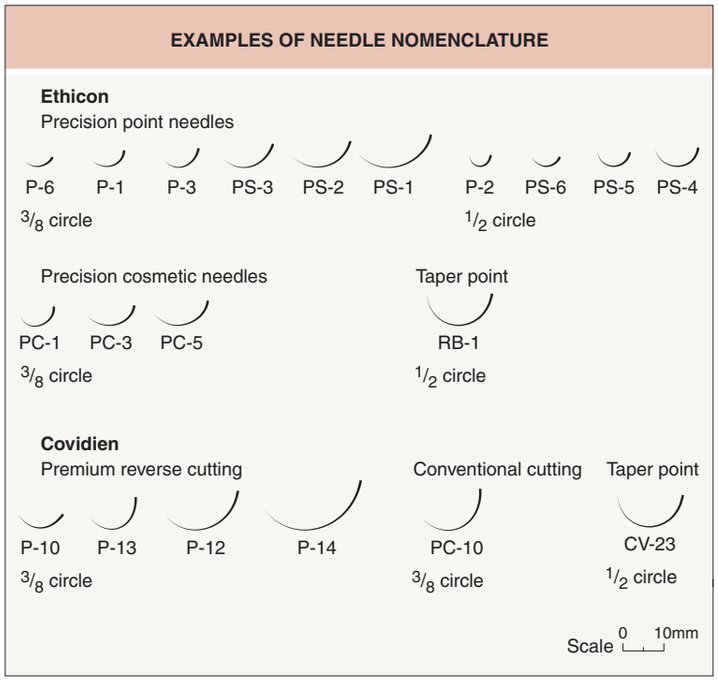


Fig. 144.3 Needle nomenclature by two representative manufacturers. P, plastic; PC, precision cosmetic; PS, plastic skin.

given repair should be utilized. In areas with thick dermis such as the back, larger needles (e.g. PS-1 or PS-2) are much easier to pass through the tissue without bending.

Instruments

Instruments that provide the greatest precision and speed for a given procedure should be selected. There is a wide variation in the cost and quality of surgical instruments. Low-quality, low-cost instruments should be avoided as they are poorly finished and, therefore, are more difficult to use and lack durability. A high-quality instrument will more than make up for its cost by performing well day after day in countless procedures. Modern instruments are a blend of surgical stainless steel with carbon alloy, chromium, nickel and tungsten carbide. Tungsten carbide is a very hard alloy that enhances the function and durability of the blades of scissors and the jaws of needle holders. Quality instruments are usually covered by a warranty which will range from 1 to 5 years or even the life of the instrument, depending on the instrument type and cost.

It is important to keep instruments in good condition by properly caring for them and keeping them sharp. For example, using delicate scissors to cut suture will dull them quickly. Rough handling of delicate forceps and needle holders during surgery or the sterilization process may cause them to become misaligned. Any instrument that is not fully functional should be removed from the surgical tray and sent to the manufacturer for repair.

Some of the authors' instruments of choice for given procedures are listed and shown in Figures 144.7 through 144.9.

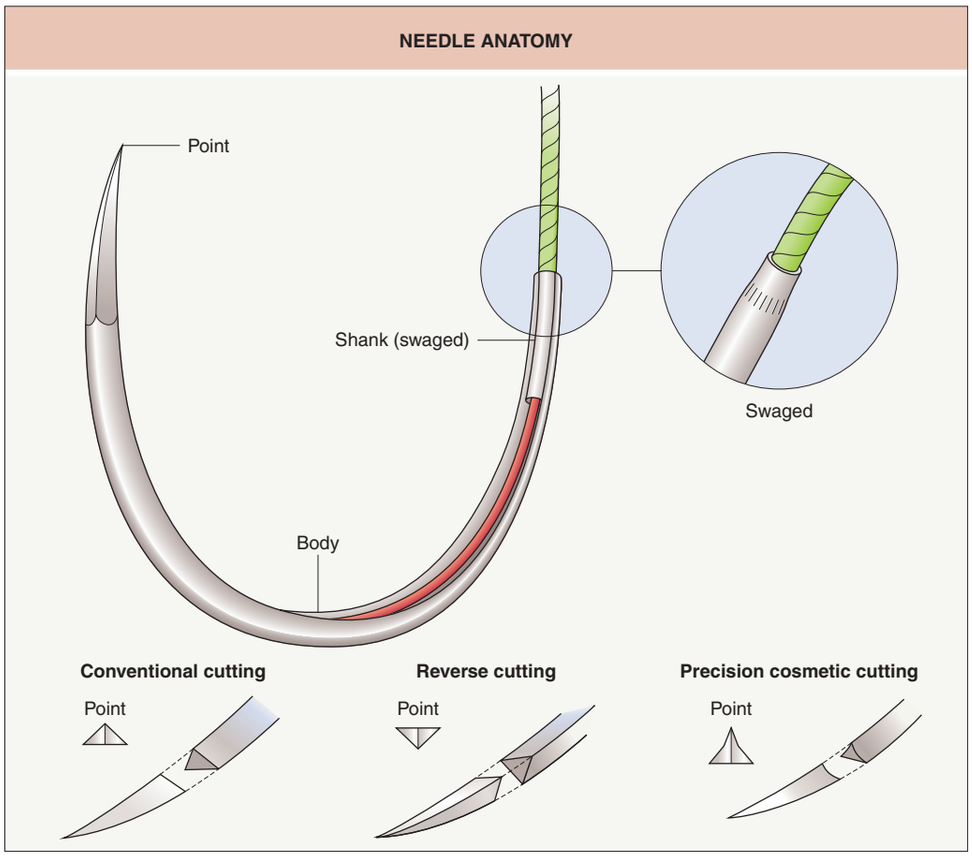


Fig. 144.4 Needle anatomy. The shank body and point are shown as are specific needle points for different types of cutting. Needles should be grasped at approximately one-third of the distance from the swaged area to the point. Avoid placement on or near the swaged area or near the tip.

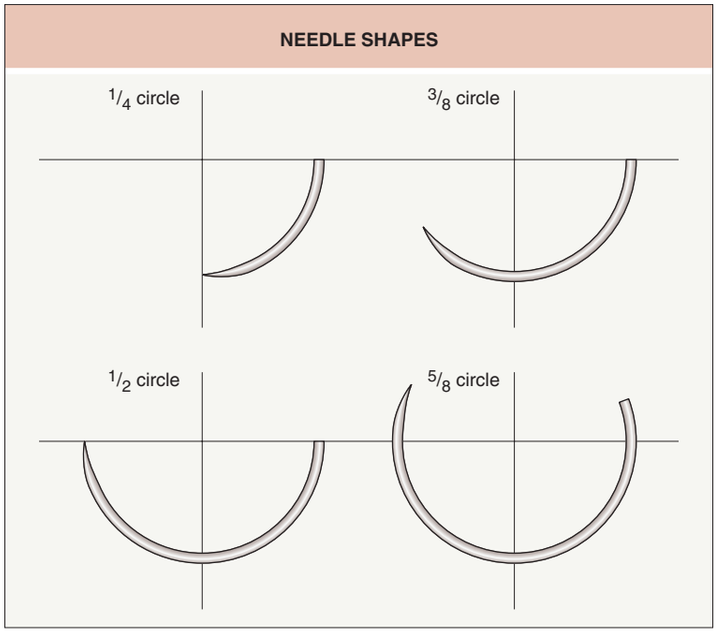


Fig. 144.5 Needle shapes. The most common curvature used in skin surgery is the 3/8 circle. The 1/2 circle curvature is useful when working in confined spaces.

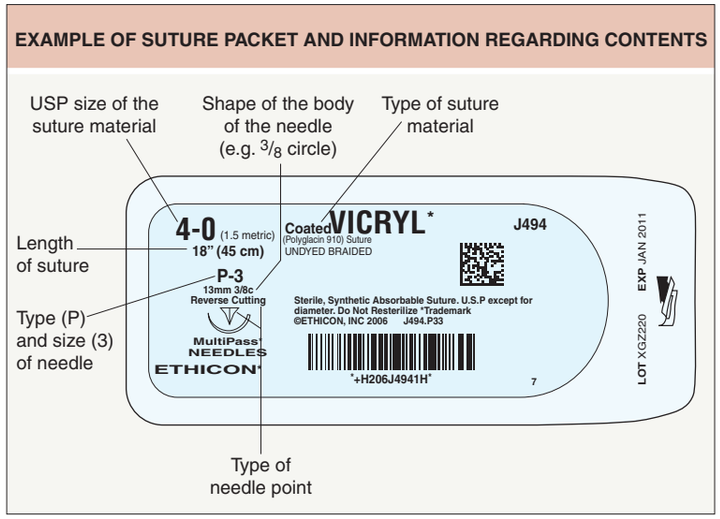


Fig. 144.6 Example of suture packet and information regarding contents.

Curettes

Developed in the late 1800s, the dermal curette has been used to treat a wide variety of cutaneous neoplasms, both benign and malignant. Common curettes are straight with a round head (Fox) or possess an oval head set at an angle from the stem (Cannon). They are labeled by size, depending upon the aperture of the cutting surface of the curette. Mancuso–Fox and Mancuso–Cannon curettes are also available, which have a ruler on the handle. For standard curettage and electrodesiccation, a set of curettes ranging from 6 mm down to 2 mm may be employed. Generally the larger curette is used first to debulk the tumor. This is followed by the smaller curette, which is used to remove small pockets of residual tumor. Smaller curettes (1–2 mm) are excellent instruments for obtaining subungual keratotic debris for fungal culture and KOH examination or detection of scabies mites. Curettes can also be used to debulk tumors, thereby better delineating their margins prior to excision[55]. With repeated use, curettes will become dull and must be periodically sharpened. There are disposable, single-use curettes; however, they tend to be very sharp and may cut into healthy tissue.



Fig. 144.7 Facial surgical instruments. Authors' tray for facial surgery/repair includes (from left to right) two curved Mosquito hemostats, suture scissors, a double-pronged and a single-pronged skin hook, delicate Webster needle holder, curved iris scissors, delicate Supercut® Shea undermining scissors, 0.9 mm Castroviejo forceps, and Siegel blade handle with #15 blade. Two towel clamps are at the top.



Fig. 144.8 Trunk or extremity surgical instruments. Authors' tray for larger procedures in thicker skin includes (from left to right) curved Mosquito hemostats, suture scissors, skin hooks, Mayo–Hegar needle holder, curved iris scissors, Supercut® Metzenbaum undermining scissors (excellent when extensive undermining is anticipated; otherwise, baby Metzenbaum or Shea scissors are sufficient), Adson toothed forceps, and #3 handle with #10 blade. Two towel clamps are at the top.

Scalpels

The choice of scalpel handle and blade is based on the surgical site and personal preference of the surgeon (Fig. 144.10). The flat, standard #3 handle is the one used most frequently in dermatologic surgery as it is durable, inexpensive, and adequate for the majority of cutaneous procedures. This instrument is available with or without a ruler on the handle. Ergonomic refinements have led to the introduction of several additional handles that offer more precise control and better grip, e.g. the thinner, longer, grooved #7 handle. The Siegel handle, which is a thin, round, knurled and well-balanced handle, is well suited for Mohs micrographic surgery. It is easily rolled with the fingers to facilitate very subtle adjustments in the cutting angle. For small procedures, such as those on the eyelid and/or ear, some surgeons prefer short, round, knurled blade handles that hold slender specialized mini-blades (see below).

The most commonly used blades in dermatologic surgery are #15, #10, and #11. The #15 blade is the most popular blade. It is gently curved and is appropriate for the majority of skin surgery. The #10 blade is a wide blade, similar in shape, but larger than the #15 blade; it is favored when cutting through sites with thick dermis such as the back. The #11 blade is tapered to a sharp point; it is used to create stab incisions for drainage procedures, the removal of milia, precise standing cone removal, and "through and through" excisions. It is often used with the cutting surface up, which is opposite to the positioning of the #10 and #15 blades. Scalpel blades are made of either stainless steel or sharper, more expensive, Teflon®-coated carbon steel. Disposable scalpels attached to plastic handles are available, but they are not weighted and are usually less sharp.

Needle holders

Needle holders for facial and hand surgery are small and light with narrow, fine jaws, while larger needle holders with wide sturdy jaws are designed for work on the trunk and proximal extremities. The jaws of needle holders are either smooth or serrated (Fig. 144.11). Serrations prevent twisting of larger needles (e.g. Ethicon PS-2 and FS-2) during suturing. Smooth jaws are less damaging to fine-caliber needles (e.g. Ethicon P-3) and will not tear finer sutures (6–0), but suture needles may slip if not grasped carefully. Alloy inserts of tungsten carbide serve to increase the strength and hardness of the jaws and these inserts improve the grip on needles in smooth-jawed needle holders



Fig. 144.9 Eyelid tray. Tray setup for eyelid surgery includes (bottom row, left to right) hand-held electrocautery, #3 blade handle, iris scissors, Westcott (or Castroviejo) scissors, Castroviejo needle holder, and two 0.5 mm Castroviejo forceps, in addition to (top row, left to right) Castroviejo calipers (used for measuring dimensions of eyelid skin grafts and planning tarsoconjunctival flaps[54]), 2-pronged delicate skin hooks, 4-pronged skin hooks (rakes), and curved Mosquito clamp.



Fig. 144.10 Scalpel handles and blades. From left to right: #3 handle with #10 blade, Siegel handle (authors' preference) with #15 blade, and Beaver handle with #64 blade.

(see Fig. 144.11). Instruments with tungsten carbide inserts are readily identified by their gold finger handles; they are more expensive but are typically guaranteed for five years. There are also small needle holders that have delicate serrated jaws, which allow for a good grip on fine needles without shredding fine sutures. Large needles should not be used with fine needle holders as this may lead to damage to the inserts of these delicate instruments.

Popular models such as the 4.5- to 5-inch long Webster and Halsey needle holders, which have smooth or delicately serrated jaws and tapered tips, are ideal for the small needles and fine suture materials that are commonly used for cutaneous facial surgery (see Figs. 144.7 and 144.11). However, use of these instruments for procedures on the trunk will quickly lead to their misalignment. The Crile-Wood needle holder has a gently tapered blunt tip; it is designed to hold larger needles and is more appropriate for skin surgery on the trunk or extremities. Baumgartner and Mayo–Hegar holders are durable, strong drivers with short tips and serrated jaws, providing a mechanical advantage with larger needles in thicker skin (see Figs. 144.8 and 144.11). The Olsen–Hegar needle holder has suture-cutting scissors behind the jaws and is convenient to use when working alone although it is easy to inadvertently cut the suture when attempting to regrasp the needle.

Scissors

Surgical scissors are required for cutting skin, undermining the subcutis and deeper fascial layers, cutting sutures, and removing wound dressings (Fig. 144.12). Scissors may have long or short handles, and the blades are straight or curved and serrated or smooth. The tips may be sharp or blunt. Scissors used in cutaneous surgery can be either completely stainless steel (most popular, least expensive) or have tungsten carbide inserts to strengthen the blades.

Gradle scissors are small, delicate, sharp-tipped, and tapered to a very fine point with a gentle curve. Due to their sharpness and precision, Supercut® Gradle scissors are ideal for removing thin stages during Mohs micrographic surgery and for removing skin tags. Gradle scissors must be used with care, and they should never be used to cut sutures. With improper use, they are quickly dulled, the cutting surfaces are nicked, and the tips are easily malpositioned.

Tissue scissors have relatively short handles and sharp tips. They are available in straight or curved models, with or without the serrations that prevent tissue motion during cutting. Of the various models available, the authors prefer curved Supercut® iris scissors to cut tissue and for sharp dissection. Supercut® iris scissors have the sharpest edge and they are easily recognized by their black handles. These scissors have a fine beveled angle at the cutting edge, and they are available with smooth edges or one serrated edge. The "razor-like" edge of these scissors enables the surgeon to cut tissue in a smooth, easy motion.

Westcott and Castroviejo scissors are delicate, spring-loaded tissue scissors with very sharp tips (see Fig. 144.9). The configuration of their handle and spring-loaded action make them ideal for manipulation in small delicate sites. For this reason, they are popular with oculoplastic surgeons. They should only be used for cutting thin tissue, such as that encountered in eyelid surgery, or they will dull quickly.

Large, less expensive scissors are sufficient for cutting sutures. Tissue scissors should never be used to cut sutures. Specially designed suture-removal scissors with a half-moon hook on the lower blade are available



Fig. 144.11 Comparison of delicate Webster and Mayo–Hegar needle holders. This Webster needle holder (right) features tungsten carbide jaw inserts which add strength and improve the grip on fine needles in smooth-jawed needle holders. The serrated jaws of the larger Mayo–Hegar needle holder (left) provide a firm grip on large needles, but may shred fine suture and optimally should only be used with 2–0 to 4–0 suture.



Fig. 144.12 Standard scissors. From left to right: Supercut® Gradle scissors, Supercut® iris scissors, and Supercut® baby Metzenbaum scissors. *Courtesy Glenn Goldman, MD.*

and the small hooked tip easily grasps the loop and prevents accidental sticks.

Undermining scissors are usually blunt-tipped (for safety) and have longer handles (for comfort). They are available in different sizes to accommodate the various anatomic regions in which skin surgery is performed. Baby Metzenbaum scissors have a high handle-to-blade length ratio, and, with the resultant small blade arc, they have become the most widely used scissor for sharp or blunt undermining (see Fig. 144.12). Larger Metzenbaum scissors are appropriate for extensive undermining in fascial planes on the scalp, trunk, and extremities (see Fig. 144.8). Stevens tenotomy scissors and Supercut® Shea undermining scissors are utilized for more superficial, delicate undermining (see Fig. 144.7). The tips of these scissors allow for sharp, less traumatic undermining.

For bandage-cutting, 5.5-inch Lister scissors are the most popular, with their angled blades and large blunt tips that easily slide under a dressing without damaging the underlying skin. The Universal scissor is also a popular choice. The serrated edges and larger rings provide greater cutting power.

Forceps

Proper forceps are essential for delicate, safe handling of tissue and suture needles during skin surgery. The most useful forceps in skin surgery are lightweight and have fine tips. The tips may be toothed, serrated, or smooth. Serrated forceps can exert excessive pressure on tissues, resulting in crush injury. Toothed forceps have opposing fine teeth and thus exert less pressure overall. Only toothed forceps should be used to grasp the epidermis and superficial dermis. For cutaneous surgery, the most popular tissue forceps (Adson) has 1×2 teeth. Some forceps have both distal teeth for handling of tissue and a more proximal raised platform for firmly grasping suture needles, allowing the surgeon to avoid manual handling of sharp needles.

Forceps are available with delicate (≤0.9 mm), regular (1–1.5 mm), or heavy (≥1.6 mm) tips. Adson forceps are the standard large forceps used for excisional surgery on the trunk and proximal extremities. Bishop–Harmon forceps and Foerester forceps are very lightweight, fine-tipped, and ideal for delicate work on the face and hand. Because these forceps are easily bent and misaligned, they must be handled with care, and they should not be used for manipulating the thicker skin of the trunk or proximal extremities. Castroviejo forceps usually feature a suturing platform and offer the delicate tip of a Bishop–Harmon forceps, but with a sturdier build and wider grip (see Fig. 144.7).

Both epilating and jewelers' forceps have fine, sharp points and are useful for suture removal. Splinter forceps have fine, extra-fine or superfine delicate pointed tips, and they are used in hair transplants, for splinter removal, and for removing embedded sutures.

Hemostats

Hemostats are used to grasp bleeding vessels prior to ligation. The most popular hemostat is the Halsted Mosquito model which is available in 3.5-inch and 5-inch lengths, either curved or straight, and either delicate- or regular-tipped. A modified instrument known as an Allis clamp is particularly helpful during cyst or lipoma removal (Fig. 144.13). It has finger grips and a locking mechanism similar to a hemostat, however, the jaws have opposing sharp teeth that grasp tissue firmly. Since these teeth can devitalize tissue, the Allis clamp is only used to provide traction on tissue that is being excised, such as a cyst wall.

Skin hooks

Skin hooks enable the surgeon to handle tissue with minimal trauma, and they are particularly useful for elevating flaps and reflecting skin edges during undermining[55]. Many surgeons also use skin hooks to visualize bleeding vessels for hemostasis and for placement of dermal sutures. Skin hooks possess a sharp tip that has the potential to inflict a perioperative sharps injury. Thus, these instruments should be handled with caution and the tips shielded on the tray when not in use as is done with scalpels and needles.

Skin hooks are available in single-, double- or multiple-pronged patterns. The multiple-pronged instruments are used mainly for rhytidectomies and larger truncal procedures in which large flaps are being elevated. Single-pronged hooks are used most frequently for undermining delicate skin or for placing sutures. The single shepherd hook – which has a more circular shape – holds tissue better than does the single standard hook, but it does not release as easily. Some surgeons prefer the double-pronged skin hook due to its lower risk of puncture injury to the operator or assistant.

Special Instruments

For delicate work near the eye, the dermatologic surgeon needs fine instruments that allow for precise cutting and carefully controlled tissue manipulation. The Beaver handle, which comes in a variety of sizes, can be rolled with one's fingertips, providing greater precision and control (see Fig. 144.10). Beaver handles are fitted with specialized smaller, sharper blades. The #64 blade has a rounded tip that one may prefer for work around the eye. The #67 and #65 blades are smaller versions of the #15 and #11 blades, respectively. However, these mini-blades dull more rapidly than do the standard #15 blades. Angled Beaver blades (Beaver® 6600) are useful for taking Mohs stages or biopsies in the ear canal.

The Castroviejo needle holder is ideal for suturing the delicate skin near the eye. This needle holder has spring handles and an optional



Fig. 144.13 Allis clamps. The inset highlights the sharp teeth which can firmly grasp a cyst or lipoma to facilitate removal.

self-locking device. Castroviejo and Westcott scissors (see above) provide meticulous control when cutting eyelid skin. Lightweight forceps, such as Bishop–Harmon, Foerester or Castroviejo, aid in achieving the delicate handling of tissues necessary in this region. Plastic, Teflon®, and metal eye shields may be used to protect the globe when the lid margin will be breached. Plastic shields are popular as they do not conduct heat or electricity from electrosurgical devices. However, they must never be used with lasers; instead a non-reflective stainless steel shield should be employed.

Chalazion clamps are commonly used for immobilizing earlobes, lips, and tongues during procedures on these areas and provide excellent hemostasis in these highly vascularized tissues. Nail nippers, splitters, and elevators are necessary for nail surgery and are reviewed in Ch. 149.

Antiseptics and Sterilization

A summary of sterilization methods is presented in Table 144.4[56].

Additional figures available in our eBook (see inside front cover for access code).

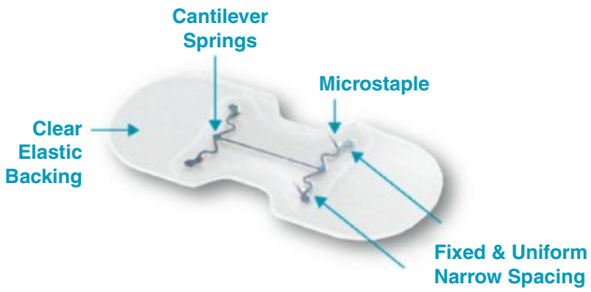
STERILIZATION METHODS		
Method	**Advantages**	**Disadvantages**
Steam autoclave	Most popular in office; easiest; safest	Must use 20–30 min at 2 atm pressure and 121°C; corrosive; may dull sharp instruments
Chemiclave	Lower humidity than steam; less dulling of sharp instruments; instruments are drier	Special chemical needed (mixture of formaldehyde, methyl ethyl ketone, acetone, and alcohols)
Dry heat (oven)	Inexpensive; no corrosion or dulling	High temperature, longer time (1 h at 171°C; 6 h at 121°C); cannot use cloth, paper, or plastic
Gas sterilization	Good for large volumes (mostly used in hospitals)	Expensive equipment; prolonged times (1 day for paper, 7 days for polyvinyl chloride); toxic and mutagenic gas
Cold sterilization: glutaraldehyde or ortho-phthalaldehyde solutions	Simple; inexpensive; used for heat-sensitive equipment (e.g. endoscopes)	Irritating to skin (glutaraldehyde); not recommended as only method; not always effective against bacterial spores (ortho-phthalaldehyde has superior sporicidal activity)

Table 144.4 Sterilization methods.

REFERENCES

1. Artandi C. A revolution in sutures. *Surg Gynecol Obstet*. 1980;150:235–236.
2. Snyder CC. On the history of the suture. *Plast Reconstr Surg*. 1976;58:401–406.
3. Goldenberg IS. Catgut, silk, and silver: the story of surgical sutures. *Surgery*. 1959;46:908–912.
4. Wangensteen OH, Wangensteen SD, Klinger CF. Wound management of Ambroise Pare and Dominique Larrey, great French military surgeons of the 16th and 19th centuries. *Bull Hist Med*. 1972;46:207–234.
5. Toledo-Pereyra LH. Galen's contribution to surgery. *J Hist Med Allied Sci*. 1973;28:357–375.
6. Melle GJ. Early history of the ligature. *S Afr Med J*. 1934;8:290–292.
7. Gudger EW. Stitching wounds with the mandibles of ants and beetles. *JAMA*. 1925;84:1861–1864.
8. Ahmad A, O'Leary JP. Observations on early suture materials: the first stitch in time. *Am Surg*. 1997;63:1027–1028.
9. Levenson SM, Geever EF, Crowley LV, Oates JF, Berard CW, Rosen H. The healing of rat skin wounds. *Ann Surg*. 1965;161:293–308.
10. Usher FC, Allen JE, Crosthwait RW, Cogan JE. Polypropylene monofilament. A new, biologically inert suture for closing contaminated wounds. *JAMA*. 1962;179:780–782.
11. Bucknall TE. Factors influencing wound complications: a clinical and experimental study. *Ann R Coll Surg Engl*. 1983;65:71–77.
12. Bennett RG. Selection of wound closure materials. *J Am Acad Dermatol*. 1988;18:619–637.
13. Holmlund DE. Physical properties of surgical suture materials: stress-strain relationship, stress-relaxation and irreversible elongation. *Ann Surg*. 1976;184:189–193.
14. Herrmann JB. Tensile strength and knot security of surgical suture materials. *Am Surg*. 1971;37:209–217.
15. Postlethwait RW, Willigan DA, Ulin AW. Human tissue reaction to sutures. *Ann Surg*. 1975;181:144–150.
16. Garrett AB. Wound closure materials. *Cutaneous Surgery*. Philadelphia: W.B. Saunders; 1994.
17. Jenkins H, Hrdina LS, Owens Jr FM, Swisher FM. Absorption of surgical gut (catgut): iii. duration in the tissues after loss of tensile strength. *Arch Surg*. 1942;45:74–102.
18. Webster RC, McCollough EG, Giandello PR, Smith RC. Skin wound approximation with new absorbable suture material. *Arch Otolaryngol*. 1985;111:517–519.
19. Guyuron B, Vaughan C. A comparison of absorbable and nonabsorbable suture materials for skin repair. *Plast Reconstr Surg*. 1992;89:234–236.
20. Bingham JL, Brown MR, Mellette JRJ. Reducing the coefficient of friction for fast-absorbing gut suture. *Dermatol Surg*. 2009;35:2004.
21. Postlethwait RW. Polyglycolic acid surgical suture. *Arch Surg*. 1970;101:489–494.
22. Conn J, Oyasu R, Welsh M, Beal JM. Vicryl (polyglactin 910) synthetic absorbable sutures. *Am J Surg*. 1974;128:19–23.
23. Craig PH, Williams JA, Davis KW, et al. A biologic comparison of polyglactin 910 and polyglycolic acid synthetic absorbable sutures. *Surg Gynecol Obstet*. 1975;141:1–10.
24. Aston SJ, Rees TD. Vicryl sutures. *Aesth Plast Surg*. 1976;1:289–293.
25. Fosko SW, Heap D. Surgical pearl: an economical means of skin closure with absorbable suture. *J Am Acad Dermatol*. 1998;39:248–250.
26. Lerwick E. Studies on the efficacy and safety of polydioxanone monofilament absorbable suture. *Surg Gynecol Obstet*. 1983;156:51–55.
27. Molea G, Schonauer F, Bifulco G, D'Angelo D. Comparative study on biocompatibility and absorption times of three absorbable monofilament suture materials (polydioxanone, poliglecaprone 25, glycomer 631). *Br J Plast Surg*. 2000;53:137–141.
28. Chantarasak ND, Milner RH. A comparison of scar quality in wounds closed under tension with PGA (Dexon) and polydioxanone (PDS). *Br J Plast Surg*. 1989;42:687–691.
29. Rodeheaver GT, Powell TA, Thacker JG, Edlich RF. Mechanical performance of monofilament synthetic absorbable sutures. *Am J Surg*. 1987;154:544–547.
30. Katz AR, Mukherjee DP, Kaganov AL, Gordon S. A new synthetic monofilament absorbable suture made from polytrimethylene carbonate. *Surg Gynecol Obstet*. 1985;161:213–222.
31. Ethicon Inc. *Wound Closure Manual*. 2007.
32. Niessen FB, Spauwen PH, Kon M. The role of suture material in hypertrophic scar formation: Monocryl vs. Vicryl-Rapide. *Ann Plast Surg*. 1997;39:254–260.
33. Regan T, Lawrence N. Comparison of poliglecaprone-25 and polyglactin-910 in cutaneous surgery. *Dermatol Surg*. 2013;39:1340–1344.
34. Rosenzweig LB, Abdelmalek M, Ho J, Hruza GJ. Equal cosmetic outcomes with 5-0 poliglecaprone-25 versus 6-0 polypropylene for superficial closures. *Dermatol Surg*. 2010;36:1126–1129.
35. Lewin JM, Ostad A, Brauer JA. Surgical corner: a poliglecaprone 25-only approach to wound closure: cosmetic and financial advantages. *J Drugs Dermatol*. 2013;12:341–342.
36. Naghshineh N, Ota KS, Tang L, et al. A double-blind controlled trial of polyglytone 6211 versus poliglecaprone 25 for use in body contouring. *Ann Plast Surg*. 2010;65:124–128.
37. Elek SD, Conen PE. The virulence of Staphylococcus pyogenes for man; a study of the problems of wound infection. *Br J Experimental Pathol*. 1957;38:573–586.
38. Nilsson T. Mechanical properties of Prolene and Ethilon sutures after three weeks in vivo. *Scand J Plast Reconstr Surg*. 1982;16:11–15.

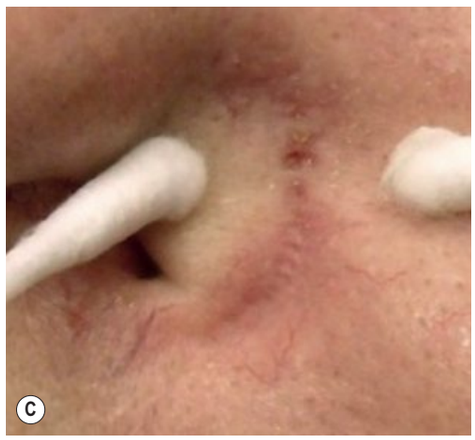
39. Nilsson T. Mechanical properties of Prolene, Ethilion and surgical steel loops. *Scand J Plast Reconstr Surg*. 1981;15:111–115.
40. Miller JM, Kimmel LE. Clinical evaluation of monofilament polypropylene suture. *Am Surg*. 1967;33:666–670.
41. Bang RL, Mustafa MD. Comparative study of skin wound closure with polybutester (Novafil) and polypropylene. *J R Coll Surg Edinb*. 1989;34:205–207.
42. Alam M, Posten W, Martini MC, et al. Aesthetic and functional efficacy of subcuticular running epidermal closures of the trunk and extremity: a rater-blinded randomized control trial. *Arch Dermatol*. 2006;142:1272–1278.
43. Cordova K, Sweeney S, Jellinek NJ. The elegant ellipse—running subcuticular closures. *Dermatol Surg*. 2013;39:804–807.
44. Campbell JP, Swanson NA. The use of staples in dermatologic surgery. *J Dermatol Surg Oncol*. 1982;8:680–690.
45. Eisen DB, Zhuang AR, Hasan A, et al. 5-0 polypropylene versus 5-0 fast absorbing plain gut for cutaneous wound closure: a randomized evaluator blind trial. *Arch Dermatol Res*. 2020;312:179–185.
46. Pourang A, Crispin MK, Clark AK, et al. Use of 5-0 fast absorbing gut versus 6-0 fast absorbing gut during cutaneous wound closure on the head and neck: a randomized evaluator-blinded split-wound comparative effectiveness trial. *J Am Acad Dermatol*. 2019;81:213–218.
47. Maw JL, Quinn JV, Wells GA, et al. A prospective comparison of octylcyanoacrylate tissue adhesive and suture for the closure of head and neck incisions. *J Otolaryngol*. 1997;26:26–30.
48. Quinn J, Wells G, Sutcliffe T, et al. A randomized trial comparing octylcyanoacrylate tissue adhesive and sutures in the management of lacerations. *JAMA*. 1997;277:1527–1530.
49. Taube M, Porter RJ, Lord PH. A combination of subcuticular suture and sterile Micropore tape compared with conventional interrupted sutures for skin closure. A controlled trial. *Ann R Coll Surg Engl*. 1983;65:164–167.
50. Katz KH, Desciak EB, Maloney ME. The optimal application of surgical adhesive tape strips. *Dermatol Surg*. 1999;25:686–688.
51. Bernstein G. Needle basics. *J Dermatol Surg Oncol*. 1985;11:1177–1178.
52. Rotunda AM, Hu XY, Brodsky M. Advantages of the half-circle suture needle for reconstructing small cutaneous surgical wounds. *Dermatol Surg*. 2014;40:592–595.
53. Travelute CR, Cartee TV. Straight suture needle for full-thickness skin graft fixation on the ear. *J Drugs Dermatol*. 2013;12:104–105.
54. Baker SR. *Local Flaps in Facial Reconstruction*. 3rd ed. Philadelphia: Elsevier Health Sciences; 2014.
55. Johnson TM, Tromovitch TA, Swanson NA. Combined curettage and excision: a treatment method for primary basal cell carcinoma. *J Am Acad Dermatol*. 1991;24: 613–617.
56. Sebben JE. Sterilization and care of surgical instruments and supplies. *J Am Acad Dermatol*. 1984;11:381–392.



eFig. 144.1 MicroMend® skin closure device. It mimics a butterfly closure and can be removed by the patient. *Courtesy KitoTech Medical, Seattle, WA.*







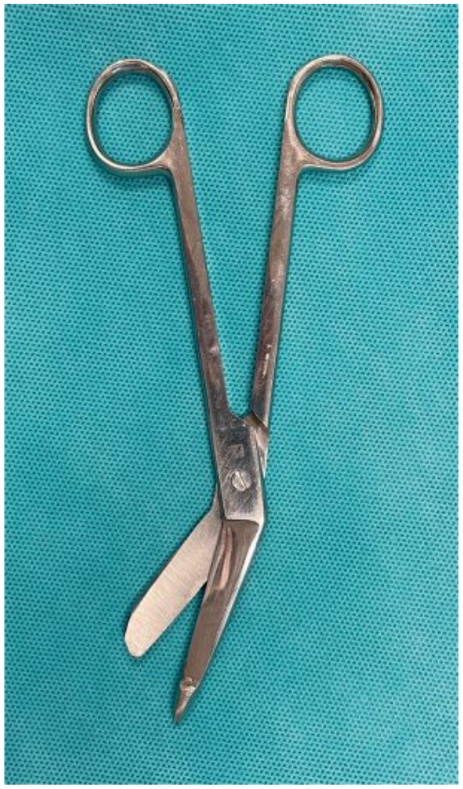
eFig. 144.2 Suture reactions and abscesses. A Suture abscess with obvious central pustule and inflammatory rim. **B** Secondarily infected suture reaction (*Staphylococcus aureus*). **C** Extruding ("spitting") suture; note the small sinus tract.



eFig. 144.3 Two different sizes of Olsen–Hegar scissors/needle holders.



eFig. 144.4 Suture-removal scissors (with groove to grab suture) and forceps.
Instruments courtesy George Tiemann & Company, Hauppauge, NY.



eFig. 144.5 Lister bandage-cutting scissors.



eFig. 144.6 Chalazion clamp. Chalazion clamps can be utilized to immobilize soft tissue and minimize bleeding in well vascularized areas such as the lip or tongue. The screw on the shaft is tightened until adequate hemostasis is achieved.



eFig. 144.7 Blade remover. *Instrument courtesy George Tiemann & Company, Hauppauge, NY.*

145 Dressings

Afsaneh Alavi, Hadar Lev-Tov and Robert S. Kirsner

Chapter Contents

Moist Healing Environment 2501
History of Wound Dressings 2501
Functions of a Wound Dressing 2501
Traditional Wound Dressings 2502
First and Second Intention Healing 2502
Role of Debridement 2503
Wound Cleansers 2503
Topical Antimicrobials and Dressings that Contain Antimicrobial Agents 2503
Moisture-Retentive Dressings 2505
Advanced Wound Therapies 2510
Compression Therapy 2514
Future Directions 2515

Key features

- Wound dressings have evolved from simple wound coverings to more active wound management tools that directly interact with the wound environment
- No perfect dressing exists for all wounds but when used appropriately, dressings can improve healing time and cosmesis as well as reduce pain and infections
- Semipermeable or occlusive dressings provide a moist environment, retain wound fluid that contains growth factors conducive to healing, and promote a low tissue oxygen tension that stimulates angiogenesis and deposition of collagen
- The major types of moisture-retentive dressings include films, foams, hydrogels, alginates, gelling fibers, hydrocolloids, and superabsorbents

INTRODUCTION

Dermatologists are involved in the care of a variety of acute and chronic wounds including surgical incisions. The range of treatment options is substantial and expanding, providing therapeutic flexibility. Appropriate wound dressing selection requires an understanding of the properties of various dressings, as well as their advantages and disadvantages. As the wound heals, the ideal dressing may change based on the amount of exudate, necrotic tissue, and pain or the presence or absence of infection (Table 145.1).

MOIST HEALING ENVIRONMENT

Providing a moist wound environment is an important principle of wound healing. There are several mechanisms by which moisture assists the healing process, the most basic of which is reduced tissue desiccation and prevention of crust formation. Studies by Winter[1] demonstrated that uncovered, air-dried wounds re-epithelialized at a slower rate (see below). This slower rate has been attributed to the requirement of the regenerating epidermis to migrate below an overlying crust and other dry fibrous tissue to a region of moisture where live cells survive. It is only in such an environment that epidermal cells can move toward bridging the defect of the wound; therefore, the thicker the crust, the deeper the migration that is required. While scarring is associated with deep wounds and the loss of adnexal structures, improved cosmetic outcome has been observed following the use of occlusive dressings[2].

By reducing moisture transmission, moisture-retentive dressings optimize healing via several possible mechanisms. These include providing a moist environment (Fig. 145.1), increasing the availability of growth factors and matrix materials, and maintaining an electrical gradient within the wound, which also promotes healing.

HISTORY OF WOUND DRESSINGS

The use of wound dressings dates back to antiquity. For at least 4000 years, fabrics such as linen were employed, until woven absorbent cotton gauze was introduced in 1871. The Edwin Smith Surgical Papyrus, which is one of the earliest medical treatises (circa 1615 BCE), describes the use of linen strips and plaster to dress wounds, stating that closed wounds would heal more quickly than open wounds[2]. Ancient documents disclose how lint was used to pack and fill open wounds and how bandages were used to re-approximate wounds in order to facilitate healing. Linen strips were sometimes coated with grease or oil in order to prevent adherence to wounds or with honey to create a semi-occlusive and adherent dressing[3].

Until Lister connected the presence of pus with infection, pus had been viewed as beneficial ("laudable pus"). However, this association became linked so strongly that it was held that one is always indicative of the other, which is not always true. The association significantly interfered with the acceptance of occlusive dressings, despite better and faster healing, due to the fear of an increased number of bacteria under the dressing. Although the work of Pasteur, Koch, and Lister in the late 1800s on the cause of bacterial infections spurred the investigation of specific therapies for wound management, it was not until the mid-1900s that the understanding of wound healing changed.

Despite the teaching of the Smith Papyrus, it was believed that wounds healed faster if kept dry and uncovered. However, in 1948, Oscar Gilje described a "moist chamber effect" for wound healing[4]. Two years later, Schilling and colleagues studied common minor wounds with highly occlusive or semi-occlusive nylon films and found semi-occlusive dressings to be more effective for healing than open treatment. The finding that semi-occlusive dressings were more effective than the highly occlusive dressings is thought to have set back further study. In 1962, George Winter conducted the landmark study on moist wound healing, demonstrating a 30% greater benefit of occlusive dressings compared with air drying of wounds[1]. Many studies conducted since Winter's seminal work, including in the porcine model of wound healing, have supported the benefits of moist wound healing by occlusive dressings[5].

FUNCTIONS OF A WOUND DRESSING

The essential function of every dressing is to optimize the healing environment, but because the process of wound repair is dynamic (see Ch. 141), each stage may require a different dressing. While an ideal wound dressing would have many positive features (see Table 145.1), they should at the minimum protect the wound from trauma, bacterial invasion, or exposure to caustic substances; this is especially important during the acute inflammatory stage when promotion of granulation tissue formation and epithelialization is crucial. In addition, the dressing should be composed of a material that does not shed fibers or other material into the wound that could lead to foreign body reactions or irritant or allergic contact dermatitis[6]. The "ideal" dressing that meets all of these requirements for every wound type does not yet exist (Table 145.2). However, given the array of dressings available, it is possible to achieve one's goal.

TRADITIONAL WOUND DRESSINGS

Wound dressings can be categorized either by the dressing technique and how the dressing is utilized relative to the wound (see below) or by the composition and structure of the dressing[2]. Naturally occurring materials such as cotton, silk, linen, or cellulose-based substances have a long history of use and have been produced in various combinations for maximum clinical usefulness.

The basic cotton gauze bandages in use today are frequently composed of cotton plus cellulose acetate (added for increased absorbency) and are manufactured with or without various substances incorporated into the fabric. Gauze bandages are inexpensive and easy to use but have limited moisture-retentive capacity and may adhere to the wound; the moisture retentive properties can be enhanced by impregnation with hydrophobic coatings. White petrolatum and other ointments such as soft paraffin wax (e.g. Vaseline® gauze, Aquaphor® gauze, Adaptic™ dressing), with or without antimicrobial agents such as povidone-iodine (Betadine®), sulfadiazine, bismuth tribromophenate (Xeroform™ dressing), framycetin or chlorhexidine, are examples of impregnated substances. Balsam of Peru is found in the tulle gras dressing used predominantly in Western Europe. These medicated dressings are often composites of rayon, nylon, or gauze and are used for malodorous wounds such as chronic ulcers. Activated charcoal cloths (with or without antibacterial silver salt) are also used to control odor.

Because these impregnated dressings have less adherence to the wound, they are placed directly against the wound bed. In addition, they are less painful to remove and can be molded into the depression of deeper wounds for the purpose of filling dead space and providing absorption. The disadvantage of this type of dressing is the potential for maceration of the wound and the surrounding skin, should the dressing remain in place for an extended period of time. While traditional dressings such as gauze are relatively inexpensive and readily available, they require frequent replacement, which is time-consuming and can be costly due to the expense of nursing care[7].

SELECTION OF APPROPRIATE DRESSINGS	
Wound factor	**Dressing**
Exudate	
• Provides moisture	Hydrogel
• Maintains moisture	Film, hydrocolloid
• Absorbs moisture	Foam, alginate, gelling fibers, superabsorbent
Pain	
• Reduces pain	Hydrogel, soft silicone, contact layers
Bleeding	
• Contains hemostatic agents	Alginates
Superficial infection	
• Reduces number of microorganisms	Impregnated with silver, chlorhexidine, polyhexamethylene biguanide, iodine, honey, copper oxide, dialkylcarbamoyl chloride, or methylene blue plus gentian violet as antiseptics

Table 145.1 Selection of appropriate dressings. Availability and cost are two additional factors that are not wound-related.

Primary dressings are those that are in contact with the wound whereas *secondary* dressings cover the primary dressing and/or secure the primary dressing in place. Most conventional dressings are "layered" and are constructed as either "pressure" or "non-pressure" dressings. A layered dressing is usually created in three parts: (1) the contact or interface layer, which is usually a non-adherent, fluid-permeable material that makes direct contact with the wound; (2) the absorbent layer, usually a cotton pad, gauze or other such material, which is placed on top of the contact layer to "wick in" and retain wound exudate and help the dressing mold to the shape of the wound; and (3) the outer layer or wrap, often tape or other banding material for retention of the underlying layers. Each layer is placed in close approximation to the prior one, without gaps or air pockets, and should increase in size and degree of overlap, from wound bed to outermost layer.

A "pressure" dressing has more bulk added to the absorbent layer and is used to assist in hemostasis and to act as a bolster. Usually applied immediately after a surgical procedure such as debridement or graft placement (enhances graft–wound bed interaction), a pressure dressing is changed to a lighter dressing within 24 hours. In addition to limiting bleeding, the pressure dressing also reduces local edema. However, it is important to be aware of the amount of pressure exerted upon the wound bed so as not to create localized ischemia, potentially resulting in tissue necrosis[8].

FIRST AND SECOND INTENTION HEALING

Typically, primary closure is employed for postsurgical wound defects that are clean and free of debris. Aseptically placed sutures provide hemostasis, reduce the possibility of wound infection, and may improve

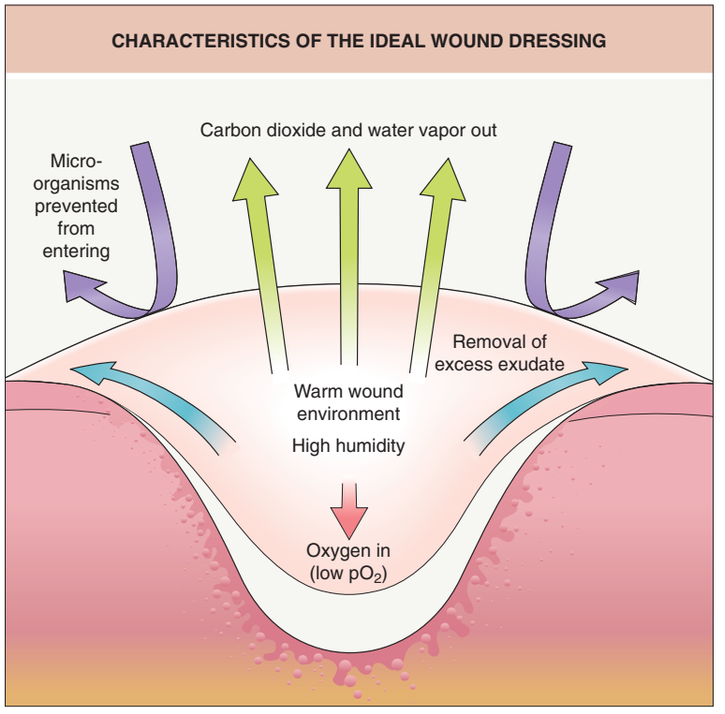


Fig. 145.1 Characteristics of the ideal wound dressing. *Courtesy Gregg M. Menaker, MD.*

CHARACTERISTICS OF AN IDEAL DRESSING – COMPARISON OF MOISTURE-RETENTIVE DRESSINGS					
	Comfort	**Absorbency**	**Pain relief**	**Easy to re-apply**	**Debridement**
Films	+		+		+
Foams	+	++	+	+	
Hydrogels	++	+	++	+	++
Alginates	++	+++		+	+
Hydrocolloids	+	++	+	+	+
Superabsorbents	+	+++		+	

Table 145.2 Characteristics of an ideal dressing – comparison of moisture-retentive dressings[e1].

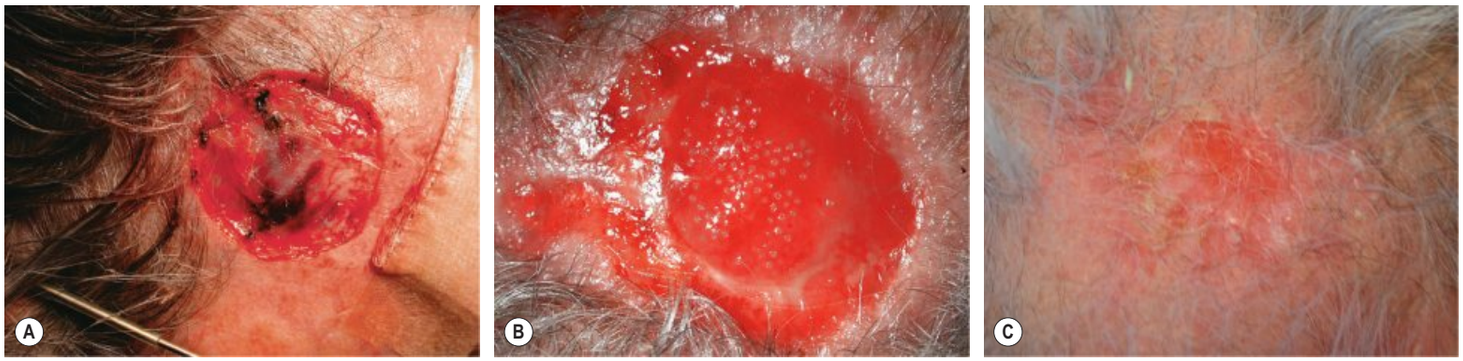


Fig. 145.2 Second intention healing. A Surgical wound immediately following Mohs micrographic surgery; a semi-occlusive dressing will be applied. **B** Three weeks following surgery. Note the abundance of pink–red granulation tissue. **C** Fully re-epithelialized wound six weeks following surgery. *Courtesy Gregg M. Menaker, MD.*

the ultimate cosmetic result. After suture removal, the use of external splinting tape (e.g. Steri-Strips™) or tension-relieving dressings (e.g. embrace®) supports the tissues, enabling favorable collagen remodeling that may limit scar formation and hypertrophy. Use of an antimicrobial ointment under the dressing does not reduce the rate of infections but does increase the risk of contact dermatitis, while the use of any ointment did not reduce complications[9,10].

Second intention healing is often employed following cutaneous surgical techniques such as tangential biopsy, curettage, cryosurgery, laser surgery, and excision in concave sites (Fig. 145.2). In such cases, moisture in the wound bed is the key to optimal healing. A semi-occlusive dressing is the treatment of choice, with the topical application of ointment directly on the wound. Monitoring the wound for signs of infection and preventing the wound bed from drying until re-epithelialization has occurred are usually sufficient measures for the management of this type of surgical wound[11].

ROLE OF DEBRIDEMENT

Debridement is the removal of necrotic, contaminated, or foreign material from a wound or from areas adjacent to the wound. Although data from controlled trials are limited, it is considered a key component of wound management due to its purported ability to induce acute healing and reduce microorganisms[12]. Five types of debridement exist: surgical, mechanical, autolytic, enzymatic, and biologic. Although *surgical* debridement is often the fastest and most direct way of removing unhealthy tissue, it may not be the method of choice for all patients. Factors such as the frequent need for analgesics, possible bleeding, the extent of non-viable tissue, patient preferences, and the practitioner's level of expertise need to be considered. An example of *mechanical* debridement is the wet-to-dry dressing that is employed for wounds with significant necrotic tissue, but it does not distinguish between viable and non-viable tissue.

In *autolytic* debridement, occlusive dressings provide a moist wound environment which promotes the lytic activity of enzymes present in accumulated wound fluid. This assists in the clearance of residual debris during early wound healing. *Enzymatic* (chemical) debridement involves the topical application of an enzymatic agent and this can be used to supplement autolytic debridement. Currently, one agent is FDA-approved: collagenase (Santyl®) ointment. It assists in the removal of devitalized tissue and aids in granulation tissue formation and re-epithelialization.

Biologic debridement employs fly larvae (maggots) and has been used for centuries to debride chronic ulcers. Nowadays, the most commonly used maggots are those of the green bottle fly, *Lucilia sericata*. Maggots digest necrotic tissue via collagenases and trypsin-like enzymes, thereby exposing healthy tissue. They also have antimicrobial effects, including secretion of antibacterial compounds (e.g. phenylacetic acid, phenylacetaldehyde) in addition to ingestion and subsequent killing of Gram-positive bacteria (including MRSA) and, to a lesser extent, Gram-negative bacteria. In a clinical trial of 267 patients with leg ulcers, larval therapy led to faster debridement than hydrogel therapy, but larval therapy has not been shown to improve healing rates or decrease bacterial load[13,14].

WOUND CLEANSERS

The removal of loose debris from the wound surface is termed *wound cleansing* and is a component of local wound care[15]. Optimal wound cleansers should have low cytotoxicity and they include water, isotonic normal saline (0.9% sodium chloride), and in some cases, dilute acetic acid or other mild acid solutions. Isotonic normal saline is a good cleanser for the majority of wounds and a Cochrane collaboration review found clean tap water as a suitable alternative[16].

Wound cleansing can be performed via several methods: compresses (gauze squeezed so no excess fluid), soaking (saturated gauze), cleansing sprays, and high-pressure irrigation. Irrigation can cause trauma to the wound bed and is not recommended for deep wounds unless one makes sure no cleansing fluid is retained within a "pocket" in the wound.

TOPICAL ANTIMICROBIALS AND DRESSINGS THAT CONTAIN ANTIMICROBIAL AGENTS

The presence of bacteria in wounds may delay acute wound healing, depending upon the quantity, species, and variants of bacteria as well as their organization within the wound (e.g. biofilms). They may also contribute to delayed healing of chronic wounds, but because resident bacteria are often held in check by host resistance, most chronic wounds heal with bacteria present. That said, bacteria do compete with adjacent cells for oxygen and nutrients and they can also produce toxins that delay healing. Bacteria within wounds can also form biofilms which are complex adherent accretions that are difficult for antibiotics to penetrate. Clinically differentiating a wound in bacterial balance from a wound where bacteria are delaying healing remains a challenge.

While a clean wound created with good aseptic technique (e.g. sutured surgical excision) does not require topical antimicrobials[9,10], they may be needed for some acute and chronic wounds with critical colonization. Topical antimicrobial agents include antiseptics and antibiotics. Antiseptics non-selectively destroy or inhibit the growth of microorganisms, whereas antibiotics are only effective against specific bacteria[17]. Due to the emergence of bacterial resistance and the risk of development of allergic contact dermatitis, topical *antibiotics* are typically reserved for superficial cutaneous infections such as impetigo. Mupirocin, retapamulin, ozenoxacin and fusidic acid are indicated for the treatment of cutaneous infections due to *Staphylococcus aureus* or *Streptococcus pyogenes*[18,19]. Silver sulfadiazine has broader antimicrobial coverage, but a pseudo-eschar can form and may delay healing[19,20]. Triple antibiotic cream or ointment formulations available over the counter may contain combinations of polymyxin, gramicidin, bacitracin, and/or neomycin; however, the latter two are amongst the most common allergens in North America (see Ch. 14).

Because *antiseptics* often affect cellular metabolism (including cell wall formation), they are less often associated with the emergence of resistant organisms. The antimicrobial activity and cellular toxicities of various antiseptics are listed in Table 145.3[17,21]. ***Silver*** has been used since ancient times for treating wound infections due to its antimicrobial activity. When in contact with wound fluid, silver metallic salt (Ag^0) becomes ionized (Ag^+) and highly active against bacteria.

DRESSINGS THAT CONTAIN ANTISEPTICS				
Antimicrobial agent	**Examples of dressings**	**Coverage spectrum**	**Advantages**	**Disadvantages**
Silver	Acticoat® Flex 7 Silver, Actisorb® Silver 220, Algicell® Ag (alginate), Aquacel® Ag, Contreet® Biatain Ag Foam, ColActive® Plus Ag, Mepilex® Ag, Opticell™ AG+ (gelling fiber), PolyMem®/ PolyMem MAX Silver, SilvaSorb® (hydrogel), Silvercel® (alginate), Silverlon®, Tegaderm™ Ag (alginate), UrgoTul® Ag/Silver, UrgoTul® SSD	Broad-spectrum antibacterial, including MRSA and VRE	• Release antibacterial levels of silver for 3–7 days • Appear to decrease the levels of matrix metalloproteinases that are upregulated in non-healing, chronic wounds • Microbial resistance is rare • Variety of products available for different wound situations • Infrequent application required	• Silver may stain tissues (localized argyria) • Relatively expensive • Slows acute wound healing
Chlorhexidine or polyhexamethylene biguanide (PHMB), a chlorhexidine derivative	Bactigras™ (chlorhexidine), GemCore360° (PHMB), Kendall™ AMD foam (PHMB), Kerlix™ AMD gauze (PHMB), PuraPly® AM (PHMB)	Broad-spectrum antibacterial and antifungal	• Low tissue toxicity • Different forms available, including foam, ribbons, and gauze • Comforting so recommended for painful wounds	• May cause stinging and ICD • Cytotoxicity – cornea, inner ear (in the setting of tympanic membrane rupture), and cartilage • Systemic and local hypersensitivity reactions
Povidone-iodine* Cadexomer-iodine polymer* Other iodophors	Inadine®, Betadine® cream applied to gauze, Iodoflex™, Iodosorb® (gel), Ioplex®	Broad-spectrum antimicrobial – bacteria, fungi, viruses	• Less irritating to skin than iodine alone • Cadexomer-iodine polymer does not inhibit wound healing	• May cause stinging • ICD, ACD • Povidone-iodine can inhibit wound healing
Honey	Activon Tulle, First Honey® Manuka, MEDIHONEY® Calcium (alginate), MEDIHONEY® gel	Broad-spectrum antimicrobial – bacteria, fungi, viruses	• Low tissue toxicity • Autolytic debridement	• May cause maceration • ACD to propolis
Methylene blue and gentian violet	Hydrofera Blue® Classic, READY, READY-Transfer	Broad-spectrum antibacterial, including MRSA and VRE, and anti-candidal	• Less irritating • Good absorptive capacity for cavity wounds	• Bacteriostatic
Methylene blue, gentian violet, and silver	RTD™ (Retro-Tech Dressing)	Broad-spectrum antibacterial, including MRSA and VRE, and anti-candidal	• See silver above • See methylene blue and gentian violet above	• See silver above • See methylene blue and gentian violet above
Hypertonic saline	Mesalt®	Broad-spectrum antibacterial	• Less irritating to skin	
Copper oxide	MedCu®	Broad spectrum antibacterial, antifungal and antiviral	• Can be incorporated into fabric, including masks	
Dialkylcarbamoyl chloride (DACC)	Cutimed® Sorbact® (contact layer)	Broad spectrum, anti-candidal	• Reduces inflammation by trapping bacteria rather than killing bacteria • Variety of dressing types available	• Bacteriostatic

*Not to be used in young children, pregnant or lactating women, or individuals with a known iodine sensitivity; to be used cautiously in patients with thyroid disorders.

Table 145.3 Dressings that contain antiseptics. ACD, allergic contact dermatitis; ICD, irritant contact dermatitis; MRSA, methicillin-resistant *Staphylococcus aureus*; VRE, vancomycin-resistant enterococci. From refs 18, 19, 23–25, 27, 31, 33, 36, e2, e3.

The bactericidal action of ionized silver can be explained by the binding of silver ions to tissue proteins or by reactions with chloride anions, which then bind to bacterial DNA and RNA and alter bacterial cell walls and nuclear membranes[22]. Silver also has anti-inflammatory effects and may have angiogenic properties. In addition, silver ions decrease the levels of matrix metalloproteinases (MMPs) that are often upregulated in non-healing wounds. Despite these effects, a recent Cochrane review found no significantly higher healing rates with silver dressings, suggesting that short-term use is optimal[23,24]. Newer dressings, in which high-density polyethylene mesh is impregnated with nanocrystalline silver (Fig. 145.3)[25], can release antibacterial levels of silver for 3–7 days[26].

Chlorhexidine gluconate is a biguanide antiseptic with a wide range of antimicrobial activity against Gram-positive and Gram-negative bacteria, yeasts, and molds, but it is recommended for intact skin not open wounds as it works by disturbing the cytoplasmic membrane[27]. Despite data that it can inhibit re-epithelialization, chlorhexidine-containing dressings have been used in wounds and burns with reported benefit[28]. Because there can be associated cytotoxicity, especially to the cornea, inner ear (in the setting of tympanic membrane rupture), and cartilage, exposure to these structures should be avoided[29]. Systemic and local hypersensitivity reactions have also been observed. A chlorhexidine derivative, polyhexamethylene biguanide (PHMB), appears to be safer and has been added to several wound dressings including gauze, ribbons, foam, and hydrogels.

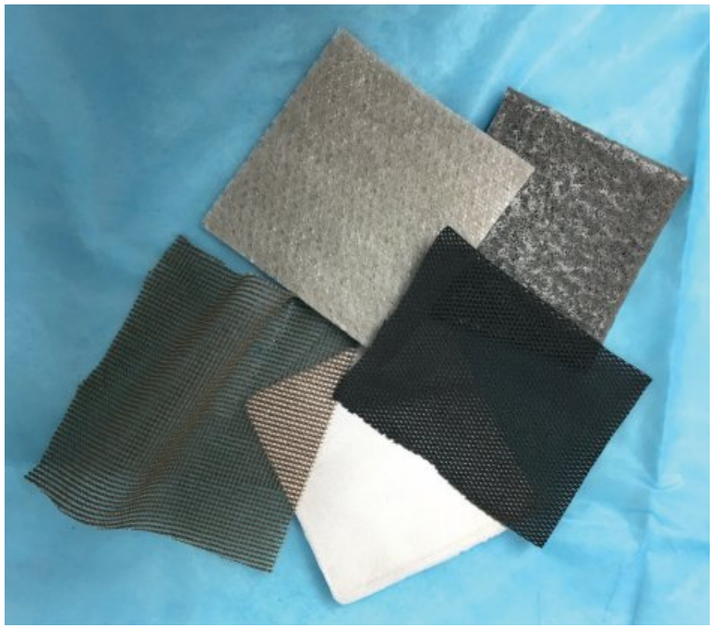


Fig. 145.3 A variety of silver dressings. Clockwise from 2 o'clock, Silvercel®, PolyMem® MAX® Silver, Acticoat® Flex 7 Silver, ColActive® Plus Ag, and Restore® Silver.

Iodine is a broad-spectrum antiseptic that is available in different formulations[30]. However, povidone-iodine, a commonly used antiseptic, can inhibit wound healing. In contrast, newer formulations such as cadexomer-iodine polymer, which slowly releases iodine from dextran beads, do not slow healing and have not been found to have toxic effects on keratinocytes. The starch lattice in the cadexomer-iodine polymer is highly absorptive (1 gram absorbs up to 7 ml of fluid) and as the fluid is absorbed, the iodine is slowly released[31]. The iodine confers antimicrobial activity for several days, but is in a low enough concentration that cytotoxic effects are avoided. The frequency of dressing changes is determined by the rate of iodine release, which is largely dependent on wound exudate[32].

Studies in patients with venous leg ulcers have shown a significant decrease in ulcer size when cadexomer-iodine was compared to hydrocolloid and paraffin gauze dressings[33]. When compared to other treatments for diabetic foot ulcers, cadexomer-iodine was associated with a cost benefit[34]. Because iodine can be absorbed systemically, caution is required when using these dressings in patients with a history of thyroid disease. They should not be used in young children, pregnant or lactating women, or patients with known iodine sensitivity.

While first used centuries ago, ***honey*** has experienced a resurgence due to recognition of its antimicrobial properties. The latter is related to honey's high osmolality, which minimizes the availability of water to bacteria[35]. Manuka honey, a commonly used type of honey, also contains flavonoids and aromatic acids that have antimicrobial properties. In addition, honey exhibits an anti-odor effect by decreasing the wound pH; release of hydrogen peroxide and glucuronic acid stimulates macrophages/monocytes, promotes inflammatory cytokine production, and provides analgesic and antibacterial effects[36]. A Cochrane review found that topical treatment of superficial and partial-thickness burns with honey may improve healing when compared to some conventional dressings[37,38].

Methylene blue and ***gentian violet***, two organic dyes, have been combined in a polyvinyl alcohol sponge to produce an antimicrobial dressing (Hydrofera Blue® Classic, READY, READY-Transfer)[39]. These dyes are not released from the dressing, thus avoiding previously reported tissue toxicities. The dressing has broad-spectrum activity against Gram-positive bacteria, Gram-negative bacteria, and *Candida* spp. These two organic dyes have also been combined with silver in a polymer matrix-containing foam dressing (RTD™).

Copper oxide has demonstrated broad-spectrum bactericidal as well as pro-angiogenic effects and therefore has been incorporated into a dressing[40]. In wounded diabetic mice treated with copper oxide dressings, enhanced angiogenesis post-wounding was observed along with upregulation of proangiogenic factors, including placental growth factor, hypoxia-inducible factor-1 alpha, and vascular endothelial growth factor[41].

Dialkylcarbamoyl chloride (DACC) is a highly hydrophobic fatty acid derivative that can irreversibly bind bacteria via hydrophobic interactions. DACC has been incorporated into a variety of dressings and in a controlled clinical trial reduced the short-term incidence of postsurgical skin infections compared to a standard dressing[42].

MOISTURE-RETENTIVE DRESSINGS

Moisture-retentive dressings, traditionally called passive dressings, are distinct from active dressings, with the former commonly divided into six major groups: films, foams, hydrogels, alginates/gelling fibers, hydrocolloids, and the most recent addition, superabsorbent dressings (Fig. 145.4; Table 145.4). In choosing the most appropriate dressing for a particular wound, it is important to strike a moisture balance, i.e. not too dry and not too wet.

Films

Polymer films are thin, self-adhesive, transparent sheets of polyurethane or other synthetic semipermeable material (Fig. 145.5). These dressings are gas permeable, allowing for the exchange of oxygen, carbon dioxide and water vapor, but impermeable to larger molecule efflux, due to their pore size. Therefore, bacteria, proteins and wound fluid are prevented from moving across the dressing. Its permeability to water vapor allows for the release of insensible water and sweat from the skin. This provides the potential advantage of preventing maceration of the wound and surrounding skin. The semi-occlusive nature of this dressing allows for passage of oxygen to the wound, which had been considered to be an important feature when these dressings were initially introduced. Since then, evidence has indicated that low pO_2 levels (similar to those that actually exist under the dressings) facilitate healing.

Advantages/disadvantages

The advantages of this type of dressing include translucency, thereby allowing direct visualization of the wound without removal of the dressing; permeability to water vapor; and tendency to reduce postoperative pain. They enhance re-epithelialization of graft donor sites, with a reported increase in healing rates of 25%–45%[43]. One disadvantage of film dressings is that they are difficult to place properly, requiring uniform tension on the film to prevent wrinkling and its adherence to itself (similar to what is experienced with Saran™ Plastic Wrap). As the film usually only adheres to intact skin, a 1–2 cm application margin is recommended. In addition, due to shearing forces, it is best to avoid using films on thin or fragile skin.

Films may adhere to the wound as drying progresses, thereby risking disruption or stripping of the newly formed epithelium that is not yet tightly bound to the underlying dermal layer. It is also possible to traumatize newly grafted skin tissue during dressing changes. For these reasons, it is advisable to allow the film dressing to remain in place until it spontaneously falls off, which occurs after 1–2 weeks[44]. Any wrinkling of the film during placement can create a conduit for bacterial penetration and leakage of wound exudate. It is therefore recommended that for exudative wounds the film have a complete 2–3 cm adhesion margin to prevent this leakage.

Another disadvantage of film dressings is that they are non-absorbent; therefore, wound fluid can accumulate under the dressing layer, especially with highly exudative wounds. This is often the case during the first 7–10 days after the creation of a wound, with the adherent properties of film dressings making frequent changing undesirable.

Foams

Polymer foams are semi-occlusive, bilaminate, and polyurethane- or silicone-based dressings. They consist of a hydrophilic foam with a hydrophobic backing, which can prevent leakage, provide a barrier against bacterial penetration, and provide the moist environment afforded by films, but with the addition of some absorbency (Fig. 145.6). The inner layer is composed of an absorbent, gas-permeable polyurethane foam mesh, which lies adjacent to the wound. The outer layer is a semipermeable, non-absorbent membrane composed of polyurethane, polyester, silicone or Gore-Tex®, surrounded by a polyoxyethylene glycol foam. This layer protects against outside bacterial contamination to some extent and against the drying out of the underlying layers.

Foam dressings are typically non-adherent, thereby requiring secondary dressing layers to ensure secure placement with a good seal. The quality of the seal is important to prevent leakage, desiccation, and problems with adherence. There are, however, some foams available with an adhesive surface and/or border, usually surrounding a central absorptive core. Ideally, once a foam dressing has absorbed some amount of exudate, it should be able to retain that fluid, even if exposed to pressure. Some brands are described as having such a quality.

Advantages/disadvantages

Although absorbent, there is usually a limit to the amount of wound exudate this type of dressing can absorb. Therefore, it should be changed every 1–3 days. The permeability of foams to both gas and water vapor makes them suitable for mild to moderately exudative wounds, although some brands may accommodate highly exudative wounds.

Silicone-based rubber foams, known as silastic foams, are composed of a silicone mixture to which a stannous octoate catalyst has been added. This type molds and contours to the shape of the wound and therefore can be used for packing cavities or deep ulcers such as pilonidal sinuses. The additional advantages are absorbency, non-adherence, increased comfort for the patient, a tendency to be less expensive, and dressing changes that do not generally require skilled nursing care[45].

The disadvantages of foam dressings are the inability to use them with dry wounds, their opacity, which prevents visual monitoring of the wound, and the need for frequent changing, perhaps as often as every day. Infrequent changing could risk incorporation of the dressing

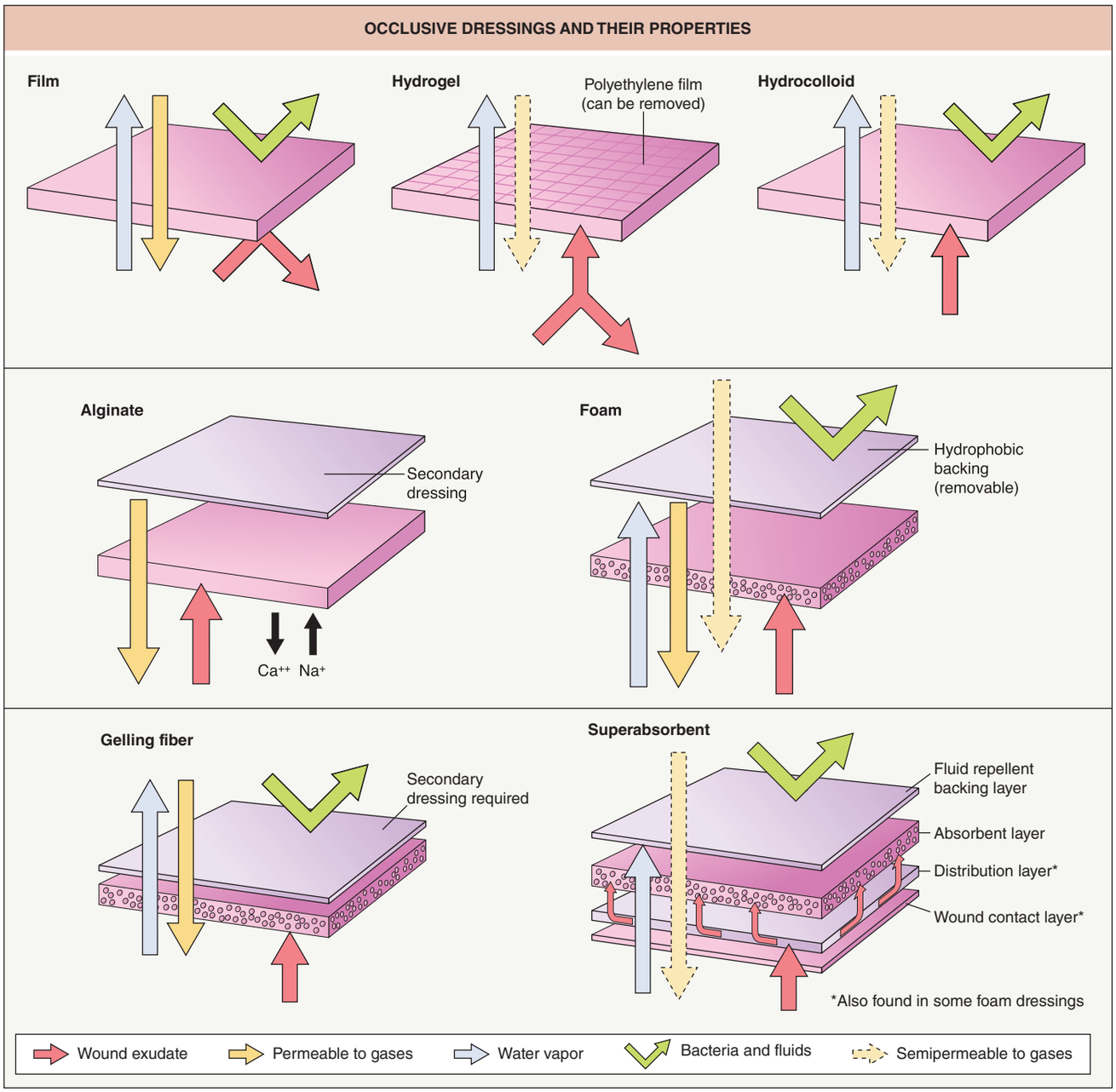


Fig. 145.4 Occlusive dressings and their properties. The six major dressings are polymer films, polymer foams, hydrogels, alginates/gelling fibers, hydrocolloids, and superabsorbents. *Courtesy Gregg M. Menaker, MD.*

material into the wound itself. There is also the possibility of an undesirable drying effect of the wound if drainage is insufficient to maintain a moist environment.

Hydrogels

As their name implies, hydrogels are composed primarily of water – up to 96% of the content. This dressing type consists of a cross-linked hydrophilic polymer network composed of polyvinyl alcohol, polyacrylamide, polyethylene oxide or polyvinyl pyrrolidone; it is produced as sheets, amorphous gels (pre-mixed or dry), or as impregnated dressings (Fig. 145.7). Hydrogels are semitransparent (allowing visual inspection of the wound), have a high absorptive capacity (between 100% and 200% of their volume), and are able to maintain a moist wound environment. The absorptive action is delayed in its onset and increases slowly as it provides for continuous, long-term absorption. Hydrogels are described as semi-adherent or completely non-adherent, depending upon the type, and therefore require a secondary dressing to hold them in place[46]. The latter is necessary, as hydrogels provide a poor bacterial barrier and selectively permit Gram-negative organisms to proliferate[47].

In general, the *sheet form* of a hydrogel dressing is constructed by sandwiching the hydrophilic polymer between two removable thin sheets of polyethylene film, with some types containing a supportive inner gel mesh. For application to the wound, the film on the contact side is removed, leaving the outer film in place. With this mode of application, the dressing is semipermeable to gases (including oxygen) and water vapor. If the outer film is also removed, then the dressing becomes permeable to fluid as well; as a result, exudate can pass to a secondary gauze dressing. The polymer sheets can be removed easily without trauma to the wound bed.

The *amorphous type* of hydrogel is composed of a cornstarch-derived, polymerized compound that forms a gel upon hydration at the time of its use. It is available commercially in a powdered or pre-mixed form, is applied wet to the wound defect, requires a secondary outer dressing, and requires water application to the surface for removal.

Advantages/disadvantages

One significant advantage of hydrogel dressings is a reduction in postoperative pain and inflammation. Another is that hydrogels have been shown to accelerate the rate of wound healing when compared to gauze

MOISTURE-RETENTIVE DRESSINGS						
Dressing type	**Examples**	**Composition**	**Permeability**	**Indicated uses**	**Advantages**	**Disadvantages**
Films	Bioclusive™, Blisterfilm™ Transparent Film Dressing (TFD), Carrafilm™, Derma View II, Mefilm®, Mepore® Film, Opsite™, Polyskin® II, Tegaderm™ Film, Transeal® TFD	Thin polyurethane sheet	Semipermeable	• Intravenous sites • Skin tears • Split-thickness graft donor sites • Laser resurfacing • Mohs surgery defects • Holding pinch grafts in place for venous leg ulcers	• Translucent • Permeable to water vapour • Pain reduction • Creates bacterial barrier	• Difficult to position properly • May adhere to wound as it dries • Possible exudate accumulation • Non-absorbent
Foam	*Adherent and non-adherent*: Allevyn™, Biatain™, Biopatch®, CuraFoam™, Flexzan®, Hydrasorb®, Lyofoam®, Mepilex®, Optifoam®, PolyMem®, Reston™, Sof-Foam™	Bilaminate polyurethane or silicone	Semipermeable	• Chronic wounds • Surgical excisions • Dermabrasion • Burns • Mohs surgery defects • Laser resurfacing	• Absorbent • Permeable to water vapour • Conforms to wound shape • Thermally insulates • Comfortable	• Opaque • Cannot be used on dry wounds • Possible undesirable drying effect on inadequately exudative wounds
Hydrogels	*Hydrogel sheets*: ActiFormCool®, AquaDerm™, Aquaflo®, AquaSite®, CarraDres™, CarraSorb™ M Freeze Dried Gel, Flexigel®, Vigilon® *Amorphous gels*: Biolex® Wound Gel, Carrasyn® Hydrogel, Hydrogel GRX®, Hypergel®, Intrasite™ Gel, Normlgel®, Tegagel™ Hydrogel Wound Filler *Impregnated dressings*: AquaSite™ gauze, Curafil® gauze, Curagel®, DermaGauze™, Tegagel™ Hydrogel Wound Filler with gauze	Hydrophilic polymer sheets, gel, and impregnated dressings	Semipermeable with outer membrane in place	• Dry wounds • Dermabrasion • Laser resurfacing • Superficial thermal burns • Chemical peels • Graft donor sites • Partial thickness wounds	• Semitransparent • Donates fluid to necrotic tissue • Soothing, cushioning and cooling effect, reduction of postoperative pain • Available in sheets, powdered or pre-mixed amorphous gels • Low trauma at dressing changes • Reportedly helpful for pruritus	• No spontaneous sucking ability • Absorption is slow • Requires secondary dressing • Caution in infected wounds
Alginates	Algicate Ag, AlgiCell®/ Algicell® Ag, AlgiSite™ M, Algosteril®, CarraGinate™, CarraSorb™ H, Fibracol® Plus (collagen [90%]–alginate [10%]), Kalginate™, Kaltostat®, Maxorb®, MedVance™, Melgisorb® Plus/Melgisorb® Ag, Sorbsan®/Sorbsan® Silver	Seaweed-based complex polysaccharide	Semipermeable	• Chronic highly exudative wounds • Full-thickness burns • Surgical wounds • Split-thickness graft donor sites • Mohs surgery defects	• Highly absorbent with spontaneous sucking ability • Hemostatic properties • Non-adherent • Conforms to wound shape • Soluble for low trauma dressing changes with normal saline	• Requires a secondary dressing to prevent desiccation • Gel has unpleasant appearance and odor • Mild burning sometimes reported upon application
Gelling fibers	Aquacel®, Exufiber®, Opticell®	Polyvinyl alcohol, sodium carboxymethyl cellulose, chitosan-based polysaccharide polymers	Semipermeable	• Moderate to highly exudative wounds	• Handles heavy exudate • Locks in exudate to reduce maceration • When removed, does not fall apart	• If no exudate, can adhere to wound • Requires a secondary dressing
Hydrocolloids	Allevyn™, Comfeel®, DuoDERM®,DynaDerm®, Exuderm®, Hydrocol® II, MedVance™, Nu-Derm®, Primacol®, RepliCare™, Restore®, Tegaderm™ Hydrocolloid, Tegasorb™	Starch or plastic woven polymer, dextran, polyethylene glycol, water	Semipermeable	• Chronic ulcers • Burns • Traumatic wounds • Surgical wounds • Dermabrasion • Inflammatory disorders (e.g. lichen simplex chronicus)	• Capillary action facilitates debris removal • Conforms to wound shape • Directly adheres to wound site and is easy to use • Increased patient comfort • Thermal insulation	• Risk of maceration of surrounding skin • Possible wound trauma with dressing change • Gel has unpleasant appearance and odor • Opaque • Caution in infected wounds • Collected exudate often confused with wound infection • Excessive granulation tissue (prolonged use)

Table 145.4 Moisture-retentive dressings[40,49].

Continued

MOISTURE-RETENTIVE DRESSINGS						
Dressing type	**Examples**	**Composition**	**Permeability**	**Indicated uses**	**Advantages**	**Disadvantages**
Superabsorbent	Flivasorb®, KerraMax®, Mextra®, OptiLock®, Sorbion®	Polyacrylic acid polymers	Semipermeable	• Moderate to highly exudative wounds	• Handles heavy exudate • Locks in exudate to reduce maceration • When removed, does not fall apart	• Caution when applied under compression • May adhere to wound if exudate dries
Contact layers	Adaptic Touch™, Cutimed Sorbact WCL, Mepitel® One, UrgoTul®	Flexible polyester mesh	Permeable (non-occlusive)	• Contact layer for wounds	• Non-adherent • Less pain with dressing change	• Not recommended for stage 1 pressure ulcers, third-degree burns or wounds with eschar
Silicone dressings	Mepilex® (foam), Mepitel® (film), Mepilex® Transfer (foam), Mepitel® Border (foam)	Silicone-based	Semipermeable Suitable as primary or secondary dressings	• Bullous disorders including epidermolysis bullosa • Fragile skin	• Absorbent • Non-adherent	• Opaque

Table 145.4 Moisture-retentive dressings[40,49].



Fig. 145.5 A transparent film dressing is used to occlude a dry wound. This example is Tegaderm™.

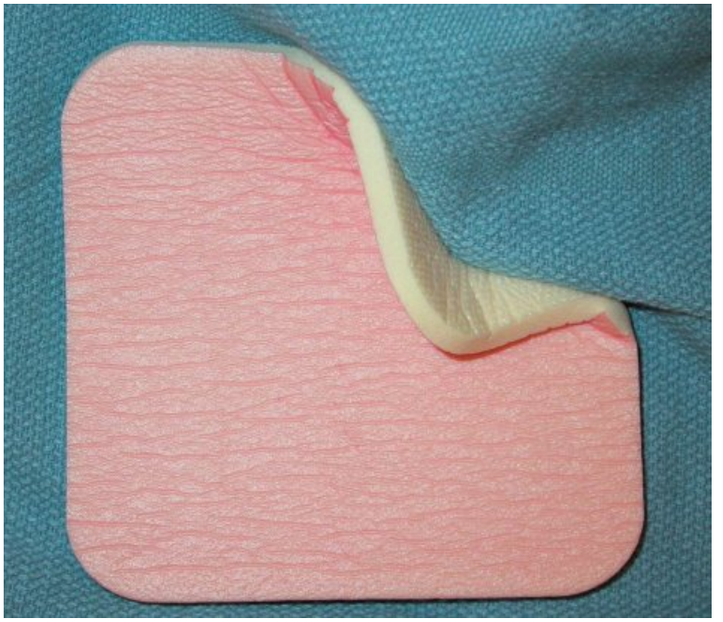


Fig. 145.6 Polymer foam dressing. It consists of hydrophilic foam with a hydrophobic backing (pink).

dressings and non-adherent dressings such as Telfa™. For example, the rate of re-epithelialization of split-thickness porcine wounds was 25%–45% faster with hydrogels, and 100% of the hydrogel-treated wounds healed by postoperative day 4 compared with 32% of open-air (control) wounds[48]. Hydrogels have also been credited with faster healing rates in studies of dermabrasion and hair transplant donor and recipient sites, when compared to standard non-adherent dressings[49].

Hydrogels are not recommended for infected wounds. In addition, the semi- or non-adherent nature of hydrogels often results in more frequent dressing changes than is needed with other occlusive dressings.

Alginates

Highly absorbent alginate dressings are composed of a natural, complex polysaccharide derived from various types of algae or kelp (seaweed). An extraction process produces a sodium salt form of alginic acid and, during a second step, sodium ions are exchanged for calcium, zinc, and magnesium. The end result is an alginate fiber; non-woven mats or twists of this fiber are then made into a dressing (Fig. 145.8). Upon application of the dressing, a reverse ion exchange occurs between the calcium within the alginate fibers and the sodium from blood or the wound exudate. This results in the formation of a soluble sodium alginate gel that fills and completely covers the wound in a non-adherent manner, providing a moist wound healing environment. The extent and rate of gel formation depends on the amount of wound exudate. Alginate dressing materials also have hemostatic properties, believed to be the result of the release of free calcium by the fibers during the ion exchange. This release of calcium augments the clotting cascade, producing the hemostatic advantage.

Because alginate gel dressings are highly absorbent, they can remain in place at the wound site for several days at a time, thereby minimizing dressing changes. To secure an alginate dressing, a secondary dressing is required. A dressing change is indicated when the dressing has been in place for several days or when exudate soaks through to the secondary dressing[50]. Removal of the dressing in a dried state can re-injure the wound.

Advantages/disadvantages

Alginate dressings are soluble and can be removed by saline irrigation, permitting less painful dressing changes. They have been shown to encourage wound healing and are metabolized by the body, should residual material remain at the wound. Despite concerns about the potential toxicity of alginates, they have been used for over 50 years without any commonly reported complications. However, removal of the secondary outer dressing is necessary to visually inspect the wound and to monitor for desiccation.

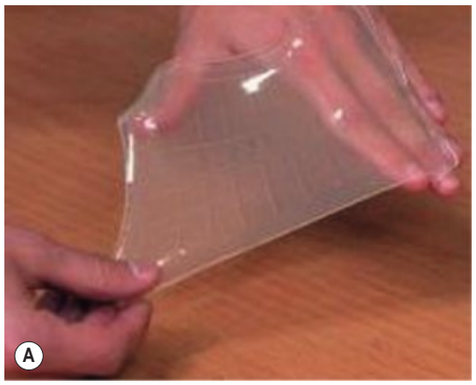




Fig. 145.7 Hydrogels. **A** Hydrogel sheet. **B** Premixed amorphous hydrogel.



Fig. 145.9 Hydrocolloid dressing placed over a healing wound on the ankle. This example is DuoDERM®.



Fig. 145.8 Collagen–alginate complex dressing. Alginate dressings have hemostatic effects and can be used post-debridement.

Gelling Fibers (Hydrofibers)

Highly absorptive hydrofibers are another category of dressings with similarities to alginates. They are composed of carboxymethyl cellulose fibers that interact with wound fluid, turn into a gel, and aid in autolytic debridement[51]. Gelling fibers are up to three times more absorbent than alginates. An additional advantage over alginates is their vertical uptake of wound fluid, thereby decreasing the risk of peri-wound maceration.

Hydrocolloids

Colloid is a Greek term for a two-phase system comprised of a uniform dispersion of one phase of matter (unfilterable small particles) into another phase of matter or matrix. Mutually attractive charges exist between the particles, which contributes to the diffusible properties of colloids. Colloids are characterized by the strength of attraction of the particles to the continuous medium and to the proportion of water within that medium. This property accounts for the absorptive and expansive capacity of colloid gels, which function as a semipermeable membrane. Gel swelling occurs because the particle concentration of the gel is usually higher than that of the surrounding medium, thereby drawing water from the surroundings into the gel.

Hydrocolloid dressings were first employed as ostomy products and are now available in multiple forms. The most commonly used hydrocolloid dressings (e.g. DuoDERM®) are available as sheets with an inner adhesive layer consisting of a hydrophilic colloid base that is a mixture of pectin, karaya, guar or carboxymethyl cellulose plus an adhesive containing polyisobutylene, styrene isoprene, or ethylene vinyl acetate (Fig. 145.9). The outer layer is composed of a thin semipermeable material such as polyurethane. A gel is formed in the presence of wound exudate, and as a unit, the dressing is semipermeable to water vapor and gases[52].

Another type of hydrocolloid dressing is a synthetic, non-adherent, high-density plastic woven polymer (e.g. N-Terface®). Fluid is able to flow through this matrix to be absorbed by an overlying dressing without adherence to the new epithelial surface.

Advantages/disadvantages

When in sheet form, these dressings can be cut and conformed to the shape of the wound. They are waterproof and adhere directly; as a result, they do not require a secondary dressing. In addition, these dressings have a cushioning or pressure-relieving effect (especially at bony sites), which increases as the dressing absorbs exudate. The resulting colloidal gel that forms prevents the dressing from adhering to the wound base. Accumulation of the exudate itself in a moist, semipermeable environment becomes a source of phagocytic cells and endogenous enzymes. This feature, along with the gel, results in autolytic debridement that can be washed away with saline irrigation of the wound bed[53]. Because hydrocolloids are impermeable to water, oxygen, and carbon dioxide, they are popular "waterproof" dressings[54].

Due to their semipermeable outer barrier, hydrocolloids have also been shown to stimulate angiogenesis and increase the rate of healing by as much as 40% when compared to open-air controls. A comparison of hydrocolloids versus wet-to-dry saline gauze dressings in the treatment of decubitus ulcers found that hydrocolloids do not require as many dressing changes as traditional wound dressings. Although the cost of individual hydrocolloid dressings was greater than gauze dressings and the healing rates were the same, the savings were in the cost of nursing time. In addition, the dressing changes tend to be simple and painless for the patient[55].

Disadvantages of hydrocolloids include maceration of the skin surrounding the wound, a potential for irritant or allergic contact dermatitis (e.g. to adhesives), and the risk of forming excessive granulation tissue. Similar to alginate dressings, the end product of hydrocolloids is a thick, yellow–brown, often foul-smelling gel resembling purulent discharge[56]. The patient needs to be educated regarding the distinction.

Superabsorbent Dressings

This expanding category of dressings is characterized by enhanced absorption, with exudate pulled up and often laterally into the construct of the dressing. By using a larger interface surface, more viscous drainage can be absorbed. Superabsorbent dressings contain particles composed of three-dimensional networks of polyacrylic acid polymers that are crosslinked by covalent bonds and swell upon contact with aqueous solutions. As water enters the dressing, the carboxylic acid groups of the polymer ionize and are electrostatically repelled from each other; this results in significant space for water and each particle can absorb hundreds of times its own weight in fluid. Superabsorbent dressings are indicated for exudative wounds and can also aid healing by trapping bacteria[57] and proteolytic enzymes[58]. If overlying pressure is placed (e.g. compression), it is important to remember that these dressings swell over time and this can increase pressure on the wound, potentially inhibiting healing[59].

Contact Layers

Contact layers are single-layer constructs that are applied directly to the wound surface. They are non-absorbent, non-adherent, woven polyethylene mesh dressings impregnated with different materials such as petrolatum, hydrocolloid, and silicone. These contact layers serve as primary dressings and are covered by a secondary dressing[60]. Wound exudate can flow through them while they protect the wound bed from the trauma of dressing changes. Contact layers are commonly used to secure and protect advanced tissue products (see below) and may stay in place for up to two weeks while the secondary dressings are changed more frequently.

Composite Dressings

The designs of occlusive dressings are constantly changing with the goal of improved and simplified care for a greater range of wounds. Several newer types of composite dressings, which combine two or more types of semi-occlusive dressings into one product, are commercially available. They have three components: (1) a semi- or non-adherent layer that contacts the wound (like a hydrogel, hydrocolloid, foam or alginate; Fig. 145.10); (2) an absorptive layer; and (3) an outer layer (like a film with an adhesive border). This maximizes the efficiency and comfort of the dressing by expanding absorbency as well as lessening the chance of maceration[61]. Other features include the lack of need for secondary retention dressings and better waterproof coverings, which enable the patient to shower or bathe.

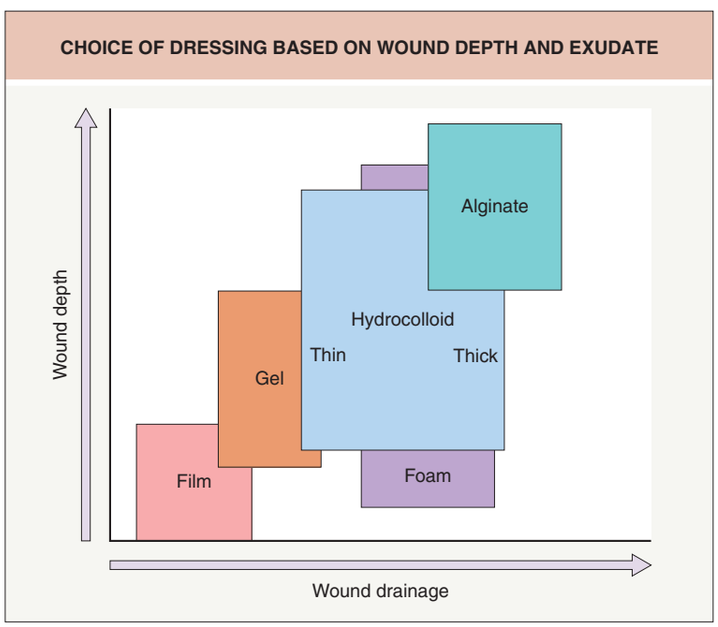


Fig. 145.10 Choice of dressing based on wound depth and exudate. *Courtesy Gregg M. Menaker, MD.*

ADVANCED WOUND THERAPIES

Scientific and clinical advances have increased the therapeutic options for chronic wounds. For example, topical growth factors and tissue-engineered skin equivalents can be combined with standard treatments[62–64].

Topical Growth Factors

Growth factors are critical to the wound healing process, as they stimulate fibroblasts, promote angiogenesis, and encourage migration of keratinocytes. Fluid from acute wounds contains multiple growth factors including platelet-derived growth factor (PDGF) and epidermal growth factor (EGF). Maintaining contact of this fluid with the underlying wound bed via the use of occlusive dressings has been shown to augment wound healing. A topical formulation of recombinant human PDGF, becaplermin (Regranex®) gel, has been shown to increase the complete closure rate of diabetic foot ulcers by 43%. Its current FDA indication is for non-healing diabetic neuropathic foot ulcers[65]. Unfortunately, *in vivo* results with other growth factors failed to translate into improved wound healing in human clinical trials, highlighting the complex microenvironment of a chronic wound.

Tissue-Engineered Skin Equivalents or Skin Substitutes

Advances during the 1970s in tissue culture techniques for keratinocytes and fibroblasts, including the ability to generate large quantities of these cells, resulted in the production of a new group of wound dressings. A variety of tissue-engineered skin equivalents, both cellular and acellular, are commercially available and Table 145.5 outlines some of these products. A true skin substitute provides both the physiologic and mechanical functions akin to an autologous skin graft. Advantages of tissue-engineered dressings include no painful donor sites and the potential for providing coverage of large areas.

Chronic wounds treated with engineered dressings often undergo an "edge effect", characterized by promotion of epithelialization from the edge of the ulcer toward its center, likely due to a release of cytokines by the donor cells[66]. There are currently three types of skin substitutes: epidermal grafts, dermal replacements (acellular or cellular), and composite grafts (with both an epidermal and dermal component). Tissue-engineered dressings can also be classified as autologous, allogeneic (human donor), or xenogeneic (usually bovine or porcine). Currently, the primary allogeneic sources are cadaveric dermis and neonatal foreskin. *Cellular and tissue-based products*, which includes skin equivalents and substitutes, is a term used by the FDA to signify those products regulated by the Center for Biologics Evaluation and Research.

Epidermal Grafts

The first cultured epidermal autografts were successfully cultivated in 1975 by Rheinwald and Green. They have been used successfully in a variety of clinical situations including burns, chronic ulcers, vitiligo, and postsurgical wounds.

Epicel® represents an epidermal autograft in which a skin biopsy is obtained from the patient and then the *autologous* keratinocytes are co-cultured with irradiated murine fibroblasts that serve as a feeder layer[67]. A sheet of keratinocytes two to eight cells thick forms and is attached to petrolatum gauze. The graft is then sutured in place and the gauze backing is removed at 1 week when the keratinocytes have attached to the wound. Skin biopsies obtained 6–12 months post-grafting show anchoring fibrils and neovascularization. This epidermal autograft is approved for use in partial- and full-thickness burns. Disadvantages include the several-week period required to culture the keratinocytes, graft fragility, a short shelf life, and the cost of processing.

For decades, the roofs of suction blisters created in uninvolved skin have been used to repigment vitiligo. More recently, an automated system for epidermal autologous grafting was introduced that uses heat and suction to produce small epidermal microdomes, with consistent cleavage at the lamina lucida[68]. Advantages include no requirement for anesthesia or a highly skilled surgeon, performance in an outpatient setting, minimal donor site pain, and lack of scarring. The grafts have been applied to a variety of chronic and acute wounds and pathergy has not been observed in patients with pyoderma gangrenosum.

TISSUE-ENGINEERED SKIN EQUIVALENTS			
Examples (name and description)	**Possible uses**	**Advantages**	**Disadvantages**
Single layer – viable cells			
Autologous			
Epicel® – sheet of cultured **keratinocytes** (derived from a skin biopsy) attached to petrolatum gauze [commercially available, FDA-approved for burns ≥30% BSA]	Partial- and full-thickness burns, congenital melanocytic nevus excision sites, pyoderma gangrenosum (non-inflammatory; see Ch. 26)	• Small donor site wound • Capable of self-repair • Single application is often sufficient • Permanent and cosmetically acceptable • Good adherence	• Very expensive • Minimal shelf life; must be used soon after delivery from manufacturer • Several-week culture period • Needs biopsy of normal skin • Contraindicated if history of anaphylaxis due to vancomycin, amikacin, or amphotericin
Allogeneic			
Dermagraft® – neonatal foreskin **fibroblasts** grown on a biodegradable mesh; FDA-approved for diabetic foot ulcers (see Table 145.6)	Diabetic foot ulcers	High level of evidence for effectiveness	• Fragile construct – sensitive to physical manipulation
Single layer – acellular or non-viable cells			
Xenogeneic (see Table 145.6 for additional information)			
Porcine collagen			
Oasis® Wound Matrix, Ultra Tri-Layer Matrix – porcine intestinal collagen type I and extracellular matrix (Fig. 145.11)	Chronic ulcers, including diabetic and venous, burns, skin tears, split-thickness graft donor sites, post-laser resurfacing	• Long shelf life* • Non-human origin avoids human pathogen transmission* • Immediately available* • Reduces pain of some wounds* • Stored at room temperature	• Expensive* • May adhere to wound strongly enough to damage new epithelium • Usually needs multiple applications • May have higher infection rate
Permacol® – acellular porcine dermal collagen (approved as surgical implant)	Used primarily for surgical repairs, e.g. abdominal, hernia	Stored at room temperature	
Biobrane® – acellular porcine collagen type I		Stored at room temperature	
Bovine collagen			
INTEGRA® Dermal Regeneration Template – bovine tendon collagen and shark chondroitin	FDA-approved for burns and diabetic foot ulcers	• High level of evidence of effectiveness for diabetic foot ulcers • Stored at room temperature • Flexible	• Possible bovine allergy
Matriderm® – bovine collagen types I, III and V plus solubilized elastin		• Stored at room temperature • Flexible	• Possible bovine allergy
Allogeneic (see Table 145.6 for additional information)			
AlloDerm® Regenerative Tissue Matrix, GRAFTJACKET NOW™ Acellular Dermal Matrix – cadaveric decellularized dermis	Burns and split-thickness skin graft sites	• Decreased pain • Immediate availability • Single application	• Theoretical risk of transmission of human pathogens
Human amniotic membrane (HAM) – inner layer of the amniotic sac	Diabetic foot ulcers	• Non-immunogenic • Applied without immobilization • Long shelf life (cryopreserved)	• Does not survive in chronic wounds after 2–4 weeks
Composite – cellular			
Xenogeneic & allogeneic			
Apligraf® – neonatal foreskin keratinocytes and fibroblasts plus bovine collagen type I; bilayered; FDA-approved for venous ulcers and diabetic foot ulcers	Diabetic foot ulcers (>6 weeks) and venous ulcers (>4 weeks) Epidermolysis bullosa	• High level of evidence • Self-repair ability • Single application (can be repeated up to 5 times) • Stored at room temperature • Immediately available (no several-week culture period as with autologous keratinocyte products)	• Several-week shelf life • Possible transmission of infectious diseases because of human donors but sources are screened
StrataGraft® – cultured human keratinocytes (NIKS cells) and dermal fibroblasts in murine collagen; FDA approved for deep partial-thickness burns	Deep partial- and full-thickness burns, chronic non-healing ulcers	• Promotes self-repair • Single application may be sufficient • Immediately available • Long shelf life (can be cryopreserved)	• Expensive • Avoid in patients with glycerin intolerance • Possible transmission of infectious diseases because of human donors but sources are screened
*Applies to all xenogeneic products.			

Table 145.5 Tissue-engineered skin equivalents. BSA, body surface area; min, minutes; NIKS cells, spontaneously immortalized human keratinocyte cell line. From refs 46, 56, 58, 60, 61, 63, e4–e6.

Dermal Replacements

There are two types of dermal replacements: xenogeneic and allogeneic (Table 145.6). Neither of these is permanent: DNA analysis of wounds after the application of non-autologous skin substitutes shows almost complete disappearance of the grafted cells after two months[69]. The goal of these dermal grafts is to provide a temporary biologic scaffold in order to stimulate the healing process. They are placed over the wound, extending slightly onto normal skin, and then bolstered into place. Secondary dressings must be applied. It is advisable to keep the primary dressing in place for up to a week following its placement and to follow the individualized product instructions. The major component of dermal replacements is collagen; other elements of the extracellular matrix, e.g. glycosaminoglycans (GAGs), may be included and in the case of cellular products, fibroblasts.

Xenogeneic

Although other sources are available, xenogeneic grafts are usually composed of porcine or bovine collagen (see Table 145.6). The advantages of these products are: (1) their ability to effect hemostasis and to provide immediate closure as well as cosmetically acceptable scars with second intention healing; (2) safety from potential human pathogen transmission due to their animal origin; and (3) an adequate shelf life, facilitating off-the-shelf access.

Oasis® Wound Matrix and Biobrane® are examples of acellular matrices derived from porcine collagen (Fig. 145.11). They have significant elasticity, enabling a full range of motion of the covered body part, and there is no requirement for dressing changes once it has adhered to the wound bed. However, Biobrane® may adhere to the wound so tightly that it can damage newly developed epithelium[70].

INTEGRA® Dermal Regeneration Template is composed of two layers: an outer silicone layer overlies a layer composed of bovine tendon

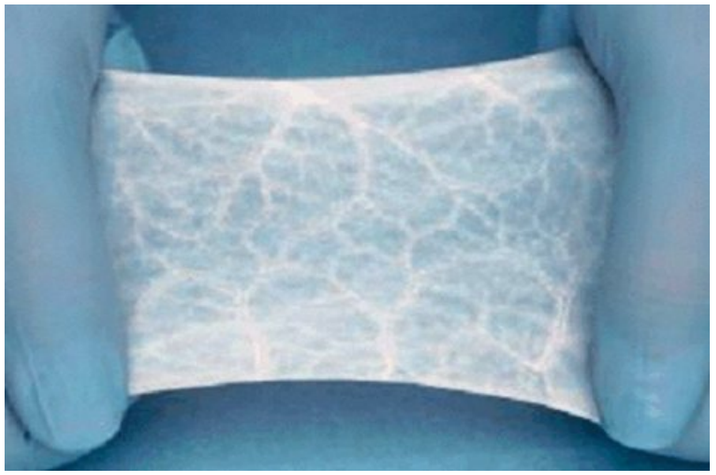


Fig. 145.11 An acellular xenogeneic dressing. This particular wound matrix is derived from porcine small intestine submucosa (Oasis®) and serves as a dermal graft.

SELECTED DERMAL REPLACEMENT GRAFTS		
	Description	**Comments**
Xenogeneic		
Biobrane®	Bilayer dressing: inner nylon mesh fabric coated with **porcine** type I collagen ("dermis") bonded to a semipermeable silicone film membrane ("epidermis")	• Tissue ingrowth into the nylon fabric following binding of collagen to fibrin • Trilaminar nylon (better for clean, partial-thickness burn wounds or donor sites) and monofilament nylon (better for meshed autografts) • Approved for partial-thickness burns
Oasis® Wound Matrix, Ultra Tri-Layer Matrix	Derived from porcine small intestine submucosa (mucosa and muscle removed) **Porcine** type I collagen, extracellular matrix (e.g. hyaluronic acid, fibronectin), and growth factors (FGF, TGF-β)	• In study of 120 patients with venous leg ulcers, after 12 weeks of treatment, 55% of Oasis® + compression group healed vs 34% in compression alone group; at 6 months, 100% and 70% remained healed, respectively • Approved for venous, diabetic and pressure ulcers, second-degree burns, graft donor sites, surgical wounds, and full-thickness skin injuries
INTEGRA® Dermal Regeneration Template	Bilayer dressing: **bovine** tendon collagen admixed with **shark** cartilage-derived, modified GAGs ("dermis") plus an outer silicone membrane	• Debridement required prior to graft placement with sutures or staples • Outer silicone cover removed after several weeks; in large wounds, replaced by ultrathin autograft (two-step process) • In a controlled trial of diabetic foot ulcers, improved time and rate of wound closure when compared to standard of care treatment • Approved for life-threatening third-degree burns and diabetic ulcers
Allogeneic		
AlloDerm® Regenerative Tissue Matrix*	Human cadaveric skin, chemically treated and purified to remove epidermis, all cellular components, and pathogens Cryopreserved (shelf life of 6 months)	• Repopulation of host fibroblasts and endothelial cells seen within 10 days of grafting • Approved for repair or replacement of damaged or inadequate integumental tissue, e.g. breast reconstruction
Dermagraft®	Neonatal foreskin fibroblasts are seeded onto a 3-D scaffold of biodegradable polyglactin mesh	• Similar time to graft take and similar fibroblast function as TransCyte™ (see below) • In 245 patients with diabetic ulcers, significant improvement in wound closure by week 12: Dermagraft® 30% versus conventional therapy 18% • Approved for full-thickness diabetic foot ulcers present >6 weeks that are deep but do not involve tendons, muscle or bone; HDE for ulcers in epidermolysis bullosa
Xenogeneic & allogeneic		
Transcyte™	Biobrane® (see above) plus neonatal foreskin fibroblasts	• Requires ~2 weeks for graft take • Fibroblasts initially secrete extracellular matrix (including collagen) and growth factors that stimulate granulation tissue and epithelialization but then die • In a controlled trial of excised burns, easier to use and similar outcomes when compared to human cadaveric skin • Approved for deep partial- and full-thickness burns

*Additional allogeneic grafts include those derived from human umbilical cord (EpiCord®) and placental membranes (AmnioBand® EpiFix™, Grafix®, NuShield®). Other acellular dermal matrices (ADMs) that may be used for venous and diabetic ulcers as well as breast reconstruction include AlloMax™, AlloPatch®, DermACELL™, DermaMatrix™, Flex HD®, Strattice™, SurgiMend®, and TheraSkin®.

Table 145.6 Selected dermal replacement grafts. FGF, fibroblast growth factor; GAGs, glycosaminoglycans; HDE, humanitarian device exemption; TGF-β, transforming growth factor-β. *From refs 46, 57, 60, 61, 63, e4–e11. Courtesy Gregg M. Menaker, MD.*

collagen and shark cartilage GAGs. The latter is thought to simulate dermal matrix. Because INTEGRA® has a complicated application procedure, the FDA requires that all physicians complete a company-sponsored training program.

Allogeneic

Allogeneic dermal grafts are composed of cadaveric dermis or neonatal foreskin fibroblasts (see Table 145.6). The advantages of these products include their ability to provide immediate closure and cosmetically acceptable scars with second intention healing, in addition to an adequate shelf life, facilitating off-the-shelf access. However, there is a risk of graft rejection due to T cell recognition of donor T cells[71]. Examples include AlloDerm® Regenerative Tissue Matrix which consists of decellularized cadaveric dermis and GRAFTJACKET NOW™ Acellular Dermal Matrix which is derived from processed acellular cadaveric skin (see Table 145.5). The FDA currently categorizes both AlloDerm® and GRAFTJACKET NOW™ as banked human tissue for transplantation. Dermagraft® is a biodegradable scaffold seeded with neonatal foreskin fibroblasts and is FDA-approved for the treatment of diabetic foot ulcers[72].

Composite Grafts

Engineered composite grafts are bilayered skin equivalents. Current products consist of an epidermal layer composed of human keratinocytes and a dermal layer composed of bovine collagen matrix seeded with human fibroblasts. In Apligraf®, both cell types are derived from human neonatal foreskins (Fig. 145.12). This composite graft produces its own matrix proteins and growth factors and, if wounded, it can repair itself. Although FDA-approved for venous leg ulcers and diabetic foot ulcers, Apligraf® has been used to treat acute and chronic wounds that failed to heal by standard means, including those due to epidermolysis bullosa, pyoderma gangrenosum, burns, and surgical excisions. Whereas several applications of the material may be required to completely heal chronic wounds, a single application may be sufficient to initiate a satisfactory healing response. Chronic venous ulcers that were randomized to receive compression plus Apligraf® healed in a shorter time period compared to compression alone, especially in the case of larger defects[72,73].

More recent evidence suggests that Apligraf® modulates an array of cellular pathways in the epidermis at the wound's edge, ultimately transforming a chronic wound into an acute one[74]. In venous leg ulcers, Apligraf® also stimulates antifibrotic changes within the wound bed[75]. This includes decreased expression of gene targets of profibrotic TGF-β1, increased levels of the TGF-β inhibitor decorin, and upregulation of fibroblast-derived matrix metallopeptidase 8.

A point-of-care delivery system named RECELL® was recently developed that allows delivery of autologous skin to the wound bed via a cell spray containing keratinocytes, melanocytes, Langerhan cells, and papillary dermal fibroblasts[76]. This onsite cell harvesting device can create 1 ml of cell suspension from a 1 cm^2 piece of split-thickness donor tissue; the former can then be sprayed onto an area of up to 80 cm^2. The maximum per device is 24 ml of cell suspension. In a randomized controlled study in burn patients that compared standard split-thickness skin grafts (STSGs) versus the application of RECELL® Spray-On Skin™ cells to widely meshed STSGs, the cell spray had similar efficacy and safety but decreased the donor site area by ~30%[77].

Apligraf® and similar products are costly, but they have an excellent safety profile as well as the advantage of accelerating healing and reducing long-term costs.

Negative Pressure Wound Therapy (NPWT)

NPWT, developed in the 1990s, is based on the delivery of sub-atmospheric pressure to the wound bed. In this vacuum-assisted closure (VAC) system, a polyurethane or polyvinyl alcohol foam is cut and placed on the wound surface. The foam is then sealed over by a transparent drape in order to provide a closed airtight system (Fig. 145.13). A vacuum pump, connected to this space via a plastic tube, provides a negative pressure environment. NPWT removes interstitial fluid, stimulates angiogenesis, and enhances circulation as well as lymphatic drainage. There is evidence to support the use of NPWT for acute postsurgical wounds[78]. Although there is some evidence that NPWT improves healing of diabetic foot ulcers, more information regarding appropriate patient selection, duration of treatment, and use of combined treatments is required[79].

Nowadays there are portable, often single-use, systems that can deliver effective negative pressure to a variety of low-to-moderately exudative wounds. Some of these systems use superabsorbent dressings, rather than a canister, to retain wound exudate[80]. The dressing is placed under a sealed film covering and is linked to a battery-operated, portable pump that can be harnessed around the thigh, allowing for patient mobility[80]. Single-use NPWT systems appear to lead to similar, if not improved, wound healing and they reduce the cost of care given the outpatient setting[81]. Another modification is lavage of the wound bed by a wound cleanser or antiseptic while the NPWT is functioning[82].

Oxygen Therapy

Because multiple studies have pointed to hypoxia as one of the major factors leading to a delay in wound healing, both hyperbaric oxygen therapy (HBOT) and topical oxygen therapy have been utilized.

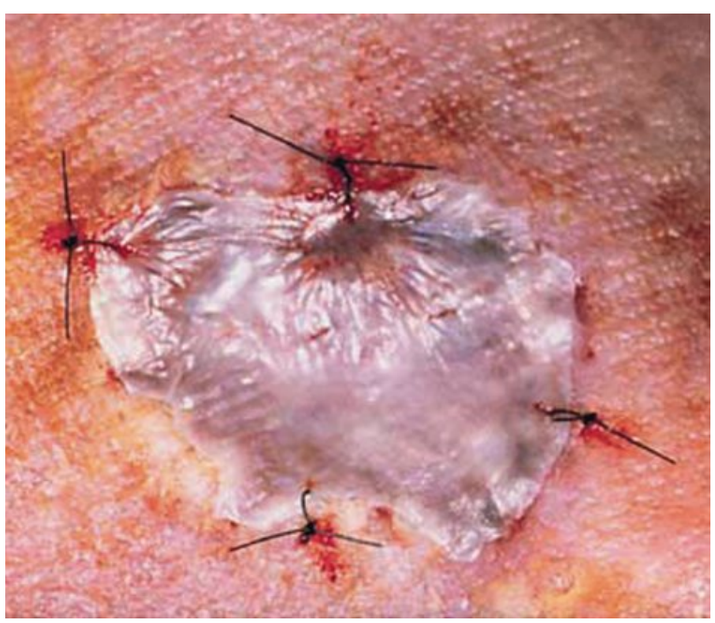


Fig. 145.12 Example of an engineered composite (xenogeneic and allogeneic) graft sutured into place (Apligraf®). *Courtesy Gregg M. Menaker, MD.*



Fig. 145.13 Negative pressure wound therapy. In negative pressure wound therapy, a polyurethane (this patient) or polyvinyl alcohol foam is cut and placed on the wound surface. The foam is then sealed over by a transparent drape. A vacuum pump, connected via a plastic tube, provides a negative pressure environment. The sterile polyurethane foam has large pores and stimulates granulation tissue.

In HBOT, oxygen is administered at pressures greater than one atmosphere. Patients are placed in a pressure chamber where they breathe oxygen at this increased pressure. Systemic HBOT sessions last 45–120 minutes and are conducted once or twice daily for 20–30 sessions. This oxygenation of hypoxic tissue induces vasoconstriction and reduces edema and congestion. At a cellular level, there is increased fibroblast replication, collagen synthesis, and neovascularization as well as upregulation of growth factors.

To screen for a potential response to HBOT, the patient has transcutaneous oxygen levels measured in the peri-wound region both at baseline and while breathing 100% oxygen; at least a doubling of the levels is preferred. While a systematic review concluded that there was short-term but not long-term improvement of diabetic ulcers with HBOT[83], randomized controlled trials with small sample sizes reported the effectiveness of HBOT[84]. A data analysis of 6259 patients did not support the use of HBOT for diabetic foot ulcers, highlighting the need for large randomized controlled trials[85]. Additional methods for oxygenation of wounds include topical pressurized oxygen, topical continuous diffusion of oxygen, and dressings that release oxygen, but proper selective application of these interventions is required[86].

COMPRESSION THERAPY

Based on substantial scientific and clinical evidence, compression therapy represents the mainstay of treatment for all cutaneous manifestations of chronic venous insufficiency, from varicose veins and edema to lipodermatosclerosis and venous leg ulcers. The physiologic effects of compression include acceleration of the velocity of venous flow, augmentation of venous return toward the heart, reduction of venous reflux and edema, promotion of oxygenation to the surrounding dermis, and stimulation of fibrinolysis[87]. Compression therapy is also employed following lower extremity surgical procedures.

Types of Compression

There are several different methods of compression therapy, ranging from stockings and compression bandages to devices such as intermittent pneumatic compression systems (Table 145.7). Compression stockings are graded from Class I to IV based upon the pressure at the ankle (see Table 105.4) whereas compression bandages are classified as either long stretch (elastic with substantial extensibility) or short stretch (inelastic with limited extensibility). Multiple factors influence the sub-bandage pressure including: (1) the tension or amount of force that is used to stretch the bandage during application; (2) the width of the bandage – wider bandages are associated with decreased compression; (3) the size of the leg – a larger circumference leads to reduced pressure; and (4) the number of layers of compression – a higher number increases pressure[88]. This is reflected in a modified Laplace law[89]:

$$\text{Sub-bandage pressure (mmHg)} = \frac{\text{tension (KgF)} \times \text{number of layers} \times \text{a constant}}{\text{limb circumference (cm)} \times \text{bandage width (cm)}}$$

In addition to the type of bandage material and the method of wrapping, the amount of pressure also depends on muscle contraction.

Although the definitive optimal pressure required to prevent capillary leakage secondary to venous hypertension has not been delineated, an ankle pressure of 30–40 mmHg is recommended for leg ulcers[90]. The higher compression pressure of 40 mmHg should be considered for persons with an ankle–brachial index (ABI) of 0.8 to 1.3, indicating adequate vascular supply (see Table 105.8). In patients with predominantly venous disease, but coexisting arterial compromise (ABI = 0.66–0.8), modifications in the form of inelastic (rather than elastic) compression and fewer layers of compression is recommended[91,92]. Individuals with an ABI of 0.5 to 0.65 should have further modifications, e.g. one or two layers of a tubular bandage that can be easily removed. Inappropriate compression bandaging in patients with arterial disease can lead to ischemia and is therefore potentially harmful. Patients with congestive heart failure (CHF) may have difficulty tolerating compression therapy because compression of the lower extremities may increase preload volume and worsen CHF.

Compression stockings

With graduated compression stockings, the patient is afforded some independence in the application of the device. However, for arthritic

TYPES OF COMPRESSION SYSTEMS			
Compression system	**Examples**	**Advantages**	**Disadvantages**
Long stretch (elastic) bandages	ACE™, Biflex® (also short), Dauerbinde® K, SurePress®	• Base of the toes to knees • Low working pressure • High resting pressure • 100%–200% extensibility • Can be applied as spiral or figure-of-eight • Inexpensive; washable and reusable forms available	• Tend to unravel • Do not provide a sustained compression • Risk of incorrect application • Can lose elasticity with continued use
Short stretch (inelastic) bandages	Zinc paste (Viscopaste®/Unna boot), Actio®, Biflex® (also long), Comprilan®, Panelast®, Porelast®	• Comfortable so better tolerated • Minimal interference with daily activities • Some (e.g. Viscopaste®) can generate high working pressure	• Can lose compression after application • Not good for highly exudative wounds • Viscopaste®/Unna boot needs to be applied by well-trained staff
Devices	CircAid® (with Velcro®), FarrowWrap® (with Velcro®), Sigvaris CoolFLEX® (with metal fastening clasps)	• Adjustable compression • Easy to put on and remove	• Expensive • Bulky
Multicomponent bandages	Coban™ 2, Coban™ 2 Lite, Profore® (5 layers), Profore® Lite (4 layers), Actico®2 C	• Higher compression and sustained high compression • Graduated compression • Reduced ("Lite") compression available for patients with mixed venous and arterial disease	• Needs to be applied by well-trained staff
Intermittent compression devices	Lympha Press® (pneumatic pump)	• Enhance fibrinolytic activity	• Expensive • Requires being immobile for a few hours per day
Tubular system	Tubigrip® (contains latex) EdemaWear® Medigrip LF™	• Easy to use • Tubular bandage doubled back over limb to increase compression	• Low compression (unless that is what is desired because of coexisting arterial disease)

Table 145.7 Types of compression systems. LF, latex free. From refs 70, 73, 83, e12–e14.



Fig. 145.14 Unna boot. Non-elastic compression therapy with a zinc-impregnated compression wrap.

and/or elderly patients, application can be difficult unless the stockings have zippers or Velcro® fasteners. Although compression stockings are commonly used as maintenance therapy, recent studies have observed that they are comparable to bandaging systems for the treatment of venous leg ulcers, including producing similar healing rates[93]. A systematic review found no significant differences between compression stockings and compression bandages with respect to ulcer healing, time to ulcer healing, or ulcer recurrence[94]. In general, compression stockings are more tolerable, less costly, and less bulky. Patient education and demonstration can lead to increased compliance.

Compression bandages

In the 1880s, Paul Gerson Unna introduced a bandage, now referred to as the Unna boot, for the treatment of venous leg ulcers and selected eczematous dermatoses. It was originally a cotton bandage impregnated with zinc oxide, gelatin, and glycerin paste. Applied in a semi-rigid state, the Unna boot confers (semi-rigid) compression, along with the advantages of a moisture-retaining occlusive dressing (Fig. 145.14). It should be applied by a qualified medical professional and changed once a week unless heavy drainage from the wound necessitates more frequent replacement. Correct application of the Unna boot prevents excessive or abnormal pressure to the limb, compromised circulation, skin breakdown, additional ulcer formation, or further limb deterioration (Video 145.1). Over a century later, the Unna boot is still a frequently employed compression bandage for venous leg ulcers[95].

Medicated paste bandages such as the Unna boot can be used alone (inelastic) or underneath an additional layer of cohesive bandaging (e.g. Coban™ [elastic]), especially on the lower extremities. By creating an absorptive, protective contact layer, they can also address the stasis dermatitis often associated with leg ulcers. In addition to preservatives, these open-weave cotton bandages are impregnated with: (1) zinc oxide paste, calamine, or ichthammol, all of which have a soothing action on irritated skin; (2) coal tar, which has an anti-inflammatory effect; or (3) clioquinol, which has deodorizing and antibacterial actions. Preservative-free zinc oxide products are commercially available as are combinations of zinc oxide with each of the above components or calamine plus clioquinol.

Short stretch (inelastic) versus long stretch (elastic) bandages

Elastic bandages provide both easy stretchability and a sustained squeeze on tissue (see Table 145.7). This is because these bandages recoil back to their original length due to the presence of elastomeric fibers. In contrast, inelastic bandages such as the Unna boot and short stretch bandage (more commonly used in Europe) form a rigid covering that resists lateral expansion of the calf muscle during active contractions. Of note, contractions of the calf muscle act as a pump that generates a propelling force to promote venous return (see Fig. 105.2).

Compression bandages may be composed of a single component or multiple combined components. In a meta-analysis[96], short stretch bandages were found to be as efficacious in promoting healing of venous leg ulcers as more complex multi-component bandaging systems, in both ambulatory and non-ambulatory patients. However, Cochrane reviews suggest that the evidence supports multi-component systems (over single-component systems) and systems with an elastic component (over those with an inelastic bandage)[97]. Lastly, tubular systems (Tubigrip®, EdemaWear®) provide low compression and can be used by patients with reduced ABIs (see above).

Compression devices

Intermittent pneumatic compression (IPC) devices deliver sequential pressure to the limb. IPC is a beneficial adjunct to other forms of compression in the treatment of venous leg ulcers, especially for non-ambulatory patients[98,99]. When the calf muscle pump is not active, the use of a dynamic compression system is more beneficial than a passive system[99–101]. Portable IPC devices that are relatively easy to operate are available for home use. In a randomized controlled trial, patients with lymphedema and venous leg ulcers healed faster and with less pain when a 4-layer compression system was combined with daily home-based IPC as compared to 4-layer compression alone[102]. Both self-adjustable Velcro® devices and hybrid systems are alternative compression therapy choices that may increase compliance.

FUTURE DIRECTIONS

Wound dressings are an essential component of wound care, compression therapy for venous leg ulcers, and pressure redistribution for pressure ulcers. Over the past century, dressings have moved from a passive to more active role with improvements in moisture-retentive products and delivery systems. However, incorporation of active ingredients into traditional dressings increases their cost and raises regulatory issues as to whether a dressing is a drug or a medical device. Advances based on growth factors, cellular therapy, and skin substitutes will continue, but selection of the most appropriate dressing for a given clinical scenario will remain the key decision for the physician.

Additional figures and references available in our eBook (see inside front cover for access code).

REFERENCES

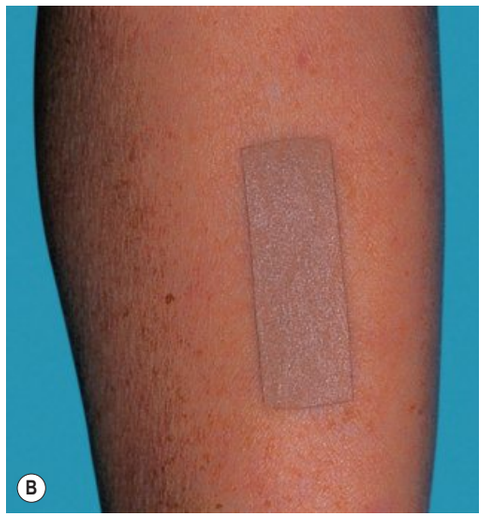
1. Winter GD. Formation of the scab and the rate of epithelization of superficial wounds in the skin of the young domestic pig. *Nature*. 1962;193:293–294.
2. Bennett R. Dressings and miscellaneous surgical materials. In: *Fundamentals of Cutaneous Surgery*. St. Louis: Mosby; 1987.
3. Cho CY, Lo JS. Dressing the part. *Dermatol Clin*. 1998;16:25–47.
4. Gilje O. On taping (adhesive tape treatment) of leg ulcers. *Acta Derm Venereol*. 1948;28:454–467.
5. Eaglstein WH, Mertz PM. New methods for assessing epidermal wound healing: the effects of triamcinolone acetonide and polyethelene film occlusion. *J Invest Dermatol*. 1978:71:382–4.
6. Cunningham B, Berstein L, Woodley DT. Wound dressings. In: Roenigk RK, Roenigk HH, eds. *Roenigk & Roenigk's Dermatologic Surgery: Principles and Practice*. 2nd ed. New York: Marcel Dekker; 1996:131–148.
7. Matthews D. Dressing of open wounds and burns with tulle gras. *Lancet*. 1941;1:43.
8. Ersek RA. Ischemic necrosis and elastic net bandages. *Tex Med*. 1982;78:47–49.
9. Smack DP, Harrington AC, Dunn C, et al. Infection and allergy incidence in ambulatory surgery patients using white petrolatum vs bacitracin ointment. A randomized controlled trial. *JAMA*. 1996;26:972–977.
10. Dixon AJ, Dixon MP, Dixon JP. Randomized clinical trial of the effect of applying ointment to surgical wounds before occlusive dressing. *B J Surg*. 2006;93:937–943.
11. Zitelli J. Wound healing by first and second intention. In: Roenigk RK, Roenigk HH, eds. *Roenigk & Roenigk's Dermatologic Surgery: Principles and Practice*. 2nd ed. New York: Marcel Dekker; 1996:101–130.
12. Lipsky BA, Berendt AR, Cornia PB, et al. 2012 Infectious Diseases Society of America clinical practice guideline for the diagnosis and treatment of diabetic foot infections. *Clin Infect Dis*. 2012;54:e132–e173.
13. Beasley WD, Hirst G. Making a meal of MRSA-the role of biosurgery in hospital-acquired infection. *J Hosp Infect*. 2004;56:6–9.
14. Dumville JC, Worthy G, Soares MO, et al. VenUS II: a randomised controlled trial of larval therapy in the management of leg ulcers. *Health Technol Assess*. 2009;13:1–182, iii–iv.
15. Witkowski JA, Parish LC. Wound cleansers. *Clin Dermatol*. 1996;14:89–93.
16. Fernandez R, Griffiths R. Water for wound cleansing. *Cochrane Database Syst Rev*. 2012(2):CD003861.
17. Scimeca CL, Bharara M, Fisher TK, et al. An update on pharmacological interventions for diabetic foot ulcers. *Foot Ankle Spec*. 2010;3:285–302.
18. Sutherland R, Boon RJ, Griffin KE, et al. Antibacterial activity of mupirocin (pseudomonic acid), a new antibiotic for topical use. *Antimicrob Agents Chemother*. 1985;27:495–498.
19. Lipsky BA, Hoey C. Topical antimicrobial therapy for treating chronic wounds. *Clin Infect Dis*. 2009;49:1541–1549.
20. Frank C, Bayoumi I, Westendorp C. Approach to infected skin ulcers. *Can Fam Physician*. 2005;51:1352–1359.
21. Harding KG, Jones V, Price P. Topical treatment: which dressing to choose. *Diabetes Metab Res Rev*. 2000;16(Suppl. 1):S47–50.
22. Woo KY, Ayello EA, Sibbald RG. Silver versus other antimicrobial dressings: best practices! *Surg Technol Int*. 2008;17:50–71.

23. Vermeulen H, van Hattem JM, Storm-Versloot MN, Ubbink DT. Topical silver for treating infected wounds. *Cochrane Database Syst Rev*. 2007:CD005486.
24. O'Meara S, Al-Kurdi D, Ologun Y, Ovington LG. Antibiotics and antiseptics for venous leg ulcers. *Cochrane Database Syst Rev*. 2010(10):CD003557.
25. Strohal R, Schelling M, Takacs M, et al. Nanocrystalline silver dressings as an efficient anti-MRSA barrier: a new solution to an increasing problem. *J Hosp Infect*. 2005;60:226–230.
26. Carter MJ, Tingley-Kelley K, Warriner 3rd RA. Silver treatments and silver-impregnated dressings for the healing of leg wounds and ulcers: a systematic review and meta-analysis. *J Am Acad Dermatol*. 2010;63:668–679.
27. Ikeda T, Tazuke S, Watanabe M. Interaction of biologically active molecules with phospholipid membranes. I. Fluorescence depolarization studies on the effect of polymeric biocide bearing biguanide groups in the main chain. *Biochim Biophys Acta*. 1983;735:380–386.
28. Abdel-Sayed P, Dorian Tornay D, Nathalie Hirt-Burri N, et al. Implications of chlorhexidine use in burn units for wound healing. *Burns*. 2020;46:1150–1156.
29. Best AJ, Nixon MF, Taylor GJ. Brief exposure of 0.05% chlorhexidine does not impair non-osteoarthritic human cartilage metabolism. *J Hosp Infect*. 2007;67:67–71.
30. Cooper RA. Iodine revisited. *Int Wound J*. 2007;4:124–137.
31. Brough R, Jones C. Iatrogenic iodine as a cause of hypothyroidism in infants with end-stage renal failure. *Pediatr Nephrol*. 2006;21:400–402.
32. Li W, Dasgeb B, Phillips T, et al. Wound-healing perspectives. *Dermatol Clin*. 2005;23:181–192.
33. Hansson C. The effects of cadexomer iodine paste in the treatment of venous leg ulcers compared with hydrocolloid dressing and paraffin gauze dressing. Cadexomer Iodine Study Group. *Int J Dermatol*. 1998;37:390–396.
34. Apelqvist J, Ragnarson Tennvall G. Cavity foot ulcers in diabetic patients: a comparative study of cadexomer iodine ointment and standard treatment. An economic analysis alongside a clinical trial. *Acta Derm Venereol*. 1996;76:231–235.
35. Molan PC. The role of honey in the management of wounds. *J Wound Care*. 1999;8:415–418.
36. Moore OA, Smith LA, Campbell F, et al. Systematic review of the use of honey as a wound dressing. *BMC Complement Altern Med*. 2001;1:2.
37. Jull AB, Rodgers A, Walker N. Honey as a topical treatment for wounds. *Cochrane Database Syst Rev*. 2008(4):CD005083.
38. Jull A, Walker N, Parag V, et al. Honey as Adjuvant Leg Ulcer Therapy trial collaborators. Randomized clinical trial of honey-impregnated dressings for venous leg ulcers. *Br J Surg*. 2008;95:175–182.
39. Shi L, Ermis R, Kiedaisch B, Carson D. The effect of various wound dressings on the activity of debriding enzymes. *Adv Skin Wound Care*. 2010;23:456–462.
40. Borkow G, Okon-Levy N, Gabbay J. Copper oxide impregnated wound dressing: biocidal and safety studies. *Wounds*. 2010;22:301–310.
41. Borkow G, Gabbay J, Dardik R, et al. Molecular mechanisms of enhanced wound healing by copper oxide-impregnated dressings. *Wound Repair Regen*. 2010;18:266–275.
42. Bua N, Smith GE, Totty JP, et al. Dialkylcarbamoyl chloride dressings in the prevention of surgical site infections after nonimplant vascular surgery. *Ann Vasc Surg*. 2017;44:387–394.
43. Hien NT, Prawer SE, Katz HI. Facilitated wound healing using transparent film dressing following Mohs micrographic surgery. *Arch Dermatol*. 1988;124:903–906.
44. Rosdy M, Clauss LC. Cytotoxicity testing of wound dressings using normal human keratinocytes in culture. *J Biomed Mater Res*. 1990;24:363–377.
45. Vermeulen H, Ubbink DT, Goossens A, et al. Systematic review of dressings and topical agents for surgical wounds healing by secondary intention. *Br J Surg*. 2005;92:665–672.
46. Eisenbud D, Hunter H, Kessler L, Zulkowski K. Hydrogel wound dressings: where do we stand in 2003? *Ostomy Wound Manage*. 2003;49:52–57.
47. Mertz PM, Marshall DA, Eaglstein WH. Occlusive wound dressings to prevent bacterial invasion and wound infection. *J Am Acad Dermatol*. 1985;12:662–668.
48. Geronemus RG, Robins P. The effect of two new dressings on epidermal wound healing. *J Dermatol Surg Oncol*. 1982;8:850–852.
49. Mandy SH. A new primary wound dressing made of polyethylene oxide gel. *J Dermatol Surg Oncol*. 1983;9:153–155.
50. Thomas S. Alginate dressings in surgery and wound management–Part 1. *J Wound Care*. 2000;9:56–60.
51. Broussard KC, Powers JG. Wound dressings: selecting the most appropriate type. *Am J Clin Dermatol*. 2013;14:449–459.
52. Cassidy St C, Peter SD, Lacey S, et al. Biobrane versus Duoderm for the treatment of intermediate thickness burns in children: a prospective, randomized trial. *Burns*. 2005;31:890–893.
53. Bolton LL, Johnson CL, Van Rijswijk L. Occlusive dressings: therapeutic agents and effects on drug delivery. *Clin Dermatol*. 1991;9:573–583.
54. Powers JG, Morton LM, Phillips TJ. Dressings for chronic wounds. *Dermatol Ther*. 2013;26:197–206.
55. Xakellis GC, Chrischilles EA. Hydrocolloid versus saline-gauze dressings in treating pressure ulcers: a cost-effectiveness analysis. *Arch Phys Med Rehabil*. 1992;73:463–469.
56. Gilchrist B, Reed C. The bacteriology of chronic venous ulcers treated with occlusive hydrocolloid dressings. *Br J Dermatol*. 1989;121:337–344.
57. Larko E, Persson A, Blom K. Effect of superabsorbent dressings in a 3D acellular tissue model of Pseudomonas aeruginosa biofilm. *J Wound Care*. 2015;24:206–210.
58. Wiegand C, White RJ. Binding and inhibition of protease enzymes, including MMPs, by a superabsorbent dressing in vitro. *J Wound Care*. 2013;22:221–224.
59. Ousey K, Atkin L, White R. Superabsorbent wound dressings: a literature review. *Wounds UK*. 2013;9:52–60.
60. Stoica AE, Chiscov C, Grumezescu AM. Nanomaterials for wound dressings: an up-to-date overview. *Molecules*. 2020;25:2699.
61. Hansbrough JF, Franco ES. Skin replacements. *Clin Plast Surg*. 1998;25:407–423.
62. Colletta V, Dioguardi D, Di Lonardo A, et al. A trial to assess the efficacy and tolerability of Hyalofill-F in non-healing venous leg ulcers. *J Wound Care*. 2003;12:357–360.
63. Veves A, Falanga V, Armstrong DG, et al. Apligraf Diabetic Foot Ulcer Study. Graftskin, a human skin equivalent, is effective in the management of noninfected neuropathic diabetic foot ulcers: a prospective randomized multicenter clinical trial. *Diabetes Care*. 2001;24:290–295.
64. Wieman TJ, Smiell JM, Su Y. Efficacy and safety of a topical gel formulation of recombinant human platelet-derived growth factor-BB (becaplermin) in patients with chronic neuropathic diabetic ulcers. A phase III randomized placebo-controlled double-blind study. *Diabetes Care*. 1998;21:822–827.
65. Margolis DJ, Kantor J, Santanna J, et al. Effectiveness of platelet releasate for the treatment of diabetic neuropathic foot ulcers. *Diabetes Care*. 2001;24:483–488.
66. Kirsner RS, Falanga V, Kerdel FA, et al. Skin grafts as pharmacological agents: pre-wounding of the donor site. *Br J Dermatol*. 1996;135:292–296.
67. Cutting KF, Westgate SJ. Super-absorbent dressings: how do they perform in vitro? *Br J Nurs*. 2012;21:14–19.
68. Maderal AD, Kirsner RS. Clinical and economic benefits of autologous epidermal grafting. *Cureus*. 2016;8:e875.
69. Khachemoune A, Bello YM, Phillips TJ. Factors that influence healing in chronic venous ulcers treated with cryopreserved human epidermal cultures. *Dermatol Surg*. 2002;28:274–280.
70. Bello YM, Falabella AF. Use of skin substitutes in dermatology. *Dermatol Clin*. 2001;19:555–561.
71. Yang JY, Tsai YC, Noordhoff MS. Clinical comparison of commercially available Biobrane preparations. *Burns*. 1989;15:197–203.
72. Benichou G, Yamada Y, Yun SH, et al. Immune recognition and rejection of allogeneic skin grafts. *Immunotherapy*. 2011;3:757–770.
73. Falanga V, Margolis D, Alvarez O, et al. Rapid healing of venous ulcers and lack of clinical rejection with an allogeneic cultured human skin equivalent. Human Skin Equivalent Investigators Group. *Arch Dermatol*. 1998;134:293–300.
74. Stone RC, Stojandinovic O, Rosa AM, et al. A bioengineered living cell construct activates an acute wound healing response in venous leg ulcers. *Sci Trans Med*. 2017;9:8611.
75. Stone RC, Stojandinovic O, Sawaya A, et al. A bioengineered living cell construct activates metallothionein/zinc/MMP8 and inhibits TGFβ to stimulate remodeling of fibrotic venous leg ulcers. *Wound Repair Regen*. 2020;28:164–176.
76. Sood R, Roggy DE, Zieger MJ, et al. A comparative study of spray keratinocytes and autologous meshed split-thickness skin graft in the treatment of acute burn injuries. *Wounds*. 2015;27:31–40.
77. Holmes JH, Molnar JA, Shupp JW, et al. Demonstration of the safety and effectiveness of the RECELL® System combined with split-thickness meshed autografts for the reduction of donor skin to treat mixed-depth burn injuries. *Burns*. 2019;45:772–782.
78. Armstrong DG, Lavery LA. Diabetic Foot Study Consortium. Negative pressure wound therapy after partial diabetic foot amputation: a multicentre, randomised controlled trial. *Lancet*. 2005;366:1704–1710.
79. Jeffcoate WJ, Lipsky BA, Berendt AR, et al. Unresolved issues in the management of ulcers of the foot in diabetes. *Diabet Med*. 2008;25:1380–1389.
80. Hudson DA, Adams KG, Huyssteen AV, et al. Simplified negative pressure wound therapy: clinical evaluation of an ultraportable, no-canister system. *Int Wound J*. 2015;12:195–201.
81. Burke J, Morley R, Khanbhai M. Using portable negative pressure wound therapy devices in the home care setting. *Smart Homecare Technology and TeleHealth*. 2014;2014:129–135.
82. Kim PJ, Attinger C, Constantine C, et al. Negative pressure wound therapy with instillation: international consensus guidelines update. *Int Wound J*. 2020;17:175–186.
83. Kranke P, Bennett MH, Martyn-St James M, et al. Hyperbaric oxygen therapy for chronic wounds. *Cochrane Database Syst Rev*. 2012(4):CD004123.
84. O'Reilly D, Pasricha A. Hyperbaric oxygen therapy for diabetic ulcers: systematic review and meta-analysis. *Int J Technol Assess Health Care*. 2013;29:269–281.
85. Margolis DJ, Gupta J, Hoffstad O, et al. Lack of effectiveness of hyperbaric oxygen therapy for the treatment of diabetic foot ulcer and the prevention of amputation: a cohort study. *Diabetes Care*. 2013;36:2160.
86. Hu J, Guo S, Hu H, et al. Systematic review of the efficacy of topical haemoglobin therapy for wound healing. *Int Wound J*. 2020;17:1323–1330.
87. de Araujo T, Valencia I, Federman DG, Kirsner RS. Managing the patient with venous ulcers. *Ann Intern Med*. 2003;138:326–334.
88. Partsch H. Compression therapy of the legs. A review. *J Dermatol Surg Oncol*. 1991;17:799–805.
89. Melhuish JM, Clark M, Williams R, Harding KG. The physics of sub-bandage pressure measurement. *J Wound Care*. 2000;9:308–310.
90. Stemmer R, Marescaux J, Furderer C. [Compression therapy of the lower extremities particularly with compression stockings]. *Hautarzt*. 1980;31:355–365.
91. Woo KY, Alavi A, Evans R, et al. New advances in compression therapy for venous leg ulcers. *Surg Technol Int*. 2013;23:61–68.
92. Mosti G, Iabichella ML, Partsch H. Compression therapy in mixed ulcers increases venous output and arterial perfusion. *J Vasc Surg*. 2012;55:122–128.
93. Ashby RL, Gabe R, Ali S, et al. Clinical and cost-effectiveness of compression hosiery versus compression bandages in treatment of venous leg ulcers (Venous leg Ulcer Study IV, VenUS IV): a randomised controlled trial. *Lancet*. 2014;383:871–879.
94. Mauck KF, Asi N, Elraiyah TA, et al. Comparative systematic review and meta-analysis of compression modalities for the promotion of venous ulcer healing and reducing ulcer recurrence. *J Vasc Surg*. 2014;60:71S–90S.
95. Kikta MJ, Schuler JJ, Meyer JP, et al. A prospective, randomized trial of Unna's boots versus hydroactive dressing in the treatment of venous stasis ulcers. *J Vasc Surg*. 1988;7:478–483.
96. Nelson EA, Harrison MB. Canadian Bandage Trial Team. Different context, different results: venous ulcer healing and the use of two high-compression technologies. *J Clin Nurs*. 2014;23:768–773.
97. O'Meara S, Cullum N, Nelson EA, Dumville JC. Compression for venous leg ulcers. *Cochrane Database Syst Rev*. 2012(11):CD000265.
98. Obermayer A, Gostl K, Walli G, Benesch T. Chronic venous leg ulcers benefit from surgery: long-term results from 173 legs. *J Vasc Surg*. 2006;44:572–579.
99. Partsch H. Intermittent pneumatic compression in immobile patients. *Int Wound J*. 2008;5:389–397.
100. Diamantopoulos I, Lever MJ. Can an intermittent pneumatic compression system monitor venous filling in the leg? *J Med Eng Technol*. 2008;32:221–227.
101. Alavi A, Sibbald RG, Phillips TJ, et al. What's new: management of venous leg ulcers. Treating venous leg ulcers. *J Am Acad Dermatol*. 2016;74:643–664.
102. Alvarez OM, Markowitz L, Parker R, et al. Faster healing and a lower rate of recurrence of venous ulcers treated with intermittent pneumatic compression: results of a randomized controlled trial. *Eplasty*. 2020;20:e6.



eFig. 145.1 Activated charcoal cloth impregnated with silver (Actisorb® Silver 220). The envelope is spun bonded nylon.



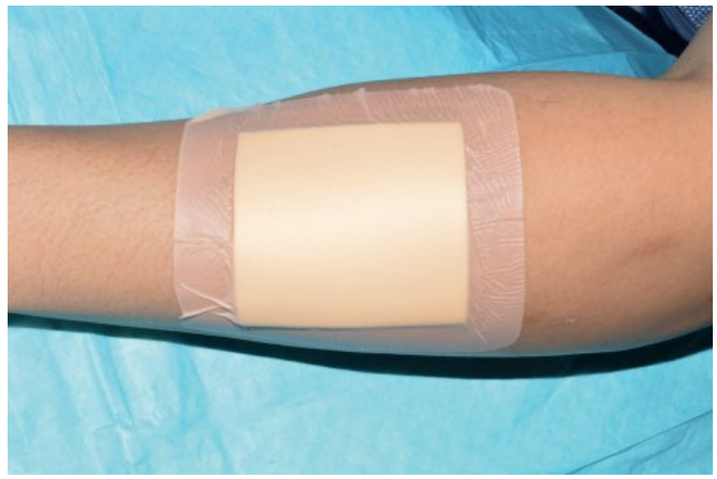




eFig. 145.2 Pressure dressing. A Ointment applied over sutures to prevent the contact layer from adhering directly to the wound. **B** Three layers of paper tape comprise the contact layer. **C** Rolled gauze or a cotton dental roll can be used to: (i) provide pressure for hemostasis; (ii) aid in conforming the dressing to the wound; and (iii) absorb excess exudate. The entire dressing is secured with additional layers of tape. *Courtesy Gregg M. Menaker, MD*.



eFig. 145.3 A polymer film is used to occlude a wound that has been covered by cotton gauze. *Courtesy Gregg M. Menaker, MD*.



eFig. 145.4 A foam dressing.





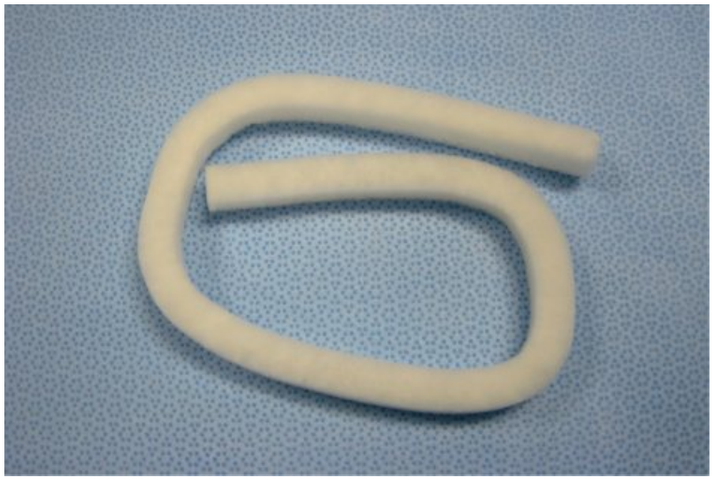
eFig. 145.5 Occlusive dressings for post-laser resurfacing. A In this side-by-side comparison, the patient's left face is dressed with a foam dressing. **B** In this side-by-side comparison, the patient's right face is dressed using the open technique.



eFig. 145.6 Example of an alginate.



eFig. 145.8 Graduated compression stockings being applied.



eFig. 145.7 Example of a collagen–alginate complex dressing. The rope form can be used to pack deep wounds. *Courtesy Gregg M. Menaker, MD.*

Video 145.1 Unna Boot Dressing.

EREFERENCES

e1. Eaglstein WH, Davis SC, Mehle AL, Mertz PM. Optimal use of an occlusive dressing to enhance healing. Effect of delayed application and early removal on wound healing. *Arch Dermatol*. 1988;124:392–395.
e2. Glesinger R, Cohen AD, Bogdanov-Berezovsky A, et al. A randomized controlled trial of silver sulfadiazine, biafine, and saline-soaked gauze in the treatment of superficial partial-thickness burn wounds in pigs. *Acad Emerg Med*. 2004;11:339–342.
e3. Storm-Versloot MN, Vos CG, Ubbink DT, Vermeulen H. Topical silver for preventing wound infection. *Cochrane Database Syst Rev*. 2010:CD006478.
e4. Cordts PR, Hanrahan LM, Rodriguez AA, et al. A prospective, randomized trial of Unna's boot versus Duoderm CGF hydroactive dressing plus compression in the management of venous leg ulcers. *J Vasc Surg*. 1992;15:480–486.
e5. Mostow EN, Haraway GD, Dalsing M, et al. Effectiveness of an extracellular matrix graft (OASIS Wound Matrix) in the treatment of chronic leg ulcers: a randomized clinical trial. *J Vasc Surg*. 2005;41:837–843.
e6. Smith Jr. DJ. Use of Biobrane in wound management. *J Burn Care Rehabil*. 1995;16:317–320.
e7. Heimbach D, Luterman A, Burke J, et al. Artificial dermis for major burns. A multi-center randomized clinical trial. *Ann Surg*. 1988;208:313–320.
e8. Eisenbud D, Huang NF, Luke S, Silberklang M. Skin substitutes and wound healing: current status and challenges (part 1 of 2). *Wounds*. 2004;16:2–17.
e9. Driver VR, Lavery LA, Reyzelman AM, et al. A clinical trial of Integra Template for diabetic foot ulcer treatment. *Wound Repair Regen*. 2015;23:891–900.
e10. Marston WA, Hanft J, Norwood P, Pollak R. The efficacy and safety of Dermagraft in improving the healing of chronic diabetic foot ulcers. *Diabetes Care*. 2003;26:1701–1705.
e11. Purdue GF, Hunt JL, Still JM, et al. A multicenter clinical trial of a biosynthetic skin replacement, Dermagraft-TC, compared with cryopreserved human cadaver skin for temporary coverage of excised burn wounds. *J Burn Care Rehabil*. 1997;18:52–57.
e12. Gohel MS, Barwell JR, Taylor M, et al. Long term results of compression therapy alone versus compression plus surgery in chronic venous ulceration (ESCHAR): randomised controlled trial. *BMJ*. 2007;335:83.
e13. Fletcher A, Cullum N, Sheldon TA. A systematic review of compression treatment for venous leg ulcers. *BMJ*. 1997;315:576–580.
e14. Cullum N, Nelson EA, Fletcher AW, Sheldon TA. Compression bandages and stockings for venous leg ulcers. *Cochrane Database Syst Rev*. 2000:CD000265.

Biopsy Techniques and Basic Excisions 146

Suzanne Olbricht

Chapter Contents

Key Concepts 2517
Indications/Contraindications 2523
Preoperative History and Considerations 2524
Techniques 2524
Variations/Unusual Situations 2530
Postoperative Care 2531
Complications 2532
Future Trends 2532

Key features

- Choice of a particular biopsy technique is based upon the anatomic site, type of skin lesion, desired histologic information, and patient preference
- Wound closure is accomplished via suturing (primary intention) or second intention
- Choice of a specific suturing technique depends upon the needs of the wound (e.g. eversion of the edges), with the goal being an optimal functional and aesthetic result
- Excision *in toto* with repair is a common surgical procedure for dermatologists and it is accomplished through a series of well-defined steps
- Postoperative care and instructions minimize the risk of complications

INTRODUCTION

The cornerstone of dermatologic diagnosis is the correlation of clinical and histologic findings. A biopsy procedure is required in order to obtain tissue for pathologic examination and, fortunately, the skin is more accessible than most other tissues. Modern instruments and techniques allow cutaneous biopsies to be performed efficiently with minimal tissue distortion. In some situations, a biopsy procedure is also curative, either coincidentally or intentionally. Knowledge of basic excisional surgical techniques can minimize cosmetic and functional impairment. A well-planned and timely skin biopsy may also circumvent the need for more invasive procedures. Even critically ill patients can undergo a skin biopsy with minimal risk.

KEY CONCEPTS

Site Selection

Performance of a biopsy that will yield accurate and relevant histologic information depends upon the selection of an appropriate lesion or site within a lesion (Table 146.1).

The anticipated depth of the lesion to be biopsied must also be considered. A superficial lesion, e.g. an actinic keratosis versus squamous cell carcinoma *in situ*, can be assessed via a thinner horizontal biopsy that extends to the papillary dermis. On the other hand, accurate diagnosis of a subcutaneous nodule, e.g. panniculitis versus polyarteritis nodosa, requires a biopsy that extends into the deeper portions of the subcutaneous fat. Occasionally, fascia must be obtained, e.g. morphea profunda versus eosinophilic fasciitis. Disorders that primarily affect the collagen and elastic fibers within the dermis may have subtle histologic findings (e.g. atrophoderma of Pasini and Pierini) and longitudinally sectioned wedge biopsies that include both the affected area as well as adjacent normal-appearing skin prove most helpful.

Biopsy Technique Selection

Seven major methods are employed to biopsy skin: curettage, snip or scissors biopsy, shave biopsy, saucerization biopsy, punch biopsy, incisional biopsy, and excision *in toto* (Table 146.2). Depending upon the type of lesion and its size, several of these procedures are also curative, especially excision *in toto*. However, these methods differ with regard to the quality and quantity of skin obtained. Lesional characteristics and operator experience are factors that influence the choice of a particular procedure.

Curettage is frequently used to remove clinically benign epidermal lesions such as verrucae or seborrheic keratoses as well as actinic keratoses (AKs) and basal cell carcinomas (BCCs), especially the superficial type. The curettings can also be used to confirm the clinical diagnosis, but histologic interpretation may prove challenging if the tissue specimen is fragmented and its orientation becomes problematic. *Snip or scissors biopsy* is an efficient technique for assessing pedunculated lesions as well as removing benign growths (e.g. acrochordons, filiform warts).

The *shave biopsy* usually provides a specimen consisting of epidermis, papillary dermis, and sometimes reticular dermis (particularly in elevated lesions). It is a popular biopsy technique for recontouring papular, clinically benign lesions (e.g. irritated or unwanted compound and dermal melanocytic nevi, fibrous papules of the nose) where histologic confirmation is desired. Shave biopsy is also a useful procedure for diagnosing superficial carcinomas, e.g. nodular and superficial BCCs, squamous cell carcinoma (SCC) *in situ*, and lentigo maligna. However, for lentigo maligna, palpation beforehand to exclude induration and a possible desmoplastic component is recommended.

When tissue is procured via a *saucerization procedure*, the depth of the biopsy specimen is intentionally deeper due to angulation of the blade. This technique is often used to biopsy melanocytic nevi with atypical features when the differential diagnosis includes a thin melanoma[1]. Its advantage is that it allows histologic examination of the entire lesion or a large portion of the lesion, which increases diagnostic accuracy (as compared to partial punch biopsy). Saucerization is also performed to confirm the clinical diagnosis of minimally invasive SCC or keratoacanthoma and to distinguish the former from a hypertrophic AK.

BIOPSY SITE SELECTION	
Lesion/disorder	**Appropriate site**
Tumor	Thickest portion; avoid necrotic tissue
Blister	Edge of lesion, including perilesional skin (see Fig. 29.12)
Ulcerated/necrotic lesion	Edge of ulcer or necrosis plus adjacent skin
Generalized polymorphous eruption	Characteristic well-developed lesion of recent onset. If multiple biopsies are obtained, include different morphologies
Small vessel vasculitis	Characteristic lesion of recent onset
Livedo racemosa	Pale center of broken ring. Multiple biopsies increase diagnostic yield

Table 146.1 Biopsy site selection.

SELECTION OF TYPE OF BIOPSY TECHNIQUE				
Method	**Indication**	**Type of specimen obtained**	**Anesthetic technique (Fig. 146.1)**	**Closure**
Curettage	• Lesions involving the epidermis (e.g. SKs, AKs, verrucae) • Confirm clinical diagnosis of BCC prior to definitive treatment	Epidermal sheet or fragments of epidermis and dermis	Wheal	Second intention
Scissors biopsy	• Pedunculated lesion	Tissue above connection to the epidermis	None or wheal	Second intention
Shave biopsy	• Lesions involving the epidermis ± superficial dermis • Elevated lesion	Epidermis, papillary dermis, and occasionally reticular dermis (elevated lesions)	Wheal	Second intention
Saucerization biopsy	• Lesions involving the epidermis and dermis • Atypical melanocytic nevus versus thin melanoma • Hypertrophic AK versus minimally invasive SCC	Similar to a shave biopsy, but specimen is thicker (i.e. contains reticular dermis)	Wheal or deep infiltration	Second intention
Punch biopsy	• Process (e.g. tumor, inflammation) involves the dermis • Depressed lesion	Epidermis, dermis, and sometimes subcutaneous fat	Wheal or deep infiltration	Primary intention; simple suture
Incisional biopsy	• Process (e.g. tumor, inflammation) involves the subcutaneous fat or fascia • Large-sized tumors • Subtle disorders of dermal connective tissue	Epidermis, dermis, and subcutaneous fat Can include fascia where needed	Deep infiltration	Primary intention; layered closure
Excision *in toto*	• Biopsy intended to be definitive treatment • Strong clinical suspicion of cutaneous malignancy (e.g. invasive melanoma)	Epidermis, dermis, and subcutaneous fat Can include fascia where needed	Deep infiltration	Primary intention; layered closure

Table 146.2 Selection of type of biopsy technique. AKs, actinic keratoses; BCC, basal cell carcinoma; SCC, squamous cell carcinoma; SKs, seborrheic keratoses.

The *punch biopsy* supplies a cylindrical to conically shaped specimen consisting of epidermis, dermis, and sometimes subcutaneous fat. The volume of tissue sampled correlates with the size of the punch biopsy instrument. The diameter of the metal "barrel" can vary from 2 to 8 mm; the wider the diameter, the greater the likelihood of obtaining subcutaneous fat. However, the thickness of the dermis must be kept in mind in addition to the amount of subcutaneous fat required to address possible clinical diagnoses. Punch biopsies are particularly helpful for examining processes within the dermis such as tumors or inflammation (see Table 146.2). In the case of tumors, sampling a majority of the lesion is desirable, so that for large-sized tumors, multiple punch biopsies may be required.

The *incisional* biopsy removes a wedge of tissue from the center or edge of a lesion (see Site Selection) and is the best option for obtaining deep subcutaneous fat or fascia for histologic examination. It is also used to sample a significant portion of large-sized tumors. Excision *in toto* removes the entire lesion and includes epidermis, dermis, and subcutaneous fat. For these reasons, it is often utilized when the leading clinical diagnosis is invasive cutaneous melanoma.

Specimen Handling

Transportation of the biopsy specimen to the laboratory differs according to the processing and type of examination required. Most specimens are placed in formalin, but, occasionally, special carrier media are necessary (Table 146.3). Fresh tissue specimens are sent on saline-moistened gauze and promptly delivered to the laboratory; the laboratory must be in reasonable proximity and have the capability of quickly processing the tissue. Occasionally, fresh or frozen tissue is sent overnight with cold packs or on dry ice, respectively, to a more distant laboratory (see Fig. 76.10). When handling small or thin biopsy specimens, it is important to confirm that they are clearly within the formalin solution and not adhering to the upper portions of the container or lid to prevent desiccation artifact.

A protocol must be established within the clinician's practice to ensure that specimens and results are appropriately tracked and assigned to the correct patient. Immediately after the biopsy specimen has been obtained, it should be placed in a container prelabeled with the patient's name and other identifying information. If multiple biopsies are to be performed, pre-labeling the containers alphabetically and with the respective sites avoids confusion. A specimen log book (Table 146.4) ensures notification of the results to the patient and disposition of recommended care.

SPECIMEN HANDLING		
Proposed laboratory test	**Carrier medium**	**Comments**
Routine microscopy, immunohistochemistry, PCR assay	10% neutral buffered formalin	Fixation process begins immediately
Direct immunofluorescence	Michel's medium -or- Fresh*	Depends on laboratory preference or availability
Flow cytometry	Fresh*	Lymphoma cutis
Culture for bacteria, mycobacteria or fungi	Fresh* -or- Minced in sterile culture/carrier medium appropriate for organism (mincing usually performed by laboratory)	
Culture for viruses	Viral transport medium (e.g. M4RT®)	
Electron microscopy	Glutaraldehyde	

*Laboratory must be in close proximity and specimen placed on saline-moistened gauze, but need to avoid bacteriostatic saline solution when culturing for microbes.

Table 146.3 Specimen handling. PCR, polymerase chain reaction.

Patient Preparation

A discussion of the reason(s) to do the biopsy, the site to be biopsied, and the technique to be used can be brief and to the point. Informed consent requires a discussion of the major risks, which include bleeding, discomfort, infection, and scarring (see Ch. 151). Bleeding can usually be controlled by firm pressure at the site of the wound, but may require more aggressive forms of hemostasis. Discomfort is usually minimal, although some sites such as the forehead, fingers, and feet may throb.

Infection is unusual. Except when the area to be biopsied is already infected or the site is mucosal, the skin can be prepared by application of an antiseptic agent and the procedure is then considered to be a *clean* procedure. For clean procedures of non-mucosal, non-infected sites, preoperative prophylactic antibiotics are currently not recommended, even in patients with artificial valves or joints (with the possible exception of sites at high risk of infection, e.g. groin, during

LOG BOOK FOR BIOPSY SPECIMENS			
Date	2/21/22	2/21/22	2/22/22
Patient initials with birthdate versus full name	TMF 4/4/87	John Doe	James Brown
Anatomic site	right cheek	right thigh	left scalp
Specimen pick-up (+/– initials)	√	√	√
Histopathologic diagnosis	BCC	Reactive changes	Pilar cyst
Patient informed/plan if needed	Called 2/28/22 / surgery SO*	Released to EMR†	Letter sent†

*SO, surgeon's initials.
†In the era of EMRs, patients can choose to have personal online portals; letters generated are included in the electronic record (for those who decline the portal).

Table 146.4 Log book for biopsy specimens. Specimen pick-up can be completed by courier service. BCC, basal cell carcinoma; EMR, electronic medical record.

SITE PREPARATION PROTOCOL	
Sequential steps	**Comments**
Mark site with surgical pen or ink	Local anesthesia may obscure site, especially when the erythematous color is due to vasodilation or when there is a minimally elevated dermal tumor
Time out for patient and site identification	JCAHO universal protocol for patient safety
Photograph site or record landmarks	Up to ~15% of biopsy sites may be later incorrectly identified by the patient and ~5% by the surgeon[8]
Clip hair as needed	Shaving hair increases incidence of infection
Cleanse skin surface	Antiseptic agents listed in Table 146.6
Drape	Gauze (small biopsies) or sterile towels
Anesthetize	Local instillation of anesthetic agent

Table 146.5 Site preparation protocol. JCAHO, Joint Commission on Accreditation of Healthcare Organizations.

ANTISEPTIC AGENTS		
Agent	**Advantages**	**Disadvantages**
Povidone–iodine (Betadine®)	Broad antimicrobial spectrum, including fungi	Irritant and allergic contact dermatitis Residual color May cross-react with iodine in radiocontrast media and iodides in medications
Chlorhexidine (Hibiclens®)	Broad antimicrobial coverage Limited systemic absorption Prolonged suppression of bacterial growth	Keratitis due to ocular exposure Cochlear damage if enters middle ear Irritant and allergic contact dermatitis Contact urticaria Very rarely, anaphylaxis
Isopropyl alcohol	Inexpensive Denatures protein, including bacterial cell walls Immediate (but not prolonged) effect	Weak antimicrobial activity Flammable in the setting of cautery Skin irritant Skin must remain wet for 2 minutes for maximum effect
Chlorhexidine–isopropyl alcohol combination (ChloraPrep®)	Combination provides both short-term and long-term effects Evidence it is more effective than povidone–iodine[10]	Those of either agent alone (see above)
Hexachlorophene (pHisoHex®)	Strong effect against Gram-positive cocci	Little effect on Gram-negative organisms or fungi Teratogen Absorbed through skin with potential neurotoxicity in infants
Soap and water	Traditional preoperative handwashing regimen Disinfects hands as well as alcohol-based rubs[64] Better against *Clostridium difficile* and Norwalk virus	At operative site, cumbersome and messy No prolonged antisepsis
Hydrogen peroxide	Readily available Inexpensive	No significant antiseptic properties Cytotoxic to keratinocytes *in vitro*

Table 146.6 Antiseptic agents.

the first 2 years after joint placement)[2–4]. The overall goal is a reduction in the emergence of antibiotic-resistant bacteria and in one study, for example, preoperative prophylactic antibiotics increased nasal carriage of methicillin-resistant *Staphylococcus aureus*[5]. Tables 151.2 and 151.3 review the guidelines for antibiotic prophylaxis as well as regimens for both oral and non-oral sites. If preoperative antibiotics are given, they are administered within a 2-hour window before the incision; there is debate as to whether or not a second dose is administered 6 hours later and under which circumstances antibiotics should be continued for 48–72 hours[6]. When pretreated with a 5-day regimen of intranasal mupirocin ointment (twice daily) and a total body wash with chlorhexidine soap (daily avoiding the eyes and ears), nasal carriers of *S. aureus* were observed to have fewer postoperative infections[7].

Most patients are primarily interested in discussing whether or not there will be visible scarring. This is best predicted by the type of biopsy to be performed and the anatomic site. Generally, patients can be reassured that small biopsies may be done without grossly noticeable permanent "marks".

Many patients are anxious about the needle sticks required for administration of the local anesthesia and the pain of the procedure. The patient's cooperation is easily obtained in an organized and peaceful environment with a calm and reassuring staff. A well-informed, comfortable patient in a supine position will tolerate the procedure without difficulty.

Site Preparation and Anesthesia

Effective site preparation is most efficient if a standard clinical protocol has been established (Table 146.5). Marking and photographing the site[8,9], cleansing the skin (Table 146.6)[10], and draping are important procedures prior to the instillation of local anesthesia. Local anesthesia is adequate for all skin biopsies and is reviewed in detail in Chapter 143.

When the local anesthetic agent is instilled into a deep compartment (i.e. subcutaneous fat; Fig. 146.1A), 5 to 10 minutes is required for anesthesia to develop on the surface of the skin. Gentle massage of the site may assist in spreading the agent subepidermally and achieving good anesthesia. Injection of the agent superficially, creating an edematous wheal, has immediate efficacy but is more painful (Fig. 146.1B). Since a punch or shave biopsy requires very little agent and therefore a very short injection time, superficial instillation is the technique often used. In addition, a wheal is helpful prior to a shave biopsy as the lesion is further elevated from the plane of the surrounding skin. Of note,

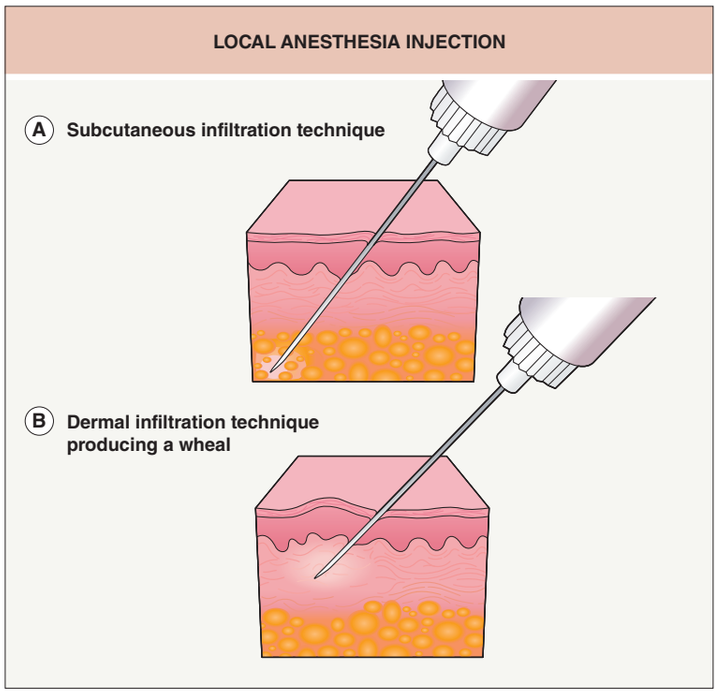


Fig. 146.1 Local anesthesia injection. A Deep infiltration. **B** Superficial infiltration.

METHODS OF HEMOSTASIS

Method	Comments
Compression	• Appropriate for small-diameter, superficial wounds • Folded dry sponge with tightly applied bandage
Styptics: aluminum chloride hexahydrate (Drysol™, Xerac AC™), silver nitrate, or ferric subsulfate (Monsel's solution)*	• Apply pressure to diminish active bleeding • Then apply styptic with cotton-tipped swab and pressure to wound bed for 30 sec–2 min
Absorbable hemostatic sponge: Gelfoam®, Instat®, Oxycel®	• Apply pressure to diminish active bleeding • Then place sponge in wound and bandage in place with pressure • Warn patient of presence of "foreign body"
Electrocoagulation and heat cautery	• Reviewed in Chapter 140
Sutures	• When used for wound closure, generally creates sufficient hemostasis in the sidewalls of the wound • Figure-of-eight suture, utilizing an absorbable suture (Fig. 146.2), may be required for a large-caliber vessel

*Ferric subsulfate (Monsel's solution) can result in a tattoo.

Table 146.7 Methods of hemostasis.

since epinephrine (adrenaline) requires up to 15 minutes to produce maximal vasoconstriction and thereby minimize bleeding[11], lidocaine without epinephrine is sufficient for an immediate biopsy. Regardless of other considerations, it is critical to have the local anesthesia in the compartment that is to be biopsied, i.e. a superficial wheal may be entirely adequate as anesthesia for a shave biopsy but will not suffice for an incisional wedge biopsy that extends into the subcutaneous fat.

Hemostasis

All biopsy procedures require attention to hemostasis of the wound bed (Table 146.7; see Table 151.5). While styptics and absorbable hemostatic sponges are used for those wounds healing by second intention, suturing provides sufficient hemostasis for punch biopsy sites. Wounds created during an incisional biopsy or excision *in toto* may require electrocoagulation for hemostasis before closure (see Ch. 140). The endpoint is no active bleeding in the wound bed. Bleeding within the dermis in the sides of the wound can be controlled by suturing and does not need cautery. At times, to produce hemostasis, a large actively bleeding vessel may need to be identified, grasped with a hemostat, and tied off with an absorbable suture and a figure-of-eight suture (Fig. 146.2).

Wound Closure

Closure of wounds created by a biopsy procedure may occur by either second or primary intention healing. Second intention healing repairs wounds by the processes of granulation tissue formation, epidermal cell migration, and contraction (see Ch. 141). These processes occur simultaneously, beginning within the first few days after surgery and continuing until the wound has completely re-epithelialized. For the remainder of the patient's life, maturation of the scar occurs, with gradual improvement in color, texture, and contour. Indications, disadvantages, and contraindications for second intention healing are outlined in Table 146.8.

Closure of the wound via suturing is regarded as primary intention healing. The same processes of granulation tissue formation, epithelial migration, and contraction occur; however, they are significantly reduced, because the sides of the wound are already apposed. Processes related to fibroblast activity and collagen deposition play a more important role in primary intention healing, allowing adequate tensile strength to develop to keep the wound closed[12]. These scars also undergo maturation throughout the remainder of the patient's life. Both second and primary intention healing are promoted by appropriate wound care and dressings.

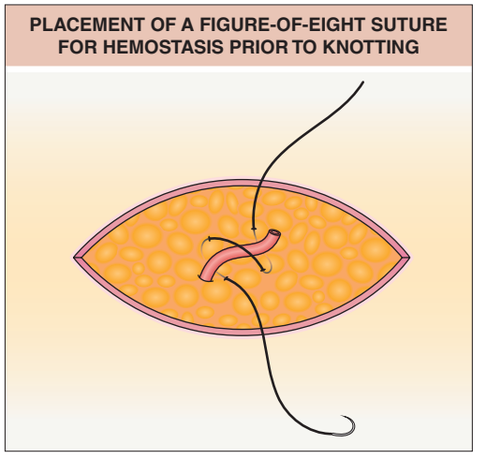


Fig. 146.2 Placement of a figure-of-eight suture for hemostasis prior to knotting.

For primary intention healing, wounds may be closed either by placement of a simple full-thickness suture or by layered closure. In a layered closure, subepidermal buried sutures appose subcutaneous and dermal tissue, provide alignment of the wound edges, set up the wound edges for eversion, and assist with hemostasis by occluding any vessels bleeding within the edge of the wound. In addition, the subepidermal sutures supply strength to handle tension within the closure. Although subepidermal sutures are generally absorbable, they remain intact within the tissue for 8 to 12 weeks, the period during which the scar is slowly acquiring tensile strength. As a result, they prevent dehiscence and spread of the scar. Epidermal or skin sutures appose the epidermal edges and complete eversion. They can also correct minor degrees of misalignment in the closure. Satisfying these objectives via conscious placement of sutures improves the function and appearance of the scar[13,14].

Knotting is the means for stabilizing the placement of the suture, usually produced with an instrument tie (Fig. 146.3). The first throw of the knot is started by pulling the long end of the suture tight with the fingers of the non-dominant hand and looping it around the needle holder once or twice. The needle holder then grasps the short end and pulls it through the loops. The loops are pulled across the wound so that they lie flat. These steps are then repeated to produce the second throw of the knot, but this time with the loop in the opposite direction around the needle holder. When this second loop is pulled across the wound, a square knot is created. Depending on the memory and thickness of

SECOND INTENTION HEALING – INDICATIONS, DISADVANTAGES AND CONTRAINDICATIONS
Indications
• Shallow wounds • In combination with a primary closure in which the deepest portion is closed primarily • Concave sites, e.g. medial canthus, conchal bowl, alar crease, temple • Mucosal sites, e.g. conjunctivae, lip, genitalia • Infected, necrotic, or easily infected sites • Sites under significant tension because of physical exercise or size of the wound • Preferred by patient – simple, no sutures, normal activities
Disadvantages
• Sometimes prolonged healing time, especially on distal lower extremities • Scarring which may be depressed and angulated or circular, especially if not in concave site
Contraindications
• Relative: wound into muscle or fascia • Relative: wound at a free margin – contraction can lead to distortion, e.g. ectropion, elevated alar rim (see Fig. 148.9) • Absolute: inability to stop bleeding without a suture

Table 146.8 Second intention healing – indications, disadvantages and contraindications.

the suture material (see Ch. 144), three to six throws may be required to properly secure the knot. Care is taken to ensure that the knot lies flat without significant tension or tightness[15]. Sometimes, a loose loop is left in the second throw, to allow the suture to adjust to any wound swelling that may develop.

Sutures commonly used for subepidermal placement are composed of synthetic absorbable materials such as braided polyglactin (Vicryl®) or monofilament polydioxanone (PDS®). The *interrupted buried dermal suture* (Fig. 146.4A) is designed such that the suture is in the dermis and fat and the knot is inverted (buried). The needle enters the undermined deep surface of the wound (not the sidewall) and passes up into the dermis. After crossing the wound, it enters the opposite side of the wound at the same level in the dermis and then exits the deep surface. The knot is then tied and the ends of the suture cut. When the suture material is released, the knot settles within the deep portion of the wound, minimizing tissue reaction to the suture and extrusion through the wound. Enough buried dermal sutures are placed such that tension is eliminated and the deep tissues are completely apposed. In order to facilitate eversion, this basic suture may be modified, creating a *buried vertical mattress suture*[16]. The suture is nearest to the skin surface (within the superficial dermis) at a point 3–4 mm lateral to the wound edge, and then it exits the wound deeper in the dermis (Fig. 146.4B). A very subtle dimple may be appreciated above the suture where it lies superficially in the dermis.

On occasion, a *running dermal suture* is used to close the deep component. This suture is begun similarly to the interrupted buried dermal suture, but, after tying, only the short end of the suture is cut. The needle then draws the suture through the subcutaneous fat and dermis on one side, passing to the other side, and then continuing along the length of the wound. At each step, the suture is pulled tightly to appose the edges. At the end of the wound, the knot is achieved by tying the loose end to the last loop. This suture is only used when there is little tension in the wound, as rupture of the suture material anywhere along the suture line would release the suture for the entire length of the wound, allowing dehiscence or spread of the scar.

Monofilament nylon (Ethilon®) or polypropylene (Prolene®) are commonly used epidermal sutures. The *simple interrupted epidermal suture* is placed by passing the needle through the epidermis into the superficial dermis in a plane just superior to the buried suture, across the wound, into the dermis on the opposite side and then up through the epidermis (Fig. 146.4C). Eversion is assisted by placing the suture closer to the wound edge but relatively deeper in the wound so that the epidermal surface does not roll. Using the curve of the needle to create the path for the suture also facilitates eversion. If there are no buried sutures, the suture apposes the edges for the full depth of the wound (e.g. for closure of punch biopsies).

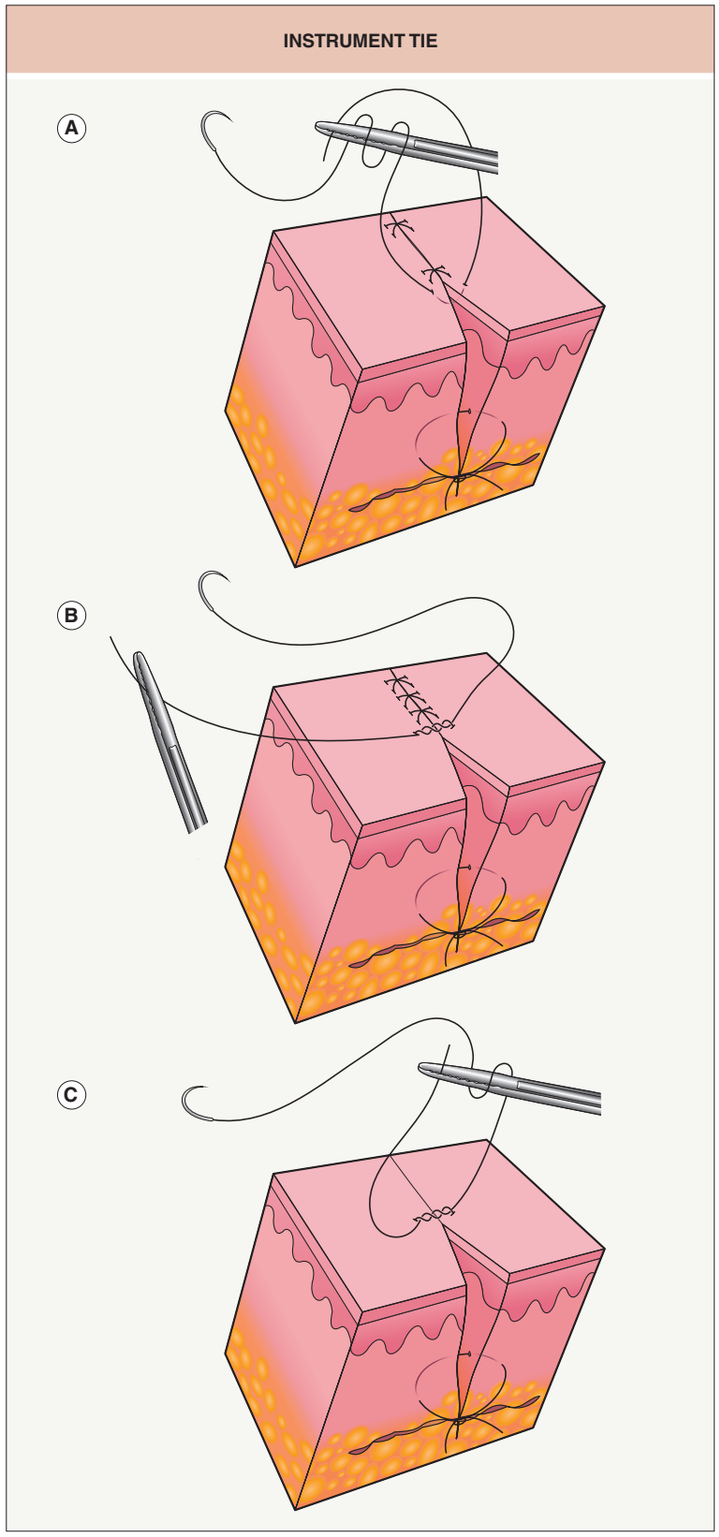


Fig. 146.3 Instrument tie. A The suture is looped around the needle holder, then the needle holder grasps the short end and pulls it through the loops to create a knot. **B** The suture is drawn over the wound so that the knot lies flat across the wound. **C** A loop is made around the needle holder in the opposite direction. The needle holder then grabs the short end and pulls it through so that the knot lies flat on the skin surface.

The *vertical mattress suture* (Fig. 146.4D) is sometimes used for wounds in thicker skin where eversion may be difficult and when a single suture apposing the deep and superficial edges is desired. This suture has four points of entry into the skin. It is started by passing the needle through the epidermis 5–8 mm lateral to the wound edge, exiting from the deep portion of the wound. It re-enters the opposite side of the wound in the same deep position, and exits from the epidermis equidistant

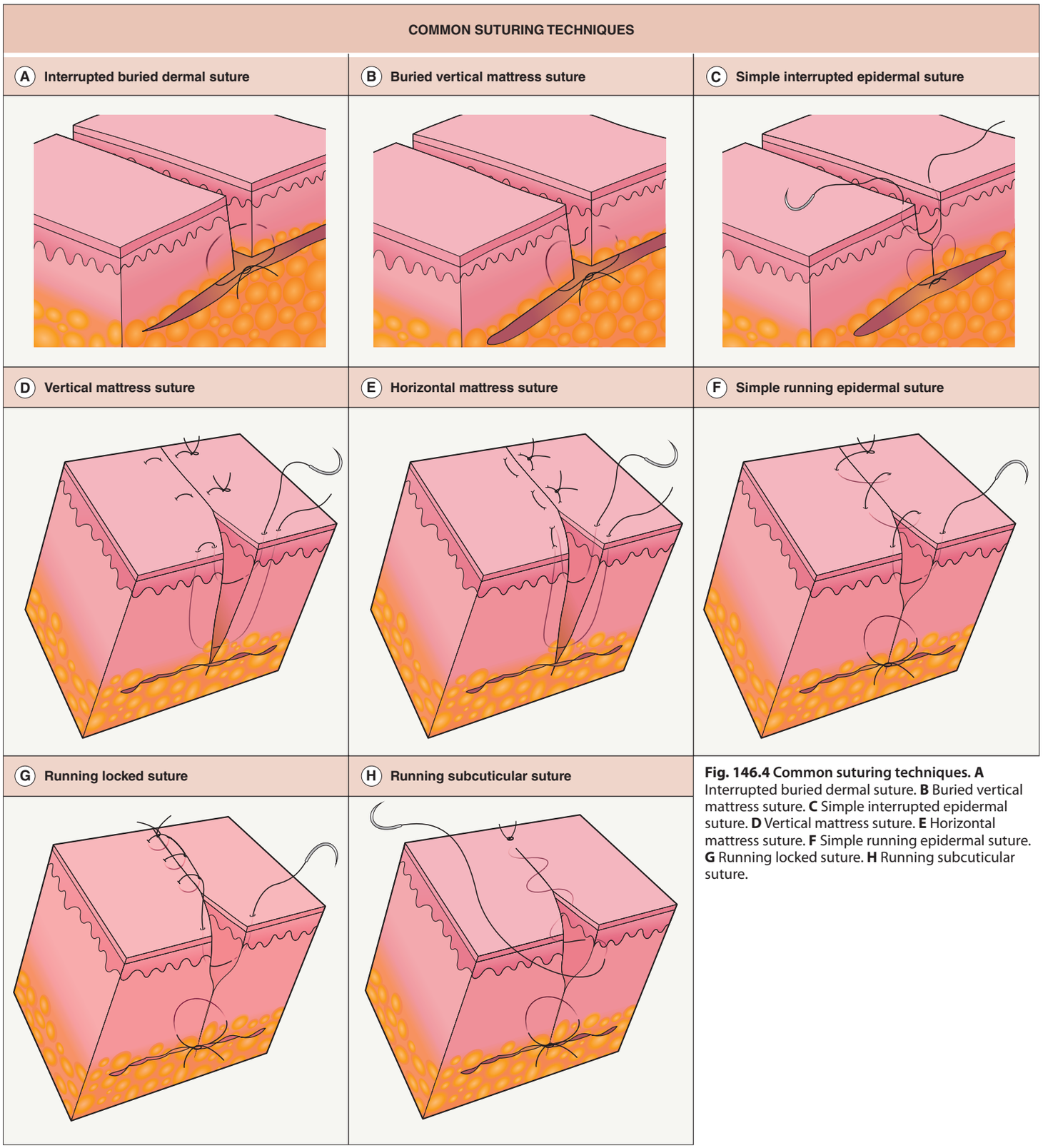


Fig. 146.4 Common suturing techniques. A Interrupted buried dermal suture. **B** Buried vertical mattress suture. **C** Simple interrupted epidermal suture. **D** Vertical mattress suture. **E** Horizontal mattress suture. **F** Simple running epidermal suture. **G** Running locked suture. **H** Running subcuticular suture.

from the wound edge as the entry point. The needle is reversed and the epidermis is re-entered *closer* to the wound edge; it is then drawn through the upper dermis before crossing the wound, entering the dermis and finally exiting close to the wound edge. Once tied, the knot is positioned on one side of the wound, not over the line of closure.

A *horizontal mattress suture* can be used in thinner skin such as the neck or the dorsum of the hand, and it also has four points of entry into the skin. The first two points of entry are the same as in the vertical mattress suture (Fig. 146.4E), but closer to the wound edge (i.e. 3–5 mm). However, after the needle is reversed, the third point of entry into the epidermis is 3–4 mm from the exit point, on the same side of the wound edge and equidistant from the wound edge. The suture is then drawn through the upper dermis, crosses the wound, enters the opposite sidewall in the same dermal position and finally exits at the same distance from the wound edge, 3–4 mm from the first entry point. This knot, when tied, is also positioned on one side of the wound, not over the line of closure (Video 146.1).

Since sutures of both the vertical mattress and horizontal mattress sutures must be removed within 1–2 weeks (depending upon the site), they are not good sutures to use as the sole means of closure in a wound

with tension. Of note, a variant, the running combined simple and vertical mattress suture, also everts well and saves surgical time[17].

In the presence of buried sutures that have produced even alignment of the epidermal edges, a *simple running epidermal suture* can be used to complete the closure (Video 146.2). This running suture may be passed via the dermis and the epidermis in a fashion similar to the simple interrupted epidermal suture (Fig. 146.4F). In addition, the needle may be passed under the superficial loop of the previous suture, thus creating the *running locked suture* (Fig. 146.4G). This suture can assist with hemostasis and will not completely unravel if the suture breaks under wound tension. Irrespective of the epidermal suture that is chosen, track marks can appear due to tension, inadequate undermining, and ineffective buried dermal sutures, as well as poor placement of the epidermal sutures.

Alternatively, the suture may be placed entirely within the upper dermis, referred to as a *running subcuticular suture* (Fig. 146.4H, Video 146.3). This suture is placed with the needle and non-absorbable suture passing in and out of the upper dermis in a plane horizontal to the surface. Two knots are tied, one on each end of the wound, and they are the only visible portions of the suture. A fully buried running subcuticular suture with absorbable suture can also be placed. Running sutures are frequently used to save time, but they can accentuate minor misalignments of the wound edges[18].

Non-absorbable sutures that pass through to the surface of the skin should be removed as they can cause tissue inflammation and create a less than optimal functional and cosmetic result. To remove a suture, the thread is severed near the knot with either fine-tipped scissors or a #11 blade. The knot is then pulled over the line of closure so that the wound edges are not pulled apart. Sutures on the face are generally removed after 5–7 days, and sutures elsewhere at 10–14 days. If buried dermal sutures are used, the epidermal sutures may be removed at the earlier times. Sometimes, absorbable suture material is used for superficial closures, especially in the simple running epidermal suture, precluding the need for suture removal. Sterile adhesive tapes such as Steri-Strips™ or tissue glue (Dermabond®) are also occasionally used instead of epidermal sutures to avoid the need for suture removal, but they are ineffective in producing eversion and in dealing with tension. When compared to traditional epidermal sutures, adhesive tapes in one study produced an equivalent result in overall scar cosmesis, *if* subcutaneous closure had been achieved with no tension and there was perfect alignment of the surface[19]. Of note, in another study, no differences in cosmetic outcome were observed when adhesive tapes plus dermal sutures were compared to dermal sutures alone[20]. The use of adhesive tapes after suture removal may, however, reduce the amount of scar spreading when they are left in position for several weeks[21]. Table 146.9 outlines alternatives to sutures for wound closure[22–25].

WOUND CLOSURE – ALTERNATIVES TO SUTURING	
Adhesive tapes (Steri-Strips™)	• For perfectly apposed lacerations or wound edges under little tension • Often used with a liquid adhesive, e.g. Mastisol® • May be used for epidermal closure after subcutaneous closure completed by suturing
MicroMend® wound closures	• Metal clips are incorporated into adhesive bandage • For wounds that are fairly well apposed and under only modest tension • Available OTC for lacerations
Staples*	• Highest tensile strength • Good for wounds under tension
Tissue glues (e.g. 2-octyl cyanoacrylate [Dermabond®], fibrinogen [Tisseel™], hydrogel [Duraseal™])	• Can be considered for epidermal closure of wounds under little tension • Less effective than dermal suturing for minimizing dehiscence[24] • Side effects include allergic contact dermatitis, sensation of heat when applied
Laser welding (Nd:YAG, CO_2 lasers)	• Experimental and used infrequently in the clinical setting
Photochemical welding (Rose Bengal plus green light)	• Experimental

*Also requires skin stapler and staple remover.

Table 146.9 Wound closure – alternatives to suturing. OTC, over-the-counter.

EXAMPLES OF DISORDERS ASSESSED VIA BIOPSY OF NORMAL SKIN	
Disease	**Comments**
Neurologic • Small fiber neuropathy • Cerebral autosomal dominant arteriopathy with subcortical infarcts and leukoencephalopathy (CADASIL) • Neuroaxonal dystrophy • Peripheral autonomic neuropathy	• Pathologic metrics for diagnosis of small fiber neuropathy based on 3 mm punch biopsy at the ankle
Intravascular lymphoma	• Incisional biopsy recommended
Systemic amyloidosis	• Punch biopsy of abdominal fat pad (versus needle aspiration of subcutaneous fat)

Table 146.10 Examples of disorders assessed via biopsy of normal skin. Tissue can also be used (as comparison) to confirm mosaicism and to assist in diagnosing inherited disorders (e.g. muscular dystrophies, sarcoglycanopathies).

INDICATIONS/CONTRAINDICATIONS

A biopsy is indicated when the clinical diagnosis of a cutaneous disorder is unclear or must be substantiated before a course of treatment is undertaken. Inflammatory disorders are often biopsied to assist in the differentiation of multiple processes that may have a similar clinical appearance. Infectious processes are biopsied to detect the causative organism in tissue sections and/or to obtain tissue for culture. Lesions suspicious for malignancy are biopsied in order to develop a surgical plan appropriate for the tumor type. Biopsies of normal skin may also be performed to assist in the diagnosis of systemic diseases or to obtain tissue for genetic studies (Table 146.10)[26–28]. Skin biopsies may even be performed prenatally.

Most patients can safely undergo a skin biopsy, so contraindications are not absolute. A skin biopsy may save the patient from a more invasive procedure if the disease process can be determined via histologic examination of the skin. Patients who are immunosuppressed because of medications (e.g. prednisone, chemotherapy, tacrolimus) or underlying diseases (e.g. HIV infection, lymphoma, leukemia) often require biopsies because of the complicated interplay between the underlying disorders and the side effects of therapy (e.g. infections, drug reactions).

In addition, there are no cutaneous or mucosal sites where a biopsy is contraindicated. Diagnostically, it is more useful to biopsy a lesion from the hand or the face that provides accurate information than it is to biopsy a late-stage, nonspecific lesion on the arm. Biopsies can be done on the legs of patients with diabetes mellitus as well as the digits of patients with vascular compromise, although greater attention to postoperative care is often necessary. For patients with coagulation or platelet disorders (due to either underlying diseases or medications), it may be preferable to biopsy a site that can be compressed to produce hemostasis. For example, if an arm or leg were biopsied, postoperative bleeding can be controlled by pressure applied by an elastic circumferential bandage.

In certain anatomic sites, it may be necessary to exercise caution to avoid injuring a vital structure (see Chs. 142 & 151). The temporal nerve lies in a superficial location, just beneath thin dermis and subcutaneous fat, midway between the eyebrow and the temporal hairline. The spinal accessory nerve also courses superficially at the posterior edge of the sternocleidomastoid muscle, approximately one-third of the distance between the mastoid process and the inferior attachments of the muscle. Severing these nerves leads to motor dysfunction; thus, these sites are best biopsied in a superficial manner. The temporal and thyroid arteries are also relatively superficial; cutting them leads to temporary difficulty with hemostasis but without long-term adverse effect.

Some lesions require special consideration before performing a biopsy. A mass that is pulsatile may indicate large arterial vessel involvement, a situation requiring additional clinical evaluation prior to biopsy and special surgical arrangements in case of bleeding. A post-traumatic cephalic mass or cystic midline lesion may need preoperative radiologic examination to identify any possible connection to the intracranial

PREOPERATIVE HISTORY
Allergies
Medications, including nutritional supplements and over-the-counter preparations (see Ch. 133)
Past reactions to local anesthesia
Difficulties with hemostasis during previous procedures
Past problems with wound healing, e.g. infection, keloid formation
Pacemaker or implantable cardioverter-defibrillator (ICD)
Disease or past replacement of the cardiac valves
Past orthopedic surgery with joint replacement
Hypertension
Diabetes mellitus
Immunosuppression
Infection or vascular compromise at the biopsy site
Smoking habits and willingness to discontinue
Possible pregnancy

Table 146.11 Preoperative history.

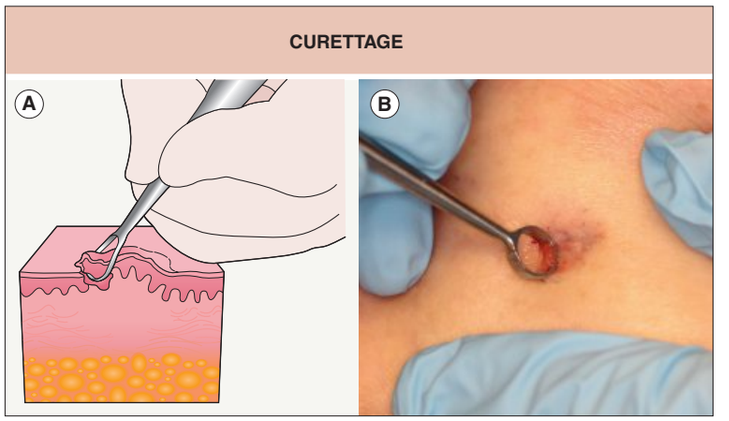


Fig. 146.5 Curettage. A Diagram. **B** Demonstration of technique.

or intraspinal space[29]. Excision of a benign lesion, e.g. epidermoid inclusion cyst, on the upper trunk or shoulders of a patient who tends to form keloids must be carefully discussed, weighing the possibility of keloid formation against how bothersome the lesion is. Hypertrophic scars, on the other hand, are common and resolve with time and/or pressure as well as corticosteroid injections, and need not interfere with the performance of a biopsy.

PREOPERATIVE HISTORY AND CONSIDERATIONS

While there are no absolute contraindications to performing a biopsy, a clinician will want to be aware of certain features of a patient's medical and surgical history in order to formulate an adequate surgical plan and to predict the need to manage possible complications. Table 146.11 summarizes information pertinent to the issues previously discussed. In particular, patients who are taking medications or have underlying disorders that lead to abnormalities in coagulation or platelet function should be identified in advance. Almost all procedures can be done despite a patient receiving warfarin, heparin, clopidogrel, apixaban, rivaroxaban[30], or aspirin if the site of the biopsy is planned carefully and the options for hemostasis are readily available. The bleeding time may also be affected by alcohol ingestion, oral vitamin E, and nonsteroidal anti-inflammatory drugs, in addition to a number of alternative therapies, including garlic, gingko, ginger, ginseng, feverfew, fish oil, and green tea[31] (Table 133.3). While biopsies may be done safely during pregnancy[32], the emotional turmoil surrounding a coincidental miscarriage or pregnancy mishap is great enough to defer elective procedures (e.g. shave biopsy of an unwanted intradermal nevus) to the postpartum period, whereas biopsies of atypical pigmented lesions in which the differential diagnosis includes melanoma are not deferred. Biopsies and excisions can also be done safely under local anesthesia in children as long as they can cooperate.

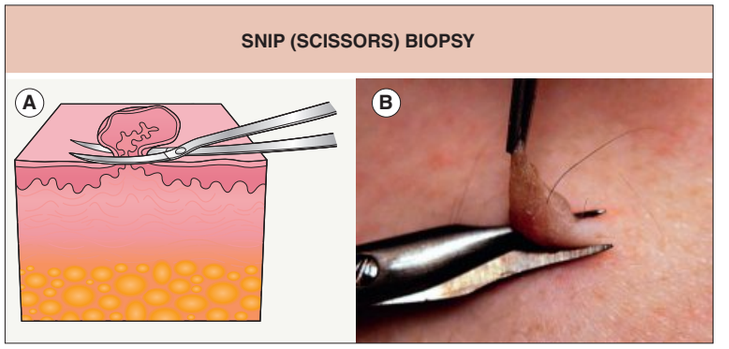


Fig. 146.6 Snip (scissors) biopsy. A Diagram. **B** Demonstration of technique.

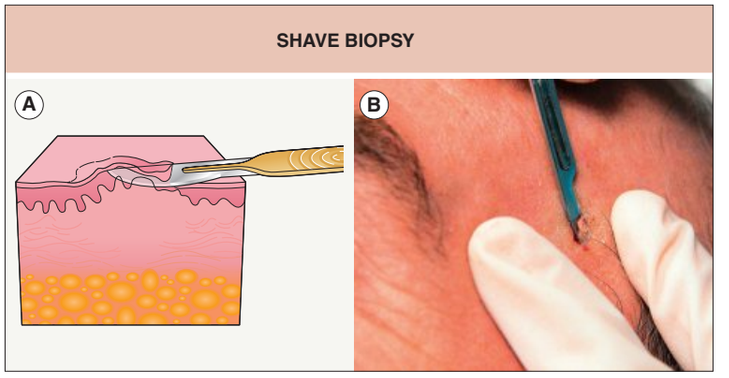


Fig. 146.7 Shave biopsy. A Diagram. **B** Demonstration of technique.

TECHNIQUES

Curettage

Local anesthesia is achieved by wheal formation (see Fig. 146.1). Depending upon the size and thickness of the lesion, a curette 3–5 mm in diameter is held like a pencil and drawn with pressure across the lesion (if epidermal) or through the lesion (e.g. presumed BCC). With one smooth movement and moderate pressure (as well as opposing traction by the non-dominant hand), an epidermal sheet or ball of tissue may be obtained (Fig. 146.5). In the case of incomplete removal, further fragments may be obtained by repeated curettage. This type of biopsy assumes that healing will be by second intention. Hemostasis may be obtained by a styptic, electrodesiccation, absorbable hemostatic sponge, or pressure. The resulting scar is usually minimal in the case of epidermal lesions or of no significant concern in the case of a BCC, since later definitive treatment will produce the final scar.

Snip or Scissors Biopsy

Pedunculated lesions can be biopsied via a snip or scissors biopsy (Fig. 146.6). Local anesthesia is obtained by wheal formation in the upper dermis just under the narrow attachment of the lesion to the skin surface. For tumors with a very narrow neck, this type of biopsy can be done quickly without anesthesia. Scissors, usually fine iris scissors or sharp Gradle scissors, are used to separate the lesion from its base at the level of the skin surface. A toothed forceps is often used to handle the tissue. Healing is by second intention, and a styptic, electrodesiccation, absorbable hemostatic sponge, or pressure may be required for hemostasis. Scarring produced by this type of biopsy procedure is a small, subtle, often hypopigmented macule.

Shave Biopsy and Saucerization Biopsy

Shave biopsy is the most commonly used technique for obtaining a skin specimen for histologic examination (Fig. 146.7). A local anesthetic is used to produce a wheal under the lesion so that it is elevated above the plane of the surrounding skin. A #15 blade on a blade handle is used (almost parallel to the skin surface) to cut the specimen from its bed. Alternatively, only the blade without the blade handle is used. Cutaneous surgeons generally hold the blade or the blade handle like a pencil, to facilitate control of small movements. It is helpful to begin

on one edge by holding the blade vertically and incising only through the epidermis. The blade is then turned to a horizontal position and a smooth sawing motion is used to complete the removal of the specimen. A good specimen may also be obtained by a single-edged razor blade held in a semi-curved shape[33].

The goal is a shallow, saucer-shaped defect and a single piece of unfragmented tissue; edges should be smooth. Forceps may be used to hold the specimen while *in situ* in order to supply traction against the movement of the blade and then to remove the entire specimen and place it in the appropriate container. However, the tissue must be handled gently so that crush artifact does not confuse the microscopic appearance. Toothed, as opposed to smooth or ridged, forceps minimize crushing of the tissue. The specimen should include full-thickness epidermis and superficial dermis. The most common error when first performing shave biopsies is to remove only keratotic debris or the upper portion of the epidermis. The latter is especially true in areas with thick stratum corneum (e.g. palms, soles). Therefore, the dermatologist needs to appreciate the angulation of the blade that is required in order to obtain the full thickness of the epidermis plus some of the superficial dermis. Observation of the wound bed and review of the tissue sections will help refine the skills needed to perform this procedure.

In a saucerization procedure, the depth of the biopsy specimen is intentionally deeper due to the angulation of the blade, which may or may not be attached to a handle (Fig. 146.8). Fat may even be included in the base of the specimen in sites with a thin dermis, but in general the biopsy extends to at least the mid reticular dermis. Both saucerization and shave biopsy sites heal by second intention. As with curettage and snip biopsy, hemostasis is easily obtained with a styptic, electrodesiccation, absorbable hemostatic sponge, and/or pressure. With practice and skill, as well as choosing the appropriate lesion to biopsy in this manner, the resulting mature scar is flat or slightly depressed with slight hypopigmentation.

Punch Biopsy

A punch biopsy is routinely used to sample processes within the mid to deep dermis or depressed lesions. As discussed above, the volume of tissue obtained varies depending upon the diameter of the metal "barrel". For example, the specimen obtained with a 2 mm punch biopsy is very small and may not yield sufficient pathologic findings for an accurate diagnosis. In one study, however, where 2 mm punch biopsy specimens (examined by a dermatopathologist) were compared to excisional specimens, an accurate diagnosis (primarily AKs, BCCs, SCCs, inflammatory dermatoses) was made in 79 of 84 cases[34]. For most punch biopsies, an instrument with a 3 to 4 mm diameter is adequate. Occasionally, a 6 or 8 mm punch biopsy is performed to increase the likelihood of obtaining subcutaneous fat. However, as stated previously, the thickness of the dermis and the amount of subcutaneous fat required to establish the diagnosis must be kept in mind.

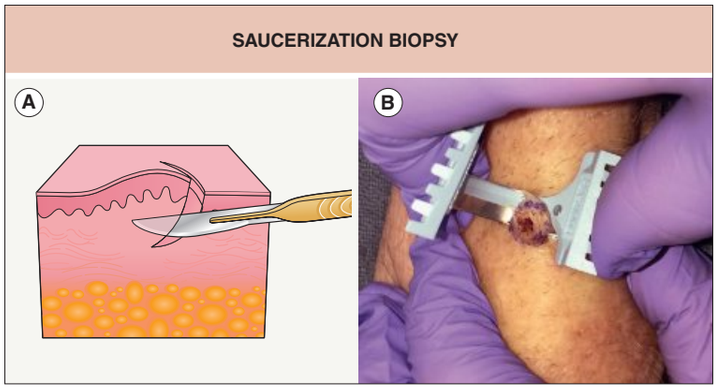


Fig. 146.8 Saucerization biopsy. A Diagram. **B** Demonstration of technique.

Disposable punch biopsy instruments are generally used. Reusable stainless steel instruments are available but must be sterilized following each procedure and sharpened frequently. Toothed forceps, scissors, needle holder, and suture material are also required. Local anesthesia is achieved with either superficial or deep infiltration of the agent.

An optimal aesthetic result is obtained when the round punch biopsy instrument is used to produce an oval-shaped defect that can be closed without "dog-ear" formation when sutured into a straight line parallel to the other skin lines in the region. This is accomplished with traction produced by stretching or spreading the skin with the index finger and thumb of one hand in a direction perpendicular to the desired wound closure line; the punch is then pushed into the skin and rotated in one direction with the other hand (Fig. 146.9). Back-and-forth twisting is not recommended as epidermis may be sheared off. Generally, the instrument is pushed and rotated until the subcutaneous plane is reached, as indicated by loss of the resistance encountered while cutting through the dermis. At times, the punch biopsy is utilized to just incise the skin superficially as when the skin is very thin (e.g. on the ear). The punch biopsy instrument is then removed and forceps are used (peripherally at one superficial edge) to gently extricate the specimen from the wound. Scissors may be needed to detach the base of the specimen, which can then be transferred to the appropriate prelabeled container. In the case of fibrotic tumors or disorders, pressure may need to be applied to the surrounding skin to elevate the biopsy specimen.

Although a punch biopsy wound can be left to heal by second intention after achieving hemostasis, the resulting scar may be depressed and takes several weeks to heal. Usually this wound is closed primarily, and the resulting scar is generally white or hypopigmented and has a linear or cruciate configuration. On the trunk or extremities, one or two simple interrupted epidermal sutures of 4–0 nylon or polypropylene monofilament suture achieve closure and hemostasis. On the face, neck, or hands, the resulting scar may be less apparent if 5–0 or 6–0 simple interrupted sutures are utilized. Some physicians use fast-absorbing gut for patients who are unable to return for suture removal. However, it is also reasonable to have the patient return for a face-to-face discussion of the biopsy results, since the biopsy is being done to establish a diagnosis and determine a treatment plan. Sutures on the face are removed at 5–7 days, and on the trunk or extremities, at 10–14 days. A pathology report is usually available within 7 days.

Table 146.12 highlights special considerations when performing a punch biopsy on the face.

Incisional Biopsy

Large lesions in which the characteristic pathology is within the dermis or subcutis are often biopsied via an incisional or wedge biopsy

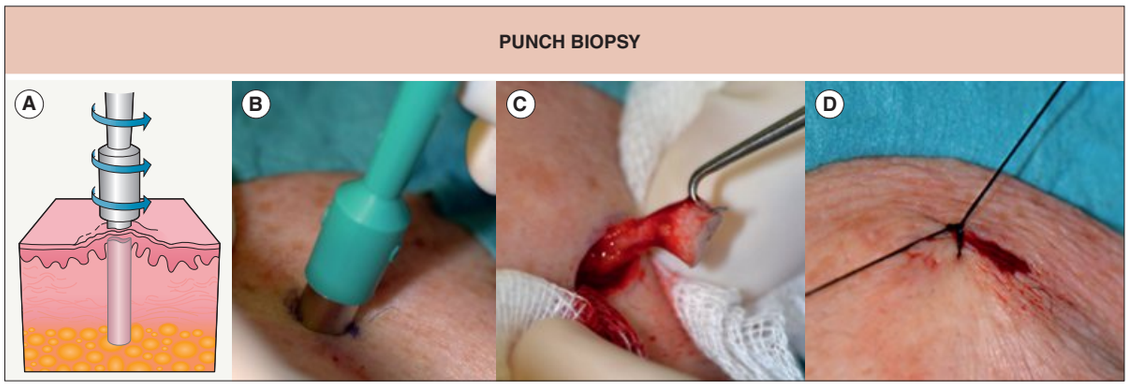


Fig. 146.9 Punch biopsy. A Diagram. **B** Punch biopsy instrument rotated into the skin. **C** The biopsy specimen is gently removed with a skin hook placed peripherally and superficially in order to avoid crush artifact. **D** Closure of the biopsy wound with a simple epidermal suture. *Photographs courtesy Luis Requena, MD.*

SPECIAL CONSIDERATIONS FOR A PUNCH BIOPSY ON THE FACE
• Position patient in a supine position with draping or gauze to protect the eyes from light or inadvertent damage by suture or instrument • Use a 3 mm punch biopsy instrument (if possible); a 4 mm punch biopsy wound can produce standing cones when closed • Choose a site with low visibility (if possible), e.g. in the shadows of the face, at cosmetic unit boundaries, or off/beyond the center of the face • Protect underlying tissue with an anesthetic wheal • Tailor depth of excision to depth of pathology rather than rotating and pushing the punch biopsy instrument to its hub • Control bleeding with suture(s) – simple interrupted sutures of monofilament 5–0 or 6–0 nylon or polypropylene • Protect with bandage and remove sutures at 5–7 days

Table 146.12 Special considerations for a punch biopsy on the face.

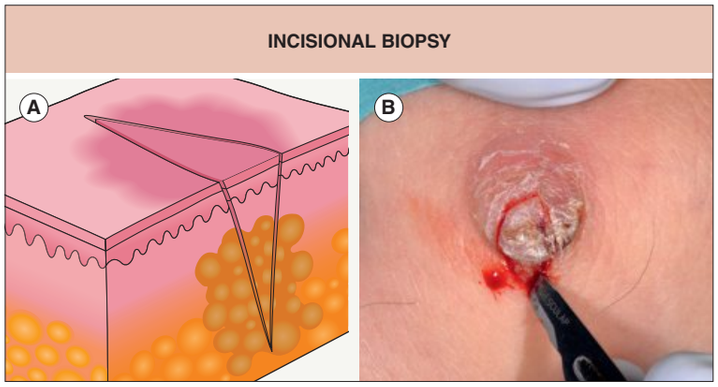


Fig. 146.10 Incisional biopsy. A Diagram. **B** Demonstration of the procedure.

(Fig. 146.10). The specimen may be entirely lesional or may contain an edge of clinically normal skin, which allows comparison of involved versus uninvolved skin as well as examination for any microscopically apparent early changes at the edge of the lesion. The goal is to obtain a wedge of tissue 3–4 mm wide and as deep as necessary. The tissue should be in one piece for accurate orientation of the specimen during preparation; depending upon the possible diagnoses, longitudinal sectioning may be requested. The length of the wedge varies, but should be long enough to avoid cutaneous cone formation in the final closure.

Local anesthesia is obtained by deep and slow infiltration of the agent. It is advisable to wait 10 to 15 minutes after instillation to allow for complete anesthesia and to obtain the maximal vasoconstrictive effect of epinephrine. With a #15 blade (mounted on a blade handle) held perpendicular to the skin surface, a superficial incision into the epidermis scores one long side of the wedge using a light touch and one long motion, facilitated by traction by the non-dominant hand or an assistant. The second long side is then scored similarly. These lines are then redrawn with the blade held in the same manner but with firm pressure, incising into deep tissue, first one side, then the other. The incision is continued until the desired depth has been reached, usually in one or two more cutting movements. The incision is angled toward the center axis so that deep within the tissue, the two incisions meet and complete the separation of the tissue. A forceps is used to lift the tissue out of the wound. If the tissue is still connected at its base, the blade or tissue scissors may be used to complete the detachment.

Hemostasis is best achieved by point electrocoagulation. Large arterioles may require tying off with absorbable suture. An incisional biopsy wound is generally closed with suturing. In some circumstances, such as a site compromised by necrosis or infection, second intention healing may be the best option, even if it is slow and prolonged (see Table 146.8). Deep interrupted sutures of absorbable suture material, 4–0 or 5–0 in caliber, with the knot inverted are utilized to close the subcutis and the dermis (see Fig. 146.4). The epidermis is then closed with simple interrupted sutures of nylon or polypropylene monofilament. The size of the epidermal suture varies depending upon the site; the face is generally closed with 6–0 suture and other sites by 4–0 or 5–0 suture.

EXCISION OF COMMON BENIGN CUTANEOUS LESIONS	
Lesion	**Comments**
Epidermoid inclusion cyst	Dissection facilitated by injection of liberal amount of local anesthesia into surrounding tissue; allows surgeon to work in plane between resulting edema and cyst wall[65] Fusiform excision should include any poral opening or scarring attaching the cyst to the surface Fusiform excision may be smaller than the area deformed by the cyst, but enough of the redundant expanded tissue should be excised so that the scar lies flat
Pilar cyst	See epidermoid inclusion cyst; dissection usually easier
Lipoma	The extent can be appreciated by palpation, then marked with surgical marking pen. A linear incision is made in the middle of the skin covering the lipoma. The tumor is more firm and dense than the surrounding normal subcutaneous fat
Dermatofibroma	Patient needs to be warned that scar may be more noticeable than original lesion, especially on the lower extremities
Melanocytic nevi	See text

Table 146.13 Excision of common benign cutaneous lesions.

Excisional Biopsy (Excision *in toto*)

Excision represents the workhorse of dermatologic surgery[35]. The procedure is designed to remove entire lesions for histopathologic examination as well as for surgical cure. Lesions such as a clinically typical BCC or an unsightly or troublesome subepidermal lesion presumed to be benign are commonly biopsied as well as excised in this fashion (Table 146.13). Atypical pigmented lesions highly suspicious for invasive melanoma are typically excised *in toto* as a biopsy procedure because the degree of atypia and depth of invasion may not be uniform; the excision allows the pathologist to examine the entire lesion and decreases the likelihood of sampling error. In addition, excision is frequently the treatment of choice after the diagnosis of a cutaneous malignancy has been established by a previous biopsy. The excision specimen is again submitted for histologic examination in order to confirm the diagnosis and for comment as to whether the margins of the specimen are clear of tumor. Some surgeons will place a nick or a suture in one edge of the specimen to assist in orientation. Although the basic concepts discussed above with regard to an incisional biopsy also pertain to this procedure, an excision *in toto* is more complicated because it is intended to be the final definitive procedure. Therefore, margins required for cure, as well as cosmetic and functional challenges with respect to the final scar, must be carefully considered in advance.

Recommended margins for removal of an entire lesion depend on the clinical diagnosis. Most benign lesions can be removed completely by including a 1–2 mm margin of normal-appearing skin around the circumference of the tumor. A small, clinically well-demarcated BCC or SCC is generally, though not always, cured with 4–5 mm margins[36,37]. Atypical nevi are frequently excised with 3–4 mm margins. While 4 mm may not be required for complete removal of the lesion, it may save some patients from a second procedure since it is standard practice to re-excise a nevus with severe atypia that is still present at the margins microscopically. The suggested margin for melanoma *in situ* is 5 mm although excision of lentigo maligna may require wider margins. For invasive melanoma, the recommended margin depends on the Breslow depth, e.g. 1 cm margins for tumors ≤1.0 mm in depth (see Ch. 113). The depth of the defect to be created must also be planned in advance[38]. Primary closure is facilitated when the base of the surgical wound lies within subcutaneous fat. In the case of melanomas, the excision should include full-thickness skin and subcutis with fascia often visible at the wound base.

Although an excision is often referred to as an ellipse, the actual shape is fusiform (Fig. 146.11). The optimal geometry of the wound varies depending on the contour of the site and the elasticity and thickness of the skin[39]. The angle at each end of the excision varies from 30 to 75 degrees[40]. In order to minimize standing cone formation, each side of the fusiform shape is three to four times as long as it is

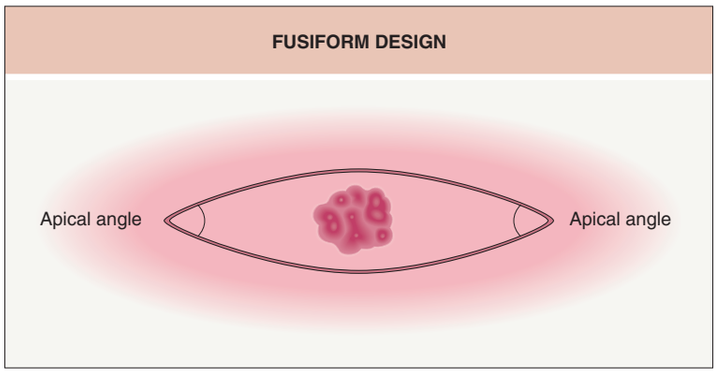


Fig. 146.11 Fusiform design.

wide. The central axis becomes the line of closure and dictates where the surface scar will be visible. A mature scar should appear as a thin line, although some spreading may be seen on the upper trunk and shoulders. From a cosmetic standpoint, an optimal scar results when the line of closure is placed within major skin folds, superficial skin tension lines, wrinkles, or boundaries between distinct cosmetic units (see Ch. 142). Movement of underlying muscles may distort the line of closure, but this can be predicted in advance and the excision plan adjusted. For hair-bearing areas, the line of closure should follow the normal patterns of hair growth.

The process of excision and repair can be divided into a series of steps (Fig. 146.12, Video 146.4). Local anesthesia is best obtained by injection into the subcutaneous tissue. The planned excision, which is delineated with surgical marking dye *prior* to injection, is ringed by the anesthetic agent, with the needle pointed outward to include the area needed for undermining. After ensuring that anesthesia has developed, the site is cleansed and draped with sterile towels or drapes. The excision is begun by stabilizing the site either with the non-dominant hand or by an assistant. As with an incisional biopsy, the epidermis is scored on both sides by drawing lightly with a #15 blade (mounted on a blade handle) along the lines chosen to create the fusiform shape. With continued traction, the incision is completed to the base of the wound by drawing the blade with increased pressure. Unlike with the incisional biopsy, the blade is held vertically throughout the procedure so that the edges of the wound are perpendicular to the skin surface, not angled inward to create a wedge. Completing the incision in one to two strokes after scoring minimizes ragged edges. Care is taken at both apical angles to completely incise to the same depth as that reached at the center of the wound. When the fusiform incision is complete, to either the level of the subcutaneous fat or the fascial plane, the specimen sits up from its base like an island. The specimen is then dissected from the base of the wound using scissors or a blade and the specimen is transferred to the appropriate container. The end result of the excision is a fusiform-shaped wound with vertical sides and a flat even base consisting of subcutaneous fat or fascia. Hemostasis is achieved by electrocoagulation.

The remainder of the procedure deals with the creation of a cosmetically acceptable and functional closure. In order to free tissue for movement into the wound, undermining is performed at the edges of the wound with either scissors or a scalpel. A favorite technique is to use scissors with rounded tips for insertion and then spreading of the tissue to produce blunt dissection in the plane of undermining, a procedure advocated because of the belief that it is less likely to cut arteries or nerves. Using the same scissors, but with a snipping or cutting motion to sharply dissect, is also safe and more effective in generating a smooth, less ragged unit of skin[41]. Sometimes, the two techniques are combined, with spreading followed by snipping of the intervening tethering strands. Undermining can also be done with a blade, sweeping horizontally from the depth of the wound into the surrounding tissues. Regardless of the technique chosen, good exposure and visualization is achieved by maintaining adequate hemostasis as the dissection proceeds, with undermining done in a controlled fashion. Tactile confirmation of the position of the tips of the scissors is also helpful.

In order to fill the defect with skin that matches with regard to thickness, the level of undermining is almost always at the same depth as the base of the wound, i.e. within the subcutaneous fat or at the fascial plane. Rarely, when there are superficially located arteries and nerves to be avoided, the plane of undermining is more superficial than the base of the wound. The use of curved scissors with the tips pointed upwards may facilitate staying in the appropriate plane.

The goals of undermining are to mobilize a unit of skin to be moved into the defect[42] in order to reduce wound closure tension[43], to allow proper wound edge eversion[44], and to provide a wide area for distribution of redundant tissue over the base of the wound (see Fig. 147.1). Undermining around the entire wound to a distance that is at least the diameter of the wound may be required to meet these goals. When little undermining is done, apposed wound edges are pulled inward and redundant tissue bunches up in the wound bed. This redundant tissue has a force and mass that may apply pressure to the healing wound and produce a wide atrophic scar (Fig. 146.13). During closure, wide undermining disperses the redundant tissue over a large area of wound bed. It may also serve to create a plate-like horizontal scar that distributes the forces of contraction and stabilizes the final result (see Fig. 147.2). Undermining must include the apical angles, where it facilitates the rotation that occurs as the two sides of the fusiform shape are brought together. The adequacy of the width of undermining can be tested either by picking up both wound edges with toothed forceps or skin hooks and opposing them or by placing a large temporary suture. The temporary suture may also supply some intraoperative tissue expansion that will facilitate closure. Braided polyester (e.g. Ethibond®) suture is commonly used for this purpose since it is soft and will not cut through tissue. If, with these tests, the wound edges cannot be draped easily for closure, undermining can be extended.

Once undermining is adequate and after again ensuring that the wound is dry, subcutaneous and epidermal sutures are placed to complete the closure. As with the incisional biopsy, deep interrupted sutures of absorbable suture material (4–0 or 5–0 in caliber, with the knot inverted) close the subcutis and the dermis. If the wound is thick or under tension, optimal closure may entail two layers of subcutaneous sutures. The epidermis is then closed with simple interrupted or running sutures with a smaller caliber. For a fusiform excision *in toto*, the end result of the procedure is a straight or curved line of closure that has the wound edges completely apposed and everted. The line of closure sits above the surrounding skin, sometimes described as having the appearance of the ridge line of a tent or a mountain range. The healing of a tensionless everted wound edge results in a flat, hairline scar.

Cutaneous Cone (Dog-Ear) Repair

Closure of a fusiform excision may create cutaneous cones, i.e. tissue redundancies that distort the normal contour of the skin at the apical angles[45]. These cutaneous cones are also referred to as "dog-ears" and may consist of standing cones, lying cones, inverted cones, or protruding cones. Inverted cones can be the most difficult to diagnose, as the appearance is that of a subtle dimple rather than a protrusion. Regardless of their subtle nature, these redundancies will distort the final scar unless they are repaired. Cutaneous cones are also produced by tissue movement during flap closures.

Standing cones primarily result from geometric factors (Fig. 146.14). They may appear in closures of fusiform excisions (with sides of equal length) when the sides are of insufficient length compared to the width of the excision. The resulting apical angles are too wide to rotate in and maintain a flat contour to the skin surface. For this reason, linear closure of a circle, an oval, or an ellipse will always create standing cones. Also, cutaneous cones always form during closure of fusiform shapes that have sides of unequal length; redundant tissue becomes apparent on the longer side. Notably, when an excision is performed on a convex surface, standing cones may occur despite seemingly small apical angles. With suture placement, collagen bundles are pulled together and act as rigid rods that will not lie flat on a curved surface.

In addition to geometric forces, protrusions are produced when there is excessive subcutaneous tissue in the base of the wound at the apices (as compared to the center of the wound). A lack of adequate undermining at the apices will then magnify these protrusions. This process is usually called "boating" or "pseudo dog-ear" formation. It is important to distinguish boating from true standing cone formation because repair

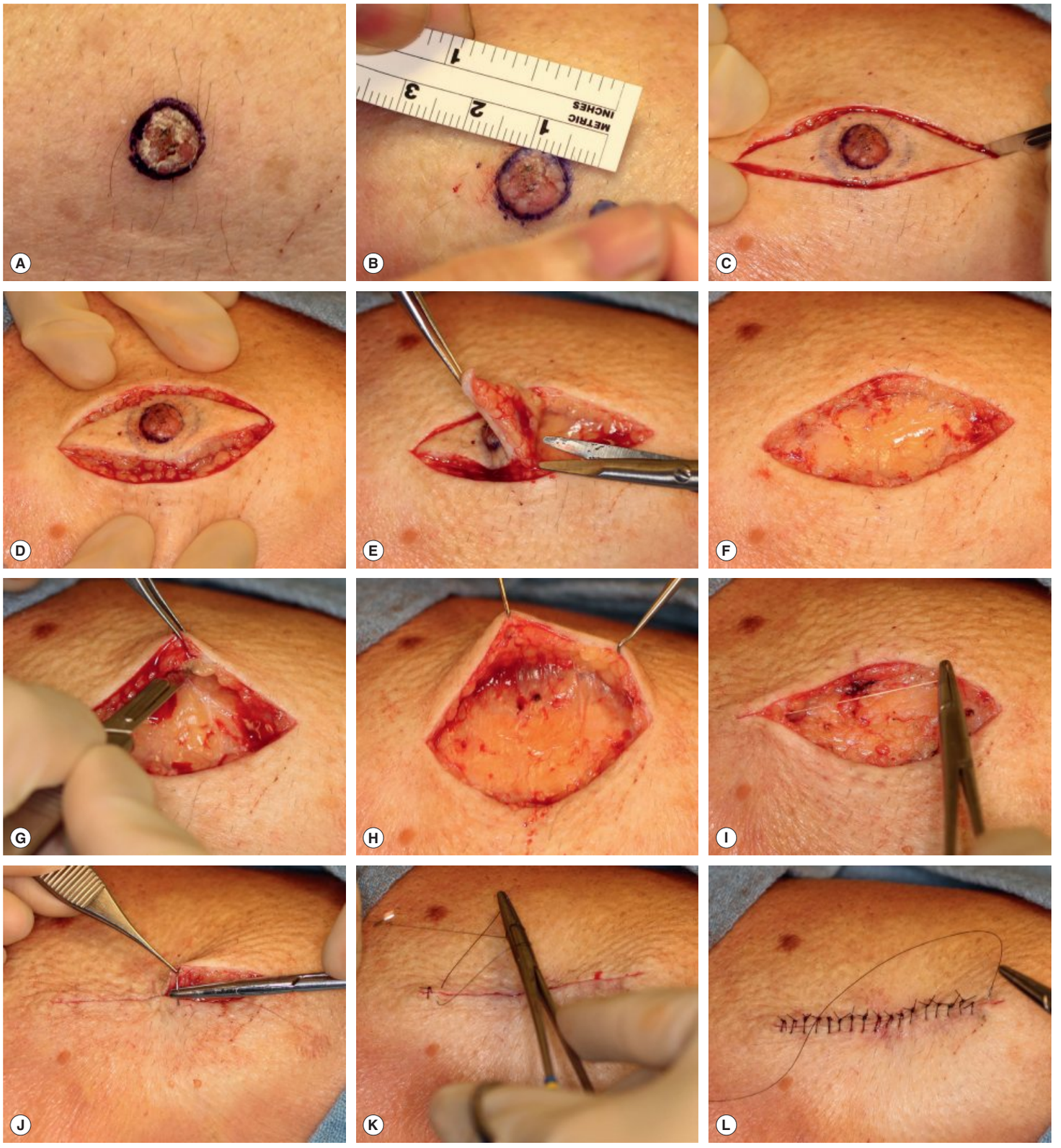


Fig. 146.12 Fusiform excision of a squamous cell carcinoma. A,B After the lesion and appropriate margins are marked, the site is anesthetized, prepped with an antiseptic agent, and draped with sterile towels. **C** Stabilizing the site with traction, the epidermis on one side of the fusiform design is scored using a #15 blade and then the opposite side is scored. **D** The incision is completed into the appropriate plane in the subcutaneous tissue and the specimen then sits up in the middle of the wound like an island. **E,F** The base of the specimen is dissected with scissors or a blade. **G,H** The wound edges are then undermined in the same plane as the base of the wound with blunt-tipped scissors or a blade. Electrodesiccation or electrocoagulation is used to address small actively bleeding vessels to achieve hemostasis. **I,J** The subepidermal space is closed with buried sutures. **K,L** The epidermal edges are apposed by simple interrupted sutures.

of the former requires removal of the excess subcutaneous tissue and appropriate undermining as opposed to the techniques described below.

Many standing cones are small and can be repaired via a closure that employs the rule of halves (Fig. 146.15). The midpoint of each side is apposed with a suture, bisecting the wound. Each unclosed half is then bisected again and the closure is continued until all tissue has been apposed. For a fusiform shape with unequal sides, repair of standing cones in this manner produces a curved line of closure. The curvature is directly proportional to the size of the dog-ear. If the wound is in a site such as the forehead, which lacks loose tissue to free up and mobilize,

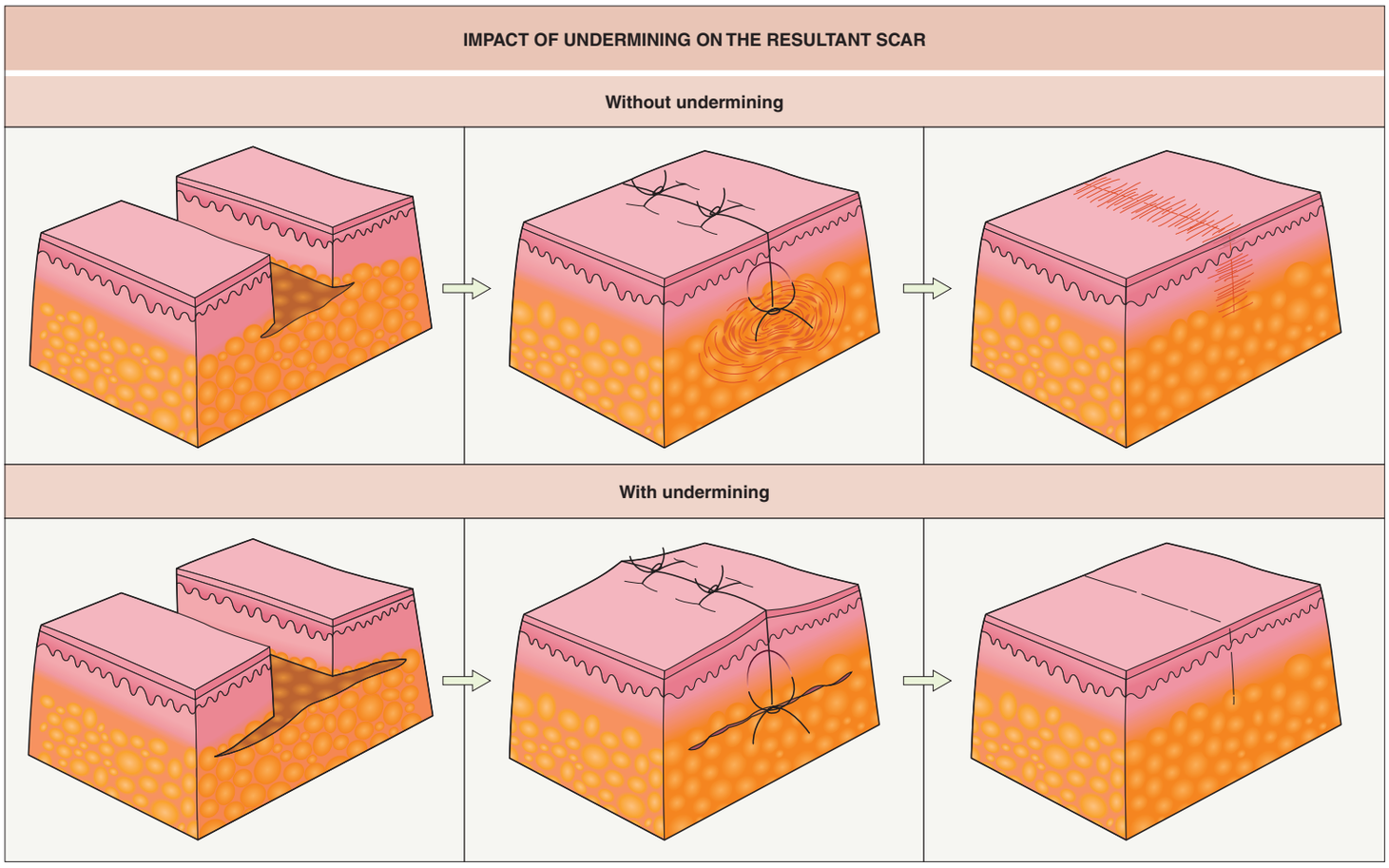


Fig. 146.13 Impact of undermining on the resultant scar. Without undermining, there is tension on the wound and eversion of the wound edges does not occur. Another consequence is spreading of the scar.

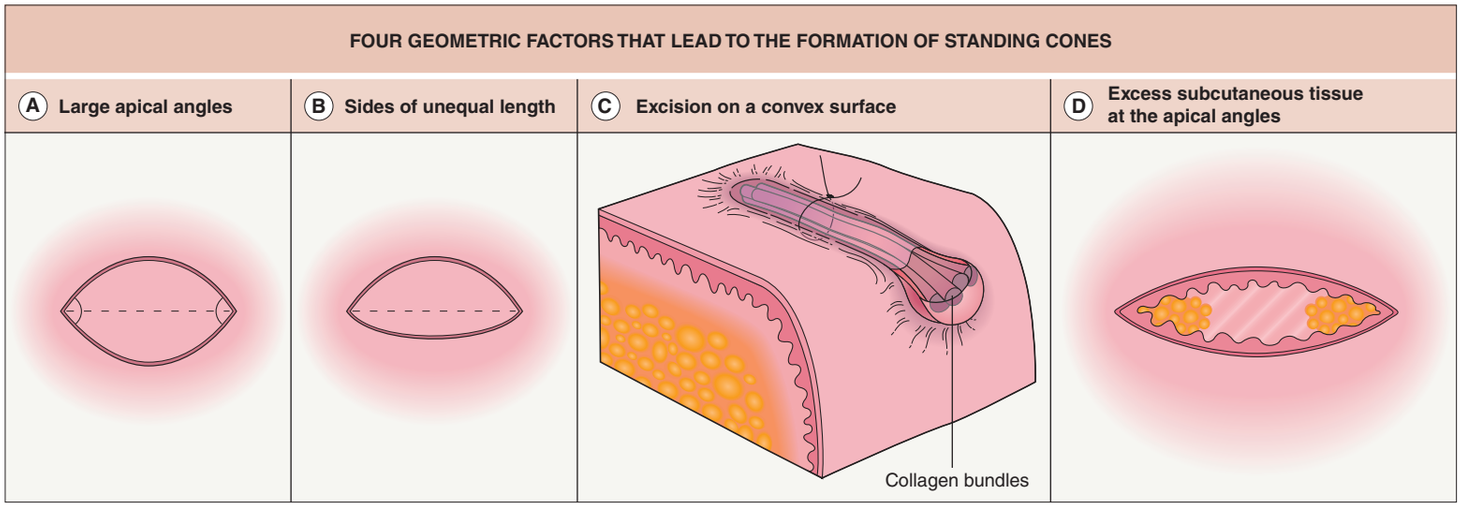


Fig. 146.14 Four geometric factors that lead to the formation of standing cones.

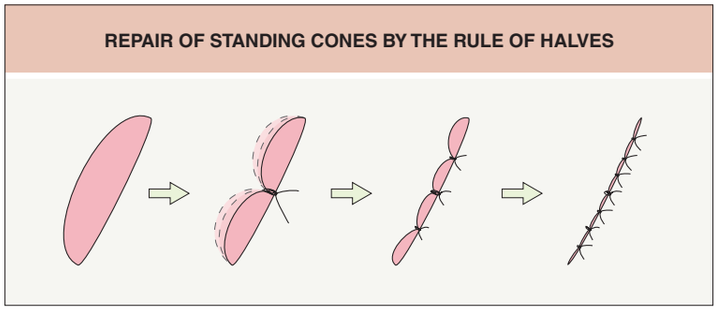


Fig. 146.15 Repair of standing cones by the rule of halves.

the line of closure may remain straight; however, there will be noticeable gathering on one side of the line and a depressed contour on the opposite side of the line where the skin is thinned as it was stretched to fit.

Simple straight, curvilinear, or angled excisions of standing cones will also restore the desired contour of the site, even though they lengthen the scar (Fig. 146.16). The first step is to close the center portion of the wound with subcutaneous sutures. It is helpful to continue to appose subcutaneous tissue from the center of the wound outward until the standing cones become visible. Epidermal sutures may also need to be placed since any gaping at the center of the wound will underestimate the size of the dog-ears. After undermining, one limb of the standing cone is cut through to the base of the wound along the line that is desired for final closure. Undermining is repeated until the

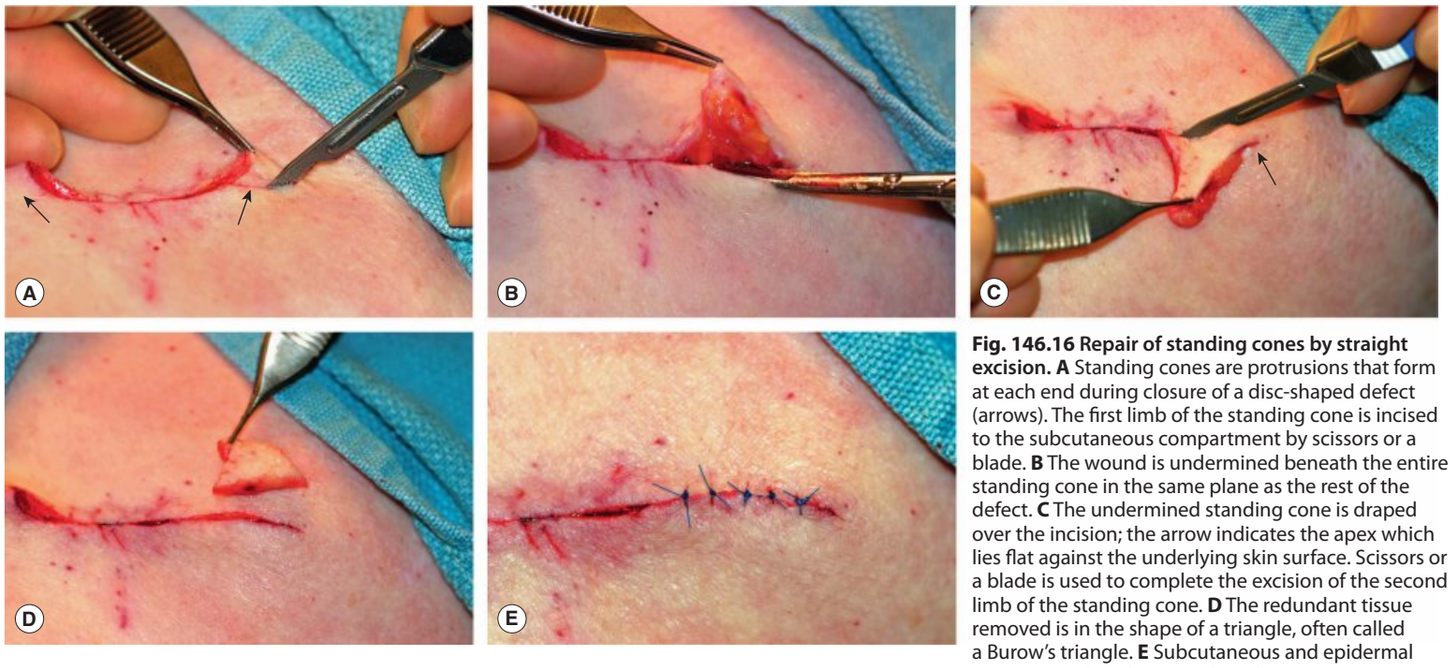


Fig. 146.16 Repair of standing cones by straight excision. A Standing cones are protrusions that form at each end during closure of a disc-shaped defect (arrows). The first limb of the standing cone is incised to the subcutaneous compartment by scissors or a blade. **B** The wound is undermined beneath the entire standing cone in the same plane as the rest of the defect. **C** The undermined standing cone is draped over the incision; the arrow indicates the apex which lies flat against the underlying skin surface. Scissors or a blade is used to complete the excision of the second limb of the standing cone. **D** The redundant tissue removed is in the shape of a triangle, often called a Burow's triangle. **E** Subcutaneous and epidermal sutures are placed to complete the closure.

excess tissue can be draped over the cut edge. The new apical angle will lie flat if the limb has been adequately cut and if undermining has been sufficient. The second limb of the standing cone is then addressed by cutting from the wound to the new apical angle. The excess tissue that is removed will be in the shape of a triangle that is referred to as a Burow's triangle[46]. An alternative method, helpful for novices wanting to create a straight line closure, is bisection of the standing cone, laying each half out along the skin surface and then cutting the two triangles of excess tissue. Closure is then completed with subcutaneous and epidermal sutures.

An *M-plasty* is a dog-ear repair that shortens the total scar length (Fig. 146.17). Depending upon the site, M-plasty scars may also fit within prominent lines and folds more accurately. This procedure is particularly helpful in sites that are not flat. The first step, as above, is to close the center portion of the wound and adequately undermine the apical angle. *Both* lateral limbs are cut at an obtuse angle from the end of the wound to about halfway toward the apex of the redundancy. The excess tissue is then draped over the cut edge and an M is now apparent. Cutting from the central tip to the two new apical angles removes two pieces of tissue that are also triangular in shape. The area of these two triangles is equal to the area of the single triangle that would have been removed if a simple excision of the standing cone had been performed. Once the central tip lies in a good position, then a standard closure is performed. If the tip needs to be advanced to approximate the wound edges and fill the defect, a *half-buried horizontal mattress suture* (also called a *tip stitch* or *three-corner stitch*) is used (see Fig. 146.17E). Care must be taken with the three-corner stitch, as necrosis of the tip can occur with too much tension.

A dog-ear may also be displaced to a distant site. After closure of the central portion of the wound, an incision is made perpendicular to the dog-ear to an appropriate site where there is enough redundant tissue such that it can be removed as a triangle (Fig. 146.18). Undermining is required over a wide area so that tissue can be moved without tension. This procedure is also referred to as a Burow's advancement flap (see Ch. 147). It is commonly used to avoid dog-ear repair in a free margin or in a cosmetically or functionally sensitive area.

Finessing closure of fusiform excisions may require changing the axis of the line of closure so that the scar blends better with the prominent lines and folds of the site. Changing the axis will produce dog-ears that can be repaired by any of these methods.

VARIATIONS/UNUSUAL SITUATIONS

A *disc excision* (with straight or angled edges) may be performed either for biopsy purposes or for biopsy and definitive treatment. This option is chosen when healing by second intention is preferred[47] or when it is desirable to remove the tumor first and then repair the dog-ears during the closure. Second intention healing may be advantageous when the risk of adverse reactions with primary closure is high. For example, excisions of even small tumors on the anterior lower leg that are closed primarily can produce wounds with tension and wounds that are more likely than those at other sites to dehisce, become infected, or be painful. This is especially true if undermining is inadequate and weight-bearing and limb dependency is not minimized for the first 5–7 postoperative days.

Another option for wounds with too much tension on the anterior lower leg is the placement of a skin graft, but postoperative care requires leg elevation and the absolute avoidance of weight-bearing. Alternatively, the wound can be closed, either partially or completely, with a *purse-string suture*[48,49]. The latter is a running suture that is placed around the entire perimeter of the disc. After its placement, tension is applied to the ends of the suture until maximum constriction is obtained and then the ends are knotted. Advantages of the pursestring suture are speed, distribution of tension circumferentially, and amelioration of the need for the removal of excess normal skin in order to complete a fusiform excision. Since the time for complete re-epithelialization of a wound undergoing second intention healing is related to the diameter of the largest circle that can be drawn within the wound, even closure of a wound by 30% can result in a significant reduction in healing time. This smaller wound can also be grafted if desired.

When wounds heal by second intention, postoperative care is less burdensome, as the patient may resume normal activities almost immediately while dressing and bandaging the wound daily. However, compared to a linear excision, re-epithelialization requires a significantly longer period of time; the latter varies directly with the size of the wound and can range from 2 weeks to several months on the distal lower extremities. The patient also needs to consider the resultant scar, i.e. a depressed circular scar versus a graft versus a linear scar.

Removal of melanocytic nevi on the upper trunk and shoulders via disc excision or saucerization (angled edges) results in a smaller, often more cosmetically acceptable scar than does a fusiform excision. Also, the excision of tumors in sites such as the ear may be amenable to disc excision followed by second intention healing.

Performing a disc excision and then repairing the dog-ears during the closure allows the surgeon to pay particular attention to the issue of appropriate curative margins without dealing simultaneously with the cosmetic and functional issues of the closure. Once the tumor has been removed and the area widely undermined, the line of closure can be determined, that is, the closure with the least amount of tension that fits into the dominant lines of the site[50,51]. The central portion of the

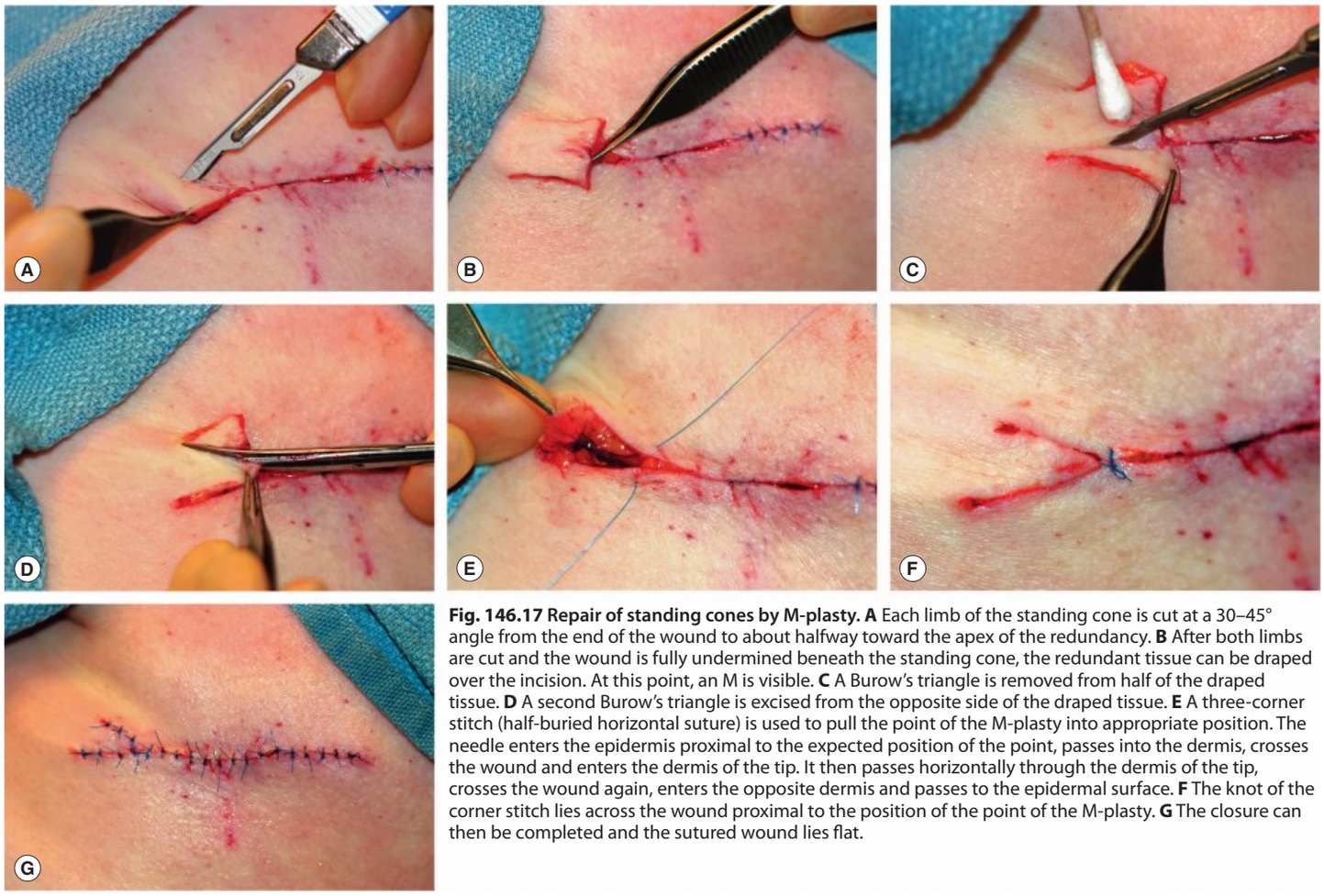


Fig. 146.17 Repair of standing cones by M-plasty. A Each limb of the standing cone is cut at a 30–45° angle from the end of the wound to about halfway toward the apex of the redundancy. **B** After both limbs are cut and the wound is fully undermined beneath the standing cone, the redundant tissue can be draped over the incision. At this point, an M is visible. **C** A Burow's triangle is removed from half of the draped tissue. **D** A second Burow's triangle is excised from the opposite side of the draped tissue. **E** A three-corner stitch (half-buried horizontal suture) is used to pull the point of the M-plasty into appropriate position. The needle enters the epidermis proximal to the expected position of the point, passes into the dermis, crosses the wound and enters the dermis of the tip. It then passes horizontally through the dermis of the tip, crosses the wound again, enters the opposite dermis and passes to the epidermal surface. **F** The knot of the corner stitch lies across the wound proximal to the position of the point of the M-plasty. **G** The closure can then be completed and the sutured wound lies flat.

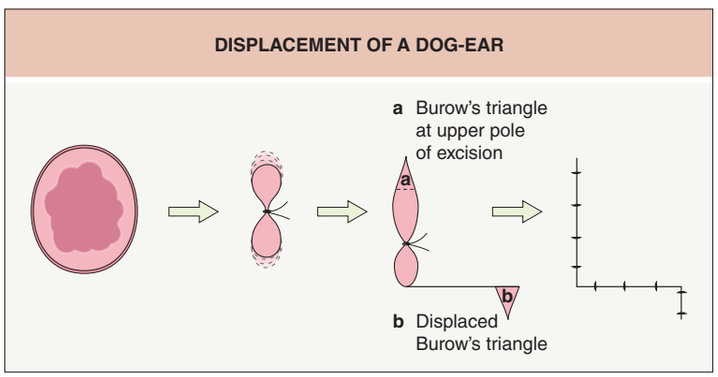


Fig. 146.18 Displacement of a dog-ear.

wound is apposed by subcutaneous and epidermal sutures or by a large simple interrupted temporary suture and then the dog-ears are repaired. Since the cosmetic and functional issues are addressed after excision of the tumor and undermining, the resulting scar can be optimized.

The shape of the excision can also be modified via a procedure known as an *S-plasty*[52]. Most useful on convex surfaces, this variation increases the total length of the scar while keeping the linear distance between the two apices constant. In a simple fusiform excision, the tension is located primarily in the center of the wound and is exerted along a single vector that is perpendicular to the axis of the wound. On the other hand, an S-plasty redirects and redistributes tension into multiple vectors along the wound, thereby minimizing tension in the center of the wound; in addition, the central tension vector is perpendicular to the primary tension vectors at the apices of the wound. Because much of the tension is displaced from the area of maximal convexity, the likelihood of a central depression or dehiscence is reduced.

POSTOPERATIVE CARE

Wound care and bandaging both play an important role in minimizing the risk of complications and in obtaining optimal cosmetic and functional results. Wound care removes surface debris and promotes re-epithelialization. A good bandage supports and stabilizes the wound in the closed position, wicks away excessive blood or tissue fluid, supplies pressure to the wound for hemostasis, and protects the wound from the dryness and bacterial contamination of the external environment.

A small shallow wound that is to heal by second intention is cared for by daily cleansing of the site with mild soap and water, application of petrolatum[53], and coverage with an adhesive bandage such as a Band-Aid® (with a central non-adherent area). There is little to no evidence that topical antibiotic ointments are better than petrolatum. In addition, bacitracin and Neosporin® (bacitracin, polymyxin B +/– neomycin) ointments are associated with a substantial risk of developing contact dermatitis. Topical mupirocin is also not recommended because of the high prevalence of antibiotic resistance[54]. A liquid adhesive bandage was reported to be effective as well as easy to use[55] in a trial focusing on minor cuts and abrasions. A large shallow wound that is to close by second intention may need a bandage fashioned specifically for that site, usually consisting of layers composed of petrolatum, Telfa®, gauze or cotton, and then tape or other means of adhering the bandage at the site.

A layered bandage is also required for a sutured wound. A liquid adhesive (e.g. Mastisol®) is applied to the skin surface surrounding the sutures. Petrolatum is applied in a thin line onto the wound edge. Sterile tapes such as Steri-Strips™ may be placed perpendicular to the line of closure. The final layer is rolled gauze or cotton, which is then taped in place with paper tape, Scanpor® tape, Kind Removal® Silicone Tape, or Hy-Tape® ("pink" tape). Elastic dressing (e.g. Coban®) can be used for compression, but should be released and reapplied if it is used circumferentially, so that vascular compromise distally does not occur.

Patients need oral and written instructions regarding the care the wound will require at home. Most simple wounds are cleansed daily with soap and water and redressed until the sutures are removed or the wound has completely re-epithelialized. Patients should understand that they need to remove any crusting or debris from the wound as they cleanse it and they may prefer to use cotton-tipped swabs or gauze. Instructions regarding bandages should likewise be clear. Leaving the wound open to the air or allowing it to become dry retards re-epithelialization and may compromise the final appearance or the scar[56].

Bandages that minimize the need for wound care are preferred by many patients. In addition, the stability and protection afforded by a bandage that stays in place for a week or more may further optimize the results, especially for wounds closed primarily. These bandages may be constructed in layers as discussed above and should be kept dry to prevent maceration of the covered skin. On the trunk and extremities, a bandage can be made of a polyurethane foam dressing (e.g. Cutinova Hydro®) covered by a water repellent film (e.g. Bioclusive®), precluding the need for any care and allowing ease of movement and a normal regimen for bathing.

Once the sutures have been removed and the wound cleaned, the use of liquid adhesive and sterile tapes for another week or two further stabilizes the wound. Many specialized bandaging systems are available for complicated wounds (see Ch. 145).

SHORT-TERM AND LONG-TERM COMPLICATIONS OF BIOPSY PROCEDURES AND EXCISIONS
Short-term complications
• Irritant or allergic contact dermatitis to topical antibiotics and/or tapes and bandages • Hemorrhage • Poor wound healing; dehiscence of closed wounds • Pain • Infection • Pruritus, paresthesias
Long-term complications
• Atrophic scars (thin, depressed, spread) • Hypertrophic scars (red, thickened) • Keloids • Distortion of normal structures (e.g. ectropion, elevated nasal ala, notching of the lip or helix of the ear) • Hyper- or hypopigmentation • Hypoesthesia, anesthesia • Paralysis (e.g. due to injury to facial nerve branches)

Table 146.14 Short-term and long-term complications of biopsy procedures and excisions.

COMPLICATIONS

Short-term complications of biopsies and excisions are few in number and engender limited morbidity (Table 146.14)[57]. In addition, the smaller the procedure, the fewer the complications, which explains why shave biopsies and snip biopsies are quite safe. Bleeding is the most common complication and may occur from the time of the procedure to after the patient has returned home, but usually within the first 24 hours. Taking care to achieve hemostasis during the procedure minimizes adverse bleeding events even for patients taking anticoagulants and antiplatelet medications[58].

Infection occurs rarely, i.e. in <1% of most procedures[59], in contrast to the development of irritant or allergic contact dermatitis which is more common. The latter is usually due to adhesives and less often topical antibiotics (see above)[60]. Dermatitis can frequently be managed with a change in the wound care regimen but if there are significant symptoms or risk of postinflammatory hyperpigmentation, topical corticosteroids may be applied. Biopsies performed on the lower limbs, limbs affected by lymphedema, intertriginous areas, and ears are most susceptible to infections. If an infection develops, culture and oral antibiotics may be required.

Pain is generally minimal. When it occurs 3–5 days after the procedure, infection is the most likely cause, even in the absence of erythema, tenderness, and purulence. Very rarely, paresthesias may result and can persist for several months, especially on the forehead and scalp. Wounds that are closed primarily may dehisce because of tension, hematoma formation, poor wound healing, or infection. These wounds are thereafter managed for second intention healing and a delayed reconstruction can be undertaken, if needed, once the attendant inflammation has resolved.

Long-term complications (see Table 146.14) generally consist of functionally or cosmetically adverse scarring[61]. Depressed scars may occur if not enough subcutaneous tissue is brought into the line of closure. Atrophic and widened scars occur in areas where there is intermittent stretching of the scar as it overlies major muscle groups. Careful surgical technique that includes adequate undermining, minimization of tension at the line of closure, and the use of multiple subcutaneous sutures can reduce the likelihood of this complication.

Scars may pursue a prolonged course of healing with erythematous thickening at the line of closure. These hypertrophic scars do resolve with time. To speed their resolution, practitioners often advise massage or inject triamcinolone acetonide (10–40 mg/ml) into the scars. Silicone dressings are also recommended, but they are probably no more effective than non-silicone gel dressings[62]. In addition, scars may have a fragile surface (due to reduced dermal–epidermal attachments), pruritus, or paresthesias, most of which resolve with time.

A true keloidal scar is one that grows beyond the boundaries of the original surgical injury and appears as a thickened erythematous or hyperpigmented nodule or plaque (see Ch. 98). It occurs in predisposed individuals who may have a history of previous keloid formation. Keloidal scarring is most commonly observed when procedures are performed on the upper trunk and shoulders and may be very difficult to treat.

FUTURE TRENDS

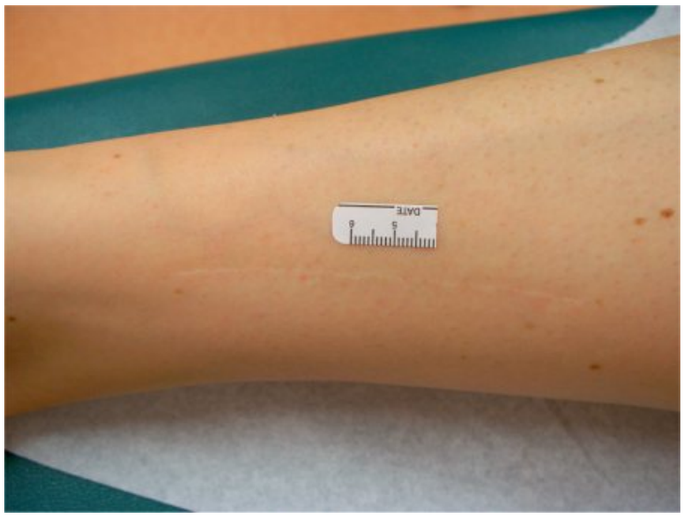
For the foreseeable future, histologic examination of tissue specimens will remain the mainstay of dermatologic diagnostic testing. Excisions likewise will be frequently utilized, both to remove a specimen for diagnosis as well as to clear pathologic tissue completely. Hopefully, in the future, there will be improved means of anesthesia[63] and improved wound care with the development of affordable agents that speed healing and minimize scarring. Advances in dermoscopy, confocal laser microscopy, and ultrasound allow visualization of microscopic tissue architecture and cellular detail *in vitro*, but for diagnostic purposes, this technology has not replaced standard biopsy techniques. However, they may direct site selection for biopsies, improving diagnostic accuracy.

Additional figure available in our eBook (see inside front cover for access code).

REFERENCES

1. Doolan BJ, Robinson AJ, Wolfe R, et al. Accuracy of partial biopsies in the management of cutaneous melanoma. *Australas J Dermatol*. 2019;60:209–213.
2. Messingham MJ, Arpey CJ. Update on the use of antibiotics in cutaneous surgery. *Dermatol Surg*. 2005;31:1068–1078.
3. Wilson W, Taubert KA, Gewitz M, et al. Prevention of infective endocarditis: guidelines from the American Heart Association. *Circulation*. 2007;116:1736–1754.
4. Meyer GW, Artis AL. Antibiotic prophylaxis for orthopedic prostheses and GI procedures: report of a survey. *Am J Gastroenterol*. 1997;92:989–991.
5. McMurray CL, Hardy KJ, Verlander NQ, Hawkey PM. Antibiotic surgical prophylaxis increases nasal carriage of antibiotic resistant staphylococci. *J Med Microbiol*. 2015;64:1489–1495.
6. Classen DC, Evans RS, Pestotnik SL, et al. The timing of prophylactic administration of antibiotics and the risk of surgical wound infection. *N Engl J Med*. 1992;326:281–286.
7. Bode LGM, Kluytmans AJW, Wertheim HFL, et al. Preventing surgical-site infections in nasal carriers of Staphylococcus aureus. *N Engl J Med*. 2010;362:9–17.
8. McGuinness JL, Goldstein G. The value of preoperative biopsy site photography for identifying cutaneous lesions. *Dermatol Surg*. 2010;36:194–197.
9. Alam M, Lee A, Ibrahimi OA, et al. A multistep approach to improving biopsy site identification in dermatology: physician, staff and patient roles based on Delphi consensus. *JAMA Dermatol*. 2014;150:550–558.
10. Darouiche RA, Wall MJ, Itani KMF, et al. Chlorhexidine-alcohol versus povidone-iodine for surgical site antisepsis. *N Engl J Med*. 2010;362:18–26.

11. Lui S, Carpenter RL, Chiu AA, et al. Epinephrine prolongs duration of subcutaneous infiltration of local anesthesia in a dose related manner. *Reg Anesth*. 1995;20:378–384.
12. Baum CL, Arpey CJ. Normal cutaneous wound healing: clinical correlation with cellular and molecular events. *Dermatol Surg*. 2005;31:674–686.
13. Perry AW, McShane RH. Fine tuning of the skin edges in the closure of surgical wounds: controlling inversion and eversion with the path of the needle. *J Dermatol Surg Oncol*. 1981;7:471–476.
14. Miller CJ, Antunes MB, Sobanko JF. Surgical technique for optimal outcomes: Part II. Repairing tissue: suturing. *J Am Acad Dermatol*. 2015;72:389–402.
15. Annunziata CC, Drake DB, Woods JA, et al. Technical considerations in knot construction. *J Emerg Med*. 1997;15:351–356.
16. Zitelli JA, Moy RL. Buried vertical mattress suture. *J Dermatol Surg Oncol*. 1989;15:17–19.
17. Krunic AL, Weitzul S, Taylor RS. Running combined simple and vertical mattress suture: a rapid skin-everting stitch. *Dermatol Surg*. 2005;31:325–329.
18. Wong NL. Review of continuous sutures in dermatology surgery. *J Dermatol Surg Oncol*. 1993;19:923–931.
19. Yang S, Ozog D. Comparison of traditional superficial cutaneous sutures versus adhesive strips in layered dermatologic closures on the back—a prospective, randomized, split-scar study. *Dermatol Surg*. 2015;41:1257–1263.
20. Custis T, Armstrong AW, King TH, et al. Effect of adhesive strips and dermal sutures vs dermal sutures only on wound closure: a randomized clinical trial. *JAMA Dermatol*. 2015;151:862–867.
21. Hodges JM. Management of facial lacerations. *South Med J*. 1976;69:1413–1418.
22. Kamegaya Y, Farinelli WA, Vila Echague AV, et al. Evaluation of photochemical tissue bonding for closure of skin incisions and excisions. *Lasers Surg Med*. 2005;37:264–270.
23. Biancari F, Tiozzo V. Staples versus sutures for closing leg wounds after vein graft harvesting for coronary artery bypass surgery. *Cochrane Database Syst Rev*. 2010(5):CD008057.
24. Coulthard P, Esposito M, Worthington HV, et al. Tissue adhesives for closure of surgical incisions. *Cochrane Database Syst Rev*. 2010(5):CD004287.
25. Dumville JC, Coulthard P, Worthington HV, et al. Tissue adhesives for closure of surgical incisions. *Cochrane Database Syst Rev*. 2014(11):CD004287.
26. Hautz T, Zelger BG, Weissenbacher A, et al. Standardizing skin biopsy sampling to assess rejection in vascularized composite allotransplantation. *Clin Transplant*. 2013;27:E81–E90.
27. Lauria G, Hsieh ST, Johansson O, et al. European Federation of Neurological Societies/Peripheral Nerve Society Guideline on the use of skin biopsy in the diagnosis of small fiber neuropathy. Report of a joint task force of the European Federation of Neurological Societies and the Peripheral Nerve Society. *Eur J Neurol*. 2010;17:903–912.
28. Rozenbaum D, Tung J, Xue Y, et al. Skin biopsy in the diagnosis of intravascular lymphoma: a retrospective diagnostic accuracy study. *J Am Acad Dermatol*. 2021;85:665–670.
29. Baldwin HE, Berck CM, Lynfield YL. Subcutaneous nodules of the scalp: preoperative management. *J Am Acad Dermatol*. 1991;25:819–830.
30. Chang TW, Arpey CJ, Baum CL, et al. Complications with new oral anticoagulants dabigatran and rivaroxaban in cutaneous surgery. *Dermatol Surg*. 2015;41:784–793.
31. Chang LK, Whitaker DC. The impact of herbal medicines on dermatologic surgery. *Dermatol Surg*. 2001;27:759–763.
32. Li JN, Nijhawan RI, Srivastava D. Cutaneous surgery in patients who are pregnant or breastfeeding. *Dermatol Clin*. 2019;37:307–317.
33. Harvey DT, Fenske NA. The razor blade biopsy technique. *Dermatol Surg*. 1995;21:345–347.
34. Todd P, Garioch JJ, Humphreys S, et al. Evaluation of the 2-mm punch biopsy in dermatological diagnosis. *Clin Exp Dermatol*. 1996;21:11–13.
35. Dunlavey E, Leshin B. The simple excision. *Dermatol Clin*. 1998;16:49–64.
36. Wolf DJ, Zitelli JA. Surgical margins for basal cell carcinoma. *Arch Dermatol*. 1987;123:340–344.
37. Brodland DG, Zitelli JA. Surgical margins for excision of primary cutaneous squamous cell carcinoma. *J Am Acad Dermatol*. 1992;27:241–248.
38. Takenouchi T, Nomoto S, Ito M. Factors influencing the linear depth of invasion of primary basal cell carcinoma. *Dermatol Surg*. 2001;27:393–396.
39. Chretien-Marquet B, Caillou V, Brasnu DN, et al. Description of cutaneous excision and suture using a mathematical model. *Plast Reconstr Surg*. 1999;103:145–150.
40. Moody BR, McCarthy JE, Sengelmann RD. The apical angle: a mathematical analysis of the ellipse. *Dermatol Surg*. 2001;27:61–63.
41. Boyer JD, Zitelli JA, Brodland DG. Undermining in cutaneous surgery. *Dermatol Surg*. 2001;27:75–78.
42. Mackay DR, Saggers GC, Kotwal N, et al. Stretching skin: undermining is more important than intraoperative tissue expansion. *Plast Reconstr Surg*. 1990;86:722–730.
43. McGuire MF. Studies of the excisional wound: I. Biomechanical effects of undermining and wound orientation on closing tension and work. *Plast Reconstr Surg*. 1980;66:419–427.
44. Zitelli JA. Tips for a better ellipse. *J Am Acad Dermatol*. 1990;22:101–103.
45. Gormley DE. The dog-ear: causes, prevention, and correction. *J Dermatol Surg Oncol*. 1977;3:194–198.
46. Gormley DE. A brief analysis of the Burow's wedge/triangle principle. *J Dermatol Surg Oncol*. 1985;11:121–123.
47. Zitelli JA. Wound healing by secondary intention. A cosmetic appraisal. *J Am Acad Dermatol*. 1983;9:407–415.
48. Harrington AC, Montemarano A, Welch M, et al. Variations of the pursestring suture in skin cancer reconstruction. *Dermatol Surg*. 1999;25:277–281.
49. Romiti R, Randle HW. Complete closure by purse-string suture. *Dermatol Surg*. 2002;28:1070–1072.
50. Davis TS. The circular excision. *Ann Plast Surg*. 1980;4:21–25.
51. Spicer TE. Techniques of facial lesion excision and closure. *J Dermatol Surg Oncol*. 1982;8:551–556.
52. Paolo B, Stefania R, Massimiliano C, et al. Modified S-plasty: an alternative to the elliptical excision to reduce the length of suture. *Dermatol Surg*. 2003;29:394–398.
53. Czarnowicki T, Malajian D, Khattri S, et al. Petrolatum: barrier repair and antimicrobial responses underlying this "inert" moisturizer. *J Allergy Clin Immunol*. 2016;137:1091–1102. e1–7.
54. Dadashi M, Hajikhani B, Darban-Sarokhalil D, et al. Mupirocin resistance in *Staphylococcus aureus*: a systemic review and meta-analysis. *J Glob Antimicrob Resist*. 2020;20:238–247.
55. Eaglstein WH, Sullivan TP, Giordano PA, et al. A liquid adhesive bandage for the treatment of minor cuts and abrasions. *Dermatol Surg*. 2002;28:263–267.
56. Eaglstein WH. Moist wound healing with occlusive dressings: a clinical focus. *Dermatol Surg*. 2001;27:175–181.
57. Salasche SJ. Acute surgical complications: cause, prevention and treatment. *J Am Acad Dermatol*. 1986;15:1163–1185.
58. Otley C, Olbricht SM, Frank EW, et al. Risks of perioperative anticoagulation in dermatologic surgery. *Arch Dermatol*. 1996;132:161–165.
59. Futoryan T, Grande D. Postoperative wound infection rates in dermatology surgery. *Dermatol Surg*. 1995;21:509–514.
60. Gette MT, Marks JC, Maloney ME. Frequency of postoperative allergic contact dermatitis to topical antibiotics. *Arch Dermatol*. 1992;128:365–367.
61. Hayes CM, Whitaker DC. Complications of cutaneous surgery. *Adv Dermatol*. 1994;9:161–177.
62. De Oliveira GV, Nunes TA, Magna LA, et al. Silicone versus nonsilicone gel dressings: a controlled trial. *Dermatol Surg*. 2001;27:721–726.
63. Greenbaum SS. Iontophoresis as a tool for anesthesia in dermatologic surgery: an overview. *Dermatol Surg*. 2001;27:1027–1030.
64. Nthumba PM, Stepita-Poenaru E, Poenaru D, et al. Cluster-randomized, crossover trial of the efficacy of plain soap and water versus alcohol-based rub for surgical hand preparation in a rural hospital in Kenya. *Br J Surg*. 2010;97:1621–1628.
65. Salasche SJ, Giancola JM, Trookman NS. Surgical pearl: hydroexpansion with local anesthesia. *J Am Acad Dermatol*. 1995;33:510–512.



eFig. 146.1 Flat hairline scar on the distal lower extremity due to significant undermining and an everted wound edge. *Courtesy Jean L. Bolognia, MD and Stephen Ariyan, MD*.

147 Flaps

David G. Brodland

Key features

- A cookbook approach to flap reconstruction is not realistic
- The mnemonic STARTS lists basic reconstruction options: simple side-to-side closures, transposition flaps, advancement flaps, rotation flaps, tissue importation flaps, and skin grafts
- Understanding the dynamics of a flap optimizes its execution
- For reconstruction, the simplest approach that achieves the desired result is often best
- Extensive undermining, everted wound edges, meticulous hemostasis without excessive electrocoagulation, and technical precision are important in achieving an outstanding result

INTRODUCTION

Cutaneous reconstruction has played an important role in the establishment of dermatologic surgery as a vital discipline within dermatology. An in-depth understanding of reconstructive techniques, combined with a dermatologist's intimate familiarity with skin, enables optimal aesthetic and functional results. Equally important is an in-depth understanding of the tissue dynamics of flaps, why they work, what problems each flap type can address, and their limitations. A cookbook approach to flap reconstruction is not realistic because of the many variables relating to the characteristics of the defect, the donor skin, the patient, and the surgeon. It is better to develop a foundation of basic concepts from which the individual can build his or her skills and unique style of reconstruction.

BACKGROUND

At the patient's side, it is always helpful to have an on-demand recall of flap options. With experience, this is automatic, but those with less experience may find the mnemonic STARTS helpful (Table 147.1). It is incumbent upon the surgeon to synthesize the many factors that may affect the choice of the most appropriate flap for a defect. The characteristics of the wound, qualities of the adjacent skin, the functional aspects of the affected anatomic site, the pertinent aesthetic considerations, the anatomic borders in proximity to the defect, and the age and expectations of the patient all contribute to deciding the most appropriate reconstruction.

The most important goal in reconstruction is functional aesthetics. This means that the reconstruction should first and foremost maintain all vital functions and accomplish this aesthetically. Not all aesthetic reconstructions are functional, but all functional reconstructions can be aesthetic.

STARTS MNEMONIC
Simple side-to-side closure
Transposition flaps
Advancement flaps
Rotation flaps
Tissue importation flaps
Skin grafts

Table 147.1 STARTS mnemonic.

Fundamentals of Flap Design and Suturing Technique

Technical precision, including suturing technique, may be the most important variable in achieving an outstanding result. The first important step is to prepare the wound edges of both the defect and the flap. All incisions should be made at a 90° angle to the skin surface such that the wall of the defect and the edge of the flap are square. Secondly, the wound base should be made a uniform depth. Whether reconstructing with an elliptical side-to-side closure or with any of the more intricate flaps, the contour of the wound base will persist and may affect the long-term appearance of the wound. Likewise, the thickness of the flap should be uniform. Although the optimal plane of flap dissection is somewhere between the upper mid subcutaneous and deep subcutaneous tissue, the ideal thickness of a flap varies and must be determined on a case-by-case basis. Flaps constructed too thinly can develop vascular compromise or may lead to an unnatural appearance. Conversely, a very thick flap may be bulky, have decreased mobility or be more difficult to manipulate while suturing, and it may unintentionally damage underlying neurovascular structures or muscles. Hair-bearing skin mandates attention to the level of the hair follicles.

Widespread undermining of the subcutaneous tissue adjacent to both the defect and the donor site defect is important for creating a broad "plate-like scar" (Fig. 147.1). This results in an even distribution of scar contraction over a greater area and diffuses the effects of contraction such that it is not focused on the flap itself or the incision lines of the flap (Fig. 147.2). Undermining should be uniform and complete, including the areas of low tissue tension such as the tips of an ellipse or the pivot points of flaps[1,2].

Next, meticulous pinpoint hemostasis with complete visualization of all undermined skin with the help of an assistant is critical. Excessive postoperative bleeding within a sutured wound often results in an inferior outcome. It should be emphasized, however, that extensive tissue injury caused by electrosurgical hemostasis should be avoided as fervently as postoperative bleeding, since this can contribute equally to unwanted results. With a well-prepared wound and flap that are characterized by uniformity in thickness, sharply squared edges, well-loosened tissue margins, and excellent hemostasis, the wound is ready for suturing.

An adequately undermined flap may still lead to distortion of delicate structures if the flap is large, heavy, or moves under considerable tension. A flap suspension suture may be necessary to avoid distortion or displacement of delicate tissue. These sutures are placed in fixed or rigid structures underlying the flap. Periosteal sutures represent a common anchoring technique and they are placed from the periosteum through the undersurface of the flap into the deep dermis[3]. When this suture is placed in the undersurface of the flap, it should correspond topographically to its desired location relative to the periosteal suture. More than one suspension suture may be needed and should be placed in a direction parallel to the flap blood supply to avoid vascular compromise of the flap.

Whether it is a side-to-side closure or a flap, eversion of the skin edges (along with undermining) is also essential (see Fig. 147.1). Given their longer period of effectiveness, as compared to epidermal sutures, the author prefers the use of subcutaneous ("buried") vertical mattress sutures to achieve eversion (see Ch. 146)[4,5].

Flap Movement Characteristics

It is helpful to broadly characterize flap types according to their mechanism of skin movement and rearrangement. By understanding the dynamics of each flap, it is easier to select one that will provide

functionally aesthetic results. Upon consideration of the unique characteristics of the defect, the donor skin, and the functional and aesthetic issues of reconstruction in the context of the mechanics of flap tissue movement, a rational decision regarding the method of closure can be made. The components that flaps share include the flap body, the pedicle or vascular base, primary and secondary defects, and, as an integral part of flap dynamics, the primary and secondary movements (Table 147.2, Fig. 147.3)[6].

Most tissue movement results in some degree of tension. This tension creates vectors of force that tend to return moving skin back to its original position. The primary movement of a flap creates a primary tension vector, while the secondary movement (during closure of the donor site defect) creates a secondary tension vector. Consideration of these forces and the effects of these forces on adjacent tissue and even the blood supply of the flap is the primary factor in selecting one flap over another[7]. The most perfectly executed flap that, via tension vectors, results in the distortion of a free margin (e.g. a lip or eyelid) is of little value to the patient or the goal of aesthetic restoration. Therefore, the initial and most important skill required for the proper execution of flaps is the ability to anticipate the direction and amount of tension created by a particular flap and to predict what effects this tension will have on adjacent structures (see Figs. 147.2 & 147.3). Secondarily, judicious use of tension sutures is helpful.

There are four broad categories of flaps based upon how the tissue is rearranged to achieve closure (Table 147.3). In the first category, one or both Burow's triangles that would be removed if the wound were closed by a simple side-to-side closure are displaced. The second includes the flaps that reconfigure defects, while the third includes flaps that reorient tissue from adjacent pools of laxity into the defect. Finally, there is a category of flaps that enables defect closure by tissue importation.

Burow's triangle displacement flaps

Flaps that displace Burow's triangles to a "convenient" location distant from the defect include the single tangent advancement flap (Burow's flap), the bilateral single tangent advancement flap (A-to-T flap), the double tangent advancement flap (U-flap), the bilateral double tangent advancement flap (H-flap), and rotation flaps (e.g. the dorsal nasal or Rieger flap, Mustarde flap, helical advancement flap) (Fig. 147.4).

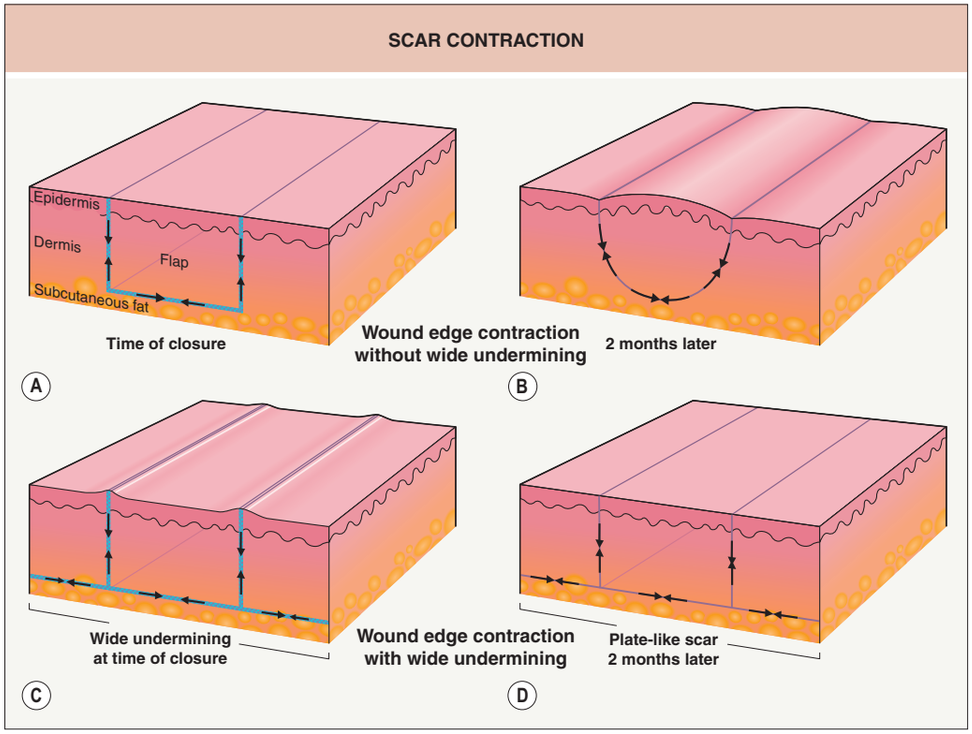


Fig. 147.1 Scar contraction. A Sutured wound without wound edge eversion and without undermining of the surrounding tissue. **B** The results of scar contraction, leading to inversion of the scars and trapdoor deformity of the flap. **C** A wound sutured with eversion and wide undermining. **D** The canceling effect of scar contraction and wound eversion as well as the diffusion of scar contraction in the deep, undermined wound plane ("plate-like" scar).

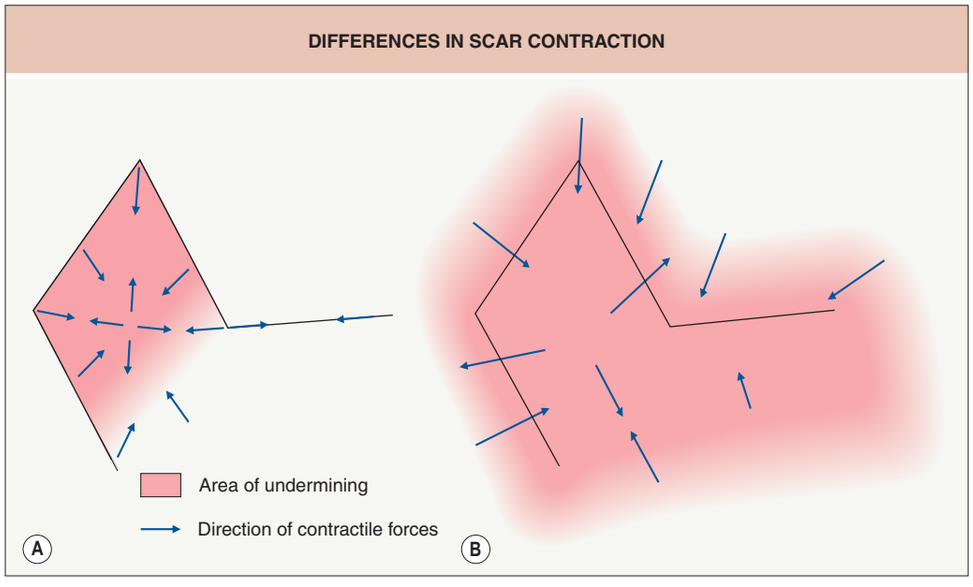


Fig. 147.2 Differences in scar contraction. Depiction of differences between wounds that are undermined and those that are not undermined prior to suture placement. **A** The contraction forces are focused on the margins of the flap in a wound that was not widely undermined. **B** Broad diffusion of contractile forces that are not concentrated at the flap margins, making trapdoor deformity ("pincushioning") less likely in the widely undermined flap.

DEFINITIONS OF FLAP COMPONENTS	
Body	The skin being advanced, transposed, rotated, interpolated, or imported into the primary defect
Pedicle (vascular base)	The conduit of the vascular supply that will remain intact and maintain the vascularization of the body of the flap intraoperatively and for the early postoperative period
Primary defect	The area deficient in skin that will be reconstructed by the movement of the body of the flap
Secondary defect (donor site defect)	The area devoid of skin created by the movement of the body of the flap
Primary flap movement	The movement of the flap body into the defect
Secondary flap movement	The tissue movement necessary to close the void or donor site defect created by the movement of the body of the flap
Primary tension vector	The direction of the force tending to counteract the movement of the body of the flap
Secondary tension vector	The direction of the force created by the closure of the donor site defect

Table 147.2 Definitions of flap components. See Fig. 147.3 for illustration of these definitions.

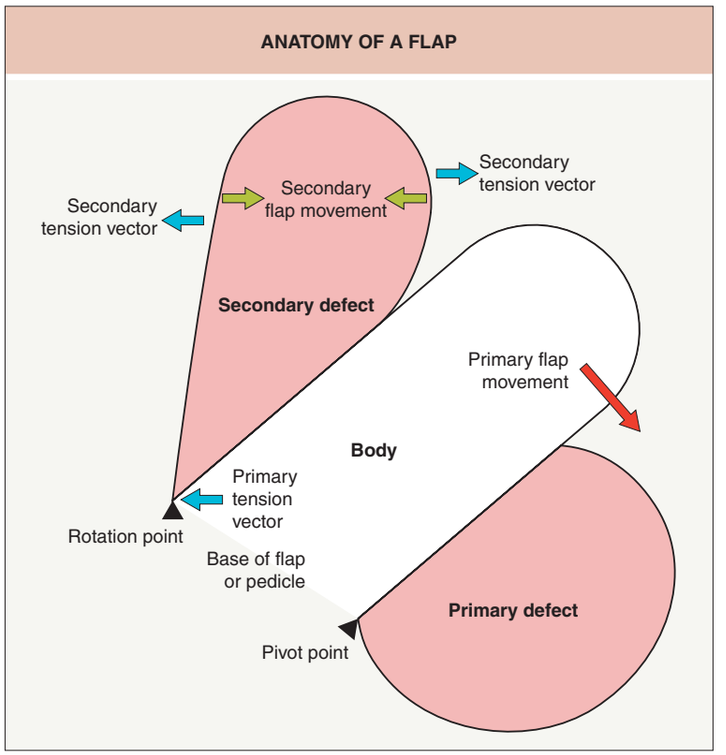


Fig. 147.3 Anatomy of a flap. Definitions of the components of a flap are outlined in Table 147.2.

CLASSIFICATION OF FLAPS BASED ON DESIGN CHARACTERISTICS					
Flap category	**Flap variations**	**Synonyms**	**Mechanism of tissue movement**	**Advantages**	**Disadvantages**
Burow's triangle displacement flaps	Single tangent adv flap	Burow's flap	• Tissue advancement: dependent upon intrinsic tissue elasticity	• Enables closures adjacent to vital structures through displacement of Burow's triangles • Single tangent flaps have excellent blood supply	• Depends on intrinsic skin laxity of the flap skin • Requires extensive undermining • Double tangent flaps have a more limited blood supply
	Bilateral single tangent adv flap	A-to-T flap, O-to-T flap			
	Double tangent adv flap	U-flap			
	Bilateral double tangent adv flap	H-flap			
	Curvilinear tangent adv flap	Rotation flap, Karapandzic flap, Mustarde flap			
Defect reconfiguration flaps	Pedicled V-to-Y flap	Kite flap, myocutaneous pedicle flap, island pedicle flap	• Tissue advancement: dependent upon intrinsic elasticity of subcutaneous pedicle • Tissue movement results in reconfiguration of the defect	• Tissue-conservative due to reconfiguration of the defect without removal of Burow's triangle	• Blood supply is limited to the subcutaneous pedicle • Use limited to locations with spongy, elastic subcutaneous tissue
Tissue reorientation flaps	Rhombic transposition flap	Limberg flap, Dufourmentel flap, Webster's 30° flap, banner flap	• Reorientation of adjacent tissue laxity	• Effective for tight closures • Directional tissue gain can be achieved in direction of tissue deficit	• Depends on laxity adjacent to the defect • Multidirectional incisions; difficult to place all in RSTL
	Bilobed transposition flap				
	Nasolabial transposition flap	Melolabial fold flap			
	Nasolabial flap with a twist (Spear's flap)*				
Tissue importation flaps	Forehead flap	Indian flap	• Importation of tissue from a distant site	• Coverage of large wounds • Can provide vascularity for coverage of avascular grafts such as cartilage grafts	• Two-stage flap • Vascular supply limited to narrow pedicle
	Nasolabial interpolation flap	Melolabial interpolation flap			
	Retroauricular pedicled flap	Pin back flap			
	Subcutaneous tunneling island pedicle flap**				
	Modified Hughes flap Abbe cross-lip flap				

*This flap has features of both reorientation and tissue importation flaps.
**Can be single stage flap.

Table 147.3 Classification of flaps based on design characteristics. adv, advancement; RSTL, relaxed skin tension lines.

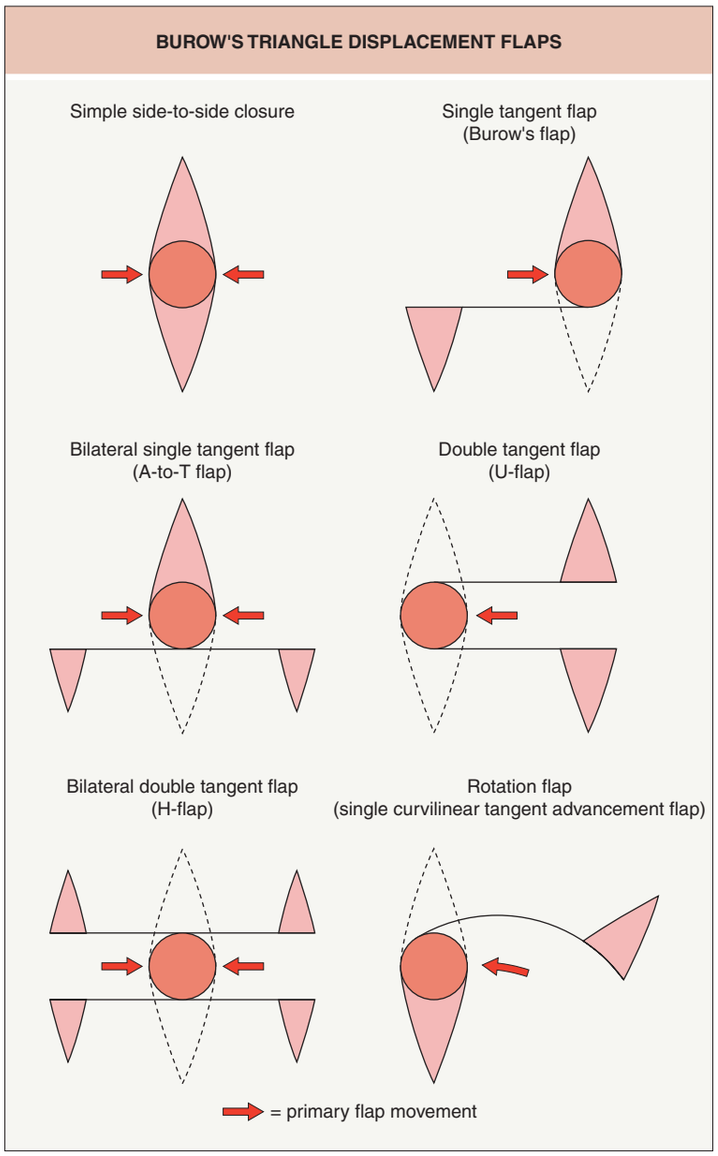


Fig. 147.4 Burow's triangle displacement flaps.

These flaps displace Burow's triangles along straight or curved incision(s) tangential to the wound[8].

The key features of these flaps are: (1) they displace Burow's triangles to a distant site; (2) there is limited reorientation of tissue; and (3) their movement is dependent upon the intrinsic elasticity of the skin. Just as a simple side-to-side closure performed in stiff, inelastic skin would result in a tense closure, so would a Burow's triangle displacement-type flap. When the surrounding skin is elastic and "loose", the wound edges can be closed under minimal tension in both a side-to-side closure and with these flaps. Thus, the only advantage that these flaps confer over a side-to-side closure in tight skin is that a larger area of skin is typically undermined, which releases the flap from the tethering effect of the subcutaneous tissue. This allows for a modest decrease in wound closure tension. The primary utility of these flaps is in defects where, for functional or aesthetic reasons, it is inconvenient to remove a Burow's triangle immediately adjacent to the defect. An example of this is a defect above or below the eye in which displacement of the Burow's triangle is useful to avoid removing a triangle from the eyebrow or eyelid (Fig. 147.5).

Defect reconfiguration flaps

The pedicled V-to-Y advancement flap is unique in that it is an advancement of tissue with its vascular base as a pedicle of subcutaneous tissue and muscle oriented in a plane perpendicular to the skin and at 90° to the more traditional advancement or rotation flaps. In this case, the tissue redundancy created at the pivot point of the flap is buried in the subcutaneous plane at the advancing edge of the flap (see below). Fundamentally, the pedicled V-to-Y flap reconfigures the typical roundish shape of the wound to a sharp, angled, geometric shape that is easily closed without standing cones or distortion of surrounding structures (Fig. 147.6). Movement of this flap is entirely dependent on the elasticity of the tissue that comprises the vascular pedicle of the flap.

Tissue reorientation flaps

Tissue reorientation flaps are characterized by the lifting of skin from an adjacent donor site and reorienting it through the transposition of the flap over a peninsula of skin between the donor site and the defect. There is a pivot point at the base of this flap (see Fig. 147.3). The tissue movement depends on the presence of *laxity in adjacent tissue*. Although intrinsic elasticity of the flap skin may facilitate the ease of execution, without ample laxity in the donor site, the transposition cannot be performed. Some of the flaps that fall into this category include the rhombic transposition flap (see Fig. 147.2), the bilobed transposition flap, and the nasolabial transposition flap (see Table 147.3).

To better understand the reorientation of tissue that occurs in these flaps, a review of the most basic tissue reorientation flap, the Z-plasty, is helpful. Z-plasties transpose two angular flaps, placing them in a complementary fashion into the defects of the other flap (Fig. 147.7). This reorientation of tissue ultimately results in the lengthening of the skin in the direction of the middle arm of the Z-plasty (Fig. 147.8). There is a complementary decrease in the length of skin perpendicular to this same arm. The amount of lengthening is proportional to the angles of the flap(s). Put another way, tissue gain in the direction of the middle arm is proportional to the width of the base of the flaps. This is effectively the mechanism of tissue reorientation in transposition flaps. Upon careful examination, Z-plasties can be found within the design of transposition flaps (Fig. 147.9). Therefore, just as with Z-plasties, transposition flaps work because the reorientation of the tissue results in lengthening of tissue in the direction of the skin deficit at the expense of the laxity in the donor site.

It is helpful to understand the utility of these principles of reorientation – an example of this would be a defect on the nasal tip (Fig. 147.10). The skin is typically very tight in this area, making simple side-to-side closure in the vertical direction difficult. Side-to-side closure in the horizontal direction is impractical because of the distortion that would occur to the free margin of the ala. When one looks for donor sites, there is typically a substantial amount of laxity on the mid nasal dorsum and nasal sidewall. A bilobed flap allows utilization of this laxity through tissue reorientation using two lobes[9]. The underlying mechanism of tissue reorientation is a series of Z-plasties inherent in this flap. Since tissue gain in Z-plasties is in the direction of the middle arm of the Z-plasty, a substantial reorientation and lengthening of tissue in the desirable direction for repair of the defect occurs without distortion[10]. In contrast to the Burow's triangle displacement flap, this flap does not rely upon intrinsic elasticity of the flap skin. This is key to avoiding distortion of the alar rim.

Tissue importation flaps

Large defects, or defects in areas where tissue laxity is lacking, may be reconstructed by importing vascularized skin from a site that is not adjacent to the defect (see Table 147.3)[11]. Tissue importation flaps are typically derived from a distant donor site with ample tissue laxity and, most importantly, an excellent blood supply. This blood supply may be based on a particular artery (e.g. paramedian forehead flap based on the supratrochlear artery) or by a rich, random-pattern blood supply (e.g. the retroauricular pedicle flap).

These flaps are typically two-staged flaps requiring a period of vascular ingrowth from the wound bed of the defect. This period ranges from 2 to 6 weeks, with 3 weeks being the most commonly reported time point for transection of the pedicle. In the head and neck region, defect sites where tissue importation flaps are commonly employed include the nose, ear, eyelid, and lip.

There are also single-staged tissue importation flaps. These are tunneled flaps in which skin from a non-adjacent site with a subcutaneous and muscular pedicle is passed through a "tunnel" to the defect site. The pedicle lies within the tunnel providing blood supply to the flap.

The appropriate selection and execution of these four broad flap categories are discussed in more detail below.

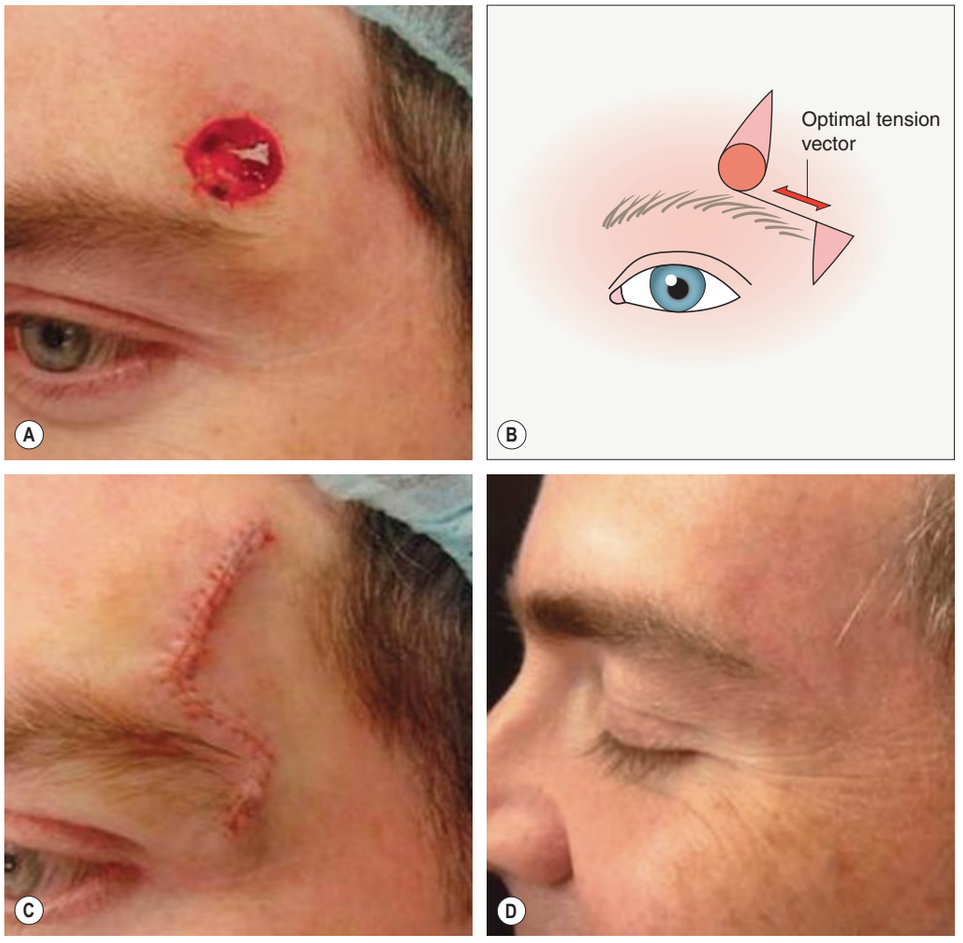


Fig. 147.5 Single tangent advancement flap (Burow's flap). A The wound extends to the brow. **B** Determine the tension vector that will cause the least distortion and make the tangential incision parallel to this optimal tension vector. Both Burow's triangles (displaced and adjacent to defect) are oriented perpendicular to the optimal tension vector. **C** Closure with a single tangent advancement flap with the tangent extending lateral to the brow and displacing a Burow's triangle to the temple and lateral orbit. **D** The eyebrow is entirely preserved.

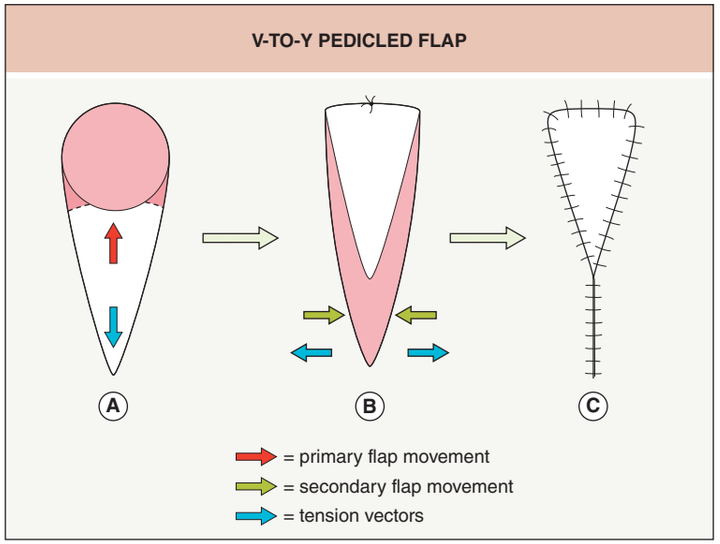


Fig. 147.6 The pedicled V-to-Y flap. Reconfiguration of the defect (pink shaded area) in **A** to the defect in **B**. The shaded secondary defect in **B** is comprised entirely of acute angles which are easily closed primarily (**C**). Also see Fig. 147.20.

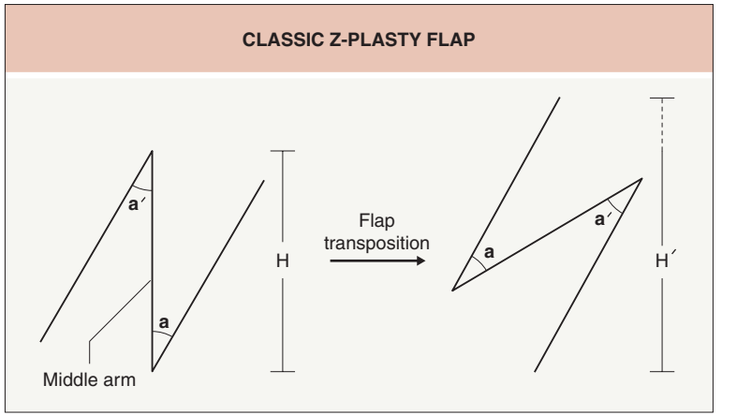


Fig. 147.7 Classic Z-plasty flap. The directional tissue gain (dotted line) is depicted (H to H′) after flap transposition in the direction of the middle arm of the Z-plasty.

DESCRIPTION OF TECHNIQUE

Burow's Triangle Displacement Flaps

Single tangent advancement flaps (STAFs) and rotation flaps

There are several variants of Burow's triangle displacement flaps that are differentiated by the number of Burow's triangle displacements, or the configuration of the tangential line extending to the displaced triangle (see Fig. 147.4). Ideally, the design of these flaps should, when possible, place surgical scars at cosmetic subunit borders and within relaxed skin tension lines. Therefore, when a defect is located near an arcing junction of a cosmetic subunit or if the relaxed skin tension lines are curved such as on the cheek (Fig. 147.11), then the Burow's triangle displacement flap, classically known as the rotation flap, may be an excellent option[12]. On the other hand, when the cosmetic subunit junctions or relaxed skin tension lines are relatively straight, the STAF, or "Burow's advancement flap", may be optimal. A variation, the crescentic advancement flap, can be employed when the anatomic structures are naturally curved (Fig. 147.12).



Fig. 147.8 Classic Z-plasty flap. A Defect close to the eyelid margin. The middle arm of this Z-plasty flap is composed of the defect *plus* the Burow's triangles excised above and below it to facilitate the transposition of the flaps (*). The medial flap is transposed over the lateral flap (arrows). **B** The wound is closed via a Z-plasty closure with the transposition of flaps at the upper medial and lower lateral aspects of the wound. This is done to lengthen tissue in the direction of the palpebral margin in order to prevent ectropion as demonstrated at the 4-month postoperative visit (**C**).

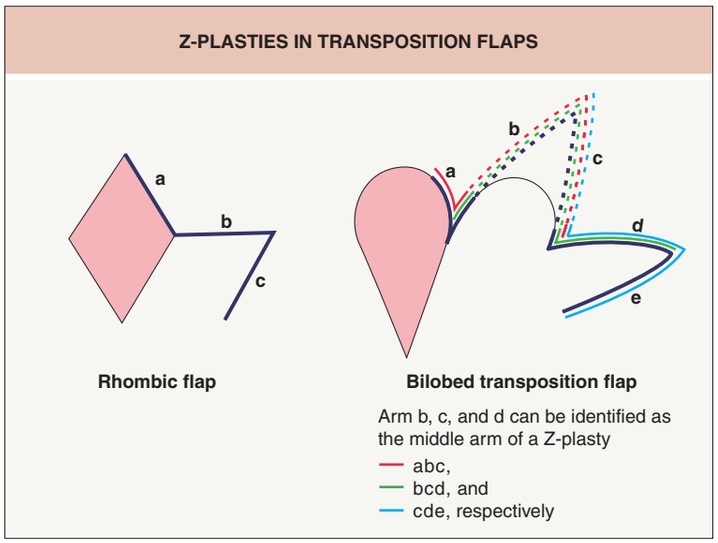


Fig. 147.9 Z-plasties in transposition flaps. Z-plasties are highlighted within the designs of both the rhombic and the bilobed transposition flap. Note in the rhombic flap the middle arm of the Z-plasty is line (b) and is the direction of anticipated tissue lengthening. In the bilobed transposition flap diagram, there is a series of three Z-plasties all contributing to tissue gain in the desired direction of the defect.

Once the need to displace a Burow's triangle so as to avoid a vital structure is established, the incision lines should be planned in the optimal location. The incision, whether straight or arced, should extend to the point of preferred triangle displacement. The triangle should then be excised, commensurate in depth to the thickness of the flap. After undermining and hemostasis, the first point of suturing is the closure of the displaced Burow's triangle. The second point of suturing is then the closure of the other Burow's triangle. The remainder of the flap can then be completely sutured into the defect with even distribution of the remaining edges of the flap to the defect's wound edges.

Double tangent advancement flaps (DTAFs)

DTAFs displace both Burow's triangles along parallel tangents (see Fig. 147.4). Therefore, these flaps are typically peninsular in configuration with an isolated vascular base at the distal ends of the tangents. The execution of this flap is very similar to that of an STAF, except that one must be mindful of the more limited vascular supply (Fig. 147.13). This isolated vascular supply necessitates limiting the length of the flap to three to four times its width. As with other advancement flaps, the first closure points are at the site of the displaced Burow's triangles. Suturing the advancing flap with even distribution of the flap along the recipient tissue margins completes the execution of this flap[8].

Site-Specific Variations of Burow's Triangle Displacement Flaps

Helical advancement flaps

Helical advancement flaps are often discussed as a unique entity, but they are merely variants of Burow's triangle displacement flaps. The characteristics of the helix are unique owing to its highly distortable free margin that is curved in nearly every dimension and its limited pool of adjacent tissue laxity[13,14]. The common variant of the helical advancement flap is directly analogous to the DTAF in that parallel tangents are incised from the helical defect along the anterior rim of the helix and the posterior helix. Another variant is an STAF in which a single incision is made along the anterior helical rim while a non-displaced Burow's triangle is excised directly posterior to the defect onto the posterior ear. Both the DTAF variant and this STAF variant can be either a single flap (derived superior or inferior to the defect) or two flaps (derived both above and below the defect). As with all Burow's triangle displacement flaps, the helical advancement flap displaces the Burow's triangle to a more convenient location. Most of these flaps derive donor skin inferiorly. The donor pool from the superior helix is typically less abundant but can be very beneficial, both in large mid-helical defects when two flaps are used and in defects of the superior helix[15].

A common use of the helical advancement flap is for a small to medium-sized defect on the mid helix not involving the cartilage (Fig. 147.14). While a wedge closure of the ear could be considered, displacing the anterior triangle by utilizing the lax skin of the lower helix and earlobe obviates the need to do a wedge resection of the auricular cartilage and avoids disruption of its delicate architecture. Burow's triangles can easily be displaced to the earlobe, which facilitates the advancement of the helical skin into the defect. Despite the resultant decrease in the size of the earlobe, the aesthetic impact tends to be minimal as long as the anterior profile of the ear is maintained. Since the earlobe is most visible on the lateral view and because the opposite earlobe is not simultaneously visible, subtle changes in size tend to go unnoticed.

With a more superiorly located defect, the donor pool is at the anterior aspect of the helical rim. Although the extent of tissue movement from the anterior helix is often less than can be expected on the inferior helix, this varies greatly and must be determined for each case.

With the helical advancement flap variant, which is a *double* tangent flap or "U-flap", the parallel lines are well hidden in the helical groove or on the helical rim and on the ear posteriorly. A possible disadvantage is the very narrow flap base with its attenuated blood supply. However, the helical rim has a rich vascular supply and is more forgiving even when tension on the wound edges is considerable. Nevertheless, under tension there is a risk of distal necrosis of this type of helical advancement flap.

Notably, the helical advancement flap variant with a *single* tangential incision does not have the same narrow base. Its posterior Burow's triangle is excised directly posterior to the defect. The same anterior



Fig. 147.10 Bilobed flap. A Defect on the nasal tip adjacent to the free margin of the ala. Bilobed flap reconstruction with minimal distortion of the alar rim (**B**) and long-term result (**C**).



Fig. 147.11 Rotation flap. Large defect (**A**) on the medial cheek and lower eyelid reconstructed with a rotation flap (Mustarde flap) with displacement of the superior Burow's triangle laterally along the curvilinear tangent which follows the relaxed skin tension lines (**B**). **C** Final results with no distortion of the eyelid and incision lines nicely camouflaged along cosmetic subunit borders and relaxed skin tension lines.

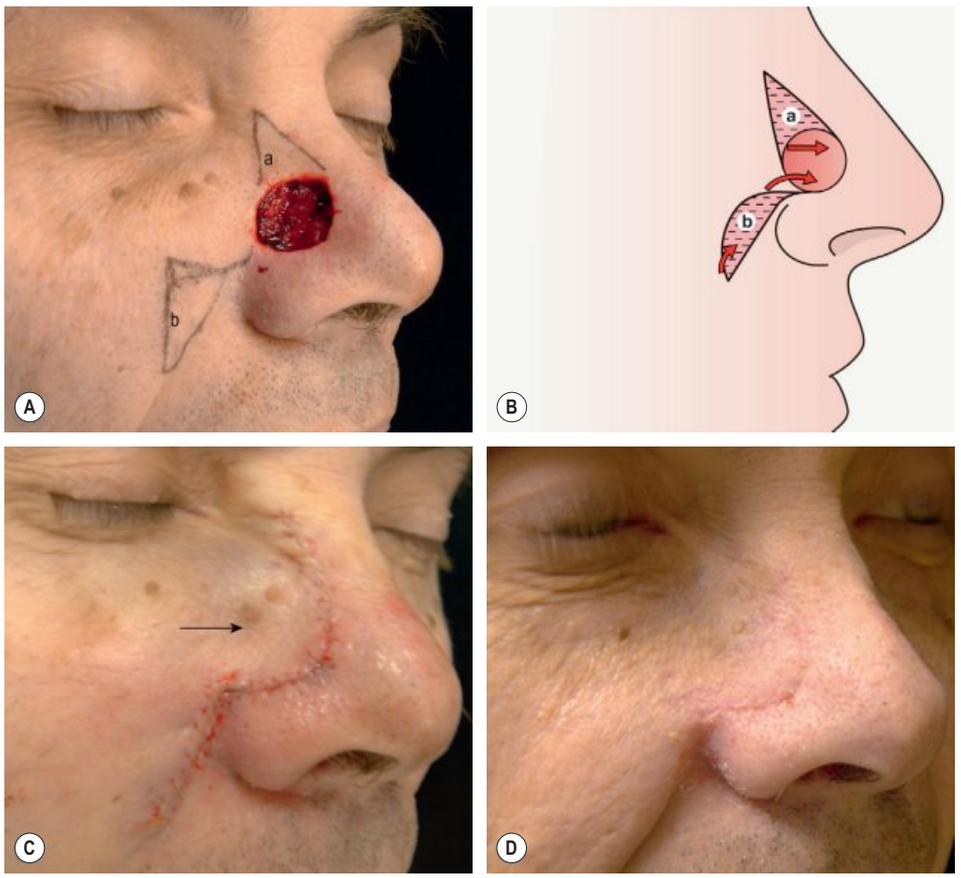


Fig. 147.12 Crescentic advancement flap. A Medium-sized defect on the right inferior nasal sidewall. A single tangent advancement flap (Burow's flap) is planned with a crescent-shaped Burow's triangle on the medial cheek. **B** The crescent (b) fits nicely into the naturally curved anatomic configuration of the alar crease and creates a "wound edges of unequal length" situation which further contributes to the advancement of skin onto the nose. **C** Flap sutured in place; note the subtle indentation (arrow) that corresponds to a periosteal suture placed at the nasofacial sulcus in order to prevent tenting and to recreate the sulcus. **D** Four-month postoperative appearance.



Fig. 147.13 Double tangent advancement flap. A Defect with preoperative plan to advance skin from lateral to the defect, incorporating the residual brow. **B** Sutured flap realigning the brow. **C** Six months postoperatively with reconstitution of the brow. This technique was used to reconstruct and preserve the continuity of the eyebrow in this patient.

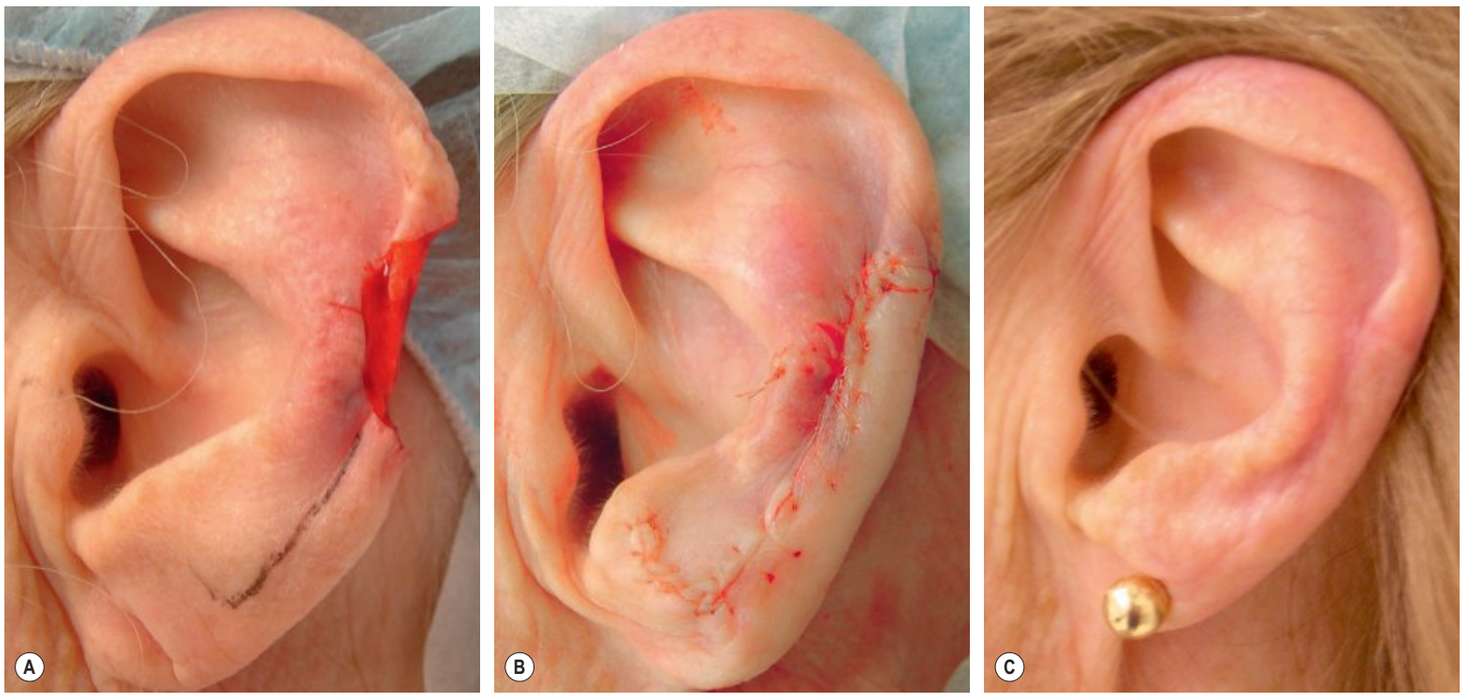


Fig. 147.14 Helical rim advancement flap. A Defect of the mid helix involving a small amount of cartilage. A single tangential incision is planned inferiorly within the helical groove to the earlobe. A Burow's triangle excision is planned directly behind the defect on the posterior ear. The flap will be raised by dissection of the skin from the posterior ear above the perichondrium. The displaced Burow's triangle will be removed from the earlobe and the skin of the flap will be redraped through upward advancement into the defect. **B** The flap is sutured after a very small wedge of cartilage has been removed to reconstitute the helical rim of cartilage. **C** Three-month postoperative appearance.

incision is made along the helical rim (see Fig. 147.14), but the base of the flap now becomes the entire posterior ear. The flap can be dissected from the cartilage posteriorly and redraped with advancement over the defect. Equally excellent cosmetic results can be obtained with this variant and with very little downside.

Dorsal nasal flap

The dorsal nasal flap (Rieger flap) is a specialized, site-specific variant of the Burow's triangle displacement flap that is useful for reconstructing moderately sized distal nasal defects. The basic design of this flap is predicated upon the fact that it is often inconvenient or unfeasible to remove a large Burow's triangle on the nasal tip. The design of this flap displaces a Burow's triangle from the nasal tip to the glabella along an incisional arc that extends from the more inferior aspect of the defect (above the alar crease) to the nasofacial sulcus and finally onto the glabella (Fig. 147.15).

The dorsal nasal flap relies on the rich blood supply of the medial canthal plexus that is largely supplied by the angular and infratrochlear arteries. This rotation flap employs a "back-cut" which slightly alters the dynamics of the flap, with the back-cut serving as the displaced Burow's triangle. However, this maneuver simultaneously narrows the base of the flap which improves its ease of rotational movement. Based on the rich vascular supply of the medial canthus, the narrowed base is robustly supplied by the angular artery. The back-cut also enables the incorporation of some glabellar skin into the flap, contributing to the closure of the secondary defect and reducing distortional tension on the nasal tip.

The most important aspect in the execution of the dorsal nasal flap is creation of a broad-enough arc by extending to the nasofacial sulcus, but skirting the medial canthal skin, *en route* to the glabella. The second key element is the plane of dissection when elevating the flap. While the portions of the flap that will be covering the nasal defect can be trimmed and thinned to match the native skin and defect, the body of the flap must be dissected at the level of the perichondrium and periosteum. This assures adequate blood supply from the canthal plexus. When these principles are observed, this flap is robust and can reconstruct moderately large nasal tip defects without distortion and with an excellent tissue match.

While the surgeon must be aware of important variables that can substantially affect the successful use of any flap, this is especially true

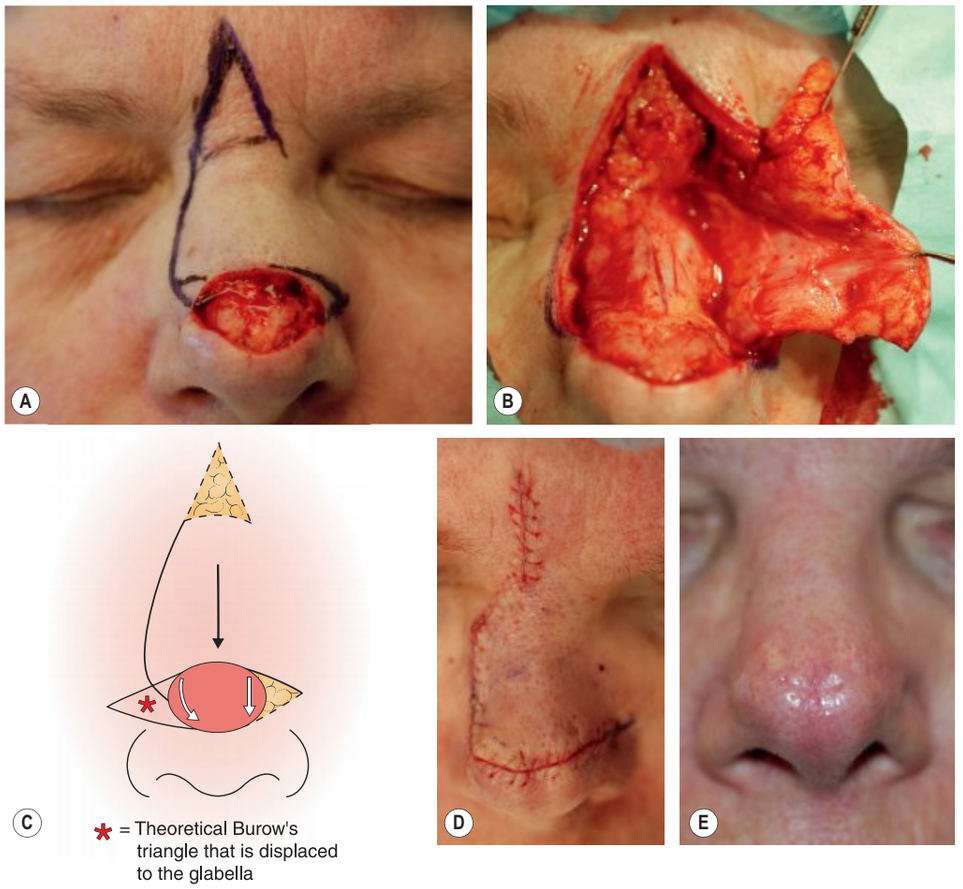


Fig. 147.15 Dorsal nasal (Rieger) flap. A Moderate-sized defect of the nasal tip. **B** The flap is incised and reflected demonstrating the deep plane of dissection just above the nasal periosteum. The flap will be redraped over the tip of the nose with primary closure of the displaced Burow's triangle on the glabella. **C** Displaced Burow's triangles (*) are depicted as is downward tissue advancement via rotation of nasal tissue on a lateral base. **D** Flap sutured into place. **E** Result four months postoperatively.

in the case of the dorsal nasal flap. The ideal situation is a patient with very non-sebaceous and elastic or "loose" skin of the nasal dorsum. Characteristics that raise concern about whether this flap can be successfully executed include thick, inflexible, and highly sebaceous skin. Also, prior surgeries on the nose or the medial canthus should be viewed as a potential source of compromised vascular supply. Distortion of the distal nose structures may occur if there is severe structural compromise of the free margin or the cartilage of the nasal tip and consideration should be given to other reconstructive options (e.g. a tissue importation flap). The dorsal nasal flap should be reserved for defects that are too large to be reconstructed with a small local flap such as the bilobed flap, yet smaller than a defect for which a tissue importation flap would be more ideally suited. The most difficult aspect of successfully executing a dorsal nasal flap is anticipating and dealing with the secondary motion inherent in this flap. The more curved the flap, the greater the secondary defect on the nasal sidewall/nasofacial sulcus.

Other Site-Specific Flaps

Alar rotation flap (ARF) and spiral rotation flap (SRF)

There are two flaps which, like the dorsal nasal flap, are rotation flaps with back-cuts that are particularly useful for alar defects. The ARF is best suited for smaller defects limited to the ala while the SRF is useful for larger defects involving both the ala and lower nasal sidewall.

When defects are limited to the ala, the **ARF** is a good alternative to full-thickness skin grafts; the ideal defect is <75% of the vertical height of the ala and is located on the mid to medial ala. Classically, the superior edge of the defect is near the alar crease. The flap design displaces the triangle laterally along an arcing incision that is made within the crease and extends off the nose onto the apical triangle at the junction of the nose, cheek, and upper lip (Fig. 147.16). This incision is further extended a short distance along the nasolabial fold to where the back-cut is made. The size of the back-cut should be proportional to the defect, i.e. about the size of a Burow's triangle had it been excised superior to the defect. The flap, which is thick and incorporates the rich blood supply of the lateral ala, is then elevated. A diminutive Burow's triangle is excised inferolateral to the alar defect.

The key suture of the ARF is placed at the alar–labial junction to close the back-cut defect. This nicely recreates the alar–labial junction. The second key stitch closes the alar defect. With the flap in position, the surgeon looks to incorporate enough of the back-cut portion of the flap onto the ala to replace the tissue volume of the defect. This is important because the ala is typically highly sensitive to tissue loss and the back-cut creates the opportunity to incorporate tissue from the apical triangle onto the nose. This restores and preserves the normal tissue volume of the ala.

An analogous flap may be used for alar defects located near the alar rim. The design of the flap is simply inverted and the arcing incision is made along the alar rim to the alar–labial junction where the back-cut is similar to that just described, but is inverted. A diminutive Burow's triangle is excised superior to the defect and the flap is rotated onto the nose and into the defect in the same fashion.

The **SRF** is an excellent way to reconstruct defects involving the ala and the lower nasal sidewall[16]. It enables reconstruction of the ala and alar crease in a single stage. The design is that of a 270° rotation flap with a back-cut on the medial cheek, and it represents an alternative to the nasolabial transposition flap.

An arcing incision is made from the inferomedial aspect of the wound onto the nasal sidewall and extended laterally onto the upper medial cheek (Fig. 147.17). The arc is extended inferiorly to the nasolabial fold. From there a back-cut incision is made superiorly along the fold. The proportions of the flap are important and the flap can be conceptualized as having three parts: (1) the alar portion; (2) the body; and (3) the tail. The alar portion of the flap will reconstruct the alar portion of the defect and is equal in size to this area. The body and tail of the flap are equal in size to the vertical dimension of the entire defect. This proportional sizing of the flap assures successful restoration of the nasal defect, with the skin of the medial cheek ultimately serving as the donor site. Just as with the ARF, the back-cut tissue, which in an SRF is the tail of the flap, is incorporated

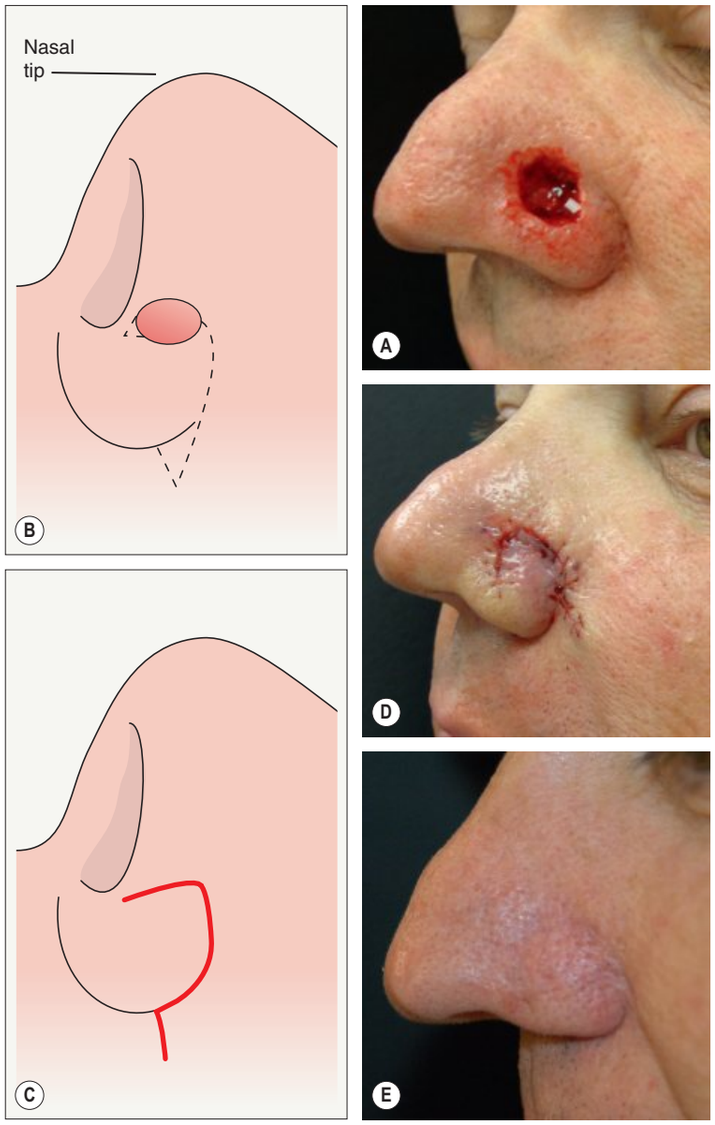


Fig. 147.16 Alar rotation flap (ARF). A These flaps are best suited for mid to medial defects that are <75% of the vertical height of the ala. **B** The design is a rotation flap with a back-cut incised within the alar crease to the apical triangle at the alar–labial junction. **C** Closure of the back-cut recreates the crease at the alar–labial junction. **D** Incorporation of the back-cut skin onto the ala prevents distortion of the ala. **E** Long-term follow-up.

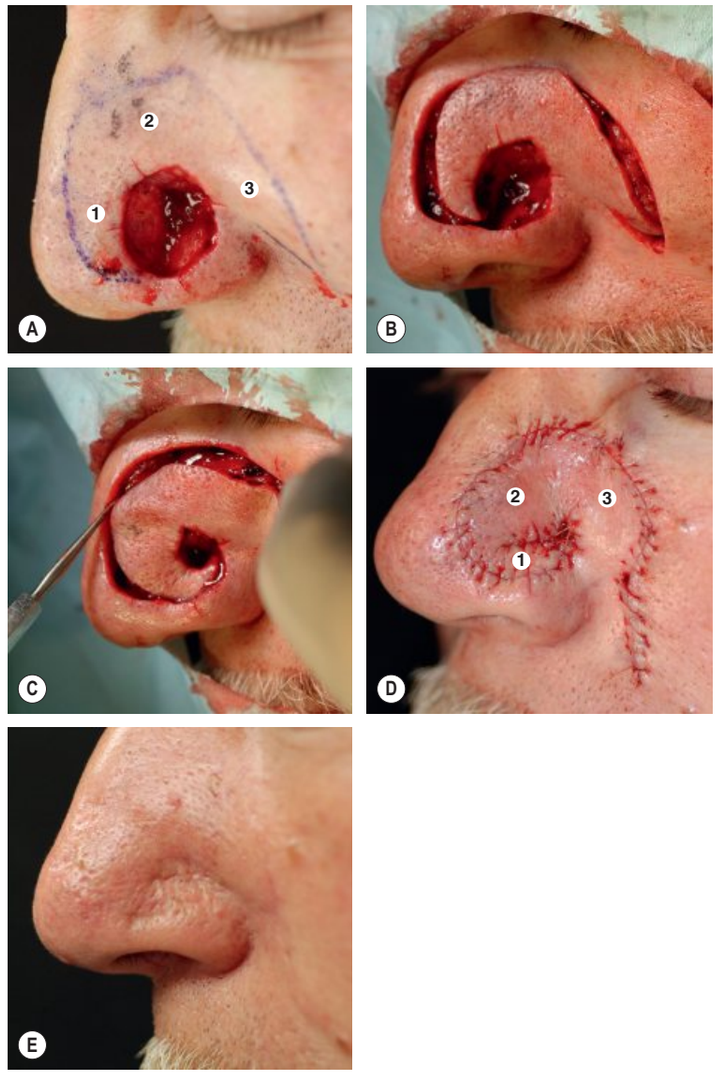


Fig. 147.17 Spiral rotation flap (SRF). A These flaps are well suited for larger defects involving the ala, alar crease, and lower nasal sidewall. The flap (outlined in ink) can be conceptualized as having three parts: (1) the alar portion (equals the size of the alar defect); (2) the body; and (3) the tail; the latter two components equal the size of the entire wound. **B** Incision of the flap with a back-cut on the medial cheek along the melolabial junction. **C** After undermining, with the flap base created at the inner aspect of the spiral flap, demonstration of the spiral rotation of the flap into the alar portion of the defect. **D** Sutured flap. **E** Three-month follow-up.

as much as possible into the closure. Some of the tail will be trimmed, but incorporation of as much of this tissue as possible helps to restore the tissue volume on the nose. This restoration, in turn, prevents distortion of the free margin and other structures.

The method of undermining and raising of an SRF deserves mention. The alar portion is completely detached from the underlying tissue as is the tail. The perimeter of the flap body is undermined to enable rotation and advancement. Vascular supply of the flap is based upon the rich vascular plexus of the lateral ala and upper lateral lip located beneath the "inner" edge of the spiral. In this way, the flap is similar to the pedicled V-to-Y flap since its base is largely deep to the flap and care must be taken to preserve this base.

Cheiloplasty of the lip

Cheiloplasty of the lip is a special form of the simple elliptical closure. It is used in small to moderate-sized defects of the lip that involve the vermilion or the vermilion border. It is traditionally taught as a wedge closure with a full-thickness excision of skin, mucosa, submucosa, and musculature. However, when tissue-conserving excisions (e.g. Mohs micrographic surgery) are employed and much of the orbicularis oris muscle is preserved, a subtotal wedge excision of the muscle (cheiloplasty) is preferred due to its simplicity as well as the decreased chance of lip dysfunction and other complications[17].

Careful realignment of the vermilion border is essential. Prior to excision of the tumor, hash marks are made with a scalpel along the vermilion border as precise reference points. The hash marks enable precise realignment of the vermilion border (Fig. 147.18).

The surgeon surveys the amount (if any) of redundant soft tissue that forms when the wound edges are approximated. Usually, the apex of the wedge (after removal of redundant muscle) is obtuse, creating a very slight trough in the lip in an anterior-to-posterior direction. In our experience, the less muscle that is removed, the less likely a noticeable notch in the vermilion lip will form and the function of the lip is beautifully maintained. After excision of Burow's triangles on the external lip and the internal lip (see Fig. 147.18B), and after undermining the cutaneous portion of the defect, the key suture is the one that reapproximates the medial and lateral muscle edges. This is best done by the placement of a "figure-of-eight" suture, which is similar to a horizontal mattress suture and snares the bellies of the anterior edge of the orbicularis oris muscle and precisely approximates them (see Fig. 147.18C–E). Upon healing, the ridge created by this approximation becomes a functional and aesthetic component of the lip and recreates

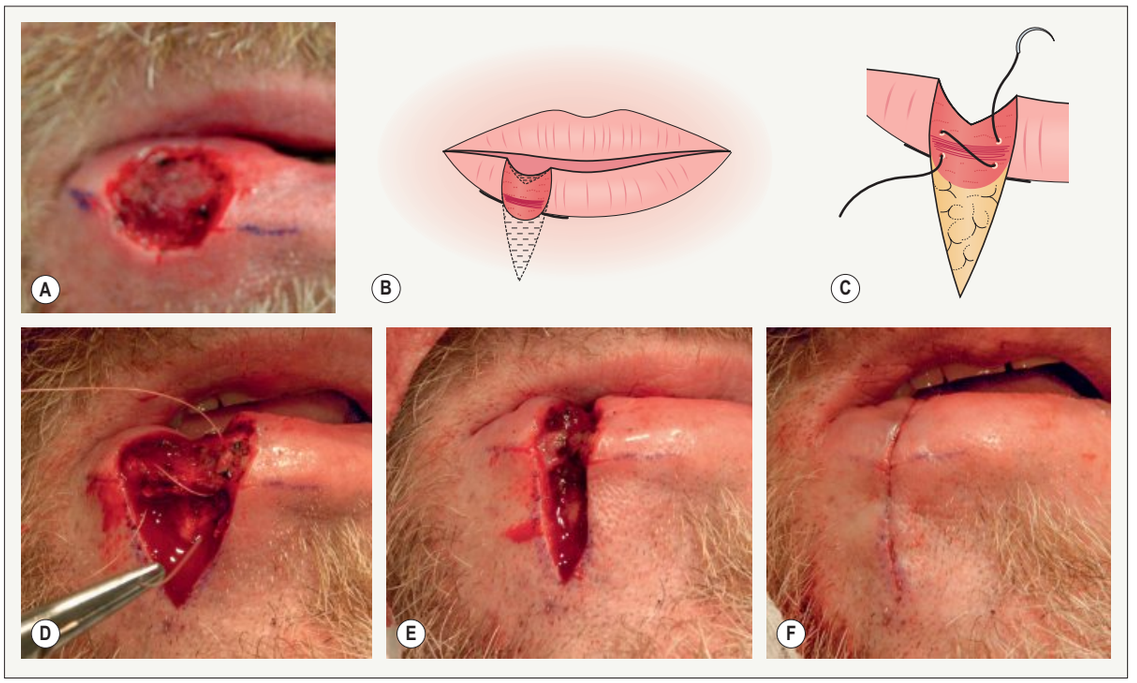


Fig. 147.18 Wedge closure of the lip. A Typical defect after Mohs surgical excision of a squamous cell carcinoma. Note indelible ink lines and nicks in the skin that demarcate the vermilion border, facilitating precise realignment. **B** Burow's triangles are excised intraorally and extraorally perpendicular to the vermilion border. After determining the minimal amount of muscle that must be removed to avoid excessive redundancy when the wound edges are approximated, an obtuse wedge of muscle is removed. **C** The anterior margin of the orbicularis oris muscle is identified medially and laterally. A "figure-of-eight" stitch is placed to reapproximate the muscle margins. **D** "Figure-of-eight" suture in place prior to reapproximation of muscle edges. **E** Realignment of the anterior edge of the orbicularis oris muscle. **F** Wound closure prior to the placement of superficial epidermal sutures. Note the near perfect realignment of the vermilion border and the well-proportioned recapitulation of the lower lip.

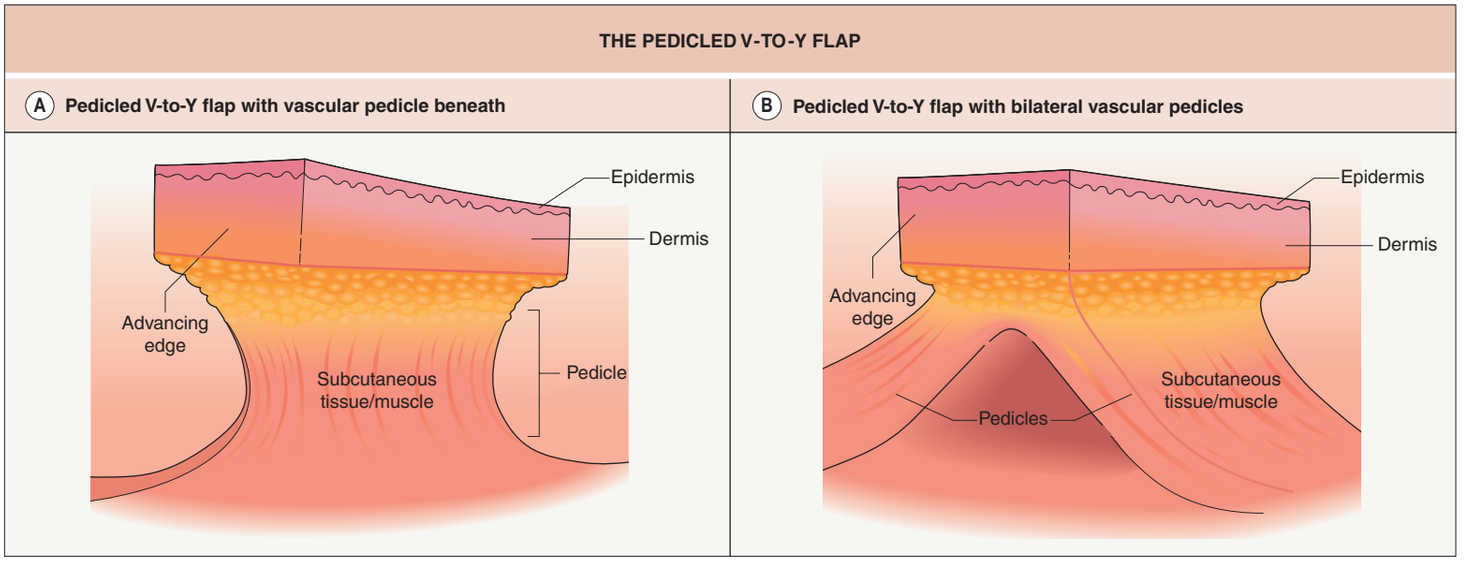


Fig. 147.19 The pedicled V-to-Y flap. A Vascular pedicle derived immediately beneath the island of skin. **B** Vascular pedicles derived from tissue lateral to the island of skin.

the appropriate muscular bulge at the vermilion border. Adjustment of the wound edges to perfectly realign the previously placed hash marks with epidermal sutures will ensure a perfectly realigned vermilion border. Some surgeons use braided rather than monofilament sutures to minimize irritation of the mucosal portion of the other lip.

Defect Reconfiguration (Pedicled V-to-Y) Flaps

The pedicled V-to-Y flap (PVYF) is a unique advancement flap in that the creation of an island of epidermis and dermis eliminates any blood supply from the rich vascular plexus within the deep dermis and superficial subcutaneous skin[18]. In effect, the vascular supply is isolated to the subcutaneous tissue. The two variations in pedicle design hinge upon whether the pedicle is created immediately beneath the island or from the subcutaneous tissue lateral to the island (Fig. 147.19). The variant with the vascular pedicle immediately beneath the island of skin is created by dissecting away surrounding superficial subcutaneous tissue and eliminating the tethering effects of the tissue adjacent to the pedicle. The PVYF with laterally based pedicles is created by tunneling immediately beneath the island while carefully maintaining vascularized sheets of subcutaneous and muscle tissue, either bilaterally or unilaterally to the side of the island (Fig. 147.20). Selection of which pedicle variation is best depends upon the site. PVYFs in locations with elastic, spongy subcutaneous tissue do well with deep pedicles whereas lateral pedicles are preferred for defects within tighter skin with less spongy subcutaneous tissue and with a good lateral blood supply; the latter often comes in the form of facial muscle[19].

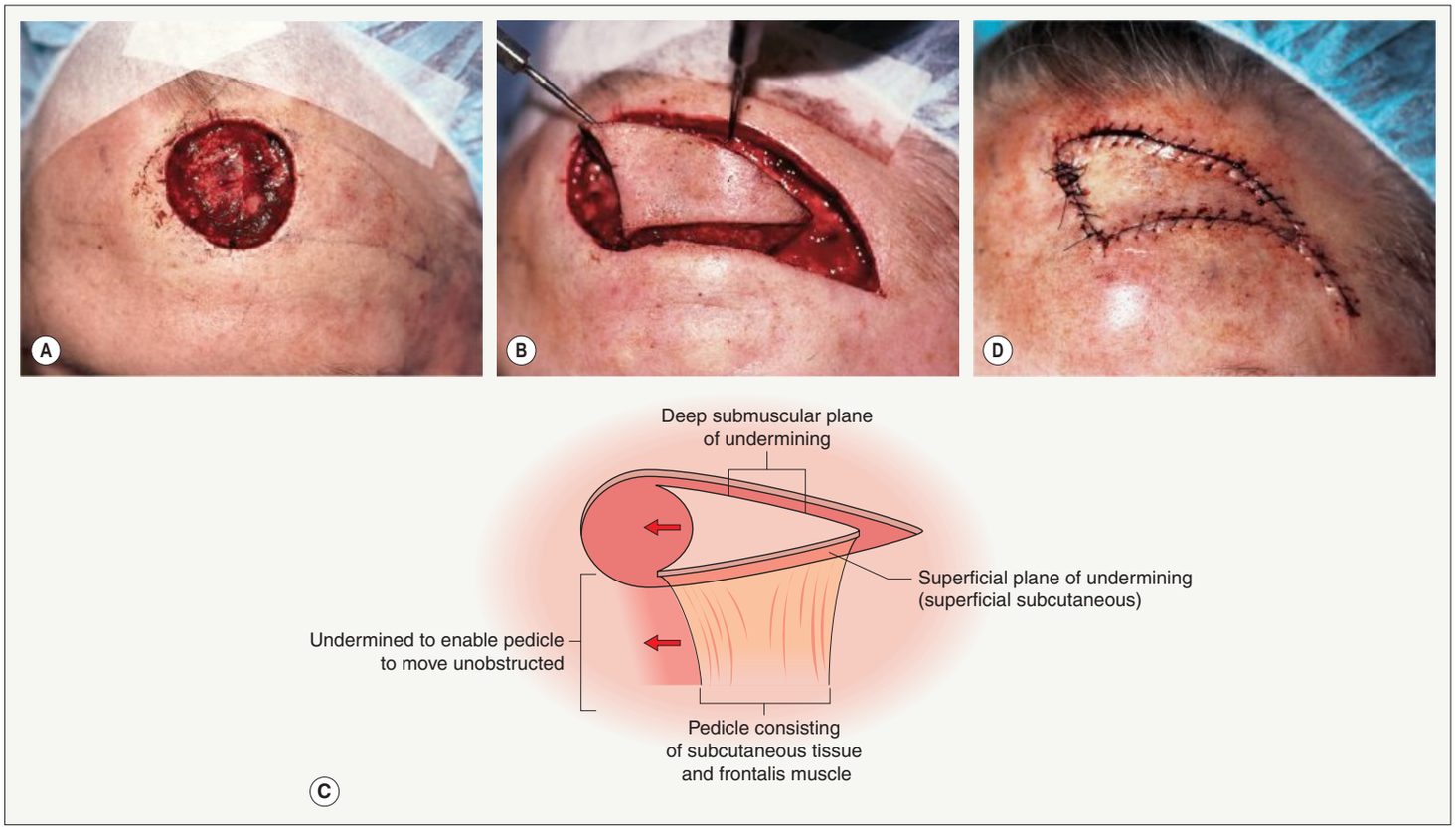


Fig. 147.20 The pedicled V-to-Y flap. A Large mid-upper forehead defect. **B** Intraoperatively, the pedicled V-to-Y flap is designed with a single inferior muscular pedicle based on the rich blood supply of the supratrochlear and supraorbital arteries. **C** The frontalis muscle serves as the inferiorly based pedicle for the flap. This muscular pedicle is constructed via undermining in the subcutis beginning at the lower edge of the flap (superficial plane) and undermining in the submuscular plane which is begun at the superior edge of the flap (deep plane). The skin medial to the pedicle must also be undermined to facilitate its advancement in the direction of the defect. **D** The defect is now comprised of acute angles which are easier to close primarily.

In general, it is appropriate to think of the PVYF as an advancement of what would be one of the Burow's triangles in a simple side-to-side closure. The PVYF is an extremely tissue-efficient flap in which little or no tissue is discarded and yet often provides outstanding clinical results. The mechanism for tissue conservation involves a reconfiguration of the roundish defect into an angular shape (see Fig. 147.6). The original shape of the defect is reconfigured behind the advancing island to a defect of equal area, but very angular in shape that can be closed without tissue redundancy.

It is conceptually useful to recognize that a PVYF (especially with the pedicle based immediately beneath the island) is essentially a rotation flap turned perpendicular to the surface of the skin (Fig. 147.21). Whereas, in a rotation flap, the vascular source lies parallel with the skin, the analogous vascular supply of the PVYF runs perpendicular to the skin. Similarly, the plane of tissue movement in the traditional rotation flap is parallel with the skin, but is perpendicular to the skin in a PVYF. Once this analogy between a rotation flap and a PVYF is understood, it is easy to see that movement of the PVYF is facilitated by the same factors that facilitate movement of a rotation flap. For example, excision of the Burow's triangle facilitates the rotation and advancement of the rotation flap. Likewise, the advancement of a PVYF is facilitated by the removal of the tissue analogous to the Burow's triangle, i.e. any subcutaneous tissue at the base of the defect (Fig. 147.21B). Without its removal, the subcutaneous tissue left in the wound base serves as a physical impedance to the advancing flap.

Another technique for enhancing rotation flap mobility, the back-cut, is also applicable to the PVYF. A back-cut for a rotation flap releases some of the restraining tension of the flap and is helpful in its mobilization. The equivalent of a back-cut can also improve the mobility of a PVYF. This is done by incising the subcutaneous pedicle at the trailing edge of the flap in a direction beveled slightly into the pedicle (see Fig. 147.21B).

In order to enable eversion of the skin edges of a PVYF, the island is very slightly undermined at the dermal–subcutaneous junction to facilitate its eversion. In addition, the skin surrounding the flap is widely undermined in the superficial subcutaneous tissue. The flap is then advanced into the defect, with closure of the donor site behind the flap in a V-to-Y fashion and closure of all skin edges.

Pedicled V-to-Y flap variation: the pincer flap

Altering the shape of the pedicled flap or the nature of the pedicle affords advantages in site-specific reconstructions. For example, the pincer flap is used to reconstruct the cupid's bow of the upper lip (Fig. 147.22). In the pincer flap, the shape of the flap is altered by extending its lateral incisions outside of the lateral margins of the defect, thereby creating peninsular extensions of the flap. These, unlike the body of the flap, are detached from the underlying tissue so they can be folded inwardly in a "pincer" fashion, thus forming a teardrop-shaped flap (see Fig. 147.22B). Upon suturing, this curved advancing edge recreates and preserves the curvaceous vermilion border at the cupid's bow. In addition to preserving function, it beautifully avoids disruption of an aesthetically critical facial feature.

Tissue Reorientation Flaps

Transposition flaps are among the most useful flaps because of their ability to tap into adjacent tissue reservoirs and repair defects in anatomic locations with minimal laxity. These flaps allow for repair of even large defects with minimal or no skin tension and without distortion of important surrounding anatomic structures. The classic transposition flap is the rhombic flap, with other useful transposition flap variants being the bilobed flap and the single-staged nasolabial transposition flap[20]. All these reorientation flaps are fundamentally based upon the Z-plasty.

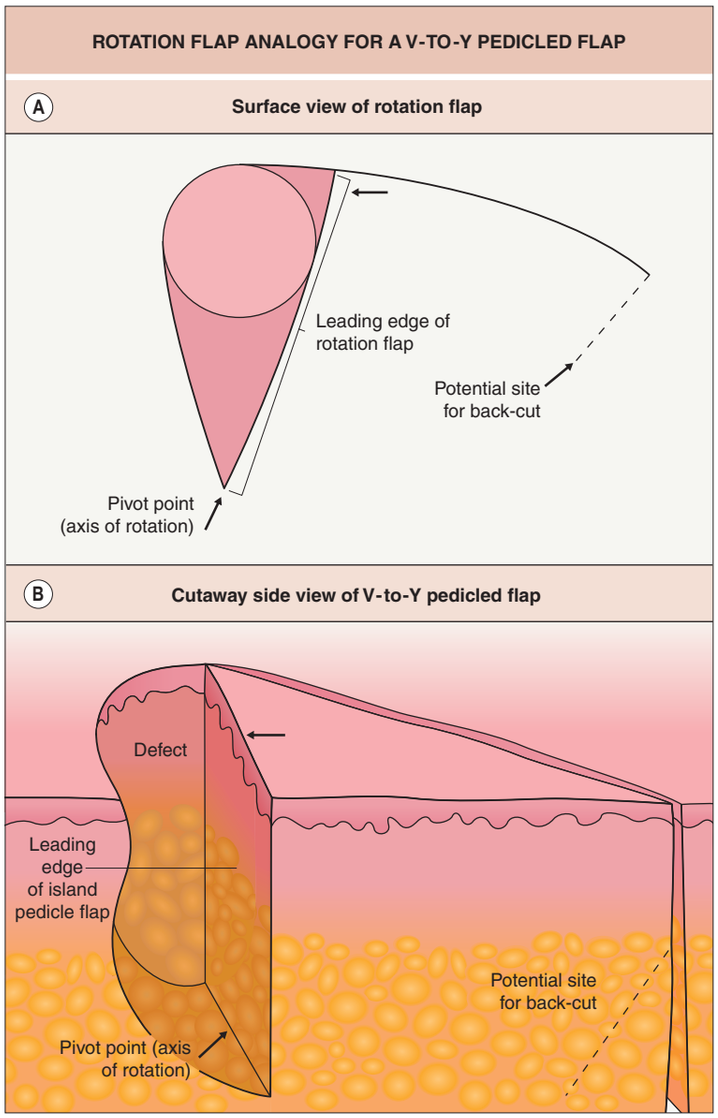


Fig. 147.21 Rotation flap analogy for the pedicled V-to-Y flap. A A rotation flap with standard removal of a Burow's triangle adjacent to the defect and the site of a potential back-cut which would facilitate flap movement. **B** Side view of a defect and the pedicled V-to-Y flap. The plane of rotation is perpendicular to the skin surface. The shaded area is where the equivalent of a Burow's triangle has been removed to facilitate flap movement. The dotted line is analogous to the back-cut of a rotation flap. Note the similarities between a rotation flap and the pedicled V-to-Y flap.

Rhombic transposition flap

The classic rhombic flap, originally described by Limberg in 1963, was based on the concept of placing the tension vector of the secondary defect nearly perpendicular to that of the primary defect (Fig. 147.23A). After closure of the donor site, the Limberg flap allowed for repair of the primary defect with essentially no wound edge tension. Dufourmentel added important modifications that made the closure of the donor site easier by placing the secondary defect at an acute angle (60°) to the primary defect. Thus, the flap passes through a shorter arc in order to be positioned within the primary defect (Fig. 147.23B). Webster modified the rhombic flap further by making the angle of the secondary defect even more acute (30°) to further facilitate closure of the secondary defect (Fig. 147.23C). The smaller flap size of the Webster variant allows the surgeon to position the flap in almost any location relative to the primary defect in order to tap into the most lax skin available. However, as the angle of the secondary defect becomes more acute, more of the wound tension is transferred from the donor site to the primary defect. Care must be taken to ensure that the tension on the flap does not compromise its vascular supply and flap viability. Another important concept to bear in mind is that as more tension is transferred to the primary defect, nearby anatomic structures will be more prone to distortion.

Careful planning is required prior to incising the rhombic transposition flap in order to ensure that the donor site comes from an area adjacent to the defect with adequate tissue laxity. This donor site, most commonly, parallels the relaxed skin tension lines. The Burow's triangle is removed at the pivot point prior to insetting of the flap. This ensures more accurate incision lines and allows more precise suture placement in order to distribute the flap tension evenly. After undermining and hemostasis, the first suture is placed to close the secondary defect. Next, the flap is inset into the defect, trimmed to fit, and sutured.

Although extremely versatile, there are specific areas where the rhombic flap provides reliable and reproducible results. The lateral upper two-thirds of the nose and the lateral forehead are ideally suited for the rhombic flap because of the frequent difficulty in closing defects in these areas primarily (Fig. 147.24). The adjacent tissue laxity available on the nasal sidewall and the lateral cheek provide ample reservoirs of donor tissue. Large defects of the central cheek may be closed by the rhombic flap when simpler options are not possible. One significant drawback of this flap is the difficulty in concealing the geometric shape of the incision lines.

Bilobed transposition flap

The bilobed flap is essentially two transposition flaps in series, and it is one of the most useful flaps for repair of defects of the lower one-third of the nose. The easily distorted alar rim can be protected from distortional tension by virtue of the inherent series of Z-plasties within this flap, with the Z-plasties serving to reorient skin in the direction of the alar rim. The bilobed flap was first described by Esser in 1918 and important modifications to the flap were described by Zitelli in 1989[9]. Zitelli modified the classic flap to decrease the pivot angle of the flap from 180° to 90–100° (Fig. 147.25). This simple modification helps to minimize two of the most common problems associated with the bilobed flap – a trapdoor deformity (pincushioning) of the primary lobe and the tendency for standing cones to form at the pivot point of the flap.

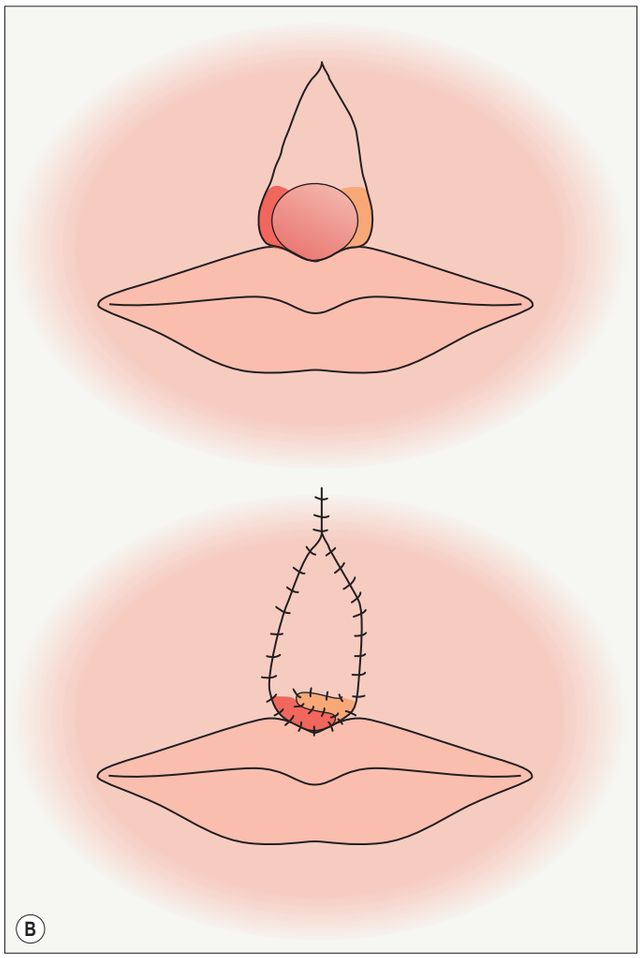
Careful planning is required for the bilobed flap to ensure minimal distortion of surrounding structures. Fig. 147.25B depicts a reliable method for planning the incisions of the bilobed flap. Drawing with a sterile marker on the patient ensures that the incision lines are placed in such a way as to maximize both functional and aesthetic results. For nasal defects, the flap should be designed so that the tertiary defect is closed perpendicular to the alar rim. This ensures that the contralateral ala is not lifted during closure of the tertiary defect. On the side of the flap where the pivot point is located, the plane of undermining is carried to the nasofacial groove in order to facilitate mobilization of the flap with no distortion of surrounding structures. Closure of the tertiary site is followed by closure of the Burow's triangle adjacent to the defect. Next, the flap is inset and sutured into the defect. The secondary flap is then trimmed to match the secondary defect and sutured in place (Fig. 147.26).

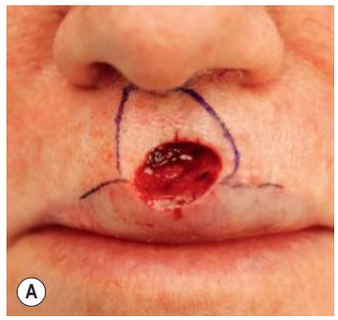
Defects of the lower one-third of the nose measuring 0.5–1.5 cm are the ideal size for the bilobed flap. Smaller defects can often be closed in a primary fashion and larger defects may need either a skin graft or a two-staged tissue importation flap. Although the bilobed flap is most commonly used for the distal third of the nose, it may be used in other anatomic sites, especially when there is potential for distortion of a free margin. Bilobed flaps can be combined with other flaps to repair relatively large defects located adjacent to the alar rim. This avoids distortion and enables the use of a smaller flap. Video 147.1 illustrates the combination of a bilobed flap and an island pedicle flap.

Trilobed flap and rhombic flap with Z-plasty

Useful variants of the rhombic and bilobed flaps include the trilobed flap and the rhombic flap with Z-plasty[21,22]. These flaps expand on the concept that transposition flaps which are arranged in series include more Z-plasties and, therefore, enable greater tissue movement without distortion of free margins. Again, the most common site for these flaps is the distal nose. In particular, they are useful for defects located very distally on the nasal tip (Fig. 147.27), for defects on delicate, easily distortable noses, or for defects that are larger than what a bilobed flap can effectively close.

The only difference between a bilobed and trilobed flap and a rhombic flap with a single or multiple Z-plasties is the size of the second subsequent lobe(s). The latter uses a diminutive lobe (the Z-plasty) that, when transposed into the defect, only partially fills it. The remainder of the tertiary defect(s) is closed primarily.





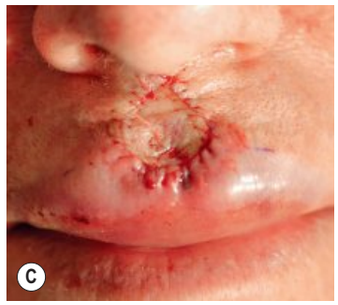




Fig. 147.22 Pincer flap. A This variant is site-specific for the cupid's bow. **B** The pedicled V-to-Y flap with pincer-like extensions on the lateral edges of the defect (shading). These "pincers" are folded upon one another to recreate the teardrop shape of the philtrum and cupid's bow. **C** Pincer flap sewn into place with side-lighting to show the recreation of the concavity of the philtrum at the cupid's bow. **D** Four-month follow-up.

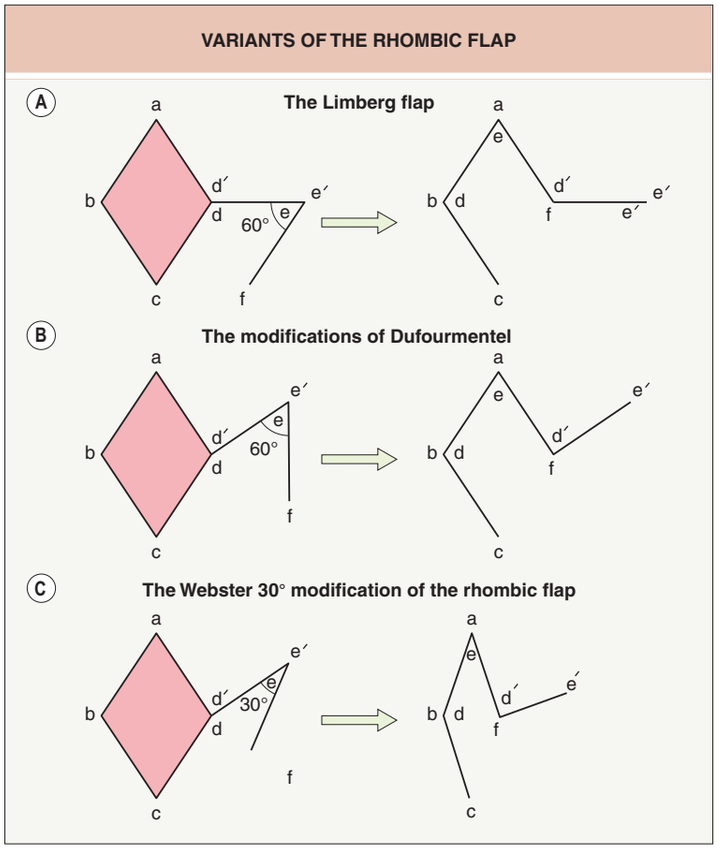


Fig. 147.23 Variants of the rhombic flap. A The Limberg flap is the standard rhombic flap. **B** The modifications of Dufourmentel. **C** The Webster 30° modification of the rhombic flap.

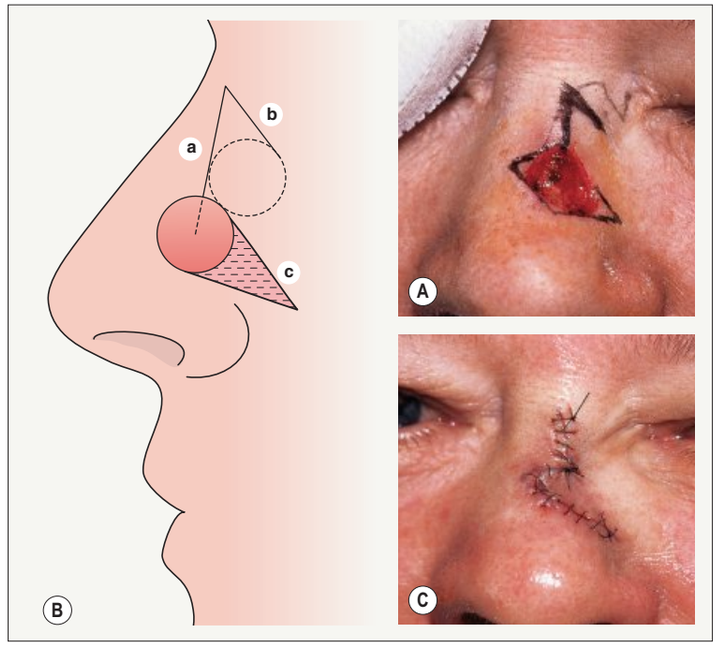


Fig. 147.24 Rhombic transposition flap on the upper lateral nose. A, B Key to the correct design of this flap is identification of the center point of the defect. The first incision for the flap is made in a line (a) along a vector radiating from the central point into the donor skin. The second incision (b) is made at an angle between 45° and 60° to this radiating incision, keeping in mind that the width of the flap must equal the width of the defect. Next, a 30° Burow's triangle is excised such that the flap side of the incision (c) is parallel to the lateral edge of the rhombic flap (b). **C** The tip of the flap is trimmed to fit the defect and the wound edges are sutured.

Nasolabial transposition flap

The single-staged nasolabial (melolabial) flap is a transposition flap variation that can be used to reconstruct defects of the nasal sidewall or large alar defects. Traditional designs of the nasolabial flap resulted in significant blunting of the nasofacial sulcus and frequently in a trapdoor deformity, often requiring one or more postoperative revisions. This is perhaps why this flap has been underutilized in reconstruction of the nose. In 1990, Zitelli described several modifications of the traditional design that helped to minimize the need for surgical revisions[23]. The flap should be designed to include the preplanned excision of the Burow's triangle along the lateral nasal sidewall (Fig. 147.28). The donor site should parallel the nasolabial fold and, once incised and elevated, should be widely undermined; the recipient site should be undermined in the submuscular plane on the nose.

The first stitch is a periosteal suture placed in the undersurface of the flap corresponding to the new location of the nasofacial sulcus. This is secured to the periosteum of the lateral nasal sidewall, thus recreating the sulcus while eliminating tension on the flap. The periosteal sutures also minimize secondary flap movement that might pull the ala laterally. The distal flap should then be thinned and sutured in place. Tacking sutures are placed in the undersurface of the flap in an attempt to recreate the alar crease and to prevent collapse of the internal nasal valve. The tip of the flap is finally trimmed to match the defect and sutured in place.

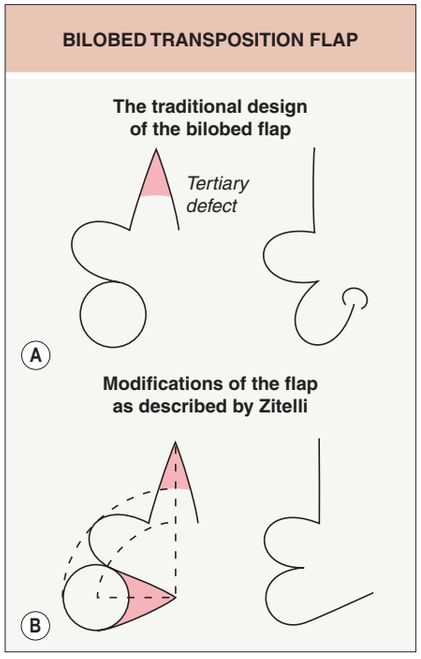


Fig. 147.25 Bilobed transposition flap. A The traditional design of the bilobed flap results in tissue protrusion at the pivot point. **B** Modifications of the bilobed flap as described by Zitelli.

Tissue Importation Flaps

Tissue importation flaps are a loosely associated group of flaps that employ the concept of transferring tissue from a distant reservoir into a defect when other adjacent repair options are unsatisfactory. The flap itself is supported by either: (1) a single vessel as with an axial flap; or (2) a rich plexus of subcutaneous perforating vessels that enter the flap pedicle through underlying muscle (random pattern flap). Tissue importation flaps are ordinarily two- or three-stage procedures. The first stage includes the initial planning and implementation of the flap. The vascular pedicle is left in place after the first stage to ensure adequate blood supply. The second stage involves the separation of the pedicle and insetting of the proximal flap. Tissue importation flaps are most useful for reconstruction of large defects and are especially valuable when cartilage grafting is required to rebuild normal anatomic substructure and preserve proper function.

Forehead flaps

The *paramedian forehead flap* is classically an axial flap based on the supratrochlear artery[24,25]. It is the most useful flap for reconstruction of subtotal and total nasal defects. The excellent vascular supply supports both the flap and any cartilage grafts that are used to rebuild the cartilage framework of the nose (see Ch. 148). The paramedian forehead flap also provides excellent color and texture match and often exceeds the cosmetic results of a skin graft.

An important concept in flap design includes the enlargement of the nasal defect to encompass the entire cosmetic unit when possible. This makes the junction of the flap and the remaining nasal skin less conspicuous and is more likely to result in an excellent cosmetic outcome. If necessary, proper mucosal lining is ensured by using a nasal mucosal flap, a turndown flap, or a split-thickness skin graft (Fig. 147.29). If cartilage support is required, conchal or nasal septal cartilage is used to rebuild the normal cartilage framework (see Ch. 148). Next, a foil template of the defect is constructed and used to outline the flap on the forehead. A 4×4-inch gauze is used to simulate the length of the pedicle.

For tissue importation, the design of the pedicle is a critical step since it is the conduit for blood supply to the flap. Classically, the paramedian forehead flap is considered an axial flap based upon the supratrochlear artery (STA). Doppler identification of its precise location is often done to assure inclusion of the STA and optimization of blood flow. However, the need to meticulously include the Doppler-identified artery has recently been challenged. In a study that compared flaps based on a Doppler-localized STA versus paramidline forehead flaps based medial

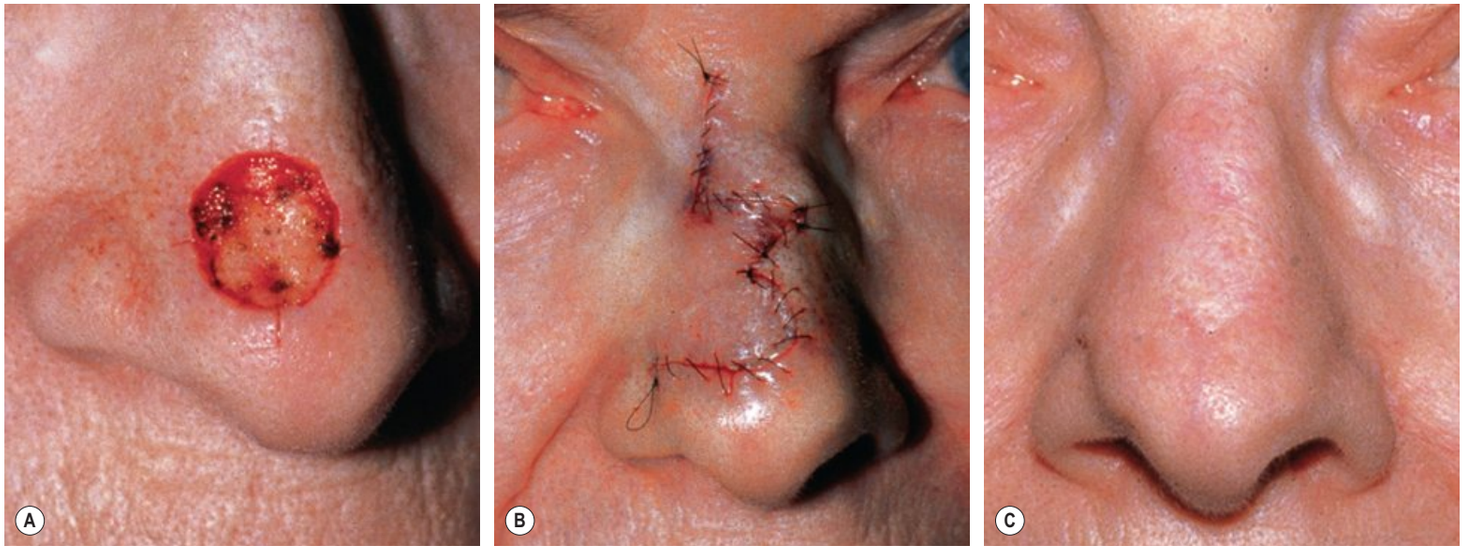


Fig. 147.26 Bilobed flap. A Distal nose defect. **B** Defect reconstructed with a bilobed transposition flap. **C** Cosmetic result at 1 year postoperatively.

to the STA without the use of Doppler (see Fig. 147.29E), similar clinical results were observed[26]. Furthermore, histologic examination of the proximal and distal portions of the pedicle found little differences in vascular composition when the two groups were compared. The only histologic difference was more blood vessels in the pedicles of the paramidline forehead flaps than in the STA-based flaps.

The *paramidline forehead flap* design utilizes the exact midline of the glabella for the medial pedicle incision. The lateral incision is made 1.2 cm lateral to this without respect to the location of the STA. All other aspects of the forehead flap execution are the same as with the STA-centered flap design (see Fig. 147.29E).

Irrespective of how the forehead flap is designed, flap procurement is begun by incising the distal flap (on the upper forehead) in the subcutaneous plane, and as dissection progresses inferiorly, it is gradually deepened. That is, the distal one-third of the flap is dissected in the superficial subcutaneous plane, with deepening over the middle one-third to just above the periosteum in the proximal one-third (just above the brow). When dissecting the glabellar portion of the pedicle, care must be taken to ensure that the axial arteries are not severed as they exit the supraorbital foramen. Bilaterally, the forehead donor site is undermined in the subgaleal plane and then closed in a layered fashion. The widest part of the forehead defect may not close, but heals well by second intention. Finally, the distal end of the flap is thinned to match the thickness of the remaining nasal skin before it is inset.

The second stage of the forehead flap is typically performed 3 weeks later (see Fig. 147.29G). The pedicle is severed near its base and closed primarily. After carefully trimming and thinning the proximal edge of the nasal flap as well as freshening its margin, it is inset into the defect.

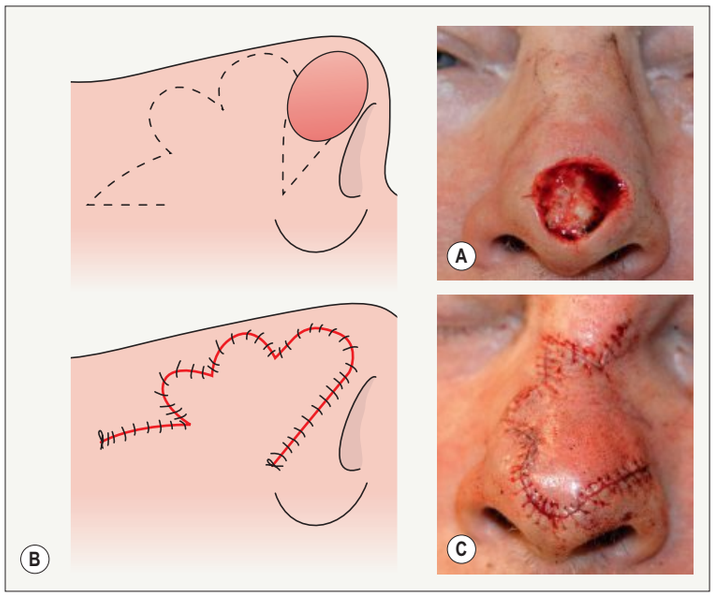


Fig. 147.27 Trilobed flap. A Large subtotal defect of the nasal tip. **B** Trilobed flap with tertiary lobe oriented perpendicular to the alar rim. These three lobes are transposed inferiorly and sequentially into the defects. A total of five Z-plasties are incorporated within this design enabling nearly tension-free redistribution of skin from the upper nose to the nasal tip. **C** Closed wound with minimal distortion of the nasal tip and alar structures.

Nasolabial interpolation flap

The nasolabial (melolabial) interpolation flap has been utilized primarily for defects of the nasal ala. This flap is especially useful for large defects and complex defects involving the alar rim. In certain circumstances, the flap may be utilized for the repair of nasal tip defects when the latter are moderate in size and a paramedian forehead flap is less optimal[27,28].

When utilizing the nasolabial interpolation flap for the repair of alar defects, excision of the remainder of the cosmetic unit of the ala ensures a better aesthetic and functional result (Fig. 147.30). After providing any necessary cartilage support, a foil template is made of the contralateral ala and then it is flipped over and placed on the ipsilateral nasolabial skin. A 4 × 4-inch gauze can be utilized to ensure proper flap length. The flap on the cheek is incised and dissected to a well-vascularized pedicle deep in the subcutis.

The flap can be based either superiorly or inferiorly. The former is best for larger or more medial defects (see Fig. 147.30), but in men, this design is limited by hair-bearing skin. In women, longer flaps can be designed affording greater reach medially. The inferiorly based flap, incised from the nasofacial sulcus, is more limited in length and width. However, the skin is more delicate and free of hair follicles, often resulting in better skin match. The flap is twisted on its pedicle, trimmed, and sutured into place. The donor defect is closed up to the base of the pedicle.

Three weeks later, the patient returns for separation of the pedicle (see Fig. 147.30C,D). The surgeon amputates, trims, and sutures the flap and the cheek to ensure recreation of the normal complex anatomic features of this aesthetically important area. Fusiform excision of the

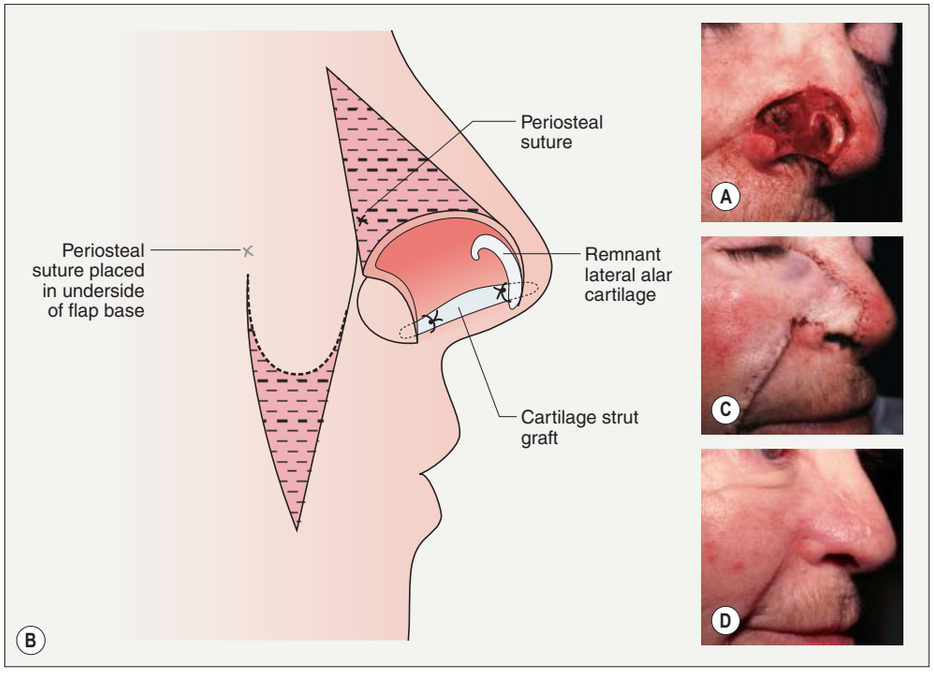


Fig. 147.28 Nasolabial transposition flap. A Large nasal defect involving loss of cartilage and extending to the intranasal skin. **B** Excision of a Burow's triangle on the nasal sidewall is oriented towards the medial canthal tendon. The lateral incision of the flap should extend no higher than the apex of alar skin over which the flap is to be transposed. In this case, an auricular cartilage strut graft is placed along the alar rim and inserted into medial and lateral dermal pockets and anchored with deep sutures into the wound base. The points of placement of the periosteal sutures into the undersurface of the advancing flap are indicated with an X. The distal flap is aggressively defatted. **C** The flap is trimmed to fit the defect, wrapped around the alar rim and folded onto itself, reforming the rim. **D** Cosmetic result at 6 months postoperatively.

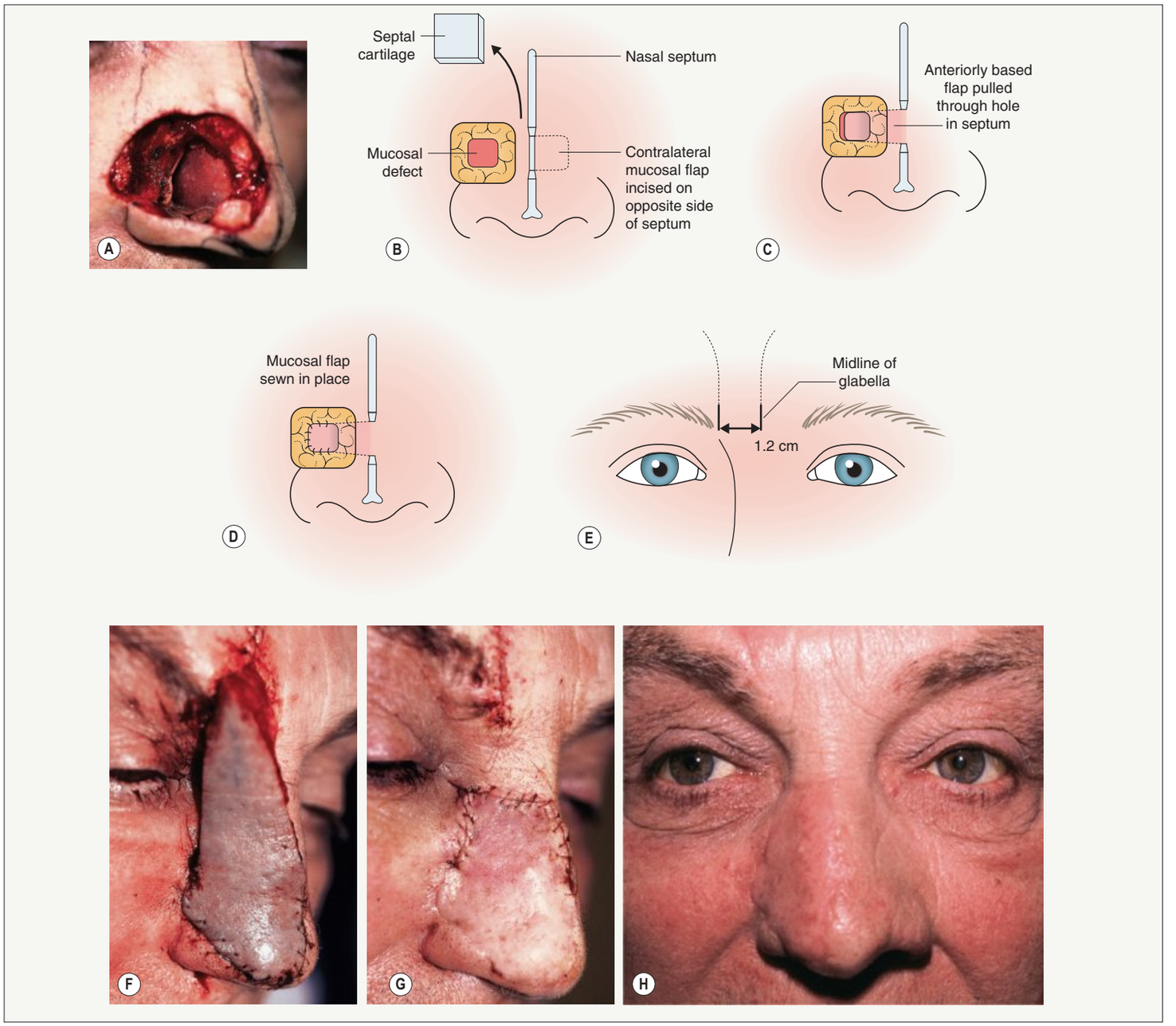


Fig. 147.29 Paramidline forehead flap. A Large full-thickness defect of the right half of the distal nose. **B** The mucosal defect is reconstructed with a contralateral septal mucosal pull-through flap. A U-shaped incision is made in the contralateral septal mucosa, based anteriorly and correctly sized to cover the defect. In addition, a 15 mm^2 cartilage graft is harvested from the nasal septum and used to reconstitute the structural integrity of the nasal sidewall. (Note that the remainder of the nasal sidewall cosmetic subunit and the right nasal tip subunit will be excised prior to reconstruction with the forehead flap.) **C** The mucosal flap is delivered through the septal defect into the right nasal vestibule. **D** The mucosal flap is sutured into place. **E** The design of the pedicle uses the midline of the glabella as the medial incision point; the lateral incision is made 1.2 cm lateral to the midline. Using a template, the forehead flap is then incised and raised on this 1.2 cm-wide pedicle. **F** Immediately postoperatively. **G** Immediately after takedown of flap 3 weeks later. **H** Early cosmetic results with no revision 2 months postoperatively.

pedicle stump provides for the most aesthetically pleasing repair of the cheek donor site.

Retroauricular flap

The two-staged retroauricular flap is useful for large defects of the helical rim, antihelix, and scapha (Fig. 147.31). The retroauricular flap is a random pattern flap without a single vascular pedicle. Nonetheless, because of the rich blood supply of scalp skin, this represents one of the best vascularized random pattern tissue importation flaps and easily supports cartilage grafts (if needed)[13,14].

After providing cartilage support (if needed; see Ch. 148), a foil template of the defect is fashioned and placed on the skin of the postauricular scalp. The distal flap may originate anywhere from the retroauricular sulcus to the posterior surface of the ear, depending on how far anteriorly it must reach. The incisions are then made, extending posteriorly to the hairline. The flap is dissected in a subcutaneous plane and the tip judiciously thinned to match the thickness of the skin at the defect. The flap is sutured into place being sure to minimize tension as the flap curls around the anterior helical rim. The use of bolster sutures can be very helpful in recreating the curve of the antihelix. Three weeks later, the pedicle is severed near the scalp and inset. The donor site can be closed primarily, with a skin graft, or left to heal by second intention.

Spear's flap

The inverted nasolabial (melolabial) pedicle flap, described by Spear[29], is useful for reconstruction of full-thickness defects of the ala that involve the attachment point of the lateral ala to the cheek (Fig. 147.32).

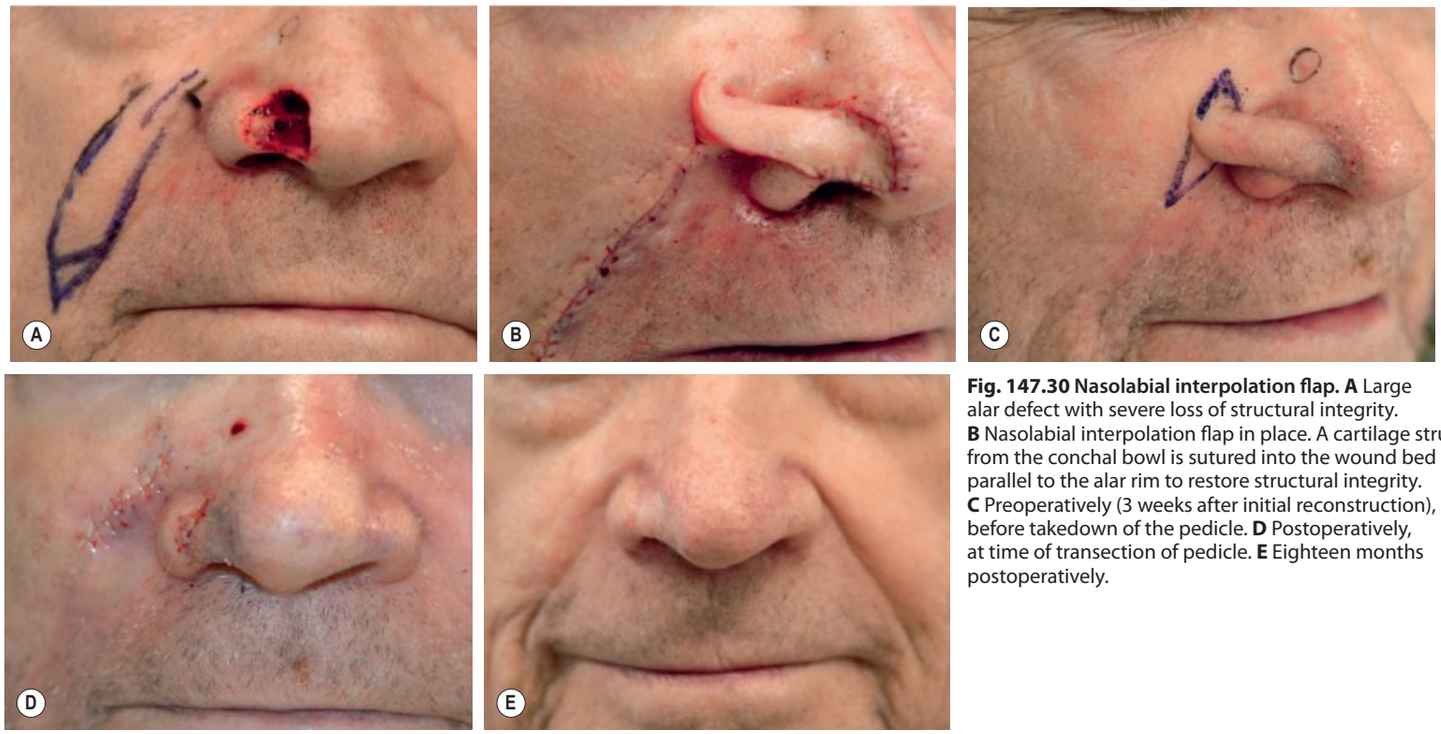


Fig. 147.30 Nasolabial interpolation flap. A Large alar defect with severe loss of structural integrity. **B** Nasolabial interpolation flap in place. A cartilage strut from the conchal bowl is sutured into the wound bed parallel to the alar rim to restore structural integrity. **C** Preoperatively (3 weeks after initial reconstruction), before takedown of the pedicle. **D** Postoperatively, at time of transection of pedicle. **E** Eighteen months postoperatively.

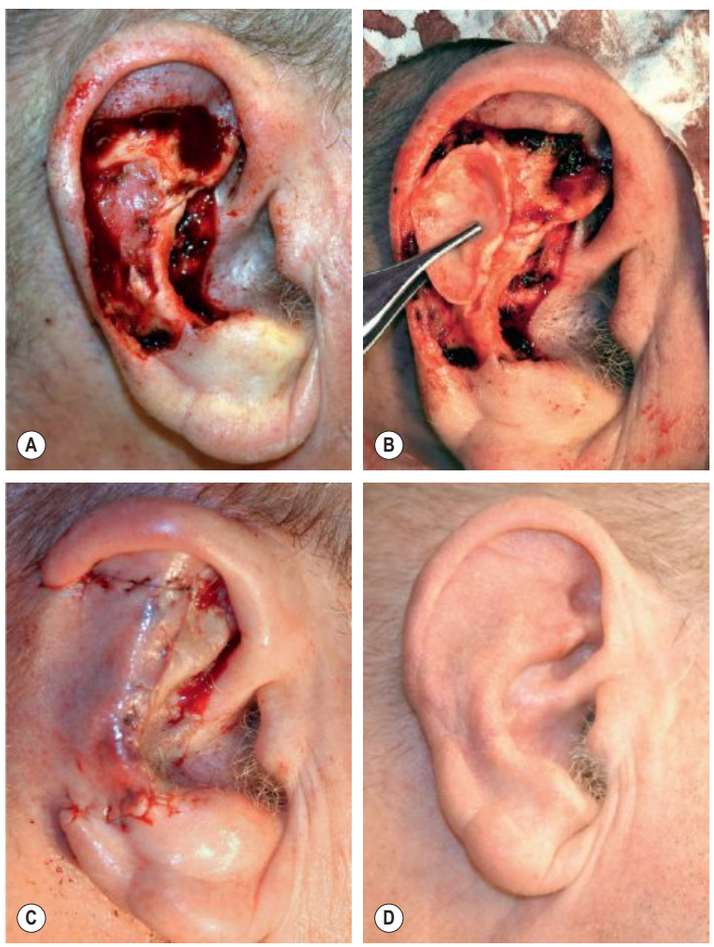


Fig. 147.31 Retroauricular flap. A Large defect of the anterior ear including substantial loss of cartilage of the mid antihelix and helical rim. **B** A cartilage graft harvested from the contralateral conchal bowl is used to restore structural integrity of the infrastructure of the auricle. **C** Closure of the retroauricular flap with resurfacing of the helix and antihelix. A split-thickness skin graft is used to resurface the crus of the antihelix and a portion of the conchal bowl. The pedicle from the retroauricular skin will be divided at 3 weeks. **D** Reconstructive results at 4 months.

The design of the Spear's flap is planned in a manner similar to that of the single-staged nasolabial interpolation flap, with the use of a foil template made from the contralateral ala. This template is placed upside down on the skin of the cheek lateral to the nasolabial fold and the flap is incised to a point just lateral to the superior edge of the defect. The flap is then dissected to a well-vascularized pedicle deep in the subcutis. Next, the flap is twisted on its pedicle and the edge of the mucosal defect adjacent to the nasal tip is sutured to the under-turned skin of the medial edge of the flap. The lateral portion of the under-turned flap is then sutured to the lateral mucosal defect. By folding the flap upon itself, the alar rim and the external surface of the ala are recreated, and the tip of the flap is carefully trimmed to match the contralateral ala. The surface of the flap is closed in a layered fashion. As with the other nasolabial flaps, the donor site is closed after widely undermining the skin of the cheek. Occasionally, a standing cone is created superolaterally to the new ala and it needs to be excised and sutured to complete the repair. Postoperatively, the newly formed ala may be positioned too far laterally and may require repositioning using a Z-plasty transposition of the alar base medially in a revision performed two or more months later.

Tunneled flaps

Tunneled flaps are variants of tissue importation flaps in that skin from a non-adjacent site is used to reconstruct a defect. They can be single-stage flaps, but may require revision because of the deformation the pedicle can create along the path of the tunnel. Examples of these flaps include the nasolabial to lip pull-through flap, the paranasal to ala flap, and the retroauricular pull-through flap (flip-flop flap)[30–32].

These flaps are based upon a pedicle that, like the PVYF but unlike other tissue importation flaps, is composed entirely of subcutaneous and muscular tissues and includes an axial vascular bundle within the pedicle. The flap skin and its pedicle are then passed through a tunnel of intervening skin (or cartilage) to the defect. As a result, it is a higher-risk flap than most PVYFs and tissue importation flaps. The initial key step is finding suitably vascular locations for these flaps. Sites most often chosen for flap placement include the nose, lip, and ear. Of note, the subcutaneous tunneling island pedicle flap (IPF) is not a traditional advancing IPF and technically is not a defect reconfiguration flap. Rather, it is a type of tissue importation flap (see Table 147.3).

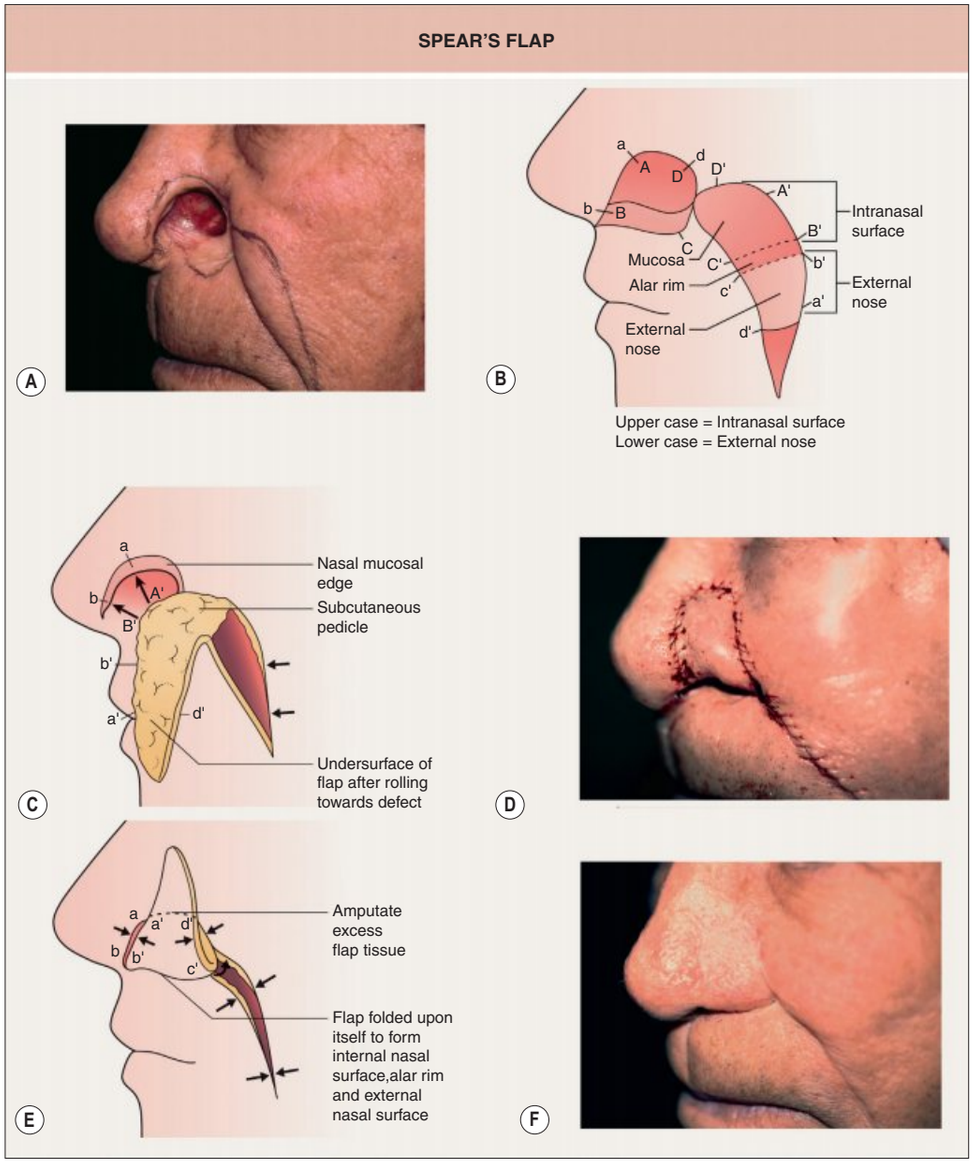


Fig. 147.32 Spear's flap. A Nasal defect involving the entire nasal ala and a portion of the nasal sidewall with the plans marked for a nasolabial transposition flap with a twist as described by Spear. **B** Flap incised prior to rolling towards defect. **C** Initial movements of flap. **D** Flap in place having been twisted on a subcutaneous pedicle sutured into the mucosal side of the defect and folded upon itself followed by suturing of the cutaneous side of the defect. **E** Corresponding schematic demonstrating placement of the flap and amputation of the distal portion. **F** Early results after second revision.

First, the donor skin is identified in an area with a suitably vascular pedicle. Careful measurements of both the defect and the length of the subcutaneous pedicle are necessary so that the latter reaches the defect under minimal tension. Next, the island is incised and a pedicle deep to the island is developed. It may be helpful to elevate the skin overlying the prospective pedicle to visualize its development. Once an adequate pedicle is developed, the skin between the base of the pedicle and the defect is undermined, creating a tunnel. The tunnel must be large enough for the tissue to pass and not be compressed; cautious defatting of the tunnel walls is often helpful to ensure ample room. This defatting also decreases the degree of fullness of the intervening skin created by the bulk of the pedicle. The length of the pedicle should be limited to three to four times its diameter, unless it is an axial flap. It is prudent to anticipate a 10%–20% "shortening" of the pedicle as it is rotated and stretched through the tunnel into the defect.

Larger alar defects can likewise be repaired with the *paranasal to ala tunneled flap* (Fig. 147.33). This flap also uses skin from the medial cheek, with a pedicle developed from the paranasal subcutaneous tissue and muscle. A short tunnel is developed between the flap and the defect through which the flap is passed. As noted previously, debulking of the soft tissue around the tunnel facilitates the passing of the flap and pedicle through it. The donor site is closed primarily and the flap is inset and sutured into the wound.

In the *retroauricular pull-through flap (flip-flop flap)*, an island of skin is pulled through a "tunnel" (created either by the surgeon or in the process of cancer removal) that goes through the cartilage of the conchal bowl in order to repair the anterior surface of the ear (Fig. 147.34). The principles of developing the pedicle and assuring that adequate space exists within the tunnel apply to this flap as well. The flap itself originates from the postauricular skin and is pedicled upon the rich vascular plexus of the retroauricular sulcus. It is flipped like a book page on its pedicle, pulled through to the anterior surface of the ear, and sutured. The donor site may heal by second intention, be closed (partially or completely) primarily, or grafted.

Combination Flaps

Not all defects can be conveniently closed with a single flap. There are times when a combination of closure techniques is employed, either because the defect is too large or because the defect involves more than one cosmetic subunit. These types of wounds are better closed using a combination of flaps or flaps plus grafts (see Fig. 147.31). Combination closures for very large defects are usually employed when a flap is able to close a significant portion, but not all, of the defect. In that situation, a full-thickness graft may be used to supplement a flap and complete the coverage of a defect. Grafts can be harvested from any of the common donor sites, depending on tissue match and the adequacy of donor skin (see Ch. 148). When reconstructing a wound after Mohs micrographic surgery (i.e. a high degree of certainty of cancer-free margins exists), tissue adjacent to the wound can be safely used as "Burow's grafts".

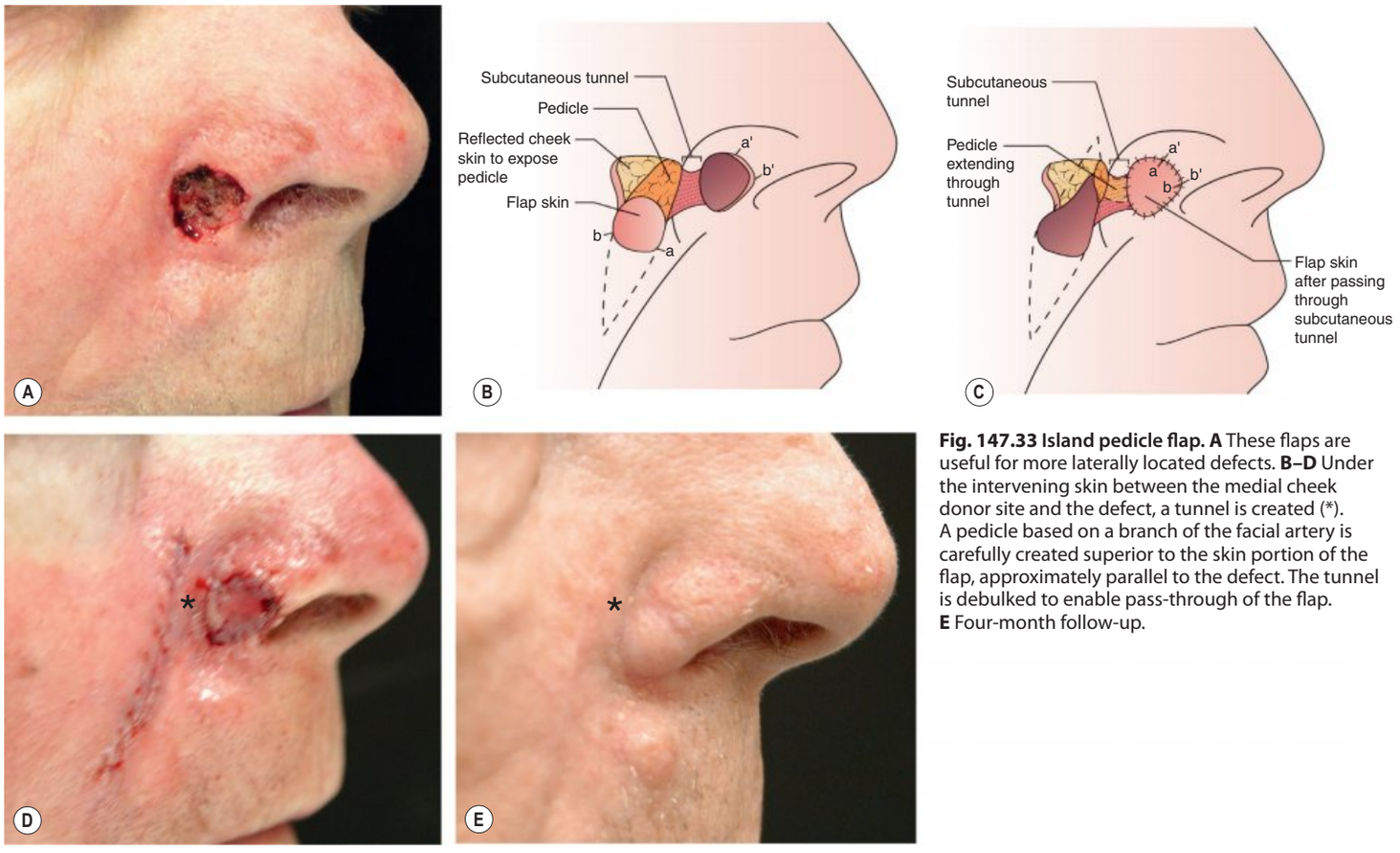


Fig. 147.33 Island pedicle flap. A These flaps are useful for more laterally located defects. **B–D** Under the intervening skin between the medial cheek donor site and the defect, a tunnel is created (*). A pedicle based on a branch of the facial artery is carefully created superior to the skin portion of the flap, approximately parallel to the defect. The tunnel is debulked to enable pass-through of the flap. **E** Four-month follow-up.

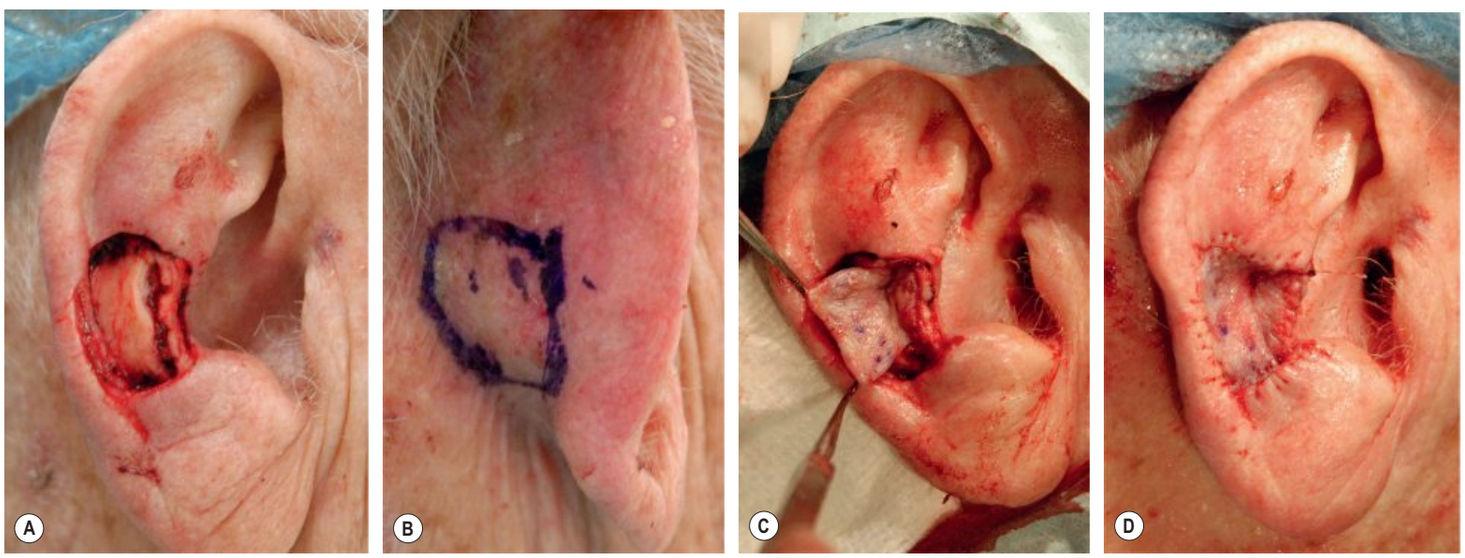


Fig. 147.34 Retroauricular pull-through flap (flip-flop flap). A This flap is ideally suited for large deep defects of the anterior ear, especially when cartilage is lost or compromised. **B** The donor site is designed for a book page-like flap movement, with the posterior-most portion of the flap sutured into the posterior-most aspect of the defect nearest the helix. **C** The flap being passed through the cartilage defect is based upon retroauricular subcutaneous and muscular tissue. **D** Flap sutured into place.

The Burow's triangle(s) of a flap can be defatted and trimmed to fit the remaining defect rather than being discarded.

Sometimes, flap and graft combinations are used to reconstruct defects that involve more than one cosmetic subunit. In such a wound, a flap is used to reconstruct one cosmetic subunit while a full-thickness skin graft is used to reconstruct the other, maintaining the "separateness" of each cosmetic subunit. The principle of maintaining the boundaries between cosmetic subunits is very useful in achieving a much less noticeable cosmetic result. If flaps or grafts are applied across cosmetic subunits, the aesthetic disruption that occurs becomes more visible.

There are also defects that involve multiple cosmetic subunits that are best repaired individually with different flaps. The same principle applies in that maintaining the integrity of individual cosmetic subunits is an important consideration in achieving a more natural and less noticeable result. These types of closures require creativity and sometimes ingenious methods to accomplish complete closure.

Table 147.4 summarizes previously discussed flaps and areas of the face where the specific flaps are most useful for providing excellent functional and aesthetic results.

COMMON LOCATIONS FOR FLAP TYPES
Burow's triangle displacement flaps
Burow's flap (single tangent advancement flap) and bilateral single tangent advancement flap (A-to-T flap)
• Distal, lateral nasal sidewall • Upper lateral lip • Infranasal upper lip • Eyebrow and suprabrow forehead • Mid helix
Unilateral or bilateral double tangent advancement flap (U- or H-flap)
• Forehead • Helix • Large defect of upper lip
Rotation flap(s)
• Upper cheek • Medial chin • Nasal dorsum (Rieger flap) • Lower eyelid
Defect reconfiguration flaps
Pedicled V-to-Y flap
• Upper lateral and mid upper cutaneous lip • Mucosal lip • Lateral chin and lower lip • Distal nasal sidewall • Preauricular cheek • Eyebrow
Tissue reorientation flaps
Rhombic transposition flap
• Nasal sidewall • Temple and lateral forehead • Lateral canthus and lateral lower lid • Lateral chin and lower lip • Superior and anterior helix
Bilobed transposition flap
• Nasal tip and supratip • Lower lateral lip • Periocular skin
Nasolabial transposition flap
• Alar defects, especially those involving the lateral portion of the ala • Lateral alar crease and distal nasal sidewall
Tissue importation flaps
Paramedian/paramidline forehead flap
• Large nasal defects • Moderate-size nasal tip defects • Nasal defects with loss of cartilage and/or nasal lining • Large medial canthus defects
Nasolabial (melolabial) interpolation flap
• Nasal ala and alar rim • Nasal tip • Mid upper lip
Melolabial flap with a twist (Spear's flap)
• Full-thickness alar defects involving the junction of the lateral ala and the cheek/upper lip
Retroauricular flap
• Large defects of the anterior ear or helix • Full-thickness defects requiring cartilage graft reconstruction
Subcutaneous tunneling island pedicle flap
• Inferior nasal defects • Medial upper lip • Conchal bowl and antihelical ear (flip-flop flap)

Table 147.4 Common locations for flap types.

POSTOPERATIVE CARE

Postoperative care after flap surgery varies from practice to practice. Some surgeons have the patient change the bandage once to several times a day, cleansing the wound at each bandage change. Others apply a bandage for a day or two and leave the sutured wounds open to air thereafter. Still others apply a single bandage at the time of the surgery and leave it undisturbed for up to a week. Regardless of how the postoperative care is accomplished, there are common goals to achieve during the postoperative period.

One of these common goals is to prevent postoperative bleeding. The first 48 hours is the time period during which bleeding and hematomas most commonly occur. Efforts to reduce these complications include meticulous intraoperative hemostasis and the postoperative application of pressure to the wound. Pressure can be applied by using taping techniques, pressure wraps, or specialized pressure garments. Normally, pressure becomes less important after 24 to 48 hours. In the patient at higher risk for bleeding, it may be necessary to maintain pressure for a more prolonged period of time. In some patients with a very high risk of postoperative bleeding, it may be helpful to use a tie-over bolster dressing directly over the wound to ensure constant firm pressure throughout the postoperative period.

Another common goal in the postoperative care of flaps is to reduce the risk of infection. All forms of infection can complicate the postoperative course and affect the cosmetic and functional results. Prevention of postoperative infections is covered in Chapter 151. However, good surgical technique and observance of sterile technique during reconstruction is paramount. One novel approach, particularly well-suited for cutaneous reconstructions, is the direct infiltration of the unclosed wound preoperatively with local anesthesia containing antibiotics. The benefit of intralesional nafcillin and clindamycin has been studied and this procedure is used routinely in some practices prior to reconstruction[33,34].

An additional important goal in the postoperative care of flap reconstruction is protection of the flap tissue from all environmental insults, including contamination, physical injury, temperature extremes, excessive movement and stretching of the sutured skin during the early postoperative period, and ultraviolet radiation. This is best accomplished by occlusive bandaging techniques and thorough education of the patient.

Presented here are the details of postoperative flap care as routinely implemented in one surgical practice. After the completion of flap reconstruction, a light bandage consisting of hypoallergenic tape over Steri-Strips™ is placed directly over the incision lines. The tape completely covers the sutured skin resulting in complete occlusion of the wound. A "bulky" secondary bandage is then applied on top of this thin primary bandage. The bulky bandage consists of rolled or fluffed absorbent gauze, which is affixed with hypoallergenic paper tape, using a technique of taping which applies downward pressure. This is accomplished by the placement of one end of the tape on the skin of one side of the wound and stretching it over the top of the bulky gauze and then attaching the other end to the opposite side of the flap under tension. This is repeated numerous times with thin, 1-cm-wide strips of tape until the bulky gauze is entirely covered and firmly affixed by the tape. The patient is instructed to remove the bulky secondary bandage 24 to 48 hours after surgery, leaving the thin, flat primary bandage in place. This bandage is left undisturbed and kept dry for the remainder of the week.

The patient returns to the office after 1 week for bandage removal, suture removal, and evaluation of the wound. Any evidence of hematoma, infection, or other complication is addressed. The skin is cleansed and another thin bandage consisting of Steri-Strips™ and hypoallergenic tape is applied for one more week. The patient is instructed again to keep this bandage dry and to remove it in 1 week (i.e. 2 weeks after the surgery). The patient is encouraged to contact the physician during the postoperative period if there are any problems and to return in 3 months for a final evaluation of the wound healing process. Minor revisions may be made at that time to optimize the aesthetic and functional results.

COMPLICATIONS

In the immediate postoperative period, the potentially serious sequelae are primarily postoperative bleeding and infection. Both adverse events

are rare if meticulous surgical technique is used[35]. Nonetheless, failure to recognize either complication and intervene appropriately can lead to disastrous postoperative results. Postoperative bleeding that results in a hematoma requires immediate attention. The most effective intervention is an immediate return to the operating suite to remove the sutures, evacuate the hematoma, locate and ligate the bleeding vessel, and re-suture the wound. Failure to do so risks flap necrosis. If a postoperative infection is present, immediate oral antibiotics and drainage of any abscess are required.

In the mid-postoperative period, the most common complication requiring intervention is the development of a hypertrophic scar or trapdoor deformity. This usually becomes evident about 4 to 8 weeks after surgery and occasionally develops despite wide undermining, appropriate flap thinning, and meticulous suturing technique at the time of surgery. Often, the patient is advised to aggressively massage the site many times per day. Massage and tincture of time often promote adequate remodeling of the healing wound. Occasionally, active intervention is necessary. Varying concentrations of intralesional triamcinolone acetonide injections may be helpful (5–40 mg/ml), depending upon the scar's location and thickness.

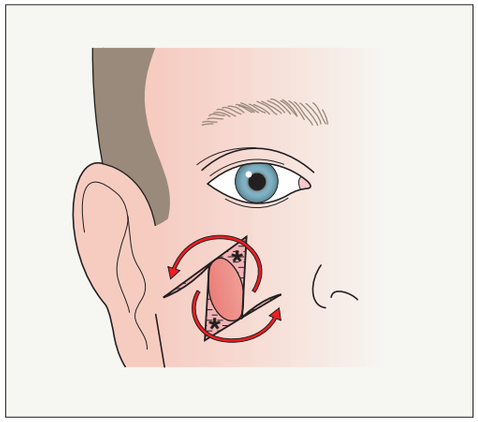
Late postoperative complications include persistent trapdoor deformity, surface irregularities, blunting or ablation of the junction between cosmetic units, and surface telangiectasia. Persistent trapdoor deformity and minor surface irregularities can be addressed as early as 6–12 weeks postoperatively with the use of a scalpel to plane the surface and dermabrasion or dermasanding to blend the planed surface. In order to redefine the junction between cosmetic units that may have been ablated by the placement of a flap (e.g. the alar crease in a nasolabial transposition flap), incising the area, thinning the subcutis, and re-suturing the skin edges to recreate the natural fold is usually all that is required. Laser ablation of telangiectasia around the incision lines of large nasal flaps can be done for any unremitting perincisional blood vessels.

Sometimes, regardless of proper patient selection, flap planning and suturing technique, some amount of postoperative refinements may be necessary. These vary from simple procedures to correct surface irregularities to more complicated interventions requiring further scalpel surgery. The key to a successful outcome from a postoperative intervention is recognizing the circumstances where an intervention would be helpful and then choosing the appropriate intervention. Understanding the normal sequence of healing after a surgical procedure helps the surgeon to decide when and by what means to intervene in this process.

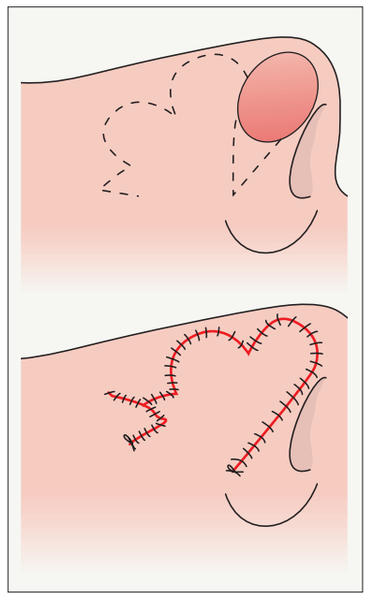
Additional figures available in our eBook (see inside front cover for access code).

REFERENCES

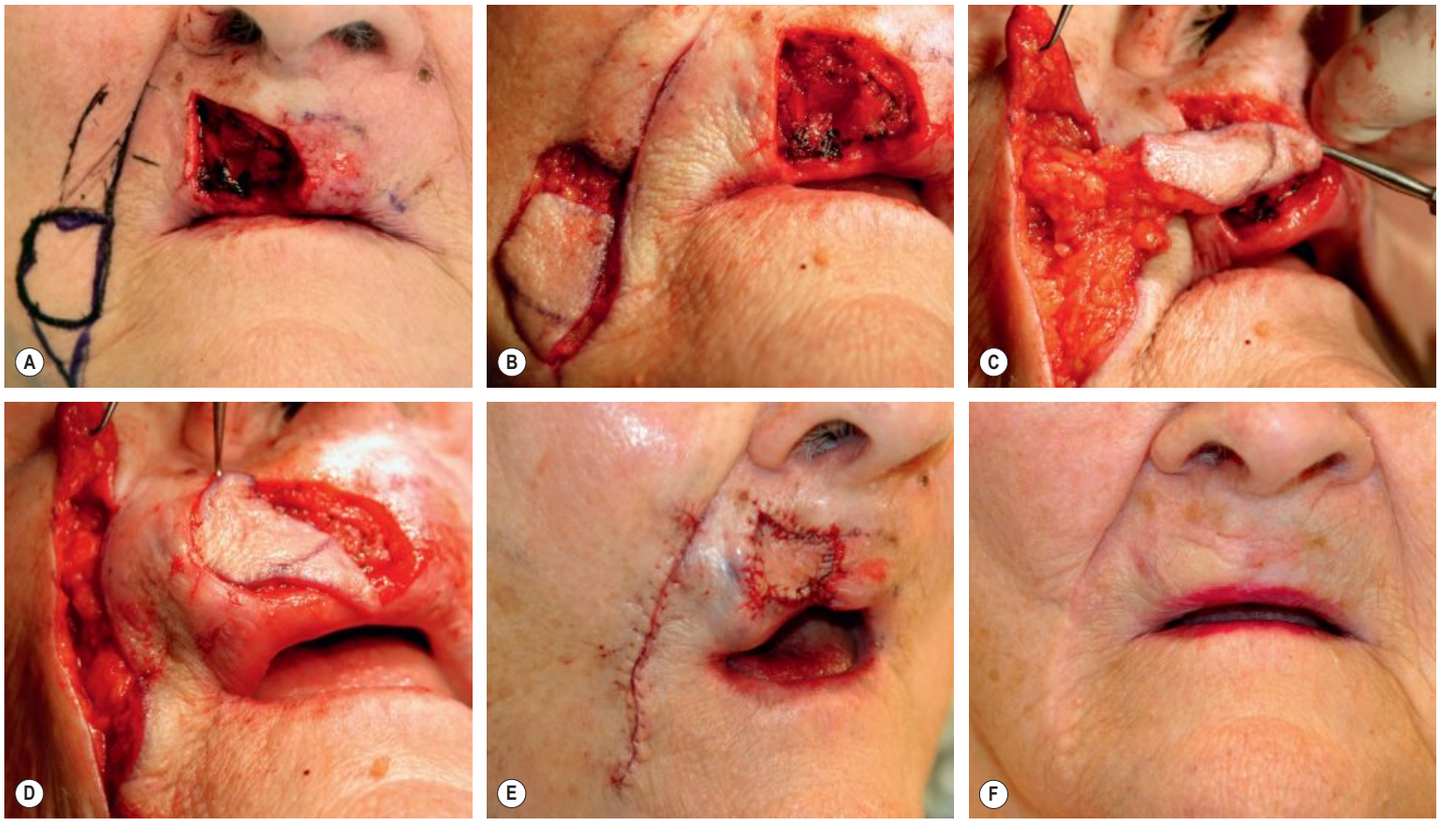
1. Zitelli JA. Tips for a better ellipse. *J Am Acad Dermatol*. 1990;22:101–103.
2. Boyer JD, Zitelli JA, Brodland DG. Undermining in cutaneous surgery. *Dermatol Surg*. 2001;27:65–68.
3. Zitelli JA. Tips for wound closure: pearls for minimizing dog-ears and applications of periosteal sutures. *Dermatol Clin*. 1989;7:123–128.
4. Zitelli JA, Moy RL. Buried vertical mattress suture. *J Dermatol Surg Oncol*. 1989;15:17–19.
5. Brodland DG. Complex cutaneous closures. In: Ratz JL, ed. *Textbook of Dermatologic Surgery*. Philadelphia: Lippincott-Raven; 1998.
6. Brodland DG. Fundamentals of flap and graft wound closure in cutaneous surgery. *Cutis*. 1994;53:192–200.
7. Dzubow LM. Flap dynamics. *J Dermatol Surg Oncol*. 1991;17:116–130.
8. Brodland DG. Advancement flaps. In: Roenigk RK, Roenigk Jr HH, eds. *Dermatologic Surgery: Principles and Practice*. 2nd ed. New York: Marcel Dekker; 1996.
9. Zitelli JA. The bilobed flap for nasal reconstruction. *Arch Dermatol*. 1989;125:957–959.
10. Miller CJ. Design principles for transposition flaps: the rhombic (single-lobed), bilobed and trilobed flaps. *Dermatol Surg*. 2014;40(Suppl. 9):S43–52.
11. Burget GC, Menick FJ. *Aesthetic Reconstruction of the Nose*. St. Louis: CV Mosby; 1994.
12. Goldman GD. Rotation flaps. *Dermatol Surg*. 2005;31:1006–1013.
13. Brodland DG. Auricular reconstruction. *Dermatol Clin*. 2005;23:23–41.
14. Brodland DG. Advanced reconstruction of the ear: a framework for successful wound closure. *Dermatol Surg*. 2014;40(Suppl. 9):S571–585.
15. Antia NH, Buch VI. Chondrocutaneous advancement flap for the marginal defect of the ear. *Plast Reconstr Surg*. 1967;39:472–477.
16. Stoner JG, Stoner JG. Spiral subcutaneous island pedicle flap for repair of alar defects. In: Ratner D, Cohen JL, Brodland DG, eds. *Reconstructive Conundrums in Dermatologic Surgery: The Nose*. Oxford: Wiley Blackwell; 2014:71–74.
17. Zitelli JA, Brodland DG. A regional approach to reconstruction of the upper lip. *J Dermatol Surg Oncol*. 1991;17:143–148.
18. Dzubow LM. Subcutaneous island pedicle flaps. *J Dermatol Surg Oncol*. 1986;12:591–596.
19. Pharis DB, Papadapoulos DJ. Superiorly based nasolabial interpolation flap for repair of nasal tip defects. *Dermatol Surg*. 2000;26:19–24.
20. Borges AF. The rhombic flap. *Plast Reconst Surg*. 1981;67:458–466.
21. Albertini JG, Hansen JP. Trilobed flap reconstruction for distal nasal skin defects. *Dermatol Surg*. 2010;36:1726–1735.
22. Rotunda AM, Bennett RG. Nasal tip wound repair using a rhombic transposition flap with a double Z-plasty at its base. In: Ratner D, Cohen JL, Brodland DG, eds. *Reconstructive Conundrums in Dermatologic Surgery: The Nose*. Oxford: Wiley Blackwell; 2014:63–67.
23. Zitelli JA. The nasolabial flap as a single-staged procedure. *Arch Dermatol*. 1990;126:1445–1448.
24. Brodland DG. Paramedian forehead flap reconstruction for nasal defects. *Dermatol Surg*. 2005;31:1046–1052.
25. Jellinek NJ, Nguyen TH, Albertino JG. Paramedian forehead flap: advances, procedural nuances and variations in technique. *Dermatol Surg*. 2014;40(Suppl. 9):S30–S42.
26. Stigall LE, Bramlette TB, Zitelli JA, Brodland DG. The paramidline forehead flap: a clinical and microanatomic study. *Dermatol Surg*. 2016;42:764–771.
27. Cook J. Repair of an alar defect. In: Ratner D, Cohen JL, Brodland DG, eds. *Reconstructive Conundrums in Dermatologic Surgery: The Nose*. Oxford: Wiley Blackwell; 2014:107–112.
28. Fisher GH. Reconstruction of a full thickness soft triangle defect. In: Ratner D, Cohen JL, Brodland DG, eds. *Reconstructive Conundrums in Dermatologic Surgery: The Nose*. Oxford: Wiley Blackwell; 2014:113–117.
29. Spear SL, Kroll SS, Romm S. A new twist to the nasolabial flap for reconstruction of lateral alar defects. *Plast Reconstr Surg*. 1987;79:915–920.
30. Kearney C, Sheridan A, Vinciullo C, Elliott T. A tunneled and turned-over nasolabial flap for reconstruction of full thickness nasal ala defects. In: Ratner D, Cohen JL, Brodland DG, eds. *Reconstructive Conundrums in Dermatologic Surgery: The Nose*. Oxford: Wiley Blackwell; 2014:119–126.
31. Cook JL. Tunneled and transposed island pedicle flaps in facial reconstruction. *Dermatol Surg*. 2014;40(9S):516–529.
32. Hollmig ST, Leach BC, Cook J. Single-stage interpolation flaps in facial reconstruction. *Dermatol Surg*. 2014;40(Suppl. 9):S562–569.
33. Griego RD, Zitelli JA. Intra-incisional prophylactic antibiotics for dermatologic surgery. *Arch Dermatol*. 1998;134:688–692.
34. Huether MJ, Griego RD, Brodland DG, Zitelli JA. Clindamycin for intralesional antibiotic prophylaxis in dermatologic surgery. *Arch Derm*. 2002;138:1145–1148.
35. Merritt BG, Lee NY, Brodland DG, et al. The safety of Mohs surgery. A prospective multicenter cohort study. *J Am Acad Dermatol*. 2012;67:1302–1309.



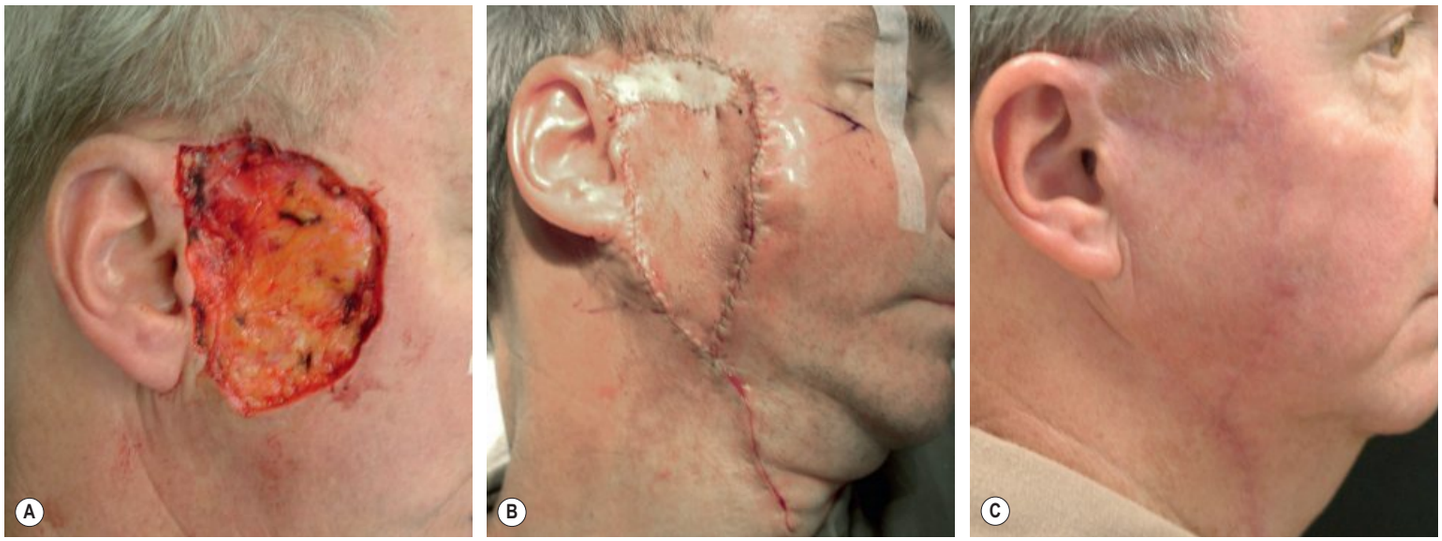
eFig. 147.1 The middle arm of this Z-plasty flap is composed of the defect *plus* the Burow's triangles excised above and below it to facilitate the transposition of the flaps (hatched). The medial flap is transposed over the lateral flap.



eFig. 147.2 Rhombic flap with Z-plasty. This flap is designed similarly to a bilobed flap but it has a Z-plasty in series with the secondary lobe. This can be viewed as a diminutive third lobe analogous to a trilobed flap. Upon closure, the diminutive lobe is transposed into the defect of the secondary lobe, partially filling it. The remainder of the defect is closed primarily as is the donor site of the Z-plasty on the nasal sidewall.



eFig. 147.3 Nasolabial to lip pull-through flap, a subcutaneous tunneling island pedicle flap (IPF). A Large upper lip defect with donor skin identified for a tunneling IPF. **B** Incision of the island and development of the pedicle. **C** Adequate length of the pedicle is assured. **D** The IPF is passed through the tunnel. Cautious defatting of the tunnel lessens the bulk effect of the pedicle plus the overlying skin. **E** Flap sewn in place with the donor site closed primarily. **F** Appearance at 1 year.



eFig. 147.4 Combination flap and graft. A Large defect of the preauricular cheek. **B** Partial closure of the lower 75% of the defect with the pedicled V-to-Y flap. The remaining defect is closed with a full-thickness skin graft derived from an extension of the wound inferior to the donor site of the flap on the anterior neck. **C** Reconstructive results 3 months postoperatively.



eFig. 147.5 Combination flap closure of multiple cosmetic subunits. A Deep defect involving the upper cutaneous lip and the lateral ala, including the alar rim. **B** Combination of the pedicled V-to-Y flap to reconstruct the cutaneous lip plus a nasolabial interpolation flap to reconstruct the lateral alar rim. **C** Division and debulking of the interpolation flap pedicle at 2.5 months with contouring of the ala and the alar crease. **D** Immediately postoperative. **E** Six months postoperatively.

148 Grafts

Désirée Ratner and Priya Mahindra Nayyar

Chapter Contents

Wound Healing Considerations 2556
Full-Thickness Skin Grafts 2557
Split-Thickness Skin Grafts 2561
Composite Grafts 2565
Free Cartilage Grafts 2566

Key features

- Free skin grafts are pieces of skin that have been severed from their local blood supply and transferred to another location
- Grafts for soft tissue reconstruction can be divided into four types: full-thickness skin grafts, split-thickness skin grafts, composite grafts, and free cartilage grafts
- In dermatologic surgery, grafts are most commonly used to repair defects created after removal of skin cancers; grafts also provide coverage and more rapid healing of leg ulcers
- The clinical situation determines the type of graft to be placed
- A working knowledge of the indications, techniques, donor site considerations, postoperative care, and postoperative complications of all types of skin grafting is essential for optimal soft tissue reconstruction

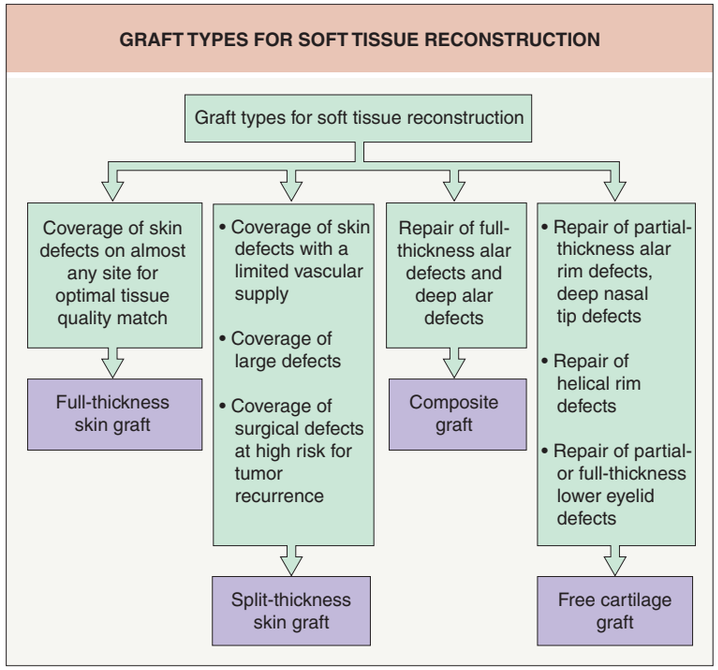


Fig. 148.1 Graft types for soft tissue reconstruction.

INTRODUCTION AND BACKGROUND

Skin grafting procedures originated approximately 2500 to 3000 years ago, when surgeons of the Hindu Tilemaker caste replaced noses amputated as punishment for theft and adultery with skin grafts harvested from the gluteal region[1]. It was not until the nineteenth century that skin grafting was reintroduced. In 1869, Reverdin's account of pinch grafting for leg ulcers was published; in subsequent decades, Ollier and Thiersch's accounts of thin split-thickness skin grafting, and Wolfe and Krause's accounts of full-thickness skin grafting, appeared in the literature. While these and other nineteenth-century surgeons used skin grafts to address only the most difficult problems of surgical management, skin grafting has since evolved into a reconstructive option that is routinely, and sometimes preferentially, used for the surgical repair of skin defects.

Free skin grafts are pieces of skin which have been severed from their blood supply and transferred to another location. They can be divided into four types: full-thickness skin grafts (FTSGs), split-thickness skin grafts (STSGs), composite grafts, and free cartilage grafts (Fig. 148.1; Tables 148.1 and 148.2)[2,3]. FTSGs are composed of the entire epidermis and the full thickness of dermis, including adnexal structures such as hair follicles and sweat glands. STSGs are composed of the full thickness of the epidermis and partial thickness of dermis. These can be subdivided into thin, medium, and thick grafts, depending on the amount of dermis included in the graft. Composite grafts are composed of at least two different tissue types, usually skin and cartilage. Free cartilage grafts consist of cartilage with its overlying perichondrium.

WOUND HEALING CONSIDERATIONS

Wound healing after skin grafting proceeds through a unique series of events[2,4]. The first 24-hour period following graft placement is termed the stage of plasmatic imbibition, during which fibrin glue attaches the graft to its recipient bed, allowing it to take up the underlying wound exudate and to become edematous, gaining up to 40% in weight. The graft thereby remains hydrated and obtains a supply of nutrients, which maintains graft vessel patency until revascularization begins. The fibrin beneath the graft is subsequently replaced by granulation tissue, which attaches the graft permanently to its bed.

With proper apposition of the graft to its bed, revascularization may proceed. Anastomoses begin to form within 48–72 hours of grafting between the recipient bed and pre-existing vessels in the dermis of the graft, a process known as inosculation. Vascular proliferation occurs next, with sprouting and budding of vessels in the graft and its bed. Even relatively avascular tissue may be grafted, as long as the avascular area is small and surrounded by a rich vascular supply. Through a process known as the bridging phenomenon, vascular connections arising from the vascularized part of the recipient bed allow blood flow to occur through pre-existing graft vasculature, so that nutrients reach the part of the graft overlying the avascular area. Full circulation is restored to the graft within 4–7 days.

Restoration of the lymphatic circulation parallels restoration of the blood supply over the first week. Epidermal proliferation occurs between the 4th and 8th day post-transplant and persists for several weeks. Degeneration of sebaceous and eccrine glands may occur initially, but subsequent glandular regeneration may allow partial function to be maintained. Graft reinnervation and return of sensory nerve function may begin as early as 2–4 weeks after grafting, although patients do not usually regain full sensation for many months.

If extension of the ischemic period occurs, decreased graft survival may result (Table 148.3). Hematoma or seroma formation, infection, or mechanical shear forces may disrupt the fragile vascular connections between the graft and its bed. These complications tend to affect FTSGs (which have a greater volume to nourish and revitalize) more than STSGs.

COMPARISON OF GRAFT TYPES USED IN SOFT TISSUE RECONSTRUCTION								
Graft type	**Tissue match**	**Nutritional requirements**	**Requirement for recipient bed vascularity**	**Infection risk**	**Graft contraction risk**	**Durability**	**Sensation**	**Adnexal functions**
FTSG	Good to excellent	High	High	Low	Low	Good to excellent	Good	Excellent
STSG	Poor to fair	Low	Low	Low	High	Fair to good	Fair	Poor
Composite	Good	High	Very high	Moderate	Low	Fair	Fair	Good
Free cartilage	NA	Moderate	High	Moderate	Migration or deformation possible, with subsequent resorption	Good	NA	NA

Table 148.1 Comparison of graft types used in soft tissue reconstruction. FTSG, full-thickness skin graft; NA, not available; STSG, split-thickness skin graft.

INDICATIONS, CONTRAINDICATIONS, ADVANTAGES, AND DISADVANTAGES OF GRAFT TYPES USED IN SOFT TISSUE RECONSTRUCTION				
Graft type	**Indications**	**Contraindications**	**Advantages**	**Disadvantages**
Full-thickness skin graft (FTSG)	Coverage of skin defects, usually located on the face or scalp, requiring an optimal tissue quality match	Avascular graft bed	Excellent color and texture match Minimal graft contraction	Time consuming Donor site requires closure Requires meticulous technique
Split-thickness skin graft (STSG)	Coverage of large defects and defects with a limited vascular supply or at sites at high risk for tumor recurrence	Defects near free margins Facial defects in cosmetically sensitive areas	Increased chance of survival Ease of application Ability to cover large defects Able to act as a "window" to detect recurrence of high-risk tumors	Suboptimal cosmetic appearance Decreased durability Presence of granulating donor site wound Greater graft contraction Special equipment required to harvest larger grafts
Perichondrial cutaneous graft	Repair of deep nasal tip and alar defects, especially those with exposed cartilage	Avascular graft bed	Thicker than FTSG Contract less than FTSG Increased chance of survival under conditions of vascular compromise (compared to FTSG)	
Composite graft	Repair of full-thickness alar defects or nasal tip defects (<2 cm in diameter) with cartilage loss	Defects >2 cm in diameter	Single-stage procedure May yield good functional and aesthetic results when used to repair appropriately sized defects	Greater risk of graft failure under conditions of vascular compromise Graft size limitations (<2 cm) Limited donor tissue available Donor site may require flap or complex closure Increased risk of infection and graft displacement
Free cartilage graft	Repair of defects of nasal ala, tip or sidewall, ear or eyelid requiring restoration of structural support or preservation of contour of free margins	None	Provide structural support for selected facial and ear defects	Donor site may be painful Increased risk of postoperative infection Increased risk of graft displacement

Table 148.2 Indications, contraindications, advantages, and disadvantages of graft types used in soft tissue reconstruction.

Even after the ischemic period is past, other factors may decrease the vascular supply nourishing the undersurface of the graft[2,3,5]. The most important of these is cigarette smoking or use of other nicotine-containing products,[5] but diabetes mellitus, protein deprivation, and severe trace element or vitamin deficiencies may also increase the risk of graft failure. Certain systemic medications, such as corticosteroids, chemotherapeutic agents, other immunosuppressive drugs and anticoagulants, may interfere with wound healing as well.

Other causes of graft failure include: insufficient vascularity due to necrotic debris within the recipient bed, hematoma, seroma, an avascular wound bed, previous radiotherapy, infection, excessive graft tension, mechanical shearing forces, and improper postoperative care (see Table 148.3)[2,3]. The most common infectious agents associated with graft failure include coagulase-positive staphylococci, β-hemolytic streptococci, and *Pseudomonas* spp. Pseudomonal infections are particularly common in auricular grafts. For all of these reasons, a thorough preoperative evaluation, meticulous intraoperative technique, and good postoperative care are essential to maximize graft survival.

FULL-THICKNESS SKIN GRAFTS

Indications/Contraindications

FTSGs are most commonly used to repair facial defects resulting from skin cancer removal. They may be used to repair defects at virtually any site, as long as the recipient bed has a sufficiently rich vascular supply to promote capillary regrowth and fibroblasts to supply collagen for graft adherence. Small avascular areas may be grafted due to the bridging phenomenon. Larger avascular areas, including patches of exposed bone, cartilage, tendon or nerve devoid of periosteum, perichondrium, peritenon or perineurium, respectively, are unable to support FTSGs. For this reason, FTSGs should not be placed over larger areas of avascular tissue.

Under the proper circumstances, FTSGs can provide excellent color, texture, and thickness match for facial defects because they include the full thickness of epidermis and dermis. Wound contraction is minimized since the full thickness of dermis is present, and adnexal structures remain intact[6]. FTSGs may be especially useful for the cosmetically and functionally acceptable repair of defects of the nasal tip, dorsum, ala and lateral sidewall, as well as the lower eyelid and ear (Fig. 148.2)[7].

Preoperative History and Donor Site Considerations

A thorough preoperative evaluation that includes questions regarding bleeding tendencies, alcohol use, use of anticoagulant medications (including aspirin and nonsteroidal anti-inflammatory drugs), and a history of hypertension can help assess the risk of excessive bleeding and clot formation beneath the graft[2,3]. Diabetes mellitus, nutritional deficiencies, cigarette smoking, or the use of other nicotine-containing

CAUSES OF GRAFT FAILURE	
Poor graft–bed contact	Hematoma
	Seroma
	Shearing forces due to excessive postoperative activity
	Shearing forces due to inadequate immobilization of graft
Poor recipient bed vascularity	Inadequate vascular bed (e.g. previous radiotherapy)
	Exposed cartilage, bone, tendon
	Nicotine-induced vasoconstriction
Infection	Coagulase-positive *Staphylococcus* spp.
	Beta-hemolytic *Streptococcus* spp.
	Pseudomonas spp.
Host factors	Diabetes mellitus
	Immunosuppression
	Poor general health
	Nutritional deficiencies, including hypoalbuminemia
	Systemic conditions with vascular compromise
Technique	Rough handling of tissue
	Excessive devitalized tissue in recipient bed due to cautery
	Increased tension on graft due to inadequate size
	Inadequate hemostasis
	Inadequate trimming of adipose layer
	Placement of upside-down graft (more common with STSG)
	Inadequate anchoring (composite and free cartilage grafts)

Table 148.3 Causes of graft failure. STSG, split-thickness skin graft.



Fig. 148.2 Full-thickness skin graft. A Full-thickness skin graft taken from the preauricular region was used to repair this defect of the right upper anterior ear. **B** Eight-week postoperative result.

products may increase the risk of graft failure, and any history of these should be identified preoperatively.

Selection of a donor site for full-thickness skin grafting depends upon the color, texture, thickness, and sebaceous qualities of the skin surrounding the defect (Tables 148.4 and 148.5). Most FTSGs are taken from sun-exposed areas above the shoulders whose color, vascular pattern, texture, and distribution of adnexal structures best match the skin surrounding facial defects. The thinnest grafts are usually harvested from the upper eyelid or the postauricular sulcus. Medium-thickness grafts are often harvested from the preauricular and cervical regions, while thicker grafts may be taken from the supraclavicular or clavicular region, conchal bowl, or nasolabial fold. Donor skin thickness, irrespective of site, will vary from one patient to another. It is therefore important to examine all sites carefully to find the best possible tissue match. This approach will ensure optimal donor site selection for each individual patient and surgical defect.

DONOR SITE CONSIDERATIONS FOR FULL-THICKNESS SKIN GRAFTS	
• Pattern of sun exposure • Color • Vascular pattern • Texture • Sebaceous quality	• Skin thickness • Skin consistency • Sufficient tissue available for harvesting • Ability to camouflage donor site scar

Table 148.4 Donor site considerations for full-thickness skin grafts.

SUMMARY OF POSSIBLE FULL-THICKNESS SKIN GRAFT DONOR SITES FOR DEFECTS IN DIFFERENT LOCATIONS	
Defect sites	**Donor sites**
Nasal dorsum, sidewalls, tip	Preauricular region, supraclavicular region or lateral neck (if large)
Nasal tip, ala	Preauricular region, conchal bowl, nasolabial fold
Junction of nasal dorsum/tip	Burow's graft
Ear	Postauricular sulcus, preauricular cheek
Lower eyelid/ medial canthus	Upper eyelid, postauricular sulcus
Scalp	Supraclavicular region, lateral neck, inner upper arm
Forehead	Burow's graft, supraclavicular region, lateral neck, inner upper arm (if large)

Table 148.5 Summary of possible full-thickness skin graft donor sites for defects in different locations.

A regional approach may, at times, be used to obtain the best possible match for a given defect. Grafts taken from redundant upper eyelid skin may be used to repair lower eyelid defects, providing a good color and texture match in addition to a well-camouflaged donor site scar. Grafts used for lower eyelid defects should be oversized by 100%–200% to allow for contraction and to avoid ectropion. Due to its relatively large size and inconspicuous location, postauricular skin may also be useful as a donor site for eyelid and auricular defects. Because postauricular skin is relatively non-sun-exposed, grafts harvested from this region may not provide a good color or texture match for other facial defects.

Preauricular skin is more versatile and can be used to repair most nasal defects, since the thickness and degree of sun exposure of these areas tend to be comparable. Donor site scars in this region can be easily camouflaged, as in facelift surgery, to provide a cosmetically desirable result. Even bearded individuals have a 1–2 cm hairless zone in the preauricular region. Care must be taken not to harvest hair-bearing skin in grafts taken from this area. Accidentally including mature follicular units may produce undesirable hair growth within the graft. Hair-bearing skin from the temporoparietal region may be used to repair eyebrow defects, where survival of the follicular units after transplantation may produce a superior cosmetic result. Skin from the nasolabial fold or the conchal bowl can sometimes be used to graft small nasal tip or ala defects with good tissue match[8]. At times, sufficient skin laxity may be present, particularly on the nose or forehead, to allow for partial defect closure, utilizing the adjacent Burow's triangle as a FTSG to repair the remainder of the defect, providing an excellent tissue match[9–11].

For larger defects requiring FTSGs of sun-damaged skin, such as the forehead and scalp vertex, the supraclavicular region or lateral neck can be used as donor sites. Again, care must be taken not to harvest

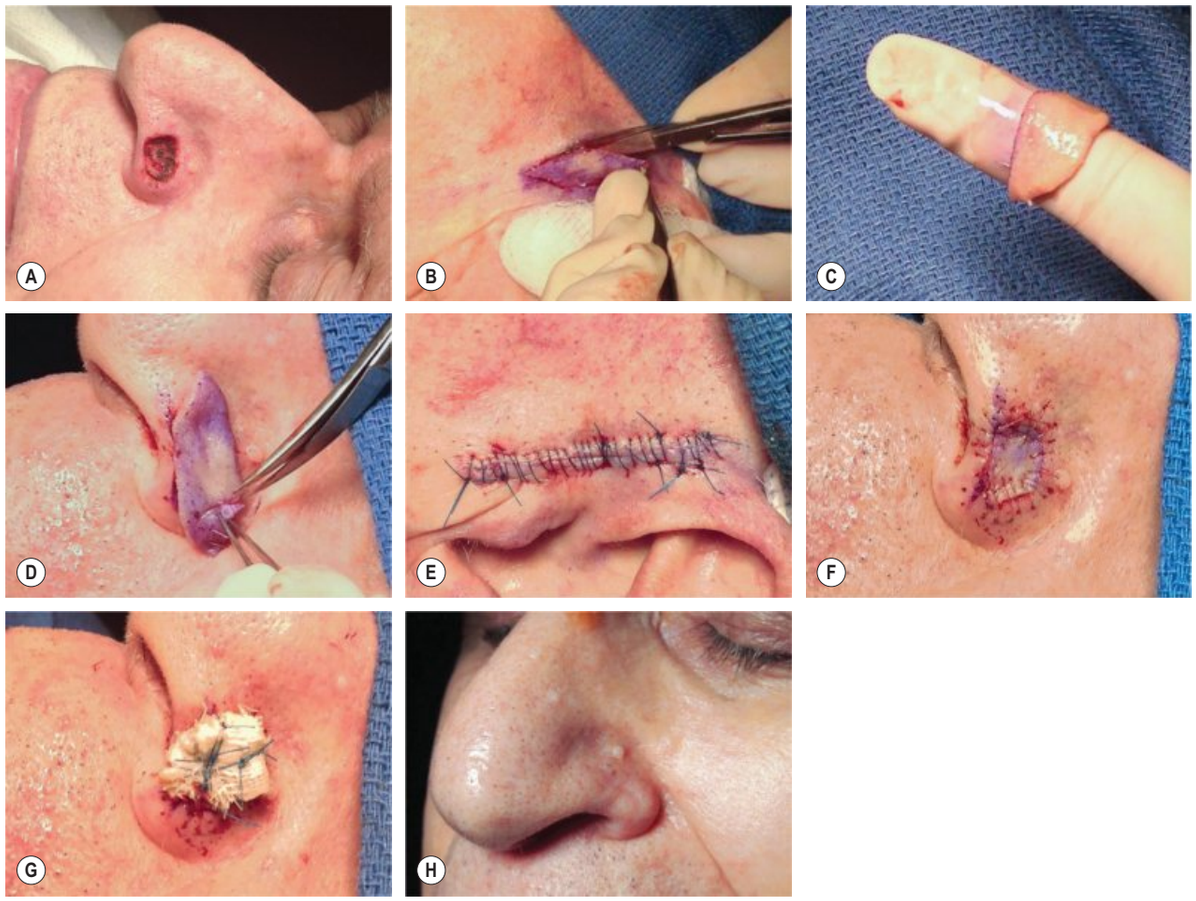


Fig. 148.3 Placement of a full-thickness skin graft. A Defect of the left nasal ala, measuring 1.8 × 1.2 cm, is present after removal of basal cell carcinoma via Mohs micrographic surgery. A preauricular donor site will provide the best match based upon color, sebaceous quality, degree of photodamage, and thickness. **B** With a sterile marker, a template has been made from the periphery of the recipient site and the template is then used to produce an inked margin at the donor site (center of wedge). Next, Burow's triangles are outlined on either side of the template. Marking the donor site prior to injecting local anesthesia prevents incorrect sizing due to tissue stretch from lidocaine infiltration. The donor site is excised with a scalpel to the level of the subcutaneous fat. **C** The graft is carefully defatted with curved iris scissors so that only the white, glistening surface of the dermis remains. **D** The full-thickness skin graft is trimmed with curved iris scissors to ensure a perfect fit. **E** The preauricular donor site is closed primarily. **F** Full-thickness skin graft sewn into place with 6–0 fast-absorbing gut sutures. **G** Xeroform™ bolster sewn into place over the full-thickness skin graft with 5–0 polypropylene tie-over sutures. **H** Sixteen-week postoperative result. The graft shows good color and texture match with the surrounding skin.

unwanted hair along with the graft. These donor sites are often more difficult to camouflage, especially in areas that might not always be covered by clothing, and must be carefully oriented. Although their color and texture match may be suboptimal, areas below the neck with thin, redundant skin, such as the upper inner arms, forearms and inguinal area, can also be considered as donor sites.

Description of Technique

Varying techniques for harvesting and placing FTSGs have been described[2,3,9–11]. To perform a FTSG, a template of the defect is first made, using any flexible material, such as gauze, Telfa™ or aluminum foil, which can be bent to conform to the defect (Fig. 148.3A). After marking the periphery of the recipient site with a sterile marker, the template material is pressed against the defect, and the resulting outline of the inked margin serves as a guide to cut a perfect template. The template is applied to the donor site, and inking material is applied around it (Fig. 148.3B). The graft should be 3%–5% larger than the true template to allow for the natural contraction and shrinkage of the graft after it has been harvested. Often, just cutting around the outside of the inked margin accounts for this extra "safety" skin. For eyelid defects, grafts should be oversized significantly to minimize the risk of ectropion. Marking the donor site prior to local anesthesia prevents incorrect sizing due to tissue stretch from lidocaine infiltration. It is important to note that a donor site ellipse with a 3:1 ratio may not always be required, allowing for smaller donor defects[12].

After the donor site is marked, local anesthesia is injected into the donor and recipient sites. Epinephrine (adrenaline) may be used without compromising graft survival. If waterproof ink is not available for template marking, the outline of the template may be scored on the donor site with a needle. The donor site and recipient beds are then scrubbed with an antibacterial preparation such as povidone–iodine (especially around the eyes and ears) or chlorhexidine, excess scrub is removed, and sites are draped with sterile towels.

The donor site is excised with a scalpel to the level of the subcutaneous fat (Video 148.1). The graft is placed in a sterile bowl or Petri dish containing sterile normal saline, where it may remain for up to 1–2 hours. Grafts may be utilized up to 24 hours after harvesting if refrigerated or kept on ice. Before suturing the graft into place, defatting should occur. This is an essential step, since direct contact between the graft and its bed promotes connections between existing vessels as well as new vessel growth and nutritional support from the base of the defect. Adipose tissue adherent to the graft is poorly vascularized and is therefore not an effective medium for vessel growth between the graft and its bed.

When defatting is performed, the graft is placed dermal-side-up on the fingers or in the palm. All fat is trimmed from the underside using sharp scissors (Video 148.2). Fat is adequately removed when all of the yellow globular material is gone, leaving a white glistening dermal surface (Fig. 148.3C, Video 148.3). If indicated, part of the dermis can also be trimmed to allow for differences in recipient site depth, although adnexal structures may be removed in the process, potentially altering the cosmetic result. The graft is then placed dermis-down in its bed, and rotated and trimmed if necessary, to achieve a perfect fit (Fig. 148.3D, Videos 148.4 and 148.5). While one surgeon is trimming the graft, another may close the donor site, usually in a linear layered

fashion with bilateral removal of standing cones (Fig. 148.3E). For conchal bowl donor sites, a 2- or 3-mm punch biopsy instrument may be used to remove full-thickness discs of cartilage, thereby facilitating second intention healing from the underlying dermis.

Contouring of donor skin in FTSGs may be challenging, particularly when repairing defects on the nasal tip, ala, lateral nasal sidewall, helical rim, and eyelid[13]. Graft contouring often requires multiple trial placements within the recipient bed, as well as multiple trimmings, to obtain an optimal result. Removal of cartilage not needed for structural support from the recipient site may increase the chance of graft survival, particularly for auricular defects, without compromising the aesthetic appearance of the repair[14].

Securing the Graft

Perimeter sutures, basting sutures, support dressings, or a combination of any or all of these can be used to anchor the FTSG. Depending upon the graft's size, four to eight interrupted 4–0 or 5–0 absorbable or non-absorbable sutures may be placed at opposite edges of the graft periphery (e.g. at 3, 6, 9 and 12 o'clock) to tack down its four quadrants. A simple running suture, such as 6–0 fast-absorbing chromic gut suture, may then be placed around the graft's perimeter (Fig. 148.3F, Video 148.6). Great care is taken to achieve perfect epidermal wound approximation. The running suture is placed in almost epicuticular fashion, passing the needle first through the graft and then through the surrounding skin. Placing the suture slightly higher in the dermis on the graft side and slightly deeper in the dermis of the surrounding skin makes suture placement easier, prevents tenting of the graft edges, and maximizes graft–recipient bed contact.

Using tissue adhesives in full-thickness skin grafting has been investigated. In a pilot study, it was found that applying cyanoacrylate tissue adhesive to secure FTSGs to their recipient bed wound edges produced cosmetic results essentially identical to those achieved with suturing[15]. Because these adhesives set virtually instantaneously, the graft must be perfectly trimmed and aligned before adhesive application, since fine adjustments in positioning the graft's edges are not easily made. Tissue adhesives may represent a time-saving alternative for securing the periphery of certain grafts, particularly those in relatively immobile areas such as the temple, forehead, and distal nose.

Basting or quilting sutures, usually simple interrupted 6–0 fast-absorbing gut sutures, can occasionally be placed to secure the central portion of the graft. They can be useful in securing large grafts to provide extra support against movement, as well as grafts placed on a concave surface where tenting could possibly occur. All sutures should be snug, but not strangulating, so as not to compromise graft survival.

Immobilization of the graft over its bed can be maximized with pressure dressings. Classically, tie-over bolster dressings have been employed to immobilize grafts, using anchoring stents to ensure direct contact between the graft and its bed[2,3]. These stents may consist of various materials including Xeroform™ gauze (bismuth tribromophenate-petrolatum-impregnated gauze), cotton balls, foam rubber, sponges, plastic beads, or disks. Although sutures or skin staples are usually employed to anchor the stent, adhesive wound closure tapes or Steri-Strips™ can also be applied to exert even pressure on the bolster[16]. Adherence of the dressing to the graft, which tends to pull the graft from its bed at the time of dressing removal, is minimized by first applying petrolatum ointment, a non-adherent contact dressing, or Xeroform™ gauze to the graft site. Pressure or tie-over dressings help immobilize the newly placed graft during the critical period of revascularization, thereby preventing hematoma or seroma formation. While such dressings may not be necessary to secure very small FTSGs[17], a recent literature review found that graft take, cosmetic outcomes, and postoperative complications after use of either tie-over bolsters or quilting sutures were comparable[18].

The simplest bolster consists of Xeroform™ gauze alone, which is molded and placed to apply pressure to the graft. One end of each peripheral non-absorbable suture is cut long, to a length of approximately 3–6 cm, and its opposing suture is left uncut (Video 148.7). The suture ends can then be tied over the dressing two at a time (i.e. 12 o'clock to 6 o'clock and 3 o'clock to 9 o'clock) to secure the bolster (Fig. 148.3G, Video 148.8). Alternatives to tie-over sutures include the running bolster suture, staples, and the "Lilliputian" technique[19,20]. A light dressing consisting of Telfa™ and Hypafix® may be placed over the graft. A pressure dressing should be placed over the donor site for 24 hours.

Postoperative Care

After the pressure dressings are removed, careful wound care should be performed once to twice daily. One method is to gently clean both the donor site and the area immediately surrounding the bolster with hydrogen peroxide to remove all crusts, followed by application of petrolatum ointment (Vaseline®). The bolster is not disturbed until dressing removal at 1 week, at which point the bolster and all tie-over sutures are removed. Steri-Strips™ may be applied to the donor site as needed after suture removal.

The ideal graft is light pink when the bolster is removed. Its color may range, however, from pink or red to darker blue or purple, depending on the extent of graft revascularization. Patients should be cautioned about these color changes beforehand. A bluish tinge may be a sign of ecchymosis rather than graft failure. At the 1-week time point, a white graft is a sign that the graft has not revascularized and will fail, requiring the underlying wound to heal secondarily. A black graft signals necrosis and is also undesirable. It is possible that the entire epidermal surface may become black and necrotic and then slough without adversely affecting the graft's dermal portion, as re-epithelialization can occur from adnexal structures and the epithelial edges, with an acceptable cosmetic result. Therefore, eschars should not be debrided, since they can serve as natural dressings under which healing will progress. Patients should be counseled that the graft's vascular supply remains fragile for weeks. For this reason, trauma, including direct shower water to the area, and excessive activity should be avoided for an additional 1 to 2 weeks.

When there is a good color and texture match between the FTSG and the surrounding skin, the cosmetic result is excellent (Fig. 148.3H).

Variations/Unusual Situations

Purse-string suture

The purse-string suture is a subcuticular stitch placed around the periphery of a circular or oval surgical defect[21]. This type of suture allows partial defect closure by advancing skin from the entire periphery of the wound and may help to cover areas of exposed cartilage or bone at the wound edges that could inhibit graft take. In addition, the graft required to cover the remainder of the defect is greatly reduced in size due to an ~50% decrease in the defect area. Because of this reduced defect size, the graft needed to complete the repair may be harvested from traditional preauricular, postauricular or supraclavicular donor sites, which provide the best color, texture, and thickness match for most sun-exposed areas. Furthermore, FTSG placement decreases the risk of significant wound contraction, resulting in better cosmetic and functional results than would be produced by split-thickness skin grafting or second intention healing.

Large scalp defects extending to bone can present a significant management challenge, which can be handled by placing a purse-string suture followed by a galeal hinge flap[22]. After purse-string placement, the galea aponeurotica adjacent to the scalp defect is scored with a scalpel, and a partial-thickness galeal flap of sufficient size to cover all or a portion of the exposed periosteum or bone may be dissected free and transposed into place, using the same motion as turning a page of a book. This hinged galeal tissue serves to recreate the vascular bed required for successful graft placement and thus permits repair of deep and often difficult scalp defects in a single operative session.

Burow's grafts

Defects of the nasal sidewall and dorsum, and sometimes of the forehead, lateral neck or other areas, may be repaired with Burow's grafts[9–11]. Because Burow's grafts utilize skin adjacent to the defect, they tend to provide a cosmetically superior match compared to grafts harvested from distant locations. In general, these grafts are harvested from the skin superior to the defect if on the nose, and medial or lateral to the defect if on the forehead. The Burow's triangle is excised (see Ch. 146) and the resulting donor defect is closed primarily, thereby partially decreasing the original defect size. The triangle is defatted, trimmed, and sutured into the defect. Operating time is decreased because a separate donor site is not required. Burow's grafts tend to be limited in size. When insufficient laxity is present for partial donor site closure, or if the Burow's triangle is not sufficiently large to cover the remaining defect, alternative donor sites should be sought.

Deep nasal defects

Deep postsurgical defects on the nose may, at times, pose a challenge for repair. Delaying FTSG placement for 12 to 14 days may increase the likelihood of graft survival over defects of the nasal tip and ala with denuded cartilage[2,3]. Also, when tissue loss is deep in these areas, delaying skin grafting for 7 to 14 days may allow granulation tissue to fill in the defect such that a better contour may ultimately be achieved[2,3]. Because the early granulating wound produces an excellent vascular bed, delayed grafting may be considered in patients with reduced wound bed vascularity, e.g. those who smoke or have had previous radiotherapy. At the time of delayed graft placement, the wound bed is debrided by rubbing with dry gauze and the wound edges refreshed by scraping them with a scalpel oriented perpendicular to the wound edges. Prophylactic antibiotics are often prescribed when placing delayed grafts.

If a depressed defect is anticipated, but immediate reconstruction is preferred, dermal grafts can be used as tissue filler prior to FTSG placement[24]. Dermal grafts can effectively fill the defect, with little risk of resorption, and eliminate the need for a more complicated repair choice. The "drumhead" graft repair of deep nasal alar defects involves application of an overlying rigid plastic suspension coupled with an undersized graft, thereby preventing graft depression and nasal valve collapse; a cut portion of the periphery of the sterile plastic packaging from a suture packet can serve as the plastic suspension[25]. It enables the graft to remain apposed to the recipient bed, suspended as it would be in its natural form if it were supported both by soft tissue and by nasal cartilage. A bolster can be placed overlying the graft.

Perichondrial cutaneous grafts (PCCGs) are actually composite grafts composed of full-thickness skin and subjacent perichondrium; PCCGs may be used as substitutes for FTSGs when reconstructing deep nasal tip and alar defects, particularly those with exposed cartilage[26,27]. PCCGs are harvested from the conchal bowl, utilizing the subperichondrial plane as the plane of dissection. The cartilage is not removed, making this graft more analogous to a FTSG than a cartilage-containing composite graft. The advantages of PCCGs over FTSGs include the following: PCCGs are thicker, have a greater chance of survival under conditions of vascular compromise, contract less than FTSGs, and may achieve better skin texture match on the distal nose due to the sebaceous nature of conchal bowl skin.

Postoperative Complications

Complications of full-thickness skin grafting can be divided into short-term problems of graft failure and long-term functional and cosmetic problems[2,3]. Short-term problems include infection, hematoma, seroma, and shearing of the graft over its bed. These problems are significant when they occur, but can usually be avoided. Infection after grafting of facial defects, in particular, is not often encountered, and oral antibiotics are not routinely given postoperatively. Nevertheless, it is important to be gentle while handling tissue intraoperatively and to minimize devitalized tissue created by electrocoagulation to minimize the risk of infection. Prophylactic oral antibiotics covering *Staphylococcus* and *Streptococcus* spp. may be helpful in selected patients, especially those with diabetes mellitus, immunosuppression, or a prolonged intraoperative time. Grafts on the ears, fingers, and legs may benefit from prophylactic antibiotics, as these sites can be prone to postoperative wound infections.

Hematoma and seroma formation can be avoided by meticulous intraoperative hemostasis, pressure dressings, and postoperative caution. After consultation with the patient's internist, cardiologist, or primary care physician, patients may be instructed to avoid aspirin for 10 days before surgery, nonsteroidal anti-inflammatory drugs for 5 days before surgery, and alcohol for 2 days before and 2 days after surgery. In the past, patients taking antithrombotic medications were advised to discontinue them before surgery if their internist or cardiologist was in agreement. The current recommendations for management have, however, changed. While the risk of bleeding complications increases slightly if oral anticoagulants are not discontinued, most dermatologic surgeons do not routinely request that these medications be discontinued preoperatively, since the risk of morbidity from hemorrhagic complications is minimal compared to that of the thrombotic events potentially associated with their discontinuation[28]. Patients are also advised not to engage in vigorous activity, heavy lifting, or bending for at least 2 weeks postoperatively. The latter measures help to inhibit graft movement and supplement the bolster's effectiveness in minimizing shearing of the graft over its bed.

Long-term complications of FTSGs consist of cosmetic and functional problems. It is imperative to stress to the patient prior to graft placement that FTSGs usually take months to look natural. Preoperative counseling may help to alleviate fears concerning the graft's appearance during the first weeks after bolster removal. Make-up can usually be applied 3–4 weeks after grafting. It is important to note that FTSGs are often depressed during their first 2–4 weeks. This depression will usually correct itself within 4–6 weeks.

Although careful donor site selection will minimize the color, texture, and contour deformities that can occur, patient and physician satisfaction with the cosmetic result may not be complete after healing has finished. Spot dermabrasion or laser resurfacing has traditionally been performed at 6 weeks to 6 months after grafting to correct differences in elevation between the graft and its surrounding skin, as well as to improve color and texture mismatch[29]. While studies have focused on pulsed dye laser (PDL) treatment of postsurgical scars rather than FTSGs or STSGs, a meta-analysis found an average 72% rate of improvement or no recurrence of hypertrophic scars and keloids with PDL therapy[30]. Graft hyperpigmentation can be addressed with a brief course of topical hydroquinone and/or tretinoin.

Functional complications of FTSGs occur primarily as a result of wound contraction. Grafts contract secondary to the centripetal movement of unopposed elastic fibers. A variable amount of shrinkage can therefore be expected, depending upon donor site thickness and elasticity[6,31]. In one study, it was found that the area of FTSGs contracted by a mean of 38% by 16 weeks after placement, with grafts applied to the periorbital area and nose contracting more than those on the scalp and temples[32]. Contraction usually increases as graft thickness decreases, and it is thought to occur in the fibrous layer under the graft, either in the bed itself or in the layer of scar tissue wedged between the graft and its bed[6]. Complications due to graft contraction are usually minimal in FTSGs. If wound contraction does produce functional or cosmetic abnormalities, revisional surgery may be needed.

Future Directions

For defects with an inadequate vascular bed, full-thickness skin grafting may not be possible, necessitating repair with a less cosmetically elegant STSG. High-density, porous, polyethylene implants have therefore been designed which permit ingrowth of fibroneovascular tissue without changing the size or shape of the implant[33]. When these prefabricated implants were placed in rabbits, it was found that they developed sufficient vascularity to sustain FTSGs. This technology holds promise for patients with deep nasal and ear defects, in whom an anatomically correct structure could be implanted, after which time would be allowed for fibrovascular tissue ingrowth, with full-thickness skin grafting performed later for a superior cosmetic result.

Progress is also being made on incorporating complex blood vessels into bioengineered skin equivalents, while 3D printing techniques have been investigated as a means of generating skin equivalents. Recently, a vascularized, perfusable skin graft was fabricated via 3D printing utilizing a bioink that contained human foreskin dermal fibroblasts, endothelial cells, and placental pericytes suspended in rat tail type I collagen to form a dermis. This was followed by 3D printing with a second bioink containing human foreskin keratinocytes to form an epidermis. *In vitro*, the keratinocytes replicated and matured to form a multilayered barrier while the endothelial cells and pericytes self-assembled into interconnected microvascular networks[34]. With these advances in technology, it seems possible that, at some point, 3D printing of complex tissue-like constructs to use as skin grafts could become routine.

SPLIT-THICKNESS SKIN GRAFTS

Split-thickness skin grafts (STSGs) consist of epidermis and a portion of the dermis. These grafts vary in thickness from ~0.005 to 0.030 inches (0.13–0.78 mm), and are classified as thin, medium, or thick, depending upon the amount of dermis included within the graft (Table 148.6).

CLASSIFICATION OF SPLIT-THICKNESS SKIN GRAFTS	
Thin	0.005–0.012 in/0.13–0.30 mm
Medium	0.012–0.018 in/0.30–0.46 mm
Thick	0.018–0.030 in/0.46–0.76 mm

Table 148.6 Classification of split-thickness skin grafts.

Indications/Contraindications

STSGs contain less tissue requiring revascularization than FTSGs and are therefore more likely to survive when placed on almost any recipient bed, including those with a limited vascular supply. As a result, these grafts may be placed over periosteum, perichondrium, peritenon, and perineurium. STSGs are also used to cover large defects (Fig. 148.4A), particularly those that cannot be covered by a flap or would heal too slowly by second intention, as well as refractory venous leg ulcers[2,3]. STSGs may be useful for covering surgical defects in sites at high risk for tumor recurrence, since recurrent tumor is usually visible when growing through split-thickness skin. If the tumor has not recurred after 1–2 years, the graft can be removed and definitive reconstruction performed.

Advantages of STSGs over FTSGs include their improved chance of survival under conditions of vascular compromise, their ease of application, their ability to cover large defects, and their ability to act as a "window" for recurrence of high-risk lesions. The principal disadvantages of STSGs include their suboptimal cosmetic appearance, the presence of a granulating donor site wound requiring postoperative care, greater contraction, and the special equipment required to harvest larger grafts. Furthermore, because of their relative thinness, STSGs may be less durable than FTSGs, necessitating regrafting or partial healing by second intention.

While thicker STSGs tend to be cosmetically superior to thinner ones, poor color and texture match with the surrounding skin often occurs after STSG placement. STSGs tend to be pale or white in color, hairless, and smooth, with impaired sweating due to the fact that adnexal structures are not removed in their entirety with the graft and do not survive. The contrast between the STSG and its surrounding skin can therefore produce a "tire-patch" appearance (Fig. 148.4B), which is more pronounced than that seen with FTSGs.

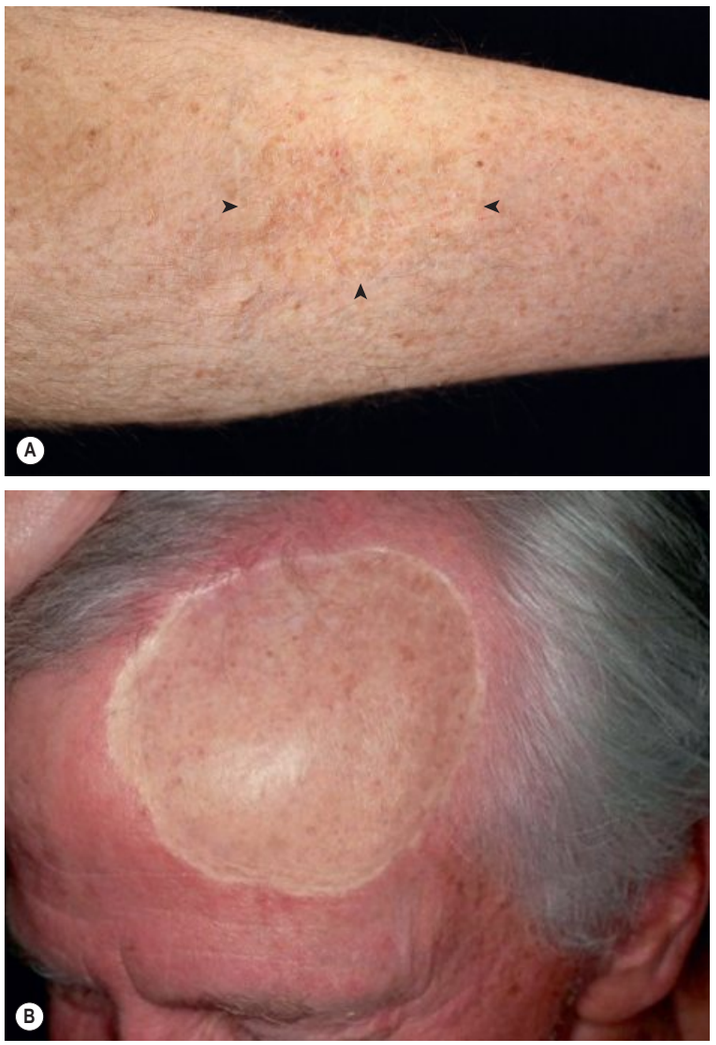


Fig. 148.4 Split-thickness skin grafts (STSGs). A A relatively thick STSG placed on the medial aspect of the lower extremity with excellent cosmetic results; arrowheads denote the edges of the graft. **B** STSG placed on the forehead and scalp several years prior, following excision of a cutaneous melanoma. Note the relative hypopigmentation, altered texture, and depression of the STSG compared to the normal surrounding skin. *Courtesy Jean L. Bolognia, MD.*

Preoperative History and Donor Site Considerations

Donor scar cosmesis should be taken into consideration when selecting a split-thickness donor site. The ease of postoperative care and the type of instrument used to harvest the graft may also help dictate donor site choice. Ideally, STSGs should be harvested from a site where a broad area of skin can be removed while still being concealed beneath clothing. The most common donor sites include the anterior, medial, and lateral portions of the upper thigh, the inner and outer aspects of the upper arm, and the inner aspect of the forearm. Lower back and abdominal skin can also be harvested. The anteromedial thigh is most frequently used as the donor site for STSGs, as harvesting and wound care are convenient, and wounds in this location do not interfere with ambulation. Donor site wounds on the buttocks tend to require assisted postoperative care, although their scars are ideally placed from a cosmetic standpoint. Power-driven dermatomes and large freehand knives require large flat donor surfaces, which may limit donor sites to the thighs, abdomen, and buttocks, while smaller grafts can be harvested freehand or with a power-driven dermatome.

Description of Grafting Techniques

A wide variety of techniques for harvesting and placing STSGs have been described[2,3]. The instruments used to harvest STSGs can be classified into freehand and electric dermatomes. Freehand dermatomes include scalpel blades, double-edged razor blades, and knives such as the Weck blade. Although acceptable grafts can be obtained using these freehand devices, considerable technical expertise is required to harvest them.

A standard #15, #15c, or #10 blade can be an effective tool for harvesting small STSGs of medium thickness. After a template of the defect is made, the donor site is marked, anesthetized with 1% or 2% lidocaine, or with a dilute lidocaine solution if the tumescent technique is to be employed, and scored lightly with the blade. The graft is then harvested by orienting the blade parallel to the skin and gently sweeping it just below the level of the epidermis, so that the blade is visible beneath the skin (Fig. 148.5). It is helpful to have an assistant apply traction to the donor site while the graft is harvested. Several blades may be required for harvesting, as blade sharpness diminishes quickly with multiple passes. This technique may be especially useful in harvesting small medium-thickness STSGs to repair auricular and postauricular defects.

Power-driven dermatomes became the standard method of harvesting larger STSGs after Brown developed the first such instrument in the 1940s. Electric dermatomes designed to harvest STSGs of varying thicknesses and widths, from several centimeters up to nearly 15 cm, are now commonly employed, and lithium ion battery-powered units are also available. Although STSGs can be obtained easily and reliably with any of these devices when properly used, graft quality is technique-dependent, and substantial irregularity in graft thickness and width may occur. The Zimmer dermatome, which was originally powered by compressed water-pumped nitrogen and subsequently modified into an electrically powered version, tends to harvest uniform grafts of predetermined width and thickness such that consistent graft quality tends to be less dependent on the operator's technique. Multipurpose motor systems now exist which include a control box, foot switch, and autoclavable motor that can be used not only with dermatomes,

but also with diamond fraises for dermabrasion, adjustable skin graft meshers, and other types of surgical handpieces, allowing a wide array of procedures to be performed using a single unit.

After the dermatome is prepared, the donor and recipient sites are anesthetized, prepped and draped in the usual sterile fashion. If chlorhexidine surgical scrub is used, a saline wash is employed to remove any excess scrub. The donor site is lubricated in advance with sterile mineral oil or another lubricant to ease travel of the dermatome over the skin. The handpiece is held on the donor site at an angle of 30–45°. A throttle control is pressed to start the cut, and the unit is guided forward using light downward pressure to ensure that the cutting edge remains in continuous contact with the donor site. An assistant applies tension by pulling the skin away from the donor area to create a flat, even surface. As the dermatome glides over the donor skin, the graft emerges from the pocket of the dermatome, and is lifted away from the machine with tissue forceps or hemostats (Fig. 148.6A). Once a sufficiently large graft has been harvested, the dermatome is pulled away from the skin and the graft is placed in sterile saline or on sterile saline-soaked gauze (Fig. 148.6B). A modified harvesting technique using tumescent anesthesia and placement of a polyurethane membrane over the donor site has been reported to prevent graft shrinkage and dehydration and to facilitate graft fixation at the recipient site[35].



Fig. 148.5 Freehand harvesting of a small split-thickness skin graft from the upper outer arm. The blade is oriented parallel to the skin, and gently swept just below the level of the epidermis, so that it is just visible through the graft. An assistant applies traction to the donor site to facilitate harvesting.

Securing the Graft

As in the case of FTSGs, STSGs should be secured so that infection, hematoma or seroma formation, and mechanical shearing forces can be prevented. Both the perimeter and the central portion of the graft must be secured for adequate nutritional support and to ensure graft survival. The edges of STSGs need not be as closely approximated to the surrounding wound edges as those of FTSGs, since overlapping skin will slough without affecting the ultimate cosmetic result. After the graft has been placed with the dermal side adherent to the recipient bed, its perimeter may be secured with sutures or staples. Centrally placed basting sutures may also be helpful in ensuring apposition of the graft to its bed. Once the graft has been secured and its bolster sewn into place, a non-adhesive dressing or pressure dressing may be applied as an additional precaution. Sutures or staples are removed after 7–10 days.

Donor Site Care

Harvesting STSGs creates a second wound, the donor defect, which often causes more postoperative discomfort than the grafted area itself.

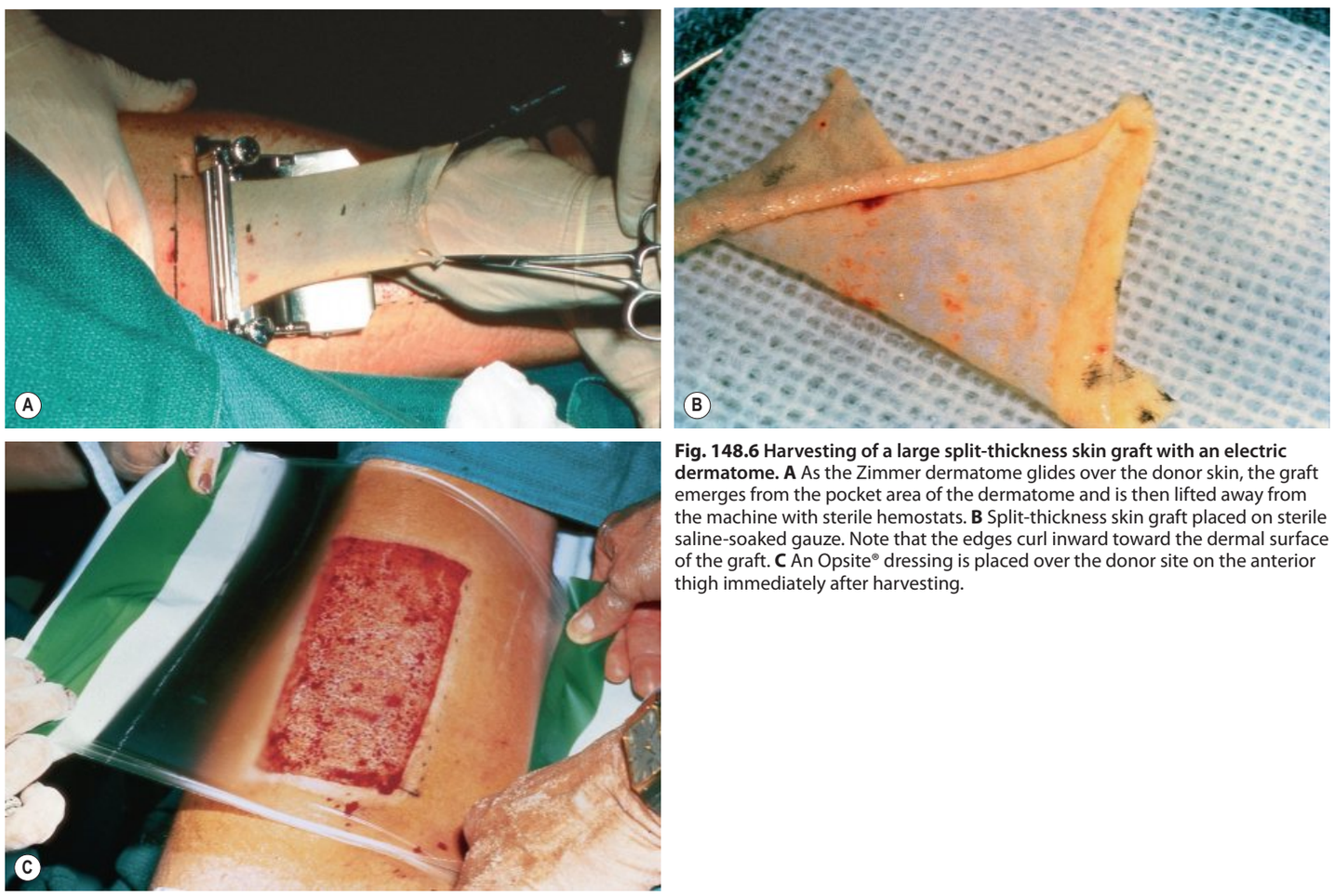


Fig. 148.6 Harvesting of a large split-thickness skin graft with an electric dermatome. A As the Zimmer dermatome glides over the donor skin, the graft emerges from the pocket area of the dermatome and is then lifted away from the machine with sterile hemostats. **B** Split-thickness skin graft placed on sterile saline-soaked gauze. Note that the edges curl inward toward the dermal surface of the graft. **C** An Opsite® dressing is placed over the donor site on the anterior thigh immediately after harvesting.

This partial-thickness wound heals by second intention. While STSG donor sites were once treated with bulky occlusive dressings left in place for 10–14 days, the advent of transparent, vapor-permeable dressings such as Opsite® has improved both patient comfort and ease of care in the postoperative period (Fig. 148.6C)[36]. These dressings are advantageous because they allow the serosanguineous drainage that inevitably accumulates at the donor site to collect, keeping the wound moist and thereby shortening healing time. Because these dressings are transparent, the wound can easily be observed for complications during healing. In one review, these dressings were associated with the fastest healing rates, low infection rates, the least amount of pain, and lower cost when compared with other dressings[37].

After the skin around the donor site area is cleaned and dried, a thin coat of an adhesive such as Mastisol® is applied around the wound and allowed to dry. An Opsite® dressing is then placed over the wound. Paper tape is placed around the perimeter of the Opsite®, followed by a gauze dressing and an elastic bandage (e.g. Ace™ wrap).

Variations/Unusual Situations

Meshing the graft with scalpel slits may be performed to allow drainage of accumulated blood or serosanguineous material that could otherwise inhibit graft–bed contact. This technique may also be used to expand the surface area of STSGs. A meshing machine may be utilized to expand the graft's surface area further by ratios ranging from 3:1 to 9:1. Meshing can facilitate coverage of a large recipient area with smaller donor grafts. Expanded meshed grafts placed experimentally on contaminated recipient beds have been found to exhibit increased take as compared to non-meshed donor skin[38].

Postoperative Care

During the first 24 hours after grafting, a large amount of serosanguineous fluid may accumulate beneath the donor site dressing. Patients need to be forewarned about this possibility so that they do not become alarmed. If necessary, the fluid can be drained with a needle and syringe, and an Opsite® patch applied. Alternatively, a new Opsite® dressing can be placed. The dressing can then be left in place until healing is complete. Depending on the STSG's thickness, the donor site should fully re-epithelialize in 7–21 days. The scar usually evolves in color from pink to white over a period of months.

Complications

The complications of split-thickness skin grafting can be divided into early complications, which stem from failure of engraftment, and late complications[2,3]. Failure of engraftment may result from hematoma or seroma formation, infection, or shearing forces. Late complications can be divided into cosmetic and functional problems (Fig. 148.7).

Color and texture mismatch of STSGs with the surrounding skin is predictable and expected. Grafts often remain erythematous for months to years after placement. More importantly, they may exhibit significant postoperative hyperpigmentation or hypopigmentation. Darker-skinned patients are especially prone to graft hyperpigmentation, despite observance of preventive measures. Patients should therefore minimize graft exposure to the sun without sunscreens for 6 months, and wear sunscreens consistently thereafter. The absence of adnexal structures predisposes to xerosis and a build-up of keratinous debris. The resultant scaling, pruritus, and dryness can be minimized with liberal emollient use.

Functional considerations are of paramount concern, since STSGs contract more than FTSGs and can create forces powerful enough to produce joint contracture if placed over or near joints. Contraction of facial grafts, especially near the nasal ala, the eyelid, the helical rim and the free margins of the vermilion border, may produce significant cosmetic deformities, including alar retraction, ectropion, helical rim distortion, and vermilion border distortion, respectively. Hypertrophic scarring of the graft and donor sites may also occur, which can be treated with corticosteroid-impregnated tape, intralesional corticosteroids, or pulsed dye laser. Graft fragility and breakdown can occur in areas of trauma, particularly in sites such as the lower leg, or in areas with little underlying soft tissue support, such as those directly overlying perichondrium or periosteum. These complications are not always avoidable, but forewarning patients may reduce unnecessary trauma to the area. Lastly, bullae can occur within graft sites, presumably related to decreased anchoring properties of the basement membrane zone (see Ch. 33).

Future Directions

In recent years, biosynthetic and tissue-engineered living skin replacements have been the focus of research in skin transplantation[39–41]. Cultured human keratinocytes have been seeded onto type I collagen membranes petrolatum gauze to reconstitute the epidermis, enabling

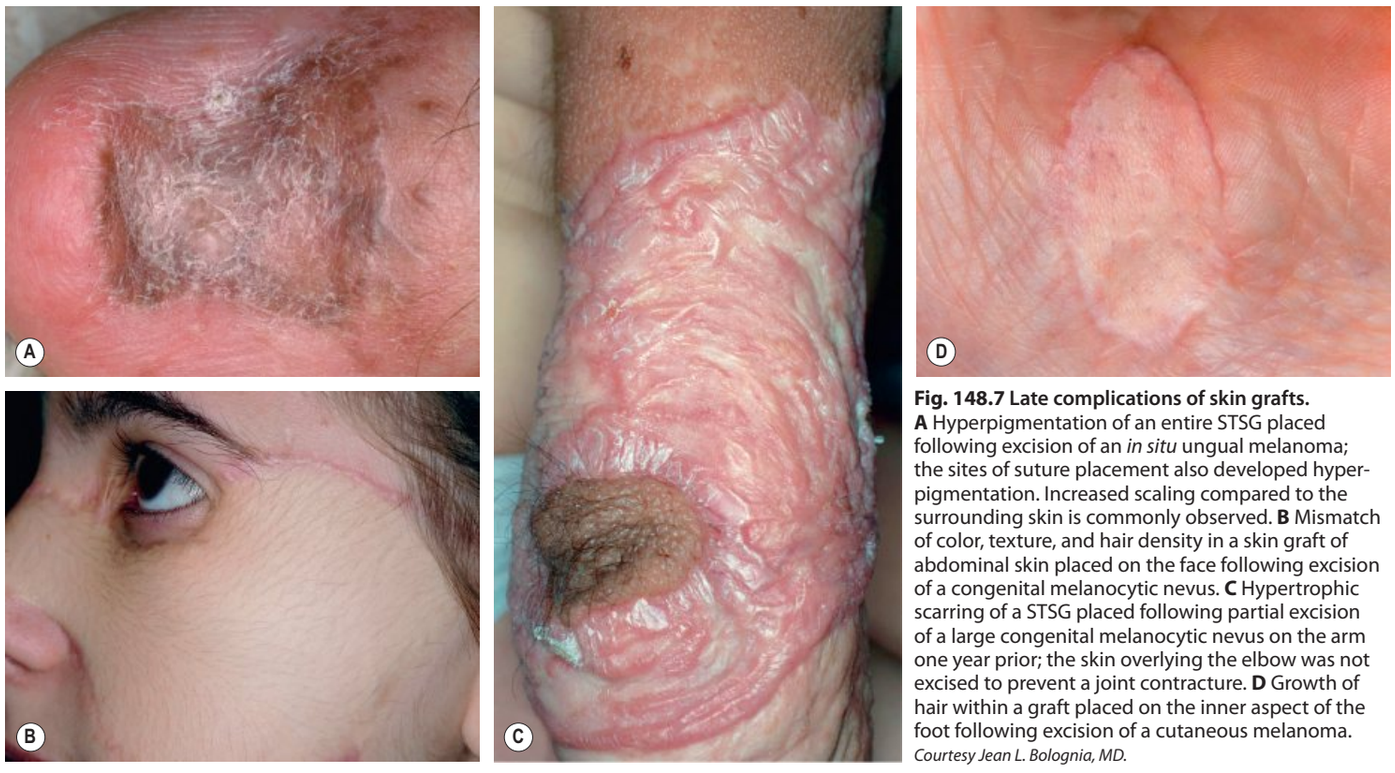


Fig. 148.7 Late complications of skin grafts. **A** Hyperpigmentation of an entire STSG placed following excision of an *in situ* ungual melanoma; the sites of suture placement also developed hyperpigmentation. Increased scaling compared to the surrounding skin is commonly observed. **B** Mismatch of color, texture, and hair density in a skin graft of abdominal skin placed on the face following excision of a congenital melanocytic nevus. **C** Hypertrophic scarring of a STSG placed following partial excision of a large congenital melanocytic nevus on the arm one year prior; the skin overlying the elbow was not excised to prevent a joint contracture. **D** Growth of hair within a graft placed on the inner aspect of the foot following excision of a cutaneous melanoma. *Courtesy Jean L. Bolognia, MD.*

transfer of actively proliferating keratinocytes onto partial-thickness wounds. Human epidermal tissues mimicking the biochemical and morphologic properties of human skin have been established *in vitro* by growing human keratinocytes on a dermal fibroblast-containing collagen gel. Such skin-equivalent cultures are being used to reconstitute the epidermis in patients with full-thickness burn wounds and chronic ulcers (see Ch. 145).

Artificial dermis is now routinely used prior to full-thickness grafting, and an acellular allograft dermal matrix has been shown to provide a good bed for STSGs in patients with full- and partial-thickness burns. A tissue-engineered human skin equivalent, i.e. a bilayered product containing living human fibroblasts, keratinocytes and bovine collagen, is commercially available for the repair of surgical defects and coverage of lower leg ulcers that would previously have been repaired with STSGs. Dermal–epidermal composites using autologous keratinocytes and human allodermis may in the future be used for grafting full-thickness wounds in patients with burns, leg ulcers, or surgical wounds.

COMPOSITE GRAFTS

Indications/Contraindications

Composite grafts are modified FTSGs, consisting of two or more tissue layers. In dermatologic surgery, these grafts are usually composed of skin and cartilage, although they may be composed of skin and fat or skin and perichondrium[3,26,42–48]. Composite grafts are especially useful for repairing full-thickness alar rim defects, as well as nasal tip defects with cartilage loss[46,47]. Full-thickness nasal mucosal defects can be repaired using composite grafts to provide mucosal lining and structural support with a nasolabial or forehead flap placed thereafter to reconstruct the overlying soft tissue defect (see Fig. 147.29). As discussed earlier, conchal bowl composite grafts or PCCGs, consisting of skin and perichondrium, may be used (with or without an underlying cartilage graft) for deeper nasal defects requiring skin coverage, especially defects with exposed cartilage[48].

Preoperative History and Considerations

Composite grafts require rapid revascularization to survive. Early re-establishment of circulation occurs via direct vessel anastomoses between the subdermal plexus of the graft and the subdermal plexus of the wound edge. Since composite grafts are dependent upon this bridging phenomenon for their survival, they are of necessity limited in size, with no point being more than 1 cm from a vascular source, as the risk of central necrosis increases significantly at graft diameters >2 cm[3,47]. Composite grafts for nasal ala and ear reconstruction are possible because of the rich vascular supply of the nose and ear, and because of the small surface areas generally involved. Composite grafts, like FTSGs, are threatened by excessive shearing forces of the graft over its bed, which prevent revascularization.

Composite grafts pass through four stages as they heal[3,47]. After graft placement, the tissue blanches completely. By 6 hours, the graft becomes pale pink, signifying anastomosis of the graft vessels with those of the recipient site. At 12–24 hours, the graft appears dusky blue, reflecting venous congestion, and by 3–7 days, it should be pink, indicating graft survival.

Donor Site Considerations for Composite Grafts

The complexity of nasal ala anatomy makes reconstruction of full-thickness defects in this area difficult. There may be insufficient nasal skin to develop adequate local flaps, and nasolabial flaps, which provide reasonable defect coverage, generate other cosmetic deformities. Loss of alar tissue support also creates a functional deficit, as the alar skin is liable literally to "blow in the breeze" on inspiration and expiration. Composite grafts provide an excellent cosmetic and functional alternative for repair of full-thickness alar rim defects <2 cm in diameter[46]. Grafts taken from the earlobe have been used successfully for this type of repair, although grafts taken from the cartilaginous portion of the ear are more frequently used[43,46].

Donor sites for harvesting auricular composite grafts include the helical crus, helical rim, and conchal bowl (see Ch. 142)[46–48]. Small alar defects with cartilage loss can be elegantly repaired using the helical crus as donor site, while more substantial defects may require repair using the helical rim or conchal bowl, since the crus may not provide sufficient inner lining for the graft. Donor defects involving the helical crus can be repaired with minimal scar formation, while wedge excisions are usually necessary to repair helical rim donor sites. Conchal bowl donor sites heal by second intention.

The advantages of auricular composite grafts in repairing full-thickness alar rim defects relate mainly to the presence of cartilage, which provides structural support and stability, with prevention of alar distortion during inspiration and at rest[46,48]. Disadvantages include a higher risk of graft failure with an increased number of tissue layers, substantial graft size limitations, and limited donor tissue availability. Nevertheless, these grafts, when properly applied, can yield outstanding results. In one animal study, maintaining an intact skin-to-cartilage interface and an equivalent skin-to-cartilage ratio improved composite graft survival; however, when cartilage size exceeded skin size, or when skin and cartilage were separated before transfer, survival decreased, highlighting the importance of an intact skin-to-cartilage interface in optimizing graft survival[49].

Composite grafts used for full-thickness nasal mucosal repair are usually obtained from the triangular fossa, scapha, conchal cavum, cymba, or helical crus (see Fig. 142.13). The appropriate donor site is that which best matches the contour of the surgical defect. These donor sites are usually allowed to heal by second intention, with good aesthetic outcomes.

Description of Technique

Composite grafts used for alar repair are performed as follows (Fig. 148.8)[42,46,48]: the donor and recipient sites are anesthetized using local anesthesia, and prepped with an antiseptic solution. If the alar tissue is scarred and retracted, the area must be vigorously debrided to assure the best possible blood supply for the graft. The defect is then

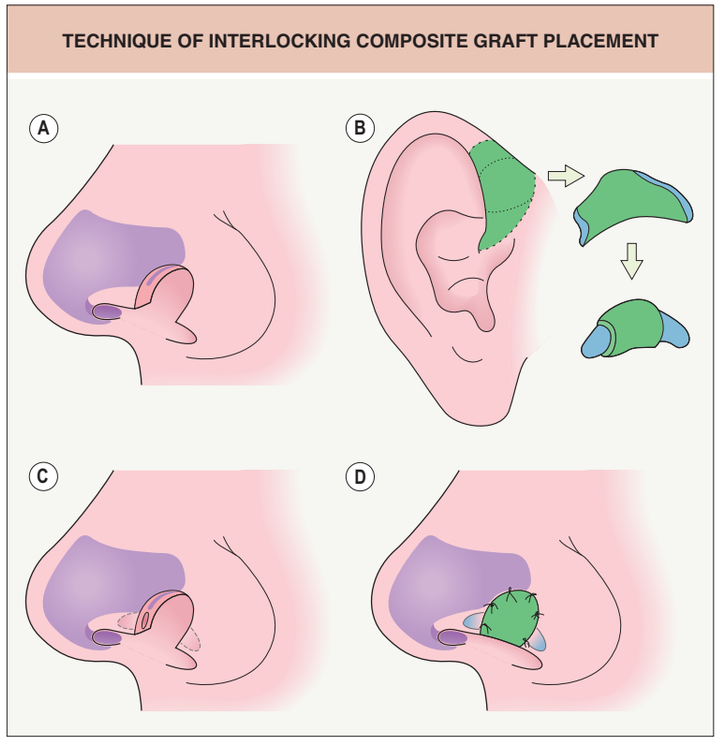


Fig. 148.8 Technique of interlocking composite graft placement. A A full-thickness nasal ala defect extending through both skin and cartilage requires repair. **B** Donor site at the crus of the helix. An area of skin ~5%–10% greater in area than the actual defect is marked out, with cartilaginous wings marked out on either side. After the graft is harvested, the skin is removed on both sides to expose the cartilaginous portion of the graft, such that two cartilaginous pegs with their overlying perichondrium (blue color) frame the lateral aspects of the graft. **C** A pocket is undermined on either side of the recipient site into which the cartilaginous pegs will be placed. **D** The cartilaginous pegs are inserted into the holes prepared within the alar tissue on either side of the defect. The graft is then sutured into place.

measured and a template made as described previously. The donor site is marked and anesthetized, and the graft is harvested. The tissue is handled very gently and placed in sterile saline until ready for placement.

Due to the fragility of composite grafts, a tongue-in-groove technique is recommended to maximize graft stability and increase graft survival[46]. Two cartilaginous wings are marked out and anesthetized on either side of the donor site prior to graft harvesting. After the graft is harvested, the skin overlying these two cartilaginous wings is removed, leaving the cartilage with its overlying perichondrium (Fig. 148.8B). These wings are then inserted into pockets prepared within the alar tissue of both sides of the defect (Fig. 148.8C) such that the graft interlocks with its recipient bed (Fig. 148.8D). Interlocking the graft with its bed may help to minimize shearing forces and provide a larger surface area for revascularization.

The graft is sutured into place in two layers. The undersurface of the graft, which replaces the inner lining of the nose, can be secured first using a 6–0 absorbable suture. The skin is then closed with a 6–0 non-absorbable suture, taking very small tissue bites to minimize vessel strangulation and to maximize the number of potential vessels available for reanastomosis. The needle should pass through the mucosal portion of the graft first, then through the outer epithelial edge of the graft, so that the knots are tied externally, and are not buried between the graft and its recipient bed. The cartilage does not need to be sutured, as it will heal on its own. A Vaseline® gauze or Xeroform™ dressing can then be placed in the nasal vestibule for support, and petrolatum ointment applied to the external suture line. A non-stick dressing is then applied to protect the graft from external injury.

Conchal bowl composite grafts used for reconstruction of deep alar defects are harvested in essentially the same way as composite grafts taken from the helical crus[47]. Potential advantages of the conchal bowl technique include increased bulk, which may be superior in filling deep partial-thickness alar defects, and an excellent cosmetic match for the sebaceous skin of the nose.

Donor Site Closure[48]

Helical crus defects can often be closed in a side-to-side fashion. A simple advancement, rotation, or transposition flap may also be utilized to take advantage of loose preauricular skin. Helical rim defects are usually closed with an ear wedge resection. Auricular grafts obtained from the triangular fossa, scapha, conchal bowl, or cymba heal well by second intention. Conchal bowl defects may heal more rapidly if a 2 or 3 mm punch biopsy instrument is used to remove small plugs of conchal cartilage, which allows healing by second intention from the dermis on the opposite side.

Variations/Unusual Situations

When securing composite grafts onto the nasal ala, delayed intranasal knot tying has been recommended by some authors to facilitate wound closure by improving visualization, allowing gentler manipulation of tissue, and enabling precise suture placement in a confined space[50]. When placing intranasal sutures, the needle of the 6–0 fast-absorbing chromic gut suture is first passed through the nasal mucosa, and then through the corresponding location on the "mucosal" side of the graft. Sutures are placed at 1–2 mm intervals along the defect and graft, and their free ends are held separately by hemostats to prevent tangling. After all intranasal sutures have been placed, the composite graft is placed into the alar defect and the cartilaginous wings inserted. The most internal intranasal sutures are then tied first, followed by the more accessible external sutures.

Postoperative Care

To minimize edema, ice packs should be applied to the grafted area as often as possible for up to several days postoperatively. Oral antibiotics are generally advisable because of the high bacterial colonization around the nares and the higher risk of failure with composite grafts. Sutures are removed after 1 week.

Complications

As with other types of grafts, there is a risk of necrosis in the early stages of healing, and contraction, textural changes, atrophy, and contour irregularities thereafter. If the graft survives but the cosmetic result is suboptimal, dermabrasion or laser resurfacing may be performed 6 weeks to 6 months postoperatively to correct textural differences between the graft and the surrounding skin, and to improve the color match between them. Resurfacing of the entire cosmetic unit may provide superior cosmetic results. In the event of composite graft failure, a two-stage revision with placement of a cheek interpolation flap may be performed or, alternatively, a second composite grafting procedure may be undertaken.

Conchal bowl donor sites are at somewhat greater risk of postoperative bleeding than other areas if left to heal by second intention. Application of pressure dressings over the front and back of the ear to "sandwich" the conchal cartilage with placement of hemostatic foam over the donor site may decrease this risk. Other types of complications at auricular donor sites are rare[51].

The ear is also prone to infection with *Pseudomonas* spp., which reside in the external auditory meatus. Cleaning the ear with a dilute vinegar solution, applying topical gentamicin ointment, and oral quinolone antibiotics are all helpful prophylactic measures which should be considered after harvesting auricular cartilage. If infection is suspected, oral quinolone antibiotics should be started immediately, and therapy guided thereafter by the results of cultures and sensitivities. If the infection does not resolve with appropriate antibiotics, the presence of a fungal infection, most often secondary to *Candida*, should be excluded.

FREE CARTILAGE GRAFTS

Indications/Contraindications

Free cartilage grafts are used most commonly in dermatologic surgery to reconstruct the nasal ala, tip and sidewall, the ear, and the eyelid[42,44,51–53]. These grafts may be used to restore the architecture of an anatomic site that has undergone significant cartilage loss. Free cartilage grafts are also useful in stabilizing the position and contour of free margins against the forces of contraction during wound healing.

Nasal Ala

Partial-thickness alar defects extending into deep soft tissue or approaching the alar rim often lead to rim collapse, producing a functional as well as a cosmetic deficit. Placement of cartilage grafts, consisting of cartilage with its overlying perichondrium, can be used to avert this potential problem[51–53]. The grafted cartilage provides a rigid but flexible framework that braces the alar rim against collapse during inspiration and expiration. Cartilage grafts may be used in conjunction with flaps and FTSGs to maintain airway patency and to minimize the risk of alar retraction during healing (Fig. 148.9)[44,51–53].

The usefulness of the free cartilage graft lies in its ability to prevent alar retraction. It is possible that long-term survival of the cartilage itself may not ultimately be important, as the mere presence of the rigid framework of the graft in the initial stages of wound healing seems to be sufficient to inhibit alar retraction.

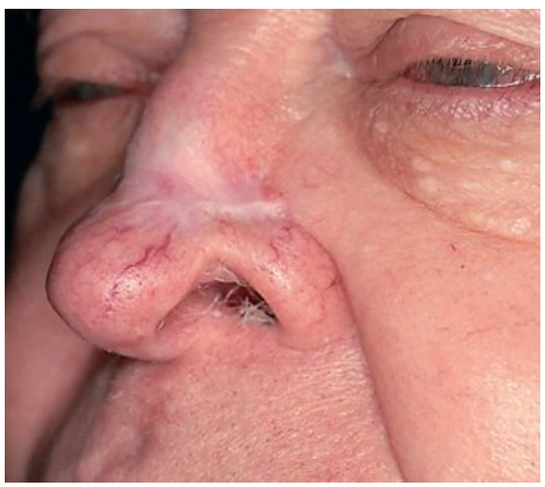


Fig. 148.9 Distortion of the nasal alar rim due to scar retraction from second intention healing following removal of a basal cell carcinoma. Use of free cartilage grafts or composite grafts composed of skin and cartilage can help to prevent this complication. *Courtesy Jean L. Bolognia, MD.*

Nasal Sidewall and Tip

Deep nasal sidewall defects may, at times, involve loss of the upper lateral nasal cartilage. Nasal valve obstruction may result, which becomes noticeable with inspiration and resolves on expiration. Delayed nasal valve obstruction can also occur if unresisted scar contracture collapses the remaining cartilaginous structure of the nasal sidewall. Replacing lost cartilage at the time of reconstruction can avert these potential problems. Similarly, loss of cartilage at the distal nasal tip necessitates structural support replacement for optimal function and cosmesis.

Ear

Auricular defects involving cartilage loss are generally repaired for cosmetic, rather than functional, reasons. Cartilage grafts may be used as braces along the helical rim to minimize the risk of contracture, and may also be used in the conchal bowl to assist in hearing-aid placement[42].

Preoperative History and Donor Site Considerations

Potential donor sites for free cartilage grafts include the conchal bowl, the auricular helix, the antihelix, nasal septum, and ribs[42]. The conchal bowl and antihelix are the donor sites most frequently used by dermatologic surgeons[44,48,53]. Conchal cartilage is elastic, has a high degree of memory, and has varied contours that can be matched to the desired alar contour. Although an anterior approach to the conchal bowl may be used, the posterior approach results in better camouflage of the donor site scar and preservation of the shape of the ear. If the antihelix is used as a donor site, it is recommended that subtotal resection of the antihelical cartilage be performed, leaving a complete rim of intact helical cartilage to prevent distortion.

Description of Technique

Nasal ala

The techniques for alar batten cartilage grafting have been well described[42,44,48,51]. The alar batten provides a rigid but flexible cartilaginous framework to brace against alar rim collapse. The length of the cartilage graft is determined by measuring the distance between the lateral and medial borders of the defect at the alar rim, and adding to that measurement an extra 4–5 mm. The conchal bowl donor site is incised anteriorly or posteriorly, whereas the antihelical donor site is incised anteriorly. The skin overlying the cartilage is then undermined with blunt-scissor dissection to expose the perichondrial surface. The desired length of cartilage is incised with a scalpel (Fig. 148.10A), and a second incision is made exactly parallel to the first, creating a cartilaginous strip that may be 3–6 mm in width, depending upon the desired width of the graft (Video 148.9). Alternatively, a larger disk or oblong-shaped piece may be harvested to match the base of the defect. The cartilage is easily separated from the overlying skin with sharp-scissor dissection. The graft is placed in sterile saline while the donor site is reapproximated with non-absorbable sutures.

The cartilage graft is secured by undermining the soft tissue of the recipient bed medially and laterally with a hemostat or blunt-scissor dissection, and the ends of the graft are inserted into the undermined pockets such that the graft interlocks with its bed (Fig. 148.10B, Videos 148.10 and 148.11). The graft is anchored to its bed with one or two 5–0 absorbable sutures for additional security (Video 148.12). A disk- or oblong-shaped cartilage graft also requires suturing for secure placement.

After the graft has been anchored, a nasolabial transposition flap or FTSG is sutured into place to complete the closure (Fig. 148.10C,D, and see Videos 148.1, 148.2, 148.3, 148.4, 148.5, 148.6). A standard tie-over bolster is placed over the FTSG and secured with 5–0 non-absorbable sutures (see Videos 148.7, 148.8). Sutures are removed at 1 week.



Fig. 148.10 Harvesting and placement of a free cartilage graft. A The posterior conchal bowl donor site has been incised to the level of the perichondrium. The desired length of cartilage was incised with the scalpel, and a second incision made parallel to the first to isolate a cartilaginous strip with its overlying perichondrium. **B** The ends of the cartilaginous strip with its overlying perichondrium have been inserted into pockets undermined on either side of the recipient bed, such that the graft interlocks with its recipient bed on the left nasal ala. The graft is sutured to the underlying dermis with one 5–0 absorbable suture for additional security. **C** A full-thickness skin graft has been sutured into place over the free cartilage graft. **D** Eight-week postoperative view of the full-thickness skin graft and underlying free cartilage graft on the left nasal ala. The alar rim remains in perfect alignment.

Nasal sidewall and tip

Free cartilage grafts used for nasal sidewall and tip reconstruction are harvested in much the same way as free cartilage grafts for alar reconstruction[42]. Nasal sidewall grafts tend to be wider and broader than alar grafts, since they must brace a broader area against the forces of inspiration. Alternatively, multiple cartilaginous strips can be placed perpendicular to the lateral nasal sidewall, and then secured with absorbable or non-absorbable sutures to brace the side of the nose against collapse. After the cartilaginous structure is in place, a flap or FTSG may be performed to cover the remaining cutaneous defect.

Nasal tip grafts for distal nasal reconstruction are organized to provide both proximal and distal structural support, thus optimizing the aesthetic and functional result[42,51,52]. The proximal grafts consist of bilateral batten grafts secured to the lateral cartilages with 5–0 or 6–0 non-absorbable sutures. On top of these may be sewn a dorsal nasal cartilage graft. A columellar strut of cartilage often provides distal support, on top of which may be sewn an additional tip graft. Alar batten grafts secured to the columellar strut and lateral alar soft tissue provide alar rim support. A paramedian forehead flap or melolabial interpolation flap may be placed thereafter to provide coverage of the cutaneous defect.

Ear

If conchal cartilage is used to repair a large helical defect, the cartilage graft should match the defect as closely as possible in size and shape[42]. Harvesting and placing a narrow strip of cartilage matching the helical defect alone will result in helical rim collapse under the forces of wound contraction. If necessary, a partial wedge closure of the defect may be performed to decrease the size of the defect requiring replacement of structural support. The cartilage graft is secured by sewing it to the intact cartilaginous framework with 5–0 absorbable or non-absorbable sutures. The graft is then generally covered with a pedicled retroauricular advancement flap.

Eyelid

Partial-thickness lower eyelid defects with loss of the tarsal plate, as well as full-thickness lower eyelid defects, may be repaired with cartilage grafts. Stabilization of the eyelid margin with free cartilage grafts provides structural support, minimizing the risk of ectropion and preventing corneal desiccation. The technique for performing free cartilage grafts to repair full-thickness and partial-thickness lower eyelid defects is beyond the scope of this chapter, but is well described by Otley and Sherris[42].

Postoperative Care

Regardless of the site of cartilage grafting, care must be taken postoperatively to minimize movement of the graft. Routine wound care is performed to the flap or skin graft overlying the free cartilage graft. Trauma to the area should be minimized.

Complications

Postoperative complications following cartilage grafting are rare. There is a risk of postoperative infection at conchal bowl donor sites, particularly with Gram-negative bacilli, which reside within the external auditory meatus. Appropriate bacterial and fungal cultures of any exudate should be obtained if infection is suspected. Empiric therapy with quinolone antibiotics should be initiated, and modified as sensitivities dictate. When prophylactic antibiotics and appropriate operative technique are used, the risk of suppurative chondritis is extremely low[54].

Postoperative tenderness, swelling, and erythema may herald inflammatory chondritis or perichondritis, which should be treated with cool compresses and nonsteroidal anti-inflammatory drugs for several weeks or even months postoperatively.

Later complications may include graft resorption, displacement or deformation after placement, and extrusion. Surgical revision may be required if these complications occur. Auricular and nasal recipient sites are subject to trauma and are therefore at increased risk of graft displacement and resorption. Every effort should therefore be made intraoperatively to utilize grafts of sufficient thickness and stiffness to resist the forces of trauma and wound contracture, and to anchor these grafts to maximize their stability.

Future Trends

While autologous cartilage is considered the optimal grafting material due to its pliability, accessibility, and ease of harvesting under local anesthesia, its supply may be limited, and harvesting may entail additional morbidity. Other implantable materials for nasal reconstruction have been investigated, including porous, high-density polyethylene implants, which have been well tolerated as replacements for native cartilage in patients requiring rhinoplasty or nasal reconstruction[55,56].

Tissue engineering has been used to generate autologous cartilage implants to fill defects of the nose or outer ear[57]. Chondrocytes can be stimulated with growth factors to increase their proliferative rate and extracellular matrix production. Such chondrocytes, when implanted in a resorbable synthetic scaffold, can thereby be induced to produce three-dimensional aggregates of cartilage. In one study, collagen lattices containing cultured chondrocytes implanted into rabbit auricular cartilage generated new cartilage within 5 weeks[57]. *In vitro* engineering of human cartilage could be the ideal replacement method, without the risk of infection and with the possibility of reconstructing large defects with different configurations. In a first-in-human trial, autologous chondrocytes harvested from the nasal septum were cultured in media with autologous serum and seeded onto collagen type I and type III membranes[58]. After 4 weeks, the resulting engineered cartilage grafts, 25 × 25 × 2 mm, were successfully implanted beneath forehead or nasolabial flaps, just as native auricular cartilage would have been, with comparable aesthetic and functional results. These and newer implantable materials should become increasingly available over time, and will undoubtedly be useful for surgeons who perform nasal reconstruction.

CONCLUSIONS

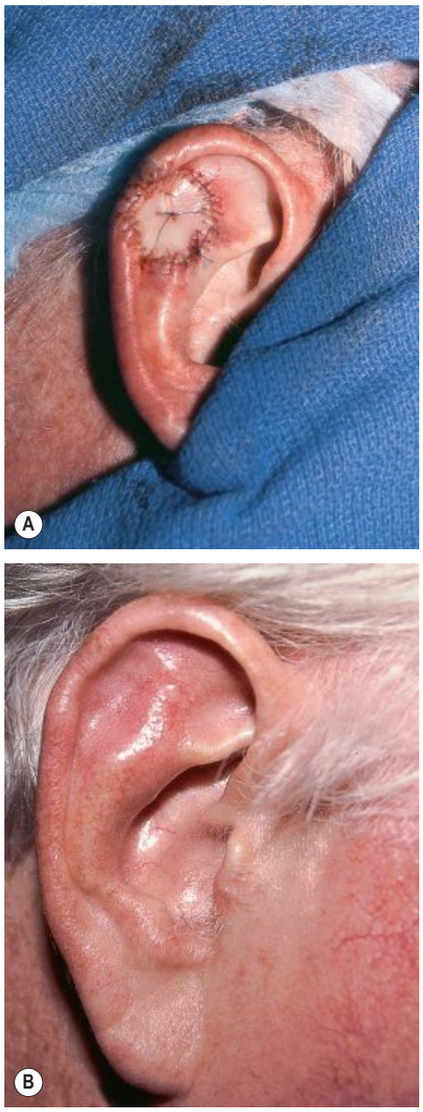
A working knowledge of the indications, techniques, donor site considerations, and postoperative complications of all types of skin grafts is necessary for soft tissue reconstruction. As the incidence of skin cancer continues to rise, increasing numbers of patients are likely to undergo reconstructive procedures requiring full-thickness skin and/or cartilage grafting. Lower extremity ulcers are another common problem, and split-thickness skin grafting remains an effective, reasonable treatment for such patients. With proper defect assessment, reconstructive planning, and attention to detail preoperatively, intraoperatively and postoperatively, optimal cosmetic and functional results can be achieved using the full range of grafting techniques, a thorough understanding of which is therefore invaluable for all physicians performing reconstructive surgery.

Additional figures available in our eBook (see inside front cover for access code).

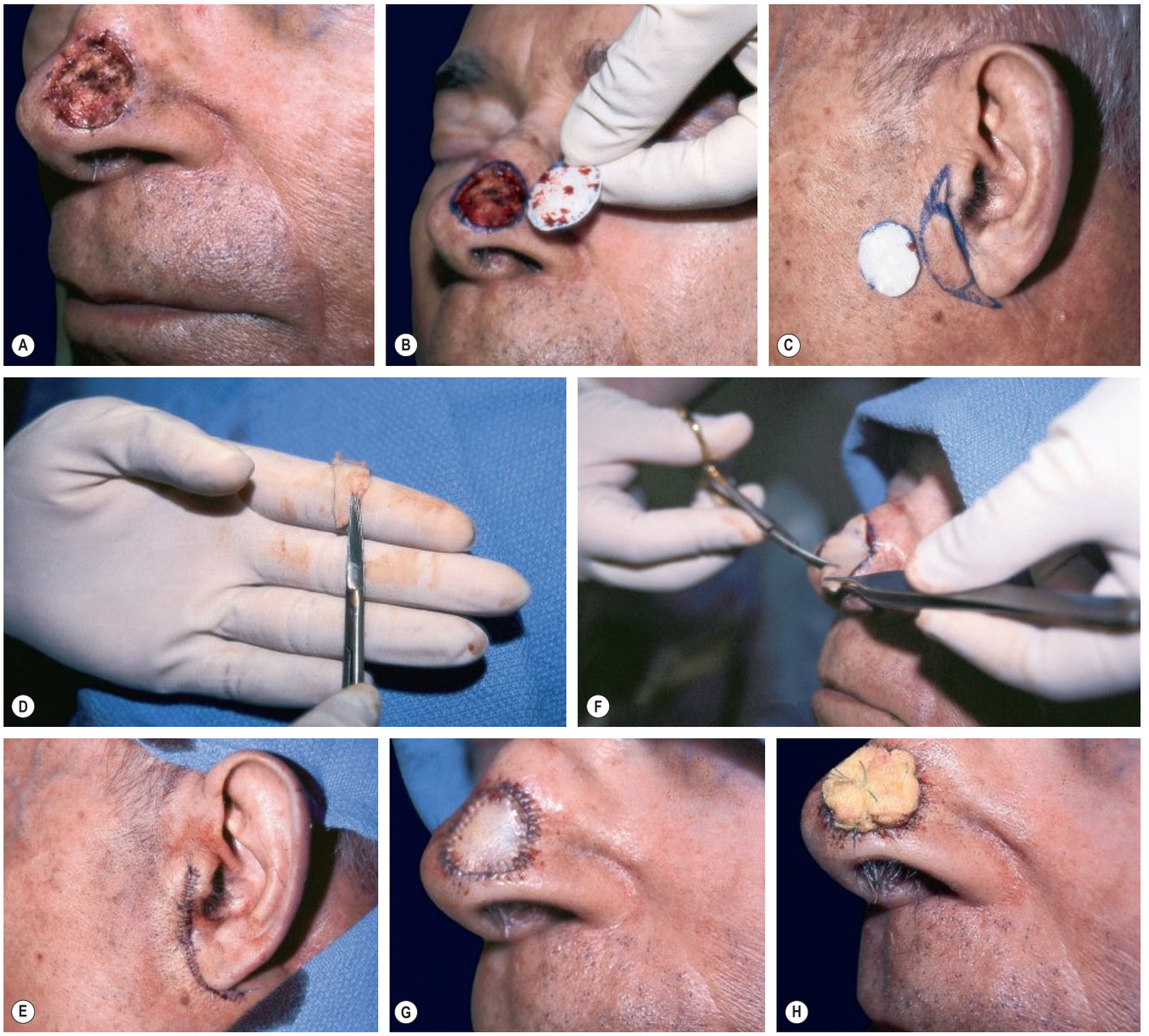
REFERENCES

1. Hauben DJ, Baruchin A, Mahler A. On the history of the free skin graft. *Ann Plast Surg*. 1982;9:242–245.
2. Ratner D. Skin grafting. *Semin Cutan Med Surg*. 2003;22:295–305.
3. Adams DC, Ramsey ML. Grafts in dermatologic surgery: review and update on full- and split-thickness grafts, free cartilage grafts and composite grafts. *Dermatol Surg*. 2005;31:1055–1067.
4. Smahel J. The healing of skin grafts. *Clin Plast Surg*. 1977;4:409–424.
5. Goldminz D, Bennett RG. Cigarette smoking and flap and full-thickness graft necrosis. *Arch Dermatol*. 1991;127:1012–1015.
6. Walden JL, Garcia H, Hawkins H, et al. Both dermal matrix and epidermis contribute to an inhibition of wound contraction. *Ann Plast Surg*. 2000;45:162–166.
7. Gloster Jr. HM. The use of full-thickness skin grafts to repair nonperforating nasal defects. *J Am Acad Dermatol*. 2000;42:1041–1050.
8. Rohrer TE, Dzubow LM. Conchal bowl skin grafting in nasal tip reconstruction: clinical and histologic evaluation. *J Am Acad Dermatol*. 1995;33:476–481.
9. Zitelli JA. Burow's grafts. *J Am Acad Dermatol*. 1987;17:271–279.
10. Krishnan R, Hwang L, Orengo I. Dog-ear graft technique. *Dermatol Surg*. 2001;27:312–314.
11. Kaufman AJ. Adjacent-tissue skin grafts for reconstruction. *Dermatol Surg*. 2004;30:1349–1353.
12. Wang Q, Cai M, Wu YL, Zhang GC. Mathematical guide to minimize donor site in full-thickness skin grafting. *Dermatol Surg*. 2009;35:1364–1367.
13. Hill TG. Contouring of donor skin in full-thickness skin grafting. *J Dermatol Surg Oncol*. 1987;13:883–888.
14. Larson PO, Ragi G, Mohs FE, Snow SN. Excision of exposed cartilage for management of Mohs surgery defects of the ear. *J Dermatol Surg Oncol*. 1991;17:749–752.
15. Craven NM, Telfer NR. An open study of tissue adhesive in full-thickness skin grafting. *J Am Acad Dermatol*. 1999;40:607–611.

16. Orengo I, Lee MW. Surgical pearl: the "unsuture" technique for skin grafts. *J Am Acad Dermatol*. 1998;38:758–759.
17. Langtry JA, Kirkham P, Martin IC, Fordyce A. Tie-over bolster dressings may not be necessary to secure small full thickness skin grafts. *Dermatol Surg*. 1998;24:1350–1353.
18. Kromka W, Cameron M, Fathi R. Tie-over bolster dressings vs basting sutures for the closure of full-thickness skin grafts: a review of the literature. *J Cut Med Surg*. 2018;22:602–606.
19. Adams DC, Ramsey ML, Marks VJ. The running bolster suture for full-thickness skin grafts. *Dermatol Surg*. 2004;30:92–94.
20. Srivastava D, Kouba DJA. "Lilliputian" technique for rapid and efficient securing of bolster dressings over full-thickness skin grafts. *Dermatol Surg*. 2009;35:1280–1281.
21. Brady JG, Grande DJ, Katz AE. The purse-string suture in facial reconstruction. *J Dermatol Surg Oncol*. 1992;18:812–816.
22. Halpern ME, Adams C, Ratner D. Galeal hinge flaps: a useful technique for immediate repair of scalp defects extending to periosteum. *Dermatol Surg*. 2009;35:1127–1130.
23. Robinson JK, Dillig G. The advantages of delayed nasal full-thickness skin grafting after Mohs micrographic surgery. *Dermatol Surg*. 2002;28:845–851.
24. Meyers S, Rohrer T, Grande D. Use of dermal grafts in reconstructing deep nasal defects and shaping the ala nasi. *Dermatol Surg*. 2001;27:300–305.
25. Draper BL, Wentzell JM. The "drumhead" graft repair of deep nasal alar defects. *Dermatol Surg*. 2007;33:17–22.
26. Gloster Jr HM, Brodland DG. The use of perichondrial cutaneous grafts to repair defects of the lower third of the nose. *Br J Dermatol*. 1997;136:43–46.
27. Thibault MJ, Bennett RG. Success of delayed full-thickness skin grafts after Mohs micrographic surgery. *J Am Acad Dermatol*. 1995;32:1004–1009.
28. Callahan S, Goldsberry A, Kim G, Yoo S. The management of antithrombotic medication in skin surgery. *Dermatol Surg*. 2012;38:1417–1426.
29. Nehal KS, Levine VJ, Ross B, Ashinoff R. Comparison of high-energy pulsed carbon dioxide laser resurfacing and dermabrasion in the revision of surgical scars. *Dermatol Surg*. 1998;24:647–650.
30. Leventhal D, Furr M, Reiter D. Treatment of keloids and hypertrophic scars: a meta-analysis and review of the literature. *Arch Facial Plast Surg*. 2006;8:362–368.
31. Stephenson AJ, Griffiths RW, La Hausse-Brown TP. Patterns of contraction in human full thickness skin grafts. *Br J Plast Surg*. 2000;53:397–402.
32. Michelotti B, Mathis R, Roberts J, et al. Periorbital Mohs reconstruction: characterization of tumor histology, anatomic location, and factors influencing postoperative complications. *Dermatol Surg*. 2014;40:1084–1093.
33. Can Z, Ercocen AR, Apaydin I, et al. Tissue engineering of high density porous polyethylene implant for three-dimensional reconstruction: an experimental study. *Scand J Plast Reconstr Surg Hand Surg*. 2000;34:9–14.
34. Baltazar T, Merola J, Catarino C, et al. Three dimensional bioprinting of a vascularized and perfusable skin graft using human keratinocytes, fibroblasts, pericytes, and endothelial cells. *Tissue Eng Part A*. 2020;26:227–238.
35. Kneiling M, Breuninger H, Schippert W, et al. A modified, improved, easy and fast technique for split-thickness skin grafting. *Brit J Dermatol*. 2011;165:581–584.
36. Field LM. Harvesting split-thickness grafts in direct continuity with "op-site" membrane biologic dressings [letter]. *Dermatol Surg*. 1995;21:357–359.
37. Rakel BA, Bermel MA, Abbott LI, et al. Split-thickness skin graft donor site care: a quantitative synthesis of the research. *Appl Nurs Res*. 1998;11:174–182.
38. Nappi JF, Falcone RE, Ruberg RL. Meshed skin grafts versus sheet skin grafts on a contaminated bed. *J Dermatol Surg Oncol*. 1984;10:380–381.
39. Horch RE, Debus M, Wagner G, Stark GB. Cultured human keratinocytes on type I collagen membranes to reconstitute the epidermis. *Tissue Eng*. 2000;6:53–67.
40. Suzuki S, Shin-ya K, Kawai K, Nishimura Y. Application of artificial dermis prior to full-thickness skin grafting for resurfacing the nose. *Ann Plast Surg*. 1999;43:439–442.
41. Metcalfe AD, Ferguson MW. Bioengineering skin using mechanisms of regeneration and repair. *Biomaterials*. 2007;28:5100–5103.
42. Otley CC, Sherris DA. Spectrum of cartilage grafting in cutaneous reconstructive surgery. *J Am Acad Dermatol*. 1998;39:982–992.
43. Haas AF, Glogau RG. A variation of composite grafting for reconstruction of full-thickness nasal alar defects. *Arch Dermatol*. 1994;130:978–980.
44. Adams C, Ratner D. Composite and free cartilage grafting. *Dermatol Clin*. 2005;23:129–140. vii.
45. Geyer AS, Pasternack F, Adams C, Ratner D. Use of a skin-fat composite graft to prevent alar notching: an alternative to the delayed postoperative repair. *Dermatol Surg*. 2005;31:602–607.
46. Ratner D, Katz A, Grande DJ. An interlocking auricular composite graft. *Dermatol Surg*. 1995;21:789–792.
47. Weisberg NK, Becker DS. Repair of nasal ala defects with conchal bowl composite grafts. *Dermatol Surg*. 2000;26:1047–1051.
48. Haug MD, Rieger UM, Gubisch W. Managing the ear as a donor site for composite graft in nasal reconstruction: update on technical refinements and donor site management in 110 cases. *Ann Plast Surg*. 2009;63:171–175.
49. Lu GN, Tawfik O, Sykes K, et al. Association of skin and cartilage variables with composite graft healing in a rabbit model. *JAMA Facial Plastic Surg*. 2019;21:44–49.
50. Albertini JG, Ramsey ML. Surgical pearl: delayed intranasal knot tying for composite grafts of the ala. *J Am Acad Dermatol*. 1998;39:787–788.
51. Otley CC. Alar batten cartilage grafting. *Dermatol Surg*. 2000;26:969–972.
52. Byrd DR, Otley CC, Nguyen TH. Alar batten cartilage grafting in nasal reconstruction: functional and cosmetic results. *J Am Acad Dermatol*. 2000;43:833–836.
53. Zopf DA, Iams W, Kim JC, et al. Full-thickness skin graft overlying a separately harvested auricular cartilage graft for alar reconstruction. *JAMA Facial Plastic Surg*. 2013;15:131–134.
54. Kaplan AL, Cook JL. The incidences of chondritis and perichondritis associated with the surgical manipulation of auricular cartilage. *Dermatol Surg*. 2004;30:58–62. discussion 62.
55. Williams JD, Romo III T, Sclafani AP, Cho H. Porous high-density polyethylene implants in auricular reconstruction. *Arch Otolaryngol Head Neck Surg*. 1997;123:578–583.
56. Naumann A, Rotter N, Buija J, Aigner J. Tissue engineering of autologous cartilage transplants for rhinology. *Am J Rhinol*. 1998;12:59–63.
57. Sterodimas A, DeFaria J, Correa WE, Pitangiy I. Tissue engineering in plastic surgery: an up-to-date review of the current literature. *Ann Plast Surg*. 2009;62:97–103.
58. Fulco I, Miot S, Haug MD, et al. Engineered autologous cartilage tissue for nasal reconstruction after tumour resection: an observational first-in-human trial. *Lancet*. 2014;384:337–346.



eFig. 148.1 Full-thickness skin graft. A Full-thickness skin graft taken from the preauricular region was used to repair this defect of the right upper anterior ear. **B** Eight-week postoperative result.



eFig. 148.2 Placement of a full-thickness skin graft. A A 1.7 × 2 cm defect of the nasal tip is present after removal of recurrent basal cell carcinoma with Mohs micrographic surgery. A preauricular donor site provides the best match in this case for color, sebaceous quality, degree of photodamage, and thickness. **B** After marking the periphery of the recipient site with a marking pen, the template material is pressed against the defect. The resulting outline of the inked margin serves as a guide to cut a perfect template, seen here adjacent to the nasal defect. **C** The template has been applied to the preauricular donor site, and inking material applied around it. Burow's triangles are outlined on either side of the template to close the site primarily. Marking the donor site prior to local anesthesia prevents incorrect sizing due to tissue stretch from lidocaine infiltration. **D** The graft is carefully defatted with curved iris scissors so that only the white, glistening surface of the dermis remains. **E** The preauricular donor site is closed primarily. **F** The full-thickness skin graft is trimmed with curved iris scissors to ensure a perfect fit. **G** Full-thickness skin graft sewn into place with 6–0 fast-absorbing chromic gut sutures. **H** Xeroform™ bolster sewn into place over full-thickness skin graft with 5–0 polypropylene tie-over sutures.

149 Nail Surgery

Bertrand Richert and Phoebe Rich

Chapter Contents

Surgical Anatomy of the Nail Unit 2570
Preoperative Evaluation and Patient Preparation 2571
Anesthesia of the Nail Unit 2571
Instruments for Nail Surgery 2572
Nail Plate Avulsion 2573
Biopsy Techniques 2574
Surgical Procedures for Disorders of the Nail Unit 2575
Postoperative Care 2579
Complications of Nail Surgery 2580

Key features

- A thorough understanding of the anatomy and physiology of the nail unit is a prerequisite for performing successful nail surgery
- The nail matrix forms the nail plate; any damage to the matrix (including from surgical procedures) can cause permanent nail dystrophy
- Because there is no subcutaneous tissue in the nail unit, the dermis of the nail bed sits on the periosteum of the distal digit
- Preoperative evaluation prior to nail surgery is essential and should include appropriate diagnostic imaging

INTRODUCTION

An accurate diagnosis of nail disorders often requires clinicopathologic correlation. When performing a biopsy of the nail unit, it is important that: (1) the most appropriate surgical procedure be performed correctly; (2) there is precise handling of the specimen in the histopathology laboratory; and (3) a dermatopathologist with knowledge of the nuances of nail pathology examine the tissue[1,2]. A range of disorders require nail surgery, from nail tumors to ingrown toenails. As with surgical procedures performed elsewhere, the major goals include establishing a diagnosis and/or providing treatment safely and with minimal pain or scarring[3]. Because dermatologists are the physicians who understand and manage nail disorders, they are well suited to perform nail surgery. A solid grasp of the anatomy and physiology of the nail unit is a prerequisite for successful nail surgery. Additional requirements for an optimal outcome include a well-prepared patient, adequate anesthesia, proper surgical technique, and hemostasis (Table 149.1).

SURGICAL ANATOMY OF THE NAIL UNIT

Basic Anatomy

The components of the nail unit are the nail plate, nail matrix, nail bed, hyponychium, and proximal and lateral nail folds.

The **nail matrix** rests on the midportion of the distal phalanx and has a broad crescent shape (Fig. 149.1). It is covered in large part by the proximal nail fold and extends on average half the distance from the nail fold to the central crease of the distal interphalangeal (DIP) joint. On the great toe, the lateral horns of the matrix can extend as far as the midline of the lateral aspect of the digit or even farther (Fig. 149.2). This is an important concept, especially when performing a phenol matricectomy for ingrown nails or a lateral longitudinal biopsy. The distal portion of the nail matrix is visible through the proximal nail plate on the thumbs and sometimes other fingers as the white half-moon-shaped structure called the lunula. While the proximal portion of the matrix produces the upper third of the nail plate, the distal portion provides the lower two-thirds (see Fig. 149.2). Consequently, surgery involving the distal matrix has a very low risk of producing nail dystrophy, as the upper layers of the nail plate will cover the defect[4,5].

The **nail bed**, sometimes referred to as the sterile matrix, extends from the distal lunula to the hyponychium. A rich vascular supply leads to the pink color that is visible through the translucent nail plate. The nail bed is composed of longitudinal ridges and grooves which interlock with opposing structures on the undersurface of the nail plate, contributing to the tight adhesion of the plate to the bed. Surgery of the nail bed rarely leads to permanent dystrophy of the nail apparatus, but it may result in mild onycholysis. An important feature of the nail bed is that there is no subcutaneous tissue beneath it. The dermis of the nail bed sits directly on the periosteum of the distal digit. The lack of subcutaneous tissue in the nail unit explains why nail surgical specimens should extend to the level of the periosteum.

The **hyponychium** begins at the most distal part of the nail bed, where the nail plate detaches to form its free edge and just proximal to the distal groove; it then becomes contiguous with the volar skin of the digit. Just proximal to the hyponychium is the onychodermal band, the area of maximal attachment between the nail plate and its bed which seals and protects the nail unit from environmental factors. Trauma- or disease-induced disruption of the onychodermal band can result in onycholysis, followed by bacterial and fungal contamination. The **proximal nail fold** covers and protects most of the matrix and the newly formed plate. The most distal portion of the proximal nail fold gives rise to the cuticle, which adheres tightly to the proximal nail plate, thereby sealing and protecting the nail pocket from environmental pathogens and irritants.

The **lateral folds** ensheath the lateral aspects of the plate. Proximally, they merge with the proximal nail fold and distally with the hyponychium. The proximal and lateral nail folds are collectively called the paronychium. The term perionychium refers to the paronychium plus the hyponychium and nail bed[5].

The insertion of the **extensor tendon** of the digit onto the phalanx is just proximal to the most proximal portion of the matrix. In an adult, this is ~12 mm proximal to the cuticle. Except in the most extensive nail surgical procedures such as nail unit ablation, this tendon is not observed within the surgical field.

Innervation

Paired palmar and dorsal nerves course along the lateral sides of the digit in close approximation to the digital arteries (see Fig. 149.1). In general, the index, middle and ring fingertips get their innervation from the palmar digital nerves whereas the thumb and little (fifth) finger are innervated by the dorsal nerves[6]. This is an important consideration when performing a digital block.

Vascular Supply

The paired proper digital arteries, which run along the lateral and volar sides of the digit, comprise the main blood supply to the nail unit (see Fig. 149.1). They anastomose to form three arcades: (1) the superficial arcade – supplies the area overlying the DIP joint; (2) the proximal arcade – supplies the proximal nail fold and matrix; and (3) the distal arcade – supplies the nail bed and hyponychium.

PREREQUISITES FOR SUCCESSFUL NAIL SURGERY
1. Understanding of nail anatomy and physiology
2. Proper patient selection and preparation
3. Adequate anesthesia
4. Hemostasis
5. A nail condition that has eluded diagnosis by routine clinical inspection, history, diagnostic imaging, and/or microbiologic evaluation
6. A dermatopathologist who is familiar with the histopathologic idiosyncrasies of the nail unit

Table 149.1 Prerequisites for successful nail surgery.

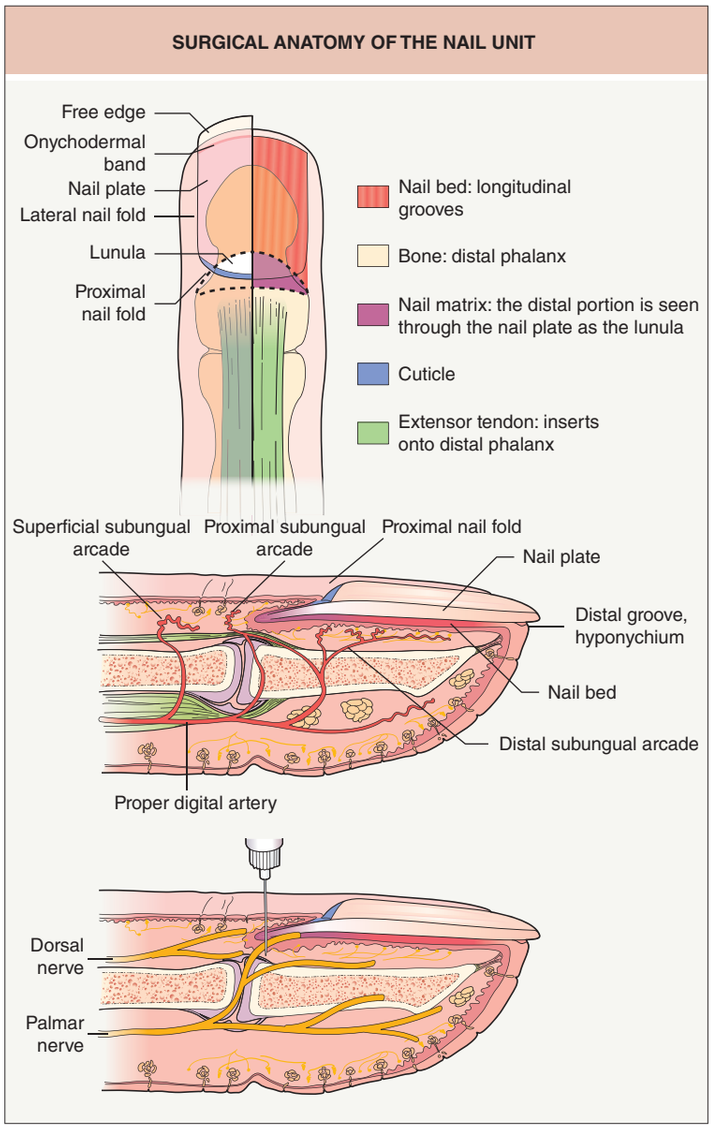


Fig. 149.1 Surgical anatomy of the nail unit. There are three arcades of blood vessels as well as both a dorsal and palmar nerve. In the distal digital block, after local anesthesia is injected around the dorsal nerve branch, the needle is advanced vertically towards the palmar surface where additional anesthesia is injected around the palmar nerve (see Fig. 149.3A).

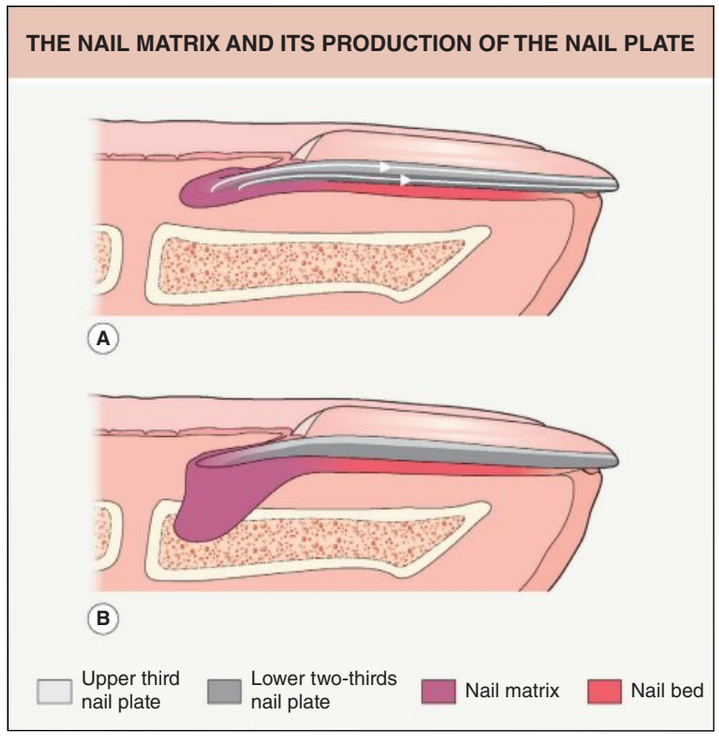


Fig. 149.2 The nail matrix and its production of the nail plate. A The proximal portion of the matrix produces the upper third of the nail plate (light gray) and its distal part the lower two-thirds (dark gray). **B** On the great toe, the lateral horns of the matrix can extend as far as the midline of the lateral aspect of the digit or even farther.

PREOPERATIVE EVALUATION AND PATIENT PREPARATION

A thorough and efficient preoperative evaluation is required prior to nail surgery. Screening for underlying diseases, especially those that predispose to peripheral vascular disease (e.g. diabetes mellitus, Raynaud phenomenon, atherosclerosis), should be done, in addition to a review of medications, allergies (e.g. povidone–iodine, antibiotics, narcotics, anesthetics, latex), smoking history, and past surgical procedures, in particular the presence of prosthetic heart valves and joint replacements (see Table 151.2). Diagnostic imaging can detect underlying bony defects as well as define space-occupying lesions and their anatomic relationships prior to nail surgery. A full "procedure, alternatives, and risks" (PAR) discussion should include the possibility of bleeding, pain, infection, and permanent nail dystrophy. Information regarding work disruption should be provided. Premedication is not particularly useful, except in those who are very anxious. No systemic drugs, including anticoagulants and antiplatelet agents, should be discontinued. Prophylactic antibiotics are only indicated for individuals with high-risk cardiac conditions or prosthetic joint replacements at high risk for infection (see Tables 151.2 & 151.3). While not mandatory, clinical photographs of the preoperative nail may prove worthwhile. The digit is then prepped with alcohol, chlorhexidine, or povidone–iodine and sterilely draped.

ANESTHESIA OF THE NAIL UNIT

The choice of anesthetic will depend on the pain expected postoperatively. Plain 1% or 2% lidocaine and ropivacaine (2 mg/ml) have a more rapid onset while 0.5% bupivacaine provides adequate anesthesia after 15 minutes; there is a longer duration of anesthesia with the latter two local anesthetics (see Ch. 143). Multiple studies involving thousands of patients support the premise that lidocaine with epinephrine (adrenaline) can be safely injected into digits, as long as patients have no history of peripheral vascular compromise and the recommended volume is injected (see below)[7]. However, as nail surgery is usually performed with a tourniquet, there is little need for the vasoconstrictive effect of epinephrine.

Pain during anesthesia comes from several factors: the needle prick, rapid injection, and acidity of the anesthetic. In order to reduce these side effects, the surgeon should use thin needles (30-gauge), inject very slowly, and buffer the lidocaine (see Ch. 143).

Anesthesia can be administered as a nerve block (distal digital block) or as infiltrative anesthesia (wing procedure). In the *distal digital block*, the needle is inserted vertically, 1 cm lateral and proximal to the junction of the proximal and lateral folds; here 0.5 ml of the anesthetic is injected in order to anesthetize the dorsal nerve branch (Fig. 149.3A). The needle is then advanced vertically towards the palmar surface,

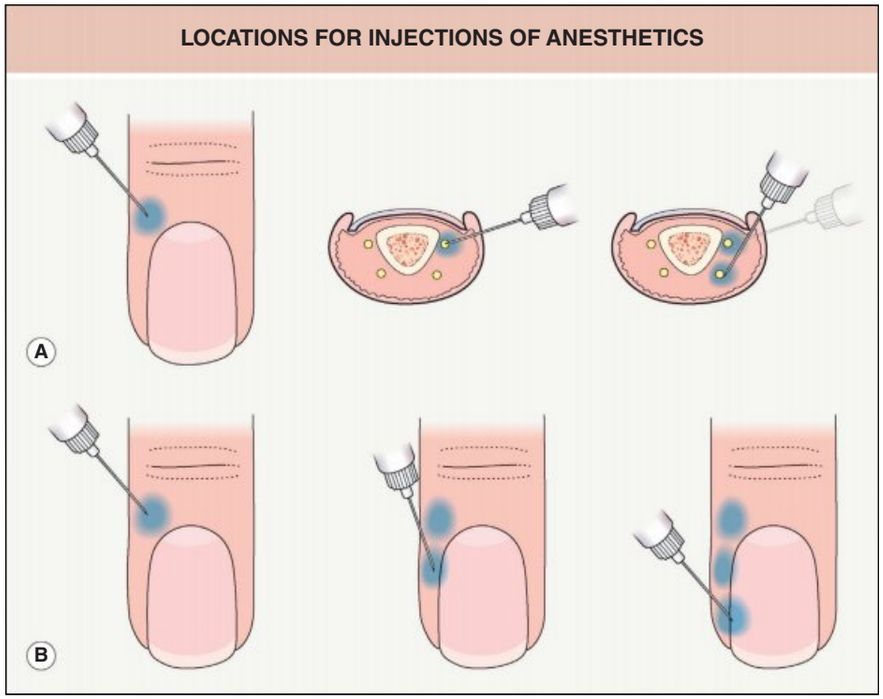


Fig. 149.3 Locations for injections of anesthetics. A Distal digital nerve block. **B** Infiltrative wing procedure.

where an additional 0.5 ml is injected around the palmar nerve branch. The procedure is then repeated on the opposite side to obtain full anesthesia of the nail unit. This nerve block has several advantages over the proximal digital (ring) block: (1) the onset of action is quicker; (2) less volume of anesthetic is required; (3) less risk of injuring the neurovascular bundles at the base of the finger; and (4) the injection is more comfortable.

In the *wing procedure*, anesthetic is injected to produce a dermal wheal at the most proximal portion of the lateral nail fold. The anesthetic progressively diffuses distally within the lateral nail fold, thus resembling a wing. Moving distally around the nail, anesthetic is repeatedly injected into the distal edge of the previously anesthetized skin until the surgical field is adequately numbed (Fig. 149.3B). The associated tissue edema provides a certain degree of hemostasis[8]. Injecting a longer-acting anesthetic (e.g. bupivacaine) postoperatively provides prolonged anesthesia and reduces bleeding after removal of the tourniquet due to the extra liquid-based pressure on the lateral digital arteries[9].

INSTRUMENTS FOR NAIL SURGERY

Most of the instruments used in nail surgery are standard instruments used in cutaneous surgery. A few specific instruments are needed in order to make nail surgery easier to perform. An *elevator* allows atraumatic detachment of the plate from the bed and several types are available, such as the Freer nail elevator or Locke elevator (Fig. 149.4). *Nail nippers* are essential for cutting the nail plate. When cutting thick nails, the dual-action nail nipper is invaluable. The English nail splitter is very popular but has a major drawback: its thicker lower jaw induces lateral onycholysis ahead of the cutting line. Straight nail nippers with their sharp, thinner, beveled jaws are less traumatic (Fig. 149.5).

As nail surgery requires a bloodless surgical field, a tourniquet, applied for a maximum of 20 minutes, is very useful. Several options are available. The Penrose drain, clamped with a sturdy hemostat, is commonly used but studies have shown that it delivers high and unreliable pressure that has the potential for lateral nerve damage, and thus it is not recommended for digits. A sterile glove, half a size smaller than the adequate size, can be employed; the corresponding fingertip of the glove is pierced with scissors and then rolled back to the base of the proximal phalanx (Fig. 149.6). This technique exsanguinates the digit and delivers an acceptable pressure around 500 mmHg. The remainder of the glove serves as a sterile field[9]. T-Ring®, a digital tourniquet specifically designed to ensure hemostasis with the lowest efficient pressure (~150 mmHg), is commercially available. Its limitation is cost (currently $10 USD per unit).

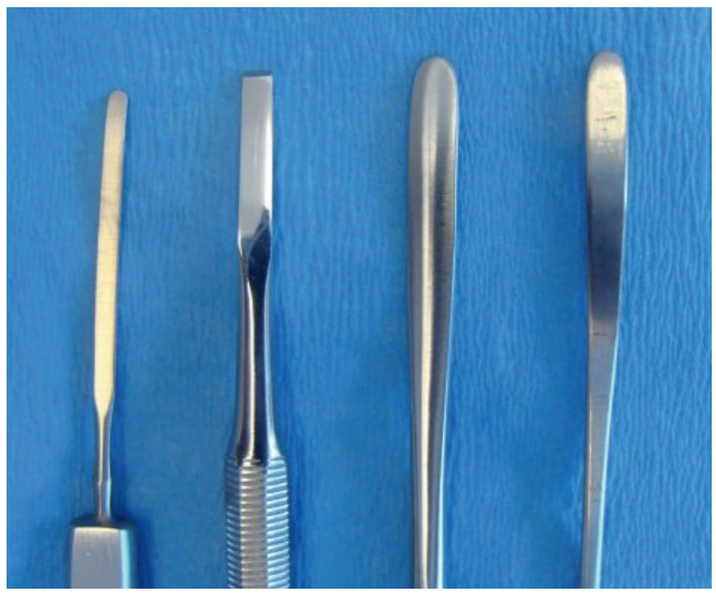


Fig. 149.4 Different types of nail elevators. From left to right, McKenty periosteal elevator, dental spatula, Freer nail elevator, and dura mater elevator.

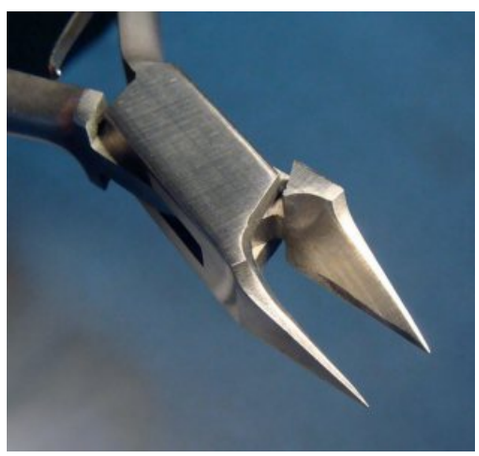


Fig. 149.5 Sharp-pointed and beveled nail nippers.

NAIL PLATE AVULSION

Nail avulsion is the most basic procedure in nail surgery and is a prelude to most other nail unit procedures. It allows visualization of the nail bed and matrix, thus providing good exposure for biopsy or excision (Fig. 149.7). Except for patients with retronychia, total nail avulsion should be discouraged because as the counterpressure exerted by the nail plate disappears, the distal wall and pulp raise upward in combination with a shrinkage of the nail bed. The result is more bulky soft tissue at the end of the digit and an increased risk of distal embedding during nail regrowth. Partial nail avulsion is therefore preferred[10], with the remaining normal nail plate reducing the risk of distal embedding[1]. Partial nail avulsion serves as an adjuvant therapeutic intervention in onychomycosis as it reduces the fungal mass, especially of a dermatophytoma (Fig. 149.8). In addition, nail avulsion is an early step in chemical matricectomy (see below), may be performed to drain an acute paronychia, and is a must when exploring pigmented lesions within the nail matrix. There are two approaches to nail avulsion – distal and proximal, although the latter is rarely used.



Fig. 149.6 Sterile glove used as a tourniquet and sterile field. One fingertip of the glove is pierced with scissors and rolled back to the base of the proximal phalanx.

For *distal nail plate avulsion*, an elevator is first pushed under the proximal nail fold and slid back and forth from one side to the other in order to detach the fold from the plate (Fig. 149.9A). The elevator is then inserted under the free edge of the nail plate in a distal to proximal direction to free the plate from its bed (Fig. 149.9B). As the instrument reaches the matrix area where the attachment of the nail plate is looser, a decrease in resistance is felt. To loosen the entire plate, the instrument is inserted under the plate at several sites, advancing from the hyponychium to the matrix. Lateral motions across the nail bed should not be done to loosen the nail plate as this can injure the fragile longitudinal nail bed ridges. The plate is then grasped on one lateral edge by a hemostat or a nail puller, rotated (Fig. 149.9C), and pulled off the nail bed.

If the avulsion is performed to explore the entire matrix area, avulsion alone will not suffice. Two releasing incisions, ~1 cm in length, are made at each junction of the proximal and lateral nail folds, angling laterally and proximally. This allows the nail fold to be reflected so that the matrix can be inspected (Fig. 149.10). When performing a biopsy or excisional surgery, skin hooks or sutures help to maintain the reflection of the proximal nail fold. At the end of the procedure, the fold is placed back into its original position and secured with simple interrupted sutures or adhesive strips. The nail plate, if not needed for

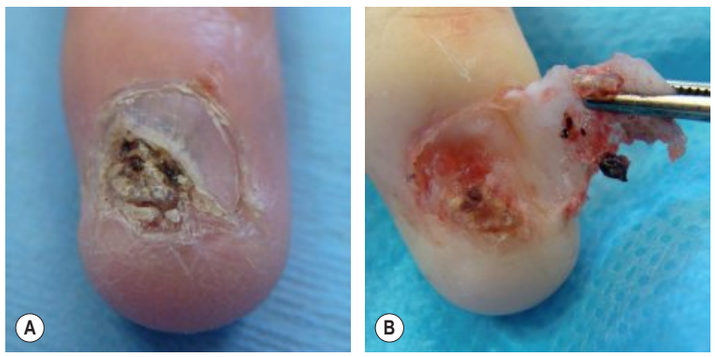


Fig. 149.7 Lateral avulsion of the plate to expose the nail bed. A Keratotic lesion suspicious for squamous cell carcinoma is extending from under the nail plate. **B** Lateral avulsion allows examination of the nail bed and biopsy of the tumor.

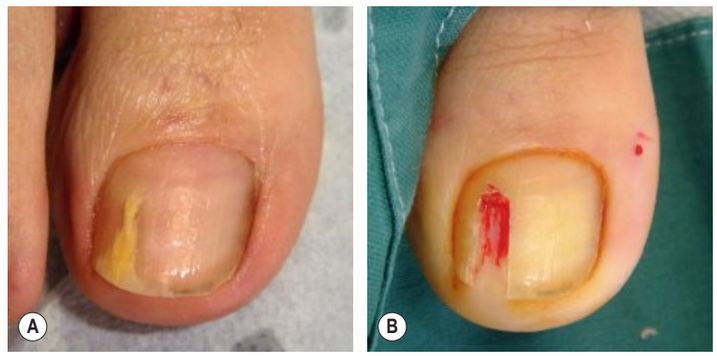


Fig. 149.8 Treatment of a dermatophytoma. A Yellow spike due to a dermatophytoma. **B** Partial avulsion of the nail plate and removal of the fungal mass.

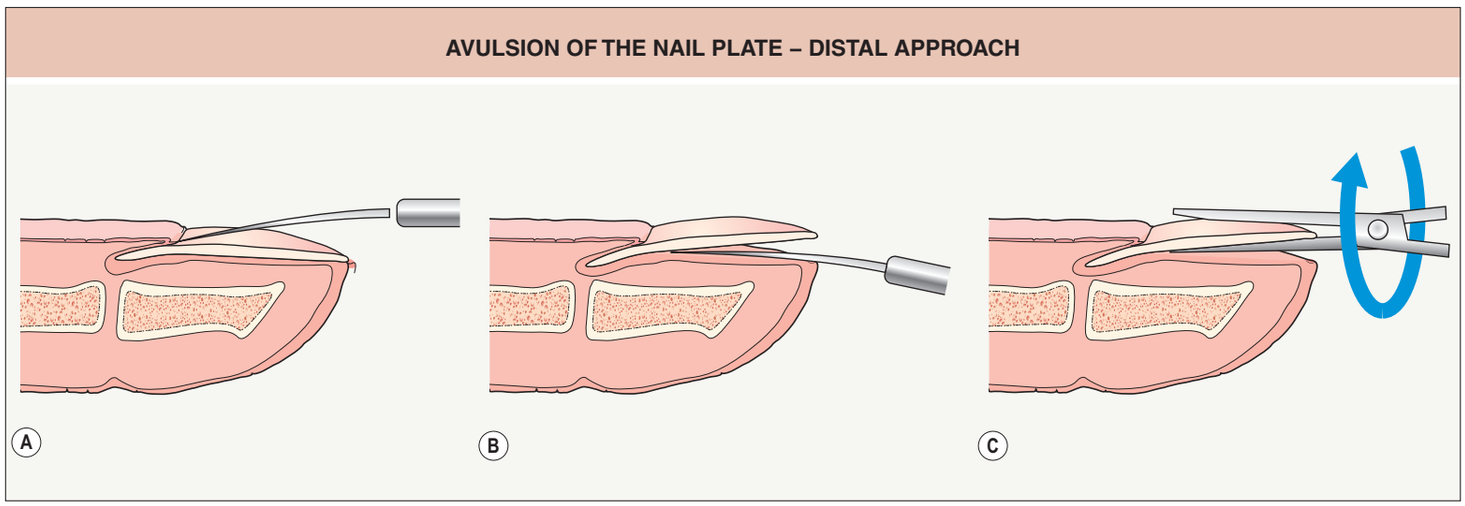


Fig. 149.9 Avulsion of the nail plate – distal approach. A An elevator is first pushed under the proximal nail fold, moving back and forth from one side to the other in order to detach the fold from the plate. **B** The elevator is then inserted under the free edge of the plate in a distal to proximal direction to free the plate from its bed. **C** The plate is then grasped by a hemostat or a nail puller and rotated off the nail bed.

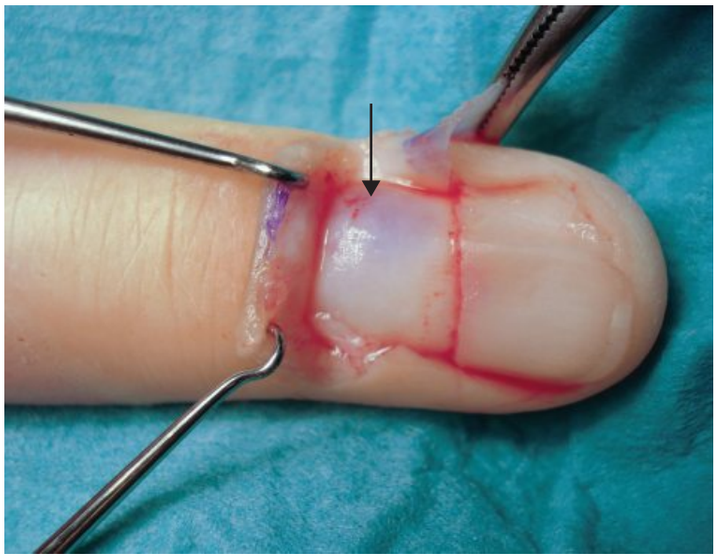


Fig. 149.10 Visualization of a glomus tumor within the proximal nail matrix. Following two oblique incisions at the junction of the lateral and proximal nail folds, retraction of the proximal nail fold, and proximal lateral avulsion of the nail plate, the entire nail matrix is exposed. The glomus tumor within the matrix (arrow) is identified prior to removal.

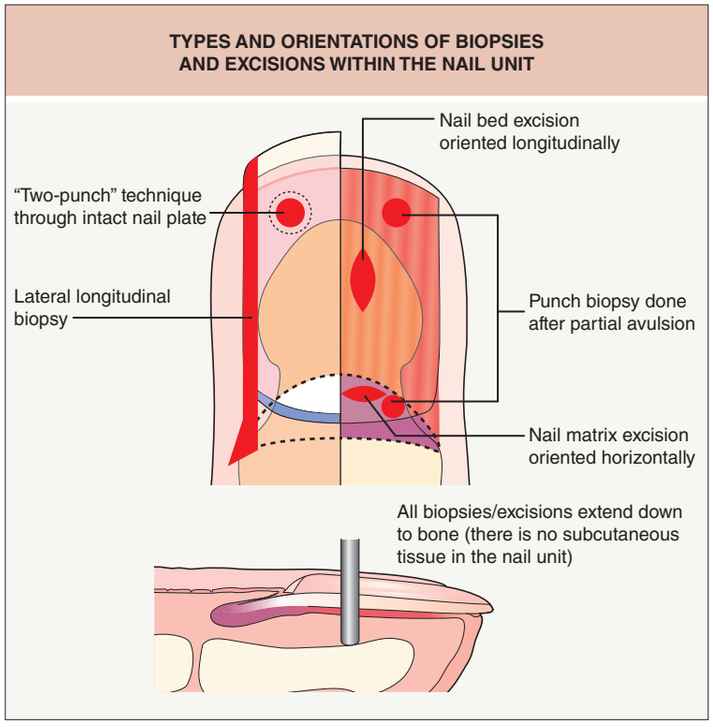


Fig. 149.11 Types and orientations of biopsies and excisions within the nail unit.

CLINICAL FEATURES OF NAIL BED DISORDERS IN WHICH A BIOPSY MAY FACILITATE DIAGNOSIS AND SUBSEQUENT TREATMENT	
Diagnosis	**Clinical features**
Malignant tumors of the nail bed	
Squamous cell carcinoma, Bowen disease	Hyperkeratosis, dyschromia, onycholysis, destruction of the nail plate
Keratoacanthoma	Multiple or solitary, nail plate destruction, mass, erosion, granulation tissue, pain
Melanoma	Pigmentation of the nail bed, erosion, destruction of the nail plate; 25% are amelanotic
Metastatic carcinomas	Mass, pseudo-clubbing, nail dystrophy, dusky red color, ± pain
Basal cell carcinoma	Rare, variable clinical appearance
Benign tumors of the nail bed	
Pyogenic granuloma	Exuberant friable mass, needs to be distinguished from amelanotic melanoma
Glomus tumor	Spontaneous pain, blue–red mass
Epidermoid cyst	Mass, nail plate deformity
Fibroma	Mass, elevation, distortion of the nail (if presses on matrix, distal groove; if underneath nail plate, elevation of plate)
Exostosis	Mass, elevation of the nail plate, tenderness
Osteochondroma	Enlargement of digit, elevation or destruction of the nail plate
Enchondroma	Mass, alteration of the nail plate, pain
Infectious conditions of the nail bed	
Onychomycosis	Hyperkeratosis, dyschromia, nail dystrophy, onycholysis
Verruca vulgaris	Verrucous mass, sometimes painful, nail plate deformity or destruction, must distinguish from verrucous or squamous cell carcinoma
Crusted scabies	Hyperkeratosis of hyponychium
Inflammatory dermatoses involving the nail bed	
Psoriasis	Onycholysis, hyperkeratosis, splinter hemorrhages, oil drop discoloration
Lichen planus	Violaceous discoloration, atrophy of nail bed; if nail matrix is involved, trachyonychia, hapalonychia (soft nails), dorsal pterygium
Other nail bed conditions	
Hemorrhage, trauma	Red–violet to black discoloration under nail plate; persistent or non-migrating discoloration needs to be distinguished from melanoma

Table 149.2 Clinical features of nail bed disorders in which a biopsy may facilitate diagnosis and subsequent treatment.

pathologic examination or culture, should be repositioned to cover and protect the wound during the early stages of the healing process. It can be secured by sutures or adhesive. Although the plate will not reattach and is eventually shed, it provides protection and minimizes discomfort during the immediate postoperative period.

BIOPSY TECHNIQUES

To minimize scarring and offer the best functional and cosmetic outcome, nail surgical procedures should follow a few rules. Within the nail bed, the incision should be oriented longitudinally, whereas within the matrix it should ideally be oriented horizontally (Fig. 149.11). The surgical approach depends upon the location of the pathology within the nail unit.

Nail Bed Biopsy

Nail bed biopsy is a simple and safe technique for the diagnosis of a variety of nail bed disorders, from onycholysis to tumors (Table 149.2). The nail plate is usually partially avulsed prior to the nail bed biopsy (Fig. 149.12A). If the defect is >4 mm, re-approximation of the edges is recommended. However, the nail bed is fragile and suturing of the margins may be difficult. To facilitate closure of the wound, generous lateral undermining should be performed at the level of the periosteum. Nonetheless, it is amazing how very large defects of the nail bed (e.g. after Mohs surgery) may regenerate totally by second intention[1].

For the removal of tumors such as onychopapillomas, elliptical excisional biopsies of the nail bed along a longitudinal axis are recommended (Fig. 149.12B,C). Closure is performed with absorbable sutures (e.g. Vicryl®) (Fig. 149.12D).

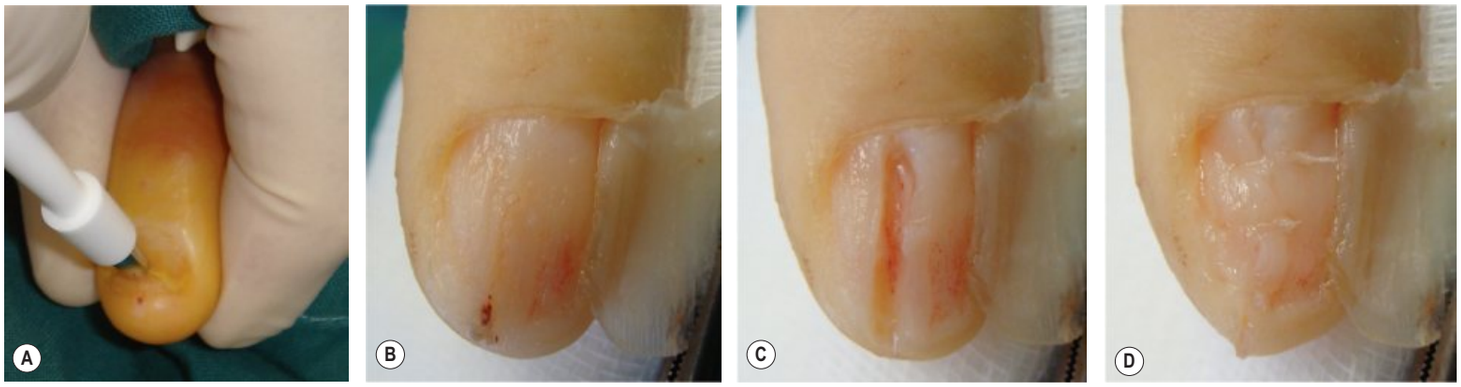


Fig. 149.12 Nail bed biopsy – punch biopsy versus longitudinal excisional biopsy. A After partial nail avulsion, the punch biopsy instrument is rotated with pressure until there is contact with bone. **B** Lateral avulsion of the nail plate exposes an onychopapilloma along the nail bed. **C** Longitudinal incision allows delicate dissection of the tumor from the bone. **D** Suturing of the nail bed; the nail plate will be returned to its original location and secured to the lateral fold.

Nail Matrix Biopsy

Nail matrix biopsy has one major indication: determination of the cause of longitudinal melanonychia (see Ch. 71). The biopsy must be taken from the nail matrix because that is where the pigment is generated. Fortunately, in ~95% of patients, the pigment's origin is within the *distal* matrix[11]. Since the latter synthesizes the ventral portion of the nail plate (see Fig. 149.2), the primary sequela is a nail plate thinned from below. If the pigment origin is located within the *proximal* matrix, then nail plate dystrophy will result, usually as a longitudinal fissure; this is because the proximal matrix generates the dorsal (upper) one-third of the nail plate.

In order to expose the entire matrix area, both retraction of the proximal nail fold and proximal nail avulsion are performed (Fig. 149.13). Once the matrix is exposed, the appropriate surgical technique is chosen based upon the width and shape of the pigmented band. The entire pigmented area is removed to ensure complete histologic examination.

- If the pigment origin is roundish and fits within a 3 mm punch biopsy trephine, it can be removed with that instrument. However, two caveats apply: (1) the trephine should be advanced down to bone, with the specimen severed at the level of the periosteum; and (2) the specimen should be harvested with delicate curved, fine-tipped scissors. Handling fragile matrix tissue with forceps will crush it and induce artifacts[12]. The defect does not need to be sutured.
- If the pigment origin has a longitudinal orientation, then a narrow elliptical excision down to the bone is recommended. Delicate lateral undermining allows closure of the defect with 5-0 absorbable sutures.
- If the pigment origin involves a wide area of the matrix, a tangential excision is indicated. This technique virtually "shaves" the matrix, removing the matrix epidermis and a small portion of dermis. It allows the pathologist to examine the entire lesion, but the margins are usually difficult to assess. The resultant specimens have been shown to provide adequate tissue for accurate histopathologic diagnosis. In general, postoperative nail plate dystrophy is not observed even if nearly the entire *distal* matrix has been removed. In contrast, tangential excision of the *proximal* matrix results in nail thinning and brittleness in most patients, but rarely pterygium. It is noteworthy that this technique avoids mutilating surgery, especially since the cause of longitudinal melanonychia is often a benign process[13]. Lastly, the nail plate is put back in place and secured to the lateral nail fold.
- When the pigmented streak is located within the lateral third of the nail plate, a lateral longitudinal biopsy (see next section) is appropriate.

Lateral Longitudinal Biopsy

This procedure permits examination of the entire nail apparatus including the proximal nail fold, matrix, nail bed, nail plate, and hyponychium. It is especially helpful in diseases involving the proximal portion of the nail apparatus (often presenting as alterations of the surface of the nail plate) and for inflammatory disorders in which all these structures are affected concomitantly. Obvious clinical involvement of the lateral aspect of at least one nail is required. The patient must be warned that this type of biopsy will narrow the nail permanently due to the partial amputation of the lateral horn of the matrix. In order to avoid postoperative lateral deviation, the specimen should be <3 mm in width[14].

The incision begins halfway between the cuticle and the crease of the DIP joint and extends distally through the proximal nail fold, then the nail plate and its bed until the hyponychium is reached. A second parallel incision is made in the lateral nail groove, joining the initial incision at the fingertip (Fig. 149.14A). Proximally, the incision curves laterally in order to remove the lateral horn of the matrix[15]. The latter is especially important with the great toenail (see Fig. 149.2). The specimen is then carefully detached from the bone with delicate scissors. Detaching the matrix from the bone at the proximal tip of the biopsy specimen is a critical step, and care should be taken to avoid curving the scissors upward too soon and foreshortening the specimen[16]. Residual lateral nail matrix tissue leads to nail spicule formation (Fig. 149.15). The defect is re-approximated with horizontal mattress sutures in order to recreate a lateral nail fold (Fig. 149.14B). This technique may be utilized for various tumors, including longitudinal melanonychia of the lateral third of the nail plate.

Proximal Nail Fold Biopsy

Lesions of the proximal nail fold can be biopsied via shave, punch, or incisional techniques as well as excised *en bloc*, similar to cutaneous lesions elsewhere. A Freer elevator may be inserted beneath the proximal nail fold to shield the matrix from inadvertent damage from the scalpel (Fig. 149.16).

SURGICAL PROCEDURES FOR DISORDERS OF THE NAIL UNIT

Acute Paronychia

Unless there is spontaneous drainage, acute paronychia requires prompt surgical intervention. In addition to the associated pain, long-standing pressure on the matrix from the collection of pus may impair normal regrowth of the nail plate, especially in children. Incision of the proximal nail fold is discouraged as this can lead to retraction and distortion of the fold. If the abscess is under the proximal nail fold or around the base of the nail ("runaround"), avulsion of the proximal third of the nail plate will allow immediate drainage and bacterial culture (Fig. 149.17A–C). This also allows for the nail pocket to be rinsed with an antiseptic solution. Avulsion of a lateral strip of nail plate can be done if the abscess is within the lateral nail fold.

Chronic Paronychia

When medical treatment of chronic paronychia fails (see Ch. 71), surgical treatment can be considered (Fig. 149.18A). There are two recommended procedures: (1) *en bloc crescentic excision*; and (2) *square-flap technique*. In the former, a Freer elevator is inserted under the proximal nail fold in order to protect the matrix. A #15 surgical blade is then used to excise *en bloc* a crescent-shaped, full-thickness piece of skin that is 4 mm at its greatest width, extending from one lateral nail fold to the other (Fig. 149.18B). A beveled incision angled

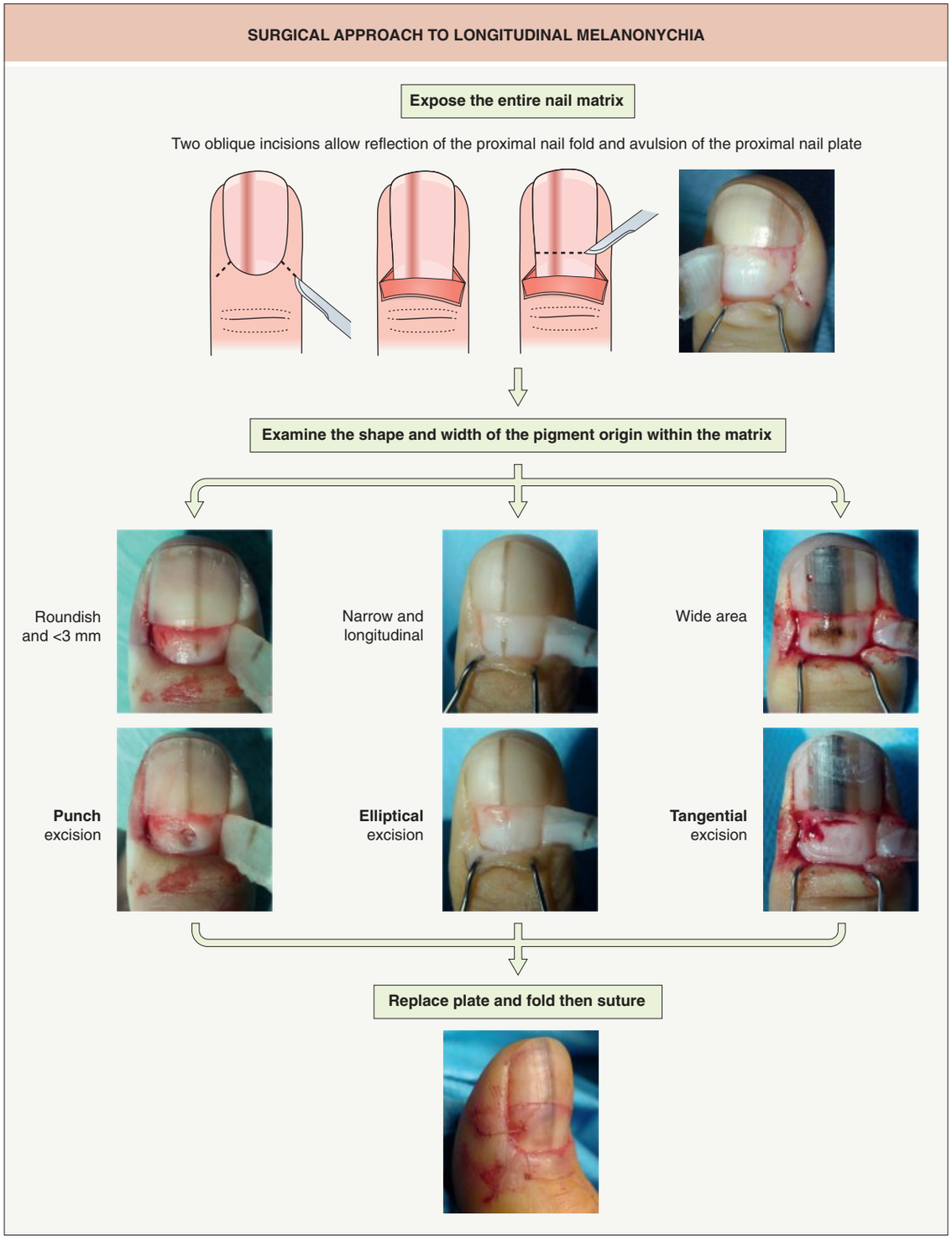


Fig. 149.13 Surgical approach to longitudinal melanonychia. Following two oblique incisions at the junction of the lateral and proximal nail folds, retraction of the proximal nail fold, and proximal lateral avulsion of the plate, the entire matrix, including the origin of the pigmented band, is visualized. The type of biopsy depends upon the size and shape of the pigment origin. At the conclusion of the procedure, the plate and the proximal nail fold are placed back in their original positions and secured. A fourth option is a lateral longitudinal biopsy when the pigmented streak is located within the lateral third of the nail plate (see Fig. 149.14A).

at 45° prevents removal of the nail-producing tissues of the proximal nail fold responsible for the normal shine of the nail plate[17]. Complete healing by second intention restores the proximal nail fold with its cuticle within 8–10 days (Fig. 149.18C). The cosmetic outcome is excellent, with only a greater portion of the nail plate and lunula visible. In the square-flap technique, two lateral oblique releasing incisions allow the proximal nail fold to be tilted backwards exposing its fibrotic undersurface. All fibrotic material is removed and the flap returned to its original position and sutured. The major advantage of this procedure is that lengthening of the visible nail plate does not occur[18].

Ingrown Toenail

There is an ongoing debate regarding both the treatment and the cause of this painful condition, i.e. is the nail itself or the surrounding tissues at fault? There are two major surgical approaches: (1) narrow the nail plate; or (2) debulk surrounding soft tissues. The surgeon must select the most appropriate approach on an individual basis[19].

Lateral matricectomy via chemical cautery represents the easiest and most useful technique for patients with laterally ingrown toenails. The key is to destroy the portion of the nail matrix associated with the ingrown part of the nail. Two successive systematic Cochrane reviews found that the use of phenol (88%) was the most effective therapeutic approach in terms of morbidity and success rate (based upon recurrences at 6+ months), as compared to excisional surgical procedures[20]. In most large studies, the success rate has been 95% or greater[21–23]. Phenol has three relevant properties: it is necrotizing, a disinfectant, and an anesthetic. This leads to a very comfortable postoperative period, as phenol induces demyelination of terminal nerve endings for several weeks[24].



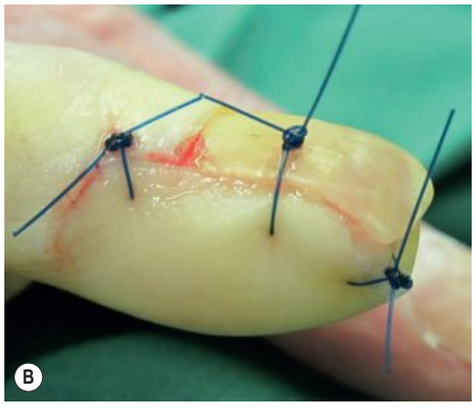


Fig. 149.14 Lateral longitudinal biopsy. **A** Note the downward curve of the proximal portion of the excision; this ensures removal of the lateral horn of the matrix. **B** Sutures are placed to close the defect and the lateral fold is re-created. *Courtesy Marie Caucanas, MD.*



Fig. 149.15 Lateral nail spicule due to incomplete removal of the lateral horn of the matrix. Note the straight line of the incision and compare to Fig. 149.14.



Fig. 149.16 Biopsy of the proximal nail fold via a crescent-shaped incision. Insertion of an elevator protects the underlying nail matrix.







Fig. 149.17 Surgical treatment of acute paronychia. **A** Swelling of the proximal fold with abscess formation. **B** Following detachment of the proximal nail fold from the nail plate with an elevator, accumulated pus is released and can be cultured. **C** Avulsion of the proximal third of the nail plate allows full drainage and rinsing of the nail pocket with antiseptics.



Fig. 149.18 Surgical treatment of chronic paronychia. A Loss of the cuticle, rolled proximal nail fold, and dystrophy of the nail plate with yellowing, ridging, and roughness. **B** Crescent-shaped resection of the proximal nail fold, extending from one lateral nail fold to the other. Note the beveled 45° angle of the incision. **C** Appearance on postoperative day 8.

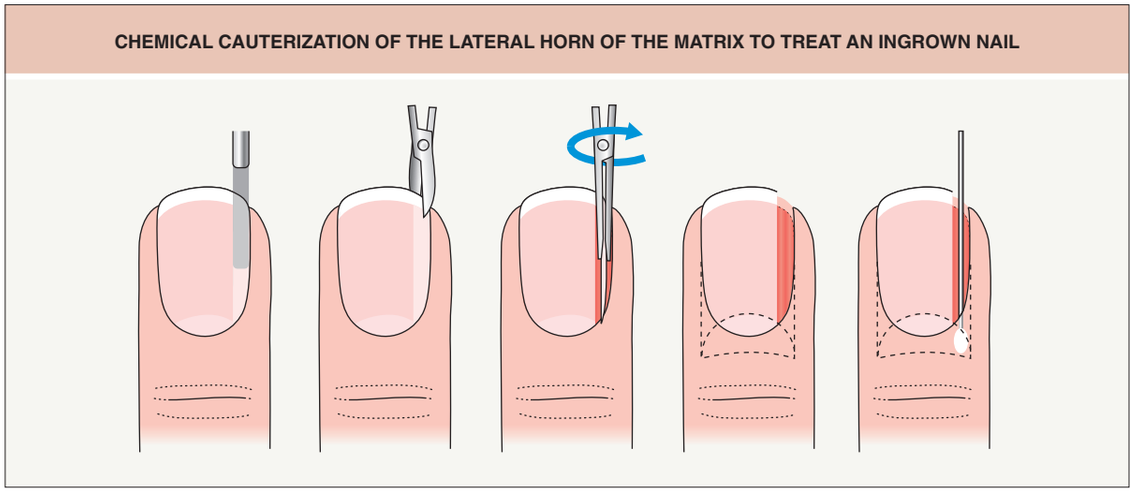


Fig. 149.19 Chemical cauterization of the lateral horn of the matrix to treat an ingrown nail. A strip of nail plate ~3 to 5 mm in width is elevated, cut, and then avulsed up to its origin under the proximal nail fold. The cauterant, usually 88% phenol, is applied onto the exposed lateral horn of the matrix and bed with a wisp of cotton wool (see Videos 149.1–149.5).

After anesthesia is established, a tourniquet is placed to ensure a completely bloodless field. Granulation tissue, if present, is curetted for a better view of the lateral part of the nail plate, so as to avoid excessive nail plate removal. A lateral or bilateral (if the condition affects both sides) strip of nail plate ~3 to 5 mm in width is avulsed up to its origin under the proximal nail fold (Fig. 149.19). *Phenol* (88%) is applied onto the exposed lateral horn of the matrix and bed with a wisp of cotton wool, urethral swab, nasopharyngeal swab, or the elevator itself (Videos 149.1–149.5). Cotton swabs should not be oversoaked as this may result in cauterant spilling onto periungual tissue or seeping under the remaining nail plate (and leading to unwanted destruction). Phenol acts by coagulating tissue proteins and a bloodless field is mandatory at this point otherwise the phenol coagulates blood proteins rather than matrix epithelium. This is the most common reason for recurrences.

Based upon histologic studies in cadavers, the ideal application time is four minutes[25]. Curettage of the matrix prior to applying the cauterant does not increase the success rate[26], and rinsing with alcohol merely dilutes the phenol but does not neutralize it[27]. Bleeding after removal of the tourniquet will inactivate the cauterant. Phenol is safe in diabetics[28] and children[29] and for recalcitrant ingrown nails from epidermal growth factor receptor (EGFR) inhibitors[30]. The major drawback of this technique is oozing for 2 to 4 weeks. This may promote infection, especially in patients with poor hygiene. However, in view of the numerous phenol matricectomies performed, infections remain very rare. Pincer nails, characterized by hypercurvature of both sides of the nail, can also be managed with bilateral phenol matricectomy.

Trichloracetic acid (100%) is an excellent alternative as success rates and postoperative morbidity are similar to phenol[31]. Application time is one minute[32]. For distal embedding and very hypertrophic and exuberant lateral folds, wide debulking with second intention healing is easy to perform and very effective with an excellent cosmetic outcome[33,34]. The main drawback is the prolonged healing time.

Tumors and Cysts

The clinical features of the following tumors and cysts are discussed in Chapter 71.

Fibrokeratoma

For subungual fibrokeratomas, reflection of the proximal nail fold following two oblique incisions is mandatory to expose the cul-de-sac. In most instances, the fibrokeratoma originates either at the most proximal portion of the cul-de-sac or from the undersurface of the proximal nail fold. The tumor should be delicately dissected using fine scissors until reaching its base, where it is severed. Injury to the matrix is quite unlikely as the nail plate remains in place. The proximal nail fold is then returned to its original position and secured with 5-0 sutures. Incomplete resection leads to recurrence[35]. Fibrokeratomas of the nail bed are rare and should be excised via a longitudinal ellipse after plate avulsion.

Subungual exostosis

After nail avulsion, either dissection with preservation of the nail bed or *en bloc* resection of the tumor with a bone rongeur followed by second intention healing works well. Both procedures should expose spongious bone[36,37] and be performed under full aseptic conditions.

Glomus tumor

After avulsion of the plate, the tumor is gently extirpated with fine curved scissors via a longitudinally or transversally oriented incision; the orientation depends upon whether the tumor is within the nail bed (longitudinal) or the nail matrix (transverse) (see Fig. 149.11). The incision is closed with interrupted absorbable sutures and the nail plate is placed back and secured to the lateral folds (Fig. 149.20).

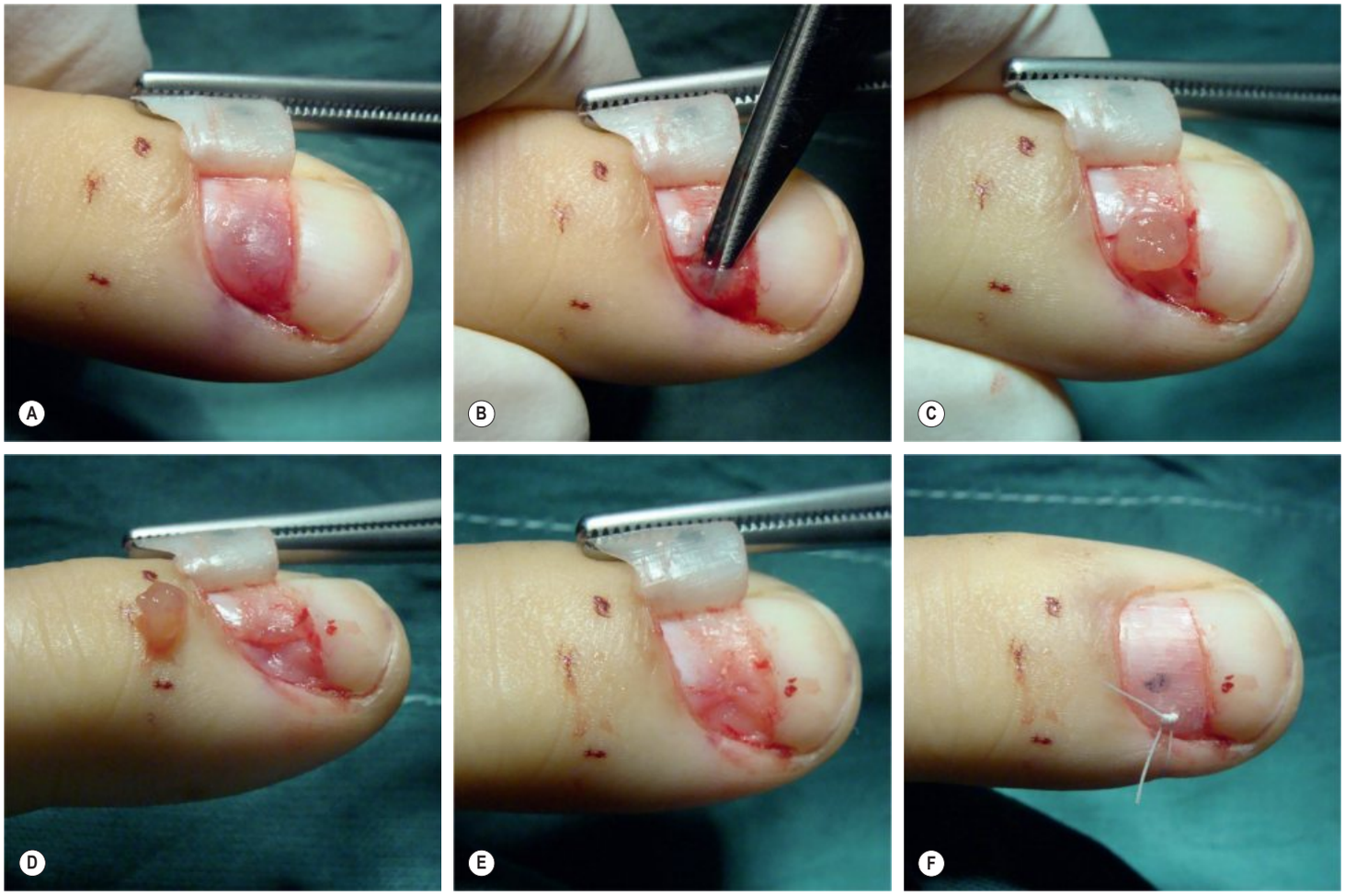


Fig. 149.20 Removal of a nail bed glomus tumor. A Proximal lateral avulsion of the nail plate exposes the tumor within the nail bed. **B** A longitudinal incision allows delicate dissection of the tumor from the bone with smooth-tipped curved scissors. **C, D** Extirpation of the tumor. **E** Suturing of the nail bed. **F** The nail plate is returned to its original location and secured to the lateral fold.

Onychomatricoma

A delicate distal (to proximal) avulsion, taking care not to tear the digitations, exposes a villous tumor resting on the matrix. The proximal nail fold is tilted backwards. The tumor is tangentially excised from the matrix with a Teflon™-coated blade[38,39]. To avoid any adherence between the ventral aspect of the proximal fold and the matrix that could result in a pterygium, the surgeon can slide some tulle gras into the nail pocket and secure it with two sutures for three weeks. Lastly, the proximal nail fold is placed back into its original location and the two lateral incisions sutured closed.

Digital myxoid cyst (pseudocyst)

For pseudocysts resting over the DIP joint (type A), the best option is drainage followed by cryotherapy (double freeze-thaw). When located in the dorsal nail fold and pressing onto the underlying matrix (type B), drainage followed by compressive dressings for several weeks is associated with a high success rate. The same procedure is recommended for myxoid pseudocysts expanding under the matrix (type C). If the patient has experienced several relapses with the conservative approach or wishes to undergo a definitive procedure, methylene blue-guided surgery to ligate the joint fluid leak is an elegant, comfortable, and efficient technique[40]. Sometimes a proximal nail fold flap is raised to dissect the pseudocyst.

Squamous cell carcinoma

The goal is to preserve the digit and its function[41]. Surgical excision with histologic control of the margins is recommended, including performing Mohs micrographic surgery[42]. Closure may be accomplished via a flap, graft, or second intention healing. Recurrence is possible as human papillomavirus is causative in about up to two-thirds of patients[43,44]. If bony involvement is demonstrated radiographically or histologically, amputation of the distal phalanx is indicated.

Melanoma

In several series with long-term follow-up as well as in a meta-analysis[45], *in situ* or thin melanomas (Breslow depth ≤0.5 mm) treated with *en bloc* removal of the nail unit, with >6 mm margins, has resulted in an excellent survival rate (100%)[46–48]. Because the dermis of the matrix and nail bed rests directly on bone, ensuring that the deep margin is clear of tumor requires greater attention. Closure is obtained with second intention healing or a full-thickness graft (see Fig. 148.7A). For deeper melanomas, there is accumulating evidence to support recommending digit-sparing surgery versus amputation[49–51].

Hemostasis

Intraoperative hemostasis is ensured with a tourniquet. Postoperative bleeding varies depending upon the type of surgery. For limited bleeding, application of a cotton-tipped applicator dipped in 35% aluminum chloride will suffice. If bleeding is moderate, oxidized cellulose or gelatin sterile sponges work well. For severe postoperative bleeding, injection of local anesthetic (0.5 ml) into the lateral aspect of the digit at the level of the digital artery will act as a volumetric tourniquet, until clotting occurs. The use of a bulky dressing for at least 48 hours combined with elevation of the limb limits the risk of excessive postoperative bleeding[52].

POSTOPERATIVE CARE

Proper dressings can reduce postoperative pain and throbbing and minimize complications. The dressing should be nonadherent, absorbent, and perfectly fitted so it remains in place. Applying large amounts of ointment (possibly containing antiseptics) covered with a nonadherent dressing such as petrolatum-impregnated gauze (e.g. Vaseline™ gauze,

Tulle gras, Adaptic®), or with added antiseptics (e.g. Xeroform™ gauze, Bactigras®, Betadine Tulle®), will protect the wound from drying and will allow an easy and painless removal. If postoperative bleeding is noticed, a bulky dressing made of two or three loose layers of mesh gauze will absorb bleeding and provide protection against trauma. A bandage or tube gauze such as Xspan® secures the dressing in place. Given the likelihood of postoperative edema, the dressing should not be too constrictive.

Postoperative pain management relies on two major interventions: elevation of the limb for 48 hours and analgesics. The latter should be adapted to the expected pain from the surgery. Acetaminophen and/or nonsteroidal anti-inflammatory drugs (NSAIDs) are usually enough, but for some painful procedures, narcotic analgesics are sometimes prescribed. Keeping the limb elevated will minimize throbbing. Bleeding into the dressing can result in the bandage sticking to the surgical site. If this occurs, soaking the bandage will loosen it prior to its removal. Written instructions on how to perform postoperative care at home are highly recommended. Patients should also be informed about long-term paresthesias, especially at the digit tip, that can follow nail surgery and may last up to six months[53].

COMPLICATIONS OF NAIL SURGERY

Nail surgery is safe and effective. However, as with any surgical procedure, complications may occur. General complications are similar to those observed at other anatomic sites, e.g. hematomas, infection, necrosis, bleeding, keratin implantation cysts, tumor recurrence, and hypertrophic scars or keloids. Nail surgery-specific complications include lateral deviation of the plate after partial ablation of the nail apparatus, nail dystrophy, distal embedding of the plate, and formation of nail spicules (see Fig. 149.15). In addition, nail surgery can lead to pyogenic granuloma formation, complex regional pain syndrome (reflex sympathetic dystrophy)[54], and deep infections such as osteomyelitis and septic arthritis (Table 149.3). When the principles of nail surgery are carefully followed by the surgeon and if the patient adheres to the specific instructions from the physician regarding wound care and postoperative treatment regimens, significant complications are rare[52,55]. If necessary, the dermatologic surgeon should involve fellow dermatologists, hand surgeons, or infectious disease specialists who may be able to offer their assistance and expertise with difficult cases.

COMPLICATIONS OF NAIL SURGERY
Short-term (within 14 days of surgery)
• Bleeding, pain, infection (including septic arthritis, osteomyelitis), pyogenic granuloma
Long-term (>3 months following surgery)
• *Neurologic:* Paresthesias (common) Complex pain syndrome (reflex sympathetic dystrophy) (very rare)
• *Dystrophy:* Lateral deviation of the plate (if lateral removal >3 mm) Plate dystrophy, e.g. splits, ridges, grooves, thinning, from matrix scarring Pterygium due to scarring within the proximal fold and matrix Onycholysis due to nail bed scarring Cuticle retraction due to cuticle scarring
• *Distal embedding* from nail shedding and dorsal distortion of the pulp
• *Nail spicules* due to incomplete removal of the lateral horns of the matrix
• *Recurrence of tumor* because of incomplete removal
• *Implantation cyst* (common after full-thickness grafting)
• *Hypertrophic scars and keloids* (latter very rare even in populations at risk)

Table 149.3 Complications of nail surgery.

Additional tables on Patient evaluation prior to nail surgery, Nail unit tumors: radiographic findings and surgical treatments, and Etiologies of a pseudo-Hutchinson sign, available in our eBook (see inside front cover for access code).

REFERENCES

1. Richert B. Basic nail surgery. *Dermatol Clin*. 2006;24:313–322.
2. André J, Sass U, Richert B, Theunis A. Nail pathology. *Clin Dermatol*. 2013;31:526–539.
3. Rich P. Nail biopsy: indications and methods. *Dermatol Surg*. 2001;27:229–234.
4. Fleckman P, Allan C. Surgical anatomy of the nail unit. *Dermatol Surg*. 2001;27:257–260.
5. Haneke E. Surgical anatomy of the nail apparatus. *Dermatol Clin*. 2006;24:291–296.
6. Haneke E. Surgical anatomy of the nail apparatus. In: Richert B, di Chiacchio N, Haneke E, eds. *Nail Surgery*. London: Informa; 2010. p. 1–15.
7. Ilicki J. Safety of epinephrine in digital nerve blocks: a literature review. *J Emerg Med*. 2015;49:799–809.
8. Jellinek NJ, Vélez NF. Nail surgery: best way to obtain effective anesthesia. *Dermatol Clin*. 2015;33:265–271.
9. Richert B. Instrumention. In: Richert B, di Chiacchio N, Haneke E, editors. *Nail Surgery*. London: Informa; 2010. p. 11–15.
10. Collins SC, Cordova K, Jellinek NJ. Alternatives to complete nail plate avulsion. *J Am Acad Dermatol*. 2008;59:619–626.
11. Baran R, Kechijian P. Longitudinal melanonychia (melanonychia striata): diagnosis and management. *J Am Acad Dermatol*. 1989;21:1165–1175.
12. Jellinek N. Nail matrix biopsy of longitudinal melanonychia: diagnostic algorithm including the matrix shave biopsy. *J Am Acad Dermatol*. 2007;56:803–810.
13. Richert B, Theunis A, Norrenberg S, André J. Tangential excision of pigmented nail matrix lesions responsible for longitudinal melanonychia: evaluation of the technique on a series of 30 patients. *J Am Acad Dermatol*. 2013;69:96–104.
14. De Berker DA, Baran R. Acquired malalignment: a complication of lateral longitudinal nail biopsy. *Acta Derm Venereol*. 1998;78:468–470.
15. Krull E. Biopsy techniques. In: Krull E, Zook E, Baran R, Haneke E, eds. *Nail Surgery: A Text and Atlas*. Philadelphia: Lippincott Williams & Wilkins; 2001. p. 55–81.
16. de Berker DA. Lateral longitudinal nail biopsy. *Australas J Dermatol*. 2001;42:142–144.
17. Baran R, Bureau H. Surgical treatment of recalcitrant chronic paronychias of the fingers. *J Dermatol Surg Oncol*. 1981;7:106–107.
18. Ferreira Vieira d'Almeida L, Papaiordanou F, Araújo Machado E, et al. Chronic paronychia treatment: square flap technique. *J Am Acad Dermatol*. 2016;75:398–403.
19. Richert B. Surgical management of ingrown toenails – an update overdue. *Dermatol Ther*. 2012;25:498–509.
20. Eekhof JA, Van Wijk B, Knuistingh Neven A, van der Wouden JC. Interventions for ingrowing toenails. *Cochrane Database Syst Rev*. 2012;4:CD001541.
21. Bostanci S, Ekmekçi P, Gürgey E. Chemical matricectomy with phenol for the treatment of ingrowing toenail: a review of the literature and follow-up of 172 treated patients. *Acta Derm Venereol*. 2001;81:181–183.
22. Di Chiacchio N, Belda Jr W, Di Chiacchio NG, et al. Nail matrix phenolization for treatment of ingrowing nail: technique report and recurrence rate of 267 surgeries. *Dermatol Surg*. 2010;36:534–537.
23. Vaccari S, Dika E, Balestri R, et al. Partial excision of matrix and phenolic ablation for the treatment of ingrowing toenail: a 36-month follow-up of 197 treated patients. *Dermatol Surg*. 2010;36:1288–1293.
24. Boberg JS, Frederiksen MS, Harton FM. Scientific analysis of phenol nail surgery. *J Am Podiatr Med Assoc*. 2002;92:575–579.
25. Becerro de Bengoa Vallejo R, Losa Iglesias ME, Viejo Tirado F, Serrano Pardo R. Cauterization of the germinal nail matrix using phenol applications of differing durations: a histologic study. *J Am Acad Dermatol*. 2012;67:706–711.
26. Tassara G, Machado MA, Gouthier MAD. Treatment of ingrown nail: comparison of recurrence rates between the nail matrix phenolization classical technique and phenolization associated with nail matrix curettage – is the association necessary? *An Bras Dermatol*. 2011;86:1046–1048.
27. Cordoba Diaz D, Losa Iglesias ME, Cordoba Diaz M, Becerro de Bengoa Vallejo R. Evidence of the efficacy of alcohol lavage in the phenolization treatment of ingrown toenails. *J Eur Acad Dermatol Venereol*. 2011;25:794–798.
28. Felton PM, Weaver TD. Phenol and alcohol chemical matrixectomy in diabetic versus nondiabetic patients. A retrospective study. *J Am Podiatr Med Assoc*. 1999;89:410–412.
29. Islam S, Lin EM, Drongowski R, et al. The effect of phenol on ingrown toenail excision in children. *J Pediatr Surg*. 2005;40:290–292.
30. Dika E, Balestri R, Vaccari S, et al. Successful treatment of pyogenic granulomas following gefitinib therapy with partial matricectomy and phenolization. *J Dermatolog Treat*. 2009;20:374–375.
31. André MS, Caucanas M, André J, Richert B. Treatment of ingrowing toenails with phenol 88% or trichloroacetic acid 100%: a comparative, prospective, randomized, double-blind study. *Dermatol Surg*. 2018;44:645–650.
32. Kim S-H, Ko H-C, Oh C-K, et al. Trichloroacetic acid matricectomy in the treatment of ingrowing toenails. *Dermatol Surg*. 2009;35:973–979.
33. Chapeskie H, Kovac JR. Case series: soft-tissue nail-fold excision: a definitive treatment for ingrown toenails. *Can J Surg*. 2010;53:282–286.
34. Rosa IP, Di Chiacchio N, Di Chiacchio NG, Caetano L. "Super u" – a technique for the treatment of ingrown nail. *Dermatol Surg*. 2015;41:652–653.
35. Ballan A, Zeinaty P, Tomb R, et al. Acquired ungual fibrokeratoma: a systematic review of the literature. *Int J Dermatol*. 2021;60:533–539.
36. Haneke E, Di Chiacchio N, Richert B. Surgery of the bony phalanx. In: Richert B, di Chiacchio N, Haneke E, eds. *Nail Surgery*. London: Informa; 2010. p. 149–164.
37. De Berker DA, Langtry J. Treatment of subungual exostoses by elective day case surgery. *Br J Dermatol*. 1999;140:915–918.
38. Di Chiacchio N, Richert B, Haneke E. Surgery of the matrix. In: Richert B, di Chiacchio N, Haneke E, eds. *Nail Surgery*. London: Informa; 2010. p. 103–132.
39. Cogrel O. Shave biopsy for a digital onychomatricoma. *Ann Dermatol Venereol*. 2014;141:634–635.
40. de Berker D, Lawrence C. Ganglion of the distal interphalangeal joint (myxoid cyst): therapy by identification and repair of the leak of joint fluid. *Arch Dermatol*. 2001;137:607–610.
41. Lecerf P, Richert B, Theunis A, André J. A retrospective study of squamous cell carcinoma of the nail unit diagnosed in a Belgian general hospital over a 15-year period. *J Am Acad Dermatol*. 2013;69:253–261.
42. Dika E, Piraccini BM, Balestri R, et al. Mohs surgery for squamous cell carcinoma of the nail: report of 15 cases.

Our experience and a long-term follow up. *Br J Dermatol*. 2012;167:1310–1314.
43. Dika E, Venturoli S, Patrizi A, et al. The detection of human papillomavirus-16 in squamous cell carcinoma of the nail unit: a case series. *J Am Acad Dermatol*. 2017;76:354–356.
44. Shimizu A, Kuriyama Y, Hasegawa M, et al. Nail squamous cell carcinoma: a hidden high-risk human papillomavirus reservoir for sexually transmitted infections. *J Am Acad Dermatol*. 2019;81:1358–1370.
45. Jo G, Cho SI, Choi S, Mun JH. Functional surgery versus amputation for in situ or minimally invasive nail melanoma: a meta-analysis. *J Am Acad Dermatol*. 2019;81:917–922.
46. Nakamura Y, Ohara K, Kishi A, et al. Effects of non-amputative wide local excision on the local control and prognosis of in situ and invasive subungual melanoma. *J Dermatol*. 2015;42:861–866.
47. Neczyporenko F, André J, Torosian K, et al. Management of in situ melanoma of the nail apparatus with functional surgery: report of 11 cases and review of the literature. *J Eur Acad Dermatol Venereol*. 2014;28:550–557.
48. Goettmann S, Moulonguet I, Zaraa I. In situ nail unit melanoma: epidemiological and clinic-pathologic features with conservative treatment and long-term follow-up. *J Eur Acad Dermatol Venereol*. 2018;32:2300–2306.
49. Moehrle M, Metzger S, Schippert W, et al. "Functional" surgery in subungual melanoma. *Dermatol Surg*. 2003;29:366–374.
50. Montagner S, Belfort FA, Belda Junior W, Di Chiacchio N. Descriptive survival study of nail melanoma patients treated with functional surgery versus distal amputation. *J Am Acad Dermatol*. 2018;79:147–149.
51. Tanaka K, Nakamura Y, Mizutani T, et al. Confirmatory trial of non-amputative digit preservation surgery for subungual melanoma: Japan Clinical Oncology Group study (JCOG1602, J-NAIL study protocol). *BMC Cancer*. 2019;19:1002.
52. Richert B, Dahdah M. Complications of nail surgery. In: Nouri K, ed. *Complications in Dermatologic Surgery*. Philadelphia: Mosby; 2008. p. 137–158.
53. Walsh ML, Shipley DV, de Berker DA. Survey of patients' experiences after nail surgery. *Clin Exp Dermatol*. 2009;34:e154–e156.
54. Guerrero-González GA, Di Chiacchio NG, D'Apparecida Machado-Filho C, Di Chiacchio N. Complex regional pain syndrome after nail surgery. *Dermatol Surg*. 2016;42:1116–1118.
55. Moossavi M, Scher RK. Complications of nail surgery: a review of the literature. *Dermatol Surg*. 2001;27:225–228.

PATIENT EVALUATION PRIOR TO NAIL SURGERY
History

• Medical history
  • Diabetes mellitus
  • Peripheral artery disease
  • Autoimmune connective tissue disease
  • Raynaud phenomenon
  • Arthritis
  • Prosthetic joints or heart valves
  • Bleeding diathesis
• Drug history
  • Allergies
  • Use of anticoagulants, antiplatelet agents (salicylates, thienopyridines, NSAIDs)
  • Use of herbal medicine
• Cutaneous history
  • History of the nail condition (duration, progression, exposures, trauma)
  • Psoriasis, lichen planus or other cutaneous disorders with nail manifestations
  • Previous malignancies
• Previous fungal, bacterial and/or viral cultures or diagnostic tests
  • Occupation and hobbies

Examination
• All 20 nails, good lighting and magnification • Mucous membranes, hair, and scalp • Pertinent cutaneous examination • Peripheral pulses, especially in toenail surgery
Laboratory tests
• Radiography, diagnostic imaging studies (e.g. MRI) • Mycology, microbiology or virology studies
"Procedure, alternatives and risks" discussion (see Table 149.3)
• Possibility of permanent dystrophy • Possibility of no diagnosis • Length of time for nail to regrow • Bleeding, infection, and pain, as with any surgery

eTable 149.1 Patient evaluation prior to nail surgery. MRI, magnetic resonance imaging; NSAIDs, nonsteroidal anti-inflammatory drugs.

ETIOLOGIES OF A PSEUDO-HUTCHINSON SIGN
Pigment present in paronychium
• Normal variant for Fitzpatrick skin phototypes IV, V and VI • Laugier–Hunziker syndrome, Peutz–Jeghers syndrome • Radiation exposure • Malnutrition • Medications (e.g. minocycline, zidovudine [AZT]) • Postinflammatory • Benign melanocytic nevi, lentigines • Regressing nevoid melanosis in childhood • Subungual hematoma
Pigment visible through paronychium
• Neoplasms (benign nevi, squamous cell carcinoma, basal cell carcinoma) • Subungual hematoma

eTable 149.3 Etiologies of a pseudo-Hutchinson sign.

NAIL UNIT TUMORS: RADIOGRAPHIC FINDINGS AND SURGICAL TREATMENTS		
Tumor	**Radiographic findings**	**Surgical treatment**
Subungual exostosis	Radiopaque bone growth that is well circumscribed	Nail plate avulsion followed by surgical removal (can use bone rongeur)[e1]
Keratoacanthoma	Cup-shaped radiolucent defect (early)	Surgical excision[e2]
Enchondroma	Central round radiolucent defect	Surgical excision*
Squamous cell carcinoma	Radiolucent defect (late)	Microscopically controlled (Mohs) surgery)[e3–e5]
Glomus tumor	Occasional radiolucent defect; can visualize via MRI	Surgical excision (nail bed – longitudinal axis; nail matrix – horizontal axis)[e6]
Myxoid cyst	Osteoarthritis	Cryosurgery, surgical excision (can use nail elevator to protect matrix)[e7]

*Performed primarily by other surgical subspecialists.

e1.Carrol RE, Chance JT, Inan Y. Subungual exostosis of the hand. *J Hand Surg Br.* 1992;17:569–574.
e2.Baran R, Gottman S. Distal digital keratoacanthoma: a report of 12 cases and review of the literature. *Br J Dermatol.* 1998;139:512–515.
e3.Jellinek NJ. Primary malignant tumors of the nail unit. *Adv Dermatol.* 2005;21:33–64.
e4.Berker DA, Dahl MG, Malcolm AJ, Lawrence CM. Micrographic surgery for subungual squamous cell carcinoma. *Br J Plast Surg.* 1996;49:414–419.
e5.Goldminz D, Bennett RG. Mohs micrographic surgery of the nail unit. *J Dermatol Surg Oncol.* 1992;18:721–726.
e6.Baran R, Dawber RPR, de Berker D, eds. *Diseases of the Nails and their Management.* 3rd edn. London: Blackwell; 2001.
e7.Salasche SJ. Myxoid cysts of the proximal nail fold: a surgical approach. *J Dermatol Surg Oncol.* 1984;10:35–39.

eTable 149.2 Nail unit tumors: radiographic findings and surgical treatments.

150 Mohs Micrographic Surgery

Charlene Lam and Allison T. Vidimos

Chapter Contents

Introduction 2582
History 2583
Training in Mohs Micrographic Surgery 2584
Appropriate Use Criteria and Cost-Effective Care 2584
Indications 2584
Contraindications 2589
Preoperative History and Considerations 2589
Technique 2589
Variations/Refinements 2589
Challenges and Pitfalls 2590
Reconstruction 2593
Postoperative Care 2593
Complications 2593
Future Trends 2593

Synonyms: ■ Mohs surgery ■ Chemosurgery ■ Mohs chemosurgery (fresh tissue technique and fixed tissue technique)

Key features

- Based upon the concept of contiguous spread of a tumor from a single focus
- 100% microscopic tissue margin examination
- Highest evidence-based cure rate for cutaneous malignancies, but success is dependent on resources and skills of the surgeon and histotechnician
- Same physician serves as both surgeon and pathologist
- Precise excision of cancerous tissue
- Preservation of the maximum amount of non-cancerous tissue
- Total tissue control and precise mapping
- Immediate re-excision of residual cancerous tissue as indicated
- Reconstruction typically performed by Mohs surgeon
- Exceedingly low complication rate

INTRODUCTION

Mohs micrographic surgery (MMS) is a specialized method for skin cancer removal that combines surgery with pathology resulting in an excellent cure rate. The goals are to remove only the cancerous tissue while viewing the complete margin, thereby preserving the maximum amount of normal tissue (i.e. tissue-sparing). From a functional, aesthetic and reconstructive perspective, tissue-sparing is especially important for skin cancers in the periorbital, nasal, auricular, perioral, digital, and anogenital areas. MMS is also the preferred treatment method for skin cancers that are clinically poorly defined, recurrent, and/or have a higher risk of recurrence because of histologic features or anatomic location (Table 150.1).

There are four major components: surgical excision, histopathologic examination, precise mapping, and wound management. The *surgical* component consists of removing a disc of tissue with a beveled surgical margin (Fig. 150.1A). The disc of tissue, or "layer", ensures that the entire 360° of tumor margin is circumferentially removed and examined. The *histopathologic* component involves cryopreserving this disc and cutting it in a horizontal fashion, then mounting sections onto glass slides, followed by staining and microscopic examination for residual tumor. This processing technique differs from standard excisions in which specimens are formalin-fixed, paraffin-embedded (FFPE) and cut in a "bread-loaf" fashion (Fig. 150.1B). Precise *mapping* entails marking any residual tumor on the map of the excision with the remaining positive area of tumor re-excised as indicated. This three-step process is repeated until there is no residual tumor identified microscopically. During this procedure, the Mohs surgeon has complete control of the excised tissue, including laboratory processing and interpretation of the tissue sections, as well as precise mapping. In the fourth step, *wound management*, the tumor-free defect is surgically closed or allowed to heal by second intention.

INDICATIONS FOR MOHS MICROGRAPHIC SURGERY FOR NON-MELANOMA SKIN CANCER (KERATINOCYTE CARCINOMA)
Tumor characteristics[1]

• Recurrent
• High-risk* anatomic location (Area H): "Mask areas" of the face (central face, eyelids, eyebrows, nose, lips, chin, ear, and periauricular skin/sulci, temple; Fig. 150.2), anogenital region, hands, feet, nail units, ankles, and nipples/areola
• Medium-risk† anatomic location (Area M): Face outside of area H, scalp, neck, pretibial leg
• Aggressive histologic subtype:
  • BCC: morpheaform (sclerosing), micronodular, basosquamous (metatypical), infiltrating
  • SCC: Breslow depth >2 mm, Clark level >III, deeply penetrating, poorly differentiated or undifferentiated‡, spindle cell, sclerosing, small cell, clear cell, lymphoepithelioma-like, sarcomatoid, acantholytic¶
• Perineural invasion
• Large size (>2 cm diameter)
• Poorly defined clinical borders (lateral and/or deep)
• Rapid growth
• Positive margin on recent excision

Characteristics of background skin
• Prior exposure to ionizing radiation • Chronic scar (Marjolin ulcer)
Patient characteristics
• Immunocompromised: solid organ transplant recipient, chronic lymphocytic leukemia, HIV infection, pharmacologic immunosuppression • Underlying genetic syndrome, e.g. xeroderma pigmentosum, basal cell nevus syndrome, Bazex–Dupré–Christol syndrome • Patient known to have previous high-risk tumors without other known health risk factors
*High risk for recurrence. †Medium risk for recurrence. ‡High degree of nuclear polymorphism, high mitotic rate, or low degree of keratinization. ¶Not included in the Appropriate Use Criteria (AUC) criteria[1].

Table 150.1 Indications for Mohs micrographic surgery for non-melanoma skin cancer (keratinocyte carcinoma). BCC, basal cell carcinoma; SCC, squamous cell carcinoma.

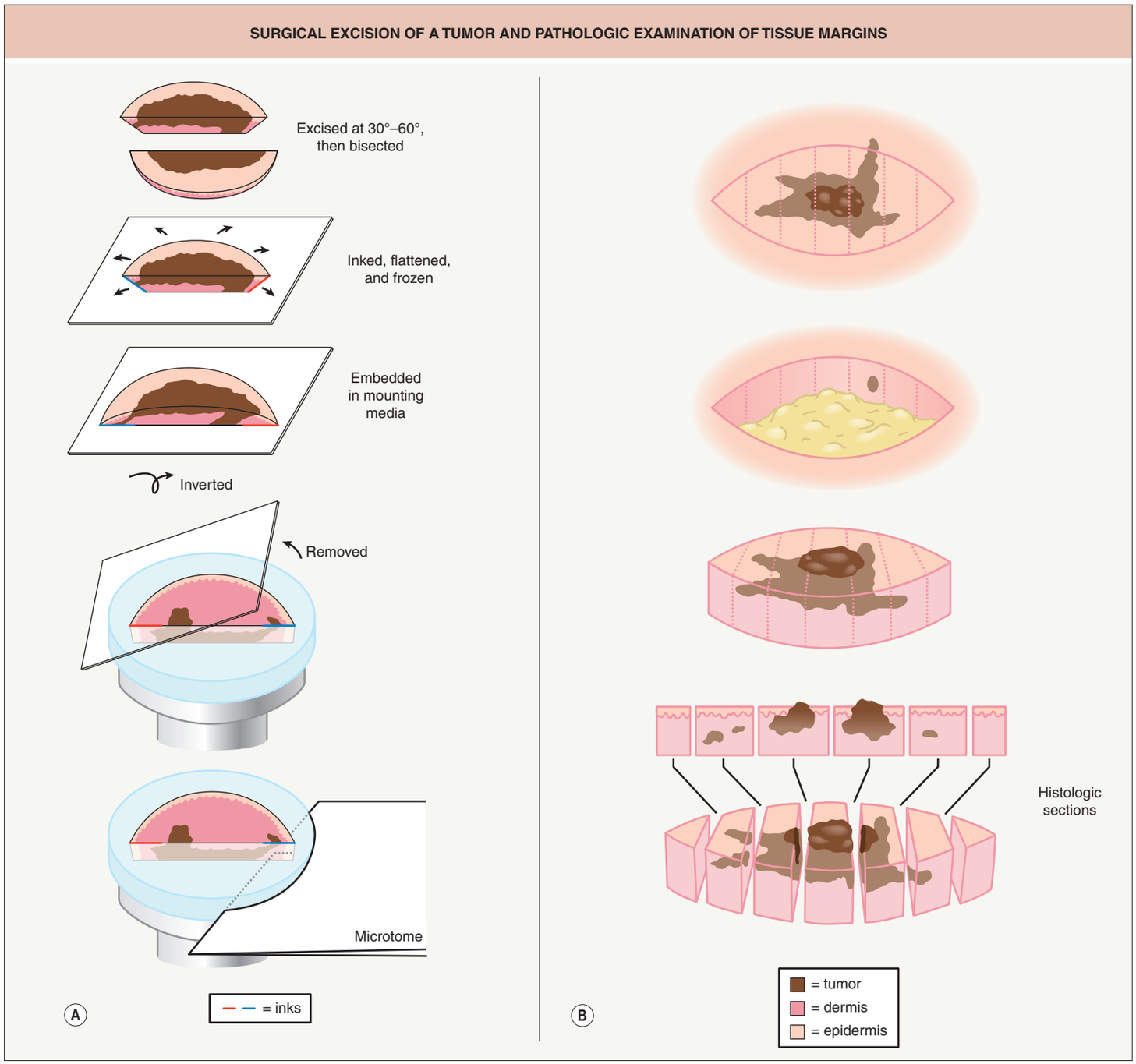


Fig. 150.1 Surgical excision of a tumor and pathologic examination of tissue margins. A Mohs micrographic surgery in which 100% of the total margin is examined. Following excision with a narrow margin, the specimen is flattened so that when the tissue is horizontally sectioned, the skin edge is in the same plane as the deep margin. Note the inversion of the tissue prior to sectioning. **B** Standard elliptical excision with vertical tissue sectioning ("bread loafing"). Histologically, the margins may appear clear even though there is still residual tumor.

HISTORY

Originally termed *chemosurgery*, MMS was developed by Dr Frederic E. Mohs at the University of Wisconsin-Madison and first published in 1941[2]. His original clinical technique involved the application of a zinc chloride paste to cancerous tissue 24 hours prior to surgical removal of the tumor. The paste fixed and isolated the tumor *in vivo*. Subsequently, the tumor was excised and processed in a manner similar to the technique used today. However, if there were residual tumor at the margins, zinc chloride paste was re-applied to cancerous margins for 24 hours prior to any further tissue resection. These steps were repeated until complete tumor clearance was obtained[3].

Limitations of this process include a long incubation period and tissue necrosis from the zinc chloride paste which renders wounds unsuitable for surgical reconstruction. The latter led to Dr Mohs' second major innovation – an objective analysis of second intention wound healing. Historically, surgical dogma held that second intention healing produced inferior cosmetic results compared to reconstruction, the surgeon's "first intention for healing". The acceptable, and at times superior, cosmetic outcome associated with second intention healing, particularly on concave surfaces, imparts its rightful place among valid reconstructive techniques.

Over 40 years ago, the zinc chloride-based, fixed tissue technique evolved into the fresh-frozen tissue technique[3], which was popularized by Tromovitch and Stegman[4]. The fresh-frozen section technique eliminated the need for the escharotic zinc chloride paste, and it allowed complete tumor clearance via multiple resections in a single day. Furthermore, without a zinc chloride-induced necrotic base, immediate

surgical reconstruction could be performed. The fresh tissue technique has now become the standard protocol for MMS.

TRAINING IN MOHS MICROGRAPHIC SURGERY

Training in MMS involves all aspects of cutaneous oncology, tumor resection, tissue preparation, histologic interpretation, and reconstruction. The substantial clinical, surgical, and histopathologic training received during a dermatology residency provides the background for specialized training in MMS. One of the unique advantages of Mohs surgical training is the degree of expertise in clinicopathologic correlation, which derives from dual training in both clinical and pathologic tumor assessment. The dermatologic surgeon must also acquire a mastery of cutaneous and soft tissue anatomy as well as reconstruction. MMS training programs differ depending upon the country, with a one-year Accreditation Council for Graduate Medical Education (ACGME) fellowships available in the US[5].

Both the American Board of Dermatology (ABD) and the American Osteopathic Board of Dermatology offer subspecialty certification in Micrographic Dermatologic Surgery. After 2025, a prerequisite for the ABD certifying examination will be completion of an ACGME-approved Micrographic Surgery and Dermatologic Oncology fellowship.

APPROPRIATE USE CRITERIA AND COST-EFFECTIVE CARE

In 2012, there was a multi-society collaboration to develop appropriate use criteria (AUC) for MMS[1]. For each of 270 clinical scenarios, a panel of surgical and medical dermatologists examined the rational use of MMS, taking into account multiple factors including size, behavior, and location (Fig. 150.2)[1,6]. In addition, tumors that did not require MMS, e.g. small basal cell carcinomas on the trunk, were identified (www.aad.org/education/appropriate-use-criteria/mohs-surgery-auc). The National Comprehensive Cancer Network (NCCN) guidelines for the treatment of cutaneous malignancies is also available as a reference[7].

Studies on the cost-effectiveness of MMS have produced variable results and conclusions, depending on the study location and methods[8,9]. When standard excision with FFPE sections and immediate repair is compared with MMS, the costs are either similar or the former is slightly less expensive than MMS. However, the cost-effectiveness of MMS is enhanced when the following factors are taken into account: the physical location of the surgical procedure (office-based vs. ambulatory surgery center or hospital), specimen processing (frozen vs. permanent sections), type and extent of reconstruction required (smaller defect size due to tissue-sparing vs. standard wide local excision), and the need for additional surgery for tumor recurrences[8–12]. Hopefully, application of MMS AUC[1] will lead to even greater cost savings.

INDICATIONS

Most skin cancers are locally invasive and, depending on their location, can invade vital structures such as the eye, nose, lips and ears, leading to significant tissue destruction. With time and neglect, metastasis may develop. The majority of non-melanoma skin cancers are low-risk and do not fulfill the criteria outlined in Table 150.1. For such tumors, cost-efficient superficial ablative techniques (e.g. electrodesiccation and curettage) or simple excision can be performed. Currently, ~25% of skin cancers are treated with MMS in the US[10]. MMS is well suited for skin cancers at high risk for recurrence and for those tumors located in regions requiring tissue conservation and complete margin control[10]. This includes large lesions in cosmetically sensitive areas.

Factors that identify a "high risk" skin cancer include clinical and histologic characteristics of the tumor, anatomic site, and history of prior treatment(s) (see Table 150.1). Because of the complete histologic examination of surgical margins, MMS allows tracking of unpredictable superficial or deep projections of tumor (see Fig. 150.1A). MMS is very useful for tracking tumors that involve embryonic fusion planes, the periorbital region, nerves, and bone. It is these deep and irregular tumor extensions that are primarily responsible for the higher recurrence rates observed with other techniques. Importantly, the indications for MMS are not absolute, and any treatment decision needs to be made in collaboration with the patient's preferences (e.g. local vs. general anesthesia for extensive procedures), performance status, and understanding of alternative treatment options and associated cure rates.

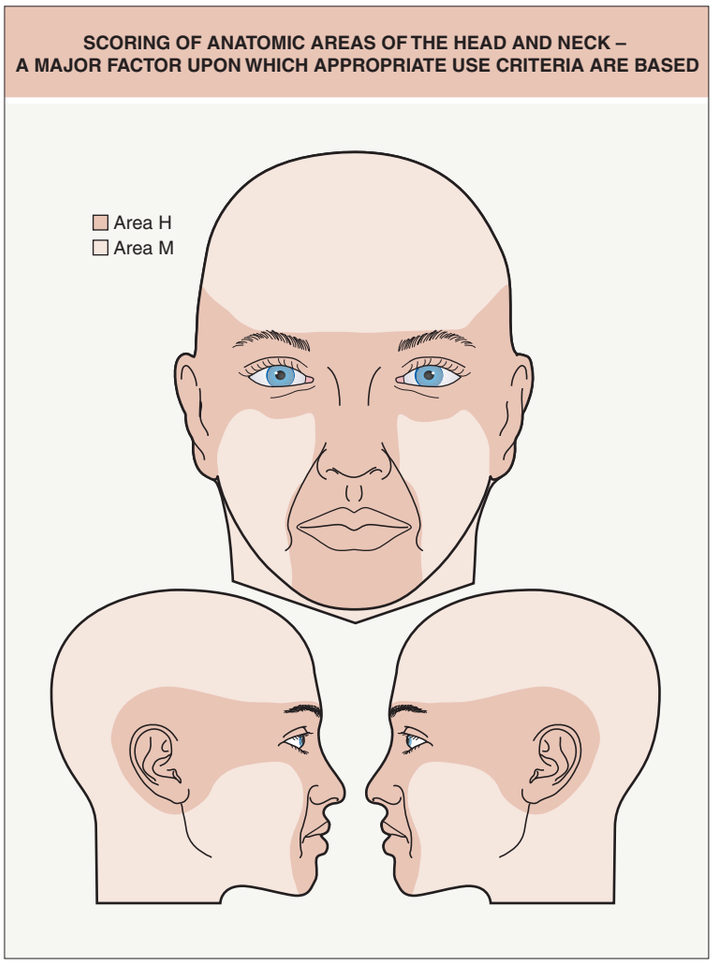


Fig. 150.2 Scoring of anatomic areas of the head and neck – a major factor upon which appropriate use criteria are based. Area H represents the anatomic sites with the highest risk for recurrence and the greatest need for tissue sparing, followed by Area M. The majority of the trunk and extremities is labeled as Area L (lowest need for tissue sparing and risk of recurrence), with the hand, foot, ankle, nail unit, nipple/areola, and anogenital region representing additional Area H sites and the shins an Area M site[1]. See www.aad.org/education/appropriate-use-criteria/mohs-surgery-auc as well as the Mohs AUC app.

The use of MMS for the more commonly managed cutaneous malignancies will be reviewed first, followed by its use for unusual neoplasms (Table 150.2).

Basal Cell Carcinoma

For primary BCCs, cure rates of 87% to 95% can be obtained with superficial ablative therapies and excision, especially on the trunk and extremities. In a meta-analysis by Rowe et al.[13], the 5-year cure rate for *primary* BCC treated with MMS was 99%, as compared to 90% to 93% using standard treatments (Table 150.3). For *recurrent* BCC treated with MMS, the 5-year cure rate was 90%–94% as compared to 80% for standard treatments (surgical excision, radiotherapy, cryotherapy, electrodesiccation and curettage)[14].

MMS provides superior cure rates for high-risk BCCs that are more likely to recur, including those that are large in size (>2 cm) or have aggressive histologic subtypes (e.g. basosquamous carcinoma[38]) or perineural invasion[39,40].

Squamous Cell Carcinoma

MMS offers the highest cure rates for patients with high-risk primary or recurrent SCCs. The local recurrence rates, based on a retrospective review of MMS versus non-MMS modalities for primary SCC, are outlined in Table 150.3[16].

MMS is indicated for management of SCCs with one or more risk factors for recurrence or metastasis (see Table 150.1). These indications include large SCCs (>2 cm), recurrent tumors, incompletely excised SCCs, and tumors with ill-defined clinical margins, rapid growth, an aggressive histologic subtype, and/or perineural invasion (Fig. 150.3), as well as SCCs arising in chronic scar tissue (Marjolin ulcer)[41]. Immunosuppressed patients, including those with solid organ transplants and chronic lymphocytic leukemia, as well as patients receiving medications such as voriconazole and unopposed vemurafenib, can develop rapidly growing SCCs that benefit from MMS.

In addition, SCCs arising in high-risk anatomic sites may be managed with MMS. For example, tumors of the lip have a high propensity for recurrence and metastasis with cure rates as high as 92% achieved with MMS[42]. MMS is also well suited for SCCs occurring in anogenital areas and on the digits, where tissue conservation is important. When compared with conventional methods, MMS for the treatment of penile SCC offers comparable survival rates. Prior to MMS, SCCs involving the nail unit were often treated with amputation or radiation. MMS provides an excellent choice for treatment of periungual and subungual SCC without osseous involvement, with cure rates of up to 96%[43].

Erythroplasia of Queyrat (EQ) is a term used for SCC *in situ* (SCCIS) arising in anogenital mucosae, especially in men. An erythematous thin plaque is typically seen on the inner surface of the foreskin, glans penis, and/or coronal sulcus of an uncircumcised man (see Chs. 73 & 108). In women, differentiated vulvar intraepithelial neoplasia (dVIN) and high-grade squamous intraepithelial lesion (HSIL) are the preferred terms, with oncogenic human papillomaviruses (HPVs) often playing an etiologic role in the latter. HPV infection also increases the risk of anogenital SCC in immunosuppressed individuals (e.g. HIV-infected).

MMS is an effective treatment for EQ, with a 5-year cure rate of 90%[17]. When excising EQ of the glans penis, Mohs layers should be very thin in order to minimize entry into and resection of the corpus spongiosum and cavernosum. If either is entered, achieving hemostasis can be challenging. EQ can often extend into the urethra and differentiation of SCCIS from transitional epithelium is often difficult on frozen sections. With deep extension along the urethra, collaboration with a urologist and completion of the surgery under general anesthesia are recommended.

CUTANEOUS TUMORS TREATED WITH MOHS MICROGRAPHIC SURGERY AND REPORTED CURE RATES	
Cutaneous tumors	**Cure rates (5-year)**
Basal cell carcinoma	99% (primary tumors)[13] 90%–93% (recurrent tumors)[14]
Squamous cell carcinoma	92%–99% (primary tumors)[15] 90% (locally recurrent tumors)[16]
Erythroplasia of Queyrat	90%[17]
Cutaneous melanoma *in situ*, including lentigo maligna	67%–100%[19–24]
Atypical fibroxanthoma	93%–100%[25]
Dermatofibrosarcoma protuberans	97%–100%[26–29]
Merkel cell carcinoma	84%[30]
Microcystic adnexal carcinoma	90%[31–33]
Sebaceous carcinoma	89%[34]
Extramammary Paget disease	92%–97%[35,36]
Leiomyosarcoma (superficial)	87%[37]

Table 150.2 Cutaneous tumors treated with Mohs micrographic surgery and reported cure rates. For eccrine porocarcinoma, angiosarcoma and lymphoepithelioma-like carcinoma, efficacy based only upon case reports. For mucinous eccrine carcinoma, increased efficacy relative to wide excision not established. Some surgeons also use Mohs surgery for invasive cutaneous melanoma.

FIVE-YEAR CURE RATES FOR PRIMARY BCC AND SCC		
Treatment modality	**5-year cure rate**	
	BCC (%)	**SCC (%)**
Surgical excision	90	92
Electrodesiccation & curettage	92	96
Radiation	91	90
Cryotherapy	93	N/A
All non-Mohs modalities	91	92
Mohs micrographic surgery	99	97

Table 150.3 Five-year cure rates for primary basal cell carcinoma (BCC) and squamous cell carcinoma (SCC) by treatment modality. Based upon refs 1 and 4. There is some inherent bias in these data as the studies quoted in this table did not all use the same patient selection criteria. For example, techniques such as electrodesiccation and curettage appear to have higher cure rates for SCC than does excision to the adipose layer, but it is likely that patients who had curettage selected as a definitive treatment had superficial tumors. N/A, not available.

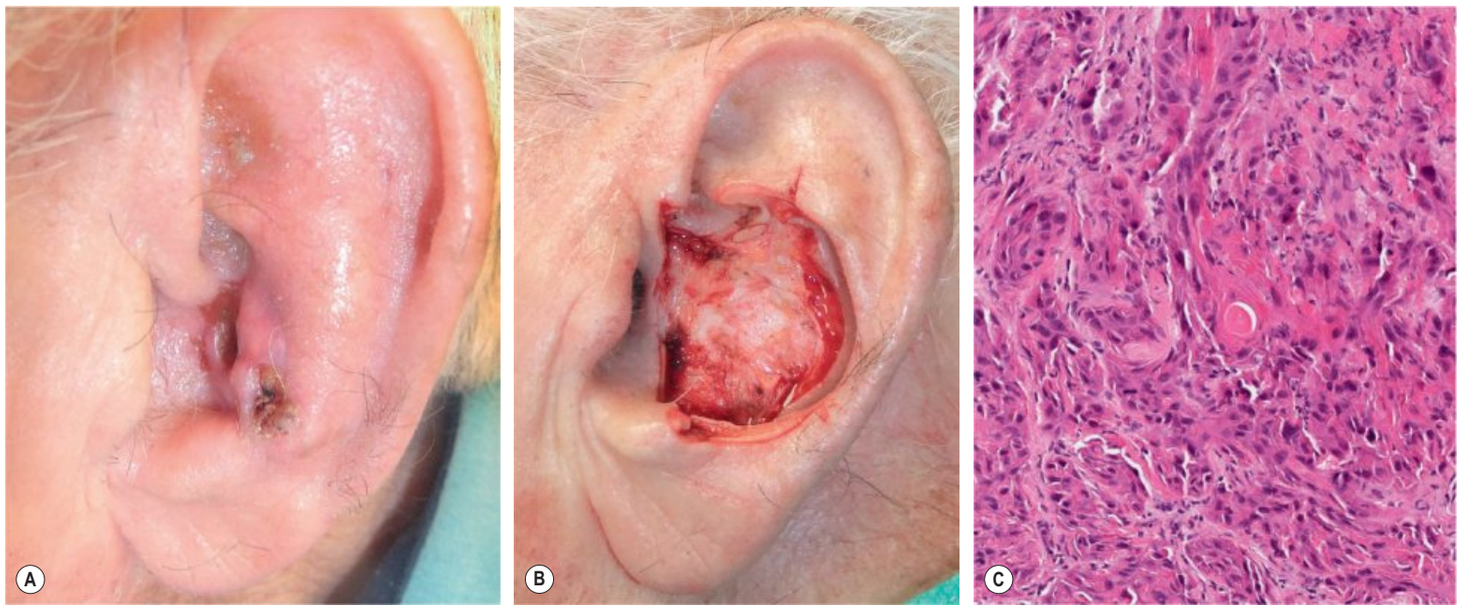


Fig. 150.3 Recurrent, biopsy-proven, moderately differentiated squamous cell carcinoma (SCC) of the left conchal bowl. A Prior to Mohs micrographic surgery. **B** Tumor extirpation resulted in a through-and-through defect of the ear. **C** Histologic features of this aggressive SCC include nests and cords of polygonal cells with enlarged, pleomorphic nuclei and only small foci of keratinization.

Keratoacanthomas (KAs) classically grow quickly and then can spontaneously involute. However, management of KAs remains controversial[18]. Microscopically, some KAs are difficult to distinguish from SCC and there are reports of non-regressing and metastatic KAs, implying that the tumor was actually an SCC. Currently, most KAs are considered to be well-differentiated SCCs. MMS may be particularly beneficial for large lesions, as well as those occurring in anatomically sensitive areas.

Verrucous carcinoma is considered a variant of SCC, and it can be associated with HPV infection. Tumors most commonly occur in the oral cavity, on the plantar foot, or on the penis (see Ch. 108). While generally considered a low-grade carcinoma, there are reports of metastasis. Histopathologic interpretation of frozen sections can be challenging because the tumor cells are very well differentiated with minimal nuclear atypia, making distinction from pseudoepitheliomatous hyperplasia, verruca vulgaris, or condyloma acuminatum challenging. In patients with a clear-cut clinical diagnosis verified by histologic examination, the irregular architectural pattern of verrucous carcinoma may aid in evaluating the margins of excision by MMS.

Cutaneous Melanoma

Melanoma in situ *(lentigo maligna) of the head and neck region*

Treatment of melanoma *in situ* (MIS), in particular lentigo maligna (LM), of the head and neck region is a subject of debate. Controversies include width of surgical margins, MMS versus standard surgical excision, and use of pre- or postoperative topical imiquimod. Even within MMS, there are different techniques, from classic MMS with frozen sections to "slow Mohs" utilizing "rush" permanent sections. Reasons for the debate include: (1) the difficulty in distinguishing atypical melanocytes of photodamaged skin from melanoma cells (Fig. 150.4), especially in frozen sections stained with H&E or antibodies that recognize melanosomes; and (2) the natural history and prognosis of LM. The first can lead to residual tumor or unnecessary excision of photodamaged skin while the second can complicate determining an impact on survival.

Current NCCN guidelines recommend surgical treatment with margins of 0.5–1.0 cm, allowing for narrower margins depending upon anatomical and functional considerations[44]. However, LM treated with surgical excision alone may require wider margins as lesions tend to be ill-defined with subclinical spread[44] and a local recurrence rate of 6%–20% has been reported with standard excision[45]. Although still employed in a minority of patients, the use of MMS to treat cutaneous melanoma has increased over the past two decades, from 2.6% (2001) to 7.9% (2016)[46].

There are no randomized controlled trials comparing wide local excision (WLE) versus MMS to treat MIS of the head and neck region. Database studies, including a retrospective review of a prospective database that compared H&E-based MMS with WLE[24], reported comparable rates of overall and melanoma-specific survival. In the retrospective review, there was also no difference in recurrence rates[24]. Studies from single institutions have also observed low recurrence rates[21–23], e.g. <1% with a mean follow-up of 2.8–3.7 years[21,22].

As noted previously, distinguishing atypical melanocytes of photodamaged skin from melanoma cells in frozen sections can prove challenging. In addition to similar cellular features, processing artifacts (e.g. freeze-induced vacuolization within keratinocytes that resembles vacuolization in melanocytes) may lead to misinterpretation[47]. Detection of a transition zone between photodamaged skin and MIS in FFPE vertical sections can assist in determining clear margins, but this is not possible with *en face* processing of LM margins. To address this potential problem, a prospective cohort study (n = 167) was conducted that examined the accuracy of MIS margin assessment with MMS and H&E-stained frozen sections; the authors reported an accuracy rate of 95%[48]. The latter was determined by excising an additional 1 mm margin followed by its examination by a dermatopathologist. Other approaches include: (1) vertically processing the central debulk plus a narrow margin[22]; (2) obtaining shallow biopsies from the patient's normal-appearing adjacent skin or both perilesional and distant skin[49]; and (3) examination of FFPE tissue margins to confirm that the final MMS margin is negative[50,51].

Potential improvements include immunohistochemical (IHC) staining with antibodies that recognize melanocyte-specific transcription factors (e.g. MITF) rather than melanosomal proteins (e.g. Melan-A/MART-1) (Table 150.4). This prevents staining of melanosome-containing keratinocytes and overestimating the density of melanocytes within photodamaged skin[52] as well as falsely diagnosing pigmented actinic keratoses as LM. Of note, in a survey of Mohs surgeons, only 36% felt comfortable interpreting MART-1-stained frozen sections and a need for additional education was noted as was recognition that formal training is not offered in all fellowship training programs[53].

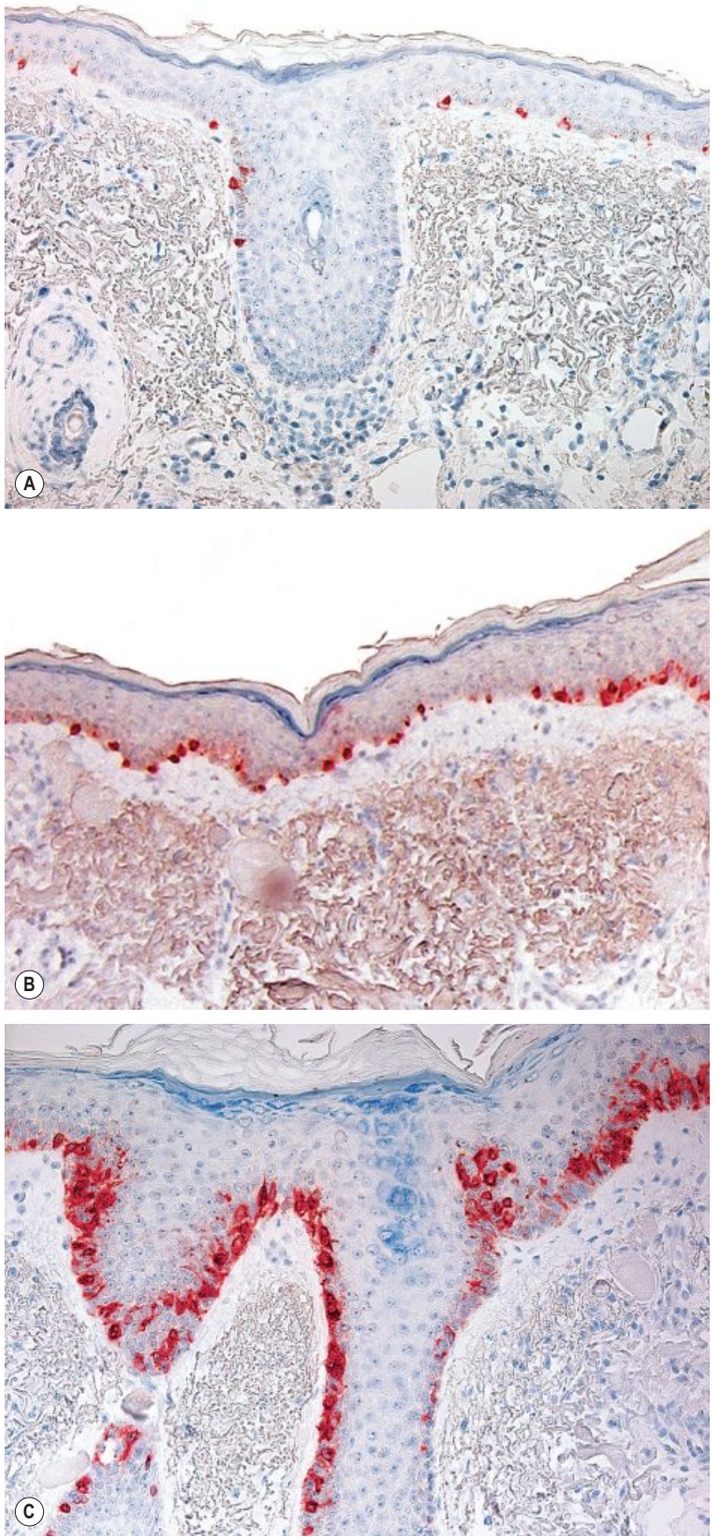
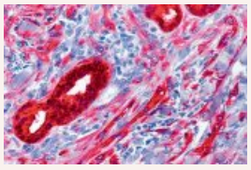


Fig. 150.4 Immunostaining with Melan-A/MART-1. A Normal density of melanocytes. **B** Melanocytic hyperplasia with scattered atypical melanocytes in sun-damaged skin. **C** Lentigo maligna with atypical melanocytic proliferation, some pagetoid spread, and adnexal extension. *Courtesy Clark C. Otley, MD, and Randall K. Roenigk, MD.*

SPECIAL AND IMMUNOHISTOCHEMICAL STAINS USED IN MOHS MICROGRAPHIC SURGERY							
	SCC*	**BCC**	**DFSP**	**EMPD**	**Sebaceous carcinoma**	**Melanoma†**	**MAC**
Special stains	–	Toluidine blue	–	PAS	Oil red O‡	–	Toluidine blue[e1]
Immunohistochemical stains	AE1/AE3 (inset) 	AE1/AE3, Ber-EP4	CD34	CK7, CEA	Adipophilin, CK (e.g. AE1/AE3)	MITF, Melan-A/MART-1 (Fig. 150.4), Mel-5, SOX10, HMB45	CK (e.g. AE1/AE3)

*To detect perineural invasion and high-risk histologic subtypes, e.g. infiltrating, spindle cell, single cell.
†Includes lentigo maligna and other types of melanoma *in situ*.
‡Being replaced by adipophilin stain.

Table 150.4 Special and immunohistochemical stains used in Mohs micrographic surgery. AE1/AE3, pankeratin marker; Ber-EP4, stains cellular glycoproteins in BCCs, sweat glands, and some hair follicles; BCC, basal cell carcinoma; CEA, carcinoembryonic antigen; CK7, cytokeratin 7; DFSP, dermatofibrosarcoma protuberans; EMPD, extramammary Paget disease; MAC, microcystic adnexal carcinoma; MART-1, melanoma antigen recognized by T cells; MITF, microphthalmia transcription factor (nuclear stain); PAS, periodic acid Schiff; SCC, squamous cell carcinoma. *Photomicrograph: Courtesy Luis Requena, MD.*

Invasive melanoma

Based on large randomized controlled trials (RCTs), WLE with recommended margins is the gold standard for treatment of invasive melanoma (see Ch. 113). In patients undergoing sentinel lymph node biopsy, the WLE is routinely performed in tandem[54]. Cutaneous melanomas in general are well-defined, with the exception of some cases of LM and acrolentiginous melanoma. For locally recurrent melanomas, ill-defined or amelanotic melanomas, or melanomas in anatomic sites such as the genitalia, digits, eyelids, nose and ears, a multidisciplinary approach that includes MMS can be considered. There is also some evidence suggesting the utility of MMS for thin melanomas[11,19,55,56].

Staged excisions ("slow Mohs") for melanoma

One variant of MMS is staged excisions ("slow Mohs")[50,51,57] in which the tissue specimen is sent for "rush" FFPE sections that are read by a dermatopathologist the next day. The wound is kept open and covered with a pressure dressing. Some surgeons debulk the visible tumor and determine its depth via vertical processing while assessing the peripheral margin in an *en face* fashion, whereas others cut the tissue radially, allowing the pathologist to appreciate the transition from tumor to actinically damaged skin. If there is residual melanoma, another layer is removed until a negative (tumor-free) margin is achieved. The obvious major disadvantage is the inconvenience of a multi-day procedure. Reported recurrence rates range from <1% to 7.3%, with follow-up ranging from 3 to 57 months[45,58].

Additional staged-excision techniques include the square technique[59], geometric staged excision[60], and the spaghetti technique[61]. In the ***square technique***, two closely spaced, parallel blades are used to create a square-shaped defect (thin and frame-like) with the tumor and presumed adequate margins left intact. If the excised peripheral tissue has clear margins, then the central square is removed surgically[59]. When the square technique was used to treat 834 melanomas, the mean margin required for histologic clearance was 9.33 mm for MIS and 13.7 mm for invasive melanoma. With a median follow-up of 9.3 years, the projected recurrence rate was 2.2% at 10 years[62].

In the ***geometric staged excision***[60], the entire specimen is excised in a geometric pattern; the margins are inked and strips are cut off along the margins. The cut strips are oriented, processed and cut *en face* while the central portion is cut vertically to determine tumor depth. As a result, the entire peripheral margin is examined, which is where the tumor may extend a significant distance from the clinically apparent lesion. In addition, the vertical sections of the central portion confirms or adjusts the tumor thickness. Some dermatopathologists prefer this method because it may be easier to process the tissue for examination of the entire peripheral epidermal and dermal margin[63,64]. In the ***spaghetti technique***, thin strips at the peripheral margin of the visible tumor are excised in stages until the whole tumor is mapped out, then the central lesion is removed. This allows for closure between each stage. A local recurrence rate of 4.76% at a median follow-up of 25 months has been reported[61].

A potential disadvantage of the square and geometric pattern techniques is that a few extra millimeters of skin are sacrificed in order to provide the straight lateral margins. For small tumors, this difference is marginal but if several layers are required and/or the tumor is irregularly shaped, reconstruction can become more complex.

Currently, evidence-based support for the use of MMS to treat cutaneous melanoma is limited by single institution experiences, inclusion of heterogenous tumor types, variable (and sometimes limited) observation periods, and outcome measures based upon local recurrence rates. Given the natural history of LM, the latter can be problematic. Whether a multi-center, randomized, controlled, prospective trial comparing WLE with MIS will ever be conducted remains uncertain.

Uncommon or Rare Cutaneous Neoplasms

Due to the relative rarity of these uncommon tumors, the efficacy of MMS is based primarily on case series from a single institution or case reports.

Atypical fibroxanthoma/pleomorphic dermal sarcoma

Atypical fibroxanthoma (AFX) is a dermal-based mesenchymal neoplasm that develops within photodamaged skin and has minimal, if any, metastatic potential (see Ch. 116). Tumors with similar pathologic features but which demonstrate subcutaneous invasion, necrosis, and/or lymphovascular or perineural invasion are associated with a worse outcome and are referred to as pleomorphic dermal sarcoma (PDS). Typically, AFX presents as a nodule in the head and neck region of an elderly person with significant actinic damage. Its histologic features are said to be relatively easy to identify in frozen sections. For AFX, MMS has been reported to result in lower recurrence rates and greater tissue preservation whereas in PDS, the data is limited[65].

Dermatofibrosarcoma protuberans

Dermatofibrosarcoma protuberans (DFSP) is a slowly growing, locally aggressive soft tissue sarcoma that most often arises on the trunk of young to middle-aged adults (see Ch. 116). It typically extends in an irregular fashion beyond the clinically visible tumor margins. Based upon pooled raw data collected over a 20-year period, recurrence rates following WLE have ranged from 6% to 60% versus 1% to 3% following MMS[26,66–68]. A possible explanation for this difference is the inclusion of patients with primary DFSP, recurrent DFSP, and DFSP with fibrosarcomatous changes, which can lead to biased results as patients with more aggressive disease tended to have WLE (compared to MMS)[66–68]. Of note, a recent retrospective, multicenter study comparing MMS vs. WLE for DFSP on the trunk and extremities found no difference in outcomes[69] while emphasizing the need for complete resection with precise margin control[70]. In the head and neck region, MMS can be advantageous given the potential for conserving tissue while offering margin control[71].

DFSP is often a large-sized tumor and as a result, MMS can be a time-consuming procedure. If tumor identification proves difficult in frozen sections, staged excision ("slow Mohs"; see above), utilizing anti-CD34 IHC staining, can be performed[72,73].

Merkel cell carcinoma

Merkel cell carcinoma (MCC) is a very aggressive malignancy, often arising in older adults with photodamage or who are immunosuppressed (see Ch. 115)[74]. Clinically, the tumor usually presents as a pink–red to violaceous papulonodule that favors the head and neck region. Microscopically, the tumor cells are aggregated into large sheets, allowing them to be easily identified in frozen sections. NCCN guidelines recommend WLE plus sentinel lymph node biopsy (SLNB) followed by radiotherapy to the primary site and regional lymph nodes (unless the lesion is low risk [≤1 cm on the trunk or an extremity with no lymphovascular invasion and negative surgical margins in the setting of a negative SLNB]; (see Fig. 115.19). However, a database study found that patients who underwent MMS were less likely to have a sentinel lymph node biopsy performed[75]. That said, when 22 MCCs were removed via MMS, positive margins were noted in 57% of the cases despite the surgical margins taken meeting or exceeding NCCN guidelines of 1–2 cm margins; however, 92% of the positive cases involved the deep margin[76].

Microcystic adnexal carcinoma

Microcystic adnexal carcinoma (MAC) is a locally aggressive tumor that typically involves the face of older adults (Fig. 150.5). Histologically, it has an infiltrative growth pattern with frequent perineural invasion (Fig. 150.6). With an overall recurrence rate reported in the literature approaching 40%, MMS offers an advantage. Based upon several studies, a five-year cure rate of 90% has been observed following MMS (see Table 150.2)[31]. In one of these studies, defects following MMS were four times larger than clinical estimates[32].

Sebaceous carcinoma

Sebaceous carcinoma can develop in any site that contains sebaceous glands, but it has a predilection for periocular skin. MMS is often employed for tumors in the latter location. Based upon a review of the literature, WLE of sebaceous carcinomas was associated with a local recurrence rate of 4%–37% and a nodal metastatic rate of 3%–28%[77]. In comparison, MMS had a local recurrence rate of 11% (2 of 18 patients) with nodal metastases developing in 1 patient[34]. A more recent

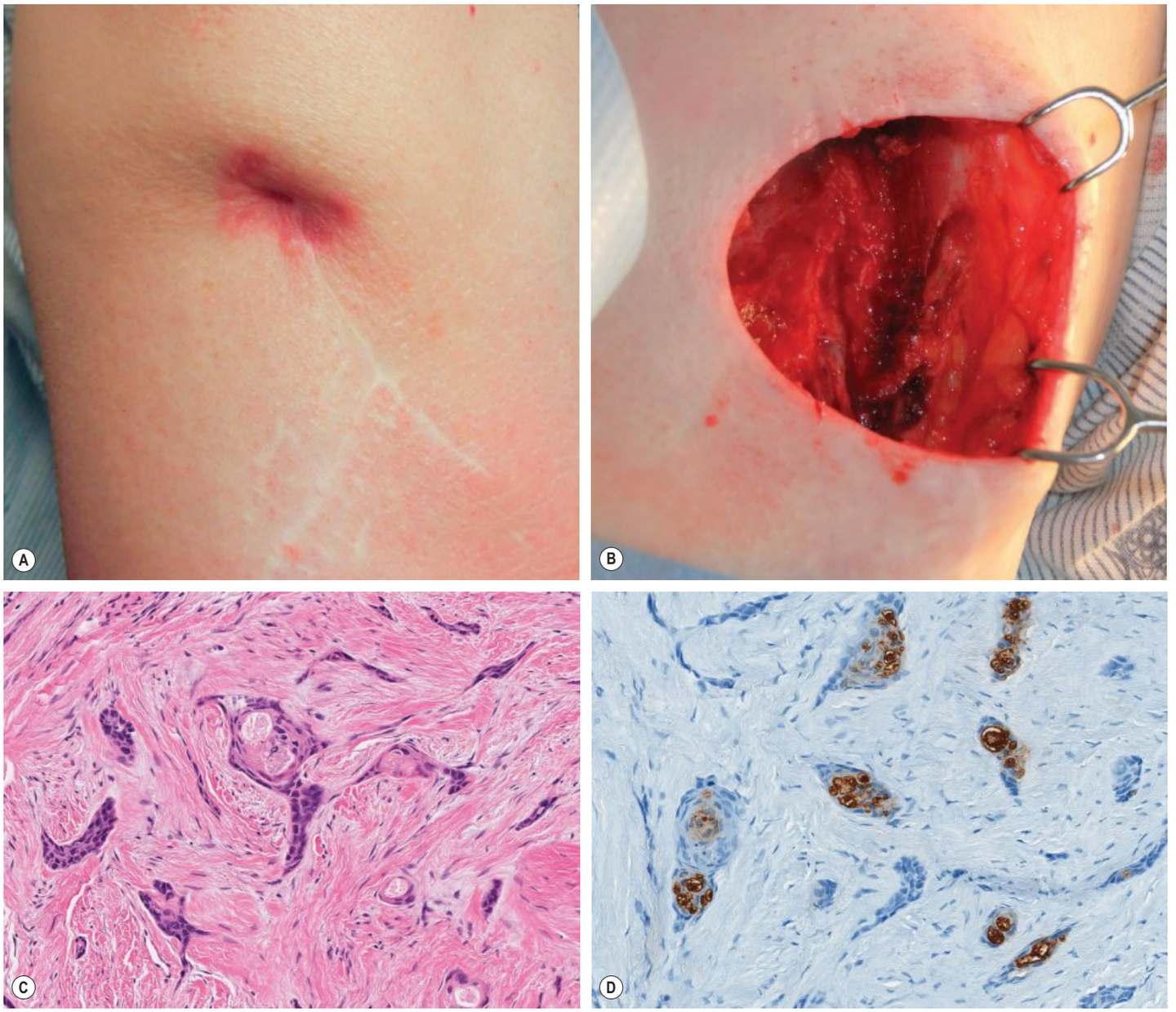


Fig. 150.5 Recurrent basal cell carcinoma (BCC) plus microcystic adnexal carcinoma (MAC). A Recurrent, biopsy-proven BCC of the right upper lateral arm that had been previously treated four times (electrodesiccation and curettage; excision; Mohs micrographic surgery [MMS] twice) over a twenty-year period. An indurated nodule was present at the scar site. **B** Defect after two MMS stages; there was deep infiltration of the subcutaneous tissue, muscle, and periosteum of the humerus. **C** Histologically, small infiltrative basaloid tumor strands embedded within a desmoplastic stroma were seen; there was also ductal differentiation. Because the possibility of a coexisting MAC was raised, the tissue was thawed and submitted for formalin-fixed paraffin-embedded (FFPE) sections. **D** Immunohistochemical staining of FFPE sections demonstrated CEA-positivity of ductal cells, supporting the diagnosis of MAC.

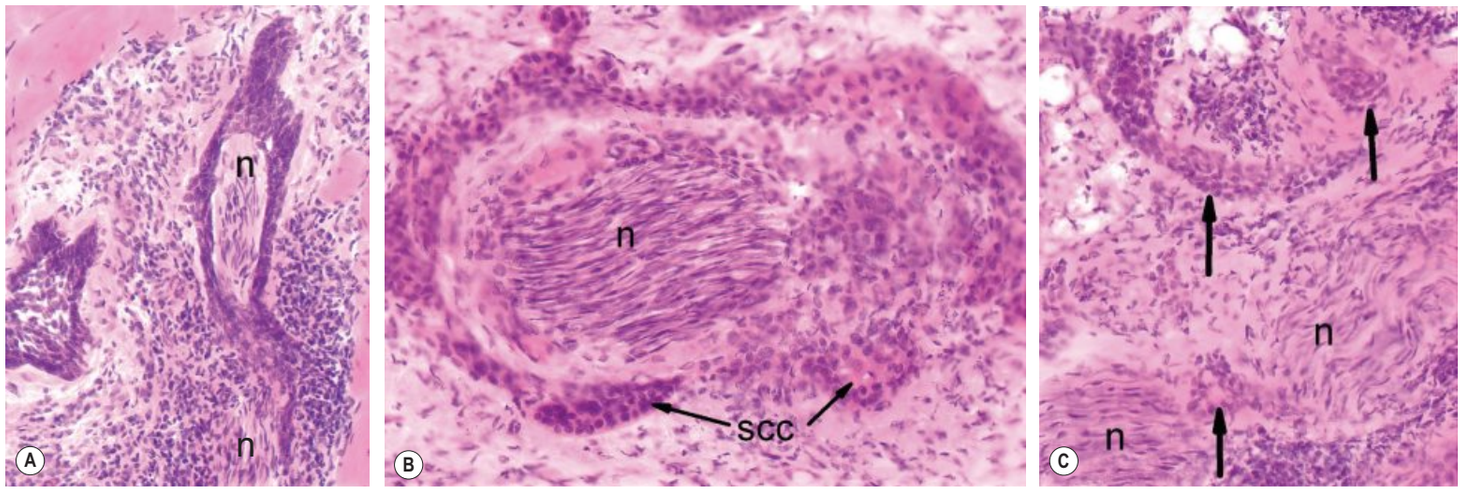


Fig. 150.6 Perineural involvement by various cutaneous tumors (frozen sections). A Basal cell carcinoma with a halo of basal cells enveloping a cutaneous nerve (n). **B** Squamous cell carcinoma (SCC) surrounding nerve fiber (n). **C** Microcystic adnexal carcinoma with perineural invasion by dominant pilar structures (arrows) in the deep subcutaneous portion of the tumor; n, nerve. *Reproduced with permission from Snow S. Atlas of Mohs Surgery Frozen Sections. Madison, WI: Scope Publishing, 2010.*

retrospective review of 45 sebaceous carcinomas treated with MMS found no local recurrences, metastases, or disease-specific deaths, with a mean follow-up of 3.6 years[78]. One challenge associated with these tumors is discontiguous growth, which can thwart any method of histologic margin evaluation. The removal of an extra safety margin of tissue for permanent sections is a reasonable strategy.

Other adnexal carcinomas

This group consists of the uncommon tumors that have sweat gland (eccrine, apocrine), sebaceous gland, or follicular differentiation and includes mucinous carcinoma, eccrine porocarcinoma, adenoid cystic carcinoma, papillary adenocarcinoma, and trichilemmal carcinoma (see Ch. 111). These tumors are usually locally destructive with extensive unpredictable local tissue invasion and therefore have a high rate of local recurrence following excision. Typically, their microscopic features are readily recognizable in frozen sections so they are amenable to MMS[79]. Rapid IHC staining can aid in diagnosis (see Table 150.4).

Miscellaneous tumors

MMS has been utilized for other malignant neoplasms, including angiosarcoma, lymphoepithelioma-like carcinoma, leiomyosarcoma and extramammary Paget disease, as well as cutaneous breast metastases[35–37,80,81]. Occasionally MSS is employed for benign tumors that have a predilection for recurrence such as infantile digital fibroma, desmoplastic trichoepithelioma, and granular cell tumor. Rarely, it is used to eradicate drug-resistant cutaneous fungal infections.

CONTRAINDICATIONS

Discontiguous tumors can lead to the problem of false-negative margins, both with MMS and with WLE. Therefore, this feature is not an absolute contraindication. When the tumor cells cannot reliably be identified in frozen sections this is a relative contraindication. If patients are unwilling or unable to undergo surgery that is time intensive, then standard excision or a non-surgical approach such as radiotherapy may be a better option. However, for some patients with serious medical problems, MMS done under local anesthesia may be safer than surgery performed under general anesthesia[82–84].

PREOPERATIVE HISTORY AND CONSIDERATIONS

A history and focused skin examination should be performed at the time of consultation, which can be the same day as the surgical procedure. The pathology report should be reviewed and, if the diagnosis appears questionable, the histologic sections should be re-examined. Indications for antibiotic prophylaxis should be evaluated and then reviewed with the patient's primary physician, cardiologist or orthopedic surgeon if necessary (see Table 151.2)[85]. Similarly, the management of any implanted electronic medical device as well as anticoagulants and antiplatelet agents needs to be addressed (see Ch. 151).

A thorough review of allergies, including past reactions to antibiotics, local anesthetics, povidone–iodine preparations, latex and adhesives, is conducted. MMS routinely employs only local anesthetics (see Ch. 143), but depending upon the patient oral anxiolytics may also be prescribed. Although lidocaine allergy is rare, the surgeon should be prepared for an emergency response if required.

Upon completion of the medical evaluation, the Mohs surgeon should explain the nature of the tumor, therapeutic options, the key features of MMS, and repair options. In order to prevent wrong-site surgery, photographs of biopsy sites are strongly encouraged. Visualization and confirmation of the biopsy site with the patient are essential[86]. Following informed consent, a standardized time-out is taken prior to the procedure. Patients should be encouraged to continue regular medications and eat a light meal on the morning of surgery, unless conscious sedation is planned.

Individuals with extremely large, recurrent, fixed, deeply invasive tumors and/or clinical signs of perineural invasion can benefit from preoperative radiologic imaging[87,88]. For detection of perineural invasion and intracranial extension (including meningeal), magnetic resonance imaging (MRI) represents the most sensitive imaging modality. However, detection of small nerve involvement is limited and immediate post-resection changes may distort findings. A computed tomography (CT) scan is more sensitive in identifying subtle bone erosion while both CT and MRI are used to evaluate regional lymph nodes.

Very complex cases requiring a multidisciplinary approach should be evaluated preoperatively by other subspecialties (e.g. oculoplastics, otolaryngology, neurosurgery, plastic surgery, radiation oncology) as needed. Following removal of the tumor by or with the assistance of the Mohs surgeon, the most appropriate specialist performs the repair.

TECHNIQUE

Table 150.5 provides a flow sheet for performing MMS and Fig. 150.7 depicts the procedure. (Also see Video 150.1)

VARIATIONS/REFINEMENTS

There are several modifications/variations of MMS that are used to improve: the speed of tissue processing[89]; the efficiency of tumor removal; and the recognition of individual tumor cells for better margin control. For descriptions of staged-excision ("slow Mohs") techniques, see the Cutaneous Melanoma section.

The *single section method* can be used for smaller tumors[90]. It consists of a highly beveled specimen with relaxing incisions on the superior, tumor-bearing portion to allow all peripheral edges to fold outward into a single plane. This method is particularly useful for tumors in which a shallow Mohs layer can be taken and then the surgical defect

allowed to heal by second intention. The unaltered examination of the complete deep margin also reduces the possibility of missed deep margins due to tissue subdivision.

A *non-beveled 90° incision* can be used for MMS on the extremities. The resulting vertical edges are ideal for reconstruction. Although a traditional beveled edge can be trimmed prior to reconstruction, a true, sharp, straight 90° angle is more difficult to obtain. Disadvantages include excision of more tissue and the necessity to manipulate the specimen to make the tissue flatten into a single plane.

In *wide excision MMS* ("wide Mohs"), a larger, clinically tumor-free margin (5–20 mm) is taken. It can be used for tumors that have a high propensity for recurrence or metastases (including satellite metastases), in particular melanoma, Merkel cell carcinoma, and cutaneous sarcomas[17]. In these scenarios, margin control is prioritized over tissue sparing[5].

During MMS, *rapid immunohistochemical (IHC) staining* can be utilized to assist in histologic evaluation (see Table 150.4)[91]. Some surgeons find it especially helpful for challenging and high-risk tumors[52,92,93]. However, there has been rather limited adoption of IHC staining by Mohs surgeons due to the additional cost and time required as well as concerns regarding reliability. In a 2013 survey of Mohs surgeons, only 22% of the respondents (n = 378) incorporated IHC staining into their practice following fellowship training[53].

CHALLENGES AND PITFALLS

The success of the procedure is dependent upon the precision and meticulousness of each step. Recurrences following MMS have been linked to inherent tumor characteristics such as morphology, size or location as well as errors in the procedure[94]. Errors encountered during MMS can be divided into technical (e.g. excess epidermal tissue in the central portion of the layer pushed down to cut margin and interpreted as tumor, incorrect bevel angle or relaxing incisions) and pathologic interpretation (Fig. 150.8)[95,96]. A limitation of MMS arises when the invasiveness of the tumor prevents continued tracking and consultation with the appropriate surgical specialist is indicated.

There are several clinical scenarios in which it is appropriate to send tissue for FFPE including: (1) a second opinion is required during removal of a cutaneous melanoma; (2) further assessment is needed of an aggressive, deep, or histologically unusual tumor; (3) confirmation of the presence of a different tumor than was diagnosed preoperatively (Figs. 150.5 and 150.9); (4) a significant amount of tissue is available for complete staging of the primary tumor; (5) unusual histologic findings in the frozen sections require a second opinion; (6) frozen section interpretation is insufficient to assess the tissue margin reliably; (7) a tumor diagnosed solely by frozen section prior to surgery, i.e. no preoperative biopsy was sent for routine histology; or (8) special stains

MOHS MICROGRAPHIC SURGERY (MMS) FLOW SHEET
Preoperative assessment
• Upon arrival, the patient's demographic information is confirmed, allergies, pertinent medications and vital signs are recorded, and the preoperative biopsy is reviewed • Any prophylactic antibiotic, anti-anxiety drug or cardiac device is either administered or managed as needed • The tumor is closely examined (Fig. 150.7A) and the clinical margin is marked (e.g. with gentian violet) • Reference to diagrams, landmarks and photographs is made to ensure correct site identification and every patient is asked to confirm the tumor location with a mirror[86] • The planned procedure and possible reconstruction are reviewed and consent obtained
Preparation of the site and first Mohs surgery layer

• The site is then wiped with alcohol, local anesthetic (see Ch. 143) is infiltrated, and the site is prepped with chlorhexidine or povidone–iodine
• The central portion of the tumor is de-bulked with a curette to further define subclinical tumor extension (Fig. 150.7B); this step may be omitted when tumors are very small or on thin eyelid skin
• The first MMS layer includes all clinically evident tumor plus a small margin of normal-appearing tissue (Fig. 150.7C)
  • Depending on the histologic subtype and likelihood of subclinical tumor extensions, the margin of normal skin may range from 1 to 10 mm
  • For shallow tumors or those at sites favorable for second intention healing, the first MMS layer is planned as a shallow excision
  • For deep tumors or at sites where second intention healing is not a good option, a full-thickness excision to subcutaneous fat is performed
• For recurrent tumors, the most thorough approach is to resect all tissue involved by the previous treatments, including the primary site and reconstruction scar; if the recurrence is clearly isolated to only one site and/or complete resection would cause difficulties, then a localized resection of the clinically recurrent area can be considered
• When excising the MMS layer, the scalpel is held at a 30–60° angle to the skin surface to create a beveled incision (Fig. 150.7C)
• Before the layer is completely removed, both the layer and the adjacent surrounding tissue are marked with shallow scalpel cuts or a marking pen to help orient the specimen to the defect[e2] (Fig. 150.7D)
• The layer is removed and placed on a transfer card or marked gauze while maintaining correct orientation relative to the defect (Fig. 150.7E)
• Hemostasis is obtained using electrocoagulation or thermocautery as indicated
• A sterile pressure dressing is placed on the wound and the patient is discharged to a waiting room while the tissue is processed

Handling of the tissue specimen
• A map of the specimen is drawn that is relative to anatomic landmarks including the skin notches (Fig. 150.7H) • The specimen is sectioned precisely in order to fit on the cryostat chuck and microscope slide (Fig. 150.7F) • Attention must be paid to maintaining proper numbering, inking and mapping of specimens • All cut margins, except the epidermal edge, are inked systematically with different colored dyes and recorded on the specimen map (Fig. 150.7G,H) • The technician prepares the tissue pieces for freezing by flattening them so that the epidermis lies in the same plane as the dermis and deep margins, using one of several available techniques; if any edge or portion of the specimen curves upward, relaxing cuts are placed on the top surface of the specimen • The technician embeds the tissue piece (deep surface upward) on a chuck with embedding medium and freezes it in the cryostat • Frozen sections are then cut, mounted on slides, and stained with hematoxylin and eosin (H&E)   • Toluidine blue stain can also be used because it is rapid and the purplish metachromatic stromal staining helps to distinguish BCCs from adnexal structures
Histopathologic assessment and additional layers
• The surgeon examines the frozen sections and marks any residual tumor foci on the specimen map (Fig. 150.7J) • If further resection is required, the surgeon precisely removes additional tissue in the area of residual tumor, using the map and skin notches present on the patient for orientation (Fig. 150.7K) • This process is repeated until all tissue margins are microscopically free of tumor • Once the tumor is completely removed, the final defect is measured and photographed and wound management options are discussed and implemented

Table 150.5 Mohs micrographic surgery (MMS) flow sheet. MSS requires a high-complexity approved laboratory, e.g. by CLIA (www.cms.gov/regulations-and-guidance/legislation/clia). Fig. 150.7 depicts the procedure. BCCs, basal cell carcinomas.

are required that cannot be performed reliably on frozen sections[97]. In addition, when there is histologic evidence of a second neoplasm or the histologic features of the tumor being removed via MMS and the preoperative diagnosis differ, the original FFPE sections should be reviewed.

Although infrequent, cutaneous neoplasms can invade bone. This may be the consequence of previous inadequate treatment, anatomic site (e.g. embryonic fusion planes, areas with thin overlying skin such as the scalp, sternum, and distal phalanx), tumor biology, and patient comorbidities (e.g. chronic lymphocytic leukemia, solid transplant-related immunosuppression). In addition, tumors with perineural invasion can gain access into bone via bony foramina. When tumors invade bone, the following strategies are used to control its growth and potentially effect a cure: (1) establish the diagnosis and mode of invasion of the tumor histologically; (2) obtain radiologic imaging to determine the macroscopic extent of bone involvement and status of the regional lymph nodes (see above); and (3) refer to a related subspecialist for bone

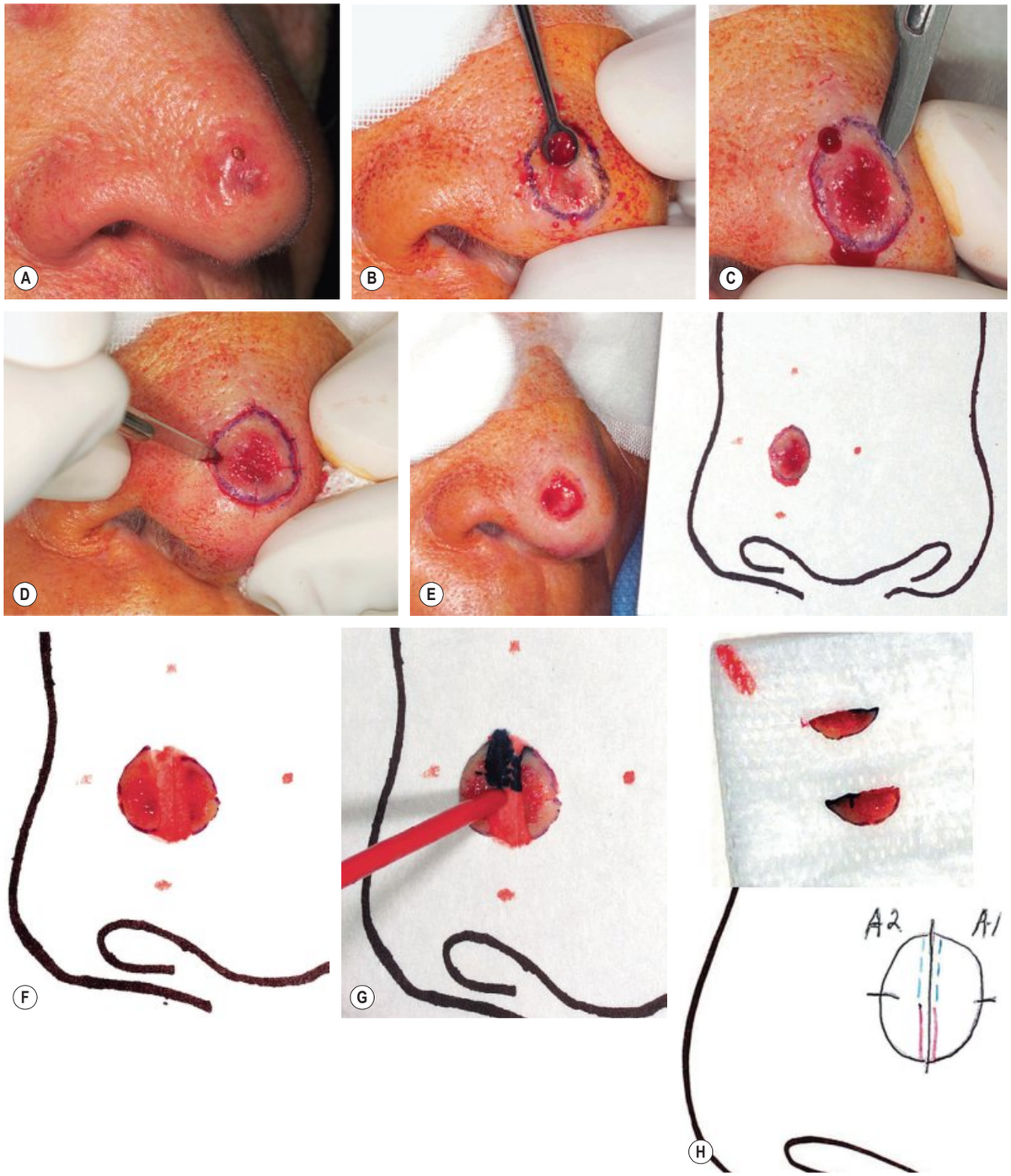


Fig. 150.7 Mohs micrographic surgery technique. A Preoperative appearance of a basal cell carcinoma on the nose. **B** Debulking of the tumor via curettage. **C** Beveled excision (with scalpel at a 45° angle) of all clinically evident tumor plus a small margin of normal-appearing skin. **D** Placement of skin notches at 3, 6, 9 and 12 o'clock positions in the specimen and adjacent surrounding tissue. **E** Orientation of the excised specimen on an anatomic card. **F** Specimen sectioned into two pieces and flattened. **G** Marking of the cut margins of the specimen with red and blue inks. **H** Matching Mohs map and tissue specimen ready for histologic preparation. A red mark on the gauze denotes the location of the first specimen with the second specimen always placed below. Different systems are used but precision is common to all.

Continued

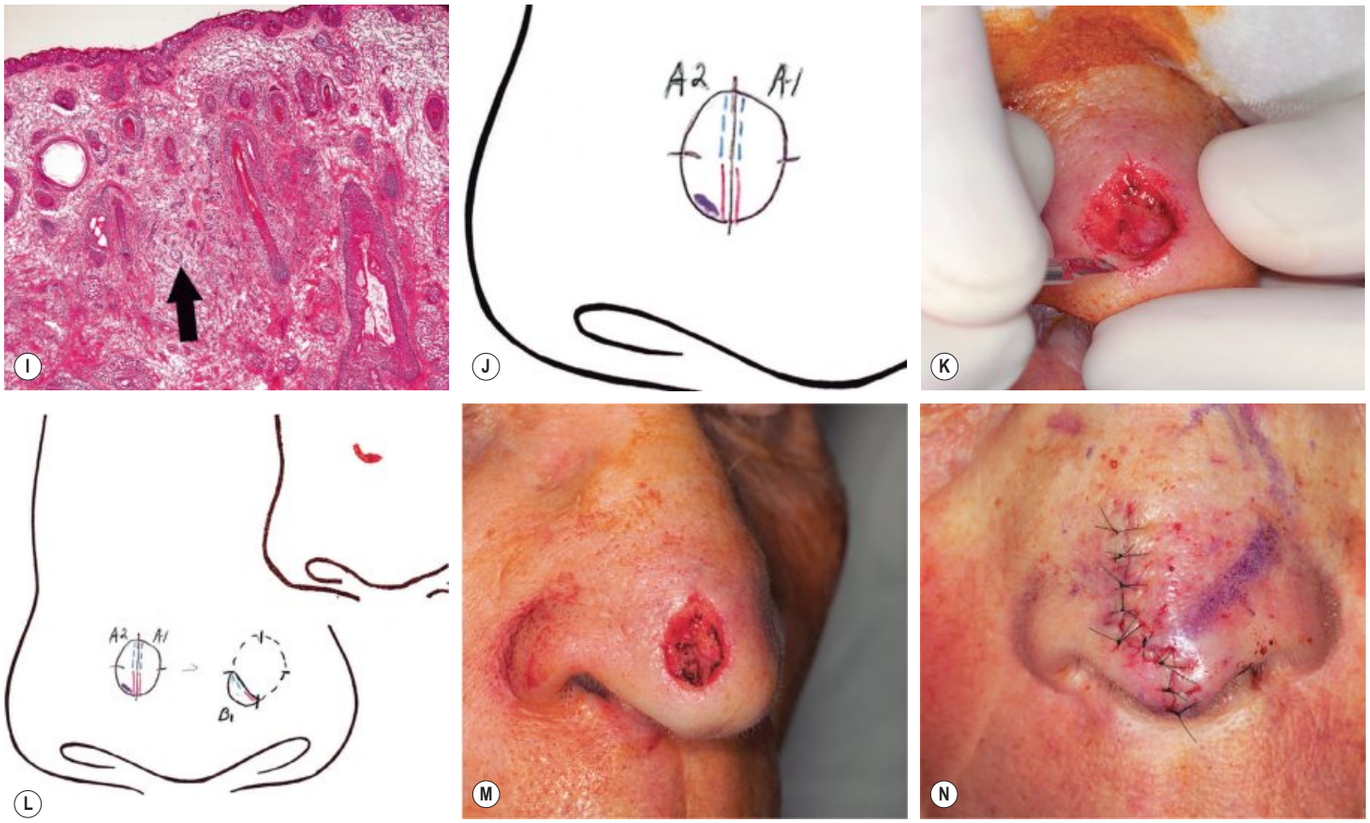


Fig. 150.7 Mohs micrographic surgery technique. (cont'd) **I** Histopathologic section with positive tumor denoted by the arrow. **J** Mohs map marked with purple at the site of cancer at the margin. **K** Re-excision of the area of residual basal cell carcinoma. **L** Mohs map from the second layer with corresponding tissue. **M, N** Postoperative tumor-free defect and repair. *Courtesy Clark C. Otley, MD, and Randall K. Roenigk, MD.*

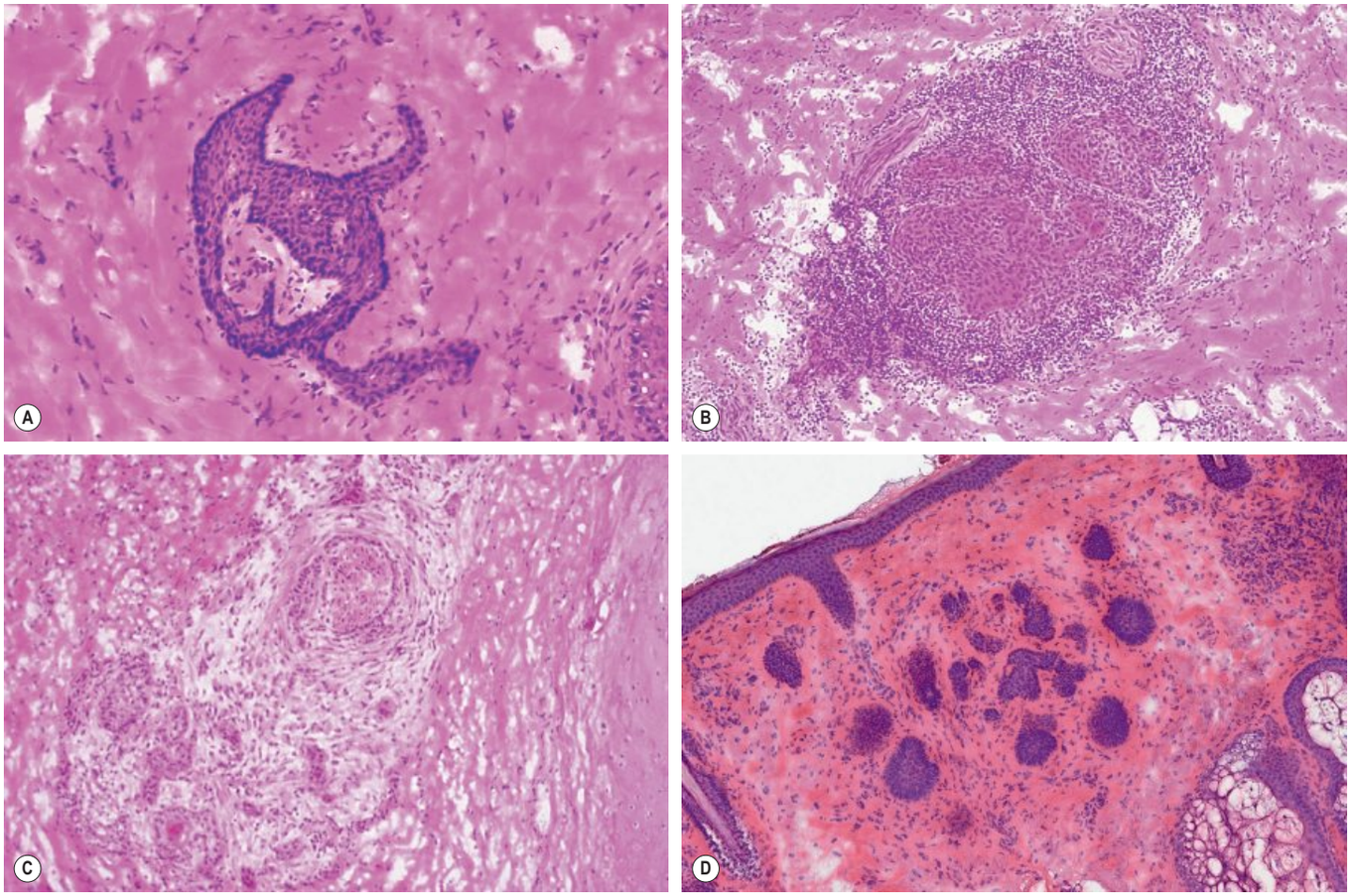


Fig. 150.8 Histopathologic challenges in Mohs surgery. A Folliculocentric basaloid proliferation may mimic basal cell carcinoma; however, the lack of clefting adjacent to the cells, apoptosis, or mitotic figures as well as the presence of a fibrous sheath permits distinction. **B** Dense inflammation can obscure tumor cells, as seen here with a squamous cell carcinoma in a patient with chronic lymphocytic leukemia. **C** Careful evaluation is required to identify subtle foci of perineural squamous cell carcinoma. **D** Follicular remnants can mimic basaloid islands. *A–C, Courtesy Clark C. Otley, MD, and Randall K. Roenigk, MD.*

resection as indicated. In difficult tumors with perineural invasion, additional Mohs layers may be taken to assure a tumor-free plane.

Small foci of sinus, nasal, or scalp bone may be excised locally with a bone rongeur or a chisel and mallet. Even when bone is exposed during tumor surgery, second intent healing is possible. If more than 1 cm of bone is exposed, burring, abrasion, or chiseling of spots 1 cm apart to reach bleeding spots can facilitate granulation. The procedure should be done with the patient recumbent to minimize the extremely rare risk of air embolus into the cavernous sinus (to date 2 cases reported). If sufficient granulation tissue can be stimulated to cover the exposed facial or scalp bone relatively quickly, cellulitis and osteomyelitis rarely occur[98]. Other options include coverage with an acellular dermal matrix or a split-thickness skin graft. These three methods of wound management are frequently preferred over more complex flaps that may delay detection of recurrent tumor. Close clinical surveillance is imperative.

RECONSTRUCTION

After complete tumor clearance, multiple options exist for management of tissue defects. The management strategy takes into account anatomic location, patient comorbidities, tumor severity, and the aesthetic needs of the patient. With guidance from the Mohs surgeon, patients are able to select the best options for reconstruction.

Surgical defects that heal by second intention may result in excellent cosmetic results especially in concave regions. Second intention healing can also be used for recurrent tumors in which flaps or grafts might hinder surveillance. Patients must be willing to attend to the area over a 2- to 8-week healing period. Typically, wound care regimens involve cleansing the wound daily with a saline solution or soapy water, applying a layer of ointment, and then covering with a non-adherent dressing. Wound care after cutaneous reconstruction is similar to second intention wound care, although limited to 1–2 weeks. A discussion of cutaneous reconstruction can be found in Chapters 146–148.

POSTOPERATIVE CARE

In addition to those given preoperatively (see Table 151.3), antibiotics may be given postoperatively for wound infection prophylaxis if surgery is extensive as well as for any debilitated patient for whom proper wound care is a concern[85]. Additionally, surgical reconstruction on highly sebaceous noses and distal lower extremities (below the knee) plus those near the nares and mouth may require prophylactic antibiotics. Pain control is assessed on a case-by-case basis. Substantial pain following MMS is uncommon. Acetaminophen is usually sufficient for postoperative discomfort, especially for smaller defects and simple repairs. Oral narcotic analgesics may be prescribed for patients with low pain thresholds, large tumors, complex reconstruction, or wounds in anatomic locations of high tension (e.g. scalp) or sensitivity (e.g. lip, nose, ear)[99]. One randomized controlled trial found the combination of acetaminophen and ibuprofen superior in controlling postoperative pain compared to acetaminophen with codeine and acetaminophen alone[99].

Ongoing surveillance at least annually for new primary and recurrent cancer is recommended for all patients, given that 50% of patients with keratinocyte carcinomas will experience another skin cancer during the subsequent 5 years.

COMPLICATIONS

Complications and adverse events from MMS are uncommon and the procedure has an undetectable mortality rate[100,101]. A large, multicenter, prospective cohort study of adverse events in MMS found that the rate of adverse events was <1%, with the majority being minor[100].

Intraoperative considerations include anxiety, pain (with local anesthesia injection), bleeding, nerve damage, and allergic reactions. If warranted, oral midazolam can be given in the range of 5–15 mg for healthy adults. Knowledge of vascular, muscular, and neural anatomy, especially within the "danger zones" of the face (see Ch. 142), helps to avoid and anticipate specific complications. Hemorrhage is a potential risk during surgery and is minimized with meticulous hemostasis and pressure bandaging. The superficial temporal artery is the most common major artery that may be transected, and its transection usually requires suture ligation. Epinephrine (adrenaline) included in the local anesthetic temporarily improves hemostasis. To date, there is no evidence that patients taking aspirin or warfarin for serious medical problems experience increased risks of serious hemorrhage or bleeding complications following MMS. In addition, while there is a significantly increased risk of bleeding complications in patients on thienopyridines (e.g. clopidogrel, ticlopidine) undergoing dermatologic surgery, these medications are typically continued due to the possible risk of internal thrombotic complications[102,103].



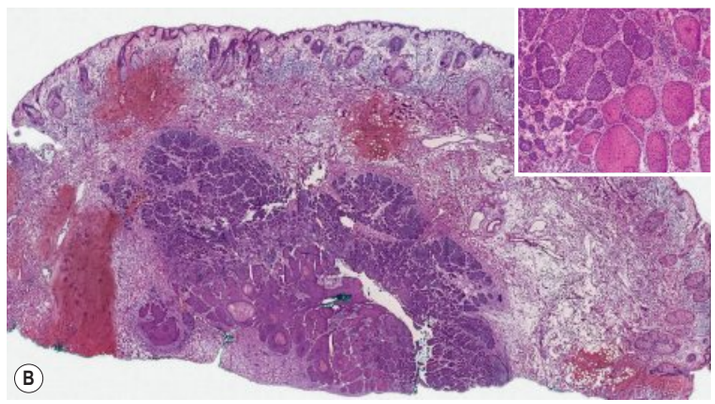


Fig. 150.9 Collision tumor – basal cell carcinoma (BCC) and squamous cell carcinoma (SCC). A A biopsy-proven micronodular/nodular BCC on the ear. **B** Frozen sections demonstrated distinct aggregates of uniform basaloid cells as well as variably large, irregular complexes of polygonal cells with eosinophilic cytoplasm and enlarged, partly pleomorphic nuclei (*inset*).

Injury to cutaneous sensory nerves occurs during all cutaneous surgery. Transection of significant motor nerves is occasionally necessary for removal of deeply invasive tumors, especially in the temporal region. Whenever possible, the surgeon should inform the patient before surgery of any possible loss of function or sensation.

Additional postoperative complications include infection, dehiscence, partial- or full-thickness necrosis, and seroma formation (see Ch. 151). Based upon several studies, the infection rate post MMS is very low (0.7%)[101,104,105].

FUTURE TRENDS

The history of MMS is one of continuous innovation and improvement. Potential enhancements include perioperative tumor definition via noninvasive imaging (e.g. reflectance confocal microscopy, optical coherence tomography) in order to visualize subclinical tumor involvement, use of rapid immunostains that enhance diagnostic sensitivity and specificity, new indications for MMS based upon evidence-based

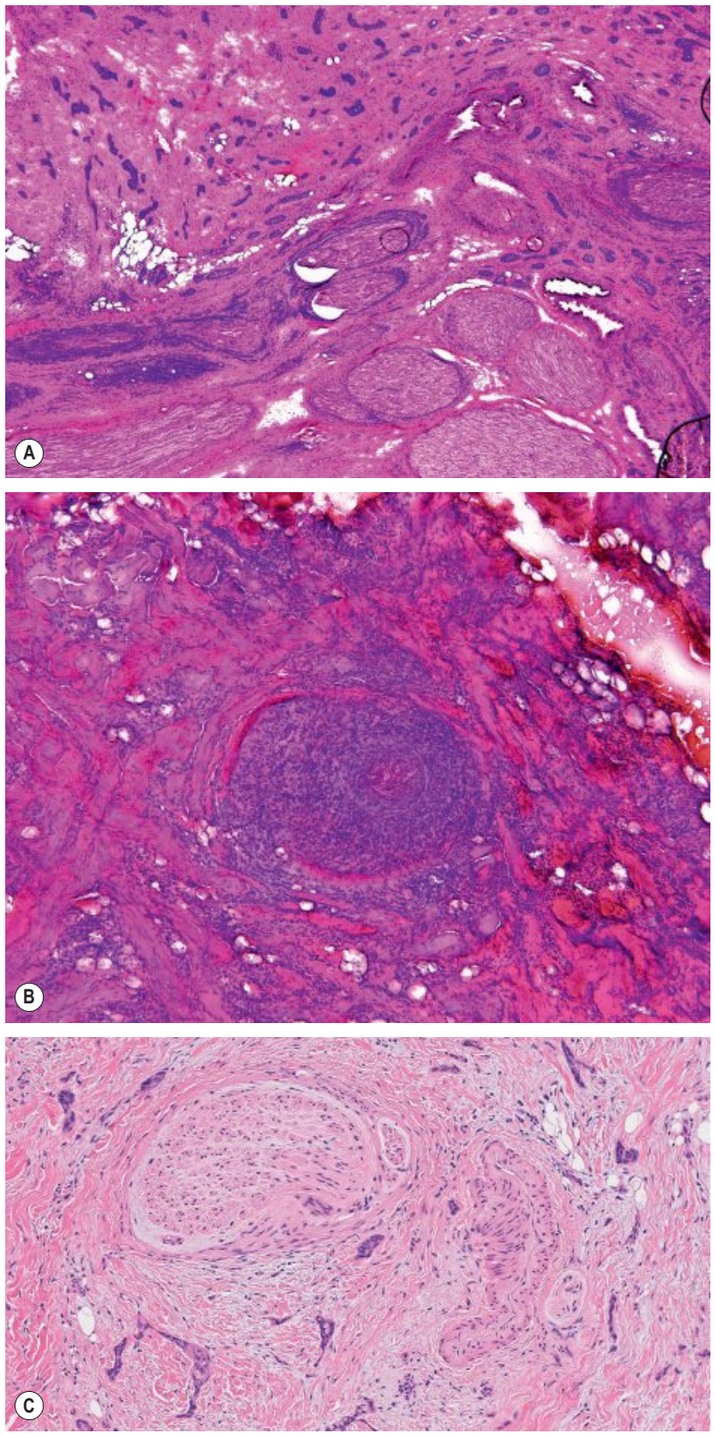
medicine, and further refinements of practice guidelines centered on patient-related outcomes[1]. With the increase in the incidence of skin cancer, the demand for MMS will continue to rise. Given the risk of overuse of MMS, it is important to be mindful of its appropriate use, other viable treatment options, and shared decision-making with patients[1,5]. Current ongoing, large, multicenter database studies aim to further establish MMS as the treatment of choice for high-risk cutaneous neoplasms due to high cure rates, tissue sparing potential, safety, low complication rate, convenience of an outpatient procedure, and cost effectiveness[20,28–30,33].

Additional figures and table on Mohs Micrographic Surgery - Challenges, Pitfalls, and Recommendations available in our eBook (see inside front cover for access code).

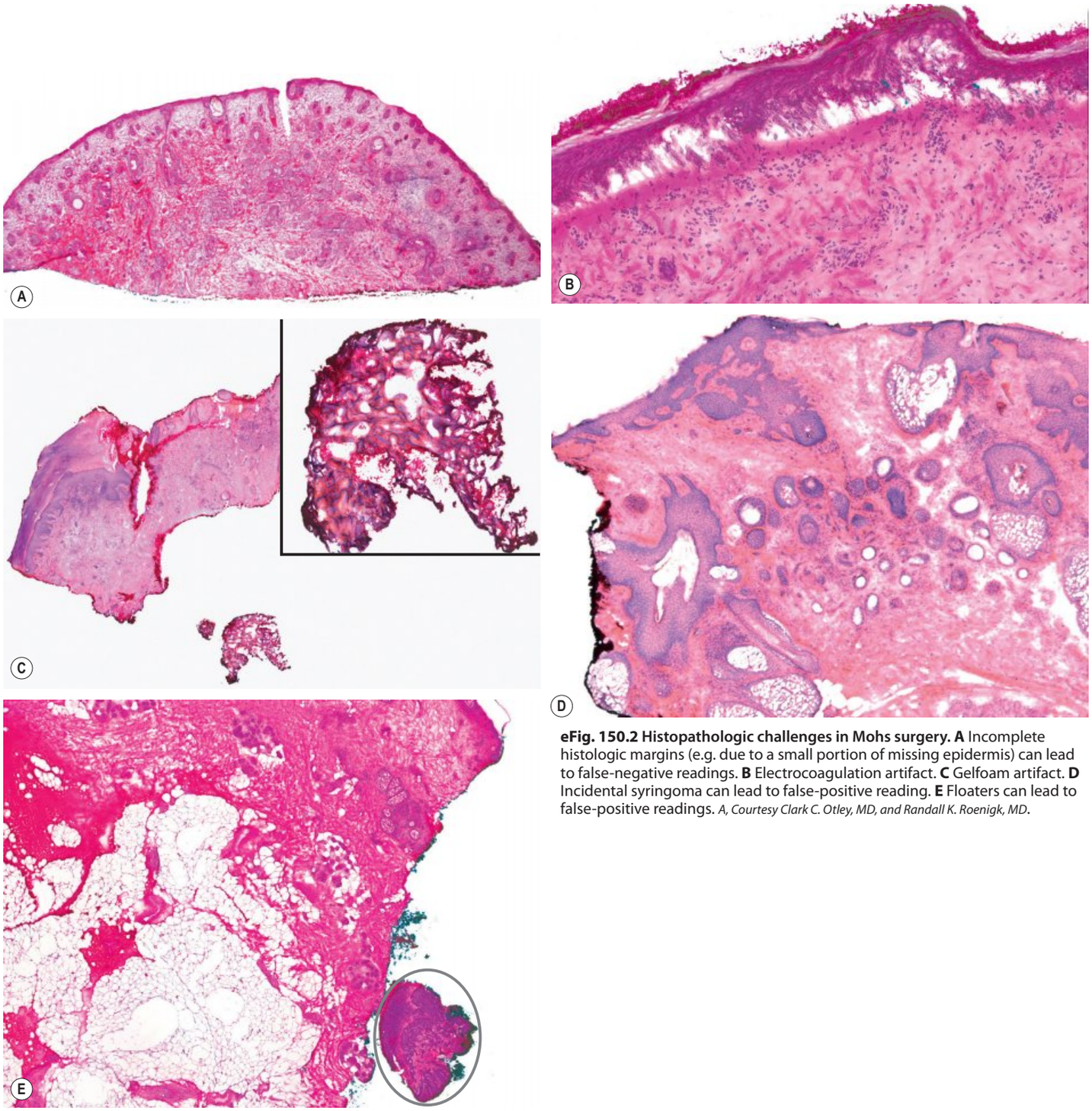
REFERENCES

1. Connolly SM, Baker DR, Coldiron BM, et al. AAD/ACMS/ASDSA/ASMS 2012 appropriate use criteria for Mohs micrographic surgery: a report of the American Academy of Dermatology, American College of Mohs Surgery, American Society for Dermatologic Surgery Association, and the American Society for Mohs Surgery. *J Am Acad Dermatol*. 2012;67:531–550.
2. Mohs FE. Chemosurgery: A microscopically controlled method of cancer excision. *Arch Surg*. 1941;42:279–295.
3. Trost LB, Bailin PL. History of Mohs surgery. *Dermatol Clin*. 2011;29:135–139.
4. Tromovitch TA, Stegeman SJ. Microscopically controlled excision of skin tumors: chemosurgery (Mohs): fresh tissue technique. *Arch Dermatol*. 1974;110:231–232.
5. Hanke CW, Moy RL, Roenigk RK, et al. Current status of surgery in dermatology. *J Am Acad Dermatol*. 2013;69:972–1001.
6. Coldiron B. Commentary: Implementation of the appropriate-use criteria will not increase Mohs micrographic surgery utilization. *J Am Acad Dermatol*. 2014;71:36–37.
7. National Comprehensive Cancer Network. (www.nccn.org/guidelines/category_1).
8. Tierney EP, Hanke CW. Cost effectiveness of Mohs micrographic surgery: review of the literature. *J Drugs Dermatol*. 2009;8:914–922.
9. Seidler AM, Bramlette TB, Washington CV, et al. Mohs versus traditional surgical excision for facial and auricular nonmelanoma skin cancer: an analysis of cost-effectiveness. *Dermatol Surg*. 2009;35:1776–1787.
10. Rogers HW, Coldiron BM. Analysis of skin cancer treatment and costs in the United States Medicare population, 1996–2008. *Dermatol Surg*. 2013;39:35–42.
11. Cook J, Zitelli JA. Mohs micrographic surgery: a cost analysis. *J Am Acad Dermatol*. 1998;39:698–703.
12. Ravitskiy L, Brodland DG, Zitelli JA. Cost analysis: Mohs micrographic surgery. *Dermatol Surg*. 2012;38:585–594.
13. Rowe DE, Carroll RJ, Day Jr. CL. Long-term recurrence rates in previously untreated (primary) basal cell carcinoma: implications for patient follow-up. *J Dermatol Surg Oncol*. 1989;15:315–328.
14. Rowe DE, Carroll RJ, Day CL. Mohs surgery is the treatment of choice for recurrent (previously treated) basal cell carcinoma. *J Dermatol Surg Oncol*. 1989;15:424–431.
15. Roenigk RK, Roenigk HH. Current surgical management of skin cancer in dermatology. *J Dermatol Surg Oncol*. 1990;16:136–151.
16. Chren M, Linos E, Torres JS, et al. Tumor recurrence 5 years after treatment of cutaneous basal cell carcinoma and squamous cell carcinoma. *J Invest Dermatol*. 2013;133:1188–1196.
17. Mikhail GR. Cancers, precancers, and pseudocancers on the male genitalia. A review of clinical appearances, histopathology, and management. *J Dermatol Surg Oncol*. 1980;6:1027–1035.
18. Kwiek B, Schwartz RA. Keratoacanthoma (KA): An update and review. *J Am Acad Dermatol*. 2016;74:1220–1233.
19. Bricca GM, Brodland DG, Ren D, Zitelli JA. Cutaneous head and neck melanoma treated with Mohs micrographic surgery. *J Am Acad Dermatol*. 2005;52:92–100.
20. Bene NI, Healy C, Coldiron BM. Mohs micrographic surgery is accurate 95.1% of the time for melanoma in situ: a prospective study of 167 cases. *Dermatol Surg*. 2008;34:660–664.
21. Valentín-Nogueras SM, Brodland DG, Zitelli JA, et al. Mohs micrographic surgery using MART-1 immunostain in the treatment of invasive melanoma and melanoma in situ. *Dermatol Surg*. 2016;42:733–744.
22. Etzkorn JR, Sobanko JF, Elenitsas R, et al. Low recurrence rates for in situ and invasive melanomas using Mohs micrographic surgery with melanoma antigen recognized by T cells 1 (MART-1) immunostaining: tissue processing methodology to optimize pathologic staging and margin assessment. *J Am Acad Dermatol*. 2015;72:840–850.
23. Newman J, Beal M, Schram SE, Lee PK. Mohs micrographic surgery for lentigo maligna and lentigo maligna melanoma using Mel-5 immunostaining: an update from the University of Minnesota. *Dermatol Surg*. 2013;39:1794–1799.
24. Nosrati A, Berliner JG, Goel S, et al. Outcomes of melanoma in situ treated with mohs micrographic surgery compared with wide local excision. *JAMA Dermatol*. 2017;153:436–441.
25. Tolkachjov SN, Kelley BF, Aladhdab F, et al. Atypical fibroxanthoma: systemic review and meta-analysis of treatment with Mohs micrographic surgery or excision. *J Am Acad Dermatol*. 2018;79:929–934.
26. Lowe GC, Onajin O, Baum CL, et al. A comparison of Mohs micrographic surgery and wide local excision for treatment of dermatofibrosarcoma protuberans with long-term follow-up: the Mayo Clinic experience. *Dermatol Surg*. 2017;43:98–106.
27. Ratner D, Thomas CO, Johnson TM, et al. Mohs micrographic surgery for the treatment of dermatofibrosarcoma protuberans. Results of a multiinstitutional series with an analysis of the extent of microscopic spread. *J Am Acad Dermatol*. 1997;37:600–613.
28. Gloster HM, Harris KR, Roenigk RK. A comparison between Mohs micrographic surgery and wide surgical excision for the treatment of dermatofibrosarcoma protuberans. *J Am Acad Dermatol*. 1996;35:82–87.
29. Snow SN, Gordon EM, Larson PO, et al. Dermatofibrosarcoma protuberans: a report on 29 patients treated by Mohs micrographic surgery with long-term follow-up and review of the literature. *Cancer*. 2004;101:28–38.
30. Boyer JD, Zitelli JA, Brodland DG, D'Angelo G. Local control of primary Merkel cell carcinoma: review of 45 cases treated with Mohs micrographic surgery with and without adjuvant radiation. *J Am Acad Dermatol*. 2002;47:885–892.
31. Leibovitch I, Huilgol SC, Selva D, et al. Microcystic adnexal carcinoma: treatment with Mohs micrographic surgery. *J Am Acad Dermatol*. 2005;52:295–300.
32. Chiller K, Passaro D, Scheuller M, et al. Microcystic adnexal carcinoma: forty-eight cases, their treatment, and their outcome. *Arch Dermatol*. 2000;136:1355–1359.
33. Snow S, Madjar DD, Hardy S, et al. Microcystic adnexal carcinoma: report of 13 cases and review of the literature. *Dermatol Surg*. 2001;27:401–408.
34. Spencer JM, Nossa R, Tse DT, Sequeira M. Sebaceous carcinoma of the eyelid treated with Mohs micrographic surgery. *J Am Acad Dermatol*. 2001;44:1004–1009.
35. O'Connor WJ, Lim KK, Zalla MJ, et al. Comparison of Mohs micrographic surgery and wide excision for extramammary Paget's disease. *Dermatol Surg*. 2003;29:723–727.
36. Damavandy AA, Terushkin V, Zitelli JA, et al. Intraoperative immunostaining for cytokeratin-7 during Mohs micrographic surgery demonstrates low local recurrence rates in extramammary Paget's disease. *Dermatol Surg*. 2018;44:354–364.
37. Humphreys TR, Finkelstein DH, Lee JB. Superficial leiomyosarcoma treated with Mohs micrographic surgery. *Dermatol Surg*. 2004;30:108–112.
38. Leibovitch I, Huilgol SC, Selva D, et al. Basosquamous carcinoma: treatment with Mohs micrographic surgery. *Cancer*. 2005;104:170–175.
39. Paoli J, Daryoni D, Wennberg AM, et al. 5-year recurrence rates of Mohs micrographic surgery for aggressive and recurrent facial basal cell carcinoma. *Acta Derm Venereol*. 2011;91:689–693.
40. Ratner D, Lowe L, Johnson TM, Fader DJ. Perineural spread of basal cell carcinomas treated with Mohs micrographic surgery. *Cancer*. 2000;88:1605–1613.
41. Leibovitch I, Huilgol SC, Selva D, et al. Cutaneous squamous carcinoma in situ (Bowen's disease): treatment with Mohs micrographic surgery. *J Am Acad Dermatol*. 2005;52:253–260.
42. Holmkvist KA, Roenigk RK. Squamous cell carcinoma of the lip treated with Mohs micrographic surgery: outcome at 5 years. *J Am Acad Dermatol*. 1998;38:960–966.
43. Zaiac MN, Weiss E. Mohs micrographic surgery of the nail unit and squamous cell carcinoma. *Dermatol Surg*. 2001;27:246–251.
44. Coit DG, Thompson JA, Albertini MR, et al. Cutaneous Melanoma, Version 2.2019, NCCN Clinical Practice Guidelines in Oncology. *J Natl Compr Canc Netw*. 2019;17:367–402.
45. Beaulieu D, Fathi R, Srivastava D, et al. Current perspectives on Mohs micrographic surgery for melanoma. *Clin Cosmet Investig Dermatol*. 2018;11:309–320.
46. Lee MP, Sobanko JF, Shin TM, et al. Evolution of Excisional Surgery Practices for Melanoma in the United States. *JAMA Dermatol*. 2019;155:1244–1251.
47. Connolly KL, Nehal KS, Busam KJ. Lentigo maligna and lentigo maligna melanoma: contemporary issues in diagnosis and management. *Melanoma Manag*. 2015;2:171–178.
48. Bene NI, Healy C, Coldiron BM. Mohs micrographic surgery is accurate 95.1% of the time for melanoma in situ: a prospective study of 167 cases. *Dermatol Surg*. 2008;34:660–664.
49. Albertini JG, Elston DM, Libow LF, et al. Mohs micrographic surgery for melanoma: a case series, a comparative study of immunostains, an informative case report, and a unique mapping technique. *Dermatol Surg*. 2002;28:656–665.
50. Cohen LM, McCall MW, Zax RH. Mohs micrographic surgery for lentigo maligna and lentigo maligna melanoma. A follow-up study. *Dermatol Surg*. 1998;24:673–677.
51. Kim J, Taube JM, McCalmont TH, et al. Quantitative comparison of MiTF, Melan-A, HMB-45 and Mel-5 in solar lentigines and melanoma in situ. *J Cutan Pathol*. 2011;38:775–779.
52. Christensen KN, Hochwalt PC, Hocker TL, et al. Comparison of MITF and Melan-A immunohistochemistry during Mohs surgery for lentigo maligna-type melanoma *in situ* and lentigo maligna melanoma. *Dermatol Surg*. 2016;42:167–175.
53. Trimble JS, Cherpelis BS. Rapid immunostaining in Mohs: current applications and attitudes. *Dermatol Surg*. 2013;39:56–63.
54. Swetter SM, Tsao H, Bichakjian CK, et al. Guidelines of care for the management of primary cutaneous melanoma. *J Am Acad Dermatol*. 2019;80:208–250.
55. Bricca GM, Brodland DG, Ren D, Zitelli JA. Cutaneous head and neck melanoma treated with Mohs micrographic surgery. *J Am Acad Dermatol*. 2005;52:92–100.
56. Cheraghlou S, Christensen SR, Agogo GO, Girardi M. Comparison of survival after Mohs micrographic surgery vs wide margin excision for early-stage invasive melanoma. *JAMA Dermatol*. 2019;155:1252–1259.
57. Zalla MJ, Lim KK, Dicaudo DJ, Gagnot MM. Mohs micrographic excision of melanoma using immunostains. *Dermatol Surg*. 2000;26:771–784.
58. Bub JL, Berg D, Slee A, Odland PB. Management of lentigo maligna and lentigo maligna melanoma with staged excision: a 5-year follow-up. *Arch Dermatol*. 2004;140:552–558.
59. Johnson TM, Headington JT, Baker SR, Lowe L. Usefulness of the staged excision for lentigo maligna and lentigo maligna melanoma: the "square" procedure. *J Am Acad Dermatol*. 1997;37:758–764.
60. Abdelmalek M, Loosemore MP, Hurt MA, Hruza G. Geometric staged excision for the treatment of lentigo maligna and lentigo maligna melanoma: a long-term experience with literature review. *Arch Dermatol*. 2012;148:599–604.
61. Gaudy-Marqueste C, Perchenet AS, Tasei AM, et al. The "spaghetti technique": an alternative to Mohs surgery or staged surgery for problematic lentiginous melanoma (lentigo maligna and acral lentiginous melanoma). *J Am Acad Dermatol*. 2011;64:113–118.
62. Moyer JS, Rudy S, Boonstra PS, et al. Efficacy of staged excision with permanent section margin control for cutaneous head and neck melanoma. *JAMA Dermatol*. 2017;153:282–288.
63. Whalen J, Leone D. Mohs micrographic surgery for the treatment of malignant melanoma. *Clin Dermatol*. 2009;27:597–602.
64. Trotter MJ. Melanoma margin assessment. *Clin Lab Med*. 2011;31:289–300.

65. Soleymani T, Aasi SZ, Novoa R, Hollmig ST. Atypical Fibroxanthoma and Pleomorphic Dermal Sarcoma: Updates on Classification and Management. *Dermatol Clin*. 2019;37:253–259.
66. Foroozan M, Sei JF, Amini M, et al. Efficacy of Mohs micrographic surgery for the treatment of dermatofibrosarcoma protuberans: systematic review. *Arch Dermatol*. 2012;148:1055–1063.
67. Bogucki B, Neuhaus I, Hurst EA. Dermatofibrosarcoma protuberans: a review of the literature. *Dermatol Surg*. 2012;38:537–551.
68. Loghdey MS, Varma S, Rajpara SM, et al. Mohs micrographic surgery for dermatofibrosarcoma protuberans (DFSP): A single-centre series of 76 patients treated by frozen-section Mohs micrographic surgery with a review of the literature. *J Plast Reconstr Aesthet Surg*. 2014;67:1315–1321.
69. Houdek MT, Tsoi KM, Mallett KE, et al. Surgical outcomes of primary dermatofibrosarcoma protuberans: A retrospective, multicenter study. *Ann Surg Oncol*. 2022;29:8632–8638.
70. van Houdt WJ. Margins in DFSP reconsidered: primum non nocere. *Ann Surg Oncol*. 2020;27:634–636.
71. Badhey A, Tikhtman R, Tang A. Management of dermatofibrosarcoma protuberans. *Curr Op Otolaryngol Head Neck Surg*. 2021;29:278–282.
72. Tan WP, Barlow RJ, Robson A, et al. Dermatofibrosarcoma protuberans: 35 patients treated with Mohs micrographic surgery using paraffin sections. *Br J Dermatol*. 2011;164:363–366.
73. Chaput B, Filleron T, Le Guellec S, et al. Dermatofibrosarcoma protuberans: margins reduction using slow-Mohs micrographic surgery. Experience with 35 patients. *Ann Chir Plast Esthet*. 2014;59:219–225.
74. O'Connor WJ, Roenigk RK, Brodland DG. Merkel cell carcinoma. Comparison of Mohs micrographic surgery and wide excision in eighty-six patients. *Dermatol Surg*. 1997;23:929–933.
75. Shaikh WR, Sobanko JF, Etzkorn JR, et al. Utilization patterns and survival outcomes after wide local excision or Mohs micrographic surgery for Merkel cell carcinoma in the United States, 2004–2009. *J Am Acad Dermatol*. 2018;78:175–177. e173.
76. Wilkerson E, Knackstedt R, Vidimos A, et al. A retrospective cohort study of comprehensive peripheral and deep margin assessment in merkel cell carcinoma: standard margins may be unreliable. *J Am Acad Dermatol*. 2021;84:570–572.
77. Kyllo RL, Brady KL, Hurst EA. Sebaceous carcinoma: review of the literature. *Dermatol Surg*. 2015;41:1–15.
78. Brady KL, Hurst EA. Sebaceous carcinoma treated with Mohs micrographic surgery. *Dermatol Surg*. 2017;43:281–286.
79. Tolkachjov SN. Adnexal carcinomas treated with Mohs micrographic surgery. *Dermatol Surg*. 2017;43:1199–1207.
80. Bernstein SC, Roenigk RK. Leiomyosarcoma of the skin: treatment of 34 cases. *Dermatol Surg*. 1996;22:631–635.
81. Lam C, Wilkinson M, Billingsley E. Mohs micrographic surgery for cutaneous metastasis of breast cancer. *Dermatol Surg*. 2013;39:1537–1539.
82. Alam M, Ricci D, Havey J, et al. Safety of peak serum lidocaine concentration after Mohs micrographic surgery: a prospective cohort study. *J Am Acad Dermatol*. 2010;63:87–92.
83. Mason SE, Noel-Storr A, Ritchie CW. The impact of general and regional anesthesia on the incidence of post-operative cognitive dysfunction and post-operative delirium: a systematic review with meta-analysis. *J Alzheimers Dis*. 2010;22:67–79.
84. Pedersen T, Eliasen K, Henriksen E. A prospective study of mortality associated with anaesthesia and surgery: risk indicators of mortality in hospital. *Acta Anaesthesiol Scand*. 1990;34:176–182.
85. Maragh SL, Otley CC, Roenigk RK, Phillips PK. Antibiotic prophylaxis in dermatologic surgery: updated guidelines. *Dermatol Surg*. 2005;31:83–91.
86. Alam M, Lee A, Ibrahimi OA, et al. A multistep approach to improving biopsy site identification in dermatology: physician, staff, and patient roles based on a Delphi consensus. *JAMA Dermatol*. 2014;150:550–558.
87. Vidimos AT, Stultz TW. Imaging in cutaneous oncology: radiology for dermies. *Dermatol Clin*. 2011;29:243–260.
88. Humphreys TR, Shah K, Wysong A, et al. The role of imaging in the management of patients with nonmelanoma skin cancer: When is imaging necessary? *J Am Acad Dermatol*. 2017;76:591–607.
89. Todd MM, Lee JW, Marks VJ. Rapid toluidine blue stain for Mohs' micrographic surgery. *Dermatol Surg*. 2005;31:244–245.
90. Randle HW, Zitelli J, Brodland DG, Roenigk RK. Histologic preparation for Mohs micrographic surgery. The single section method. *J Dermatol Surg Oncol*. 1993;19:522–524.
91. Trimble JS, Cherpelis BS. Rapid immunostaining in Mohs: current applications and attitudes. *Dermatol Surg*. 2013;39:56–63.
92. El Tal AK, Abrou AE, Stiff MA, Mehregan DA. Immunostaining in Mohs micrographic surgery: a review. *Dermatol Surg*. 2010;36:275–290.
93. Miller CJ, Sobanko JF, Zhu X, et al. Special stains in Mohs surgery. *Dermatol Clin*. 2011;29:273–286.
94. Campbell T, Armstrong AW, Schupp CW, et al. Surgeon error and slide quality during Mohs micrographic surgery: is there a relationship with tumor recurrence? *J Am Acad Dermatol*. 2013;69:105–111.
95. Bouzari N, Olbricht S. Histologic pitfalls in the Mohs technique. *Dermatol Clin*. 2011;29:261–272.
96. Mehrany K, Weenig RH, Pittelkow MR, et al. High recurrence rates of squamous cell carcinoma after Mohs' surgery in patients with chronic lymphocytic leukemia. *Dermatol Surg*. 2005;31:38–42.
97. American Academy of Dermatology. Position statement on appropriate uses of paraffin sections in association with Mohs micrographic surgery 2011. (www.aad.org/forms/policies/Uploads/PS/PS-Appropriate Uses of Paraffin Sections in Association with Mohs Mircographic Surgery.pdf).
98. Snow SN, Stiff MA, Bullen R, et al. Second-intention healing of exposed facial-scalp bone after Mohs surgery for skin cancer: review of ninety-one cases. *J Am Acad Dermatol*. 1994;31:450–454.
99. Sniezek PJ, Brodland DG, Zitelli JA. A randomized controlled trial comparing acetaminophen, acetaminophen and ibuprofen, and acetaminophen and codeine for postoperative pain relief after Mohs surgery and cutaneous reconstruction. *Dermatol Surg*. 2011;37:1007–1013.
100. Alam M, Ibrahim O, Nodzenski M, et al. Adverse events associated with Mohs micrographic surgery: multicenter prospective cohort study of 20,821 cases at 23 centers. *JAMA Dermatol*. 2013;149:1378–1385.
101. Merritt BG, Lee NY, Brodland DG, et al. The safety of Mohs surgery: a prospective multicenter cohort study. *J Am Acad Dermatol*. 2012;67:1302–1309.
102. Cook-Norris RH, Michaels JD, Weaver AL, et al. Complications of cutaneous surgery in patients taking clopidogrel-containing anticoagulation. *J Am Acad Dermatol*. 2011;65:584–591.
103. Bordeaux JS, Martires KJ, Goldberg D, et al. Prospective evaluation of dermatologic surgery complications including patients on multiple antiplatelet and anticoagulant medications. *J Am Acad Dermatol*. 2011;65:576–583.
104. Whitaker DC, Grande DJ, Johnson SS. Wound infection rate in dermatologic surgery. *J Dermatol Surg Oncol*. 1988;14:525–528.
105. Busam KJ, Hester K, Charles C, et al. Detection of clinically amelanotic malignant melanoma and assessment of its margins by in vivo confocal scanning laser microscopy. *Arch Dermatol*. 2001;137:923–929.



eFig. 150.1 Perineural involvement by various cutaneous tumors. A Basal cell carcinoma with a halo of basal cells enveloping a cutaneous nerve (frozen section). **B** Squamous cell carcinoma surrounding nerve fiber (frozen section). **C** Microcystic adnexal carcinoma with perineural invasion (formalin-fixed).



eFig. 150.2 Histopathologic challenges in Mohs surgery. A Incomplete histologic margins (e.g. due to a small portion of missing epidermis) can lead to false-negative readings. **B** Electrocoagulation artifact. **C** Gelfoam artifact. **D** Incidental syringoma can lead to false-positive reading. **E** Floaters can lead to false-positive readings. *A, Courtesy Clark C. Otley, MD, and Randall K. Roenigk, MD.*

MOHS MICROGRAPHIC SURGERY – CHALLENGES, PITFALLS, AND RECOMMENDATIONS		
	Challenges/pitfalls	**Recommendations**
Technical		
Tissue characteristics	• Photodamaged skin is more fragile and will tear and fragment • Sebaceous skin	• Careful curettage • Iris scissors to remove layer
	• Complex tissue location (e.g. inner ear) and components such as muscle, cartilage and bone (latter must be decalcified before sectioning)	• Iris scissors to remove layer • 15c blade to remove layer • "Hockey stick" beaver blade
	• Fatty tissue requires intense freezing, which can lead to an increase in epidermal freeze artifacts, tissue fractures, and specimen chipping	• Define tumor with curette and only remove what is necessary
Debulking	• Curettage may cause irregular borders, epidermal loss, or induce floaters* • Within layer, excess epidermal tissue centrally can be pushed down to cut margin and interpreted as tumor	• Only curette when indicated • Saline irrigation • Cut off any attached tumor
Excising	• Cutting into cancerous tissue if bevel <15°	• Bevel angle of 30° to 45°
	• Tissue has thick and tall edges if bevel angle >45°	• Use relaxing incisions on tissue to allow the epidermis to lie flat
	• Cutting marginal surfaces when making the relaxing incisions	• Make relaxing incisions near the center of the layer
Electrocoagulation	• Excessive electrocoagulation can cause elongation of the nuclei and cytoplasm of epidermal keratinocytes in addition to basement membrane retraction artifact	• Use of lidocaine with epinephrine (adrenaline) allows constriction of blood vessels and less need for electrocoagulation
Orienting	• Tissue rotation	• Double hash or asymmetric hash marks
	• Induction of floaters when making hash marks	• Saline irrigation • Ink marker[e2]
Mapping	• Inaccurate mapping	• Consistency
Sectioning	• Tissue lacerations mistaken for hash marks	• Caution when grasping tissue with forceps
Inking	• Placing ink on wrong margin	• Per CLIA requirements, inking performed by either surgeon or other qualified laboratory personnel
	• Inadequate inking	• Consistent process
	• Ink running into the wrong section	• High quality ink
Tissue flattening and freezing	• Ice crystal formation if specimen frozen too slowly, leading to cracks and hole in the specimen	• Appropriate temperature is –22° to –30°C
	• Curling of tissue if blades are not cold enough	• Cold cutting blades
Cutting	• Tearing or curling of tissue	• Sharp blades • Check blade for nicks
	• Specimen too thin or too thick	• Loose screws can result in a thick specimen • Adjust blade angle
	• Floaters	• Clean blades
	• Chatter or incomplete sections due to dull blades	• Change blades
Slide fixation	• Artifact due to short dehydration time	• Appropriate dehydration time
	• Tissue doesn't attach or falls off due to defects on the slides	• Check for defects on the slide; use charged or adhesive coated slides
	• Errors in labeling	• Proper labeling
Staining[e3]	• Weak or excessive staining	• Identify problematic step
	• Artifacts due to not enough time for dehydration	• Complete dehydration
	• Floaters if staining solution is contaminated	• Change staining solution frequently
Cover slipping	• Bubbles	• Align with length of slide and closely roll onto slide
	• Water beads	• May have skipped xylene clearing step while staining[e3]
Pathologic interpretation (Fig. 150.8)		
Floater[e4,*]	• Curettage	• Wipe blade between cuts when separating the layer into subunits • Change blade between layers • Saline irrigation after excision
	• Orientation marks	• Process layer in one piece • Ink marker
	• Cutting	• Keep the blades clean
	• Inking	• Change inking solution frequently

eTable 150.1 Mohs micrographic surgery – challenges, pitfalls and recommendations.

Continued

MOHS MICROGRAPHIC SURGERY – CHALLENGES, PITFALLS, AND RECOMMENDATIONS		
	Challenges/pitfalls	**Recommendations**
Missing epidermis[94,e5] = false negative	• Aggressive curettage	• Attention to margin of tumor
	• Incomplete margin around site of debulking	• Bevel blade
	• Tissue edges do not lie flat	• Relaxing cuts
Dermal tissue drop-out[94,e5] = false negative	• Inadequate freezing of tissue	• Freeze tissue appropriately • Assure full section is cut
Inflammation vs tumor	• Inflammation can obscure or resemble the tumor, especially SCCs	• Examine deeper section within block • Immunostaining • Awareness of patient's comorbidities (e.g. CLL)
Unexpected pathology	• Frozen pathology incongruent with biopsy report • Superficial or partial biopsy[e6,e7]	• Confirmation of biopsy site • Collision tumor (Fig. 150.9) • Send tissue for FFPE sections • Immunostaining
BCC vs benign entities	• Tangentially sectioned hair follicles mimic BCC • Benign folliculocentric proliferation	• Examine multiple sections • Look for retraction and stromal changes of BCC
BCC vs other neoplasms	• Trichoepithelioma, spiradenoma, cylindroma, MAC, and metastatic breast cancer may resemble BCC	• Examine multiple sections • Thaw the block and send for FFPE sections • Immunostaining
AK vs SCCIS vs SCC	• Misreading AK for SCCIS or reverse	• Standardize definition of AK and SCCIS
	• Missing SCC clumps within the dermis	• Evaluate the dermis carefully for cells of SCC • Immunostaining
SCC vs benign conditions	• Healing wound and biopsy sites mistaken for SCC	• Identify biopsy site grossly and microscopically
	• Tangential sectioning of epidermis resembling SCC	• Examine multiple sections for lumina, fragments of hair, and hair papillae
SCC vs other neoplasms	• Inflamed seborrheic keratosis or verruca vulgaris mistaken for SCC • Adnexal tumor mistaken for SCC	• Examine multiple sections • Thaw the block and send for FFPE sections • Immunostaining
Perineural invasion	• Missing perineural invasion • Mistaken as peritumoral fibrosis, reparative perineural proliferation, or epithelial sheath neuroma	• High index of suspicion in invasive SCC • Examine multiple sections • Consider processing final full margin via FFPE sections • Immunostaining
Infiltrative tumors	• Missing subtle cords and nests of infiltrative BCC or MAC within the dermis	• Toluidine blue staining[e1] • Send for FFPE sections (Fig. 150.5D)
Melanoma	• Difficulty recognizing atypical melanocytes • Lack of cellular detail	• Immunostaining • Discuss with dermatopathologist • "Slow Mohs" or geometric staged excision
Other tumors	• Skip areas in Merkel cell carcinoma, EMPD, and sebaceous carcinoma • Scar mistaken for DFSP • Normal pilar apparatus mistaken for leiomyosarcoma	• Awareness of potential for false-negative clear margin in multifocal tumors • Consider an additional excision of margins for FFPE sections • Immunostaining
*Floaters are dislodged pieces of tissue that occur during excision, embedding, cutting or staining that can hinder histologic interpretation in frozen sections.		

eTable 150.1 Mohs micrographic surgery – challenges, pitfalls and recommendations. AK, actinic keratosis; BCC, basal cell carcinoma; CLL, chronic lymphocytic leukemia; DFSP, dermatofibrosarcoma protuberans; EMPD, extramammary Paget disease; FFPE, formalin-fixed, paraffin-embedded; MAC, microcystic adnexal carcinoma; SCC, squamous cell carcinoma; SCCIS, squamous cell carcinoma *in situ*. *Adapted from Bernstein SC, Roenigk RK. Leiomyosarcoma of the skin: treatment of 34 cases. Dermatol Surg 1996;22:631–5; and Bouzari N, Olbricht S. Histologic pitfalls in the Mohs technique. Dermatol Clin 2011;29:261–72.*

E-REFERENCES

e1. Wang SQ, Goldberg LH, Nemeth A. The merits of adding toluidine blue-stained slides in Mohs surgery in the treatment of a microcystic adnexal carcinoma. *J Am Acad Dermatol*. 2007;56:1067–1069.
e2. Bagheri S, King T, Justiniano H, Eisen DB. Maintaining tissue orientation during mohs micrographic surgery: scalpel versus marker. *Dermatol Surg*. 2011;37: 1412–1416.
e3. Larson K, Ho HH, Anumolu PL, Chen TM. Hematoxylin and eosin tissue stain in Mohs micrographic surgery: a review. *Dermatol Surg*. 2011;37:1089–1099.
e4. Alam M, Shah AD, Ali S, et al. Floaters in Mohs micrographic surgery. *Dermatol Surg*. 2013;39:1317–1322.
e5. Lee KC, Higgins 2nd HW, Dufresne Jr. RG. Tumor recurrence after Mohs micrographic surgery. *J Am Acad Dermatol*. 2014;70:385–386.
e6. Mehregan DR, Dooley VN. How to get the most out of your skin biopsies. *Int J Dermatol*. 2007;46:727–733.
e7. Fernandez EM, Helm T, Ioffreda M, Helm KF. The vanishing biopsy: the trend toward smaller specimens. *Cutis*. 2005;76:335–339.

151 Surgical Complications and Optimizing Outcomes

Stacy L. McMurray and Anna S. Clayton

Key features

- A thorough preoperative assessment of the patient is required to increase the probability of a successful outcome for any surgical procedure
- Attention to detail, selection of the simplest procedures that will produce the desired result, and meticulous intraoperative technique will prevent many complications
- Anticipation of avoidable complications and careful management of unavoidable ones optimize results
- Clear communication between patient and surgeon must begin before the start of the procedure and continue through every stage, including the recovery and healing phases
- Because many complications do not manifest until several days to months postoperatively, patients must be monitored periodically to ensure that all parties are satisfied with the final outcome

INTRODUCTION

Surgical complications are deviations from the original planned outcome, usually resulting from multiple interrelated events (Fig. 151.1). Although complications in dermatologic surgery are uncommon[1,2], potential complications can often be avoided or minimized with careful planning and meticulous technique.

Complications vary widely, from impacting cosmetic appearance to life-threatening. Life-threatening emergencies in cutaneous surgery are rare, but the surgeon must be prepared to deal with problems such as cardiac arrhythmias and anaphylaxis. Proper, well-maintained resuscitation equipment must be readily available, and staff should maintain Basic Life Support (BLS) training, including the use of an automated external defibrillator (AED). Physicians in offices where extensive cutaneous surgery is performed should also have Advanced Cardiac Life Support (ACLS) training.

A thorough preoperative assessment, including history and directed physical examination, can identify pre-existing conditions that may impact healing. Informed consent obtained at this time, and again just prior to the procedure, ensures that the patient has realistic expectations. This education minimizes future misunderstandings regarding known risks of the procedure.

Prevention of an unsatisfactory outcome starts during the planning stage and continues with good intraoperative surgical technique and postoperative care. Anticipation of avoidable complications and management of unavoidable ones optimizes results. Throughout the process, it is essential to involve patients in their care.

DISCUSSION

Preoperative Assessment

A thorough preoperative assessment is a valuable tool for identifying conditions that could lead to surgical complications. A simple preoperative questionnaire can be completed by the patient at the time of the initial evaluation. "Yes" or "no" answers to specific questions can indicate a need for further evaluation or for a change in the operative plan (Fig. 151.2).

Potential for bleeding

Although some bleeding is expected during any surgical procedure, excessive bleeding is a common complication. The discovery of a bleeding disorder prior to surgery allows for correction of the condition if it is reversible, or changing plans for surgery if it is not. The bleeding disorder may be due to abnormalities in the *coagulation cascade*, *platelets*, or both. Platelet disorders result from abnormalities in *production*, *survival*, or *function*.

Laboratory evaluation

If the history does not suggest a bleeding disorder and the patient is otherwise well, laboratory testing is usually unnecessary. Appropriate screening tests should be checked if there is suspicion for a hereditary or acquired bleeding disorder. A platelet count only identifies a quantitative abnormality. The bleeding-time test measures platelet function, but accurate determination of results is operator-dependent. An *in vitro* bleeding-time assay, the platelet function analyzer 100 (PFA-100), provides an easy method for rapidly assessing platelet function. Unlike the bleeding time, the PFA-100 can be performed on a collected blood specimen. Additional screening tests include a PT (prothrombin time) and an aPTT (activated partial thromboplastin time) to determine defects in the extrinsic and intrinsic coagulation pathways, respectively. The international normalization ratio (INR) is discussed in the next section.

Medications and dietary supplements

The preoperative assessment should include a review of medications and dietary supplements (see Table 133.3), in particular antiplatelet and anticoagulant medications. When these drugs are prescribed for cardiac or neurologic indications, discontinuation can potentially lead to serious events (e.g. coronary artery stent thrombosis). In general, surgeons should not discontinue these medications but should instead focus on intraoperative precautions, such as meticulous hemostasis and minimal undermining[3,4].

Aspirin and aspirin-containing products are well-documented sources of bleeding problems. Platelet aggregation is irreversibly altered when aspirin acetylates cyclooxygenase. Patients taking aspirin for general health benefits, rather than specific medical indications, may discontinue the aspirin from ≥10 days *before* until 5–7 days *after* surgery. *Nonsteroidal anti-inflammatory drugs* affect the same enzyme, although the block is neither as severe nor irreversible[5]. If possible, the patient should stop these medications 1–4 days prior to surgery, depending on the half-life of the drug.

Dipyridamole suppresses platelet aggregation by inhibiting phosphodiesterase and increasing cyclic adenosine monophosphate (cAMP) levels within platelets. It is used in combination with aspirin for secondary prevention of thromboembolic events. The antiplatelet effect of dipyridamole is less than that of aspirin, and it does not appear to increase bleeding complications[6].

Thienopyridines (e.g. *clopidogrel*, *ticlopidine*, *prasugrel*) irreversibly inhibit platelet aggregation via inhibition of $P2Y_{12}$, a platelet ADP receptor. *Cilostazol* is a selective type 3 phosphodiesterase inhibitor with weaker $P2Y_{12}$ inhibition; it is typically used for claudication. Normal platelet function usually returns 5–7 days after discontinuation. Despite the slightly increased risk of complications in patients receiving $P2Y_{12}$ inhibitors, these medications can typically be continued without significant issues[7,8].

Several studies have been published in the vascular, oral, orthopedic, and dermatologic surgery literature supporting the viewpoint that surgery can be performed without stopping *warfarin*. An INR should be checked prior to surgery. Most authors advocate an upper limit of 3 or 3.5[8–12]. The safety of dermatologic surgery with INRs >3.5 has not been well studied, though one study found a poor correlation between bleeding complications and INR levels, with complications also occurring in the setting of in-range INRs[13]. If warfarin is discontinued in consultation with the prescribing physician, it should be held for 4–5 days preoperatively. If a patient on warfarin develops significant

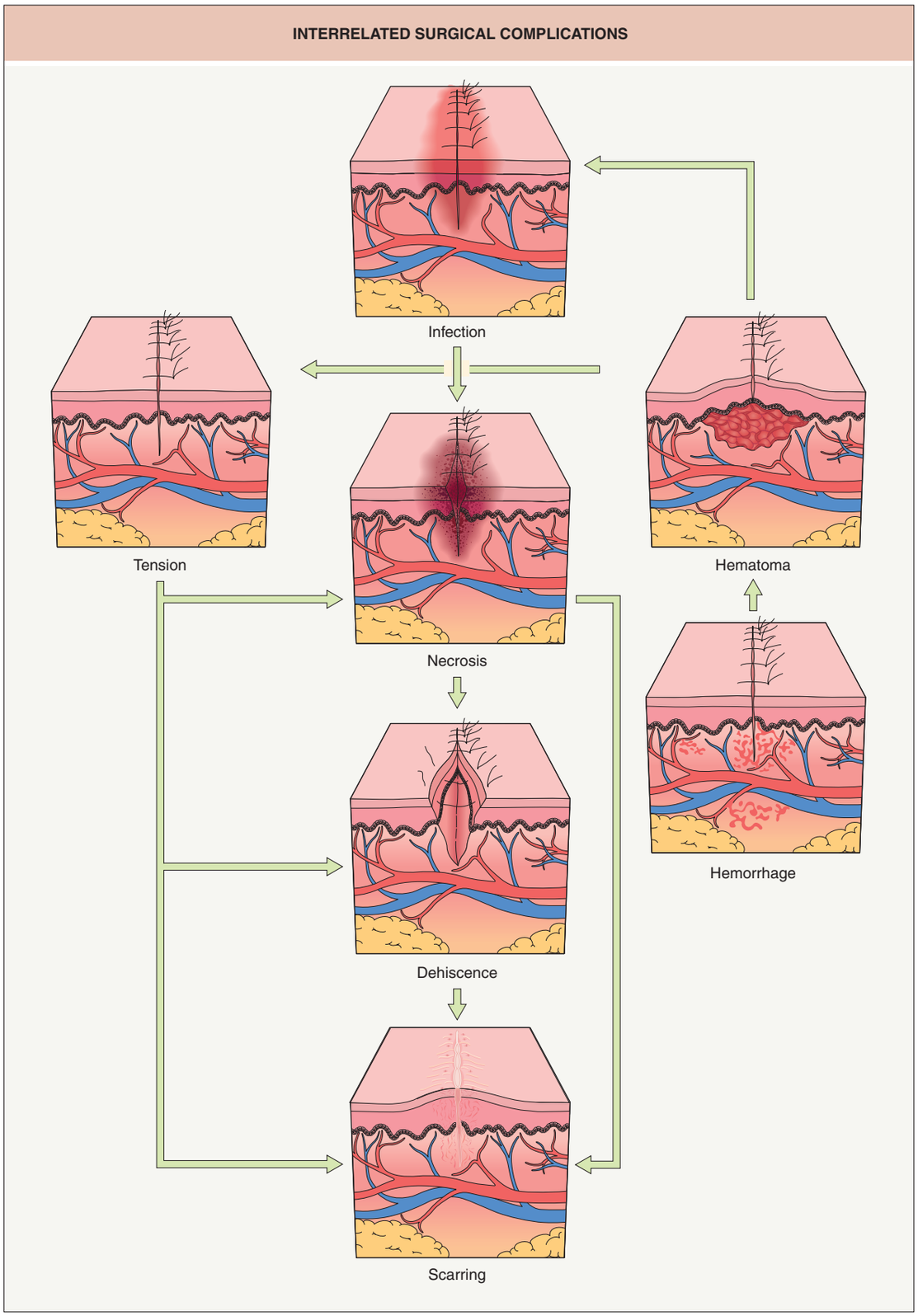


Fig. 151.1 Interrelated surgical complications.

postoperative bleeding, the anticoagulation can be reversed with one or more of the following: oral or intravenous vitamin K, fresh frozen plasma, and four-factor prothrombin complex concentrate.

Factor Xa inhibitors *apixaban* and *rivaroxaban* are often used as alternatives to warfarin while the direct thrombin inhibitor *dabigatran* is occasionally used as an alternative; this group of drugs is referred to as DOACs (direct oral anticoagulants; see Table 22.8 and Fig. 22.6). Literature remains sparse regarding these agents in dermatologic surgery. One large randomized trial of invasive, non-dermatologic procedures found similar rates of bleeding complications with warfarin versus dabigatran, but both medications were held preoperatively[14]. A more recent single-center, retrospective analysis found that patients receiving a DOAC at the time of Mohs micrographic surgery had a significantly greater risk for developing postoperative hemorrhagic complications compared to patients treated with traditional oral anticoagulants[15]. The authors recommend similar intraoperative precautions with these medications (see above). Idarucizumab is approved for reversing dabigatran, and andexanet alfa is a specific antidote for apixaban and rivaroxaban, but this is less of an issue because of their shorter half-lives of ≤12 hours.

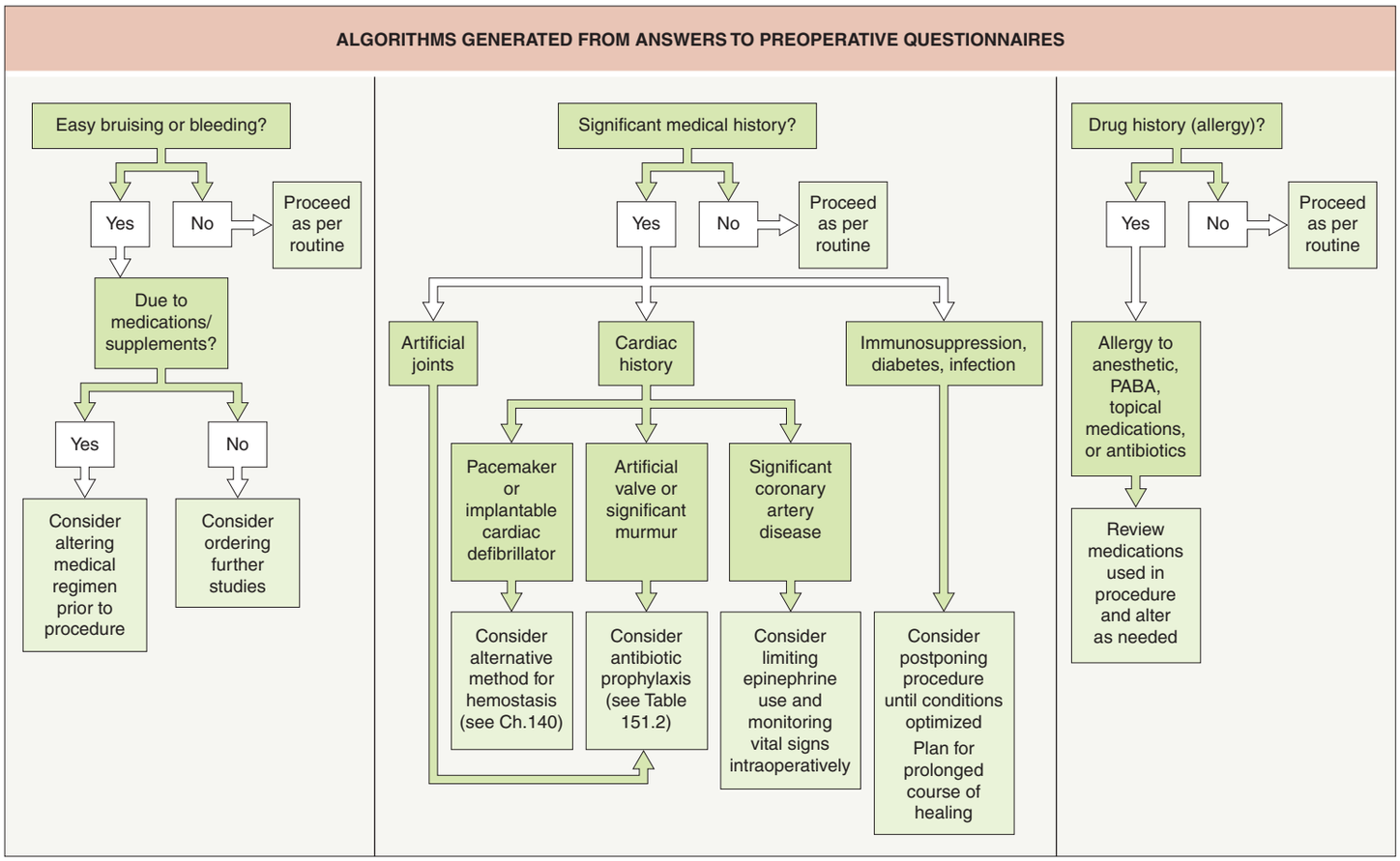


Fig. 151.2 Algorithms generated from answers to preoperative questionnaires. PABA, para-aminobenzoic acid.

Heparin acts as an antithrombin factor. Intravenous, unfractionated heparin has a short half-life of ~1 hour and can be rapidly reversed by intravenous protamine sulfate. *Low-molecular-weight heparin* (LMWH) has a half-life of 3–5 hours and is administered subcutaneously. Either form can be used to bridge patients in whom discontinuing warfarin preoperatively has been deemed necessary. LMWH is discontinued 24 hours prior to surgery, whereas unfractionated heparin is stopped five hours preoperatively. Either form of heparin is then restarted, together with warfarin, 24 hours post-procedure, with the heparin discontinued after a therapeutic INR has been attained.

Complementary and alternative therapies can inhibit platelet function or enhance anticoagulation. Common agents include *vitamin E*, *garlic*, and *eicosapentaenoic acid* (fish oil). Table 133.3 has a more comprehensive list of *dietary supplements* that have effects on platelet function and coagulation[16]. Patients should discontinue these supplements prior to surgery. More recently, enhanced bleeding has been observed in patients receiving *ibrutinib*, a Bruton tyrosine kinase (BTK) inhibitor used to treat lymphomas and chronic lymphocytic leukemia. This is thought to be related to the role of BTK and other kinases in platelet signaling pathways. This is less of an issue with second- and third-generation BTK inhibitors, e.g. acalabrutininib, zanubrutinib, pirtobrutinib.

Ethanol is a potent vasodilator that inhibits platelet aggregation and platelet granule release, as well as accentuating the increase in bleeding time caused by aspirin[17]. Excessive alcohol consumption may also decrease the patient's attention to optimal wound protection. Patients should be advised to avoid alcohol consumption during the immediate perioperative period.

Wound healing

The principles of wound healing are covered in detail in Chapter 141. To forestall complications due to poor wound healing, close attention should be paid to pre-existing medical conditions and medications that affect wound healing. Postponing surgery may be a wise decision for some patients. If the procedure cannot be postponed, the patient should be forewarned that the postoperative healing phase could be prolonged. Any chronic debilitating illness can predispose patients to secondary infections.

Systemic *corticosteroids* can delay healing and predispose patients to secondary infections. Patients on other immunosuppressive medications such as cyclosporine may also be prone to infections and prolonged healing. *Inhibitors of vascular endothelial growth factor* (VEGF), including monoclonal antibodies (e.g. *bevacizumab*) and oral tyrosine kinase inhibitors (e.g. *sorafenib*), have been associated with delayed healing and wound dehiscence (see Fig. 102.16). These agents should be held for at least 4–6 weeks prior to surgical procedures[18,19].

Cigarette smoking interferes with wound healing in a dose-dependent manner, and flaps or grafts are particularly susceptible[20–22]. Ideally, patients should avoid smoking for at least 3 weeks before surgery, but one study found that over 85% of smokers continued smoking preoperatively despite instructions to stop. At a minimum, patients should be strongly encouraged to decrease consumption to less than half a pack per day or switch to nicotine replacement patches for at least 2 weeks preoperatively and 1 week postoperatively[23,24]. Compared to cigarettes, the patches do not result in the high peak blood nicotine levels that lead to peripheral vasoconstriction and reduced wound tissue oxygen tension.

There is literature to support delaying cosmetic procedures for up to one year after cessation of *isotretinoin* therapy due to the risk of poor wound healing and the formation of excessive granulation tissue[25–27]. However, most reported problems have been individual case reports involving resurfacing procedures after courses of isotretinoin for acne therapy. More recent data from larger cohort studies suggest that procedures, including laser hair removal, dermabrasion, and laser resurfacing for acne scars, may be safe to perform during or shortly after a course of isotretinoin therapy[28–32].

Reactivation of herpes simplex virus (HSV) infection can dramatically interfere with the postoperative course. Patients with a history of herpes labialis or other facial herpetic infections should receive prophylactic antiviral therapy prior to dermabrasion, laser resurfacing, chemical peels, or surgery involving known trigger area(s). Antiviral therapy, such as oral valacyclovir 500 mg twice daily, should start on the day of the procedure and continue for 10 days postoperatively or until the skin has re-epithelialized[33]. Alternative regimens include oral famciclovir 250 mg three times daily or oral acyclovir 200 mg five times daily.

Prophylactic antibiotics

Antibiotic prophylaxis is administered to prevent surgical site infection, bacterial endocarditis, or infection in implanted prosthetic devices. The risk and consequences of infection must be weighed against the risk and cost of the antibiotic.

Wounds are placed into four general categories (Table 151.1). The majority of dermatologic surgical procedures are clean or clean-contaminated and do not need prophylaxis. However, prophylactic antibiotics may be helpful in certain clean-contaminated wounds. For example, antibiotics can be considered for procedures involving the oronasal mucosa, axilla, or anogenital region, although there are no controlled studies. Procedures that approach the ear canal may be at higher risk for infection with Gram-negative organisms. Long procedures are also more likely to develop wound infections: the infection rate almost doubles with each hour of operation. Prophylactic antibiotics are recommended for procedures at increased risk for surgical site infection, including surgery on the lower extremities or in the groin, wedge excisions of the lip or ear, flaps on the nose, all skin grafts, and in patients with extensive inflammatory skin disease[34]. When possible, prophylactic antibiotics should be prescribed in anticipation of these types of repairs. Unless the patient is in a special group (see below), some surgeons limit prophylactic antibiotics to just excisions on the lower extremities and ears, especially if the cartilage is exposed. Antibiotics are therapeutic, not prophylactic, for contaminated and infected wounds.

WOUND CLASSIFICATION		
Class	**Attributes**	**% that develop infections**
Clean	Immaculate technique Non-inflammatory	1–4
Clean-contaminated	Small breaks in technique Gastrointestinal, respiratory, or genitourinary tracts entered without gross contamination	5–15
Contaminated	Major breaks in technique Gross contamination from gastrointestinal, genitourinary, or respiratory tracts	6–25
Dirty and/or infected	Wound with acute bacterial infection ± pus	>25

Table 151.1 Wound classification[1]. Technique in the table refers to sterile surgical technique.

Two special patient groups should be considered for antibiotic prophylaxis: (1) those at risk for infective endocarditis; and (2) those at risk for bloodborne infection of total joint replacements (Table 151.2)[34]. In patients with total joint replacements or specific cardiac diseases, no prophylaxis is indicated if the surgical procedure is in a non-infected cutaneous site. In general, prophylactic antibiotics are no longer recommended by the American Academy of Orthopedic Surgeons and American Dental Association for patients with prosthetic joint replacements undergoing dental procedures; possible exceptions, including mucosal incision in a patient with a history of joint surgery complications, are outlined in Table 151.2[35,36]. However, to date, recommendations specific to dermatologic procedures are lacking. Table 151.3 summarizes suggestions for antibiotic prophylaxis regimens. If any question arises, consider consultation with the patient's cardiologist, internist, or orthopedic surgeon.

Implantable electronic medical devices

Cardiac defibrillators and pacemakers

The electrosurgical instruments often used in cutaneous procedures have the potential to interfere with the function of pacemakers and implantable cardioverter-defibrillators (ICDs), though the risk is quite low with modern devices (see Ch. 140)[37]. Alternatives to electrosurgery include battery-operated and AC-powered *thermal cautery units* that do not produce high-frequency electromagnetic interference (EMI) or electrical currents traversing the body. *Bipolar instruments* (e.g. forceps) concentrate the current across the tips, minimizing the chance of interference. If conventional electrosurgery is used, the active tip should not be applied within 5 cm of the implanted device whenever possible. Electrocoagulation should also be kept at as low a setting as possible and delivered in bursts lasting <5 seconds to minimize the chance of prolonged inhibition[38].

If conventional electrosurgery is used in a patient with an ICD, a contingency plan should be in place to deal with an arrhythmia should it occur, and an AED should be immediately available. If the device is deactivated or its function altered for the procedure, it is the surgeon's responsibility to ensure that patients return to their cardiologists within a reasonable time period for readjustment and evaluation.

Deep brain stimulators

There are few reports of patients undergoing dermatologic surgery who have an implanted deep brain stimulator (DBS). These devices are used to treat Parkinson disease and can be turned off with an external magnet if the resultant tremor does not interfere with surgery. Bipolar forceps or electrocautery are preferred to limit EMI. If a monopolar device is necessary, the dispersive plate should be positioned so that the pulse generator and lead wires are not located between the plate and the surgical site[39].

ANTIBIOTIC PROPHYLAXIS FOR DERMATOLOGIC SURGERY – PATIENT GROUPS AT RISK FOR INFECTIVE ENDOCARDITIS AND INFECTION OF TOTAL JOINT REPLACEMENTS
High-risk cardiac conditions (infected skin or breach of oral mucosa)
• Prosthetic heart valve or prosthetic material used in valve repair • History of infective endocarditis • Unrepaired cyanotic congenital heart disease (includes palliative shunts and conduits) • Completely repaired congenital heart defects with prosthetic materials or devices* • Repaired congenital heart disease with residual defects at or adjacent to site of prosthetic patch or prosthetic device • Cardiac transplant recipients who develop cardiac valvulopathy
Prosthetic joint replacements *(infected skin, breach of oral mucosa†; non-infected site at high risk of surgical site infection†)*
• First 2 years after joint placement • Previous prosthetic joint infections • Type 1 diabetes mellitus • Immunosuppression (HIV infection, medications, underlying malignancy) • Malnourishment • Hemophilia
*First 6 months after procedure (surgical or catheter intervention). †The American Academy of Orthopedic Surgeons (AAOS) and American Dental Association no longer recommend the general use of prophylactic antibiotics in patients with prosthetic joints undergoing dental procedures, but they can be considered for patients with a history of complications associated with their joint replacement surgery who are undergoing procedures such as gingival manipulation or mucosal incision[35,36]; however, to date, there are no AAOS recommendations specific to non-infected, high-risk sites.

Table 151.2 Antibiotic prophylaxis for dermatologic surgery – patient groups at risk for infective endocarditis and infection of total joint replacements. HIV, human immunodeficiency virus. Adapted from the American Heart Association, the American Dental Association, the American Academy of Orthopedic Surgeons, and reference 34.

RECOMMENDATIONS FOR ANTIBIOTIC PROPHYLAXIS IN PATIENTS AT RISK FOR INFECTIVE ENDOCARDITIS AND INFECTION OF TOTAL JOINT REPLACEMENTS			
Surgical site/ procedure	**Allergy**	**Antibiotic**	**Dose†**
Non-oral – wedge excisions of lip or ear, nasal flaps, all grafts	None	Cephalexin* or dicloxacillin*	2 g PO
		– *or* –	
		cefazolin/ceftriaxone*	1 g IM/IV
Non-oral – wedge excisions of lip or ear, nasal flaps, all grafts	Penicillin	Clindamycin or azithromycin/ clarithromycin*	600 mg PO 500 mg PO
		– *or* –	
		clindamycin	600 mg IM/IV
Oral mucosa breached	None	Amoxicillin	2 g PO
		– *or* –	
		cefazolin/ceftriaxone or ampicillin	1 g IV/IM 2 g IV/IM
Oral mucosa breached	Penicillin	Clindamycin or azithromycin/ clarithromycin	600 mg PO 500 mg PO
		– *or* –	
		clindamycin	600 mg IM/IV
Lesions in the groin or on the legs	None	Cephalexin* or TMP–SMX DS	2 g PO 1 tablet PO
		– *or* –	
		ceftriaxone*	1–2 g IV
Lesions in the groin or on the legs	Penicillin	TMP–SMX DS or levofloxacin*	1 tablet PO 500 mg PO
		– *or* –	
		clindamycin and gentamicin	600 mg and 2 mg/kg IV

*In communities with increased risk for methicillin-resistant *Staphylococcus aureus*, consider prophylaxis with TMP–SMX DS (1 tab PO) or clindamycin (600 mg PO).
†Give single dose (PO, IM or IV) 30–60 minutes before procedure.

Table 151.3 Recommendations for antibiotic prophylaxis in patients at risk for infective endocarditis and infection of total joint replacements[34]. IM, intramuscular; IV, intravenous; PO, by mouth; TMP–SMX DS, trimethoprim–sulfamethoxazole double-strength.

Cochlear implants

Cochlear implants (CIs) provide a sense of sound by direct stimulation of the auditory nerve. They consist of an external part that sits behind the ear and another part implanted below the skin. While potential for EMI exists, there are limited studies examining electrosurgery in patients with CIs. The British Cochlear Implant Group and CI manufacturer guidelines recommend against the use of monoterminal electrosurgery in the head and neck region; biterminal electrosurgery can be used safely if not within 1 to 2 cm of the CI[39]. A conservative approach may be prudent, with use of electrosurgical instruments below the clavicles and only electrocautery in the vicinity of the implant.

Nerve stimulators

Implantable nerve stimulators (e.g. vagal nerve, sacral nerve, phrenic nerve, spinal cord stimulators) are now available for a variety of indications. There are also implantable neurostimulators (e.g., NeuroPace® RNS® System) for epilepsy. Some of these devices can be temporarily turned off during electrosurgery without adverse effects. Electrocautery is recommended when possible to minimize risk of EMI. Other techniques to minimize interference include use of bipolar forceps and positioning of dispersive pads away from the implanted device. When in doubt, the authors advise consultation with the prescribing physician for further recommendations.

Allergies

True allergic reactions to local anesthetics may be type I (immediate) or type IV (delayed-type hypersensitivity) (see Ch. 143). Patients with a type IV sensitivity to one major group of local anesthetics (ester or amide) are usually not allergic to members of the other group. Type I reactions are more commonly associated with the ester anesthetics and their para-aminobenzoic acid (PABA) metabolite. Although the lack of cross-reactivity between ester and amide anesthetics is true for type IV sensitivity, it has not been adequately studied for anaphylaxis. If there is a possible history of a type I amide allergy, referral to an allergist for a progressive challenge protocol can be considered. It is important to consider the possibility that the allergic reaction is due to the preservative (e.g. methylparaben, metabisulfite). Use of preservative-free anesthetics can resolve this problem.

Epinephrine (adrenaline) is a vasoconstrictive agent commonly added to local anesthetics to reduce bleeding and prolong the duration of anesthesia. Patients occasionally report a history of an "allergy" to local anesthetic, describing their symptoms as palpitations, headache, tachycardia, tachypnea, or tremor (see Ch. 143). Such reports likely represent reactions to epinephrine given in high doses or inadvertently injected intravascularly. Since the half-life of epinephrine in serum is short, specific therapy for these reactions is usually not necessary. In order to avoid them, the lowest dosage and concentration of epinephrine (<1:100 000) should be used, and injection of significant amounts intravascularly should be avoided using proper infiltration technique[40].

Another common systemic side effect often mistaken as an allergic reaction is the vasovagal reaction. The patient recalls becoming pale, sweaty, and lightheaded, perhaps even fainting. Hypotension can occur, but in contrast to a true toxic or allergic reaction, the pulse is slow and regular (see Table 143.2). Urinary incontinence and abnormal limb movements may occur during a vasovagal reaction and are not diagnostic of seizure activity[41]. Treatment consists of keeping the patient supine or in the Trendelenburg position and giving reassurance. Once the patient has recovered, they can gradually sit up and ambulate.

Chlorhexidine gluconate is a frequently utilized surgical skin preparation (see Table 146.6). It is a broad-spectrum antibacterial of the halogenated phenol class. Despite its very weak sensitizing potential, it has been reported to cause allergic contact dermatitis[36,42]. Similar reactions have occurred with the iodophor povidone–iodine (Betadine®)[43]. Both compounds can be skin irritants, especially when occluded. Care must be taken to remove all traces of cleanser prior to dressing application.

Topical antibiotics can cause allergic contact dermatitis. Although neomycin is the most common sensitizer, bacitracin can also cause sensitization. Co-reactivity against both neomycin and bacitracin is common. Cross-sensitivity between neomycin, gentamicin, kanamycin, streptomycin, and tobramycin can occur. Mupirocin or erythromycin ointment are alternatives if the patient is allergic to both neomycin and bacitracin. As there is no convincing evidence that topical antibiotic ointments prevent infection, plain petrolatum ointment may be the best agent for wound dressing.

Informed consent

The lines of communication should be open between the surgeon and the patient before the procedure begins. The physician should explain the condition, how it affects overall health, risks and benefits of the procedure, and treatment alternatives in layman's terms. Common complications (e.g. bleeding, infection, allergic reactions, scarring) and strategies for dealing with them should also be discussed. In turn, the patient must accept responsibility for preoperative preparation and postoperative wound care. When complications arise, as they inevitably will, the surgeon should be honest with the patient about treatment options and outcomes.

Intraoperative Considerations

Contamination

The risk of infection in cutaneous surgery is very low. Two often-cited studies estimated the risk at 2.3%–2.4%[44,45], but more recent data suggest the rate is likely <1%[46,47]. Wound infections usually do not become evident until 4–8 days postoperatively, but in most cases the infection truly begins at the time of surgery. The surgical team should prepare the surgical field and wear the correct protective equipment to reduce the incidence of infection.

The skin cannot be sterilized, but the majority of the resident flora and pathogenic bacteria can be removed with mechanical cleansing and antiseptic agents. The extent of skin preparation varies with the invasiveness and complexity of the proposed surgical procedure. A 2-second wipe with 70% isopropyl alcohol or a 10-second cleansing with an iodophor swab is adequate for superficial biopsies. Chlorhexidine is the most frequently utilized preoperative preparation for skin surgery. It produces rapid destruction of a wide range of Gram-positive and Gram-negative bacteria, and it binds with the protein of the stratum corneum, providing residual action. However, chlorhexidine is irritating to the conjunctiva and toxic to the cornea, tympanic membrane, and middle ear; caution must be exercised in these areas. Iodophors are another excellent antiseptic; one advantage is that the prepared area is readily apparent because of the brownish-orange color. They are effective against Gram-positive and Gram-negative bacteria and some fungal spores, but iodophors have a slower and shorter duration of action than chlorhexidine. As noted earlier, they can cause irritant or allergic contact dermatitis. There are also rare reports of anaphylaxis to chlorhexidine used as a surgical scrub.

Use of a surgical mask may help protect the patient from surgical personnel with active upper respiratory tract infections. The mask protects the surgical team from contamination by saliva droplets or blood from the patient. It is also essential to protect the eyes from accidental splashes of body fluid. Appropriate personal protective equipment is advocated in all surgical situations as part of universal precautions. In cases where sterility is not necessary, non-sterile examination gloves can be used. Recent data suggest that Mohs micrographic surgery can be performed as a clean procedure with low infection rates[48].

For all surgical procedures, proper handling of sharps is essential. Needles should never be recapped, and blades should not be changed by hand. Despite best intentions, needlestick injuries may still occur, and surgeons must have a plan for testing and treatment when appropriate (Table 151.4). The current recommendations for treating needlestick injuries are available online from the National Institute for Occupational Safety and Health (OSHA) or from the Clinicians' Post-Exposure Prophylaxis Hotline (PEPline) at 1-888-448-4911.

Bleeding and hemostasis

Hemostasis can be approached based on the amount of bleeding encountered (Fig. 151.3). Bleeding that occurs during shave biopsies can be controlled through the use of mechanical pressure, topical hemostatic agents such as aluminum chloride, or electrodesiccation. Bleeding during more extensive procedures may require suturing, use of other hemostatic agents (Table 151.5), electrocoagulation, or a combination of techniques.

Intraoperative bleeding can obscure the surgical site and can be bothersome to both the surgeon and the patient. If bleeding continues after closure, it may result in a hematoma that can lead to infection, increased tension on wound edges, dehiscence, flap necrosis, and graft loss (see Fig. 151.1). A careful history assists in identifying patients prone to bleeding. When not contraindicated (e.g. procedures on toes or fingers in patients with peripheral vascular disease), use of epinephrine with the anesthetic is helpful (see Ch. 143). Suction provides good visualization in an otherwise bloody field. An assistant can place traction across the wound surface or pressure at the periphery of the site. Frequent blotting with sponges or cotton-tipped applicators also helps to keep the field clear.

Bleeding should be controlled promptly; individual small vessels should be isolated and precisely cauterized (to avoid excessive char) or ligated. It may be prudent to ligate visible vessels lying adjacent to the wound bed as they might be nicked or partially cut during the procedure. Large vessels noted in the surgical wound should be tied off or cauterized at both visualized ends if the surgeon is sure there is adequate collateral circulation to the area. Tying off visible vessel ends using a figure-of-eight technique with an absorbable suture provides reliable hemostasis (see Fig. 146.2). Of note, bleeding, which may not be apparent at the time of the closure, may develop once the effect of epinephrine diminishes. The surgeon must ensure that the surgical field is as dry as possible prior to closure. Particular attention should be paid to apices, where visualization can be more difficult, or cut muscle that can steadily ooze.

If, at the beginning of the procedure, bleeding is more than usual, undermining should be minimized, and a linear closure should be

TRANSMISSION OF VIRAL INFECTIONS VIA NEEDLESTICK INJURIES

Viral infection		Transmission risk	Postexposure prophylaxis (PEP)	Comments	Follow-up laboratory evaluation
Human immunodeficiency virus (HIV)		0.3%	• 3 (or more) antiretroviral drugs* • Preferably begun within hours of exposure • Four-week course, if tolerated • Discontinued if source patient determined to be HIV-negative	• HIV testing: rapid test for HIV Ab or p24 Ag/HIV Ab test • Expert consultation, especially if source patient has resistant disease, exposed person is pregnant or breastfeeding • Counseling, including prevention of secondary transmission, drug toxicities	HIV testing: • baseline, 6 weeks, 12 weeks, and 6 months postexposure unless 4th-generation p24 Ag/HIV Ab test utilized, then baseline, 6 weeks, and 4 months (see Fig. 78.3) • at any time if acute retroviral syndrome suspected
Hepatitis B virus (HB, Hep B)	Source patient: HBsAg + HBeAg –	1%–6%	• *If unvaccinated, incomplete series*†, *or known vaccine non-responder*, HBIG ×1 and first dose of Hep B vaccine series, both within 24 hours • *If known responder to Hep B vaccine*‡, no treatment	• If antibody response of exposed person unknown, test for anti-HBs Ab • Similar protocol if exposed person pregnant or breastfeeding • Refrain from donating blood, plasma, organs, tissue, or semen	Anti-HBs Ab titer 2 months after completing vaccine series (4 months if received HBIG)
	Source patient: HBsAg + HBeAg +	~20%–30%			
Hepatitis C virus (Hep C, HCV)		1.8%	Not recommended	• Risk may be limited to hollow-bore needlesticks • Test source patient for anti-HCV Ab¶	Anti-HCV Ab titer¶ and serum ALT level: • baseline and 4–6 months HCV RNA levels: 4–6 weeks

*Currently recommended 3-drug regimen (2016): raltegravir 400 mg po twice daily (or dolutegravir 50 mg daily) plus Truvada®, 1 tablet po once daily (contains tenofovir 300 mg and emtricitabine 200 mg).
†Complete series = 3 doses.
‡Serum HBs Ab ≥ 10 mIU/ml.
¶Confirm positive ELISA results with supplemental test, e.g. recombinant immunoblot assay.

Table 151.4 Transmission of viral infections via needlestick injuries. Ab, antibody; Ag, antigen; HBIG, hepatitis B immune globulin; s, surface. *Adapted from Updated U.S. Public Health Service Guidelines for the Management of Occupational Exposures to HBV, HCV, and HIV and Recommendations for Postexposure Prophylaxis. MMWR 2013;62(RR10);1–19; Kuhar DT, Henderson DK, Struble KA, et al. Updated US Public Health Service guidelines for the management of occupational exposures to human immunodeficiency virus and recommendations for postexposure prophylaxis. Infect Control Hosp Epidemiol 2013;34:875–92.*

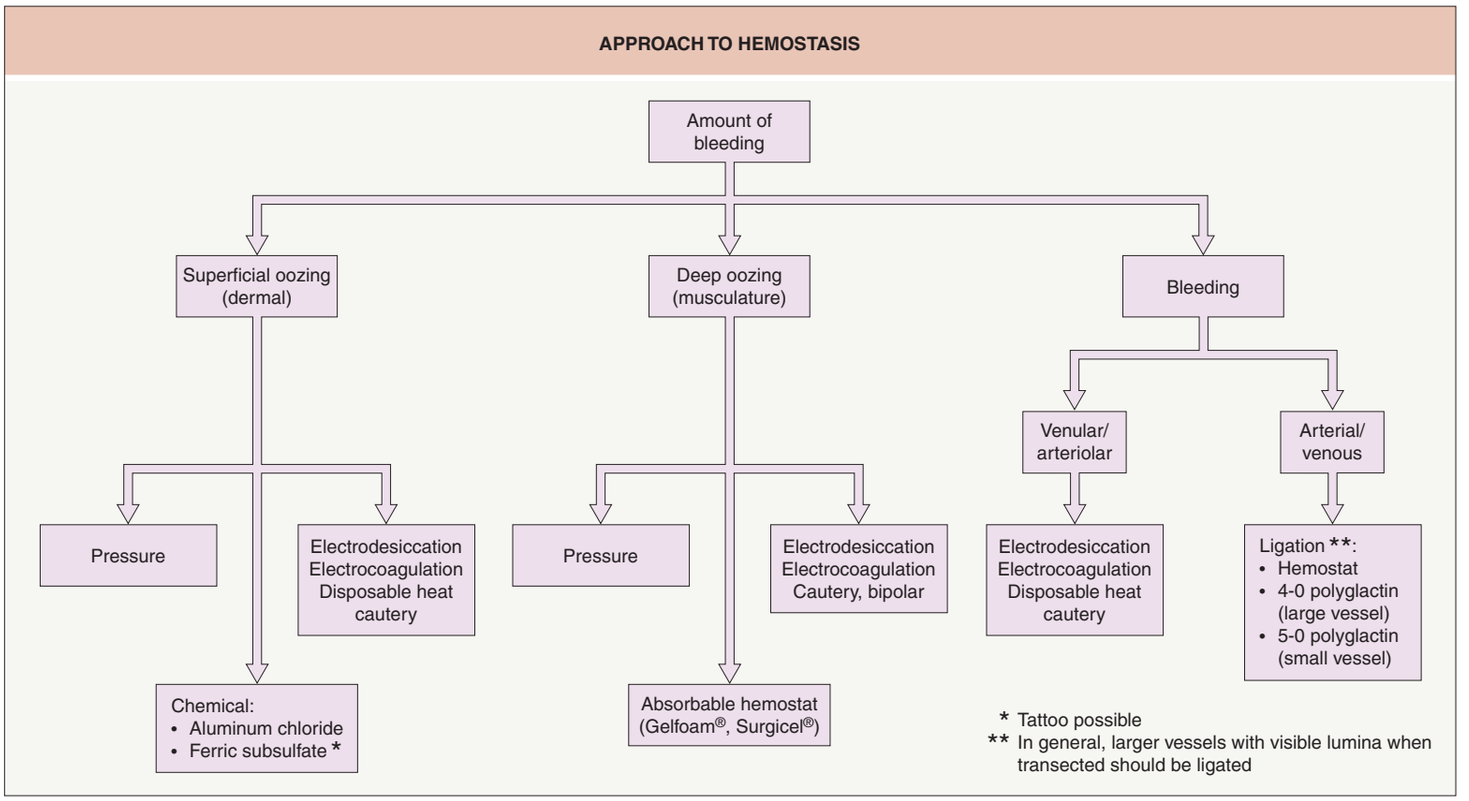


Fig. 151.3 Approach to hemostasis. *Courtesy Glenn Goldman, MD.*

HEMOSTATIC AGENTS			
Generic name	**Trade name®,™**	**Advantages**	**Disadvantages**
Bone wax	Bone wax	Effectively controls bony surface bleeding (skull)	Impedes bacterial clearance; nidus for infection
Gelatin foams, gelatin sponges	Gelfoam, Gelfilm, Surgifoam	Non-antigenic; absorbed within 4–6 weeks; controls small vessel and bony bleeding	Significant swelling occurs
Oxidized cellulose	Surgicel	Low pH has antimicrobial effect; dissolves in 2–6 weeks	May cause foreign body reaction; may not combine with thrombin
Microfibrillar collagen	Avitene, Helistat, Instat, Collastat	Swelling not significant; absorbed in <8 weeks	Less effective in thrombocytopenic patients
Thrombin	Thrombin-JMI, Evithrom, Recothrom	Fast; controls minor capillary and small venule bleeding	Do not use in individuals who react to human blood products
Thrombin with gelatin	Surgiflo, Floseal	Controls moderate arterial bleeding	Can swell up to 20%; needs contact with blood which serves as fibrinogen source
Fibrin sealants	Tisseel, Evicel, Vistaseal	Controls venous oozing from raw surfaces	Can be denatured by antiseptics containing alcohol, iodine, or heavy metal ions
Ferric subsulfate (20% solution)	Monsel's solution	Inexpensive; low pH resists bacterial contamination	Can cause tattoo/discoloration; for superficial oozing
Silver nitrate (applicator sticks)		Easily stored; some bacteriostatic properties	Tattoo risk; for superficial oozing
Aluminum chloride (20%–40% solution)	Drysol (20%)	Inexpensive	Some formulations flammable; may delay wound healing; for superficial oozing
Powders composed of hydrophilic polymers with potassium salts	QR powder	Fast, inexpensive	Can only be used on wounds healing by second intention
Powders composed of microporous polysaccharide hemospheres	Arista AH	Absorbed by body so can be used on wounds that will be closed	

Table 151.5 Hemostatic agents.

considered over a flap or graft. Blood easily accumulates unnoticed in non-visualized "dead space". Drain placement should be considered for larger flaps or complex multilayered linear closures to avoid hematoma formation. Drains can be open or closed systems. An open system, such as a Penrose drain, lacks an enclosed network or collecting system. It is a passive drain that allows fluids to flow by gravity into gauze. For dermatologic surgery, a fenestrated small Penrose drain can often suffice (Fig. 151.4). It should be removed after 24–48 hours, once the chance for hematoma formation has diminished. Closed systems, such as the Mini-Flap wound suction drain and the Jackson–Pratt drain, are sealed,

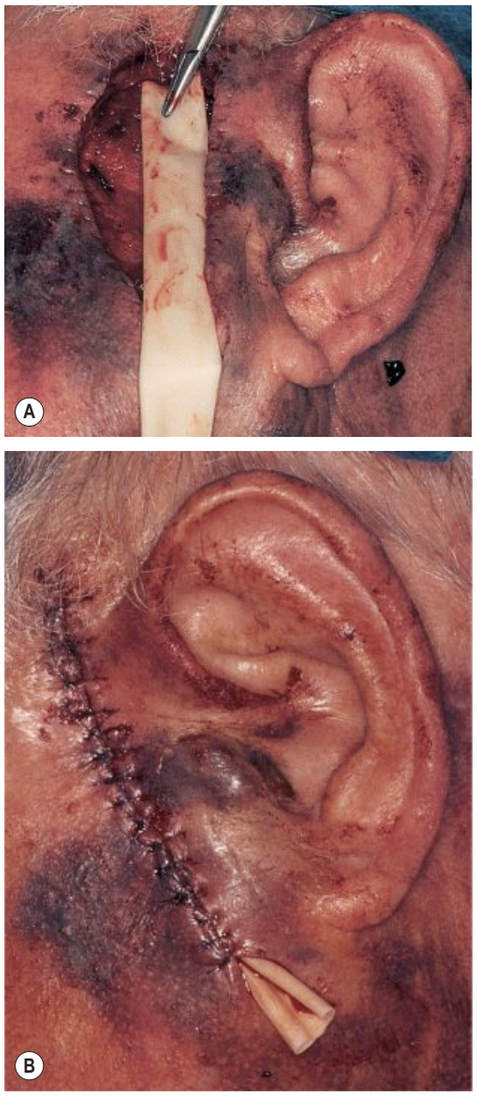


Fig. 151.4 Placement of Penrose drain because of excessive bleeding. *Courtesy Thomas Stasko, MD.*



Fig. 151.5 Postoperative appearance of wound closed under tension with resulting necrosis. *Courtesy Thomas Stasko, MD.*

with a draining tube connected to a container. Active suction draws the fluid from the tissue cavity into the container. In open wounds that bleed despite adequate attempts at hemostasis, hemostatic agents such as gelatin foams (Gelfoam®), oxidized cellulose (Oxycel®, Surgicel®), microfibrillar collagen (Avitene™, Collastat®), or topical thrombin can be applied to the wound. These agents provide a matrix to speed coagulation (see Table 151.5)[49,50]. Caution should be exercised when using oxidized cellulose because excessive amounts can result in foreign body reactions[51].

Tissue injury

Some tissue injury is unavoidable during invasive procedures. Gentle handling of the wound edges minimizes trauma and allows the viable tissue to heal more rapidly. Skin hooks or single-toothed forceps should be used to grasp tissue without crushing it. Indiscriminate and excessive electrocoagulation should be avoided. Large areas of charred and necrotic tissue within the wound increase the risk of poor healing and infection[52].

Tension

Excessive tension at the closure site can lead to tissue necrosis and dehiscence (see Fig. 151.1). Postoperatively, tension can cause increased discomfort for the patient once the local anesthesia has dissipated. Surgeons tend to tighten surface sutures when wounds gape open, but such action can result in "train track" scars. Closures should be planned to minimize wound tension. Buried absorbable sutures should bear the tension, minimizing the need for tight surface sutures. Adequate undermining and appropriate orientation of the closure will help achieve maximal tissue movement. Instead of a linear closure, a flap or graft can minimize tension in appropriate circumstances. Relaxing incisions can also be performed 2–3 cm from the wound edge, parallel to the incision site, to share tension over a larger area. If the defect cannot be completely closed due to excessive tension, partial closure can be performed, and the remainder of the wound allowed to heal secondarily. If the site is chosen well (usually in concave areas), this method yields excellent cosmetic results. Intraoperative or preoperative tissue expansion may also allow for the safe closure of large defects[44]. If a wound appears too tight at the time of closure, it probably is.

Necrosis

Necrosis is usually the result of a hematoma, an infection, or wound tension compromising blood flow to the skin edge (see Fig. 151.1). Although pale tissue at a flap or wound edge may be a warning of compromised perfusion, actual necrosis will not become evident until the postoperative period (Fig. 151.5). The factors leading to necrosis, however, begin preoperatively. The hazards of smoking have been discussed previously, but they cannot be overemphasized. Smoking decreases perfusion and increases the risk of necrosis. Patients should be counseled repeatedly to stop, or at least decrease, their exposure to tobacco and nicotine-containing products (e.g. e-cigarettes).

The blood supply to the skin arises primarily from the subdermal plexus. Extensive superficial undermining may damage this plexus and the segmental arteries supplying it. Hematoma formation and even normal postoperative edema can compromise blood flow via pressure on this plexus. Sutures tied too tightly may also decrease perfusion. The use of a loop stitch, leaving space between the first and second loops of the surgeon's knot, allows for tissue expansion from postsurgical edema, decreasing the risk of tissue necrosis.

Surgical dogma long held that epinephrine was contraindicated in digits and other areas of limited collateral circulation. However, several reviews and one large series of 3110 consecutive patients have demonstrated that injecting anesthesia with epinephrine into digital skin is safe[45–47,53]. It would be reasonable, though not requisite, to use a more dilute epinephrine concentration in these areas (e.g. 1:500 000 instead of 1:100 000). Caution should still be exercised in patients with Raynaud phenomenon or other peripheral vascular disease.

Flap tips can become necrotic because of an inadequate blood supply. Exceeding the 3:1 length-to-base ratio decreases circulation to the distal tip. When correcting redundancies caused by rotation at the flap base, the surgeon must ensure that the pedicle is not narrowed excessively. Correction of the redundancy can be delayed to protect the vascular supply.

Grafts may become necrotic if an adequate blood supply from the wound bed is not established. In general, full-thickness skin grafts require more nutrients than split-thickness grafts (see Ch. 148). Areas with a poor or absent vascular supply, such as exposed bone, exposed cartilage, or sites of previous therapeutic radiation, often cannot support full-thickness grafts and may not fully support even split-thickness grafts. In particular, sites with greater than 1 cm^2 of exposed

bone or cartilage have a greater incidence of graft failure. Delaying graft placement for about 10 days may improve graft take.

The graft must also be well-apposed to the wound bed. Strict hemostasis is required to prevent blood from accumulating in the space between the graft and the wound. However, excessive electrocoagulation should be avoided because of the resultant necrotic debris. Absorbable hemostatic agents may also interfere with engrafting. The placement of basting sutures and tie-down bolsters increases contact between the graft and the wound bed (see Ch. 148).

Nerve deficits

The preoperative evaluation should include a quick survey of neurologic function in the areas potentially affected by the proposed procedure (e.g. lifting eyebrows, tightly closing eyelids, smiling). During surgery, sensory and motor nerves may be injured or cut (see Ch. 142). It is essential to document – and, more importantly, make the patient aware of – pre-existing deficits before infiltrating the anesthetic (see Ch. 143). Local anesthesia or nerve blocks can cause temporary deficits lasting 6–12 hours. However, full evaluation of nerve injuries may not be possible until several weeks after surgery.

Skin surgery will result in the transection of cutaneous nerves. Patients frequently note temporary *sensory* deficits at the site of primary closures or flaps and almost all will experience hypoesthesia in skin grafts. Most areas have diverse sensory innervation, and unless a major nerve is injured, there are very few significant permanent deficits. Sensory nerves often do regenerate, but this may take months to occur. The patient should be aware preoperatively that there may be paresthesias in the area as it heals. Occasionally, normal sensation never returns. Areas most prone to noticeable sensory defects are the digits, the forehead, and the scalp.

Injury to *motor* nerves can be more alarming, since this can result in paralysis of the denervated muscles. The closer the injury to the nerve root, the more severe the consequence. Thankfully, most of the larger branches of the facial nerve are deep to the muscle fascia and well protected. As a result, injuries to the main trunk of the facial nerve (or its zygomatic and buccal branches) rarely occur in dermatologic surgery.

The area of highest consequence on the cheek lies lateral to a line drawn from the lateral canthus of the eye to the angle of the mouth and medial to where the nerve divides into five major branches near the surface of the parotid gland (Fig. 151.6). Medial to this area, innervation is usually diverse enough to render the results of transection of a single nerve mild. Lateral to this area, the main trunk lies deep within the parotid gland and is relatively well protected[54]. Unless the procedure is a deep excision of an infiltrative skin cancer, the majority of cutaneous surgeons are unlikely to cause significant motor nerve injury except in the following important danger zones:

- The *temporal branch of the facial nerve* courses very superficially as it crosses the zygomatic arch and traverses the temple. Here it is covered only by the superficial temporalis fascia, with very little subcutaneous fat. The nerve lies deep to the superficial temporal artery. Paralysis of the frontalis muscle, manifesting as an inability to elevate the forehead, results from transection of the nerve in this location (Fig. 151.7A). This loss is often of only cosmetic concern; however, if there is pre-existing brow ptosis, the paralysis may result in a severe ptosis that interferes with vision and requires surgical correction with a browpexy.
- The *zygomatic branch of the facial nerve*. Damage to this nerve, although less common than damage to the temporal branch, impairs the function of the orbicularis oculi muscles. This can lead to an inability to completely appose the upper and lower eyelids and subsequent corneal desiccation.
- The *mandibular branch of the facial nerve* is subject to injury as it crosses the mandible, near the facial artery and vein. It is covered at this point only by skin and thin, variably present, platysma muscle. This nerve innervates the lip depressors, and injury can cause asymmetry visible when the patient smiles or grimaces. In addition, mouth function may be compromised, resulting in drooling.
- The *spinal accessory nerve* can be damaged as it exits from behind the sternocleidomastoid muscle at Erb's point in the posterior triangle of the neck. Damage paralyzes the trapezius muscle leading to winging of the scapula and difficulty abducting the arm. Pain frequently accompanies injury to the spinal accessory nerve.

The surgeon must be aware of these danger zones (see Fig. 151.6). Injury is sometimes unavoidable, especially if a neoplasm involves the nerve. Early consultation, even preoperatively, with the appropriate specialties (neurology, neurosurgery, radiation oncology) may allow for optimal management of the problems. Regeneration of motor nerves is possible but unpredictable. When major motor branches are cut, surgical reapproximation or nerve grafts may be necessary. Muscle stimulation may prevent atrophy while awaiting return of function. At times it may be practical to simply address the functional problems created, such as placing gold weights to allow eye closure (Fig. 151.7B).

Unsatisfactory scarring

Although scars do not acquire their final appearance until many months following surgery, operative techniques can greatly affect the appearance. Though scar spreading may be unavoidable in certain anatomic areas (e.g. upper trunk, shoulders), use of longer-lasting absorbable or non-absorbable sutures in the deeper layers of the closure can reduce the risk[55].

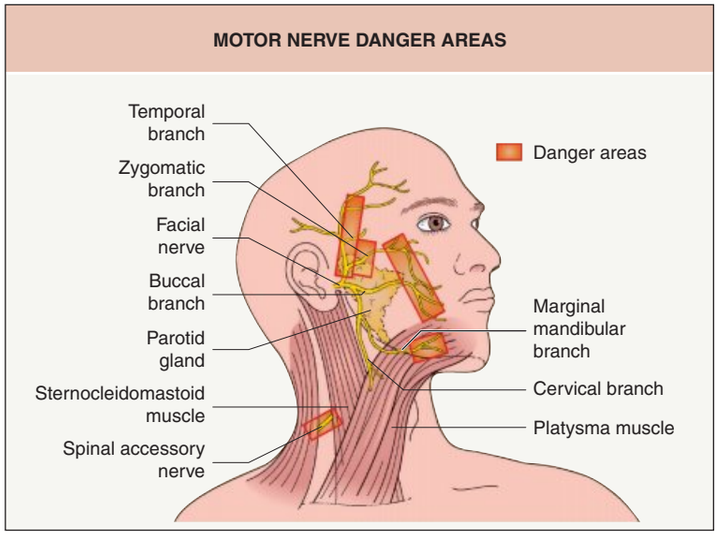


Fig. 151.6 Motor nerve danger areas.

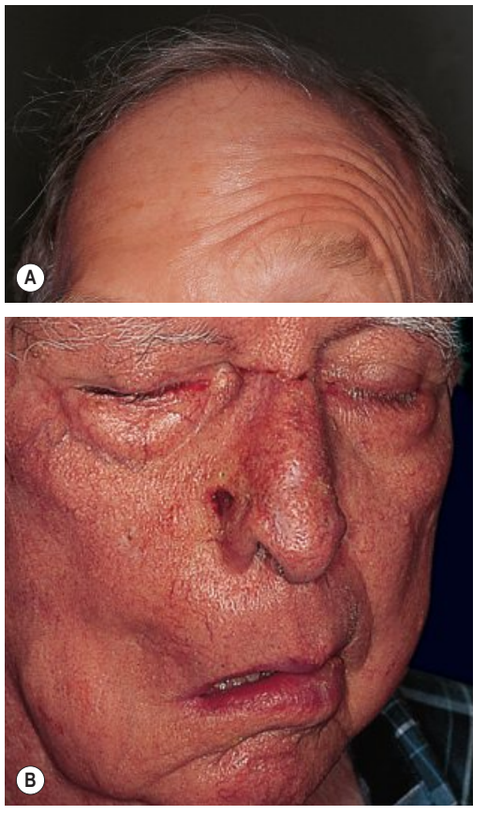


Fig. 151.7 Damage to the facial nerve. A Loss of the ability to elevate the right forehead due to transection of the right temporal branch. **B** Loss of function of the main branch of the right facial nerve. The ability to close the right eye has been restored by the placement of a gold weight in the eyelid. *Courtesy Thomas Stasko, MD.*



Fig. 151.8 "Trapdoor" or "pincushion" appearance of a flap reconstruction. *Courtesy Thomas Stasko, MD.*

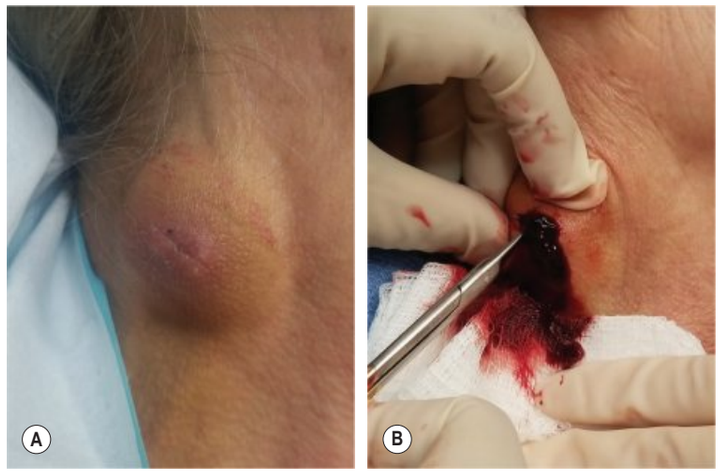


Fig. 151.9 Hematoma. A Postoperative hematoma formation. **B** Evacuation of gelatin-like clot.

A trapdoor or pincushion-like appearance may develop in transposition flaps (Fig. 151.8). Wide undermining at the time of repair, squaring off the corners, and basting sutures may reduce the incidence of this complication[56]. Removing excess subcutaneous tissue underneath the flap and trimming the flap to minimize redundancy may also help.

Postoperative Considerations

Before the patient leaves the office, detailed wound care instructions should be reviewed with the patient and caregiver(s). The surgeon must provide easily understood, written postoperative wound care instructions that include answers to the most commonly asked questions – for example, "How do I know if it is infected?", "How much bleeding is too much bleeding?", "When can I take a shower/bath?", "When can I play golf/tennis?". The patient should also have a direct method of contacting the physician or a suitable representative 24 hours a day if questions or concerns arise. A little foresight and education can greatly reduce the number of midnight calls and allow rapid identification and correction of complications. It is imperative that the contact physician be available and responsive. It is helpful for the physician or designee to call every patient postoperatively to check in and answer questions.

Bleeding/hematoma/ecchymosis

Some cases of postoperative bleeding will occur despite exhaustive preoperative evaluation, preparation, and careful intraoperative hemostasis. Most bleeding occurs within the first 24 hours, with the majority occurring within 6 hours. During this period, clots are fragile, and movement can easily dislodge them. As epinephrine from the local anesthetic dissipates, small vessel bleeding may increase. A pressure dressing applied immediately after the procedure helps prevent this problem. The patient should be instructed to leave the dressing in place for at least 24 hours. If the surgical procedure was more involved than a superficial shave or punch biopsy, the dressing should consist of multiple layers: petrolatum, then a non-adherent contact layer (e.g. Telfa™, CURAD® Non-Stick Pads), followed by a bulky absorbent layer (e.g. gauze, cotton, sponges, eye pads). An outer layer of tape or stretchable wrap (e.g. Ace Wrap®, Coban®) then covers all of these. The bandage should provide pressure but not cause ischemia.

A small amount of bleeding is normal; however, bleeding which soaks the dressing needs attention. The patient should be instructed to remove the old dressing, as saturated dressings no longer provide meaningful pressure, and apply firm pressure without release for 15–20 minutes as timed *by the clock*. If pressure stops the bleeding, then the dressing should be reinforced with additional gauze and tape. If bleeding persists at a reduced level, pressure should be reapplied for an additional 15–20 minutes. If bleeding persists, then the patient needs to be evaluated by the surgeon.

The surgeon can once again attempt direct pressure. If this fails, the wound should be exposed and the area re-anesthetized and explored. If a single bleeding vessel is identified, it can be electrocoagulated or ligated. Frequently, a single source is not identified. Bleeding can occur in multiple areas and each must be addressed. A drain may be helpful if a very dry surgical field cannot be achieved. If possible, surgical procedures should be scheduled early in the day to prevent late-night bleeding events.

If blood collects in the dead space of a wound, a hematoma forms. Hematomas can lead to dehiscence or necrosis due to pressure, and they may act as a nidus for infection (see Fig. 151.1). Hematomas consist of gelatin-like clots that are usually too firm to evacuate without removing sutures. The presenting symptom may be an acute, throbbing pain (large hematomas) or a pressure sensation (smaller hematomas). Early, expanding hematomas should be evacuated after re-anesthetizing the site. After evacuation (Fig. 151.9), the area should be irrigated, and any residual bleeding controlled. The wound may be re-closed, with particular attention to closing any dead space. Placing a drain is often appropriate. Many surgeons advocate empiric antibiotics after hematoma evacuation, because of an increased risk of infection.

If the hematoma goes unnoticed and untreated for several days, the clot becomes organized (Fig. 151.10A). It is then thick, fibrous, and adherent to the surrounding tissue. If large or actively expanding, it should still be evacuated (Fig. 151.10B). In most circumstances, the resulting wound should be allowed to heal by second intention with possible delayed closure or scar revision (Fig. 151.10C).

Small, organized hematomas can be allowed to resorb without evacuation. If, around 1–2 weeks later, there is significant liquefaction leading to a fluctuant mass, the fluid can be aspirated with a large bore (16- to 18-gauge) needle. Warm compresses applied for 30- to 60-minute intervals several times daily speed resolution.

Bromelain (bromelin), found in the pineapple plant, has long been used as a medicinal. One placebo-controlled study found that oral bromelain decreased the time required for resorption of surgery-associated hematoma. The recommended dose was 500 mg immediately postoperatively and then three to four times a day on an empty stomach until the hematoma resolved. Patients not allergic to pineapple reported no side effects[15].

Ecchymoses occur when there is leakage of a small amount of blood into the interstitial space. Significant bruising is common following surgical procedures involving areas with loose distensible tissue, such as the periorbital area, the neck, or the upper chest in the elderly. It can be alarming to the patient who is not counseled to expect this possibility. The involved area changes color from deep purple, black and blue, to green, and then to yellow as the hemoglobin is degraded to bilirubin. The ecchymosis can extend widely, usually migrating to dependent areas. The concern is mainly cosmetic as ecchymoses are temporary with most resolving without sequelae.

Infection

Although most cases of infection begin at the time of surgery, postoperative contamination is possible without good wound care. Blood-soaked dressings are breeding grounds for bacteria. Patients and caregivers

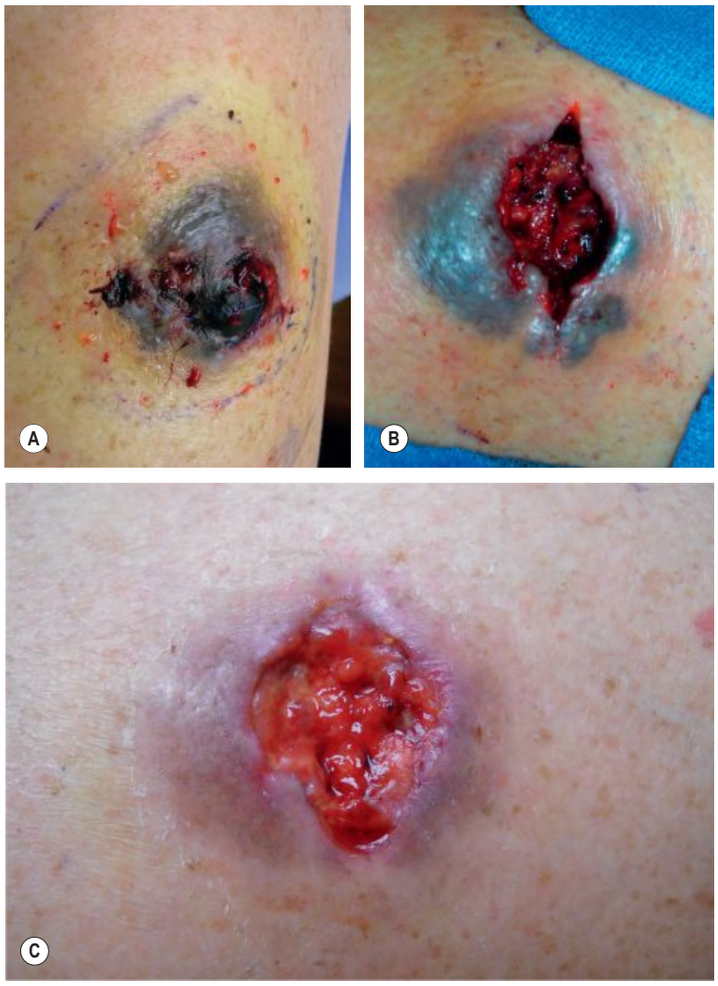


Fig. 151.10 Evacuation of an organized hematoma. Prior to (**A**) and immediately after (**B**) evacuation of the clot. **C** After 2 weeks of healing by second intention.

should be instructed to wash their hands carefully prior to changing any dressings or cleaning the wound site. Excessive exposure or manipulation of the wound site during the first 24–48 hours after the procedure should be avoided.

Infection usually does not become evident until 4–8 days after surgery. The patient may note increasing erythema (Fig. 151.11) and worsening pain and tenderness. Ascending red streaks (lymphangitis), swelling, and a purulent discharge may develop. Systemic symptoms of fever and chills indicate spread of the infection.

The area should be treated with rest, elevation, and heat. If the infection appears significant, sutures should be removed, and the defect left open. Abscesses should be drained, and the discharge sent for culture, primarily bacterial and occasionally also fungal. Deep cavities should be packed lightly with iodoform gauze with the packing changed daily until drainage stops. Antibiotics should be initiated based on the most likely causative organism(s) and then adjusted according to culture results.

Staphylococcus aureus is the most frequent culprit in the skin. A first-generation cephalosporin, a β-lactamase-resistant penicillin, or a penicillin/β-lactamase inhibitor combination would be an appropriate choice (see Ch. 127). If *Pseudomonas aeruginosa* is suspected, as in postoperative chondritis of the external ear, a fluoroquinolone would be appropriate. Rapid spread, systemic symptoms, or extensive lymphangitis may require parenteral antibiotics, more aggressive wound care, and possible hospitalization.

Given the rise in the incidence of methicillin-resistant *S. aureus* (MRSA), the surgeon should be aware of the rates of MRSA in the local community. After culture of the site, if there is a high index of suspicion for MRSA infection, empiric coverage with oral doxycycline, trimethoprim–sulfamethoxazole, or clindamycin should be considered.



Fig. 151.11 Wound infection and necrosis at full-thickness skin graft site. *Courtesy Thomas Stasko, MD.*



Fig. 151.12 Contact dermatitis to antibiotic ointment. *Courtesy Thomas Stasko, MD.*



Fig. 151.13 Inflammatory suture reaction. *Courtesy Thomas Stasko, MD.*

Penicillins and cephalosporins are considered safe during pregnancy by the American Academy of Pediatrics (formerly FDA category B). When indicated, safe second-line alternatives include erythromycin and clindamycin[57]. Tetracyclines (previous category D) are contraindicated beyond 15 weeks of gestation due to fetal risk of discoloration of teeth and inhibition of bone growth[58].

Contact dermatitis, candidiasis, or dermatophyte infections may mimic bacterial infection. Contact dermatitis due to topical antibiotics frequently presents with pruritus rather than pain and with erythema in all the areas of cream or ointment application (Fig. 151.12). Contact dermatitis from bandage adhesives will usually be strikingly limited to the area of adhesive contact. Inflammatory suture reactions can occur without infection (Fig. 151.13).

Necrosis

The earliest sign of necrosis may be pallor or cyanosis at the periphery of the flap or graft. Early intervention could include judicious suture removal or replacement to reduce tension, elevation to reduce edema and thereby improve blood flow, and gentle heat to the area to improve circulation. Treatment with hyperbaric oxygen may be considered in the face of early necrosis of a large or vital reconstruction.

Once necrosis is established, minimal cleaning and debridement should be undertaken until the full extent of necrosis is clearly demarcated. Vigorous debridement may extend the process further. An eschar

eventually forms and then separates from the wound base as the latter heals by second intention (Fig. 151.14). If infection is present, it should be treated appropriately. Delayed scar revision is an option if the site does not heal with an acceptable appearance.

Dehiscence

Wound edges separate because of excessive tension, infection, or necrosis (see Fig. 151.1; Fig. 151.15). Dehiscence most often occurs at the time of suture removal. Scar tensile strength never exceeds 80% of the strength of uncut skin, and maximum tensile strength is not achieved until months after the procedure. At 2 weeks after surgery, tensile strength is less than 10% of normal (Fig. 151.16)[59]. Patients should be told specifically which activities they may or may not undertake (i.e. no lifting more than "x" pounds, no running, no jogging, no sit-ups, etc.).

If prolonged support is needed, sutures may be removed in stages. Adhesive strips provide some short-lived support for 1–2 days after suture removal. If the wound opens at suture removal because of excessive tension or too much activity (Fig. 151.17), the surgeon can consider resuturing if there is no infection, hematoma, or necrosis. If dehiscence is due to another underlying complication, such as infection or hematoma, that condition should be treated first.

Wound appearance

Postoperative wound appearance may be a source of anxiety for both patient and surgeon. Problems range from simple (e.g. a spitting subcutaneous suture) to more complex (e.g. a trapdoor deformity or spread scar). A key to dealing with most of these problems is continued and open communication. The patient who does not feel free to express concerns in the office may all too readily do so elsewhere.

Buried sutures should be absorbed uneventfully by the body within the time period specified by the manufacturer. Unfortunately, nature does not always adhere to package inserts. As digestion of the suture takes place, pustules reflecting sterile abscesses or papules due to granulomatous inflammation can appear along the suture track (Figs. 151.18 & 151.19). In addition, sutures may extrude or be "spit" from the skin intact (Fig. 151.20); while some authors believe this is more likely to occur if the sutures are placed too superficially within the dermis, even deeply placed sutures can be extruded in some patients. These events may occur anywhere from 1 to 4 months postoperatively, most commonly at about 6 weeks. The pustules can be opened with a sterile needle and the remaining suture gently removed. Sometimes, the papules are deeper. If the appearance is consistent with a suture reaction, the patient can be reassured then instructed to gently massage the site. If the suture is protruding, it can be removed. The ultimate appearance of the scar is usually unaffected by this process.

In sites with severe photodamage (e.g. the shins in women), atypical squamous proliferations can appear at the margins of completely

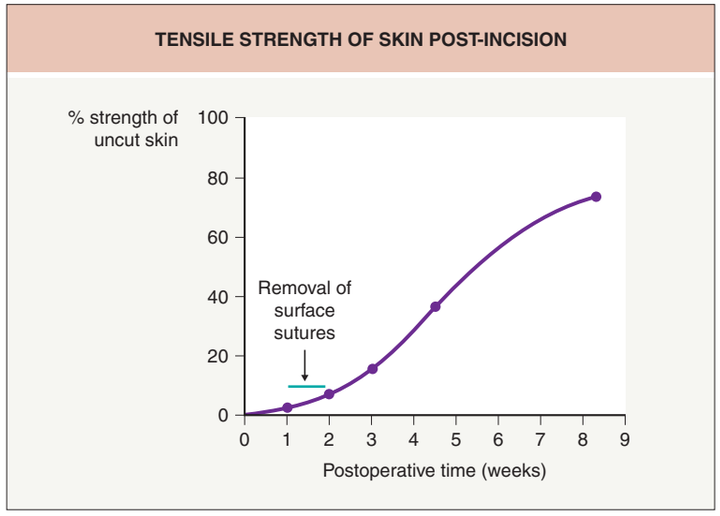


Fig. 151.16 Tensile strength of skin post-incision.



Fig. 151.14 Necrosis of a full-thickness skin graft. Two weeks after placement. *Courtesy Thomas Stasko, MD.*



Fig. 151.17 Wound dehiscence after suture removal.

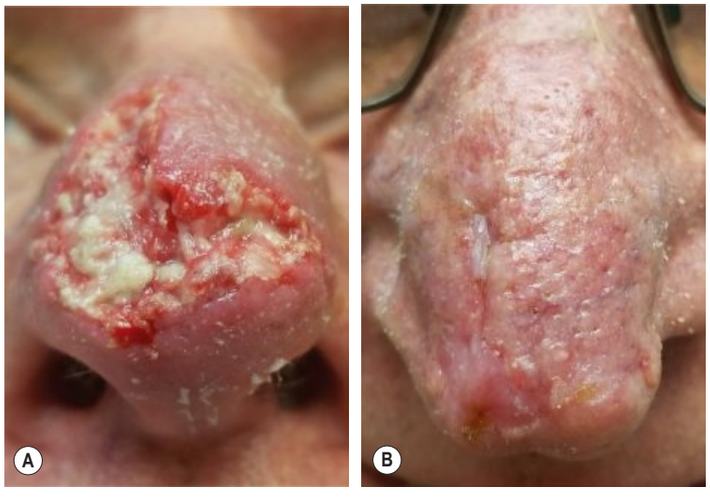


Fig. 151.15 Dehiscence and necrosis of a bilateral advancement flap of the nasal tip. A Initial dehiscence. **B** Follow-up after second intention healing with application of petrolatum; no additional interventions were performed.



Fig. 151.18 Granulomatous reaction to suture placement. Dull pink nodule with obvious spitting suture at the end of the incision line. *Courtesy Jean L. Bolognia, MD.*

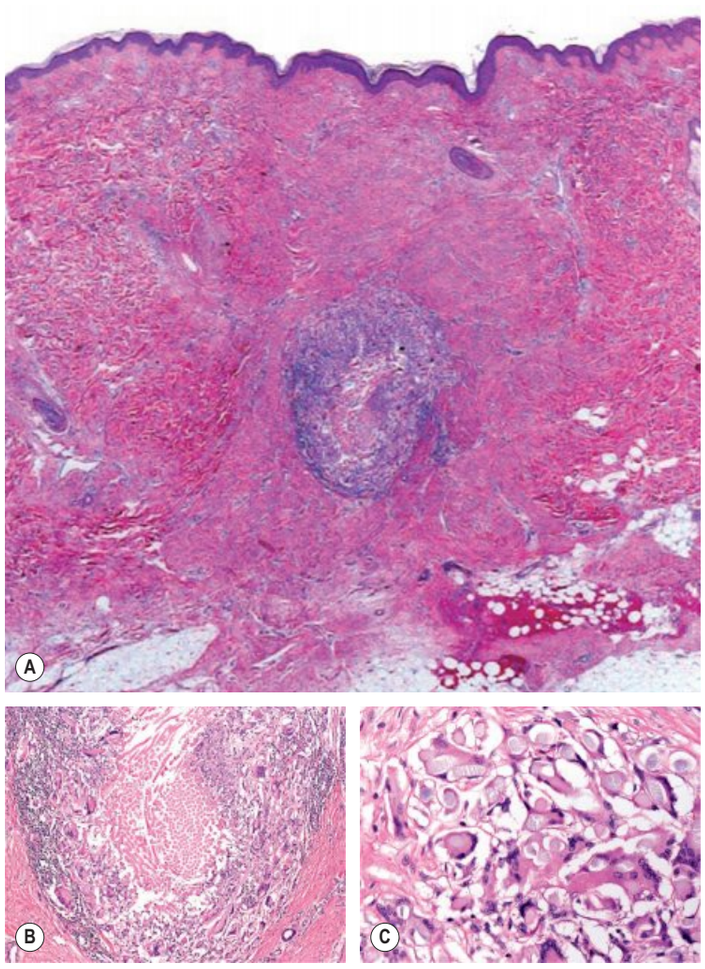


Fig. 151.19 Histologic features of a granulomatous reaction to braided suture material. A, B The suture material present within the dermis is cut both *en face* and longitudinally. On higher power, histiocytes and multinucleated giant cells surround the suture (**B**) and the giant cells have engulfed the suture material (**C**). *Courtesy Lorenzo Cerroni, MD.*

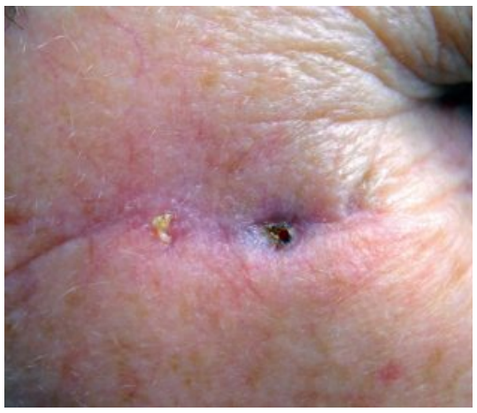


Fig. 151.20 Spitting absorbable suture within the incision line.

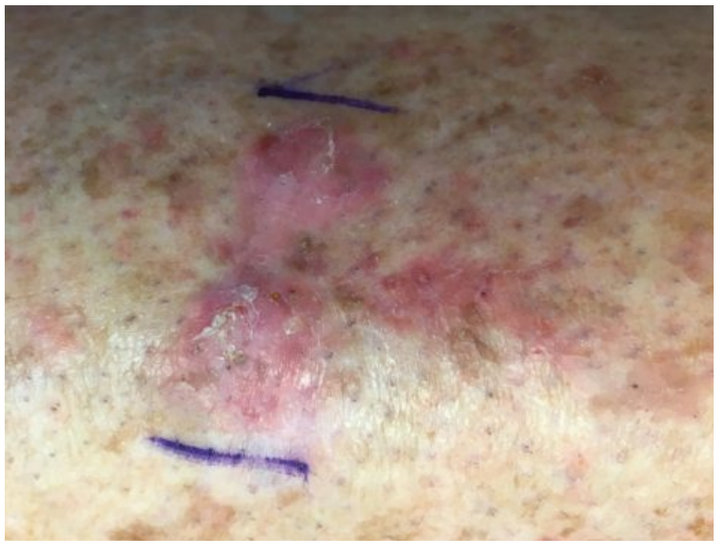


Fig. 151.21 Atypical squamous proliferations on the shin of a woman with severe photodamage. The nodules arose following complete surgical excision of a squamous cell carcinoma. Biopsy of one lesion confirmed the clinical diagnosis and the nodules resolved following two intralesional injections of triamcinolone and topical halbetasol. *Courtesy Jean L. Bolognia, MD.*



Fig. 151.22 Suture "tracks" in a spread scar. *Courtesy Thomas Stasko, MD.*



Fig. 151.23 Hypertrophic scar. One month after excisional surgery. *Courtesy Thomas Stasko, MD.*

excised skin cancers (Fig. 151.21). These lesions are likely triggered by inflammation and growth factors involved in wound repair. A biopsy can be performed, especially if the original tumor was a squamous cell carcinoma or keratoacanthoma. Treatment options include intralesional injections of triamcinolone, 5-fluorouracil, and methotrexate (see Table 108.9) or oral acitretin for more extensive involvement.

Suture tracks (railroad tracking) are caused by tight sutures left in place too long (Fig. 151.22). The best way to avoid this appearance is to minimize wound tension with proper placement of buried sutures in order to allow for early suture removal.

Some anatomic sites are more prone to the development of keloids and hypertrophic scars (Fig. 151.23), and some individuals may have a genetic predisposition to keloid development. Intervention at the early stages of a hypertrophic scar can yield a more acceptable result. High-potency topical or intralesional corticosteroids may decrease the thickness of the scar and the accompanying pain and pruritus. However, there is a risk of telangiectasias, atrophy, or widening of the scar[60]. Anecdotally, smaller hypertrophic scars may respond to simple massage, though the ideal duration and frequency have not been defined[61]. Silicone gel sheeting applied to the scars and worn for

12–24 hours per day for at least 2 months has been shown to improve the appearance of hypertrophic scars and keloids[62]. Simple occlusion and hydration may be just as effective without silicone[63]. One study using topical onion extract found that it was ineffective in improving erythema or pruritus of postsurgical scars, while petrolatum-based ointment alone did improve appearance[64].

Scar appearance can be improved by dermabrasion or ablative laser resurfacing. When performed during the 4- to 8-week interval following the initial injury, it superimposes the mechanisms of second intention wound healing on the remodeling phase of the primary scar. This appears to re-establish a normal-appearing epidermis across initial scar boundaries[65]. Lasers (e.g. carbon dioxide (CO_2) laser, 585 nm pulsed dye laser) may be used to improve the appearance of scars as well as in the treatment of hypertrophic scars and keloids (see Ch. 137)[66].

Keloids develop more frequently on the earlobes, neck, and trunk. In predisposed individuals, even superficial shave biopsies can result in keloids. Patients at risk should be counseled about this prior to the procedure. There are several treatment options for keloids and they have varying degrees of success (see Ch. 98).

Even well-approximated wound edges can produce spread scars. Scar spreading is more common on the back, chest, and shoulders, especially in younger patients. Patients who need excisions in these areas should be counseled preoperatively about the possibility that an initially thin scar may widen over time. Most widening occurs within 6 months after the surgery.

Corticosteroid injections can improve the appearance of a trapdoor deformity in the area of a flap. The patient should also be instructed to massage the area. Revision can be considered if these interventions do not produce an acceptable cosmetic result. Multiple small Z-plasties along the scar line, "defatting", and peripheral undermining can also improve the appearance[67]. However, patience often produces the best results.

Patients should be warned about the possibility of hyper- or hypopigmentation. Pigmentary variations are more pronounced in individuals with darker skin phototypes. The wound site should be strictly protected from UV exposure. Early epidermal hyperpigmentation can be improved with topical hydroquinone, though this is ineffective unless combined with UV protection.

CONCLUSIONS

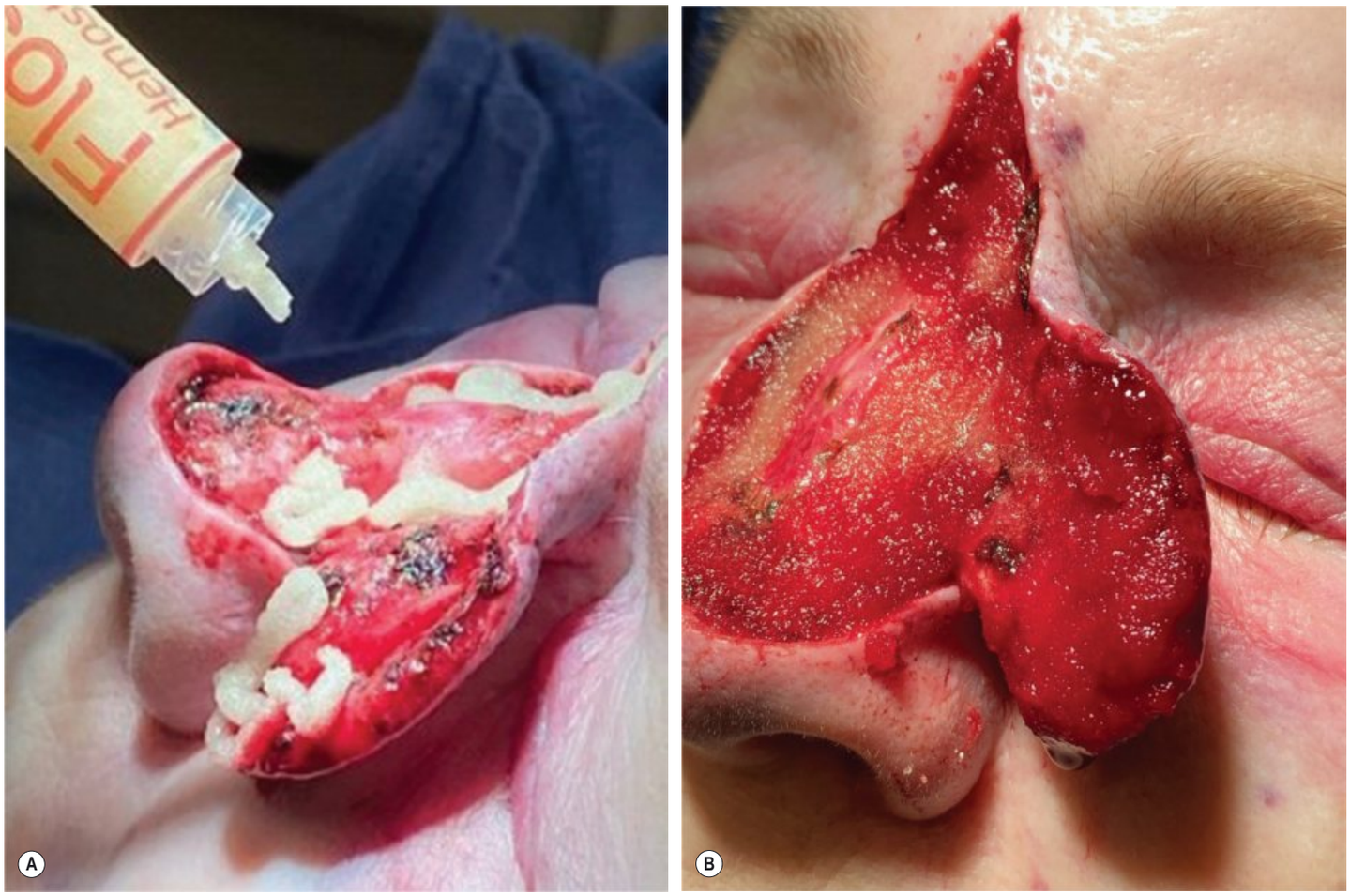
Avoiding complications requires planning and careful evaluation at each stage of the procedure: preoperative, intraoperative, and postoperative. Despite the best intentions, careful planning, and the most expert hands, complications still occur. The surgeon must remember to treat the patient, not just the condition. The patient who feels abandoned may not be happy with any outcome, no matter how technically perfect.

Additional figures available in our eBook (see inside front cover for access code).

REFERENCES

1. Cook JL, Perone JB. A prospective evaluation of the incidence of complications associated with Mohs micrographic surgery. *Arch Dermatol*. 2003;139:143–152.
2. Starling J 3rd, Thosani MK, Coldiron BM. Determining the safety of office-based surgery: what 10 years of Florida data and 6 years of Alabama data reveal. *Dermatol Surg*. 2012;38:171–177.
3. Callahan S, Goldsberry A, Kim G, Yoo S. The management of antithrombotic medication in skin surgery. *Dermatol Surg*. 2012;38:1417–1426.
4. Lewis KG, Dufresne RG Jr. A meta-analysis of complications attributed to anticoagulation among patients following cutaneous surgery. *Dermatol Surg*. 2008;34:160–164. discussion 164–5.
5. Salasche SJ. Acute surgical complications: cause, prevention, and treatment. *J Am Acad Dermatol*. 1986;15:1163–1185.
6. Di Vincenzo V, Cappelletti L, Acciai N, et al. The effect of dipyridamole and aspirin on postoperative blood loss after myocardial revascularization. *J Cardiothorac Anesth*. 1989;3(Suppl 1):88.
7. Cook-Norris RH, Michaels JD, Weaver AL, et al. Complications of cutaneous surgery in patients taking clopidogrel-containing anticoagulation. *J Am Acad Dermatol*. 2011;65:584–591.
8. Bordeaux JS, Martires KJ, Goldberg D, et al. Prospective evaluation of dermatologic surgery complications including patients on multiple antiplatelet and anticoagulant medications. *J Am Acad Dermatol*. 2011;65:576–583.
9. Ah-Weng A, Natarajan S, Velangi S, Langtry JA. Preoperative monitoring of warfarin in cutaneous surgery. *Br J Dermatol*. 2003;149:386–389.
10. Alcalay J. Cutaneous surgery in patients receiving warfarin therapy. *Dermatol Surg*. 2001;27:756–758.
11. Alcalay J, Alkalay R. Controversies in perioperative management of blood thinners in dermatologic surgery: continue or discontinue? *Dermatol Surg*. 2004;30:1091–1094. discussion 1094.
12. Caliendo FJ, Halpern VJ, Marini CP, et al. Warfarin anticoagulation in the perioperative period: is it safe? *Ann Vasc Surg*. 1999;13:11–16.
13. Blasdale C, Lawrence CM. Perioperative international normalized ratio level is a poor predictor of postoperative bleeding complications in dermatological surgery patients taking warfarin. *Br J Dermatol*. 2008;158:522–526.
14. Healey JS, Eikelboom J, Douketis J, et al. Periprocedural bleeding and thromboembolic events with dabigatran compared with warfarin: results from the Randomized Evaluation of Long-Term Anticoagulation Therapy (RE-LY) randomized trial. *Circulation*. 2012;126:343–348.
15. Eilers RE Jr, Goldenberg A, Cowan NL, et al. A retrospective assessment of postoperative bleeding complications in anticoagulated patients following Mohs micrographic surgery. *Dermatol Surg*. 2018;44:504–511.
16. Dinehart SM, Henry L. Dietary supplements: altered coagulation and effects on bruising. *Dermatol Surg*. 2005;31:819–826. discussion 826.
17. Deykin D, Janson P, McMahon L. Ethanol potentiation of aspirin-induced prolongation of the bleeding time. *N Engl J Med*. 1982;306:852–854.
18. Scappaticci FA, Fehrenbacher L, Cartwright T, et al. Surgical wound healing complications in metastatic colorectal cancer patients treated with bevacizumab. *J Surg Oncol*. 2005;91:173–180.
19. Erinjeri JP, Fong AJ, Kemeny NE, et al. Timing of administration of bevacizumab chemotherapy affects wound healing after chest wall port placement. *Cancer*. 2011;117:1296–1301.
20. Smith JB, Fenske NA. Cutaneous manifestations and consequences of smoking. *J Am Acad Dermatol*. 1996;34:717–732; quiz 733–4.
21. Goldminz D, Bennett RG. Cigarette smoking and flap and full-thickness graft necrosis. *Arch Dermatol*. 1991;127:1012–1015.
22. Jensen JA, Goodson WH, Hopf HW, Hunt TK. Cigarette smoking decreases tissue oxygen. *Arch Surg*. 1991;126:1131–1134.
23. Gill JF, Yu SS, Neuhaus IM. Tobacco smoking and dermatologic surgery. *J Am Acad Dermatol*. 2013;68:167–172.
24. Sorensen LT. Wound healing and infection in surgery: the pathophysiological impact of smoking, smoking cessation, and nicotine replacement therapy: a systematic review. *Ann Surg*. 2012;255:1069–1079.
25. Rubenstein R, Roenigk HH Jr, Stegman SJ, Hanke CW. Atypical keloids after dermabrasion of patients taking isotretinoin. *J Am Acad Dermatol*. 1986;15:280–285.
26. Zachariae H. Delayed wound healing and keloid formation following argon laser treatment or dermabrasion during isotretinoin treatment. *Br J Dermatol*. 1988;118:703–706.
27. Bernestein LJ, Geronemus RG. Keloid formation with the 585-nm pulsed dye laser during isotretinoin treatment. *Arch Dermatol*. 1997;133:111–112.
28. Bagatin E, dos Santos Guadanhim LR, Yarak S, et al. Dermabrasion for acne scars during treatment with oral isotretinoin. *Dermatol Surg*. 2010;36:483–489.
29. Picosse FR, Yarak S, Cabral NC, Bagatin E. Early chemabrasion for acne scars after treatment with oral isotretinoin. *Dermatol Surg*. 2012;38:1521–1526.
30. Chandrashekar BS, Varsha DV, Vasanth V, et al. Safety of performing invasive acne scar treatment and laser hair removal in patients on oral isotretinoin: a retrospective study of 110 patients. *Int J Dermatol*. 2014;53:1281–1285.
31. Moradi A, Aghaei S, Safaee-Ardekani G, Moradi M. Co-administration of NLite and Er:YAG laser with isotretinoin. *Lasers Surg Med*. 2009;41:34–35.
32. Yoon JH, Park EJ, Kwon IH, et al. Concomitant use of an infrared fractional laser with low-dose isotretinoin for the treatment of acne and acne scars. *J Dermatolog Treat*. 2014;25:142–146.
33. Gilbert S, McBurney E. Use of valacyclovir for herpes simplex virus-1 (HSV-1) prophylaxis after facial resurfacing: a randomized clinical trial of dosing regimens. *Dermatol Surg*. 2000;26:50–54.
34. Wright TI, Baddour LM, Berbari EF, et al. Antibiotic prophylaxis in dermatologic surgery: advisory statement 2008. *J Am Acad Dermatol*. 2008;59:464–473.
35. Rethman MP, Watters W 3rd, Abt E, et al. The American Academy of Orthopaedic Surgeons and the American Dental Association clinical practice guideline on the prevention of orthopaedic implant infection in patients undergoing dental procedures. *J Bone Joint Surg Am*. 2013;95:745–747.
36. Sollecito TP, Abt E, Lockhart PB, et al. The use of prophylactic antibiotics prior to dental procedures in patients with prosthetic joints: evidence-based clinical practice guideline for dental practitioners: a report of the American Dental Association Council on Scientific Affairs. *J Am Dent Assoc*. 2015;146:11–16. e8.
37. El-Gamal HM, Dufresne RG, Saddler K. Electrosurgery, pacemakers and ICDs: a survey of precautions and complications experienced by cutaneous surgeons. *Dermatol Surg*. 2001;27:385–390.
38. LeVasseur JG, Kennard CD, Finley EM, Muse RK. Dermatologic electrosurgery in patients with implantable cardioverter-defibrillators and pacemakers. *Dermatol Surg*. 1998;24:233–240.
39. Tripathi SV, Hurst EA. Pacemakers, deep brain stimulators, cochlear implants, and nerve stimulators: a review of common devices encountered in the dermatologic surgery patient. *Dermatol Surg*. 2019;45:1228–1236.
40. Thomas RM, Amonette RA. Emergencies in skin surgery. In: Roenigk RK, Roenigk HHJ, eds. *Dermatologic Surgery Principles and Practice*. 2nd ed. New York: Marcel Dekker; 1996, pp. 77–89.
41. Brigo F, Nardone R, Ausserer H, et al. The diagnostic value of urinary incontinence in the differential diagnosis of seizures. *Seizure*. 2013;22:85–90.
42. Ljunggren B, Moller H. Eczematous contact allergy to chlorhexidine. *Acta Derm Venereol*. 1972;52:308–310.
43. Marks JG, Jr. Allergic contact dermatitis to povidone-iodine. *J Am Acad Dermatol*. 1982;6:473–475.
44. Greenbaum SS, Greenbaum CH. Intraoperative tissue expansion using a Foley catheter following excision of a basal cell carcinoma. *J Dermatol Surg Oncol*. 1990;16:45–48.
45. Denkler K. A comprehensive review of epinephrine in the finger: to do or not to do. *Plast Reconstr Surg*. 2001;108:114–124.
46. Krunic AL, Wang LC, Soltani K, et al. Digital anesthesia with epinephrine: an old myth revisited. *J Am Acad Dermatol*. 2004;51:755–759.
47. Thomson CJ, Lalonde DH, Denkler KA, Feicht AJ. A critical look at the evidence for and against elective epinephrine use in the finger. *Plast Reconstr Surg*. 2007;119:260–266.

48. Rogers HD, Desciak EB, Marcus RP, et al. Prospective study of wound infections in Mohs micrographic surgery using clean surgical technique in the absence of prophylactic antibiotics. *J Am Acad Dermatol*. 2010;63:842–851.
49. Achneck HE, Sileshi B, Jamiolkowski RM, et al. A comprehensive review of topical hemostatic agents: efficacy and recommendations for use. *Ann Surg*. 2010;251:217–228.
50. Ho J, Hruza G. Hydrophilic polymers with potassium salt and microporous polysaccharides for use as hemostatic agents. *Dermatol Surg*. 2007;33:1430–1433.
51. Billingsley EM, Maloney ME. Considerations in achieving hemostasis. In: Robinson JK, Arndt KA, Leboit PE, Wintroub BU, eds. *Atlas of Cutaneous Surgery*. Philadelphia: WB Saunders; 1996:67–73.
52. Alam M, Ibrahim O, Nodzenski M, et al. Adverse events associated with Mohs micrographic surgery: multicenter prospective cohort study of 20,821 cases at 23 centers. *JAMA Dermatol*. 2013;149:1378–1385.
53. Lalonde D, Bell M, Benoit P, et al. A multicenter prospective study of 3,110 consecutive cases of elective epinephrine use in the fingers and hand: the Dalhousie Project clinical phase. *J Hand Surg Am*. 2005;30:1061–1067.
54. Salasche SJ, Bernstein G, Senkarik M. *Surgical Anatomy of the Skin*. Norwalk: Appleton & Lange; 1988.
55. McDonald M, Stasko T. Prevention of unsatisfactory scarring. In: Harahap M, ed. *Surgical Techniques for Cutaneous Scar Revision*. New York: Marcel Dekker; 2000:53–80.
56. Kaufman AJ, Kiene KL, Moy RL. Role of tissue undermining in the trapdoor effect of transposition flaps. *J Dermatol Surg Oncol*. 1993;19:128–132.
57. Goldberg D, Maloney M. Dermatologic surgery and cosmetic procedures during pregnancy and the post-partum period. *Dermatol Ther*. 2013;26:321–330.
58. Li JN, Nijhawan RI, Srivastava D. Cutaneous surgery in patients who are pregnant or breastfeeding. *Dermatol Clin*. 2019;37:307–317.
59. Stasko T. *Complications of Cutaneous Procedures*. 2nd ed. New York: Marcel Dekker; 1996.
60. Ketchum LD, Smith J, Robinson DW, Masters FW. The treatment of hypertrophic scar, keloid and scar contracture by triamcinolone acetonide. *Plast Reconstr Surg*. 1966;38:209–218.
61. Shin TM, Bordeaux JS. The role of massage in scar management: a literature review. *Dermatol Surg*. 2012;38:414–423.
62. Berman B, Flores F. Comparison of a silicone gel-filled cushion and silicone gel sheeting for the treatment of hypertrophic or keloid scars. *Dermatol Surg*. 1999;25:484–486.
63. Ricketts CH, Martin L, Faria DT, et al. Cytokine mRNA changes during the treatment of hypertrophic scars with silicone and nonsilicone gel dressings. *Dermatol Surg*. 1996;22:955–959.
64. Jackson BA, Shelton AJ. Pilot study evaluating topical onion extract as treatment for postsurgical scars. *Dermatol Surg*. 1999;25:267–269.
65. Harmon CB, Yarborough JM. Scar revision by dermabrasion. In: Roenigk RK, Roenigk HHJ, eds. *Dermatologic Surgery Principles and Practice*. 2nd ed. New York: Marcel Dekker; 1996:911–921.
66. Alster T, Zaulyanov L. Laser scar revision: a review. *Dermatol Surg*. 2007;33:131–140.
67. Koranda FC, Webster RC. Trapdoor effect in nasolabial flaps. Causes and corrections. *Arch Otolaryngol*. 1985;111:421–424.



eFig. 151.1 Topical application of the hemostatic agent Floseal®, which contains human thrombin and gelatin granules, to the wound bed (A) to reduce postoperative bleeding (B). *Courtesy William G. Stebbins, MD.*



eFig. 151.2 Organized hematoma of the upper back. *Courtesy Thomas Stasko, MD.*



eFig. 151.3 Organized hematoma of the chest healing by second intention following evacuation. *Courtesy William G. Stebbins, MD.*



eFig. 151.4 Ecchymoses of the cheeks following dorsal nasal flap repair.



eFig. 151.5 Sterile pustule and granulomatous reaction to suture placement.

Evaluation of Beauty and the Aging Face 152

Naissan O. Wesley and Thomas E. Rohrer

Chapter Contents

Evaluation of Beauty 2611
Anatomic Basis for the Aging Appearance. 2613
Photoaging 2613
Pigmentary System 2614
Volume Changes – the Loss of Subcutaneous Fat 2614
Changes in Facial Musculature 2615
Changes in Underlying Cartilage and Bone 2616
Inherent Loss of Elasticity 2616
Sex and Gender Differences. 2616
Ethnic Differences 2616
Combination Therapies. 2617

INTRODUCTION

"It is amazing how complete is the delusion that beauty is goodness."
~Leo Tolstoy

"The only lasting beauty is the beauty of the heart." "The beauty you see in me is a reflection of you." "Beauty surrounds us."
~Rumi

"Perhaps the mission of an artist is to interpret beauty to people – the beauty within themselves."
~Langston Hughes

"In diversity, there's beauty and there's strength."
~Maya Angelou

Nancy Etcoff, in *Survival of the Prettiest: The Science of Beauty*, explains that beauty is a universal component of the human experience which promotes pleasure, rivets attention, and impels action that helps ensure survival of our genes[1].

Striving to be more beautiful is not a new phenomenon. Human preoccupation with beauty and a youthful appearance dates back as far as recorded history. Anthropologists have determined that over 40 000 years ago, red ochre paints were used in southern Africa for facial and body ornamentation[2]. In 5 BCE, the Roman author Ovid wrote *The Art of Beauty*, the first known book on beauty and cosmetics, detailing the use of black eye shadow made from wood ash and golden eye shadow made from saffron.

Few human traits are as ingrained as beauty. It is thought to be hardwired into our brains and can even be detected in infants. Studies have shown that by the age of 3 months, babies stare longer at attractive faces than those deemed to be less attractive. Also, 1-year-old toddlers will play longer with attractive dolls than with plain dolls[3]. In functional magnetic resonance imaging studies where subjects were shown photographs of attractive men and women, viewing beautiful faces activated reward circuitry within the brain and dopamine pathways[4]. Studies have shown that humans can make judgements on facial attractiveness in 100 msec, and with longer exposure times the judgment is not changed, only strengthened[5]. There is even a dedicated special area of the ventral stream of the temporal lobe of the brain that helps humans with the task of recognizing faces quickly called the fusiform face area[6]. This area is highly specialized in the task of facial recognition in all humans and is thought to have evolved to aid our ancestors in rapidly assessing the trustworthiness of other humans.

If examined from an evolutionary standpoint, this innate attraction to beauty certainly makes sense. Beauty has been interpreted in terms of reproductive potential as it provides an advantage in selecting or being selected as a mate for sexual reproduction. Attraction to beauty also makes sense from a disease perspective. It is said that "beauty is a burden that only the healthy can carry". In other words, the sickly are by nature less attractive. Those with an ideal physique and youthful proportions are much more likely to be healthy and be able to reproduce. By choosing an attractive healthy mate, one is increasing the odds that his or her genes will be passed on.

In one study, 20 subjects were asked to grade graduates from a 1920s high school yearbook on their attractiveness. When the actual lifespans of these graduates were determined, facial attractiveness correlated with increased lifespan. Correlations between beauty and health help to explain why, from an evolutionary standpoint, the notion of beauty may become an innate concept within a species[7].

Besides being considered a more ideal mate, attractiveness may also have a number of other benefits. Nancy Etcoff has stated that people tend to respond positively to good-looking people without expectation of reward, and, further, that good-looking people tend to be less penalized for everything from shoplifting to cheating at exams[1]. In the same workplace, attractive people were found to earn up to 12% higher wages as compared to co-workers who were considered average-looking[2]. Also, pharmaceutical representatives have been shown to have a 1.9% increase in sales for every unit increase in the Likert Scale for attractiveness. While the average height of a man in the US is 5′ 7″ (170.2 cm), the average height of Fortune 500 CEOs is 6′ 1″ (185.4 cm). Statistically, US Presidents have also been found to be significantly taller than their constituents. Lastly, even West Point graduates who had higher scores on an attractiveness scale rose to higher military ranks.

The advent of more accessible photography with smartphone devices and app filters has further exemplified what an important role light and shadows play in the appearance of attractiveness. Renowned makeup artist Kevyn Aucoin recognized the importance of highlights and shadows in his work. Part of aesthetic dermatology work involves restoring or optimizing highlights and shadows with procedures to achieve a more attractive appearance.

EVALUATION OF BEAUTY

Recognizing beauty and understanding its significance may be far easier than actually defining it[8]. Anthropometry represents the quantitative measurement of facial features and an assessment of resultant ratios. It is based on proportional relationships of the face that are known as the neoclassical canons, which have been studied and revised for centuries. As originally proposed by Leonardo da Vinci, the ideal face can be divided horizontally into three equal parts; these parts are composed of the distances between: (1) the frontal hairline and the inferior edge of the frontal bone; (2) the supraorbital margin and the base of the nose; and (3) the base of the nose and the inferior aspect of the chin (Fig. 152.1A)[9]. In general, mathematically idealized facial proportions translate into a symmetric, oval- or heart-shaped face, with prominent cheekbones, tapered jaw line, narrow nasal base, and thin lips. These proportions, however, are largely based on facial features in White women and ethnic variations of these "ideal" proportions should be emphasized.

Some of the other features that are consistently shown to be rated as beautiful across nationalities include symmetry and averageness. Symmetry could be considered the optimal outcome of development from a two-celled embryo, dividing perfectly every single time. The closer the ability to do so in the face of various environmental pressures, the higher the genetic quality of those cells. In fact, symmetry is positively related to growth rate, survivability, and fitness across species[10]. When

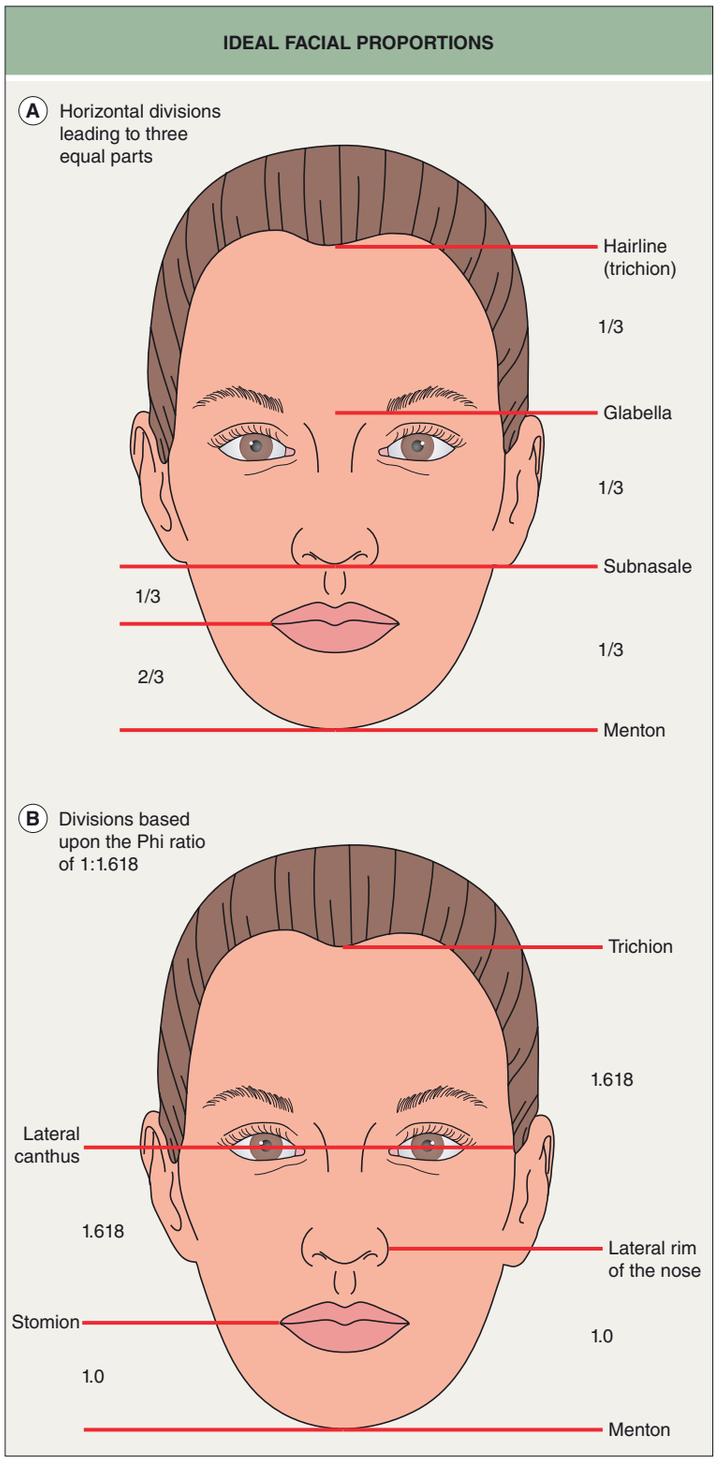


Fig. 152.1 The "ideal" face. A Horizontal divisions leading to three equal parts creates an "ideal" face. These three parts are composed of the distances between: (1) the frontal hairline and the inferior edge of the frontal bone; (2) the supraorbital margin and the base of the nose; and (3) the base of the nose and the inferior aspect of the chin. The divisions were originally proposed by Leonardo da Vinci. **B** Ideal facial proportions based upon the Phi ratio of 1 : 1.618. *Adapted from Milutinovic J, Zelic K, Nedeljkovic N. Evaluation of facial beauty using anthropometric proportions. Scientific World J 2014:2014:428250.*

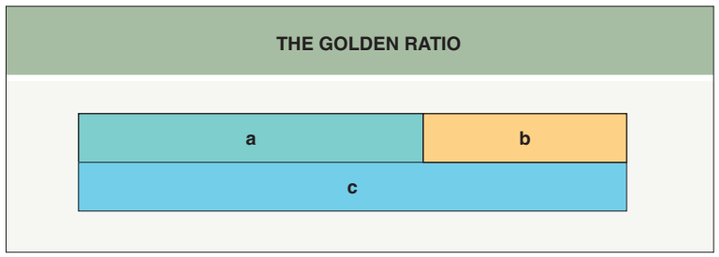


Fig. 152.2 The golden ratio based upon Phi. Phi is the unique point on a line that divides the line into two lines in such a manner that the ratio of the smaller portion (b) to the larger portion (a) is the same as the ratio of the larger portion (a) to the whole line (c). In other words, "b" is to "a" as "a" is to "c". This ratio is a repeating number that is rounded off to 1 : 1.618. A triangle composed of lines with lengths in the Phi ratio is referred to as a golden triangle.

images are manipulated to make them more or less symmetric, the more symmetric image is usually chosen as the more attractive one[11]. Averageness is also seen as being attractive and can also be viewed as being genetically more diverse and stronger. As different populations are subjected to different pathogens, they are more likely to acquire protective mutations against those pathogens. The greater the genetic mixing, the more inherited protective mutations and adaptability to the environment one is likely to have[12]. Facial averageness has been positively correlated with medical health[13]. In sum, both symmetry and averageness can be seen as being genetically healthy and therefore make sense to be markers of what is considered beautiful to a species.

A more exact mathematical method for calculating beauty across nature via mathematical proportions is the concept of "Phi", or the golden ratio. A ratio of 1 : 1.618 was described by ancient Greeks as a mathematical method for calculation of the optimal proportions for all structures in nature (Fig. 152.1B). In fact, some authorities believe that the neoclassical canons (see above) are modifications of Phi. Phi represents the unique point on a line that divides the line into two lines in such a manner that the ratio of the smaller portion to the larger portion is the same as the ratio of the larger portion to the whole line (Fig. 152.2). This ratio is a repeating number that is rounded off to 1 : 1.618. Of note, there are innumerable examples of the use of the Phi ratio in nature and art, including the Parthenon, the Great Pyramid of Giza, the sculpture Venus de Milo, the length of each section of our finger, the shell of a nautilus, pinecones, and the petals of a sunflower.

A triangle composed of lines with lengths in the Phi ratio is referred to as a golden triangle. When expanded, one can even create golden pentagons and golden decagons. Stephen Marquardt trademarked the "Phi mask", a facial mask composed of proportions that incorporate the 1 : 1.618 ratio, to describe the mathematically ideal attractive face. Although the Phi mask has been applied to persons of all races and ethnicities, Marquardt recognized that ethnic variations exist and has incorporated modifications for three different ethnic groups – White, Asian, and African. However, pitfalls against using the mask to denote attractiveness among all ethnic groups, particularly in sub-Saharan Africans, East Asians, and White women, has been described[14].

A novel model to describe or measure attractiveness has been described by Steven Dayan. It can be employed when description of natural beauty, both at baseline and after a cosmetic procedure, is desired. In this model, "attractiveness consists of a 3-dimensional area defined by beauty, genuineness, and self-esteem. When all three variables are at a maximum, a desirable attractive appearance is achieved that can be interpreted as 'natural'. Similar to the time-space dilemma, attractiveness is relative, dynamic, and highly dependent on the position of the projector and the interpreter. The 3D cube of attractiveness is therefore contained within a 4th dimension that takes into account the perspective of the judger"[15]. Similarly, Dayan et al.[16] also demonstrated in a pilot observational study that visually blind individuals can detect beauty, supporting the idea that beauty may rely on primal forms of messaging that are subconsciously appreciated.

As there is no single ideal of beauty, ethnic variations should be celebrated and recognized such that not every person is treated with aesthetic procedures to look the same and potentially look "pretty" but lose their unique beauty. For example, when a surgeon has perfected a rhinoplasty of one size and shape, e.g. a thin upsloped nose, it may look attractive in a White woman and others with similar features, but look unattractive in those without those features, especially in individuals from other ethnic groups.

It should be noted that sometimes features that are unique and do not conform to the neoclassical canons or golden ratio, including prominent brows, eyes, nose shape or lips, as well as confidence, persona, hair, the way the body is decorated with clothing or adorned with body art, health, and the beauty that exudes from within, can uniquely make people look more attractive.



Fig. 152.3 Rhytides of the aging face. Rhytides form as a result of UV radiation-induced damage, loss of skin elasticity, repetitive movement of underlying facial musculature, changes in volume from fat redistribution, and bone as well as cartilage resorption.

ANATOMIC BASIS FOR THE AGING APPEARANCE

Knowledge of facial anatomy and anatomic changes that occur with aging is essential for properly evaluating and treating the aesthetic patient. With aging, both the golden ratio (Phi) and the neoclassical canons start to shift. The upper one-third of the face *elongates* due to recession of the frontal hairline and brow ptosis, while proportionately the middle third remains relatively stable (but may elongate with nasal tip ptosis). However, midface volume loss can occur as a result of fat redistribution and skeletal changes. The lower third of the face becomes *shortened* with perioral fat redistribution and significant resorption of the bony mandible, which may also lead to shifts in dentition, further affecting aesthetics of the lower face and smile.

The appearance of the aging face is multifactorial and does not appear to simply be a matter of sagging from the effect of years of gravitational forces pulling the face downwards. Rather, a complex ongoing alteration in proportions occurs as one ages. Notably, studies by Rohrich and Pessa[17] have shown that there is not one large confluent layer of subcutaneous fat in the face but rather multiple distinct compartments that act independently from one another (see below, Volume changes). For example, the malar fat pad in the mid cheek is composed of three separate compartments; as these compartments change in size, the ligaments separating the compartments become more evident and a smooth, rounded, youthful appearance transforms into the multicontoured aged face.

After examining numerous photographs of patients as they aged, Lambros[18] concluded that there is actually very little positional change in the midface region. Despite the common perception that the face drops inferiorly with age, he noted that the eyelid–cheek margin did not change with advancing years, nor did facial nevi of the midface descend with age. Just as individual water molecules simply move up and down rather than actually traveling with waves at sea, the wave of downward motion "seen" in an aging face may simply represent shifts in subcutaneous tissue.

Rhytides also play a key role in producing an aged appearance. The underlying causes of rhytides are multiple and include ultraviolet radiation-induced damage, loss of skin elasticity, repetitive movement of underlying facial musculature, changes in volume from fat redistribution, and bone as well as cartilage resorption (Fig. 152.3).

PHOTOAGING

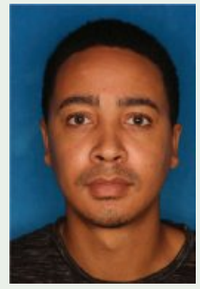
Cumulative exposure to sunlight and environmental pollution/toxins is a major factor in aging skin. Clinical signs of cutaneous photoaging include: rhytides, lentigines, keratoses, telangiectasias, loss of translucency, loss of elasticity, and a sallow color[19,20]. The Fitzpatrick Scale of Skin Phototypes (see Table 0.6) serves as a good indicator of the potential for developing signs of photoaging.

A simple systematic classification of patient photoaging types (types I through IV) was developed by Dr Richard Glogau (Table 152.1)[21]. However, the generalizations outlined in this table are influenced by the amount of cumulative sun exposure and usually apply at a later age and to a lesser degree in those with more darkly pigmented skin. Type I refers to younger patients with no rhytides, even when the face is animated by talking or expression. Type II refers to patients with "wrinkles in motion", who demonstrate the influence the underlying musculature has on the skin.

GLOGAU PHOTOAGING CLASSIFICATION – WRINKLE SCALE

Type I – "No wrinkles"

- Early photoaging
  - Skin uniform in color to mild pigmentary changes
  - No keratoses
- Wrinkles
  - No wrinkles, even at the corners of the eyes and mouth
- Patient age (yrs) – 20s or 30s
- Minimal or no makeup



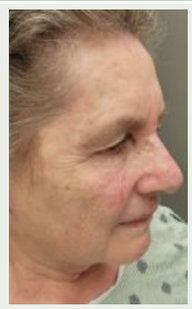
Type II – "Wrinkles in motion"

- Early to moderate photoaging
  - Early solar lentigines visible
  - Keratoses palpable but not visible
- Wrinkles
  - *When the face is at rest*, the patient appears similar to type I
  - *When the face is animated by expression*, parallel lines appear – first at the corners of the mouth, then parallel to the melolabial folds, then at the corners of the eyes, and finally over the malar cheeks
- Patient age (yrs) – late 30s or 40s
- Usually wears some foundation



Type III – "Wrinkles at rest"

- Advanced photoaging
  - Obvious dyschromia, telangiectasias
  - Visible keratoses
- Wrinkles
  - Present even when not moving facial muscles
- Patient age (yrs) – 50s or older
- Wears heavy foundation



Type IV – "Only wrinkles"

- Severe photoaging
  - Yellow–gray color of skin
  - Prior skin malignancies
- Wrinkles
  - Wrinkled throughout with no normal skin
  - Total replacement of normal skin with minute, rhomboid and geometric rhytides may be most obvious in the perioral skin
- Patient age (yrs) – 60s to 70s
- Can't wear makeup – "cakes and cracks"

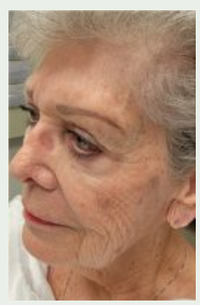


Table 152.1 Glogau photoaging classification – wrinkle scale. Changes appear at a later age and to a lesser degree in those with more darkly pigmented skin. yrs, years. *Adapted from Glogau RG. Chemical peeling and aging skin. J Geriatr Dermatol 1994;2:30–5.*

As the photoaging process advances, there is greater damage to collagen and elastic fibers. Of note, collagen production is maintained by dynamic mechanical tension placed on fibroblasts by intact collagen fibers. With age and particularly sun-related damage, type I collagen (most prevalent form with a half-life of 15 years) becomes more and more fragmented. As more collagen becomes fragmented, there is less stretching tension placed on fibroblasts and they respond by making more metalloproteases and less collagen. This creates a vicious cycle of increasing collagen loss and subsequent thinning of the skin[22]. Eventually, with substantial breakdown of collagen and elastic fibers, the wrinkles produced by dynamic movement of the face persist, even when the face is at rest.

Generally, by the sixth or later decade of life, there are visible parallel lines lateral to the eyes ("crow's feet"), at the corners of the mouth, and radiating down from the lower eyelids onto the malar cheeks, as well as around the upper and lower lips. These patients appear lined, even when their face is at rest, and are classified as type III, "wrinkles at rest". The repetitive effect of underlying muscular expression is now permanently "ingrained" into the skin, i.e. lines are readily visible even without active muscular contraction.

With continued photoaging, the wrinkles gradually spread to cover the majority of the facial skin, while the dermis becomes totally engorged with accumulations of poorly staining ground substance, giving a thickened, coarse quality to the skin. This is classified as photoaging type IV, "only wrinkles".

PIGMENTARY SYSTEM

The Fitzpatrick skin phototype classification scheme is based upon the skin's response to UV light (Table 0.6)[23]. The patient's skin phototype also serves as a good indicator of the potential for developing dyschromia following epidermal/papillary dermal injury.

VOLUME CHANGES – THE LOSS OF SUBCUTANEOUS FAT

A major component of aesthetic disharmony in the aging face is the loss or redistribution of subcutaneous fat. Detailed studies by Rohrich and Pessa[17], utilizing cadaver dissections and staining techniques, have demonstrated that facial fat (unlike fat elsewhere in the body) is partitioned into discrete compartments which may age independently of one another (Fig. 152.4). Redistribution and loss of these fat pads contribute to formation of the nasojugal fold, malar crease, nasolabial fold, pre-jowl sulcus, and marionette lines as well as wasting of the temples, superior brow, and buccal fat (Fig. 152.5).

While in some areas (e.g. the submental region and buccal fat pad), unwanted subcutaneous fat may lend itself to removal via liposuction, cryolipolysis, or deoxycholic acid injection, in general, there is now a new appreciation that removal of fat should be done with caution due to the flattening or hollowing of contours that could result and possibly lead to a more aged appearance. Due to a loss of subcutaneous fat, the older face has a flattened quality to the cheekbones, a sunken appearance to the lips, a bulging of the inferior fat pads of the eye, and, in general, a loss of the fullness and roundness of youth. Experienced aesthetic surgeons have recognized this and are moving away from excessive fat removal to a combination of fat repositioning and restoration, along with SMAS (superficial musculoaponeurotic system) repositioning, restoration of bony loss with implants or injectable fillers, and skin resurfacing or optimization. Dr Steven Hoefflin has written: "In the aging face it is not the tightness of the SMAS or skin that makes the difference, but the quantity and position of subcutaneous fat"[24].

As an example, the routine removal of the infraorbital fat as a part of blepharoplasty, which often accentuated the deep grooves between the lower eyelid and the cheek, has become outdated. Now surgeons prefer to utilize an arcus marginalis release and mobilize the fat medially and anteriorly to fill in the groove and return a more youthful appearance to the lower eyelids through restoration of lower lid convexity. Similarly, repositioning of the premalar fat has become an important part of routine face-lifting, reversing the aged appearance that comes from flattening of the cheekbone contours.

In the 1950s, Dr Ulrich Hinderer, a plastic surgeon, devised facial lines that aided in the optimal placement of cheek implants. In addition to cheek implants, Hinderer's lines can be used to guide the optimal placement of soft tissue fillers and fat transfers in order to create midface volume restoration or enhancement. These lines are drawn: (1) from the lateral canthus to the lateral commissure; and (2) from the mid tragus to the mid nasal ala (Fig. 152.6). These lines demarcate three different regions of the midface: the zygomaticomalar, the anteromedial, and the submalar. The region immediately above where the lines intersect in the zygomaticomalar region is the area of maximal light reflection and is where the apex of the cheek should be, particularly in women.

An optimal S-curve, which is seen in young rather than older individuals, can be achieved via injection of soft tissue fillers into the midface[25]. Improvement in patients' feelings of facial attractiveness has been observed following restoration of midface volume loss by soft tissue fillers (Fig. 152.7; see Ch. 158)[26].

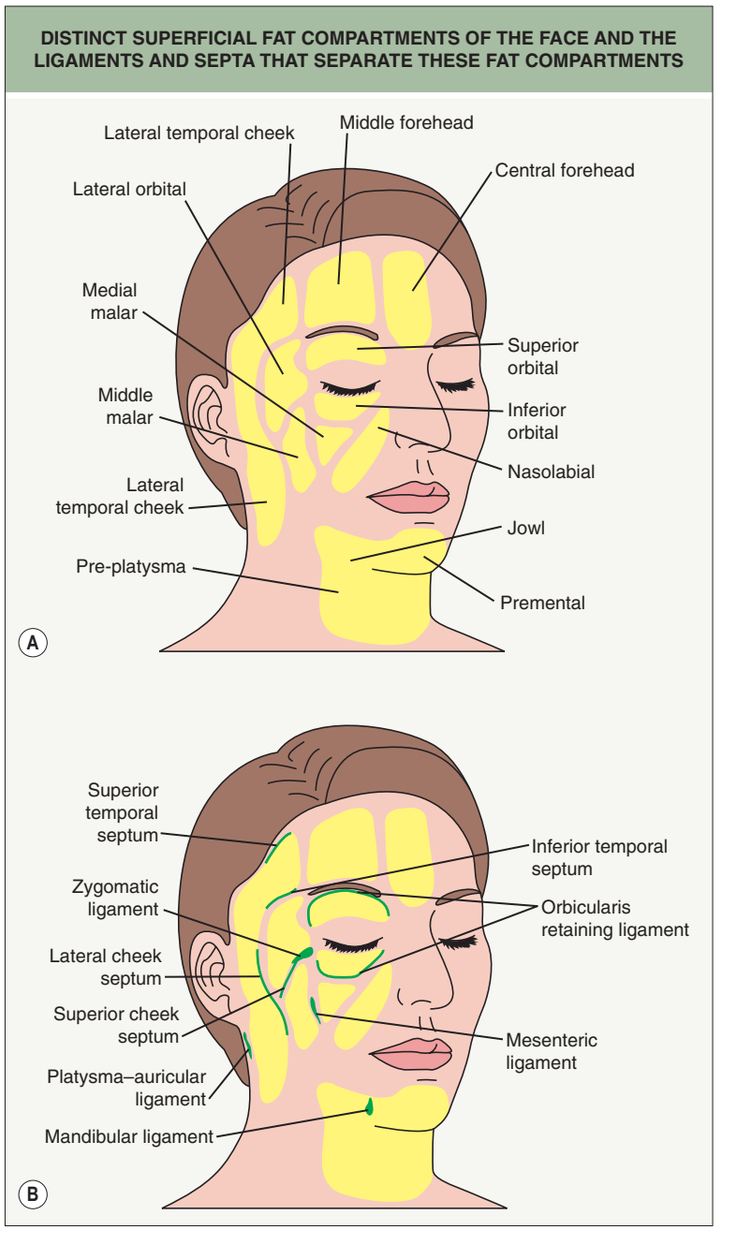


Fig. 152.4 Distinct superficial fat compartments of the face and the ligaments and septa that separate these fat compartments. A The superficial fat compartments of the face are separated by delicate fascial tissue and septa. With aging, volume loss and volume shifts appear to occur at different rates in different compartments, leading to irregularities in facial contour; this is in distinction to the smooth transitions between facial concavities and convexities associated with a youthful appearance and beauty. **B** Where the adjacent compartments meet, the septa converge to form retaining ligaments. In addition, facial muscles (e.g. the zygomaticus major muscle) attach through these fibrous septa to overlying superficial fat compartments. *Adapted from Shiffman MA, Di Giuseppe A, Cosmetic Surgery: Art and Techniques. Springer, 2013.*



Fig. 152.5 Laser resurfacing. A Before a full-face ablative resurfacing procedure. **B** After the procedure, she looks "better" but not "younger", because no attention has been paid to volume changes.

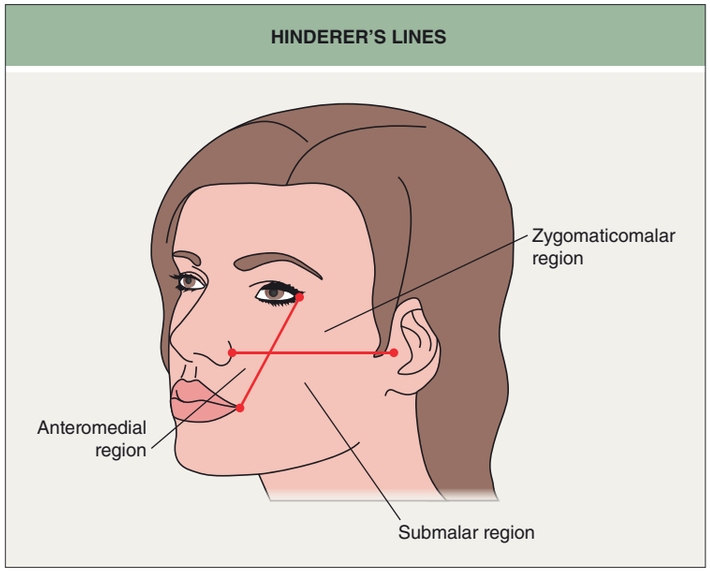


Fig. 152.6 Hinderer's lines. These lines are drawn: (1) from the lateral canthus to the lateral commissure; and (2) from the mid tragus to the mid nasal ala. They can be used to guide the optimal placement of soft tissue fillers and fat transfers (as well as cheek implants) in order to create midface volume enhancement.

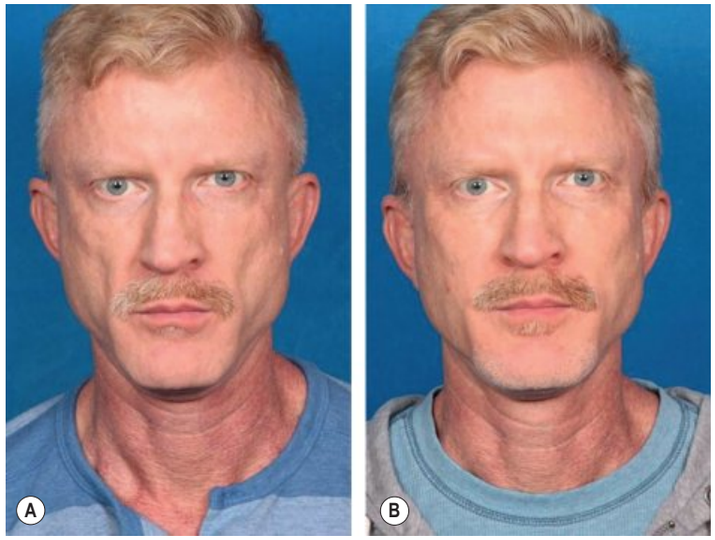


Fig. 152.7 Restoration of midface volume loss by soft tissue fillers. A Before soft tissue filler injection. **B** After injection. Even replacing small amounts of volume in the midface can lead to a natural look and provide the patient with a more youthful and attractive appearance.

CHANGES IN FACIAL MUSCULATURE

Perhaps nothing has driven home the impact of facial musculature on facial aging like the introduction of botulinum toxin type A (BoNT-A) for selective chemical denervation of muscles of the face. Paralysis or partial weakening of the glabellar corrugator/procerus complex, the forehead frontalis muscle, and the lateral orbicularis muscles has revolutionized the management of the upper third of the aging face. In addition, judicious use and careful placement of neuromodulators into the orbicularis oris, depressor anguli oris, masseters, and platysmal neck bands can aid in managing creases, wrinkling, and banding of the lower face and neck (see Ch. 159).

Brow position is closely associated with emotional states, and the medial and lateral portions of the brow function independently in this regard. Surgeons must be conscious of the strong impact that brow shape and position can have on appearance and even interpersonal relationships. For example, people tend to treat you better if you do not have a glabellar scowl, if your eyebrows arch properly (if you are female), and if the relationship between the lateral and medial brow is flattering.

In young women, the arch of the brow has been found to be most attractive when located above the lateral limbus (Fig. 152.8). Photographs of patients following botulinum exotoxin A injection were rated by 40 subjects to be 40% less angry, 49% less fearful, 10% less sad, and 71% more happy than photographs of the same patients prior to their injections[27]. In a small series of 10 patients suffering from depression, nine reported significant improvement in their symptoms to the point of no longer feeling depressed two months following botulinum toxin injection[28]. It may be that when people feel that they are more attractive, they become more confident and have more positive interactions with others. Alam et al.[29] postulated that muscular manipulations which

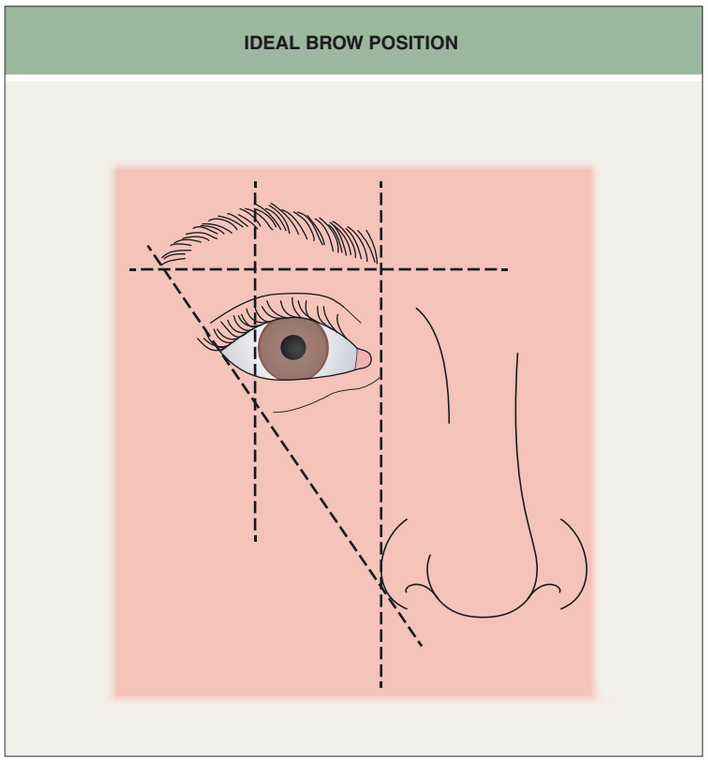


Fig. 152.8 Ideal brow position. In young women, the arch of the brow has been found to be most attractive when it peaks above the lateral limbus.

result in more positive facial expressions may lead to more positive emotional states. Likewise, reducing external signs of anger, fear, and sadness may reduce internal negative emotions.

CHANGES IN UNDERLYING CARTILAGE AND BONE

Due to changes in the underlying cartilage, the aging nose elongates and the tip droops. The aging mouth is affected by bony resorption and remodeling of the maxilla, while the chin sharpens and protrudes. The ears appear to lengthen as the lobes droop. The tarsal plate softens and no longer holds the lower lid margin in its proper position or curve. Various surgical procedures address these problems, including tip rhinoplasty, tarsal lid tightening, canthoplasty, and chin implants. Both dental implant procedures and maxillofacial surgery can address intrinsic changes affecting the lower face while BoNT-A injected into the depressor septi nasi and dilator naris muscles temporarily improves nasal tip ptosis. In addition, soft tissue fillers can be used to correct the aging changes associated with bony resorption and may result in a more natural appearance and feel than an implant. For example, these fillers may be placed in the nasal dorsum, jawline, marionette lines, pre-jowl sulcus, mentum, ear lobes, tear troughs, and midface (see above).

The diagnostic eye of the cosmetic surgeon should not overlook the contribution of the underlying hard structures of the face, particularly when assessing for the presence (or, more commonly, absence) of facial symmetry. Patients often present with requests for the treatment of facial problems without appreciating the contribution of underlying structures to their facial asymmetry. Recognizing, photographing, and discussing pre-existing facial asymmetry due to underlying bony or cartilaginous structural differences is an important component of setting realistic patient expectations.

INHERENT LOSS OF ELASTICITY

As the facial soft tissue ages, both the skin and the underlying supporting structures, while sagging under the effects of gravity, also lose their inherent resiliency or ability to resist stretching. Skin laxity occurs as a result of a decreased underlying framework, a thinned and damaged dermis, and a breakdown in elastic and collagen fibers[22].

SEX AND GENDER DIFFERENCES IN CHARACTERISTICS OF ATTRACTIVE HUMAN FACES

Idealized female facial features	Idealized male facial features
A larger, smooth forehead	Wider face
Eyebrows that have an arch or gull-wing shape	An overhanging, horizontal brow with minimal arch
Eyes that are set wider apart, creating a bigger look	Deeper set eyes that look closer together
Prominent cheekbones, a smaller nose	A somewhat larger nose
A heart-shaped taper to the lower face, with a smaller lower : upper face ratio	A squared lower face and prominent jawline with a more equal ratio of lower : upper face
Full vermilion lips	A wider mouth A beard or coarser texture to the lower facial skin, and laryngeal prominence of the thyroid cartilage (Adam's apple)

Table 152.2 Sex and gender differences in characteristics of attractive human faces. These characteristics are cross-culturally persistent.

In the lower third of the face, a facelift procedure may be essential for a successful aesthetic outcome. Redraping, repositioning, and judicious removal of skin and soft tissue that has lost its elasticity can lead to the restoration of a youthful appearance that sometimes cannot be achieved with a combination of resurfacing, fillers, fat transfer, and/or BoNT-A. However, while facelift procedures have been shown to decrease the estimated age of a person by a mean of 3.1 years (range, −4.0 to 9.4 years), they did not consistently improve attractiveness in one study when assessed at least six months postoperatively[30]. Recognizing what an individual views as ideal beauty is as important as using a multifaceted corrective approach.

SEX AND GENDER DIFFERENCES

The idealized female face tends to exhibit several characteristics that are reproducible from culture to culture and across the ages. Attractive masculine faces tend to have a very different set of characteristics (Table 152.2), although they have not been studied as extensively as those of women.

When compared to women, the skin of men tends to have higher sebum content, less transepidermal water loss (TEWL), and a lower pH[31]. In both sexes, hydration decreases and pH increases with aging, but not to the same degree in men as in women. An age-associated decrease in sebum content also occurs in women, but it is minor in men[32].

Facial hair patterns can also play a role in camouflaging the appearance of aging in men, particularly the presence of marionette lines and pre-jowl sulci, the loss of jawline definition, and submental fullness or neck skin laxity. In one study, women viewed facial hair in men as a sign of attractiveness[33].

Ideals of beauty may also differ depending on how a person self-identifies their gender. Cisgender, transgender, nonbinary, genderfluid, or transitioning patients may desire a more masculine, feminine, or androgynous appearance depending on the ideal. Care should be taken to know a patient's gender identification and then align specific goals with the procedures being planned.

ETHNIC DIFFERENCES

According to the American Society of Plastic Surgeons, more than 4.8 million cosmetic procedures were performed on ethnic minority patients in 2019, an increase of 410% since 2000. Based upon US Census Bureau projections, by the year 2056, >50% of the US population will be of non-White descent. While mathematical anthropometric measurements of the ideal facial structure have been determined, most of these measurements were based on the White face. Future anthropometric facial analyses need to take into account not only ethnocentric variations in facial structure and the effects of aging, but also ethnically diverse perceptions of beauty. Ethnic patients do not necessarily desire a "westernized" look, as what constitutes beauty is influenced by racial, cultural, and

OBJECTIVE DIFFERENCES IN SKIN STRUCTURE AND PHYSIOLOGY BASED ON ETHNICITY		
Evidence supports:	**Insufficient evidence* for:**	**Inconclusive:**
• Increased melanin content and melanosomal dispersion in more darkly pigmented skin • Multinucleated and larger fibroblasts in Black skin compared with White skin • Larger mast cell granules, increased PLS, and increased tryptase localized to PLS in Black compared to White skin • Variable blood vessel reactivity	Ethnic differences in: • Skin elastic recovery/extensibility • Skin microflora • Facial pore size†	Ethnic differences in: • Transepidermal water loss • Water content • Corneocyte desquamation • Lipid content • Barrier function‡ • pH‡)

*Categorized under this heading because only two studies or fewer examined these variables.
†Sugiyama-Nakagiri Y, Sugata K, Hachiya A, et al. Ethnic differences in the structural properties of facial skin. J Dermatol Sci 2009;53:135–9.
‡Voegeli R, Gierschendorf J, Summers B, Rawlings AV. Facial skin mapping: from single point bio-instrumental evaluation to continuous visualization of skin hydration, barrier function, skin surface pH, and sebum in different ethnic skin types. Int J Cosmet Sci 2019;41:411–24.

Table 152.3 Objective differences in skin structure and physiology based on ethnicity. PLS, parallel-linear striations (seen within mast cells by electron microscopy). *Adapted from Wesley NO, Maibach HI. Racial (ethnic) differences in skin properties: the objective data. Am J Clin Dermatol 2003;4:843–60.*

environmental factors. Descriptions of ethnocentric variability in these ideals have begun to appear in the dermatologic literature[34].

The cosmetic concerns of ethnic patients also vary due to inherent differences in skin structure and physiology (Table 152.3)[34a], mechanisms of aging, and facial anatomy (Fig. 152.9)[35]. In more darkly pigmented individuals, the initial signs of aging may consist of midface volume shifts rather than the solar lentigines and rhytides seen in lightly pigmented individuals. Due to the protective effects of melanin, lentigines and facial rhytides can appear decades later in darkly pigmented individuals. However, dyschromia can be a significant cosmetic concern in these patients.

COMBINATION THERAPIES

Optimal improvement in appearance can more often be obtained by combining procedures. Topical agents to even out skin tone and rhytids such as tretinoin, α-hydroxy acids, hydroquinone, antioxidants, peptides, and growth factors can be employed in addition to treatments for actinic keratoses (e.g. 5-fluorouracil, imiquimod, tirbanibulin, photodynamic therapy) which can inhibit or reverse UV radiation-associated changes in aging skin. Treating diseases such as acne and melasma also improves overall facial appearance. At the other end of the therapeutic spectrum, rhytidectomy, blepharoplasty, brow lift, and suction-assisted lipectomy often provide dramatic results in facial rejuvenation. The choice of specific therapies rests on the ability of the surgeon to look at the face, analyze the anatomic components of the aging appearance, and then prioritize them, matching the risk : benefit ratios of various procedures to each element with the priorities of the patient in mind. Is the predominant problem photodamage, dynamic rhytides, sagging, or the loss or shift of facial volume? Often there are also overriding constraints, e.g. the "downtime", surgical risk, cost, likelihood of benefit, that all weigh in on the selection of the appropriate therapy. However, underlying all these choices must be a rational analysis of the various elements that comprise the aging face. The more an aesthetic surgeon is able to specifically tailor treatments to the individual patient, the more likely the outcome will be aesthetically optimal and be associated with a higher degree of patient satisfaction.

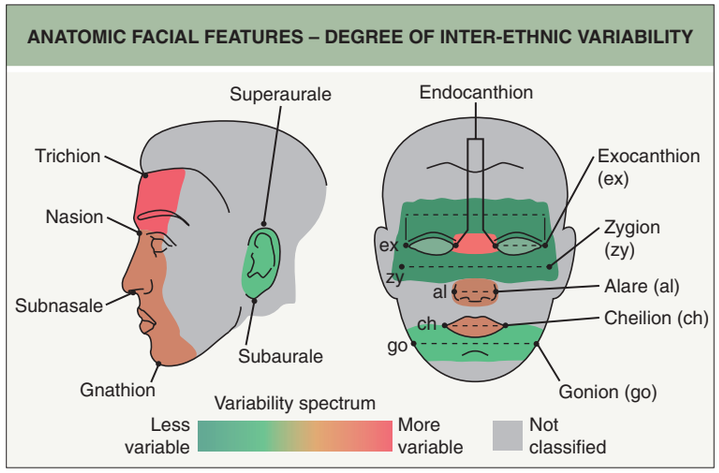


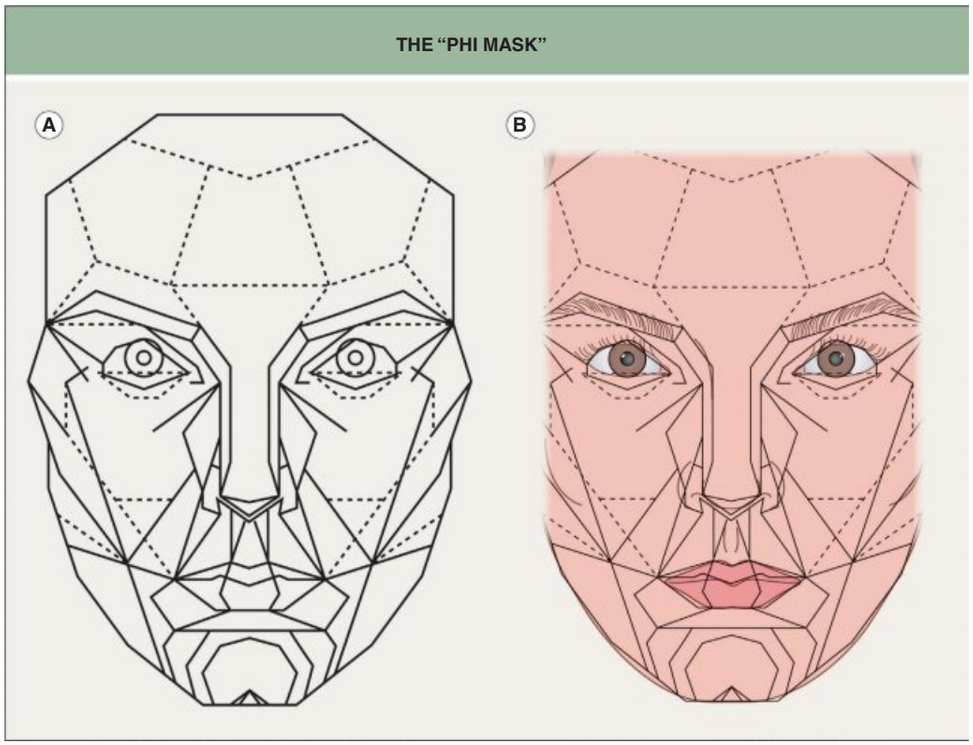
Fig. 152.9 Anatomic facial features – degree of inter-ethnic variability. These measurements are derived from the neoclassical canons. *Adapted from Fang F, Clapham PJ, Chung KC. A systematic review of interethnic variability in facial dimensions. Plast Reconstr Surg 2011;127:874–81.*

Additional figures and table on Facial analysis of women of different ethnic groups, available in our eBook (see inside front cover for access code).

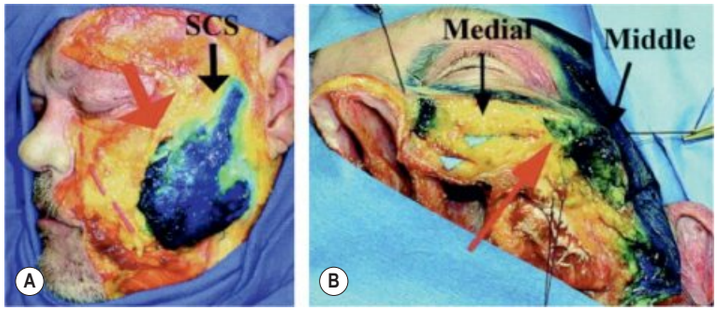
REFERENCES

1. Etcoff N. *Survival of the Prettiest: the Science of Beauty*. New York: Doubleday; 1999.
2. Luftman D, Ritvo E. *The Beauty Prescription: The Complete Formula For Looking and Feeling Beautiful*. McGraw-Hill; 2008:8.
3. Langlois JH, Roggman LA, Casey RJ, et al. Infant preferences for attractive faces: rudiments of a stereotype. *Dev Psychol*. 1987;23:363–369.
4. Aharon I, Etcoff N, Ariely D, et al. Beautiful faces have variable reward value: fMRI and behavioral evidence. *Neuron*. 2001;32:537–551.
5. Willis J, Todorov A. First impressions: making up your mind after a 100-ms exposure to a face. *Psychol Sci*. 2006;17:592–598.
6. Kanwisher N, McDermott J, Chun MM. The fusiform face area: a module in human extrastriate cortex specialized for face perception. *J Neurosci*. 1997;17:4302–4311.
7. Henderson JJA. Facial attractiveness predicts longevity. *Evol Hum Behav*. 2003;24:351–356.
8. Alam M, Dover JS. On beauty: evolution, psychosocial considerations, and surgical enhancement. *Arch Dermatol*. 2001;137:795–807.
9. Milutinovic J, Zelic K, Nedeljkovic N. Evaluation of facial beauty using anthropometric proportions. *Scientific World J*. 2014;2014:428250.
10. Møller AP, Zamora-Muñoz C. Antennal asymmetry and sexual selection in a cerambycid beetle. *Anim Behav*. 1997;54:1509–1515.
11. Mealey L, Bridgstock R, Townsend GC. Symmetry and perceived facial attractiveness: a monozygotic co-twin comparison. *J Pers Soc Psychol*. 1999;76:151–158.
12. Kock RA, Woodford MH, Rossiter PB. Disease risks associated with the translocation of wildlife. *Rev Sci Tech*. 2010;29:329–350.
13. Rhodes G, Zebrowitz LA, Clark A, et al. Do facial averageness and symmetry signal health? *Evol Hum Behav*. 2001;22:31–46.
14. Holland E. Marquardt's Phi mask: pitfalls of relying on fashion models and the golden ratio to describe a beautiful face. *Aesth Plast Surg*. 2008;32:200–208.
15. Dayan S, Romero DH. Introducing a novel model: the special theory of relativity for attractiveness to define a natural and pleasing outcome following cosmetic treatments. *J Cosmet Dermatol*. 2018;17:925–930.
16. Dayan SH, Cristel RT, Gandhi ND, et al. Perception of beauty in the visually blind: a pilot observational study. *Dermatol Surg*. 2020;46:1317–1322.
17. Rohrich R, Pessa J. The fat compartments of the face: anatomy and clinical implications for cosmetic surgery. *J Plast Reconstr Surg*. 2007;119:2219–2227.
18. Lambros V. Observations on periorbital and midface aging. *Plast Reconstr Surg*. 2007;120:1367–1376.
19. Balin A, Pratt L. Physiological consequences of human skin aging. *Cutis*. 1989;43:431–436.
20. Montagna W, Carlisle K, Kirchner S. *Epidermal and Dermal Histological Markers of Photodamaged Human Facial Skin*. Shelton, CT: Richardson-Vicks; 1988.

21. Glogau RG. Chemical peeling and aging skin. *J Geriatr Dermatol*. 1994;2:30–35.
22. Fisher GJ, Varani J, Voorhees JJ. Looking older: fibroblast collapse and therapeutic implications. *Arch Dermatol*. 2008;144:666–672.
23. Fitzpatrick T. The validity and practicality of sun-reactive skin types I through VI. *Arch Dermatol*. 1988;124:869–871.
24. Hoefflin SM. The youthful face: tight is not right, repositioning is right. *Plast Reconstr Surg*. 1998;101:1417.
25. Glogau RG., Tan SR. Filler esthetics. In: Carruthers J, Carruthers A, editors. Soft Tissue Augmentation. In: Dover JS, Alam M, series editors. *Procedures in Cosmetic Dermatology*. Edinburgh: Elsevier Saunders; 2005. p. 11–18.
26. Taub AF. Cheek augmentation improves feelings of facial attractiveness. *J Drugs Dermatol*. 2012;11:1077–1080.
27. Heckmann M, Teichmann B, Schröder U, et al. Pharmacologic denervation of frown muscles enhances baseline expression of happiness and decreases baseline expression of anger, sadness, and fear. *J Am Acad Dermatol*. 2003;49:213–216.
28. Finzi E, Wasserman E. Treatment of depression with botulinum toxin A: a case series. *Dermatol Surg*. 2006;32:645–649.
29. Alam M, Barrett KC, Hodapp RM, Arndt KA. Botulinum toxin and the facial feedback hypothesis: can looking better make you feel happier? *J Am Acad Dermatol*. 2008;58:1061–1072.
30. Zimm AJ, Modabber M, Fernandes V, et al. Objective assessment of perceived age reversal and improvement in attractiveness after aging face surgery. *JAMA Facial Plast Surg*. 2013;15:405–410.
31. Luebberding S, Krueger N, Kerscher M. Skin physiology in men and women: in vivo evaluation of 300 people including TEWL, SC hydration, sebum content and skin surface pH. *Int J Cosmet Sci*. 2013;35:477–483.
32. Luebberding S, Krueger N, Kerscher M. Age-related changes in male skin: quantitative evaluation of one hundred and fifty male subjects. *Skin Pharmacol Physiol*. 2014;27:9–17.
33. Dixson BJ, Rantala MJ. The role of facial and body hair distribution in women's judgments of men's sexual attractiveness. *Arch Sex Behav*. 2016;45:877–889.
34. Talakoub L, Wesley NO. Differences in perceptions of beauty and cosmetic procedures performed in ethnic patients. *Semin Cutan Med Surg*. 2009;28:115–129.
34a. Young MM, Franken A, du Plessis JL. Transepidermal water loss, stratum corneum hydration, and skin surface pH of female African and Caucasian nursing students. *Skin Res Technol*. 2019;25:88–95.
35. Fang F, Clapham PJ, Chung KC. A systematic review of interethnic variability in facial dimensions. *Plast Reconstr Surg*. 2011;127:874–881.



eFig. 152.1 The "Phi mask". A By incorporating the 1:1.618 ratio into numerous golden triangles and hexagons, the Phi mask reflects the mathematically ideal face. **B** The Phi mask superimposed on the human face.



eFig. 152.2 Multiple distinct subcutaneous fat compartments of the face. A, B The middle cheek (blue) fat compartment lies between the medial (yellow) and lateral temporal cheek (yellow) fat compartments. The superior border is defined by the superior cheek septum (SCS; green). A zone of fixation (red arrow) is noted where this compartment adjoins the middle compartment and inferior orbital (yellow) compartment. *From Rohrich R, Pessa J. The fat compartments of the face: anatomy and clinical implications for cosmetic surgery. J Plast Reconstr Surg 2007;119:2219–27.*

FACIAL ANALYSIS OF WOMEN OF DIFFERENT ETHNIC GROUPS

	White	African-American	Latino-American			Southern Chinese
			Caribbean	Central	South	
Horizontal proportions*	1:1:1	1:1.2:1.3 or 1:1.2:1.2				
Nasofrontal angle	125°–147°	127.6° or 136.8°–137.4°	110°	137°	136°	137.9° (119–166)
Nasofacial angle	31°–40°	33.4° or 38.9°	41°	44°	46°	36.4° (20–46)
Alar width:intercanthal distance	1:1	1.2:1	1.2:1	1:1	1.1:1	>1:1
Columella:lobule	2:1	1.3:1 or 1:1.2 or 1:1.3	1.5:1	1.1:1	1.5:1	1.2:1
Nasolabial angle	90°–120°	73.9° or 85.6°–90.3°	110°	99°	100°	87.8° (55–108)

*Horizontal proportions derived from relationship of: trichion to glabella, glabella to subnasale, subnasale to gnathion ratio.

eTable 152.1 Facial analysis of women of different ethnic groups. *Adapted from Powell N, Humphreys B. Proportions of the Aesthetic Face. New York: Thieme-Stratton, 1984, and Wen YF, Wong HM, Lin R, et al. Inter-ethnic/racial facial variations: A systematic review and Bayesian meta-analysis of photogrammetric studies. PLoS One 2015;10:e0134525.*

Cosmetics and Cosmeceuticals 153

Zoe Diana Draelos

Synonyms: ■ Cosmeceuticals – bioactive cosmetics, functional cosmetics ■ Skin care products – moisturizers, cleansers, astringents ■ Hair care products – shampoos, conditioners ■ Nail products – nail polish, nail sculptures ■ Cosmetics – facial foundation, blush, eyeshadow, mascara, lipstick

Key features

- Colored cosmetics and skin care products have an important role in the prevention of dermatologic disease and the maintenance of skin health
- Hair is a non-living structure whose appearance and behavior can be improved via the use of shampoos and conditioners
- Nail cosmetics primarily adorn the nails, but improper use can lead to nail disease
- Cosmeceuticals are non-prescription products designed to improve the functioning of the skin, primarily by targeting the aging process
- Skin, hair, and nail care products have a profound impact on these structures, and they should be part of the working knowledge of every dermatologist

INTRODUCTION

Cosmetics and skin care products are assuming an increasingly important role within dermatology as the sophistication of raw materials and the resulting formulations provide for the development of products that impact the functioning of the skin. It was traditionally thought that the stratum corneum was a non-living, biologically inert layer of the skin upon which skin care products and cosmetics impinge. It was also thought that the stratum corneum was a complete barrier unaffected by the application of non-prescription topical agents. An improved understanding of stratum corneum function, primarily obtained through the use of non-invasive bioengineering techniques, has demonstrated that the stratum corneum can be dramatically influenced by non-prescription topical agents, and that these agents can indeed penetrate the stratum corneum and influence skin function.

Recognition of the biologic importance of the stratum corneum to skin health led to the development of a new category of skin care product, referred to as the cosmeceutical[1]. A cosmeceutical is a scientifically designed, useful product intended for external application to the human body that has desirable aesthetic effects and meets rigid chemical, physical, and medical standards[2]. Even though many cosmeceuticals currently exist for use on the skin, hair and nails, there is no regulatory description that acknowledges the current scientific sophistication of these formulations. Rather, a cosmetic is defined by the US Federal Food, Drug and Cosmetic Act, written in 1938, as "articles intended to be rubbed, poured, sprinkled, or sprayed on, introduced into, or otherwise applied to the human body or any part thereof for cleansing, beautifying, promoting attractiveness, or altering the appearance", without affecting structure or function[3].

Cosmeceuticals are now a reality due to the ever-expanding dermatologic knowledge base, which has rendered obsolete the prior outdated clear distinction between cosmetics and drugs[4]. It is somewhat bewildering to realize that water is a cosmeceutical given that water profoundly influences the structure and function of the viable epidermis. Many substances can function as cosmeceuticals if entry into and through the stratum corneum is facilitated via the use of penetration enhancers, such as propylene glycol, isopropyl myristate, or pyrrolidone derivatives. Propylene glycol profoundly alters the barrier characteristics of the stratum corneum, while isopropyl myristate is capable of penetrating into the lipid bilayer of cell membranes. Pyrrolidone derivatives interact with both keratin and stratum corneum lipids to drive substances into the skin. These enhancers are commonly found in cosmetic formulations; however, improved understanding of skin physiology allowed recognition of their profound effects on the skin, which were previously unknown.

DISCUSSION

Skin Care Products

The three basic categories of skin care products are cleansers, moisturizers, and astringents. Cleansers are designed to remove sebum, desquamating corneocytes, bacteria, fungi and environmental dirt from the face and body, while leaving the intercellular lipid barrier intact. Astringents represent a subset of cleansers designed to supplement the failure of the cleanser to perform its intended function. Moisturizers are designed to minimize the barrier damage induced by cleansing. Thus, these three skin care products work together to balance the hygiene needs of the skin with the important task of preserving barrier function.

Cleansers

The development of soaps designed to cleanse the skin has been the single most important advance in decreasing disease worldwide. Even though soap is ubiquitous in the developed world, one of the main goals of global health organizations is to introduce the concept of cleansing with soap to regions of the world where contagious diseases run rampant. In basic chemical terms, soap is a fatty acid salt resulting from a reaction between a fat and an alkali[5]. The soap solubilizes sebum and environmental dirt, such that it can be rinsed away with water. The mechanics of rubbing soap over the skin with the hand or a bathing implement results in the physical removal of desquamating scales, bacteria and fungi from the skin surface. In high-income countries, where bathing has become a daily ritual, excessive use of soap has resulted in dermatologic conditions such as xerotic eczema. This has led to the development of cleansers with skin conditioning benefits that are chemically not true soaps, and they are referred to as detergents.

Cleansers, whether formulated as bars or liquids, can be divided into three basic types: *soaps, syndets and combars* (Table 153.1). True soaps are composed of long-chain fatty acid alkali salts with a pH between 9 and 10. This alkaline pH raises the pH of the skin following cleansing, resulting in stratum corneum barrier disruption and the resultant feeling of tightness following bathing. Alkalinization of the skin disrupts the natural acid mantle, which may be significant in dermatitic skin. Recognition of the need to preserve skin pH at 5.4 led to the development of *syn*thetic *det*ergents, known as syndets, such as sodium cocoyl isethionate. Syndet cleansers, also known as beauty cleansers, contain less than 10% soap and are designed with a pH of 5.5–7.0 so as to minimize cutaneous alkalinization[6]. The third type of cleanser, known as a combar, is composed of an alkaline soap to which surface-active agents with a pH of 9–10 have been added. Combars are milder cleansers than true soaps but induce more thorough cleansing than syndets. For example, true soap is a good cleansing choice for excessively oily or dirty skin, while a combar is a good cleanser for normal skin with a moderate amount of environmental dirt. Syndets would be the least damaging to the cutaneous barrier in persons with xerosis or any form of dermatitis.

The many brands of cleansers currently on the market fall into one of the three aforementioned groups, yet there must be something unique, for marketing purposes, about each cleanser. The unique aspects of each cleanser are created through the addition of specialty

CATEGORIES OF CLEANSING PRODUCTS		
Product type	**Composition**	**Product examples®,™**
Bar soap	True soap in bar form; pH 9–10	Ivory Bar Soap (Procter & Gamble)
Syndet bar cleanser	Synthetic detergents (no soap), in bar form; pH 5–7	Basis Sensitive Skin Bar (Beiersdorf)
		Cetaphil Gentle Cleansing Bar (Galderma)
		Dove Bar (Unilever)
		Olay Quench Moisturizing Bar (Procter & Gamble)
Syndet liquid	Synthetic detergents, in liquid form; pH 5.5–7	Dove Body Wash (Unilever)
		Olay Foaming Face Wash (Procter & Gamble)
Combar soap	Combination of true soap and synthetic detergent; pH 9–10	Dial Antibacterial Bar Soap (Henkel Corporation)
		Irish Spring Original Bar Soap (Colgate-Palmolive)
Body wash	Emulsion system applied with a puff, allowing synthetic detergent cleansing combined with enhanced skin moisturization and emolliency	Aveeno Daily Moisturizing Body Wash (Johnson & Johnson)
		Cetaphil Ultra Gentle Body Wash (Galderma)
		Dove Deep Moisture Body Wash (Unilever)
		Olay Moisture Ribbons Plus Body Wash (Procter & Gamble)
Lipid-free cleanser	Cleans without fats; may contain glycerin, cetyl alcohol, stearyl alcohol, sodium lauryl sulfate and, occasionally, propylene glycol	Aquanil Cleanser (Person & Covey)
		CeraVe Hydrating Cleanser (L'Oréal)
		Cetaphil Gentle Skin Cleanser (Galderma)
Cleansing cream	Waxes and mineral oil with detergent action from borax	Noxzema Original Deep Cleansing Cream (Unilever)*
		Pond's Cold Cream (currently contains sodium borate)
Astringent/toner	Alcohol-based product that may contain witch hazel, salicylic acid or glycolic acid	Clarifying Lotion 2, 3, 4 (Clinique)
Moisturizing astringent/toner	Glycerin-based humectant moisturizer	Clarifying Lotion 1 (Clinique)
Exfoliant cleanser	Glycolic acid- or salicylic acid-containing cleanser	Oil-Free Acne Wash (Neutrogena)
Abrasive cleanser	Hydrated silica grains within the syndet cleanser	Clinique 7 Day Scrub Cream (Estée Lauder)
		Olay Age Defying Daily Renewal Skin Cleanser (Procter & Gamble)
		Cetaphil Extra Gentle Daily Scrub (Galderma)
*Does not contain borax.		

Table 153.1 Categories of cleansing products.

additives (Table 153.2). Common cleanser additives include various fragrances as well as foaming agents designed to alter the aesthetics of the lather, but the most dermatologically relevant additives are antibacterial agents. The most widely used antibacterial in both bar and liquid cleansers is benzalkonium chloride, a quaternary ammonium compound that disrupts the cellular membrane of microbes. It is bacteriostatic against Gram-positive and some Gram-negative bacteria in addition to being fungistatic. However, benzalkonium chloride is not active against nonenveloped viruses, and some species of *Staphylococcus aureus* contain a gene that leads to resistance to quaternary ammonium compounds[7].

Another important dermatologic need with regard to skin cleansing is minimization of skin barrier dysfunction. Unfortunately, surfactants cannot distinguish unwanted sebum and oil-soluble dirt from intercellular lipids. Thus, increases in transepidermal water loss are typically noted in direct proportion to the cleansing ability of the cleanser. An attempt to provide cleansing and barrier restoration in the same product has led to the development of body washes. Since body washes are liquids, incorporating both hydrophilic and lipophilic ingredients emulsified into a single phase, it is possible to cleanse and moisturize simultaneously while allowing for rinsing away of the surfactants. Body washes must be used with a puff to introduce both water and air into the cleanser emulsion in sufficient quantity to allow cleansing and moisturization to occur. The syndet detergents, primarily ammonium laureth sulfate, solubilize oil-soluble dirt into the rinse water for removal during the cleansing phase when the body wash concentration is high and the water concentration low, while occlusive moisturizing substances (e.g. petrolatum) and emollients (e.g. soybean oil) are left behind to retard transepidermal water loss and improve skin smoothness during the rinse phase when the body wash concentration is low and the water concentration is high.

Other cleanser variants for persons with dry, dermatitic skin include lipid-free, non-foaming cleansers and cold creams. These products are excellent at removing cosmetics and low levels of environmental dirt. Lipid-free cleansers are non-foaming, soap-free liquid products applied to dry or moistened skin, rubbed to produce minimal lather, and rinsed or wiped away. They possess low surfactant capabilities, and they can only remove bacteria through mechanical means, yet they are important in persons with barrier disruption[8]. The classic cleanser for dry, dermatitic skin is cold cream, which combines the effect of a lipid solvent, such as wax or mineral oil, with detergent action from borax[9]. However, not all formulations of cold creams contain borax (sodium borate).

Occasionally, a dermatologic need arises for specialty cleansers designed to offer a skin benefit beyond pure removal of sebum and environmental dirt. For example, it may be desirable to induce corneocyte disadhesion in older patients requiring an exfoliant cleanser. This can be accomplished through the addition of chemical exfoliants, such as salicylic or glycolic acid, to the cleanser formulations discussed previously. Exfoliant cleansers containing benzoyl peroxide or salicylic acid are sometimes used as an adjunct in topical acne treatment. Exfoliation can also be induced mechanically through the incorporation of fine abrasive particles (such as aluminum oxide, hydrated silica grains, ground fruit pits, or sodium tetraborate decahydrate granules) in a liquid syndet cleanser to remove skin scale. Lastly, mechanical exfoliation can be encouraged by using specially woven face cloths, designed to remove skin scale without inducing epidermal damage.

The development of novel detergents and cleansing specialty additives has created a confusing plethora of consumer products, yet the goal remains the same: to allow adequate skin hygiene without barrier damage. Our next concern is the discussion of moisturizers, designed to replace skin sebum and natural moisturizing factors in instances where the stratum corneum barrier has been damaged from exuberant cleansing.

SPECIALTY SOAP FORMULATIONS	
Type of soap	**Unique ingredients**
Superfatted soap	Increased oil and fat, representing up to 10%
Castile soap	Olive oil used as main fat
Deodorant soap	Antibacterial agents
French milled soap	Additives to reduce alkalinity
Floating soap	Extra air trapped during mixing process
Oatmeal soap	Ground oatmeal added (coarsely ground to produce abrasive soap; finely ground for gentle cleanser)
Acne soap	Sulfur, resorcinol, benzoyl peroxide and/or salicylic acid added
Facial soap	Smaller bar size, no special ingredients
Bath soap	Larger bar size, no special ingredients
Aloe vera soap	Aloe vera added to soap, no special skin benefit
Vitamin E soap	Vitamin E added, no special skin benefit
Cocoa butter soap	Cocoa butter used as major fat
Nut or fruit oil soap	Nut or fruit oils used as major fat
Transparent soap	Glycerin and sucrose added
Abrasive soap	Pumice, coarse oatmeal, maize meal, ground nut kernels, dried herbs, or flowers added
High impact soap	Strong, high-concentration fragrance added to scent skin after cleansing
Soap-free soap	Contains synthetic detergents (syndet bar)

Table 153.2 Specialty soap formulations.

DIFFERENT TYPES OF MOISTURIZERS		
Moisturizer type	**Composition**	**Product examples®,™**
Oil only	Petrolatum	Vaseline petroleum jelly (Unilever)
Oil-in-water emulsion	Water, petrolatum	Eucerin Original Healing Cream (Beiersdorf)
		Vanicream (Pharmaceutical Specialties)
Polymer-based	Water, polyglycerylmeth-acrylate, petrolatum	Cetaphil Moisturizing Cream (Galderma)
Vegetable oil and wax	Castor oil, corn oil, ozokerite, beeswax, paraffin, carnauba wax	Norwegian Formula Lip Moisturizer (Neutrogena)
Glycerin-rich	Water, glycerin, petrolatum	Norwegian Formula Hand Cream (Neutrogena)
		Curél Daily Moisture Original Lotion (Kao Corporation)
Dimethicone and ceramides	Water, petrolatum, dimethicone, ceramides	CeraVe Moisturizing Cream (L'Oréal)
		EpiCeram (Primus Pharmaceuticals)

Table 153.3 Different types of moisturizers. Additional prescription moisturizers are available, e.g. ones based upon glycyrrhetinic acid plus shea butter (Atopiclair® cream) or castor oil (Promiseb™ cream); a complete list is provided in Table 129.12.

Moisturizers

The term "moisturizer" is somewhat misleading to the consumer, who assumes that the cream or lotion puts moisture or water back into the skin[10]. Moisturizers do not put water back into the skin externally, nor do they get incorporated into the intracellular lipids. Moisturizers simply attempt to retard transepidermal water loss and create an optimal environment for restoration of the stratum corneum barrier[11]. The optimal water content for the stratum corneum is between 10% and 30%, depending on the measurement technique employed, and moisturizers can function to raise the cutaneous water content through occlusion or humectancy via a variety of active agents (Table 153.3)[12].

Occlusive moisturizers prevent evaporative water loss to the environment by placing an oily substance on the skin surface through which water cannot penetrate, thus replenishing the stratum corneum moisture by water movement from the lower viable epidermal and dermal layers[13]. There are many different classes of chemicals that can function as occlusive moisturizers[14], for example, hydrocarbon oils and waxes (petrolatum, mineral oil, paraffin, squalene), silicones (cyclomethicone, dimethicone), vegetable oils (castor oil, corn oil, grape seed oil, soybean oil), animal oils (mink oil, emu oil), fatty acids (lanolin acid, stearic acid), fatty alcohols (lanolin alcohol, cetyl alcohol), polyhydric alcohols (propylene glycol), wax esters (lanolin, beeswax, stearyl stearate), vegetable waxes (carnauba wax, candelilla wax), phospholipids (lecithin), and sterols (cholesterol, ceramides)[15].

The most effective occlusive moisturizer is petrolatum, since it reduces transepidermal water loss by 99%[16]. Total occlusion of the stratum corneum is undesirable, since transepidermal water loss is the cellular signal that initiates barrier repair and the resulting synthesis of intercellular lipids[17,18]. Complete cessation of transepidermal water loss results in no barrier repair, allowing water loss to return to its pretreatment level once complete occlusion has been removed[17–19]. Petrolatum allows barrier repair while permeating throughout the interstices of the stratum corneum[20].

Another technique for rehydrating the stratum corneum is the use of humectants. Humectants are substances that attract moisture; they include glycerin, honey, sodium lactate, urea, propylene glycol, sorbitol, pyrrolidone carboxylic acid, gelatin, hyaluronic acid, and some vitamins and proteins[14,21]. The body utilizes hyaluronic acid and other glycosaminoglycans in the dermis as biologic humectants to prevent desiccation of the skin. Humectants can only hydrate the skin from the environment when the ambient humidity exceeds 70%. Consequently, rehydration of the stratum corneum generally occurs by water that is attracted from the deeper epidermal and dermal tissues. Most moisturizers combine both occlusive and humectant moisturizing ingredients, since water drawn by a humectant to a damaged stratum corneum barrier will be lost to the atmosphere unless trapped by an occlusive[22,23]. Humectants also help to improve the smoothness of xerotic skin by inducing corneocyte swelling and minimizing voids between the desquamating corneocytes[24].

In summary, remoisturization of the skin must occur in four steps:

- initiation of barrier repair (see Ch. 124)[25]
- alteration of surface cutaneous moisture partition coefficient
- onset of dermal–epidermal moisture diffusion
- synthesis of intercellular lipids[26].

Moisturizers attempt to increase stratum corneum water content through the principles of occlusion and humectancy. The discovery of aquaporin-3 channels in the skin and their modulation by glycerin and urea has increased research into osmotic cell balance as another mechanism for moisturization.

Astringents

Occasionally, patients use skin care products that either correct the deficiencies of the cleanser or supplement the effects of the moisturizer. These products are known as astringents or toners (see Table 153.1). They are used after cleansing but before moisturizing, and they are left on the face following use. Astringents are usually liquids wiped over the face with a cotton ball. Originally, astringents were intended to remove soap scum left behind on the face from the use of lye-based soaps and hard water. If left behind, this soap scum could cause irritant contact dermatitis. The original astringents were fragranced isopropyl alcohol or propylene glycol solutions designed to remove oil-soluble residue. The development of synthetic detergents and treated water has made this original intent obsolete, yet astringents remain popular.

Currently, astringents are used to remove the oily residue left behind after cleansing of the face with lipid-free cleansers or cleansing creams, discussed previously. Oily complexion astringents are formulated to remove any remaining sebum from the face following synthetic detergent cleansing or to deliver keratolytics, such as salicylic acid, glycolic acid or witch hazel. Some astringents designed for dry skin contain a humectant liquid moisturizer, such as propylene glycol or glycerin, and skin soothing agents, such as allantoin, guaiazulene or quaternium-19[27].

FUNCTIONS OF FACIAL FOUNDATION
• Add facial color
• Blend facial color
• Camouflage pigmentation irregularities
• Normalize facial skin
• Provide sun protection
• Act as a treatment product

Table 153.4 Functions of facial foundation.

A complete cosmetic-counter facial treatment routine involves a cleanser followed by an astringent and then a moisturizer. Once the skin has been prepared in this manner, colored cosmetics are applied.

Colored Facial Cosmetics

Colored facial cosmetics are intended to adorn the eyes, lips, and cheeks with color for the purposes of creating a fashionable appearance, highlighting certain desirable features, and camouflaging facial flaws. Colored cosmetics are of importance to the dermatologist for their role in maintaining skin health, inducing dermatitis, and camouflaging surgical defects.

Facial foundations

Formulation

Facial foundations are the first cosmetic applied to the face following the use of a moisturizer and are basically pigmented moisturizers worn for 8 hours or longer before removal. Consequently, this class of colored facial cosmetics has the greatest impact on the integrity of the skin. Facial foundations are available for every complexion type and skin color, fulfilling the needs listed in Table 153.4.

There are four basic facial foundation formulations: oil-based, water-based, oil-free, and water-free or anhydrous forms[28]. Oil-based products are designed for dry skin, while water-based products can be adapted for all skin types. Oil-free formulations are used in oily skin foundations, while anhydrous forms are extremely long-wearing and used for camouflage or theatrical purposes.

Oil-based foundations are water-in-oil emulsions containing pigments suspended in oil (e.g. mineral oil) or lanolin alcohol. Vegetable oils (grape seed, coconut, sesame, safflower) and synthetic esters (isopropyl myristate, octyl palmitate, isopropyl palmitate) may also be incorporated. The water evaporates from the foundation following application, leaving the pigment in oil on the face. This creates a moist skin feeling, especially desirable in dry complected patients. Because the color is fully developed within the oily phase of the formulation, oil-based foundations do not shift color as they mix with sebum. These foundations are easy to apply, since the pigment can continue to be spread over the face for up to 5 minutes, prior to setting.

Water-based facial foundations are oil-in-water emulsions containing a small amount of oil, in which the pigment is emulsified, and a relatively large quantity of water. The primary emulsifier is usually a soap, such as triethanolamine, or a non-ionic surfactant. The secondary emulsifier, present in a smaller quantity, is usually glyceryl stearate or propylene glycol stearate. These popular foundations are appropriate for minimally dry to normal skin. Since the pigment is already developed in oil, this foundation type is also not subject to color drift. The amount of time the product can be moved over the face, known in the industry as playtime, is shorter than with oil-based foundations.

Oil-free facial foundations contain no animal, vegetable, or mineral oils. They contain other oily substances, such as dimethicone or cyclomethicone. These foundations are usually designed for oily complected individuals, since they leave the skin with a dry feeling. Dimethicone is non-comedogenic, non-acnegenic and hypoallergenic, accounting for the tremendous popularity of this type of facial foundation formulation. Both water-based and oil-free foundations are usually packaged in a bottle.

Water-free, or anhydrous, foundations are waterproof. Vegetable oil, mineral oil, lanolin alcohol and synthetic esters form the oil phase, which may be mixed with waxes to form a cream. High concentrations of pigment can be incorporated into the formulation, yielding an opaque facial foundation. The coloring agents are based on titanium dioxide with iron oxides, occasionally in combination with ultramarine blue. Titanium dioxide acts both as a facial concealing agent and sunscreen. These products can be dipped from a jar, squeezed from a tube, wiped from a compact, or stroked from a stick. Water-free foundations are well suited for use in people who require facial camouflaging. They can be combined with a high-coverage powder foundation to increase the opacity of the cosmetic.

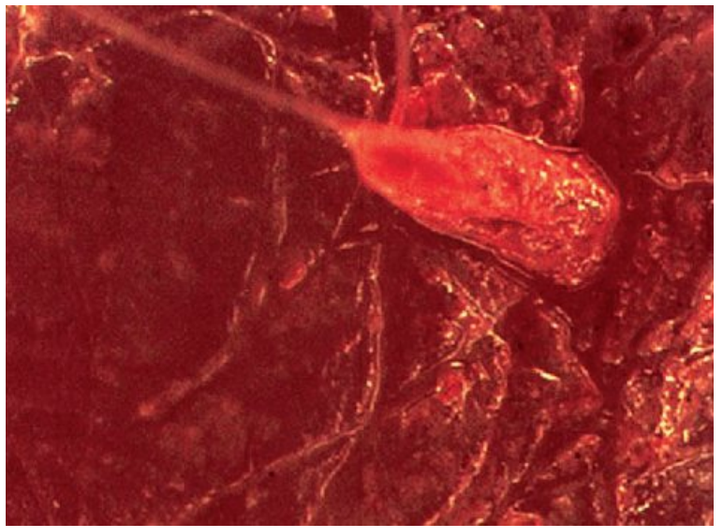


Fig. 153.1 Migration of iron oxide particles in facial foundation to follicular ostia. As seen by video microscopy (400×), this migration tends to occur as sebum and eccrine secretions mix with the cosmetic film.

Application and cutaneous effects

Facial foundations must be evenly applied to create the optimal cosmetic appearance and achieve the secondary benefit of sun protection. The iron oxide pigment and other covering agents, e.g. titanium dioxide, zinc oxide and kaolin, are physical particulates that block both UVA and UVB radiation (see Ch. 132). A facial foundation *without* any added organic sunscreen ingredients, such as ecamsule, octyl methoxycinnamate, oxybenzone or avobenzone, usually has a sun(burn) protection factor (SPF) of at least 4. Facial foundations that have greater coverage in order to camouflage underlying pigmentation defects usually possess an SPF of at least 8. The inclusion of additional sunscreen agents to a facial foundation can raise its SPF to 15. Thus, facial foundation is an excellent, cosmetically elegant facial photoprotectant.

An even, cosmetically acceptable application of facial foundation begins with a proper color match to the skin at the jawline and application with the fingertips. A dab of foundation should be placed on the forehead, nose, cheeks, and chin, and then blended with a light circular motion until it is evenly spread over the entire face, including the lips. Finally, a puff or sponge should be used, stroking in a downward direction, to remove any streaks and to flatten vellus facial hair. Special care should be taken to rub the foundation into the hairline, over the tragus, and beneath the chin. Foundation should also be blended around the eyes, and it may even be applied to the entire upper eyelid if desired. The foundation should be allowed to set or dry until it can no longer be removed with light touch. If additional coverage is desired, a second layer of foundation can be applied.

The most common adverse dermatologic effect related to the use of facial foundation is a condition patients describe as "breakouts". Patients typically note small follicular papules 48 hours after using a new facial foundation. The appearance resembles that of acne; however, the 48-hour time course is inconsistent with a diagnosis of acne. This condition may represent a follicular irritant contact dermatitis, since facial foundations tend to migrate to the follicular ostia as they mix with eccrine secretions and sebum, which break down the cosmetic film (Fig. 153.1). This observation may explain why facial foundations that have been found on clinical testing to be non-comedogenic and non-acnegenic cause acneiform eruptions in individuals with self-diagnosed sensitive skin. Overall, however, facial foundations are an infrequent cause of dermatologic problems.

COVERING ABILITY OF FACE POWDER INGREDIENTS
• Titanium dioxide*
• Kaolin (hydrated aluminum silicate)
• Magnesium carbonate
• Magnesium stearate
• Zinc stearate
• Prepared chalk
• Zinc oxide*
• Rice starch
• Precipitated chalk
• Talc (hydrated magnesium silicate)
*Hardness greater than platinum, gold, and silver so capable of producing black dermographism.

Table 153.5 Covering ability of face powder ingredients. Listed in order of increasing opacity.

PIGMENTS ALLOWED BY THE US FDA IN EYE SHADOW COSMETICS
• Iron oxides
• Titanium dioxide (alone, or combined with mica)
• Copper, aluminum, and silver powder
• Ultramarine blue, violet, and pink
• Manganese violet
• Carmine
• Chrome oxide and hydrate
• Iron blue
• Bismuth oxychloride (alone, or on mica or talc)
• Mica

Table 153.6 Pigments allowed by the US Food and Drug Administration (FDA) in eye shadow cosmetics.

Powders

One of the ways of preventing migration of facial foundation, improving its sun protective capabilities, and increasing oil absorption is to apply powder over the foundation. Facial powders contain predominantly talc (hydrated magnesium silicate) and increased amounts of covering pigments. The covering pigments used in face powder are listed in order of increasing opaqueness in Table 153.5. It is generally accepted that the optimum opacity is achieved with a particle size of 0.25 mcg. Black dermographism from earrings and rings can result when face powders contain ingredients, e.g. zinc oxide, that are harder than platinum, silver or gold.

Facial powders usually also contain magnesium carbonate and/or kaolin (hydrated aluminum silicate) to absorb oil and perspiration. Full-coverage face powders with increased pigments and light-reflective particles are usually packaged as a cake in a compact and applied to the face with a puff, loose in a jar and dusted over the face with a brush, or stroked over the face from an automatic brush dispenser. These face powders with increased pigments can be used as a facial foundation and are known as mineral make-ups. They are recommended for persons with sensitive skin and rosacea as they contain no liquids, fewer preservatives, and fewer ingredients. As a result, there is decreased potential for allergic and irritant contact dermatitis. Specially pigmented powders are used to redden the cheeks, known as blushes, and to color the eyelids, known as eye shadows.

Facial blushes

Facial blushes are typically powders designed to simulate rosy cheeks, occasionally an unwanted finding in rosacea patients. Blushes have the same basic formulation as face powders, except for the presence of different surface characteristics that can vary from a matte dull finish to a frosted shine or metallic glow, depending on current fashion trends[29]. Some of the rough-edged particles designed to produce light reflection can cause irritation in people with sensitive skin. Powder blush can be used to absorb facial oil and blend the facial erythema of rosacea across the cheeks, as well as to add color to a sallow face by dusting on the central chin, cheeks, nasal tip, and forehead.

Eye shadows

Eye shadows are similar to powder blushes in formulation and surface characteristics, except that the color variation is broader, but limited in the US by the Food and Drug Administration (FDA) to the purified natural colors or inorganic pigments listed in Table 153.6[30]. Eye shadow can be used to camouflage misshapen eyes, provide sun protection to the upper eyelid, and minimize the appearance of unwanted periorbital pigmentation. Eye shadows are a common concern to dermatologists, since they may be responsible for eyelid dermatitis. They may contain the same light-reflective particles as blushes and cause pruritus of the eyelids due to irritant contact dermatitis until discontinued (Fig. 153.2).

In one series, the North American Contact Dermatitis Group determined that 12% of cosmetic reactions occurred on the eyelid, but only 4% could be linked to eye make-up use[31]. When allergic contact dermatitis is due to eye shadows, the most common culprits are the red pigments used in pinkish eye shadows. Unfortunately, it can be difficult to determine the etiology of allergic contact eyelid dermatitis with routine patch testing[32], since many substances can be transferred to the eye area by the hands, complicating the dermatologic evaluation[33]. However, eye shadows are a rare cause of eye infections, since the dry powder cake does not support bacterial growth.



Fig. 153.2 Upper eyelid dermatitis. Upper eyelid dermatitis may be exacerbated by the use of heavily pigmented, light-reflective eye shadows.

Mascaras

Mascaras are eyelash cosmetics, as opposed to eye shadows which are eyelid cosmetics. Mascaras are designed to color, camouflage, elongate and thicken the eyelashes, which frame the eyes. They must be carefully formulated to allow easy and even application without smudging, irritancy or toxicity. Some of the coloring agents employed include iron oxide to produce black, ultramarine blue to create navy, and umber, burnt sienna, or synthetic brown oxide to create brown[34].

Most modern mascaras are formulated as liquids, then stored in a tube with a multitufted applicator brush or comb. The applicator is inserted into the tube between uses, providing numerous opportunities to inoculate bacteria into the cosmetic. The most dangerous bacterial infection is a corneal infection due to *Pseudomonas aeruginosa*, which can permanently diminish visual acuity[35,36]. *Staphylococcus epidermidis, S. aureus* and fungal organisms may also proliferate in contaminated mascaras[37,38]. Infections are more common if the globe is traumatized by the infected mascara wand. Even though mascaras contain antibacterials, it is still wise to discard all mascara tubes after three months and not allow multiple persons to use the same mascara tube[39].

There are several mascara formulations that are less likely to support bacterial and fungal growth (Table 153.7). Mascaras are available as water- or solvent-based and as a water/solvent hybrid. Water-based mascaras are easily removed with water and less likely to cause eye area irritation, but the presence of water provides a welcome medium for bacterial growth. Solvent-based mascaras are manufactured without water, must be removed with a special cleanser, and are more irritating; however, they are less likely to support bacterial growth and are therefore the formulation of choice for individuals who are carriers of *Staphylococcus* or *Streptococcus* spp[40]. The water/solvent hybrid mascaras are an attempt to provide a water-resistant cosmetic with the

DIFFERENT TYPES OF MASCARA FORMULATIONS		
Mascara formulation	**Composition**	**Advantages/Disadvantages**
Water-based	Waxes, pigments, resins	Easy to remove with water; runs with tearing; supports bacterial growth
Solvent-based waterproof	Petroleum distillates, pigments, waxes	Must be removed with solvent; waterproof; does not support bacterial growth
Water-resistant water/solvent hybrid	Oil-in-water emulsion, pigments	Removal with water and cleanser; resists running with tearing; less likely to support bacterial growth
Compressed cake	Pigments, talc	Removal with water; runs with tearing; least allergenic; does not support bacterial growth

Table 153.7 Different types of mascara formulations.

CAMOUFLAGE FOR ABNORMALITIES OF FACIAL PIGMENTATION OR COLOR		
Facial color	**Disease process**	**Undercover foundation color**
Red	Rosacea, psoriasis, lupus erythematosus, port-wine birthmark, telangiectasias	Green
Yellow	Solar elastosis, chemotherapy, dialysis	Purple
Brown hyperpigmentation	Melasma, lentigines, nevi	White
Hypopigmentation and depigmentation	Postinflammatory, congenital, vitiligo	Brown

Table 153.8 Camouflage for abnormalities of facial pigmentation or color.

benefits of both. Recent analyses of waterproof mascaras, as well as long-lasting lipsticks, have found high levels of fluorine, suggesting the presence of per and polyfluoroalkyl substances (PFAS).

Another dermatologic side effect of the use of mascara is conjunctival pigmentation, resulting from the washing of mascara into the conjunctival sac by lacrimal fluid[41]. This colored particulate matter can be observed on the inferior tarsal (palpebral) conjunctiva. Histologically, the pigment is seen within macrophages and extracellularly in association with a variable lymphocytic infiltrate. Electron microscopy suggests that ferritin, carbon, and iron oxides are present within the tissues[42]. Unfortunately, there is no treatment for the condition, which is usually asymptomatic.

Specialty mascaras are available for curling and elongating the eyelashes. These mascaras contain pigmented polymers that polymerize on the eyelash as they dry. The polymer then shrinks, curling the eyelash and placing a thin, long-wearing, pigmented film around the hair which thickens and elongates the lash. In addition, a prescription cosmeceutical containing bimatoprost 0.03% (Latisse®; originally indicated for the treatment of glaucoma) is available to elongate eyelashes via prostaglandin modulation (see Ch. 129)[43]. Side effects include iris and eyelid pigmentation, which may be permanent.

Lipsticks

Lipstick is a lip cosmetic designed to frame the teeth. Traditional lipsticks are mixtures of waxes, oils and pigments in various concentrations to yield the characteristics of the final product. For example, a lipstick designed to remain on the lips for a prolonged period of time is composed of high wax, low oil, and high pigment concentrations, whereas a product designed for a smooth creamy feel on the lips is composed of low wax and high oil concentrations[44]. The waxes commonly incorporated into lipstick formulations are white beeswax, candelilla wax, carnauba wax, ozokerite wax, lanolin wax, ceresin wax and other synthetic waxes. Usually, lipsticks contain a combination of these waxes carefully selected and blended to achieve the desired melting point. Oils for pigment dispersion are then selected, such as castor oil, white mineral oil, lanolin oil, hydrogenated vegetable oils or oleyl alcohol, to form a film suitable for application to the lips[45,46].

Newer lipstick formulations contain long-wearing polymers that create a waterproof film over the lips that remains in place indefinitely until worn away with speech or eating. These long-wearing lip products can cause cheilitis, due to their non-moisturizing formulations. In addition, lip products are marketed that claim to plump the lips. These products contain irritants, such as capsaicin, that create a mild irritant contact dermatitis resulting in short-lived lip edema.

Certain common lipstick ingredients can cause problems in the sensitized patient[47]. Castor oil, found in almost all lipsticks due to its excellent ability to dissolve bromo acid dyes, can cause allergic contact dermatitis[48]. Even the bromo acid dyes, such as eosin (D & C Red No. 21), found in indelible lipsticks can cause allergic contact dermatitis[49]. Other lipstick ingredients reported to cause allergic contact dermatitis include: waxes (e.g. propolis[50]), preservatives (e.g. propyl gallate[51], benzoic acid[52]), sunscreens (e.g. oxybenzone[53], benzophenone-3[54]), colors (e.g. lithol rubine BCA [Pigment Red 57-1][55]), fragrances (e.g. peppermint oil), vitamin E, and ricinoleic acid[56].

Facial cosmetics for camouflaging

All of the colored cosmetics previously discussed are used in combination for facial camouflaging purposes in order to minimize facial defects while accentuating attractive facial features. Camouflage cosmetics are used by paramedical aestheticians, dermatologists, plastic surgeons, and cosmetic consultants[57]. Their successful use requires a well-formulated, quality product applied with the skill of a stage make-up technician and the artistic abilities of a painter[58]. Facial defects requiring camouflaging are defects of pigmentation and/or contour[59].

Pigmentation defects represent abnormalities limited to the color of the skin, whereas contour defects are defined as areas where the facial skin is hypertrophic or atrophic, with textural changes due to the absence of appendageal structures. Table 153.8 lists examples of pigmentary abnormalities frequently encountered by dermatologists that arise from inflammatory disorders, systemic diseases, or extrinsic effects (e.g. sun exposure). Pigmentation defects or discolorations can be camouflaged either by applying an opaque cosmetic that allows none of the abnormal underlying skin tones to be appreciated or by applying foundations of complementary colors. For example, red discoloration can be camouflaged by applying a green foundation, since green is the complementary color to red. The blending of red skin with green foundation yields a brown tone, which can be readily covered by a more conventional facial foundation. Furthermore, yellow skin tones can be blended with a complementary-colored purple foundation to also yield brown tones.

The camouflaging of facial contour abnormalities is based on the principle that dark colors make protuberances appear to recede while light colors make surface depressions appear shallower. Creating an even-appearing surface on a scarred face is achieved through artistic shading. Powdered blush-type products are best suited for this purpose. Areas of the face that need to be lightened should be brushed with a light pink or peach pearled blush or buffer. Areas of the face that need to be darkened should be brushed with a deep plum or bronze matte-finish blush or highlighter.

Hair Care Products

Some of the material discussed previously is applicable to hair care products, since shampoos can be likened to skin cleansers, while conditioners are analogous to skin moisturizers.

Hair shampoos

Shampoos are simply designed to cleanse the hair; however, this is a complicated task considering that the average woman has 4–8 m^2 of hair surface area to clean[60]. Shampoos are intended to remove sebum, sweat components, desquamated stratum corneum, styling products, and environmental dirt from the hair and scalp[61]. They contain detergents, foaming agents, conditioners, thickeners, opacifiers, softeners, sequestering agents, fragrances, preservatives, and specialty additives[62]. Synthetic detergents remove sebum and dirt; however, excessive removal of sebum leaves the hair dull, susceptible to static electricity, and difficult to comb, creating the need for hair conditioners[63].

Shampoo detergents can be chemically classified as anionics, cationics, non-ionics, amphoterics, and natural surfactants (Table 153.9)[64]. The basic difference between bar soap and shampoo is the addition of a higher concentration of sequestering agents to chelate magnesium and calcium ions, preventing the formation of other salts or insoluble soaps known as soap scum. Without sequestering agents, shampoos would leave the hair dull and contribute to scalp pruritus. There are many different types of shampoo, designed to meet various hair cleansing needs (Table 153.10). Nowadays, a number of shampoos claim to be sulfate-free, meaning the requisite cleansing detergent is not sodium lauryl sulfate or sodium laureth sulfate.

A more recent development is dry shampoo, which consists of a powder that is dusted on the scalp while avoiding the hair, and then is brushed out. The powder absorbs oil and is removed without water contact. The advantage of dry shampoos is the prolongation of the effect of artificial hair coloring agents that occurs when water contact is avoided.

Hair conditioners

The need for hair conditioners arises from the inability of shampoos to remove just enough sebum to leave the hair clean, without removing too much sebum and thus creating dry, unmanageable, dull hair[65]. Conditioners are also required because permanent waving, permanent coloring, and other chemical hair treatments damage the cuticle, making the hair harsh, brittle, and difficult to disentangle (Table 153.11; Fig. 153.3)[66]. Hair conditioners are designed to reverse this hair damage by improving sheen, decreasing brittleness, decreasing porosity, increasing strength, and repairing degradation in hair proteins[67,68].

Hair conditioners improve manageability by decreasing static electricity. Following combing or brushing, the hair shafts become negatively charged, causing the hairs to repel one another. Conditioners deposit positively charged ions on the hair shaft, neutralizing the electrical charge. They also improve manageability by reducing hair shaft combing friction by as much as 50%, leading to enhanced disentangling. Conditioners also smooth the cuticular scale to increase hair shine (Fig. 153.4)[69,70]. Maximum hair shine is produced by large-diameter, elliptical hair shafts with a sizable medulla and intact, overlapping cuticular scales[71]. Hair that lacks shine is missing its cuticle (Fig. 153.5).

Special hair conditioner formulations attempt to repair split-ends by temporarily reapproximating the frayed remnants of remaining medulla and cortex. This is accomplished by including hydrolyzed animal proteins that can minimally penetrate the hair shaft, enhancing hair tensile strength by 5% until the hair is next shampooed. There are several types of conditioners formulated for a variety of needs (Table 153.12). Leave-in conditioners are specially designed for Afro-textured hair in order to maintain hair water content despite the unavoidable loss that occurs following hair straightening[72].

Safety issues

Hair care products are generally safe, especially since they are rinsed from the hair and skin by water. However, patients can develop allergic contact dermatitis, in particular to paraphenylenediamine (PPD) which is contained in permanent hair dyes. The dermatitis more commonly affects the face and neck rather than the scalp alone[73]. Gradual coloring with metallic dyes and temporary coloring can be used in patients who are allergic to PPD, but they need to be warned of possible cross-reactions to chemically related topical and systemic medications (see Table 153.11)[74].

In addition to applying chemical relaxers to "permanently" straighten curly or kinky hair, a semi-permanent technique, known by several names including Brazilian hair straightening, keratin blowout and Brazilian keratin treatment, can be utilized, with straightening effects lasting for 10–16 weeks. A keratin- and formaldehyde-containing solution is applied to the hair followed by the use of a heated straightening iron. The health concern is the release of toxic levels of formaldehyde gas. In solution, formaldehyde can be in equilibrium with methylene glycol and it has multiple chemical names; therefore hair products labeled as "formaldehyde-free" but containing methylene glycol, formalin, methanal, methyl aldehyde, methylene oxide, oxomethane, oxymethylene, oxymethyline, formic aldehyde or formol are still an issue. In contrast, Japanese hair straightening (also known as thermal reconditioning) utilizes ammonium thioglycolate in combination with a heated straightening iron and is permanent (see Table 153.11).

SHAMPOO DETERGENTS		
Surfactant type	**Chemical class**	**Characteristics**
Anionics	Lauryl sulfates, laureth sulfates, sarcosines, sulfosuccinates	Deep cleansing; may leave hair harsh
Cationics	Long-chain amino esters, ammonio esters	Poor cleansing; poor lather; impart softness and manageability
Non-ionics	Polyoxyethylene fatty alcohols, polyoxyethylene sorbitol esters, alkanolamides	Mildest cleansing; impart manageability
Amphoterics	Betaines, sultaines, imidazolinium derivatives	Non-irritating to eyes; mild cleansing; impart manageability
Natural surfactants	Sarsaparilla, soapwort, soap bark, ivy, agave	Poor cleansing; excellent lather

Table 153.9 Shampoo detergents.

SPECIALTY SHAMPOOS		
Shampoo type	**Function**	**Unique ingredients**
Oily hair	Provide excellent cleansing to remove sebum with minimal conditioning	Strong surfactants such as sodium lauryl sulfate or the sulfosuccinates
Dry hair	Provide mild cleansing and excellent conditioning	Milder surfactants such as sodium laureth sulfate Sulfate-free formulations based on betaine and sulfosuccinates
Conditioning	Contain added conditioners to enhance shine and minimize static electricity	Hydrolyzed proteins designed to penetrate the hair shaft
Baby	Utilize mild detergents that anesthetize the conjunctiva to prevent stinging, burning, and irritation	Detergents from the amphoteric group such as the betaines
Medicated	Designed to treat dandruff and seborrheic dermatitis through the use of keratolytics as well as antiproliferative and anti-inflammatory agents	Tar, salicylic acid, sulfur, selenium disulfide, ketoconazole, and zinc pyrithione
Professional	Designed for use following hair coloring to reduce hair shaft swelling	Cationic acidic shampoos to neutralize residual hair shaft alkalinity following permanent hair coloring
Dry	Absorb oil without water contact, prolonging the effect of permanent, semipermanent, and temporary hair coloring agents	Absorbent powder

Table 153.10 Specialty shampoos.

CHEMICAL HAIR TREATMENTS: COLORING, PERMANENT WAVING, AND RELAXING				
Treatment	**Definition**	**Chemicals used**	**Process**	**Adverse effects**
Permanent coloring	Color persists indefinitely (until new growth appears)	• H_2O_2 (referred to as the developer or oxidizing agent) • Ammonia • Dye (e.g. *p*-phenylenediamine [PPD], aminophenols)	• H_2O_2 lightens ("lifts") the previous color by oxidizing melanin, and it causes the dye to "develop" and deposit color • Alkaline pH leads to swelling and disruption of the cuticle, allowing the dye to penetrate into the cortex • To dye dark hair to a light blonde color, the hair must first be bleached (e.g. with a mixture of ammonium persulfate and H_2O_2)	• Dull, brittle hair (especially with permanent color) • Allergic contact dermatitis, in particular to PPD • In patients allergic to PPD, potential cross reactivity to textile dyes, sulfonamides, benzocaine, procaine, para-aminobenzoic acid • Staining of the skin and seborrheic keratoses
Demi-permanent coloring	Color lasts 2–3 months (12–24 shampoos)	• Low concentration of H_2O_2 • Non-ammonia alkali (e.g. monoethanolamine) • Dye (e.g. *p*-phenylenediamine, aminophenols)	• Similar to permanent color (but to a lesser degree)	
Semi-permanent coloring	Color lasts 4–6 weeks (6–12 shampoos)	• No H_2O_2 • Mild non-ammonia alkali • Azo dyes, henna, polymerized dyes, aminophenols ± *p*-phenylenediamine	• Small dye particles both coat the cuticle and penetrate into the cortex, or dye polymers coat the cuticle • The hair is not lightened	
Gradual coloring	Color slowly builds up over time	• Metallic dyes (e.g. salts of lead, bismuth or silver)	• Dye particles slowly accumulate in the cuticle, darkening the hair within a limited (brown–black) range	
Temporary coloring	Color is removed with 1–2 shampoos	• Azo and other FD&C dyes	• Dye coats the cuticle of the hair shaft (particles are too large to penetrate the cuticle)	
Permanent waving ("perm")*	Chemical treatments "permanently" curl hair (until new growth appears)	• Ammonium or sodium thioglycolate (pH 9–10; "alkaline perm") –or – • Glycerol monothioglycolate (pH 6.5–8; "acid perm"; requires application of heat) – *or* – • Bisulfites or mercaptamine (low/neutral pH, "thioglycolate-free perms")	• The hair is wrapped around rods and the chemical solution is applied to break disulfide bonds between keratin polypeptide chains • Neutralizing solution is then used to reform the disulfide bridges, and the hair takes the shape of the rod	• Dull, brittle hair (especially with alkaline perms) • Irritant contact dermatitis • Allergic contact dermatitis, in particular to glycerol monothioglycolate • Glycerol monothioglycolate may be retained in hair for up to 3 months
Chemical relaxing (lanthionizing)*	Chemical treatments "permanently" straighten hair that is curly or kinky (until new growth appears)	• Sodium hydroxide (lye) – *or* – • Guanidine hydroxide (calcium hydroxide cream + guanidine carbonate activator solution; "no-lye" relaxers) – *or* – • Ammonium thioglycolate ("thio" relaxers)	• Disulfide bonds between keratin polypeptide chains are broken and reformed in a similar manner to permanent waving • Relaxer cream is brushed onto the hair, which is mechanically smoothened section by section; this is followed by use of a neutralizing shampoo	• Dull, brittle hair (breakage may be substantial, especially with sodium hydroxide) • Irritant contact dermatitis/chemical burns • Scarring from sodium hydroxide chemical burns • Allergic contact dermatitis

*Permanent waving or relaxing should be performed before coloring hair, since the former procedures can produce irreversible color loss; to minimize damage to the cuticle, it is best to wait 2–4 weeks before color is applied.

Table 153.11 Chemical hair treatments: coloring, permanent waving, and relaxing. See the text for a description of Brazilian and Japanese hair straightening techniques. FD&C, Federal Food, Drug and Cosmetic Act; H_2O_2, hydrogen peroxide.

Nail Care Products

There are a variety of nail care products (Table 153.13). The focus of this section is on nail polish and the use of nail sculptures while nail changes associated with a manicure or a pedicure are outlined in Table 71.11.

Nail polish

Nail polish is a cosmetic designed to temporarily place a pigmented layer over the natural nail plate. It consists of pigments suspended in a volatile solvent to which film-forming agents have been added[75]. Nitrocellulose is the most commonly employed primary film-forming agent in nail lacquer. It produces a shiny, tough film that adheres well to the nail plate. The film is somewhat oxygen-permeable, thus allowing gas exchange between the atmosphere and the nail plate, which is required to maintain nail strength. It also decreases nail water vapor loss from 1.6 to 0.4 mg/cm^2/h, preventing nail plate dehydration[76].

A resin, such as tosylamide formaldehyde (also referred to as toluene sulfonamide–formaldehyde resin), must be added to the nitrocellulose to decrease hardness, but some individuals are sensitive to this substance, which is found on the standard dermatology patch test tray. This resin has been eliminated in hypoallergenic nail enamels, which instead contain a polyester resin or cellulose acetate butyrate, but allergic contact dermatitis is still possible and the enamel is less durable[77].

A professional nail enamel application requires three layers of polish: a base coat, a pigmented nail enamel, and a top coat. The base coat ensures good adhesion to the nail plate and prevents polish chipping. The second layer is the actual pigmented nail enamel, while the third layer or top coat provides gloss and resistance to chipping. A newer professional nail enamel application technique is known as nail shellac. Nail shellacs utilize either an ultraviolet light-cured pigmented polymer, identical to that used in nail sculptures (discussed below), or an LED-cured polymer to create a thin, hard pigmented film over the natural nail plate.

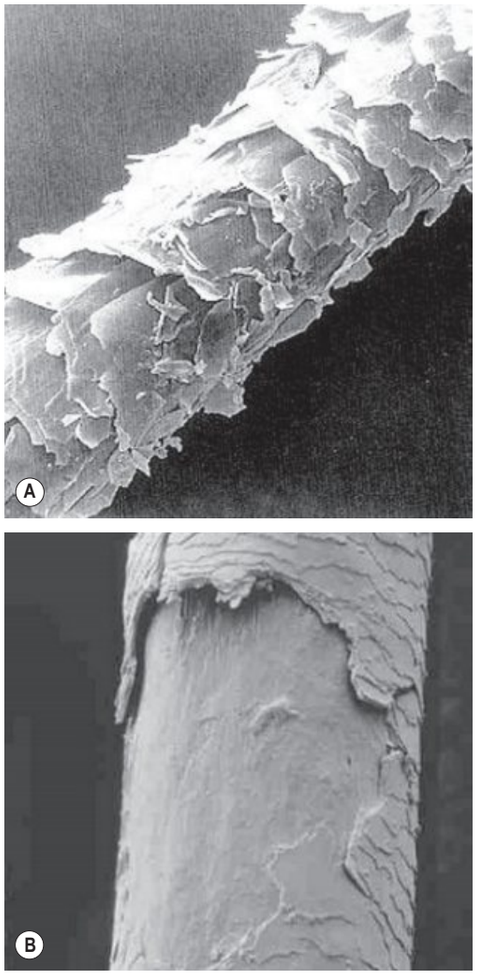


Fig. 153.3 Electron photomicrographs of chemically damaged hair shafts. A Loose cuticle, compared to the tightly overlapping cuticle of normal hairs (see Fig. 153.5). **B** Missing cuticle with exposed cortex.

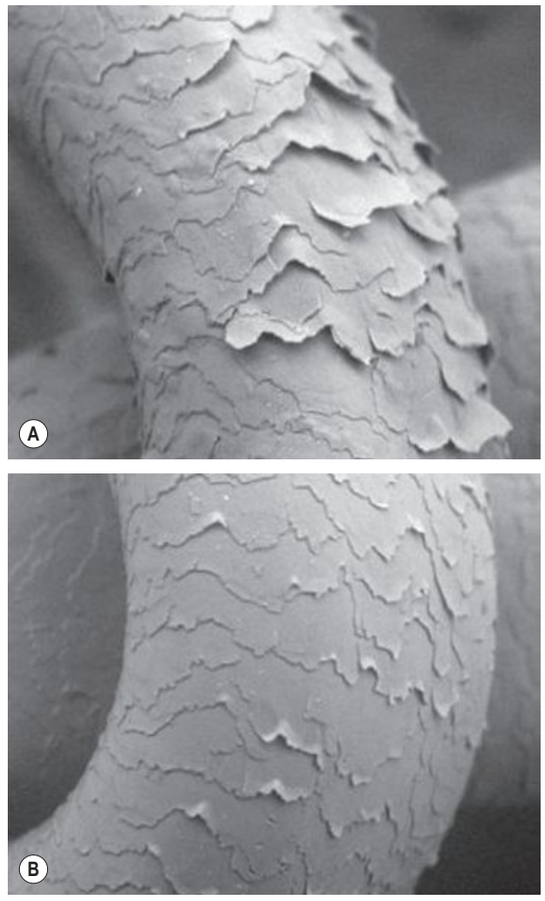


Fig. 153.4 Electron photomicrographs demonstrating the effect of hair conditioners. A Unconditioned hair shaft with uplifted cuticle. **B** Conditioned hair shaft with tightly adherent cuticle.

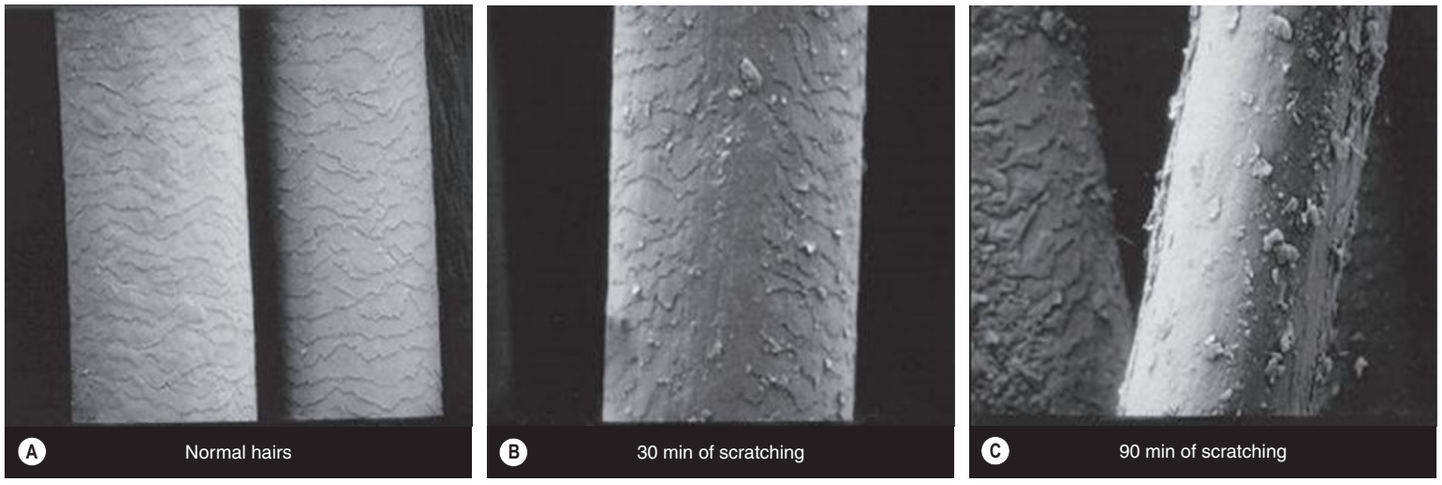


Fig. 153.5 Electron photomicrographs demonstrating the progressive removal of the hair cuticle as a result of scratching. The most common cause of cuticle removal is scratching and this leads to dull fragile hair. Note that the normal hairs have a tightly overlapping cuticle.

Problems associated with nail enamels include nail plate discoloration and allergic contact dermatitis. Nail staining is most commonly seen following the use of deep red nail polishes containing D & C Reds No. 6, 7, 34, or 5 Lake[78]. The nail plate will be stained yellow after 7 days of continuous nail polish wear and will fade without treatment in approximately 14 days, once the enamel has been removed (Fig. 153.6)[79]. Allergic contact dermatitis is seen in persons sensitive to tosylamide formaldehyde, who may develop proximal nail fold erythema and edema, fingertip tenderness and swelling, and/or eyelid dermatitis[80]. In one series, the North American Contact Dermatitis Group determined that 4% of positive patch tests were due to tosylamide formaldehyde resin allergy[32].

Nail sculptures (artificial nails)

Nail polish is designed to color the nail plate. It may make the nail somewhat stronger due to the presence of the resin layer, but it cannot elongate fingernails. Since long fingernails are considered attractive by some women, this has led to the development of an industry dedicated to the application of nail prostheses. These nail prostheses, known as nail sculptures, are applied over the natural fingernails and toenails (Table 153.14).

Nail sculptures are formed by mixing liquid ethyl or isobutyl methacrylate monomers with powdered polymethyl methacrylate polymer. This mixture polymerizes in the presence of a benzoyl peroxide accelerator and a formable acrylic is produced, which hardens in 7–9 minutes[81]. Usually, hydroquinone, monomethyl ether of hydroquinone, or pyrogallol is added to slow down polymerization[82].

Many patients are not aware that the finished nail sculptures require more care than natural fingernails. With continued wear of the sculpture, the acrylic loosens from the natural nail, especially around the edges. These loose edges must be clipped and new acrylic applied approximately every 3 weeks to prevent infection and onycholysis[83,84]. However, damage to the natural nail plate is inevitable with the use of nail sculptures (Fig. 153.7). After 2 to 4 months of wear, the natural nail plate becomes yellowed, dry, thin, and bendable. This is due to interference with the nail's normal vapor exchange, nail plate trauma during the removal process, and damage to the underlying nail bed[85]. For this reason, it is not advisable to wear sculptured nails for more than 3 months consecutively, allowing 1 month between applications (Fig. 153.8). Oftentimes nail sculptures are adorned with nail polishes to create special visual effects (Table 153.15).

Allergic contact dermatitis is an important dermatologic issue, since isobutyl, ethyl, and tetrahydrofurfuryl methacrylate are strong sensitizers[86,87]. However, the polymerized, cured acrylic is not sensitizing, only the liquid monomer[88]. Therefore, a careful operator who avoids skin contact with the uncured acrylic can avoid sensitizing the patient. Patch testing should be performed in suspected sensitized individuals with methyl methacrylate (2% in petrolatum) and ethyl acrylate (0.1% in petrolatum) as a screen and then, if additional analysis is required, the meth(acrylate) series for artificial nails, including 2-hydroxyethyl methacrylate (2-HEMA), 2-hydroxypropyl methacrylate (2-HPMA), and triethyleneglycol diacrylate (TREGDA). Patch tests consisting of monomers should be avoided as this may lead to sensitization[89].

HAIR CONDITIONERS		
Type	**Use**	**Indication**
Instant	Apply following shampoo; rinse	Minimally damaged hair; aids wet combing
Deep	Apply for 20–30 minutes; shampoo; rinse	Chemically damaged hair
Leave-in	Apply to towel-dried hair; style	Prevents hair-dryer or hair-straightening damage; aids in combing and styling
Rinse	Apply following shampoo; rinse	Aids in disentangling if creamy rinse; removes soap residue if clear rinse

Table 153.12 Hair conditioners.

Hydroxy Acid Cosmeceuticals

The discussion so far has focused on products intended to function purely in a cosmetic realm, yet there are cosmeceuticals in the current marketplace known as hydroxy acids. These hydroxy acids address the scaliness and roughness of aged skin that is not due to an inherently lower stratum corneum water content[90]. The roughness associated with mature skin may be due to abnormal desquamation associated with a possible failure in intercellular communication[91]. This observation has led to the enormous popularity of α- and β-hydroxy acids.

Alpha-hydroxy acids

This group of organic carboxylic acids is distinguished by a substituted hydroxy group covalently bonded to the α-carbon of a carboxylic acid. The linear, aliphatic nature of the α-hydroxy acid (AHA) structure accounts for its water-soluble or hydrophilic properties (Fig. 153.9). The three subcategories of AHA consist of: (1) monocarboxylic acids – glycolic (2-hydroxyethanoic acid), lactic (2-hydroxy-propanoic acid), and mandelic acid (2-hydroxy-2-phenylethanoic acid); (2) dicarboxylic acids – malic (2-hydroxy-1,4-butanedioic acid) and tartaric acid (2,3-dihydroxy-1,4-butanedioic acid); and (3) tricarboxylic acids – citric acid (2-hydroxy-1,2,3-propanetricarboxylic acid). The intricacies of the formulation are more important than the nature of the AHA, since the exfoliative effect is similar[92].

AHAs induce immediate epidermal effects through corneocyte disadhesion, which is thought to require disruption of ionic bonding[93,94]. The corneocyte disadhesion occurs initially in the stratum corneum at the level of the stratum granulosum; once the cutaneous barrier has been disrupted, this is followed by dermal penetration[95].



Fig. 153.6 Yellow nail staining due to wearing deeply pigmented red and orange nail polishes. This type of staining is common and reversible.

NAIL COSMETICS			
Nail cosmetic	**Main ingredients**	**Function**	**Adverse reactions**
Nail polish	Nitrocellulose, tosylamide formaldehyde resin*, plasticizers (e.g. dibutyl phthalate, camphor), solvents, colorants	Add color and shine to nail plates	Allergic contact dermatitis to tosylamide formaldehyde resin Nail plate staining
Nail hardener	Formaldehyde, acetates, acrylics or other resins	Increase nail strength and prevent breakage	Allergic contact dermatitis to formaldehyde
Nail enamel remover	Acetone, alcohol, ethyl acetate or butyl acetate	Remove nail polish	Irritant contact dermatitis
Cuticle remover	Sodium or potassium hydroxide	Destroy keratin that forms excess cuticular tissue on nail plate	Irritant contact dermatitis Paronychia
Nail bleach	Hydrogen peroxide	Remove nail plate stains	Irritant contact dermatitis
Nail white	White pigments	Whiten free nail edge	Practically none
Nail polish drier	Vegetable oils, alcohols or silicone derivatives	Speed drying time of nail polish	Practically none
Nail buffing cream	Pumice, talc or kaolin	Smooth ridges in nails	Practically none
Nail moisturizer	Occlusives, humectants, lactic acid	Increase water content of nails	Practically none

*Also referred to as toluene sulfonamide–formaldehyde resin.

Table 153.13 Nail cosmetics. A nail wrap is a thin sheet of material (e.g. linen, silk, fiberglass) that is glued to a torn or split nail plate as a means of repair.

NAIL SCULPTURE APPLICATION
Nail sculpture application is an involved process requiring approximately 2 hours to sculpt 10 fingernails. The basic process is as follows: • All nail polish and oils are removed from the nail. • The nail is roughened with a coarse emery board, pumice stone, or grinding drill to create an optimal surface for sculpted nail adhesion; this can damage the nail plate surface. • An antifungal and antibacterial liquid, such as decolorized iodine, is applied to the entire nail plate to minimize onychomycosis and paronychia. • The loose edges of the cuticle are trimmed, removed or pushed back, depending on the operator; this can lead to paronychia and nail dystrophy. • A flexible template is fitted beneath the natural nail plate, upon which the elongated sculpted nail will be built, or a preformed plastic nail tip is used for this purpose. • The acrylic is mixed and applied with a brush to cover the entire natural nail plate and extended onto the template or preformed nail tip to obtain the desired nail length. • The final sculpture is sanded to a high shine. • Nail polish, jewels, decals, decorative metal strips, or airbrushed designs may be added.

Table 153.14 Nail sculpture application. UV- or LED-cured gel-based *extensions* also contain photoinitiators. For dip powder manicures, primed nails are dipped into colored acrylic powder following by application of an activator polish which does not require UV light for curing.

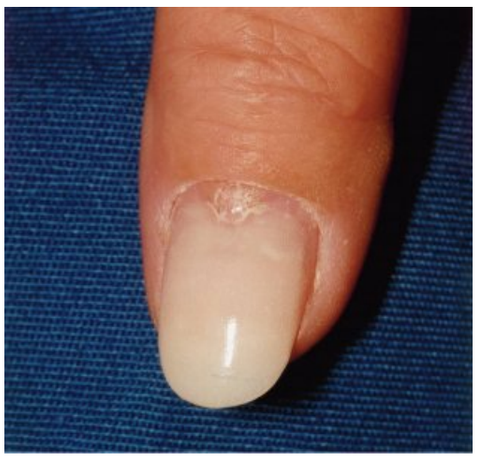


Fig. 153.7 Onychodystrophy of the central nail due to wearing a nail prosthesis. The nail prosthesis grows out with the nail plate and new polymer must be applied to the proximal nail fold. The polymer has damaged the cells of the central nail matrix.



Fig. 153.8 Continuous use of a nail prosthesis can result in dramatic nail plate damage.

NAIL POLISH – SPECIAL EFFECTS		
Special polish categories	**Technology**	**Advantages/ Disadvantages**
Polish strips	Polish applied to an adhesive layer with removable backing	No mess, must be cut to fit the nail and pressed in place
Color changing polish	Polish contains molecules that change with temperature or UV light exposure from a non-conjugated to conjugated configuration	Can be used to determine if UV light exposure has occurred/color change cannot be completely controlled
Textured polish	Polyethylene terephthalate fibers give 3D woven fiber effect or glass beads give a caviar finish	Can create unique fashion effects
Magnetic polish	Contains magnetic particles, such as iron oxide, that align when exposed to a magnetic field	Can create one-of-a-kind nail effects/metal allergy a possibility
Crackle polish	Top coat nail polish contains ethyl alcohol that evaporates rapidly creating surface tension change and crackle effect	Can create two-tone nail polish effect/less durable nail polish

Table 153.15 Nail polish – special effects. UV, ultraviolet.

CHEMICAL STRUCTURE OF GLYCOLIC ACID

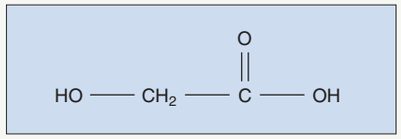


Fig. 153.9 The chemical structure of glycolic acid, accounting for its hydrophilic properties.

The epidermal effects of AHAs are a thinned stratum corneum with acanthosis and decreased melanogenesis. The dermal effects of AHAs are delayed and include increased synthesis of glycosaminoglycans, prevention of topical corticosteroid atrophy, and increased dermal thickness, possibly due to enhanced production of collagen via fibroblast proliferation, in a dose-dependent manner[96,97].

Disruption of corneocyte adhesion is ultimately valuable in a large variety of dermatologic conditions (Table 153.16)[98]. For example, AHAs can be incorporated into an acne treatment regimen, given their ability to induce epidermolysis and dislodge comedones; however, AHAs cannot enter the milieu of the pore[99]. Monthly glycolic acid peels have been shown to be of benefit in the treatment of rosacea[100]. Sloughing of corneocytes and smoothing of seborrheic keratoses, verrucae and calluses have also been reported[101,102]. Glycolic acid preparations, either formulated as topicals or short-contact peels, appear to be appropriate for both lightly and darkly pigmented skin[103]. Lastly, AHAs have been purported to function as anti-inflammatory agents and antioxidants by alleviating the erythema associated with cutaneous ultraviolet light exposure[104]. Glycolic acid appears to confer an SPF of ~2.4 to the skin[105].

Beta-hydroxy acid

A similar, but chemically different, member of the hydroxy acid family is salicylic acid (ortho-hydrobenzoic acid), the only so-called β-hydroxy acid (BHA). Salicylic acid is an organic aromatic carboxylic acid with a hydroxy group in the beta position (Fig. 153.10).

Salicylic acid is unique among the hydroxy acids, since it can enter the milieu of the sebaceous unit, inducing exfoliation in the oily areas of the face[106]. For this reason, it has been used for years as a comedolytic in over-the-counter (OTC) preparations designed to improve comedonal acne[107,108]. Salicylic acid is approved for the treatment of acne as an OTC drug, monographed by the FDA at a level of 2% or less. It is also an excellent keratolytic, inducing exfoliation of calluses, corns and warts[109]. Salicylic acid is incorporated into many shampoos designed to remove undesquamated corneocytes from the scalp of patients with seborrheic dermatitis and psoriasis[110].

Salicylic acid is thought to function through solubilization of intercellular cement, thereby reducing corneocyte adhesion. It appears to eliminate the stratum corneum layer by layer from the outermost level downward[111]. This is in contrast to the α-hydroxy acids, which appear

DERMATOLOGIC USES OF HYDROXY ACIDS AS TOPICAL PREPARATIONS AND PEELS
Skin conditions
• Photodamaged skin • Ichthyosis • Xerotic eczema • Acne • Acne rosacea • Seborrheic keratoses (improves appearance) • Actinic keratoses • Lentigines (improves appearance) • Verrucae
Cutaneous effects
• Moisturizing exfoliant • Skin peeling agent • Penetration enhancer • Preventative for corticosteroid-induced skin atrophy

Table 153.16 Dermatologic uses of hydroxy acids as topical preparations and peels.

CHEMICAL STRUCTURE OF SALICYLIC ACID

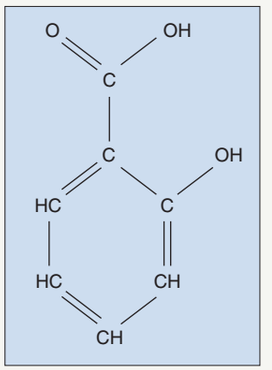


Fig. 153.10 The chemical structure of salicylic acid, accounting for its lipophilic properties.

POPULAR INGREDIENTS IN COSMECEUTICAL FORMULATIONS		
Cosmeceutical category	**Ingredient**	**Comments**
Antioxidant carotenoids	Retinol	Oxidized to retinaldehyde and then retinoic acid for activity
	Astaxanthin	Found in high concentration in salmon
	Lutein	Extensive conjugated double bonds in polyene side chain
Antioxidant flavonoids	Soy	Contains genestein and diadzein which function as phytoestrogens and protect against lipid peroxidation
	Curcumin	Active ingredient is tetrahydrocurcumin – quenches oxygen radicals and inhibits NF-κB
	Silymarin	Milk thistle plant extract; contains antioxidants silybin, silydianin, silychristin
	Pycnogenol®	French marine bark extract; contains antioxidants taxifolin, catechin, procyanidins
Antioxidant polyphenols	Green tea	Contains antioxidant polyphenols: epicatechin, epicatechin-3-gallate, epigallocatechin, epigallocatechin-3-gallate
	Pomegranate	Extract contains pantothenic acid, polyphenols
Endogenous antioxidants	Vitamin E	Primary antioxidant in skin
	Vitamin C	Secondary antioxidant in skin
	Ubiquinone (coenzyme Q10)	Tertiary antioxidant in skin
Anti-inflammatory	Aloe vera	Mucilage contains choline, choline salicylate
	Ginkgo	Contains bilobalides, ginkgolides, ginkgolic acid
Pigment lighteners	Vitamin C	May interrupt melanogenesis by interacting with copper ions
	Licorice extract	Contains liquiritin and isoliquertin, which disperse melanin, and glabridin, which inhibits tyrosinase
	Kojic acid	A hydrophilic fungal derivative; inhibits tyrosinase activity *in vitro*
	Aloesin	Naturally occurring hydroxymethylchromone; inhibits tyrosinase by competitive inhibition
	Arbutin	A naturally occurring gluconopyranoside; decreases tyrosinase activity and may inhibit melanosomal maturation
Peptides	Signal peptides	Peptides composed of amino acids attached to palmitic acid, a penetration enhancer; mimic peptides including fragments of collagens 1 and 3; an example is the palmitoylated derivative of the collagen pentapeptide Lys-Thr-Thr-Lys-Ser (Pal-KTTKS)
	Carrier peptides	Carry ingredients, such as copper (Cu), with a plasma protein fragment; an example is Gly-His-Lys (GHK)-Cu
	Neurotransmitter peptides	Purported to inhibit release of acetylcholine at the neuromuscular junction and relax muscles; an example is acetyl hexapeptide-3
Human stem cell-conditioned media	Growth factors	Growth factors (e.g. fibroblast growth factor [FGF], epidermal growth factor [EGF], keratinocyte growth factor [KGF]) released into the media of cultured neonatal foreskin fibroblasts are added to moisturizers
Microbiome ingredients	Prebiotics	Sugars (e.g. fructo-oligosaccharides [FOS], galacto-oligosaccharides [GOS]) or plant oils that promote the growth of beneficial bacteria on the skin surface
	Probiotics	Dairy propionic acid bacteria (PAB) such as lactobacilli and bifidobacteria; the bacteria are usually sonicated unless product is sold refrigerated
	Postbiotics	Non-viable bacterial products or metabolic by-products from probiotic bacteria (e.g. enzymes, peptides, peptido-glycan-derived muropeptides, polysaccharides, cell surface proteins, organic acids)

Table 153.17 Popular ingredients in cosmeceutical formulations. These are in addition to the hydroxy acids. NF-κB, nuclear factor kappa-light-chain-enhancer of activated B cells. Adapted from refs 113–117.

to diminish cellular cohesion between the corneocytes at the lowest levels of the stratum corneum. This difference is probably due in part to the water-soluble characteristics of the α-hydroxy acids, which readily penetrate into the stratum corneum, and the oil-soluble characteristics of salicylic acid, which remains on the stratum corneum.

Topical application of salicylic acid can also take the form of short-contact cutaneous peels. Salicylic acid can be used alone in concentrations of 10%–50% or combined with the α-hydroxy acid lactic acid in Jessner's solution (see Table 154.4). Salicylic acid will remain in solution at concentrations of ≤20% in 95% ethyl alcohol; however, at concentrations of 30% and above, it precipitates, necessitating shaking of the solution prior to use. In contrast to glycolic acid peels, salicylic acid is a self-neutralizing peel that ends with the formation of white salicylic acid crystals on the skin[112]. The crystals are easily rinsed from the skin surface with water, but they remain in the follicular ostia, providing a prolonged keratolytic effect.

Additional Cosmeceuticals

As a group, cosmeceuticals can offer other skin benefits in addition to those previously described for the hydroxy acids (Table 153.17; Fig. 153.11).



Fig. 153.11 Lightening of facial lentigines. **A** Numerous facial lentigines due to photodamage. **B** Lightening of lentigines after treatment with a formulation containing kojic acid, emblica extract, and glycolic acid.

FUTURE DIRECTIONS

Improved understanding of the physiology of the stratum corneum is leading to new dermatologic developments within the realm of cosmetics and skin care products. This has spurred the growth in cosmeceuticals that promise to improve cutaneous function and enhance appearance. In addition, technology that was originally developed for skin keratin can be directly transferred to hair and nail keratin. Future research will undoubtedly explore methods of preventing cutaneous inflammation, which represents a common thread between dermatologic disease and potential adverse effects of cosmetics.

REFERENCES

1. Draelos ZD. Cosmeceuticals: what's real, what's not. *Dermatol Clin*. 2019;37:107–115.
2. Epstein H. Factors in formulating cosmeceutical vehicles. *Cosmet Toilet*. 1997;112:91–99.
3. Federal Food, Drug, and Cosmetic Act (sections [21 USC 301–392]).
4. Lavrijsen APM, Vermeer BJ. Cosmetics and drugs: is there a need for a third group: cosmeceutics? *Br J Dermatol*. 1991;124:503–504.
5. Willcox MJ, Crichton WP. The soap market. *Cosmet Toilet*. 1989;104:61–63.
6. Wortzman MS, Scott RA, Wong PS, et al. Soap and detergent bar rinsability. *J Soc Cosmet Chem*. 1986;37:89–97.
7. Buffet-Bataillon S, Tattevin P, Bonnaure-Mallet M, Jolivet-Gougeon A. Emergence of resistance to antimicrobial agents: the role of quaternary ammonium compounds - a critical review. *Int J Antimicrob Agents*. 2012;39:381–389.
8. Mills OH, Berger RS, Baker MD. A controlled comparison of skin cleansers in photoaged skin. *J Geriatric Dermatol*. 1993;1:173–179.
9. Jass HE. Cold creams. In: deNaarre MG, editor. *The Chemistry and Manufacture of Cosmetics*, vol. III. 2nd ed. Wheaton, IL: Allured Publishing; 1975:237–249.
10. Baker CG. Moisturization: new methods to support time proven ingredients. *Cosmet Toilet*. 1987;102:99–102.
11. Lynde CW. Moisturizers: what they are and how they work. *Skin Therapy Lett*. 2001;6:3–5.
12. Ghali FE. Improved clinical outcomes with moisturization in dermatologic disease. *Cutis*. 2005;76(6 Suppl.):13–18.
13. Wilhelm KP, Cua AB, Maibach HI. Skin aging. Effect on transepidermal water loss, stratum corneum hydration, skin surface pH, and casual sebum content. *Arch Dermatol*. 1991;127:1806–1809.
14. Lodén M. Role of topical emollients and moisturizers in the treatment of dry skin barrier disorders. *Am J Clin Dermatol*. 2003;4:771–788.
15. de Jager MW, Gooris GS, Ponec M, Bouwstra JA. Lipid mixtures prepared with well-defined synthetic ceramides closely mimic the unique stratum corneum lipid phase behavior. *J Lipid Res*. 2005;46:2649–2656.
16. Friberg SE, Ma Z. Stratum corneum lipids, petrolatum and white oils. *Cosmet Toilet*. 1993;107:55–59.
17. Jass HE, Elias PM. The living stratum corneum: implications for cosmetic formulation. *Cosmet Toilet*. 1991;106:47–53.
18. Holleran W, Feingold K, Man MQ, et al. Regulation of epidermal sphingolipid synthesis by permeability barrier function. *J Lipid Res*. 1991;32:1151–1158.
19. Buraczewska I, Berne B, Lindberg M, et al. Changes in skin barrier function following long-term treatment with moisturizers, a randomized controlled trial. *Br J Dermatol*. 2007;156:492–498.
20. Ghadially R, Halkier-Sorensen L, Elias PM. Effects of petrolatum on stratum corneum structure and function. *J Am Acad Dermatol*. 1992;26:387–396.
21. Spencer TS. Dry skin and skin moisturizers. *Clin Dermatol*. 1988;6:24–28.
22. Rieger MM, Deem DE. Skin moisturizers II. The effects of cosmetic ingredients on human stratum corneum. *J Soc Cosmet Chem*. 1974;25:253–262.
23. Idson B. Dry skin: moisturizing and emolliency. *Cosmet Toilet*. 1992;107:69–78.
24. Robbins CR, Fernee KM. Some observations on the swelling of human epidermal membrane. *JSCC*. 1983;37:21–34.
25. Bouwstra J, Pilgram G, Gooris G, et al. New aspects of the skin barrier organization. *Skin Pharmacol Appl Skin Physiol*. 2001;14(Suppl. 1):52–62.
26. Jackson EM. Moisturizers: what's in them? How do they work? *Am J Contact Dermatitis*. 1992;3:162–168.
27. Wilkinson JB, Moore RJ. Astringents and skin toners. In: *Harry's Cosmeticology*. 7th ed. New York: Chemical Publishing; 1982:74–81.
28. Draelos ZK. *Cosmetics in Dermatology*. Edinburgh: Churchill Livingstone; 1995:1–14.
29. Schlossman ML, Feldman AJ. Fluid foundation and blush make-up. In: deNavarre MG, ed. *The Chemistry and Manufacture of Cosmetics*. Wheaton, IL: Allured Publishing; 1988:748–751.
30. Lanzet M. Modern formulations of coloring agents: facial and eye. In: Frost P, Horowitz SN, eds. *Principles of Cosmetics for the Dermatologist*. St Louis: Mosby; 1982:138–139.
31. Adams RM, Maibach HI. A five-year study of cosmetic reactions. *J Am Acad Dermatol*. 1985;13:1062–1069.
32. Wolf R, Perluk H. Failure of routine patch test results to detect eyelid dermatitis. *Cutis*. 1992;49:133–134.
33. Rietschel RL, Warshaw EM, Sasseville D, et al. Common contact allergens associated with eyelid dermatitis: data from the North American Contact Dermatitis Group 2003-2004 study period. *Dermatitis*. 2007;18:78–81.
34. Wilkinson JB, Moore RJ. Coloured make-up preparations. In: *Harry's Cosmeticology*. 7th ed. New York: Chemical Publishing; 1982:341–347.
35. Wilson LA, Ahearn DG. Pseudomonas-induced corneal ulcer associated with contaminated eye mascaras. *Am J Ophthalmol*. 1977;84:112–119.
36. MMWR Reports. Pseudomonas aeruginosa corneal infection related to mascara applicator trauma. *Arch Dermatol*. 1990;126:734.
37. Ahearn DG, Wilson LA. Microflora of the outer eye and eye area cosmetics. *Develop Ind Microbiol*. 1976;17:23–28.

38. Kuehne JW, Ahearn DG. Incidence and characterization of fungi in eye cosmetics. *Develop Ind Microbiol*. 1971;12:1973–1977.
39. Bhadauria B, Ahearn DG. Loss of effectiveness of preservative systems of mascaras with age. *Appl Environ Microbiol*. 1980;39:665–667.
40. Ahern DG, Wilson LA, Julian AJ, et al. Microbial growth in eye cosmetics: contamination during use. *Develop Ind Microbiol*. 1974;15:211–216.
41. Alevi D, Donnenfeld E, Perry H. Mascara-induced conjunctival pigmentation. *JAMA Ophthalmol*. 2016;134:e162720.
42. Platia EV, Michels RG, Green WR. Eye-cosmetic-induced conjunctival pigmentation. *Ann Ophthalmol*. 1978;10:501–504.
43. Tosti A, Pazzaglia M, Voudouris S, Tosti G. Hypertrichosis of the eyelashes caused by bimatoprost. *J Am Acad Dermatol*. 2004;51(5 Suppl.):S149–150.
44. Cunningham J. Color cosmetics. In: Williams DF, Schmitt WH, eds. *Chemistry and Technology of the Cosmetics and Toiletries Industry*. London: Blackie; 1992:143–149.
45. deNavarre MG. Lipstick. In: deNavarre MG, ed. *The Chemistry and Manufacture of Cosmetics*. 2nd ed. Wheaton, IL: Allured Publishing; 1975:778.
46. Boelcke U. Requirements for lipstick colors. *J Soc Cosmet Chem*. 1961;12:468.
47. Sulzberger MD, Boodman J, Byrne LA, Mallozzi ED. Acquired specific hypersensitivity to simple chemicals. Cheilitis with special reference to sensitivity to lipsticks. *Arch Dermatol*. 1938;37:597–615.
48. Sai S. Lipstick dermatitis caused by castor oil. *Contact Dermatitis*. 1983;9:75.
49. Calnan CD. Allergic sensitivity to eosin. *Acta Allergol*. 1959;13:493–499.
50. Walgrave SE, Warshaw EM, Glesne LA. Allergic contact dermatitis from propolis. *Dermatitis*. 2005;16:209–215.
51. Cronin E. Lipstick dermatitis due to propyl gallate. *Contact Dermatitis*. 1980;6:213–214.
52. Calnan CD. Amyldimethylamino benzoic acid causing lipstick dermatitis. *Contact Dermatitis*. 1980;6:233.
53. Aguirre A, Izu R, Gardeazabal J, et al. Allergic contact cheilitis from a lipstick containing oxybenzone. *Contact Dermatitis*. 1992;27:267–268.
54. Schram SE, Glesne LA, Warshaw EM. Allergic contact cheilitis from benzophenone-3 in lip balm and fragrance/flavorings. *Dermatitis*. 2007;18:221–224.
55. Hayakawa R, Fujimoto Y, Kaniwa M. Allergic pigmented lip dermatitis from lithol rubine BCA. *Am J Contact Dermatitis*. 1994;5:34–37.
56. Sai S. Lipstick dermatitis caused by ricinoleic acid. *Contact Dermatitis*. 1983;9:524.
57. Rayner V. *Clinical Cosmetology: A Medical Approach to Esthetics Procedures*. Albany, NY: Milady Publishing; 1993:116–122.
58. Buchman H. *Stage Makeup*. New York: Watson-Guptill; 1979:15–18.
59. Draelos ZK. Cosmetic camouflaging techniques. *Cutis*. 1993;52:362–364.
60. Bouillon C. Shampoos and hair conditioners. *Clin Dermatol*. 1988;6:83–92.
61. Robbins CR. Interaction of shampoo and creme rinse ingredients with human hair. In: *Chemical and Physical Behavior of Human Hair*. 2nd ed. New York: Springer-Verlag; 1988:122–167.
62. Fox C. An introduction to the formulation of shampoos. *Cosmet Toilet*. 1988;103:25–58.
63. Zviak C, Vanlerberghe G. Scalp and hair hygiene. In: Zviak C, ed. *The Science of Hair Care*. New York: Marcel Dekker; 1986:49–86.
64. Rieger M. Surfactants in shampoos. *Cosmet Toilet*. 1988;103:59–72.
65. Garcia ML, Epps JA, Yare RS, Hunter LD. Normal cuticle-wear patterns in human hair. *J Soc Cosmet Chem*. 1978;29:155–175.
66. Corbett JF. Hair conditioning. *Cutis*. 1979;23:405–413.
67. Zviak C, Bouillon C. Hair treatment and hair care products. In: Zviak C, ed. *The Science of Hair Care*. New York: Marcel Dekker; 1986:115–116.
68. Rook A. The clinical importance of 'weathering' in human hair. *Br J Dermatol*. 1976;95:111–112.
69. Price VH. The role of hair care products. In: Orfanos CE, Montagna W, Stuttgen G, eds. *Hair Research*. Berlin: Springer-Verlag; 1981:501–506.
70. Robinson VNE. A study of damaged hair. *J Soc Cosmet Chem*. 1976;27:155–161.
71. Zviak C, Bouillon C. Hair treatment and hair care products. In: Zviak C, ed. *The Science of Hair Care*. New York: Marcel Dekker; 1986:134–137.
72. Douglas A, Onalaja AA, Taylor SC. Hair care products used by women of African descent: review of ingredients. *Cutis*. 2020;105:183–188.
73. Ojo EO, Gowda A, Nedorost S. Scalp dermatitis in patients sensitized to components of hair products. *Dermatitis*. 2019;30:264–267.
74. LaBerge L, Pratt M, Fong B, et al. A 10-year review of p-phenylenediamine and related para-amino compounds at the Ottawa Patch Test Clinic. *Dermatitis*. 2011;22:332–334.
75. Wing HJ. Nail preparations. In: deNavarre MG, ed. *The Chemistry and Manufacture of Cosmetics*. Wheaton, IL: Allured Publishing; 1988:983–1005.
76. Mast R. Nail products. In: Whittam JH, ed. *Cosmetic Safety: A Primer for Cosmetic Scientists*. New York: Marcel Dekker; 1987:265–313.
77. Schlossman ML. Nail-enamel resins. *Cosmetic Technol*. 1979;1:53.
78. Samman PD. Nail disorders caused by external influences. *J Soc Cosmet Chem*. 1977;28:351.
79. Daniel DR, Osmet LS. Nail pigmentation abnormalities. *Cutis*. 1980;25:595–607.
80. Scher RK. Cosmetics and ancillary preparations for the care of the nails. *J Am Acad Dermatol*. 1982;6:523–528.
81. Dinani N, George S. Nail cosmetics: a dermatological perspective. *Clin Exp Dermatol*. 2019;44:599–605.
82. Viola LJ. Fingernail elongators and accessory nail preparations. In: Balsam MS, Sagarin E, eds. *Cosmetics, Science and Technology*. 2nd ed. New York: Wiley-Interscience; 1972:543–552.
83. Goodwin P. Onycholysis due to acrylic nail applications. *J Exp Dermatol*. 1976;1:191–192.
84. Lane CW, Kost LB. Sensitivity to artificial nails. *Arch Dermatol*. 1956;74:671–672.
85. Baden H. Cosmetics and the nail. In: *Diseases of the Hair and Nails*. Chicago: Yearbook Publishers; 1987:99–102.
86. Marks JG, Bishop ME, Willis WF. Allergic contact dermatitis to sculptured nails. *Arch Dermatol*. 1979;115:100.
87. Fisher AA. Cross reactions between methyl methacrylate monomer and acrylic monomers presently used in acrylic nail preparations. *Contact Dermatitis*. 1980;6:345–347.
88. Fisher AA, Franks A, Glick H. Allergic sensitization of the skin and nails to acrylic plastic nails. *J Allergy*. 1957;28:84.
89. Sasseville D. Acrylates. Contact allergen of the year. *Dermatitis*. 2012;23:3–5.
90. Potts RO, Buras EM, Chrisman DA. Changes with age in the moisture content of human skin. *J Invest Dermatol*. 1984;82:97–100.
91. Wepierre J, Marty JP. Percutaneous absorption and lipids in elderly skin. *J Appl Cosmetol*. 1988;6:79–92.
92. Stiller MJ, Bartolone J, Stern R, et al. Topical 8% glycolic acid and 8% l-Lactic acid creams for the treatment of photodamaged skin. *Arch Dermatol*. 1996;132:631–636.
93. Dietre CM, Griffin TD, Murphy GF, et al. Effects of alpha-hydroxy acids on photoaged skin. *J Am Acad Dermatol*. 1996;34:187–195.
94. Berardesca E, Maibach H. AHA mechanism of action. *Cosmet Toilet*. 1995;110:30–31.
95. Van Scott EJ, Yu RJ. Hyperkeratinization, corneocyte cohesion and alpha hydroxy acids. *J Am Acad Dermatol*. 1984;11:867–879.
96. Bernstein EF, Uitto J. Connective tissue alterations in photoaged skin and the effects of alpha hydroxy acids. *J Geriatric Dermatol*. 1995;3(Suppl):7A–18A.
97. Lavker RM, Kaidbey K, Leyden JJ. Effects of topical ammonium lactate on cutaneous atrophy from a potent topical corticosteroid. *J Am Acad Dermatol*. 1992;26:535–544.
98. Van Scott EJ, Yu RJ. Alpha hydroxy acids: procedures for use in clinical practice. *Cutis*. 1989;43:222–228.
99. Van Scott EJ, Yu RJ. Alpha hydroxy acids: therapeutic potentials. *Can J Dermatol*. 1989;1:108–112.
100. Briden ME, Rendon-Pellerano MI. Treatment of rosacea with glycolic acid. *J Geriatric Dermatol*. 1996;4(Suppl):17B–21B.
101. Klaus MV. Evaluation of ammonium lactate in the treatment of seborrheic keratoses. *J Am Acad Dermatol*. 1977;22:199–203.
102. Siskin SB. The effects of ammonium lactate 12% lotion versus no therapy in the treatment of dry skin of the heels. *Int J Dermatol*. 1993;32:905–907.
103. Kakita LS, Petratos MA. The use of glycolic acid in Asian and darker skin types. *J Geriatric Dermatol*. 1996;4(Suppl):8B–11B.
104. Perricone NV. An alpha hydroxy acid acts as an antioxidant. *J Geriatric Dermatol*. 1993;1:101–104.
105. Perricone NV, DiNardo JC. Photoprotective and antiinflammatory effects of topical glycolic acid. *Dermatol Surg*. 1996;22:435–437.
106. Davies M, Marks R. Studies on the effect of salicylic acid on the normal stratum corneum. *Br J Dermatol*. 1980;103:191–196.
107. DiNardo JC. A comparison of salicylic acid, salicylic acid with glycolic acid and benzoyl peroxide in the treatment of acne. *Cosmet Dermatol*. 1995;8:12.
108. Kligman A, Kligman AM. Salicylic acid as a peeling agent for the treatment of acne. *Cosmet Dermatol*. 1997;10:44–47.
109. Huber C, Christopher E. Keratolytic effect of salicylic acid. *Arch Dermatol Res*. 1977;257:293–297.
110. Draelos ZD. Salicylic acid in the dermatologic armamentarium. *Cosmet Dermatol*. 1997;10(Suppl. 4):7–8.
111. Roberts DL, Marshall R, Marks R. Detection of the action of salicylic acid on the normal stratum corneum. *Br J Dermatol*. 1980;103:191–196.
112. Kligman D, Kligman AM. Salicylic acid peels for the treatment of photoaging. *Dermatol Surg*. 1998;24:325–328.
113. Singh M, Griffiths CE. The use of retinoids in the treatment of photoaging. *Dermatol Ther*. 2006;19:297–305.
114. Serri R, Iorizzo M. Cosmeceuticals: focus on topical retinoids in photoaging. *Clin Dermatol*. 2008;26:633–635.
115. Mehta RC, Fitzpatrick RE. Endogenous growth factors as cosmeceuticals. *Dermatol Ther*. 2007;20:350–359.
116. Leonard SS, Cutler D, Ding M, et al. Antioxidant properties of fruit and vegetable juices: more to the story than ascorbic acid. *Ann Clin Lab Sci*. 2002;32:193–200.
117. Ortonne JP, Passeron T. Melanin pigmentary disorders: treatment update. *Dermatol Clin*. 2005;23:209–226.

Chemical and Mechanical Skin Resurfacing 154

Gary D. Monheit and Katherine Hrynewycz

Chapter Contents

Preoperative History and Considerations *2633*
Chemical Resurfacing Procedures *2636*
Mechanical Resurfacing Procedures *2643*
Postoperative Care *2646*
Complications *2647*

Synonyms: ■ Chemical resurfacing: chemical peeling, chemexfoliation ■ Mechanical resurfacing: dermabrasion (includes dermasanding) ■ Jessner's peel: Combes' peel ■ Baker–Gordon peel: deep phenol peel ■ Microneedling: percutaneous collagen induction

Key features

- Chemical peeling, dermabrasion, and laser ablation are the three main methods of skin resurfacing
- Chemical and mechanical resurfacing procedures have a long history of safety and efficacy in ameliorating various skin conditions and improving cutaneous photoaging
- Resurfacing procedures represent one part of a comprehensive skin care program that should include photoprotective measures and topical medical and/or cosmeceutical agents
- Each resurfacing procedure injures the skin to a specific depth to promote the regrowth of new skin with improved surface characteristics
- The degree of clinical improvement, the length of the recovery period, and the risk of complications are all proportionate to the depth of tissue injury chosen and skin type
- Selection of suitable patients and proper choice of resurfacing procedure are critical to success
- Both dermabrasion and the "TCA CROSS" technique are methods for treating acne scars
- Microdermabrasion and microneedling are additional approaches for facial rejuvenation
- Prolonged erythema, pigmentary or textural irregularities, infection, delayed healing, and scarring are potential complications of resurfacing
- Resurfacing procedures are a rewarding part of dermatologic practice, both for the patient and for the physician

INTRODUCTION AND HISTORY

Resurfacing procedures to improve the health and appearance of the skin have been utilized by humans for thousands of years. The ancient Egyptians applied various chemicals to the skin and may have even used abrasives like sandpaper to obtain a smoother skin surface[1,2]. Resurfacing methods within the practice of dermatology were initially described over 100 years ago. Early on, chemical cauterants were used primarily for proliferative lesions and skin disorders, with pioneers such as Hebra and Jessner discovering the usefulness of acidic and basic compounds for skin exfoliation. Over the past several decades, the role of chemexfoliation has expanded dramatically to include textural and cosmetic revisions. Our society's increasing emphasis on a youthful image and aesthetic appearance has resulted in an explosion in public demand for commercial skin care products, professional assistance from physicians and non-physicians to assure proper medical and cosmeceutical skin therapy, and procedural intervention. However, the development and application of safe and effective procedures needs to be based upon sound reproducible data.

All ablative resurfacing procedures injure the skin, in a controlled fashion, to a specific depth and thereby promote the growth of new skin with improved surface characteristics. The three fundamental methods used to create this controlled injury are chemical resurfacing (chemical peeling), mechanical resurfacing (motorized dermabrasion or manual dermasanding), and laser resurfacing (see Ch. 137). Chemical resurfacing entails the application of acidic or basic abrasive chemical substances that can destroy selective levels of the epidermis or dermis. Mechanical resurfacing involves smoothing the skin surface with an abrasive surface which physically removes portions of the epidermis and dermis.

In general, skin resurfacing procedures can be classified as superficial, medium-depth, or deep, according to their level of injury (Table 154.1). Skin resurfacing is usually performed only on the face and neck, in part because of the critical aesthetic value of this area. Caution must be exercised in treating the neck, arms, and trunk due to a propensity for complications; only superficial procedures should be performed on the lower one-third of the neck and other non-facial areas. Resurfacing of sites such as the hands and arms has yielded less predictable and less impressive results as well as a higher risk for scarring.

In comparison to the other resurfacing modalities available for skin rejuvenation, chemical resurfacing probably has the longest and most well-documented history[1]. Experimentation with various peeling compounds in the late nineteenth and early twentieth centuries led to sporadic reports in the medical literature describing their use. The initial reports were met with skepticism, but further investigation by both dermatologists and plastic surgeons verified their effectiveness in facial skin rejuvenation and as a treatment for skin disorders. Subsequently, chemical peeling experienced a tremendous growth in popularity and has become an important part of our armamentarium in the management of various cosmetic as well as non-cosmetic skin problems. Currently, chemical peeling is the third most commonly employed cosmetic procedure, after injectable neurotoxins and soft tissue fillers.

Since Kromayer's original report of motorized dermabrasion in 1905, there has been considerable growth not only in chemical resurfacing procedures, but also in mechanical resurfacing. Mechanical resurfacing is most often known as dermabrasion, but it refers to any procedure that involves surgical planing of the skin using an abrasive surface. The use of dermabrasion was originally limited to the treatment of scars, but its role expanded during the latter half of the twentieth century to include a multitude of indications including improvement of elevated skin grafts and rejuvenation of photodamaged skin[2]. Recent adaptations of the traditional techniques of dermabrasion have led to the development of a less invasive procedure, known as microdermabrasion[3]. Dermasanding, which is a manual technique of dermabrasion utilizing abrasive paper, has been in use for centuries, but recently has experienced a resurgence[4,5]. Although overshadowed by ablative and non-ablative laser resurfacing (see Ch. 137), mechanical resurfacing procedures remain a popular option for both patients and physicians.

PREOPERATIVE HISTORY AND CONSIDERATIONS

Indications

The preoperative consultation is important in identifying at-risk patients who are best avoided or who require an extra-cautious approach, as well

CLASSIFICATION OF ABLATIVE SKIN RESURFACING METHODS
Superficial – very light
• Low-potency formulations of glycolic acid or other α-hydroxy acids • 10%–20% TCA (weight-to-volume formulation) • Tretinoin • 20% salicylic acid • Jessner's solution (see Table 154.4)
• Microdermabrasion
Superficial – light
• 50%–70% glycolic acid • Jessner's solution (greater number of coats than for very light peel) • 25%–30% TCA • Solid CO_2 slush • 30% salicylic acid
• Microdermabrasion
Medium-depth
• Jessner's–35% TCA (most popular combination) • 70% glycolic acid – 35% TCA • Solid CO_2–35% TCA (most potent combination) • 40% TCA (not recommended) • 88% phenol (rarely used)
• Conservative manual dermasanding • Erbium:YAG laser resurfacing • Conservative fractional CO_2 laser resurfacing • Ablative fractional erbium:YAG laser resurfacing
Deep
• Unoccluded or occluded Baker–Gordon phenol peel (see Table 154.6) • TCA in concentrations >50% (not recommended)
• Wire-brush or diamond-fraise dermabrasion • Aggressive manual dermasanding • Manual dermasanding or motorized dermabrasion after a medium-depth peel • Aggressive erbium:YAG laser resurfacing • CO_2 laser resurfacing • Combination erbium:YAG/CO_2 laser resurfacing • Ablative fractional CO_2 laser resurfacing

Table 154.1 Classification of ablative skin resurfacing methods. Although this classification represents an oversimplification because the depth of injury actually varies somewhat along a continuum for each different type of resurfacing procedure, it is helpful when discussing the various options with a patient. The lighter shade represents chemical methods and the darker shade mechanical methods. TCA, trichloroacetic acid.

MAJOR INDICATIONS FOR CHEMICAL AND MECHANICAL SKIN RESURFACING
• Actinically damaged skin and rhytides • Scarring • Multiple pre-neoplastic or neoplastic epidermal lesions (e.g. actinic keratoses, lentigines) • Acne, rhinophyma • Pigmentary dyschromias (including tattoos) • Demarcation lines secondary to other resurfacing procedures

Table 154.2 Major indications for chemical and mechanical skin resurfacing.

CONTRAINDICATIONS TO CHEMICAL AND MECHANICAL SKIN RESURFACING
Absolute
• Poor physician–patient relationship • Lack of psychological stability and mental preparedness • Unrealistic expectations • Poor general health and nutritional status • Isotretinoin therapy within the last 6 months*,† • Complete absence of intact pilosebaceous units on the face • Active infection or open wounds such as HSV, excoriations, or open acne cysts
Relative
• Medium-depth or deep resurfacing procedure within the last 3–12 months* • Recent facial surgery involving extensive undermining, such as a rhytidectomy* • History of abnormal scar formation or delayed wound healing • History of therapeutic radiation exposure • History of certain skin diseases (e.g. rosacea, seborrheic dermatitis, atopic dermatitis, psoriasis, vitiligo) or active retinoid dermatitis • Fitzpatrick skin types IV, V and VI*
*These contraindications apply only to medium-depth and deep resurfacing procedures. †General consensus for mechanical dermabrasion and fully ablative laser surgery.

Table 154.3 Contraindications to chemical and mechanical skin resurfacing. HSV, herpes simplex virus.

as in selecting patients who are ideal candidates for intervention. The dermatologist must evaluate the prospective patient and his or her skin condition carefully, in order to determine if a chemical or mechanical resurfacing procedure is indicated. When resurfacing is deemed appropriate, selection of the proper procedure for each patient is critical to assure that the desired results are achieved in a safe and effective manner. The depth of the injury that must be created by resurfacing to achieve significant improvement is related to the degree of skin surface irregularities and their depth. There are six major indications for resurfacing (Table 154.2).

Pre-neoplastic or neoplastic skin lesions can certainly be removed or improved with resurfacing procedures. Those originating in the epidermis, such as actinic keratoses, lentigines, and seborrheic keratoses are more amenable to treatment than those with a dermal extension or origin. Although some dermatologic conditions may be aggravated by resurfacing, acne and pigmentary dyschromias such as melasma respond favorably to superficial chemical peeling or microdermabrasion, especially when accompanied by appropriate cosmeceutical products and sunscreens. Another indication for chemical and mechanical skin resurfacing is to blend the effects of other procedures, e.g. ablative laser resurfacing of periocular or perioral rhytides, by preventing or eliminating lines of demarcation.

Photoaging is probably the single condition for which skin resurfacing procedures are most often performed. For patients with photoaging, the Glogau system (see Ch. 152) is helpful in deciding upon the most appropriate skin rejuvenation program. It classifies patients into one of four groups based on degree of severity. Patients in category I are often young with minimal to mild photoaging and are best managed with superficial chemical peels or microdermabrasion in conjunction with topical medications or cosmeceuticals (e.g. retinoids, glycolic acids, exfoliants, antioxidants, vitamin C, vitamin E). Patients in category II would likely benefit from a medium-depth chemical peel as well as long-term medical therapy to include a retinoid and/or an α-hydroxy acid (AHA). Individuals in category III typically need prolonged medical treatment in conjunction with one of the following: a medium-depth chemical peel (with or without dermasanding), a deep chemical peel, dermabrasion, or laser resurfacing. For patients with category IV photoaging, interventions utilized for category III individuals are also recommended, but the addition of an invasive surgical operation such as a rhytidectomy or blepharoplasty is often required to achieve the desired results. Nowadays, reconstruction of facial form and correction of deep furrows with injectable neurotoxins and soft tissue fillers is such that resurfacing techniques represent a final stage in the combination approach to facial rejuvenation (see Chs. 158 and 159).

Contraindications and Patient Selection

When evaluating a patient for chemical or mechanical resurfacing, a careful history and physical examination are important to assess the skin problems which prompted his or her presentation and to identify any factors that may contribute to intraoperative or postoperative difficulties (Table 154.3). It is best not to inject soft tissue fillers on the same day as a chemical peel. The patient should also be asked about prior resurfacing procedures, rhytidectomy (facelift), or oral isotretinoin therapy within the last six months, as these can increase the risk of complications following medium-depth and deep resurfacing[6,7].

Although some clinicians no longer require a six-month waiting period post isotretinoin administration, the authors still adhere to this recommendation. Any history of abnormal scar formation or therapeutic radiation exposure warrants extreme caution when considering a patient for skin resurfacing. Individuals with prior radiation exposure should be examined closely for the presence of intact facial hair to ensure that there are enough pilosebaceous units to promote re-epithelialization[8].

Another important element of the patient's history is the presence or absence of a prior herpes simplex viral (HSV) infection. Because recurrence of oral HSV can be triggered by a resurfacing procedure, especially in the perioral and periorbital regions, antiviral therapy (e.g. valacyclovir) is administered prophylactically (see below). Risk factors for HIV infection or viral hepatitis should be identified, and in the authors' opinion, routine laboratory screening is recommended in individuals undergoing dermabrasion with a powered engine. A history of abnormal wound healing from trauma or previous procedures, such as hypertrophic scarring or dyschromia, may be a contraindication to peeling or dermabrasion. The general health and nutritional status of the patient is also an important consideration, especially for medium-depth and deep resurfacing procedures, to ensure timely and complete healing.

Patients with certain cutaneous disorders, such as rosacea, seborrheic dermatitis, atopic dermatitis, psoriasis or vitiligo, may be at increased risk for postoperative complications, including disease exacerbation, prolonged erythema, contact dermatitis, or even delayed healing. In particular, individuals with rosacea have vasomotor instability and may develop an exaggerated inflammatory response to the resurfacing procedure. Caution should also be exercised for patients with autoimmune connective tissue diseases, including cutaneous lupus and systemic sclerosis, as the trauma of chemical peeling may exacerbate the disease. Evaluation of the patient's Fitzpatrick skin type (see Ch. 0) is helpful in predicting the chance of postoperative hyper- or hypopigmentation. Individuals with Fitzpatrick skin types I or II are at low risk for dyspigmentation after medium-depth or deep resurfacing, whereas those with types III through VI are at greater risk for these complications[9].

The patient should understand that chemical and mechanical resurfacing procedures cannot reliably reduce pore size, and their ability to improve lax skin or deeper wrinkles and scars is limited and depends upon the type of intervention being performed. While dermabrasion may sometimes eliminate telangiectasias, chemical peels cannot accomplish this and can even unmask them by removing the pigmentary irregularities. The patient must fully understand the potential benefits, limitations and risks of the procedure, and an informed consent must be signed.

A test spot (e.g. along the lateral hair line) may be useful in some patients to assess their suitability for resurfacing and may be particularly helpful when there is a great deal of concern about the chances of postoperative pigmentary dyschromias[10]; test spots are definitely recommended for individuals with skin types III–VI. Of note, while a favorable test spot result does not guarantee a positive outcome following full-face resurfacing, an unfavorable test spot result is useful in identifying high-risk patients. The latter include those at risk for postinflammatory hyperpigmentation, spotting, irregular coloration, hypopigmentation, or poor or delayed healing. If the dermatologist feels any uncertainty about the patient's suitability or the likelihood of a favorable result, the procedure should not be performed.

Pre-treatment photographs – full-face frontal, lateral and oblique views as well as problem areas – are essential for documenting baseline appearance. They also allow for accurate assessment of postoperative improvement.

Preoperative and Intraoperative Preparations

Another purpose of the preoperative consultation is to ensure that the patient is adequately prepared for the procedure. Almost every patient desiring facial rejuvenation for cutaneous photoaging would benefit from botulinum toxin injections to alleviate dynamic wrinkles (see Ch. 159). These injections appear to enhance the results of deeper resurfacing procedures by immobilizing the muscles implicated in the development of dynamic rhytides during the critical time of postoperative collagen remodeling. In patients with photoaging, it is recommended that botulinum toxin injections be administered as an adjunctive therapy at least 3 days prior to medium-depth or deep chemical peels, dermabrasion, or laser resurfacing.

Due to the significant morbidity associated with herpetic infections during the healing period, patients who undergo medium-depth or deep resurfacing (see Table 154.1) should be treated prophylactically with an antiviral agent, regardless of whether there is a history of HSV infections[11]. These drugs are not routinely given to patients having a superficial chemical peel or microdermabrasion, because the injury is generally not sufficient to activate the virus. However, preventive therapy may be considered in conjunction with superficial resurfacing in patients with a strong personal history of recurrent HSV infections. Recommended prophylaxis consists of acyclovir 400 mg three times daily, valacyclovir 500 mg twice daily or famciclovir 250 mg twice daily, beginning on the day of the procedure. It is advisable to administer the drug for at least 10 to 14 days thereafter[12]. The reason for such a long duration of therapy is that viral replication is possible only in intact epidermal cells, making clinical infection unlikely during the first few days postoperatively. The risk of an eruption increases dramatically with the onset of re-epithelialization and remains high until healing is complete.

It is important that the patient adhere to a strict skin care regimen during the immediate preoperative and postoperative periods to achieve optimal results. The authors treat patients with topical tretinoin on a nightly basis prior to the procedure. Retinoids increase epidermal proliferation and presumably lead to more rapid re-epithelialization after the chemical peel. Because of the tendency for retinoids to cause irritation within 1 to 2 weeks of starting therapy (i.e. retinoid dermatitis), a retinoid formulation with lower irritation potential should be used in patients with sensitive skin. The retinoid should be discontinued one week prior to the chemical peel. In patients with active retinoid dermatitis, resurfacing should be delayed because this condition may lead to a prolongation in postoperative erythema. Decreasing the frequency of application or switching to a less irritating retinoid will allow the inflammation to subside, so that the procedure can be performed[13].

All-*trans*-retinoic acid, or tretinoin, has been classified as a superficial chemical peeling agent, but it is best considered as an integral component of a complete skin rejuvenation program. With chronic use, this drug has been shown to improve actinically damaged skin both clinically and histologically[14]. The use of tretinoin prior to chemical peeling, dermabrasion, or laser resurfacing speeds epidermal healing and enhances the effects of the procedure[13,14]. For chemical peels in particular, use of preoperative topical tretinoin to reduce areas of hyperkeratosis and decrease the thickness of the stratum corneum allows for greater penetration of the peel solution, resulting in a more homogeneous peel and a deeper peel. Use of tretinoin is restricted, however, during the postoperative healing period, until there is diminished inflammatory erythema and complete re-epithelialization with a fully mature epidermis.

Hydroquinone inhibits the enzyme tyrosinase and can reduce the production of epidermal melanin during the healing phase. Patients with skin type III or higher may benefit from twice-daily application of 2% to 4% topical hydroquinone during the preoperative and postoperative (post-healing) periods – even if there is no history of pigmentary abnormalities[9]. It is also necessary to use hydroquinone in patients of any skin type when peeling is done to treat pigmentary dyschromias such as melasma or postinflammatory hyperpigmentation[9]. While a Wood's lamp was used in the past to localize melanin pigment to either the epidermis or dermis (i.e. epidermal versus dermal melasma), histopathologic studies and confocal microscopy have shown that there is often a mixture of the two forms in an individual patient. Nonetheless, in both melasma and postinflammatory hyperpigmentation, increased melanin within the epidermis responds better to superficial peels than does dermal pigment. The use of non-inflammatory peeling agents, e.g. salicylic acid, is preferred for disorders such as melasma as there is less tendency for postinflammatory hyperpigmentation (Fig. 154.1).

All patients undergoing any type of skin resurfacing procedure must adhere to strict photoprotective measures during the postoperative period. This issue is critical in patients whose Fitzpatrick skin type is III or higher, in patients with pigmentary abnormalities, in patients taking exogenous estrogens, and in all patients having medium-depth or deep resurfacing. Specific methods to minimize sun exposure and proper use of sun blocks should be discussed. Patients are also counseled to avoid tobacco use, as smoking in the postoperative period may interfere with the healing process, thereby limiting the effectiveness of the resurfacing and increasing the risk of poor wound healing.

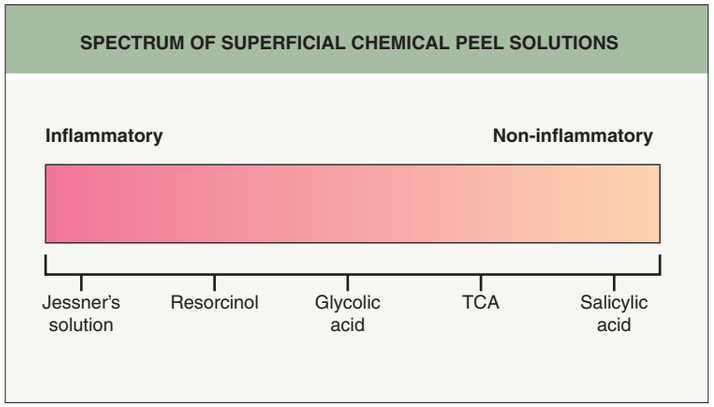


Fig. 154.1 Spectrum of superficial chemical peel solutions. Inflammatory chemical peel solutions are used primarily for photoaging, while non-inflammatory chemical peel solutions are best for Fitzpatrick skin types III–VI, melasma, and postinflammatory hyperpigmentation. TCA, trichloroacetic acid.

The need for intraoperative sedation and analgesia is also discussed with the patient preoperatively, so that plans are made accordingly. Superficial resurfacing procedures usually require only "talkesthesia," a technique that is extremely helpful in awake patients undergoing a procedure, i.e. talking calmly to the patient with encouragement during the procedure. Medium-depth chemical or mechanical resurfacing usually requires a limited degree of perioperative sedation and analgesia, which may include the application of topical amide anesthetics and regional blocks of the supraorbital, infraorbital, and mental nerves (see Ch. 143), as well as oral diazepam, intramuscular meperidine hydrochloride, and/or intramuscular hydroxyzine hydrochloride. Although deep resurfacing procedures can be accomplished entirely with nerve blockade, local injections of lidocaine, and mild sedatives, some patients require intravenous or general (endotracheal tube) anesthesia. Application of the tumescent technique (see Ch. 156) to resurfacing has allowed many patients to undergo deep resurfacing procedures without the additional risks of intravenous or general anesthesia[15]. The patient's inherent pain tolerance, level of anxiety, concomitant medical conditions, and willingness to pay the extra costs of heavier sedation are important topics to discuss during the preoperative consultation that is used to plan for appropriate anesthesia.

Preoperatively, the patient must be given specific instructions to follow, both for the day of the procedure and for postoperative care. These should be carefully reviewed verbally prior to the procedure, with the same instructions provided in written form. On the day of the procedure, the patient washes his or her face with a gentle cleanser and preferably avoids the application of any cosmetics. Individuals undergoing procedures requiring minimal or no sedation are encouraged to eat a light breakfast, but patients receiving deeper anesthesia should have nothing by mouth except for their usual medications. Particularly for medium-depth and deep resurfacing procedures, the dermatologist should meet with the patient and his or her family preoperatively to re-establish rapport, answer last-minute questions, discuss perioperative and postoperative expectations and instructions, and assure compliance with antiviral prophylaxis as needed.

CHEMICAL RESURFACING PROCEDURES

Although there is currently a wide variety of resurfacing procedures available for facial rejuvenation, chemical peeling remains a popular choice for both patient and physician. In comparison to some of the newer options, chemical peels have a longstanding safety and efficacy record, are performed with ease, are low in cost, and have a predictable and relatively quick recovery time. Various acidic and basic compounds are used to produce a controlled skin injury and are classified as superficial, medium-depth, and deep peeling agents, according to their level of penetration, destruction, and inflammation (see Table 154.1). In general, superficial peels cause epidermal injury and occasionally extend into the papillary dermis, medium-depth peels cause injury through the papillary dermis to the upper reticular dermis, and deep peels cause injury down to the mid-reticular dermis[16].

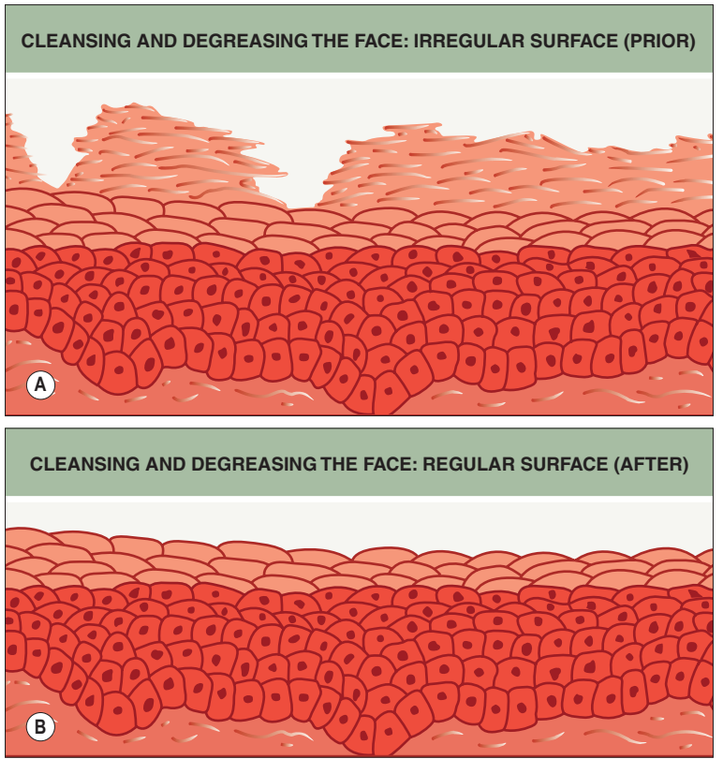


Fig. 154.2 Cleansing and degreasing the face. A Irregular surface (prior). **B** Clean, regular surface (after).

Prior to the application of peeling solutions, the skin surface must be vigorously cleansed to remove residual oils, debris, and excess stratum corneum. The authors use gauze pads with an effective detergent cleanser, followed by rinsing with water and drying. Because of the defatting and degreasing properties of acetone, gauze pads moistened with an acetone preparation are then used to cleanse the skin even further. Finally, the cleansed skin is palpated immediately prior to peeling to check for the presence of residual oil and if any is felt, the process is repeated. *The importance of cleansing prior to the peeling procedure cannot be overemphasized*. A thorough and evenly distributed cleansing and degreasing of the face assures uniform penetration of the peeling solution and leads to an even result without skipping areas (Fig. 154.2).

The effect of a chemical peel is dependent upon the agent used, its concentration, and the techniques employed before and during its application. Each wounding agent used in peels has unique chemical properties and causes a specific pattern of injury to the skin[15–20]. It is important for the physician using these solutions to be familiar with their cutaneous effects and proper methods of application, to assure correct depth of injury. The marketplace has been flooded with numerous proprietary formulations of peeling agents with each product claiming unique advantages. These products are often expensive and have not been shown to be safer or more effective than the conventional solutions. Their advantage rests in the prepackaging of materials and ease for the physician. The following discussion on superficial, medium-depth, and deep peeling will therefore focus on the specific chemical agents that are responsible for producing the various patterns of injury rather than proprietary products.

Superficial Chemical Peeling

Superficial chemical peels are indicated in the management of acne and its postinflammatory sequelae, mild photoaging (Glogau I and II), and epidermal lesions such as lentigines and keratoses, as well as melasma and other pigmentary dyschromias[21]. A series of peels is usually necessary to obtain optimal results[22]. The frequency of peels and degree of exposure to the peeling agent may be increased gradually as necessary. Results are enhanced by medical or cosmeceutical therapy, including a retinoid, antioxidants and, if necessary, a bleaching agent. All superficial chemical peels share the advantages

JESSNER'S SOLUTION (COMBES' FORMULA)	
Resorcinol	14 g
Salicylic acid	14 g
85% lactic acid	14 g
95% ethanol (q.s.ad)	100 ml

Table 154.4 Jessner's solution (Combes' formula). q.s.ad, a sufficient quantity up to.

of only mild stinging and burning during application as well as minimal time (a few days) needed for recovery.

Superficial chemical peels are divided into two varieties – very light and light (see Table 154.1). With *very light* peels, the injury is usually limited to the stratum corneum and only creates exfoliation; however, the injury may extend into the stratum granulosum. The agents used for these peels include low-potency formulations of glycolic acid, 10%–20% trichloroacetic acid (TCA), tretinoin, 20% salicylic acid, and Jessner's solution (Table 154.4)[23–25]. *Light* peels injure the entire epidermis down to the basal layer, stimulating the regeneration of a fresh new epithelium. Agents used for light peels include 50%–70% glycolic acid, 25%–30% TCA, Jessner's solution (greater number of coats than for very light peels), 30% salicylic acid, and solid CO_2 slush[23,24]. During the application of superficial peeling agents, there may be mild stinging followed by a level I frosting, defined as the appearance of erythema and streaky whitening on the surface (Fig. 154.3).

Alpha-hydroxy acids (AHAs) are naturally found in foods and have been used widely in skin rejuvenation regimens since the early 1990s. The depth of injury is determined by the specific AHA used, its pH, the concentration of free acid, the volume applied to the skin, and the duration of contact. In low concentrations, AHAs have been shown to decrease the cohesion of corneocytes at the junction of the stratum corneum and the stratum granulosum[26]. Higher concentrations are associated with complete epidermolysis. With chronic use of AHA-containing products on a daily basis, there is an increase in skin thickness, acid glycosaminoglycans (mucopolysaccharides), and the density of collagen, as well as an improvement in elastic fiber quality[19]. The most popular of the AHAs, **glycolic acid**, is available in a variety of over-the-counter preparations and can be purchased by physicians in buffered as well as unbuffered concentrations as high as 70% for chemical peels. Twice monthly or every other week applications of 40%–70% glycolic acid (with cotton swabs, a sable brush, or 2×2-inch gauze pads) have been used most often for acne, mild photoaging, and melasma[27]. The time of application is critical for glycolic acid, as it must be rinsed off with water or neutralized with 5% sodium bicarbonate after 2 to 4 minutes. It is the only peeling agent that is time-dependent, requiring neutralization to end its action.

Application of 10%–20% **TCA** with either a saturated gauze pad or sable brush produces erythema and a very light frost within 15 to 45 seconds. The depth of penetration of the peeling solution is related to the number of coats applied. Epidermal protein denaturation results in exfoliation without vesiculation. Concentrations of TCA up to 25% can be used alone as a superficial peeling agent but may create an injury and inflammation that extends partially into the upper dermis. **Jessner's solution** is a combination of keratolytic ingredients that has been used for over 100 years in the treatment of inflammatory and comedonal acne as well as hyperkeratotic skin disorders (see Table 154.4). Jessner's solution has intense keratolytic activity, initially causing loss of corneocyte cohesion within the stratum corneum and subsequently creating intercellular and intracellular edema within the upper epidermis if application is continued[28]. The mode of application for the Jessner's peel is similar to that of the 10%–20% TCA peel. The clinical endpoint of treatment is erythema with blotchy frosting (when used prior to application of TCA in medium-depth peels) or a more uniform frosting (when used alone for superficial peels). While Jessner's peel can be used in extrafacial sites, care must be taken to restrict the total amount of peel solution, as salicylic acid is absorbed systemically.

Salicylic acid, also referred to as a β-hydroxy acid, is one of the ingredients in Jessner's solution. It can be used alone for superficial chemical peeling and is a preferred therapy for comedonal acne and inflammatory rosacea as it is lipophilic and concentrates within the pilosebaceous apparatus (Fig. 154.4)[25]. Salicylic acid is quite effective as an adjunctive therapy for both open and closed comedones and for resolving post-acne erythema. As noted previously, salicylic acid produces less inflammation than other superficial peeling agents (see Fig. 154.1) and therefore is associated with a lower risk of postinflammatory hyperpigmentation. Salicylic acid is the preferred peeling agent for removing the excess pigmentation in melasma and postinflammatory hyperpigmentation. It is safer and more effective in reducing epidermal pigment, especially when combined with a bleaching agent (e.g. hydroquinone) and sunscreens.



Fig. 154.3 Levels of frosting. A Level I frosting as found with light chemical peeling: erythema with streaky frosting. **B** Level II frosting: erythema with diffuse white frosting. **C** Level III frosting: solid white enamel frosting.



Fig. 154.4 Salicylic acid peels. These peels are effective for the treatment of acne, including comedones. Repetitive peels over 6 weeks combined with medical acne treatment will hasten resolution of the condition. Note the perifollicular frosting seen with salicylic acid, a lipophilic chemical.

Prior to the initial treatment, the patient must understand that the net effect of repetitive superficial chemical peels never approaches the beneficial effect obtained with a single medium-depth or deep peel. The improvements in cutaneous photoaging following superficial peels are usually subtle because there is little to no effect on the dermis. These peels thus cannot produce an appreciable effect on textural changes such as deep wrinkles and furrows, which originate within the dermis. Nonetheless, their ease of use and minimal downtime makes these "lunchtime" peels rewarding for patients with realistic expectations and are a favorite of busy patients. Superficial peels are best employed in combination with cosmeceutical agents and other minimal- to no-downtime procedures such as botulinum toxin A injections, microneedling, and intense pulsed light treatments. Desired and expected results include a "brightened" skin appearance with a more uniform color and texture.



Fig. 154.5 Jessner's–35% trichloroacetic acid (TCA) chemical peel. A Before treatment. **B** 3 days after treatment. **C** 6 days after treatment. **D** 2 months after treatment.

Medium-Depth Chemical Peeling

Medium-depth chemical peels consist of controlled damage through the epidermis and into the papillary dermis, with variable extension to the upper reticular dermis. Both medium-depth and deep chemical peels produce epidermal necrosis plus papillary dermal edema and homogenization with a sparse lymphocytic infiltrate within the first several days[15]. Postoperatively, over a period of 3 months, there is increased collagen production with expansion of the papillary dermis and the development of a mid-dermal band of thicker collagen fibers. These changes correlate with the clinical improvement in texture, fine lines, and color observed over time (Fig. 154.5).

For many years, 40%–50% TCA was the prototypical medium-depth peeling agent because of its ability to ameliorate fine wrinkles, actinic changes, and "pre-neoplasias". TCA as a single agent for medium-depth peeling has fallen out of favor because of the high risk of complications, especially scarring and pigmentary alterations, when used in strengths approaching 50% and higher[29]. Today, most medium-depth chemical peels are performed utilizing 35% TCA in combination with Jessner's solution, 70% glycolic acid, or solid CO_2 as the "priming" agent. These combination peels have been found to be as effective as 50% TCA alone, but safer with fewer risks[30]. The level of penetration is better controlled with these combination peels, thereby preventing the "hot spots" seen with higher concentrations of TCA that can produce dyschromia and scarring.

Brody and Hailey[31] developed the use of solid CO_2 to freeze the skin prior to the application of 35% TCA. This causes epidermal necrosis and significant dermal edema, thereby allowing deeper penetration of the TCA in selected areas. This technique is particularly useful for effacing the edges of mild acne scars and destroying thicker epidermal growths. Monheit[28] then described a combination medium-depth peel in which Jessner's solution is first applied, followed by 35% TCA, with comparable clinical results. Similarly, Coleman and Futrell[32] have demonstrated the usefulness of 70% glycolic acid prior to the application of 35% TCA for medium-depth peeling. Jessner's solution and glycolic acid both appear to effectively weaken the epidermal barrier and allow deeper, more uniform and more controlled penetration of 35% TCA.

Current indications for medium-depth chemical peeling include Glogau group II cutaneous photoaging, epidermal lesions such as actinic keratoses, pigmentary dyschromias, and mild acne scarring, as well as blending of the effects of deeper resurfacing procedures. The most popular of the medium-depth peels for facial rejuvenation is the Jessner's–35% TCA peel. This peel has been widely accepted because of its broad range of uses, the large number of individuals in whom it is indicated, its ease of modification according to the patient or situation, and its excellent safety profile.

The Jessner's–35% TCA peel is particularly useful for the improvement of mild to moderate photoaging (Fig. 154.6). It freshens sallow, atrophic skin and softens fine rhytides, with minimal risk of textural or pigmentary complications. Collagen remodeling occurs for as long as 3 to 4 months postoperatively during which time there is continued improvement in texture and rhytides. Deep furrows, however, are not eliminated with this peel and there is no significant skin retraction as is seen with ablative fractional laser resurfacing or deep chemical peels. When used in conjunction with a retinoid, bleaching agent, and sunscreens, a single Jessner's–35% TCA peel lessens pigmentary dyschromias and lentigines more effectively than repetitive superficial peels. Epidermal growths such as actinic keratoses



Fig. 154.6 Medium-depth chemical peel used to treat moderate photoaging of the skin. A Preoperative, demonstrating actinic keratoses plus aging textural changes. **B** Application of 35% trichloroacetic acid (TCA) directly after Jessner's solution. **C** White enamel frosting (level III) from 35% TCA. **D** Desquamation and inflammation 4 days after peel. **E** Final results 6 months later.

also respond well to this peel. In fact, the Jessner's–35% TCA peel has been found to be as effective as topical 5-fluorouracil in removing both grossly visible and clinically undetectable actinic keratoses while having the added advantages of lower morbidity and greater improvement in associated photoaging[33,34].

Another indication for the Jessner's–35% TCA peel is to blend the effects of other resurfacing procedures with the surrounding skin[35]. Patients who have undergone ablative fractional CO_2 laser resurfacing, deep chemical peeling or dermabrasion to a localized area such as the periorbital or perioral region often develop a sharp line of demarcation between the treated and untreated skin. The treated skin may appear hypopigmented (also known as pseudohypopigmentation) in comparison to the untreated photodamaged skin. These irregularities are often conspicuous and are troubling to the patient. A Jessner's–35% TCA peel performed on the adjacent untreated skin helps to blend the treated area into its surroundings. For example, a patient with advanced photoaging in the periorbital region and moderate photoaging on the remaining face may desire fractional CO_2 laser resurfacing only around the eyes. In this patient, medium-depth chemical peeling of the areas not treated with the laser would improve the photoaging in these regions and avoid a line of demarcation[36] (Fig. 154.7). Similarly, a patient with acne or surgical scars having spot or regional dermabrasion or ablative fractional laser resurfacing to a facial cosmetic unit would benefit from a Jessner's–35% TCA peel to the remainder of that cosmetic unit or to the rest of the face. It is important to note that when used in combination with other resurfacing procedures such as laser ablation or dermabrasion, the peel should be performed first, in order to avoid accidental application of the peeling agent onto previously abraded or laser-treated areas, which may lead to scarring (Fig. 154.8).

Using either cotton-tipped applicators or gauze pads, a single, even coat of Jessner's solution is applied first to the forehead, then the cheeks, nose and chin, and, lastly, the eyelids. Proper application of Jessner's solution causes minimal discomfort and creates a faint frost within a background of mild erythema (Fig. 154.9A)[37]. After waiting 1 to 2 minutes for the Jessner's solution to completely dry, 35% TCA is applied evenly with one to four cotton-tipped applicators (Fig. 154.9B). The ultimate effectiveness of this peel is directly dependent upon the depth of penetration of the peeling solutions, and this depth is a function of the adequacy of degreasing and the amount of both solutions applied. The use of cotton swabs, particularly for the application of TCA, is advantageous because it allows the surgeon to quantitatively vary the amount of solution applied according to the patient's specific needs. *The amount of TCA delivered to the skin surface is determined by the number of applicators used, their degree of saturation, the amount of pressure applied to the skin surface, and the duration of their contact with the skin*. Four moist cotton-tipped applicators are applied in broad strokes over the forehead and on the medial cheeks. Two mildly soaked cotton-tipped applicators can be used across the lips and chin, and one damp cotton-tipped applicator on the eyelids (Fig. 154.9C). In addition to location, these parameters are varied based on skin thickness and degree of photodamage.

When applying TCA, anatomic areas of the face are peeled sequentially from the forehead to the temple to the cheeks and finally to the lips and eyelids. Careful feathering of the solution into the hairline and around the rim of the jaw and brow conceals the demarcation line between peeled and non-peeled skin. Areas of wrinkled skin are stretched taut with the help of an assistant, to allow even application of the solution into the folds and troughs. This technique is particularly

helpful on the skin of the upper and lower lips. For perioral rhytides, TCA is applied with the wooden portion of a cotton-tipped applicator and extended onto the vermilion border (Fig. 154.9D).

Eyelid skin must be treated delicately and carefully to avoid over-application to this thinner skin and to prevent exposure of the eyes to the TCA solution. The patient should be positioned with the head elevated at 30°. Excess peel solution on the cotton tip should be squeezed out so that the applicator is semi-dry. With the eyes closed, a single applicator is rolled gently from the periorbital skin onto the upper eyelid skin without going below the superior aspect of the tarsal plate. Another semi-dry applicator is then rolled onto the lower eyelid skin within 2 to 3 mm of the lid margin while the patient is looking superiorly.



Fig. 154.7 Combination of medium-depth peel of the face plus CO_2 laser ablative resurfacing of the periorbital region. A Before treatment. **B** After treatment.

Excess peel solution should never be left on the lids because it can roll into the eyes. Any tears should be immediately dried with a cotton-tipped applicator because they may pull the solution into the eye by capillary action (see Fig. 154.9C). Tears can also travel down the cheek and carry TCA onto the neck, resulting in a linear streak.

The white frost from TCA application appears on the treated area within 30 seconds to 2 minutes. This response is representative of keratocoagulation and indicates that the TCA's physiologic reaction is complete. The Jessner's–35% TCA combination takes longer to frost than phenol preparations, but a shorter period of time than the superficial peeling agents. The desired endpoint for medium-depth peeling is level II to level III frosting. Level II frosting is defined as uniform white-coated frosting with a background of erythema (see Fig. 154.3B). Level III frosting, which is associated with penetration to the reticular dermis, is a solid white enamel frosting with no background of erythema (see Fig. 154.3C). A deeper level III frosting should be restricted solely to areas of thick skin and heavy actinic damage. Most medium-depth chemical peels achieve a level II frosting and this is especially important over the eyelids and areas of sensitive skin. Areas with a greater tendency to form scars, such as the zygomatic arch and the bony prominences of the jawline and chin, should receive no greater than level II frosting.

Before re-treating an area, the surgeon should wait at least 3 to 4 minutes after the application of TCA, to ensure that frosting has reached its peak. Each cosmetic unit is then assessed, and areas of incomplete or uneven frosting are carefully re-treated with a thin application of TCA. Additional applications of TCA increase the depth of penetration as well as the risk of complications, so one should apply more solution only to the underfrosted areas. In other words, do not apply 35% TCA to fully frosted areas as this may cause inflammation beyond the level expected and potentially lead to scarring. Thicker keratoses do not frost as well as the surrounding skin, so vigorous rubbing of the lesion may be needed for adequate TCA penetration. If necessary, thicker epidermal lesions may be treated with liquid nitrogen cryotherapy for several seconds prior to the application of TCA. As will be discussed later, mechanical abrasion can also be performed in selected areas at the completion of the Jessner's–35% TCA chemical peel, to enhance the results.

Although there is an immediate burning sensation as the peel solution is applied, the discomfort begins to subside as frosting occurs and resolves fully by the time of discharge. If necessary, a topical amide anesthetic can be applied under occlusion prior to a medium-depth peel for pain relief[38]. Cool saline compresses offer symptomatic relief at the conclusion of the peel. Unlike the compresses utilized in glycolic acid peels, the saline following a TCA peel simply provides relief and does not "neutralize" the acid.

TCA CROSS

The "TCA CROSS" (TCA *c*hemical *r*econstruction *o*f *s*kin *s*cars) technique is an innovative approach to deep ice-pick and fibrotic acne scars (Fig. 154.10A). Rather than a peel or method of exfoliation, it is



Fig. 154.8 Combination procedure utilizing perioral–periorbital CO_2 laser resurfacing with Jessner's–35% trichloroacetic acid (TCA) peel to the remainder of the face. The peel will blend the color and texture of the laser-treated areas. **A** Preoperative: the eyelids and lips need deeper resurfacing than do the cheeks, which require only medium-depth injury. **B** Four days postoperative: note difference in the rate of healing between laser- and peel-treated areas. **C** One year postoperative.

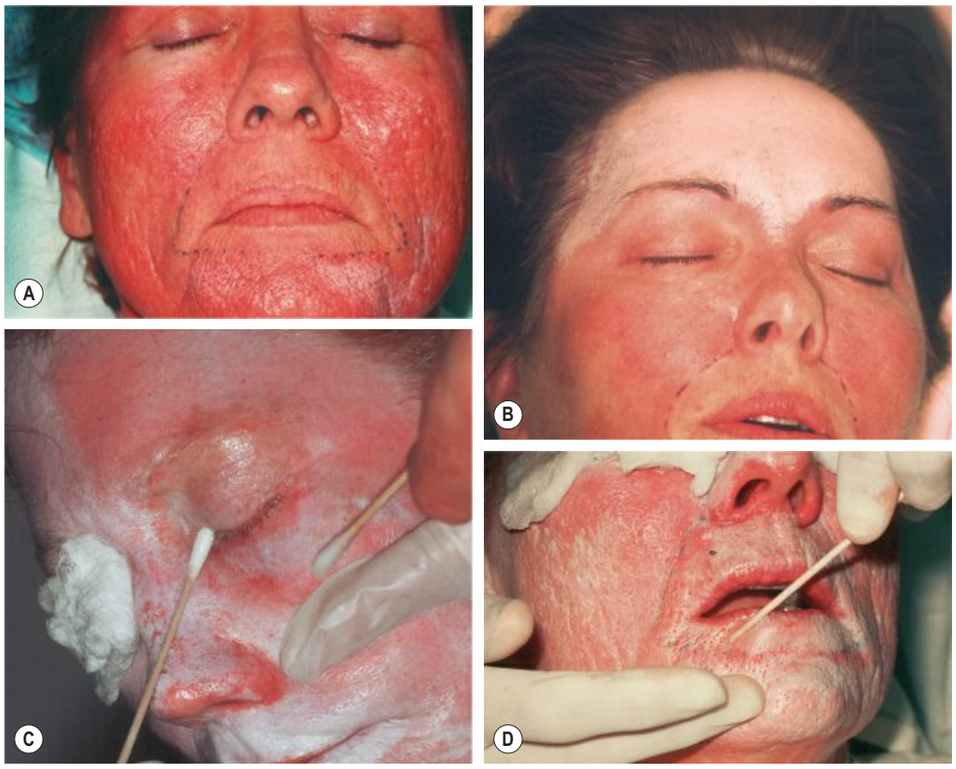


Fig. 154.9 Technical aspects of the Jessner's–35% trichloroacetic acid (TCA) peel. A Appearance of level I frosting after application of Jessner's solution – erythema with blotchy frosting. **B** 35% TCA applied, after Jessner's solution dries, with an even application using cotton-tipped applicators (one to four). A level III or white enamel frosting is obtained. **C** Eyelids are treated with one cotton-tipped applicator moistened with 35% TCA. A dry applicator is used to absorb tears during eyelid peeling. **D** Lip rhytides are peeled with saturated cotton-tipped applicators. The wooden shaft is used to rub peel solution further into the lip rhytides.



Fig. 154.10 "TCA CROSS" technique used as a destructive method for ice-pick scars. A Preoperative with ice-pick scars of the nose and cheek. **B** Frosting limited to just the ice-pick scars. **C** Postoperative.

the use of 90% TCA as a full-thickness destructive tool. When applied to an ice-pick scar, it destroys the epidermis and its deep dermal tunnel, creating a full-thickness skin wound which will heal with the formation of new collagen, thus filling the depressed scar. This method offers a simpler approach to these full-thickness depressions in which the alternatives are surgical: punch grafts, excision, and scar revision. The procedure is performed independently of other resurfacing procedures such as peeling, laser resurfacing or dermabrasion.

After the face is cleansed and degreased with acetone (see above), the ice-pick and depressed fibrotic scars to be treated are outlined with a skin marker and photographed. This serves as a guide for further treatment sessions. The 90% TCA is applied to the interior of the ice-pick scar with a toothpick, being careful not to drip the acid onto normal skin as this could lead to additional scarring. Of note, this is a full-thickness destruction of skin and not a peel, so the TCA should be applied *only* to the interior of the scar itself[39]. Each of the scars is treated until a brilliant white frosting appears (Fig. 154.10B). A topical antibiotic is then placed on each treated site. The procedure is performed with no anesthesia or sedation, as it only produces a brief stinging equivalent to the sensation of cryosurgery.

Healing occurs over the next 2 to 3 weeks, with granulation tissue, fibroplasia, and remodeling of new collagen, which will elevate and soften the depressed scars (Fig. 154.10C). The procedure is then repeated 3 to 6 times at 6-week intervals until substantial elevation has been achieved. This can be followed by a more superficial resurfacing procedure such as medium-depth peeling, laser resurfacing, or dermabrasion to smooth the more superficial scars and blend them with other treated areas.

The physician must warn the patient about potential dyschromia, especially in Fitzpatrick skin types III through VI, as skin destruction of this depth can depigment the treated areas. The multiple procedures may not be able to raise all the scars to the surface but they will surely provide improvement. The TCA CROSS technique does add another simple therapeutic option for treating scars.

Deep Chemical Peeling

Patients in Glogau groups III and IV may require deep chemical peeling, motorized dermabrasion, or laser resurfacing to improve their greater degree of skin damage. Deep chemical peeling leads to production of new collagen and ground substance down to a level in proportion to the depth of the peel. Deep chemical peels create an injury through the papillary dermis and into the superficial reticular dermis, which may extend into the mid-reticular dermis. For deep peeling, either TCA in concentrations >50% or a phenol-containing preparation is used. Because of the risk of scarring and other complications with such potent concentrations of TCA, this agent is not recommended for deep chemical peeling. Therefore, solutions containing phenol remain the preferred formulation for deep chemical peels[40–46].

A deep chemical peel is one of the most permanent cutaneous rejuvenation procedures (Table 154.5)[46]. Histologically, it leads to a dense neocollagenesis zone with new elastic fibers that increases over 6 weeks (Fig. 154.11). The classic Baker–Gordon formula is outlined

DEEP PHENOL–CROTON OIL CHEMICAL PEELS	
• Phenol–croton oil formulas lead to deeper penetration than full-strength phenol* (see Table 154.6 for composition of Baker–Gordon formula) • Used for rejuvenation of severely photoaged skin (Glogau III and IV), with significant improvement or even elimination of deep furrows as well as other textural and pigmentary irregularities the expected result (Fig. 154.11)	
Potential specific complications and contraindications	
Cutaneous	• Scarring (Fig. 154.12), a "plastic" or alabaster appearance with an effacement of normal skin texture, hypopigmentation (greater problem in darker skin phototypes and men), persistent postoperative erythema for months
Systemic	• Cardiotoxicity
Contraindications	• History of cardiac arrhythmias or taking a medication known to precipitate arrhythmias
Relative contraindications	• History of hepatic or renal disease (phenol undergoes hepatic and renal elimination)
Preoperative evaluation and procedure	
Preoperative evaluation	• CBC, LFTs, BUN, crt, electrolytes, baseline electrocardiogram
Procedure	• Before administration of anesthesia (general or deep sedation), patient is examined while in a seated position and appropriate landmarks are noted • After thorough cleansing and degreasing of skin, chemical agent is applied sequentially to six aesthetic units: forehead, perioral region, right cheek, left cheek, nose, and periorbital region • The peel is extended slightly beyond the mandibular rim to conceal the demarcation between treated and untreated skin, but should not be extended to the vertical neck because of the risk of scarring in this area • Periorbital skin is treated cautiously and conservatively to avoid overpenetration, which can lead to ectropion or scarring; notably, diluting a phenol compound with water may increase its penetration so mineral oil (rather than water) should be used to flush the eyes if contact occurs • Cotton-tipped applicators are used; the technique is similar to that for a Jessner's–35% TCA peel (see text), but less solution is used because frosting occurs very rapidly • Following application, there is a burning sensation that lasts for 15–20 seconds, subsides for 20 minutes, and then returns for the next 6 to 8 hours • A 15-minute time interval between the treatment of each cosmetic area is recommended so the entire procedure requires 60 to 90 minutes
*Pure, undiluted 88% phenol is rarely used because it causes rapid and complete coagulation of epidermal keratin proteins and this blocks further penetration.	

Table 154.5 Deep phenol–croton oil chemical peels. BUN, blood urea nitrogen; CBC, complete blood count; crt, creatinine; IV, intravenous; LFTs, liver function tests; PAC, premature atrial contraction; PVC, premature ventricular contraction. Data from references 40–46.

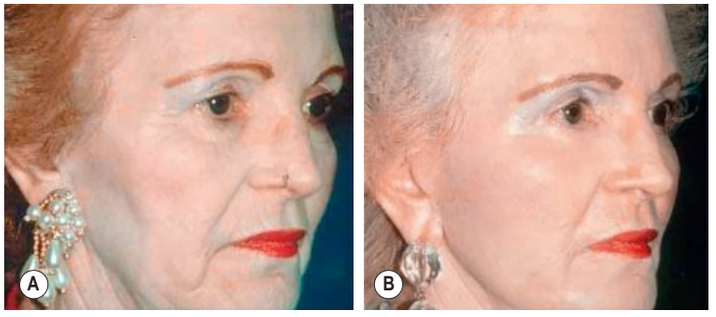


Fig. 154.11 Deep phenol–croton oil peel. A Before treatment. **B** 3 months after treatment with obvious reduction in rhytides.

THE BAKER–GORDON FORMULA		
Ingredient	**Amount**	**Comments**
88% liquid phenol, USP	3 ml	Final concentration of phenol is 50%–55%
Tap water	2 ml	Dilution increases penetration
Septisol® liquid soap (0.25% hexachlorophene)	8 drops	A surfactant that reduces skin tension, allowing more even penetration
Croton oil	3 drops*	A vesicant and epidermolytic agent that enhances phenol absorption Efficacy may be more related to the amount of croton oil than it is to that of phenol[40,42]
*Using 1 or 2 drops of croton oil, rather than the 3 in the Baker–Gordon formula, can limit the risk of phenol complications such as textural effacement or hypopigmentation.		

Table 154.6 The Baker–Gordon formula. The mixture or suspension of ingredients is freshly prepared and must be stirred vigorously prior to application due to its poor miscibility. USP, United States Pharmacopeia.

in Table 154.6. While it was originally thought that phenol was the active agent, in 1996 Hetter proposed, based upon careful data and animal studies, that croton oil was the active agent[40]. Others have subsequently confirmed the correlation of croton oil concentration with depth of wounding and there are various formulas of the Hetter peel (Table 154.7). While the expanded range of phenol–croton oil peels has increased their clinical applications and safety, performance of deep chemical peels requires experience.

The deep peel is indicated for moderate to severe photodamage (Glogau IV) and extensive rhytides in patients with skin types I–III. Associated lightening is an unwanted side effect in darker skin phototypes. Care must be taken in choosing the appropriate patient given the prolonged recovery and need for close monitoring to ensure proper healing. In addition, sedation and pain control, including the use of opioids, nonsteroidal anti-inflammatory drugs (NSAIDs) and benzodiazepines, are required during and after the procedure. A dull to moderately severe discomfort begins during the procedure and extends for up to 4 hours afterwards.

The peel solution should be freshly mixed and it separates easily without agitation. The face is divided into 6 cosmetic units and application time for each unit is 20 minutes such that the duration of a full-face treatment is 1½ to 2 hours. Because absorption occurs, this time spacing is required to limit serum phenol concentrations as it has both cardiac and renal toxicities. Intravenous hydration is administered prior to and during the procedure to assist in reducing phenol levels and the patient is monitored for cardiac arrhythmias.

After thorough cleansing with a detergent and acetone, the phenol–croton oil peel solution is applied with cotton-tip applicators, utilizing the correct number of passes and pressure to produce a visible solid white frosting. The latter appears very quickly after application and gradually resolves into a gray color with edema within an hour. While tape occlusion is the classic approach for creating deeper penetration, a lighter version is the *untaped* phenol–croton oil peel which heals faster and lessens the risk of overpenetration and scarring (Fig. 154.12). For the following 2 to 3 weeks, mild debriding soaks and ointments are

HETTER CHEMICAL PEELS WITH VARYING CONCENTRATIONS OF PHENOL AND CROTON OIL			
Type of peel	**Phenol (%)**	**Croton oil (%)**	**Cosmetic unit/indication**
Light	2.5	0.1	Eyelids, neck
Medium-depth	33	0.7	Cheeks, nose, chin; *not* for eyelids
Deep	33	1.1	Full-face except eyelids
Very deep (Baker–Gordon formula)	50	2.1	Lip rhagades, severe photodamage with pale skin

Table 154.7 Hetter chemical peels with varying concentrations of phenol and croton oil.



Fig. 154.12 Complications from a Baker–Gordon phenol peel. There was prolonged non-healing, resulting in hypopigmentation and marbled scarring.

regularly applied. Prolonged postoperative care is required, along with medical supervision to assess for healing and early signs of potential complications (see below). Post-peel erythema may last as long as 6 weeks while collagen rejuvenation is occurring.

MECHANICAL RESURFACING PROCEDURES

For over 50 years, dermabrasion utilizing a rotating abrasive surface attached to a power-driven hand engine was considered the premier skin resurfacing procedure for facial scars. It has generally been regarded as a deep resurfacing modality based on its depth of injury and its prolonged healing time. The original descriptions of modern dermabrasion involved the use of a wire brush (which remains in use today), but there has been a movement toward more superficial methods of mechanical resurfacing. In 1957, the diamond fraise was introduced and became the preferred instrument for dermabrasion by some surgeons because it is less aggressive and more forgiving than the wire brush[47]. There has also been a resurgence of interest in manual dermasanding, which allows for more deliberate and controlled skin planing[4,5]. Microdermabrasion and microneedling are the mechanical resurfacing procedures developed most recently and represent the most conservative forms of mechanical resurfacing[3].

Microdermabrasion

Because microdermabrasion removes the stratum corneum and superficial spinous layer and the injury rarely extends past the basal layer, this modality is considered superficial in depth. Whether it is classified as very light or light in comparison to other superficial resurfacing procedures depends upon the technique and aggressiveness of the operator. The microdermabrasion unit's handpiece is a closed system, which propels aluminum oxide crystals at the skin at high speeds and simultaneously removes them with suction. These units were developed commercially in the mid-1990s and are currently in widespread use in both physicians' offices and non-medical aesthetic spas. Variants of this superficial resurfacing modality include hydrafacials and DermaSweep™ (DermaSweep, Inc.).

ADVANTAGES OF MANUAL DERMASANDING OVER MOTORIZED DERMABRASION
• Greater control over depth of injury, particularly on the lips and orbital rims • Blending of abraded areas into adjacent unabraded areas accomplished more easily and with better results • Lower cost and greater simplicity of instrumentation and set-up • Risk of aerosolizing infectious particles is far less • Possibly lower incidence of postinflammatory hypopigmentation

Table 154.8 Advantages of manual dermasanding over motorized dermabrasion.

Microdermabrasion may be indicated for acneiform conditions, pigmentary dyschromias, and as a "lunchtime" procedure for facial rejuvenation in all skin types[48], but in general it is not considered effective for improving the appearance of rhytides[49,50]. Both the patient and physician must understand that the degree of objective improvement with microdermabrasion may be limited. It is best used in conjunction with a regimen of topical "cosmeceuticals" including a retinoid, a bleaching agent, antioxidants and sunscreen, with the repeated superficial exfoliation of microdermabrasion enhancing the overall efficacy of the therapeutic program.

Ideal candidates for microdermabrasion typically desire facial rejuvenation without downtime. Appropriately selected patients have a subjective perception of improvement usually exceeding the objective signs depicted with photographs. Patients often report that their skin has a smoother texture and that cosmetics are easier to apply and they blend in with their skin more easily. Microdermabrasion has also been successfully combined with intense pulsed light (IPL) therapy to enhance penetration of the light.

Although the role of microdermabrasion in facial rejuvenation grew dramatically after its initial development, the scientific data to justify its use were lacking until more recently. An increase in epidermal and dermal thickness, flattening of the rete pegs, papillary dermal hyalinization, and newly deposited collagen and elastic fibers have all been observed[51]. Following microdermabrasion, there also appears to be a significant alteration in epidermal barrier function[52]. In addition, investigators have observed an elevation of transcription factors, cytokines, and matrix metalloproteinases following microdermabrasion[53]. This can lead to an enhancement of the effectiveness of topical agents. Microdermabrasion can also be used in combination with very light chemical peels (e.g. DermaSweep™).

Manual Dermasanding

Manual dermasanding involves abrading the skin by hand using silicon carbide sandpaper or wallscreen that is commercially available at any hardware store. It is gaining in popularity for skin resurfacing because it has several advantages over power-driven dermabrasion (Table 154.8). Its classification as a wounding agent is entirely dependent upon the type of paper used, the force applied by the surgeon, and the duration of contact with the skin. Although manual dermasanding can be used to produce a wound as deep as with wire-brush dermabrasion or several passes with a pulsed CO_2 laser, it is probably most commonly used as a medium-depth or "minimally deep" resurfacing modality.

Manual dermasanding can be used to resurface an entire face, but because it is so labor-intensive it is most often utilized for resurfacing localized regions to minimize the appearance of a scar[54] or to blend or enhance the effects of a medium-depth chemical peel or a combination procedure[55]. It can be used following a fractional laser resurfacing to feather the transition into hair-bearing areas that are inaccessible to the laser. Manual dermasanding of the eyebrows and hairline and gently abrading the upper neck at the inferior aspect of the laser-irradiated zone are all effective at minimizing lines of demarcation between treated and untreated skin (Fig. 154.13). It can also be useful immediately after laser resurfacing for stubborn rhytides, particularly in the perioral region; manual dermasanding can improve the outcome by producing a slightly greater depth of injury in a controlled fashion where further thermal injury would be risky. It will also remove adherent necrotic debris and thermal damage after laser resurfacing, thus enhancing the healing process. Similarly, a medium-depth chemical peel can be immediately followed by manual dermasanding of the more troublesome areas to enhance results as well as along the borders of the peeled skin to blend the effects.



Fig. 154.13 Dermasanding. Manual dermasanding utilizing G-320 grit silicon carbide sandpaper to blend CO_2 laser resurfacing into the eyebrow area. The sterilized sandpaper has been wrapped around rolled-up gauze pads and moistened with saline or soap-free cleanser for lubrication.

Our clinical experience suggests that dermasanding after a Jessner's–35% TCA peel may yield impressive postoperative results that approach those seen with either motorized dermabrasion or fractional CO_2 laser resurfacing in patients with cutaneous photoaging (Fig. 154.14). This combination is particularly helpful in patients who may not tolerate the greater degree of sedation often necessary with CO_2 laser resurfacing or who cannot afford the additional fees to cover anesthesia services.

The necessary materials for manual dermasanding include silicon carbide sandpaper or wallscreen. Both may be purchased in a variety of grades: fine grade (G-400), medium grade (G-220–320), and coarse grade (G-180). The sandpaper is easier to use because of its flexibility; it is also more easily cut into smaller pieces, which can be steam autoclaved. A 1.5-inch (4 cm) × 3-inch (8 cm) piece of sterilized sandpaper is wrapped around either the barrel of a 3 ml syringe or a rolled-up gauze pad and moistened with saline or a soap-free cleanser for lubrication. A 1% solution of lidocaine with epinephrine (adrenaline) may be used if additional anesthesia is necessary. The skin is stretched and both back-and-forth and circular motions are used to gradually abrade the skin, layer by layer, until the hills and valleys are softened or adjacent areas are blended to the desired degree. Coarser grades (G-320) may be used initially for "debulking", followed by finer grades (G-400) later in the procedure. The fine grade is used to blend delicate areas of skin such as around the eyelids. At the completion of the procedure, the dark-colored silicon carbide particles remaining on the skin surface should be rinsed off because there is a risk of their becoming implanted, creating a pigmented tattoo.



Fig. 154.14 Medium-depth chemical peel plus manual dermasanding. Jessner's–35% trichloroacetic acid was applied to the face followed immediately by manual dermasanding of the cutaneous lips and chin. **A** Preoperative with obvious perioral rhytides. **B** Postoperative with significant improvement.

Motorized Dermabrasion

Although various abrasive materials have long been used for mechanical resurfacing, the development of a power-driven unit to facilitate the procedure was revolutionary. Some of the units most commonly used today are the Bell Handengine (Bell Handengine®, Inc.), the AEV-12 hand engine (Ellis International), and the Osada surgical handpiece (Osada, Inc.). A topical refrigerant spray was routinely used to produce anesthesia and to harden the skin as it is abraded (Fig. 154.15). The spray immobilizes the topographic features so that there is no distortion by the pressure of the abrasive instrument. Concerns regarding potential harm to the environment from cryogenic sprays have limited the availability of topical refrigerant sprays in several countries, including the US. Utilizing liquid nitrogen or agents that cryopreserve tissue specimens is *not* recommended because they create a colder temperature that can lead to hypopigmentation and/or scarring. Options include tumescent anesthesia as a means of firming the tissue or use of the diamond fraise without a cryogen.



Fig. 154.15 Mechanical dermabrasion. This technique is performed with a diamond fraise over rigid skin cooled with a topical refrigerant spray. More recently, the latter has been replaced by tumescent anesthesia.

The two abrasive instruments most often employed with these motor-driven units are the wire brush and the diamond fraise. The wire brush has numerous small-caliber, stainless steel wires that project circumferentially from the curved side of a cylindrical hub. A diamond fraise consists of a stainless-steel cylinder to which industrial-grade diamonds are bonded to create the abrasive surface. Compared with wire-brush instruments, diamond fraises are manufactured with a greater variety in their shape, width of abrasive surface, wheel diameter, and coarseness

of grit. While there continues to be considerable controversy regarding which one of these instruments is superior[47], surgeons generally agree that the wire brush is more aggressive. The wire brush cuts more quickly and more deeply into the skin with each stroke, thereby posing a greater risk for injury and requiring more skill to operate. Although the diamond fraise is generally safer and more forgiving, it may not yield the degree of improvement possible with the wire brush, especially for more stubborn conditions such as acne scarring.

Because dermabrasion with either instrument is highly technique-dependent and the learning curve is steep, there may be considerable variability in the clinical results obtained by different operators. To be adequately trained, it is very important for beginner dermabraders to receive hands-on instruction from an experienced operator. The proper techniques for motorized dermabrasion have also been the subject of comprehensive reviews in the literature[47]. Careful evaluation of the depth of injury throughout the procedure is critical to assure a sufficient depth for optimal results without penetrating beyond the desired level and risking scar formation. Because of the potential for aerosolization of infectious particles during dermabrasion, appropriate precautions are mandatory to protect the operating room staff (see Ch. 136). This includes protective masks, face shields, and an air evacuation system.

Although the resurgence of manual dermasanding and the development of laser technology have led to a decline in the number of motorized dermabrasion procedures, it remains a reliable treatment for moderate-to-severe acne scarring (Fig. 154.16). Dermabrasion selectively planes off the "hilltops" that surround the atrophic "valleys", whereas chemical peeling and laser resurfacing may produce an injury of equivalent depth in both areas. This explains that while it is possible to efface the edges of atrophic scars with the CO_2 laser or the solid CO_2–35% TCA peel[31], it may prove more difficult to achieve desired results (compared to dermabrasion).

The physician must choose the scars most amenable to dermabrasion alone. These include shallow fibrotic scars, hypertrophic scars and undulating, rolling scars, in addition to atrophic and boxcar scars. Deeper fibrotic scars, ice-pick scars, and scars with significant tissue loss may require a lifting or filling procedure prior to dermabrasion. In these patients, the results are significantly enhanced by performing one or more of the following adjunctive procedures 4 to 6 weeks preoperatively: punch or scalpel excision, TCA CROSS technique, punch grafting, dermal grafting, fat grafting, or scar undermining (subcision)[56].

Subcision

Deeper fibrotic scars can be excised or they can be elevated prior to resurfacing[57]. Subcision represents a surgical option for elevating scars in which the scars are outlined, photographed, cleansed, and injected with local anesthesia. A specialized undermining needle (e.g. Nokor™) or a tri-beveled 18-gauge needle is inserted at an acute angle through an incision at the edge of the scar (Fig. 154.17). The needle is then advanced under the scar, horizontally and parallel to the skin surface. Fan-like motions break fibrotic dermal scar bands, releasing the overlying skin to raise upward. A pressure dressing is placed to evacuate blood from the pocket that is created under the scar. During wound healing, this pocket fills with new collagen fibers leading to scar elevation[58]. The procedure is usually repeated 2 to 5 times. Sometimes to further enhance filling in of the scar, a dermal graft harvested from the retroauricular area can be inserted with jeweler's forceps into the pocket generated by the Nokor™ needle.

Microneedling

Microneedling represents a minimally invasive procedure in which the device contains multiple fine-gauge needles 0.5–3 mm in length that penetrate the skin and trigger wound healing. One goal is to induce dermal remodeling and skin rejuvenation via increased production of collagen and elastin[59,60]. The devices vary from manually operated to battery- or electric-powered and are designed as rollers, automated pens, and patches in which the operator can often toggle between different lengths of needles. Clinical indications include acne, surgical, traumatic and burn scars, photoaging, striae, skin laxity, dyschromias, alopecia, and potentially transdermal drug delivery (Table 154.9).

Preoperatively, a topical anesthetic may be applied and multiple sessions are frequently needed to obtain desired results. Transient erythema is the most common side effect and rarely hypersensitivity reactions, scar formation, or dyspigmentation occur. Advantages include relatively low cost, wide spectrum of applications, overall ease of use, and favorable side effect profile including its relative safety in skin of color[61]. However, there is a lack of high-quality, prospective, randomized controlled trials comparing microneedling with other resurfacing modalities.

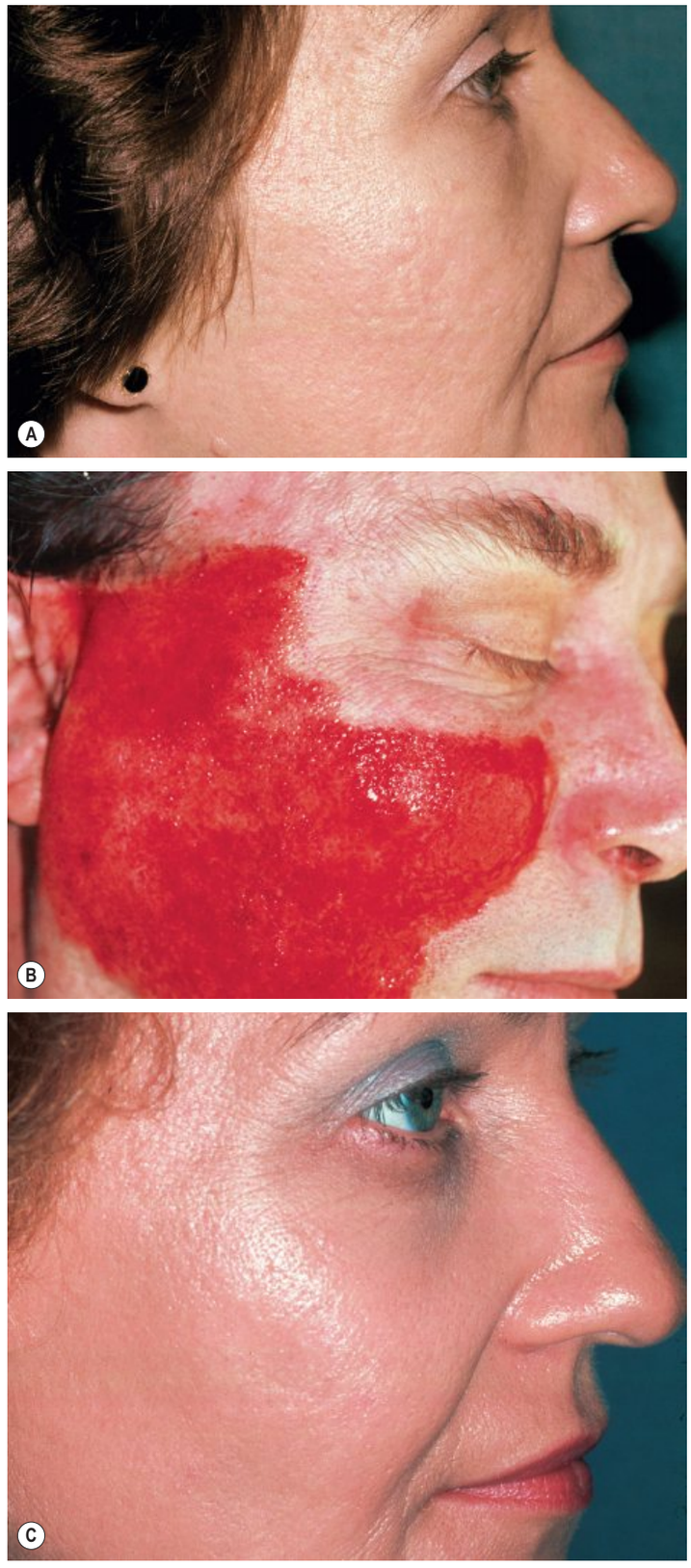


Fig. 154.16 Full-face dermabrasion performed for acne scars. A Preoperative: shallow and atrophic scars that are most amenable to dermabrasion. **B** Postoperative: dermabrasion prior to biosynthetic dressing. **C** Three months postoperative.

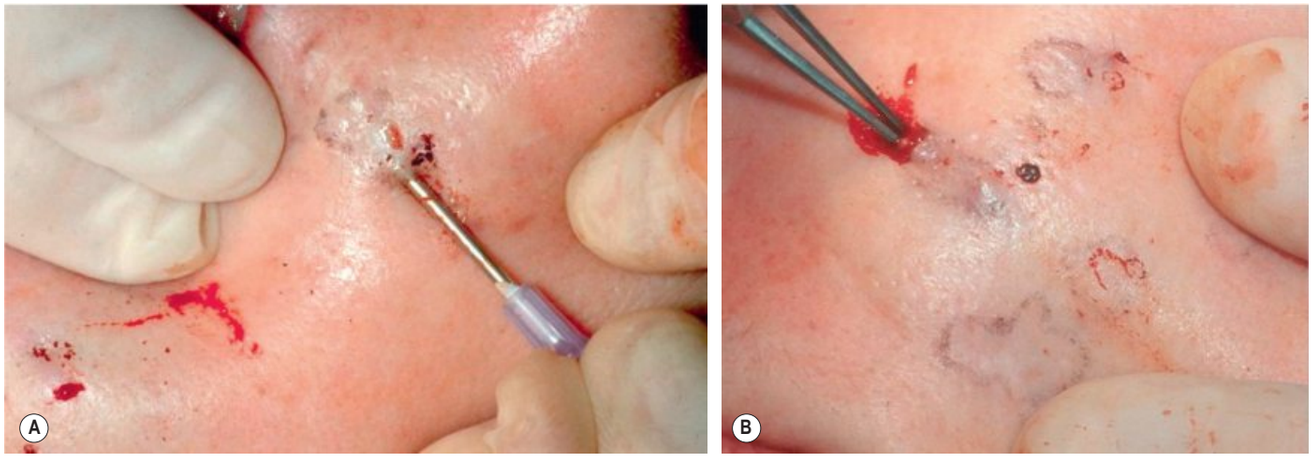


Fig. 154.17 Treatment of facial scars by subcision. A Scars to be treated have been outlined with a skin marker, photographed, and anesthetized. A Nokor™ needle is inserted into the dermis underneath a scar and advanced horizontally parallel to the skin surface. **B** To further enhance filling in of the scar, a dermal graft can be inserted with jeweler's forceps into the pocket generated by the Nokor™ needle.

EXAMPLES OF DRUGS DELIVERED TRANSDERMALLY VIA MICRONEEDLING	
Drug	**Treatment/indication(s)**
Anesthetics (topical)	Enhance anesthetic effect prior to minimally invasive procedures
Bimatoprost	Hypopigmentation
Bleomycin	Refractory verrucae vulgares
Botulinum toxin	Increased pore size, skin texture irregularities
Corticosteroids	Scars, bulky flaps
Cosmeceuticals	Melasma (transexamic acid), photoaging, skin texture irregularities
Platelet rich plasma (PRP)	Alopecia (e.g. androgenetic), photoaging

Table 154.9 Examples of drugs delivered transdermally via microneedling.

A promising variant is radiofrequency (RF) microneedling in which thermal-assisted microneedles stimulate new collagen formation by inflaming and destroying the dermis or subcutaneous tissue. Because the energy source is an electric current and the energy is not emitted until the dermal–epidermal junction is breached, there is minimal risk of hyperpigmentation[62]. Indications are those of traditional microneedling and cellulite improvement. See Chapter 137 and Table 137.1 for additional details.

POSTOPERATIVE CARE

Because superficial resurfacing procedures generally do not extend beyond the epidermis, the dermal wound healing mechanisms are not activated. In contrast, medium-depth and deep resurfacing procedures stimulate the following four stages of dermal wound healing (see Ch. 141): (1) inflammation and coagulation; (2) re-epithelialization; (3) fibroplasia and matrix formation; and (4) collagen remodeling.

Because the pronounced edema following medium-depth and deep resurfacing procedures may minimize the appearance of scars, rhytides and other irregularities, the patient's initial perception of his or her improvement may be exaggerated. As swelling subsides postoperatively, patients should be reassured and advised that collagen remodeling continues for several months and leads to further clinical improvement. At some point in the postoperative course, patients often want to know when another resurfacing procedure can be performed if it is necessary. The presence of persistent postoperative erythema may indicate continued collagen remodeling and may serve as a warning that a similar resurfacing procedure performed prematurely could produce scarring. To assure their safety, patients undergoing medium-depth resurfacing should not undergo another medium-depth or deep procedure for the next 3 to 9 months. An individual having a deep resurfacing procedure should avoid another one for at least 12 months postoperatively. Touch-up procedures for revision of a prior suboptimal outcome are also best avoided during these time periods, especially if erythema is still present.

Healing time is generally proportional to the depth of the resurfacing procedure. *Superficial* resurfacing procedures cause minimal downtime and necessitate little postoperative care. They usually produce mild erythema and desquamation that last from 1 to 4 days depending on the wounding agent and the techniques used. Regular washing with a mild cleanser and the use of routine moisturizers and sunscreens are generally sufficient during the healing period.

Following *medium-depth* resurfacing procedures, there is a considerably longer healing time and more intensive postoperative care is necessary. Follow-up visits are scheduled regularly to monitor the patient's postoperative course. After a medium-depth chemical peel, occlusive dressings are not necessary because the epidermis, which is not removed intraoperatively, functions as a biologic dressing until peeling occurs. Because areas of medium-depth peeling which have been enhanced by manual dermasanding do not possess residual epidermis, occlusive dressings may be used on these areas during the first 3 postoperative days.

The patient is instructed to soak the areas four times daily with warm compresses and to apply an emollient after each soak and during the intervening periods as necessary. A solution of 0.25% acetic acid (one tablespoon of white vinegar added to one pint of warm water) is preferred for the soaks because the mild acidity is physiologic for healing granulation tissue. It is also a mild debridant and has antibacterial effects, especially against *Pseudomonas* spp. and other Gram-negative organisms. Occlusive emollients, such as petrolatum, Aquaphor® or Eucerin® ointment, speed the process of re-epithelialization and lessen the tendency for delayed healing[63]. These emollients are also helpful in wound debridement and in the prevention of crust formation and infection. Showers, soaks, and emollients are continued for a week postoperatively.

Following medium-depth resurfacing, edema begins to appear almost immediately and progressively worsens during the first 48 hours. It can even be severe enough to close the eyelids and impair the patient's visual fields. If tolerated, aspirin or other NSAIDs can be administered, preoperatively and during the first 24 hours postoperatively, to alleviate discomfort and reduce swelling. After a medium-depth chemical peel such as the Jessner's–35% TCA peel, there is initially a brawny, dusky erythema which is followed by the formation of a brownish crust that begins to separate from the skin surface between days 4 and 8 postoperatively. Although the initial darkening can be disturbing to the patient, it represents an expected separation of the epidermis. The underlying, newly formed epithelium is brightly erythematous but fades to a pink color that resembles a sunburn (see Fig. 154.6D). By postoperative day 7 to 10, re-epithelialization has occurred and the erythema can be camouflaged with cosmetics. Within 2 to 4 weeks after the procedure, the erythema usually resolves fully, and retinoids and sunscreens can be restarted as tolerated.

Deep resurfacing procedures, such as the Baker–Gordon phenol peel or dermabrasion, require a follow-up visit the next day, several visits during the first week, and very close monitoring thereafter. At each visit, instructions for wound care are reviewed with the patient

and any questions are answered. The immediate postoperative course after deep resurfacing is similar to that following medium-depth procedures, except that edema and erythema may be even more severe and persistent. NSAIDs can provide some relief, but an intramuscular corticosteroid injection is often administered on the day of surgery, even though its effects on wound healing are not completely understood. Pruritus may occur during the healing phase following a resurfacing procedure of any depth but is particularly prevalent after deeper resurfacing. This problem can be alleviated by the use of emollients, ice packs, NSAIDs, and antihistamines until the pruritus spontaneously resolves. Milia formation, which commonly occurs 3 to 4 weeks after deep chemical peeling or mechanical resurfacing, is easily managed with needle extraction.

Patients undergoing deep mechanical resurfacing with either motorized dermabrasion or manual dermasanding can have an occlusive hydrogel biosynthetic dressing (e.g. Vigilon®, 2nd Skin®) applied immediately after the procedure. In patients undergoing a Baker–Gordon phenol peel, occlusive tape or a biosynthetic dressing is usually utilized postoperatively. Occlusive tape dressings must be removed on the first postoperative day and this procedure may require analgesia and sedation. For this reason, the authors prefer untaped phenol peels with application of ointment or bio-occlusive dressings. Whenever a biosynthetic dressing is used, it must be removed daily and replaced with a new one for the first 2 or 3 days postoperatively so that the face can be gently debrided with saline soaks and moistened cotton tips. The patient should be instructed to regularly apply an occlusive ointment to areas around the mouth, eyelids, and hairline that are not adequately covered by the dressing. Occlusive biosynthetic dressings have been shown to enhance collagen synthesis and hasten re-epithelialization in superficial wounds. They also minimize the amount of discomfort and obviate the need for repeated soaks by the patient during the first few days after the procedure.

By the third day following deep mechanical or chemical resurfacing, the patient begins open wound care with 0.25% acetic acid soaks four to six times daily and regular applications of an occlusive ointment. By the 7th to the 14th day postoperatively, re-epithelialization is usually complete and the ointment is replaced by a heavy moisturizer. The marked edema and erythema typically seen after dermabrasion or dermasanding generally resolve after several weeks. The erythema resulting from deep peeling may be more persistent but is rarely present beyond 2 to 4 months. Strict sun avoidance is critical for 3 to 6 months after dermabrasion or deep chemical peeling. The patient typically restarts sunscreens and retinoid therapy within a couple of weeks of re-epithelialization, as tolerated.

COMPLICATIONS

Complications may occur following any method of skin resurfacing involving injury to any depth but are more common after medium-depth and deep procedures. It is far simpler to prevent the development of a complication than to manage it once it has occurred. Complications may be prevented by proper selection of suitable patients and appropriate resurfacing modalities, precise intraoperative technique, and proper patient management before and after the procedure (see Table 154.3). The dissatisfied patient represents a complication even when the cosmetic result is favorable. An explanation of realistic results and review of photographs of "average" rather than best results during the pre-treatment consultation is recommended. Any information provided at this time is included within informed consent.

Improper wound care, trauma to healing areas resulting from overzealous debridement, compulsive picking or scratching, and premature use of irritating substances such as depilatories or wax for the removal of hair can each cause the depth of injury to extend beyond the threshold of safety. As discussed below, the development of infection in the postoperative period can also extend the depth of injury and increase the risk of permanent sequelae.

With specific regard to chemical peeling, excessive injury to the skin can result from poor technique during application or problems with the chemical agents utilized. The degree of frosting is monitored closely to assure that the agent has been applied evenly and that the injury extends to the proper depth (Table 154.10). Although it does not always correlate completely with the depth of injury, the level of frosting is a very valuable guide for determining the appropriate endpoint of treatment

CLINICAL SIGNS THAT REFLECT DEPTH OF WOUNDING
• Level of frosting (see Fig. 154.3)
• Time for frosting to appear
• Time for frosting to disappear
• Skin turgor
• Epidermal slide*
*Sliding of the epidermis off the dermis due to separation of the two tissues.

Table 154.10 Clinical signs that reflect depth of wounding.

(see Fig. 154.3). Injuring the skin too deeply during a chemical peel, as suggested by an excessive degree of frosting, may result not only from over-application but also from the use of excessively concentrated peeling solutions. The latter error can be caused by the surgeon's choice of an improper peeling agent, such as 50% TCA, or it can be related to unexpected disturbances in a solution's pharmacologic mixture. For Baker–Gordon peels, a new batch should be mixed by the surgeon prior to each procedure to be certain that the preparation is made correctly; the other peeling solutions are available in various formulations and strengths for purchase directly from medical supply dealers. Reputable dealers mix and label these solutions properly according to standard *weight-to-volume* formulas. It should be noted that the latter accurately reflect the TCA percentages cited in the medical literature, while volume-to-volume and weight-to-weight preparations of TCA do not.

Storage of peeling solutions in proper containers away from sunlight and immediate replacement of expired solutions are important measures to ensure chemical stability of the agents being used[64]. Immediately prior to peeling, an ample volume of the solution should be poured from the primary storage container into a smaller, secondary cup. The peeling agent is applied directly to the skin surface from this cup and the excess subsequently discarded to avoid contamination of the storage container and to avoid the accidental transfer of concentrated crystals from the neck of the storage container to the patient's skin.

Errors during mechanical resurfacing procedures may also lead to an injury of excessive depth and a higher risk of adverse sequelae. This problem can result from poor technique in the handling of the instruments or from failure to recognize the appropriate treatment endpoint. The beginner should first start by conservatively dermasanding small areas to get a comfortable feel for the skin's response to this type of injury. As knowledge and experience is gained, one can then progress on to diamond fraise dermabrasion and later to the use of the wire brush. Observation of experienced surgeons and hands-on training are invaluable. The beginner should always err on the side of conservatism, while still yielding favorable results, to avoid excessively deep tissue injury that could produce long-term complications.

During chemical peeling or mechanical resurfacing, intraoperative exposure of vital structures to the resurfacing agent may occur and can have serious adverse consequences. Extreme care must be exercised when dermabrading with a power-driven, rotating instrument, assuring that the dominant hand maintains complete control continuously and free skin edges (e.g. eyelid, lip) are not caught up in the wire brush or diamond fraise, as the latter may result in tearing of the skin. During chemical peeling, the moistened applicator should never be passed over the central face, in order to avoid inadvertent exposure of a vulnerable surface such as the eye to the solution. There should always be appropriate fluids readily available to rinse the area in case such an exposure does occur. In particular, saline is used to dilute TCA, mineral oil is used to dilute phenol solutions, and sodium bicarbonate is used to neutralize glycolic acid.

Adverse systemic effects related to a resurfacing procedure are very uncommon but can usually be traced to an identifiable causative factor in the perioperative period. Peeling with phenol solutions has been associated with systemic toxicities, so these procedures must be performed slowly and only on properly selected, healthy patients in an appropriate clinical setting. The use of Jessner's solution poses a theoretical risk of systemic salicylate or resorcinol toxicity, but this is probably not clinically significant when application is limited to the face and neck. Undoubtedly, the most common cause of systemic problems related to resurfacing procedures is an adverse allergic or physiologic reaction to a medication used for anesthesia. It is imperative that the surgeon knows all the physiologic effects and the potential adverse consequences of each drug administered systemically, unless there is an

attending anesthesiologist who assumes this responsibility. Fortunately, the chemical and mechanical resurfacing procedures utilized most often can be performed with little or no sedation.

It is important to make a distinction between a true complication and an expected side effect of a resurfacing procedure. With medium-depth and deep resurfacing, transient erythema, flushing, increased skin temperature, pruritus, edema, and milia formation are typical occurrences, so they should not be classified as true complications. Patient reassurance may be all that is necessary, since these problems usually resolve spontaneously. True complications that may develop within a treated area include infection, delayed wound healing, persistent erythema, scarring, and pigmentary or textural abnormalities[65,66]. Any of these true complications can occur despite proper patient and procedure selection, perfect surgical technique, and appropriate management before and after the operation.

Infection is an uncommon complication that develops during the postoperative period and may be caused by bacterial, viral, or fungal organisms. An important preventive measure is the repeated use of soaks for adequate wound debridement. Frequent postoperative visits are also helpful to assure early recognition and treatment of any infection so that scarring does not result. An infection may present with delayed wound healing, ulcerations, excessive necrotic material and crusting, purulent drainage, or odor. An acneiform eruption or pustular folliculitis can also be a manifestation of infection and should be treated as such. Infection with streptococcal and staphylococcal organisms can occur under biosynthetic membranes or thick, occlusive ointments, so these are best avoided, except in the immediate postoperative period. Other organisms, such as *Escherichia coli* or *Pseudomonas* spp., may infect the area if there is improper wound care. *Candida* infections can also occur and are sometimes related to the use of prophylactic antibiotics or occlusive wound care. Clinical suspicion of a wound infection necessitates immediate institution of empiric antimicrobial therapy, laboratory culture for identification of the organism(s), and wound debridement as necessary[67].

Herpes simplex viral infections can occur during the healing period following medium-depth or deep resurfacing and have the potential for devastating sequelae. An outbreak can even occur in patients on the recommended 10- to 14-day prophylactic antiviral regimen. The keys to avoiding scar formation are rapid recognition and aggressive therapy begun early in the course of the infection. The dosage of antiviral drug should be increased to the recommended maximum in cases of active herpetic infections.

Persistent erythema beyond 2 months after a medium-depth procedure may be precipitated by the use of topical or systemic retinoid therapy, contact with various allergens or irritants, an underlying skin condition, genetic susceptibility, or the presence of active infection[65,68]. Persistent erythema may indicate the impending development of scar formation. Especially when indurated, it should be treated promptly and aggressively. Management includes massage therapy, topical, intralesional or even systemic corticosteroids, silicone gel sheeting, and pulsed dye laser therapy. In most cases, scarring can be prevented. Mild scarring may even fade away spontaneously. Rarely, ectropion or eclabium can occur when aggressive resurfacing creates scarring or excessive tightening of periorbital or perioral skin, respectively, in a susceptible patient.

Textural abnormalities, skin atrophy, and dyspigmentation are additional complications that may occur with medium-depth and deep resurfacing procedures. The return of normal pigmentation in patients with Fitzpatrick skin type IV or higher is less predictable, so an extra measure of caution is necessary. Postoperative hyperpigmentation may be prevented and/or treated after re-epithelialization with a topical retinoid, a 4%–8% hydroquinone preparation, and strict photoprotection, but the hypopigmentation that can follow deeper resurfacing is typically permanent. Another potential pigmentary problem following deeper resurfacing procedures is a conspicuous demarcation line separating the untreated and treated areas. Although this problem can usually be avoided with adequate planning and proper technique, the approach to its management should focus on lightening the pigment in the adjacent untreated areas.

CONCLUSIONS AND FUTURE TRENDS

The sheer number of patients demanding medical therapy or procedural intervention to rejuvenate their skin mandates that dermatologists be well versed in this area. The field of resurfacing is constantly changing, with the development of new techniques and procedures as well as fluctuations in patient demands and expectations. In all areas of cosmetic surgery, there has been a recent trend in favor of less invasive procedures. Dermatologists often choose to learn and implement only a handful of resurfacing procedures that best fulfill the needs of their practice and meet the demands of their patient population.

Additional figures available in our eBook (see inside front cover for access code).

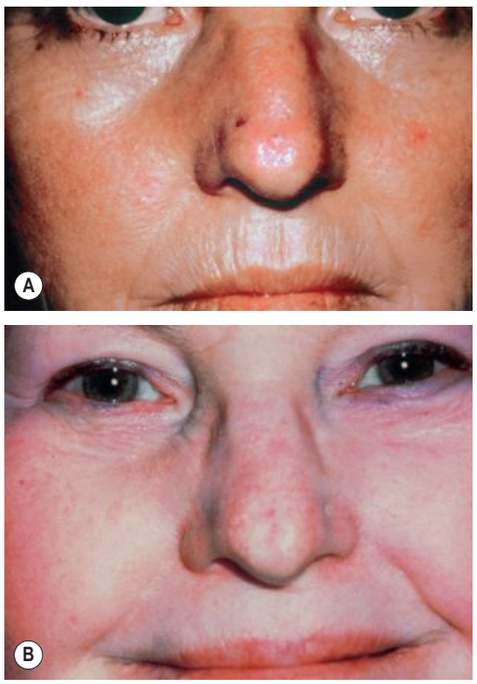
REFERENCES

1. Brody HJ, Monheit GD, Resnik SS, Alt TH. A history of chemical peeling. *Dermatol Surg*. 2000;26:405–409.
2. Lawrence N, Mandy S, Yarborough J, Alt T. History of dermabrasion. *Dermatol Surg*. 2000;26:95–101.
3. Tsai RY, Wang CN, Chan HL. Aluminum oxide crystal microdermabrasion. A new technique for treating facial scarring. *Dermatol Surg*. 1995;21:539–542.
4. Harris DR, Noodleman FR. Combining manual dermasanding with low strength trichloroacetic acid to improve actinically injured skin. *J Dermatol Surg Oncol*. 1994;20:436–442.
5. Chiarello SE. Tumescent dermasanding with cryospraying. A new wrinkle on the treatment of rhytids. *Dermatol Surg*. 1996;22:601–610.
6. Dingman DL, Hartog J, Siemionow M. Simultaneous deep-plane face lift and trichloroacetic acid peel. *Plast Reconstr Surg*. 1994;93:86–93, discussion 94–5.
7. Rubenstein R, Roenigk HH, Stegman SJ, Hanke CW. Atypical keloids after dermabrasion of patients taking isotretinoin. *J Am Acad Dermatol*. 1986;15:280–285.
8. Wolfe SA. Chemical face peeling following therapeutic irradiation. *Plast Reconstr Surg*. 1982;69:859–862.
9. Monheit GD. Chemical peeling for pigmentary dyschromias. *Cosmet Dermatol*. 1995;8:10–15.
10. Swinehart JM. Test spots in dermabrasion and chemical peeling. *J Dermatol Surg Oncol*. 1990;16:557–563.
11. Gilbert S, McBurney E. Use of valacyclovir for herpes simplex virus-1 (HSV-1) prophylaxis after facial resurfacing: a randomized clinical trial of dosing regimens. *Dermatol Surg*. 2000;26:50–54.
12. Monheit GD. Facial resurfacing may trigger the herpes simplex virus. *Cosmet Dermatol*. 1995;8:9–16.
13. Monheit GD. Skin preparation: an essential step before chemical peeling or laser resurfacing. *Cosmet Dermatol*. 1996;9:13–14.
14. Yamamoto O, Bhawan J, Hara M, Gilchrest BA. Keratinocyte degeneration in human facial skin: documentation of new ultrastructural markers for photodamage and their improvement during topical tretinoin therapy. *Exp Dermatol*. 1995;4:9–19.
15. Goodman G. Dermabrasion using tumescent anesthesia. *J Dermatol Surg Oncol*. 1994;20:802–807.
16. Stegman SJ. A study of dermabrasion and chemical peels in an animal model. *J Dermatol Surg Oncol*. 1980;6:490–497.
17. Stegman SJ. A comparative histologic study of the effects of three peeling agents and dermabrasion on normal and sun-damaged skin. *Aesthetic Plast Surg*. 1982;6:123–125.
18. Nelson BR, Fader DJ, Gillard M, et al. Pilot histologic and ultrastructural study of the effects of medium-depth chemical facial peels on dermal collagen in patients with actinically damaged skin. *J Am Acad Dermatol*. 1995;32:472–478.
19. Ditre CM, Griffin TD, Murphy GF, et al. Effects of alpha-hydroxy acids on photoaged skin: a pilot clinical, histologic, and ultrastructural study. *J Am Acad Dermatol*. 1996;34:187–195.
20. Fitzpatrick RE, Tope WD, Goldman MP, Satur NM. Pulsed carbon dioxide laser, trichloroacetic acid, Baker-Gordon phenol, and dermabrasion: a comparative clinical and histologic study of cutaneous resurfacing in a porcine model. *Arch Dermatol*. 1996;132:469–471.
21. Lee H, Kim IH. Salicylic acid peels for the treatment of acne vulgaris in Asian patients. *Dermatol Surg*. 2003;29:1196–1199.
22. Bauman L. Chemical peeling. In: Bauman L, ed. *Cosmetic Dermatology: Principles and Practice*. 1st ed. New York: McGraw-Hill; 2002:173–186.
23. Rubin M, Tung R. *Procedures in Cosmetic Dermatology Series: Chemical Peels*. Philadelphia: Saunders; 2010.
24. Clark CP. Office-based skin care and superficial peels: the scientific rationale. *Plast Reconstr Surg*. 1999;104:854–864, discussion 865–6.
25. Kligman D, Kligman AM. Salicylic acid peels for the treatment of photoaging. *Dermatol Surg*. 1998;24:325–328.
26. Van Scott EJ, Yu RJ. Hyperkeratinization, corneocyte cohesion, and alpha hydroxy acids. *J Am Acad Dermatol*. 1984;11:867–879.
27. Slavin JW. Considerations in alpha hydroxy acid peels. *Clin Plast Surg*. 1998;25:45–52.
28. Monheit GD. The Jessner's + TCA peel: a medium depth chemical peel. *J Dermatol Surg Oncol*. 1989;15:945–950.
29. Brody HJ. Trichloroacetic acid application in chemical peeling, operative techniques. *Plast Reconstr Surg*. 1995;2:127–128.
30. Leonhardt JM, Rossy K, Lawrence N. Trichloroacetic acid (TCA peels). In: Rubin MG, Tung R, eds. *Chemical Peels*. Philadelphia: Saunders; 2010.
31. Brody HJ, Hailey CW. Medium-depth chemical peeling of the skin: a variation of superficial chemosurgery. *J Dermatol Surg Oncol*. 1986;12:1268–1275.
32. Coleman WP, Futrell JM. The glycolic acid trichloroacetic acid peel. *J Dermatol Surg Oncol*. 1994;20:76–80.
33. Witheiler DD, Lawrence N, Cox SE, et al. Long-term efficacy and safety of Jessner's solution and 35% trichloroacetic acid vs 5% fluorouracil in the treatment of widespread facial actinic keratoses. *Dermatol Surg*. 1997;23:191–196.

34. Spira M, Freeman R, Arfai P, et al. Clinical comparison of chemical peeling dermabrasion, and 5-fu for senile keratoses. *Plast Reconstr Surg*. 1970;46:61–66.
35. Monheit GD. Combinations of therapy. In: Tung R, Rubin M, eds. *Chemical Peels*. 2nd ed. Philadelphia: Elsevier; 2011:133–150.
36. Monheit GD, Zeitouni NC. Skin resurfacing for photoaging: laser resurfacing versus chemical peeling. *Cosmet Dermatol*. 1997;10:11–22.
37. Monheit GD, Prather CL. Chemical peels for precancerous skin lesions. In: Macfarlane D, ed. *Skin Cancer Management: A Practical Approach*. New York: Springer; 2010:27–39.
38. Koppel RA, Coleman KM, Coleman WP. The efficacy of EMLA versus ELA-Max for pain relief in medium-depth chemical peeling: a clinical and histopathologic evaluation. *Dermatol Surg*. 2000;26:61–64.
39. Lee JB, Chung WG, Kwahck H, Lee KH. Focal treatment of acne scars with trichloroacetic acid: chemical reconstruction of skin scars method. *Dermatol Surg*. 2002;28:1017–1021.
40. Hetter GP. An examination of the phenol-croton oil peel: Part I. Dissecting the formula. *Plast Reconstr Surg*. 2000;105:227–239, discussion 249–51.
41. Baker TJ, Gordon HL. The ablation of rhytides by chemical means: a preliminary report. *J Fla Med Assoc*. 1961;48:451–454.
42. Hetter GP. An examination of the phenol-croton oil peel: Part IV. Face peel results with different concentrations of phenol and croton oil. *Plast Reconstr Surg*. 2000;105:1061–1083, discussion 1084–7.
43. Alt T. Occluded Baker/Gordon chemical peel. Review and update. *J Dermatol Surg Oncol*. 1989;15:980–993.
44. Wexler MR, Halon DA, Teitelbaum A, et al. The prevention of cardiac arrhythmias produced in an animal model by the topical application of a phenol preparation in common use for face peeling. *Plast Reconstr Surg*. 1984;73:595–598.
45. Beeson WH. The importance of cardiac monitoring in superficial and deep chemical peeling. *J Dermatol Surg Oncol*. 1987;13:949–950.
46. Beeson WH, McCollough EG. Chemical face peeling without taping. *J Derm Surg*. 1985;11:985–990.
47. Alt TH. Facial dermabrasion: advantages of the diamond fraise technique. *J Dermatol Surg Oncol*. 1987;13:618–624.
48. Bernard RW, Beran SJ, Rusin L. Microdermabrasion in clinical practice. *Clin Plast Surg*. 2000;27:571–577.
49. Shim EK, Barnette D, Hughes K, Greenway HT. Microdermabrasion: a clinical and histopathologic study. *J Dermatol Surg*. 2001;27:524–530.
50. Coimbra M, Rohrich RJ, Chao J, Brown SA. A prospective controlled assessment of microdermabrasion for damaged skin and fine rhytides. *Plast Reconstr Surg*. 2004;113:1438–1443, discussion 1444.
51. Freedman BM, Rueda-Pedraza E, Waddell SP. The epidermal and dermal changes associated with microdermabrasion. *J Dermatol Surg*. 2001;27:1031–1033, discussion 1033–4.
52. Rajan P, Grimes PE. Skin barrier changes induced by aluminum oxide and sodium chloride microdermabrasion. *J Dermatol Surg*. 2002;28:390–393.
53. Karimipour DJ, Kang S, Johnson TM, et al. Microdermabrasion: a molecular analysis following a single treatment. *J Am Acad Dermatol*. 2005;52:215–223.
54. Zisser M, Kaplan B, Moy RL. Surgical pearl: manual dermabrasion. *J Am Acad Dermatol*. 1995;33:105–106.
55. Lusthaus S, Benmeir P, Neuman A, et al. The use of sandpaper in chemical peeling combined with dermabrasion of the face. *Ann Plast Surg*. 1993;31:281–282.
56. Goodman GJ. Postacne scarring: a review of its pathophysiology and treatment. *Dermatol Surg*. 2000;26:857–871.
57. Alam M, Omura N, Kaminer MS. Subcision for acne scarring: technique and outcomes in 40 patients. *Dermatol Surg*. 2005;31:310–317, discussion 317.
58. Orentreich DS, Orentreich N. Subcutaneous incisionless (subcision) surgery for the correction of depressed scars and wrinkles. *Dermatol Surg*. 1995;21:6543–6549.
59. Hou A, Cohen B, Haimovic A, Elbuluk N. Microneedling: a comprehensive review. *Dermatol Surg*. 2017;43:321–329.
60. Fernandes D. Minimally invasive percutaneous collagen induction. *Oral Maxillofac Surg Clin North Am*. 2005;17:51–63.
61. Cohen BE, Elbuluk N. Microneedling in skin of color: a review of uses and efficacy. *J Am Acad Dermatol*. 2016;74:348–355.
62. Alster TS, Lupton JR. Nonablative cutaneous remodeling using radiofrequency devices. *Clin Dermatol*. 2007;25:487–491.
63. Collawn SS, Boissy RE, Gamboa M, Vasconez LO. Ultrastructural study of the skin after facial chemical peels and the effect of moisturization on wound healing. *Plast Reconstr Surg*. 1998;101:1374–1379, discussion 1380.
64. Spinowitz AL, Rumsfield J. Stability-time profile of trichloroacetic acid at various concentrations and storage conditions. *J Dermatol Surg Oncol*. 1989;15:974–975.
65. Brody HJ. Complications of chemical peeling. *J Dermatol Surg Oncol*. 1989;15:1010–1019.
66. Demas PN, Bridenstine JB. Diagnosis and treatment of postoperative complications after skin resurfacing. *J Oral Maxillofac Surg*. 1999;57:837–841.
67. Giandoni MB, Grabski WJ. Cutaneous candidiasis as a cause of delayed surgical wound healing. *J Am Acad Dermatol*. 1994;30:981–984.
68. Maloney BP, Millman B, Monheit G, McCollough EG. The etiology of prolonged erythema after chemical peel. *Dermatol Surg*. 1998;24:337–341.



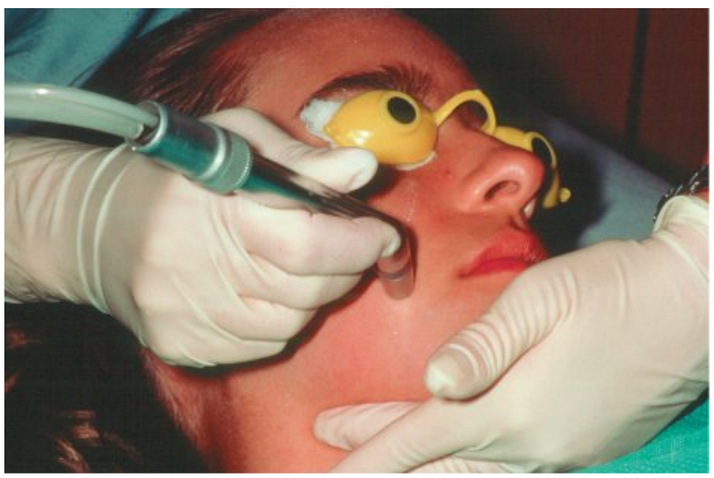
eFig. 154.1 Jessner's–35% trichloroacetic acid (TCA) chemical peel. A Patchy (level I) frosting following application of Jessner's solution. **B** After Jessner's solution dries, application of TCA leads to white enamel (level III) frosting.



eFig. 154.2 Advanced photoaging in the form of perioral rhytides treated with a Baker–Gordon phenol peel. A Preoperative: perioral rhytides, textural and pigmentary changes, and keratoses. **B** Postoperative: 2 years later. Note the phenol peel maintains correction for many years.



eFig. 154.4 Scars to be treated by subcision are outlined with a skin marker and photographed. This serves as a guide for further treatment sessions.



eFig. 154.3 Microdermabrasion. Aluminum oxide crystals are propelled at high speeds within a closed system and removed with suction.



eFig. 154.5 Microneedling of the face in a 40-year-old woman with skin texture irregularities, melasma, and acne scarring. A, B Before treatment. **C, D** After three sessions of microneedling performed at 4- to 6-week intervals. No other light- or energy-based procedures, toxins, or soft tissue fillers were utilized during this period.

155 Phlebology and Treatment of Leg Veins

Mitchel P. Goldman and Robert A. Weiss

Chapter Contents

Venous Anatomy, Physiology, and Pathophysiology 2650
Physical Examination of the Phlebology Patient 2651
Laboratory Evaluation of the Superficial Venous System. 2652
Compression in Sclerotherapy and Venous Disease 2653
Sclerosing Solutions. 2654
Techniques for Treating Telangiectasias and Reticular Veins. 2656
Larger Varicose Veins 2657
Postsclerotherapy Compression 2660
Complications 2660
Ambulatory Phlebectomy 2662
Targeting the Saphenofemoral Junction 2663

Key features

- Superficial telangiectasias, reticular veins, and varicose veins of the lower extremities are interconnected and develop after impairment of venous return
- Poor venous return results from venous valvular incompetence or primary muscle pump failure
- A pretreatment physical examination to assess the extent and cause of the venous abnormalities should be performed with the patient in a standing position
- The physical examination should be supplemented by duplex ultrasonography when saphenous vein reflux is suspected
- Both preoperative and postoperative compression are important in the management of venous insufficiency
- Sclerosing agents should destroy the entire vascular wall, producing permanent fibrosis of the vessel
- The minimal concentration and volume of sclerosing agent needed to achieve the desired results should be used
- All affected portions of the superficial venous system should be treated, ideally in one session and starting with the most proximal
- Large veins should be treated before smaller veins, and veins should be treated from proximal to distal
- FDA-approved sclerosing agents include sodium tetradecyl sulfate and polidocanol, both liquid and microfoam formulations
- Hypertonic saline (11.7%–23.4%) and glycerin (72% mixed 2:1 with 1% lidocaine, with or without epinephrine) are not FDA-approved for vein sclerosis, making their usage off-label
- The most common local side effects following injection of sclerosing agents are hyperpigmentation and telangiectatic matting and much less often cutaneous ulcers
- Patients generally require one to three sclerosant injection treatment sessions, spaced at 6- to 8-week intervals
- Utilizing tumescent anesthesia, incompetent saphenous veins and large tributaries over 4 mm in diameter can be effectively treated by ambulatory phlebectomy, radiofrequency or laser thermal ablation, or cyanoacrylate adhesive closure

INTRODUCTION

Varicose and telangiectatic leg veins increase in extent and severity with increasing age. The evolution of safe and effective treatment options has made sclerotherapy, ambulatory phlebectomy, endovenous laser ablation (LA), and radiofrequency (RF) ablation expanding areas within dermatologic surgery[1]. The utilization of improved diagnostic modalities, more efficient sclerosing agents, and simplified surgical techniques has rendered the treatment of venous disease safe, efficient, and highly satisfying for both patient and physician. This chapter presents the most recent advances in sclerotherapy, ambulatory phlebectomy, endovenous LA, RF ablation, and cyanoacrylate adhesive closure (CAC) as they relate to the management of telangiectasias, reticular veins and varicose veins, both non-saphenous and saphenous.

VENOUS ANATOMY, PHYSIOLOGY, AND PATHOPHYSIOLOGY

The peripheral venous system functions both as a reservoir to store extra blood (e.g. during pregnancy) and as a conduit to return blood from the periphery to the heart and lungs. The correct function of the venous system depends on a complex series of pumps and valves that are individually frail, yet the system as a whole performs well under extremely adverse conditions[2] (Fig. 155.1). Superficial veins carry less than 5% of venous blood, while the deep venous system carries 95% of venous blood.

The *superficial* venous system is a complicated, variable network of interconnecting veins[3]. A few of the larger truncal superficial

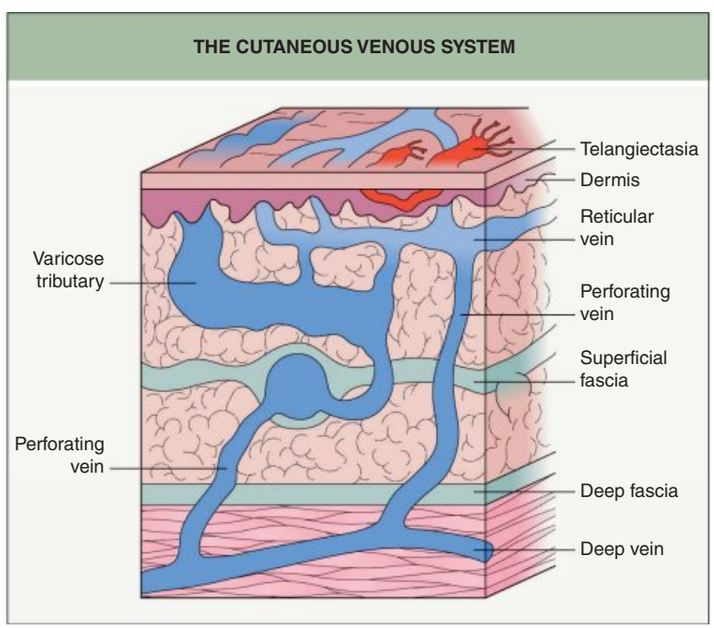


Fig. 155.1 The cutaneous venous system. The deep venous system drains the superficial venous system, which, in turn, is fed from the skin surface by telangiectasias within the dermis. The latter drain via reticular veins into the larger venous channels located in the reticular dermis and subcutaneous compartments. *Redrawn from Somjen GM, Ziegenbein R, Johnston AH, Royle JP. Anatomical examination of leg telangiectases with duplex scanning. J Dermatol Surg Oncol 1993;19:940.*

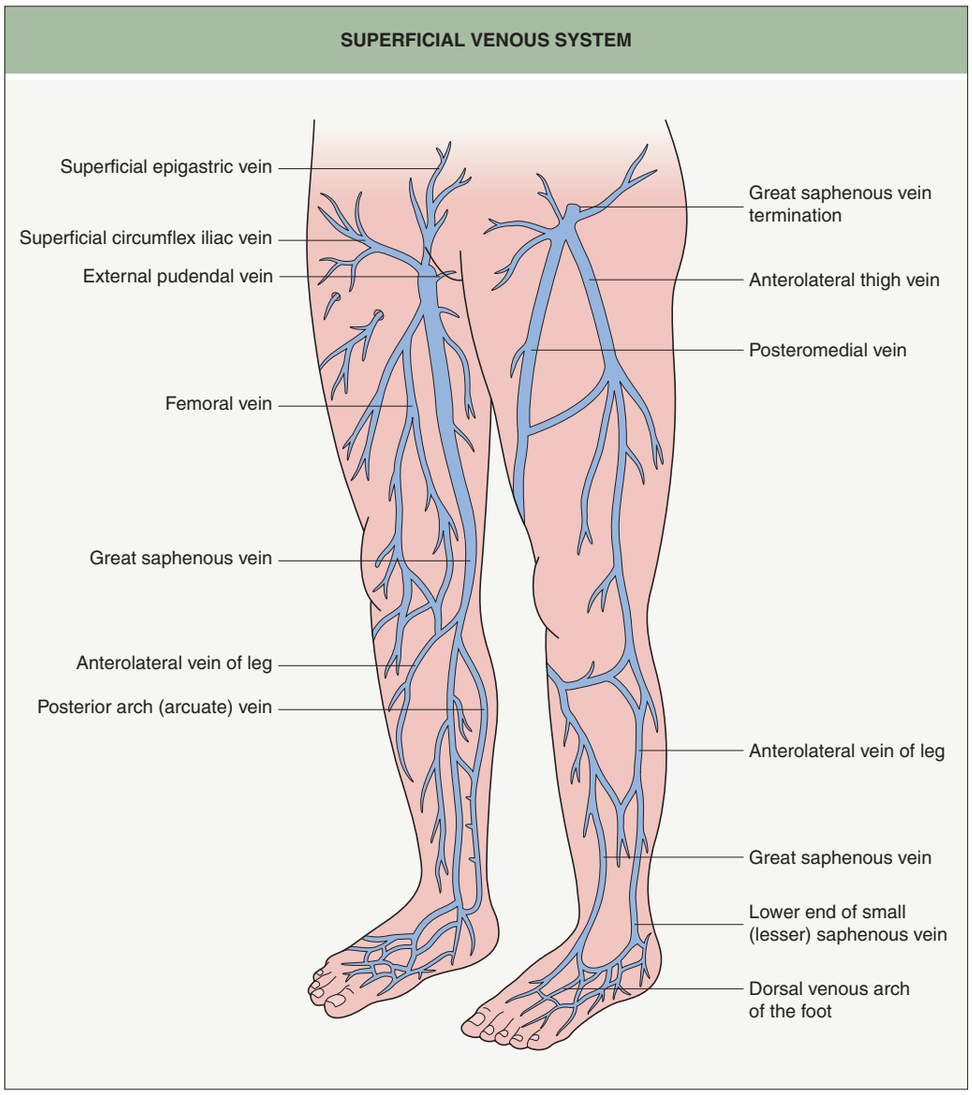


Fig. 155.2 Superficial venous system. Lateral and medial views of the distribution of the major axial trunks of the superficial venous system, the great and small saphenous veins, and associated tributaries. The anterolateral thigh vein was previously referred to as the lateral circumflex vein.

veins are fairly constant in location. These truncal superficial veins serve as a conduit to pass blood centrally into the deep venous system. The two principal named superficial veins are the small saphenous vein (SSV), which runs from the ankle to the knee, and the great saphenous vein (GSV), which runs from the ankle to the groin[4] (Fig. 155.2).

An interconnecting system of *perforating* veins that pass through the deep fascia connects the superficial veins to the deep veins of the calf or thigh (Figs. 155.1, 155.3 & 155.4). All venous blood eventually is received by the deep venous system on its way back to the right atrium.

Blood is propelled back to the heart via the pumping action of the foot and calf muscles, which squeeze blood out of a venous segment through one-way valves when muscle contractions increase the pressure within the fascial muscle compartment (Fig. 155.5). Venous pathology can result from primary muscle pump failure due to venous obstruction (thrombotic or non-thrombotic) or from venous valvular incompetence[5].

A genetic predisposition for the development of varicose veins has been observed, with both autosomal dominant and recessive patterns of inheritance described. Approximately 70% of patients can identify superficial venous disease as a familial trait. Hormonal influences from pregnancy or estrogen and progesterone supplementation are believed to be additional predisposing factors.

In summary, telangiectasias, reticular veins, and varicose veins reflect hereditary and hormonal factors as well as static gravitational pressures and dynamic muscular forces transmitted through failed venous valves. While genetic traits cannot be altered, the influence of hemodynamic forces and hydrostatic pressure can be modified, both by sclerotherapy and surgical techniques.

PHYSICAL EXAMINATION OF THE PHLEBOLOGY PATIENT

The purpose of the clinical examination is to survey the main venous trunks and determine where the primary or highest points of reflux are located. During the examination, the patient should be standing, preferably on a platform. It is important to determine the grade of venous insufficiency[6]. The recommended CEAP classification system is based on clinical manifestations (C), etiologic factors (E), anatomic distribution of disease (A), and the underlying pathophysiologic findings (P) (Table 155.1)[7]. The venous severity scoring (VSS) system is based on three elements: the number of anatomic segments affected, grading of symptoms and signs, and disability. The consensus statement on this approach to clinical assessment was published worldwide in 25 journals and books in eight languages.

For the practicing physician, CEAP is an instrument for establishing the correct diagnosis, guiding treatment, and assessing prognosis. It is important to stress that CEAP is a descriptive classification, while VSS and quality-of-life (QoL) scores represent instruments for longitudinal clinical research and assessing outcomes. In modern phlebologic practice, the vast majority of patients will have a duplex scan of the venous system of the leg, which will provide data on E, A, and P. In basic CEAP, the single highest descriptor should be used for clinical class; e.g. a patient with varicose veins, swelling and lipodermatosclerosis

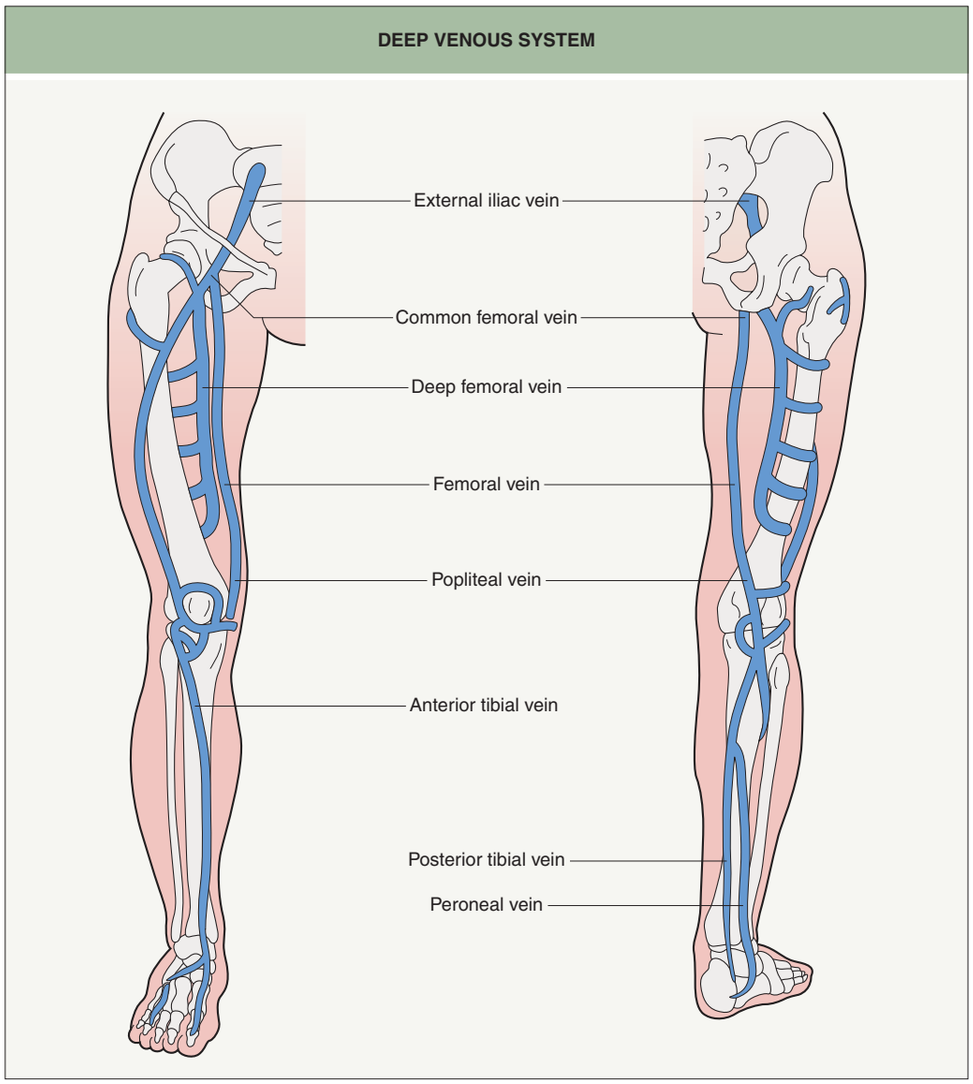


Fig. 155.3 Deep venous system. The major drainage vessel for below the knee is the popliteal vein, while the femoral vein is the major portal of drainage in the inguinal area (great saphenous distribution).

will be C4b (see Table 155.1). However, use of just the C-classification provides no advantage over previous classification schemes that were based solely on clinical appearance. Even in basic CEAP, where a duplex scan is performed, classification of E, A, and P with multiple descriptors is recommended. For A (anatomic classification), the simple superficial (s), perforator (p), and deep (d) descriptors should be used; e.g. a symptomatic patient with stasis dermatitis, primary disease of the superficial and deep veins, and reflux would be classified as C4aS; Ep; As,d; Pr. While venous disease is complex, it can be described using this system, and clinicians are encouraged to use all four components of CEAP.

A disposable sclerotherapy garment is an excellent means for preserving patient modesty while gaining full access to the entire lower extremity. A two-step examination stool also aids in the clinical assessment. The medial plantar and ankle regions are examined for the presence of specific skin changes, including clusters of telangiectatic veins (referred to as "corona phlebectasia"), hemosiderin deposition, livedoid vasculopathy (atrophie blanche), lipodermatosclerosis, and/or active or healed ulceration (see Ch. 105). These findings suggest a chronic state of venous insufficiency located in either the saphenous veins or the deep venous systems. The lateral posterior malleolar region is similarly examined. Skin changes in this area most often indicate small saphenous vein insufficiency.

There are three branch veins that are important for evaluating the saphenofemoral junction (SFJ)[8]. Attention is first directed toward the anterior abdominal wall. The presence of varices in this area ("caput medusae") indicates insufficiency of the superficial epigastric vein (see Fig. 155.2); this is always abnormal and should alert the phlebologist to underlying deep venous obstruction, usually in the iliofemoral segment (see Fig. 155.3). The posteromedial thigh vein and the anterolateral thigh vein are often also insufficient in patients with GSV insufficiency and this usually presents as dilated reticular veins and telangiectasias within the involved anatomic zones[7].

LABORATORY EVALUATION OF THE SUPERFICIAL VENOUS SYSTEM

Vascular testing is indicated for symptomatic patients in whom the source of reflux is unclear by physical examination as well as several other clinical situations (Table 155.2). In the past, a key instrument was a handheld Doppler device, which detects increased or decreased frequency shifts from ultrasound waves that are reflected from blood cells coming toward or going away from the Doppler ultrasound probe, respectively[9]. Handheld Doppler devices have 4 MHz probes that penetrate more deeply (up to 8 cm) and 8 MHz probes that penetrate more superficially (0.5–2 cm).

When utilizing a Doppler device, the examiner places the probe over the vein in question and then compresses distal to the probe to create a flux sound (Fig. 155.6A)[10]. Because the veins have one-way valves, if a vein is normal there will be no reflux or reversal of flow upon release of the distal compression. If a reflux sound is heard after release of the distal compression, this is abnormal and diagnostic of venous valvular insufficiency (Fig. 155.6B). It is best to hold the probe at a 30° to 45° angle[11]. Reversal of blood flow, as the patient increases abdominal pressure with the Valsalva maneuver, indicates incompetent valves from the SFJ to the distal-most site of the probe. When placed on the medial superior thigh over the GSV a few centimeters distal to the

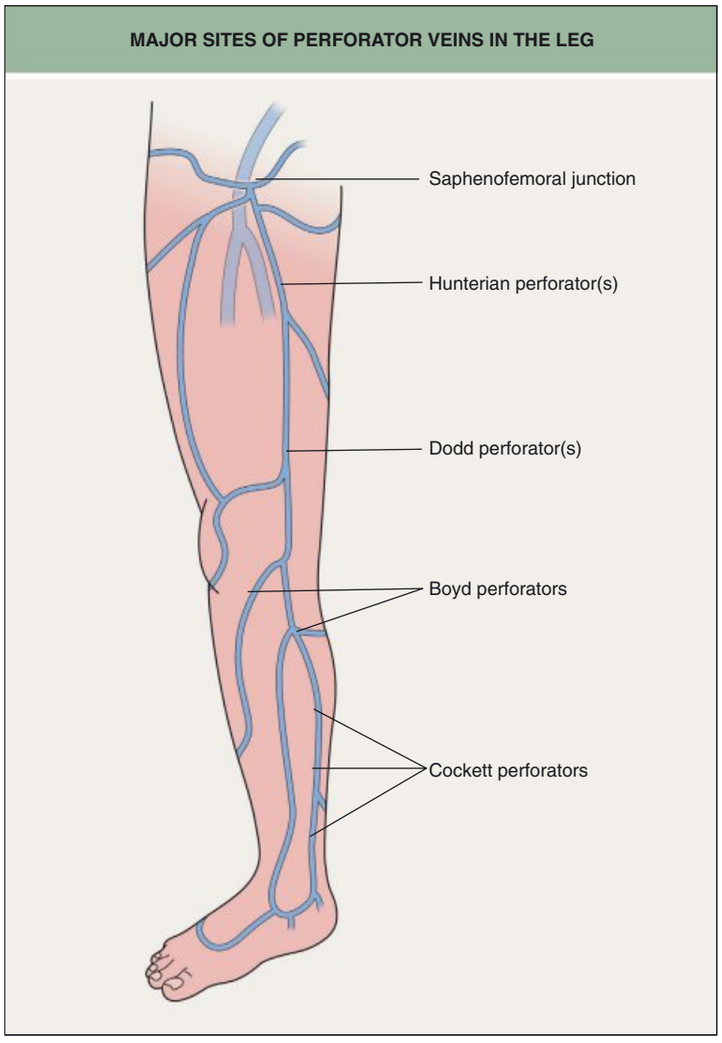


Fig. 155.4 Major sites of perforator veins in the leg. Posteriorly, additional perforating vein sites include the popliteal fossa, midportion of the gastrocnemius muscle belly, and two near the ankle.

SFJ, reversal of blood flow for >0.5 seconds indicates an incompetent SFJ. These patients require endovenous RF or laser closure of the GSV before any treatment of the distal varicose, reticular, and/or telangiectatic leg veins.

Nowadays, most vein experts utilize duplex ultrasonography (also referred to as duplex scanning) which is a faster, highly accurate, non-invasive technique that can provide both anatomic and physiologic information regarding the venous system[12] (Table 155.3). It is the modality of choice, not only for pretreatment assessment of varicose veins, but also for guidance during endovenous RF and laser procedures and for performing follow-up studies. Duplex examination of normal veins involves the use of a 7.5–12 MHz high-resolution B-mode scanner. In B-mode (brightness mode) ultrasonography, a linear array of transducers simultaneously scans a plane through the body and creates a two-dimensional image on a screen (Fig. 155.7). This type of scanning is more commonly known as 2D mode. Velocity information is presented as a color-coded overlay superimposed on a B-mode image and is called color Doppler.

COMPRESSION IN SCLEROTHERAPY AND VENOUS DISEASE

Graduated compression has many benefits in patients with venous disease including providing symptomatic relief, hastening venous ulcer healing, and minimizing the risk of venous ulcer recurrence[13,14]. By reducing the diameter of veins, compression therapy increases flow velocity and decreases the chance of thrombus formation. Following sclerotherapy (which is essentially a *controlled* thrombophlebitic reaction), compression reduces the diameter of the resulting thrombosis of the treated vein, which minimizes the inflammatory reaction, thereby decreasing the extent and incidence of post-treatment hyperpigmentation, recanalization of the vein, and telangiectatic matting. Compression also increases the contact between the sclerosant and the endothelial lining of the vessel wall, potentiating pan-vessel obliteration. There are three main types of graduated compression: graduated elastic compression stockings or bandages, inelastic compression garments or bandages, and pneumatic compression pumps[15]. Compression bandages are not recommended, as they are difficult to apply in a graduated manner and hold their compression for only a few hours after application.

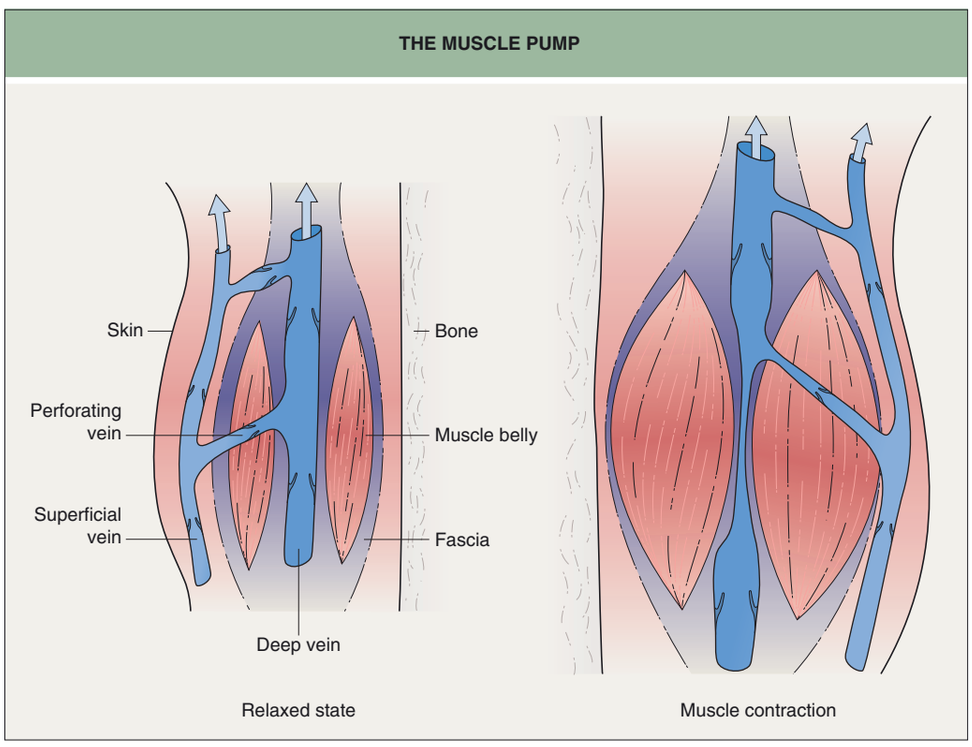


Fig. 155.5 The muscle pump, or "peripheral heart". The pump is located primarily in the calves. During muscle contraction, compression of veins transports blood to the heart by means of the deep venous system. *Adapted from Goldman MP, et al. Sclerotherapy, 5th ed. London: Mosby, 2011.*

Graduated elastic compression stockings are most commonly employed following sclerotherapy. They come in four classes, based on the pressure generated by the stocking at the level of the ankle, ranging from 20–30 mmHg (class I) to 50–60 mmHg (class IV) (see Ch. 105)[16]. Most sclerotherapy patients wear thigh-high or pantyhose stockings. In addition, most manufacturers now offer so-called "fashion hose" which approximate 18 mmHg pressure and are sheer, leading to greater patient compliance. In a multicenter study performed by Weiss et al.[17], 20–30 mmHg graduated compression stockings were shown to increase sclerotherapeutic efficacy and diminish post-treatment hyperpigmentation. At least 3 days of compression were necessary to produce this positive effect and 3 weeks of daytime wear was found to be the optimal time required for maximal effect[17].

We recommend that all patients wear graduated compression stockings for 1 week ("24/7") after the procedure. It is important for the patient to wear the stockings 24 hours a day, even while in the shower and when sleeping. If one removes the stockings in the shower, the superficial veins dilate. If one removes the stockings at night, the superficial system also dilates. Because stockings are worn around-the-clock for the first week, it is recommended that all patients wear thigh-high stockings, as these are more hygienic and easier to use than pantyhose, which extend up to the waist.

CEAP CLASSIFICATION OF CHRONIC VENOUS DISORDERS
Clinical classification (C)
C0: no visible or palpable signs of venous disease C1: telangiectasias or reticular veins C2: varicose veins C3: edema C4a: hemosiderin pigmentation, eczematous dermatitis (stasis dermatitis) C4b: lipodermatosclerosis, livedoid vasculopathy (atrophie blanche) C5: healed venous ulcer C6: active venous ulcer S: symptoms including aches, pains, tightness, skin irritation, heaviness, muscle cramps, and other complaints attributable to venous dysfunction A: asymptomatic
Etiologic classification (E)
Ec: congenital Ep: primary Es: secondary (post-thrombotic) En: no venous etiology identified
Anatomic classification (A)
As: superficial veins Ap: perforator veins Ad: deep veins An: no venous location identified
Pathophysiologic classification (P)
Pr: reflux Po: obstruction Pr,o: reflux and obstruction Pn: no venous pathophysiology identified

Table 155.1 CEAP (Clinical, Etiologic, Anatomic, Pathophysiologic) classification of chronic venous disorders.

SCLEROSING SOLUTIONS

The optimal sclerosing agent is one that induces pan-endothelial destruction or removal[18]. Thrombosis alone will not obliterate vessels because intact endothelium contains tissue plasminogen activator that can dissolve thrombi, leading to recanalization. The ideal sclerosing agent should possess no systemic toxicity and produce local endothelial destruction that fully extends to the adventitia with minimal thrombus formation[19]. The resultant vascular destruction induces an inflammatory reaction which leads to fibrosis and eventual obliteration of the vessel.

INDICATIONS FOR VASCULAR TESTING
1. Any varicosity greater than 2 mm in diameter extending the length of the calf or thigh 2. Presence of a "starburst" cluster of telangiectasias over sites of perforating veins (medial distal calf, mid-posterior calf, medial knee, medial mid-thigh) 3. Evidence of incompetent perforating veins (they connect the superficial and deep venous systems), e.g. lichen aureus 4. Varicose veins, either truncal or saphenous 5. Clinical signs of venous insufficiency (see Ch. 105) 6. Symptomatic veins of any diameter 7. History of deep venous thrombosis and/or thrombophlebitis 8. History of previous venous surgery or sclerotherapy with poor results or recurrence of varicosities

Table 155.2 Indications for vascular testing.

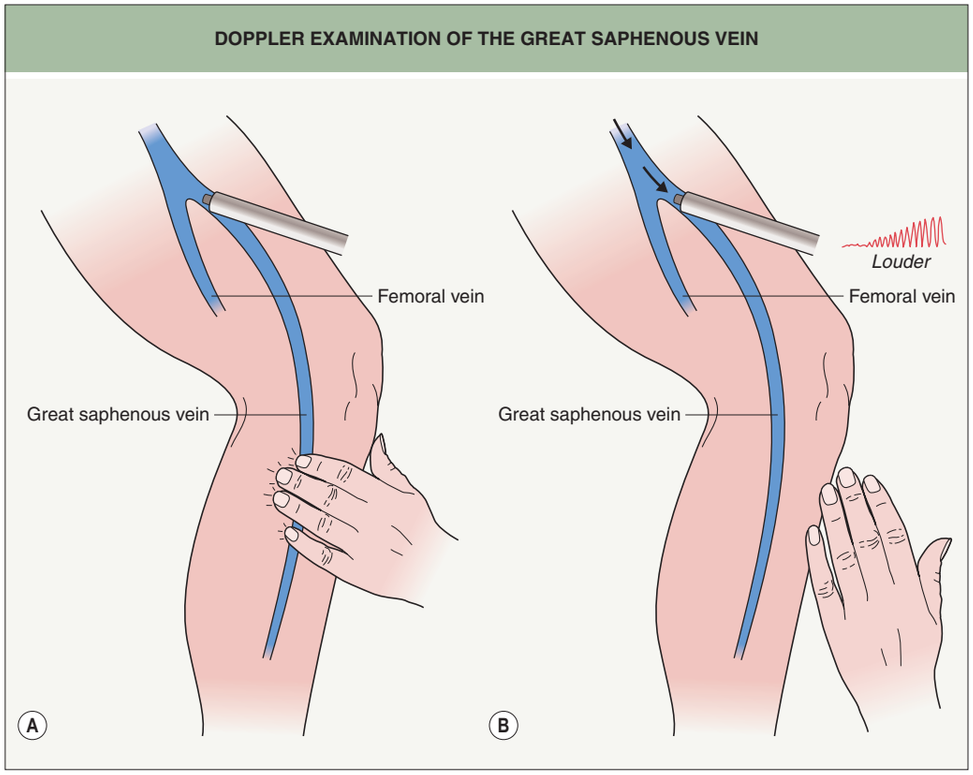


Fig. 155.6 Doppler examination of the great saphenous vein and detection of reflux. A The Doppler probe is held at a 30° to 45° angle and distally the vein is compressed by the examiner. **B** Detection of reflux following the release of distal compression denotes venous valvular insufficiency. *Courtesy Neil Sadick, MD.*

COMPARISON OF DOPPLER ULTRASOUND DEVICE AND DUPLEX ULTRASOUND SCANNER FOR PRESCLEROTHERAPY EVALUATION		
	Doppler	**Duplex**
Portability	Yes	Yes
Easy to use	Yes	Yes
Information obtained	1. Patency, competence of venous valves 2. Detection of deep venous thrombosis in thigh	1. Patency, competence of venous valves 2. Detection of deep venous thrombosis with greater accuracy (thigh > calf) 3. Velocity of reflux 4. Anatomy and anomalies of venous system (e.g. number of great saphenous veins) 5. Termination of small saphenous vein 6. Thrombosis versus sclerosis
Reliability	Less reliable because of blind, non-timed, pulsed sound beam	More reliable because of actual visualization of venous anatomy

Table 155.3 Comparison of Doppler ultrasound device and duplex ultrasound scanner for presclerotherapy evaluation.



Fig. 155.7 Duplex ultrasonography. In the two-dimensional (2D) B-mode duplex image, reverse flow (shown in blue) is seen coming from a branch of the great saphenous vein (GSV) that is superior to the GSV.

There are several important points to remember when choosing a particular sclerosing solution and determining the appropriate sclerosant concentration (Table 155.4)[20]:

1. If the sclerosant is too weak, insufficient endothelial damage will occur, leading to thrombosis secondary to varicose vessel wall damage. However, there will be no fibrosis and recanalization of the vessel occurs.
2. Too strong a solution may lead to uncontrolled destruction of vascular endothelium as well as additional vessel wall layers, which may eventuate in hyperpigmentation, neoangiogenesis (telangiectatic matting), and ulceration secondary to sclerosant extravasation. Excessive inflammation can also develop, leading to painful superficial thrombophlebitis.
3. Choose the minimal sclerosant concentration (MSC) that will cause irreversible damage to the cellular wall of the abnormal vessel.

Sclerosing agents are classified into three groups based upon the mechanism whereby they cause injury to the endothelium (Table 155.5):

1. ***Hyperosmotic agents*** **–** the osmotic agents include hypertonic saline, hypertonic saline–dextrose, and non-chromated glycerin. Their primary mechanism of action involves endothelial cell damage via dehydration (Fig. 155.8A).
2. ***Chemical irritants*** – the chemical irritants include chromated glycerin (glycerin plus potassium chromate) and polyiodide iodide. They injure cells by acting as corrosives; their cauterizing effect is thought to be due to the associated heavy metal (Fig. 155.8B).
3. ***Detergent sclerosants*** – the detergent sclerosants include sodium tetradecyl sulfate, polidocanol, ethanolamine oleate, and sodium morrhuate. This group of agents causes vascular injury by altering the surface tension around endothelial cells (Fig. 155.8C).

A GUIDE FOR THE SELECTION OF SCLEROSING SOLUTION CONCENTRATION AND VOLUME BY VESSEL TYPE		
Vessel	**Solution concentration**	**Volume (per region)**
Telangiectatic matting (after previous treatment)	Glycerin, 72%, diluted 2:1 with 1% lidocaine with 1:100 000 epinephrine	0.1–0.2 ml
Telangiectasias (up to 1 mm)	Glycerin, 72%, diluted 2:1 with 1% lidocaine with 1:100 000 epinephrine	0.1–0.3 ml
	Sodium tetradecyl sulfate, 0.1%–0.25% Polidocanol, 0.25%–0.5%	
	Hypertonic saline, 11.7%	
	Hypertonic saline, 10%, and dextrose, 25%	
Venulectasias (1–2 mm)	Sodium tetradecyl sulfate, 0.25%–0.5% Glycerin, 72%	0.2–0.5 ml
	Polidocanol, 0.5%–0.75%	
	Hypertonic saline, 11.7%–23.4% Hypertonic saline, 10%, and dextrose, 25%	
Reticular veins (2–4 mm subcutaneous blue veins)	Sodium tetradecyl sulfate, 0.1%–0.25%, *foam*	0.5 ml (may increase to 1–3 ml if filling of reticular vein by foam is observed)
	Polidocanol, 0.25%–0.5%, *foam*	
Non-saphenous varicose veins (3–8 mm)	Sodium tetradecyl sulfate, 0.5%–1%, *foam*	0.5 ml for liquids, 3 ml of foam per injection site in a large-capacity vein
	Polidocanol, 1–3%*	
Saphenous varicose trunks (usually >5 mm)	Polidocanol *foam* (Varithena®), 1%	0.5 ml for liquids (low-volume injection critical at high concentrations), 3 ml with foam
	Sodium tetradecyl sulfate, 1%–3%, *foam*	
	Polidocanol, 3%–5%†	
*1% is the highest concentration available in the US. †Not available in the US.		

Table 155.4 A guide for the selection of sclerosing solution concentration and volume by vessel type. The sclerosing agents are listed in order of preference.

The only agents that are Food and Drug Administration (FDA)-approved for sclerotherapy in the US are sodium tetradecyl sulfate, sodium morrhuate (fatty acids in cod liver oil), and polidocanol[21], including the 1% foam formulation (Varithena® [Boston Scientific]). Hypertonic saline is approved as an abortifacient rather than for the treatment of varicose veins. Glycerin is approved as a hyperosmotic agent for the treatment of acute intracerebral edema and acute angle glaucoma. Polyiodide iodide, a chemical irritant, lacks FDA approval for any indication. Glycerin (50%–72%), hypertonic saline (11.7%–23.4%), polidocanol (0.25%–5%), and sodium tetradecyl sulfate (0.1%–3%) are the current sclerosants of choice in the US.

Determining the minimal volume and concentration of the most appropriate sclerosing agent is a key factor in producing effective sclerotherapy results. This concept, termed the minimal sclerosant concentration (MSC), will enable the sclerotherapist to achieve maximal results while minimizing the complication profile[22,23]. A guide to suggested sclerosing agents and initial choices of sclerosant concentrations and volumes for instillation as related to vessel type and diameter is presented in Table 155.4.

IMPORTANT CHARACTERISTICS OF SCLEROSING SOLUTIONS					
Sclerosing solution (brand name)	**Class**	**Allergenicity**	**Risks**	**FDA approval**	**Dose limitation**
Hypertonic saline [11.7%–23.4%®]	Hyperosmotic	None	Pain* and cramping Necrosis of skin Hyperpigmentation	Yes, as abortifacient [18%–30%]	6–10 ml
Hypertonic saline [10%] and dextrose [25%] (Sclerodex®)	Hyperosmotic	Low (due only to added phenethyl alcohol)	Pain* (much less than with hypertonic saline alone)	No (sold in Canada)	10 ml of undiluted solution
Sodium tetradecyl sulfate (Sotradecol® [US], Fibrovein®, Thromboject®)	Detergent	Very rare anaphylaxis	Pain* with perivascular injection Necrosis of skin (with higher concentrations) Hyperpigmentation	Yes	10 ml of 3%
Polidocanol (Asclera® [US], Asklerol®, Aethoxysklerol®, Aetoxisclerol®, Sklerovein™, Varithena® [US])	Detergent	Very rare anaphylaxis	Lowest risk of pain Necrosis usually from arteriole injection Hyperpigmentation (with higher concentrations) Disulfiram-like reaction	Yes	5 ml of 3% (depends on body weight, see ref. 5)
Sodium morrhuate (Scleromate®)	Detergent	Anaphylaxis, highest risk	Pain* Necrosis of skin Hyperpigmentation	Yes	10 ml
Ethanolamine oleate	Detergent	Urticaria, anaphylaxis	Pain* Necrosis of skin Hyperpigmentation Viscous, difficult to inject Acute renal failure Hemolytic reactions	Yes (used primarily for esophageal varices)	10 ml
Polyiodide iodide (Varigloban®, Variglobin®, Sclerodine®)	Chemical irritant	Anaphylaxis Iodine hypersensitivity reactions	Pain* Necrosis of skin Dark brown color makes intravascular placement more difficult to confirm	No	5 ml of 3%
Glycerin [72%] with chromium potassium [8%] (Chromex®, Scleremo®); glycerin [172%] diluted 2:1 with 1% lidocaine, with or without epinephrine	Chemical irritant (plain glycerin may be an osmotic agent as well)	Very rare anaphylaxis (none for glycerin alone)	Pain* and cramping Low risk of hyperpigmentation Viscous, difficult to inject Hematuria with injections >10 ml	Yes (for treatment of acute intracerebral edema and acute angle glaucoma)	10 ml

*Includes burning.

Table 155.5 Important characteristics of sclerosing solutions. Sclerosing agents are classified into three groups: hyperosmotic agents, detergents and chemical irritants.

It is also important to have a working knowledge of the complication profile of each sclerosing solution (see Table 155.5). For example, hypertonic saline, an osmotic sclerosant, is associated with burning and cramping on injection and an increased incidence of ulcerative necrosis secondary to extravasation.

Sodium tetradecyl sulfate and polidocanol have been associated with a low incidence of allergic reactions, ranging from urticaria to anaphylaxis (<0.01%). However, with increasing usage, it is now thought that the risk of type I (i.e. immediate hypersensitivity) reactions is actually extremely low. In fact, after over 35 years of use in over 100 000 patients, the authors have never seen an allergic reaction except for one case of urticaria. Hyperpigmentation has been reported in 5%–30% of patients treated with all sclerosing solutions except glycerin, which has a <1% incidence of pigmentation. In the authors' experience, the incidence of hyperpigmentation is related more to the concentration of the sclerosing agent as well as patient skin type, vessel type, and other vascular fragility factors[24–26].

Creating foaming detergent solutions by mixing them with air or CO_2 (typically in a mixture of 1 ml of solution with 4 ml of air or CO_2) has been found to increase the potency of the sclerosing solution twofold while decreasing its adverse effect profile fourfold. Foam displaces blood and remains for an extended time in the target vessel. This makes the sclerosing solution more efficient, so that it may be utilized at lower concentrations. The use of CO_2 rather than room air allows the gas–sclerosant bubbles to break down faster, minimizing the possibility of gas embolization into the arterial circulation via a patent foramen ovale. Of note, the detergent moiety in the foam is broken down within seconds and/or within centimeters of its injection. As a result, the foam bubbles that reach the heart are purely air with no toxicity, similar to the release of air bubbles after a SCUBA dive.

TECHNIQUES FOR TREATING TELANGIECTASIAS AND RETICULAR VEINS

The treatment of telangiectasias and reticular veins is most commonly performed for cosmetic improvement, but up to 50% of these patients also report a variety of symptoms from dull aching legs to throbbing pain over the telangiectasia[27,28]. Telangiectasias are best defined as nearly flat, red to blue vessels 0.1–1 mm in diameter (Table 155.6). Venulectasias are blue- to violet-colored vessels, sometimes distended above the skin surface and most often 1–2 mm in diameter. Reticular veins have a cyanotic blue to blue–green hue and are visually 2–4 mm in diameter. When a complex of reticular veins is located on the lateral thigh, it is felt to be a vestige of embryonal development known as the lateral subdermal plexus[29,30].

The treatment of telangiectasias and reticular veins is undertaken only after all sources of reflux have been addressed, as it is important to treat proximal sites of reflux first and to treat larger vessels before smaller veins. Alone or in combination with laser or intense pulsed light technology, sclerotherapy of small-diameter vessels is the most common challenge faced by the dermatologic surgeon who performs sclerotherapy. Preoperative photographic documentation and full informed consent outlining all possible risks and complications as well as treatment expectations should be obtained prior to therapy[31,32].

Materials employed in the treatment of telangiectasias and reticular veins are relatively simple. They may include:

- cotton balls soaked with 70% isopropyl alcohol
- protective gloves
- 3 and 5 ml disposable syringes
- Female-to-female adaptor for mixing air with detergent solution
- 30-gauge disposable ½-inch transparent hub needles

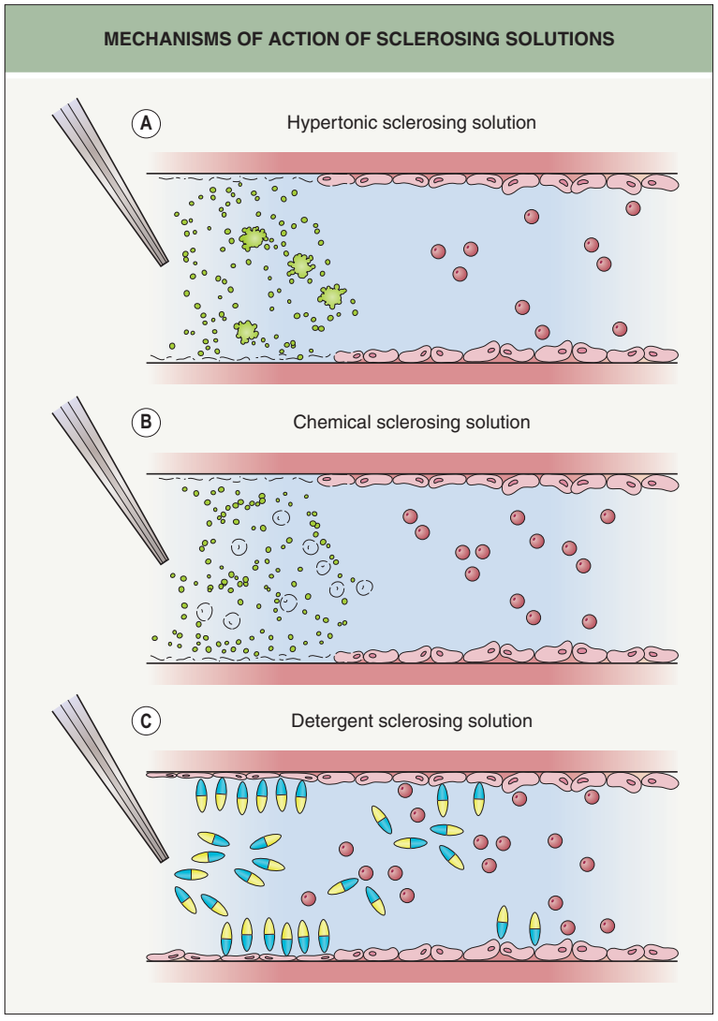


Fig. 155.8 Mechanisms of action of sclerosing solutions. A Hypertonic, which induces endothelial damage via a gradient dehydration effect. **B** Chemical, which injures cells by acting as a corrosive. **C** Detergent, where the hydrophobic portion of the detergent molecule (blue) attaches to the endothelial cell wall while the hydrophilic portion (yellow) draws water into the cell, leading to an overhydrated maceration effect. *Adapted from Goldman MP, et al. Sclerotherapy, 5th edn. London: Mosby, 2011.*

- magnifying lens (2–3×), possibly with cross-polarized light
- nitroglycerin paste for prolonged blanching
- bronchodilator inhaler in case of bronchospasm
- 1:1000 epinephrine (adrenaline) in case of anaphylaxis.

Flow sheets with segmental numerical division of the legs are helpful in documenting areas that are treated at each session. Because successful sclerotherapy that results in pan-luminal endofibrosis can take up to 6 weeks, it is recommended that treatment sessions should not be repeated for at least this interval of time.

There are four variable components that may be employed in the treatment of telangiectatic and reticular veins including[33–35]:

1. ***Aspiration.*** Aspiration of a small amount of blood into the needle hub may ensure that the dermatologic surgeon has adequately cannulated the vein. Of note, the vein may collapse if aspiration is too strong.
2. ***Direct puncture without aspiration.*** This technique relies on the feeling associated with perforating the vein wall. Although it is slightly more precarious for beginners, this technique can be mastered with time.
3. ***Air bolus variant*** (Fig. 155.9A). Injection of <0.5 ml of air prior to introduction of the sclerosant will displace blood in the vein. Once intravascular access is confirmed, the sclerosant can be safely injected. Air inadvertently introduced into the tissues is not as damaging as the sclerosant might be. Too strong of a push may lead to truncal distention and rupture. The small air bolus technique is ideal for hypertonic saline, as even slight extravasation of solution will cause ulceration.
4. ***Empty vein variant.*** In an attempt to remove as much blood as possible, the leg is elevated and kneading with gentle pressure is performed before the sclerosant is injected. The persistence of varicose veins after treatment is usually due to recanalization of the intramural thrombus that develops, and the empty vein technique may reduce the amount of thrombus. This concept is more important when treating larger veins. Other advantages of this technique are that an empty vein has minimal volume and therefore the endothelium is exposed to a concentration of sclerosant similar to that injected. Also, a smaller volume of sclerosant is necessary to ensure contact with the endothelial surface and lower concentrations of sclerosant may be employed since there is less blood in the vein to dilute the solution[36]. Foamed sclerosing agents, discussed later, displace blood from veins, thereby automatically resulting in the empty vein technique and enhanced efficacy.

Injection Technique

Injection is performed utilizing one or more of the previously described techniques. The needle may be bent at an angle of 30°. Hand traction is used by either the dermatologic surgeon or an assistant to keep the skin taut (Fig. 155.9B). Large vessels are injected before smaller vessels, i.e. injection of the reticular veins feeding smaller telangiectasias or venules may eradicate the latter, minimizing side effects such as hyperpigmentation. Areas of vascular arborization (Fig. 155.10) should be treated before single discrete linear vessels are cannulated[37].

The utilization of alcohol in swabbing the skin prior to injection will decrease the index of refraction of light and thus make the vessels more visible at the skin surface. In addition, cross-polarized light can be used to enhance vessel visualization by eliminating reflection of light from the skin surface. Brisk cannulation of veins causes minimal vascular trauma, less vasoconstriction, and less chance of extravasation of blood. Injection pressure is kept to a minimum by performing the injection slowly to prevent vascular distention and to allow adequate time for the sclerosing agent to interact with the endothelium. A small amount of sclerosant is used at each injection site (0.1–0.4 ml) to minimize side effects such as telangiectatic matting, post-sclerosis pigmentation, and ulcerative necrosis due to extravasation. The sclerosing injection is stopped when the solution has filled the targeted veins and the injector no longer sees the vessel clearing of blood. Injections are carried out at approximately 3–6 cm intervals until the entire vessel has been treated.

Treatment Protocol

Treatment sessions are scheduled at 6- to 8-week intervals to allow enough time for full endosclerosis to occur, for post-treatment inflammation to resolve, and to evaluate the results of the previous treatment session. Most patients will require one to three treatment sessions to clear their legs of unwanted telangiectatic and reticular vessels. If a poor response is seen at the end of this treatment schedule, the dermatologic surgeon may:

- increase the concentration of sclerosant
- switch to another sclerosant
- re-examine the patient to find a possible source of reflux previously missed.

Lasers and Intense Pulsed Light Sources for Treatment of Telangiectasias

Laser and intense pulsed light (IPL) therapy of lower extremity vessels may have a synergistic effect when used in combination with sclerotherapy (see Ch. 137).

LARGER VARICOSE VEINS

The treatment of large-diameter blood vessels requires greater and more precise attention to detail regarding anatomy and points of reflux[38]. Contraindications to treatment of large-diameter veins include pregnancy, lactation, allergy to the sclerosing agent, a hypercoagulable state (see Table 105.9 for causes of thrombophilia), non-ambulation, and non-compliance[39]. A foamed detergent is currently recommended

CLASSIFICATION OF VEINS AND CLINICAL APPROACH TO TREATMENT OF VENOUS PATHOLOGY

	Type	Description	Diameter (mm)	Color	Treatment	
	I	Telangiectasias (spider veins) Telangiectatic matting	0.1–1	Usually red network	• Microsclerotherapy • Intense pulsed light • Laser (e.g. pulsed dye, 1064 nm Nd:YAG)	
	II	Venulectasias	1–2	Violaceous	• Sclerotherapy • Laser (e.g. 1064 nm Nd:YAG)	
	III	Reticular varicosities	2–4	Cyanotic blue to blue–green	• Sclerotherapy • Ambulatory phlebectomy • Laser (e.g. 1064 nm Nd:YAG)	
	IV	Varicosities (secondary saphenous branch or perforator-related)	3–8	• Blue to blue–green	• Ambulatory phlebectomy • Sclerotherapy	
	V	Saphenous varicosities (truncal or axial varicosities including main saphenous trunks and first-generation branch varicosities)	≥5	• Blue to blue–green • May be palpable and not visible	• Ambulatory phlebectomy • Endovenous radio-frequency closure • Sclerotherapy • Endovenous laser ablation (EVLA)	

Table 155.6 Classification of veins and clinical approach to treatment of venous pathology. Nd:YAG, neodymium-doped yttrium aluminum garnet.
Photographs courtesy Jean L. Bolognia, MD.

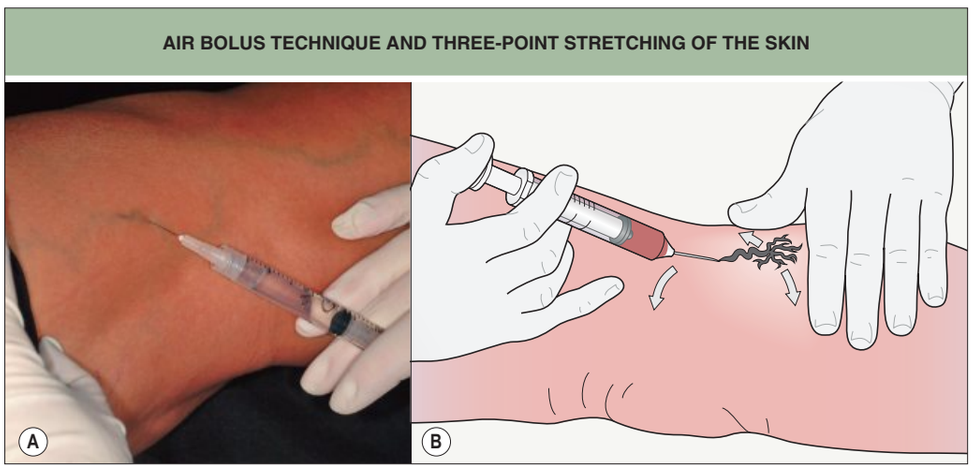


Fig. 155.9 Air bolus technique and three-point stretching of the skin. A Injection of an air bolus (<0.5 ml) prior to injection of sclerosant can displace blood in the vein and ensure intravascular needle location. Air inadvertently introduced into the tissues is not as damaging as the sclerosant might be. **B** Three-point stretching of the skin allows for more accurate cannulation of the vessel. *B, Redrawn from Goldman MP, et al. Sclerotherapy, 5th edn. London: Mosby, 2011.*

as the sclerosing agent (see below), with the concentration determined by the size of the vein to be injected (see Table 155.4).

Factors of importance in the treatment of large-diameter veins include:

1. An understanding of the precise anatomy of the varicosity under consideration for treatment.
2. Adherence to a rational treatment plan in which injections begin at the highest point of reflux, with progression to the next highest point in a proximal-to-distal direction.
3. Determination of the most significant reflux point[40,41].

The dermatologic surgeon must determine whether reflux originates in the deep venous system, the SFJ, saphenopopliteal junction (SPJ), GSV,



Fig. 155.10 Treatment of arborizing feeder veins. This therapeutic approach (arrow) diminishes the number of injections required in a given sclerotherapy session, thus minimizing potential side effects. *Courtesy Jean L. Bolognia, MD.*

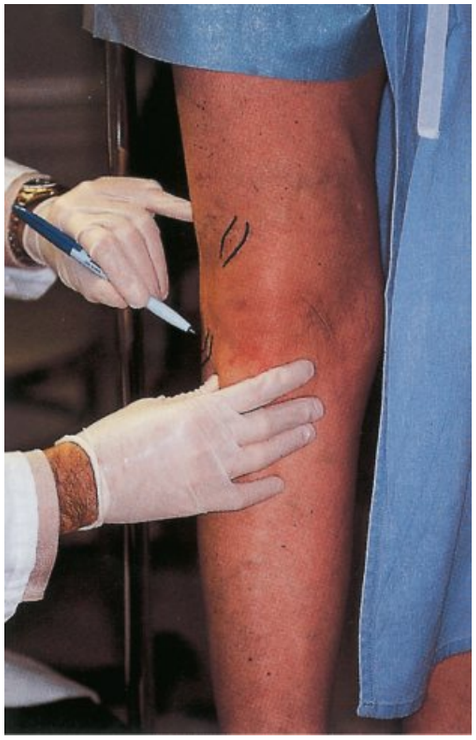


Fig. 155.11 Initial step prior to large-vein sclerotherapy. Marking of treatment sites in a standing position by indelible marker. *Courtesy Neil Sadick, MD.*

SSV, or a perforator (see Fig. 155.2 & 155.3). The veins which represent the primary source of reflux must be treated before secondary sources of reflux are treated. Guidance via duplex ultrasonography (see Table 155.3) is often helpful in the therapeutic approach to larger-diameter vessels, particularly in those patients where the anatomy is so intricate that the point of reflux would otherwise be difficult to detect.

Several slightly modified techniques and/or positions for large-vein sclerotherapy have been described. Three positions for treating large-diameter vessels are: (1) the standing supine elevation direct cannulation technique; (2) the multiple precannulation sites (MPS) technique; and (3) the supine cannulation (SC) technique[41,42].

In the *standing supine elevation direct cannulation* technique, the patient stands at first, causing the varices to bulge and become more visible (Fig. 155.11)[30]. Injection points are marked at primary sites of reflux into the superficial venous system and approximately every 3–4 cm along the vein to be treated. The patient is then placed in a supine or prone position, the vein is emptied to maximize sclerosant–endothelial contact, and a small volume of sclerosant is injected at each of the marked points along the vein to be treated. A 27- to 30-gauge needle on a 3 ml syringe is often employed for this technique. The needle is advanced while aspirating into the syringe until aspiration of dark venous blood indicates penetration of the lumen. Concentrated sclerosant (0.5–1.5 ml) is injected at each site, followed by massage to ensure maximum sclerosant–endothelial contact. The vein will appear visually contracted at the end of the treatment. Leg elevation for a minute following the injection of foam allows the larger veins to contract. This may result in further spread and better contact of the sclerosant with the endothelium, improving the clinical results.

In the *multiple precannulation sites* (MPS) variation, the patient initially stands so as to induce the varices to bulge and become more visible. Injection points are marked at proximal *and* distal sites along the distended vein. The veins are subsequently cannulated with either a 23-gauge butterfly needle and tubing or a plastic intravenous cannula and extension tubing at *both* the proximal and distal sites[43].

The butterfly needles or cannulas must be firmly secured, as the patient then moves to the treatment table and elevates the extremity undergoing treatment. After an intravascular position has been verified, 2–3 ml of sclerosant is infused into the cannula and subsequently into the vein while the surrounding area is observed for swelling or other evidence of extravasation. In most patients, a single proximal and a single distal injection point are sufficient to sclerose a large tortuous vessel[44].

The authors routinely use the *supine cannulation* (SC) position, as it is faster and has less risk of a vasovagal reaction when compared to the upright position. Larger veins are treated proximally to distally with an appropriate concentration of sclerosing solution (see Table 155.4). Foamed detergent solutions are recommended for sclerosis of larger varicose veins, and if foaming with room air or CO_2 is chosen (see next section), this is performed just prior to injection[45].

Foamed Detergent Solutions

Polidocanol 1% injectable foam (Varithena®)

Polidocanol 1% injectable foam (Varithena®) is FDA-approved for the treatment of incompetent GSVs, accessory saphenous veins, and visible varicosities of the GSV system above and below the knee. Physicians administering this polidocanol 1% foam must be experienced with venous procedures, possess a detailed working knowledge of duplex ultrasonography of veins, and be trained in its administration. The formulation is based upon a patented technology that produces cohesive, low-nitrogen microfoam coupled with a microfoam-generating device which injects an O_2:CO_2 (65:35) gas mixture with <0.8% nitrogen, leading to small bubbles (median diameter <100 microns). The resulting microfoam produces endothelial destruction with a very low polidocanol concentration of 1% in a 1:7 ratio of liquid:gas phases. The cohesive microfoam fills the vein lumen leading to circumferential contact and displacement of blood resulting in more efficient vein sclerosis.

Spontaneous foaming with room air

Before the approval of polidocanol 1% foam (Varithena®), a detergent solution such as sodium tetradecyl sulfate or polidocanol was foamed to a thick consistency by rapidly agitating it with room air in a ratio of solution to gas of 1: 4. As noted previously, using foam is advantageous when treating larger varicosities. For instance, an increased quantity of solution can be injected over longer segments of veins. Also, a foamed sclerosing solution retains more of its potency, as the full concentration of the sclerosant is present on each microbubble, residing on the outer micelle. Due to persistence and increased potency, foamed agents reduce the number of required treatments and allow treatment of larger vessels.

In contrast, for smaller vessels, non-foamable glycerin and hypertonic saline are rapidly diluted, acting only within their concentration gradients and thus limiting the extent and intensity of sclerosing action. It is not practical to treat large veins with glycerin or hypertonic saline, as more frequent injections would be necessary, and the potency rapidly diminishes due to the concentration being rapidly diluted by blood within the treated vein.

Duplex Ultrasonography

In addition to delineating vascular anatomy, duplex ultrasonography (see Fig. 155.7) can be used to assess the vascular response to sclerotherapy, including that of large non-junctional varicose veins. Incomplete endosclerosis has a pattern of intravascular thrombosis (multiple echoes), with the vein lumen remaining partially patent. When sclerotherapy has been successful, the vein wall is thickened and non-compressible (non-echogenic)[38,46]. Duplex ultrasonography can also provide guidance during sclerotherapy with *foamed* sclerosing agents. The distribution of foamed sclerosant as it flows into the targeted vein is easily visible as a sparkling echo. This also decreases the chance for inadvertent arterial injection.

POSTSCLEROTHERAPY COMPRESSION

Cotton-roll pads or foam pads may be applied along the entire course of the treated vessels and held in place by a compression garment. Graduated compression stockings that are class I (20–30 mmHg) or preferably class II (30–40 mmHg) are suggested for all patients following sclerotherapy of telangiectasias and reticular veins[17]. Patients should be instructed to walk for 30 minutes after each treatment session in order to minimize thromboembolic events as well as to decrease the diameter of the superficial veins. The optimal duration of compression was shown in a more recent study to be a minimum of 3 weeks of daytime wear, although 3 days of daytime compression led to better results than did no compression[17]. After large-vein sclerotherapy, we recommend 7 days of uninterrupted compression (24/7), during which the patient may bathe or shower by either placing a large plastic bag over the compression bandage or stocking or just allowing the stocking to get wet and then drying it with a hairdryer. After the first 7 days, the compression pads or cotton rolls are discarded and patients are permitted to remove the stocking, as needed, for bathing and sleeping. Ambulation is begun immediately post-treatment.

COMPLICATIONS

There are three major considerations when anticipating and managing complications of sclerotherapy (Table 155.7). The first is that fastidious technique will minimize the incidence of side effects. Second is an appropriate understanding of maneuvers that may be instituted if something is thought to have gone wrong. Finally, an appreciation of the management options available for adverse sequelae can minimize the intensity of complications when they occur[47].

SCLEROTHERAPY COMPLICATIONS	
Cutaneous complications	**Extracutaneous complications**
Early	**Early**
• Localized urticaria • Urticarial or morbilliform eruptions • Bruising • Edema • Ischemia/necrosis (e.g. due to arterial injection, vasospasm, extravasation)	• Systemic allergic reactions (e.g. anaphylaxis) • Scotomata (with foam sclerosants) • Migraine with aura • Vasovagal syncope
Delayed	**Delayed**
• Superficial thrombophlebitis • Ulceration (secondary to ischemia/necrosis) • Hyperpigmentation • Telangiectatic matting (neoangiogenesis) • Hypertrichosis • Compression-related problems (folliculitis, irritant contact dermatitis)	• Deep venous thrombosis/pulmonary embolus • Nerve damage

Table 155.7 Sclerotherapy complications.

Postsclerotherapy Pigmentation

The incidence of postsclerotherapy hyperpigmentation (Fig. 155.12) varies from 5% to 30%[26,45,48,49]. The purple–brown discoloration has been shown to be due to extravascular deposits of hemosiderin[50]. Hypercoagulability syndromes such as antithrombin III, protein C or protein S deficiencies, use of nonsteroidal anti-inflammatory drugs (NSAIDs), high total body iron stores, use of minocycline, or vessel fragility, commonly noted in the elderly, may predispose to this adverse sequela[51]. Methods to minimize the incidence of postsclerotherapy pigmentation are outlined in Table 155.8. Although various treatment modalities have been tried for this complication, only the Q-switched ruby laser has shown any degree of reproducible success[52–54]. The hyperpigmentation usually resolves over 6–12 months. If it persists, the dermatologic surgeon should search for a vessel with persistent reflux into the area or an underlying predisposition.

Telangiectatic Matting

Blushes or nets composed of very fine telangiectasias may occur around sites of previously injected veins or sites of previous surgical interruption, e.g. ligation or ambulatory phlebectomy (Fig. 155.13). They may occur from days to months after treatment and are seen in 5%–15% of patients[26,45,55]. Sites of predilection include the thighs, medial malleolus, and medial and lateral calves. Risk factors include obesity, use of estrogen-containing

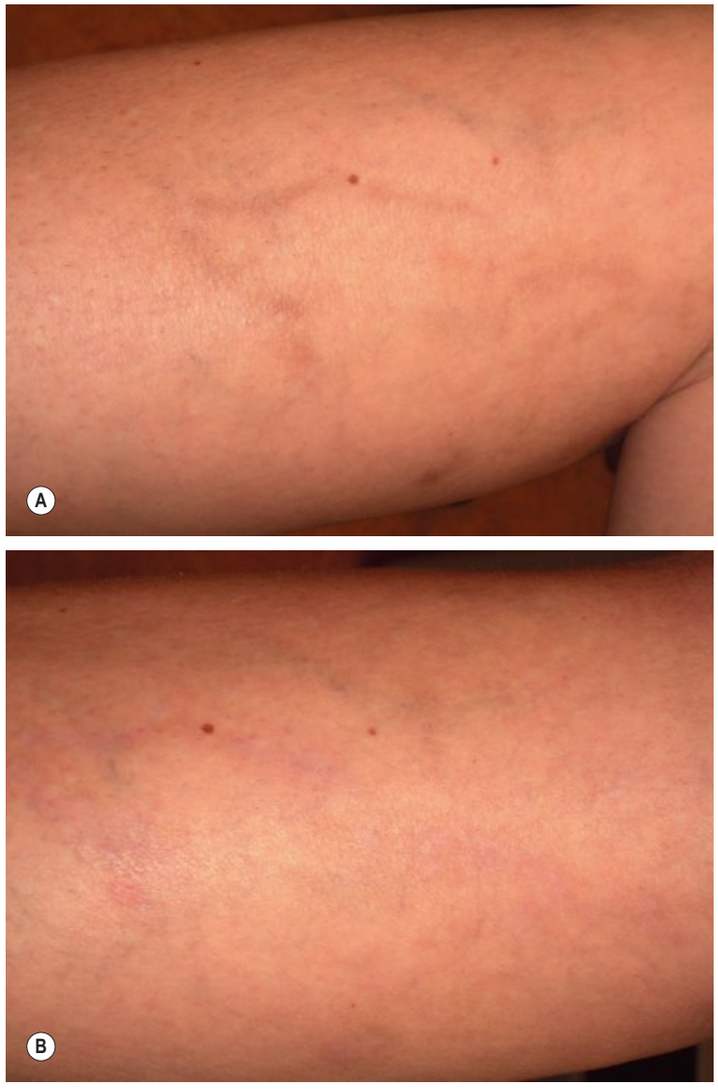


Fig. 155.12 Sclerotherapy-induced hyperpigmentation. A Development of hyperpigmentation along the course of a 3–4 mm diameter reticular vein three months after treatment with sodium tetradecyl sulfate 0.5% foam. **B** Six months after treatment with the Q-switched ruby laser at 6 J/cm^2, 5 mm diameter spot. Note complete resolution of hyperpigmentation. The melanocytic nevus serves as a landmark.

medications, and pregnancy. Excessive postsclerotherapy inflammation may also predispose individuals to this complication, due to inadequate compression or exceeding the MSC of the sclerosing solution.

Generally, telangiectatic matting resolves within 3–12 months without specific treatment. Persistence should lead the dermatologic surgeon to attempt to locate a source of reflux in the area (usually a feeding reticular vein), although matting may be a sign of underlying saphenous vein insufficiency. Low injection pressure utilizing the MSC is the most effective way to minimize this complication. Additional measures include the use of no more than 1 ml of sclerosant per injection site, limiting the injection blanch to 1–2 cm, encouraging normalization of weight, and discontinuation of oral contraceptives for 1 month prior and 2 months following sclerotherapy. Short-wavelength lasers (595–600 nm) and intense pulsed light sources as well as reinjection of vessels utilizing a glycerin solution are the most effective ways of managing this problem (see Table 155.4)[56].

Ulceration

Cutaneous necrosis may occur with any sclerosing agent (although the authors have never seen this with glycerin). It may be the result of extravasation of a sclerosing agent into the perivascular tissues, which is especially common with the use of hypertonic saline, non-foamed sodium tetradecyl sulfate, or polidocanol that is >1% in concentration; injection into a dermal arteriole or an arteriovenous anastomosis; reactive vasospasm of such a vessel; or excessive cutaneous pressure created by compression techniques[57]. If there is extravasation of hypertonic saline into the perivascular tissue, infiltration of the area with normal saline may dilute the sclerosant. A hemorrhagic bulla may form at the site within 12–24 hours and later progress to an ulcer. If a porcelain-white area appears within the skin immediately after injection, this indicates arteriole injection or spasm. To reduce the likelihood of ulceration, the physician may rub a small amount of 2% nitroglycerin ointment into the area until a reactive hyperemia is seen. Since most ulcerations are less than 4 mm in diameter, second intention healing usually results in an acceptable scar. Larger ulcerations may be excised (as early as possible) and closed for faster healing and a smaller scar. Application of topical silicone gel (e.g. Stratacel® [Stratpharma]) may reduce the pain associated with the ulcer and speed the rate of healing[58].

METHODS TO MINIMIZE POSTSCLEROTHERAPY HYPERPIGMENTATION
Pretreatment planning
• Evaluate for a hypercoagulable state in patients with a history of venous thrombosis (see Table 105.9) • Avoid treating patients with known defects in iron transport (e.g. hemochromatosis) • Avoid concomitant use of minocycline, aspirin, or NSAIDs
Treatment technique
• Eliminate high-pressure reflux before treating smaller vessels • Select a sclerosant with the least inflammatory effects • Use a sclerosant concentration appropriate for the vessel size (see Table 155.4) • Minimize intravascular pressure by elevating the leg during treatment • Direct treatment at the deepest site in a telangiectatic cluster • Minimize risk of vessel rupture (e.g. by slow injection) • Avoid excessive syringe pressure
Post-treatment care
• Apply compression immediately after treatment • Remove postsclerotherapy thrombi as early as possible

Table 155.8 Methods to minimize postsclerotherapy hyperpigmentation. NSAIDs, nonsteroidal anti-inflammatory drugs.

Systemic Allergic Reaction

True allergic reactions following sclerotherapy treatments are extremely rare. Delayed hypersensitivity reactions, which may be urticarial or morbilliform in nature, can occur from 8 to 16 hours after treatment. Type I immediate reactions, varying from urticaria to bronchospasm to anaphylaxis eventuating in cardiovascular collapse, have been rarely reported. Intrinsically, only hypertonic saline has no potential to act as an allergen. However, the presence of additives such as benzoate or lidocaine may lead to the development of hypersensitivity reactions.

Sodium tetradecyl sulfate has a surprisingly low allergic potential (<0.01%). The most commonly reported hypersensitivity reactions are morbilliform eruptions developing 30–90 minutes after injection[59]. Reactions to polidocanol are similarly rare (<0.01%). Both urticarial and morbilliform reactions have been reported, as well as an extremely rare anaphylaxis-related fatality[59].

Antihistamines and oral corticosteroids (e.g. prednisone 40–60 mg/day for 7–10 days) can be used for the milder reactions, whereas intravenous corticosteroids and subcutaneous epinephrine are often required for more severe reactions.

Arterial Injection

The most feared complication in sclerotherapy is inadvertent injection into an artery. Arterial injection of a sclerosing agent produces a sludge embolus that obstructs small arteries as well as the microcirculation. The most common location for an arterial injection to occur is the popliteal fossa, when attempting to inject the SSV. After an intra-arterial injection, the patient usually notes immediate pain, but not always.

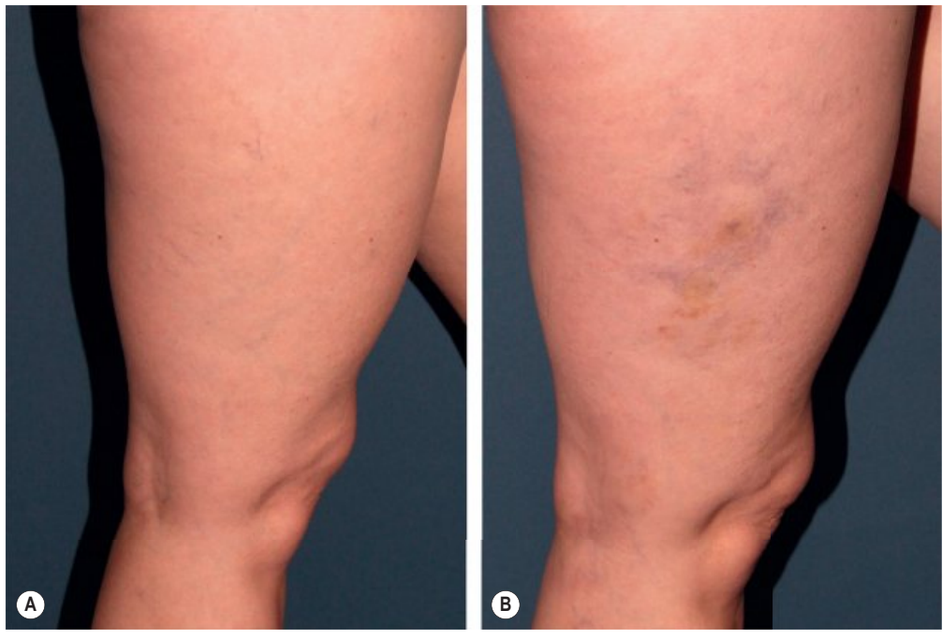


Fig. 155.13 Telangiectatic matting (neoangiogenesis). **A** Prior to vein surgery. **B** After vein surgery – development of telangiectatic matting at the site of the scar.

A dusky cyanotic hue and pallor in the distribution of the injected artery usually occurs within a few minutes to several hours. Arterial pulsations of the posterior tibial or dorsalis pedis arteries are usually not affected. Sloughing of superficial tissues may result in significant scarring or may even require amputation[60].

Arterial injection is a true sclerotherapy emergency. Immediate intervention has been advocated but has never been proven to affect outcome. Procaine (1%), administered via periarterial infiltration, forms a complex with sodium tetradecyl sulfate, rendering it inactive; however, procaine is not effective for polidocanol. Cooling of the limb to minimize tissue anoxia, followed by immediate heparinization for 7–10 days and administration of intravenous dextran (10%, 500 mg daily) for 3 days is recommended. Thrombolysis and the utilization of long-term vasodilator therapy (e.g. calcium channel blockers) should be considered.

Miscellaneous Complications

Localized urticaria following injection is common and is most likely related to mast cell degranulation and cytokine release. No treatment is indicated, although pretreatment with an H_1 antihistamine or immediate application of a class I ultra-potent topical corticosteroid may ameliorate the erythema, if bothersome to the patient. Compression stocking-related problems such as ulcers, pressure bullae, contact dermatitis and folliculitis may be minimized by adherence to appropriate compression application and fitting guidelines[47].

Nerve damage may occur secondary to direct injection of sclerosant or as a result of perivascular inflammation around nerve sheaths. The saphenous and sural veins of the inner leg and foot are high-risk sites and special care should be taken when injecting these locations. The utilization of NSAIDs may shorten the duration of symptoms[61].

Superficial thrombophlebitis develops 1–3 weeks after injection, presenting as a tender erythematous induration of the injected vein. This complication is observed less often if compression is maintained for an adequate period of time following sclerotherapy. When superficial thrombophlebitis occurs, the thrombus should be evacuated and adequate compression, frequent ambulation, and aspirin or an NSAID instituted. The concomitant presence of deep vein thrombosis (DVT) must be considered[47], and a search for underlying causes for thrombophlebitis other than the sclerotherapy, such as an internal malignancy, may be warranted.

AMBULATORY PHLEBECTOMY

Ambulatory phlebectomy is an in-office surgical procedure designed for the complete removal of diseased venous segments by means of hook avulsion of the targeted vessel. It was developed in the 1950s by the Swiss dermatologist Robert Mueller[62]. All superficial veins, except for the groin termination of the GSV, may be easily avulsed utilizing this technique. Large veins – in particular, well-demarcated branches of the GSV, SSV or perforators – can be avulsed through microstab incisions[62,63].

Preoperative Considerations

Doppler and duplex ultrasonography are necessary to confirm the competence of the SFJ and the SPJ, as well as that of the deep venous system[64]. The varicose veins to be removed are outlined with an indelible marking pen with the patient in a standing position. Marking of appropriate venous segments is the most important aspect of this procedure because it allows rapid isolation of desired venous segments to be removed. Because of potential shift of the vein up to 1 to 2 cm when moving from an upright vertical to a transverse horizontal position, the patient is then asked to lie in the operative position and confirmation of venous position by transepidermal illumination (Veinlite® [TransLite LLC] or Venoscope® II [Venoscope LLC]) with separate marking over the veins is performed. This double-marking technique has been found to be helpful in determining positional shift[65,66] (Fig. 155.14).

Anesthesia and Intraoperative Materials for Ambulatory Phlebectomy

Tumescent anesthesia has several advantages when performing ambulatory phlebectomy. These include: (1) rapid anesthesia of an extensive segment of diseased vein; (2) compression of the vein, allowing it to be removed through a 2–3 mm incision; and (3) easier location of the vein owing to the temporary swelling and firmness of the soft tissues which press the vein against the skin. In addition, tumescent anesthesia reduces blood loss, diminishes bruising, eliminates multiple needle sticks, and produces greater postoperative comfort. Most commonly, tumescent anesthesia comprised of 0.05% lidocaine with 1:1 000 00 epinephrine is employed (see Table 156.3)[67,68].



Fig. 155.14 Double-marking technique for ambulatory phlebectomy. Outlining of the varicose veins while the patient is standing (black ink) and then while the patient is lying down in the operative position (green ink) utilizing transillumination.

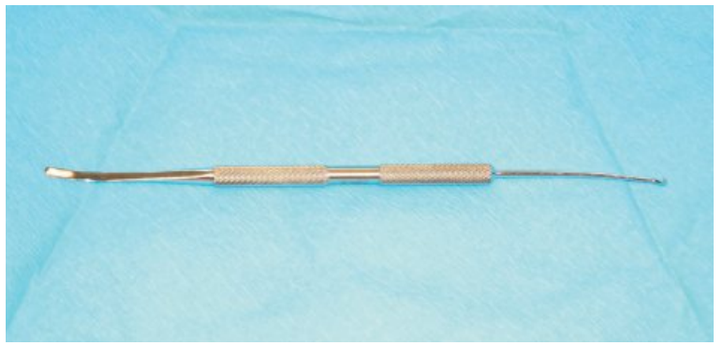


Fig. 155.15 Phlebectomy hook. A classic Mueller type of hook at one end and a Varady dissector at the other end ("Goldman hook").

Instrumentation for ambulatory phlebectomy should include several varied hook devices, which come in small, medium, and large diameters (sizes 2 to 4) from various manufacturers. The ideal hook should have a comfortable grip to prevent fatigue and a sharp harpoon to catch the adventitia of the vein[62,69] (Fig. 155.15).

Ambulatory Phlebectomy Technique

Microincisions measuring from 1 to 3 mm in length and parallel to the long axis of the extremity are made with an 18- or 16-gauge hypodermic needle or a #11 blade. The microincisions are made vertically and should follow the relaxed skin tension lines. The interval between incisions varies between 3 and 5 cm according to the type of vein being removed. Separation of the vein from the surrounding adventitia may be accomplished by utilizing an iris scissor or blunt probe and should also follow the skin tension lines[66].

The vein is then exteriorized utilizing the phlebectomy hook. Next, the exteriorized vein is clamped proximally and distally and pushed or pulled, depending on operator preference, from each end until the vein is avulsed (Fig. 155.16). A gentle rotation or rolling motion of the clamp in the same and/or opposite direction pulls and frees the vein from its secondary connective tissue sheath. The process is repeated at 3–5 cm intervals along the entire length of the marked vein, until the entire diseased vein has been removed or adequate interruption has been made[70,71].

Special care is required in difficult anatomic zones such as the knees, ankles, and feet. The "hooking" should be gentle and slow. Once the vein is hooked, it should come out easily. If it is difficult and if removal of the vein requires a lot of traction, it is possible that a fascial strand structure

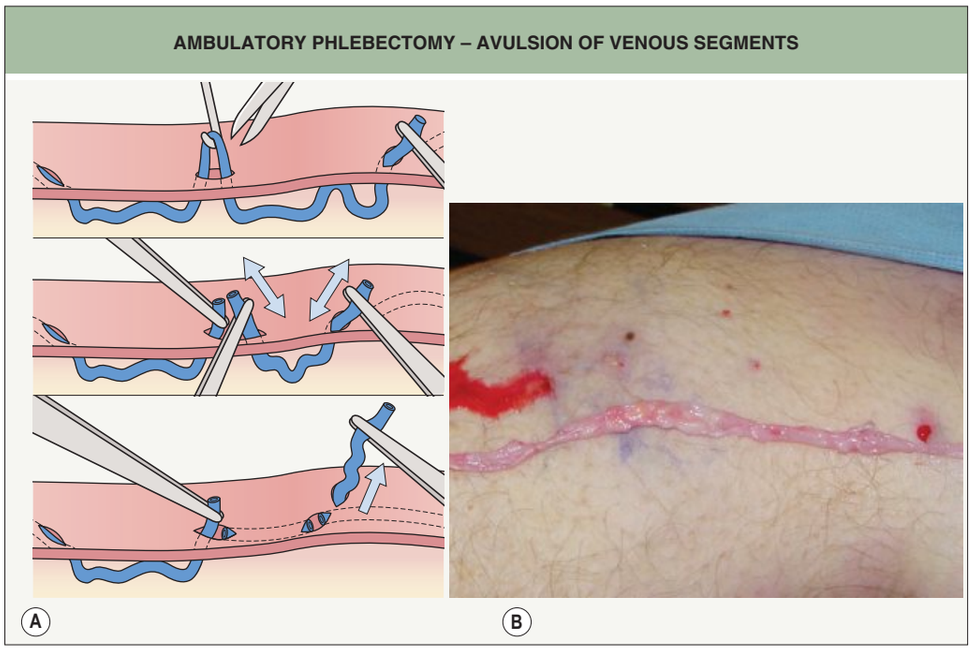


Fig. 155.16 Ambulatory phlebectomy – avulsion of venous segments. A After pinpoint incisions, the dilated vein is hooked at several sites and incised; the venous segments are clamped both proximally and distally and then pulled and rolled to free them from their attachments to the surrounding adventitia. **B** Avulsed segment of the varicose vein next to pinpoint incisions. *A, Redrawn from Ricci S, Georgiev M, Goldman MP. Ambulatory Phlebectomy: A Practical Guide to Stab Avulsion Variectomey, 2nd edn. London: Taylor & Francis, 2005.*

has been hooked. The hook should be removed, reintroduced, and another attempt made. Ambitious "hooking" in the ankle and foot region should be avoided in order to eliminate complications such as swelling, hematoma, and lymphatic and nerve damage. Phlebectomy in the pretibial area should also be performed very carefully because many lymphatic vessels are normally located in this area. Aggressive damage to lymphatic vessels can result in a lymphocele. Phlebectomy in the popliteal area should be particularly gentle since the skin of the back of the knee is very soft and microincisions are very easily enlarged by overzealous "hooking".

Postoperative Considerations for Ambulatory Phlebectomy

Postoperatively, the area is cleansed and antibiotic ointment applied to the puncture sites. The leg is then wrapped, first with cotton gauze and then with an elastic compression dressing extending from the dorsum of the foot to the groin. This dressing helps to promote hemostasis, reduces swelling of the foot and leg, and speeds wound healing. The bandage is removed in 24 hours and a class II (30–40 mmHg) graduated compression stocking is then worn continuously for 1 week (24/7) and after that during waking hours for 2–4 weeks.

Walking while the patient is still in the office is encouraged to help mold the pressure wrap and to uncover any persistent bleeding. This allows the patient to quickly return to a normal gait, thus generating normal function of the calf muscle pump and minimizing potential thromboembolic complications.

Complications of Ambulatory Phlebectomy

Ambulatory phlebectomy satisfactorily removes varicosities of different sizes and results in a series of micro-scars that are cosmetically pleasing to the patient and dermatologic surgeon. The entire procedure can be performed under local tumescent anesthesia on an ambulatory basis[72,73]. Complications may be divided according to the system that has been affected (Table 155.9). The most common complication is the development of a lymphocele, which presents as a firm subcutaneous nodule. Simple aspiration of yellow–clear lymphatic fluid with a 22-gauge needle should be performed every week, with immediate compression over the drained area. Resolution typically occurs after two to three drainage sessions.

COMPLICATIONS OF AMBULATORY PHLEBECTOMY
Anesthetic complications
• Allergic reaction • Purpura at injection site
Vascular complications
• Bleeding, seroma • Superficial thrombophlebitis • Deep venous thrombosis/pulmonary embolus • Telangiectatic matting • Lymphocele • Persistent edema
Neurologic complications
• Nerve damage around the ankle • Hypesthesia (temporary) • Dysesthesia (temporary or permanent) • Traumatic neuroma
Cutaneous complications (other than vascular sequelae)
• Skin necrosis (blistering, ulceration) related to the procedure or compression bandage • Postoperative infection (e.g. cellulitis) • Hypo- or hyperpigmentation of the microincision • Dimpling • Tattooing with marking pen ink • Talc granuloma

Table 155.9 Complications of ambulatory phlebectomy.

TARGETING THE SAPHENOFEMORAL JUNCTION (SFJ)

Whereas saphenofemoral ligation and stripping was previously the only reliable method to address SFJ incompetence, this surgical procedure has gradually been replaced due to the development of a variety of minimally invasive procedures. Foremost amongst these are endovenous laser ablation and endovenous radiofrequency ablation; when compared to conventional surgery, they are equally or more efficacious with lower complication profiles[74]. Additional techniques, e.g. endovenous steam ablation, catheter-directed or ultrasound-guided foam sclerotherapy, mechanochemical endovenous ablation, are also available as are new products, e.g. polidocanol 1% foam (Varithena®), cyanoacrylate adhesive (VenaSeal™ [Medtronic]).

Endovenous Laser Ablation (EVLA)

In endovenous laser ablation (EVLA), the mechanism of action varies depending upon the wavelength of the laser (Table 155.10). Those wavelengths that primarily target tissue water (e.g. 1320 nm Nd:YAG laser) have proven to be superior to those that primarily target hemoglobin (810–1064 nm)[75,76]. Prior to EVLA, the patient is evaluated clinically in both a standing and a supine position and double-marked,

as with ambulatory phlebectomy (see above). Tumescent anesthesia is then delivered along the course of the vein to be treated and may be introduced within the fascial sheath aided by duplex ultrasonography.

A laser fiber with a 600 micron diameter is inserted into the vein (Fig. 155.17A). When the laser is on, a helium–neon (He:Ne) aiming beam is continuously illuminated, helping to ensure that the laser fiber is in the superficial venous system. Correct placement of the laser fiber tip approximately 2 cm distal to the SFJ is confirmed via direct visualization with duplex ultrasonography and secondarily by laser fiber measurement and viewing of the He:Ne aiming beam through the skin. Utilization of an automated catheter drawback system, set at 1 mm/second, provides uniform heating of the vessel (Fig. 155.17B).

Endovenous laser treatment is stopped when the distal tip of the fiber reaches a point 1 to 3 cm from the vein entry site. This can also be confirmed with direct visualization of the aiming beam through the skin or by duplex ultrasonography. Total laser application time is then recorded. Repeat duplex ultrasonography of the saphenous vein is performed to confirm successful treatment. The terminal portion of the vein (immediately adjacent to the point of entry) is thermocoagulated. If the vein had been accessed through phlebectomy, then it is tied with a 3-0 polyglactin 910 suture. If clinically indicated, ambulatory phlebectomy and/or sclerotherapy of tributaries are then performed, either immediately or, more commonly, two months later since most distal varicosities resolve once the refluxing GSV or SSV has been treated.

Endovenous Radiofrequency Closure (Ablation)

An endovenous catheter-based approach is employed in which a specially designed, insulated electrode that is 7 cm in length delivers radiofrequency (RF) energy-induced heat directly to the vein wall (ClosureFast™ catheter [Medtronic]; Fig. 155.18). The endovenous electrode is held in place while energy heats it to a temperature of 120°C. The elevated temperature remains localized to a narrow rim around the active electrode. Proper use of the RF device does require close, stable contact between the active electrode and the vessel wall and the procedure requires tumescent anesthesia to allow contact of the vein wall with the central 7 cm metal core. By strictly controlling the temperature, boiling, vaporization and carbonization of the tissue are avoided. Twenty years of clinical experience suggest that RF endovenous closure, like EVLA, is highly effective at occluding saphenous veins and abolishing reflux. Of note, it is associated with a rapid reduction in lower extremity pain, fatigue, aching, and CEAP clinical class.

General anesthesia is the most significant risk factor for developing DVT and the failure to use tumescent local anesthesia is the major risk factor for developing skin burns. In our clinical practices, tumescent anesthesia is always employed and no skin injuries or thrombi have been observed to date. Some bruising from tumescent anesthesia can occur and anesthesia of the treated portion of the leg may persist for 8 to 24 hours. It is advisable to limit endovenous RF treatment to the GSV segment above the knee to minimize the risk of paresthesias due to injury of the saphenous nerve. Collectively, two of our patients have developed focal numbness (4 cm in diameter) on the lower medial leg, which resolved within 6 months.

ENDOVENOUS LASER ABLATION (EVLA) – MECHANISM OF ACTION		
Wavelength (nm)	**Target**	**Mechanism of action**
810–1064	Hemoglobin	• Heating of blood causes thermal destruction and contraction of the vein wall
1320, 1440, 1550	Water	• Direct targeting of tissue water results in a more controlled, uniform heating of the vein wall • The presence of red blood cells within the vessel is not required

Table 155.10 Endovenous laser ablation (EVLA) – mechanism of action. The mechanism of action of EVLA is dependent on the wavelength of the laser and the subsequent selective target.

Combination with Ambulatory Phlebectomy

Based upon our experience in over 2000 patients, the combination of endovenous ablation techniques with ambulatory phlebectomy can be very effective in eliminating saphenous reflux along with varicose tributaries. Indeed, the two procedures may even provide a synergistic effect as single isolated phlebectomies have shown benefit in reducing GSV incompetence[77]. As outlined above, following double-marking of the varicose veins, the area surrounding the GSV and distal tributaries that are to be treated is infiltrated with tumescent anesthesia. Usually 20 cm inferior to the SFJ (mid medial thigh), the GSV can be accessed through a 2–3 mm incision. The GSV is then treated with the endovenous ablation technique (RF or laser) and the varicose tributaries are removed via standard ambulatory phlebectomy technique. A ligature is placed on the exposed portion of the GSV.

At the conclusion of surgery, the entire leg is wrapped in a short stretch compression bandage over copious padding that has been placed on the sites where the varicose veins were removed via phlebectomy. The tiny incisions are not sutured as these open 2–3 mm incisions allow for drainage of the anesthetic solution over the next 24 hours. This helps to minimize swelling and bruising. The patient is seen the next day, the compression bandage is removed, and the leg is examined

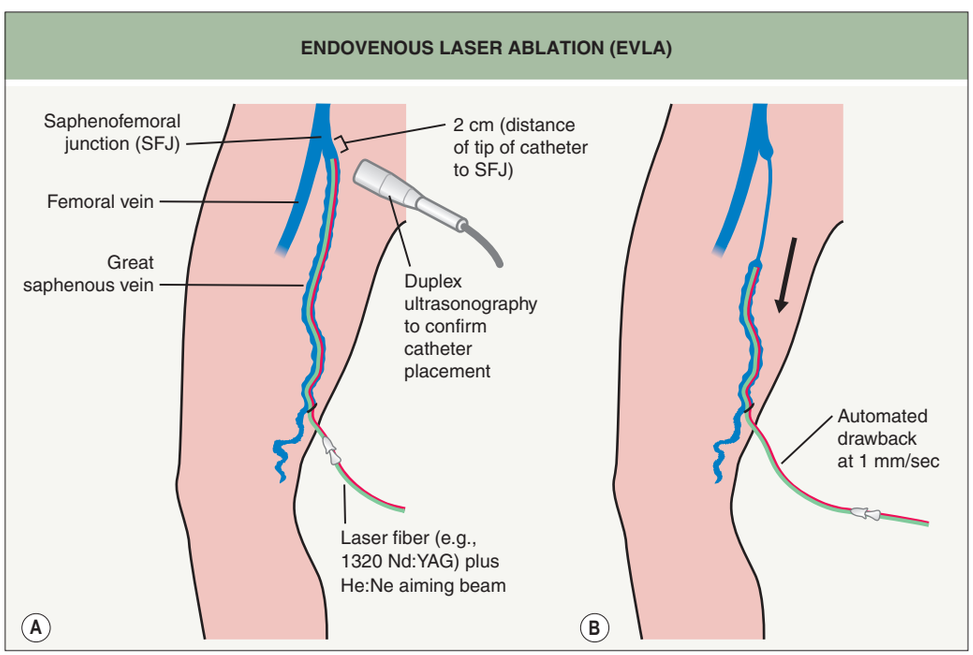


Fig. 155.17 Endovenous laser ablation (EVLA). **A** The laser fiber is inserted into the vein and when the laser is on, a helium–neon (He:Ne) aiming beam is continuously illuminated, helping to ensure that the laser fiber is in the superficial venous system. Correct placement of the laser fiber tip is confirmed via duplex ultrasonography and secondarily by laser fiber measurement and viewing of the He:Ne aiming beam through the skin. **B** Utilization of an automated catheter drawback system provides uniform heating of the vessel.

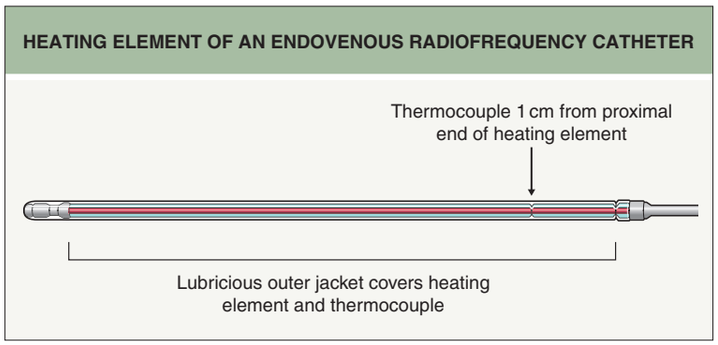


Fig. 155.18 Heating element of an endovenous radiofrequency catheter (ClosureFast™ catheter). After heating to 120°C, 7-cm segments of the varicose vein are treated.

for hematoma formation or other adverse sequelae. All incisions are covered with antibacterial ointment and an adhesive bandage, e.g. BAND-AID®. A class II (30–40 mmHg) graduated compression stocking is applied to the leg. The latter is left on 24 hours a day for 1 week (as compared to 3 days if only RF ablation is performed).

The major complications of endovenous laser or RF treatment plus ambulatory phlebectomy are temporary pigmentation over the treated vein, temporary nerve damage, hematoma, localized superficial thrombophlebitis, and temporary lymphocele. All other adverse effects are extremely rare. For a complete discussion, see reference 78.

Comparative Clinical Trials

Multiple randomized clinical trials have now established the equivalent efficacy of endovenous laser ablation and endovenous RF closure when each is compared to conventional surgery[28,74,79]. The cost effectiveness of these two minimally invasive procedures also appears to be comparable to surgery[80] with superior complication profiles[81]. As a result, endovenous laser and RF ablation have increasingly become first-line therapies[82,83].

Other Endovenous Procedures for the Treatment of Saphenofemoral Junction Incompetence

Ultrasound-guided foam sclerotherapy (UGFS) is a technique whereby the GSV is sclerosed with a foaming agent such as sodium tetradecyl sulfate or polidocanol utilizing ultrasonography for guidance. This procedure can be effective at abolishing SFJ incompetence and improving clinical outcome in patients with venous disease[84–86]. When compared to conventional surgery, UGFS has been equally efficacious in ameliorating reflux, but multiple treatment sessions may be required[74,85]. *Endovenous thermal ablation with steam* is a more recently introduced technique that has been utilized to achieve both radiologic and clinical improvement of SFJ incompetence[87]. Initial reports have suggested that it is not inferior to EVLA[88].

Several novel techniques have been developed for closure of the GSV that do not require tumescent anesthesia. Injection of *polidocanol endovenous microfoam 1%* (Varithena®; see above section for details) has led to improvement in both clinical symptomatology due to SFJ incompetence as well as aesthetic appearance[89]. Similarly, a proprietary *cyanoacrylate adhesive* (VenaSeal™) has been developed for permanent closure of incompetent superficial truncal leg veins and was approved by the FDA in 2015. The adhesive is delivered via a hydrophobic catheter advanced to a point 5 cm below the SFJ. *Mechanochemical endovenous ablation* is a technique that combines a rotating wire and the infusion of liquid sclerosant to simultaneously induce endothelial injury. It is currently undergoing comparative trials with radiofrequency ablation[90].

CONCLUSIONS

Sclerotherapy, ambulatory phlebectomy, and endovenous vein ablation techniques are excellent treatments for both cosmetic and symptomatic venous disease[91]. Although they all require some additional training and knowledge of superficial venous anatomy and physiology, remarkable medical and cosmetic improvements in the sensation and appearance of legs can be achieved. Thus, the dermatologic surgeon now can treat all forms of varicose and telangiectatic leg veins from the largest to the smallest.

Additional figure available in our eBook (see inside front cover for access code).

REFERENCES

1. Goldman MP, Guex JJ, Weiss RA. *Sclerotherapy Treatment of Varicose and Telangiectatic Leg Veins*. 6th ed. London: Elsevier; 2016.
2. Boisseau MR. Venous valves in the legs: hemodynamic and biological problems and relationship to physiopathology. *J Mal Vasc*. 1997;22:122–127.
3. Griton P, Vanet P, Cloarec M. Anatomic and functional features of venous valves. *J Mal Vasc*. 1997;22:97–100.
4. Labropoulos N, Giannoukas AD, Nicolaides AN, et al. The role of venous reflux and calf muscle pump function in nonthrombotic chronic venous insufficiency. Correlation with severity of signs and symptoms. *Arch Surg*. 1996;131:403–406.
5. Labropoulos N, Delis K, Mansour MA, et al. Prevalence and clinical significance of posterolateral thigh perforator vein incompetence. *J Vasc Surg*. 1997;26:743–748.
6. Butie A. Clinical examination of varicose veins. *Dermatol Surg*. 1995;21:52–56.
7. Kistner RL, Eklof B, Masuda EM. Diagnosis of chronic venous disease of the lower extremities: the "CEAP" classification. *Mayo Clin Proc*. 1996;71:338–345.
8. Furderer CR, Marescaux J, Pavis d'Escurac X, Stemmer R. Junctions of the saphenous vein. Anatomy and treatment concepts. *Phlebologie*. 1986;39:3–14.
9. Weiss RA. Evaluation of the venous system by Doppler ultrasound and photoplethysmography or light reflection rheography before sclerotherapy. *Semin Dermatol*. 1993;12:78–87.
10. Weiss RA. Vascular studies of the legs for venous or arterial disease. *Dermatol Clin*. 1994;12:175–190.
11. Weiss RA, Weiss MA. Continuous wave venous Doppler examination for pretreatment diagnosis of varicose and telangiectatic veins. *Dermatol Surg*. 1995;21:58–62.
12. Thibault PK. Duplex examination. *Dermatol Surg*. 1995;21:77–82.
13. Nelson EA, Bell-Syer SE. Compression for preventing recurrence of venous ulcers. *Cochrane Database Syst Rev*. 2012(8):CD002303.
14. O'Meara S, Cullum N, Nelson EA, Dumville JC. Compression for venous leg ulcers. *Cochrane Database Syst Rev*. 2012(11):CD000265.
15. Veraart JC, Neumann H. Interface pressure measurements underneath elastic and non-elastic bandages. *Phlebologie*. 1996;1(Suppl):56–59.
16. Veraart JC, Koster D, Neumann H. Compression therapy and the pressure in the deep venous system. *Phlebologie*. 1996;1(Suppl):68–73.
17. Weiss RA, Sadick NS, Goldman MP, Weiss MA. Post-sclerotherapy compression: controlled comparative study of duration of compression and its effects on clinical outcome. *Dermatol Surg*. 1999;25:105–108.
18. Carlin MC, Ratz JL. Treatment of telangiectasia: comparison of sclerosing agents. *J Dermatol Surg Oncol*. 1987;13:1181–1184.
19. Sadick NS. Advances in sclerosing solutions. *Cosmet Dermatol*. 1996;20:313–316.
20. Sadick NS. Hyperosmolar versus detergent sclerosing agents in sclerotherapy. Effect on distal vessel obliteration. *J Dermatol Surg Oncol*. 1994;20:313–316.
21. Goldman MP. A comparison of sclerosing agents. Clinical and histologic effects of intravascular sodium morrhuate, ethanolamine oleate, hypertonic saline (11.7%), and sclerodex in the dorsal rabbit ear vein. *J Dermatol Surg Oncol*. 1991;17:354–362.
22. Sadick NS. Sclerotherapy of varicose and telangiectatic leg veins. Minimal sclerosant concentration of hypertonic saline and its relationship to vessel diameter. *J Dermatol Surg Oncol*. 1991;17:65–70.
23. Weiss RA, Goldman MP. Advances in sclerotherapy. *Dermatol Clin*. 1995;13:431–445.
24. Sadick NS. Treatment of varicose and telangiectatic leg veins with hypertonic saline: a comparative study of heparin and saline. *J Dermatol Surg Oncol*. 1990;16:24–28.
25. Sadick NS, Farber B. A microbiologic study of diluted sclerotherapy solutions. *J Dermatol Surg Oncol*. 1993;19:450–454.
26. Leach BC, Goldman MP. Comparative trial between sodium tetradecyl sulfate and glycerin in the treatment of telangiectatic leg veins. *Dermatol Surg*. 2003;29:612–614, discussion 615.
27. Weiss MA, Weiss RA, Goldman MP. Sclerotherapy: how minor varicosities cause leg pain. *Contemp Ob Gyn*. 1991;36:113–125.
28. Brittenden J, Cooper D, Dimitrova M, et al. Five-year outcomes of a randomized trial of treatments for varicose veins. N Eng. *J Med*. 2019;381:912–922.
29. Weiss MA, Weiss RA. Sclerotherapy. *Curr Opin Dermatol*. 1997;4:167–174.
30. Goldman MP, Weiss RA, Bergan JJ. Diagnosis and treatment of varicose veins: a review. *J Am Acad Dermatol*. 1994;31:393–413, quiz 414–16.
31. Goldman MP, Bennett RG. Treatment of telangiectasia: a review. *J Am Acad Dermatol*. 1987;17:167–182.
32. Baccaglini H, Spreafico G, Castro C, Sorrentino P. Consensus conference on sclerotherapy of varicose veins of the lower limbs. *Phlebologie*. 1997;12:2–16.
33. Guex JJ. Microsclerotherapy. *Semin Dermatol*. 1993;12:129–134.
34. Duffy DM. Sclerotherapy. *Clin Dermatol*. 1992;10:373–380.
35. Bodian EL. Techniques of sclerotherapy for sunburst venous blemishes. *J Dermatol Surg Oncol*. 1985;11:696–704.
36. Duffy DM. Small vessel sclerotherapy: an overview. *Adv Dermatol*. 1988;3:221–242.

37. Goldman MP. Advances in sclerotherapy treatment of varicose and telangiectatic leg vein. *Am J Cosmet Surg*. 1992;9:235–240.
38. Zummo M, Forrestal M. Sclerotherapy of the long saphenous vein – a prospective duplex controlled comparative study. *Phlebologie*. 1995;1(Suppl):571–573.
39. Baccaglini U, Spreafico G, Castoro C, Sorrentino P. Sclerotherapy of varicose veins of the lower limbs. Consensus paper. North American Society of Phlebology. *Dermatol Surg*. 1996;22:883–889.
40. Cornu-Thenard A, de Cottreau H, Weiss RA. Sclerotherapy. Continuous wave Doppler-guided injections. *Dermatol Surg*. 1995;21:867–870.
41. de Groot WP. Practical phlebology. Sclerotherapy of large veins. *J Dermatol Surg Oncol*. 1991;17:589–595.
42. Gallagher PG. Varicose veins–primary treatment with sclerotherapy. A personal appraisal. *J Dermatol Surg Oncol*. 1992;18:39–42.
43. Marley WM, Marley NF. Sclerotherapy treatment of varicose veins. *Semin Dermatol*. 1993;12:98–101.
44. Orbach EJ. Sclerotherapy of varicose veins. Utilization of intravenous air-block technique. *Am J Surg*. 1944;66:362–366.
45. Barrett JM, Allen B, Ockelford A, Goldman MP. Microfoam ultrasound-guided sclerotherapy of varicose veins in 100 legs. *Dermatol Surg*. 2004;30:6–12.
46. Raymond-Martimbeau P. Advanced sclerotherapy treatment of varicose veins with duplex ultrasonographic guidance. *Semin Dermatol*. 1993;12:123–128.
47. Leibaschoff G, Brizzio E, Ferreira J, Banf J. Prevention of iatrogenic complications in the treatment of varicosities. *Am J Cosmet Surg*. 1994;11:51–53.
48. Georgiev M. Postsclerotherapy hyperpigmentations: a one-year follow-up. *J Dermatol Surg Oncol*. 1990;16:608–610.
49. Georgiev M. Postsclerotherapy hyperpigmentations. Chromated glycerin as a screen for patients at risk (a retrospective study). *J Dermatol Surg Oncol*. 1993;19:649–652.
50. Thibault P, Wlodarczyk J. Postsclerotherapy hyperpigmentation. The role of serum ferritin levels and the effectiveness of treatment with the copper vapor laser. *J Dermatol Surg Oncol*. 1992;18:47–52.
51. Goldman MP. Postsclerotherapy hyperpigmentation. Treatment with a flashlamp-excited pulsed dye laser. *J Dermatol Surg Oncol*. 1992;18:417–422.
52. Goldman MP, Kaplan RP, Duffy DM. Postsclerotherapy hyperpigmentation: a histologic evaluation. *J Dermatol Surg Oncol*. 1987;13:547–550.
53. Scott C, Seiger E. Postsclerotherapy pigmentation. Is serum ferritin level an accurate indicator? *Dermatol Surg*. 1997;23:281–282. discussion 283.
54. Tafazzoli A, Rostan EF, Goldman MP. Q-switched ruby laser treatment for postsclerotherapy hyperpigmentation. *Dermatol Surg*. 2000;26:653–656.
55. Goldman MP, Sadick NS, Weiss RA. Cutaneous necrosis, telangiectatic matting, and hyperpigmentation following sclerotherapy. Etiology, prevention, and treatment. *Dermatol Surg*. 1995;21:19–29, quiz 31–2.
56. Davis LT, Duffy DM. Determination of incidence and risk factors for postsclerotherapy telangiectatic matting of the lower extremity: a retrospective analysis. *J Dermatol Surg Oncol*. 1990;16:327–330.
57. Zimmet SE. The prevention of cutaneous necrosis following extravasation of hypertonic saline and sodium tetradecyl sulfate. *J Dermatol Surg Oncol*. 1993;19:641–646.
58. Zimmet SE. Hyaluronidase in the prevention of sclerotherapy-induced extravasation necrosis. A dose-response study. *Dermatol Surg*. 1996;22:73–76.
59. Weiss RA, Weiss MA. Incidence of side effects in the treatment of telangiectasias by compression sclerotherapy: hypertonic saline vs. polidocanol. *J Dermatol Surg Oncol*. 1990;16:800–804.
60. Biegeleisen K, Neilsen RD, O'Shaughnessy A. Inadvertent intra-arterial injection complicating ordinary and ultrasound-guided sclerotherapy. *J Dermatol Surg Oncol*. 1993;19:953–958.
61. Thibault PK, Wlodarczyk J. Correlation of serum ferritin levels and postsclerotherapy pigmentation. A prospective study. *J Dermatol Surg Oncol*. 1994;20:684–686.
62. Goldman MP, Georgiev M, Ricci S. *Ambulatory Phlebectomy: A Practical Guide for Treating Varicose Veins*. 2nd ed. New York: Taylor & Francis; 2005.
63. Garde C. Cryosurgery of varicose veins. *J Dermatol Surg Oncol*. 1994;20:56–58.
64. Georgiev M, Ricci S, Carbone D, et al. Stab avulsion of the short saphenous vein. Technique and duplex evaluation. *J Dermatol Surg Oncol*. 1993;19:456–464.
65. Neumann HA. Ambulant minisurgical phlebectomy. *J Dermatol Surg Oncol*. 1992;18:53–54.
66. Weiss RA, Goldman MP. Transillumination mapping prior to ambulatory phlebectomy. *Dermatol Surg*. 1998;24:447–450.
67. Olivencia JA. Maneuver to facilitate ambulatory phlebectomy. *Dermatol Surg*. 1996;22:654–655.
68. Smith SR, Goldman MP. Tumescent anesthesia in ambulatory phlebectomy. *Dermatol Surg*. 1998;24:453–456.
69. Ramelet AA. Muller phlebectomy. A new phlebectomy hook. *J Dermatol Surg Oncol*. 1991;17:814–816.
70. Sadick NS, Schanzer H. Combined high ligation and stab avulsion for varicose veins in an outpatient setting. *Dermatol Surg*. 1998;24:475–479.
71. Sadick NS. Multifocal pull-through endovascular cannulation technique of ambulatory phlebectomy. *Dermatol Surg*. 2002;28:32–37.
72. Ramelet AA. Complications of ambulatory phlebectomy. *Dermatol Surg*. 1997;23:947–954.
73. Olivencia JA. Complications of ambulatory phlebectomy. Review of 1000 consecutive cases. *Dermatol Surg*. 1997;23:51–54.
74. Nesbitt C, Bedenis R, Bhattacharya V, Stansby G. Endovenous ablation (radiofrequency and laser) and foam sclerotherapy versus open surgery for great saphenous vein varices. *Cochrane Database Syst Rev*. 2014(7):CD005624.
75. Goldman MP, Mauricio M, Rao J. Intravascular 1320-nm laser closure of the great saphenous vein: a 6- to 12-month follow-up study. *Dermatol Surg*. 2004;30:1380–1385.
76. Weiss RA, Munavalli G, Bellew SG, Beasley K. Comparison of endovenous saphenous vein obliteration techniques: 810 nm versus 1320 nm versus radiofrequency. *Lasers Surg Med*. 2005;S17:34.
77. Pittaluga P, Chastanet S, Locret T, Barbe R. The effect of isolated phlebectomy on reflux and diameter of the great saphenous vein: a prospective study. *Eur J Vasc Endovasc Surg*. 2010;40:122–128.
78. Goldman MP, Weiss RA. Ambulatory phlebectomy and endolumenal closure of varicose veins. In: Robinson JK, Hanke CW, Siegel DM, Fratila A, eds. *Surgery of the Skin: Procedural Dermatology*. 2nd ed. Philadelphia: Elsevier Mosby; 2010:589–600.
79. Rasmussen LH, Lawaetz M, Bjoern L, et al. Randomized clinical trial comparing endovenous laser ablation, radiofrequency ablation, foam sclerotherapy and surgical stripping for great saphenous varicose veins. *Br J Surg*. 2011;98:1079–1087.
80. Carroll C, Hummel S, Leaviss J, et al. Clinical effectiveness and cost-effectiveness of minimally invasive techniques to manage varicose veins: a systematic review and economic evaluation. *Health Technol Assess*. 2013;17: i–xvi, 1–141.
81. Dzieciuchowicz L, Espinosa G, Paramo JA. Haemostatic activation and inflammatory response after three methods of treatment of great saphenous vein incompetence. *Phlebology*. 2014;29:154–163.
82. Wallace T, El-Sheikha J, Nandhra S, et al. Long-term outcomes of endovenous laser ablation and conventional surgery for great saphenous varicose veins. *Br J Surg*. 2018;105:1759–1767.
83. Hwang JH, Park SW, Chang IS, et al. Endovenous thermal ablation of recurrent varicose veins due to residual great saphenous venous insufficiency after saphenous venous surgery: a comparative study. *Dermatol Surg*. 2018;44:1287–1294.
84. Chen CH, Chiu CS, Yang CH. Ultrasound-guided foam sclerotherapy for treating incompetent great saphenous veins – results of 5 years of analysis and morphologic evolvement study. *Dermatol Surg*. 2012;38:851–857.
85. Shadid N, Ceulen R, Nelemans P, et al. Randomized clinical trial of ultrasound-guided foam sclerotherapy versus surgery for the incompetent great saphenous vein. *Br J Surg*. 2012;99:1062–1070.
86. dos Santos JB, Junior WC, Porta RMP, et al. Catheter-directed foam sclerotherapy with tumescence of the great saphenous vein versus ultrasound-guided foam sclerotherapy: A randomized controlled trial. *Phlebology*. 2020;35:84–91.
87. Mlosek RK, Wozniak W, Gruszecki L, Stapa RZ. The use of a novel method of endovenous steam ablation in treatment of great saphenous vein insufficiency: own experiences. *Phlebology*. 2014;29:58–65.
88. van den Bos RR, Malskat WS, De Maeseneer MG, et al. Randomized clinical trial of endovenous laser ablation versus steam ablation (LAST trial) for great saphenous varicose veins. *Br J Surg*. 2014;101:1077–1083.
89. Todd 3rd KL, Wright D. VANISH-2 Investigator Group. The VANISH-2 study: a randomized, blinded, multicenter study to evaluate the efficacy and safety of polidocanol endovenous microfoam 0.5% and 1.0% compared with placebo for the treatment of saphenofemoral junction incompetence. *Phlebology*. 2014;29:608–618.
90. van Eekeren RR, Boersma D, Holewijn S, et al. Mechanochemical endovenous Ablation versus RADiOfrequeNcy Ablation in the treatment of primary great saphenous vein incompetence (MARADONA): study protocol for a randomized controlled trial. *Trials*. 2014;15:121.
91. Alam M, Nguyen T. *Treatment of Leg Veins*. Philadelphia: Saunders; 2006.



eFig. 155.1 Macular brown discoloration overlying veins that have been injected with hypertonic saline. *Courtesy Jean L. Bolognia, MD.*

Body Contouring: Liposuction and Non-invasive Modalities

156

Kyle M. Coleman and William P. Coleman III

Chapter Contents

Consultation 2667
Liposuction 2667
Liposuction Instrumentation 2671
Liposuction Variations 2672
Non-Cosmetic Liposuction 2672
Postoperative Care 2673
Complications of Liposuction. 2673
Non-invasive Body Contouring. 2673
Cellulite 2675

Synonyms: ■ Liposculpture ■ Tumescent liposuction ■ Lipoplasty ■ Lipolysis

Key features

- Liposuction is indicated for spot reduction of localized adiposities
- Liposuction is ideally suited for healthy patients who are near their ideal body weight
- The tumescent local anesthetic technique is the safest approach to anesthesia for liposuction
- Non-invasive technologies offer the benefits of less downtime compared to liposuction
- Careful selection of the appropriate treatment for each patient is necessary to achieve the best results

INTRODUCTION AND BACKGROUND

Liposuction is an effective method for surgically improving localized areas of excess subcutaneous fat. Liposuction has undergone many changes since initial reports in the late 1970s[1–3]. Modern liposuction is performed using dilute local anesthesia, via the tumescent technique, together with small cannulas connected to a vacuum aspirator. When performed correctly using the tumescent techniques, liposuction can be safely performed in an office setting with very few complications. Substantial amounts of fat can be aspirated with minimal blood loss and excellent aesthetic results. Patient selection remains paramount in achieving good results.

Liposuction is currently among the most common invasive cosmetic procedures performed in the US. However, recent survey data have shown a decrease in the number of liposuctions being performed. This is likely due to the increased availability of non-invasive technologies that are currently approved by the FDA for the treatment of localized adiposity. These technologies generally have fewer side effects than tumescent liposuction but deliver more modest results. When choosing between liposuction and non-invasive treatments, it is important that patients have realistic expectations.

CONSULTATION

As with any other medical or surgical consultation, a pertinent review of past medical history, medications, and allergies is essential. The review of systems should be comprehensive enough to exclude any underlying abnormalities which would preclude or modify treatments[4]. Social and psychiatric histories may reveal details which would make the patient an inappropriate candidate for cosmetic treatments.

The physical examination for body contouring should be performed with the patient completely unclothed in the body areas of concern to them. The patient should be examined standing up so that the full effects of gravity are apparent. Physical examination consists of both observation and palpation to reveal the thickness and firmness of underlying fatty tissue. The physician should look for asymmetries, scars, hernias, musculoskeletal abnormalities, dimples, skin laxity, and overlying cutaneous lesions. During this examination, it is important to point out any of these features that may affect results. This will add to the patient's understanding about what may or may not be able to be achieved through body contouring procedures. It is important to accurately describe individual body parts in words that the patient will understand. A diagram of typical anatomic sites may prove helpful (see Fig. 156.6). Also, it is important to remember that patients have a different vantage point; photography and/or full-length mirrors may be helpful during the consultation to ensure their understanding.

A frank discussion about the patient's goals should also be had; many patients have unrealistic expectations with regard to body contouring procedures. Patients should also appreciate the pros and cons of the currently available options for body contouring. Patients undergoing non-invasive treatments must understand that results are inferior to tumescent liposuction and that multiple treatments will likely be required. Patients undergoing liposuction procedures must recognize the surgical risks as well as the need for external compression garments.

The presence of obesity and/or poor muscle tone are warning signs that the patient may not be an appropriate candidate. Generally, obese patients do not make good candidates for body contouring procedures. These patients may have underlying disorders that place them at higher procedural risk; also, due to their excess weight, these procedures will often create minimal, if any, improvement.

Occasionally, patients, mostly male, present with a large amount of visceral fat. Palpation of the abdominal tissues reveals a firm underlying musculature with very little fat on the pinch test. These patients are not only poor candidates for body contouring procedures but are also at increased risk for cardiovascular disease. It is important to recommend consultation with a primary care physician and appropriate nutritional experts.

LIPOSUCTION

Indications and Contraindications

Tumescent liposuction is indicated for improving localized adiposities. Certain areas of subcutaneous fat are often not fully responsive to diet and exercise alone, and there are no exercises capable of spot reduction of adiposity.

Most liposuction patients complain that the troublesome areas of fat excess "run in the family". Furthermore, areas of excess subcutaneous fat can be resistant to caloric restriction or exercise. Tumescent liposuction is able to specifically target these localized areas of excess subcutaneous fat as a complement to, not a replacement for, diet and exercise.

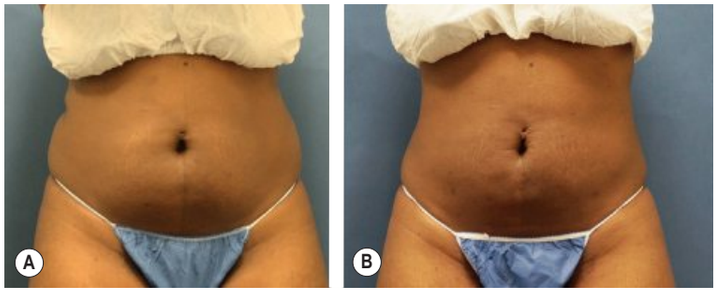


Fig. 156.1 Liposuction of the upper and lower abdomen. A Preoperative. **B** Postoperative, showing improved contours. *Courtesy K.M. Coleman, MD.*

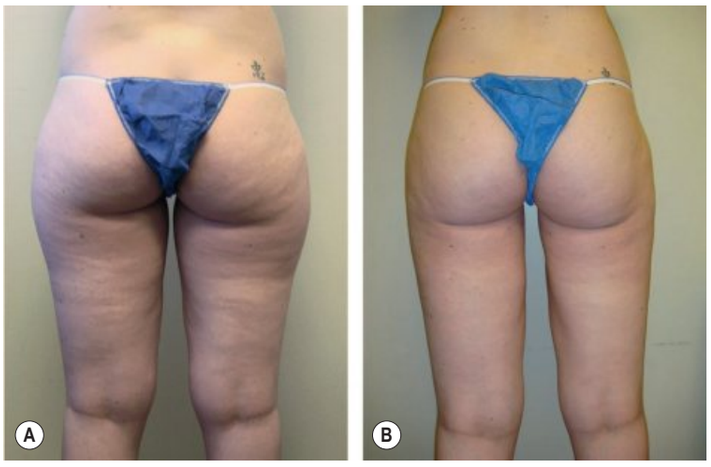


Fig. 156.2 Liposuction of the inner and outer thighs and hips. A Preoperative. **B** Postoperative, showing improved contours. *Courtesy K.M. Coleman, MD.*

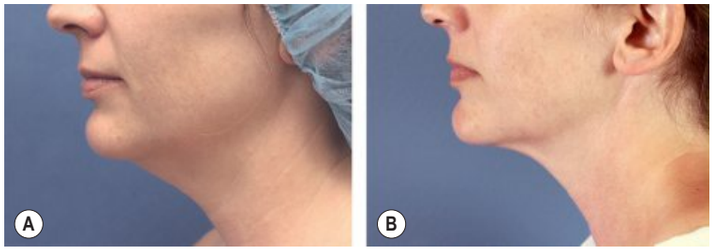


Fig. 156.3 Liposuction of the neck and jowls. A Preoperative. **B** Postoperative, showing improved appearance. *Courtesy K.M. Coleman, MD.*

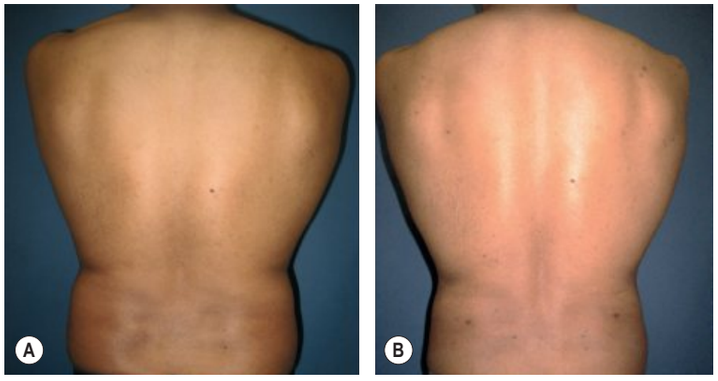


Fig. 156.4 Liposuction of male flanks. A Preoperative. **B** Postoperative, showing the improvement. *Courtesy K.M. Coleman, MD.*

Liposuction can be used to treat localized areas of adiposities throughout the body. Common areas improved by liposuction include the abdomen (Fig. 156.1) and inner and outer thighs (Fig. 156.2). Other sites include the neck and jowls (Fig. 156.3), male and female breasts, back, flanks (Fig. 156.4), hips (Fig. 156.2), buttocks, upper arms, knees (Fig. 156.5), calves, and ankles (Fig. 156.6). Genetic predisposition determines the location of excess fat storage in each individual.

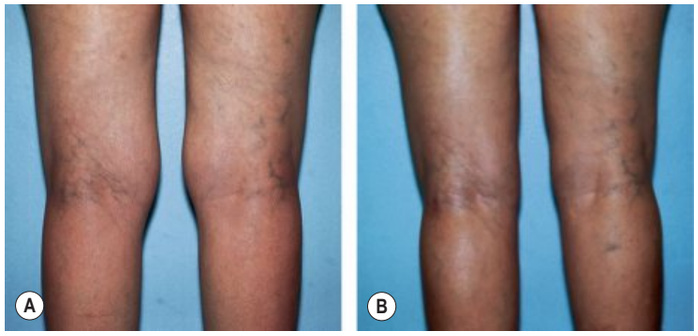


Fig. 156.5 Liposuction of the medial knees. A Preoperative. **B** Postoperative, showing more even contours. *Courtesy W.P. Coleman III, MD.*

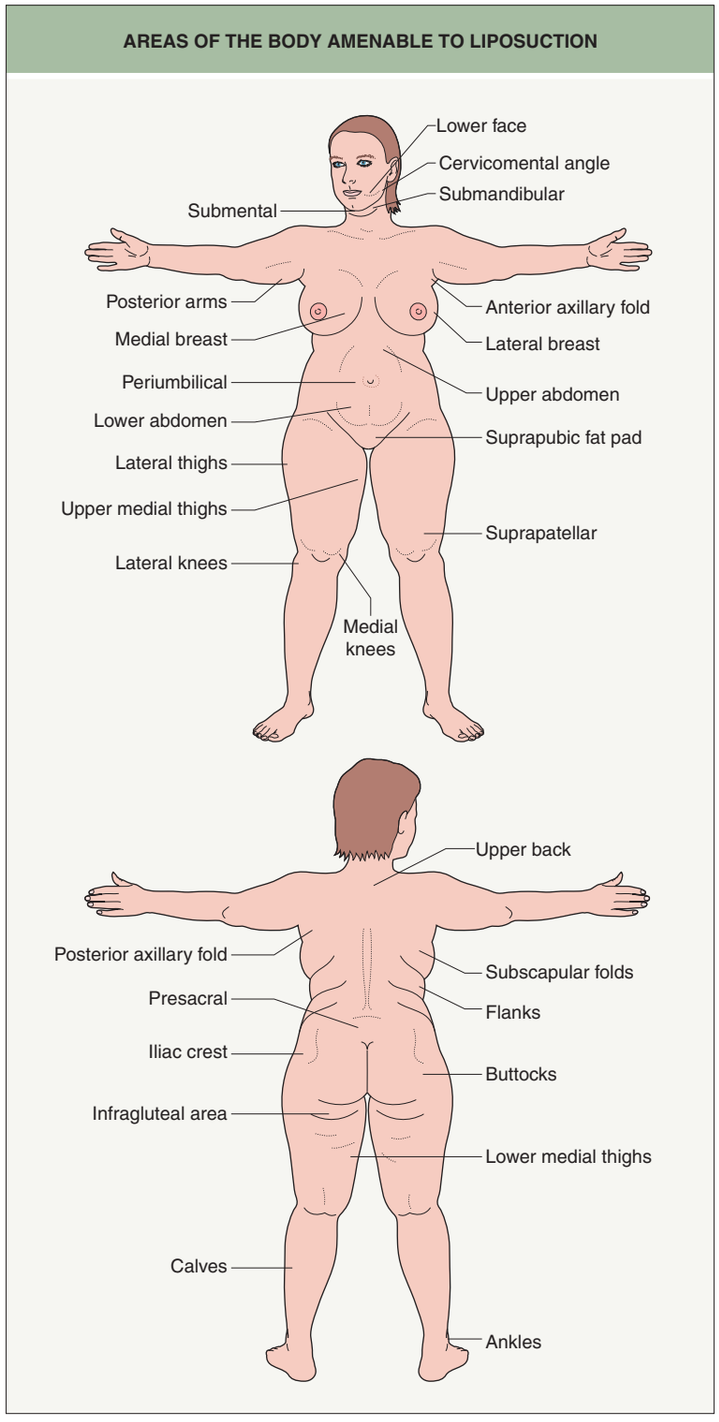


Fig. 156.6 Areas of the body amenable to liposuction.

NON-COSMETIC INDICATIONS FOR LIPOSUCTION
Lipomas
Familial multiple lipomatosis
Adiposis dolorosa (Dercum disease)
Gynecomastia
Pseudogynecomastia
Insulin-induced lipohypertrophy
"Buffalo hump" due to Cushing syndrome
Lipodystrophy in HIV-infected patients
Axillary hyperhidrosis (Fig. 156.7)
Flap undermining
Lymphedema following axillary lymphadenectomy

Table 156.1 Non-cosmetic indications for liposuction. ART, antiretroviral therapy.



Fig. 156.7 Superficial liposuction of the axilla is performed for improvement of hyperhidrosis. *Courtesy W.P. Coleman III, MD.*

In general, operating on over 10% of the body increases liposuction risks. Guidelines of care published by dermatologic organizations recommend fat extractions of less than 4500–5000 ml[5,6]. This volume should be considered as an uppermost limit; beyond this, profound fluid shifts may occur, resulting in cardiovascular compromise. Many experienced liposuction surgeons rarely, if ever, remove anywhere near 5000 ml in a single session. Larger extractions also necessitate larger infiltrations of local anesthetics. When the tumescent technique is employed, guidelines of care recommend not exceeding a lidocaine dose of 55 mg/kg[7–10]. In slender patients, this should probably be adjusted down to 45 mg/kg. These dose limits also restrict the number of areas that can be treated during a single liposuction procedure.

If, in the physician's judgment, it is risky to treat all of the areas that concern the patient, serial liposuction should be recommended. These separate surgeries can be spaced days or months apart, according to the patient's preference.

Non-cosmetic indications for liposuction include pseudogynecomastia and aspiration of lipomas[11–13] (Table 156.1). Liposuction can be effective for debulking larger tumors with a minimal scar. It can also be used as an alternative for treating axillary hyperhidrosis by destroying eccrine and apocrine glands (Fig. 156.7)[13].

Contraindications are outlined in Table 156.2.

The Preoperative Visit

A carefully planned preoperative visit is usually scheduled two or more weeks prior to the actual date of the surgery. Generally, a complete blood count and a complete metabolic profile are obtained; a prothrombin time and partial thromboplastin time may be indicated based on history. Some physicians also perform a urinalysis and tests for infectious diseases such as viral hepatitis and HIV.

Detailed pre- and postoperative instructions should be provided to the patient during this visit. Preoperative instructions should include a list of over-the-counter medications that should be avoided. Aspirin, non-steroidal anti-inflammatory drugs (e.g. ibuprofen), vitamin E, fish oil, and alcohol are common anticoagulants that patients should carefully avoid preoperatively. Herbal remedies may also have anticoagulant activity and should be avoided for 2 weeks preoperatively.

CONTRAINDICATIONS TO TUMESCENT LIPOSUCTION
Absolute
Severe obesity
Individuals seeking liposuction as a weight-loss procedure
Body dysmorphic syndrome
Untreated psychiatric illness
Excessive scarring in the areas to be improved
Hernia in area of proposed treatment
Relative
Moderate obesity
Poor wound healing (including Ehlers–Danlos syndrome)
Hypertrophic or keloidal scarring
Coagulation or bleeding disorders
Allergy to lidocaine
Adverse reaction to epinephrine (e.g. tachycardia)
Significant medical illnesses
Unstable psychiatric illnesses
Hernia in area of proposed treatment

Table 156.2 Contraindications to tumescent liposuction.

Drugs that affect the hepatic cytochrome P450 system should be discontinued if possible (see later). In addition, patients should be counseled about proper nutrition. Trying to lose weight rapidly or eating excessively should both be discouraged. Some patients benefit from nutritional counseling on a pre- and postoperative basis.

Description of Techniques

Tumescent anesthesia

The technique of using tumescent local anesthesia for liposuction was developed by the dermatologist Dr Jeffrey Klein. In 1987, Klein published his technique for the infiltration of a dilute solution of lidocaine with epinephrine (adrenaline) into fat, allowing for liposuction to be performed under local anesthesia[7]. Due to significantly reduced bleeding, the previous common complications of seroma and hematoma became uncommon[14]. Bruising was also minimized. The procedure has proven to be remarkably safe.

Klein demonstrated that dilute concentrations of lidocaine with epinephrine are not absorbed into the circulation to the same degree as higher 1%–2% concentrations of lidocaine, even when the total doses are equal. He confirmed that using only dilute solutions of lidocaine with epinephrine safely allowed lidocaine dosages of up to 35 mg/kg body weight[8]. This advance allowed larger amounts of fat to be removed with only local anesthesia.

A typical tumescent anesthetic formulation is shown in Table 156.3. Dilute solutions of lidocaine with epinephrine provide safe local anesthesia with excellent vasoconstriction. Sodium bicarbonate is added to adjust the solution to a more physiologic pH. The combination of a dilute solution of lidocaine with the vasoconstrictive effect of epinephrine ensures minimal systemic absorption of lidocaine[15].

The tumescent technique provides a number of advantages (Table 156.4). Local anesthesia persists for up to 24 hours after tumescent liposuction, reducing the need for postoperative analgesia[16]. The extensive vasoconstriction produced by dilute epinephrine reduces the volume of whole blood for each liter of pure fat removed by liposuction to less than 12 ml[14,16]. With rapid postoperative recovery, patients can return to their normal lives quickly. Improved aesthetic results are also seen with tumescent liposuction because smaller cannulas can be used, reducing irregularities of the skin[17].

An important advantage is the decrease in anesthetic risk observed with tumescent anesthesia for liposuction, as compared to intravenous or general anesthesia[18–21]. Systemic anesthesia can be associated with a significant risk of serious complications[22]. More recent research has indicated that the maximum safe dosage of lidocaine, when used with the tumescent technique for liposuction, is 55 mg/kg[9,10]. Klein recommends an upper limit of 45 mg/kg for thinner individuals[17].

Fresh tumescent anesthetic solution must be correctly and carefully prepared in a sterile fashion prior to each procedure by a trained healthcare professional. Standardization is important in order to avoid confusion and limit risk. The concentration of lidocaine or epinephrine can be varied depending on the anatomic site. The standard formula of

TYPICAL TUMESCENT ANESTHETIC FORMULATION (LIDOCAINE 0.05%, EPINEPHRINE 1 : 1 000 000)
50 ml 1% plain lidocaine (500 mg)
1 ml 1 : 1000 epinephrine from ampule (1 mg)
10 ml sodium bicarbonate (8.4% $NaHCO_3$ solution)
1 liter normal saline (0.9% NaCl solution)

Table 156.3 Typical tumescent anesthetic formulation (lidocaine 0.05%, epinephrine 1 : 1 000 000).

ADVANTAGES OF TUMESCENT LIPOSUCTION
Complete regional anesthesia without the need for nerve blocks
Local anesthesia persists for up to 24 hours, reducing the need for postoperative analgesia
Minimizes blood loss
Minimal postoperative ecchymoses
Rapid postoperative recovery
Smaller cannulas can be used, reducing skin irregularities
Decreased anesthetic risk compared to intravenous or general anesthesia

Table 156.4 Advantages of tumescent liposuction.

0.05% lidocaine with 1 : 1 000 000 epinephrine plus sodium bicarbonate works well for most sites (see Table 156.3). Occasionally, fibrous areas such as the periumbilical area or breast require a higher concentration of lidocaine, up to 0.1%.

Proper infiltration of tumescent anesthesia is important. The skin is prepped with an antimicrobial scrub. Insertion sites for the infiltration needles are anesthetized with small wheals of 1% lidocaine with epinephrine. The prepared tumescent anesthetic bags are suspended from an intravenous pole. Infiltration tubing is connected to the anesthetic bags and then passed through a peristaltic pump. Air is expressed from the infiltration tubing and a small-gauge, blunt-tipped infiltrating cannula or spinal needle is connected. Warming the anesthetic solution to body temperature prior to infiltration may reduce the pain of infiltration.

The anesthetic fluid may initially be infiltrated into the subcutaneous fat using 20-gauge spinal needles. More extensive infiltration is then performed using a blunt-tipped 16- to 18-gauge infiltrating cannula (Fig. 156.8). These small-diameter infiltration cannulas can be passed through tiny incisions created in the skin with a #15c or #11 blade or a 1–2 mm punch. A peristaltic pump facilitates infiltration of the anesthetic fluid into the subcutaneous fat compartment. The cannula must be repositioned to ensure an even distribution of the tumescent anesthetic. Needle movement is associated with increased pain; consequently, a gentle, slow infiltration technique is preferred. In certain areas with more sensitivity, infiltration must be done even more slowly. An infiltration speed of 100 ml/min is usually well tolerated.

Once sufficient tumescent anesthetic has been infiltrated, the surgeon should wait at least 15 minutes to allow for maximal vasoconstrictive effect of the epinephrine. An overlying blanching of the skin will gradually appear. The patient is then properly "tumesced" and ready for aspiration of adipose tissue. Allowing up to an hour between conclusion of infiltration and the onset of suctioning may result in fat removal with even less infranate.

Drug interactions must be considered when using any form of anesthesia[23]. Caution must be exercised with patients on β-blockers, especially non-selective ones. Although rapid absorption of epinephrine may result in hypertension and bradycardia in these patients, when the epinephrine is absorbed slowly, as in the case of tumescent anesthesia, there is minimal risk.

Tumescent anesthesia and certain sedatives may have significant interactions[23]. Some sedatives (such as diazepam) can reduce the rate of lidocaine metabolism after liposuction. Lidocaine is rapidly eliminated by hepatic metabolism, but a number of drugs can inhibit lidocaine metabolism, possibly leading to an increase in lidocaine toxicity[17]. Examples of such drugs are provided in Table 156.5. These medications should be avoided or discontinued prior to liposuction, or the total dose of lidocaine should be reduced.

Surgeons performing tumescent anesthesia should understand the symptoms of lidocaine toxicity and potential treatments (see Ch. 143).



Fig. 156.8 Infiltration of tumescent anesthetic into the previously marked patient. Concentric circles denote areas of increased fat. Sterile towels are positioned to absorb leaking fluid. *Courtesy W.P. Coleman III, MD.*

EXAMPLES OF POSSIBLE DRUG INTERACTIONS WITH LIDOCAINE	
Drug	**Comments**
Anesthetics	
• Bupivacaine	Lidocaine is displaced from plasma binding proteins by bupivacaine
• Halothane plus nitrous oxide	Increase in lidocaine plasma concentration (lowers maximum safe dose)
Amiodarone	Sinus bradycardia, seizures; competes with lidocaine for binding to CYP3A4
Tramadol	Lowers seizure threshold
Phenytoin	Additive cardiac depressant effects
Benzodiazepines, e.g. alprazolam, diazepam	Inhibit lidocaine metabolism
Azole and triazole antifungals, e.g. ketoconazole, itraconazole, fluconazole	Inhibit lidocaine metabolism

Table 156.5 Examples of possible drug interactions with lidocaine. *Adapted from Klein JA. Lidocaine toxicity and drug interactions. In: Tumescent Technique. Tumescent Anesthesia and Microcannular Liposuction. St. Louis: Mosby; 2000.*

Because bupivacaine cardiac toxicity can be subtle, is not preceded by convulsions, and is often unresponsive to resuscitation efforts, bupivacaine is contraindicated for liposuction[24]. In contrast, lidocaine usually gives warning signs of CNS toxicity long before the onset of dangerous cardiotoxic effects. Prilocaine has been used in Europe for tumescent anesthesia instead of lidocaine[25]. However, rigorous comparative studies have not been performed; and, in the US, prilocaine does not have Food and Drug Administration (FDA) approval to be marketed for local anesthesia for dermatologic surgical procedures. Prilocaine can also produce methemoglobinemia[25].

Liposuction surgical technique

The patient is taken to the preoperative area, where he or she changes into surgical garments. Vital signs including blood pressure and heart rate are obtained. Photographs from multiple views should then be taken if they have not been done preoperatively. Areas should be completely unclothed so as not to distort the surgical site(s).

Next, the surgeon marks the patient, who is standing to allow for the effects of gravity. Marking can be done according to the custom of the surgeon, but should be devised so that the subsequent distortion by local anesthetic infiltration will not obscure the various thicknesses of the adiposity. One way to mark is to use concentric circles, as in a topographic map (see Fig. 156.8). Existing dimples and dents should also be outlined for later identification during surgery so that they can be avoided.

The previously marked patient is then positioned on the surgical table. If significant sedation is to be employed, intravenous lines and monitoring devices such as pulse oximeters and cardiac monitors can be utilized. While patients undergoing the tumescent technique usually require very little ancillary sedation, most patients do appreciate pre-sedation with mild oral sedatives such as lorazepam. Those who are pain-sensitive can receive minor additional sedation such as 25 mg of meperidine intramuscularly, a dose which does not impair protective reflexes.

Once the patient is relaxed, tumescent infiltration can begin (see Fig. 156.8). Peristaltic pumps can be regulated for a comfortable rate of infiltration, e.g. 100 ml/min. Of note, more aggressive forms of systemic anesthesia and deeper sedation put patients at higher risk for abdominal perforation. Another disadvantage of deep sedation is that, because of concerns about total anesthesia time, there is usually little or no delay between infiltration and the onset of the procedure leading to less vasoconstriction. As noted previously, significant vasoconstriction from the infiltration of the tumescent fluid does not occur for at least 10–15 minutes after infiltration.

LIPOSUCTION INSTRUMENTATION

The basic instruments required for liposuction are suction cannulas, tubing, and an aspirator[26]. Liposuction can be performed using many different types of cannulas and aspirators. The number of holes arranged along the shaft of the cannula is probably unimportant, although two or more holes increase the flow of fat through the instrument. The most important parameter for choosing cannulas is size: the smallest possible cannula should be employed. Smaller-diameter cannulas (≤3 mm) create smaller tunnels through the fat and achieve smoother results (Fig. 156.9). In addition, smaller-diameter cannulas penetrate the fat more easily and create less tissue trauma. Longer cannulas allow the surgeon to work from fewer skin insertion sites, leaving fewer scars, while shorter cannulas are easier to control as they pass through subcutaneous tissue. The tiny incisions required for insertion of 3 mm cannulas leave nearly invisible scars in most patients, but can be an issue if the patient has a tendency towards keloid formation or hyperpigmentation.

Liposuction is based on the technique of criss-crossing tunnels (from multiple insertion sites) through the subcutaneous tissue. Each area to be suctioned should be tunneled from at least two different directions, but often three or four are more effective. Multiple small tunnels ultimately provide the smoothest contraction of the overlying skin and the most thorough removal of fat. Subsequent contraction of the fatty layer occurs much like a wet sponge contracting into a dry one (Fig. 156.10).

The liposuction aspirate should be yellow or slightly blood-tinged (Fig. 156.11). A red aspirate in the suction tubing indicates excessive bleeding and the surgeon should immediately move on to a different tunnel. The surgeon's instrument hand acts as the piston moving the instrument in and out of the tissue smoothly. The free hand pulls, presses, and squeezes the skin to facilitate penetration of the cannula and provides important tactile information about the thickness of the underlying fat. The final surgical endpoint should be a skin thickness in the suctioned areas which is similar to that of the surrounding untreated skin.

Cannula insertion sites are routinely left open rather than being sutured closed. Closing insertion sites with sutures leads to an increase in postoperative edema due to decreased drainage. The authors generally prefer the use of a #15c blade to create insertion sites leading to less visible scarring. Klein[17] has advocated the use of small 1–2 mm openings made with a punch biopsy instrument.

Liposuction Devices

Ultrasound-assisted

External ultrasound involves preoperative use of an ultrasonic probe over the areas to be suctioned, in an attempt to liquefy or loosen the fat. However, double-blind studies found no benefit to this approach[27]. *Internal* ultrasonic liposuction employs a probe or cannula with an ultrasonic vibration at the tip. These instruments have been shown to liquefy fat prior to suction. Although this makes subsequent liposuction easier, studies have shown increased potential for seromas and burns[28].



Fig. 156.9 A variety of small-diameter liposuction cannulas. The presence of two or more holes increases the flow of fat through the instrument, and while longer cannulas allow the surgeon to work from fewer skin insertion sites, shorter cannulas are easier to control. *Courtesy W.P. Coleman III, MD.*

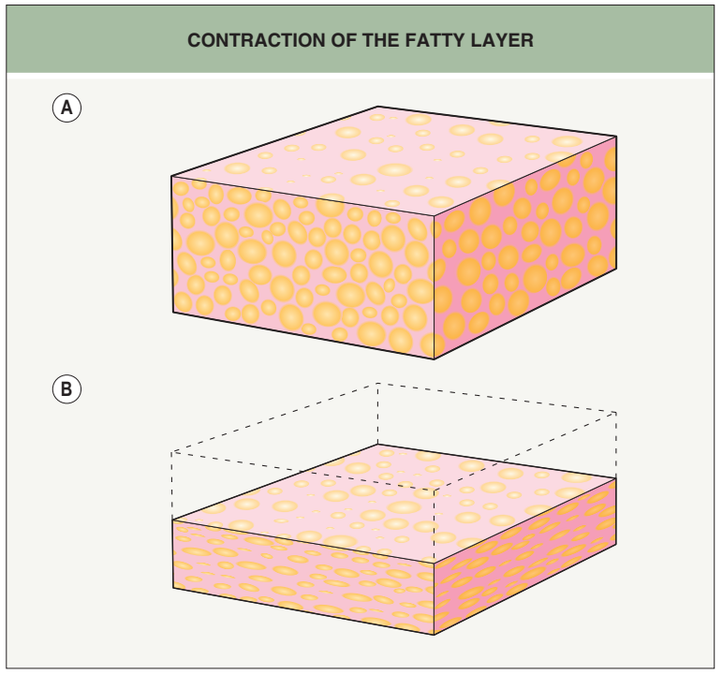


Fig. 156.10 Contraction of the fatty layer. A Immediately after liposuction, the fatty layer resembles a wet sponge. With subsequent subtraction of the fat cells, the thickness of the subcutaneous tissue decreases. **B** Much like a dry sponge, the subcutaneous tissue has compacted.



Fig. 156.11 Bloodless liposuction aspirate. Typical, nearly bloodless liposuction aspirate using the tumescent technique. *Courtesy W.P. Coleman III, MD.*

Ultrasonic probes pass through the tissue like a "hot knife through butter" and do not provide the usual tactile feedback from tissue resistance that manual cannulas do. This makes it difficult for the surgeon to determine in exactly what level of the fat the cannula is located and increases the possibility of intra-abdominal perforation or "end hits" to the opposing dermis. These devices should only be used by experienced surgeons and may be advantageous for skin tightening or if there is excessive fibrous tissue, e.g. gynecomastia.

Power-assisted

These instruments feature a motorized cannula, which moves in a back and forth or swirling motion (Fig. 156.12). The short, motorized strokes vary according to the instrument and allow the surgeon to precisely sculpt small areas of excess fat. Powered liposuction instruments also allow easier penetration of fat, when compared to manual cannulas, but retain some feel of tissue resistance[29]. Studies have shown that powered liposuction increases the fat aspirated (per minute) by 30% or more[29]. There have been no significant complications reported with the use of this approach, although some early users described an increase in seromas. Powered instruments create a larger tunnel than a manual instrument of the same diameter; this should be taken into account when choosing the appropriate size cannula.

Laser-assisted

Laser-assisted devices are designed to transmit infrared laser energy, via a fiber, subcutaneously during liposuction in order to generate heat. Early iterations of these devices had very low power and showed very little difference compared to manual liposuction[30]. Diode and Nd:YAG laser liposuction devices are available from several manufacturers in a variety of wavelengths. Newer devices have higher power and longer wavelengths that are more selective for fat, potentially increasing their efficacy. Benefits include emulsification of fat to make aspiration easier, decreased blood loss[31], and potential for increased skin tightening. The laser fibers can cause burns if used incorrectly, although newer devices have real time temperature feedback mechanisms to reduce this risk. Laser liposuction does take more time to perform and increases costs. Skin tightening seems to be the main purported advantage to these devices. Although this has been difficult to quantify, studies using subcutaneous laser alone have shown significant improvement in skin laxity[32]. However, manual liposuction alone also produces significant tightening and external energy-based tightening devices may provide the same effect.

Radiofrequency-assisted

Several newer devices have employed subcutaneous radiofrequency technology in order to try to increase skin tightening. Some of these devices use monopolar radiofrequency while others use bipolar technology. The purported advantage over laser- and ultrasound-assisted liposuction is better control of the heat produced. Radiofrequency-assisted liposuction has been shown to be safe, but when compared to manual liposuction, enhanced skin contraction is still unproven and a direct comparison trial will be difficult. However, several studies have shown that there is potential for this technology to aid in skin contraction[33].

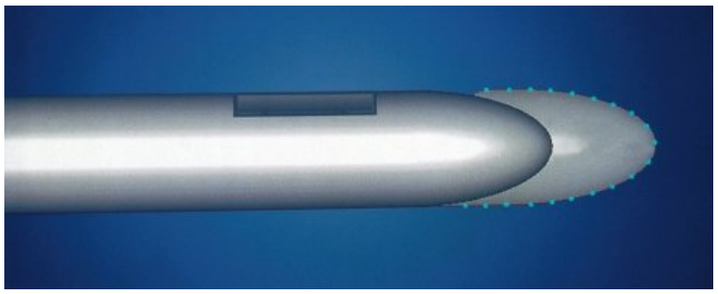


Fig. 156.12 Reciprocating powered cannula. This reciprocating powered cannula has a 3 mm to-and-fro motion. *From Coleman WP III, Katz B, Bruck M, et al. The efficacy of powered liposuction. Dermatol Surg 2001;27:735–8.*

Water-assisted

These devices employ powerful streams of water directed into the fat layer to create tunnels to facilitate fat removal. Proponents of this approach claim that this reduces the volume of tumescent fluid required. This makes very little sense since the anesthetic effect of the fluid takes several minutes to take effect, long after the tunnel has already been bored by the water jet. There may be potential benefits with this technology when performing fat transplantation as the fat cells may be better preserved than through physical avulsion, but this remains speculative.

Manual liposuction versus device-assisted

The major potential advantage of these devices is skin tightening; however, as stated previously, this is difficult to assess. In patients with more laxity or fibrous tissue, there may be some advantage. However, in individuals with good skin quality, these devices are likely unnecessary as manual liposuction alone provides good skin contraction. Also, it is important to recognize the increased cost associated with using these devices, including disposable costs. Each surgeon needs to determine which instrument he or she is most comfortable with and stick with the approach that is most successful. Each instrument can have a steep learning curve. Excellent liposuction results may be achieved with any of these devices, but only if the surgeon is experienced and well trained.

LIPOSUCTION VARIATIONS

Guidelines of care published by dermatologic organizations recommend that liposuction be performed as a solo procedure and not combined with other techniques[5,6]. However, there are cases in which liposuction is employed as a fundamental part of a combined surgical procedure. For instance, in rhytidectomy, liposuction of the neck and pre-tunneling of the cheeks are often performed prior to flap dissection and advancement. In patients in whom the neck alone is to be treated, liposuction may be combined with submental resection and platysmal plication, with each surgical component contributing to the final result. External light-based and radiofrequency devices may also be combined with neck liposuction to improve skin contraction.

In other anatomic sites, skin excision may be combined with liposuction. Where there is a significant abdominal panniculus, a suprapubic incision may be used to remove excess skin in conjunction with liposuction of the rest of the abdomen. However, in most patients with a moderate panniculus, this may be unnecessary because of the significant skin retraction that occurs after liposuction of the lower abdomen. Experience shows that most patients who consult for abdominoplasty achieve excellent results with liposuction alone. Abdominoplasty is a much more aggressive procedure, with significantly increased morbidity and mortality. The final scar is significant and often unattractive as well.

Liposuction is an excellent option for improvement of pseudogynecomastia in men. In these patients, the breast enlargement results primarily from excess fat rather than the excess glandular tissue present in true gynecomastia. Aggressive liposuction is required to remove what is usually thicker and more fibrotic fat. Powered or ultrasonic liposuction is sometimes useful in tunneling through this more fibrous fat. In patients with true gynecomastia, the glandular tissue must also be removed, usually through a submammary or periareolar incision, to obtain sufficient flattening of the breast. Liposuction can also be used for moderate breast reduction in females. The best results are seen in women with soft breasts. Very firm glandular breasts of younger patients do not respond well to liposuction, nor do ptotic breasts, which may sag more after the procedure. These patients are better served with excisional breast reduction.

NON-COSMETIC LIPOSUCTION

Liposuction may also be used for non-cosmetic indications (see Table 156.1). The chief among these are hyperhidrosis and lipoma removal[11]. When topical preparations are ineffective, botulinum toxin injections, sympathectomy, external focused microwave, and liposuction can be performed. For axillary hyperhidrosis, subdermal liposuction is used aggressively to remove as much of the subdermal fat in the axilla

as possible (see Fig. 156.7). Since many of the eccrine and apocrine sweat glands reside in the upper fat, liposuction can diminish sweating postoperatively. The goal is to make the patient sweat normally, but not to become anhidrotic. Preoperatively, a starch iodine test identifies the areas of greatest sweating (see Ch. 39). The liposuction should be aggressive enough to create some subdermal fibrosis, in an attempt to eliminate as many dermal eccrine and apocrine structures as possible. Patients are usually comfortable within 24 hours and able to resume normal activities within 2–3 days. Often, there is immediate diminished sweating with a rebound 2–3 weeks postoperatively, followed by a gradual decrease in sweating as fibrosis develops in the subdermal region.

Larger lipomas can also be reduced efficiently using liposuction. The goal here is to flatten out the lipoma but not necessarily remove the entire lesion. The advantage of liposuction over standard excisional surgery is that the former leads to a much smaller scar. As with any adiposity, the lipoma is tunneled in a criss-cross direction until flat. Subsequent healing and fibrosis usually flattens the remaining lipoma further, resulting in a normal contour. It is difficult to suction smaller lipomas and these are best removed through direct puncture excision. However, lipomas the size of a golf ball or larger are excellent candidates for liposuction. Since the entire lesion is not surgically removed, lipomas treated in this fashion may be more likely to recur; the patient should be made aware of this possibility. Liposuction should be reserved for lesions that are in cosmetically sensitive areas or those of a size which would necessitate a larger incision.

POSTOPERATIVE CARE

Following liposuction, patients are usually quite comfortable during the initial postoperative period. It is important to remind patients, well before the procedure takes place, that they are going to have significant drainage for the first day following liposuction surgery. Barrier protection is recommended for car seats, furniture, and bed linens during this period.

The patient's insertion sites may be coated with petrolatum or antibiotic ointment prior to application of absorbent materials. Modern absorbent pads are capable of absorbing significant amounts of drainage from the insertion sites thereby decreasing the need for patients to change pads. Most individuals will experience continued drainage for 24–48 hours following liposuction. Patients are advised to take their first shower with the absorbent bandages and the tape in place, as the shower assists in the removal of the tape.

Following the application of sufficient amount and layers of absorbent pads, a compression garment or a compression bandage is fitted. Numerous styles of postoperative liposuction compression garments are available. Postoperative compression minimizes bruising and aids in drainage. Gravitational drainage minimizes postoperative edema. It is important to use firm compression immediately following tumescent liposuction[34]. Compression assists patients in feeling more secure and decreases pain by restricting movement of the treated tissue. Many patients actually enjoy the comfort and feel of a compression garment due to the soreness sometimes associated with movement in the immediate postoperative period. Patients with pre-existing laxity or large amounts of fat removal may benefit from a longer period of compression.

Infections have occasionally been reported with liposuction and oral antibiotics may provide prophylaxis against more serious infections. Of note, lidocaine is bactericidal[35]. This may explain, in part, the relatively few infections seen with tumescent liposuction. Careful local wound care and cleanliness are essential in producing a good liposuction outcome.

Most patients can return to work within 48 hours following their liposuction. It is important to ask the patients to ambulate regularly beginning the day after surgery. This movement encourages drainage as well as remodeling of the subcutaneous tissue. Movement has the additional benefit of increasing lymphatic drainage through intermittent pumping action of skeletal muscles. Light exercise may begin 24–48 hours after surgery, but patients should be advised to start at 25% of their normal routine. Generally, patients are back to normal exercise routines after the first postoperative week.

All patients are given a set of written postoperative liposuction instructions including important phone numbers should the patient need to contact the physician. These postoperative instructions remind the patient that swelling and firmness beneath the skin and a reduced sensation in the skin are common. This will usually resolve over the first 3 to 4 weeks after the surgery. The postoperative instructions also remind patients that the final results are not seen until 6–12 months following the liposuction.

Patients return for their first postoperative appointment 1 day following liposuction. This visit is important to check for problems and reassure the patient. The next visit usually occurs during the first 3 weeks. It is often necessary to remind patients that improvement from liposuction is a gradual process. This postoperative visit is a good opportunity for encouraging patients to exercise, maintain an active and healthy lifestyle, and eat a reasonable diet. Patients are seen for 3-month and 6-month follow-up visits. If touch-ups are required, it is wise to wait 1 year before proceeding to be certain that the final results have been achieved. Secondary liposuctions that are performed too early in the postoperative period may lead to skin irregularities.

COMPLICATIONS OF LIPOSUCTION

Complications of liposuction must be differentiated from common sequelae. After liposuction, it is common to have prolonged swelling, areas of numbness, bruising, and red incisions. Infections, hematomas, and seromas are rare complications that require medical attention but can usually be resolved rapidly.

Serious complications of liposuction are closely linked to the type of sedation employed. There have been a number of deaths from liposuction in patients who had moderate or deep sedation[18,19,36]. The authors are not aware of any deaths from liposuction in patients who underwent the procedure with true tumescent local anesthesia[37].

Deep vein thrombosis and pulmonary embolism postoperatively are surgical complications generally associated with non-ambulatory patients and prolonged procedures under general anesthesia. An advantage of the tumescent local anesthetic technique is that patients are ambulatory immediately after surgery, thus minimizing the risk of this potential problem. Patients who are obese and inactive are more at risk for the development of this complication; this should be taken into consideration during the preoperative evaluation.

Abdominal perforation is one of the leading causes of liposuction death[38]. This is exclusively a complication of liposuction under general anesthesia[20]. Deeply sedated patients have decreased muscle tone and are unable to alert the physician to the pain of penetration of the liposuction cannula. Occult abdominal hernias may contribute to this complication. The treating physician should be aware of any abdominal scars and palpate for hernias during the preoperative visit.

General anesthesia also increases risks of respiratory failure and cardiac death[22]. Besides the direct effect of systemic anesthesia, fluid overload may contribute to these problems. Anesthesiologists who are not accustomed to working with patients who have been infiltrated with tumescent anesthetic fluids may inadvertently overhydrate the patient with additional intravenous fluids. A significant amount of the saline infused subcutaneously is absorbed systemically, automatically correcting for surgical fluid losses. Compounding this problem is the discovery that intravenous fluid bags are typically overfilled by at least 10%, leading to further errors in calculating fluid replacement in liposuction[39].

The keys to avoiding complications in liposuction lie in proper patient selection, appropriate patient evaluation, realistic patient expectations, monitoring according to the degree of sedation, good surgical technique, avoidance of excessive fat removal or overzealous additional simultaneous procedures, and adequate postoperative care.

NON-INVASIVE BODY CONTOURING

Liposuction is now a mature procedure and most patients obtain predictable results[40,41]. However, as with all cosmetic procedures, there is a general trend toward trying to accomplish similar results with less invasive techniques. Several non-invasive modalities are currently approved for the treatment of localized subcutaneous fat (Table 156.6). Some of these treatments, such as injection lipolysis, have been in existence for many years, but recently have garnered more interest; other technologies, such as external ultrasonic devices, external cryolipolysis, external radiofrequency, and low-level light treatments, are relative newcomers to the field.

NON-INVASIVE BODY CONTOURING MODALITIES	
Non-invasive modality	**Mechanism of action**
Injection lipolysis (deoxycholate)	Fat cell membrane disruption (adipocytolysis)
High-intensity focused ultrasound	Thermal destruction of adipocytes
Non-thermal focused ultrasound	Cavitation disruption of adipocytes
Cryolipolysis	Cold-induced apoptosis/panniculitis
Radiofrequency (mono-, uni-, bi-, tri-polar)	Thermal destruction of adipocytes
Low level light therapy	Photochemical membrane pore creation (theoretical)

Table 156.6 Non-invasive body contouring modalities.

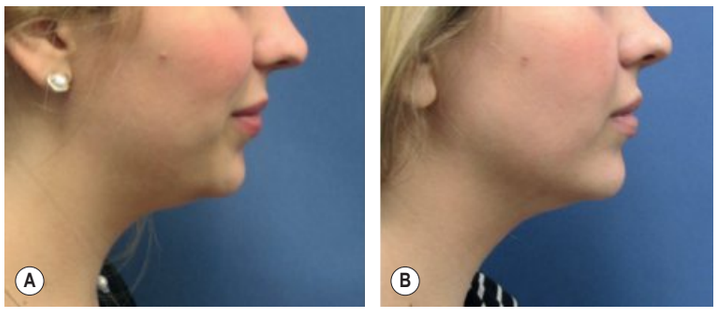


Fig. 156.13 Phosphatidylcholine/deoxycholate injection to the submental area. A Pre-treatment. **B** 1 month post-treatment, showing improved contour of the neck. *Courtesy K.M. Coleman, MD.*

Injection Lipolysis

Mesotherapy, which was originally developed in the 1950s, has re-emerged as a treatment for localized adiposities. Most commonly, this technique involves the subcutaneous injection of a formulation containing phosphatidylcholine plus a detergent solvent that leads to the dissolution of fat cells[42]. More recent work has shown that the detergent solvent, usually deoxycholic acid, is more likely the active ingredient in this solution[43]. Deoxycholic acid works by causing adipocytolysis, leading to a decrease in fat volume via contraction and remodeling. In 2015, deoxycholic acid was approved by the FDA for the reduction of moderate to severe submental fullness. The injections consist of small aliquots (0.1–0.2 ml) placed ~1 cm apart from each other[44]. Treatment volume used varies depending on the amount of adiposity present. Most patients will require several treatments, at least one month apart, for best results. Of note, many physicians are lengthening the time between sessions to allow post-treatment edema to subside more completely prior to the next set of injections. Full results are not apparent until 12 weeks post-therapy (Fig. 156.13).

Post-treatment sequelae include edema, ecchymoses, decreased sensation, and hair loss. For most patients, edema is self-limited but in some instances, persistent edema may occur necessitating treatment with intralesional triamcinolone acetonide or anti-inflammatory medications. Post-treatment edema tends to lessen with subsequent deoxycholic acid injections.

There have been several reports of off-label use of deoxycholic acid, including for jowls, pre- and post-axillary bra fat, suprapatellar fat pads, and small truncal adiposities[45,46]. The therapeutic efficacy of deoxycholic acid injections is limited to smaller adiposities. Its use for larger areas has not been established and would not be clinically or financially feasible.

Low Level Light Therapy (LLLT)

An external 635 nm diode laser (Zerona™; Erchonia) is FDA-cleared for fat reduction around the waist. Theoretically, this device reduces the size of subcutaneous fat by induction of a photochemical reaction which creates small pores in the adipocyte cell membrane[47]. However, early reports of the results of these treatments had only short follow-up times and no weight control. In addition, several studies have shown that the minimal results produced seem to abate over time, with long-term results still in question as well.

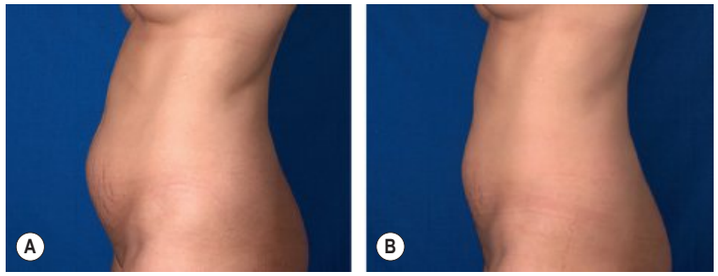


Fig. 156.14 Non-thermal focused ultrasound (UltraShape™) treatment of the abdomen. A Pre-treatment. **B** 42 days post-treatment.

High-Intensity Focused Ultrasound

High-frequency ultrasound, HIFU (LipoSonix™; Innovations Medical), relies upon ultrasound-induced thermal destruction of adipocytes. This device is based on technology currently employed in the treatment of malignant tumors, in particular prostate cancer. The ultrasound has a focal depth of 1.3 cm and creates tissue temperatures up to about 70°C. The thermal destruction of adipocytes at this depth leads to tissue contraction and reduction of adiposities over an 8- to 12-week period[48]. The FDA cleared this technology for non-invasive waist circumference reduction in 2011 and reduction in waist circumference from a single treatment has been reported to be about 2–3 cm. Patients complain of discomfort during the treatments which can be moderate to severe in some. The most common sequelae from HIFU include post-procedural pain, numbness, edema, and ecchymoses.

Non-thermal Focused Ultrasound

Non-thermal, external ultrasound (UltraShape Power®; Candela™) produces targeted cavitation of fat cells without producing significant heating; this allows the device to achieve lipolysis without creating damage to blood vessels and nerves[49,50]. Disruption of the adipocytes leads to release of fatty acids. The device has been cleared by the FDA for abdominal circumference reduction. Treatments are performed every 2 weeks; generally, 3 treatments are recommended. During treatment, patients experience minimal if any discomfort. The focal depth of the ultrasound is 1.5 cm and care should be taken over bony prominences to avoid reflection of the waves.

Post-procedural sequelae are rare and are likely related to technique. Blistering can result from inadequate contact with the device or treatment over a bony area. Patients may resume all activities immediately after treatments and generally have no pain, edema, or bruising. Patients are advised to avoid excessive fat consumption during the first 2 days post-procedure. Treatment results appear gradually with improvement over a 6- to 8-week period. After 3 treatments, an average reduction in waist circumference of 3–5 cm has been reported (Fig. 156.14).

Cryolipolysis

Cryolipolysis (Coolsculpting®; Zeltiq Aesthetics) involves the targeted production of adipocyte apoptosis via thermal energy extraction (without damage to the epidermis). Porcine and human trials have shown significant reduction in subcutaneous fat. This device utilizes vacuum suction to elevate tissue into contact with cooling plates within the device[51,52]. There are now several different applicators to fit different body types and areas. The treatment involves placing the treatment applicator over the selected area and starting the vacuum and cooling process; the applicator remains in place for 1 hour. Separate body areas can be treated at the same time or sequentially. Current recommendations are to retreat the area in 1 month, with results occurring gradually over a period of 2–3 months.

During the treatment, there is mild discomfort. Immediately after treatment, the treated area is cold and indurated; this resolves over about thirty minutes (Fig. 156.15). A randomized trial has shown that vigorous massage of the treated tissue can lead to greater reduction in

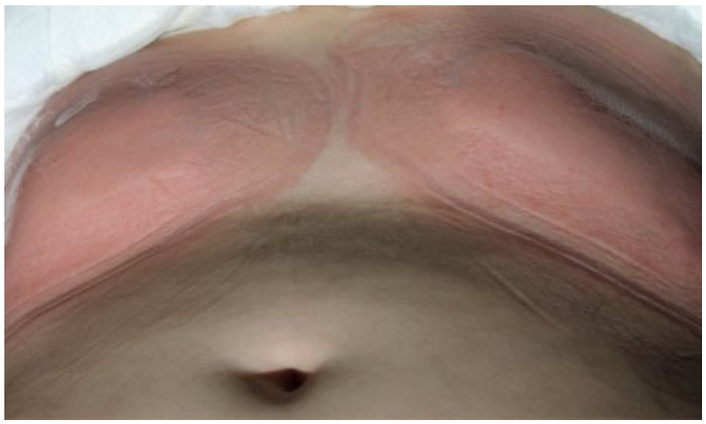


Fig. 156.15 Immediate post-treatment response of cryolipolysis. The treated skin is elevated, cold to the touch, clay-like, and erythematous.

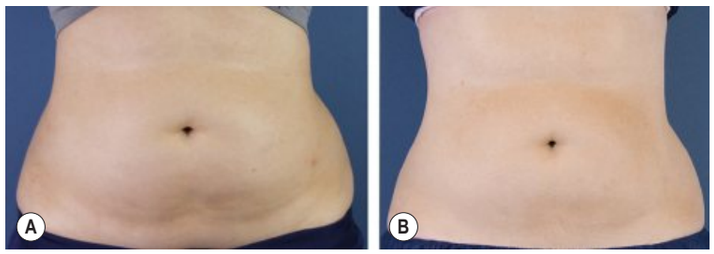


Fig. 156.16 Cryolipolysis (Coolsculpting®) of the abdomen. A Pre-treatment. **B** 6 months later, after 2 treatments. *Courtesy K.M. Coleman, MD.*

adiposities. Commonly, there is some erythema for the first few hours; patients complain of transient pain, numbness, bruising, and edema, which all generally resolve over 2 weeks. Rarely, prolonged pain can occur; this usually responds to oral anti-inflammatory agents. There have been several reports of paradoxical adipose hyperplasia which may require liposuction for correction[53]. Results of these treatments is highly dependent on proper patient selection and proper application of the device (Fig. 156.16). Multiple treatment tips are usually needed to adequately treat an area.

Radiofrequency

Radiofrequency devices utilize an oscillating electrical field to create heat in target tissues; lower frequencies are able to penetrate more deeply. Several radiofrequency devices are available for multiple aesthetic uses. Devices can be monopolar or unipolar (1 electrode), bipolar, or multipolar. For fat reduction, results with radiofrequency devices have been mixed with some newer devices reportedly more successful.

A selective, contactless radiofrequency device (Vanquish Me™; BTL Aesthetics) uses focused field radiofrequency to target adiposities. A prospective trial showed a 4.93 cm reduction in abdominal circumference after 4 weekly treatments; however, 3 patients showed no reduction at all[54]. Use of a vacuum-assisted bipolar device that utilizes software to maintain constant temperature control (Evolve®; Inmode) led to a 2.7 cm decrease in abdominal circumference after 6 weekly treatments[55]. Currently, this device combines non-vacuum bipolar heads with suction-assisted heads in order to treat more superficial adiposity and skin laxity.

CELLULITE

Cellulite is a common problem for most women with variable presentations. It can present as dimples, rippling of the skin, and/or superficial adiposities. The morphology of cellulite stems from superficial fat deposits, skin laxity, and perpendicular dermal bands which lead to dimpling. For years, treatment options have been less than satisfying in their durability and effectiveness. However, more recently introduced technologies have shown promise for providing durable improvement in the appearance of cellulite (Table 156.7).

CELLULITE TREATMENT OPTIONS	
Treatment	**Mechanism of action**
Manual subcision*	Manual release of dermal bands
External radiofrequency	Skin tightening, reduction of superficial adiposity
Subdermal side-firing (1440 nm Nd:YAG) laser	Release of dermal bands, skin tightening, reduction of adiposity
Subdermal radiofrequency	Skin tightening, reduction of adiposity
Vacuum-assisted subcision	Controlled release of dermal bands
Injectable collagenase	Lysis of dermal bands
*Sometimes followed by injection of fillers such as calcium hydroxylapatite and poly-L-lactic acid microspheres.	

Table 156.7 Cellulite treatment options.

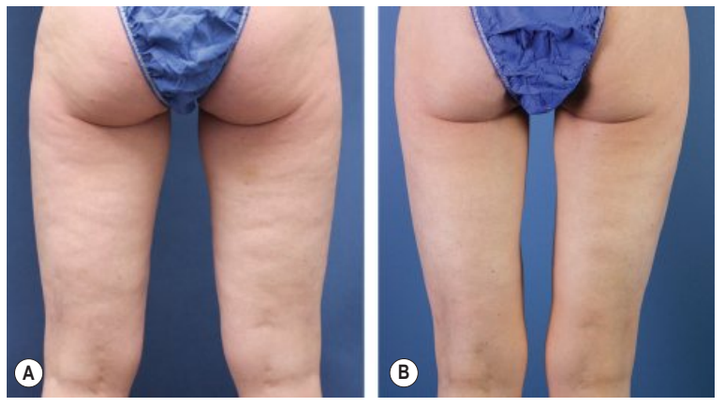


Fig. 156.17 Subdermal laser treatment (Cellulaze®) of posterior thigh cellulite. A Pre-treatment. **B** 6 months post-treatment. *Courtesy K.M. Coleman, MD.*

External Devices

There are several commercially available external treatments that attempt to improve cellulite. Most of them are minimally, if at all, effective in providing long-term improvement. For example, body wraps and massages can temporarily improve the appearance of cellulite, but there is no durable improvement. Most of the devices employed for the external treatment of cellulite rely on radiofrequency-induced heat to tighten skin and reduce superficial adiposity. Because these devices only address two of the three causes of cellulite – laxity and superficial adiposity – their effectiveness is limited. They require numerous treatment sessions to produce any improvement and results tend to not be durable.

Rapid Acoustic Pulse™ technology, which utilizes high intensity, high frequency, ultrashort acoustic wave pulses, is said to be capable of disrupting fascial connections, rendering the dimpling less evident. However, the results may not be durable beyond the treatment period.

Subdermal Devices

Since cellulite is created by subdermal bands and adiposity, these devices target the subdermal plane. This approach is minimally invasive and generally performed with tumescent anesthesia. The first device that incorporated subdermal treatment of cellulite was the 1440 nm side-firing laser (Cellulaze®; Cynosure). Its laser fibers are designed to refract the beam into two perpendicular beams which allow for treatment in two directions. One beam treats skin laxity and superficial adiposity while the second helps to cut the cellulite bands. Although results have been mixed, some authors have reported very good results that were durable (Fig. 156.17)[56]. Other subdermal technologies such as radiofrequency devices can be used in patients with cellulite; however, they address the laxity and superficial adiposity without cutting the dermal bands.

Subcision

Manual subcision of cellulite dimples has long been effective in some physicians' hands. When performed by those experienced in this technique, durable results have been observed. Subcision is generally performed with an 18-gauge filter needle under local anesthesia.

The needle is used to horizontally cut the dermal bands and release the dimples.

Vacuum-assisted subcision

Since manual subcision can be technically challenging and time-consuming, attempts have been made to enhance effectiveness and reproducibility. With a vacuum-assisted subcision device (cellfina®; Merz Aesthetics), the vacuum secures and elevates the tissue with the dimple, allowing for insertion of an oscillating blade into the correct tissue plane to release the dermal bands[57]. This leads to more exact targeting of the dermal bands and more rapid treatments. Results have been reported as very durable, lasting up to several years. As these vacuum-assisted devices only target dermal bands, they work best for dimpled cellulite and are not very effective in patients with laxity or rippled cellulite.

Fat Transfer and Fillers

For severe dimpling of cellulite, subcision of dimples alone may not be sufficient. Placement of fat or fillers can help to further smooth these lesions. Based upon their collagen stimulatory properties, fillers such as calcium hydroxylapatite and poly-L-lactic acid microspheres are also being used to treat cellulite[58]. They are injected in a dilute fashion in order to improve skin laxity.

Collagenase

Injectable collagenase (Qwo®; Endo Pharmaceuticals) is the most recent addition to the therapeutic armamentarium for cellulite, and it has shown some promise in clinical trials[59]. In order to release dimpling, the collagenase is injected into dermal bands. There is no need for anesthesia and serial injections are performed every 3 to 4 weeks per current protocols. However, the latter may undergo further revisions. Based upon early results, improvement may be durable (up to at least 2 years). A significant drawback is the potential for developing large ecchymoses that lead to hemosiderin deposition in some patients.

CONCLUSION

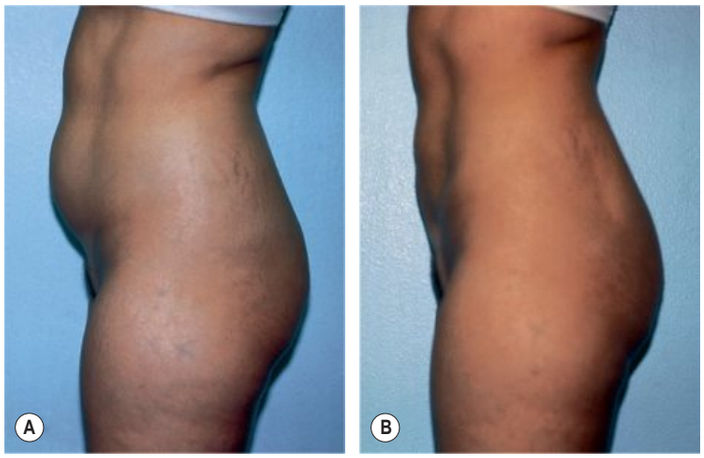
Technology is constantly providing physicians with new ways to minimize localized adiposities. Regardless of what instrumentation is used, it is likely that in the future liposuction will remain one of the most popular and predictable cosmetic procedures. As more non-invasive treatments become available, it is important to recognize the pros and cons of each of these devices. No matter which type of treatment is performed, the single most important aspect in choosing a therapy is patient selection.

Additional figures available in our eBook (see inside front cover for access code).

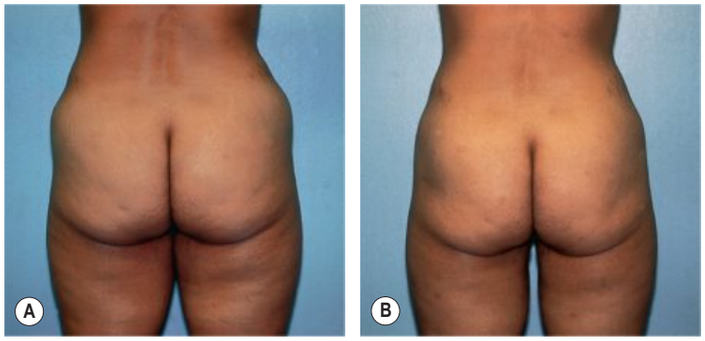
REFERENCES

1. Fischer A, Fischer G. First surgical treatment for molding body's cellulite with three 5 mm incisions. *Bull Int Acad Cosmet Surg*. 1976;3:35.
2. Illouz YG. Body contouring by lipolysis: a 5-year experience with over 3000 cases. *Plast Reconstr Surg*. 1983;72:591–597.
3. Fournier PF, Otteni FM. Lipodissection in body sculpturing: the dry procedure. *Plast Reconstr Surg*. 1983;72:598–609.
4. Flynn TC, Narins RS. Preoperative evaluation of the liposuction patient. *Dermatol Clin*. 1999;17:729–734.
5. Coleman III WP, Glogau RG, Klein JA, et al. Guidelines of care of liposuction. *J Am Acad Dermatol*. 2001;45:438–447.
6. Lawrence N, Clark RE, Flynn TC, Coleman III WP. American Society for Dermatologic Surgery Guidelines of Care for Liposuction. *Dermatol Surg*. 2000;26:265–269.
7. Klein JA. Tumescent technique for liposuction surgery. *Am J Cosmet Surg*. 1987;4:263–267.
8. Klein JA. Tumescent technique for regional anesthesia permits lidocaine doses of 35 mg/kg for liposuction. *J Dermatol Surg Oncol*. 1990;16:248–263.
9. Ostad A, Kageyama N, Moy RL. Tumescent anesthesia with a lidocaine dose of 55 mg/kg is safe for liposuction. *Dermatol Surg*. 1996;22:921–927.
10. Coleman III WP. Tumescent anesthesia with a lidocaine dose of 55 mg/kg is safe for liposuction (editorial). *Dermatol Surg*. 1996;22:919.
11. Coleman III WP. Noncosmetic applications of liposuction. *J Dermatol Surg Oncol*. 1988;14:1085–1090.
12. Chastain MA, Chastain JB, Coleman III WP. HIV lipodystrophy: review of the syndrome and report of a case treated with liposuction. *Dermatol Surg*. 2001;27:497–500.
13. Coleman III WP, Letessier S, Hanke CW. Liposuction. In: Coleman III WP, Hanke CW, Alt TH, Asken S, eds. *Cosmetic Surgery of the Skin*. St Louis: Mosby; 1997:178–205.
14. Lillis PJ. Liposuction surgery under local anesthesia: limited blood loss and minimal lidocaine absorption. *J Dermatol Surg Oncol*. 1988;14:1145–1148.
15. Klein JA. Anesthetic formulation of tumescent solutions. *Dermatol Clin*. 1999;17:751–759.
16. Klein JA. Tumescent technique for local anesthesia improves safety in large-volume liposuction. *Plast Reconstr Surg*. 1993;92:1085–1098; discussion 1099–1100.
17. Klein JA. *Tumescent Technique. Tumescent Anesthesia and Microcannular Liposuction*. St Louis: Mosby; 2000.
18. Coleman III WP, Hanke CW, Glogau RG. Does the specialty of the physician affect fatality rates in liposuction? A comparison of specialty specific data. *Dermatol Surg*. 2000;26:611–615.
19. Rao RB, Ely SF, Hoffman RS. Deaths related to liposuction. *N Engl J Med*. 1999;30:1471–1475.
20. Coleman III WP, Hanke CW, Lillis P, et al. Does the location of the surgery or the specialty of the physician affect malpractice claims in liposuction? *Dermatol Surg*. 1999;25:343–347.
21. Hanke CW, Bernstein G, Bullock S. Safety of tumescent liposuction in 15,336 patients. National survey results. *Dermatol Surg*. 1995;21:459–462.
22. Forrest JB, Rehder K, Cahalan MK, Goldsmith CH. Multicenter study of general anesthesia. III. Predictors of severe perioperative adverse outcomes. *Anesthesiology*. 1992;76:3–15.
23. Klein JA, Kassarjdian N. Lidocaine toxicity with tumescent liposuction. A case report of probable drug interactions. *Dermatol Surg*. 1997;23:1169–1174.
24. Klein JA. Intravenous fluids and bupivacaine are contraindicated in tumescent liposuction. *Plast Reconstr Surg*. 1998;102:2516–2519.
25. Breuninger H, Wehner-Caroli J. Subcutaneous infusion anesthesia with prilocaine diluted with Ringer's lactate. *Hautarzt*. 1998;49:709–713.
26. Bernstein G. Instrumentation for liposuction. *Dermatol Clin*. 1999;17:735–749.
27. Lawrence N, Coleman III WP. Ultrasonic-assisted liposuction. Internal and external. *Dermatol Clin*. 1999;17:761–771.
28. Lawrence N, Coleman III WP. The biologic basis of ultrasonic liposuction. *Dermatol Surg*. 1997;23:1197–1200.
29. Coleman III WP, Katz B, Bruck M, et al. The efficacy of powered liposuction. *Dermatol Surg*. 2001;27:735–738.
30. Prado A, Andrades P, Danilla S, et al. A prospective, randomized, double-blind, controlled clinical trial comparing laser-assisted lipoplasty with suction-assisted lipoplasty. *Plast Reconstr Surg*. 2006;118:1032–1045.
31. Abdelaal MM, Aboelatta YA. Comparison of blood loss in laser lipolysis vs traditional liposuction. *Aesthet Surg J*. 2014;34:907–912.
32. Sarnoff DS. Evaluation of the safety and efficacy of a novel 1440nm Nd:YAG laser for neck contouring and skin tightening without liposuction. *J Drugs Dermatol*. 2013;12:1382–1388.
33. Theodorou SJ, Del Vecchio D, Chia CT. Soft tissue contraction in body contouring with radiofrequency-assisted liposuction: a treatment gap solution. *Aesthet Surg J*. 2018;38:S74–S83.
34. Klein JA. Post-tumescent liposuction care. Open drainage and bimodal compression. *Dermatol Clin*. 1999;17:881–889.
35. Klein JA. Antibacterial effects of tumescent lidocaine. *Plast Reconstr Surg*. 1999;104:1934–1936.
36. Grazer FM, de Jong RH. Fatal outcomes from liposuction: census survey of cosmetic surgeons. *Plast Reconstr Surg*. 2000;105:436–446; discussion 447–8.
37. Hanke W, Cox SE, Kuznets N, Coleman 3rd WP. Tumescent liposuction report performance measurement initiative: national survey results. *Dermatol Surg*. 2004;7:967–977.
38. Talmor M, Hoffman LA, Lieberman M. Intestinal perforation after suction lipoplasty: a case report and review of the literature. *Ann Plast Surg*. 1997;38:169–172.
39. Coleman IV WP, Flynn TC, Coleman KL. When one liter does not equal 1000 milliliters: implications for the tumescent technique. *Dermatol Surg*. 2000; 26:1024–1028.
40. Yoho RA, Romaine JJ, O'Neil D. Review of the liposuction, abdominoplasty, and face-lift mortality and morbidity risk literature. *Dermatol Surg*. 2005;31:733–743.
41. Shiffman MA, Di Giuseppe A. *Liposuction: Principles and Practice*. Berlin: Springer-Verlag; 2006.
42. Rotunda AM, Kolodney MS. Mesotherapy and phosphatidylcholine injections: historical clarification and review. *Dermatol Surg*. 2006;32:465–480.
43. Rotunda AM, Weiss SR, Rivkin LS. Randomized double-blind clinical trial of subcutaneously injected deoxycholate versus a phosphatidylcholine-deoxycholate combination for the reduction of submental fat. *Dermatol Surg*. 2009;35:792–803.
44. Rzany B, Griffiths T, Walker P, et al. Reduction of unwanted submental fat with ATX-101 (deoxycholic acid), an adipocytolytic injectable treatment: results from a phase III, randomized, placebo-controlled study. *Br J Dermatol*. 2014;170:445–453.
45. Montes J, Santos E, Chillar A. Jowl reduction with deoxycholic acid. *Dermatol Surg*. 2020;46:78–85.
46. Zarbafian M, Fabi S. Off-label uses of deoxycholic acid in body contouring. *Dermatol Surg*. 2020;46:S2–S7.
47. Neira R, Arroyave J, Ramirez H, et al. Fat liquefaction: effect of low-level laser energy on adipose tissue. *Plast Reconstr Surg*. 2002;110:912–922.
48. Jewell ML, Weiss RA, Baxter RA, et al. Safety and tolerability of high-intensity focused ultrasonography for noninvasive body sculpting: 24-week data from a randomized, sham-controlled study. *Aesthet Surg J*. 2012;32:868–876.
49. Teitelbaum SA, Burns JL, Kubota J, et al. Noninvasive body contouring by focused ultrasound: safety and efficacy of the Contour I device in a multicenter, controlled, clinical study. *Plast Reconstr Surg*. 2007;120:779–789.
50. Moreno-Moraga J, Valero-Altés T, Riquelme AM, et al. Body contouring by non-invasive transdermal focused ultrasound. *Lasers Surg Med*. 2007;39:315–323.
51. Manstein D, Laubach H, Watanabe K, et al. Selective cryolysis: a novel method of non-invasive fat removal. *Lasers Surg Med*. 2008;40:595–604.
52. Zelickson B, Egbert BM, Preciado J, et al. Cryolipolysis for noninvasive fat cell destruction: initial results from a pig model. *Dermatol Surg*. 2009;35:1462–1470.
53. Hedayati B, Juhász M, Chu S, et al. Adverse events associated with cryolipolysis: a systematic review of the literature. *Dermatol Surg*. 2020;46:S8–S13.
54. Fajkošová K, Machovcová A, Onder M, et al. Selective radiofrequency therapy as a non-invasive approach for contactless body contouring and circumferential reduction. *J Drugs Dermatol*. 2014;13:291–296.

55. Boisnic S, Divaris M, Nelson AA, et al. A clinical and biological evaluation of a novel, noninvasive radiofrequency device for the long-term reduction of adipose tissue. *Lasers Surg Med*. 2014;46:94–103.
56. Alexiades M, Munavalli G, Goldberg D, et al. Prospective multicenter clinical trial of a temperature-controlled subcutaneous microneedle fractional bipolar radiofrequency system for the treatment of cellulite. *Dermatol Surg*. 2018;44:1262–1271.
57. Kaminer M, Coleman W, Weiss R, et al. Multicenter pivotal study of vacuum-assisted precise tissue release for the treatment of cellulite. *Dermatol Surg*. 2015;41:336–347.
58. Coleman KM, Pozner J. Combination therapy for rejuvenation of the outer thigh and buttock: a review and our experience. *Dermatol Surg*. 2016;42(Suppl 2): S124–130.
59. Sadick N, Goldman M, Liu G. Collagenase *Clostridium histolyticum* for the treatment of edematous fibrosclerotic panniculopathy (cellulite): a randomized trial. *Dermatol Surg*. 2019;45:1047–1056.



eFig. 156.1 Liposuction of the upper and lower abdomen. A Preoperative. **B** Postoperative, showing improved contours. *Courtesy W.P. Coleman III, MD.*



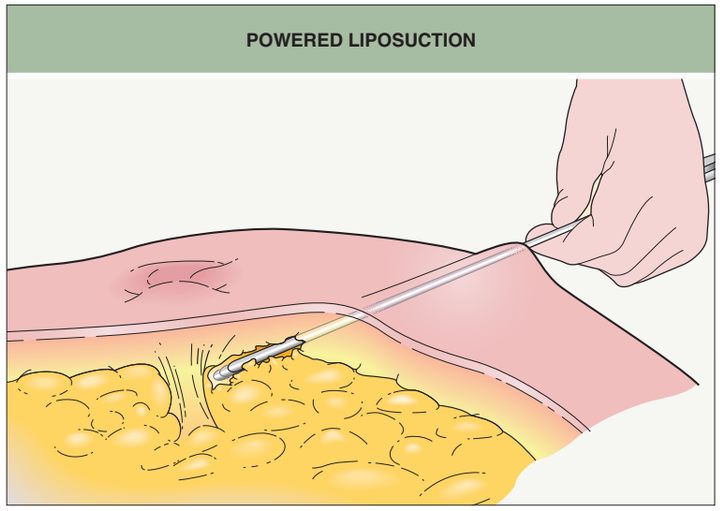
eFig. 156.2 Liposuction of the inner and outer thighs and hips. A Preoperative. **B** Postoperative, showing improved contours. *Courtesy W.P. Coleman III, MD.*



eFig. 156.3 Liposuction of the neck and jowls. A Preoperative. **B** Postoperative, showing improved appearance. *Courtesy W.P. Coleman III, MD.*



eFig. 156.4 Peristaltic pump for infiltration of tumescent anesthetic mixtures. *Courtesy K.M. Coleman, MD.*



eFig. 156.5 Powered liposuction. Using powered liposuction to more precisely sculpt small areas of fat around the umbilicus.



eFig. 156.6 Examples of liposuction compression garments. *Courtesy Miller Medical, Tucson, AZ.*

157 Hair Restoration

Marc R. Avram and Nicole E. Rogers

Key features

- A mainstay of correcting androgenic alopecia is transplantation of follicles harvested from the non-alopecic posterior scalp as 1–4 hair follicular units
- Follicular unit grafts can be obtained either manually or mechanically and are placed into small "recipient" sites (0.5–1 mm in diameter) produced by a blade or needle
- There are two major surgical methods: (1) elliptical donor harvesting (follicular unit transplantation [FUT]); and (2) follicular unit excision (FUE)
- Patient expectations and continued progression of androgenic alopecia, as well as donor site hair density, quantity and quality, are key considerations
- Although men and women have different patterns of androgenic alopecia, properly selected patients can undergo successful hair transplantation

INTRODUCTION

Hair frames our face and its length, color, and style reflect our personality and how we perceive ourselves. The framing preserves a youthful facial appearance by shortening the face and returning the viewer's focus to the center of the face. While hair is one of the few physical characteristics we can easily control, the inability to correct hair loss can lead to concerns regarding appearance and psychological stress. In the case of androgenetic alopecia, some individuals accept hair thinning as an unavoidable aging phenomenon, whereas others actively seek medical and/or surgical treatment options.

HISTORICAL PERSPECTIVE

The first hair transplantation procedure for male pattern hair loss was successfully performed in the 1950s, using large punch autografts. Alternative techniques such as hair-bearing flaps and scalp reductions were also performed in an effort to redistribute hair or reduce the size of bald scalp. However, because of unsightly large "plugs", unnatural orientation of hair, and obvious scars revealed by continued hair loss, these techniques were largely abandoned in favor of follicular unit grafts. The latter are placed into small "recipient" sites (0.5–1 mm in diameter) produced by a blade or needle. Follicular unit grafts can be obtained either manually or mechanically.

MALE AND FEMALE PATTERN HAIR LOSS (ANDROGENETIC ALOPECIA)

Pathogenesis

Miniaturization of terminal pigmented anagen hairs to fine hypopigmented vellus hairs is the hallmark of androgenetic alopecia (AGA; Fig. 157.1). Androgens, in particular testosterone and dihydrotestosterone (DHT), are required for the progressive reduction in hair follicle size with each cycle. The enzyme 5α-reductase, which is inhibited by drugs such as finasteride, converts testosterone to DHT (see Fig. 69.10). In addition to 5α-reductase isoenzymes, multiple androgen-metabolizing enzymes actually reside within the hair follicle itself, providing an explanation for "end-organ" sensitivity (see Ch. 69).

Stem cells, which reside in the hair follicle bulge, are responsible for hair follicle cycling and when these cells are destroyed, there is loss of the follicle. In mice, combining bulge cells with neonatal dermal cells can give rise to a hair follicle as well as the sebaceous gland and epidermis[1]. Within the hair follicle, stem cells give rise to secondary germ cells with each hair cycle; the latter cells represent a progenitor population that is responsible for the production of the hair shaft during anagen (but undergoes apoptosis at the end of anagen)[2]. In a study that compared bald scalp with hair-bearing scalp in men, the stem cell population was maintained in the bald scalp but there was a marked reduction in progenitor cells, suggesting that study of this second population of cells could provide further insight into male pattern hair loss[3].

In gene expression arrays, increased expression of the gene that encodes prostaglandin D2 synthetase was observed in bald scalp as compared to haired scalp in men with AGA[4]; the latter enzyme converts prostaglandin H2 (PGH2) to PGD2. Balding scalp was also found to have increased levels of PGD2, and PGD2 was shown to inhibit hair growth in explants of human hair follicles. This inhibition of hair growth by PGD2 required interactions with one of its receptors, pointing to a potential therapeutic target.

Population studies have pointed to a polygenic inheritance pattern, with both maternal and paternal genetic influences. Of the associated genes identified to date, the androgen receptor gene (*AR*), present on the long arm of the X chromosome (Xq11–12), has been identified as a major determinant of hair loss in men (AGA2)[5–7]. Within exon 1 of *AR* is the *AR*-CAG polymorphism, which refers to the number of repeat sequences of cytosine–adenine–guanine (CAG) present, with the normal range of CAG repeats being 10–40. The number of CAG repeats appears to *inversely* correlate with the degree of androgen sensitivity. Men with fewer CAG repeats have an increased risk of developing AGA and a higher cellular sensitivity to androgens; they also demonstrate a greater response to finasteride treatment[8]. In contrast, men with >40 repeats appear to be protected and have androgen insensitivity[9]. Variants in *AR* may influence hair loss in women as well[10].

AR also has single nucleotide polymorphisms (rs6152; see Ch. 54) and White men with the A (adenine) allele have a low likelihood of developing AGA[11] while those with the G (guanine) allele have a 70% lifetime risk of developing AGA, which increases to >80% if there is a positive paternal family history. Other implicated genes include *EDA2R*, which encodes the ectodysplasin A2 receptor and is also found on the X chromosome (see Ch. 63)[12], as well as genes located at 20p11 (AGA3)[13] and 3q26 (AGA1)[14]. As more insight is gained into the interplay of these genes, it may be possible to diagnose AGA at an early age and predict who may benefit from therapy. Of note, it is important for patients to realize that while a family history of AGA provides useful information, it does not predict the rate and extent of hair loss in a particular individual.

Clinical Features

The diagnosis of AGA is usually straightforward, especially in men. This is based upon the characteristic pattern, the miniaturization of hairs, and the lack of clinical inflammation or scalp symptoms (see Ch. 69). Occasionally, an unusual presentation requires clinicopathologic correlation, and if there is evidence of perifollicular erythema, the possibility of a scarring (cicatricial) alopecia needs to be excluded[15]. In women, patterned alopecia may first become clinically apparent as a result of a superimposed telogen effluvium, perhaps following a febrile illness or birth of a child. These patients require an evaluation for telogen effluvium as outlined in Table 69.4 and possible hyperandrogenemia (e.g. serum free testosterone, DHEA-S), especially in the setting of hirsutism and/or recalcitrant acne vulgaris or any signs of virilization. Female pattern hair loss has to be distinguished from other causes of alopecia, including diffuse alopecia areata, early lichen planopilaris (LPP), frontal fibrosing

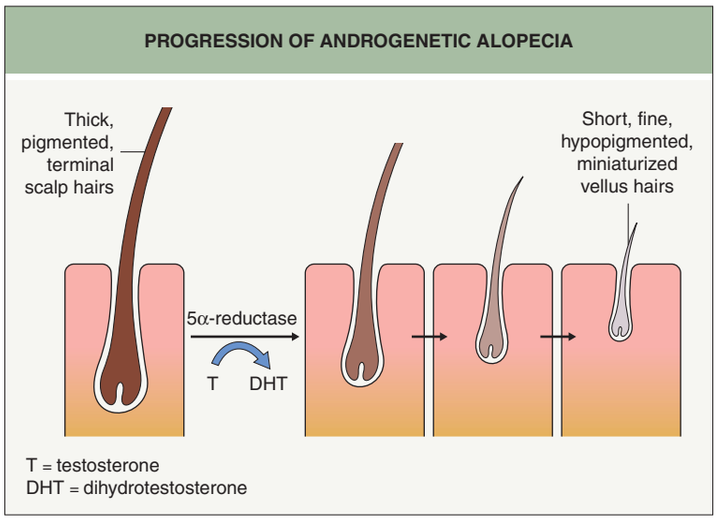


Fig. 157.1 Progression of androgenetic alopecia. Testosterone is metabolized into dihydrotestosterone (DHT) by the enzyme 5α-reductase and this conversion can occur within the hair follicle. *Courtesy Dowling B. Stough, MD.*

alopecia (FFA), or fibrosing alopecia in a pattern distribution (FAPD), and central centrifugal cicatricial alopecia (CCCA); as a result, histologic evaluation may be required.

There are grading systems for AGA that allow assessment of severity, progression and response to therapy. In men, the Norwood classification (Fig. 157.2) is used more often than the Hamilton classification system. Patterned hair loss in women is classically given a Ludwig grade (I, II or III; Fig. 157.3), even though the hair loss often has a Christmas tree pattern. Occasionally, the classification scheme for men is used if women present with vertex thinning or deep bitemporal recession.

Treatment (Other Than Transplant Surgery)

Medical therapies

Topical minoxidil as a 5% solution is FDA-approved for men[16] whereas the 2% solution and 5% foam are approved for both women and men. In general, the therapeutic effects are modest, but it may prove beneficial as an adjunct to hair transplantation[17]. Topical minoxidil can be helpful during the postoperative period to enhance and hasten growth of transplanted hairs. Minoxidil has multiple known mechanisms of action, but its effect on hair follicles is generally attributed to its vasodilatory or angiogenic properties and perhaps its effect on potassium channels[18].

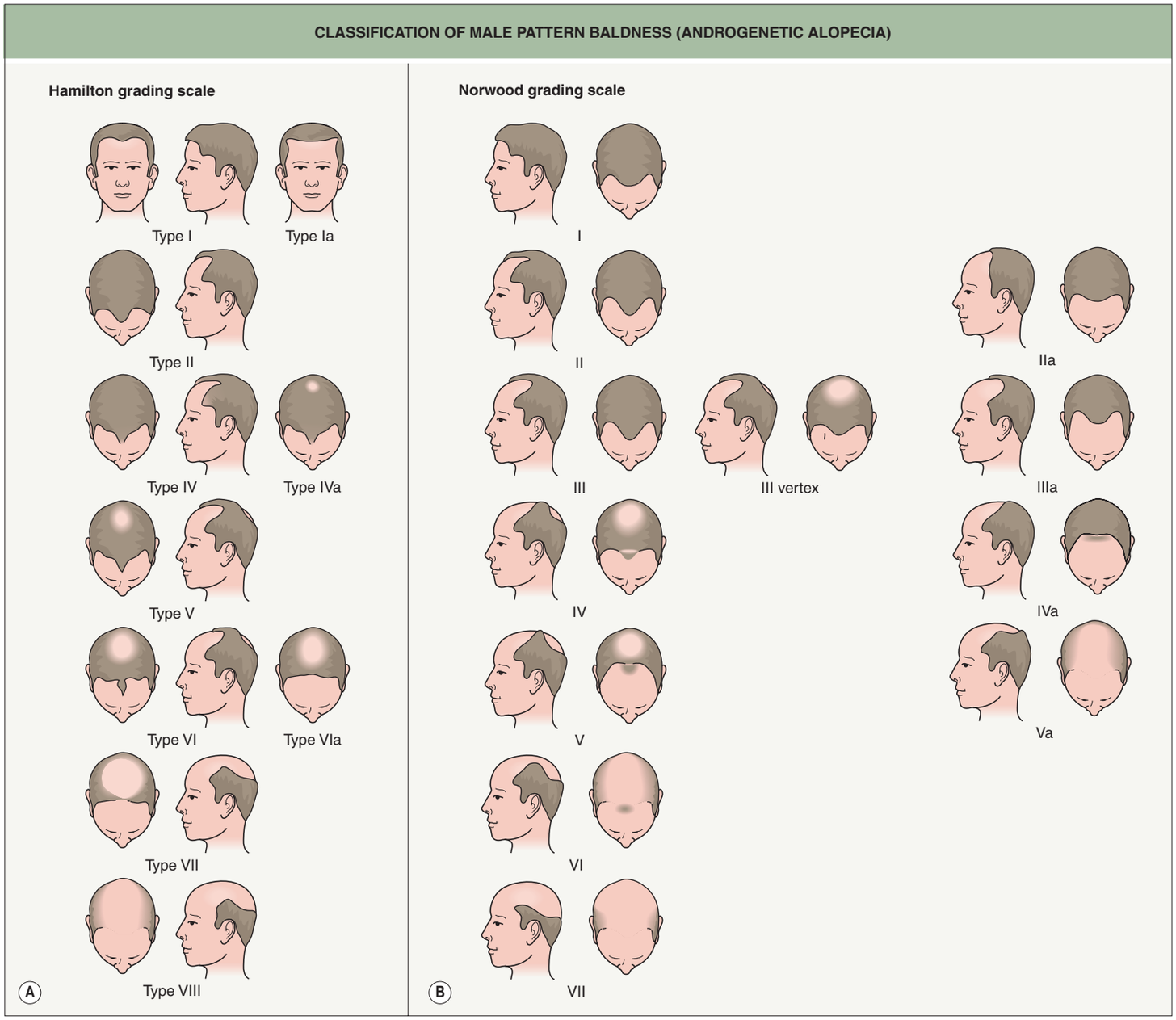


Fig. 157.2 Classification of male pattern baldness (androgenetic alopecia). A Hamilton grading scale. **B** Norwood grading scale. *Adapted from Hamilton JB. Male hormone stimulation is prerequisite and incitant in common baldness. Am J Anat 1942;71:451–80; and Norwood OT. Male pattern baldness: classification and incidence. South Med J 1975;68:1359–65.*

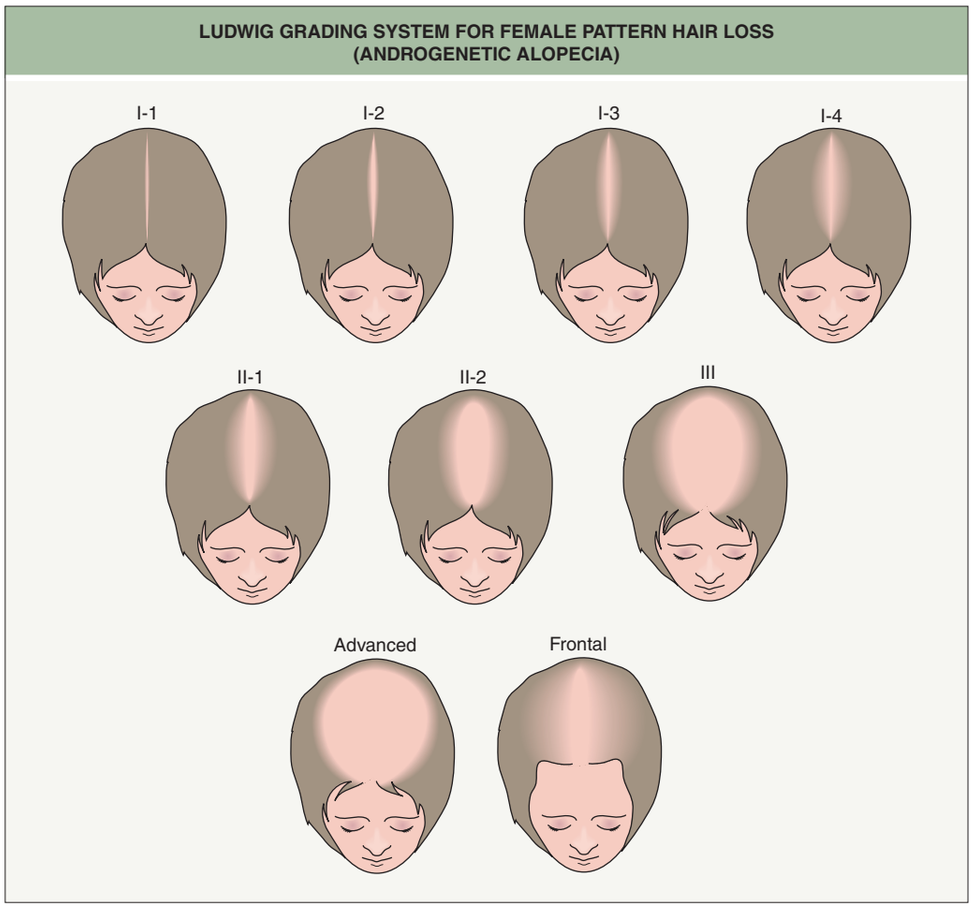


Fig. 157.3 Ludwig grading scale for female pattern hair loss (androgenetic alopecia). Midline hair loss in a Christmas tree pattern is a clue to androgenetic alopecia in women but is not depicted in the Ludwig grading scale. The Sinclair grading scale has five stages: normal (1); widening of the central part (2) plus volume loss lateral to the part (3); bald spot anteriorly (4); and advanced (5).

Increased proliferation of dermal papilla cells[19], an increase in hair caliber, a decrease in the rate of apoptosis of cells in the germinative pool, and more time spent in the anagen phase have all been observed[20]. A possible explanation for the variability in therapeutic responses amongst individuals is differing levels of sulfotransferase activity (which catalyzes minoxidil sulfate) within their hair follicles. There is evidence that aspirin may inhibit this sulfotransferase activity[21].

There has been growing interest in the use of *low-dose oral minoxidil* for AGA in both men and women[22]. Doses vary from 0.625 to 2.5 mg once or twice daily, with lower doses in women and lower doses initially. Multiple studies have demonstrated safety and efficacy in the treatment of male and female pattern hair loss.

Side effects of minoxidil include unwanted hypertrichosis of the cheeks or forehead, headache, ankle edema, and for topical preparations, allergic or irritant contact dermatitis. With regard to the latter, propylene glycol in the vehicle is often the culprit and it has been removed from the 5% foam product (Rogaine®). Facial hypertrichosis is more commonly observed with oral minoxidil and the risk may be greater in those with a genetic propensity for dark facial hair. In women, oral spironolactone can be prescribed to potentially reduce this side effect, in addition to its use as a treatment for female pattern hair loss (see Ch. 69). Fetal hypertrichosis has also been reported and so use of minoxidil is discouraged in pregnant or breastfeeding women. Lastly, reported cardiovascular side effects from oral minoxidil (uncommon with low doses) include hypotension, tachycardia, and pericarditis.

Finasteride inhibits type II 5α-reductase, which converts testosterone to DHT and is present in hair follicles (see Fig. 69.10). Oral finasteride (1 mg daily) is FDA-approved for men with AGA. In a randomized trial of 1553 men given either finasteride 1 mg or placebo for 1 year (with a blinded extension for a second year), significantly greater hair counts in the balding vertex were observed in those receiving finasteride[23]. Five-year results from the same study demonstrated that hair growth peaked at 1–2 years, but hair counts still remained well above baseline for 90% of patients[24]. Although finasteride was FDA-approved for stimulating the growth of vertex hairs, it also stimulates regrowth of frontal scalp hairs[25]. Its use in combination with hair transplantation has yielded statistically greater hair counts 48 weeks after surgery in comparison to the control/placebo group[26]. There is also some evidence that finasteride may work better in men with higher levels of DHT (such as those in their mid-twenties)[27].

Patients are advised to allow at least 6 months before expecting to see a therapeutic effect. If they discontinue the finasteride, the AGA will return to its pre-treatment appearance. Because finasteride is metabolized extensively in the liver, it should be used with caution in patients who have known liver disease[28]. Finasteride also artificially lowers the serum prostate-specific antigen (PSA) level by ~50%[29]. Therefore, both the primary care physician and the patient need to be made aware of this effect. Although early data from prostate cancer trials suggested that finasteride might increase the histologic grade (i.e. severity) of prostate cancer,[30] subsequent analyses suggested a detection bias[31].

Overall, the drug is well tolerated. Side effects that occur in <2% of men taking finasteride include decreased libido, erectile dysfunction and ejaculation disorder, compared with their occurrence in 1% of the placebo group. Rarer side effects include gynecomastia, breast tenderness, and depression[32]. In a double-blind, placebo-controlled, multicenter trial in young men, no changes in spermatogenesis or semen production were observed[33]. However, there have been two reports of severe azoospermia leading to impaired fertility[34]. While the authors feel comfortable prescribing finasteride for men who are planning to have children, it should be discontinued if there are fertility issues, before embarking upon more invasive infertility treatments. Sexual dysfunction, even after discontinuation of finasteride, has been reported, but with selection bias, recall bias, and lack of control for confounding factors[35]. Prolonged libido effects in conjunction with other findings such as brain fog and depression have been collectively coined "post-finasteride syndrome"; Merck has updated its packaging to reflect this possibility but the diagnosis remains controversial and poorly understood. Most recently, the FDA added suicidal ideation and behavior to the package insert despite the lack of reasonable evidence of a causal link. Patients who are reluctant to take oral finasteride may benefit from a compounded (off-label) formulation of topical finasteride[36].

We encourage surgical candidates to stabilize their hair loss by taking finasteride, or another medical therapy, for 6 to 12 months prior to hair transplantation. Most men benefit from combination therapy (Fig. 157.4). Patients who report sexual dysfunction side effects should discontinue oral finasteride and, after an interval of 1–2 weeks, try every second- or third-day dosing.



Fig. 157.4 Combination of hair transplantation and oral finasteride (1 mg daily). A 38-year-old man with male pattern hair loss (baseline). **B** Appearance following 1 year of finasteride plus hair transplantation (500 grafts).

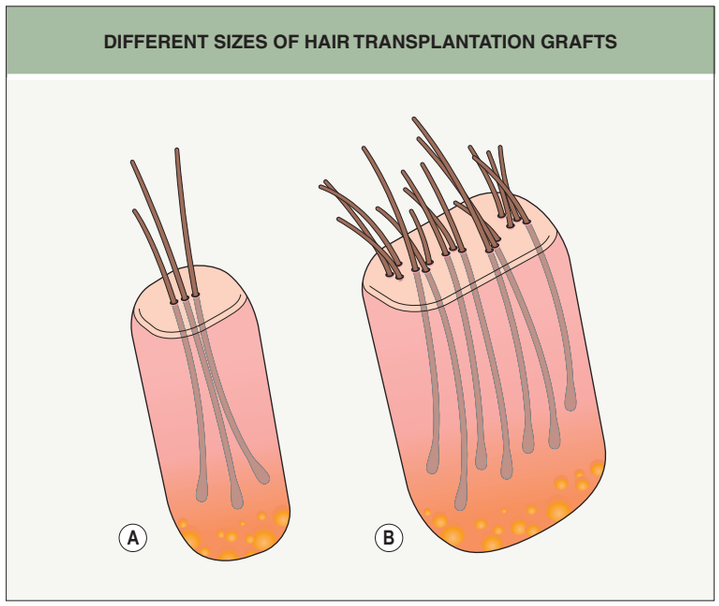


Fig. 157.5 Different sizes of hair transplantation grafts. A The newer technique uses 1- to 4-hair follicular unit grafts. **B** The older technique uses larger 10- to 15-hair grafts.

Finasteride is not FDA-approved for women with AGA, and at a dosage of 1 mg daily, no improvement was observed in clinical trials[37]. Of note, finasteride can cause feminization of the male fetus. In an uncontrolled series of post-menopausal women, higher doses of 2.5 mg and 5 mg daily led to improvement in hair density in 62% and 81% of patients, respectively[38,39]. Excellent tolerability has been observed in women on long-term finasteride, with minimal-to-no side effects[40].

Dutasteride differs slightly from finasteride in that it blocks both type I and type II 5α-reductase isoenzymes. It has been used off-label at a dosage of 0.5 mg daily for AGA in men who did not respond to finasteride, and increased hair counts were observed in a randomized, placebo-controlled trial[41]. However, the drug's half-life is 5 weeks, compared with 6–8 hours for finasteride. Thus, side effects are longer-lasting (several months) and more difficult to reverse. In a double-blind, placebo-controlled trial, men who received oral dutasteride (0.5 mg daily) versus placebo for 1 year had significant decreases from baseline in sperm count: by 28.6% at 26 weeks, 25% at 52 weeks, and 23% at 24 weeks after the trial ended[42]. Sperm motility was also reduced at the latter time point. This potentially irreversible drop in sperm count and motility is an issue for men who still desire to have children.

Low-level light therapy

Photo-biostimulation via low-level light therapy (LLLT) is another possible treatment for hair loss. This was initially based upon the observation that laser hair removal can sometimes trigger paradoxical hair growth in the surrounding skin[43]. Based upon their approval by the FDA as a medical device (rather than a drug), multiple LLLT products are commercially available. The patient combs light (650–700 nm) through the hair two to three times per week or wears a laser cap for a prescribed amount of time daily, with the expectation of hair growth. However, there have only been a limited number of published studies examining the effects of LLLT on hair growth[44,45]. Patient expectations should be managed, and while it is very safe (e.g. can be used in pregnant women), the authors seldom recommend it as monotherapy but rather utilize in combination with minoxidil, platelet-rich plasma, or finasteride[46].

Platelet-rich plasma

Platelet rich plasma (PRP) has emerged as an appealing therapy for hair loss given its autologous nature. It was first described in conjunction with hair surgery to increase growth of transplanted follicles[47]. This technique involves obtaining 10–40 ml of the patient's blood followed by centrifugation in order to achieve a platelet-rich concentration that is 4–7× baseline. Activated platelets have been shown to release platelet-derived growth factor, epidermal growth factor, transforming growth factor, and vascular endothelial growth factor[48]. The PRP is then injected into areas of alopecia, either alone or in combination with adjuvants such as calcium chloride or calcium gluconate. Numerous proprietary PRP "kits" have been developed for dental, orthopedic, and now dermatologic applications.

While most studies have focused on its use for AGA, PRP has also shown some promise in the treatment of alopecia areata[49] and LPP[50]. In one clinical trial in patients with AGA, three monthly injections followed by a booster injection 3 months later led to more rapid hair thickening and regrowth than did injections every 2 months over 6 months[51]. However, in a randomized controlled trial of patients with AGA, injection of PRP versus saline into two equivalent sites on the scalp resulted in similar results[52]. This and other studies have led some to question the effectiveness of PRP[53]. More research is therefore needed to further refine optimal dosing and treatment guidelines.

HAIR TRANSPLANTATION

Hair transplantation is a procedure performed in an outpatient setting under local anesthesia. It is based on the theory of donor dominance, i.e. terminal hair from the unaffected posterior scalp will continue its growth pattern even when transplanted to the balding frontal scalp[54]. Unfortunately, until the 1990s, hair transplants often had an unnatural appearance due to unsightly and obvious "plugs", sometimes likened to a "Barbie-doll" appearance. Over the past two decades, there has been a revolutionary movement away from 3–4 mm grafts containing 15–30 hair follicles to grafts containing groupings of one to four hair follicles, referred to as individual follicular units (Fig. 157.5). This has resulted in the transplanted hair having a more natural appearance (Figs. 157.6 & 157.7).

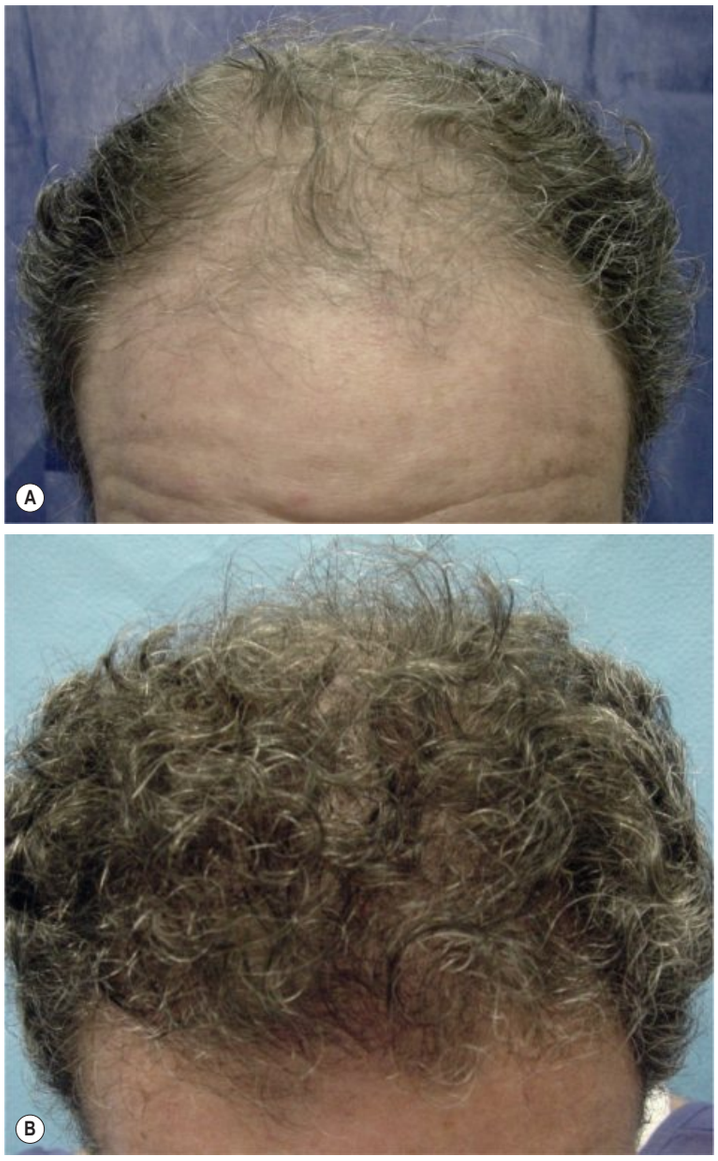


Fig. 157.6 Hair transplantation for male pattern hair loss. A Norwood IV pattern (baseline). **B** Appearance following transplantation of 900 hair grafts, each with one to three hairs.



Fig. 157.7 Hair transplantation for female pattern hair loss. A Ludwig II pattern (baseline). **B** Appearance following transplantation of 750 hair grafts, each with one to three hairs.

The net perceived density from a hair transplant is equal to the number of successfully transplanted follicles minus ongoing hair loss. In order to maximize long-term results, all patients undergoing this surgical procedure are encouraged to continue topical minoxidil, low-dose oral minoxidil, and/or oral finasteride (see above). Halting or at least slowing the miniaturization process allows for the perception of greater hair density.

Candidate Selection

As with all surgical procedures, the preoperative consultation is key to the success of the procedure. The consultation establishes whether the patient is an appropriate candidate for hair transplantation, both from a medical and a psychological perspective. In addition, it allows for an assessment of areas of greatest concern and whether the patient has realistic expectations of what a hair transplant can achieve.

A complete medical, surgical, and hair loss history is obtained, including previous hair transplants and scalp surgeries as well as scar formation. The etiology of the hair loss is determined, primarily via physical examination of the scalp. Occasionally, additional sites need to be examined and/or clinicopathologic correlation is required. The stage of patterned hair loss also needs to be established (see Figs. 157.2 & 157.3). All medications, prescription, over-the-counter and herbal, are reviewed with regard to their effects on hair growth and hemostasis (see Chs. 21 & 133).

The basic criteria for assessing the appropriateness of a candidate for hair transplantation are outlined in Table 157.1. In particular, the density of donor hair in the occipital scalp and the caliber of the hair need to be appraised, as both have an impact on the perceived density of the transplant (Table 157.2). Obviously, greater donor density and more grafts to transplant as well as thicker hairs rather than fine hairs lead to a fuller-appearing transplant.

Key Concepts

Both men and women should be made aware that AGA represents an ongoing process, i.e. it will progress despite undergoing hair transplantation. Medications (e.g. oral finasteride, minoxidil) or PRP and LLLT can help to maximize hair density from a transplant by minimizing ongoing hair loss. However, in planning for the transplant procedure, the surgeon should always assume that in the future these medications may be discontinued (see Table 157.2). Also, the progressive nature of AGA means that additional hair transplants may be required. The physician should therefore emphasize *before* the procedure how ongoing hair loss will affect the density and cosmetic appearance of the transplant as well as how this influences the placement of the grafts so as to assure a long-term natural appearance.

The number of expected procedures to accomplish both short- and long-term goals should be reviewed, as well as the limits on available

FIVE BASIC CRITERIA FOR ASSESSING CANDIDATES FOR HAIR TRANSPLANTATION	
Age	Patients over the age of 25 years are preferable. While patients younger than 25 years of age often seek consultation, there is a hesitancy to operate. The predictive value of future hair loss is much lower for individuals between 15 and 25 years of age. Even with the theoretical safety net of finasteride, physicians should carefully choose candidates under 25 years of age. This subgroup also tends to desire a return to a full head of hair as opposed to a mature pattern of restoration that is routinely performed in older age groups.
Hair shaft caliber	The caliber of the hair shaft is crucial. Those with large-caliber hair shafts (greater than 70 microns) obtain much denser coverage than individuals with corn silk quality hair. This can be demonstrated mathematically in that very small volume increases in hair shaft diameter result in exponential increases in surface area coverage.
Donor hair	A variety of instruments are available to measure donor hair density. Measuring a 0.25 cm^2 field and multiplying by four is the preferred method. Patients seeking hair transplantation who have >80 follicular units/cm^2 are excellent candidates. Those with donor hair density <40 follicular units/cm^2 are considered poor candidates.
Degree of baldness	The degree of baldness is perhaps the most important criterion in candidate selection. Those with complete baldness of the frontal scalp as opposed to baldness limited to the vertex are excellent candidates. When frontal baldness is corrected, this creates the most dramatic positive change in appearance.
Hair color	Follicular unit grafting has made hair color less of an issue than when punch grafts were employed. Color contrast between hair and skin can make grafts apparent if not transplanted with great care. Individuals with "salt-and-pepper" hair, red hair, or blonde hair are preferential to those with jet-black hair. Black-haired individuals are not exempt as hair transplant candidates, but should receive only one-hair follicular units in the frontal hairline for the most natural result. Proper technique eliminates most problems with dark-haired candidates.

Table 157.1 Five basic criteria for assessing candidates for hair transplantation. *Courtesy Dowling B. Stough, MD.*

HAIR TRANSPLANTATION – CLINICAL FINDINGS AND REALISTIC EXPECTATIONS		
Clinical findings	**Realistic expectations**	**Comment**
• High donor density • Large-caliber (thick) hair • Stabilized hair loss via topical minoxidil, low-dose oral minoxidil, and/or oral finasteride	1000–1500 graft sessions will create the perception of increased hair density	Need to plan the procedure *assuming* the patient may stop the medication(s) and the hair loss will resume
• Poor donor density • Thin-caliber (fine) hair • Ongoing hair loss	1000–1500 graft sessions may create little increase in *perceived* density	Although the transplant will result in more hair, this may not be apparent due to ongoing hair loss and thin-caliber hair

Table 157.2 Hair transplantation – clinical findings and realistic expectations. The net density from a transplant = number of follicles transplanted minus ongoing hair loss.

donor hairs. Reasons for preferring to transplant primarily the frontal scalp as opposed to the vertex need to be explained – the vertex can consume donor grafts and it exhibits a continued 360° progression of hair loss which can lead to a peripheral rim of bald scalp which will appear unnatural over time. In addition, transplanting the frontal scalp, not the vertex, produces the maximum cosmetic impact. Therefore, transplanting the vertex should be approached with caution, particularly in younger patients. Concentrating the transplants in the frontal scalp will allow maximum long-term density with minimal long-term cosmetic risk.



Fig. 157.8 Occipital scalp scar secondary to elliptical donor harvesting. *Courtesy Dowling B. Stough, MD.*

Patients have to realize that elliptical donor harvesting will lead to a permanent scar of the posterior scalp (Fig. 157.8). The scar is of no practical concern unless the patient has his or her hair closely cut. If the patient expresses an interest in having closely cropped hair, follicular unit extraction (FUE) should be considered (see below). However, the possibility of small "white dots" following FUE should also be discussed. Lastly, the patient must appreciate the need for a conservative approach to placement of the anterior hairline so that it will have a natural appearance over a lifetime as the temporal and posterior hairlines recede.

Staff Training for Manual Hair Transplantation

Contemporary hair transplantation is a team procedure, and an efficient, high-quality transplant requires a well-trained surgical team. Assistant technicians should be motivated and interested in learning and mastering the procedure. In addition, they need to be able to do repetitive tasks without tiring, losing concentration, or becoming frustrated. Technicians are utilized primarily for cutting and planting. The first task involves sectioning of the donor strip into slivers, followed by further meticulous sectioning into follicular units and prompt placement into chilled saline or other holding solution (Fig. 157.9). After the physician creates recipient sites, technicians can help insert the follicular unit grafts into the scalp. Recipient sites are generally designed at a density of 35–40 follicular units/cm^2 but a lower density may be employed in areas where there is already pre-existing hair growth.

During the procedure, the physician closely monitors the quality of graft creation and placement. It is recommended that physicians learning the procedure have a staff member train at the same time. In order to avoid repetitive strain syndrome, technicians should position their elbows or forearms on a firm, supportive surface while using wrist and finger movements to plant grafts. Rotation of duties can also prove helpful.

Donor Region

The amount of available donor hair is the primary limiting factor in hair transplantation. In general, there are 65–85 follicular groupings/cm^2 in the occipital donor scalp[55]. If there are <40 follicular units/cm^2, the patient is considered a poor candidate (see Table 157.1). The mid-occipital scalp between the upper and lower occipital protuberances is the recommended donor site, given its density of hair and the ability to camouflage the donor scar due to the lack of involvement by AGA. If the harvesting is done too superiorly on the occiput, progressive AGA may reveal the surgical sites. Of note, donor density does not correlate with the extent of current or future hair loss in the frontal scalp or vertex. Harvesting of donor hair is performed via two different techniques: (1) elliptical donor harvesting; and (2) FUE (Table 157.3).

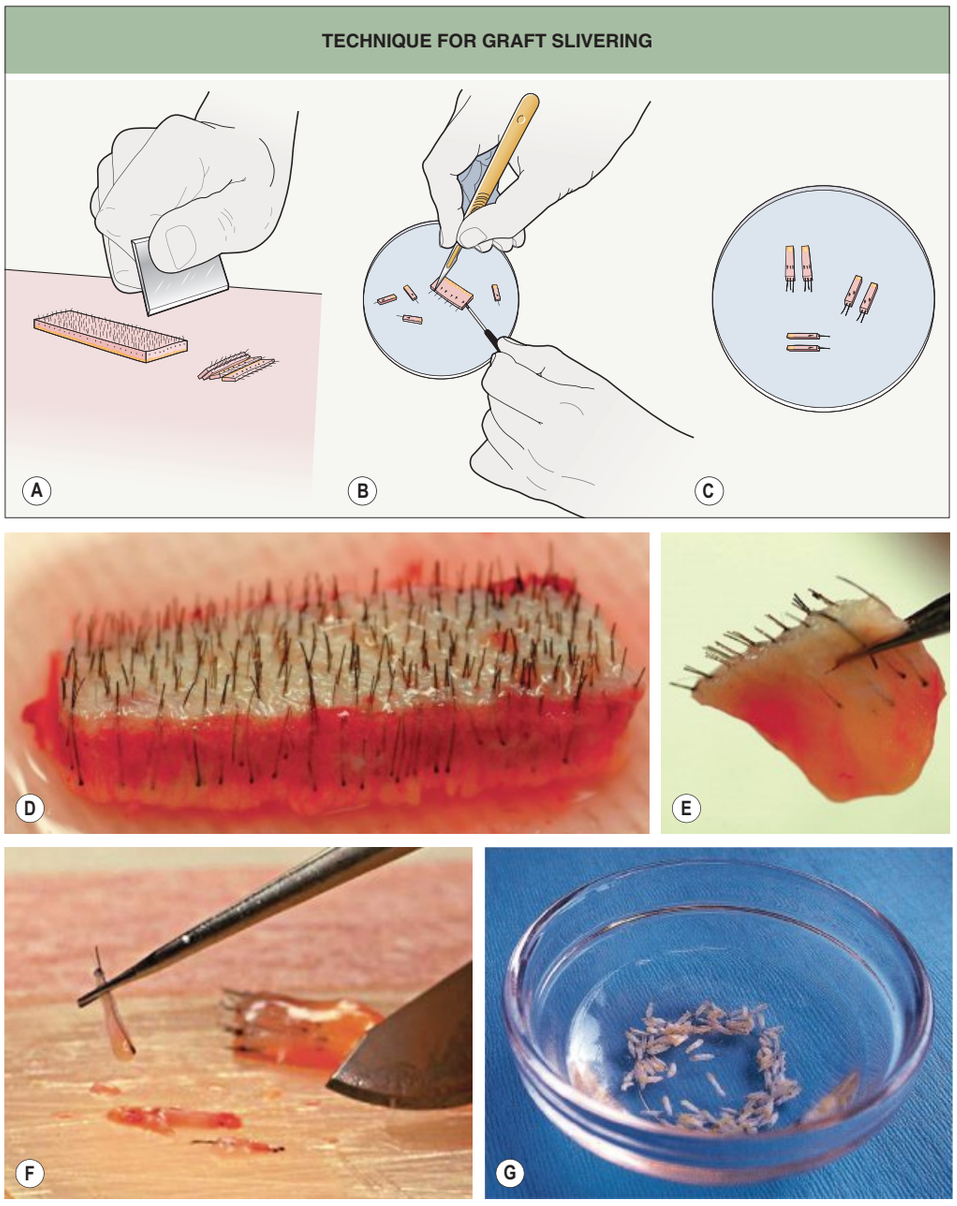


Fig. 157.9 Technique for graft slivering. A Donor slivering which produces slivers 2 mm wide by 10 mm long. **B** Slivers being sectioned into follicular units. **C** Follicular unit grafts are placed into dish with saline and separated into one-, two- and three-haired follicular units. **D** A portion of donor strip prior to slivering. **E** Appearance of a sliver. **F** A single follicular unit produced by microscopic dissection of a sliver. **G** Follicular unit grafts are stored in isotonic saline to maintain their viability. *Courtesy Dowling B. Stough, MD.*

COMPARISON OF ELLIPTICAL DONOR HARVESTING VERSUS FOLLICULAR UNIT EXTRACTION		
	Elliptical donor harvesting	**Follicular unit extraction**
Visible scar if short hair cut	Yes	No
Transection of hair follicles	Minimal	Variable
Time required to perform harvest	10–20 minutes	30–90 minutes
Time needed to create grafts	Lengthy	Minimal
Quality of resulting transplant	Excellent	Excellent

Table 157.3 Comparison of elliptical donor harvesting versus follicular unit extraction.

Elliptical donor harvesting (follicular unit transplantation [FUT])

Elliptical donor harvesting is still performed in a large number of patients because it allows for the safe and rapid removal of a large number of hair follicles, with minimal transection of hairs[56]. In addition, if patients will never wear their hair closely cropped, the resultant linear scar is not a concern and in contrast to follicular unit extractions, there is no need to trim hairs to 1 mm prior to the procedure. Elliptical donor harvesting is also referred to as follicular unit transplantation (FUT) or follicular unit strip surgery (FUSS).

The length and width of the donor ellipse depends on the number of follicular groupings required for the patient. For example, if 1000 follicular groupings are needed for the frontal scalp and a patient has an average donor density of 75 follicular units/cm^2, a 13.5 cm by 1 cm strip should contain approximately 1000 follicular grafts. It is important to remember that if a greater number of grafts are required, the ellipse should be lengthened rather than widened since increasing the width of a donor ellipse creates more wound tension which may lead to a hypertrophic or wide scar.

Ideal local anesthesia is obtained by infiltrating 1% lidocaine with epinephrine (adrenaline) superficially into the dermis. Once anesthesia has been achieved, bacteriostatic normal saline can be injected to provide further anesthesia, hemostasis, and dermal turgor. Turgor helps to reduce the transection of hair follicles. The blade(s) should be oriented parallel to the exiting follicles to avoid transection of hair follicles. The incision should be into the subcutaneous fat, and not deeper, in order to avoid transecting the occipital arteries (Fig. 157.10). Lateral retraction around the ellipse using fine skin hooks creates good visibility for the surgeon harvesting the ellipse (Fig. 157.11). The ellipse can be removed by scissors or a scalpel, carefully avoiding damage to any follicles in the subcutaneous tissue.



Fig. 157.10 Elliptical donor harvesting. To avoid transection of the hair follicles, the double blades should be oriented parallel to the exiting follicles. The incision should extend into the subcutaneous fat but not deeper (~5 mm into the scalp). Some surgeons prefer a single blade for performing the ellipse.



Fig. 157.11 Elliptical donor harvesting. Lateral retraction using fine skin hooks exerts tension away from the excision and creates good visibility. The ellipse can be removed by scissors or a scalpel, being careful to avoid damage to any follicles in the subcutaneous tissue.

If the incision does not go any deeper than the subcutaneous fat layer, the ellipse can be removed without the use of electrocoagulation or thermal coagulation. Also, if the donor ellipse is <1 cm in width, it can often be primarily repaired without undermining. Some surgeons utilize a two-layer closure with absorbable sutures while others perform a single-layer closure. Staples or sutures can be utilized and then removed 7–10 days postoperatively. In some patients in which there is good surgical technique and optimal wound healing, the donor area from a single strip procedure may be more natural-appearing than with FUE. However, one cannot predict donor site healing following strip harvesting.

Follicular grafts

Hair naturally grows in groupings of 1–4 hair follicles, referred to as follicular units (see Fig. 157.5)[57]. During the 1960s to 1990s, 3–4 mm grafts that contained multiple follicular units were employed, leading to an unnatural appearance with obvious bundles of hair. Nowadays, each graft contains one follicular grouping with 1–4 hair follicles. Thus, these grafts mimic the normal grouping of scalp hairs and create a natural appearance.

When an ellipse is harvested, surgical teams carefully separate 500–2000 follicular units from the donor strip over 1–3 hours (see Fig. 157.9). Cutting instruments vary but include #11 and #15 blades as well as #10 prep blades. Good lighting, comfortable chairs, and well-designed instruments are prerequisites for producing follicular units with minimal follicular transection. Most surgeons believe microscopic dissection or magnification reduces transection of follicles during the separation process (Fig. 157.12).



Fig. 157.12 Use of magnification to separate follicular units from the donor strip.

It is important to create intact, minimally traumatized follicular units and place the transplanted hair into the recipient sites as efficiently and quickly as possible. As soon as the follicular unit grafts are separated from the donor ellipse, they must be put into a holding solution until they are placed into the recipient sites. Commercially available holding solutions can enhance survival of these hair follicles, in part by reducing apoptosis[58]. If grafts desiccate for even a few minutes they will die and not grow. One of the advantages of the FUE technique is that following visual inspection, harvested grafts can be transplanted immediately.

The number of follicular units required for each surgery depends on the extent of hair loss, available donor hair, and density of pre-existing terminal hair follicles in the recipient area. This can vary from 100 to 2500 follicular groupings per procedure. Larger cases may be done over two days to avoid technician fatigue and reduce the chance of undesirable sequelae.

Follicular unit excision (FUE)

In the FUE technique, single follicular units consisting of groupings of 1–4 hair follicles are surgically removed from the occipital scalp. Tiny punch devices (~0.75–1.2 mm in diameter) are used to remove the grafts[59,60]. The incisions are so small that they usually leave no visible scar after they heal; however sometimes small "white dots" are seen. For patients who like to have closely cropped hair, FUE is generally preferred. It is also an option for patients who have significant tension or extensive scarring from previous elliptical donor harvesting.

Although manual FUE requires more time than elliptical donor harvesting, the introduction of automated mechanical instruments and robotic technology has led to a reduction in extraction times. Important considerations when performing manual FUE are outlined in Table 157.4. Potential disadvantages of FUE include a higher rate of transection of follicular groupings when compared to strip harvesting as well as the risk of "thinning out" the donor area due to repeated extractions[61]. In one small series, the number of lifetime follicles was similar for FUT and FUE[62].

Numerous devices exist for performing FUE[59,60]. Earlier devices utilized manual or motorized dull punches to gently extract the grafts in order to avoid damage to bulb anatomy. Subsequently, motorized, sharp punches

MANUAL FOLLICULAR UNIT EXTRACTION (FUE) – PROCEDURAL CONSIDERATIONS
• The incision should follow the **follicular exit angle** from the scalp, taking into account individual hair follicle characteristics and the observation that follicles grow in a curve with the concavity of the follicle on the acute angle side of the follicle.
• Because the length of the trimmed hair dictates the *apparent* **angle of hair growth**, hair follicles must be trimmed to the preferred length of ~1 mm so as to identify the *true* angle of emergence; if the hair follicle is trimmed too long, the apparent angle is more acute than the true angle and if the hair is trimmed too short, tumescence can conceal both the follicle and its angle of hair growth. Cross polarization may assist in visualizing the hair growth angle.
• To minimize initial **wound size**, one can first incise shallowly perpendicular to the skin surface followed by a deeper incision directed along the angle of hair growth; if an incision with a cylindrical punch follows the angle of hair growth, the wound will be an ellipse.
• Optimally, the targeted follicles should be in the center of the punch instrument or needle, and because hair grows at an acute angle, the inferior side of the punch instrument will first contact the skin.
• If the **axial force** created by the inferior side of the punch instrument is too great, the bulb of the follicle may be displaced inferiorly and amputated; a predominantly tangential force, rotation, or oscillation minimizes follicle displacement as does skin tension applied via tumescence or skin traction.
• To avoid graft torsion, **frictional forces** between the punch instrument and the skin must be minimized by using a very sharp, well-designed instrument with a thin wall and by minimizing incision depth.
• In order to free up intact follicles, deeper incisions are required if the ORS is strongly attached to surrounding adipose tissue and if the ORS is weakly attached to the IRS.
• Because of **follicular splay** within a grouping, use of a punch instrument with a greater diameter may be required to excise intact grafts and minimize follicle transection rates; with manual harvesting, one can expect an average 2.10–2.25 follicles/graft with a 0.8–0.9 mm punch instrument.

Table 157.4 Manual follicular unit extraction (FUE) – procedural considerations. IRS, inner root sheath; ORS, outer root sheath.

were employed to speed up excisions. Punch instruments with a flared or trumpet shape were introduced more recently to try to reduce transection of hair bulbs. Robotic systems such as ARTAS® (Venus Concepts) can be used to minimize physician fatigue and eliminate the need to acquire all the surgical skills needed to dissect grafts.

With FUE, the surgeon can target follicular groups of a specific size or hairs with a specific diameter or pigmentation. Single hairs may be harvested for eyebrow restoration, or larger 3–4 hair groupings may be targeted to add density over the mid scalp. Because of minimal scarring, harvesting from the beard region or other terminal hair-bearing areas is also an option. In addition, harvesting can be done even after multiple strip surgeries have led to a very tight donor area.

For optimal cosmetic results and to preserve symmetry, one should irregularly harvest from the entire *safe donor area* (SDA) rather than from just a small shaven area. Of note, the surgeon should not be pressured to over-harvest, lest the donor area be depleted. Unfortunately, patients sometimes seek less expensive "black market" hair transplants and then can present with donor and/or recipient site necrosis and soft tissue infections, resulting in few options for repair.

Hairline Design and Recipient Site Creation

In men, the hairline defines the cosmetic success of a hair transplant. Most women have stable frontal, temporal and posterior hairlines, making recreation of a hairline unnecessary. As with hair graft creation, hairline design should mimic, as closely as possible, what occurs in nature. However, patients and physicians often try to mimic the hairline a patient had before their male pattern hair loss began. Even with follicular unit transplants, this approach to hairline design often leads to cosmetic failure. This is due to not considering the slow steady recession of the temporal and posterior hairlines in addition to the frontal hairline.

The design of the frontal hairline should be such that over time it will remain balanced with the temporal and posterior hairlines.



Fig. 157.13 Immediate postoperative appearance with graft placement and hairline design. *Courtesy Dowling B. Stough, MD.*

This requires recreating a frontal hairline which is higher and more receded than the one which was present before the process began. Initially, some patients will resist the idea of a higher, more receded hairline, but explaining and demonstrating with a mirror how their temporal and posterior hairlines preclude a low frontal hairline usually changes their opinion.

Rather than considering the hairline to be a fixed boundary, it should be thought of as a natural transition zone of gradually increasing density from skin to terminal hair-bearing skin. This ill-defined "feathering zone" is created by placing, in an irregular pattern, follicular unit grafts (with 1–4 follicles) along the newly created hairline (Fig. 157.13)[63]. Dense packing of grafts should not be performed along the frontal hairline because a densely packed hairline has an unnatural appearance. The level at which the hairline is placed varies from individual to individual and it is important to examine each patient in a global, 360° manner before determining placement of the hairline.

While male pattern hair loss is progressive, transplanted hair will have long-term growth. Therefore, when evaluating patients, the surgeon must assume that all patients will progress to the highest grade of involvement, i.e. the worst-case scenario. As noted previously, for several reasons, including the progressive nature of AGA leading to an unnatural appearance, transplanting into the vertex should be approached with caution.

Anesthesia and Recipient Site Creation

A combination of supraorbital/supratrochlear nerve blocks, field blocks, and local infiltration with 1% lidocaine with epinephrine is performed. Hemostasis is essential for good visibility when creating recipient sites and for graft placement. The epinephrine in the local anesthetic (placed into the dermis, not the subcutaneous space) is usually adequate for providing excellent hemostasis. While most surgeons use "off-the-shelf" 1% lidocaine with 1 : 100 000 epinephrine, concentrations of the latter may range from 1 : 50 000 to 1 : 500 000.

Recipient sites should mimic the natural 30–45° angle of hair growth on the scalp (Fig. 157.14). There are a variety of needles, in particular 18, 19, 20 and 21 gauge needles, that are used to make recipient sites for 4, 3, 2, and single hair groupings, respectively. When creating recipient sites, surgeons must be careful not to transect existing hair follicles. Most advocate using magnification to place recipient sites in order to limit the loss of existing hair during surgery[64]. The key to success is to arrange recipient sites in a random, irregular pattern with 10–30 sites/cm^2, depending on the density of existing hair on the scalp.

Graft Placement and Postoperative Course

Microvascular forceps are used by surgical assistants to place the grafts. These forceps gently grasp the follicular units by their perifollicular tissue, avoiding trauma to the hair follicles. Placement of the grafts into recipient sites is often the most challenging component of the hair

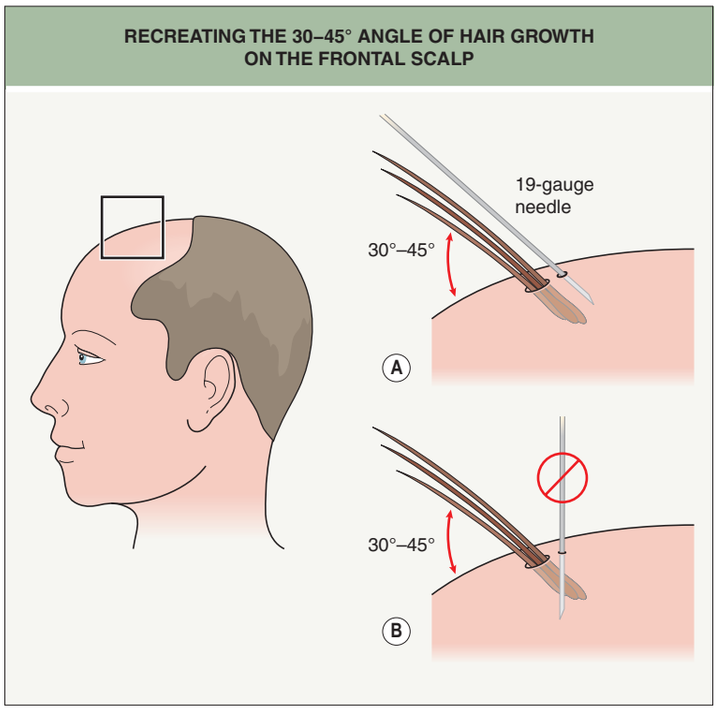


Fig. 157.14 Recreating the 30–45° angle of hair growth on the frontal scalp. Correct (**A**) versus incorrect technique (**B**). Grafts should not be oriented perpendicular to the scalp surface.

HAIR TRANSPLANTATION – POSTOPERATIVE INSTRUCTIONS	
Day of the procedure	• Apply non-adherent dressing overnight • Oral acetaminophen (paracetamol) 300 mg/codeine 30 mg every 4–6 hours as needed with food* • Oral prednisone 40 mg daily for 3 days to reduce frontal scalp edema • Resume regular activities, but no heavy lifting or strenuous exercise until staples/sutures removed • Sleep with head elevated
Postoperative days 1–3	• Day 1 – remove dressing • Shower each day and allow water to run over grafts • Comb hair without allowing comb's teeth to hit perifollicular crusts • Do not pick or scratch at perifollicular crusts • Apply emollient to the donor site(s) daily • Days 1, 2 – continue prednisone (see above)
Postoperative days 4–7	• Resume light exercise • Follow instructions outlined above for showering, combing, and emollient application
Postoperative days 7–10	• Staples/sutures removed • Resume regular exercise regimen • Perifollicular crusts gradually disappear
*In general, only required on the day of surgery.	

Table 157.5 Hair transplantation – postoperative instructions. Patients should not wear a hairpiece for at least 2 weeks after the procedure.

transplant procedure, both for novice and experienced hair transplant teams. The major challenges include hemostasis and "popping" of grafts from recipient sites after they are placed. However, it is difficult to predict which patient will have "popping" grafts. This phenomenon is overcome by applying light pressure over a placed graft for 5–15 seconds with a saline-soaked cotton swab before placing the next graft.

After the procedure, an overnight dressing is placed to protect the grafts. The entire dressing should be non-adherent and removed by the patient the next morning (Table 157.5). Staples or sutures are removed during a 7- to 10-day postoperative visit. The transplanted hair begins to appear 3–6 months after the procedure and is fully grown by 9–14 months. Patients must be warned of the possibility of post-transplant telogen effluvium.

Complications

Medical and surgical complications from a hair transplant procedure are unusual. The extensive vascular supply to the scalp results in rapid wound healing and a low risk of infection. In addition to reactions to medications and vasovagal episodes, complications include excessive swelling (~5%), postoperative bleeding (<0.5%), folliculitis, a temporary headache, and temporary pruritus or numbness of the scalp. Persistent problems include permanent numbness in the donor or recipient sites, abnormal scarring around the grafts, hypertrophic scarring of the donor site, and poor growth of hair grafts. The latter can be minimized by keeping the grafts constantly moist.

Hypopigmentation often occurs at extraction sites within the donor region but its occurrence is not predicable. It is often larger in diameter than the punch instrument used to obtain the graft. Scalp micropigmentation has been used to successfully camouflage this hypopigmentation. Telogen effluvium of nonreplaced hair, also referred to as "shock" hair loss, is an uncommon complication that in the authors' experience resolves on its own. It stems from overharvesting of grafts in a specific region. In general, *maximal* harvesting during a single procedure should be 25% of the total number of follicular units. Because the number of safely harvested grafts depends on the density of follicular groupings and hair caliber, individuals with fine hair and older individuals (number of follicular groupings decreases with age) who undergo harvesting of higher numbers of follicular groupings are at risk for this complication. Lastly, a hair transplant-triggered flare of LPP has been reported. It is unclear if a hair transplant actually triggered a flare of LPP or subclinical preexisting disease became more active.

Corrective Hair Transplant Surgery

When patients present for corrective surgery due to previous transplantation of 3–4 mm punch grafts that have led to unnatural large "plugs", i.e. a "pluggy" transplant, three major options exist: (1) add a large number of follicular unit grafts containing one to four hairs between the larger plugs; (2) surgically remove the large grafts; and/or (3) perform laser-assisted hair removal. Which option is best suited for an individual patient is determined during the consultation.

Adding follicular unit grafts

Transplantation of a large number of follicular unit grafts containing one to four hair follicles – in front of, in between, and behind large grafts – will soften the "pluggy" appearance (Fig. 157.15). This option is appealing for many patients because it allows for both cosmetic improvement and increased density (Fig. 157.16). Unfortunately, some patients with an unnatural hairline have a depleted donor supply from previous transplant procedures while others are reluctant to have another surgery following the emotional trauma from the initial transplant.

Surgical removal of grafts

Some hairlines are so cosmetically inappropriate that there is no worthwhile corrective option other than surgically removing the grafts. This option is also indicated for large grafts with perifollicular white scar tissue. The grafts can be removed by either a 2–4 mm punch instrument or an elliptical excision. Another option is to perform FUEs from larger grafts via 1 mm punch instruments. The latter procedure reduces the "pluggy" appearance of the larger grafts while allowing a more natural appearing graft to remain.

In general, scars on the scalp heal well with minimal evidence of the surgical procedure. However, all patients should be warned that cosmetically evident scars develop in a small minority of cases. If unacceptable scars do arise, pulsed dye, ablative, non-ablative, or fractional ablative laser treatments can be used to help improve the cosmetic appearance.

Laser-assisted removal of large grafts

As with other parts of the body, lasers only remove pigmented terminal hair follicles (see Ch. 137)[65]. Typically 5–10 treatments are needed to permanently remove the majority of follicles. Similar to FUE of larger

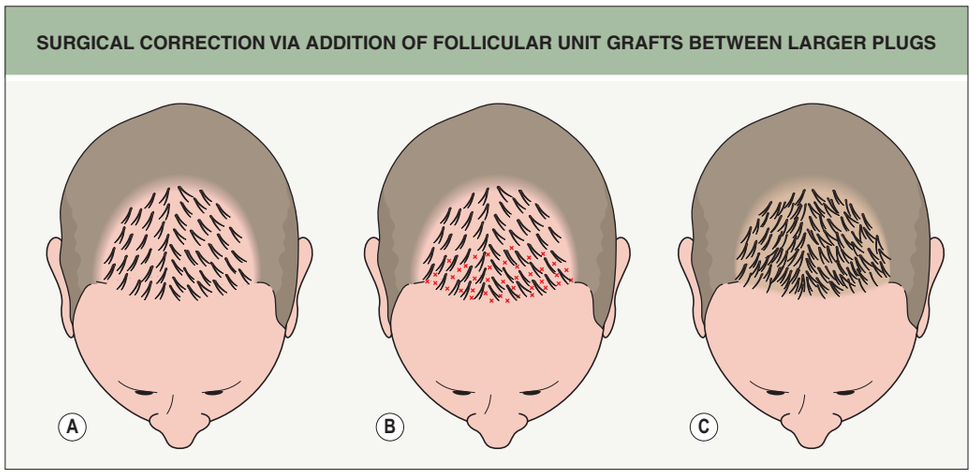


Fig. 157.15 Surgical correction via addition of follicular unit grafts between larger plugs. A Previous transplantation of 3–4 mm punch grafts can lead to unnatural large "plugs" of hair. **B**, **C** Addition of follicular unit grafts between and in front of the larger grafts softens the hairline and the overall appearance.



Fig. 157.16 Corrective hair transplant surgery. A Widely scattered large plugs with significant contrast between the lightly pigmented scalp and the black hairs. **B** Softened and improved appearance after the transplantation of 1000 follicular unit grafts containing one to three hairs.

grafts, laser-assisted removal eliminates the majority, but not all, of the hairs, thus providing a substantial cosmetic improvement of the unnatural plugs while retaining some of the transplanted hair for a more natural appearance. Laser therapy is an excellent option for patients who want to improve their cosmetic appearance in a safe, non-invasive manner.

Hypertrophic or broad scars in the donor region

All patients have a permanent scar from elliptical donor harvesting, but the majority of scars are 1–2 mm wide and are of no practical concern (see Fig. 157.8). That said, patients should be made aware of this permanent donor scar *before* they have a transplant. If the patient expresses a possible interest in having their hair cut short, FUE should be considered (see above).

When wide donor scars occur, they can be a major cosmetic problem without an easy solution for repair. Scar revision leads to variable improvement. Pulsed dye, non-ablative, or fractional ablative lasers may be used to help reduce the thickness and erythema of hypertrophic scars. The best method for minimizing the risk of a wide scar is to keep the width of the donor strip to ≤1 cm. While this does not guarantee a fine, thin scar, it does reduce the risk of a wide scar. Another option is to transplant a large number of follicular groupings into the scar in an attempt to provide camouflage.

Hair Transplantation in Scarring Alopecias

Hair transplantation can be successfully performed to improve the appearance of scarring due to previous cosmetic or cranial procedures. However, if there is any concern regarding active inflammation, a biopsy specimen should be obtained. Any inflammation, whether from a primary scalp dermatosis, infection or previous surgery, must be resolved completely before hair is transplanted. In the case of inflammatory scalp dermatoses, patients should have no evidence of inflammation for at least 6 months off therapy before the transplant procedure is performed.

Patients undergoing surgery for cicatricial alopecias such as LPP, FFA, or CCCA must understand that even if their disease is quiet at the time of surgery, any subsequent flares may compromise the future growth of the grafts. In other words, when there is any active inflammation, the transplanted hair may not grow and all patients should be informed of this *before* their first transplant. Of note, in a retrospective review of 51 patients who received hair transplants for FFA, most of them lost grafts over the following 5 years but there was still very high patient satisfaction[66].

Compared to sites without scarring, the yield is less when hair is transplanted into scar tissue. How large the difference will be varies from patient to patient. In general, more transplant sessions are needed in patients with scarring alopecia.

Hair Transplantation in African-Americans

In addition to pattern hair loss in men and women of African ancestry, traction alopecia and CCCA are also commonly seen in women (see Ch. 69)[67]. If there is a question regarding the precise diagnosis, clinicopathologic correlation is recommended prior to transplantation. For CCCA, there should be no evidence of inflammation for 6 months (off therapy) before the transplant procedure is performed. While patients can wear wigs or hair pieces, hair transplantation is the only way to permanently fill in the areas of alopecia (Fig. 157.17A).

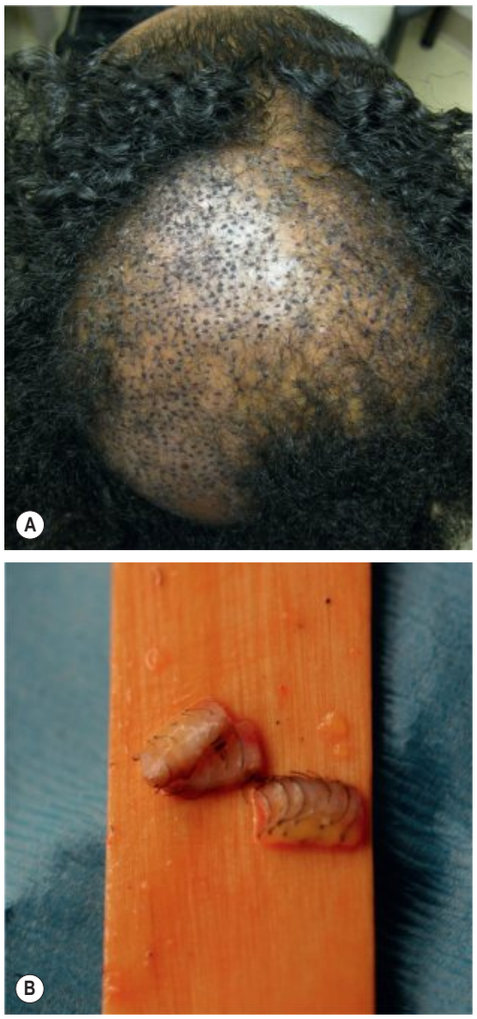


Fig. 157.17 Hair transplantation for central centrifugal cicatricial alopecia. **A** Appearance 1 week following transplantation of 1200 follicular unit grafts in an African-American woman. **B** Cross-section of Afro hair follicles demonstrating their characteristic C-shaped curve.

When transplanting Afrocentric type 4 hair, it is important to note that the curl of the follicles and the C-shaped curve of the hairs make separation of the follicles slightly more difficult (Fig. 157.17B). Rather than using a straight blade, the blade must be bent in order to not transect the hair follicles. Also, the grafts may be slightly larger, requiring a larger bore needle (e.g. 16 gauge) to create recipient sites. Lastly, there is an increased risk of keloid or hypertrophic scar formation in patients with darker skin phototypes, more often in the donor region than in the recipient sites. Injecting triamcinolone acetonide suspension prior to donor site closure may help lessen the risk of such scar formation.

FUTURE TRENDS

Regeneration and cloning of hair follicles represents the next step in revolutionizing hair transplantation. With an unlimited supply of hairs, there will no longer be constraints based upon the density of hairs in the donor region. Keratinocyte tubulogenesis has been induced by cultured dermal papilla cells[68]; bone marrow- and umbilical cord-derived mesenchymal stem cells were shown to be a reservoir for follicle regeneration[69]; and epidermal wounding, with upregulation of Wnt proteins, led to hair follicle regeneration in adult mouse skin[70]. In addition, erythropoietin has been found to promote the growth of dermal papilla cells as well as to prolong the anagen phase of cultured human hair follicles[71]. Lastly, ongoing research utilizing a mouse model for AGA should provide insights into mechanisms of disease and therapies[72].

Acknowledgment

The authors wish to thank Dowling B. Stough, MD, for his contribution to this chapter in the previous editions.

Additional figures available in our eBook (see inside front cover for access code).

REFERENCES

1. Blanpain C, Lowry WE, Geoghegan A, et al. Self-renewal, multipotency, and the existence of two cell populations within an epithelial stem cell niche. *Cell*. 2004;118:635–648.
2. Ito M, Kizawa K, Hamada K, Cotsarelis G. Hair follicle stem cells in the lower bulge form the secondary germ, a biochemically distinct but functionally equivalent progenitor cell population, at the termination of catagen. *Differentiation*. 2004;72:548–557.
3. Garza LA, Yang C-C, Zhao T, et al. Bald scalp in men with androgenetic alopecia retains hair follicle stem cells but lacks CD200-rich and CD34-positive hair follicle progenitor cells. *J Clin Invest*. 2011;121:613–622.
4. Garza LA, Liu Y, Yang Z, et al. Prostaglandin D2 inhibits hair growth and is elevated in bald scalp of men with androgenetic alopecia. *Sci Transl Med*. 2012;4:126ra34.
5. Ellis J, Stebbing M, Harrap S. Polymorphism of the androgen receptor gene is associated with male pattern baldness. *J Invest Dermatol*. 2001;116:452–455.
6. Hillmer A, Hanneken S, Tirzmann S, et al. Genetic variation in the human androgen gene is the major determinant of common early onset androgenetic alopecia. *Am J Hum Genet*. 2005;77:140–148.
7. Levy-Nissenbaum E, Bar-Natan M, Frydman M, Pras E. Confirmation of the association between male pattern baldness and the androgen receptor gene. *Eur J Dermatol*. 2005;15:339–340.
8. Wakisaka N, Taira Y, Ishikawa M, et al. Effectiveness of finasteride on patients with male pattern baldness who have different androgen receptor gene polymorphisms. *J Investig Dermatol Symp Proc*. 2005;10:293–294.
9. Sinclair R, Greenland KJ, Egmond S, et al. Men with Kennedy disease have a reduced risk of androgenetic alopecia. *Br J Dermatol*. 2007;157:290–294.
10. Sawaya ME, Shalita AR. Androgen receptor polymorphisms (CAG repeat lengths) in androgenetic alopecia, hirsutism and acne. *J Cutan Med Surg*. 1998;3:9–15.
11. Hayes V, Severi G, Eggleton S, et al. The E211 G >A androgen receptor polymorphism is associated with a decreased risk of metastatic prostate cancer and androgenetic alopecia. *Cancer Epidemiol Biomarkers Prev*. 2005;14:993–996.
12. Prodi DA, Pirastu N, Maninchedda G, et al. EDA2R is associated with androgenetic alopecia. *J Invest Dermatol*. 2008;128:2268–2270.
13. Hillmer AM, Brockschmidt FF, Hanneken S, et al. Susceptibility variants for male-pattern baldness on chromosome 20p11. *Nat Genet*. 2008;40:1279–1281.
14. Hillmer AM, Flaquer A, Hanneken S, et al. Genome-wide scan and fine-mapping linkage study of androgenetic alopecia reveals a locus on chromosome 3q26. *Am J Hum Genet*. 2008;82:737–743.
15. Chiang YZ, Tosti A, Chaudry IH, et al. Lichen planopilaris following hair transplantation and face lift surgery. *Br J Dermatol*. 2012;166:666–670.
16. Olsen EA, Whiting D, Bergfeld W, et al. A multicenter, randomized, placebo-controlled double-blind clinical trial of a novel formulation of 5% topical minoxidil topical foam vs. placebo in the treatment of androgenetic alopecia in men. *J Am Acad Dermatol*. 2007;57:767–774.
17. Avram MR, Cole JP, Gandelman M, et al. The potential role of minoxidil in the hair transplantation setting. *Dermatol Surg*. 2002;28:894–900.
18. Messenger AG, Rundegren J. Minoxidil: mechanisms of action on hair growth. *Br J Dermatol*. 2004;150:186–194.
19. Han JH, Kwon OS, Chung JH, et al. Effect of minoxidil on proliferation and apoptosis in dermal papilla cells of human hair follicle. *J Dermatol Sci*. 2004;34:91–98.
20. Abell E. Histologic response to topically applied minoxidil. *Curr Ther Res*. 1984;36:1098–1106.
21. Goren A, Sharma A, Dhurat R, et al. Low-dose daily aspirin reduces topical minoxidil efficacy in androgenetic alopecia patients. *Dermatol Ther*. 2018;31:e12741.
22. Randolph M, Tosti A. Oral minoxidil treatment for hair loss: a review of efficacy and safety. *J Am Acad Dermatol*. 2021;84:737–746.
23. Kaufman KD, Olsen EA, Whiting D, et al. Finasteride in the treatment of men with androgenetic alopecia. *J Am Acad Dermatol*. 1998;39:578–589.
24. Finasteride Male Pattern Hair Loss Study Group. Long-term (5-year) multinational experience with finasteride 1 mg in the treatment of men with androgenetic alopecia. *Eur J Dermatol*. 2002;12:38–49.
25. Leyden J, Dunlap F, Miller B, et al. Finasteride in the treatment of men with frontal male pattern hair loss. *J Am Acad Dermatol*. 1999;40:930–937.
26. Leavitt M, Perez-Meza D, Rao NA, et al. Effects of finasteride (1 mg) on hair transplant. *J Dermatol Surg*. 2005;31:1268–1276.
27. Camacho FM, Garcia-Hernandez MJ, Fernandez-Crehuet JL. Value of hormonal levels in patients with male androgenetic alopecia treated with finasteride: better response in patients under 26 years old. *Br J Dermatol*. 2008;158:1121–1124.
28. McClellan KJ, Markham A. Finasteride: a review of its use in male pattern hair loss. *Drugs*. 1999;57:111–126.
29. D'Amico AV, Roehrborn CH. Effect of 1 mg/day finasteride on concentrations of serum prostate-specific antigen in men with androgenetic alopecia: a randomized controlled trial. *Lancet Oncol*. 2007;8:21–25.
30. Thompson IM, Goodman PJ, Tangen CM, et al. The influence of finasteride on the development of prostate cancer. *N Engl J Med*. 2003;349:215–224.
31. Cohen YC, Liu KS, Heyden NL, et al. Detection bias due to the effect of finasteride on prostate volume: a modeling approach for analysis of the Prostate Cancer Prevention Trial. *J Natl Cancer Inst*. 2007;99:1366–1374.
32. Propecia (package insert). Whitehouse Station, NJ: Merck & Co; 2004.

33. Overstreet JS, Fug VL, Gould J, et al. Chronic treatment with finasteride daily does not affect spermatogenesis or semen production in young men. *J Urol*. 1999;162:1295–1300.
34. Liu KE, Binsaleh S, Lo KC, Jarvi K. Propecia-induced spermatogenic failure: a report of two cases. *Fertil Steril*. 2008;90:849.
35. Irwig MS, Kolukula S. Persistent sexual side effects of finasteride for male pattern hair loss. *J Sex Med*. 2011;8:1747–1753.
36. Lee SW, Juhasz M, Mobasher P, et al. Systematic review of topical finasteride in the treatment of androgenetic alopecia in men and women. *J Drugs Dermatol*. 2018;17:457–463.
37. Price VH, Roberts JL, Hordinsky M, et al. Lack of efficacy of finasteride in postmenopausal women with androgenetic alopecia. *J Am Acad Dermatol*. 2000;43:768–776.
38. Iorizzo M, Vincenzi C, Voudouris S, et al. Finasteride treatment of female pattern hair loss. *Arch Dermatol*. 2006;142:298–302.
39. Yo JH, Jung JY, Choi JW, et al. 5 mg/day finasteride treatment for normoandrogenic Asian women with female pattern hair loss. *J Eur Acad Dermatol Venereol*. 2011;25:211–214.
40. Seale LR, Eglini AN, McMichael AJ. Side effects related to 5-alpha-reductaste inhibitor treatment of hair loss in women: a review. *J Drugs Dermatol*. 2016;15:414–419.
41. Eun HC, Kwon OS, Yeon JH, et al. Efficacy, safety, and tolerability of dutasteride 0.5 mg once daily in male patients with male pattern hair loss: a randomized, double-blind, placebo-controlled phase III study. *J Am Acad Dermatol*. 2010;63:252–258.
42. Amory JK, Wang C, Swerdloff RS, et al. The effect of 5-alpha-reductase on semen parameters and serum hormones in healthy men. *J Clin Endocrinol Metab*. 2007;92:1659–1665.
43. Desai S, Mahmoud BH, Bhatia AC, Hamzavi IH. Paradoxical hypertrichosis after laser therapy: a review. *Dermatol Surg*. 2010;36:291–298.
44. Avram MR, Rogers NE. The use of low-level light for hair growth: part I. *J Cosmet Laser Ther*. 2009;11:110–117.
45. Leavitt M, Charles G, Heyman E, Michaels D. HairMax LaserComb laser phototherapy device in the treatment of male androgenetic alopecia: a randomized, double-blind, sham device-controlled, multicentre trial. *Clin Drug Invest*. 2009;29:283–292.
46. Keene SA. Illuminating current pitfalls in optimal photobiomodulation device development and assessment for treating hair loss. *Exp Dermatol*. 2016;25:758–759.
47. Uebel CO, da Silva JB, Cantarelli D, Martins P. The role of platelet plasma growth factors in male pattern baldness surgery. *Plast Reconstr Surg*. 2006;118:1458–1466.
48. Lubkowska A, Dolegowska B, Banfi G. Growth factor contents in PRP and their applicability in medicine. *J Biol Regul Homeost Agents*. 2012;26:3S–22S.
49. Trink A, Sorbellini E, Bezzola P, et al. A randomized, double-blind, placebo- and active-controlled, half-head study to evaluate the effects of platelet-rich plasma on alopecia areata. *Br J Dermatol*. 2013;169:690–694.
50. Bolanca Z, Goren A, Getaldic-Svarc B, et al. Platelet-rich plasma as a novel treatment for lichen planopilaris. *Dermatol Ther*. 2016;29:233–235.
51. Hausauer A, Jones D. Evaluating the efficacy of different platelet-rich plasma regimens for management of androgenetic alopecia: a single-center, blinded, randomized clinical trial. *Dermatol Surg*. 2018;44:1191–1200.
52. Shapiro J, Ho A, Sukhdeo K, et al. Evaluation of platelet-rich plasma as a treatment for androgenetic alopecia: a randomized controlled trial. *J Am Acad Dermatol*. 2020;83:1298–1303.
53. Bigby M, Grimalt R. Platelet-rich plasma lacks evidence of clinically significant improvement of androgenetic alopecia. *J Am Acad Dermatol*. 2021;84:1183–1185.
54. Orentreich N. Autografts in alopecias and other selected dermatological conditions. *Ann NY Acad Sci*. 1959;83:463–479.
55. Jimenez F, Ruifernández JM. Distribution of human hair in follicular units. A mathematical model for estimating the donor size in follicular unit transplantation. *Dermatol Surg*. 1999;25:294–298.
56. Avram M, Rogers N. Contemporary hair transplantation. *Dermatol Surg*. 2009;35:1705–1719.
57. Harris JA. Follicular unit extraction. *Facial Plast Surg*. 2008;24:404–413.
58. Rose PT, Nusbaum AG, Nusbaum BP, Morgan MB. A comparison of apoptotic activity for follicular unit extraction of hair grafts stored in different holding solutions. *Dermatol Surg*. 2020;46:721–723.
59. Onda M, Igawa HH, Inoue K, Tanino R. Novel technique of follicular unit extraction with a powered punching device. *Dermatol Surg*. 2008;34:1683–1688.
60. Avram MR, Watkins SA. Robotic follicular unit extraction in hair transplantation. *Dermatol Surg*. 2014;40:1319–1327.
61. Avram MR, Rogers N, Watkins S. Side effects from follicular unit extraction in hair transplantation. *J Cutan Aesthet Surg*. 2014;7:177–179.
62. Josephitis D, Shapiro R. A side-by-side study of FUT vs. FUE graft availability in the same patients and its implications on lifetime donor supply and management. *Hair Transplant Forum Intl*. 2019;29(177):182–185.
63. Stough DB, Schell BJ, Weyrich R. The role of facial proportion in hair restoration surgery. *Ann Plast Surg*. 1997;38:129–136.
64. Avram MR. Polarized light-emitting diode magnification for optimal recipient site creation during hair transplant. *Dermatol Surg*. 2005;31:1124–1127.
65. Grossman MC, Dierickx C, Farinelli W, et al. Damage to hair follicles by normal mode ruby laser pulses. *J Am Acad Dermatol*. 1996;35:889–894.
66. Vano-Galvan S, Villodres E, Pigem R, et al. Hair transplant in frontal fibrosing alopecia: a multicenter review of 51 patients. *J Am Acad Dermatol*. 2019;81:865–866.
67. Callender VD, McMichael AJ, Cohen GF. Medical and surgical therapies for alopecias in black women. *Dermatol Ther*. 2004;17:164–176.
68. Chermnykh ES, Vorotelyak EA, Gnedeva KY, et al. Dermal papilla cells induce keratinocyte tubulogenesis in culture. *Histochem Cell Biol*. 2010;133:567–576.
69. Yoo BY, Shin YH, Yoon HH, et al. Application of mesenchymal stem cells derived from bone marrow and umbilical cord in human hair transplantation. *J Dermatol Sci*. 2010;60:74–83.
70. Ito M, Yang Z, Andl T, et al. Wnt-dependent de novo hair follicle regeneration in adult mouse skin after wounding. *Nature*. 2007;447:316–320.
71. Kang BM, Shin SH, Kwack MH, et al. Erythropoietin promotes hair shaft growth in cultured human hair follicles and modulates hair growth in mice. *J Dermatol Sci*. 2010;59:86–90.
72. Crabtree JS, Kilbourne EJ, Peano BJ, et al. A mouse model of androgenetic alopecia. *Endocrinology*. 2010;151:2373–2380.

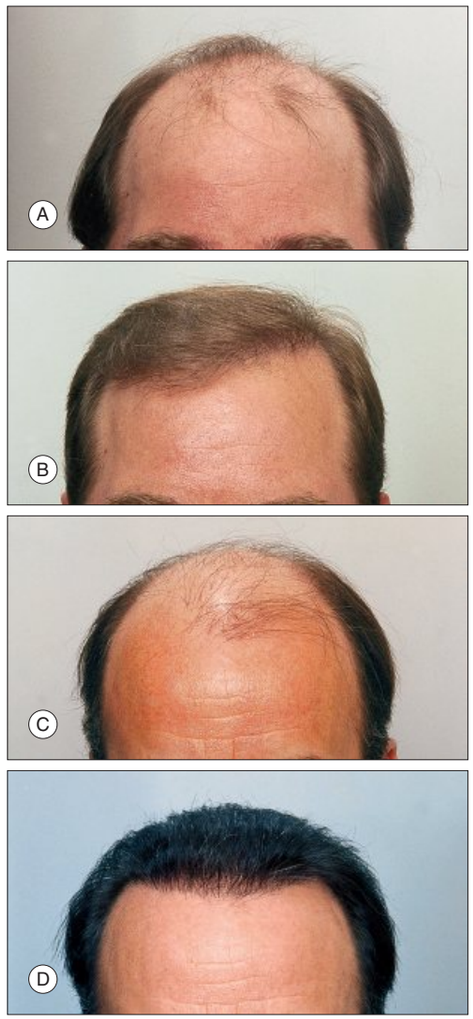


eFig. 157.1 The natural hairline. This is the natural hairline of a 32-year-old White man. *Courtesy Dowling B. Stough, MD*.

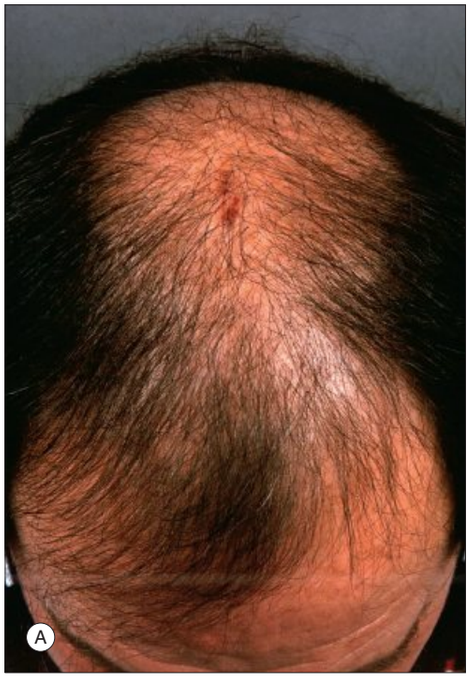


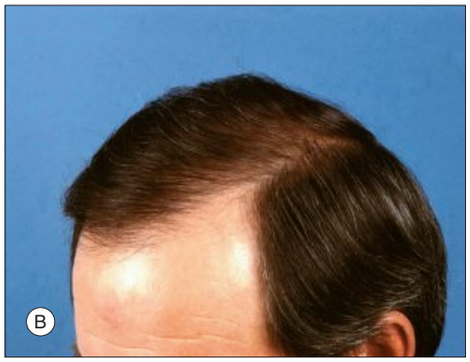


eFig. 157.2 Comparison of two patients who had received 1500 follicular unit grafts. Because of larger hair caliber and 1+ curl, the patient in **A** appears to have better coverage when compared to the patient in **B**.



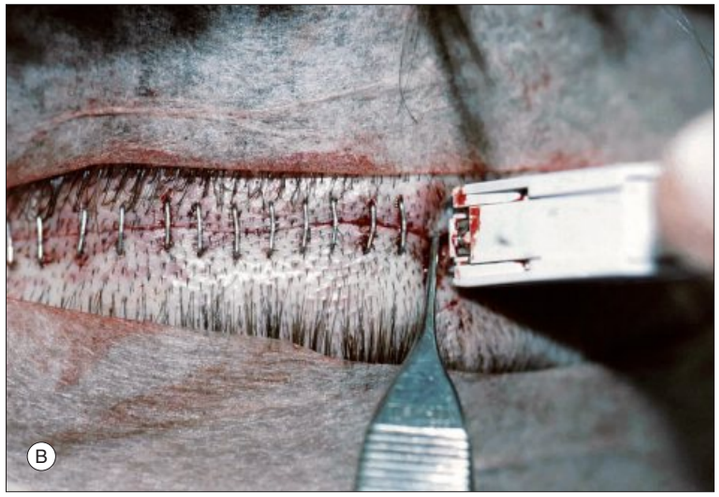
eFig. 157.3 Maximizing recipient density. Before (**A**, **C**) and after (**B**, **D**) photographs of patients following a single transplant session. *Courtesy Dowling B. Stough, MD*.





eFig. 157.4 A 40-year-old man with Norwood IV pattern alopecia. A, B The patient underwent a total of 2500 grafts; his vertex was not transplanted. This patient's hairline was started 3 years prior to its completion. *Courtesy Dowling B. Stough, MD.*





eFig. 157.5 Donor strip harvesting. A The donor strip prior to closure. **B** The donor area closure with staples. *Courtesy Dowling B. Stough, MD.*

Injectable Soft Tissue Augmentation 158

Amelia K. Hausauer and Derek H. Jones

Chapter Contents

Historical Perspective 2692
General Injection Protocols 2692
Injectable Soft Tissue Filler Materials 2694
Platelet-Rich Plasma 2699
Complications 2699

Key features

- Fillers are used to soften the appearance of superficial wrinkles and to recontour and smooth the deep folds of the face
- Other indications include reducing the appearance of atrophic, traumatic, and acne scars; lip augmentation; and volumizing the face in areas of lipoatrophy or senescence-associated fat loss
- Agents include hyaluronic acid derivatives, synthetic materials, autologous fat, and platelet-rich plasma
- Selection of an agent depends on the size, depth, and location of the volume deficiency as well as the cost and longevity of the product
- Agents are injected into the dermis, subcutaneous fat, or supra-periosteal space via a needle or cannula; various techniques, such as serial puncture, linear threading, fanning, cross-hatching or depot injection, are utilized and require an understanding of anatomy and best injection practices
- Fillers can be used as monotherapy or as an adjunct to other rejuvenating injectable techniques or surgical procedures in order to maximize longevity and aesthetic correction
- Complications are technique-dependent or material-related, and include hypersensitivity reactions, granuloma formation, bacterial biofilms, contour irregularities, and vascular occlusion, in addition to common injection-related phenomena such as pain, edema, and purpura

CAUSES OF CUTANEOUS DEFECTS AND CONTOUR CHANGES AMENABLE TO FILLERS FOR CORRECTION
Chronologic aging
• Loss of subcutaneous fat • Gravity • Bone resorption (e.g. mandible, maxilla, zygoma)
Photodamage
• Degradation of collagen, elastin, hyaluronic acid, and other components of the extracellular matrix leading to decreased skin turgor and rhytides
Other
• Exercise-induced lipoatrophy • Scarring (e.g. due to acne, varicella, trauma, surgery) • Inflammation (e.g. lipoatrophy due to lupus panniculitis or other panniculitides; see Ch. 100) • Lipodystrophy (inherited, acquired, drug-induced; see Ch. 101)

Table 158.1 Causes of cutaneous defects and contour changes amenable to fillers for correction.

SOFT TISSUE AUGMENTATION INDICATIONS
FDA-approved (see Table 158.4 for indications for specific products)
• Moderate to severe facial wrinkles and folds, such as nasolabial folds • Submucosal implantation for lip augmentation and perioral rhytides • Deep injection for cheek augmentation to restore age-related volume loss in the midface • Volumization of the dorsal hands • Chin augmentation to improve prominence and profile • HIV-associated lipoatrophy • Acne scars
Off-label
• Non-dynamic rhytides and folds – nasojugal folds, marionette lines, glabellar folds, etched-in radial cheeks lines, horizontal neck rhytides • Volume deficits – lipoatrophy (including buttocks and body deficits), sunken temples, tear trough deformity, atrophic earlobes • Structural prominences – jawline, nasal bridge, lateral eyebrow elevation • Distensible scars – trauma, surgery • Skin laxity • Nipple contouring

Table 158.2 Soft tissue augmentation indications. FDA, US Food and Drug Administration.

Interventions for the aging face can be broadly categorized into the four "R's" of facial rejuvenation: **R**esurfacing (chemical peels, dermabrasion, and ablative and non-ablative lasers); **R**edraping (the various pulling and lifting facial surgical procedures); **R**elaxing (chemodenervation with paralytic agents); and **R**eplacement/**R**econtouring (the use of filling agents for superficial and deep soft tissue augmentation). This fourth "R" has witnessed remarkable growth as patient demand for safe and effective minimally invasive aesthetic techniques has increased. In concert, the number of available dermal fillers and agents for soft tissue augmentation has expanded exponentially. More recently, there has been a shift from filling wrinkles and lines to replacing volume loss associated with atrophied fat and bone[1].

Patients often do not adequately appreciate the degree and significance of their volume deficit and must first be educated about the underlying anatomy of what is producing their "wrinkle". In addition to explaining the significance of volume deficits adjacent to the areas of primary concern, a distinction must be made between dynamic versus static lines as well as cutaneous changes due to photodamage versus those due to chronologic aging (senescence) (Table 158.1). Although these defects often appear in combination, they must be assessed individually. Patients should be made aware of newer, commercially available injectable products so that the physician is able to personalize their treatment and cater to subtle nuances of their faces. Many of the newer products have unique characteristics and indications that make them more suitable for certain patients (Table 158.2).

While the type of defect is clearly important, so are its size, depth, and location, in addition to the appearance and integrity of the adjacent tissue. A discussion regarding therapeutic options should include alternatives such as surgery (e.g. rhytidectomy, excision), resurfacing (see Ch. 137), and chemodenervation agents (see Ch. 159), as well as no intervention at all. Patients should understand the indications, technique, advantages, disadvantages, and inherent risks of each procedure, and they should be given an estimate of the financial cost and "downtime". As with any treatment, the degree of overall success is largely proportional to the creation (and achievement) of realistic and appropriate goals and expectations. Patients undergoing elective rhytide effacement and optimization with injectable fillers must realize that replacing lost or atrophic subcutaneous tissue is often temporary. Monotherapy with

one agent may not be adequate, and multiple agents may be required. All wrinkles are not created equal; they come in many shapes and sizes, and there is no one filler agent that is suitable for all defects. The choice of an appropriate dermal or subcutaneous implant requires knowledge of the available options and their characteristics.

HISTORICAL PERSPECTIVE

Dating back to 1893, Neuber used blocks of autologous fat harvested from the arms for tissue augmentation of depressed facial defects. Eighteen years later, Brunings first described using the syringe technique to transfer free fat. Then, in 1953, Baronders published a review of permanent soft tissue augmentation with liquid silicone. Finally, in 1981, bovine collagen became the first US Food and Drug Administration (FDA)-approved xenogeneic agent for soft tissue augmentation, and it remained the standard filler for over 20 years (Table 158.3).

In 1981, Zyderm® I was the first bovine collagen filler, followed by Zyderm® II and Zyplast®. As a group, they have a long safety track record having been used in more than a million patients[2]. All three were derived from a closed US cattle herd carefully monitored to prevent transmission of bovine spongiform encephalitis, a prion-mediated disease. Cutaneous hypersensitivity reactions occurred in 3% of patients; therefore, pre-treatment skin testing became mandatory[3]. The longevity of these bovine collagen fillers was ~2–3 months. Bovine collagen is historically important as it set the standard against which the next generation of soft tissue fillers was initially compared.

In an attempt to reduce the risk of hypersensitivity reactions, a series of dermal fillers were developed that did not require skin testing, some of which were longer lasting – CosmoDerm®/CosmoPlast® (bioengineered human collagen); Evolence® (porcine type I collagen, potentially lasting up to one year)[4]; and a family of injectables from preserved particulate cadaveric connective tissue (Dermalogen®, Cymetra®, and Fascian®). With the exception of Renuva®, an allograft adipose matrix, most are no longer commercially available due to high manufacturing costs and low demand.

In 2003, the FDA approved Restylane®, which ushered in a new era of agents made from hyaluronic acid (HA). Many of the HA formulations proved to be superior in longevity compared to their collagen predecessors and had more feasible manufacturing. Globally, HA quickly became the most popular soft tissue filler. Currently available FDA-approved formulations of HA are outlined in Table 158.4. Historic HA formulations that are no longer available in the US are listed in Table 158.3.

TEMPORARY SOFT TISSUE FILLERS THAT ARE NO LONGER AVAILABLE IN THE US
Bovine-derived collagen
• Zyderm® I, Zyderm® II, Zyplast®
Porcine-derived collagen
• Evolence®
Non-cadaveric human collagen
• CosmoDerm® 1, CosmoDerm® 2, CosmoPlast®
Autologous human collagen
• Autologen®
Cadaveric human collagen
• Dermalogen®, Cymetra®
Cadaveric fascia lata
• Fascian®
Cadaveric adipose matrix
• Renuva®
Porcine-derived gelatin
• Fibrel®
Avian-derived hyaluronic acid
• Hylaform®, Hylaform Plus®
Non-animal stabilized hyaluronic acid
• Captique®, Elevess®, Prevelle Silk®
Autologous fibroblast therapy
• Isolagen®

Table 158.3 Temporary soft tissue fillers that are no longer available in the US. This is due to discontinuation by the manufacturer or decreased demand because of popularity of other products.

GENERAL INJECTION PROTOCOLS

Prior to performing any filler procedure, injectors must have a firm grasp of vascular anatomy to ensure safety and help guide optimal injection techniques and product selection. This forms the foundation of all treatments; its importance cannot be overemphasized, since accidental injection into facial arteries can have catastrophic consequences, as outlined by the American Society for Dermatologic Surgery (ASDS) Task Force on evidence-based guidelines for prevention and treatment of adverse events from injectable fillers[5]. While intravascular injection is possible at any location on the face (e.g. lips' labial arteries), the nose, glabella, forehead, superior nasolabial fold, and medial cheek are considered significant danger zones, from highest to lowest, for vascular complications, visual compromise, and cerebrovascular events[6,7].

Studying anatomy and appreciating its variability are the underpinnings of all injection techniques, which vary by location, and represent a life-long learning endeavor. The facial artery is a branch of the external carotid artery that crosses the jawline periosteally at the antegonial notch just anterior to the border of the masseter muscle (see Fig. 142.3). It takes a circuitous course deeply from the lower lateral cheek to the nasolabial fold, branching off as the inferior and superior labial arteries, then becoming the angular artery near the superior nasolabial fold (see Fig. 142.15). More superficially, the angular artery runs along the medial cheek/lateral nose in variable patterns[8]. It anastomoses with four arteries: (1) dorsal nasal artery; (2) distal ophthalmic artery, which connects to the retinal and cerebral vasculature; (3) supratrochlear artery; and (4) supraorbital artery; the two latter arteries are end branches of the distal ophthalmic artery. The supratrochlear and supraorbital arteries traverse the supraorbital ridge periosteally at the glabella and medial brow, respectively, then run superiorly toward the scalp. These pathways explain the danger zones referenced above[5].

There is no one completely safe injection protocol only safer strategies based upon location, which are briefly outlined here.

Nose, Glabella, and Forehead

These three regions present the highest risk. Therefore, to minimize the potential for disastrous outcomes, only the most experienced injectors should approach treatment in these areas. Although rare, the chance of blindness is greatest with nasal injections into the dorsal nasal artery. Based on cadaveric studies, the safest plane on the dorsal nose appears to be pre-periosteal or pre-perichondrial[9]. Yet, due to vascular variability, the dorsal nasal artery may lie on the midline periosteum[10].

The glabella also carries higher risk because of the periosteal exit of the supratrochlear and supraorbital arteries. Injecting deeply within this region is contraindicated. Experts may consider correcting glabellar rhytides that do not respond to neuromodulators with intradermal injections using small needles. However, the vessels are variable, potentially running more superficially, especially in those with thin tissue[11,12]. These arteries course cephalad to caudal and surface superficially within the frontalis muscle superior to the brow. Consequently, forehead correction is safest with cannulas placed in the pre-periosteal, subgaleal plane at least 2 cm superior to the orbital rim and in a horizontal direction, perpendicular to the vasculature.

Nasolabial Fold, Cheek

Two additional danger zones are: (1) the superior nasolabial fold where the angular artery becomes subcutaneous; and (2) the cheek medial to the midpupillary line (medial cheek), where the infraorbital artery runs periosteally and the angular artery subcutaneously. Both needles and cannulas are FDA-approved for injection in these regions, but given the different vascular depths and pathways, a cannula with a minimum size of 25-gauge (G) may be safer (see below)[13–16]. In contrast, the lateral cheek along the zygomatic prominence is considered less risky, although the zygomaticofacial artery does sit on the periosteum. Injection along the periosteum with a needle or cannula is appropriate[5].

FDA-APPROVED INDICATIONS FOR SOFT TISSUE FILLERS CURRENTLY EMPLOYED IN THE US	
Trade name (®,™)	**FDA-approved indication**
Hyaluronic acid	
Restylane, Restylane-L*	• moderate to severe facial wrinkles and folds • lip augmentation
Restylane Refyne* Restylane Defyne*	• moderate to severe facial wrinkles and folds • augmentation of the chin region (Defyne only)
Restylane Silk* Restylane Kysse*	• lip augmentation • correction of perioral rhytides
Restylane Lyft* (formerly Perlane-L)	• moderate to severe facial folds and wrinkles • age-related volume loss and augmentation of the midface • volumization of the dorsal hands
Restylane Contour*	• cheek augmentation
Juvéderm Ultra, Juvéderm Ultra XC*	• moderate to severe facial wrinkles and folds • lip and perioral augmentation
Juvéderm Ultra Plus, Juvéderm Ultra Plus XC*	• moderate to severe facial wrinkles and folds
Juvéderm Voluma XC*	• age-related volume loss in the midface • augmentation of chin region
Juvéderm Vobella XC*	• lip augmentation • correction of perioral rhytides
Juvéderm Vollure XC*	• moderate to severe facial wrinkles and folds
Juvéderm Volux XC*	• improving jawline definition
Belotero Balance, Belotero Balance + *	• moderate to severe facial wrinkles and folds
Resilient HA (RHA) 2, 3, 4*	• moderate to severe dynamic facial wrinkles and folds
RHA Redensity*	• moderate to severe dynamic perioral wrinkles
Synthetic†	
Polymethylmethacrylate microspheres plus bovine collagen (Bellafill)*	• correction of nasolabial folds • acne scars
Poly-L-lactic acid‡ (Sculptra and Sculptra Aesthetic)	• HIV-associated lipoatrophy • shallow-to-deep smile lines (nasolabial folds), contour deficiencies, and other facial wrinkles
Calcium hydroxylapatite‡ (Radiesse)	• HIV-associated lipoatrophy • moderate to severe facial wrinkles and folds • volumization of the dorsal hands
Calcium hydroxylapatite plus lidocaine (Radiesse +)*	• moderate to severe facial wrinkles and folds
Silicone	• none¶
Autologous	
Autologous fat	• not regulated as long as not modified in any way
Azficel-T (LAVIV)	• moderate to severe nasolabial fold wrinkles in adults

*Contains 0.3% lidocaine.
†Bellafill® contains bovine collagen.
‡Plus carboxymethyl-cellulose.
¶Silikon 1000 is FDA-approved for intraocular use.

Table 158.4 FDA-approved indications for soft tissue fillers currently employed in the US. In general, soft tissue fillers are approved for use in adults and not in the pediatric population. FDA, US Food and Drug Administration. For updates, see www.fda.gov.

SOFT TISSUE AUGMENTATION: PREINJECTION CONSIDERATIONS
Medical background

• Medications (anticoagulants, antiplatelet agents)
• Medical history
  • Autoimmune connective tissue disease, e.g. systemic sclerosis
  • Granulomatous disorders, e.g. sarcoidosis
  • Scarring conditions (e.g. keloids) or tendency to form hypertrophic scars
  • Previous facial herpes simplex viral infection
  • Previous hypersensitivity reactions/allergies
• Pregnancy and lactation
• Surgical history, including cosmetic procedures
  • Rhytidectomy, blepharoplasty
  • Reconstructive surgery
  • Facial implants
  • Previous injections of soft tissue fillers and neurotoxins

Defect parameters
• Location • Volume required • Alternative and simultaneous treatments
Patient goals

• Defect of concern
• Expectations regarding
  • Degree of correction
  • Product longevity
• Recuperation time (“downtime”)
• Risk/benefit ratio

Table 158.5 Soft tissue augmentation: preinjection considerations.

Temple

Periosteal depots, deep to the superficial temporal vessels, are used to correct an atrophic temple. The needle is injected inside the “safe zone” whose border is 1 cm superior to the superior orbital rim, 1 cm lateral to the temporal fusion line, and 2.5 cm superior to the zygomatic arch where the middle temporal vein lies[17,18].

Lips

Injections should be superficial, as the labial arteries usually course more deeply between the mucosa and orbicularis oris at the wet–dry border[19].

Chin, Jawline

Because the facial artery crosses the mandible just anterior to the border of the masseter muscle, injections along the rami in this region must sit above the bone. Periosteal injection at the gonial angle appears to be safer when sharpening the contour and widening the jaw or the midline mandible to create anterior or inferior chin projection[20].

Consultation and Evaluation

With a firm knowledge of anatomy, injectors can then approach patient consultation and evaluation. Baseline asymmetry, subjective defects, and realistic expectations should be discussed with the patient (Table 158.5). To fully appreciate the depth and scope of the defect, patients should be placed in a gravity-dependent or seated position with adequate lighting. The latter should be at an acute angle in order to accentuate surface irregularities and deficits. A careful patient selection process will assist in determining ideal candidates for soft tissue augmentation. Contraindications include prior allergy to the filler material or its constituents (e.g. lidocaine). Pre-existing conditions in the planned treatment area such as dermatitis, acne, or infection may require postponement of the procedure. The expected level of improvement and longevity are also key discussion points.

Prior to the procedure, patients should be instructed to abstain from all *nonessential* medications that can inhibit coagulation and platelet aggregation. For example, aspirin is avoided for 10–14 days and NSAIDs for 5–7 days in order to decrease the risk of bleeding and bruising. In addition, omega-3 fatty acids, fish oil, and a number of over-the-counter supplements should be discontinued (see Table 133.3). Prior to the procedure, written consent is obtained and both make-up and cutaneous debris are removed[21]. Pre- and post-treatment photographs are strongly recommended.

Preparation

Clean technique is critical in preventing contamination during the initial handling, mixing, and injecting of the filler. The skin is cleansed with alcohol, chlorhexidine (avoiding the ear canal and eye), hypochlorous acid or other antimicrobial agent, and gloves are changed after intraoral manipulation. Percutaneous injections of fillers can be painful, necessitating the consideration of adding anesthesia to the treatment protocol. Although the physician can combine fillers with an anesthetic, most commercial products are now premixed with lidocaine (see Table 158.4). Some injectable products may require nerve blocks and/or regional anesthesia (see Ch. 143). More commonly, however, ice or topical anesthetic preparations are sufficient.

Injection Techniques

Proper placement of the filler material is crucial. Common injection techniques include serial puncture, linear threading, fanning, cross-hatching, and depot injection[22]. In the *serial puncture technique*, small amounts of filler are sequentially deposited along the wrinkle or fold. The injections are placed close to one another so that the filler can blend in a continuous fashion; post-injection massage can also help to blend the filler so that it is evenly distributed. Using the *linear threading technique*, the full length of the needle/cannula is inserted into the proper dermal or subcutaneous plane, and the filler is injected in a retrograde manner as the needle is withdrawn. Conversely, the material can be injected as the needle is advanced (anterograde), creating blunt dissection within the tissue space. The *fanning technique* involves multiple passes in different, but evenly spaced, directions without withdrawing the needle/cannula from its original site of insertion. The *cross-hatching* or *radial injection technique* involves evenly spaced, linear injections in a grid-like pattern; this technique is used for filling large areas and for the oral commissures[23]. Finally, *depot injections* are useful when placing volumizing fillers within the subcutaneous fat or along the periosteum. Occasionally, small depot aliquots are also placed along the infraorbital ridge, with a movement toward using cannulas in this region. Massage immediately after depot placement of filler helps to blend the product into the natural contour of the region.

Additional important recommendations[5]:

- *Inject small volumes slowly, under low pressure*. When there is arterial cannulation or compression from deposition adjacent to arteries, large volume, high pressure boluses may be more detrimental.
- *Retract the syringe plunger (reflux test) prior to injection*. If positive for blood, then intravascular placement is possible. Stop straight away and reposition. However, a negative reflux test does not exclude possible intravascular injection[15,24].
- *Continually move the needle or cannula tip to minimize the risk of prolonged intravascular injection of a larger bolus*.

Needles and Cannulas

Evolving consensus supports the use of blunt-tipped cannulas, especially those with a larger bore (e.g. 25 G)[25], to reduce the risk of vascular injury. Cadaveric and reflux studies suggest that larger diameter cannulas are less likely to perforate vasculature, when compared to smaller diameter cannulas (e.g. 27 G) or needles[14–16]. This is of particular importance in areas (e.g. cheeks, lips) where both needles and cannulas are FDA-approved. Blunt-tipped cannulas are best suited for injecting in the subdermal plane and are not appropriate for intradermal injections. One of the authors (DJ) demonstrates high-risk anatomy and the use of cannulas in Video 158.1.

INJECTABLE SOFT TISSUE FILLER MATERIALS

There is an ever-expanding array of fillers for soft tissue augmentation (see Table 158.4). Table 158.6 lists the characteristics of the ideal filler. While soft tissue fillers can be subdivided based upon derivation, depth of placement or duration of effect, most physicians develop preferences based upon location of desired augmentation.

Hyaluronic Acid Derivatives

Hyaluronic acid derivatives are currently the most commonly employed soft tissue fillers (Table 158.7). The term *hyaluronic acid* is derived from the Greek word for glass, *hyalos*, and is so named because of its clear appearance. Hyaluronic acid (HA) is a key glycosaminoglycan (GAG; previously referred to as mucopolysaccharides) within the extrafibrillar matrix of the dermis (see Ch. 95). It is a ubiquitous component of connective tissue and is conserved amongst mammals, making it species-nonspecific. Within connective tissue, HA forms a gelatinous matrix that surrounds collagen and elastic fibers and creates volume via its water-binding capability. HA also plays a role in cellular migration and therefore it is important in the development and remodeling of tissues. A direct correlation exists between the amount of HA in the dermis and its water content as well as between HA content and the viscoelastic properties of the extracellular matrix. The concentration of naturally occurring HA within the skin decreases with age, resulting in a decreased ability to retain water, rendering the dermis less voluminous and increasing its propensity to wrinkle.

The HA molecule consists of a polysaccharide chain comprised of numerous repeating disaccharides of N-acetylglucosamine and D-glucuronic acid. The longer the chain, the higher the molecular weight. All currently available, FDA-approved HA fillers are derived from bacterial (*Streptococcus*) fermentation. "Raw" or non-crosslinked HA is supplied as a powder, forming a viscous liquid when exposed to water. If injected in this unmodified state, exogenous HA imparts a duration of correction of only 12 to 24 hours. In order to increase tissue residence time, HA molecules must be stabilized via chemical crosslinking of the polysaccharide chains; this modification slows enzymatic breakdown and provides an acceptable duration of correction. Most commercially available, FDA-approved HAs are crosslinked by BDDE (1,4-*b*uane*d*iol *d*iglycidyl *e*ther), with each filler differing in its manufacturing process.

Following the initial crosslinking, HA exists as a gel similar in consistency to Jell-O®. Subsequent post-crosslinking modifications, which vary depending upon the specific product, impart different attributes. For example, with the Restylane® family, the gelatin is passed through a sieve that creates microscopic particles of identical shape and size. Restylane® (approved in 2003) is then suspended in phosphate-buffered saline at a concentration of 20 mg/ml with 100 000 gel particles/ml. By comparison, Restylane® Lyft (formerly Perlane-L®) has a larger mean gel particle size with 10 000 particles/ml. Refyne, Defyne, Contour, and Kysse are more recent additions to the Restylane® family (see Table 158.4).

The Juvéderm® family relies on a proprietary technology that creates particles of random shapes and sizes. Juvéderm® products (first approved in 2006) have an HA concentration of 24 mg/ml, with Juvéderm® Ultra Plus being more heavily crosslinked than Juvéderm® Ultra (Fig. 158.1). Belotero Balance® is a monophasic, non-particulate gel crosslinked in two consecutive reactions, resulting in a cohesive HA

PARTIAL LIST OF THE CHARACTERISTICS OF THE IDEAL FILLER SUBSTANCE	
• FDA-approved • Non-allergenic (minimal risk of hypersensitivity, no pretesting required) • Non-carcinogenic and non-teratogenic • User-friendly product (e.g. easy flow, ergonomic syringe) • Versatile syringe volumes (e.g. touch-up syringes) • Easy storage (no need for refrigeration) • Long shelf-life	• Affordable • Long-lasting • Predictable level of correction • Painless • Minimal recuperation • Minimal adverse sequelae (e.g. infection, ecchymosis) • No migration • No overt cutaneous change (undetectable) • Correctable post-injection (e.g. with hyaluronidase)

Table 158.6 Partial list of the characteristics of the ideal filler substance. FDA, US Food and Drug Administration.

BENEFITS OF HYALURONIC ACID DERIVATIVES
• Identical in all species and all tissue types • Minimal risk of hypersensitivity reaction (no skin test required) • Room temperature storage • Biodegradable • Long-lasting and stable • High degree of safety (biocompatible, resorbable, reversible)

Table 158.7 Benefits of hyaluronic acid derivatives.



Fig. 158.1 Hyaluronic acid – volumization in a patient with lean body mass. A Pre-treatment. **B** One week following injection of large volumes of Juvéderm® Ultra Plus to the cheeks and Juvéderm® Ultra to the brow area, nasolabial folds, and oral commissures.

gel with varying zones of crosslinking density. The HA concentration in Belotero Balance® (approved in 2011) is 22.5 mg/ml.

The pivotal, phase III trials leading to FDA approval of Restylane®, Juvéderm®, and Belotero Balance® were six-month, randomized, blinded, multicenter, split-face, controlled trials (RCTs) that compared Zyplast® collagen to the respective HA for the treatment of moderate to severe nasolabial folds[26–28]. At six months, all three HA fillers demonstrated superiority over Zyplast® collagen, with inter-study design and results having more similarities than differences (Fig. 158.2A). The HA products have been shown to be safe in all skin types. Further studies, focusing on repeat treatment after six months, suggest that less volume is required to regain optimal correction[28–30]. Often, an extended duration of 1–2 years or more was observed (Fig. 158.2B).

For the treatment of moderate to severe wrinkles and folds, HA products are usually injected into the immediate subdermal plane or superficial subcutis. If injected too superficially into the dermis, contour irregularity as well as a bluish discoloration due to the Tyndall effect may occur. The latter results from the optical scatter of different wavelengths of light encountering a clear substance. Recent studies suggest that Belotero Balance®, if injected more superficially (intradermally), integrates more smoothly into the dermis as compared to the Restylane® and Juvéderm® families. The former is also less likely to create a Tyndall effect[31]. This makes Belotero Balance® particularly well suited for treatment of superficial, etched-in lines such as vertical lip lines (Fig. 158.3 & 158.4)[32]. Both Restylane® and Juvéderm® Ultra are FDA-approved for lip augmentation (Fig. 158.5), although Belotero Balance® is often used off-label for this indication[33].

In 2013, Juvéderm Voluma® XC ("Voluma") was the first HA filler to be FDA-approved for deep injection for cheek augmentation as a means of restoring age-related volume loss in the mid face (Video 158.2). This filler consists of a 20 mg/ml mixture of low- and high-molecular-weight HA. Voluma® differs from other HA fillers in that the lower-molecular-weight component, composed of shorter polysaccharide chains, allows for more efficient crosslinking (Vycross® technology). This, in turn, produces a highly cohesive gel with greater lift capability. Results from the pivotal phase III multicenter, single-blinded RCT showed significant improvement in moderate to severe, age-related midfacial volume loss at six months (compared to the no-treatment control group; Fig. 158.6). Data suggest that nearly half of the patients maintained correction up to 24 months, emphasizing its long-term effectiveness.

Reported adverse events with Voluma® were similar to other HA fillers and included swelling, tenderness and purpura, which resolved within a week in the majority of individuals[34]. Recent data have



Fig. 158.2 Correction of nasolabial folds. A Comparison of bovine collagen (Zyplast®) to hyaluronic acid (Juvéderm® Ultra Plus). **B** Demonstration of long-term effect with repeated injection of hyaluronic acid (Juvéderm®). *Adapted from Smith SR, Jones D, Thomas JA, et al. Duration of wrinkle correction following repeat treatment with Juvederm hyaluronic acid fillers. Arch Dermatol Res. 2010;302:757–62.*



Fig. 158.3 Treatment of superficial, etched-in lines with Belotero Balance®. **A** Pre-treatment. **B** Two weeks post-treatment.

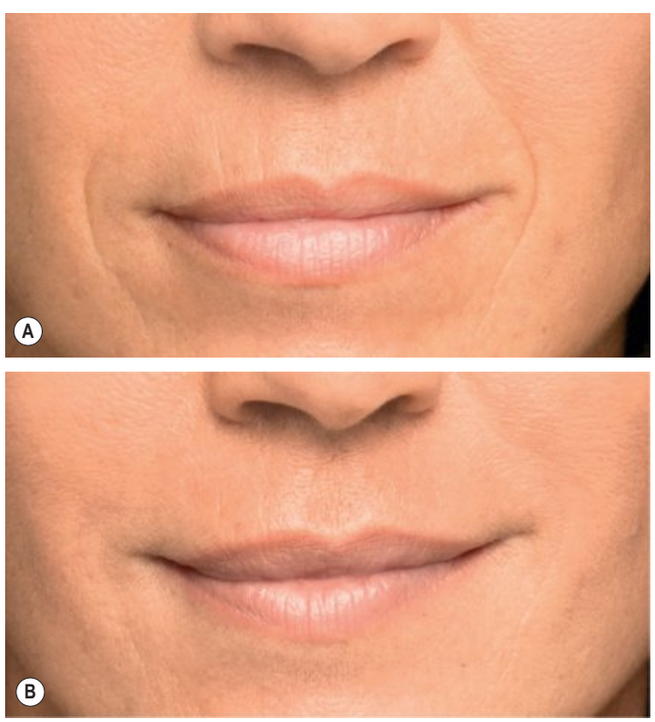


Fig. 158.4 Treatment of superficial lines with Belotero Balance®. A Pre-treatment. **B** Two weeks post-treatment.





Fig. 158.5 Hyaluronic acid – lip and perioral augmentation. A Prior to injection of Restylane® into the perioral area. **B** Three months post-injection with correction maintained. *Courtesy Seth L. Matarasso, MD.*



Fig. 158.6 Restoration of midface volume with Juvéderm Voluma® XC. **A** Pre-treatment. **B** Six months post-treatment. *From Jones D, Murphy DK. Volumizing hyaluronic acid filler for midface volume deficit: 2-year results from a pivotal single-blind randomized controlled study. Dermatol Surg. 2013;39:1602–12.*

pointed to an increased incidence of delayed adverse events (e.g. edema, nodules) in up to 1% of treated individuals. They occur months after injection, possibly due to the degradation process triggering an inflammatory response, either spontaneously or after an immunologic trigger[35]. Juvéderm Voluma® XC is intended for injection into deeper subcutaneous and periosteal planes and should not be injected intradermally; nor should it be injected into the lip or glabellar areas.

In 2016 and 2017, two additional fillers based upon Vycross® technology received FDA approval. Vobella XC® is indicated for lip augmentation and correction of perioral rhytides in adults over the age of 21 years, whereas Vollure XC® corrects moderate to severe wrinkles and folds such as the nasolabial fold (see Table 158.4). Unlike previously FDA-approved products with these indications, Vollure® is the first HA filler reported to last up to 18 months within the nasolabial folds in the pivotal trials.

The most recently introduced family of products in the US (approved in 2017 but distributed in 2020) is Resilient HA (RHA®). They contain 23 mg/ml and are produced with similar, but fewer modifications than other HA families. Double-blind RCTs of RHA® 2–4 had a primary six-month endpoint and were compared to control HA filler or no

treatment of nasolabial folds; based upon follow-up through 64 weeks, there was non-inferiority[36,37].

A unique feature of HA is its reversibility, and complications from HA fillers can often be easily corrected. Injections of hyaluronidase (Vitrase®, Hylenex®) can dissolve previously injected HA; this is very helpful if the filler has been misplaced, there is a complication post-injection (e.g. vascular occlusion, delayed granulomatous reaction), or there is impending vascular necrosis. An *in vitro*, dose-response study suggested that Juvéderm® was more resistant to hyaluronidase when compared to Restylane®. In the authors' experience, 10 units (U) of hyaluronidase (Vitrase®) per 0.1 cc of Juvéderm or 5 U per 0.1 cc of Restylane® may be the most appropriate dose to dissolve the HA[38]. Up to 30–40 U of Vitrase® may be required per 0.1 cc of Voluma®[39]. The need for the greater amount of hyaluronidase for correction of these products likely reflects their more highly crosslinked nature.

All currently FDA-approved HA families have a product that is pre-packaged admixed with lidocaine, which significantly reduces pain on injection (see Table 158.4).

Poly-L-Lactic Acid

Polymerized poly-L-lactic acid (PLLA; Sculptra®) augments soft tissue by stimulating the production of collagen. In 2004, it was FDA-approved for the correction of HIV-associated facial lipoatrophy. Five years later, the FDA approved Sculptra® Aesthetic for the correction of shallow-to-deep nasolabial fold contour deficiencies and other facial wrinkles. It is often injected off-label for panfacial rejuvenation in immunocompetent individuals with limited lipoatrophy, improvement of nonfacial skin laxity[40], and nonsurgical gluteal augmentation[41]. However, effects are often subtle with many treatments required for optimal results.

Sculptra® is powdered lyophilized suture material (Vicryl® [polyglactin 910]); the freeze-dried preparations of PLLA can be stored at room temperature. Based upon early study designs, the current aesthetic label recommends that each vial be reconstituted two hours prior to deep dermal injection with a total of 5 ml of liquid: 4 ml of sterile water and 1 ml of lidocaine. This results in a thick suspension of 4.45% PLLA. Refinements in protocol have led to the common off-label practice of a >24-hour hydration time with higher dilutions, e.g. addition of up to 9–11 ml of liquid (or higher for the body), to generate a more uniform suspension and reduce the risk of papule formation[42].

Immediately prior to injection, the mixture is vigorously agitated. A 25–26 G needle is used to place the filler in the subcutaneous plane and care is taken to avoid overcorrection. Intradermal injection can result in visible papules. Frequent needle changes may be necessary, as the material has a tendency to form clumps and clog the bore. There may be the appearance of some immediate augmentation from saline in the reconstituted solution and some edema. However, to achieve optimal correction and prolonged neocollagenesis, the recommended protocol is a series of three or more sessions at 3- to 6-week intervals. Persistence of augmentation varies, but some improvement can be seen for up to 1.5 to 2 years.

Palpable, but not visible, papulonodules develop in some patients, and a granulomatous reaction at sites of injection can also arise. All of these complications tend to persist for months to years before resolving. To try to minimize papule formation, the following can be done: use greater dilution volumes, increase the time interval between reconstitution and injection, avoid intradermal injection, inject smaller aliquots per site, and vigorously massage the injected areas to eliminate any lumpiness. In addition to massaging during and post-treatment, it is often recommended that the patient follow the "rule of 5 s": massage for 5 minutes 5 times daily for 5 days. That said, a small study found that this advice had no significant impact on nodule formation or treatment outcomes[43].

Calcium Hydroxylapatite

In 2006, Radiesse® was FDA approved for the correction of moderate to severe facial folds and wrinkles (e.g. nasolabial folds) and for the correction of signs of HIV-associated lipoatrophy. Correction of volume loss of the dorsal hands was a later indication, receiving FDA approval in 2015[44]. It is safe in all skin types (Fig. 158.7)[42,45,46]. Radiesse® is a milky white suspension comprised of two components: (1) an aqueous gel carrier containing glycerin, sodium carboxymethylcellulose, and water; and (2) 25–45 micron microsphere particles of calcium hydroxylapatite (CaH). CaH is a non-allergenic (inert) bioceramic that is identical to the primary mineral constituents found in bone and teeth. This biocompatible product contains no human, bacterial, or animal products and poses minimal risk for hypersensitivity reactions. Utilization of the product was initially limited due to the significant discomfort and throbbing after injection, so the FDA approved the practice of pre-mixing Radiesse® with 2% lidocaine immediately prior to injection. Subsequently, a lidocaine-containing version, Radiesse® (+), became available. The material is deposited deeply at the dermal–subcutaneous junction. Injection provides immediate results, and no overcorrection or undercorrection is required[1].

As the gel carrier correction gradually resolves, it is replaced by new collagen formation stimulated by the scaffold of calcium hydroxylapatite particles. While histologic studies have demonstrated the presence of CaH and neocollagenesis for up to 78 weeks, the duration of clinical correction has not been well documented beyond 12 months[1]. Lip augmentation is contraindicated, as mucosal granulomas may form and the constant motion of the lip and compression from contraction of the orbicularis oris may cause migration and clumping of the filler (Fig. 158.8)[47]. Off-label uses of this product include revolumizing the face of immunocompetent individuals[1,47] as well as improving skin laxity via biostimulation with dilute and hyperdilute mixtures injected over repeated sessions[48].

Since Radiesse® is radio-opaque, the patient should be informed that it may be visible on radiographs as well as CT scans. However, there is no evidence that calcium hydroxylapatite particles obscure underlying structures or mask abnormal pathology[49].

Lipotransfer

Historically, autologous fat has always been considered one of the safest fillers, with estimates of success as high as 70%, but two concerns have remained. The original *en bloc* technique required excision of the donor tissue and a resultant second defect; essentially, patients traded one



Fig. 158.7 Treatment of age-related facial lipoatrophy with Radiesse®.
A Pre-treatment. **B** Post-treatment (2 weeks).



Fig. 158.8 Formation of papules and nodules due to placement of Radiesse® into the lip. A, B The size can vary from a few millimeters to over a centimeter. *A, Courtesy Seth L. Matarasso, MD.*



Fig. 158.9 Lipotransfer and subcision to correct scarring due to previous surgical excision of a cyst. A Pre-treatment. **B** Post-treatment.

defect for another. Furthermore, the non-particulate solid nature of the tissue required implantation, with the potential for incisional scars. The arrival of tumescent liposuction in the 1980s solved many of these existing problems. A by-product of liposuction, the suctioned fat was easily accessible and could be reinjected through small cannulas/needles, leading to a resurgence of autologous fat grafting (AFG).

Areas amenable to AFG include the nasolabial folds, cheeks, infraorbital region, marionette lines, and lips. Scars as well as stable disease processes associated with idiopathic facial subcutaneous atrophy (e.g. linear morphea, Parry–Romberg syndrome) can also benefit (Fig. 158.9). The dorsal hands often share all of the signs of aging found in sun-exposed areas, and replacing fat in the dorsal hands masks the appearance of protruding tendons and blood vessels, imparting a more youthful appearance. Adipose transfer has also been shown to be effective in treating HIV-associated lipoatrophy in patients who have a suitable donor reserve.

There is great variability in the techniques used to procure, purify, and inject adipose tissue, resulting in great variability in outcomes. Table 158.8 reviews basic concepts, but a detailed discussion of the evolving nuances is beyond the scope of this chapter.

LIPOTRANSFER
Advantages
• Biocompatibility with avoidance of allergy • Abundant graft supply • Three-dimensional volumization • Potential long-standing correction
Disadvantages
• Need for donor fat harvesting • Percentage of graft that survives is unpredictable • Inability to remove after placement • Requires a two-step procedure: harvesting and insertion of the fat • Significant “downtime”, e.g. post-procedural edema • Rare risk of fat emboli and vision changes including blindness
Key components of procedure

• Anesthesia – general or local tumescent (see Ch. 143)
• Fat harvesting
  • From easy-to-access areas that are relatively insensitive to dietary fluctuation – upper outer buttock/flank, medial knee
  • Donor fat aspirated with a 12–14 G, single-holed microcannula mounted on a conventional hypodermic (10–20 ml) Luer-Lok® syringe or by traditional liposuction methods (see Ch. 156)
  • Processing via different methods (e.g. sterile saline washing; centrifugation to separate excess fluid, erythrocytes, and nonviable cells; use of an FDA-cleared filtration system such as PUREGRAFT)
  • Limited postoperative morbidity
• Fat re-injection
  • Processed, pure supernatant injected into subcutaneous plane using a large-bore (16–18 G) cannula/needle
  • Great variability in technique – multiple passes with layering of small fat droplets, intramuscular placement, superficial nanofat*
  • Repeat smaller volume injections over time have greater viability than a single large implantation; passive diffusion within the recipient bed cannot sustain the latter
  • Massage to disperse and contour
• Postoperative care
  • Systemic antibiotics
  • Pain management, avoiding aspirin-containing products

*Nanofat is highly emulsified and the adipocytes are mechanically disrupted such that there are no viable cells; the injection contains adipose-derived stem cells and growth factors.

Table 158.8 Key features of lipotransfer[7,50–56].

Silicone

Silicone (polydimethylsiloxane) consists of repeating units of dimethylsiloxane terminated with trimethylsiloxane. Centistoke (cs) refers to the viscosity of silicone oil and is directly related to the chain length of the repeating units. A 1 cs product is equivalent in consistency to water, a 350 cs product is similar in consistency to mineral oil, and a 1000 cs product is similar in texture to honey. While silicone has had a tumultuous history and continues to be controversial, it has largely been replaced by HA, PLLA, and CaH fillers.

Medical grade (350 cs) liquid silicone was never approved by the FDA for injection into humans and such use remains prohibited in the US. However, there is an FDA indication for AdatoSil® (5000 cs; approved in 1994) and Silikon® (1000 cs; approved in 1997) which is intraocular injection to produce tamponade to treat retinal detachment. Under the US FDA Modernization Act of 1997, physicians gained the right to use medical devices in an off-label manner, so after years of being banned for cosmetic implantation, physicians could legally use these FDA-approved and standardized silicone oils.

Silikon® 1000 is the most appropriate form of injectable liquid silicone currently available for off-label soft tissue augmentation. It is injected in a microdroplet, serial puncture method, most often for severe HIV-associated lipoatrophy (Fig. 158.10). As placement of the product results in permanent augmentation, there is very little margin

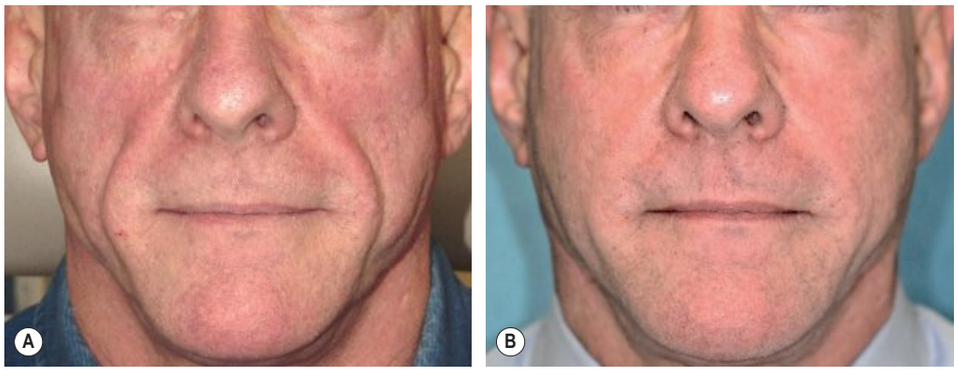


Fig. 158.10 Correction of HIV lipoatrophy with injectable silicone (Silikon® [1000 cs]). **A** Pre-treatment. **B** Five years post-treatment.

for error, and experience plus meticulous technique are essential. Since HIV-associated facial volume loss has become less common and there are safer alternative fillers with excellent outcomes, it is the authors' opinion that even when expertly injected, the incidence of adverse events is too high to justify its continued use. These complications include facial edema, overcorrection, superficial beading, movement of the product to a distant site (drift)[57,58], and granulomatous or inflammatory reactions with delayed firmness and nodules. In a 10-year retrospective follow-up of patients treated for HIV-associated facial lipoatrophy, adverse events were observed in 7%[58].

Polymethylmethacrylate (PMMA) Microspheres

Bellafill® (formerly Artefill®) is the only FDA-approved soft tissue filler that is a non-resorbable implant. It is indicated for the correction of nasolabial folds and acne scars. Polymethylmethacrylate (PMMA) microspheres are suspended in a solution of 3.5% bovine collagen and 0.3% lidocaine; the collagen serves as a carrier and is degraded within 1–3 months following injection. As a result, Bellafill® is currently the only commercially available filler in the US that requires skin testing for bovine collagen hypersensitivity. The remaining intact, inert, non-biodegradable 30–40 micron PMMA beads, similar to Lucite™ or Plexiglas™, are large enough to avoid phagocytosis but small enough to promote permanent augmentation. Once the host's collagen has encapsulated the microspheres, the augmentation has been purported to be permanent[42,59].

Bellafill® is a third-generation product whose predecessors were Arteplast® and Artecoll®. Improvements include PMMA particles that are more uniform in size and rounder with a smoother surface. Microspheres <20 microns, which were responsible for a high incidence of granuloma formation in previous generations, have been removed. However, even with this newer formulation which has a higher safety profile[59], there continues to be a risk of disfiguring delayed granulomas. The latter occur more commonly with off-label use[60], and in our experience, inevitably recur and never fully resolve. While the results may be permanent and therefore more economical, so are any adverse effects, which may require serial treatment with intralesional injections of 5-fluorouracil plus triamcinolone, oral antibiotics, or surgical excision[61].

PLATELET-RICH PLASMA

Platelet-rich plasma (PRP), an autologous solution with a high concentration of platelets and fibrin in a small volume of plasma, may be used to enhance one's complexion and less often as an injectable filler. Given the high number of growth factors implicated in extracellular matrix remodeling that it contains, PRP has become an increasingly popular option for rejuvenation. While the quality of published studies has appeared to lag behind quantity, there is a growing number of small RCTs, albeit with different designs, that have reported benefit from intralesional PRP.

One split-face, randomized, rater-blinded study of 20 Asian patients found good to moderate improvement in lower eyelid wrinkles and skin tone after three injection sessions (compared to saline control)[62]. One month after a single PRP session, an 89% increase in collagen density was observed histologically compared to baseline and 93% more collagen induction compared to the saline control injections[63]. However, the latter also led to improvement, possibly due to a needling effect. In another study of a single session of PRP versus saline in which photographs were reviewed at six months, masked subjects, but not two expert dermatologists, saw significantly better fine and coarse skin texture[64]. The authors argued that this discrepancy may stem from the failure of imaging to detect nuanced changes and patients' intimate understanding of their own skin topography. A more recent three-session, saline-controlled trial found statistically significant improvement in wrinkles, texture, and pores using a VISIA® system[65]; the latter may better detect subtle changes in the skin canvas than does global photography. An *in vitro* arm of this trial demonstrated that PRP mitigated ultraviolet B-induced matrix metalloproteinase-1 and tyrosinase upregulation and induced fibrillin and tropoelastin (precursor to elastin) expression. Perhaps this may explain the effects of PRP on skin photoaging and its enhancement of visible complexion metrics. Histologic improvement of solar elastosis following PRP injections has also been reported[66].

Taken together, these results support a potential role for PRP in improving skin texture, softening fine lines, and ameliorating degenerative soft tissue changes. While meaningful changes may be seen with a single treatment, more robust aesthetic outcomes seem to come from a series of sessions. However, the studies to date remain small, with a wide variation in protocols and outcome measures, many of which are subjective. There is a need for rigorous, larger scale RCTs to better standardize therapy[67]. Lastly, the combination of PRP plus HA fillers and platelet-rich fibrin matrix (derived from a true clot but often misclassified in the literature) should be investigated for any synergistic biostimulatory activity.

COMPLICATIONS

The popularity of soft tissue fillers is in part due to their favorable side-effect profile. Common injection-related phenomena include erythema, swelling, pain, and bruising. These generally resolve within a week without treatment. The erythema and swelling often appear immediately after injection. Minimizing the number of skin punctures and applying ice may reduce pain, erythema, and swelling[68]. To limit bruising, patients should be instructed to abstain from medications that inhibit platelet aggregation for at least 7–10 days prior to injection. Vigorous exercise with its associated blood pressure elevation should also be avoided for the first 24 hours after the injections. The use of a small-gauge needle, slow injection technique with small aliquots of product as well as blunt cannulas and fewer puncture sites may further minimize bruising. However, bruises are often inevitable and treatment with intense pulsed light or pulsed dye and potassium titanyl phosphate (KTP) lasers may be effective therapies, as they all can target the hemoglobin chromophore contained in the extravasated blood[69]. Superficial bruising from fillers often lightens substantially within a day following laser- or light-based treatment.

More serious complications from soft tissue fillers may occur and include: (1) nodules, beading, and Tyndall effect from superficial placement; (2) infection; (3) hypersensitivity reactions; (4) delayed nodule formation; and (5) vascular compromise (Fig. 158.11A; Table 158.9). Inappropriate placement of fillers may result in the development of papulonodules, which are palpable and often visible. Injecting too superficially with an HA filler may lead to beading as well as blue–gray discoloration due to the Tyndall effect. Hyaluronidase

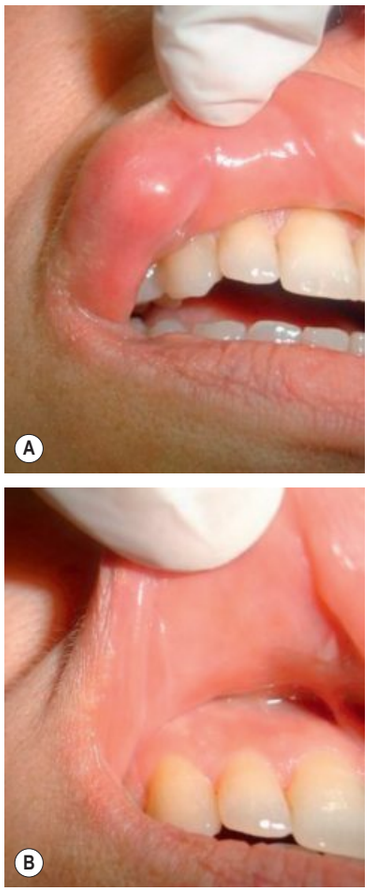


Fig. 158.11 Foreign body reaction to hyaluronic acid. A Nodule due to granulomatous inflammation arose six weeks after injection. **B** Resolution following intralesional hyaluronidase and triamcinolone. *Courtesy Mahmoud Abdallah, MD.*

can be used to treat these complications (see above; Fig. 158.11B). Vitrase® and Hylenex® are the two FDA-approved formulations of hyaluronidase that may be used off-label for dissolving unwanted previously injected HA. Hylenex® is a genetically engineered human recombinant hyaluronidase, whereas Vitrase® is ovine testicle-derived hyaluronidase. In the ophthalmologic literature, the reported incidence of allergic reactions to hyaluronidase is ~1 in 2000. While to date no cases of allergy or anaphylaxis have been reported in the dermatologic literature, a preliminary intradermal skin test with a few units can be considered to exclude hypersensitivity. Because there is a theoretical risk of cross-reactivity in patients who are allergic to honeybees and yellow jackets, patients who have had severe reactions or anaphylaxis to bee stings should be skin tested prior to treatment[70]. Persistent papules can also occur following injection of PMMA microspheres, poly-L-lactic acid, and silicone. Methods to reduce this complication are outlined in Table 158.9.

Any time there is a breach in the integrity of the skin, infection can occur. To minimize the risk, the skin should be cleansed with an antimicrobial agent such as isopropyl alcohol, chlorhexidine (avoiding the ear canal and eye), or hypochlorous acid prior to injection. Patients with an infection may present with tender erythematous fluctuant nodules or abscesses. These skin findings may be accompanied by systemic symptoms such as fever. When an infection is suspected, a microbiological culture of exudate, if present, should be obtained and/or the lesion biopsied for histopathologic examination and tissue culture. Therapeutic interventions include incision and drainage and empiric broad-spectrum antibiotics such as dual therapy with a macrolide (e.g. clarithromycin) and quinolone until the culture results are available[5,71]. Trauma from injections may also trigger a recurrence of herpes simplex viral infection. Prophylactic antiviral treatment (e.g. valacyclovir) should be considered if a patient has a history of a post-procedure recurrence and when treating the perioral area in a patient with a history of recurrent herpes labialis[69].

Prior to the introduction of HA fillers, hypersensitivity reactions were more commonly observed (see above). There are a few reported cases of hypersensitivity reactions to HA (Fig. 158.12), and these may be due to residual proteins or impurities from the manufacturing process or they may be due to low-molecular-weight HA fragments[71]. Hypersensitivity reactions to HA fillers often resolve spontaneously after several months, but resolution may be accelerated by application of tacrolimus ointment, intralesional corticosteroids, intralesional hyaluronidase, and/or incision and drainage[68].

Delayed nodules are variable in their etiology and difficult to precisely diagnose without histopathologic and/or culture results. They may be secondary to a hypersensitivity reaction, soft tissue infection, development of a biofilm, or formation of a foreign body granuloma (see Table 158.9). Although delayed nodules occur more commonly with permanent fillers such as PMMA or silicone (hence our recommendation to avoid their routine use), they can develop following injection of temporary fillers including HA. Hypothetically, delayed nodules secondary to an *immune reaction* may be triggered by residual proteins in the product or, in the case of HA fillers, by low-molecular-weight fragments of HA[71]. As noted above, these fragments provide a theoretical explanation for the increased incidence of delayed reactions (~1%–4%) seen with the Vycross® fillers, which consist of a mixture of both high- and low-molecular-weight HA[34,72–75].

There are some data to suggest a greater risk of delayed reactions after influenza-like illnesses, following vaccinations, and during cold and flu season[72,76,77]. More recently, delayed filler reactions have been observed following administration of SARS-CoV-2 mRNA vaccines. These reactions were typically mild to moderate and resolved within a few days, often without treatment. In a case series, the ACE (angiotensin-converting enzyme) inhibitor lisinopril at a dose of 5–10 mg daily led to a rapid reduction in edema[78].

Biofilms may also cause delayed nodules. When filler is injected, it can become coated with colonies of bacteria that secrete a protective and adhesive matrix. This results in a low-grade chronic infection resistant to antibiotics and the immune system. Often bacterial cultures will be negative as standard culturing techniques are not sensitive enough to detect this type of infection. Delayed nodules due to formation of biofilms can present as a "sterile" inflammatory nodule, an abscess or other form of soft tissue infection, or a foreign body granuloma[71]. In order to try to prevent biofilm formation, it is important to cleanse the skin with an antimicrobial agent (e.g. chlorhexidine [avoiding the ear canal and eye]) prior to injection. Infectious delayed nodules may be related to biofilms, but can also be due to less common organisms such as atypical mycobacteria.

As all synthetic fillers represent foreign bodies, an intense host response can occur resulting in the formation of *foreign body granulomas*. Although infrequent, this presentation is more common with permanent fillers and has been well documented histologically (see Fig. 94.11)[79].

While there are several therapeutic interventions for delayed nodules (see Table 158.9), they should be guided by clinical judgment (e.g. inflammatory versus non-inflammatory, sterile versus infected) as well as culture results and/or histopathologic findings when available. Treatment options for removal of as much of the filler as possible include intralesional hyaluronidase (if an HA filler), incision and drainage, and excision. Delayed nodules are often immune-mediated and can be treated with a 1- to 2-week course of oral corticosteroids (e.g. prednisone 30 mg daily). If there is concern regarding an active infection, empiric oral antibiotics are advisable (see above)[5]. Additional therapies employed for delayed nodules include topical or intralesional corticosteroids, oral immunosuppressants, and lasers (see Table 158.9)[80].

While the majority of adverse events are reversible, vascular complications can be devastating and often irreversible (Table 158.10). Tissue necrosis may occur if filler is injected directly into the vasculature, resulting in ischemic or embolic phenomena. Of particular concern are the arteries in the mid central face that connect to the ophthalmic circulation, i.e. where the facial artery continues as the angular artery immediately superior to the nasolabial fold (see above). The angular artery then branches into the lateral nasal artery and other collateral vessels, which connect the internal and external carotid artery systems[95] (see Fig. 142.15).

Signs and symptoms of vascular compromise include pain, arborizing blanching, duskiness, and reticulated erythema that may extend along the artery and its branches (Fig. 158.13). Over time, this can progress to a necrotic eschar, ulceration, and scarring. Treatment should be instituted immediately at the first sign of vascular compromise[68]. If blanching occurs while injecting, immediately discontinue[5]. If the complication occurs with an HA filler, injection of hyaluronidase is recommended.

COMPLICATIONS FROM SOFT TISSUE FILLERS	
Complication	**Prevention and management strategies**
• Injection site reactions (erythema, swelling, pain, bruising)	• Avoid anticoagulants and antiplatelet agents such as aspirin • Consider cannulas to minimize bruising • Smaller needles may reduce pain and bruising • Ice application for swelling and pain • Intense pulsed light or vascular lasers can be used to treat bruising
• Nodules, beading, and Tyndall effect	• Avoid superficial placement; inject smoothly • Treat with massage, hyaluronidase (if HA filler), or aspiration/excision
• Persistent papules	• More common with certain products • For Bellafill®, inject smoothly • For Sculptra®, greater volume dilution • For silicone, use microdroplet technique
• Infection	• Pre-cleanse the skin with an antimicrobial agent, e.g. chlorhexidine* • Consider incision and drainage and/or antibiotics if infection occurs
• Herpes simplex virus reactivation	• Treat with oral antiviral medication if: (1) history of post-procedure reactivation; (2) injecting the perioral area in a patient with a positive history of herpes labialis; or (3) evidence of active outbreak
• Hypersensitivity†	• Avoid injection in patients with known sensitivity • Skin test for bovine collagen in the case of Bellafill® • Hypersensitivity after HA fillers often resolves spontaneously, but consider treatment with tacrolimus ointment, intralesional corticosteroids, intralesional hyaluronidase, and/or incision and drainage

• Delayed nodules:
  • Inflammatory/immune-mediated (hypersensitivity)
  • Biofilm-related
  • Infectious
  • Foreign body granuloma
	• Pre-cleanse the skin with an antimicrobial agent prior to injection, e.g. chlorhexidine*
	• Incision and drainage plus culture and/or biopsy for histopathologic examination
	• Hyaluronidase (if HA filler) or surgical excision
	• Oral broad-spectrum antibiotics for 2–6 weeks, e.g. clarithromycin, minocycline
	• For non-infectious etiologies, consider topical, oral or intralesional corticosteroids; intralesional 5-fluorouracil; oral immunosuppressants; or laser therapy

• Vascular compromise (necrosis, blindness)	• Injectors should have a thorough knowledge of facial vascular anatomy and the depth at which a filler should be placed • Aspirate before injecting • Use a cannula or smaller gauge needle in high-risk areas • Inject product slowly and in small aliquots; use low pressure to prevent retrograde injection • Discontinue the injection immediately if blanching occurs or if the patient complains of significant pain or vision changes • If vascular compromise of the skin occurs, begin warm compresses, massage, and oral aspirin; if HA filler, inject hyaluronidase along artery and its branches (for additional measures, see Table 158.10) • If blindness or visual compromise occurs, see protocol in Table 158.10

*Avoid the ear canal and eye.
†Dermal perivascular and periappendageal mononuclear infiltrate, with infiltration of the implanted filler by neutrophils, lymphocytes, histiocytes, and eosinophils.

Table 158.9 Complications from soft tissue fillers. HA, hyaluronic acid.

Different formulations of hyaluronidase are available, which makes it difficult to establish standardized dosing. Variable doses have been reported in the literature, from 10–30 units per $2 \times 2\,cm^2$ area along the artery and its branches[96] up to a total of 1500 units injected within the affected region[97]. Larger doses may be required for higher cross-linked fillers such as Voluma®[38]. As outlined in Tables 158.9 and 158.10, additional conservative measures can also be initiated. A thorough assessment and detailed treatment plan should be instituted for each patient. Immediate and ongoing care with frequent monitoring ensures optimal outcomes and decreases the risk of permanent complications[89].

Although very rare, more serious complications can occur secondary to *embolism* of the filler into the ocular circulation, leading to blindness and/or ophthalmoplegia, or into the brain, causing a cerebrovascular accident. Blindness may occur when there is sufficient pressure and retrograde arterial displacement of injected material from the peripheral vessels into the ocular circulation[98].

The anatomic sites most commonly associated with visual complications include the nose, glabella, forehead, and nasolabial fold[99], with the first three sites accounting for 85% of reported cases in a recent review. Here, the filler can travel through the branches of the internal carotid system (e.g. supratrochlear, supraorbital, dorsal nasal artery) to the ophthalmic artery, which further branches into the retinal artery. Alternatively, at sites such as the nasolabial fold, the filler can enter the ocular circulation via rich anastomoses between the external and internal carotid systems (see Ch. 142).



Fig. 158.12 Pustular and granulomatous reaction to injections of hyaluronic acid (Restylane®). *Courtesy Julie V. Schaffer, MD.*

MANAGEMENT OF SUSPECT VASCULAR OCCLUSION/INJURY WITH OR WITHOUT VISUAL COMPROMISE FOLLOWING INJECTION OF FILLER
Hyaluronic acid filler with blindness or visual compromise – time is crucial
• Halt injection at first signs of visual compromise, usually occurring unilaterally during or immediately post injection

• *Prior* to intervention, evaluate and document visual status in each eye independently including:
  • ability to read letters (Snellen chart, near card, magazine print)
  • ability to count fingers
  • ability to perceive hand motion
  • presence of light perception
  • extraocular muscle function
  • pupillary light response
• Photograph face in frontal position

• Immediately contact an ophthalmologist familiar with management of such cases   • As swift care is crucial and to avoid a delay in care, highly recommend establishing a pre-existing relationship and plan with an oculoplastic surgeon, ophthalmologist, and/or retina specialist
• Prompt hyaluronidase injections with >150 units into the treated region, ischemic skin, and along arterial paths leading to the eye • Consider injecting similar doses at the supraorbital and supratrochlear foramina • Repeat in quick succession as needed
• Retrobulbar and peribulbar hyaluronidase injections may be beneficial, but remain controversial

• Additional conservative measures:
  • Breathing into a paper bag to increase CO_2
  • Ocular massage with firm manual pressure to globe for 5–15 seconds alternating with rapid release for a total of 5 minutes; wait a few minutes, then repeat. Cyclical pressure inducing rapid reperfusion may dislodge embolus
  • Topical timolol (0.5%) and oral acetazolamide (500 mg) may decrease intraocular pressure

Hyaluronic acid filler with blindness or visual compromise and CNS involvement
• If signs or symptoms of CNS involvement, contact 911 and your local emergency stroke services • If no overt signs or symptoms, always evaluate for CNS involvement after addressing visual compromise
Hyaluronic acid filler without blindness/visual compromise
• Halt injection if "flash" in the syringe (vascular regurgitation) or tissue blanching or reticulation in treatment area (Fig. 158.13)

• Prompt high-dose hyaluronidase injection into skin at occlusion site as well as peripheral regions
  • Unanimously supported intervention[81–91], but optimal dosing unclear and based on anatomic region and product
  • Hundreds of units, perhaps pulsed in 15-minute intervals (500 units in increments of 125 units superior to single bolus)[92]

• Additional conservative measures:
  • Skin massage
  • Intralesional or systemic corticosteroids
  • Warm compresses
  • Oral aspirin
  • Nitroglycerin less beneficial
  • Hyperbaric oxygen for wound healing

Calcium hydroxylapatite
• Preliminary evidence of filler dissolution with sodium thiosulfate injection (0.1–0.2 ml of 250 mg/ml)[93,94], but its use for vascular occlusion remains unknown

Table 158.10 Management of suspect vascular occlusion/injury with or without visual compromise following injection of filler. Recommendations adapted from evidence-based guidelines from the American Society for Dermatologic Surgery (ASDS) Task Force[5]. Of note, there is no current standard of care for managing iatrogenic retinal embolism from hyaluronic acid filler (conditional recommendations, low certainty evidence). For vascular occlusion *sans* ocular event, the recommendations are strong with more moderate certainty evidence. CNS, central nervous system.



Fig. 158.13 Evolving vascular occlusion following injection of Juvéderm® Ultra XC into the cheek. Note the arborizing blanching, duskiness, and reticulated erythema that is observed in addition to pain.

The signature feature of ocular embolism is immediate visual impairment, which may be accompanied by ocular pain, nausea, and vomiting. Such events represent an ophthalmologic emergency. If any of these signs or symptoms occur, the patient should be sent urgently for ophthalmologic consultation, since treatment aimed at recanalizing the affected vessel(s) and restoring tissue perfusion needs to be performed within a short window of time. The most frequently cited interval is 90 minutes, but more recent investigations have suggested an interval as short as 10–15 min[100]. Therefore, a predetermined and detailed action plan is required. In an attempt to restore vision, prebulbar and retrobulbar injections of hyaluronidase can be performed immediately[7], but this intervention remains controversial (see Table 159.10)[101–103]. Because treatment of embolic blindness is usually unsuccessful, prevention is of critical importance[98].

When performed with care, soft tissue augmentation is a highly effective and safe procedure. To ensure the best outcomes while minimizing any adverse events, a thorough understanding of facial anatomy as well as proper injection technique are imperative. Injectors should be aware of both prevention and management strategies to minimize complications and improve patient outcomes (see Tables 158.9 and 158.10).

CONCLUSION

The vast array of available filler products, and those that are on the horizon, are only one means to improve tissue loss associated with aging and trauma. The optimal result may be best achieved by combining fillers of different depth, origin, and durability with other aesthetic procedures. The science of soft tissue augmentation is continuously evolving. Keeping abreast of advances and perfecting a few techniques will be most advantageous for patients; it is not only what is injected, but how it is injected, that determines the degree of success. Finally, regardless of the treatment chosen, it is the combination of clinical judgment, realistic expectations, meticulous preparation, and surgical skill that provides optimal results.

Copyright notice

Derek H. Jones retains copyright to his original photographs in Chapter 158.

Additional figures available in our eBook (see inside front cover for access code).

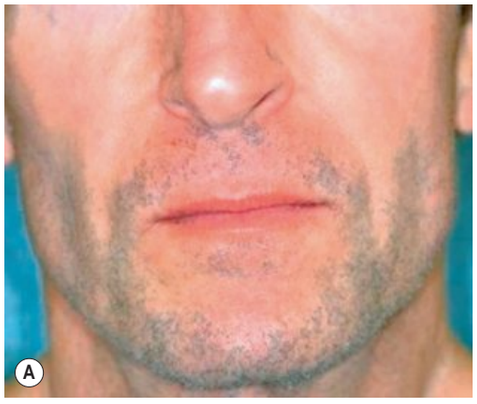
REFERENCES

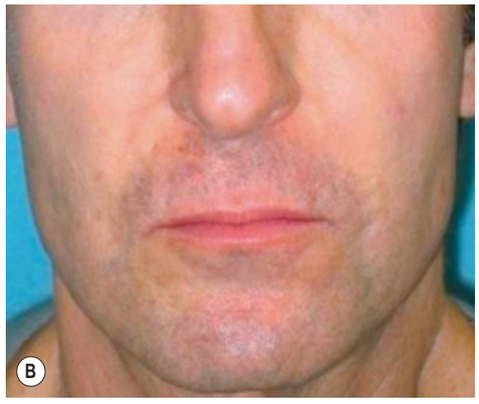
1. Moers-Carpi M, Storck R, Howell D, et al. Physician and patient satisfaction after use of calcium hydroxylapatite for cheek augmentation. *Dermatol Surg*. 2012;38:1217–1222.
2. Ashinoff R. Overview: soft tissue augmentation. *Clin Plast Surg*. 2000;27:479–487.
3. Moody BR, Sengelmann RD. Topical tacrolimus in the treatment of bovine collagen hypersensitivity. *Dermatol Surg*. 2001;27:789–791.
4. Narins RS, Brandt FS, Lorenc ZP, et al. Twelve-month persistency of a novel ribose-cross-linked collagen dermal filler. *Dermatol Surg*. 2008;34(Suppl. 1):S31–S39.
5. Jones D, Fitzgerald R, Cox SE, et al. Preventing and treating adverse events of injectable fillers: evidence-based recommendations from the American Society for Dermatologic Surgery Multidisciplinary Task Force. *Dermatol Surg*. 2021;47:214–226.
6. Beleznay K, Carruthers JDA, Humphrey S, et al. Update on avoiding and treating blindness from fillers: a recent review of the world literature. *Aesthet Surg J*. 2019;39:662–674.
7. Beleznay K, Carruthers JDA, Humphrey S, Jones D. Avoiding and treating blindness from fillers: a review of the world literature. *Dermatol Surg*. 2015;41:1097–1117.
8. Kim Y-S, Choi D-Y, Gil Y-C, et al. The anatomical origin and course of the angular artery regarding its clinical implications. *Dermatol Surg*. 2014;40:1070–1076.
9. Choi D, Bae J, Youn K, et al. Topography of the dorsal nasal artery and its clinical implications for augmentation of the dorsum of the nose. *J Cosmet Dermatol*. 2018;17:637–642.
10. Lee W, Kim JS, Oh W, et al. Nasal dorsum augmentation using soft tissue filler injection. *J Cosmet Dermatol*. 2019;18:1245–1260.
11. Cho KH, Dalla Pozza E, Toth G, et al. Pathophysiology study of filler-induced blindness. *Aesthet Surg J*. 2019;39:96–106.
12. Cotofana S, Alfertshofer M, Frank K, et al. Relationship between vertical glabellar lines and the supratrochlear and supraorbital arteries. *Aesthet Surg J*. 2020;40:1341–1348.
13. Goodman GJ, Roberts S, Callan P. Experience and management of intravascular injection with facial fillers: results of a multinational survey of experienced injectors. *Aesth Plast Surg*. 2016;40:549–555.
14. Pavicic T, Webb KL, Frank K, Gotkin RH, et al. Arterial wall penetration forces in needles versus cannulas. *Plast Reconstr Surg*. 2019;143:504e–512e.
15. Tseng FW, Bommareddy K, Frank K, et al. Descriptive analysis of 213 positive blood aspiration cases when injecting facial soft tissue fillers. *Aesthet Surg J*. 2021;41:616–624.
16. Alam M, Kakar R, Dover JS, et al. Risk of vascular occlusion associated with usig needles vs cannulas for filler injection. *JAMA Dermatol*. 2021;157:174–180.
17. Carruthers J, Humphrey S, Beleznay K, Carruthers A. A suggested injection zone for soft tissue fillers in the temple. *Dermatol Surg*. 2017;43:756–757.
18. Cotofana S, Gaete A, Hernandez CA, et al. The six different injection techniques for the temple relevant for soft tissue filler augmentation procedures - clinical anatomy and danger zones. *J Cosmet Dermatol*. 2020;19:1570–1579.
19. Cotofana S, Alfertshofer M, Schenck TL, et al. Anatomy of the superior and inferior labial arteries revised: an ultrasound investigation and implication for lip volumization. *Aesthet Surg J*. 2020;40:1327–1335.
20. Cotofana S, Lachman N. Arteries of the face and their relevance for minimally invasive facial procedures: an anatomical review. *Plast Reconstr Surg*. 2019;413:416–426. Erratum in: *Plast Reconstr Surg.* 2019;143:1282–3.
21. Bacigalupi R, Clark J, Lupo MP. An overview of injectable fillers with special consideration to the periorbital area. *Cosmet Dermatol*. 2012;25:421–426.
22. Rohrich RJ, Nguyen AT, Kenkel JM. Lexicon for soft tissue implants. *Dermatol Surg*. 2009;35(Suppl. 2):1605–1611.
23. Rohrich RJ, Ghavami A, Crosby MA. The role of hyaluronic acid fillers (Restylane) in facial cosmetic surgery: review and technical considerations. *Plast Reconstr Surg*. 2007;120(Suppl. 6):41S–54S.
24. Fitzgerald R, Bertucci V, Sykes JM, Duplechain JK. Adverse reactions to injectable fillers. *Facial Plast Surg*. 2016;32:532–555.
25. Pavicic T, Webb KL, Frank K, Gotkin RH, et al. Arterial wall penetration forces in needles versus cannulas. *Plast Reconstr Surg*. 2019;143(3):504e–512ee.
26. Narins RS, Brandt F, Leyden J, et al. A randomized, double-blind, multicenter comparison of the efficacy and tolerability of Restylane versus Zyplast for the correction of nasolabial folds. *Dermatol Surg*. 2003;29:588–595.
27. Baumann LS, Shamban AT, Lupo MP, et al. Comparison of smooth-gel hyaluronic acid dermal fillers with cross-linked bovine collagen: a multicenter, double-masked, randomized, within-subject study. *Dermatol Surg*. 2007;33(Suppl. 2):S128–135.
28. Narins RS, Coleman 3rd WP, Donofrio LM, et al. Improvement in nasolabial folds with a hyaluronic acid filler using a cohesive polydensified matrix technology: results from an 18-month open-label extension trial. *Dermatol Surg*. 2010;36(Suppl. 3):1800–1808.
29. Narins RS, Dayan SH, Brandt FS, Baldwin EK. Persistence and improvement of nasolabial fold correction with nonanimal-stabilized hyaluronic acid 100,000 gel particles/mL filler on two retreatment schedules: results up to 18 months on two retreatment schedules. *Dermatol Surg*. 2008;34(Suppl. 1):S2–S8, discussion S8.
30. Smith SR, Jones D, Thomas JA, et al. Duration of wrinkle correction following repeat treatment with Juvederm hyaluronic acid fillers. *Arch Dermatol Res*. 2010;302:757–762.
31. Micheels P, Besse S, Flynn TC, et al. Superficial dermal injection of hyaluronic acid soft tissue fillers: comparative ultrasound study. *Dermatol Surg*. 2012;38:1162–1169.
32. Black J, Gross TM, Murcia CL, Jones DH. Cohesive polydensified matrix hyaluronic acid for treatment of etched-in fine facial lines: a 6-month open label clinical trial. *Dermatol Surg*. 2018;44:1002–1011.
33. Glogau R, Bank D, Brandt F, et al. A randomized, evaluator-blinded, controlled study of the effectiveness and safety of small gel particle hyaluronic acid for lip augmentation. *Dermatol Surg*. 2012;38:1180–1182.
34. Jones D, Murphy DK. Volumizing hyaluronic acid filler for midface volume deficit: 2-year results from a pivotal single-blind randomized controlled study. *Dermatol Surg*. 2013;39:1602–1612.
35. Humphrey S, Jones DH, Carruthers JD, et al. Retrospective review of delayed adverse events secondary to treatment with a smooth, cohesive 20 mg/ml hyaluronic acid filler in 4500 patients. *J Am Acad Dermatol*. 2020;83:86–95.
36. Monheit G, Kaufman-Janette J, Josepha JH, et al. Efficacy and safety of two resilient hyaluronic acid fillers in the treatment of moderate-to-severe nasolabial folds: a 64-week, prospective, multicenter, controlled, randomized, double-blinded, and within-subject study. *Dermatol Surg*. 2020;46:1521–1529.
37. Kaufman-Janette J, et al. Efficacy and safety of a new resilient hylauronic acid dermal filler, in the correction of moderate-to-severe nasolabial folds: a 64-week, prospective, multicenter, controlled, randomized, double-blind and within-subject study. *J Cosmet Dermatol*. 2019;18:1244–1253.
38. Jones D, Tezel A, Borell M. In-vitro resistance to degradation of HA by ovine testicular hyaluronidase. *Dermatol Surg*. 2010;36:804–809.
39. Shumate G, Chopra R, Jones D, et al. In vivo degradation of crosslinked hyaluronic acid fillers by exogenous hyaluronidases. *Dermatol Surg*. 2018;44:1075–1083.
40. Mazzuco R, Dal'Forno T, Hexsel D. Poly-L-lactic acid for nonfacial skin laxity. *Dermatol Surg*. 2020;46(Suppl 1):S86–S88.
41. Lin M, Dubin DP, Khorasani H. Poly-L-lactic acid for minimally invasive gluteal augmentation. *Dermatol Surg*. 2020;46:386–394.
42. Jones D. Volumizing the face with soft tissue fillers. *Clin Plast Surg*. 2011;38:379–390.
43. Wu D, Goldman MP. The efficacy of massage in reducing nodules formation after poly-L-lactic acid administration for facial volume loss: a randomized, evaluator-blinded clinical trial. *Dermatol Surg*. 2016;42:1266–1272.
44. Goldman M, Moradi A, Katz B, et al. Safety and efficacy of calcium hydroxylapatite dermal filler for hand treatment. *J Am Acad Dermatol*. 2015;72(5):AB20.
45. Smith S, Busso M, McClaren M, Bass LS. A randomized, bilateral, prospective comparison of calcium hydroxylapatite microspheres versus human-based collagen for the correction of nasolabial folds. *Dermatol Surg*. 2007;33(Suppl. 2):S112–S121.
46. Carruthers A, Carruthers J. Evaluation of injectable calcium hydroxylapatite for the treatment of facial lipoatrophy associated with human immunodeficiency virus. *Dermatol Surg*. 2008;34:1486–1499.
47. Busso M, Moers-Carpi M, Storck R, et al. Multicenter, randomized trial assessing the effectiveness and safety of calcium hydroxylapatite for hand rejuvenation. *Dermatol Surg*. 2010;36:790–797.
48. Goldie K, Peeters W, Alghoul M, et al. Global Consensus Guidelines for injection of diluted and hyperdiluted calcium hydroxylapatite for skin tightening. *Dermatol Surg*. 2018;44(suppl 1):S32–S41.
49. Carruthers A, Liebeskind M, Carruthers J, Forster B. Radiographic and computed tomographic studies of calcium hydroxylapatite for treatment of HIV-associated facial lipoatrophy and correction of nasolabial folds. *Dermatol Surg*. 2008;34(s1):S78–S84.
50. Tzikas TL. Autologous fat grafting for midface rejuvenation. *Facial Plast Surg Clin North Am*. 2006;14:229–240.
51. Glogau RG. Microlipoinjection. Autologous fat grafting. *Arch Dermatol*. 1988;124:1340–1343.
52. Pinski KS, Roenigk Jr. HH. Autologous fat transplantation. Long-term follow-up. *J Dermatol Surg Oncol*. 1992;18:179–184.
53. Moscatello DK, Dougherty M, Narins RS, Lawrence N. Cryopreservation of human fat for soft tissue augmentation: viability requires use of cryoprotectant and controlled freezing and storage. *Dermatol Surg*. 2005;31:1506–1510.
54. Carpaneda CA, Ribeiro MT. Percentage of graft viability versus injected volume in adipose autotransplants. *Aesthetic Plast Surg*. 1994;18:17–19.
55. Sadick NS, Hudgins LC. Fatty acid analysis of transplanted adipose tissue. *Arch Dermatol*. 2001;137:723–727.
56. Drake L, Dinehart S, Farmer E, et al. Guidelines of care for soft tissue augmentation: fat transplantation. American Academy of Dermatology. *J Am Acad Dermatol*. 1996;34:690–694.
57. Duffy DM. The silicone conundrum: a battle of anecdotes. *Dermatol Surg*. 2002;28:590–594.
58. Jones DH, Carruthers A, Brody HJ, et al. Ten-year and beyond follow-up after treatment with highly purified liquid-injectable silicone for HIV-associated facial lipoatrophy: a report of 164 patients. *Dermatol Surg*. 2019;45:941–948.
59. Cohen SR, Berner CF, Busso M, et al. Artefill: a long lasting injectable wrinkle filler material – summary of the US Food and Drug Administration trials and a progress report on 4- to 5- year outcomes. *Plast Reconstr Surg*. 2006;118:64S–76S.
60. Kakar R, Minokadeh A, Jones DH. Delayed inflammatory nodules with off-label use of Food and Drug Administration-approved polymethylmethacrylate. *Dermatol Surg*. 2021;47:1030–1031.
61. Jones D. Treatment of delayed reactions to dermal fillers. *Dermatol Surg*. 2014;40:1180.
62. Kang BK, Shin MK, Lee JH, Kim NI. Effects of platelet-rich plasma on wrinkles and skin tone in Asian lower eyelid skin: preliminary results from a prospective randomised, split-face trial. *Eur J Dermatol*. 2014;24:100–101.
63. Abuaf OK, Yildiz H, Baloglu H, et al. Histologic evidence of new collagen formulation using platelet rich plasma in skin rejuvenation: a prospective controlled clinical study. *Ann Dermatol*. 2016;28:718–724.
64. Alam M, Hughart R, Champlain A, et al. Effect of platelet rich plasma injection for rejuvenation of photoaged facial skin: a randomized clinical trial. *JAMA Dermatol*. 2018;154:1447–1452.
65. Du R, Lei T. Effects of autologous platelet-rich plasma injections on facial skin rejuvenation. *Exp Ther Med*. 2020;19:3024–3030.
66. Diaz-Ley B, Cuevast J, Alonso-Castro L, et al. Benefits of plasma rich in growth factors (PRGF) in skin photodamage: clinical response and histological assessment. *Dermatol Ther*. 2015;28:258–263.
67. Hausauer AK, Humphrey S. The physician's guide to platelet-rich plasma in dermatologic surgery part II: clinical evidence. *Dermatol Surg*. 2020;46:447–456.
68. Alam M, Gladstone H, Kramer EM, et al. ASDS Guidelines of care: injectable fillers. *Dermatol Surg*. 2008;34(Suppl. 1):S115–S148.
69. Funt D, Pavicic T. Dermal fillers in aesthetics: an overview of adverse events and treatment approaches. *Clin Cosmet Investig Dermatol*. 2013;6:295–316.
70. Keller EC, Kaminer MS. Use of hyaluronidase in patients with bee allergy. *Dermatol Surg*. 2014;40:1145–1147.
71. Glashofer MD, Flynn TC. Complications of temporary fillers. In: Carruthers J, Carruthers A, eds. *Soft Tissue Augmentation*. Toronto: Elsevier Saunders; 2013:179–187.
72. Humphrey S, Jones DH, Carruthers JD, et al. Retrospective review of delayed adverse events secondary to treatment with a smooth, cohesive 20 mg/ml hyaluronic acid filler in 4500 patients. *J Am Acad Dermatol*. 2020;83:86–95.

73. Jones D, Bank D. Five-year postmarket safety experience with the optimal balance technology of hyaluronic acid filler. *Dermatol Surg*. 2020;46:145–147.
74. Artzi O, Loizides C, Verner I, Landau M. Resistant and recurrent late reaction to hyaluronic acid-based gel. *Dermatol Surg*. 2016;42:31–37.
75. Sadeghpour M, Quatrano NA, Bonati LM, et al. Delayed-onset nodules to differentially crosslinked hyaluronic acids: comparative incidence and risk assessment. *Dermatol Surg*. 2019;45:1085–1094.
76. Beleznay K, Carruthers JD, Carruthers A, et al. Delayed-onset nodules secondary to a smooth cohesive 20 mg/mL hyaluronic acid filler: cause and management. *Dermatol Surg*. 2015;41:929–939.
77. Turkmani MG, De Boulle K, Philipp-Dormston WG. Delayed hypersensitivity reaction to hyaluronic acid dermal filler following influenza-like illness. *Clin Cosmet Investig Dermatol*. 2019;12:277–283.
78. Munavalli GG, Knutsen-Larson S, Lupo MP, Geronemus RG. Oral angiotensin-converting enzyme inhibitors for treatment of delayed inflammatory reactions to dermal hyaluronic acid fillers following COVID-19 vaccination—a model for inhibition of angiotensin II-induced cutaneous inflammation. *JAAD Case Rep*. 2021;10:63–68.
79. Molina-Ruiz AM, Requena L. Foreign body granulomas. *Dermatol Clin*. 2015;33:497–523.
80. Ledon JA, Savas JA, Yang S, et al. Inflammatory nodules following soft tissue filler use: a review of causative agents, pathology and treatment options. *Am J Clin Dermatol*. 2013;14:401–411.
81. Glaich AS, Cohen JL, Goldberg LH. Injection necrosis of the glabella: protocol for prevention and treatment after use of dermal fillers. *Dermatol Surg*. 2006;32:276–281.
82. Lee W, Oh W, Oh SM, Yang EJ. Comparative effectiveness of different interventions of perivascular hyaluronidase. *Plast Reconstr Surg*. 2020;145:957–964.
83. Rauso R, Zerbinati N, Franco R, et al. Cross-linked hyaluronic acid filler hydrolysis with hyaluronidase: different settings to reproduce different clinical scenarios. *Dermatol Ther*. 2020;33:e13269.
84. Li J, Xu Y, Wang Y, et al. The role of hyaluronidase for the skin necrosis caused by hyaluronic acid injection-induced embolism: a rabbit auricular model study. *Aesthetic Plast Surg*. 2019;43:1362–1370.
85. Ciancio F, Tarico MS, Giudice G, Perrotta RE. Early hyaluronidase use in preventing skin necrosis after treatment with dermal fillers: report of two cases. *F1000Res*. 2018;7:1388.
86. Fang M, Rahman E, Kapoor KM. Managing complications of submental artery involvement after hyaluronic acid filler injection in chin region. *Plast Reconstr Surg Glob Open*. 2018;6:e1789.
87. Juhász ML, Marmur ES. Temporal fossa defects: techniques for injecting hyaluronic acid filler and complications after hyaluronic acid filler injection. *J Cosmet Dermatol*. 2015;14:254–259.
88. Cohen JL, Biesman BS, Dayan SH, et al. Treatment of hyaluronic acid filler-induced impending necrosis with hyaluronidase: consensus recommendations. *Aesthet Surg J*. 2015;35:844–849.
89. Beleznay K, Humphrey S, Carruthers JD, Carruthers A. Vascular compromise from soft tissue augmentation: experience with 12 cases and recommendations for optimal outcomes. *J Clin Aesthet Dermatol*. 2014;7:37–43.
90. Alam M, Hughart R, Geisler A, et al. Effectiveness of low doses of hyaluronidase to remove hyaluronic acid filler nodules: a randomized clinical trial. *JAMA Dermatol*. 2018;154:765–772.
91. Alam M, Dover JS. Management of complications and sequelae with temporary injectable fillers. *Plast Reconstr Surg*. 2007;120(6 Suppl):98S–105S.
92. Lee W, Oh W, Oh SM, Yang EJ. Comparative effectiveness of different interventions of perivascular hyaluronidase. *Plast Reconstr Surg*. 2020;145(4):957–964.
93. Robinson DM. In vitro analysis of the degradation of calcium hydroxylapatite dermal filler: a proof-of-concept study. *Dermatol Surg*. 2018;44:S5–S9.
94. Rullan PP, Olson R, Lee KC. The use of intralesional sodium thiosulfate to dissolve facial nodules from calcium hydroxylapatite. *Dermatol Surg*. 2020;46:1366–1368.
95. DeLorenzi C. Complications of injectable fillers, part 2: vascular complications. *Aesthet Surg J*. 2014;34:584–600.
96. Dayan S, Arkins JP, Mathison CC. Management of impending necrosis associated with soft tissue filler injections. *J Drugs Dermatol*. 2011;10:1007–1012.
97. DeLorenzi C. Complications of injectable fillers, part I. *Aesthet Surg J*. 2013;3:561–575.
98. Park SW, Woo SJ, Park KH, et al. Iatrogenic retinal artery occlusion caused by cosmetic facial filler injections. *Am J Ophthalmol*. 2012;154:653–662.
99. Ozturk CN, Li Y, Tung R, et al. Complications following injection of soft-tissue fillers. *Aesthet Surg J*. 2012;33:862–877.
100. Tobalem S, Schutz JS, Chronopoulos A. Central retinal artery occlusion – rethinking retinal survival time. *BMC Ophthalmol*. 2018;18:101.
101. Lee W, Koh IS, Oh W, Yang EJ. Ocular complications of soft tissue filler injections: a review of literature. *J Cosmet Dermatol*. 2020;19:772–781.
102. Surek CC, Said SA, Perry JD, Zins JE. Retrobulbar injection for hyaluronic acid gel filler-induced blindness: a review of efficacy and technique. *Aesth Plast Surg*. 2019;43:1034–1040.
103. Paap MK, Milman T, Ugradar S, et al. Examining the role of retrobulbar hyaluronidase in reversing filler-induced blindness: a systematic review. *Ophthalmic Plast Reconstr Surg*. 2020;36:231–238.

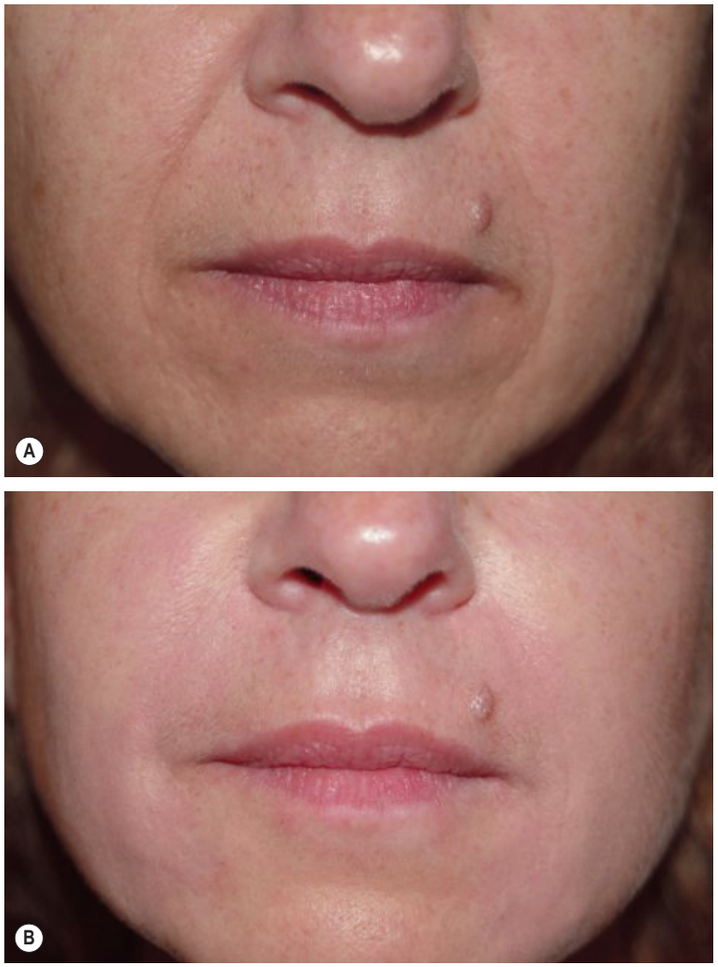


eFig. 158.1 Hyaluronic acid – augmentation of nasolabial folds, lips, and oral commissures. A, B Pre-treatment. **C, D** Following injection of Juvéderm Ultra®.





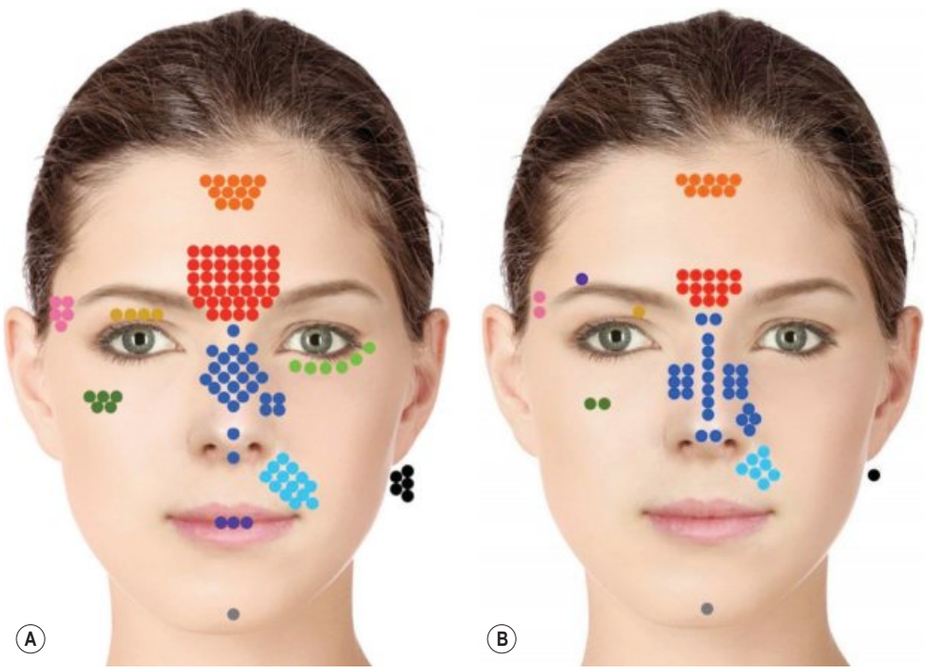
eFig. 158.2 Poly-L-lactic acid – correction of facial fat loss. A Pre-treatment in a patient with facial fat loss related to aging and lean body mass. **B** Eight months post-treatment of the cheeks (and temples) with 10 vials of Sculptra® (five treatments, two vials per treatment) over 4 months.



eFig. 158.3 Calcium hydroxylapatite – perioral augmentation. A Prior to injection of 1 ml of Radiesse®. **B** Follow-up: softening of nasolabial fold and elevation of lateral oral commissure. *Courtesy Seth L. Matarasso, MD.*



eFig. 158.4 Calcium hydroxylapatite – correction of facial fat loss. A Pre-treatment in a patient with facial fat loss related to aging and lean body mass. **B** Following injection of Radiesse® into the midface.



eFig. 158.5 Location of filler injection in reported cases of blindness. A 98 patients (2015). **B** 48 patients (2019). The black dots represent cases in which the location was simply listed as "face". *A, Reproduced with permission from Beleznay K, Carruthers JD, Humphrey S, Jones D. Avoiding and treating blindness from fillers: a review of the world literature. Dermatol Surg 2015;41:1097-117. B, Reproduced with permission from Beleznay K, Carruthers JDA, Humphrey S, et al. Update on avoiding and treating blindness from fillers: a recent review of the world literature. Aesthet Surg J 2019;39:662–74.*

Botulinum Toxin 159

Nagasai C. Adusumilli, Elizabeth Tanzi, Alastair Carruthers, Jean Carruthers and Ada Regina Trindade de Almeida

Chapter Contents

Properties of Botulinum Toxins 2705
Cosmetic Use of Botulinum Toxin Type A 2706
Medical Uses of Botulinum Toxin Type A 2714
Complications 2715
Safety 2716

Synonyms:
- Botulinum toxin type A, botulinum A exotoxin, BoNT-A; onabotulinumtoxinA – BOTOX®/BOTOX® Cosmetic; abobotulinumtoxinA – Dysport®, Azzalure®; incobotulinumtoxinA – Xeomin®/Bocouture®; prabotulinumtoxinA-xvfs – Jeuveau®; daxibotulinumtoxinA-lanm – DAXXIFY®
- Botulinum toxin type B, BoNT-B; rimabotulinumtoxinB – MYOBLOC®

Key features

- Botulinum toxin (BoNT) causes chemodenervation of muscles by blocking acetylcholine release
- BoNT is also capable of inhibiting the release of other neurotransmitters, such as substance P, noradrenaline, calcitonin gene-related peptide, and glutamate from a variety of synaptosomal and neuronal systems
- Injections of BoNT type A (BoNT-A) that weaken or relax muscles can smooth hyperfunctional lines and change the contour of the face and neck
- Adjunctive use of BoNT-A with soft-tissue augmentation or laser resurfacing is beneficial, particularly in active regions such as the perioral and periocular areas
- The cosmetic effects of BoNT-A typically last months and may increase with subsequent injections
- In addition to its effect on musculature, BoNT-A successfully denervates sweat glands, serving as an effective alternative treatment for hyperhidrosis, and it can also improve the pain, swelling, and discoloration associated with Raynaud phenomenon
- Complications (e.g. eyelid ptosis) are generally caused by diffusion of the toxin to non-targeted muscles and can be minimized by using concentrated doses and careful technique

INTRODUCTION

Botulinum toxin (BoNT) injections are commonly used to improve facial aesthetics by smoothing hyperdynamic rhytides of the face and neck. In recent years, the use of BoNT has evolved to reflect a more three-dimensional approach to facial rejuvenation, often in combination with soft-tissue augmentation or other restorative procedures. Moreover, a better understanding of its mechanism of action has led to innovative indications across a number of therapeutic fields.

PROPERTIES OF BOTULINUM TOXINS

Various strains of the bacterium *Clostridium botulinum* produce seven distinct serotypes of BoNT that affect neural function: A, B, C1, D, E, F and G[1]. Although all serotypes produce chemodenervation and atrophy of skeletal muscles by blocking acetylcholine release from motor neurons at the neuromuscular junction (Fig. 159.1), they differ with regard to cellular mechanism of action and clinical profile.

Formulations

BoNT type A (BoNT-A), the first serotype developed for use in humans, is available in seven formulations worldwide (Table 159.1). Five have been approved by the U.S. Food and Drug Administration (FDA) for the treatment of glabellar rhytides and have been assigned specific drug names to avoid confusion and reduce the potential for dosing errors: onabotulinumtoxinA (onaA; BOTOX®/BOTOX® Cosmetic), abobotulinumtoxinA (aboA; Dysport®, Azzalure®), incobotulinumtoxinA (incoA; Xeomin®/Bocouture®), prabotulinumtoxinA-xvfs (praboA; Jeuveau®), and daxibotulinumtoxinA-lanm (DAXI; DAXXIFY®). Outside of North America, BoNT-A formulations include Prosigne® and Neuronox®. One formulation of BoNT type B (BoNT-B; rimabotulinumtoxinB (rimaB; MYOBLOC®/NeuroBloc®) is also available in North America (see Table 159.1). All preparations of BoNT differ in terms of purification procedures, potency, and clinical effect and may not be used interchangeably.

Clinical Differences

Clinical differences between onaA and aboA have been debated, in particular the possibility of greater diffusion and migration by aboA[2–4]. However, digital image correlation at various time points utilizing speckle-tracking photogrammetry demonstrated no significant differences between aboA and onaA in the reduction of dynamic glabellar rhytides[5]. Similar efficacy for onaA and aboA has also been observed for non-cosmetic indications, such as facial synkinesis[6]. While suggested dosing ratios have ranged from 1 : 2 to 1 : 4 (onaA : aboA), a dosing ratio of 1 : 2.5 has been shown to increase the field of anhidrotic effect[2], and a higher dose ratio of 1 : 3 has been reported to result in greater longevity[3,7,8], as well as a faster onset of action[8]. Although no clear consensus on a conversion factor between products has been reached, current guidelines recommend a dose ratio of 1 : 2.5 or less than 1 : 3[2,9].

The first BoNT formulation without complexing proteins, incoA, has been shown to be as safe and effective as onaA for the treatment of glabellar rhytides, with a rapid onset of effect and duration of effect of up to 5 months or more[10–12]. In contrast to aboA (see above), incoA has similar dosing to onaA. Researchers had initially speculated that complexing proteins would limit diffusion of the active neurotoxin within the target muscle[13], but human and animal studies have suggested otherwise[2,14]. For example, Kerscher and colleagues found no difference in the size of the anhidrotic area after injection with incoA or onaA[2].

In a multicenter, randomized, double-blind, controlled clinical trial that enrolled 540 patients with moderate to severe glabellar rhytides, a single treatment with praboA (20 U) was found to be as safe and effective as onaA; no serious side effects were observed with this more recently approved formulation of BoNT-A[15]. One comparison study of the effectiveness of rimaB versus onaA reported similar findings[16]. Of note, rimaB was FDA-approved in 2000 for cervical dystonia but is used off-label to treat facial rhytides.

When used for the treatment of hyperkinetic lines in the face, there are several key differences between rimaB and onaA: rimaB has a more rapid onset of action but a shorter duration of effect, diffuses more widely, and is associated with greater pain and other side effects when compared to onaA[17]. That said, one study which examined seven doses of rimaB found all to be safe and effective for the treatment of hyperfunctional rhytides, with a dose-related duration of effect[18].

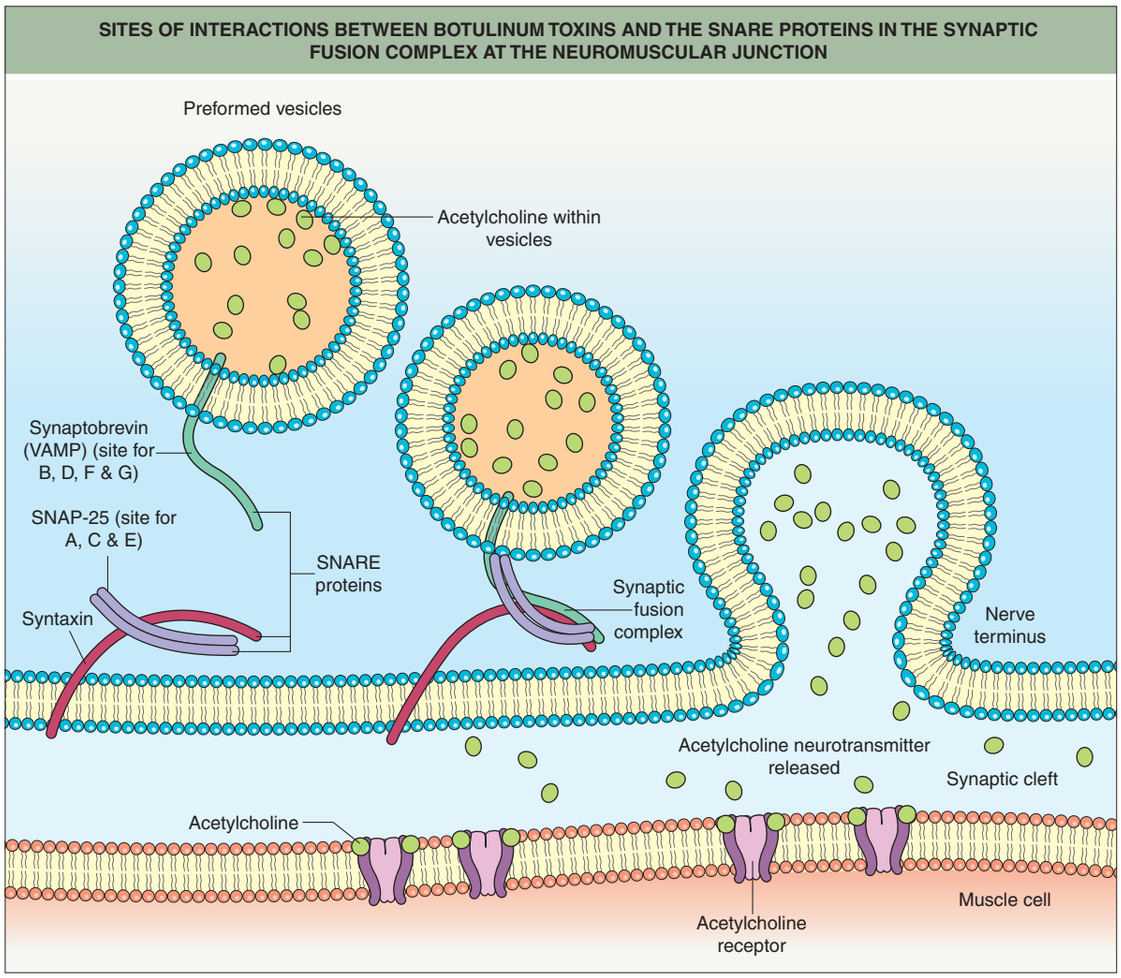


Fig. 159.1 Sites of interactions between botulinum toxins and the SNARE proteins in the synaptic fusion complex at the neuromuscular junction. Botulinum toxins A, C, and E catalyze the cleavage of the SNAP-25 protein. Botulinum toxins B, D, F, and G catalyze the cleavage of synaptobrevin (or the vesicle-associated membrane protein, VAMP). *Adapted from Rohrer TE, Beer K. Background to botulinum toxin. In: Carruthers A, Carruthers J (eds). Botulinum Toxin. Philadelphia: Saunders, 2005.*

Topical BoNT-A

Percutaneous delivery of topical BoNT has been limited by its inability to cross the stratum corneum. As a result, it has been combined with mechanical, chemical, and thermal techniques in an attempt to enhance percutaneous delivery[19–21]. Despite early promising reports of the treatment of lateral canthal rhytides (Fig. 159.2) and primary axillary hyperhidrosis[22–25] with topical formulations of BoNT-A, to date, no such formulations have been approved by the FDA. For example, in contrast to the effectiveness of injectable daxibotulinumtoxinA[26], topical daxibotulinumtoxinA gel did not meet primary endpoints for efficacy in a phase III trial. Nonetheless, topical BoNT-A remains a potential approach for the treatment of anatomic areas that are difficult to manage or particularly painful to inject.

A Note About Dosing

Most of the published information regarding the cosmetic uses of BoNT pertains to the use of onaA, followed in recent years by aboA and incoA. Data are scarce regarding other formulations of BoNT-A. Since most of our experience pertains to the use of onaA, the following discussion (including units and description of techniques) focuses on this formulation specifically. However, a conversion rate of 1 : 1 U may be considered for all 100-U product vials (incoA, Prosigne®, and Neuronox®) and 1 : 2.5 U for aboA.

COSMETIC USE OF BOTULINUM TOXIN TYPE A

Hyperkinetic lines result from the repeated contraction of muscles perpendicular to the rhytides. Weakening or relaxing these muscles with BoNT-A can smooth horizontal lines on the forehead (from frontalis contraction), vertical lines in the glabellar region between the eyebrows (from corrugator contraction), horizontal creases across the bridge of the nose (from procerus contraction), "crow's feet" and lateral lines along the lower eyelid (from lateral orbicularis oculi contraction), and perioral lines (from orbicularis oris contraction). Deep grooves or folds elsewhere that are exacerbated by muscle activity are also amenable to treatment. Patients 30–50 years of age may be most responsive to BoNT-A, because their rhytides are more likely to be caused by muscle activity rather than by the loss of skin elasticity that occurs with aging.

Injections for aesthetic indications may be given intramuscularly, subcutaneously, or intradermally. We use intradermal injections, especially in the crow's feet area, to minimize bruising. All of the usual precautions prior to any injection should be followed. The area may be chilled with ice before injection to minimize any discomfort in sensitive individuals. Alternatively, a topical anesthetic can be applied 15 to 30 minutes prior to injection to minimize discomfort.

The effects of BoNT-A injections are usually apparent within a day or two and are obvious for 3 or 4 months, although they may last for 6 months or more. In comparison to other BoNT-A formulations, injectable daxibotulinumtoxinA (DAXI) has been reported to have a longer duration of effect on glabellar lines[26]. There is also a tendency for repeated BoNT-A injections to provide more prolonged aesthetic improvement.

Glabellar Frown Lines

Frown lines in the glabellar region are caused by contraction of the corrugator supercilii and orbicularis oculi muscles, which move the brow medially, and the procerus and depressor supercilii muscles, which pull the brow inferiorly. Because the corrugator and procerus are used only to control facial expression, the goal of treatment should be to produce a significant weakening of these muscles. The treatment sites and doses should be individualized because the location, size, and use of the frown muscles vary greatly between individuals. We currently use five injection sites when treating glabellar frown lines and vary the dosage depending on the individual brow (Fig. 159.3; Table 159.2). If the extent of the frown reaches the midpupillary line, additional injection sites may be warranted (Video 159.1) The procedure effectively smooths the glabellar lines at rest and prevents their appearance when the patient attempts to frown, for an average of 3 to 4 months (Fig. 159.4)

CURRENTLY AVAILABLE BOTULINUM TOXIN FORMULATIONS AND CLINICAL USES								
	OnaA	**AboA**	**DAXI**	**IncoA**	**PraboA**	**RimaB**	**BoNT-A**	**BoNT-A**
Trade names®	BOTOX/BOTOX Cosmetic/ Vistabel/ Vistabex	Dysport, Azzalure	DAXXIFY	Xeomin/Bocouture	Jeuveau	MYOBLOC/ NeuroBloc	Prosigne/Lantox/ Redux	Neuronox/ Meditoxin/ Botulift
Manufacturer	Allergan, Inc.	Ipsen Biopharm Ltd/Medicis Pharmaceutical Corp. Galderma	Revance Therapeutics, Inc.	Merz Pharmaceuticals	Evolus, Inc.	Solstice Neurosciences, LLC	Lanzhou Institute of Biological Products	Medytox, Inc.
Active substance	BoNT-A + complex (900 kDa)	BoNT-A + complex (400 kDa)	BoNT-A free of complexing proteins (150kDa)	BoNT-A free of complexing proteins (150 kDa)	BoNT-A free of complexing proteins (900 kDa)	BoNT-B + complex (700 kDa)	BoNT-A + complex (900 kDa)	BoNT-A + complex (940 kDa)
Excipients (per vial)	HSA 500 mcg NaCl 0.9 mg	HSA 125 mcg Lactose 2.5 mg	L-histidine 0.14 mg L-histidine-HCl monohydrate 0.65 mg Polysorbate 20 0.1 mg RTP004 peptide 11.7 mcg Trehalose dihydrate 36 mg	HSA 1000 mcg Sucrose 4.7 mg	HSA 500 mcg NaCl 0.9 mg	HSA 500 mcg NaCl 0.1 M Disodium succinate 0.01 M HCl (to adjust pH) Water for injection	Gelatin 5 mg Dextran 25 mg Sucrose 25 mg	HSA 500 mcg NaCl 0.9 mg
Units per vial	50 or 100	300 or 500	50 or 100	100	100	2500, 5000, or 10 000	50 or 100	100
Indications [*FDA-approved in italics*]	*Glabellar lines*, axillary hyperhidrosis**, chronic migraine, blepharospasm, cervical dystonia*	*Glabellar lines*, cervical dystonia*, blepharospasm	*Glabellar lines*	*Blepharospasm, cervical dystonia*, cosmetic use in some countries	*Glabellar lines**	*Cervical dystonia*	Glabellar lines, hyperhidrosis, blepharospasm, cervical dystonia	Blepharospasm
*Moderate to severe glabellar lines **Severe primary axillary hyperhidrosis								

Table 159.1 Currently available botulinum toxin formulations and clinical uses. At the time of writing, BoNT/A-DP by Croma-Pharma GmbH is in Phase III trials. AboA, abobotulinumtoxinA; DAXI, daxibotulinumtoxinA; HSA, human serum albumin; IncoA, incobotulinumtoxinA; OnaA, onabotulinumtoxinA; PraboA, prabotulinumtoxinA-xvfs; RimaB, rimabotulinumtoxinB.

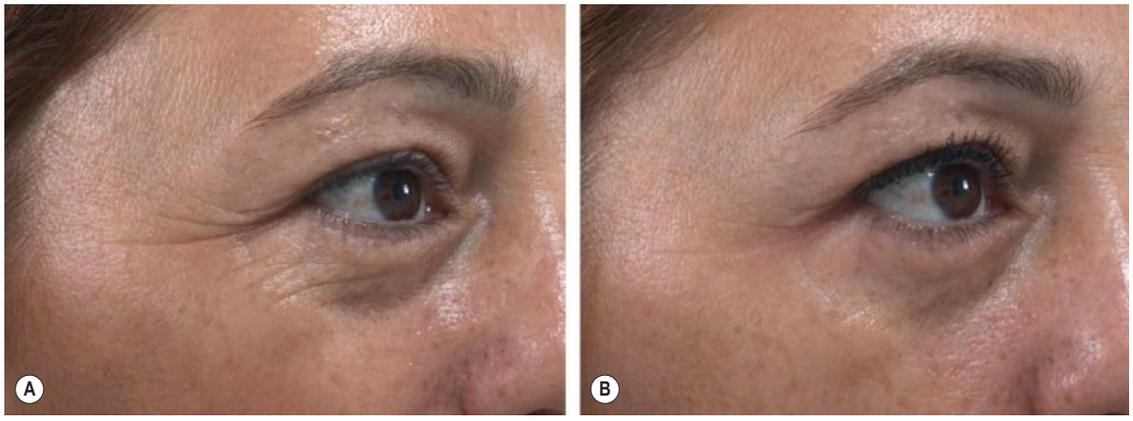


Fig. 159.2 Topical BoNT-A for lateral canthal rhytides (crow's feet). Before (**A**) and after (**B**) treatment.

Crow's Feet

Contraction of the lateral fibers of the orbicularis oculi muscle produces "crow's feet", lines that radiate from the lateral canthus. Since forceful closure of the eyelids requires orbicularis contraction, the goal of treatment is to produce weakening just in the lateral orbital area, rather than a complete paralysis of the muscle. Because the orbicularis oculi is diffusely innervated, multiple injections are required to weaken broad areas of the muscle. Doses and sites vary among clinicians – we evenly distribute the BoNT-A into two to four separate injection sites (Fig. 159.5; see Table 159.2) while others may employ up to seven injection sites (Video 159.2). Results last approximately 3 months (Fig. 159.6).

Horizontal Forehead Lines

Deep horizontal creases in the forehead are produced by the repeated contraction of the frontalis muscle. This large, vertically oriented muscle is the brow elevator; it inserts superiorly into the galea aponeurotica and inferiorly into the skin of the brow. Unfortunately, weakening the

frontalis muscle sufficiently to eliminate hyperkinetic forehead lines can result in undesired brow ptosis or a complete lack of expressiveness. Therefore, it is our practice to divide the BoNT-A amongst multiple sites distributed horizontally across the midforehead (Fig. 159.7; see Table 159.2). The goal of treatment is to only soften, rather than completely eliminate, forehead lines. Ideally, the individual will still be able to elevate the eyebrows, albeit to a lesser extent, after treatment (Fig. 159.8). We believe that the brow depressors should *always* be treated at the same time as the frontalis, and so we employ the technique described in the next section. Effects typically last from 3 to 6 months (Video 159.3).

Brow Lift and Shaping

Brow ptosis often occurs during aging, resulting in an angry, scowling expression. Notably, the shape and height of the eyebrows are

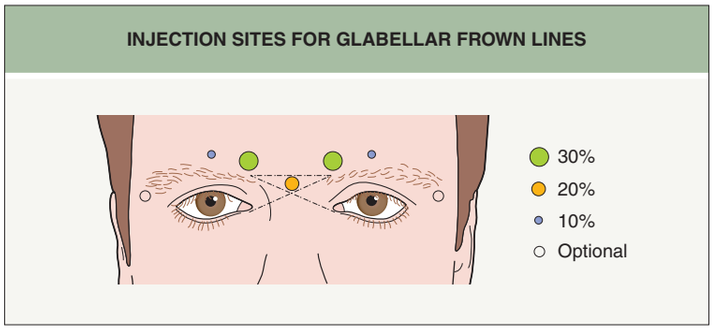


Fig. 159.3 Injection sites for glabellar frown lines. The authors currently use five injection sites when treating glabellar frown lines and vary the dosage depending on the individual brow. The injection in the midpupillary line may be omitted if eyebrow ptosis seems likely or possible. Sometimes, an injection is made above the lateral canthus or into the tail of the eyebrow.

USE OF onaA IN THE UPPER FACE: DOSING AND TECHNIQUES

Treatment area	Injection sites and tips
Glabellar rhytides	• Men: starting dose 60 U, titrate to 100 U; women: starting dose 30 U, titrate to 50 U • 7–10 U (women) or 15–20 U (men) just above the superior bony orbital rim directly above the inner canthus on each side (Fig. 159.3) • 5–10 U into procerus muscle at midline • For horizontal brows: 4–5 U 1 cm above bony supraorbital rim in the midpupillary line* • Sometimes necessary to inject above lateral canthus or into the tail of the eyebrow to improve lateral eyebrow position
Lateral canthal rhytides (crow's feet)	• 12–15 U/side, distributed amongst 2–4 sites (Fig. 159.5) • Inject when patient is *not* smiling to avoid affecting the ipsilateral zygomaticus complex (which can lead to upper lip ptosis) • Inject lateral to the lateral orbital rim; more medial injections can cause lower eyelid droop • Superficial injections (as few as possible) will avoid bruising • Avoid injecting superficial veins
Horizontal forehead rhytides	• 10–15 U amongst multiple sites horizontally across the midforehead, 2–3 cm above the eyebrows (Fig. 159.7) • 5 injection sites for broad foreheads†; 4 injection sites and a slightly lower dose for narrow foreheads
Hypertrophic orbicularis oculi muscle	• Subcutaneous injections of 2–4 U in the midpupillary line, 3 mm below the ciliary margin (Fig. 159.9) • Higher doses can result in keratoconjunctivitis sicca (dry eye)

*Injection site most likely to cause ptosis.
†More than 12 cm between the temporal fusion lines (the slight prominence at the point where the temporalis fascia joins the skull) at the midforehead level.

Table 159.2 Use of onaA in the upper face: dosing and techniques.



Fig. 159.4 Effect of BoNT-A injections for glabellar frown lines. A subject at rest (**A**) and during frowning (**B**). Same subject at rest (**C**) and attempting to frown (**D**) two weeks after BoNT-A treatment.

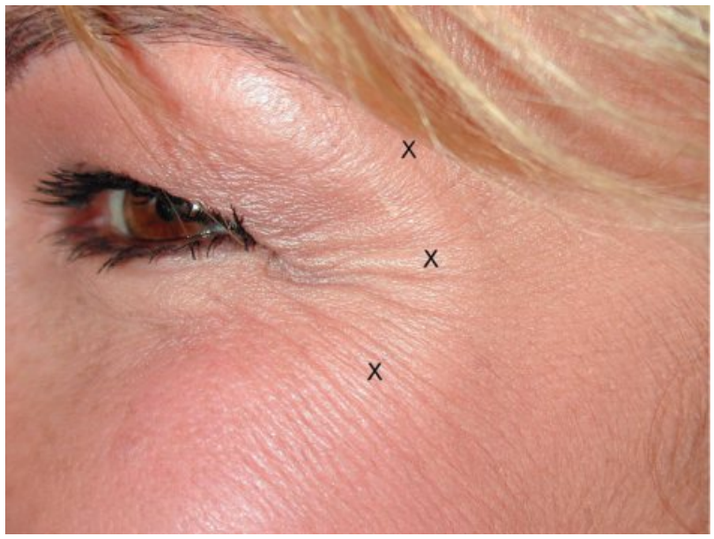


Fig. 159.5 Injection sites for lateral canthal rhytides (crow's feet). The authors inject 12–15 U of onaA per side among two to four injection sites.



Fig. 159.6 Effect of BoNT-A injections for lateral canthal rhytides (crow's feet). Subject before (**A**) and after (**B**) BoNT-A treatment.

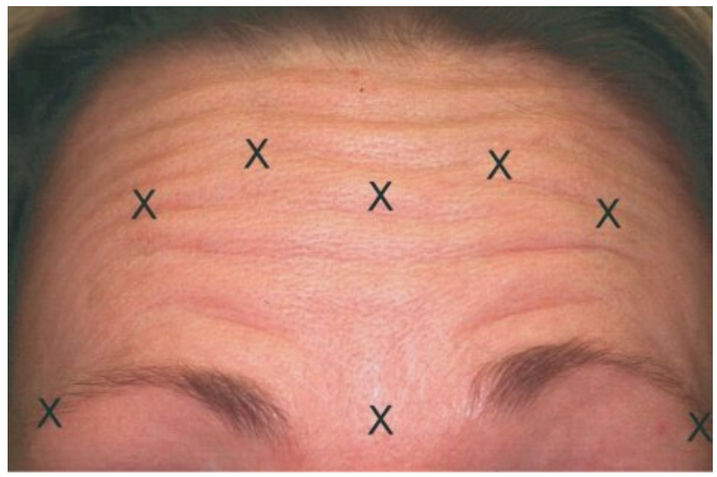


Fig. 159.7 Injection sites for horizontal forehead lines. Injection sites must be kept well above the brow. The lower X's mark the sites of injection of the brow depressors.

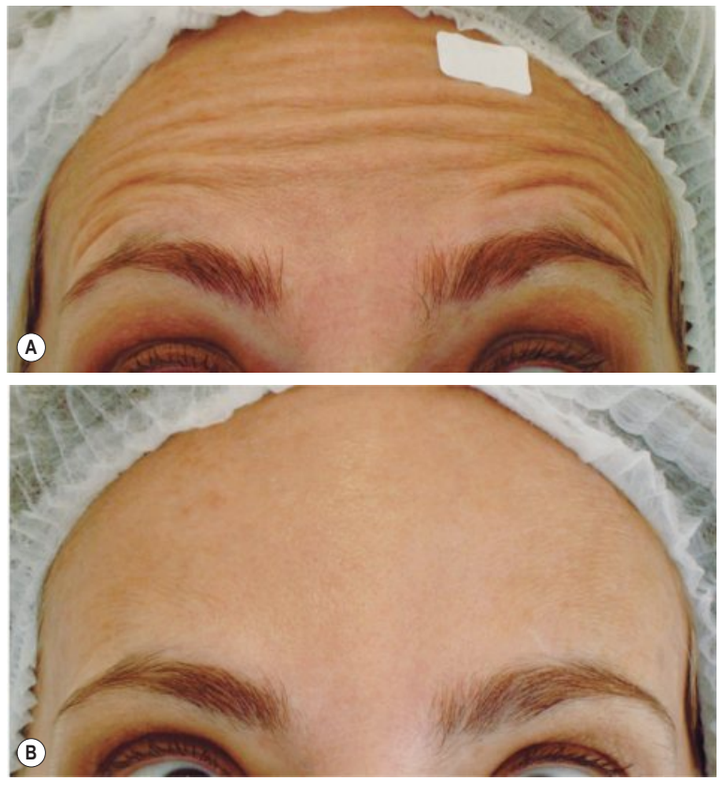


Fig. 159.8 Effect of BoNT-A injections for horizontal forehead lines. The subject elevates the brows before (**A**) and after (**B**) BoNT-A treatment.

determined by the opposing activity of the frontalis muscle, which elevates the brow, and the brow depressors. The medial brow depressors are the corrugator supercilii, the procerus, and the medial portion of the orbicularis oculi; the lateral depressor is the lateral portion of the orbicularis oculi (that is lateral to the temporal fusion line). Although we initially believed that brow lifts were a result of the inactivation of the brow depressors, subsequent research showed that central injections of 20–40 U of onaA into the glabella alone (with the most lateral injection at the midpupillary line) led to a dramatic lateral eyebrow elevation, followed by an entire brow lift that peaked 12 weeks after treatment, while too little (10 U) led to a brief fall in eyebrow position[27]. We now believe that the change in eyebrow position after glabellar injection in women is due to diffusion of the toxin into the lower frontalis muscle, which causes an improved resting tone in the remainder of the muscle and in eyebrow position.

Hypertrophic Orbicularis Oculi

The pretarsal portion of the orbicularis oculi muscle is involved in the blink reflex. Contraction of the pretarsal orbicularis during smiling tends to decrease the size of the palpebral aperture. Hypertrophy of this muscle can give a "jelly roll" appearance to the lower eyelid, enough that some individuals may complain that they look overweight. We have found that injection of 2 U (or occasionally 4 U) of onaA into the lower pretarsal orbicularis (Fig. 159.9) opens the palpebral aperture both at rest and during smiling (Fig. 159.10; see Table 159.2)[28].

Midface Injections

Contraction of the upper nasalis muscle causes fanning rhytides ("bunny lines") at the nasal root (Fig. 159.11). BoNT-A treatment weakens the upper nasalis and dramatically softens these lines. Bunny lines are typically treated in conjunction with the glabellar complex (Table 159.3).



Fig. 159.9 Injection sites for hypertrophic orbicularis oculi muscle. 2–4 U of onaA are injected into the lower pretarsal orbicularis oculi muscle.



Fig. 159.10 Effect of BoNT-A injections for hypertrophic orbicularis oculi muscle. Treatment of the lower pretarsal orbicularis opens the palpebral aperture. Note the position of the lower eyelids in the subject before (**A**) and after (**B**) BoNT-A treatment.



Fig. 159.11 Injection sites for bunny lines. 2–4 U of BoNT-A injected in each belly of the upper nasalis, at the lateral bony dorsum of the nose.

USE OF onaA IN THE MIDFACE: DOSING AND TECHNIQUES	
Treatment area	**Injection sites and tips**
Bunny lines	• 2–4 U into the upper nasalis muscle, usually 1 injection/side (Fig. 159.11) • Inject well above nasofacial groove* to avoid lip ptosis (due to relaxing the levator labii superioris muscle) • Injection followed by gentle massage
Repeated nasal flare	• 5–10 U bilaterally into lower nasalis muscle fibers covering the lateral nasal ala • Inject the most active area of contraction
Nasolabial folds	• Select patients only, e.g. those with a naturally shorter cutaneous upper lip • 1 U into each lip elevator complex above the nasofacial groove
Nasal tip droop	• 2–3 U into depressor septi nasi muscle at the base of the columella
*Refers to groove between the nose and cheek.	

Table 159.3 Use of onaA in the midface: dosing and techniques.

Some individuals repeatedly and embarrassingly dilate their nostrils in social situations. The sides of the columella/septum become visible when the nostrils are prominently flared. Contraction of the nasalis muscle accentuates the nasal flare. Small doses of BoNT-A can produce a satisfactory decrease in involuntary nostril flare in some patients for 3 to 4 months (see Table 159.3).

The nasolabial folds extend from the lateral nasal ala to a point lateral to the external angle of the mouth. Young adults have a shallow indentation, but older individuals who smile excessively or sustain photodamage can develop a permanent, deep crevice. The most common treatments for nasolabial folds have been soft-tissue fillers and laser resurfacing. Although muscle contraction contributes to the appearance of the folds, injecting BoNT-A directly into the area of the fold is not recommended, because it is likely to result in an asymmetric smile, flaccid cheek and flattening of the midface, along with a vertical lengthening of the cutaneous upper lip, leading to incomplete or disappointing results. However, for some individuals who have a naturally shorter cutaneous upper lip, very small doses of BoNT-A can be beneficial for improving nasolabial folds (see Table 159.3), particularly when the injections are given concurrently with fillers or resurfacing. Because duration of effect of this procedure is relatively long (~6 months), it is important to be very careful in patient selection and to be clear about the potential results of the procedure.

Nasal tip droop is common during aging. Contraction of the depressor septi nasi, a small muscle located at the external base of the nasal septum, pulls the tip of the nose downward. BoNT-A slightly elevates the nasal tip (see Table 159.3). Caution should be taken with individuals who already have a long non-vermilion upper lip, because of an associated risk of lip ptosis.

Vertical Lip Rhytides (Perioral Lines)

During aging, the mouth undergoes characteristic changes: the lateral portions of the lips recede to produce a "rosebud mouth"; the vertical distance between the columella and the vermilion border of the upper lip increases, and the substance of the vermilion lip rolls inside, producing the thin and disappointed lips characteristic of old age. The cutaneous upper lip lengthens, and dense vertical perioral rhytides appear. These vertical lines are commonly referred to as "smokers' lines" but they can have other causes, such as heredity, photodamage, or activities

such as playing a musical instrument that require pursing of the lips. Radial upper lip rhytides are exaggerated by the pursestring-like action of the orbicularis oris sphincter muscle of the lip. Multiple fine rhytides of the upper lip can be effectively treated with fillers such as hyaluronic acid or with mid-depth or deeper resurfacing. However, deeper rhytides may be resistant to these treatments.

BoNT-A treatment of the lip sphincter is recommended only for deep lines. Small doses that produce localized microparesis of the orbicularis oris can dramatically reduce radial lip lines and improve the appearance of the lips (Table 159.4). To maintain competence of the mouth, it is important to be conservative with dosing, and superficial injections are recommended over deep injections (Fig. 159.12) (Video 159.4). Even with conservative dosing, however, BoNT-A treatment of perioral lines may result in lip sphincter weakening that subtly affects mouth function. This procedure may not be desirable for musicians who play wind instruments and professional singers or speakers. Some patients have difficulty with lip proprioception after treatment, but eating, drinking and singing are typically not affected. BoNT-A injections for radial lip lines may be particularly useful in combination with perioral laser or electrosurgical resurfacing or in combination with a soft-tissue-augmenting agent such as hyaluronic acid (Fig. 159.13).

USE OF onaA IN THE LOWER FACE AND NECK: DOSING AND TECHNIQUES

Treatment area	Injection sites and tips
Perioral rhytides	• 4 U/lip (2 U/lip quadrant); typically 1 U/vertical lip line (Fig. 159.12) • Inject into area of muscle contraction adjacent to the creases at the vermilion border on either side of Cupid's bow • Avoid injecting lip corners (can lead to drooping of the lateral lip and drooling) as well as the midline (can lead to flattening of Cupid's bow)
Upper gum show	• 1–2 U into levator labii superioris alaeque nasi muscle (on each side of the bony nasal prominence) • Younger patients
Mouth frown	• 2–3 U into the posterior aspect of the depressor anguli oris (DAO) muscle on each side, close to the mandible (Fig. 159.15) • Additional 3 U into each mentalis muscle insertion • Asking the patient to frown can aid in identifying the DAO muscle • Not recommended for singers or musicians
Marionette lines	• 2–5 U into each DAO muscle immediately above the angle of the mandible and 1 cm lateral to the lateral oral commissure; amount injected depends upon size of the muscle • Injection must be lateral and low, at the junction of the depressor and the superior margin of the mandible • An injection too medial or too high can cause ipsilateral weakness of the depressor labii inferioris muscle and flattening of the lower lip contour when the mouth attempts to form an "O"; an injection too high may compromise sphincter function and cause mouth incompetence
Mental crease	• 3–5 U/mentalis muscle band
Peau d'orange chin	• 5–10 U into mentalis muscle at the most distal point from the orbicularis oris muscle (i.e. the prominence of the chin; Fig. 159.18)
Masseteric hypertrophy	• 20–35 U into each masseter muscle
Platysmal bands	• 5 U into contracted platysma muscle; 3 sites at 1–1.5 cm intervals for a total of 15 U/band (Fig. 159.20A) • Single treatment typically involves 2 bands and a total dose of 30 U into the neck • Recommended only for patients who have obvious platysmal bands, good cervical skin elasticity, and minimal submental fat accumulation

Table 159.4 Use of onaA in the lower face and neck: dosing and techniques.

Facial Asymmetry: Functional Muscle Imbalance

Injections of BoNT-A can be used to correct facial asymmetry resulting from facial nerve palsies, dystonias, surgery, or trauma[29]. In cases of hemiparesis, BoNT-A is used to decrease muscle activity on the unaffected side; for hyperkinesia, the affected muscles are treated.

Midfacial asymmetry may have bony tissue, soft tissue, innervational or muscular causes. BoNT-A treatment can be invaluable for patients with facial asymmetry caused by neuromuscular abnormalities. In hemifacial spasm, repeated clonic and tonic facial movements draw the facial midline over toward the hyperfunctional side. BoNT-A treatment of the hyperfunctional zygomaticus, risorius and masseter muscles allows the face to be centered at rest. Hypofunctional asymmetry, such as that seen in Bell palsy due to unilateral seventh nerve dysfunction, can be relieved by small doses of BoNT-A injected into muscles on the normally functioning side. Only 1–2 U of onaA into the zygomaticus, risorius, and orbicularis oris muscles and 5–10 U into the masseter muscle are needed to restore facial symmetry (Fig. 159.14).

For patients with asymmetric jaw movement, intraoral injection of 10–15 U of onaA into the internal pterygoid on the hyperfunctional side can relax the jaw and relieve discomfort. Unilateral surgical or traumatic injury of the orbicularis oris or the risorius muscle can cause the mouth to be pulled off-center by the unopposed actions of the partner muscles on the uninjured side. Chemodenervation of the risorius immediately lateral to the corner of the mouth on the uninjured side re-centers the mouth when the face is at rest. Similarly, facial asymmetry is evident in individuals with congenital or acquired unilateral weakness of the depressor anguli oris (DAO) muscle, who are unable to depress the corner of one side of the mouth. In these cases as well, BoNT-A treatment of the partner muscle restores aesthetic balance.

Mouth Frown

The frowning expression created when the lateral corners of the mouth are permanently angled downward can create an impression of disapproval and unpleasantness. The DAO muscle pulls down the corner of the mouth in opposition to the zygomaticus major and minor muscles. BoNT-A can be used to weaken the DAO and reset muscular balance (Fig. 159.15), allowing the zygomaticus to elevate the corners of the mouth and return them to a horizontal position (Fig. 159.16). The effects of this procedure may be potentiated with repeated treatment.

It is always important to be cautious when injecting toxin close to the mouth. A misplaced injection could result in complications, including a flaccid cheek, incompetent mouth, or asymmetric smile. This treatment is not recommended for singers or musicians, or for patients who use their perioral muscle with intensity. With this procedure, as for others in the perioral area, the most pleasing results may be obtained with BoNT-A injections in combination with laser resurfacing.

Melomental Folds (Marionette Lines)

Melomental folds ("drool grooves" or marionette lines) extending from the down-turned corner of the mouth to the lateral mentum

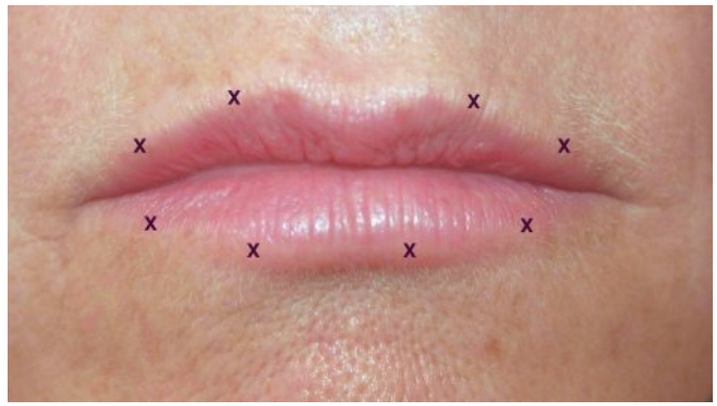


Fig. 159.12 Injection sites for perioral rhytides. The authors typically inject 1 U of onaA per lip line.



Fig. 159.13 Effect of BoNT-A injections for radial lip lines. This treatment is particularly efficacious when used in combination with a soft-tissue-augmenting agent such as hyaluronic acid. Before (**A**) and after (**B**) BoNT-A treatment.



Fig. 159.14 Left-sided Bell palsy. Before (**A**) and after (**B**) BoNT-A treatment of the right side, with improvement in asymmetry. The authors typically inject 1–2 U of onaA into the zygomaticus, risorius, and orbicularis oris muscles and 5–10 U into the masseter muscle.

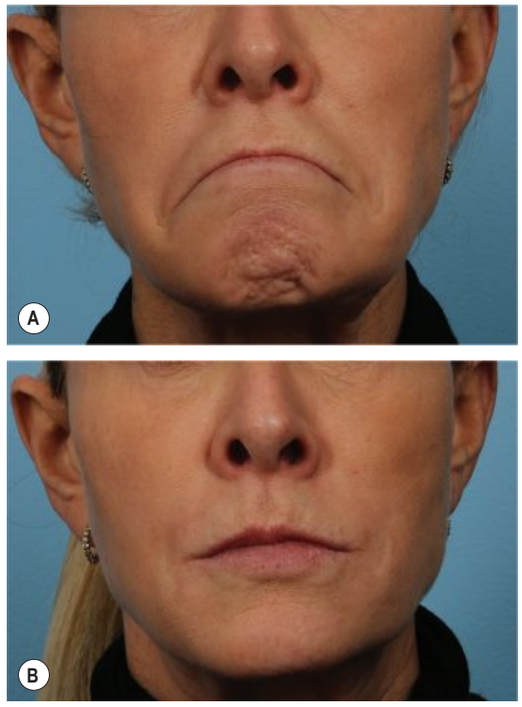


Fig. 159.16 Effect of BoNT-A injections for mouth frown. Before (**A**) and after (**B**) BoNT-A treatment. The authors typically inject 2–3 U of onaA into the posterior aspect of the depressor anguli oris muscle and 3 U into each insertion of the mentalis muscle.



Fig. 159.15 Injection sites for mouth frown.

involuntarily produce a sad expression and give the appearance of advancing age. Because contraction of the DAO muscle exacerbates the melomental folds, BoNT-A treatment is a useful adjunct to soft-tissue augmentation (see Table 159.4). Best results in this area are obtained with combined therapy as BoNT-A treatment prevents the repeated molding and contortion of the implant, enhancing and extending the duration of the soft-tissue augmentation. When performing a comprehensive approach to the entire aging face, BoNT-A treatment of the DAO muscle is often included (Video 159.5)

Mental Crease

The convexity between the lower lip and the prominence of the chin is called the mental crease. Contraction of the mentalis muscle can produce a deep groove in this region. This area is closely tethered to the bony mentum (chin), and soft-tissue augmentation of the mental crease is often unsuccessful because the filling agent visibly beads. BoNT-A injections at the level of the crease may also give unsatisfactory results because the orbicularis oris is weakened, sometimes resulting in an incompetent mouth. However, injection of the mentalis muscle gives a satisfactory softening of the crease while avoiding complications from weakening of the orbicularis oris (see Table 159.4). Injections into the mentalis are especially valuable in individuals who have had previous trauma or surgery to this area (Fig. 159.17).

Peau d'Orange (Apple Dumpling) Chin

An "orange peel" appearance of the chin during aging results from the loss of dermal collagen and subcutaneous fat at the mentum.



Fig. 159.17 Effect of BoNT-A injections on a mental crease. Subject puckers before (**A, B**) and two weeks after (**C, D**) chemodenervation of a traumatically damaged mentalis muscle with BoNT-A.



Fig. 159.19 Effect of BoNT-A injections on masseteric hypertrophy. Subject before (**A**) and after (**B**) BoNT-A treatment. The authors inject 20–35 U onaA into each masseter muscle.

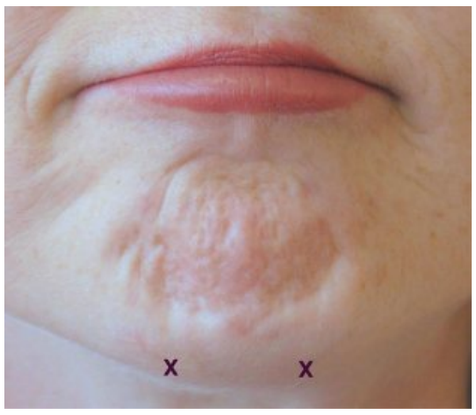


Fig. 159.18 Injection sites for a *peau d'orange* chin. The authors inject 5–10 U of onaA into the mentalis muscle at these sites.

The appearance worsens when the mentalis and depressor labii inferioris muscles are used together with the orbicularis oris muscle during mastication or speech. *Peau d'orange* chin is frequently seen asymmetrically during and after recovery from unilateral facial paresis (Bell palsy). Previous treatment options have included soft-tissue augmentation to fill in the tissue gaps and ablative and non-ablative laser resurfacing. Depending upon the patient's aesthetic need for chin augmentation, BoNT-A and soft-tissue augmentation can be used together, or BoNT-A can be used alone to improve the appearance of the chin (Fig. 159.18; see Table 159.4) (Video 159.6). Following treatment, the chin is massaged to facilitate diffusion of the toxin.

Masseteric Hypertrophy

A number of studies have observed a reduction of muscle thickness in Asian and White[30] patients with masseteric hypertrophy who were treated with BoNT-A. Reductions in muscle bulk ranged from 20% to 50% and lasted from 3 to 6 months, depending upon the doses used. Effective sculpting of the jawline can be achieved (Fig. 159.19; see Table 159.4). When investigated in a White versus East Asian population, smaller doses were required for aesthetic improvement in the former versus the latter, and patients experienced a 6- to 7-month improvement in symptoms of bruxism[30].

Platysmal Bands

Platysmal bands are formed when the anterior fibers of the platysma separate into two discrete vertical bands. The bands often tighten and become more visible when the neck is animated, as when the patient speaks, exercises, or plays a musical instrument. The emergence of platysmal bands during aging is often accompanied by other senescent changes, including loss of cervical skin elasticity and accumulation of submental fat. BoNT chemodenervation of the anterior part of the platysma muscle can soften the platysmal bands (Fig. 159.20) and produce a gentle anterior neck lift. However, in aging necks with jowl formation and bone resorption, BoNT-A treatment of the platysma may emphasize, rather than soften, the muscle cords. Thus, chemodenervation of the platysma is recommended only for patients who have obvious platysmal bands, good cervical skin elasticity, and minimal submental fat accumulation.

Large doses of BoNT-A must be used cautiously in the neck. The platysma is external to the larynx and the muscles of deglutition and neck flexion. Doses from 75–100 U of onaA can produce weakness in the neck flexors and dysphagia, and we have reported one patient treated with only 60 U in her neck who developed such profound dysphagia that she required a nasogastric tube until she could swallow again[31]. Therefore, we recommend that the physician proceed with caution and inject no more than 30–40 U of onaA spread over multiple sites per cervical treatment session (see Table 159.4).

Adjunctive Use

BoNT-A is beneficial in many patients as adjunctive therapy in order to enhance or prolong the results of other cosmetic procedures. Prior to surgery, BoNT-A treatment to chemodenervate specific muscles can facilitate subsequent manipulation of tissues during the surgery and permit a greater surgical correction or a better concealment of the surgical incision. BoNT-A can also be used to reduce tension exerted on a wound or surgical incision by the underlying muscles, thereby promoting better healing with less scar formation[32].

Combination treatment with lasers, light-based modalities, and soft-tissue augmentation offers a synergistic approach to the treatment of facial aging. BoNT-A in conjunction with ablative resurfacing leads to optimal improvement of dynamic rhytides, with superior and longer-lasting outcomes[33]. Regular postoperative injections, given every 6 to 12 months, prolong the effects of resurfacing, and many clinicians

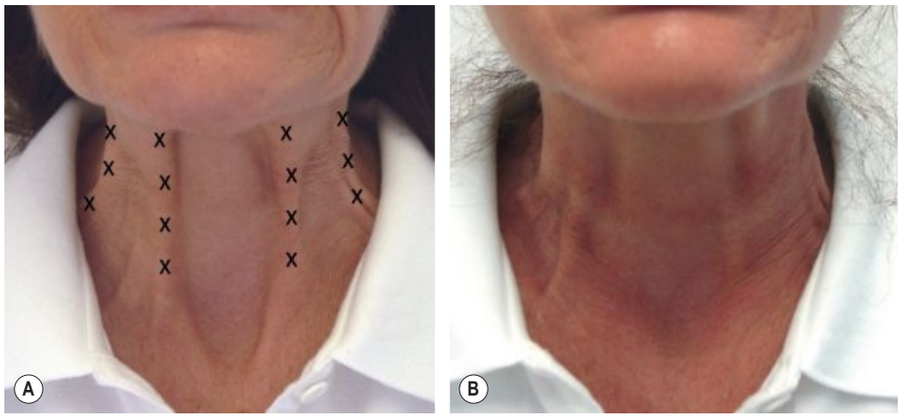


Fig. 159.20 Effect of BoNT-A injections on platysmal bands. Before (**A**) and after (**B**) treatment. Each band is injected in three sites at 1 to 1.5 cm intervals with 3–4 U of onaA per site.

now use BoNT-A injections as part of their standard laser resurfacing protocol. Likewise, combination treatment with BoNT-A and intense pulsed light (IPL) leads to greater global aesthetic benefits, with a reduction in fine lines and rhytides and improvement in skin tone, texture and erythema, compared to IPL alone[34]. Of note, BoNT-A injections delivered immediately into areas of moderate to severe edema due to laser resurfacing procedures or IPL can lead to increased and unwanted neurotoxin diffusion. Therefore, caution is recommended in this situation[34], especially since neurotoxin injections are often performed as a second procedure due to concern regarding neurotoxin inactivation by heat-producing lasers or light- and energy-based devices[34].

BoNT-A is also frequently used in combination with soft-tissue augmentation, where it prevents the distortion of the filler and prolongs the beneficial effects of tissue augmentation. Preceding the injection of filling agents by approximately 1 week, BoNT-A may work on several levels, including reducing the dynamic component of rhytide formation in newly remodeled skin and allowing more permanent eradication of rhytides[32]. Together, BoNT-A and fillers produce greater aesthetic improvements of longer duration than either modality alone[35].

MEDICAL USES OF BOTULINUM TOXIN TYPE A

Hyperhidrosis

Dramatically effective with minimal side effects, BoNT-A was approved for the treatment of axillary hyperhidrosis in Canada and the US in 2001 and 2004, respectively, and a high level of efficacy has been established in clinical trials for this indication (level A recommendation)[36,37]. Along with a decrease in perspiration lasting from 6 to 24 months, injections can improve quality of life and decrease body odor for up to 7 months[38,39].

Studies comparing onaA with aboA or incoA have shown similar levels of safety and efficacy[40,41], with a non-significant trend toward a more rapid onset of action with aboA[41]. RimaB, while effective, is associated with a greater amount of pain on injection and systemic adverse events (e.g. xerostomia, flu-like symptoms)[42].

Typically, 50–150 U of onaA per axilla are divided among 10–20 injection sites spaced 1.5–2 cm apart (Video 159.7). BoNT-A is injected intradermally or immediately subdermally. Injections are usually repeated at 6- to 12-month intervals, although, in the experience of the authors, most subjects are far below their pre-injection degree of hyperhidrosis when they present for reinjection. Alternatively, BoNT-A topically applied in large doses (200 U) has been shown to be safe and may prove to be an effective method for treating axillary hyperhidrosis[43].

The efficacy of BoNT-A in palmar hyperhidrosis is less assured (level B, probably effective), with a limited number of blinded, prospective trials[36,37]. Some consider BoNT-A only after failure of traditional treatment approaches, due to the necessity of anesthesia and the high doses required[38]. Typical doses of onaA for the palm range from 50–200 U distributed among 50–100 injection sites, including the distal wrist crease and the thenar and hypothenar eminences. Although studies show significant decreases in sweat production for 3–4 months (Fig. 159.21), most patients experience some degree of hand weakness that can last up to 2 weeks, with the thumb–index finger pinch significantly affected[44].



Fig. 159.21 Effect of BoNT-A injections on palmar hyperhidrosis. Only the right palm was treated as the right hand is the primary one used in social interactions. Small residual areas of sweating may be treated at a follow-up visit 2–4 weeks later.

Given that sweating, as well as friction, can exacerbate Hailey–Hailey disease, injections of BoNT-A into lesional skin can lead to clinical improvement. One approach is to utilize a total of 100 U, injecting 2 U into every cm^2 of involved skin.

Raynaud Phenomenon

BoNT-A is an increasingly utilized treatment for Raynaud phenomenon, defined as an exacerbated, transient vasospasm of the digital arteries, particularly in the hands, that is triggered by cold or emotional stress (see Ch. 43). Patients may experience three phases of skin discoloration: white (resulting from vasoconstriction and interruption of regional vascular flow), blue (cyanosis corresponding to blood de-oxygenation), and red (when reperfusion occurs). Pain and paresthesia due to sensory nerve ischemia may occur during an attack, and the condition may progress to ulcerations and gangrene[45].

BoNT-A injections appear to target both neural and vascular abnormalities responsible for the clinical manifestations of the syndrome, leading to a significant decrease in pain and improvements in color, mobility, blood flow and oxygen saturation, as well as healing of persistent digital ulcers[46–49]. BoNT-A is believed to work via two mechanisms: at the level of the vessel, promoting vasodilation due to the blockade of norepinephrine and acetylcholine release, and at the nerve, blocking receptors, and neurotransmitters that stimulate both pain (substance P, calcitonin gene-related peptide, and glutamate) and vasoconstriction[46].

Injection may be performed into the palmar region, wrists, and/or fingers. There is no consensus yet with regard to dose, dilution, or injection sites. The simplest technique involves 5 U onaA into the medial and lateral aspects of each finger at its base, using insulin syringes (BD Ultrafine II, 0.3 ml) for a total of 50 U onaA per hand. Some clinicians avoid injecting the thumb unless there is significant symptomatic involvement. Response can be perceived within days to a week with remarkable improvement of numbness and pain. Side effects, which are minimal and temporary, include local pain triggering a vasospastic attack.

These results warrant further investigation of clinical effect and optimal dosing with larger controlled trials.

Migraine

In 2011, the FDA approved onaA for chronic migraine prophylaxis. In addition to inhibiting release of acetylcholine from nerve endings (see Fig. 159.1), it can inhibit the release of glutamate, substance P, and calcitonin gene-related peptide (CGRP)[50]. The pathogenic role of the latter has led to the approval of several monoclonal antibodies (e.g. erenumab) and oral medications (e.g. ubrogepant) for migraine prophylaxis or treatment that target CGRP.

Typically, 100 U of onaA are distributed within the brow, temple and occipital regions, in addition to injections into any trigger sites. Historically, there have been mixed results, but a recent meta-analysis of randomized, double-blind, placebo-controlled trials reported a reduction in episode frequency and improved quality of life for up to three months after injections[50]. However, because the clinical effects on facial muscles are readily detectable, this has led to the criticism that trials are not truly blinded.

Depression

Research indicates that BoNT injections – and subsequent inability to frown – correlates with an improvement in symptoms of depression[51,52], suggesting that muscles of facial expression may play a role in mood regulation. A double-blind, randomized, placebo-controlled trial of 30 patients with major depression found that scores on the Hamilton Depression Rating Scale, Beck Depression Inventory, and Clinical Global Impressions Scale decreased by an average of 47% after one treatment with BoNT-A in the glabella, compared to a 9% reduction in patients who received saline[53]. Results were maintained over the 16-week follow-up period. In a second randomized, placebo-controlled trial, half of the patients with major depression responded to BoNT-A injections to the corrugator and procerus muscles, with an ~50% reduction in scores on the Montgomery–Åsberg Depression Rating Scale[52]. Only 15% of patients who received placebo reported such improvement.

COMPLICATIONS

BoNT-A occasionally affects non-targeted muscles or glandular tissue in the areas surrounding the injection, which can result in effects such as eyelid ptosis (Fig. 159.22), lower eyelid laxity, epiphora (excessive tearing), diplopia, brow ptosis, decreased strength of eye closure, dry eye, mouth incompetence, difficulties in speech, and the inability to whistle. Use of both careful injection technique to target the toxin to the appropriate muscles and concentrated low doses to limit its diffusion to non-targeted muscles or glands are recommended to prevent the occurrence of these adverse effects[53]. In general, a higher concentration allows for more accurate placement, greater duration of effect and fewer side effects, since lower concentrations may encourage the spread of toxin. Of note, there is an area of denervation associated with each point of injection of about 1–1.5 cm (diameter, 2–3 cm) that is due to toxin spread.

A quizzical or "cockeyed" appearance can occur in the brow when the lateral fibers of the frontalis muscle have not been injected adequately and these untreated lateral fibers pull upward on the brow (Fig. 159.23). Brow ptosis may last upwards of 3 months, while upper eyelid ptosis can persist for 2–12 weeks. When upper eyelid ptosis occurs, options include: (1) thrice daily 0.5% apraclonidine eyedrops, an α_2-adrenergic agonist used for glaucoma, which leads to contraction of the Müller muscle and a 1–2 mm elevation of the upper eyelid[54]; (2) oral pyridostigmine bromide (60 mg 3–4 times daily), an anticholinesterase drug used for myasthenia gravis that inhibits acetylcholine breakdown, whose side effects include hypersalivation, blurred vision, muscle cramps, vomiting, and diarrhea[54]; and (3) precise injections of 0.5–1 U of BoNT-A into the subdermal plane just above the eyelash line at the extreme medial and lateral aspects of the upper eyelid, thereby reducing the strength of the orbicularis oculi muscle and allowing the Müller muscle and the levator muscle to become less opposed[55].

Bruising, diplopia, ectropion, a drooping lateral lower eyelid, and an asymmetric smile (caused by the spread of toxin to the zygomaticus major) are also reported complications of BoNT-A injections in the periorbital area. Transient local bruising, ptosis, dry eyes, diplopia, and facial droop can occur with injections into the cheek.



Fig. 159.23 Cockeyed eyebrow. Untreated lateral fibers of the frontalis muscle pull upward on the lateral brow. The result is a quizzical appearance.



Fig. 159.22 Blepharoptosis. Diffusion of toxin into the levator of the upper eyelid resulted in eyelid ptosis (**A**) with partial recovery after 3 weeks (**B**) and complete recovery after 5 weeks (**C**). See text for therapeutic options.

Complications of the lower face involve effects on muscle function and facial expression, usually due to use of BoNT-A in large doses. Injections placed too close to the mouth, injection into the mental fold, and interaction with the orbicularis oris muscle can all result in a flaccid cheek, incompetent mouth, or asymmetric smile. Large doses (>100 U) of onaA in the platysma have resulted in reports of dysphagia and weakness of the neck flexors.

Although one of the greatest concerns associated with the use of BoNT-A is the formation of neutralizing antibodies leading to non-response of subsequent injections, the overall risk is actually low (<1%) when BoNT-A is used at recommended doses for cosmetic applications. Of note, the protein content in current lots of BoNT-A is significantly lower than in previous batches and has been shown to be less antigenic than the original product. Although antibody formation has occurred with current lots of BoNT-A[56], it is usually associated with the use of large doses for therapeutic, rather than cosmetic, purposes[57]. The lack of complexing proteins in incoA reduces the antigenicity[56] but does not appear to eliminate it entirely[58]. Injecting the lowest effective doses, with the longest feasible intervals between injections, minimizes the potential for immunogenicity.

Allergic reactions to BoNT-A are rare but have been described in the literature. Additional reactions include serious or non-serious cutaneous eruptions[59] as well as granulomas[60]. After large doses for therapeutic purposes, anaphylactic reactions and severe respiratory failure have occurred[61,62].

SAFETY

No long-term adverse effects have been reported, and no systemic safety problems have been associated with FDA-approved uses of BoNT. A review of the long-term safety of BoNT-A for cosmetic purposes revealed no serious adverse events (AEs) in over 850 treatment sessions for up to 9 years[63]. An interim analysis of 768 patients enrolled in phase 3 clinical trials, who received up to six treatments of aboA, found that multiple treatments over 17 months were well tolerated[64]. A large-scale, comprehensive phase III program of onaA for crow's feet and glabellar rhytides comprising three trials, 684 patients, and up to four treatment cycles found no serious treatment-related AEs, evidence of distant spread of the toxin, or immunogenicity over a 12-month period[65]. Side effects were mostly mild and included hematoma, headache, and injection-site hemorrhage. Treating both the crow's feet region and glabellar rhytides at the same time did not result in an increased incidence of AEs, and side effects appeared to decline with repeated treatments.

However, the risk of serious complications increases with higher doses: in an analysis of 1031 AE reports submitted to the FDA, 407 occurred with higher therapeutic doses, including 28 deaths and other serious cardiovascular complications[59]. The FDA could not determine a causal relationship between the fatalities and BoNT-A injections, especially since 26 patients who died had underlying cardiovascular diseases with an elevated mortality risk. Notably, no deaths or cardiovascular complications were associated with cosmetic doses. Similarly, another investigation of 658 FDA-submitted AEs, which included 180 cases of aspiration, dysphagia and/or pneumonia and 16 deaths, involved only therapeutic doses in already compromised individuals[66]. As a result, the FDA requested safety label changes with black box warnings and a *r*isk *e*valuation and *m*itigation *s*trategy (REMS), including a consumer guide outlining the risks associated with treatment, for all BoNT products[67].

FUTURE TRENDS

The use of BoNT continues to evolve, with new applications that deepen our understanding of clinical effect and mechanism of action. There have been anecdotal reports of tighter, smoother skin after BoNT-A injections, as well as a lower incidence of acne[68]. Current research indicates that BoNT-A acts on the biological behavior of fibroblasts, including reducing production of matrix metalloproteinases (MMPs), responsible for the slow degradation of type I collagen, and stimulating the production of procollagen I. Collagen production and degradation has been investigated *in vitro* by measuring procollagen type I carboxy-terminal peptide (PIP) and MMPs, respectively. Levels of PIP increased significantly when fibroblasts were grown in the presence of BoNT, with upregulation of type I collagen and a decrease in MMPs[69]. In an *in vivo* investigation of the effects of BoNT on photodamaged skin, mice were pretreated with BoNT-A and subsequently irradiated with ultraviolet B light[70]. Compared to control mice, those injected with BoNT-A had significantly decreased secretion of inflammatory cytokines associated with photodamage and postinflammatory hyperpigmentation.

Intradermal injection of BoNT-A has been used with success to treat oily skin and enlarged pores. When the T-zone (forehead and nose) was injected in a series of 20 patients, 17 reported an improvement in skin oiliness[71]. Significantly lower sebum production was noted in 25 patients treated with 3 to 5 U of aboA in each of ten injection sites across the forehead, as measured by a sebometer[72]. The authors speculated that blockade of local acetylcholine receptors in the pilosebaceous unit with BoNT-A could result in altered rates of sebum production.

SUMMARY

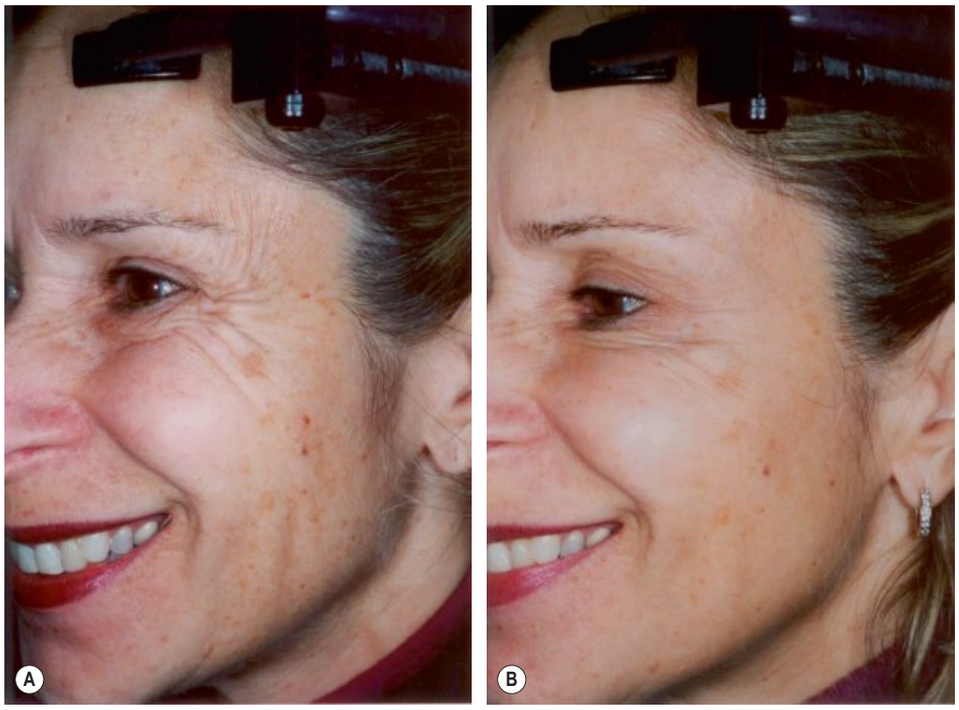
BoNT-A remains the treatment of choice for smoothing hyperkinetic lines in the face and neck, creating a more pleasant and youthful appearance. Alone or in combination with surgery, soft-tissue augmentation, or ablative and non-ablative laser resurfacing, BoNT-A treatment is both an art and a science, with its use in facial sculpting and enhancing, along with dermatologic correction. Intramuscular injections of BoNT-A have also become first-line therapeutic options for a number of disorders characterized by muscular hyperactivity, such as strabismus, blepharospasm, hemifacial spasm, and cervical dystonia. In addition, the ability of BoNT to block acetylcholine release and other neurotransmitters from autonomic nerve endings innervating glandular tissue or smooth muscle has led to its use for hyperhidrosis, migraine prophylaxis, and Raynaud phenomenon. Easy to use, minimally invasive, and well tolerated, BoNT carries an impressive safety record, and there is no doubt its number of indications will continue to grow.

Additional figures available in our eBook (see inside front cover for access code).

REFERENCES

1. Jankovic J, Hallett M, eds. *Therapy with Botulinum Toxin*. New York: Marcel Dekker; 1994.
2. Hexsel D, Brum C, do Prado DZ, et al. Field effect of two commercial preparations of botulinum toxin type A: a prospective, double-blind, randomized clinical trial. *J Am Acad Dermatol*. 2012;67:226–232.
3. Kerscher M, Roll S, Becker A, Wigger-Alberti W. Comparison of the spread of three botulinum toxin type A preparations. *Arch Dermatol Res*. 2012;304:155–161.
4. Hexsel D, Dal'Forno T, Hexsel C, et al. A randomized pilot study comparing the action halos of two commercial preparations of botulinum toxin type A. *Dermatol Surg*. 2008;34:52–59.
5. Wilson AJ, Chang B, Taglienti AJ, et al. A quantitative analysis of onabotulinumtoxinA, abobotulinumtoxinA, and incobotulinumtoxinA: a randomized, double-blind, prospective clinical trial of comparative dynamic strain reduction. *Plast Reconstr Surg*. 2016;137:1424–1433.
6. Thomas AJ, Larson MO, Braden S, et al. Effect of 3 commercially available botulinum toxin neuromodulators on facial synkinesis: a randomized clinical trial. *JAMA Facial Plast Surg*. 2018;20:141–147.
7. Monheit G, Pickett A. Basic science: abobotulinum toxin A. In: Carruthers A, Carruthers J, Dover JS, Alam M, eds. *Procedures in Cosmetic Dermatology: Botulinum Toxin. 3rd ed. New York: Saunders Elsevier*; 201326–34.
8. Nettar KD, Yu KC, Bapna S, et al. An internally controlled, double-blind comparison of the efficacy of onabotulinumtoxinA and abobotulinumtoxinA. *Arch Facial Plast Surg*. 2011;13:380–386.
9. Karsai S, Raulin C. Current evidence on the unit equivalence of different botulinumneurotoxinA formulations and recommendations for clinical practice in dermatology. *Dermatol Surg*. 2009;35:1–8.
10. Sattler G, Callander MJ, Grablowitz D, et al. Noninferiority of incobotulinumtoxinA, free from complexing proteins, compared with another botulinum toxin type A in the treatment of glabellar frown lines. *Dermatol Surg*. 2010;36:2146–2154.
11. Carruthers A, Carruthers J, Coleman 3rd WP, et al. Multicenter, randomized, phase III study of a single dose of incobotulinumtoxinA, free from complexing proteins, in the treatment of glabellar frown lines. *Dermatol Surg*. 2013;39:551–558.
12. Prager W, Bee EK, Havermann I, Zschocke I. Onset, longevity, and patient satisfaction with incobotulinumtoxinA for the treatment of glabellar frown lines: a single-arm, prospective clinical study. *Clin Interv Aging*. 2013;8:449–456.
13. Frevert J, Sattler G. Basic science: xeomin. In: Carruthers A, Carruthers J, Dover JS, Alam M, eds. *Procedures in Cosmetic Dermatology: Botulinum Toxin*. 3rd ed. New York: Saunders Elsevier; 2013:35–42.
14. Carli L, Montecucco C, Rossetto O. Assay of diffusion of different botulinum neurotoxin type A formulations injected in the mouse leg. *Muscle Nerve*. 2009;40:374–380.

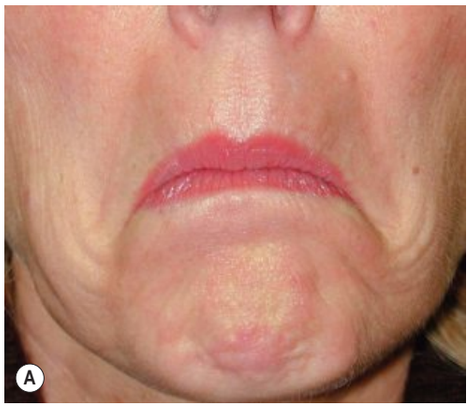
15. Rzany BJ, Ascher B, Avelar RL, et al. A multicenter, randomized, double-blind, placebo-controlled, single-dose, phase III, non-inferiority study comparing prabotulinumtoxinA and onabotulinumtoxinA for the treatment of moderate to severe glabellar lines in adult patients. *Aesthet Surg J*. 2020;40:413–429.
16. Won CH, Lee HM, Lee WS, et al. Efficacy and safety of a novel botulinum toxin type A product for the treatment of moderate to severe glabellar lines: a randomized, double-blind, active-controlled multicenter study. *Dermatol Surg*. 2013;39:171–178.
17. Matarasso SL. Comparison of botulinum toxin types A and B: a bilateral and double-blind randomized evaluation in the treatment of canthal rhytides. *Dermatol Surg*. 2003;29:7–13.
18. Carruthers A, Carruthers J, Flynn TC, Leong MS. Dose-finding, safety, and tolerability study of botulinum toxin type B for the treatment of hyperfunctional glabellar lines. *Dermatol Surg*. 2007;33:S60–S68.
19. Bar-Ilan E, Koren A, Shehadeh W, et al. An enhanced transcutaneous delivery of botulinum toxin for the treatment of Hailey-Hailey disease. *Dermatol Ther*. 2020;33:e13184.
20. Friedman O, Koren A, Niv R, et al. The toxic edge: a novel treatment for refractory erythema and flushing of rosacea. *Lasers Surg Med*. 2019;51:325–331.
21. Junsuwan N, Manuskiatti W, Phothong W, Wanitphakdeedecha R. Fractional CO_2 laser-assisted botulinum toxin type A delivery for the treatment of primary palmar hyperhidrosis. *Lasers Med Sci*. 2021;36:233–236.
22. Waugh JM, Glogau RG. Topical neurotoxin. In: Carruthers A, Carruthers J, Dover JS, Alam M, eds. *Procedures in Cosmetic Dermatology: Botulinum Toxin*. 3rd ed. New York: Saunders Elsevier; 2013:67–71.
23. Brandt F, O'Connell C, Cazzaniga A, Waugh JM. Efficacy and safety evaluation of a novel botulinum toxin topical gel for the treatment of moderate to severe lateral canthal lines. *Dermatol Surg*. 2010;36(Suppl. 4):2111–2118.
24. Glogau R, Blitzer A, Brandt F, et al. Results of a randomized, double-blind, placebo-controlled study to evaluate the efficacy and safety of a botulinum toxin type A topical gel for the treatment of moderate-to-severe lateral canthal lines. *J Drugs Dermatol*. 2012;11:38–45.
25. Clinical trial to evaluate ANT-1207 in participants with primary axillary hyperhidrosis. <https://clinicaltrials.gov/ct2/show/NCT02479139>
26. Bertucci V, Solish N, Kaufman-Janette J, et al. DaxibotulinumtoxinA for injection has a prolonged duration of response in the treatment of glabellar lines: pooled data from two multicenter, randomized, double-blind, placebo-controlled, phase 3 studies (SAKURA 1 and SAKURA 2). *J Am Acad Dermatol*. 2020;82:838–845.
27. Carruthers A, Carruthers J. Eyebrow height after botulinum toxin type A to the glabella. *Dermatol Surg*. 2007;33:S26–S31.
28. Flynn TC, Carruthers JA, Carruthers JA. Botulinum-A toxin treatment of the lower eyelid improves infraorbital rhytides and widens the eye. *Dermatol Surg*. 2001;27:703–708.
29. deMaio M. Facial asymmetries. In: deMaio M, Rzany B, eds. *Botulinum Toxin in Aesthetic Medicine*. Berlin: Springer-Verlag; 2007:93–101.
30. Liew S, Dart A. Nonsurgical reshaping of the lower face. *Aesthet Surg J*. 2008;28:251–257.
31. Carruthers J, Carruthers A. Practical cosmetic Botox techniques. *J Cutan Med Surg*. 1999;3(Suppl. 4):S49–S52.
32. Fagien S. Botox for the treatment of dynamic and hyperkinetic facial lines and furrows: adjunctive use in facial aesthetic surgery. *Plast Reconstr Surg*. 2003;112:40S–52S.
33. Zimbler M, Undavia S. Update on the effect of botulinum toxin pretreatment on laser resurfacing results. *Arch Facial Plast Surg*. 2012;14:156–158.
34. Giordano CN, Matarasso SL, Ozog DM. Injectable and topical neurotoxins in dermatology: indications, adverse events, and controversies. *J Am Acad Dermatol*. 2017;76:1027–1042.
35. Beer KR. Combined treatment for skin rejuvenation and soft-tissue augmentation of the aging face. *J Drugs Dermatol*. 2011;10:125–132.
36. Naumann M, Dressler D, Hallett M, et al. Evidence-based review and assessment of botulinum neurotoxin for the treatment of secretory disorders. *Toxicon*. 2013;67:141–152.
37. Lakraj AA, Moghimi N, Jabbari B. Hyperhidrosis: anatomy, pathophysiology and treatment with emphasis on the role of botulinum toxins. *Toxins (Basel)*. 52013821–840.
38. Nawrocki S, Cha J. The etiology, diagnosis, and management of hyperhidrosis: a comprehensive review: therapeutic options. *J Am Acad Dermatol*. 2019;81:669–680.
39. Heckmann M, Teichmann B, Pause BM, Plewig G. Amelioration of body odor after intracutaneous axillary injection of botulinum toxin A. *Arch Dermatol*. 2003;139:57–59.
40. Talarico-Filho S, Mendonça DO, Nascimento M, et al. A double-blind, randomized, comparative study of two type A botulinum toxins in the treatment of primary axillary hyperhidrosis. *Dermatol Surg*. 2007;33:S44–S50.
41. El Kahky HM, Diab HM, Aly DG, Farag NM. Efficacy of onabotulinum toxin A (Botox) versus abobotulinum toxin A (Dysport) using a conversion factor (1:2.5) in treatment of primary palmar hyperhidrosis. *Dermatol Res Pract*. 2013:686329.
42. Glaser DA, Mattox AR. Focal axillary hyperhidrosis. In: Carruthers A, Carruthers J, Dover JS, Alam M, eds. *Procedures in Cosmetic Dermatology: Botulinum Toxin*. 3rd ed. New York: Saunders Elsevier; 2013:160–168.
43. Lueangarun S, Sermsilp C, Tempark T. Topical botulinum toxin type A liposomal cream for primary axillary hyperhidrosis: a double-blind, randomized, split-site, vehicle-controlled study. *Dermatol Surg*. 2018;44:1094–1101.
44. Mariwalla K, Solish N. Palmo-plantar hyperhidrosis. In: Carruthers A, Carruthers J, Dover JS, Alam M, eds. *Procedures in Cosmetic Dermatology: Botulinum Toxin*. 3rd ed. New York: Saunders Elsevier; 2013:169–174.
45. Levien TL. Advances in the treatment of Raynaud's phenomenon. *Vasc Health Risk Manag*. 2010;6:167–177.
46. Kossintseva I, Barankin B. Improvement in both Raynaud disease and hyperhidrosis in response to botulinum toxin type A treatment. *J Cutan Med Surg*. 2008;12:189–193.
47. Fregene A, Ditmars D, Siddiqui A. Botulinum toxin type A: a treatment option for digital ischemia in patients with Raynaud's phenomenon. *J Hand Surg Am*. 2009;34:446–452.
48. Neumeister MW. Botulinum toxin type A in the treatment of Raynaud's phenomenon. *J Hand Surg Am*. 2010;35:2085–2092.
49. Smith L, Polsky D, Franks Jr. AG. Botulinum toxin-A for the treatment of Raynaud syndrome. *Arch Dermatol*. 2012;148:426–428.
50. Bruloy E, Sinna R, Grolleau JL, et al. Botulinum toxin versus placebo: a meta-analysis of prophylactic treatment for migraine. *Plast Reconstr Surg*. 2019;143:239–250.
51. Wollmer MA, de Boer C, Kalak N, et al. Facing depression with botulinum toxin: a randomized controlled trial. *J Psychiatr Res*. 2012;46:574–581.
52. Finzi E, Rosenthal NE. Treatment of depression with onabotulinumtoxinA: a randomized, double-blind, placebo controlled trial. *J Psych Res*. 2014;52:1–6.
53. Klein AW. Complications, adverse reactions, and insights with the use of botulinum toxin. *Dermatol Surg*. 2003;29:549–556.
54. Karami M, Taheri A, Mansoori P. Treatment of botulinum toxin-induced eyelid ptosis with anticholinesterases. *Dermatol Surg*. 2007;33:1392–1395.
55. Fagien S. Temporary management of upper lid ptosis, lid malposition, and eyelid fissure asymmetry with botulinum toxin type A. *Plast Recons Surg*. 2004;114:1892–1902.
56. Hefter H, Hartmann C, Kahlen U, et al. Prospective analysis of neutralising antibody titres in secondary non-responders under continuous treatment with a botulinumtoxin type A preparation free of complexing proteins–a single cohort 4-year follow-up study. *Br Med J Open*. 2012:2 pii:e000646.
57. Mejia NI, Vuong KD, Jankovic J. Long-term botulinum toxin efficacy, safety, and immunogenicity. *Mov Disord*. 2005;20:592–597.
58. Dressler D. IncobotulinumtoxinA (Xeomin®) can produce antibody-induced therapy failure in a patient pretreated with abobotulinumtoxinA (Dysport®). *J Neural Transm*. 2014;121:769–771.
59. Coté TR, Mohan AK, Polder JA, et al. Botulinum toxin type A injections: adverse events reported to the US Food and Drug Administration in therapeutic and cosmetic cases. *J Am Acad Dermatol*. 2005;53:407–415.
60. Ahbib S, Lachapelle JM, Marot L. Sarcoidal granulomas following injections of botulinum toxin A (Botox) for corrections of wrinkles. *Ann Dermatol Venereol*. 2006;133:43–45.
61. LeWitt PA, Trosch RM. Idiosyncratic adverse reactions to intramuscular botulinum toxin type A injection. *Mov Disord*. 1997;12:1064–1067.
62. Li M, Goldberger BA, Hopkins C. Fatal case of BOTOX-related anaphylaxis? *J Forensic Sci*. 2005;50:169–172.
63. Carruthers J, Carruthers A. Complications of botulinum toxin type A. *Facial Plast Surg Clin North Am*. 2007;15:51–54.
64. Monheit GD, Cohen JL. J Long-term safety of repeated administrations of a new formulation of botulinum toxin type A in the treatment of glabellar lines: interim analysis from an open-label extension study. *J Am Acad Dermatol*. 2009;61:421–425.
65. Carruthers J, Rivkin A, Donofrio L, et al. A multicenter, randomized, double-blind, placebo-controlled study to evaluate the efficacy and safety of repeated onabotulinumtoxinA treatments in subjects with crow's feet lines and glabellar lines. *Dermatol Surg*. 2015;41:702–711.
66. US Food and Drug Administration. Early communication about an ongoing safety review Botox and Botox Cosmetic (botulinum toxin type A) and Myobloc (botulinum toxin type B). *Plast Surg Nurs*. 2008;28:150–151.
67. Kuehn BM. FDA requires black box warnings on labeling for botulinum toxin products. *JAMA*. 2009;301:2316.
68. Brin MF, Boodhoo TI, Pogoda JM, et al. Safety and tolerability of onabotulinumtoxinA in the treatment of facial lines: a meta-analysis of individual patient data from global clinical registration studies in 1678 participants. *J Am Acad Dermatol*. 2009;61:961–970.
69. Oh SH, Lee Y, Seo YJ, et al. The potential effect of botulinum toxin type A on human dermal fibroblasts: an in vitro study. *Dermatol Surg*. 2012;38:1689–1694.
70. Jung JA, Kim BJ, Kim MS, et al. Protective effect of botulinum toxin against ultraviolet-induced skin pigmentation. *Plast Reconstr Surg*. 2019;144:347–356.
71. Shah AR. Use of intradermal botulinum toxin to reduce sebum production and facial pore size. *J Drugs Dermatol*. 2008;7:847–850.
72. Rose AE, Goldberg DJ. Safety and efficacy of intradermal injection of botulinum toxin for the treatment of oily skin. *Dermatol Surg*. 2013;39:443–448.



eFig. 159.1 Crow's feet. Subject with crow's feet before (**A**) and 3 weeks after BoNT-A treatment (**B**).

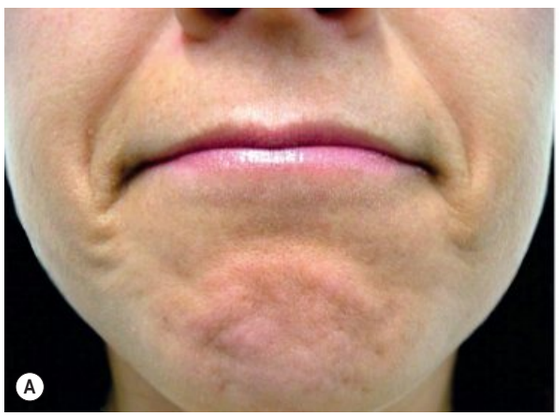


eFig. 159.2 Partial right frontalis paralysis after surgery for removal of a forehead osteoma. Before (**A**, **B**) and 2 weeks after glabellar (**C**, **D**) lateral orbicularis and left frontalis injections.



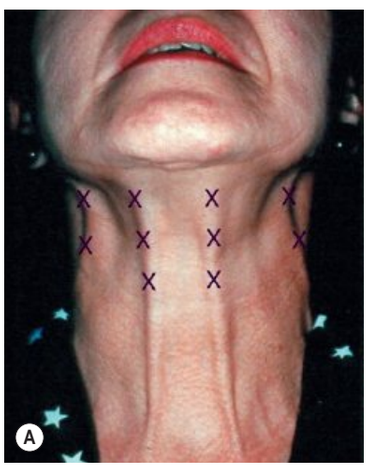


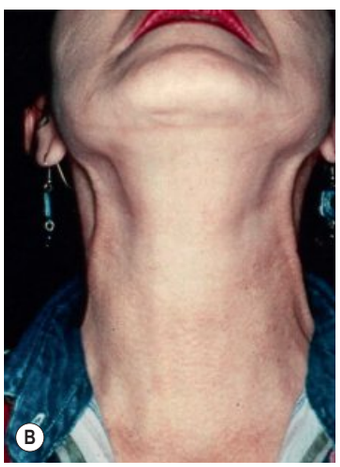
eFig. 159.3 Mouth frown. The subject before (**A**) and after BoNT-A treatment (**B**) of the depressor anguli oris muscle.





eFig. 159.4 Effect of BoNT-A injections for mouth frown. Before (**A**) and after (**B**) BoNT-A treatment. The authors typically inject 2–3 U of onaA into the posterior aspect of the depressor anguli oris muscle and 3 U into each insertion of the mentalis muscle.





eFig. 159.5 Injection sites for platysmal bands. Before (**A**) and after treatment (**B**). Each band is injected in three sites at 1 to 1.5 cm intervals with 3–4 U of BoNT-A (onabotulinumtoxinA) per site. *Courtesy M. Carney, MD.*



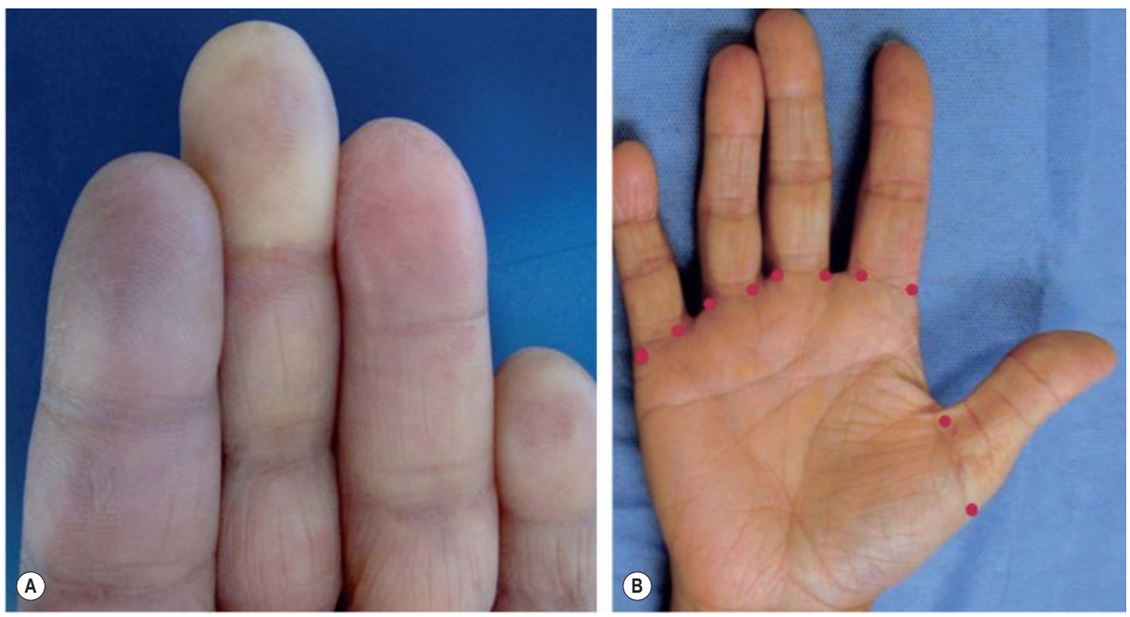
eFig. 159.6 Injection sites for horizontal necklace lines. Aliquots of 1 to 2 U of BoNT-A (onabotulinumtoxinA) are injected into the deep intradermal plane at 2 to 3 cm intervals.



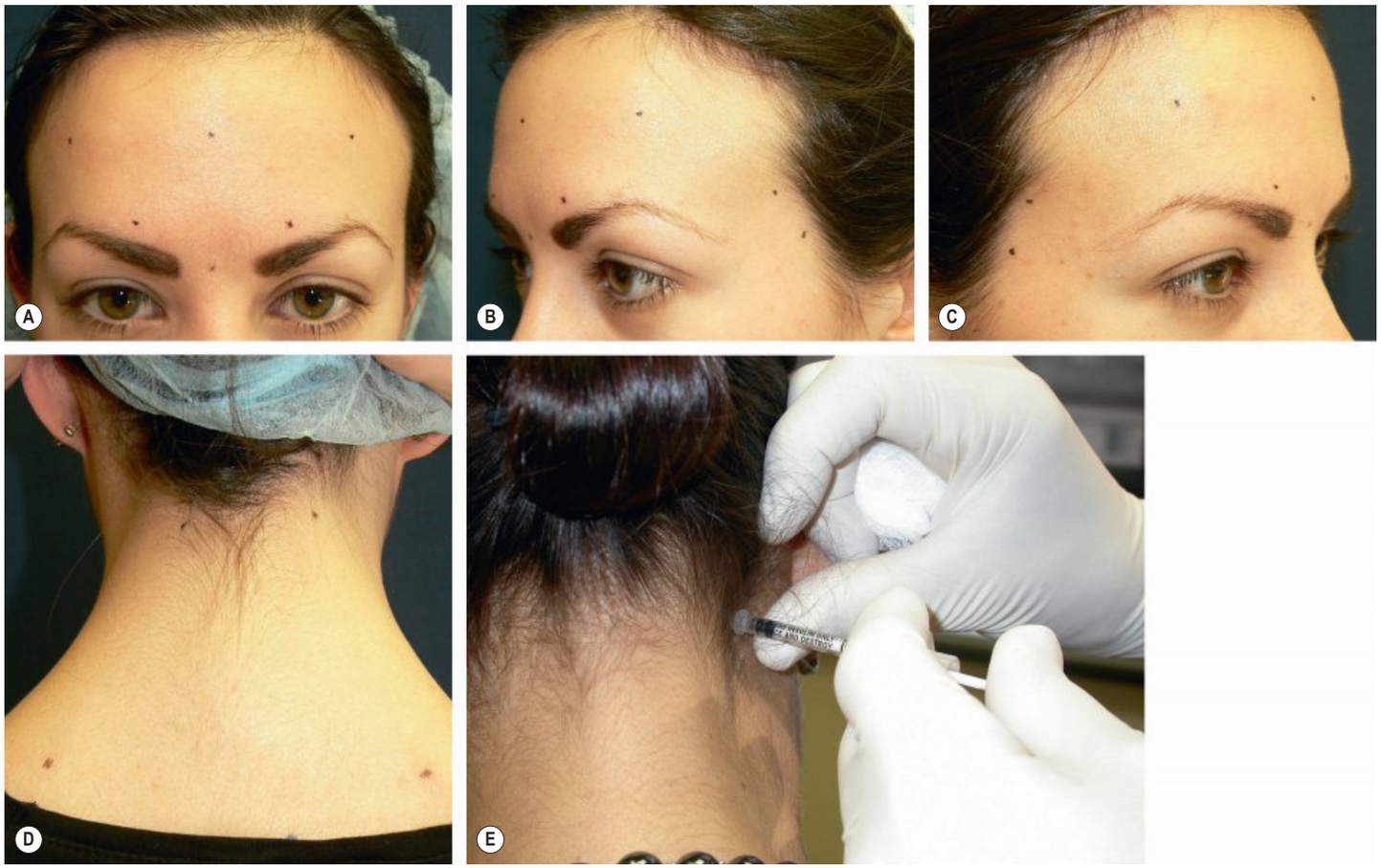
eFig. 159.7 Intense pulsed light plus BoNT-A injections. Subject before (**A**) and after combined therapy (**B**).



eFig. 159.8 Injection sites for palmar hyperhidrosis. The authors inject 100 to 150 U BoNT-A (onabotulinumtoxinA) per hand (depending on size) in approximately 100 injection sites.



eFig. 159.9 Raynaud phenomenon. A Pallor of fingers due to vasoconstriction and interruption of regional vascular flow as well as blue-colored cyanosis corresponding to blood de-oxygenation. **B** Injection of BoNT-A into the bases of the fingers restores normal circulation. Some clinicians do not inject the thumb unless it has significant disease.



eFig. 159.10 A–E Injection sites for migraine. The authors usually inject 100 U BoNT-A (onaA) distributed between the brow, temples, and occipital areas.